P-694

NASA SP-7037 (287)
February 1993

AERONAUTICAL ENGINEERING

1992 CUMULATIVE INDEX

(NASA-SP-7037(287)) AERONAUTICAL ENGINEERING: A CUMULATIVE INDEX TO A CONTINUING BIBLIOGRAPHY (SUPPLEMENT 287) (NASA) 694 p

N93-23038

Unclas

00/01 0157794

NASA STI PROGRAM
SCIENTIFIC & TECHNICAL INFORMATION

SUPPLEMENTS COVERED IN THIS ISSUE

Document	*Page Range*	*Date*	*Coverage*
NASA SP-7037(275)	1-58	February 1992	January 1992
NASA SP-7037(276)	59-168	March 1992	February 1992
NASA SP-7037(277)	169-240	April 1992	March 1992
NASA SP-7037(278)	241-306	May 1992	April 1992
NASA SP-7037(279)	307-418	June 1992	May 1992
NASA SP-7037(280)	419-514	July 1992	June 1992
NASA SP-7037(281)	515-606	August 1992	July 1992
NASA SP-7037(282)	607-698	September 1992	August 1992
NASA SP-7037(283)	699-782	October 1992	September 1992
NASA SP-7037(284)	783-930	November 1992	October 1992
NASA SP-7037(285)	931-1014	December 1992	November 1992
NASA SP-7037(286)	1015-1144	January 1993	December 1992

NASA SP-7037 (287)
February 1993

AERONAUTICAL ENGINEERING

1992 CUMULATIVE INDEX

National Aeronautics and Space Administration
Scientific and Technical Information Program
Washington, DC 1993

This publication was prepared by the NASA Center for AeroSpace Information,
800 Elkridge Landing Road, Linthicum Heights, MD 21090-2934, (301) 621-0390.

INTRODUCTION

WHAT THIS CUMULATIVE INDEX IS

This publication is a cumulative index to the abstracts contained in NASA SP-7037(275) through NASA SP-7037(286) of *Aeronautical Engineering: A Continuing Bibliography.* NASA SP-7037, and its supplements have been compiled through the cooperative efforts of the American Institute of Aeronautics and Astronautics (AIAA), and the National Aeronautics and Space Administration (NASA). Entries prepared by the two contributing organizations are identified as follows:

1. NASA entries by their *STAR* accession numbers (N92-10000).
2. AIAA entries by their *IAA* accession numbers (A92-10000 series).

HOW THIS CUMULATIVE INDEX IS ORGANIZED

This Cumulative Index includes a subject, personal author, corporate source, foreign technology, contract number, report number, and accession number index.

HOW TO USE THE SUBJECT INDEX

Two types of cross-references appear in the subject index:

1. Use (U) references indicate that the subject term is not "postable," i.e., not a valid term, and that the following term or terms are used instead. For example:

   AIRCRAFT PROTUBERANCES
   U PROTUBERANCES
   FLIGHT PERFORMANCE
   U FLIGHT CHARACTERISTICS

2. Narrower Term (NT) references refer the user to more specific headings in the same subject area, under which additional material on the subject may be found. For example:

   FLOW RESISTANCE
   NT AERODYNAMIC DRAG
   NT FRICTION DRAG
   NT SUPERSONIC DRAG

In addition, a searcher may use the title or title and title extension in the index to narrow further his quest for particular items; this is because subject terms may include documents on different aspects of the same subject term. For example:

AIRLINE OPERATIONS
All-weather operations, including pilot role, instrument landing systems and guidance aids.
Airport congestion as constraint on air travel, considering runway capacity and adjusted demand.

HOW TO USE THE PERSONAL AUTHOR INDEX

All personal authors used in the abstract-section citations in the individual Supplements appear in the index. Differences in translation schemes may require multiple searching on the index for variants of an author's name. For example:

EMELIANOV, M. D.
and
YEMELYANOV, M. D.

HOW TO USE THE CORPORATE SOURCE INDEX

The corporate source index entries are abridged versions of the corporate sources used in the abstract-section citations in the individual Supplements. The corporate source supplementary (organizational component) does not appear in the index. For example:

BOEING CO., SEATTLE, WASH. MILITARY AIRCRAFT SYSTEMS DIV. (Source citation entry)
BOEING CO., SEATTLE, WASH. (Source index entry)

PAGE ii INTENTIONALLY BLANK

HOW TO USE THE FOREIGN TECHNOLOGY INDEX

The foreign technology index identifies research performed outside of the United States. Listings in this index are arranged alphabetically by country of intellectual origin. For example:

CHINA, PEOPLE'S REPUBLIC OF

HOW TO USE THE CONTRACT NUMBER INDEX

All contract numbers that are identified in the abstract-section citations in the individual Supplements appear in this index. Changes by agencies in the style in which contract numbers are presented may require multiple searching for variants. For example:

AF 33(615)-71-C-1758
F33615-71-C-1758

HOW TO USE THE REPORT NUMBER INDEX

All report numbers that have been assigned by the corporate source, monitoring agency or cataloging activity appear in this index. Variations in cataloging may result in different report number series. For example:

TP-924
ONERA-TP-924

HOW TO USE THE ACCESSION NUMBER INDEX

All documents that were acquired, indexed, and announced in *STAR* during the year which have been assigned a unique identification number appear in this index. For example:

N92-10001
N92-10002

IDENTIFICATION OF DESIRED SUPPLEMENT

The abstract and descriptive cataloging for any accession number selected from the indexes may be found in the appropriate Supplement. The page-number range of each Supplement appears on the inside front cover of this index. Once the range of page numbers containing the selected accession number is located in the second column, the desired supplement number will be found in the first column. For example:

Page 250 will be found in Supplement 278

AVAILABILITY OF DOCUMENTS

Information concerning the availability of documents announced in *Aeronautical Engineering Supplements* is found in the Introduction to the most currently issued *Supplement*.

FEDERAL DEPOSITORY LIBRARY PROGRAM

In order to provide the general public with greater access to U.S. Government publications, Congress established the Federal Depository Library Program under the Government Printing Office (GPO), with 53 regional depositories responsible for permanent retention of material, inter-library loan, and reference services. At least one copy of nearly every NASA and NASA-sponsored publication, either in printed or microfiche format, is received and retained by the 53 regional depositories. A list of the regional GPO libraries, arranged alphabetically by state, appears on the inside back cover. These libraries are *not* sales outlets. A local library can contact a Regional Depository to help locate specific reports, or direct contact may be made by an individual.

PUBLIC COLLECTIONS OF NASA DOCUMENTS

An extensive collection of NASA and NASA-sponsored publications is maintained by the British Library Lending Division, Boston Spa, Wetherby, Yorkshire, England for public access. The British Library Lending Division also has available many of the non-NASA publications cited in *STAR*. European requesters may purchase facsimile copy or microfiche of NASA and NASA-sponsored documents, those identified by both the symbols # and * from ESA — Information Retrieval Service European Space Agency, 8-10 rue Mario-Nikis, 75738 CEDEX 15, France.

TABLE OF CONTENTS

	Page
Subject Index	A-1
Personal Author Index	B-1
Corporate Source Index	C-1
Foreign Technology Index	D-1
Contract Number Index	E-1
Report Number Index	F-1
Accession Number Index	G-1

AERONAUTICAL ENGINEERING / *A Continuing Bibliography*
1992 Cumulative Index

February 1993

Typical Subject Index Listing

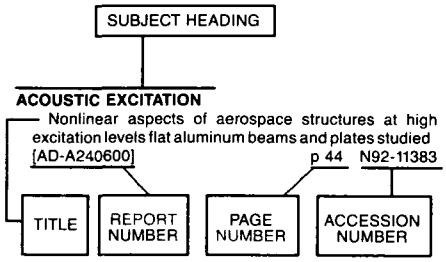

The subject heading is a key to the subject content of the document. The title is used to provide a description of the subject matter. When the title is insufficiently descriptive of document content, a title extension is added, separated from the title by three hyphens. The accession number and the page number are included in each entry to assist the user in locating the abstract in the abstract section. If applicable, a report number is also included as an aid in identifying the document. Under any one subject heading, the accession numbers are arranged in sequence.

A

A-300 AIRCRAFT
Ageing airplane repair assessment program for Airbus A300 p 838 N92-30123
A-310 AIRCRAFT
The TSE 310 troubleshooting expert prototype for the Airbus A-310 commercial aircraft p 307 A92-25180
Comparison of recent results from different wind tunnel facilities along with comparisons of measured flight results and wind tunnel based predictions
[AIAA PAPER 92-3985] p 1060 A92-56809
A-320 AIRCRAFT
New Airbus Industrie airliners on course for long-haul era p 308 A92-26792
Design for validation p 601 A92-33607
British Airways Airbus A320 pilots' autothrust survey
[SAE PAPER 912225] p 636 A92-40023
Utilizing the fault monitoring system for the A320 aircraft p 700 A92-43157
The A320 laminar fin programme
[ONERA, TP NO. 1992-23] p 849 A92-48586
A320 flight control from the pilot's point of view p 1083 A92-56028
Flight simulation and digital flight controls p 884 N92-28526
Preparation for a new plane (A 320): Experience reviewed p 1010 N92-30954
Flight crew integration in the maintenance chain of a commercial aircraft (A 320) p 1012 N92-30957
A-7 AIRCRAFT
Fatigue management for the A-7P p 363 N92-18593
Ground collision avoidance using a variable incidence altitude measurement system for the A-7 aircraft
[AD-A243880] p 352 N92-19259
ABERRATION
Optical design of dual combiner head-up displays p 414 A92-24628
Binary optic-corrected conformal windows for optical seekers
[AIAA PAPER 92-2802] p 779 A92-41340
ABILITIES
Profile of an effective engineering manager
[AD-A246525] p 781 N92-27528
ABLATION
Low-to-high altitude predictions of three-dimensional ablative reentry flowfields
[AIAA PAPER 92-0366] p 394 A92-26227
Stability and inherent precision of two methods for solving motion and ablation equations for fireball-forming bodies in the earth atmosphere p 929 A92-46595
Ablation performance characterization of thermal protection materials using a Mach 4.4 Sled Test
[AIAA PAPER 92-3055] p 893 A92-48713
Aerothermal ablation behavior of selected candidate external insulation materials
[AIAA PAPER 92-3056] p 893 A92-48714
Ablation and temperature sensors for flight measurements in reentry body heat shields p 227 N92-15004
ABLATIVE MATERIALS
Ablative control mechanism in nozzle thermo-protection
[AIAA PAPER 92-3054] p 889 A92-48712
The IRS plasma wind tunnels for the investigation of thermal protection materials for reentry vehicles p 208 N92-15009
Postflight aerothermodynamic analysis of Pegasus(tm) using computational fluid dynamic techniques
[NASA-CR-186017] p 445 N92-21188
ABORT APPARATUS
Evolution of ejection systems --- Russian book p 262 A92-21684
ABRASION
Effects of the abrasiveness of test and training site soils on parachute life
[AD-A252389] p 1038 N92-32900
ABRASION RESISTANCE
Sand erosion behavior of GFRP p 576 A92-32662
ABRASIVES
Precision drilling of ceramic-coated components with abrasive-waterjets
[ASME PAPER 91-GT-232] p 149 A92-15641
ABSORBERS (MATERIALS)
Evaluation of the applicability of Helmholtz resonators for low frequency acoustic liners
[PB92-138544] p 605 N92-23588
ABSORPTIVITY
Improvement in transmission loss of aircraft double wall with resonators p 1011 A92-53091
ABSTRACTS
FAA vertical flight research, engineering, and development bibliography, 1962 - 1991
[FAA/ARD-30] p 462 N92-21210
AC GENERATORS
270-Vdc/hydrid 115-Vac electric power generating system technology demonstrator evolution to a dual-channel, more electric aircraft technology development testbed
[SAE PAPER 912183] p 655 A92-40003
270-Vdc/hybrid 115 Vac electric power generating system technology demonstrator
[SAE PAPER 912051] p 861 A92-45435
ACCELERATED LIFE TESTS
Designing through test
[AIAA PAPER 91-3822] p 232 A92-17664
Transgressions in a pilot-helicopter system p 358 A92-27394
Performance of aluminum honeycomb panels with structural defects and core anomalies. II - Specimen description and test results p 591 A92-36156
Ceramics for engines p 578 N92-22517
In-service evaluation of 2090 aluminum-lithium alloy on F/A-18 aircraft
[AD-A248472] p 986 N92-30321
ACCELERATION
Separation of relaminarised boundary layers
[CUED/A-AERO/TR-16] p 592 N92-22209
ACCELERATION (PHYSICS)
Lift development of delta wings undergoing constant acceleration from rest p 9 A92-13209
Airfoil boundary layer measurements at low Re in an accelerating flow from a nonzero velocity p 62 A92-13673
Experimental results and numerical modeling of solidification during aircraft high-g arcs
[AIAA PAPER 92-0843] p 493 A92-29609
Determination of the mean duration of normal acceleration loads at the center of mass of aircraft during a flight in a turbulent atmosphere p 480 A92-30192
An estimate of the influence of the compressor stability margin on the pick-up time of a turbojet engine p 654 A92-37423
Expansion tube experiments for the investigation of ram-accelerator-related combustion and gasdynamic problems
[AIAA PAPER 92-3246] p 904 A92-48845
Simulation analysis of the influence of variation in some selected design and control parameters on the acceleration time of a turbojet engine p 970 A92-52890
Rotorcraft acceleration and climb performance model
[SCT-90RR-30] p 116 N92-13059
Low-noise oscillators for airborne radar applications
[AD-A242264] p 300 N92-17258
Measurement of derivatives due to acceleration in heave and sideslip p 364 N92-18785
Evaluation of human response to structural vibrations induced by sonic booms
[NASA-CR-189584] p 697 N92-26130
ACCELERATION STRESSES (PHYSIOLOGY)
Two crew stations for dynamic flight simulation p 572 A92-35443
ACCELERATORS
Computational studies of a superdetonative ram accelerator mode p 399 A92-28529
Accelerators and decelerators for large hypersonic aircraft p 665 A92-36952
Theoretical and experimental investigation of the thermodynamics of the thermally choked ram accelerator p 604 N92-22137
ACCELEROMETERS
Coherence multiplexed polarimetric fibre sensor arrays for aerospace applications p 370 A92-27785
Calibration of an aircraft control surface using a tri-axial accelerometer package p 555 A92-35942
Testability of the PAALS auto-align sensor system --- Precision Accelerometer Alignment and Leveling System p 965 A92-49310
Research on measurement and control of helicopter rotor response using blade-mounted accelerometers 1990-91 p 1057 A92-56316
Short time force measurement system p 208 N92-15001
Evaluation of electrolytic tilt sensors for measuring model angle of attack in wind tunnel tests
[NASA-TM-4315] p 297 N92-16283
ACCEPTABILITY
Qualification test report. Fuel pump test stand 3C3965G05
[AD-A242929] p 280 N92-17552
Validation of simulation systems for aircraft acceptance testing p 852 N92-28531
ACCESS CONTROL
A modeling strategy for large-scale optimization based on analysis and visualization principles
[AD-A246570] p 777 N92-26620
ACCESSORIES
An eight month gearbox development program
[AIAA PAPER 92-3368] p 850 A92-48941
ACCIDENT INVESTIGATION
JAS 39 Gripen progress report p 112 A92-16058
ACCIDENT PREVENTION
Requirements for an aircraft mishap analysis system p 16 A92-11170
Manually flown windshear recovery technique p 27 A92-11386
Closing the loop on helicopter crashworthiness design requirements p 107 A92-14392

Management decisions have an impact on flight safety
p 92 A92-15175
Who or what saved the day? A comparison of traditional and glass cockpits p 833 A92-44931
Stop, look and learn from accident investigation
p 834 A92-44996
The effectiveness of training programs for preventing aircrew 'error' p 834 A92-44997
Organizational factors in human factors accident investigation p 834 A92-45000
Human factors and simulation p 951 A92-53236

ACCIDENTS
A report on enhancements for existing and future helicopters supporting operations of the Canadian oil and gas industry
[CTN-91-60126] p 636 N92-25350

ACCOUNTING
MassInfo - An intelligent mass properties information system p 928 A92-47628

ACCUMULATIONS
The effect of hoar-frosted wings on the Fokker 50 take-off characteristics p 451 N92-21692

ACCUMULATORS
Microgravity nucleation and particle coagulation experiments support
[NASA-CR-190159] p 502 N92-21385

ACCURACY
Relative accuracy of wind tunnel calibration speeds
p 484 A92-32056
On the calculation of repeatable accuracy, with special reference to GPS p 955 A92-49383
Mobile Microwave Landing System (MMLS): Operational requirements for setup accuracy
[AD-A241844] p 103 N92-13052
The effect of droplet sizing uncertainty on ice accretions p 679 N92-24874
An adaptive correction technique for Differential Global Positioning System p 726 N92-26623

ACOUSTIC ATTENUATION
Active control of sound transmission through elastic plates using piezoelectric actuators p 53 A92-11052
Inter-noise 90; Proceedings of the International Conference on Noise Control Engineering, Goteborg, Sweden, Aug. 13-15, 1990. Vols. 1 & 2
[ISBN 91-7848-224-0] p 693 A92-39042
Airport noise contours - Converting from NNI to Leq
p 686 A92-39053
Computation of aircraft noise exposure using digitized topography data p 687 A92-39058
Active control of pulsed flow for low frequency noises attenuation p 694 A92-39109
Improvement in transmission loss of aircraft double wall with resonators p 1011 A92-53091
Theoretical models for duct acoustic propagation and radiation p 236 N92-14782
A lightweight loudspeaker for aircraft communications and active noise control p 1125 N92-32964

ACOUSTIC DUCTS
Theoretical and experimental methods in acoustics of ducts and mufflers - A critical review
p 693 A92-39068
Theoretical models for duct acoustic propagation and radiation p 236 N92-14782
Design and performance of duct acoustic treatment
p 236 N92-14783
Experimental validation of a line-duct acoustics model including flow
[NLR-TP-90223-U] p 927 N92-28695

ACOUSTIC EMISSION
Combination of different unsteady quantity measurements for gas turbine blade fault diagnosis
[ASME PAPER 91-GT-201] p 149 A92-15624
Progress towards fiber optic smart structures at UTIAS
p 368 A92-24781
Ultimate strength prediction of ASTM D - 3039 tensile specimens from acoustic emission amplitude data
[AIAA PAPER 92-0258] p 394 A92-25716
Acoustic emission monitoring of a ground durability and damage tolerance test --- for aircraft structures
p 492 A92-28737
Acoustic emission during changes in the aerodynamic load on the surface of a fan blade p 511 A92-30318

ACOUSTIC EXCITATION
Comparative study of fatigue in various materials and designs under sonic loading p 287 A92-21003
Generation of several wave packets in the boundary layer of a wing profile p 424 A92-30136
Investigation on effects on enhancing lift by acoustic excitation p 693 A92-38923
Coupled propeller contributions to aircraft noise and vibration p 694 A92-39085
Propeller sound excitation on an aircraft fuselage using a loudspeaker ring p 643 A92-39087
Effect of acoustic excitation on stalled flows over an airfoil p 703 A92-41267
Suppression of fatigue-inducing cavity acoustic modes in turbofan engines p 925 A92-46809
The engineering prediction for aircraft noise
p 1010 A92-50206
Forcing level effects of internal acoustic excitation on the improvement of airfoil performance
p 1136 A92-56162
Nonlinear aspects of aerospace structures at high excitation levels flat aluminum beams and plates studied
[AD-A240600] p 44 N92-11383
Prediction of response of aircraft panels subjected to acoustic and thermal loads
[NASA-CR-190305] p 678 N92-24345

ACOUSTIC FATIGUE
Fatigue due to noise-induced pressure
[ASME PAPER 91-GT-150] p 148 A92-15588
Suppression of fatigue-inducing cavity acoustic modes in turbofan engines p 925 A92-46809
Sonic fatigue analysis and anti-sonic fatigue design of aircraft structure p 848 A92-47666
Research on sonic fatigue calculation and test for aircraft panel p 958 A92-50203
Acoustic testing at elevated temperatures
p 981 A92-51405
Acoustic fatigue life prediction for nonlinear structures with multiple resonant modes
[NASA-CR-190471] p 1000 N92-30988

ACOUSTIC FREQUENCIES
Numerical methods in elastoacoustics in the nonmodal domain
[ONERA, TP NO. 1991-232] p 415 A92-26383

ACOUSTIC IMPEDANCE
Evaluation of the applicability of Helmholtz resonators for low frequency acoustic liners
[PB92-138544] p 605 N92-23588

ACOUSTIC INSTABILITY
Relationship between the instability waves and noise of high-speed jets p 924 A92-45835

ACOUSTIC MEASUREMENT
Importance of an accurate prediction of shock curvature for high-speed rotor noise p 414 A92-25578
An optical microphone for the detection of hidden helicopters
[AIAA PAPER 92-0377] p 395 A92-26235
Sound transmission through a high-temperature acoustic probe tube p 415 A92-26406
A survey of the broadband shock associated noise prediction methods
[AIAA PAPER 92-0501] p 415 A92-26930
Broadband shock associated noise from supersonic jets measured by a ground observer
[AIAA PAPER 92-0502] p 416 A92-26931
Broadband shock associated noise from supersonic jets measured by a ground observer p 1135 A92-54909
The design of a subsonic low-noise, low-turbulence wind tunnel for acoustic measurements
[AIAA PAPER 92-3883] p 1094 A92-56726
A survey of the broadband shock associated noise prediction methods
[NASA-TM-105365] p 237 N92-14797
Ablation and temperature sensors for flight measurements in reentry body heat shields
p 227 N92-15004
The acoustic flashlight
[MBB-Z-0359-90-PUB] p 239 N92-15938
Human response to helicopter noise: A test of A-weighting
[AD-A243719] p 304 N92-17506
Method and apparatus for acoustic plate mode liquid-solid phase transition detection
[DE92-003778] p 401 N92-18705
A sophisticated, multi-channel data acquisition and processing system for high frequency noise research
[NASA-CR-189137] p 696 N92-24688
Experimental validation of a line-duct acoustics model including flow
[NLR-TP-90223-U] p 927 N92-28695
Lateral spread of sonic boom measurements from US Air Force boomfile flight tests p 1140 N92-33883

ACOUSTIC MICROSCOPES
Characterization of diffusion bonds using an acoustic microscope p 491 A92-28686

ACOUSTIC PROPAGATION
Acoustic isolation of layers p 54 A92-12345
Experimental study of the effects of atmospheric turbulence on sound propagation over the ground
[ONERA, TP NO. 1991-211] p 415 A92-26363
Noise from turbine generators - Noise control, propagation, and assessment p 686 A92-39044
Solutions of acoustic field problems using parallel computers p 925 A92-45929
Basic experiments on the directivity of the sound radiation emitted by a turboshaft engine
[ONERA, TP NO. 1992-36] p 926 A92-48597
Experimental study of noise generation and propagation in a turbofan model p 1136 A92-56169
Aeroacoustics of flight vehicles: Theory and practice. Volume 2: Noise control
[NASA-RP-1258-VOL-2] p 235 N92-14779
Theoretical models for duct acoustic propagation and radiation p 236 N92-14782
Nonlinear acoustic propagation of shock waves through the atmosphere with molecular relaxation
p 511 N92-20360

ACOUSTIC PROPERTIES
Experimental characteristics comparison between two scale-model propellers p 24 A92-10962
Numerical methods in elastoacoustics in the nonmodal domain
[ONERA, TP NO. 1991-232] p 415 A92-26383
A distributed vaporization time-lag model for gas turbine combustor dynamics
[AIAA PAPER 92-3465] p 865 A92-49014
Measurement of acoustic properties of the composite materials constituting the main rotor hub of the Agusta-Westland helicopter EH-101 (civil version)
p 1010 A92-49475
Vibroacoustic simulation of an airplane structure
p 629 N92-24871
Steady-state acoustical noise measurements in aviation systems
[AD-A247831] p 780 N92-27924
Exposures from headset interference tones
[AD-A247175] p 1136 N92-32697

ACOUSTIC RETROFITTING
Silent solutions --- noise suppression for Stage 3 corporate fleets p 970 A92-53120

ACOUSTIC SCATTERING
Sound produced by an aerodynamic source adjacent to a partly coated, finite elastic plate
p 414 A92-25365
Acoustic scattering by a disk or annulus linking two concentric cylindrical shells. I - Theory and results for heavy exterior fluid loading. II - Results for heavy exterior fluid loading on both shells p 696 A92-40588
A numerical study of fuselage scattering effects on rotor noise p 511 N92-20428
Steady state risetimes of shock waves in the atmosphere p 1140 N92-33882

ACOUSTIC SIMULATION
Loudness of shaped sonic booms
p 695 A92-39238
The Dornier 328 Acoustic Test Cell (ATC) for interior noise tests and selected test results
[AIAA PAPER 92-2164] p 1137 N92-32951

ACOUSTICS
Screech noise source structure of a supersonic rectangular jet
[AIAA PAPER 92-0503] p 331 A92-26932
Jet noise classical theory and experiments
p 54 N92-10602
Critical problems of computational aeroacoustics
p 167 N92-13857
Application of analysis techniques for low frequency interior noise and vibration of commercial aircraft
[NASA-CR-189555] p 481 N92-20376
Passive acoustic range estimation of helicopters
[AD-A248033] p 926 N92-28302
Nonlinear analyses of composite aerospace structures in sonic fatigue
[NASA-CR-190565] p 854 N92-30209
NAS (Numerical Aerodynamic Simulation Program) technical summaries, March 1989 - February 1990
[NASA-TM-107960] p 1013 N92-31852

ACQUISITION
When should we start high-rate production of the B-2? An analysis based on flight test results
[RAND/P-7757] p 697 N92-25204

ACRYLIC RESINS
Minimum surface treatments for adhesively bonded repairs p 754 A92-42501

ACTIVATION ANALYSIS
Surface activation of Concorde by Be-7
p 605 N92-23295

ACTIVE CONTROL
Active control of sound transmission through elastic plates using piezoelectric actuators p 53 A92-11052
Experimental active control of a two-dimensional truss
p 47 A92-11346
Experimental demonstration of active vibration control for flexible structures p 50 A92-11442
Alleviation of whirl-flutter on tilt-rotor aircraft using active controls p 133 A92-14423
Active suppression of rotating stall and surge in axial compressors
[ASME PAPER 91-GT-87] p 122 A92-15552
Active control of rotating stall in a low speed axial compressor
[ASME PAPER 91-GT-88] p 122 A92-15553
Active stabilization of multistage axial-compressor aerodynamic system instabilities
[ASME PAPER 91-GT-403] p 76 A92-15733

EH101 helicopter development p 112 A92-16060
Active control for gas turbine combustors p 128 A92-16585
Helicopter air resonance modeling and suppression using active control p 204 A92-18625
A numerical study of secondary fuel injection techniques for active control of combustion instability in a ramjet [AIAA PAPER 92-0777] p 374 A92-27114
A study of active flutter suppression for a wing/store system p 379 A92-27826
Optimal output feedback for linear time-periodic systems p 412 A92-28142
Parameter identification of compressor dynamics during closed-loop operation p 508 A92-29313
Compressor modeling and active control of stall/surge p 508 A92-29315
Active vibration control using fixed order dynamic compensation with frequency shaped cost functionals p 508 A92-29324
Thermal control for hypersonic vehicle propulsion p 468 A92-29356
Model development for active surge control/rotating stall avoidance in aircraft gas turbine engines p 468 A92-29375
An integrated, full-range surge control/rotating stall avoidance compressor control system p 469 A92-29376
Analysis of open loop higher harmonic control at high airspeeds on a modern four-bladed articulated rotor [AIAA PAPER 92-2450] p 542 A92-34477
Vibration reduction in helicopter rotors using an active control surface located on the blade [AIAA PAPER 92-2451] p 564 A92-34478
AIAA Dynamics Specialists Conference, Dallas, TX, Apr. 16, 17, 1992, Technical Papers p 565 A92-35651
A summary of the Active Flexible Wing program [AIAA PAPER 92-2080] p 565 A92-35652
Flutter suppression for the Active Flexible Wing - Control system design and experimental validation [AIAA PAPER 92-2097] p 566 A92-35666
Multifunction tests of a frequency domain based flutter suppression system [AIAA PAPER 92-2096] p 566 A92-35667
Rolling Maneuver Load Alleviation using active controls [AIAA PAPER 92-2099] p 566 A92-35670
Rotary-wing aeroservoelastic problems [AIAA PAPER 92-2107] p 567 A92-35678
A general gust and maneuver load analysis method to account for the effects of active control saturation and nonlinear aerodynamics [AIAA PAPER 92-2126] p 567 A92-35693
Full authority active control system design for a high performance helicopter p 567 A92-35732
Multivariable methods for helicopter flight control law design - A review p 568 A92-35748
Preliminary evaluation of new control laws on the experimental fly-by-wire Dauphin helicopter p 568 A92-35756
Active control of helicopter ground and air resonance p 568 A92-35762
Evaluation of a constant feedback gain for closed loop higher harmonic control p 568 A92-35768
Generalized higher harmonic control - Ten years of Aerospatiale experience p 569 A92-35769
The development and testing of an active control of structural response system for the EH101 helicopter p 569 A92-35775
Eigenstructure assignment for handling qualities in helicopter flight control law design p 570 A92-35786
Active control of the hydraulic forces of a body by a splitter plate p 591 A92-36351
Exploratory design studies of actively controlled wings using integrated multidisciplinary synthesis p 641 A92-36828
Aeroservoelasticity p 642 A92-37577
Theoretical and experimental methods in acoustics of ducts and mufflers - A critical review p 693 A92-39068
A survey of active control in aircraft cabins p 643 A92-39084
Active control of structurally-coupled sound fields generated by localized force inputs p 694 A92-39106
Active control of pulsed flow for low frequency noises attenuation p 694 A92-39109
Active control of airborne noise transmitted through a ribbed panel p 695 A92-39111
NOISE-CON 90; Proceedings of the 10th National Conference on Noise Control Engineering, University of Texas, Austin, Oct. 15-17, 1990 [ISBN 0-931784-21-2] p 695 A92-39226
Active vibration control of smart structural materials p 673 A92-39281
Modern developments in shear flow control with swirl p 703 A92-41265
Gust load alleviation control design for the accuracy of an aeroelastic active control model p 745 A92-43134
ACT wind tunnel experiment on gust load alleviation. II - Wind tunnel test with active support facility p 745 A92-43135
Active control of vortex structures in a separating flow over an airfoil [AIAA PAPER 92-2728] p 804 A92-45563
International Congress on Recent Developments in Air- and Structure-Borne Sound and Vibration, Auburn University, AL, Mar. 6-8, 1990, Proceedings. Vols. 1 & 2 p 924 A92-45876
On-line performance evaluation of multiloop digital control systems p 873 A92-46739
Active control of blade vortex interaction p 814 A92-46944
A new method of helicopter rotor blade motion control p 875 A92-47786
A theoretical study of sensor-actuator schemes for rotating stall control [AIAA PAPER 92-3486] p 878 A92-49025
Development of active control technology for the next generation of combat aircraft p 975 A92-50008
Carefree handling systems for helicopters p 975 A92-50010
Dynamics and control of hypersonic aeropropulsive/aeroelastic vehicles [AIAA PAPER 92-4326] p 1073 A92-55170
ATTAS flight test and simulation results of the advanced gust management system LARS [AIAA PAPER 92-4343] p 1079 A92-55332
Active control of asymmetric vortical flows around cones using injection and heating [AIAA PAPER 92-4426] p 1025 A92-55350
Experimental evaluation of a 50-percent thick airfoil with blowing and suction boundary layer control [AIAA PAPER 92-4500] p 1026 A92-55368
Numerical simulations of flutter and its suppression by active control [AIAA PAPER 92-4652] p 1082 A92-55396
Synthesis of gust load alleviation with flutter margin augmentation p 1082 A92-56021
Optimization of aeroelastic system with active control p 1083 A92-56022
Smart structures in the active control of blade vortex interaction p 1085 A92-56314
Experimental investigation of helicopter coupled rotor/body control p 1086 A92-56318
Analysis of open loop higher harmonic control at high airspeeds on a modern four-bladed articulated rotor [NASA-TM-103876] p 21 N92-11000
The development of a requirement specification for an experimental active flight control system for a variable stability helicopter: An Ada simulation in JSD p 135 N92-12466
Hydraulic actuator system for rotor control p 224 N92-14363
Approximation methods for control of acoustic/structure models with piezoceramic actuators [NASA-CR-189578] p 234 N92-15658
Loading and vibration reduction through active aerodynamic control [AD-A242321] p 283 N92-17243
Experimental validation of structural optimization methods [NASA-TM-104203] p 404 N92-19258
Active control of the flow past a cylinder executing rotary motions p 349 N92-19623
Performance tests of a cryogenic hybrid magnetic bearing for turbopumps [NASA-TM-105627] p 473 N92-20523
Active flow control for twenty-first century high-performance aircraft with applications to land and sea vehicles p 447 N92-21504
Helicopter active rotor control p 570 N92-22157
Dynamic simulation of a solid fuelled gas turbine system p 592 N92-22315
Static aeroelastic analysis of ACT wind tunnel model aircraft [NAL-TM-624] p 632 N92-25366
Vibration tests and structural modeling of an aircraft model for active control technology experiments [NAL-TM-626] p 662 N92-25401
Multifunction tests of a frequency domain based flutter suppression system [NASA-TM-107615] p 662 N92-25607
Low power magnetic bearing design for high speed rotating machinery p 772 N92-27739
An evaluation of some strategies for vibration control of flexible rotors p 773 N92-27800
Self-adaptive aeropropulsion components-enhancing axial compressor performance [AD-A246123] p 743 N92-27817
Integrated Design Analysis and Optimisation of Aircraft Structures [AGARD-LS-186] p 851 N92-28469
The use and effectiveness of piloted simulation in transport aircraft research and development p 886 N92-28549
A summary of the active flexible wing program [NASA-TM-107655] p 962 N92-31264
Rolling maneuver load alleviation using active controls [NASA-TM-107654] p 962 N92-31351
Active control of the separation region on a two-dimensional airfoil [AD-A249739] p 948 N92-31622
Control of unsteady separated flow associated with the dynamic stall of airfoils [NASA-CR-190688] p 950 N92-32177
Active control of sound transmission through stiff lightweight composite fuselage constructions p 1137 N92-32957
Active control of interior noise in a large scale cylinder using piezoelectric actuators p 1137 N92-32958
Active vibrations and noise control for turboprop application research program activities p 1138 N92-32962
Active synchrophasing of propeller unbalance p 1138 N92-32963
A lightweight loudspeaker for aircraft communications and active noise control p 1125 N92-32964
Active control of compressor surge and stall [AD-A252771] p 1126 N92-33498

ACTS

ACTS aeronautical experiments [AIAA PAPER 92-2042] p 485 A92-29956

ACTUATOR DISKS

Current topics connected with rotating stall p 521 A92-35913
On the limitations of Froude's actuator disc concept [ETN-91-90136] p 81 N92-11973
The role of crack growth in defect assessment [PNR-90798] p 501 N92-20909
Powder processing of aero-engine components [PNR-90813] p 756 N92-27044

ACTUATORS

Active control of sound transmission through elastic plates using piezoelectric actuators p 53 A92-11052
Static aeroelastic control using strain actuated adaptive structures p 26 A92-11122
Experimental active control of a two-dimensional truss p 47 A92-11346
Robust stabilization with positive real uncertainty - Beyond the small gain theorem p 50 A92-11444
Fault tolerant control based on a new accommodation filter p 51 A92-11453
Numerical simulation of the actuation system for the ALDF's propulsion control valve --- Aircraft Landing Dynamics Facility p 41 A92-13204
High-performance fighter fly-by-wire flight control actuation system --- for YF-23A prototype [AIAA PAPER 92-1123] p 563 A92-33277
Adaptive response control of wing structures carrying heavy tip weights [AIAA PAPER 92-2527] p 583 A92-34374
A study on the feasibility of using adaptive structures in the attenuation of vibration characteristics of rotary wings [AIAA PAPER 92-2452] p 541 A92-34415
An analytical and experimental investigation of flutter suppression via piezoelectric actuation [AIAA PAPER 92-2106] p 567 A92-35677
Application of a double actuator electronic fuel control unit on a small gas turbine engine [SAE PAPER 912160] p 655 A92-39993
Basic design concepts for smart actuators for aerospace plane control p 752 A92-41193
On the characteristics of servo actuators attached to a model spaceplane for dynamic wind-tunnel test p 762 A92-43213
Fault tolerant EHA architectures --- electro-hydrostatic actuator p 763 A92-43885
Development of the DDV actuation system on the IDF aircraft [SAE PAPER 912080] p 844 A92-45455
Potential for integrated optical circuits in advanced aircraft with fiber optic control and monitoring systems p 856 A92-46246
Simple fly-by-wire actuator p 876 A92-48491
Variable displacement electro-hydrostatic actuator --- for flight control systems p 876 A92-48492
C-141 and C-130 power-by-wire flight control systems p 876 A92-48493
Electric actuation system duty cycles --- in fly-by-wire/power-by-wire control p 877 A92-48494
A theoretical study of sensor-actuator schemes for rotating stall control [AIAA PAPER 92-3486] p 878 A92-49025

An analytical and experimental study to investigate flutter suppression via piezoelectric actuation
[NASA-TM-893240] p 156 N92-12173
Hydraulic actuator system for rotor control
p 224 N92-14363
F/A-18 stabilator: Equivalent set of point forces required for pneumatic bag load case simulation
[AD-A242637] p 206 N92-15073
Approximation methods for control of acoustic/structure models with piezoceramic actuators
[NASA-CR-189578] p 234 N92-15658
Helicopter active rotor control p 570 N92-22157
Active noise control: Piezoceramic actuators in fluid/structure interaction models
[NASA-CR-190328] p 685 N92-26125
Assessment of valve actuator motor rotor degradation by Fourier Analysis of current waveform
[DE92-013233] p 909 N92-28814
Electromechanical systems with transient high power response operating from a resonant AC link
[NASA-TM-105716] p 870 N92-28985
Combined load test apparatus for flat panels
[NASA-CASE-LAR-14698-1] p 911 N92-30028
Nonlinear stability and control study of highly maneuverable high performance aircraft, phase 2
[NASA-CR-190667] p 978 N92-30922
An analytical and experimental investigation of flutter suppression via piezoelectric actuation
[NASA-TM-107653] p 962 N92-31174
Active control of interior noise in a large scale cylinder using piezoelectric actuators p 1137 N92-32958
Active vibrations and noise control for turboprop application research program activities
p 1138 N92-32962
Simulation model of a twin-tail, high performance airplane
[NASA-TM-107601] p 1088 N92-33537

ADA (PROGRAMMING LANGUAGE)
Flight test results of an Ada coded INS/GPS open loop Kalman filter design p 100 A92-16958
Flight test of a GPS-aided low-cost inertial navigation system programmed in Ada p 101 A92-16973
Formal specification and verification of Ada software
[AIAA PAPER 91-3713] p 230 A92-17585
Applications of an automated programming system
[AIAA PAPER 91-3767] p 231 A92-17629
ARINC and the avionics of commercial aircraft. II
p 637 A92-37072
Design and implementation of a generic Kalman filter in Ada p 858 A92-48475
Avionics software reusability observations and recommendations p 921 A92-48502
Process/object-oriented Ada software design for an experimental helicopter p 164 N92-12461
Technical evaluation report on the 52nd Symposium on Software for Guidance and Control
[AGARD-AR-302] p 303 N92-17498
Software Engineering Laboratory (SEL) Ada performance study report
[NASA-TM-105510] p 412 N92-18125
A model of the ADA avionics real-time system: An example of the benefits of the hardware/software codesign approach in development of real-time systems
[AD-A248893] p 967 N92-30524
Development statistics for the UH-1 Ada feasibility study
[AD-A252404] p 982 N92-30547
Experience with Ada on the F-18 High Alpha Research Vehicle Flight Test Program
[NASA-TM-104259] p 1062 N92-34039

ADAPTIVE CONTROL
On-line adaptive control of unstable aircraft wing flutter p 27 A92-11374
New robust adaptive control system using multiple regularization parameters p 51 A92-11455
Application of quantitative feedback theory (QFT) to flight control problems p 27 A92-11499
Identification of aerodynamic coefficients using computational neural networks
[AIAA PAPER 92-0172] p 255 A92-23783
Adaptive simulator motion software with supervisory control p 412 A92-28136
Computational mechanics today p 399 A92-28464
On the adaptive control of missile autopilots
p 477 A92-29102
Robust adaptive nonlinear control of high performance aircraft p 478 A92-29188
A system identification model for adaptive nonlinear control p 508 A92-29248
Real-time simulation and adaptive PID control of QSK-06A control for gas turbine p 470 A92-29740
Robustness of control systems with nonlinear parametric correction for certain types of perturbations
p 509 A92-30311
Effect of adaptive material properties on static aeroelastic control
[AIAA PAPER 92-2526] p 539 A92-34373
Adaptive response control of wing structures carrying heavy tip weights
[AIAA PAPER 92-2527] p 583 A92-34374
Design of adaptive fast-sampling digital controllers for active flutter suppression
[AIAA PAPER 92-2105] p 567 A92-35676
An adaptive flight control for use in connection with helicopter engine failure p 745 A92-43159
Inspection of stability deterioration with an adaptive regulator p 776 A92-43178
Temporal adaptive Euler/Navier-Stokes algorithm involving unstructured dynamic meshes
p 812 A92-46887
Unstructured and adaptive mesh generation for high Reynolds number viscous flows p 816 A92-47042
On multiple grid method p 1006 A92-49585
Stability of an adaptive controller for aircraft. I - Analysis via Liapunov theory p 976 A92-51940
Discrete event fuzzy airport control
p 1046 A92-55973
An approach to the organization of an adaptive man-machine system for flight vehicle control
p 1133 A92-57445
Project of an adaptive multiaxial autopilot with learning pilot control
[ETN-92-90592] p 205 N92-15072
Adaptive control of nonlinear systems with applications to the control of flexible robot arms
[AD-A244409] p 413 N92-19397
Nonlinear stability and control study of highly maneuverable high performance aircraft, phase 2
[NASA-CR-189911] p 382 N92-19841
Aeroelastic behavior of an adaptive lifting surface
p 443 N92-20378
Identification of aerodynamic coefficients using computational neural networks
[AD-A244711] p 447 N92-21753
An evaluation of some strategies for vibration control of flexible rotors p 773 N92-27800
Nonlinear stability and control study of highly maneuverable high performance aircraft, phase 2
[NASA-CR-190667] p 978 N92-30922
A learning enhanced flight control system for high performance aircraft
[AD-A252520] p 1086 N92-32435

ADAPTIVE FILTERS
Evaluation of an adaptive unstructured remeshing technique for integrated fluid-thermal-structural analysis
p 37 A92-10445
Polish radar technology. V - Adaptive MTI filters for uniform and staggered sampling p 40 A92-12293
Adaptive airborne MTI with two-dimensional motion compensation p 102 A92-17240
Adaptive suppression of biodynamic interference in helmet-mounted displays and head teleoperation
p 197 A92-18611
The application of lattice-structure adaptive filters to clutter-suppression for scanning radar
p 403 N92-19154

ADDING CIRCUITS
Repetitive High Energy Pulsed Power (RHEPP) temperature monitoring system utilizing Luxtron fluoroptic sensors and thermocouples technical reference manual
[DE92-013461] p 999 N92-30893

ADDITION RESINS
Vinyl capped addition polyimides
[NASA-CASE-LEW-15027-2] p 579 N92-24053

ADDITIVES
Static tests for the evaluation of fuel additives
[AIAA PAPER 92-0686] p 389 A92-27053
Properties of aircraft fuels and related materials
[AD-A240650] p 35 N92-11213
Levitation of YBa2Cu3O(7-x) superconductor in a variable magnetic field p 771 N92-27735

ADHESION
Adhesive shear strength of impact ice --- inside wind tunnel p 30 A92-11068
Preliminary evaluation of adhesion strength measurement devices for ceramic/titanium matrix composite bonds
[NASA-TM-105803] p 932 N92-31267

ADHESION TESTS
KGR-1 thick adherend specimen evaluation for the determination of adhesive mechanical properties
p 994 A92-51513
Preliminary evaluation of adhesion strength measurement devices for ceramic/titanium matrix composite bonds
[NASA-TM-105803] p 932 N92-31267

ADHESIVE BONDING
Numerical comparison of experimentally measured ultrasound through a multilayered specimen
p 510 A92-28682
Thin bondline measurement of adhesively bonded metallic aircraft structures using an ultrasonic analyzer
p 491 A92-28684
The reinforcing effect of composite patch repairs on metallic aircraft structures p 419 A92-30498
The evolution from bonded F27 aircraft to Arall structures p 699 A92-41177
Minimum surface treatments for adhesively bonded repairs p 754 A92-42501
The evaluation of non-tank surface treatments for aluminium bonding repairs p 761 A92-42502
Stress field sensitivity of a composite patch repair as a result of varying patch thickness p 763 A92-44630
Basic study of adhesive bonding for fiber-composites - Adhesive bonding technologies on jet engine parts
p 764 A92-44733
Non-chromated anodize process for corrosion resistance and adhesive bonding p 892 A92-47341
Use of adhesive bonded attachments for a composite aircraft fuel tank p 785 A92-47414
Characterization of stainless steel pretreatments for adhesive bonding p 994 A92-51546
Preliminary evaluation of adhesion strength measurement devices for ceramic/titanium matrix composite bonds
[NASA-TM-105803] p 932 N92-31267

ADHESIVES
Low VOC primer for structural bonding --- volatile organic compound p 892 A92-47338
KGR-1 thick adherend specimen evaluation for the determination of adhesive mechanical properties
p 994 A92-51513
A damage tolerance assessment of bonded repairs to CF-18 composite components. Part 1: Adhesive properties
[DREP-TM-88-25-PT-1] p 143 N92-12060
Preliminary evaluation of adhesion strength measurement devices for ceramic/titanium matrix composite bonds
[NASA-TM-105803] p 932 N92-31267

ADIABATIC CONDITIONS
A study on the interaction between a bow shock wave generated by a blunt body and a turbulent boundary layer p 8 A92-12424
Theoretical and experimental investigation of the thermodynamics of the thermally choked ram accelerator p 604 N92-22137
Hypersonic flow past radiation-cooled surfaces
[MBB-FE-202-S-PUB-0468-A] p 832 N92-29713

ADIABATIC FLOW
The 3-D Navier-Stokes flow and temperature field computation for a forced mixer nozzle
p 770 N92-27482

ADVECTION
Development of a new flux splitting scheme
p 596 N92-23352
Development of new flux splitting schemes --- computational fluid dynamics algorithms
p 682 N92-25809
Special Course on Unstructured Grid Methods for Advection Dominated Flows
[AGARD-R-787] p 771 N92-27671

AERIAL PHOTOGRAPHY
Automated thematic processing of aircraft scanner data gathered over pasture territory in Turkmenia
p 406 A92-25330
A high resolution multispectral video system
p 587 A92-35479
Computer-Controlled Navigation System/General Positioning System (CCNS/GPS) - A guidance, positioning, and management system for remote sensing flights
p 840 A92-47630
The use of photogrammetry in aviation equipment flight testing p 994 A92-51649

AERIAL RECONNAISSANCE
Reconfigurable Mobile System - Ground, sea and air applications p 218 A92-19986
Aerobureau - Strategic television airmobile reports via satellite p 218 A92-19988
A small light-weight rotor platform for ground observation and pollution control p 1057 A92-56329

AERIAL RUDDERS
Low-speed wind tunnel testing of the lateral control force for the upper rudder surface of a joined-wing airfoil
p 711 A92-43228
Low-speed wind tunnel testing of a joined-wing airfoil
p 711 A92-43229
Design of a fighter aircraft vertical tail enhanced buffet environment survivability p 551 N92-23235

AEROACOUSTICS
Aeroacoustical modification of a propeller
p 24 A92-10961
Prediction of high-resolution flowfields for rotorcraft aeroacoustics p 53 A92-11053

Development of a shock noise prediction code for high-speed helicopters - The subsonically moving shock
p 165 A92-14384
Acoustic predictions using measured pressures from a model rotor in the DNW p 165 A92-14385
Removal of spurious reflections from computational fluid dynamic solutions with the complex cepstrum
p 235 A92-20729
Unsteady aerodynamic methods for turbomachinery aeroelastic and aeroacoustic applications
[AIAA PAPER 92-0011] p 252 A92-23730
Computation of supersonic jet mixing noise for an axisymmetric CD nozzle using k-epsilon turbulence model
[AIAA PAPER 92-0500] p 414 A92-26328
Numerical methods in elastoacoustics in the nonmodal domain
[ONERA, TP NO. 1991-232] p 415 A92-26383
A survey of the broadband shock associated noise prediction methods
[AIAA PAPER 92-0501] p 415 A92-26930
An aeroacoustic model about the rotating stall of a compressor p 416 A92-27855
Transition control of instability waves over an acoustically excited flexible surface p 416 A92-28037
Acoustic characteristics and dynamic structural loading of an ASTOVL aircraft in hover
[AIAA PAPER 92-0370] p 416 A92-28190
Secondary instability mechanisms in compressible, axisymmetric boundary layers
[AIAA PAPER 92-0743] p 343 A92-28224
Investigation of the effect of an ultrasonic acoustic field on boundary layer separation on an airfoil
p 511 A92-30205
Active noise reduction p 603 A92-32980
Theoretical and experimental methods in acoustics of ducts and mufflers - A critical review
p 693 A92-39068
Active control of pulsed flow for low frequency noises attenuation p 694 A92-39109
NOISE-CON 90; Proceedings of the 10th National Conference on Noise Control Engineering, University of Texas, Austin, Oct. 15-17, 1990
[ISBN 0-931784-21-2] p 695 A92-39226
Helicopter far-field acoustic levels as a function of reduced rotor speeds p 695 A92-39228
Loudness of shaped sonic booms
p 695 A92-39238
A review of computational/experimental methodology developments in aeroacoustics p 695 A92-39241
Mixed volume boundary element approach for aerodynamics p 617 A92-39934
Acoustic sources in a tripped flow past a resonator tube p 778 A92-41266
A perspective on helicopter noise p 780 A92-43160
High-speed propeller noise prediction - A multidisciplinary approach p 924 A92-45831
The relationship between mode localization and energy transmission parameters in the vibration of coupled structures p 925 A92-45921
Solutions of acoustic field problems using parallel computers p 925 A92-45929
Research on helicopter rotors - Progress in aerodynamics, aeroelasticity and acoustics
[ONERA, TP NO. 1992-27] p 849 A92-48589
Influence of geometrical parameters on helicopter rotor high speed impulsive noise
[ONERA, TP NO. 1992-40] p 926 A92-48601
Acoustic spinning-mode analysis by iterative threshold method applied to a helicopter turboshaft engine
[ONERA, TP NO. 1992-41] p 926 A92-48602
Research and studies on quiet helicopters
[ONERA, TP NO. 1992-59] p 926 A92-48618
Direct evaluation of aeroacoustic theory in a jet
p 1010 A92-50296
Forcing level effects of internal acoustic excitation on the improvement of airfoil performance
p 1136 A92-56162
Experimental study of noise generation and propagation in a turbofan model p 1136 A92-56169
Design of a variable contraction for a full-scale automotive wind tunnel
[AIAA PAPER 92-3929] p 1096 A92-56760
Aeroacoustics of flight vehicles: Theory and practice. Volume 1: Noise sources
[NASA-RP-1258-VOL-1] p 54 N92-10598
Development of unsteady aerodynamic analyses for turbomachinery aeroelastic and aeroacoustic applications
[NASA-CR-4400] p 12 N92-10979
A comparative analysis of XV-15 tiltrotor hover test data and WOPWOP predictions incorporating the fountain effect
[NASA-CR-189455] p 114 N92-11992
Critical problems of computational aeroacoustics
p 167 N92-13857
Aeroacoustics of flight vehicles: Theory and practice. Volume 2: Noise control
[NASA-RP-1258-VOL-2] p 235 N92-14779
Jet noise suppression p 236 N92-14784
Computation of supersonic jet mixing noise for an axisymmetric CD nozzle using k-epsilon turbulence model
[NASA-TM-105338] p 237 N92-14795
A survey of the broadband shock associated noise prediction methods
[NASA-TM-105365] p 237 N92-14797
Linear acoustics in gas mixtures with rate processes
p 238 N92-15013
Thermoacoustic refrigeration p 595 N92-22720
Experimental study of the mechanism of sound generation by rotating stall in centrifugal turbomachines
p 605 N92-23726
Operational noise data for OH-58D Army helicopters
[AD-A246822] p 926 N92-28292
The design of test-section inserts for higher speed aeroacoustic testing in the Ames 80- by 120-foot wind tunnel
[NASA-TM-103915] p 927 N92-28909
Performance of uncoated AFRSI blankets during multiple Space Shuttle flights
[NASA-TM-103892] p 890 N92-29104
CFD methods development considerations for unsteady aerodynamic analysis
[NASA-TM-107644] p 947 N92-31239
High speed turboprop aeroacoustic study (counterrotation). Volume 2: Computer programs
[NASA-CR-185242] p 1011 N92-31248
Fourth Aircraft Interior Noise Workshop
[NASA-CP-10103] p 1136 N92-32948
Acoustic loads prediction on jet aircraft
p 1136 N92-32949

AEROASSIST
Aeroassist flight experiment heating-rate sensitivity study p 3 A92-10427
Aerobrake aerothermodynamic environment predictions in support of the Aeroassist Flight Experiment
[TABES PAPER 91-278] p 519 A92-34683
Aerobang - A new synergetic plane-change maneuver
[AAS PAPER 91-418] p 753 A92-43356
Thermochemical nonequilibrium flow computations of flow around the aeroassist flight experiment
p 713 A92-44368
Aerodynamic heating on AFE due to nonequilibrium flow with variable entropy at boundary layer edge
p 183 N92-15020
An alternative concept for aeroassisted orbit transfers
[AD-A243409] p 287 N92-17325
Simulation of real-gas effects on pressure distributions for aeroassist flight experiment vehicle and comparison with prediction
[NASA-TP-3157] p 501 N92-20677
Thermal response of rigid and flexible insulations and reflective coating in an aeroconvective heating environment
[NASA-TM-103925] p 852 N92-28721
Stagnation-point heat-transfer rate predictions at aeroassist flight conditions
[NASA-TP-3208] p 1001 N92-31281

AEROBRAKING
Aeroassist flight experiment heating-rate sensitivity study p 3 A92-10427
A ballistic investigation of the aerodynamic characteristics of a blunt vehicle at hypersonic speeds in carbon dioxide and air
[AIAA PAPER 92-0328] p 322 A92-25775
Monte Carlo simulation of entry in the Martian atmosphere
[AIAA PAPER 92-0494] p 329 A92-26324
Plasmadynamic effects in thermochemical nonequilibrium aerobrake flows
[AIAA PAPER 92-0573] p 333 A92-26980
Aerobrake guidance law synthesis using feedback linearization p 485 A92-29304
A six-degree-of-freedom guidance and control analysis of Mars aerocapture
[AIAA PAPER 92-0736] p 486 A92-31676
Computation of near-wake, aerobrake flowfields
p 441 A92-32181
Aerobrake aerothermodynamic environment predictions in support of the Aeroassist Flight Experiment
[TABES PAPER 91-278] p 519 A92-34683
Earth aerobraking strategies for manned return from Mars p 752 A92-41535
Plasmadynamic effects in thermochemical nonequilibrium aerobrake flows p 705 A92-41538
Free-flight trim-angle predictions for the aeroassist flight experiment p 705 A92-41540
A parametric analysis of radiative structure in aerobrake shock layers
[AIAA PAPER 92-2970] p 816 A92-46985
Laminar hypersonic flow over a compression using the HANA code
[AIAA PAPER 92-2896] p 820 A92-47872

AEROCAPTURE
A six-degree-of-freedom guidance and control analysis of Mars aerocapture
[AIAA PAPER 92-0736] p 486 A92-31676

AERODYNAMIC BALANCE
Forward flight trim calculation and frequency response validation of a high-order helicopter simulation model
p 132 A92-14337
Aerodynamic balance range of aircraft of different configurations p 134 A92-16801
Optimization of the aerodynamic balance and parameters of the horizontal tail surfaces of the three-surface aircraft configuration with allowance for the capabilities of the stability and control augmentation system p 134 A92-16803
Force measurement on rotating, ablating models using an air bearing balance p 483 A92-31174
Nonparametric methods of regression analysis in problems related to the processing of aerodynamic balance calibration tests p 602 A92-36417
Periodic trim solutions with hp-version finite elements in time p 874 A92-46931
Computational aspects of helicopter trim analysis and damping levels from Floquet theory p 875 A92-46933
Dual strain gage balance system for measuring light loads
[NASA-CASE-LAR-14419-1] p 42 N92-10185
An experimental analysis of lateral jet injection into confined swirling crossflows p 156 N92-12199
Investigation of the influence of rotary aerodynamics on the study of high angle of attack dynamics of the F-15B using bifurcation analysis
[AD-A243969] p 348 N92-19367
Model rotor icing tests in the NASA. Lewis Icing Research Tunnel p 450 N92-21688
Wind tunnel magnetic Suspension Systems at the University of Southampton, England
p 751 N92-27804
A simulation model of a single rotor helicopter
p 979 N92-31865
Aerodynamic centre of wing-body combinations
[ESDU-92024] p 1036 N92-32479
Computational aspects of helicopter trim analysis and damping levels from Floquet theory
[NASA-CR-190736] p 1087 N92-33107

AERODYNAMIC BRAKES
Aerodynamic heating on AFE due to nonequilibrium flow with variable entropy at boundary layer edge
p 183 N92-15020
Stretched skin concept for the entry aerodynamic decelerator system of planetary probes
p 576 N92-23836

AERODYNAMIC CHARACTERISTICS
An experimental study of subsonic separated flow over parawings p 4 A92-10901
Aerodynamic design of propeller by numerical optimization p 24 A92-10957
Aerodynamic modification of a propeller
p 4 A92-10958
Experimental characteristics comparison between two scale-model propellers p 24 A92-10962
Effect of riblets on turbulence in the wake of an airfoil
p 5 A92-11051
Derivation of aircraft linear state equations from implicit nonlinear equations p 27 A92-11361
Applying mu-synthesis to missile autopilot design
p 28 A92-11564
Comparative analysis of the lift-drag ratio and heat flows toward the surface of wave riders of different configurations p 7 A92-12173
Experimental and theoretical study of the improvement of the aerodynamic characteristics of supersonic flow past bodies with surface injection of a gas jet with particles
p 8 A92-12204
The background and the development of the TAL-WAR (Rose) shape blimp with the articulated thruster
[AIAA PAPER 91-3692] p 17 A92-12749
Flight in a steady wind field p 131 A92-13696
AHS, Annual Forum, 47th, Phoenix, AZ, May 6-8, 1991, Proceedings. Vols. 1 & 2 p 59 A92-14326
LH wind tunnel testing - Key to advanced aerodynamic design p 104 A92-14331
Value of survivability enhancement techniques
p 59 A92-14349
The helicopter air-to-air value-driven engagement model (HAVDEM) - Prototype development
p 105 A92-14353
Aerodynamic design of a Coanda induced force and thruster anti-torque system p 109 A92-14419
Transient aerodynamic behaviours associated with stepwise incidence variation of airfoils
p 66 A92-15327

Investigation of unsteady excitation effects on aerodynamic properties of airfoils p 66 A92-15335
Time-dependent aerodynamic analysis of ducted and unducted propfans at angle of attack
[ASME PAPER 91-GT-190] p 74 A92-15616
Design of a small axial compressor for high efficiency over a wide operating range
[ASME PAPER 91-GT-195] p 124 A92-15620
Propulsion requirements for high altitude long endurance flight
[ASME PAPER 91-GT-393] p 127 A92-15723
Aerodynamic measuring techniques for transonic and supersonic flow in cascades and turbomachines
[ONERA, TP NO. 1991-170] p 137 A92-16135
Changing the structure and improving the aerodynamic characteristics of supersonic flow past bodies through ejection of a gas jet with particles p 78 A92-16680
Flight test of a half-scale unmanned air vehicle
p 193 A92-20208
Incompressible steady aerodynamics using a standard finite element code p 174 A92-20218
Turbulent boundary-layer characteristics over a flat-plate/wedge configuration at Mach 6
p 176 A92-20761
Effects of gas-surface interaction models on aerodynamic characteristics p 244 A92-21718
PAR-WIG performance prediction during acceleration from water-borne to air-borne p 291 A92-21721
Analysis of circular elastic membrane wings
p 245 A92-21722
A computational study on directional stability of chine-shaped forebodies at high-alpha
[AIAA PAPER 92-0030] p 249 A92-22152
Aerodynamic characteristics of a wing near its tip using panel method p 251 A92-22524
Computational aerodynamic simulation on HOPE
p 251 A92-22635
An efficient calculation method of subsonic aerodynamic characteristics for a Space Shuttle orbiter in the reentry attitude p 252 A92-23383
A study of flow past bodies of revolution with a Riabushinskii generatrix p 252 A92-23502
Measurements of lateral aerodynamics characteristics of forebodies at high angle of attack in subsonic and transonic flows
[AIAA PAPER 92-0174] p 255 A92-23785
On one method of constructing adaptive difference grids in aerodynamics problems p 311 A92-24902
End plate interference effects on the aerodynamics of a circular cylinder in uniform flow p 313 A92-25097
Variable-complexity aerodynamic optimization of an HSCT wing using structural wing-weight equations
[AIAA PAPER 92-0212] p 317 A92-25685
Aerodynamic applications of pressure-sensitive paint
[AIAA PAPER 92-0264] p 394 A92-25720
Comprehensive helicopter rotor instrumentation - A retrofit approach using miniature transducers
[AIAA PAPER 92-0268] p 369 A92-25724
Effect of viscous drag on optimum spanwise lift distribution
[AIAA PAPER 92-0287] p 319 A92-25740
Aerodynamic characteristics of a hypersonic viscous optimized waverider at high altitudes
[AIAA PAPER 92-0306] p 320 A92-25755
A ballistic investigation of the aerodynamic characteristics of a blunt vehicle at hypersonic speeds in carbon dioxide and air
[AIAA PAPER 92-0328] p 322 A92-25775
Aerodynamic characteristics of a propeller powered high lift semispan wing
[AIAA PAPER 92-0388] p 323 A92-26244
Computational analysis of high-speed ejection seats
[AIAA PAPER 92-0403] p 324 A92-26256
The effects of blowing on delta wing vortices during dynamic pitching at high angles of attack
[AIAA PAPER 92-0407] p 325 A92-26260
Finite wing aerodynamics with simulated glaze ice
[AIAA PAPER 92-0414] p 325 A92-26265
A fast implicit upwind solution algorithm for three-dimensional unstructured dynamic meshes
[AIAA PAPER 92-0447] p 328 A92-26291
A multibody approach to modeling tilt-wing rotorcraft dynamics
[AIAA PAPER 92-0487] p 328 A92-26318
Aerodynamic computations of high-speed transonic propellers
[ONERA, TP NO. 1991-218] p 330 A92-26370
Elements of airplane performance --- Book
[ISBN 90-6275-608-5] p 357 A92-26550
Theoretical study on the unsteady aerodynamic characteristics of an oscillating cascade with tip clearance (In the case of loaded cascade) p 331 A92-26797
Hover evaluation of an integrated pneumatic lift/reaction-drive rotor system
[AIAA PAPER 92-0630] p 333 A92-27010
Determination of duty factors from experimental data in local interaction theory p 338 A92-27645
An approach to the low-speed longitudinal aerodynamic characteristics of the joined wing configuration
p 339 A92-27909
An experimental investigation of the inlet exit flow field improved by aerodynamic grid p 343 A92-28477
Computational fluid dynamics and aircraft design
p 457 A92-28875
System identification requirements for high-bandwidth rotorcraft flight control system design
p 479 A92-29332
The effect of wing twist optimized in the framework of the plane cross section hypothesis on the aerodynamic characteristics of a wing-body combination at hypersonic speeds p 424 A92-30129
Problems of strength and aeroelasticity of present-day propfans p 471 A92-30133
Calculating the steady-state nonlinear aerodynamic characteristics of thin wings near the interface between two fluids p 426 A92-30181
Analysis of the stability of the lateral motion of aircraft
p 480 A92-30191
The aerodynamic characteristics of grid fin wings
p 427 A92-30201
Aerodynamic characteristics of slender sharp-leading-edge delta wings with air scooping through the air intake at hypersonic velocities. I
p 427 A92-30206
Dynamics of the three-dimensional angular motions of rotating flight vehicles in the presence of the aerodynamic hysteresis of the moment characteristic
p 428 A92-30371
An approximate method for calculating flow past solid wings of small aspect ratio based on a nonlinear theory of a continuous vortex surface p 428 A92-30373
Calculation of the aerodynamic characteristics of bodies of revolution in incompressible flow by the vortex surface method p 428 A92-30375
Low speed aerodynamic performance of a capsule-shaped flying object p 430 A92-30559
Experimental and computational investigation of wind tunnel effects on airfoil flow fields
[AIAA PAPER 92-0672] p 431 A92-30624
CFD state-of-the-art in the U.S.S.R
p 495 A92-31486
Evaluation of the aerodynamic effects of commuter class (type 1-1/2) anti-icing fluids on small general aviation airplanes
[AIAA PAPER 92-0643] p 459 A92-31675
Analytical and experimental studies of the aerodynamic characteristics of a delta wing at a slip angle at high supersonic velocities p 437 A92-31854
Aerodynamic characteristics of a blunt delta wing with air bleed through an intake at supersonic and hypersonic velocities. II p 437 A92-31855
A parametric study of the lift-drag ratio of blunt cones
p 437 A92-31860
Flow past a highly curved wing with tangential jet ejection p 438 A92-31868
The total drag of a body in the flow of a viscous heat-conducting gas p 439 A92-31873
Computational studies of the aerodynamic characteristics of delta wings with a subsonic leading edge p 439 A92-31874
Experimental investigation of the air bypass effect in the shock-wave region on the aerodynamic characteristics of a wing profile p 439 A92-31877
Experimental investigation of the optimal deflection of a single-slotted flap with different degrees of extension on a modern supercritical profile p 439 A92-31879
Aerodynamic characteristics of the combination of a wing with a cambered middle surface with a fuselage
p 439 A92-31880
Some characteristics of transonic flow past an airfoil in the case of developed separation
p 440 A92-31885
Mathematical modeling of nonstationary viscous flow over a solid angle of finite span p 440 A92-31890
Lift characteristics of an infinite-span cylindrical wing of a thick symmetric profile at low subsonic velocities
p 440 A92-31897
Observation and comparison of rainfall measured at a high sample rate p 505 A92-32073
Dynamics of an optimized rotor blade at off-design flight conditions p 461 A92-32250
Low-speed cruise aerodynamics of the stopped rotor/disk rotorcraft concept
[AIAA PAPER 92-1067] p 517 A92-33240
Fully integrated aerodynamic/dynamic optimization of helicopter rotor blades
[AIAA PAPER 92-2374] p 542 A92-34544
A design optimization procedure for high-speed prop-rotors
[AIAA PAPER 92-2375] p 542 A92-34545
EUROFAR airframe aerodynamic design
p 546 A92-35750
Wind tunnel study of aerodynamic characteristics of base combustion p 666 A92-36967
Aerodynamic analysis and modification design of NPU airfoils p 613 A92-38270
The effect of a velocity gradient on the aerodynamic forces of a circular cylinder with tangential blowing
p 614 A92-38859
A calculation of influence of vortex breakdown on aerodynamic characteristics for slender wings
p 616 A92-38920
Some practical aspects of viscous drag reduction concepts
[SAE PAPER 912129] p 618 A92-39976
1991-92 AHS Technical Committee highlights - Aerodynamics p 623 A92-40391
Design of wing profiles with tangential suction or injection p 624 A92-40602
A correlation study of the wing-body interference factor for high angles of attack p 700 A92-41179
Estimation of overall drag coefficient of an aerospace plane p 700 A92-41188
Multi-constraint wing optimization p 701 A92-41197
Prediction of vortex shedding from forebodies with chines p 702 A92-41228
Flow over a twin-tailed aircraft at angle of attack. I - Spatial characteristics p 702 A92-41229
Study on calculating the subsonic and supersonic aerodynamic characteristics of slender wing-body combinations at large angles of attack
p 706 A92-41926
An aerodynamic hypothesis for the wing aeroelasticity problem p 761 A92-42665
Aerodynamics of two-shock bodies derived by the gasdynamic design method p 707 A92-42683
Construction of a wing profile with a flap modeled by a point vortex p 707 A92-42726
Flow of a rarefied gas over a cylinder at angle of sideslip p 708 A92-42738
Gasdynamic design --- Russian book
[ISBN 5-02-029715-1] p 708 A92-42777
A quick automatic method for computing performance of ducted-propeller p 736 A92-42800
Three-dimensional visualizations of the aerodynamic characteristics of delta wings for the transition from subsonic to supersonic leading edges in supersonic-hypersonic flow p 709 A92-43073
Aircraft Symposium, 28th, Tokyo, Japan, Nov. 7-9, 1990, Proceedings p 699 A92-43095
Hypersonic testing technology of HOPE (H-II orbiting plane) p 747 A92-43096
Analysis of the aerodynamic performance of rotors with the boundary element method p 709 A92-43119
The progress of a STOL project p 699 A92-43137
Measurement of magnus derivatives with an elastically forced oscillation rig p 749 A92-43172
Design - Analysis and experimental verification of a propeller working in the low Reynolds number range
p 710 A92-43174
Analysis of the aerodynamic characteristics of a simple remotely piloted research vehicle (RPRV)
p 710 A92-43191
Aerodynamic design of an advanced turboprop using Euler codes p 737 A92-43196
Aerodynamic design tool development for the calculation code of hypersonic flow p 711 A92-43198
The effectiveness of the warp shape airfoil of a supersonic transport p 711 A92-43203
Experimental study of the aerodynamic characteristics at Mach 3 of an air-intake model p 711 A92-43204
Motion estimation for cable-mount dynamic wind-tunnel test p 749 A92-43210
On the characteristics of servo actuators attached to a model spaceplane for dynamic wind-tunnel test
p 762 A92-43213
Aerodynamic characteristics of a hypersonic aircraft
p 711 A92-43226
Effectiveness of aircraft aerodynamic performance on each part of a joined wing p 712 A92-43230
Aerodynamic characteristics of a high-speed composite airfoil p 712 A92-43231
Reevaluation of the motion of an airship
p 731 A92-43243
Aerodynamic characteristics of curved delta wings in the case of subsonic separated flow
p 712 A92-44121
Spaceplane longitudinal aerodynamic parameter estimation by cable-mount dynamic wind-tunnel test
[SAE PAPER 911980] p 788 A92-45385
Experimental studies on aerodynamic characteristics of SSTO vehicle at low subsonic speeds
[SAE PAPER 911981] p 788 A92-45386
Computational aerodynamics - The next generation
[SAE PAPER 911988] p 788 A92-45390

Aerodynamic development of boundary layer control system for NAL QSTOL research aircraft 'ASKA'
[SAE PAPER 912010] p 843 A92-45410
Aerodynamic characteristics near the tip of a finite wing by a panel method
[SAE PAPER 912020] p 790 A92-45413
A calculation of penetration of the jet issuing normally into a cross flow across a wall boundary layer
[SAE PAPER 912029] p 790 A92-45419
Experimental and numerical study of aerodynamic characteristics for second generation SST
[SAE PAPER 912056] p 844 A92-45439
AIAA Applied Aerodynamics Conference, 10th, Palo Alto, CA, June 22-24, 1992, Technical Papers. Pts. 1 & 2
p 791 A92-45476
Rapid synthesis for evaluating missile maneuverability parameters
[AIAA PAPER 92-2615] p 873 A92-45488
Aerodynamic characteristics of hoar frost roughness
p 808 A92-45829
Streamlines, vorticity lines, and vortices around three-dimensional bodies p 808 A92-45845
Comparison of six robustness tests evaluating missile autopilot robustness to uncertain aerodynamics
p 873 A92-46737
Flow over a twin-tailed aircraft at angle of attack. II - Temporal characteristics p 810 A92-46781
Comment on 'Canard-wing interaction in unsteady supersonic flow' p 812 A92-46820
Aerodynamic sensitivities for subsonic lifting-surface
p 819 A92-47695
The A320 laminar fin programme
[ONERA, TP NO. 1992-23] p 849 A92-48586
Aerodynamic performance of a full-scale lifting ejector system in a STOVL fighter aircraft
[AIAA PAPER 92-3094] p 824 A92-48738
Pulse jet one-way valve performance
[AIAA PAPER 92-3169] p 863 A92-48790
On multiple grid method p 1006 A92-49585
Fourier functional analysis for unsteady aerodynamic modeling p 935 A92-50313
An aerodynamical analysis of 'seesaw' type rotor for autogyro p 937 A92-52034
Method of large particles in arbitrary curvilinear orthogonal coordinates for the solution of problems of hydro and aerodynamics p 937 A92-52035
Brownian-motion limited aerodynamic focusing of heavy molecules p 995 A92-52722
Influence of atmospheric rarefaction on aerodynamic characteristics of flying vehicles p 938 A92-52750
Aerodynamic characteristics of a standard corrugated body in a free-molecular flow p 940 A92-52818
Estimation of aerodynamic characteristics from flight-test data. I - Multicollinearity in the equation error method p 960 A92-53007
Maximum likelihood algorithm and its application to parameter identification of closed-loop flight vehicles
p 1008 A92-53023
Calculations for aerodynamic characteristics of HOPE type vehicle in subsonic and hypersonic flow
p 1018 A92-53560
Aerodynamic study of H-II Orbiting Plane, HOPE
p 1103 A92-53639
Aerodynamic airfoils design by quasi-solutions method of inverse boundary-value problems
p 1020 A92-53998
A comparison of the calculated and experimental off-design performance of a radial flow turbine
[AIAA PAPER 92-3069] p 1020 A92-54004
An experimental investigation of the flow in a diffusing S-duct
[AIAA PAPER 92-3622] p 1021 A92-54090
Particle image velocimetry measurements of the aerodynamics of a wind turbine p 1115 A92-54337
An analysis of boundary layer for droplet aerodynamic stripped in high speed gas flow p 1116 A92-54563
Stability, control and gust response characteristics of an ultralight freewing airplane
[AIAA PAPER 92-4342] p 1079 A92-55331
Aerodynamic parameters of the X-31 drop model estimated from flight-data at high angles of attack
[AIAA PAPER 92-4357] p 1080 A92-55343
Parameter identification of AV-8B wingborne aerodynamics for flight simulator model updates
[AIAA PAPER 92-4506] p 1027 A92-55373
Aerodynamic analysis of the Pioneer unmanned air vehicle
[AIAA PAPER 92-4635] p 1027 A92-55382
State-space representation of aerodynamic characteristics of an aircraft at high angels of attack
[AIAA PAPER 92-4651] p 1028 A92-55395
New 1.27-m leg of the National Aerospace Laboratory hypersonic wind tunnel p 1092 A92-56003
Experimental investigation of the boundary layer in a corner formed by two circular arc airfoils
p 1029 A92-56046
Numerical simulation of supersonic unsteady flow using a panel method p 1030 A92-56048
On the effect of canards on NAL spaceplane model (0 order) in low speed area p 1030 A92-56052
Low-speed wind tunnel testing for the high-speed propeller at high shaft angle of attack
p 1030 A92-56054
A physical approach to the estimation of aerodynamic characteristics from flight data p 1030 A92-56058
A low speed wind tunnel investigation of the direct side force control of a joined-wing aircraft with overhanging fin p 1084 A92-56079
Direct simulation of low-density flow over airfoils
p 1030 A92-56159
The achievement of aerodynamic goals on the EH101 project through the 'single site' concept
p 1058 A92-56342
Predicted aerodynamic characteristics for HL-20 lifting-body using the aerodynamic preliminary analysis system (APAS)
[AIAA PAPER 92-3941] p 1033 A92-56771
Description of a pressure measurement technique for obtaining surface static pressures of a radial turbine
[AIAA PAPER 92-4006] p 1123 A92-56829
Numerical simulation of unsteady flow in a hypersonic shock tunnel facility
[AIAA PAPER 92-4029] p 1034 A92-56851
Effect of a simulated glaze ice shape on the aerodynamic performance of a rectangular wing
[AIAA PAPER 92-4042] p 1035 A92-56861
An integrated analytical aeropropulsive/aeroelastic model for the dynamic analysis of hypersonic vehicles
[AIAA PAPER 92-4567] p 1035 A92-57034
Technical evaluation report, AGARD Fluid Dynamics Panel Symposium on Effects of Adverse Weather on Aerodynamics
[NASA-TM-105192] p 2 N92-10002
Subsonic wind tunnel testing handbook
[AD-A240263] p 13 N92-10986
Effect of twin fins on isolated tailplane lift-curve slope
[ESDU-91009] p 80 N92-11969
On simple aerodynamic sensitivity derivatives for use in interdisciplinary optimization
[NASA-TM-104145] p 82 N92-11985
Computer programs for the calculation of dual sting pitch and roll angles required for an articulated sting to obtain angles of attack and sideslip on wind-tunnel models
[NASA-TM-104161] p 138 N92-12007
Wind tunnel investigation of the interaction and breakdown characteristics of slender wing vortices at subsonic, transonic, and supersonic speeds
[NASA-TP-3114] p 82 N92-12994
An experimental investigation of vortex flaps on a canard combat-aircraft configuration p 87 N92-13023
Steady and unsteady aerodynamics of a pitching straked wing model at high angles of attack p 87 N92-13024
Some characteristics and effects of the F/A-18 LEX vortices p 88 N92-13025
Multiple roll attractors of a delta wing at high incidence p 88 N92-13026
An aircraft model for the AIAA controls design challenge
[NASA-CR-186019] p 117 N92-13064
A 3-degree-of-freedom flight simulator evaluation of unsteady aerodynamics effects
[AD-A241540] p 139 N92-13079
Formulation of the linear model from the nonlinear simulation for the F18 HARV p 117 N92-13842
Design of transonic compressor cascades using hodograph method p 202 N92-13973
A fast implicit upwind solution algorithm for three-dimensional unstructured dynamic meshes
[NASA-TM-104186] p 185 N92-15050
Piloted simulation study of a balloon-assisted deployment of an aircraft at high altitude
[NASA-TM-104245] p 272 N92-15986
STS-40 descent BET products: Development and results
[NASA-CR-189570] p 286 N92-16012
Aerodynamic development of the X-31 aircraft for the high angle of attack region
[MBB-FE211-S-PUB-452] p 275 N92-17313
Hi-alpha forebody design. Part 2: Determination of body shapes for positive directional stability
[NASA-CR-189850] p 359 N92-18038
Technical evaluation report on the Fluid Dynamics Panel Specialists' Meeting on Effects of Adverse Weather on Aerodynamics
[AGARD-AR-306] p 352 N92-18242
The Goldstein Engineering Research Laboratory
[AERO-REPT-8906] p 308 N92-18322
X-31 enhancement of aerodynamics for maneuvering beyond stall p 363 N92-18779
Prediction of aerodynamic phenomena limiting aircraft manoeuvrability p 364 N92-18781
Parametric effects of some aircraft components on high-alpha aerodynamic characteristics
p 364 N92-18782
Transformation of flightmechanical design requirements for modern fighters into aerodynamic characteristics
p 365 N92-18794
Experimental investigation into the effects of riblets on compressor cascade performance
[AD-A243881] p 377 N92-19235
Identification of aerodynamic models for maneuvering aircraft
[NASA-CR-190039] p 348 N92-19359
Development of a steady potential solver for use with linearized, unsteady aerodynamic analyses
[NASA-TM-105288] p 473 N92-20525
The status of the US VAWT program
[DE92-002931] p 505 N92-21040
Serrated trailing edges for improving lift and drag characteristics of lifting surfaces
[NASA-CASE-LAR-13870-1-CU] p 463 N92-21587
Multi-colored layers for visualizing aerodynamic flow effects
[NASA-CASE-LAR-13742-1] p 447 N92-21588
The adverse aerodynamic impact of very small leading-edge ice (roughness) buildups on wings and tails
p 451 N92-21691
The effect of hoar-frosted wings on the Fokker 50 take-off characteristics p 451 N92-21692
A summary of NASA research on effects of heavy rain on airfoils p 452 N92-21694
Aerodynamic effects of de/anti-icing fluids and description of a facility and test technique for their assessment p 452 N92-21697
Wind tunnel investigation of the aerodynamic effects of aircraft ground deicing/anti-icing fluids and criteria for aerodynamic acceptance p 452 N92-21698
Identification of aerodynamic coefficients using computational neural networks
[AD-A244711] p 447 N92-21753
Compressing the compressor
[PNR-90824] p 476 N92-21848
The aerodynamics of ship superstructures
p 503 N92-21953
Analytical modeling of SH-2F helicopter shipboard operation p 464 N92-21961
Heat transfer characteristics of hypersonic waveriders with an emphasis on the leading edge effects
[NASA-CR-189586] p 525 N92-22215
First approach to an integrated fin design
p 551 N92-23236
Introduction to Special Course on Engineering Methods in Aerodynamic Analysis and Design of Aircraft
p 552 N92-23951
Configuration development --- preliminary aircraft design p 552 N92-23953
Panel methods for aerodynamic analysis and design
p 552 N92-23955
Aircraft drag analysis methods p 552 N92-23957
An incremental strategy for calculating consistent discrete CFD sensitivity derivatives
[NASA-TM-104207] p 625 N92-24681
Dynamics of aerospace shuttles p 667 N92-24760
VORVISC: A vortex lattice method with viscous and compressibility corrections for full aircraft configurations including propulsion p 626 N92-24857
Wind-tunnel investigation of aerodynamic and stability characteristics of a forward swept wing X-29 model
p 627 N92-24862
Description of a pressure measurement technique for obtaining surface static pressures of a radial turbine
[NASA-TM-105643] p 680 N92-24959
Longitudinal and lateral-directional aerodynamic characteristics of a wing-cone configuration at Mach numbers from 2.5 to 4.5
[NASA-TM-4337] p 630 N92-24977
The natural flow wing-design concept
[NASA-TP-3193] p 631 N92-25202
Assessment of potential aerodynamic benefits from spanwise blowing at the wing tip
[NASA-TM-107847] p 631 N92-25261
Algorithm and code development for unsteady three-dimensional Navier-Stokes equations
[NASA-CR-190077] p 692 N92-25264
A low-speed wind tunnel study of vortex interaction control techniques on a chine-forebody/delta-wing configuration
[NASA-CR-189616] p 632 N92-25510
Navier-Stokes analysis of turbine blade heat transfer and performance p 768 N92-27468
Wind tunnel magnetic Suspension Systems at the University of Southampton, England
p 751 N92-27804
Technical evaluation report on the Flight Mechanics Panel Symposium on Flying Qualities
[AGARD-AR-311] p 733 N92-27870

Computations of unsteady flows around airfoil sections by explicit and implicit methods solving the Euler and Navier-Stokes equations p 720 N92-27948
NPSNET: Flight simulation dynamic modeling using quaternions
[AD-A247484] p 923 N92-28245
Studies in general aviation aerodynamics
[NASA-CR-190431] p 827 N92-28511
Experimental and computational ice shapes and resulting drag increase for a NACA 0012 airfoil
[NASA-TM-105743] p 828 N92-28674
Identification of aerodynamic models for maneuvering aircraft
[NASA-CR-190444] p 852 N92-28720
Explicit Navier-Stokes computation of turbomachinery flows
[AD-A249284] p 909 N92-28879
A comparison of the calculated and experimental off-design performance of a radial flow turbine
[NASA-CR-189207] p 831 N92-29402
Spatial and temporal adaptive procedures for the unsteady aerodynamic analysis of airfoils using unstructured meshes
[NASA-TM-107635] p 831 N92-29445
Computation of three-dimensional effects on two dimensional wings
[NASA-CR-190576] p 832 N92-29691
Influence of structural and aerodynamic modeling on flutter analysis and structural optimization
[AD-A248487] p 978 N92-30323
Joint computational and experimental aerodynamics research on a hypersonic vehicle
[DE92-013439] p 943 N92-30367
Two-dimensional aerodynamic characteristics of several polygon-shaped cross-sectional models applicable to helicopter fuselages
[NASA-TP-3233] p 944 N92-30394
Lewis icing research tunnel test of the aerodynamic effects of aircraft ground deicing/anti-icing fluids
[NASA-TP-3238] p 952 N92-30395
Vortex flow aerodynamics
[AGARD-AR-299] p 946 N92-30947
A demonstration of passive blade twist control using extension-twist coupling
[NASA-TM-107642] p 1001 N92-31155
Extension of the integral equation formulation of linearized time dependent subsonic flow
[AD-A250654] p 947 N92-31171
CFD methods development considerations for unsteady aerodynamic analysis
[NASA-TM-107644] p 947 N92-31239
Wind tunnel aerodynamic characteristics of a transport-type airfoil in a simulated heavy rain environment
[NASA-TP-3184] p 948 N92-31532
A computational examination of directional stability for smooth and chined forebodies at high-alpha
[NASA-CR-4465] p 950 N92-32114
Transonic wind tunnel test of a 14 percent thick oblique wing
[NASA-TM-102230] p 950 N92-32213
Turbine disk cavity aerodynamics and heat transfer
p 1124 N92-32265
A critical evaluation of a three-dimensional Navier-Stokes CFD as a tool to design supersonic turbine stages p 1124 N92-32268
User's manual for AeroFcn: A FORTRAN program to compute aerodynamic parameters
[NASA-TM-104237] p 1133 N92-32507
An examination of several high resolution schemes applied to complex problems in high speed flows
[AD-A250814] p 1124 N92-32632
Effect of afterbody geometry on aerodynamic characteristics of isolated nonaxisymmetric afterbodies at transonic Mach numbers
[NASA-TP-3236] p 1041 N92-33706
Analysis of spacecraft entry into Mars atmosphere
p 1105 N92-33763
Numerical investigation of the effects of icing on fixed and rotary wing aircraft
[NASA-CR-190542] p 1044 N92-34105
Analysis of iced wings
[NASA-TM-105773] p 1042 N92-34144

AERODYNAMIC COEFFICIENTS
Application of nonlinear control strategies to aircraft at high angle of attack p 26 A92-11329
On-line state estimation and parameter identification for flight p 50 A92-11429
Parallel computation of aerodynamic influence coefficients for aeroelastic analysis on a transputer network p 53 A92-12367
Cascade flutter analysis with transient response aerodynamics p 154 A92-15972
Aerodynamic sensitivity analysis methods for the compressible Euler equations p 233 A92-19619
Identification of aerodynamic coefficients using computational neural networks
[AIAA PAPER 92-0172] p 255 A92-23783
Measurements of lateral aerodynamics characteristics of forebodies at high angle of attack in subsonic and transonic flows
[AIAA PAPER 92-0174] p 255 A92-23785
Experimental investigation of the coefficients of the normal-force derivatives for rectangular wings with translational oscillations p 423 A92-30127
Measurement on hypersonic dynamic stable coefficients of a winged vehicle p 430 A92-30550
Free-flight trim-angle predictions for the aeroassist flight experiment p 705 A92-41540
Local bridging to predict aerodynamic coefficients in hypersonic, rarefied flow p 705 A92-41541
Research on state equations of unsteady aerodynamics p 709 A92-43132
Aerodynamic drag as determined from flight test data of the STOL research aircraft Asuka
p 709 A92-43145
Flight simulation of a spaceplane p 752 A92-43190
Wind tunnel tests on the motion of a spaceplane simulation for cable mount p 752 A92-43192
Determination of aerodynamic sensitivity coefficients based on the three-dimensional full potential equation
[AIAA PAPER 92-2670] p 798 A92-45525
LU-SGS implicit scheme for entry vehicle flow computation and comparison with aerodynamic data
[AIAA PAPER 92-2671] p 798 A92-45526
On the aerodynamics/dynamics of store separation from hypersonic aircraft
[AIAA PAPER 92-2722] p 807 A92-45595
Optimum cruise lift coefficient in initial design of jet aircraft p 845 A92-46806
Time domain numerical calculations of unsteady vortical flows about a flat plate airfoil p 936 A92-50473
Approximate aerodynamic analysis for complicated bodies in rarefied gas flows p 938 A92-52754
The relation among the general unsteady aerodynamic coefficients of a wing in subsonic and supersonic speed
p 941 A92-53022
Application of recursive partially unknown system identification to aerodynamic coefficients estimation
[AIAA PAPER 92-4504] p 1081 A92-55371
Measurements of longitudinal static aerodynamic coefficients with cable mount system
p 1093 A92-56013
A physical approach to the estimation of aerodynamic characteristics from flight data p 1030 A92-56058
Millisecond aerodynamic force measurement with side-jet model in the ISL shock tunnel
[AIAA PAPER 92-3963] p 1097 A92-56790
High Reynolds number testing in support of transport airplane development
[AIAA PAPER 92-3982] p 1099 A92-56807
Maximum lift of wings with trailing-edge flaps at low speeds
[ESDU-91014] p 81 N92-11970
Effect of solidity and inclination on propeller-nacelle force coefficients
[NASA-TM-4316] p 90 N92-13038
Formulation of the linear model from the nonlinear simulation for the F18 HARV p 117 N92-13842
A multiblock flow solver for inviscid hypersonic flows
p 181 N92-14986
Applicability of bridging methods to hypersonic rarefied flow aerodynamics of reentry vehicles
p 184 N92-15032
Transitional flows around re-entry bodies
p 184 N92-15035
Computation of aerodynamic coefficients on Hermes-Ariane5 configuration p 184 N92-15040
A method of estimating a flow breakdown boundary for aerofoils and swept wings in transonic flows
[ESDU-91021] p 258 N92-15970
Excrescence drag magnification factors at the drag-rise condition for aerofoils with a specified form of upper-surface pressure distribution
[ESDU-91029] p 259 N92-15973
Dynamic stall on wind turbine blades
[DE92-001157] p 262 N92-17874
An initial investigation into methods of computing transonic aerodynamic sensitivity coefficients
[NASA-CR-190040] p 348 N92-19545
Invariant boundary conditions for cascade flows
p 498 N92-20147
Identification of aerodynamic coefficients using computational neural networks
[AD-A244711] p 447 N92-21753
Wind-tunnel investigation of aerodynamic and stability characteristics of a forward swept wing X-29 model
p 627 N92-24862
Rarefied-flow aerodynamics
[NASA-CR-190452] p 715 N92-27191
Experimental and computational ice shapes and resulting drag increase for a NACA 0012 airfoil
[NASA-TM-105743] p 828 N92-28674
Calculation of support interferences on the aerodynamic coefficients for a wind tunnel calibration model
[ESA-TT-1247] p 830 N92-29159
Determination of aerodynamic sensitivity coefficients for wings in transonic flow
[NASA-CR-190570] p 832 N92-29657
Preliminary subsonic aerodynamic model for simulation studies of the HL-20 lifting body
[NASA-TM-4302] p 978 N92-31175
Lift and rolling moment due to spoilers on wings with trailing-edge flaps deflected at subsonic speeds
[ESDU-92002-SUPPL] p 1037 N92-32782
Further wind tunnel investigation of the SM701 airfoil with aileron and turbulators
[NASA-CR-190702] p 1038 N92-33063
Parametric investigation of single-expansion-ramp nozzles at Mach numbers from 0.60 to 1.20
[NASA-TP-3240] p 1042 N92-34193

AERODYNAMIC CONFIGURATIONS
Control theory for optimum design of aerodynamic shapes p 6 A92-11328
The background and the development of the TAL-WAR (Rose) shape blimp with the articulated thruster
[AIAA PAPER 91-3692] p 17 A92-12749
Design and performance of advanced blading for a high-speed HP compressor
[ASME PAPER 91-GT-374] p 76 A92-15718
Three-dimensional solution-adaptive grid generation on composite configurations p 172 A92-18352
Numerical calculation of subsonic and supersonic aerodynamic loads around complex configuration vehicle
p 175 A92-20488
Navier-Stokes computations for aerodynamic configurations at high angles of attack
p 246 A92-21981
Aerodynamic design and optimization in one shot
[AIAA PAPER 92-0025] p 248 A92-22147
A parametric study of the aeroelastic stability of a binary wing-with-engine nacelle flutter system in incompressible flow p 270 A92-22472
Forebody vortex control p 251 A92-22517
Application of a universe-series code for inviscid flow over complex 3-dimensional configurations
[AIAA PAPER 92-0150] p 253 A92-23765
Application of the multiplier penalty function method to the optimum design of wing configurations of aerospace vehicle p 356 A92-25013
Construction of aerodynamic profiles
p 315 A92-25299
An interactive boundary-layer approach to multielement airfoils at high lift
[AIAA PAPER 92-0404] p 324 A92-26257
Multibody interference at transonic Mach numbers
[AIAA PAPER 92-0651] p 334 A92-27023
Finite element Navier-Stokes solver for unstructured grids p 398 A92-28035
Aerodynamic design optimization using sensitivity analysis and computational fluid dynamics
p 340 A92-28044
Estimation of propulsion-induced effects on transonic flows over a hypersonic configuration
[AIAA PAPER 92-0523] p 341 A92-28197
Aerodynamic wing-nacelle integration
p 458 A92-30134
Combined method for the solution of plane direct problems of flow past bodies with jets
p 427 A92-30200
Numerical computation of compressible flow around an object of complex shape p 429 A92-30517
Study on effectiveness of the front wedge shape in hypersonic flow p 430 A92-30552
Low speed aerodynamic performance of a capsule-shaped flying object p 430 A92-30559
High angle of attack aerodynamics - Subsonic, transonic, and supersonic flows --- Book
[ISBN 0-387-97672-8] p 431 A92-30850
Numerical simulation of three-dimensional supersonic flow around aerodynamic configurations
p 434 A92-31492
An improved PNS scheme for predicting complex three-dimensional hypersonic flows
[AIAA PAPER 92-0753] p 436 A92-31679
Aero-propulsive effects on configuration shaping
[AIAA PAPER 91-5064] p 459 A92-31691
An aerodynamic design study of a series of lifting bodies at angles of attack from 10 to 53 degrees at Mach numbers from 2.30 to 4.62 p 442 A92-32500
An inverse method for the design of transonic wings
[AIAA PAPER 92-1025] p 517 A92-33206
Chaotic and nonlinear dynamic response of aerosurfaces with structural nonlinearities
[AIAA PAPER 92-2547] p 518 A92-34517

Shape optimization of three-dimensional structures with adaptive meshing
[AIAA PAPER 92-2434] p 586 A92-34548
Analysis, development, and integration of the mechanical components of a vehicle powered by photo-voltaic cells
[TABES PAPER 91-503] p 606 A92-34692
Computational fluid dynamics as a tool for aerodynamic analysis of ejection seats p 519 A92-35444
Tail rotor aerodynamic features recorded in flight
p 546 A92-35752
High alpha aerodynamic control by tangential fuselage blowing p 611 A92-36848
An information system for the numerical simulation of 3D Euler flows around aircraft p 613 A92-37554
Recent advances in maneuver loads analysis
p 642 A92-37576
Measurement and analysis of the flow field above a wing/body configuration p 616 A92-38917
Computational analysis of drag reduction techniques for afterbody/nozzle/empennage configurations
[SAE PAPER 912127] p 618 A92-39974
European Fighter Aircraft (EFA) programme status report p 646 A92-40043
Design optimization of natural laminar flow bodies in compressible flow p 701 A92-41219
The design of fully-optimized configurations by using the iterative optimum-optimorum theory --- shape of delta wings of minimum drag p 709 A92-43072
Aerodynamic design of a nonplanar airfoil by an inverse method with Navier-Stokes equations
p 711 A92-43197
Transonic visualization test for the airframe shape improvement of a spaceplane p 752 A92-43200
Experimental study of the aerodynamic characteristics at Mach 3 of an air-intake model p 711 A92-43204
Aerodynamics of lifting configurations --- Russian book
p 712 A92-44125
Recent developments at the Shoeburyness STOVL test facility p 881 A92-45314
An improved approach for the computation of transonic/supersonic flows with applications to aerospace configurations
[AIAA PAPER 92-2613] p 793 A92-45487
The design of a system of codes for industrial calculations of flows around aircraft and other complex aerodynamic configurations
[AIAA PAPER 92-2619] p 917 A92-45492
Aerodynamic shape optimization of hypersonic configurations including viscous effects
[AIAA PAPER 92-2635] p 795 A92-45506
Commercial turbofan engine exhaust nozzle flow analyses using PAB3D
[AIAA PAPER 92-2701] p 801 A92-45543
Predicted pressure distribution on a prop-fan blade through Euler analysis p 810 A92-46791
Numerical simulation of multizone two-dimensional transonic flows using the full Navier-Stokes equations
p 815 A92-46955
Gridding strategies and associated results for winged entry vehicles p 918 A92-47051
An unstructured mesh generation algorithm for three-dimensional aeronautical configurations
p 918 A92-47053
Single block mesh generation for a fuselage plus two lifting surfaces p 817 A92-47054
New concepts for multi-block grid generation for flow domains around complex aerodynamic configurations
p 817 A92-47079
Generation of unstructured grids within a hybrid multi-block environment p 818 A92-47090
Aerodynamic studies on space plane configuration at hypersonic speed p 1019 A92-53641
Current European research activities in helicopter interactional aerodynamics p 1058 A92-56330
Unsteady aerodynamic calculations for general configurations by the double-point method
[NAL-TR-1101T] p 12 N92-10980
Determination of vortex-breakdown criteria by solving the Euler and Navier-Stokes equations
p 87 N92-13018
Vortex control: Further encounters p 87 N92-13020
Technical activities of the configuration aeroelasticity branch
[NASA-TM-104146] p 159 N92-13458
Experiences with optimizing airfoil shapes for maximum lift over drag p 90 N92-13838
Aerodynamic shape optimization of arbitrary hypersonic vehicles p 194 N92-13954
Aerothermodynamics for Space Vehicles
[ESA-SP-318] p 180 N92-14973
Aerothermodynamic configuration of first generation aerospace planes (of Buran-type) and first flight results
p 211 N92-14975
Aerothermodynamic development of the CARINA re-entry vehicle: CFD analyses and experimental tests
p 211 N92-14980
Steps towards an efficient and accurate method solving the Euler equations around a re-entry configuration at super- and hypersonic speed p 181 N92-14987
Interference heating near fin/body junctions on hypersonic vehicles p 182 N92-14996
Computational aerothermodynamic methods for industrial applications to re-entry and hypersonic cruise problems p 227 N92-15027
Aerothermodynamics for United States advanced programs p 184 N92-15039
Computation of aerodynamic coefficients on Hermes-Ariane5 configuration p 184 N92-15040
Grid impact on 3D hypersonic flows
p 184 N92-15041
Evolution and development of hypersonic configurations 1958-1990
[AD-A242768] p 197 N92-15069
CAR 88: A method to calculate subsonic and supersonic, steady and unsteady, potential flow about complex configurations
[NLR-TR-88154-U] p 400 N92-18221
X-31: Discussion of steady state and rotary derivatives
p 365 N92-18789
Analysis of lossy composite terminating structures
[NASA-CR-189901] p 404 N92-19217
Vortex characteristics of C5A/B, C141B and C130E aircraft applicable to ATC terminal flight operations tower fly-by-data
[PB92-114586] p 449 N92-20318
The adverse aerodynamic impact of very small leading-edge ice (roughness) buildups on wings and tails
p 451 N92-21691
The evolution of the bypass engine
[PNR-90832] p 476 N92-21850
Recent developments at the Shoeburyness (England) STOVL Test Facility
[PNR-90806] p 572 N92-22096
PAN AIR: A computer program for predicting subsonic or supersonic linear potential flows about arbitrary configurations using a higher order panel method. Volume 1: Theory document (version 3.0)
[NASA-CR-3251] p 526 N92-22648
PAN AIR: A computer program for predicting subsonic or supersonic linear potential flows about arbitrary configurations using a higher order panel method. Volume 2: User's manual (version 3.0)
[NASA-CR-3252] p 527 N92-22865
NASA aerodynamics program
[NASA-TM-4368] p 609 N92-24678
A study of transonic aerodynamic analysis methods for use with a hypersonic aircraft synthesis code
[NASA-CR-189854] p 625 N92-24803
Longitudinal and lateral-directional aerodynamic characteristics of a wing-cone configuration at Mach numbers from 2.5 to 4.5
[NASA-TM-4337] p 630 N92-24977
High-alpha vortex decoupling investigations on a chine forebody/Delta wing configuration at transonic Mach numbers
[NASA-CR-189642] p 715 N92-26651
Distributed acoustic receptivity in laminar flow control configurations
[NASA-CR-4438] p 765 N92-26680
Application of S1BYL2 to the AGARD WG18 compressor test cases p 768 N92-27452
Transonic wind tunnel investigation of limit cycle oscillations on fighter type wings p 721 N92-27959
Constrained spanload optimization for minimum drag of multi-lifting-surface configurations
[NLR-TP-89126-U] p 828 N92-28660
Aerodynamic design optimization using sensitivity analysis and computational fluid dynamics
[NASA-CASE-LAR-14815-1-CU] p 910 N92-29830
Euler solver for arbitrary configurations: Further applications p 949 N92-31888
A method for designing blended wing-body configurations for low wave drag
[NASA-TP-3261] p 1036 N92-32480
New concepts for multi-block grid generation for flow domains around complex aerodynamic configurations
[NLR-TP-91046-U] p 1037 N92-32730
Investigation of advancing front method for generating unstructured grid
[NASA-CR-190902] p 1128 N92-34043

AERODYNAMIC DRAG

Base pressure on an axisymmetric finned body during forced rotation in the autorotation regime
p 7 A92-12165
Drag balance for hypervelocity impulse facilities
p 207 A92-18375
Flight test of a half-scale unmanned air vehicle
p 193 A92-20208
Inviscid drag prediction for transonic transport wings using a full-potential method p 174 A92-20212
Simulation of GRM drag compensation system --- Geopotential Research Mission p 285 A92-21023
Minimum induced drag of a wing in a circular open wind tunnel p 251 A92-22521
Prediction of drag at subsonic and transonic speeds using Euler methods
[AIAA PAPER 92-0169] p 255 A92-23780
A flight test study to determine aircraft propulsive efficiency and aerodynamic drag using two parameter identification methods and Lock's propeller model
[AIAA PAPER 92-0170] p 271 A92-23781
The use of variable camber to reduce drag, weight and costs of transport aircraft p 313 A92-25096
A turbulence model for iced airfoils and its validation
[AIAA PAPER 92-0417] p 326 A92-26267
Multibody interference at transonic Mach numbers
[AIAA PAPER 92-0651] p 334 A92-27023
Effect of viscosity on the drag of slender axisymmetric bodies in hypersonic flow p 425 A92-30154
The feasibility of reducing induced wing drag by using crescent planform wings p 425 A92-30167
Supersonic and hypersonic boundary-layer transition induced by discrete trips p 522 A92-36023
Computational analysis of drag reduction techniques for afterbody/nozzle/empennage configurations
[SAE PAPER 912127] p 618 A92-39974
Unsteady aerodynamic loading produced by a sinusoidally oscillating delta wing p 701 A92-41223
Accurate prediction of drag using Euler methods
p 703 A92-41246
Minimum-drag bodies moving in locality-law media
p 779 A92-42732
Aerodynamic drag of a cylinder in two-phase flow
p 707 A92-42735
The design of fully-optimized configurations by using the iterative optimum-optimorum theory --- shape of delta wings of minimum drag p 709 A92-43072
Low density heat transfer phenomena
[AIAA PAPER 92-2899] p 820 A92-47875
Estimation of lift and drag characteristics of an aircraft from flight data p 959 A92-51942
Non-slender shapes of minimum drag
p 937 A92-52029
An aerodynamical analysis of 'seesaw' type rotor for autogyro p 937 A92-52034
Remarks on the relation between lift induced drag and vortex drag p 941 A92-53079
Drag computation by vortex methods
p 1031 A92-56161
Resolution of Navier-Stokes equations around profiles: Drag evolution
[ONERA-RTS-86/1685-AY-156A] p 43 N92-11310
Aerodynamic shape optimization of arbitrary hypersonic vehicles p 194 N92-13954
The effects of winglets on low aspect ratio wings at supersonic Mach numbers
[NASA-CR-4407] p 178 N92-13996
A unified viscous theory of lift and drag of 2-D thin airfoils and 3-D thin wings
[NASA-CR-4414] p 178 N92-13997
A turbulence model for iced airfoils and its validation
[NASA-TM-105373] p 186 N92-15052
Trim drag reduction concepts for horizontal takeoff single-stage-to-Orbit vehicles
[NASA-TM-102687] p 206 N92-15076
Experiments and analysis concerning the use of external burning to reduce aerospace vehicle transonic drag
[NASA-TM-105397] p 279 N92-17546
Dynamic stall on wind turbine blades
[DE92-001157] p 262 N92-17874
An experimental study of a sting-mounted circulation control wing
[AD-A243912] p 346 N92-18895
Notes on the cause of parachute critical velocity
[AD-A244417] p 347 N92-19085
Dynamical systems analysis of an aerodynamic decelerator's behavior during the initial opening process
[AD-A244194] p 348 N92-19394
Evaluation of NACA0012 airfoil test results in the NAL two-dimensional transonic wind tunnel
[NAL-TR-1109T] p 445 N92-21287
Serrated trailing edges for improving lift and drag characteristics of lifting surfaces
[NASA-CASE-LAR-13870-1-CU] p 463 N92-21587
Experimental investigation of heavy rainfall effect on a 2-D high lift airfoil p 452 N92-21696
Aircraft drag analysis methods p 552 N92-23957
A study of transonic aerodynamic analysis methods for use with a hypersonic aircraft synthesis code
[NASA-CR-189854] p 625 N92-24803
Performance degradation due to hoar frost on lifting surfaces p 628 N92-24866

An experimental investigation of the surface flow and wake dynamics associated with transverse flow over wavy cylinders p 681 N92-25547
Reynolds number dependence of the drag coefficient for laminar flow through fine-scale screens
[DE92-002930] p 765 N92-26698
Aerodynamic drag on the bullet trains
p 766 N92-26911
Flow around an isolated surface roughness in the laminar boundary layer p 766 N92-26913
Application of riblet surface to pipe flow
p 766 N92-26915
Special Course on Skin Friction Drag Reduction
[AGARD-R-786] p 717 N92-27706
Basic concepts on boundary layers
p 717 N92-27707
Drag reduction: An industrial challenge
p 717 N92-27708
Aircraft drag reduction p 717 N92-27709
Boundary layer transition: Prediction, application to drag reduction p 717 N92-27711
Turbulent skin-friction drag reduction by active and passive means, part 1 p 718 N92-27714
Experimental and computational ice shapes and resulting drag increase for a NACA 0012 airfoil
[NASA-TM-105743] p 828 N92-28674
Methods for direct simulation of transition in hypersonic boundary layers 2 p 912 N92-30064
High Reynolds number test of the Boeing TR77 airfoil in the Langley 0.3-meter transonic cryogenic tunnel
[NASA-TM-4189] p 947 N92-31246
Further wind tunnel investigation of the SM701 airfoil with aileron and turbulators
[NASA-CR-190702] p 1038 N92-33063
Applications of a direct/iterative design method to complex transonic configurations
[NASA-TP-3234] p 1039 N92-33484
Analysis of the flight performance of the 155 mm M864 base burn projectile
[BRL-TR-3083] p 1041 N92-33699
Parametric investigation of single-expansion-ramp nozzles at Mach numbers from 0.60 to 1.20
[NASA-TP-3240] p 1042 N92-34193
Method of reducing drag in aerodynamic systems
[NASA-CASE-LEW-14791-1] p 1043 N92-34243

AERODYNAMIC FORCES

Nonstationary forces on a wing airfoil
p 4 A92-10825
Vibration of a wing of finite span in subsonic flow at small distances from a solid boundary p 9 A92-12808
Blade defect force investigation in a compressor cascade p 10 A92-13233
Step response of unsteady aerodynamics acting on a plane swept wing in incompressible flow for finite state modeling p 63 A92-14031
Dynamic response of a variable-speed rotor during rapid shaft tilt p 132 A92-14400
Prediction of generalized aerodynamic forces following linearized supersonic theory
[ONERA, TP NO. 1991-114] p 76 A92-16093
Aerodynamic damping of blade vibrations in turbomachines --- Russian book p 200 A92-18198
Application of aeroservoelastic modeling using minimum-state unsteady aerodynamic approximations
p 204 A92-18622
Use of neural networks in control of high alpha maneuvers
[AIAA PAPER 92-0048] p 282 A92-22164
Compressor blade row unsteady aerodynamic response to attached and separated flow forcing functions
[AIAA PAPER 92-0147] p 253 A92-23763
Approach to side force alleviation through modification of the pointed forebody geometry p 309 A92-24418
On the prediction of unsteady forces on gas turbine blades. I - Description of the approach. II - Analysis of the results p 311 A92-24724
Experimental studies of a two-element airfoil with large separation
[AIAA PAPER 92-0267] p 317 A92-25723
Aerodynamic characteristics of a hypersonic viscous optimized waverider at high altitudes
[AIAA PAPER 92-0306] p 320 A92-25755
Theoretical study on the unsteady aerodynamic characteristics of an oscillating cascade with tip clearance (In the case of loaded cascade) p 331 A92-26797
Obtaining the velocity field required for the calculation of propeller unsteady forces using 'traditional' approximate methods and CFD
[AIAA PAPER 92-0520] p 331 A92-26945
A numerical method for analyzing the nonlinear flutter of wings at high angles of attack p 338 A92-27827
The mean power of forces and moments in unsteady aerodynamics p 421 A92-28949
Dynamic stability of elastic vehicles with unsteady aerodynamic force modeling p 509 A92-29326
A pressure-drag-determination method for aerodynamic-interference problems p 425 A92-30157
Aerodynamic effect of compression shocks on an oscillating aileron in transonic flow p 440 A92-31898
Time simulation of flutter with large stiffness changes
[AIAA PAPER 92-2394] p 585 A92-34467
Extending a transonic small disturbance code to treat swept vertical surfaces
[AIAA PAPER 92-2503] p 518 A92-34498
An analytical evaluation of the aerodynamic forces acting on a circular cylinder in a uniform shear flow
p 522 A92-35995
Active control of the hydraulic forces of a body by a splitter plate p 591 A92-36351
A note on the Kutta condition in Glauert's solution of the thin aerofoil problem p 613 A92-37933
The effect of a velocity gradient on the aerodynamic forces of a circular cylinder with tangential blowing
p 614 A92-38859
Delay of wing vortex bursting by using favorable interaction of vortices p 615 A92-38910
Numerical simulation of separation flow on bodies of revolution at high angle of attack using Euler equations
p 616 A92-38919
A method for determining the internal force characteristics of a model in external supersonic flow
p 706 A92-42682
Spectrogram diagnosis of aircraft disasters
[SAE PAPER 912041] p 836 A92-45425
Joint computational/experimental aerodynamics research on a hypersonic vehicle. I - Experimental results p 812 A92-46890
Joint computational/experimental aerodynamics research on hypersonic vehicle. II - Computational results p 812 A92-46891
Stability and dynamic coupling of elastic vehicles with unsteady aerodynamic forces considered
p 1102 A92-53545
Experimental investigation of the stability of a clearance-excited rotor system with optimal parameters
p 1114 A92-54223
ATTAS flight test and simulation results of the advanced gust management system LARS
[AIAA PAPER 92-4343] p 1079 A92-55332
Parameter identification of unsteady aerodynamic forces for elastic vehicles
[AIAA PAPER 92-4505] p 1027 A92-55372
State-space representation of aerodynamic characteristics of an aircraft at high angels of attack
[AIAA PAPER 92-4651] p 1028 A92-55395
Calculations of aerodynamic forces on a wing with thrust using B.E.M p 1030 A92-56049
Millisecond aerodynamic force measurement with side-jet model in the ISL shock tunnel
[AIAA PAPER 92-3963] p 1097 A92-56790
Susceptibility of a parallelogram type skin friction balance to rotational motion
[AD-A241348] p 139 N92-13078
Dynamic characteristics and stability analysis of space shuttle main engine oxygen pump p 224 N92-14366
Short time force measurement system
p 208 N92-15001
Experimental ice shape and performance characteristics for a multi-element airfoil in the NASA Lewis Icing Research Tunnel
[NASA-TM-105380] p 261 N92-17347
Dynamic wind tunnel tests on control of forebody vortices with suction p 380 N92-18793
Aeroservoelastic stability of aircraft at high incidence
p 381 N92-18795
Investigation of the influence of rotary aerodynamics on the study of high angle of attack dynamics of the F-15B using bifurcation analysis
[AD-A243969] p 348 N92-19367
A study in dynamic control of a super maneuver with neural networks p 463 N92-21510
Aerodynamic interference between stores
[AD-A247207] p 715 N92-27172
Propulsion simulator for magnetically suspended wind tunnel models p 750 N92-27801
Wind tunnel magnetic Suspension Systems at the University of Southampton, England
p 751 N92-27804
Unsteady transonic aerodynamics of pointed bodies of revolution in supersonic freestream p 719 N92-27946
Direct coupling of fluid structure in transonic aeroelasticity p 721 N92-27954
Numerical simulation of shock-stall flutter of an airfoil using the Navier-Stokes equations p 746 N92-27956
Time simulation of flutter with large stiffness changes
[NASA-TM-107650] p 963 N92-32111

AERODYNAMIC HEAT TRANSFER

Recombination-dominated nonequilibrium heat transfer to arbitrarily catalytic hypersonic vehicles
p 2 A92-10426
Aeroassist flight experiment heating-rate sensitivity study p 3 A92-10427
Experimental and theoretical study of the improvement of the aerodynamic characteristics of supersonic flow past bodies with surface injection of a gas jet with particles
p 8 A92-12204
Heat transfer in supersonic flow past a single crater
p 63 A92-13741
Calculation of the base pressure and enthalpy behind a step in the path of two supersonic streams with allowance for the effect of boundary layers and heat fluxes
p 63 A92-13748
Engineering method for calculating surface pressures and heating rates on vehicles with embedded shocks
[AIAA PAPER 91-5060] p 171 A92-17842
Numerical simulation of total temperature separation in jets
[AIAA PAPER 92-0535] p 396 A92-26952
Calculation of heat transfer and friction for a blunt body in the path of supersonic flow of a chemically equilibrium air-xenon mixture p 336 A92-27532
Radiant heat transfer in supersonic three-dimensional and axisymmetric flow of air past evaporating bodies
p 337 A92-27533
Calculation of three-dimensional flow past blunt cones near the plane of symmetry for different flow regimes in the shock layer and in the presence of gas injection from the surface p 337 A92-27593
Three-dimensional buoyancy-induced flow and heat transfer around the wheel outboard of an aircraft
p 397 A92-27773
A computational study of flow past bodies and heat transfer for isentropic compression flows
p 425 A92-30158
Numerical study of coupled heat transfer under conditions of filtering and film cooling of blunt anisotropic bodies p 610 A92-36552
Similarity and resistance in near-sonic flows for given heat conduction p 708 A92-43065
Heat transfer to a delta wing and two waverider wings in rarefied hypersonic flow p 937 A92-52748
Force and heat transfer on a disc in rarefied flow
p 939 A92-52764
Effect of porosity in transpiration cooling system
p 1112 A92-53786
Quantitative heat transfer measurements in hypersonic wind tunnels by means of infrared thermography
p 1115 A92-54321
Interference heating near fin/body junctions on hypersonic vehicles p 182 N92-14996
Infrared measurements of aerodynamic heating in hypersonic wind tunnel p 208 N92-15002
Heat transfer measurements in ONERA supersonic and hypersonic wind tunnels using passive and active infrared thermography p 208 N92-15003

AERODYNAMIC HEATING

Fundamentals of applied aerogasdynamics. II - Viscous flow past bodies. Control devices --- Russian book
p 64 A92-14281
Effect of nose shape on three-dimensional stagnation region streamlines and heating rates
[AIAA PAPER 91-5032] p 171 A92-17822
Analysis of cooling systems for hypersonic aircraft
[AIAA PAPER 91-5063] p 216 A92-17843
Three-dimensional thermal structural analysis of a swept cowl leading edge subjected to skewed shock-shock interference heating p 174 A92-20306
Application of the LAURA code for slender-vehicle aerothermodynamics p 310 A92-24652
An engineering aerodynamic heating method for hypersonic flow
[AIAA PAPER 92-0499] p 329 A92-26327
Approximate analysis of aerodynamic heating at hypersonic speed p 430 A92-30551
Thermal protection analysis of Mars-earth return vehicles p 497 A92-32183
Comparison of heating calculations with experimental data on a modified Shuttle Orbiter p 441 A92-32184
Axial compression corner flow with shock impingement p 441 A92-32196
Earth atmospheric entry studies for manned Mars missions p 442 A92-32251
Structural tailoring/analysis for hypersonic components - Executive system development
[AIAA PAPER 92-2471] p 583 A92-34360
Thermoviscoplastic analysis of engine cowl leading edge subjected to oscillating shock-shock interaction
[AIAA PAPER 92-2537] p 583 A92-34381
Thermoviscoplastic response of thin plates subjected to intense local heating
[AIAA PAPER 92-2538] p 584 A92-34382
Nonlinear flutter of orthotropic composite panel under aerodynamic heating
[AIAA PAPER 92-2132] p 589 A92-35699
Thermal management for a Mach 5 cruise aircraft using endothermic fuel p 736 A92-41225

Thermal structures - Four decades of progress
p 729 A92-41239
Engineering aerodynamic heating method for hypersonic flow p 705 A92-41539
A study of aerophysical and dynamic characteristics using an axisymmetric flight test vehicle with a reusable nose section p 707 A92-42684
Hypersonic testing technology of HOPE (H-II orbiting plane) p 747 A92-43096
Experimental studies on aerodynamic heating and thermal protection in hypersonic flight
p 709 A92-43101
Aerodynamic heating measurement in hypersonic flow
p 709 A92-43102
A thin metal model for aerodynamic heating tests of shock wave interaction p 709 A92-43103
Thermal measurement test in a shock wind tunnel
p 748 A92-43104
Aerodynamic heating in three-dimensional shock wave turbulent boundary layer interaction induced by sweptback sharp fins in hypersonic flows
[SAE PAPER 912044] p 791 A92-45428
Effect of the grid system on heat transfer computations for high speed flows p 900 A92-47071
Numerical experiments on unsteady shock reflection processes using the thin-layer Navier-Stokes equations
p 818 A92-47155
Heat transfer characteristics of hypersonic waveriders with an emphasis on leading edge effects
[AIAA PAPER 92-2920] p 821 A92-47892
Ablation performance characterization of thermal protection materials using a Mach 4.4 Sled Test
[AIAA PAPER 92-3055] p 893 A92-48713
Three-dimensional optimal reentry trajectory and aerodynamic heating history of the Space Shuttle
p 984 A92-49582
Aerodynamic heating characteristics of space planes tested by NAL hypersonic wind tunnel
p 1017 A92-53547
Numerical simulations of shock reflections by a TVD scheme p 1018 A92-53558
Spaceplane aerodynamic heating and thermal protection design method p 1102 A92-53578
HOPE re-entry experimental vehicle
p 1103 A92-55098
Active control of asymmetric vortical flows around cones using injection and heating
[AIAA PAPER 92-4426] p 1025 A92-55350
Aerothermodynamic test of spaceplane by thin-skin method p 1093 A92-56043
Numerical simulation of hypersonic viscous flow for the design of H-2 orbiting plane (HOPE-2)
[NAL-TR-1093] p 11 N92-10009
The effect of a type 3 and type 4 shock/shock interaction on heat transfer in the stagnation region
p 160 N92-13867
Aerodynamic heating on AFE due to nonequilibrium flow with variable entropy at boundary layer edge
p 183 N92-15020
Development and application of computational aerothermodynamics flowfield computer codes
[NASA-CR-190294] p 624 N92-24229
A simplified method for thermal analysis of a cowl leading edge subject to intense local shock-wave-interference heating
[NASA-TP-3167] p 679 N92-24797
Finite element methods for integrated aerodynamic heating analysis
[NASA-CR-190353] p 633 N92-25959

AERODYNAMIC INTERFERENCE

The aerodynamic interference between a flapped tanker aircraft and a receiver aircraft during air-to-air refuelling
p 29 A92-13199
Two-dimensional adaptive-wall tests in the NASA Ames two- by two-foot transonic wind tunnel
p 30 A92-13201
Wall interference assessment/correction for transonic airfoil data p 30 A92-13214
On vortex interference for canard configuration
p 64 A92-14071
High speed wind tunnel wall interference research progress at Nanjing Aeronautical Institute
p 136 A92-15338
The canard-wing interference and stall safety of light canard aircraft p 111 A92-15341
Interference effects of very high bypass ratio nacelle installations on a low-wing transport
[ASME PAPER 91-GT-241] p 75 A92-15646
Wall interference calculation in a transonic test section including simulation of discrete slots
[AIAA PAPER 92-0032] p 249 A92-22153
Wind tunnel boundary interference prediction and correction
[AIAA PAPER 92-0036] p 249 A92-22157
Identification of aerodynamic effectiveness and interference effects of direct-lift-control flaps from flight data
[AIAA PAPER 92-0171] p 271 A92-23782
Numerical simulation of inviscid flow over a complicated body using an overlapping grid technique
p 313 A92-25043
Application of the wall pressure method to wall interference corrections for model tests at high angle of attack in high speed wind tunnel p 315 A92-25134
Experimental results on a wall interference correction method with interface measurements
[AIAA PAPER 92-0570] p 333 A92-26978
Multibody interference at transonic Mach numbers
[AIAA PAPER 92-0651] p 334 A92-27023
Ground facility interference on aircraft configurations with separated flow
[AIAA PAPER 92-0673] p 384 A92-27042
Aerodynamic wing-nacelle integration
p 458 A92-30134
A pressure-drag-determination method for aerodynamic-interference problems p 425 A92-30157
Theoretical model to calculate aerodynamic interference effects between rotor and wing of tiltrotors
p 521 A92-35788
A correlation study of the wing-body interference factor for high angles of attack p 700 A92-41179
Wind tunnel wall corrections for unsteady flow applying steady wall adaptation and CFD-techniques
p 706 A92-42533
Whirl-flutter stability of a pusher configuration in nonuniform flow p 845 A92-46813
An improved wall correction method for the longitudinal stability p 978 A92-53388
A simple three component velocity measurement method using a rotated split-film sensor
p 1115 A92-54333
Application of a wall pressure method in a wind tunnel test section with adjustable longitudinal slots
p 1091 A92-54336
Evaluation of sidewall interference in the NAL two-dimensional transonic wind tunnel
p 1092 A92-56011
A shock tunnel experiment on aerodynamic interference induced by RCS jet p 1029 A92-56042
Analysis of helicopter rotor-fuselage interference with time averaged pressure distribution
p 1032 A92-56331
Wind tunnel blockage effects on slender wings undergoing large amplitude motions
[AIAA PAPER 92-3926] p 1096 A92-56757
Experimental study of an independently deflected wingtip mounted on a semispan wing
[NASA-TM-102842] p 13 N92-10983
Model representation in the PANCOR wall interference assessment code
[NASA-TM-104152] p 31 N92-11022
Wind tunnel tests on A4, A4.1, and A4.2 2-D airfoil models in the IAR 5-ft. wind tunnel: Boeing Commercial Airplane Company and Institute for Aerospace Research collaborative work program
[NRC-IAR-C3] p 81 N92-11975
A derivation of gross thrust for a sea-level jet engine test cell
[NRC-30165] p 130 N92-12001
Wall interference calculation in a transonic wind tunnel with discrete slots p 83 N92-12995
Water tunnel flow visualization studies of a canard-configured X-31A-like fighter aircraft model
[AD-A241362] p 90 N92-13037
Interference heating near fin/body junctions on hypersonic vehicles p 182 N92-14996
A wall interference assessment/correction system
[NASA-CR-189785] p 259 N92-15974
Atmospheric pressure flow reactor: Gas phase chemical kinetics under tropospheric conditions without wall effects
[NASA-CASE-MSC-21384-1] p 297 N92-16243
User guide for WIACX: A transonic wind-tunnel wall interference assessment and correction procedure for the NTF
[NASA-TM-104168] p 261 N92-17547
Aircraft aerodynamics and stability and control during air-to-air refueling
[AERO-REPT-9017] p 380 N92-18321
Installation effects of wing-mounted turbofan nacelle-pylons on a 1/17-scale, twin-engine, low-wing transport model
[NASA-TP-3168] p 346 N92-19002
Asymptotic theory of transonic wind tunnel wall interference
[AD-A244075] p 403 N92-19080
Comparison of a two-dimensional adaptive-wall technique with analytical wall interference correction techniques
[NASA-TP-3132] p 444 N92-20494
Evaluation of NACA0012 airfoil test results in the NAL two-dimensional transonic wind tunnel
[NAL-TR-1109T] p 445 N92-21287
Survey of experimental techniques for performance prediction p 552 N92-23954
A simplified method for thermal analysis of a cowl leading edge subject to intense local shock-wave-interference heating
[NASA-TP-3167] p 679 N92-24797
An analysis of the sidewall boundary layer effect in two-dimensional wind tunnel testing p 626 N92-24856
Aerodynamic interference between stores
[AD-A247207] p 715 N92-27172
Evaluation of measured-boundary-condition methods for 3D subsonic wall interference
[NLR-TR-88072-U] p 832 N92-29884
An investigation into the interface between three closely spaced axi-symmetric bodies at subsonic speed
[CRANFIELD-AERO-9114] p 948 N92-31514

AERODYNAMIC LOADS

Computation of steady and unsteady control surface loads in transonic flow p 5 A92-11066
The aerodynamic interference between a flapped tanker aircraft and a receiver aircraft during air-to-air refuelling
p 29 A92-13199
Fickle effect of nose microasymmetry on the high-alpha aerodynamics p 10 A92-13217
Estimation of the size of separation zone in a turbine stage under small load p 10 A92-13235
An integrated airloads-inflow model for use in rotor aeroelasticity and control analysis p 64 A92-14328
A full scale airframe high cycle fatigue test methodology and its application to the SH-2G helicopter
p 105 A92-14345
Analysis of rotor blade dynamics using experimental UH-60A airloads obtained at the DNW
p 107 A92-14394
The effect of steady aerodynamic loading on the flutter stability of turbomachinery blading
[ASME PAPER 91-GT-130] p 71 A92-15574
Formulation of a simplified model of rotor-horizontal stabilizer interactions and comparison with experimental measurements
[ONERA, TP NO. 1991-157] p 77 A92-16125
Theoretical study and prediction of BVI noise including close interactions
[ONERA, TP NO. 1991-174] p 165 A92-16138
A lifting line theory for supersonic flow applications
[AIAA PAPER 91-5058] p 171 A92-17841
Static aeroelastic analysis for generic configuration wing p 174 A92-20201
Numerical calculation of subsonic and supersonic aerodynamic loads around complex configuration vehicle
p 175 A92-20488
Unsteady Euler analysis of the flowfield of a propfan at an angle of attack p 242 A92-21070
Prediction of periodic loadings on single rotation propfan with off-axis inflow p 277 A92-21071
The FALSTAFF program - A standard spectrum for simulating the service loading of aircraft with prevailing maneuver loads p 284 A92-21922
Response of symmetrically laminated rectangular plates subjected to heating p 296 A92-24186
Approach to side force alleviation through modification of the pointed forebody geometry p 309 A92-24418
The calculation of the static elastic aerodynamic distribution for the rolling maneuver aircraft
p 379 A92-25010
Multiple line-vortex model of vortex flows around body of revolution at high angles of attack up to 60 degrees
p 314 A92-25104
Numerical investigation of performance degradation of wings and rotors due to icing
[AIAA PAPER 92-0412] p 325 A92-26264
An unsteady Euler scheme for the analysis of ducted propellers
[AIAA PAPER 92-0522] p 332 A92-26947
Evaluation of methods for estimating store carriage loads
[AIAA PAPER 92-0675] p 379 A92-27043
Determination of duty factors from experimental data in local interaction theory p 338 A92-27645
Acoustic characteristics and dynamic structural loading of an ASTOVL aircraft in hover
[AIAA PAPER 92-0370] p 416 A92-28190
Structural and aerodynamic analysis of a large-scale advanced propeller blade p 375 A92-28517
Determination of the mean duration of normal acceleration loads at the center of mass of aircraft during a flight in a turbulent atmosphere p 480 A92-30192
Generation of loads for finite-element models of large aircraft p 459 A92-30209
Acoustic emission during changes in the aerodynamic load on the surface of a fan blade p 511 A92-30318
High aerodynamic loads on an airfoil submerged in an unsteady stream p 432 A92-31183

A procedure for calculating the static aeroelasticity characteristics of flight vehicles by the influence coefficient method using three-dimensional finite element schemes
p 460 A92-31896
Analytical aeroelastic stability considerations and conversion loads for an XV-15 tilt-rotor in a wind tunnel simulation
[AIAA PAPER 92-2258] p 540 A92-34413
Blade root torsional dampers to reduce hub loads
[AIAA PAPER 92-2449] p 541 A92-34476
Unsteady aerodynamic characteristics of a dual-element airfoil
[AIAA PAPER 92-2508] p 518 A92-34501
Optimizing tuning masses for helicopter rotor blade vibration reduction including computed airloads and comparison with test data
[AIAA PAPER 92-2376] p 542 A92-34546
Rolling Maneuver Load Alleviation using active controls
[AIAA PAPER 92-2099] p 566 A92-35670
Maneuver load control using optimized feedforward commands
[AIAA PAPER 92-2100] p 567 A92-35671
Identification of helicopter component loads using multiple regression
[AIAA PAPER 92-2110] p 544 A92-35681
Buffet load measurements on an F/A-18 vertical fin at high-angle-of-attack
[AIAA PAPER 92-2127] p 520 A92-35694
Calculation of pitch-link loads in deep stall using state-of-the-art methodology p 520 A92-35753
General model of isolated helicopter blade for stability investigation p 547 A92-35774
The effects of inner wake modelling on blade airloads
p 521 A92-35784
Low profile microsensor for aerodynamic pressure measurement p 555 A92-35949
Turbomachinery unsteady load predictions with nonuniform inflow p 611 A92-36972
Recent advances in maneuver loads analysis
p 642 A92-37576
Unsteady aerodynamic loading produced by a sinusoidally oscillating delta wing p 701 A92-41223
Improved measurement of the dynamic loads acting on rotating parachutes p 702 A92-41236
Coalescence of aeroelastic modes in flutter analysis
p 758 A92-41241
Recent airfoil tests in NAL 2D high Reynolds number wind tunnel p 748 A92-43171
Unsteady airloading panel method for propfans
p 780 A92-44512
Prediction of rotor unsteady airloads using vortex filament theory
[AIAA PAPER 92-2610] p 792 A92-45484
Design load predictions on a fighter-like aircraft wing
p 811 A92-46797
Time-average loading on a two-dimensional airfoil in a large amplitude motion p 811 A92-46805
Statistical prediction of maximum buffet loads on the F/A-18 vertical fin p 811 A92-46816
Aerodynamic parametric studies and sensitivity analysis for rotor blades in axial flight p 816 A92-46959
Engine flight load reliability analysis
p 968 A92-49827
Investigation of the tail buffeting of the C-101
p 942 A92-53253
Methodology for calculating aerodynamic sensitivity derivatives p 1024 A92-54911
Tow-tank study of nonlinear aerodynamics of a 2-D airfoil
[AIAA PAPER 92-4499] p 1026 A92-55367
Response of helicopter blades to a sharp collective increase p 1084 A92-56282
Finite-element analysis and multibody dynamics issues in rotorcraft dynamic analysis p 1055 A92-56286
Simulation of helicopter see-saw rotor motion
p 1055 A92-56287
Numerical simulation of unsteady rotor wakes
p 1032 A92-56352
CH-53E/AV-8B aircraft sling load recovery system analysis
[AD-A239950] p 21 N92-10022
Experimental study of an independently deflected wingtip mounted on a semispan wing
[NASA-TM-102842] p 13 N92-10983
Studies of aerothermal loads generated in regions of shock/shock interaction in hypersonic flow
[NASA-CR-181893] p 43 N92-11319
Multi-disciplinary optimization of aeroservoelastic systems
[NASA-CR-188983] p 44 N92-11377
A review of aeronautical fatigue investigations in Sweden during the period May 1989 to April 1991
[FFA-TN-1991-24] p 158 N92-12313
Review of aircraft dynamic loads due to flow separation p 85 N92-13008
Multiple roll attractors of a delta wing at high incidence p 88 N92-13026
Numerical simulation of vortex flows past impulsively started wings p 88 N92-13028
Effect of solidity and inclination on propeller-nacelle force coefficients
[NASA-TM-4316] p 90 N92-13038
Flight operations for higher harmonic control research
[AD-A242478] p 196 N92-15067
Numerical simulation of VAWT stochastic aerodynamic loads produced by atmospheric turbulence: VAWT-SAL code
[DE92-000597] p 229 N92-15392
A comparison of spanwise aerodynamic loads estimated from measured bending moments versus direct pressure measurements on horizontal axis wind turbine blades
[DE92-001158] p 301 N92-16458
Wind loads on a mirage III O aircraft mounted above a ground plane
[AD-A243004] p 275 N92-17266
Dynamic stall on wind turbine blades
[DE92-001157] p 262 N92-17874
An overview: Challenges in wind technology development
[DE92-001190] p 302 N92-17875
Fatigue life behaviour of composite structures
p 390 N92-18577
Aerodynamic and flowfield hysteresis of slender wing aircraft undergoing large-amplitude motions
p 364 N92-18780
Non-linear airloads hypersurface representation: A time domain perspective p 346 N92-18783
CH-46 and OH-58 transmission stress wave analysis
[AD-A244321] p 365 N92-18826
The NREL teetering hub rotor code: Final results and conclusions
[DE92-001187] p 410 N92-19633
Optimizing tuning masses for helicopter rotor blade vibration reduction including computed airloads and comparison with test data
[NASA-TM-104194] p 367 N92-19846
Blade-mounted trailing edge flap control for BVI noise reduction
[NASA-CR-4426] p 512 N92-21173
Simulation of iced wing aerodynamics
p 450 N92-21686
Adaptive active flutter suppression of wings in subsonic and transonic flight regimes p 553 N92-24010
Progress in integrated analysis with adaptive unstructured meshing p 683 N92-25914
Computational structures technology at Grumman: Current practice/future needs p 684 N92-25930
Computer program for calculating in-flight aircraft-store interface reaction loads
[AD-A245782] p 731 N92-26896
Computational method to predict thermodynamic, transport, and flow properties for the modified Langley 8-foot high-temperature tunnel
[NASA-TM-4374] p 767 N92-27193
Progress of magnetic suspension and balance systems for wind tunnels in the USSR p 751 N92-27803
NLR inviscid transonic unsteady loads prediction methods in aeroelasticity p 720 N92-27947
Computation of flutter boundaries in the time and frequency domain p 720 N92-27952
Reduction and analysis of F-111C flight data
[AD-A250341] p 853 N92-28771
Status of the FAA flight loads monitoring program
p 914 N92-30113
Yaw dynamics of horizontal axis wind turbines
[DE92-001245] p 1004 N92-30837
Vortex flow aerodynamics
[AGARD-AR-299] p 946 N92-30947
A summary of the active flexible wing program
[NASA-TM-107655] p 962 N92-31264
Rolling maneuver load alleviation using active controls
[NASA-TM-107654] p 962 N92-31351
Aerodynamic centre of wing-body combinations
[ESDU-92024] p 1036 N92-32479
Turbulence-induced loads on a teetered rotor
p 1042 N92-34029

AERODYNAMIC NOISE

High-speed impulsive noise and aerodynamic results for rectangular and swept rotor blade tip tests in S1-Modane wind tunnel
[ONERA, TP NO. 1991-124] p 76 A92-16102
Aerodynamic and acoustic calculations of transonic nonlifting hovering rotors
[ONERA, TP NO. 1991-178] p 77 A92-16140
The jet edge-tone feedback cycle - Linear theory for the operating stages p 392 A92-24758
Sound produced by an aerodynamic source adjacent to a partly coated, finite elastic plate
p 414 A92-25365
Direct computation of the sound from a compressible co-rotating vortex pair
[AIAA PAPER 92-0374] p 414 A92-26232
Flow visualization of a prop-fan leading-edge vortex
[AIAA PAPER 92-0386] p 323 A92-26242
Computation of supersonic jet mixing noise for an axisymmetric CD nozzle using k-epsilon turbulence model
[AIAA PAPER 92-0500] p 414 A92-26328
Reducing the background noise level in the test section of a wind tunnel for transonic flow velocities
p 511 A92-30143
An experimental study of tone-like noise in the flow past a wing at low flow velocities p 425 A92-30160
Analytical study on plate edge noise. I - Trailing edge noise caused by vorticity waves p 511 A92-32502
An experimental study of the noise of flow past a wing at low velocities p 603 A92-33771
Rotor blade-vortex interaction noise reduction and vibration using higher harmonic control
p 604 A92-35778
Research on aircraft engines p 558 A92-35912
Noise from turbine generators - Noise control, propagation, and assessment p 686 A92-39044
Noise generated by wind turbines p 686 A92-39045
Theoretical and experimental methods in acoustics of ducts and mufflers - A critical review
p 693 A92-39068
Active control of pulsed flow for low frequency noises attenuation p 694 A92-39109
Acoustic sources in a tripped flow past a resonator tube p 778 A92-41266
Relationship between the instability waves and noise of high-speed jets p 924 A92-45835
Direct evaluation of aeroacoustic theory in a jet
p 1010 A92-50296
Aeroacoustics of flight vehicles: Theory and practice. Volume 1: Noise sources
[NASA-RP-1258-VOL-1] p 54 N92-10598
Rotor noise p 54 N92-10600
Jet noise classical theory and experiments
p 54 N92-10602
Airframe noise p 55 N92-10605
Annoyance caused by advanced turboprop aircraft flyover noise: Comparison of different propeller configurations
[NASA-TP-3104] p 56 N92-11758
Flyover-noise measurement and prediction
p 236 N92-14786
Computation of supersonic jet mixing noise for an axisymmetric CD nozzle using k-epsilon turbulence model
[NASA-TM-105338] p 237 N92-14795
The acoustic flashlight
[MBB-Z-0359-90-PUB] p 239 N92-15938
An evaluation of some alternative approaches for reducing fan tone noise
[NASA-TM-105356] p 416 N92-18282
A numerical study of fuselage scattering effects on rotor noise p 511 N92-20428
Experimental study of the mechanism of sound generation by rotating stall in centrifugal turbomachines
p 605 N92-23726
Analysis of rotor vibratory loads using higher harmonic pitch control
[NASA-CR-189591] p 696 N92-24251
Turbine drive system of the high pressure LOX turbopump test facility
[DE92-783191] p 680 N92-25342
Boundary layer induced noise in aircraft
[CUED/A-AERO/TR-18] p 927 N92-29201
Fourth Aircraft Interior Noise Workshop
[NASA-CP-10103] p 1136 N92-32948
Acoustic loads prediction on jet aircraft
p 1136 N92-32949
Advanced subsonic transport approach noise: The relative contribution of airframe noise
[NASA-TM-104112] p 1140 N92-34148

AERODYNAMIC STABILITY

Aeroelastic stability analysis of aerial propellers
p 24 A92-10955
V-22 pilot-in-the-loop aeroelastic stability analysis
p 133 A92-14422
Dynamics of helicopters with dissimilar blades
p 133 A92-14427
Active stabilization of multistage axial-compressor aerodynamic system instabilities
[ASME PAPER 91-GT-403] p 76 A92-15733
Aerodynamic balance range of aircraft of different configurations p 134 A92-16801
The response of a helicopter to windshear
p 269 A92-21470
A parametric study of the aeroelastic stability of a binary wing-with-engine nacelle flutter system in incompressible flow p 270 A92-22472

Rapid prediction of high-alpha unsteady aerodynamics of slender-wing aircraft p 309 A92-24412
Characteristics of the phugoid motion of nonmaneuverable aircraft p 480 A92-30190
Coupled rotor-fuselage dynamics and aeroelasticity in turning flight
[AIAA PAPER 92-2109] p 544 A92-35680
Bearingless rotor aeromechanical stability measurements and correlations using nonlinear aerodynamics p 547 A92-35772
Whirl-flutter stability of a pusher configuration in nonuniform flow p 845 A92-46813
Aeromechanical stability of hingeless helicopter rotors in forward flight p 874 A92-46923
Experimental observations of instability modes in a rectangular jet p 1135 A92-54908
Aerodynamic model identification of a spaceplane model from a cable-mount dynamic wind-tunnel test p 1093 A92-56114
Dynamics of helicopters with dissimilar blades in forward flight p 1056 A92-56288
Blade instability of horizontally stoppable rotors p 1085 A92-56308
CH-53E/AV-8B aircraft sling load recovery system analysis
[AD-A239950] p 21 N92-10022
Rotorcraft system identification
[AGARD-AR-280] p 22 N92-11001
Investigation of the aeroelastic stability of the AFW wind-tunnel model using CAP-TSD
[NASA-TM-104142] p 81 N92-11977
Performance improvements and fuel cost savings due to leading edge modification of a vintage delta wing jet fighter
[FFA-TN-1991-22] p 114 N92-11993
A numerical solution of implicit nonlinear equations of motion for rotor blades p 115 N92-13053
China's first variable stability aircraft: The BW-1-Gets its pre-acceptance flight tests
[AD-A240941] p 116 N92-13062
Formulation of the linear model from the nonlinear simulation for the F18 HARV p 117 N92-13842
A simplified method for predicting the stability of aerodynamically excited turbomachinery p 224 N92-14364
Trim drag reduction concepts for horizontal takeoff single-stage-to-Orbit vehicles
[NASA-TM-102687] p 206 N92-15076
Periodic trim solutions with HP-version finite elements in time
[NASA-CR-189778] p 282 N92-17019
Assessment of rotorcraft system identification as applied to the AH-64 p 274 N92-17160
Aerodynamic development of the X-31 aircraft for the high angle of attack region
[MBB-FE211-S-PUB-452] p 275 N92-17313
Non-linear airloads hypersurface representation: A time domain perspective p 346 N92-18783
X-31: Discussion of steady state and rotary derivatives p 365 N92-18789
Transformation of flightmechanical design requirements for modern fighters into aerodynamic characteristics p 365 N92-18794
Aeroservoelastic stability of aircraft at high incidence p 381 N92-18795
Notes on the cause of parachute critical velocity
[AD-A244417] p 347 N92-19085
Proposal for a low cost close air support aircraft for the year 2000: The Raptor
[NASA-CR-190023] p 367 N92-19496
Current status of computational methods for transonic unsteady aerodynamics and aeroelastic applications
[NASA-TM-104191] p 446 N92-21432
Wind-tunnel static and free-flight investigation of high-angle-of-attack stability and control characteristics of a model of the EA-6B airplane
[NASA-TP-3194] p 631 N92-25276
Current status of computational methods for transonic unsteady aerodynamics and aeroelastic applications p 718 N92-27937
Transonic wind tunnel test of a 14 percent thick oblique wing
[NASA-TM-102230] p 950 N92-32213
Dynamic interactions between hypersonic vehicle aerodynamics and propulsion system performance
[NASA-CR-190638] p 1038 N92-33304
Implementation of a personal computer based parameter estimation program
[AD-A252914] p 1061 N92-33502

AERODYNAMIC STALLING

A numerical simulation of separated flows around bodies p 8 A92-12423
Poststall airfoil response to a periodic freestream p 10 A92-13218
An analysis of pitch and plunge effects on unsteady airfoil behavior p 65 A92-14359
Investigation of unsteady excitation effects on aerodynamic properties of airfoils p 66 A92-15335
The canard-wing interference and stall safety of light canard aircraft p 111 A92-15341
Computational study of stall flutter in linear cascades
[ASME PAPER 91-GT-5] p 67 A92-15503
The role of tip clearance in high-speed fan stall
[ASME PAPER 91-GT-83] p 69 A92-15550
Nonlinear stall flutter and divergence analysis of cantilevered graphite/epoxy wings p 219 A92-20746
Effect of turbulence modeling on dynamic stall of a NACA0012 airfoil
[AIAA PAPER 92-0027] p 248 A92-22149
Compressibility effects on the dynamic stall of a three-dimensional wing
[AIAA PAPER 92-0191] p 256 A92-23800
Leading edge velocity field of an oscillating airfoil in compressible dynamic stall
[AIAA PAPER 92-0193] p 257 A92-23802
Navier-Stokes computation of airfoil in stall using algebraic Reynolds-stress model
[AIAA PAPER 92-0195] p 257 A92-23803
Study of role of unsteady separation in formation of dynamic stall vortex
[AIAA PAPER 92-0196] p 257 A92-23804
Navier-Stokes calculations of inboard stall delay due to rotation p 309 A92-24410
Concerning a basic assumption for aeroelasticity in turbomachinery p 373 A92-26920
Nonlinear large amplitude aeroelastic behavior of composite rotor blades at large static deflection
[AIAA PAPER 92-2257] p 540 A92-34412
Oscillating airfoil velocity field during large amplitude dynamic stall p 622 A92-40171
Design and development of a compressible dynamic stall facility p 747 A92-41215
Effect of acoustic excitation on stalled flows over an airfoil p 703 A92-41267
Chaotic stall response of helicopter rotor in forward flight p 730 A92-43046
Indicial method calculating dynamic stall on a vertical axis wind turbine p 714 A92-44528
Numerical simulations of separated flows around oscillating airfoil for dynamic stall phenomena
[SAE PAPER 911991] p 788 A92-45393
Static and dynamic flow field development about a porous suction surface wing
[AIAA PAPER 92-2628] p 795 A92-45500
A LEX blowing technique for post-stall lateral control of trapezoidal wings
[AIAA PAPER 92-2714] p 802 A92-45553
Exploratory investigation of a spanwise blowing concept for tip-stall control on cranked-arrow wings
[AIAA PAPER 92-2637] p 806 A92-45576
Chaotic oscillation in helicopter blade stall response p 846 A92-46922
Analysis of the onset of dynamic stall p 1024 A92-54919
The vortical structure in the wake during dynamic stall
[AIAA PAPER 92-4496] p 1026 A92-55364
Comparative numerical study of two turbulence models for airfoil static and dynamic stall
[AIAA PAPER 92-4649] p 1028 A92-55394
Flutter and stall response of a helicopter blade with structural nonlinearity p 1055 A92-56178
Helicopter tail rotor stall flutter p 1056 A92-56290
Measurements of the dynamic stall vortex convection speed p 1032 A92-56351
Performance evaluation of a transonic wind tunnel compressor
[AIAA PAPER 92-3927] p 1096 A92-56758
Numerical investigation of the effect of leading edge geometry on dynamic stall of airfoils
[AD-A239949] p 12 N92-10015
Formulation of the linear model from the nonlinear simulation for the F18 HARV p 117 N92-13842
Wichita State University 1986 aviation safety research projects
[DOT/FAA/CT-91/4] p 263 N92-16986
Dynamic stall on wind turbine blades
[DE92-001157] p 262 N92-17874
An overview: Challenges in wind technology development
[DE92-001190] p 302 N92-17875
X-31 enhancement of aerodynamics for maneuvering beyond stall p 363 N92-18779
Recent results from data analysis of dynamic stall on wind turbine blades
[DE92-001200] p 505 N92-20245
Laser velocimetry measurements of oscillating airfoil dynamic stall flow field
[AD-A244546] p 502 N92-21297
High angle of attack: Aerodynamics p 528 N92-23956
Navier-Stokes simulation of dynamic stall on a rotating airfoil p 626 N92-24853
Pressure-based high-order TVD methodology for dynamic stall control
[AD-A247056] p 774 N92-27918
A computational investigation of airfoil stall flutter
[AD-A247302] p 947 N92-31300
Control of unsteady separated flow associated with the dynamic stall of airfoils
[NASA-CR-190688] p 950 N92-32177
Aeroelasticity of bluff bodies p 1089 N92-34165

AERODYNAMICS

A simplified model for aerodynamic flows around streamlined models p 63 A92-13816
Aerodynamics and heat transfer investigations on a high Reynolds number turbine cascade
[ASME PAPER 91-GT-157] p 148 A92-15593
Stability of a viscous compressible shear layer with a temperature drop p 79 A92-16684
A perspective on aerospace CFD p 169 A92-20145
A boundary integral formulation for the kinetic field in aerodynamics. I - Mathematical analysis p 243 A92-21504
Future experimental needs to support applied aerodynamics - A transonic perspective
[AIAA PAPER 92-0156] p 254 A92-23771
Future experimental needs in low-speed aerodynamics
[AIAA PAPER 92-0157] p 254 A92-23772
A comparison of optimization-based approaches for a model computational aerodynamics design problem p 316 A92-25636
A modern view of Theodore Theodorsen --- Book
[ISBN 0-930403-85-1] p 307 A92-26250
Computational study of the aerodynamics and control by blowing of asymmetric vortical flows over delta wings
[AIAA PAPER 92-0410] p 325 A92-26263
An analytical approach to grid sensitivity analysis --- of NACA wing sections
[AIAA PAPER 92-0660] p 334 A92-27031
A boundary integral formulation for the kinetic field in aerodynamics. II - Applications to unsteady 2D flows p 339 A92-28005
Applications of an implicit, upwind Navier-Stokes code, CRAFT, to steady/unsteady reacting, multi-phase flowfields
[AIAA PAPER 92-0837] p 422 A92-29603
Fluid Dynamics Conference, 22nd, Osaka, Japan, Nov. 15, 1990, Proceedings p 494 A92-30501
The unstructured upwind method p 429 A92-30522
Semiconductor laser Doppler anemometer for applications in aerodynamic research p 495 A92-31173
Twenty-five years of aerodynamic research with infrared imaging p 497 A92-32232
Heat transfer effects on aerodynamics and implications for wind-tunnel tests p 497 A92-32240
A general gust and maneuver load analysis method to account for the effects of active control saturation and nonlinear aerodynamics
[AIAA PAPER 92-2126] p 567 A92-35693
Efficient direct solvers for large-scale computational fluid dynamics problems p 690 A92-37534
Aerospace - Collected translations of selected papers p 608 A92-38266
Flight-vehicle materials, structures, and dynamics - Assessment and future directions. Vol. 3 - Ceramics and ceramic-matrix composites --- Book
[ISBN 0-7918-0661-8] p 668 A92-39852
Structural features of a heated round turbulent jet in a cross-flow p 676 A92-40148
Analysis of airship lateral maneuverability
[AIAA PAPER 91-1274] p 743 A92-41212
High-Reynolds-number test requirements in low-speed aerodynamics p 787 A92-45263
International Pacific Air and Space Technology Conference and Aircraft Symposium, 29th, Gifu, Japan, Oct. 7-11, 1991, Proceedings
[SAE P-246] p 783 A92-45376
Applied Computational Aerodynamics - Case studies
[AIAA PAPER 92-2661] p 845 A92-45580
Forebody flow control on a full-scale F/A-18 aircraft
[AIAA PAPER 92-2674] p 806 A92-45583
Flight deck aerodynamics of a nonaviation ship p 810 A92-46790
Forebody vortex control using small, rotatable strakes p 811 A92-46798
Aerodynamic parametric studies and sensitivity analysis for rotor blades in axial flight p 816 A92-46959
Grid adaptation to multiple functions for applied aerodynamic analysis p 817 A92-47045
On-line identification and control of linearized aircraft dynamics p 1082 A92-55911
Future requirements for hypersonic aerodynamic and aerothermodynamic facilities
[AIAA PAPER 92-3903] p 1094 A92-56738
Transonic turbine blade cascade testing facility
[AIAA PAPER 92-4034] p 1101 A92-56856

Recent advances on a finite element algorithm for computational aerodynamics: Transonics-hypersonics
[DE91-018176] p 11 N92-10010
Parameter identification for nonlinear aerodynamic systems
[NASA-CR-188985] p 53 N92-10347
The effects of Reynolds number, rotor incidence angle and surface roughness on the heat transfer distribution in a large-scale turbine rotor passage
[NASA-CR-184260] p 42 N92-11297
Phenomenological modeling of the wake produced by a straight two dimensional base in subsonic flow
[REPT-90/59] p 82 N92-11982
Vortex Flow Aerodynamics
[AGARD-CP-494] p 83 N92-12996
The use of artificial neural networks in experimental data acquisition and aerodynamic design p 90 N92-13848
An evaluation of preliminary Doppler global velocimetry measurements p 90 N92-13849
Review of aerodynamic design in the Netherlands
p 193 N92-13929
A comparison of two closely-related approaches to aerodynamic design optimization p 193 N92-13933
Recent progress in inverse methods in France
p 201 N92-13938
Research on inverse, hybrid and optimization problems in engineering sciences with emphasis on turbomachine aerodynamics: Review of Chinese advances
p 201 N92-13939
The research progress on Hodograph Method of aerodynamic design at Tsinghua University
p 177 N92-13974
International aviation (selected articles)
[AD-A241119] p 170 N92-13993
JPRS report: Science and technology. USSR: Space
[JPRS-USP-91-007] p 211 N92-14101
Experimental research of the aerodynamics of nozzles and plumes at hypersonic speeds
[NASA-CR-187316] p 185 N92-15048
Wichita State University 1986 aviation safety research projects
[DOT/FAA/CT-91/4] p 263 N92-16986
Identification techniques: Frequency domain methods
p 273 N92-17158
Modification of Jindivik air intake duct with an auxiliary intake static aerodynamic tests
[AD-A243002] p 275 N92-17234
An alternative concept for aeroassisted orbit transfers
[AD-A243409] p 287 N92-17325
Flow visualization and wake analysis for standard and modified configurations of the AN/ALQ-78 antenna pod
[AD-A243552] p 260 N92-17339
Hi-alpha forebody design. Part 1: Methodology base and initial parametrics
[NASA-CR-189849] p 358 N92-18024
Software Engineering Laboratory (SEL) Ada performance study report
[NASA-TM-105510] p 412 N92-18125
Window cooling for high speed flight
[AD-D015145] p 344 N92-18193
Aerodynamic control of fighter aircraft by manipulation of forebody vortices p 380 N92-18791
Forebody vortex control aeromechanics
p 380 N92-18792
Transformation of flightmechanical design requirements for modern fighters into aerodynamic characteristics
p 365 N92-18794
The 8th Symposium on Turbulent Shear Flows. Volume 1: Sessions 1-18
[AD-A243809] p 402 N92-18933
Linearized aerodynamic and control law models of the X-29A airplane and comparison with flight data
[NASA-TM-4356] p 381 N92-19174
Towards understanding software: 15 years in the SEL
p 413 N92-19423
Secondary instability of high-speed flows and the influence of wall cooling and suction
[NASA-CR-4427] p 406 N92-19844
Activities of NRC-CNRC, Institute for Aerospace Research
[CTN-92-60431] p 420 N92-20204
Pressure and velocity measurements about an airfoil during a parallel blade-vortex interaction
p 446 N92-21429
Techfest 18 Proceedings
[NIAR-92-1] p 420 N92-21501
Aerodynamic design with CFD p 447 N92-21514
Effects of Adverse Weather on Aerodynamics
[AGARD-CP-496] p 449 N92-21679
The effect of wing ice contamination on essential flight characteristics p 449 N92-21681
Dynamic performance of an aircraft on its landing gear: Test and evaluation on a dihedral p 466 N92-21970
A theoretical investigation of the induced drag of wing of finite aspect ratio
[CUED/A-AERO/TR-17(1991)] p 525 N92-22193
Overview of the subsonic propulsion technology session p 560 N92-22531
Integrated Design Analysis and Optimisation of Aircraft Structures
[AGARD-R-784] p 550 N92-23227
JPRS report: Science and technology. Central Eurasia: Space
[JPRS-USP-92-002] p 575 N92-23705
Special Course on Engineering Methods in Aerodynamic Analysis and Design of Aircraft
[AGARD-R-783] p 552 N92-23950
Configuration development --- preliminary aircraft design p 552 N92-23953
High angle of attack: Aerodynamics
p 528 N92-23956
NASA aerodynamics program
[NASA-TM-4368] p 609 N92-24678
Proceedings of the 3rd Canadian Symposium on Aerodynamics
[CTN-92-60420] p 625 N92-24849
Experimental investigation of nozzle/plume aerodynamics at hypersonic speeds
[NASA-CR-190074] p 664 N92-25162
Joint computational and experimental aerodynamics research on a reentry vehicle
[DE91-017315] p 667 N92-25315
Prediction and analysis of wing flutter at transonic speeds p 662 N92-25555
Transonic turbine blade cascade testing facility
[NASA-TM-105646] p 667 N92-26129
Theoretical principles of a Euler method for the calculation of three dimensional flows
[F+W-TF-2012] p 767 N92-27045
Rarefied-flow aerodynamics
[NASA-CR-190452] p 715 N92-27191
Experimental investigation of turbulence behavior in shock wave/turbulent boundary layer interactions
[AD-A247792] p 774 N92-27886
Comparison of Euler and full potential methods for unsteady transonic flow calculations
p 719 N92-27943
Experimental aerodynamic facilities of the Aerodynamics Research and Concepts Assistance Branch
[AD-A247489] p 883 N92-28248
Integrating aerodynamics and structures in the minimum weight design of a supersonic transport wing
[NASA-TM-107586] p 850 N92-28435
Application of piloted simulation to high-angle-of-attack flight-dynamics research for fighter aircraft
p 886 N92-28551
Boundary conditions for Euler equations at internal block faces of multi-block domains using local grid refinement
[NLR-TP-90134-U] p 908 N92-28712
Nonlinear normal and axial force indicial responses for a two dimensional airfoil
[AD-A247196] p 830 N92-28888
Parameter identification for nonlinear aerodynamic systems
[NASA-CR-190264] p 830 N92-29329
Second-order shock-expansion theory extended to include real gas effects
[AD-A247191] p 831 N92-29539
Aerodynamic design optimization using sensitivity analysis and computational fluid dynamics
[NASA-CASE-LAR-14815-1-CU] p 910 N92-29830
A preliminary experimental investigation of local isotropy in high-Reynolds-number turbulence
p 912 N92-30042
Non-linear interactions in homogeneous turbulence with and without background rotation p 912 N92-30044
Selection of opening model for parachute scaling studies
[AD-A250882] p 943 N92-30239
Ultra high bypass Nacelle aerodynamics inlet flow-through high angle of attack distortion test
[NASA-CR-189149] p 943 N92-30298
Research and technology, 1991. Langley Research Center
[NASA-TM-4331] p 1013 N92-30733
Yaw dynamics of horizontal axis wind turbines
[DE92-001245] p 1004 N92-30837
Nonlinear stability and control study of highly maneuverable high performance aircraft, phase 2
[NASA-CR-190667] p 978 N92-30922
Nonlinear aerodynamics and the design of wing tips
[NASA-CR-190649] p 946 N92-31157
Overview of the NASA Dryden Flight Research Facility aeronautical flight projects
[NASA-TM-104254] p 962 N92-31261
In-flight leading-edge extension vortex flow-field survey measurements on a F-18 aircraft at high angle of attack
[NASA-TM-4398] p 947 N92-31276
Automatic design of transonic airfoils to reduce the shock induced pressure drag p 949 N92-31863
Axisymmetric bluff-body flow: A vortex solver for thin shells
[DE92-016748] p 1003 N92-31933
A continuing study of altitude determination deficiencies of the Service Aircraft Instrumentation Package (SAIP)
[AD-A245952] p 968 N92-32051
Dynamic interactions between hypersonic vehicle aerodynamics and propulsion system performance
[NASA-CR-190638] p 1038 N92-33304
On the anomalies in single-jet hover suckdown data
[NASA-TM-102261] p 1038 N92-33306
Implementation of a personal computer based parameter estimation program
[AD-A252914] p 1061 N92-33502
Research and technology, 1990
[NASA-TM-107967] p 1143 N92-33948

AEROELASTIC RESEARCH WINGS

Application of aeroservoelastic modeling using minimum-state unsteady aerodynamic approximations
p 204 A92-18622
Static aeroelastic analysis for generic configuration wing p 174 A92-20201
Application of analytical and design tools for fighter wing aeroelastic tailoring
[AIAA PAPER 92-2373] p 542 A92-34543
AIAA Dynamics Specialists Conference, Dallas, TX, Apr. 16, 17, 1992, Technical Papers p 565 A92-35651
A summary of the Active Flexible Wing program
[AIAA PAPER 92-2080] p 565 A92-35652
Simulation and model reduction for the AFW program
[AIAA PAPER 92-2081] p 572 A92-35653
Further investigations of the aeroelastic behavior of the AFW wind-tunnel model using transonic small disturbance theory
[AIAA PAPER 92-2082] p 565 A92-35654
The multiple-function multi-input/multi-output digital controller system for the AFW wind tunnel model
[AIAA PAPER 92-2083] p 565 A92-35655
On-line analysis capabilities developed to support the AFW wind-tunnel tests
[AIAA PAPER 92-2084] p 572 A92-35656
Flutter suppression digital control law design and testing for the AFW wind tunnel model
[AIAA PAPER 92-2095] p 566 A92-35668
A flutter suppression system using strain gages applied to Active Flexible Wing Technology - Design and test
[AIAA PAPER 92-2098] p 566 A92-35669
Rolling Maneuver Load Alleviation using active controls
[AIAA PAPER 92-2099] p 566 A92-35670
Maneuver load control using optimized feedforward commands
[AIAA PAPER 92-2100] p 567 A92-35671
New time-domain technique for flutter boundary identification
[AIAA PAPER 92-2102] p 588 A92-35673
Predicted and measured in-flight wing deformations of a forward-swept-wing aircraft p 548 A92-35936
Investigation of the aeroelastic stability of the AFW wind-tunnel model using CAP-TSD
[NASA-TM-104142] p 81 N92-11977
Extension of the integral equation formulation of linearized time dependent subsonic flow
[AD-A250654] p 947 N92-31171
A summary of the active flexible wing program
[NASA-TM-107655] p 962 N92-31264
Flutter suppression digital control law design and testing for the AFW wind-tunnel model
[NASA-TM-107652] p 962 N92-31350
Rolling maneuver load alleviation using active controls
[NASA-TM-107654] p 962 N92-31351

AEROELASTICITY

Aeroelastic stability analysis of aerial propellers
p 24 A92-10955
Extensions to the minimum-state aeroelastic modeling method p 20 A92-11081
Static aeroelastic control using strain actuated adaptive structures p 26 A92-11122
Parallel computation of aerodynamic influence coefficients for aeroelastic analysis on a transputer network p 53 A92-12367
Aeroelastic analysis of wings using the Euler equations with a deforming mesh p 10 A92-13215
Step response of unsteady aerodynamics acting on a plane swept wing in incompressible flow for finite state modeling p 63 A92-14031
An integrated airloads-inflow model for use in rotor aeroelasticity and control analysis p 64 A92-14328
Recent rotorcraft aeroelastic testing in the Langley Transonic Dynamics Tunnel p 136 A92-14377
Experimental investigation of helicopter vibration reduction using rotor blade aeroelastic tailoring
p 107 A92-14396
V-22 pilot-in-the-loop aeroelastic stability analysis
p 133 A92-14422

Evaluation of an advanced finite element analysis for rotor blades p 109 A92-14426
Optimization of the flutter load by material orientation p 146 A92-15222
Aeroelastic tailoring of aeronautical composite wing structures p 146 A92-15343
Computational study of stall flutter in linear cascades [ASME PAPER 91-GT-5] p 67 A92-15503
Optical measurements of unducted fan flutter [ASME PAPER 91-GT-19] p 147 A92-15510
The effect of steady aerodynamic loading on the flutter stability of turbomachinery blading [ASME PAPER 91-GT-130] p 71 A92-15574
Aeroservoelastic stabilization techniques for hypersonic flight vehicles [AIAA PAPER 91-5056] p 203 A92-17839
Cabin structural vibration and noise for transport aircraft p 192 A92-17876
Aerodynamic damping of blade vibrations in turbomachines --- Russian book p 200 A92-18198
Experimental and theoretical analysis of composite I-beams with elastic couplings p 216 A92-18377
Parameter insensitive control utilizing eigenspace methods --- for flutter suppression in aeroelastic vehicles p 204 A92-18615
Flutter analysis of anisotropic panels with patched cracks p 219 A92-20216
Nonlinear stall flutter and divergence analysis of cantilevered graphite/epoxy wings p 219 A92-20746
Time domain flutter analysis of cascades using a full-potential solver p 176 A92-20747
Linear panel flutter of an elliptic cylindrical shell p 291 A92-21216
Integrated flight control law synthesis for an aeroelastic forward-swept wing aircraft [AIAA PAPER 92-0046] p 281 A92-22163
An experimental system to investigate subsonic aeroelastic behavior of lifting surfaces [AIAA PAPER 92-0061] p 250 A92-22176
A parametric study of the aeroelastic stability of a binary wing-with-engine nacelle flutter system in incompressible flow p 270 A92-22472
The Civil Rotorcraft Initiative - An action agenda p 241 A92-22707
Static aeroelastic tailoring of composite aircraft swept wings modelled as thin-walled beam structures p 294 A92-23114
Unsteady aerodynamic methods for turbomachinery aeroelastic and aeroacoustic applications [AIAA PAPER 92-0011] p 252 A92-23730
Transonic aeroelasticity analysis using state-space unsteady aerodynamic modeling p 310 A92-24422
The calculation of the static elastic aerodynamic distribution for the rolling maneuver aircraft p 379 A92-25010
Aeroelastic analysis of swept, anhedral, and tapered tip rotor blades p 316 A92-25577
Concerning a basic assumption for aeroelasticity in turbomachinery p 373 A92-26920
Measurements of the inflow to a vibrating rotor blade [AIAA PAPER 92-0634] p 333 A92-27012
A numerical method for analyzing the nonlinear flutter of wings at high angles of attack p 338 A92-27827
Aeroelastic analysis of advanced propellers using an efficient Euler solver [AIAA PAPER 92-0488] p 341 A92-28194
Dynamic stability of elastic vehicles with unsteady aerodynamic force modeling p 509 A92-29326
On automatic control of aeroelastic vehicles p 509 A92-29327
Problems of strength and aeroelasticity of present-day propfans p 471 A92-30133
Effect of shock waves on the critical rate of bending-torsional flutter of an airfoil p 494 A92-30208
Reduction of computational models in strength problems p 496 A92-31858
A procedure for calculating the static aeroelasticity characteristics of flight vehicles by the influence coefficient method using three-dimensional finite element schemes p 460 A92-31896
Integrated aeroelastic control optimization of laminated composite lifting surfaces p 481 A92-32248
Impact of structural optimization with aeroelastic/multidisciplinary constraints on helicopter rotor design [AIAA PAPER 92-1001] p 535 A92-33193
Multidisciplinary design optimization of a large transport aircraft wing [AIAA PAPER 92-1002] p 536 A92-33194
Effect of adaptive material properties on static aeroelastic control [AIAA PAPER 92-2526] p 539 A92-34373
AIAA/ASME/ASCE/AHS/ASC Structures, Structural Dynamics and Materials Conference, 33rd, Dallas, TX, Apr. 13-15, 1992, Technical Papers. Pt. 3 - Structural dynamics I p 584 A92-34389
Dynamic response to time-dependent excitations of cantilevered aircraft wing structures modelled as thin-walled beams [AIAA PAPER 92-2213] p 584 A92-34403
Experimental and theoretical study for nonlinear aeroelastic behavior of a flexible rotor blade [AIAA PAPER 92-2253] p 584 A92-34410
Nonlinear large amplitude aeroelastic behavior of composite rotor blades at large static deflection [AIAA PAPER 92-2257] p 540 A92-34412
Analytical aeroelastic stability considerations and conversion loads for an XV-15 tilt-rotor in a wind tunnel simulation [AIAA PAPER 92-2258] p 540 A92-34413
A new aeroelastic model for composite rotor blades with straight and swept tips [AIAA PAPER 92-2259] p 541 A92-34414
A study on the feasibility of using adaptive structures in the attenuation of vibration characteristics of rotary wings [AIAA PAPER 92-2452] p 541 A92-34415
Joined-wing model vibrations using PC-based modal testing and finite element analysis [AIAA PAPER 92-2260] p 541 A92-34417
AIAA/ASME/ASCE/AHS/ASC Structures, Structural Dynamics and Materials Conference, 33rd, Dallas, TX, Apr. 13-15, 1992, Technical Papers. Pt. 4 - Structural dynamics II p 584 A92-34451
Time simulation of flutter with large stiffness changes [AIAA PAPER 92-2394] p 585 A92-34467
FAMUSS - A new aeroservoelastic modeling tool [AIAA PAPER 92-2395] p 541 A92-34468
NACA 0012 benchmark model experimental flutter results with unsteady pressure distributions [AIAA PAPER 92-2396] p 517 A92-34469
Aircraft aeroservoelastic compensation using constrained optimization [AIAA PAPER 92-2399] p 564 A92-34470
Aeroelasticity - Advances and future directions [AIAA PAPER 92-2446] p 585 A92-34475
Vibration reduction in helicopter rotors using an active control surface located on the blade [AIAA PAPER 92-2451] p 564 A92-34478
Aeroelastic response and blade loads of a composite rotor in forward flight [AIAA PAPER 92-2566] p 564 A92-34480
Aeroelastic response of helicopters with flexible fuselage modeling [AIAA PAPER 92-2567] p 564 A92-34481
Parametric studies for tiltrotor aeroelastic stability in high-speed flight [AIAA PAPER 92-2568] p 565 A92-34482
Extending a transonic small disturbance code to treat swept vertical surfaces [AIAA PAPER 92-2503] p 518 A92-34498
Three-dimensional time-marching aeroelastic analyses using an unstructured-grid Euler method [AIAA PAPER 92-2506] p 542 A92-34500
A design optimization procedure for high-speed prop-rotors [AIAA PAPER 92-2375] p 542 A92-34545
New complex pole and gust response approximations for integrated aeroservoelastic synthesis [AIAA PAPER 92-2377] p 565 A92-34547
Aeroelastic optimization of an advanced geometry helicopter rotor [AIAA PAPER 92-2360] p 543 A92-34592
Analysis of cascades using a two dimensional Euler aeroelastic solver [AIAA PAPER 92-2370] p 556 A92-34598
Multifunction tests of a frequency domain based flutter suppression system [AIAA PAPER 92-2096] p 566 A92-35667
Development and analysis of flight flutter prediction methods [AIAA PAPER 92-2101] p 588 A92-35672
Robustness characteristics of fast-sampling digital controllers for active flutter suppression [AIAA PAPER 92-2104] p 567 A92-35675
An analytical and experimental investigation of flutter suppression via piezoelectric actuation [AIAA PAPER 92-2106] p 567 A92-35677
Rotary-wing aeroservoelastic problems [AIAA PAPER 92-2107] p 567 A92-35678
Coupled rotor-fuselage dynamics and aeroelasticity in turning flight [AIAA PAPER 92-2109] p 544 A92-35680
An experimental and analytical investigation of wing flutter on a trail rotor V/STOL aircraft [AIAA PAPER 92-2112] p 544 A92-35682
A numerical classical flutter analysis of advanced propellers [AIAA PAPER 92-2118] p 557 A92-35687
Role of shock dynamics in transonic flutter [AIAA PAPER 92-2121] p 520 A92-35690
A new method for transonic static aeroelasticity problems [AIAA PAPER 92-2123] p 589 A92-35691
Temperature and initial curvature effects in low-density panel flutter [AIAA PAPER 92-2128] p 589 A92-35695
The use of Stodola modes in rotor-blade aeroelastic studies p 590 A92-35729
A piloted comparison of elastic and rigid blade-element rotor models using parallel processing technology p 546 A92-35751
Evaluation of a constant feedback gain for closed loop higher harmonic control p 568 A92-35768
Bearingless rotor aeromechanical stability measurements and correlations using nonlinear aerodynamics p 547 A92-35772
Theoretical and experimental study of a model rotor p 547 A92-35781
Trends of research on cascade flutter p 558 A92-35914
Limit cycle oscillation and flight flutter testing p 570 A92-35939
Aeroelastic tailoring analysis for advanced turbo propellers with composite blades p 558 A92-36358
Nonstationary aerohydroelasticity of spherical bodies --- Russian book [ISBN 5-02-014006-6] p 670 A92-36611
Comparison of two flutter analysis methods for elastic aircraft p 660 A92-37394
Aeroservoelasticity p 642 A92-37577
Robust frequency design of linear stationary systems in aeroautoelastics p 690 A92-37791
Integral equation methods for linear and nonlinear aerodynamics p 617 A92-39949
Comparison of elastic and rigid blade-element rotor models using parallel processing technology for piloted simulations [SAE PAPER 912120] p 608 A92-39968
Aeroelasticity and the Tiltrotor VTOL aircraft p 647 A92-40389
1991-92 AHS Technical Committee highlights - Dynamics p 647 A92-40393
Extension and validation of an unsteady wake model for rotors p 702 A92-41224
Application of Active Flexible Wing technology to the Agile Falcon p 729 A92-41233
Transonic aeroelasticity analysis for rotor blades p 758 A92-41238
Coalescence of aeroelastic modes in flutter analysis p 758 A92-41241
Structural and aerodynamic data transformation using inverse isoparametric mapping p 758 A92-41242
Transition of the flutter mode of a two-dimensional section with an external store p 758 A92-41244
A model of a deformable aeroplane with a wing of low aspect ratio and movable control surfaces for studying natural vibrations p 744 A92-41528
An aerodynamic hypothesis for the wing aeroelasticity problem p 761 A92-42665
Helicopter aeroelastic stability and response - Current topics and future trends p 730 A92-43100
Dynamic response and aeroelastic analysis of a propeller blade of a prop-fan engine p 762 A92-43109
Optimization of blade structure to reduce rotor vibration p 730 A92-43118
Research on state equations of unsteady aerodynamics p 709 A92-43132
Gust load alleviation control design for the accuracy of an aeroelastic active control model p 745 A92-43134
ACT wind tunnel experiment on gust load alleviation. II - Wind tunnel test with active support facility p 745 A92-43135
Response characteristics of a wing in supersonic flow near flutter boundary [SAE PAPER 911999] p 789 A92-45401
On-line performance evaluation of multiloop digital control systems p 873 A92-46739
Integrated aeroservoelastic wing synthesis by nonlinear programming/approximation concepts p 873 A92-46752
Navier-Stokes computations on swept-tapered wings, including flexibility p 810 A92-46786
An aeroelastic analysis with a generalized dynamic wake p 847 A92-46932
Research on helicopter rotors - Progress in aerodynamics, aeroelasticity and acoustics [ONERA, TP NO. 1992-27] p 849 A92-48589
Advances in aircraft modal identification [ONERA, TP NO. 1992-47] p 877 A92-48608
Helicopter rotor blade aeroelasticity in forward flight with an implicit structural formulation p 958 A92-50315
Solution of Euler equations with unstructured mesh - 3-D case p 941 A92-52973
Design variables and constraint derivatives in aeroelastic tailoring p 997 A92-53074

Stability and dynamic coupling of elastic vehicles with unsteady aerodynamic forces considered
p 1102 A92-53545
FREPS - A forced response prediction system for turbomachinery blade rows
[AIAA PAPER 92-3072] p 1130 A92-54006
Rotary wing structural dynamics and aeroelasticity --- Book
[ISBN 1-56347-031-4] p 1052 A92-54550
Aeroelastic modal characteristics of mistuned blade assemblies - Mode localization and loss of eigenstructure p 1117 A92-54921
Vortical flow computations on a flexible blended wing-body configuration p 1024 A92-54922
Getting up to speed in hypersonic structures
p 1117 A92-55127
Dynamics and control of hypersonic aeropropulsive/aeroelastic vehicles
[AIAA PAPER 92-4326] p 1073 A92-55170
New literal approximations for the longitudinal dynamic characteristics of flexible flight vehicles
[AIAA PAPER 92-4411] p 1075 A92-55205
E-6 flutter investigation and experience
[AIAA PAPER 92-4601] p 1077 A92-55280
Automated procedures for aircraft aeroservoelastic compensation
[AIAA PAPER 92-4606] p 1077 A92-55284
Parameter identification of unsteady aerodynamic forces for elastic vehicles
[AIAA PAPER 92-4505] p 1027 A92-55372
Numerical simulations of flutter and its suppression by active control
[AIAA PAPER 92-4652] p 1082 A92-55396
An example of whirl flutter analysis
p 1052 A92-56015
Propeller-nacelle whirl flutter analysis and wind tunnel test p 1052 A92-56016
Optimization of composite material wing of fighter type aircrafts p 1053 A92-56018
Analysis and wind tunnel test of low aspect wing gust load alleviation p 1053 A92-56020
Synthesis of gust load alleviation with flutter margin augmentation p 1082 A92-56021
Optimization of aeroelastic system with active control
p 1083 A92-56022
Measurements of blade flapping motion on a wind tunnel model p 1093 A92-56023
Generalized aerodynamics analysis by the boundary element method p 1030 A92-56050
Aeroelastic effects of spoiler surfaces on a low-aspect-ratio rectangular wing p 1030 A92-56154
Dynamic analysis of rotor blades with root retention design variations p 1054 A92-56156
Multidisciplinary optimization of aeroservoelastic systems using reduced-size models
p 1054 A92-56176
Flutter and stall response of a helicopter blade with structural nonlinearity p 1055 A92-56178
Demonstration of structural optimization applied to wind-tunnel model design p 1119 A92-56181
Simulation of helicopter see-saw rotor motion
p 1055 A92-56287
Dynamics of helicopters with dissimilar blades in forward flight p 1056 A92-56288
Aeroelasticity of a coaxial helicopter rotor
p 1057 A92-56309
A time-dependent tip loss formula for rotor blade dynamic analysis p 1057 A92-56310
A finite element method for shear stresses calculation in composite blade models p 1121 A92-56322
An approach for increasing aeroelastic divergence dynamic pressure of wind-tunnel models
[AIAA PAPER 92-4002] p 1099 A92-56825
Buffet test in the National Transonic Facility
[AIAA PAPER 92-4032] p 1100 A92-56854
An integrated analytical aeropropulsive/aeroelastic model for the dynamic analysis of hypersonic vehicles
[AIAA PAPER 92-4567] p 1035 A92-57034
Development of unsteady aerodynamic analyses for turbomachinery aeroelastic and aeroacoustic applications
[NASA-CR-4405] p 12 N92-10979
Three dimensional numerical method for resolving small transonic perturbations in unstructured mesh
[ONERA-RT-56/3064-RY-006-R] p 13 N92-10989
Perfect compressible two dimensional boundary layer strong fluid coupling in the case of sharp leading edge profiles. Unsteady case of isolated profiles and steady case of blade grids
[ONERA-RT-43/1621-RY-006-R] p 43 N92-11311
Multi-disciplinary optimization of aeroservoelastic systems
[NASA-CR-188983] p 44 N92-11377
Investigation of the aeroelastic stability of the AFW wind-tunnel model using CAP-TSD
[NASA-TM-104142] p 81 N92-11977
An experimental study of the sensitivity of helicopter rotor blade tracking to root pitch adjustment in hover
[NASA-TM-4313] p 61 N92-12989
A numerical solution of implicit nonlinear equations of motion for rotor blades p 115 N92-13053
Planform curvature effects on flutter characteristics of a wing with 56 deg leading-edge sweep and panel aspect ratio of 1.14
[NASA-TP-3116] p 115 N92-13054
Control augmented structural optimization of aeroelasticity tailored fiber composite wings
[AD-A241464] p 135 N92-13075
Technical activities of the configuration aeroelasticity branch
[NASA-TM-104146] p 159 N92-13458
International aviation (selected articles)
[AD-A241119] p 170 N92-13993
The benchmark aeroelastic models program: Description and highlights of initial results
[NASA-TM-104180] p 185 N92-15049
Structural dynamics division research and technology accomplishments for F.Y. 1991 and plans for F.Y. 1992
[NASA-TM-104188] p 261 N92-17509
Response of structures to galloping excitation: Background and approximate estimation
[ESDU-91010] p 399 N92-18091
Semi-empirical model for prediction of unsteady forces on an airfoil with application to flutter
[NASA-TM-105414] p 346 N92-18760
Aeroservoelastic stability of aircraft at high incidence
p 381 N92-18795
Investigation of the effects of aeroelastic deformations on the radar cross section of aircraft
[AD-A243889] p 402 N92-18940
Engine Structures Modeling Software System (ESMOSS)
[NASA-CR-187227] p 404 N92-19277
A study of the aeroelastic behaviour of helicopter rotor blades featuring swept tips p 367 N92-19701
Aeroelastic behavior of an adaptive lifting surface
p 443 N92-20378
Unsteady-pressure and dynamic-deflection measurements on an aeroelastic supercritical wing
[NASA-TM-4278] p 445 N92-20654
Current status of computational methods for transonic unsteady aerodynamics and aeroelastic applications
[NASA-TM-104191] p 446 N92-21432
A historical overview of tiltrotor aeroelastic research at Langley Research Center
[NASA-TM-107578] p 502 N92-21460
Materials and Structures Research Department: Scientific report (1990)
[ETN-92-90727] p 466 N92-22000
Further investigations of the aeroelastic behavior of the AFW wind-tunnel model using transonic small disturbance theory
[NASA-TM-107576] p 526 N92-22240
Determining structural performance
p 560 N92-22519
Three-dimensional time-marching aeroelastic analyses using an unstructured-grid Euler method
[NASA-TM-107567] p 527 N92-23116
Integrated Design Analysis and Optimisation of Aircraft Structures
[AGARD-R-784] p 550 N92-23227
Sensitivity analysis of dynamic aeroelastic responses
p 571 N92-23229
Application of analytical and design tools for fighter wing aeroelastic tailoring p 550 N92-23231
The structural optimization system OPTSYS: Current status and applications p 550 N92-23232
Application of an automated multidisciplinary analysis and optimisation system to the design of aircraft structures p 551 N92-23233
Multidisciplinary optimization studies using ASTROS
p 571 N92-23234
Proceedings of the 3rd Canadian Symposium on Aerodynamics
[CTN-92-60420] p 625 N92-24849
Nonliner aspects of transonic aeroelasticity
p 628 N92-24864
Flowfield in the vicinity of the F/A-18 vertical fin at high-angle-of-attack p 628 N92-24865
Algorithm and code development for unsteady three-dimensional Navier-Stokes equations
[NASA-CR-190077] p 692 N92-25264
Static aeroelastic analysis of ACT wind tunnel model aircraft
[NAL-TM-624] p 632 N92-25366
Vibration tests and structural modeling of an aircraft model for active control technology experiments
[NAL-TM-626] p 662 N92-25401
Large scale optimization using ASTROS: An overview
p 649 N92-25921
Transonic Unsteady Aerodynamics and Aeroelasticity
[AGARD-CP-507] p 718 N92-27936
Current status of computational methods for transonic unsteady aerodynamics and aeroelastic applications
p 718 N92-27937
Unstructured-grid methods development for unsteady aerodynamic and aeroelastic analyses
p 718 N92-27938
Unsteady aerodynamics for aeroelasticity at the Flight Dynamics Directorate p 718 N92-27939
Recent applications of linear and nonlinear unsteady aerodynamics for aeroelastic analysis
p 718 N92-27940
Comparison of Euler and full potential methods for unsteady transonic flow calculations
p 719 N92-27943
NLR inviscid transonic unsteady loads prediction methods in aeroelasticity p 720 N92-27947
Transonic aeroelastic calculations in both the time and frequency domains p 720 N92-27950
Aeroelastic calculations for fighter aircraft using the transonic small disturbance equation
p 720 N92-27951
Analysis of unsteady aerodynamic and flutter characteristics of an aeroelastic model in transonic flow
p 720 N92-27953
Direct coupling of fluid structure in transonic aeroelasticity p 721 N92-27954
Investigation of the aeroelastic stability of the AFW wind-tunnel model using CAP-TSD p 721 N92-27955
Numerical simulation of shock-stall flutter of an airfoil using the Navier-Stokes equations p 746 N92-27956
Transonic aeroelastic computations on wings using Navier-Stokes equations p 721 N92-27957
Development of a method to predict transonic limit cycle oscillation characteristics of fighter aircraft
p 746 N92-27958
The benchmark aeroelastic models program: Description and highlights of initial results
p 721 N92-27960
Practical architecture of design optimisation software for aircraft structures taking the MBB-Lagrange code as an example p 851 N92-28471
Structural optimization of aircraft p 851 N92-28472
Mathematical optimization: A powerful tool for aircraft design p 851 N92-28474
Buffet test in the National Transonic Facility
[NASA-CR-189595] p 888 N92-29352
Modeling and analysis methodology for aeroelastically tailored chordwise deformable wings
[NASA-CR-189620] p 961 N92-30304
Influence of structural and aerodynamic modeling on flutter analysis and structural optimization
[AD-A248487] p 978 N92-30323
MBB-LAGRANGE: A general structural reliability and optimization structural system
[MBB/FW321/S/PUB/467] p 998 N92-30423
Composite beam analysis linear analysis of naturally curved and twisted anisotropic beams
[AD-A252652] p 999 N92-30766
An analytical and experimental investigation of flutter suppression via piezoelectric actuation
[NASA-TM-107653] p 962 N92-31174
Flutter suppression digital control law design and testing for the AFW wind-tunnel model
[NASA-TM-107652] p 962 N92-31350
Time simulation of flutter with large stiffness changes
[NASA-TM-107650] p 963 N92-32111
Strong coupling between inviscid fluid and boundary layer of sharp leading edges: Two-dimensional stationary and turbulent cases for isolated profiles and guard vanes
[ONERA-RT-44/1621-RY-016-R] p 1125 N92-32776
Pressure measurements on a rectangular wing with a NACA0012 airfoil during conventional flutter
[NASA-TM-104211] p 1042 N92-34147
Introduction to Flutter of Winged Aircraft, volume 2
[VKI-LS-1992-01-VOL-2] p 1088 N92-34161
Aeroelasticity of bluff bodies p 1089 N92-34165
Unsteady wind tunnel tests p 1089 N92-34166
Flutter in the transonic flight regime
p 1089 N92-34167

AEROLOGY

A ionospheric-sounding experiment from an aircraft
p 160 A92-13809

AEROMANEUVERING

Rotorcraft Maneuverability and Agility Survivability Sensitivity Analysis (RMASSA) p 161 A92-14351

AERONAUTICAL ENGINEERING

Developing undergraduate gas turbine and turbomachinery courses
[AIAA PAPER 91-2509] p 56 A92-12700
Technology in the lives of an aircraft designer
[AIAA PAPER 91-3069] p 192 A92-20000
A modern view of Theodore Theodorsen --- Book
[ISBN 0-930403-85-1] p 307 A92-26250
Advances of cryogenics in aeronautics and astronautics p 398 A92-27908

Tying it all together - The NASA/USRA University Advanced Design Program
[AIAA PAPER 92-1040] p 605 A92-33221
Facing the crisis in aircraft design education
p 606 A92-34770
Modern aircraft design. Vol. 1 (2nd Edition) --- Book
p 647 A92-40897
BA's 777 p 958 A92-51580
777 shaping up p 959 A92-52300
Study of alternatives: Dayton's Aviation heritage, Ohio
[PB91-202275] p 2 N92-10972
A review of aeronautical fatigue investigations in Sweden during the period May 1989 to April 1991
[FFA-TN-1991-24] p 158 N92-12313
International aviation (selected articles)
[AD-A241119] p 170 N92-13993
Review of investigations on aeronautical fatigue in the Federal Republic of Germany
[ETN-92-90317] p 225 N92-14397
Dynamic flying investigations on 1/13.5 NALLA model (Longitudinal Results)
[NAL-PD-FC-9113] p 359 N92-18073
The Goldstein Engineering Research Laboratory
[AERO-REPT-8906] p 308 N92-18322
Techfest 18 Proceedings
[NIAR-92-1] p 420 N92-21501
Aeronautical research in the United States: Challenges for the 1990's p 420 N92-21502
DLR-news: Announcements of the German Research Institute for Aeronautics and Astronautics
p 698 N92-25413
Naval Postgraduate School aircraft synthesis program (user's manual)
[AD-A246198] p 777 N92-26458
Development of telemetry for the agility flight test of a radio controlled fighter model
[AD-A248653] p 753 N92-27994
NASA/DOD Aerospace Knowledge Diffusion Research Project. Paper 13: The information-seeking habits and practices of engineers
[NASA-TM-107931] p 782 N92-28114
Aeronautical Engineering Group publications, 1950 - present
[AERO-REPT-8907] p 910 N92-29683
Numerical optimization in Germany: A non-exhaustive survey on current activities with emphasis on aeronautics
[MBB/FE211/S/PUB/474] p 932 N92-30675
United States Air Force summer research program 1991. Volume 1: Program management report
[AD-A248763] p 1142 N92-32338
NASA authorization, 1993, volume 1
[GPO-55-260-VOL-1] p 1142 N92-33147
Activities report of the National Aerospace Laboratory
[ETN-92-92053] p 1143 N92-33694
Research and technology, 1990
[NASA-TM-107967] p 1143 N92-33948

AERONAUTICAL SATELLITES

Ranging and positioning experiments for aircraft using Engineering Test Satellite V p 102 A92-17242
Experiments on aeronautical satellite communications using ETS-V p 395 A92-26779
High gain airborne antenna for satellite communications p 354 A92-26780
Characteristics of a future aeronautical satellite communications system
[AIAA PAPER 92-2058] p 453 A92-29889
ACTS aeronautical experiments
[AIAA PAPER 92-2042] p 485 A92-29956
Experiments on aeronautical satellite communications using ETS-V satellite p 639 A92-40187
High gain airborne antenna for satellite communications p 639 A92-40188
History of aeronautical satellite communications
p 1046 A92-56088
Aeronautical satellite communications system
p 1046 A92-56089
Evaluation report of an experimental Satcom operation by a Japan Airline's B747 passenger plane
p 1046 A92-56092
Aeronautical satellite system test and implementation
p 676 N92-24095
Inmarsat aeronautical mobile satellite system: Internetworking issues p 677 N92-24098
System considerations, projected requirements and applications for aeronautical mobile satellite communications for air traffic services
p 677 N92-24163
Aeronautical mobile satellite service: Air traffic control applications p 677 N92-24164
Spectrum sharing between AMSS(R) and MSS
p 677 N92-24165
Future developments in aeronautical satellite communications p 678 N92-24167

AERONAUTICS

Sound generation by a stenosis in a pipe
p 415 A92-26405
Iberia's Aeronautical Mapping Application (ACAI)
p 637 A92-37073
1991 report to the aerospace profession; SETP Symposium, 35th, Beverly Hills, CA, Sept. 26-28, 1991, Proceedings p 645 A92-40028
Aircraft Symposium, 28th, Tokyo, Japan, Nov. 7-9, 1990, Proceedings p 699 A92-43095
A review of UK aviation policy
[TT-9107] p 61 N92-12988
Techfest 18 Proceedings
[NIAR-92-1] p 420 N92-21501
Research and technology, 1991
[NASA-TM-105320] p 516 N92-22659
DLR-News: Announcements of the German Research Institute for Aeronautics and Astronautics
p 698 N92-26086
An international aerospace information system: A cooperative opportunity
[NASA-TM-108171] p 1142 N92-33237
Research and technology, 1990
[NASA-TM-107967] p 1143 N92-33948

AEROSOLS

Twenty years of airborne research at the University of Washington p 161 A92-14925
Measured and calculated optical property profiles in the mixed layer and free troposphere p 1129 A92-54630
Meeting Review: Airborne Aerosol Inlet Workshop
[NASA-CR-189814] p 301 N92-17393
Lower stratospheric measurement issues workshop report p 409 N92-19127

AEROSPACE ENGINEERING

Testing capabilities at AEDC for development of hypersonic vehicles
[AIAA PAPER 91-5027] p 483 A92-31686
Constraint-based component-modeling for knowledge-based design
[AIAA PAPER 92-1192] p 600 A92-33304
AIAA/ASME/ASCE/AHS/ASC Structures, Structural Dynamics and Materials Conference, 33rd, Dallas, TX, Apr. 13-15, 1992, Technical Papers. Pt. 4 - Structural dynamics II p 584 A92-34451
Designing a better engineer p 606 A92-34771
Why composites wait in the wings
p 577 A92-35475
Composite materials for aerospace applications
p 577 A92-36377
International Aerospace Symposium 90, Nagoya, Japan, Nov. 26, 27, 1990, Proceedings p 607 A92-38201
1991-92 AHS Technical Committee highlights - Manufacturing and product assurance
p 609 A92-40396
Shot peening - Theory and applications --- Book
[ISBN 2-907669-18-4] p 676 A92-40400
Engineering and technology Japanese aircraft/spacecraft p 699 A92-41781
Acoustic transmission through a 2-D orthotropic multi-layered infinite cylindrical shell p 780 A92-44197
Super plastic forming technology applied to aeroengine and space equipment p 764 A92-44732
Applied aerodynamics education - Design and science
[AIAA PAPER 92-2662] p 928 A92-45581
Aerospace pressurization system design
[SAE AIR 1168/7] p 849 A92-48022
Aircraft Symposium, 29th, Gifu, Japan, Oct. 7-9, 1991, Proceedings p 1015 A92-56001
The wind tunnel, its evolution for aerospace test purposes, perspective for curriculum development
[AIAA PAPER 92-4017] p 1100 A92-56839
Development and integration of modern laboratories in aerospace education
[AIAA PAPER 92-4022] p 1141 A92-56844
Computers in aeronautics and space research at the Lewis Research Center
[NASA-TM-105096] p 53 N92-11642
Eighty years of aerospace technique through ATMA bulletins
[ETN-91-90097] p 57 N92-11963
NASA reliability preferred practices for design and test
[NASA-TM-4322] p 157 N92-12286
JPRS report: Science and technology. USSR: Space
[JPRS-USP-91-007] p 211 N92-14101
Proceedings of the USAF Structural Integrity Program Conference
[AD-A242943] p 279 N92-17204
Techfest 18 Proceedings
[NIAR-92-1] p 420 N92-21501
JPRS report: Science and technology. Central Eurasia: Engineering and equipment
[JPRS-UEQ-92-002] p 592 N92-22298
Research and technology, 1991
[NASA-TM-105320] p 516 N92-22659
JPRS report: Science and technology. Central Eurasia: Space
[JPRS-USP-92-002] p 575 N92-23705
DLR-news: Announcements of the German Research Institute for Aeronautics and Astronautics
p 698 N92-25413
DLR-News: Announcements of the German Research Institute for Aeronautics and Astronautics
p 698 N92-26086
Rarefied-flow aerodynamics
[NASA-CR-190452] p 715 N92-27191
System requirements specification for SMART structures mode p 777 N92-27830
AFRAPT Program at Texas A and M University research for advanced aircraft engine structures
[AD-A247040] p 743 N92-28076
NASA/DOD Aerospace Knowledge Diffusion Research Project. Paper 14: An analysis of the technical communications practices reported by Israeli and US aerospace engineers and scientists
[NASA-TM-107924] p 782 N92-28183
The basic research simulator programme and the industrial and aerospace community: Opportunities for cooperative research
[LR-662] p 887 N92-28579
DLR research reports and communications
[ETN-92-91391] p 929 N92-29218
Trends in aeropropulsion research and their impact on engineering education
[NASA-TM-105682] p 972 N92-31172
An international aerospace information system: A cooperative opportunity
[NASA-TM-108171] p 1142 N92-33237
Research and technology, 1990
[NASA-TM-107967] p 1143 N92-33948

AEROSPACE ENVIRONMENTS

Atmospheric disturbance model for aircraft and space capable vehicles
[AIAA PAPER 92-0294] p 407 A92-25747

AEROSPACE INDUSTRY

Damage assessment for composite smart structures
p 140 A92-13601
Industry warms to CFD p 392 A92-24908
Advanced materials for aircraft engine applications
p 390 A92-28251
36th Roy Chadwick Lecture - Manufacturing breakout 1941-1991: Development in aerospace industry manufacturing techniques p 419 A92-28941
Overview and major characteristics of future aeronautical and space systems
[AIAA PAPER 92-2441] p 585 A92-34472
International Aerospace Symposium 90, Nagoya, Japan, Nov. 26, 27, 1990, Proceedings p 607 A92-38201
Robotics application in aerospace manufacturing
p 671 A92-38216
Self reliance in aerospace structures
p 758 A92-41190
Engineering and technology Japanese aircraft/spacecraft p 699 A92-41781
Fiber optic systems for mobile platforms IV; Proceedings of the Meeting, San Jose, CA, Sept. 18, 1990
[SPIE-1369] p 779 A92-42601
Working together in the development of the B777
p 1015 A92-56080
NASA reliability preferred practices for design and test
[NASA-TM-4322] p 157 N92-12286
Military and civil software standards and guidelines for guidance and control p 163 N92-12452
Aerospace technology: Technical data and information on foreign test facilities
[GAO/NSIAD-90-71FS] p 139 N92-13076
Proceedings of the USAF Structural Integrity Program Conference
[AD-A242943] p 279 N92-17204
Impact and promise of NASA aeropropulsion technology p 559 N92-22511

AEROSPACE MEDICINE

Testing and evaluation of the Vanner electrical inverters, models 24-1500 and SP 00112
[AD-A241914] p 299 N92-17216

AEROSPACE PLANES

Advanced SCRAM-LACE system concept for single-stage-to-orbit space plane
[IAF PAPER 91-272] p 32 A92-12599
H2/air subsystem combustion kinetics in aerospaceplane powerplants
[IAF PAPER 91-276] p 25 A92-12600
Slush hydrogen (SLH2) technology development for application to the National Aerospace Plane (NASP)
p 144 A92-13432
Test results of the expander cycle air turbo ramjet for a future space plane
[IAF PAPER 91-271] p 120 A92-14709
'Spaceplanes' R&D status of Japan
[AIAA PAPER 91-5002] p 209 A92-17802

A geometric approach to regulator and tracker design for an aerospace plane
[AIAA PAPER 91-5054] p 203 A92-17837
Hydrogen exhaust gas disposition by afterburning
[AIAA PAPER 91-5075] p 200 A92-17848
Hypersonic materials p 212 A92-18002
Spaceplane system studies p 285 A92-22632
Flight simulation and its application
p 284 A92-22634
Computational aerodynamic simulation on HOPE
p 251 A92-22635
Fiber optics for the National Aero-Space Plane
p 386 A92-24780
HOPE looks to CFD for help --- NASDA's H-II Orbiting Plane p 386 A92-24910
On the skip flight of a spaceplane
p 387 A92-25503
Computational studies of a superdetonative ram accelerator mode p 399 A92-28529
Air flow under a flight-vehicle engine
p 429 A92-30528
Safety test on the rolling angles of a winged vehicle in hypersonic speed p 480 A92-30549
Flight vehicles of the future p 419 A92-31525
French research and technology program on advanced hypersonic propulsion
[AIAA PAPER 91-5003] p 471 A92-31683
Aero-propulsive effects on configuration shaping
[AIAA PAPER 91-5064] p 459 A92-31691
Wide-range combustion chamber of ramjet
[AIAA PAPER 91-5094] p 472 A92-31696
Preliminary sizing methodology for hypersonic vehicles
p 460 A92-32233
Numerical simulation of hypersonic viscous flow for the design of H-II orbiting plane (HOPE)
p 612 A92-37549
X-31 flight test update p 645 A92-40034
International Conference on Aerospace Trends...2001 - From Aeroplane to Aerospace Plane, Thiruvananthapuram, India, June 27, 28, 1991, Proceedings p 751 A92-41184
Estimation of overall drag coefficient of an aerospace plane p 700 A92-41188
Basic design concepts for smart actuators for aerospace plane control p 752 A92-41193
Hypersonic testing technology of HOPE (H-II orbiting plane) p 747 A92-43096
Experimental studies on aerodynamic heating and thermal protection in hypersonic flight
p 709 A92-43101
Flight simulation of a spaceplane p 752 A92-43190
Wind tunnel tests on the motion of a spaceplane simulation for cable mount p 752 A92-43192
Aerodynamic design of a nonplanar airfoil by an inverse method with Navier-Stokes equations
p 711 A92-43197
Transonic visualization test for the airframe shape improvement of a spaceplane p 752 A92-43200
Motion estimation for cable-mount dynamic wind-tunnel test p 749 A92-43210
Estimation of spaceplane longitudinal stability and control derivatives from dynamic wind tunnel test
p 752 A92-43211
Estimation of spaceplane model inertia characteristics
p 752 A92-43212
On the characteristics of servo actuators attached to a model spaceplane for dynamic wind-tunnel test
p 762 A92-43213
International Pacific Air and Space Technology Conference and Aircraft Symposium, 29th, Gifu, Japan, Oct. 7-11, 1991, Proceedings
[SAE P-246] p 783 A92-45376
Estimation of spaceplane lateral-directional stability and control derivatives from dynamic wind tunnel test
[SAE PAPER 911979] p 872 A92-45384
Spaceplane longitudinal aerodynamic parameter estimation by cable-mount dynamic wind-tunnel test
[SAE PAPER 911980] p 788 A92-45385
Aerospace plane hydrogen scramjet boosting
[SAE PAPER 912071] p 891 A92-45451
Effects of wing planform on HSCT off-design aerodynamics --- High Speed Civil Transport
[AIAA PAPER 92-2629] p 844 A92-45501
Thrust/speed effects on long-term dynamics of aerospace planes p 889 A92-46766
Aerospace plane guidance using time-scale decomposition and feedback linearization
p 984 A92-50498
Thermal-structural panel buckling tests
p 993 A92-51409
Development study on air turbo-ramjet engine for space plane p 1065 A92-53487
Conceptual design of scramjet engine
p 1065 A92-53490
Key design considerations for scramjet powered space plane p 1066 A92-53491
Performance analysis of idealized scramjet
p 1066 A92-53493
Fabrication test and evaluation of graphite/PMR-15 polyimide for HOPE primary structure
p 1105 A92-53516
Aerodynamic heating characteristics of space planes tested by NAL hypersonic wind tunnel
p 1017 A92-53547
Calculations for aerodynamic characteristics of HOPE type vehicle in subsonic and hypersonic flow
p 1018 A92-53560
Spaceplane aerodynamic heating and thermal protection design method p 1102 A92-53578
Space plane navigation simulation
p 1103 A92-53603
Concepts of flight experiments for HOPE development
p 1103 A92-53635
Aerodynamic study of H-II Orbiting Plane, HOPE
p 1103 A92-53639
Aerodynamic studies on space plane configuration at hypersonic speed p 1019 A92-53641
An advanced scramjet propulsion concept for a 350 MG SSTO space plane - External nozzle performance
[AIAA PAPER 92-3719] p 1067 A92-54134
HOPE re-entry experimental vehicle
p 1103 A92-55098
Current status of R&D on materials for super/hypersonic transports p 1106 A92-56002
A shock tunnel experiment on aerodynamic interference induced by RCS jet p 1029 A92-56042
Aerothermodynamic test of spaceplane by thin-skin method p 1093 A92-56043
On the effect of canards on NAL spaceplane model (0 order) in low speed area p 1030 A92-56052
Lateral control of spaceplane at hypersonic flight
p 1104 A92-56069
Aerodynamic model identification of a spaceplane model from a cable-mount dynamic wind-tunnel test
p 1093 A92-56114
Evaluation of a IMU with optical fiber gyros in dynamic windtunnel tests p 1104 A92-56121
Tests results on Air Turbo Ramjet for a future space plane
[IAF PAPER 92-0657] p 1071 A92-57098
Combined exo/endoatmospheric transport alternatives
[IAF PAPER 92-0663] p 1104 A92-57102
Thermographic gust wind tunnel measurements
[ONERA-RF-31/3409-PY] p 81 N92-11972
Aerospace plane technology: Research and development efforts in Japan and Australia
[AD-A241641] p 62 N92-12991
The effect of a type 3 and type 4 shock/shock interaction on heat transfer in the stagnation region
p 160 N92-13867
Rapid near-optimal aerospace plane trajectory generation and guidance
[NASA-CR-189469] p 205 N92-14066
History of EPOS air-launched spaceplane project
p 211 N92-14103
Aerothermodynamic configuration of first generation aerospace planes (of Buran-type) and first flight results
p 211 N92-14975
Weight evaluation and sensitivity analysis for space plane. Part 2: TSTO
[NAL-TM-602-PT-2] p 287 N92-17754
Conceptual design of two-stage-to-orbit hybrid launch vehicle
[NASA-CR-190006] p 486 N92-20666
Conceptional design to heat-resistant airframe of HOPE p 575 N92-23820
Large thin composite thermostructural parts
p 576 N92-23821
Design challenges for the National Aero-Space Plane
p 551 N92-23822
The future challenge for aeropropulsion
[NASA-TM-105613] p 658 N92-25164
Assessment of flying-quality criteria for air-breathing aerospacecraft
[NASA-CR-4442] p 663 N92-25982
An experimental investigation of a 2-D scramjet inlet at flow Mach numbers of 8 to 25 and stagnation temperatures of 800 to 4,100 K p 739 N92-26586
Robust intelligent flight control for hypersonic vehicles
[NASA-CR-185680] p 746 N92-28209
Saenger: The reference concept and its technological requirements - aerothermodynamics
[MBB-FE-202-S-PUB-0463-A] p 890 N92-29629
Technology programme: Aerothermodynamics and propulsion integration. Numerical and experimental aerothermodynamics
[MBB-FE-202-S-PUB-0464-A] p 831 N92-29648
Aerothermodynamics and propulsion integration in the Saenger technology programme
[MBB-FE-202-S-PUB-0469-A] p 831 N92-29649
Aerothermodynamic challenges of the Saenger space-transportation system
[MBB-FE-202-S-PUB-0462-A] p 890 N92-29680

AEROSPACE SAFETY

The icing of the elevator of the DLR icing research aircraft of Do 28 type
[DLR-MITT-91-12] p 953 N92-31813

AEROSPACE SCIENCES

Whither scientific ballooning?
[AIAA PAPER 91-3676] p 1 A92-11021
Total quality treatment for science and technology --- in USAF p 697 A92-36950
Eighty years of aerospace technique through ATMA bulletins
[ETN-91-90097] p 57 N92-11963
An international aerospace information system: A cooperative opportunity
[NASA-TM-108171] p 1142 N92-33237

AEROSPACE SYSTEMS

Aerospace software engineering in the United Kingdom p 233 A92-19405
Aerospace software in Sweden p 233 A92-19406
New insulation constructions for aerospace wiring applications. Volume 1: Testing and evaluation
[AD-A240638] p 22 N92-11006
New insulation constructions for aerospace wiring applications. Volume 2: The 270 VDC arc tracking testing with power controllers
[AD-A240639] p 23 N92-11007
Machine Intelligence for Aerospace Electronic Systems
[AGARD-CP-499] p 164 N92-12517
RAMREQ: A computerized tool for the definition of RAM (Reliability, Availability, Maintainability) requirements of complex systems p 412 N92-18647
Ground collision avoidance using a variable incidence altitude measurement system for the A-7 aircraft
[AD-A243880] p 352 N92-19259
A system approach to aircraft optimization
p 550 N92-23228
Research and technology, 1990
[NASA-TM-107967] p 1143 N92-33948

AEROSPACE TECHNOLOGY TRANSFER

Emerging technologies for gas turbine engines - U.A.V. synergies
[AIAA PAPER 92-3757] p 867 A92-49114
777 - The airlines' higher-order technology airplane
p 1052 A92-55104
Proceedings of the USAF Structural Integrity Program Conference
[AD-A242943] p 279 N92-17204
An international aerospace information system: A cooperative opportunity
[NASA-TM-108171] p 1142 N92-33237

AEROSPACE VEHICLES

A perspective on aerospace CFD p 169 A92-20145
Rapid prediction of high-alpha unsteady aerodynamics of slender-wing aircraft p 309 A92-24412
Application of the multiplier penalty function method to the optimum design of wing configurations of aerospace vehicle p 356 A92-25013
Fiber-coupled position sensors for aerospace applications p 370 A92-27776
Analysis, development, and integration of the mechanical components of a vehicle powered by photo-voltaic cells
[TABES PAPER 91-503] p 606 A92-34692
An improved approach for the computation of transonic/supersonic flows with applications to aerospace configurations
[AIAA PAPER 92-2613] p 793 A92-45487
Navier-Stokes simulation for the winged space vehicle 'HOPE' at subsonic, transonic, and supersonic regimes
p 1018 A92-53559
New methods in robust control
[AD-A240221] p 29 N92-11018
Aerospace technology: Technical data and information on foreign test facilities
[GAO/NSIAD-90-71FS] p 139 N92-13076
Experiments and analysis concerning the use of external burning to reduce aerospace vehicle transonic drag
[NASA-TM-105397] p 279 N92-17546
A multi-loop guidance scheme using singular perturbation and linear quadratic regulator techniques simultaneously p 481 N92-20148
Advanced electromagnetic methods for aerospace vehicles
[NASA-CR-188630] p 488 N92-20193
Cryogenic hydrogen-induced air-liquefaction technologies for combined-cycle propulsion applications
p 487 N92-21526
NASA aerodynamics program
[NASA-TM-4368] p 609 N92-24678
Hypersonic aerospace vehicle leading edge cooling using heat pipe, transpiration and film cooling techniques
p 780 N92-26733

Surface generation and editing operations applied to structural support of aerospace vehicle fuselages
p 777 N92-27831
Advanced electromagnetic methods for aerospace vehicles
[NASA-CR-190650] p 1001 N92-31156

AEROTHERMOCHEMISTRY

Rate parameters for coupled vibration-dissociation in a generalized SSH approximation --- Schwarz, Slawsky, and Herzfeld p 235 A92-20301
Plasmadynamic effects in thermochemical nonequilibrium aerobrake flows
[AIAA PAPER 92-0573] p 333 A92-26980
Applications of an implicit, upwind Navier-Stokes code, CRAFT, to steady/unsteady reacting, multi-phase flowfields
[AIAA PAPER 92-0837] p 422 A92-29603
Characteristic-based algorithms for flows in thermochemical nonequilibrium p 670 A92-36846
An exploration of chemically reacting viscous hypersonic flow p 612 A92-37550
Plasmadynamic effects in thermochemical nonequilibrium aerobrake flows p 705 A92-41538
Thermochemical nonequilibrium flow computations of flow around the aeroassist flight experiment
p 713 A92-44368
Heat pipe and surface mass transfer cooling of hypersonic vehicle structures p 763 A92-44380
Computation of 3-D hypersonic flows in chemical non-equilibrium including transport phenomena
[AIAA PAPER 92-2876] p 820 A92-47858
Numerical simulation of chemical and thermal nonequilibrium flows behind compression shocks
[AIAA PAPER 92-2879] p 820 A92-47860
Aerothermal ablation behavior of selected candidate external insulation materials
[AIAA PAPER 92-3056] p 893 A92-48714
Thermally and chemically nonequilibrium hypersonic flow in three-dimensional geometry
p 1019 A92-53580
Aerothermodynamics for Space Vehicles
[ESA-SP-318] p 180 N92-14973
Hypersonic viscous shock layer in thermochemical nonequilibrium p 183 N92-15014
Influence of chemical modeling on the solution of hypersonic shock layers p 183 N92-15016
Numerical simulation of thermochemical non-equilibrium viscous flows around reentry bodies
p 227 N92-15029
Modelling of chemical and physical effects with respect to flows around reentry bodies
[MBB-FE-211/S/PUB/0465/A] p 347 N92-19296

AEROTHERMODYNAMICS

Aerothermodynamic systems engineering and design
[SAE AIR 1168/3] p 36 A92-10039
Aeroassist flight experiment heating-rate sensitivity study p 3 A92-10427
Evaluation of an adaptive unstructured remeshing technique for integrated fluid-thermal-structural analysis
p 37 A92-10445
Wave engine aerothermodynamic design
[ASME PAPER 91-GT-4] p 120 A92-15502
A numerical procedure of three-dimensional design problem in turbomachinery
[ASME PAPER 91-GT-144] p 72 A92-15583
Comparison of time-resolved turbine rotor blade heat transfer measurements and numerical calculations
[ASME PAPER 91-GT-268] p 151 A92-15666
Jet engine fault detection with discrete operating points gas path analysis p 129 A92-17200
Thrust nozzle test facility at DLR Cologne
[AIAA PAPER 91-5024] p 206 A92-17818
Application of the STAPAT II code to hypersonic vehicle aerothermodynamics
[AIAA PAPER 91-5035] p 209 A92-17824
Turbulent boundary-layer characteristics over a flat-plate/wedge configuration at Mach 6
p 176 A92-20761
Hypersonic flow simulations using DSMC (direct simulation Monte Carlo) p 323 A92-26216
Enthalpy damping for high Mach number Euler solutions p 330 A92-26402
Sound transmission through a high-temperature acoustic probe tube p 415 A92-26406
Thermal management systems for high Mach airbreathing propulsion
[AIAA PAPER 92-0515] p 373 A92-26941
An experimental/computational study of sharp fin induced shock wave/turbulent boundary layer interactions at Mach 5 - Experimental results
[AIAA PAPER 92-0749] p 335 A92-27093
Approximate analysis of aerodynamic heating at hypersonic speed p 430 A92-30551
Acquisition of an aerothermodynamic data base by means of a winged experimental reentry vehicle
p 486 A92-30685
An improved PNS scheme for predicting complex three-dimensional hypersonic flows
[AIAA PAPER 92-0753] p 436 A92-31679
Thermal protection analysis of Mars-earth return vehicles p 497 A92-32183
Axial compression corner flow with shock impingement p 441 A92-32196
Ground test facilities for aerothermal and aero-optical evaluation of hypersonic interceptors
[AIAA PAPER 92-1074] p 573 A92-33244
Aerobrake aerothermodynamic environment predictions in support of the Aeroassist Flight Experiment
[TABES PAPER 91-278] p 519 A92-34683
Thermal structures and materials for high-speed flight; Collection of Papers of the 1st Thermal Structures Conference, University of Virginia, Charlottesville, Nov. 13-15, 1990
[ISBN 1-56347-017-9] p 590 A92-35847
Numerical simulation of hypersonic viscous flow for the design of H-II orbiting plane (HOPE)
p 612 A92-37549
Thermal structures - Four decades of progress
p 729 A92-41239
Evaluation of the ATD-GASP for endo-leap applications --- Aerothermal Technology Development of Generalized Aerodynamic Simulation Programs
[AIAA PAPER 92-2771] p 704 A92-41318
Multiple aperture window and seeker concepts for endo KEW applications
[AIAA PAPER 92-2806] p 752 A92-41344
Study of the flow field and molecular radiation heating around a reentry vehicle p 711 A92-43227
Direct simulation of re-entry flows with ionization
p 713 A92-44367
Laminar heat transfer to blunt cones in high-enthalpy hypervelocity flows p 713 A92-44372
Thermal radiation effects on a shocked particle-laden gas p 780 A92-44377
Aerothermodynamics of a 1.6-meter-diameter sphere in hypersonic rarefied flow p 808 A92-45840
Energy analysis of high-speed flight systems
p 925 A92-46430
Waves and thermodynamics in high Mach number propulsive ducts p 809 A92-46431
Analysis of thermo-chemical nonequilibrium models for carbon dioxide flows
[AIAA PAPER 92-2852] p 892 A92-47835
Examination of ultraviolet radiation theory for bow shock rocket experiments
[AIAA PAPER 92-2871] p 901 A92-47853
Characteristics of the Shuttle Orbiter leeside flow during a reentry condition
[AIAA PAPER 92-2951] p 821 A92-47915
Aerothermodynamic calculations for the Space Shuttle Orbiter
[AIAA PAPER 92-2953] p 821 A92-47917
Naval aircraft/engine mission payoff analyses
[AIAA PAPER 92-3473] p 865 A92-49019
Pseudostream function formulation - A method of solving three-dimensional aerodynamic analysis and design problems in turbomachinery p 996 A92-52981
Radiative heat transfer from nonequilibrium shock layer to a hypersonic reentry body p 1019 A92-53579
Thermally and chemically nonequilibrium hypersonic flow in three-dimensional geometry
p 1019 A92-53580
Performance benefits of adaptive in-flight propulsion system optimization
[AIAA PAPER 92-3749] p 1068 A92-54149
Evaluation of a multigrid-based Navier-Stokes solver for aerothermodynamic computations
[AIAA PAPER 92-4563] p 1027 A92-55375
Aerothermodynamic test of spaceplane by thin-skin method p 1093 A92-56043
Future requirements for hypersonic aerodynamic and aerothermodynamic facilities
[AIAA PAPER 92-3903] p 1094 A92-56738
Hypersonic aerodynamic/aerothermodynamic testing capabilities at Langley Research Center
[AIAA PAPER 92-3937] p 1096 A92-56767
The trisonic wind tunnel Muenchen and its involvement in the German SAeNGER-programme
[AIAA PAPER 92-4019] p 1100 A92-56841
A database of aerothermal measurements in hypersonic flow for CFD validation
[AIAA PAPER 92-4023] p 1034 A92-56845
Laboratory simulation of aerothermodynamic phenomena - A review
[AIAA PAPER 92-4025] p 1104 A92-56847
The German Hypersonics Technology Programme - Status report 1992
[IAF PAPER 92-0867] p 1105 A92-57258
Technologies for the National Aero-Space Plane
[IAF PAPER 92-0868] p 1105 A92-57259
Numerical simulation of hypersonic viscous flow for the design of H-2 orbiting plane (HOPE-2)
[NAL-TR-1093] p 11 N92-10009
Application of infrared thermography to thermal flux measurement in wind tunnels
[AAAF-NT-89-12] p 31 N92-11020
Studies of aerothermal loads generated in regions of shock/shock interaction in hypersonic flow
[NASA-CR-181893] p 43 N92-11319
An assessment and application of turbulence models for hypersonic flows
[NASA-TM-105124] p 82 N92-11984
Experimental simulation and diagnostics of high-enthalpy real-gas flows
[AD-A241286] p 166 N92-13822
Aerothermodynamics for Space Vehicles
[ESA-SP-318] p 180 N92-14973
Aerothermodynamic challenges for ESA programmes
p 180 N92-14974
Aerothermodynamic configuration of first generation aerospace planes (of Buran-type) and first flight results
p 211 N92-14975
Analysis tools of ONERA and DLR for the aerothermodynamics of reentry vehicles
p 211 N92-14977
Aerothermodynamic development of the CARINA re-entry vehicle: CFD analyses and experimental tests
p 211 N92-14980
Experimental study of hypersonic shock wave boundary layer interactions by means of infrared technique
p 182 N92-14994
Interference heating near fin/body junctions on hypersonic vehicles p 182 N92-14996
Hypersonic aerothermodynamic computations using a point-implicit TVD method p 183 N92-15006
Linear acoustics in gas mixtures with rate processes
p 238 N92-15013
Hypersonic viscous shock layer in thermochemical nonequilibrium p 183 N92-15014
FALKE and COBRA technology development in aerodynamics and aerothermodynamics
p 183 N92-15017
Aerodynamic heating on AFE due to nonequilibrium flow with variable entropy at boundary layer edge
p 183 N92-15020
High enthalpy testing in the Aachen (Fed. Republic of Germany) shock tunnel TH 2 p 208 N92-15021
Computational aerothermodynamic methods for industrial applications to re-entry and hypersonic cruise problems p 227 N92-15027
Numerical simulation of thermochemical non-equilibrium viscous flows around reentry bodies
p 227 N92-15029
Behaviour and modelling of the aerothermodynamics of ballistic entry vehicles in the high altitude flow regimes
p 184 N92-15031
Parallelization of a Direct Simulation Monte Carlo (DSMC) code for fluid dynamics p 227 N92-15033
Aerothermodynamics for United States advanced programs p 184 N92-15039
Computation of aerodynamic coefficients on Hermes-Ariane5 configuration p 184 N92-15040
Aerothermodynamic challenges of the Saenger space-transportation system p 184 N92-15042
Aerothermodynamic radiation studies
[NASA-CR-185666] p 284 N92-15998
Application of program LAURA to perfect gas shock tube flows: A parametric study
[NASA-TM-104190] p 298 N92-17002
Reaction speed constant for the reactions between N + O2 and between O + N2
[ETN-92-90861] p 347 N92-19252
Modelling of chemical and physical effects with respect to flows around reentry bodies
[MBB-FE-211/S/PUB/0465/A] p 347 N92-19296
Postflight aerothermodynamic analysis of Pegasus(tm) using computational fluid dynamic techniques
[NASA-CR-186017] p 445 N92-21188
The NASA hypersonic research engine program
p 474 N92-21521
Development and application of computational aerothermodynamics flowfield computer codes
[NASA-CR-190294] p 624 N92-24229
An engineering method for interactive inviscid-boundary layers in three-dimensional hypersonic flows
[NASA-TM-107838] p 632 N92-25279
Progress in integrated analysis with adaptive unstructured meshing p 683 N92-25914
A high angle of attack inviscid shuttle orbiter computation
[NASA-TM-107606] p 685 N92-25964
Computational method to predict thermodynamic, transport, and flow properties for the modified Langley 8-foot high-temperature tunnel
[NASA-TM-4374] p 767 N92-27193

Presentation of a computational code for 3-D compressible flow in complex channels and cavities
p 769 N92-27475
Aerothermodynamics of nozzle flows for advanced hypersonic propulsion systems p 769 N92-27478
Steady and Transient Performance Prediction of Gas Turbine Engines
[AGARD-LS-183] p 868 N92-28458
Saenger: The reference concept and its technological requirements - aerothermodynamics
[MBB-FE-202-S-PUB-0463-A] p 890 N92-29629
Technology programme: Aerothermodynamics and propulsion integration. Numerical and experimental aerothermodynamics
[MBB-FE-202-S-PUB-0464-A] p 831 N92-29648
Aerothermodynamics and propulsion integration in the Saenger technology programme
[MBB-FE-202-S-PUB-0469-A] p 831 N92-29649
Aerothermodynamic challenges of the Saenger space-transportation system
[MBB-FE-202-S-PUB-0462-A] p 890 N92-29680
Hypersonic flow past radiation-cooled surfaces
[MBB-FE-202-S-PUB-0468-A] p 832 N92-29713
Acquisition of an aerothermodynamic data base by means of a winged experimental reentry vehicle
[MBB/FE202/S/PUB/461] p 787 N92-30232
Research on aero-thermodynamic distortion induced structural dynamic response of multistage compressor blading
[AD-A250865] p 974 N92-32059
Perspectives on hypersonic viscous and nonequilibrium flow research
[NASA-CR-190817] p 1039 N92-33413

AEROTHERMOELASTICITY
Aerothermoelastic analysis of a NASP-like vertical fin
[AIAA PAPER 92-2400] p 541 A92-34471
Nonlinear flutter of orthotropic composite panel under aerodynamic heating
[AIAA PAPER 92-2132] p 589 A92-35699

AFRICA
Future air navigation systems for Africa
p 532 A92-33439

AFTERBODIES
Propulsion aspects of hypersonic turbo-ramjet-engines with special emphasis on nozzle/aftbody integration
[ASME PAPER 91-GT-395] p 127 A92-15725
Optimization of bluff body for minimum drag in ground proximity p 431 A92-31154
Simulation of 3-D shear flows around a nozzle-afterbody at high speeds p 519 A92-34826
Computational analysis of drag reduction techniques for afterbody/nozzle/empennage configurations
[SAE PAPER 912127] p 618 A92-39974
The effect of afterbody devices on drag reduction
p 942 A92-53097
Experimental results for a hypersonic nozzle/afterbody flow field
[AIAA PAPER 92-3915] p 1032 A92-56747
Viscous computations of cold air/air flow around scramjet nozzle afterbody
[NASA-CR-4406] p 13 N92-10982
Aerodynamic centre of wing-body combinations
[ESDU-92024] p 1036 N92-32479
Effect of afterbody geometry on aerodynamic characteristics of isolated nonaxisymmetric afterbodies at transonic Mach numbers
[NASA-TP-3236] p 1041 N92-33706

AFTERBURNING
Weak extinction limits of large scale flameholders
[ASME PAPER 91-GT-234] p 125 A92-15643
F-14/F110 engine integration p 112 A92-16055
Thermal imaging of afterburning plumes
p 129 A92-17179
Hydrogen exhaust gas disposition by afterburning
[AIAA PAPER 91-5075] p 200 A92-17848
Effect of carbon particles and mixing on afterburning of exhaust plumes
[AIAA PAPER 92-0767] p 387 A92-27107
Experimental investigation on the mechanism of flame stabilization in afterburner with V-gutter flameholder
p 487 A92-29725

AGING
The FAA aging airplane program plan for transport aircraft p 838 N92-30128
Ageing aircraft research in the Netherlands
p 838 N92-30129
Survey of French activities concerning structural airworthiness and aging aircraft p 838 N92-30130
Transport Canada aging aircraft activities
p 838 N92-30131

AGING (MATERIALS)
The aging aircraft fleet - A challenge for nondestructive inspection p 145 A92-13657
Industry seeks tonic for aging aircraft
p 308 A92-28492
Nortec 30 Eddyscan - Portable flaw imaging for aging aircraft p 492 A92-28745
Structural airworthiness of aging Boeing jet transports - 747 fuselage fatigue test program
[AIAA PAPER 92-1128] p 537 A92-33280
Effective maintenance practices to manage system aging p 1119 A92-56215
Human factors evaluation of the work environment of operators engaged in the inspection and repair of aging aircraft
[AD-A246445] p 724 N92-27914
Turbine aircraft engine operational trending and JT8D static component reliability study
[DOT/FAA/CT-91/10] p 870 N92-28686
The 1991 International Conference on Aging Aircraft and Structural Airworthiness
[NASA-CP-3160] p 912 N92-30106
Structural integrity of future aging airplanes
p 913 N92-30107
Performance of fuselage pressure structure
p 913 N92-30109
Federal Aviation Administration aging aircraft nondestructive inspection research plan
p 914 N92-30116
Evaluation of the effects of the environment on the behavior of the primary structures of composite material aircraft in service: Historic and current situation
p 1110 N92-33048
Isothermal aging of IM7/8320 and IM7/5260
[NASA-TM-107666] p 1110 N92-33423
Current nondestructive inspection methods for aging aircraft
[DOT/FAA/CT-91/5] p 1126 N92-33480

AGREEMENTS
Agreements/subagreements applicable to Wallops, 12 Nov. 1991 p 575 N92-22598
Ageing aircraft research in the Netherlands
p 838 N92-30129

AGRICULTURAL AIRCRAFT
High altitude solar power platform --- aircraft design analysis
[NASA-TM-103578] p 506 N92-21546
Trajectories and stability of trailing vortices very near the ground
[NRC-32151] p 716 N92-27344

AH-64 HELICOPTER
Manufacture of a primary flight structure using thermoplastics p 1 A92-10197
Flight testing the handling qualities requirements of ADS-33C - Lessons learned at ATTC
p 104 A92-14339
The design and manufacture of an advanced thermoplastic horizontal stabilator for the AH-64A
p 59 A92-14354
Design optimization of rotor blades for improved performance and vibration p 106 A92-14389
Flight simulation modeling in support of engine/airframe integration p 1055 A92-56279
Assessment of rotorcraft system identification as applied to the AH-64 p 274 N92-17160
Modeling methods for high-fidelity rotorcraft flight mechanics simulation
[NASA-TM-103842] p 482 N92-21440
The use of a dedicated testbed to evaluate simulator training effectiveness p 884 N92-28533
Cost/benefit analysis of the AH-64 (Apache) helicopter Automated Test Equipment (ATE)
[AD-A252909] p 1101 N92-33398
Developing robust support structures for high-technology subsystems: The AH-64 Apache helicopter
[AD-A252773] p 1017 N92-33499
On the calculation of the response of helicopters to control inputs
[NASA-CR-190812] p 1088 N92-33536

AILERONS
Aerodynamic effect of compression shocks on an oscillating aileron in transonic flow p 440 A92-31898
The equations governing the motion of wing-aileron structural systems constructed from advanced anisotropic composite materials
[AIAA PAPER 92-2469] p 564 A92-34359
Optimization of aeroelastic system with active control
p 1083 A92-56022
Application of automation for structural-composites production p 1119 A92-56109
A preliminary look at an optimal multivariable design for propulsion-only flight control of jet-transport aircraft
[NASA-CR-186014] p 663 N92-25734
Evaluation of high lift devices of the quiet STOL experimental aircraft ASKA
[NAL-TR-1102] p 733 N92-28153
Further wind tunnel investigation of the SM701 airfoil with aileron and turbulators
[NASA-CR-190702] p 1038 N92-33063

AIR
Brush seal leakage performance with gaseous working fluids at static and low rotor speed conditions
[NASA-TM-105400] p 297 N92-16265

AIR BREATHING BOOSTERS
Potential hypersonic vehicles applications
[AIAA PAPER 91-5086] p 169 A92-17854
Challenging power-density requirements for future fighter APUs
[SAE PAPER 912177] p 655 A92-40002

AIR BREATHING ENGINES
Review of propulsion applications and numerical simulations of the pulsed detonation engine concept
p 129 A92-17177
Supersonic inlet flow computation
p 171 A92-17502
Hypersonic airbreathing propulsion activities for Saenger
[AIAA PAPER 91-5040] p 200 A92-17828
Numerical and experimental investigation of airframe-integrated inlet for high velocities
p 243 A92-21072
Spaceplane system studies p 285 A92-22632
Thermal management of air-breathing propulsion systems
[AIAA PAPER 92-0514] p 373 A92-26940
Thermal management systems for high Mach airbreathing propulsion
[AIAA PAPER 92-0515] p 373 A92-26941
An investigation on flame stability by fuel permeability in a flame holder made of porous ceramic material
p 375 A92-28435
Laser-initiated conical detonation wave for supersonic combustion p 375 A92-28531
Strain-induced extinction of hydrogen-air counterflow diffusion flames - Effects of steam, CO2, N2, and O2 additives to air
[AIAA PAPER 92-0877] p 487 A92-29639
On the experimental investigation of air-breathing engine of new schemes p 469 A92-29711
Air flow under a flight-vehicle engine
p 429 A92-30528
Study of cavity pumping in supersonic internal flow
p 429 A92-30538
A parametric study of airbreathing Pulsed Detonation Engine
[AIAA PAPER 92-0392] p 471 A92-31660
Design considerations for nozzles of hypersonic airbreathing propulsion
[AIAA PAPER 91-5019] p 471 A92-31685
The National Aerospace Plane program and the APL role p 666 A92-37375
The thermodynamic approach in the study of large systems - Application to high-velocity airbreathing propulsion p 654 A92-37824
Mechanics and thermodynamics of propulsion (2nd revised and enlarged edition) --- Book
[ISBN 0-201-14659-2] p 672 A92-38275
Trends in propulsion technology p 757 A92-41186
High-speed flight propulsion systems --- Book
[ISBN 1-56347-011-X] p 862 A92-46426
Introduction --- propulsion system performance for hypersonic vehicles p 862 A92-46427
Propulsion systems from takeoff to high-speed flight
p 889 A92-46428
Propulsion system performance and integration for high Mach air breathing flight p 862 A92-46429
Energy analysis of high-speed flight systems
p 925 A92-46430
Laser-initiated conical detonation wave for supersonic combustion. III
[AIAA PAPER 92-3247] p 893 A92-48846
Restart of theory of air-breathing engines
[AIAA PAPER 92-3472] p 906 A92-49018
Development study on air turbo-ramjet engine for space plane p 1065 A92-53487
Flowpath and sensitivity analyses of high speed propulsion systems
[AIAA PAPER 92-3806] p 1069 A92-54178
Interaction between chemical reaction and turbulence in supersonic nonpremixed H2-air combustion
p 1117 A92-54931
Development of local nonintrusive measurements of inlet and exhaust flows for the ground testing of air-breathing engines
[AIAA PAPER 92-3899] p 1122 A92-56735
Laser-driven hypersonic air-breathing propulsion simulator
[AIAA PAPER 92-3922] p 1095 A92-56753
Effects of oxygen dissociation on hypervelocity combustion experiments
[AIAA PAPER 92-3964] p 1098 A92-56791
Airbreathing engine selection criteria for SSTO propulsion system
[IAF PAPER 92-0658] p 1071 A92-57099

Optimization of two stage reusable space transportation systems with rocket and airbreathing propulsion concepts
[IAF PAPER 92-0863] p 1104 A92-57254
The German Hypersonics Technology Programme - Status report 1992
[IAF PAPER 92-0867] p 1105 A92-57258
Trim drag reduction concepts for horizontal takeoff single-stage-to-Orbit vehicles
[NASA-TM-102687] p 206 N92-15076
Experiments and analysis concerning the use of external burning to reduce aerospace vehicle transonic drag
[NASA-TM-105397] p 279 N92-17546
Advanced ramjet concepts program
p 474 N92-21520
Airbreathing combined cycle engine systems
p 475 N92-21523
H2 fueled flightweight ramjet construction and test
p 475 N92-21531
System controls challenges of hypersonic combined-cycle engine powered vehicles
p 475 N92-21533
NASA's hypersonic propulsion program: History and direction p 476 N92-21535
Symposium on High Speed Airbreathing Propulsion: The Solid Fuel Combustion Chamber and Beyond
[ETN-92-90685] p 575 N92-22268
High speed airbreathing propulsion in Europe
p 575 N92-22277
Some comments on turbulence modeling from an industrial perspective p 678 N92-24531
Assessment of flying-quality criteria for air-breathing aerospacecraft
[NASA-CR-4442] p 663 N92-25982
Aerothermodynamics of nozzle flows for advanced hypersonic propulsion systems p 769 N92-27478
Robust intelligent flight control for hypersonic vehicles
[NASA-CR-185680] p 746 N92-28209
Users manual for updated computer code for axial-flow compressor conceptual design
[NASA-CR-189171] p 924 N92-30207
Trends in aeropropulsion research and their impact on engineering education
[NASA-TM-105682] p 972 N92-31172
Laser-initiated conical detonation wave for supersonic combustion, part 3
[AD-A250522] p 989 N92-32076

AIR CARGO
Airport activity statistics of certificated route air carriers: Calendar year 1990
[AD-A241483] p 93 N92-13045
Organic Matrix Composite Helicopter Internal/External Cargo Pallet System (OMC INTEX)
[AD-A251127] p 961 N92-30878

AIR CONDITIONING EQUIPMENT
Evolutionary upgrade and application of the C-130H simple-cycle refrigeration system
[SAE PAPER 911439] p 270 A92-21836

AIR COOLING
Discharge coefficients of cooling holes with radiused and chamfered inlets
[ASME PAPER 91-GT-269] p 151 A92-15667
A method for estimating the efficiency of gas turbine blade cooling systems p 657 A92-40606
Rotational coherent anti-Stokes Raman spectroscopy measurements in a rotating cavity with axial throughflow of cooling air - Oxygen concentration measurements
p 990 A92-49574
High-temperature combustor and seal for a water piston propulsor
[AD-A242493] p 229 N92-15385
Cooled high-temperature radial turbine program 2
[NASA-CR-189122] p 1073 N92-34236

AIR DATA SYSTEMS
Optical velocity sensor for air data applications
p 368 A92-24575
Failure detection and fault management techniques for flush airdata sensing systems
[AIAA PAPER 92-0263] p 369 A92-25719
Atmospheric analysis for airdata calibration on research aircraft
[AIAA PAPER 92-0293] p 369 A92-25746
Inertial reference units with integrated air speed determination for helicopters p 554 A92-35764
Development of a pneumatic high-angle-of-attack flush airdata sensing system
[SAE PAPER 912142] p 651 A92-39980
Air data measurement for hypersonic vehicles
[SAE PAPER 912143] p 651 A92-39981
Utilizing the fault monitoring system for the A320 aircraft p 700 A92-43157
Absolute fiber optic pressure transducer for aircraft air data measurement p 858 A92-48501
A fault-tolerant Air Data/Inertial Reference System
p 967 A92-51011
Some important factors in turbulence in flight measurement p 1063 A92-54324
A new system for recording unstable aerodynamic phenomena in NAVSWC Hypervelocity Wind Tunnel No. 9 p 1091 A92-54325
High angle-of-attack flush airdata sensing system
p 1064 A92-56172
Development of a pneumatic high-angle-of-attack flush airdata sensing (HI-FADS) system
[NASA-TM-104241] p 118 N92-11994
Results of the space shuttle vehicle ascent air data system probe calibration test using a 0.07-scale external tank forebody model (68T) in the AEDC 16-foot transonic wind tunnel (IA-310), volume 1
[NASA-CR-167696] p 286 N92-17167
Results of the space shuttle vehicle ascent air data system probe calibration test using a 0.07-scale external tank forebody model (68T) in the AEDC 16-foot transonic wind tunnel (IA-310), volume 2
[NASA-CR-167697] p 286 N92-17214
A simple and low cost system to measure delay times in pneumatic systems
[NLR-TP-90174-U] p 859 N92-28644

AIR DEFENSE
Heuristic route optimization: A model for force level route planning p 164 N92-12520
Avionics standardization in the USAF: 1980 to 1990
p 198 N92-14048
A-2000: Close air support aircraft design team
[NASA-CR-190022] p 463 N92-21567
National airspace system. Air defense and law enforcement surveillance operational concept NAS-SR-135
[DOT/FAA/SE-92/3] p 953 N92-31211
DoD key technologies plan
[AD-A253692] p 1142 N92-33238

AIR DROP OPERATIONS
Conceptual design and analysis of a special operations transport
[AIAA PAPER 92-1066] p 536 A92-33239
Trajectory analysis of the G-11 family of clustered parachutes to determine minimum altitude
[AD-A243375] p 261 N92-17404

AIR DUCTS
Design and off-design point characteristics of Separated Core Ultra High Bypass Engine (SCUBE)
[AIAA PAPER 92-3776] p 867 A92-49120
Modification of Jindivik air intake duct with an auxiliary intake static aerodynamic tests
[AD-A243002] p 275 N92-17234

AIR FILTERS
Engine air particle separator panels for helicopter engine protection p 545 A92-35735
The development of an engine air particle separator system for the CH-47 helicopter p 545 A92-35736
Application of CFD in the design of gas turbine engine components p 741 N92-27461

AIR FLOW
Surface flow visualization of rotating propeller
p 4 A92-10959
An analysis of the flow-pattern at the exit of a single-stage turbine p 10 A92-13234
Aerating fuel nozzle design influences on airflow features p 129 A92-17176
An experimental investigation of the combustion of a hydrogen jet injected parallel in a supersonic air stream
[AIAA PAPER 91-5102] p 212 A92-17861
Linear panel flutter of an elliptic cylindrical shell
p 291 A92-21216
Numerical analysis of airflow in aircraft cabins
[SAE PAPER 911441] p 245 A92-21837
Development and application of a particle image velocimeter for high-speed flows
[AIAA PAPER 92-0004] p 292 A92-22129
Experimental measurement of the vortex development downstream of a lobed forced mixer
[ASME PAPER 90-GT-27] p 295 A92-23299
Aerodynamic effects on fuel spray structure - Experiment and theory
[AIAA PAPER 92-0227] p 317 A92-25691
Flow field measurement and visualization using projected smoke trails
[AIAA PAPER 92-0384] p 323 A92-26241
Radiant heat transfer in supersonic three-dimensional and axisymmetric flow of air past evaporating bodies
p 337 A92-27533
Numerical simulation of two incoming streams in a dual-combustion ramjet combustor p 375 A92-28419
The aviation kerosene burning in the non-uniform air flow p 487 A92-29728
Air flow under a flight-vehicle engine
p 429 A92-30528
Airflow effects about PMS probes on the DLR Falcon --- Particle Measuring System for atmospheric research aircraft p 467 A92-32060
Commercial airplane air distribution system development through the use of computational fluid dynamics
[AIAA PAPER 92-0987] p 535 A92-33182
Fokker 50 flameouts in icing conditions
p 548 A92-35940
Aerodynamic drag of a cylinder in two-phase flow
p 707 A92-42735
The main wing boundary layer separation pattern of STOL research aircraft Asuka p 709 A92-43144
Laminar heat transfer to blunt cones in high-enthalpy hypervelocity flows p 713 A92-44372
Computational fluid dynamics applications in airplane cabin ventilation system design
[SAE PAPER 911992] p 788 A92-45394
The effect of molecular relaxation processes in air on the rise time of sonic booms p 898 A92-45883
Flight deck aerodynamics of a nonaviation ship
p 810 A92-46790
Segmental heat transfer in a pin fin channel with ejection holes p 900 A92-47267
Rotational coherent anti-Stokes Raman spectroscopy measurements in a rotating cavity with axial throughflow of cooling air - Oxygen concentration measurements
p 990 A92-49574
Time domain numerical calculations of unsteady vortical flows about a flat plate airfoil p 936 A92-50473
Aerodynamic heating characteristics of space planes tested by NAL hypersonic wind tunnel
p 1017 A92-53547
A study of the airwake aerodynamics over the flight deck of an AOR model ship
[AD-A241008] p 89 N92-13034
Stabilized square parachute
[AD-D015014] p 90 N92-13036
SIMOUN and Scirocco wind tunnel nozzle viscous flow study p 208 N92-14999
NASA's rotary engine technology enablement program: 1983-1991
[NASA-TM-105562] p 378 N92-20033
The aerodynamics of ship superstructures
p 503 N92-21953
Measurement of the flow distribution over the flight deck of an aircraft carrier p 504 N92-21955
Active thermal isolation for temperature responsive sensors
[NASA-CASE-LAR-14612-1] p 911 N92-29954
Method of measuring cross-flow vortices by use of an array of hot-film sensors
[NASA-CASE-LAR-14824-1-SB] p 998 N92-30390
Exploratory experimental investigation of a wave propeller
[AD-A252175] p 949 N92-32062

AIR INTAKES
An efficient method for calculating three-dimensional transonic flow past air intakes p 7 A92-12178
Development and bench test of high-temperature combustion chamber with structural ceramic components
[ASME PAPER 91-GT-315] p 126 A92-15691
A simple model to simulate subsonic intakes and propelling nozzles of aircraft gas turbine engines
[ASME PAPER 91-GT-392] p 153 A92-15722
A global approach in evaluating inlet/engine compatibility
[ASME PAPER 91-GT-402] p 127 A92-15732
Engine air inlet and de-icing system - At -30 C in the icing tunnel of NRC Ottawa p 92 A92-17252
Influence of flight parameters on air intake internal flow distortions due to gun blast-air interaction
p 310 A92-24426
Analysis of an advanced ducted propeller subsonic inlet
[AIAA PAPER 92-0274] p 318 A92-25728
The effect of air-compressor adjustment by means of air-bleed on the reserve of its stable operation
p 471 A92-29973
Aerodynamic characteristics of slender sharp-leading-edge delta wings with air scooping through the air intake at hypersonic velocities. I
p 427 A92-30206
Numerical computation of supersonic intakes
p 430 A92-30539
Aerodynamic characteristics of a blunt delta wing with air bleed through an intake at supersonic and hypersonic velocities. II p 437 A92-31855
A method for determining the internal force characteristics of a model in external supersonic flow
p 706 A92-42682
Experimental study of the aerodynamic characteristics at Mach 3 of an air-intake model p 711 A92-43204
Wind tunnel test of a supersonic air intake
p 711 A92-43205
Viscous flow analysis of advanced particle separators
p 737 A92-44517
Configuration effects on the ingestion of hot gas into the engine intake p 842 A92-45315

Automatic control of test parameters for intake measurements in a low-speed wind tunnel
p 1091 A92-54341
Supersonic wind tunnel test of airintake/airframe integrated models p 1028 A92-56006
Humidity effects on gas turbine performance
[NRC-30241] p 130 N92-11998
Study of detached turbulent flow in an air intake by means of high speed tomography and laser velocimetry
[REPT-90/55] p 157 N92-12216
Analysis of an advanced ducted propeller subsonic inlet
[NASA-TM-105393] p 179 N92-14002
Meeting Review: Airborne Aerosol Inlet Workshop
[NASA-CR-189814] p 301 N92-17393
CFD contributions during hypersonic airplane intake design p 769 N92-27472

AIR JETS
Feedback mechanism of self-oscillations in the case of an underexpanded supersonic jet impinging on a plane obstacle p 79 A92-16682
Computation of normal impinging jets in cross-flow and comparison with experiment p 250 A92-22446
An investigation on the characteristics of combustor with oblique air jet p 375 A92-28434
Structural features of a heated round turbulent jet in a cross-flow p 676 A92-40148
Use of the TMS-65 heating equipment at airports to create fog-dispersal zones above the runway to facilitate takeoff p 775 A92-44084
Acoustic control of combustor primary zone air-jet mixing
[AIAA PAPER 92-3651] p 1067 A92-54104
Numerical simulation of the reactive flow in advanced (HSR) combustors using KIVA-2
[NASA-CR-188996] p 26 N92-11014

AIR LAUNCHING
An air-launched balloon system for a 230 lb gross inflation
[AIAA PAPER 91-3689] p 16 A92-11032
History of EPOS air-launched spaceplane project
p 211 N92-14103

AIR LAW
No end to incidents in airspace? III
p 262 A92-23172
The law in Australia relating to negligence of aircrew and engineers p 606 A92-33463
Aviation products liability and navigation - Recent developments and future directions p 697 A92-39563
Airline deregulation - Impact on human factors
p 834 A92-44999
Annals of air and space law. Vol. 16
p 1012 A92-51450
Winds of change: Domestic air transport since deregulation
[NRC-SR-230] p 92 N92-13040
National airspace system. Air defense and law enforcement surveillance operational concept NAS-SR-135
[DOT/FAA/SE-92/3] p 953 N92-31211
Re-engining for real stage 3 compliance
[PNR-90872] p 1072 N92-33748

AIR NAVIGATION
Strategic vs tactical air traffic control utilizing ADS and earth reference area NAV p 96 A92-16631
Operational and economic benefits of area navigation from the perspective of a major air carrier
p 96 A92-16632
The DOT/DOD Federal Radionavigation Plan
p 96 A92-16637
From Russia and beyond --- equipment and areas of coverage for Loran navigation outside NAS
p 96 A92-16638
Aircraft navigation using Global Positioning System improved with geostationary satellites
p 99 A92-16934
Potential impact of GPS and automatic dependent surveillance on air lane separation in the North Atlantic Organized Track System p 99 A92-16935
Integrated use of GPS and GLONASS in civil aviation navigation. I - Coverage and data models
p 99 A92-16950
Ranging and positioning experiments for aircraft using Engineering Test Satellite V p 102 A92-17242
Report of the working group Future CNS Systems - Applications and impact on the German air transport system p 266 A92-21325
Processing and displaying radio navigation data --- Russian book p 266 A92-21683
Potential impact of FANS - Far-reaching and positive --- Future Air Navigation Systems p 267 A92-23296
Transition to cooperative ATM system requires commitment --- Air Traffic Management
p 267 A92-23297
FANS implementation planning under way in Canada
p 267 A92-23298
Navigation and flight management systems - Thoughts of a user p 354 A92-26848
The cockpit of a modern aircraft - The Airbus A340 considered as an example p 357 A92-26849
LOS rate estimation in inertial navigation using landmarks p 453 A92-29360
Navigation - Land, sea, air, and space --- Book
[ISBN 0-87942-257-2] p 496 A92-31778
The technological revolution in oceanic air traffic control p 531 A92-33431
Future air traffic control and navigation systems; Proceedings of the AIAA International Civil Aviation Seminar, Paris, France, June 12, 1991
[AIAA SP-050-1991] p 532 A92-33433
Air transportation - The global vision
p 532 A92-33434
The ICAO Future Air Navigation System
p 532 A92-33435
FANS technology and the future of air traffic services
p 532 A92-33436
The view from the airport p 532 A92-33438
Future air navigation systems for Africa
p 532 A92-33439
A view from the Pacific Basin --- air traffic
p 532 A92-33440
International standardization p 533 A92-33441
Growing need to replace ILS can best be met by MLS
p 534 A92-36124
GPS interferometric attitude and heading determination - Flight test results p 650 A92-39561
Aviation products liability and navigation - Recent developments and future directions p 697 A92-39563
The status of Loran's implementation in the National Airspace System (NAS) p 638 A92-39565
Receiver autonomous integrity monitoring (RAIM) - Techniques, performance and potential
p 638 A92-39567
Future considerations for vertical flight
p 608 A92-40383
The Automatic Dependent Surveillance (ADS) system
p 724 A92-41208
A computerized flight inspection system --- for testing of basic air navigation ground facilities
p 726 A92-43881
Computer-Controlled Navigation System/General Positioning System (CCNS/GPS) - A guidance, positioning, and management system for remote sensing flights
p 840 A92-47630
Navigation charts on trial - How safe is safe?
p 1012 A92-49380
Ideal proportional navigation p 976 A92-50497
A new aspect of future air navigation systems - How Secondary Surveillance Radar Mode S could protect civil aviation p 1012 A92-51424
GPS tests during approach at Singapore and Roissy
p 956 A92-53240
Height keeping performance requirements for reducing vertical separation minima used for air traffic control
p 1046 A92-56081
The electronic aeronautical chart for general aeronautics: A system specification
[ILR-MITT-263(1991)] p 20 N92-10997
Engineering Graphical Analysis Tool (EGAT) development program p 164 N92-12542
NASA TSRV essential flight control system requirements via object oriented analysis
[NASA-CR-189573] p 381 N92-19499
General maintenance handbook for airway facilities
[PB92-147586] p 640 N92-25518
An adaptive correction technique for Differential Global Positioning System p 726 N92-26623
Loran-C performance assurance assessment program
[NASA-CR-190469] p 840 N92-28718
DLR research reports and communications
[ETN-92-91391] p 929 N92-29218
European studies to investigate the feasibility of using 1000 ft vertical separation minima above FL 290. Part 1: Overview of organisation, techniques employed, and conclusions
[NLR-TP-91062-U-PT-1] p 841 N92-29605
The 1991 Federal Aviation Administration plan for research, engineering and development
p 1142 N92-32453
CTAS: Computer intelligence for air traffic control in the terminal area
[NASA-TM-103959] p 1044 N92-33080
Integrated Russian VLF/Omega receiver design
[PB92-193390] p 1051 N92-33809

AIR POLLUTION
Size and critical supersaturation for condensation of jet engine exhaust particles p 161 A92-15884
Studies on the effect of high-flying air-traffic on the atmosphere
[IAF PAPER 91-737] p 301 A92-22495
Low volatile organic compound paints
[DE91-017984] p 35 N92-11203
EDMS: Microcomputer pollution model for civilian airports and Air Force bases, (user's guide)
[AD-A240528] p 45 N92-11578
The atmospheric effects of stratospheric aircraft: A first program report
[NASA-RP-1272] p 408 N92-19121
Natural cycles, gases p 408 N92-19123
Designing a methodology for future air travel scenarios p 409 N92-19125
Ozone response to aircraft emissions: Sensitivity studies with two-dimensional models p 409 N92-19126
Environmentally sound
[PNR-90776] p 506 N92-21743
NASA High Speed Research Program, Emissions Scenarios Committee report of meetings on 26 September 1991 and 9 January 1992
[NASA-CR-190379] p 1004 N92-32147

AIR QUALITY
EDMS: Microcomputer pollution model for civilian airports and Air Force bases, (user's guide)
[AD-A240528] p 45 N92-11578

AIR SAMPLING
SHARP: Subsonic High Altitude Research Platform
[NASA-CR-190004] p 648 N92-25263
A preliminary design and analysis of an advanced heat-rejection system for an extreme altitude advanced variable cycle diesel engine installed in a high-altitude advanced research platform
[NASA-CR-186021] p 871 N92-29427

AIR START
Kalman filter mechanization for INS airstart
p 574 A92-33602
Research on altitude simulation of starting for a single-spool small turbojet p 969 A92-49836
The application of a theoretical blade sailing model to predict the behaviour of articulated helicopter rotors
p 960 A92-52849

AIR TO AIR MISSILES
A calculating method of the kill probability attack area for AAM p 975 A92-50212
Ideal proportional navigation p 976 A92-50497

AIR TO AIR REFUELING
The aerodynamic interference between a flapped tanker aircraft and a receiver aircraft during air-to-air refuelling
p 29 A92-13199
Handling and performance considerations when conducting air-to-air refuelling of large aircraft by the probe and drogue system p 548 A92-35937
F-14 dual hydraulic failure flying qualities evaluation
p 645 A92-40029
Aircraft aerodynamics and stability and control during air-to-air refueling
[AERO-REPT-9017] p 380 N92-18321

AIR TRAFFIC
Flight test investigation of the wake vortices generated by helicopters p 270 A92-21925
Studies on the effect of high-flying air-traffic on the atmosphere
[IAF PAPER 91-737] p 301 A92-22495
No end to incidents in airspace? III
p 262 A92-23172
A view from the Pacific Basin --- air traffic
p 532 A92-33440
International standardization p 533 A92-33441
High speed VSTOL on the horizon - The answer to congestion?
[SAE PAPER 911976] p 843 A92-45383
A systematic formulation, as an approach to air traffic
[MBB-Z-0371-91-PUB] p 19 N92-10996
Airport activity statistics of certificated route air carriers: Calendar year 1990
[AD-A241483] p 93 N92-13045
FAA air traffic activity: FY 1990. Addendum
[AD-A241484] p 93 N92-13046
Evaluation of triple simultaneous parallel ILS approaches spaced 4300 feet apart, phase 4a
[ACD-340] p 191 N92-14034
Public-sector aviation issues: Graduate research award papers, 1989 - 1990
[PB91-242271] p 308 N92-19662
UK airmisses involving commercial air transport: September - December 1990
[ETN-92-91050] p 452 N92-21746
An aircraft Earth station for general aviation
p 678 N92-24194
Tilt rotors and the Port Authority of New York and New Jersey Airport System
[RAND-R-3971/1-PA-SUMM] p 636 N92-25262
Implementation and operational experience with a new arrival traffic management system at the Frankfurt ATC-Center p 728 N92-27905
FAA aviation forecasts
[AD-A250412] p 837 N92-29182

European studies to investigate the feasibility of using 1000 ft vertical separation minima above FL 290. Part 1: Overview of organisation, techniques employed, and conclusions
[NLR-TP-91062-U-PT-1] p 841 N92-29605
Analysis of delay reducing and fuel saving sequencing and spacing algorithms for arrival traffic
[NASA-TM-103880] p 1044 N92-33194

AIR TRAFFIC CONTROL
Managing Europe's air traffic system
p 19 A92-11876
The European ATC challenge p 19 A92-11877
Polish radar technology. III - Weather channel for primary surveillance radar p 40 A92-12291
Analysis and design optimization of monopulse receivers for secondary surveillance radar p 40 A92-12299
Distributed artificial intelligence approach to air traffic control p 161 A92-13436
Classification of radar clutter using neural networks
p 145 A92-14252
Legal capacity of Eurocontrol to ensure smooth aviation in Europe p 167 A92-16134
Madrid's double airport p 138 A92-16231
The future of Loran-C navigation, instrument approaches and flight following for air traffic management
p 95 A92-16630
Strategic vs tactical air traffic control utilizing ADS and earth reference area NAV p 96 A92-16631
A simulator and performance criteria for evaluation of ground and space-based ATC surveillance
p 96 A92-16639
An electronically scanned precision runway monitor
p 98 A92-16654
TCAS in the 1990s --- Traffic alert and Collision Avoidance System p 98 A92-16657
New practical method for measurement error determination in radar systems under real traffic conditions p 155 A92-17238
Ranging and positioning experiments for aircraft using Engineering Test Satellite V p 102 A92-17242
Z-Basic algorithm for collision avoidance system
p 188 A92-18482
The application of neural networks to drone control
p 205 A92-19273
Potential impact of FANS - Far-reaching and positive --- Future Air Navigation Systems p 267 A92-23296
Transition to cooperative ATM system requires commitment --- Air Traffic Management
p 267 A92-23297
FANS implementation planning under way in Canada
p 267 A92-23298
Quantitative estimation of secondary surveillance radar information p 353 A92-24943
The avoidance of collisions for Newtonian bodies with hidden variables p 353 A92-24945
European studies to investigate the feasibility of using 1000 ft vertical separation minima above FL 290. II - Precision radar data analysis and collision risk assessment p 353 A92-24946
Behind the screens --- development of Central Flow Management Unit for air traffic control
p 353 A92-25520
The real TCAS --- traffic alert and collision avoidance system p 350 A92-25521
Advanced ASDE provides new eyes and ears for controllers p 453 A92-29506
Greater RNAV utilization could expand system capacity p 448 A92-29507
Automatic Dependent Surveillance (ADS) Pacific Engineering Trials (PET)
[AIAA PAPER 92-1812] p 453 A92-29760
Low earth orbit satellite concepts for air traffic control applications
[AIAA PAPER 92-1927] p 453 A92-29856
Radio Technical Commission for Aeronautics, Technical Symposium, Washington, DC, Nov. 18-20, 1991, Proceedings p 531 A92-33426
A European perspective on the co-operative air traffic management concept p 531 A92-33427
Perspectives on the cooperative air traffic management concept - Far East/Pacific point of view
p 606 A92-33428
CATMAC - A way to integrate ground ATC and airborne systems p 531 A92-33429
An aircraft manufacturer's perspective
p 515 A92-33430
The technological revolution in oceanic air traffic control p 531 A92-33431
Profile negotiation - A concept for integrating airborne and ground-based automation for managing arrival traffic
p 531 A92-33432
Future air traffic control and navigation systems; Proceedings of the AIAA International Civil Aviation Seminar, Paris, France, June 12, 1991
[AIAA SP-050-1991] p 532 A92-33433
Air transportation - The global vision
p 532 A92-33434
The ICAO Future Air Navigation System
p 532 A92-33435
FANS technology and the future of air traffic services
p 532 A92-33436
Harmonisation and integration of air traffic control in Europe p 532 A92-33437
The view from the airport p 532 A92-33438
Future air navigation systems for Africa
p 532 A92-33439
European ATC integration faces dual challenges
p 534 A92-36076
Maximum-miss aircraft collision avoidance
p 660 A92-37077
GPS - Can it contribute to European ATC?
p 637 A92-38380
Runway incursions and airport surface traffic automation
[SAE PAPER 912123] p 635 A92-39970
Implementing data link across the Pacific
[SAE PAPER 912235] p 638 A92-40027
Computation of aircraft geometric height under radar surveillance p 639 A92-40239
Future considerations for vertical flight
p 608 A92-40383
The Automatic Dependent Surveillance (ADS) system
p 724 A92-41208
Microwave landing system modeling with application to air traffic control automation p 725 A92-41220
Introduction to the traffic alert and collision avoidance system (TCAS) III p 734 A92-43150
The traffic alert and collision avoidance system (TCAS) for air navigation p 734 A92-43151
Mode S data link pilot-system interface - A blessing in de skies or a beast of burden? p 839 A92-44920
Who or what saved the day? A comparison of traditional and glass cockpits p 833 A92-44931
Perspective versus plan view air traffic control (ATC) displays - Survey and empirical results
p 896 A92-44967
Real targets, unreal displays - The inadvertent suppression of critical radar data p 839 A92-44969
Real-time control tower simulation for evaluation of airport surface traffic automation p 879 A92-44976
Operational evaluation of a tower workstation for clearance delivery p 879 A92-44981
Putting the control back in air traffic control - An enhanced Universal Development Simulation System
p 916 A92-44982
Full model simulation of the National Airspace System - Research and training platform p 880 A92-45042
Empirical foundations and sensitivity testing - Is it enough for the 90's? p 835 A92-45054
Terminal area traffic management
p 955 A92-50122
Monopulse secondary surveillance radar and the mode-S surveillance system p 956 A92-53239
Discrete event fuzzy airport control
p 1046 A92-55973
Height keeping performance requirements for reducing vertical separation minima used for air traffic control
p 1046 A92-56081
History of aeronautical satellite communications
p 1046 A92-56088
A data processing system for oceanic air traffic control p 1046 A92-56090
An experimental program concerning a satellite data link for oceanic ATC p 1046 A92-56093
A consideration on air traffic control processing capability in terminal area p 1047 A92-56110
The 1990 Airport Surveillance Radar Wind Shear Processor (ASR-WSP) operational test at Orlando International Airport
[AD-A239852] p 18 N92-10019
Solid-State Radar Beacon Decoder (SSRBD) Operational Test and Evaluation (OT/E) integration test plan
[DOT/FAA/CT-TN91/30] p 19 N92-10020
Air-to-air visual acquisition handbook
[ATC-151] p 93 N92-13042
FAA air traffic activity: FY 1990. Addendum
[AD-A241484] p 93 N92-13046
Aircraft accident report: Northwest Airlines, Inc., Flights 1482 and 299. Runway incursion and collision, Detroit Metropolitan/Wayne County Airport, Romulus, Michigan, December 3, 1990
[PB91-910405] p 187 N92-14006
Electronic systems in transportation
[TP-9983] p 189 N92-14009
A strategy for exploiting the full potential of MLS based terminal procedures in Canada p 190 N92-14025
A Taxi And Ramp Management And Control system (TARMAC) p 207 N92-14027
A unique approach to aircraft conflict resolution using artificial intelligence techniques p 190 N92-14029
Evaluation of triple simultaneous parallel ILS approaches spaced 4300 feet apart, phase 4a
[ACD-340] p 191 N92-14034
Data Multiplexing Network (DMN) phase 3 equipment Operational Test and Evaluation (OT and E)/integration test report
[DOT/FAA/CT-TN91/50] p 221 N92-14270
Rotorcraft low altitude IFR benefit/cost analysis: Operations analysis
[SCT-90RR-44] p 191 N92-15061
Terminal Doppler weather radar test bed operation, Orlando: January-June 1990
[AD-A242890] p 301 N92-17028
An investigation of air transportation technology at the Massachusetts Institute of Technology, 1990-1991
p 265 N92-17985
High Capacity Voice Recorder (HCVR) Operational Test and Evaluation (OT and E)/integration test plan
[DOT/FAA/CT-TN91/55] p 402 N92-18959
The COMPAS system in the ATC environment
[DLR-MITT-91-08] p 354 N92-19041
Design principles of automation aids for ATC approach control p 354 N92-19042
COMPAS system concept p 354 N92-19043
Evaluation of the COMPAS experimental system
p 355 N92-19044
Experiences developed in transfering the experimental COMPAS system to an operational prototype version
p 355 N92-19045
Steps toward acceptance p 355 N92-19046
Evaluation of the COMPAS operational system
p 355 N92-19047
Extension of the Frankfurt COMPAS for general application p 355 N92-19048
The impact of COMPAS on the future Cooperative Air Traffic Management Concept (CATMAC)
p 355 N92-19049
The role of planning systems in future air traffic management p 355 N92-19050
JPL's Real-Time Weather Processor project (RWP) metrics and observations at system completion
p 413 N92-19428
Estimating the probability of vertical overlap from the paired aircraft data obtained in the European vertical data collection using the program DGLDiF
[NLR-TR-88108-U] p 356 N92-19491
The Center/TRACON Automation System (CTAS): A video presentation
[NASA-TM-103887] p 356 N92-20029
Vortex characteristics of C5A/B, C141B and C130E aircraft applicable to ATC terminal flight operations tower fly-by-data
[PB92-114586] p 449 N92-20318
Television Microwave Link (TML) Operational Test and Evaluation (OT/E)/integration test report
[DOT/FAA/CT-TN91/57] p 500 N92-20653
Evaluation of triple simultaneous parallel ILS approaches spaced 5000 feet apart, phase 4.b
[DOT/FAA/CT-91/31] p 456 N92-21404
Flight deck benefits of integrated data link communication
[NASA-TP-3219] p 456 N92-21459
Cockpit weather information needs
p 449 N92-21503
UK airmisses involving commercial air transport: September - December 1990
[ETN-92-91050] p 452 N92-21746
Technical feasibility of digital three-dimensional cellular communications for air traffic control applications. Volume 1: Introduction and summary
[AD-A244573] p 534 N92-22104
Technical feasibility of digital three-dimensional cellular communications for air traffic control applications. Volume 2: Example system design details
[AD-A244574] p 534 N92-22105
Technical feasibility of digital three-dimensional cellular communications for air traffic control applications. Volume 3: Ground network architecture
[AD-A244575] p 534 N92-22106
Aircraft accident report: Runway collision of USAir Flight 1493, Boeing 737 and Skywest Flight 5569 Fairchild Metroliner, Los Angeles International Airport, Los Angeles, CA, February 1, 1991
[PB91-910409] p 530 N92-23596
System considerations, projected requirements and applications for aeronautical mobile satellite communications for air traffic services
p 677 N92-24163
Aeronautical mobile satellite service: Air traffic control applications p 677 N92-24164
Spectrum sharing between AMSS(R) and MSS
p 677 N92-24165
Nationwide system delay study of the microwave landing system in the New York terminal area, volume 1
[DOT/FAA/CT-TN91/59-VOL-1] p 640 N92-25098

General maintenance handbook for airway facilities
[PB92-147586] p 640 N92-25518
Flight test of avionic and air-traffic control systems
[ETN-92-91063] p 640 N92-25590
ATTAS experimental cockpit and ATMOS for flight control components and systems investigations
p 641 N92-25595
Testing of an experimental FMS p 648 N92-25596
Rotorcraft terminal ATC route standards
[SCT-90RR-33] p 641 N92-26101
JTIDS electromagnetic compatibility in the 960-1215 MHz band
[AD-A247834] p 773 N92-27864
Knowledge-based planning for controlled airspace flight operation as part of a cockpit assistant
p 727 N92-27895
On board planning of 4D-trajectories
p 728 N92-27897
Implementation and operational experience with a new arrival traffic management system at the Frankfurt ATC-Center p 728 N92-27905
A formal definition of the object-oriented paradigm for requirements analysis
[AD-A246814] p 729 N92-28132
FAA aviation forecasts
[AD-A250412] p 837 N92-29182
NARSIM: A real-time simulator for air traffic control research
[NLR-TP-90147-U] p 888 N92-29204
Application of VME-technology on an airborne data link processor unit
[NLR-MP-88040-U] p 841 N92-29615
Remote sensing of trapping layer base height using ATIS transmissions
[AD-A250074] p 1004 N92-31362
The 1991 Federal Aviation Administration plan for research, engineering and development
p 1142 N92-32453
Safety study of TCAS 2 for logic version 6.04
[DOT/FAA/RD-92/22] p 1047 N92-32537
Airport Surveillance Radar (ASR-9) wind shear processor: 1991 test at Orlando, Florida
[AD-A252246] p 1124 N92-32686
Air traffic control: FAA's advanced automation system contract
[GAO/IMTEC-91-25] p 1048 N92-32861
CTAS: Computer intelligence for air traffic control in the terminal area
[NASA-TM-103959] p 1044 N92-33080
Simulation test and evaluation of TCAS 2 logic version 6.04
[DOT/FAA/RD-92/23] p 1048 N92-33098
Analysis of delay reducing and fuel saving sequencing and spacing algorithms for arrival traffic
[NASA-TM-103880] p 1044 N92-33194
Design and evaluation of an advanced air-ground data-link system for air traffic control
[NASA-TM-103899] p 1050 N92-33407
Radar clutter classification
[ISBN-0-315-57981-1] p 1126 N92-33440
Controller response to conflict resolution advisory prototype
[PB92-190032] p 1050 N92-33596
Impacts of technology on the capacity needs of the US national airspace system
[NASA-CR-4470] p 1045 N92-34192
Human factors issues in the use of artificial intelligence in air traffic control. October 1990 Workshop
[NASA-CR-190925] p 1051 N92-34203

AIR TRAFFIC CONTROLLERS (PERSONNEL)
Managing Europe's air traffic system
p 19 A92-11876
Data-link communication between controllers and pilots - A review and synthesis of the simulation literature
p 94 A92-14045
Airport Surface Traffic Automation p 95 A92-16228
Quantitative estimation of secondary surveillance radar information p 353 A92-24943
The real TCAS --- traffic alert and collision avoidance system p 350 A92-25521
Advanced ASDE provides new eyes and ears for controllers p 453 A92-29506
Perspective versus plan view air traffic control (ATC) displays - Survey and empirical results
p 896 A92-44967
The role of planning systems in future air traffic management p 355 N92-19050
Controller memory enhancement: Field facility concepts and techniques
[DOT/FAA/CT-TN92/7] p 640 N92-24799
Exposures from headset interference tones
[AD-A247175] p 1136 N92-32697
Design and evaluation of an advanced air-ground data-link system for air traffic control
[NASA-TM-103899] p 1050 N92-33407
Controller response to conflict resolution advisory prototype
[PB92-190032] p 1050 N92-33596
Human factors issues in the use of artificial intelligence in air traffic control. October 1990 Workshop
[NASA-CR-190925] p 1051 N92-34203

AIR TRANSPORTATION
Air transport research in Germany p 61 A92-17095
Report of the working group Future CNS Systems - Applications and impact on the German air transport system p 266 A92-21325
The real TCAS --- traffic alert and collision avoidance system p 350 A92-25521
Trends in the selection of airliners
p 417 A92-28183
An aircraft manufacturer's perspective
p 515 A92-33430
Air transportation - The global vision
p 532 A92-33434
Australian aeronautics, 1989-90 p 515 A92-33460
Halfway around the world is far enough
p 516 A92-33462
Prospects for a commercial STOL transportation system p 634 A92-38207
The helicopter commuter - A perspective on regular passenger transportation by rotary wing
p 634 A92-38208
Opening closed skies - The prospects for further liberalization of trade in international air transport services p 697 A92-39244
Civil aircraft design in relation to airworthiness
p 635 A92-39303
Assurance of safety in the aging aircraft fleet
p 635 A92-39305
Auxiliary power system requirements for commercial air transports - Past, present and future
[SAE PAPER 912188] p 656 A92-40007
A helicopter transportation system
p 723 A92-43161
Small and cost-effective airship for transportation
p 731 A92-43244
Safety vs. economy, system-theoretic approach to the problem analysis p 916 A92-45002
Judgement training for Alaskan pilots
p 835 A92-45048
Trends in commercial aircraft design - What evolution factors and what approach?
[ONERA, TP NO. 1992-25] p 786 A92-48587
Managing simulator wiring information and deriving system continuity p 964 A92-49287
Air transports in the 21st century
p 1015 A92-55103
Personal air transport: State of the art
[PB91-204768] p 18 N92-10991
Winds of change: Domestic air transport since deregulation
[NRC-SR-230] p 92 N92-13040
Electronic systems in transportation
[TP-9983] p 189 N92-14009
Aircraft accident reports: Brief format. US civil and foreign aviation issue number 4 of 1989 accidents
[PB90-916904] p 263 N92-17133
Discussion for possibility of some aerodynamic ground effect craft
[NAL-TM-619] p 300 N92-17757
Joint University Program for Air Transportation Research, 1990-1991
[NASA-CP-3131] p 242 N92-17984
An investigation of air transportation technology at the Massachusetts Institute of Technology, 1990-1991
p 265 N92-17985
Investigation of air transportation technology at Ohio University, 1990-1991 p 265 N92-17990
Investigation of air transportation technology at Princeton University, 1990-1991 p 266 N92-17995
Bibliography of technical reports, 1980 - 1990
[PB92-110691] p 417 N92-18814
Kappa Group: The initial guess. A proposal in response to a commercial air transportation study
[NASA-CR-189981] p 366 N92-19374
Aircraft gas turbine emissions: Their nature, technology for reduction, and a pollution comparison with channel tunnel transport
[ETN-92-91056] p 559 N92-22406
Aviation system: Capital investment plan
p 636 N92-25297
An analysis of fixed wing tactical airlifter characteristics using an intra-theater airlift computer model
[AD-A246908] p 732 N92-27719
Human factors evaluation of the work environment of operators engaged in the inspection and repair of aging aircraft
[AD-A246445] p 724 N92-27914
The Eurofar program: An European overview on advanced VTOL civil transportation system
[MBB-UD-0611-91-PUB] p 952 N92-30418
Allocation and recovery of federal airport and airway costs, 1991
[AD-A249436] p 983 N92-30777
NASA High Speed Research Program, Emissions Scenarios Committee report of meetings on 26 September 1991 and 9 January 1992
[NASA-CR-190379] p 1004 N92-32147
The impact of air transport on the environment
[PNR-90876] p 1129 N92-33751
Impacts of technology on the capacity needs of the US national airspace system
[NASA-CR-4470] p 1045 N92-34192

AIR WATER INTERACTIONS
Relating the microwave radar cross section to the sea surface stress - Physics and algorithms
p 597 A92-35028

AIRBORNE EQUIPMENT
Windshear detection and avoidance - Airborne systems survey p 17 A92-11382
Manually flown windshear recovery technique
p 27 A92-11386
Computer-aided equipment layout for the fuselage of maneuverable aircraft p 113 A92-16833
Digital technology applied to airborne receivers
p 98 A92-16927
Concepts for replacing shipboard TACAN with differential GPS p 101 A92-16971
Radar troubleshooting assistant expert system
[AIAA PAPER 91-3764] p 231 A92-17626
A new 1553 all-bus instrumentation monitor
p 198 A92-19252
Aerobureau - Strategic television airmobile reports via satellite p 218 A92-19988
On the accuracy of an aircraft-borne ambient electric-field measuring system p 186 A92-20127
A new thermometric instrument for airborne measurements in clouds p 368 A92-24918
Real-time decision aiding - Aircraft guidance for wind shear avoidance
[AIAA PAPER 92-0290] p 350 A92-25743
Airborne in situ computation of the wind shear hazard index
[AIAA PAPER 92-0291] p 351 A92-25744
ETS-V/EMSS mobile satellite communication experiments p 395 A92-26776
A consistency test of airborne GPS using multiple monitor stations p 454 A92-30651
High altitude airborne remote sensing mission using the advanced microwave precipitation radiometer (AMPR)
p 574 A92-34893
Development of a 3-D remote sensing radar
p 597 A92-34908
X-band side-looking airborne radar for remote sensing
p 554 A92-34976
Mechanical design of an airborne imaging microwave radiometer p 554 A92-35276
Rotor aeromechanics research with the RAE research Lynx - The experimental facility and test programme
p 547 A92-35767
State-of-the-art airborne video recording
p 555 A92-35932
The development of multiple-input models for airborne noise prediction p 695 A92-39243
Modulation transfer function degradation in segmented windows p 733 A92-41431
Utilizing the fault monitoring system for the A320 aircraft p 700 A92-43157
Map projections and airborne moving map displays
p 966 A92-49327
Time Resolved Lidar Fluorosensor operating from helicopter p 1121 A92-56296
Pulsed field system for detecting the presence of a target in a subsurface environment
[AD-D015074] p 296 N92-16174
The imaging spectrometer p 599 N92-23387
Quick-look system p 599 N92-23393
Development of a helicopter-borne 8-channel ranging scatterometer
[PB92-141977] p 599 N92-23441
A high gain antenna system for airborne satellite communication applications p 677 N92-24096
Flight test of ARINC 741 configuration low gain SATCOM system on Boeing 747-400 aircraft p 677 N92-24097
Life cycle costs of the C-130 electrical power system upgrade
[AD-A246759] p 786 N92-28348
Applications of ASICs to avionics
[AGARD-AG-329] p 859 N92-28376
Simplified signal processing for an airborne CO2 Doppler lidar p 1000 N92-31023
Spectrum modal analysis for the detection of low-altitude windshear with airborne Doppler radar
[NASA-CR-4457] p 953 N92-31549
High temperature aircraft research furnace facilities
[NASA-CR-184384] p 1101 N92-33826

AIRBORNE LASERS
Interactive graphics method for removal of helicopter motions from laser profile data p 598 A92-35109
Intra-flight laser data links - Technology focus p 725 A92-41472
Theoretical simulation of a 2 micron airborne solid state laser anemometer p 1000 N92-31059
AIRBORNE RADAR
Multiple phase centre DPCA for airborne radar --- Displaced Phase Centre Antenna p 95 A92-16257
X-band side-looking airborne radar for remote sensing p 554 A92-34976
Motion errors in an airborne synthetic aperture radar system p 840 A92-48416
An airborne multimode radar display processor p 965 A92-49308
Integrating a radar/ESM antenna suite with the S-70 helicopter --- Electronic Surveillance Measures p 957 A92-49333
Detection and imaging of moving objects with synthetic aperture radar. I - Optimal detection and parameter estimation theory p 955 A92-50033
The B-2 radar p 956 A92-53102
Low-noise oscillators for airborne radar applications [AD-A242264] p 300 N92-17258
AIRBORNE RADAR APPROACH
94 GHz MMW imaging radar system [SAE PAPER 912208] p 651 A92-40015
AIRBORNE SURVEILLANCE RADAR
Developments in airborne surveillance and control systems p 98 A92-16655
Adaptive airborne MTI with two-dimensional motion compensation p 102 A92-17240
Monopulse secondary surveillance radar and the mode-S surveillance system p 956 A92-53239
AIRBORNE/SPACEBORNE COMPUTERS
Verification of flight software by embedding software simulation in simulation of external environment p 232 A92-19084
Development of a multi-computer in-flight data acquisition and analysis system for general aviation aircraft [AIAA PAPER 92-1037] p 553 A92-33218
Flight management system integration on the F-117A [AIAA PAPER 92-1077] p 563 A92-33246
F15E terrain following system development [AIAA PAPER 92-1079] p 563 A92-33248
The Mission Computer/Electronic Display Subsystem for the United States Air Force C-17A transport aircraft [AIAA PAPER 92-1244] p 553 A92-33337
Flight testing of the Boeing 747-400 Central Maintenance Computer system p 555 A92-35950
ARINC and the avionics of commercial aircraft. II p 637 A92-37072
Airborne Data Acquisition and Relay System p 839 A92-47574
NAECON 91; Proceedings of the IEEE National Aerospace and Electronics Conference, Dayton, OH, May 20-24, 1991. Vols. 1-3 [ISBN 0-7803-0084-X] p 786 A92-48426
A high performance general purpose processing element for avionic applications p 920 A92-48440
Is the avionics system of the Hermes Spaceplane centralized or decentralized? p 984 A92-49258
An ultrareliable integrated digital computer for helicopters p 964 A92-49273
Computer software in civil aircraft p 1006 A92-49302
An advanced flight path management system for low-altitude helicopter flight p 975 A92-49330
Dead reckoning for aircraft in distributed interactive simulation [AIAA PAPER 92-4171] p 1008 A92-52456
The B-2 radar p 956 A92-53102
Recent developments in data acquisition and control systems at the Aircraft Research Association Limited p 1091 A92-54323
Advanced information processing system: Inter-computer communication services [NASA-CR-187556] p 53 N92-11706
Integrated Communications, Navigation, Identification, Avionics (ICNIA) expert system for fault tolerant avionics p 118 N92-12539
A development-memory approach for enhancing avionics software logistics p 119 N92-12540
Behavior-based fault monitoring [AD-A241254] p 164 N92-13746
International aviation (selected articles) [AD-A241119] p 170 N92-13993
Getting expert systems off the ground: Lessons learned from integrating model-based diagnostics with prototype flight hardware p 220 N92-14217
Formulation of a strategy for monitoring control integrity in critical digital control systems [NASA-TM-104158] p 206 N92-15075
The proposed revision to RTCA DO178A and its influence on system design [PNR-90821] p 510 N92-21847
Advanced Transport Operating System (ATOPS) control display unit software description [NASA-CR-189606] p 652 N92-24689
Application of VME-technology on an airborne data link processor unit [NLR-MP-88040-U] p 841 N92-29615
Experience with Ada on the F-18 High Alpha Research Vehicle Flight Test Program [NASA-TM-104259] p 1062 N92-34039
AIRCRAFT
Registration of aircraft in the aircraft registrar using the 'Leasing Decree' of the Federal Minister of Transport of February 12, 1991 p 56 A92-11215
International Pacific Air and Space Technology Conference and Aircraft Symposium, 29th, Gifu, Japan, Oct. 7-11, 1991, Proceedings [SAE P-246] p 783 A92-45376
AIRCRAFT ACCIDENT INVESTIGATION
Requirements for an aircraft mishap analysis system p 16 A92-11170
Fair weather convection and light aircraft accidents [IAF PAPER ST-91-004] p 186 A92-20651
Canada making many changes in wake of Dryden crash report p 529 A92-33799
Analysis of accidents during instrument approaches p 529 A92-34253
Loss of cabin pressurization in U.S. naval aircraft - 1969-90 p 634 A92-37168
Salvaging the wreckage - Multidistrict litigation and aviation p 697 A92-39245
Review of aviation record p 634 A92-39302
How to promote error tolerance in complex systems in the context of ships and aircraft p 673 A92-39308
Engine reliability p 654 A92-39309
Learning from aircraft accidents and incidents p 635 A92-39310
Windscreen departure p 723 A92-42500
An aircraft landing accident caused by visually induced spatial disorientation p 834 A92-44993
The development of an intelligent human factors data base as an aid for the investigation of aircraft accidents p 928 A92-44994
Stop, look and learn from accident investigation p 834 A92-44996
The effectiveness of training programs for preventing aircrew 'error' p 834 A92-44997
The effect on aircraft evacuations of passenger behaviour and smoke in the cabin p 834 A92-44998
Organizational factors in human factors accident investigation p 834 A92-45000
Judgement training for Alaskan pilots p 835 A92-45048
Rejected takeoffs - Causes, problems, and consequences p 835 A92-45052
ICAO Flight Safety and Human Factors Programme p 835 A92-45055
Mandatory psychological testing of pilots as a requirement for licensing in Norway? p 835 A92-45081
On travelling wave vibration of high-speed duplex helical gears p 990 A92-49580
Takeoff Performance Monitoring System display options [AIAA PAPER 92-4138] p 967 A92-52433
Midair collision - The links in a chain p 951 A92-52645
Aircraft accident report: MarkAir, Inc., Boeing 737-2X6C, N670MA, controlled flight into terrain, Unalakleet, Alaska, 2 June 1990 [PB91-910402] p 92 N92-13039
Aircraft accident report: Northwest Airlines, Inc., Flights 1482 and 299. Runway incursion and collision, Detroit Metropolitan/Wayne County Airport, Romulus, Michigan, December 3, 1990 [PB91-910405] p 187 N92-14006
Aircraft accident/incident summary report: Midair collision involving Lycoming Air Services Piper Aerostar PA-60 and Sun Company Aviation Department Bell 412, Merion, Pennsylvania, April 4, 1991 [PB91-910407] p 187 N92-15055
Aircraft accident reports: Brief format US civil and foreign aviation issue number 2 of 1989 accidents [PB90-916902] p 263 N92-15978
Aircraft accident reports: Brief format US civil and foreign aviation issue number 3 of 1989 accidents [PB90-916903] p 263 N92-15979
Aircraft accident reports: Brief format. US civil and foreign aviation issue number 4 of 1989 accidents [PB90-916904] p 263 N92-17133
Aircraft accident report: Northwest Airlines, Inc., Flights 1482 and 299. Runway incursion and collision, Detroit Metropolitan/Wayne County Airport, Romulus, Michigan, December 3, 1990 [PB91-910405] p 264 N92-17213
Freezing precipitation on lifting surfaces [NRC-32124] p 448 N92-20156
UK airmisses involving commercial air transport: September - December 1990 [ETN-92-91050] p 452 N92-21746
Aircraft accident reports: Brief format U.S. Civil and Foreign Aviation Issue Number 5 of 1989 accidents [PB90-916905] p 452 N92-21833
Aircraft accident report: Unstabilized approach and loss of control NPA, Inc. dba United Express Flight 2415, British Aerospace BA-3101, N41OUE, Tri-Cities Airport, Pasco, Washington, December 26, 1989 [PB91-910406] p 453 N92-21873
Aircraft accident report: Runway collision of USAir Flight 1493, Boeing 737 and Skywest Flight 5569 Fairchild Metroliner, Los Angeles International Airport, Los Angeles, CA, February 1, 1991 [PB91-910409] p 530 N92-23596
Aircraft accident report: Ryan International Airlines DC-9-15, N565PC, loss of control on takeoff, Cleveland-Hopkins International Airport, Cleveland, Ohio, February 17, 1991 [PB91-910410] p 530 N92-23597
Examination of aircraft warning and caution lights after shock testing [NLR-TP-89284-U] p 952 N92-30474
Aircraft accident report: Explosive decompression - loss of cargo door in flight, United Airlines Flight 811, Boeing 747-122, N4713U, Honolulu, Hawaii, February 24, 1989 [PB92-910402] p 953 N92-31159
Aircraft accident report: L'Express Airlines, Inc., Flight 508, Beech C99, N7217L weather encounter and crash near Birmingham, Alabama, July 10, 1991 [PB92-910401] p 1043 N92-32455
Development of rating instruments and procedures for aviation mishap investigation [AD-A253072] p 1044 N92-33288
Aircraft accident/incident summary report: Controlled flight into terrain Bruno's Inc., Beechjet, N25BR, Rome, Georgia, 11 December 1991 [PB92-910404] p 1044 N92-34081
AIRCRAFT ACCIDENTS
Pre-flight risk assessment in emergency medical service (EMS) helicopters p 16 A92-11171
Analysis of general aviation accidents during operations under instrument flight rules p 16 A92-11172
A DFW microburst model based on DL-191 data p 17 A92-11380
Manually flown windshear recovery technique p 27 A92-11386
Rates and risk factors for accidents and incidents versus violations for U.S. airmen p 91 A92-14048
TCAS in the 1990s --- Traffic alert and Collision Avoidance System p 98 A92-16657
Aging aircraft programme entails major effort and expense p 169 A92-20023
Analysis of changes in the pilot population and general aviation accidents p 187 A92-20722
Precipitation development in Colorado Front Range snowstorms - 15 November 1987 case study p 301 A92-23008
The problem of aging aircraft - Is mandatory retirement the answer? p 308 A92-27448
Severe turbulence with a low-level jet ahead of a squall line p 407 A92-27939
Understanding and predicting microbursts p 407 A92-27953
Fire-fighting foams must meet newly-developed ICAO standard p 448 A92-29508
The application of high spectral and spatial resolution imaging spectrometers for locating downed aircraft p 598 A92-35132
Civil aircraft design in relation to airworthiness p 635 A92-39303
Aircraft accidents and human factors p 723 A92-43219
Spectrogram diagnosis of aircraft disasters [SAE PAPER 912041] p 836 A92-45425
Navigation charts on trial - How safe is safe? p 1012 A92-49380
Human factors and simulation p 951 A92-53236
Effect of atmospheric disturbances on airplane response [AIAA PAPER 92-4340] p 1078 A92-55329
Severe turbulence and maneuvering from airline flight records [AIAA PAPER 92-4341] p 1078 A92-55330
Aircraft accident report: MarkAir, Inc., Boeing 737-2X6C, N670MA, controlled flight into terrain, Unalakleet, Alaska, 2 June 1990 [PB91-910402] p 92 N92-13039

Development of an emergency underwater escape breathing system for CH124 seaking aircrew
[DCIEM-87-TR-11] p 92 N92-13041
Onboard cabin water spray system under various discharge configurations
[DOT/FAA/CT-TN91/42] p 93 N92-13043
Aircraft accident report: Northwest Airlines, Inc., Flights 1482 and 299. Runway incursion and collision, Detroit Metropolitan/Wayne County Airport, Romulus, Michigan, December 3, 1990
[PB91-910405] p 187 N92-14006
Aircraft accident/incident summary report: Midair collision involving Lycoming Air Services Piper Aerostar PA-60 and Sun Company Aviation Department Bell 412, Merion, Pennsylvania, April 4, 1991
[PB91-910407] p 187 N92-15055
Aircraft accident reports: Brief format US civil and foreign aviation issue number 2 of 1989 accidents
[PB90-916902] p 263 N92-15978
Aircraft accident reports: Brief format US civil and foreign aviation issue number 3 of 1989 accidents
[PB90-916903] p 263 N92-15979
Aircraft accident reports: Brief format. US civil and foreign aviation issue number 4 of 1989 accidents
[PB90-916904] p 263 N92-17133
Aircraft accident report: Northwest Airlines, Inc., Flights 1482 and 299. Runway incursion and collision, Detroit Metropolitan/Wayne County Airport, Romulus, Michigan, December 3, 1990
[PB91-910405] p 264 N92-17213
Airplane crashes on the runway. Fine modeling of the behavior after burning of a frame submitted to linear crushing
[IMFL-90-64] p 353 N92-19350
Public-sector aviation issues: Graduate research award papers, 1989 - 1990
[PB91-242271] p 308 N92-19662
The effect of wing ice contamination on essential flight characteristics p 449 N92-21681
Aircraft accident reports: Brief format U.S. Civil and Foreign Aviation Issue Number 5 of 1989 accidents
[PB90-916905] p 452 N92-21833
Aircraft accident report: Unstabilized approach and loss of control NPA, Inc. dba United Express Flight 2415, British Aerospace BA-3101, N41OUE, Tri-Cities Airport, Pasco, Washington, December 26, 1989
[PB91-910406] p 453 N92-21873
Aircraft accident report: Runway collision of USAir Flight 1493, Boeing 737 and Skywest Flight 5569 Fairchild Metroliner, Los Angeles International Airport, Los Angeles, CA, February 1, 1991
[PB91-910409] p 530 N92-23596
Aircraft accident report: Ryan International Airlines DC-9-15, N565PC, loss of control on takeoff, Cleveland-Hopkins International Airport, Cleveland, Ohio, February 17, 1991
[PB91-910410] p 530 N92-23597
World commercial aircraft accidents: 1st edition, 1946-1991
[DE92-009801] p 636 N92-24713
Analysis of helicopter accident risk exposure near heliports, airports, and unimproved sites
[SCT-91RR-13] p 637 N92-26028
Composite profiles of helicopter mishaps at heliports and airports
[AD-A248887] p 724 N92-28052
Drop test: Cessna Golden Eagle 421B
[DOT/FAA/CT-TN91/32] p 837 N92-28900
Aircraft accident report: Explosive decompression - loss of cargo door in flight, United Airlines Flight 811, Boeing 747-122, N4713U, Honolulu, Hawaii, February 24, 1989
[PB92-910402] p 953 N92-31159
Canadian aircrew sea water survival, 1952-1987
[DCIEM-88-RR-39] p 954 N92-32219
Aircraft accident report: L'Express Airlines, Inc., Flight 508, Beech C99, N7217L weather encounter and crash near Birmingham, Alabama, July 10, 1991
[PB92-910401] p 1043 N92-32455
Development of rating instruments and procedures for aviation mishap investigation
[AD-A253072] p 1044 N92-33288

AIRCRAFT ANTENNAS
Multiple phase centre DPCA for airborne radar --- Displaced Phase Centre Antenna p 95 A92-16257
High gain airborne antenna for satellite communications p 354 A92-26780
A parallel-series-fed microstrip array with high efficiency and low cross-polarization p 496 A92-31630
Radiation and coupling between antennas mounted on a complex metallic structure p 760 A92-42315
Using the single point excitation technique to measure aperture impedance over a broad frequency range p 761 A92-42320
Single slotted array achieves multimode performance p 726 A92-44428
Scattering mechanism and RCS reduction of antennas p 726 A92-44850
IsoDoppler and mocomp corrections improve MTI radar p 898 A92-45774
SATCOM antenna siting study on P-3C aircraft, volume 1
[NASA-CR-189514] p 221 N92-14262
SATCOM antenna siting study on P-3C aircraft, volume 2
[NASA-CR-189515] p 221 N92-14263
Electronically steerable antenna for aircraft p 229 N92-15272
Automated composite ellipsoid modelling for high frequency GTD analysis
[NASA-CR-189853] p 275 N92-17316
Finite difference time domain grid generation from AMC helicopter models
[NASA-TM-107679] p 1128 N92-34017

AIRCRAFT APPROACH SPACING
Height keeping performance requirements for reducing vertical separation minima used for air traffic control p 1046 A92-56081
A compensatory algorithm for the slow-down effect on constant-time-separation approaches
[NASA-TM-4285] p 23 N92-10024
A Taxi And Ramp Management And Control system (TARMAC) p 207 N92-14027
Evaluation of triple simultaneous parallel ILS approaches spaced 4300 feet apart, phase 4a
[ACD-340] p 191 N92-14034
Estimating the probability of vertical overlap from the paired aircraft data obtained in the European vertical data collection using the program DGLDiF
[NLR-TR-88108-U] p 356 N92-19491
Evaluation of triple simultaneous parallel ILS approaches spaced 5000 feet apart, phase 4.b
[DOT/FAA/CT-91/31] p 456 N92-21404
MLS mathematical modeling study of Philadelphia International Airport runway 27L
[DOT/FAA/CT-TN91/54] p 573 N92-22503
Analysis of delay reducing and fuel saving sequencing and spacing algorithms for arrival traffic
[NASA-TM-103880] p 1044 N92-33194

AIRCRAFT BRAKES
The development and test of thermoplastic composite speed brake p 272 A92-24178
Three-dimensional buoyancy-induced flow and heat transfer around the wheel outboard of an aircraft p 397 A92-27773
Quantification of aircraft carbon brake wear using regression analysis and periodic wave forms
[SAE PAPER 912174] p 644 A92-39999
Characterization of thermal performance of wheel outboard of an aircraft p 849 A92-48352

AIRCRAFT CARRIERS
Concepts for replacing shipboard TACAN with differential GPS p 101 A92-16971
Self-compensating carrier aircraft recovery system p 448 A92-32238
A study of the airwake aerodynamics over the flight deck of an AOR model ship
[AD-A241008] p 89 N92-13034
Neural network and fuzzy logic technology for naval flight control
[AD-A242650] p 206 N92-15074
Deck motion criteria for carrier aircraft operations p 464 N92-21952
Ship airwake measurement and modeling options for rotorcraft applications p 503 N92-21954
Measurement of the flow distribution over the flight deck of an aircraft carrier p 504 N92-21955
Integration of flight and carrier landing aid systems for shipboard operations p 456 N92-21958
Approach and landing assisted by onboard image processing p 457 N92-21959
Approach and landing guidance p 457 N92-21960
Analytical modeling of SH-2F helicopter shipboard operation p 464 N92-21961
Helicopter/ship analytic dynamic interface p 464 N92-21962
Evaluating fixed wing aircraft in the aircraft carrier environment p 464 N92-21963
Some implications for advanced STOVL operation from invincible class ships p 466 N92-21971
Revolution at sea: Aircraft options for the year 2030 p 466 N92-21974
Aircraft ship operations
[AGARD-AR-312] p 850 N92-28468

AIRCRAFT COMMUNICATION
Data-link communication between controllers and pilots - A review and synthesis of the simulation literature p 94 A92-14045
Automatic link establishment - The key to reliable helicopter NOE communications p 94 A92-14403
A prelude to interoperability - Comments on the lack of Federal Radionavigation Plan procedures for assessing the potential of a candidate system to fit into the mix of domestic radionavigation systems p 97 A92-16651
Digital technology applied to airborne receivers p 98 A92-16927
SATZAP - A novel approach to GPS integrity p 99 A92-16947
Implementation of a RAIM monitor in a GPS receiver and an integrated GPS/IRS p 99 A92-16948
Design and implementation of a total flight test system p 189 A92-19278
Report of the working group Future CNS Systems - Applications and impact on the German air transport system p 266 A92-21325
Potential impact of FANS - Far-reaching and positive --- Future Air Navigation Systems p 267 A92-23296
FANS implementation planning under way in Canada p 267 A92-23298
ARINC and commercial aircraft avionics. I p 353 A92-25655
ACTS aeronautical experiments
[AIAA PAPER 92-2042] p 485 A92-29956
Implementing data link across the Pacific
[SAE PAPER 912235] p 638 A92-40027
Intra-flight laser data links - Technology focus p 725 A92-41472
RFI effects analysis of an airport-installed HF transmitter on aircraft COMM/NAV receivers p 725 A92-42313
Using satellite communication for aircraft Automatic Dependent Surveillance p 725 A92-42486
Navigation experiment on an aircraft using the GPS-INS navigation system. I - Introduction to the system p 726 A92-43122
Navigation experiment on aircraft flight using the GPS-INS navigation system. II - Test results p 726 A92-43123
Helicopters for public services, including rescue, fire fighting, and medical emergency p 723 A92-43163
An investigation of the desensitizing effects by high power HF broadcast transmitters on HF airborne receivers p 726 A92-43937
Data Link integration in commercial transport operations p 839 A92-44919
Airborne/shipborne PSK telemetry data link p 839 A92-47511
World Administrative Radio Conference ends favourably for air transport sector p 956 A92-52650
Aeronautical satellite communications system p 1046 A92-56089
Aircraft satellite communication systems p 1046 A92-56091
A consideration on air traffic control processing capability in terminal area p 1047 A92-56110
Integrated Communications, Navigation, Identification, Avionics (ICNIA) expert system for fault tolerant avionics p 118 N92-12539
The impact of cockpit automation on crew coordination and communication. Volume 1: Overview, LOFT evaluations, error severity, and questionnaire data
[NASA-CR-177587] p 93 N92-13044
Rotorcraft low altitude IFR benefit/cost analysis: Operations analysis
[SCT-90RR-44] p 191 N92-15061
Proportional plus integral control of aircraft for automated maneuvering formation flight
[AD-A243792] p 382 N92-19505
Flight deck benefits of integrated data link communication
[NASA-TP-3219] p 456 N92-21459
Cockpit weather information needs p 449 N92-21503
A TMS320-based modem for the aeronautical-satellite core data service p 594 N92-22562
Design considerations for general aviation mobile satellite terminals p 594 N92-22572
Aeronautical mobile satellite service: An overview p 594 N92-22573
Aeronautical satellite system test and implementation p 676 N92-24095
Flight test of ARINC 741 configuration low gain SATCOM system on Boeing 747-400 aircraft p 677 N92-24097
Inmarsat aeronautical mobile satellite system: Internetworking issues p 677 N92-24098
Low cost, electronically steered phased array for general aviation p 677 N92-24099
General maintenance handbook for airway facilities
[PB92-147586] p 640 N92-25518
Mid-range UV communications --- ultraviolet radiation
[AD-D015213] p 770 N92-27615
Advances in Fibre-Optic Technology in Communications and for Guidance and Control
[AGARD-LS-184] p 774 N92-28084
Fiber optic data busses for aircraft p 736 N92-28093

An analysis of aircrew communication patterns and content
[AD-A246618] p 907 N92-28253
Proceedings of the Workshop on Advanced Network and Technology Concepts for Mobile, Micro, and Personal Communications
[NASA-CR-190459] p 1000 N92-30923
The 1991 Federal Aviation Administration plan for research, engineering and development
p 1142 N92-32453
A lightweight loudspeaker for aircraft communications and active noise control p 1125 N92-32964
Feasibility of measuring transverse electric noise at VLF and LF on an ice cap
[AD-A252280] p 1129 N92-33220

AIRCRAFT COMPARTMENTS

Flammability, smoke and toxic gas combustion products of composites used in aircraft cabins p 14 A92-10257
New thermoplastic composites for aircraft structures and interiors p 34 A92-10271
Acoustic isolation of layers p 54 A92-12345
Reliability of helicopter composite dynamic components p 145 A92-14344
Numerical analysis of airflow in aircraft cabins
[SAE PAPER 911441] p 245 A92-21837
Commercial airplane air distribution system development through the use of computational fluid dynamics
[AIAA PAPER 92-0987] p 535 A92-33182
Design of advanced composite components for maintainability based on inservice experience
[AIAA PAPER 92-1085] p 537 A92-33251
Noise level reduction inside helicopter cabins
p 545 A92-35733
A survey of active control in aircraft cabins
p 643 A92-39084
Laboratory testing of a high transmission loss aircraft cabin structure p 663 A92-39229
Display trends in aircraft cockpits p 734 A92-43217
The effect on aircraft evacuations of passenger behaviour and smoke in the cabin p 834 A92-44998
Computational fluid dynamics applications in airplane cabin ventilation system design
[SAE PAPER 911992] p 788 A92-45394
A340 handling, cockpit design improve on predecessor A320 p 849 A92-47969
Aerospace pressurization system design
[SAE AIR 1168/7] p 849 A92-48022
Cockpit crew research p 951 A92-51440
Investigation of a method for determining machining stress in polymethylmethacrylate (PMMA) of airplane canopies p 986 A92-53096
Aluminium-lithium alloys - Application on helicopters
p 1106 A92-56326
Design method of a helicopter cockpit
p 1058 A92-56337
Onboard cabin water spray system under various discharge configurations
[DOT/FAA/CT-TN91/42] p 93 N92-13043
Interior noise p 236 N92-14785
Interior noise prediction methodology: ATDAC theory and validation
[NASA-CR-187626] p 697 N92-25368
Vibro-acoustic FE analyses of the Saab 2000 aircraft
p 1137 N92-32952
Advanced Study for Active Noise Control in Aircraft (ASANCA)
[AIAA PAPER 92-2092] p 1137 N92-32956

AIRCRAFT CONFIGURATIONS

Fickle effect of nose microasymmetry on the high-alpha aerodynamics p 10 A92-13217
Rotorcraft Maneuverability and Agility Survivability Sensitivity Analysis (RMASSA) p 161 A92-14351
Optimization of the aerodynamic balance and parameters of the horizontal tail surfaces of the three-surface aircraft configuration with allowance for the capabilities of the stability and control augmentation system p 134 A92-16803
A configuration development strategy for the NASP
[AIAA PAPER 91-5044] p 210 A92-17830
Engineering method for calculating surface pressures and heating rates on vehicles with embedded shocks
[AIAA PAPER 91-5060] p 171 A92-17842
Forebody vortex flow control on the F-16C using tangential slot and jet nozzle blowing
[AIAA PAPER 92-0019] p 247 A92-22141
Experimental necessities for subsonic transport configuration development
[AIAA PAPER 92-0158] p 254 A92-23773
Approach to side force alleviation through modification of the pointed forebody geometry p 309 A92-24418
Numerical simulations of flow fields over aircrafts
p 313 A92-25042
Calculation of the carriage loads of tandem stores on a fighter aircraft
[AIAA PAPER 92-0283] p 319 A92-25736
Low aspect ratio wing code validation experiment
[AIAA PAPER 92-0402] p 324 A92-26255
The NASA Computational Aerosciences Program - Toward teraFLOPS computing
[AIAA PAPER 92-0558] p 411 A92-26968
Embedded meshes of controllable quality synthesised from elementary geometric features
[AIAA PAPER 92-0663] p 411 A92-27034
Ground facility interference on aircraft configurations with separated flow
[AIAA PAPER 92-0673] p 384 A92-27042
Cartesian Euler method for arbitrary aircraft configurations p 340 A92-28039
Tiger development status --- Franco-German antitank helicopter p 458 A92-29672
Dornier 328 - A Daimler for commuters
p 458 A92-30091
Airbus - The family expands p 419 A92-30092
Determination of the objective-function gradient in the problem of minimizing stress concentration using the finite element method p 494 A92-30170
Generation of loads for finite-element models of large aircraft p 459 A92-30209
Preliminary sizing methodology for hypersonic vehicles
p 460 A92-32233
Design for the relief of thermal stresses in a large high-speed wing
[AIAA PAPER 92-1082] p 536 A92-33250
Three-dimensional time-marching aeroelastic analyses using an unstructured-grid Euler method
[AIAA PAPER 92-2506] p 542 A92-34500
Determining design gust loads for nonlinear aircraft similarity between methods based on matched filter theory and on stochastic simulation
[AIAA PAPER 92-2369] p 518 A92-34597
Mass-transporter p 543 A92-34650
The computation of three-dimensional flows using unstructured grids p 612 A92-37539
Single engine testing of the F-14A(PLUS) airplane in the power approach configuration p 645 A92-40036
Current growth in the aeronautics p 701 A92-41196
Analysis of airship lateral maneuverability
[AIAA PAPER 91-1274] p 743 A92-41212
Downwash for joined-wing airframe with control surface deflections p 702 A92-41235
A method for determining the internal force characteristics of a model in external supersonic flow
p 706 A92-42682
The concept of an unmanned flying vehicle at high altitude p 731 A92-43242
Reevaluation of the motion of an airship
p 731 A92-43243
An overview of US Navy and Marine Corps V/STOL
p 783 A92-45303
Prediction and measurement of jet flowfield features for ASTOVL aircraft p 787 A92-45318
Update of the X-29 high-angle-of-attack program
[SAE PAPER 912006] p 783 A92-45407
An economic approach to accurate wing design
[SAE PAPER 912008] p 789 A92-45408
High speed aerodynamics of upper surface blowing aircraft configurations
[AIAA PAPER 92-2611] p 793 A92-45485
Two-point optimization of complete three-dimensional airplane configuration
[AIAA PAPER 92-2618] p 844 A92-45491
Effects of wing planform on HSCT off-design aerodynamics --- High Speed Civil Transport
[AIAA PAPER 92-2629] p 844 A92-45501
Prismatic grid generation with an efficient algebraic method for aircraft configurations
[AIAA PAPER 92-2721] p 803 A92-45559
Viscous flow past a nacelle isolated and in proximity of a flat plate
[AIAA PAPER 92-2723] p 803 A92-45560
Whirl-flutter stability of a pusher configuration in nonuniform flow p 845 A92-46813
Grid generation and compressible flow computations about a high-speed civil transport configuration
p 919 A92-47055
A geometry-integrated approach to multiblock grid generation p 919 A92-47083
Investigations of propulsion integration interference effects on a transport aircraft configuration
[AIAA PAPER 92-3097] p 849 A92-48739
Reduction of the side force on pointed forebodies through add-on tip devices p 1024 A92-54918
The flow field characteristics about a fighter configuration at high angles of attack
[AIAA PAPER 92-4358] p 1025 A92-55344
Model flight tests of a spin-resistant trainer configuration p 1054 A92-56158
Wing mass formula for twin fuselage aircraft
p 1054 A92-56171
Comparison of recent results from different wind tunnel facilities along with comparisons of measured flight results and wind tunnel based predictions
[AIAA PAPER 92-3985] p 1060 A92-56809
Static internal performance of ventral and rear nozzle concepts for short-takeoff and vertical-landing aircraft
[NASA-TP-3103] p 12 N92-10975
China's first variable stability aircraft: The BW-1-Gets its pre-acceptance flight tests
[AD-A240941] p 116 N92-13062
Aerodynamic aircraft design methods and their notable applications: Survey of the activity in Japan
p 193 N92-13930
On a global aerodynamic optimization of a civil transport aircraft p 193 N92-13931
Design of 3-dimensional complex airplane configurations with specified pressure distribution via optimization
p 194 N92-13948
Development of an analytical method to predict helicopter main rotor performance in icing conditions
[NASA-CR-189110] p 258 N92-15967
Estimation of airborne performance in landing
[ESDU-91032] p 272 N92-15988
Rotorcraft System Identification
[AGARD-LS-178] p 273 N92-17153
Finite element analysis of ASTOVL fighter structure
[AD-A243724] p 275 N92-17513
Parametric effects of some aircraft components on high-alpha aerodynamic characteristics
p 364 N92-18782
X-31: Discussion of steady state and rotary derivatives
p 365 N92-18789
Forebody vortex control aeromechanics
p 380 N92-18792
Kappa Group: The initial guess. A proposal in response to a commercial air transportation study
[NASA-CR-189981] p 366 N92-19374
Proposal for a low cost close air support aircraft for the year 2000: The Raptor
[NASA-CR-190023] p 367 N92-19496
Preliminary design studies of an advanced general aviation aircraft
[NASA-CR-190024] p 461 N92-20064
Manx: Close air support aircraft preliminary design
[NASA-CR-189992] p 463 N92-21565
Aircraft Ship Operations
[AGARD-CP-509] p 464 N92-21951
Preconsiderations on aircraft integration
p 599 N92-23402
Configuration development --- preliminary aircraft design p 552 N92-23953
Panel methods for aerodynamic analysis and design
p 552 N92-23955
Aircraft drag analysis methods p 552 N92-23957
Geometry acquisition and grid generation: Recent experiences with complex aircraft configurations
p 691 N92-24400
VORVISC: A vortex lattice method with viscous and compressibility corrections for full aircraft configurations including propulsion p 626 N92-24857
The natural flow wing-design concept
[NASA-TP-3193] p 631 N92-25202
SHARP: Subsonic High Altitude Research Platform
[NASA-CR-190004] p 648 N92-25263
Interior noise prediction methodology: ATDAC theory and validation
[NASA-CR-187626] p 697 N92-25368
Multiblock grid generation for jet engine configurations
p 659 N92-25720
A preliminary look at an optimal multivariable design for propulsion-only flight control of jet-transport aircraft
[NASA-CR-186014] p 663 N92-25734
Comparison of Janus and field test aircraft detection ranges for the line-of-sight forward heavy system
[AD-A246047] p 770 N92-27600
Recent applications of linear and nonlinear unsteady aerodynamics for aeroelastic analysis
p 718 N92-27940
Development of telemetry for the agility flight test of a radio controlled fighter model
[AD-A248653] p 753 N92-27994
Full mission simulation: A view into the future
p 884 N92-28537
Calculation of unsteady subsonic and supersonic flow about oscillating wings and bodies by new panel methods
[NLR-TP-89119-U] p 827 N92-28659
Modular simulation of HEI fragments and blast pressure
[AD-A248205] p 910 N92-29191
High speed research system study. Advanced flight deck configuration effects
[NASA-CR-189650] p 967 N92-30965
Extension of the integral equation formulation of linearized time dependent subsonic flow
[AD-A250654] p 947 N92-31171

ASTOVL combat aircraft design synthesis and optimization
[CRANFIELD-AERO-9201] p 963 N92-31515
The F-18 high alpha research vehicle: A high-angle-of-attack testbed aircraft
[NASA-TM-104253] p 1060 N92-33404
Applications of a direct/iterative design method to complex transonic configurations
[NASA-TP-3234] p 1039 N92-33484
Dynamic response of induced pressures, suckdown, and temperatures for two tandem jet STOVL configurations
[NASA-TM-103934] p 1039 N92-33581
On the estimation of jet-induced fountain lift and additional suckdown in hover for two-jet configurations
[NASA-TM-102268] p 1040 N92-33618
Effect of afterbody geometry on aerodynamic characteristics of isolated nonaxisymmetric afterbodies at transonic Mach numbers
[NASA-TP-3236] p 1041 N92-33706

AIRCRAFT CONSTRUCTION MATERIALS
High temperature thermoplastic and polyimide processing using CARE-MOLD wash-out tooling p 36 A92-10259
Light metal materials for aircraft structure p 140 A92-13444
Reliability of helicopter composite dynamic components p 145 A92-14344
Producibility Demonstrator Program - Technological preeminence through concurrent engineering p 146 A92-14449
Weathering test of AFRP composites for the application of helicopter fuselage --- Aramide Fiber Reinforced Plastic p 142 A92-15309
Current stabilizing of fastened composite joints to improve non-sparking lightning current performance p 213 A92-20130
The use of finite difference electromagnetic analysis in the design and verification of modern aircraft p 192 A92-20136
The compatibility and tradeoffs of titanium and composites p 288 A92-22758
Weight estimating guide for advanced composites p 289 A92-23418
Composites usage on the RAH-66 Comanche p 457 A92-29669
A critical appraisal of thermomechanical processing of structural titanium alloys p 488 A92-30611
Lifting surface design using the principle of passive control of elastic characteristics p 480 A92-31865
The first fifty years of composite materials in aircraft construction p 461 A92-32325
Development of an advanced composite material on vertical stabilizer of F-X aircraft p 579 A92-32555
Agile responsive effective support - Design and testing of the ARES concept demonstrator aircraft
[AIAA PAPER 92-1038] p 536 A92-33219
Study of materials and structures for the High-Speed Civil Transport
[AIAA PAPER 92-1080] p 536 A92-33249
Design of advanced composite components for maintainability based on inservice experience
[AIAA PAPER 92-1085] p 537 A92-33251
The equations governing the motion of wing-aileron structural systems constructed from advanced anisotropic composite materials
[AIAA PAPER 92-2469] p 564 A92-34359
Overview and major characteristics of future aeronautical and space systems
[AIAA PAPER 92-2441] p 585 A92-34472
Why composites wait in the wings p 577 A92-35475
Smart structures for helicopters p 516 A92-35727
Crashworthiness of truncated composite cones under side loads p 590 A92-35746
A survey of composite structure technology at the Aerospatiale Helicopter Division p 546 A92-35754
Thermal structures and materials for high-speed flight; Collection of Papers of the 1st Thermal Structures Conference, University of Virginia, Charlottesville, Nov. 13-15, 1990
[ISBN 1-56347-017-9] p 590 A92-35847
Flight-vehicle materials, structures, and dynamics - Assessment and future directions. Vol. 3 - Ceramics and ceramic-matrix composites --- Book
[ISBN 0-7918-0661-8] p 668 A92-39852
1991-92 AHS Technical Committee highlights - Structures and materials p 609 A92-40397
New titanium applications on the Boeing 777 airplane p 754 A92-41119
The evolution from bonded F27 aircraft to Arall structures p 699 A92-41177
Technological excellence in honeycomb sandwich and composite structures for aerospace applications p 757 A92-41180
Development of intermetallic materials for aerospace systems p 754 A92-41874
Metal matrix composite fabrication processes for high performance aerospace structures p 760 A92-42145
Composite makers sense changes p 754 A92-42345
Experimental operation of aircraft-engine turbine blade materials p 737 A92-43233
Thermal fiber-reinforced-plastic composite technology for aircraft structures p 755 A92-43237
Al-Li alloys find their niche p 755 A92-43685
Structural concept of main wings of high altitude unmanned aerial vehicle and basic properties of thermoplastic composites as candidate material
[SAE PAPER 912053] p 843 A92-45437
Composites in manufacturing - Case studies
[ISBN 0-87263-406-X] p 784 A92-47403
The impact of advanced materials on small turbine engines
[SAE PAPER 911207] p 862 A92-48021
Addressing the challenge of aircraft component design and manufacture from metal matrix composites p 985 A92-50007
Moldless composite aircraft wing structural design modifications p 958 A92-51527
Steels for aerospace applications p 986 A92-52983
Damage tolerance and durability design of composite aircraft structures p 996 A92-53067
A review of some computer programs of composites p 1009 A92-53069
Safety factor and reliability for composite laminates p 996 A92-53070
New materials drive high-performance aircraft p 1105 A92-55134
Current status of R&D on materials for super/hypersonic transports p 1106 A92-56002
Detailed analysis and test correlation of a stiffened composite wing panel p 1121 A92-56324
Critical appraisal of the McDonnell Douglas closure model for predicting fatigue crack growth
[ARL-STRUC-R-444] p 44 N92-11376
Mechanical qualification tests for materials used in the fabrication of aircraft parts
[CEAT-M5-5443/01] p 195 N92-14042
The two-bay crack problem in fuselages built in GLARE and ARALL
[LR-653] p 196 N92-14044
Bulging of fatigue cracks in a pressurized aircraft fuselage
[LR-655] p 196 N92-14045
Rapid repair of integrally stiffened carbon fibre composite structures by bolted aluminium elements
[MBB-FE202-S-PUB-0453-A] p 290 N92-17310
A guide for the consideration of composite material impacts on airframe costs
[AD-A243928] p 417 N92-19466
Materials and process directions for advanced aero-engine design
[PNR-90814] p 378 N92-19938
Fatigue in single crystal nickel superalloys
[AD-A244815] p 489 N92-21015
The search for new materials
[PNR-90777] p 490 N92-21744
Materials and Structures Research Department: Scientific report (1990)
[ETN-92-90727] p 466 N92-22000
Report on aerospace structures and structural materials R and D in Europe
[PB92-123553] p 550 N92-22785
Conceptional design to heat-resistant airframe of HOPE p 575 N92-23820
Towards GLARE: The development of a fatigue insensitive and damage tolerant aircraft material
[ETN-92-91301] p 648 N92-24966
Ceramic composites: Enabling aerospace materials
[NASA-TM-105599] p 756 N92-27378
The effect of jet fuel exposure on advanced aerospace composites. Part 1: Thermal and chemical analysis
[AD-A246559] p 756 N92-27531
Apparatus for elevated temperature compression or tension testing of specimens
[NASA-CASE-LAR-14775-1] p 912 N92-30099
Low-velocity impact loading on fibre reinforced aluminum laminates (ARALL) and other aircraft sheet materials
[ETN-92-91613] p 987 N92-30414
Activities of the Aeronautical Research Laboratory p 1013 N92-30768
Organic Matrix Composite Helicopter Internal/External Cargo Pallet System (OMC INTEX)
[AD-A251127] p 961 N92-30878
Residual strength of repaired graphite/epoxy laminates after 5 years of outdoor exposure p 1108 N92-32577
Damage tolerance certification methodology for composite structures p 1108 N92-32579
Examples of advanced near-net shape manufacturing techniques for aerospace
[MBB-Z-0399-91-PUB] p 1125 N92-32742
Isothermal aging of IM7/8320 and IM7/5260
[NASA-TM-107666] p 1110 N92-33423
Advanced airframe structural materials: A primer and cost estimating methodology
[AD-A253371] p 1062 N92-34182

AIRCRAFT CONTROL
Flying the A340 iron bird p 20 A92-10666
Application of nonlinear control strategies to aircraft at high angle of attack p 26 A92-11329
Aircraft control under conditions of windshear p 27 A92-11384
Aircraft control in a downburst on takeoff and landing p 27 A92-11385
Design of localizer capture and track hold for a transport airplane - An H(infinity)/LTR approach p 52 A92-11583
H(infinity) robust control synthesis for a fighter performing a coordinated bank turn p 29 A92-11585
An assessment of robustness of variable structure control systems for advanced aircraft manoeuvres p 29 A92-11595
Computation of vectoring nozzle performance p 10 A92-13213
Development and future view of the technology for fly-by-light control system elements p 131 A92-14027
Results of flight tests of the Boeing Sikorsky Fantail demonstrator p 106 A92-14376
Day/Night Adverse weather Pilotage System (D/NAPS) p 94 A92-14429
Analysis of criteria predicting the tendency of pilot induced oscillation for linear non-linear system p 133 A92-15340
X-29 high angle of attack p 111 A92-16052
Aircraft ground vibration test by means of flight control surfaces
[ONERA, TP NO. 1991-96] p 133 A92-16079
Consideration of the time lag of engine processes in the problem of VTOL aircraft control synthesis p 134 A92-16807
Hydraulic pumps - The key to power generation p 215 A92-17348
An alternative derivation of the modified gain function of Song and Speyer p 232 A92-18464
Retrospective essay on nonlinearities in aircraft flight control p 204 A92-18601
Dynamics of hang-gliders p 204 A92-18608
Optimal control problems with maximum functional p 232 A92-18616
Application of stochastic robustness to aircraft control systems p 204 A92-18620
The application of neural networks to drone control p 205 A92-19273
A new method for increasing maximum flight endurance p 280 A92-21006
Aircraft flight controls design using output feedback p 280 A92-21180
Computational investigation of slot blowing for fuselage forebody flow control
[AIAA PAPER 92-0020] p 248 A92-22142
Aircraft control at high-alpha by tangential blowing
[AIAA PAPER 92-0021] p 281 A92-22143
Use of neural networks in control of high alpha maneuvers
[AIAA PAPER 92-0048] p 282 A92-22164
Fluid power conversion p 357 A92-25372
An experiment on the weight vs control relations of subsonic airplanes p 357 A92-25502
2-D and 3-D minimum-time-to-turn flights via parameter optimization
[AIAA PAPER 92-0731] p 379 A92-27083
Adaptive simulator motion software with supervisory control p 412 A92-28136
Flight investigation of variations in rotorcraft control and display dynamics for hover p 379 A92-28151
Abstract model and controller design for an unstable aircraft p 380 A92-28153
Washout filters in the bifurcation control of high alpha flight dynamics p 476 A92-29061
Meeting VSTOL aircraft performance requirements using scheduled H(infinity) controllers p 477 A92-29094
Fuzzy controller design and stability analysis for an aircraft model p 478 A92-29124
Synthesis of robust nonlinear autopilots using differential game theory p 478 A92-29330
Tiltrotor control law design for rotor loads alleviation using modern control techniques p 478 A92-29331
Robust optimal control with a worst case time domain performance criterion p 509 A92-29368
The analysis and approximate representation of the optimal control law for a maneuverable aircraft p 479 A92-30131
Estimation of the optimal load characteristics of aircraft control levers p 479 A92-30150
Comments on 'Fuzzy logic for control of roll and moment for a flexible wing aircraft' p 480 A92-30995

Aircraft control and simulation --- Book
[ISBN 0-471-61397-5] p 480 A92-31021
Improving the efficiency of passenger aircraft during the landing approach p 460 A92-31893
A second-order control optimization method for nonlinear dynamic systems and its use for calculating optimal aircraft trajectories p 460 A92-31894
The ATF YF-23 Vehicle Management System
[AIAA PAPER 92-1076] p 563 A92-33245
Aircraft aeroservoelastic compensation using constrained optimization
[AIAA PAPER 92-2399] p 564 A92-34470
A summary of the Active Flexible Wing program
[AIAA PAPER 92-2080] p 565 A92-35652
On-line analysis capabilities developed to support the AFW wind-tunnel tests
[AIAA PAPER 92-2084] p 572 A92-35656
Rotary-wing aeroservoelastic problems
[AIAA PAPER 92-2107] p 567 A92-35678
A general gust and maneuver load analysis method to account for the effects of active control saturation and nonlinear aerodynamics
[AIAA PAPER 92-2126] p 567 A92-35693
A digital Doppler Rate of Descent Indicator (DRODI) p 555 A92-35927
Calibration of an aircraft control surface using a tri-axial accelerometer package p 555 A92-35942
United 232 - Coping with the 'one-in-a-billion' loss of all flight controls p 530 A92-36349
Aircraft control for take-off in windshear p 660 A92-36990
Aeroservoelasticity p 642 A92-37577
A separated algorithm and application to flight test p 690 A92-38273
B-2 handling, automation tailored to two-pilot crew p 643 A92-39725
Application of linearization analysis to aircraft dynamics p 661 A92-39902
Controls for agility research in the NASA High-Alpha Technology Program
[SAE PAPER 912148] p 661 A92-39984
Wavelength-multiplexed fiber-optic position encoder for aircraft control systems p 734 A92-42602
Development of fly-by-light systems for commercial aircraft p 744 A92-42605
Flight evaluations on in-flight simulation of unstable aircraft p 744 A92-43115
Three-dimensional game for two aircraft p 744 A92-43129
Path angular control of the STOL research aircraft Asuka p 745 A92-43146
Inspection of stability deterioration with an adaptive regulator p 776 A92-43178
The relationship between the weight and flight characteristics of a transonic aircraft p 731 A92-43189
A study of the pilot's associate system p 745 A92-43218
Advanced display system for an aircraft payload p 735 A92-43221
747-400 upper rudder control system p 731 A92-43546
Safety vs. economy, system-theoretic approach to the problem analysis p 916 A92-45002
Hot gas ingestion characteristics and flow visualization of a vectored thrust STOVL concept p 860 A92-45316
An acrobatic airship 'Acrostat'
[SAE PAPER 911994] p 843 A92-45396
Development of the DDV actuation system on the IDF aircraft
[SAE PAPER 912080] p 844 A92-45455
A design of strongly stabilizing controller
[SAE PAPER 912081] p 917 A92-45456
Analysis of a pneumatic forebody flow control concept about a full aircraft geometry
[AIAA PAPER 92-2678] p 799 A92-45530
A new milestone in automatic aircraft control - Fly-by-light systems transmit commands optoelectronically p 784 A92-45699
Fiber optic controls for aircraft engines - Issues and implications p 856 A92-46244
Potential for integrated optical circuits in advanced aircraft with fiber optic control and monitoring systems p 856 A92-46246
X-29 H-infinity controller synthesis p 873 A92-46749
Forebody vortex control using small, rotatable strakes p 811 A92-46798
Study on two variable control plan for twin spool turbojet engine p 862 A92-47697
Aircraft stabilization at large angles of attack p 875 A92-47785
Fiber-optic position transducers for aircraft controls p 857 A92-48041
The propulsive-only flight control problem p 876 A92-48487
Artificial intelligence techniques applied to vehicle management system diagnostics p 965 A92-49315
Development of active control technology for the next generation of combat aircraft p 975 A92-50008
Optimal discrete-time static output-feedback design - A W-domain approach p 1007 A92-50499
Negative state weighting in the linear quadratic regulator for aircraft control p 1007 A92-50513
Flap control simulation p 980 A92-51398
Stability of an adaptive controller for aircraft. I - Analysis via Liapunov theory p 976 A92-51940
Parameter estimation of an augmented airplane with unsteady aerodynamics modelling p 1073 A92-53546
A simulator evaluation of various manual control concepts for fly-by-wire transport aircraft
[AIAA PAPER 92-4328] p 1073 A92-55172
Robust dynamic inversion control laws for aircraft control
[AIAA PAPER 92-4329] p 1073 A92-55173
Neural networks for feedback linearization in aircraft control
[AIAA PAPER 92-4391] p 1074 A92-55192
Identification and control of aircraft dynamics using radial basis function neural networks
[AIAA PAPER 92-4393] p 1074 A92-55194
Aircraft ride quality controller design using new robust root clustering theory for linear uncertain systems
[AIAA PAPER 92-4399] p 1075 A92-55199
Robust sampled data eigenstructure assignment using the delta operator
[AIAA PAPER 92-4400] p 1075 A92-55200
Design of robust Quantitative Feedback Theory controllers for pitch attitude hold systems
[AIAA PAPER 92-4409] p 1075 A92-55203
A robust gain scheduler interpolated into multiple models by membership functions
[AIAA PAPER 92-4553] p 1131 A92-55265
Automated procedures for aircraft aeroservoelastic compensation
[AIAA PAPER 92-4606] p 1077 A92-55284
Nonlinear model-following control application to airplane control (1992 AIAA Controls Design Challenge)
[AIAA PAPER 92-4625] p 1077 A92-55302
Quantitative Feedback Theory approach to AIAA Controls Design Challenge
[AIAA PAPER 92-4626] p 1077 A92-55303
AIAA Atmospheric Flight Mechanics Conference, Hilton Head Island, SC, Aug. 10-12, 1992, Technical Papers. Pts. 1-2 p 1078 A92-55326
Stability, control and gust response characteristics of an ultralight freewing airplane
[AIAA PAPER 92-4342] p 1079 A92-55331
Optimal trajectories for an unmanned air-vehicle in the horizontal plane
[AIAA PAPER 92-4344] p 1079 A92-55333
Development of a high-angle-of-attack stability and control prediction code
[AIAA PAPER 92-4354] p 1079 A92-55340
Dynamic derivative data for high angle of attack simulation
[AIAA PAPER 92-4355] p 1079 A92-55341
Analytical development of an equivalent system mismatch function
[AIAA PAPER 92-4422] p 1080 A92-55346
Computer aided evaluation of aircraft handling qualities and flight control system robustness
[AIAA PAPER 92-4423] p 1080 A92-55347
Flight test results using a low order equivalent systems technique to estimate flying qualities
[AIAA PAPER 92-4425] p 1080 A92-55349
High angle-of-attack control enhancement on a forward swept wing aircraft
[AIAA PAPER 92-4427] p 1080 A92-55351
Vortical flow control on a wing-body combination using tangential blowing
[AIAA PAPER 92-4430] p 1081 A92-55354
An identification procedure for a system with a choice of feedback structures p 1132 A92-55426
Application of fuzzy control to aircraft guidance p 1083 A92-56033
Using the simulation modeling method to estimate the reliability of the crew-flight vehicle system p 1133 A92-57444
An approach to the organization of an adaptive man-machine system for flight vehicle control p 1133 A92-57445
Development of digital/optical rotary position transducer
[NAL-TR-1106] p 29 N92-10028
Maximized gust loads for a nonlinear airplane using matched filter theory and constrained optimization
[NASA-TM-104138] p 23 N92-11010
Application of Eigenstructure Assignment to the control of powered lift combat aircraft
[RAE-TM-FS-1009] p 135 N92-12004
Vortex control: Further encounters p 87 N92-13020
Control of forebody vortices by suction at the nose of the RAE high incidence research model p 87 N92-13022
An aircraft model for the AIAA controls design challenge
[NASA-CR-186019] p 117 N92-13064
Electronic systems in transportation
[TP-9983] p 189 N92-14009
Introduction to neural computing and categories of neural network applications to guidance, navigation and control p 234 N92-14674
Aircraft ground test and subscale model results of axial thrust loss caused by thrust vectoring using turning vanes
[NASA-TM-4341] p 273 N92-17071
Development of high angle of attack control laws for an unstable, non-minimum phase aircraft using variations of the quantitative feedback technique
[AD-A243698] p 282 N92-17096
Loading and vibration reduction through active aerodynamic control
[AD-A242321] p 283 N92-17243
A robust digital flight control system for an unfanned research vehicle using discrete quantitative feedback theory
[AD-A243638] p 283 N92-17748
Identification of the stability and control derivatives of a DLC-flap system for VSRA
[NAL-TR-1116] p 283 N92-17917
Investigation of air transportation technology at Princeton University, 1990-1991 p 266 N92-17995
Neural networks for aircraft system identification p 303 N92-17998
Optimal aircraft performance during microburst encounter p 266 N92-17999
Dynamic flying investigations on 1/13.5 NALLA model (Longitudinal Results)
[NAL-PD-FC-9113] p 359 N92-18073
Aircraft aerodynamics and stability and control during air-to-air refueling
[AERO-REPT-9017] p 380 N92-18321
X-31 enhancement of aerodynamics for maneuvering beyond stall p 363 N92-18779
Characterization of unsteady aerodynamic phenomena at high angles p 364 N92-18787
X-31: Discussion of steady state and rotary derivatives p 365 N92-18789
Aerodynamic control of fighter aircraft by manipulation of forebody vortices p 380 N92-18791
Application of nonlinear QFT to flight control design for high angle of attack maneuvers with thrust vectoring
[AD-A243821] p 381 N92-19241
Ground collision avoidance using a variable incidence altitude measurement system for the A-7 aircraft
[AD-A243880] p 352 N92-19259
CDI sensitivity and crosstrack error on nonprecision approaches
[AD-A243981] p 356 N92-19391
Proposal for a low cost close air support aircraft for the year 2000: The Raptor
[NASA-CR-190023] p 367 N92-19496
Proportional plus integral control of aircraft for automated maneuvering formation flight
[AD-A243792] p 382 N92-19505
Integrated aerodynamic-structural-control wing design p 349 N92-19698
Design and evaluation of a robust dynamic neurocontroller for a multivariable aircraft control problem
[NASA-TM-105579] p 481 N92-20586
Some interesting phenomena from Lavi test flights relating to aircraft stability and control
[IAITIC-91-1017] p 482 N92-20849
Blade-mounted trailing edge flap control for BVI noise reduction
[NASA-CR-4426] p 512 N92-21173
High-speed civil transport flight- and propulsion-control technological issues
[NASA-CR-186015] p 482 N92-21253
Computer-aided design of flight control systems
[AD-A244657] p 483 N92-21752
Fiber optics for controls p 570 N92-22529
Design of an integrated airframe/propulsion control system architecture
[NASA-CR-182004] p 602 N92-22643
Design of an integrated airframe/propulsion control system architecture
[NASA-CR-182007] p 602 N92-22644
Configuration development --- preliminary aircraft design p 552 N92-23953

Wind-tunnel static and free-flight investigation of high-angle-of-attack stability and control characteristics of a model of the EA-6B airplane
[NASA-TP-3194] p 631 N92-25276
Arrangements and methods for the survey of aircraft radio components and systems p 652 N92-25603
Application of nonlinear feedback control theory to supermaneuverable aircraft
[NASA-CR-190336] p 663 N92-25648
A preliminary look at an optimal multivariable design for propulsion-only flight control of jet-transport aircraft
[NASA-CR-186014] p 663 N92-25734
F-111C flight dynamic model aerodynamic data-base development and verification
[AD-A246356] p 715 N92-26947
High lift aircraft
[AD-D015215] p 732 N92-27185
Effects of cockpit lateral stick characteristics on handling qualities and pilot dynamics
[NASA-CR-4443] p 878 N92-28584
Some longitudinal handling qualities design guidelines for active control technology transport aircraft
[NLR-TP-90129-U] p 878 N92-28652
Feedback control laws for highly maneuverable aircraft
[NASA-CR-190535] p 879 N92-29654
On-line analysis capabilities developed to support the AFW wind-tunnel tests
[NASA-TM-107651] p 961 N92-30752
High speed research system study. Advanced flight deck configuration effects
[NASA-CR-189650] p 967 N92-30965
Preliminary subsonic aerodynamic model for simulation studies of the HL-20 lifting body
[NASA-TM-4302] p 978 N92-31175
A summary of the active flexible wing program
[NASA-TM-107655] p 962 N92-31264
Design and analysis issues of integrated control systems for high-speed civil transports
[NASA-CR-186022] p 979 N92-31656
A background to the handling qualities of aircraft
[ESDU-92006] p 1087 N92-32780
Simulation model of a twin-tail, high performance airplane
[NASA-TM-107601] p 1088 N92-33537
Nonlinear dynamic-inversion flight control of supermaneuverable aircraft p 1062 N92-33953
Piloted evaluation of an integrated propulsion and flight control simulator
[NASA-TM-105797] p 1088 N92-34107
Improved articulated fin/wing control system statement of government interests
[AD-D015268] p 1088 N92-34131

AIRCRAFT DESIGN

Control theory for optimum design of aerodynamic shapes p 6 A92-11328
Application of waverider-based configurations to hypersonic vehicle design
[AIAA PAPER 91-3304] p 32 A92-12742
Computation of three-dimensional turbulent vortical flows on bodies at high incidence p 9 A92-13203
H-76B Fantail demonstrator composite fan blade fabrication p 145 A92-14356
Development of a reclined crashworthy crewseat for rotorcraft p 105 A92-14370
Rotorcraft airframe structural optimization for combined vibration and fatigue constraints p 106 A92-14390
Concurrent engineering at Boeing Helicopters p 162 A92-14393
V-22 Osprey tiltrotor blade fold/wing stow system design and testing p 109 A92-14420
Corrosion prevention field test utilizing water displacement compounds p 110 A92-14436
A basis for ice formation design p 146 A92-14556
From the history of Soviet aviation - Aircraft of the Il'iushin design bureau (2nd revised and enlarged edition) --- Russian book p 61 A92-15022
Aircraft design experience p 110 A92-15326
A development of computer support system for wing design p 162 A92-15332
1990 report to the aerospace profession; Society of Experimental Test Pilots, Symposium, 34th, Beverly Hills, CA, Sept. 27-29, 1990, Proceedings p 111 A92-16051
F-117A flight test program p 112 A92-16061
Design is the name of the game - Comparison of the F5D Skylancer to the F4D Skyray p 167 A92-16062
NASA research program directed at reducing supersonic transport noise p 61 A92-16150
Mirage 2000-5 - Dassault's delta described p 113 A92-16622
Maximum mass allowance to justify passenger-carrying aircraft modification p 113 A92-16802
Dornier Do 328 - A start in the world market p 113 A92-17093
The long-distance Airbus A340 - Europe's largest aircraft p 113 A92-17094
ASNT and aerospace - What about the next 50 years? p 215 A92-17293
Operational design factors for NASP derived vehicles
[AIAA PAPER 91-5081] p 210 A92-17851
Dornier 328 first flight p 192 A92-19924
Technology in the lives of an aircraft designer
[AIAA PAPER 91-3069] p 192 A92-20000
Analysis technique for lightning attachment zoning of aircraft p 186 A92-20126
The use of finite difference electromagnetic analysis in the design and verification of modern aircraft p 192 A92-20136
Direct-inverse transonic wing-design method in curvilinear coordinates including viscous interaction p 193 A92-20202
Four decades of transonic fighter design p 193 A92-20203
Beriev Be-42 - A unique jet-propelled seaplane p 269 A92-21010
Fluid power distribution and control p 292 A92-21733
Condor, an all-electric airplane p 269 A92-21734
Gust effects on a flexible aircraft p 270 A92-22474
Weight estimating guide for advanced composites p 289 A92-23418
Future experimental needs to support applied aerodynamics - A transonic perspective
[AIAA PAPER 92-0156] p 254 A92-23771
On the threshold - The outlook for supersonic and hypersonic aircraft p 356 A92-24402
Agility as a contributor to design balance p 356 A92-24405
Europe presents a united CFD front p 392 A92-24909
Tilting at targets --- tilt rotor aircraft development p 357 A92-25074
The stealth master p 307 A92-25175
Fleet modernization - One approach p 307 A92-25371
Fluid power conversion p 357 A92-25372
A comparison of optimization-based approaches for a model computational aerodynamics design problem p 316 A92-25636
Lighter than air - An illustrated history of the airship (Revised edition) --- Book p 418 A92-25680
Variable-complexity aerodynamic optimization of an HSCT wing using structural wing-weight equations
[AIAA PAPER 92-0212] p 317 A92-25685
Prediction of average downwash gradient for canard configurations
[AIAA PAPER 92-0284] p 319 A92-25737
Non-planar wing design by Navier-Stokes inverse computation
[AIAA PAPER 92-0285] p 319 A92-25738
A methodology for the analysis and modeling of thrust vectoring usage
[AIAA PAPER 92-0389] p 357 A92-26245
The 'derivative' and 'synthetic' approaches in aircraft design p 358 A92-27901
The stability analysis of the nonlinear shimmy p 358 A92-27902
Aerodynamic design optimization using sensitivity analysis and computational fluid dynamics p 340 A92-28044
Computational fluid dynamics and aircraft design p 457 A92-28875
36th Roy Chadwick Lecture - Manufacturing breakout 1941-1991: Development in aerospace industry manufacturing techniques p 419 A92-28941
Dornier 328 - A Daimler for commuters p 458 A92-30091
Aerodynamic wing-nacelle integration p 458 A92-30134
Selection of efficient primary-structure/force configurations for aircraft lifting surfaces subjected to displacement constraints p 458 A92-30140
Stability of stiffened panels with allowance for plasticity under nonstationary heating and loading p 493 A92-30152
Perspectives in aerospace design --- Book
[ISBN 1-56347-010-1] p 459 A92-31606
Aero-propulsive effects on configuration shaping
[AIAA PAPER 91-5064] p 459 A92-31691
Approximate determination of the effect of deviations of wing and tail geometry from design parameters on the drag coefficient of subsonic aircraft p 460 A92-31878
Approximate closed-form buckling solutions for the optimization of aircraft structures p 579 A92-32578
Recent advances in restraint technology p 535 A92-32979
Preliminary results from the High Speed Airframe Integration Research project
[AIAA PAPER 92-1004] p 536 A92-33196
An inverse method for the design of transonic wings
[AIAA PAPER 92-1025] p 517 A92-33206
Agile responsive effective support - Design and testing of the ARES concept demonstrator aircraft
[AIAA PAPER 92-1038] p 536 A92-33219
The U-2A flight test program
[AIAA PAPER 92-1086] p 537 A92-33252
System design from mission definition to flight validation
[AIAA PAPER 92-1091] p 605 A92-33256
The use of large teams in conceptual aircraft design
[AIAA PAPER 92-1092] p 605 A92-33257
Multidisciplinary design environment development for air vehicle engineering
[AIAA PAPER 92-1113] p 605 A92-33269
Application of a local panel buckling constraint within automated multidisciplinary structural analysis and design
[AIAA PAPER 92-1116] p 537 A92-33271
Design for Corrosion Prevention
[AIAA PAPER 92-1127] p 577 A92-33279
Structural design for durability - Lessons learned from service and test data
[AIAA PAPER 92-1129] p 537 A92-33281
Concepts for a future aircraft design environment
[AIAA PAPER 92-1188] p 600 A92-33300
An interactive system for aircraft design and optimization
[AIAA PAPER 92-1190] p 600 A92-33302
Design sheet - An environment for facilitating flexible trade studies during conceptual design
[AIAA PAPER 92-1191] p 600 A92-33303
Integration of supportability elements into the conceptual design process
[AIAA PAPER 92-1194] p 600 A92-33306
Application of multidisciplinary optimization to conceptual aircraft design at Rockwell International - A status report
[AIAA PAPER 92-1196] p 537 A92-33307
Design tradeoffs on engine-integrated hypersonic vehicles
[AIAA PAPER 92-1205] p 537 A92-33313
The Mission Computer/Electronic Display Subsystem for the United States Air Force C-17A transport aircraft
[AIAA PAPER 92-1244] p 553 A92-33337
The C-17 - Modern airlift technology
[AIAA PAPER 92-1262] p 538 A92-33342
Low Reynolds number, long endurance aircraft design
[AIAA PAPER 92-1263] p 538 A92-33343
ACSYNT - A standards-based system for parametric, computer aided conceptual design of aircraft
[AIAA PAPER 92-1268] p 601 A92-33345
New way of flying (1990 Sir Charles Kingsford Smith Lecture) p 515 A92-33461
AIAA/ASME/ASCE/AHS/ASC Structures, Structural Dynamics and Materials Conference, 33rd, Dallas, TX, Apr. 13-15, 1992, Technical Papers. Pt. 5 - Design engineering/design optimization, materials, work-in-progress p 585 A92-34522
Application of analytical and design tools for fighter wing aeroelastic tailoring
[AIAA PAPER 92-2373] p 542 A92-34543
A design optimization procedure for high-speed prop-rotors
[AIAA PAPER 92-2375] p 542 A92-34545
A structural design and optimization tool for ducted rotor/wing blades
[AIAA PAPER 92-2361] p 543 A92-34593
An expert system to aid real world finite element analysis
[AIAA PAPER 92-2488] p 601 A92-34604
Mass-transporter p 543 A92-34650
Facing the crisis in aircraft design education p 606 A92-34770
Designing a better engineer p 606 A92-34771
An experimental and analytical investigation of wing flutter on a trail rotor V/STOL aircraft
[AIAA PAPER 92-2112] p 544 A92-35682
The aerodynamic assistant - A tool for V/STOL aircraft conceptual design p 545 A92-35737
The V-22 Osprey - A significant flight test challenge p 546 A92-35766
Flight testing of the Boeing 747-400 Central Maintenance Computer system p 555 A92-35950
Composite materials for aerospace applications p 577 A92-36377
Exploratory design studies of actively controlled wings using integrated multidisciplinary synthesis p 641 A92-36828
Dimensional characterization of a large aircraft structure by photogrammetry p 607 A92-37061
Use of the thrust-weight diagram versus transport cargo in the initial dimensioning of passenger-transport aircraft p 642 A92-37074
The National Aerospace Plane program and the APL role p 666 A92-37375

Numerical simulation of hypersonic viscous flow for the design of H-II orbiting plane (HOPE)
p 612 A92-37549
An information system for the numerical simulation of 3D Euler flows around aircraft p 613 A92-37554
Recent advances in maneuver loads analysis
p 642 A92-37576
The quiet STOL research aircraft ASUKA
p 642 A92-38206
Prospects for a commercial STOL transportation system p 634 A92-38207
New processes in commercial airplane design
p 607 A92-38218
Production technologies and aircraft design
p 608 A92-38220
Civil aircraft design in relation to airworthiness
p 635 A92-39303
Aircraft structural design p 643 A92-39304
Analysis for the application of hybrid laminar flow control to a long-range subsonic transport aircraft
[SAE PAPER 912113] p 617 A92-39964
Noise abatement procedures vs. safety
[SAE PAPER 912137] p 635 A92-39977
Agility and high angle of attack - An Air Force research perspective
[SAE PAPER 912145] p 608 A92-39983
Concorde flight testing - Powerplant and performance flying
[SAE PAPER 912192] p 644 A92-40009
Concorde, fifteen years on the front line
[SAE PAPER 912193] p 644 A92-40010
Aging aircraft and structural airworthiness
[SAE PAPER 912212] p 635 A92-40016
Sikorski (S-76) High Intensity Radiated Fields (HIRF) test
[SAE PAPER 912214] p 652 A92-40017
The Pond Racer preliminary flight test report
p 645 A92-40031
Rafale: Program update - Development of a naval version p 645 A92-40035
The Hummingbird experience at Lockheed Georgia
p 646 A92-40041
European Fighter Aircraft (EFA) programme status report p 646 A92-40043
Conceptual design and analysis of a special operations transport p 646 A92-40387
Aeroelasticity and the Tiltrotor VTOL aircraft
p 647 A92-40389
1991-92 AHS Technical Committee highlights - Handling qualities p 662 A92-40395
Modern aircraft design. Vol. 1 (2nd Edition) --- Book
p 647 A92-40897
Some aspects of advanced aircraft development
p 729 A92-41176
International Conference on Aerospace Trends...2001 - From Aeroplane to Aerospace Plane, Thiruvananthapuram, India, June 27, 28, 1991, Proceedings p 751 A92-41184
Current growth in the aeronautics p 701 A92-41196
Automation of flight vehicle design --- Russian book
[ISBN 5-217-01447-4] p 776 A92-42780
The design of fully-optimized configurations by using the iterative optimum-optimorum theory --- shape of delta wings of minimum drag p 709 A92-43072
Some consideration for evaluation of structural integrity of aging aircraft p 762 A92-43107
Optimum structural design of a cantilevered rectangular elastic wing with a gust load alleviation system
p 762 A92-43133
Operational progress of the STOL research aircraft Asuka p 730 A92-43138
Design - Analysis and experimental verification of a propeller working in the low Reynolds number range
p 710 A92-43174
The relationship between the weight and flight characteristics of a transonic aircraft
p 731 A92-43189
The effectiveness of the warp shape airfoil of a supersonic transport p 711 A92-43203
Small and cost-effective airship for transportation
p 731 A92-43244
Joint Aviation Authorities: Development of an international standard for safety regulation - The first steps are being taken by the JAA p 781 A92-43548
Al-Li alloys find their niche p 755 A92-43685
Composite material stub-blade wing joint
p 763 A92-44618
An overview of US Navy and Marine Corps V/STOL
p 783 A92-45303
Jet-powered V/STOL aircraft - Lessons learned
p 841 A92-45304
Military utility of medium speed V/STOL designs
p 841 A92-45308
Evolution of ASTOVL aircraft design
p 842 A92-45311
International Pacific Air and Space Technology Conference and Aircraft Symposium, 29th, Gifu, Japan, Oct. 7-11, 1991, Proceedings
[SAE P-246] p 783 A92-45376
The high speed challenge for rotary wing aircraft
[SAE PAPER 911974] p 842 A92-45381
The fatigue scatter factors and reduction factors in the design of aircraft and helicopter's structural lives
[SAE PAPER 911984] p 843 A92-45387
The impact of CFD on the airplane design process - Today and tomorrow
[SAE PAPER 911989] p 788 A92-45391
Computational aerodynamics in aircraft design - Challenges and opportunities for Euler/Navier-Stokes methods
[SAE PAPER 911990] p 788 A92-45392
An acrobatic airship 'Acrostat'
[SAE PAPER 911994] p 843 A92-45396
Ducted fan VTOL for working platform
[SAE PAPER 911995] p 843 A92-45397
Results and lessons learned from the STOL and Maneuver Demonstration Program
[SAE PAPER 912005] p 843 A92-45406
Aerodynamic development of boundary layer control system for NAL QSTOL research aircraft 'ASKA'
[SAE PAPER 912010] p 843 A92-45410
Aero-structural integrated design of forward swept wing
[SAE PAPER 912021] p 790 A92-45414
Feasibility study on a microwave-powered unmanned aerial vehicle for the communication relay utilization
[SAE PAPER 912052] p 843 A92-45436
Structural concept of main wings of high altitude unmanned aerial vehicle and basic properties of thermoplastic composites as candidate material
[SAE PAPER 912053] p 843 A92-45437
Experimental and numerical study of aerodynamic characteristics for second generation SST
[SAE PAPER 912056] p 844 A92-45439
Integrated wiring system
[SAE PAPER 912058] p 897 A92-45440
Effects of wing planform on HSCT off-design aerodynamics --- High Speed Civil Transport
[AIAA PAPER 92-2629] p 844 A92-45501
Determination of aerodynamic sensitivity coefficients based on the three-dimensional full potential equation
[AIAA PAPER 92-2670] p 798 A92-45525
Analysis of a pneumatic forebody flow control concept about a full aircraft geometry
[AIAA PAPER 92-2678] p 799 A92-45530
Surface grid generation in a parameter space
[AIAA PAPER 92-2717] p 803 A92-45556
Applied Computational Aerodynamics - Case studies
[AIAA PAPER 92-2661] p 845 A92-45580
Applied aerodynamics education - Design and science
[AIAA PAPER 92-2662] p 928 A92-45581
Integrated aeroservoelastic wing synthesis by nonlinear programming/approximation concepts
p 873 A92-46752
Design load predictions on a fighter-like aircraft wing
p 811 A92-46797
System for generating sequences of phased gust or taxi loadings p 845 A92-46800
Optimum cruise lift coefficient in initial design of jet aircraft p 845 A92-46806
Minimizing supersonic wave drag with physical constraints at design and off-design Mach numbers
p 811 A92-46808
Wing mass formula for subsonic aircraft
p 845 A92-46812
Optimization of constant altitude-constant airspeed flight of turbojet aircraft p 845 A92-46815
Filament winding of composite isogrid fuselage structures p 784 A92-47405
Design and test of aircraft aft fuselage structure using postbuckled shear panels p 848 A92-47406
Design and use of aramid fiber in aircraft structures
p 784 A92-47407
The effect of composite material allowable changes on VTOL airframe weights p 848 A92-47629
The airplane --- F-117 aircraft p 849 A92-47759
A340 handling, cockpit design improve on predecessor A320 p 849 A92-47969
B-1B excels in conventional role p 786 A92-47971
US Navy revisits escape modules p 849 A92-47975
Trends in commercial aircraft design - What evolution factors and what approach?
[ONERA, TP NO. 1992-25] p 786 A92-48587
Computational icing analysis for aircraft inlets
[AIAA PAPER 92-3178] p 836 A92-48793
Fighter airframe/propulsion integration - A General Dynamics perspective
[AIAA PAPER 92-3332] p 850 A92-48915
Emerging airframe/propulsion integration technologies at General Electric
[AIAA PAPER 92-3335] p 850 A92-48917
Emerging technologies for gas turbine engines - U.A.V. synergies
[AIAA PAPER 92-3757] p 867 A92-49114
Managing simulator wiring information and deriving system continuity p 964 A92-49287
A study on mechanical model of the helicopter 'ground resonance' p 955 A92-50214
The 'White Pelican' project - Design and construction of the world's largest paper airplane
p 931 A92-51400
Cost effective close tolerance plastic master models
p 958 A92-51538
BA's 777 p 958 A92-51580
Successful transfer of technology from a research and development laboratory to an Aerospatiale production unit p 931 A92-51808
777 shaping up p 959 A92-52300
Simulation software flowdown in the aircraft design process - Problems and solutions
[AIAA PAPER 92-4160] p 1008 A92-52450
Anti-fatigue optimization design by artificial intelligence strategy p 996 A92-53013
A review of some computer programs of composites
p 1009 A92-53069
Investigation of the tail buffeting of the C-101
p 942 A92-53253
Integrated system to support computer analysis in conceptual aerospace design p 1130 A92-53596
Aerodynamic airfoils design by quasi-solutions method of inverse boundary-value problems
p 1020 A92-53998
An experimental investigation of the flow in a diffusing S-duct
[AIAA PAPER 92-3622] p 1021 A92-54090
Optimization of a 2D scramjet-vehicle using CFD and simplified approximate flow analysis techniques
[AIAA PAPER 92-3673] p 1022 A92-54116
Mikoyan's market-buster p 1052 A92-54981
777 - The airlines' higher-order technology airplane
p 1052 A92-55104
Turning up the heat on aircraft structures --- design and analysis for high-temperature conditions
p 1052 A92-55131
Continuous flying quality improvement - The measure and the payoff
[AIAA PAPER 92-4327] p 1073 A92-55171
PAYCOS, a multidisciplinary sizing code for hypersonic vehicles
[AIAA PAPER 92-4564] p 1132 A92-55376
Whirl flutter analysis and application to aircraft design
p 1053 A92-56017
A development of hypermedia type database system for instruction of aircraft conceptual design
p 1132 A92-56113
Application of advanced multidisciplinary analysis and optimization methods to vehicle design synthesis
p 1054 A92-56160
Wing mass formula for twin fuselage aircraft
p 1054 A92-56171
High angle-of-attack flush airdata sensing system
p 1064 A92-56172
Solutions to supportability concerns related to reduced-signature aircraft p 1055 A92-56220
New aircraft technologies - Challenges for dependability p 1120 A92-56225
Electronics/avionics integrity - Definition, measurement and improvement p 1120 A92-56252
Research needs for a commercial passenger tiltrotor
p 1056 A92-56298
The Eurofar program - An European overview on advanced VTOL civil transportation system
p 1016 A92-56299
A simulation study of tiltrotor vertical takeoff procedures using conventional and variable diameter rotor systems
p 1056 A92-56301
Technology exploitation for in-service support of future rotorcraft p 1016 A92-56327
Roles of wind tunnel tests and CFD analyses in the design of energy-efficient SST
[AIAA PAPER 92-3923] p 1133 A92-56754
A multi-diagnostic approach to testing V/STOL craft
[AIAA PAPER 92-4008] p 1099 A92-56831
CFD validation experiments for hypersonic flows
[AIAA PAPER 92-4024] p 1034 A92-56846
Combined exo/endoatmospheric transport alternatives
[IAF PAPER 92-0663] p 1104 A92-57102
Development of unsteady aerodynamic analyses for turbomachinery aeroelastic and aeroacoustic applications
[NASA-CR-4405] p 12 N92-10979
Practical input optimization for aircraft parameter estimation experiments p 114 N92-11989
NASA reliability preferred practices for design and test
[NASA-TM-4322] p 157 N92-12286

An aircraft model for the AIAA controls design challenge
[NASA-CR-186019] p 117 N92-13064
Control augmented structural optimization of aeroelasticity tailored fiber composite wings
[AD-A241464] p 135 N92-13075
Review of aerodynamic design in the Netherlands
p 193 N92-13929
Aerodynamic aircraft design methods and their notable applications: Survey of the activity in Japan
p 193 N92-13930
Design of 3-dimensional complex airplane configurations with specified pressure distribution via optimization
p 194 N92-13948
Extended mapping and characteristics techniques for inverse aerodynamic design p 194 N92-13949
Application of direct inverse analogy method (DIVA) and viscous design optimization techniques
p 176 N92-13951
Research on inverse methods and optimization in Italy
p 202 N92-13956
An inverse method for the aerodynamic design of three-dimensional aircraft engine nacelles
p 194 N92-13958
Vortex generator design for aircraft inlet distortion as a numerical optimization problem p 194 N92-13959
An inverse method with regularity condition for transonic airfoil design p 177 N92-13969
Analysis and design of planar and non-planar wings for induced drag minimization
[NASA-CR-189509] p 179 N92-13999
Avionics technology beyond 2000
p 200 N92-14058
Numerical investigations in three-dimensional internal flows
[NASA-CR-189467] p 221 N92-14313
Design and performance of duct acoustic treatment
p 236 N92-14783
Quiet aircraft design and operational characteristics
p 236 N92-14787
Energy height method for flight path optimisation. Addendum A: Numerical method suitable for rapid use on IBM PC compatible computers
[ESDU-91016-ADD] p 272 N92-15987
Identification of high-level functional/system requirements for future civil transports
[NASA-CR-189561] p 276 N92-15991
A CLIPS-based tool for aircraft pilot-vehicle interface design p 303 N92-16605
Finite element analysis of ASTOVL fighter structure
[AD-A243724] p 275 N92-17513
Hi-alpha forebody design. Part 1: Methodology base and initial parametrics
[NASA-CR-189849] p 358 N92-18024
Hi-alpha forebody design. Part 2: Determination of body shapes for positive directional stability
[NASA-CR-189850] p 359 N92-18038
Use of stepwise regression techniques and kinematic compatibility for the analysis of EAP flight data
p 365 N92-18790
Transformation of flightmechanical design requirements for modern fighters into aerodynamic characteristics
p 365 N92-18794
Kappa Group: The initial guess. A proposal in response to a commercial air transportation study
[NASA-CR-189981] p 366 N92-19374
Proposal for a low cost close air support aircraft for the year 2000: The Raptor
[NASA-CR-190023] p 367 N92-19496
Preliminary design studies of an advanced general aviation aircraft
[NASA-CR-190024] p 461 N92-20064
Structural dynamics and vibrations of damped, aircraft-type structures
[NASA-CR-4424] p 499 N92-20194
Design of a turbofan powered regional transport aircraft
[NASA-CR-190130] p 461 N92-20280
NASA advanced aeronautics design solar powered remotely piloted vehicle
[NASA-CR-190007] p 462 N92-20665
An evaluation of in-cabin safety features in passenger aircraft
[ETN-92-90656] p 449 N92-20794
Alpha Group: The Behemoth Apteryx. Final design proposal
[NASA-CR-190026] p 462 N92-20951
The SnoDog: Preliminary design of a close air support aircraft
[NASA-CR-189990] p 462 N92-21489
Techfest 18 Proceedings
[NIAR-92-1] p 420 N92-21501
Aerodynamic design with CFD p 447 N92-21514
System controls challenges of hypersonic combined-cycle engine powered vehicles
p 475 N92-21533
The Langley turbo-prop commuter design: A complete project description
[NASA-CR-189987] p 463 N92-21540
High altitude solar power platform --- aircraft design analysis
[NASA-TM-103578] p 506 N92-21546
Manx: Close air support aircraft preliminary design
[NASA-CR-189992] p 463 N92-21565
The Guardian: Preliminary design of a close air support aircraft
[NASA-CR-189991] p 463 N92-21566
A-2000: Close air support aircraft design team
[NASA-CR-190022] p 463 N92-21567
The search for new materials
[PNR-90777] p 490 N92-21744
Variable-camber systems integration and operational performance of the AFTI/F-111 mission adaptive wing
[NASA-TM-4370] p 570 N92-22194
The NASA aircraft icing research program
p 549 N92-22534
Supersonic throughflow fans for high-speed aircraft
p 561 N92-22541
Time-optimal reorientation maneuvers of an aircraft
p 549 N92-22605
Design of an integrated airframe/propulsion control system architecture
[NASA-CR-182004] p 602 N92-22643
Design of an integrated airframe/propulsion control system architecture
[NASA-CR-182007] p 602 N92-22644
A system approach to aircraft optimization
p 550 N92-23228
Sensitivity analysis of dynamic aeroelastic responses
p 571 N92-23229
Application of multidisciplinary optimization methods to the design of a supersonic transport
p 550 N92-23230
Application of analytical and design tools for fighter wing aeroelastic tailoring p 550 N92-23231
Application of an automated multidisciplinary analysis and optimisation system to the design of aircraft structures p 551 N92-23233
Design of a fighter aircraft vertical tail enhanced buffet environment survivability p 551 N92-23235
Efficient and robust design optimization of transonic airfoils p 528 N92-23717
Special Course on Engineering Methods in Aerodynamic Analysis and Design of Aircraft
[AGARD-R-783] p 552 N92-23950
Introduction to Special Course on Engineering Methods in Aerodynamic Analysis and Design of Aircraft
p 552 N92-23951
Computational procedures for preliminary design
p 552 N92-23952
Configuration development --- preliminary aircraft design p 552 N92-23953
Panel methods for aerodynamic analysis and design
p 552 N92-23955
High angle of attack: Aerodynamics
p 528 N92-23956
Aircraft drag analysis methods p 552 N92-23957
Geometry acquisition and grid generation: Recent experiences with complex aircraft configurations
p 691 N92-24400
An interactive multi-block grid generation system
p 691 N92-24419
An incremental strategy for calculating consistent discrete CFD sensitivity derivatives
[NASA-TM-104207] p 625 N92-24681
Aerodynamic design and analysis of a light aircraft propeller p 629 N92-24876
Variable geometry sailplanes Minisigma
p 629 N92-24877
The natural flow wing-design concept
[NASA-TP-3193] p 631 N92-25202
The NASA/industry Design Analysis Methods for Vibrations (DAMVIBS) Program: A government overview
[NASA-TM-107579] p 680 N92-25267
Interior noise prediction methodology: ATDAC theory and validation
[NASA-CR-187626] p 697 N92-25368
Development of pre- and post-processor system for structural analysis
[NAL-TM-628] p 681 N92-25403
Computational Structures Technology for Airframes and Propulsion Systems
[NASA-CP-3142] p 683 N92-25911
Computational structures technology and UVA Center for CST p 683 N92-25912
Computer codes developed and under development at Lewis p 692 N92-25913
CSM activities at the NASA Langley Research Center
p 683 N92-25916
Overview of computational structural methods for modern military aircraft p 684 N92-25928
Aircraft optimization by a system approach: Achievements and trends
[NASA-TM-107622] p 650 N92-25995
Gamma Group-The Pale Horse: A proposal in response to a commercial air transportation study ort study
[NASA-CR-190019] p 731 N92-26435
Naval Postgraduate School aircraft synthesis program (user's manual)
[AD-A246198] p 777 N92-26458
NAL Dornier 228-200 flight research airplane: Present status and outline of the installed equipment
[NAL-TM-637] p 732 N92-27429
CFD contributions during hypersonic airplane intake design p 769 N92-27472
System requirements specification for SMART structures mode p 777 N92-27830
Surface generation and editing operations applied to structural support of aerospace vehicle fuselages
p 777 N92-27831
Evaluation of landing configuration by flight test of the quiet STOL experimental aircraft ASKA
[NAL-TR-1113] p 733 N92-28191
Integrating aerodynamics and structures in the minimum weight design of a supersonic transport wing
[NASA-TM-107586] p 850 N92-28435
Practical architecture of design optimisation software for aircraft structures taking the MBB-Lagrange code as an example p 851 N92-28471
Structural optimization of aircraft p 851 N92-28472
Multidisciplinary design and optimization
[AGARD-PAPER-2] p 851 N92-28473
Mathematical optimization: A powerful tool for aircraft design p 851 N92-28474
Use of a virtual cockpit for the development of a future transport aircraft p 886 N92-28547
Application of piloted simulation to high-angle-of-attack flight-dynamics research for fighter aircraft
p 886 N92-28551
Constrained spanload optimization for minimum drag of multi-lifting-surface configurations
[NLR-TP-89126-U] p 828 N92-28660
Quaternion and Euler angles in kinematics
[NAL-TM-636] p 909 N92-28836
Aerodynamic characteristics obtained from alpha sweep test of the quiet STOL experimental aircraft ASKA
[NAL-TR-1112] p 853 N92-28901
Improving designer productivity --- artificial intelligence
[NASA-TM-103929] p 854 N92-29417
Concurrent engineering in design of aircraft structures
[MBB-FE-2-S-PUB-472] p 854 N92-29650
Numerical investigations in three-dimensional internal flows
[NASA-CR-190498] p 998 N92-30380
MBB-LAGRANGE: A general structural reliability and optimization structural system
[MBB/FW321/S/PUB/467] p 998 N92-30423
Multidisciplinary optimization of fiber composite aircraft structures
[MBB/FW321/S/PUB/476] p 961 N92-30424
High speed research system study. Advanced flight deck configuration effects
[NASA-CR-189650] p 967 N92-30965
ASTOVL combat aircraft design synthesis and optimization
[CRANFIELD-AERO-9201] p 963 N92-31515
Collection of papers of the 31st Israel Annual Conference on Aviation and Astronautics
[ITN-92-85124] p 932 N92-31861
Integrated computer systems in aircraft design and manufacture: Difficulties and implications
p 1010 N92-31864
An installed nacelle design code using a multiblock Euler solver. Volume 1: Theory document
[NASA-CR-189652-VOL-1] p 950 N92-32226
An installed nacelle design code using a multiblock Euler solver. Volume 2: User guide
[NASA-CR-189652-VOL-2] p 951 N92-32228
A method for designing blended wing-body configurations for low wave drag
[NASA-TP-3261] p 1036 N92-32480
Eighth DOD/NASA/FAA Conference on Fibrous Composites in Structural Design, part 1
[NASA-CP-3087-PT-1] p 1106 N92-32513
Design, evaluation and experimental effort toward development of a high strain composite wing for Navy aircraft p 1107 N92-32514
Development of thermoplastic components for structural validation p 1107 N92-32522
Global/local methods research using the CSM testbed
p 1107 N92-32528
Computational methods for global/local analysis
[NASA-TM-107591] p 1125 N92-33104
An investigation of switched reluctance rotor position estimation using neural networks
[AD-A252846] p 1061 N92-33414

Applications of a direct/iterative design method to complex transonic configurations
[NASA-TP-3234] p 1039 N92-33484
Survey and analysis of research on supersonic drag-due-to-lift minimization with recommendations for wing design
[NASA-TP-3202] p 1040 N92-33656
Activities report of the National Aerospace Laboratory
[ETN-92-92053] p 1143 N92-33694
The Rolls-Royce Trent
[PNR-90875] p 1061 N92-33750
Introduction to Flutter of Winged Aircraft, volume 2
[VKI-LS-1992-01-VOL-2] p 1088 N92-34161
Flutter models: Their design, manufacture, and ground testing p 1089 N92-34164
Flutter analyses using high speed computers. Part 1: Flutter analyses for large aircraft p 1089 N92-34168

AIRCRAFT DETECTION
Nonlinear aircraft tracking filter utilizing control variable estimation p 302 A92-21179
Selection of the time parameters of the probing pulse during the nonstationary irradiation of flight vehicles p 454 A92-31951
Characteristics of the energy analysis of optical radar in the case of nonstationary irradiation of flying objects p 454 A92-31955
Innovation in the laser warning sensor field p 554 A92-35742
Data processing in navigation complexes --- Russian book
[ISBN 5-217-01060-6] p 725 A92-42789
Study on an induction method for a flying object, taking accelerating targets into account p 744 A92-43127
Aircraft evasive maneuvers against flying objects p 744 A92-43128
Three-dimensional game for two aircraft p 744 A92-43129
Distance and angle measuring method using laser light and rereflection plates p 762 A92-43206
The role of stealth in naval aviation and joint/combined operations
[AD-A240595] p 22 N92-11005
Modeling radar clutter
[AD-A240965] p 158 N92-13351
Aircraft tracking for structural fatigue p 361 N92-18584
Aircraft tracking optimization of parameters selection p 361 N92-18585
Parametric bicubic spline and CAD tools for complex targets shape modelling in physical optics radar cross section prediction p 403 N92-19151
The Lockheed F-117A
[RAND-P-7746-RGS] p 731 N92-26673
Comparison of Janus and field test aircraft detection ranges for the line-of-sight forward heavy system
[AD-A246047] p 770 N92-27600
National airspace system. Air defense and law enforcement surveillance operational concept NAS-SR-135
[DOT/FAA/SE-92/3] p 953 N92-31211

AIRCRAFT ENGINES
Renewed interest in pulsed engines may be linked to 'black' aircraft p 24 A92-10600
The INFO-ROC technique - A method for comparing and optimizing inspection systems p 144 A92-13563
Nondestructive depth profiling of the protective coating on a turbine blade p 144 A92-13641
Distortion tolerance of the T800-LHT-800 turboshaft engine p 120 A92-14409
The role of laminar-turbulent transition in gas turbine engines p 120 A92-14868
Intermetallic and ceramic matrix composites for 815 to 1370 C (1500 to 2500 F) gas turbine engine applications p 141 A92-15128
Isothermal flow fields in a research combustor for lean blowout studies
[ASME PAPER 91-GT-37] p 121 A92-15520
Minimization of the number of cooling holes in internally cooled turbine blades
[ASME PAPER 91-GT-52] p 121 A92-15530
Two-phase flow correlations in air/oil systems of aero engines
[ASME PAPER 91-GT-54] p 121 A92-15532
The efficiencies of single-stage centrifugal compressors for aircraft applications
[ASME PAPER 91-GT-77] p 122 A92-15546
Stall inception in axial flow compressors
[ASME PAPER 91-GT-86] p 69 A92-15551
Three dimensional flow in a linear compressor cascade at design conditions
[ASME PAPER 91-GT-114] p 70 A92-15565
Multi-blade row Navier-Stokes simulations of fan-bypass configurations
[ASME PAPER 91-GT-148] p 73 A92-15586
The impact load on containment rings during a multiple blade shed in aircraft gas turbine engines
[ASME PAPER 91-GT-163] p 123 A92-15598
Turbine blade tip clearance improvement
[ASME PAPER 91-GT-164] p 123 A92-15599
Gas turbine main shaft internal flow and heat transfer
[ASME PAPER 91-GT-165] p 123 A92-15600
On-line distortion analysis system for inlet-engine testing
[ASME PAPER 91-GT-166] p 136 A92-15601
Analytical investigation of the rules of component matching in turbojet engines
[ASME PAPER 91-GT-170] p 123 A92-15605
Study of external dynamic flap loads on a 6 percent B-1B model
[ASME PAPER 91-GT-236] p 125 A92-15645
Integrated flight/propulsion control for flight critical applications - A propulsion system perspective
[ASME PAPER 91-GT-284] p 125 A92-15679
Development and bench test of high-temperature combustion chamber with structural ceramic components
[ASME PAPER 91-GT-315] p 126 A92-15691
Lean blowout in a research combustor at simulated low pressures
[ASME PAPER 91-GT-359] p 137 A92-15713
A propulsion perspective of the next generation supersonic transport
[ASME PAPER 91-GT-385] p 126 A92-15719
The selective bleed variable cycle engine --- aircraft propulsion
[ASME PAPER 91-GT-388] p 126 A92-15720
A simple model to simulate subsonic intakes and propelling nozzles of aircraft gas turbine engines
[ASME PAPER 91-GT-392] p 153 A92-15722
Optimal thermal management system for HALE UAV --- High Altitude Long Endurance Unmanned Air Vehicles
[ASME PAPER 91-GT-396] p 111 A92-15726
A low noise propulsion concept for the supersonic transport
[ASME PAPER 91-GT-397] p 127 A92-15727
Liquid cooled turbocharged propulsion system for HALE application
[ASME PAPER 91-GT-399] p 127 A92-15729
Inlet planar waves - A current perspective
[ASME PAPER 91-GT-400] p 76 A92-15730
Development of a freejet capability for evaluating inlet-engine compatibility
[ASME PAPER 91-GT-401] p 137 A92-15731
A global approach in evaluating inlet/engine compatibility
[ASME PAPER 91-GT-402] p 127 A92-15732
Three-dimensional calculations of reactive flows in aircraft combustion chambers performed using two combustion models
[ONERA, TP NO. 1991-110] p 154 A92-16089
Consideration of the time lag of engine processes in the problem of VTOL aircraft control synthesis p 134 A92-16807
Effect of inertia forces on the characteristics of a long hydrodynamic vibration damper in the mixed flow regime p 154 A92-16811
A method for determining the optimal composition of the measured parameters in diagnosing gas turbine engines p 128 A92-16819
Effect of Eulerian inertia forces on the stressed state of the rotating components of aircraft turbomachines p 128 A92-16828
A test bench for evaluating powerplant electrization p 138 A92-16830
Effect of the blade height of the nozzle ring of axial-flow microturbines on the flow velocity factor and exit angle p 128 A92-16831
The long-distance Airbus A340 - Europe's largest aircraft p 113 A92-17094
Engine air inlet and de-icing system - At -30 C in the icing tunnel of NRC Ottawa p 92 A92-17252
Numerical simulation for various flowfields of aero-engine components p 200 A92-17503
Hydrogen exhaust gas disposition by afterburning
[AIAA PAPER 91-5075] p 200 A92-17848
A probabilistic method for monitoring the remaining life of aircraft gas turbine engine components using the temperature limit criterion p 201 A92-18292
Large chord turbine cascade testing at engine Mach and Reynolds number p 173 A92-18771
Short fatigue crack growth from blunt notches in an aero-engine alloy p 212 A92-19760
Thermo-mechanical fatigue crack growth in aircraft engine materials p 213 A92-19799
Performance improvements of an F-15 airplane with an integrated engine-flight control system p 205 A92-20204
Evaluation of a bounded high-resolution scheme for combustor flow computations p 201 A92-20734
Holographic-interferometry methods employed for vibration-strength testing of aviation-engine workpieces p 219 A92-20771
Air transport research in Germany p 241 A92-21014
Computational fluid dynamics based three-dimensional turbofan inlet/fan cowl analysis system p 243 A92-21075
Role of dynamic simulation in fighter engine design and development p 277 A92-21080
Development and tribological properties of new cyclotriphosphazene high temperature lubricants for aircraft gas turbine engines p 287 A92-21327
Condor, an all-electric airplane p 269 A92-21734
The position of the unsteady flow computation in the compressor and turbine design and analysis process
[AIAA PAPER 92-0015] p 278 A92-22137
Applications of IMI 834 in aeroengines - A collaborative IMI/MTU programme p 288 A92-22754
Ti-6Al-4V forgings with enhanced fatigue characteristics for engine and airframe applications p 288 A92-22757
The compatibility and tradeoffs of titanium and composites p 288 A92-22758
The beta-CEZ - A high performance titanium alloy for aerospace engines p 289 A92-22760
Nonlinear transient analysis of composite ATP blade model p 294 A92-23111
Prediction of low cycle fatigue life of engine cases p 295 A92-23385
Expert system for real-time aircraft monitoring p 410 A92-24411
Quasi-static analysis of roller bearing p 391 A92-24732
Predication of fastening capacity of screwed joint structure with cone assembly p 391 A92-24737
The jet screen ignition scheme and its experimental verification p 388 A92-24744
Aeroengine sensor failure detection by Bayesian multiple hypothesis testing p 391 A92-24747
A simplified method of transient mathematical model for non-augmentation engine p 372 A92-24750
Thermal management of air-breathing propulsion systems
[AIAA PAPER 92-0514] p 373 A92-26940
Experimental techniques for the assessment of fuel thermal stability
[AIAA PAPER 92-0685] p 389 A92-27052
A numerical study of secondary fuel injection techniques for active control of combustion instability in a ramjet
[AIAA PAPER 92-0777] p 374 A92-27114
Optically powered and interrogated rotary position sensor for aircraft engine control applications p 370 A92-27777
Transient behavior of supersonic flow through inlets p 340 A92-28043
Advanced materials for aircraft engine applications p 390 A92-28251
Numerical simulation of two incoming streams in a dual-combustion ramjet combustor p 375 A92-28419
Experimental investigation on the structure of flow field and the total pressure loss in an atomizing channel injector p 375 A92-28436
Structural and aerodynamic analysis of a large-scale advanced propeller blade p 375 A92-28517
A technique for quantitatively measuring microstructurally induced ultrasonic noise p 510 A92-28720
Brazing method helps repair aircraft gas-turbine nozzles p 492 A92-29504
CUSAE '91; Proceedings of the 1st China-USSR Seminar on Aero Engines, Nanjing, People's Republic of China, Apr. 15-20, 1991 p 469 A92-29709
The effect of air-compressor adjustment by means of air-bleed on the reserve of its stable operation p 471 A92-29973
Restoration of aircraft engine nozzle block blades by vacuum arc brazing with controlled current p 471 A92-30381
Wide-range combustion chamber of ramjet
[AIAA PAPER 91-5094] p 472 A92-31696
GE, Snecma consider venture to develop uprated Perm PS-90 p 472 A92-32297
Russians say D-30F6 engine used in MiG-31 is highly reliable p 472 A92-32298
Saturn/Lyulka diversifies business to cope with Russian economic crisis p 472 A92-32299
Thermally sprayed coating systems for surface protection and clearance control applications in aero engines p 488 A92-32394
An analysis of impact resistance of composite blades for aircraft engines (Analysis with two dimensional and three dimensional finite elements) p 579 A92-32562
Integration of artificial intelligence and numerical optimization techniques for the design of complex aerospace systems
[AIAA PAPER 92-1189] p 600 A92-33301

System reliability and risk assessment
[AIAA PAPER 92-2345] p 582 A92-34320
Ceramics and ceramic matrix composites - Aerospace potential and status
[AIAA PAPER 92-2445] p 577 A92-34474
A real-time rain-flow method of cycle counting and its program design for aeroengine service loads
p 557 A92-35560
Experimental research on blade containment
p 557 A92-35561
Life prediction of local stress-strain method
p 588 A92-35564
Energy analysis of aeroengine and its significance
p 557 A92-35569
Statistical analysis and prediction of aeroengine deterioration p 557 A92-35570
Technical history of aircraft engines
p 558 A92-35911
Research on aircraft engines p 558 A92-35912
Combustion research and design technology of aircraft engines p 558 A92-35915
Research and development of aircraft engine materials p 577 A92-35916
An aircraft controller and its development
p 558 A92-35917
Engine maintenance technology and its development
p 516 A92-35918
Development trends of recent aircraft engines
p 558 A92-35919
Perspective on future aircraft engines
p 558 A92-35921
Fokker 50 flameouts in icing conditions
p 548 A92-35940
Research flight test of a scaled unmanned air vehicle
p 549 A92-35944
AV-8B V/STOL performance analysis
p 549 A92-35948
A method for determining equivalent stresses in aviation gas turbine engine blades p 559 A92-36421
Optimal measurement and health index selection for gas turbine performance status and fault diagnosis
[ASME PAPER 91-GT-294] p 653 A92-36889
An approach for evaluation of gas turbine deposition
[ASME PAPER 91-GT-214] p 653 A92-36890
An investigation in the variance in particle surface interactions and their effects in gas turbines
[ASME PAPER 91-GT-380] p 653 A92-36891
Coating effect on particle trajectories and turbine blade erosion p 653 A92-36892
TMFSLAM - Design analysis tool for coated structures
[ASME PAPER 91-GT-141] p 690 A92-36895
A new method for calculating burst speed of aeroengine disks
[ASME PAPER 91-GT-121] p 670 A92-36899
Advanced propulsion systems for large subsonic transports p 653 A92-36977
Research and development of turbofan engine for supersonic aircraft p 654 A92-38025
Fretting fatigue p 672 A92-38225
Aerospace - Collected translations of selected papers
p 608 A92-38266
A dynamic digital model for the turbojet with pulse-monitored fueller p 654 A92-38267
Monolithic ceramics p 668 A92-39854
Design considerations for a generic E.V.M. --- Engine Vibration Monitoring
[SAE PAPER 912095] p 651 A92-39952
Future military APU requirements
[SAE PAPER 912176] p 655 A92-40001
Challenging power-density requirements for future fighter APUs
[SAE PAPER 912177] p 655 A92-40002
Single lever power management of turboprop engines
[SAE PAPER 912200] p 656 A92-40013
Reactive mixing layer between pressure reflecting boundaries p 656 A92-40144
Thermal oxidation stability of aviation turbine fuels --- Book
[ISBN 0-8031-1248-3] p 669 A92-40409
A method for estimating the efficiency of gas turbine blade cooling systems p 657 A92-40606
A model of the operation of the pulsejet engine and a study of its characteristics p 657 A92-40608
Heat transfer on a cylindrical surface in the cavities of gas turbine engine rotors p 657 A92-40609
Low-frequency vibrations of the shutters of the variable Laval nozzle of gas turbine engines p 657 A92-40610
A method for estimating the technological and economic efficiency of measures enhancing the reliability of aviation gas turbine engines p 657 A92-40621
Pusher turboprop installation technology for the Embraer CBA-123 vector
[SAE PAPER 911030] p 658 A92-40943
Some aspects of advanced aircraft development
p 729 A92-41176
Trends in propulsion technology p 757 A92-41186
The turbo-ramjet Griffon p 782 A92-41820
Airlines could reap big saving with new Pratt common core p 736 A92-42400
A fiber optic temperature sensor for aerospace applications p 761 A92-42607
Operational progress of the STOL research aircraft Asuka p 730 A92-43138
The main wing boundary layer separation pattern of STOL research aircraft Asuka p 709 A92-43144
Experimental operation of aircraft-engine turbine blade materials p 737 A92-43233
Research on a low-noise engine for a high-speed VTOL aircraft p 737 A92-43239
Viscous flow analysis of advanced particle separators
p 737 A92-44517
Super plastic forming technology applied to aeroengine and space equipment p 764 A92-44732
Numerical simulation of impact resistance on composite blade p 738 A92-44734
Elevated temperature crack growth in aircraft engine materials p 891 A92-45234
VSTOL engine design evolution - Growth of the Pegasus engine for Harrier p 860 A92-45306
Current technology propulsion systems meet the STOVL window of opportunity p 860 A92-45307
A USAF assessment of STOVL fighter options
p 842 A92-45310
Auxiliary power units for current and future aircraft
[SAE PAPER 912059] p 862 A92-45441
Fiber optic controls for aircraft engines - Issues and implications p 856 A92-46244
High-speed flight propulsion systems --- Book
[ISBN 1-56347-011-X] p 862 A92-46426
Introduction --- propulsion system performance for hypersonic vehicles p 862 A92-46427
Propulsion systems from takeoff to high-speed flight
p 889 A92-46428
Mathematical modeling of the flight of passenger aircraft in the case of engine failure p 875 A92-47777
Concept of a one-dimensional model of the dynamic behavior of a gas turbine p 862 A92-47791
CIS engines. I - The range revealed
p 786 A92-47821
Investigation of the structural inhomogeneity of a titanium alloy p 893 A92-47958
The impact of advanced materials on small turbine engines
[SAE PAPER 911207] p 862 A92-48021
Optics in aircraft engines p 926 A92-48500
Design and test of an Active Tip Clearance System for centrifugal compressors
[AIAA PAPER 92-3189] p 863 A92-48801
Aero mechanics in the twenty-first century
[AIAA PAPER 92-3194] p 863 A92-48805
Prediction of a high bypass ratio engine exhaust nozzle flowfield
[AIAA PAPER 92-3259] p 864 A92-48855
A simplified real-time engine model for developing aeroengine control system
[AIAA PAPER 92-3321] p 864 A92-48904
Measurement of scalar flowfield at exit of combustor sector using Raman diagnostics
[AIAA PAPER 92-3350] p 894 A92-48927
Experimental pyrometer system for a gas turbine engine
[AIAA PAPER 92-3482] p 859 A92-49022
Design issues in a fiber optic sensor system architecture for aircraft engine control
[AIAA PAPER 92-3483] p 866 A92-49023
Subsonic flight test evaluation of a propulsion system parameter estimation process for the F100 engine
[AIAA PAPER 92-3745] p 866 A92-49110
Generators inside small engines
[AIAA PAPER 92-3755] p 867 A92-49113
Engine aircraft systems integration course
[AIAA PAPER 92-3762] p 928 A92-49117
Conceptual study of separated core ultra high bypass engine
[AIAA PAPER 92-3775] p 867 A92-49119
Analytical and experimental studies of heat pipe radiation cooling of hypersonic propulsion systems
[AIAA PAPER 92-3809] p 867 A92-49128
Ignition delays, heats of combustion, and reaction rates of aluminum alkyl derivatives used as ignition and combustion enhancers for supersonic combustors
[AIAA PAPER 92-3841] p 894 A92-49134
Compensating for manufacturing and life-cycle variations in aircraft engine control systems
[AIAA PAPER 92-3869] p 868 A92-49139
Engine flight load reliability analysis
p 968 A92-49827
Effect of thermodynamic parameters on performance and cost of turbine engines p 969 A92-49834
Research on aircraft life cycle cost reduction
p 1012 A92-49835
The role of PM in the design of lightweight aircraft engine components p 991 A92-50137
Technical tools of test automation for gas-turbine engines based on cluster CAMAC modules with an increased number of channels p 980 A92-51348
Analysis of propulsion system dynamics in the validation of a high-order state space model of the UH-60
[AIAA PAPER 92-4150] p 959 A92-52441
The numerical simulation of flow about installed aero engine nacelle using a finite element Euler solver on unstructured meshes p 941 A92-52848
High temperature MMCs for aero-engines - Challenge and potential p 986 A92-52982
Numerical simulation of three-dimensional turbulent flows in combustion chambers p 970 A92-53276
Transient response of the rotor-support system of aeroengines p 997 A92-53293
Aircraft engines and gas turbines (2nd revised and enlarged edition) --- Book
[ISBN 0-262-11162-4] p 970 A92-53336
Simulation research on the dynamic characteristics of steam-injected gas turbine p 971 A92-53389
Japan pushes high speed research
p 1015 A92-53434
Viscosity characteristics of synthetic aviation oils at low temperatures p 1105 A92-53875
The VRT gas turbine combustor - Phase II
[AIAA PAPER 92-3471] p 1067 A92-54035
Thermal paints for shock/boundary layer interaction in inlet flows
[AIAA PAPER 92-3626] p 1113 A92-54093
Improvements in teaching aircraft engine design
[AIAA PAPER 92-3758] p 1141 A92-54152
CIS engines - The range revealed. II
p 1069 A92-54546
Development of ITS90 small gas turbine engine
p 1070 A92-55500
Test data models to characterize turbine engine operation in altitude test facilities
[AIAA PAPER 92-3917] p 1095 A92-56749
An acceptance process for the evaluation of inlet distortion
[AIAA PAPER 92-3918] p 1032 A92-56750
Development and validation of a freejet technique for inlet-engine compatibility testing
[AIAA PAPER 92-3921] p 1033 A92-56752
Smoothing CFM56 engine removal rate at USAir
[AIAA PAPER 92-3928] p 1070 A92-56759
Turbine engine performance test and evaluation techniques
[AIAA PAPER 92-3977] p 1071 A92-56803
A conceptual study for future engine test facility
[AIAA PAPER 92-3992] p 1099 A92-56815
Numerical simulation of the reactive flow in advanced (HSR) combustors using KIVA-2
[NASA-CR-188996] p 26 N92-11014
Properties of aircraft fuels and related materials
[AD-A240650] p 35 N92-11213
An inverse method for the aerodynamic design of three-dimensional aircraft engine nacelles
p 194 N92-13958
The effects of manufacturing tolerances on the vibration of aero-engine rotor-damper assemblies
p 222 N92-14349
Probabilistic lifing approach for aero engine disks made of powder nickel base alloys containing ceramic defects
p 226 N92-14424
Programs at Wright-Patterson Air Force Base
p 228 N92-15092
Analysis of aircraft engine blade subject to ice impact
[NASA-TM-105336] p 229 N92-15402
Safety considerations in testing a fuel-rich aeropropulsion gas generator
[NASA-TM-105258] p 279 N92-17061
Proceedings of the USAF Structural Integrity Program Conference
[AD-A242943] p 279 N92-17204
Qualification test report. Fuel pump test stand 3C3965G05
[AD-A242929] p 280 N92-17552
Local extinction mechanisms in non-premixed turbulent combustion
[AD-A242027] p 290 N92-17682
An analysis of the aircraft engine Component Improvement Program (CIP): A life cycle cost approach
[AD-A243346] p 280 N92-17729
Hydrogen fueled subsonic-ram-combustor model tests for an air-turbo-ram engine
[NAL-TR-1064T] p 280 N92-17855
Institute for experimental fluid mechanics: Results for 1990
[IB-222-90-A-46] p 400 N92-18244
Introduction: Needs and approaches to reliability and quality assurance in design and manufacture
p 402 N92-19005

Materials and process directions for advanced aero-engine design
[PNR-90814] p 378 N92-19938
Superplastic applications in aero engines
[PNR-90788] p 473 N92-20436
ETOPS: A developing scene
[PNR-90844] p 473 N92-20459
The 60 years of Bristol engines
[PNR-90845] p 473 N92-20460
High-speed civil transport flight- and propulsion-control technological issues
[NASA-CR-186015] p 482 N92-21253
H2-fueled high-bypass turbofan p 475 N92-21529
Emissions from aircraft: Standards and potential for improvement
[PNR-90768] p 476 N92-21740
Environmentally sound
[PNR-90776] p 506 N92-21743
Aircraft gas turbine emissions: Their nature, technology for reduction, and a pollution comparison with channel tunnel transport
[ETN-92-91056] p 559 N92-22406
Aeropropulsion 1987
[NASA-CP-3049] p 559 N92-22510
Impact and promise of NASA aeropropulsion technology p 559 N92-22511
High-temperature polymer matrix composites
p 578 N92-22513
Development of a new generation of high-temperature composite materials p 578 N92-22515
Aeropropulsion structures p 559 N92-22518
Determining structural performance
p 560 N92-22519
Life prediction technologies for aeronautical propulsion systems p 560 N92-22520
Optical measurement systems p 594 N92-22527
Overview of the subsonic propulsion technology session p 560 N92-22531
Aircraft engine hot section technology: An overview of the HOST Project p 561 N92-22535
NASA thrusts in high-speed aeropropulsion research and development: An overview p 561 N92-22538
Coupled multi-disciplinary simulation of composite engine structures in propulsion environment
[NASA-TM-105575] p 596 N92-23267
Evaluation of the applicability of Helmholtz resonators for low frequency acoustic liners
[PB92-138544] p 605 N92-23588
Some comments on turbulence modeling from an industrial perspective p 678 N92-24531
The future challenge for aeropropulsion
[NASA-TM-105613] p 658 N92-25164
Multiblock grid generation for jet engine configurations
p 659 N92-25720
Thermally sprayed coating systems for surface protection and clearance control applications in aero engines
[PNR-90802] p 741 N92-27422
Three dimensional calculations of reactive flows within aircraft combustion chambers including some combustion models p 770 N92-27490
Self-adaptive aeropropulsion components-enhancing axial compressor performance
[AD-A246123] p 743 N92-27817
AFRAPT Program at Texas A and M University research for advanced aircraft engine structures
[AD-A247040] p 743 N92-28076
An appraisal of cost-effectiveness models used in the Air Force and Navy aircraft engine component improvement programs
[AD-A245910] p 743 N92-28162
Steady and Transient Performance Prediction of Gas Turbine Engines
[AGARD-LS-183] p 868 N92-28458
Practical considerations in designing the engine cycle
p 869 N92-28460
Steady and transient performance calculation method for prediction, analysis, and identification
p 869 N92-28461
Inlet distortion effects in aircraft propulsion system integration p 869 N92-28464
Engine performance and health monitoring models using steady state and transient prediction methods
p 870 N92-28467
Turbine aircraft engine operational trending and JT8D static component reliability study
[DOT/FAA/CT-91/10] p 870 N92-28686
Flight evaluation of an extended engine life mode on an F-15 airplane
[NASA-TM-104240] p 871 N92-29659
Current and future developments in civil aircraft non-destructive evaluation from an operator's point of view p 787 N92-30122
Statistics on aircraft gas turbine engine rotor failures that occurred in US commercial aviation during 1989
[DOT/FAA/CT-92/5] p 971 N92-30303
Trends in aeropropulsion research and their impact on engineering education
[NASA-TM-105682] p 972 N92-31172
Polymer blends, volume 1
[AD-A252112] p 987 N92-31419
Research into improving the durability of the hot section in the aircraft turbine engine
[AD-A250342] p 973 N92-31439
Analytical and experimental studies of heat pipe radiation cooling of hypersonic propulsion systems
[DE92-013428] p 973 N92-31817
Liquid lubricants for advanced aircraft engines
[NASA-TM-104531] p 1109 N92-32863
Bird ingestion into large turbofan engines
[DOT/FAA/CT-91/17] p 1043 N92-33005
Statistics on aircraft gas turbine engine rotor failures that occurred in US commercial aviation during 1988
[DOT/FAA/CT-91/28] p 1071 N92-33105
Re-engining for real stage 3 compliance
[PNR-90872] p 1072 N92-33748
The impact of air transport on the environment
[PNR-90876] p 1129 N92-33751
Joint study on the computerisation of in-field aero engines vibration diagnosis
[PNR-90799] p 1072 N92-33815
Fatigue crack growth of small corner defects from blunt notches in an aeroengine alloy
[PNR-90860] p 1111 N92-34019

AIRCRAFT EQUIPMENT

A ionospheric-sounding experiment from an aircraft
p 160 A92-13809
Radiometric properties of the NS001 Thematic Mapper Simulator aircraft multispectral scanner
p 155 A92-17110
Autonomously aided strapdown attitude reference system p 204 A92-18610
Avionics systems of the 21st century
p 467 A92-28874
Relating the microwave radar cross section to the sea surface stress - Physics and algorithms
p 597 A92-35028
A high resolution multispectral video system
p 587 A92-35479
Approach flight trials in the Netherlands for the Navstar GPS Joint Program Office International Test Program
p 533 A92-35928
Aircraft hydraulic systems (3rd revised and enlarged edition) --- Book
[ISBN 0-89464-562-5] p 642 A92-38316
Flexible heat pipe cold plates for aircraft thermal control
[SAE PAPER 912105] p 674 A92-39959
Comparison of R2SPG waveforms with simulated EMP --- Repetitive Random Square-wave Pulse Generator
p 760 A92-42317
Singlemode fiber optic rotary joint for aircraft applications p 779 A92-42606
Advanced display system for an aircraft payload
p 735 A92-43221
Demonstration performance of an aircraft liquid crystal display p 735 A92-43224
Remote measurements of supercooled integrated liquid water during WISP/FAA aircraft icing program
p 915 A92-46788
Advanced pneumatic impulse ice protection system (PIIP) for aircraft p 845 A92-46807
Design criteria and analysis of the dynamic behavior of high speed, heavily loaded and precision epicyclic gears for aircraft use
[AIAA PAPER 92-3491] p 906 A92-49028
Concept evaluation of the UH-60 externally mounted rescue hoist
[AD-A240545] p 22 N92-11004
Corrosion and your aircraft
[NRC-30465] p 114 N92-11991
Integrated Communications, Navigation, Identification, Avionics (ICNIA) expert system for fault tolerant avionics
p 118 N92-12539
Onboard cabin water spray system under various discharge configurations
[DOT/FAA/CT-TN91/42] p 93 N92-13043
Validation and verification flight test for TCAS-2 logic changes (MOPS Change 6)
[DOT/FAA/CT-TN91/46] p 268 N92-15981
Design of a fiber optic image transmission link
[AD-A243686] p 304 N92-17088
Cockpit weather information needs
p 449 N92-21503
Radiant energy power source for jet aircraft
[DE92-008726] p 648 N92-24556
Aircraft photovoltaic power-generating system
p 775 N92-26581
Evaluation of head impact kinematics for passengers seated behind interior walls
[AD-A252651] p 952 N92-30551
A cable detection lidar system for helicopters
p 1001 N92-31068
Airborne experimental FLIR program
p 1064 N92-32447
PDES application protocol suite for composites (PAS-C). Functional needs report for the PAS-C program
[AD-A247886] p 1108 N92-32629
Method of reducing drag in aerodynamic systems
[NASA-CASE-LEW-14791-1] p 1043 N92-34243

AIRCRAFT FUEL SYSTEMS

Evaluation of the fungicide properties of antifreeze additives for jet fuels p 141 A92-15070
High temperature, thermally stable JP fuels - An overview
[AIAA PAPER 92-0683] p 389 A92-27050
Experimental techniques for the assessment of fuel thermal stability
[AIAA PAPER 92-0685] p 389 A92-27052
Application of a double actuator electronic fuel control unit on a small gas turbine engine
[SAE PAPER 912160] p 655 A92-39993
Non-curing fuel and water resistant sealant compositions p 985 A92-51906
Separation of external stores: Comparison of results
[F+W-TF-2058] p 732 N92-26944

AIRCRAFT FUELS

Methyl-tert-butyl ether as a component of aviation gasolines p 34 A92-12146
Evaluation of the fungicide properties of antifreeze additives for jet fuels p 141 A92-15070
The aviation kerosene burning in the non-uniform air flow p 487 A92-29728
Thermal oxidation stability of aviation turbine fuels --- Book
[ISBN 0-8031-1248-3] p 669 A92-40409
Microbiological spoilage of aviation turbine fuel. II - Evaluation of a suitable biocide p 891 A92-45600
Calculation of fuel sloshing and its coupling vibration with a tank p 991 A92-50204
Properties of aircraft fuels and related materials
[AD-A240650] p 35 N92-11213
Structural considerations for aircraft payload Modification: P-3C zero fuel weight increase
[AD-A242690] p 196 N92-15068
Advanced thermally stable, jet fuels development program annual report. Volume 1: Model and experiment system development
[AD-A249625] p 988 N92-31462

AIRCRAFT GUIDANCE

Managing Europe's air traffic system
p 19 A92-11876
Polish radar technology. II - Adaptive radar AVIA CM
p 39 A92-12290
Day/Night Adverse weather Pilotage System (D/NAPS) p 94 A92-14429
Results of a test program for the use of differential GPS for approach guidance p 101 A92-16969
Real-time decision aiding - Aircraft guidance for wind shear avoidance
[AIAA PAPER 92-0290] p 350 A92-25743
Energy-heading transients in atmospheric flight guidance for airbreathing hypersonic vehicles
[AIAA PAPER 91-5065] p 480 A92-31692
Approach flight trials in the Netherlands for the Navstar GPS Joint Program Office International Test Program
p 533 A92-35928
The appropriate concern for possible aberrations in landing guidance signals p 839 A92-44932
Approach guidance in a downburst
p 873 A92-46741
Computer-Controlled Navigation System/General Positioning System (CCNS/GPS) - A guidance, positioning, and management system for remote sensing flights
p 840 A92-47630
Flight management system back-up navigation for the A330/A340 aircraft p 975 A92-49326
A fuel-optimal 4D guidance algorithm
p 978 A92-53095
A general approach to optimal real-time guidance of dynamic systems based on nonlinear programming
[AIAA PAPER 92-4378] p 1131 A92-55182
Concepts for pilot interaction with an automated NOE obstacle-avoidance system
[AIAA PAPER 92-4472] p 1076 A92-55232
Application of fuzzy control to aircraft guidance
p 1083 A92-56033
Change and reliability of the DC-9-81 digital flight guidance system p 1084 A92-56086
Passive range estimation for rotorcraft low-altitude flight
[NASA-TM-103897] p 2 N92-10003
Tracking performance requirements for rotorcraft instrument approaches to reduced minima. Phase 1: Preliminary study
[NRC-32137-PHASE-1] p 102 N92-11988

A methodology for software specification and development based on simulation p 135 N92-12458
DME growth elements and their use with MLS p 189 N92-14018
A unique approach to aircraft conflict resolution using artificial intelligence techniques p 190 N92-14029
Image-based ranging and guidance for rotorcraft [NASA-CR-184829] p 191 N92-14036
Rapid near-optimal aerospace plane trajectory generation and guidance [NASA-CR-189469] p 205 N92-14066
Method of guiding an in-flight vehicle to a designed flight path [AD-D015061] p 268 N92-17707
Flying an aircraft as a problem-solving process: About the Instrument-Failure-Simulator (IFS) as a test for pilot-candidates [DLR-FB-91-23] p 455 N92-20902
Approach and landing guidance p 457 N92-21960
Testing concept of a movement area guidance p 641 N92-25597
Status of automatic guidance systems for rotorcraft in low altitude flight p 727 N92-27894
Trajectory optimization for hypersonic aircraft guidance p 728 N92-27898
Reference mode effect on the auditory display of aircraft bank angle [AD-A247825] p 728 N92-27916
Advances in Fibre-Optic Technology in Communications and for Guidance and Control [AGARD-LS-184] p 774 N92-28084
On the optimization of windshear warning and guidance systems [NLR-TP-90196-U] p 837 N92-29703
High speed research system study. Advanced flight deck configuration effects [NASA-CR-189650] p 967 N92-30965
Development of new flight procedures for the Microwave Landing System (MLS) [NLR-TP-91156-U] p 1047 N92-32830
CTAS: Computer intelligence for air traffic control in the terminal area [NASA-TM-103959] p 1044 N92-33080

AIRCRAFT HAZARDS
Evaluation of a technique to quantify microburst windshear hazard potential to aircraft p 17 A92-11379
Stochastic prediction techniques for wind shear hazard assessment p 48 A92-11381
Windshear detection and avoidance - Airborne systems survey p 17 A92-11382
Optimal trajectories and guidance trajectories for aircraft flight through windshears p 27 A92-11383
Aircraft control under conditions of windshear p 27 A92-11384
Aircraft control in a downburst on takeoff and landing p 27 A92-11385
Rates and risk factors for accidents and incidents versus violations for U.S. airmen p 91 A92-14048
Lightning standards for aircraft protection p 91 A92-14688
Lightning activity in microburst producing storm cells [ONERA, TP NO. 1991-98] p 161 A92-16080
Nonlinear triggered lightning models for use in finite difference calculations p 230 A92-20128
Whole aircraft lightning indirect effects evaluation using low level injection techniques p 192 A92-20134
LEWICE/E - An Euler based ice accretion code [AIAA PAPER 92-0037] p 316 A92-25676
United 232 - Coping with the 'one-in-a-billion' loss of all flight controls p 530 A92-36349
Aircraft-triggered lightning - Processes following strike initiation that affect aircraft p 836 A92-46784
Stochastic prediction techniques for wind shear hazard assessment p 1007 A92-50505
An impact dynamics investigation on some problems in bird strike on windshields of high-speed aircrafts p 986 A92-53330
A data fusion algorithm for multi-sensor microburst hazard assessment [AIAA PAPER 92-4339] p 1063 A92-55328
LEWICE/E: An Euler based ice accretion code [NASA-TM-105389] p 179 N92-14001
Study of the engine bird ingestion experience of the Boeing 737 aircraft [DOT/FAA/CT-89/16] p 187 N92-15053
Thermal energy test apparatus [AD-A243526] p 305 N92-17537
Freezing precipitation on lifting surfaces [NRC-32124] p 448 N92-20156
Numerical simulation of an aircraft anti-icing system incorporating a rivulet model for the runback water p 448 N92-20303
Effects of Adverse Weather on Aerodynamics [AGARD-CP-496] p 449 N92-21679
Flight in adverse environmental conditions p 449 N92-21680
The effect of hoar-frosted wings on the Fokker 50 take-off characteristics p 451 N92-21692
NASA's aircraft icing technology program [NASA-TM-104518] p 527 N92-23105
A cable detection lidar system for helicopters p 1001 N92-31068
Preliminary screening procedures and criteria for replacements for Halons 1211 and 1301 [AD-A252912] p 1126 N92-33501

AIRCRAFT HYDRAULIC SYSTEMS
Will hydraulic systems meet tomorrow's aircraft power requirements? p 21 A92-13246
Hydraulic pumps - The key to power generation p 215 A92-17348
Fluid power distribution and control p 292 A92-21733
High-performance fighter fly-by-wire flight control actuation system --- for YF-23A prototype [AIAA PAPER 92-1123] p 563 A92-33277
Steady state and quasi-transient analysis of aircraft hydraulic system with network theory p 642 A92-37391
F-14 dual hydraulic failure flying qualities evaluation p 645 A92-40029

AIRCRAFT ICING
Self-induced flow in a stepped rotating tube [ASME PAPER 91-GT-276] p 152 A92-15673
Engine air inlet and de-icing system - At -30 C in the icing tunnel of NRC Ottawa p 92 A92-17252
Heat transfer measurements from a smooth NACA 0012 airfoil p 218 A92-20215
Roughness effects on heat transfer from a NACA 0012 airfoil p 219 A92-20217
Study of theoretical and wind tunnel results on flight performance degradation due to leading edge rime ice accretion [AIAA PAPER 92-0038] p 262 A92-22158
Development of an improved model for runback water on aircraft surfaces [AIAA PAPER 92-0042] p 270 A92-22160
Industrial measurement of microphysical parameters - Application to natural and simulated icing clouds --- for aircraft icing p 262 A92-23302
A theoretical analysis utilizing the LEWICE and EPPLER numerical analyses to predict flight performance degradation under icing conditions [AIAA PAPER 92-0134] p 263 A92-23754
Examination of a numerical icing-severity scale [AIAA PAPER 92-0164] p 263 A92-23777
Investigation of the diffuser flow quality in an icing research wind tunnel p 382 A92-24406
Volume spectra in supercooled clouds for several research flights [AIAA PAPER 92-0167] p 350 A92-25683
Proposal for a 3-D, vectorized, adaptable, algorithm for modeling the randomness, unsteadiness, and microphysical properties of ice accretion [AIAA PAPER 92-0299] p 351 A92-25751
Development of a sensor for the detection of aircraft wing contaminants [AIAA PAPER 92-0300] p 369 A92-25752
Laboratory evaluation of a sensor for detection of aircraft wing contaminants [AIAA PAPER 92-0301] p 369 A92-25753
Aircraft icing [ONERA, TP NO. 1991-202] p 351 A92-26359
Helium bubble flow visualization of the spanwise separation on a NACA 0012 with simulated glaze ice [AIAA PAPER 92-0413] p 341 A92-28192
Comparison of two-dimensional and three-dimensional droplet trajectory calculations in the vicinity of finite wings [AIAA PAPER 92-0645] p 342 A92-28215
Cold-cycle pressure-jet helicopters: Ventures, designs, and developments. III - Costs and developments p 458 A92-29675
Analysis of iced wings [AIAA PAPER 92-0416] p 423 A92-29972
Experimental and numerical investigation of anti-icing phenomena on a NACA 0012 assembly [AIAA PAPER 92-0531] p 459 A92-31669
Fokker 50 flameouts in icing conditions p 548 A92-35940
Flying on thin ice p 634 A92-38375
Aircraft ground deicing [SAE PAPER 912222] p 635 A92-40021
EIPOS for ice-formation control on aircraft in flight - An alternative technique p 647 A92-40545
Measurements in a leading-edge separation bubble due to a simulated airfoil ice accretion p 723 A92-41262
On the possibility of freezing and sticking phenomena in a transport during the ground taxiing and takeoff run and on the preventions of the hazard [SAE PAPER 912042] p 836 A92-45426
BUWICE - An interactive icing program applied to engine inlets [AIAA PAPER 92-3179] p 922 A92-48794
Effect of a deicing device on the induced drag of a lifting airfoil p 959 A92-51947
Predicting droplet impingement on yawed wings p 1043 A92-56180
Low energy ice protection for helicopters p 1059 A92-56348
Experimental ice shape and performance characteristics for a multi-element airfoil in the NASA Lewis Icing Research Tunnel [NASA-TM-105380] p 261 N92-17347
Particle trajectory computer program for icing analysis of axisymmetric bodies [NASA-CR-189134] p 352 N92-19276
Icing simulation: A survey of computer models and experimental facilities p 450 N92-21684
A review of icing research at the Royal Aerospace Establishment p 451 N92-21689
Wind tunnel investigation of a wing-propeller model performance degradation due to distributed upper-surface roughness and leading edge shape modification p 451 N92-21690
The adverse aerodynamic impact of very small leading-edge ice (roughness) buildups on wings and tails p 451 N92-21691
Preparation of the ice certification of the Dornier 328 regional airliner by numerical simulation and by ground test p 451 N92-21693
Progress report on analysis of differential attenuation radar data obtained during WISP-91 [PB92-133800] p 503 N92-21828
The NASA aircraft icing research program p 549 N92-22534
NASA's aircraft icing technology program [NASA-TM-104518] p 527 N92-23105
Comparison of two-dimensional and three-dimensional droplet trajectory calculations in the vicinity of finite wings [NASA-TM-105617] p 596 N92-23154
Aircraft accident report: Ryan International Airlines DC-9-15, N565PC, loss of control on takeoff, Cleveland-Hopkins International Airport, Cleveland, Ohio, February 17, 1991 [PB91-910410] p 530 N92-23597
The icing of the wing upper side and bottom side of the icing research aircraft of the DLR p 724 N92-26349
Numerical investigation of the effects of icing on fixed and rotary wing aircraft [NASA-CR-190542] p 1044 N92-34105

AIRCRAFT INDUSTRY
Soviet aerospace in turmoil --- miltary to civil production conversion p 2 A92-13220
A holistic approach to support p 60 A92-14413
How to support the 'little guy' --- helicopter maintenance p 60 A92-14437
Nondestructive testing developments in the aircraft industry p 214 A92-17288
High costs force avionics links p 276 A92-22000
The stealth master p 307 A92-25175
Industry seeks tonic for aging aircraft p 308 A92-28492
Airbus - The family expands p 419 A92-30092
Australian aeronautics, 1989-90 p 515 A92-33460
German-GUS cooperation in civil aviation p 785 A92-47592
Airline industry safety management systems and feedback p 951 A92-51439
AIAA/AHS Flight Simulation Technologies Conference, Hilton Head Island, SC, Aug. 24-26, 1992, Technical Papers p 981 A92-52426
Russian realities --- changes in aviation industry infrastructure p 932 A92-53250
Aircraft Symposium, 29th, Gifu, Japan, Oct. 7-9, 1991, Proceedings p 1015 A92-56001
China's first variable stability aircraft: The BW-1-Gets its pre-acceptance flight tests [AD-A240941] p 116 N92-13062
International aviation (selected article) [AD-A240986] p 170 N92-13991
Application of MSC/DYNA to shock and impact problems in aircraft industry [MBB-UD-0593-91-PUB] p 225 N92-14382
Polymer infiltration studies [NASA-CR-190204] p 578 N92-22486
Fundamentals of structural optimisation p 851 N92-28470
The 1991 International Conference on Aging Aircraft and Structural Airworthiness [NASA-CP-3160] p 912 N92-30106
NDE research efforts at the FAA Center for Aviation Systems Reliability p 914 N92-30119

Current and future developments in civil aircraft non-destructive evaluation from an operator's point of view p 787 N92-30122
Research and technology, 1991. Langley Research Center
[NASA-TM-4331] p 1013 N92-30733
NASA High Speed Research Program, Emissions Scenarios Committee report of meetings on 26 September 1991 and 9 January 1992
[NASA-CR-190379] p 1004 N92-32147
Examples of advanced near-net shape manufacturing techniques for aerospace
[MBB-Z-0399-91-PUB] p 1125 N92-32742

AIRCRAFT INSTRUMENTS
Functionally integrated aircraft instrumentation for the next generation commercial helicopter p 117 A92-14402
A state-of-the-art data acquisition system p 217 A92-19231
Pneumatic distortion compensation for aircraft surface pressure sensing devices p 218 A92-20206
Optical design of dual combiner head-up displays p 414 A92-24628
Automated thematic processing of aircraft scanner data gathered over pasture territory in Turkmenia p 406 A92-25330
Failure detection and identification for aircraft sensors p 370 A92-27832
Bell's OH-58D proves its reliability p 458 A92-29670
Airborne tests of flux measurement by the relaxed eddy accumulation technique p 504 A92-32052
Airflow effects about PMS probes on the DLR Falcon --- Particle Measuring System for atmospheric research aircraft p 467 A92-32060
Modifications to and data correction methods for some radiometers used on aircraft p 467 A92-32062
The design and operational characteristics of a heated radome for air motion measurement p 467 A92-32064
Use of relative humidity sensors for planes measurement p 467 A92-32080
An airborne Doppler lidar for meteorological research p 467 A92-32082
A new aircraft universal lightweight digital dropsonde p 467 A92-32089
An airborne cryogenic frost-point hygrometer p 467 A92-32090
Design and preliminary tests of a new airborne thermometer p 468 A92-32097
Feature extraction from two-dimensional images using fractal analysis p 496 A92-32130
The U-2A flight test program
[AIAA PAPER 92-1086] p 537 A92-33252
A study of the precision characteristics of a gyroscopic gravimeter p 581 A92-33778
Air data measurement for hypersonic vehicles
[SAE PAPER 912143] p 651 A92-39981
A sensitive fast-response probe to measure turbulence and heat flux from any airplane p 775 A92-42097
Civil development and certification of a helicopter automatic approach and hover system on the Sikorsky S-76
[SAE PAPER 911975] p 872 A92-45382
Avionics flight systems for the 21st century
[SAE PAPER 912033] p 784 A92-45421
Functional mock-up tests for flight control system of the NAL QSTOL research aircraft 'ASKA'
[SAE PAPER 912036] p 881 A92-45422
Through the looking glass --- effectiveness of electronic flight instrument systems p 856 A92-46449
Common airborne instrumentation system (CAIS) --- time-division multiplexed data acquisition system p 856 A92-47538
Mechanisms of high-current pulses in lightning and long-spark stepped leaders p 1116 A92-54678
Modified Doppler detects wind shear more reliably p 1015 A92-55099
The use and misuse of aircraft and missile RCS statistics
[AD-A239892] p 41 N92-10141
Tracking performance requirements for rotorcraft instrument approaches to reduced minima. Phase 1: Preliminary study
[NRC-32137-PHASE-1] p 102 N92-11988
A development-memory approach for enhancing avionics software logistics p 119 N92-12540
Limitations of a holographic 3-D pixel projector for cockpit displays
[AD-A241295] p 119 N92-13067
High Intensity Radiated Fields (HIRF) project plan
[DOT/FAA/CT-TN91/1] p 297 N92-16181
Instrumentation and data processing p 273 N92-17155
An evaluation of four F-16 vertical velocity indicator configurations
[AD-A243629] p 370 N92-18014
Concept design phase expendable holographic sensor to measure ocean small angle optical scattering
[AD-A245067] p 501 N92-20997
Advanced Transport Operating System (ATOPS) color displays software description: MicroVAX system
[NASA-CR-189603] p 556 N92-22395
An investigation into the feasibility of providing a proximity warning device for search and rescue helicopters
[ETN-92-91057] p 530 N92-22408
Recommended system concept p 599 N92-23383
The imaging spectrometer p 599 N92-23387
Quick-look system p 599 N92-23393
Preconsiderations on aircraft integration p 599 N92-23402
Microwave temperature profiler for clear air turbulence prediction
[NASA-CASE-NPO-18115-1-CU] p 916 N92-29148
Sensor fault detection on board an aircraft with observer and polynomial classifier
[DLR-FB-91-34] p 859 N92-29870
The rise of active-element phased-array radar
[RAND-P-7747-RGS] p 999 N92-30755
Estimation of aircraft attitude by angular rate measurements p 963 N92-31881
A continuing study of altitude determination deficiencies of the Service Aircraft Instrumentation Package (SAIP)
[AD-A245952] p 968 N92-32051

AIRCRAFT LANDING
Optimal trajectories and guidance trajectories for aircraft flight through windshears p 27 A92-11383
Aircraft control in a downburst on takeoff and landing p 27 A92-11385
U-parameter design example - Robust flight control for wind-shear protection p 28 A92-11502
Design of the flare control law for longitudinal autopilot using H(infinity) synthesis p 28 A92-11562
Several results of lidar measurements of the characteristics of oblique visibility at an airfield p 45 A92-12844
Numerical simulation of the actuation system for the ALDF's propulsion control valve --- Aircraft Landing Dynamics Facility p 41 A92-13204
The new airport aeronautic meteorological codes p 160 A92-13855
Integration of flight and carrier landing aid systems for shipboard operations
[ONERA, TP NO. 1991-113] p 134 A92-16092
Wide area differential GPS p 101 A92-16966
New siting techniques for the ILS glide slope p 188 A92-17422
Nonlinear landing gear behavior at touchdown p 192 A92-19606
Fair weather convection and light aircraft accidents
[IAF PAPER ST-91-004] p 186 A92-20651
GPS integrated system application in aircraft approach landing p 266 A92-21466
Improving the efficiency of passenger aircraft during the landing approach p 460 A92-31893
Effect of wind shear on airspeed during airplane landing approach p 481 A92-32242
A digital Doppler Rate of Descent Indicator (DRODI) p 555 A92-35927
Aircraft noise - The calculation of the noise exposure by aircraft in the Netherlands p 687 A92-39054
F-14 dual hydraulic failure flying qualities evaluation p 645 A92-40029
V-22 full scale development testing p 646 A92-40038
MLS system error model identification and synthesis p 639 A92-40232
The landing equipment of a high-tech aircraft p 730 A92-43149
An aircraft landing accident caused by visually induced spatial disorientation p 834 A92-44993
Simulation of triple simultaneous parallel ILS approaches p 880 A92-45025
Thrust laws for microburst wind shear penetration p 873 A92-46750
Mathematical modeling of the effect of windshear on the dynamics of a landing aircraft p 875 A92-47784
Roll metrics for handling qualities - The landing approach p 976 A92-50520
Differential GPS/inertial navigation approach/landing flight test results p 956 A92-51009
The application of imaging sensors to aircraft landings in adverse weather p 1045 A92-54902
A fuzzy logic based F/A-18 automatic carrier landing system
[AIAA PAPER 92-4392] p 1074 A92-55193
An investigation of the automation of emergency landings for helicopters p 1083 A92-56026
Optimal control of tiltrotor aircraft following power failure p 1085 A92-56303
Evaluation of two high-speed runway exits
[DOT/FAA/CT-TN91/36] p 31 N92-11021
Prototype runway hold-short lighting system
[DOT/FAA/CT-TN91/43] p 31 N92-11028
Mobile Microwave Landing System (MMLS): Operational requirements for setup accuracy
[AD-A241844] p 103 N92-13052
A Taxi And Ramp Management And Control system (TARMAC) p 207 N92-14027
Neural network and fuzzy logic technology for naval flight control
[AD-A242650] p 206 N92-15074
Visual approach data collection at San Francisco International Airport (SFO)
[DOT/FAA/CT-90/23] p 354 N92-18112
A summary of NASA research on effects of heavy rain on airfoils p 452 N92-21694
Ship airwake measurement and modeling options for rotorcraft applications p 503 N92-21954
Integration of flight and carrier landing aid systems for shipboard operations p 456 N92-21958
Approach and landing assisted by onboard image processing p 457 N92-21959
Approach and landing guidance p 457 N92-21960
Analytical modeling of SH-2F helicopter shipboard operation p 464 N92-21961
Helicopter/ship analytic dynamic interface p 464 N92-21962
Evaluating fixed wing aircraft in the aircraft carrier environment p 464 N92-21963
A review of Australian activity on modelling the helicopter/ship dynamic interface p 465 N92-21967
Helicopter handling: Experience and new developments p 465 N92-21969
Nationwide system delay study of the microwave landing system in the New York terminal area, volume 1
[DOT/FAA/CT-TN91/59-VOL-1] p 640 N92-25098
Radar multipath study for rain-on-radome experiments at the Aircraft Landing Dynamics Facility
[NASA-TM-101657] p 680 N92-25137
High lift aircraft
[AD-D015215] p 732 N92-27185
Aircraft ship operations
[AGARD-AR-312] p 850 N92-28468
S-76B certification for vertical take-off and landing operations from confined areas
[NLR-TP-90286-U] p 852 N92-28714
Trial of a slant visual range measuring device p 1000 N92-31043
Flight testing and simulation of an F-15 airplane using throttles for flight control
[NASA-TM-104255] p 1087 N92-32864
CTAS: Computer intelligence for air traffic control in the terminal area
[NASA-TM-103959] p 1044 N92-33080

AIRCRAFT LAUNCHING DEVICES
Accelerators and decelerators for large hypersonic aircraft p 665 A92-36952
United States Navy ski jump experience and future applications p 465 N92-21968

AIRCRAFT MAINTENANCE
The maintenance economy and economic life of structures p 37 A92-10673
Advanced technology for aviation maintenance training - An industry status report and development plan p 47 A92-11180
Organizational context for aircraft maintenance and inspection p 2 A92-11181
Eddy current imaging of aircraft using real time image signal processing p 144 A92-13594
The aging aircraft fleet - A challenge for nondestructive inspection p 145 A92-13657
Maintenance, Malfunction Information Report system p 60 A92-14414
Spares support of your Rotary-Wing Jenny p 60 A92-14435
How to support the 'little guy' --- helicopter maintenance p 60 A92-14437
Malfunction/discrepancy reporting p 60 A92-14438
Implanted component faults and their effects on gas turbine engine performance
[ASME PAPER 91-GT-41] p 121 A92-15524
Enhanced visual technique for rapid inspection of aircraft structures p 214 A92-17290
Rapid ultrasonic scanning of aircraft structures p 215 A92-17292
ASNT and aerospace - What about the next 50 years? p 215 A92-17293
National research program for nondestructive inspection of aging aircraft p 169 A92-17294
Some results on metal and composite patch reinforcement of aluminum honeycomb panel p 216 A92-18830
Retrofit provides navigation enhancement for older aircraft p 198 A92-20025
Historical development of eddy current testing in aircraft maintenance p 292 A92-21900

A cognitive temporal model for the planning in aircraft maintenance p 307 A92-25178
The TSE 310 troubleshooting expert prototype for the Airbus A-310 commercial aircraft p 307 A92-25180
Industry seeks tonic for aging aircraft p 308 A92-28492
Neutron radiography with SNRS p 492 A92-28747
An advanced neutron radiography system p 492 A92-28748
Analysis of the efficiency of some structural-inspection strategies in aircraft maintenance p 419 A92-30141
Restoration of aircraft engine nozzle block blades by vacuum arc brazing with controlled current p 471 A92-30381
Damage tolerance and repair experience of composite structures
[AIAA PAPER 92-1256] p 515 A92-33339
Smart structures for helicopters p 516 A92-35727
Engine maintenance technology and its development p 516 A92-35918
Flight testing of the Boeing 747-400 Central Maintenance Computer system p 555 A92-35950
Blade repair with adaptive vision tracking
[ASME PAPER 91-GT-208] p 607 A92-36897
Seeing beneath the surface with NDE p 671 A92-36948
Aircraft maintenance support system p 607 A92-38217
Ageing airliner census - Still flying safely p 634 A92-38374
Assurance of safety in the aging aircraft fleet p 635 A92-39305
Aging aircraft and structural airworthiness
[SAE PAPER 912212] p 635 A92-40016
Composite material repairs to metallic airframe components p 699 A92-41237
Environmental evaluation of repairs to fuselage lap joints p 699 A92-41534
Maintenance scheduling for critical parts of aircraft p 699 A92-42054
Windscreen departure p 723 A92-42500
Aircraft reliability and maintainability p 700 A92-43141
Study on the maintainability and inspection of the STOL research aircraft Asuka p 700 A92-43148
Quality management of landing gear with pulling support system p 762 A92-43156
A study of a ground support equipment (GSE) network p 748 A92-43158
Stress field sensitivity of a composite patch repair as a result of varying patch thickness p 763 A92-44630
Reliability centered maintenance for metallic airframes based on a stochastic crack growth approach p 897 A92-45242
Structural risk assessment in the Israel Air Force for fleet management p 836 A92-46779
Advanced composite components in airline service status and repair p 785 A92-47416
A field repair of advanced helicopter vertical fin structure p 785 A92-47417
Industrial practice in aeronautical maintenance p 786 A92-47774
The application of multimedia expert systems to the depot level maintenance environment p 922 A92-48557
Managing simulator wiring information and deriving system continuity p 964 A92-49287
Low cost HIRF troubleshooting and verification method for digital avionics systems p 990 A92-49304
Are we doing HIRF testing sensibly? --- avionics certification in commercial aircraft p 931 A92-49305
Aging aircraft and airworthiness p 931 A92-51399
Working together in the development of the B777 p 1015 A92-56080
Engine condition monitoring system for B747-400 p 1064 A92-56082
Current repair technologies for jet engine components p 1016 A92-56085
The operational status of automated aircraft washing system p 1016 A92-56087
Solutions to supportability concerns related to reduced-signature aircraft p 1055 A92-56220
Field test of an advanced maintenance-system p 1016 A92-56221
Program plan: National aging aircraft research program
[DOT/FAA/CT-88/32-1] p 18 N92-10992
Corrosion and your aircraft
[NRC-30465] p 114 N92-11991
A knowledge-based assistant for diagnosis in aircraft maintenance p 61 N92-12538
Implementing total quality management at the intermediate level of aircraft maintenance
[AD-A241768] p 62 N92-12992
A proposed composite repair methodology for primary structure
[NRC-LTR-ST-1658] p 115 N92-13056
Avionics modernization/upgrades in the late 1990s p 199 N92-14055
Fatigue of repaired composite structures p 214 N92-14411
Methodology for assessment of skin repairs on Airbus aircraft p 226 N92-14428
Aging Aircraft NDI Development and Demonstration Center (AANC): An overview
[DE92-002358] p 241 N92-15962
Rapid repair of integrally stiffened carbon fibre composite structures by bolted aluminium elements
[MBB-FE202-S-PUB-0453-A] p 290 N92-17310
Development of a knowledge base for use in an Expert System Advisor for Aircraft Maintenance Scheduling (ESAAMS)
[AD-A243435] p 305 N92-17687
An analysis of the aircraft engine Component Improvement Program (CIP): A life cycle cost approach
[AD-A243346] p 280 N92-17729
Fatigue testing and tear down operations on Airbus A320 forward fuselage p 360 N92-18579
Durability and damage tolerance testing and fatigue life management: A CF-18 experience p 361 N92-18581
The G-222 aircraft individual tracking programme p 361 N92-18582
Structural airworthiness of aging Boeing jet transports p 362 N92-18590
Aircraft fatigue management in the Royal Air Force p 363 N92-18591
Managing airborne assets through loads monitoring p 363 N92-18594
Approach to crew training in support of the USAF Aircraft Structural Integrity Program (ASIP) p 363 N92-18595
Structured Hypermedia Application Development Model (SHADM): A structured model for technical documentation application design
[AD-A244268] p 417 N92-19336
Finite element analysis of a riveted repair on a curved composite panel
[AD-A243916] p 404 N92-19384
Public-sector aviation issues: Graduate research award papers, 1989 - 1990
[PB91-242271] p 308 N92-19662
A review of aging aircraft technology: An IAI perspective
[IAITIC-91-1018] p 461 N92-20500
The Guardian: Preliminary design of a close air support aircraft
[NASA-CR-189991] p 463 N92-21566
Advisory Circular: Corrosion control for aircraft
[FAA-AC-43-4A] p 420 N92-21834
Human factors evaluation of the work environment of operators engaged in the inspection and repair of aging aircraft
[AD-A246445] p 724 N92-27914
Application of knowledge-based systems for diagnosis of aircraft systems
[NLR-TP-90192-U] p 837 N92-28655
Report on the workshop on Ion Implantation and Ion Beam Assisted Deposition
[AD-A250561] p 927 N92-28923
Generation of spectra and stress histories for fatigue and damage tolerance analysis of fuselage repairs
[AD-A250390] p 854 N92-29180
Bearing servicing tool
[NASA-CASE-MSC-21881-1] p 912 N92-30082
The 1991 International Conference on Aging Aircraft and Structural Airworthiness
[NASA-CP-3160] p 912 N92-30106
Maintaining the safety of an aging fleet of aircraft p 837 N92-30108
Current DOT research on the effect of multiple site damage on structural integrity p 913 N92-30112
Inspection of aging aircraft: A manufacturer's perspective p 914 N92-30117
The FAA aging airplane program plan for transport aircraft p 838 N92-30128
Ageing aircraft research in the Netherlands p 838 N92-30129
Survey of French activities concerning structural airworthiness and aging aircraft p 838 N92-30130
Transport Canada aging aircraft activities p 838 N92-30131
Aging commuter aeroplanes: Fatigue evaluation and control methods p 915 N92-30132
A manufacturer's approach to ensure long term structural integrity p 838 N92-30133
Model analysis and expert system development for planning and scheduling teleoperations for aircraft turnaround functions, volume 1
[AD-A251037] p 932 N92-30253
Model analysis and expert system development for planning and scheduling teleoperations for aircraft turnaround functions. Volume 2: Top user's guide
[AD-A251083] p 932 N92-30258
Laser induced fluorescence detection of gums in jet fuels
[AD-A252685] p 987 N92-30767
Flight crew integration in the maintenance chain of a commercial aircraft (A 320) p 1012 N92-30957
GNAS Maintenance Control Center (GMCC) Design Qualification Test and Evaluation (DQT/E) test procedures
[DOT/FAA/CT-TN91/40] p 983 N92-30976
GNAS Maintenance Control Center (GMCC) Design Qualification Test and Evaluation (DQT/E) test report
[DOT/FAA/CT-TN91/39] p 932 N92-31615
Aging fleet: Maintaining airworthiness p 953 N92-31862
Developing robust support structures for high-technology subsystems: The AH-64 Apache helicopter
[AD-A252773] p 1017 N92-33499

AIRCRAFT MANEUVERS

On-line state estimation and parameter identification for flight p 50 A92-11429
Results of flight tests of the Boeing Sikorsky Fantail demonstrator p 106 A92-14376
Enhanced energy maneuverability for attack helicopters using continuous, variable (C-V) rotor speed control p 132 A92-14421
The flight test pilot's display - A CRT system for test maneuvers p 118 A92-16057
Problem of the optimal correction of a flight test program for an aircraft system p 113 A92-16809
Control concept for maneuvering in hypersonic flight
[AIAA PAPER 91-5055] p 203 A92-17838
Z-Basic algorithm for collision avoidance system p 188 A92-18482
Analysis of aircraft performance during lateral maneuvering for microburst avoidance p 205 A92-20207
Control surfaces correlation in DLC maneuvers p 280 A92-21301
Control surfaces correlation in DSFC maneuvers --- Direct Side-Force Control p 281 A92-21307
The FALSTAFF program - A standard spectrum for simulating the service loading of aircraft with prevailing maneuver loads p 284 A92-21922
Use of neural networks in control of high alpha maneuvers
[AIAA PAPER 92-0048] p 282 A92-22164
A new method for calculation of helicopter maneuvering flight p 282 A92-23382
Dynamics of an aircraft-towed body during release
[AIAA PAPER 92-0130] p 295 A92-23750
Future experimental needs in high-alpha vehicle dynamics
[AIAA PAPER 92-0159] p 254 A92-23774
Center of pressure calculations for a bent-axis vehicle
[AIAA PAPER 92-0168] p 254 A92-23779
Agility as a contributor to design balance p 356 A92-24405
The calculation of the static elastic aerodynamic distribution for the rolling maneuver aircraft p 379 A92-25010
A methodology for the analysis and modeling of thrust vectoring usage
[AIAA PAPER 92-0389] p 357 A92-26245
Target pitch angle for the microburst escape maneuver
[AIAA PAPER 92-0730] p 379 A92-27082
The analysis and approximate representation of the optimal control law for a maneuverable aircraft p 479 A92-30131
Characteristics of the phugoid motion of nonmaneuverable aircraft p 480 A92-30190
YF-22A prototype Advanced Tactical Fighter demonstration/validation flight test program overview
[AIAA PAPER 92-1087] p 537 A92-33253
The effectiveness of Coriolis dampening of convection during aircraft high-g arcs p 581 A92-33847
Rolling Maneuver Load Alleviation using active controls
[AIAA PAPER 92-2099] p 566 A92-35670
Maneuver load control using optimized feedforward commands
[AIAA PAPER 92-2100] p 567 A92-35671
The use of inverse simulation for conceptual design p 546 A92-35738
X-29 high angle of attack flight test procedures, results, and lessons learned p 548 A92-35934
Handling and performance considerations when conducting air-to-air refuelling of large aircraft by the probe and drogue system p 548 A92-35937
Possible utilization of GPS in precision approach maneuvers p 637 A92-37075

Maximum-miss aircraft collision avoidance
p 660 A92-37077
Recent advances in maneuver loads analysis
p 642 A92-37576
Measures of merit for aircraft dynamic maneuvering
p 642 A92-37825
Inverse and optimal control for desired outputs
p 661 A92-39894
Controls for agility research in the NASA High-Alpha Technology Program
[SAE PAPER 912148] p 661 A92-39984
Aircraft evasive maneuvers against flying objects
p 744 A92-43128
An adaptive flight control for use in connection with helicopter engine failure p 745 A92-43159
Toward an integrated multimodal approach to flight simulation p 880 A92-45026
Results and lessons learned from the STOL and Maneuver Demonstration Program
[SAE PAPER 912005] p 843 A92-45406
Parameter identification of linear systems based on smoothing p 873 A92-46742
Fighter airframe/propulsion integration - A McDonnell Aircraft perspective
[AIAA PAPER 92-3333] p 850 A92-48916
Some problems on atmospheric turbulence spectrum and aircraft response p 975 A92-50235
Dynamics and control of maneuverable towed flight vehicles p 976 A92-50508
Estimation of lift and drag characteristics of an aircraft from flight data p 959 A92-51942
Developmental evaluation of a centrifuge flight simulator as an enhanced maneuverability flying qualities tool
[AIAA PAPER 92-4157] p 982 A92-52447
Dead reckoning for aircraft in distributed interactive simulation
[AIAA PAPER 92-4171] p 1008 A92-52456
Midair collision - The links in a chain
p 951 A92-52645
Invertibility and trajectory control for nonlinear maneuvers of aircraft
[AIAA PAPER 92-4410] p 1075 A92-55204
An efficient algorithm for optimal aircraft trajectories
[AIAA PAPER 92-4412] p 1076 A92-55206
Severe turbulence and maneuvering from airline flight records
[AIAA PAPER 92-4341] p 1078 A92-55330
Aerodynamic parameters of the X-31 drop model estimated from flight-data at high angles of attack
[AIAA PAPER 92-4357] p 1080 A92-55343
Flight simulator fidelity assessment in a rotorcraft lateral translation maneuver
[AIAA PAPER 92-4424] p 1092 A92-55348
Force production mechanisms of a tangential jet on bodies at high alpha
[AIAA PAPER 92-4648] p 1082 A92-55393
Optimization approach for helicopter maneuverability with a point mass model p 1083 A92-56025
High angle-of-attack flush airdata sensing system
p 1064 A92-56172
The solution of the helicopter flight dynamics tasks by the methods of optimal control theory
p 1085 A92-56284
A study of helicopter rotor/fuselage response in low-speed manoeuvres - Comparison of theory with flight p 1086 A92-56334
Development of a 1/7th scale fighter UAV for flight research
[AD-A240703] p 23 N92-11008
Monitoring load experience of individual aircraft
[NLR-TP-90084-U] p 196 N92-15065
Investigation of advanced aircraft performance measures of merit including new agility metrics
[AD-A242016] p 272 N92-15990
Target pitch angle for the microburst escape maneuver p 266 N92-17996
A parametric approach to spectrum development
p 360 N92-18578
Manoeuvring Aerodynamics
[AGARD-CP-497] p 363 N92-18778
X-31 enhancement of aerodynamics for maneuvering beyond stall p 363 N92-18779
Prediction of aerodynamic phenomena limiting aircraft manoeuvrability p 364 N92-18781
Application of nonlinear QFT to flight control design for high angle of attack maneuvers with thrust vectoring
[AD-A243821] p 381 N92-19241
Identification of aerodynamic models for maneuvering aircraft
[NASA-CR-190039] p 348 N92-19359
Proportional plus integral control of aircraft for automated maneuvering formation flight
[AD-A243792] p 382 N92-19505
Center of pressure calculations for a bent-axis vehicle
[DE92-005186] p 498 N92-20143
Control integration concept for hypersonic cruise-turn maneuvers
[NASA-TP-3136] p 481 N92-20195
Some interesting phenomena from Lavi test flights relating to aircraft stability and control
[IAITIC-91-1017] p 482 N92-20849
Time-optimal reorientation maneuvers of an aircraft
p 549 N92-22605
Application of nonlinear feedback control theory to supermaneuverable aircraft
[NASA-CR-190336] p 663 N92-25648
Development of the Basic Flight Instruction Tutoring System (BFITS)
[AD-A246458] p 751 N92-27836
Reference mode effect on the auditory display of aircraft bank angle
[AD-A247825] p 728 N92-27916
Identification of aerodynamic models for maneuvering aircraft
[NASA-CR-190444] p 852 N92-28720
Feedback control laws for highly maneuverable aircraft
[NASA-CR-190535] p 879 N92-29654
Rolling maneuver load alleviation using active controls
[NASA-TM-107654] p 962 N92-31351
Optimal trajectories for an unmanned air vehicle
p 963 N92-31880
Rapid development of the X-31 simulation to support flight-testing
[NASA-TM-104256] p 1060 N92-33149
The F-18 high alpha research vehicle: A high-angle-of-attack testbed aircraft
[NASA-TM-104253] p 1060 N92-33404
Nonlinear dynamic-inversion flight control of supermaneuverable aircraft p 1062 N92-33953

AIRCRAFT MODELS

Application of nonlinear control strategies to aircraft at high angle of attack p 26 A92-11329
Robust stabilization of a helicopter model
p 28 A92-11501
Robust autopilot design for aircraft with multiple lateral-axes controls using H(infinity) synthesis
p 28 A92-11563
Experimental determination of the center of mass, the principal central axes of inertia and moments of inertia --- aircrafttt models applied to real aircraf
p 40 A92-12346
The background and the development of the TAL-WAR (Rose) shape blimp with the articulated thruster
[AIAA PAPER 91-3692] p 17 A92-12749
Numerical modeling technique for field-to-cable coupling through advanced composite material
p 146 A92-14684
Recent development of wind-tunnel test techniques at ONERA
[ONERA, TP NO. 1991-135] p 137 A92-16110
Multidisciplinary modeling and simulation of a generic hypersonic vehicle
[AIAA PAPER 91-5015] p 232 A92-17813
On the accuracy of an aircraft-borne ambient electric-field measuring system p 186 A92-20127
The use of finite difference electromagnetic analysis in the design and verification of modern aircraft
p 192 A92-20136
System-identification of airplanes using the 'estimation before modelling' technique p 269 A92-21007
Use of neural networks in control of high alpha maneuvers
[AIAA PAPER 92-0048] p 282 A92-22164
Examination of a numerical icing-severity scale
[AIAA PAPER 92-0164] p 263 A92-23777
A multibody approach to modeling tilt-wing rotorcraft dynamics
[AIAA PAPER 92-0487] p 328 A92-26318
Calculations of hot gas ingestion for a STOVL aircraft model
[AIAA PAPER 92-0385] p 374 A92-28191
Washout filters in the bifurcation control of high alpha flight dynamics p 476 A92-29061
Fuzzy controller design and stability analysis for an aircraft model p 478 A92-29124
An electromagnetic suspension system for aerodynamic studies p 483 A92-30409
Aircraft control and simulation --- Book
[ISBN 0-471-61397-5] p 480 A92-31021
Investigation of the aerodynamic features of flows past models using thin-film capacitance-type sensors of pressure oscillations p 440 A92-31884
The Second Goldstein Lecture: Modern developments in fluid dynamics - An addendum p 442 A92-32323
FAMUSS - A new aeroservoelastic modeling tool
[AIAA PAPER 92-2395] p 541 A92-34468
Aeroelastic response of helicopters with flexible fuselage modeling
[AIAA PAPER 92-2567] p 564 A92-34481
Acoustic results of the Boeing model 360 whirl tower test p 603 A92-35741
Theoretical and experimental study of a model rotor
p 547 A92-35781
Comparison of elastic and rigid blade-element rotor models using parallel processing technology for piloted simulations
[SAE PAPER 912120] p 608 A92-39968
1991-92 AHS Technical Committee highlights - Dynamics p 647 A92-40393
Identification of the transfer function between turbulence and aircraft p 743 A92-41226
A model of a deformable aeroplane with a wing of low aspect ratio and movable control surfaces for studying natural vibrations p 744 A92-41528
Gasdynamic design --- Russian book
[ISBN 5-02-029715-1] p 708 A92-42777
In-flight simulation of backside operating models using direct lift controller
[SAE PAPER 912069] p 872 A92-45450
Aircraft spoiler effects under wind shear
[AIAA PAPER 92-2642] p 796 A92-45509
Parameter identification of linear systems based on smoothing p 873 A92-46742
Pitch rate/sideslip effects on leading-edge extension vortices of an F/A-18 aircraft model
p 874 A92-46810
A study on mechanical model of the helicopter 'ground resonance' p 955 A92-50214
Fourier functional analysis for unsteady aerodynamic modeling p 935 A92-50313
Cost effective close tolerance plastic master models
p 958 A92-51538
Simulation software flowdown in the aircraft design process - Problems and solutions
[AIAA PAPER 92-4160] p 1008 A92-52450
Solution of Euler equations with unstructured mesh - 3-D case p 941 A92-52973
Preliminary assessment of the robustness of dynamic inversion based flight control laws
[AIAA PAPER 92-4330] p 1074 A92-55174
Quantitative Feedback Theory approach to AIAA Controls Design Challenge
[AIAA PAPER 92-4626] p 1077 A92-55303
Intelligent control law tuning for AIAA Controls Design Challenge
[AIAA PAPER 92-4631] p 1132 A92-55306
Analytical development of an equivalent system mismatch function
[AIAA PAPER 92-4422] p 1080 A92-55346
Computer aided evaluation of aircraft handling qualities and flight control system robustness
[AIAA PAPER 92-4423] p 1080 A92-55347
Flight simulator fidelity assessment in a rotorcraft lateral translation maneuver
[AIAA PAPER 92-4424] p 1092 A92-55348
Buffet test in the National Transonic Facility
[AIAA PAPER 92-4032] p 1100 A92-56854
Model representation in the PANCOR wall interference assessment code
[NASA-TM-104152] p 31 N92-11022
Control of forebody vortices by suction at the nose of the RAE high incidence research model
p 87 N92-13022
Water tunnel flow visualization studies of a canard-configured X-31A-like fighter aircraft model
[AD-A241362] p 90 N92-13037
An aircraft model for the AIAA controls design challenge
[NASA-CR-186019] p 117 N92-13064
Preservation and utilization of finite element models of USAF aircraft structures
[AD-A241657] p 160 N92-13470
SATCOM antenna siting study on P-3C aircraft, volume 2
[NASA-CR-189515] p 221 N92-14263
FALKE and COBRA technology development in aerodynamics and aerothermodynamics
p 183 N92-15017
Development and evaluation of a finite element model for a fiber composite helicopter fuselage
[MBB-UD-0584-90-PUB] p 196 N92-15066
Hot-wire surveys in the vortex wake downstream of a three-percent fighter aircraft model at high angles of attack
[AD-A241869] p 259 N92-15975
Development of high angle of attack control laws for an unstable, non-minimum phase aircraft using variations of the quantitative feedback technique
[AD-A243698] p 282 N92-17096
Rotorcraft System Identification
[AGARD-LS-178] p 273 N92-17153
Instrumentation and data processing
p 273 N92-17155
Neural networks for aircraft system identification
p 303 N92-17998

Dynamic flying investigations on 1/13.5 NALLA model (Longitudinal Results)
[NAL-PD-FC-9113] p 359 N92-18073
Measurement of derivatives due to acceleration in heave and sideslip p 364 N92-18785
Identification of aerodynamic models for maneuvering aircraft
[NASA-CR-190039] p 348 N92-19359
A guide for the consideration of composite material impacts on airframe costs
[AD-A243928] p 417 N92-19466
A study of the aeroelastic behaviour of helicopter rotor blades featuring swept tips p 367 N92-19701
Calculations of hot gas ingestion for a STOVL aircraft model
[NASA-TM-105437] p 350 N92-19993
Bistatic image processing for a 32 x 19 inch model aircraft using scattered fields obtained in the OSU-ESL compact range
[NASA-CR-189932] p 499 N92-20197
Analytical modeling of SH-2F helicopter shipboard operation p 464 N92-21961
Static aeroelastic analysis of ACT wind tunnel model aircraft
[NAL-TM-624] p 632 N92-25366
Vibration tests and structural modeling of an aircraft model for active control technology experiments
[NAL-TM-626] p 662 N92-25401
Progress of magnetic suspension and balance systems for wind tunnels in the USSR p 751 N92-27803
Development of telemetry for the agility flight test of a radio controlled fighter model
[AD-A248653] p 753 N92-27994
NACA0012 airfoil data corrected for sidewall boundary-layer effects in the NAL two-dimensional transonic wind tunnel
[NAL-TM-640T] p 722 N92-28151
Estimation of cable-mounted model inertia characteristics for dynamic wind-tunnel test
[NAL-TM-641] p 722 N92-28152
Force measurements on AGARD calibration model-B at transonic speeds in the NAL two-dimensional wind tunnel
[NAL-TM-639] p 722 N92-28190
A gust generation method for full configuration aircraft tests in a low speed wind tunnel. Part 1: Design and preliminary experiments
[NAL-TR-1115-PT-1] p 722 N92-28192
Integrating aerodynamics and structures in the minimum weight design of a supersonic transport wing
[NASA-TM-107586] p 850 N92-28435
Identification of aerodynamic models for maneuvering aircraft
[NASA-CR-190444] p 852 N92-28720
Model analysis and expert system development for planning and scheduling teleoperations for aircraft turnaround functions, volume 1
[AD-A251037] p 932 N92-30253
Model analysis and expert system development for planning and scheduling teleoperations for aircraft turnaround functions. Volume 2: Top user's guide
[AD-A251083] p 932 N92-30258
Two-dimensional aerodynamic characteristics of several polygon-shaped cross-sectional models applicable to helicopter fuselages
[NASA-TP-3233] p 944 N92-30394
Simulation model of a twin-tail, high performance airplane
[NASA-TM-107601] p 1088 N92-33537
Static and dynamic flow visualization studies of two double-delta wing models at high angles of attack
[AD-A252878] p 1040 N92-33678
Effect of afterbody geometry on aerodynamic characteristics of isolated nonaxisymmetric afterbodies at transonic Mach numbers
[NASA-TP-3236] p 1041 N92-33706
Flutter models: Their design, manufacture, and ground testing p 1089 N92-34164

AIRCRAFT NOISE

Development of a shock noise prediction code for high-speed helicopters - The subsonically moving shock p 165 A92-14384
A neural network for the identification of measured helicopter noise p 162 A92-14387
Stage 2 noise certification of the Sikorsky S-76A and S-76C helicopters p 91 A92-14388
Environmental impact of a future supersonic transport aircraft
[ONERA, TP NO. 1991-132] p 161 A92-16108
Interior noise reduction program for the Dornier 328 p 114 A92-17254
Broadband shock-associated noise from supersonic jets in flight p 235 A92-18683
The Civil Rotorcraft Initiative - An action agenda p 241 A92-22707
Helicopter/heliport operations - Environmental implications p 241 A92-22708
Review on the abatement of helicopter noise p 406 A92-25501
An optical microphone for the detection of hidden helicopters
[AIAA PAPER 92-0377] p 395 A92-26235
The price of success - Mitigation and litigation in airport growth p 417 A92-27450
Models of space-averaged energetics of plates p 398 A92-28031
Identification of helicopter noise using a neural network p 416 A92-28032
Improved noise rejection in automatic carrier landing systems p 380 A92-28154
NATO CCMS aircraft noise study on receiver technology p 686 A92-39050
Noise from military airfields in the United Kingdom p 686 A92-39052
Airport noise contours - Converting from NNI to Leq p 686 A92-39053
Aircraft noise - The calculation of the noise exposure by aircraft in the Netherlands p 687 A92-39054
DANSIM - Danish Airport Noise Simulation Model - Basic principles, experience, and improvements p 687 A92-39055
Comparison of aircraft noise indices for noise zoning at military airfields p 687 A92-39056
DANSIM applications - Development of airport noise reduction strategies and environmental policy p 687 A92-39057
Computation of aircraft noise exposure using digitized topography data p 687 A92-39058
Calculation of aircraft noise contours taking into account the lateral flight track dispersion p 687 A92-39059
Advanced method for single event aircraft noise analysis p 693 A92-39060
A noise survey around Oslo Airport Fornebu p 687 A92-39061
Distribution of maximum levels of aircraft noise around their mean value p 693 A92-39062
Interdependencies of aircraft-/airport-noise and urban- and regional-planning standards p 688 A92-39063
Determination of aircraft noise levels while the engine is running on the ground - An approach from the point of urbanization and architecture p 688 A92-39064
Do we really need 57 ways of rating aircraft noise? p 688 A92-39065
Summary of Dornier 328 interior noise control study p 643 A92-39083
A survey of active control in aircraft cabins p 643 A92-39084
Coupled propeller contributions to aircraft noise and vibration p 694 A92-39085
Evaluation of sound transmission into aircraft fuselages by a reciprocity technique p 694 A92-39086
Noise inside aircraft fuselages subjected to airborne excitation p 643 A92-39089
A mobile system for measuring airport noise p 688 A92-39099
A model for the effects of aircraft overflight noise on the reproductive success of raptorial birds p 688 A92-39101
Trading number of operations versus loudness of aircraft p 688 A92-39102
Temporal change of noisiness of helicopter noise p 689 A92-39103
Temporal change of timbre of helicopter noise p 694 A92-39104
Active control of airborne noise transmitted through a ribbed panel p 695 A92-39111
Laboratory testing of a high transmission loss aircraft cabin structure p 663 A92-39229
Some experiences with community response to low levels of aircraft noise p 689 A92-39235
Aircraft noise and the elderly p 689 A92-39236
Annoyance from aircraft overflights in wilderness p 689 A92-39239
Relating the annoyance of aircraft overflights to their audibility by outdoor recreationists p 689 A92-39240
The development of multiple-input models for airborne noise prediction p 695 A92-39243
Noise abatement procedures vs. safety
[SAE PAPER 912137] p 635 A92-39977
A perspective on helicopter noise p 780 A92-43160
Basic experiments on the directivity of the sound radiation emitted by a turboshaft engine
[ONERA, TP NO. 1992-36] p 926 A92-48597
Research and studies on quiet helicopters
[ONERA, TP NO. 1992-59] p 926 A92-48618
Shimmy of nose undercarriage wheels p 959 A92-51948
Progress towards quieter civil helicopters p 1011 A92-52847
Path identification in structural acoustics p 1059 A92-56346
Aeroacoustics of flight vehicles: Theory and practice. Volume 1: Noise sources
[NASA-RP-1258-VOL-1] p 54 N92-10598
Rotor noise p 54 N92-10600
Airframe noise p 55 N92-10605
Annoyance caused by advanced turboprop aircraft flyover noise: Comparison of different propeller configurations
[NASA-TP-3104] p 56 N92-11758
A new simulator for assessing subjective effects of sonic booms
[NASA-TM-104150] p 56 N92-11759
Development of an annoyance model based upon elementary auditory sensations for steady-state aircraft interior noise containing tonal components
[NASA-TM-104147] p 166 N92-13758
Human response to aircraft noise p 236 N92-14780
Interior noise p 236 N92-14785
Flyover-noise measurement and prediction p 236 N92-14786
Propeller-driven-small airplane noise certification
[LR-650] p 237 N92-14798
Human response to helicopter noise: A test of A-weighting
[AD-A243719] p 304 N92-17506
An evaluation of some alternative approaches for reducing fan tone noise
[NASA-TM-105356] p 416 N92-18282
Re-engining appears to offer best payback for young: Chapter 2 compliant aircraft
[PNR-90848] p 378 N92-19939
Application of analysis techniques for low frequency interior noise and vibration of commercial aircraft
[NASA-CR-189555] p 481 N92-20376
The impact of aircraft noise control technology
[PNR-90846] p 512 N92-20461
Annoyance caused by aircraft en route noise
[NASA-TP-3165] p 512 N92-20479
Sonic booms produced by US Air Force and US Navy aircraft: Measured data
[AD-A244804] p 512 N92-21719
Risk to hearing from overflight noise of military aircraft
[ISVR-TR-194] p 604 N92-22241
Overview of NASA PTA propfan flight test program p 561 N92-22536
Propulsion challenges and opportunities for high-speed transport aircraft p 561 N92-22540
The future challenge for aeropropulsion
[NASA-TM-105613] p 658 N92-25164
Steady-state acoustical noise measurements in aviation systems
[AD-A247831] p 780 N92-27924
Operational noise data for OH-58D Army helicopters
[AD-A246822] p 926 N92-28292
Boundary layer induced noise in aircraft
[CUED/A-AERO/TR-18] p 927 N92-29201
Aviation noise: Costs of phasing out noisy aircraft
[GAO/RCED-91-128] p 1011 N92-31454
Fourth Aircraft Interior Noise Workshop
[NASA-CP-10103] p 1136 N92-32948
MD-80 aft cabin noise control: A case history p 1137 N92-32950
The Dornier 328 Acoustic Test Cell (ATC) for interior noise tests and selected test results
[AIAA PAPER 92-2164] p 1137 N92-32951
Use of SEA to predict structure-borne noise in aircraft p 1137 N92-32955
Advanced Study for Active Noise Control in Aircraft (ASANCA)
[AIAA PAPER 92-2092] p 1137 N92-32956
Active control of interior noise in a large scale cylinder using piezoelectric actuators p 1137 N92-32958
Active vibrations and noise control for turboprop application research program activities p 1138 N92-32962
Active synchrophasing of propeller unbalance p 1138 N92-32963
A lightweight loudspeaker for aircraft communications and active noise control p 1125 N92-32964
Building vibrations induced by noise from rotorcraft and propeller aircraft flyovers
[NASA-TM-104170] p 1138 N92-33160
Advanced subsonic transport approach noise: The relative contribution of airframe noise
[NASA-TM-104112] p 1140 N92-34148
Impacts of technology on the capacity needs of the US national airspace system
[NASA-CR-4470] p 1045 N92-34192

AIRCRAFT PARTS

X-ray computed tomography of composites p 36 A92-10143
Flight service evaluation of composite helicopter components p 106 A92-14372
An advanced neutron radiography system p 492 A92-28748

Maintenance scheduling for critical parts of aircraft
p 699 A92-42054
Using the single point excitation technique to measure aperture impedance over a broad frequency range
p 761 A92-42320
Tooling for C-17 composite parts p 900 A92-47412
Durability analysis for a main bulkhead subjected to load on the body of an aircraft p 848 A92-47664
Economic life analysis for replacing components
p 785 A92-47670
RTM - Simultaneous design and tooling reduces cost and lead time p 994 A92-51537
Structural design and testing results of composite landing gear components p 1057 A92-56328
Damage tolerant design of critical aircraft structural components
[AIAA PAPER 92-4041] p 1123 A92-56860
Tribology needs for future space and aeronautical systems
[NASA-TM-104525] p 214 N92-15191
Aging Aircraft NDI Development and Demonstration Center (AANC): An overview
[DE92-002358] p 241 N92-15962
Computered tomography: Experimental data acquisition and parallelization of reconstruction algorithm
[DE92-005151] p 499 N92-20301
A sensitivity analysis on component reliability from fatigue life computations
[AD-A247430] p 908 N92-28425

AIRCRAFT PERFORMANCE
Performance and handling qualities criteria for low cost real time rotorcraft simulators - A methodology development p 136 A92-14365
Computer aiding for low-altitude helicopter flight
p 94 A92-14444
Aircraft design experience p 110 A92-15326
Mirage 2000-5 - Dassault's delta described
p 113 A92-16622
RAH-66 Comanche - A cut above the rest
p 61 A92-16675
Analysis of aircraft performance during lateral maneuvering for microburst avoidance
p 205 A92-20207
Thermal management of hypersonic aircraft using noncryogenic fuels
[SAE PAPER 911443] p 270 A92-21839
A flight test study to determine aircraft propulsive efficiency and aerodynamic drag using two parameter identification methods and Lock's propeller model
[AIAA PAPER 92-0170] p 271 A92-23781
Single lever power management of turboprop engines
p 372 A92-25373
Elements of airplane performance --- Book
[ISBN 90-6275-608-5] p 357 A92-26550
High density fuel qualification for a gas turbine engine
[AIAA PAPER 92-0684] p 389 A92-27051
Robustness analysis of a model reference adaptive control system p 412 A92-27859
Meeting VSTOL aircraft performance requirements using scheduled H(infinity) controllers p 477 A92-29094
Robust adaptive nonlinear control of high performance aircraft p 478 A92-29188
Perspectives in aerospace design --- Book
[ISBN 1-56347-010-1] p 459 A92-31606
A study of altitude-constrained supersonic cruise transport concepts
[AIAA PAPER 92-1027] p 536 A92-33208
Sentinel 1000 flight test programme overview and preliminary results
[AIAA PAPER 92-1229] p 538 A92-33326
Flight testing a high performance kit built aircraft
[AIAA PAPER 92-1240] p 538 A92-33333
New way of flying (1990 Sir Charles Kingsford Smith Lecture) p 515 A92-33461
Aircraft performance --- Book
[ISBN 0-521-36264-4] p 538 A92-33919
AV-8B V/STOL performance analysis
p 549 A92-35948
Concorde flight testing - Powerplant and performance flying
[SAE PAPER 912192] p 644 A92-40009
The Pond Racer preliminary flight test report
p 645 A92-40031
X-31 flight test update p 645 A92-40034
Single engine testing of the F-14A(PLUS) airplane in the power approach configuration p 645 A92-40036
MD-11 status report p 646 A92-40040
Effect of thrust vectoring on level-turn performance
p 729 A92-41243
Aircraft Symposium, 28th, Tokyo, Japan, Nov. 7-9, 1990, Proceedings p 699 A92-43095
The progress of a STOL project p 699 A92-43137
Effectiveness of aircraft aerodynamic performance on each part of a joined wing p 712 A92-43230
International Powered Lift Conference, London, England, Aug. 29-31, 1990, Proceedings
[ISBN 0-903409-68-2] p 783 A92-45302
Jet-powered V/STOL aircraft - Lessons learned
p 841 A92-45304
ASTOVL flexibility in the 21st century
p 783 A92-45309
A progress report on ASTOVL control concept studies under the VAAC programme p 871 A92-45319
The experimental and computational study of jet impingement flowfields with reference to VSTOL aircraft performance p 787 A92-45324
Optimization of constant altitude-constant airspeed flight of turbojet aircraft p 845 A92-46815
Study on two variable control plan for twin spool turbojet engine p 862 A92-47697
Naval aircraft/engine mission payoff analyses
[AIAA PAPER 92-3473] p 865 A92-49019
Estimation of lift and drag characteristics of an aircraft from flight data p 959 A92-51942
Takeoff Performance Monitoring System display options
[AIAA PAPER 92-4138] p 967 A92-52433
Regional challenge --- flight test of Canadair Regional Jet p 961 A92-53121
Identification and control of aircraft dynamics using radial basis function neural networks
[AIAA PAPER 92-4393] p 1074 A92-55194
Height keeping performance requirements for reducing vertical separation minima used for air traffic control
p 1046 A92-56081
Engine condition monitoring system for B747-400
p 1064 A92-56082
Multidisciplinary optimization of aeroservoelastic systems using reduced-size models
p 1054 A92-56176
The Eurofar program - An European overview on advanced VTOL civil transportation system
p 1016 A92-56299
First level release of 2GCHAS for comprehensive helicopter analysis p 1133 A92-56339
The compound helicopter - A concept revisited
p 1058 A92-56341
Comparison of recent results from different wind tunnel facilities along with comparisons of measured flight results and wind tunnel based predictions
[AIAA PAPER 92-3985] p 1060 A92-56809
Investigation of advanced aircraft performance measures of merit including new agility metrics
[AD-A242016] p 272 N92-15990
System identification methods for handling-qualities evaluation p 274 N92-17165
Discussion for possibility of some aerodynamic ground effect craft
[NAL-TM-619] p 300 N92-17757
Example of statistical techniques applied to cruise performance guarantees (Student's t distribution)
[ESDU-91018] p 276 N92-17843
Example of statistical techniques applied to autoland touchdown dispersion (confidence intervals for normal and skew distributions)
[ESDU-91019] p 268 N92-17844
Variability of standard aircraft performance parameters
[ESDU-91020] p 276 N92-17847
Optimal aircraft performance during microburst encounter p 266 N92-17999
Statistical methods applicable to analysis of aircraft performance data
[ESDU-91017] p 359 N92-18096
A preliminary flight test on a basic performance of the flight research airplane Do 228: Velocity vs glide path angle
[NAL-TM-613] p 359 N92-18482
A parametric approach to spectrum development
p 360 N92-18578
Analysis of the effects of removing nose ballast from the F-15 eagle
[AD-A244044] p 366 N92-19178
Proposal for a low cost close air support aircraft for the year 2000: The Raptor
[NASA-CR-190023] p 367 N92-19496
Preliminary design studies of an advanced general aviation aircraft
[NASA-CR-190024] p 461 N92-20064
Control integration concept for hypersonic cruise-turn maneuvers
[NASA-TP-3136] p 481 N92-20195
NASA advanced aeronautics design solar powered remotely piloted vehicle
[NASA-CR-190007] p 462 N92-20665
Active flow control for twenty-first century high-performance aircraft with applications to land and sea vehicles p 447 N92-21504
A-2000: Close air support aircraft design team
[NASA-CR-190022] p 463 N92-21567
Wind tunnel investigation of a wing-propeller model performance degradation due to distributed upper-surface roughness and leading edge shape modification
p 451 N92-21690
A summary of NASA research on effects of heavy rain on airfoils p 452 N92-21694
Survey of experimental techniques for performance prediction p 552 N92-23954
A summary of XB-70 sonic boom signature data
[NASA-CR-189630] p 696 N92-24800
F-111C flight dynamic model aerodynamic data-base development and verification
[AD-A246356] p 715 N92-26947
Technical evaluation report on the Flight Mechanics Panel Symposium on Flying Qualities
[AGARD-AR-311] p 733 N92-27870
Effects of cockpit lateral stick characteristics on handling qualities and pilot dynamics
[NASA-CR-4443] p 878 N92-28584
The 1991 International Conference on Aging Aircraft and Structural Airworthiness
[NASA-CP-3160] p 912 N92-30106
Performance of fuselage pressure structure
p 913 N92-30109
The design and development of a portable, DSP micro-processor based, high-accuracy data acquisition system
[NRC-32146] p 1134 N92-32851
Simulation model of a twin-tail, high performance airplane
[NASA-TM-107601] p 1088 N92-33537
The Rolls-Royce Trent
[PNR-90875] p 1061 N92-33750
Numerical investigation of the effects of icing on fixed and rotary wing aircraft
[NASA-CR-190542] p 1044 N92-34105

AIRCRAFT PILOTS
Cockpit distractions - Precursors to emergencies
p 16 A92-11178
Helicopter control response types for hover and low-speed near-earth tasks in degraded visual conditions
p 132 A92-14338
The helicopter air-to-air value-driven engagement model (HAVDEM) - Prototype development
p 105 A92-14353
Analysis of changes in the pilot population and general aviation accidents p 187 A92-20722
Transgressions in a pilot-helicopter system
p 358 A92-27394
Nonstationary manual control. III p 776 A92-43187
A study of the pilot's associate system
p 745 A92-43218
Research on a helicopter information control system
p 735 A92-43220
The development of a real time visual flight simulator for tactical operations research and measurement
p 880 A92-45027
A training program for airline line instructors
p 835 A92-45044
Empirical foundations and sensitivity testing - Is it enough for the 90's? p 835 A92-45054
Knowledge-sensitive task manipulation - Acquiring knowledge from pilots flying a motion-based flight simulator p 916 A92-45064
Mandatory psychological testing of pilots as a requirement for licensing in Norway?
p 835 A92-45081
An approach to the organization of an adaptive man-machine system for flight vehicle control
p 1133 A92-57445
An experimental study of organismic principles of the functioning of the crew-transport aircraft system
p 1133 A92-57446
Pilot's Automated Weather Support System (PAWSS) concepts demonstration project. Phase 1: Pilot's weather information requirements and implications for weather data systems design
[NASA-CR-188228] p 46 N92-11593
Soviet electronic display systems under research and manufactured for the civil aviation aircraft of the 1990's
[AD-A240933] p 119 N92-13066
MULTIRAD
[AD-A244211] p 412 N92-19247
A mathematical model of a tilt-wing aircraft for piloted simulation
[NASA-TM-103864] p 368 N92-19847
The Flight Simulation Facility at the Wichita State University p 484 N92-21511
Limitations on helicopter operations in the aeronaval environment p 466 N92-21973
Global positioning system supported pilot's display
p 534 N92-22436
Status of automatic guidance systems for rotorcraft in low altitude flight p 727 N92-27894
ICAAS piloted simulation evaluation
p 735 N92-27906

Use of a commercially available flight simulator during aircrew performance testing
[AD-A245922] p 883 N92-28407
Aircraft simulation and pilot proficiency: From surrogate flying towards effective training p 884 N92-28532
The use of a dedicated testbed to evaluate simulator training effectiveness p 884 N92-28533
Introduction to cognitive processes of expert pilots
[DOT/FAA/RD-92/12] p 952 N92-30980

AIRCRAFT POWER SUPPLIES
Electronic control of a turbine power unit
p 470 A92-29741
The engine inside p 558 A92-36126
The computer analysis of the prediction of aircraft electrical power supply system reliability
p 690 A92-37950
The use of high voltage direct current in aircraft electrical systems - A Navy perspective
[SAE PAPER 912173] p 655 A92-39998
270-Vdc/hydrid 115-Vac electric power generating system technology demonstrator evolution to a dual-channel, more electric aircraft technology development testbed
[SAE PAPER 912183] p 655 A92-40003
High speed civil transport electrical power system technology requirements
[SAE PAPER 912185] p 655 A92-40005
Advanced power generation systems for more electric aircraft
[SAE PAPER 912186] p 656 A92-40006
Secondary power system preliminary design
[SAE PAPER 912189] p 656 A92-40008
A criterion for estimating the economic and operational efficiency of the power distribution systems of commercial aircraft p 657 A92-40611
Efficiency of a 5V/5mW power by light power supply for avionics applications p 734 A92-42603
Using helicopters for the erection of power transmission lines p 723 A92-43162
Auxiliary power units for advanced fighters
p 737 A92-43545
Electric power generating system for the Boeing 777 airplane
[SAE PAPER 912050] p 861 A92-45434
Auxiliary power units for current and future aircraft
[SAE PAPER 912059] p 862 A92-45441
An artificial intelligence approach for the verification of requirements for aircraft electrical power systems
p 863 A92-48481
A new resonant link aircraft power generating system
p 970 A92-50528
New-type of ultralight flexible a-Si solar cell and its application on an airplane p 970 A92-53181
Nonflammable hydraulic power system for tactical aircraft. Volume 2: Equipment and systems test and evaluation
[AD-A239805] p 35 N92-10100

AIRCRAFT PRODUCTION
Manufacturing techniques - Split torque path helicopter transmission p 110 A92-14452
Rotor revolutions in the Far East - Helicopters in China, Mongolia, and Siberia p 241 A92-22711
Weaving an aircraft p 392 A92-24911
36th Roy Chadwick Lecture - Manufacturing breakout 1941-1991: Development in aerospace industry manufacturing techniques p 419 A92-28941
Dornier 328 now in flight testing p 457 A92-29418
New processes in commercial airplane design
p 607 A92-38218
Production technologies and aircraft design
p 608 A92-38220
Aircraft structural design p 643 A92-39304
Concorde, fifteen years on the front line
[SAE PAPER 912193] p 644 A92-40010
Enhanced vision system option on future aircraft
[SAE PAPER 912204] p 651 A92-40014
1991-92 AHS Technical Committee highlights - Manufacturing and product assurance
p 609 A92-40396
Some aspects of advanced aircraft development
p 729 A92-41176
The evolution from bonded F27 aircraft to Arall structures p 699 A92-41177
Minimum surface treatments for adhesively bonded repairs p 754 A92-42501
Assembling the future p 783 A92-44895
Automatic function testing in the aircraft production
p 1015 A92-56083
Development of an automatic drilling system. II
p 1118 A92-56107
B-2 program: Trends in manufacturing
[AD-A242141] p 242 N92-15963
From IGES to STEP
[REPT-3.1.6] p 603 N92-23881
High-speed civil transport issues and technology program
[NASA-CR-186020] p 962 N92-31208

AIRCRAFT PRODUCTION COSTS
Manufacturing cost model for composites
p 1012 A92-51565
Lynx - A 50 year product? p 1056 A92-56307

AIRCRAFT RELIABILITY
Mind that restyle --- failure analysis of aircraft composite structures p 91 A92-13700
Continuation of the AHS round robin on fatigue reliability and damage tolerance p 59 A92-14341
Safe life reliability - Evaluation of new statistical methods p 104 A92-14343
Performance and handling qualities criteria for low cost real time rotorcraft simulators - A methodology development p 136 A92-14365
Main concepts of providing the static/fatigue strength of helicopters in the USSR p 110 A92-14455
ASNT and aerospace - What about the next 50 years?
p 215 A92-17293
National research program for nondestructive inspection of aging aircraft p 169 A92-17294
Designing through test
[AIAA PAPER 91-3822] p 232 A92-17664
Damage tolerance of the fighter aircraft 37 Viggen. I - Analytical assessment. II - Experimental verification
p 192 A92-19819
Methodology for the assessment of material quality effects on airframe fatigue durability p 213 A92-19820
Dornier 328 first flight p 192 A92-19924
Aging aircraft programme entails major effort and expense p 169 A92-20023
F27 aging aircraft programme emphasizes corrosion prevention p 186 A92-20024
Retrofit provides navigation enhancement for older aircraft p 198 A92-20025
Transgressions in a pilot-helicopter system
p 358 A92-27394
The problem of aging aircraft - Is mandatory retirement the answer? p 308 A92-27448
A theoretical study on helicopter alert time without maintenance p 358 A92-27836
Bell's OH-58D proves its reliability
p 458 A92-29670
The V-22 Osprey - Preparing for fleet operations
p 458 A92-29671
Structural airworthiness of aging Boeing jet transports - 747 fuselage fatigue test program
[AIAA PAPER 92-1128] p 537 A92-33280
C.A.T.C.H. - Computer aided test conductor handbook: A method for reducing cost, time and effort in an aircraft test and certification program p 602 A92-35943
Civil aircraft design in relation to airworthiness
p 635 A92-39303
Assurance of safety in the aging aircraft fleet
p 635 A92-39305
Engine reliability p 654 A92-39309
Aging aircraft and structural airworthiness
[SAE PAPER 912212] p 635 A92-40016
1991-92 AHS Technical Committee highlights - Test and evaluation p 609 A92-40398
Simulation of commercial-aircraft reliability
p 759 A92-42057
Statistical analysis of field data for aircraft warranties
p 760 A92-42077
Some consideration for evaluation of structural integrity of aging aircraft p 762 A92-43107
Aircraft reliability and maintainability
p 700 A92-43141
Flight tests on the structures of the STOL research aircraft Asuka p 730 A92-43143
The fatigue scatter factors and reduction factors in the design of aircraft and helicopter's structural lives
[SAE PAPER 911984] p 843 A92-45387
Research on aircraft life cycle cost reduction
p 1012 A92-49835
Aging aircraft and airworthiness p 931 A92-51399
Working together in the development of the B777
p 1015 A92-56080
Solutions to supportability concerns related to reduced-signature aircraft p 1055 A92-56220
New aircraft technologies - Challenges for dependability p 1120 A92-56225
Program plan: National aging aircraft research program
[DOT/FAA/CT-88/32-1] p 18 N92-10992
Robotic non-destructive inspection of aircraft, phase 1
[AD-A240777] p 44 N92-11367
Fatigue Management
[AGARD-CP-506] p 360 N92-18571
A probabilistic procedure for aircraft fleet management
p 360 N92-18576
Structural airworthiness of aging Boeing jet transports
p 362 N92-18590
Tornado structural fatigue life assessment of the German Air Force p 363 N92-18592
Fatigue management for the A-7P
p 363 N92-18593
Tactical Rubidium Frequency Standard (TRFS)
[AD-A243934] p 401 N92-18897
ETOPS: A developing scene
[PNR-90844] p 473 N92-20459
A review of aging aircraft technology: An IAI perspective
[IAITIC-91-1018] p 461 N92-20500
Design of an integrated airframe/propulsion control system architecture
[NASA-CR-182004] p 602 N92-22643
Test plan for the international aircraft operator information system
[DOT/FAA/CT-91/18] p 781 N92-26830
Estimating the reliability of a system on the basis of sample paths
[AD-A248585] p 774 N92-28171
A sensitivity analysis on component reliability from fatigue life computations
[AD-A247430] p 908 N92-28425
The 1991 International Conference on Aging Aircraft and Structural Airworthiness
[NASA-CP-3160] p 912 N92-30106
Structural integrity of future aging airplanes
p 913 N92-30107
Performance of fuselage pressure structure
p 913 N92-30109
Current DOT research on the effect of multiple site damage on structural integrity p 913 N92-30112
Federal Aviation Administration aging aircraft nondestructive inspection research plan
p 914 N92-30116
NDE research efforts at the FAA Center for Aviation Systems Reliability p 914 N92-30119
Survey of French activities concerning structural airworthiness and aging aircraft p 838 N92-30130
Transport Canada aging aircraft activities
p 838 N92-30131
Aging fleet: Maintaining airworthiness
p 953 N92-31862
A background to the handling qualities of aircraft
[ESDU-92006] p 1087 N92-32780
Flight flutter testing p 1089 N92-34163

AIRCRAFT RUNUP
Heavy metal --- fighter aircraft test rigs
p 207 A92-18100

AIRCRAFT SAFETY
Application of smart structures to aircraft health monitoring p 20 A92-11123
Requirements for an aircraft mishap analysis system
p 16 A92-11170
Sensors and systems to enhance aviation safety against weather hazards p 160 A92-14265
Lightning standards for aircraft protection
p 91 A92-14688
The canard-wing interference and stall safety of light canard aircraft p 111 A92-15341
Lightning protection for the Dornier 328
p 113 A92-17253
ASNT and aerospace - What about the next 50 years?
p 215 A92-17293
Analysis technique for lightning attachment zoning of aircraft p 186 A92-20126
Evolution of ejection systems --- Russian book
p 262 A92-21684
The Civil Rotorcraft Initiative - An action agenda
p 241 A92-22707
Damping down the fires --- in civil transport aircraft
p 350 A92-25075
Energy attenuation for crashworthy seating systems - Past, present, and possible future development
p 544 A92-35452
Why not a safety rating? --- in Australian civil aviation
p 530 A92-36200
Maximum-miss aircraft collision avoidance
p 660 A92-37077
Ageing airliner census - Still flying safely
p 634 A92-38374
Review of aviation record p 634 A92-39302
Assurance of safety in the aging aircraft fleet
p 635 A92-39305
Aircraft ground deicing
[SAE PAPER 912222] p 635 A92-40021
Zonal analysis - The final step in system safety assessment p 760 A92-42071
Windscreen departure p 723 A92-42500
Some consideration for evaluation of structural integrity of aging aircraft p 762 A92-43107
Joint Aviation Authorities: Development of an international standard for safety regulation - The first steps are being taken by the JAA p 781 A92-43548
Stop, look and learn from accident investigation
p 834 A92-44996

Wing leading edge design with composites to meet bird strike requirements p 848 A92-47404
Internationalization of telemetry systems p 920 A92-47535
Safety in the sky - Designing bomb-resistant baggage containers p 836 A92-47775
Continuous flying quality improvement - The measure and the payoff
[AIAA PAPER 92-4327] p 1073 A92-55171
Working together in the development of the B777 p 1015 A92-56080
Change and reliability of the DC-9-81 digital flight guidance system p 1084 A92-56086
Program plan: National aging aircraft research program
[DOT/FAA/CT-88/32-1] p 18 N92-10992
Corrosion and your aircraft
[NRC-30465] p 114 N92-11991
A review of UK aviation policy
[TT-9107] p 61 N92-12988
Winds of change: Domestic air transport since deregulation
[NRC-SR-230] p 92 N92-13040
Helicopter rejected takeoff airspace requirements
[SCT-91RR-28] p 116 N92-13058
Soviet electronic display systems under research and manufactured for the civil aviation aircraft of the 1990's
[AD-A240933] p 119 N92-13066
Lightning protection requirements for aircraft: A proposed specification
[RAE-TM-FS(F)-632-REV-ISSUE] p 187 N92-14007
Passenger knowledge of airline safety information
[CRANFIELD-AERO-9111] p 187 N92-15054
High Intensity Radiated Fields (HIRF) project plan
[DOT/FAA/CT-TN91/1] p 297 N92-16181
Wichita State University 1986 aviation safety research projects
[DOT/FAA/CT-91/4] p 263 N92-16986
Program plans: Aviation safety research
[NIAR-91-30] p 264 N92-17587
Discussion for possibility of some aerodynamic ground effect craft
[NAL-TM-619] p 300 N92-17757
Joint University Program for Air Transportation Research, 1990-1991
[NASA-CP-3131] p 242 N92-17984
An investigation of air transportation technology at the Massachusetts Institute of Technology, 1990-1991 p 265 N92-17985
The Operational Loads Monitoring System, OLMS p 361 N92-18586
Life management approach for USAF aircraft p 362 N92-18587
Structural airworthiness of aging Boeing jet transports p 362 N92-18590
Aircraft fatigue management in the Royal Air Force p 363 N92-18591
An evaluation of in-cabin safety features in passenger aircraft
[ETN-92-90656] p 449 N92-20794
Preliminary design and lay-out of an infant restraint system p 449 N92-21513
Effects of Adverse Weather on Aerodynamics
[AGARD-CP-496] p 449 N92-21679
National airspace system: System effectiveness operational concept NAS-SR-138
[DOT/FAA/SE-92/2] p 535 N92-23096
Aviation system: Capital investment plan p 636 N92-25297
A report on enhancements for existing and future helicopters supporting operations of the Canadian oil and gas industry
[CTN-91-60126] p 636 N92-25350
Ingress, emergency egress, and emergency evacuation testing of army aircraft
[AD-A246398] p 724 N92-27750
Human factors evaluation of the work environment of operators engaged in the inspection and repair of aging aircraft
[AD-A246445] p 724 N92-27914
Avionic data bus integration technology
[DOT/FAA/CT-91/19] p 736 N92-27973
Composite profiles of helicopter mishaps at heliports and airports
[AD-A248887] p 724 N92-28052
Maintaining the safety of an aging fleet of aircraft p 837 N92-30108
Status of the FAA flight loads monitoring program p 914 N92-30113
Damage tolerance for commuter aircraft p 914 N92-30114
Federal Aviation Administration aging aircraft nondestructive inspection research plan p 914 N92-30116
Evaluation of head impact kinematics for passengers seated behind interior walls
[AD-A252651] p 952 N92-30551
Aircraft accident report: Explosive decompression - loss of cargo door in flight, United Airlines Flight 811, Boeing 747-122, N4713U, Honolulu, Hawaii, February 24, 1989
[PB92-910402] p 953 N92-31159
Aviation safety: Changes needed in FAA's service difficulty reporting program
[GAO/RCED-91-24] p 953 N92-31453
Aging fleet: Maintaining airworthiness p 953 N92-31862
Report of the aviation safety review of Department of Energy helicopter operations
[DE92-016346] p 954 N92-31928
The 1991 Federal Aviation Administration plan for research, engineering and development p 1142 N92-32453
Aircraft accident report: L'Express Airlines, Inc., Flight 508, Beech C99, N7217L weather encounter and crash near Birmingham, Alabama, July 10, 1991
[PB92-910401] p 1043 N92-32455
A review and discussion of flight management system incidents reported to the aviation safety reporting system
[AD-A252438] p 1043 N92-32941
Accomplishments under the Airport Improvement Program, FY 1991
[AD-A253046] p 1101 N92-33434
Aircraft accident/incident summary report: Controlled flight into terrain Bruno's Inc., Beechjet, N25BR, Rome, Georgia, 11 December 1991
[PB92-910404] p 1044 N92-34081

AIRCRAFT SPECIFICATIONS
First flight for Airbus A340 p 21 A92-12750
Beriev Be-42 - A unique jet-propelled seaplane p 269 A92-21010
Polymer blends, volume 1
[AD-A252112] p 987 N92-31419

AIRCRAFT SPIN
Wichita State University 1986 aviation safety research projects
[DOT/FAA/CT-91/4] p 263 N92-16986
Surface pressure measurements on the wing of a wind tunnel model during steady rotation
[AD-A243047] p 260 N92-17281

AIRCRAFT STABILITY
Experimental determination of the center of mass, the principal central axes of inertia and moments of inertia --- aircrafttt models applied to real aircraf p 40 A92-12346
Supersonic boundary-layer stability analysis on an aircraft wing p 9 A92-13207
Analysis of criteria predicting the tendency of pilot induced oscillation for linear non-linear system p 133 A92-15340
X-29 high angle of attack p 111 A92-16052
Optimization of the aerodynamic balance and parameters of the horizontal tail surfaces of the three-surface aircraft configuration with allowance for the capabilities of the stability and control augmentation system p 134 A92-16803
Regulation of relaxed static stability aircraft p 203 A92-18463
Dynamics of hang-gliders p 204 A92-18608
Roll-performance criteria for high augmented aircraft p 204 A92-18623
Forward-look wind-shear detection for microburst recovery p 378 A92-24408
The stability analysis of the nonlinear shimmy p 358 A92-27902
A new approach to determining control surface's moments of inertia with test-twice vibrations approach p 379 A92-27914
Abstract model and controller design for an unstable aircraft p 380 A92-28153
Hover control of a PVTOL using nonlinear regulator theory p 478 A92-29171
Estimating the probability of a safe flight for an aircraft flying under the effect of disturbances p 479 A92-30132
Dynamics of helicopter tip-over during taxiing p 479 A92-30149
Analysis of the stability of the lateral motion of aircraft p 480 A92-30191
Aircraft control and simulation --- Book
[ISBN 0-471-61397-5] p 480 A92-31021
Digital time series analysis for flutter test data
[AIAA PAPER 92-2103] p 589 A92-35674
Robustness characteristics of fast-sampling digital controllers for active flutter suppression
[AIAA PAPER 92-2104] p 567 A92-35675
An analytical and experimental investigation of flutter suppression via piezoelectric actuation
[AIAA PAPER 92-2106] p 567 A92-35677
Dynamics of helicopters in ground resonance with and without blade dissimilarities
[AIAA PAPER 92-2108] p 544 A92-35679
Helicopter in-flight frequency response test techniques p 548 A92-35938
A separated algorithm and application to flight test p 690 A92-38273
A review of recent programs and future plans for rotorcraft in-flight simulation at Ames Research Center
[SAE PAPER 912121] p 608 A92-39969
An automated workstation for the half-scale testing of the flight vehicle stabilization circuit p 664 A92-40622
Flight evaluations on in-flight simulation of unstable aircraft p 744 A92-43115
An acrobatic airship 'Acrostat'
[SAE PAPER 911994] p 843 A92-45396
Computational aspects of helicopter trim analysis and damping levels from Floquet theory p 875 A92-46933
Analysis of the VISTA longitudinal simulation capability for a cruise flight condition p 876 A92-48488
Robust flight control systems - A parameter space design p 976 A92-50503
Aircraft longitudinal dynamics equations including wind shear effects p 977 A92-51946
Nonlinear dynamic stability characteristics of recovery bodies p 977 A92-52041
Static and dynamic flight-path stability of airplanes p 977 A92-52043
Algorithmic improvements for simulator motion drive
[AIAA PAPER 92-4158] p 1007 A92-52448
The VISTA/F-16 programmable feel system
[AIAA PAPER 92-4172] p 977 A92-52457
A study on the stability of aircraft at high angles-of-attack and state vector propagation sensitivity p 978 A92-53394
Parameter estimation of an augmented airplane with unsteady aerodynamics modelling p 1073 A92-53546
AIAA Atmospheric Flight Mechanics Conference, Hilton Head Island, SC, Aug. 10-12, 1992, Technical Papers. Pts. 1-2 p 1078 A92-55326
Stability, control and gust response characteristics of an ultralight freewing airplane
[AIAA PAPER 92-4342] p 1079 A92-55331
Development of a high-angle-of-attack stability and control prediction code
[AIAA PAPER 92-4354] p 1079 A92-55340
Navier-Stokes prediction of large-amplitude delta-wing roll oscillations characterizing wing rock
[AIAA PAPER 92-4428] p 1080 A92-55352
Stochastic self-induced roll oscillations of slender delta wing at high angles of attack
[AIAA PAPER 92-4498] p 1081 A92-55366
Application of recursive partially unknown system identification to aerodynamic coefficients estimation
[AIAA PAPER 92-4504] p 1081 A92-55371
Parameter identification of AV-8B wingborne aerodynamics for flight simulator model updates
[AIAA PAPER 92-4506] p 1027 A92-55373
Aerodynamic analysis of the Pioneer unmanned air vehicle
[AIAA PAPER 92-4635] p 1027 A92-55382
Motion analysis of 2-dimensional flat plate in ground effect p 1030 A92-56053
Flight research p 194 N92-13981
Formulation of a strategy for monitoring control integrity in critical digital control systems
[NASA-TM-104158] p 206 N92-15075
Identification of the stability and control derivatives of a DLC-flap system for VSRA
[NAL-TR-1116] p 283 N92-17917
Dynamic flying investigations on 1/13.5 NALLA model (Longitudinal Results)
[NAL-PD-FC-9113] p 359 N92-18073
Aircraft aerodynamics and stability and control during air-to-air refueling
[AERO-REPT-9017] p 380 N92-18321
Some interesting phenomena from Lavi test flights relating to aircraft stability and control
[IAITIC-91-1017] p 482 N92-20849
Evaluating fixed wing aircraft in the aircraft carrier environment p 464 N92-21963
F-111C flight dynamic model aerodynamic data-base development and verification
[AD-A246356] p 715 N92-26947
Hot-gas reingestion engine response considerations
[PNR-90810] p 740 N92-27042
Nonlinear stability and control study of highly maneuverable high performance aircraft, phase 2
[NASA-CR-190667] p 978 N92-30922
Vortex flow aerodynamics
[AGARD-AR-299] p 946 N92-30947

AIRCRAFT STRUCTURES
New thermoplastic composites for aircraft structures and interiors p 34 A92-10271
The study on the composite-patching repairs for metallic aircraft structures p 36 A92-10285

Applied fracture mechanics research in the aerospace field p 37 A92-10375
Computer simulation of weapon blast pressures on flexible surfaces p 39 A92-12115
Light metal materials for aircraft structure p 140 A92-13444
Laser-based ultrasonics on GR/epoxy composite - Interferometric detection p 144 A92-13554
Evaluation of thermoplastic matrix composites for use in energy-absorbing helicopter subfloors p 141 A92-14374
Committees, their importance to the structures of the Helicopter Association International p 59 A92-14411
Corrosion prevention field test utilizing water displacement compounds p 110 A92-14436
Certifying composite helicopter structures p 110 A92-14443
Effect of the wake flow on the soundproofing of aircraft structures p 166 A92-16824
A study of a version of the boundary conditions of a two-dimensional spline in surface and line modeling p 163 A92-16826
The designer-FEM model interface based on the data base management concept p 163 A92-16832
Lightning protection for the Dornier 328 p 113 A92-17253
Enhanced visual technique for rapid inspection of aircraft structures p 214 A92-17290
Rapid ultrasonic scanning of aircraft structures p 215 A92-17292
Cabin structural vibration and noise for transport aircraft p 192 A92-17876
Rolling in the tolerance p 216 A92-18005
Some results on metal and composite patch reinforcement of aluminum honeycomb panel p 216 A92-18830
Fatigue and damage tolerance verification of aircraft structures p 217 A92-19677
Aging aircraft programme entails major effort and expense p 169 A92-20023
Forebody vortex control with miniature, rotatable nose-boom strakes
[AIAA PAPER 92-0022] p 281 A92-22144
Efficient evaluation of the flexibility of tapered I-beams accounting for shear deformations p 295 A92-23269
Progress towards fiber optic smart structures at UTIAS p 368 A92-24781
Smart skins and fiber-optic sensors application and issues p 368 A92-24785
Weaving an aircraft p 392 A92-24911
Ultimate strength prediction of ASTM D - 3039 tensile specimens from acoustic emission amplitude data
[AIAA PAPER 92-0258] p 394 A92-25716
Development of a sensor for the detection of aircraft wing contaminants
[AIAA PAPER 92-0300] p 369 A92-25752
A superelement simplified analysis for the vibration systems of the complex structures p 398 A92-27903
Models of space-averaged energetics of plates p 398 A92-28031
Investigation on opening and ejection of an aircraft canopy by using a solid rocket engine p 358 A92-28489
Thermal imaging of graphite/epoxy composite samples with fabricated defects p 491 A92-28655
Thin bondline measurement of adhesively bonded metallic aircraft structures using an ultrasonic analyzer p 491 A92-28684
X-ray computed tomographic inspection of castings p 492 A92-28725
Nortec 30 Eddyscan - Portable flaw imaging for aging aircraft p 492 A92-28745
The reinforcing effect of composite patch repairs on *metallic aircraft structures* p 419 A92-30498
Structures and materials technologies for hypersonic vehicles - Lessons from Hermes experience
[AIAA PAPER 91-5098] p 486 A92-31697
Structural materials for NASP
[AIAA PAPER 91-5101] p 486 A92-31698
A study of flow of a fluid film on the surface of a plate *in the case of slot injection* p 496 A92-31892
A procedure for calculating the static aeroelasticity characteristics of flight vehicles by the influence coefficient method using three-dimensional finite element schemes p 460 A92-31896
Airflow effects about PMS probes on the DLR Falcon --- Particle Measuring System for atmospheric research aircraft p 467 A92-32060
Surfprep flash-lamp depaint system evaluation p 497 A92-32411
Design, analysis, testing, and certification of composite primary structure for the Piaggio P-180 Avanti p 535 A92-32553
Approximate closed-form buckling solutions for the optimization of aircraft structures p 579 A92-32578
Study of materials and structures for the High-Speed Civil Transport
[AIAA PAPER 92-1080] p 536 A92-33249
Dynamic synthesis of mechanical systems with a finite number of degrees of freedom p 603 A92-33790
Coupled analysis of independently modeled finite *element subdomains*
[AIAA PAPER 92-2235] p 581 A92-34289
A Rayleigh-Ritz design methodology for cutouts in composite structures
[AIAA PAPER 92-2278] p 582 A92-34297
An independent refinement and integration procedure in multiregion finite element analysis
[AIAA PAPER 92-2290] p 582 A92-34307
The equations governing the motion of wing-aileron structural systems constructed from advanced anisotropic composite materials
[AIAA PAPER 92-2469] p 564 A92-34359
Experimental and analytical study of the effects of floor location on response of composite fuselage frames
[AIAA PAPER 92-2473] p 539 A92-34362
Response of plate-like structures to correlated random pressure fluctuations
[AIAA PAPER 92-2378] p 584 A92-34452
Time simulation of flutter with large stiffness changes
[AIAA PAPER 92-2394] p 585 A92-34467
Computational structures technology
[AIAA PAPER 92-2442] p 585 A92-34473
Chaotic and nonlinear dynamic response of aerosurfaces with structural nonlinearities
[AIAA PAPER 92-2547] p 518 A92-34517
Structural optimization at Aerospatiale Aircraft
[AIAA PAPER 92-2371] p 601 A92-34542
Application of analytical and design tools for fighter wing aeroelastic tailoring
[AIAA PAPER 92-2373] p 542 A92-34543
New complex pole and gust response approximations for integrated aeroservoelastic synthesis
[AIAA PAPER 92-2377] p 565 A92-34547
Combined compressive and shear buckling analysis of hypersonic aircraft sandwich panels
[AIAA PAPER 92-2487] p 586 A92-34603
Removing aircraft surface coatings p 516 A92-35574
Low profile microsensor for aerodynamic pressure measurement p 555 A92-35949
Performance of aluminum honeycomb panels with structural defects and core anomalies. II - Specimen description and test results p 591 A92-36156
Dimensional characterization of a large aircraft structure by photogrammetry p 607 A92-37061
Laboratory testing of a high transmission loss aircraft cabin structure p 663 A92-39229
Aircraft structural design p 643 A92-39304
Inspection of composite structures p 676 A92-40882
The evolution from bonded F27 aircraft to Arall structures p 699 A92-41177
Technological excellence in honeycomb sandwich and composite structures for aerospace applications p 757 A92-41180
Thermal structures - Four decades of progress p 729 A92-41239
Structure-borne noise transmission in the Propfan Test Assessment aircraft p 778 A92-41240
On the three-dimensional vibration analysis of simultaneously skewed and twisted cantilevered parallelepipeds p 759 A92-41801
The evaluation of non-tank surface treatments for *aluminium bonding repairs* p 761 A92-42502
Bayesian reliability analysis in connection with the evaluation of multiple-site damage p 762 A92-43126
A study of aircraft surface coating technology p 700 A92-43147
WIG transportation efficiency considering the influence of no-load situation p 781 A92-43241
The concept of an unmanned flying vehicle at high altitude p 731 A92-43242
Stringer subsystem automation p 700 A92-43246
Development of an automatic metal sheet working machine for interior structure p 700 A92-43247
Analysis and testing of a composite sandwich shell horizontal tail p 755 A92-44617
International Congress on Recent Developments in Air- *and Structure-Borne Sound and Vibration*, Auburn University, AL, Mar. 6-8, 1990, Proceedings. Vols. 1 & 2 p 924 A92-45876
The relationship between mode localization and energy transmission parameters in the vibration of coupled structures p 925 A92-45921
Strength evaluation and safety of machine/structure. III - Case examples on strength and safety evaluation of machine/structure 3.2 aircraft (airframe) p 882 A92-47303
Low VOC primer for structural bonding --- volatile organic compound p 892 A92-47338
Design and use of aramid fiber in aircraft structures p 784 A92-47407
Resin transfer molding of a complex composite aircraft structure p 784 A92-47410
Tooling for C-17 composite parts p 900 A92-47412
Use of adhesive bonded attachments for a composite aircraft fuel tank p 785 A92-47414
Research of environmental spectrum for aircraft structure p 785 A92-47655
Cptimal maintenance program of damage tolerance structure p 785 A92-47660
Sonic fatigue analysis and anti-sonic fatigue design of aircraft structure p 848 A92-47666
A failure analysis for landing gear structural system p 849 A92-47667
Addressing the challenge of aircraft component design and manufacture from metal matrix composites p 985 A92-50007
Research on sonic fatigue calculation and test for aircraft panel p 958 A92-50203
Combined application of the energy method and the *weighted residual method - A new way to construct the* finite elements p 991 A92-50239
Thermal-structural panel buckling tests p 993 A92-51409
Impact damage tolerance of helicopter sandwich structures p 958 A92-51506
New thermoplastic polyimide composite for supersonic aircraft structures p 985 A92-51512
KGR-1 thick adherend specimen evaluation for the determination of adhesive mechanical properties p 994 A92-51513
Characterization of stainless steel pretreatments for adhesive bonding p 994 A92-51546
Development of composite structures with enhanced damage tolerance p 985 A92-51555
Damage tolerance and durability design of composite aircraft structures p 996 A92-53067
From fatigue test life to structure safe life p 997 A92-53099
Calculation of the exerting force necessary to form the aircraft hull plate in the symmetry plate bender with three rolls and the feeding value of the centre roll p 998 A92-53297
New materials drive high-performance aircraft p 1105 A92-55134
New literal approximations for the longitudinal dynamic *characteristics of flexible flight vehicles*
[AIAA PAPER 92-4411] p 1075 A92-55205
E-6 flutter investigation and experience
[AIAA PAPER 92-4601] p 1077 A92-55280
Optimization of composite material wing of fighter type aircrafts p 1053 A92-56018
Application of X-ray image radiography system for aircraft p 1118 A92-56084
Development of aircraft bonded structure and the NDI method p 1016 A92-56100
Mechanical properties of laminate aluminum matrix composites p 1106 A92-56102
Titanium alloy casting for aerospace p 1106 A92-56103
Effects of spectrum variations on fatigue crack growth p 1123 A92-57399
Nonlinear aspects of aerospace structures at high excitation levels flat aluminum beams and plates studied
[AD-A240600] p 44 N92-11383
Corrosion and your aircraft
[NRC-30465] p 114 N92-11991
A proposed composite repair methodology for primary structure
[NRC-LTR-ST-1658] p 115 N92-13056
Detailed analysis and test correlation of a stiffened composite wing panel
[NASA-TM-104154] p 159 N92-13460
Preservation and utilization of finite element models of USAF aircraft structures
[AD-A241657] p 160 N92-13470
Mechanical qualification tests for materials used in the fabrication of aircraft parts
[CEAT-M5-5443/01] p 195 N92-14042
Structural considerations for aircraft payload Modification: P-3C zero fuel weight increase
[AD-A242690] p 196 N92-15068
Rapid repair of integrally stiffened carbon fibre composite structures by bolted *aluminium elements*
[MBB-FE202-S-PUB-0453-A] p 290 N92-17310
Explicit finite element method for transparency impact analysis
[AD-A243527] p 264 N92-17478
Institute for experimental fluid mechanics: Results for 1990
[IB-222-90-A-46] p 400 N92-18244
Fatigue Management
[AGARD-CP-506] p 360 N92-18571
The development of fatigue management requirements and techniques p 360 N92-18572

Fatigue safety factor: Assessment of associated safety level p 401 N92-18573
Probabilistic design and fatigue management based on probabilistic fatigue models with reliability updating p 360 N92-18574
Aging aircraft structural damage analysis p 360 N92-18575
A probabilistic procedure for aircraft fleet management p 360 N92-18576
Fatigue life behaviour of composite structures p 390 N92-18577
Aircraft tracking optimization of parameters selection p 361 N92-18585
Life management approach for USAF aircraft p 362 N92-18587
Structural airworthiness of aging Boeing jet transports p 362 N92-18590
Aircraft fatigue management in the Royal Air Force p 363 N92-18591
Tornado structural fatigue life assessment of the German Air Force p 363 N92-18592
Fatigue management for the A-7P p 363 N92-18593
Managing airborne assets through loads monitoring p 363 N92-18594
Approach to crew training in support of the USAF Aircraft Structural Integrity Program (ASIP) p 363 N92-18595
Development and characterization of Powder Metallurgy (PM) 2XXX series Al alloy products and Metal Matrix Composite (MMC) 2XXX Al/SiC materials for high temperature aircraft structural applications
[NASA-CR-187631] p 390 N92-19290
Finite element analysis of a riveted repair on a curved composite panel
[AD-A243916] p 404 N92-19384
Integrated aerodynamic-structural-control wing design p 349 N92-19698
Manx: Close air support aircraft preliminary design
[NASA-CR-189992] p 463 N92-21565
The Guardian: Preliminary design of a close air support aircraft
[NASA-CR-189991] p 463 N92-21566
A-2000: Close air support aircraft design team
[NASA-CR-190022] p 463 N92-21567
Advisory Circular: Corrosion control for aircraft
[FAA-AC-43-4A] p 420 N92-21834
Materials and Structures Research Department: Scientific report (1990)
[ETN-92-90727] p 466 N92-22000
Report on aerospace structures and structural materials R and D in Europe
[PB92-123553] p 550 N92-22785
Integrated Design Analysis and Optimisation of Aircraft Structures
[AGARD-R-784] p 550 N92-23227
Application of an automated multidisciplinary analysis and optimisation system to the design of aircraft structures p 551 N92-23233
First approach to an integrated fin design p 551 N92-23236
A fin optimisation study p 551 N92-23237
Structural optimization of aircraft practice and trends p 551 N92-23239
Prediction of response of aircraft panels subjected to acoustic and thermal loads
[NASA-CR-190305] p 678 N92-24345
Vibroacoustic simulation of an airplane structure p 629 N92-24871
The NASA/industry Design Analysis Methods for Vibrations (DAMVIBS) Program: A government overview
[NASA-TM-107579] p 680 N92-25267
Computational Structures Technology for Airframes and Propulsion Systems
[NASA-CP-3142] p 683 N92-25911
Computational structures technology and UVA Center for CST p 683 N92-25912
Computer codes developed and under development at Lewis p 692 N92-25913
A brief overview of computational structures technology related activities at NASA Lewis Research Center p 683 N92-25915
CSM activities at the NASA Langley Research Center p 683 N92-25916
Analysis and design technology for high-speed aircraft structures p 684 N92-25918
Large scale optimization using ASTROS: An overview p 649 N92-25921
Overview of computational structural methods for modern military aircraft p 684 N92-25928
A preliminary study on damage detection using piezoelectric film
[AD-A246350] p 733 N92-28118
Integrated Design Analysis and Optimisation of Aircraft Structures
[AGARD-LS-186] p 851 N92-28469
Practical architecture of design optimisation software for aircraft structures taking the MBB-Lagrange code as an example p 851 N92-28471
Structural optimization of aircraft p 851 N92-28472
Multidisciplinary design and optimization
[AGARD-PAPER-2] p 851 N92-28473
Paint removal using cryogenic processes
[AD-A247668] p 895 N92-28912
Concurrent engineering in design of aircraft structures
[MBB-FE-2-S-PUB-472] p 854 N92-29650
The 1991 International Conference on Aging Aircraft and Structural Airworthiness
[NASA-CP-3160] p 912 N92-30106
Structural integrity of future aging airplanes p 913 N92-30107
Maintaining the safety of an aging fleet of aircraft p 837 N92-30108
Performance of fuselage pressure structure p 913 N92-30109
Fracture mechanics research at NASA related to the aging commercial transport fleet p 913 N92-30110
Preliminary results on the fracture analysis of multi-site cracking of lap joints in aircraft skins p 913 N92-30111
Current DOT research on the effect of multiple site damage on structural integrity p 913 N92-30112
Damage tolerance for commuter aircraft p 914 N92-30114
Inspection of aging aircraft: A manufacturer's perspective p 914 N92-30117
NDE research efforts at the FAA Center for Aviation Systems Reliability p 914 N92-30119
Aging aircraft NDI Development and Demonstration Center (AANC): An overview --- nondestructive inspection p 915 N92-30120
Nondestructive inspection perspectives p 915 N92-30121
Current and future developments in civil aircraft non-destructive evaluation from an operator's point of view p 787 N92-30122
Nonlinear analyses of composite aerospace structures in sonic fatigue
[NASA-CR-190565] p 854 N92-30209
In-service evaluation of 2090 aluminum-lithium alloy on F/A-18 aircraft
[AD-A248472] p 986 N92-30321
MBB-LAGRANGE: A general structural reliability and optimization structural system
[MBB/FW321/S/PUB/467] p 998 N92-30423
Multidisciplinary optimization of fiber composite aircraft structures
[MBB/FW321/S/PUB/476] p 961 N92-30424
Activities of the Aeronautical Research Laboratory p 1013 N92-30768
Aging fleet: Maintaining airworthiness p 953 N92-31862
Analysis of three icing test flights reaching the aircraft-referred icing degree of severe
[ESA-TT-1254] p 954 N92-31943
A Protection And Detection Surface (PADS) for damage tolerance p 1107 N92-32523
Global/local methods research using the CSM testbed p 1107 N92-32528
Evaluation of composite components on the Bell 206L and Sikorsky S-76 helicopters p 1107 N92-32575
Damage tolerance certification methodology for composite structures p 1108 N92-32579
Detection of honeycomb damage using hexagonal grid discontinuities
[DREP-89-9] p 1109 N92-32846
Aspects of compression in aerospace composites: Future requirements p 1109 N92-33036
Evaluation of the effects of the environment on the behavior of the primary structures of composite material aircraft in service: Historic and current situation p 1110 N92-33048
Computational methods for global/local analysis
[NASA-TM-107591] p 1125 N92-33104
Lightning strike tests of composite connectors
[AD-A252281] p 1044 N92-33249
Development of 3D electromagnetic modeling tools for airborne vehicles
[NASA-CR-190810] p 1126 N92-33307
Current nondestructive inspection methods for aging aircraft
[DOT/FAA/CT-91/5] p 1126 N92-33480
Inspection of fabricated fuselage panels using electronic shearography
[DOT/FAA/CT-TN92/26] p 1127 N92-33627
Activities report of the National Aerospace Laboratory
[ETN-92-92053] p 1143 N92-33694
Effects of constraint on crack growth under aircraft spectrum loading
[NASA-TM-107677] p 1128 N92-34178
Advanced airframe structural materials: A primer and cost estimating methodology
[AD-A253371] p 1062 N92-34182

AIRCRAFT SURVIVABILITY

Value of survivability enhancement techniques p 59 A92-14349
Effects of ionizing and nonionizing radiation on aircraft p 295 A92-23301
Controlling radar signature p 967 A92-52018
The challenge of commercial aircraft survivability p 931 A92-52022
The SnoDog: Preliminary design of a close air support aircraft
[NASA-CR-189990] p 462 N92-21489
Aging fleet: Maintaining airworthiness p 953 N92-31862

AIRCRAFT TIRES

Aircraft landing-induced tire spinup p 193 A92-20209
Reduced basis technique for evaluating the sensitivity coefficients of the nonlinear tire response
[AIAA PAPER 92-2530] p 583 A92-34376
Determination of tire-wheel interface loads for aircraft wheels
[AIAA PAPER 92-2482] p 543 A92-34599
Cut progression during dynamometer testing of foreign object damaged type VII extra high pressure aircraft tires
[SAE PAPER 912155] p 644 A92-39990
Runway drainage characteristics related to tire friction performance
[SAE PAPER 912156] p 664 A92-39991
26 x 6.6 radial-belted aircraft tire performance
[SAE PAPER 912157] p 644 A92-39992
Finite element analysis of tire critical speeds p 762 A92-42949
Behavior of aircraft tire coupons under various loading conditions
[AD-A241416] p 116 N92-13063
Foreign object damage to tires operating in a wartime environment
[AD-A247195] p 724 N92-27682

AIRCRAFT WAKES

The dynamic character of the wake of an axisymmetric body at an angle of attack
[AIAA PAPER 91-3268] p 8 A92-12741
Effect of the wake flow on the soundproofing of aircraft structures p 166 A92-16824
Numerical and experimental analysis of vortex sheets behind lifting surfaces
[AIAA PAPER 92-0409] p 325 A92-26262
Effect of wing tip vortices on a trailing aircraft p 935 A92-50303
Computation of vortex wake flows and control of their effects on trailing wings
[AIAA PAPER 92-4429] p 1025 A92-55353
On aircraft wake properties and some methods for stimulating decay and breakdown of tip vortices p 87 N92-13021
Numerical simulation of vortex flows past impulsively started wings p 88 N92-13028
Analytical/numerical matching and periodic inversion: Two advances in free wake analysis p 178 N92-13994
An experimental study of a turbulent wing-body junction and wake flow
[AD-A243388] p 260 N92-17222
Vortex characteristics of C5A/B, C141B and C130E aircraft applicable to ATC terminal flight operations tower fly-by-data
[PB92-114586] p 449 N92-20318
Trajectories and stability of trailing vortices very near the ground
[NRC-32151] p 716 N92-27344
Viscous effects on a vortex wake in ground effect
[NASA-CR-190400] p 907 N92-28361

AIRFIELD SURFACE MOVEMENTS

Airport Surface Traffic Automation p 95 A92-16228
Madrid's double airport p 138 A92-16231
An electronically scanned precision runway monitor p 98 A92-16654
Dynamics of helicopter tip-over during taxiing p 479 A92-30149
Runway incursions and airport surface traffic automation
[SAE PAPER 912123] p 635 A92-39970
A proposed method for evaluating runway roughness p 748 A92-43125
Real-time control tower simulation for evaluation of airport surface traffic automation p 879 A92-44976
Use of high-fidelity simulation in the development of an F/A-18 active ground collision avoidance system
[AIAA PAPER 92-4140] p 959 A92-52434
Evaluation of two high-speed runway exits
[DOT/FAA/CT-TN91/36] p 31 N92-11021

Surface painted taxiway markings at Seattle-Tacoma International Airport
[DOT/FAA/CT-TN91/49] p 32 N92-11029
Electronic systems in transportation
[TP-9983] p 189 N92-14009
A Taxi And Ramp Management And Control system (TARMAC) p 207 N92-14027
Runway exit designs for capacity improvement demonstrations. Phase 2: Computer model development
[NASA-CR-190166] p 484 N92-21162
Testing concept of a movement area guidance
p 641 N92-25597

AIRFOIL FENCES
Studies of gas turbine heat transfer: Airfoil surfaces and end-wall cooling effects
[AD-A244055] p 376 N92-19097

AIRFOIL OSCILLATIONS
Dynamic characterization and identification of nonlinear systems application to aeronautical structures
p 39 A92-11830
A numerical simulation of separated flows around bodies p 8 A92-12423
Investigation of unsteady excitation effects on aerodynamic properties of airfoils p 66 A92-15335
Analysis of criteria predicting the tendency of pilot induced oscillation for linear non-linear system
p 133 A92-15340
Inviscid-viscous coupled solution for unsteady flows through vibrating blades. II - Computational results
[ASME PAPER 91-GT-126] p 71 A92-15571
An experiment on unsteady flow over an oscillating airfoil
[ASME PAPER 91-GT-181] p 73 A92-15613
The position of the unsteady flow computation in the compressor and turbine design and analysis process
[AIAA PAPER 92-0015] p 278 A92-22137
Unsteady Euler solution for oscillatory airfoil and oscillating flap
[AIAA PAPER 92-0131] p 252 A92-23751
Leading edge velocity field of an oscillating airfoil in compressible dynamic stall
[AIAA PAPER 92-0193] p 257 A92-23802
Time marching integral equation method for the solutions of unsteady transonic flows p 314 A92-25129
Theoretical study on the unsteady aerodynamic characteristics of an oscillating cascade with tip clearance (In the case of loaded cascade) p 331 A92-26797
Oscillating two-dimensional hypersonic airfoils at small angles of attack p 340 A92-28042
Unsteady airfoil flow solutions on moving zonal grids
[AIAA PAPER 92-0543] p 342 A92-28200
Characteristics of the phugoid motion of nonmaneuverable aircraft p 480 A92-30190
Experiment on pitching moments of separated flow around airfoil profiles p 429 A92-30527
Unsteady transonic Euler solutions using finite elements
[AIAA PAPER 92-2504] p 518 A92-34499
Unsteady aerodynamic characteristics of a dual-element airfoil
[AIAA PAPER 92-2508] p 518 A92-34501
Chaotic and nonlinear dynamic response of aerosurfaces with structural nonlinearities
[AIAA PAPER 92-2547] p 518 A92-34517
An investigation of cascade flutter using a two-dimensional full-potential solver
[AIAA PAPER 92-2119] p 558 A92-35688
The numerical simulation of transonic inviscid flow over oscillating airfoils p 616 A92-38918
Oscillating airfoil velocity field during large amplitude dynamic stall p 622 A92-40171
Vortex interaction in the wake behind an oscillating airfoil p 623 A92-40175
Data analysis for unsteady turbulence measurements over airfoils p 701 A92-41214
Design and development of a compressible dynamic stall facility p 747 A92-41215
Comment on 'Transition effects on airfoil dynamics and implications for subscale tests' p 703 A92-41247
Experimental and numerical investigations on separated flows around pitching airfoils p 710 A92-43166
Buffeting characteristics of a transonic airfoil
p 711 A92-43202
Numerical simulations of separated flows around oscillating airfoil for dynamic stall phenomena
[SAE PAPER 911991] p 788 A92-45393
Experimental investigation of the flowfield of an oscillating airfoil
[AIAA PAPER 92-2622] p 793 A92-45494
Airfoil pressure measurements during oblique shock wave-vortex interaction in a Mach 3 stream
[AIAA PAPER 92-2631] p 795 A92-45503
Spatial and temporal adaptive procedures for the unsteady aerodynamic analysis of airfoils using unstructured meshes
[AIAA PAPER 92-2694] p 800 A92-45540
Time accurate computation of unsteady transonic flows around an airfoil with oscillating flap on dynamic grid
[AIAA PAPER 92-2733] p 805 A92-45567
A numerical study of control surface buzz using computational fluid dynamic methods
[AIAA PAPER 92-2654] p 806 A92-45578
Nonuniform motion of leading-edge vortex breakdown on ramp pitching delta wings p 808 A92-45828
Self-induced roll oscillations of low-aspect-ratio rectangular wings p 874 A92-46802
Numerical solutions of unsteady oscillating flows past an airfoil
[AIAA PAPER 92-3212] p 825 A92-48817
Analysis of the onset of dynamic stall
p 1024 A92-54919
Vortical flow computations on a flexible blended wing-body configuration p 1024 A92-54922
The vortical structure in the wake during dynamic stall
[AIAA PAPER 92-4496] p 1026 A92-55364
Tow-tank study of nonlinear aerodynamics of a 2-D airfoil
[AIAA PAPER 92-4499] p 1026 A92-55367
Understanding and development of a prediction method of transonic limit cycle oscillation characteristics of fighter aircraft
[AIAA PAPER 92-4501] p 1026 A92-55369
Computing high-speed flows past an oscillating cylinder near a vertical wall
[AIAA PAPER 92-4653] p 1028 A92-55397
On the structure of unsteady shock induced separation of the transonic airfoil in the NAL two-dimensional wind tunnel p 1029 A92-56010
Wind tunnel blockage effects on slender wings undergoing large amplitude motions
[AIAA PAPER 92-3926] p 1096 A92-56757
Numerical investigation of the effect of leading edge geometry on dynamic stall of airfoils
[AD-A239949] p 12 N92-10015
Downwash measurements on a pitching canard-wing configuration
[AD-A239956] p 12 N92-10016
Aerodynamic coefficients of a symmetrical airfoil in an oscillating flow
[AD-A241073] p 89 N92-13035
Unsteady flows in rotor-stator cascades
[AD-A241593] p 158 N92-13410
Non-linear airloads hypersurface representation: A time domain perspective p 346 N92-18783
A quantitative study of unsteady compressible flow on an oscillating airfoil
[AD-A244572] p 445 N92-21012
Laser velocimetry measurements of oscillating airfoil dynamic stall flow field
[AD-A244546] p 502 N92-21297
A computational investigation of airfoil stall flutter
[AD-A247302] p 947 N92-31300
Flutter in the transonic flight regime
p 1089 N92-34167

AIRFOIL PROFILES
Unsteady incompressible viscous flow past an airfoil
p 3 A92-10662
The just attached shock-wave at the leading edge of a profile p 3 A92-10663
Nonstationary forces on a wing airfoil
p 4 A92-10825
Effect of riblets on turbulence in the wake of an airfoil
p 5 A92-11051
Numerical solution of steady incompressible viscous flows over airfoils p 8 A92-12649
Solution of the Reynolds-averaged Navier-Stokes equations for transonic aerofoil flows p 9 A92-13198
Wall interference assessment/correction for transonic airfoil data p 30 A92-13214
Poststall airfoil response to a periodic freestream
p 10 A92-13218
Finite difference numerical prediction of aerodynamics of an airfoil flying over wavy wall p 64 A92-14033
Transient aerodynamic behaviours associated with stepwise incidence variation of airfoils
p 66 A92-15327
Computation of the potential flow through cascades using the conformal mapping and the singularity method
p 66 A92-15356
Eigenvalue calculation procedure for an Euler/Navier-Stokes solver with application to flows over airfoils p 170 A92-17429
Complex variable boundary element method for external potential flows p 172 A92-18353
Algebraic turbulence modeling for unstructured and adaptive meshes p 216 A92-18362
Numerical study on using sulfur hexafluoride as a wind tunnel test gas p 216 A92-18373
Influences of wind tunnel parameters on airfoil characteristics at high subsonic speeds
p 173 A92-18769
Heat transfer measurements from a smooth NACA 0012 airfoil p 218 A92-20215
Roughness effects on heat transfer from a NACA 0012 airfoil p 219 A92-20217
Vibration characteristics of pretwisted aerofoil cross-section blade packets under rotating conditions
p 219 A92-20756
Optimization of the three-dimensional shape of lifting bodies of small aspect ratio at hypersonic velocities
p 244 A92-21602
Adaptation methods for viscous flows
p 246 A92-21982
Navier-Stokes analysis of blunt trailing edge airfoils
[AIAA PAPER 92-0024] p 248 A92-22146
Aerodynamic design and optimization in one shot
[AIAA PAPER 92-0025] p 248 A92-22147
Nonequilibrium algebraic turbulence modeling considerations for transonic airfoils and wings
[AIAA PAPER 92-0026] p 248 A92-22148
An experimental system to investigate subsonic aeroelastic behavior of lifting surfaces
[AIAA PAPER 92-0061] p 250 A92-22176
Computation of transonic flow over an airfoil at large Reynolds numbers p 252 A92-23414
Grid studies for thin-layer Navier-Stokes computations of airfoil flowfields
[AIAA PAPER 92-0184] p 256 A92-23794
Navier-Stokes computation of airfoil in stall using algebraic Reynolds-stress model
[AIAA PAPER 92-0195] p 257 A92-23803
Prediction of turbulent flow behavior over a slotted flap p 309 A92-24407
Separation control using moving surface effects - A numerical simulation p 309 A92-24419
A new method for solving the kernel equations of transonic flows - An auxiliary kernel method
p 410 A92-25108
The study of inverse boundary layer algorithm for transonic flows over aerofoils p 315 A92-25140
Construction of aerodynamic profiles
p 315 A92-25299
Analysis of a 2-D airfoil motion flying in-proximity-to a wavy-wall surface-lifting surface-scheme
p 315 A92-25506
An interactive boundary-layer approach to multielement airfoils at high lift
[AIAA PAPER 92-0404] p 324 A92-26257
Efficient simulation of incompressible viscous flow over single and multi-element airfoils
[AIAA PAPER 92-0405] p 324 A92-26258
Automatic grid generation for iced airfoil flowfield predictions
[AIAA PAPER 92-0415] p 326 A92-26266
A turbulence model for iced airfoils and its validation
[AIAA PAPER 92-0417] p 326 A92-26267
A comparative study of turbulence models for overset grids
[AIAA PAPER 92-0437] p 327 A92-26284
Unsteady pressure field and vorticity production over a pitching airfoil p 330 A92-26416
Calculation of compressible boundary layer flow about airfoils by a finite element/finite difference method
[AIAA PAPER 92-0524] p 332 A92-26948
A variational method for solving the problem of motion of a profile of complex geometry in a fluid
p 397 A92-27482
Effect of airfoil (trailing-edge) thickness on the numerical solution of panel methods based on the Dirichlet boundary condition p 340 A92-28041
Optimized control of structured grids
p 429 A92-30520
Multi-block airfoil profile of grid formation
p 429 A92-30523
Experiment on pitching moments of separated flow around airfoil profiles p 429 A92-30527
The Bauer-Garabedian-Korn airfoil test in a two-dimensional wind tunnel p 429 A92-30532
Experimental and computational investigation of wind tunnel effects on airfoil flow fields
[AIAA PAPER 92-0672] p 431 A92-30624
Flow near the trailing edge of an airfoil
p 431 A92-31151
High aerodynamic loads on an airfoil submerged in an unsteady stream p 432 A92-31183
Time marching integral equation method for unsteady transonic flows around airfoils p 433 A92-31489
A new adaptive algorithm for turbulent flows
p 434 A92-31547
Optimization of a lifting surface for minimum induced drag p 437 A92-31853
Approximate determination of the effect of deviations of wing and tail geometry from design parameters on the drag coefficient of subsonic aircraft p 460 A92-31878
A numerical solution of inviscid transonic flow using the Boltzmann equation p 443 A92-32504

Unsteady transonic Euler solutions using finite elements
[AIAA PAPER 92-2504] p 518 A92-34499
Dynamic characteristics of a Benchmark models program supercritical wing
[AIAA PAPER 92-2368] p 571 A92-34596
Unsteady flow past an airfoil pitching at a constant rate p 610 A92-36826
Multipoint inverse airfoil design method based on conformal mapping p 610 A92-36827
A note on the Kutta condition in Glauert's solution of the thin aerofoil problem p 613 A92-37933
A flow visualization experiment on the unsteady flow around two-dimensional airfoil p 615 A92-38913
The numerical simulation of separation control using moving surface effect p 616 A92-38924
Bifurcation analysis of airfoils in incompressible flow p 623 A92-40580
Numerical predictions of transonic viscous flows around aerofoils through an Euler/boundary layer interaction method p 624 A92-40600
Prediction of separation point in compressible turbulent boundary layers by Green's lag-entrainment method p 700 A92-41178
Curvature effects for three-dimensional compressible boundary-layer stability p 701 A92-41207
Drag reduction of bluff bodies through momentum injection p 702 A92-41231
Wake effects on the prediction of transonic viscous flows around airfoils p 702 A92-41232
Domain-decomposition algorithm applied to multielement airfoil grids p 703 A92-41261
Measurements in a leading-edge separation bubble due to a simulated airfoil ice accretion p 723 A92-41262
Effect of acoustic excitation on stalled flows over an airfoil p 703 A92-41267
Computer simulation of an unsteady flow around an airfoil with a spoiler p 710 A92-43167
Recent airfoil tests in NAL 2D high Reynolds number wind tunnel p 748 A92-43171
Wing test at the cryogenic wind tunnel of the National Defense Academy p 749 A92-43199
The effectiveness of the warp shape airfoil of a supersonic transport p 711 A92-43203
Low-speed wind tunnel testing of a joined-wing airfoil p 711 A92-43229
Effectiveness of aircraft aerodynamic performance on each part of a joined wing p 712 A92-43230
Aerodynamic characteristics of a high-speed composite airfoil p 712 A92-43231
Measurements of the velocity and vorticity fields around a pitching airfoil
[AIAA PAPER 92-2626] p 794 A92-45498
Application of an unstructured Navier-Stokes solver to multi-element airfoils operating at transonic maneuver conditions
[AIAA PAPER 92-2638] p 796 A92-45507
Aircraft spoiler effects under wind shear
[AIAA PAPER 92-2642] p 796 A92-45509
Multi-point inverse design of an infinite cascade of airfoils
[AIAA PAPER 92-2650] p 797 A92-45517
Separation control on high Reynolds number multi-element airfoils
[AIAA PAPER 92-2636] p 806 A92-45575
Temporal adaptive Euler/Navier-Stokes algorithm involving unstructured dynamic meshes p 812 A92-46887
Analysis of motion of airfoil flying over wavy-wall surface (lifting surface method) p 818 A92-47100
The design and testing of an airfoil with hybrid laminar flow control
[ONERA, TP NO. 1992-22] p 822 A92-48585
Critical Mach number estimates for dense gases p 933 A92-49498
Design and optimization of airfoils in non-stalling incompressible flow with a prescribed range of the angle of attack p 933 A92-49556
A review of scale effects in unsteady aerodynamics p 934 A92-50121
A fast conformal mapping algorithm with no FFT p 1007 A92-50471
Effect of a deicing device on the induced drag of a lifting airfoil p 959 A92-51947
A direct viscous-inviscid interaction method for the flow calculation around airfoils p 936 A92-52028
Aerodynamic airfoils design by quasi-solutions method of inverse boundary-value problems p 1020 A92-53998
Analysis of the onset of dynamic stall p 1024 A92-54919
Grid studies for thin-layer Navier-Stokes computations of airfoil flowfields p 1025 A92-54935
Experimental evaluation of a 50-percent thick airfoil with blowing and suction boundary layer control
[AIAA PAPER 92-4500] p 1026 A92-55368
Direct simulation of low-density flow over airfoils p 1030 A92-56159
Forcing level effects of internal acoustic excitation on the improvement of airfoil performance p 1136 A92-56162
Two-fence concept for efficient trapping of vortices on airfoils p 1031 A92-56165
Downwash measurements on a pitching canard-wing configuration
[AD-A239956] p 12 N92-10016
Resolution of Navier-Stokes equations around profiles: Drag evolution
[ONERA-RTS-86/1685-AY-156A] p 43 N92-11310
Hydrodynamic flow visualization around an oscillating vane. Extension of study to the case of higher incidences and amplitudes and the starting off phase from permanent regime
[ONERA-RT-56/1369-AN] p 43 N92-11312
Wind tunnel tests on A4, A4.1, and A4.2 2-D airfoil models in the IAR 5-ft. wind tunnel: Boeing Commercial Airplane Company and Institute for Aerospace Research collaborative work program
[NRC-IAR-C3] p 81 N92-11975
Flapping inertia for selected rotor blades
[NASA-TM-104125] p 115 N92-13057
Review of aerodynamic design in the Netherlands p 193 N92-13929
Inverse airfoil design procedure using a multigrid Navier-Stokes method p 193 N92-13932
Analysis and design of transonic airfoils using streamwise coordinates p 194 N92-13955
Airfoil optimization with efficient gradient calculations p 177 N92-13960
Design optimization of transonic airfoils p 177 N92-13961
The benchmark aeroelastic models program: Description and highlights of initial results
[NASA-TM-104180] p 185 N92-15049
A turbulence model for iced airfoils and its validation
[NASA-TM-105373] p 186 N92-15052
Control of unsteady separated flow associated with the dynamic pitching of airfoils
[NASA-CR-189758] p 258 N92-15966
A method of estimating a flow breakdown boundary for aerofoils and swept wings in transonic flows
[ESDU-91021] p 258 N92-15970
Unsteady-flow-field predictions for oscillating cascades
[NASA-TM-105283] p 348 N92-19437
WP 4b compressible flow simulation: Information System for flow simulation based on the Navier-Stokes equation (ISNaS). Requirements grid generation for the ISNaS compressible flow solver
[NLR-TR-88103-U] p 405 N92-19490
Influence of airfoil geometry on delta wing leading-edge vortices and vortex-induced aerodynamics at supersonic speeds
[NASA-TP-3105] p 350 N92-20038
The FM-007: An advanced jet commuter for HUB to spoke transportation
[NASA-CR-189988] p 461 N92-20267
Fully integrated aerodynamic/dynamic optimization of helicopter rotor blades
[NASA-TM-104226] p 461 N92-20417
Blade-mounted trailing edge flap control for BVI noise reduction
[NASA-CR-4426] p 512 N92-21173
Grid generation and flow solution method for Euler equations on unstructured grids
[NASA-TM-4295] p 528 N92-23533
The benchmark aeroelastic models program: Description and highlights of initial results p 721 N92-27960
Automatic design of transonic airfoils to reduce the shock induced pressure drag p 949 N92-31863

AIRFOILS

Design and testing of a controlled diffusion airfoil cascade for industrial axial flow compressor application
[ASME PAPER 90-GT-140] p 6 A92-11286
Airfoil boundary layer measurements at low Re in an accelerating flow from a nonzero velocity p 62 A92-13673
Fundamental research in helicopter rotor blade-vortex interaction modeling p 65 A92-14358
An analysis of pitch and plunge effects on unsteady airfoil behavior p 65 A92-14359
Advanced ice protection systems test in the NASA Lewis Icing Research Tunnel p 108 A92-14406
Wind tunnel wall effects in a linear oscillating cascade
[ASME PAPER 91-GT-133] p 72 A92-15576
The experimental approach to the LEBU on turbulent drag reduction p 243 A92-21469
New nonequilibrium turbulence model for calculating flows over airfoils p 330 A92-26403
Zonal flow analysis method for two-dimensional airfoils p 330 A92-26435
Results of an icing test on a NACA 0012 airfoil in the NASA Lewis Icing Research Tunnel
[AIAA PAPER 92-0647] p 334 A92-27021
Analysis of a 2-D airfoil motion flying in-proximity-to a wavy-wall surface - Finite difference method p 421 A92-29517
Manufacture of XD gamma titanium aluminide airfoils via investment casting and machining p 494 A92-30603
An experimental study of the noise of flow past a wing at low velocities p 603 A92-33771
Aerodynamic analysis and modification design of NPU airfoils p 613 A92-38270
Investigation on effects on enhancing lift by acoustic excitation p 693 A92-38923
Subsonic and transonic low-Reynolds-number airfoils with reduced pitching moments p 701 A92-41211
Optimum hypersonic wings and wave riders p 706 A92-42531
An experimental investigation of the oblique blade-vortex interaction p 712 A92-43447
Computational evaluation of an airfoil with a Gurney flap
[AIAA PAPER 92-2708] p 802 A92-45550
Compressible Navier-Stokes solutions for a suction boundary control airfoil
[AIAA PAPER 92-2710] p 802 A92-45551
Active control of vortex structures in a separating flow over an airfoil
[AIAA PAPER 92-2728] p 804 A92-45563
Visualization of stopping flow over airfoils
[AIAA PAPER 92-2730] p 804 A92-45564
Prediction of the viscous transonic aerodynamic performance of supercritical aerofoil sections
[AIAA PAPER 92-2653] p 805 A92-45569
A compact higher order Euler solver for unstructured grids with curved boundaries
[AIAA PAPER 92-2696] p 807 A92-45590
An unstructured approach to the design of multiple-element airfoils
[AIAA PAPER 92-2709] p 807 A92-45592
Calculation of potential flow around airfoils using a discrete vortex method p 808 A92-45827
Time-average loading on a two-dimensional airfoil in a large amplitude motion p 811 A92-46805
Advanced pneumatic impulse ice protection system (PIIP) for aircraft p 845 A92-46807
Effect of model cooling on periodic transonic flow p 813 A92-46900
Experimental investigation of the parallel vortex-airfoil interaction at transonic speeds p 813 A92-46901
Unstructured and adaptive mesh generation for high Reynolds number viscous flows p 816 A92-47042
Anisotropic control of mesh generation based upon a Voronoi type method p 918 A92-47043
Adaptive parallel meshes with complex geometry p 918 A92-47050
Multi-block grid generation around wing-body-engine-pylon configurations p 817 A92-47060
3-D numerical grid generation for the transonic flow analysis about multi-bodies p 817 A92-47061
Orthogonal grids for multiple airfoils p 818 A92-47096
The numerical simulation of compressible flow around an airfoil at high angle of attack p 818 A92-47686
Airfoil wake and linear theory gust response including sub and superresonant flow conditions
[AIAA PAPER 92-3074] p 823 A92-48724
Flexible manufacturing in repair of gas turbine engine components
[AIAA PAPER 92-3524] p 786 A92-49049
On central-difference and upwind schemes p 1007 A92-50466
The wall interference correction and test data processing methods for airfoil wind tunnel test with endplates p 942 A92-53087
Preliminary airfoil testing experience in the NDA cryogenic wind tunnel p 1091 A92-54326
Shock detection on airfoils by means of piezo foil- and hot film arrays p 1115 A92-54334
The use of silicon microsensors in smart skins for aerodynamic research p 1116 A92-54348
Comparative numerical study of two turbulence models for airfoil static and dynamic stall
[AIAA PAPER 92-4649] p 1028 A92-55394
Evaluation of sidewall interference in the NAL two-dimensional transonic wind tunnel p 1092 A92-56011
BGK1 airfoil oilflow tests in the NAL two-dimensional wind tunnel. II p 1029 A92-56044
High subsonic wind tunnel test of a two-dimensional hybrid-laminar-flow-control airfoil with slotted surface p 1029 A92-56045

Experimental investigation of the boundary layer in a corner formed by two circular arc airfoils
p 1029 A92-56046
Design and wind tunnel test of low-Reynolds-number airfoil p 1029 A92-56047
Sound produced by vortex-airfoil interaction
p 1136 A92-56345
High-lift testing at high Reynolds numbers
[AIAA PAPER 92-3986] p 1033 A92-56810
Dual strain gage balance system for measuring light loads
[NASA-CASE-LAR-14419-1] p 42 N92-10185
Perfect compressible two dimensional boundary layer strong fluid coupling in the case of sharp leading edge profiles. Unsteady case of isolated profiles and steady case of blade grids
[ONERA-RT-43/1621-RY-006-R] p 43 N92-11311
The BCAC/IAR collaborative research program to investigate the sidewall boundary layer effects in the IAR/NRC 2-D High Reynolds Number Test Facility
[NRC-HSA-434] p 81 N92-11976
Experiences with optimizing airfoil shapes for maximum lift over drag p 90 N92-13838
Inverse airfoil design procedure using a multigrid Navier-Stokes method p 193 N92-13932
Application of direct inverse analogy method (DIVA) and viscous design optimization techniques
p 176 N92-13951
Study of a new airfoil used in reversible axial fans
p 177 N92-13970
Aerodynamics p 202 N92-13977
Airfoil Vibration Dampers program
[NASA-CR-184276] p 225 N92-14391
Results of an Icing test on a NACA 0012 airfoil in the NASA Lewis Icing Research Tunnel
[NASA-TM-105374] p 185 N92-15051
Experimental study of a vortex subjected to imposed strain
[NASA-CR-189757] p 258 N92-15969
Simplified method for the prediction of aerofoil excrescence drag magnification factor for turbulent boundary layers at subcritical Mach numbers
[ESDU-91028] p 259 N92-15972
Excrescence drag magnification factors at the drag-rise condition for aerofoils with a specified form of upper-surface pressure distribution
[ESDU-91029] p 259 N92-15973
Use of Navier-Stokes analysis in section design
[AD-A242074] p 299 N92-17168
Experimental ice shape and performance characteristics for a multi-element airfoil in the NASA Lewis Icing Research Tunnel
[NASA-TM-105380] p 261 N92-17347
Semi-empirical model for prediction of unsteady forces on an airfoil with application to flutter
[NASA-TM-105414] p 346 N92-18760
Thrust vector control of an overexpanded supersonic nozzle using pin insertion and rotating airfoils
[AD-A243891] p 387 N92-18942
Comparison of a two-dimensional adaptive-wall technique with analytical wall interference correction techniques
[NASA-TP-3132] p 444 N92-20494
Fatigue in single crystal nickel superalloys
[AD-A244815] p 489 N92-21015
The status of the US VAWT program
[DE92-002931] p 505 N92-21040
Evaluation of NACA0012 airfoil test results in the NAL two-dimensional transonic wind tunnel
[NAL-TR-1109T] p 445 N92-21287
Pressure and velocity measurements about an airfoil during a parallel blade-vortex interaction
p 446 N92-21429
The adverse aerodynamic impact of very small leading-edge ice (roughness) buildups on wings and tails
p 451 N92-21691
A summary of NASA research on effects of heavy rain on airfoils p 452 N92-21694
The measurement of water film thickness on airfoils in heavy rain conditions using conductance sensors
p 452 N92-21695
Experimental investigation of heavy rainfall effect on a 2-D high lift airfoil p 452 N92-21696
Aerodynamic effects of de/anti-icing fluids and description of a facility and test technique for their assessment p 452 N92-21697
The NASA Langley laminar-flow-control experiment on a swept, supercritical airfoil: Evaluation of initial perforated configuration
[NASA-TM-4309] p 525 N92-22196
SERI advanced wind turbine blades
[DE92-001216] p 598 N92-22971
Improved shock-capturing of Jameson's scheme for the Euler equations
[PB92-148758] p 596 N92-23251
Efficient and robust design optimization of transonic airfoils p 528 N92-23717
An incremental strategy for calculating consistent discrete CFD sensitivity derivatives
[NASA-TM-104207] p 625 N92-24681
Periodic Euler and Navier-Stokes solutions about oscillating airfoils p 626 N92-24850
Navier-Stokes simulation of dynamic stall on a rotating airfoil p 626 N92-24853
Performance degradation due to hoar frost on lifting surfaces p 628 N92-24866
Aerodynamic design and analysis of a light aircraft propeller p 629 N92-24876
Prediction and analysis of wing flutter at transonic speeds p 662 N92-25555
An outline of a numerical scheme for calculating two-dimensional time linearised transonic flow using the Green's function method
[AD-A246349] p 764 N92-26258
Distributed acoustic receptivity in laminar flow control configurations
[NASA-CR-4438] p 765 N92-26680
Modeling of heavy-gas effects on airfoil flows
[NASA-CR-190357] p 716 N92-27558
Computations of unsteady flows around airfoil sections by explicit and implicit methods solving the Euler and Navier-Stokes equations p 720 N92-27948
Further investigation of the effect of model cooling on periodic transonic flow p 721 N92-27961
Experimental and computational ice shapes and resulting drag increase for a NACA 0012 airfoil
[NASA-TM-105743] p 828 N92-28674
Results of a low power ice protection system test and a new method of imaging data analysis
[NASA-TM-105745] p 828 N92-28696
Study of the leading-edge vortex dynamics in the unsteady flow over an airfoil
[AD-A247532] p 829 N92-28865
Nonlinear normal and axial force indicial responses for a two dimensional airfoil
[AD-A247196] p 830 N92-28888
Fatigue in single crystal nickel superalloys
[AD-A248190] p 896 N92-29408
Spatial and temporal adaptive procedures for the unsteady aerodynamic analysis of airfoils using unstructured meshes
[NASA-TM-107635] p 831 N92-29445
Computation of three-dimensional effects on two dimensional wings
[NASA-CR-190576] p 832 N92-29691
Active thermal isolation for temperature responsive sensors
[NASA-CASE-LAR-14612-1] p 911 N92-29954
Experimental investigation of the flowfield of an oscillating airfoil
[NASA-TM-105675] p 833 N92-30182
Numerical calculations of two-dimensional single and multi-material flow fields with CCICE
[DE92-015778] p 1000 N92-30903
High Reynolds number test of the Boeing TR77 airfoil in the Langley 0.3-meter transonic cryogenic tunnel
[NASA-TM-4189] p 947 N92-31246
Digital analysis of wind tunnel imagery to measure fluid thickness
[NASA-CR-189234] p 983 N92-31252
Fatigue in single crystal nickel superalloys
[AD-A250068] p 987 N92-31360
A surface definition code for turbine blade surfaces
[DE92-010574] p 1004 N92-31498
Wind tunnel aerodynamic characteristics of a transport-type airfoil in a simulated heavy rain environment
[NASA-TP-3184] p 948 N92-31532
Active control of the separation region on a two-dimensional airfoil
[AD-A249739] p 948 N92-31622
Automatic design of transonic airfoils to reduce the shock induced pressure drag p 949 N92-31863
Exploratory experimental investigation of a wave propeller
[AD-A252175] p 949 N92-32062
Control of unsteady separated flow associated with the dynamic stall of airfoils
[NASA-CR-190688] p 950 N92-32177
Further wind tunnel investigation of the SM701 airfoil with aileron and turbulators
[NASA-CR-190702] p 1038 N92-33063
Investigation of advancing front method for generating unstructured grid
[NASA-CR-190902] p 1128 N92-34043
Analysis of iced wings
[NASA-TM-105773] p 1042 N92-34144
Pressure measurements on a rectangular wing with a NACA0012 airfoil during conventional flutter
[NASA-TM-104211] p 1042 N92-34147

AIRFRAME MATERIALS

Manufacture of a primary flight structure using thermoplastics p 1 A92-10197
Prediction of long-term creep rupture properties for an aluminium alloy for airframe applications
p 141 A92-15206
Fatigue due to noise-induced pressure
[ASME PAPER 91-GT-150] p 148 A92-15588
Methodology for the assessment of material quality effects on airframe fatigue durability p 213 A92-19820
A critical appraisal of thermomechanical processing of structural titanium alloys p 488 A92-30611
Experimental and analytical study of the effects of floor location on response of composite fuselage frames
[AIAA PAPER 92-2473] p 539 A92-34362
Thermal structures and materials for high-speed flight; Collection of Papers of the 1st Thermal Structures Conference, University of Virginia, Charlottesville, Nov. 13-15, 1990
[ISBN 1-56347-017-9] p 590 A92-35847
Advances in aircraft component superplastic forming/diffusion bonding technology
[SAE PAPER 912216] p 674 A92-40018
Contribution of individual load cycles to crack growth under aircraft spectrum loading p 891 A92-45236
Reliability centered maintenance for metallic airframes based on a stochastic crack growth approach
p 897 A92-45242
Buckling, postbuckling and crippling of thin walled composite airframe structures under compression
p 899 A92-46940
The effect of composite material allowable changes on VTOL airframe weights p 848 A92-47629
Experimental investigation on flutter characteristics of composite torsion-box p 996 A92-53055
Present status of Al-Li alloys p 1106 A92-56105
Modern helicopter technologies at MBB and the application in future programmes p 1016 A92-56304
A proposed composite repair methodology for primary structure
[NRC-LTR-ST-1658] p 115 N92-13056
Conceptional design to heat-resistant airframe of HOPE p 575 N92-23820
Structural assessment of ultralightweight composites
p 1107 N92-32525
Out of plane analysis for composite structures
p 1107 N92-32527
Advanced airframe structural materials: A primer and cost estimating methodology
[AD-A253371] p 1062 N92-34182

AIRFRAMES

Fundamentals of applied aerogasdynamics. I - Aerodynamics of wings (profiles), airframes, and their combinations --- Russian book p 64 A92-14280
A full scale airframe high cycle fatigue test methodology and its application to the SH-2G helicopter
p 105 A92-14345
Analysis of crash-resistant fuel systems and airframe structure interaction in a crash environment
p 105 A92-14369
Rotorcraft airframe structural optimization for combined vibration and fatigue constraints p 106 A92-14390
Finite element correlation of the U.S. Army/BHTI ACAP composite airframe helicopter p 108 A92-14399
Metal fibers and fabrics as shielding materials for composites, missiles and airframes p 141 A92-14680
A comparison of cooling methods for the airframe nozzle of a single-stage-to-orbit aircraft
[AIAA PAPER 91-5036] p 210 A92-17825
Fatigue crack initiation and small crack growth in several airframe alloys p 212 A92-19754
Ti-6Al-4V forgings with enhanced fatigue characteristics for engine and airframe applications p 288 A92-22757
IMPAC - An integrated methodology for propulsion and airframe control p 477 A92-29118
The NASA/Industry Design Analysis Methods for Vibrations (DAMVIBS) Program - Boeing helicopters airframe finite element modeling
[AIAA PAPER 92-2202] p 539 A92-34392
The NASA/Industry Design Analysis Methods for Vibrations (DAMVIBS) Program - Sikorsky Aircraft - Advances toward interacting with the airframe design process
[AIAA PAPER 92-2204] p 540 A92-34394
A method for the construction of safe S-N curves
p 586 A92-34759
Aerospace - Collected translations of selected papers
p 608 A92-38266
Composite material repairs to metallic airframe components p 699 A92-41237
Space Shuttle airframe inspection trend-analysis report p 759 A92-42052
Transonic visualization test for the airframe shape improvement of a spaceplane p 752 A92-43200
Reevaluation of the motion of an airship
p 731 A92-43243

The large scale test control systems designed and built by the Boeing Company to support the 757 and 767 major fatigue tests
[SAE PAPER 911985] p 881 A92-45388
Durability analysis for a main bulkhead subjected to load on the body of an aircraft p 848 A92-47664
Manufacturing cost model for composites p 1012 A92-51565
Supersonic wind tunnel test of airintake/airframe integrated models p 1028 A92-56006
Aluminium-lithium alloys - Application on helicopters p 1106 A92-56326
Airframe noise p 55 N92-10605
Propulsive lift noise p 55 N92-10606
Preservation and utilization of finite element models of USAF aircraft structures
[AD-A241657] p 160 N92-13470
Experiences at Langley Research Center in the application of optimization techniques to helicopter airframes for vibration reduction
[NASA-TM-104193] p 299 N92-17033
The NASA/industry design analysis methods for vibrations (DAMVIBS) program: Accomplishments and contributions
[NASA-TM-104192] p 299 N92-17034
Proceedings of the USAF Structural Integrity Program Conference
[AD-A242943] p 279 N92-17204
Fatigue Management
[AGARD-CP-506] p 360 N92-18571
Probabilistic design and fatigue management based on probabilistic fatigue models with reliability updating p 360 N92-18574
The Operational Loads Monitoring System, OLMS p 361 N92-18586
Large area QNDE inspection for airframe integrity p 362 N92-18588
Recent fracture mechanics results from NASA research related to the aging commercial transport fleet p 362 N92-18589
Investigation of the effects of aeroelastic deformations on the radar cross section of aircraft
[AD-A243889] p 402 N92-18940
Airplane crashes on the runway. Fine modeling of the behavior after burning of a frame submitted to linear crushing
[IMFL-90-64] p 353 N92-19350
A guide for the consideration of composite material impacts on airframe costs
[AD-A243928] p 417 N92-19466
Structural dynamics and vibrations of damped, aircraft-type structures
[NASA-CR-4424] p 499 N92-20194
Baseline vibration measurements of remotely piloted helicopters for higher harmonic control research
[AD-A244669] p 482 N92-21360
Hypersonic propulsion research p 561 N92-22543
Conceptional design to heat-resistant airframe of HOPE p 575 N92-23820
The NASA/industry Design Analysis Methods for Vibrations (DAMVIBS) Program: A government overview
[NASA-TM-107579] p 680 N92-25267
Computational Structures Technology for Airframes and Propulsion Systems
[NASA-CP-3142] p 683 N92-25911
Computational structures technology and UVA Center for CST p 683 N92-25912
CSM activities at the NASA Langley Research Center p 683 N92-25916
Overview of mechanics of materials branch activities in the computational structures area p 684 N92-25917
Computational structures technology at Grumman: Current practice/future needs p 684 N92-25930
Airframe life prediction p 649 N92-25931
Thermal QNDE detection of airframe disbonds p 914 N92-30118
Structural assessment of ultralightweight composites p 1107 N92-32525
PDES application protocol suite for composites (PAS-C). Functional needs report for the PAS-C program
[AD-A247886] p 1108 N92-32629
Current nondestructive inspection methods for aging aircraft
[DOT/FAA/CT-91/5] p 1126 N92-33480
Thermal-structural test facilities at NASA Dryden
[NASA-TM-104249] p 1062 N92-34202

AIRLINE OPERATIONS
How to support the 'little guy' --- helicopter maintenance p 60 A92-14437
A constraint satisfaction approach to operative management of aircraft routing p 350 A92-25181
Radio Technical Commission for Aeronautics, Technical Symposium, Washington, DC, Nov. 18-20, 1991, Proceedings p 531 A92-33426
Why not a safety rating? --- in Australian civil aviation p 530 A92-36200
Aviation meteorology p 685 A92-38383
ELS pilot evaluation --- Electronic Library System
[SAE PAPER 912107] p 691 A92-39960
Flight operations safety management
[SAE PAPER 912124] p 635 A92-39971
Airlines could reap big saving with new Pratt common core p 736 A92-42400
Airline deregulation - Impact on human factors p 834 A92-44999
A training program for airline line instructors p 835 A92-45044
Industrial practice in aeronautical maintenance p 786 A92-47774
Terminal area traffic management p 955 A92-50122
A study on the marginal analysis method for the airline yield management p 951 A92-53018
Regional airline and equipment review - Evolution, trends, and future prospects p 1015 A92-55102
A comparison between the consequences of the liberal and non-liberal UK-Europe bilaterals
[TT-9101] p 18 N92-10018
Program plan: National aging aircraft research program
[DOT/FAA/CT-88/32-1] p 18 N92-10992
Parameter identification studies on the NASA/Ames Research Center Advanced Concepts Flight Simulator
[NASA-TM-105126] p 31 N92-11024
Prototype runway hold-short lighting system
[DOT/FAA/CT-TN91/43] p 31 N92-11028
Surface painted taxiway markings at Seattle-Tacoma International Airport
[DOT/FAA/CT-TN91/49] p 32 N92-11029
A review of UK aviation policy
[TT-9107] p 61 N92-12988
Aircraft accident report: MarkAir, Inc., Boeing 737-2X6C, N670MA, controlled flight into terrain, Unalakleet, Alaska, 2 June 1990
[PB91-910402] p 92 N92-13039
Winds of change: Domestic air transport since deregulation
[NRC-SR-230] p 92 N92-13040
New York Downtown Manhattan (Wall Street) Heliport: Operations analysis
[DOT/FAA/RD-91/12] p 139 N92-13077
Aircraft accident report: Northwest Airlines, Inc., Flights 1482 and 299. Runway incursion and collision, Detroit Metropolitan/Wayne County Airport, Romulus, Michigan, December 3, 1990
[PB91-910405] p 187 N92-14006
A strategy for exploiting the full potential of MLS based terminal procedures in Canada p 190 N92-14025
Quiet aircraft design and operational characteristics p 236 N92-14787
Passenger knowledge of airline safety information
[CRANFIELD-AERO-9111] p 187 N92-15054
Rotorcraft low altitude IFR benefit/cost analysis: Operations analysis
[SCT-90RR-44] p 191 N92-15061
Aircraft accident reports: Brief format US civil and foreign aviation issue number 2 of 1989 accidents
[PB90-916902] p 263 N92-15978
Identification of high-level functional/system requirements for future civil transports
[NASA-CR-189561] p 276 N92-15991
Aircraft accident report: Northwest Airlines, Inc., Flights 1482 and 299. Runway incursion and collision, Detroit Metropolitan/Wayne County Airport, Romulus, Michigan, December 3, 1990
[PB91-910405] p 264 N92-17213
Investigation on freezing and sticking phenomena of slush on airplane surfaces when taxiing on the ground and the succeeding take-off run phase
[NAL-TR-1026] p 352 N92-18182
Public-sector aviation issues: Graduate research award papers, 1989 - 1990
[PB91-242271] p 308 N92-19662
Aircraft accident report: Ryan International Airlines DC-9-15, N565PC, loss of control on takeoff, Cleveland-Hopkins International Airport, Cleveland, Ohio, February 17, 1991
[PB91-910410] p 530 N92-23597
Tilt rotors and the Port Authority of New York and New Jersey Airport System
[RAND-R-3971/1-PA-SUMM] p 636 N92-25262
Drag reduction: An industrial challenge p 717 N92-27708
European studies to investigate the feasibility of using 1000 ft vertical separation minima above FL 290. Part 1: Overview of organisation, techniques employed, and conclusions
[NLR-TP-91062-U-PT-1] p 841 N92-29605
Structural integrity of future aging airplanes p 913 N92-30107
Communication: An important element of maintenance and repair p 838 N92-30124
Aviation safety: Changes needed in FAA's service difficulty reporting program
[GAO/RCED-91-24] p 953 N92-31453
Aviation noise: Costs of phasing out noisy aircraft
[GAO/RCED-91-128] p 1011 N92-31454
An assessment of the B-747's capability to operate on rough surfaces
[AD-A250134] p 963 N92-31793
Aircraft accident report: L'Express Airlines, Inc., Flight 508, Beech C99, N7217L weather encounter and crash near Birmingham, Alabama, July 10, 1991
[PB92-910401] p 1043 N92-32455
Statistics on aircraft gas turbine engine rotor failures that occurred in US commercial aviation during 1988
[DOT/FAA/CT-91/28] p 1071 N92-33105
Workshop on Aeronautical Decision Making (ADM). Volume 1: Executive summary
[DOT/FAA/RD-92/14-VOL-1] p 1142 N92-33305
Impacts of technology on the capacity needs of the US national airspace system
[NASA-CR-4470] p 1045 N92-34192

AIRPORT BEACONS
Airport Surface Traffic Automation p 95 A92-16228

AIRPORT LIGHTS
Prototype runway hold-short lighting system
[DOT/FAA/CT-TN91/43] p 31 N92-11028
Airport smart power lighting system
[DOT/FAA/CT-TN91/12] p 573 N92-22966

AIRPORT PLANNING
Madrid's double airport p 138 A92-16231
German airports - Capacity crisis p 61 A92-17097
Airport terminals p 283 A92-21125
The price of success - Mitigation and litigation in airport growth p 417 A92-27450
Airfield construction (3rd revised and enlarged edition) --- Russian book
[ISBN 5-277-01070-X] p 670 A92-36606
Interdependencies of aircraft-/airport-noise and urban- and regional-planning standards p 688 A92-39063
Determination of aircraft noise levels while the engine is running on the ground - An approach from the point of urbanization and architecture p 688 A92-39064
Simulation of triple simultaneous parallel ILS approaches p 880 A92-45025

AIRPORT SECURITY
Airport X-ray screening technology becomes a viable explosives detector p 836 A92-47925

AIRPORT SURFACE DETECTION EQUIPMENT
Advanced ASDE provides new eyes and ears for controllers p 453 A92-29506

AIRPORTS
Legal problems in aircraft towing using the PTS procedure p 56 A92-11214
The view from the airport p 532 A92-33438
Noisemap 6.0 - The USAF microcomputer program for airport noise analysis p 686 A92-39051
Noise from military airfields in the United Kingdom p 686 A92-39052
Airport noise contours - Converting from NNI to Leq p 686 A92-39053
Aircraft noise - The calculation of the noise exposure by aircraft in the Netherlands p 687 A92-39054
DANSIM - Danish Airport Noise Simulation Model - Basic principles, experience, and improvements p 687 A92-39055
Comparison of aircraft noise indices for noise zoning at military airfields p 687 A92-39056
A noise survey around Oslo Airport Fornebu p 687 A92-39061
A mobile system for measuring airport noise p 688 A92-39099
Some experiences with community response to low levels of aircraft noise p 689 A92-39235
Airport technology international 1992 p 664 A92-39514
Noise abatement procedures vs. safety
[SAE PAPER 912137] p 635 A92-39977
RFI effects analysis of an airport-installed HF transmitter on aircraft COMM/NAV receivers p 725 A92-42313
Use of the TMS-65 heating equipment at airports to create fog-dispersal zones above the runway to facilitate takeoff p 775 A92-44084
Real-time control tower simulation for evaluation of airport surface traffic automation p 879 A92-44976
Putting the control back in air traffic control - An enhanced Universal Development Simulation System p 916 A92-44982
Grooved runway surface texture before and after rubber removal p 1093 A92-56111
Surface painted taxiway markings at Seattle-Tacoma International Airport
[DOT/FAA/CT-TN91/49] p 32 N92-11029

EDMS: Microcomputer pollution model for civilian airports and Air Force bases, (user's guide)
[AD-A240528] p 45 N92-11578
A review of UK aviation policy
[TT-9107] p 61 N92-12988
Airport activity statistics of certificated route air carriers: Calendar year 1990
[AD-A241483] p 93 N92-13045
Electronic systems in transportation
[TP-9983] p 189 N92-14009
A strategy for exploiting the full potential of MLS based terminal procedures in Canada p 190 N92-14025
Evaluation of advanced microwave landing system procedures in the New York terminal area
[DOT/FAA/ND-91/1] p 354 N92-18967
Comparative evaluation of internally and externally lighted taxiway guidance signs
[DOT/FAA/CT-TN92/2] p 573 N92-22237
Tilt rotors and the Port Authority of New York and New Jersey Airport System
[RAND-R-3971/1-PA-SUMM] p 636 N92-25262
Analysis of helicopter accident risk exposure near heliports, airports, and unimproved sites
[SCT-91RR-13] p 637 N92-26028
Composite profiles of helicopter mishaps at heliports and airports
[AD-A248887] p 724 N92-28052
Allocation and recovery of federal airport and airway costs, 1991
[AD-A249436] p 983 N92-30777
GNAS Maintenance Control Center (GMCC) Design Qualification Test and Evaluation (DQT/E) test procedures
[DOT/FAA/CT-TN91/40] p 983 N92-30976
Trial of a slant visual range measuring device
p 1000 N92-31043
GNAS Maintenance Control Center (GMCC) Design Qualification Test and Evaluation (DQT/E) test report
[DOT/FAA/CT-TN91/39] p 932 N92-31615
Global positioning system runway incursion program static ground tests
[DOT/FAA/CT-TN91/44] p 957 N92-31838
Airport Surveillance Radar (ASR-9) wind shear processor: 1991 test at Orlando, Florida
[AD-A252246] p 1124 N92-32686
Air traffic control: FAA's advanced automation system contract
[GAO/IMTEC-91-25] p 1048 N92-32861
Performance of insulated pavements at Newton Fields, Jackman, Maine
[CRREL-92-9] p 1101 N92-32903
ILS mathematical modeling study of an ILS localizer and glide slope proposed for runway 32R, Moffett Field Airport, California
[DOT/FAA/CT-TN92/28] p 1048 N92-33308
Accomplishments under the Airport Improvement Program, FY 1991
[AD-A253046] p 1101 N92-33434
Criteria for use of seal coats on airport pavements
[DOT/FAA/RD-92/18] p 1102 N92-34247

AIRSHIPS
The background and the development of the TAL-WAR (Rose) shape blimp with the articulated thruster
[AIAA PAPER 91-3692] p 17 A92-12749
Stratospheric lighter-than-air powered platform
p 110 A92-15334
Developments in airborne surveillance and control systems p 98 A92-16655
Lighter than air - An illustrated history of the airship (Revised edition) --- Book p 418 A92-25680
Boundary layer flows around an airship
p 430 A92-30560
Sentinel 1000 flight test programme overview and preliminary results
[AIAA PAPER 92-1229] p 538 A92-33326
Flying qualities testing on the modern technology airship p 570 A92-35933
Analysis of airship lateral maneuverability
[AIAA PAPER 91-1274] p 743 A92-41212
An acrobatic airship 'Acrostat'
[SAE PAPER 911994] p 843 A92-45396
ILS mathematical modeling study of an ILS localizer and glide slope proposed for runway 32R, Moffett Field Airport, California
[DOT/FAA/CT-TN92/28] p 1048 N92-33308

AIRSPACE
No end to incidents in airspace? III
p 262 A92-23172
Heliport VFR airspace design based on helicopter performance
[SCT-90RR-34] p 103 N92-13049
Helicopter rejected takeoff airspace requirements
[SCT-91RR-28] p 116 N92-13058
Helicopter physical and performance data
[SCT-91RR-27] p 116 N92-13060
Operational survey: VFR heliport approaches and departures
[SCT-91RR-26] p 190 N92-14033
Monitoring operational concept
[DOT/FAA/SE-91/3] p 268 N92-15980
COMPAS system concept p 354 N92-19043
Impacts of technology on the capacity needs of the US national airspace system
[NASA-CR-4470] p 1045 N92-34192

AIRSPEED
Effects of variations in head-up display airspeed and altitude representations on basic flight performance
p 46 A92-11204
Flying qualities evaluation of the V22 tiltrotor
p 131 A92-14334
Effect of wind shear on airspeed during airplane landing approach p 481 A92-32242
Inertial reference units with integrated air speed determination for helicopters p 554 A92-35764
Influence of air velocity on the habit of ice crystal growth from the vapor p 668 A92-38111
Velocity dependence of high angle of attack longitudinal flying qualities criteria
[SAE PAPER 912149] p 662 A92-39985
A note on thrust control for jetliner during approach
p 1053 A92-56061
Theoretical simulation of a 2 micron airborne solid state laser anemometer p 1000 N92-31059

ALGEBRA
An analytical approach to grid sensitivity analysis for NACA four-digit wing sections
[NASA-CR-190251] p 631 N92-25175

ALGORITHMS
New robust adaptive control system using multiple regularization parameters p 51 A92-11455
A method of centers based on barrier functions for solving optimal control problems with continuum state and control constraints p 52 A92-11467
Real-time estimation of gas turbine engine damage using a control based Kalman filter algorithm
[ASME PAPER 91-GT-216] p 124 A92-15633
A fast implicit upwind solution algorithm for three-dimensional unstructured dynamic meshes
[AIAA PAPER 92-0447] p 328 A92-26291
Simulation of hypersonic flows on unstructured grids
p 434 A92-31496
An unstructured mesh generation algorithm for three-dimensional aeronautical configurations
p 918 A92-47053
A fast, uncoupled, compressible, two-dimensional, unsteady boundary layer algorithm with separation for engine inlets
[AIAA PAPER 92-3082] p 823 A92-48729
Interface of an uncoupled boundary layer algorithm with an inviscid core flow algorithm for unsteady supersonic engine inlets
[AIAA PAPER 92-3083] p 823 A92-48730
Recent advances on a finite element algorithm for computational aerodynamics: Transonics-hypersonics
[DE91-018176] p 11 N92-10010
A compensatory algorithm for the slow-down effect on constant-time-separation approaches
[NASA-TM-4285] p 23 N92-10024
A comparison of airborne wake vortex detection measurements with values predicted from potential theory
[NASA-TP-3125] p 18 N92-10994
Real-time fault diagnosis for propulsion systems
[NASA-TM-105303] p 26 N92-11017
Resolution of the Navier-Stokes equations applied to the computation of the laminar flow around a two dimensional wing profile
[CERT-RT-65/5604-35] p 43 N92-11307
Practical input optimization for aircraft parameter estimation experiments p 114 N92-11989
Locally linear neural networks for aerospace navigation systems p 103 N92-12530
Advanced rotorcraft control using parameter optimization
[NASA-CR-189502] p 135 N92-13073
Comparison of polynomial approximations and artificial neural nets for response surfaces in engineering optimization p 165 N92-13835
Critical problems of computational aeroacoustics
p 167 N92-13857
Aerodynamic shape optimization of arbitrary hypersonic vehicles p 194 N92-13954
Analysis and design of transonic airfoils using streamwise coordinates p 194 N92-13955
Automated problem resolution prototype in automated en route air traffic control p 190 N92-14028
A unique approach to aircraft conflict resolution using artificial intelligence techniques p 190 N92-14029
Image-based ranging and guidance for rotorcraft
[NASA-CR-184829] p 191 N92-14036
Rapid near-optimal aerospace plane trajectory generation and guidance
[NASA-CR-189469] p 205 N92-14066
Analysis of objects in binary images
[NASA-CR-4420] p 234 N92-14598
Progress with multigrid schemes for hypersonic flow problems
[NASA-CR-189579] p 185 N92-15047
A fast implicit upwind solution algorithm for three-dimensional unstructured dynamic meshes
[NASA-TM-104186] p 185 N92-15050
The problem of multiple solutions in area navigation and computed centerline operations with the microwave landing system
[AD-A242757] p 191 N92-15058
Project of an adaptive multiaxial autopilot with learning pilot control
[ETN-92-90592] p 205 N92-15072
Supersonic propulsion simulation by incorporating component models in the large perturbation inlet (LAPIN) computer code
[NASA-TM-105193] p 279 N92-15993
Failure detection and fault management techniques for flush airdata sensing systems
[NASA-TM-4335] p 276 N92-17128
A numerical study of the stability of the swept attachment line boundary layer
[AERO-REPT-9103] p 345 N92-18293
Evaluation of the COMPAS experimental system
p 355 N92-19044
A comparative study of numerical versus analytical waverider solutions
[AD-A244183] p 347 N92-19304
An algorithm for robust eigenstructure assignment using the linear quadratic regulator
[AD-A244267] p 412 N92-19335
Robust control system design with application to high performance helicopters p 382 N92-19621
A walk through the planned CS building
[NASA-CR-189963] p 386 N92-19675
A multi-loop guidance scheme using singular perturbation and linear quadratic regulator techniques simultaneously p 481 N92-20148
Bistatic image processing for a 32 x 19 inch model aircraft using scattered fields obtained in the OSU-ESL compact range
[NASA-CR-189932] p 499 N92-20197
Computered tomography: Experimental data acquisition and parallelization of reconstruction algorithm
[DE92-005151] p 499 N92-20301
MATGRID: A program for generation of C-H and C-O topology grids around wing/body configurations. Mathematical definition document
[FFA-TN-1990-19] p 444 N92-20468
Timing analysis of parallel algorithms on a MIMD multiprocessor
[ITN-92-85153] p 510 N92-20905
Measurement of LORAN-C envelope to cycle difference in the far field
[PB92-128909] p 455 N92-21263
Three-dimensional simulations of hypersonic flows
[MBB-UK-0155-89-PUB] p 447 N92-21703
Three-dimensional multigrid algorithm for the Euler and the thin-layer Navier-Stokes equations
[PB92-134329] p 602 N92-22216
PC based flight path reconstruction using UD factorization filtering algorithm
[NAL-PD-FC-9201] p 534 N92-22389
Grid generation and flow solution method for Euler equations on unstructured grids
[NASA-TM-4295] p 528 N92-23533
Computations of unsteady multistage turbomachinery flows p 562 N92-23671
Adaptive active flutter suppression of wings in subsonic and transonic flight regimes p 553 N92-24010
Periodic Euler and Navier-Stokes solutions about oscillating airfoils p 626 N92-24850
Observations on computational methodologies for use in large-scale, gradient-based, multidisciplinary design incorporating advanced CFD codes
[NASA-TM-104206] p 630 N92-24956
CAD product data exchange: Conversions for curves and surfaces
[ISBN-90-6275-723-9] p 648 N92-24964
Constraint-based scheduling
[NASA-TM-107873] p 692 N92-25190
Algorithm and code development for unsteady three-dimensional Navier-Stokes equations
[NASA-CR-190077] p 692 N92-25264
TCGRID: A three dimensional C-grid generator for turbomachinery p 659 N92-25716
Computational Fluid Dynamics --- numerical methods and algorithm development
[NASA-CP-10078] p 660 N92-25808

Development of new flux splitting schemes --- computational fluid dynamics algorithms
p 682 N92-25809
Algorithmic development in structures technology
p 684 N92-25924
Algorithms for blending surface generation
[AD-A245686] p 777 N92-26524
Interface of an uncoupled boundary layer algorithm with an inviscid core flow algorithm for unsteady supersonic engine inlets
[NASA-TM-105684] p 739 N92-27037
On the computation of unsteady turbomachinery flows. Part 1: Euler equations in vibrating cascades
p 768 N92-27460
Computation and visualization of specific flow phenomena in turbomachinery application
p 741 N92-27463
Unsteady Euler calculations in 3D internal aerodynamics p 768 N92-27470
A fast, uncoupled, compressible, two-dimensional, unsteady boundary layer algorithm with separation for engine inlets
[NASA-TM-105686] p 770 N92-27653
A frontal approach for node generation in Delaunay triangulations p 771 N92-27680
Design of bearings for rotor systems based on stability
p 773 N92-27799
An evaluation of some strategies for vibration control of flexible rotors p 773 N92-27800
Fundamentals of structural optimisation
p 851 N92-28470
Wave drag determination in the transonic full-potential flow code MATRICS
[NLR-TP-90062-U] p 828 N92-28709
A rotorcraft flight database for validation of vision-based ranging algorithms
[NASA-TM-103906] p 841 N92-29103
Aerodynamic design optimization using sensitivity analysis and computational fluid dynamics
[NASA-CASE-LAR-14815-1-CU] p 910 N92-29830
A gridless Euler/Navier-Stokes solution algorithm for complex two-dimensional applications
[NASA-TM-107631] p 944 N92-30570
Implicit upwind-Euler solution algorithms for unstructured-grid applications
[NASA-TM-107645] p 945 N92-30691
Subsonic flight test evaluation of a performance seeking control algorithm on an F-15 airplane
[NASA-TM-4400] p 973 N92-31275
Spectrum modal analysis for the detection of low-altitude windshear with airborne Doppler radar
[NASA-CR-4457] p 953 N92-31549
Low density real gas flows about hypersonic vehicles
[AD-A250048] p 949 N92-31777
A comparison of the performance of two gust front detection algorithms using a length-based scoring technique
[AD-A250862] p 1004 N92-32103
A parameter optimization approach to controller partitioning for integrated flight/propulsion control application
[NASA-TM-105826] p 979 N92-32241
Safety study of TCAS 2 for logic version 6.04
[DOT/FAA/RD-92/22] p 1047 N92-32537
An examination of several high resolution schemes applied to complex problems in high speed flows
[AD-A250814] p 1124 N92-32632
Airport Surveillance Radar (ASR-9) wind shear processor: 1991 test at Orlando, Florida
[AD-A252246] p 1124 N92-32686
The use of Kalman filtering techniques to improve the accuracy of flight test data
[NRC-32139] p 1064 N92-32850
Analysis of delay reducing and fuel saving sequencing and spacing algorithms for arrival traffic
[NASA-TM-103880] p 1044 N92-33194
Computational algorithms for increased control of depth-viewing volume for stereo three-dimensional graphic displays
[NASA-TM-4379] p 1065 N92-34109

ALIGNMENT
Error estimation of INS ground alignment through observability analysis p 639 A92-40226
Testability of the PAALS auto-align sensor system --- Precision Accelerometer Alignment and Leveling System
p 965 A92-49310
Study of optical techniques for the Ames unitary wind tunnels. Part 1: Schlieren
[NASA-CR-189951] p 385 N92-19218
Multi-channel fiber optic rotary joint for single-mode fiber
[AD-D015273] p 927 N92-29095

ALL-WEATHER LANDING SYSTEMS
Helicopter fog flying trials p 530 A92-35759
EVS could expand all-weather landing capability of airliners p 556 A92-36125
94 GHz MMW imaging radar system
[SAE PAPER 912208] p 651 A92-40015
Autonomous landing - Functional requirements
p 840 A92-48470
The application of imaging sensors to aircraft landings in adverse weather p 1045 A92-54902

ALLOCATIONS
National Aeronautics and Space Administration
p 238 N92-14927
Allocation and recovery of federal airport and airway costs, 1991
[AD-A249436] p 983 N92-30777

ALTERNATING CURRENT
Advanced techniques in current signature analysis
[DE92-007680] p 679 N92-24892
Electromechanical systems with transient high power response operating from a resonant AC link
[NASA-TM-105716] p 870 N92-28985

ALTERNATING DIRECTION IMPLICIT METHODS
A semi-elliptic analysis for 2-D viscous flows through cascade configurations p 3 A92-10688
Numerical analysis of a thermal deicer
[AIAA PAPER 92-0527] p 357 A92-26950
Navier-Stokes and Euler solutions for an unmanned aerial vehicle
[AIAA PAPER 92-2609] p 792 A92-45483
An unfactored implicit scheme for 3D inviscid transonic flows
[AIAA PAPER 92-2668] p 798 A92-45523

ALTIMETERS
Probability distributions that are important when assessing barometric aiding to GPS p 100 A92-16952
A Kalman filter mechanization for the baro-inertial vertical channel p 673 A92-39558
C-29A aircraft altimeter errors
[AD-A240486] p 23 N92-11011
Estimation of aircraft attitude by angular rate measurements p 963 N92-31881
The utility of analog vertical velocity information during instrument flight with a Head-Up Display (HUD)
[AD-A252863] p 1065 N92-33277

ALTIMETRY
GPS interferometric attitude and heading determination - Flight test results p 650 A92-39561

ALTITUDE
Operational survey: VFR heliport approaches and departures
[SCT-91RR-26] p 190 N92-14033
A continuing study of altitude determination deficiencies of the Service Aircraft Instrumentation Package (SAIP)
[AD-A245952] p 968 N92-32051
User's manual for AeroFcn: A FORTRAN program to compute aerodynamic parameters
[NASA-TM-104237] p 1133 N92-32507

ALTITUDE CONTROL
Balloon altitude control by valving - A review and comparison of actual flight data and vertical performance analysis results
[AIAA PAPER 91-3669] p 14 A92-11016
Baro-inertial loop for the USAF Standard RLG INU
p 97 A92-16647
Eliminating pilot-caused altitude deviations - A human factors approach p 834 A92-45041
Nonlinear model-following control application to airplane control (1992 AIAA Controls Design Challenge)
[AIAA PAPER 92-4625] p 1077 A92-55302
European studies to investigate the feasibility of using 1000 ft vertical separation minima above FL 290. Part 1: Overview of organisation, techniques employed, and conclusions
[NLR-TP-91062-U-PT-1] p 841 N92-29605

ALTITUDE SIMULATION
Research on altitude simulation of starting for a single-spool small turbojet p 969 A92-49836
Turbine engine hot-part temperature measurement techniques
[AIAA PAPER 92-3960] p 1122 A92-56788

ALTITUDE TESTS
Turbine engine performance test and evaluation techniques
[AIAA PAPER 92-3977] p 1071 A92-56803
Acoustic interactions between an altitude test facility and jet engine plumes: Theory and experiments
[NASA-CR-190423] p 738 N92-26405

ALUMINIDES
Corrosion damage and regeneration of aluminide coatings on aircraft turbine blades p 142 A92-15244
A preliminary study of the microstructure-property relationships in cast gamma titanium aluminide alloys
p 487 A92-30596
Manufacture of XD gamma titanium aluminide airfoils via investment casting and machining
p 494 A92-30603
Development of intermetallic materials for aerospace systems p 754 A92-41874
Axial alignment of short-fiber titanium aluminide composites by directional solidification
p 892 A92-46838

ALUMINUM
Some results on metal and composite patch reinforcement of aluminum honeycomb panel
p 216 A92-18830
Performance of aluminum honeycomb panels with structural defects and core anomalies. II - Specimen description and test results p 591 A92-36156
Anodize and prime your aluminum without environmental headaches p 892 A92-47340
Nonlinear aspects of aerospace structures at high excitation levels flat aluminum beams and plates studied
[AD-A240600] p 44 N92-11383
Surface residual stress analysis of metals and alloys
[AD-A248372] p 895 N92-28426

ALUMINUM ALLOYS
Aerospace Arall - A challenge for the aircraft designer
p 33 A92-10232
Light metal materials for aircraft structure
p 140 A92-13444
The microstructural stability of TiC reinforced rapidly solidified Al-Fe-V-Si composite structures
p 141 A92-15169
Prediction of long-term creep rupture properties for an aluminium alloy for airframe applications
p 141 A92-15206
Corrosion damage and regeneration of aluminide coatings on aircraft turbine blades p 142 A92-15244
Proof test and fatigue crack growth modeling on 2024-T3 aluminum alloy p 213 A92-19828
Mechanical and fracture behaviour of Ti-6Al-2Sn-4Zr-2Mo-0.1Si alloys p 288 A92-22755
Ti-6Al-4V forgings with enhanced fatigue characteristics for engine and airframe applications p 288 A92-22757
A fatigue crack growth threshold p 389 A92-26667
Fretting fatigue p 672 A92-38225
Self reliance in aerospace structures
p 758 A92-41190
The evaluation of non-tank surface treatments for aluminium bonding repairs p 761 A92-42502
Aluminides modified by palladium - Protection of new parts by local finishing
[ONERA, TP NO. 1992-49] p 893 A92-48610
Mechanical properties of laminate aluminum matrix composites p 1106 A92-56102
The two-bay crack problem in fuselages built in GLARE and ARALL
[LR-653] p 196 N92-14044
Bulging of fatigue cracks in a pressurized aircraft fuselage
[LR-655] p 196 N92-14045
Development and characterization of Powder Metallurgy (PM) 2XXX series Al alloy products and Metal Matrix Composite (MMC) 2XXX Al/SiC materials for high temperature aircraft structural applications
[NASA-CR-187631] p 390 N92-19290
Durability and damage tolerance of aluminum castings
[AD-A245237] p 490 N92-21159
Surface residual stress analysis of metals and alloys
[AD-A248372] p 895 N92-28426
Tensile and interlaminar properties of GLARE (trade name) laminates
[AD-A250188] p 895 N92-28921
Short cracks and durability analysis of the Fokker 100 wing/fuselage structure
[NLR-TP-90336-U] p 910 N92-29603
In-service evaluation of 2090 aluminum-lithium alloy on F/A-18 aircraft
[AD-A248472] p 986 N92-30321
Low-velocity impact loading on fibre reinforced aluminum laminates (ARALL) and other aircraft sheet materials
[ETN-92-91613] p 987 N92-30414
Mechanical behavior and processing of aluminum metal matrix composites
[AD-A249918] p 987 N92-30874
Effects of constraint on crack growth under aircraft spectrum loading
[NASA-TM-107677] p 1128 N92-34178

ALUMINUM COMPOUNDS
Ignition delays, heats of combustion, and reaction rates of aluminum alkyl derivatives used as ignition and combustion enhancers for supersonic combustors
[AIAA PAPER 92-3841] p 894 A92-49134
Thermomechanical fatigue behavior of a silicone carbide fiber-reinforced calcium aluminosilicate glass-ceramic matrix composite
[AD-A249870] p 988 N92-31823

ALUMINUM OXIDES
Effect of sustained high temperature exposure on the mechanical properties of Nicalon/Al2O3 composites
p 668 A92-39672
Fabrication and testing of corrosion resistant coatings --- for turbine engine components
[DE92-003553] p 490 N92-21063

Properties of a TZP/Al2O3 composite after long-term exposure at 1000 C
[AD-A246407] p 757 N92-27752

ALUMINUM-LITHIUM ALLOYS
Al-Li alloys find their niche p 755 A92-43685
Present status of Al-Li alloys p 1106 A92-56105
Aluminium-lithium alloys - Application on helicopters p 1106 A92-56326
In-service evaluation of 2090 aluminum-lithium alloy on F/A-18 aircraft
[AD-A248472] p 986 N92-30321

AMBIENT TEMPERATURE
Experimental study of performance degradation of a rotating system in the NASA Lewis RC icing tunnel
[NASA-CR-190684] p 1102 N92-34141

AMBIPOLAR DIFFUSION
Monte Carlo simulation of reentry flows with ionization
[AIAA PAPER 92-0493] p 328 A92-26323

AMORPHOUS MATERIALS
The effect of physical aging on the creep response of a thermoplastic composite
[AD-A243600] p 290 N92-17932

AMORPHOUS SILICON
New-type of ultralight flexible a-Si solar cell and its application on an airplane p 970 A92-53181

AMPHIBIOUS AIRCRAFT
A quick automatic method for computing performance of nonducted propeller with constant-revolutional-speed p 393 A92-25505
Analysis of a 2-D airfoil motion flying in-proximity-to a wavy-wall surface-lifting surface-scheme p 315 A92-25506

AMPHIBIOUS VEHICLES
High-temperature combustor and seal for a water piston propulsor
[AD-A242493] p 229 N92-15385

AMPLIFICATION
A robust gain scheduler interpolated into multiple models by membership functions
[AIAA PAPER 92-4553] p 1131 A92-55265

AMPLIFIERS
A state-of-the-art data acquisition system p 217 A92-19231

AMPLITUDES
Hydrodynamic flow visualization around an oscillating vane. Extension of study to the case of higher incidences and amplitudes and the starting off phase from permanent regime
[ONERA-RT-56/1369-AN] p 43 N92-11312

ANALOG CIRCUITS
What is an ASIC? p 859 N92-28377

ANALOG COMPUTERS
An automated workstation for the half-scale testing of the flight vehicle stabilization circuit p 664 A92-40622

ANALOG DATA
The utility of analog vertical velocity information during instrument flight with a Head-Up Display (HUD)
[AD-A252863] p 1065 N92-33277

ANALYSIS (MATHEMATICS)
A wing rock model for the F-14A aircraft
[AD-A243109] p 275 N92-17300
Implementation of a personal computer based parameter estimation program
[AD-A252914] p 1061 N92-33502

ANALYTIC FUNCTIONS
Application of holomorphic vectors theory in three-dimensional potential flow problem p 292 A92-21923

ANCHORS (FASTENERS)
Evaluation of grounding and mooring points for Army aircraft
[AD-A250749] p 953 N92-31193

ANECHOIC CHAMBERS
Wall pressure wavenumber-frequency spectrum beneath a turbulent boundary layer measured with transducer arrays calibrated with an acoustical method
[ONERA, TP NO. 1991-212] p 329 A92-26364
Precision analysis on static measurement of radar cross section p 370 A92-27906
The design of a subsonic low-noise, low-turbulence wind tunnel for acoustic measurements
[AIAA PAPER 92-3883] p 1094 A92-56726
Annoyance caused by aircraft en route noise
[NASA-TP-3165] p 512 N92-20479

ANEMOMETERS
Study of interactions on anemoclinometric sensors
[REPT-90/30] p 138 N92-12006
Calibration data for improved correction of UVW propeller anemometers
[DE92-002935] p 297 N92-16281
Measured and predicted rotor performance for the SERI advanced wind turbine blades
[DE92-001215] p 598 N92-23119

ANGLE OF ATTACK
Application of nonlinear control strategies to aircraft at high angle of attack p 26 A92-11329
A numerical simulation of separated flows around bodies p 8 A92-12423
The dynamic character of the wake of an axisymmetric body at an angle of attack
[AIAA PAPER 91-3268] p 8 A92-12741
Computation of three-dimensional turbulent vortical flows on bodies at high incidence p 9 A92-13203
Experimental investigation on the effect of crescent planform on lift and drag p 9 A92-13206
Lift development of delta wings undergoing constant acceleration from rest p 9 A92-13209
Experimental investigation on gas-particle flow in cascades p 62 A92-13300
An analysis of pitch and plunge effects on unsteady airfoil behavior p 65 A92-14359
Time-dependent aerodynamic analysis of ducted and unducted propfans at angle of attack
[ASME PAPER 91-GT-190] p 74 A92-15616
X-29 high angle of attack p 111 A92-16052
MiG-29 prototype and development flight tests - General overview and high angle of attack investigation p 113 A92-16064
Stratified flow around an axisymmetric body at small angle of attack p 172 A92-18385
Hypersonic flows over slender circular cones at small angles of attack p 173 A92-19068
Evaluations of X-29 high-AOA regime show promise for future fighters p 192 A92-19925
Model oscillations at high angle of attack in a low speed wind tunnel test
[IAF PAPER ST-91-001] p 175 A92-20649
Instabilities of flows over bodies at large incidence p 176 A92-20738
Surface flow patterns on an ogive-cylinder at incidence p 176 A92-20762
Unsteady Euler analysis of the flowfield of a propfan at an angle of attack p 242 A92-21070
Navier-Stokes computations for aerodynamic configurations at high angles of attack p 246 A92-21981
An experimental study of pneumatic vortex flow control on high angle of attack forebody model
[AIAA PAPER 92-0018] p 247 A92-22140
Aircraft control at high-alpha by tangential blowing
[AIAA PAPER 92-0021] p 281 A92-22143
A computational study on directional stability of chine-shaped forebodies at high-alpha
[AIAA PAPER 92-0030] p 249 A92-22152
Future experimental needs in high-alpha vehicle dynamics
[AIAA PAPER 92-0159] p 254 A92-23774
Rapid prediction of high-alpha unsteady aerodynamics of slender-wing aircraft p 309 A92-24412
Experimental studies of a two-element airfoil with large separation
[AIAA PAPER 92-0267] p 317 A92-25723
Controlling unsteady lift using unsteady trailing-edge flap motions
[AIAA PAPER 92-0275] p 318 A92-25729
Unique high-alpha roll dynamics of a sharp-edged 65 deg delta wing
[AIAA PAPER 92-0276] p 318 A92-25730
Pitch-up motions of delta wings
[AIAA PAPER 92-0278] p 318 A92-25732
The evaluation of canard couplings at high angles of attack
[AIAA PAPER 92-0281] p 318 A92-25735
The anchored and loose vortex systems of finite wings
[AIAA PAPER 92-0318] p 321 A92-25765
Effects of tip Reynolds number and tip asymmetry on vortex wakes of axisymmetric bodies at various angles of attack
[AIAA PAPER 92-0406] p 324 A92-26259
The effects of blowing on delta wing vortices during dynamic pitching at high angles of attack
[AIAA PAPER 92-0407] p 325 A92-26260
Effect of upstream disturbance on flow asymmetry
[AIAA PAPER 92-0408] p 325 A92-26261
Computational study of the aerodynamics and control by blowing of asymmetric vortical flows over delta wings
[AIAA PAPER 92-0410] p 325 A92-26263
Some thoughts on conical flow asymmetry
[AIAA PAPER 92-0427] p 326 A92-26275
Cross-flow separation on a prolate spheroid at angles of attack
[AIAA PAPER 92-0428] p 326 A92-26276
Separation-induced self-excited structural oscillations
[AIAA PAPER 92-0486] p 328 A92-26317
The formation and structure of plasma wakes behind large high-voltage space platforms in ionosphere
[AIAA PAPER 92-0577] p 407 A92-26984
Effects of nose bluntness and angle of attack on slender bodies in hypersonic flows
[AIAA PAPER 92-0638] p 334 A92-27016
Evaluation of methods for estimating store carriage loads
[AIAA PAPER 92-0675] p 379 A92-27043
Holographic flowfield density measurements in swept shock wave/boundary-layer interactions
[AIAA PAPER 92-0746] p 335 A92-27092
Hypersonic flow of a viscous gas past sharp elliptical cones at angles of attack and slip p 336 A92-27531
A numerical method for analyzing the nonlinear flutter of wings at high angles of attack p 338 A92-27827
Turbulence model effects on separated flow about a prolate spheroid p 340 A92-28036
High-alpha application of variable-gain output feedback control p 380 A92-28152
Model attitude measurements at NASA Langley Research Center
[AIAA PAPER 92-0763] p 398 A92-28226
Numerical modeling of self-oscillations for a small-aspect-ratio delta wing using measurements of roll motion at large angles of attack p 424 A92-30138
High angle of attack aerodynamics - Subsonic, transonic, and supersonic flows --- Book
[ISBN 0-387-97672-8] p 431 A92-30850
Calculation of real-gas effects on blunt-body trim angles p 432 A92-31169
Combined effect of nose bluntness and angle of attack on slender bodies in viscous hypersonic flows
[AIAA PAPER 92-0755] p 436 A92-31680
Singularity bypass algorithms in the numerical solution of equations of body motion relative to a center of mass in the atmosphere in the presence of disturbances p 437 A92-31857
An aerodynamic design study of a series of lifting bodies at angles of attack from 10 to 53 degrees at Mach numbers from 2.30 to 4.62 p 442 A92-32500
Buffet load measurements on an F/A-18 vertical fin at high-angle-of-attack
[AIAA PAPER 92-2127] p 520 A92-35694
X-29 high angle of attack flight test procedures, results, and lessons learned p 548 A92-35934
X-29 high angle-of-attack flight test air data comparisons of an inertial navigation system and noseboom probe p 549 A92-35945
High alpha aerodynamic control by tangential fuselage blowing p 611 A92-36848
Solution of Euler equations for fighter forebody-inlet combinations at high angles of attack p 613 A92-38269
Nonlinear control law with application to high angle-of-attack flight p 661 A92-39904
Development of a pneumatic high-angle-of-attack flush airdata sensing system
[SAE PAPER 912142] p 651 A92-39980
Agility and high angle of attack - An Air Force research perspective
[SAE PAPER 912145] p 608 A92-39983
Velocity dependence of high angle of attack longitudinal flying qualities criteria
[SAE PAPER 912149] p 662 A92-39985
Effects of attack angle on leg portion of the horseshoe vortex around the idealized wing p 623 A92-40177
Calculation of rotational derivatives in the case of local interaction between flow and a body surface p 624 A92-40746
A correlation study of the wing-body interference factor for high angles of attack p 700 A92-41179
Flow over a twin-tailed aircraft at angle of attack. I - Spatial characteristics p 702 A92-41229
Symmetry breaking in vortex flows on conical bodies p 703 A92-41278
Prediction of shock pattern dynamics at hypersonic angle of attack maneuvers of endo-KEW missile forebodies
[AIAA PAPER 92-2768] p 704 A92-41317
Free-flight trim-angle predictions for the aeroassist flight experiment p 705 A92-41540
Update of the X-29 high-angle-of-attack program
[SAE PAPER 912006] p 783 A92-45407
Numerical investigation into high-angle-of-attack leading-edge vortex flow
[AIAA PAPER 92-2600] p 791 A92-45477
Effect of canard deflection on close-coupled canard-wing-body aerodynamics
[AIAA PAPER 92-2602] p 792 A92-45479
The effects of nozzle exit geometry on forebody vortex control using blowing
[AIAA PAPER 92-2603] p 792 A92-45480
High speed aerodynamics of upper surface blowing aircraft configurations
[AIAA PAPER 92-2611] p 793 A92-45485
Coupled numerical simulation of the external and engine inlet flows for the F-18 at large incidence
[AIAA PAPER 92-2621] p 793 A92-45493
Experimental investigation of the flowfield of an oscillating airfoil
[AIAA PAPER 92-2622] p 793 A92-45494

Vortex trapping on a 60 degree delta wing
[AIAA PAPER 92-2639] p 796 A92-45508
Aircraft spoiler effects under wind shear
[AIAA PAPER 92-2642] p 796 A92-45509
Unsteady pressure and load measurements on an F/A-18 vertical fin at high-angle-of-attack
[AIAA PAPER 92-2675] p 798 A92-45529
Active control of vortex structures in a separating flow over an airfoil
[AIAA PAPER 92-2728] p 804 A92-45563
Visualization of stopping flow over airfoils
[AIAA PAPER 92-2730] p 804 A92-45564
Experimental investigation of vortex dynamics on delta wings
[AIAA PAPER 92-2731] p 804 A92-45565
Full-scale high angle-of-attack tests of an F/A-18
[AIAA PAPER 92-2676] p 806 A92-45584
Measurements of the unsteady vortex flow over a wing-body at angle of attack
[AIAA PAPER 92-2729] p 808 A92-45598
Flow over a twin-tailed aircraft at angle of attack. II - Temporal characteristics p 810 A92-46781
Outflow boundary conditions using Duhamel's equation p 813 A92-46913
Hypersonic plasma predictions at nonzero angle of attack
[AIAA PAPER 92-3027] p 925 A92-47028
The numerical simulation of compressible flow around an airfoil at high angle of attack p 818 A92-47686
Some exact and numerical results for plane steady sheared flow of an incompressible inviscid fluid
p 821 A92-48019
An experimental investigation on aft bypass supersonic inlet performance at high angle of attack and yaw
p 862 A92-48268
Thrust vectoring characteristics of the F-18 high alpha research vehicle at angles of attack from 0 to 70 deg
[AIAA PAPER 92-3095] p 877 A92-48737
An inviscid/viscous coupling approach for vortex flow field calculations p 933 A92-49510
Design and optimization of airfoils in non-stalling incompressible flow with a prescribed range of the angle of attack p 933 A92-49556
Rarefied gas flow around a disc with different angles of attack p 938 A92-52753
Monte Carlo simulation of the hypersonic mon- and diatomic gas flow past a disk at an angle of attack
p 939 A92-52770
Measurement of angle of attack using a five-hole arrow head pitot tube p 941 A92-53009
A study on the stability of aircraft at high angles-of-attack and state vector propagation sensitivity
p 978 A92-53394
Full Navier-Stokes calculations on the installed F/A-18 inlet at a high angle of attack
[AIAA PAPER 92-3175] p 1020 A92-54012
Unsteady blade pressures on a propfan - Predicted and measured compressibility effects
[AIAA PAPER 92-3774] p 1023 A92-54161
Evaluation of electrolytic tilt sensors for wind tunnel model angle-of-attack (AOA) measurements
p 1116 A92-54344
Development of a high-angle-of-attack stability and control prediction code
[AIAA PAPER 92-4354] p 1079 A92-55340
Dynamic derivative data for high angle of attack simulation
[AIAA PAPER 92-4355] p 1079 A92-55341
Effects of the roll angle on cruciform wing-body configurations at high incidences
[AIAA PAPER 92-4356] p 1079 A92-55342
The flow field characteristics about a fighter configuration at high angles of attack
[AIAA PAPER 92-4358] p 1025 A92-55344
High angle-of-attack control enhancement on a forward swept wing aircraft
[AIAA PAPER 92-4427] p 1080 A92-55351
Force production mechanisms of a tangential jet on bodies at high alpha
[AIAA PAPER 92-4648] p 1082 A92-55393
Comparative numerical study of two turbulence models for airfoil static and dynamic stall
[AIAA PAPER 92-4649] p 1028 A92-55394
State-space representation of aerodynamic characteristics of an aircraft at high angels of attack
[AIAA PAPER 92-4651] p 1028 A92-55395
Low-speed wind tunnel testing for the high-speed propeller at high shaft angle of attack
p 1030 A92-56054
Lateral control of spaceplane at hypersonic flight
p 1104 A92-56069
High angle-of-attack flush airdata sensing system
p 1064 A92-56172
Aerodynamic calculation of an elliptic ring wing
[AIAA PAPER 91-0068] p 1035 A92-57035
Transonic and supersonic Euler computations of vortex-dominated flow fields about a generic fighter
[NASA-TP-3156] p 11 N92-10011
Development of a pneumatic high-angle-of-attack flush airdata sensing (HI-FADS) system
[NASA-TM-104241] p 118 N92-11994
Computer programs for the calculation of dual sting pitch and roll angles required for an articulated sting to obtain angles of attack and sideslip on wind-tunnel models
[NASA-TM-104161] p 138 N92-12007
In-flight flow visualization and pressure measurements at low speeds on the NASA F-18 high alpha research vehicle p 85 N92-13009
Control of forebody vortices by suction at the nose of the RAE high incidence research model
p 87 N92-13022
Steady and unsteady aerodynamics of a pitching straked wing model at high angles of attack p 87 N92-13024
Effect of solidity and inclination on propeller-nacelle force coefficients
[NASA-TM-4316] p 90 N92-13038
Hypersonic flow past delta wing flow simulated by Navier-Stokes solutions p 180 N92-14981
Contribution of fin and tailplane to sideforce and yawing moment derivatives due to sideslip at supersonic speeds at low angles of attack
[ESDU-91031] p 259 N92-15971
Hot-wire surveys in the vortex wake downstream of a three-percent fighter aircraft model at high angles of attack
[AD-A241869] p 259 N92-15975
Evaluation of electrolytic tilt sensors for measuring model angle of attack in wind tunnel tests
[NASA-TM-4315] p 297 N92-16283
Development of high angle of attack control laws for an unstable, non-minimum phase aircraft using variations of the quantitative feedback technique
[AD-A243698] p 282 N92-17096
A wing rock model for the F-14A aircraft
[AD-A243109] p 275 N92-17300
Aerodynamic development of the X-31 aircraft for the high angle of attack region
[MBB-FE211-S-PUB-452] p 275 N92-17313
Model incidence measurement using SAAB ELOPTOPOS system
[NLR-TP-89182-U] p 385 N92-18416
Manoeuvring Aerodynamics
[AGARD-CP-497] p 363 N92-18778
X-31 enhancement of aerodynamics for maneuvering beyond stall p 363 N92-18779
Parametric effects of some aircraft components on high-alpha aerodynamic characteristics
p 364 N92-18782
Analysis of unsteady force, pressure, and flow-visualization data for a pitching straked wing model at high angles of attack p 364 N92-18784
Measurement of derivatives due to acceleration in heave and sideslip p 364 N92-18785
Wind tunnel force measurements and visualization on a 60-deg delta wing in oscillation, stepwise motion, and gusts p 364 N92-18786
Characterization of unsteady aerodynamic phenomena at high angles p 364 N92-18787
X-31: Discussion of steady state and rotary derivatives
p 365 N92-18789
An experimental study of a sting-mounted circulation control wing
[AD-A243912] p 346 N92-18895
Application of nonlinear QFT to flight control design for high angle of attack maneuvers with thrust vectoring
[AD-A243821] p 381 N92-19241
Identification of aerodynamic models for maneuvering aircraft
[NASA-CR-190039] p 348 N92-19359
Investigation of the influence of rotary aerodynamics on the study of high angle of attack dynamics of the F-15B using bifurcation analysis
[AD-A243969] p 348 N92-19367
Investigation of a semi-empirical method to predict limit cycle oscillations of modern fighter aircraft
[NLR-TP-90087-U] p 481 N92-20475
High angle of attack: Aerodynamics
p 528 N92-23956
Normal force of low aspect ratio wing-body combinations up to high angles of attack at supersonic speeds
[ESDU-91042] p 553 N92-24009
Flowfield in the vicinity of the F/A-18 vertical fin at high-angle-of-attack p 628 N92-24865
Wind-tunnel static and free-flight investigation of high-angle-of-attack stability and control characteristics of a model of the EA-6B airplane
[NASA-TP-3194] p 631 N92-25276
Grid generation for a complex aircraft configuration
p 649 N92-25714
A high angle of attack inviscid shuttle orbiter computation
[NASA-TM-107606] p 685 N92-25964
High-alpha vortex decoupling investigations on a chine forebody/Delta wing configuration at transonic Mach numbers
[NASA-CR-189642] p 715 N92-26651
A study of juncture flow in the NASA Langley 0.3-meter transonic cryogenic tunnel
[NASA-CR-190430] p 773 N92-27880
Flow visualization studies of a sideslipping, canard-configured X-31A-Like fighter aircraft model
[AD-A245940] p 829 N92-28883
Nonlinear normal and axial force indicial responses for a two dimensional airfoil
[AD-A247196] p 830 N92-28888
Study of optical techniques for the Ames unitary wind tunnels. Part 3: Angle of attack
[NASA-CR-190541] p 888 N92-29655
Ultra high bypass Nacelle aerodynamics inlet flow-through high angle of attack distortion test
[NASA-CR-189149] p 943 N92-30298
In-flight leading-edge extension vortex flow-field survey measurements on a F-18 aircraft at high angle of attack
[NASA-TM-4398] p 947 N92-31276
Transonic wind tunnel test of a 14 percent thick oblique wing
[NASA-TM-102230] p 950 N92-32213
Static and dynamic flow visualization studies of two double-delta wing models at high angles of attack
[AD-A252878] p 1040 N92-33678
Prediction and control of asymmetric vortical flows around slender bodies using Navier-Stokes equations
p 1127 N92-33968

ANGLES (GEOMETRY)
Ground collision avoidance using a variable incidence altitude measurement system for the A-7 aircraft
[AD-A243880] p 352 N92-19259
Feasibility study of hypersonic clinometric measurements at R3Ch
[ONERA-RSF-136/1865-AY-728-] p 829 N92-28789

ANGULAR ACCELERATION
Blade instability of horizontally stoppable rotors
p 1085 A92-56308

ANGULAR MOMENTUM
Dynamics of the three-dimensional angular motions of rotating flight vehicles in the presence of the aerodynamic hysteresis of the moment characteristic
p 428 A92-30371
Effect of atmospheric disturbances on airplane response
[AIAA PAPER 92-4340] p 1078 A92-55329

ANGULAR VELOCITY
Calculation of rotational derivatives in the case of local interaction between flow and a body surface
p 624 A92-40746
Nonlinear inversion flight control for a supermaneuverable aircraft p 873 A92-46751
Symptom of payload-induced flight instability
p 873 A92-46761
Computation of the hydrodynamic forces and moments on a body of revolution with and without appendages
[AD-A243033] p 298 N92-16978
FCS skewed sensors array: Practical considerations
p 968 N92-31868

ANISOTROPIC MEDIA
A viscoplastic theory for anisotropic materials
[ONERA, TP NO. 1992-90] p 391 A92-24721
Linear analysis of naturally curved and twisted anisotropic beam p 899 A92-46936
Oscillations of an anisotropic rotor on an elastic anisotropic support p 1057 A92-56311

ANISOTROPIC PLATES
Flutter analysis of anisotropic panels with patched cracks p 219 A92-20216
Initial postbuckling response of an unsymmetrically laminated rectangular plate p 1108 N92-32586

ANISOTROPIC SHELLS
Dynamic analysis of rotor flex-structure based on nonlinear anisotropic shell models p 899 A92-46946
Sensitivity of tire response to variations in material and geometric parameters p 900 A92-47128

ANISOTROPY
Anisotropic control of mesh generation based upon a Voronoi type method p 918 A92-47043
Life prediction and constitutive models for engine hot section anisotropic materials program
[NASA-CR-189223] p 1072 N92-33479
Continuation of tailored composite structures of ordered staple thermoplastic material
[NASA-CR-189671] p 1110 N92-33613

ANNOTATIONS
Magnetic suspension and balance systems: A comprehensive, annotated bibliography
[NASA-TM-4318] p 32 N92-11030

ANNULAR DUCTS
Experimental performance of three design factors for ventral nozzles for SSTOVL aircraft
[AIAA PAPER 92-3789] p 1069 A92-54168
Experimental performance of three design factors for ventral nozzles for SSTOVL aircraft
[NASA-TM-105697] p 742 N92-27669

ANNULAR FLOW
Experimental investigation of coannular jet flow with swirl along a centerbody p 172 A92-18367
Numerical modelling for gas duct in tuboannular combustor p 371 A92-24738
Loss prediction of annular cascade flow based upon S1/S2 stream surface Navier-Stokes analysis p 338 A92-27802
Calculations of the dilution system in an annular gas turbine combustor p 494 A92-31164
Pressure oscillation in the leakage annulus between a shrouded impeller and its housing due to impeller-discharge-pressure disturbances p 580 A92-32942
An experimental and computational investigation of an annular reverse-flow combustor
[UTIAS-338] p 129 N92-11996
Validation of a CANARI code by the computation of three dimensional turbulent flow in turbine valve p 741 N92-27462
Laser anemometer measurements and computations in an annular cascade of high turning core turbine vanes
[NASA-TP-3252] p 830 N92-28980

ANNULAR NOZZLES
The enhancement of mixing in high-speed heated jets using a counterflowing nozzle
[AIAA PAPER 92-3262] p 825 A92-48857

ANNULI
Computational and experimental investigation of annulus heat transfer with swirl
[AIAA PAPER 92-4060] p 1119 A92-56143
The problem of static pressure measurement in turbomachinery annuli using traversable instrumentation
[PNR-90791] p 591 N92-22099

ANODIC COATINGS
Anodize and prime your aluminum without environmental headaches p 892 A92-47340
Non-chromated anodize process for corrosion resistance and adhesive bonding p 892 A92-47341

ANTARCTIC REGIONS
Hunting phenomena of the balloon motions observed over Antarctica
[AIAA PAPER 91-3667] p 14 A92-11014
Long duration ballooning in Antarctica - An operational perspective
[AIAA PAPER 91-3679] p 15 A92-11023
Polar patrol balloon
[AIAA PAPER 91-3688] p 15 A92-11031

ANTENNA ARRAYS
Telemetry antenna patterns for single and multi-element arrays p 188 A92-19216
ETS-V/EMSS mobile satellite communication experiments p 395 A92-26776
A parallel-series-fed microstrip array with high efficiency and low cross-polarization p 496 A92-31630
High gain airborne antenna for satellite communications p 639 A92-40188
Beam scanning error of phased array antenna p 676 A92-40189
Single slotted array achieves multimode performance p 726 A92-44428
Flight test of ARINC 741 configuration low gain SATCOM system on Boeing 747-400 aircraft p 677 N92-24097
Compact range test applications, phase 2
[AD-A248790] p 999 N92-30583

ANTENNA COMPONENTS
DRES unmanned aerial vehicle data link research
[AD-A244272] p 365 N92-19030

ANTENNA COUPLERS
Antennas on complex platforms p 494 A92-31084
Decoupling of antennas using periodic structures p 725 A92-42634

ANTENNA DESIGN
Telemetry antenna patterns for single and multi-element arrays p 188 A92-19216
Finite element analysis of large wavelength antenna radome problems for leading edge and radar phased arrays p 267 A92-23984
Characteristics of a future aeronautical satellite communications system
[AIAA PAPER 92-2058] p 453 A92-29889
High-frequency techniques for antenna analysis p 494 A92-31071
Antennas on complex platforms p 494 A92-31084
Acceptance of two identical radars in the absence of a precision reference p 533 A92-35931
Transfer function between airborne VLF transmit and receive loop antenna p 1045 A92-54754
SATCOM antenna siting study on P-3C aircraft, volume 1
[NASA-CR-189514] p 221 N92-14262
SATCOM antenna siting study on P-3C aircraft, volume 2
[NASA-CR-189515] p 221 N92-14263
Electronically steerable antenna for aircraft p 229 N92-15272
A high gain antenna system for airborne satellite communication applications p 677 N92-24096
Low cost, electronically steered phased array for general aviation p 677 N92-24099
ILS mathematical modeling study of an ILS localizer and glide slope proposed for runway 32R, Moffett Field Airport, California
[DOT/FAA/CT-TN92/28] p 1048 N92-33308

ANTENNA RADIATION PATTERNS
Telemetry antenna patterns for single and multi-element arrays p 188 A92-19216
Finite element analysis of large wavelength antenna radome problems for leading edge and radar phased arrays p 267 A92-23984
High gain airborne antenna for satellite communications p 354 A92-26780
High-frequency techniques for antenna analysis p 494 A92-31071
Antennas on complex platforms p 494 A92-31084
A parallel-series-fed microstrip array with high efficiency and low cross-polarization p 496 A92-31630
Beam scanning error of phased array antenna p 676 A92-40189
Radiation and coupling between antennas mounted on a complex metallic structure p 760 A92-42315
Decoupling of antennas using periodic structures p 725 A92-42634
SATCOM antenna siting study on P-3C aircraft, volume 2
[NASA-CR-189515] p 221 N92-14263
Antenna pattern measurement facilities
[AD-A248964] p 982 N92-30329

ANTENNAS
Joint Federal Aviation Administration (FAA)/Civil Aviation Authority (CAA) Microwave Landing System (MLS) Area Navigation (RNAV) flight evaluations
[DOT/FAA/CT-TN91/17] p 268 N92-15983
Flow visualization and wake analysis for standard and modified configurations of the AN/ALQ-78 antenna pod
[AD-A243552] p 260 N92-17339
Advanced electromagnetic methods for aerospace vehicles
[NASA-CR-190650] p 1001 N92-31156

ANTHROPOMETRY
An anthropometric evaluation of the TH-57 Jetranger helicopter p 46 A92-11164

ANTIFREEZES
Evaluation of the fungicide properties of antifreeze additives for jet fuels p 141 A92-15070

ANTIFRICTION BEARINGS
The application of a cylindrical-spherical floating ring bearing as a device to control stability of turbogenerators p 224 N92-14371

ANTIICING ADDITIVES
Aircraft ground deicing
[SAE PAPER 912222] p 635 A92-40021
Microbiological spoilage of aviation turbine fuel. II - *Evaluation of a suitable biocide* p 891 A92-45600
Technical evaluation report, AGARD Fluid Dynamics Panel Symposium on Effects of Adverse Weather on Aerodynamics
[NASA-TM-105192] p 2 N92-10002

ANTIMISSILE MISSILES
Multiple aperture window and seeker concepts for endo KEW applications
[AIAA PAPER 92-2806] p 752 A92-41344
Transient aerodynamics of a high dynamic pressure shroud separation for a ground-based interceptor missile
[AIAA PAPER 92-2820] p 705 A92-41348

ANTIOXIDANTS
Advanced thermally stable jet fuel development program. Volume 2: Compositional factors affecting thermal degradation of jet fuels
[AD-A252656] p 987 N92-31399

APOLLO PROJECT
NASA engineers and the age of Apollo
[NASA-SP-4104] p 929 N92-28344

APOLLO SOYUZ TEST PROJECT
Issues in developing control zones for international space operations p 1141 A92-56602

APPLICATION SPECIFIC INTEGRATED CIRCUITS
Applications of ASICs to avionics
[AGARD-AG-329] p 859 N92-28376
What is an ASIC? p 859 N92-28377
A radar signal processing ASIC and a VME interface circuit p 859 N92-28380

APPLICATIONS PROGRAMS (COMPUTERS)
Failure environment analysis tool (FEAT) development status
[AIAA PAPER 91-3803] p 232 A92-17654
Application of the STAPAT II code to hypersonic vehicle aerothermodynamics
[AIAA PAPER 91-5035] p 209 A92-17824
The Software Factory, version 5.0
[AIAA PAPER 92-0590] p 411 A92-26992
A review of some computer programs of composites p 1009 A92-53069
Numerical simulation of the reactive flow in advanced (HSR) combustors using KIVA-2
[NASA-CR-188996] p 26 N92-11014
Investigation of the aeroelastic stability of the AFW wind-tunnel model using CAP-TSD
[NASA-TM-104142] p 81 N92-11977
A methodology for software specification and development based on simulation p 135 N92-12458
Process/object-oriented Ada software design for an experimental helicopter p 164 N92-12461
Pilot's associate: Evolution of a functional prototype p 118 N92-12531
Helicopter main-rotor speed effects: A comparison of predicted ranges of detection from the aural detection program ICHIN and the electronic detection program ARCAS
[NASA-TM-104134] p 166 N92-12598
Numerical simulation of vortex street-edge interaction p 88 N92-13027
A 3-degree-of-freedom flight simulator evaluation of *unsteady aerodynamics effects*
[AD-A241540] p 139 N92-13079
Verification of NISA 2 and ENDURE fracture mechanics capability
[NRC-ST-621] p 159 N92-13453
Getting expert systems off the ground: Lessons learned from integrating model-based diagnostics with prototype flight hardware p 220 N92-14217
Airfoil Vibration Dampers program
[NASA-CR-184276] p 225 N92-14391
F/A-18 stabilator: Equivalent set of point forces required for pneumatic bag load case simulation
[AD-A242637] p 206 N92-15073
Numerical simulation of VAWT stochastic aerodynamic loads produced by atmospheric turbulence: VAWT-SAL code
[DE92-000597] p 229 N92-15392
Simplified method for the prediction of aerofoil excrescence drag magnification factor for turbulent boundary layers at subcritical Mach numbers
[ESDU-91028] p 259 N92-15972
Advanced flight software reconfiguraton p 287 N92-17350
An application of the object-oriented paradigm to a flight simulator
[AD-A243624] p 384 N92-18012
Prediction of far-field harmonic noise from propellers
[ESDU-91033] p 416 N92-18074
The 3D inelastic analysis methods for hot section components
[NASA-CR-189089] p 402 N92-18971
Performance and stability analysis of the non-linear dynamics of a simple powered lifting hypersonic vehicle flying on a minor circle
[AD-A243933] p 366 N92-19192
Impact of a process improvement program in a production software environment: Are we any better? p 413 N92-19422
Towards understanding software: 15 years in the SEL p 413 N92-19423
The NREL teetering hub rotor code: Final results and conclusions
[DE92-001187] p 410 N92-19633
A novel approach in formulation of special transition elements: Mesh interface elements
[NASA-CR-189050] p 501 N92-20954
Runway exit designs for capacity improvement demonstrations. Phase 2: Computer model development
[NASA-CR-190166] p 484 N92-21162
Cooperative planning in aviation contexts p 456 N92-21509
Modernized MBB panel code: User's guide including background theory
[PB92-136431] p 526 N92-22233
A two-stroke diesel engine simulation program
[NASA-CR-185155] p 562 N92-22647
PAN AIR: A computer program for predicting subsonic or supersonic linear potential flows about arbitrary configurations using a higher order panel method. Volume 1: Theory document (version 3.0)
[NASA-CR-3251] p 526 N92-22648
Multidisciplinary optimization studies using ASTROS p 571 N92-23234

Analysis of EMP response of structures using frequency domain electromagnetic interaction codes
[AD-A245758] p 765 N92-26592
Hypersonic code efficiency and validation studies
[NASA-CR-190680] p 948 N92-31533
Three-dimensional compressible turbulent computations for a nondiffusing S-duct
[NASA-CR-4391] p 951 N92-32240
Potential flow theory and operation guide for the panel code PMARC
[NASA-TM-102851] p 1036 N92-32422
Computations of unsteady multistage compressor flows in a workstation environment
[NASA-TM-103839] p 1071 N92-32452
User's manual for AeroFcn: A FORTRAN program to compute aerodynamic parameters
[NASA-TM-104237] p 1133 N92-32507
Safety study of TCAS 2 for logic version 6.04
[DOT/FAA/RD-92/22] p 1047 N92-32537
Further development of the CANAERO computer code to include propulsor modelling
[DREA-CR-90-425] p 1038 N92-32811
Advanced software development workstation: Effectiveness of constraint-checking --- spaceflight simulation and planning
[NASA-CR-190712] p 1134 N92-32865
Experience with Ada on the F-18 High Alpha Research Vehicle Flight Test Program
[NASA-TM-104259] p 1062 N92-34039

APPROACH
Effect of wind shear on airspeed during airplane landing approach p 481 A92-32242
Analysis of stand-alone differential GPS for precision approach p 638 A92-38381
Microwave landing system modeling with application to air traffic control automation p 725 A92-41220
A re-analysis of the causes of Boeing 727 'black hole landing' crashes p 833 A92-44985
Differential GPS/inertial navigation approach/landing flight test results p 956 A92-51009
Helicopter physical and performance data
[SCT-91RR-27] p 116 N92-13060
Microwave landing system autoland system analysis
[NASA-CR-189551] p 191 N92-15060
Flight evaluation of curved MLS precision approaches in a twin otter aircraft, phase 2
[AD-A243025] p 268 N92-17568
Visual approach data collection at San Francisco International Airport (SFO)
[DOT/FAA/CT-90/23] p 354 N92-18112
Evaluation of triple simultaneous parallel ILS approaches spaced 5000 feet apart, phase 4.b
[DOT/FAA/CT-91/31] p 456 N92-21404
Effective cueing during approach and touchdown: Comparison with flight p 886 N92-28552

APPROACH AND LANDING TESTS (STS)
Note on flight measured control effectiveness of the quiet STOL experimental aircraft ASKA
[NAL-TR-1103] p 746 N92-28154
Evaluation of landing configuration by flight test of the quiet STOL experimental aircraft ASKA
[NAL-TR-1113] p 733 N92-28191

APPROACH CONTROL
The new airport aeronautic meteorological codes p 160 A92-13855
Airport Surface Traffic Automation p 95 A92-16228
GPS for precision approaches p 139 A92-16648
Precision approach using GPS and GLONASS p 97 A92-16649
Design and flight test of a differential GPS/inertial navigation system for approach/landing guidance p 97 A92-16650
Wide area differential GPS p 101 A92-16966
Results of a test program for the use of differential GPS for approach guidance p 101 A92-16969
Integrated navigation for approach guidance using differential GPS p 101 A92-16970
GPS integrated system application in aircraft approach landing p 266 A92-21466
Forward-look wind-shear detection for microburst recovery p 378 A92-24408
A note on thrust control for jetliner during approach p 457 A92-29518
Improving the efficiency of passenger aircraft during the landing approach p 460 A92-31893
Approach guidance in a downburst p 873 A92-46741
GPS tests during approach at Singapore and Roissy p 956 A92-53240
Application of fuzzy control to aircraft guidance p 1083 A92-56033
Tracking performance requirements for rotorcraft instrument approaches to reduced minima. Phase 1: Preliminary study
[NRC-32137-PHASE-1] p 102 N92-11988
Aircraft accident report: MarkAir, Inc., Boeing 737-2X6C, N670MA, controlled flight into terrain, Unalakleet, Alaska, 2 June 1990
[PB91-910402] p 92 N92-13039
FAA air traffic activity: FY 1990. Addendum
[AD-A241484] p 93 N92-13046
DME growth elements and their use with MLS p 189 N92-14018
A Taxi And Ramp Management And Control system (TARMAC) p 207 N92-14027
Evaluation of triple simultaneous parallel ILS approaches spaced 4300 feet apart, phase 4a
[ACD-340] p 191 N92-14034
The COMPAS system in the ATC environment
[DLR-MITT-91-08] p 354 N92-19041
Design principles of automation aids for ATC approach control p 354 N92-19042
COMPAS system concept p 354 N92-19043
Evaluation of the COMPAS experimental system p 355 N92-19044
Experiences developed in transfering the experimental COMPAS system to an operational prototype version p 355 N92-19045
Steps toward acceptance p 355 N92-19046
Evaluation of the COMPAS operational system p 355 N92-19047
Extension of the Frankfurt COMPAS for general application p 355 N92-19048
The impact of COMPAS on the future Cooperative Air Traffic Management Concept (CATMAC) p 355 N92-19049
Attributes of winged manned space vehicles and their relationship to ground site characteristics and facilities p 487 N92-20776
Enhanced displays, flight controls, and guidance systems for approach and landing p 456 N92-21957
Approach and landing assisted by onboard image processing p 457 N92-21959
Approach and landing guidance p 457 N92-21960
Development of new flight procedures for the Microwave Landing System (MLS)
[NLR-TP-91156-U] p 1047 N92-32830

APPROACH INDICATORS
Curved landing approaches using ILS and Loran C p 94 A92-13854
Infra-red offers new landing aid competition p 198 A92-18937
A compensatory algorithm for the slow-down effect on constant-time-separation approaches
[NASA-TM-4285] p 23 N92-10024

APPROPRIATIONS
National Aeronautics and Space Administration p 238 N92-14923
National Aeronautics and Space Administration p 238 N92-14925
National Aeronautics and Space Administration p 238 N92-14927
New Ways: Tiltrotor aircraft and magnetically levitated vehicles
[OTA-SET-507] p 238 N92-14933
National Aeronautics and Space Administration research and development p 238 N92-15937
National Aeronautics and Space Administration p 417 N92-18309
National Aeronautics and Space Administration Authorization Act, 1993
[S-2558-IS] p 698 N92-25606
Departments of Veterans Affairs and Housing and Urban Development, and independent agencies appropriations for 1993, part 6
[GAO-55-636-PT-6] p 1141 N92-32505
NASA authorization, 1993, volume 1
[GPO-55-260-VOL-1] p 1142 N92-33147

APPROXIMATION
Extensions to the minimum-state aeroelastic modeling method p 20 A92-11081
A study of a version of the boundary conditions of a two-dimensional spline in surface and line modeling p 163 A92-16826
A method for estimating the minimum distance between two flight vehicles during their separation p 486 A92-30139
Slenderness approximations in RCS estimation - The simplest 2-D case p 533 A92-33622
Taylor series approximation of geometric shape variation for the Euler equations p 899 A92-46916
Approximate analysis for failure probability of structural systems p 901 A92-47671
New literal approximations for the longitudinal dynamic characteristics of flexible flight vehicles
[AIAA PAPER 92-4411] p 1075 A92-55205
Comparison of polynomial approximations and artificial neural nets for response surfaces in engineering optimization p 165 N92-13835
Design optimization of transonic airfoils p 177 N92-13961
Approximation methods for control of acoustic/structure models with piezoceramic actuators
[NASA-CR-189578] p 234 N92-15658
Approximate truncated balanced realizations for infinite dimensional systems p 602 N92-22493
Efficient and robust design optimization of transonic airfoils p 528 N92-23717
An approximate viscous shock layer technique for calculating chemically reacting hypersonic flows about blunt-nosed bodies p 1041 N92-33837

ARAMID FIBER COMPOSITES
Design and use of aramid fiber in aircraft structures p 784 A92-47407

ARC DISCHARGES
New insulation constructions for aerospace wiring applications. Volume 2: The 270 VDC arc tracking testing with power controllers
[AD-A240639] p 23 N92-11007

ARC HEATING
Numerical prediction of the flow characteristics in an arc wind tunnel
[AIAA PAPER 92-4016] p 1100 A92-56838
Flow contamination and flow quality in arc heaters used for hypersonic testing
[AIAA PAPER 92-4028] p 1100 A92-56850
Initial calibration of the HEAT-H2 arc-heated wind tunnel
[AD-A245072] p 484 N92-20898

ARC LAMPS
Simulation of high heat flux levels with graphite heating and arc lamps p 980 A92-51402

ARC SPRAYING
Development of a new generation of high-temperature composite materials p 578 N92-22515

ARC WELDING
Restoration of aircraft engine nozzle block blades by vacuum arc brazing with controlled current p 471 A92-30381
Blade repair with adaptive vision tracking
[ASME PAPER 91-GT-208] p 607 A92-36897
Stainless steel welding shines through on wind tunnel project p 1123 A92-57039

ARCHITECTURE
Determination of aircraft noise levels while the engine is running on the ground - An approach from the point of urbanization and architecture p 688 A92-39064

ARCHITECTURE (COMPUTERS)
The designer-FEM model interface based on the data base management concept p 163 A92-16832
Digital technology applied to airborne receivers p 98 A92-16927
A parallel architecture adapted to onboard multiexpert systems p 276 A92-23040
From concept to model: Conception and evaluation of an architecture for a distributed system with SAHARA - Some reflections on results of the utilization of SAHARA in the framework of the Electronic Copilot
[ONERA, TP NO. 1991-216] p 411 A92-26368
Advancing airlift avionics - C-17 avionics suite
[AIAA PAPER 92-1243] p 553 A92-33336
Transmission vibration monitoring - A single board computer architecture p 554 A92-35765
ARINC and the avionics of commercial aircraft. II p 637 A92-37072
Evaluation and comparison of triple and quadruple flight control architectures p 745 A92-43884
Fault tolerant EHA architectures --- electro-hydrostatic actuator p 763 A92-43885
Future directions in computing and CFD
[AIAA PAPER 92-2734] p 917 A92-45489
A high performance general purpose processing element for avionic applications p 920 A92-48440
Global memory in the Pave Pace architecture p 920 A92-48447
A fault-tolerant network architecture for integrated avionics p 965 A92-49297
Flight management system back-up navigation for the A330/A340 aircraft p 975 A92-49326
Neural networks for feedback linearization in aircraft control
[AIAA PAPER 92-4391] p 1074 A92-55192
Advanced information processing system: Inter-computer communication services
[NASA-CR-187556] p 53 N92-11706
An independent review of the Multi-Path Redundant Avionics Suite (MPRAS) architecture assessment and characterization report
[NASA-CR-188126] p 163 N92-12440
A NASA/RAE cooperation in the development of a real-time knowledge based autopilot p 164 N92-12528
AI for RPVs, Sensor Driven Airborne Replanner (SDAR), for a Robotic Aircraft Sensor Platform (RASP) p 114 N92-12534
Engineering Graphical Analysis Tool (EGAT) development program p 164 N92-12542

Evolution of avionic systems architecture, from the 1950's to the present p 198 N92-14047
Mixed approach towards modular avionics conflicting requirements p 199 N92-14051
Avionics software evolution p 199 N92-14052
Avionics technology beyond 2000 p 200 N92-14058
Architecture for Survivable System Processing (ASSP) p 220 N92-14210
Artificial Neural Network Approaches in Guidance and Control
[AGARD-LS-179] p 234 N92-14673
Introduction to neural computing and categories of neural network applications to guidance, navigation and control p 234 N92-14674
Implementation of an object-oriented flight simulator D.C. electrical system on a hypercube architecture
[AD-A243700] p 284 N92-17097
Ultra High Speed Numerical Wind Tunnel (UHSNWT) initiative at National Aerospace Laboratory numerical simulator - second generation
[NAL-TR-1108] p 384 N92-18037
NASA TSRV essential flight control system requirements via object oriented analysis
[NASA-CR-189573] p 381 N92-19499
Data processing aspects of the Hermes Flight Control Center p 513 N92-20629
Design of an integrated airframe/propulsion control system architecture
[NASA-CR-182004] p 602 N92-22643
Design of an integrated airframe/propulsion control system architecture
[NASA-CR-182007] p 602 N92-22644
Parallel knowledge based systems architectures for in-flight mission management p 728 N92-27904
Core avionics and standardization
[AD-A248326] p 735 N92-27925
Application of VME-technology on an airborne data link processor unit
[NLR-MP-88040-U] p 841 N92-29615
A model of the ADA avionics real-time system: An example of the benefits of the hardware/software codesign approach in development of real-time systems
[AD-A248893] p 967 N92-30524
Fly-by-light technology development plan
[NASA-CR-181954] p 1086 N92-32778
The development of an airborne information management system for flight test
[NASA-TM-104251] p 1065 N92-32866

AREA NAVIGATION
Greater RNAV utilization could expand system capacity p 448 A92-29507
The problem of multiple solutions in area navigation and computed centerline operations with the microwave landing system
[AD-A242757] p 191 N92-15058

ARIANE LAUNCH VEHICLE
Computation of aerodynamic coefficients on Hermes-Ariane5 configuration p 184 N92-15040

ARMED FORCES (FOREIGN)
Aircraft fatigue management in the Royal Air Force p 363 N92-18591

ARMED FORCES (UNITED STATES)
Total quality treatment for science and technology --- in USAF p 697 A92-36950
Avionics standardization in the USAF: 1980 to 1990 p 198 N92-14048
The V-22 tilt rotor: A comparison with existing Coast Guard aircraft
[AD-A245843] p 650 N92-26039
Decision-making guide for the proposed Coast Guard differential global positioning system
[AD-A246046] p 957 N92-32054
United States Air Force summer research program 1991. Volume 1: Program management report
[AD-A248763] p 1142 N92-32338

ARRAYS
Method of measuring cross-flow vortices by use of an array of hot-film sensors
[NASA-CASE-LAR-14824-1-SB] p 998 N92-30390
FCS skewed sensors array: Practical considerations p 968 N92-31868

ARRESTING GEAR
Self-compensating carrier aircraft recovery system p 448 A92-32238

ARROW WINGS
Computational studies of transonic flow past a swept wing and the boundary layer characteristics p 438 A92-31872
The effectiveness of the warp shape airfoil of a supersonic transport p 711 A92-43203
Exploratory investigation of a spanwise blowing concept for tip-stall control on cranked-arrow wings
[AIAA PAPER 92-2637] p 806 A92-45576
Proposal for a low cost close air support aircraft for the year 2000: The Raptor
[NASA-CR-190023] p 367 N92-19496

ARTIFICIAL INTELLIGENCE
Using new aggregation operators in rule-based intelligent control p 51 A92-11456
Distributed artificial intelligence approach to air traffic control p 161 A92-13436
Preliminary design of axial compressors using artificial intelligence and numerical optimization techniques
[ASME PAPER 91-GT-334] p 126 A92-15699
An intelligent pilot vehicle interface for a day/night *adverse weather pilotage system (D/NAPS)*
[AIAA PAPER 91-3729] p 197 A92-17596
Probabilistic reasoning for intelligent wind shear avoidance p 302 A92-21181
AI technology and application development on the Shuttle project p 302 A92-23693
Real-time decision aiding - Aircraft guidance for wind shear avoidance
[AIAA PAPER 92-0290] p 350 A92-25743
Identification of helicopter noise using a neural network p 416 A92-28032
Integration of artificial intelligence and numerical optimization techniques for the design of complex aerospace systems
[AIAA PAPER 92-1189] p 600 A92-33301
Advanced training systems for the next decade and beyond
[AIAA PAPER 92-1626] p 690 A92-38699
Airport X-ray screening technology becomes a viable explosives detector p 836 A92-47925
An artificial intelligence approach for the verification of requirements for aircraft electrical power systems p 863 A92-48481
Developing intelligent automatic test equipment p 922 A92-48569
Verification and validation testing of the pilot's associate p 966 A92-49318
The design and simulation of an intelligence flight control system p 976 A92-50237
Anti-fatigue optimization design by artificial intelligence strategy p 996 A92-53013
Machine Intelligence for Aerospace Electronic Systems
[AGARD-CP-499] p 164 N92-12517
Locally linear neural networks for aerospace navigation systems p 103 N92-12530
AI for RPVs, Sensor Driven Airborne Replanner (SDAR), for a Robotic Aircraft Sensor Platform (RASP) p 114 N92-12534
Engineering Graphical Analysis Tool (EGAT) development program p 164 N92-12542
The use of artificial neural networks in experimental data acquisition and aerodynamic design p 90 N92-13848
Knowledge based system applications for guidance and control
[AGARD-AR-284] p 205 N92-14065
Automated planning with special relevance to associate systems technology and mission planning
[AD-A241924] p 303 N92-17438
A connectionist approach to autonomous robotic navigation p 454 N92-20356
Towards coherent hypermedia navigation by pragmatic dialogue modeling
[PB92-114735] p 455 N92-20818
Improving designer productivity --- artificial intelligence
[NASA-TM-103929] p 854 N92-29417
CTAS: Computer intelligence for air traffic control in the terminal area
[NASA-TM-103959] p 1044 N92-33080
Human factors issues in the use of artificial intelligence in air traffic control. October 1990 Workshop
[NASA-CR-190925] p 1051 N92-34203

ARTIFICIAL SATELLITES
Fuzzy guidance system evaluation p 778 N92-27903

ASCENT
Determination of balloon drag
[AIAA PAPER 91-3666] p 5 A92-11013
Results of the space shuttle vehicle ascent air data system probe calibration test using a 0.07-scale external tank forebody model (68T) in the AEDC 16-foot transonic wind tunnel (IA-310), volume 1
[NASA-CR-167696] p 286 N92-17167
Results of the space shuttle vehicle ascent air data system probe calibration test using a 0.07-scale external tank forebody model (68T) in the AEDC 16-foot transonic wind tunnel (IA-310), volume 2
[NASA-CR-167697] p 286 N92-17214

ASIA
Future considerations for vertical flight p 608 A92-40383

ASPECT RATIO
Lift development of delta wings undergoing constant acceleration from rest p 9 A92-13209
Combined compressive and shear buckling analysis of hypersonic aircraft sandwich panels
[AIAA PAPER 92-2487] p 586 A92-34603
Effect of twin fins on isolated tailplane lift-curve slope
[ESDU-91009] p 80 N92-11969
The BCAC/IAR collaborative research program to investigate the sidewall boundary layer effects in the IAR/NRC 2-D High Reynolds Number Test Facility
[NRC-HSA-434] p 81 N92-11976
Numerical simulation of vortex flows past impulsively started wings p 88 N92-13028
The effects of winglets on low aspect ratio wings at *supersonic Mach numbers*
[NASA-CR-4407] p 178 N92-13996
Simulation of iced wing aerodynamics p 450 N92-21686
A theoretical investigation of the induced drag of wing of finite aspect ratio
[CUED/A-AERO/TR-17(1991)] p 525 N92-22193

ASPHALT
Alternate/modified binders for asphalt airfield pavements
[AD-A242829] p 285 N92-17260
Criteria for use of seal coats on airport pavements
[DOT/FAA/RD-92/18] p 1102 N92-34247

ASSEMBLING
Assembling the future p 783 A92-44895

ASSESSMENTS
Structural risk assessment in the Israel Air Force for fleet management p 836 A92-46779

ASSOCIATIVE PROCESSING (COMPUTERS)
A novel associative memory for high level control functions p 52 A92-11472

ASTROLOY (TRADEMARK)
Crack initiation and the short-to-long crack growth transition in a Ni-base superalloy p 213 A92-19767

ASTRONAUTICS
Collection of papers of the 31st Israel Annual Conference on Aviation and Astronautics
[ITN-92-85124] p 932 N92-31861
An international aerospace information system: A cooperative opportunity
[NASA-TM-108171] p 1142 N92-33237

ASTRONOMY
United States Air Force summer research program 1991. Volume 1: Program management report
[AD-A248763] p 1142 N92-32338

ASYMMETRY
Effect of upstream disturbance on flow asymmetry
[AIAA PAPER 92-0408] p 325 A92-26261
Asymmetric vortex flow over circular cones p 86 N92-13014
Prediction and control of asymmetric vortical flows around slender bodies using Navier-Stokes equations p 1127 N92-33968

ASYMPTOTIC METHODS
A simplified model for aerodynamic flows around streamlined models p 63 A92-13816
Development of a combined fast method for studying the plane motions of rigid bodies in the atmosphere around the center of mass in the presence of perturbations p 304 A92-23563
An algebraic model for dissipation in supersonic boundary layers
[AIAA PAPER 92-0311] p 320 A92-25759
Boundary layer on slender wings of small aspect ratio p 441 A92-31963
Asymptotic defect boundary-layer theory applied to hypersonic flows p 610 A92-36839
The subsonic and transonic flow around the leading edge of a thin airfoil with a parabolic nose
[AIAA PAPER 92-2649] p 797 A92-45516
Asymptotic theory of transonic wind tunnel wall interference
[AD-A244075] p 403 N92-19080
Nonlinear system design: Adaptive feedback linearization with unmodeled dynamics
[AD-A248484] p 1009 N92-30335

ASYMPTOTIC PROPERTIES
Asymptotics of the upper branch of the neutral curve at subsonic and transonic external flow velocities p 79 A92-16705

ASYMPTOTIC SERIES
Multiple line-vortex model of vortex flows around body of revolution at high angles of attack up to 60 degrees p 314 A92-25104

ATMOSPHERIC ATTENUATION
Radar multipath study for rain-on-radome experiments at the Aircraft Landing Dynamics Facility
[NASA-TM-101657] p 680 N92-25137
A numerical model for sonic boom propagation through an inhomogeneous, windy atmosphere p 1138 N92-33876

ATMOSPHERIC BOUNDARY LAYER
A data base for flight in the wake of a ship
[AIAA PAPER 92-0295] p 319 A92-25748

Surface-layer gusts for aircraft operation
p 774 A92-42095
Simple models for the description of turbulence in the atmospheric boundary layer
[DLR-FB-90-17] p 410 N92-19292
Measurements in the inhomogeneous convective boundary layer using three powered gliders
p 775 N92-26350

ATMOSPHERIC CHEMISTRY
Impact of heterogeneous chemistry on model-calculated ozone change due to high speed civil transport aircraft
p 45 A92-12941
Twenty years of airborne research at the University of Washington p 161 A92-14925
Digital ozonesondes - Examples of results from the EMEFS experiments of 1988 and 1990
p 468 A92-32140
Hypersonic flows with air chemistry over a reentry vehicle at high altitudes p 1017 A92-53549
High-speed civil transport aircraft emissions
p 408 N92-19122
Designing a methodology for future air travel scenarios p 409 N92-19125
Lower stratospheric measurement issues workshop report p 409 N92-19127
Reaction speed constant for the reactions between N + O2 and between O + N2
[ETN-92-90861] p 347 N92-19252

ATMOSPHERIC CIRCULATION
Mesoscale dynamics of cold fronts - Structures described by dropsoundings in Fronts 87
p 230 A92-18902
Airdata calibration techniques for measuring atmospheric wind profiles p 856 A92-46792
Simplified signal processing for an airborne CO2 Doppler lidar p 1000 N92-31023

ATMOSPHERIC COMPOSITION
Airborne tests of flux measurement by the relaxed eddy accumulation technique p 504 A92-32052
Meeting Review: Airborne Aerosol Inlet Workshop
[NASA-CR-189814] p 301 N92-17393
Natural cycles, gases p 408 N92-19123
Designing a methodology for future air travel scenarios p 409 N92-19125
Lower stratospheric measurement issues workshop report p 409 N92-19127

ATMOSPHERIC CORRECTION
Methods for determining atmospheric correction for radio-rangefinder measurements of inclined trajectories
p 775 A92-44070

ATMOSPHERIC EFFECTS
Flight service evaluation of composite helicopter components p 106 A92-14372
Determination of aircraft noise levels while the engine is running on the ground - An approach from the point of urbanization and architecture p 688 A92-39064
The effect of atmospheric turbulence on the external store separation from an aircraft p 934 A92-50233
A study of the airwake aerodynamics over the flight deck of an AOR model ship
[AD-A241008] p 89 N92-13034
The atmospheric effects of stratospheric aircraft: A first program report
[NASA-RP-1272] p 408 N92-19121
Lower stratospheric measurement issues workshop report p 409 N92-19127
A study of atmospheric optical scattering parameters at 1.5 and 2 micron region for solid state Doppler lidar applications p 1001 N92-31067
High-Speed Research: Sonic Boom, volume 1
[NASA-CP-3172] p 1061 N92-33874

ATMOSPHERIC ELECTRICITY
Stratospheric electrodynamics from superpressure balloons - A technical challenge for small payload environments
[AIAA PAPER 91-3674] p 14 A92-11019
Expert knowledge techniques applied to the analysis of electric field mill data p 408 A92-27991
Mechanisms of high-current pulses in lightning and long-spark stepped leaders p 1116 A92-54678

ATMOSPHERIC ENTRY
A unified nonequilibrium model for hypersonic flows
p 3 A92-10575
Shuttle Entry Air Data System - An experimental investigation of calibration for ascent flight
[AIAA PAPER 92-0133] p 286 A92-23753
A ballistic investigation of the aerodynamic characteristics of a blunt vehicle at hypersonic speeds in carbon dioxide and air
[AIAA PAPER 92-0328] p 322 A92-25775
Monte Carlo simulation of entry in the Martian atmosphere
[AIAA PAPER 92-0494] p 329 A92-26324
Singularity bypass algorithms in the numerical solution of equations of body motion relative to a center of mass in the atmosphere in the presence of disturbances
p 437 A92-31857
Vibrational relaxation effects in hypersonic flows of a viscous gas p 609 A92-36550
Thermal deformation of a polymer heat shield material on the descent trajectory p 754 A92-42655
Direct simulation of hypersonic rarefied flows about atmospheric re-entry vehicles p 710 A92-43169
Study of the flow field and molecular radiation heating around a reentry vehicle p 711 A92-43227
Direct simulation of re-entry flows with ionization
p 713 A92-44367
A parametric analysis of radiative structure in aerobrake shock layers
[AIAA PAPER 92-2970] p 816 A92-46985
Decoupled predictions of radiative heating in air using a particle simulation method
[AIAA PAPER 92-2971] p 816 A92-46986
Gridding strategies and associated results for winged entry vehicles p 918 A92-47051
Computation of 3-D hypersonic flows in chemical non-equilibrium including transport phenomena
[AIAA PAPER 92-2876] p 820 A92-47858
Influence of atmospheric rarefaction on aerodynamic characteristics of flying vehicles p 938 A92-52750
Enhancements and applications of DSMC for hypersonic rarefied flows p 939 A92-52761
Concepts of flight experiments for HOPE development
p 1103 A92-53635
Three-dimensional calculation of radiative field in hypersonic air shock layers p 1023 A92-54498
HOPE re-entry experimental vehicle
p 1103 A92-55098
NASA aerodynamics program
[NASA-TM-4368] p 609 N92-24678

ATMOSPHERIC ENTRY SIMULATION
Simulation of hypersonic flows on unstructured grids
p 434 A92-31496

ATMOSPHERIC IONIZATION
Monte Carlo simulation of reentry flows with ionization
[AIAA PAPER 92-0493] p 328 A92-26323

ATMOSPHERIC MODELS
Impact of heterogeneous chemistry on model-calculated ozone change due to high speed civil transport aircraft
p 45 A92-12941
Atmospheric disturbance model for aircraft and space capable vehicles
[AIAA PAPER 92-0294] p 407 A92-25747
Some issues on modeling atmospheric turbulence experienced by helicopter rotor blades
p 647 A92-40885
Meeting Review: Airborne Aerosol Inlet Workshop
[NASA-CR-189814] p 301 N92-17393
Ozone response to aircraft emissions: Sensitivity studies with two-dimensional models p 409 N92-19126
On the optimization of windshear warning and guidance systems
[NLR-TP-90196-U] p 837 N92-29703
Remote sensing of trapping layer base height using ATIS transmissions
[AD-A250074] p 1004 N92-31362
A numerical model for sonic boom propagation through an inhomogeneous, windy atmosphere
p 1138 N92-33876

ATMOSPHERIC MOISTURE
Retrieval of total precipitable water over high latitude regions using radiometric measurements near 90 and 183 GHz p 505 A92-32129

ATMOSPHERIC OPTICS
Aero-optical testing in the NSWC Hypervelocity Tunnel No. 9
[AIAA PAPER 92-2797] p 747 A92-41336
Visibility in the atmosphere and flight safety --- Russian book
[ISBN 5-286-00416-4] p 775 A92-42785
JPRS report: Science and technology. USSR: Engineering and equipment
[JPRS-UEQ-91-010] p 593 N92-22397
Agreements/subagreements applicable to Wallops, 12 Nov. 1991 p 575 N92-22598

ATMOSPHERIC PHYSICS
Agreements/subagreements applicable to Wallops, 12 Nov. 1991 p 575 N92-22598

ATMOSPHERIC PRESSURE
A Kalman filter mechanization for the baro-inertial vertical channel p 673 A92-39558
C-29A aircraft altimeter errors
[AD-A240486] p 23 N92-11011
Atmospheric pressure flow reactor: Gas phase chemical kinetics under tropospheric conditions without wall effects
[NASA-CASE-MSC-21384-1] p 297 N92-16243

ATMOSPHERIC RADIATION
Manned orbital balloon flight - Available techniques
[AIAA PAPER 91-3675] p 15 A92-11020

ATMOSPHERIC SCATTERING
A study of atmospheric optical scattering parameters at 1.5 and 2 micron region for solid state Doppler lidar applications p 1001 N92-31067

ATMOSPHERIC SOUNDING
Recent developments in the use of thin-film polyethylene balloons for meteorological applications
p 16 A92-11033
Mesoscale dynamics of cold fronts - Structures described by dropsoundings in Fronts 87
p 230 A92-18902
Atmospheric analysis for airdata calibration on research aircraft
[AIAA PAPER 92-0293] p 369 A92-25746
Airborne tests of flux measurement by the relaxed eddy accumulation technique p 504 A92-32052
Use of relative humidity sensors for planes measurement p 467 A92-32080
An airborne cryogenic frost-point hygrometer
p 467 A92-32090
Retrieval of total precipitable water over high latitude regions using radiometric measurements near 90 and 183 GHz p 505 A92-32129

ATMOSPHERIC TEMPERATURE
Hunting phenomena of the balloon motions observed over Antarctica
[AIAA PAPER 91-3667] p 14 A92-11014
A new thermometric instrument for airborne measurements in clouds p 368 A92-24918
Modeling the effect of helicopter downwash on warm fog p 775 A92-44081

ATMOSPHERIC TURBULENCE
A new method for simulating atmospheric turbulence for rotorcraft applications p 162 A92-14368
The response of a helicopter to windshear
p 269 A92-21470
International standardisation of regulations for gust loading calculations p 270 A92-22473
Gust effects on a flexible aircraft p 270 A92-22474
Atmospheric disturbance model for aircraft and space capable vehicles
[AIAA PAPER 92-0294] p 407 A92-25747
Experimental study of the effects of atmospheric turbulence on sound propagation over the ground
[ONERA, TP NO. 1991-211] p 415 A92-26363
Severe turbulence with a low-level jet ahead of a squall line p 407 A92-27939
Understanding and predicting microbursts
p 407 A92-27953
Determination of the mean duration of normal acceleration loads at the center of mass of aircraft during a flight in a turbulent atmosphere p 480 A92-30192
Effects of ambient turbulence on the decay of a trailing vortex wake p 442 A92-32245
Windshear detection p 652 A92-40883
Some issues on modeling atmospheric turbulence experienced by helicopter rotor blades
p 647 A92-40885
Adequacy of modeling turbulence and related effects on helicopter response p 730 A92-41263
A sensitive fast-response probe to measure turbulence and heat flux from any airplane p 775 A92-42097
Selected models of aircraft navigation space
p 839 A92-45373
The effect of atmospheric turbulence on the external store separation from an aircraft p 934 A92-50233
Some problems on atmospheric turbulence spectrum and aircraft response p 975 A92-50235
Effect of atmospheric disturbances on airplane response
[AIAA PAPER 92-4340] p 1078 A92-55329
ATTAS flight test and simulation results of the advanced gust management system LARS
[AIAA PAPER 92-4343] p 1079 A92-55332
The modelling of turbulence and downbursts for flight simulators
[UTIAS-339] p 161 N92-12373
Numerical simulation of VAWT stochastic aerodynamic loads produced by atmospheric turbulence: VAWT-SAL code
[DE92-000597] p 229 N92-15392
Simple models for the description of turbulence in the atmospheric boundary layer
[DLR-FB-90-17] p 410 N92-19292
Nonlinear acoustic propagation of shock waves through the atmosphere with molecular relaxation
p 511 N92-20360
A new method for simulating atmospheric turbulence for rotorcraft applications p 464 N92-21956
The modelling of turbulence and downbursts for flight simulators
[ISBN-0-315-59945-6] p 749 N92-27645

Response of helicopters to gusts
[NLR-TP-90159-U] p 879 N92-28653
Atmospheric turbulence spectra and correlation functions
[NLR-TP-89217-U] p 915 N92-28689
High-Speed Research: Sonic Boom, volume 1
[NASA-CP-3172] p 1061 N92-33874
Wave equations and computational models for sonic boom propagation through a turbulent atmosphere
p 1139 N92-33877
Simulations of sonic boom ray tube area fluctuations for propagation through atmospheric turbulence including caustics via a Monte Carlo method
p 1139 N92-33878
Analysis of sonic boom data to quantify distortions of shock profiles p 1139 N92-33879
The effect of turbulence on the loudness of minimized sonic boom signatures p 1139 N92-33880
Model experiment to study the effect of turbulence on risetime and waveform of N waves
p 1139 N92-33881
Steady state risetimes of shock waves in the atmosphere p 1140 N92-33882
Preliminary results from the White Sands Missile Range sonic boom propagation experiment
p 1140 N92-33884
Turbulence-induced loads on a teetered rotor
p 1042 N92-34029

ATMOSPHERICS
Probability of cycle jumps in Omega receivers and other phase locked loop applications
[PB92-128891] p 455 N92-21279

ATOMIC EXCITATIONS
Improving sample introduction for total wear metal determination by atomic emission spectroscopy
p 389 A92-26850

ATOMIC RECOMBINATION
Recombination-dominated nonequilibrium heat transfer to arbitrarily catalytic hypersonic vehicles
p 2 A92-10426

ATOMIZERS
The influence of spray angle on the continuous- and discrete-phase flowfield downstream of an engine combustor swirl cup
[AIAA PAPER 92-3231] p 863 A92-48832

ATOMIZING
Interfacial instability between a liquid film and the surrounding compressible gas
[AIAA PAPER 92-0461] p 395 A92-26302
Experimental investigation on the structure of flow field and the total pressure loss in an atomizing channel injector p 375 A92-28436
On performance calculation of centrifugal dish atomizer combustor p 654 A92-37390
Near-injector structure of non-evaporating pressure-atomized sprays at various ambient densities
p 681 N92-25571

ATTACK AIRCRAFT
Technology developments applied to the AH-1W SuperCobra
[AIAA PAPER 91-3071] p 21 A92-11607
Enhanced energy maneuverability for attack helicopters using continuous, variable (C-V) rotor speed control
p 132 A92-14421
Graceful degradation of GPS/INS performance with fewer than four satellites p 97 A92-16644
Flight management system integration on the F-117A
[AIAA PAPER 92-1077] p 563 A92-33246
Rafale: Program update - Development of a naval version p 645 A92-40035
Aircraft route optimization using adaptive simulated annealing p 922 A92-48565
Computational icing analysis for aircraft inlets
[AIAA PAPER 92-3178] p 836 A92-48793
Flight management system of the F-117A
p 1082 A92-55910
An experimental investigation of vortex flaps on a canard combat-aircraft configuration p 87 N92-13023
Scorpion: Close Air Support (CAS) aircraft
[NASA-CR-189974] p 462 N92-20664
The SnoDog: Preliminary design of a close air support aircraft
[NASA-CR-189990] p 462 N92-21489
Time-optimal reorientation maneuvers of an aircraft
p 549 N92-22605

ATTENUATION
Method and apparatus for acoustic plate mode liquid-solid phase transition detection
[DE92-003778] p 401 N92-18705

ATTITUDE (INCLINATION)
That all-important interface p 100 A92-16953
INS alignment using GPS Phase III user equipment computed corrections p 100 A92-16955
Model attitude measurements at NASA Langley Research Center
[AIAA PAPER 92-0763] p 398 A92-28226
Numerical simulation of vortex flows past impulsively started wings p 88 N92-13028
Evaluation of electrolytic tilt sensors for measuring model angle of attack in wind tunnel tests
[NASA-TM-4315] p 297 N92-16283
Target pitch angle for the microburst escape maneuver p 266 N92-17996
GPS/INS integration for improved aircraft attitude estimates
[AD-A243947] p 356 N92-19604

ATTITUDE CONTROL
A proposal for a dynamic test platform for inertial units and/or GPS p 138 A92-16653
Autonomously aided strapdown attitude reference system p 204 A92-18610
GPS interferometric attitude and heading determination - Initial flight test results p 454 A92-30023
Analyzing the flared landing task with pitch-rate flight control systems p 661 A92-39905
Study of the flight control of remotely piloted helicopters p 745 A92-43183
Numerical analysis of RCS jet in hypersonic flights
[SAE PAPER 912063] p 791 A92-45445
Nonlinear inversion flight control for a supermaneuverable aircraft p 873 A92-46751
The propulsive-only flight control problem
p 876 A92-48487
Design of robust Quantitative Feedback Theory controllers for pitch attitude hold systems
[AIAA PAPER 92-4409] p 1075 A92-55203
An autorotation-entry control for a helicopter with a fuzzy controller p 1083 A92-56032
V-22 propulsion system design p 1070 A92-56300
An evaluation of four F-16 vertical velocity indicator configurations
[AD-A243629] p 370 N92-18014
Characterization of unsteady aerodynamic phenomena at high angles p 364 N92-18787
Description and simulation results of the Italsat AOCS advanced flight simulator p 667 N92-24472
Fuzzy guidance system evaluation
p 778 N92-27903

ATTITUDE GYROS
Estimation of aircraft attitude by angular rate measurements p 963 N92-31881

ATTITUDE INDICATORS
Measurement of position and attitude using laser and retro-reflectors p 1047 A92-56120
Evaluation of electrolytic tilt sensors for measuring model angle of attack in wind tunnel tests
[NASA-TM-4315] p 297 N92-16283
GPS interferometric attitude and heading determination: Initial flight test results p 269 N92-17994
Estimation of aircraft attitude by angular rate measurements p 963 N92-31881

ATTITUDE STABILITY
A multibody analog of the dual-spin problem
p 49 A92-11426
Pitch-heave dynamics models for an air cushion vehicle
[ISBN-0-315-51095-1] p 716 N92-27624

AUDIO FREQUENCIES
Do we really need 57 ways of rating aircraft noise?
p 688 A92-39065
Exposures from headset interference tones
[AD-A247175] p 1136 N92-32697

AUDITORY DEFECTS
Risk to hearing from overflight noise of military aircraft
[ISVR-TR-194] p 604 N92-22241

AUDITORY PERCEPTION
NATO CCMS aircraft noise study on receiver technology p 686 A92-39050
A noise survey around Oslo Airport Fornebu
p 687 A92-39061
Temporal change of noisiness of helicopter noise
p 689 A92-39103
Temporal change of timbre of helicopter noise
p 694 A92-39104
Human response to aircraft noise p 236 N92-14780
Human response to helicopter noise: A test of A-weighting
[AD-A243719] p 304 N92-17506

AUSTENITIC STAINLESS STEELS
Characterization of stainless steel pretreatments for adhesive bonding p 994 A92-51546

AUSTRALIA
Aerospace plane technology: Research and development efforts in Japan and Australia
[AD-A241641] p 62 N92-12991

AUTOCLAVES
Enhanced diagnostic system for autoclaves and bonding presses p 145 A92-14381

AUTOGYROS
Instrumented blade experiments using a light autogiro
p 555 A92-35773
An aerodynamical analysis of 'seesaw' type rotor for autogyro p 937 A92-52034

AUTOMATA THEORY
Route planning --- in real-time of avionics systems
p 1006 A92-49317

AUTOMATED EN ROUTE ATC
Polish radar technology. II - Adaptive radar AVIA CM
p 39 A92-12290
Profile negotiation - A concept for integrating airborne and ground-based automation for managing arrival traffic
p 531 A92-33432
Automated problem resolution prototype in automated en route air traffic control p 190 N92-14028

AUTOMATED RADAR TERMINAL SYSTEM
The European ATC challenge p 19 A92-11877
Evaluation of triple simultaneous parallel ILS approaches spaced 4300 feet apart, phase 4a
[ACD-340] p 191 N92-14034
Evaluation of triple simultaneous parallel ILS approaches spaced 5000 feet apart, phase 4.b
[DOT/FAA/CT-91/31] p 456 N92-21404
Safety study of TCAS 2 for logic version 6.04
[DOT/FAA/RD-92/22] p 1047 N92-32537

AUTOMATIC CONTROL
Managing Europe's air traffic system
p 19 A92-11876
Jet engine test system including expert system for diagnosis
[ASME PAPER 91-GT-408] p 137 A92-15737
A low-altitude breakthrough system using optimal path terrain following p 205 A92-20483
On the adaptive control of missile autopilots
p 477 A92-29102
On automatic control of aeroelastic vehicles
p 509 A92-29327
Frequency domain testing of helicopter dynamics using automated input signals p 545 A92-35731
Nonparametric methods of regression analysis in problems related to the processing of aerodynamic balance calibration tests p 602 A92-36417
An estimate of the influence of the compressor stability margin on the thrust of a turbojet engine
p 654 A92-37424
A new milestone in automatic aircraft control - Fly-by-light systems transmit commands optoelectronically
p 784 A92-45699
Automatic document generation with case on a DOD avionics project p 1005 A92-49299
The design and simulation of an intelligence flight control system p 976 A92-50237
Dynamics and control of maneuverable towed flight vehicles p 976 A92-50508
Automatic control of test parameters for intake measurements in a low-speed wind tunnel
p 1091 A92-54341
The operational status of automated aircraft washing system p 1016 A92-56087
Development of an automatic drilling system. II
p 1118 A92-56107
Issues in developing control zones for international space operations p 1141 A92-56602
Pilot's Automated Weather Support System (PAWSS) concepts demonstration project. Phase 1: Pilot's weather information requirements and implications for weather data systems design
[NASA-CR-188228] p 46 N92-11593
Machine Intelligence for Aerospace Electronic Systems
[AGARD-CP-499] p 164 N92-12517
Heuristic route optimization: A model for force level route planning p 164 N92-12520
The impact of cockpit automation on crew coordination and communication. Volume 1: Overview, LOFT evaluations, error severity, and questionnaire data
[NASA-CR-177587] p 93 N92-13044
Dual mode shock absorber and method
[PATENT-1-265-541] p 115 N92-13055
Automated planning with special relevance to associate systems technology and mission planning
[AD-A241924] p 303 N92-17438
An exploration of function analysis and function allocation in the commercial flight domain
[NASA-CR-4374] p 368 N92-19871
The Center/TRACON Automation System (CTAS): A video presentation
[NASA-TM-103887] p 356 N92-20029
Proceedings of the 53rd Symposium on Air Vehicle Mission Control and Management
[AGARD-AR-310] p 1010 N92-32229
Air traffic control: FAA's advanced automation system contract
[GAO/IMTEC-91-25] p 1048 N92-32861
A workstation-based evaluation of a far-field route planner for helicopters
[NASA-TM-102882] p 1051 N92-33609

Human factors issues in the use of artificial intelligence in air traffic control. October 1990 Workshop
[NASA-CR-190925] p 1051 N92-34203

AUTOMATIC FLIGHT CONTROL
Flying qualities evaluation of the V22 tiltrotor
p 131 A92-14334
Flight test control --- Russian book
p 136 A92-15021
V-22 flight test p 112 A92-16056
Optimization of the aerodynamic balance and parameters of the horizontal tail surfaces of the three-surface aircraft configuration with allowance for the capabilities of the stability and control augmentation system p 134 A92-16803
Retrospective essay on nonlinearities in aircraft flight control p 204 A92-18601
Flight investigation of variations in rotorcraft control and display dynamics for hover p 379 A92-28151
Pilot activated automatic recovery system on the F-117A
[AIAA PAPER 92-1126] p 563 A92-33278
An evaluation of a simple PID controller designed using optimal control theory when applied to helicopter stabilisation p 569 A92-35785
Limit cycle oscillation and flight flutter testing
p 570 A92-35939
Development of pitot static flightline testing
p 556 A92-35953
Analyzing the flared landing task with pitch-rate flight control systems p 661 A92-39905
Integrated flight control systems - Architectural considerations for future aircraft concepts
p 872 A92-45322
Comparison of six robustness tests evaluating missile autopilot robustness to uncertain aerodynamics
p 873 A92-46737
Robust discrete controller design for an unmanned research vehicle (URV) using discrete quantitative feedback theory p 877 A92-48495
Vision-based obstacle detection for rotorcraft flight
p 967 A92-52465
Automatic formation flight control
[AIAA PAPER 92-4473] p 1076 A92-55233
Flight management system of the F-117A
p 1082 A92-55910
Resonance and control response tests using a control stimulation drive
[MBB-UD-0586-90-PUB] p 134 N92-12003
Microwave landing system autoland system analysis
[NASA-CR-189551] p 191 N92-15060

AUTOMATIC LANDING CONTROL
Airport Surface Traffic Automation p 95 A92-16228
A simulator and performance criteria for evaluation of ground and space-based ATC surveillance
p 96 A92-16639
Design and flight test of a differential GPS/inertial navigation system for approach/landing guidance
p 97 A92-16650
Improved noise rejection in automatic carrier landing systems p 380 A92-28154
Shuttle autoland status summary
[AIAA PAPER 92-1273] p 666 A92-38478
A fuzzy logic based F/A-18 automatic carrier landing system
[AIAA PAPER 92-4392] p 1074 A92-55193
An investigation of the automation of emergency landings for helicopters p 1083 A92-56026
Synthesis of a MLS automatic landing control law for the NAL experimental research aircraft Do-228
p 1084 A92-56062
Approach and landing assisted by onboard image processing p 457 N92-21959
CTAS: Computer intelligence for air traffic control in the terminal area
[NASA-TM-103959] p 1044 N92-33080

AUTOMATIC PILOTS
Design of the flare control law for longitudinal autopilot using H(infinity) synthesis p 28 A92-11562
Robust autopilot design for aircraft with multiple lateral-axes controls using H(infinity) synthesis
p 28 A92-11563
Applying mu-synthesis to missile autopilot design
p 28 A92-11564
Design of localizer capture and track hold for a transport airplane - An H(infinity)/LTR approach
p 52 A92-11583
Enhanced autopilot design through hardware-in-the-loop simulation p 204 A92-19103
Automated mission planning - A striking capability
p 412 A92-28494
On the adaptive control of missile autopilots
p 477 A92-29102
Synthesis of robust nonlinear autopilots using differential game theory p 478 A92-29330
Pilot activated automatic recovery system on the F-117A
[AIAA PAPER 92-1126] p 563 A92-33278
PDFIII - A flight control system for EW UAV's
[TABES PAPER 91-315] p 565 A92-34688
An evaluation of a simple PID controller designed using optimal control theory when applied to helicopter stabilisation p 569 A92-35785
Control system optimization using genetic algorithms
p 661 A92-39900
Experimental investigation of in-flight oscillation on helicopters and its prevention p 977 A92-53089
Automatic formation flight control
[AIAA PAPER 92-4473] p 1076 A92-55233
Gain scheduled linear PID autopilot for the AIAA Controls Design Challenge aircraft
[AIAA PAPER 92-4629] p 1078 A92-55304
Flight management system of the F-117A
p 1082 A92-55910
A module-level testing environment for safety-critical software systems p 1132 A92-56293
A NASA/RAE cooperation in the development of a real-time knowledge based autopilot
p 164 N92-12528
Project of an adaptive multiaxial autopilot with learning pilot control
[ETN-92-90592] p 205 N92-15072
Multiple input sliding mode control for autonomous diving and steering of underwater vehicles
[AD-A241935] p 283 N92-17442
DRES unmanned aerial vehicle data link research
[AD-A244272] p 365 N92-19030
Flight-determined benefits of integrated flight-propulsion control systems
[NASA-TM-4393] p 742 N92-27587

AUTOMATIC TEST EQUIPMENT
Inspection of compressor discs by ultrasonic leaky waves using an automated C-scan system
p 144 A92-13584
A procedure for automated gas turbine blade fault identification based on spectral pattern analysis
[ASME PAPER 91-GT-259] p 151 A92-15661
Fault Tree Interpreter --- expert system shell for rule-based expert systems development for control of ATE
[AIAA PAPER 91-3789] p 232 A92-17645
Realistic real-time ground testing
[AIAA PAPER 92-0197] p 284 A92-23805
Aircraft maintenance support system
p 607 A92-38217
Recent manufacturing advances for spiral bevel gears
[SAE PAPER 912229] p 674 A92-40024
The application of multimedia expert systems to the depot level maintenance environment
p 922 A92-48557
Developing intelligent automatic test equipment
p 922 A92-48569
A microprocessor-based automation test system for the experiment of the multi-stage compressor
p 997 A92-53100
Automatic production test equipment (APTE) for the B-2 p 997 A92-53107
A common engineering-to-manufacturing-to-field test strategy to achieve systems readiness beyond the '90s
p 931 A92-53111
Recent developments in data acquisition and control systems at the Aircraft Research Association Limited
p 1091 A92-54323
Automatic function testing in the aircraft production
p 1015 A92-56083

AUTOMATIC WEATHER STATIONS
Visibility measurements for the Automated Surface Observing System (ASOS) p 468 A92-32095

AUTOMATION
Automated mission planning - A striking capability
p 412 A92-28494
Stringer subsystem automation p 700 A92-43246
Development of an automatic metal sheet working machine for interior structure p 700 A92-43247
Application of automation for structural-composites production p 1119 A92-56109
Design principles of automation aids for ATC approach control p 354 N92-19042

AUTOMOBILE ENGINES
Development of natural gas rotary engines
[PB92-149665] p 765 N92-26816

AUTONOMOUS NAVIGATION
RAIM - Will it meet the RTCA GPS minimum operational performance standards? --- Receiver Autonomous Integrity Monitoring p 96 A92-16635
In-flight demonstration of hybrid GPS/Loran RAIM
p 96 A92-16643
Integrated use of GPS and GLONASS in civil aviation navigation. I - Coverage and data models
p 99 A92-16950
Comparison of fixed and variable threshold RAIM algorithms p 100 A92-16951
Autonomous landing - Functional requirements
p 840 A92-48470
Inertial navigation sensor integrated motion analysis for autonomous vehicle navigation p 995 A92-52470
Analysis of image-based navigation system for rotorcraft low-altitude flight p 1046 A92-55968
Adaptive tactical navigation program
p 102 N92-12529
A connectionist approach to autonomous robotic navigation p 454 N92-20356
A rotorcraft flight database for validation of vision-based ranging algorithms
[NASA-TM-103906] p 841 N92-29103
Techniques for autonomous navigation
[DE92-013458] p 957 N92-31746

AUTONOMY
Board-autonomous flight trajectory measurement by example of an ILS measuring system
p 641 N92-25601

AUTOREGRESSIVE PROCESSES
Preliminary study of algorithm for real-time flutter monitoring
[SAE PAPER 912001] p 897 A92-45403
An identification procedure for a system with a choice of feedback structures p 1132 A92-55426
Real-time processing of radar return on a parallel computer
[NASA-CR-4456] p 1043 N92-32606

AUTOROTATION
Base pressure on an axisymmetric finned body during forced rotation in the autorotation regime
p 7 A92-12165
Plotting the universal characteristic of a compressor in low-rpm and autorotation regimes p 657 A92-40607
Optimization approach for helicopter maneuverability with a point mass model p 1083 A92-56025
An autorotation-entry control for a helicopter with a fuzzy controller p 1083 A92-56032

AUXILIARY POWER SOURCES
Garrett GTP50-1 multipurpose small power unit technology demonstrator program
[ASME PAPER 91-GT-328] p 153 A92-15698
The engine inside p 558 A92-36126
Future military APU requirements
[SAE PAPER 912176] p 655 A92-40001
Challenging power-density requirements for future fighter APUs
[SAE PAPER 912177] p 655 A92-40002
Auxiliary power system requirements for commercial air transports - Past, present and future
[SAE PAPER 912188] p 656 A92-40007
Secondary power system preliminary design
[SAE PAPER 912189] p 656 A92-40008
A criterion for estimating the economic and operational efficiency of the power distribution systems of commercial aircraft p 657 A92-40611
Auxiliary power units for advanced fighters
p 737 A92-43545
Auxiliary power units for current and future aircraft
[SAE PAPER 912059] p 862 A92-45441
Space Shuttle Orbiter auxiliary power unit status
[SAE PAPER 912060] p 889 A92-45442
Design of the Boeing 777 electric system
p 1070 A92-55902
Interior noise prediction methodology: ATDAC theory and validation
[NASA-CR-187626] p 697 N92-25368

AVAILABILITY
HiRel - Reliability/availability integrated workstation tool p 1120 A92-56257
RAMREQ: A computerized tool for the definition of RAM (Reliability, Availability, Maintainability) requirements of complex systems p 412 N92-18647

AVALANCHE DIODES
Optical velocity sensor for air data applications
p 368 A92-24575
Semiconductor laser Doppler anemometer for applications in aerodynamic research
p 495 A92-31173

AVIATION METEOROLOGY
Polish radar technology. III - Weather channel for primary surveillance radar p 40 A92-12291
Several results of lidar measurements of the characteristics of oblique visibility at an airfield
p 45 A92-12844
The new airport aeronautic meteorological codes
p 160 A92-13855
Sensors and systems to enhance aviation safety against weather hazards p 160 A92-14265
Integration of flight and carrier landing aid systems for shipboard operations
[ONERA, TP NO. 1991-113] p 134 A92-16092
Fair weather convection and light aircraft accidents
[IAF PAPER ST-91-004] p 186 A92-20651

Probabilistic reasoning for intelligent wind shear avoidance p 302 A92-21181
Precipitation development in Colorado Front Range snowstorms - 15 November 1987 case study p 301 A92-23008
Forward-look wind-shear detection for microburst recovery p 378 A92-24408
Real-time decision aiding - Aircraft guidance for wind shear avoidance
[AIAA PAPER 92-0290] p 350 A92-25743
Airborne in situ computation of the wind shear hazard index
[AIAA PAPER 92-0291] p 351 A92-25744
Experimental evaluation of candidate graphical microburst alert displays
[AIAA PAPER 92-0292] p 369 A92-25745
Atmospheric disturbance model for aircraft and space capable vehicles
[AIAA PAPER 92-0294] p 407 A92-25747
Visibility measurements for the Automated Surface Observing System (ASOS) p 468 A92-32095
Aviation meteorology p 685 A92-38383
Shear progress --- wind shear handling and recognition technologies for aviation p 609 A92-40880
Visibility in the atmosphere and flight safety --- Russian book
[ISBN 5-286-00416-4] p 775 A92-42785
Modeling the effect of helicopter downwash on warm fog p 775 A92-44081
Thrust laws for microburst wind shear penetration p 873 A92-46750
Remote measurements of supercooled integrated liquid water during WISP/FAA aircraft icing program p 915 A92-46788
Optimal recovery from microburst wind shear
[AIAA PAPER 92-4338] p 1078 A92-55327
A data fusion algorithm for multi-sensor microburst hazard assessment
[AIAA PAPER 92-4339] p 1063 A92-55328
Severe turbulence and maneuvering from airline flight records
[AIAA PAPER 92-4341] p 1078 A92-55330
Pilot's Automated Weather Support System (PAWSS) concepts demonstration project. Phase 1: Pilot's weather information requirements and implications for weather data systems design
[NASA-CR-188228] p 46 N92-11593
Alert generation and cockpit presentation for an integrated microburst alerting system p 265 N92-17988
JPL's Real-Time Weather Processor project (RWP) metrics and observations at system completion p 413 N92-19428
Cockpit weather information needs p 449 N92-21503
Effects of Adverse Weather on Aerodynamics
[AGARD-CP-496] p 449 N92-21679
Flight in adverse environmental conditions p 449 N92-21680
Experimental evaluation of candidate graphical microburst alert displays
[NASA-CR-189633] p 735 N92-27424

AVIATION PSYCHOLOGY
The development of an intelligent human factors data base as an aid for the investigation of aircraft accidents p 928 A92-44994
Workshop on integrated Crew Resource Management (CRM)
[DOT/FAA/RD-92/5] p 781 N92-27518

AVIONICS
Applications of advanced composites in a 3/4 air transportable rack p 36 A92-10314
Flying the A340 iron bird p 20 A92-10666
Flight testing the avionics system of the V-22 Osprey p 117 A92-14378
Functionally integrated aircraft instrumentation for the next generation commercial helicopter p 117 A92-14402
Day/Night Adverse weather Pilotage System (D/NAPS) p 94 A92-14429
Integrated flight/propulsion control for flight critical applications - A propulsion system perspective
[ASME PAPER 91-GT-284] p 125 A92-15679
Implementation of a RAIM monitor in a GPS receiver and an integrated GPS/IRS p 99 A92-16948
INS alignment using GPS Phase III user equipment computed corrections p 100 A92-16955
Real-time microfocus radiography for electronic failure analysis p 214 A92-17289
An intelligent pilot vehicle interface for a day/night adverse weather pilotage system (D/NAPS)
[AIAA PAPER 91-3729] p 197 A92-17596
Knowledge maintenance in an evolving system using a deep structure representation
[AIAA PAPER 91-3941] p 231 A92-17605
Advanced avionics system development environment
[AIAA PAPER 91-3944] p 231 A92-17608
Putting ten pounds of avionics in a one pound package (Can we do it again?)
[AIAA PAPER 91-3766] p 197 A92-17628
Applications of an automated programming system
[AIAA PAPER 91-3767] p 231 A92-17629
An alternative method for acquiring avionic bus data in a class I PCM telemetry system p 217 A92-19202
Observability under recurrent loss of data p 302 A92-21191
Clever cockpits p 241 A92-21700
Condor, an all-electric airplane p 269 A92-21734
High costs force avionics links p 276 A92-22000
AI technology and application development on the Shuttle project p 302 A92-23693
Optical velocity sensor for air data applications p 368 A92-24575
Anglo-American avionics p 307 A92-25575
ARINC and commercial aircraft avionics. I p 353 A92-25655
From concept to model: Conception and evaluation of an architecture for a distributed system with SAHARA - Some reflections on results of the utilization of SAHARA in the framework of the Electronic Copilot
[ONERA, TP NO. 1991-216] p 411 A92-26368
Durability analysis using fracture mechanics for avionics integrity p 396 A92-26799
The Software Factory, version 5.0
[AIAA PAPER 92-0590] p 411 A92-26992
A new method for orientation calculation of the electromagnetic helmet-mounted sighting unit p 370 A92-27837
Avionics systems of the 21st century p 467 A92-28874
Applications of composite material systems to avionic systems packaging p 576 A92-32564
Suit study - The impact of VMS in subsystem integration
[AIAA PAPER 92-1078] p 563 A92-33247
F15E terrain following system development
[AIAA PAPER 92-1079] p 563 A92-33248
ES-3A flight test program
[AIAA PAPER 92-1230] p 538 A92-33327
Advancing airlift avionics - C-17 avionics suite
[AIAA PAPER 92-1243] p 553 A92-33336
The Mission Computer/Electronic Display Subsystem for the United States Air Force C-17A transport aircraft
[AIAA PAPER 92-1244] p 553 A92-33337
Never make the same mistake twice - Using configuration control and error analysis to improve software quality p 601 A92-33603
Test Engineering Language for Avionic Systems p 554 A92-35763
Instrumented blade experiments using a light autogiro p 555 A92-35773
ARINC and the avionics of commercial aircraft. II p 637 A92-37072
A novel avionic sensor for fly-by-light controls p 650 A92-38128
Requirements for high flux cooling of future avionics systems
[SAE PAPER 912104] p 673 A92-39958
ELS pilot evaluation --- Electronic Library System
[SAE PAPER 912107] p 691 A92-39960
Multidimensional ELS user interface --- Electronic Library System
[SAE PAPER 912108] p 691 A92-39961
ELS for the A340 --- Electronic Library System
[SAE PAPER 912111] p 651 A92-39963
Cost effectiveness of environmental stress screening (ESS) - A case history p 760 A92-42084
Design-for-reliability through durability analysis p 760 A92-42086
Code Division Multiple Access (CDMA) system candidate for integrated modular avionics p 725 A92-42604
Utilizing the fault monitoring system for the A320 aircraft p 700 A92-43157
Development of the D-size liquid crystal flat panel display for aircraft p 734 A92-43208
Evaluation test on the simulator of the liquid crystal flat display. II p 734 A92-43209
Avionics flight systems for the 21st century
[SAE PAPER 912033] p 784 A92-45421
Through the looking glass --- effectiveness of electronic flight instrument systems p 856 A92-46449
Modular avionics - A commercial perspective p 858 A92-48427
RTOK elimination with TSMM --- Rerurn Tested OK reproduction using time stress measurement module p 902 A92-48446
Liquid flow-through cooling for avionics applications p 902 A92-48448
Rapid systems integration of navigation avionics p 858 A92-48473
Systems simulation of an advanced avionics COMSEC unit p 921 A92-48485
Applying advanced digital simulation techniques in designing fault tolerant systems p 921 A92-48489
Avionics software reusability observations and recommendations p 921 A92-48502
Expert Avionics Code Modification p 921 A92-48513
Using design of experiments to improve product and process integrity p 928 A92-48555
IEEE/AIAA Digital Avionics Systems Conference, 10th, Los Angeles, CA, Oct. 14-17, 1991, Proceedings
[ISBN 0-7803-0115-3] p 964 A92-49251
Testing and analysis of a 'smart' interface to connect two complex avionics bus systems without significant modification to the software of either system p 964 A92-49254
Is the avionics system of the Hermes Spaceplane centralized or decentralized? p 984 A92-49258
Application of syndrome pattern-matching approach to fault isolation in avionic systems p 1005 A92-49261
Digital flight control systems - Some new commercial twists p 974 A92-49264
Avionics systems engineering education p 1012 A92-49269
Liquid cooled approaches for high density avionics p 989 A92-49274
High performance heat sink for surface mount applications --- in avionics system design p 989 A92-49275
Progressive avionics packaging technologies p 989 A92-49276
Next-generation avionics packaging and cooling 'test results from a prototype system' p 989 A92-49277
The Office of Naval Research initiative on ultradependable multicomputers and electronic systems p 1005 A92-49278
JIAWG module fault coverage metrics methodology p 989 A92-49279
A new approach to embedded computer performance measurement --- in avionics p 1005 A92-49288
An integrated analysis and simulation tool for avionics system development p 1005 A92-49289
A fault-tolerant network architecture for integrated avionics p 965 A92-49297
Automatic document generation with case on a DOD avionics project p 1005 A92-49299
The Catalyst software engineering environment --- in avionics p 1005 A92-49300
MLS/RNAV control display unit development p 965 A92-49303
Low cost HIRF troubleshooting and verification method for digital avionics systems p 990 A92-49304
Are we doing HIRF testing sensibly? --- avionics certification in commercial aircraft p 931 A92-49305
Testability of the PAALS auto-align sensor system --- Precision Accelerometer Alignment and Leveling System p 965 A92-49310
Fault tolerant avionics display system p 965 A92-49312
Route planning --- in real-time of avionics systems p 1006 A92-49317
The data flow simulator, a tool for system simulation --- in digital avionics p 1006 A92-49329
An advanced flight path management system for low-altitude helicopter flight p 975 A92-49330
Systems commonality - Integrated avionics for the MH-47E and the MH-60K p 966 A92-49331
The army special operations aircraft integrated avionics subsystem - An operational perspective p 966 A92-49332
Operating principles for integrated sensor processing p 966 A92-49336
The concept exploration stage of a dependable avionic system p 1006 A92-49339
GPS integration improves mission capabilities of CH-47D aircraft p 966 A92-49340
Architectures and GPS/INS integration - Impact on mission accomplishment p 967 A92-51003
A fault-tolerant Air Data/Inertial Reference System p 967 A92-51011
The use of photogrammetry in aviation equipment flight testing p 994 A92-51649
Application of resin and metal matrix composites to advanced avionics enclosure p 985 A92-51921
Application of advanced composites in SEM-E heatsinks for the thermal management of avionics p 986 A92-51922
Detailed investigation of causes of avionics field failures p 995 A92-51925
Automatic production test equipment (APTE) for the B-2 p 997 A92-53107
Standardizing operational flight data handling p 1009 A92-53109
Change and reliability of the DC-9-81 digital flight guidance system p 1084 A92-56086

Aeronautical satellite communications system
p 1046 A92-56089
Electronics/avionics integrity - Definition, measurement and improvement p 1120 A92-56252
Engineering reliability and maintainability review - A regimen for discovering production deficiencies
p 1120 A92-56254
HiRel - Reliability/availability integrated workstation tool p 1120 A92-56257
Test and integration concept for complex helicopter avionic systems p 1064 A92-56292
Modern helicopter technologies at MBB and the application in future programmes p 1016 A92-56304
An independent review of the Multi-Path Redundant Avionics Suite (MPRAS) architecture assessment and characterization report
[NASA-CR-188126] p 163 N92-12440
Military and civil software standards and guidelines for guidance and control p 163 N92-12452
Process/object-oriented Ada software design for an experimental helicopter p 164 N92-12461
Machine Intelligence for Aerospace Electronic Systems
[AGARD-CP-499] p 164 N92-12517
Expert system for the Tornado ground-based check-out system p 118 N92-12536
Integrated Communications, Navigation, Identification, Avionics (ICNIA) expert system for fault tolerant avionics
p 118 N92-12539
A development-memory approach for enhancing avionics software logistics p 119 N92-12540
Engineering Graphical Analysis Tool (EGAT) development program p 164 N92-12542
Behavior-based fault monitoring
[AD-A241254] p 164 N92-13746
General aviation activity and avionics survey, calendar year 1989
[PB91-179234] p 169 N92-13926
Evolution of avionic systems architecture, from the 1950's to the present p 198 N92-14047
Avionics standardization in the USAF: 1980 to 1990
p 198 N92-14048
Historical perspective on the evolution of avionics standards p 198 N92-14049
Avionics standardization in Europe
p 199 N92-14050
Mixed approach towards modular avionics conflicting requirements p 199 N92-14051
Avionics software evolution p 199 N92-14052
Common avionics baseline: The product of the joint integrated avionics working group p 199 N92-14053
Avionics systems development: Technological trends, conflicts, and cost issues in a changing European environment p 199 N92-14054
Avionics modernization/upgrades in the late 1990s
p 199 N92-14055
Avionics reliability, durability, and integrity: Can they be independent of application? p 200 N92-14056
Avionics technology beyond 2000
p 200 N92-14058
Testing of the high accuracy inertial navigation system in the Shuttle Avionics Integration Lab
p 210 N92-14087
Architecture for Survivable System Processing (ASSP)
p 220 N92-14210
The problem of multiple solutions in area navigation and computed centerline operations with the microwave landing system
[AD-A242757] p 191 N92-15058
Structural considerations for aircraft payload Modification: P-3C zero fuel weight increase
[AD-A242690] p 196 N92-15068
Development of a calibrated software reliability model for flight and supporting ground software for avionic systems p 234 N92-15870
A CLIPS-based tool for aircraft pilot-vehicle interface design p 303 N92-16605
AGSSS: The Airborne Graphics Software Support System; an Ada/PHIGS-based display editor for the rapid development of cockpit display software systems
[AD-A243224] p 277 N92-17221
Validation of flight critical control systems
[AGARD-AR-274] p 382 N92-20026
Activities of NRC-CNRC, Institute for Aerospace Research, Flight Research Lab.
[CTN-92-60432] p 420 N92-20205
Space software is first of all software
p 509 N92-20590
Scorpion: Close Air Support (CAS) aircraft
[NASA-CR-189974] p 462 N92-20664
Flight test of ARINC 741 configuration low gain SATCOM system on Boeing 747-400 aircraft p 677 N92-24097
Flight test of avionic and air-traffic control systems
[ETN-92-91063] p 640 N92-25590
Ground and satellite supported flight trajectory measurement by example of the avionics flight test system AFES p 641 N92-25600
Arrangements and methods for the survey of aircraft radio components and systems p 652 N92-25603
Knowledge-based planning for controlled airspace flight operation as part of a cockpit assistant
p 727 N92-27895
ICAAS piloted simulation evaluation
p 735 N92-27906
Core avionics and standardization
[AD-A248326] p 735 N92-27925
Avionic data bus integration technology
[DOT/FAA/CT-91/19] p 736 N92-27973
Applications of ASICs to avionics
[AGARD-AG-329] p 859 N92-28376
Applications of silicon hybrid multi-chip modules to avionics p 859 N92-28379
A model of the ADA avionics real-time system: An example of the benefits of the hardware/software codesign approach in development of real-time systems
[AD-A248893] p 967 N92-30524
Analysis of data from a DO-178A software development process p 1134 N92-32880
SATWG networked quality function deployment
p 1134 N92-33339
Study objectives: Will commercial avionics do the job? Improvements needed? p 1065 N92-33340

AWACS AIRCRAFT

Developments in airborne surveillance and control systems p 98 A92-16655

AXIAL COMPRESSION LOADS

Axial compression corner flow with shock impingement p 441 A92-32196

AXIAL FLOW

Unsteady viscous flow in a high speed core compressor
[ASME PAPER 91-GT-91] p 70 A92-15555
The numerical simulation of a high-speed axial flow compressor
[ASME PAPER 91-GT-272] p 75 A92-15669
Design and performance of advanced blading for a high-speed HP compressor
[ASME PAPER 91-GT-374] p 76 A92-15718
Navier-Stokes calculations of inboard stall delay due to rotation p 309 A92-24410
An engineering aerodynamic heating method for hypersonic flow
[AIAA PAPER 92-0499] p 329 A92-26327
Radiant heat transfer in supersonic three-dimensional and axisymmetric flow of air past evaporating bodies
p 337 A92-27533
Numerical analysis of techniques for efficient generation of vorticity in supersonic flows
[AIAA PAPER 92-0828] p 422 A92-29596
Power spectrum of ring modes of pressure fluctuations at the surface of a cylinder in axial flow
p 603 A92-33770
Engineering aerodynamic heating method for hypersonic flow p 705 A92-41539
Study of a new airfoil used in reversible axial fans
p 177 N92-13970
Boundary layer flow in axial compressors (theoretical part)
[ETN-92-91006] p 501 N92-21232
A comparison of predicted and measured inlet distortion flows in a subsonic axial inlet flow compressor rotor
[NASA-TM-105427] p 633 N92-26104

AXIAL FLOW TURBINES

An Axial Turbobrake
[ASME PAPER 91-GT-1] p 147 A92-15501
Turbulence modelling for secondary flow prediction in a turbine cascade
[ASME PAPER 91-GT-57] p 68 A92-15535
3-D loss prediction based on secondary flow and blade shear layer interaction
[ASME PAPER 91-GT-59] p 68 A92-15536
Effects of stator wakes and spanwise nonuniform inlet conditions on the rotor flow of an axial turbine stage
[ASME PAPER 91-GT-93] p 70 A92-15557
The effect of blade tip geometry on the tip leakage flow in axial turbine cascades
[ASME PAPER 91-GT-135] p 72 A92-15577
A direct optimization procedure for spanwise work distribution in non-free vortex turbine stages
[ASME PAPER 91-GT-204] p 124 A92-15626
Effect of the blade height of the nozzle ring of axial-flow microturbines on the flow velocity factor and exit angle
p 128 A92-16831
Three-dimensional calculation of low-frequency unsteady transonic flow in axial turbine stages
p 174 A92-19110
3D LDA measurement in an axial fan rotor
p 391 A92-24730
An investigation in the variance in particle surface interactions and their effects in gas turbines
[ASME PAPER 91-GT-380] p 653 A92-36891
Coating effect on particle trajectories and turbine blade erosion p 653 A92-36892
Reynolds stress distribution downstream of a turbine cascade p 614 A92-38861
Advanced CFD simulation and testing of compressor blading in the multistage environment
[AIAA PAPER 92-3040] p 822 A92-48701
Establishing two-dimensional flow in a large-scale planar turbine cascade
[AIAA PAPER 92-3066] p 823 A92-48720
Investigation of three-dimensional flow field in a turbine including rotor/stator interaction. I - Design development and performance of the research facility
[AIAA PAPER 92-3325] p 883 A92-48908
Investigation of three-dimensional flow field in a turbine including rotor/stator interaction. II - Three-dimensional flow field at the exit of the nozzle
[AIAA PAPER 92-3326] p 826 A92-48909
Experimental modeling of film-cooled axial turbine tip seals
[AIAA PAPER 92-4058] p 1119 A92-56141
Computer code for preliminary sizing analysis of axial-flow turbines
[NASA-CR-4430] p 473 N92-20196
Users manual and modeling improvements for axial turbine design and performance computer code TD2-2
[NASA-CR-189118] p 716 N92-27376

AXISYMMETRIC BODIES

The dynamic character of the wake of an axisymmetric body at an angle of attack
[AIAA PAPER 91-3268] p 8 A92-12741
Stratified flow around an axisymmetric body at small angle of attack p 172 A92-18385
Formation of shocks within axisymmetric nozzles
p 176 A92-20760
A method of calculation for the radius of curvature of the attached shock waves in front of a sharp-nosed axi-symmetrical body placed in a uniform stream
p 243 A92-21319
Effects of tip Reynolds number and tip asymmetry on vortex wakes of axisymmetric bodies at various angles of attack
[AIAA PAPER 92-0406] p 324 A92-26259
Computation of laminar flow over a long slender axisymmetric blunted cone in hypersonic flow
[AIAA PAPER 92-0756] p 336 A92-27098
Breakdown of an axisymmetric laminar wake
p 424 A92-30145
Effect of viscosity on the drag of slender axisymmetric bodies in hypersonic flow p 425 A92-30154
Linear stability of three-dimensional boundary layers over axisymmetric bodies at incidence
p 431 A92-31157
Unsteady hypersonic boundary layers for slender axisymmetric bodies with large injection rates
p 524 A92-36100
Spectral solution of inviscid supersonic flows over wedges and axisymmetric cones p 524 A92-36359
Quick calculation of three-dimensional supersonic flow past nearly axisymmetric bodies p 624 A92-40605
Design optimization of natural laminar flow bodies in compressible flow p 701 A92-41219
Prediction of vortex shedding from forebodies with chines p 702 A92-41228
The inviscid stability of supersonic flow past heated or cooled axisymmetric bodies p 712 A92-44363
Enhancements to viscous-shock-layer technique
[AIAA PAPER 92-2897] p 820 A92-47873
A Navier-Stokes solution of Hull-ring wing-thruster interaction p 221 N92-14310
Behaviour and modelling of the aerothermodynamics of ballistic entry vehicles in the high altitude flow regimes
p 184 N92-15031
Particle trajectory computer program for icing analysis of axisymmetric bodies
[NASA-CR-189134] p 352 N92-19276
Comparison of two-dimensional and three-dimensional droplet trajectory calculations in the vicinity of finite wings
[NASA-TM-105617] p 596 N92-23154
Normal force of low aspect ratio wing-body combinations up to high angles of attack at supersonic speeds
[ESDU-91042] p 553 N92-24009
An investigation into the interface between three closely spaced axi-symmetric bodies at subsonic speed
[CRANFIELD-AERO-9114] p 948 N92-31514
Aerodynamic centre of wing-body combinations
[ESDU-92024] p 1036 N92-32479

AXISYMMETRIC FLOW

Axisymmetric potential flow calculations. II - Design mode p 8 A92-12399
Estimation of the size of separation zone in a turbine stage under small load p 10 A92-13235

On the nonlinear stability of a high-speed, axisymmetric boundary layer p 78 A92-16457
Mach 4 and Mach 8 axisymmetric nozzles for a high-enthalpy shock tunnel p 78 A92-16668
Similarity solutions for supersonic axisymmetric flows p 173 A92-18387
Analysis of transonic flow past an axisymmetric convex corner p 312 A92-25015
Euler calculations of axisymmetric under-expanded jets by an adaptive-refinement method
[AIAA PAPER 92-0321] p 321 A92-25768
Analysis of hypersonic nozzles including vibrational nonequilibrium and intermolecular force effects
[AIAA PAPER 92-0330] p 322 A92-25777
Direct numerical simulation of laminar breakdown in high-speed, axisymmetric boundary layers
[AIAA PAPER 92-0742] p 343 A92-28223
Swirl effects on confined flows in axisymmetric geometries p 399 A92-28513
An inverse inviscid method for the design of quasi-three dimensional turbomachinery cascades p 523 A92-36033
An experimental and numerical study of confined axisymmetric jet with a bluff body p 621 A92-40106
Effect of tabs on the evolution of an axisymmetric jet p 656 A92-40151
Hybrid Navier-Stokes/Monte Carlo method for reacting flow calculations p 705 A92-41537
Processing of axisymmetric flow interferograms with density profile bends or discontinuities p 993 A92-51316
The behaviour of the pressure temperature and density in an inviscid unsteady transonic axisymmetric flow with shock waves p 1018 A92-53553
Detecting 3-D, turbulent separation regions using unsteady computerized thermographic technique p 1023 A92-54308
Numerical simulation of transient hypervelocity flow in an expansion tube
[NASA-CR-189615] p 592 N92-22228
Axisymmetric bluff-body flow: A vortex solver for thin shells
[DE92-016748] p 1003 N92-31933

AZIMUTH
Error estimation of INS ground alignment through observability analysis p 639 A92-40226

B

B-1 AIRCRAFT
Study of external dynamic flap loads on a 6 percent B-1B model
[ASME PAPER 91-GT-236] p 125 A92-15645
B-1B excels in conventional role p 786 A92-47971

B-47 AIRCRAFT
Life management approach for USAF aircraft p 362 N92-18587

B-70 AIRCRAFT
A summary of XB-70 sonic boom signature data
[NASA-CR-189630] p 696 N92-24800

BACKGROUND NOISE
Reducing the background noise level in the test section of a wind tunnel for transonic flow velocities p 511 A92-30143

BACKSCATTERING
Bistatic image processing for a 32 x 19 inch model aircraft using scattered fields obtained in the OSU-ESL compact range
[NASA-CR-189932] p 499 N92-20197
Concept design phase expendable holographic sensor to measure ocean small angle optical scattering
[AD-A245067] p 501 N92-20997
Development of a helicopter-borne 8-channel ranging scatterometer
[PB92-141977] p 599 N92-23441

BACKWARD FACING STEPS
Control of turbulent flow on a backward-facing step
[AIAA PAPER 92-0066] p 250 A92-22179
Experimental investigation of a supersonic combustion flowfield employing staged transverse injection behind a rearward-facing step
[AIAA PAPER 92-0090] p 292 A92-22196
Evaluation of parallel injector configurations for Mach 2 combustion p 376 A92-28533
Supersonic flow over an axisymmetric backward-facing step p 705 A92-41542
The flow over a backward-facing step under controlled perturbation - Laminar separation p 705 A92-41653
Predictions of a turbulent backward-facing-step flow with a cubic pressure-strain model
[AIAA PAPER 92-2647] p 796 A92-45514
LDA measurements in a Mach 2 flow over a rearward facing step with staged transverse injection
[AIAA PAPER 92-2692] p 800 A92-45539
A study of the flammability limit of the backward facing step flow combustion
[AIAA PAPER 92-3846] p 895 A92-49136
Turbulent diffusion flame properties behind a backward-facing step p 985 A92-50255
Flow modification over a backward facing step
[AD-A241351] p 158 N92-13406
An experimental investigation of the separating/reattaching flow over a backstep
[NASA-CR-190426] p 716 N92-27399

BAGGAGE
Safety in the sky - Designing bomb-resistant baggage containers p 836 A92-47775

BALANCE
Further developments relating to the NASA Langley Research Center 13-inch magnetic suspension and balance system
[NASA-CR-188995] p 31 N92-11023
Present status of the MIT/NASA Langley 6-inch MSBS p 750 N92-27802
Progress of magnetic suspension and balance systems for wind tunnels in the USSR p 751 N92-27803

BALANCING
Identification of dynamic characteristics of flexible rotors as dynamic inverse problem p 220 N92-13962
Mechanical design of a rotary balance system for NASA. Langley Research Center's vertical spin tunnel p 664 N92-25090
Active synchrophasing of propeller unbalance p 1138 N92-32963

BALL BEARINGS
Performance of hybrid ball bearings in oil and jet fuel p 900 A92-47176
Rotor support for the STME oxygen turbopump
[AIAA PAPER 92-3282] p 904 A92-48872

BALLAST (MASS)
Analysis of the effects of removing nose ballast from the F-15 eagle
[AD-A244044] p 366 N92-19178

BALLISTIC RANGES
An experimental study of the flow past spheres at transonic speeds and high Reynolds numbers p 312 A92-25002
Test on high enthalpy hypersonic flow using a ballistic range p 747 A92-43097

BALLISTICS
A ballistic investigation of the aerodynamic characteristics of a blunt vehicle at hypersonic speeds in carbon dioxide and air
[AIAA PAPER 92-0328] p 322 A92-25775
Determination of physicochemical constant in the wake of a body from ballistic experiments p 609 A92-36549

BALLOON FLIGHT
NASA test flights with increased flight stress indices
[AIAA PAPER 91-3665] p 20 A92-11012
Determination of balloon drag
[AIAA PAPER 91-3666] p 5 A92-11013
Hunting phenomena of the balloon motions observed over Antarctica
[AIAA PAPER 91-3667] p 14 A92-11014
Balloon altitude control by valving - A review and comparison of actual flight data and vertical performance analysis results
[AIAA PAPER 91-3669] p 14 A92-11016
Overpressurized zero pressure balloon system
[AIAA PAPER 91-3671] p 14 A92-11018
Manned orbital balloon flight - Available techniques
[AIAA PAPER 91-3675] p 15 A92-11020
Whither scientific ballooning?
[AIAA PAPER 91-3676] p 1 A92-11021
International survey of scientific ballooning support organizations
[AIAA PAPER 91-3677] p 1 A92-11022
Long duration ballooning in Antarctica - An operational perspective
[AIAA PAPER 91-3679] p 15 A92-11023
The NASA long duration balloon project
[AIAA PAPER 91-3680] p 15 A92-11024
A valve-down technique for small balloons
[AIAA PAPER 91-3681] p 15 A92-11025
Small balloon ballistic tracing and behavior anomalies
[AIAA PAPER 91-3682] p 15 A92-11026
Kestrel balloon launch system
[AIAA PAPER 91-3684] p 15 A92-11027
Design of a trans-global manned balloon system with relevance to scientific ballooning
[AIAA PAPER 91-3687] p 15 A92-11030
Polar patrol balloon
[AIAA PAPER 91-3688] p 15 A92-11031
An air-launched balloon system for a 230 lb gross inflation
[AIAA PAPER 91-3689] p 16 A92-11032
Recent developments in the use of thin-film polyethylene balloons for meteorological applications p 16 A92-11033
Added mass of high-altitude balloons
[AIAA PAPER 91-3693] p 16 A92-11034
China-Soviet long duration balloon flight project
[AIAA PAPER 91-3678] p 1 A92-11036
Oscillations of balloon-flight altitude p 836 A92-46660

BALLOON SOUNDING
AIAA International Balloon Technology Conference, Albuquerque, NM, Oct. 8-10, 1991, Technical Papers p 1 A92-11001
Stratospheric electrodynamics from superpressure balloons - A technical challenge for small payload environments
[AIAA PAPER 91-3674] p 14 A92-11019
Recent developments in the use of thin-film polyethylene balloons for meteorological applications p 16 A92-11033

BALLOONS
AIAA International Balloon Technology Conference, Albuquerque, NM, Oct. 8-10, 1991, Technical Papers p 1 A92-11001
Structural behavior of scientific balloons - Finite element simulation and verification
[AIAA PAPER 91-3668] p 20 A92-11015
Operational evaluation of recently developed balloon fabrication methods
[AIAA PAPER 91-3670] p 1 A92-11017

BANDWIDTH
Control of a helicopter engine in low altitude flight p 562 N92-23122
Sensor compatibility/optimal sensor combinations p 599 N92-23403

BARIUM COMPOUNDS
Levitation of YBa2Cu3O(7-x) superconductor in a variable magnetic field p 771 N92-27735

BAROMETERS
Baro-inertial loop for the USAF Standard RLG INU p 97 A92-16647

BAROTROPIC FLOW
Thrust vector control of an overexpanded supersonic nozzle using pin insertion and rotating airfoils
[AD-A243891] p 387 N92-18942

BASE FLOW
Base pressure measurements on a cone at Mach numbers from M sub infinity = 5 to 7 p 173 A92-18770
Calculation of high speed base flows
[AIAA PAPER 92-2679] p 799 A92-45531
Secondary instability of high-speed flows and the influence of wall cooling and suction
[NASA-CR-4427] p 406 N92-19844
Analysis of the flight performance of the 155 mm M864 base burn projectile
[BRL-TR-3083] p 1041 N92-33699

BASE PRESSURE
Base pressure in supersonic flow - Further thoughts about a theory p 331 A92-26442
A study of the base pressure behind circular steps p 426 A92-30196
Base pressure measurements on a cone at hypersonic Mach numbers: A contribution to aerothermodynamics for space vehicles p 181 N92-14992
Simulation of real-gas effects on pressure distributions for aeroassist flight experiment vehicle and comparison with prediction
[NASA-TP-3157] p 501 N92-20677
Progress of magnetic suspension and balance systems for wind tunnels in the USSR p 751 N92-27803
Analysis of the flight performance of the 155 mm M864 base burn projectile
[BRL-TR-3083] p 1041 N92-33699

BASIC (PROGRAMMING LANGUAGE)
Z-Basic algorithm for collision avoidance system p 188 A92-18482

BAYES THEOREM
Aeroengine sensor failure detection by Bayesian multiple hypothesis testing p 391 A92-24747
Study on the reliability evaluation of engine fuel accessories p 392 A92-24749
Bayesian reliability analysis in connection with the evaluation of multiple-site damage p 762 A92-43126
Radar clutter classification
[ISBN-0-315-57981-1] p 1126 N92-33440

BAYS (STRUCTURAL UNITS)
An analysis of fixed wing tactical airlifter characteristics using an intra-theater airlift computer model
[AD-A246908] p 732 N92-27719

BEACONS
Effect of guard band reduction on marker beacon receiver performance
[DOT/FAA/CT-TN92/18] p 1002 N92-31617

BEAM INJECTION
Formation and sustainment of a very low aspect ratio tokamak using coaxial helicity injection: Helicity Injected Torus (HIT) experiment
[DE92-014311] p 1136 N92-32595

BEAMS (SUPPORTS)
Control design via TAM and H-infinity approaches - A flexible beam case study p 51 A92-11445
Static aeroelastic tailoring of composite aircraft swept wings modelled as thin-walled beam structures p 294 A92-23114
Efficient evaluation of the flexibility of tapered I-beams accounting for shear deformations p 295 A92-23269
On the behavior of pretwisted beams with irregular cross-sections p 495 A92-31564
New, unusual and nonclassical behavior of thin-walled composite structures p 580 A92-32746
Helicopter rotor blade aeroelasticity in forward flight with an implicit structural formulation p 958 A92-50315
Nonlinear aspects of aerospace structures at high excitation levels flat aluminum beams and plates studied [AD-A240600] p 44 N92-11383
Aeroelastic behavior of an adaptive lifting surface p 443 N92-20378
Thrust test fixture [AD-D015259] p 983 N92-31192
BEARING (DIRECTION)
An alternative derivation of the modified gain function of Song and Speyer p 232 A92-18464
GPS interferometric attitude and heading determination - Flight test results p 650 A92-39561
A method of passive range determination using only two bearing measurements [AD-D015182] p 455 N92-20834
Reference mode effect on the auditory display of aircraft bank angle [AD-A247825] p 728 N92-27916
BEARING ALLOYS
Rolling element bearing member [PATENT-1-271-213] p 158 N92-13434
BEARINGLESS ROTORS
LH wind tunnel testing - Key to advanced aerodynamic design p 104 A92-14331
Variation in hover aeromechanical stability trends with bearingless main rotor design p 109 A92-14425
Bearingless main rotor system composite component fabrication techniques p 110 A92-14453
Calculation of pitch-link loads in deep stall using state-of-the-art methodology p 520 A92-35753
Bearingless rotor aeromechanical stability measurements and correlations using nonlinear aerodynamics p 547 A92-35772
BEARINGS
The basics of powder lubrication in high-temperature powder-lubricated dampers [ASME PAPER 91-GT-248] p 150 A92-15653
Hydraulic actuator system for rotor control p 224 N92-14363
Ceramic technology for Advanced Heat Engines Project [DE92-002397] p 289 N92-16128
Full-scale transmission testing to evaluate advanced lubricants [NASA-TM-105668] p 764 N92-26560
Dynamics of a split torque helicopter transmission [NASA-TM-105681] p 910 N92-29136
Bearing servicing tool [NASA-CASE-MSC-21881-1] p 912 N92-30082
BEDS (GEOLOGY)
Aerodynamic roughness measured in the field and simulated in a wind tunnel [NASA-CR-4422] p 347 N92-19354
BEECHCRAFT AIRCRAFT
Resin transfer molding of a complex composite aircraft structure p 784 A92-47410
Aircraft accident/incident summary report: Controlled flight into terrain Bruno's Inc., Beechjet, N25BR, Rome, Georgia, 11 December 1991 [PB92-910404] p 1044 N92-34081
BELL AIRCRAFT
The NASA/Industry Design Analysis Methods for Vibrations (DAMVIBS) Program - Bell Helicopter Textron accomplishments [AIAA PAPER 92-2201] p 539 A92-34391
An evaluation of IFR approach techniques: Generic helicopter simulation compared with actual flight p 886 N92-28550
Evaluation of composite components on the Bell 206L and Sikorsky S-76 helicopters p 1107 N92-32575
BENARD CELLS
Experimental study of convection effects around the phase charge interface p 1111 A92-53755
BEND TESTS
Tensile and interlaminar properties of GLARE (trade name) laminates [AD-A250188] p 895 N92-28921
BENDING MOMENTS
Simulation of vibrational status of gas-turbine engine p 470 A92-29731
Non-homogeneous bars under tension, pure bending and thermal loads p 495 A92-31198
Helicopter rotor blade aeroelasticity in forward flight with an implicit structural formulation p 958 A92-50315
A comparison of spanwise aerodynamic loads estimated from measured bending moments versus direct pressure measurements on horizontal axis wind turbine blades [DE92-001158] p 301 N92-16458
Loading and vibration reduction through active aerodynamic control [AD-A242321] p 283 N92-17243
Airplane crashes on the runway. Fine modeling of the behavior after burning of a frame submitted to linear crushing [IMFL-90-64] p 353 N92-19350
BENDING THEORY
On the behavior of pretwisted beams with irregular cross-sections p 495 A92-31564
BENDING VIBRATION
Effect of shock waves on the critical rate of bending-torsional flutter of an airfoil p 494 A92-30208
Coupled vibrations of turbomachine blades p 738 A92-44545
BERNOULLI THEOREM
Structural considerations for aircraft payload Modification: P-3C zero fuel weight increase [AD-A242690] p 196 N92-15068
BERYLLIUM ISOTOPES
Surface activation of Concorde by Be-7 p 605 N92-23295
BIAS
The effect of droplet sizing uncertainty on ice accretions p 679 N92-24874
BIBLIOGRAPHIES
Magnetic suspension and balance systems: A comprehensive, annotated bibliography [NASA-TM-4318] p 32 N92-11030
Bibliography of technical reports, 1980 - 1990 [PB92-110691] p 417 N92-18814
FAA vertical flight research, engineering, and development bibliography, 1962 - 1991 [FAA/ARD-30] p 462 N92-21210
JPRS report: Science and technology. USSR: Engineering and equipment [JPRS-UEQ-92-001] p 592 N92-22296
JPRS report: Science and technology. Central Eurasia: Engineering and equipment [JPRS-UEQ-92-002] p 592 N92-22298
JPRS report: Science and technology. USSR: Engineering and equipment [JPRS-UEQ-91-010] p 593 N92-22397
Research and technology, 1991 [NASA-TM-105320] p 516 N92-22659
JPRS report: Science and technology. Central Eurasia: Space [JPRS-USP-92-002] p 575 N92-23705
Dredging research program: Global positioning system bibliography [AD-A248954] p 729 N92-28079
BINARY ALLOYS
Composite strengthening of Nb-Ti base alloys p 577 A92-36380
BINARY DATA
Binary optical filters for scale invariant pattern recognition [NASA-TM-103902] p 853 N92-28910
BINDERS (MATERIALS)
Alternate/modified binders for asphalt airfield pavements [AD-A242829] p 285 N92-17260
BIODYNAMICS
Adaptive suppression of biodynamic interference in helmet-mounted displays and head teleoperation p 197 A92-18611
BIOGRAPHY
A modern view of Theodore Theodorsen --- Book [ISBN 0-930403-85-1] p 307 A92-26250
BIOT METHOD
Aerodynamic calculation of an elliptic ring wing [AIAA PAPER 91-0068] p 1035 A92-57035
On aircraft wake properties and some methods for stimulating decay and breakdown of tip vortices p 87 N92-13021
BIRD-AIRCRAFT COLLISIONS
Effect of some load factors of bird impact on blade response p 371 A92-24740
Effect of different force-functions and initial shock pressure on blade response p 374 A92-27913
The selection of bird impact load types --- on turbojet compressor and turbofan fan blades p 448 A92-29732
Wing leading edge design with composites to meet bird strike requirements p 848 A92-47404
Bird impact analysis of aircraft windshield transparency p 958 A92-50236
An impact dynamics investigation on some problems in bird strike on windshields of high-speed aircrafts p 986 A92-53330
A study of dynamic response to bird impact on arc windshields of aircrafts p 952 A92-53340
Study of the engine bird ingestion experience of the Boeing 737 aircraft [DOT/FAA/CT-89/16] p 187 N92-15053
Explicit finite element method for transparency impact analysis [AD-A243527] p 264 N92-17478
Bird ingestion into large turbofan engines [DOT/FAA/CT-91/17] p 1043 N92-33005
Engine bird ingestion experience of the Boeing 737 aircraft: Expanded data base [DOT/FAA/CT-91/32] p 1045 N92-34151
BIRDS
A model for the effects of aircraft overflight noise on the reproductive success of raptorial birds p 688 A92-39101
Bird ingestion into large turbofan engines [DOT/FAA/CT-91/17] p 1043 N92-33005
BIT ERROR RATE
Experiments on aeronautical satellite communications using ETS-V p 395 A92-26779
BLADE SLAP NOISE
Acoustic predictions using measured pressures from a model rotor in the DNW p 165 A92-14385
High-speed impulsive noise and aerodynamic results for rectangular and swept rotor blade tip tests in S1-Modane wind tunnel [ONERA, TP NO. 1991-124] p 76 A92-16102
Acoustic emission during changes in the aerodynamic load on the surface of a fan blade p 511 A92-30318
Noise level reduction inside helicopter cabins p 545 A92-35733
Some aerodynamic mechanisms of impulsive noise during blade-vortex-interaction p 604 A92-35782
1991-92 AHS Technical Committee highlights - Acoustics p 696 A92-40390
Noise of two high-speed model counter-rotation propellers at takeoff/approach conditions p 925 A92-46799
Influence of geometrical parameters on helicopter rotor high speed impulsive noise [ONERA, TP NO. 1992-40] p 926 A92-48601
Experimental study of the equivalent sound source center of the propeller rotating noise p 1011 A92-53257
A calculation method to predict helicopter noise and its verification p 1135 A92-56074
The application of experimental data to blade wake interaction noise prediction [NASA-CR-189461] p 237 N92-14789
BLADE TIPS
Lifting line predictions for a swept tip rotor blade p 65 A92-14424
Optical measurements of unducted fan flutter [ASME PAPER 91-GT-19] p 147 A92-15510
Stator averaged, rotor blade-to-blade near wall flow in a multistage axial compressor with tip clearance variation [ASME PAPER 91-GT-30] p 67 A92-15514
Computation of flow past a turbine blade with and without tip clearance [ASME PAPER 91-GT-56] p 68 A92-15534
The role of tip clearance in high-speed fan stall [ASME PAPER 91-GT-83] p 69 A92-15550
Three-dimensional flow and mixing in a axial flow compressor with different rotor tip clearances [ASME PAPER 91-GT-89] p 70 A92-15554
Effects of simulated rotation on tip leakage in a planar cascade of turbine blades. I - Tip gap flow [ASME PAPER 91-GT-127] p 71 A92-15572
Effects of simulated rotation on tip leakage in a planar cascade of turbine blades. II - Downstream flow field and blade loading [ASME PAPER 91-GT-128] p 71 A92-15573
The effect of blade tip geometry on the tip leakage flow in axial turbine cascades [ASME PAPER 91-GT-135] p 72 A92-15577
Turbine blade tip clearance improvement [ASME PAPER 91-GT-164] p 123 A92-15599
Rotordynamic evaluation of an advanced multi-squeeze film damper - Imbalance response and bladeless simulation [ASME PAPER 91-GT-242] p 149 A92-15647
High-speed impulsive noise and aerodynamic results for rectangular and swept rotor blade tip tests in S1-Modane wind tunnel [ONERA, TP NO. 1991-124] p 76 A92-16102
Aerodynamic and acoustic calculations of transonic nonlifting hovering rotors [ONERA, TP NO. 1991-178] p 77 A92-16140
A simplified model for the interaction of a rotor tip vortex with an airframe [AIAA PAPER 92-0320] p 321 A92-25767
Numerical analysis of helicopter rotor blades p 430 A92-30558

Performance of a high-pressure-ratio centrifugal compressor influenced by distribution of tip clearance of the mixed-flow impeller p 498 A92-32509
Navier-Stokes analysis of blade tip shape in hover p 521 A92-35758
Design and manufacturing of torsional flexible blade models p 547 A92-35780
On the influence of blade-vortex-interactions on vortex structure p 521 A92-35783
Numerical simulations of the flow through cascades with tip clearance p 523 A92-36038
The use of optical sensors and signal processing gas turbine engines p 856 A92-46247
Experimental and numerical study of flow around helicopter rotor blade tips p 814 A92-46948
Experimental modeling of film-cooled axial turbine tip seals
[AIAA PAPER 92-4058] p 1119 A92-56141
A time-dependent tip loss formula for rotor blade dynamic analysis p 1057 A92-56310
Experimental study of an independently deflected wingtip mounted on a semispan wing
[NASA-TM-102842] p 13 N92-10983
Detailed noise measurements on the SR-7A propeller: Tone behavior with helical tip Mach number
[NASA-TM-105206] p 304 N92-16705
Tiltrotor research aircraft composite blade repairs: Lessons learned
[NASA-TM-103875] p 367 N92-19563
TCGRID: A three dimensional C-grid generator for turbomachinery p 659 N92-25716
Turbine blade tip and seal clearance excitation forces
[NASA-CR-184341] p 973 N92-31910

BLADE-VORTEX INTERACTION
Fundamental research in helicopter rotor blade-vortex interaction modeling p 65 A92-14358
Acoustic predictions using measured pressures from a model rotor in the DNW p 165 A92-14385
Computation of the BVI noise for the BO105 Model Rotor in forward flight and comparison with wind tunnel tests p 165 A92-14386
3-D loss prediction based on secondary flow and blade shear layer interaction
[ASME PAPER 91-GT-59] p 68 A92-15536
A viscous flow study of shock-boundary layer interaction, radial transport, and wake development in a transonic compressor
[ASME PAPER 91-GT-69] p 68 A92-15539
The role of tip clearance in high-speed fan stall
[ASME PAPER 91-GT-83] p 69 A92-15550
Numerical prediction of wakes in cascades and compressor rotors including the effects of mixing. II - Rotor passage flow and wakes including the effects of spanwise mixing
[ASME PAPER 91-GT-222] p 74 A92-15639
Modelling of unsteady transitional boundary layers
[ASME PAPER 91-GT-282] p 152 A92-15677
Theoretical study and prediction of BVI noise including close interactions
[ONERA, TP NO. 1991-174] p 165 A92-16138
Sound produced by an aerodynamic source adjacent to a partly coated, finite elastic plate p 414 A92-25365
Vortex modeling for rotor aerodynamics - The 1991 Alexander A. Nikolsky Lecture p 315 A92-25576
An experimental and analytical study of the interaction of a vortex with an airframe
[AIAA PAPER 92-0319] p 321 A92-25766
A simplified model for the interaction of a rotor tip vortex with an airframe
[AIAA PAPER 92-0320] p 321 A92-25767
Experimental investigation of the perpendicular rotor blade-vortex interaction at transonic speeds p 340 A92-28047
Calculation of pitch-link loads in deep stall using state-of-the-art methodology p 520 A92-35753
Rotor blade-vortex interaction noise reduction and vibration using higher harmonic control p 604 A92-35778
Some aerodynamic mechanisms of impulsive noise during blade-vortex-interaction p 604 A92-35782
On the influence of blade-vortex-interactions on vortex structure p 521 A92-35783
Delay of wing vortex bursting by using favorable interaction of vortices p 615 A92-38910
Vortex interaction in the wake behind an oscillating airfoil p 623 A92-40175
An experimental investigation of the oblique blade-vortex interaction p 712 A92-43447
Boundary-layer measurements during a parallel blade-vortex interaction
[AIAA PAPER 92-2623] p 794 A92-45495
Experimental investigation of the parallel vortex-airfoil interaction at transonic speeds p 813 A92-46901
Active control of blade vortex interaction p 814 A92-46944
Experimental and numerical study of flow around helicopter rotor blade tips p 814 A92-46948
An Eulerian/Lagrangian method for computing blade/vortex impingement p 814 A92-46952
Three-dimensional blade vortex interactions p 815 A92-46953
Effects of leading and trailing edge flaps on the aerodynamics of airfoil/vortex interactions p 815 A92-46957
Progress towards quieter civil helicopters p 1011 A92-52847
Smart structures in the active control of blade vortex interaction p 1085 A92-56314
BVI impulsive noise reduction by higher harmonic pitch control - Results of a scaled model rotor experiment in the DNW p 1136 A92-56344
Sound produced by vortex-airfoil interaction p 1136 A92-56345
Blade-vortex noise on a helicopter main rotor. Study of the strong two dimensional incompressible interaction
[ONERA-RT-96/5094-PY] p 511 N92-20388
Blade-mounted trailing edge flap control for BVI noise reduction
[NASA-CR-4426] p 512 N92-21173
Pressure and velocity measurements about an airfoil during a parallel blade-vortex interaction p 446 N92-21429
Prediction of helicopter noise: Adaptation of noise load calculations to the blade-vortex interaction
[ONERA-RS-97/5094-PY] p 513 N92-21736
A new method for simulating atmospheric turbulence for rotorcraft applications p 464 N92-21956
Numerical simulations of wakes, blade-vortex interaction, flutter, and flutter suppression by feedback control p 597 N92-23997
Aerodynamic design and analysis of a light aircraft propeller p 629 N92-24876
A gust generation method for full configuration aircraft tests in a low speed wind tunnel. Part 1: Design and preliminary experiments
[NAL-TR-1115-PT-1] p 722 N92-28192

BLADES
On the behavior of pretwisted beams with irregular cross-sections p 495 A92-31564

BLASIUS FLOW
Leading-edge receptivity for blunt-nose bodies
[NASA-CR-190563] p 1036 N92-32648

BLAST LOADS
Computer simulation of weapon blast pressures on flexible surfaces p 39 A92-12115
Composite cylinder blast overpressure testing p 529 A92-32984
Modular simulation of HEI fragments and blast pressure
[AD-A248205] p 910 N92-29191

BLIND LANDING
Control and display combinations for blind vertical landings p 661 A92-39903

BLOWDOWN WIND TUNNELS
Study on transonic cascade performance by use of newly built facility p 136 A92-15328
Isothermal flow fields in a research combustor for lean blowout studies
[ASME PAPER 91-GT-37] p 121 A92-15520
Wind-tunnel studies of F/A-18 tail buffet p 310 A92-24421
Buffet load measurements on an F/A-18 vertical fin at high-angle-of-attack
[AIAA PAPER 92-2127] p 520 A92-35694
Quantitative heat transfer measurements in hypersonic wind tunnels by means of infrared thermography p 1115 A92-54321
A new system for recording unstable aerodynamic phenomena in NAVSWC Hypervelocity Wind Tunnel No. 9 p 1091 A92-54325
The Langley 15-inch Mach 6 High Temperature Tunnel
[AIAA PAPER 92-3938] p 1096 A92-56768
Experimental investigation of heavy rainfall effect on a 2-D high lift airfoil p 452 N92-21696
Replacement of the NAL high pressure air storage system
[NAL-TM-634] p 888 N92-28835
Production of periodical Mach number variations in high subsonic flow in a blow down wind tunnel, and its influence on profile measurements
[ETN-92-91492] p 833 N92-29889

BLOWERS
Validation of a 3D Navier-Stokes code on experimental compressor bladings
[ONERA, TP NO. 1991-229] p 330 A92-26381
Design analysis of the T-800 inlet particle separator/air oil cooler blower p 579 A92-32556

BLOWING
Computational investigation of slot blowing for fuselage forebody flow control
[AIAA PAPER 92-0020] p 248 A92-22142
Aircraft control at high-alpha by tangential blowing
[AIAA PAPER 92-0021] p 281 A92-22143
The dynamics and control of fluctuating pressure loads in the reattachment region of a supersonic free shear layer
[AIAA PAPER 92-0178] p 255 A92-23788
The effects of blowing on delta wing vortices during dynamic pitching at high angles of attack
[AIAA PAPER 92-0407] p 325 A92-26260
Unsteady circulation control aerodynamics of a circular cylinder with periodic jet blowing p 330 A92-26401
Calculation of three-dimensional flow past blunt cones near the plane of symmetry for different flow regimes in the shock layer and in the presence of gas injection from the surface p 337 A92-27593
Unsteady hypersonic boundary layers for slender axisymmetric bodies with large injection rates p 524 A92-36100
High alpha aerodynamic control by tangential fuselage blowing p 611 A92-36848
The effect of a velocity gradient on the aerodynamic forces of a circular cylinder with tangential blowing p 614 A92-38859
Design of wing profiles with tangential suction or injection p 624 A92-40602
The effects of nozzle exit geometry on forebody vortex control using blowing
[AIAA PAPER 92-2603] p 792 A92-45480
Pulsating spanwise blowing on a fighter aircraft
[AIAA PAPER 92-4359] p 1025 A92-55345
High angle-of-attack control enhancement on a forward swept wing aircraft
[AIAA PAPER 92-4427] p 1080 A92-55351
Vortical flow control on a wing-body combination using tangential blowing
[AIAA PAPER 92-4430] p 1081 A92-55354
Experimental evaluation of a 50-percent thick airfoil with blowing and suction boundary layer control
[AIAA PAPER 92-4500] p 1026 A92-55368
Force production mechanisms of a tangential jet on bodies at high alpha
[AIAA PAPER 92-4648] p 1082 A92-55393
Experimental investigation of the effects of blowing on bursting of strake vortices
[AD-A240256] p 13 N92-10985

BLOWOUTS
Lean blowout in a research combustor at simulated low pressures
[ASME PAPER 91-GT-359] p 137 A92-15713

BLUFF BODIES
Flow visualization and wake analysis for complex three-dimensional bluff bodies at subcritical through critical Reynolds numbers
[AIAA PAPER 92-0155] p 253 A92-23770
Experimental investigation of a three-dimensional bluff-body wake
[AIAA PAPER 92-0429] p 326 A92-26277
Flow about cylinders with helical surface protrusions
[AIAA PAPER 92-0540] p 332 A92-26957
Optimization of bluff body for minimum drag in ground proximity p 431 A92-31154
Change of flow about an elongated rectangular cylinder in a range of Reynolds numbers of 200 to 0.7 x 10 exp 4 p 522 A92-35997
An experimental and numerical study of confined axisymmetric jet with a bluff body p 621 A92-40106
The natural and forced formation of spot-like Lambda-structures caused by vortex dislocations in a wake p 621 A92-40111
Drag reduction of bluff bodies through momentum injection p 702 A92-41231
Direct simulation of vortex shedding in dilute gas flows past bluff bodies p 939 A92-52766
Axisymmetric bluff-body flow: A vortex solver for thin shells
[DE92-016748] p 1003 N92-31933
Aeroelasticity of bluff bodies p 1089 N92-34165

BLUNT BODIES
Recombination-dominated nonequilibrium heat transfer to arbitrarily catalytic hypersonic vehicles p 2 A92-10426
A spatial marching technique for the inviscid blunt body problem p 4 A92-10691
A study on the interaction between a bow shock wave generated by a blunt body and a turbulent boundary layer p 8 A92-12424
Base pressure measurements on a cone at Mach numbers from M sub infinity = 5 to 7 p 173 A92-18770
Navier-Stokes analysis of blunt trailing edge airfoils
[AIAA PAPER 92-0024] p 248 A92-22146

Numerical simulation of supersonic separated flow over blunt cones at high angles of attack p 313 A92-25039
Singular perturbation theory of hypersonic flow over blunt bodies p 313 A92-25048
Numerical simulation and analysis for hypersonic flow with separation over blunt cone at angle of attack p 314 A92-25126
Multidomain spectral solutions of high-speed flows over blunt cones
[AIAA PAPER 92-0324] p 322 A92-25771
Monte Carlo simulation of reentry flows with ionization
[AIAA PAPER 92-0493] p 328 A92-26323
An approximate viscous shock layer technique for calculating nonequilibrium hypersonic flows about blunt-nosed bodies
[AIAA PAPER 92-0498] p 329 A92-26326
Effects of nose bluntness and angle of attack on slender bodies in hypersonic flows
[AIAA PAPER 92-0638] p 334 A92-27016
Computation of laminar flow over a long slender axisymmetric blunted cone in hypersonic flow
[AIAA PAPER 92-0756] p 336 A92-27098
Calculation of heat transfer and friction for a blunt body in the path of supersonic flow of a chemically equilibrium air-xenon mixture p 336 A92-27532
Calculation of three-dimensional flow past blunt cones near the plane of symmetry for different flow regimes in the shock layer and in the presence of gas injection from the surface p 337 A92-27593
Effective treatments of the singular line boundary problem for three dimensional grids
[AIAA PAPER 92-0545] p 342 A92-28202
Flow of a viscous twisted fluid film on the surface of a blunt body in supersonic flow of a gas p 424 A92-30146
Calculation of real-gas effects on blunt-body trim angles p 432 A92-31169
Combined effect of nose bluntness and angle of attack on slender bodies in viscous hypersonic flows
[AIAA PAPER 92-0755] p 436 A92-31680
A parametric study of the lift-drag ratio of blunt cones p 437 A92-31860
Active control of the hydraulic forces of a body by a splitter plate p 591 A92-36351
Numerical study of coupled heat transfer under conditions of filtering and film cooling of blunt anisotropic bodies p 610 A92-36552
Nonstationary viscous shock layer in supersonic motion over an inhomogeneity p 708 A92-42737
Laminar heat transfer to blunt cones in high-enthalpy hypervelocity flows p 713 A92-44372
Integrated electric density and scaling law for hypersonic blunt-body wakes p 714 A92-44865
Shock interaction induced by two hemisphere-cylinders
[SAE PAPER 912043] p 790 A92-45427
Decoupled predictions of radiative heating in air using a particle simulation method
[AIAA PAPER 92-2971] p 816 A92-46986
Thermal and chemical nonequilibrium viscous shock layer flows over a blunt body at high altitudes p 938 A92-52749
Hypersonic merged layer blunt body flows with wakes p 939 A92-52757
Hypersonic flows with air chemistry over a reentry vehicle at high altitudes p 1017 A92-53549
Experimental investigation on turbulent phenomena in three-dimensional shock wave/turbulent boundary layer interaction induced by blunt fin p 1018 A92-53557
Interaction between a body flying at a supersonic velocity and a point explosion p 1019 A92-53867
Approximate aerodynamic analysis of jet interaction
[AIAA PAPER 92-4640] p 1027 A92-55387
Three-dimensional shock wave-turbulent boundary layer interaction induced by blunt body and protuberance p 1029 A92-56009
On the footprints of three-dimensional separated vortex flows around blunt bodies: Attempts of defining and analyzing complex flow structures p 84 N92-13005
Hypersonic flow past delta wing flow simulated by Navier-Stokes solutions p 180 N92-14981
An improved method for simulating supersonic flow past a wedge shaped body
[NAL-TR-1097] p 345 N92-18239
Simulation of real-gas effects on pressure distributions for aeroassist flight experiment vehicle and comparison with prediction
[NASA-TP-3157] p 501 N92-20677
Case 7.4: Blunt nose delta wing Euler-boundary layer calculation p 525 N92-22184
Heat transfer characteristics of hypersonic waveriders with an emphasis on the leading edge effects
[NASA-CR-189586] p 525 N92-22215
Hypersonic laminar flow computations over a blunt leading edged delta wing at three different chord Reynolds numbers
[FFA-TN-1991-40] p 528 N92-23168
Second-order shock-expansion theory extended to include real gas effects
[AD-A247191] p 831 N92-29539
Two-dimensional aerodynamic characteristics of several polygon-shaped cross-sectional models applicable to helicopter fuselages
[NASA-TP-3233] p 944 N92-30394
An examination of several high resolution schemes applied to complex problems in high speed flows
[AD-A250814] p 1124 N92-32632
An approximate viscous shock layer technique for calculating chemically reacting hypersonic flows about blunt-nosed bodies p 1041 N92-33837
Computation and stability analysis of laminar flow over a blunt cone in hypersonic flow p 1041 N92-33839

BLUNT LEADING EDGES

Experimental studies of the interaction of converging axisymmetric shock waves with sharp and blunt cones in supersonic flow p 63 A92-13749
Improved nonequilibrium viscous shock-layer scheme for hypersonic blunt-body flowfields p 310 A92-24653
Aerodynamic characteristics of a blunt delta wing with air bleed through an intake at supersonic and hypersonic velocities. II p 437 A92-31855
A heat flow peak on the upwind surface of a blunt-leading-edge delta wing p 438 A92-31862
Aerodynamically blunt and sharp bodies
[AIAA PAPER 92-2727] p 808 A92-45597
The effect of rounding the leading edges on the characteristics of separated flow past delta wings of low aspect ratio
[RAE-LIB-TRANS-2164] p 257 N92-15964
Leading-edge receptivity for blunt-nose bodies
[NASA-CR-190563] p 1036 N92-32648

BLURRING

Aero-optical testing in the NSWC Hypervelocity Tunnel No. 9
[AIAA PAPER 92-2797] p 747 A92-41336

BO-105 HELICOPTER

Frequency-domain identification of BO 105 derivative models with rotor degrees of freedom p 104 A92-14327
System identification requirements for high-bandwidth rotorcraft flight control system design p 479 A92-29332
The DLR test aircraft in FZ-BS VFW614/ATTAS, Dornier DO228-101, MBB BO 105-S-3 p 648 N92-25591

BOATTAILS

Transonic Navier-Stokes computations for a spinning body of revolution
[AD-A241015] p 180 N92-14972
Effect of afterbody geometry on aerodynamic characteristics of isolated nonaxisymmetric afterbodies at transonic Mach numbers
[NASA-TP-3236] p 1041 N92-33706

BODIES OF REVOLUTION

Subsonic axisymmetric viscoelastic flow past thin tapered bodies of revolution p 6 A92-12134
Computation of three-dimensional turbulent vortical flows on bodies at high incidence p 9 A92-13203
Changing the structure and improving the aerodynamic characteristics of supersonic flow past bodies through ejection of a gas jet with particles p 78 A92-16680
Three-dimensional linear stability approach to transition on wings and bodies of revolution at incidence p 172 A92-18361
Surface flow patterns on an ogive-cylinder at incidence p 176 A92-20762
An investigation on detached shock waves ahead of bodies of revolution at transonic speeds p 251 A92-23381
A study of flow past bodies of revolution with a Riabushinskii generatrix p 252 A92-23502
Some thoughts on conical flow asymmetry
[AIAA PAPER 92-0427] p 326 A92-26275
Bodies of revolution with minimal wave drag at transonic gas flow velocities p 424 A92-30135
Calculation of the aerodynamic characteristics of bodies of revolution in incompressible flow by the vortex surface method p 428 A92-30375
Analysis of slender bodies of revolution with curved-ground effect and waving-water effect p 524 A92-36151
Numerical simulation of separation flow on bodies of revolution at high angle of attack using Euler equations p 616 A92-38919
Calculation of rotational derivatives in the case of local interaction between flow and a body surface p 624 A92-40746
On the measurement of subsonic flow around an appended body of revolution at cryogenic conditions in the NTF p 880 A92-45265
Measurements of the unsteady vortex flow over a wing-body at angle of attack
[AIAA PAPER 92-2729] p 808 A92-45598
Vortex formation over a close-coupled canard-wing-body configuration in unsymmetrical flow p 85 N92-13010
Transonic Navier-Stokes computations for a spinning body of revolution
[AD-A241015] p 180 N92-14972
Computation of the hydrodynamic forces and moments on a body of revolution with and without appendages
[AD-A243033] p 298 N92-16978
Asymptotic theory of transonic wind tunnel wall interference
[AD-A244075] p 403 N92-19080
Unsteady transonic aerodynamics of pointed bodies of revolution in supersonic freestream p 719 N92-27946
Second-order shock-expansion theory extended to include real gas effects
[AD-A247191] p 831 N92-29539

BODY KINEMATICS

Representation of geometric stiffening in multibody system simulation p 217 A92-19463
Rigid and flexible joint modelling in multibody dynamics using finite elements p 671 A92-37559
Special Rotation Vectors quaternions in three components
[AIAA PAPER 92-4168] p 1008 A92-52454
Evaluation of head impact kinematics for passengers seated behind interior walls
[AD-A252651] p 952 N92-30551

BODY-WING AND TAIL CONFIGURATIONS

New Airbus Industrie airliners on course for long-haul era p 308 A92-26792
Analysis of junction flowfields using the incompressible Navier-Stokes equations
[AIAA PAPER 92-0519] p 331 A92-26944
Approximate determination of the effect of deviations of wing and tail geometry from design parameters on the drag coefficient of subsonic aircraft p 460 A92-31878
Single block mesh generation for a fuselage plus two lifting surfaces p 817 A92-47054
On a global aerodynamic optimization of a civil transport aircraft p 193 N92-13931

BODY-WING CONFIGURATIONS

Evaluation of Euler solvers for transonic wing-fuselage geometries p 174 A92-20214
Measurements of the flow around a lifting-wing/body junction p 175 A92-20726
Effect of leading-edge cross-sectional geometry on slender wing unsteady aerodynamics
[AIAA PAPER 92-0173] p 255 A92-23784
An approach to the design of wings - The role of mathematics, physics and economics
[AIAA PAPER 92-0286] p 319 A92-25739
Influence of wing shapes on the surface pressure fluctuations of a wing-body junction
[AIAA PAPER 92-0433] p 327 A92-26280
An experimental study of a turbulent wing-body junction and wake flow
[AIAA PAPER 92-0434] p 327 A92-26281
A one-equation turbulence model for aerodynamic flows
[AIAA PAPER 92-0439] p 327 A92-26285
The effect of wing twist optimized in the framework of the plane cross section hypothesis on the aerodynamic characteristics of a wing-body combination at hypersonic speeds p 424 A92-30129
Turbulent flow in the wake of an idealized wing-body junction
[AIAA PAPER 92-0282] p 435 A92-31652
Aerodynamic characteristics of the combination of a wing with a cambered middle surface with a fuselage p 439 A92-31880
Characteristics of transonic flow past a configuration comprising a wing and a fuselage with a large midsection ratio p 439 A92-31882
Effect of the fuselage midsection ratio on the character of wing-fuselage aerodynamic interference p 439 A92-31883
Experimental study of a low Reynolds number tandem airfoil configuration p 442 A92-32241
The equations governing the motion of wing-aileron structural systems constructed from advanced anisotropic composite materials
[AIAA PAPER 92-2469] p 564 A92-34359
Use of the thrust-weight diagram versus transport cargo in the initial dimensioning of passenger-transport aircraft p 642 A92-37074
An experimental evaluation of some turbulence models from a three-dimensional turbulent boundary layer around a wing-body junction p 620 A92-40087
A correlation study of the wing-body interference factor for high angles of attack p 700 A92-41179
Effect of canard deflection on close-coupled canard-wing-body aerodynamics
[AIAA PAPER 92-2602] p 792 A92-45479

Three-dimensional orthogonal-to-surface structured grid generation with transonic Navier-Stokes flow solutions for a commercial transport configuration
[AIAA PAPER 92-2616] p 793 A92-45490
Practical design optimization of wing/body configurations using the Euler equations
[AIAA PAPER 92-2633] p 795 A92-45505
Transonic calculations for wings with deflected control surfaces
[AIAA PAPER 92-2617] p 805 A92-45572
Measurements of the unsteady vortex flow over a wing-body at angle of attack
[AIAA PAPER 92-2729] p 808 A92-45598
Multi-block grid generation around wing-body-engine-pylon configurations
p 817 A92-47060
Effects of a leading-edge fillet on the flow past an appendage-body junction p 935 A92-50301
Vortical flow computations on a flexible blended wing-body configuration p 1024 A92-54922
Effects of the roll angle on cruciform wing-body configurations at high incidences
[AIAA PAPER 92-4356] p 1079 A92-55342
Optimization of aeroelastic system with active control
p 1083 A92-56022
Navier-Stokes simulation of a close-coupled canard-wing-body configuration p 1031 A92-56163
Transonic and supersonic Euler computations of vortex-dominated flow fields about a generic fighter
[NASA-TP-3156] p 11 N92-10011
Vortical flow simulation by using structured and unstructured grids p 83 N92-12999
Analysis of results of an Euler-equation method applied to leading-edge vortex flow p 84 N92-13000
On the simulation of compressible turbulent flows past delta wing, delta wing-body and delta wing-canard
p 84 N92-13003
Definition of the unsteady vortex flow over a wing/body configuration
[NASA-CR-180083] p 178 N92-13995
An experimental study of a turbulent wing-body junction and wake flow
[AD-A243388] p 260 N92-17222
MATGRID: A program for generation of C-H and C-O topology grids around wing/body configurations. Mathematical definition document
[FFA-TN-1990-19] p 444 N92-20468
Normal force of low aspect ratio wing-body combinations up to high angles of attack at supersonic speeds
[ESDU-91042] p 553 N92-24009
A study of transonic aerodynamic analysis methods for use with a hypersonic aircraft synthesis code
[NASA-CR-189854] p 625 N92-24803
Algorithm and code development for unsteady three-dimensional Navier-Stokes equations
[NASA-CR-190077] p 692 N92-25264
Vibration tests and structural modeling of an aircraft model for active control technology experiments
[NAL-TM-626] p 662 N92-25401
On a multi-block method for transonic turbulent flows past a wing-fuselage configuration p 632 N92-25569
Observation and measurements of flow structures in the stagnation region of a wing-body junction
p 714 N92-26616
Subsonic investigations of vortex interaction control for enhanced high-alpha aerodynamics of a chine forebody/Delta wing configuration
[NASA-CR-189641] p 715 N92-26652
Pressure-based high-order TVD methodology for dynamic stall control
[AD-A247056] p 774 N92-27918
Analysis of results of an Euler-equation method applied to leading-edge vortex flow
[NLR-TP-90368-U] p 827 N92-28657
An experimental study of the relationship between velocity and pressure fluctuations in a wing-body junction
[AD-A249628] p 946 N92-31122
Aerodynamic centre of wing-body combinations
[ESDU-92024] p 1036 N92-32479
A method for designing blended wing-body configurations for low wave drag
[NASA-TP-3261] p 1036 N92-32480
Survey and analysis of research on supersonic drag-due-to-lift minimization with recommendations for wing design
[NASA-TP-3202] p 1040 N92-33656

BOEING AIRCRAFT
H-76B Fantail demonstrator composite fan blade fabrication p 145 A92-14356
Concurrent engineering at Boeing Helicopters
p 162 A92-14393
Delivered with feeling --- computer-based design of flight control system for Boeing 777 p 134 A92-16621
Feeling normal --- evaluation of advanced control systems for future Boeing 777 p 134 A92-16623
Systems engineering as applied to the Boeing 777
[AIAA PAPER 92-1010] p 515 A92-33198
Design of advanced composite components for maintainability based on inservice experience
[AIAA PAPER 92-1085] p 537 A92-33251
The NASA/Industry Design Analysis Methods for Vibrations (DAMVIBS) Program - Boeing helicopters airframe finite element modeling
[AIAA PAPER 92-2202] p 539 A92-34392
Acoustic results of the Boeing model 360 whirl tower test p 603 A92-35741
New titanium applications on the Boeing 777 airplane
p 754 A92-41119
Electric power generating system for the Boeing 777 airplane
[SAE PAPER 912050] p 861 A92-45434
Boeing Helicopters Advanced Rotorcraft Transmission (ART) Program summary of component tests
[AIAA PAPER 92-3364] p 905 A92-48937
BA's 777 p 958 A92-51580
777 shaping up p 959 A92-52300
Design of the Boeing 777 electric system
p 1070 A92-55902
Structural airworthiness of aging Boeing jet transports
p 362 N92-18590
Structural integrity of future aging airplanes
p 913 N92-30107
Performance of fuselage pressure structure
p 913 N92-30109
Lewis icing research tunnel test of the aerodynamic effects of aircraft ground deicing/anti-icing fluids
[NASA-TP-3238] p 952 N92-30395
Study objectives: Will commercial avionics do the job? Improvements needed? p 1065 N92-33340

BOEING 720 AIRCRAFT
An integrated real-time turbine engine flight test system p 201 A92-19275

BOEING 727 AIRCRAFT
Design and analysis of reengine Boeing 727-100 center inlet S duct by a reduced Navier-Stokes code
[AIAA PAPER 92-1221] p 517 A92-33320
A re-analysis of the causes of Boeing 727 'black hole landing' crashes p 833 A92-44985
Design and analysis of vortex generators on reengined Boeing 727-100QF center inlet S-duct by a reduced Navier-Stokes code
[AIAA PAPER 92-2700] p 800 A92-45542
Application of analysis techniques for low frequency interior noise and vibration of commercial aircraft
[NASA-CR-189555] p 481 N92-20376

BOEING 737 AIRCRAFT
Aircraft accident report: MarkAir, Inc., Boeing 737-2X6C, N670MA, controlled flight into terrain, Unalakleet, Alaska, 2 June 1990
[PB91-910402] p 92 N92-13039
Measurements of fuselage skin strains and displacements near a longitudinal lap joint in a pressurized aircraft
[NASA-TM-104163] p 159 N92-13455
Study of the engine bird ingestion experience of the Boeing 737 aircraft
[DOT/FAA/CT-89/16] p 187 N92-15053
A graphical weather system design for the NASA transport systems research vehicle B-737
[NASA-TM-104205] p 556 N92-22504
Engine bird ingestion experience of the Boeing 737 aircraft: Expanded data base
[DOT/FAA/CT-91/32] p 1045 N92-34151

BOEING 747 AIRCRAFT
An experiment on the weight vs control relations of subsonic airplanes p 357 A92-25502
A fast implicit upwind solution algorithm for three-dimensional unstructured dynamic meshes
[AIAA PAPER 92-0447] p 328 A92-26291
Structural airworthiness of aging Boeing jet transports - 747 fuselage fatigue test program
[AIAA PAPER 92-1128] p 537 A92-33280
Halfway around the world is far enough
p 516 A92-33462
Mass-transporter p 543 A92-34650
Flight testing of the Boeing 747-400 Central Maintenance Computer system p 555 A92-35950
747-400 upper rudder control system
p 731 A92-43546
Crew transportation for the 1990s. I - Commercializing manned flight with today's propulsion
p 889 A92-46726
GPS tests during approach at Singapore and Roissy
p 956 A92-53240
Engine condition monitoring system for B747-400
p 1064 A92-56082
Aeronautical satellite communications system
p 1046 A92-56089
Evaluation report of an experimental Satcom operation by a Japan Airline's B747 passenger plane
p 1046 A92-56092
A fast implicit upwind solution algorithm for three-dimensional unstructured dynamic meshes
[NASA-TM-104186] p 185 N92-15050
Flight test of ARINC 741 configuration low gain SATCOM system on Boeing 747-400 aircraft p 677 N92-24097
Implicit upwind-Euler solution algorithms for unstructured-grid applications
[NASA-TM-107645] p 945 N92-30691
Aircraft accident report: Explosive decompression - loss of cargo door in flight, United Airlines Flight 811, Boeing 747-122, N4713U, Honolulu, Hawaii, February 24, 1989
[PB92-910402] p 953 N92-31159
An assessment of the B-747's capability to operate on rough surfaces
[AD-A250134] p 963 N92-31793
Structural assessment of ultralightweight composites
p 1107 N92-32525

BOEING 757 AIRCRAFT
Parameter identification studies on the NASA/Ames Research Center Advanced Concepts Flight Simulator
[NASA-TM-105126] p 31 N92-11024

BOEING 767 AIRCRAFT
Parameter identification studies on the NASA/Ames Research Center Advanced Concepts Flight Simulator
[NASA-TM-105126] p 31 N92-11024

BOILING
Flow pattern characterization and heat transfer behavior in a boiling two-phase flow in an inclined pipe
p 493 A92-29722
Observational study of pool boiling under microgravity
p 757 A92-41060
Boiling and condensation in microfin tubes
p 682 N92-25660

BOLIDES
Stability and inherent precision of two methods for solving motion and ablation equations for fireball-forming bodies in the earth atmosphere p 929 A92-46595

BOLTED JOINTS
Preliminary finite element analysis of unloaded and loaded notched composite laminated plates
[NRC-LTR-ST-1806] p 159 N92-13454
Rapid repair of integrally stiffened carbon fibre composite structures by bolted aluminium elements
[MBB-FE202-S-PUB-0453-A] p 290 N92-17310

BOLTZMANN TRANSPORT EQUATION
A numerical solution of inviscid transonic flow using the Boltzmann equation p 443 A92-32504
Motion of a sphere in a gas - Numerical solution of the linearized Boltzmann equation p 591 A92-36194
Transitional flows around re-entry bodies
p 184 N92-15035

BOMBER AIRCRAFT
B-2 handling, automation tailored to two-pilot crew
p 643 A92-39725
The B-2 radar p 956 A92-53102
Automatic production test equipment (APTE) for the B-2 p 997 A92-53107
B-2 program: Trends in manufacturing
[AD-A242141] p 242 N92-15963
When should we start high-rate production of the B-2? An analysis based on flight test results
[RAND/P-7757] p 697 N92-25204

BOMBS (ORDNANCE)
Safety in the sky - Designing bomb-resistant baggage containers p 836 A92-47775

BONDING
Thermodynamic structural analysis of high speed propulsion systems
[IAF PAPER 91-278] p 120 A92-14711
Development of aircraft bonded structure and the NDI method p 1016 A92-56100
Large area QNDE inspection for airframe integrity
p 362 N92-18588

BOOLEAN ALGEBRA
The avoidance of collisions for Newtonian bodies with hidden variables p 353 A92-24945

BOOMS (EQUIPMENT)
X-29 high angle-of-attack flight test air data comparisons of an inertial navigation system and noseboom probe
p 549 A92-35945
Effect of a nose-boom on forebody vortex flow
p 812 A92-46818

BOOSTER ROCKET ENGINES
Optimal launch trajectory of a hypersonic research vehicle
[AIAA PAPER 92-4302] p 1103 A92-55310

BOREHOLES
Cutting treatment by drilling of fiber bound synthetic materials
[MBB-UD-0609-91-PUB] p 988 N92-31716

BORESIGHT ERROR
Aero-optical testing in the NSWC Hypervelocity Tunnel No. 9
[AIAA PAPER 92-2797] p 747 A92-41336

BORIC ACIDS
Non-chromated anodize process for corrosion resistance and adhesive bonding p 892 A92-47341
BORING MACHINES
Cutting treatment by drilling of fiber bound synthetic materials
[MBB-UD-0609-91-PUB] p 988 N92-31716
BORON
Swirl and fuel composition effects on boron combustion in solid-fuel ramjets p 668 A92-36964
BORON-EPOXY COMPOSITES
The study on the composite-patching repairs for metallic aircraft structures p 36 A92-10285
The reinforcing effect of composite patch repairs on metallic aircraft structures p 419 A92-30498
Environmental evaluation of repairs to fuselage lap joints p 699 A92-41534
BOUNDARIES
A frontal approach for node generation in Delaunay triangulations p 771 N92-27680
Validation of three-dimensional incompressible spatial direct numerical simulation code: A comparison with linear stability and parabolic stability equation theories for boundary-layer transition on a flat plate
[NASA-TP-3205] p 943 N92-30295
Development of 3D electromagnetic modeling tools for airborne vehicles
[NASA-CR-190810] p 1126 N92-33307
BOUNDARY CONDITIONS
A study of a version of the boundary conditions of a two-dimensional spline in surface and line modeling
p 163 A92-16826
Modeling the ventilated wind tunnel wall
[AIAA PAPER 92-0035] p 249 A92-22156
Control of turbulent flow on a backward-facing step
[AIAA PAPER 92-0066] p 250 A92-22179
Boundary singularities in steady potential compressible flow through plane two-dimensional channels
p 336 A92-27384
Estimation of propulsion-induced effects on transonic flows over a hypersonic configuration
[AIAA PAPER 92-0523] p 341 A92-28197
Two-dimensional heat transfer from a rectangular fin with asymmetrical thermal boundary conditions
p 498 A92-32524
Outflow boundary conditions for Euler analysis of flow in turbine scroll p 591 A92-36037
A numerical study of flow of a viscous gas in a Laval nozzle in the narrow channel approximation
p 706 A92-42680
Bleed-boundary conditions for numerically simulated mixed-compression supersonic inlet flow
p 713 A92-44520
Critical effects of downstream boundary conditions on vortex breakdown
[AIAA PAPER 92-2601] p 792 A92-45478
A new automatic grid generation environment for CFD applications
[AIAA PAPER 92-2720] p 803 A92-45558
Viscous flow past a nacelle isolated and in proximity of a flat plate
[AIAA PAPER 92-2723] p 803 A92-45560
A compact higher order Euler solver for unstructured grids with curved boundaries
[AIAA PAPER 92-2696] p 807 A92-45590
Ritz vectors synthesis versus modal synthesis for fluid-structure interaction modeling p 898 A92-45885
The method of determinant equations in the applied theory of optimal systems - Systems with 'rigid' constraints and with fixed boundary conditions p 917 A92-46629
Outflow boundary conditions using Duhamel's equation p 813 A92-46913
Application of non-reflecting boundary conditions to three-dimensional Euler equation calculations for thick strut cascades
[AIAA PAPER 92-3045] p 822 A92-48705
Pseudostream function formulation - A method of solving three-dimensional aerodynamic analysis and design problems in turbomachinery p 996 A92-52981
Design of 3-dimensional complex airplane configurations with specified pressure distribution via optimization
p 194 N92-13948
Annular seals of high energy centrifugal pumps: Presentation of full scale measurement
p 224 N92-14362
Invariant boundary conditions for cascade flows
p 498 N92-20147
Grid generation for a complex aircraft configuration
p 649 N92-25714
Development and validation of a characteristic boundary condition for a cell-centered Euler method
[NLR-TP-90144-U] p 828 N92-28692
Boundary conditions for Euler equations at internal block faces of multi-block domains using local grid refinement
[NLR-TP-90134-U] p 908 N92-28712
Evaluation of measured-boundary-condition methods for 3D subsonic wall interference
[NLR-TR-88072-U] p 832 N92-29884
Validation of three-dimensional incompressible spatial direct numerical simulation code: A comparison with linear stability and parabolic stability equation theories for boundary-layer transition on a flat plate
[NASA-TP-3205] p 943 N92-30295
BOUNDARY ELEMENT METHOD
Complex variable boundary element method for external potential flows p 172 A92-18353
A boundary element method for the potential, compressible aerodynamics of bodies in arbitrary motion
p 314 A92-25098
Analysis of tenon and mortise contact problems by boundary element methods p 587 A92-35554
Mixed volume boundary element approach for aerodynamics p 617 A92-39934
Analysis of the aerodynamic performance of rotors with the boundary element method p 709 A92-43119
Calculations of aerodynamic forces on a wing with thrust using B.E.M p 1030 A92-56049
Generalized aerodynamics analysis by the boundary element method p 1030 A92-56050
Development of an integrated BEM approach for hot fluid structure interaction: BEST-FSI: Boundary Element Solution Technique for Fluid Structure Interaction
[NASA-CR-189202] p 574 N92-22211
Turbulent mixing in supersonic jets
p 715 N92-27054
Hyperbolic grid generation with BEM source terms
[NLR-TP-90334-U] p 923 N92-28635
Nonlinear analyses of composite aerospace structures in sonic fatigue
[NASA-CR-190565] p 854 N92-30209
BOUNDARY INTEGRAL METHOD
A boundary integral formulation for the kinetic field in aerodynamics. I - Mathematical analysis
p 243 A92-21504
Calculation methods of three-dimensional boundary layers p 245 A92-21978
Recent progress in finite element method and boundary integral equation method for nonviscous transonic flows
p 314 A92-25127
A boundary integral formulation for the kinetic field in aerodynamics. II - Applications to unsteady 2D flows
p 339 A92-28005
Knowledge-based nonlinear boundary integral models of compressible viscous flows over arbitrary bodies - Taking CFD back to basics p 617 A92-39941
A new integral equation for potential compressible aerodynamics of rotors in forward flight
p 815 A92-46958
A complete boundary integral formulation for steady compressible inviscid flows governed by nonlinear equations p 934 A92-50211
A boundary integral formulation for unsteady transonic potential flows p 719 N92-27942
BOUNDARY LAYER CONTROL
Optimal boundary control of nonsteady incompressible flow with an application to viscous drag reduction
p 39 A92-11344
Performance improvements of compressor cascades by controlling the profile and sidewall boundary layers
[ASME PAPER 91-GT-260] p 75 A92-15662
Detection of flow state in an unsteady separating flow
p 219 A92-20741
Numerical investigation of supersonic mixed-compression inlet using an implicit upwind scheme p 243 A92-21073
Preliminary investigation of inlet dynamic distortion and it's passive control p 245 A92-21742
Flow characteristic and flow control of high aspect ratio and highly curved S-bend diffuser p 245 A92-21743
Separation control using moving surface effects - A numerical simulation p 309 A92-24419
Problems of laminar-turbulent transition control in a boundary layer p 312 A92-24979
Control of laminar boundary layer separation
p 393 A92-24980
Design of a hybrid laminar flow control nacelle
[AIAA PAPER 92-0400] p 373 A92-26253
Control of strong shock-turbulent boundary layer interaction in rectangular channels p 422 A92-29714
Control of the development of boundary layer disturbances p 423 A92-30126
Investigating the feasibility of controlling the laminar-turbulent transition by means of laminarizing plates p 493 A92-30161
Flight studies of the riblet effect on drag variation
p 438 A92-31871
Boundary-layer-separation control p 440 A92-31886
The numerical simulation of separation control using moving surface effect p 616 A92-38924
Laminar flow control of subsonic boundary layers by suction and heat transfer strips p 617 A92-39338
Analysis for the application of hybrid laminar flow control to a long-range subsonic transport aircraft
[SAE PAPER 912113] p 617 A92-39964
Application of laminar flow control to high-bypass-ratio turbofan engine nacelles
[SAE PAPER 912114] p 618 A92-39965
Application of linear stability theory in laminar flow design
[SAE PAPER 912116] p 618 A92-39967
Some practical aspects of viscous drag reduction concepts
[SAE PAPER 912129] p 618 A92-39976
A study of three dimensional turbulent boundary layer separation and vortex flow control using the reduced Navier Stokes equations p 621 A92-40105
Drag reduction of bluff bodies through momentum injection p 702 A92-41231
Aerodynamic development of boundary layer control system for NAL QSTOL research aircraft 'ASKA'
[SAE PAPER 912010] p 843 A92-45410
Compressible Navier-Stokes solutions for a suction boundary control airfoil
[AIAA PAPER 92-2710] p 802 A92-45551
An investigation of passive control methods for shock-induced separation at hypersonic speeds
[AIAA PAPER 92-2725] p 808 A92-45596
Gortler instability and supersonic quiet nozzle design
p 813 A92-46902
The design and testing of an airfoil with hybrid laminar flow control
[ONERA, TP NO. 1992-22] p 822 A92-48585
Experimental evaluation of a 50-percent thick airfoil with blowing and suction boundary layer control
[AIAA PAPER 92-4500] p 1026 A92-55368
Results from computational analysis of a mixed compression supersonic inlet
[NASA-TM-104475] p 12 N92-10976
Proceedings of the Seminar on Investigation and Control of Boundary-Layer Transition
[NAL-SP-11] p 400 N92-18483
Active flow control for twenty-first century high-performance aircraft with applications to land and sea vehicles p 447 N92-21504
The NASA Langley laminar-flow-control experiment on a swept, supercritical airfoil: Evaluation of initial perforated configuration
[NASA-TM-4309] p 525 N92-22196
Distributed acoustic receptivity in laminar flow control configurations
[NASA-CR-4438] p 765 N92-26680
Special Course on Skin Friction Drag Reduction
[AGARD-R-786] p 717 N92-27706
Basic concepts on boundary layers
p 717 N92-27707
Aircraft drag reduction p 717 N92-27709
Laminar-turbulent transition: Fundamentals
p 717 N92-27710
Boundary layer transition: Prediction, application to drag reduction p 717 N92-27711
Turbulent skin-friction drag reduction by active and passive means, part 1 p 718 N92-27714
Evaluation of high lift devices of the quiet STOL experimental aircraft ASKA
[NAL-TR-1102] p 733 N92-28153
Boundary layer induced noise in aircraft
[CUED/A-AERO/TR-18] p 927 N92-29201
Active control of the separation region on a two-dimensional airfoil
[AD-A249739] p 948 N92-31622
Method of reducing drag in aerodynamic systems
[NASA-CASE-LEW-14791-1] p 1043 N92-34243
BOUNDARY LAYER EQUATIONS
Fundamentals of applied aerogasdynamics. II - Viscous flow past bodies. Control devices --- Russian book
p 64 A92-14281
Numerical solution of the boundary-layer equations for a general aviation fuselage p 174 A92-20211
Axisymmetric analogy for three-dimensional viscous flow problems p 244 A92-21617
Introduction to three dimensional boundary layers
p 245 A92-21977
Calculation methods of three-dimensional boundary layers p 245 A92-21978
A numerical method for solving the circulation control airfoil with wall jet p 314 A92-25103
The study of inverse boundary layer algorithm for transonic flows over aerofoils p 315 A92-25140
An approach to the design of wings - The role of mathematics, physics and economics
[AIAA PAPER 92-0286] p 319 A92-25739
Characteristics of transonic flow past a configuration comprising a wing and a fuselage with a large midsection ratio p 439 A92-31882
Asymptotic defect boundary-layer theory applied to hypersonic flows p 610 A92-36839

Non-equilibrium hypersonic flow simulations using the second-order boundary layer equations
p 612 A92-37551
Wake effects on the prediction of transonic viscous flows around airfoils p 702 A92-41232
Performance predictions for centrifugal compressor impellers p 759 A92-41836
A bi-directional marching finite element algorithm for three-dimensional boundary layer separation flow computations p 942 A92-53288
Computational fluid dynamics p 177 N92-13979
Analysis tools of ONERA and DLR for the aerothermodynamics of reentry vehicles
p 211 N92-14977
Proceedings of the Seminar on Investigation and Control of Boundary-Layer Transition
[NAL-SP-11] p 400 N92-18483
Two-dimensional transonic flow calculation by interaction of Euler and boundary layer equations
[PB92-136449] p 448 N92-21784
Case 7.4: Blunt nose delta wing Euler-boundary layer calculation p 525 N92-22184
Fundamental aspects of boundary layers and transition in turbomachines p 658 N92-24337
Boundary layer computations using a generalized formulation p 679 N92-24873

BOUNDARY LAYER FLOW
Recombination-dominated nonequilibrium heat transfer to arbitrarily catalytic hypersonic vehicles
p 2 A92-10426
Correlation of separation shock motion with pressure fluctuations in the incoming boundary layer
p 5 A92-11061
Boundary-layer and wake measurements on a swept, circulation-control wing p 9 A92-13205
On the nonlinear stability of a high-speed, axisymmetric boundary layer p 78 A92-16457
Magnetohydrodynamic boundary layer flow over a rotating disk p 304 A92-21338
On velocity profile models for predicting end wall boundary layers and their blade force defects in axial compressor cascades p 311 A92-24877
Design of a hybrid laminar flow control nacelle
[AIAA PAPER 92-0400] p 373 A92-26253
Turbulence modeling for high speed flows
[AIAA PAPER 92-0436] p 327 A92-26283
Calculation of compressible boundary layer flow about airfoils by a finite element/finite difference method
[AIAA PAPER 92-0524] p 332 A92-26948
Numerical analysis of shock-induced separation alleviation using vortex generators
[AIAA PAPER 92-0751] p 335 A92-27095
Assessment of three models of turbulence in a shock-boundary layer interaction of a heated wall
p 423 A92-29999
Effect of compressibility on the value of the acceptable roughness Reynolds number p 427 A92-30197
Numerical analysis on laminar flow control of transonic airfoils p 430 A92-30557
Boundary layer flows around an airship
p 430 A92-30560
A computational exploration of the importance of three-dimensionality, boundary layer development, and flow chemistry to the prediction of scramjet nozzle performance
[AIAA PAPER 91-5059] p 472 A92-31689
Twenty-five years of aerodynamic research with infrared imaging p 497 A92-32232
Numerical studies of supersonic flow over a compression corner p 442 A92-32324
Asymptotic defect boundary-layer theory applied to hypersonic flows p 610 A92-36839
Compressible turbulent boundary layers with heat addition by homogeneous condensation
p 611 A92-36843
Performance of turbulence models to predict supersonic boundary layer flows p 613 A92-37553
Experiments on turbulent flow due to an enclosed rotating disk p 615 A92-38863
Boundary-layer receptivity due to a wall suction and control of Tollmien-Schlichting waves
p 616 A92-39333
Bursts and sources of pressure fluctuation in turbulent boundary layers p 619 A92-40055
Three-dimensional vortical structure of a large-scale coherent vortex in a turbulent boundary layer
p 619 A92-40056
Evolution of three-dimensionality in stable and unstable curved mixing layers p 619 A92-40059
Evolution of coherent structures during transition in a flat-plate boundary layer p 621 A92-40126
Influence of suction through a slot on a turbulent boundary layer p 622 A92-40127
Models of turbulence in a hypersonic boundary layer
p 705 A92-41817
A calculation of penetration of the jet issuing normally into a cross flow across a wall boundary layer
[SAE PAPER 912029] p 790 A92-45419
Boundary-layer measurements during a parallel blade-vortex interaction
[AIAA PAPER 92-2623] p 794 A92-45495
Surface and flow field measurements in a symmetric crossing shock wave/turbulent boundary layer flow
[AIAA PAPER 92-2634] p 806 A92-45574
Discrete modes and continuous spectra in supersonic boundary layers p 809 A92-46264
Computation of turbulent, separated, unswept compression ramp interactions p 813 A92-46897
Generation of efficient multiblock grids for Navier-Stokes computations p 919 A92-47081
A new method for predicting the end wall boundary layers and the blade force defects inside the passage of axial compressor cascades p 819 A92-47691
Interface of an uncoupled boundary layer algorithm with an inviscid core flow algorithm for unsteady supersonic engine inlets
[AIAA PAPER 92-3083] p 823 A92-48730
Effects of vortex generators on the growth of a compressible shear layer
[AIAA PAPER 90-1979] p 934 A92-50269
An analysis of boundary layer for droplet aerodynamic stripped in high speed gas flow p 1116 A92-54563
Boundary layer study on nozzle wall at hypersonic velocities
[AIAA PAPER 92-4013] p 1034 A92-56836
Numerical modeling of transonic juncture flow
[AIAA PAPER 92-4036] p 1035 A92-56858
The measurement of plate vibration and sound radiation from a turbulent boundary layer manipulator
[AD-A240127] p 42 N92-10206
Airframe noise p 55 N92-10605
Studies of aerothermal loads generated in regions of shock/shock interaction in hypersonic flow
[NASA-CR-181893] p 43 N92-11319
Wind tunnel tests on A4, A4.1, and A4.2 2-D airfoil models in the IAR 5-ft. wind tunnel: Boeing Commercial Airplane Company and Institute for Aerospace Research collaborative work program
[NRC-IAR-C3] p 81 N92-11975
The BCAC/IAR collaborative research program to investigate the sidewall boundary layer effects in the IAR/NRC 2-D High Reynolds Number Test Facility
[NRC-HSA-434] p 81 N92-11976
Preliminary investigation of the shock-boundary layer interaction in a simulated fan passage
[AD-A242656] p 185 N92-15045
Control of unsteady separated flow associated with the dynamic pitching of airfoils
[NASA-CR-189758] p 258 N92-15966
Results of measured temperature distribution on an adiabatic wing model with radiation thermometer
[NAL-TM-610] p 261 N92-17755
Window cooling for high speed flight
[AD-D015145] p 344 N92-18193
Marching with the parabolized Navier-Stokes equations. Problem 1: Numerical study of hypersonic viscous cone flow
[AERO-REPT-9007] p 344 N92-18231
A numerical study of the stability of the swept attachment line boundary layer
[AERO-REPT-9103] p 345 N92-18293
Calculation of hypersonic non-equilibrium viscous flow using second order boundary layer theory
[MBB-FE122-S-PUB-434] p 345 N92-18316
Proceedings of the Seminar on Investigation and Control of Boundary-Layer Transition
[NAL-SP-11] p 400 N92-18483
Boundary layer flow in axial compressors (theoretical part)
[ETN-92-91006] p 501 N92-21232
Boundary layer flow in axial compressors (theoretical part)
[ETN-92-91007] p 501 N92-21233
Boundary layer flow in axial compressors (theoretical part)
[ETN-92-91008] p 502 N92-21234
Pressure and velocity measurements about an airfoil during a parallel blade-vortex interaction
p 446 N92-21429
A three-dimensional, compressible, laminar boundary-layer method for general fuselages. Volume 1: Numerical method
[NASA-CR-4292-VOL-1] p 679 N92-24547
An analysis of the sidewall boundary layer effect in two-dimensional wind tunnel testing p 626 N92-24856
Laminar-turbulent transition process in the presence of simulated wall roughness p 626 N92-24858
On the coupling of Euler/boundary-layer equations
p 627 N92-24859
A scheme for two dimensional Euler and boundary layer interactive solutions p 627 N92-24860
Performance degradation due to hoar frost on lifting surfaces p 628 N92-24866
Turbulence modeling for hypersonic flight
[NASA-CR-190313] p 630 N92-24898
Observation and measurements of flow structures in the stagnation region of a wing-body junction
p 714 N92-26616
Interface of an uncoupled boundary layer algorithm with an inviscid core flow algorithm for unsteady supersonic engine inlets
[NASA-TM-105684] p 739 N92-27037
NACA0012 airfoil data corrected for sidewall boundary-layer effects in the NAL two-dimensional transonic wind tunnel
[NAL-TM-640T] p 722 N92-28151
Air ejector experiments using the two-dimensional supersonic cascade tunnel: Zero secondary flow performance
[NAL-TM-632] p 887 N92-28829
Stability and transition of hypersonic boundary-layer flows
[AD-A250279] p 948 N92-31555
Three-dimensional compressible turbulent computations for a nondiffusing S-duct
[NASA-CR-4391] p 951 N92-32240
Strong coupling between inviscid fluid and boundary layer of sharp leading edges: Two-dimensional stationary and turbulent cases for isolated profiles and guard vanes
[ONERA-RT-44/1621-RY-016-R] p 1125 N92-32776

BOUNDARY LAYER SEPARATION
Airfoil boundary layer measurements at low Re in an accelerating flow from a nonzero velocity
p 62 A92-13673
Influence of the entropy layer on the separation length in hypersonic aerodynamics in the triple-deck framework. II p 63 A92-13815
Control of hypersonic aerodynamic forces with surface blowing p 172 A92-18363
Wedge-induced turbulent boundary-layer separation on a roughened surface at Mach 6.0 p 175 A92-20379
Detection of flow state in an unsteady separating flow
p 219 A92-20741
Turbulent boundary-layer characteristics over a flat-plate/wedge configuration at Mach 6
p 176 A92-20761
Calculation of the parameters of separated flow behind a plane rounded body in the path of two supersonic flows p 244 A92-21624
Effects of trailing-edge flap on buffet characteristics of a supercritical airfoil p 378 A92-24413
Separation control using moving surface effects - A numerical simulation p 309 A92-24419
Control of laminar boundary layer separation
p 393 A92-24980
Experimental studies of a two-element airfoil with large separation
[AIAA PAPER 92-0267] p 317 A92-25723
Numerical investigation of a transverse jet for supersonic aerodynamic control
[AIAA PAPER 92-0639] p 334 A92-27017
Numerical analysis of shock-induced separation alleviation using vortex generators
[AIAA PAPER 92-0751] p 335 A92-27095
Numerical investigation of laminar separated trailing-edge flows p 339 A92-28026
Incompressible flow past a flat plate aerofoil with leading edge separation bubble p 421 A92-28943
Numerical methods in the theory of boundary layer interaction with nonviscous flow p 426 A92-30185
Transverse correlation of the spectral components of pressure fluctuations on a plate ahead of a step
p 426 A92-30187
Investigation of the effect of an ultrasonic acoustic field on boundary layer separation on an airfoil
p 511 A92-30205
Effects of sweepback on unsteady separation in Mach 5 compression ramp interactions
[AIAA PAPER 92-0430] p 435 A92-31663
Unsteady separation in sharp fin-induced shock wave/turbulent boundary layer interaction at Mach 5
[AIAA PAPER 92-0748] p 436 A92-31678
Computational studies of transonic flow past a swept wing and the boundary layer characteristics
p 438 A92-31872
Boundary-layer-separation control p 440 A92-31886
Computational study of incipient leading-edge separation on a supersonic delta wing
p 442 A92-32237
The experimental investigation on the diffuser flow distortion p 519 A92-35543
Prediction for the incipient separation of fin-generated three-dimensional shock wave turbulent boundary layer interactions p 615 A92-38909
The numerical simulation of separation control using moving surface effect p 616 A92-38924

A study of three dimensional turbulent boundary layer separation and vortex flow control using the reduced Navier Stokes equations p 621 A92-40105
Measurements in a leading-edge separation bubble due to a simulated airfoil ice accretion p 723 A92-41262
Computation of saddle point of attachment p 703 A92-41276
Basic experiment on a supersonic vortex flow around a missile body p 705 A92-41545
BGK airfoil oil flow test in a two-dimensional transonic wind tunnel p 711 A92-43201
Navier-Stokes solutions of transonic nozzle flow with shock-induced flow separations p 713 A92-44515
Separation control on high Reynolds number multi-element airfoils
[AIAA PAPER 92-2636] p 806 A92-45575
An investigation of passive control methods for shock-induced separation at hypersonic speeds
[AIAA PAPER 92-2725] p 808 A92-45596
Simplified linear stability transition prediction method for separated boundary layers p 812 A92-46883
Separation and vortex formation in turbulent flows
[ONERA, TP NO. 1992-7] p 822 A92-48579
A bi-directional marching finite element algorithm for three-dimensional boundary layer separation flow computations p 942 A92-53288
Dynamical scaling of a model unsteady separating flow p 1117 A92-54932
On the structure of unsteady shock induced separation of the transonic airfoil in the NAL two-dimensional wind tunnel p 1029 A92-56010
Forcing level effects of internal acoustic excitation on the improvement of airfoil performance p 1136 A92-56162
Physics of vortical flows p 1031 A92-56166
Small two-dimensional surface excrescences on aircraft wings approaching separation p 1031 A92-56170
Numerical investigation of the effect of leading edge geometry on dynamic stall of airfoils
[AD-A239949] p 12 N92-10015
Review of aircraft dynamic loads due to flow separation p 85 N92-13008
In-flight flow visualization and pressure measurements at low speeds on the NASA F-18 high alpha research vehicle p 85 N92-13009
An experimental study of the flow over a sharp-edged delta wing at subsonic and transonic speeds p 85 N92-13011
Vortex generator design for aircraft inlet distortion as a numerical optimization problem p 194 N92-13959
Navier-Stokes analysis of turbulent boundary layer and wake for two-dimensional lifting bodies p 221 N92-14309
Flow over a delta wing at hypersonic speeds p 181 N92-14993
Proceedings of the Seminar on Investigation and Control of Boundary-Layer Transition
[NAL-SP-11] p 400 N92-18483
Optimization of tangential mass injection for minimizing flow separation in a scramjet inlet
[AD-A243868] p 376 N92-18867
The 8th Symposium on Turbulent Shear Flows. Volume 1: Sessions 1-18
[AD-A243809] p 402 N92-18933
Active flow control for twenty-first century high-performance aircraft with applications to land and sea vehicles p 447 N92-21504
Case 7.4: Blunt nose delta wing Euler-boundary layer calculation p 525 N92-22184
Separation of relaminarised boundary layers
[CUED/A-AERO/TR-16] p 592 N92-22209
Navier-Stokes simulation of dynamic stall on a rotating airfoil p 626 N92-24853
Visualization of boundary-layer development on turbomachine blades with liquid crystals
[NASA-CR-190433] p 742 N92-27519
Aircraft drag reduction p 717 N92-27709
An experimental study of the relationship between velocity and pressure fluctuations in a wing-body junction
[AD-A249628] p 946 N92-31122
Active control of the separation region on a two-dimensional airfoil
[AD-A249739] p 948 N92-31622
The calculation of incompressible separated turbulent boundary layers p 1003 N92-31886

BOUNDARY LAYER STABILITY

Triple-deck structure p 3 A92-10690
Supersonic boundary-layer stability analysis on an aircraft wing p 9 A92-13207
Effect of suction on the stability of supersonic boundary layers. I - Second-mode waves. II - First-mode waves p 174 A92-19611
Wave motions in a three-dimensional boundary layer p 244 A92-21629
The effects of suction on the nonlinear stability of the three-dimensional boundary layer above a rotating disc p 393 A92-25366
The effect of successive distortions of the boundary layer in a supersonic flow
[AIAA PAPER 92-0309] p 320 A92-25757
On hypersonic boundary-layer stability
[AIAA PAPER 92-0737] p 335 A92-27088
Evolution of perturbations in a supersonic boundary layer p 337 A92-27596
Transition control of instability waves over an acoustically excited flexible surface p 416 A92-28037
Direct numerical simulation of laminar breakdown in high-speed, axisymmetric boundary layers
[AIAA PAPER 92-0742] p 343 A92-28223
Flame sheet algorithm for use in numerical modeling of ramjet combustion instability p 390 A92-28503
Control of the development of boundary layer disturbances p 423 A92-30126
Generation of several wave packets in the boundary layer of a wing profile p 424 A92-30136
Asymptotic form of the lower branch of the neutral curve in a transonic boundary layer p 427 A92-30204
Linear stability of three-dimensional boundary layers over axisymmetric bodies at incidence p 431 A92-31157
Secondary instabilities in compressible boundary layers p 435 A92-31639
Numerical studies of transverse curvature effects on transonic flow stability p 524 A92-36186
Application of laminar flow control to the High Speed Civil Transport - The NASA Supersonic Laminar Flow Control Program
[SAE PAPER 912115] p 643 A92-39966
Application of linear stability theory in laminar flow design
[SAE PAPER 912116] p 618 A92-39967
Curvature effects for three-dimensional compressible boundary-layer stability p 701 A92-41207
Susceptibility of a supersonic boundary layer to acoustic perturbations p 707 A92-42730
The inviscid stability of supersonic flow past heated or cooled axisymmetric bodies p 712 A92-44363
Prediction of laminar boundary layer using cubic splines
[AIAA PAPER 92-2702] p 801 A92-45544
Effect of a bulge on the subharmonic instability of subsonic boundary layers p 898 A92-45833
Effect of a fan of rarefaction waves on the development of disturbances in a supersonic boundary layer p 809 A92-46519
Gortler instability and supersonic quiet nozzle design p 813 A92-46902
The calculation of three-dimensional compressible boundary layer stability on swept wings p 818 A92-47684
Linear stability of supersonic cone boundary layers p 1024 A92-54910
Numerical simulation of swept-wing flows
[NASA-CR-189457] p 180 N92-14969
A numerical study of the stability of the swept attachment line boundary layer
[AERO-REPT-9103] p 345 N92-18293
Proceedings of the Seminar on Investigation and Control of Boundary-Layer Transition
[NAL-SP-11] p 400 N92-18483
Laminar-turbulent transition: Fundamentals p 717 N92-27710

BOUNDARY LAYER TRANSITION

Boundary-layer transition across a stratocumulus cloud edge in a coastal zone p 45 A92-10489
Comparative studies of flow around a wing profile in two wind tunnels p 7 A92-12170
The role of laminar-turbulent transition in gas turbine engines p 120 A92-14868
Modelling of unsteady transitional boundary layers
[ASME PAPER 91-GT-282] p 152 A92-15677
A quiet-flow Ludwieg tube for experimental study of high speed boundary layer transition
[AIAA PAPER 91-5026] p 207 A92-17819
Effect of suction on the stability of supersonic boundary layers. I - Second-mode waves. II - First-mode waves p 174 A92-19611
Leading edge velocity field of an oscillating airfoil in compressible dynamic stall
[AIAA PAPER 92-0193] p 257 A92-23802
Problems of laminar-turbulent transition control in a boundary layer p 312 A92-24979
A numerical calculation of three dimensional incompressible laminar, transition and turbulent boundary layers p 393 A92-25138
Transition control of instability waves over an acoustically excited flexible surface p 416 A92-28037
Direct numerical simulation of laminar breakdown in high-speed, axisymmetric boundary layers
[AIAA-PAPER 92-0742] p 343 A92-28223
Control of the development of boundary layer disturbances p 423 A92-30126
An experimental study of tone-like noise in the flow past a wing at low flow velocities p 425 A92-30160
Investigating the feasibility of controlling the laminar-turbulent transition by means of laminarizing plates p 493 A92-30161
The effect of the angle-of-attack on laminar-turbulent boundary transition near the lower surface of triangular plates in a supersonic gas flow p 426 A92-30180
Effect of the longitudinal and transverse riblets of a flat plate on laminar-to-turbulent transition p 428 A92-30210
Characteristics of transonic flow past a configuration comprising a wing and a fuselage with a large midsection ratio p 439 A92-31882
Structure of a boundary layer on the lower surface of a wing in flight and in a wind tunnel p 440 A92-31899
A method of boundary layer laminarization on an oscillating wing p 441 A92-31969
Liquid crystal coatings for surface shear-stress visualization in hypersonic flows p 496 A92-32177
Earth atmospheric entry studies for manned Mars missions p 442 A92-32251
Supersonic and hypersonic boundary-layer transition induced by discrete trips p 522 A92-36023
A comparison of transition Reynolds number measured in a wind tunnel and in flight p 522 A92-36026
Aerodynamic analysis and modification design of NPU airfoils p 613 A92-38270
Turbine blade heat transfer prediction using coupled turbulent Prandtl number and transition models
[SAE PAPER 912152] p 674 A92-39987
Evolution of three-dimensionality in stable and unstable curved mixing layers p 619 A92-40059
A new method for visualization and measurement of turbulent flow patterns p 619 A92-40063
Evolution of coherent structures during transition in a flat-plate boundary layer p 621 A92-40126
Comment on 'Transition effects on airfoil dynamics and implications for subscale tests' p 703 A92-41247
Concepts for the stability analysis of NLF-experiments on swept wings
[AIAA PAPER 92-2706] p 801 A92-45548
Simplified linear stability transition prediction method for separated boundary layers p 812 A92-46883
Problems and solutions for transition detection in cryogenic wind tunnels by infrared imaging p 1090 A92-54319
A quiet-flow Ludwieg tube for experimental study of high speed boundary layer transition
[AIAA PAPER 92-3885] p 1094 A92-56727
Supersonic and hypersonic quiet tunnel technology at NASA Langley
[AIAA PAPER 92-3908] p 1094 A92-56743
The ASU Transition Research Facility
[AIAA PAPER 92-3910] p 1094 A92-56744
Tohoku University low-turbulence wind tunnel
[AIAA PAPER 92-3913] p 1095 A92-56746
Perfect compressible two dimensional boundary layer strong fluid coupling in the case of sharp leading edge profiles. Unsteady case of isolated profiles and steady case of blade grids
[ONERA-RT-43/1621-RY-006-R] p 43 N92-11311
Control aspects of the transition from transversal to transonic flow, step effects
[ETN-91-90106] p 82 N92-11981
Simplified method for the prediction of aerofoil excrescence drag magnification factor for turbulent boundary layers at subcritical Mach numbers
[ESDU-91028] p 259 N92-15972
The effect of freestream turbulence on the vortical flow over a delta wing p 261 N92-17681
Results of measured temperature distribution on an adiabatic wing model with radiation thermometer
[NAL-TM-610] p 261 N92-17755
Boundary-layer transition and heat transfer on slender delta wings
[AERO-REPT-8904] p 262 N92-17849
Deterministic multi-zone ice accretion modeling p 265 N92-17987
Proceedings of the Seminar on Investigation and Control of Boundary-Layer Transition
[NAL-SP-11] p 400 N92-18483
Hypersonic wakes
[ETN-92-91082] p 349 N92-19925
Boundary Layers in Turbomachines
[VKI-LS-1991-06] p 658 N92-24336
Fundamental aspects of boundary layers and transition in turbomachines p 658 N92-24337
Investigations of blade row interaction and boundary layer transition phenomena in a multistage aero engine low-pressure turbine by measurements with hot-film probes and surface-mounted hot-film gauges p 658 N92-24338

Aspects of unsteady blade-surface boundary layers and transition in axial turbomachines p 658 N92-24340
Research activities on CFD at the Ship Research Institute p 766 N92-26908
Three dimensional boundary layer transition on a yawed cylinder p 766 N92-26909
Aerodynamic drag on the bullet trains p 766 N92-26911
Flow around an isolated surface roughness in the laminar boundary layer p 766 N92-26913
Application of riblet surface to pipe flow p 766 N92-26915
Cross-flow instabilities and pressure gradients in boundary layers p 767 N92-26922
Turbulent heat flux measurements in a transitional boundary layer
[NASA-TM-105623] p 716 N92-27377
Basic concepts on boundary layers p 717 N92-27707
Laminar-turbulent transition: Fundamentals p 717 N92-27710
Boundary layer transition: Prediction, application to drag reduction p 717 N92-27711
The eddy structures in bounded shear flows p 717 N92-27712
The FML compressor as a drive system for the LFSWT: A narrative p 751 N92-27978
Turbulent spot generation and growth rates in a transonic boundary layer
[AD-A250221] p 909 N92-29118
Validation of three-dimensional incompressible spatial direct numerical simulation code: A comparison with linear stability and parabolic stability equation theories for boundary-layer transition on a flat plate
[NASA-TP-3205] p 943 N92-30295
Stability and transition of hypersonic boundary-layer flows
[AD-A250279] p 948 N92-31555
Leading-edge receptivity for blunt-nose bodies
[NASA-CR-190563] p 1036 N92-32648
High speed transition prediction
[NASA-CR-190836] p 1039 N92-33424

BOUNDARY LAYERS
On the nonlinear stability of a high-speed, axisymmetric boundary layer p 78 A92-16457
Tangential mass addition for shock/boundary-layer interaction control in scramjet inlets p 80 A92-17197
Analysis of an advanced ducted propeller subsonic inlet
[AIAA PAPER 92-0274] p 318 A92-25728
An interactive boundary-layer approach to multielement airfoils at high lift
[AIAA PAPER 92-0404] p 324 A92-26257
Boundary-layer receptivity of sound with roughness p 604 A92-36006
New model for predicting end wall boundary layer in an axial cascade p 611 A92-37389
An adaptive grid method for computing the high speed 3D viscous flow about a re-entry vehicle
[AIAA PAPER 92-2685] p 799 A92-45534
Alleviation of side force on tangent-ogive forebodies using passive porosity
[AIAA PAPER 92-2711] p 802 A92-45552
Active control of vortex structures in a separating flow over an airfoil
[AIAA PAPER 92-2728] p 804 A92-45563
Aerodynamic characteristics of hoar frost roughness p 808 A92-45829
Rayleigh imaging and flow tagging in ground test facilities p 1115 A92-54330
Approximate Riemann solver for hypervelocity flows p 1117 A92-54934
A hypersonic wind tunnel test of a mixed-compression air inlet model p 1028 A92-56007
BGK1 airfoil oilflow tests in the NAL two-dimensional wind tunnel. II p 1029 A92-56044
Experimental investigation of the boundary layer in a corner formed by two circular arc airfoils p 1029 A92-56046
Physics of vortical flow p 86 N92-13016
A study of the airwake aerodynamics over the flight deck of an AOR model ship
[AD-A241008] p 89 N92-13034
Analysis of an advanced ducted propeller subsonic inlet
[NASA-TM-105393] p 179 N92-14002
The aerodynamic effect of fillet radius in a low speed compressor cascade
[NASA-TM-105347] p 202 N92-14063
Aerodynamic heating on AFE due to nonequilibrium flow with variable entropy at boundary layer edge p 183 N92-15020
Simplified method for the prediction of aerofoil excrescence drag magnification factor for turbulent boundary layers at subcritical Mach numbers
[ESDU-91028] p 259 N92-15972
Excrescence drag magnification factors at the drag-rise condition for aerofoils with a specified form of upper-surface pressure distribution
[ESDU-91029] p 259 N92-15973
Optimization of tangential mass injection for minimizing flow separation in a scramjet inlet
[AD-A243868] p 376 N92-18867
On the instability of boundary layers on heated flat plates
[NASA-CR-187581] p 347 N92-19250
Wind tunnel investigation of the aerodynamic effects of aircraft ground deicing/anti-icing fluids and criteria for aerodynamic acceptance p 452 N92-21698
Two-dimensional transonic flow calculation by interaction of Euler and boundary layer equations
[PB92-136449] p 448 N92-21784
Separation of relaminarised boundary layers
[CUED/A-AERO/TR-16] p 592 N92-22209
Inlets, ducts, and nozzles p 593 N92-22523
Boundary Layers in Turbomachines
[VKI-LS-1991-06] p 658 N92-24336
Fundamental aspects of boundary layers and transition in turbomachines p 658 N92-24337
Aspects of unsteady blade-surface boundary layers and transition in axial turbomachines p 658 N92-24340
An engineering method for interactive inviscid-boundary layers in three-dimensional hypersonic flows
[NASA-TM-107838] p 632 N92-25279
An experimental investigation of the surface flow and wake dynamics associated with transverse flow over wavy cylinders p 681 N92-25547
Visualization of boundary-layer development on turbomachine blades with liquid crystals
[NASA-CR-190433] p 742 N92-27519
The eddy structures in bounded shear flows p 717 N92-27712
A study of juncture flow in the NASA Langley 0.3-meter transonic cryogenic tunnel
[NASA-CR-190430] p 773 N92-27880
Calculation of unsteady transonic flows with mild separation by viscous-inviscid interaction
[NASA-TP-3197] p 827 N92-28477
Boundary layer induced noise in aircraft
[CUED/A-AERO/TR-18] p 927 N92-29201
A preliminary experimental investigation of local isotropy in high-Reynolds-number turbulence p 912 N92-30042
Validation of three-dimensional incompressible spatial direct numerical simulation code: A comparison with linear stability and parabolic stability equation theories for boundary-layer transition on a flat plate
[NASA-TP-3205] p 943 N92-30295
Swept shock/boundary layer interaction experiments in support of CFD code validation
[NASA-CR-190583] p 1036 N92-32494
Leading-edge receptivity for blunt-nose bodies
[NASA-CR-190563] p 1036 N92-32648
An approximate viscous shock layer technique for calculating chemically reacting hypersonic flows about blunt-nosed bodies p 1041 N92-33837

BOUNDARY LUBRICATION
Lubricant evaluation and performance 2
[AD-A247464] p 895 N92-28398

BOUNDARY VALUE PROBLEMS
Synthesis of wing profiles from chord velocity diagrams using quasi-solutions for inverse boundary value problems p 80 A92-16815
On an adaptive numerical method for solution of high gradient problems p 410 A92-24905
Effective treatments of the singular line boundary problem for three dimensional grids
[AIAA PAPER 92-0545] p 342 A92-28202
Slenderness approximations in RCS estimation - The simplest 2-D case p 533 A92-33622
Construction of a wing profile with a flap modeled by a point vortex p 707 A92-42726
Flow and shape correction problems for thin profiles in incompressible stream p 707 A92-42736
Numerical analysis of flow through oscillating cascade sections p 713 A92-44513
Aerodynamic airfoils design by quasi-solutions method of inverse boundary-value problems p 1020 A92-53998
Steady flow of a fluid-solid mixture in a circular cylinder
[DE91-018698] p 41 N92-10174
Extended mapping and characteristics techniques for inverse aerodynamic design p 194 N92-13949
Hypersonic aerothermodynamic computations using a point-implicit TVD method p 183 N92-15006
Case 7.4: Blunt nose delta wing Euler-boundary layer calculation p 525 N92-22184
Boundary conditions for Euler equations at internal block faces of multi-block domains using local grid refinement
[NLR-TP-90134-U] p 908 N92-28712
Integration of wall interference assessment and wall adaptation
[NLR-TP-91119-U] p 1101 N92-32734
Computational aspects of helicopter trim analysis and damping levels from Floquet theory
[NASA-CR-190736] p 1087 N92-33107

BOW WAVES
A study on the interaction between a bow shock wave generated by a blunt body and a turbulent boundary layer p 8 A92-12424
Shock interaction induced by two hemisphere-cylinders
[SAE PAPER 912043] p 790 A92-45427
Examination of ultraviolet radiation theory for bow shock rocket experiments
[AIAA PAPER 92-2871] p 901 A92-47853
Preliminary results from the White Sands Missile Range sonic boom propagation experiment p 1140 N92-33884

BRAGG ANGLE
Analytical and experimental studies of the aerodynamic characteristics of a delta wing at a slip angle at high supersonic velocities p 437 A92-31854

BRAKES (FOR ARRESTING MOTION)
An Axial Turbobrake
[ASME PAPER 91-GT-1] p 147 A92-15501
Accelerators and decelerators for large hypersonic aircraft p 665 A92-36952
Test results for rotordynamic coefficients of the SSME HPOTP turbine interstage seal with two swirl brakes p 223 N92-14357

BRANCHING (MATHEMATICS)
Washout filters in the bifurcation control of high alpha flight dynamics p 476 A92-29061
Two-parameter bifurcation analysis of axial flow compressor dynamics p 421 A92-29355
Chaotic motion in mechanical and engineering systems p 695 A92-39480
Bifurcation analysis of airfoils in incompressible flow p 623 A92-40580

BRAYTON CYCLE
Power performance of a nonisentropic Brayton cycle p 54 A92-11281
General performance characteristics of real heat engine p 1011 A92-50401
Detonation duct gas generator demonstration program
[AIAA PAPER 92-3174] p 1066 A92-54011
An advanced scramjet propulsion concept for a 350 MG SSTO space plane - External nozzle performance
[AIAA PAPER 92-3719] p 1067 A92-54134

BRAZING
Brazing method helps repair aircraft gas-turbine nozzles p 492 A92-29504
Restoration of aircraft engine nozzle block blades by vacuum arc brazing with controlled current p 471 A92-30381
Joining a Ni-based creep-resistant (ODS) alloy by brazing p 1116 A92-54867
Evaluation and qualification of diffusion braze repair techniques for superalloy gas turbine components
[NRC-LTR-ST-1839] p 504 N92-22028

BRIDGMAN METHOD
Fundamental studies on Marangoni convection related to Bridgman crystal growth p 1111 A92-53758

BRIGHTNESS DISCRIMINATION
Comparative evaluation of internally and externally lighted taxiway guidance signs
[DOT/FAA/CT-TN92/2] p 573 N92-22237

BRIGHTNESS DISTRIBUTION
Demonstration performance of an aircraft liquid crystal display p 735 A92-43224
The C-17 Multifunction Display - A building block for avionic systems p 1063 A92-55907

BRIGHTNESS TEMPERATURE
Retrieval of total precipitable water over high latitude regions using radiometric measurements near 90 and 183 GHz p 505 A92-32129

BRISTOL-SIDDELEY BS 53 ENGINE
VSTOL engine design evolution: Growth of the Pegasus engine for Harrier
[PNR-90805] p 739 N92-27039

BROADBAND
Broadband shock-associated noise from supersonic jets in flight p 235 A92-18683
A survey of the broadband shock associated noise prediction methods
[AIAA PAPER 92-0501] p 415 A92-26930
Integrating a radar/ESM antenna suite with the S-70 helicopter --- Electronic Surveillance Measures p 957 A92-49333
The design of broadband radar absorbing surfaces
[AD-A240521] p 42 N92-11235
A survey of the broadband shock associated noise prediction methods
[NASA-TM-105365] p 237 N92-14797

BROADCASTING
An investigation of the desensitizing effects by high power HF broadcast transmitters on HF airborne receivers p 726 A92-43937
DLR-News: Announcements of the German Research Institute for Aeronautics and Astronautics p 698 N92-26086
Remote sensing of trapping layer base height using ATIS transmissions
[AD-A250074] p 1004 N92-31362
Decision-making guide for the proposed Coast Guard differential global positioning system
[AD-A246046] p 957 N92-32054
BROWNIAN MOVEMENTS
Brownian-motion limited aerodynamic focusing of heavy molecules p 995 A92-52722
In situ measurement of particle formation in heated jet fuels: A new application of photon correlation spectroscopy
[DE92-003641] p 488 N92-20132
BRUSH SEALS
Performance characteristics of brush seals for limited-life engines
[ASME PAPER 91-GT-281] p 152 A92-15676
Simple effective thickness model for circular brush seals
[AIAA PAPER 92-3192] p 903 A92-48803
Effects of material choices on brush seal performance p 1116 A92-54650
Army research concerns in engine sealing p 228 N92-15089
Seal development activities at Allison Turbine Division p 228 N92-15093
Seal related development activities at EG/G p 228 N92-15095
Brush seal leakage performance with gaseous working fluids at static and low rotor speed conditions
[NASA-TM-105400] p 297 N92-16265
BUBBLES
Helium bubble flow visualization of the spanwise separation on a NACA 0012 with simulated glaze ice
[AIAA PAPER 92-0413] p 341 A92-28192
Incompressible flow past a flat plate aerofoil with leading edge separation bubble p 421 A92-28943
Observational study of pool boiling under microgravity p 757 A92-41060
Measurements in a leading-edge separation bubble due to a simulated airfoil ice accretion p 723 A92-41262
Laminar separation bubbles and airfoil design at low Reynolds numbers
[AIAA PAPER 92-2735] p 797 A92-45515
Helium bubble flow visualization of the spanwise separation on a NACA 0012 with simulated glaze ice
[NASA-TM-105742] p 714 N92-26612
On the origin and acoustical behaviour of cloud cavitation
[ISBN-90-9004317-9] p 1125 N92-33066
BUCKLING
Approximate closed-form buckling solutions for the optimization of aircraft structures p 579 A92-32578
Application of a local panel buckling constraint within automated multidisciplinary structural analysis and design
[AIAA PAPER 92-1116] p 537 A92-33271
Combined compressive and shear buckling analysis of hypersonic aircraft sandwich panels
[AIAA PAPER 92-2487] p 586 A92-34603
Buckling, postbuckling and crippling of thin walled composite airframe structures under compression p 899 A92-46940
Thermal-structural panel buckling tests p 993 A92-51409
Initial postbuckling response of an unsymmetrically laminated rectangular plate p 1108 N92-32586
BUDGETS
National Aeronautics and Space Administration Authorization Act, 1993
[S-2558-IS] p 698 N92-25606
BUFFETING
Effects of trailing-edge flap on buffet characteristics of a supercritical airfoil p 378 A92-24413
Wind-tunnel studies of F/A-18 tail buffet p 310 A92-24421
Buffet load measurements on an F/A-18 vertical fin at high-angle-of-attack
[AIAA PAPER 92-2127] p 520 A92-35694
Numerical investigation of tail buffet on F-18 aircraft
[AIAA PAPER 92-2673] p 798 A92-45528
Unsteady pressure and load measurements on an F/A-18 vertical fin at high-angle-of-attack
[AIAA PAPER 92-2675] p 798 A92-45529
Flow over a twin-tailed aircraft at angle of attack. II - Temporal characteristics p 810 A92-46781
Statistical prediction of maximum buffet loads on the F/A-18 vertical fin p 811 A92-46816
Investigation of the tail buffeting of the C-101 p 942 A92-53253
Review of aircraft dynamic loads due to flow separation p 85 N92-13008
Vortex control: Further encounters p 87 N92-13020
Scale model measurements of fin buffet due to vortex bursting on F/A-18 p 365 N92-18788
Design of a fighter aircraft vertical tail enhanced buffet environment survivability p 551 N92-23235
Buffet test in the National Transonic Facility
[NASA-CR-189595] p 888 N92-29352
BUILDINGS
A walk through the planned CS building
[NASA-CR-189963] p 386 N92-19675
Development of a wind chamber for model testing of tornado forces on structures
[PB92-104165] p 386 N92-19940
Building vibrations induced by noise from rotorcraft and propeller aircraft flyovers
[NASA-TM-104170] p 1138 N92-33160
BULKHEADS
Durability analysis for a main bulkhead subjected to load on the body of an aircraft p 848 A92-47664
Surface generation and editing operations applied to structural support of aerospace vehicle fuselages p 777 N92-27831
BUOYANCY
Heat transfer in rotating serpentine passages with trips normal to the flow
[ASME PAPER 91-GT-265] p 151 A92-15663
Three-dimensional buoyancy-induced flow and heat transfer around the wheel outboard of an aircraft p 397 A92-27773
Convective flow analysis on the KC-135 aircraft
[AIAA PAPER 92-0844] p 493 A92-29610
Heat transfer in rotating serpentine passages with trips skewed to the flow
[NASA-TM-105581] p 499 N92-20235
BUOYS
Comparison of aircraft synthetic aperture radar and buoy spectra during NORCSEX '88 p 597 A92-34878
BURAN SPACE SHUTTLE
Aerothermodynamic configuration of first generation aerospace planes (of Buran-type) and first flight results p 211 N92-14975
BURGER EQUATION
On an adaptive numerical method for solution of high gradient problems p 410 A92-24905
BURNERS
NLR experience with high velocity burner rig testing, 1979-1989
[NLR-TP-89152-U] p 385 N92-18415
BURNING RATE
Combustion of solid fueled ramjet. I
[AIAA PAPER 92-3727] p 894 A92-49105
Free-radicals aided combustion with scramjet applications
[IAF PAPER 92-0659] p 1106 A92-57100
Nonstationary gasdynamics p 220 N92-13985
Rotary engine performance limits predicted by a zero-dimensional model
[NASA-CR-189129] p 474 N92-20650
Analysis of the flight performance of the 155 mm M864 base burn projectile
[BRL-TR-3083] p 1041 N92-33699
BURNING TIME
National Aerospace Plane flight test - External burning on the F/A-18 p 645 A92-40032
The influence of a retarding rocket on parameter limits for reentry trajectories p 211 N92-15037
BY-PRODUCTS
Monitoring jet fuel degradation using quartz crystal microbalances
[DE92-004730] p 489 N92-20858
BYPASS RATIO
Extension of a three-dimensional Euler method for calculating the flowfield around bypass engines with fan and core jet p 62 A92-13690
Multi-blade row Navier-Stokes simulations of fan-bypass configurations
[ASME PAPER 91-GT-148] p 73 A92-15586
Interference effects of very high bypass ratio nacelle installations on a low-wing transport
[ASME PAPER 91-GT-241] p 75 A92-15646
Experimental investigation of the air bypass effect in the shock-wave region on the aerodynamic characteristics of a wing profile p 439 A92-31877
Advanced propulsion systems for large subsonic transports p 653 A92-36977
Application of laminar flow control to high-bypass-ratio turbofan engine nacelles
[SAE PAPER 912114] p 618 A92-39965
An experimental investigation on aft bypass supersonic inlet performance at high angle of attack and yaw p 862 A92-48268
Design and off-design point characteristics of Separated Core Ultra High Bypass Engine (SCUBE)
[AIAA PAPER 92-3776] p 867 A92-49120
Turbofan with a small bypass ratio for first stage of a two-stage to-orbit vehicle p 968 A92-49833
Further calculations of the performance of turbofan engines incorporating a wave rotor
[AD-A240867] p 131 N92-13072
Installation effects of wing-mounted turbofan nacelle-pylons on a 1/17-scale, twin-engine, low-wing transport model
[NASA-TP-3168] p 346 N92-19002
Extension of a three dimensional Euler-code for the investigation of the flow field around bypass engines with fan and core jet
[DLR-FB-91-13] p 503 N92-21699
The evolution of the bypass engine
[PNR-90832] p 476 N92-21850
BYPASSES
Numerical investigation of supersonic inlet with realistic bleed and bypass systems p 713 A92-44519
Conceptual study of separated core ultra high bypass engine
[AIAA PAPER 92-3775] p 867 A92-49119
Ultra high bypass Nacelle aerodynamics inlet flow-through high angle of attack distortion test
[NASA-CR-189149] p 943 N92-30298

C

C (PROGRAMMING LANGUAGE)
Applications of an automated programming system
[AIAA PAPER 91-3767] p 231 A92-17629
On-line performance evaluation of multiloop digital control systems p 873 A92-46739
C BAND
Terminal Doppler weather radar test bed operation, Orlando: January-June 1990
[AD-A242890] p 301 N92-17028
C-130 AIRCRAFT
Evolutionary upgrade and application of the C-130H simple-cycle refrigeration system
[SAE PAPER 911439] p 270 A92-21836
C-130 glass cockpit system development program
[AIAA PAPER 92-1050] p 553 A92-33230
C-141 and C-130 power-by-wire flight control systems p 876 A92-48493
Testing and evaluation of the Vanner electrical inverters, models 24-1500 and SP 00112
[AD-A241914] p 299 N92-17216
Life cycle costs of the C-130 electrical power system upgrade
[AD-A246759] p 786 N92-28348
C-135 AIRCRAFT
Measurements and correlation of two-phase pressure drop under microgravity conditions p 37 A92-10435
Demonstration of gas liquid separation under the microgravity by aircraft KC-135
[SAE PAPER 912024] p 897 A92-45416
Modifications to the rapid melt/rapid quench and transparent polymer video furnaces for the KC-135
[NASA-CR-184215] p 157 N92-12231
Life management approach for USAF aircraft p 362 N92-18587
Materials processing in low gravity
[NASA-CR-184280] p 499 N92-20198
High temperature aircraft research furnace facilities
[NASA-CR-184384] p 1101 N92-33826
C-141 AIRCRAFT
A revolution in air transport - Acquiring the C-141 Starlifter p 607 A92-38101
C-141 and C-130 power-by-wire flight control systems p 876 A92-48493
Testing and evaluation of the Vanner electrical inverters, models 24-1500 and SP 00112
[AD-A241914] p 299 N92-17216
Life management approach for USAF aircraft p 362 N92-18587
C-160 AIRCRAFT
Analysis and modeling of lightning strikes to the F106B, CVF580, and C160 aircraft p 186 A92-20129
C-5 AIRCRAFT
Life management approach for USAF aircraft p 362 N92-18587
CABIN ATMOSPHERES
Effectiveness of an onboard water spray system during an oxygen enriched cabin fire
[DOT/FAA/CT-TN91/51] p 264 N92-17149
CABLES (ROPES)
Measurements of longitudinal static aerodynamic coefficients with cable mount system p 1093 A92-56013
Aerodynamic model identification of a spaceplane model from a cable-mount dynamic wind-tunnel test p 1093 A92-56114

Estimation of cable-mounted model inertia characteristics for dynamic wind-tunnel test
[NAL-TM-641] p 722 N92-28152
CALCULUS OF VARIATIONS
Automated trajectory synthesis for hypersonic vehicles using energy management and variational calculus techniques p 210 A92-19061
CALIBRATING
5,000-hour stability tests of metal sheathed thermocouples at respective temperatures of 538 C and 875 C
[ASME PAPER 91-GT-182] p 148 A92-15614
Radiometric properties of the NS001 Thematic Mapper Simulator aircraft multispectral scanner
p 155 A92-17110
Shuttle Entry Air Data System - An experimental investigation of calibration for ascent flight
[AIAA PAPER 92-0133] p 286 A92-23753
Atmospheric analysis for airdata calibration on research aircraft
[AIAA PAPER 92-0293] p 369 A92-25746
Nonparametric methods of regression analysis in problems related to the processing of aerodynamic balance calibration tests p 602 A92-36417
Airdata calibration techniques for measuring atmospheric wind profiles p 856 A92-46792
Thrust stand design principles
[AIAA PAPER 92-3976] p 1098 A92-56802
The cryogenic balance design and balance calibration methods
[AIAA PAPER 92-4001] p 1122 A92-56824
Study of interactions on anemoclinometric sensors
[REPT-90/30] p 138 N92-12006
Development of a calibrated software reliability model for flight and supporting ground software for avionic systems p 234 N92-15870
Calibration data for improved correction of UVW propeller anemometers
[DE92-002935] p 297 N92-16281
Results of the space shuttle vehicle ascent air data system probe calibration test using a 0.07-scale external tank forebody model (68T) in the AEDC 16-foot transonic wind tunnel (IA-310), volume 1
[NASA-CR-167696] p 286 N92-17167
Results of the space shuttle vehicle ascent air data system probe calibration test using a 0.07-scale external tank forebody model (68T) in the AEDC 16-foot transonic wind tunnel (IA-310), volume 2
[NASA-CR-167697] p 286 N92-17214
High accuracy fuel flowmeter. Phase 2C and 3: The mass flowrate calibration of high accuracy fuel flowmeters
[NASA-CR-187108] p 406 N92-19775
Initial calibration of the HEAT-H2 arc-heated wind tunnel
[AD-A245072] p 484 N92-20898
Criteria for the operation of federally-owned secondary calibration laboratories (ionizing radiation)
[PB92-112481] p 485 N92-21777
Calculation of support interferences on the aerodynamic coefficients for a wind tunnel calibration model
[ESA-TT-1247] p 830 N92-29159
Comparison of two-way satellite time transfer and GPS common-view time transfer between OCA and TUG
p 1050 N92-33356
Calibration of GPS antennas
[ETN-92-92034] p 1051 N92-33693
CALORIMETERS
Heat flux sensor research and development: The cool film calorimeter
[NASA-CR-189789] p 298 N92-17006
CAMBER
Modeling and analysis methodology for aeroelastically tailored chordwise deformable wings
[NASA-CR-189620] p 961 N92-30304
CAMBERED WINGS
Analysis of flexible-membrane and jet-flapped airfoils using velocity singularities p 10 A92-13216
The use of variable camber to reduce drag, weight and costs of transport aircraft p 313 A92-25096
Aerodynamic characteristics of the combination of a wing with a cambered middle surface with a fuselage
p 439 A92-31880
An experimental study of a sting-mounted circulation control wing
[AD-A243912] p 346 N92-18895
Variable-camber systems integration and operational performance of the AFTI/F-111 mission adaptive wing
[NASA-TM-4370] p 570 N92-22194
Survey and analysis of research on supersonic drag-due-to-lift minimization with recommendations for wing design
[NASA-TP-3202] p 1040 N92-33656
CAMERAS
AI for RPVs, Sensor Driven Airborne Replanner (SDAR), for a Robotic Aircraft Sensor Platform (RASP)
p 114 N92-12534
Image-based ranging and guidance for rotorcraft
[NASA-CR-184829] p 191 N92-14036
Model incidence measurement using SAAB ELOPTOPOS system
[NLR-TP-89182-U] p 385 N92-18416
Study of optical techniques for the Ames unitary wind tunnels. Part 2: Light sheet and vapor screen
[NASA-CR-190217] p 573 N92-22195
Study of optical techniques for the Ames unitary wind tunnels. Part 3: Angle of attack
[NASA-CR-190541] p 888 N92-29655
CANADA
Activities of NRC-CNRC, Institute for Aerospace Research, Flight Research Lab.
[CTN-92-60432] p 420 N92-20205
CANADAIR AIRCRAFT
Regional challenge --- flight test of Canadair Regional Jet p 961 A92-53121
CANARD CONFIGURATIONS
On vortex interference for canard configuration
p 64 A92-14071
The canard-wing interference and stall safety of light canard aircraft p 111 A92-15341
Aerodynamic balance range of aircraft of different configurations p 134 A92-16801
A simplified method for simulating steady, unsteady flow around canard wing configuration p 311 A92-24876
The evaluation of canard couplings at high angles of attack
[AIAA PAPER 92-0281] p 318 A92-25735
Prediction of average downwash gradient for canard configurations
[AIAA PAPER 92-0284] p 319 A92-25737
An approach to the low-speed longitudinal aerodynamic characteristics of the joined wing configuration
p 339 A92-27909
European Fighter Aircraft (EFA) programme status report p 646 A92-40043
Effect of canard deflection on close-coupled canard-wing-body aerodynamics
[AIAA PAPER 92-2602] p 792 A92-45479
Quantification of canard and wing interactions using spatial correlation velocimetry
[AIAA PAPER 92-2687] p 807 A92-45588
Comment on 'Canard-wing interaction in unsteady supersonic flow' p 812 A92-46820
On the effect of canards on NAL spaceplane model (0 order) in low speed area p 1030 A92-56052
Navier-Stokes simulation of a close-coupled canard-wing-body configuration p 1031 A92-56163
On the simulation of compressible turbulent flows past delta wing, delta wing-body and delta wing-canard
p 84 N92-13003
Vortex formation over a close-coupled canard-wing-body configuration in unsymmetrical flow p 85 N92-13010
An experimental investigation of vortex flaps on a canard combat-aircraft configuration p 87 N92-13023
Water tunnel flow visualization studies of a canard-configured X-31A-like fighter aircraft model
[AD-A241362] p 90 N92-13037
On a global aerodynamic optimization of a civil transport aircraft p 193 N92-13931
Analysis of an advanced fighter aircraft using jet flap techniques and the vortex lattice method
[AD-A244051] p 366 N92-19185
Proposal for a low cost close air support aircraft for the year 2000: The Raptor
[NASA-CR-190023] p 367 N92-19496
The FM-007: An advanced jet commuter for HUB to spoke transportation
[NASA-CR-189988] p 461 N92-20267
The Guardian: Preliminary design of a close air support aircraft
[NASA-CR-189991] p 463 N92-21566
Longitudinal and lateral-directional aerodynamic characteristics of a wing-cone configuration at Mach numbers from 2.5 to 4.5
[NASA-TM-4337] p 630 N92-24977
Visualisation in water of vortex flow over sharp-edged canard configurations
[ARL-FLIGHT-MECH-R-189] p 632 N92-25410
CANONICAL FORMS
A Lie Bracket solution of the optimal thrust magnitude on a singular arc in atmospheric flight
[AIAA PAPER 92-4345] p 1079 A92-55334
CANOPIES
Investigation on opening and ejection of an aircraft canopy by using a solid rocket engine
p 358 A92-28489
Parachute canopy control simulation - A solution for aircrew emergency training p 572 A92-35428
Methods for predicting successful ejection seat canopy penetration p 544 A92-35441
Investigation of a method for determining machining stress in polymethylmethacrylate (PMMA) of airplane canopies p 986 A92-53096
Selection of opening model for parachute scaling studies
[AD-A250882] p 943 N92-30239
CANTILEVER BEAMS
Flexure-torsion behavior of sheat-deformable beams with applications to aircraft wing sections
[AIAA PAPER 92-2467] p 582 A92-34357
Adaptive response control of wing structures carrying heavy tip weights
[AIAA PAPER 92-2527] p 583 A92-34374
Dynamic response to time-dependent excitations of cantilevered aircraft wing structures modelled as thin-walled beams
[AIAA PAPER 92-2213] p 584 A92-34403
Effects of T-tabs and large deflections in double cantilever beam specimen tests p 673 A92-39009
Behavior of thin-walled beams made of advanced composite materials and incorporating non-classical effects p 673 A92-39944
On the three-dimensional vibration analysis of simultaneously skewed and twisted cantilevered parallelepipeds p 759 A92-41801
Structural optimization of a cantilevered beam subject to combined static loadings p 1118 A92-56024
CANTILEVER PLATES
Nonlinear stall flutter and divergence analysis of cantilevered graphite/epoxy wings p 219 A92-20746
Effect of different force-functions and initial shock pressure on blade response p 374 A92-27913
CAPACITORS
Suppression of radiating harmonics Electro-Impulse Deicing (EIDI) systems
[DOT/FAA/CT-TN90/33] p 405 N92-19764
CAPACITY
German airports - Capacity crisis p 61 A92-17097
CARBON
Effect of carbon particles and mixing on afterburning of exhaust plumes
[AIAA PAPER 92-0767] p 387 A92-27107
Quantification of aircraft carbon brake wear using regression analysis and periodic wave forms
[SAE PAPER 912174] p 644 A92-39999
CARBON DIOXIDE
Analysis of thermo-chemical nonequilibrium models for carbon dioxide flows
[AIAA PAPER 92-2852] p 892 A92-47835
Brush seal leakage performance with gaseous working fluids at static and low rotor speed conditions
[NASA-TM-105400] p 297 N92-16265
Emissions from aircraft: Standards and potential for improvement
[PNR-90768] p 476 N92-21740
CARBON DIOXIDE LASERS
Simplified signal processing for an airborne CO2 Doppler lidar p 1000 N92-31023
CARBON FIBER REINFORCED PLASTICS
Manufacture of a primary flight structure using thermoplastics p 1 A92-10197
Thermal properties of high performance thermoplastic composites based on poly(ether ketone ketone) (PEKK)
p 34 A92-10238
Processing parameters for carbon/PMR-15 composite flat panels p 34 A92-11812
LDF thermoplastic composites technology
p 34 A92-13243
Damage assessment for composite smart structures
p 140 A92-13601
Weathering test of AFRP composites for the application of helicopter fuselage --- Aramide Fiber Reinforced Plastic p 142 A92-15309
Design and testing leading to certification of the Airbus A340 nose landing gear doors p 272 A92-24192
Development of an advanced composite material on vertical stabilizer of F-X aircraft p 579 A92-32555
Design analysis of the T-800 inlet particle separator/air oil cooler blower p 579 A92-32556
Robotics application in aerospace manufacturing
p 671 A92-38216
A method to determine propagation direction of compressive fracture in carbon-fibre composites
p 672 A92-38770
Repair operation on a composite material structure
p 700 A92-43153
Automation of composite material structure installation
p 700 A92-43248
Measurement of acoustic properties of the composite materials constituting the main rotor hub of the Agusta-Westland helicopter EH-101 (civil version)
p 1010 A92-49475
Induction bonding procedures for graphite reinforced thermoplastic assemblies p 994 A92-51545
Fabrication test and evaluation of graphite/PMR-15 polyimide for HOPE primary structure
p 1105 A92-53516
Structural design and testing results of composite landing gear components p 1057 A92-56328

Rapid repair of integrally stiffened carbon fibre composite structures by bolted aluminium elements
[MBB-FE202-S-PUB-0453-A] p 290 N92-17310
Conceptional design to heat-resistant airframe of HOPE p 575 N92-23820
CFRP stiffened panels under compression
p 1109 N92-33044

CARBON FIBERS
Design, analysis, and testing of integrally stiffened composite centre fuselage skin for future fighter aircraft
p 535 A92-32554
Materials and structures for Hermes
p 666 A92-38213
A field repair of advanced helicopter vertical fin structure p 785 A92-47417
Polymer infiltration studies
[NASA-CR-189773] p 289 N92-17004
Design, analysis, and testing of integrally stiffened composite centre fuselage skin for future fighter aircraft
[MBB-FE2-PUB-S-450] p 359 N92-18333
Polymer infiltration studies
[NASA-CR-190204] p 578 N92-22486
Stretched skin concept for the entry aerodynamic decelerator system of planetary probes
p 576 N92-23836
Polymer blends, volume 1
[AD-A252112] p 987 N92-31419
Jet fuel absorption and dynamic mechanical analysis of carbon fibre composites p 1110 N92-33050

CARBON-CARBON COMPOSITES
Critical appraisal of the McDonnell Douglas closure model for predicting fatigue crack growth
[ARL-STRUC-R-444] p 44 N92-11376
Large thin composite thermostructural parts
p 576 N92-23821

CARCINOGENS
Carcinogenic hydrocarbons emission with gas-turbine engines exhaust gases p 504 A92-29726

CARGO
Trajectory analysis of the G-11 family of clustered parachutes to determine minimum altitude
[AD-A243375] p 261 N92-17404
An analysis of fixed wing tactical airlifter characteristics using an intra-theater airlift computer model
[AD-A246908] p 732 N92-27719

CARGO AIRCRAFT
An airlifter for the long haul p 358 A92-28493
A helicopter transportation system
p 723 A92-43161
Tooling for C-17 composite parts p 900 A92-47412
Organic Matrix Composite Helicopter Internal/External Cargo Pallet System (OMC INTEX)
[AD-A251127] p 961 N92-30878

CARRIAGES
Cryogenic test rig with an aerodynamic magnetically levitated carriage p 750 N92-27792

CARRIER WAVES
Whole aircraft lightning indirect effects evaluation using low level injection techniques p 192 A92-20134

CARTESIAN COORDINATES
Traveling on the curved earth p 19 A92-10474
A finite difference solution of the Euler equations on non-body-fitted Cartesian grids p 818 A92-47153
Universal weaving for turbine engine composite preforms
[AD-A237667] p 202 N92-14059
Cartesian based grid generation/adaptive mesh refinement p 682 N92-25722

CASCADE CONTROL
Achieving fault tolerance in multichannel control systems --- for avionics p 974 A92-49296

CASCADE FLOW
A semi-elliptic analysis for 2-D viscous flows through cascade configurations p 3 A92-10688
Design and testing of a controlled diffusion airfoil cascade for industrial axial flow compressor application
[ASME PAPER 90-GT-140] p 6 A92-11286
Blade defect force investigation in a compressor cascade p 10 A92-13233
Experimental investigation on gas-particle flow in cascades p 62 A92-13300
Computation of the potential flow through cascades using the conformal mapping and the singularity method
p 66 A92-15356
Computational study of stall flutter in linear cascades
[ASME PAPER 91-GT-5] p 67 A92-15503
Design method for subsonic and transonic cascade with prescribed Mach number distribution
[ASME PAPER 91-GT-18] p 67 A92-15509
Turbine cascade calculations through a fractional step Navier-Stokes algorithm
[ASME PAPER 91-GT-55] p 68 A92-15533
Turbulence modelling for secondary flow prediction in a turbine cascade
[ASME PAPER 91-GT-57] p 68 A92-15535
A 3D FEM variational aerodynamic calculation and performance analysis of a leaned turbine stator cascade
[ASME PAPER 91-GT-79] p 69 A92-15548
An investigation of a strong shock-wave turbulent boundary layer interaction in a supersonic compressor cascade
[ASME PAPER 91-GT-92] p 70 A92-15556
Three dimensional flow in a linear compressor cascade at design conditions
[ASME PAPER 91-GT-114] p 70 A92-15565
Similarity transformations for compressor blading
[ASME PAPER 91-GT-123] p 70 A92-15568
Effects of simulated rotation on tip leakage in a planar cascade of turbine blades. I - Tip gap flow
[ASME PAPER 91-GT-127] p 71 A92-15572
Effects of simulated rotation on tip leakage in a planar cascade of turbine blades. II - Downstream flow field and blade loading
[ASME PAPER 91-GT-128] p 71 A92-15573
The effect of steady aerodynamic loading on the flutter stability of turbomachinery blading
[ASME PAPER 91-GT-130] p 71 A92-15574
The effect of blade tip geometry on the tip leakage flow in axial turbine cascades
[ASME PAPER 91-GT-135] p 72 A92-15577
Aerodynamics and heat transfer investigations on a high Reynolds number turbine cascade
[ASME PAPER 91-GT-157] p 148 A92-15593
Unsteady lifting surface theory for a rotating transonic cascade of swept blades
[ASME PAPER 91-GT-178] p 73 A92-15610
Analysis and prediction of transonic turbine blade losses
[ASME PAPER 91-GT-183] p 73 A92-15615
Unsteady Navier-Stokes simulation of transonic cascade flow using an unfactored implicit upwind relaxation scheme with inner iterations
[ASME PAPER 91-GT-223] p 74 A92-15637
Numerical prediction of wakes in cascades and compressor rotors including the effects of mixing. I - Cascade wakes including the effects of incidence and freestream turbulence
[ASME PAPER 91-GT-225] p 74 A92-15638
Numerical prediction of wakes in cascades and compressor rotors including the effects of mixing. II - Rotor passage flow and wakes including the effects of spanwise mixing
[ASME PAPER 91-GT-222] p 74 A92-15639
Film cooling research on the endwall of a turbine nozzle guide vane in a short duration annular cascade. I - Experimental technique and results
[ASME PAPER 91-GT-252] p 150 A92-15657
Film cooling research on the endwall of a turbine nozzle guide vane in a short duration annular cascade. II - Analysis and correlation of results
[ASME PAPER 91-GT-253] p 150 A92-15658
Performance improvements of compressor cascades by controlling the profile and sidewall boundary layers
[ASME PAPER 91-GT-260] p 75 A92-15662
Inlet flow angle determination of transonic compressor cascades
[ASME PAPER 91-GT-274] p 75 A92-15671
Film cooling on a gas turbine rotor blade
[ASME PAPER 91-GT-279] p 152 A92-15675
Blade row interaction in a multistage low-pressure turbine
[ASME PAPER 91-GT-283] p 125 A92-15678
Simple formulae for optimal solidity of two-dimensional compressor cascades based on diffusion concept
[ASME PAPER 91-GT-308] p 126 A92-15687
Transonic and supersonic inviscid computations in cascades using adaptive unstructured meshes
[ASME PAPER 91-GT-312] p 75 A92-15689
Transonic cascade flow prediction using the Navier-Stokes equations
[ASME PAPER 91-GT-313] p 76 A92-15690
Design and analysis of a high pitch to chord ratio cascade representative of ducted propfans
[ASME PAPER 91-GT-335] p 126 A92-15700
Cascade flutter analysis with transient response aerodynamics p 154 A92-15972
Aerodynamic measuring techniques for transonic and supersonic flow in cascades and turbomachines
[ONERA, TP NO. 1991-170] p 137 A92-16135
Large chord turbine cascade testing at engine Mach and Reynolds number p 173 A92-18771
Explicit Navier-Stokes computation of cascade flows using the k-epsilon turbulence model
p 175 A92-20727
Time domain flutter analysis of cascades using a full-potential solver p 176 A92-20747
Solution of the problem of three-dimensional flow past the blade rows of turbomachines with allowance for viscosity effects p 244 A92-21618
Unsteady aerodynamic methods for turbomachinery aeroelastic and aeroacoustic applications
[AIAA PAPER 92-0011] p 252 A92-23730
Aerodynamics of loaded cascades in subsonic flows subject to unsteady three-dimensional vortical disturbances
[AIAA PAPER 92-0146] p 253 A92-23762
Multigrid Navier-Stokes calculations for three dimensional cascades
[AIAA PAPER 92-0190] p 256 A92-23799
Measurements of the pressure and velocity distribution in low-speed turbomachinery by means of high-frequency pressure transducers p 391 A92-24723
Design of turbomachinery blading in transonic flows by the circulation method p 311 A92-24725
On velocity profile models for predicting end wall boundary layers and their blade force defects in axial compressor cascades p 311 A92-24877
Pressure wave propagation studies for oscillating cascades
[AIAA PAPER 92-0145] p 316 A92-25682
The effect of blade solidity on the aerodynamic loss of a transonic turbine cascade
[AIAA PAPER 92-0393] p 323 A92-26248
Theoretical study on the unsteady aerodynamic characteristics of an oscillating cascade with tip clearance (In the case of loaded cascade) p 331 A92-26797
A deforming grid variational principle and finite element method for computing unsteady small disturbance flows in cascades
[AIAA PAPER 92-0665] p 335 A92-27036
Loss prediction of annular cascade flow based upon S1/S2 stream surface Navier-Stokes analysis
p 338 A92-27802
Calculation of three-dimensional transonic turbine cascade flow p 344 A92-28519
Inviscid and viscous transonic flows in cascades using an implicit upwind algorithm p 344 A92-28522
Navier-Stokes solution of transonic cascade flows using nonperiodic C-type grids p 344 A92-28523
The unresolved unsteady flow in multistage compressor blade rows p 421 A92-29472
Analysis of effects of freestream turbulence on cascade performance p 422 A92-29716
Studying method of measuring flow-field between stages in axial-flow compressor p 423 A92-29720
Generalized expression of chorochronic periodicity in turbomachinery blade-row interaction
p 423 A92-30000
Numerical analysis of three-dimensional unsteady turbulent flows in a turbine stage p 443 A92-32501
Analysis of cascades using a two dimensional Euler aeroelastic solver
[AIAA PAPER 92-2370] p 556 A92-34598
An investigation of cascade flutter using a two-dimensional full-potential solver
[AIAA PAPER 92-2119] p 558 A92-35688
Finite element Euler calculations of unsteady transonic cascade flows
[AIAA PAPER 92-2120] p 520 A92-35689
Trends of research on cascade flutter
p 558 A92-35914
Numerical simulations in turbomachinery; Proceedings of the Symposium, ASME and JSME Joint Fluids Engineering Conference, 1st, Portland, OR, June 23-27, 1991
[ISBN 0-7918-0714-2] p 522 A92-36028
An inverse inviscid method for the design of quasi-three dimensional turbomachinery cascades
p 523 A92-36033
Inviscid and viscous quasi-three-dimensional flow solutions in a transonic turbine cascade
p 523 A92-36035
Unsteady Navier-Stokes simulation of turbulent flows through a supersonic compressor cascade
p 523 A92-36036
Outflow boundary conditions for Euler analysis of flow in turbine scroll p 591 A92-36037
Numerical simulations of the flow through cascades with tip clearance p 523 A92-36038
Turbomachinery unsteady load predictions with nonuniform inflow p 611 A92-36972
New model for predicting end wall boundary layer in an axial cascade p 611 A92-37389
Reynolds stress distribution downstream of a turbine cascade p 614 A92-38861
Renormalization group based algebraic turbulence model for three-dimensional turbomachinery flows
p 703 A92-41268
Secondary flow investigation inside the passage of a compressor cascade p 706 A92-42124
Calculation of transonic flow in turbomachine cascades p 708 A92-43067
Numerical analysis of flow through oscillating cascade sections p 713 A92-44513

Row-by-row off-design performance calculation method for turbines p 737 A92-44514
Multi-point inverse design of an infinite cascade of airfoils
[AIAA PAPER 92-2650] p 797 A92-45517
Effect of flow rate on loss mechanisms in a backswept centrifugal impeller p 897 A92-45606
The application of particle image velocimetry (PIV) in a short-duration transonic annular turbine cascade
[ASME PAPER 91-GT-221] p 899 A92-46825
A new method for predicting the end wall boundary layers and the blade force defects inside the passage of axial compressor cascades p 819 A92-47691
Experience with the Johnson-King turbulence model in a transonic turbine cascade flow solver
p 821 A92-48207
Numerical computations of transonic flows through cascades
[AIAA PAPER 92-3041] p 822 A92-48702
Application of non-reflecting boundary conditions to three-dimensional Euler equation calculations for thick strut cascades
[AIAA PAPER 92-3045] p 822 A92-48705
Establishing two-dimensional flow in a large-scale planar turbine cascade
[AIAA PAPER 92-3066] p 823 A92-48720
Development of an efficient analysis for high Reynolds number inviscid/viscid interactions in cascades
[AIAA PAPER 92-3073] p 823 A92-48723
Wake mixing and performance measurements in a linear compressor cascade with crenulated trailing edges
[AIAA PAPER 92-3188] p 824 A92-48800
A turbulence model based on RNG for quasi-three-dimensional cascade flows --- renormalization group methods
[AIAA PAPER 92-3312] p 825 A92-48898
A Navier-Stokes analysis of a controlled-diffusion compressor cascade at increasing inlet-flow angles
[AIAA PAPER 92-3313] p 825 A92-48899
Full field flow visualization and computer-aided velocity measurements in a bank of cylinders in a wind tunnel
p 991 A92-50040
Transonic turbine blade cascade testing facility
[AIAA PAPER 92-4034] p 1101 A92-56856
Experimental unsteady pressures on an oscillating cascade with supersonic leading edge locus
[AIAA PAPER 92-4035] p 1035 A92-56857
Supercritical blade design on stream surfaces of revolution with an inverse method p 220 N92-13950
Design of transonic compressor cascades using hodograph method p 202 N92-13973
The aerodynamic effect of fillet radius in a low speed compressor cascade
[NASA-TM-105347] p 202 N92-14063
Preliminary investigation of the shock-boundary layer interaction in a simulated fan passage
[AD-A242656] p 185 N92-15045
Thermal nonequilibrium effects on turbine cascade aerodynamics
[AD-A244049] p 404 N92-19183
Unsteady-flow-field predictions for oscillating cascades
[NASA-TM-105283] p 348 N92-19437
Invariant boundary conditions for cascade flows
p 498 N92-20147
Transonic turbine blade cascade testing facility
[NASA-TM-105646] p 667 N92-26129
Validation of a CANARI code by the computation of three dimensional turbulent flow in turbine valve
p 741 N92-27462
Computation of the unsteady transonic 2D cascade flow by an Euler algorithm with interactive grid generation
p 719 N92-27944
Explicit Navier-Stokes computation of turbomachinery flows
[AD-A249284] p 909 N92-28879
Laser anemometer measurements and computations in an annular cascade of high turning core turbine vanes
[NASA-TP-3252] p 830 N92-28980
Development of a multigrid transonic potential flow code for cascades
[NASA-CR-190480] p 830 N92-29361
Examination of the main error factors with regards to secondary losses in compression and turbine cascades by variations of the blade picture ratio
[ETN-92-91493] p 871 N92-29927

CASCADE WIND TUNNELS
Study on transonic cascade performance by use of newly built facility p 136 A92-15328
On the prediction of unsteady forces on gas turbine blades. I - Description of the approach. II - Analysis of the results p 311 A92-24724
Air ejector experiments using the two-dimensional supersonic cascade tunnel: Zero secondary flow performance
[NAL-TM-632] p 887 N92-28829

CASING
A numerical investigation of axial flow compressor casing treatment p 942 A92-53381
Diffuser casing upgrade for an advanced turbofan
[NLR-TP-90097-U] p 870 N92-28711

CASSINI MISSION
A low-power, high-efficiency Ka-band TWTA
p 671 A92-38163

CAST ALLOYS
Manufacture of XD gamma titanium aluminide airfoils via investment casting and machining
p 494 A92-30603
Low cycle fatigue of cast nickel base turbine rotors
p 226 N92-14405
Durability and damage tolerance of aluminum castings
[AD-A245237] p 490 N92-21159

CASTING
Titanium alloy casting for aerospace
p 1106 A92-56103
Present and future trends in turbine blade material and manufacturing technology
[PNR-90825] p 488 N92-20164

CASTINGS
X-ray computed tomographic inspection of castings
p 492 A92-28725

CATALYSTS
Safety considerations in testing a fuel-rich aeropropulsion gas generator
[NASA-TM-105258] p 279 N92-17061
Cryogenic hydrogen-induced air-liquefaction technologies for combined-cycle propulsion applications
p 487 N92-21526

CATAPULTS
JPATS escape system development
p 543 A92-35434
Dynamic performance of an aircraft on its landing gear: Test and evaluation on a dihedral p 466 N92-21970

CATHODE RAY TUBES
Development of the D-size liquid crystal flat panel display for aircraft p 734 A92-43208
The C-17 Multifunction Display - A building block for avionic systems p 1063 A92-55907

CAUCHY INTEGRAL FORMULA
Complex variable boundary element method for external potential flows p 172 A92-18353

CAUCHY PROBLEM
Application of special series for studying nonstationary transonic gas flows p 311 A92-24904
Increasing the accuracy of the Godunov scheme for calculating steady-state supersonic gas flows by solving the generalized Riemann problem p 1035 A92-57499
Performance prediction and design of maximum thrust planar supersonic nozzles using a flux-difference-splitting technique p 738 N92-26480

CAVITATION FLOW
Turbine disk temperatures resulting from the hot mainstream at engine conditions
[AIAA PAPER 92-0398] p 373 A92-26252
Helium bubble flow visualization of the spanwise separation on a NACA 0012 with simulated glaze ice
[AIAA PAPER 92-0413] p 341 A92-28192
Inverse solution of 3D incompressible turbulent boundary layer with separated bubbles
p 522 A92-35992
Separated and cavitation flows - Principal properties and computational models --- Russian book
[ISBN 5-02-014005-8] p 610 A92-36600
Laminar separation bubbles and airfoil design at low Reynolds numbers
[AIAA PAPER 92-2735] p 797 A92-45515
Pressure measurements in high speed water tunnels
[DE92-004891] p 386 N92-19978
Helium bubble flow visualization of the spanwise separation on a NACA 0012 with simulated glaze ice
[NASA-TM-105742] p 714 N92-26612
On the origin and acoustical behaviour of cloud cavitation
[ISBN-90-9004317-9] p 1125 N92-33066

CAVITIES
Window cooling for high speed flight
[AD-D015145] p 344 N92-18193
Turbine disk cavity aerodynamics and heat transfer
p 1124 N92-32265

CAVITY FLOW
Shock-boundary layer interaction control with low-profile vortex generators and passive cavity
[AIAA PAPER 92-0064] p 250 A92-22178
Unsteady incompressible flow computations with quadrilateral elements p 394 A92-26219
Evaluation of shear layer cavity resonance mechanisms by numerical simulation
[AIAA PAPER 92-0555] p 333 A92-26965
Flowfield simulation about the SOFIA Airborne Observatory
[AIAA PAPER 92-0656] p 342 A92-28217
Study of cavity pumping in supersonic internal flow
p 429 A92-30538
Navier-Stokes study of supersonic cavity flowfield with passive control p 442 A92-32239
Experimental investigation of supersonic flow over two cavities in tandem p 610 A92-36830
Passive control of supersonic cavity flowfields
[SAE PAPER 912153] p 619 A92-39988
Navier-Stokes cavity solutions based on second-order turbulence modeling
[AIAA PAPER 92-2765] p 704 A92-41314
Numerical study on a supersonic open cavity flow with geometric modification of aft bulkhead
[AIAA PAPER 92-2627] p 794 A92-45499
Heat transfer to a cylinder submerged in a rectangular cavity in supersonic flow --- to simulate electrical cables routed through Space Shuttle Solid Rocket Booster External Tank
[AIAA PAPER 92-2949] p 901 A92-47913
Rotational coherent anti-Stokes Raman spectroscopy measurements in a rotating cavity with axial throughflow of cooling air - Oxygen concentration measurements
p 990 A92-49574
Numerical investigation of unsteady supersonic cavity flowfield with passive control p 88 N92-13029
Measurements of fluctuating pressure in a rectangular cavity in transonic flow at high Reynolds numbers
[NASA-TM-4363] p 633 N92-25752
Turbine disk cavity aerodynamics and heat transfer
p 1124 N92-32265

CAVITY RESONATORS
Bias of an optical passive ring-resonator gyro caused by the misalignment of the polarization axis in the polarization-maintaining fiber resonator
p 652 A92-40262

CELESTIAL NAVIGATION
On the overdetermined celestial fix p 19 A92-10475
Visual photometric experiment data processing system
[AD-A248657] p 729 N92-27964

CEMENTS
Preliminary evaluation of adhesion strength measurement devices for ceramic/titanium matrix composite bonds
[NASA-TM-105803] p 932 N92-31267

CENTER OF GRAVITY
Weight, center of gravity and modal test report for NTF fan blade set no. 3
[NASA-CR-189583] p 498 N92-20072

CENTER OF MASS
Experimental determination of the center of mass, the principal central axes of inertia and moments of inertia --- aircrafttt models applied to real aircraf
p 40 A92-12346
Development of a combined fast method for studying the plane motions of rigid bodies in the atmosphere around the center of mass in the presence of perturbations
p 304 A92-23563
Determination of the mean duration of normal acceleration loads at the center of mass of aircraft during a flight in a turbulent atmosphere p 480 A92-30192
Singularity bypass algorithms in the numerical solution of equations of body motion relative to a center of mass in the atmosphere in the presence of disturbances
p 437 A92-31857
Computational analysis of inertial effects on the stability of an ACES-II ejection seat p 543 A92-35436
The problem of body motion in a medium with resistance p 604 A92-36416

CENTER OF PRESSURE
Center of pressure calculations for a bent-axis vehicle
[AIAA PAPER 92-0168] p 254 A92-23779
Center of pressure calculations for a bent-axis vehicle
[DE92-005186] p 498 N92-20143

CENTERBODIES
Experimental investigation of coannular jet flow with swirl along a centerbody p 172 A92-18367

CENTRAL PROCESSING UNITS
Active flow control for twenty-first century high-performance aircraft with applications to land and sea vehicles p 447 N92-21504
Development of pre- and post-processor system for structural analysis
[NAL-TM-628] p 681 N92-25403

CENTRIFUGAL COMPRESSORS
Investigation of the flow at the exit of an unshrouded centrifugal impeller and comparison with the 'classical' jet-wake theory
[ASME PAPER 90-GT-124] p 6 A92-11287
Impeller flow field measurement and analysis
[ASME PAPER 90-GT-146] p 38 A92-11288
Wave engine aerothermodynamic design
[ASME PAPER 91-GT-4] p 120 A92-15502
Experimental study of the swirling flow in the internal volute of a centrifugal compressor
[ASME PAPER 91-GT-7] p 67 A92-15505

Preliminary experience with an expert system providing initial centrifugal compressor sizing for performance prediction and analysis
[ASME PAPER 91-GT-28] p 162 A92-15513
Surge dynamics in a free-spool centrifugal compressor system
[ASME PAPER 91-GT-31] p 68 A92-15515
Dynamic analysis technique of rotating centrifugal impeller
[ASME PAPER 91-GT-50] p 148 A92-15528
An improved method for aerodynamic design of centrifugal impeller blades
[ASME PAPER 91-GT-76] p 69 A92-15545
The efficiencies of single-stage centrifugal compressors for aircraft applications
[ASME PAPER 91-GT-77] p 122 A92-15546
NASA low-speed centrifugal compressor for 3-D viscous code assessment and fundamental flow physics research
[ASME PAPER 91-GT-140] p 72 A92-15580
Analytical investigation of the rules of component matching in turbojet engines
[ASME PAPER 91-GT-170] p 123 A92-15605
A calculation procedure for three-dimensional turbulent flow in a centrifugal impeller with any blade geometry
[ASME PAPER 91-GT-171] p 73 A92-15606
Deterministic blade row interactions in a centrifugal compressor stage
[ASME PAPER 91-GT-273] p 75 A92-15670
LDV measurements of a mixed-flow impeller at design and near stall
[ASME PAPER 91-GT-310] p 153 A92-15688
Development of T-100 multipurpose small power unit
[ASME PAPER 91-GT-327] p 153 A92-15697
Some rotordynamic problems in small turbo-engines p 470 A92-29736
A study on the rotating stall of centrifugal compressors. II - Effect of vaneless diffuser inlet shape on rotating stall p 497 A92-32508
Performance of a high-pressure-ratio centrifugal compressor influenced by distribution of tip clearance of the mixed-flow impeller p 498 A92-32509
A refined analytical method for designing high pressure ratio centrifugal impellers p 591 A92-36032
Unsteady flow within centrifugal compressor channels under rotating stall and surge
[ASME PAPER 91-GT-85] p 670 A92-36901
Plotting the universal characteristic of a compressor in low-rpm and autorotation regimes p 657 A92-40607
Performance predictions for centrifugal compressor impellers p 759 A92-41836
Effect of flow rate on loss mechanisms in a backswept centrifugal impeller p 897 A92-45606
Magnetic bearing design and control optimization for a four-stage centrifugal compressor p 900 A92-47188
Active magnetic bearings give systems a lift p 901 A92-48201
Design and test of an Active Tip Clearance System for centrifugal compressors
[AIAA PAPER 92-3189] p 863 A92-48801
Navier-Stokes investigation of a transonic centrifugal compressor stage using an algebraic Reynolds stress model
[AIAA PAPER 92-3311] p 825 A92-48897
Mixed flow compressor surge margin gain using a manifolded diffuser system
[AIAA PAPER 92-3753] p 1068 A92-54151
A survey of instabilities within centrifugal pumps and concepts for improving the flow range of pumps in rocket engines
[NASA-TM-105439] p 387 N92-18280
Turbocharged pressurized combustion system
[PB92-142579] p 756 N92-26521
Dynamic control of aerodynamic instabilities in gas turbine engines p 870 N92-28466
Explicit Navier-Stokes computation of turbomachinery flows
[AD-A249284] p 909 N92-28879
A 4-spot time-of-flight anemometer for small centrifugal compressor velocity measurements
[NASA-TM-105717] p 909 N92-29105
Explicit Navier-Stokes computation of turbomachinery flows
[AD-A248458] p 911 N92-29933
Numerical simulation of turbomachinery flows with advanced turbulence models p 1124 N92-32270
Effects of curvature and rotation on turbulence in the NASA low-speed centrifugal compressor impeller p 1124 N92-32292

CENTRIFUGAL FORCE
Optical measurements of unducted fan flutter
[ASME PAPER 91-GT-19] p 147 A92-15510
Effect of Eulerian inertia forces on the stressed state of the rotating components of aircraft turbomachines p 128 A92-16828
Impact response of composite UHB propeller blades
[SAE PAPER 912046] p 861 A92-45430
An analysis of the effect of centrifugal force on the impact resistance of composite fan blades for turbo-fan engines
[SAE PAPER 912047] p 861 A92-45431
Surface heat transfer and flow properties of vortex arrays induced artificially and from centrifugal instabilities p 1121 A92-56371
Behavior of aircraft tire coupons under various loading conditions
[AD-A241416] p 116 N92-13063
Analysis of Euler's and stress tensor methods for calculating power consumption of high speed centrifugal fans and turbocompressors
[DE92-728396] p 298 N92-16325
Calculation of local power consumptions and efficiencies of centrifugal fans and turbocompressors
[DE92-728402] p 298 N92-16326
Experimental study of the mechanism of sound generation by rotating stall in centrifugal turbomachines p 605 N92-23726

CENTRIFUGAL PUMPS
Annular seals of high energy centrifugal pumps: Presentation of full scale measurement p 224 N92-14362
A survey of instabilities within centrifugal pumps and concepts for improving the flow range of pumps in rocket engines
[NASA-TM-105439] p 387 N92-18280
Experimental study of the mechanism of sound generation by rotating stall in centrifugal turbomachines p 605 N92-23726

CENTRIFUGES
Professor Jesse W. Beams and the first practical magnetic suspension p 771 N92-27723

CENTRIFUGING STRESS
Design and performance of the centrifuge-based Dynamic Flight Simulator
[AIAA PAPER 92-4156] p 981 A92-52446

CEPSTRAL ANALYSIS
Removal of spurious reflections from computational fluid dynamic solutions with the complex cepstrum p 235 A92-20729

CERAMIC COATINGS
Compressor coating effects on gas turbine engine performance p 25 A92-11282
Thermal barrier coating life prediction model development
[ASME PAPER 91-GT-40] p 147 A92-15523
Precision drilling of ceramic-coated components with abrasive-waterjets
[ASME PAPER 91-GT-232] p 149 A92-15641
Protective coatings of thermal barrier type p 214 A92-20349
Fabrication and testing of corrosion resistant coatings --- for turbine engine components
[DE92-003553] p 490 N92-21063

CERAMIC FIBERS
Mechanical testing of glass-ceramic matrix composites
[ONERA, TP NO. 1991-182] p 388 A92-26351
Probabilistic lifing approach for aero engine disks made of powder nickel base alloys containing ceramic defects p 226 N92-14424
High temperature dynamic engine seal technology development
[NASA-TM-105641] p 596 N92-23435
Ceramic composites: Enabling aerospace materials
[NASA-TM-105599] p 756 N92-27378

CERAMIC MATRIX COMPOSITES
Intermetallic and ceramic matrix composites for 815 to 1370 C (1500 to 2500 F) gas turbine engine applications p 141 A92-15128
Design and analysis of ceramic and CMC components for advanced gas turbines
[ASME PAPER 91-GT-156] p 142 A92-15592
Ceramic matrix composites and its application in gas turbine engines
[ASME PAPER 91-GT-338] p 143 A92-15702
Mechanical testing of glass-ceramic matrix composites
[ONERA, TP NO. 1991-182] p 388 A92-26351
Ultrasonic NDE for ceramic- and metal-matrix composite material characterization p 491 A92-28690
Flight vehicles of the future p 419 A92-31525
Ceramics and ceramic matrix composites - Aerospace potential and status
[AIAA PAPER 92-2445] p 577 A92-34474
Effect of sustained high temperature exposure on the mechanical properties of Nicalon/Al2O3 composites p 668 A92-39672
Flight-vehicle materials, structures, and dynamics - Assessment and future directions. Vol. 3 - Ceramics and ceramic-matrix composites --- Book
[ISBN 0-7918-0661-8] p 668 A92-39852
Fabrication and properties of fiber-reinforced ceramic composites made by directed metal oxidation p 669 A92-39861
High-temperature durability considerations for HSCT combustor
[NASA-TP-3162] p 289 N92-17070
Ceramic composites: Enabling aerospace materials
[NASA-TM-105599] p 756 N92-27378
Thermomechanical fatigue behavior of a silicone carbide fiber-reinforced calcium aluminosilicate glass-ceramic matrix composite
[AD-A249870] p 988 N92-31823

CERAMICS
Life time prediction for ceramic gas turbine components
[ASME PAPER 91-GT-96] p 122 A92-15560
Impact design methods for ceramic components in gas turbine engines
[ASME PAPER 91-GT-115] p 123 A92-15566
Ceramic component processing development for advanced gas-turbine engines
[ASME PAPER 91-GT-120] p 142 A92-15567
Development of silicon nitride rotors for the ATTAP program at Garrett Ceramic Components --- Advanced Turbine Technology Applications Project
[ASME PAPER 91-GT-154] p 142 A92-15590
Gas-generator with high-temperature path ceramic components
[ASME PAPER 91-GT-152] p 148 A92-15594
The use of NDE as a process development tool for ceramic engine components
[ASME PAPER 91-GT-290] p 152 A92-15682
Development and bench test of high-temperature combustion chamber with structural ceramic components
[ASME PAPER 91-GT-315] p 126 A92-15691
Advanced ceramic engine technology for gas turbines
[ASME PAPER 91-GT-368] p 153 A92-15716
An investigation on flame stability by fuel permeability in a flame holder made of porous ceramic material p 375 A92-28435
The use of CT for dimensional measurements of green and sintered ceramic components p 490 A92-28592
Ceramics and ceramic matrix composites - Aerospace potential and status
[AIAA PAPER 92-2445] p 577 A92-34474
Flight-vehicle materials, structures, and dynamics - Assessment and future directions. Vol. 3 - Ceramics and ceramic-matrix composites --- Book
[ISBN 0-7918-0661-8] p 668 A92-39852
Monolithic ceramics p 668 A92-39854
Study of grinding process and strength for ceramic heat insulated engine
[SME PAPER MR91-177] p 897 A92-45260
Ceramic regenerator program
[NASA-CR-189053] p 225 N92-14374
Probabilistic lifing approach for aero engine disks made of powder nickel base alloys containing ceramic defects p 226 N92-14424
Ceramic technology for Advanced Heat Engines Project
[DE92-002397] p 289 N92-16128
Fiber-sensor design for turbine engines
[DE92-003539] p 376 N92-18230
Evaluation of an innovative high-temperature ceramic wafer seal for hypersonic engine applications p 578 N92-22205
Ceramics for engines p 578 N92-22517
Small engine technology programs p 560 N92-22532
Evaluation of the elevated-temperature mechanical reliability of a HIPed silicon nitride
[DE92-007838] p 579 N92-23223
The cost of silicon nitride powder: What must it be to compete?
[DE92-008710] p 669 N92-25223
Advanced Turbine Technology Applications Project (ATTAP)
[NASA-CR-189142] p 682 N92-25649
Properties of a TZP/Al2O3 composite after long-term exposure at 1000 C
[AD-A246407] p 757 N92-27752
Preliminary evaluation of adhesion strength measurement devices for ceramic/titanium matrix composite bonds
[NASA-TM-105803] p 932 N92-31267

CERTIFICATION
A computer programme for the certification of helicopter vertical take-off and landing operations and an application to the S-76B helicopter p 106 A92-14379
Stage 2 noise certification of the Sikorsky S-76A and S-76C helicopters p 91 A92-14388
Design, analysis, testing, and certification of composite primary structure for the Piaggio P-180 Avanti p 535 A92-32553
S-76B certification for vertical take-off and landing operations from confined areas p 530 A92-35760

Concorde flight testing - Powerplant and performance flying
[SAE PAPER 912192] p 644 A92-40009
MD-11 status report p 646 A92-40040
Are we doing HIRF testing sensibly? --- avionics certification in commercial aircraft p 931 A92-49305
AS 332 MKII - Development and certification p 1059 A92-56343
Flyover-noise measurement and prediction p 236 N92-14786
Propeller-driven-small airplane noise certification
[LR-650] p 237 N92-14798
Fatigue life behaviour of composite structures p 390 N92-18577
Suppression of radiating harmonics Electro-Impulse Deicing (EIDI) systems
[DOT/FAA/CT-TN90/33] p 405 N92-19764
Regulations and their changes for certification of civil aircraft in icing conditions p 450 N92-21683
Preparation of the ice certification of the Dornier 328 regional airliner by numerical simulation and by ground test p 451 N92-21693
The proposed revision to RTCA DO178A and its influence on system design
[PNR-90821] p 510 N92-21847
Impact of regulation changes on engine design and certification
[PNR-90789] p 559 N92-22098
Validation of simulation systems for aircraft acceptance testing p 852 N92-28531
The use of load enhancement factors in the certification of composite aircraft structures
[NLR-TP-90068-U] p 852 N92-28649
S-76B certification for vertical take-off and landing operations from confined areas
[NLR-TP-90286-U] p 852 N92-28714

CESSNA AIRCRAFT
Drop test: Cessna Golden Eagle 421B
[DOT/FAA/CT-TN91/32] p 837 N92-28900

CH-46 HELICOPTER
CH-46 and OH-58 transmission stress wave analysis
[AD-A244321] p 365 N92-18826

CH-47 HELICOPTER
The development of an engine air particle separator system for the CH-47 helicopter p 545 A92-35736
GPS integration improves mission capabilities of CH-47D aircraft p 966 A92-49340
Rotorcraft In-Flight Simulation Research at NASA Ames Research Center: A Review of the 1980's and plans for the 1990's
[NASA-TM-103873] p 853 N92-28926

CHALLENGER (ORBITER)
Performance of uncoated AFRSI blankets during multiple Space Shuttle flights
[NASA-TM-103892] p 890 N92-29104

CHANNEL FLOW
Compressibility effects in thin channels with injection p 216 A92-18369
An efficient Euler solver for predominantly supersonic flows with embedded subsonic pockets
[AIAA PAPER 92-0323] p 322 A92-25770
Boundary singularities in steady potential compressible flow through plane two-dimensional channels p 336 A92-27384
Control of strong shock-turbulent boundary layer interaction in rectangular channels p 422 A92-29714
Computations of a transonic flow about an airfoil in a wind tunnel with porous walls p 423 A92-30128
The Berlin oil channel for drag reduction research p 571 A92-34219
On the mechanics of 3-D turbulent boundary layers p 620 A92-40068
Embedded longitudinal vortex arrays, velocity and temperature fields, loss and heat transfer augmentation p 621 A92-40121
Transition to turbulence in curved channel flow p 621 A92-40125
Heat transfer in a channel with built-in wing-type vortex generators p 757 A92-41082
A numerical study of flow of a viscous gas in a Laval nozzle in the narrow channel approximation p 706 A92-42680
Segmental heat transfer in a pin fin channel with ejection holes p 900 A92-47267
Total losses in turbulent flows inside conical diffusers p 819 A92-47782
Experimental investigation of liquid carbonhydrogen fuel combustion in channel at supersonic velocities
[AIAA PAPER 92-3429] p 894 A92-48986
Detonation duct gas generator demonstration program
[AIAA PAPER 92-3174] p 1066 A92-54011
Physics of vortical flows p 1031 A92-56166
A weakly nonlinear theory for wave-vortex interactions in curved channel flow
[NASA-TP-3158] p 347 N92-19175
Laser-spectroscopic measurement techniques for hypersonic, turbulent wind tunnel flows
[NASA-TM-103928] p 405 N92-19596
Structure of three-dimensional turbulent boundary layers p 999 N92-30654

CHANNELS
Multi-channel fiber optic rotary joint for single-mode fiber
[AD-D015273] p 927 N92-29095

CHANNELS (DATA TRANSMISSION)
Development and future view of the technology for fly-by-light control system elements p 131 A92-14027
An alternative method for acquiring avionic bus data in a class I PCM telemetry system p 217 A92-19202
MIL-STD-1553 data bus/PCM multiplexer system p 188 A92-19211
Evaluating the use of satellite communications in the government of Canada p 594 N92-22577
Avionic data bus integration technology
[DOT/FAA/CT-91/19] p 736 N92-27973
Fiber optic data busses for aircraft p 736 N92-28093

CHAOS
Chaotic and nonlinear dynamic response of aerosurfaces with structural nonlinearities
[AIAA PAPER 92-2547] p 518 A92-34517
Chaotic motion in mechanical and engineering systems p 695 A92-39480
Chaotic stall response of helicopter rotor in forward flight p 730 A92-43046
Chaotic oscillation in helicopter blade stall response p 846 A92-46922
Chaotic dynamic behavior in a simplified rotor blade lag model p 846 A92-46926
A double chaotic attractor in transonic flow p 1019 A92-53561
Studies in chaos using stochastic methods
[AD-A246919] p 780 N92-27171

CHAPLYGIN EQUATION
Boundary singularities in steady potential compressible flow through plane two-dimensional channels p 336 A92-27384
Design of transonic compressor cascades using hodograph method p 202 N92-13973

CHARGE COUPLED DEVICES
A high-performance LLLTV CCD camera for nighttime pilotage p 855 A92-46227
Development of an electronic high speed camera system for the quantitative analysis of unsteady flows
[MPIS-100/1991] p 300 N92-17344
Model incidence measurement using SAAB ELOPTOPOS system
[NLR-TP-89182-U] p 385 N92-18416

CHARTS
The electronic aeronautical chart for general aeronautics: A system specification
[ILR-MITT-263(1991)] p 20 N92-10997
Design considerations for IAP charts: Approach course track and communication frequencies
[AD-A241482] p 103 N92-13051

CHEBYSHEV APPROXIMATION
An inviscid stability analysis of unbounded supersonic mixing layer flows p 443 N92-20332

CHECKOUT
Expert system for the Tornado ground-based check-out system p 118 N92-12536
Comparison of three controllers applied to helicopter vibration
[NASA-TM-102192] p 878 N92-28457
An evaluation of decelerating IFR approaches utilizing a helicopter flight simulator
[CTN-92-60348] p 1048 N92-32845

CHEMICAL ANALYSIS
The effect of jet fuel exposure on advanced aerospace composites. Part 1: Thermal and chemical analysis
[AD-A246559] p 756 N92-27531

CHEMICAL BONDS
H-N2 interaction energies, transport cross sections, and collision integrals p 1135 A92-54660

CHEMICAL COMPOSITION
Swirl and fuel composition effects on boron combustion in solid-fuel ramjets p 668 A92-36964
Flow characterization in the NASA Ames 16-inch Shock Tunnel
[AIAA PAPER 92-3810] p 1090 A92-54180
Flow contamination and flow quality in arc heaters used for hypersonic testing
[AIAA PAPER 92-4028] p 1100 A92-56850
High-speed civil transport aircraft emissions p 408 N92-19122
Advanced thermally stable jet fuel development program. Volume 2: Compositional factors affecting thermal degradation of jet fuels
[AD-A252656] p 987 N92-31399

CHEMICAL EQUILIBRIUM
A non-linearly stable implicit finite element algorithm for hypersonic aerodynamics p 433 A92-31487
Non-equilibrium hypersonic flow simulations using the second-order boundary layer equations p 612 A92-37551
Integrated electric density and scaling law for hypersonic blunt-body wakes p 714 A92-44865
High enthalpy nozzle flows p 182 N92-15000
Influence of chemical modeling on the solution of hypersonic shock layers p 183 N92-15016
Effects of chemical equilibrium on turbine engine performance for various fuels and combustor temperatures
[NASA-TM-105399] p 562 N92-23254

CHEMICAL REACTIONS
Interaction between chemical reaction and turbulence in supersonic nonpremixed H2-air combustion p 1117 A92-54931
Poly 1, 2, 4-triazoles via aromatic nucleophilic displacement
[NASA-CASE-LAR-14440-1] p 35 N92-10066
Reaction speed constant for the reactions between N + O2 and between O + N2
[ETN-92-90861] p 347 N92-19252
Simulation of the flow on a space glider. Stagnation point calculation using the 2D Navier-Stokes equations including chemical effects p 624 N92-24393
TVD finite-difference solutions of nonequilibrium vibrationally relaxing and chemically reacting gaseous flows p 626 N92-24854
Modeling of the reactant conversion rate in a turbulent shear flow p 829 N92-28820
Effect of walls on the supersonic reacting mixing layer p 912 N92-30065
Turbulent reacting flows and supersonic combustion
[AD-A251065] p 986 N92-30256

CHEMILUMINESCENCE
Shock enhancement and control of hypersonic combustion
[AD-A248558] p 896 N92-29580

CHEMISORPTION
Solid-vapor adsorption refrigeration system development
[PB92-164383] p 771 N92-27715

CHILDREN
Preliminary design and lay-out of an infant restraint system p 449 N92-21513

CHINA
Research on inverse, hybrid and optimization problems in engineering sciences with emphasis on turbomachine aerodynamics: Review of Chinese advances p 201 N92-13939

CHINESE AIRCRAFT
The 'derivative' and 'synthetic' approaches in aircraft design p 358 A92-27901

CHIPS (ELECTRONICS)
Putting ten pounds of avionics in a one pound package (Can we do it again?)
[AIAA PAPER 91-3766] p 197 A92-17628
Built-in testable error detection and correction p 394 A92-25846
Thermal management of high heat flux electronic components in space and aircraft systems, phase 1
[AD-A239982] p 41 N92-10157
What is an ASIC? p 859 N92-28377

CHIPS (MEMORY DEVICES)
A high performance general purpose processing element for avionic applications p 920 A92-48440

CHLORIDES
Poly 1, 2, 4-triazoles via aromatic nucleophilic displacement
[NASA-CASE-LAR-14440-1] p 35 N92-10066

CHLORINE FLUORIDES
Nonflammable hydraulic power system for tactical aircraft. Volume 2: Equipment and systems test and evaluation
[AD-A239805] p 35 N92-10100

CHOLESKY FACTORIZATION
A parallel-vector algorithm for rapid structural analysis on high-performance computers
[NASA-TM-102614] p 595 N92-22649

CHROMIUM ALLOYS
Cyclic hot corrosion of Haynes 230 alloy p 754 A92-41091
High-temperature metal matrix composite p 1105 A92-53878
High temperature strain gage technology for hypersonic aircraft development applications
[NASA-CR-189101] p 592 N92-22239

CHROMIUM STEELS
Creep-fatigue crack growth in Jethete M152 at 550 C under mixed mode conditions p 288 A92-21490
Rolling element bearing member
[PATENT-1-271-213] p 158 N92-13434

CHUTES
Fire bombing and fire bombers
[CA-PATENT-1-268-164] p 1061 N92-33582
CINEMATOGRAPHY
High-speed cinematography of supersonic mixing layers
[AIAA PAPER 92-3545] p 1112 A92-54044
CIRCUIT PROTECTION
New insulation constructions for aerospace wiring applications. Volume 2: The 270 VDC arc tracking testing with power controllers
[AD-A240639] p 23 N92-11007
CIRCUIT RELIABILITY
Durability analysis using fracture mechanics for avionics integrity p 396 A92-26799
On upsets of analog portions of digital flight control systems due to electromagnetic interference
[SAE PAPER 912144] p 651 A92-39982
CIRCULAR CONES
Similarity solutions for supersonic axisymmetric flows p 173 A92-18387
Hypersonic flows over slender circular cones at small angles of attack p 173 A92-19068
Theoretical analysis of the effect of the porous walls of a wind tunnel on transonic flow past bodies of cone-cylinder type p 427 A92-30202
A method for calculating the separated flow past a circular cone, taking viscous-inviscid interaction into account p 427 A92-30203
Comparison of interferometric measurements with 3-D Euler computations for circular cones in supersonic flow
[AIAA PAPER 92-2691] p 800 A92-45538
Asymmetric vortex flow over circular cones p 86 N92-13014
CIRCULAR CYLINDERS
Pressure on a cylinder with a screen in transverse flow p 6 A92-12164
Flat-ended circular cylinder in hypersonic rarefied flow p 174 A92-20304
End plate interference effects on the aerodynamics of a circular cylinder in uniform flow p 313 A92-25097
Unsteady incompressible flow computations with quadrilateral elements p 394 A92-26219
Unsteady circulation control aerodynamics of a circular cylinder with periodic jet blowing p 330 A92-26401
A study of the base pressure behind circular steps p 426 A92-30196
Cylinder-induced shock-wave boundary-layer interaction p 433 A92-31188
Large eddy simulation of unsteady turbulent wake of a circular cylinder using the finite element method p 587 A92-34825
An analytical evaluation of the aerodynamic forces acting on a circular cylinder in a uniform shear flow p 522 A92-35995
The effect of a velocity gradient on the aerodynamic forces of a circular cylinder with tangential blowing p 614 A92-38859
Hypersonic turbulent separated flow past an unswept circular cylinder on a flat plate p 615 A92-38908
Aerodynamic drag of a cylinder in two-phase flow p 707 A92-42735
Flow of a rarefied gas over a cylinder at angle of sideslip p 708 A92-42738
Flow around two square cylinders in staggered arrangements p 761 A92-42797
Numerical approximation of hypersonic shocks in a finite-element method using flux-corrected transport (FCT) p 708 A92-43060
Shock interaction induced by two hemisphere-cylinders
[SAE PAPER 912043] p 790 A92-45427
The unsteady interaction of a 3-dimensional vortex filament with a cylinder p 813 A92-46934
Steady flow of a fluid-solid mixture in a circular cylinder
[DE91-018698] p 41 N92-10174
Flow around two circular cylinders arranged perpendicular to each other
[PB91-238279] p 297 N92-16225
Active control of the flow past a cylinder executing rotary motions p 349 N92-19623
An experimental investigation of the surface flow and wake dynamics associated with transverse flow over wavy cylinders p 681 N92-25547
The three-dimensional stability of the Foeppl vortices p 949 N92-31889
CIRCULATION
Window cooling for high speed flight
[AD-D015145] p 344 N92-18193
Modelling the vaporiser and primary zone flows for a modern gas turbine combustion chamber p 742 N92-27484
CIRCULATION CONTROL AIRFOILS
Boundary-layer and wake measurements on a swept, circulation-control wing p 9 A92-13205
Two-dimensional, incompressible aerofoil design and analysis p 247 A92-21987
A numerical method for solving the circulation control airfoil with wall jet p 314 A92-25103
Unsteady circulation control aerodynamics of a circular cylinder with periodic jet blowing p 330 A92-26401
Navier-Stokes methods to predict circulation control airfoil performance p 442 A92-32243
An experimental study of a sting-mounted circulation control wing
[AD-A243912] p 346 N92-18895
CIRCULATION CONTROL ROTORS
Hover evaluation of an integrated pneumatic lift/reaction-drive rotor system
[AIAA PAPER 92-0630] p 333 A92-27010
CIRCULATION DISTRIBUTION
Breaking down the delta wing vortex: The role of vorticity in the breakdown process p 86 N92-13017
CIRRUS CLOUDS
A comparison of measured and modeled broadband fluxes from aircraft data during the ICE '89 field experiment p 1003 A92-49771
CITIES
Tilt rotors and the Port Authority of New York and New Jersey Airport System
[RAND-R-3971/1-PA-SUMM] p 636 N92-25262
CIVIL AVIATION
Soviet aerospace in turmoil --- military to civil production conversion p 2 A92-13220
The practical application of new technology to the civil rotorcraft need p 108 A92-14410
Committees, their importance to the structures of the Helicopter Association International p 59 A92-14411
Maintenance, Malfunction Information Report system p 60 A92-14414
The Eurofar vehicle overview p 108 A92-14416
Flight safety; Proceedings of the Conference, London, England, Nov. 21, 1991 p 92 A92-16050
Legal capacity of Eurocontrol to ensure smooth aviation in Europe p 167 A92-16134
Aircraft navigation using Global Positioning System improved with geostationary satellites p 99 A92-16934
GPS availability. I - Availability of service achievable for different categories of civil users. II - Evaluation of state probabilities for 21-satellite and 24-satellite constellations p 99 A92-16949
Integrated use of GPS and GLONASS in civil aviation navigation. I - Coverage and data models p 99 A92-16950
Infra-red offers new landing aid competition p 198 A92-18937
Analysis of changes in the pilot population and general aviation accidents p 187 A92-20722
Pratt & Whitney PW300 for general aviation p 277 A92-21012
High costs force avionics links p 276 A92-22000
The Civil Rotorcraft Initiative - An action agenda p 241 A92-22707
Quantitative estimation of secondary surveillance radar information p 353 A92-24943
Anglo-American avionics p 307 A92-25575
Radio Technical Commission for Aeronautics, Technical Symposium, Washington, DC, Nov. 18-20, 1991, Proceedings p 531 A92-33426
A European perspective on the co-operative air traffic management concept p 531 A92-33427
Perspectives on the cooperative air traffic management concept - Far East/Pacific point of view p 606 A92-33428
An aircraft manufacturer's perspective p 515 A92-33430
The technological revolution in oceanic air traffic control p 531 A92-33431
The ICAO Future Air Navigation System p 532 A92-33435
International standardization p 533 A92-33441
Mass-transporter p 543 A92-34650
European ATC integration faces dual challenges p 534 A92-36076
Growing need to replace ILS can best be met by MLS p 534 A92-36124
Why not a safety rating? --- in Australian civil aviation p 530 A92-36200
Ageing airliner census - Still flying safely p 634 A92-38374
Flying on thin ice p 634 A92-38375
Analysis of stand-alone differential GPS for precision approach p 638 A92-38381
GPS/GLONASS user systems in Sweden p 638 A92-38384
Safety at sea and in the air - Taking stock together; Proceedings of the Conference, London, England, Nov. 13-15, 1990
[ISBN 0-903409-78-X] p 634 A92-39301
Civil aircraft design in relation to airworthiness p 635 A92-39303
Aircraft structural design p 643 A92-39304
Airport technology international 1992 p 664 A92-39514
Future considerations for vertical flight p 608 A92-40383
1991-92 AHS Technical Committee highlights - Aircraft design p 608 A92-40392
ICAO Flight Safety and Human Factors Programme p 835 A92-45055
Effects of wing planform on HSCT off-design aerodynamics --- High Speed Civil Transport
[AIAA PAPER 92-2629] p 844 A92-45501
Industrial practice in aeronautical maintenance p 786 A92-47774
Safety in the sky - Designing bomb-resistant baggage containers p 836 A92-47775
Trends in commercial aircraft design - What evolution factors and what approach?
[ONERA, TP NO. 1992-25] p 786 A92-48587
Computer software in civil aircraft p 1006 A92-49302
Capacity as a consideration for providing aeronautical mobile satellite air traffic services in the U.S. domestic airspace p 956 A92-51007
A new aspect of future air navigation systems - How Secondary Surveillance Radar Mode S could protect civil aviation p 1012 A92-51424
World Administrative Radio Conference ends favourably for air transport sector p 956 A92-52650
Progress towards quieter civil helicopters p 1011 A92-52847
A study on the marginal analysis method for the airline yield management p 951 A92-53018
Regional airline and equipment review - Evolution, trends, and future prospects p 1015 A92-55102
Air transports in the 21st century p 1015 A92-55103
777 - The airlines' higher-order technology airplane p 1052 A92-55104
Research needs for a commercial passenger tiltrotor p 1056 A92-56298
The Eurofar program - An European overview on advanced VTOL civil transportation system p 1016 A92-56299
Personal air transport: State of the art
[PB91-204768] p 18 N92-10991
A systematic formulation, as an approach to air traffic
[MBB-Z-0371-91-PUB] p 19 N92-10996
Military and civil software standards and guidelines for guidance and control p 163 N92-12452
Aircraft accident report: MarkAir, Inc., Boeing 737-2X6C, N670MA, controlled flight into terrain, Unalakleet, Alaska, 2 June 1990
[PB91-910402] p 92 N92-13039
Airport activity statistics of certificated route air carriers: Calendar year 1990
[AD-A241483] p 93 N92-13045
Soviet electronic display systems under research and manufactured for the civil aviation aircraft of the 1990's
[AD-A240933] p 119 N92-13066
General aviation activity and avionics survey, calendar year 1989
[PB91-179234] p 169 N92-13926
FAA statistical handbook of aviation: Calendar year 1989
[PB91-202051] p 170 N92-13927
Aircraft accident reports: Brief format US civil and foreign aviation issue number 3 of 1989 accidents
[PB90-916903] p 263 N92-15979
Aircraft accident report: Northwest Airlines, Inc., Flights 1482 and 299. Runway incursion and collision, Detroit Metropolitan/Wayne County Airport, Romulus, Michigan, December 3, 1990
[PB91-910405] p 264 N92-17213
Variability of standard aircraft performance parameters
[ESDU-91020] p 276 N92-17847
Feasibility of systematic recycling of aircraft Halon extinguishing agents
[DOT/FAA/CT-91/21] p 352 N92-18259
Public-sector aviation issues: Graduate research award papers, 1989 - 1990
[PB91-242271] p 308 N92-19662
The environmental impact of commercial aviation: The evolution of exhaust emissions legislation and control technology
[PNR-90847] p 505 N92-20574
High-speed civil transport flight- and propulsion-control technological issues
[NASA-CR-186015] p 482 N92-21253
Aeronautical research in the United States: Challenges for the 1990's p 420 N92-21502
Regulations and their changes for certification of civil aircraft in icing conditions p 450 N92-21683

Aircraft accident reports: Brief format U.S. Civil and Foreign Aviation Issue Number 5 of 1989 accidents
[PB90-916905] p 452 N92-21833
Aircraft accident report: Unstabilized approach and loss of control NPA, Inc. dba United Express Flight 2415, British Aerospace BA-3101, N41OUE, Tri-Cities Airport, Pasco, Washington, December 26, 1989
[PB91-910406] p 453 N92-21873
Aeronautical mobile satellite service: An overview
p 594 N92-22573
Symposium on Marketing for Technological Products
[MBB-UE-0014-90-PUB] p 606 N92-23928
Tilt rotors and the Port Authority of New York and New Jersey Airport System
[RAND-R-3971/1-PA-SUMM] p 636 N92-25262
Aviation system: Capital investment plan
p 636 N92-25297
Computational Structures Technology for Airframes and Propulsion Systems
[NASA-CP-3142] p 683 N92-25911
Preliminary structural sizing of a Mach 3.0 high-speed civil transport model
[NASA-CR-189631] p 685 N92-25960
An adaptive correction technique for Differential Global Positioning System p 726 N92-26623
Piloted Simulation Effectiveness
[AGARD-CP-513] p 786 N92-28522
Flight simulation and digital flight controls
p 884 N92-28526
Validation of simulation systems for aircraft acceptance testing p 852 N92-28531
FAA aviation forecasts
[AD-A250412] p 837 N92-29182
European studies to investigate the feasibility of using 1000 ft vertical separation minima above FL 290. Part 1: Overview of organisation, techniques employed, and conclusions
[NLR-TP-91062-U-PT-1] p 841 N92-29605
Current and future developments in civil aircraft non-destructive evaluation from an operator's point of view p 787 N92-30122
Communication: An important element of maintenance and repair p 838 N92-30124
Ageing aircraft research in the Netherlands
p 838 N92-30129
The Eurofar program: An European overview on advanced VTOL civil transportation system
[MBB-UD-0611-91-PUB] p 952 N92-30418
Aircraft accident report: Explosive decompression - loss of cargo door in flight, United Airlines Flight 811, Boeing 747-122, N4713U, Honolulu, Hawaii, February 24, 1989
[PB92-910402] p 953 N92-31159
High-speed civil transport issues and technology program
[NASA-CR-186020] p 962 N92-31208
Design and analysis issues of integrated control systems for high-speed civil transports
[NASA-CR-186022] p 979 N92-31656
Federal aviation regulations. Part 91: General operating and flight rules
[PB92-197334] p 1017 N92-33176
Isothermal aging of IM7/8320 and IM7/5260
[NASA-TM-107666] p 1110 N92-33423
Engine bird ingestion experience of the Boeing 737 aircraft: Expanded data base
[DOT/FAA/CT-91/32] p 1045 N92-34151
Impacts of technology on the capacity needs of the US national airspace system
[NASA-CR-4470] p 1045 N92-34192

CL-41 AIRCRAFT
Tutor aft fuselage and empennage full-scale fatigue test: Resolution of horizontal stabilizer installation difficulties
[NRC-LTR-ST-1804] p 114 N92-11990

CLASSIFICATIONS
Modelling aspects and robustness issues in rotorcraft system identification p 274 N92-17159
Radar clutter classification
[ISBN-0-315-57981-1] p 1126 N92-33440

CLASSIFIERS
A multi-layer neural network classifier for radar clutter
p 291 A92-21691
Sensor fault detection on board an aircraft with observer and polynomial classifier
[DLR-FB-91-34] p 859 N92-29870
Radar clutter classification
[ISBN-0-315-57981-1] p 1126 N92-33440

CLEAN ENERGY
Wind energy program overview
[DE91-002178] p 689 N92-25498

CLEANING
Removing aircraft surface coatings
p 516 A92-35574

CLEAR AIR TURBULENCE
Windshear detection p 652 A92-40883
Severe turbulence and maneuvering from airline flight records
[AIAA PAPER 92-4341] p 1078 A92-55330
Microwave temperature profiler for clear air turbulence prediction
[NASA-CASE-NPO-18115-1-CU] p 916 N92-29148

CLEARANCES
The use of optical sensors and signal processing gas turbine engines p 856 A92-46247
Design and test of an Active Tip Clearance System for centrifugal compressors
[AIAA PAPER 92-3189] p 863 A92-48801
Eddy current transducing system
[DE91-018924] p 401 N92-18515
Turbine blade tip and seal clearance excitation forces
[NASA-CR-184341] p 973 N92-31910

CLIMATE CHANGE
NASA High Speed Research Program, Emissions Scenarios Committee report of meetings on 26 September 1991 and 9 January 1992
[NASA-CR-190379] p 1004 N92-32147

CLIMATOLOGY
Meeting Review: Airborne Aerosol Inlet Workshop
[NASA-CR-189814] p 301 N92-17393

CLIMBING FLIGHT
Key design considerations for scramjet powered space plane p 1066 A92-53491
Rotorcraft acceleration and climb performance model
[SCT-90RR-30] p 116 N92-13059
Operational survey: VFR heliport approaches and departures
[SCT-91RR-26] p 190 N92-14033
Variability of standard aircraft performance parameters
[ESDU-91020] p 276 N92-17847
Numerical methods for the simulation of complex multi-body flows with applications for the integrated Space Shuttle vehicle p 945 N92-30741
Application of the Chimera overlapped grid scheme to simulation of Space Shuttle ascent flows
p 945 N92-30742

CLOCKS
LORAN-C data reduction at the US Naval Observatory
p 1050 N92-33358

CLOSURE LAW
Second moment closure predictions of jet-on-jet impingement flows p 675 A92-40102
A compressible Navier-Stokes solver with two-equation and Reynolds stress turbulence closure models
[NASA-CR-4440] p 681 N92-25376

CLOSURES
Sound generation by a stenosis in a pipe
p 415 A92-26405

CLOUD COVER
The 1988 Australian Winter Storms Experiment - Case study: 6 August 1988 p 301 A92-23009
Global positioning system supported pilot's display
p 534 N92-22436

CLOUD GLACIATION
Industrial measurement of microphysical parameters - Application to natural and simulated icing clouds --- for aircraft icing p 262 A92-23302
Influence of air velocity on the habit of ice crystal growth from the vapor p 668 A92-38111

CLOUD PHYSICS
Twenty years of airborne research at the University of Washington p 161 A92-14925
Industrial measurement of microphysical parameters - Application to natural and simulated icing clouds --- for aircraft icing p 262 A92-23302
Feature extraction from two-dimensional images using fractal analysis p 496 A92-32130

CLOUDS
Propagation of shock waves through clouds
[AERO-REPT-9104] p 400 N92-18317

CLOUDS (METEOROLOGY)
A new thermometric instrument for airborne measurements in clouds p 368 A92-24918
Progress report on analysis of differential attenuation radar data obtained during WISP-91
[PB92-133800] p 503 N92-21828

CLUSTER ANALYSIS
Aircraft ride quality controller design using new robust root clustering theory for linear uncertain systems
[AIAA PAPER 92-4399] p 1075 A92-55199

CLUTCHES
Thermal mechanical analysis of sprag clutches
[NASA-CR-190686] p 1128 N92-34207

CLUTTER
Polish radar technology. V - Adaptive MTI filters for uniform and staggered sampling p 40 A92-12293
Classification of radar clutter using neural networks
p 145 A92-14252
Adaptive airborne MTI with two-dimensional motion compensation p 102 A92-17240
Simulation of radar clutter and jet engine modulation using digital quadrature modulator p 216 A92-19091
A multi-layer neural network classifier for radar clutter
p 291 A92-21691
The application of lattice-structure adaptive filters to clutter-suppression for scanning radar
p 403 N92-19154
Spectrum modal analysis for the detection of low-altitude windshear with airborne Doppler radar
[NASA-CR-4457] p 953 N92-31549
Radar clutter classification
[ISBN-0-315-57981-1] p 1126 N92-33440

CMOS
Built-in testable error detection and correction
p 394 A92-25846

COAGULATION
Microgravity nucleation and particle coagulation experiments support
[NASA-CR-190159] p 502 N92-21385
Microgravity nucleation and particle coagulation experiments support
[NASA-CR-189899] p 502 N92-21433

COANDA EFFECT
Aerodynamic design of a Coanda induced force and thruster anti-torque system p 109 A92-14419

COASTING FLIGHT
Using helicopters for coastal alert p 723 A92-43164
Space shuttle entry terminal area energy management
[NASA-TM-104744] p 308 N92-19930

COASTS
Boundary-layer transition across a stratocumulus cloud edge in a coastal zone p 45 A92-10489
Comparison of aircraft synthetic aperture radar and buoy spectra during NORCSEX '88 p 597 A92-34878

COATING
Thermal response of rigid and flexible insulations and reflective coating in an aeroconvective heating environment
[NASA-TM-103925] p 852 N92-28721

COATINGS
The design of broadband radar absorbing surfaces
[AD-A240521] p 42 N92-11235
Criteria for use of seal coats on airport pavements
[DOT/FAA/RD-92/18] p 1102 N92-34247

COAXIAL CABLES
Whole aircraft lightning indirect effects evaluation using low level injection techniques p 192 A92-20134

COAXIAL FLOW
Effect of carbon particles and mixing on afterburning of exhaust plumes
[AIAA PAPER 92-0767] p 387 A92-27107

COBALT ALLOYS
Evaluation and qualification of diffusion braze repair techniques for superalloy gas turbine components
[NRC-LTR-ST-1839] p 504 N92-22028

COCKPIT SIMULATORS
Flying the A340 iron bird p 20 A92-10666
Utilization of a research simulator for the development of new flight control concepts
[ONERA, TP NO. 1991-161] p 137 A92-16128
Concept for future cockpits p 118 A92-16148
Feeling normal --- evaluation of advanced control systems for future Boeing 777 p 134 A92-16623
Experimental evaluation of candidate graphical microburst alert displays
[AIAA PAPER 92-0292] p 369 A92-25745
Flight test of avionic and air-traffic control systems
[ETN-92-91063] p 640 N92-25590
ATTAS experimental cockpit and ATMOS for flight control components and systems investigations
p 641 N92-25595
Experimental evaluation of candidate graphical microburst alert displays
[NASA-CR-189633] p 735 N92-27424
Transport delay measurements: Methodology and analysis for the F-16C combat engagement trainer, the display for advanced research and training, and the F-16A limited field of view
[AD-A248519] p 888 N92-29505

COCKPITS
Cockpit distractions - Precursors to emergencies
p 16 A92-11178
A model for evaluation and training in aircrew coordination and cockpit resource management
p 46 A92-11191
Navy Aircrew Common Ejection Seat (NACES) program summary p 104 A92-13465
Tomorrow's cockpit displays p 117 A92-13699
MIDIS - A microcomputer flight decision simulator
p 136 A92-13845
Development of a reclined crashworthy crewseat for rotorcraft p 105 A92-14370
Integrated flight/propulsion control for flight critical applications - A propulsion system perspective
[ASME PAPER 91-GT-284] p 125 A92-15679
Helicopter NVG testing in the United Kingdom
p 112 A92-16053

The flight test pilot's display - A CRT system for test maneuvers p 118 A92-16057
Concept for future cockpits p 118 A92-16148
DARPA high resolution display technologies p 218 A92-19977
The cockpit of a modern aircraft - The Airbus A340 considered as an example p 357 A92-26849
Recent advances in restraint technology p 535 A92-32979
C-130 glass cockpit system development program [AIAA PAPER 92-1050] p 553 A92-33230
Display trends in aircraft cockpits p 734 A92-43217
A study of the pilot's associate system p 745 A92-43218
Current status and future tasks of a cockpit liquid crystal display p 735 A92-43222
Lessons learned about information management within the Pilot's Associate program p 916 A92-44909
Mode S data link pilot-system interface - A blessing in de skies or a beast of burden? p 839 A92-44920
Who or what saved the day? A comparison of traditional and glass cockpits p 833 A92-44931
Empirical foundations and sensitivity testing - Is it enough for the 90's? p 835 A92-45054
A340 handling, cockpit design improve on predecessor A320 p 849 A92-47969
Artificial intelligence in the helicopter cockpit of the future p 964 A92-49271
MLS/RNAV control display unit development p 965 A92-49303
Extreme wide field-of-view displays and the enclosed cockpit p 965 A92-49313
Cockpit crew research p 951 A92-51440
Design method of a helicopter cockpit p 1058 A92-56337
Identification of high-level functional/system requirements for future civil transports [NASA-CR-189561] p 276 N92-15991
AGSSS: The Airborne Graphics Software Support System; an Ada/PHIGS-based display editor for the rapid development of cockpit display software systems [AD-A243224] p 277 N92-17221
Assessment of cockpit interface concepts for data link retrofit [NASA-CR-187615] p 268 N92-17512
Alert generation and cockpit presentation for an integrated microburst alerting system p 265 N92-17988
An evaluation of four F-16 vertical velocity indicator configurations [AD-A243629] p 370 N92-18014
An exploration of function analysis and function allocation in the commercial flight domain [NASA-CR-4374] p 368 N92-19871
Activities of NRC-CNRC, Institute for Aerospace Research, Flight Research Lab. [CTN-92-60432] p 420 N92-20205
The Flight Simulation Facility at the Wichita State University p 484 N92-21511
Knowledge-based planning for controlled airspace flight operation as part of a cockpit assistant p 727 N92-27895
Use of a virtual cockpit for the development of a future transport aircraft p 886 N92-28547
Effects of cockpit lateral stick characteristics on handling qualities and pilot dynamics [NASA-CR-4443] p 878 N92-28584
Tasking and communication flows in the F/A-18D cockpit: Issues, problems, and possible solutions [AD-A245977] p 853 N92-28802
High speed research system study. Advanced flight deck configuration effects [NASA-CR-189650] p 967 N92-30965

CODE DIVISION MULTIPLE ACCESS
Code Division Multiple Access (CDMA) system candidate for integrated modular avionics p 725 A92-42604

COEFFICIENT OF FRICTION
Fretting fatigue p 672 A92-38225
Wall functions for the kappa-epsilon turbulence model in generalized nonorthogonal curvilinear coordinates [NASA-CR-190368] p 685 N92-25962

COEFFICIENTS
Determination of rotordynamic coefficients for labyrinth seals and application to rotordynamic design calculations p 223 N92-14360
Computation of aerodynamic coefficients on Hermes-Ariane5 configuration p 184 N92-15040
A semi empirical method for the analytical representation of stationary measured profile coefficients for applications of rotary wing aerodynamics [ETN-92-91491] p 832 N92-29741

COGNITION
Introduction to cognitive processes of expert pilots [DOT/FAA/RD-92/12] p 952 N92-30980
Workshop on Aeronautical Decision Making (ADM). Volume 1: Executive summary [DOT/FAA/RD-92/14-VOL-1] p 1142 N92-33305

COGNITIVE PSYCHOLOGY
A cognitive temporal model for the planning in aircraft maintenance p 307 A92-25178

COHERENT RADAR
Bistatic scattering on a monostatic radar range p 849 A92-48408

COLD FLOW TESTS
Effect of carbon particles and mixing on afterburning of exhaust plumes [AIAA PAPER 92-0767] p 387 A92-27107
Experimental study of a two-dimensional scramjet inset, M(freestream) = 10.1-25.1 p 611 A92-36974
Scale model test results of a multi-slotted vectoring 2DCD ejector nozzle [AIAA PAPER 92-3264] p 864 A92-48859
Test description and preliminary pitot-pressure surveys for Langley Test Technique Demonstrator at Mach 6 [AIAA PAPER 92-3940] p 1096 A92-56770
Viscous computations of cold air/air flow around scramjet nozzle afterbody [NASA-CR-4406] p 13 N92-10982

COLD FRONTS
Mesoscale dynamics of cold fronts - Structures described by dropsoundings in Fronts 87 p 230 A92-18902

COLD ROLLING
Rolling in the tolerance p 216 A92-18005

COLD SURFACES
Experimental studies of hypersonic shock-wave boundary-layer interactions [NASA-CR-190731] p 950 N92-32162

COLD WEATHER
Aircraft ground deicing [SAE PAPER 912222] p 635 A92-40021

COLLIMATION
Antenna pattern measurement facilities [AD-A248964] p 982 N92-30329

COLLISION AVOIDANCE
TCAS in the 1990s --- Traffic alert and Collision Avoidance System p 98 A92-16657
Potential impact of GPS and automatic dependent surveillance on air lane separation in the North Atlantic Organized Track System p 99 A92-16935
Z-Basic algorithm for collision avoidance system p 188 A92-18482
The avoidance of collisions for Newtonian bodies with hidden variables p 353 A92-24945
European studies to investigate the feasibility of using 1000 ft vertical separation minima above FL 290. II - Precision radar data analysis and collision risk assessment p 353 A92-24946
The real TCAS --- traffic alert and collision avoidance system p 350 A92-25521
Heterodyne techniques in the I.R. bandwidth for laser obstacle detection p 533 A92-35740
The obstacle avoidance radar - A safety mean for low altitude flights in adverse weather conditions p 554 A92-35743
Maximum-miss aircraft collision avoidance p 660 A92-37077
Code Division Multiple Access (CDMA) system candidate for integrated modular avionics p 725 A92-42604
Introduction to the traffic alert and collision avoidance system (TCAS) III p 734 A92-43150
The traffic alert and collision avoidance system (TCAS) for air navigation p 734 A92-43151
Collision probability estimate method for impact generated low earth orbit space debris clouds [AAS PAPER 91-369] p 752 A92-43269
Use of high-fidelity simulation in the development of an F/A-18 active ground collision avoidance system [AIAA PAPER 92-4140] p 959 A92-52434
Midair collision - The links in a chain p 951 A92-52645
Height keeping performance requirements for reducing vertical separation minima used for air traffic control p 1046 A92-56081
Air-to-air visual acquisition handbook [ATC-151] p 93 N92-13042
Validation and verification flight test for TCAS-2 logic changes (MOPS Change 6) [DOT/FAA/CT-TN91/46] p 268 N92-15981
Ground collision avoidance using a variable incidence altitude measurement system for the A-7 aircraft [AD-A243880] p 352 N92-19259
UK airmisses involving commercial air transport: September - December 1990 [ETN-92-91050] p 452 N92-21746
Use of high-fidelity simulation in the development of an F/A-18 active ground collision avoidance system p 837 N92-28530
A cable detection lidar system for helicopters p 1001 N92-31068
Safety study of TCAS 2 for logic version 6.04 [DOT/FAA/RD-92/22] p 1047 N92-32537
Simulation test and evaluation of TCAS 2 logic version 6.04 [DOT/FAA/RD-92/23] p 1048 N92-33098

COLLISIONS
Aircraft accident report: Northwest Airlines, Inc., Flights 1482 and 299. Runway incursion and collision, Detroit Metropolitan/Wayne County Airport, Romulus, Michigan, December 3, 1990 [PB91-910405] p 187 N92-14006
Aircraft accident report: Northwest Airlines, Inc., Flights 1482 and 299. Runway incursion and collision, Detroit Metropolitan/Wayne County Airport, Romulus, Michigan, December 3, 1990 [PB91-910405] p 264 N92-17213
Aircraft accident report: Runway collision of USAir Flight 1493, Boeing 737 and Skywest Flight 5569 Fairchild Metroliner, Los Angeles International Airport, Los Angeles, CA, February 1, 1991 [PB91-910409] p 530 N92-23596

COLLOCATION
An inviscid stability analysis of unbounded supersonic mixing layer flows p 443 N92-20332

COLOR INFRARED PHOTOGRAPHY
A high resolution multispectral video system p 587 A92-35479

COLORADO
Precipitation development in Colorado Front Range snowstorms - 15 November 1987 case study p 301 A92-23008

COLUMBIA (ORBITER)
Shuttle Infrared Leeside Temperature Sensing (SILTS) experiment - STS-35 and STS-40 preliminary results [AIAA PAPER 92-0126] p 286 A92-23746

COMBAT
Effectiveness of V-22 tiltrotors in support of land combat operations p 60 A92-14442
The development of a real time visual flight simulator for tactical operations research and measurement p 880 A92-45027
Verification and validation testing of the pilot's associate p 966 A92-49318
Generic helicopter for multiship simulations [AIAA PAPER 92-4151] p 959 A92-52442
Investigation of advanced aircraft performance measures of merit including new agility metrics [AD-A242016] p 272 N92-15990
ICAAS piloted simulation evaluation p 735 N92-27906
Transport delay measurements: Methodology and analysis for the F-16C combat engagement trainer, the display for advanced research and training, and the F-16A limited field of view [AD-A248519] p 888 N92-29505
DoD key technologies plan [AD-A253692] p 1142 N92-33238

COMBINED CYCLE POWER GENERATION
Influence of air liquefaction cycle on performance of combined cycle engine p 372 A92-24878
Japan pushes high speed research p 1015 A92-53434
H2 fueled flightweight ramjet construction and test p 475 N92-21531
System controls challenges of hypersonic combined-cycle engine powered vehicles p 475 N92-21533

COMBINED STRESS
Determination of the energy absorption of composite structures under combined loadings p 145 A92-14441
Combined compressive and shear buckling analysis of hypersonic aircraft sandwich panels [AIAA PAPER 92-2487] p 586 A92-34603
Structural optimization of a cantilevered beam subject to combined static loadings p 1118 A92-56024
Combined load test apparatus for flat panels [NASA-CASE-LAR-14698-1] p 911 N92-30028

COMBUSTIBLE FLOW
Simultaneous coherent anti-Stokes Raman spectroscopy measurements in hydrogen-fueled supersonic combustion p 287 A92-21052
The jet screen ignition scheme and its experimental verification p 388 A92-24744
UV laser spectroscopic measurements in jet engine combustion exit flows [AIAA PAPER 92-0513] p 396 A92-26939
Combustion instability related to vortex shedding in dump combustors and their passive control p 374 A92-27354
A numerical study of the effects of geometry on the performance of a supersonic combustor [AIAA PAPER 92-0624] p 342 A92-28213

Applications of an implicit, upwind Navier-Stokes code, CRAFT, to steady/unsteady reacting, multi-phase flowfields
[AIAA PAPER 92-0837] p 422 A92-29603
Diagonal implicit scheme for computing flows with finite rate chemistry p 488 A92-32253
On performance calculation of centrifugal dish atomizer combustor p 654 A92-37390
Second moment closure predictions of jet-on-jet impingement flows p 675 A92-40102
Numerical simulations of the transdetonative ram accelerator combusting flow field on a parallel computer
[AIAA PAPER 92-3249] p 894 A92-48848
Mixing and combustion effects in a sliding-wedge ram accelerator with hydrogen injection
[AIAA PAPER 92-3251] p 890 A92-48849
A numerical study of two-phase flow in gas turbine combustors
[AIAA PAPER 92-3468] p 905 A92-49015
A study of the flammability limit of the backward facing step flow combustion
[AIAA PAPER 92-3846] p 895 A92-49136
Experiments on the structure of an annular compressible reacting shear layer p 969 A92-50311
Instrumentation key to NASP combustor tests p 1092 A92-55100
Numerical simulation of the reactive flow in advanced (HSR) combustors using KIVA-2
[NASA-CR-188996] p 26 N92-11014
Laser based, non-intrusive measurement system for analysis of jet engine flows
[AD-A242398] p 279 N92-17011
Local extinction mechanisms in non-premixed turbulent combustion
[AD-A242027] p 290 N92-17682
Fractal image compression of Rayleigh, Raman, LIF and LDV data in turbulent reacting flows
[AD-A246960] p 767 N92-27352
Modelling the vaporiser and primary zone flows for a modern gas turbine combustion chamber p 742 N92-27484
Turbulent reacting flows and supersonic combustion
[AD-A251065] p 986 N92-30256
Contribution to the modelling of turbulent combustion in the case of stabilisation by flame-lock
[ESA-TT-1229] p 988 N92-31942
Theories of turbulent combustion in high speed flows
[AD-A253032] p 1111 N92-33624

COMBUSTION
Supersonic reacting internal flowfields p 155 A92-16989
Expansion tube experiments for the investigation of ram-accelerator-related combustion and gasdynamic problems
[AIAA PAPER 92-3246] p 904 A92-48845
Advanced nozzle and engine components test facility
[AIAA PAPER 92-3993] p 1099 A92-56816
Airplane crashes on the runway. Fine modeling of the behavior after burning of a frame submitted to linear crushing
[IMFL-90-64] p 353 N92-19350
Cryogenic hydrogen-induced air-liquefaction technologies for combined-cycle propulsion applications p 487 N92-21526
Experimental investigation of nozzle/plume aerodynamics at hypersonic speeds
[NASA-CR-190074] p 664 N92-25162
Development of natural gas rotary engines
[PB92-149665] p 765 N92-26816
A new unsteady mixing model to predict NO(x) production during rapid mixing in a dual-stage combustor
[NASA-CR-189155] p 971 N92-30569

COMBUSTION CHAMBERS
Numerical simulations of unsteady reactive flows in a combustion chamber p 39 A92-11761
Calculation of gas combustion regimes in a counterflow vortex chamber p 34 A92-12209
Isothermal flow fields in a research combustor for lean blowout studies
[ASME PAPER 91-GT-37] p 121 A92-15520
Reliability analysis of a structural ceramic combustion chamber
[ASME PAPER 91-GT-155] p 123 A92-15591
CFD analysis of jet mixing in low NO(x) flametube combustors
[ASME PAPER 91-GT-217] p 124 A92-15634
Weak extinction limits of large scale flameholders
[ASME PAPER 91-GT-234] p 125 A92-15643
Development and bench test of high-temperature combustion chamber with structural ceramic components
[ASME PAPER 91-GT-315] p 126 A92-15691
Development of T-100 multipurpose small power unit
[ASME PAPER 91-GT-327] p 153 A92-15697
Lean blowout in a research combustor at simulated low pressures
[ASME PAPER 91-GT-359] p 137 A92-15713
Low-frequency pressure oscillations in a model ramjet combustor p 154 A92-16026
Three-dimensional calculations of reactive flows in aircraft combustion chambers performed using two combustion models
[ONERA, TP NO. 1991-110] p 154 A92-16089
Lean low NO(x) combustion concept evaluation p 143 A92-16583
The role of primary jet injection on mixing in gas turbine combustion p 128 A92-16584
Active control for gas turbine combustors p 128 A92-16585
Isothermal modeling of gas turbine combustors - Computational study p 129 A92-17203
Hypersonic airbreathing propulsion activities for Saenger
[AIAA PAPER 91-5040] p 200 A92-17828
Evaluation of a bounded high-resolution scheme for combustor flow computations p 201 A92-20734
A computational investigation of mixing and reacting flows in supersonic combustors
[AIAA PAPER 92-0626] p 278 A92-23817
Numerical modelling for gas duct in tuboannular combustor p 371 A92-24738
Characterization of a two-phase flow field downstream of a 3x-scale gas turbine co-axial, counter-swirling, combustor dome swirl cup
[AIAA PAPER 92-0229] p 393 A92-25693
A new unsteady mixing model to predict NO(x) production during rapid mixing in a dual-stage combustor
[AIAA PAPER 92-0233] p 372 A92-25696
Two and three dimensional parabolized Navier-Stokes code for scramjet combustor, nozzle, and film cooling analysis
[AIAA PAPER 92-0391] p 372 A92-26247
CARS temperature measurements and validation of a computing code on a gas-turbine combustor
[ONERA, TP NO. 1991-224] p 373 A92-26376
A numerical study of secondary fuel injection techniques for active control of combustion instability in a ramjet
[AIAA PAPER 92-0777] p 374 A92-27114
Premixed, turbulent combustion of axisymmetric sudden expansion flows p 397 A92-27770
A numerical study of the effects of geometry on the performance of a supersonic combustor
[AIAA PAPER 92-0624] p 342 A92-28213
Numerical simulation of two incoming streams in a dual-combustion ramjet combustor p 375 A92-28419
An investigation on the characteristics of combustor with oblique air jet p 375 A92-28434
An improved computation for gas-turbine combustion chamber flow p 375 A92-28479
Flame sheet algorithm for use in numerical modeling of ramjet combustion instability p 390 A92-28503
Evaluation of parallel injector configurations for Mach 2 combustion p 376 A92-28533
Hydrocarbon-fueled scramjet combustor investigation p 376 A92-28535
Numerical analysis of techniques for efficient generation of vorticity in supersonic flows
[AIAA PAPER 92-0828] p 422 A92-29596
Experimental investigation on the mechanism of flame stabilization in afterburner with V-gutter flameholder p 487 A92-29725
Calculations of the dilution system in an annular gas turbine combustor p 494 A92-31164
Wide-range combustion chamber of ramjet
[AIAA PAPER 91-5094] p 472 A92-31696
Energy analysis of aeroengine and its significance p 557 A92-35569
Combustion research and design technology of aircraft engines p 558 A92-35915
Development trends of recent aircraft engines p 558 A92-35919
Similarity and scale effects in solid-fuel ramjet combustors p 666 A92-36965
On performance calculation of centrifugal dish atomizer combustor p 654 A92-37390
Influence of inlet conditions on the flowfield in a model gas turbine combustor p 672 A92-38866
LDV measurements of the flowfield in a simulated combustor with axial and side inlets p 672 A92-38867
Auxiliary power units for advanced fighters p 737 A92-43545
Flow establishment in a generic scramjet combustor p 737 A92-44525
Aerospace plane hydrogen scramjet boosting
[SAE PAPER 912071] p 891 A92-45451
Mixing in the dome region of a staged gas turbine combustor
[AIAA PAPER 92-3089] p 903 A92-48734
Experimental study of cross-stream mixing in a rectangular duct
[AIAA PAPER 92-3090] p 903 A92-48735
An experimental investigation of high-aspect-ratio cooling passages
[AIAA PAPER 92-3154] p 890 A92-48780
The influence of spray angle on the continuous- and discrete-phase flowfield downstream of an engine combustor swirl cup
[AIAA PAPER 92-3231] p 863 A92-48832
Numerical simulation of turbine 'hot spot' alleviation using film cooling
[AIAA PAPER 92-3309] p 904 A92-48896
Measurement of scalar flowfield at exit of combustor sector using Raman diagnostics
[AIAA PAPER 92-3350] p 894 A92-48927
A distributed vaporization time-lag model for gas turbine combustor dynamics
[AIAA PAPER 92-3465] p 865 A92-49014
A numerical study of two-phase flow in gas turbine combustors
[AIAA PAPER 92-3468] p 905 A92-49015
Prediction of gas turbine combustor flow by a finite element code
[AIAA PAPER 92-3469] p 906 A92-49016
Combustion of solid fueled ramjet. II
[AIAA PAPER 92-3728] p 894 A92-49106
Analytical design and demonstration of a low-cost expendable turbine engine combustor
[AIAA PAPER 92-3754] p 867 A92-49112
Numerical simulation of three-dimensional turbulent flows in combustion chambers p 970 A92-53276
Some thermodynamical aspects in the optimization of supersonic combustors p 1065 A92-53486
Detailed numerical analysis of standing oblique detonation p 1111 A92-53550
Applied analytical combustion/emissions research at the NASA Lewis Research Center - A progress report
[AIAA PAPER 92-3338] p 1067 A92-54025
The VRT gas turbine combustor - Phase II
[AIAA PAPER 92-3471] p 1067 A92-54035
Acoustic control of combustor primary zone air-jet mixing
[AIAA PAPER 92-3651] p 1067 A92-54104
Instrumentation key to NASP combustor tests p 1092 A92-55100
Combustion and core noise p 55 N92-10607
Numerical simulation of the reactive flow in advanced (HSR) combustors using KIVA-2
[NASA-CR-188996] p 26 N92-11014
An experimental and computational investigation of an annular reverse-flow combustor
[UTIAS-338] p 129 N92-11996
An experimental analysis of lateral jet injection into confined swirling crossflows p 156 N92-12199
High-temperature combustor and seal for a water piston propulsor
[AD-A242493] p 229 N92-15385
Redesign of flight space shuttle main engine nozzle G-15 seal area based on the thermal analysis and flow models p 212 N92-15877
Safety considerations in testing a fuel-rich aeropropulsion gas generator
[NASA-TM-105258] p 279 N92-17061
High-temperature durability considerations for HSCT combustor
[NASA-TP-3162] p 289 N92-17070
Local extinction mechanisms in non-premixed turbulent combustion
[AD-A242027] p 290 N92-17682
Hydrogen fueled subsonic-ram-combustor model tests for an air-turbo-ram engine
[NAL-TR-1064T] p 280 N92-17855
Optimization of tangential mass injection for minimizing flow separation in a scramjet inlet
[AD-A243868] p 376 N92-18867
Component-specific modeling --- jet engine hot section components
[NASA-CR-189088] p 377 N92-19726
Transport phenomena and interfacial kinetics in multiphase combustion systems
[AD-A244849] p 489 N92-20695
Inlet technology p 447 N92-21528
NASA's hypersonic propulsion program: History and direction p 476 N92-21535
Symposium on High Speed Airbreathing Propulsion: The Solid Fuel Combustion Chamber and Beyond
[ETN-92-90685] p 575 N92-22268
Aircraft engine hot section technology: An overview of the HOST Project p 561 N92-22535
Effects of chemical equilibrium on turbine engine performance for various fuels and combustor temperatures
[NASA-TM-105399] p 562 N92-23254
Turbocharged pressurized combustion system
[PB92-142579] p 756 N92-26521

A parametric numerical study of mixing in a cylindrical duct
[NASA-TM-105695] p 738 N92-26553
Modelling the vaporiser and primary zone flows for a modern gas turbine combustion chamber
p 742 N92-27484
Three dimensional calculations of reactive flows within aircraft combustion chambers including some combustion models p 770 N92-27490
Experimental study of cross-stream mixing in a rectangular duct
[NASA-TM-105694] p 742 N92-27652
An analysis of combustion studies in shock expansion tunnels and reflected shock tunnels
[NASA-TP-3224] p 895 N92-28374
Applied analytical combustion/emissions research at the NASA Lewis Research Center
[NASA-TM-105731] p 890 N92-29343
A new unsteady mixing model to predict NO(x) production during rapid mixing in a dual-stage combustor
[NASA-CR-189155] p 971 N92-30569
Laser-initiated conical detonation wave for supersonic combustion, part 3
[AD-A250522] p 989 N92-32076
The impact of air transport on the environment
[PNR-90876] p 1129 N92-33751

COMBUSTION CHEMISTRY
Weak extinction limits of large scale flameholders
[ASME PAPER 91-GT-234] p 125 A92-15643
Three-dimensional calculations of reactive flows in aircraft combustion chambers performed using two combustion models
[ONERA, TP NO. 1991-110] p 154 A92-16089
A numerical investigation of hydrogen combustion in Mach 2 flow
[AIAA PAPER 92-0341] p 388 A92-25787
Evaluation of NO(x) mechanisms for lean, premixed combustion
[ASME PAPER 91-GT-257] p 668 A92-36900
Hypersonic mixing and combustion studies in the hypulse facility p 737 A92-44526
Interaction between chemical reaction and turbulence in supersonic nonpremixed H2-air combustion
p 1117 A92-54931
Transport phenomena and interfacial kinetics in multiphase combustion systems
[AD-A244849] p 489 N92-20695
DLR-News: Announcements of the German Research Institute for Aeronautics and Astronautics
p 698 N92-26086
Three dimensional calculations of reactive flows within aircraft combustion chambers including some combustion models p 770 N92-27490
An analysis of combustion studies in shock expansion tunnels and reflected shock tunnels
[NASA-TP-3224] p 895 N92-28374

COMBUSTION CONTROL
Lean low NO(x) combustion concept evaluation
p 143 A92-16583
Active control for gas turbine combustors
p 128 A92-16585
Combustion instability related to vortex shedding in dump combustors and their passive control
p 374 A92-27354
Dynamic simulation of a solid fuelled gas turbine system p 592 N92-22315
Shock enhancement and control of hypersonic combustion
[AD-A248558] p 896 N92-29580

COMBUSTION EFFICIENCY
An investigation of fuel nozzles for combustion performance p 278 A92-21745
A numerical study of isothermal flows of a slit V-gutter
[AIAA PAPER 92-0100] p 293 A92-22203
A new unsteady mixing model to predict NO(x) production during rapid mixing in a dual-stage combustor
[AIAA PAPER 92-0233] p 372 A92-25696
An experimental study of supersonic H2 combustion and heat transfer in a circular duct p 388 A92-25997
An investigation on the characteristics of combustor with oblique air jet p 375 A92-28434
Calculation of combustion efficiency of dump combustor in ramjet engine p 375 A92-28480
Wide-range combustion chamber of ramjet
[AIAA PAPER 91-5094] p 472 A92-31696
Swirl and fuel composition effects on boron combustion in solid-fuel ramjets p 668 A92-36964
Solid-fuel ramjet fuel regression rate/thrust modulation
p 666 A92-36966
Measurement of scalar flowfield at exit of combustor sector using Raman diagnostics
[AIAA PAPER 92-3350] p 894 A92-48927
A new vane swirler as applied to dual-inlet side-dump combustor
[AIAA PAPER 92-3654] p 906 A92-49085
A study of the flammability limit of the backward facing step flow combustion
[AIAA PAPER 92-3846] p 895 A92-49136
Hydrogen fueled subsonic-ram-combustor model tests for an air-turbo-ram engine
[NAL-TR-1064T] p 280 N92-17855
The coherent flamelet model for propulsion applications p 756 N92-27486
A new unsteady mixing model to predict NO(x) production during rapid mixing in a dual-stage combustor
[NASA-CR-189155] p 971 N92-30569

COMBUSTION PHYSICS
Renewed interest in pulsed engines may be linked to 'black' aircraft p 24 A92-10600
Engineering model for analysis of scramjet combustor performance with finite-rate chemistry
p 129 A92-17202
Effects of unsteady shock impingement on high-speed gaseous mixing
[AIAA PAPER 91-5091] p 172 A92-17857
Numerical simulation of interaction of diffusion flame with vortex pair in a recirculation zone p 390 A92-28433
A model of the operation of the pulsejet engine and a study of its characteristics p 657 A92-40608
Planar fluorescence imaging of a transverse jet in a supersonic crossflow p 755 A92-44501
Pulse jet one-way valve performance
[AIAA PAPER 92-3169] p 863 A92-48790
A distributed vaporization time-lag model for gas turbine combustor dynamics
[AIAA PAPER 92-3465] p 865 A92-49014
Combustion of solid fueled ramjet. I
[AIAA PAPER 92-3727] p 894 A92-49105
Combustion and core noise p 55 N92-10607
Local extinction mechanisms in non-premixed turbulent combustion
[AD-A242027] p 290 N92-17682
Aircraft engine hot section technology: An overview of the HOST Project p 561 N92-22535
A two-stroke diesel engine simulation program
[NASA-CR-185155] p 562 N92-22647
Three-dimensional modeling of diesel engine intake flow, combustion and emissions
[NASA-CR-189126] p 658 N92-24539
Computational method to predict thermodynamic, transport, and flow properties for the modified Langley 8-foot high-temperature tunnel
[NASA-TM-4374] p 767 N92-27193
An analysis of combustion studies in shock expansion tunnels and reflected shock tunnels
[NASA-TP-3224] p 895 N92-28374
A new unsteady mixing model to predict NO(x) production during rapid mixing in a dual-stage combustor
[NASA-CR-189155] p 971 N92-30569
Collection of papers of the 31st Israel Annual Conference on Aviation and Astronautics
[ITN-92-85124] p 932 N92-31861
Contribution to the modelling of turbulent combustion in the case of stabilisation by flame-lock
[ESA-TT-1229] p 988 N92-31942

COMBUSTION PRODUCTS
Flammability, smoke and toxic gas combustion products of composites used in aircraft cabins p 14 A92-10257
Carcinogenic hydrocarbons emission with gas-turbine engines exhaust gases p 504 A92-29726
Nonstationary gasdynamics p 220 N92-13985
Natural cycles, gases p 408 N92-19123
Three-dimensional modeling of diesel engine intake flow, combustion and emissions
[NASA-CR-189126] p 658 N92-24539

COMBUSTION STABILITY
Low-frequency pressure oscillations in a model ramjet combustor p 154 A92-16026
One-dimensional analysis of liquid-fueled combustion instability p 143 A92-17188
An experimental study of supersonic H2 combustion and heat transfer in a circular duct p 388 A92-25997
A numerical study of secondary fuel injection techniques for active control of combustion instability in a ramjet
[AIAA PAPER 92-0777] p 374 A92-27114
Combustion instability related to vortex shedding in dump combustors and their passive control
p 374 A92-27354
An experimental investigation of the swirling combustor for integral liquid fuel ramjet p 557 A92-35541
Acoustic control of combustor primary zone air-jet mixing
[AIAA PAPER 92-3651] p 1067 A92-54104
Dynamic simulation of a solid fuelled gas turbine system p 592 N92-22315

COMBUSTION TEMPERATURE
Simultaneous coherent anti-Stokes Raman spectroscopy measurements in hydrogen-fueled supersonic combustion p 287 A92-21052
Wind tunnel study of aerodynamic characteristics of base combustion p 666 A92-36967
Hydrogen fueled subsonic-ram-combustor model tests for an air-turbo-ram engine
[NAL-TR-1064T] p 280 N92-17855

COMMAND AND CONTROL
Developments in airborne surveillance and control systems p 98 A92-16655
Multisensor data fusion and decision support for airborne target identification p 454 A92-31063
Gulf Range Drone Control Upgrade System Mobile Control System p 882 A92-47567
Information Management Engineering (IME) laboratory: A database development facility
[AD-A243191] p 305 N92-17369
DRES unmanned aerial vehicle data link research
[AD-A244272] p 365 N92-19030
SIMNET plan view display user manual
[AD-A244617] p 510 N92-21392

COMMAND GUIDANCE
Control concept for maneuvering in hypersonic flight
[AIAA PAPER 91-5055] p 203 A92-17838
Global Positioning System telecommand link
p 839 A92-47566

COMMERCIAL AIRCRAFT
Dornier Do.328 special - Examining the high-speed commuter p 21 A92-11882
Maximum mass allowance to justify passenger-carrying aircraft modification p 113 A92-16802
The TSE 310 troubleshooting expert prototype for the Airbus A-310 commercial aircraft p 307 A92-25180
Fleet modernization - One approach
p 307 A92-25371
ARINC and commercial aircraft avionics. I
p 353 A92-25655
Supersonic nozzle mixer ejector p 376 A92-28536
Commercial airplane air distribution system development through the use of computational fluid dynamics
[AIAA PAPER 92-0987] p 535 A92-33182
Study of materials and structures for the High-Speed Civil Transport
[AIAA PAPER 92-1080] p 536 A92-33249
Design for the relief of thermal stresses in a large high-speed wing
[AIAA PAPER 92-1082] p 536 A92-33250
New processes in commercial airplane design
p 607 A92-38218
Assurance of safety in the aging aircraft fleet
p 635 A92-39305
ELS pilot evaluation --- Electronic Library System
[SAE PAPER 912107] p 691 A92-39960
Auxiliary power system requirements for commercial air transports - Past, present and future
[SAE PAPER 912188] p 656 A92-40007
Secondary power system preliminary design
[SAE PAPER 912189] p 656 A92-40008
Aging aircraft and structural airworthiness
[SAE PAPER 912212] p 635 A92-40016
MD-11 status report p 646 A92-40040
A criterion for estimating the economic and operational efficiency of the power distribution systems of commercial aircraft p 657 A92-40611
Simulation of commercial-aircraft reliability
p 759 A92-42057
RFI effects analysis of an airport-installed HF transmitter on aircraft COMM/NAV receivers p 725 A92-42313
Development of fly-by-light systems for commercial aircraft p 744 A92-42605
The 1991 Cierva Lecture - Aberdeen and its influence on the evolution of the commercial IFR twin engined helicopter p 723 A92-43446
EICAS in an integrated cockpit --- Engine Indication Crew Alerting System p 855 A92-44922
Avionics flight systems for the 21st century
[SAE PAPER 912033] p 784 A92-45421
Aircraft Command in Emergency Situations (ACES)
[SAE PAPER 912039] p 835 A92-45424
Airbus A319 - Completion of the standard fuselage family p 848 A92-47591
Modular avionics - A commercial perspective
p 858 A92-48427
Digital flight control systems - Some new commercial twists p 974 A92-49264
Are we doing HIRF testing sensibly? --- avionics certification in commercial aircraft p 931 A92-49305
Critical digital systems - A fly-by-light consideration
p 974 A92-49324
A low maintenance and highly reliable fly-by-light architecture p 975 A92-49325
Aging aircraft and airworthiness p 931 A92-51399
The challenge of commercial aircraft survivability
p 931 A92-52022
Silent solutions --- noise suppression for Stage 3 corporate fleets p 970 A92-53120
Air transports in the 21st century
p 1015 A92-55103

The application of direct transcription to commercial aircraft trajectory optimization
[AIAA PAPER 92-4528] p 1077 A92-55246
Research needs for a commercial passenger tiltrotor
p 1056 A92-56298
High Reynolds number testing in support of transport airplane development
[AIAA PAPER 92-3982] p 1099 A92-56807
High-lift testing at high Reynolds numbers
[AIAA PAPER 92-3986] p 1033 A92-56810
Buffet test in the National Transonic Facility
[AIAA PAPER 92-4032] p 1100 A92-56854
A comparison between the consequences of the liberal and non-liberal UK-Europe bilaterals
[TT-9101] p 18 N92-10018
Program plan: National aging aircraft research program
[DOT/FAA/CT-88/32-1] p 18 N92-10992
Parameter identification studies on the NASA/Ames Research Center Advanced Concepts Flight Simulator
[NASA-TM-105126] p 31 N92-11024
Winds of change: Domestic air transport since deregulation
[NRC-SR-230] p 92 N92-13040
Development of an annoyance model based upon elementary auditory sensations for steady-state aircraft interior noise containing tonal components
[NASA-TM-104147] p 166 N92-13758
Background issues for on-line aircraft documentation
p 119 N92-13858
International aviation (selected article)
[AD-A240986] p 170 N92-13991
Quiet aircraft design and operational characteristics
p 236 N92-14787
Identification of high-level functional/system requirements for future civil transports
[NASA-CR-189561] p 276 N92-15991
Aircraft accident report: Northwest Airlines, Inc., Flights 1482 and 299. Runway incursion and collision, Detroit Metropolitan/Wayne County Airport, Romulus, Michigan, December 3, 1990
[PB91-910405] p 264 N92-17213
Discussion for possibility of some aerodynamic ground effect craft
[NAL-TM-619] p 300 N92-17757
Structural airworthiness of aging Boeing jet transports
p 362 N92-18590
Designing a methodology for future air travel scenarios p 409 N92-19125
Ozone response to aircraft emissions: Sensitivity studies with two-dimensional models p 409 N92-19126
Annoyance caused by aircraft en route noise
[NASA-TP-3165] p 512 N92-20479
UK airmisses involving commercial air transport: September - December 1990
[ETN-92-91050] p 452 N92-21746
Effects of turbine cooling assumptions on performance and sizing of high-speed civil transport
[NASA-TM-105610] p 562 N92-23537
World commercial aircraft accidents: 1st edition, 1946-1991
[DE92-009801] p 636 N92-24713
Tilt rotors and the Port Authority of New York and New Jersey Airport System
[RAND-R-3971/1-PA-SUMM] p 636 N92-25262
Structural analysis for preliminary design of High Speed Civil Transport (HSCT) p 684 N92-25926
Application of integrated structural analysis to the high speed civil transport p 684 N92-25927
Gamma Group-The Pale Horse: A proposal in response to a commercial air transportation study ort study
[NASA-CR-190019] p 731 N92-26435
Drag reduction: An industrial challenge
p 717 N92-27708
Generation of spectra and stress histories for fatigue and damage tolerance analysis of fuselage repairs
[AD-A250390] p 854 N92-29180
FAA aviation forecasts
[AD-A250412] p 837 N92-29182
Structural integrity of future aging airplanes
p 913 N92-30107
Fracture mechanics research at NASA related to the aging commercial transport fleet p 913 N92-30110
Status of the FAA flight loads monitoring program
p 914 N92-30113
Nondestructive inspection perspectives
p 915 N92-30121
Statistics on aircraft gas turbine engine rotor failures that occurred in US commercial aviation during 1989
[DOT/FAA/CT-92/5] p 971 N92-30303
Aviation safety: Changes needed in FAA's service difficulty reporting program
[GAO/RCED-91-24] p 953 N92-31453
Aviation noise: Costs of phasing out noisy aircraft
[GAO/RCED-91-128] p 1011 N92-31454
Aircraft accident report: L'Express Airlines, Inc., Flight 508, Beech C99, N7217L weather encounter and crash near Birmingham, Alabama, July 10, 1991
[PB92-910401] p 1043 N92-32455
Fly-by-light technology development plan
[NASA-CR-181954] p 1086 N92-32778
Flight service environmental effects on composite materials and structures p 1110 N92-33054
Statistics on aircraft gas turbine engine rotor failures that occurred in US commercial aviation during 1988
[DOT/FAA/CT-91/28] p 1071 N92-33105
Study objectives: Will commercial avionics do the job? Improvements needed? p 1065 N92-33340
Current nondestructive inspection methods for aging aircraft
[DOT/FAA/CT-91/5] p 1126 N92-33480
The Rolls-Royce Trent
[PNR-90875] p 1061 N92-33750
Advanced subsonic transport approach noise: The relative contribution of airframe noise
[NASA-TM-104112] p 1140 N92-34148

COMMERCIAL SPACECRAFT
Crew transportation for the 1990s. I - Commercializing manned flight with today's propulsion
p 889 A92-46726

COMMONALITY
Common airborne instrumentation system (CAIS) --- time-division multiplexed data acquisition system
p 856 A92-47538

COMMUNICATING
Communication: An important element of maintenance and repair p 838 N92-30124

COMMUNICATION CABLES
Numerical modeling technique for field-to-cable coupling through advanced composite material
p 146 A92-14684

COMMUNICATION EQUIPMENT
Engineering Graphical Analysis Tool (EGAT) development program p 164 N92-12542
General maintenance handbook for airway facilities
[PB92-147586] p 640 N92-25518
Mid-range UV communications --- ultraviolet radiation
[AD-D015213] p 770 N92-27615
DoD key technologies plan
[AD-A253692] p 1142 N92-33238

COMMUNICATION NETWORKS
A prelude to interoperability - Comments on the lack of Federal Radionavigation Plan procedures for assessing the potential of a candidate system to fit into the mix of domestic radionavigation systems p 97 A92-16651
CATMAC - A way to integrate ground ATC and airborne systems p 531 A92-33429
Using satellite communication for aircraft Automatic Dependent Surveillance p 725 A92-42486
Feasibility study on a microwave-powered unmanned aerial vehicle for the communication relay utilization
[SAE PAPER 912052] p 843 A92-45436
Capacity as a consideration for providing aeronautical mobile satellite air traffic services in the U.S. domestic airspace p 956 A92-51007
Aeronautical satellite communications system
p 1046 A92-56089
Aircraft satellite communication systems
p 1046 A92-56091
Revolution at sea: Aircraft options for the year 2030
p 466 N92-21974
Technical feasibility of digital three-dimensional cellular communications for air traffic control applications. Volume 1: Introduction and summary
[AD-A244573] p 534 N92-22104
Technical feasibility of digital three-dimensional cellular communications for air traffic control applications. Volume 2: Example system design details
[AD-A244574] p 534 N92-22105
Technical feasibility of digital three-dimensional cellular communications for air traffic control applications. Volume 3: Ground network architecture
[AD-A244575] p 534 N92-22106
Evaluating the use of satellite communications in the government of Canada p 594 N92-22577
System considerations, projected requirements and applications for aeronautical mobile satellite communications for air traffic services
p 677 N92-24163
Aeronautical mobile satellite service: Air traffic control applications p 677 N92-24164
Future developments in aeronautical satellite communications p 678 N92-24167
An aircraft Earth station for general aviation
p 678 N92-24194
Current activities and future plans for GPS applications p 640 N92-24735
Proceedings of the Workshop on Advanced Network and Technology Concepts for Mobile, Micro, and Personal Communications
[NASA-CR-190459] p 1000 N92-30923
GNAS Maintenance Control Center (GMCC) Design Qualification Test and Evaluation (DOT/E) test report
[DOT/FAA/CT-TN91/39] p 932 N92-31615

COMMUNICATION SATELLITES
Low earth orbit satellite concepts for air traffic control applications
[AIAA PAPER 92-1927] p 453 A92-29856
Growing need to replace ILS can best be met by MLS
p 534 A92-36124
Capacity as a consideration for providing aeronautical mobile satellite air traffic services in the U.S. domestic airspace p 956 A92-51007
SATCOM antenna siting study on P-3C aircraft, volume 1
[NASA-CR-189514] p 221 N92-14262
Flight test of ARINC 741 configuration low gain SATCOM system on Boeing 747-400 aircraft p 677 N92-24097
Description and simulation results of the Italsat AOCS advanced flight simulator p 667 N92-24472
Proceedings of the Workshop on Advanced Network and Technology Concepts for Mobile, Micro, and Personal Communications
[NASA-CR-190459] p 1000 N92-30923
Decision-making guide for the proposed Coast Guard differential global positioning system
[AD-A246046] p 957 N92-32054

COMMUNICATION THEORY
Improving the LAMP Mk 3 SH-60B HF communication system
[AD-A245970] p 910 N92-29344

COMMUNITIES
Some experiences with community response to low levels of aircraft noise p 689 A92-39235
Reducing environmental noise impacts: A USAREUR noise management program handbook
[AD-A240797] p 237 N92-14791

COMMUTER AIRCRAFT
Dornier Do.328 special - Examining the high-speed commuter p 21 A92-11882
Lightning protection for the Dornier 328
p 113 A92-17253
Interior noise reduction program for the Dornier 328
p 114 A92-17254
On-board data acquisition system for Embraer's CBA123 p 198 A92-19251
Dornier 328 - A Daimler for commuters
p 458 A92-30091
Summary of Dornier 328 interior noise control study
p 643 A92-39083
Coupled propeller contributions to aircraft noise and vibration p 694 A92-39085
The FM-007: An advanced jet commuter for HUB to spoke transportation
[NASA-CR-189988] p 461 N92-20267
The Langley turbo-prop commuter design: A complete project description
[NASA-CR-189987] p 463 N92-21540
Damage tolerance for commuter aircraft
p 914 N92-30114

COMPARISON
Comparison of LDA and LTA applications for propeller tests in wind tunnels
[NLR-MP-88031-U] p 827 N92-28658

COMPATIBILITY
Development of a freejet capability for evaluating inlet-engine compatibility
[ASME PAPER 91-GT-401] p 137 A92-15731

COMPENSATORS
Design of compensators for linear parameter-varying feedback systems by the gain scheduling technique
p 507 A92-29101
Active vibration control using fixed order dynamic compensation with frequency shaped cost functionals
p 508 A92-29324

COMPETITION
A comparison between the consequences of the liberal and non-liberal UK-Europe bilaterals
[TT-9101] p 18 N92-10018
Winds of change: Domestic air transport since deregulation
[NRC-SR-230] p 92 N92-13040

COMPILERS
Process/object-oriented Ada software design for an experimental helicopter p 164 N92-12461
Parallel knowledge based systems architectures for in-flight mission management p 728 N92-27904

COMPLEX COMPOUNDS
Solid-vapor adsorption refrigeration system development
[PB92-164383] p 771 N92-27715

COMPLEX SYSTEMS
Applying advanced digital simulation techniques in designing fault tolerant systems p 921 A92-48489
State and time granularity in system description: An example
[REPT-91-040] p 603 N92-22673

COMPLEX VARIABLES
Complex variable boundary element method for external potential flows p 172 A92-18353
COMPONENT RELIABILITY
Malfunction/discrepancy reporting p 60 A92-14438
Transmission overhaul and component replacement predictions using Weibull and renewal theory p 155 A92-17201
Failure detection and identification for aircraft sensors p 370 A92-27832
Cost effectiveness of environmental stress screening (ESS) - A case history p 760 A92-42084
Advanced Rotorcraft Transmission program summary [AIAA PAPER 92-3363] p 905 A92-48936
An ultrareliable integrated digital computer for helicopters p 964 A92-49273
Liquid cooled approaches for high density avionics p 989 A92-49274
Progressive avionics packaging technologies p 989 A92-49276
The Office of Naval Research initiative on ultradependable multicomputers and electronic systems p 1005 A92-49278
JIAWG module fault coverage metrics methodology p 989 A92-49279
Damage tolerant design of critical aircraft structural components [AIAA PAPER 92-4041] p 1123 A92-56860
A sensitivity analysis on component reliability from fatigue life computations [AD-A247430] p 908 N92-28425
Component performance requirements p 869 N92-28462
Turbine aircraft engine operational trending and JT8D static component reliability study [DOT/FAA/CT-91/10] p 870 N92-28686
COMPOSITE MATERIALS
Flammability, smoke and toxic gas combustion products of composites used in aircraft cabins p 14 A92-10257
High temperature thermoplastic and polyimide processing using CARE-MOLD wash-out tooling p 36 A92-10259
Light metal materials for aircraft structure p 140 A92-13444
Continuation of the AHS round robin on fatigue reliability and damage tolerance p 59 A92-14341
Producibility Demonstrator Program - Technological preeminence through concurrent engineering p 146 A92-14449
Automated composite lay-up p 146 A92-14450
Metal fibers and fabrics as shielding materials for composites, missiles and airframes p 141 A92-14680
Numerical modeling technique for field-to-cable coupling through advanced composite material p 146 A92-14684
Optimization of the flutter load by material orientation p 146 A92-15222
Development and design with advanced materials --- Book [ISBN 0-444-88706-7] p 296 A92-24176
Fiber optic sensors for smart skins applications p 392 A92-24778
Composites usage on the RAH-66 Comanche p 457 A92-29669
Structures and materials technologies for hypersonic vehicles - Lessons from Hermes experience [AIAA PAPER 91-5098] p 486 A92-31697
Structural materials for NASP [AIAA PAPER 91-5101] p 486 A92-31698
Lifting surface design using the principle of passive control of elastic characteristics p 480 A92-31865
The first fifty years of composite materials in aircraft construction p 461 A92-32325
The initial development of an expert system for designing composite material wing structures p 599 A92-32542
Design, analysis, testing, and certification of composite primary structure for the Piaggio P-180 Avanti p 535 A92-32553
Design, analysis, and testing of integrally stiffened composite centre fuselage skin for future fighter aircraft p 535 A92-32554
Applications of composite material systems to avionic systems packaging p 576 A92-32564
Agile responsive effective support - Design and testing of the ARES concept demonstrator aircraft [AIAA PAPER 92-1038] p 536 A92-33219
Design of advanced composite components for maintainability based on inservice experience [AIAA PAPER 92-1085] p 537 A92-33251
The equations governing the motion of wing-aileron structural systems constructed from advanced anisotropic composite materials [AIAA PAPER 92-2469] p 564 A92-34359
Analysis, development, and integration of the mechanical components of a vehicle powered by photo-voltaic cells [TABES PAPER 91-503] p 606 A92-34692
Why composites wait in the wings p 577 A92-35475
Large-amplitude finite element flutter analysis of composite panels in hypersonic flow [AIAA PAPER 92-2130] p 589 A92-35697
Nonlinear flutter of orthotropic composite panel under aerodynamic heating [AIAA PAPER 92-2132] p 589 A92-35699
Experimenting a new composite rotor on an Aerospatiale Dauphin helicopter p 546 A92-35744
Aeroelastic tailoring analysis for advanced turbo propellers with composite blades p 558 A92-36358
Composite materials for aerospace applications p 577 A92-36377
Materials and structures for Hermes p 666 A92-38213
Active vibration control of smart structural materials p 673 A92-39281
Behavior of thin-walled beams made of advanced composite materials and incorporating non-classical effects p 673 A92-39944
1991-92 AHS Technical Committee highlights - Structures and materials p 609 A92-40397
Inspection of composite structures p 676 A92-40882
Composite material repairs to metallic airframe components p 699 A92-41237
Engineering and technology Japanese aircraft/spacecraft p 699 A92-41781
Composite makers sense changes p 754 A92-42345
Composite material stub-blade wing joint p 763 A92-44618
Stress field sensitivity of a composite patch repair as a result of varying patch thickness p 763 A92-44630
Dynamic analysis of rotor flex-structure based on nonlinear anisotropic shell models p 899 A92-46946
Composites in manufacturing - Case studies [ISBN 0-87263-406-X] p 784 A92-47403
The effect of composite material allowable changes on VTOL airframe weights p 848 A92-47629
Advanced experimental design applied to damage tolerance of composite materials p 993 A92-51505
Application of advanced composites in SEM-E heatsinks for the thermal management of avionics p 986 A92-51922
Structural optimization and vibration control of composite rotor blades p 960 A92-53056
A review of some computer programs of composites p 1009 A92-53069
Safety factor and reliability for composite laminates p 996 A92-53070
Design variables and constraint derivatives in aeroelastic tailoring p 997 A92-53074
New materials drive high-performance aircraft p 1105 A92-55134
Design and testing of a composite hingeless hub for rotary-wing aircraft p 1053 A92-56075
Application of automation for structural-composites production p 1119 A92-56109
State-of-the-art materials for future gas turbine engines p 1070 A92-56122
A proposed composite repair methodology for primary structure [NRC-LTR-ST-1658] p 115 N92-13056
The effect of physical aging on the creep response of a thermoplastic composite [AD-A243600] p 290 N92-17932
Design, analysis, and testing of integrally stiffened composite centre fuselage skin for future fighter aircraft [MBB-FE2-PUB-S-450] p 359 N92-18333
A guide for the consideration of composite material impacts on airframe costs [AD-A243928] p 417 N92-19466
Materials and process directions for advanced aero-engine design [PNR-90814] p 378 N92-19938
Computered tomography: Experimental data acquisition and parallelization of reconstruction algorithm [DE92-005151] p 499 N92-20301
The search for new materials [PNR-90777] p 490 N92-21744
Airframe life prediction p 649 N92-25931
Composite strength statistics from fiber strength statistics [AD-A245616] p 755 N92-26383
The effect of jet fuel exposure on advanced aerospace composites. Part 1: Thermal and chemical analysis [AD-A246559] p 756 N92-27531
Structural optimization of aircraft p 851 N92-28472
Mathematical optimization: A powerful tool for aircraft design p 851 N92-28474
The use of load enhancement factors in the certification of composite aircraft structures [NLR-TP-90068-U] p 852 N92-28649
Modeling and analysis methodology for aeroelastically tailored chordwise deformable wings [NASA-CR-189620] p 961 N92-30304
Low-velocity impact loading on fibre reinforced aluminum laminates (ARALL) and other aircraft sheet materials [ETN-92-91613] p 987 N92-30414
A demonstration of passive blade twist control using extension-twist coupling [NASA-TM-107642] p 1001 N92-31155
Advanced electromagnetic methods for aerospace vehicles [NASA-CR-190650] p 1001 N92-31156
Evaluation of composite components on the Bell 206L and Sikorsky S-76 helicopters p 1107 N92-32575
Supportability evaluation of thermoplastic and thermoset composites p 1108 N92-32576
PDES application protocol suite for composites (PAS-C). Functional needs report for the PAS-C program [AD-A247886] p 1108 N92-32629
Active control of sound transmission through stiff lightweight composite fuselage constructions p 1137 N92-32957
The Utilization of Advanced Composites in Military Aircraft [AGARD-R-785] p 1109 N92-33033
Aspects of compression in aerospace composites: Future requirements p 1109 N92-33036
Evaluation of the effects of the environment on the behavior of the primary structures of composite material aircraft in service: Historic and current situation p 1110 N92-33048
Fluid effects: Thermoset and thermoplastic matrix composites p 1110 N92-33049
Flight service environmental effects on composite materials and structures p 1110 N92-33054
Lightning strike tests of composite connectors [AD-A252281] p 1044 N92-33249
COMPOSITE PROPELLANTS
Solid fuel ramjet infrared signature [AD-A246299] p 753 N92-26362
COMPOSITE STRUCTURES
Three-dimensional finite-element analysis of interlaminar stresses in thick composite laminates p 39 A92-11791
Processing parameters for carbon/PMR-15 composite flat panels p 34 A92-11812
Mind that restyle --- failure analysis of aircraft composite structures p 91 A92-13700
Reliability of helicopter composite dynamic components p 145 A92-14344
The design and manufacture of an advanced thermoplastic horizontal stabilator for the AH-64A p 59 A92-14354
Flight service evaluation of composite helicopter components p 106 A92-14372
Enhanced diagnostic system for autoclaves and bonding presses p 145 A92-14381
Studying dynamic behavior of X380 helicopter equipped with a new 5-blade composite rotor p 108 A92-14398
Finite element correlation of the U.S. Army/BHTI ACAP composite airframe helicopter p 108 A92-14399
Determination of the energy absorption of composite structures under combined loadings p 145 A92-14441
Certifying composite helicopter structures p 110 A92-14443
Bearingless main rotor system composite component fabrication techniques p 110 A92-14453
Aeroelastic tailoring of aeronautical composite wing structures p 146 A92-15343
Status of the NH90 European Helicopter Program p 113 A92-16676
Experimental and theoretical analysis of composite I-beams with elastic couplings p 216 A92-18377
Experimental investigation of periodically excited rotating composite rotor blades p 218 A92-20213
Flutter analysis of anisotropic panels with patched cracks p 219 A92-20216
An analysis of impact resistance of composite fan blade p 293 A92-22523
An analysis of impact resistance of composite blades for turbo-fan engines p 294 A92-23109
Nonlinear transient analysis of composite ATP blade model p 294 A92-23111
Static aeroelastic tailoring of composite aircraft swept wings modelled as thin-walled beam structures p 294 A92-23114
Development and design with advanced materials --- Book [ISBN 0-444-88706-7] p 296 A92-24176
Design and testing leading to certification of the Airbus A340 nose landing gear doors p 272 A92-24192
Weaving an aircraft p 392 A92-24911

Ultimate strength prediction of ASTM D - 3039 tensile specimens from acoustic emission amplitude data
[AIAA PAPER 92-0258] p 394 A92-25716
The detection of damage and the measurement of strain within composites by means of embedded optical fiber sensors p 491 A92-28669
New, unusual and nonclassical behavior of thin-walled composite structures p 580 A92-32746
Composite cylinder blast overpressure testing p 529 A92-32984
Damage tolerance and repair experience of composite structures
[AIAA PAPER 92-1256] p 515 A92-33339
A Rayleigh-Ritz design methodology for cutouts in composite structures
[AIAA PAPER 92-2278] p 582 A92-34297
Structural tailoring/analysis for hypersonic components - Executive system development
[AIAA PAPER 92-2471] p 583 A92-34360
Coupled 2D-3D finite element method for analysis of a skin panel with a discontinuous stiffener
[AIAA PAPER 92-2474] p 583 A92-34363
Dynamic response to time-dependent excitations of cantilevered aircraft wing structures modelled as thin-walled beams
[AIAA PAPER 92-2213] p 584 A92-34403
Nonlinear large amplitude aeroelastic behavior of composite rotor blades at large static deflection
[AIAA PAPER 92-2257] p 540 A92-34412
A new aeroelastic model for composite rotor blades with straight and swept tips
[AIAA PAPER 92-2259] p 541 A92-34414
Application of composite rotor blade stability analysis to extension-twist coupled blades
[AIAA PAPER 92-2254] p 564 A92-34479
Aeroelastic response and blade loads of a composite rotor in forward flight
[AIAA PAPER 92-2566] p 564 A92-34480
AIAA/ASME/ASCE/AHS/ASC Structures, Structural Dynamics and Materials Conference, 33rd, Dallas, TX, Apr. 13-15, 1992, Technical Papers. Pt. 5 - Design engineering/design optimization, materials, work-in-progress p 585 A92-34522
Crashworthiness of truncated composite cones under side loads p 590 A92-35746
A survey of composite structure technology at the Aerospatiale Helicopter Division p 546 A92-35754
Exploratory design studies of actively controlled wings using integrated multidisciplinary synthesis p 641 A92-36828
Inspection of composite structures p 676 A92-40882
The evolution from bonded F27 aircraft to Arall structures p 699 A92-41177
Technological excellence in honeycomb sandwich and composite structures for aerospace applications p 757 A92-41180
Helicopter aeroelastic stability and response - Current topics and future trends p 730 A92-43100
Aerodynamic characteristics of a high-speed composite airfoil p 712 A92-43231
Automation of composite material structure installation p 700 A92-43248
Analysis and testing of a composite sandwich shell horizontal tail p 755 A92-44617
Stress field sensitivity of a composite patch repair as a result of varying patch thickness p 763 A92-44630
Numerical simulation of impact resistance on composite blade p 738 A92-44734
An analysis of the effect of centrifugal force on the impact resistance of composite fan blades for turbo-fan engines
[SAE PAPER 912047] p 861 A92-45431
Finite elements analysis of flexural edge wave for composite fan blades
[SAE PAPER 912048] p 861 A92-45432
Approach for analysis and design of composite rotor blades p 899 A92-46801
Filament winding of composite isogrid fuselage structures p 784 A92-47405
Design and test of aircraft aft fuselage structure using postbuckled shear panels p 848 A92-47406
Design and use of aramid fiber in aircraft structures p 784 A92-47407
Design of helicopter composite structures for crashworthiness p 848 A92-47408
Resin transfer molding of a complex composite aircraft structure p 784 A92-47410
Tooling for C-17 composite parts p 900 A92-47412
The role of nonmetallic fasteners in aircraft wings and other composite structures p 784 A92-47413
Use of adhesive bonded attachments for a composite aircraft fuel tank p 785 A92-47414
Advanced composite components in airline service status and repair p 785 A92-47416
A field repair of advanced helicopter vertical fin structure p 785 A92-47417
Moldless composite aircraft wing structural design modifications p 958 A92-51527
Development of composite structures with enhanced damage tolerance p 985 A92-51555
Manufacturing cost model for composites p 1012 A92-51565
Integral wing/fuel box p 958 A92-51569
Experimental investigation on flutter characteristics of composite torsion-box p 996 A92-53055
Damage tolerance and durability design of composite aircraft structures p 996 A92-53067
Study of dynamic strength on composite wing p 996 A92-53071
Fabrication test and evaluation of graphite/PMR-15 polyimide for HOPE primary structure p 1105 A92-53516
Computed tomography (CT) as a nondestructive test method used for composite helicopter components p 1121 A92-56276
Influence of cross section variations on the structural behaviour of composite rotor blades p 1121 A92-56320
Detailed analysis and test correlation of a stiffened composite wing panel p 1121 A92-56324
Composite blades for helicopter main and tail rotors developed by Mil Design Bureau p 1057 A92-56325
Transverse shear effect on flutter of composite panels p 1122 A92-56607
New insulation constructions for aerospace wiring applications. Volume 1: Testing and evaluation
[AD-A240638] p 22 N92-11006
Behavior of aircraft tire coupons under various loading conditions
[AD-A241416] p 116 N92-13063
Control augmented structural optimization of aeroelasticity tailored fiber composite wings
[AD-A241464] p 135 N92-13075
Detailed analysis and test correlation of a stiffened composite wing panel
[NASA-TM-104154] p 159 N92-13460
Universal weaving for turbine engine composite preforms
[AD-A237667] p 202 N92-14059
Rapid repair of integrally stiffened carbon fibre composite structures by bolted aluminium elements
[MBB-FE202-S-PUB-0453-A] p 290 N92-17310
Fatigue life behaviour of composite structures p 390 N92-18577
Analysis of lossy composite terminating structures
[NASA-CR-189901] p 404 N92-19217
Finite element analysis of a riveted repair on a curved composite panel
[AD-A243916] p 404 N92-19384
Tiltrotor research aircraft composite blade repairs: Lessons learned
[NASA-TM-103875] p 367 N92-19563
Integrated aerodynamic-structural-control wing design p 349 N92-19698
Optimization of composite sandwich cover panels subjected to compressive loadings
[NASA-TP-3173] p 489 N92-20679
Manufacturing development of pultruded composite panels
[NASA-CR-181780] p 578 N92-22637
RTM: Cost-effective processing of composite structures p 578 N92-22678
Coupled multi-disciplinary simulation of composite engine structures in propulsion environment
[NASA-TM-105575] p 596 N92-23267
Computer codes developed and under development at Lewis p 692 N92-25913
A brief overview of computational structures technology related activities at NASA Lewis Research Center p 683 N92-25915
Overview of mechanics of materials branch activities in the computational structures area p 684 N92-25917
Airframe life prediction p 649 N92-25931
Composite fuselage technology (summary of year 2)
[NASA-CR-190434] p 731 N92-26655
Computed Tomography (CT) as a nondestructive test method used for composite helicopter components
[MBB-UD-0603-91-PUB] p 910 N92-29873
Nonlinear analyses of composite aerospace structures in sonic fatigue
[NASA-CR-190565] p 854 N92-30209
Multidisciplinary optimization of fiber composite aircraft structures
[MBB/FW321/S/PUB/476] p 961 N92-30424
Organic Matrix Composite Helicopter Internal/External Cargo Pallet System (OMC INTEX)
[AD-A251127] p 961 N92-30878
Eighth DOD/NASA/FAA Conference on Fibrous Composites in Structural Design, part 1
[NASA-CP-3087-PT-1] p 1106 N92-32513
Design, evaluation and experimental effort toward development of a high strain composite wing for Navy aircraft p 1107 N92-32514
Development of thermoplastic components for structural validation p 1107 N92-32522
PDES application protocol suite for composites (PAS-C). Functional needs report for the PAS-C program
[AD-A247886] p 1108 N92-32629
Active control of sound transmission through stiff lightweight composite fuselage constructions p 1137 N92-32957
The Utilization of Advanced Composites in Military Aircraft
[AGARD-R-785] p 1109 N92-33033
Aspects of compression in aerospace composites: Future requirements p 1109 N92-33036
CFRP stiffened panels under compression p 1109 N92-33044
Evaluation of the effects of the environment on the behavior of the primary structures of composite material aircraft in service: Historic and current situation p 1110 N92-33048
Fluid effects: Thermoset and thermoplastic matrix composites p 1110 N92-33049
Flight service environmental effects on composite materials and structures p 1110 N92-33054
Computational methods for global/local analysis
[NASA-TM-107591] p 1125 N92-33104
Global/local interlaminar stress analysis of a grid-stiffened composite panel
[NASA-CR-190822] p 1125 N92-33139
Lightning strike tests of composite connectors
[AD-A252281] p 1044 N92-33249
Continuation of tailored composite structures of ordered staple thermoplastic material
[NASA-CR-189671] p 1110 N92-33613

COMPRESSED GAS

Composite cylinder blast overpressure testing p 529 A92-32984

COMPRESSIBILITY

Compressibility effects on the dynamic stall of a three-dimensional wing
[AIAA PAPER 92-0191] p 256 A92-23800
Compressibility effects on the growth and structure of homogeneous turbulent shear flow p 675 A92-40052
Turbulence modeling for hypersonic flight
[NASA-CR-190313] p 630 N92-24898
Natural flow wing
[NASA-CASE-LAR-14281-1] p 829 N92-28729
Turbulent spot generation and growth rates in a transonic boundary layer
[AD-A250221] p 909 N92-29118

COMPRESSIBILITY EFFECTS

Compressibility effects in thin channels with injection p 216 A92-18369
Leading edge velocity field of an oscillating airfoil in compressible dynamic stall
[AIAA PAPER 92-0193] p 257 A92-23802
A boundary element method for the potential, compressible aerodynamics of bodies in arbitrary motion p 314 A92-25098
Effect of compressibility on the value of the acceptable roughness Reynolds number p 427 A92-30197
Compressibility effects in turbulent far wakes p 622 A92-40140
Unsteady blade pressures on a propfan - Predicted and measured compressibility effects
[AIAA PAPER 92-3774] p 1023 A92-54161
An experimental study of the flow over a sharp-edged delta wing at subsonic and transonic speeds p 85 N92-13011
Control of unsteady separated flow associated with the dynamic stall of airfoils
[NASA-CR-190688] p 950 N92-32177
Numerical simulation of turbulence at the back of the airplane
[ETN-92-91664] p 1037 N92-32769
Theories of turbulent combustion in high speed flows
[AD-A253032] p 1111 N92-33624

COMPRESSIBLE BOUNDARY LAYER

A quiet-flow Ludwieg tube for experimental study of high speed boundary layer transition
[AIAA PAPER 91-5026] p 207 A92-17819
On the calculation of the compressible boundary layer on a nonplanar delta wing with supersonic leading edges p 252 A92-23409
A Navier-Stokes solver for stretched triangular grids
[AIAA PAPER 92-0183] p 256 A92-23793
Calculation of compressible boundary layer flow about airfoils by a finite element/finite difference method
[AIAA PAPER 92-0524] p 332 A92-26948
Compressible laminar boundary layers for perfect and real gases in equilibrium at Mach numbers to 30
[AIAA PAPER 92-0757] p 336 A92-27099
Evolution of perturbations in a supersonic boundary layer p 337 A92-27596

Secondary instability mechanisms in compressible, axisymmetric boundary layers
[AIAA PAPER 92-0743] p 343 A92-28224
Nonadiabatic and three-dimensional effects in compressible turbulent boundary layers
p 431 A92-31156
Secondary instabilities in compressible boundary layers p 435 A92-31639
Compressible turbulent boundary layers with heat addition by homogeneous condensation
p 611 A92-36843
The calculation of a compressible boundary layer past a pointed body and a delta wing p 622 A92-40173
Analysis of turbulence models for hypersonic boundary layers p 623 A92-40182
Numerical predictions of transonic viscous flows around aerofoils through an Euler/boundary layer interaction method p 624 A92-40600
Prediction of separation point in compressible turbulent boundary layers by Green's lag-entrainment method
p 700 A92-41178
Curvature effects for three-dimensional compressible boundary-layer stability p 701 A92-41207
Wake effects on the prediction of transonic viscous flows around airfoils p 702 A92-41232
The inviscid compressible Goertler problem in three-dimensional boundary layers p 809 A92-46441
The calculation of three-dimensional compressible boundary layer stability on swept wings
p 818 A92-47684
A fast, uncoupled, compressible, two-dimensional, unsteady boundary layer algorithm with separation for engine inlets
[AIAA PAPER 92-3082] p 823 A92-48729
An experimental examination of the effects of incoming boundary layer modifications on the dynamics of a turbulent compression corner interaction
[AIAA PAPER 92-3667] p 1022 A92-54111
A three-dimensional, compressible, laminar boundary-layer method for general fuselages. Volume 2: User's manual
[NASA-CR-4292-VOL-2] p 678 N92-24344
A three-dimensional, compressible, laminar boundary-layer method for general fuselages. Volume 1: Numerical method
[NASA-CR-4292-VOL-1] p 679 N92-24547
A fast, uncoupled, compressible, two-dimensional, unsteady boundary layer algorithm with separation for engine inlets
[NASA-TM-105686] p 770 N92-27653
Turbulent spot generation and growth rates in a transonic boundary layer
[AD-A250221] p 909 N92-29118
Methods for direct simulation of transition in hypersonic boundary layers 2 p 912 N92-30064

COMPRESSIBLE FLOW

Simple turbulence models for supersonic flows - Bodies at incidence and compression corners p 5 A92-11059
Inviscid spatial stability of a three-dimensional compressible mixing layer p 39 A92-11816
Euler flow predictions for an oscillating cascade using a high resolution wave-split scheme
[ASME PAPER 91-GT-198] p 74 A92-15623
Thermal details in a rotor-stator cavity at engine conditions with a mainstream
[ASME PAPER 91-GT-275] p 151 A92-15672
Turbulent flow calculations using unstructured and adaptive meshes p 153 A92-15823
Solution of the compressible Euler equations for steady flows around helicopter rotor blades by an implicit space-centered method
[ONERA, TP NO. 1991-177] p 77 A92-16139
Stability of a viscous compressible shear layer with a temperature drop p 79 A92-16684
Asymptotics of the upper branch of the neutral curve at subsonic and transonic external flow velocities
p 79 A92-16705
Analysis of transonic flow over plane compressor cascades using the large-particle method
p 79 A92-16812
Aerodynamic sensitivity analysis methods for the compressible Euler equations p 233 A92-19619
Sonic eddy - A model for compressible turbulence
p 176 A92-20739
Numerical investigation of supersonic mixed-compression inlet using an implicit upwind scheme p 243 A92-21073
A hot-wire anemometer in compressible subsonic flow
p 244 A92-21623
An assessment of particle velocimetry potential in hypersonic flow
[AIAA PAPER 92-0010] p 247 A92-22135
An efficient upwind relaxation-sweeping algorithm for three-dimensional Navier-Stokes equations
[AIAA PAPER 92-0023] p 248 A92-22145
Organized structure in a Mach 5/Mach 3 turbulent shear layer
[AIAA PAPER 92-0180] p 256 A92-23790
Transonic aeroelasticity analysis using state-space unsteady aerodynamic modeling p 310 A92-24422
A wave-model-based refinement criterion for adaptive-grid computation of compressible flows
[AIAA PAPER 92-0322] p 321 A92-25769
Direct computation of the sound from a compressible co-rotating vortex pair
[AIAA PAPER 92-0374] p 414 A92-26232
Predictions of compressible viscous flows at all Mach number using pressure correction, collocated primitive variables and non-orthogonal meshes
[AIAA PAPER 92-0426] p 326 A92-26274
Laser velocimetry seed particles within compressible, vortical flows p 395 A92-26413
Resonance of circular shock waves
p 395 A92-26795
Numerical simulation of total temperature separation in jets
[AIAA PAPER 92-0535] p 396 A92-26952
Transition to turbulence in confined, compressible mixing layers. I - 3D numerical simulations with excitation of random, broadband white noise
[AIAA PAPER 92-0553] p 332 A92-26964
Boundary singularities in steady potential compressible flow through plane two-dimensional channels
p 336 A92-27384
Three-dimensional compressible flows in turbo-machinery solved by the pseudostream function formulation p 338 A92-27801
Numerical experiments on a new class of nonoscillatory schemes
[AIAA PAPER 92-0421] p 341 A92-28193
A computational study of flow past bodies and heat transfer for isentropic compression flows
p 425 A92-30158
Numerical computation of compressible flow around an object of complex shape p 429 A92-30517
Semi-inverse marching characteristics scheme for supersonic flows p 432 A92-31187
Interference flows past cylinder-fin-sting-cavity assemblies p 442 A92-32236
Numerical studies of transverse curvature effects on transonic flow stability p 524 A92-36186
Evaluation of a finite volume method for compressible shear layers p 610 A92-36834
Similarity in supersonic mixing layers
p 611 A92-36842
High alpha aerodynamic control by tangential fuselage blowing p 611 A92-36848
A new finite element formulation for computational fluid dynamics. X - The compressible Euler and Navier-Stokes equations p 612 A92-37552
Performance of turbulence models to predict supersonic boundary layer flows p 613 A92-37553
Numerical simulation of separation flow on bodies of revolution at high angle of attack using Euler equations
p 616 A92-38919
Knowledge-based nonlinear boundary integral models of compressible viscous flows over arbitrary bodies - Taking CFD back to basics p 617 A92-39941
Simulation and modeling of homogeneous compressible turbulence under isotropic mean compression
p 622 A92-40134
Design and development of a compressible dynamic stall facility p 747 A92-41215
Design optimization of natural laminar flow bodies in compressible flow p 701 A92-41219
Visualization and analysis of hypersonic flows and comparison to experimental data
[AIAA PAPER 92-2774] p 704 A92-41320
Viscous simulation method for unsteady flows past multicomponent configurations p 714 A92-44671
Critical effects of downstream boundary conditions on vortex breakdown
[AIAA PAPER 92-2601] p 792 A92-45478
A nonlinear relaxation/quasi-Newton algorithm for the compressible Navier-Stokes equations
[AIAA PAPER 92-2643] p 796 A92-45510
Shock fitting with a finite volume approximation to the Euler equations
[AIAA PAPER 92-2646] p 796 A92-45513
Effect of throat contouring on two-dimensional converging-diverging nozzles using URS method
[AIAA PAPER 92-2659] p 797 A92-45520
Comparison of interferometric measurements with 3-D Euler computations for circular cones in supersonic flow
[AIAA PAPER 92-2691] p 800 A92-45538
Navier-Stokes analysis and experimental data comparison of compressible flow in a diffusing S-duct
[AIAA PAPER 92-2699] p 800 A92-45541
Transonic unsteady inviscid and viscous flow's simulation around 2-D moving bodies
[AIAA PAPER 92-2704] p 801 A92-45546
Parallel computing strategies for block multigrid implicit solution of the Euler equations p 812 A92-46894
Computation of turbulent, separated, unswept compression ramp interactions p 813 A92-46897
A new integral equation for potential compressible aerodynamics of rotors in forward flight
p 815 A92-46958
Unstructured and adaptive mesh generation for high Reynolds number viscous flows p 816 A92-47042
Anisotropic control of mesh generation based upon a Voronoi type method p 918 A92-47043
Grid generation and compressible flow computations about a high-speed civil transport configuration
p 919 A92-47055
A finite difference solution of the Euler equations on non-body-fitted Cartesian grids p 818 A92-47153
The numerical simulation of compressible flow around an airfoil at high angle of attack p 818 A92-47686
Numerical simulation of chemical and thermal nonequilibrium flows behind compression shocks
[AIAA PAPER 92-2879] p 820 A92-47860
Interface of an uncoupled boundary layer algorithm with an inviscid core flow algorithm for unsteady supersonic engine inlets
[AIAA PAPER 92-3083] p 823 A92-48730
Experiments on the enhancement of compressible mixing via streamwise vorticity. I - Optical measurements
[AIAA PAPER 92-3549] p 906 A92-49064
Improved artificial dissipation schemes for the Euler equations p 933 A92-49508
The simulation of inviscid, compressible flows using an upwind kinetic method on unstructured grids
p 933 A92-49515
A complete boundary integral formulation for steady compressible inviscid flows governed by nonlinear equations p 934 A92-50211
Effects of vortex generators on the growth of a compressible shear layer
[AIAA PAPER 90-1979] p 934 A92-50269
A general explicit or semi-explicit algorithm for compressible and incompressible flows
p 937 A92-52682
Experiments on separation at a compression corner in rarefied hypersonic flows p 938 A92-52755
An experimental investigation of the flow in a diffusing S-duct
[AIAA PAPER 92-3622] p 1021 A92-54090
Mach 3 wind tunnel test of mixed compression supersonic inlet
[AIAA PAPER 92-3625] p 1021 A92-54092
Assessment of compressibility corrections to the k-epsilon model in high-speed shear layers
p 1024 A92-54905
Measurements of turbulence in hypersonic flow
p 1092 A92-56005
A hypersonic wind tunnel test of a mixed-compression air inlet model p 1028 A92-56007
Wind tunnel test of M = 2.5 mixed compression inlet
p 1028 A92-56008
Perfect compressible two dimensional boundary layer strong fluid coupling in the case of sharp leading edge profiles. Unsteady case of isolated profiles and steady case of blade grids
[ONERA-RT-43/1621-RY-006-R] p 43 N92-11311
On the simulation of compressible turbulent flows past delta wing, delta wing-body and delta wing-canard
p 84 N92-13003
Evaluation of rotordynamic coefficients of look-through labyrinths by means of a three volume bulk flow model
p 223 N92-14356
Control of unsteady separated flow associated with the dynamic pitching of airfoils
[NASA-CR-189758] p 258 N92-15966
Resolution of the Euler equations applied to a helicopter rotor in forward flight
[ONERA-RSF-2/3731-AY-004A] p 406 N92-19976
A quantitative study of unsteady compressible flow on an oscillating airfoil
[AD-A244572] p 445 N92-21012
Laser velocimetry measurements of oscillating airfoil dynamic stall flow field
[AD-A244546] p 502 N92-21297
Three-dimensional compressible turbulent computations for a diffusing S-duct
[NASA-CR-4392] p 526 N92-22249
Modeling of linear isentropic flow systems
p 593 N92-22495
A compressible Navier-Stokes solver with two-equation and Reynolds stress turbulence closure models
[NASA-CR-4440] p 681 N92-25376
Wall functions for the kappa-epsilon turbulence model in generalized nonorthogonal curvilinear coordinates
[NASA-CR-190368] p 685 N92-25962

Interface of an uncoupled boundary layer algorithm with an inviscid core flow algorithm for unsteady supersonic engine inlets
[NASA-TM-105684] p 739 N92-27037
Turbulent mixing in supersonic jets
p 715 N92-27054
Presentation of a computational code for 3-D compressible flow in complex channels and cavities
p 769 N92-27475
The 3-D Navier-Stokes flow and temperature field computation for a forced mixer nozzle
p 770 N92-27482
Special Course on Unstructured Grid Methods for Advection Dominated Flows
[AGARD-R-787] p 771 N92-27671
Navier-Stokes analysis and experimental data comparison of compressible flow within ducts
[NASA-TM-105796] p 972 N92-30972
Automatic design of transonic airfoils to reduce the shock induced pressure drag p 949 N92-31863
Three-dimensional compressible turbulent computations for a nondiffusing S-duct
[NASA-CR-4391] p 951 N92-32240
User's manual for AeroFcn: A FORTRAN program to compute aerodynamic parameters
[NASA-TM-104237] p 1133 N92-32507
Navier-Stokes analysis and experimental data comparison of compressible flow in a diffusing S-duct
[NASA-TM-105683] p 1072 N92-33746

COMPRESSION LOADS
Coupled 2D-3D finite element method for analysis of a skin panel with a discontinuous stiffener
[AIAA PAPER 92-2474] p 583 A92-34363
Buckling, postbuckling and crippling of thin walled composite airframe structures under compression
p 899 A92-46940
Effects of elevated temperature on the viscoplastic modeling of graphite/polymeric composites
[NASA-TM-104160] p 35 N92-11149
Optimization of composite sandwich cover panels subjected to compressive loadings
[NASA-TP-3173] p 489 N92-20679
Natural flow wing
[NASA-CASE-LAR-14281-1] p 829 N92-28729
Apparatus for elevated temperature compression or tension testing of specimens
[NASA-CASE-LAR-14775-1] p 912 N92-30099
Initial postbuckling response of an unsymmetrically laminated rectangular plate p 1108 N92-32586
Aspects of compression in aerospace composites: Future requirements p 1109 N92-33036
CFRP stiffened panels under compression
p 1109 N92-33044

COMPRESSION RATIO
An estimate of the influence of the compressor stability margin on the thrust of a turbojet engine
p 654 A92-37424

COMPRESSION TESTS
Apparatus for elevated temperature compression or tension testing of specimens
[NASA-CASE-LAR-14775-1] p 912 N92-30099
The Utilization of Advanced Composites in Military Aircraft
[AGARD-R-785] p 1109 N92-33033
Aspects of compression in aerospace composites: Future requirements p 1109 N92-33036
CFRP stiffened panels under compression
p 1109 N92-33044

COMPRESSION WAVES
Wave engine aerothermodynamic design
[ASME PAPER 91-GT-4] p 120 A92-15502

COMPRESSIVE STRENGTH
Combined compressive and shear buckling analysis of hypersonic aircraft sandwich panels
[AIAA PAPER 92-2487] p 586 A92-34603
A method to determine propagation direction of compressive fracture in carbon-fibre composites
p 672 A92-38770
The Utilization of Advanced Composites in Military Aircraft
[AGARD-R-785] p 1109 N92-33033
Aspects of compression in aerospace composites: Future requirements p 1109 N92-33036

COMPRESSOR BLADES
Fracture analysis on compressor blades
p 37 A92-10672
Compressor coating effects on gas turbine engine performance p 25 A92-11282
Blade defect force investigation in a compressor cascade p 10 A92-13233
An improved method for aerodynamic design of centrifugal impeller blades
[ASME PAPER 91-GT-76] p 69 A92-15545
Computation of 3D flow phenomena in axial flow compressor blade rows
[ASME PAPER 91-GT-78] p 69 A92-15547
Unsteady viscous flow in a high speed core compressor
[ASME PAPER 91-GT-91] p 70 A92-15555
The influence of blade leaning on the performance of an integrated OGV-diffuser system
[ASME PAPER 91-GT-104] p 122 A92-15561
Three dimensional flow in a linear compressor cascade at design conditions
[ASME PAPER 91-GT-114] p 70 A92-15565
Similarity transformations for compressor blading
[ASME PAPER 91-GT-123] p 70 A92-15568
The effect of steady aerodynamic loading on the flutter stability of turbomachinery blading
[ASME PAPER 91-GT-130] p 71 A92-15574
The torsional stability of a compressor cascade
[ASME PAPER 91-GT-180] p 123 A92-15612
Performance improvements of compressor cascades by controlling the profile and sidewall boundary layers
[ASME PAPER 91-GT-260] p 75 A92-15662
Design and performance of advanced blading for a high-speed HP compressor
[ASME PAPER 91-GT-374] p 76 A92-15718
Detuning from the natural resonances of the blade in the computer-aided design of blade rows for axial-flow compressors p 80 A92-16818
Method for the prediction of supersonic compressor blade performance p 277 A92-21078
Applications of IMI 834 in aeroengines - A collaborative IMI/MTU programme p 288 A92-22754
Compressor blade row unsteady aerodynamic response to attached and separated flow forcing functions
[AIAA PAPER 92-0147] p 253 A92-23763
Validation of a 3D Navier-Stokes code on experimental compressor bladings
[ONERA, TP NO. 1991-229] p 330 A92-26381
The unresolved unsteady flow in multistage compressor blade rows p 421 A92-29472
Analysis of effects of freestream turbulence on cascade performance p 422 A92-29716
Calculation of 3D flow field in a single transonic compressor stage p 422 A92-29719
Studying method of measuring flow-field between stages in axial-flow compressor p 423 A92-29720
The selection of bird impact load types --- on turbojet compressor and turbofan fan blades
p 448 A92-29732
Research on damage tolerance of compressor blade
p 588 A92-35556
Experimental research on blade containment
p 557 A92-35561
Arbitrary blade section design based on viscous considerations - Blade optimization p 523 A92-36030
Unsteady Navier-Stokes simulation of turbulent flows through a supersonic compressor cascade
p 523 A92-36036
Secondary flow investigation inside the passage of a compressor cascade p 706 A92-42124
Possibility of increasing durability of blades with damages p 761 A92-42654
Advanced CFD simulation and testing of compressor blading in the multistage environment
[AIAA PAPER 92-3040] p 822 A92-48701
Wake mixing and performance measurements in a linear compressor cascade with crenulated trailing edges
[AIAA PAPER 92-3188] p 824 A92-48800
A Navier-Stokes analysis of a controlled-diffusion compressor cascade at increasing inlet-flow angles
[AIAA PAPER 92-3313] p 825 A92-48899
Supercritical blade design on stream surfaces of revolution with an inverse method p 220 N92-13950
Experimental investigation of the unsteady pressure field around an oscillating blade
[MITT-90-01] p 768 N92-27407
Application of S1BYL2 to the AGARD WG18 compressor test cases p 768 N92-27452
Examination of the main error factors with regards to secondary losses in compression and turbine cascades by variations of the blade picture ratio
[ETN-92-91493] p 871 N92-29927
Research on aero-thermodynamic distortion induced structural dynamic response of multistage compressor blading
[AD-A250865] p 974 N92-32059
An improved compressor performance prediction model
[PNR-90873] p 1072 N92-33749

COMPRESSOR EFFICIENCY
Experimental study of the swirling flow in the internal volute of a centrifugal compressor
[ASME PAPER 91-GT-7] p 67 A92-15505
Surge dynamics in a free-spool centrifugal compressor system
[ASME PAPER 91-GT-31] p 68 A92-15515
3-D loss prediction based on secondary flow and blade shear layer interaction
[ASME PAPER 91-GT-59] p 68 A92-15536
A viscous flow study of shock-boundary layer interaction, radial transport, and wake development in a transonic compressor
[ASME PAPER 91-GT-69] p 68 A92-15539
The efficiencies of single-stage centrifugal compressors for aircraft applications
[ASME PAPER 91-GT-77] p 122 A92-15546
Active suppression of rotating stall and surge in axial compressors
[ASME PAPER 91-GT-87] p 122 A92-15552
Active control of rotating stall in a low speed axial compressor
[ASME PAPER 91-GT-88] p 122 A92-15553
An investigation of a strong shock-wave turbulent boundary layer interaction in a supersonic compressor cascade
[ASME PAPER 91-GT-92] p 70 A92-15556
Design of a small axial compressor for high efficiency over a wide operating range
[ASME PAPER 91-GT-195] p 124 A92-15620
Performance improvements of compressor cascades by controlling the profile and sidewall boundary layers
[ASME PAPER 91-GT-260] p 75 A92-15662
An estimate of the influence of the compressor stability margin on the pick-up time of a turbojet engine
p 654 A92-37423
An estimate of the influence of the compressor stability margin on the thrust of a turbojet engine
p 654 A92-37424
Steady and transient performance calculation method for prediction, analysis, and identification
p 869 N92-28461

COMPRESSOR ROTORS
Inspection of compressor discs by ultrasonic leaky waves using an automated C-scan system
p 144 A92-13584
Quasi-three-dimensional characteristics method for a supersonic compressor rotor
[ASME PAPER 91-GT-81] p 69 A92-15549
Numerical prediction of wakes in cascades and compressor rotors including the effects of mixing. I - Cascade wakes including the effects of incidence and freestream turbulence
[ASME PAPER 91-GT-225] p 74 A92-15638
Numerical prediction of wakes in cascades and compressor rotors including the effects of mixing. II - Rotor passage flow and wakes including the effects of spanwise mixing
[ASME PAPER 91-GT-222] p 74 A92-15639
Applications of IMI 834 in aeroengines - A collaborative IMI/MTU programme p 288 A92-22754
A method for measuring high-subsonic two-dimensional periodic flow field using a single-hole high-response cylindrical pressure probe p 588 A92-35567
Numerical verification of NISA 2 finite element analysis of the cracked 5th stage compressor disc of J-85 jet engine
[NRC-LTR-ST-1792] p 129 N92-11997
Effects of inlet distortion on the development of secondary flows in a subsonic axial inlet compressor rotor p 89 N92-13030
Application of CFD in the design of gas turbine engine components p 741 N92-27461
NASA. Lewis Research Center supersonic throughflow fan program
[NASA-TM-103248] p 972 N92-31250
Research on aero-thermodynamic distortion induced structural dynamic response of multistage compressor blading
[AD-A250865] p 974 N92-32059

COMPRESSORS
A small five-hole spherical pressure probe for compressor experiments p 38 A92-10970
Evaluation of metal hydride compressors for applications in Joule-Thomson cryocoolers p 296 A92-23835
Influence of flight parameters on air intake internal flow distortions due to gun blast-air interaction
p 310 A92-24426
Reduction of torque pulsation of Stirling engine-compressor system p 992 A92-50785
Lower-end dynamic characteristics of a magnetically coupled free-piston Stirling engine/compressor system
p 992 A92-50795
Performance evaluation of a transonic wind tunnel compressor
[AIAA PAPER 92-3927] p 1096 A92-56758
Small engine components test facility compressor testing cell at NASA Lewis Research Center
[AIAA PAPER 92-3980] p 1098 A92-56806
Supercritical blade design on stream surfaces of revolution with an inverse method p 220 N92-13950
The aerodynamic effect of fillet radius in a low speed compressor cascade
[NASA-TM-105347] p 202 N92-14063

Experimental investigation into the effects of riblets on compressor cascade performance
[AD-A243881] p 377 N92-19235
Currently available fuel gas booster compressor equipment for small gas turbine engines
[PB92-127026] p 499 N92-20265
Benchmark performance analysis of an ECM-modulated air-to-air heat pump with a reciprocating compressor
[DE92-004478] p 500 N92-20341
Cryogenic hydrogen-induced air-liquefaction technologies for combined-cycle propulsion applications
p 487 N92-21526
Thermoacoustic refrigeration p 595 N92-22720
Methodology for the determination of criticality codes and recertification intervals for Tank Mounted Air Compressors (TMAC) and Base Mounted Air Compressors (BMAC)
[NASA-CR-189268] p 770 N92-27649
Solid-vapor adsorption refrigeration system development
[PB92-164383] p 771 N92-27715
Computation of the unsteady transonic 2D cascade flow by an Euler algorithm with interactive grid generation
p 719 N92-27944
The FML compressor as a drive system for the LFSWT: A narrative p 751 N92-27978
Calculation of installation effects within performance computer programs p 869 N92-28465
Small engine components test facility compressor testing cell at NASA Lewis Research Center
[NASA-TM-105685] p 982 N92-30508
Repetitive High Energy Pulsed Power (RHEPP) temperature monitoring system utilizing Luxtron fluoroptic sensors and thermocouples technical reference manual
[DE92-013461] p 999 N92-30893
Navier-Stokes analysis and experimental data comparison of compressible flow within ducts
[NASA-TM-105796] p 972 N92-30972
Active control of compressor surge and stall
[AD-A252771] p 1126 N92-33498
An improved compressor performance prediction model
[PNR-90873] p 1072 N92-33749
Method of reducing drag in aerodynamic systems
[NASA-CASE-LEW-14791-1] p 1043 N92-34243

COMPUTATION

Calculation methods on equivalence ratio of multi-propellant for propulsion system
p 893 A92-48269
Critical problems of computational aeroacoustics
p 167 N92-13857
Analysis of Euler's and stress tensor methods for calculating power consumption of high speed centrifugal fans and turbocompressors
[DE92-728396] p 298 N92-16325
Calculation of local power consumptions and efficiencies of centrifugal fans and turbocompressors
[DE92-728402] p 298 N92-16326
Special Course on Engineering Methods in Aerodynamic Analysis and Design of Aircraft
[AGARD-R-783] p 552 N92-23950
Computational procedures for preliminary design
p 552 N92-23952
Overview of computational structural methods for modern military aircraft p 684 N92-25928
Constrained spanload optimization for minimum drag of multi-lifting-surface configurations
[NLR-TP-89126-U] p 828 N92-28660
Second-order shock-expansion theory extended to include real gas effects
[AD-A247191] p 831 N92-29539
A computational examination of directional stability for smooth and chined forebodies at high-alpha
[NASA-CR-4465] p 950 N92-32114
Computational methods for global/local analysis
[NASA-TM-107591] p 1125 N92-33104
Computation and stability analysis of laminar flow over a blunt cone in hypersonic flow p 1041 N92-33839

COMPUTATIONAL FLUID DYNAMICS

Biennial Fluid Dynamics Symposium on Advanced Problems and Methods in Fluid Mechanics, 19th, Kozubnik, Poland, Sept. 3-8, 1989, Selected Papers
p 37 A92-10654
Viscous flow solutions for slender bodies of revolution at incidence p 4 A92-10692
Emergence of coherent patterns of vortex stretching during reconnection - A scattering paradigm
p 38 A92-11041
Implicit flux-split Euler schemes for unsteady aerodynamic analysis involving unstructured dynamic meshes p 5 A92-11057
Numerical investigation of bleed on three-dimensional turbulent interactions due to sharp fins
p 5 A92-11062
Finite element solutions of the Euler equations for transonic external flows p 5 A92-11063
Computation of steady and unsteady control surface loads in transonic flow p 5 A92-11066
Flow analysis and design of three-dimensional wind tunnel contractions p 5 A92-11067
Kernel function occurring in supersonic unsteady potential flow p 6 A92-11080
Computational investigation of circular-to-rectangular transition ducts
[AIAA PAPER 91-3342] p 6 A92-11605
Axisymmetric potential flow calculations. II - Design mode p 8 A92-12399
A numerical simulation of separated flows around bodies p 8 A92-12423
Numerical solution of steady incompressible viscous flows over airfoils p 8 A92-12649
Euler code evaluation of a transatmospheric vehicle at supersonic speeds p 9 A92-13202
Supersonic boundary-layer stability analysis on an aircraft wing p 9 A92-13207
Secondary separation from a slender wing
p 62 A92-13448
Extension of a three-dimensional Euler method for calculating the flowfield around bypass engines with fan and core jet p 62 A92-13690
A simplified model for aerodynamic flows around streamlined models p 63 A92-13816
A basis for ice formation design p 146 A92-14556
Computation of the potential flow through cascades using the conformal mapping and the singularity method
p 66 A92-15356
Computational study of stall flutter in linear cascades
[ASME PAPER 91-GT-5] p 67 A92-15503
Computation of flow past a turbine blade with and without tip clearance
[ASME PAPER 91-GT-56] p 68 A92-15534
Computation of 3D flow phenomena in axial flow compressor blade rows
[ASME PAPER 91-GT-78] p 69 A92-15547
NASA low-speed centrifugal compressor for 3-D viscous code assessment and fundamental flow physics research
[ASME PAPER 91-GT-140] p 72 A92-15580
Three-dimensional Navier-Stokes computation of turbomachinery flows using an explicit numerical procedure and a coupled k-epsilon turbulence model
[ASME PAPER 91-GT-146] p 72 A92-15584
Subsonic propulsion system installation analysis and optimization
[ASME PAPER 91-GT-167] p 111 A92-15602
CFD analysis of jet mixing in low NO(x) flametube combustors
[ASME PAPER 91-GT-217] p 124 A92-15634
Unsteady Navier-Stokes simulation of transonic cascade flow using an unfactored implicit upwind relaxation scheme with inner iterations
[ASME PAPER 91-GT-223] p 74 A92-15637
Validation of a numerical method for unsteady flow calculations
[ASME PAPER 91-GT-271] p 151 A92-15668
The numerical simulation of a high-speed axial flow compressor
[ASME PAPER 91-GT-272] p 75 A92-15669
Transonic and supersonic inviscid computations in cascades using adaptive unstructured meshes
[ASME PAPER 91-GT-312] p 75 A92-15689
Transonic cascade flow prediction using the Navier-Stokes equations
[ASME PAPER 91-GT-313] p 76 A92-15690
Design and analysis of a high pitch to chord ratio cascade representative of ducted propfans
[ASME PAPER 91-GT-335] p 126 A92-15700
Computations of unsteady multistage compressor flows in a workstation environment
[ASME PAPER 91-GT-336] p 163 A92-15701
The NASP Program - An update p 61 A92-16059
Three-dimensional calculations of reactive flows in aircraft combustion chambers performed using two combustion models
[ONERA, TP NO. 1991-110] p 154 A92-16089
Solution of the compressible Euler equations for steady flows around helicopter rotor blades by an implicit space-centered method
[ONERA, TP NO. 1991-177] p 77 A92-16139
Aerodynamic and acoustic calculations of transonic nonlifting hovering rotors
[ONERA, TP NO. 1991-178] p 77 A92-16140
On the interaction between first- and second-mode waves in a supersonic boundary layer
p 78 A92-16462
Unsteady blade-surface pressures on a large-scale advanced propeller - Prediction and data
p 80 A92-17178
Eigenvalue calculation procedure for an Euler/Navier-Stokes solver with application to flows over airfoils p 170 A92-17429
CFD application to 2D/3D flow fields in Scramjet engine p 170 A92-17501
Supersonic inlet flow computation
p 171 A92-17502
Numerical simulation for various flowfields of aero-engine components p 200 A92-17503
Multidisciplinary modeling and simulation of a generic hypersonic vehicle
[AIAA PAPER 91-5015] p 232 A92-17813
Three dimensional hypersonic inlets - Low speed performance
[AIAA PAPER 91-5021] p 171 A92-17817
A quiet-flow Ludwieg tube for experimental study of high speed boundary layer transition
[AIAA PAPER 91-5026] p 207 A92-17819
Numerical and experimental study of jet impingement or interaction effects at hypersonic and supersonic speeds
[AIAA PAPER 91-5038] p 171 A92-17826
The value of sub-scale flight tests in the development of NASP vehicles
[AIAA PAPER 91-5048] p 210 A92-17834
A lifting line theory for supersonic flow applications
[AIAA PAPER 91-5058] p 171 A92-17841
Three-dimensional solution-adaptive grid generation on composite configurations p 172 A92-18352
Complex variable boundary element method for external potential flows p 172 A92-18353
Numerical prediction of subsonic turbulent flows over slender bodies at high incidence p 172 A92-18358
Algebraic turbulence modeling for unstructured and adaptive meshes p 216 A92-18362
Prediction of steady and unsteady asymmetric vortical flows around circular cones p 172 A92-18372
Similarity solutions for supersonic axisymmetric flows
p 173 A92-18387
Analysis of spiraling vortical flows around slender delta wings moving in an inviscid medium p 173 A92-18900
Three-dimensional calculation of low-frequency unsteady transonic flow in axial turbine stages
p 174 A92-19110
Some Aspects of uncertainty in computational fluid dynamics results p 233 A92-19609
Aerodynamic sensitivity analysis methods for the compressible Euler equations p 233 A92-19619
A perspective on aerospace CFD p 169 A92-20145
CFD helps the Air Force fly right p 169 A92-20146
Soviet CFD - An international perspective
p 233 A92-20150
Numerical solution of the boundary-layer equations for a general aviation fuselage p 174 A92-20211
Engineering calculations of three-dimensional inviscid hypersonic flowfields p 175 A92-20378
Removal of spurious reflections from computational fluid dynamic solutions with the complex cepstrum
p 235 A92-20729
Upwind scheme for solving the Euler equations on unstructured tetrahedral meshes p 175 A92-20735
Nonequilibrium hypersonic inviscid steady flows
p 176 A92-20737
Instabilities of flows over bodies at large incidence
p 176 A92-20738
Estimation of the maximum instantaneous distortion --- of inlet pressure in aircraft engines p 242 A92-21051
Numerical investigation of supersonic mixed-compression inlet using an implicit upwind scheme p 243 A92-21073
Computational fluid dynamics based three-dimensional turbofan inlet/fan cowl analysis system
p 243 A92-21075
An improvement of the double-point method for unsteady subsonic flow p 243 A92-21315
A boundary integral formulation for the kinetic field in aerodynamics. I - Mathematical analysis
p 243 A92-21504
Optimization of the three-dimensional shape of lifting bodies of small aspect ratio at hypersonic velocities
p 244 A92-21602
Numerical analysis of airflow in aircraft cabins
[SAE PAPER 911441] p 245 A92-21837
Computational methods in viscous aerodynamics --- Book p 245 A92-21976
The finite volume approach for the Navier-Stokes equations p 246 A92-21980
Navier-Stokes computations for aerodynamic configurations at high angles of attack
p 246 A92-21981
Adaptation methods for viscous flows
p 246 A92-21982
Experiences with finite element methods for the velocity-vorticity formulation of three-dimensional, viscous, incompressible flows p 246 A92-21984
Computational investigation of slot blowing for fuselage forebody flow control
[AIAA PAPER 92-0020] p 248 A92-22142

Navier-Stokes analysis of blunt trailing edge airfoils
[AIAA PAPER 92-0024] p 248 A92-22146
A computational study on directional stability of chine-shaped forebodies at high-alpha
[AIAA PAPER 92-0030] p 249 A92-22152
Modeling the ventilated wind tunnel wall
[AIAA PAPER 92-0035] p 249 A92-22156
Wind tunnel boundary interference prediction and correction
[AIAA PAPER 92-0036] p 249 A92-22157
Steady supersonic and hypersonic flow computations using Eulerian and new Lagrangian formulations
[AIAA PAPER 92-0055] p 249 A92-22170
Computational vorticity capturing - Application to helicopter rotor flows
[AIAA PAPER 92-0056] p 250 A92-22171
A simple numerical criterion for vortex breakdown
[AIAA PAPER 92-0057] p 250 A92-22172
Control of turbulent flow on a backward-facing step
[AIAA PAPER 92-0066] p 250 A92-22179
Parallel algorithms for panel methods --- in fluid dynamics p 293 A92-22346
Computation of normal impinging jets in cross-flow and comparison with experiment p 250 A92-22446
On the calculation of the compressible boundary layer on a nonplanar delta wing with supersonic leading edges p 252 A92-23409
Computation of transonic flow over an airfoil at large Reynolds numbers p 252 A92-23414
A study on vortex flow control of inlet distortion in the re-engined 727-100 center inlet duct using computational fluid dynamics
[AIAA PAPER 92-0152] p 253 A92-23767
Future experimental needs to support applied aerodynamics - A transonic perspective
[AIAA PAPER 92-0156] p 254 A92-23771
Experimental necessities for subsonic transport configuration development
[AIAA PAPER 92-0158] p 254 A92-23773
One view of experimental aerodynamics
[AIAA PAPER 92-0160] p 254 A92-23775
What we need in experimental aerodynamics - One engineering educator's view
[AIAA PAPER 92-0161] p 241 A92-23776
Prediction of drag at subsonic and transonic speeds using Euler methods
[AIAA PAPER 92-0169] p 255 A92-23780
A Navier-Stokes solver for stretched triangular grids
[AIAA PAPER 92-0183] p 256 A92-23793
Grid studies for thin-layer Navier-Stokes computations of airfoil flowfields
[AIAA PAPER 92-0184] p 256 A92-23794
Implementation of Vigneron's streamwise pressure gradient approximation in the PNS equations
[AIAA PAPER 92-0189] p 256 A92-23798
Multigrid Navier-Stokes calculations for three dimensional cascades
[AIAA PAPER 92-0190] p 256 A92-23799
Navier-Stokes computation of airfoil in stall using algebraic Reynolds-stress model
[AIAA PAPER 92-0195] p 257 A92-23803
Hot gas environment around STOVL aircraft in ground proximity. II - Numerical study p 371 A92-24403
Comparison of two Navier-Stokes codes for attached transonic wing flows p 309 A92-24414
Flow over an all-body hypersonic aircraft - Experiment and computation p 310 A92-24651
Multizonal Navier-Stokes solutions for the multibody Space Shuttle configuration p 310 A92-24667
A simplified method for simulating steady, unsteady flow around canard wing configuration p 311 A92-24876
On one method of constructing adaptive difference grids in aerodynamics problems p 311 A92-24902
Application of special series for studying nonstationary transonic gas flows p 311 A92-24904
Industry warms to CFD p 392 A92-24908
Europe presents a united CFD front p 392 A92-24909
HOPE looks to CFD for help --- NASDA's H-II Orbiting Plane p 386 A92-24910
On marching algorithms for solving stationary problems p 311 A92-24976
Numerical simulation of 2-D separated flows caused by suddenly change of the body section p 312 A92-25004
Computations of the flow past bodies and wings using Euler equations p 312 A92-25038
Numerical simulation of supersonic separated flow over blunt cones at high angles of attack p 313 A92-25039
Study of numerical computation of inviscid flow field about complex configuration of re-entry vehicle p 313 A92-25041
Numerical simulations of flow fields over aircrafts p 313 A92-25042
Numerical simulation of inviscid flow over a complicated body using an overlapping grid technique p 313 A92-25043
Numerical simulation and analysis for hypersonic flow with separation over blunt cone at angle of attack p 314 A92-25126
Recent progress in finite element method and boundary integral equation method for nonviscous transonic flows p 314 A92-25127
Time marching integral equation method for the solutions of unsteady transonic flows p 314 A92-25129
Numerical simulation of twin-jet impingement on a flat plate coupled with cross-flow p 315 A92-25374
A comparison of optimization-based approaches for a model computational aerodynamics design problem p 316 A92-25636
Evaluation of two flow analyses for subsonic diffuser design
[AIAA PAPER 92-0273] p 317 A92-25727
A three-dimensional supersonic turbulent boundary layer generated by an isentropic compression
[AIAA PAPER 92-0310] p 320 A92-25758
Turbulence amplification through a shock wave
[AIAA PAPER 92-0313] p 320 A92-25761
An analytical and computational investigation of shock-induced vortical flows
[AIAA PAPER 92-0316] p 321 A92-25763
A simplified model for the interaction of a rotor tip vortex with an airframe
[AIAA PAPER 92-0320] p 321 A92-25767
An efficient Euler solver for predominantly supersonic flows with embedded subsonic pockets
[AIAA PAPER 92-0323] p 322 A92-25770
Multidomain spectral solutions of high-speed flows over blunt cones
[AIAA PAPER 92-0324] p 322 A92-25771
Analysis of hypersonic nozzles including vibrational nonequilibrium and intermolecular force effects
[AIAA PAPER 92-0330] p 322 A92-25777
A numerical investigation of hydrogen combustion in Mach 2 flow
[AIAA PAPER 92-0341] p 388 A92-25787
Hypersonic flow simulations using DSMC (direct simulation Monte Carlo) p 323 A92-26216
Unsteady incompressible flow computations with quadrilateral elements p 394 A92-26219
Low-to-high altitude predictions of three-dimensional ablative reentry flowfields
[AIAA PAPER 92-0366] p 394 A92-26227
Maximum lift prediction for multielement wings
[AIAA PAPER 92-0401] p 324 A92-26254
Computational analysis of high-speed ejection seats
[AIAA PAPER 92-0403] p 324 A92-26256
Efficient simulation of incompressible viscous flow over single and multi-element airfoils
[AIAA PAPER 92-0405] p 324 A92-26258
Numerical and experimental analysis of vortex sheets behind lifting surfaces
[AIAA PAPER 92-0409] p 325 A92-26262
Computational study of the aerodynamics and control by blowing of asymmetric vortical flows over delta wings
[AIAA PAPER 92-0410] p 325 A92-26263
Numerical investigation of performance degradation of wings and rotors due to icing
[AIAA PAPER 92-0412] p 325 A92-26264
Automatic grid generation for iced airfoil flowfield predictions
[AIAA PAPER 92-0415] p 326 A92-26266
A fast implicit upwind solution algorithm for three-dimensional unstructured dynamic meshes
[AIAA PAPER 92-0447] p 328 A92-26291
An approximate viscous shock layer technique for calculating nonequilibrium hypersonic flows about blunt-nosed bodies
[AIAA PAPER 92-0498] p 329 A92-26326
Theoretical and experimental studies of helicopter rotor/fuselage interaction
[ONERA, TP NO. 1991-198] p 329 A92-26357
Aerodynamic computations of high-speed transonic propellers
[ONERA, TP NO. 1991-218] p 330 A92-26370
CARS temperature measurements and validation of a computing code on a gas-turbine combustor
[ONERA, TP NO. 1991-224] p 373 A92-26376
Validation of a 3D Navier-Stokes code on experimental compressor bladings
[ONERA, TP NO. 1991-229] p 330 A92-26381
New nonequilibrium turbulence model for calculating flows over airfoils p 330 A92-26403
Laser velocimetry seed particles within compressible, vortical flows p 395 A92-26413
Zonal flow analysis method for two-dimensional airfoils p 330 A92-26435
Preconditioned upwind methods to solve incompressible Navier-Stokes equations p 395 A92-26436
Numerical investigation of unsteady transonic nozzle flows p 331 A92-26443
Navier-Stokes computations for turbulent transonic projectile with a two layer model combining the ASM model of turbulence and the k-epsilon model near the wall
[AIAA PAPER 92-0518] p 331 A92-26943
Analysis of junction flowfields using the incompressible Navier-Stokes equations
[AIAA PAPER 92-0519] p 331 A92-26944
Obtaining the velocity field required for the calculation of propeller unsteady forces using 'traditional' approximate methods and CFD
[AIAA PAPER 92-0520] p 331 A92-26945
Unsteady flowfield simulation of ducted prop-fan configurations
[AIAA PAPER 92-0521] p 332 A92-26946
An unsteady Euler scheme for the analysis of ducted propellers
[AIAA PAPER 92-0522] p 332 A92-26947
Numerical simulation of total temperature separation in jets
[AIAA PAPER 92-0535] p 396 A92-26952
Evaluation of shear layer cavity resonance mechanisms by numerical simulation
[AIAA PAPER 92-0555] p 333 A92-26965
The NASA Computational Aerosciences Program - Toward teraFLOPS computing
[AIAA PAPER 92-0558] p 411 A92-26968
Numerical investigation of a transverse jet for supersonic aerodynamic control
[AIAA PAPER 92-0639] p 334 A92-27017
An analytical approach to grid sensitivity analysis --- of NACA wing sections
[AIAA PAPER 92-0660] p 334 A92-27031
Three-dimensional adaptive grid generation with applications in nonlinear fluid dynamics
[AIAA PAPER 92-0661] p 397 A92-27032
An experimental/computational study of sharp fin induced shock wave/turbulent boundary layer interactions at Mach 5 - Experimental results
[AIAA PAPER 92-0749] p 335 A92-27093
Numerical analysis of shock-induced separation alleviation using vortex generators
[AIAA PAPER 92-0751] p 335 A92-27095
Finite-element algorithm for chemically reacting hypersonic flow
[AIAA PAPER 92-0754] p 336 A92-27097
Computation of laminar flow over a long slender axisymmetric blunted cone in hypersonic flow
[AIAA PAPER 92-0756] p 336 A92-27098
A numerical method for simulating the fluid-dynamic and heat-transfer changes in a jet engine injector feed-arm due to fouling
[AIAA PAPER 92-0768] p 374 A92-27108
A study on the superconvergence of Multhopp's discretization in vortex-lattice methods p 336 A92-27381
Three-dimensional compressible flows in turbo-machinery solved by the pseudostream function formulation p 338 A92-27801
Loss prediction of annular cascade flow based upon S1/S2 stream surface Navier-Stokes analysis p 338 A92-27802
A new calculating method for the flowfield in turbomachinery - The study on the application of the vorticity-velocity equations for the numerical solution of the flowfield in turbomachinery p 338 A92-27803
The computation of transonic viscous flow p 338 A92-27831
Numerical simulation of the flow around rectangular cylinder p 339 A92-27851
A boundary integral formulation for the kinetic field in aerodynamics. II - Applications to unsteady 2D flows p 339 A92-28005
Numerical investigation of laminar separated trailing-edge flows p 339 A92-28026
Algebraic turbulence modeling for adaptive unstructured grids p 398 A92-28033
Finite element Navier-Stokes solver for unstructured grids p 398 A92-28035
Turbulence model effects on separated flow about a prolate spheroid p 340 A92-28036
Aerodynamic design optimization using sensitivity analysis and computational fluid dynamics p 340 A92-28044
Numerical simulation of vortex unsteadiness on a slender body at high incidence p 340 A92-28062
Calculations of hot gas ingestion for a STOVL aircraft model
[AIAA PAPER 92-0385] p 374 A92-28191
Aeroelastic analysis of advanced propellers using an efficient Euler solver
[AIAA PAPER 92-0488] p 341 A92-28194
Estimation of propulsion-induced effects on transonic flows over a hypersonic configuration
[AIAA PAPER 92-0523] p 341 A92-28197

A numerical study of the effects of geometry on the performance of a supersonic combustor
[AIAA PAPER 92-0624] p 342 A92-28213
Direct numerical simulation of laminar breakdown in high-speed, axisymmetric boundary layers
[AIAA PAPER 92-0742] p 343 A92-28223
An improved computation for gas-turbine combustion chamber flow p 375 A92-28479
Calculation of three-dimensional transonic turbine cascade flow p 344 A92-28519
Navier-Stokes solution of transonic cascade flows using nonperiodic C-type grids p 344 A92-28523
Three-dimensional viscous analysis of a Mach 5 inlet and comparison with experimental data p 344 A92-28526
Unsteady analysis of hot streak migration in a turbine stage p 399 A92-28537
Computational fluid dynamics and aircraft design p 457 A92-28875
Numerical simulation of slot injection into a turbulent supersonic stream
[AIAA PAPER 92-0827] p 421 A92-29595
Numerical analysis of techniques for efficient generation of vorticity in supersonic flows
[AIAA PAPER 92-0828] p 422 A92-29596
Navier-Stokes computation of hypersonic near wakes with foreign gas injection
[AIAA PAPER 92-0838] p 422 A92-29604
Convective flow analysis on the KC-135 aircraft
[AIAA PAPER 92-0844] p 493 A92-29610
Calculation of 3D flow field in a single transonic compressor stage p 422 A92-29719
Generalized expression of chorochronic periodicity in turbomachinery blade-row interaction p 423 A92-30000
Fluid Dynamics Conference, 22nd, Osaka, Japan, Nov. 15, 1990, Proceedings p 494 A92-30501
Numerical computation of compressible flow around an object of complex shape p 429 A92-30517
Optimized control of structured grids p 429 A92-30520
Multi-block airfoil profile of grid formation p 429 A92-30523
Computation of scramjet inlet flow p 430 A92-30541
Numerical computation and experimental study of shock wave reflection p 430 A92-30542
Numerical analysis on laminar flow control of transonic airfoils p 430 A92-30557
Boundary layer flows around an airship p 430 A92-30560
Experimental and computational investigation of wind tunnel effects on airfoil flow fields
[AIAA PAPER 92-0672] p 431 A92-30624
High angle of attack aerodynamics - Subsonic, transonic, and supersonic flows --- Book
[ISBN 0-387-97672-8] p 431 A92-30850
Calculations of the dilution system in an annular gas turbine combustor p 494 A92-31164
Use of finite volume schemes for transition simulation p 432 A92-31185
Freestream capturing for moving coordinates in three dimensions p 432 A92-31186
On hypersonic flow over two-dimensional aerofoils p 433 A92-31425
Numerical investigation of the high-speed conical flow past a sharp fin p 433 A92-31468
CFD state-of-the-art in the U.S.S.R p 495 A92-31486
Time marching integral equation method for unsteady transonic flows around airfoils p 433 A92-31489
Three-dimensional flow computation for two interacting, moving droplets
[AIAA PAPER 92-0343] p 496 A92-31655
A parametric study of airbreathing Pulsed Detonation Engine
[AIAA PAPER 92-0392] p 471 A92-31660
A numerical investigation of vortex flow control through small geometry modifications at the strake/wing junction of a cropped double-delta wing
[AIAA PAPER 92-0411] p 435 A92-31661
Viscous supersonic flow computations over a delta-rectangular wing with slanting surfaces p 441 A92-32178
Numerical computation of improved transonic potential method p 441 A92-32234
Evaluation of a Navier-Stokes prediction of a jet in a crossflow p 441 A92-32235
Interference flows past cylinder-fin-sting-cavity assemblies p 442 A92-32236
Computational study of incipient leading-edge separation on a supersonic delta wing p 442 A92-32237
Navier-Stokes study of supersonic cavity flowfield with passive control p 442 A92-32239
Navier-Stokes methods to predict circulation control airfoil performance p 442 A92-32243
Diagonal implicit scheme for computing flows with finite rate chemistry p 488 A92-32253
Numerical analysis of three-dimensional unsteady turbulent flows in a turbine stage p 443 A92-32501
Commercial airplane air distribution system development through the use of computational fluid dynamics
[AIAA PAPER 92-0987] p 535 A92-33182
Navier-Stokes analysis of helicopter plume flowfield for infrared calculations
[AIAA PAPER 92-0983] p 580 A92-33185
Three-dimensional time-marching aeroelastic analyses using an unstructured-grid Euler method
[AIAA PAPER 92-2506] p 542 A92-34500
Unsteady aerodynamic characteristics of a dual-element airfoil
[AIAA PAPER 92-2508] p 518 A92-34501
Analysis of cascades using a two dimensional Euler aeroelastic solver
[AIAA PAPER 92-2370] p 556 A92-34598
Aerobrake aerothermodynamic environment predictions in support of the Aeroassist Flight Experiment
[TABES PAPER 91-278] p 519 A92-34683
Large eddy simulation of unsteady turbulent wake of a circular cylinder using the finite element method p 587 A92-34825
Simulation of 3-D shear flows around a nozzle-afterbody at high speeds p 519 A92-34826
Computational fluid dynamics as a tool for aerodynamic analysis of ejection seats p 519 A92-35444
A direct-problem calculation method for gas turbines with bowed and twisted blades p 519 A92-35571
A circumferential non-uniform effect model for multistage axial-flow compressor throughflow p 588 A92-35572
Role of shock dynamics in transonic flutter
[AIAA PAPER 92-2121] p 520 A92-35690
A new method for transonic static aeroelasticity problems
[AIAA PAPER 92-2123] p 589 A92-35691
Complete Euler-solution for a rotor in hover and a propeller in forward flight p 520 A92-35755
Navier-Stokes analysis of blade tip shape in hover p 521 A92-35758
Combustion research and design technology of aircraft engines p 558 A92-35915
Numerical simulations in turbomachinery; Proceedings of the Symposium, ASME and JSME Joint Fluids Engineering Conference, 1st, Portland, OR, June 23-27, 1991
[ISBN 0-7918-0714-2] p 522 A92-36028
Arbitrary blade section design based on viscous considerations - Background information p 523 A92-36029
Unsteady hypersonic boundary layers for slender axisymmetric bodies with large injection rates p 524 A92-36100
Analysis of slender bodies of revolution with curved-ground effect and waving-water effect p 524 A92-36151
Numerical studies of transverse curvature effects on transonic flow stability p 524 A92-36186
Active control of the hydraulic forces of a body by a splitter plate p 591 A92-36351
Numerical simulation of opposing sonic jets p 524 A92-36357
Aeroelastic tailoring analysis for advanced turbo propellers with composite blades p 558 A92-36358
Separated and cavitation flows - Principal properties and computational models --- Russian book
[ISBN 5-02-014005-8] p 610 A92-36600
Evaluation of a finite volume method for compressible shear layers p 610 A92-36834
Accelerated convergence to steady state by gradual far-field damping p 610 A92-36835
Locally implicit hybrid algorithm for steady and unsteady viscous flows p 610 A92-36836
Spatial adaptation of unstructured meshes for unsteady aerodynamic flow computations p 610 A92-36838
Numerical simulation of droplet deformation in convective flows p 670 A92-36844
Characteristic-based algorithms for flows in thermochemical nonequilibrium p 670 A92-36846
Two- and three-dimensional grid generation by an algebraic homotopy procedure p 611 A92-36861
Efficient direct solvers for large-scale computational fluid dynamics problems p 690 A92-37534
Computational methods for shock waves in three-dimensional supersonic flow p 611 A92-37537
The computation of three-dimensional flows using unstructured grids p 612 A92-37539
Numerical simulation of hypersonic viscous flow for the design of H-II orbiting plane (HOPE) p 612 A92-37549
Non-equilibrium hypersonic flow simulations using the second-order boundary layer equations p 612 A92-37551
A new finite element formulation for computational fluid dynamics. X - The compressible Euler and Navier-Stokes equations p 612 A92-37552
An information system for the numerical simulation of 3D Euler flows around aircraft p 613 A92-37554
Recent advances in maneuver loads analysis p 642 A92-37576
Aerospace - Collected translations of selected papers p 608 A92-38266
International Symposium on Engineering Turbulence Modelling and Measurements, Dubrovnik, Yugoslavia, Sept. 24-24, 1990, Selected Papers p 672 A92-38851
A study of flow patterns and behaviours of 3D separated flow on a simplified Shuttle model p 615 A92-38906
The numerical simulation of transonic inviscid flow over oscillating airfoils p 616 A92-38918
Numerical simulation of separation flow on bodies of revolution at high angle of attack using Euler equations p 616 A92-38919
A calculation of influence of vortex breakdown on aerodynamic characteristics for slender wings p 616 A92-38920
The numerical simulation of separation control using moving surface effect p 616 A92-38924
Numerical simulation of interaction between vortexes and shocks in jet flow field p 616 A92-38925
Mixed volume boundary element approach for aerodynamics p 617 A92-39934
Knowledge-based nonlinear boundary integral models of compressible viscous flows over arbitrary bodies - Taking CFD back to basics p 617 A92-39941
Integral equation methods for linear and nonlinear aerodynamics p 617 A92-39949
Application of laminar flow control to the High Speed Civil Transport - The NASA Supersonic Laminar Flow Control Program
[SAE PAPER 912115] p 643 A92-39966
Application of linear stability theory in laminar flow design
[SAE PAPER 912116] p 618 A92-39967
Computational analysis of drag reduction techniques for afterbody/nozzle/empennage configurations
[SAE PAPER 912127] p 618 A92-39974
CFD calculations of closely coupled scissor wings - Inviscid, viscous, and vortex lattice with rollup results
[SAE PAPER 912150] p 619 A92-39986
Turbine blade heat transfer prediction using coupled turbulent Prandtl number and transition models
[SAE PAPER 912152] p 674 A92-39987
Passive control of supersonic cavity flowfields
[SAE PAPER 912153] p 619 A92-39988
Experimental and numerical investigation of a turbulent boundary layer over riblets p 622 A92-40128
Direct simulation of a supersonic reacting mixing-layer p 676 A92-40132
Simulation and modeling of homogeneous compressible turbulence under isotropic mean compression p 622 A92-40134
The effects of viscosity and diffusion on a supersonic mixing layer p 622 A92-40143
Numerical predictions of transonic viscous flows around aerofoils through an Euler/boundary layer interaction method p 624 A92-40600
Current growth in the aeronautics p 701 A92-41196
Transonic Navier-Stokes computations for an oscillating wing using zonal grids p 701 A92-41217
Numerical study of vortex-dominated flows for wings at high incidence and sideslip p 702 A92-41227
Accurate prediction of drag using Euler methods p 703 A92-41246
Navier-Stokes simulation for cone-derived waverider p 703 A92-41271
Extrapolation procedures for the time-dependent Navier-Stokes equations p 704 A92-41289
Stability of plane nonorthogonal stagnation flow p 704 A92-41291
Navier-Stokes cavity solutions based on second-order turbulence modeling
[AIAA PAPER 92-2765] p 704 A92-41314
Visualization and analysis of hypersonic flows and comparison to experimental data
[AIAA PAPER 92-2774] p 704 A92-41320
Adaptive mesh for turbulent hypersonic flow
[AIAA PAPER 92-2776] p 704 A92-41322
Navier-Stokes computations for pointed, spherical, and flat tipped shell at Mach 3 p 705 A92-41536
Hybrid Navier-Stokes/Monte Carlo method for reacting flow calculations p 705 A92-41537
Local bridging to predict aerodynamic coefficients in hypersonic, rarefied flow p 705 A92-41541
Similarity solutions for viscous vortex cores p 759 A92-41658

Flow analysis for axial compressor including secondary flow effects p 759 A92-41835
Wind tunnel wall corrections for unsteady flow applying steady wall adaptation and CFD-techniques p 706 A92-42533
Calculation of three-dimensional turbulent flow in wind tunnel entry section p 708 A92-43055
Numerical approximation of hypersonic shocks in a finite-element method using flux-corrected transport (FCT) p 708 A92-43060
Calculation of transonic flow in turbomachine cascades p 708 A92-43067
Upwind schemes for Navier-Stokes computations at subsonic through hypersonic speeds p 708 A92-43071
Aerodynamic design tool development for the calculation code of hypersonic flow p 711 A92-43198
Thermochemical nonequilibrium flow computations of flow around the aeroassist flight experiment p 713 A92-44368
Application of computational fluid dynamics to pitch/yaw thrust vectoring spherical convergent flap nozzles p 737 A92-44511
Numerical analysis of flow through oscillating cascade sections p 713 A92-44513
Numerical investigation of supersonic inlet with realistic bleed and bypass systems p 713 A92-44519
Bleed-boundary conditions for numerically simulated mixed-compression supersonic inlet flow p 713 A92-44520
Flow establishment in a generic scramjet combustor p 737 A92-44525
Nozzle design using generalized one-dimensional flow p 714 A92-44531
Swirl number effects on confined flows in a model of a dump combustor p 896 A92-45202
Experimental and analytical study of close-coupled ventral nozzles for ASTOVL aircraft p 861 A92-45325
Computational aerodynamics - The next generation [SAE PAPER 911988] p 788 A92-45390
The impact of CFD on the airplane design process - Today and tomorrow [SAE PAPER 911989] p 788 A92-45391
Computational aerodynamics in aircraft design - Challenges and opportunities for Euler/Navier-Stokes methods [SAE PAPER 911990] p 788 A92-45392
Numerical simulations of separated flows around oscillating airfoil for dynamic stall phenomena [SAE PAPER 911991] p 788 A92-45393
Computational fluid dynamics applications in airplane cabin ventilation system design [SAE PAPER 911992] p 788 A92-45394
Recent applications of the FNS zonal Method to complex flow problems [SAE PAPER 912003] p 789 A92-45404
Numerical simulation of a supersonic jet impingement on a ground [SAE PAPER 912014] p 789 A92-45412
A calculation of penetration of the jet issuing normally into a cross flow across a wall boundary layer [SAE PAPER 912029] p 790 A92-45419
Numerical simulations of hypersonic real-gas flows over space vehicles [SAE PAPER 912045] p 791 A92-45429
AIAA Applied Aerodynamics Conference, 10th, Palo Alto, CA, June 22-24, 1992, Technical Papers. Pts. 1 & 2 p 791 A92-45476
Numerical investigation into high-angle-of-attack leading-edge vortex flow [AIAA PAPER 92-2600] p 791 A92-45477
Effect of canard deflection on close-coupled canard-wing-body aerodynamics [AIAA PAPER 92-2602] p 792 A92-45479
Future directions in computing and CFD [AIAA PAPER 92-2734] p 917 A92-45489
The design of a system of codes for industrial calculations of flows around aircraft and other complex aerodynamic configurations [AIAA PAPER 92-2619] p 917 A92-45492
Practical design optimization of wing/body configurations using the Euler equations [AIAA PAPER 92-2633] p 795 A92-45505
Recent CFD applications on jet transport configurations [AIAA PAPER 92-2658] p 844 A92-45519
Investigation of solution operators for the three-dimensional Euler equations [AIAA PAPER 92-2666] p 797 A92-45522
A new approach for the calculation of transitional flows [AIAA PAPER 92-2669] p 798 A92-45524
LU-SGS implicit scheme for entry vehicle flow computation and comparison with aerodynamic data [AIAA PAPER 92-2671] p 798 A92-45526
Numerical investigation of tail buffet on F-18 aircraft [AIAA PAPER 92-2673] p 798 A92-45528
Calculation of high speed base flows [AIAA PAPER 92-2679] p 799 A92-45531
An adaptive grid method for computing the high speed 3D viscous flow about a re-entry vehicle [AIAA PAPER 92-2685] p 799 A92-45534
Spatial and temporal adaptive procedures for the unsteady aerodynamic analysis of airfoils using unstructured meshes [AIAA PAPER 92-2694] p 800 A92-45540
Navier-Stokes analysis and experimental data comparison of compressible flow in a diffusing S-duct [AIAA PAPER 92-2699] p 800 A92-45541
Surface grid generation in a parameter space [AIAA PAPER 92-2717] p 803 A92-45556
A new automatic grid generation environment for CFD applications [AIAA PAPER 92-2720] p 803 A92-45558
Computation of turbulent flow about cone-derived waverider [AIAA PAPER 92-2726] p 804 A92-45562
Time accurate computation of unsteady transonic flows around an airfoil with oscillating flap on dynamic grid [AIAA PAPER 92-2733] p 805 A92-45567
Navier-Stokes computation of wing leading edge tangential blowing for a tilt rotor in hover [AIAA PAPER 92-2608] p 805 A92-45568
Prediction of the viscous transonic aerodynamic performance of supercritical aerofoil sections [AIAA PAPER 92-2653] p 805 A92-45569
Computations of hypersonic flows around a three-dimensional concave/convex body [AIAA PAPER 92-2606] p 805 A92-45570
A transonic/supersonic/hypersonic CFD analysis of the entry Space Shuttle Orbiter [AIAA PAPER 92-2614] p 805 A92-45571
Transonic calculations for wings with deflected control surfaces [AIAA PAPER 92-2617] p 805 A92-45572
Application of the Euler method EUFLEX to a fighter-type airplane configuration at transonic speed [AIAA PAPER 92-2620] p 845 A92-45573
A numerical study of control surface buzz using computational fluid dynamic methods [AIAA PAPER 92-2654] p 806 A92-45578
Applied Computational Aerodynamics - Case studies [AIAA PAPER 92-2661] p 845 A92-45580
Comparison of two flux splitting schemes for calculation of ogive-cylinder at M = 3.5 and alpha = 18 deg [AIAA PAPER 92-2667] p 806 A92-45582
A fast, implicit unstructured-mesh Euler method [AIAA PAPER 92-2693] p 917 A92-45589
A compact higher order Euler solver for unstructured grids with curved boundaries [AIAA PAPER 92-2696] p 807 A92-45590
An unstructured approach to the design of multiple-element airfoils [AIAA PAPER 92-2709] p 807 A92-45592
On the aerodynamics/dynamics of store separation from hypersonic aircraft [AIAA PAPER 92-2722] p 807 A92-45595
Aerodynamically blunt and sharp bodies [AIAA PAPER 92-2727] p 808 A92-45597
Eigenfunction analysis of turbulent mixing phenomena p 898 A92-45826
Viscous high-speed flow computations by adaptive mesh embedding techniques p 808 A92-45839
Streamlines, vorticity lines, and vortices around three-dimensional bodies p 808 A92-45845
The inviscid compressible Goertler problem in three-dimensional boundary layers p 809 A92-46441
Smooth solutions for transonic gasdynamic equations --- Russian book [ISBN 5-02-029345-8] p 809 A92-46626
Navier-Stokes predictions for the F-18 wing and fuselage at large incidence p 810 A92-46783
Predicted pressure distribution on a prop-fan blade through Euler analysis p 810 A92-46791
Design load predictions on a fighter-like aircraft wing p 811 A92-46797
Numerical method for predicting transition in three-dimensional flows by spatial amplification theory p 812 A92-46886
Temporal adaptive Euler/Navier-Stokes algorithm involving unstructured dynamic meshes p 812 A92-46887
Joint computational/experimental aerodynamics research on a hypersonic vehicle. I - Experimental results p 812 A92-46890
Joint computational/experimental aerodynamics research on hypersonic vehicle. II - Computational results p 812 A92-46891
Outflow boundary conditions using Duhamel's equation p 813 A92-46913
Taylor series approximation of geometric shape variation for the Euler equations p 899 A92-46916
Experimental and numerical study of flow around helicopter rotor blade tips p 814 A92-46948
A unified procedure for solving rotor flowfield, performance and interference p 814 A92-46950
Efficient high-resolution rotor wake calculations using flow field reconstruction p 814 A92-46951
An Eulerian/Lagrangian method for computing blade/vortex impingement p 814 A92-46952
Three-dimensional blade vortex interactions p 815 A92-46953
Experimental and computational studies of hovering rotor flows p 815 A92-46954
Numerical simulation of multizone two-dimensional transonic flows using the full Navier-Stokes equations p 815 A92-46955
Initial validation of an unsteady Euler/Navier-Stokes flow solver for helicopter rotor airloads in forward flight p 815 A92-46956
Effects of leading and trailing edge flaps on the aerodynamics of airfoil/vortex interactions p 815 A92-46957
A new integral equation for potential compressible aerodynamics of rotors in forward flight p 815 A92-46958
Numerical grid generation in computational fluid dynamics and related fields; Proceedings of the 3rd International Conference, Universidad Politecnica de Cataluna, Barcelona, Spain, June 3-7, 1991 [ISBN 0-444-88948-5] p 918 A92-47035
Simple diagnosis for the quality of generated grid systems p 919 A92-47069
Patch-independent structured multiblock grids for CFD computations p 919 A92-47078
A geometry-integrated approach to multiblock grid generation p 919 A92-47083
The calculation of three-dimensional compressible boundary layer stability on swept wings p 818 A92-47684
The numerical simulation of compressible flow around an airfoil at high angle of attack p 818 A92-47686
A time marching method in finite volume for transonic diffuser turbulent flows p 819 A92-47690
A new method for predicting the end wall boundary layers and the blade force defects inside the passage of axial compressor cascades p 819 A92-47691
Aerodynamic sensitivities for subsonic lifting-surface p 819 A92-47695
Calculation of the aerodynamic derivatives of aircraft in the supersonic region using the Mach box method p 875 A92-47779
Analysis of thermo-chemical nonequilibrium models for carbon dioxide flows [AIAA PAPER 92-2852] p 892 A92-47835
Calculation of hypersonic, viscous, non-equilibrium flows around reentry bodies using a coupled boundary layer/Euler method [AIAA PAPER 92-2856] p 819 A92-47839
Computation of hypersonic flowfields in thermal and chemical nonequilibrium [AIAA PAPER 92-2874] p 819 A92-47856
Laminar hypersonic flow over a compression using the HANA code [AIAA PAPER 92-2896] p 820 A92-47872
Enhancements to viscous-shock-layer technique [AIAA PAPER 92-2897] p 820 A92-47873
Solution of the Burnett equations for hypersonic flows near the continuum limit [AIAA PAPER 92-2922] p 821 A92-47894
Characteristics of the Shuttle Orbiter leeside flow during a reentry condition [AIAA PAPER 92-2951] p 821 A92-47915
Aerothermodynamic calculations for the Space Shuttle Orbiter [AIAA PAPER 92-2953] p 821 A92-47917
Experience with the Johnson-King turbulence model in a transonic turbine cascade flow solver p 821 A92-48207
Calculation of fully three-dimensional separated flows with an unsteady viscous-inviscid interaction method [ONERA, TP NO. 1992-1] p 821 A92-48577
Advanced CFD simulation and testing of compressor blading in the multistage environment [AIAA PAPER 92-3040] p 822 A92-48701
Numerical computations of transonic flows through cascades [AIAA PAPER 92-3041] p 822 A92-48702
Application of non-reflecting boundary conditions to three-dimensional Euler equation calculations for thick strut cascades [AIAA PAPER 92-3045] p 822 A92-48705
FNS analysis of an axisymmetric scramjet inlet [AIAA PAPER 92-3100] p 824 A92-48742

Computational analysis of ramjet engine inlet interaction
[AIAA PAPER 92-3102] p 824 A92-48744
Development and application of a zonal k-epsilon turbulence model for complex 3-D flowfields
[AIAA PAPER 92-3176] p 903 A92-48792
Numerical solutions of unsteady oscillating flows past an airfoil
[AIAA PAPER 92-3212] p 825 A92-48817
Progress towards the development of transient ram accelerator simulation as part of the U.S. Air Force Armament Directorate Research Program
[AIAA PAPER 92-3248] p 904 A92-48847
Prediction of a high bypass ratio engine exhaust nozzle flowfield
[AIAA PAPER 92-3259] p 864 A92-48855
Comparative investigation of multiplane thrust vectoring nozzles
[AIAA PAPER 92-3263] p 864 A92-48858
A comparative study of scramjet injection strategies for high Mach numbers flows
[AIAA PAPER 92-3287] p 904 A92-48876
A turbulence model based on RNG for quasi-three-dimensional cascade flows --- renormalization group methods
[AIAA PAPER 92-3312] p 825 A92-48898
A Navier-Stokes analysis of a controlled-diffusion compressor cascade at increasing inlet-flow angles
[AIAA PAPER 92-3313] p 825 A92-48899
Vane-blade interaction in a transonic turbine. I - Aerodynamics
[AIAA PAPER 92-3323] p 825 A92-48906
Vane-blade interaction in a transonic turbine. II - Heat transfer
[AIAA PAPER 92-3324] p 904 A92-48907
A numerical study of two-phase flow in gas turbine combustors
[AIAA PAPER 92-3468] p 905 A92-49015
Prediction of gas turbine combustor flow by a finite element code
[AIAA PAPER 92-3469] p 906 A92-49016
Numerical flow simulation and analysis of a shrouded propfan rotor
[AIAA PAPER 92-3773] p 826 A92-49118
A computational study of advanced exhaust system transition ducts with experimental validation
[AIAA PAPER 92-3794] p 907 A92-49126
An inviscid/viscous coupling approach for vortex flow field calculations p 933 A92-49510
Navier-Stokes computations of horseshoe vortex flows p 990 A92-49516
A complete boundary integral formulation for steady compressible inviscid flows governed by nonlinear equations p 934 A92-50211
Transonic flow calculation of Euler equations by implicit iterating scheme with flux splitting p 934 A92-50215
Numerical investigation of axial flow compressor casing treatment p 934 A92-50216
Computational study of a supersonic mixer-ejector exhaust system p 969 A92-50252
Application of a solution adaptive grid scheme to complex three-dimensional flows p 935 A92-50309
On the application of parabolized Navier-Stokes equations to flow field simulations p 936 A92-51943
A direct viscous-inviscid interaction method for the flow calculation around airfoils p 936 A92-52028
Flow of a rarefied gas past a two-dimensional body of an arbitrary shape at small Mach numbers p 937 A92-52726
Kinetic theory model for the flow of a simple gas from a three-dimensional axisymmetric nozzle p 937 A92-52730
Hypersonic flow calculations around a 3D delta wing at low Knudsen numbers p 937 A92-52734
Thermal and chemical nonequilibrium viscous shock layer flows over a blunt body at high altitudes p 938 A92-52749
One-dimensional kinetic model for flows near a stagnation point of a highly cooled body in hypersonic rarefied streams p 938 A92-52751
Rarefied gas flow around a disc with different angles of attack p 938 A92-52753
Approximate aerodynamic analysis for complicated bodies in rarefied gas flows p 938 A92-52754
Hypersonic merged layer blunt body flows with wakes p 939 A92-52757
Rarefied gas numerical wind tunnel p 995 A92-52763
Force and heat transfer on a disc in rarefied flow p 939 A92-52764
Direct simulation of vortex shedding in dilute gas flows past bluff bodies p 939 A92-52766
Aerodynamics of complex shape bodies within a wide range of supersonic flows of rarefied gases p 939 A92-52767
Monte Carlo simulation of the hypersonic mon- and diatomic gas flow past a disk at an angle of attack p 939 A92-52770
DSMC simulation of hypersonic flows past 2-dimensional bodies p 939 A92-52772
Application of the DSMC method to hypersonic flow about a delta wing p 940 A92-52775
Monte Carlo study of vibrational relaxation processes p 940 A92-52777
Numerical and experimental investigations of rarefied gas flows through nozzles and composite systems p 940 A92-52797
Pseudostream function formulation - A method of solving three-dimensional aerodynamic analysis and design problems in turbomachinery p 996 A92-52981
Finite analytic numerical solution of Navier-Stokes equations p 996 A92-53011
Mixing for multi-stage axial-flow compressors p 996 A92-53015
Calculation of the transonic full-potential flowfield about 3D fuselage p 941 A92-53021
Nonlinear development and secondary instability of large-amplitude Goertler vortices in hypersonic boundary layers p 942 A92-53080
A bi-directional marching finite element algorithm for three-dimensional boundary layer separation flow computations p 942 A92-53288
A numerical investigation of axial flow compressor casing treatment p 942 A92-53381
A penalty-Galerkin finite element method for calculating transonic flow over wings p 943 A92-53386
Detailed numerical analysis of standing oblique detonation p 1111 A92-53550
A comparison of the calculated and experimental off-design performance of a radial flow turbine
[AIAA PAPER 92-3069] p 1020 A92-54004
Full Navier-Stokes calculations on the installed F/A-18 inlet at a high angle of attack
[AIAA PAPER 92-3175] p 1020 A92-54012
Application of computational fluid dynamics to the study of vortex flow control for the management of inlet distortion
[AIAA PAPER 92-3177] p 1020 A92-54013
Applied analytical combustion/emissions research at the NASA Lewis Research Center - A progress report
[AIAA PAPER 92-3338] p 1067 A92-54025
Computational and experimental studies of flow in multi-lobed forced mixers
[AIAA PAPER 92-3568] p 1112 A92-54057
Heat transfer measurements and CFD comparison of swept shock wave/boundary-layer interactions
[AIAA PAPER 92-3665] p 1021 A92-54110
Optimization of a 2D scramjet-vehicle using CFD and simplified approximate flow analysis techniques
[AIAA PAPER 92-3673] p 1022 A92-54116
Numerical study of the 3-D flowfield for a supersonic jet exiting into a hypersonic stream from a conical surface
[AIAA PAPER 92-3675] p 1022 A92-54118
Numerical calculations of propfan/swirl recovery vane flow field
[AIAA PAPER 92-3771] p 1022 A92-54160
Comparison between computational and experimental data for a hypersonic laser propelled vehicle
[AIAA PAPER 92-3808] p 1023 A92-54179
Flow characterization in the NASA Ames 16-inch Shock Tunnel
[AIAA PAPER 92-3810] p 1090 A92-54180
Three-dimensional calculation of radiative field in hypersonic air shock layers p 1023 A92-54498
Assessment of compressibility corrections to the k-epsilon model in high-speed shear layers p 1024 A92-54905
Numerical simulation of slot injection into a turbulent supersonic stream p 1024 A92-54914
Application of a parallel direct simulation Monte Carlo method to hypersonic rarefied flows p 1024 A92-54916
Efficient iterative methods for the transonic small disturbance equation p 1025 A92-54933
Approximate Riemann solver for hypervelocity flows p 1117 A92-54934
Grid studies for thin-layer Navier-Stokes computations of airfoil flowfields p 1025 A92-54935
Computation of vortex wake flows and control of their effects on trailing wings
[AIAA PAPER 92-4429] p 1025 A92-55353
Navier-Stokes computations for oscillating control surfaces
[AIAA PAPER 92-4431] p 1026 A92-55355
The vortical structure in the wake during dynamic stall
[AIAA PAPER 92-4496] p 1026 A92-55364
A discrete vortex model for predicting wing rock of slender wings
[AIAA PAPER 92-4497] p 1026 A92-55365
Tow-tank study of nonlinear aerodynamics of a 2-D airfoil
[AIAA PAPER 92-4499] p 1026 A92-55367
Evaluation of a multigrid-based Navier-Stokes solver for aerothermodynamic computations
[AIAA PAPER 92-4563] p 1027 A92-55375
Computations of the unsteady flow about a generic wing/pylon/finned-store configuration
[AIAA PAPER 92-4568] p 1027 A92-55377
Approximate aerodynamic analysis of jet interaction
[AIAA PAPER 92-4640] p 1027 A92-55387
Comparative numerical study of two turbulence models for airfoil static and dynamic stall
[AIAA PAPER 92-4649] p 1028 A92-55394
Computing high-speed flows past an oscillating cylinder near a vertical wall
[AIAA PAPER 92-4653] p 1028 A92-55397
Wind tunnel test of M = 2.5 mixed compression inlet p 1028 A92-56008
Generalized aerodynamics analysis by the boundary element method p 1030 A92-56050
Computational and experimental investigation of annulus heat transfer with swirl
[AIAA PAPER 92-4060] p 1119 A92-56143
Navier-Stokes simulation of a close-coupled canard-wing-body configuration p 1031 A92-56163
Euler/experiment correlation of a generic fighter p 1031 A92-56164
Application of computational fluid dynamics to sonic boom near- and mid-field prediction p 1031 A92-56173
The computation and validation of hovering rotor performance p 1055 A92-56285
Current European rotorcraft research activities on development of advanced CFD methods for the design of rotor blades (BRITE/EURAM 'DACRO' project) p 1032 A92-56332
Roles of wind tunnel tests and CFD analyses in the design of energy-efficient SST
[AIAA PAPER 92-3923] p 1133 A92-56754
A code validation strategy and facility for nonequilibrium, reacting flows
[AIAA PAPER 92-3970] p 1098 A92-56796
High-lift testing at high Reynolds numbers
[AIAA PAPER 92-3986] p 1033 A92-56810
CAN-DO, CFD-based Aerodynamic Nozzle Design and Optimization program for supersonic/hypersonic wind tunnels
[AIAA PAPER 92-4009] p 1033 A92-56832
Computational and numerical analysis of hypersonic nozzle flows with comparisons to wind tunnel calibration data
[AIAA PAPER 92-4011] p 1033 A92-56834
A database of aerothermal measurements in hypersonic flow for CFD validation
[AIAA PAPER 92-4023] p 1034 A92-56845
CFD validation experiments for hypersonic flows
[AIAA PAPER 92-4024] p 1034 A92-56846
Numerical simulation of unsteady flow in a hypersonic shock tunnel facility
[AIAA PAPER 92-4029] p 1034 A92-56851
Increasing the accuracy of the Godunov scheme for calculating steady-state supersonic gas flows by solving the generalized Riemann problem p 1035 A92-57499
Numerical simulation of hypersonic viscous flow for the design of H-2 orbiting plane (HOPE-2)
[NAL-TR-1093] p 11 N92-10009
Recent advances on a finite element algorithm for computational aerodynamics: Transonics-hypersonics
[DE91-018176] p 11 N92-10010
Viscous computations of cold air/air flow around scramjet nozzle afterbody
[NASA-CR-4406] p 13 N92-10982
Numerical simulation of the reactive flow in advanced (HSR) combustors using KIVA-2
[NASA-CR-188996] p 26 N92-11014
Modeling and numerical simulation of vortex flow in aerodynamics
[AD-B163670L] p 83 N92-12997
Recent progress in computational vortex-flow aerodynamics p 84 N92-13002
Flow modification over a backward facing step
[AD-A241351] p 158 N92-13406
Experimental simulation and diagnostics of high-enthalpy real-gas flows
[AD-A241286] p 166 N92-13822
The use of artificial neural networks in experimental data acquisition and aerodynamic design p 90 N92-13848
Navier-Stokes calculation of transonic flow past the NTF 65 deg delta wing p 91 N92-13868
Aerodynamics p 202 N92-13977
Computational fluid dynamics p 177 N92-13979
Definition of the unsteady vortex flow over a wing/body configuration
[NASA-CR-180083] p 178 N92-13995

A study on vortex flow control on inlet distortion in the re-engined 727-100 center inlet duct using computational fluid dynamics
[NASA-TM-105321] p 179 N92-13998
A Navier-Stokes solution of Hull-ring wing-thruster interaction p 221 N92-14310
Aerothermodynamics for Space Vehicles
[ESA-SP-318] p 180 N92-14973
Aerothermodynamic development of the CARINA re-entry vehicle: CFD analyses and experimental tests
p 211 N92-14980
A multiblock flow solver for inviscid hypersonic flows
p 181 N92-14986
Flow and temperature computations for space vehicles using adaptive finite element techniques
p 181 N92-14990
Linear acoustics in gas mixtures with rate processes
p 238 N92-15013
Experimental research of the aerodynamics of nozzles and plumes at hypersonic speeds
[NASA-CR-187316] p 185 N92-15048
A fast implicit upwind solution algorithm for three-dimensional unstructured dynamic meshes
[NASA-TM-104186] p 185 N92-15050
Industrial code development p 227 N92-15083
Development of a CFD code for analysis of fluid dynamic forces in seals p 228 N92-15084
Program plans: Aviation safety research
[NIAR-91-30] p 264 N92-17587
Hi-alpha forebody design. Part 1: Methodology base and initial parametrics
[NASA-CR-189849] p 358 N92-18024
Ultra High Speed Numerical Wind Tunnel (UHSNWT) initiative at National Aerospace Laboratory numerical simulator - second generation
[NAL-TR-1108] p 384 N92-18037
Hi-alpha forebody design. Part 2: Determination of body shapes for positive directional stability
[NASA-CR-189850] p 359 N92-18038
The Goldstein Engineering Research Laboratory
[AERO-REPT-8906] p 308 N92-18322
The installation of the AVRO 9 by 7 foot low-speed wind tunnel at the University of Manchester (England)
[AERO-REPT-9005] p 385 N92-18341
Proceedings of the Seminar on Investigation and Control of Boundary-Layer Transition
[NAL-SP-11] p 400 N92-18483
Numerical simulation of transient hypervelocity flow in an expansion tube
[NASA-CR-189601] p 402 N92-18965
Drag prediction using computation methods
[ONERA-RSF-82/1685-AY-154-4] p 349 N92-19682
Component-specific modeling --- jet engine hot section components
[NASA-CR-189088] p 377 N92-19726
A hierarchy for modeling high speed propulsion systems
[NASA-CR-186984] p 387 N92-19934
Use of CFD in the design of a modern multistage aero engine LP turbine design
[PNR-90862] p 472 N92-20179
Application of analysis techniques for low frequency interior noise and vibration of commercial aircraft
[NASA-CR-189555] p 481 N92-20376
Numerical simulation of vortical flow over a delta wing at subsonic and transonic speeds
[NLR-TP-90029-U] p 444 N92-20498
Air intakes for high speed vehicles
[AGARD-AR-270] p 445 N92-20797
Postflight aerothermodynamic analysis of Pegasus(tm) using computational fluid dynamic techniques
[NASA-CR-186017] p 445 N92-21188
Flow analysis and design optimization methods for nozzle afterbody of a hypersonic vehicle
[NASA-CR-4431] p 446 N92-21456
An alternative to unstructured grids for computing gas dynamic flows around arbitrarily complex two-dimensional bodies
[NASA-CR-189612] p 447 N92-21465
Aerodynamic design with CFD p 447 N92-21514
Three-dimensional simulations of hypersonic flows
[MBB-UK-0155-89-PUB] p 447 N92-21703
Contributions of MBB-FE211 to the 2nd Antibes Workshop on Hypersonic Flows
[MBB-FE211-S-PUB-449] p 524 N92-22179
Case 7.4 delta wing: Navier-Stokes calculation
p 525 N92-22182
Numerical simulation of transient hypervelocity flow in an expansion tube
[NASA-CR-189615] p 592 N92-22228
Further investigations of the aeroelastic behavior of the AFW wind-tunnel model using transonic small disturbance theory
[NASA-TM-107576] p 526 N92-22240
Three-dimensional compressible turbulent computations for a diffusing S-duct
[NASA-CR-4392] p 526 N92-22249
Improved large perturbation propulsion models for control system design (1988-1989) and large perturbation models of high velocity propulsion systems (1989-1990) and reduced order propulsion models for control system design (1990-1991)
[NASA-CR-190148] p 593 N92-22491
A hierarchy for modeling high speed propulsion systems p 559 N92-22492
High speed transport cruise drag --- scaling laws using Navier-Stokes equations
[NASA-CR-190248] p 527 N92-23103
A two-dimensional Euler solution for an unbladed jet engine configuration
[NASA-TM-105329] p 597 N92-23560
Interactive solution-adaptive grid generation procedure
[NASA-TM-105432] p 528 N92-23563
Development and application of computational aerothermodynamics flowfield computer codes
[NASA-CR-190294] p 624 N92-24229
A user guide for the EMTAC-MZ CFD code
[NASA-CR-4283] p 678 N92-24242
A three-dimensional, compressible, laminar boundary-layer method for general fuselages. Volume 2: User's manual
[NASA-CR-4292-VOL-2] p 678 N92-24344
Hypersonic configurations in slow speed flight
p 624 N92-24394
Software Surface Modeling and Grid Generation Steering Committee
[NASA-CP-3143] p 691 N92-24397
Geometry acquisition and grid generation: Recent experiences with complex aircraft configurations
p 691 N92-24400
Workshop on Engineering Turbulence Modeling
[NASA-CP-10088] p 678 N92-24514
Some comments on turbulence modeling from an industrial perspective p 678 N92-24531
A three-dimensional, compressible, laminar boundary-layer method for general fuselages. Volume 1: Numerical method
[NASA-CR-4292-VOL-1] p 679 N92-24547
An incremental strategy for calculating consistent discrete CFD sensitivity derivatives
[NASA-TM-104207] p 625 N92-24681
Proceedings of the 3rd Canadian Symposium on Aerodynamics
[CTN-92-60420] p 625 N92-24849
Periodic Euler and Navier-Stokes solutions about oscillating airfoils p 626 N92-24850
VORVISC: A vortex lattice method with viscous and compressibility corrections for full aircraft configurations including propulsion p 626 N92-24857
Laminar-turbulent transition process in the presence of simulated wall roughness p 626 N92-24858
On the coupling of Euler/boundary-layer equations
p 627 N92-24859
A scheme for two dimensional Euler and boundary layer interactive solutions p 627 N92-24860
A two-dimensional Euler solution for an unbladed jet engine configuration p 627 N92-24861
Nonliner aspects of transonic aeroelasticity
p 628 N92-24864
Automated grid generation for high-lift configurations
p 628 N92-24869
Nonunique solutions in unsteady transonic flow
p 629 N92-24872
Boundary layer computations using a generalized formulation p 679 N92-24873
Aerodynamic design and analysis of a light aircraft propeller p 629 N92-24876
Turbulence modeling for hypersonic flight
[NASA-CR-190313] p 630 N92-24898
Observations on computational methodologies for use in large-scale, gradient-based, multidisciplinary design incorporating advanced CFD codes
[NASA-TM-104206] p 630 N92-24956
An analytical approach to grid sensitivity analysis for NACA four-digit wing sections
[NASA-CR-190251] p 631 N92-25175
Assessment of potential aerodynamic benefits from spanwise blowing at the wing tip
[NASA-TM-107847] p 631 N92-25261
An engineering method for interactive inviscid-boundary layers in three-dimensional hypersonic flows
[NASA-TM-107838] p 632 N92-25279
Joint computational and experimental aerodynamics research on a reentry vehicle
[DE91-017315] p 667 N92-25315
Cartesian based grid generation/adaptive mesh refinement p 682 N92-25722
Computational Fluid Dynamics --- numerical methods and algorithm development
[NASA-CP-10078] p 660 N92-25808
Development of new flux splitting schemes --- computational fluid dynamics algorithms
p 682 N92-25809
A new Lagrangian method for real gases at supersonic speed p 633 N92-25814
Study of shock-induced combustion using an implicit TVD scheme p 669 N92-25816
A high angle of attack inviscid shuttle orbiter computation
[NASA-TM-107606] p 685 N92-25964
Research activities on CFD at the Ship Research Institute p 766 N92-26908
Three dimensional boundary layer transition on a yawed cylinder p 766 N92-26909
Aerodynamic drag on the bullet trains
p 766 N92-26911
Flow around an isolated surface roughness in the laminar boundary layer p 766 N92-26913
Application of riblet surface to pipe flow
p 766 N92-26915
Cross-flow instabilities and pressure gradients in boundary layers p 767 N92-26922
The changing role of experimentation in aeroengine R and D: The point of view of the research worker
[AD-A246372] p 740 N92-27062
Steady and unsteady 3D flow computation through a transonic turbine stage p 742 N92-27469
The 3-D Navier-Stokes flow and temperature field computation for a forced mixer nozzle
p 770 N92-27482
Modelling the vaporiser and primary zone flows for a modern gas turbine combustion chamber
p 742 N92-27484
Three dimensional calculations of reactive flows within aircraft combustion chambers including some combustion models p 770 N92-27490
A frontal approach for node generation in Delaunay triangulations p 771 N92-27680
Transonic Unsteady Aerodynamics and Aeroelasticity
[AGARD-CP-507] p 718 N92-27936
Computation of the unsteady transonic 2D cascade flow by an Euler algorithm with interactive grid generation
p 719 N92-27944
Computation of viscous phenomena in unsteady transonic flow p 720 N92-27949
The benchmark aeroelastic models program: Description and highlights of initial results
p 721 N92-27960
Viscous effects on a vortex wake in ground effect
[NASA-CR-190400] p 907 N92-28361
Analysis of results of an Euler-equation method applied to leading-edge vortex flow
[NLR-TP-90368-U] p 827 N92-28657
Calculation of unsteady subsonic and supersonic flow about oscillating wings and bodies by new panel methods
[NLR-TP-89119-U] p 827 N92-28659
Turbulence modeling: Survey of activities in Belgium and the Netherlands, and appraisal of the status and a view on the prospects
[NLR-TP-90184-U] p 908 N92-28694
Boundary conditions for Euler equations at internal block faces of multi-block domains using local grid refinement
[NLR-TP-90134-U] p 908 N92-28712
Explicit Navier-Stokes computation of turbomachinery flows
[AD-A249284] p 909 N92-28879
Applied analytical combustion/emissions research at the NASA Lewis Research Center
[NASA-TM-105731] p 890 N92-29343
Development of a multigrid transonic potential flow code for cascades
[NASA-CR-190480] p 830 N92-29361
A comparison of the calculated and experimental off-design performance of a radial flow turbine
[NASA-CR-189207] p 831 N92-29402
Spatial and temporal adaptive procedures for the unsteady aerodynamic analysis of airfoils using unstructured meshes
[NASA-TM-107635] p 831 N92-29445
Hyperbolic grid generation control by panel methods
[NLR-TP-91061-U] p 924 N92-29604
NASA Workshop on future directions in surface modeling and grid generation
[NASA-CP-10092] p 831 N92-29625
Aeronautical Engineering Group publications, 1950 - present
[AERO-REPT-8907] p 910 N92-29683
A semi empirical method for the analytical representation of stationary measured profile coefficients for applications of rotary wing aerodynamics
[ETN-92-91491] p 832 N92-29741
Aerodynamic design optimization using sensitivity analysis and computational fluid dynamics
[NASA-CASE-LAR-14815-1-CU] p 910 N92-29830

Production of periodical Mach number variations in high subsonic flow in a blow down wind tunnel, and its influence on profile measurements
[ETN-92-91492] p 833 N92-29889
Explicit Navier-Stokes computation of turbomachinery flows
[AD-A248458] p 911 N92-29933
Navier-Stokes computations of a viscous optimized waverider
[NASA-CR-189658] p 944 N92-30392
A gridless Euler/Navier-Stokes solution algorithm for complex two-dimensional applications
[NASA-TM-107631] p 944 N92-30570
Numerical optimization in Germany: A non-exhaustive survey on current activities with emphasis on aeronautics
[MBB/FE211/S/PUB/474] p 932 N92-30675
CFD contributions during hypersonic airplane intake design
[MBB/FE213/S/PUB/459] p 944 N92-30676
Implicit upwind-Euler solution algorithms for unstructured-grid applications
[NASA-TM-107645] p 945 N92-30691
MATGRID, a program for generation of C-H and C-O topology grids around wing/body configurations: Software description document
[FFA-TN-1990-20] p 945 N92-30713
Numerical methods for the simulation of complex multi-body flows with applications for the integrated Space Shuttle vehicle
[NASA-CR-190045] p 945 N92-30740
Numerical methods for the simulation of complex multi-body flows with applications for the integrated Space Shuttle vehicle p 945 N92-30741
Application of the Chimera overlapped grid scheme to simulation of Space Shuttle ascent flows
p 945 N92-30742
Delaunay triangulation and computational fluid dynamics meshes
[NASA-TM-107663] p 1010 N92-30907
Navier-Stokes analysis and experimental data comparison of compressible flow within ducts
[NASA-TM-105796] p 972 N92-30972
Development of a 3-D upwind PNS code for chemically reacting hypersonic flowfields
[NASA-CR-190182] p 946 N92-30977
CFD methods development considerations for unsteady aerodynamic analysis
[NASA-TM-107644] p 947 N92-31239
Stagnation-point heat-transfer rate predictions at aeroassist flight conditions
[NASA-TP-3208] p 1001 N92-31281
Advanced thermally stable, jet fuels development program annual report. Volume 1: Model and experiment system development
[AD-A249625] p 988 N92-31462
A general numerical model for wave rotor analysis
[NASA-TM-105740] p 1002 N92-31484
Hypersonic code efficiency and validation studies
[NASA-CR-190680] p 948 N92-31533
The structure and control of three-dimensional shock wave turbulent boundary layer interactions
[AD-A250209] p 1003 N92-31824
NAS (Numerical Aerodynamic Simulation Program) technical summaries, March 1989 - February 1990
[NASA-TM-107960] p 1013 N92-31852
The calculation of incompressible separated turbulent boundary layers p 1003 N92-31886
Euler solver for arbitrary configurations: Further applications p 949 N92-31888
A computational examination of directional stability for smooth and chined forebodies at high-alpha
[NASA-CR-4465] p 950 N92-32114
An installed nacelle design code using a multiblock Euler solver. Volume 1: Theory document
[NASA-CR-189652-VOL-1] p 950 N92-32226
Three-dimensional compressible turbulent computations for a nondiffusing S-duct
[NASA-CR-4391] p 951 N92-32240
Numerical simulation of turbomachinery flows with advanced turbulence models p 1124 N92-32270
Potential flow theory and operation guide for the panel code PMARC
[NASA-TM-102851] p 1036 N92-32422
Computations of unsteady multistage compressor flows in a workstation environment
[NASA-TM-103839] p 1071 N92-32452
Modeling and numerical simulation of vortex flow in aerodynamics
[NLR-TP-91154-U] p 1037 N92-32673
Numerical simulation of turbulence at the back of the airplane
[ETN-92-91664] p 1037 N92-32769
Further development of the CANAERO computer code to include propulsor modelling
[DREA-CR-90-425] p 1038 N92-32811
Perspectives on hypersonic viscous and nonequilibrium flow research
[NASA-CR-190817] p 1039 N92-33413
Activities report of the National Aerospace Laboratory
[ETN-92-92053] p 1143 N92-33694
Navier-Stokes analysis and experimental data comparison of compressible flow in a diffusing S-duct
[NASA-TM-105683] p 1072 N92-33746
Numerical investigation of the effects of icing on fixed and rotary wing aircraft
[NASA-CR-190542] p 1044 N92-34105
Application of computational fluid dynamics to the study of vortex flow control for the management of inlet distortion
[NASA-TM-105672] p 1128 N92-34112
Flutter in the transonic flight regime
p 1089 N92-34167

COMPUTATIONAL GEOMETRY

A method for estimating the minimum distance between two flight vehicles during their separation
p 486 A92-30139
Shape optimization of three-dimensional structures with adaptive meshing
[AIAA PAPER 92-2434] p 586 A92-34548
A geometry-integrated approach to multiblock grid generation p 919 A92-47083

COMPUTATIONAL GRIDS

Implicit flux-split Euler schemes for unsteady aerodynamic analysis involving unstructured dynamic meshes p 5 A92-11057
Three-dimensional space-marching algorithm on unstructured grids p 5 A92-11058
An efficient method for calculating three-dimensional transonic flow past air intakes p 7 A92-12178
Aeroelastic analysis of wings using the Euler equations with a deforming mesh p 10 A92-13215
The simulation of three-dimensional viscous flow in turbomachinery geometries using a solution-adaptive unstructured mesh methodology
[ASME PAPER 91-GT-124] p 71 A92-15569
Multi-blade row Navier-Stokes simulations of fan-bypass configurations
[ASME PAPER 91-GT-148] p 73 A92-15586
Turbulent flow calculations using unstructured and adaptive meshes p 153 A92-15823
Algebraic turbulence modeling for unstructured and adaptive meshes p 216 A92-18362
Upwind scheme for solving the Euler equations on unstructured tetrahedral meshes p 175 A92-20735
Computational vorticity capturing - Application to helicopter rotor flows
[AIAA PAPER 92-0056] p 250 A92-22171
Control of turbulent flow on a backward-facing step
[AIAA PAPER 92-0066] p 250 A92-22179
An AF3 algorithm for the calculation of transonic nonconservative full potential flow around axisymmetric inlet cowls p 251 A92-23380
An algorithm for predicting the flow past fuselage-mounted engine arrangements
[AIAA PAPER 92-0151] p 253 A92-23766
A Navier-Stokes solver for stretched triangular grids
[AIAA PAPER 92-0183] p 256 A92-23793
Grid studies for thin-layer Navier-Stokes computations of airfoil flowfields
[AIAA PAPER 92-0184] p 256 A92-23794
Study of role of unsteady separation in formation of dynamic stall vortex
[AIAA PAPER 92-0196] p 257 A92-23804
On one method of constructing adaptive difference grids in aerodynamics problems p 311 A92-24902
On an adaptive numerical method for solution of high gradient problems p 410 A92-24905
Analysis of an advanced ducted propeller subsonic inlet
[AIAA PAPER 92-0274] p 318 A92-25728
A wave-model-based refinement criterion for adaptive-grid computation of compressible flows
[AIAA PAPER 92-0322] p 321 A92-25769
Predictions of compressible viscous flows at all Mach number using pressure correction, collocated primitive variables and non-orthogonal meshes
[AIAA PAPER 92-0426] p 326 A92-26274
A comparative study of turbulence models for overset grids
[AIAA PAPER 92-0437] p 327 A92-26284
Quality assessment of two- and three-dimensional unstructured meshes and validation of an upwind Euler flow solver
[AIAA PAPER 92-0444] p 328 A92-26288
A fast implicit upwind solution algorithm for three-dimensional unstructured dynamic meshes
[AIAA PAPER 92-0447] p 328 A92-26291
Numerical investigation of a transverse jet for supersonic aerodynamic control
[AIAA PAPER 92-0639] p 334 A92-27017
An analytical approach to grid sensitivity analysis --- of NACA wing sections
[AIAA PAPER 92-0660] p 334 A92-27031
Three-dimensional adaptive grid generation with applications in nonlinear fluid dynamics
[AIAA PAPER 92-0661] p 397 A92-27032
Embedded meshes of controllable quality synthesised from elementary geometric features
[AIAA PAPER 92-0663] p 411 A92-27034
Finite element Navier-Stokes solver for unstructured grids p 398 A92-28035
Cartesian Euler method for arbitrary aircraft configurations p 340 A92-28039
Unsteady airfoil flow solutions on moving zonal grids
[AIAA PAPER 92-0543] p 342 A92-28200
Effective treatments of the singular line boundary problem for three dimensional grids
[AIAA PAPER 92-0545] p 342 A92-28202
Navier-Stokes solution of transonic cascade flows using nonperiodic C-type grids p 344 A92-28523
Optimized control of structured grids
p 429 A92-30520
Orthogonal grids around difficult bodies
p 432 A92-31160
Navier-Stokes simulation of flow through a highly contoured subsonic diffuser p 433 A92-31491
Extending a transonic small disturbance code to treat swept vertical surfaces
[AIAA PAPER 92-2503] p 518 A92-34498
Three-dimensional time-marching aeroelastic analyses using an unstructured-grid Euler method
[AIAA PAPER 92-2506] p 542 A92-34500
Structural optimization at Aerospatiale Aircraft
[AIAA PAPER 92-2371] p 601 A92-34542
Shape optimization of three-dimensional structures with adaptive meshing
[AIAA PAPER 92-2434] p 586 A92-34548
Spatial adaptation of unstructured meshes for unsteady aerodynamic flow computations p 610 A92-36838
The computation of three-dimensional flows using unstructured grids p 612 A92-37539
Panel method control in 3-D hyperbolic grid generation
p 617 A92-39940
Structural and aerodynamic data transformation using inverse isoparametric mapping p 758 A92-41242
Domain-decomposition algorithm applied to multielement airfoil grids p 703 A92-41261
Adaptive mesh for turbulent hypersonic flow
[AIAA PAPER 92-2776] p 704 A92-41322
Navier-Stokes computations for pointed, spherical, and flat tipped shell at Mach 3 p 705 A92-41536
Aerodynamic design of an advanced turboprop using Euler codes p 737 A92-43196
Numerical simulation of aerothermal loads in hypersonic engine inlets due to shock impingement
[AIAA PAPER 92-2605] p 792 A92-45482
Future directions in computing and CFD
[AIAA PAPER 92-2734] p 917 A92-45489
Coupled numerical simulation of the external and engine inlet flows for the F-18 at large incidence
[AIAA PAPER 92-2621] p 793 A92-45493
Shock fitting with a finite volume approximation to the Euler equations
[AIAA PAPER 92-2646] p 796 A92-45513
Recent CFD applications on jet transport configurations
[AIAA PAPER 92-2658] p 844 A92-45519
Spatial and temporal adaptive procedures for the unsteady aerodynamic analysis of airfoils using unstructured meshes
[AIAA PAPER 92-2694] p 800 A92-45540
Commercial turbofan engine exhaust nozzle flow analyses using PAB3D
[AIAA PAPER 92-2701] p 801 A92-45543
Numerical simulations using a dynamic solution-adaptive grid algorithm, with applications to unsteady internal flows
[AIAA PAPER 92-2719] p 803 A92-45557
A new automatic grid generation environment for CFD applications
[AIAA PAPER 92-2720] p 803 A92-45558
Comparison of two flux splitting schemes for calculation of ogive-cylinder at M = 3.5 and alpha = 18 deg
[AIAA PAPER 92-2667] p 806 A92-45582
A fast, implicit unstructured-mesh Euler method
[AIAA PAPER 92-2693] p 917 A92-45589
An unstructured approach to the design of multiple-element airfoils
[AIAA PAPER 92-2709] p 807 A92-45592
Viscous high-speed flow computations by adaptive mesh embedding techniques p 808 A92-45839
Mesh adaption for 2D transsonic Euler flows on unstructured meshes p 816 A92-47038
Mesh adaptivity with the quadtree method
p 816 A92-47041

Unstructured and adaptive mesh generation for high Reynolds number viscous flows p 816 A92-47042
Anisotropic control of mesh generation based upon a Voronoi type method p 918 A92-47043
Grid adaptation to multiple functions for applied aerodynamic analysis p 817 A92-47045
Adaptive parallel meshes with complex geometry p 918 A92-47050
Gridding strategies and associated results for winged entry vehicles p 918 A92-47051
An unstructured mesh generation algorithm for three-dimensional aeronautical configurations p 918 A92-47053
Single block mesh generation for a fuselage plus two lifting surfaces p 817 A92-47054
Grid generation and compressible flow computations about a high-speed civil transport configuration p 919 A92-47055
Grid sensitivity in low Reynolds number hypersonic continuum flows p 817 A92-47057
Multi-block grid generation around wing-body-engine-pylon configurations p 817 A92-47060
3-D numerical grid generation for the transonic flow analysis about multi-bodies p 817 A92-47061
Interactive algebraic mesh generation for twin jet transport aircraft p 817 A92-47064
Interactive generation of structured/unstructured surface meshes using adaptivity p 919 A92-47066
Effect of the grid system on heat transfer computations for high speed flows p 900 A92-47071
Generation of efficient multiblock grids for Navier-Stokes computations p 919 A92-47081
The construction, application and interpretation of three-dimensional hybrid meshes p 919 A92-47089
Orthogonal grids for multiple airfoils p 818 A92-47096
Numerical study of secondary separation in glancing shock/turbulent boundary layer interactions
[AIAA PAPER 92-3666] p 907 A92-49087
On multiple grid method p 1006 A92-49585
Application of an unsteady Navier-Stokes solver to transonic turbine design p 935 A92-50273
Application of a solution adaptive grid scheme to complex three-dimensional flows p 935 A92-50309
Method of large particles in arbitrary curvilinear orthogonal coordinates for the solution of problems of hydro and aerodynamics p 937 A92-52035
The numerical simulation of flow about installed aero engine nacelle using a finite element Euler solver on unstructured meshes p 941 A92-52848
Solution of Euler equations with unstructured mesh - 3-D case p 941 A92-52973
Comparison of turbulence models for powered-lift flow fields
[AIAA PAPER 92-3674] p 1022 A92-54117
Grid studies for thin-layer Navier-Stokes computations of airfoil flowfields p 1025 A92-54935
Three dimensional numerical method for resolving small transonic perturbations in unstructured mesh
[ONERA-RT-56/3064-RY-006-R] p 13 N92-10989
Comparison of solution of various Euler solvers and one Navier-Stokes solver for the flow about a sharp-edged cropped delta wing
[AD-B163639L] p 83 N92-12998
Vortical flow simulation by using structured and unstructured grids p 83 N92-12999
Design optimization of transonic airfoils p 177 N92-13961
Computational fluid dynamics p 177 N92-13979
Analysis of an advanced ducted propeller subsonic inlet
[NASA-TM-105393] p 179 N92-14002
Progress with multigrid schemes for hypersonic flow problems
[NASA-CR-189579] p 185 N92-15047
A fast implicit upwind solution algorithm for three-dimensional unstructured dynamic meshes
[NASA-TM-104186] p 185 N92-15050
Zonal solutions for a double-ellipse in a hypersonic flowfield
[AERO-REPT-9009] p 345 N92-18233
Accurate, productive aerodynamic simulation on patched mesh systems
[AD-A243977] p 405 N92-19386
Numerical simulation of vortical flow over a delta wing at subsonic and transonic speeds
[NLR-TP-90029-U] p 444 N92-20498
A novel approach in formulation of special transition elements: Mesh interface elements
[NASA-CR-189050] p 501 N92-20954
An alternative to unstructured grids for computing gas dynamic flows around arbitrarily complex two-dimensional bodies
[NASA-CR-189612] p 447 N92-21465
Cases 6.1 and 6.8 double ellipsoid: Navier-Stokes calculation p 525 N92-22181
Three-dimensional compressible turbulent computations for a diffusing S-duct
[NASA-CR-4392] p 526 N92-22249
Methodology for sensitivity analysis, approximate analysis, and design optimization in CFD for multidisciplinary applications --- computational fluid dynamics
[NASA-CR-190201] p 595 N92-22662
Three-dimensional time-marching aeroelastic analyses using an unstructured-grid Euler method
[NASA-TM-107567] p 527 N92-23116
Grid generation and flow solution method for Euler equations on unstructured grids
[NASA-TM-4295] p 528 N92-23533
Interactive solution-adaptive grid generation procedure
[NASA-TM-105432] p 528 N92-23563
A user guide for the EMTAC-MZ CFD code
[NASA-CR-4283] p 678 N92-24242
Geometry acquisition and grid generation: Recent experiences with complex aircraft configurations p 691 N92-24400
Domain modeling and grid generation for multi-block structured grids with application to aerodynamic and hydrodynamic configurations p 691 N92-24411
An interactive multi-block grid generation system p 691 N92-24419
On constructing three-dimensional overlapping grids with CMPGRD p 691 N92-24424
A multiblock grid generation technique applied to a jet engine configuration p 692 N92-24428
Periodic Euler and Navier-Stokes solutions about oscillating airfoils p 626 N92-24850
A two-dimensional Euler solution for an unbladed jet engine configuration p 627 N92-24861
Automated grid generation for high-lift configurations p 628 N92-24869
Boundary layer computations using a generalized formulation p 679 N92-24873
An analytical approach to grid sensitivity analysis for NACA four-digit wing sections
[NASA-CR-190251] p 631 N92-25175
Workshop on Grid Generation and Related Areas
[NASA-CP-10089] p 659 N92-25712
Grid management p 632 N92-25713
An interactive grid generation technique for turbomachinery p 659 N92-25717
TIGER: Turbomachinery interactive grid generation p 659 N92-25718
TIGGERC: Turbomachinery interactive grid generator energy distributor and restart code p 659 N92-25719
Multiblock grid generation for jet engine configurations p 659 N92-25720
Cartesian based grid generation/adaptive mesh refinement p 682 N92-25722
Grid generation research at OSU p 633 N92-25723
Integrating aerodynamic surface modeling for computational fluid dynamics with computer aided structural analysis, design, and manufacturing p 682 N92-25727
Progress in integrated analysis with adaptive unstructured meshing p 683 N92-25914
Finite element methods for integrated aerodynamic heating analysis
[NASA-CR-190353] p 633 N92-25959
Three-dimensional upwind scheme for solving the Euler equations on unstructured tetrahedral grids --- tetrahedral grids p 714 N92-26585
Eulerian computational methods
[DE92-008017] p 765 N92-26853
An integrated CFD system for 3D turbomachinery applications p 741 N92-27464
Predictions and measurements of 3D viscous flow in a transonic turbine nozzle guide vane row p 741 N92-27466
Navier-Stokes analysis of turbine blade heat transfer and performance p 768 N92-27468
Special Course on Unstructured Grid Methods for Advection Dominated Flows
[AGARD-R-787] p 771 N92-27671
A frontal approach for node generation in Delaunay triangulations p 771 N92-27680
Unstructured-grid methods development for unsteady aerodynamic and aeroelastic analyses p 718 N92-27938
Computations of unsteady flows around airfoil sections by explicit and implicit methods solving the Euler and Navier-Stokes equations p 720 N92-27948
Transonic aeroelastic computations on wings using Navier-Stokes equations p 721 N92-27957
Wave drag determination in the transonic full-potential flow code MATRICS
[NLR-TP-90062-U] p 828 N92-28709
Boundary conditions for Euler equations at internal block faces of multi-block domains using local grid refinement
[NLR-TP-90134-U] p 908 N92-28712
Spatial and temporal adaptive procedures for the unsteady aerodynamic analysis of airfoils using unstructured meshes
[NASA-TM-107635] p 831 N92-29445
Hyperbolic grid generation control by panel methods
[NLR-TP-91061-U] p 924 N92-29604
Progress in unstructured-grid methods development for unsteady aerodynamic applications
[NASA-TM-107643] p 944 N92-30393
CFD contributions during hypersonic airplane intake design
[MBB/FE213/S/PUB/459] p 944 N92-30676
Implicit upwind-Euler solution algorithms for unstructured-grid applications
[NASA-TM-107645] p 945 N92-30691
Numerical methods for the simulation of complex multi-body flows with applications for the integrated Space Shuttle vehicle
[NASA-CR-190045] p 945 N92-30740
Application of the Chimera overlapped grid scheme to simulation of Space Shuttle ascent flows p 945 N92-30742
Trajectory fitting in function space with application to analytic modeling of surfaces
[NASA-TP-3232] p 945 N92-30747
Direct simulation of high-speed mixing layers
[NASA-TP-3186] p 945 N92-30909
Hypersonic code efficiency and validation studies
[NASA-CR-190680] p 948 N92-31533
Axisymmetric bluff-body flow: A vortex solver for thin shells
[DE92-016748] p 1003 N92-31933
A method for designing blended wing-body configurations for low wave drag
[NASA-TP-3261] p 1036 N92-32480
New concepts for multi-block grid generation for flow domains around complex aerodynamic configurations
[NLR-TP-91046-U] p 1037 N92-32730
Research on some centered implicit methods for calculating transonic flows by solving Navier-Stokes equations
[ONERA-RSF-24/1408-AY-150A] p 1037 N92-32773
Development of 3D electromagnetic modeling tools for airborne vehicles
[NASA-CR-190810] p 1126 N92-33307
Investigation of advancing front method for generating unstructured grid
[NASA-CR-190902] p 1128 N92-34043

COMPUTER AIDED DESIGN

A basis for ice formation design p 146 A92-14556
A development of computer support system for wing design p 162 A92-15332
Subsonic propulsion system installation analysis and optimization
[ASME PAPER 91-GT-167] p 111 A92-15602
Interactive engine system dynamics analysis
[ASME PAPER 91-GT-193] p 124 A92-15619
Numerical optimization of helicopter rotor blade airfoils using unsteady aerodynamic calculations
[ONERA, TP NO. 1991-187] p 78 A92-16141
Delivered with feeling --- computer-based design of flight control system for Boeing 777 p 134 A92-16621
Feeling normal --- evaluation of advanced control systems for future Boeing 777 p 134 A92-16623
Design and flight test of a differential GPS/inertial navigation system for approach/landing guidance p 97 A92-16650
Detuning from the natural resonances of the blade in the computer-aided design of blade rows for axial-flow compressors p 80 A92-16818
Computer-aided equipment layout for the fuselage of maneuverable aircraft p 113 A92-16833
Model based reasoning in the aerospace domain
[AIAA PAPER 91-3709] p 230 A92-17582
Applications of an automated programming system
[AIAA PAPER 91-3767] p 231 A92-17629
Multidisciplinary modeling and simulation of a generic hypersonic vehicle
[AIAA PAPER 91-5015] p 232 A92-17813
Two-dimensional, incompressible aerofoil design and analysis p 247 A92-21987
McDonnell Douglas' new light twin helicopter - The MDX p 271 A92-22710
From concept to model: Conception and evaluation of an architecture for a distributed system with SAHARA - Some reflections on results of the utilization of SAHARA in the framework of the Electronic Copilot
[ONERA, TP NO. 1991-216] p 411 A92-26368
The NASA Computational Aerosciences Program - Toward teraFLOPS computing
[AIAA PAPER 92-0558] p 411 A92-26968

Application researches on expert system used for structural layout optimization of wings
p 398 A92-27865
Antennas on complex platforms p 494 A92-31084
Preliminary sizing methodology for hypersonic vehicles
p 460 A92-32233
The initial development of an expert system for designing composite material wing structures p 599 A92-32542
Preliminary design of an intermittent smoke flow visualization system
[AIAA PAPER 92-1028] p 580 A92-33209
Tying it all together - The NASA/USRA University Advanced Design Program
[AIAA PAPER 92-1040] p 605 A92-33221
Concepts for a future aircraft design environment
[AIAA PAPER 92-1188] p 600 A92-33300
Integration of artificial intelligence and numerical optimization techniques for the design of complex aerospace systems
[AIAA PAPER 92-1189] p 600 A92-33301
An interactive system for aircraft design and optimization
[AIAA PAPER 92-1190] p 600 A92-33302
Design sheet - An environment for facilitating flexible trade studies during conceptual design
[AIAA PAPER 92-1191] p 600 A92-33303
Constraint-based component-modeling for knowledge-based design
[AIAA PAPER 92-1192] p 600 A92-33304
ACSYNT - A standards-based system for parametric, computer aided conceptual design of aircraft
[AIAA PAPER 92-1268] p 601 A92-33345
AIAA/ASME/ASCE/AHS/ASC Structures, Structural Dynamics and Materials Conference, 33rd, Dallas, TX, Apr. 13-15, 1992, Technical Papers. Pt. 5 - Design engineering/design optimization, materials, work-in-progress p 585 A92-34522
Structural optimization at Aerospatiale Aircraft
[AIAA PAPER 92-2371] p 601 A92-34542
An expert system to aid real world finite element analysis
[AIAA PAPER 92-2488] p 601 A92-34604
The aerodynamic assistant - A tool for V/STOL aircraft conceptual design p 545 A92-35737
TMFSLAM - Design analysis tool for coated structures
[ASME PAPER 91-GT-141] p 690 A92-36895
Dimensional characterization of a large aircraft structure by photogrammetry p 607 A92-37061
Use of the thrust-weight diagram versus transport cargo in the initial dimensioning of passenger-transport aircraft
p 642 A92-37074
New processes in commercial airplane design
p 607 A92-38218
Production technologies and aircraft design
p 608 A92-38220
Integral equation methods for linear and nonlinear aerodynamics p 617 A92-39949
Software package for preliminary design of helicopter
p 775 A92-41195
Automation of flight vehicle design --- Russian book
[ISBN 5-217-01447-4] p 776 A92-42780
Optimum structural design of a cantilevered rectangular elastic wing with a gust load alleviation system
p 762 A92-43133
Aerodynamic design of a nonplanar airfoil by an inverse method with Navier-Stokes equations
p 711 A92-43197
Two-point optimization of complete three-dimensional airplane configuration
[AIAA PAPER 92-2618] p 844 A92-45491
Practical design optimization of wing/body configurations using the Euler equations
[AIAA PAPER 92-2633] p 795 A92-45505
Transonic airfoil and wing design using Navier-Stokes codes
[AIAA PAPER 92-2651] p 797 A92-45518
Recent CFD applications on jet transport configurations
[AIAA PAPER 92-2658] p 844 A92-45519
Surface grid generation in a parameter space
[AIAA PAPER 92-2717] p 803 A92-45556
A new automatic grid generation environment for CFD applications
[AIAA PAPER 92-2720] p 803 A92-45558
Minimizing supersonic wave drag with physical constraints at design and off-design Mach numbers
p 811 A92-46808
Grid generation and compressible flow computations about a high-speed civil transport configuration
p 919 A92-47055
Patch-independent structured multiblock grids for CFD computations p 919 A92-47078
Developing intelligent automatic test equipment
p 922 A92-48569
Analytical design and demonstration of a low-cost expendable turbine engine combustor
[AIAA PAPER 92-3754] p 867 A92-49112
On the application of parabolized Navier-Stokes equations to flow field simulations p 936 A92-51943
A review of some computer programs of composites
p 1009 A92-53069
Development of data base system in CIEM project
p 1009 A92-53093
Integrated system to support computer analysis in conceptual aerospace design p 1130 A92-53596
Computer aided evaluation of aircraft handling qualities and flight control system robustness
[AIAA PAPER 92-4423] p 1080 A92-55347
PAYCOS, a multidisciplinary sizing code for hypersonic vehicles
[AIAA PAPER 92-4564] p 1132 A92-55376
Configuration of flexible-skirts for an ACV and its CAD
p 1118 A92-56036
A development of hypermedia type database system for instruction of aircraft conceptual design
p 1132 A92-56113
Application of advanced multidisciplinary analysis and optimization methods to vehicle design synthesis
p 1054 A92-56160
HiRel - Reliability/availability integrated workstation tool p 1120 A92-56257
Design of a variable contraction for a full-scale automotive wind tunnel
[AIAA PAPER 92-3929] p 1096 A92-56760
Computers in aeronautics and space research at the Lewis Research Center
[NASA-TM-105096] p 53 N92-11642
Process/object-oriented Ada software design for an experimental helicopter p 164 N92-12461
Control augmented structural optimization of aeroelasticity tailored fiber composite wings
[AD-A241464] p 135 N92-13075
Experiences with optimizing airfoil shapes for maximum lift over drag p 90 N92-13838
The use of artificial neural networks in experimental data acquisition and aerodynamic design p 90 N92-13848
Third International Conference on Inverse Design Concepts and Optimization in Engineering Sciences (ICIDES-3)
[NASA-CR-188125] p 170 N92-13928
Review of aerodynamic design in the Netherlands
p 193 N92-13929
Aerodynamic aircraft design methods and their notable applications: Survey of the activity in Japan
p 193 N92-13930
Research on inverse, hybrid and optimization problems in engineering sciences with emphasis on turbomachine aerodynamics: Review of Chinese advances
p 201 N92-13939
An inverse method for the aerodynamic design of three-dimensional aircraft engine nacelles
p 194 N92-13958
A CLIPS-based tool for aircraft pilot-vehicle interface design p 303 N92-16605
Investigation of air transportation technology at Princeton University, 1990-1991 p 266 N92-17995
RAMREQ: A computerized tool for the definition of RAM (Reliability, Availability, Maintainability) requirements of complex systems p 412 N92-18647
Parametric bicubic spline and CAD tools for complex targets shape modelling in physical optics radar cross section prediction p 403 N92-19151
Engine Structures Modeling Software System (ESMOSS)
[NASA-CR-187227] p 404 N92-19277
Adaptive control of nonlinear systems with applications to the control of flexible robot arms
[AD-A244409] p 413 N92-19397
A walk through the planned CS building
[NASA-CR-189963] p 386 N92-19675
Application of a water droplet trajectory prediction code to the design of inlet particle separator anti-icing systems
[PNR-90839] p 474 N92-20573
Aerodynamic design with CFD p 447 N92-21514
Computer-aided design of flight control systems
[AD-A244657] p 483 N92-21752
Compressing the compressor
[PNR-90824] p 476 N92-21848
Multidisciplinary optimization studies using ASTROS
p 571 N92-23234
First approach to an integrated fin design
p 551 N92-23236
Simultaneous stress and flutter optimization for the wing of a transport aircraft equipped with four engines
p 571 N92-23238
Structural optimization of aircraft practice and trends
p 551 N92-23239
From IGES to STEP
[REPT-3.1.6] p 603 N92-23881
Software Surface Modeling and Grid Generation Steering Committee
[NASA-CP-3143] p 691 N92-24397
An interactive multi-block grid generation system
p 691 N92-24419
An incremental strategy for calculating consistent discrete CFD sensitivity derivatives
[NASA-TM-104207] p 625 N92-24681
Observations on computational methodologies for use in large-scale, gradient-based, multidisciplinary design incorporating advanced CFD codes
[NASA-TM-104206] p 630 N92-24956
CAD product data exchange: Conversions for curves and surfaces
[ISBN-90-6275-723-9] p 648 N92-24964
An analytical approach to grid sensitivity analysis for NACA four-digit wing sections
[NASA-CR-190251] p 631 N92-25175
Wind energy program overview
[DE91-002178] p 689 N92-25498
Grid generation research at OSU p 633 N92-25723
Integrating aerodynamic surface modeling for computational fluid dynamics with computer aided structural analysis, design, and manufacturing
p 682 N92-25727
Computational Structures Technology for Airframes and Propulsion Systems
[NASA-CP-3142] p 683 N92-25911
Computational structures technology and UVA Center for CST p 683 N92-25912
Computer codes developed and under development at Lewis p 692 N92-25913
CSM activities at the NASA Langley Research Center
p 683 N92-25916
Aircraft optimization by a system approach: Achievements and trends
[NASA-TM-107622] p 650 N92-25995
Algorithms for blending surface generation
[AD-A245686] p 777 N92-26524
System requirements specification for SMART structures mode p 777 N92-27830
Surface generation and editing operations applied to structural support of aerospace vehicle fuselages
p 777 N92-27831
Applications of ASICs to avionics
[AGARD-AG-329] p 859 N92-28376
What is an ASIC? p 859 N92-28377
Integrated Design Analysis and Optimisation of Aircraft Structures
[AGARD-LS-186] p 851 N92-28469
Fundamentals of structural optimisation
p 851 N92-28470
The evaluation of simulator effectiveness for the training of high speed, low level, tactical flight operations
p 885 N92-28539
Constrained spanload optimization for minimum drag of multi-lifting-surface configurations
[NLR-TP-89126-U] p 828 N92-28660
Improving designer productivity --- artificial intelligence
[NASA-TM-103929] p 854 N92-29417
MBB-LAGRANGE: A general structural reliability and optimization structural system
[MBB/FW321/S/PUB/467] p 998 N92-30423
A surface definition code for turbine blade surfaces
[DE92-010574] p 1004 N92-31498
Automatic design of transonic airfoils to reduce the shock induced pressure drag p 949 N92-31863
Integrated computer systems in aircraft design and manufacture: Difficulties and implications
p 1010 N92-31864
A parameter optimization approach to controller partitioning for integrated flight/propulsion control application
[NASA-TM-105826] p 979 N92-32241
Flutter analyses using high speed computers. Part 1: Flutter analyses for large aircraft p 1089 N92-34168
Flutter analyses using high speed computers. Part 2: Aerodynamic procedures p 1089 N92-34169

COMPUTER AIDED MANUFACTURING

Automated composite lay-up p 146 A92-14450
McDonnell Douglas' new light twin helicopter - The MDX p 271 A92-22710
Reliability aspects in computer integrated manufacturing systems p 397 A92-27838
Blade repair with adaptive vision tracking
[ASME PAPER 91-GT-208] p 607 A92-36897
Aircraft maintenance support system
p 607 A92-38217
Production technologies and aircraft design
p 608 A92-38220
Process control challenges during the manufacture of large superplastically formed/diffusion bonded structure
[SAE PAPER 912195] p 674 A92-40012
Recent manufacturing advances for spiral bevel gears
[SAE PAPER 912229] p 674 A92-40024
Stringer subsystem automation p 700 A92-43246

Development of an automatic metal sheet working machine for interior structure p 700 A92-43247
Automation of composite material structure installation p 700 A92-43248
Manufacturing technology methodology for propulsion system parts
[AIAA PAPER 92-3525] p 906 A92-49048
Manufacturing cost model for composites p 1012 A92-51565
Development of data base system in CIEM project p 1009 A92-53093
From IGES to STEP
[REPT-3.1.6] p 603 N92-23881
Improving designer productivity --- artificial intelligence
[NASA-TM-103929] p 854 N92-29417
Integrated computer systems in aircraft design and manufacture: Difficulties and implications p 1010 N92-31864

COMPUTER AIDED MAPPING
Navigation - Land, sea, air, and space --- Book
[ISBN 0-87942-257-2] p 496 A92-31778
Iberia's Aeronautical Mapping Application (ACAI) p 637 A92-37073
Noisemap 6.0 - The USAF microcomputer program for airport noise analysis p 686 A92-39051
Calculation of aircraft noise contours taking into account the lateral flight track dispersion p 687 A92-39059
Digital mapping display technology p 735 A92-43225
Map projections and airborne moving map displays p 966 A92-49327
Integration of radar altimeter, precision navigation, and digital terrain data for low-altitude flight
[AIAA PAPER 92-4420] p 1063 A92-55212

COMPUTER AIDED TOMOGRAPHY
X-ray computed tomography of composites p 36 A92-10143
NDE of advanced turbine engine components and materials by computed tomography
[ASME PAPER 91-GT-287] p 152 A92-15681
The use of CT for dimensional measurements of green and sintered ceramic components p 490 A92-28592
X-ray computed tomographic inspection of castings p 492 A92-28725
X-ray computed tomography for the aircraft/aerospace industry p 492 A92-28750
Computed tomography (CT) as a nondestructive test method used for composite helicopter components p 1121 A92-56276
Study of detached turbulent flow in an air intake by means of high speed tomography and laser velocimetry
[REPT-90/55] p 157 N92-12216
Computered tomography: Experimental data acquisition and parallelization of reconstruction algorithm
[DE92-005151] p 499 N92-20301
Computed Tomography (CT) as a nondestructive test method used for composite helicopter components
[MBB-UD-0603-91-PUB] p 910 N92-29873

COMPUTER ANIMATION
Flow visualization using computer animation p 629 N92-24870

COMPUTER ASSISTED INSTRUCTION
Advanced technology for aviation maintenance training - An industry status report and development plan p 47 A92-11180
C.A.T.C.H. - Computer aided test conductor handbook: A method for reducing cost, time and effort in an aircraft test and certification program p 602 A92-35943
Advanced training systems for the next decade and beyond
[AIAA PAPER 92-1626] p 690 A92-38699
Design specifications for the Advanced Instructional Design Advisor (AIDA), volume 2
[AD-A248202] p 923 N92-29188
Implementation of a personal computer based parameter estimation program
[AD-A252914] p 1061 N92-33502

COMPUTER DESIGN
Ultra High Speed Numerical Wind Tunnel (UHSNWT) initiative at National Aerospace Laboratory numerical simulator - second generation
[NAL-TR-1108] p 384 N92-18037

COMPUTER GRAPHICS
Helicopter control response types for hover and low-speed near-earth tasks in degraded visual conditions p 132 A92-14338
Sensor fusion for synthetic vision
[AIAA PAPER 91-3730] p 197 A92-17597
Interactive graphics method for removal of helicopter motions from laser profile data p 598 A92-35109
Iberia's Aeronautical Mapping Application (ACAI) p 637 A92-37073
Current status and future tasks of a cockpit liquid crystal display p 735 A92-43222
Interactive algebraic mesh generation for twin jet transport aircraft p 817 A92-47064
Real time presentation for RAFALE in-flight tests p 882 A92-47522
Simulation of automatic rotorcraft nap-of-the-earth flight in graphics workstation environment
[AIAA PAPER 92-4131] p 981 A92-52428
A simulation study of tiltrotor vertical takeoff procedures using conventional and variable diameter rotor systems p 1056 A92-56301
Mixed approach towards modular avionics conflicting requirements p 199 N92-14051
The multi-attribute task battery for human operator workload and strategic behavior research
[NASA-TM-104174] p 303 N92-17130
An application of the object-oriented paradigm to a flight simulator
[AD-A243624] p 384 N92-18012
Accurate, productive aerodynamic simulation on patched mesh systems
[AD-A243977] p 405 N92-19386
A walk through the planned CS building
[NASA-CR-189963] p 386 N92-19675
A graphical weather system design for the NASA transport systems research vehicle B-737
[NASA-TM-104205] p 556 N92-22504
From IGES to STEP
[REPT-3.1.6] p 603 N92-23881
TIGER: Turbomachinery interactive grid generation p 659 N92-25718
A modeling strategy for large-scale optimization based on analysis and visualization principles
[AD-A246570] p 777 N92-26620
Experimental evaluation of candidate graphical microburst alert displays
[NASA-CR-189633] p 735 N92-27424
Integrated computer systems in aircraft design and manufacture: Difficulties and implications p 1010 N92-31864
A graphical user-interface for propulsion system analysis
[NASA-TM-105696] p 1134 N92-33894
Computational algorithms for increased control of depth-viewing volume for stereo three-dimensional graphic displays
[NASA-TM-4379] p 1065 N92-34109

COMPUTER INFORMATION SECURITY
Systems simulation of an advanced avionics COMSEC unit p 921 A92-48485

COMPUTER NETWORKS
A study of a ground support equipment (GSE) network p 748 A92-43158
Advanced information processing system: Inter-computer communication services
[NASA-CR-187556] p 53 N92-11706
Architecture for Survivable System Processing (ASSP) p 220 N92-14210
Data Multiplexing Network (DMN) phase 3 equipment Operational Test and Evaluation (OT and E)/integration test report
[DOT/FAA/CT-TN91/50] p 221 N92-14270
The Flight Simulation Facility at the Wichita State University p 484 N92-21511
National airspace data interchange network analysis
[AD-A247345] p 727 N92-27217
SATWG networked quality function deployment p 1134 N92-33339

COMPUTER PROGRAM INTEGRITY
Cleanroom - An alternative software development process p 233 A92-19386
Distributed systems: Interconnection and fault tolerance studies
[AD-A252869] p 1135 N92-33920

COMPUTER PROGRAMMING
Formal specification and verification of Ada software
[AIAA PAPER 91-3713] p 230 A92-17585
Advanced avionics system development environment
[AIAA PAPER 91-3944] p 231 A92-17608
Applications of an automated programming system
[AIAA PAPER 91-3767] p 231 A92-17629
The Software Factory, version 5.0
[AIAA PAPER 92-0590] p 411 A92-26992
A real-time rain-flow method of cycle counting and its program design for aeroengine service loads p 557 A92-35560
The VISTA/F-16 programmable feel system
[AIAA PAPER 92-4172] p 977 A92-52457
A development-memory approach for enhancing avionics software logistics p 119 N92-12540
Development of a calibrated software reliability model for flight and supporting ground software for avionic systems p 234 N92-15870
A CLIPS-based tool for aircraft pilot-vehicle interface design p 303 N92-16605
Technical evaluation report on the 52nd Symposium on Software for Guidance and Control
[AGARD-AR-302] p 303 N92-17498
Software Engineering Laboratory (SEL) Ada performance study report
[NASA-TM-105510] p 412 N92-18125
Engine Structures Modeling Software System (ESMOSS)
[NASA-CR-187227] p 404 N92-19277
Development of a flight information system using the structured method
[AD-A248207] p 859 N92-29222
Analysis of data from a DO-178A software development process p 1134 N92-32880

COMPUTER PROGRAMS
A computer programme for the certification of helicopter vertical take-off and landing operations and an application to the S-76B helicopter p 106 A92-14379
Euler flow predictions for an oscillating cascade using a high resolution wave-split scheme
[ASME PAPER 91-GT-198] p 74 A92-15623
Analysis of cooling systems for hypersonic aircraft
[AIAA PAPER 91-5063] p 216 A92-17843
Some Aspects of uncertainty in computational fluid dynamics results p 233 A92-19609
Computations of the flow past bodies and wings using Euler equations p 312 A92-25038
LEWICE/E - An Euler based ice accretion code
[AIAA PAPER 92-0037] p 316 A92-25676
Prediction of ice accretion on a swept NACA 0012 airfoil and comparisons to flight test results
[AIAA PAPER 92-0043] p 316 A92-25677
Integrated numerical methods for hypersonic aircraft cooling systems analysis
[AIAA PAPER 92-0254] p 357 A92-25712
Analysis of an advanced ducted propeller subsonic inlet
[AIAA PAPER 92-0274] p 318 A92-25728
Effects of bleed and power extraction on the operating line of engines p 469 A92-29717
Comparison of heating calculations with experimental data on a modified Shuttle Orbiter p 441 A92-32184
Concepts for a future aircraft design environment
[AIAA PAPER 92-1188] p 600 A92-33300
Constraint-based component-modeling for knowledge-based design
[AIAA PAPER 92-1192] p 600 A92-33304
Extending a transonic small disturbance code to treat swept vertical surfaces
[AIAA PAPER 92-2503] p 518 A92-34498
Iberia's Aeronautical Mapping Application (ACAI) p 637 A92-37073
Noisemap 6.0 - The USAF microcomputer program for airport noise analysis p 686 A92-39051
Software package for preliminary design of helicopter p 775 A92-41195
Prediction of vortex shedding from forebodies with chines p 702 A92-41228
Evaluation of the ATD-GASP for endo-leap applications --- Aerothermal Technology Development of Generalized Aerodynamic Simulation Programs
[AIAA PAPER 92-2771] p 704 A92-41318
New systolic array for all-nearest-neighbours problem p 776 A92-41419
A progress report on ASTOVL control concept studies under the VAAC programme p 871 A92-45319
The design of a system of codes for industrial calculations of flows around aircraft and other complex aerodynamic configurations
[AIAA PAPER 92-2619] p 917 A92-45492
DYNamic Turbine Engine Compressor Code (DYNTECC) - Theory and capabilities
[AIAA PAPER 92-3190] p 923 A92-48802
Application of a solution adaptive grid scheme to complex three-dimensional flows p 935 A92-50309
Simulation software flowdown in the aircraft design process - Problems and solutions
[AIAA PAPER 92-4160] p 1008 A92-52450
Dynamic derivative data for high angle of attack simulation
[AIAA PAPER 92-4355] p 1079 A92-55341
Engine condition monitoring system for B747-400 p 1064 A92-56082
The operational status of automated aircraft washing system p 1016 A92-56087
A module-level testing environment for safety-critical software systems p 1132 A92-56293
Aerodynamic calculation of an elliptic ring wing
[AIAA PAPER 91-0068] p 1035 A92-57035
Numerical simulation of hypersonic viscous flow for the design of H-2 orbiting plane (HOPE-2)
[NAL-TR-1093] p 11 N92-10009
CH-53E/AV-8B aircraft sling load recovery system analysis
[AD-A239950] p 21 N92-10022
Development of unsteady aerodynamic analyses for turbomachinery aeroelastic and aeroacoustic applications
[NASA-CR-4405] p 12 N92-10979

Model representation in the PANCOR wall interference assessment code
[NASA-TM-104152] p 31 N92-11022
Parameter identification studies on the NASA/Ames Research Center Advanced Concepts Flight Simulator
[NASA-TM-105126] p 31 N92-11024
Calibration of the Naval Postgraduate School 3.5' x 5.0' academic wind tunnel
[AD-A240614] p 31 N92-11025
Theoretical study (Lagrangian modeling) of turbulent particulate dispersion
[ETN-91-99909] p 42 N92-11287
Resolution of the Navier-Stokes equations applied to the computation of the laminar flow around a two dimensional wing profile
[CERT-RT-65/5604-35] p 43 N92-11307
Numerical verification of NISA 2 finite element analysis of the cracked 5th stage compressor disc of J-85 jet engine
[NRC-LTR-ST-1792] p 129 N92-11997
Computer programs for the calculation of dual sting pitch and roll angles required for an articulated sting to obtain angles of attack and sideslip on wind-tunnel models
[NASA-TM-104161] p 138 N92-12007
An improved model-creation program for EM interaction analysis
[NRC-31764] p 155 N92-12153
Military and civil software standards and guidelines for guidance and control p 163 N92-12452
Adaptive tactical navigation program
p 102 N92-12529
A development-memory approach for enhancing avionics software logistics p 119 N92-12540
Air-to-air visual acquisition handbook
[ATC-151] p 93 N92-13042
Rotorcraft acceleration and climb performance model
[SCT-90RR-30] p 116 N92-13059
Preservation and utilization of finite element models of USAF aircraft structures
[AD-A241657] p 160 N92-13470
Experiences with optimizing airfoil shapes for maximum lift over drag p 90 N92-13838
Formulation of the linear model from the nonlinear simulation for the F18 HARV p 117 N92-13842
The use of artificial neural networks in experimental data acquisition and aerodynamic design p 90 N92-13848
Aerodynamic aircraft design methods and their notable applications: Survey of the activity in Japan
p 193 N92-13930
On a global aerodynamic optimization of a civil transport aircraft p 193 N92-13931
LEWICE/E: An Euler based ice accretion code
[NASA-TM-105389] p 179 N92-14001
Analysis of an advanced ducted propeller subsonic inlet
[NASA-TM-105393] p 179 N92-14002
Automated problem resolution prototype in automated en route air traffic control p 190 N92-14028
A unique approach to aircraft conflict resolution using artificial intelligence techniques p 190 N92-14029
Determination of rotordynamic coefficients for labyrinth seals and application to rotordynamic design calculations p 223 N92-14360
Application of MSC/DYNA to shock and impact problems in aircraft industry
[MBB-UD-0593-91-PUB] p 225 N92-14382
A concept for the revisions of structural inspection schedules p 226 N92-14431
Aviation Diagnostics And Maintenance (ADAM) system preliminary concept of operation and functional description
[AD-A242598] p 170 N92-14966
Viscous shock-layer equations for the calculation of reentry aerothermodynamics p 183 N92-15008
Development and evaluation of a finite element model for a fiber composite helicopter fuselage
[MBB-UD-0584-90-PUB] p 196 N92-15066
Project of an adaptive multiaxial autopilot with learning pilot control
[ETN-92-90592] p 205 N92-15072
The NASA Langley Research Center 0.3-meter transonic cryogenic tunnel microcomputer controller source code
[NASA-CR-189556] p 209 N92-15077
Industrial code development p 227 N92-15083
Development of a calibrated software reliability model for flight and supporting ground software for avionic systems p 234 N92-15870
Prediction of ice accretion on a swept NACA 0012 airfoil and comparisons to flight test results
[NASA-TM-105368] p 258 N92-15968
Supersonic propulsion simulation by incorporating component models in the large perturbation inlet (LAPIN) computer code
[NASA-TM-105193] p 279 N92-15993
Automated composite ellipsoid modelling for high frequency GTD analysis
[NASA-CR-189853] p 275 N92-17316
Viscous three-dimensional calculations of transonic fan performance
[NASA-TM-103800] p 242 N92-17346
Information Management Engineering (IME) laboratory: A database development facility
[AD-A243191] p 305 N92-17369
Program plans: Aviation safety research
[NIAR-91-30] p 264 N92-17587
An analysis of the aircraft engine Component Improvement Program (CIP): A life cycle cost approach
[AD-A243346] p 280 N92-17729
A robust digital flight control system for an unfanned research vehicle using discrete quantitative feedback theory
[AD-A243638] p 283 N92-17748
Aging aircraft structural damage analysis
p 360 N92-18575
A parametric approach to spectrum development
p 360 N92-18578
Steps toward acceptance p 355 N92-19046
Asymptotic theory of transonic wind tunnel wall interference
[AD-A244075] p 403 N92-19080
Thermal nonequilibrium effects on turbine cascade aerodynamics
[AD-A244049] p 404 N92-19183
Effect of nonuniform entrance flow profile on hypersonic nozzle pitching moment
[AD-A244050] p 377 N92-19184
Analysis of an advanced fighter aircraft using jet flap techniques and the vortex lattice method
[AD-A244051] p 366 N92-19185
Analysis of lossy composite terminating structures
[NASA-CR-189901] p 404 N92-19217
Particle trajectory computer program for icing analysis of axisymmetric bodies
[NASA-CR-189134] p 352 N92-19276
An algorithm for robust eigenstructure assignment using the linear quadratic regulator
[AD-A244267] p 412 N92-19335
Structured Hypermedia Application Development Model (SHADM): A structured model for technical documentation application design
[AD-A244268] p 417 N92-19336
Reuse metrics and measurement: A framework
p 413 N92-19432
Validation of flight critical control systems
[AGARD-AR-274] p 382 N92-20026
Advanced electromagnetic methods for aerospace vehicles
[NASA-CR-188630] p 488 N92-20193
Computer code for preliminary sizing analysis of axial-flow turbines
[NASA-CR-4430] p 473 N92-20196
MATGRID: A program for generation of C-H and C-O topology grids around wing/body configurations. Mathematical definition document
[FFA-TN-1990-19] p 444 N92-20468
Optimization of composite sandwich cover panels subjected to compressive loadings
[NASA-TP-3173] p 489 N92-20679
Flow studies in close-coupled ventral nozzles for STOVL aircraft
[NASA-TM-102554] p 445 N92-20934
Icing simulation: A survey of computer models and experimental facilities p 450 N92-21684
Method for calculating the three-dimensional water concentration coefficients and its industrial applications
p 502 N92-21685
Three-dimensional compressible turbulent computations for a diffusing S-duct
[NASA-CR-4392] p 526 N92-22249
Advanced Transport Operating System (ATOPS) color displays software description: MicroVAX system
[NASA-CR-189603] p 556 N92-22395
Overview of NASA PTA propfan flight test program
p 561 N92-22536
Advanced Transport Operating System (ATOPS) color displays software description microprocessor system
[NASA-CR-189605] p 556 N92-22645
PAN AIR: A computer program for predicting subsonic or supersonic linear potential flows about arbitrary configurations using a higher order panel method. Volume 2: User's manual (version 3.0)
[NASA-CR-3252] p 527 N92-22865
Effects of chemical equilibrium on turbine engine performance for various fuels and combustor temperatures
[NASA-TM-105399] p 562 N92-23254
Development and application of computational aerothermodynamics flowfield computer codes
[NASA-CR-190294] p 624 N92-24229
A user guide for the EMTAC-MZ CFD code
[NASA-CR-4283] p 678 N92-24242
An interactive multi-block grid generation system
p 691 N92-24419
A study of viscous interaction effects on hypersonic waveriders
[NASA-CR-189587] p 625 N92-24680
A study of transonic aerodynamic analysis methods for use with a hypersonic aircraft synthesis code
[NASA-CR-189854] p 625 N92-24803
VORVISC: A vortex lattice method with viscous and compressibility corrections for full aircraft configurations including propulsion p 626 N92-24857
Experimental evaluation of a flat wake theory for predicting rotor inflow-wake velocities
[NASA-TM-4334] p 630 N92-24882
MLS and DME/P multipath simulation model user's manual. Volume 1: Operating instructions
[DOT/FAA/CT-TN91/47] p 640 N92-24888
Prediction and analysis of wing flutter at transonic speeds p 662 N92-25555
TCGRID: A three dimensional C-grid generator for turbomachinery p 659 N92-25716
Grid generation research at OSU p 633 N92-25723
Computer codes developed and under development at Lewis p 692 N92-25913
Military engine computational structures technology
p 660 N92-25934
Naval Postgraduate School aircraft synthesis program (user's manual)
[AD-A246198] p 777 N92-26458
A modeling strategy for large-scale optimization based on analysis and visualization principles
[AD-A246570] p 777 N92-26620
The navigation data logger for a suitcase navigation system
[AD-A245997] p 727 N92-26756
Computer program for calculating in-flight aircraft-store interface reaction loads
[AD-A245782] p 731 N92-26896
Buffered serial data card
[AD-A246435] p 727 N92-26948
Computational method to predict thermodynamic, transport, and flow properties for the modified Langley 8-foot high-temperature tunnel
[NASA-TM-4374] p 767 N92-27193
Validation of a CANARI code by the computation of three dimensional turbulent flow in turbine valve
p 741 N92-27462
Viscous three-dimensional calculations of transonic fan performance p 768 N92-27467
System requirements specification for SMART structures mode p 777 N92-27830
Calculation of installation effects within performance computer programs p 869 N92-28465
Use of a virtual cockpit for the development of a future transport aircraft p 886 N92-28547
Calculation of unsteady subsonic and supersonic flow about oscillating wings and bodies by new panel methods
[NLR-TP-89119-U] p 827 N92-28659
Constrained spanload optimization for minimum drag of multi-lifting-surface configurations
[NLR-TP-89126-U] p 828 N92-28660
A method for computing the 3-dimensional flow about wings with leading-edge vortex separation. Part 2: Description of computer program VORSEP
[NLR-TR-86006-U] p 833 N92-29916
Experience with piloted simulation in the development of helicopters
[MBB-UD-0610-91-PUB] p 889 N92-30076
Users manual for updated computer code for axial-flow compressor conceptual design
[NASA-CR-189171] p 924 N92-30207
Selection of opening model for parachute scaling studies
[AD-A250882] p 943 N92-30239
A model of the ADA avionics real-time system: An example of the benefits of the hardware/software codesign approach in development of real-time systems
[AD-A248893] p 967 N92-30524
Development statistics for the UH-1 Ada feasibility study
[AD-A252404] p 982 N92-30547
Numerical calculations of two-dimensional single and multi-material flow fields with CCICE
[DE92-015778] p 1000 N92-30903
Nonlinear aerodynamics and the design of wing tips
[NASA-CR-190649] p 946 N92-31157
High speed turboprop aeroacoustic study (counterrotation). Volume 2: Computer programs
[NASA-CR-185242] p 1011 N92-31248
A surface definition code for turbine blade surfaces
[DE92-010574] p 1004 N92-31498

Integrated computer systems in aircraft design and manufacture: Difficulties and implications
p 1010 N92-31864
Euler solver for arbitrary configurations: Further applications p 949 N92-31888
Data reduction formulas for the 16-foot transonic tunnel: NASA Langley Research Center, revision 2
[NASA-TM-107646] p 984 N92-31900
An installed nacelle design code using a multiblock Euler solver. Volume 1: Theory document
[NASA-CR-189652-VOL-1] p 950 N92-32226
An installed nacelle design code using a multiblock Euler solver. Volume 2: User guide
[NASA-CR-189652-VOL-2] p 951 N92-32228
Analysis of data from a DO-178A software development process p 1134 N92-32880
Simulation test and evaluation of TCAS 2 logic version 6.04
[DOT/FAA/RD-92/23] p 1048 N92-33098
Implementation of a personal computer based parameter estimation program
[AD-A252914] p 1061 N92-33502
Distributed systems: Interconnection and fault tolerance studies
[AD-A252869] p 1135 N92-33920
Finite difference time domain grid generation from AMC helicopter models
[NASA-TM-107679] p 1128 N92-34017
Turbulence-induced loads on a teetered rotor
p 1042 N92-34029
Investigation of advancing front method for generating unstructured grid
[NASA-CR-190902] p 1128 N92-34043

COMPUTER SYSTEMS DESIGN

Advanced avionics system development environment
[AIAA PAPER 91-3944] p 231 A92-17608
Cleanroom - An alternative software development process p 233 A92-19386
Design of compensators for linear parameter-varying feedback systems by the gain scheduling technique
p 507 A92-29101
New Boeing flight test data acquisition systems
p 920 A92-47537
Design considerations for a modern telemetry processing and display system p 882 A92-47584
Global memory in the Pave Pace architecture
p 920 A92-48447
Modular techniques for dynamic fault-tree analysis
p 1120 A92-56241
The electronic aeronautical chart for general aeronautics: A system specification
[ILR-MITT-263(1991)] p 20 N92-10997
Pilot's associate: Evolution of a functional prototype
p 118 N92-12531
Getting expert systems off the ground: Lessons learned from integrating model-based diagnostics with prototype flight hardware p 220 N92-14217
Improvement of data processing system for gust wind tunnel data acquisition part: System conversion from off-line to on-line processing
[NAL-TM-611] p 285 N92-17756
Experiences developed in transfering the experimental COMPAS system to an operational prototype version
p 355 N92-19045
Extension of the Frankfurt COMPAS for general application p 355 N92-19048
Formal design and verification of a reliable computing platform for real-time control. Phase 2: Results
[NASA-TM-104196] p 602 N92-22320
Delfi: Design, development, and applicability of expert systems shells
[ISBN-90-6275-734-0] p 692 N92-25306
A brief overview of computational structures technology related activities at NASA Lewis Research Center
p 683 N92-25915
The design and development of a portable, DSP micro-processor based, high-accuracy data acquisition system
[NRC-32146] p 1134 N92-32851
The development of an airborne information management system for flight test
[NASA-TM-104251] p 1065 N92-32866
Human factors issues in the use of artificial intelligence in air traffic control. October 1990 Workshop
[NASA-CR-190925] p 1051 N92-34203

COMPUTER SYSTEMS PERFORMANCE

A new development in embedded computer performance measurement p 921 A92-48506
Verification and validation of F-15 and S/MTD unique software p 921 A92-48515
A new approach to embedded computer performance measurement --- in avionics p 1005 A92-49288
Parallel processing applications for gas turbine engine control p 25 N92-11012
Getting expert systems off the ground: Lessons learned from integrating model-based diagnostics with prototype flight hardware p 220 N92-14217
Data Multiplexing Network (DMN) phase 3 equipment Operational Test and Evaluation (OT and E)/integration test report
[DOT/FAA/CT-TN91/50] p 221 N92-14270
Development of a calibrated software reliability model for flight and supporting ground software for avionic systems p 234 N92-15870
Improvement of data processing system for gust wind tunnel data acquisition part: System conversion from off-line to on-line processing
[NAL-TM-611] p 285 N92-17756
Evaluation of the COMPAS operational system
p 355 N92-19047
Postflight aerothermodynamic analysis of Pegasus(tm) using computational fluid dynamic techniques
[NASA-CR-186017] p 445 N92-21188
Inspection of aircraft engine components using automated eddy current and pattern recognition techniques
[NRC-LTR-ST-1834] p 504 N92-22029
Trajectory optimization for hypersonic aircraft guidance p 728 N92-27898
Advanced techniques in reliability model representation and solution
[NASA-TP-3242] p 1134 N92-33483

COMPUTER SYSTEMS PROGRAMS

A development of computer support system for wing design p 162 A92-15332
Verification and validation of F-15 and S/MTD unique software p 921 A92-48515
Development and verification of software for flight safety critical systems p 164 N92-12469
Locally linear neural networks for aerospace navigation systems p 103 N92-12530
Advanced Transport Operating System (ATOPS) control display unit software description
[NASA-CR-189606] p 652 N92-24689

COMPUTER SYSTEMS SIMULATION

Verification of flight software by embedding software simulation in simulation of external environment
p 232 A92-19084
Simulation software flowdown in the aircraft design process - Problems and solutions
[AIAA PAPER 92-4160] p 1008 A92-52450

COMPUTER TECHNIQUES

Jet engine fault detection with discrete operating points gas path analysis p 129 A92-17200
Analysis technique for lightning attachment zoning of aircraft p 186 A92-20126
Opportunities for advanced speech processing in military computer-based systems p 293 A92-22299
Evaluation of two flow analyses for subsonic diffuser design
[AIAA PAPER 92-0273] p 317 A92-25727
A computerized flight inspection system --- for testing of basic air navigation ground facilities
p 726 A92-43881
Detecting 3-D, turbulent separation regions using unsteady computerized thermographic technique
p 1023 A92-54308
Calibration of the Naval Postgraduate School 3.5' x 5.0' academic wind tunnel
[AD-A240614] p 31 N92-11025
Computers in aeronautics and space research at the Lewis Research Center
[NASA-TM-105096] p 53 N92-11642
Air-to-air visual acquisition handbook
[ATC-151] p 93 N92-13042
Turbine engine diagnostics system study
[DOT/FAA/CT-91/16] p 202 N92-14064
Knowledge based system applications for guidance and control
[AGARD-AR-284] p 205 N92-14065
Artificial Neural Network Approaches in Guidance and Control
[AGARD-LS-179] p 234 N92-14673
Investigation of air transportation technology at Princeton University, 1990-1991 p 266 N92-17995
An application of the object-oriented paradigm to a flight simulator
[AD-A243624] p 384 N92-18012
Techfest 18 Proceedings
[NIAR-92-1] p 420 N92-21501
Aircraft drag analysis methods p 552 N92-23957
Integrating aerodynamic surface modeling for computational fluid dynamics with computer aided structural analysis, design, and manufacturing
p 682 N92-25727
Development of a flight information system using the structured method
[AD-A248207] p 859 N92-29222

COMPUTER VISION

Sensor fusion for synthetic vision
[AIAA PAPER 91-3730] p 197 A92-17597
Close-range photogrammetry meets machine vision; Proceedings of the Meeting, Zurich, Switzerland, Sept. 3-7, 1990
[SPIE-1395] p 994 A92-51626
Vision-based obstacle detection for rotorcraft flight
p 967 A92-52465
Vision-based stereo ranging as an optimal control problem
[AIAA PAPER 92-4418] p 1045 A92-55211
Passive range estimation for rotorcraft low-altitude flight
[NASA-TM-103897] p 2 N92-10003
A rotorcraft flight database for validation of vision-based ranging algorithms
[NASA-TM-103906] p 841 N92-29103
Vision-based range estimation using helicopter flight data
[NASA-TM-103930] p 1047 N92-32424

COMPUTERIZED SIMULATION

Numerical simulations of the structure of supersonic shear layers p 3 A92-10574
Computer simulation of weapon blast pressures on flexible surfaces p 39 A92-12115
A numerical simulation of separated flows around bodies p 8 A92-12423
Numerical simulation of the actuation system for the ALDF's propulsion control valve --- Aircraft Landing Dynamics Facility p 41 A92-13204
MIDIS - A microcomputer flight decision simulator
p 136 A92-13845
The helicopter air-to-air value-driven engagement model (HAVDEM) - Prototype development
p 105 A92-14353
A 3-D separation model for arbitrary planforms
p 65 A92-14360
A new method for simulating atmospheric turbulence for rotorcraft applications p 162 A92-14368
Effectiveness of V-22 tiltrotors in support of land combat operations p 60 A92-14442
Computer aiding for low-altitude helicopter flight
p 94 A92-14444
Numerical simulation for various flowfields of aero-engine components p 200 A92-17503
Verification of flight software by embedding software simulation in simulation of external environment
p 232 A92-19084
A processor-in-the-loop simulation using an XANALOG computer p 232 A92-19094
Enhanced autopilot design through hardware-in-the-loop simulation p 204 A92-19103
System-identification of airplanes using the 'estimation before modelling' technique p 269 A92-21007
A multi-layer neural network classifier for radar clutter
p 291 A92-21691
The FALSTAFF program - A standard spectrum for simulating the service loading of aircraft with prevailing maneuver loads p 284 A92-21922
Navier-Stokes code development for transonic flow simulations p 246 A92-21985
Wall interference calculation in a transonic test section including simulation of discrete slots
[AIAA PAPER 92-0032] p 249 A92-22153
Numerical studies of supersonic/hypersonic combustion
[AIAA PAPER 92-0094] p 293 A92-22200
Simulation of supersonic and hypersonic flows
p 251 A92-22790
A computational investigation of mixing and reacting flows in supersonic combustors
[AIAA PAPER 92-0626] p 278 A92-23817
Computer simulation model for Lucas Stirling refrigerators p 296 A92-23837
Comparison of two Navier-Stokes codes for attached transonic wing flows p 309 A92-24414
Multizonal Navier-Stokes solutions for the multibody Space Shuttle configuration p 310 A92-24667
A simplified method of transient mathematical model for non-augmentation engine p 372 A92-24750
Industry warms to CFD p 392 A92-24908
Numerical simulation of 2-D separated flows caused by suddenly change of the body section
p 312 A92-25004
A numerical method for solving the circulation control airfoil with wall jet p 314 A92-25103
Numerical simulation of twin-jet impingement on a flat plate coupled with cross-flow p 315 A92-25374
A quick automatic method for computing performance of nonducted propeller with constant-revolutional-speed
p 393 A92-25505
Three-dimensional simulation of slender delta wing rock and divergence
[AIAA PAPER 92-0280] p 318 A92-25734

Airborne in situ computation of the wind shear hazard index
[AIAA PAPER 92-0291] p 351 A92-25744
Proposal for a 3-D, vectorized, adaptable, algorithm for modeling the randomness, unsteadiness, and microphysical properties of ice accretion
[AIAA PAPER 92-0299] p 351 A92-25751
Analysis of hypersonic nozzles including vibrational nonequilibrium and intermolecular force effects
[AIAA PAPER 92-0330] p 322 A92-25777
Shock interference prediction using direct simulation Monte Carlo
[AIAA PAPER 92-0492] p 328 A92-26322
Monte Carlo simulation of entry in the Martian atmosphere
[AIAA PAPER 92-0494] p 329 A92-26324
Validation of a 3D Navier-Stokes code on experimental compressor bladings
[ONERA, TP NO. 1991-229] p 330 A92-26381
Numerical methods in elastoacoustics in the nonmodal domain
[ONERA, TP NO. 1991-232] p 415 A92-26383
Three-dimensional simulation of the Denver 11 July Storm of 1988 - An intense microburst event
p 407 A92-27958
Flowfield simulation about the SOFIA Airborne Observatory
[AIAA PAPER 92-0656] p 342 A92-28217
New developments in the computer simulation of X-ray nondestructive evaluation process p 490 A92-28588
A new method to estimate the effective geometric focal length and radius of ultrasonic focused probes
p 490 A92-28633
Real-time simulation and adaptive PID control of QSK-06A control for gas turbine p 470 A92-29740
Numerical simulation of supersonic nozzle flow
p 430 A92-30540
Numerical simulation of three-dimensional supersonic free shear layers p 431 A92-31152
Navier-Stokes simulation of flow through a highly contoured subsonic diffuser p 433 A92-31491
Joined-wing model vibrations using PC-based modal testing and finite element analysis
[AIAA PAPER 92-2260] p 541 A92-34417
Computational structures technology
[AIAA PAPER 92-2442] p 585 A92-34473
High-order state space simulation models of helicopter flight mechanics p 569 A92-35777
Some aerodynamic mechanisms of impulsive noise during blade-vortex-interaction p 604 A92-35782
Multifractal analysis of a lobed mixer flowfield utilizing the proper orthogonal decomposition
p 611 A92-36840
DANSIM - Danish Airport Noise Simulation Model - Basic principles, experience, and improvements
p 687 A92-39055
DANSIM applications - Development of airport noise reduction strategies and environmental policy
p 687 A92-39057
A review of computational/experimental methodology developments in aeroacoustics p 695 A92-39241
Measurements and simulation of the flow around a poppet valve p 675 A92-40103
Vortical flow simulation by the solution of the Navier-Stokes equations p 620 A92-40104
Simulation of turbulent velocity profiles appearing on rotating and stationary parts of subsonic compressors and turbines p 676 A92-40172
An analysis tool for UAV effectiveness evaluation
p 608 A92-40386
Simulation in the Air Force p 747 A92-41209
Simulation as applied to mission planning
p 747 A92-41210
Computation of saddle point of attachment
p 703 A92-41276
Simulation of commercial-aircraft reliability
p 759 A92-42057
Study on the lower aspect view of a helicopter simulator p 748 A92-43110
Study on the effective utilization of the current flight simulator p 748 A92-43113
Computer simulation of an unsteady flow around an airfoil with a spoiler p 710 A92-43167
Direct simulation of re-entry flows with ionization
p 713 A92-44367
Putting the control back in air traffic control - An enhanced Universal Development Simulation System
p 916 A92-44982
Numerical simulation of a supersonic jet impingement on a ground
[SAE PAPER 912014] p 789 A92-45412
Aerospace plane hydrogen scramjet boosting
[SAE PAPER 912071] p 891 A92-45451
Numerical simulation of aerothermal loads in hypersonic engine inlets due to shock impingement
[AIAA PAPER 92-2605] p 792 A92-45482
Prediction of rotor unsteady airloads using vortex filament theory
[AIAA PAPER 92-2610] p 792 A92-45484
Coupled numerical simulation of the external and engine inlet flows for the F-18 at large incidence
[AIAA PAPER 92-2621] p 793 A92-45493
A fast three-dimensional vortex method for unsteady wake calculations
[AIAA PAPER 92-2624] p 794 A92-45496
Numerical study on a supersonic open cavity flow with geometric modification of aft bulkhead
[AIAA PAPER 92-2627] p 794 A92-45499
Unsteady Navier-Stokes simulations of supersonic flow over a three-dimensional cavity
[AIAA PAPER 92-2632] p 795 A92-45504
Flight model for unmanned simulated helicopters
p 874 A92-46776
Hypersonic rarefied flow about a delta wing - direct simulation and comparison with experiment
p 812 A92-46892
Decoupled predictions of radiative heating in air using a particle simulation method
[AIAA PAPER 92-2971] p 816 A92-46986
New concepts for multi-block grid generation for flow domains around complex aerodynamic configurations
p 817 A92-47079
Numerical experiments on unsteady shock reflection processes using the thin-layer Navier-Stokes equations
p 818 A92-47155
Numerical simulation of chemical and thermal nonequilibrium flows behind compression shocks
[AIAA PAPER 92-2879] p 820 A92-47860
Laminar hypersonic flow over a compression using the HANA code
[AIAA PAPER 92-2896] p 820 A92-47872
Systems simulation of an advanced avionics COMSEC unit p 921 A92-48485
Computational icing analysis for aircraft inlets
[AIAA PAPER 92-3178] p 836 A92-48793
BUWICE - An interactive icing program applied to engine inlets
[AIAA PAPER 92-3179] p 922 A92-48794
DYNamic Turbine Engine Compressor Code (DYNTECC) - Theory and capabilities
[AIAA PAPER 92-3190] p 923 A92-48802
Progress towards the development of transient ram accelerator simulation as part of the U.S. Air Force Armament Directorate Research Program
[AIAA PAPER 92-3248] p 904 A92-48847
Numerical simulations of the transdetonative ram accelerator combusting flow field on a parallel computer
[AIAA PAPER 92-3249] p 894 A92-48848
A simplified real-time engine model for developing aeroengine control system
[AIAA PAPER 92-3321] p 864 A92-48904
Numerical study of secondary separation in glancing shock/turbulent boundary layer interactions
[AIAA PAPER 92-3666] p 907 A92-49087
The numerical simulation of the main fuel control unit of gas turbine engines
[AIAA PAPER 92-3760] p 867 A92-49115
An integrated analysis and simulation tool for avionics system development p 1005 A92-49289
Verification and validation testing of the pilot's associate p 966 A92-49318
The data flow simulator, a tool for system simulation --- in digital avionics p 1006 A92-49329
Dynamics and control of maneuverable towed flight vehicles p 976 A92-50508
JTIDS relative navigation and data registration
p 955 A92-51006
Development of a real-time simulation of a ship-correlated airwake model interfaced with a rotorcraft dynamic model
[AIAA PAPER 92-4149] p 1007 A92-52440
Numerical simulations of flutter and its suppression by active control
[AIAA PAPER 92-4652] p 1082 A92-55396
Direct simulation of low-density flow over airfoils
p 1030 A92-56159
A simulation study of tiltrotor vertical takeoff procedures using conventional and variable diameter rotor systems
p 1056 A92-56301
Short takeoff optimization for the XV-15 tiltrotor aircraft p 1056 A92-56302
Sound produced by vortex-airfoil interaction
p 1136 A92-56345
A high speed edgewise rotor using circulation control only in the reversed flow area p 1059 A92-56347
Integrated test and evaluation for hypervelocity systems
[AIAA PAPER 92-3901] p 1017 A92-56736
Application of electronically scanned pressure measurement system for engine simulation tests in the German-Dutch Wind Tunnel
[AIAA PAPER 92-4003] p 1122 A92-56826
Laboratory simulation of aerothermodynamic phenomena - A review
[AIAA PAPER 92-4025] p 1104 A92-56847
CH-53E/AV-8B aircraft sling load recovery system analysis
[AD-A239950] p 21 N92-10022
Results from computational analysis of a mixed compression supersonic inlet
[NASA-TM-104475] p 12 N92-10976
Numerical simulation of the reactive flow in advanced (HSR) combustors using KIVA-2
[NASA-CR-188996] p 26 N92-11014
Multi-disciplinary optimization of aeroservoelastic systems
[NASA-CR-188983] p 44 N92-11377
Advanced stress analysis methods applicable to turbine engine structures
[NASA-CR-187235] p 44 N92-11378
Computers in aeronautics and space research at the Lewis Research Center
[NASA-TM-105096] p 53 N92-11642
A new simulator for assessing subjective effects of sonic booms
[NASA-TM-104150] p 56 N92-11759
Investigation of the aeroelastic stability of the AFW wind-tunnel model using CAP-TSD
[NASA-TM-104142] p 81 N92-11977
An improved model-creation program for EM interaction analysis
[NRC-31764] p 155 N92-12153
A methodology for software specification and development based on simulation p 135 N92-12458
Locally linear neural networks for aerospace navigation systems p 103 N92-12530
Wall interference calculation in a transonic wind tunnel with discrete slots p 83 N92-12995
Modeling and numerical simulation of vortex flow in aerodynamics
[AD-B163670L] p 83 N92-12997
A 3-degree-of-freedom flight simulator evaluation of unsteady aerodynamics effects
[AD-A241540] p 139 N92-13079
Constant-temperature anemometry measurements in hypersonic boundary layers p 90 N92-13861
MLS system error model identification and synthesis
p 189 N92-14015
Mixed approach towards modular avionics conflicting requirements p 199 N92-14051
A multiblock flow solver for inviscid hypersonic flows
p 181 N92-14986
Piloted simulation study of a balloon-assisted deployment of an aircraft at high altitude
[NASA-TM-104245] p 272 N92-15986
Supersonic propulsion simulation by incorporating component models in the large perturbation inlet (LAPIN) computer code
[NASA-TM-105193] p 279 N92-15993
Implementation of an object-oriented flight simulator D.C. electrical system on a hypercube architecture
[AD-A243700] p 284 N92-17097
Weight evaluation and sensitivity analysis for space plane. Part 2: TSTO
[NAL-TM-602-PT-2] p 287 N92-17754
Ultra High Speed Numerical Wind Tunnel (UHSNWT) initiative at National Aerospace Laboratory numerical simulator - second generation
[NAL-TR-1108] p 384 N92-18037
Experiences developed in transfering the experimental COMPAS system to an operational prototype version
p 355 N92-19045
MULTIRAD
[AD-A244211] p 412 N92-19247
Runway exit designs for capacity improvement demonstrations. Phase 2: Computer model development
[NASA-CR-190166] p 484 N92-21162
Measurement of LORAN-C envelope to cycle difference in the far field
[PB92-128909] p 455 N92-21263
Probability of cycle jumps in Omega receivers and other phase locked loop applications
[PB92-128891] p 455 N92-21279
SIMNET plan view display user manual
[AD-A244617] p 510 N92-21392
Flight deck benefits of integrated data link communication
[NASA-TP-3219] p 456 N92-21459
Icing simulation: A survey of computer models and experimental facilities p 450 N92-21684
Simulation of iced wing aerodynamics
p 450 N92-21686
Principles and computer simulations of intercooled-turbocharged gas generator/expander engine p 592 N92-22132
Numerical simulation of transient hypervelocity flow in an expansion tube
[NASA-CR-189615] p 592 N92-22228

Dynamic simulation of a solid fuelled gas turbine system p 592 N92-22315
Modeling of linear isentropic flow systems p 593 N92-22495
NASA's aircraft icing technology program [NASA-TM-104518] p 527 N92-23105
Application of analytical and design tools for fighter wing aeroelastic tailoring p 550 N92-23231
Coupled multi-disciplinary simulation of composite engine structures in propulsion environment [NASA-TM-105575] p 596 N92-23267
Introduction to Special Course on Engineering Methods in Aerodynamic Analysis and Design of Aircraft p 552 N92-23951
Development and application of computational aerothermodynamics flowfield computer codes [NASA-CR-190294] p 624 N92-24229
Simulation of the flow on a space glider. Stagnation point calculation using the 2D Navier-Stokes equations including chemical effects p 624 N92-24393
Domain modeling and grid generation for multi-block structured grids with application to aerodynamic and hydrodynamic configurations p 691 N92-24411
Experimental evaluation of a flat wake theory for predicting rotor inflow-wake velocities [NASA-TM-4334] p 630 N92-24882
MLS and DME/P multipath simulation model user's manual. Volume 1: Operating instructions [DOT/FAA/CT-TN91/47] p 640 N92-24888
Assessment of potential aerodynamic benefits from spanwise blowing at the wing tip [NASA-TM-107847] p 631 N92-25261
On a multi-block method for transonic turbulent flows past a wing-fuselage configuration p 632 N92-25569
Application of nonlinear feedback control theory to supermaneuverable aircraft [NASA-CR-190336] p 663 N92-25648
Finite element methods for integrated aerodynamic heating analysis [NASA-CR-190353] p 633 N92-25959
Simulation of a rotorcraft in turbulent flows [AD-A245742] p 650 N92-26155
Simulation of 3D non-planar fatigue crack growth in a turbine blade root [DE92-006859] p 739 N92-26697
Reynolds number dependence of the drag coefficient for laminar flow through fine-scale screens [DE92-002930] p 765 N92-26698
Research activities on CFD at the Ship Research Institute p 766 N92-26908
Three dimensional boundary layer transition on a yawed cylinder p 766 N92-26909
Aerodynamic drag on the bullet trains p 766 N92-26911
Flow around an isolated surface roughness in the laminar boundary layer p 766 N92-26913
Application of riblet surface to pipe flow p 766 N92-26915
Cross-flow instabilities and pressure gradients in boundary layers p 767 N92-26922
Application of S1BYL2 to the AGARD WG18 compressor test cases p 768 N92-27452
The coherent flamelet model for propulsion applications p 756 N92-27486
Comparison of Janus and field test aircraft detection ranges for the line-of-sight forward heavy system [AD-A246047] p 770 N92-27600
Turbulent skin-friction drag reduction by active and passive means, part 1 p 718 N92-27714
Fuzzy guidance system evaluation p 778 N92-27903
ICAAS piloted simulation evaluation p 735 N92-27906
A time-linearization approach for unsteady transonic flows p 719 N92-27941
Dynamic simulation of compressor and gas turbine performance p 869 N92-28463
Aircraft ship operations [AGARD-AR-312] p 850 N92-28468
S-76B certification for vertical take-off and landing operations from confined areas [NLR-TP-90286-U] p 852 N92-28714
Quaternion and Euler angles in kinematics [NAL-TM-636] p 909 N92-28836
Modular simulation of HEI fragments and blast pressure [AD-A248205] p 910 N92-29191
Methods for direct simulation of transition in hypersonic boundary layers 2 p 912 N92-30064
Validation of three-dimensional incompressible spatial direct numerical simulation code: A comparison with linear stability and parabolic stability equation theories for boundary-layer transition on a flat plate [NASA-TP-3205] p 943 N92-30295
Resonance and control response tests using a control simulation device [MBB-UD-0608-91-PUB] p 978 N92-30439
Numerical methods for the simulation of complex multi-body flows with applications for the integrated Space Shuttle vehicle [NASA-CR-190045] p 945 N92-30740
Numerical methods for the simulation of complex multi-body flows with applications for the integrated Space Shuttle vehicle p 945 N92-30741
Numerical calculations of two-dimensional single and multi-material flow fields with CCICE [DE92-015778] p 1000 N92-30903
Direct simulation of high-speed mixing layers [NASA-TP-3186] p 945 N92-30909
Theoretical simulation of a 2 micron airborne solid state laser anemometer p 1000 N92-31059
A surface definition code for turbine blade surfaces [DE92-010574] p 1004 N92-31498
NAS (Numerical Aerodynamic Simulation Program) technical summaries, March 1989 - February 1990 [NASA-TM-107960] p 1013 N92-31852
Mathematical modeling and numerical simulation of the dynamics of flexible structures undergoing large overall motions [AD-A250202] p 979 N92-31967
Modeling and numerical simulation of vortex flow in aerodynamics [NLR-TP-91154-U] p 1037 N92-32673
Numerical simulation of turbulence at the back of the airplane [ETN-92-91664] p 1037 N92-32769
Simulation test and evaluation of TCAS 2 logic version 6.04 [DOT/FAA/RD-92/23] p 1048 N92-33098
Ideal efficiency of propellers based on Theodorsen's theory: A review and computer study, with extended plus simplified charts [UTIAS-TN-271] p 1071 N92-33102
Advanced techniques in reliability model representation and solution [NASA-TP-3242] p 1134 N92-33483
Simulation model of a twin-tail, high performance airplane [NASA-TM-107601] p 1088 N92-33537
Shafranov shift in low-aspect-ratio heliotron/torsatron CHS [NIFS-110] p 1138 N92-33743
Simulations of sonic boom ray tube area fluctuations for propagation through atmospheric turbulence including caustics via a Monte Carlo method p 1139 N92-33878
Subjective loudness response to simulated sonic booms p 1140 N92-33885
Dynamics and control of a five degree-of-freedom magnetic suspension system [NASA-CR-191259] p 1102 N92-34222

COMPUTERS

Use of a virtual cockpit for the development of a future transport aircraft p 886 N92-28547
A model of the ADA avionics real-time system: An example of the benefits of the hardware/software codesign approach in development of real-time systems [AD-A248893] p 967 N92-30524

CONCAVITY

Computations of hypersonic flows around a three-dimensional concave/convex body [AIAA PAPER 92-2606] p 805 A92-45570

CONCENTRATION (COMPOSITION)

Laser induced fluorescence detection of gums in jet fuels [AD-A252685] p 987 N92-30767

CONCENTRIC CYLINDERS

Acoustic scattering by a disk or annulus linking two concentric cylindrical shells. I - Theory and results for heavy exterior fluid loading. II - Results for heavy exterior fluid loading on both shells p 696 A92-40588

CONCORDE AIRCRAFT

Mind that restyle --- failure analysis of aircraft composite structures p 91 A92-13700
Concorde flight testing - Powerplant and performance flying [SAE PAPER 912192] p 644 A92-40009
Concorde, fifteen years on the front line [SAE PAPER 912193] p 644 A92-40010
Surface activation of Concorde by Be-7 p 605 N92-23295

CONCURRENT PROCESSING

Concurrent engineering at Boeing Helicopters p 162 A92-14393
Behavior-based fault monitoring [AD-A241254] p 164 N92-13746
Real-time processing of radar return on a parallel computer [NASA-CR-4456] p 1043 N92-32606

CONDENSERS (LIQUEFIERS)

Study of potassium turbine electric generator system p 1129 N92-33794

CONDENSING

Compressible turbulent boundary layers with heat addition by homogeneous condensation p 611 A92-36843
Humidity effects on gas turbine performance [NRC-30241] p 130 N92-11998
Temperature effects in FFA HYP 500 at M = 7 in a flow with strong expansion [FFA-TN-1991-27] p 443 N92-20229
Boiling and condensation in microfin tubes p 682 N92-25660
Further studies in filmwise condensation of steam on horizontal finned tubes [AD-A252705] p 1011 N92-31767

CONDUCTIVE HEAT TRANSFER

Conjugate conduction/convection/nucleate-boiling heat transfer with a high-speed boundary layer [AIAA PAPER 91-5033] p 215 A92-17823
An efficient finite element method for aircraft de-icing problems [AIAA PAPER 92-0532] p 459 A92-31670
Similarity and resistance in near-sonic flows for given heat conduction p 708 A92-43065
Assessment of calculation methods for efficiency of straight fins of rectangular profile p 1121 A92-56374
Investigation on freezing and sticking phenomena of slush on airplane surfaces when taxiing on the ground and the succeeding take-off run phase [NAL-TR-1026] p 352 N92-18182
Thermoacoustic refrigeration p 595 N92-22720

CONES

Numerical simulation of supersonic separated flow over blunt cones at high angles of attack p 313 A92-25039
Numerical simulation and analysis for hypersonic flow with separation over blunt cone at angle of attack p 314 A92-25126
On the sensitivity of transonic flow p 315 A92-25132
The lateral shock wave family on the surface of a cone-cylinder in transonic flowfield p 315 A92-25136
Multidomain spectral solutions of high-speed flows over blunt cones [AIAA PAPER 92-0324] p 322 A92-25771
Computation of laminar flow over a long slender axisymmetric blunted cone in hypersonic flow [AIAA PAPER 92-0756] p 336 A92-27098
Base pressure measurements on a cone at hypersonic Mach numbers: A contribution to aerothermodynamics for space vehicles p 181 N92-14992
Marching with the parabolized Navier-Stokes equations. Problem 1: Numerical study of hypersonic viscous cone flow [AERO-REPT-9007] p 344 N92-18231
Computation and stability analysis of laminar flow over a blunt cone in hypersonic flow p 1041 N92-33839

CONFERENCES

Biennial Fluid Dynamics Symposium on Advanced Problems and Methods in Fluid Mechanics, 19th, Kozubnik, Poland, Sept. 3-8, 1989, Selected Papers p 37 A92-10654
AIAA International Balloon Technology Conference, Albuquerque, NM, Oct. 8-10, 1991, Technical Papers p 1 A92-11001
IEEE Conference on Decision and Control, 29th, Honolulu, HI, Dec. 5-7, 1990, Proceedings. Vols. 1-6 p 47 A92-11312
Electrorheological fluids; Proceedings of the 2nd International Conference, Raleigh, NC, Aug. 7-9, 1989 p 40 A92-12625
AHS, Annual Forum, 47th, Phoenix, AZ, May 6-8, 1991, Proceedings. Vols. 1 & 2 p 59 A92-14326
Flight safety; Proceedings of the Conference, London, England, Nov. 21, 1991 p 92 A92-16050
1990 report to the aerospace profession; Society of Experimental Test Pilots, Symposium, 34th, Beverly Hills, CA, Sept. 27-29, 1990, Proceedings p 111 A92-16051
Institute of Navigation, National Technical Meeting, 47th, Phoenix, AZ, Jan. 22-24, 1991, Proceedings p 95 A92-16626
Development and design with advanced materials --- Book [ISBN 0-444-88706-7] p 296 A92-24176
CUSAE '91; Proceedings of the 1st China-USSR Seminar on Aero Engines, Nanjing, People's Republic of China, Apr. 15-20, 1991 p 469 A92-29709
Fluid Dynamics Conference, 22nd, Osaka, Japan, Nov. 15, 1990, Proceedings p 494 A92-30501
Radio Technical Commission for Aeronautics, Technical Symposium, Washington, DC, Nov. 18-20, 1991, Proceedings p 531 A92-33426

Future air traffic control and navigation systems; Proceedings of the AIAA International Civil Aviation Seminar, Paris, France, June 12, 1991
[AIAA SP-050-1991] p 532 A92-33433
AIAA/ASME/ASCE/AHS/ASC Structures, Structural Dynamics and Materials Conference, 33rd, Dallas, TX, Apr. 13-15, 1992, Technical Papers. Pt. 2 - Structures II
p 582 A92-34332
AIAA/ASME/ASCE/AHS/ASC Structures, Structural Dynamics and Materials Conference, 33rd, Dallas, TX, Apr. 13-15, 1992, Technical Papers. Pt. 3 - Structural dynamics I p 584 A92-34389
AIAA/ASME/ASCE/AHS/ASC Structures, Structural Dynamics and Materials Conference, 33rd, Dallas, TX, Apr. 13-15, 1992, Technical Papers. Pt. 4 - Structural dynamics II p 584 A92-34451
AIAA/ASME/ASCE/AHS/ASC Structures, Structural Dynamics and Materials Conference, 33rd, Dallas, TX, Apr. 13-15, 1992, Technical Papers. Pt. 5 - Design engineering/design optimization, materials, work-in-progress p 585 A92-34522
AIAA Dynamics Specialists Conference, Dallas, TX, Apr. 16, 17, 1992, Technical Papers p 565 A92-35651
Society of Flight Test Engineers, Annual Symposium, 21st, Garden Grove, CA, Aug. 6-10, 1990, Proceedings
p 516 A92-35926
Numerical simulations in turbomachinery; Proceedings of the Symposium, ASME and JSME Joint Fluids Engineering Conference, 1st, Portland, OR, June 23-27, 1991
[ISBN 0-7918-0714-2] p 522 A92-36028
International Aerospace Symposium 90, Nagoya, Japan, Nov. 26, 27, 1990, Proceedings p 607 A92-38201
International Symposium on Engineering Turbulence Modelling and Measurements, Dubrovnik, Yugoslavia, Sept. 24-24, 1990, Selected Papers p 672 A92-38851
Inter-noise 90; Proceedings of the International Conference on Noise Control Engineering, Goteborg, Sweden, Aug. 13-15, 1990. Vols. 1 & 2
[ISBN 91-7848-224-0] p 693 A92-39042
NOISE-CON 90; Proceedings of the 10th National Conference on Noise Control Engineering, University of Texas, Austin, Oct. 15-17, 1990
[ISBN 0-931784-21-2] p 695 A92-39226
Safety at sea and in the air - Taking stock together; Proceedings of the Conference, London, England, Nov. 13-15, 1990
[ISBN 0-903409-78-X] p 634 A92-39301
Mechanics Pan-America 1991; Pan-American Congress of Applied Mechanics, 2nd (PACAM II), Universidad Tecnica, Valparaiso, Chile, Jan. 2-5, 1991, Selected and Revised Proceedings p 673 A92-39930
1991 report to the aerospace profession; SETP Symposium, 35th, Beverly Hills, CA, Sept. 26-28, 1991, Proceedings p 645 A92-40028
Symposium on Turbulent Shear Flows, 8th, Technical University of Munich, Federal Republic of Germany, Sept. 9-11, 1991, Proceedings. Vols. 1 & 2
p 675 A92-40051
International Conference on Aerospace Trends...2001 - From Aeroplane to Aerospace Plane, Thiruvananthapuram, India, June 27, 28, 1991, Proceedings p 751 A92-41184
Annual Reliability and Maintainability Symposium, Orlando, FL, Jan. 29-31, 1991, Proceedings
[ISBN 0-87942-661-6] p 759 A92-42051
Biennial Fluid Dynamics Symposium on Advanced Problems and Methods in Fluid Mechanics, 19th, Kozubnik, Poland, Sept. 3-8, 1989, Selected Papers
p 761 A92-42529
Fiber optic systems for mobile platforms IV; Proceedings of the Meeting, San Jose, CA, Sept. 18, 1990
[SPIE-1369] p 779 A92-42601
Aircraft Symposium, 28th, Tokyo, Japan, Nov. 7-9, 1990, Proceedings p 699 A92-43095
High Reynolds number flows using liquid and gaseous helium
[ISBN 0-387-97475-X] p 897 A92-45261
International Powered Lift Conference, London, England, Aug, 29-31, 1990, Proceedings
[ISBN 0-903409-68-2] p 783 A92-45302
International Pacific Air and Space Technology Conference and Aircraft Symposium, 29th, Gifu, Japan, Oct. 7-11, 1991, Proceedings
[SAE P-246] p 783 A92-45376
AIAA Applied Aerodynamics Conference, 10th, Palo Alto, CA, June 22-24, 1992, Technical Papers. Pts. 1 & 2
p 791 A92-45476
International Congress on Recent Developments in Air- and Structure-Borne Sound and Vibration, Auburn University, AL, Mar. 6-8, 1990, Proceedings. Vols. 1 & 2
p 924 A92-45876
AHS International Specialists' Meeting on Rotorcraft Basic Research, Georgia Institute of Technology, Atlanta, Mar. 25-27, 1991, Proceedings p 846 A92-46919
Numerical grid generation in computational fluid dynamics and related fields; Proceedings of the 3rd International Conference, Universidad Politecnica de Cataluna, Barcelona, Spain, June 3-7, 1991
[ISBN 0-444-88948-5] p 918 A92-47035
Fiber optic and laser sensors VIII; Proceedings of the Meeting, San Jose, CA, Sept. 17-19, 1990
[SPIE-1367] p 901 A92-48026
NAECON 91; Proceedings of the IEEE National Aerospace and Electronics Conference, Dayton, OH, May 20-24, 1991. Vols. 1-3
[ISBN 0-7803-0084-X] p 786 A92-48426
IEEE/AIAA Digital Avionics Systems Conference, 10th, Los Angeles, CA, Oct. 14-17, 1991, Proceedings
[ISBN 0-7803-0115-3] p 964 A92-49251
IECEC '91; Proceedings of the 26th Intersociety Energy Conversion Engineering Conference, Boston, MA, Aug. 4-9, 1991. Vol. 5 - Renewable resource systems, stirling engines and applications, systems and cycles
[ISBN 0-89448-163-0] p 992 A92-50771
All-Union Conference on Optical Methods of Flow Research, 1st, Novosibirsk, Russia, Apr. 1991, Proceedings p 993 A92-51311
Structural testing technology at high temperature; Proceedings of the Conference, Dayton, OH, Nov. 4-6, 1991
[ISBN 0-912053-34-8] p 980 A92-51401
Risk management - Expanding horizons in nuclear power and other industries --- Book
[ISBN 1-56032-231-4] p 993 A92-51438
Close-range photogrammetry meets machine vision; Proceedings of the Meeting, Zurich, Switzerland, Sept. 3-7, 1990
[SPIE-1395] p 994 A92-51626
International SAMPE Electronics Conference, 5th, Los Angeles, CA, June 18-20, 1991, Proceedings
[ISBN 0-938994-58-1] p 985 A92-51901
AIAA/AHS Flight Simulation Technologies Conference, Hilton Head Island, SC, Aug. 24-26, 1992, Technical Papers p 981 A92-52426
ICIASF '91 - International Congress on Instrumentation in Aerospace Simulation Facilities, 14th, Rockville, MD, Oct. 27-31, 1991, Record
[ISBN 0-0783-0123-4] p 1114 A92-54301
AIAA Guidance, Navigation and Control Conference, Hilton Head Island, SC, Aug. 10-12, 1992, Technical Papers. Pts. 1-3 p 1130 A92-55151
AIAA Atmospheric Flight Mechanics Conference, Hilton Head Island, SC, Aug. 10-12, 1992, Technical Papers. Pts. 1-2 p 1078 A92-55326
Aircraft Symposium, 29th, Gifu, Japan, Oct. 7-9, 1991, Proceedings p 1015 A92-56001
Annual Reliability and Maintainability Symposium, Las Vegas, NV, Jan. 21-23, 1992, Proceedings
[ISBN 0-7803-0521-3] p 1119 A92-56201
Vortex Flow Aerodynamics
[AGARD-CP-494] p 83 N92-12996
Review of aircraft dynamic loads due to flow separation p 85 N92-13008
Third International Conference on Inverse Design Concepts and Optimization in Engineering Sciences (ICIDES-3)
[NASA-CR-188125] p 170 N92-13928
Rotordynamic Instability Problems in High-Performance Turbomachinery, 1990
[NASA-CP-3122] p 222 N92-14346
Proceedings of Damping 1991, volume 3
[AD-A241313] p 225 N92-14386
Proceedings of the USAF Structural Integrity Program Conference
[AD-A242943] p 279 N92-17204
Meeting Review: Airborne Aerosol Inlet Workshop
[NASA-CR-189814] p 301 N92-17393
Fatigue Management
[AGARD-CP-506] p 360 N92-18571
The 8th Symposium on Turbulent Shear Flows. Volume 1: Sessions 1-18
[AD-A243809] p 402 N92-18933
Techfest 18 Proceedings
[NIAR-92-1] p 420 N92-21501
Effects of Adverse Weather on Aerodynamics
[AGARD-CP-496] p 449 N92-21679
Low temperature environment operations of turboengines (design and user's problems)
p 450 N92-21682
Aircraft Ship Operations
[AGARD-CP-509] p 464 N92-21951
Symposium on High Speed Airbreathing Propulsion: The Solid Fuel Combustion Chamber and Beyond
[ETN-92-90685] p 575 N92-22268
Aeropropulsion 1987
[NASA-CP-3049] p 559 N92-22510
Integrated Design Analysis and Optimisation of Aircraft Structures
[AGARD-R-784] p 550 N92-23227
Software Surface Modeling and Grid Generation Steering Committee
[NASA-CP-3143] p 691 N92-24397
Workshop on Engineering Turbulence Modeling
[NASA-CP-10088] p 678 N92-24514
Proceedings of the 3rd Canadian Symposium on Aerodynamics
[CTN-92-60420] p 625 N92-24849
Workshop on Grid Generation and Related Areas
[NASA-CP-10089] p 659 N92-25712
Computational Structures Technology for Airframes and Propulsion Systems
[NASA-CP-3142] p 683 N92-25911
Technical evaluation report on the Flight Mechanics Panel Symposium on Flying Qualities
[AGARD-AR-311] p 733 N92-27870
Transonic Unsteady Aerodynamics and Aeroelasticity
[AGARD-CP-507] p 718 N92-27936
Turbine aircraft engine operational trending and JT8D static component reliability study
[DOT/FAA/CT-91/10] p 870 N92-28686
NASA Workshop on future directions in surface modeling and grid generation
[NASA-CP-10092] p 831 N92-29625
The 1991 International Conference on Aging Aircraft and Structural Airworthiness
[NASA-CP-3160] p 912 N92-30106
Proceedings of the Workshop on Advanced Network and Technology Concepts for Mobile, Micro, and Personal Communications
[NASA-CR-190459] p 1000 N92-30923
Collection of papers of the 31st Israel Annual Conference on Aviation and Astronautics
[ITN-92-85124] p 932 N92-31861
Proceedings of the 53rd Symposium on Air Vehicle Mission Control and Management
[AGARD-AR-310] p 1010 N92-32229
Eighth DOD/NASA/FAA Conference on Fibrous Composites in Structural Design, part 1
[NASA-CP-3087-PT-1] p 1106 N92-32513
Fourth Aircraft Interior Noise Workshop
[NASA-CP-10103] p 1136 N92-32948
Workshop on Aeronautical Decision Making (ADM). Volume 1: Executive summary
[DOT/FAA/RD-92/14-VOL-1] p 1142 N92-33305

CONFIGURATION INTERACTION

H-N2 interaction energies, transport cross sections, and collision integrals p 1135 A92-54660

CONFIGURATION MANAGEMENT

Never make the same mistake twice - Using configuration control and error analysis to improve software quality p 601 A92-33603
An investigation of air transportation technology at the Massachusetts Institute of Technology, 1990-1991
p 265 N92-17985

CONFORMAL MAPPING

Computation of the BVI noise for the BO105 Model Rotor in forward flight and comparison with wind tunnel tests
p 165 A92-14386
Computation of the potential flow through cascades using the conformal mapping and the singularity method
p 66 A92-15356
Multipoint inverse airfoil design method based on conformal mapping p 610 A92-36827
Prediction of vortex shedding from forebodies with chines p 702 A92-41228
Multi-point inverse design of an infinite cascade of airfoils
[AIAA PAPER 92-2650] p 797 A92-45517
Orthogonal grids for multiple airfoils
p 818 A92-47096
Some exact and numerical results for plane steady sheared flow of an incompressible inviscid fluid
p 821 A92-48019
A fast conformal mapping algorithm with no FFT
p 1007 A92-50471
Airfoil optimization with efficient gradient calculations
p 177 N92-13960
Use of Navier-Stokes analysis in section design
[AD-A242074] p 299 N92-17168

CONGRESSIONAL REPORTS

Aerospace technology: Technical data and information on foreign test facilities
[GAO/NSIAD-90-71FS] p 139 N92-13076
National Aeronautics and Space Administration
p 238 N92-14923
National Aeronautics and Space Administration
p 238 N92-14925
National Aeronautics and Space Administration
p 238 N92-14927
New Ways: Tiltrotor aircraft and magnetically levitated vehicles
[OTA-SET-507] p 238 N92-14933
National Aeronautics and Space Administration research and development p 238 N92-15937

National Aeronautics and Space Administration
p 417 N92-18309
National Aeronautics and Space Administration Authorization Act, 1993
[S-2558-IS] p 698 N92-25606
Departments of Veterans Affairs and Housing and Urban Development, and independent agencies appropriations for 1993, part 6
[GAO-55-636-PT-6] p 1141 N92-32505
Air traffic control: FAA's advanced automation system contract
[GAO/IMTEC-91-25] p 1048 N92-32861
NASA authorization, 1993, volume 1
[GPO-55-260-VOL-1] p 1142 N92-33147

CONICAL BODIES
Euler code evaluation of a transatmospheric vehicle at supersonic speeds p 9 A92-13202
Prediction of steady and unsteady asymmetric vortical flows around circular cones p 172 A92-18372
Improved nonequilibrium viscous shock-layer scheme for hypersonic blunt-body flowfields p 310 A92-24653
Predication of fastening capacity of screwed joint structure with cone assembly p 391 A92-24737
Asymptotic solution of the problem of ideal-fluid flow past the vertices of bodies and wings
p 427 A92-30199
A parametric study of the lift-drag ratio of blunt cones
p 437 A92-31860
Crashworthiness of truncated composite cones under side loads p 590 A92-35746
Spectral solution of inviscid supersonic flows over wedges and axisymmetric cones p 524 A92-36359
Influence of internal molecular degrees of freedom on the hypersonic rarefied gas flow about a conical body
p 938 A92-52752
Numerical study of the 3-D flowfield for a supersonic jet exiting into a hypersonic stream from a conical surface
[AIAA PAPER 92-3675] p 1022 A92-54118
Linear stability of supersonic cone boundary layers
p 1024 A92-54910

CONICAL FLOW
Asymmetric separated flows at supersonic speeds
p 176 A92-20742
Some thoughts on conical flow asymmetry
[AIAA PAPER 92-0427] p 326 A92-26275
Calculation of three-dimensional flow past blunt cones near the plane of symmetry for different flow regimes in the shock layer and in the presence of gas injection from the surface p 337 A92-27593
Numerical investigation of the high-speed conical flow past a sharp fin p 433 A92-31468
Asymmetric vortex flow over circular cones
p 86 N92-13014
A study of viscous interaction effects on hypersonic waveriders
[NASA-CR-189587] p 625 N92-24680
Natural flow wing
[NASA-CASE-LAR-14281-1] p 829 N92-28729

CONICAL INLETS
An AF3 algorithm for the calculation of transonic nonconservative full potential flow around axisymmetric inlet cowls p 251 A92-23380

CONICAL NOZZLES
Thermal imaging of afterburning plumes
p 129 A92-17179
Thrust vector control of an overexpanded supersonic nozzle using pin insertion and rotating airfoils
[AD-A243891] p 387 N92-18942
Initial calibration of the HEAT-H2 arc-heated wind tunnel
[AD-A245072] p 484 N92-20898

CONJUGATE GRADIENT METHOD
Parallel algorithms for panel methods --- in fluid dynamics p 293 A92-22346
Non-slender shapes of minimum drag
p 937 A92-52029
Iterative methods for large scale static analysis of structures on a scalable multiprocessor supercomputer
[NASA-CR-190369] p 692 N92-26018

CONNECTORS
Combined load test apparatus for flat panels
[NASA-CASE-LAR-14698-1] p 911 N92-30028
Lightning strike tests of composite connectors
[AD-A252281] p 1044 N92-33249

CONSERVATION EQUATIONS
Development of a 3-D upwind PNS code for chemically reacting hypersonic flowfields
[NASA-CR-190182] p 946 N92-30977

CONSERVATION LAWS
Freestream capturing for moving coordinates in three dimensions p 432 A92-31186
Newton's method solver for the axisymmetric Navier-Stokes equations p 703 A92-41269
Improved shock-capturing of Jameson's scheme for the Euler equations
[PB92-148758] p 596 N92-23251
TVD finite-difference solutions of nonequilibrium vibrationally relaxing and chemically reacting gaseous flows p 626 N92-24854

CONSTITUTIVE EQUATIONS
A viscoplastic model for single crystals
p 391 A92-24717
A unified numerical approach for the analysis of rotating disks including turbine rotors
[AIAA PAPER 92-2303] p 585 A92-34524

CONSTRAINTS
A method of centers based on barrier functions for solving optimal control problems with continuum state and control constraints p 52 A92-11467
Impact of structural optimization with aeroelastic/multidisciplinary constraints on helicopter rotor design
[AIAA PAPER 92-1001] p 535 A92-33193
Design variables and constraint derivatives in aeroelastic tailoring p 997 A92-53074
Constrained control allocation
[AIAA PAPER 92-4550] p 1131 A92-55262
Preliminary design and lay-out of an infant restraint system p 449 N92-21513
Application of an automated multidisciplinary analysis and optimisation system to the design of aircraft structures p 551 N92-23233
A fin optimisation study p 551 N92-23237
Constraint-based scheduling
[NASA-TM-107873] p 692 N92-25190
Advanced software development workstation: Effectiveness of constraint-checking --- spaceflight simulation and planning
[NASA-CR-190712] p 1134 N92-32865

CONSTRUCTION
Design and construction of a Helmholtz coil magnetic test cell
[AD-A249944] p 983 N92-30849

CONSTRUCTION MATERIALS
Process control challenges during the manufacture of large superplastically formed/diffusion bonded structure
[SAE PAPER 912195] p 674 A92-40012
Effects of material choices on brush seal performance
p 1116 A92-54650
Replacement of the NAL high pressure air storage system
[NAL-TM-634] p 888 N92-28835

CONTACT LOADS
Quasi-static analysis of roller bearing
p 391 A92-24732
Predication of fastening capacity of screwed joint structure with cone assembly p 391 A92-24737
Cyclic symmetric contact stress analysis of aeroengine rotor assembly p 470 A92-29733
Determination of tire-wheel interface loads for aircraft wheels
[AIAA PAPER 92-2482] p 543 A92-34599
Analysis of tenon and mortise contact problems by boundary element methods p 587 A92-35554
The static and fatigue computation of the propeller blades retention system p 995 A92-51895

CONTAINMENT
Experimental research on blade containment
p 557 A92-35561

CONTAMINANTS
Development of a sensor for the detection of aircraft wing contaminants
[AIAA PAPER 92-0300] p 369 A92-25752
Strain-induced extinction of hydrogen-air counterflow diffusion flames - Effects of steam, CO2, N2, and O2 additives to air
[AIAA PAPER 92-0877] p 487 A92-29639
Applied analytical combustion/emissions research at the NASA Lewis Research Center - A progress report
[AIAA PAPER 92-3338] p 1067 A92-54025
Applied analytical combustion/emissions research at the NASA Lewis Research Center
[NASA-TM-105731] p 890 N92-29343
Laser induced fluorescence detection of gums in jet fuels
[AD-A252685] p 987 N92-30767

CONTAMINATION
The effect of wing ice contamination on essential flight characteristics p 449 N92-21681
The effect of hoar-frosted wings on the Fokker 50 take-off characteristics p 451 N92-21692

CONTEXT FREE LANGUAGES
VHDL design and simulation for airborne graphics generation requirements --- VLSI hardware description language p 902 A92-48465

CONTINUUM FLOW
Solution of the Burnett equations for hypersonic flows near the continuum limit
[AIAA PAPER 92-2922] p 821 A92-47894
A clean air continuous flow propulsion facility
[AIAA PAPER 92-3912] p 1094 A92-56745
Behaviour and modelling of the aerothermodynamics of ballistic entry vehicles in the high altitude flow regimes
p 184 N92-15031
Applicability of bridging methods to hypersonic rarefied flow aerodynamics of reentry vehicles
p 184 N92-15032
A laser velocimeter investigation of the normal shockwave boundary layer interaction
p 500 N92-20485

CONTINUUM MECHANICS
Eulerian computational methods
[DE92-008017] p 765 N92-26853
Thermal mechanical analysis of sprag clutches
[NASA-CR-190686] p 1128 N92-34207

CONTINUUM MODELING
Reduction of computational models in strength problems p 496 A92-31858
Concept of a one-dimensional model of the dynamic behavior of a gas turbine p 862 A92-47791

CONTINUUMS
Grid sensitivity in low Reynolds number hypersonic continuum flows p 817 A92-47057
Eulerian computational methods
[DE92-008017] p 765 N92-26853

CONTOURS
Two-dimensional adaptive-wall tests in the NASA Ames two- by two-foot transonic wind tunnel
p 30 A92-13201
Adaptive parallel meshes with complex geometry
p 918 A92-47050
Analysis and design of transonic airfoils using streamwise coordinates p 194 N92-13955

CONTRACT MANAGEMENT
Preservation and utilization of finite element models of USAF aircraft structures
[AD-A241657] p 160 N92-13470

CONTRACTION
Flow analysis of rectangular wind tunnel contraction
p 312 A92-25001
Design of a variable contraction for a full-scale automotive wind tunnel
[AIAA PAPER 92-3929] p 1096 A92-56760

CONTRACTORS
Preservation and utilization of finite element models of USAF aircraft structures
[AD-A241657] p 160 N92-13470

CONTRACTS
Air traffic control: FAA's advanced automation system contract
[GAO/IMTEC-91-25] p 1048 N92-32861

CONTRAILS
Studies on the effect of high-flying air-traffic on the atmosphere
[IAF PAPER 91-737] p 301 A92-22495

CONTRAROTATING PROPELLERS
Azimuthal noise characteristics of contra-rotating propellers - Results of a wind tunnel model test
p 693 A92-39066
Noise of two high-speed model counter-rotation propellers at takeoff/approach conditions
p 925 A92-46799
Noise test of high-speed counterrotation propeller in low-speed wind tunnel p 1135 A92-56055
Effect of solidity and inclination on propeller-nacelle force coefficients
[NASA-TM-4316] p 90 N92-13038

CONTROL
Preliminary dynamic tests of a flight-type ejector
[AIAA PAPER 92-3261] p 1066 A92-54020
Preliminary dynamic tests of a flight-type ejector
[NASA-TM-105814] p 972 N92-30998

CONTROL BOARDS
Research on a helicopter information control system
p 735 A92-43220

CONTROL CONFIGURED VEHICLES
An acrobatic airship 'Acrostat'
[SAE PAPER 911994] p 843 A92-45396

CONTROL EQUIPMENT
Fundamentals of applied aerogasdynamics. II - Viscous flow past bodies. Control devices --- Russian book
p 64 A92-14281
Operation of the on-board measuring system of the STOL research aircraft Asuka p 734 A92-43139
Introduction to the traffic alert and collision avoidance system (TCAS) III p 734 A92-43150
Research on a helicopter information control system
p 735 A92-43220
Numerical investigation of unsteady supersonic cavity flowfield with passive control p 88 N92-13029
Stability and performance of notch filter control for unbalance response p 771 N92-27731

Rotorcraft In-Flight Simulation Research at NASA Ames Research Center: A Review of the 1980's and plans for the 1990's
[NASA-TM-103873] p 853 N92-28926
Controller response to conflict resolution advisory prototype
[PB92-190032] p 1050 N92-33596
Piloted evaluation of an integrated propulsion and flight control simulator
[NASA-TM-105797] p 1088 N92-34107

CONTROL SIMULATION
Numerical simulation of the actuation system for the ALDF's propulsion control valve --- Aircraft Landing Dynamics Facility p 41 A92-13204
A new approach to the real-time simulation of control systems with discontinuities p 508 A92-29291
On modelling of aero-gas turbine engine for real-time digital simulator --- of engine control system p 471 A92-29743
Aircraft control and simulation --- Book
[ISBN 0-471-61397-5] p 480 A92-31021
Parachute canopy control simulation - A solution for aircrew emergency training p 572 A92-35428
Introduction to the traffic alert and collision avoidance system (TCAS) III p 734 A92-43150
The acceleration control system design of a flight vehicle using a two-wing control method p 745 A92-43185
Wind tunnel tests on the motion of a spaceplane simulation for cable mount p 752 A92-43192
Modeling of the control systems of rotary wing aircraft (Review) p 875 A92-47783
Analysis of the VISTA longitudinal simulation capability for a cruise flight condition p 876 A92-48488
Derivation of ABCD system matrices from nonlinear dynamic simulation of jet engines
[AIAA PAPER 92-3319] p 923 A92-48903
Carefree handling systems for helicopters p 975 A92-50010
The design and simulation of an intelligence flight control system p 976 A92-50237
Flap control simulation p 980 A92-51398
Simulation software flowdown in the aircraft design process - Problems and solutions
[AIAA PAPER 92-4160] p 1008 A92-52450
The VISTA/F-16 programmable feel system
[AIAA PAPER 92-4172] p 977 A92-52457
A simulator evaluation of various manual control concepts for fly-by-wire transport aircraft
[AIAA PAPER 92-4328] p 1073 A92-55172
A consideration on air traffic control processing capability in terminal area p 1047 A92-56110
Testing of the high accuracy inertial navigation system in the Shuttle Avionics Integration Lab p 210 N92-14087
Performance and stability analysis of the non-linear dynamics of a simple powered lifting hypersonic vehicle flying on a minor circle
[AD-A243933] p 366 N92-19192
Double loop control law strategy and applications to helicopter
[CERT-2/7724-DERA] p 381 N92-19295
Computer-aided design of flight control systems
[AD-A244657] p 483 N92-21752
A wind tunnel study of the pioneer remotely piloted vehicle
[AD-A247028] p 732 N92-27335
Utility of ground simulation in flight control problem identification, solution development, and verification p 883 N92-28525
Use of high-fidelity simulation in the development of an F/A-18 active ground collision avoidance system p 837 N92-28530
Nonlinear dynamic-inversion flight control of supermaneuverable aircraft p 1062 N92-33953
Piloted evaluation of an integrated propulsion and flight control simulator
[NASA-TM-105797] p 1088 N92-34107

CONTROL STABILITY
Design of reliable control systems p 49 A92-11420
A design of continuous-time model reference adaptive control based on a function estimation of periodically time varying linear system p 51 A92-11454
Robust stabilization of a helicopter model p 28 A92-11501
U-parameter design example - Robust flight control for wind-shear protection p 28 A92-11502
VSTOL aircraft flight control system design using H(infinity) controllers and a switching strategy p 28 A92-11561
Application of stochastic robustness to aircraft control systems p 204 A92-18620
Washout filters in the bifurcation control of high alpha flight dynamics p 476 A92-29061
Linear systems with output constraints - The theory and application of maximal output admissible sets p 506 A92-29066
Integrated flight/propulsion control design for a STOVL aircraft using H-infinity control design techniques p 476 A92-29093
Fuzzy controller design and stability analysis for an aircraft model p 478 A92-29124
Frequency response specifications and sensitivity functions in quantitative feedback theory p 508 A92-29280
An estimate of the influence of the compressor stability margin on the thrust of a turbojet engine p 654 A92-37424
Robust stabilisation of multivariable feedback systems with desired performance requirement p 776 A92-42172
Inspection of stability deterioration with an adaptive regulator p 776 A92-43178
Model reference adaptive flight control system (MRAFCS) design with consideration of the balance point p 745 A92-43182
Nonstationary manual control. III p 776 A92-43187
A design of strongly stabilizing controller
[SAE PAPER 912081] p 917 A92-45456
Stability of an adaptive controller for aircraft. I - Analysis via Liapunov theory p 976 A92-51940
Robustness of a helicopter flight control system designed using eigenstructure assignment
[AIAA PAPER 92-4469] p 1076 A92-55229
Multiple delay model approach applied to the AIAA 1922 Controls Design Challenge
[AIAA PAPER 92-4630] p 1078 A92-55305
The development of a requirement specification for an experimental active flight control system for a variable stability helicopter: An Ada simulation in JSD p 135 N92-12466
Design and evaluation of a robust dynamic neurocontroller for a multivariable aircraft control problem
[NASA-TM-105579] p 481 N92-20586
A methodology for computing uncertainty bounds of multivariable systems based on sector stability theory concepts
[NASA-TP-3166] p 482 N92-21410
A simulation model of a single rotor helicopter p 979 N92-31865

CONTROL STICKS
Estimation of the optimal load characteristics of aircraft control levers p 479 A92-30150

CONTROL SURFACES
Computation of steady and unsteady control surface loads in transonic flow p 5 A92-11066
First flight for Airbus A340 p 21 A92-12750
Aircraft ground vibration test by means of flight control surfaces
[ONERA, TP NO. 1991-96] p 133 A92-16079
Aerodynamic balance range of aircraft of different configurations p 134 A92-16801
Control surfaces correlation in DLC maneuvers p 280 A92-21301
Control surfaces correlation in DSFC maneuvers --- Direct Side-Force Control p 281 A92-21307
Forebody vortex control p 251 A92-22517
A numerical method for unsteady transonic flow about wings with control surface p 314 A92-25107
A new approach to determining control surface's moments of inertia with test-twice vibrations approach p 379 A92-27914
Vibration reduction in helicopter rotors using an active control surface located on the blade
[AIAA PAPER 92-2451] p 564 A92-34478
Calibration of an aircraft control surface using a tri-axial accelerometer package p 555 A92-35942
Condor - An all electric airplane
[SAE PAPER 912184] p 644 A92-40004
Application of Active Flexible Wing technology to the Agile Falcon p 729 A92-41233
Downwash for joined-wing airframe with control surface deflections p 702 A92-41235
A model of a deformable aeroplane with a wing of low aspect ratio and movable control surfaces for studying natural vibrations p 744 A92-41528
Time accurate computation of unsteady transonic flows around an airfoil with oscillating flap on dynamic grid
[AIAA PAPER 92-2733] p 805 A92-45567
Transonic calculations for wings with deflected control surfaces
[AIAA PAPER 92-2617] p 805 A92-45572
A numerical study of control surface buzz using computational fluid dynamic methods
[AIAA PAPER 92-2654] p 806 A92-45578
F-16 failure detection isolation and estimation study p 876 A92-48490
Robustness characteristics of fast-sampling digital PI controllers for high-performance aircraft with impaired control surfaces p 877 A92-48496
Parameter estimation of an augmented airplane with unsteady aerodynamics modelling p 1073 A92-53546
Navier-Stokes computations for oscillating control surfaces
[AIAA PAPER 92-4431] p 1026 A92-55355
C-17 flight control system overview p 1082 A92-55906
Flutter analysis and wind tunnel test with respect to a low-aspect-ratio wing with free-rotational control surface p 1052 A92-56014
Lateral control of spaceplane at hypersonic flight p 1104 A92-56069
Prediction of forces and moments for hypersonic flight vehicle control effectors
[NASA-CR-188954] p 33 N92-11070
Loading and vibration reduction through active aerodynamic control
[AD-A242321] p 283 N92-17243
Use of stepwise regression techniques and kinematic compatibility for the analysis of EAP flight data p 365 N92-18790
Aerodynamic control of fighter aircraft by manipulation of forebody vortices p 380 N92-18791
Aeroservoelastic stability of aircraft at high incidence p 381 N92-18795
Integrated aerodynamic-structural-control wing design p 349 N92-19698
Dynamic performance of an aircraft on its landing gear: Test and evaluation on a dihedral p 466 N92-21970
Algorithm and code development for unsteady three-dimensional Navier-Stokes equations
[NASA-CR-190077] p 692 N92-25264
Prediction and analysis of wing flutter at transonic speeds p 662 N92-25555
Computation of three-dimensional effects on two dimensional wings
[NASA-CR-190576] p 832 N92-29691
Improved articulated fin/wing control system statement of government interests
[AD-D015268] p 1088 N92-34131

CONTROL SYSTEMS DESIGN
IEEE Conference on Decision and Control, 29th, Honolulu, HI, Dec. 5-7, 1990, Proceedings. Vols. 1-6 p 47 A92-11312
Experimental active control of a two-dimensional truss p 47 A92-11346
Gain-scheduled control of nonlinear partial differential equations p 47 A92-11347
A time approach to robustness of LTI systems with structured uncertainty and unmodelled dynamics --- linear time-invariant p 48 A92-11356
Closed-loop identification and iterative controller design p 48 A92-11362
Reduced-order robust controllers - H(infinity)-balanced truncation and optimal projection p 48 A92-11363
Optimal stabilization of discrete event systems p 48 A92-11376
Aircraft control under conditions of windshear p 27 A92-11384
Polygon interval arithmetic and design of robust control systems p 49 A92-11418
Design of reliable control systems p 49 A92-11420
A horizon-recursive form for predictors and their computation p 50 A92-11427
Design of non-overshooting feedback control systems p 50 A92-11431
Control design via TAM and H-infinity approaches - A flexible beam case study p 51 A92-11445
Fault tolerant control based on a new accommodation filter p 51 A92-11453
A design of continuous-time model reference adaptive control based on a function estimation of periodically time varying linear system p 51 A92-11454
New robust adaptive control system using multiple regularization parameters p 51 A92-11455
Using new aggregation operators in rule-based intelligent control p 51 A92-11456
Equivalence of optimal control problems and the use of parameterization methods p 52 A92-11466
Application of quantitative feedback theory (QFT) to flight control problems p 27 A92-11499
Robust controller design for an advanced fighter aircraft p 28 A92-11500
Robust stabilization of a helicopter model p 28 A92-11501
An approach to the optimal output feedback initial stabilizing gain problem p 52 A92-11553
VSTOL aircraft flight control system design using H(infinity) controllers and a switching strategy p 28 A92-11561
Design of the flare control law for longitudinal autopilot using H(infinity) synthesis p 28 A92-11562
Robust autopilot design for aircraft with multiple lateral-axes controls using H(infinity) synthesis p 28 A92-11563
Applying mu-synthesis to missile autopilot design p 28 A92-11564

A two-feedback-loop robust helicopter controller based on eigenspace techniques and H(infinity) synthesis
p 29 A92-11582
Design of localizer capture and track hold for a transport airplane - An H(infinity)/LTR approach
p 52 A92-11583
H(infinity) robust control synthesis for a fighter performing a coordinated bank turn p 29 A92-11585
An assessment of robustness of variable structure control systems for advanced aircraft manoeuvres
p 29 A92-11595
Practical robustness testing for helicopter flight control systems p 132 A92-14340
Development of an advanced piloted helicopter simulation p 105 A92-14363
Description of a tilt wing mathematical model for piloted simulation p 133 A92-14445
Flight test control --- Russian book
p 136 A92-15021
Control systems for the next century's fighter engines
[ASME PAPER 91-GT-278] p 125 A92-15674
Integrated flight/propulsion control for flight critical applications - A propulsion system perspective
[ASME PAPER 91-GT-284] p 125 A92-15679
An investigation of two cooling technologies as applied to a distributed propulsion control architecture
[ASME PAPER 91-GT-341] p 111 A92-15705
Utilization of a research simulator for the development of new flight control concepts
[ONERA, TP NO. 1991-161] p 137 A92-16128
Delivered with feeling --- computer-based design of flight control system for Boeing 777 p 134 A92-16621
Feeling normal --- evaluation of advanced control systems for future Boeing 777 p 134 A92-16623
Consideration of the time lag of engine processes in the problem of VTOL aircraft control synthesis
p 134 A92-16807
A geometric approach to regulator and tracker design for an aerospace plane
[AIAA PAPER 91-5054] p 203 A92-17837
Control concept for maneuvering in hypersonic flight
[AIAA PAPER 91-5055] p 203 A92-17838
Regulation of relaxed static stability aircraft
p 203 A92-18463
Retrospective essay on nonlinearities in aircraft flight control p 204 A92-18601
Parameter insensitive control utilizing eigenspace methods --- for flutter suppression in aeroelastic vehicles
p 204 A92-18615
Application of stochastic robustness to aircraft control systems p 204 A92-18620
Structure/control design synthesis of active flutter suppression system by goal programming
p 204 A92-18621
Application of aeroservoelastic modeling using minimum-state unsteady aerodynamic approximations
p 204 A92-18622
Nonlinear control of a twin-lift helicopter configuration
p 204 A92-18624
A stochastic regulator for integrated communication and control systems. I - Formulation of control law. II - Numerical analysis and simulation p 233 A92-19605
Performance improvements of an F-15 airplane with an integrated engine-flight control system
p 205 A92-20204
Control system design for the free drop test of external stores in a wind tunnel
[IAF PAPER ST-91-002] p 207 A92-20650
Parametric robust control by quantitative feedback theory p 302 A92-21176
Synthesis of a helicopter full-authority controller
p 280 A92-21178
Aircraft flight controls design using output feedback
p 280 A92-21180
A theory for mechanical flight control linkages
p 269 A92-21312
Quantitative Feedback Theory (QFT) applied to the design of a rotorcraft flight control system
[AIAA PAPER 92-0044] p 281 A92-22161
Combined H(2)/H(infinity) optimal control design applied to an advanced fighter aircraft
[AIAA PAPER 92-0045] p 281 A92-22162
Integrated flight control law synthesis for an aeroelastic forward-swept wing aircraft
[AIAA PAPER 92-0046] p 281 A92-22163
The application of parameter optimisation techniques to linear optimal control system design
p 302 A92-23038
A simplified method of transient mathematical model for non-augmentation engine p 372 A92-24750
High-alpha application of variable-gain output feedback control p 380 A92-28152
Abstract model and controller design for an unstable aircraft p 380 A92-28153
Improved noise rejection in automatic carrier landing systems p 380 A92-28154
Model-reference adaptive control for systems with D matrices p 506 A92-29052
Washout filters in the bifurcation control of high alpha flight dynamics p 476 A92-29061
Linear systems with output constraints - The theory and application of maximal output admissible sets
p 506 A92-29066
Integrated flight/propulsion control design for a STOVL aircraft using H-infinity control design techniques
p 476 A92-29093
Meeting VSTOL aircraft performance requirements using scheduled H(infinity) controllers p 477 A92-29094
Design and modeling issues for integrated airframe/propulsion control of hypersonic flight vehicles
p 477 A92-29115
Full envelope multivariable control of a gas turbine engine p 468 A92-29116
Decentralized hierarchical partitioning of centralized integrated controllers --- for flight propulsion in STOVLs
p 477 A92-29119
Fuzzy controller design and stability analysis for an aircraft model p 478 A92-29124
Robust control law development for a hypersonic cruise aircraft p 478 A92-29127
Controller design for the F-14 pitch axis control problem using the quantitative feedback theory approach
p 478 A92-29128
A hierarchical data structure and new capabilities of the Robust-Control Toolbox p 507 A92-29155
Hover control of a PVTOL using nonlinear regulator theory p 478 A92-29171
Loop shaping in mixed H2 and H-infinity optimal control p 507 A92-29177
Robust adaptive nonlinear control of high performance aircraft p 478 A92-29188
A system identification model for adaptive nonlinear control p 508 A92-29248
A new approach to the real-time simulation of control systems with discontinuities p 508 A92-29291
Active vibration control using fixed order dynamic compensation with frequency shaped cost functionals
p 508 A92-29324
System identification requirements for high-bandwidth rotorcraft flight control system design
p 479 A92-29332
Robust optimal control with a worst case time domain performance criterion p 509 A92-29368
Model development for active surge control/rotating stall avoidance in aircraft gas turbine engines
p 468 A92-29375
An integrated, full-range surge control/rotating stall avoidance compressor control system
p 469 A92-29376
Electronic control of a turbine power unit
p 470 A92-29741
An investigation of real-time diagnostic technique for DEEC system --- digital electronic engine control system
p 470 A92-29742
Aircraft control and simulation --- Book
[ISBN 0-471-61397-5] p 480 A92-31021
Self-compensating carrier aircraft recovery system
p 448 A92-32238
Integrated aeroelastic control optimization of laminated composite lifting surfaces p 481 A92-32248
Potential role of neural networks and fuzzy logic in flight control design and development
[AIAA PAPER 92-0999] p 600 A92-33191
High-performance fighter fly-by-wire flight control actuation system --- for YF-23A prototype
[AIAA PAPER 92-1123] p 563 A92-33277
Trajectory control for a low-lift maneuverable reentry vehicle
[AIAA PAPER 92-1146] p 574 A92-33287
New complex pole and gust response approximations for integrated aeroservoelastic synthesis
[AIAA PAPER 92-2377] p 565 A92-34547
Flutter suppression for the Active Flexible Wing - Control system design and experimental validation
[AIAA PAPER 92-2097] p 566 A92-35666
Flutter suppression digital control law design and testing for the AFW wind tunnel model
[AIAA PAPER 92-2095] p 566 A92-35668
Maneuver load control using optimized feedforward commands
[AIAA PAPER 92-2100] p 567 A92-35671
Design of adaptive fast-sampling digital controllers for active flutter suppression
[AIAA PAPER 92-2105] p 567 A92-35676
Full authority active control system design for a high performance helicopter p 567 A92-35732
The use of inverse simulation for conceptual design
p 546 A92-35738
Achievement of rotorcraft handling qualities specifications via feedback control p 568 A92-35747
Multivariable methods for helicopter flight control law design - A review p 568 A92-35748
Command following control law design by linear quadratic optimisation p 568 A92-35749
Experiences with high authority helicopter flight control
p 568 A92-35757
Improvement of helicopter robustness and performance control law using eigenstructure techniques and H-infinity synthesis p 569 A92-35776
Eigenstructure assignment for handling qualities in helicopter flight control law design p 570 A92-35786
A survey of active control in aircraft cabins
p 643 A92-39084
Control system optimization using genetic algorithms
p 661 A92-39900
Design of low-sensitivity modalized observers using left eigenstructure assignment p 661 A92-39908
Pulse response method for vibration reduction in periodic dynamic systems p 661 A92-39909
Robust flight control system design with multiple model approach p 661 A92-39910
On upsets of analog portions of digital flight control systems due to electromagnetic interference
[SAE PAPER 912144] p 651 A92-39982
Controls for agility research in the NASA High-Alpha Technology Program
[SAE PAPER 912148] p 661 A92-39984
Condor - An all electric airplane
[SAE PAPER 912184] p 644 A92-40004
Modern navigation, guidance, and control processing --- Book
[ISBN 0-13-596230-7] p 639 A92-40199
Basic design concepts for smart actuators for aerospace plane control p 752 A92-41193
Software safety analysis in heterogeneous multiprocessor control systems p 776 A92-42073
Robust stabilisation of multivariable feedback systems with desired performance requirement
p 776 A92-42172
Robust flight control system design using a multimodel approach. II p 745 A92-43180
Flight control system design p 776 A92-43181
Model reference adaptive flight control system (MRAFCS) design with consideration of the balance point p 745 A92-43182
Study of the flight control of remotely piloted helicopters p 745 A92-43183
A restructurable flight control system design using nonlinear compensation p 745 A92-43184
The acceleration control system design of a flight vehicle using a two-wing control method p 745 A92-43185
Evaluation and comparison of triple and quadruple flight control architectures p 745 A92-43884
Fault tolerant EHA architectures --- electro-hydrostatic actuator p 763 A92-43885
Specification of adaptive aiding systems - Information requirements for designers p 916 A92-44915
Integrated flight/propulsion control for supersonic STOVL aircraft p 872 A92-45320
Integrated flight control systems - Architectural considerations for future aircraft concepts
p 872 A92-45322
The large scale test control systems designed and built by the Boeing Company to support the 757 and 767 major fatigue tests
[SAE PAPER 911985] p 881 A92-45388
Ducted fan VTOL for working platform
[SAE PAPER 911995] p 843 A92-45397
Avionics flight systems for the 21st century
[SAE PAPER 912033] p 784 A92-45421
Functional mock-up tests for flight control system of the NAL QSTOL research aircraft 'ASKA'
[SAE PAPER 912036] p 881 A92-45422
Development of the DDV actuation system on the IDF aircraft
[SAE PAPER 912080] p 844 A92-45455
A design of strongly stabilizing controller
[SAE PAPER 912081] p 917 A92-45456
A new milestone in automatic aircraft control - Fly-by-light systems transmit commands optoelectronically
p 784 A92-45699
Fibre optic rotary position sensors for vehicle and propulsion controls p 855 A92-46243
Fiber optic controls for aircraft engines - Issues and implications p 856 A92-46244
Potential for integrated optical circuits in advanced aircraft with fiber optic control and monitoring systems
p 856 A92-46246
Integrated optic components for advanced turbine engine control systems p 925 A92-46248
On-line performance evaluation of multiloop digital control systems p 873 A92-46739
Approach guidance in a downburst
p 873 A92-46741
Linear quadratic minimax controllers
p 917 A92-46748
X-29 H-infinity controller synthesis
p 873 A92-46749

Nonlinear inversion flight control for a supermaneuverable aircraft p 873 A92-46751
Integrated aeroservoelastic wing synthesis by nonlinear programming/approximation concepts p 873 A92-46752
Two variations of certainty control p 918 A92-46762
Study on two variable control plan for twin spool turbojet engine p 862 A92-47697
Modeling of the control systems of rotary wing aircraft (Review) p 875 A92-47783
Nonlinear control design for slightly nonminimum phase systems - Application to V/STOL aircraft p 876 A92-48160
Robust discrete controller design for an unmanned research vehicle (URV) using discrete quantitative feedback theory p 877 A92-48495
Optics in aircraft engines p 926 A92-48500
Derivation of ABCD system matrices from nonlinear dynamic simulation of jet engines
[AIAA PAPER 92-3319] p 923 A92-48903
A simplified real-time engine model for developing aeroengine control system
[AIAA PAPER 92-3321] p 864 A92-48904
Design issues in a fiber optic sensor system architecture for aircraft engine control
[AIAA PAPER 92-3483] p 866 A92-49023
Intelligent Engine Control (IEC)
[AIAA PAPER 92-3484] p 866 A92-49024
The numerical simulation of the main fuel control unit of gas turbine engines
[AIAA PAPER 92-3760] p 867 A92-49115
Compensating for manufacturing and life-cycle variations in aircraft engine control systems
[AIAA PAPER 92-3869] p 868 A92-49139
Development of active control technology for the next generation of combat aircraft p 975 A92-50008
The design and simulation of an intelligence flight control system p 976 A92-50237
Optimal discrete-time static output-feedback design - A W-domain approach p 1007 A92-50499
Robust flight control systems - A parameter space design p 976 A92-50503
Conditions of optimality in problems of generalized control. II - Sufficient conditions of optimality p 1007 A92-51328
Flight control system design using eigenstructure assignment for rolling the aircraft around the velocity vector p 977 A92-51945
Analysis of propulsion system dynamics in the validation of a high-order state space model of the UH-60
[AIAA PAPER 92-4150] p 959 A92-52441
Piloted evaluation of an integrated propulsion and flight control simulator
[AIAA PAPER 92-4178] p 960 A92-52459
Optimal implicit model-following approach with frequency-shaped weighting and its application to design of flight control system p 977 A92-53094
A reversed-frame normalization design of robust flight control system p 1009 A92-53382
Improvement of atmospheric flight performance of a space vehicle through H infinity-control theory p 1130 A92-53785
Development of the full-envelope Performance Seeking Control algorithm
[AIAA PAPER 92-3748] p 1068 A92-54148
Performance benefits of adaptive in-flight propulsion system optimization
[AIAA PAPER 92-3749] p 1068 A92-54149
Hypervelocity Wind Tunnel 9 control system p 1092 A92-54343
AIAA Guidance, Navigation and Control Conference, Hilton Head Island, SC, Aug. 10-12, 1992, Technical Papers. Pts. 1-3 p 1130 A92-55151
Robust dynamic inversion control laws for aircraft control
[AIAA PAPER 92-4329] p 1073 A92-55173
Aircraft ride quality controller design using new robust root clustering theory for linear uncertain systems
[AIAA PAPER 92-4399] p 1075 A92-55199
Design of robust Quantitative Feedback Theory controllers for pitch attitude hold systems
[AIAA PAPER 92-4409] p 1075 A92-55203
New literal approximations for the longitudinal dynamic characteristics of flexible flight vehicles
[AIAA PAPER 92-4411] p 1075 A92-55205
Robustness of a helicopter flight control system designed using eigenstructure assignment
[AIAA PAPER 92-4469] p 1076 A92-55229
Control design of a UH-60 rotorcraft via CLTR and direct optimization
[AIAA PAPER 92-4470] p 1076 A92-55230
Automatic formation flight control
[AIAA PAPER 92-4473] p 1076 A92-55233
An algorithm for robust eigenstructure assignment using the Linear Quadratic Regulator
[AIAA PAPER 92-4478] p 1131 A92-55237
Constrained control allocation
[AIAA PAPER 92-4550] p 1131 A92-55262
A robust gain scheduler interpolated into multiple models by membership functions
[AIAA PAPER 92-4553] p 1131 A92-55265
G-Field Control of nonlinear systems
[AIAA PAPER 92-4555] p 1131 A92-55267
Enlisting industry support for a flight controls design lab
[AIAA PAPER 92-4560] p 1141 A92-55272
Propulsion system performance resulting from an Integrated Flight/Propulsion Control design
[AIAA PAPER 92-4602] p 1069 A92-55281
An framework for robust flight control design using constrained optimization
[AIAA PAPER 92-4603] p 1131 A92-55282
Automated procedures for aircraft aeroservoelastic compensation
[AIAA PAPER 92-4606] p 1077 A92-55284
Robust control design of an automatic carrier landing system
[AIAA PAPER 92-4619] p 1077 A92-55296
Nonlinear model-following control application to airplane control (1992 AIAA Controls Design Challenge)
[AIAA PAPER 92-4625] p 1077 A92-55302
Quantitative Feedback Theory approach to AIAA Controls Design Challenge
[AIAA PAPER 92-4626] p 1077 A92-55303
Multiple delay model approach applied to the AIAA 1922 Controls Design Challenge
[AIAA PAPER 92-4630] p 1078 A92-55305
Intelligent control law tuning for AIAA Controls Design Challenge
[AIAA PAPER 92-4631] p 1132 A92-55306
Computer aided evaluation of aircraft handling qualities and flight control system robustness
[AIAA PAPER 92-4423] p 1080 A92-55347
Flight test results using a low order equivalent systems technique to estimate flying qualities
[AIAA PAPER 92-4425] p 1080 A92-55349
Robust control system design with multiple model approach p 1083 A92-56029
Flight control system design using H(infinity) optimal control p 1083 A92-56030
MIMO state-feedback control system considering phase stability by -90 deg phase-locus method p 1084 A92-56066
Design of a flight control system using a feedback-error-learning-type neural network p 1132 A92-56067
Multidisciplinary optimization of aeroservoelastic systems using reduced-size models p 1054 A92-56176
Redundancy design philosophy for catastrophic loss protection p 1119 A92-56202
Experimental investigation of helicopter coupled rotor/body control p 1086 A92-56318
Control of large cryogenic tunnels
[AIAA PAPER 92-3930] p 1096 A92-56761
Development of digital/optical rotary position transducer
[NAL-TR-1106] p 29 N92-10028
Turbomachinery noise p 54 N92-10601
Initial design study of existing flight control system of RPH and feasibility study of implementing HHC on the SH-60B
[AD-A240522] p 30 N92-11019
Practical input optimization for aircraft parameter estimation experiments p 114 N92-11989
Development and verification of software for flight safety critical systems p 164 N92-12469
Machine Intelligence for Aerospace Electronic Systems
[AGARD-CP-499] p 164 N92-12517
An aircraft model for the AIAA controls design challenge
[NASA-CR-186019] p 117 N92-13064
Advanced rotorcraft control using parameter optimization
[NASA-CR-189502] p 135 N92-13073
A Taxi And Ramp Management And Control system (TARMAC) p 207 N92-14027
Hydraulic actuator system for rotor control p 224 N92-14363
Neural network and fuzzy logic technology for naval flight control
[AD-A242650] p 206 N92-15074
Model identification and control system design for the lambda unmanned research vehicle
[AD-A241859] p 299 N92-17024
Identification techniques: Model structure and time domain methods p 273 N92-17157
System identification requirements for high-bandwidth rotorcraft flight control system design p 282 N92-17166
Investigation of air transportation technology at Princeton University, 1990-1991 p 266 N92-17995
Neural networks for aircraft system identification p 303 N92-17998
Technical notes and correspondence: Stochastic robustness of linear time-invariant control systems p 303 N92-18002
Linearized aerodynamic and control law models of the X-29A airplane and comparison with flight data
[NASA-TM-4356] p 381 N92-19174
Double loop control law strategy and applications to helicopter
[CERT-2/7724-DERA] p 381 N92-19295
Adaptive control of nonlinear systems with applications to the control of flexible robot arms
[AD-A244409] p 413 N92-19397
Robust control system design with application to high performance helicopters p 382 N92-19621
Integrated aerodynamic-structural-control wing design p 349 N92-19698
A hierarchy for modeling high speed propulsion systems
[NASA-CR-186984] p 387 N92-19934
Design and evaluation of a robust dynamic neurocontroller for a multivariable aircraft control problem
[NASA-TM-105579] p 481 N92-20586
H2-fueled high-bypass turbofan p 475 N92-21529
System controls challenges of hypersonic combined-cycle engine powered vehicles p 475 N92-21533
Computer-aided design of flight control systems
[AD-A244657] p 483 N92-21752
Enhanced displays, flight controls, and guidance systems for approach and landing p 456 N92-21957
Approach and landing guidance p 457 N92-21960
Helicopter active rotor control p 570 N92-22157
Variable-camber systems integration and operational performance of the AFTI/F-111 mission adaptive wing
[NASA-TM-4370] p 570 N92-22194
Improved large perturbation propulsion models for control system design (1988-1989) and large perturbation models of high velocity propulsion systems (1989-1990) and reduced order propulsion models for control system design (1990-1991)
[NASA-CR-190148] p 593 N92-22491
A hierarchy for modeling high speed propulsion systems p 559 N92-22492
Directions in propulsion control p 560 N92-22530
Design of an integrated airframe/propulsion control system architecture
[NASA-CR-182007] p 602 N92-22644
System considerations, projected requirements and applications for aeronautical mobile satellite communications for air traffic services p 677 N92-24163
Aeronautical mobile satellite service: Air traffic control applications p 677 N92-24164
Development of flight testing of a fault tolerant fly-by-light yaw control system p 662 N92-25599
Integrated flight propulsion control research results using the NASA F-15 HIDEC Flight Research Facility
[NASA-TM-4394] p 740 N92-27379
International Symposium on Magnetic Suspension Technology, part 2
[NASA-CP-3152-PT-2] p 753 N92-27788
Robust intelligent flight control for hypersonic vehicles
[NASA-CR-185680] p 746 N92-28209
Overview on basis and use of performance prediction methods p 869 N92-28459
Use of a research simulator for the development of new concepts of flight control p 885 N92-28543
Electromechanical systems with transient high power response operating from a resonant AC link
[NASA-TM-105716] p 870 N92-28985
Results of a flight simulator experiment to establish handling quality guidelines for the design of future transport aircraft
[NLR-MP-88044-U] p 854 N92-29616
Nonlinear system design: Adaptive feedback linearization with unmodeled dynamics
[AD-A248484] p 1009 N92-30335
Resonance and control response tests using a control simulation device
[MBB-UD-0608-91-PUB] p 978 N92-30439
Flutter suppression digital control law design and testing for the AFW wind-tunnel model
[NASA-TM-107652] p 962 N92-31350
Design and analysis issues of integrated control systems for high-speed civil transports
[NASA-CR-186022] p 979 N92-31656

A parameter optimization approach to controller partitioning for integrated flight/propulsion control application
[NASA-TM-105826] p 979 N92-32241
A learning enhanced flight control system for high performance aircraft
[AD-A252520] p 1086 N92-32435
Analysis of delay reducing and fuel saving sequencing and spacing algorithms for arrival traffic
[NASA-TM-103880] p 1044 N92-33194
An investigation of switched reluctance rotor position estimation using neural networks
[AD-A252846] p 1061 N92-33414
Design of helicopter flight control systems for hover and low speed using eigenstructure assignment
p 1061 N92-33952
Human factors issues in the use of artificial intelligence in air traffic control. October 1990 Workshop
[NASA-CR-190925] p 1051 N92-34203

CONTROL THEORY
IEEE Conference on Decision and Control, 29th, Honolulu, HI, Dec. 5-7, 1990, Proceedings. Vols. 1-6
p 47 A92-11312
Control theory for optimum design of aerodynamic shapes p 6 A92-11328
A method of centers based on barrier functions for solving optimal control problems with continuum state and control constraints p 52 A92-11467
Application of quantitative feedback theory (QFT) to flight control problems p 27 A92-11499
U-parameter design example - Robust flight control for wind-shear protection p 28 A92-11502
A two-feedback-loop robust helicopter controller based on eigenspace techniques and H(infinity) synthesis
p 29 A92-11582
V-22 thrust power management control law development p 132 A92-14405
Analysis of criteria predicting the tendency of pilot induced oscillation for linear non-linear system
p 133 A92-15340
Optimal control problems with maximum functional
p 232 A92-18616
A stochastic regulator for integrated communication and control systems. I - Formulation of control law. II - Numerical analysis and simulation p 233 A92-19605
A low-altitude breakthrough system using optimal path terrain following p 205 A92-20483
Parametric robust control by quantitative feedback theory p 302 A92-21176
Quantitative Feedback Theory (QFT) applied to the design of a rotorcraft flight control system
[AIAA PAPER 92-0044] p 281 A92-22161
Integrated flight control law synthesis for an aeroelastic forward-swept wing aircraft
[AIAA PAPER 92-0046] p 281 A92-22163
Open-loop model reduction and parameter perturbation for active flutter suppression system
p 379 A92-24879
Decentralized-feedback pole placement of linear systems p 411 A92-27347
Optimal output feedback for linear time-periodic systems p 412 A92-28142
High-alpha application of variable-gain output feedback control p 380 A92-28152
Abstract model and controller design for an unstable aircraft p 380 A92-28153
Reaching conditions in variable structure systems for output feedback control p 506 A92-29037
Model-reference adaptive control for systems with D matrices p 506 A92-29052
Linear systems with output constraints - The theory and application of maximal output admissible sets
p 506 A92-29066
IMPAC - An integrated methodology for propulsion and airframe control p 477 A92-29118
A framework for the analysis of airframe/engine interactions and integrated flight/propulsion control
p 478 A92-29120
Robust control law development for a hypersonic cruise aircraft p 478 A92-29127
Controller design for the F-14 pitch axis control problem using the quantitative feedback theory approach
p 478 A92-29128
The implicit function theorem and robust root locus
p 507 A92-29134
A hierarchical data structure and new capabilities of the Robust-Control Toolbox p 507 A92-29155
Loop shaping in mixed H2 and H-infinity optimal control p 507 A92-29177
The generalized normal forms and method of resonance control of nonlinear dynamical systems
p 507 A92-29189
A system identification model for adaptive nonlinear control p 508 A92-29248
Frequency response specifications and sensitivity functions in quantitative feedback theory
p 508 A92-29280
Tiltrotor control law design for rotor loads alleviation using modern control techniques p 478 A92-29331
Application of the delta-operator in MIMO discrete-time adaptive flight control systems p 479 A92-29516
Trajectory control for a low-lift maneuverable reentry vehicle
[AIAA PAPER 92-1146] p 574 A92-33287
Multivariable methods for helicopter flight control law design - A review p 568 A92-35748
Command following control law design by linear quadratic optimisation p 568 A92-35749
Preliminary evaluation of new control laws on the experimental fly-by-wire Dauphin helicopter
p 568 A92-35756
Nonlinear control law with application to high angle-of-attack flight p 661 A92-39904
Design of low-sensitivity modalized observers using left eigenstructure assignment p 661 A92-39908
Modern navigation, guidance, and control processing --- Book
[ISBN 0-13-596230-7] p 639 A92-40199
The method of determinant equations in the applied theory of optimal systems - Systems with 'rigid' constraints and with fixed boundary conditions p 917 A92-46629
The propulsive-only flight control problem
p 876 A92-48487
H-infinity synthesis using a bilinear pole shifting transform p 1007 A92-50490
Improvement of atmospheric flight performance of a space vehicle through H infinity-control theory
p 1130 A92-53785
Flight control law synthesis using neural network theory
[AIAA PAPER 92-4390] p 1074 A92-55191
Invertibility and trajectory control for nonlinear maneuvers of aircraft
[AIAA PAPER 92-4410] p 1075 A92-55204
G-Field Control of nonlinear systems
[AIAA PAPER 92-4555] p 1131 A92-55267
Applications of robust control theory - Educational implications
[AIAA PAPER 92-4559] p 1131 A92-55271
Intelligent control law tuning for AIAA Controls Design Challenge
[AIAA PAPER 92-4631] p 1132 A92-55306
Application of Eigenstructure Assignment to the control of powered lift combat aircraft
[RAE-TM-FS-1009] p 135 N92-12004
An analytical and experimental study to investigate flutter suppression via piezoelectric actuation
[NASA-TM-893240] p 156 N92-12173
The development of a requirement specification for an experimental active flight control system for a variable stability helicopter: An Ada simulation in JSD
p 135 N92-12466
An aircraft model for the AIAA controls design challenge
[NASA-CR-186019] p 117 N92-13064
Advanced rotorcraft control using parameter optimization
[NASA-CR-189502] p 135 N92-13073
Development of high angle of attack control laws for an unstable, non-minimum phase aircraft using variations of the quantitative feedback technique
[AD-A243698] p 282 N92-17096
Transformation of flightmechanical design requirements for modern fighters into aerodynamic characteristics
p 365 N92-18794
Linearized aerodynamic and control law models of the X-29A airplane and comparison with flight data
[NASA-TM-4356] p 381 N92-19174
A methodology for computing uncertainty bounds of multivariable systems based on sector stability theory concepts
[NASA-TP-3166] p 482 N92-21410
Application of nonlinear feedback control theory to supermaneuverable aircraft
[NASA-CR-190336] p 663 N92-25648
Application of neural network to adaptive control theory for super-augmented aircraft
[AD-A246596] p 745 N92-27505
Use of high-fidelity simulation in the development of an F/A-18 active ground collision avoidance system
p 837 N92-28530
Application of piloted simulation to high-angle-of-attack flight-dynamics research for fighter aircraft
p 886 N92-28551
Inverse control problems: Mathematical preliminaries, system theoretical approaches, and their applications to aircraft dynamics
[LR-665] p 923 N92-28581
Practical method's for robust multivariable control
[AD-A248473] p 1009 N92-30322
On-line analysis capabilities developed to support the AFW wind-tunnel tests
[NASA-TM-107651] p 961 N92-30752
A simplified dynamic model of the T700 turboshaft engine
[NASA-TM-105805] p 1009 N92-30898
Nonlinear stability and control study of highly maneuverable high performance aircraft, phase 2
[NASA-CR-190667] p 978 N92-30922
Flutter suppression digital control law design and testing for the AFW wind-tunnel model
[NASA-TM-107652] p 962 N92-31350
The multiple-function multi-input/multi-output digital controller system for the AFW wind-tunnel model
[NASA-TM-107600] p 1060 N92-32536

CONTROL VALVES
A valve-down technique for small balloons
[AIAA PAPER 91-3681] p 15 A92-11025
Numerical simulation of the actuation system for the ALDF's propulsion control valve --- Aircraft Landing Dynamics Facility p 41 A92-13204
Turbine drive system of the high pressure LOX turbopump test facility
[DE92-783191] p 680 N92-25342

CONTROLLABILITY
Robust pole assignment using closed loop controllability conditions p 49 A92-11417
Robust controller design for an advanced fighter aircraft p 28 A92-11500
Achievement of rotorcraft handling qualities specifications via feedback control p 568 A92-35747
1991-92 AHS Technical Committee highlights - Handling qualities p 662 A92-40395
Frequency domain flight testing and analysis of an OH-58D helicopter p 847 A92-46943
Summary of the effects of engine throttle response on airplane formation-flying qualities
[AIAA PAPER 92-3318] p 877 A92-48902
Piloted simulation for the BK117 FBW demonstrator
p 1053 A92-56077
Mission oriented investigation of handling qualities through simulation p 1059 A92-56353
System identification methods for handling-qualities evaluation p 274 N92-17165
Aerodynamic control of fighter aircraft by manipulation of forebody vortices p 380 N92-18791
Linearized aerodynamic and control law models of the X-29A airplane and comparison with flight data
[NASA-TM-4356] p 381 N92-19174
The effect of wing ice contamination on essential flight characteristics p 449 N92-21681
A preliminary look at an optimal multivariable design for propulsion-only flight control of jet-transport aircraft
[NASA-CR-186014] p 663 N92-25734
Note on flight measured control effectiveness of the quiet STOL experimental aircraft ASKA
[NAL-TR-1103] p 746 N92-28154
The use of ground based simulation for handling qualities research: A new assessment p 885 N92-28545
Initial validation of a R/D simulator with large amplitude motion p 886 N92-28546
Application of piloted simulation to high-angle-of-attack flight-dynamics research for fighter aircraft
p 886 N92-28551
Effects of cockpit lateral stick characteristics on handling qualities and pilot dynamics
[NASA-CR-4443] p 878 N92-28584
Results of a flight simulator experiment to establish handling quality guidelines for the design of future transport aircraft
[NLR-MP-88044-U] p 854 N92-29616
A simulation model of a single rotor helicopter
p 979 N92-31865
A background to the handling qualities of aircraft
[ESDU-92006] p 1087 N92-32780

CONTROLLERS
Control design via TAM and H-infinity approaches - A flexible beam case study p 51 A92-11445
Using new aggregation operators in rule-based intelligent control p 51 A92-11456
Optimal rejection of bounded persistent disturbances in periodic systems p 51 A92-11464
Robust controller design for an advanced fighter aircraft p 28 A92-11500
VSTOL aircraft flight control system design using H(infinity) controllers and a switching strategy
p 28 A92-11561
Experimental and analytical investigation of hybrid squeeze film dampers
[ASME PAPER 91-GT-250] p 150 A92-15655
Enhancement of modal swept sine data by control of exciting forces p 215 A92-17562
Synthesis of a helicopter full-authority controller
p 280 A92-21178

Combined H(2)/H(infinity) optimal control design applied to an advanced fighter aircraft
[AIAA PAPER 92-0045] p 281 A92-22162
Robustness characteristics of fast-sampling digital controllers for active flutter suppression
[AIAA PAPER 92-2104] p 567 A92-35675
Robust wind shear stochastic controller-estimator
p 661 A92-39893
Control system optimization using genetic algorithms
p 661 A92-39900
Application of linearization analysis to aircraft dynamics p 661 A92-39902
Pulse response method for vibration reduction in periodic dynamic systems p 661 A92-39909
In-flight simulation of backside operating models using direct lift controller
[SAE PAPER 912069] p 872 A92-45450
Manual control of vehicles with time-varying dynamics
[SAE PAPER 912078] p 917 A92-45454
A design of strongly stabilizing controller
[SAE PAPER 912081] p 917 A92-45456
Robust flight control systems - A parameter space design p 976 A92-50503
Constrained control allocation
[AIAA PAPER 92-4550] p 1131 A92-55262
Propulsion system performance resulting from an Integrated Flight/Propulsion Control design
[AIAA PAPER 92-4602] p 1069 A92-55281
An framework for robust flight control design using constrained optimization
[AIAA PAPER 92-4603] p 1131 A92-55282
Discrete event fuzzy airport control
p 1046 A92-55973
New insulation constructions for aerospace wiring applications. Volume 2: The 270 VDC arc tracking testing with power controllers
[AD-A240639] p 23 N92-11007
Parallel processing applications for gas turbine engine control p 25 N92-11012
Formulation of a strategy for monitoring control integrity in critical digital control systems
[NASA-TM-104158] p 206 N92-15075
The NASA Langley Research Center 0.3-meter transonic cryogenic tunnel microcomputer controller source code
[NASA-CR-189556] p 209 N92-15077
Nonlinear stability and control study of highly maneuverable high performance aircraft, phase 2
[NASA-CR-189911] p 382 N92-19841
Design and evaluation of a robust dynamic neurocontroller for a multivariable aircraft control problem
[NASA-TM-105579] p 481 N92-20586
Welding technology transfer task/laser based weld joint tracking system for compressor girth welds
p 593 N92-22426
Multifunction tests of a frequency domain based flutter suppression system
[NASA-TM-107615] p 662 N92-25607
Stability and performance of notch filter control for unbalance response p 771 N92-27731
Fuzzy guidance system evaluation
p 778 N92-27903
Comparison of three controllers applied to helicopter vibration
[NASA-TM-102192] p 878 N92-28457
On-line analysis capabilities developed to support the AFW wind-tunnel tests
[NASA-TM-107651] p 961 N92-30752
Design and experimental validation of a flutter suppression controller for the active flexible wing
[NASA-TM-4381] p 979 N92-31240
A parameter optimization approach to controller partitioning for integrated flight/propulsion control application
[NASA-TM-105826] p 979 N92-32241
The multiple-function multi-input/multi-output digital controller system for the AFW wind-tunnel model
[NASA-TM-107600] p 1060 N92-32536
An investigation of switched reluctance rotor position estimation using neural networks
[AD-A252846] p 1061 N92-33414
Controller response to conflict resolution advisory prototype
[PB92-190032] p 1050 N92-33596
Dynamics and control of a five degree-of-freedom magnetic suspension system
[NASA-CR-191259] p 1102 N92-34222

CONVECTION
The effect of tip convection on the performance and optimum dimensions of cooling fins p 902 A92-48354
Measurements of the dynamic stall vortex convection speed p 1032 A92-56351
Analytical/numerical matching and periodic inversion: Two advances in free wake analysis
p 178 N92-13994
Direct simulation of high-speed mixing layers
[NASA-TP-3186] p 945 N92-30909

CONVECTION-DIFFUSION EQUATION
Navier-Stokes computations of horseshoe vortex flows
p 990 A92-49516
A general explicit or semi-explicit algorithm for compressible and incompressible flows
p 937 A92-52682

CONVECTIVE FLOW
Convective transport phenomena on the suction surface of a turbine blade including the influence of secondary flows near the endwall
[ASME PAPER 91-GT-35] p 147 A92-15518
Unique high-alpha roll dynamics of a sharp-edged 65 deg delta wing
[AIAA PAPER 92-0276] p 318 A92-25730
Convective flow analysis on the KC-135 aircraft
[AIAA PAPER 92-0844] p 493 A92-29610
The effectiveness of Coriolis dampening of convection during aircraft high-g arcs p 581 A92-33847
Numerical simulation of droplet deformation in convective flows p 670 A92-36844
Analysis of a dusty wall jet
[NASA-CR-189759] p 257 N92-15965
Process modeling KC-135 aircraft
[NASA-CR-184278] p 359 N92-18347
Operating ranges of meteorological wind tunnels for the simulation of convective boundary layer phenomena
[AD-A244153] p 409 N92-19195
Development of a new flux splitting scheme
p 596 N92-23352
Measurements in the inhomogeneous convective boundary layer using three powered gliders
p 775 N92-26350

CONVECTIVE HEAT TRANSFER
A method for determining the parameters of mathematical generalizations of experimental data on convective heat transfer p 41 A92-12803
Heat transfer in rotating serpentine passages with trips normal to the flow
[ASME PAPER 91-GT-265] p 151 A92-15663
Conjugate conduction/convection/nucleate-boiling heat transfer with a high-speed boundary layer
[AIAA PAPER 91-5033] p 215 A92-17823
Roughness effects on heat transfer from a NACA 0012 airfoil p 219 A92-20217
Two-dimensional effects in a triangular convecting fin
p 219 A92-20324
Measurement of convective heat-transfer coefficients on a wind tunnel model by passive and stimulated infrared thermography p 291 A92-21450
Measurement of convective heat-transfer coefficients in wind tunnels using passive and stimulated infrared thermography p 390 A92-24430
Earth atmospheric entry studies for manned Mars missions p 442 A92-32251
Heat transfer in the entrance region of semicircular ducts with internal fins p 497 A92-32264
Two-dimensional heat transfer from a rectangular fin with asymmetrical thermal boundary conditions
p 498 A92-32524
Stagnation point heat flux in hypersonic high enthalpy flow p 613 A92-38373
Optimum dimensions of convective-radiative spines using a temperature correlated profile
p 676 A92-40869
Heat transfer to a cylinder submerged in a rectangular cavity in supersonic flow --- to simulate electrical cables routed through Space Shuttle Solid Rocket Booster External Tank
[AIAA PAPER 92-2949] p 901 A92-47913
Indirect measurements of convective flow by IR thermography
[ONERA, TP NO. 1992-46] p 902 A92-48607
Analytical and experimental studies of heat pipe radiation cooling of hypersonic propulsion systems
[AIAA PAPER 92-3809] p 867 A92-49128
Enhancement of laminar boundary layer heat transfer by a vortex generator p 1118 A92-55453
Experimental modeling of film-cooled axial turbine tip seals
[AIAA PAPER 92-4058] p 1119 A92-56141
Stokes flows in superposed immiscible liquids with horizontal heating
[IAF PAPER 92-0909] p 1123 A92-57288
The effect of angle of incidence and Reynolds number on heat transfer in a linear turbine cascade
[AD-A243900] p 377 N92-19328
An engineering method for interactive inviscid-boundary layers in three-dimensional hypersonic flows
[NASA-TM-107838] p 632 N92-25279
Swept shock/boundary layer interaction experiments in support of CFD code validation
[NASA-CR-190583] p 1036 N92-32494

CONVERGENCE
A study on the superconvergence of Multhopp's discretization in vortex-lattice methods
p 336 A92-27381
Accelerated convergence to steady state by gradual far-field damping p 610 A92-36835
Progress with multigrid schemes for hypersonic flow problems
[NASA-CR-189579] p 185 N92-15047

CONVERGENT NOZZLES
Acoustic interactions between an altitude test facility and jet engine plumes: Theory and experiments
[NASA-CR-190423] p 738 N92-26405
Parametric investigation of single-expansion-ramp nozzles at Mach numbers from 0.60 to 1.20
[NASA-TP-3240] p 1042 N92-34193

CONVERGENT-DIVERGENT NOZZLES
Calculation of flow of a radiating gas in axisymmetric nozzles of specified shape p 7 A92-12179
Computation of supersonic jet mixing noise for an axisymmetric CD nozzle using k-epsilon turbulence model
[AIAA PAPER 92-0500] p 414 A92-26328
Uniqueness of solutions of the generalized Tricomi problem arising in the theory of the Laval nozzle
p 428 A92-30319
Low-frequency vibrations of the shutters of the variable Laval nozzle of gas turbine engines p 657 A92-40610
A numerical study of flow of a viscous gas in a Laval nozzle in the narrow channel approximation
p 706 A92-42680
Flow and acoustic features of a supersonic tapered nozzle p 712 A92-44328
Gortler instability and supersonic quiet nozzle design
p 813 A92-46902
A study on the impact of shroud geometry on ejector pumping performance
[AIAA PAPER 92-3260] p 864 A92-48856
Scale model test results of a multi-slotted vectoring 2DCD ejector nozzle
[AIAA PAPER 92-3264] p 864 A92-48859
Computation of supersonic jet mixing noise for an axisymmetric CD nozzle using k-epsilon turbulence model
[NASA-TM-105338] p 237 N92-14795
Static performance of a cruciform nozzle with multiaxis thrust-vectoring and reverse-thrust capabilities
[NASA-TP-3188] p 527 N92-23095
Parametric investigation of single-expansion-ramp nozzles at Mach numbers from 0.60 to 1.20
[NASA-TP-3240] p 1042 N92-34193

CONVERSION
A review of aging aircraft technology: An IAI perspective
[IAITIC-91-1018] p 461 N92-20500

CONVEXITY
Computations of hypersonic flows around a three-dimensional concave/convex body
[AIAA PAPER 92-2606] p 805 A92-45570

CONVOLUTION INTEGRALS
A fast conformal mapping algorithm with no FFT
p 1007 A92-50471

COOLERS
Thermal management of high heat flux electronic components in space and aircraft systems, phase 1
[AD-A239982] p 41 N92-10157

COOLING
Heat transfer effects on aerodynamics and implications for wind-tunnel tests p 497 A92-32240
Requirements for high flux cooling of future avionics systems
[SAE PAPER 912104] p 673 A92-39958
Next-generation avionics packaging and cooling 'test results from a prototype system' p 989 A92-49277
Window cooling for high speed flight
[AD-D015145] p 344 N92-18193
Secondary instability of high-speed flows and the influence of wall cooling and suction
[NASA-CR-4427] p 406 N92-19844
Effects of turbine cooling assumptions on performance and sizing of high-speed civil transport
[NASA-TM-105610] p 562 N92-23537
Users manual and modeling improvements for axial turbine design and performance computer code TD2-2
[NASA-CR-189118] p 716 N92-27376
Further investigation of the effect of model cooling on periodic transonic flow p 721 N92-27961

COOLING SYSTEMS
Minimization of the number of cooling holes in internally cooled turbine blades
[ASME PAPER 91-GT-52] p 121 A92-15530
Heat transfer in rotating serpentine passages with trips normal to the flow
[ASME PAPER 91-GT-265] p 151 A92-15663

Discharge coefficients of cooling holes with radiused and chamfered inlets
[ASME PAPER 91-GT-269] p 151 A92-15667
Optimal thermal management system for HALE UAV --- High Altitude Long Endurance Unmanned Air Vehicles
[ASME PAPER 91-GT-396] p 111 A92-15726
A comparison of cooling methods for the airframe nozzle of a single-stage-to-orbit aircraft
[AIAA PAPER 91-5036] p 210 A92-17825
Analysis of cooling systems for hypersonic aircraft
[AIAA PAPER 91-5063] p 216 A92-17843
Evolutionary upgrade and application of the C-130H simple-cycle refrigeration system
[SAE PAPER 911439] p 270 A92-21836
Reliability growth of coolers for advanced optical systems and instruments p 294 A92-22879
Integrated numerical methods for hypersonic aircraft cooling systems analysis
[AIAA PAPER 92-0254] p 357 A92-25712
Thermal management of air-breathing propulsion systems
[AIAA PAPER 92-0514] p 373 A92-26940
Structural tailoring/analysis for hypersonic components - Executive system development
[AIAA PAPER 92-2471] p 583 A92-34360
Flexible heat pipe cold plates for aircraft thermal control
[SAE PAPER 912105] p 674 A92-39959
A method for estimating the efficiency of gas turbine blade cooling systems p 657 A92-40606
Heat transfer on a cylindrical surface in the cavities of gas turbine engine rotors p 657 A92-40609
The effect of tip convection on the performance and optimum dimensions of cooling fins p 902 A92-48354
An experimental investigation of high-aspect-ratio cooling passages
[AIAA PAPER 92-3154] p 890 A92-48780
Reduction of torque pulsation of Stirling engine-compressor system p 992 A92-50785
Effect of porosity in transpiration cooling system p 1112 A92-53786
Thermal management of high heat flux electronic components in space and aircraft systems, phase 1
[AD-A239982] p 41 N92-10157
Heat transfer in rotating serpentine passages with trips skewed to the flow
[NASA-TM-105581] p 499 N92-20235
Hypersonic aerospace vehicle leading edge cooling using heat pipe, transpiration and film cooling techniques p 780 N92-26733
Presentation of a computational code for 3-D compressible flow in complex channels and cavities p 769 N92-27475
Contingency power for a small turboshaft engine by using water injection into turbine cooling air
[NASA-TM-105680] p 871 N92-29661
Study of potassium turbine electric generator system p 1129 N92-33794
Improved articulated fin/wing control system statement of government interests
[AD-D015268] p 1088 N92-34131

COORDINATE TRANSFORMATIONS
Freestream capturing for moving coordinates in three dimensions p 432 A92-31186

COORDINATES
Relative energy concepts in helicopter dynamics p 846 A92-46925
Multi-disciplinary optimization of aeroservoelastic systems
[NASA-CR-188983] p 44 N92-11377
Quaternion and Euler angles in kinematics
[NAL-TM-636] p 909 N92-28836
A surface definition code for turbine blade surfaces
[DE92-010574] p 1004 N92-31498
Time simulation of flutter with large stiffness changes
[NASA-TM-107650] p 963 N92-32111

COORDINATION
Monitoring operational concept
[DOT/FAA/SE-91/3] p 268 N92-15980
COMPAS system concept p 354 N92-19043

COPOLYMERS
BMI/bis (allylphenoxyphthalimide)-copolymers - A new family of resins for advanced composites with improved thermal oxidative stability p 33 A92-10213
Polymer blends, volume 1
[AD-A252112] p 987 N92-31419

CORDAGE
Behavior of aircraft tire coupons under various loading conditions
[AD-A241416] p 116 N92-13063

CORE FLOW
Extension of a three-dimensional Euler method for calculating the flowfield around bypass engines with fan and core jet p 62 A92-13690
Consideration of the effect of viscosity in the problem of porous-wall induction p 440 A92-31887
Similarity solutions for viscous vortex cores p 759 A92-41658
A fast, uncoupled, compressible, two-dimensional, unsteady boundary layer algorithm with separation for engine inlets
[AIAA PAPER 92-3082] p 823 A92-48729
Interface of an uncoupled boundary layer algorithm with an inviscid core flow algorithm for unsteady supersonic engine inlets
[AIAA PAPER 92-3083] p 823 A92-48730
Extension of a three dimensional Euler-code for the investigation of the flow field around bypass engines with fan and core jet
[DLR-FB-91-13] p 503 N92-21699
Interface of an uncoupled boundary layer algorithm with an inviscid core flow algorithm for unsteady supersonic engine inlets
[NASA-TM-105684] p 739 N92-27037
A fast, uncoupled, compressible, two-dimensional, unsteady boundary layer algorithm with separation for engine inlets
[NASA-TM-105686] p 770 N92-27653

CORES
Magnetic suspension using high temperature superconducting cores p 772 N92-27789

CORIOLIS EFFECT
Heat transfer in rotating serpentine passages with trips normal to the flow
[ASME PAPER 91-GT-265] p 151 A92-15663
Experimental results and numerical modeling of solidification during aircraft high-g arcs
[AIAA PAPER 92-0843] p 493 A92-29609
The effectiveness of Coriolis dampening of convection during aircraft high-g arcs p 581 A92-33847
An integrated development of the equations of motion for elastic hypersonic flight vehicles
[AIAA PAPER 92-4605] p 1077 A92-55283
Heat transfer in rotating serpentine passages with trips skewed to the flow
[NASA-TM-105581] p 499 N92-20235

CORNER FLOW
Analysis of transonic flow past an axisymmetric convex corner p 312 A92-25015
Structure of supersonic turbulent flow past a swept compression corner p 431 A92-31155
Semi-inverse marching characteristics scheme for supersonic flows p 432 A92-31187
Axial compression corner flow with shock impingement p 441 A92-32196
Numerical studies of supersonic flow over a compression corner p 442 A92-32324
Numerical and experimental investigation of rarefied compression corner flow
[AIAA PAPER 92-2900] p 820 A92-47876
Experimental investigation of the boundary layer in a corner formed by two circular arc airfoils p 1029 A92-56046
Investigation of a plate-ramp-configuration by means of laser Doppler anemometry at Mach 2.95
[AIAA PAPER 92-3956] p 1097 A92-56784
Turbulence modeling for hypersonic flight
[NASA-CR-190313] p 630 N92-24898

CORNERS
Fatigue crack growth of small corner defects from blunt notches in an aeroengine alloy
[PNR-90860] p 1111 N92-34019

COROTATION
Direct computation of the sound from a compressible co-rotating vortex pair
[AIAA PAPER 92-0374] p 414 A92-26232

CORRECTION
Thin-airfoil correction for panel methods p 811 A92-46811
Humidity effects on gas turbine performance
[NRC-30241] p 130 N92-11998
User guide for WIACX: A transonic wind-tunnel wall interference assessment and correction procedure for the NTF
[NASA-TM-104168] p 261 N92-17547
Comparison of a two-dimensional adaptive-wall technique with analytical wall interference correction techniques
[NASA-TP-3132] p 444 N92-20494

CORRELATION
Prediction of helicopter simulator sickness p 46 A92-11473
In situ measurement of particle formation in heated jet fuels: A new application of photon correlation spectroscopy
[DE92-003641] p 488 N92-20132

CORRELATION COEFFICIENTS
Control surfaces correlation in DLC maneuvers p 280 A92-21301
Control surfaces correlation in DSFC maneuvers --- Direct Side-Force Control p 281 A92-21307
Statistical methods applicable to analysis of aircraft performance data
[ESDU-91017] p 359 N92-18096

CORROSION
Corrosion damage and regeneration of aluminide coatings on aircraft turbine blades p 142 A92-15244
Industry seeks tonic for aging aircraft p 308 A92-28492
An advanced neutron radiography system p 492 A92-28748
Corrosion and your aircraft
[NRC-30465] p 114 N92-11991
Advisory Circular: Corrosion control for aircraft
[FAA-AC-43-4A] p 420 N92-21834
Aging fleet: Maintaining airworthiness p 953 N92-31862

CORROSION PREVENTION
Corrosion prevention field test utilizing water displacement compounds p 110 A92-14436
F27 aging aircraft programme emphasizes corrosion prevention p 186 A92-20024
The problem of aging aircraft - Is mandatory retirement the answer? p 308 A92-27448
Design for Corrosion Prevention
[AIAA PAPER 92-1127] p 577 A92-33279
An approach for evaluation of gas turbine deposition
[ASME PAPER 91-GT-214] p 653 A92-36890
A review of aging aircraft technology: An IAI perspective
[IAITIC-91-1018] p 461 N92-20500
Advisory Circular: Corrosion control for aircraft
[FAA-AC-43-4A] p 420 N92-21834
Inspection of aging aircraft: A manufacturer's perspective p 914 N92-30117
Aging fleet: Maintaining airworthiness p 953 N92-31862

CORROSION RESISTANCE
Compressor coating effects on gas turbine engine performance p 25 A92-11282
Thermally sprayed coating systems for surface protection and clearance control applications in aero engines p 488 A92-32394
Anodize and prime your aluminum without environmental headaches p 892 A92-47340
Non-chromated anodize process for corrosion resistance and adhesive bonding p 892 A92-47341
High-temperature combustor and seal for a water piston propulsor
[AD-A242493] p 229 N92-15385
Fabrication and testing of corrosion resistant coatings --- for turbine engine components
[DE92-003553] p 490 N92-21063

CORROSION TESTS
Aerospace Arall - A challenge for the aircraft designer p 33 A92-10232
NLR experience with high velocity burner rig testing, 1979-1989
[NLR-TP-89152-U] p 385 N92-18415

COSMIC DUST
Microgravity nucleation and particle coagulation experiments support
[NASA-CR-189899] p 502 N92-21433

COSMIC RAYS
Surface activation of Concorde by Be-7 p 605 N92-23295

COST ANALYSIS
Maximum mass allowance to justify passenger-carrying aircraft modification p 113 A92-16802
Retrofit provides navigation enhancement for older aircraft p 198 A92-20025
Study of materials and structures for the High-Speed Civil Transport
[AIAA PAPER 92-1080] p 536 A92-33249
Composite makers sense changes p 754 A92-42345
Avionics standardization in the USAF: 1980 to 1990 p 198 N92-14048
Rotorcraft low altitude IFR benefit/cost analysis: Operations analysis
[SCT-90RR-44] p 191 N92-15061
Kappa Group: The initial guess. A proposal in response to a commercial air transportation study
[NASA-CR-189981] p 366 N92-19374
A guide for the consideration of composite material impacts on airframe costs
[AD-A243928] p 417 N92-19466
Public-sector aviation issues: Graduate research award papers, 1989 - 1990
[PB91-242271] p 308 N92-19662
Preliminary design studies of an advanced general aviation aircraft
[NASA-CR-190024] p 461 N92-20064
Currently available fuel gas booster compressor equipment for small gas turbine engines
[PB92-127026] p 499 N92-20265
H2-fueled high-bypass turbofan p 475 N92-21529

The cost of silicon nitride powder: What must it be to compete?
[DE92-008710] p 669 N92-25223
Life cycle costs of the C-130 electrical power system upgrade
[AD-A246759] p 786 N92-28348
Allocation and recovery of federal airport and airway costs, 1991
[AD-A249436] p 983 N92-30777
Cost/benefit analysis of the AH-64 (Apache) helicopter Automated Test Equipment (ATE)
[AD-A252909] p 1101 N92-33398

COST EFFECTIVENESS
Relating economics to design parameters through a criterion function p 271 A92-22709
Cost effective solutions for titanium sheet metal forming p 293 A92-22785
The H-53E Super Stallion - A cost-effective solution to multi-service medium/heavy lift requirements p 647 A92-40388
A criterion for estimating the economic and operational efficiency of the power distribution systems of commercial aircraft p 657 A92-40611
A method for estimating the technological and economic efficiency of measures enhancing the reliability of aviation gas turbine engines p 657 A92-40621
Cost effectiveness of environmental stress screening (ESS) - A case history p 760 A92-42084
Design and analysis of vortex generators on reengined Boeing 727-100QF center inlet S-duct by a reduced Navier-Stokes code
[AIAA PAPER 92-2700] p 800 A92-45542
Cost effective close tolerance plastic master models p 958 A92-51538
The wind tunnel test 'system' of 1995 - Cost effective experimentation through a fusion of related technologies p 1091 A92-54342
Designing to cost effectiveness - Enhancing quality p 1119 A92-56209
Historical perspective on the evolution of avionics standards p 198 N92-14049
Avionics standardization in Europe p 199 N92-14050
Large area QNDE inspection for airframe integrity p 362 N92-18588
Special Course on Engineering Methods in Aerodynamic Analysis and Design of Aircraft
[AGARD-R-783] p 552 N92-23950
An appraisal of cost-effectiveness models used in the Air Force and Navy aircraft engine component improvement programs
[AD-A245910] p 743 N92-28162
Life cycle costs of the C-130 electrical power system upgrade
[AD-A246759] p 786 N92-28348
Allocation and recovery of federal airport and airway costs, 1991
[AD-A249436] p 983 N92-30777
Continuation of tailored composite structures of ordered staple thermoplastic material
[NASA-CR-189671] p 1110 N92-33613

COST ESTIMATES
Allocation and recovery of federal airport and airway costs, 1991
[AD-A249436] p 983 N92-30777
Air traffic control: FAA's advanced automation system contract
[GAO/IMTEC-91-25] p 1048 N92-32861
Advanced airframe structural materials: A primer and cost estimating methodology
[AD-A253371] p 1062 N92-34182

COST REDUCTION
Performance and handling qualities criteria for low cost real time rotorcraft simulators - A methodology development p 136 A92-14365
Potential hypersonic vehicles applications
[AIAA PAPER 91-5086] p 169 A92-17854
The use of variable camber to reduce drag, weight and costs of transport aircraft p 313 A92-25096
C.A.T.C.H. - Computer aided test conductor handbook: A method for reducing cost, time and effort in an aircraft test and certification program p 602 A92-35943
Future military APU requirements
[SAE PAPER 912176] p 655 A92-40001
Airlines could reap big saving with new Pratt common core p 736 A92-42400
Research on aircraft life cycle cost reduction p 1012 A92-49835
RTM - Simultaneous design and tooling reduces cost and lead time p 994 A92-51537
A common engineering-to-manufacturing-to-field test strategy to achieve systems readiness beyond the '90s p 931 A92-53111
Superplastic applications in aero engines
[PNR-90788] p 473 N92-20436
Conceptual design of two-stage-to-orbit hybrid launch vehicle
[NASA-CR-190006] p 486 N92-20666
Observations on computational methodologies for use in large-scale, gradient-based, multidisciplinary design incorporating advanced CFD codes
[NASA-TM-104206] p 630 N92-24956
The cost of silicon nitride powder: What must it be to compete?
[DE92-008710] p 669 N92-25223

COSTS
National Aeronautics and Space Administration p 238 N92-14923
When should we start high-rate production of the B-2? An analysis based on flight test results
[RAND/P-7757] p 697 N92-25204
Aviation noise: Costs of phasing out noisy aircraft
[GAO/RCED-91-128] p 1011 N92-31454

COUNTER ROTATION
Optical measurements of unducted fan flutter
[ASME PAPER 91-GT-19] p 147 A92-15510
Triple contra-rotating turbine and its basic analysis p 371 A92-24745
Evaluation of a Navier-Stokes prediction of a jet in a crossflow p 441 A92-32235
Wind tunnel test for a high speed propeller with coaxial contrarotation p 737 A92-43195
Basic analysis of counter-rotating turbines p 862 A92-47692
Calibration of the Naval Postgraduate School 3.5' x 5.0' academic wind tunnel
[AD-A240614] p 31 N92-11025
Programs at Wright-Patterson Air Force Base p 228 N92-15092
Areas of seal R/D at GE p 228 N92-15094
Counterrotating brushless DC permanent magnet motor
[DE92-003825] p 401 N92-18550
An analytical and computational investigation of shock-induced vortical flows with applications to supersonic combustion p 405 N92-19538
High speed turboprop aeroacoustic study (counterrotation). Volume 2: Computer programs
[NASA-CR-185242] p 1011 N92-31248

COUNTERFLOW
Calculation of gas combustion regimes in a counterflow vortex chamber p 34 A92-12209
The enhancement of mixing in high-speed heated jets using a counterflowing nozzle
[AIAA PAPER 92-3262] p 825 A92-48857
Theories of turbulent combustion in high speed flows
[AD-A253032] p 1111 N92-33624

COUNTING CIRCUITS
A real-time rain-flow method of cycle counting and its program design for aeroengine service loads p 557 A92-35560

COUPLED MODES
Coupled vibrations of turbomachine blades p 738 A92-44545
Lower-end dynamic characteristics of a magnetically coupled free-piston Stirling engine/compressor system p 992 A92-50795
Computational structures technology engine/airframe coupling p 649 N92-25935

COUPLING
Vibroacoustic simulation of an airplane structure p 629 N92-24871
Proof of concept of a magnetically coupled Stirling engine-driven heat pump
[DE92-017129] p 1129 N92-33271

COVARIANCE
A new method for simulating atmospheric turbulence for rotorcraft applications p 162 A92-14368

COWLINGS
Thermoviscoplastic analysis of engine cowl leading edge subjected to oscillating shock-shock interaction
[AIAA PAPER 92-2537] p 583 A92-34381
Operating characteristics at Mach 4 of an inlet having forward-swept, sidewall-compression surfaces
[AIAA PAPER 92-3101] p 863 A92-48743
The effect of a type 3 and type 4 shock/shock interaction on heat transfer in the stagnation region p 160 N92-13867
A simplified method for thermal analysis of a cowl leading edge subject to intense local shock-wave-interference heating
[NASA-TP-3167] p 679 N92-24797

CRACK ARREST
Tear straps in airplane fuselage
[AD-A248543] p 854 N92-29511

CRACK CLOSURE
Contribution of individual load cycles to crack growth under aircraft spectrum loading p 891 A92-45236
Effects of constraint on crack growth under aircraft spectrum loading
[NASA-TM-107677] p 1128 N92-34178

CRACK GEOMETRY
A study on crack initiation method for durability analysis p 901 A92-47663

CRACK INITIATION
Fatigue crack initiation and small crack growth in several airframe alloys p 212 A92-19754
Crack initiation and the short-to-long crack growth transition in a Ni-base superalloy p 213 A92-19767
A study on crack initiation method for durability analysis p 901 A92-47663
Monitoring fatigue cracks in gears p 1116 A92-54496
Fatigue crack growth of small corner defects from blunt notches in an aeroengine alloy
[PNR-90860] p 1111 N92-34019

CRACK PROPAGATION
A method of reliability analysis for propeller blades p 25 A92-10968
The INFO-ROC technique - A method for comparing and optimizing inspection systems p 144 A92-13563
Fatigue due to noise-induced pressure
[ASME PAPER 91-GT-150] p 148 A92-15588
Fatigue crack initiation and small crack growth in several airframe alloys p 212 A92-19754
Short fatigue crack growth from blunt notches in an aero-engine alloy p 212 A92-19760
Crack initiation and the short-to-long crack growth transition in a Ni-base superalloy p 213 A92-19767
Thermo-mechanical fatigue crack growth in aircraft engine materials p 213 A92-19799
Fracture analysis and crack propagation in pressurized fuselage structures - Experimental and numerical investigations p 217 A92-19812
Prediction of fatigue crack growth in a Ti-6Al-4V fan disk forging under spectrum loading p 213 A92-19817
Proof test and fatigue crack growth modeling on 2024-T3 aluminum alloy p 213 A92-19828
Flutter analysis of anisotropic panels with patched cracks p 219 A92-20216
Creep-fatigue crack growth in Jethete M152 at 550 C under mixed mode conditions p 288 A92-21490
Review of methods for crack growth testing in gas turbine engine disc materials p 296 A92-24193
Inclusion size effect on the fatigue crack propagation mechanism and fracture mechanics of a superalloy p 388 A92-24831
Creep fracture mechanisms in single crystal superalloys p 388 A92-25031
Simulation of arbitrary crack propagation in three-dimensions p 393 A92-25535
A fatigue crack growth threshold p 389 A92-26667
Methods for predicting successful ejection seat canopy penetration p 544 A92-35441
Fretting fatigue p 672 A92-38225
A method to determine propagation direction of compressive fracture in carbon-fibre composites p 672 A92-38770
A comparison of fatigue life prediction methodologies for rotorcraft p 647 A92-40884
Bayesian reliability analysis in connection with the evaluation of multiple-site damage p 762 A92-43126
Elevated temperature crack growth in aircraft engine materials p 891 A92-45234
Contribution of individual load cycles to crack growth under aircraft spectrum loading p 891 A92-45236
Reliability centered maintenance for metallic airframes based on a stochastic crack growth approach p 897 A92-45242
Economic life analysis for replacing components p 785 A92-47670
Aero mechanics in the twenty-first century
[AIAA PAPER 92-3194] p 863 A92-48805
Damage tolerant design of critical aircraft structural components
[AIAA PAPER 92-4041] p 1123 A92-56860
Effects of spectrum variations on fatigue crack growth p 1123 A92-57399
Critical appraisal of the McDonnell Douglas closure model for predicting fatigue crack growth
[ARL-STRUC-R-444] p 44 N92-11376
Verification of NISA 2 and ENDURE fracture mechanics capability
[NRC-ST-621] p 159 N92-13453
The two-bay crack problem in fuselages built in GLARE and ARALL
[LR-653] p 196 N92-14044
Bulging of fatigue cracks in a pressurized aircraft fuselage
[LR-655] p 196 N92-14045
Review of investigations on aeronautical fatigue in the Federal Republic of Germany
[ETN-92-90317] p 225 N92-14397
Probabilistic lifing approach for aero engine disks made of powder nickel base alloys containing ceramic defects p 226 N92-14424

Ceramic technology for Advanced Heat Engines Project
[DE92-002397] p 289 N92-16128
The G-222 aircraft individual tracking programme
p 361 N92-18582
Recent fracture mechanics results from NASA research related to the aging commercial transport fleet
p 362 N92-18589
Fatigue management for the A-7P
p 363 N92-18593
The role of crack growth in defect assessment
[PNR-90798] p 501 N92-20909
Towards GLARE: The development of a fatigue insensitive and damage tolerant aircraft material
[ETN-92-91301] p 648 N92-24966
Simulation of 3D non-planar fatigue crack growth in a turbine blade root
[DE92-006859] p 739 N92-26697
Tensile and interlaminar properties of GLARE (trade name) laminates
[AD-A250188] p 895 N92-28921
Generation of spectra and stress histories for fatigue and damage tolerance analysis of fuselage repairs
[AD-A250390] p 854 N92-29180
Preliminary results on the fracture analysis of multi-site cracking of lap joints in aircraft skins
p 913 N92-30111
Effects of constraint on crack growth under aircraft spectrum loading
[NASA-TM-107677] p 1128 N92-34178

CRACK TIPS
Numerical verification of NISA 2 finite element analysis of the cracked 5th stage compressor disc of J-85 jet engine
[NRC-LTR-ST-1792] p 129 N92-11997

CRACKING (FRACTURING)
Applied fracture mechanics research in the aerospace field p 37 A92-10375
The maintenance economy and economic life of structures p 37 A92-10673
Safe life reliability - Evaluation of new statistical methods p 104 A92-14343
X-ray computed tomographic inspection of castings
p 492 A92-28725
System reliability and risk assessment
[AIAA PAPER 92-2345] p 582 A92-34320
Possibility of increasing durability of blades with damages p 761 A92-42654
Investigation of the structural inhomogeneity of a titanium alloy p 893 A92-47958
Fatigue cracking threshold prediction of transport airplanes p 1118 A92-56094
Fatigue in single crystal nickel superalloys
[AD-A250068] p 987 N92-31360
Criteria for use of seal coats on airport pavements
[DOT/FAA/RD-92/18] p 1102 N92-34247

CRACKS
Critical appraisal of the McDonnell Douglas closure model for predicting fatigue crack growth
[ARL-STRUC-R-444] p 44 N92-11376
The two-bay crack problem in fuselages built in GLARE and ARALL
[LR-653] p 196 N92-14044
Redesign of flight space shuttle main engine nozzle G-15 seal area based on the thermal analysis and flow models p 212 N92-15877
Recent fracture mechanics results from NASA research related to the aging commercial transport fleet
p 362 N92-18589
A review of aging aircraft technology: An IAI perspective
[IAITIC-91-1018] p 461 N92-20500
Inspection of aircraft engine components using automated eddy current and pattern recognition techniques
[NRC-LTR-ST-1834] p 504 N92-22029
Add-on damping treatment for life extension of the F-15 upper-outer wing skin
[AD-A246149] p 746 N92-27577
Tear straps in airplane fuselage
[AD-A248543] p 854 N92-29511
Federal Aviation Administration aging aircraft nondestructive inspection research plan
p 914 N92-30116
Inspection of aging aircraft: A manufacturer's perspective p 914 N92-30117
Aging fleet: Maintaining airworthiness
p 953 N92-31862

CRASH INJURIES
Fatal occupational injury related to helicopters in the United States 1980-1985 p 186 A92-20720
Recent advances in restraint technology
p 535 A92-32979
Salvaging the wreckage - Multidistrict litigation and aviation p 697 A92-39245

CRASH LANDING
Closing the loop on helicopter crashworthiness design requirements p 107 A92-14392

CRASHES
Canada making many changes in wake of Dryden crash report p 529 A92-33799
A re-analysis of the causes of Boeing 727 'black hole landing' crashes p 833 A92-44985
Wichita State University 1986 aviation safety research projects
[DOT/FAA/CT-91/4] p 263 N92-16986
Effect of crash pulse shape on seat stroke requirements for limiting loads on occupants of aircraft
[NASA-TP-3126] p 399 N92-18053
Freezing precipitation on lifting surfaces
[NRC-32124] p 448 N92-20156
Preliminary design and lay-out of an infant restraint system p 449 N92-21513
Aircraft accident report: Ryan International Airlines DC-9-15, N565PC, loss of control on takeoff, Cleveland-Hopkins International Airport, Cleveland, Ohio, February 17, 1991
[PB91-910410] p 530 N92-23597
Aircraft accident/incident summary report: Controlled flight into terrain Bruno's Inc., Beechjet, N25BR, Rome, Georgia, 11 December 1991
[PB92-910404] p 1044 N92-34081

CRASHWORTHINESS
Analysis of crash-resistant fuel systems and airframe structure interaction in a crash environment
p 105 A92-14369
Development of a reclined crashworthy crewseat for rotorcraft p 105 A92-14370
Closing the loop on helicopter crashworthiness design requirements p 107 A92-14392
Crash-resistant rotorcraft preliminary design optimization p 109 A92-14417
Determination of the energy absorption of composite structures under combined loadings p 145 A92-14441
Structural testing of commercial rotorcraft seats - An overview p 544 A92-35437
Energy attenuation for crashworthy seating systems - Past, present, and possible future development
p 544 A92-35452
Crashworthiness of truncated composite cones under side loads p 590 A92-35746
Design of helicopter composite structures for crashworthiness p 848 A92-47408
Wichita State University 1986 aviation safety research projects
[DOT/FAA/CT-91/4] p 263 N92-16986
Effect of crash pulse shape on seat stroke requirements for limiting loads on occupants of aircraft
[NASA-TP-3126] p 399 N92-18053
A report on enhancements for existing and future helicopters supporting operations of the Canadian oil and gas industry
[CTN-91-60126] p 636 N92-25350
Drop test: Cessna Golden Eagle 421B
[DOT/FAA/CT-TN91/32] p 837 N92-28900
Evaluation of head impact kinematics for passengers seated behind interior walls
[AD-A252651] p 952 N92-30551

CRAY COMPUTERS
NAS (Numerical Aerodynamic Simulation Program) technical summaries, March 1989 - February 1990
[NASA-TM-107960] p 1013 N92-31852

CREEP DIAGRAMS
Prediction of long-term creep rupture properties for an aluminium alloy for airframe applications
p 141 A92-15206

CREEP PROPERTIES
Ice property/structure variations across the glaze/rime *transition*
[AIAA PAPER 92-0296] p 351 A92-25749
Effects of elevated temperature on the viscoplastic modeling of graphite/polymeric composites
[NASA-TM-104160] p 35 N92-11149
Thermoviscoplastic response of Ti-15-3 under various loading conditions
[NASA-CR-187621] p 45 N92-11391
The effect of physical aging on the creep response of a thermoplastic composite
[AD-A243600] p 290 N92-17932
Creep and fatigue research efforts on advanced materials p 593 N92-22514
Aeropropulsion structures p 559 N92-22518
Light thermal structures and materials for high speed flight p 649 N92-25922
Fatigue in single crystal nickel superalloys
[AD-A250068] p 987 N92-31360

CREEP RUPTURE STRENGTH
Prediction of long-term creep rupture properties for an aluminium alloy for airframe applications
p 141 A92-15206

CREEP STRENGTH
High temperature multiaxial creep testing of Nimonic 115 p 141 A92-15202
Creep fracture mechanisms in single crystal superalloys p 388 A92-25031
Joining a Ni-based creep-resistant (ODS) alloy by brazing p 1116 A92-54867
Diffusion bonding a creep-resistant Fe-ODS alloy
p 1117 A92-54868

CREEP TESTS
High temperature multiaxial creep testing of Nimonic 115 p 141 A92-15202
Creep-fatigue crack growth in Jethete M152 at 550 C under mixed mode conditions p 288 A92-21490
Fracture mechanics approach to creep growth in welded IN738LC gas turbine blades
[ASME PAPER 91-GT-119] p 670 A92-36893
The effect of physical aging on the creep response of a thermoplastic composite
[AD-A243600] p 290 N92-17932

CREW EXPERIMENT STATIONS
Manipulation and management of data collected at the Crew Station Research and Development Facility - A case study
[AIAA PAPER 92-4162] p 1008 A92-52451

CREW PROCEDURES (INFLIGHT)
An exploration of function analysis and function allocation in the commercial flight domain
[NASA-CR-4374] p 368 N92-19871
Workshop on integrated Crew Resource Management (CRM)
[DOT/FAA/RD-92/5] p 781 N92-27518
An analysis of aircrew communication patterns and content
[AD-A246618] p 907 N92-28253

CREW WORKSTATIONS
Two crew stations for dynamic flight simulation
p 572 A92-35443
Software reliability for flight crew training simulators
p 747 A92-41221
Manipulation and management of data collected at the Crew Station Research and Development Facility - A case study
[AIAA PAPER 92-4162] p 1008 A92-52451
AGSSS: The Airborne Graphics Software Support System; an Ada/PHIGS-based display editor for the rapid development of cockpit display software systems
[AD-A243224] p 277 N92-17221
SIMNET plan view display user manual
[AD-A244617] p 510 N92-21392

CREWS
Ingress, emergency egress, and emergency evacuation testing of army aircraft
[AD-A246398] p 724 N92-27750

CRITERIA
Airbreathing engine selection criteria for SSTO propulsion system
[IAF PAPER 92-0658] p 1071 A92-57099

CRITICAL FLOW
A model of gasdynamic loads on an oscillating nozzle shell p 80 A92-16817
Bleed-boundary conditions for numerically simulated mixed-compression supersonic inlet flow
p 713 A92-44520
Results from computational analysis of a mixed compression supersonic inlet
[NASA-TM-104475] p 12 N92-10976
Air intakes for high speed vehicles
[AGARD-AR-270] p 445 N92-20797

CRITICAL FREQUENCIES
Advanced Study for Active Noise Control in Aircraft (ASANCA)
[AIAA PAPER 92-2092] p 1137 N92-32956

CRITICAL LOADING
Testing of a titanium matrix composite landing gear
[SAE PAPER 912175] p 644 A92-40000

CRITICAL TEMPERATURE
A probabilistic method for monitoring the remaining life of aircraft gas turbine engine components using the temperature limit criterion p 201 A92-18292
Stability of a nonorthogonal stagnation flow to three-dimensional disturbances p 495 A92-31194
High speed civil transport p 649 N92-25919

CRITICAL VELOCITY
Finite element analysis of tire critical speeds
p 762 A92-42949
Notes on the cause of parachute critical velocity
[AD-A244417] p 347 N92-19085
Laser anemometer measurements and computations in an annular cascade of high turning core turbine vanes
[NASA-TP-3252] p 830 N92-28980

CROSS CORRELATION
Crossed beam correlation modeling and experimental techniques for measuring density fluctuations in hypersonic flows
[AIAA PAPER 92-2779] p 758 A92-41323

Atmospheric turbulence spectra and correlation functions
[NLR-TP-89217-U] p 915 N92-28689

CROSS COUPLING
Multiaxis control in longitudinal mode of aircraft
p 1083 A92-56027
Design of bearings for rotor systems based on stability
p 773 N92-27799

CROSS FLOW
Probe shapes for streamwise momentum and cross-stream turbulence intensity p 9 A92-13210
Probe systems for static pressure and cross-stream turbulence intensity p 10 A92-13211
Numerical solution of the boundary-layer equations for a general aviation fuselage p 174 A92-20211
Modeling the ventilated wind tunnel wall
[AIAA PAPER 92-0035] p 249 A92-22156
Computation of normal impinging jets in cross-flow and comparison with experiment p 250 A92-22446
Numerical simulation of supersonic separated flow over blunt cones at high angles of attack p 313 A92-25039
Numerical simulation and analysis for hypersonic flow with separation over blunt cone at angle of attack
p 314 A92-25126
Numerical simulation of twin-jet impingement on a flat plate coupled with cross-flow p 315 A92-25374
Cross-flow separation on a prolate spheroid at angles of attack
[AIAA PAPER 92-0428] p 326 A92-26276
A review of impinging jets in cross-flows - Experimentation and computation
[AIAA PAPER 92-0633] p 333 A92-27011
The structure and development of streamwise vortex arrays embedded in a turbulent boundary layer
[AIAA PAPER 92-0551] p 342 A92-28204
Nonadiabatic and three-dimensional effects in compressible turbulent boundary layers
p 431 A92-31156
Evaluation of a Navier-Stokes prediction of a jet in a crossflow p 441 A92-32235
Structural features of a heated round turbulent jet in a cross-flow p 676 A92-40148
Recent research into the aerodynamics of ASTOVL aircraft in ground environment p 623 A92-40549
Planar fluorescence imaging of a transverse jet in a supersonic crossflow p 755 A92-44501
A calculation of penetration of the jet issuing normally into a cross flow across a wall boundary layer
[SAE PAPER 912029] p 790 A92-45419
Computational study of transition front on a swept wing leading-edge model
[AIAA PAPER 92-2630] p 795 A92-45502
Concepts for the stability analysis of NLF-experiments on swept wings
[AIAA PAPER 92-2706] p 801 A92-45548
Eigenfunction analysis of turbulent mixing phenomena
p 898 A92-45826
Unsteady crossflow on a delta wing using particle image velocimetry p 811 A92-46804
Crossflow vortex and transition measurements by use of multielement hot films p 935 A92-50307
Mixing studies of helium in air at high supersonic speeds p 935 A92-50310
Assessment of passive porosity with free and fixed separation on a tangent ogive forebody
[AIAA PAPER 92-4494] p 1081 A92-55363
Model representation in the PANCOR wall interference assessment code
[NASA-TM-104152] p 31 N92-11022
An experimental analysis of lateral jet injection into confined swirling crossflows p 156 N92-12199
Numerical simulation of swept-wing flows
[NASA-CR-189457] p 180 N92-14969
Calculations of hot gas ingestion for a STOVL aircraft model
[NASA-TM-105437] p 350 N92-19993
CFD mixing analysis of jets injected from straight and slanted slots into confined crossflow in rectangular ducts
[NASA-TM-105699] p 738 N92-26561
Method of measuring cross-flow vortices by use of an array of hot-film sensors
[NASA-CASE-LAR-14824-1-SB] p 998 N92-30390
Structure of three-dimensional turbulent boundary layers p 999 N92-30654
The three-dimensional stability of the Foeppl vortices
p 949 N92-31889
A computational examination of directional stability for smooth and chined forebodies at high-alpha
[NASA-CR-4465] p 950 N92-32114
Unsteady response of the leading-edge vortices on a pitching delta wing p 1041 N92-33851

CROSS SECTIONS
The dimensional reconstruction of vortex cross-section images p 339 A92-27833
Influence of cross section variations on the structural behaviour of composite rotor blades
p 1121 A92-56320
Two-dimensional aerodynamic characteristics of several polygon-shaped cross-sectional models applicable to helicopter fuselages
[NASA-TP-3233] p 944 N92-30394

CRUCIFORM WINGS
Effects of the roll angle on cruciform wing-body configurations at high incidences
[AIAA PAPER 92-4356] p 1079 A92-55342

CRUISE MISSILES
Small engine technology programs
p 560 N92-22532

CRUISING FLIGHT
High speed rotorcraft - Comparison of leading concepts and technology needs p 108 A92-14415
YF-23A preliminary flight test results
p 112 A92-16063
Integrated GPS/INS for the National Aerospace Plane
p 102 A92-16975
Robust control law development for a hypersonic cruise aircraft p 478 A92-29127
Energy-heading transients in atmospheric flight guidance for airbreathing hypersonic vehicles
[AIAA PAPER 91-5065] p 480 A92-31692
A study of altitude-constrained supersonic cruise transport concepts
[AIAA PAPER 92-1027] p 536 A92-33208
Low-speed cruise aerodynamics of the stopped rotor/disk rotorcraft concept
[AIAA PAPER 92-1067] p 517 A92-33240
Control strategy for maximizing reconnaissance range of hypersonic cruise vehicles p 729 A92-41222
Thermal management for a Mach 5 cruise aircraft using endothermic fuel p 736 A92-41225
Aerobang - A new synergetic plane-change maneuver
[AAS PAPER 91-418] p 753 A92-43356
Experimental and numerical study of aerodynamic characteristics for second generation SST
[SAE PAPER 912056] p 844 A92-45439
Optimum cruise lift coefficient in initial design of jet aircraft p 845 A92-46806
Optimization of constant altitude-constant airspeed flight of turbojet aircraft p 845 A92-46815
Analysis of the VISTA longitudinal simulation capability for a cruise flight condition p 876 A92-48488
Technologies for the National Aero-Space Plane
[IAF PAPER 92-0868] p 1105 A92-57259
Example of statistical techniques applied to cruise performance guarantees (Student's t distribution)
[ESDU-91018] p 276 N92-17843

CRUSHING
Airplane crashes on the runway. Fine modeling of the behavior after burning of a frame submitted to linear crushing
[IMFL-90-64] p 353 N92-19350

CRYOGENIC COOLING
Reliability growth of coolers for advanced optical systems and instruments p 294 A92-22879
Evaluation of metal hydride compressors for applications in Joule-Thomson cryocoolers p 296 A92-23835
Computer simulation model for Lucas Stirling refrigerators p 296 A92-23837
Advances of cryogenics in aeronautics and astronautics p 398 A92-27908
Multicomponent gas sorption Joule-Thomson refrigeration
[NASA-CASE-NPO-17569-1-CU] p 228 N92-15203
Three-stage sorption type cryogenic refrigeration system and method employing heat regeneration
[NASA-CASE-NPO-18366-1-CU] p 300 N92-17674

CRYOGENIC EQUIPMENT
Resonant cryogenic chopper --- for infrared and submillimeter radiometers p 294 A92-22796
Space Cryogenics Workshop, 10th, Cleveland, OH, June 18-20, 1991, Proceedings p 295 A92-23826
Evaluation of metal hydride compressors for applications in Joule-Thomson cryocoolers p 296 A92-23835
Computer simulation model for Lucas Stirling refrigerators p 296 A92-23837

CRYOGENIC FLUIDS
Power economy in high-speed wind tunnels by choice of working fluid and temperature p 881 A92-45275
Paint removal using cryogenic processes
[AD-A247668] p 895 N92-28912

CRYOGENIC ROCKET PROPELLANTS
Advances of cryogenics in aeronautics and astronautics p 398 A92-27908

CRYOGENIC TEMPERATURE
Performance tests of a cryogenic hybrid magnetic bearing for turbopumps
[NASA-TM-105627] p 473 N92-20523

CRYOGENIC WIND TUNNELS
Experiments to evaluate hot-jet simulation capabilities in Cryogenic Wind-Tunnel testing
[AIAA PAPER 92-0567] p 384 A92-26975
Advances of cryogenics in aeronautics and astronautics p 398 A92-27908
Wing test at the cryogenic wind tunnel of the National Defense Academy p 749 A92-43199
On the measurement of subsonic flow around an appended body of revolution at cryogenic conditions in the NTF p 880 A92-45265
Power economy in high-speed wind tunnels by choice of working fluid and temperature p 881 A92-45275
Problems and solutions for transition detection in cryogenic wind tunnels by infrared imaging
p 1090 A92-54319
Preliminary airfoil testing experience in the NDA cryogenic wind tunnel p 1091 A92-54326
Control of large cryogenic tunnels
[AIAA PAPER 92-3930] p 1096 A92-56761
The cryogenic balance design and balance calibration methods
[AIAA PAPER 92-4001] p 1122 A92-56824
The NASA Langley Research Center 0.3-meter transonic cryogenic tunnel microcomputer controller source code
[NASA-CR-189556] p 209 N92-15077
Cryogenic test rig with an aerodynamic magnetically levitated carriage p 750 N92-27792
Calculation of support interferences on the aerodynamic coefficients for a wind tunnel calibration model
[ESA-TT-1247] p 830 N92-29159
High Reynolds number test of the Boeing TR77 airfoil in the Langley 0.3-meter transonic cryogenic tunnel
[NASA-TM-4189] p 947 N92-31246

CRYOGENICS
System of cryogenic security of the superconducting accelerator of relativistic nuclei-nuclotron
[DE91-643289] p 304 N92-16789
Cryogenic hydrogen-induced air-liquefaction technologies for combined-cycle propulsion applications
p 487 N92-21526
A study of juncture flow in the NASA Langley 0.3-meter transonic cryogenic tunnel
[NASA-CR-190430] p 773 N92-27880
Development of a quiet supersonic wind tunnel with a cryogenic adaptive nozzle
[NASA-CR-188055] p 751 N92-27976
Development of a quiet supersonic wind tunnel with a cryogenic adaptive nozzle p 751 N92-27977

CRYSTAL DEFECTS
A technique for quantitatively measuring microstructurally induced ultrasonic noise
p 510 A92-28720

CRYSTAL GROWTH
Experimental results and numerical modeling of solidification during aircraft high-g arcs
[AIAA PAPER 92-0843] p 493 A92-29609
Influence of air velocity on the habit of ice crystal growth from the vapor p 668 A92-38111
Fundamental studies on Marangoni convection related to Bridgman crystal growth p 1111 A92-53758

CRYSTALLOGRAPHY
Fatigue in single crystal nickel superalloys
[AD-A243453] p 290 N92-17653

CUBIC EQUATIONS
Parametric bicubic spline and CAD tools for complex targets shape modelling in physical optics radar cross section prediction p 403 N92-19151

CUES
Initial validation of a R/D simulator with large amplitude motion p 886 N92-28546
Effective cueing during approach and touchdown: Comparison with flight p 886 N92-28552

CUMULATIVE DAMAGE
Prediction of low cycle fatigue life of engine cases
p 295 A92-23385
Cut progression during dynamometer testing of foreign object damaged type VII extra high pressure aircraft tires
[SAE PAPER 912155] p 644 A92-39990
Repair operation on a composite material structure
p 700 A92-43153
Contribution of individual load cycles to crack growth under aircraft spectrum loading p 891 A92-45236
Sonic fatigue analysis and anti-sonic fatigue design of aircraft structure p 848 A92-47666
Short cracks and durability analysis of the Fokker 100 wing/fuselage structure
[NLR-TP-90336-U] p 910 N92-29603

CUMULUS CLOUDS
On the relation between cumulus cloud lines and surface shear lines p 410 N92-19667

CURING
Enhanced diagnostic system for autoclaves and bonding presses p 145 A92-14381
Addition curing thermosets endcapped with 4-amino (2.2) paracyclophane p 577 A92-33918

Composite makers sense changes
p 754 A92-42345

CURVATURE
Prediction of wake in a curved duct p 3 A92-10487
A method of calculation for the radius of curvature of the attached shock waves in front of a sharp-nosed axi-symmetrical body placed in a uniform stream
p 243 A92-21319
Importance of an accurate prediction of shock curvature for high-speed rotor noise p 414 A92-25578
Transition to turbulence in curved channel flow
p 621 A92-40125
Planform curvature effects on flutter characteristics of a wing with 56 deg leading-edge sweep and panel aspect ratio of 1.14
[NASA-TP-3116] p 115 N92-13054
Algorithms for blending surface generation
[AD-A245686] p 777 N92-26524
Effects of curvature and rotation on turbulence in the NASA low-speed centrifugal compressor impeller
p 1124 N92-32292

CURVE FITTING
Dynamic characterization and identification of nonlinear systems application to aeronautical structures
p 39 A92-11830
Trajectory fitting in function space with application to analytic modeling of surfaces
[NASA-TP-3232] p 945 N92-30747

CURVED BEAMS
Linear analysis of naturally curved and twisted anisotropic beam p 899 A92-46936
Composite beam analysis linear analysis of naturally curved and twisted anisotropic beams
[AD-A252652] p 999 N92-30766

CURVED PANELS
Response of plate-like structures to correlated random pressure fluctuations
[AIAA PAPER 92-2378] p 584 A92-34452
Temperature and initial curvature effects in low-density panel flutter
[AIAA PAPER 92-2128] p 589 A92-35695

CURVES
Surface grid generation in a parameter space
[AIAA PAPER 92-2717] p 803 A92-45556

CUTTING
Foreign object damage to tires operating in a wartime environment
[AD-A247195] p 724 N92-27682
Cutting treatment by drilling of fiber bound synthetic materials
[MBB-UD-0609-91-PUB] p 988 N92-31716

CYCLES
Natural cycles, gases p 408 N92-19123
Development of hardness cycles for fiber bound materials, using DSC: From laboratory specimens to complex high duty structural members
[MBB-Z-0409-91-PUB] p 987 N92-30969

CYCLIC LOADS
Prediction of low cycle fatigue life of engine cases
p 295 A92-23385
Cyclic symmetric contact stress analysis of aeroengine rotor assembly p 470 A92-29733
A compound fatigue investigation of plate specimen under low-cycle load superposed on high cycle load
p 587 A92-35555
Cyclic hot corrosion of Haynes 230 alloy
p 754 A92-41091
Cyclic fatigue behavior of silica fiber
p 754 A92-42040
Elevated temperature crack growth in aircraft engine materials p 891 A92-45234
Contribution of individual load cycles to crack growth under aircraft spectrum loading p 891 A92-45236
Numerical analysis of an engine turbine disk loaded with a large number of thermomechanical cycles
[ONERA, TP NO. 1992-31] p 902 A92-48592
Engine fan blade low cycle fatigue testing
[AIAA PAPER 92-3478] p 866 A92-49021
Discs low cycle fatigue life predictions for gas turbine engines in CSFR by using fractographic information
p 995 A92-51950
Thermoviscoplastic response of Ti-15-3 under various loading conditions
[NASA-CR-187621] p 45 N92-11391
Behavior of aircraft tire coupons under various loading conditions
[AD-A241416] p 116 N92-13063
Short cracks and durability analysis of the Fokker 100 wing/fuselage structure
[NLR-TP-90336-U] p 910 N92-29603
Research into improving the durability of the hot section in the aircraft turbine engine
[AD-A250342] p 973 N92-31439
Turbulence-induced loads on a teetered rotor
p 1042 N92-34029
Thermal mechanical analysis of sprag clutches
[NASA-CR-190686] p 1128 N92-34207

CYLINDERS
On the sensitivity of transonic flow
p 315 A92-25132
The lateral shock wave family on the surface of a cone-cylinder in transonic flowfield p 315 A92-25136
Composite cylinder blast overpressure testing
p 529 A92-32984

CYLINDRICAL BODIES
Numerical simulation of the flow around rectangular cylinder p 339 A92-27851
Power spectrum of ring modes of pressure fluctuations at the surface of a cylinder in axial flow
p 603 A92-33770
Comparison of two flux splitting schemes for calculation of ogive-cylinder at M = 3.5 and alpha = 18 deg
[AIAA PAPER 92-2667] p 806 A92-45582
Multiple shock-shock interference on a cylindrical leading edge p 813 A92-46899
Heat transfer to a cylinder submerged in a rectangular cavity in supersonic flow --- to simulate electrical cables routed through Space Shuttle Solid Rocket Booster External Tank
[AIAA PAPER 92-2949] p 901 A92-47913
Development of a CFD code for analysis of fluid dynamic forces in seals p 228 N92-15084
Flow visualization and wake analysis for standard and modified configurations of the AN/ALQ-78 antenna pod
[AD-A243552] p 260 N92-17339
Three dimensional boundary layer transition on a yawed cylinder p 766 N92-26909

CYLINDRICAL SHELLS
Linear panel flutter of an elliptic cylindrical shell
p 291 A92-21216
Study model for the reduction of noise through double wall cylindrical shells - Comparison with experimentation
p 694 A92-39088
Acoustic scattering by a disk or annulus linking two concentric cylindrical shells. I - Theory and results for heavy exterior fluid loading. II - Results for heavy exterior fluid loading on both shells p 696 A92-40588
Damaged stiffened shell research at NASA. Langley Research Center p 914 N92-30115

CZOCHRALSKI METHOD
Wide gap, permanent magnet biased magnetic bearing system p 773 N92-27794

D

D REGION
A ionospheric-sounding experiment from an aircraft
p 160 A92-13809

DAMAGE
Damage tolerance analysis for rotorcraft - What the issues are p 1058 A92-56336
Fatigue life behaviour of composite structures
p 390 N92-18577
Life management approach for USAF aircraft
p 362 N92-18587
Large area QNDE inspection for airframe integrity
p 362 N92-18588
AGARD/SMP Review: Damage Tolerance for Engine Structures. 4: Reliability and Quality Assurance
[AGARD-R-773] p 402 N92-19004
Introduction: Needs and approaches to reliability and quality assurance in design and manufacture
p 402 N92-19005
Manufacturing process control as a damage tolerance concept p 403 N92-19006
Development of a wind chamber for model testing of tornado forces on structures
[PB92-104165] p 386 N92-19940
Durability and damage tolerance of aluminum castings
[AD-A245237] p 490 N92-21159
World commercial aircraft accidents: 1st edition, 1946-1991
[DE92-009801] p 636 N92-24713
Foreign object damage to tires operating in a wartime environment
[AD-A247195] p 724 N92-27682
Performance of uncoated AFRSI blankets during multiple Space Shuttle flights
[NASA-TM-103892] p 890 N92-29104
Generation of spectra and stress histories for fatigue and damage tolerance analysis of fuselage repairs
[AD-A250390] p 854 N92-29180
Current DOT research on the effect of multiple site damage on structural integrity p 913 N92-30112
Aging commuter aeroplanes: Fatigue evaluation and control methods p 915 N92-30132
A Protection And Detection Surface (PADS) for damage tolerance p 1107 N92-32523
Criteria for use of seal coats on airport pavements
[DOT/FAA/RD-92/18] p 1102 N92-34247

DAMAGE ASSESSMENT
Damage assessment for composite smart structures
p 140 A92-13601
Continuation of the AHS round robin on fatigue reliability and damage tolerance p 59 A92-14341
Corrosion damage and regeneration of aluminide coatings on aircraft turbine blades p 142 A92-15244
Real-time estimation of gas turbine engine damage using a control based Kalman filter algorithm
[ASME PAPER 91-GT-216] p 124 A92-15633
Fatigue and damage tolerance verification of aircraft structures p 217 A92-19677
Damage tolerance of the fighter aircraft 37 Viggen. I - Analytical assessment. II - Experimental verification
p 192 A92-19819
Progress towards fiber optic smart structures at UTIAS
p 368 A92-24781
The detection of damage and the measurement of strain within composites by means of embedded optical fiber sensors p 491 A92-28669
Smart structures - A damage detection concept
p 491 A92-28672
Damage tolerant structural design using neural networks
[AIAA PAPER 92-1097] p 581 A92-33261
Damage tolerance and repair experience of composite structures
[AIAA PAPER 92-1256] p 515 A92-33339
Research on damage tolerance of compressor blade
p 588 A92-35556
A method for determining equivalent stresses in aviation gas turbine engine blades p 559 A92-36421
Some consideration for evaluation of structural integrity of aging aircraft p 762 A92-43107
Bayesian reliability analysis in connection with the evaluation of multiple-site damage p 762 A92-43126
Optimal maintenance program of damage tolerance structure p 785 A92-47660
Economic life analysis for replacing components
p 785 A92-47670
A neural network based postattack damage assessment system p 922 A92-48520
Fault tolerant avionics display system
p 965 A92-49312
Repair procedures for advanced composites for helicopters p 1016 A92-56277
Damage tolerant design of critical aircraft structural components
[AIAA PAPER 92-4041] p 1123 A92-56860
Study of the engine bird ingestion experience of the Boeing 737 aircraft
[DOT/FAA/CT-89/16] p 187 N92-15053
Aging aircraft structural damage analysis
p 360 N92-18575
Fatigue testing and tear down operations on Airbus A320 forward fuselage p 360 N92-18579
Durability and damage tolerance testing and fatigue life management: A CF-18 experience p 361 N92-18581
Advisory Circular: Corrosion control for aircraft
[FAA-AC-43-4A] p 420 N92-21834
Risk to hearing from overflight noise of military aircraft
[ISVR-TR-194] p 604 N92-22241
Composite fuselage technology (summary of year 2)
[NASA-CR-190434] p 731 N92-26655
A preliminary study on damage detection using piezoelectric film
[AD-A246350] p 733 N92-28118
Generation of spectra and stress histories for fatigue and damage tolerance analysis of fuselage repairs
[AD-A250390] p 854 N92-29180
Modular simulation of HEI fragments and blast pressure
[AD-A248205] p 910 N92-29191
Repair procedures for advanced composites for helicopters
[MBB-UD-0606-91-PUB] p 787 N92-29874
Current DOT research on the effect of multiple site damage on structural integrity p 913 N92-30112
Damage tolerance for commuter aircraft
p 914 N92-30114
Low-velocity impact loading on fibre reinforced aluminum laminates (ARALL) and other aircraft sheet materials
[ETN-92-91613] p 987 N92-30414
A preliminary study in the use of phase demodulation techniques for the analysis of gear vibration data
[NRC-32083] p 1002 N92-31469
Damage tolerance certification methodology for composite structures p 1108 N92-32579
Effects of the abrasiveness of test and training site soils on parachute life
[AD-A252389] p 1038 N92-32900
Bird ingestion into large turbofan engines
[DOT/FAA/CT-91/17] p 1043 N92-33005
Building vibrations induced by noise from rotorcraft and propeller aircraft flyovers
[NASA-TM-104170] p 1138 N92-33160

Lightning strike tests of composite connectors
[AD-A252281] p 1044 N92-33249

DAMPERS

Rotordynamic evaluation of an advanced multi-squeeze film damper - Imbalance response and bladeless simulation
[ASME PAPER 91-GT-242] p 149 A92-15647
The basics of powder lubrication in high-temperature powder-lubricated dampers
[ASME PAPER 91-GT-248] p 150 A92-15653
A gas operated bearing damper for turbomachinery
[ASME PAPER 91-GT-249] p 150 A92-15654
High-temperature powder-lubricated dampers for gas turbine engines p 399 A92-28528

DAMPING

Computational aspects of helicopter trim analysis and damping levels from Floquet theory p 875 A92-46933
A simplified method for predicting the stability of aerodynamically excited turbomachinery
p 224 N92-14364
Proceedings of Damping 1991, volume 3
[AD-A241313] p 225 N92-14386
Monitoring jet fuel degradation using quartz crystal microbalances
[DE92-004730] p 489 N92-20858
Landing gear mechanism including runway-roughness restrictor assembly
[CA-PATENT-1-257-618] p 1061 N92-33585

DAMPING TESTS

Airfoil Vibration Dampers program
[NASA-CR-184276] p 225 N92-14391

DASSAULT AIRCRAFT

The role of simulation for the study of APIS (piloting support by synthetic imagery) p 885 N92-28544

DATA ACQUISITION

A full mission simulation data system
p 162 A92-14367
A state-of-the-art data acquisition system
p 217 A92-19231
On-board data acquisition system for Embraer's CBA123 p 198 A92-19251
Implementation and usage of the RJ program Data Acquisition System Ground Station p 210 A92-19257
Design and implementation of a total flight test system
p 189 A92-19278
One view of experimental aerodynamics
[AIAA PAPER 92-0160] p 254 A92-23775
Operation and design considerations for unsteady data acquisition with PC-based systems in high Reynolds number hypersonic flowfields
[AIAA PAPER 92-0204] p 284 A92-23810
A knowledge acquisition approach for an on-board mission planner
[AIAA PAPER 92-1021] p 531 A92-33204
Development of a multi-computer in-flight data acquisition and analysis system for general aviation aircraft
[AIAA PAPER 92-1037] p 553 A92-33218
Double Density recording acquisition and playback
p 920 A92-47534
New Boeing flight test data acquisition systems
p 920 A92-47537
Common airborne instrumentation system (CAIS) --- time-division multiplexed data acquisition system
p 856 A92-47538
Modern techniques for monitoring airborne telemetry
p 857 A92-47560
Airborne Data Acquisition and Relay System
p 839 A92-47574
GLONASS data analysis - Interim results
p 955 A92-49382
Recent developments in data acquisition and control systems at the Aircraft Research Association Limited
p 1091 A92-54323
Some important factors in turbulence in flight measurement p 1063 A92-54324
A new system for recording unstable aerodynamic phenomena in NAVSWC Hypervelocity Wind Tunnel No. 9 p 1091 A92-54325
Preliminary airfoil testing experience in the NDA cryogenic wind tunnel p 1091 A92-54326
The wind tunnel test 'system' of 1995 - Cost effective experimentation through a fusion of related technologies
p 1091 A92-54342
Hypervelocity Wind Tunnel 9 control system
p 1092 A92-54343
Flight evaluation of navigation systems including MLS using NAL Do228 - Outline p 1047 A92-56116
Flight evaluation of navigation systems including MLS using NAL Do228 - Results of MLS
p 1047 A92-56117
Correlation of flight, tunnel and prediction data on a helicopter main rotor p 1059 A92-56350
Advanced nozzle and engine components test facility
[AIAA PAPER 92-3993] p 1099 A92-56816
The use of artificial neural networks in experimental data acquisition and aerodynamic design p 90 N92-13848
Development of a calibrated software reliability model for flight and supporting ground software for avionic systems p 234 N92-15870
Improvement of data processing system for gust wind tunnel data acquisition part: System conversion from off-line to on-line processing
[NAL-TM-611] p 285 N92-17756
Visual approach data collection at San Francisco International Airport (SFO)
[DOT/FAA/CT-90/23] p 354 N92-18112
Aircraft tracking for structural fatigue
p 361 N92-18584
Application of technology developed for flight simulation at NASA. Langley Research Center p 573 N92-22437
A sophisticated, multi-channel data acquisition and processing system for high frequency noise research
[NASA-CR-189137] p 696 N92-24688
Propeller noise research at NRC p 628 N92-24863
Operational noise data for OH-58D Army helicopters
[AD-A246822] p 926 N92-28292
Status of the FAA flight loads monitoring program
p 914 N92-30113
Acquisition of an aerothermodynamic data base by means of a winged experimental reentry vehicle
[MBB/FE202/S/PUB/461] p 787 N92-30232
Three-dimensional laser window formation
[NASA-RP-1280] p 984 N92-30307
Development statistics for the UH-1 Ada feasibility study
[AD-A252404] p 982 N92-30547
Repetitive High Energy Pulsed Power (RHEPP) temperature monitoring system utilizing Luxtron fluoroptic sensors and thermocouples technical reference manual
[DE92-013461] p 999 N92-30893
The design and development of a portable, DSP micro-processor based, high-accuracy data acquisition system
[NRC-32146] p 1134 N92-32851
The development of an airborne information management system for flight test
[NASA-TM-104251] p 1065 N92-32866
The Dornier 328 Acoustic Test Cell (ATC) for interior noise tests and selected test results
[AIAA PAPER 92-2164] p 1137 N92-32951
Pilots noise exposure during a Boeing 747-400 round trip: Ambient noise and acoustic-head recording and analysis of data p 1137 N92-32960

DATA BASE MANAGEMENT SYSTEMS

The designer-FEM model interface based on the data base management concept p 163 A92-16832
Development of data base system in CIEM project
p 1009 A92-53093
Information Management Engineering (IME) laboratory: A database development facility
[AD-A243191] p 305 N92-17369
Grid management p 632 N92-25713

DATA BASES

A data base for flight in the wake of a ship
[AIAA PAPER 92-0295] p 319 A92-25748
Acquisition of an aerothermodynamic data base by means of a winged experimental reentry vehicle
p 486 A92-30685
Constraint-based component-modeling for knowledge-based design
[AIAA PAPER 92-1192] p 600 A92-33304
Never make the same mistake twice - Using configuration control and error analysis to improve software quality p 601 A92-33603
Flight testing a digital terrain following system
p 548 A92-35929
Loss of cabin pressurization in U.S. naval aircraft - 1969-90 p 634 A92-37168
Software package for preliminary design of helicopter
p 775 A92-41195
The development of an intelligent human factors data base as an aid for the investigation of aircraft accidents
p 928 A92-44994
Establishing a database for flight in the wakes of structures p 810 A92-46782
An explanation-based-learning approach to knowledge compilation - A Pilot's Associate application
p 920 A92-48220
Automatic document generation with case on a DOD avionics project p 1005 A92-49299
Development of data base system in CIEM project
p 1009 A92-53093
A development of hypermedia type database system for instruction of aircraft conceptual design
p 1132 A92-56113
A database of aerothermal measurements in hypersonic flow for CFD validation
[AIAA PAPER 92-4023] p 1034 A92-56845
The use of artificial neural networks in experimental data acquisition and aerodynamic design p 90 N92-13848
Common avionics baseline: The product of the joint integrated avionics working group p 199 N92-14053
Identification techniques: Frequency domain methods
p 273 N92-17158
Accurate, productive aerodynamic simulation on patched mesh systems
[AD-A243977] p 405 N92-19386
Prototyping the IRDS: An airport application
[PB92-112580] p 484 N92-20448
Durability and damage tolerance of aluminum castings
[AD-A245237] p 490 N92-21159
Experimental study of a generic high-speed civil transport: Tabulated data
[NASA-TM-104216] p 525 N92-22232
Composite strength statistics from fiber strength statistics
[AD-A245616] p 755 N92-26383
A modeling strategy for large-scale optimization based on analysis and visualization principles
[AD-A246570] p 777 N92-26620
A prototype semantic integrity front end expert system for a relational database
[AD-A246084] p 781 N92-26765
Test plan for the international aircraft operator information system
[DOT/FAA/CT-91/18] p 781 N92-26830
F-111C flight dynamic model aerodynamic data-base development and verification
[AD-A246356] p 715 N92-26947
NASA/DOD Aerospace Knowledge Diffusion Research Project. Paper 14: An analysis of the technical communications practices reported by Israeli and US aerospace engineers and scientists
[NASA-TM-107924] p 782 N92-28183
Binary optical filters for scale invariant pattern recognition
[NASA-TM-103902] p 853 N92-28910
A rotorcraft flight database for validation of vision-based ranging algorithms
[NASA-TM-103906] p 841 N92-29103
Development of a flight information system using the structured method
[AD-A248207] p 859 N92-29222
Status of the FAA flight loads monitoring program
p 914 N92-30113
Communication: An important element of maintenance and repair p 838 N92-30124
Acquisition of an aerothermodynamic data base by means of a winged experimental reentry vehicle
[MBB/FE202/S/PUB/461] p 787 N92-30232
Numerical methods for the simulation of complex multi-body flows with applications for the integrated Space Shuttle vehicle p 945 N92-30741
An international aerospace information system: A cooperative opportunity
[NASA-TM-108171] p 1142 N92-33237
Simulation model of a twin-tail, high performance airplane
[NASA-TM-107601] p 1088 N92-33537
Experimental study of a generic high-speed civil transport
[NASA-TM-4382] p 1040 N92-33631
Joint study on the computerisation of in-field aero engines vibration diagnosis
[PNR-90799] p 1072 N92-33815
Engine bird ingestion experience of the Boeing 737 aircraft: Expanded data base
[DOT/FAA/CT-91/32] p 1045 N92-34151

DATA COLLECTION PLATFORMS

High-altitude lighter-than-air powered platform
[SAE PAPER 912054] p 844 A92-45438

DATA COMPRESSION

Compression techniques for video telemetry
p 188 A92-19214
Fractal image compression of Rayleigh, Raman, LIF and LDV data in turbulent reacting flows
[AD-A246960] p 767 N92-27352
The development of an airborne information management system for flight test
[NASA-TM-104251] p 1065 N92-32866

DATA CONVERSION ROUTINES

CAD product data exchange: Conversions for curves and surfaces
[ISBN-90-6275-723-9] p 648 N92-24964

DATA FLOW ANALYSIS

Development of a multi-computer in-flight data acquisition and analysis system for general aviation aircraft
[AIAA PAPER 92-1037] p 553 A92-33218
The data flow simulator, a tool for system simulation --- in digital avionics p 1006 A92-49329

DATA INTEGRATION

Aircraft maintenance support system
p 607 A92-38217
Data Link integration in commercial transport operations p 839 A92-44919

A Kalman filter integrated navigation design for the IAR Twin Otter Atmospheric Research Aircraft
[NRC-32148] p 1048 N92-32849
The use of Kalman filtering techniques to improve the accuracy of flight test data
[NRC-32139] p 1064 N92-32850

DATA LINKS
Data-link communication between controllers and pilots - A review and synthesis of the simulation literature
p 94 A92-14045
Automatic link establishment - The key to reliable helicopter NOE communications p 94 A92-14403
Concepts for replacing shipboard TACAN with differential GPS p 101 A92-16971
Reconfigurable Mobile System - Ground, sea and air applications p 218 A92-19986
Implementing data link across the Pacific
[SAE PAPER 912235] p 638 A92-40027
The Automatic Dependent Surveillance (ADS) system
p 724 A92-41208
Intra-flight laser data links - Technology focus
p 725 A92-41472
Mode S data link pilot-system interface - A blessing in de skies or a beast of burden? p 839 A92-44920
Airborne/shipborne PSK telemetry data link
p 839 A92-47511
Global Positioning System telecommand link
p 839 A92-47566
Gulf Range Drone Control Upgrade System Mobile Control System p 882 A92-47567
An experimental program concerning a satellite data link for oceanic ATC p 1046 A92-56093
Advanced information processing system: Inter-computer communication services
[NASA-CR-187556] p 53 N92-11706
Design of a fiber optic image transmission link
[AD-A243686] p 304 N92-17088
Assessment of cockpit interface concepts for data link retrofit
[NASA-CR-187615] p 268 N92-17512
DRES unmanned aerial vehicle data link research
[AD-A244272] p 365 N92-19030
Flight deck benefits of integrated data link communication
[NASA-TP-3219] p 456 N92-21459
Fiber optic data busses for aircraft
p 736 N92-28093
Application of VME-technology on an airborne data link processor unit
[NLR-MP-88040-U] p 841 N92-29615
US Coast Guard GPS Information Center (GPSIC) and its function within the Civil GPS Service (CGS)
p 1049 N92-33352
Design and evaluation of an advanced air-ground data-link system for air traffic control
[NASA-TM-103899] p 1050 N92-33407

DATA MANAGEMENT
Manipulation and management of data collected at the Crew Station Research and Development Facility - A case study
[AIAA PAPER 92-4162] p 1008 A92-52451
Development of data base system in CIEM project
p 1009 A92-53093
Prototyping the IRDS: An airport application
[PB92-112580] p 484 N92-20448
Flight deck benefits of integrated data link communication
[NASA-TP-3219] p 456 N92-21459
National airspace data interchange network analysis
[AD-A247345] p 727 N92-27217

DATA PROCESSING
The new airport aeronautic meteorological codes
p 160 A92-13855
Implementation and usage of the RJ program Data Acquisition System Ground Station p 210 A92-19257
Flight test data analysis of a low cost GPS/IMU integrated navigation system p 638 A92-39560
An integrated analysis and simulation tool for avionics system development p 1005 A92-49289
Operating principles for integrated sensor processing
p 966 A92-49336
The wall interference correction and test data processing methods for airfoil wind tunnel test with endplates
p 942 A92-53087
A data processing system for oceanic air traffic control p 1046 A92-56090
Tool supported software development experiences from the EFA project p 163 N92-12451
Avionics standardization in Europe
p 199 N92-14050
Architecture for Survivable System Processing (ASSP)
p 220 N92-14210
A concept for the revisions of structural inspection schedules p 226 N92-14431
Instrumentation and data processing
p 273 N92-17155
Identification techniques: Frequency domain methods
p 273 N92-17158
Aircraft tracking for structural fatigue
p 361 N92-18584
Simulator data integrity program: Process standard development
[AD-A242207] p 386 N92-19642
Data processing aspects of the Hermes Flight Control Center p 513 N92-20629
Propeller noise research at NRC p 628 N92-24863
Reduction and analysis of F-111C flight data
[AD-A250341] p 853 N92-28771
Analysis of data from a DO-178A software development process p 1134 N92-32880
Comparison of GLONASS and GPS time transfers between two west European time laboratories and VNIIFTRI p 1050 N92-33381

DATA PROCESSING TERMINALS
Upgrading the data processing section of the NAL Gust Wind Tunnel data processing system
[NAL-TM-635] p 888 N92-28833

DATA RECORDERS
High Capacity Voice Recorder (HCVR) Operational Test and Evaluation (OT and E)/integration test plan
[DOT/FAA/CT-TN91/55] p 402 N92-18959

DATA RECORDING
The SAS Flight Analysis and Aircraft Monitoring System p 555 A92-35941
24-bit flight test data recording format
p 900 A92-47528
Double Density recording acquisition and playback
p 920 A92-47534
New Boeing flight test data acquisition systems
p 920 A92-47537
Comparison of GLONASS and GPS time transfers between two west European time laboratories and VNIIFTRI p 1050 N92-33381

DATA REDUCTION
Aircraft tracking optimization of parameters selection
p 361 N92-18585
Automated screening of propulsion system test data by neural networks, phase 1
[NASA-CR-184329] p 753 N92-27403
Reduction and analysis of F-111C flight data
[AD-A250341] p 853 N92-28771
On-line analysis capabilities developed to support the AFW wind-tunnel tests
[NASA-TM-107651] p 961 N92-30752
Numerical calculations of two-dimensional single and multi-material flow fields with CCICE
[DE92-015778] p 1000 N92-30903
Further studies in filmwise condensation of steam on horizontal finned tubes
[AD-A252705] p 1011 N92-31767
Data reduction formulas for the 16-foot transonic tunnel: NASA Langley Research Center, revision 2
[NASA-TM-107646] p 984 N92-31900
LORAN-C data reduction at the US Naval Observatory
p 1050 N92-33358

DATA SAMPLING
Observation and comparison of rainfall measured at a high sample rate p 505 A92-32073
Selection of sampling rate for nonlinear flight trajectory controller of aircraft p 1084 A92-56070

DATA SMOOTHING
A new U-D factorization-based fixed-point smoother and application to flight test p 411 A92-27858
Smooth solutions for transonic gasdynamic equations --- Russian book
[ISBN 5-02-029345-8] p 809 A92-46626
Parameter identification of linear systems based on smoothing p 873 A92-46742

DATA STORAGE
Manipulation and management of data collected at the Crew Station Research and Development Facility - A case study
[AIAA PAPER 92-4162] p 1008 A92-52451
A development of hypermedia type database system for instruction of aircraft conceptual design
p 1132 A92-56113

DATA STRUCTURES
A hierarchical data structure and new capabilities of the Robust-Control Toolbox p 507 A92-29155
Mesh adaptivity with the quadtree method
p 816 A92-47041
The construction, application and interpretation of three-dimensional hybrid meshes p 919 A92-47089
VHDL design and simulation for airborne graphics *generation requirements --- VLSI hardware description* language p 902 A92-48465
An introduction to high speed aircraft noise prediction
[NASA-CR-189582] p 416 N92-19672
Constraint-based scheduling
[NASA-TM-107873] p 692 N92-25190

DATA SYSTEMS
Real Time Data System (RTDS) p 140 N92-12025
Improvement of data processing system for gust wind tunnel data acquisition part: System conversion from off-line to on-line processing
[NAL-TM-611] p 285 N92-17756
The navigation data logger for a suitcase navigation system
[AD-A245997] p 727 N92-26756
Automated screening of propulsion system test data by neural networks, phase 1
[NASA-CR-184329] p 753 N92-27403

DATA TRANSFER (COMPUTERS)
Critical digital systems - A fly-by-light consideration
p 974 A92-49324
Standardizing operational flight data handling
p 1009 A92-53109
From IGES to STEP
[REPT-3.1.6] p 603 N92-23881

DATA TRANSMISSION
High rate PCM data receiving, recording and relying
p 189 A92-19279
Optically powered and interrogated rotary position sensor for aircraft engine control applications
p 370 A92-27777
NAECON 91; Proceedings of the IEEE National Aerospace and Electronics Conference, Dayton, OH, May *20-24, 1991. Vols. 1-3*
[ISBN 0-7803-0084-X] p 786 A92-48426
Testing and analysis of a 'smart' interface to connect two complex avionics bus systems without significant modification to the software of either system
p 964 A92-49254
Processing complexity of two approaches to object detection and recognition p 234 N92-14677
Design of a fiber optic image transmission link
[AD-A243686] p 304 N92-17088
Flight deck benefits of integrated data link communication
[NASA-TP-3219] p 456 N92-21459
A TMS320-based modem for the aeronautical-satellite core data service p 594 N92-22562
Future developments in aeronautical satellite communications p 678 N92-24167
Buffered serial data card
[AD-A246435] p 727 N92-26948
Fiber optic data busses for aircraft
p 736 N92-28093

DC GENERATORS
270-Vdc/hydrid 115-Vac electric power generating system technology demonstrator evolution to a dual-channel, more electric aircraft technology development testbed
[SAE PAPER 912183] p 655 A92-40003
270-Vdc/hybrid 115 Vac electric power generating system technology demonstrator
[SAE PAPER 912051] p 861 A92-45435

DC 10 AIRCRAFT
Onboard cabin water spray system under various discharge configurations
[DOT/FAA/CT-TN91/42] p 93 N92-13043

DC 3 AIRCRAFT
DC-3 handling qualities flight tests: NACA - 1950
p 646 A92-40042

DC 9 AIRCRAFT
Change and reliability of the DC-9-81 digital flight guidance system p 1084 A92-56086
Maintaining the safety of an aging fleet of aircraft
p 837 N92-30108

DE HAVILLAND AIRCRAFT
Prediction of ice accretion on a swept NACA 0012 airfoil and comparisons to flight test results
[AIAA PAPER 92-0043] p 316 A92-25677
Prediction of ice accretion on a swept NACA 0012 airfoil and comparisons to flight test results
[NASA-TM-105368] p 258 N92-15968

DEATH
Fatal occupational injury related to helicopters in the United States 1980-1985 p 186 A92-20720

DEBRIS
Filter debris analysis: A concrete approach to wear diagnosis
[DREP-TM-88-20] p 222 N92-14345
Foreign object damage to tires operating in a wartime environment
[AD-A247195] p 724 N92-27682

DECCA NAVIGATION
The accuracy and coverage of Loran-C and of the Decca Navigator System - and the fallacy of fixed errors
p 353 A92-24944

DECELERATION
Blade instability of horizontally stoppable rotors
p 1085 A92-56308
Separation of relaminarised boundary layers
[CUED/A-AERO/TR-16] p 592 N92-22209

DECIMETER WAVES
A system for precise real-time differential GPS positioning in the decimeter range p 638 A92-39569

DECISION MAKING
Case-based reasoning - Taming the similarity heuristic --- for development of solutions to real world problems p 47 A92-11153
A model for evaluation and training in aircrew coordination and cockpit resource management p 46 A92-11191
IEEE Conference on Decision and Control, 29th, Honolulu, HI, Dec. 5-7, 1990, Proceedings. Vols. 1-6 p 47 A92-11312
MIDIS - A microcomputer flight decision simulator p 136 A92-13845
Rates and risk factors for accidents and incidents versus violations for U.S. airmen p 91 A92-14048
The helicopter air-to-air value-driven engagement model (HAVDEM) - Prototype development p 105 A92-14353
Management decisions have an impact on flight safety p 92 A92-15175
Specification of adaptive aiding systems - Information requirements for designers p 916 A92-44915
Getting test items to measure knowledge at the level of complexity which licensing authorities desire - Another dimension to test validity p 835 A92-45080
An experimental study of organismic principles of the functioning of the crew-transport aircraft system p 1133 A92-57446
Real Time Data System (RTDS) p 140 N92-12025
Pilot's associate: Evolution of a functional prototype p 118 N92-12531
AI for RPVs, Sensor Driven Airborne Replanner (SDAR), for a Robotic Aircraft Sensor Platform (RASP) p 114 N92-12534
New Ways: Tiltrotor aircraft and magnetically levitated vehicles
[OTA-SET-507] p 238 N92-14933
Automated planning with special relevance to associate systems technology and mission planning
[AD-A241924] p 303 N92-17438
Knowledge-based planning for controlled airspace flight operation as part of a cockpit assistant p 727 N92-27895
An appraisal of cost-effectiveness models used in the Air Force and Navy aircraft engine component improvement programs
[AD-A245910] p 743 N92-28162
Tasking and communication flows in the F/A-18D cockpit: Issues, problems, and possible solutions
[AD-A245977] p 853 N92-28802
Introduction to cognitive processes of expert pilots
[DOT/FAA/RD-92/12] p 952 N92-30980
Decision-making guide for the proposed Coast Guard differential global positioning system
[AD-A246046] p 957 N92-32054
Workshop on Aeronautical Decision Making (ADM). Volume 1: Executive summary
[DOT/FAA/RD-92/14-VOL-1] p 1142 N92-33305
Aircraft accident/incident summary report: Controlled flight into terrain Bruno's Inc., Beechjet, N25BR, Rome, Georgia, 11 December 1991
[PB92-910404] p 1044 N92-34081
Human factors issues in the use of artificial intelligence in air traffic control. October 1990 Workshop
[NASA-CR-190925] p 1051 N92-34203

DECISION THEORY
Radar clutter classification
[ISBN-0-315-57981-1] p 1126 N92-33440

DECODERS
Solid-State Radar Beacon Decoder (SSRBD) Operational Test and Evaluation (OT/E) integration test plan
[DOT/FAA/CT-TN91/30] p 19 N92-10020

DECOMMUTATORS
Real time presentation for RAFALE in-flight tests p 882 A92-47522

DECOMPOSITION
Accurate, productive aerodynamic simulation on patched mesh systems
[AD-A243977] p 405 N92-19386
A multiblock grid generation technique applied to a jet engine configuration p 692 N92-24428

DECOUPLING
TVD finite-difference solutions of nonequilibrium vibrationally relaxing and chemically reacting gaseous flows p 626 N92-24854
High-alpha vortex decoupling investigations on a chine forebody/Delta wing configuration at transonic Mach numbers
[NASA-CR-189642] p 715 N92-26651

DEFECTS
Performance of aluminum honeycomb panels with structural defects and core anomalies. II - Specimen description and test results p 591 A92-36156
Probabilistic lifing approach for aero engine disks made of powder nickel base alloys containing ceramic defects p 226 N92-14424
Development of an electromagnetic microscope for eddy current evaluation of materials
[AD-A242007] p 406 N92-19873
The role of crack growth in defect assessment
[PNR-90798] p 501 N92-20909
Metal-metal bondline NDE methods
[AD-A244429] p 503 N92-21730
Simulation of 3D non-planar fatigue crack growth in a turbine blade root
[DE92-006859] p 739 N92-26697
Thermal QNDE detection of airframe disbonds p 914 N92-30118
Inspection of fabricated fuselage panels using electronic shearography
[DOT/FAA/CT-TN92/26] p 1127 N92-33627
Fatigue crack growth of small corner defects from blunt notches in an aeroengine alloy
[PNR-90860] p 1111 N92-34019

DEFENSE INDUSTRY
The V-22: Can the nation afford to forgo its production?
[AD-A243158] p 242 N92-17477

DEFENSE PROGRAM
An overview of US Navy and Marine Corps V/STOL p 783 A92-45303
Fault tolerant avionics display system p 965 A92-49312
A common engineering-to-manufacturing-to-field test strategy to achieve systems readiness beyond the '90s p 931 A92-53111
Avionics standardization in the USAF: 1980 to 1990 p 198 N92-14048
The V-22: Can the nation afford to forgo its production?
[AD-A243158] p 242 N92-17477
The V-22 tilt rotor: A comparison with existing Coast Guard aircraft
[AD-A245843] p 650 N92-26039
Experimental aerodynamic facilities of the Aerodynamics Research and Concepts Assistance Branch
[AD-A247489] p 883 N92-28248
DoD key technologies plan
[AD-A253692] p 1142 N92-33238

DEFLECTION
Effects of T-tabs and large deflections in double cantilever beam specimen tests p 673 A92-39009
Downwash for joined-wing airframe with control surface deflections p 702 A92-41235
Experimental study of an independently deflected wingtip mounted on a semispan wing
[NASA-TM-102842] p 13 N92-10983
Hypersonic inviscid flow field simulations around reentry vehicles with flap deflection p 184 N92-15025
Unsteady-pressure and dynamic-deflection measurements on an aeroelastic supercritical wing
[NASA-TM-4278] p 445 N92-20654
Lift and rolling moment due to spoilers on wings with trailing-edge flaps deflected at subsonic speeds
[ESDU-92002-SUPPL] p 1037 N92-32782
Further wind tunnel investigation of the SM701 airfoil with aileron and turbulators
[NASA-CR-190702] p 1038 N92-33063

DEFORMATION
Investigation of the effects of aeroelastic deformations on the radar cross section of aircraft
[AD-A243889] p 402 N92-18940
Unsteady transonic aerodynamics of pointed bodies of revolution in supersonic freestream p 719 N92-27946
Transonic aeroelastic computations on wings using Navier-Stokes equations p 721 N92-27957
Modeling and analysis methodology for aeroelastically tailored chordwise deformable wings
[NASA-CR-189620] p 961 N92-30304

DEGRADATION
Ongoing development of a computer jobstream to predict helicopter main rotor performance in icing conditions p 65 A92-14407
Monitoring jet fuel degradation using quartz crystal microbalances
[DE92-004730] p 489 N92-20858
Assessment of valve actuator motor rotor degradation by Fourier Analysis of current waveform
[DE92-013233] p 909 N92-28814
Jet fuel absorption and dynamic mechanical analysis of carbon fibre composites p 1110 N92-33050
Experimental study of performance degradation of a rotating system in the NASA Lewis RC icing tunnel
[NASA-CR-190684] p 1102 N92-34141

DEGREES OF FREEDOM
The stability analysis of the nonlinear shimmy p 358 A92-27902
Dynamic synthesis of mechanical systems with a finite number of degrees of freedom p 603 A92-33790
Influence of internal molecular degrees of freedom on the hypersonic rarefied gas flow about a conical body p 938 A92-52752
Application of restructurable flight control system using nonlinear control to an airliner p 1084 A92-56068
Use of simulation in the USAF Test Pilot School curriculum p 884 N92-28535
Turbulence-induced loads on a teetered rotor p 1042 N92-34029
Dynamics and control of a five degree-of-freedom magnetic suspension system
[NASA-CR-191259] p 1102 N92-34222

DEICERS
Advanced ice protection systems test in the NASA Lewis Icing Research Tunnel p 108 A92-14406
Aircraft icing
[ONERA, TP NO. 1991-202] p 351 A92-26359
Numerical analysis of a thermal deicer
[AIAA PAPER 92-0527] p 357 A92-26950
Further developments in three-dimensional simulation of electrothermal deicing systems
[AIAA PAPER 92-0528] p 459 A92-31668
An efficient finite element method for aircraft de-icing problems
[AIAA PAPER 92-0532] p 459 A92-31670
Evaluation of the aerodynamic effects of commuter class (type 1-1/2) anti-icing fluids on small general aviation airplanes
[AIAA PAPER 92-0643] p 459 A92-31675
Advanced pneumatic impulse ice protection system (PIIP) for aircraft p 845 A92-46807
Effect of a deicing device on the induced drag of a lifting airfoil p 959 A92-51947
Technical evaluation report, AGARD Fluid Dynamics Panel Symposium on Effects of Adverse Weather on Aerodynamics
[NASA-TM-105192] p 2 N92-10002
Technical evaluation report on the Fluid Dynamics Panel Specialists' Meeting on Effects of Adverse Weather on Aerodynamics
[AGARD-AR-306] p 352 N92-18242
Suppression of radiating harmonics Electro-Impulse Deicing (EIDI) systems
[DOT/FAA/CT-TN90/33] p 405 N92-19764
Numerical simulation of an aircraft anti-icing system incorporating a rivulet model for the runback water p 448 N92-20303
Effects of Adverse Weather on Aerodynamics
[AGARD-CP-496] p 449 N92-21679
Aerodynamic effects of de/anti-icing fluids and description of a facility and test technique for their assessment p 452 N92-21697
Wind tunnel investigation of the aerodynamic effects of aircraft ground deicing/anti-icing fluids and criteria for aerodynamic acceptance p 452 N92-21698
Results of a low power ice protection system test and a new method of imaging data analysis
[NASA-TM-105745] p 828 N92-28696

DEICING
Advanced ice protection systems test in the NASA Lewis Icing Research Tunnel p 108 A92-14406
Engine air inlet and de-icing system - At -30 C in the icing tunnel of NRC Ottawa p 92 A92-17252
Development of an improved model for runback water on aircraft surfaces
[AIAA PAPER 92-0042] p 270 A92-22160
Development of an electrothermal de-icing/anti-icing model
[AIAA PAPER 92-0526] p 351 A92-26949
Numerical analysis of a thermal deicer
[AIAA PAPER 92-0527] p 357 A92-26950
Improvements to expulsive separation ice protection blankets
[AIAA PAPER 92-0533] p 358 A92-26951
Further developments in three-dimensional simulation of electrothermal deicing systems
[AIAA PAPER 92-0528] p 459 A92-31668
Experimental and numerical investigation of anti-icing phenomena on a NACA 0012 assembly
[AIAA PAPER 92-0531] p 459 A92-31669
An efficient finite element method for aircraft de-icing problems
[AIAA PAPER 92-0532] p 459 A92-31670
Flying on thin ice p 634 A92-38375
Aircraft ground deicing
[SAE PAPER 912222] p 635 A92-40021
EIPOS for ice-formation control on aircraft in flight - An alternative technique p 647 A92-40545
Low energy ice protection for helicopters p 1059 A92-56348
Technical evaluation report, AGARD Fluid Dynamics Panel Symposium on Effects of Adverse Weather on Aerodynamics
[NASA-TM-105192] p 2 N92-10002
Wichita State University 1986 aviation safety research projects
[DOT/FAA/CT-91/4] p 263 N92-16986

Technical evaluation report on the Fluid Dynamics Panel Specialists' Meeting on Effects of Adverse Weather on Aerodynamics
[AGARD-AR-306] p 352 N92-18242
Icing simulation: A survey of computer models and experimental facilities p 450 N92-21684
Preparation of the ice certification of the Dornier 328 regional airliner by numerical simulation and by ground test p 451 N92-21693
The NASA aircraft icing research program p 549 N92-22534
NASA's aircraft icing technology program
[NASA-TM-104518] p 527 N92-23105
Results of a low power ice protection system test and a new method of imaging data analysis
[NASA-TM-105745] p 828 N92-28696
Lewis icing research tunnel test of the aerodynamic effects of aircraft ground deicing/anti-icing fluids
[NASA-TP-3238] p 952 N92-30395
Digital analysis of wind tunnel imagery to measure fluid *thickness*
[NASA-CR-189234] p 983 N92-31252
Analysis of three icing test flights reaching the aircraft-referred icing degree of severe
[ESA-TT-1254] p 954 N92-31943

DELAMINATING
Three-dimensional finite-element analysis of interlaminar stresses in thick composite laminates p 39 A92-11791
Application of MSC/DYNA to shock and impact problems in aircraft industry
[MBB-UD-0593-91-PUB] p 225 N92-14382

DELPHI METHOD (FORECASTING)
A guide for the consideration of composite material *impacts on airframe costs*
[AD-A243928] p 417 N92-19466

DELTA FUNCTION
Robust sampled data eigenstructure assignment using the delta operator
[AIAA PAPER 92-4400] p 1075 A92-55200

DELTA WINGS
Modeling of the vortex structure at delta wings of low aspect ratio by the discrete vortex method p 7 A92-12203
Lift development of delta wings undergoing constant acceleration from rest p 9 A92-13209
Secondary separation from a slender wing p 62 A92-13448
Analysis of spiraling vortical flows around slender delta wings moving in an inviscid medium p 173 A92-18900
Doppler global velocimeter measurements of the vortical flow above a thin delta wing
[AIAA PAPER 92-0005] p 292 A92-22130
Aircraft control at high-alpha by tangential blowing
[AIAA PAPER 92-0021] p 281 A92-22143
On the calculation of the compressible boundary layer on a nonplanar delta wing with supersonic leading edges p 252 A92-23409
Effect of leading-edge cross-sectional geometry on slender wing unsteady aerodynamics
[AIAA PAPER 92-0173] p 255 A92-23784
The rolling-up and interaction of the leading-edge and trailing-edge vortex sheets of a delta wing p 314 A92-25101
Unique high-alpha roll dynamics of a sharp-edged 65 deg delta wing
[AIAA PAPER 92-0276] p 318 A92-25730
Pitch-up motions of delta wings
[AIAA PAPER 92-0278] p 318 A92-25732
Reduction of wing rock amplitudes using leading-edge vortex manipulations
[AIAA PAPER 92-0279] p 379 A92-25733
Three-dimensional simulation of slender delta wing rock and divergence
[AIAA PAPER 92-0280] p 318 A92-25734
Flow visualization image analysis of high-rate roll experiments on a delta wing
[AIAA PAPER 92-0317] p 321 A92-25764
The effects of blowing on delta wing vortices during dynamic pitching at high angles of attack
[AIAA PAPER 92-0407] p 325 A92-26260
Computational study of the aerodynamics and control by blowing of asymmetric vortical flows over delta wings
[AIAA PAPER 92-0410] p 325 A92-26263
Numerical investigation of vortex breakdown on a delta wing p 340 A92-28027
Numerical modeling of self-oscillations for a small-aspect-ratio delta wing using measurements of roll motion at large angles of attack p 424 A92-30138
Calculation of the rolling moment for a wing with a supersonic leading edge in the presence of sideslip p 426 A92-30186
Aerodynamic characteristics of slender sharp-leading-edge delta wings with air scooping through the air intake at hypersonic velocities. I p 427 A92-30206
Experimental investigations of the vortex flow on delta wings at high incidence p 432 A92-31172
A numerical investigation of vortex flow control through small geometry modifications at the strake/wing junction of a cropped double-delta wing
[AIAA PAPER 92-0411] p 435 A92-31661
Analytical and experimental studies of the aerodynamic characteristics of a delta wing at a slip angle at high supersonic velocities p 437 A92-31854
Aerodynamic characteristics of a blunt delta wing with air bleed through an intake at supersonic and hypersonic velocities. II p 437 A92-31855
A heat flow peak on the upwind surface of a blunt-leading-edge delta wing p 438 A92-31862
Computational studies of the aerodynamic characteristics of delta wings with a subsonic leading edge p 439 A92-31874
Viscous supersonic flow computations over a delta-rectangular wing with slanting surfaces p 441 A92-32178
Computational study of incipient leading-edge separation on a supersonic delta wing p 442 A92-32237
Low-speed flutter characteristics of some simple low-aspect-ratio delta-wing models p 460 A92-32247
Measurement and analysis of the flow field above a *wing/body configuration* p 616 A92-38917
The calculation of a compressible boundary layer past a pointed body and a delta wing p 622 A92-40173
Heat transfer in a channel with built-in wing-type vortex generators p 757 A92-41082
Numerical simulation of leading-edge vortex breakdown using an Euler code p 701 A92-41213
Unsteady aerodynamic loading produced by a *sinusoidally oscillating delta wing* p 701 A92-41223
Numerical study of vortex-dominated flows for wings at high incidence and sideslip p 702 A92-41227
Effect of tunnel walls on vortex breakdown location over delta wings p 703 A92-41279
Three-dimensional visualizations of the aerodynamic characteristics of delta wings for the transition from subsonic to supersonic leading edges in supersonic-hypersonic flow p 709 A92-43073
Aerodynamic characteristics of curved delta wings in the case of subsonic separated flow p 712 A92-44121
Flow field around thick delta wing with rounded leading edge
[SAE PAPER 912009] p 789 A92-45409
Numerical investigation into high-angle-of-attack leading-edge vortex flow
[AIAA PAPER 92-2600] p 791 A92-45477
Vortex trapping on a 60 degree delta wing
[AIAA PAPER 92-2639] p 796 A92-45508
Forebody vortex control for suppressing wing rock on a highly-swept wing configuration
[AIAA PAPER 92-2716] p 803 A92-45555
Experimental investigation of vortex dynamics on delta wings
[AIAA PAPER 92-2731] p 804 A92-45565
Prediction of leading-edge vortex breakdown on a delta wing oscillating in roll
[AIAA PAPER 92-2677] p 807 A92-45585
Nonuniform motion of leading-edge vortex breakdown on ramp pitching delta wings p 808 A92-45828
Experimental study of vortex flows over delta wings in wing-rock motion p 810 A92-46787
Unsteady crossflow on a delta wing using particle image velocimetry p 811 A92-46804
Hypersonic rarefied flow about a delta wing - direct simulation and comparison with experiment p 812 A92-46892
An inviscid/viscous coupling approach for vortex flow field calculations p 933 A92-49510
The influences of forced oscillations toward vortex-breakdown p 934 A92-50210
Hypersonic flow calculations around a 3D delta wing at low Knudsen numbers p 937 A92-52734
Heat transfer to a delta wing and two waverider wings in rarefied hypersonic flow p 937 A92-52748
Application of the DSMC method to hypersonic flow about a delta wing p 940 A92-52775
Signal processing schemes for Doppler global velocimetry p 1115 A92-54338
Navier-Stokes prediction of large-amplitude delta-wing roll oscillations characterizing wing rock
[AIAA PAPER 92-4428] p 1080 A92-55352
Vortical flow control on a wing-body combination using tangential blowing
[AIAA PAPER 92-4430] p 1081 A92-55354
A discrete vortex model for predicting wing rock of slender wings
[AIAA PAPER 92-4497] p 1026 A92-55365
Stochastic self-induced roll oscillations of slender delta wing at high angles of attack
[AIAA PAPER 92-4498] p 1081 A92-55366
Unsteady shock-vortex interaction on a flexible delta wing p 1030 A92-56157
Effects of external influences in subsonic delta wing vortices
[AIAA PAPER 92-4033] p 1034 A92-56855
Computational study of the aerodynamics and control by blowing of asymmetric vortical flows over delta wings
[NASA-CR-187979] p 14 N92-10990
Nonstationary flight aerodynamics in a turbulent environment
[ETN-91-90102] p 82 N92-11980
Performance improvements and fuel cost savings due to leading edge modification of a vintage delta wing jet fighter
[FFA-TN-1991-22] p 114 N92-11993
Wind tunnel investigation of the interaction and breakdown characteristics of slender wing vortices at subsonic, transonic, and supersonic speeds
[NASA-TP-3114] p 82 N92-12994
Comparison of solution of various Euler solvers and one *Navier-Stokes solver for the flow about a sharp-edged* cropped delta wing
[AD-B163639L] p 83 N92-12998
Vortical flow simulation by using structured and unstructured grids p 83 N92-12999
Analysis of results of an Euler-equation method applied to leading-edge vortex flow p 84 N92-13000
Experimental and numerical investigation of the vortex flow over a delta wing at transonic speed p 84 N92-13001
On the simulation of compressible turbulent flows past delta wing, delta wing-body and delta wing-canard p 84 N92-13003
Calculation of hypersonic leeside vortices over blunt *delta wings* p 84 N92-13004
Nonequilibrium turbulence modeling effects on transonic vortical flows about delta wings p 85 N92-13007
Vortex formation over a close-coupled canard-wing-body configuration in unsymmetrical flow p 85 N92-13010
An experimental study of the flow over a sharp-edged delta wing at subsonic and transonic speeds p 85 N92-13011
Breaking down the delta wing vortex: The role of vorticity in the breakdown process p 86 N92-13017
Investigation of vortex breakdown on a delta wing using Euler and Navier-Stokes equations p 87 N92-13019
Multiple roll attractors of a delta wing at high incidence p 88 N92-13026
An experimental analysis of critical factors involved in the breakdown process of leading edge vortex flows p 89 N92-13031
Navier-Stokes calculation of transonic flow past the NTF 65 deg delta wing p 91 N92-13868
Hypersonic flow past delta wing flow simulated by Navier-Stokes solutions p 180 N92-14981
Flow over a delta wing at hypersonic speeds p 181 N92-14993
The effect of rounding the leading edges on the characteristics of separated flow past delta wings of low aspect ratio
[RAE-LIB-TRANS-2164] p 257 N92-15964
An experimental investigation of leading edge vortical flow about a delta wing during wing rock
[AD-A243363] p 260 N92-17114
The effect of freestream turbulence on the vortical flow over a delta wing p 261 N92-17681
Boundary-layer transition and heat transfer on slender *delta wings*
[AERO-REPT-8904] p 262 N92-17849
Aerodynamic and flowfield hysteresis of slender wing aircraft undergoing large-amplitude motions p 364 N92-18780
Wind tunnel force measurements and visualization on a 60-deg delta wing in oscillation, stepwise motion, and gusts p 364 N92-18786
Computation of a Kelvin-Helmholtz instability for delta *wing vortex flows*
[AD-A244320] p 346 N92-18825
Identification of aerodynamic models for maneuvering aircraft
[NASA-CR-190039] p 348 N92-19359
Influence of airfoil geometry on delta wing leading-edge vortices and vortex-induced aerodynamics at supersonic speeds
[NASA-TP-3105] p 350 N92-20038
Temperature effects in FFA HYP 500 at M = 7 in a flow with strong expansion
[FFA-TN-1991-27] p 443 N92-20229
Numerical simulation of vortical flow over a delta wing at subsonic and transonic speeds
[NLR-TP-90029-U] p 444 N92-20498
A study in dynamic control of a super maneuver with neural networks p 463 N92-21510
Cases 6.1 and 6.8 double ellipsoid: Navier-Stokes *calculation* p 525 N92-22181

Case 7.4 delta wing: Navier-Stokes calculation
p 525 N92-22182
Case 7.4: Blunt nose delta wing Euler-boundary layer calculation p 525 N92-22184
Flow field over the wing of a delta-wing fighter model with vortex control devices at Mach 0.6 to 1.2
[NASA-TM-4296] p 526 N92-22506
Hypersonic laminar flow computations over a blunt leading edged delta wing at three different chord Reynolds numbers
[FFA-TN-1991-40] p 528 N92-23168
Normal force of low aspect ratio wing-body combinations up to high angles of attack at supersonic speeds
[ESDU-91042] p 553 N92-24009
A low-speed wind tunnel study of vortex interaction control techniques on a chine-forebody/delta-wing configuration
[NASA-CR-189616] p 632 N92-25510
High-alpha vortex decoupling investigations on a chine forebody/Delta wing configuration at transonic Mach numbers
[NASA-CR-189642] p 715 N92-26651
Subsonic investigations of vortex interaction control for enhanced high-alpha aerodynamics of a chine forebody/Delta wing configuration
[NASA-CR-189641] p 715 N92-26652
Analysis of results of an Euler-equation method applied to leading-edge vortex flow
[NLR-TP-90368-U] p 827 N92-28657
Identification of aerodynamic models for maneuvering aircraft
[NASA-CR-190444] p 852 N92-28720
Natural flow wing
[NASA-CASE-LAR-14281-1] p 829 N92-28729
A method for computing the 3-dimensional flow about wings with leading-edge vortex separation. Part 2: Description of computer program VORSEP
[NLR-TR-86006-U] p 833 N92-29916
Vortex flow visualization using colored and fluorescent dyes on flat plate delta wing with leading edge extension
[AD-A251139] p 1036 N92-32651
An experimental study of the flow over a sharp-edged delta wing at subsonic and transonic speeds
[NLR-TP-91117-U] p 1037 N92-32732
Static and dynamic flow visualization studies of two double-delta wing models at high angles of attack
[AD-A252878] p 1040 N92-33678
Unsteady response of the leading-edge vortices on a pitching delta wing p 1041 N92-33851

DEMODULATION
A preliminary study in the use of phase demodulation techniques for the analysis of gear vibration data
[NRC-32083] p 1002 N92-31469

DEMOGRAPHY
Analysis of changes in the pilot population and general aviation accidents p 187 A92-20722

DENSITY DISTRIBUTION
Measurement of a three-dimensional hypersonic density field
[AIAA PAPER 92-0383] p 323 A92-26240
Crossed beam correlation modeling and experimental techniques for measuring density fluctuations in hypersonic flows
[AIAA PAPER 92-2779] p 758 A92-41323
Processing of axisymmetric flow interferograms with density profile bends or discontinuities
p 993 A92-51316
Marching with the parabolized Navier-Stokes equations. Problem 2: Hypersonic viscous flow over a flat plate
[AERO-REPT-9008] p 345 N92-18232
Simulation of real-gas effects on pressure distributions for aeroassist flight experiment vehicle and comparison with prediction
[NASA-TP-3157] p 501 N92-20677

DENSITY MEASUREMENT
Evaluation of OH laser-induced fluorescence techniques for supersonic combustion diagnostics
[AIAA PAPER 92-0508] p 396 A92-26935
Crossed beam correlation modeling and experimental techniques for measuring density fluctuations in hypersonic flows
[AIAA PAPER 92-2779] p 758 A92-41323
Measurement of the freestream density for re-entry vehicles - A design study p 940 A92-52821

DEPENDENT VARIABLES
Nonlinear aircraft tracking filter utilizing control variable estimation p 302 A92-21179

DEPLOYMENT
Television Microwave Link (TML) Operational Test and Evaluation (OT/E)/integration test report
[DOT/FAA/CT-TN91/57] p 500 N92-20653

DEPOSITION
Deposition during vaporization of jet fuel in a heated tube
[AIAA PAPER 92-0687] p 390 A92-27054
Transport phenomena and interfacial kinetics in multiphase combustion systems
[AD-A244849] p 489 N92-20695
Monitoring jet fuel degradation using quartz crystal microbalances
[DE92-004730] p 489 N92-20858
Report on the workshop on Ion Implantation and Ion Beam Assisted Deposition
[AD-A250561] p 927 N92-28923

DEPOSITS
Transport phenomena and interfacial kinetics in multiphase combustion systems
[AD-A244849] p 489 N92-20695

DEPTH
Effect of short-term exposure to stereoscopic three-dimensional flight displays on real-world depth perception
[NASA-TP-3117] p 119 N92-13065

DESCENT
A unified procedure for solving rotor flowfield, performance and interference p 814 A92-46950
Dynamics of aerospace shuttles p 667 N92-24760

DESCENT TRAJECTORIES
A digital Doppler Rate of Descent Indicator (DRODI)
p 555 A92-35927
Thermal deformation of a polymer heat shield material on the descent trajectory p 754 A92-42655
A guidance law for hypersonic descent to a point
[AIAA PAPER 92-4303] p 1104 A92-55311
STS-40 descent BET products: Development and results
[NASA-CR-189570] p 286 N92-16012
Space shuttle entry terminal area energy management
[NASA-TM-104744] p 308 N92-19930

DESENSITIZING
An investigation of the desensitizing effects by high power HF broadcast transmitters on HF airborne receivers p 726 A92-43937

DESIGN ANALYSIS
Aerodynamic design of propeller by numerical optimization p 24 A92-10957
Aerodynamic modification of a propeller
p 4 A92-10958
ACES II PLUS ejection seat p 103 A92-13463
Design and analysis of ceramic and CMC components for advanced gas turbines
[ASME PAPER 91-GT-156] p 142 A92-15592
The design and testing of a radial flow turbine for aerodynamic research
[ASME PAPER 91-GT-220] p 124 A92-15636
Design and analysis of a high pitch to chord ratio cascade representative of ducted propfans
[ASME PAPER 91-GT-335] p 126 A92-15700
Design and performance of advanced blading for a high-speed HP compressor
[ASME PAPER 91-GT-374] p 76 A92-15718
Designing through test
[AIAA PAPER 91-3822] p 232 A92-17664
Computational fluid dynamics based three-dimensional turbofan inlet/fan cowl analysis system
p 243 A92-21075
Study on reliability design of turbine blade
p 371 A92-24739
Strategies for optimal design of gas turbine disks
p 371 A92-24741
Application of the multiplier penalty function method to the optimum design of wing configurations of aerospace vehicle p 356 A92-25013
A fast implicit upwind solution algorithm for three-dimensional unstructured dynamic meshes
[AIAA PAPER 92-0447] p 328 A92-26291
Shape-sensitivity analysis and design optimization of linear, thermoelastic solids p 395 A92-26433
Design analysis of the T-800 inlet particle separator/air oil cooler blower p 579 A92-32556
Preliminary results from the High Speed Airframe Integration Research project
[AIAA PAPER 92-1004] p 536 A92-33196
Conceptual design and analysis of a special operations transport
[AIAA PAPER 92-1066] p 536 A92-33239
Damage tolerant structural design using neural networks
[AIAA PAPER 92-1097] p 581 A92-33261
Design sheet - An environment for facilitating flexible trade studies during conceptual design
[AIAA PAPER 92-1191] p 600 A92-33303
Integration of supportability elements into the conceptual design process
[AIAA PAPER 92-1194] p 600 A92-33306
Exploratory design studies of actively controlled wings using integrated multidisciplinary synthesis
p 641 A92-36828
Zonal analysis - The final step in system safety assessment p 760 A92-42071
Software safety analysis in heterogeneous multiprocessor control systems p 776 A92-42073
Design-for-reliability through durability analysis
p 760 A92-42086
The role of nonmetallic fasteners in aircraft wings and other composite structures p 784 A92-47413
Analysis of a hydrocarbon scramjet with augmented preburning
[AIAA PAPER 92-3425] p 865 A92-48984
Design criteria and analysis of the dynamic behavior of high speed, heavily loaded and precision epicyclic gears for aircraft use
[AIAA PAPER 92-3491] p 906 A92-49028
Engine aircraft systems integration course
[AIAA PAPER 92-3762] p 928 A92-49117
Integrated system to support computer analysis in conceptual aerospace design p 1130 A92-53596
Aerodynamic study of H-II Orbiting Plane, HOPE
p 1103 A92-53639
Turning up the heat on aircraft structures --- design and analysis for high-temperature conditions
p 1052 A92-55131
PAYCOS, a multidisciplinary sizing code for hypersonic vehicles
[AIAA PAPER 92-4564] p 1132 A92-55376
Redundancy design philosophy for catastrophic loss protection p 1119 A92-56202
Organization and technical status of the NH90 European helicopter programme p 1016 A92-56306
Technology exploitation for in-service support of future rotorcraft p 1016 A92-56327
Predicted aerodynamic characteristics for HL-20 lifting-body using the aerodynamic preliminary analysis system (APAS)
[AIAA PAPER 92-3941] p 1033 A92-56771
Development of unsteady aerodynamic analyses for turbomachinery aeroelastic and aeroacoustic applications
[NASA-CR-4405] p 12 N92-10979
Modifications to the rapid melt/rapid quench and transparent polymer video furnaces for the KC-135
[NASA-CR-184215] p 157 N92-12231
NASA reliability preferred practices for design and test
[NASA-TM-4322] p 157 N92-12286
Control augmented structural optimization of aeroelasticity tailored fiber composite wings
[AD-A241464] p 135 N92-13075
Third International Conference on Inverse Design Concepts and Optimization in Engineering Sciences (ICIDES-3)
[NASA-CR-188125] p 170 N92-13928
Inverse airfoil design procedure using a multigrid Navier-Stokes method p 193 N92-13932
A comparison of two closely-related approaches to aerodynamic design optimization p 193 N92-13933
Research on inverse, hybrid and optimization problems in engineering sciences with emphasis on turbomachine aerodynamics: Review of Chinese advances
p 201 N92-13939
Extended mapping and characteristics techniques for inverse aerodynamic design p 194 N92-13949
Application of direct inverse analogy method (DIVA) and viscous design optimization techniques
p 176 N92-13951
An inverse method with regularity condition for transonic airfoil design p 177 N92-13969
Design of transonic compressor cascades using hodograph method p 202 N92-13973
Integration of dynamic, aerodynamic, and structural optimization of helicopter rotor blades
[NASA-CR-189018] p 195 N92-14038
Avionics reliability, durability, and integrity: Can they be independent of application? p 200 N92-14056
Proceedings of Damping 1991, volume 3
[AD-A241313] p 225 N92-14386
Airbus Industrie A330/A340: Full scale fatigue test of center fuselage and wing p 226 N92-14425
Theoretical models for duct acoustic propagation and radiation p 236 N92-14782
Design and performance of duct acoustic treatment
p 236 N92-14783
Analysis tools of ONERA and DLR for the aerothermodynamics of reentry vehicles
p 211 N92-14977
Aerothermodynamic challenges of the Saenger space-transportation system p 184 N92-15042
A fast implicit upwind solution algorithm for three-dimensional unstructured dynamic meshes
[NASA-TM-104186] p 185 N92-15050
The NASA/industry design analysis methods for vibrations (DAMVIBS) program: Accomplishments and contributions
[NASA-TM-104192] p 299 N92-17034
Use of Navier-Stokes analysis in section design
[AD-A242074] p 299 N92-17168

Design and testing of high-performance parachutes
[AGARD-AG-319] p 345 N92-18269
Advanced tactical fighter engine
[ETN-92-90840] p 376 N92-18728
Design principles of automation aids for ATC approach control p 354 N92-19042
Rarefaction wave eliminator design study
[AD-A244401] p 484 N92-20455
Holographic flow visualization in rotating turbomachinery
[PNR-90837] p 500 N92-20491
Conceptual design of two-stage-to-orbit hybrid launch vehicle
[NASA-CR-190006] p 486 N92-20666
Optimization of composite sandwich cover panels subjected to compressive loadings
[NASA-TP-3173] p 489 N92-20679
Alpha Group: The Behemoth Apteryx. Final design proposal
[NASA-CR-190026] p 462 N92-20951
Flow analysis and design optimization methods for nozzle afterbody of a hypersonic vehicle
[NASA-CR-4431] p 446 N92-21456
Design considerations for general aviation mobile satellite terminals p 594 N92-22572
Methodology for sensitivity analysis, approximate analysis, and design optimization in CFD for multidisciplinary applications --- computational fluid dynamics
[NASA-CR-190201] p 595 N92-22662
Integrated Design Analysis and Optimisation of Aircraft Structures
[AGARD-R-784] p 550 N92-23227
Application of multidisciplinary optimization methods to the design of a supersonic transport
p 550 N92-23230
Application of analytical and design tools for fighter wing aeroelastic tailoring p 550 N92-23231
The structural optimization system OPTSYS: Current status and applications p 550 N92-23232
First approach to an integrated fin design
p 551 N92-23236
Structural optimization of aircraft practice and trends
p 551 N92-23239
Efficient and robust design optimization of transonic airfoils p 528 N92-23717
Special Course on Engineering Methods in Aerodynamic Analysis and Design of Aircraft
[AGARD-R-783] p 552 N92-23950
Introduction to Special Course on Engineering Methods in Aerodynamic Analysis and Design of Aircraft
p 552 N92-23951
Computational procedures for preliminary design
p 552 N92-23952
Panel methods for aerodynamic analysis and design
p 552 N92-23955
Aircraft drag analysis methods p 552 N92-23957
Mechanical design of a rotary balance system for NASA. Langley Research Center's vertical spin tunnel
p 664 N92-25090
The 12-foot pressure wind tunnel restoration project model support systems p 664 N92-25091
The NASA/industry Design Analysis Methods for Vibrations (DAMVIBS) Program: A government overview
[NASA-TM-107579] p 680 N92-25267
A brief overview of computational structures technology related activities at NASA Lewis Research Center
p 683 N92-25915
Analysis of helicopter accident risk exposure near heliports, airports, and unimproved sites
[SCT-91RR-13] p 637 N92-26028
Low power magnetic bearing design for high speed rotating machinery p 772 N92-27739
Progress of magnetic suspension systems and magnetic bearings in the USSR p 772 N92-27740
Development of a quiet supersonic wind tunnel with a cryogenic adaptive nozzle
[NASA-CR-188055] p 751 N92-27976
Integrated Design Analysis and Optimisation of Aircraft Structures
[AGARD-LS-186] p 851 N92-28469
Fundamentals of structural optimisation
p 851 N92-28470
Practical architecture of design optimisation software for aircraft structures taking the MBB-Lagrange code as an example p 851 N92-28471
Structural optimization of aircraft p 851 N92-28472
Multidisciplinary design and optimization
[AGARD-PAPER-2] p 851 N92-28473
Mathematical optimization: A powerful tool for aircraft design p 851 N92-28474
Dynamics of a split torque helicopter transmission
[NASA-TM-105681] p 910 N92-29136
Design specifications for the Advanced Instructional Design Advisor (AIDA), volume 2
[AD-A248202] p 923 N92-29188
A preliminary design and analysis of an advanced heat-rejection system for an extreme altitude advanced variable cycle diesel engine installed in a high-altitude advanced research platform
[NASA-CR-186021] p 871 N92-29427
Technology programme: Aerothermodynamics and propulsion integration. Numerical and experimental aerothermodynamics
[MBB-FE-202-S-PUB-0464-A] p 831 N92-29648
Concurrent engineering in design of aircraft structures
[MBB-FE-2-S-PUB-472] p 854 N92-29650
Aerodynamic design optimization using sensitivity analysis and computational fluid dynamics
[NASA-CASE-LAR-14815-1-CU] p 910 N92-29830
Experience with piloted simulation in the development of helicopters
[MBB-UD-0610-91-PUB] p 889 N92-30076
Users manual for updated computer code for axial-flow compressor conceptual design
[NASA-CR-189171] p 924 N92-30207
Modeling and analysis methodology for aeroelastically tailored chordwise deformable wings
[NASA-CR-189620] p 961 N92-30304
Practical method's for robust multivariable control
[AD-A248473] p 1009 N92-30322
Influence of structural and aerodynamic modeling on flutter analysis and structural optimization
[AD-A248487] p 978 N92-30323
Composite beam analysis linear analysis of naturally curved and twisted anisotropic beams
[AD-A252652] p 999 N92-30766
Yaw dynamics of horizontal axis wind turbines
[DE92-001245] p 1004 N92-30837
Nonlinear aerodynamics and the design of wing tips
[NASA-CR-190649] p 946 N92-31157
ASTOVL combat aircraft design synthesis and optimization
[CRANFIELD-AERO-9201] p 963 N92-31515
Design and analysis issues of integrated control systems for high-speed civil transports
[NASA-CR-186022] p 979 N92-31656
Integrated computer systems in aircraft design and manufacture: Difficulties and implications
p 1010 N92-31864
Global/local interlaminar stress analysis of a grid-stiffened composite panel
[NASA-CR-190822] p 1125 N92-33139
Study objectives: Will commercial avionics do the job? Improvements needed? p 1065 N92-33340
Integrated Russian VLF/Omega receiver design
[PB92-193390] p 1051 N92-33809

DESIGN TO COST

Composite gearbox housing p 110 A92-14448
Producibility Demonstrator Program - Technological preeminence through concurrent engineering
p 146 A92-14449
Bearingless main rotor system composite component fabrication techniques p 110 A92-14453
Relating economics to design parameters through a criterion function p 271 A92-22709
New processes in commercial airplane design
p 607 A92-38218
Cost effective close tolerance plastic master models
p 958 A92-51538
Manufacturing cost model for composites
p 1012 A92-51565
Intelligent control law tuning for AIAA Controls Design Challenge
[AIAA PAPER 92-4631] p 1132 A92-55306

DESORPTION

Multicomponent gas sorption Joule-Thomson refrigeration
[NASA-CASE-NPO-17569-1-CU] p 228 N92-15203

DESTRUCTIVE TESTS

Design of helicopter composite structures for crashworthiness p 848 A92-47408
Induction bonding procedures for graphite reinforced thermoplastic assemblies p 994 A92-51545

DETECTION

Air-to-air visual acquisition handbook
[ATC-151] p 93 N92-13042
Processing complexity of two approaches to object detection and recognition p 234 N92-14677
Pulsed field system for detecting the presence of a target in a subsurface environment
[AD-D015074] p 296 N92-16174
On the optimization of windshear warning and guidance systems
[NLR-TP-90196-U] p 837 N92-29703
A simplified dynamic model of the T700 turboshaft engine
[NASA-TM-105805] p 1009 N92-30898
A cable detection lidar system for helicopters
p 1001 N92-31068

DETERIORATION

Statistical analysis and prediction of aeroengine deterioration p 557 A92-35570
Replacement of the NAL high pressure air storage system
[NAL-TM-634] p 888 N92-28835
Aging commuter aeroplanes: Fatigue evaluation and control methods p 915 N92-30132

DETERMINANTS

The method of determinant equations in the applied theory of optimal systems - Systems with 'rigid' constraints and with fixed boundary conditions p 917 A92-46629

DETONABLE GAS MIXTURES

Investigation of hypersonic ramjet propulsion cycles using a ram accelerator test facility
[IAF PAPER 91-275] p 278 A92-22482
Mixing and combustion effects in a sliding-wedge ram accelerator with hydrogen injection
[AIAA PAPER 92-3251] p 890 A92-48849

DETONATION

A parametric study of airbreathing Pulsed Detonation Engine
[AIAA PAPER 92-0392] p 471 A92-31660
High spatial resolution measurements of ram accelerator gas dynamic phenomena
[AIAA PAPER 92-3244] p 903 A92-48844
Numerical simulations of the transdetonative ram accelerator combusting flow field on a parallel computer
[AIAA PAPER 92-3249] p 894 A92-48848
Experimental investigation of nozzle/plume aerodynamics at hypersonic speeds
[NASA-CR-190074] p 664 N92-25162

DETONATION WAVES

Renewed interest in pulsed engines may be linked to 'black' aircraft p 24 A92-10600
Laser-initiated conical detonation wave for supersonic combustion. II
[AIAA PAPER 92-0088] p 292 A92-22195
Computational studies of a superdetonative ram accelerator mode p 399 A92-28529
Laser-initiated conical detonation wave for supersonic combustion p 375 A92-28531
A two-stage-diaphragm free-piston shock tube for a strong shock wave p 748 A92-43098
Laser-initiated conical detonation wave for supersonic combustion. III
[AIAA PAPER 92-3247] p 893 A92-48846
Detailed numerical analysis of standing oblique detonation p 1111 A92-53550
Interaction between a body flying at a supersonic velocity and a point explosion p 1019 A92-53867
Detonation duct gas generator demonstration program
[AIAA PAPER 92-3174] p 1066 A92-54011
Rarefaction wave eliminator design study
[AD-A244401] p 484 N92-20455
Laser-initiated conical detonation wave for supersonic combustion, part 3
[AD-A250522] p 989 N92-32076

DETONATORS

Combined VISAR and flash x ray testing techniques
[DE92-004732] p 385 N92-18290

DIAGNOSIS

JIAWG module fault coverage metrics methodology
p 989 A92-49279

DIAMINES

Vinyl capped addition polyimides
[NASA-CASE-LEW-15027-2] p 579 N92-24053

DIAPHRAGMS (MECHANICS)

Double piston shock-wave valve p 1117 A92-54938

DIELECTRICS

Poly 1, 2, 4-triazoles via aromatic nucleophilic displacement
[NASA-CASE-LAR-14440-1] p 35 N92-10066
Development of 3D electromagnetic modeling tools for airborne vehicles
[NASA-CR-190810] p 1126 N92-33307

DIESEL ENGINES

Ceramic technology for Advanced Heat Engines Project
[DE92-002397] p 289 N92-16128
A two-stroke diesel engine simulation program
[NASA-CR-185155] p 562 N92-22647
Three-dimensional modeling of diesel engine intake flow, combustion and emissions
[NASA-CR-189126] p 658 N92-24539
Heavy duty transport research needs assessment
[DE92-010622] p 767 N92-27394
A preliminary design and analysis of an advanced heat-rejection system for an extreme altitude advanced variable cycle diesel engine installed in a high-altitude advanced research platform
[NASA-CR-186021] p 871 N92-29427

DIFFERENCE EQUATIONS

A dynamic stiffness technique for the vibration analysis of stiffened shell structures p 1123 A92-56866

DIFFERENTIAL EQUATIONS
A fast implicit upwind solution algorithm for three-dimensional unstructured dynamic meshes
[AIAA PAPER 92-0447] p 328 A92-26291
Lyapunov exponents for systems described by differential equations with discontinuous right-hand sides
p 507 A92-29237
A fast implicit upwind solution algorithm for three-dimensional unstructured dynamic meshes
[NASA-TM-104186] p 185 N92-15050
Improved shock-capturing of Jameson's scheme for the Euler equations
[PB92-148758] p 596 N92-23251
Grid generation and flow solution method for Euler equations on unstructured grids
[NASA-TM-4295] p 528 N92-23533
Three-dimensional upwind scheme for solving the Euler equations on unstructured tetrahedral grids --- tetrahedral grids p 714 N92-26585
DIFFERENTIAL PRESSURE
Calibration of hemispherical-head flow angularity probes
[AIAA PAPER 92-4005] p 1122 A92-56828
DIFFRACTION PATTERNS
Processing of axisymmetric flow interferograms with density profile bends or discontinuities
p 993 A92-51316
DIFFUSERS
The influence of blade leaning on the performance of an integrated OGV-diffuser system
[ASME PAPER 91-GT-104] p 122 A92-15561
Flow characteristic and flow control of high aspect ratio and highly curved S-bend diffuser p 245 A92-21743
Investigation of the diffuser flow quality in an icing research wind tunnel p 382 A92-24406
Evaluation of two flow analyses for subsonic diffuser design
[AIAA PAPER 92-0273] p 317 A92-25727
Investigation on vortex control technique of flow separation in diffuser p 338 A92-27828
Separation control by vortex generators in subsonic diffuser p 338 A92-27829
Navier-Stokes simulation of flow through a highly contoured subsonic diffuser p 433 A92-31491
The experimental investigation on the diffuser flow distortion p 519 A92-35543
Numerical simulation of a confined transonic normal shock wave/turbulent boundary layer interaction
[AIAA PAPER 92-3668] p 826 A92-49088
Application of submerged vortex generators for separation control of a subsonic diffuser
p 933 A92-49832
Mixed flow compressor surge margin gain using a manifolded diffuser system
[AIAA PAPER 92-3753] p 1068 A92-54151
Diffuser casing upgrade for an advanced turbofan
[NLR-TP-90097-U] p 870 N92-28711
DIFFUSION
Design and testing of a controlled diffusion airfoil cascade for industrial axial flow compressor application
[ASME PAPER 90-GT-140] p 6 A92-11286
The aerodynamic effect of fillet radius in a low speed compressor cascade
[NASA-TM-105347] p 202 N92-14063
Atmospheric pressure flow reactor: Gas phase chemical kinetics under tropospheric conditions without wall effects
[NASA-CASE-MSC-21384-1] p 297 N92-16243
A study of the diffusion of slot-injected drag-reducing polymer solution in a turbulent boundary layer modified by large-eddy breakup devices
[AD-A243411] p 344 N92-18007
Design and performance of controlled-diffusion stator compared with original double-circular-arc stator
[NASA-TP-2852] p 562 N92-22863
DIFFUSION FLAMES
An experimental investigation of the combustion of a hydrogen jet injected parallel in a supersonic air stream
[AIAA PAPER 91-5102] p 212 A92-17861
Numerical simulation of interaction of diffusion flame with vortex pair in a recirculation zone p 390 A92-28433
Strain-induced extinction of hydrogen-air counterflow diffusion flames - Effects of steam, CO2, N2, and O2 additives to air
[AIAA PAPER 92-0877] p 487 A92-29639
Carcinogenic hydrocarbons emission with gas-turbine engines exhaust gases p 504 A92-29726
Studies on the mechanism of ignition and flameholding by plasma jets p 755 A92-42798
Local extinction mechanisms in non-premixed turbulent combustion
[AD-A242027] p 290 N92-17682
The coherent flamelet model for propulsion applications p 756 N92-27486
Theories of turbulent combustion in high speed flows
[AD-A253032] p 1111 N92-33624
Influence of the swirl producing construction in the flow and reaction field of turbulent diffusion flames
[ETN-92-92103] p 1127 N92-33916
DIFFUSION WELDING
Characterization of diffusion bonds using an acoustic microscope p 491 A92-28686
Process control challenges during the manufacture of large superplastically formed/diffusion bonded structure
[SAE PAPER 912195] p 674 A92-40012
Advances in aircraft component superplastic forming/diffusion bonding technology
[SAE PAPER 912216] p 674 A92-40018
Diffusion bonding a creep-resistant Fe-ODS alloy
p 1117 A92-54868
Superplastic applications in aero engines
[PNR-90788] p 473 N92-20436
DIGITAL COMMAND SYSTEMS
An aircraft controller and its development
p 558 A92-35917
Change and reliability of the DC-9-81 digital flight guidance system p 1084 A92-56086
DIGITAL COMPUTERS
An ultrareliable integrated digital computer for helicopters p 964 A92-49273
Standardizing operational flight data handling
p 1009 A92-53109
Selection of sampling rate for nonlinear flight trajectory controller of aircraft p 1084 A92-56070
Development of a conceptual design method for rotary-wing aircraft using digital computers
p 1058 A92-56340
Improvement of data processing system for gust wind tunnel data acquisition part: System conversion from off-line to on-line processing
[NAL-TM-611] p 285 N92-17756
Formal design and verification of a reliable computing platform for real-time control. Phase 2: Results
[NASA-TM-104196] p 602 N92-22320
DIGITAL DATA
Digital ozonesondes - Examples of results from the EMEFS experiments of 1988 and 1990
p 468 A92-32140
Flight testing a digital terrain following system
p 548 A92-35929
The SAS Flight Analysis and Aircraft Monitoring System p 555 A92-35941
Historical perspective on the evolution of avionics standards p 198 N92-14049
Flight deck benefits of integrated data link communication
[NASA-TP-3219] p 456 N92-21459
An efficient method for three-dimensional route planning with different strategies and constraints
p 728 N92-27901
Avionic data bus integration technology
[DOT/FAA/CT-91/19] p 736 N92-27973
Digital analysis of wind tunnel imagery to measure fluid thickness
[NASA-CR-189234] p 983 N92-31252
DIGITAL ELECTRONICS
Simulation of radar clutter and jet engine modulation using digital quadrature modulator p 216 A92-19091
Avionics systems of the 21st century
p 467 A92-28874
On upsets of analog portions of digital flight control systems due to electromagnetic interference
[SAE PAPER 912144] p 651 A92-39982
Next-generation avionics packaging and cooling 'test results from a prototype system' p 989 A92-49277
Critical digital systems - A fly-by-light consideration
p 974 A92-49324
DIGITAL FILTERS
PDFIII - A flight control system for EW UAV's
[TABES PAPER 91-315] p 565 A92-34688
The application of lattice-structure adaptive filters to clutter-suppression for scanning radar
p 403 N92-19154
The development of an airborne information management system for flight test
[NASA-TM-104251] p 1065 N92-32866
DIGITAL RADAR SYSTEMS
A digital Doppler Rate of Descent Indicator (DRODI)
p 555 A92-35927
Television Microwave Link (TML) Operational Test and Evaluation (OT/E)/integration test report
[DOT/FAA/CT-TN91/57] p 500 N92-20653
DIGITAL SIMULATION
Digital simulation and experimental modal analysis of dynamic characteristics of a propeller hub
p 38 A92-10965
Numerical simulations of unsteady reactive flows in a combustion chamber p 39 A92-11761
Numerical investigation of supersonic mixed-compression inlet using an implicit upwind scheme p 243 A92-21073
Development of an electrothermal de-icing/anti-icing model
[AIAA PAPER 92-0526] p 351 A92-26949
Numerical simulation of flow separation for rotors and fixed wings
[AIAA PAPER 92-0635] p 334 A92-27013
Finite-element algorithm for chemically reacting hypersonic flow
[AIAA PAPER 92-0754] p 336 A92-27097
Numerical simulation of the flow around rectangular cylinder p 339 A92-27851
Numerical simulation of interaction of diffusion flame with vortex pair in a recirculation zone p 390 A92-28433
Numerical simulation of slot injection into a turbulent supersonic stream
[AIAA PAPER 92-0827] p 421 A92-29595
On modelling of aero-gas turbine engine for real-time digital simulator --- of engine control system
p 471 A92-29743
Numerical simulation of three-dimensional supersonic flow around aerodynamic configurations
p 434 A92-31492
Three-dimensional flow computation for two interacting, moving droplets
[AIAA PAPER 92-0343] p 496 A92-31655
Numerical simulations in turbomachinery; Proceedings of the Symposium, ASME and JSME Joint Fluids Engineering Conference, 1st, Portland, OR, June 23-27, 1991
[ISBN 0-7918-0714-2] p 522 A92-36028
Numerical simulations of the flow through cascades with tip clearance p 523 A92-36038
The numerical simulation of transonic inviscid flow over oscillating airfoils p 616 A92-38918
Compressibility effects on the growth and structure of homogeneous turbulent shear flow p 675 A92-40052
Transition to turbulence in curved channel flow
p 621 A92-40125
Numerical simulation of leading-edge vortex breakdown using an Euler code p 701 A92-41213
Numerical simulation of unsteady hypersonic viscous flows in shock tunnel p 710 A92-43170
Numerical simulation of impact resistance on composite blade p 738 A92-44734
Numerical simulations of separated flows around oscillating airfoil for dynamic stall phenomena
[SAE PAPER 911991] p 788 A92-45393
Numerical simulations of hypersonic real-gas flows over space vehicles
[SAE PAPER 912045] p 791 A92-45429
Compressible Navier-Stokes solutions for a suction boundary control airfoil
[AIAA PAPER 92-2710] p 802 A92-45551
Numerical simulations using a dynamic solution-adaptive grid algorithm, with applications to unsteady internal flows
[AIAA PAPER 92-2719] p 803 A92-45557
Numerical simulation of multizone two-dimensional transonic flows using the full Navier-Stokes equations
p 815 A92-46955
The numerical simulation of compressible flow around an airfoil at high angle of attack p 818 A92-47686
Applying advanced digital simulation techniques in designing fault tolerant systems p 921 A92-48489
Numerical simulation of turbine 'hot spot' alleviation using film cooling
[AIAA PAPER 92-3309] p 904 A92-48896
Numerical simulation of a confined transonic normal shock wave/turbulent boundary layer interaction
[AIAA PAPER 92-3668] p 826 A92-49088
Numerical flow simulation and analysis of a shrouded propfan rotor
[AIAA PAPER 92-3773] p 826 A92-49118
High performance flight simulation at NASA Langley
[AIAA PAPER 92-4179] p 982 A92-52460
Rarefied gas numerical wind tunnel
p 995 A92-52763
The numerical simulation of flow about installed aero engine nacelle using a finite element Euler solver on unstructured meshes p 941 A92-52848
Finite analytic numerical solution of Navier-Stokes equations p 996 A92-53011
Rarefied gas numerical wind tunnel
p 1017 A92-53552
Numerical simulations of shock reflections by a TVD scheme p 1018 A92-53558
Numerical simulation of slot injection into a turbulent supersonic stream p 1024 A92-54914
Numerical simulation of unsteady flow in a hypersonic shock tunnel facility
[AIAA PAPER 92-4029] p 1034 A92-56851
Numerical simulation of vortex breakdown by solving the Euler equations for an incompressible fluid
p 41 N92-10163
Numerical simulation of vortex breakdown via 3-D Euler equations p 41 N92-10164

Hypersonic flow past delta wing flow simulated by Navier-Stokes solutions p 180 N92-14981
Development of nonlinear real-time helicopter simulation using a blade element method
[NLR-TP-90115-U] p 381 N92-18893
WP 4b compressible flow simulation: Information System for flow simulation based on the Navier-Stokes equation (ISNaS). Requirements grid generation for the ISNaS compressible flow solver
[NLR-TR-88103-U] p 405 N92-19490
Numerical simulation of vortical flow over a delta wing at subsonic and transonic speeds
[NLR-TP-90029-U] p 444 N92-20498
Three-dimensional simulations of hypersonic flows
[MBB-UK-0155-89-PUB] p 447 N92-21703
Symposium on High Speed Airbreathing Propulsion: The Solid Fuel Combustion Chamber and Beyond
[ETN-92-90685] p 575 N92-22268
Simulation of the flow on a space glider. Stagnation point calculation using the 2D Navier-Stokes equations including chemical effects p 624 N92-24393
Development of pre- and post-processor system for structural analysis
[NAL-TM-628] p 681 N92-25403

DIGITAL SYSTEMS
JAS 39 Gripen progress report p 112 A92-16058
A review of digital flight control system upsets caused by electromagnetic interference
[AIAA PAPER 91-3765] p 215 A92-17627
Failure detection of engine sensors with a bank of Kalman filters p 392 A92-24748
An investigation of real-time diagnostic technique for DEEC system --- digital electronic engine control system p 470 A92-29742
A new aircraft universal lightweight digital dropsonde p 467 A92-32089
Synthesis of optimal digital systems for the stabilization of stochastically perturbed unstable dynamic systems p 601 A92-33754
Common airborne instrumentation system (CAIS) --- time-division multiplexed data acquisition system p 856 A92-47538
Robustness characteristics of fast-sampling digital PI controllers for high-performance aircraft with impaired control surfaces p 877 A92-48496
Making fly-by-light a reality p 877 A92-48499
IEEE/AIAA Digital Avionics Systems Conference, 10th, Los Angeles, CA, Oct. 14-17, 1991, Proceedings
[ISBN 0-7803-0115-3] p 964 A92-49251
Historical perspective on the evolution of avionics standards p 198 N92-14049
Formulation of a strategy for monitoring control integrity in critical digital control systems
[NASA-TM-104158] p 206 N92-15075
Assessment of cockpit interface concepts for data link retrofit
[NASA-CR-187615] p 268 N92-17512
A robust digital flight control system for an unfanned research vehicle using discrete quantitative feedback theory
[AD-A243638] p 283 N92-17748
Formal design and verification of a reliable computing platform for real-time control. Phase 2: Results
[NASA-TM-104196] p 602 N92-22320
Avionic data bus integration technology
[DOT/FAA/CT-91/19] p 736 N92-27973
Flight simulation and digital flight controls p 884 N92-28526
The multiple-function multi-input/multi-output digital controller system for the AFW wind-tunnel model
[NASA-TM-107600] p 1060 N92-32536
The utility of analog vertical velocity information during instrument flight with a Head-Up Display (HUD)
[AD-A252863] p 1065 N92-33277

DIGITAL TECHNIQUES
Visualization and measurement of helicopter rotor flow using projected smoke filaments and digital image processing p 520 A92-35728
Computation of aircraft noise exposure using digitized topography data p 687 A92-39058
Advanced method for single event aircraft noise analysis p 693 A92-39060
Digital flight control systems - Some new commercial twists p 974 A92-49264
Low cost HIRF troubleshooting and verification method for digital avionics systems p 990 A92-49304
Application of digital measurement techniques to analysis of range shadowgraphs
[AD-A241554] p 139 N92-13080
A sophisticated, multi-channel data acquisition and processing system for high frequency noise research
[NASA-CR-189137] p 696 N92-24688
An efficient method for three-dimensional route planning with different strategies and constraints p 728 N92-27901
Simplified signal processing for an airborne CO2 Doppler lidar p 1000 N92-31023

DIGITAL TRANSDUCERS
Fiber-coupled position sensors for aerospace applications p 370 A92-27776
Wavelength-multiplexed fiber-optic position encoder for aircraft control systems p 734 A92-42602

DIHEDRAL ANGLE
Structure of the separated flow region in a dihedral corner in front of an obstacle in supersonic flow p 524 A92-36420
Dynamic performance of an aircraft on its landing gear: Test and evaluation on a dihedral p 466 N92-21970

DILUTION
Calculations of the dilution system in an annular gas turbine combustor p 494 A92-31164
Hot jet dilutor
[ETN-92-90860] p 366 N92-19225
CFD mixing analysis of jets injected from straight and slanted slots into confined crossflow in rectangular ducts
[NASA-TM-105699] p 738 N92-26561

DIMENSIONAL ANALYSIS
Approximate truncated balanced realizations for infinite dimensional systems p 602 N92-22493
Out of plane analysis for composite structures p 1107 N92-32527

DIMENSIONAL MEASUREMENT
The use of CT for dimensional measurements of green and sintered ceramic components p 490 A92-28592

DIPOLE ANTENNAS
Advanced electromagnetic methods for aerospace vehicles
[NASA-CR-188630] p 488 N92-20193

DIRECT CURRENT
The use of high voltage direct current in aircraft electrical systems - A Navy perspective
[SAE PAPER 912173] p 655 A92-39998
Implementation of an object-oriented flight simulator D.C. electrical system on a hypercube architecture
[AD-A243700] p 284 N92-17097
Counterrotating brushless DC permanent magnet motor
[DE92-003825] p 401 N92-18550
Advanced techniques in current signature analysis
[DE92-007680] p 679 N92-24892

DIRECT LIFT CONTROLS
Identification of the stability and control derivatives of a DLC-flap system for VSRA
[NAL-TR-1116] p 283 N92-17917

DIRECTION FINDING
Multisensor data fusion and decision support for airborne target identification p 454 A92-31063
A method of passive range determination using only two bearing measurements
[AD-D015182] p 455 N92-20834
An evaluation of superresolution methods for tactical radio direction finding
[AD-A246316] p 726 N92-26291

DIRECTIONAL ANTENNAS
Estimation of the P-3/SAR L-, C- and X-band antenna directivity in range direction based on corner reflector measurements within the absolute SAR calibration p 587 A92-35055
Integrating a radar/ESM antenna suite with the S-70 helicopter --- Electronic Surveillance Measures p 957 A92-49333

DIRECTIONAL CONTROL
Handling qualities of the H-76 Fantail Demonstrator p 131 A92-14335
Yaw dynamics of a coaxial rotor helicopter p 378 A92-24427
Low-speed wind tunnel testing of a joined-wing airfoil p 711 A92-43229
Numerical analysis of RCS jet in hypersonic flights
[SAE PAPER 912063] p 791 A92-45445
Model identification and control system design for the lambda unmanned research vehicle
[AD-A241859] p 299 N92-17024
CDI sensitivity and crosstrack error on nonprecision approaches
[AD-A243981] p 356 N92-19391
Fuzzy guidance system evaluation p 778 N92-27903

DIRECTIONAL SOLIDIFICATION (CRYSTALS)
Experimental results and numerical modeling of solidification during aircraft high-g arcs
[AIAA PAPER 92-0843] p 493 A92-29609
The effectiveness of Coriolis dampening of convection during aircraft high-g arcs p 581 A92-33847
Cold-crucible directional solidification of refractory metal-silicide eutectics p 755 A92-43684
Axial alignment of short-fiber titanium aluminide composites by directional solidification p 892 A92-46838
Experimental study of convection effects around the phase charge interface p 1111 A92-53755
Present and future trends in turbine blade material and manufacturing technology
[PNR-90825] p 488 N92-20164
Materials processing in low gravity
[NASA-CR-184280] p 499 N92-20198

DIRECTIONAL STABILITY
ACES II PLUS ejection seat p 103 A92-13463
A computational study on directional stability of chine-shaped forebodies at high-alpha
[AIAA PAPER 92-0030] p 249 A92-22152
Estimation of spaceplane lateral-directional stability and control derivatives from dynamic wind tunnel test
[SAE PAPER 911979] p 872 A92-45384
An experimental investigation of the effect of leading-edge extensions on directional stability and the effectiveness of forebody nose strakes
[AIAA PAPER 92-2715] p 802 A92-45554
High angle-of-attack control enhancement on a forward swept wing aircraft
[AIAA PAPER 92-4427] p 1080 A92-55351
Hi-alpha forebody design. Part 1: Methodology base and initial parametrics
[NASA-CR-189849] p 358 N92-18024
Hi-alpha forebody design. Part 2: Determination of body shapes for positive directional stability
[NASA-CR-189850] p 359 N92-18038
Thrust vectoring for lateral-directional stability
[NASA-CR-186016] p 482 N92-21357
Longitudinal and lateral-directional aerodynamic characteristics of a wing-cone configuration at Mach numbers from 2.5 to 4.5
[NASA-TM-4337] p 630 N92-24977
Wind-tunnel static and free-flight investigation of high-angle-of-attack stability and control characteristics of a model of the EA-6B airplane
[NASA-TP-3194] p 631 N92-25276
A computational examination of directional stability for smooth and chined forebodies at high-alpha
[NASA-CR-4465] p 950 N92-32114

DIRECTIVITY
A comparative analysis of XV-15 tiltrotor hover test data and WOPWOP predictions incorporating the fountain effect
[NASA-CR-189455] p 114 N92-11992

DIRICHLET PROBLEM
Effect of airfoil (trailing-edge) thickness on the numerical solution of panel methods based on the Dirichlet boundary condition p 340 A92-28041
Two-point optimization of complete three-dimensional airplane configuration
[AIAA PAPER 92-2618] p 844 A92-45491
Design of 3-dimensional complex airplane configurations with specified pressure distribution via optimization p 194 N92-13948

DISASTERS
Guidelines for integrating helicopter assets into emergency planning
[SCT-91RR-18] p 18 N92-10993

DISCHARGE COEFFICIENT
A nozzle internal performance prediction method
[NASA-TP-3221] p 1040 N92-33625

DISCOVERY (ORBITER)
STS-41 Space Shuttle mission report
[NASA-TM-105479] p 286 N92-16973

DISCRETE FUNCTIONS
Modeling of the vortex structure at delta wings of low aspect ratio by the discrete vortex method p 7 A92-12203
Study of the discrete singularly perturbed linear-quadratic control problem by a bilinear transformation p 163 A92-16072
Discrete event fuzzy airport control p 1046 A92-55973

DISCRIMINANT ANALYSIS (STATISTICS)
Binary optical filters for scale invariant pattern recognition
[NASA-TM-103902] p 853 N92-28910
Radar clutter classification
[ISBN-0-315-57981-1] p 1126 N92-33440

DISKS (SHAPES)
Rarefied gas flow around a disc with different angles of attack p 938 A92-52753
Force and heat transfer on a disc in rarefied flow p 939 A92-52764
Monte Carlo simulation of the hypersonic mon- and diatomic gas flow past a disk at an angle of attack p 939 A92-52770

DISPENSERS
Pneumatically actuated multiple store launcher
[AD-D015237] p 732 N92-27188

DISPERSING
EDMS: Microcomputer pollution model for civilian airports and Air Force bases, (user's guide)
[AD-A240528] p 45 N92-11578

DISPLACEMENT
Periodic trim solutions with hp-version finite elements in time p 874 A92-46931
Wavelength encoded fiber optic angular displacement sensor p 857 A92-48046
Poly 1, 2, 4-triazoles via aromatic nucleophilic displacement
[NASA-CASE-LAR-14440-1] p 35 N92-10066
Measurements of fuselage skin strains and displacements near a longitudinal lap joint in a pressurized aircraft
[NASA-TM-104163] p 159 N92-13455
Finite element frequency domain solution of nonlinear panel flutter with temperature effects and fatigue life analysis p 682 N92-25589
Direct coupling of fluid structure in transonic aeroelasticity p 721 N92-27954
DISPLACEMENT MEASUREMENT
Wind tunnel investigation of the aerodynamic effects of aircraft ground deicing/anti-icing fluids and criteria for aerodynamic acceptance p 452 N92-21698
DISPLAY DEVICES
Flying the A340 iron bird p 20 A92-10666
Effects of variations in head-up display airspeed and altitude representations on basic flight performance p 46 A92-11204
Tomorrow's cockpit displays p 117 A92-13699
Functionally integrated aircraft instrumentation for the next generation commercial helicopter p 117 A92-14402
The flight test pilot's display - A CRT system for test maneuvers p 118 A92-16057
EH101 helicopter development p 112 A92-16060
Concept for future cockpits p 118 A92-16148
DARPA high resolution display technologies p 218 A92-19977
Processing and displaying radio navigation data --- Russian book p 266 A92-21683
Experimental evaluation of candidate graphical microburst alert displays
[AIAA PAPER 92-0292] p 369 A92-25745
C-130 glass cockpit system development program
[AIAA PAPER 92-1050] p 553 A92-33230
An exploratory investigation into the definition of tracking standards for IFR helicopter approaches to reduced minima p 533 A92-35726
Enhanced vision system option on future aircraft
[SAE PAPER 912204] p 651 A92-40014
The traffic alert and collision avoidance system (TCAS) for air navigation p 734 A92-43151
Utilizing the fault monitoring system for the A320 aircraft p 700 A92-43157
Development of the D-size liquid crystal flat panel display for aircraft p 734 A92-43208
Evaluation test on the simulator of the liquid crystal flat display. II p 734 A92-43209
Display trends in aircraft cockpits p 734 A92-43217
Advanced display system for an aircraft payload p 735 A92-43221
Current status and future tasks of a cockpit liquid crystal display p 735 A92-43222
Demonstration performance of an aircraft liquid crystal display p 735 A92-43224
Digital mapping display technology p 735 A92-43225
Mode S data link pilot-system interface - A blessing in de skies or a beast of burden? p 839 A92-44920
Electronic presentation of instrument approach information p 855 A92-44923
Perspective versus plan view air traffic control (ATC) displays - Survey and empirical results p 896 A92-44967
Real targets, unreal displays - The inadvertent suppression of critical radar data p 839 A92-44969
Toward an integrated multimodal approach to flight simulation p 880 A92-45026
Centre for Flight Simulation Berlin Airbus 340 simulator for research and training p 880 A92-45028
A simulator study of a flight reference display for powered-lift STOL aircraft
[SAE PAPER 912067] p 855 A92-45449
Real time presentation for RAFALE in-flight tests p 882 A92-47522
Design considerations for a modern telemetry processing and display system p 882 A92-47584
MLS/RNAV control display unit development p 965 A92-49303
An airborne multimode radar display processor p 965 A92-49308
Fault tolerant avionics display system p 965 A92-49312
Extreme wide field-of-view displays and the enclosed cockpit p 965 A92-49313
Flight management system back-up navigation for the A330/A340 aircraft p 975 A92-49326
Map projections and airborne moving map displays p 966 A92-49327
Takeoff Performance Monitoring System display options
[AIAA PAPER 92-4138] p 967 A92-52433
The C-17 Multifunction Display - A building block for avionic systems p 1063 A92-55907
Flight test of a flight reference display for powered-lift STOL aircraft p 1064 A92-56059
Feasibility of using a knowledge-based system concept for in-flight primary flight display research
[NASA-TM-4279] p 17 N92-10017
Effect of short-term exposure to stereoscopic three-dimensional flight displays on real-world depth perception
[NASA-TP-3117] p 119 N92-13065
Soviet electronic display systems under research and manufactured for the civil aviation aircraft of the 1990's
[AD-A240933] p 119 N92-13066
Limitations of a holographic 3-D pixel projector for cockpit displays
[AD-A241295] p 119 N92-13067
Evaluation of triple simultaneous parallel ILS approaches spaced 4300 feet apart, phase 4a
[ACD-340] p 191 N92-14034
Aviation Diagnostics And Maintenance (ADAM) system preliminary concept of operation and functional description
[AD-A242598] p 170 N92-14966
Ferrundi Company supplies 4500 model head up display devices to India's MIG-21 aircraft
[AD-A241044] p 229 N92-15367
AGSSS: The Airborne Graphics Software Support System; an Ada/PHIGS-based display editor for the rapid development of cockpit display software systems
[AD-A243224] p 277 N92-17221
Cockpit display of hazardous weather information p 277 N92-17989
CDI sensitivity and crosstrack error on nonprecision approaches
[AD-A243981] p 356 N92-19391
NASA TSRV essential flight control system requirements via object oriented analysis
[NASA-CR-189573] p 381 N92-19499
A walk through the planned CS building
[NASA-CR-189963] p 386 N92-19675
SIMNET plan view display user manual
[AD-A244617] p 510 N92-21392
Cockpit weather information needs p 449 N92-21503
Cooperative planning in aviation contexts p 456 N92-21509
The Flight Simulation Facility at the Wichita State University p 484 N92-21511
Enhanced displays, flight controls, and guidance systems for approach and landing p 456 N92-21957
Advanced Transport Operating System (ATOPS) color displays software description: MicroVAX system
[NASA-CR-189603] p 556 N92-22395
Global positioning system supported pilot's display p 534 N92-22436
A graphical weather system design for the NASA transport systems research vehicle B-737
[NASA-TM-104205] p 556 N92-22504
Advanced Transport Operating System (ATOPS) color displays software description microprocessor system
[NASA-CR-189605] p 556 N92-22645
Quick-look system p 599 N92-23393
Advanced Transport Operating System (ATOPS) control display unit software description
[NASA-CR-189606] p 652 N92-24689
Expert system management system
[AD-A247102] p 781 N92-26863
Experimental evaluation of candidate graphical microburst alert displays
[NASA-CR-189633] p 735 N92-27424
Knowledge-based planning for controlled airspace flight operation as part of a cockpit assistant p 727 N92-27895
Reference mode effect on the auditory display of aircraft bank angle
[AD-A247825] p 728 N92-27916
Initial validation of a R/D simulator with large amplitude motion p 886 N92-28546
Tasking and communication flows in the F/A-18D cockpit: Issues, problems, and possible solutions
[AD-A245977] p 853 N92-28802
Engine monitoring display study
[NASA-CR-4463] p 979 N92-32175
Collaborative research on V/STOL control system/cockpit display tradeoffs under the NASA/MOD joint aeronautical program
[NASA-TM-103910] p 1087 N92-32788
Controller response to conflict resolution advisory prototype
[PB92-190032] p 1050 N92-33596
Computational algorithms for increased control of depth-viewing volume for stereo three-dimensional graphic displays
[NASA-TM-4379] p 1065 N92-34109
DISSIPATION
An algebraic model for dissipation in supersonic boundary layers
[AIAA PAPER 92-0311] p 320 A92-25759
On central-difference and upwind schemes p 1007 A92-50466
DISTANCE
A method for estimating the minimum distance between two flight vehicles during their separation p 486 A92-30139
Estimation of airborne performance in landing
[ESDU-91032] p 272 N92-15988
DISTANCE MEASURING EQUIPMENT
Use of distance-measuring equipment (DME) for correcting errors in position, velocity, and wind measurements from aircraft inertial navigation systems p 188 A92-18172
Interactive graphics method for removal of helicopter motions from laser profile data p 598 A92-35109
Distance and angle measuring method using laser light and rereflection plates p 762 A92-43206
Mobile Microwave Landing System (MMLS): Operational requirements for setup accuracy
[AD-A241844] p 103 N92-13052
DME growth elements and their use with MLS p 189 N92-14018
The problem of multiple solutions in area navigation and computed centerline operations with the microwave landing system
[AD-A242757] p 191 N92-15058
Joint Federal Aviation Administration (FAA)/Civil Aviation Authority (CAA) Microwave Landing System (MLS) Area Navigation (RNAV) flight evaluations
[DOT/FAA/CT-TN91/17] p 268 N92-15983
MLS and DME/P multipath simulation model user's manual. Volume 1: Operating instructions
[DOT/FAA/CT-TN91/47] p 640 N92-24888
DISTORTION
A study on vortex flow control of inlet distortion in the re-engined 727-100 center inlet duct using computational fluid dynamics
[AIAA PAPER 92-0152] p 253 A92-23767
Effects of inlet distortion on the development of secondary flows in a subsonic axial inlet compressor rotor p 89 N92-13030
Vortex generator design for aircraft inlet distortion as a numerical optimization problem p 194 N92-13959
A study on vortex flow control on inlet distortion in the re-engined 727-100 center inlet duct using computational fluid dynamics
[NASA-TM-105321] p 179 N92-13998
Evaluation of an innovative high-temperature ceramic wafer seal for hypersonic engine applications p 578 N92-22205
Eulerian computational methods
[DE92-008017] p 765 N92-26853
Ultra high bypass Nacelle aerodynamics inlet flow-through high angle of attack distortion test
[NASA-CR-189149] p 943 N92-30298
Research on aero-thermodynamic distortion induced structural dynamic response of multistage compressor blading
[AD-A250865] p 974 N92-32059
A numerical model for sonic boom propagation through an inhomogeneous, windy atmosphere p 1138 N92-33876
Analysis of sonic boom data to quantify distortions of shock profiles p 1139 N92-33879
DISTRIBUTED PARAMETER SYSTEMS
Gain-scheduled control of nonlinear partial differential equations p 47 A92-11347
Robustness of distributed systems with respect to small time delays p 47 A92-11351
Distributed artificial intelligence approach to air traffic control p 161 A92-13436
Robust frequency design of linear stationary systems in aeroautoelastics p 690 A92-37791
DISTRIBUTED PROCESSING
Parallel computation of aerodynamic influence coefficients for aeroelastic analysis on a transputer network p 53 A92-12367
From concept to model: Conception and evaluation of an architecture for a distributed system with SAHARA - Some reflections on results of the utilization of SAHARA in the framework of the Electronic Copilot
[ONERA, TP NO. 1991-216] p 411 A92-26368
Solution of the Euler and Navier-Stokes equations on MIMD distributed memory multiprocessors using cyclic reduction
[AIAA PAPER 92-0561] p 411 A92-26970
An application of distributed environment in flight simulation p 602 A92-35739

The Office of Naval Research initiative on ultradependable multicomputers and electronic systems p 1005 A92-49278
A fault-tolerant Air Data/Inertial Reference System p 967 A92-51011
Advanced information processing system: Inter-computer communication services [NASA-CR-187556] p 53 N92-11706
Application of neural network to adaptive control theory for super-augmented aircraft [AD-A246596] p 745 N92-27505
Advanced techniques in reliability model representation and solution [NASA-TP-3242] p 1134 N92-33483

DISTURBANCES
Effect of upstream disturbance on flow asymmetry [AIAA PAPER 92-0408] p 325 A92-26261
Discrete modes and continuous spectra in supersonic boundary layers p 809 A92-46264

DITCHING (LANDING)
Canadian aircrew sea water survival, 1952-1987 [DCIEM-88-RR-39] p 954 N92-32219

DIVERTERS
Scoping studies for small steady-state tokamaks for divertor testing [DE92-000740] p 238 N92-15761
Air ejector experiments using the two-dimensional supersonic cascade tunnel: Zero secondary flow performance [NAL-TM-632] p 887 N92-28829

DIVING (UNDERWATER)
Multiple input sliding mode control for autonomous diving and steering of underwater vehicles [AD-A241935] p 283 N92-17442
Canadian aircrew sea water survival, 1952-1987 [DCIEM-88-RR-39] p 954 N92-32219

DO-28 AIRCRAFT
The icing of the elevator of the DLR icing research aircraft of Do 28 type [DLR-MITT-91-12] p 953 N92-31813

DOCUMENT STORAGE
A summary of XB-70 sonic boom signature data [NASA-CR-189630] p 696 N92-24800

DOCUMENTATION
Background issues for on-line aircraft documentation p 119 N92-13858

DOCUMENTS
Automatic document generation with case on a DOD avionics project p 1005 A92-49299
Bibliography of technical reports, 1980 - 1990 [PB92-110691] p 417 N92-18814
FAA vertical flight research, engineering, and development bibliography, 1962 - 1991 [FAA/ARD-30] p 462 N92-21210
Aeronautical Engineering Group publications, 1950 - present [AERO-REPT-8907] p 910 N92-29683

DOMES (STRUCTURAL FORMS)
Characterization of a two-phase flow field downstream of a 3x-scale gas turbine co-axial, counter-swirling, combustor dome swirl cup [AIAA PAPER 92-0229] p 393 A92-25693
Mixing in the dome region of a staged gas turbine combustor [AIAA PAPER 92-3089] p 903 A92-48734

DOORS
Advanced thermoplastic nose landing gear door development p 20 A92-10275

DOPPLER EFFECT
Passive acoustic range estimation of helicopters [AD-A248033] p 926 N92-28302

DOPPLER NAVIGATION
Expanding U.S.M.C. roles for the AH-1W SuperCobra p 59 A92-14347
Stellar inertial navigation growing with the times upgrading of the LN-20 integrated inertial navigation system p 97 A92-16646
A digital P-code GPS receiver embedded in the AN/APN-217(V)5 Doppler Navigator p 102 A92-16976
Navigation - Land, sea, air, and space --- Book [ISBN 0-87942-257-2] p 496 A92-31778
A Kalman filter integrated navigation design for the IAR Twin Otter Atmospheric Research Aircraft [NRC-32148] p 1048 N92-32849

DOPPLER RADAR
Characteristics of thunderstorm-generated low altitude wind shear - A survey based on nationwide terminal Doppler weather radar testbed measurements p 45 A92-11378
Multiple phase centre DPCA for airborne radar --- Displaced Phase Centre Antenna p 95 A92-16257
Stellar inertial navigation growing with the times upgrading of the LN-20 integrated inertial navigation system p 97 A92-16646
Three-dimensional simulation of the Denver 11 July Storm of 1988 - An intense microburst event p 407 A92-27958
A case study of the Claycomo, Missouri microburst on July 30, 1989 p 407 A92-27961
A prototype microburst prediction product for the Terminal Doppler Weather Radar p 408 A92-27962
Aspect angle dependence of outflow strength in Denver microbursts - Spatial and temporal variations p 408 A92-27963
Enclosing shapes for single-Doppler radar features p 494 A92-30476
An airborne Doppler lidar for meteorological research p 467 A92-32082
A digital Doppler Rate of Descent Indicator (DRODI) p 555 A92-35927
IsoDoppler and mocomp corrections improve MTI radar p 898 A92-45774
Modified Doppler detects wind shear more reliably p 1015 A92-55099
Terminal Doppler weather radar test bed operation, Orlando: January-June 1990 [AD-A242890] p 301 N92-17028
Cockpit display of hazardous weather information p 277 N92-17989
Simplified signal processing for an airborne CO2 Doppler lidar p 1000 N92-31023
Theoretical simulation of a 2 micron airborne solid state laser anemometer p 1000 N92-31059
A study of atmospheric optical scattering parameters at 1.5 and 2 micron region for solid state Doppler lidar applications p 1001 N92-31067
A comparison of the performance of two gust front detection algorithms using a length-based scoring technique [AD-A250862] p 1004 N92-32103

DORNIER AIRCRAFT
Dornier Do.328 special - Examining the high-speed commuter p 21 A92-11882
Dornier Do 328 - A start in the world market p 113 A92-17093
Engine air inlet and de-icing system - At -30 C in the icing tunnel of NRC Ottawa p 92 A92-17252
Interior noise reduction program for the Dornier 328 p 114 A92-17254
Dornier 328 first flight p 192 A92-19924
Dornier 328 now in flight testing p 457 A92-29418
Dornier 328 - A Daimler for commuters p 458 A92-30091
Summary of Dornier 328 interior noise control study p 643 A92-39083
Preparation of the ice certification of the Dornier 328 regional airliner by numerical simulation and by ground test p 451 N92-21693
Preconsiderations on aircraft integration p 599 N92-23402
The DLR test aircraft in FZ-BS VFW614/ATTAS, Dornier DO228-101, MBB BO 105-S-3 p 648 N92-25591
NAL Dornier 228-200 flight research airplane: Present status and outline of the installed equipment [NAL-TM-637] p 732 N92-27429

DOSIMETERS
Criteria for the operation of federally-owned secondary calibration laboratories (ionizing radiation) [PB92-112481] p 485 N92-21777

DOWNBURSTS
Aircraft control in a downburst on takeoff and landing p 27 A92-11385
Approach guidance in a downburst p 873 A92-46741

DOWNWASH
Jet inflow simulation and its downwash effect on lifting surfaces p 9 A92-13200
High speed rotorcraft - Comparison of leading concepts and technology needs p 108 A92-14415
Downwash for joined-wing airframe with control surface deflections p 702 A92-41235
Downwash measurements on a pitching canard-wing configuration [AD-A239956] p 12 N92-10016
Analysis of a dusty wall jet [NASA-CR-189759] p 257 N92-15965
Rotorwash computer model: User's guide [DOT/FAA/RD-90/25] p 346 N92-18345

DRAG
PAR-WIG performance prediction during acceleration from water-borne to air-borne p 291 A92-21721
Results of an icing test on a NACA 0012 airfoil in the NASA Lewis Icing Research Tunnel [AIAA PAPER 92-0647] p 334 A92-27021
Non linear induced drag study of generically cambered closely coupled dual wings [SAE PAPER 912126] p 618 A92-39973
Subcritical flow studies on two-dimensional external compression supersonic inlets p 713 A92-44518
Results of an Icing test on a NACA 0012 airfoil in the NASA Lewis Icing Research Tunnel [NASA-TM-105374] p 185 N92-15051
Simplified method for the prediction of aerofoil excrescence drag magnification factor for turbulent boundary layers at subcritical Mach numbers [ESDU-91028] p 259 N92-15972
Excrescence drag magnification factors at the drag-rise condition for aerofoils with a specified form of upper-surface pressure distribution [ESDU-91029] p 259 N92-15973
Estimation of airborne performance in landing [ESDU-91032] p 272 N92-15988
The effect of wing ice contamination on essential flight characteristics p 449 N92-21681
High speed transport cruise drag --- scaling laws using Navier-Stokes equations [NASA-CR-190248] p 527 N92-23103
NACA0012 airfoil data corrected for sidewall boundary-layer effects in the NAL two-dimensional transonic wind tunnel [NAL-TM-640T] p 722 N92-28151
Note on flight measured control effectiveness of the quiet STOL experimental aircraft ASKA [NAL-TR-1103] p 746 N92-28154

DRAG CHUTES
Landing spacecraft gently on earth - The Soviet parachute systems p 33 A92-13227
Stabilized square parachute [AD-D015014] p 90 N92-13036
Design and testing of high-performance parachutes [AGARD-AG-319] p 345 N92-18269
Dynamical systems analysis of an aerodynamic decelerator's behavior during the initial opening process [AD-A244194] p 348 N92-19394

DRAG COEFFICIENTS
Determination of balloon drag [AIAA PAPER 91-3666] p 5 A92-11013
Subsonic axisymmetric viscoelastic flow past thin tapered bodies of revolution p 6 A92-12134
Diffuser efficiency estimation parameters p 79 A92-16814
Influences of wind tunnel parameters on airfoil characteristics at high subsonic speeds p 173 A92-18769
Effect of viscous drag on optimum spanwise lift distribution [AIAA PAPER 92-0287] p 319 A92-25740
Bodies of revolution with minimal wave drag at transonic gas flow velocities p 424 A92-30135
Approximate determination of the effect of deviations of wing and tail geometry from design parameters on the drag coefficient of subsonic aircraft p 460 A92-31878
An analytical evaluation of the aerodynamic forces acting on a circular cylinder in a uniform shear flow p 522 A92-35995
Estimation of overall drag coefficient of an aerospace plane p 700 A92-41188
Vortex trapping on a 60 degree delta wing [AIAA PAPER 92-2639] p 796 A92-45508
Aircraft spoiler effects under wind shear [AIAA PAPER 92-2642] p 796 A92-45509
Optimal trajectories for an unmanned air-vehicle in the horizontal plane [AIAA PAPER 92-4344] p 1079 A92-55333
Drag computation by vortex methods p 1031 A92-56161
Notes on the cause of parachute critical velocity [AD-A244417] p 347 N92-19085

DRAG DEVICES
Structural design and testing results of composite landing gear components p 1057 A92-56328

DRAG MEASUREMENT
Evaluation of sidewall interference in the NAL two-dimensional transonic wind tunnel p 1092 A92-56011
Evaluation of NACA0012 airfoil test results in the NAL two-dimensional transonic wind tunnel [NAL-TR-1109T] p 445 N92-21287

DRAG REDUCTION
Optimal boundary control of nonsteady incompressible flow with an application to viscous drag reduction p 39 A92-11344
Hub and pylon fairing integration for helicopter drag reduction p 107 A92-14391
Simulation of GRM drag compensation system --- Geopotential Research Mission p 285 A92-21023
The experimental approach to the LEBU on turbulent drag reduction p 243 A92-21469
Experimental study of pylon geometries for transport aircraft [AIAA PAPER 92-0153] p 271 A92-23768
The use of variable camber to reduce drag, weight and costs of transport aircraft p 313 A92-25096
The feasibility of reducing induced wing drag by using crescent planform wings p 425 A92-30167

Optimization of bluff body for minimum drag in ground proximity p 431 A92-31154
Possibility of reducing the wave drag of a hypersonic flight vehicle (wave rider) p 438 A92-31863
Flight studies of the riblet effect on drag variation p 438 A92-31871
Boundary-layer-separation control p 440 A92-31886
The Berlin oil channel for drag reduction research p 571 A92-34219
Wind tunnel study of aerodynamic characteristics of base combustion p 666 A92-36967
Computational analysis of drag reduction techniques for afterbody/nozzle/empennage configurations
[SAE PAPER 912127] p 618 A92-39974
Scale model test of an isolated turbofan nacelle with riblets
[SAE PAPER 912128] p 618 A92-39975
Some practical aspects of viscous drag reduction concepts
[SAE PAPER 912129] p 618 A92-39976
CFD calculations of closely coupled scissor wings - Inviscid, viscous, and vortex lattice with rollup results
[SAE PAPER 912150] p 619 A92-39986
National Aerospace Plane flight test - External burning on the F/A-18 p 645 A92-40032
Multi-constraint wing optimization p 701 A92-41197
Drag reduction of bluff bodies through momentum injection p 702 A92-41231
Comment on 'Modification of the van Driest damping function to include the effects on surface roughness' p 758 A92-41297
Gasdynamic design --- Russian book
[ISBN 5-02-029715-1] p 708 A92-42777
The design of fully-optimized configurations by using the iterative optimum-optimorum theory --- shape of delta wings of minimum drag p 709 A92-43072
The F/A-18 external burning flight test
[AIAA PAPER 91-5050] p 731 A92-44547
Experimental and numerical study of aerodynamic characteristics for second generation SST
[SAE PAPER 912056] p 844 A92-45439
Aerodynamic shape optimization of hypersonic configurations including viscous effects
[AIAA PAPER 92-2635] p 795 A92-45506
Turbulent drag reduction by laminar sublayer thickening
[AIAA PAPER 92-2707] p 801 A92-45549
Minimizing supersonic wave drag with physical constraints at design and off-design Mach numbers p 811 A92-46808
The design and testing of an airfoil with hybrid laminar flow control
[ONERA, TP NO. 1992-22] p 822 A92-48585
The A320 laminar fin programme
[ONERA, TP NO. 1992-23] p 849 A92-48586
Non-slender shapes of minimum drag p 937 A92-52029
The effect of afterbody devices on drag reduction p 942 A92-53097
Optimal design of wing shape by use of neural-network p 1054 A92-56112
Experimental study of an independently deflected wingtip mounted on a semispan wing
[NASA-TM-102842] p 13 N92-10983
Turbulent friction drag reduction: Boundary layer manipulators
[CERT-RSF-DERAT-62/5004-31] p 43 N92-11309
Aerodynamic shape optimization of arbitrary hypersonic vehicles p 194 N92-13954
The effects of winglets on low aspect ratio wings at supersonic Mach numbers
[NASA-CR-4407] p 178 N92-13996
Analysis and design of planar and non-planar wings for induced drag minimization
[NASA-CR-189509] p 179 N92-13999
Trim drag reduction concepts for horizontal takeoff single-stage-to-Orbit vehicles
[NASA-TM-102687] p 206 N92-15076
Basic hydrodynamics
[AD-A243513] p 300 N92-17387
Experiments and analysis concerning the use of external burning to reduce aerospace vehicle transonic drag
[NASA-TM-105397] p 279 N92-17546
A study of the diffusion of slot-injected drag-reducing polymer solution in a turbulent boundary layer modified by large-eddy breakup devices
[AD-A243411] p 344 N92-18007
Particle trajectory computer program for icing analysis of axisymmetric bodies
[NASA-CR-189134] p 352 N92-19276
The FM-007: An advanced jet commuter for HUB to spoke transportation
[NASA-CR-189988] p 461 N92-20267
Experimental study of the wall pressure fluctuations under a turbulent boundary layer downstream of tandem aerofoil external manipulators
[REPT-207-90-78] p 500 N92-20497
Assessment of potential aerodynamic benefits from spanwise blowing at the wing tip
[NASA-TM-107847] p 631 N92-25261
Special Course on Skin Friction Drag Reduction
[AGARD-R-786] p 717 N92-27706
Basic concepts on boundary layers p 717 N92-27707
Drag reduction: An industrial challenge p 717 N92-27708
Aircraft drag reduction p 717 N92-27709
Boundary layer transition: Prediction, application to drag reduction p 717 N92-27711
Study of turbulence structure through numerical simulations: The perspective of drag and reduction p 717 N92-27713
Turbulent skin-friction drag reduction by active and passive means, part 1 p 718 N92-27714
Constrained spanload optimization for minimum drag of multi-lifting-surface configurations
[NLR-TP-89126-U] p 828 N92-28660
Automatic design of transonic airfoils to reduce the shock induced pressure drag p 949 N92-31863
A method for designing blended wing-body configurations for low wave drag
[NASA-TP-3261] p 1036 N92-32480
Further wind tunnel investigation of the SM701 airfoil with aileron and turbulators
[NASA-CR-190702] p 1038 N92-33063
Applications of a direct/iterative design method to complex transonic configurations
[NASA-TP-3234] p 1039 N92-33484
Method of reducing drag in aerodynamic systems
[NASA-CASE-LEW-14791-1] p 1043 N92-34243

DRAINAGE
Runway drainage characteristics related to tire friction performance
[SAE PAPER 912156] p 664 A92-39991

DRILLING
Precision drilling of ceramic-coated components with abrasive-waterjets
[ASME PAPER 91-GT-232] p 149 A92-15641
Development of an automatic drilling system. II p 1118 A92-56107
Cutting treatment by drilling of fiber bound synthetic materials
[MBB-UD-0609-91-PUB] p 988 N92-31716

DRONE AIRCRAFT
The application of neural networks to drone control p 205 A92-19273
Development of a 1/7th scale fighter UAV for flight research
[AD-A240703] p 23 N92-11008
Optimal trajectories for an unmanned air vehicle p 963 N92-31880

DROOPED AIRFOILS
Studies in general aviation aerodynamics
[NASA-CR-190431] p 827 N92-28511

DROP SIZE
A piezoelectric droplet generator for use in wind tunnels p 291 A92-21374
Examination of a numerical icing-severity scale
[AIAA PAPER 92-0164] p 263 A92-23777
Aerodynamic effects on fuel spray structure - Experiment and theory
[AIAA PAPER 92-0227] p 317 A92-25691
Assessment of one-dimensional icing forecast model applied to stratiform clouds p 915 A92-46803
The influence of spray angle on the continuous- and discrete-phase flowfield downstream of an engine combustor swirl cup
[AIAA PAPER 92-3231] p 863 A92-48832
Method for calculating the three-dimensional water concentration coefficients and its industrial applications p 502 N92-21685
The effect of droplet sizing uncertainty on ice accretions p 679 N92-24874
Near-injector structure of non-evaporating pressure-atomized sprays at various ambient densities p 681 N92-25571

DROP TESTS
Control system design for the free drop test of external stores in a wind tunnel
[IAF PAPER ST-91-002] p 207 A92-20650
Aerodynamic parameters of the X-31 drop model estimated from flight-data at high angles of attack
[AIAA PAPER 92-4357] p 1080 A92-55343
Drop test: Cessna Golden Eagle 421B
[DOT/FAA/CT-TN91/32] p 837 N92-28900

DROP TOWERS
Materials processing in low gravity
[NASA-CR-184280] p 499 N92-20198

DROPS (LIQUIDS)
A piezoelectric droplet generator for use in wind tunnels p 291 A92-21374
A new thermometric instrument for airborne measurements in clouds p 368 A92-24918
Volume spectra in supercooled clouds for several research flights
[AIAA PAPER 92-0167] p 350 A92-25683
Comparison of two-dimensional and three-dimensional droplet trajectory calculations in the vicinity of finite wings
[AIAA PAPER 92-0645] p 342 A92-28215
Three-dimensional flow computation for two interacting, moving droplets
[AIAA PAPER 92-0343] p 496 A92-31655
Numerical simulation of droplet deformation in convective flows p 670 A92-36844
An analysis of boundary layer for droplet aerodynamic stripped in high speed gas flow p 1116 A92-54563
Method for calculating the three-dimensional water concentration coefficients and its industrial applications p 502 N92-21685
Comparison of two-dimensional and three-dimensional droplet trajectory calculations in the vicinity of finite wings
[NASA-TM-105617] p 596 N92-23154
Fundamental studies on droplet interactions in dense sprays
[AD-A246918] p 770 N92-27546
Experimental study of performance degradation of a rotating system in the NASA Lewis RC icing tunnel
[NASA-CR-190684] p 1102 N92-34141

DROPSONDES
Mesoscale dynamics of cold fronts - Structures described by dropsoundings in Fronts 87 p 230 A92-18902
A new aircraft universal lightweight digital dropsonde p 467 A92-32089
Precision of the long baseline acoustic navigation system used by Pegasus
[AD-A246598] p 727 N92-26795

DUAL SPIN SPACECRAFT
On the stability of a dual spin satellite with asymmetric rotor and flexible platform
[ISBN-0-315-54650-6] p 753 N92-27613

DUAL WING CONFIGURATIONS
Non linear induced drag study of generically cambered closely coupled dual wings
[SAE PAPER 912126] p 618 A92-39973

DUCT GEOMETRY
Prediction of wake in a curved duct p 3 A92-10487
Computational investigation of circular-to-rectangular transition ducts
[AIAA PAPER 91-3342] p 6 A92-11605
An experimental study of supersonic H2 combustion and heat transfer in a circular duct p 388 A92-25997
A new approach to swirl control in an S-duct p 422 A92-29710
Iterative algorithms for solving problems of the shaping of three-dimensional ducts p 428 A92-30212
Design and analysis of reengine Boeing 727-100 center inlet S duct by a reduced Navier-Stokes code
[AIAA PAPER 92-1221] p 517 A92-33320
New method of swirl control in a diffusing S-duct p 809 A92-45859
A computational study of advanced exhaust system transition ducts with experimental validation
[AIAA PAPER 92-3794] p 907 A92-49126
A parametric numerical study of mixing in a cylindrical duct
[NASA-TM-105695] p 738 N92-26553
CFD mixing analysis of jets injected from straight and slanted slots into confined crossflow in rectangular ducts
[NASA-TM-105699] p 738 N92-26561
Computational modelling of turbulent flow in S-bends p 769 N92-27480
Inlet distortion effects in aircraft propulsion system integration p 869 N92-28464

DUCTED BODIES
Design and calculation of performance of a subsonic inlet duct p 343 A92-28478
Waves and thermodynamics in high Mach number propulsive ducts p 809 A92-46431

DUCTED FAN ENGINES
An unsteady lifting surface theory for ducted fan blades
[ASME PAPER 91-GT-131] p 71 A92-15575
Multi-blade row Navier-Stokes simulations of fan-bypass configurations
[ASME PAPER 91-GT-148] p 73 A92-15586
Ducted fan VTOL for working platform
[SAE PAPER 911995] p 843 A92-45397
Conception of a UHB engine simulator for the essential characteristics of a true-scale engine --- ultrahigh bypass p 1090 A92-54322

DUCTED FANS
Supersonic throughflow fans for high-speed aircraft
p 561 N92-22541
Investigation of the flight control requirements of a half-scale ducted fan unmanned aerial vehicle
[AD-A252730] p 1087 N92-32988
DUCTED FLOW
Prediction of wake in a curved duct p 3 A92-10487
Computational investigation of circular-to-rectangular transition ducts
[AIAA PAPER 91-3342] p 6 A92-11605
Unsteady Euler calculations in 2-D internal aerodynamics with introduced vorticity
[ASME PAPER 91-GT-168] p 73 A92-15603
Time-dependent aerodynamic analysis of ducted and unducted propfans at angle of attack
[ASME PAPER 91-GT-190] p 74 A92-15616
Numerical study of branched turboprop inlet ducts using a multiple block grid procedure
[ASME PAPER 91-GT-339] p 76 A92-15703
Noise-driven flow p 173 A92-18680
A study on vortex flow control of inlet distortion in the re-engined 727-100 center inlet duct using computational fluid dynamics
[AIAA PAPER 92-0152] p 253 A92-23767
Numerical modelling for gas duct in tuboannular combustor p 371 A92-24738
Unsteady flowfield simulation of ducted prop-fan configurations
[AIAA PAPER 92-0521] p 332 A92-26946
An experimental investigation of the inlet exit flow field improved by aerodynamic grid p 343 A92-28477
Multiple normal shock wave/turbulent boundary-layer interactions p 344 A92-28527
Flow in a ventral nozzle for short takeoff and vertical landing aircraft p 376 A92-28538
Iterative algorithms for solving problems of the shaping of three-dimensional ducts p 428 A92-30212
Low speed aerodynamic performance of a capsule-shaped flying object p 430 A92-30559
Heat transfer in the entrance region of semicircular ducts with internal fins p 497 A92-32264
Navier-Stokes analysis and experimental data comparison of compressible flow in a diffusing S-duct
[AIAA PAPER 92-2699] p 800 A92-45541
Design and analysis of vortex generators on reengined Boeing 727-100QF center inlet S-duct by a reduced Navier-Stokes code
[AIAA PAPER 92-2700] p 800 A92-45542
Laser velocimetry measurements in an MHD aerodynamic duct
[AIAA PAPER 92-2986] p 899 A92-46996
An experimental investigation of the flow in a diffusing S-duct
[AIAA PAPER 92-3622] p 1021 A92-54090
CARS temperature measurements in a hypersonic propulsion test facility p 140 N92-12049
A comparison of two closely-related approaches to aerodynamic design optimization p 193 N92-13933
A study on vortex flow control on inlet distortion in the re-engined 727-100 center inlet duct using computational fluid dynamics
[NASA-TM-105321] p 179 N92-13998
CFD mixing analysis of jets injected from straight and slanted slots into confined crossflow in rectangular ducts
[NASA-TM-105699] p 738 N92-26561
High lift aircraft
[AD-D015215] p 732 N92-27185
Computational modelling of turbulent flow in S-bends
p 769 N92-27480
Modeling of heavy-gas effects on airfoil flows
[NASA-CR-190357] p 716 N92-27558
Experimental validation of a line-duct acoustics model including flow
[NLR-TP-90223-U] p 927 N92-28695
Explicit Navier-Stokes computation of turbomachinery flows
[AD-A249284] p 909 N92-28879
Navier-Stokes analysis and experimental data comparison of compressible flow within ducts
[NASA-TM-105796] p 972 N92-30972
Three-dimensional compressible turbulent computations for a nondiffusing S-duct
[NASA-CR-4391] p 951 N92-32240
Navier-Stokes analysis and experimental data comparison of compressible flow in a diffusing S-duct
[NASA-TM-105683] p 1072 N92-33746
DUCTS
Ceramic matrix composites and its application in gas turbine engines
[ASME PAPER 91-GT-338] p 143 A92-15702
A study on vortex flow control of inlet distortion in the re-engined 727-100 center inlet duct using computational fluid dynamics
[AIAA PAPER 92-0152] p 253 A92-23767
Experimental and analytical study of close-coupled ventral nozzles for ASTOVL aircraft p 861 A92-45325
A comparison of two closely-related approaches to aerodynamic design optimization p 193 N92-13933
A study on vortex flow control on inlet distortion in the re-engined 727-100 center inlet duct using computational fluid dynamics
[NASA-TM-105321] p 179 N92-13998
Atmospheric pressure flow reactor: Gas phase chemical kinetics under tropospheric conditions without wall effects
[NASA-CASE-MSC-21384-1] p 297 N92-16243
Three-dimensional compressible turbulent computations for a diffusing S-duct
[NASA-CR-4392] p 526 N92-22249
Inlets, ducts, and nozzles p 593 N92-22523
A parametric numerical study of mixing in a cylindrical duct
[NASA-TM-105695] p 738 N92-26553
Unsteady Euler calculations in 3D internal aerodynamics p 768 N92-27470
Computational modelling of turbulent flow in S-bends
p 769 N92-27480
Navier-Stokes analysis and experimental data comparison of compressible flow within ducts
[NASA-TM-105796] p 972 N92-30972
DUMMIES
Structural testing of commercial rotorcraft seats - An overview p 544 A92-35437
DUMP COMBUSTORS
Combustion instability related to vortex shedding in dump combustors and their passive control
p 374 A92-27354
Calculation of combustion efficiency of dump combustor in ramjet engine p 375 A92-28480
Swirl effects on confined flows in axisymmetric geometries p 399 A92-28513
An experimental investigation of the swirling combustor for integral liquid fuel ramjet p 557 A92-35541
Swirl number effects on confined flows in a model of a dump combustor p 896 A92-45202
A new vane swirler as applied to dual-inlet side-dump combustor
[AIAA PAPER 92-3654] p 906 A92-49085
Turbulent combustion modelling in a side dump ramjet combustor
[AIAA PAPER 92-3599] p 1112 A92-54075
DUMPING
Fire bombing and fire bombers
[CA-PATENT-1-268-164] p 1061 N92-33582
DURABILITY
Acoustic emission monitoring of a ground durability and damage tolerance test --- for aircraft structures
p 492 A92-28737
Structural design for durability - Lessons learned from service and test data
[AIAA PAPER 92-1129] p 537 A92-33281
Design-for-reliability through durability analysis
p 760 A92-42086
Damage tolerance and durability design of composite aircraft structures p 996 A92-53067
Properties of aircraft fuels and related materials
[AD-A240650] p 35 N92-11213
Avionics reliability, durability, and integrity: Can they be independent of application? p 200 N92-14056
Fatigue management for the A-7P
p 363 N92-18593
Photoelastic coating study of CT-114 coupon joint test specimen for horizontal stabilizer rear attachment fitting to vertical stabilizer rear spar
[NRC-LTR-ST-1689] p 489 N92-21018
Durability and damage tolerance of aluminum castings
[AD-A245237] p 490 N92-21159
High temperature dynamic engine seal technology development
[NASA-TM-105641] p 596 N92-23435
Research into improving the durability of the hot section in the aircraft turbine engine
[AD-A250342] p 973 N92-31439
Supportability evaluation of thermoplastic and thermoset composites p 1108 N92-32576
Residual strength of repaired graphite/epoxy laminates after 5 years of outdoor exposure p 1108 N92-32577
DUST
A study on rotor induced sand and dust environment and its harmfulness to helicopter p 960 A92-53012
Analysis of a dusty wall jet
[NASA-CR-189759] p 257 N92-15965
DYES
Multi-colored layers for visualizing aerodynamic flow effects
[NASA-CASE-LAR-13742-1] p 447 N92-21588
DYNAMIC CHARACTERISTICS
Digital simulation and experimental modal analysis of dynamic characteristics of a propeller hub
p 38 A92-10965
Dynamic behavior analysis for landing-gear with different types of dual-chamber shock-struts p 111 A92-15342
Dynamics and control of hypersonic vehicles - The integration challenge for the 1990's
[AIAA PAPER 91-5057] p 203 A92-17840
A variational method for solving the problem of motion of a profile of complex geometry in a fluid
p 397 A92-27482
Two-parameter bifurcation analysis of axial flow compressor dynamics p 421 A92-29355
Dynamic characteristics of a Benchmark models program supercritical wing
[AIAA PAPER 92-2368] p 571 A92-34596
Frequency domain testing of helicopter dynamics using automated input signals p 545 A92-35731
Lower-end dynamic characteristics of a magnetically coupled free-piston Stirling engine/compressor system
p 992 A92-50795
Simulation research on the dynamic characteristics of steam-injected gas turbine p 971 A92-53389
Identification of dynamic characteristics of flexible rotors as dynamic inverse problem p 220 N92-13962
Experiment of static and dynamic characteristics of spiral grooved seals p 223 N92-14361
Dynamic characteristics and stability analysis of space shuttle main engine oxygen pump p 224 N92-14366
Comments on frequency swept rotating input perturbation techniques and identification of the fluid force models in rotor/bearing/seal systems and fluid handling machines p 224 N92-14370
Effect of eccentricity on the static and dynamic performance of a turbulent hybrid bearing
p 225 N92-14373
Weight, center of gravity and modal test report for NTF fan blade set no. 3
[NASA-CR-189583] p 498 N92-20072
A review of Australian activity on modelling the helicopter/ship dynamic interface p 465 N92-21967
Investigation of the dynamic behaviour and the frequency response of the GG 1342 laser gyro
[ESA-TT-1236] p 595 N92-22641
Inverse control problems: Mathematical preliminaries, system theoretical approaches, and their applications to aircraft dynamics
[LR-665] p 923 N92-28581
A demonstration of passive blade twist control using extension-twist coupling
[NASA-TM-107642] p 1001 N92-31155
CSM solutions of rotating blade dynamics using integrating matrices
[NASA-CR-190577] p 1003 N92-31619
DYNAMIC CONTROL
Dynamic interpolation for linear systems
p 52 A92-11465
Active vibration control using fixed order dynamic compensation with frequency shaped cost functionals
p 508 A92-29324
The differential algebraic approach in nonlinear dynamical feedback controlled landing maneuvers
p 574 A92-33639
Nonlinear control law with application to high angle-of-attack flight p 661 A92-39904
Gust response and cross wind performance of a hovercraft with vertical wings p 1118 A92-56034
New methods in robust control
[AD-A240221] p 29 N92-11018
Neural networks for aircraft system identification
p 303 N92-17998
Ground collision avoidance using a variable incidence altitude measurement system for the A-7 aircraft
[AD-A243880] p 352 N92-19259
A study in dynamic control of a super maneuver with neural networks p 463 N92-21510
Development of telemetry for the agility flight test of a radio controlled fighter model
[AD-A248653] p 753 N92-27994
Dynamic control of aerodynamic instabilities in gas turbine engines p 870 N92-28466
Inverse control problems: Mathematical preliminaries, system theoretical approaches, and their applications to aircraft dynamics
[LR-665] p 923 N92-28581
A demonstration of passive blade twist control using extension-twist coupling
[NASA-TM-107642] p 1001 N92-31155
Design of helicopter flight control systems for hover and low speed using eigenstructure assignment
p 1061 N92-33952
Nonlinear dynamic-inversion flight control of supermaneuverable aircraft p 1062 N92-33953
Improved articulated fin/wing control system statement of government interests
[AD-D015268] p 1088 N92-34131
Dynamics and control of a five degree-of-freedom magnetic suspension system
[NASA-CR-191259] p 1102 N92-34222

DYNAMIC LOADS
Study of external dynamic flap loads on a 6 percent B-1B model
[ASME PAPER 91-GT-236] p 125 A92-15645
Acoustic characteristics and dynamic structural loading of an ASTOVL aircraft in hover
[AIAA PAPER 92-0370] p 416 A92-28190
Prediction of dynamic hub load of a rotor executing multiple sinusoidal blade pitch variations
p 846 A92-46921
Monitoring load experience of individual aircraft
[NLR-TP-90084-U] p 196 N92-15065
Recent results from data analysis of dynamic stall on wind turbine blades
[DE92-001200] p 505 N92-20245
Computational structures technology engine/airframe coupling p 649 N92-25935
Evaluation of grounding and mooring points for Army aircraft
[AD-A250749] p 953 N92-31193
DYNAMIC MODELS
Stage-by-stage poststall compression system modeling technique p 80 A92-17194
Role of dynamic simulation in fighter engine design and development p 277 A92-21080
A study of surge control using fuel pulse cutoff for dual spool turbo-jet engine p 470 A92-29737
Dynamic synthesis of mechanical systems with a finite number of degrees of freedom p 603 A92-33790
A frequency domain theory for structural identification
p 590 A92-35745
LAH main rotor model test at the DNW
p 547 A92-35771
A dynamic digital model for the turbojet with pulse-monitored fueller p 654 A92-38267
Application of linearization analysis to aircraft dynamics p 661 A92-39902
Motion estimation for cable-mount dynamic wind-tunnel test p 749 A92-43210
Estimation of spaceplane model inertia characteristics
p 752 A92-43212
System for generating sequences of phased gust or taxi loadings p 845 A92-46800
Relative energy concepts in helicopter dynamics
p 846 A92-46925
Chaotic dynamic behavior in a simplified rotor blade lag model p 846 A92-46926
Bilinear formulation applied to the stability and response of helicopter rotor blade p 847 A92-46930
An aeroelastic analysis with a generalized dynamic wake p 847 A92-46932
The use of math-dynamic models to aid the development of integrated health and usage monitoring systems
p 1006 A92-50013
Dynamics and control of maneuverable towed flight vehicles p 976 A92-50508
Development of a real-time simulation of a ship-correlated airwake model interfaced with a rotorcraft dynamic model
[AIAA PAPER 92-4149] p 1007 A92-52440
Analysis of propulsion system dynamics in the validation of a high-order state space model of the UH-60
[AIAA PAPER 92-4150] p 959 A92-52441
Experimental investigation of in-flight oscillation on helicopters and its prevention p 977 A92-53089
Modal simulation of gearbox vibration with experimental correlation
[AIAA PAPER 92-3494] p 1112 A92-54036
Dynamical scaling of a model unsteady separating flow p 1117 A92-54932
Robust identification of nonlinear aerodynamic model structure
[AIAA PAPER 92-4503] p 1081 A92-55370
Simulation of helicopter see-saw rotor motion
p 1055 A92-56287
The application of math-dynamic models to characterise a range of helicopter rotor system faults
p 1056 A92-56297
Optimal control of tiltrotor aircraft following power failure p 1085 A92-56303
The identification of coupled flapping/inflow models for hovering flight p 1058 A92-56335
Approximations for inclusion of rotor lag dynamics in helicopter flight dynamics models p 1060 A92-56354
On the limitations of Froude's actuator disc concept
[ETN-91-90136] p 81 N92-11973
Model identification and control system design for the lambda unmanned research vehicle
[AD-A241859] p 299 N92-17024
Dynamical systems analysis of an aerodynamic decelerator's behavior during the initial opening process
[AD-A244194] p 348 N92-19394
A study in dynamic control of a super maneuver with neural networks p 463 N92-21510
Analytical modeling of SH-2F helicopter shipboard operation p 464 N92-21961
Dynamic simulation of a solid fuelled gas turbine system p 592 N92-22315
Vibration tests and structural modeling of an aircraft model for active control technology experiments
[NAL-TM-626] p 662 N92-25401
Trajectory optimization for the National Aerospace Plane
[NASA-CR-190355] p 650 N92-26017
F-111C flight dynamic model aerodynamic data-base, development and verification
[AD-A246356] p 715 N92-26947
Dynamic simulation of compressor and gas turbine performance p 869 N92-28463
Explicit Navier-Stokes computation of turbomachinery flows
[AD-A249284] p 909 N92-28879
Selection of opening model for parachute scaling studies
[AD-A250882] p 943 N92-30239
A simplified dynamic model of the T700 turboshaft engine
[NASA-TM-105805] p 1009 N92-30898
Advanced thermally stable, jet fuels development program annual report. Volume 1: Model and experiment system development
[AD-A249625] p 988 N92-31462
Modal simulation of gearbox vibration with experimental correlation
[NASA-TM-105702] p 1002 N92-31485
A simulation model of a single rotor helicopter
p 979 N92-31865
Mathematical modeling and numerical simulation of the dynamics of flexible structures undergoing large overall motions
[AD-A250202] p 979 N92-31967
DYNAMIC PRESSURE
Computer simulation of weapon blast pressures on flexible surfaces p 39 A92-12115
Estimation of the maximum instantaneous distortion --- of inlet pressure in aircraft engines p 242 A92-21051
New method for boundary layer thickness control on ground plate in wind tunnel p 383 A92-25110
The unsteady flow characteristics of an S-shaped inlet at high incidence p 339 A92-27905
Experimental study of a two-dimensional random frequency generator p 483 A92-29712
NACA 0012 benchmark model experimental flutter results with unsteady pressure distributions
[AIAA PAPER 92-2396] p 517 A92-34469
Low profile microsensor for aerodynamic pressure measurement p 555 A92-35949
Improved method for estimation of the maximum instantaneous distortion values
[AIAA PAPER 92-3623] p 826 A92-49076
An approach for increasing aeroelastic divergence dynamic pressure of wind-tunnel models
[AIAA PAPER 92-4002] p 1099 A92-56825
Wall interference calculation in a transonic wind tunnel with discrete slots p 83 N92-12995
Stagnation and dynamic pressure limits for the S1 wind tunnel
[AD-A242989] p 285 N92-17297
Heat transfer characteristics of hypersonic waveriders with an emphasis on the leading edge effects
[NASA-CR-189586] p 525 N92-22215
DYNAMIC PROGRAMMING
Computer aiding for low-altitude helicopter flight
p 94 A92-14444
A stochastic regulator for integrated communication and control systems. I - Formulation of control law. II - Numerical analysis and simulation p 233 A92-19605
A constraint satisfaction approach to operative management of aircraft routing p 350 A92-25181
Optimal maintenance program of damage tolerance structure p 785 A92-47660
An efficient method for three-dimensional route planning with different strategies and constraints
p 728 N92-27901
DYNAMIC RESPONSE
Dynamic response of a variable-speed rotor during rapid shaft tilt p 132 A92-14400
Reduced basis technique for evaluating the sensitivity coefficients of the nonlinear tire response
[AIAA PAPER 92-2530] p 583 A92-34376
Dynamic response to time-dependent excitations of cantilevered aircraft wing structures modelled as thin-walled beams
[AIAA PAPER 92-2213] p 584 A92-34403
New complex pole and gust response approximations for integrated aeroservoelastic synthesis
[AIAA PAPER 92-2377] p 565 A92-34547
Vibration of gear system with web structure
p 588 A92-35573
Dynamic response of landing gears on rough repaired runway
[SAE PAPER 912154] p 644 A92-39989
Adequacy of modeling turbulence and related effects on helicopter response p 730 A92-41263
Hang-glider response to atmospheric inputs
p 874 A92-46765
Analysis of the VISTA longitudinal simulation capability for a cruise flight condition p 876 A92-48488
Study of dynamic strength on composite wing
p 996 A92-53071
A study of dynamic response to bird impact on arc windshields of aircrafts p 952 A92-53340
Stability and dynamic coupling of elastic vehicles with unsteady aerodynamic forces considered
p 1102 A92-53545
Gust response and cross wind performance of a hovercraft with vertical wings p 1118 A92-56034
Response of helicopter blades to a sharp collective increase p 1084 A92-56282
Research on measurement and control of helicopter rotor response using blade-mounted accelerometers 1990-91 p 1057 A92-56316
Engine dynamic analysis with general nonlinear finite element codes
[NASA-CR-187222] p 44 N92-11379
An analytical and experimental study to investigate flutter suppression via piezoelectric actuation
[NASA-TM-893240] p 156 N92-12173
Rotor-to-stator partial rubbing and its effects on rotor dynamic response p 224 N92-14367
Industrial code development p 227 N92-15083
Identification techniques: Frequency domain methods
p 273 N92-17158
A wing rock model for the F-14A aircraft
[AD-A243109] p 275 N92-17300
Structural dynamics division research and technology accomplishments for F.Y. 1991 and plans for F.Y. 1992
[NASA-TM-104188] p 261 N92-17509
Weight evaluation and sensitivity analysis for space plane. Part 2: TSTO
[NAL-TM-602-PT-2] p 287 N92-17754
Response of structures to galloping excitation: Background and approximate estimation
[ESDU-91010] p 399 N92-18091
Semi-empirical model for prediction of unsteady forces on an airfoil with application to flutter
[NASA-TM-105414] p 346 N92-18760
Investigation of the dynamic behaviour and the frequency response of the GG 1342 laser gyro
[ESA-TT-1236] p 595 N92-22641
Sensitivity analysis of dynamic aeroelastic responses
p 571 N92-23229
Response of helicopters to gusts
[NLR-TP-90159-U] p 879 N92-28653
Buffet test in the National Transonic Facility
[NASA-CR-189595] p 888 N92-29352
Acoustic fatigue life prediction for nonlinear structures with multiple resonant modes
[NASA-CR-190471] p 1000 N92-30988
Research on aero-thermodynamic distortion induced structural dynamic response of multistage compressor blading
[AD-A250865] p 974 N92-32059
On the calculation of the response of helicopters to control inputs
[NASA-CR-190812] p 1088 N92-33536
Dynamic response of induced pressures, suckdown, and temperatures for two tandem jet STOVL configurations
[NASA-TM-103934] p 1039 N92-33581
The dynamics of flexible multibody systems: A finite segment approach p 1128 N92-34036
Pressure measurements on a rectangular wing with a NACA0012 airfoil during conventional flutter
[NASA-TM-104211] p 1042 N92-34147
DYNAMIC STABILITY
Dynamics of hang-gliders p 204 A92-18608
Dynamic stability of elastic vehicles with unsteady aerodynamic force modeling p 509 A92-29326
Measurement on hypersonic dynamic stable coefficients of a winged vehicle p 430 A92-30550
A study on mechanical model of the helicopter 'ground resonance' p 955 A92-50214
Nonlinear dynamic stability characteristics of recovery bodies p 977 A92-52041
Static and dynamic flight-path stability of airplanes
p 977 A92-52043
Dynamic derivative data for high angle of attack simulation
[AIAA PAPER 92-4355] p 1079 A92-55341
Gust response and cross wind performance of a hovercraft with vertical wings p 1118 A92-56034
New methods in robust control
[AD-A240221] p 29 N92-11018
Dynamic characteristics and stability analysis of space shuttle main engine oxygen pump p 224 N92-14366

Wind-tunnel static and free-flight investigation of high-angle-of-attack stability and control characteristics of a model of the EA-6B airplane
[NASA-TP-3194] p 631 N92-25276

DYNAMIC STRUCTURAL ANALYSIS

Stress analysis of a propeller blade
p 38 A92-10963
Stress analysis of a propeller hub p 38 A92-10964
Digital simulation and experimental modal analysis of dynamic characteristics of a propeller hub
p 38 A92-10965
Analysis of rotor blade dynamics using experimental UH-60A airloads obtained at the DNW
p 107 A92-14394
Dynamic analysis technique of rotating centrifugal impeller
[ASME PAPER 91-GT-50] p 148 A92-15528
Representation of geometric stiffening in multibody system simulation p 217 A92-19463
Gust effects on a flexible aircraft p 270 A92-22474
Nonlinear transient analysis of composite ATP blade model p 294 A92-23111
Forced vibration of rectangular laminated plates with material damping p 294 A92-23167
Numerical methods in elastoacoustics in the nonmodal domain
[ONERA, TP NO. 1991-232] p 415 A92-26383
Dynamic analysis of annular cascade shrouded blades
p 397 A92-27856
A new approach to determining control surface's moments of inertia with test-twice vibrations approach
p 379 A92-27914
Models of space-averaged energetics of plates
p 398 A92-28031
Acoustic characteristics and dynamic structural loading *of an ASTOVL aircraft in hover*
[AIAA PAPER 92-0370] p 416 A92-28190
Relationship between the rotating stall and vibrations of a blade row p 496 A92-31988
Design analysis of the T-800 inlet particle separator/air oil cooler blower p 579 A92-32556
Application of a local panel buckling constraint within automated multidisciplinary structural analysis and design
[AIAA PAPER 92-1116] p 537 A92-33271
AIAA/ASME/ASCE/AHS/ASC Structures, Structural Dynamics and Materials Conference, 33rd, Dallas, TX, Apr. 13-15, 1992, Technical Papers. Pt. 3 - Structural dynamics I p 584 A92-34389
The NASA/Industry Design Analysis Methods for Vibrations (DAMVIBS) Program - A government overview --- of rotorcraft technology development using finite element method
[AIAA PAPER 92-2200] p 539 A92-34390
The NASA/Industry Design Analysis Methods for Vibrations (DAMVIBS) Program - Bell Helicopter Textron accomplishments
[AIAA PAPER 92-2201] p 539 A92-34391
The NASA/Industry Design Analysis Methods for Vibrations (DAMVIBS) Program - Boeing helicopters airframe finite element modeling
[AIAA PAPER 92-2202] p 539 A92-34392
The NASA/Industry Design Analysis Methods for Vibrations (DAMVIBS) program - McDonnell Douglas *Helicopter Company achievements*
[AIAA PAPER 92-2203] p 540 A92-34393
The NASA/Industry Design Analysis Methods for Vibrations (DAMVIBS) Program - Sikorsky Aircraft - Advances toward interacting with the airframe design process
[AIAA PAPER 92-2204] p 540 A92-34394
Dynamic response to time-dependent excitations of cantilevered aircraft wing structures modelled as thin-walled beams
[AIAA PAPER 92-2213] p 584 A92-34403
Experimental and theoretical study for nonlinear aeroelastic behavior of a flexible rotor blade
[AIAA PAPER 92-2253] p 584 A92-34410
AIAA/ASME/ASCE/AHS/ASC Structures, Structural Dynamics and Materials Conference, 33rd, Dallas, TX, Apr. 13-15, 1992, Technical Papers. Pt. 4 - Structural dynamics II p 584 A92-34451
Computational structures technology
[AIAA PAPER 92-2442] p 585 A92-34473
AIAA Dynamics Specialists Conference, Dallas, TX, Apr. 16, 17, 1992, Technical Papers p 565 A92-35651
A summary of the Active Flexible Wing program
[AIAA PAPER 92-2080] p 565 A92-35652
New time-domain technique for flutter boundary identification
[AIAA PAPER 92-2102] p 588 A92-35673
Digital time series analysis for flutter test data
[AIAA PAPER 92-2103] p 589 A92-35674
Rotary-wing aeroservoelastic problems
[AIAA PAPER 92-2107] p 567 A92-35678
A numerical classical flutter analysis of advanced propellers
[AIAA PAPER 92-2118] p 557 A92-35687
A frequency domain theory for structural identification
p 590 A92-35745
Inclusion principle for the Rayleigh-Ritz based substructure synthesis p 670 A92-36851
Rigid and flexible joint modelling in multibody dynamics using finite elements p 671 A92-37559
Mechanics Pan-America 1991; Pan-American Congress of Applied Mechanics, 2nd (PACAM II), Universidad Tecnica, Valparaiso, Chile, Jan. 2-5, 1991, Selected and Revised Proceedings p 673 A92-39930
On the three-dimensional vibration analysis of simultaneously skewed and twisted cantilevered parallelepipeds p 759 A92-41801
Coupled vibrations of turbomachine blades
p 738 A92-44545
Dynamic analysis of rotor flex-structure based on nonlinear anisotropic shell models p 899 A92-46946
Free vibration analysis of branched blades by the integrating matrix method p 847 A92-47122
Failure model development for an integrally bladed turbine wheel
[AIAA PAPER 92-3420] p 865 A92-48979
Calculation of fuel sloshing and its coupling vibration with a tank p 991 A92-50204
The static and fatigue computation of the propeller blades retention system p 995 A92-51895
FREPS - A forced response prediction system for turbomachinery blade rows
[AIAA PAPER 92-3072] p 1130 A92-54006
Rotary wing structural dynamics and aeroelasticity --- Book
[ISBN 1-56347-031-4] p 1052 A92-54550
Getting up to speed in hypersonic structures
p 1117 A92-55127
DAMVIBS looks at rotorcraft vibration
p 1052 A92-55128
Dynamic analysis of rotor blades with root retention design variations p 1054 A92-56156
Finite-element analysis and multibody dynamics issues *in rotorcraft dynamic analysis* p 1055 A92-56286
Influence of cross section variations on the structural behaviour of composite rotor blades
p 1121 A92-56320
A dynamic stiffness technique for the vibration analysis of stiffened shell structures p 1123 A92-56866
Variable impedance journal bearings for rotor-bearing systems p 157 N92-12270
Structural Dynamics Branch research and accomplishments for FY 1990
[NASA-TM-103747] p 230 N92-15406
Experiences at Langley Research Center in the application of optimization techniques to helicopter airframes for vibration reduction
[NASA-TM-104193] p 299 N92-17033
The NASA/industry design analysis methods for vibrations (DAMVIBS) program: Accomplishments and contributions
[NASA-TM-104192] p 299 N92-17034
Structural dynamics division research and technology accomplishments for F.Y. 1991 and plans for F.Y. 1992
[NASA-TM-104188] p 261 N92-17509
Program plans: Aviation safety research
[NIAR-91-30] p 264 N92-17587
Response of structures to galloping excitation: Background and approximate estimation
[ESDU-91010] p 399 N92-18091
Semi-empirical model for prediction of unsteady forces on an airfoil with application to flutter
[NASA-TM-105414] p 346 N92-18760
Engine Structures Modeling Software System (ESMOSS)
[NASA-CR-187227] p 404 N92-19277
Preliminary design studies of an advanced general aviation aircraft
[NASA-CR-190024] p 461 N92-20064
Structural dynamics and vibrations of damped, aircraft-type structures
[NASA-CR-4424] p 499 N92-20194
Performance tests of a cryogenic hybrid magnetic bearing for turbopumps
[NASA-TM-105627] p 473 N92-20523
The status of the US VAWT program
[DE92-002931] p 505 N92-21040
Materials and Structures Research Department: Scientific report (1990)
[ETN-92-90727] p 466 N92-22000
Determining structural performance
p 560 N92-22519
Design challenges for the National Aero-Space Plane
p 551 N92-23822
Stretched skin concept for the entry aerodynamic decelerator system of planetary probes
p 576 N92-23836
Vibration tests and structural modeling of an aircraft model for active control technology experiments
[NAL-TM-626] p 662 N92-25401
Analysis and design technology for high-speed aircraft structures p 684 N92-25918
Structures technology applications for the National AeroSpace Plane p 649 N92-25920
Large scale optimization using ASTROS: An overview
p 649 N92-25921
The benchmark aeroelastic models program: Description and highlights of initial results
p 721 N92-27960
Buffet test in the National Transonic Facility
[NASA-CR-189595] p 888 N92-29352
Acoustic fatigue life prediction for nonlinear structures with multiple resonant modes
[NASA-CR-190471] p 1000 N92-30988
A summary of the active flexible wing program
[NASA-TM-107655] p 962 N92-31264
CSM solutions of rotating blade dynamics using integrating matrices
[NASA-CR-190577] p 1003 N92-31619
Mathematical modeling and numerical simulation of the dynamics of flexible structures undergoing large overall *motions*
[AD-A250202] p 979 N92-31967
Use of SEA to predict structure-borne noise in aircraft
p 1137 N92-32955
Active vibrations and noise control for turboprop application research program activities
p 1138 N92-32962
The dynamics of flexible multibody systems: A finite segment approach p 1128 N92-34036
Introduction to Flutter of Winged Aircraft, volume 2
[VKI-LS-1992-01-VOL-2] p 1088 N92-34161
Elementary flutter analysis p 1088 N92-34162
Aeroelasticity of bluff bodies p 1089 N92-34165

DYNAMIC TESTS

A proposal for a dynamic test platform for inertial units and/or GPS p 138 A92-16653
A large-scale axial flow compressor facility and dynamic measurement techniques for rotor flow study
p 382 A92-24729
Inertia reels for aircrew restraint systems
p 529 A92-32982
Structural testing of commercial rotorcraft seats - An overview p 544 A92-35437
Two crew stations for dynamic flight simulation
p 572 A92-35443
Estimation of spaceplane longitudinal stability and control derivatives from dynamic wind tunnel test
p 752 A92-43211
Estimation of spaceplane lateral-directional stability and control derivatives from dynamic wind tunnel test
[SAE PAPER 911979] p 872 A92-45384
Spaceplane longitudinal aerodynamic parameter estimation by cable-mount dynamic wind-tunnel test
[SAE PAPER 911980] p 788 A92-45385
Preliminary dynamic tests of a flight-type ejector
[AIAA PAPER 92-3261] p 1066 A92-54020
On improvements of three-dimensional position measuring system for dynamic wind tunnel testing
p 1093 A92-56012
Water tunnel flow visualization studies of a *canard-configured X-31A-like fighter aircraft model*
[AD-A241362] p 90 N92-13037
Effect of crash pulse shape on seat stroke requirements for limiting loads on occupants of aircraft
[NASA-TP-3126] p 399 N92-18053
Dynamic wind tunnel tests on control of forebody vortices with suction p 380 N92-18793
Helicopter/ship analytic dynamic interface
p 464 N92-21962
Investigation of the dynamic behaviour and the frequency response of the GG 1342 laser gyro
[ESA-TT-1236] p 595 N92-22641
Development of hardness cycles for fiber bound materials, using DSC: From laboratory specimens to complex high duty structural members
[MBB-Z-0409-91-PUB] p 987 N92-30969
Preliminary dynamic tests of a flight-type ejector
[NASA-TM-105814] p 972 N92-30998

DYNAMICAL SYSTEMS

Optimal stabilization of discrete event systems
p 48 A92-11376
A new study on a class of discrete event dynamic *systems* p 48 A92-11377
A multibody analog of the dual-spin problem
p 49 A92-11426
Equivalence of optimal control problems and the use of parameterization methods p 52 A92-11466
Interactive engine system dynamics analysis
[ASME PAPER 91-GT-193] p 124 A92-15619
The generalized normal forms and method of resonance control of nonlinear dynamical systems
p 507 A92-29189

Parameter identification of compressor dynamics during closed-loop operation p 508 A92-29313
A Lyapunov based nonlinear control scheme for stabilizing a basic compression system using a close-coupled control valve p 508 A92-29316
Synthesis of optimal digital systems for the stabilization of stochastically perturbed unstable dynamic systems p 601 A92-33754
Dynamic synthesis of mechanical systems with a finite number of degrees of freedom p 603 A92-33790
Chaotic motion in mechanical and engineering systems p 695 A92-39480
H-infinity synthesis using a bilinear pole shifting transform p 1007 A92-50490
A general approach to optimal real-time guidance of dynamic systems based on nonlinear programming
[AIAA PAPER 92-4378] p 1131 A92-55182
Structural Dynamics Branch research and accomplishments for FY 1990
[NASA-TM-103747] p 230 N92-15406
Studies in chaos using stochastic methods
[AD-A246919] p 780 N92-27171

DYNAMOMETERS
A universal turboprop engine dynamometer test cell
[ASME PAPER 91-GT-343] p 137 A92-15706
Cut progression during dynamometer testing of foreign object damaged type VII extra high pressure aircraft tires
[SAE PAPER 912155] p 644 A92-39990

E

EAR
Exposures from headset interference tones
[AD-A247175] p 1136 N92-32697

EARLY WARNING SYSTEMS
National airspace system. Air defense and law enforcement surveillance operational concept NAS-SR-135
[DOT/FAA/SE-92/3] p 953 N92-31211

EARPHONES
Exposures from headset interference tones
[AD-A247175] p 1136 N92-32697

EARTH ATMOSPHERE
Stability and inherent precision of two methods for solving motion and ablation equations for fireball-forming bodies in the earth atmosphere p 929 A92-46595
Flowpath and sensitivity analyses of high speed propulsion systems
[AIAA PAPER 92-3806] p 1069 A92-54178
NASA High Speed Research Program, Emissions Scenarios Committee report of meetings on 26 September 1991 and 9 January 1992
[NASA-CR-190379] p 1004 N92-32147

EARTH GRAVITATION
Process modeling KC-135 aircraft
[NASA-CR-184278] p 359 N92-18347

EARTH IONOSPHERE
The formation and structure of plasma wakes behind large high-voltage space platforms in ionosphere
[AIAA PAPER 92-0577] p 407 A92-26984
Ionospheric plasma flow over large high-voltage space platforms. I - Ion-plasma-time scale interactions of a plate at zero angle of attack. II - The formation and structure of plasma wake p 779 A92-41359

EARTH ORBITAL ENVIRONMENTS
Verification of flight software by embedding software simulation in simulation of external environment p 232 A92-19084
Low earth orbit satellite concepts for air traffic control applications
[AIAA PAPER 92-1927] p 453 A92-29856
Collision probability estimate method for impact generated low earth orbit space debris clouds
[AAS PAPER 91-369] p 752 A92-43269
HOPE re-entry experimental vehicle p 1103 A92-55098

EARTH ORBITS
Issues in developing control zones for international space operations p 1141 A92-56602

EARTH ROTATION
A demonstration of centimeter-level monitoring of polar motion with the Global Positioning System p 639 N92-24302

EARTH SCIENCES
Agreements/subagreements applicable to Wallops, 12 Nov. 1991 p 575 N92-22598
Research and technology, 1990
[NASA-TM-107967] p 1143 N92-33948

EARTH SURFACE
Modification of the radiated sound directivity due to ground reflections - Application to static tests of helicopter turboshaft engines
[ONERA, TP NO. 1991-210] p 415 A92-26362

EARTH TERMINALS
The Aeronautical Mobile Satellite Service (AMSS). I - Architecture of the AMSS system p 93 A92-13851
Comparison of two-way satellite time transfer and GPS common-view time transfer between OCA and TUG p 1050 N92-33356

ECCENTRICITY
Effect of eccentricity on the static and dynamic performance of a turbulent hybrid bearing p 225 N92-14373

ECONOMIC ANALYSIS
The maintenance economy and economic life of structures p 37 A92-10673
Economic life analysis for replacing components p 785 A92-47670
Currently available fuel gas booster compressor equipment for small gas turbine engines
[PB92-127026] p 499 N92-20265
FAA aviation forecasts
[AD-A250412] p 837 N92-29182
Cost/benefit analysis of the AH-64 (Apache) helicopter Automated Test Equipment (ATE)
[AD-A252909] p 1101 N92-33398

ECONOMIC DEVELOPMENT
Wind energy program overview
[DE91-002178] p 689 N92-25498

ECONOMIC FACTORS
P120 programme - First results of the pre-development phase p 60 A92-14447
Small and cost-effective airship for transportation p 731 A92-43244
Safety vs. economy, system-theoretic approach to the problem analysis p 916 A92-45002
Aerospace plane technology: Research and development efforts in Japan and Australia
[AD-A241641] p 62 N92-12991

ECONOMICS
Aircraft tracking for structural fatigue p 361 N92-18584

EDDY CURRENTS
Eddy current imaging of aircraft using real time image signal processing p 144 A92-13594
Historical development of eddy current testing in aircraft maintenance p 292 A92-21900
Nortec 30 Eddyscan - Portable flaw imaging for aging aircraft p 492 A92-28745
Eddy current transducing system
[DE91-018924] p 401 N92-18515
Development of an electromagnetic microscope for eddy current evaluation of materials
[AD-A242007] p 406 N92-19873
Inspection of aircraft engine components using automated eddy current and pattern recognition techniques
[NRC-LTR-ST-1834] p 504 N92-22029
Inspection of fabricated fuselage panels using electronic shearography
[DOT/FAA/CT-TN92/26] p 1127 N92-33627

EDDY VISCOSITY
A turbulence model for iced airfoils and its validation
[AIAA PAPER 92-0417] p 326 A92-26267
New nonequilibrium turbulence model for calculating flows over airfoils p 330 A92-26403
Application of a new K-tau model to near wall turbulent flows p 395 A92-26437
Navier-Stokes solution of transonic cascade flows using nonperiodic C-type grids p 344 A92-28523
Renormalization group based algebraic turbulence model for three-dimensional turbomachinery flows p 703 A92-41268
A turbulence model for iced airfoils and its validation
[NASA-TM-105373] p 186 N92-15052
Towards the computation of turbulent hypersonic flows
[AERO-REPT-9106] p 345 N92-18318
The application of a Navier-Stokes CFD method to civil engine intake flows p 769 N92-27471

EDGE DETECTION
Analysis of lossy composite terminating structures
[NASA-CR-189901] p 404 N92-19217
A frontal approach for node generation in Delaunay triangulations p 771 N92-27680

EDGE LOADING
On the limitations of Froude's actuator disc concept
[ETN-91-90136] p 81 N92-11973

EDITING
Surface generation and editing operations applied to structural support of aerospace vehicle fuselages p 777 N92-27831

EDITING ROUTINES (COMPUTERS)
Automatic document generation with case on a DOD avionics project p 1005 A92-49299

EDUCATION
Developing undergraduate gas turbine and turbomachinery courses
[AIAA PAPER 91-2509] p 56 A92-12700
Tying it all together - The NASA/USRA University Advanced Design Program
[AIAA PAPER 92-1040] p 605 A92-33221
Facing the crisis in aircraft design education p 606 A92-34770
Designing a better engineer p 606 A92-34771
Advanced training systems for the next decade and beyond
[AIAA PAPER 92-1626] p 690 A92-38699
Applied Computational Aerodynamics - Case studies
[AIAA PAPER 92-2661] p 845 A92-45580
Applied aerodynamics education - Design and science
[AIAA PAPER 92-2662] p 928 A92-45581
Improvements in teaching aircraft engine design
[AIAA PAPER 92-3758] p 1141 A92-54152
Applications of robust control theory - Educational implications
[AIAA PAPER 92-4559] p 1131 A92-55271
Aerodynamics laboratory education at Purdue University - Ground testing facilities
[AIAA PAPER 92-4018] p 1100 A92-56840
The trisonic wind tunnel Muenchen and its involvement in the German SAeNGER-programme
[AIAA PAPER 92-4019] p 1100 A92-56841
Development and integration of modern laboratories in aerospace education
[AIAA PAPER 92-4022] p 1141 A92-56844
Investigation of air transportation technology at Princeton University, 1990-1991 p 266 N92-17995
Target pitch angle for the microburst escape maneuver p 266 N92-17996
Approach to crew training in support of the USAF Aircraft Structural Integrity Program (ASIP) p 363 N92-18595
MULTIRAD
[AD-A244211] p 412 N92-19247
Alpha Group: The Behemoth Apteryx. Final design proposal
[NASA-CR-190026] p 462 N92-20951
Symposium on Marketing for Technological Products
[MBB-UE-0014-90-PUB] p 606 N92-23928
Trends in aeropropulsion research and their impact on engineering education
[NASA-TM-105682] p 972 N92-31172

EFFECTIVE PERCEIVED NOISE LEVELS
Human response to helicopter noise: A test of A-weighting
[AD-A243719] p 304 N92-17506

EFFECTIVENESS
Piloted Simulation Effectiveness
[AGARD-CP-513] p 786 N92-28522
Opportunities for flight simulation to improve operational effectiveness p 883 N92-28523
Piloted simulation effectiveness development applications and limitations p 883 N92-28524
Utility of ground simulation in flight control problem identification, solution development, and verification p 883 N92-28525
Experience with piloted simulation in the development of helicopters p 884 N92-28528

EFFECTS
Effects of bleed air extraction of thrust levels on the F404-GE-400 turbofan engine
[AIAA PAPER 92-3092] p 1066 A92-54009
Effects of bleed air extraction on thrust levels on the F404-GE-400 turbofan engine
[NASA-TM-104247] p 871 N92-29425

EFFICIENCY
Flat belt continuously variable high speed drive
[DE92-008952] p 680 N92-25054

EFFLUENTS
High-speed civil transport aircraft emissions p 408 N92-19122

EGRESS
Ingress, emergency egress, and emergency evacuation testing of army aircraft
[AD-A246398] p 724 N92-27750

EIGENVALUES
Vibration characteristic analysis of a propeller blade p 38 A92-10967
Eigenvalue calculation procedure for an Euler/Navier-Stokes solver with application to flows over airfoils p 170 A92-17429
Design of low-sensitivity modalized observers using left eigenstructure assignment p 661 A92-39908
Flight control system design using eigenstructure assignment for rolling the aircraft around the velocity vector p 977 A92-51945
Aeroelastic modal characteristics of mistuned blade assemblies - Mode localization and loss of eigenstructure p 1117 A92-54921
Approximate truncated balanced realizations for infinite dimensional systems p 602 N92-22493
Design of helicopter flight control systems for hover and low speed using eigenstructure assignment p 1061 N92-33952

EIGENVECTORS
Eigenfunction analysis of turbulent mixing phenomena p 898 A92-45826
Flight control system design using eigenstructure assignment for rolling the aircraft around the velocity vector p 977 A92-51945
Robust sampled data eigenstructure assignment using the delta operator
[AIAA PAPER 92-4400] p 1075 A92-55200
Application of Eigenstructure Assignment to the control of powered lift combat aircraft
[RAE-TM-FS-1009] p 135 N92-12004
Approximate truncated balanced realizations for infinite dimensional systems p 602 N92-22493
Design of helicopter flight control systems for hover and low speed using eigenstructure assignment p 1061 N92-33952

EJECTION INJURIES
Scenario analysis of thigh gap related ejection injuries p 834 A92-44995

EJECTION SEATS
ACES II PLUS ejection seat p 103 A92-13463
Navy Aircrew Common Ejection Seat (NACES) program summary p 104 A92-13465
Computational analysis of high-speed ejection seats
[AIAA PAPER 92-0403] p 324 A92-26256
Canadian CF-18 aircraft ejection seat parachute update p 529 A92-32983
JPATS escape system development p 543 A92-35434
Computational analysis of inertial effects on the stability of an ACES-II ejection seat p 543 A92-35436
Methods for predicting successful ejection seat canopy penetration p 544 A92-35441
Computational fluid dynamics as a tool for aerodynamic analysis of ejection seats p 519 A92-35444
Scenario analysis of thigh gap related ejection injuries p 834 A92-44995

EJECTION TRAINING
JPATS escape system development p 543 A92-35434

EJECTORS
Investigation on opening and ejection of an aircraft canopy by using a solid rocket engine p 358 A92-28489
Supersonic nozzle mixer ejector p 376 A92-28536
Aerodynamic performance of a full-scale lifting ejector system in a STOVL fighter aircraft
[AIAA PAPER 92-3094] p 824 A92-48738
Preliminary dynamic tests of a flight-type ejector
[AIAA PAPER 92-3261] p 1066 A92-54020
Experimental investigation of an ejector-powered free-jet facility
[AIAA PAPER 92-3569] p 1090 A92-54058
Flow induction by pressure forces
[AIAA PAPER 92-3571] p 1067 A92-54060
Use of an approximate similarity principle for the thermal scaling of a full-scale thrust augmenting ejector
[AIAA PAPER 92-3792] p 1069 A92-54171
Supercharged ejector ramjet p 475 N92-21527
Use of an approximate similarity principle for the thermal scaling of a full-scale thrust augmenting ejector
[NASA-TM-105724] p 739 N92-26613
Air ejector experiments using the two-dimensional supersonic cascade tunnel: Zero secondary flow performance
[NAL-TM-632] p 887 N92-28829
Preliminary dynamic tests of a flight-type ejector
[NASA-TM-105814] p 972 N92-30998

ELASTIC ANISOTROPY
Composite beam analysis linear analysis of naturally curved and twisted anisotropic beams
[AD-A252652] p 999 N92-30766

ELASTIC BENDING
Calculation of the exerting force necessary to form the aircraft hull plate in the symmetry plate bender with three rolls and the feeding value of the centre roll p 998 A92-53297

ELASTIC BODIES
Ultrasonic motor utilizing elastic fin rotor p 215 A92-17414
Shape-sensitivity analysis and design optimization of linear, thermoelastic solids p 395 A92-26433
Dynamic stability of elastic vehicles with unsteady aerodynamic force modeling p 509 A92-29326
Determination of the objective-function gradient in the problem of minimizing stress concentration using the finite element method p 494 A92-30170
On the behavior of pretwisted beams with irregular cross-sections p 495 A92-31564
Stability and dynamic coupling of elastic vehicles with unsteady aerodynamic forces considered p 1102 A92-53545

ELASTIC DAMPING
Experiments on the blade loss transient response of rotor with flexible damped support
[ASME PAPER 91-GT-149] p 148 A92-15587
Integrated aeroelastic control optimization of laminated composite lifting surfaces p 481 A92-32248
FAMUSS - A new aeroservoelastic modeling tool
[AIAA PAPER 92-2395] p 541 A92-34468
Aeroelasticity - Advances and future directions
[AIAA PAPER 92-2446] p 585 A92-34475
Helicopter rotor blade aeroelasticity in forward flight with an implicit structural formulation p 958 A92-50315
Safety provision against 'ground resonance' free vibration of a coaxial helicopter p 1056 A92-56289

ELASTIC DEFORMATION
Experimental and theoretical analysis of composite I-beams with elastic couplings p 216 A92-18377
On automatic control of aeroelastic vehicles p 509 A92-29327
A new method for calculating burst speed of aeroengine disks
[ASME PAPER 91-GT-121] p 670 A92-36899
An integrated development of the equations of motion for elastic hypersonic flight vehicles
[AIAA PAPER 92-4605] p 1077 A92-55283
Alternate/modified binders for asphalt airfield pavements
[AD-A242829] p 285 N92-17260

ELASTIC PLATES
Active control of sound transmission through elastic plates using piezoelectric actuators p 53 A92-11052
Sound produced by an aerodynamic source adjacent to a partly coated, finite elastic plate p 414 A92-25365

ELASTIC PROPERTIES
Ultrasonic NDE for ceramic- and metal-matrix composite material characterization p 491 A92-28690
Lifting surface design using the principle of passive control of elastic characteristics p 480 A92-31865
The relationship between tensile and flexural strength of unidirectional composites p 891 A92-45629
Combined application of the energy method and the weighted residual method - A new way to construct the finite elements p 991 A92-50239
Oscillations of an anisotropic rotor on an elastic anisotropic support p 1057 A92-56311
A demonstration of passive blade twist control using extension-twist coupling
[NASA-TM-107642] p 1001 N92-31155
Fatigue crack growth of small corner defects from blunt notches in an aeroengine alloy
[PNR-90860] p 1111 N92-34019

ELASTIC WAVES
Pressure wave propagation studies for oscillating cascades
[AIAA PAPER 92-0145] p 316 A92-25682
A shock and an expansion wave in transonic flow p 440 A92-31961
EIPOS for ice-formation control on aircraft in flight - An alternative technique p 647 A92-40545

ELASTODYNAMICS
Electrorheological fluids; Proceedings of the 2nd International Conference, Raleigh, NC, Aug. 7-9, 1989 p 40 A92-12625
Dynamical systems analysis of an aerodynamic decelerator's behavior during the initial opening process
[AD-A244194] p 348 N92-19394

ELASTOPLASTICITY
Effect of different force-functions and initial shock pressure on blade response p 374 A92-27913

ELECTRA AIRCRAFT
Aerobureau - Strategic television airmobile reports via satellite p 218 A92-19988

ELECTRIC ARCS
New insulation constructions for aerospace wiring applications. Volume 2: The 270 VDC arc tracking testing with power controllers
[AD-A240639] p 23 N92-11007
Aerothermodynamic radiation studies
[NASA-CR-185666] p 284 N92-15998

ELECTRIC CHARGE
A test bench for evaluating powerplant electrization p 138 A92-16830

ELECTRIC CHOPPERS
Resonant cryogenic chopper --- for infrared and submillimeter radiometers p 294 A92-22796

ELECTRIC CONTROL
Variable displacement electro-hydrostatic actuator --- for flight control systems p 876 A92-48492
C-141 and C-130 power-by-wire flight control systems p 876 A92-48493
Electric actuation system duty cycles --- in fly-by-wire/power-by-wire control p 877 A92-48494

ELECTRIC CORONA
Advanced electromagnetic methods for aerospace vehicles
[NASA-CR-188630] p 488 N92-20193

ELECTRIC CURRENT
Assessment of valve actuator motor rotor degradation by Fourier Analysis of current waveform
[DE92-013233] p 909 N92-28814

ELECTRIC DISCHARGES
Study of simulated lightning discharge effects on wires of a rotorcraft
[ONERA, TP NO. 1991-173] p 92 A92-16137
Mechanisms of high-current pulses in lightning and long-spark stepped leaders p 1116 A92-54678

ELECTRIC EQUIPMENT
A new method for orientation calculation of the electromagnetic helmet-mounted sighting unit p 370 A92-27837
Life cycle costs of the C-130 electrical power system upgrade
[AD-A246759] p 786 N92-28348

ELECTRIC EQUIPMENT TESTS
Automatic function testing in the aircraft production p 1015 A92-56083
Airport smart power lighting system
[DOT/FAA/CT-TN91/12] p 573 N92-22966

ELECTRIC FIELD STRENGTH
On the accuracy of an aircraft-borne ambient electric-field measuring system p 186 A92-20127

ELECTRIC FIELDS
Stratospheric electrodynamics from superpressure balloons - A technical challenge for small payload environments
[AIAA PAPER 91-3674] p 14 A92-11019
Expert knowledge techniques applied to the analysis of electric field mill data p 408 A92-27991

ELECTRIC FILTERS
Evaluating the velocity accuracy of an integrated GPS/INS system: Flight test results
[DE92-007519] p 640 N92-25470

ELECTRIC GENERATORS
Advanced power generation systems for more electric aircraft
[SAE PAPER 912186] p 656 A92-40006
Electric power generating system for the Boeing 777 airplane
[SAE PAPER 912050] p 861 A92-45434
Generators inside small engines
[AIAA PAPER 92-3755] p 867 A92-49113
Design of the Boeing 777 electric system p 1070 A92-55902
Aircraft photovoltaic power-generating system p 775 N92-26581

ELECTRIC MOTOR VEHICLES
Heavy duty transport research needs assessment
[DE92-010622] p 767 N92-27394
Electromechanical systems with transient high power response operating from a resonant AC link
[NASA-TM-105716] p 870 N92-28985

ELECTRIC MOTORS
Ultrasonic motor utilizing elastic fin rotor p 215 A92-17414
Counterrotating brushless DC permanent magnet motor
[DE92-003825] p 401 N92-18550
Advanced techniques in current signature analysis
[DE92-007680] p 679 N92-24892
Assessment of valve actuator motor rotor degradation by Fourier Analysis of current waveform
[DE92-013233] p 909 N92-28814

ELECTRIC POTENTIAL
Analysis of a 37 kW cage-induction motor
[PB92-142116] p 597 N92-23496

ELECTRIC POWER PLANTS
JPRS report: Science and technology. USSR: Engineering and equipment
[JPRS-UEQ-91-010] p 593 N92-22397

ELECTRIC POWER SUPPLIES
270-Vdc/hydrid 115-Vac electric power generating system technology demonstrator evolution to a dual-channel, more electric aircraft technology development testbed
[SAE PAPER 912183] p 655 A92-40003
270-Vdc/hybrid 115 Vac electric power generating system technology demonstrator
[SAE PAPER 912051] p 861 A92-45435
An artificial intelligence approach for the verification of requirements for aircraft electrical power systems p 863 A92-48481
Design of the Boeing 777 electric system p 1070 A92-55902
Thermal management of high heat flux electronic components in space and aircraft systems, phase 1
[AD-A239982] p 41 N92-10157
Radiant energy power source for jet aircraft
[DE92-008726] p 648 N92-24556

ELECTRIC PROPULSION
IRS organigram p 33 N92-10053
ELECTRIC ROCKET ENGINES
IRS organigram p 33 N92-10053
ELECTRIC WIRE
Study of simulated lightning discharge effects on wires of a rotorcraft
[ONERA, TP NO. 1991-173] p 92 A92-16137
Whole aircraft lightning indirect effects evaluation using low level injection techniques p 192 A92-20134
New insulation constructions for aerospace wiring applications. Volume 1: Testing and evaluation
[AD-A240638] p 22 N92-11006
New insulation constructions for aerospace wiring applications. Volume 2: The 270 VDC arc tracking testing with power controllers
[AD-A240639] p 23 N92-11007
ELECTRICAL ENGINEERING
Research, services, and facilities (National Institute of Standards and Technology)
[PB92-109172] p 485 N92-21870
ELECTRICAL FAULTS
Digital flight control systems - Some new commercial twists p 974 A92-49264
Next-generation avionics packaging and cooling 'test results from a prototype system' p 989 A92-49277
JIAWG module fault coverage metrics methodology p 989 A92-49279
Optimal control of helicopters following power failure
[AIAA PAPER 92-4471] p 1076 A92-55231
Optimal control of tiltrotor aircraft following power failure p 1085 A92-56303
ELECTRICAL IMPEDANCE
Using the single point excitation technique to measure aperture impedance over a broad frequency range p 761 A92-42320
270-Vdc/hybrid 115 Vac electric power generating system technology demonstrator
[SAE PAPER 912051] p 861 A92-45435
Inverse problems and imaging (Pitman research notes in mathematics series Number 245)
[AD-A240333] p 53 N92-11737
ELECTRICAL INSULATION
New insulation constructions for aerospace wiring applications. Volume 1: Testing and evaluation
[AD-A240638] p 22 N92-11006
New insulation constructions for aerospace wiring applications. Volume 2: The 270 VDC arc tracking testing with power controllers
[AD-A240639] p 23 N92-11007
ELECTRICAL MEASUREMENT
Using the single point excitation technique to measure aperture impedance over a broad frequency range p 761 A92-42320
The role of crack growth in defect assessment
[PNR-90798] p 501 N92-20909
ELECTRICAL PROPERTIES
Testing and evaluation of the Vanner electrical inverters, models 24-1500 and SP 00112
[AD-A241914] p 299 N92-17216
ELECTRICITY
Thermally regenerative fuel cells
[AD-A242900] p 300 N92-17629
Air cushion vehicle conductive/semiconductive flexible skirt, and method
[AD-D015160] p 400 N92-18187
ELECTRO-OPTICS
Fiber optics for controls p 570 N92-22529
Electro optical system to measure strains at high temperature
[NASA-CR-190450] p 1127 N92-33696
ELECTROACOUSTICS
Experimental study of the effects of atmospheric turbulence on sound propagation over the ground
[ONERA, TP NO. 1991-211] p 415 A92-26363
ELECTROCHEMICAL MACHINING
Manufacture of XD gamma titanium aluminide airfoils via investment casting and machining p 494 A92-30603
ELECTROCHEMISTRY
Thermally regenerative fuel cells
[AD-A242900] p 300 N92-17629
ELECTRODES
The measurement of water film thickness on airfoils in heavy rain conditions using conductance sensors p 452 N92-21695
ELECTRODYNAMICS
Stratospheric electrodynamics from superpressure balloons - A technical challenge for small payload environments
[AIAA PAPER 91-3674] p 14 A92-11019
ELECTROLYTES
Evaluation of electrolytic tilt sensors for wind tunnel model angle-of-attack (AOA) measurements p 1116 A92-54344
ELECTROLYTIC CELLS
Evaluation of electrolytic tilt sensors for measuring model angle of attack in wind tunnel tests
[NASA-TM-4315] p 297 N92-16283
ELECTROMAGNETIC COMPATIBILITY
Radiation and coupling between antennas mounted on a complex metallic structure p 760 A92-42315
Comparison of R2SPG waveforms with simulated EMP --- Repetitive Random Square-wave Pulse Generator p 760 A92-42317
Decoupling of antennas using periodic structures p 725 A92-42634
Suppression of radiating harmonics Electro-Impulse Deicing (EIDI) systems
[DOT/FAA/CT-TN90/33] p 405 N92-19764
JTIDS electromagnetic compatibility in the 960-1215 MHz band
[AD-A247834] p 773 N92-27864
ELECTROMAGNETIC COUPLING
Numerical modeling technique for field-to-cable coupling through advanced composite material p 146 A92-14684
ELECTROMAGNETIC FIELDS
The use of finite difference electromagnetic analysis in the design and verification of modern aircraft p 192 A92-20136
Pulsed field system for detecting the presence of a target in a subsurface environment
[AD-D015074] p 296 N92-16174
Analysis of a 37 kW cage-induction motor
[PB92-142116] p 597 N92-23496
Repetitive High Energy Pulsed Power (RHEPP) temperature monitoring system utilizing Luxtron fluoroptic sensors and thermocouples technical reference manual
[DE92-013461] p 999 N92-30893
Advanced electromagnetic methods for aerospace vehicles
[NASA-CR-190650] p 1001 N92-31156
ELECTROMAGNETIC INTERACTIONS
An improved model-creation program for EM interaction analysis
[NRC-31764] p 155 N92-12153
Constraint propagation through electromagnetic interaction topologies
[NRC-31761] p 155 N92-12154
Analysis of EMP response of structures using frequency domain electromagnetic interaction codes
[AD-A245758] p 765 N92-26592
Advanced electromagnetic methods for aerospace vehicles
[NASA-CR-190650] p 1001 N92-31156
ELECTROMAGNETIC INTERFERENCE
A review of digital flight control system upsets caused by electromagnetic interference
[AIAA PAPER 91-3765] p 215 A92-17627
Coherence multiplexed polarimetric fibre sensor arrays for aerospace applications p 370 A92-27785
On upsets of analog portions of digital flight control systems due to electromagnetic interference
[SAE PAPER 912144] p 651 A92-39982
270-Vdc/hybrid 115 Vac electric power generating system technology demonstrator
[SAE PAPER 912051] p 861 A92-45435
Critical digital systems - A fly-by-light consideration p 974 A92-49324
Distributed flight control system using fiber distributed data interface (FDDI) p 976 A92-51004
Constraint propagation through electromagnetic interaction topologies
[NRC-31761] p 155 N92-12154
Design of a fiber optic image transmission link
[AD-A243686] p 304 N92-17088
Compact range test applications, phase 2
[AD-A248790] p 999 N92-30583
Fly-by-light technology development plan
[NASA-CR-181954] p 1086 N92-32778
ELECTROMAGNETIC MEASUREMENT
Inverse problems and imaging (Pitman research notes in mathematics series Number 245)
[AD-A240333] p 53 N92-11737
ELECTROMAGNETIC NOISE
Jet aircraft noise at high subsonic flight Mach numbers
[DLR-FB-91-28] p 928 N92-29997
Feasibility of measuring transverse electric noise at VLF and LF on an ice cap
[AD-A252280] p 1129 N92-33220
ELECTROMAGNETIC PULSES
Composite electromagnetic pulse threat p 146 A92-14689
Effects of ionizing and nonionizing radiation on aircraft p 295 A92-23301
Comparison of R2SPG waveforms with simulated EMP --- Repetitive Random Square-wave Pulse Generator p 760 A92-42317
Using the single point excitation technique to measure aperture impedance over a broad frequency range p 761 A92-42320
Pulsed field system for detecting the presence of a target in a subsurface environment
[AD-D015074] p 296 N92-16174
Analysis of EMP response of structures using frequency domain electromagnetic interaction codes
[AD-A245758] p 765 N92-26592
ELECTROMAGNETIC RADIATION
High-frequency techniques for antenna analysis p 494 A92-31071
Sikorski (S-76) High Intensity Radiated Fields (HIRF) test
[SAE PAPER 912214] p 652 A92-40017
High Intensity Radiated Fields (HIRF) project plan
[DOT/FAA/CT-TN91/1] p 297 N92-16181
ELECTROMAGNETIC SCATTERING
Slenderness approximations in RCS estimation - The simplest 2-D case p 533 A92-33622
Scattering mechanism and RCS reduction of antennas p 726 A92-44850
Analysis of lossy composite terminating structures
[NASA-CR-189901] p 404 N92-19217
Finite difference time domain modeling of steady state scattering from jet engines with moving turbine blades
[NASA-CR-190290] p 971 N92-30753
ELECTROMAGNETIC SHIELDING
Metal fibers and fabrics as shielding materials for composites, missiles and airframes p 141 A92-14680
Numerical modeling technique for field-to-cable coupling through advanced composite material p 146 A92-14684
Lightning standards for aircraft protection p 91 A92-14688
Testability of the PAALS auto-align sensor system --- Precision Accelerometer Alignment and Leveling System p 965 A92-49310
ELECTROMAGNETIC SPECTRA
Sensor compatibility/optimal sensor combinations p 599 N92-23403
ELECTROMAGNETIC WAVE TRANSMISSION
Methods for determining atmospheric correction for radio-rangefinder measurements of inclined trajectories p 775 A92-44070
ELECTROMAGNETISM
Lower-end dynamic characteristics of a magnetically coupled free-piston Stirling engine/compressor system p 992 A92-50795
Advanced electromagnetic methods for aerospace vehicles
[NASA-CR-188630] p 488 N92-20193
Analysis of EMP response of structures using frequency domain electromagnetic interaction codes
[AD-A245758] p 765 N92-26592
Advanced electromagnetic methods for aerospace vehicles
[NASA-CR-190650] p 1001 N92-31156
ELECTROMAGNETS
An electromagnetic suspension system for aerodynamic studies p 483 A92-30409
ELECTROMECHANICAL DEVICES
Condor, an all-electric airplane p 269 A92-21734
Condor - An all electric airplane
[SAE PAPER 912184] p 644 A92-40004
MLS/RNAV control display unit development p 965 A92-49303
Electromechanical systems with transient high power response operating from a resonant AC link
[NASA-TM-105716] p 870 N92-28985
ELECTRON BEAMS
PVD coatings for aircraft turbine blades p 216 A92-17950
A new technique for temperature and specie concentration measurements in unseeded supersonic and hypersonic gas flows
[AD-A241536] p 158 N92-13409
Materials processing in low gravity
[NASA-CR-184280] p 499 N92-20198
Composition monitoring of electron beam melting processes using diode lasers
[DE92-009527] p 669 N92-25259
ELECTRON DENSITY (CONCENTRATION)
Determination of physicochemical constant in the wake of a body from ballistic experiments p 609 A92-36549
ELECTRONIC AIRCRAFT
Making fly-by-light a reality p 877 A92-48499
ELECTRONIC CONTROL
Improvements to expulsive separation ice protection blankets
[AIAA PAPER 92-0533] p 358 A92-26951
Real-time simulation and adaptive PID control of QSK-06A control for gas turbine p 470 A92-29740
Electronic control of a turbine power unit p 470 A92-29741

An investigation of real-time diagnostic technique for DEEC system --- digital electronic engine control system
p 470 A92-29742
An aircraft controller and its development
p 558 A92-35917
Application of a double actuator electronic fuel control unit on a small gas turbine engine
[SAE PAPER 912160] p 655 A92-39993
Sikorski (S-76) High Intensity Radiated Fields (HIRF) test
[SAE PAPER 912214] p 652 A92-40017
Intelligent Engine Control (IEC)
[AIAA PAPER 92-3484] p 866 A92-49024
Utility management system for hypersonic vehicles
p 964 A92-49252
Electronically steerable antenna for aircraft
p 229 N92-15272
Fiber optics for controls p 570 N92-22529

ELECTRONIC COUNTERMEASURES
GPS/INS integration for improved aircraft attitude estimates
[AD-A243947] p 356 N92-19604

ELECTRONIC EQUIPMENT
Real-time microfocus radiography for electronic failure analysis p 214 A92-17289
Comparison of R2SPG waveforms with simulated EMP --- Repetitive Random Square-wave Pulse Generator
p 760 A92-42317
International SAMPE Electronics Conference, 5th, Los Angeles, CA, June 18-20, 1991, Proceedings
[ISBN 0-938994-58-1] p 985 A92-51901
Application of electronically scanned pressure measurement system for engine simulation tests in the German-Dutch Wind Tunnel
[AIAA PAPER 92-4003] p 1122 A92-56826
Thermal management of high heat flux electronic components in space and aircraft systems, phase 1
[AD-A239982] p 41 N92-10157
The electronic aeronautical chart for general aeronautics: A system specification
[ILR-MITT-263(1991)] p 20 N92-10997
Machine Intelligence for Aerospace Electronic Systems
[AGARD-CP-499] p 164 N92-12517
Soviet electronic display systems under research and manufactured for the civil aviation aircraft of the 1990's
[AD-A240933] p 119 N92-13066
Electronic systems in transportation
[TP-9983] p 189 N92-14009
Implementation of an object-oriented flight simulator D.C. electrical system on a hypercube architecture
[AD-A243700] p 284 N92-17097

ELECTRONIC EQUIPMENT TESTS
Radar troubleshooting assistant expert system
[AIAA PAPER 91-3764] p 231 A92-17626
Designing through test
[AIAA PAPER 91-3822] p 232 A92-17664
Realistic real-time ground testing
[AIAA PAPER 92-0197] p 284 A92-23805
Test Engineering Language for Avionic Systems
p 554 A92-35763
Low cost HIRF troubleshooting and verification method for digital avionics systems p 990 A92-49304
Are we doing HIRF testing sensibly? --- avionics certification in commercial aircraft p 931 A92-49305
Testability of the PAALS auto-align sensor system --- Precision Accelerometer Alignment and Leveling System
p 965 A92-49310
The use of photogrammetry in aviation equipment flight testing p 994 A92-51649
Field test of an advanced maintenance-system
p 1016 A92-56221
A module-level testing environment for safety-critical software systems p 1132 A92-56293
Image-supported navigation for testing instrument landing systems p 189 N92-14012
Eddy current transducing system
[DE91-018924] p 401 N92-18515
Aeronautical satellite system test and implementation
p 676 N92-24095
Cost/benefit analysis of the AH-64 (Apache) helicopter Automated Test Equipment (ATE)
[AD-A252909] p 1101 N92-33398

ELECTRONIC FILTERS
Washout filters in the bifurcation control of high alpha flight dynamics p 476 A92-29061
Stability and performance of notch filter control for unbalance response p 771 N92-27731

ELECTRONIC MODULES
A high performance general purpose processing element for avionic applications p 920 A92-48440
High performance heat sink for surface mount applications --- in avionics system design
p 989 A92-49275
Applications of silicon hybrid multi-chip modules to avionics p 859 N92-28379

ELECTRONIC PACKAGING
Applications of advanced composites in a 3/4 air transportable rack p 36 A92-10314
Putting ten pounds of avionics in a one pound package (Can we do it again?)
[AIAA PAPER 91-3766] p 197 A92-17628
Applications of composite material systems to avionic systems packaging p 576 A92-32564
Software package for preliminary design of helicopter
p 775 A92-41195
Liquid cooled approaches for high density avionics
p 989 A92-49274
High performance heat sink for surface mount applications --- in avionics system design
p 989 A92-49275
Progressive avionics packaging technologies
p 989 A92-49276
Next-generation avionics packaging and cooling 'test results from a prototype system' p 989 A92-49277
Next generation power electronics for space and aircraft. II - Packaging p 992 A92-50553
Application of resin and metal matrix composites to advanced avionics enclosure p 985 A92-51921

ELECTRONIC TRANSDUCERS
Laboratory evaluation of a sensor for detection of aircraft wing contaminants
[AIAA PAPER 92-0301] p 369 A92-25753
The use of silicon microsensors in smart skins for aerodynamic research p 1116 A92-54348
Study of interactions on anemoclinometric sensors
[REPT-90/30] p 138 N92-12006

ELECTRONIC WARFARE
PDFIII - A flight control system for EW UAV's
[TABES PAPER 91-315] p 565 A92-34688
The application of multimedia expert systems to the depot level maintenance environment
p 922 A92-48557
Standardizing operational flight data handling
p 1009 A92-53109

ELECTRONS
Prototype instrumentation and design studies
[AD-A248378] p 736 N92-28004

ELECTRORHEOLOGICAL FLUIDS
Electrorheological fluids; Proceedings of the 2nd International Conference, Raleigh, NC, Aug. 7-9, 1989
p 40 A92-12625

ELECTROSTATIC PROBES
Prototype instrumentation and design studies
[AD-A248378] p 736 N92-28004

ELEVATORS (CONTROL SURFACES)
The icing of the elevator of the DLR icing research aircraft of Do 28 type
[DLR-MITT-91-12] p 953 N92-31813

ELLIPSES
Influence of chemical modeling on the solution of hypersonic shock layers p 183 N92-15016

ELLIPSOIDS
Equilibrium solution of the Euler and Navier-Stokes equations around a double ellipsoidal shape with mono- and multi-blocks including real gas effects, part 1
p 227 N92-15030
Automated composite ellipsoid modelling for high frequency GTD analysis
[NASA-CR-189853] p 275 N92-17316
Zonal solutions for a double-ellipse in a hypersonic flowfield
[AERO-REPT-9009] p 345 N92-18233
Cases 6.1 and 6.8 double ellipsoid: Navier-Stokes calculation p 525 N92-22181

ELLIPTIC DIFFERENTIAL EQUATIONS
Concerning the functional solution of transonic flows
p 243 A92-21318
On one method of constructing adaptive difference grids in aerodynamics problems p 311 A92-24902

ELLIPTICAL ORBITS
An alternative concept for aeroassisted orbit transfers
[AD-A243409] p 287 N92-17325

EMBEDDED COMPUTER SYSTEMS
Viscous high-speed flow computations by adaptive mesh embedding techniques p 808 A92-45839
A new development in embedded computer performance measurement p 921 A92-48506
Partitioned software support concept for modular embedded computer software p 922 A92-48518
A new approach to embedded computer performance measurement --- in avionics p 1005 A92-49288
Development and verification of software for flight safety critical systems p 164 N92-12469

EMBEDDING
The detection of damage and the measurement of strain within composites by means of embedded optical fiber sensors p 491 A92-28669

EMERGENCIES
Guidelines for integrating helicopter assets into emergency planning
[SCT-91RR-18] p 18 N92-10993
Helicopter rejected takeoff airspace requirements
[SCT-91RR-28] p 116 N92-13058
Ingress, emergency egress, and emergency evacuation testing of army aircraft
[AD-A246398] p 724 N92-27750

EMERGENCY LIFE SUSTAINING SYSTEMS
Pre-flight risk assessment in emergency medical service (EMS) helicopters p 16 A92-11171

EMISSION
EDMS: Microcomputer pollution model for civilian airports and Air Force bases, (user's guide)
[AD-A240528] p 45 N92-11578
A parametric numerical study of mixing in a cylindrical duct
[NASA-TM-105695] p 738 N92-26553

EMISSION SPECTRA
Improving sample introduction for total wear metal determination by atomic emission spectroscopy
p 389 A92-26850

EMITTERS
Effect of guard band reduction on marker beacon receiver performance
[DOT/FAA/CT-TN92/18] p 1002 N92-31617

EMULSIONS
Development of fuel neutralizing agents to prevent flashback on aircraft fires
[AD-A242828] p 264 N92-17259

ENCLOSURE
Application of resin and metal matrix composites to advanced avionics enclosure p 985 A92-51921

END EFFECTORS
Robotics application in aerospace manufacturing
p 671 A92-38216

END PLATES
End plate interference effects on the aerodynamics of a circular cylinder in uniform flow p 313 A92-25097
Establishing two-dimensional flow in a large-scale planar turbine cascade
[AIAA PAPER 92-3066] p 823 A92-48720
The wall interference correction and test data processing methods for airfoil wind tunnel test with endplates
p 942 A92-53087
Contribution of tailplane-mounted twin fins to sideforce, yawing moment, and rolling moment derivatives due to sideslip
[ESDU-92007] p 1086 N92-32487

ENDOTHERMIC FUELS
Thermal management for a Mach 5 cruise aircraft using endothermic fuel p 736 A92-41225

ENERGY ABSORPTION
Evaluation of thermoplastic matrix composites for use in energy-absorbing helicopter subfloors
p 141 A92-14374
Determination of the energy absorption of composite structures under combined loadings p 145 A92-14441

ENERGY BUDGETS
Reynolds stress budget in the outwash jet arising from colliding curved wall jets p 614 A92-38860
Turbulent energy budgets in impinging zones
p 620 A92-40081

ENERGY CONSERVATION
Application of riblet surface to pipe flow
p 766 N92-26915

ENERGY CONSUMPTION
Analysis of Euler's and stress tensor methods for calculating power consumption of high speed centrifugal fans and turbocompressors
[DE92-728396] p 298 N92-16325
Calculation of local power consumptions and efficiencies of centrifugal fans and turbocompressors
[DE92-728402] p 298 N92-16326
Low power magnetic bearing design for high speed rotating machinery p 772 N92-27739

ENERGY CONVERSION
IECEC '91; Proceedings of the 26th Intersociety Energy Conversion Engineering Conference, Boston, MA, Aug. 4-9, 1991. Vol. 5 - Renewable resource systems, stirling engines and applications, systems and cycles
[ISBN 0-89448-163-0] p 992 A92-50771
DoD key technologies plan
[AD-A253692] p 1142 N92-33238

ENERGY CONVERSION EFFICIENCY
Power performance of a nonisentropic Brayton cycle
p 54 A92-11281
Kappa Group: The initial guess. A proposal in response to a commercial air transportation study
[NASA-CR-189981] p 366 N92-19374
Design and performance of controlled-diffusion stator compared with original double-circular-arc stator
[NASA-TP-2852] p 562 N92-22863
Application of CFD in the design of gas turbine engine components p 741 N92-27461

ENERGY DISSIPATION
Energy analysis of aeroengine and its significance
p 557 A92-35569

Thermal management of high heat flux electronic components in space and aircraft systems, phase 1
[AD-A239982] p 41 N92-10157
Air cushion vehicle conductive/semiconductive flexible skirt, and method
[AD-D015160] p 400 N92-18187
An investigation of the energy loss and near wake flow field of trailing edge injection p 456 N92-21839

ENERGY DISTRIBUTION
Vortex-induced energy separation in shear flows
[AIAA PAPER 92-0192] p 257 A92-23801

ENERGY METHODS
Combined application of the energy method and the weighted residual method - A new way to construct the finite elements p 991 A92-50239
Further studies of kinetic energy methods in high speed ramjet cycle analysis
[AIAA PAPER 92-3805] p 1069 A92-54177
Energy height method for flight path optimisation. Addendum A: Numerical method suitable for rapid use on IBM PC compatible computers
[ESDU-91016-ADD] p 272 N92-15987
Use of SEA to predict structure-borne noise in aircraft p 1137 N92-32955

ENERGY POLICY
Heavy duty transport research needs assessment
[DE92-010622] p 767 N92-27394

ENERGY SPECTRA
Realization of a large-scale turbulence field in a small wind tunnel p 67 A92-15487
Examination of energy spectra moments in a developing turbulent flow
[NIAR-91-28] p 399 N92-18116
Atmospheric turbulence spectra and correlation functions
[NLR-TP-89217-U] p 915 N92-28689

ENERGY STORAGE
DoD key technologies plan
[AD-A253692] p 1142 N92-33238

ENERGY TECHNOLOGY
SERI advanced wind turbine blades
[DE92-001216] p 598 N92-22971
Measured and predicted rotor performance for the SERI advanced wind turbine blades
[DE92-001215] p 598 N92-23119

ENERGY TRANSFER
Power beaming - Energy transmission at 35 GHz and higher frequencies --- for terrestrial and space applications with rectennas
[AIAA PAPER 92-2027] p 471 A92-29944
The relationship between mode localization and energy transmission parameters in the vibration of coupled structures p 925 A92-45921
Rarefied gas research at Berkeley - Current studies and future potentials
[AIAA PAPER 92-3971] p 1098 A92-56797
Propagation of shock waves through clouds
[AERO-REPT-9104] p 400 N92-18317
Presentation of a computational code for 3-D compressible flow in complex channels and cavities p 769 N92-27475
Non-linear interactions in homogeneous turbulence with and without background rotation p 912 N92-30044

ENGINE AIRFRAME INTEGRATION
Full-scale investigation of aerodynamic interactions between a rotor and fuselage p 105 A92-14361
The NASP Program - An update p 61 A92-16059
A configuration development strategy for the NASP
[AIAA PAPER 91-5044] p 210 A92-17830
Dynamics and control of hypersonic vehicles - The integration challenge for the 1990's
[AIAA PAPER 91-5057] p 203 A92-17840
Numerical and experimental investigation of airframe-integrated inlet for high velocities p 243 A92-21072
An experimental and analytical study of the interaction of a vortex with an airframe
[AIAA PAPER 92-0319] p 321 A92-25766
Design and modeling issues for integrated airframe/propulsion control of hypersonic flight vehicles p 477 A92-29115
Integrated flight/propulsion control specifications for systems with two-way coupling p 477 A92-29117
A framework for the analysis of airframe/engine interactions and integrated flight/propulsion control p 478 A92-29120
A parametric study of airbreathing Pulsed Detonation Engine
[AIAA PAPER 92-0392] p 471 A92-31660
Flowpath optimization for hypersonic vehicles
[AIAA PAPER 91-5043] p 437 A92-31688
Design tradeoffs on engine-integrated hypersonic vehicles
[AIAA PAPER 92-1205] p 537 A92-33313
EUROFAR airframe aerodynamic design p 546 A92-35750
Evolution of ASTOVL aircraft design p 842 A92-45311
ASTOVL engine control p 860 A92-45321
Investigations of propulsion integration interference effects on a transport aircraft configuration
[AIAA PAPER 92-3097] p 849 A92-48739
Internal shock interactions in propulsion/airframe integrated three-dimensional sidewall compression scramjet inlets
[AIAA PAPER 92-3099] p 824 A92-48741
Operating characteristics at Mach 4 of an inlet having forward-swept, sidewall-compression surfaces
[AIAA PAPER 92-3101] p 863 A92-48743
Fighter airframe/propulsion integration - A General Dynamics perspective
[AIAA PAPER 92-3332] p 850 A92-48915
Fighter airframe/propulsion integration - A McDonnell Aircraft perspective
[AIAA PAPER 92-3333] p 850 A92-48916
Emerging airframe/propulsion integration technologies at General Electric
[AIAA PAPER 92-3335] p 850 A92-48917
Propulsion system performance resulting from an Integrated Flight/Propulsion Control design
[AIAA PAPER 92-4602] p 1069 A92-55281
Analysis of airframe/engine interactions for a STOVL aircraft with integrated flight/propulsion control
[AIAA PAPER 92-4623] p 1052 A92-55300
Flight simulation modeling in support of engine/airframe integration p 1055 A92-56279
Test description and preliminary pitot-pressure surveys for Langley Test Technique Demonstrator at Mach 6
[AIAA PAPER 92-3940] p 1096 A92-56770
A computational and experimental investigation of a three-dimensional hypersonic scramjet inlet flow field p 11 N92-10007
Vortex generator design for aircraft inlet distortion as a numerical optimization problem p 194 N92-13959
Hypersonic airbreathing propulsion/airframe integration p 474 N92-21522
Design of an integrated airframe/propulsion control system architecture
[NASA-CR-182004] p 602 N92-22643
Design of an integrated airframe/propulsion control system architecture
[NASA-CR-182007] p 602 N92-22644
Domain modeling and grid generation for multi-block structured grids with application to aerodynamic and hydrodynamic configurations p 691 N92-24411
Computational structures technology engine/airframe coupling p 649 N92-25935
The application of flight simulation models in support of rotorcraft design and development p 884 N92-28527
Navier-Stokes computations of a viscous optimized waverider
[NASA-CR-189658] p 944 N92-30392
Application of computational fluid dynamics to the study of vortex flow control for the management of inlet distortion
[NASA-TM-105672] p 1128 N92-34112

ENGINE ANALYZERS
A method for determining the optimal composition of the measured parameters in diagnosing gas turbine engines p 128 A92-16819

ENGINE CONTROL
V-22 thrust power management control law development p 132 A92-14405
Interactive engine system dynamics analysis
[ASME PAPER 91-GT-193] p 124 A92-15619
Control systems for the next century's fighter engines
[ASME PAPER 91-GT-278] p 125 A92-15674
Integrated flight/propulsion control for flight critical applications - A propulsion system perspective
[ASME PAPER 91-GT-284] p 125 A92-15679
A global approach in evaluating inlet/engine compatibility
[ASME PAPER 91-GT-402] p 127 A92-15732
F-14/F110 engine integration p 112 A92-16055
Performance improvements of an F-15 airplane with an integrated engine-flight control system p 205 A92-20204
Aeroengine sensor failure detection by Bayesian multiple hypothesis testing p 391 A92-24747
Failure detection of engine sensors with a bank of Kalman filters p 392 A92-24748
A simplified method of transient mathematical model for non-augmentation engine p 372 A92-24750
Single lever power management of turboprop engines p 372 A92-25373
Optically powered and interrogated rotary position sensor for aircraft engine control applications p 370 A92-27777
A framework for the analysis of airframe/engine interactions and integrated flight/propulsion control p 478 A92-29120
Real-time simulation and adaptive PID control of QSK-06A control for gas turbine p 470 A92-29740
Electronic control of a turbine power unit p 470 A92-29741
On modelling of aero-gas turbine engine for real-time digital simulator --- of engine control system p 471 A92-29743
The effect of air-compressor adjustment by means of air-bleed on the reserve of its stable operation p 471 A92-29973
Rule based identifier for unknown systems p 509 A92-31430
An aircraft controller and its development p 558 A92-35917
Distributed health management systems technology for future propulsion control systems
[SAE PAPER 912167] p 655 A92-39995
Single lever power management of turboprop engines
[SAE PAPER 912200] p 656 A92-40013
British Airways Airbus A320 pilots' autothrust survey
[SAE PAPER 912225] p 636 A92-40023
Integrated flight/propulsion control for supersonic STOVL aircraft p 872 A92-45320
ASTOVL engine control p 860 A92-45321
Space Shuttle Orbiter auxiliary power unit status
[SAE PAPER 912060] p 889 A92-45442
Fiber optic controls for aircraft engines - Issues and implications p 856 A92-46244
Integrated optic components for advanced turbine engine control systems p 925 A92-46248
Fiber optic speed sensor for advanced gas turbine engine control p 857 A92-48044
Fiber-optic pressure sensor system for gas turbine engine control p 857 A92-48047
Optics in aircraft engines p 926 A92-48500
Summary of the effects of engine throttle response on airplane formation-flying qualities
[AIAA PAPER 92-3318] p 877 A92-48902
Derivation of ABCD system matrices from nonlinear dynamic simulation of jet engines
[AIAA PAPER 92-3319] p 923 A92-48903
A simplified real-time engine model for developing aeroengine control system
[AIAA PAPER 92-3321] p 864 A92-48904
Design issues in a fiber optic sensor system architecture for aircraft engine control
[AIAA PAPER 92-3483] p 866 A92-49023
Intelligent Engine Control (IEC)
[AIAA PAPER 92-3484] p 866 A92-49024
Subsonic flight test evaluation of a performance seeking control algorithm on an F-15 airplane
[AIAA PAPER 92-3743] p 878 A92-49109
Thrust stand evaluation of engine performance improvement algorithms in an F-15 airplane
[AIAA PAPER 92-3747] p 866 A92-49111
Compensating for manufacturing and life-cycle variations in aircraft engine control systems
[AIAA PAPER 92-3869] p 868 A92-49139
Piloted evaluation of an integrated propulsion and flight control simulator
[AIAA PAPER 92-4178] p 960 A92-52459
Simulation analysis of the influence of variation in some selected design and control parameters on the acceleration time of a turbojet engine p 970 A92-52890
In-flight optimization of the total propulsion system
[AIAA PAPER 92-3744] p 1068 A92-54146
In-flight performance diagnostic capability of an adaptive engine model
[AIAA PAPER 92-3746] p 1068 A92-54147
Propulsion system performance resulting from an Integrated Flight/Propulsion Control design
[AIAA PAPER 92-4602] p 1069 A92-55281
Flight simulation modeling in support of engine/airframe integration p 1055 A92-56279
Parallel processing applications for gas turbine engine control p 25 N92-11012
Control of a helicopter engine in low altitude flight p 562 N92-23122
ASTOVL engine control
[PNR-90808] p 740 N92-27040
Integrated flight propulsion control research results using the NASA F-15 HIDEC Flight Research Facility
[NASA-TM-4394] p 740 N92-27379
Subsonic flight test evaluation of a performance seeking control algorithm on an F-15 airplane
[NASA-TM-4400] p 973 N92-31275
Piloted evaluation of an integrated propulsion and flight control simulator
[NASA-TM-105797] p 1088 N92-34107

ENGINE COOLANTS
The influence of density difference between hot and coolant gas on film cooling by a row of holes - Predictions and experiments
[ASME PAPER 91-GT-255] p 151 A92-15660

Discharge coefficients of cooling holes with radiused and chamfered inlets
[ASME PAPER 91-GT-269] p 151 A92-15667
Conjugate conduction/convection/nucleate-boiling heat transfer with a high-speed boundary layer
[AIAA PAPER 91-5033] p 215 A92-17823
Analysis of cooling systems for hypersonic aircraft
[AIAA PAPER 91-5063] p 216 A92-17843
Thermal management for a Mach 5 cruise aircraft using endothermic fuel p 736 A92-41225
An experimental investigation of high-aspect-ratio cooling passages
[AIAA PAPER 92-3154] p 890 A92-48780

ENGINE DESIGN
P&W F119 - Vectored thrust for the F-22 p 25 A92-13219
The performance evaluation of aeroderivative gas turbines p 119 A92-13296
Tiger MGB - High reliability low weight --- military helicopter Main Gear Box p 109 A92-14418
Test results of the expander cycle air turbo ramjet for a future space plane
[IAF PAPER 91-271] p 120 A92-14709
Wave engine aerothermodynamic design
[ASME PAPER 91-GT-4] p 120 A92-15502
Design method for subsonic and transonic cascade with prescribed Mach number distribution
[ASME PAPER 91-GT-18] p 67 A92-15509
Computation of flow past a turbine blade with and without tip clearance
[ASME PAPER 91-GT-56] p 68 A92-15534
Future trends in turboshaft engines up to 5000 horsepower class
[ASME PAPER 91-GT-74] p 122 A92-15543
An improved method for aerodynamic design of centrifugal impeller blades
[ASME PAPER 91-GT-76] p 69 A92-15545
Three dimensional flow in a linear compressor cascade at design conditions
[ASME PAPER 91-GT-114] p 70 A92-15565
Similarity transformations for compressor blading
[ASME PAPER 91-GT-123] p 70 A92-15568
Analysis and prediction of transonic turbine blade losses
[ASME PAPER 91-GT-183] p 73 A92-15615
Interactive engine system dynamics analysis
[ASME PAPER 91-GT-193] p 124 A92-15619
A direct optimization procedure for spanwise work distribution in non-free vortex turbine stages
[ASME PAPER 91-GT-204] p 124 A92-15626
A chambered porous damper for rotor vibration control. I - Concept development
[ASME PAPER 91-GT-244] p 150 A92-15649
LDV measurements of a mixed-flow impeller at design and near stall
[ASME PAPER 91-GT-310] p 153 A92-15688
Garrett GTP50-1 multipurpose small power unit technology demonstrator program
[ASME PAPER 91-GT-328] p 153 A92-15698
Preliminary design of axial compressors using artificial intelligence and numerical optimization techniques
[ASME PAPER 91-GT-334] p 126 A92-15699
Off-design performance prediction of turbofans using gasdynamics
[ASME PAPER 91-GT-389] p 126 A92-15721
Liquid cooled turbocharged propulsion system for HALE application
[ASME PAPER 91-GT-399] p 127 A92-15729
Engineering model for analysis of scramjet combustor performance with finite-rate chemistry p 129 A92-17202
Role of dynamic simulation in fighter engine design and development p 277 A92-21080
Research on supersonic combustion
[AIAA PAPER 92-0001] p 278 A92-22126
The position of the unsteady flow computation in the compressor and turbine design and analysis process
[AIAA PAPER 92-0015] p 278 A92-22137
Cold-cycle pressure-jet helicopters - Ventures, designs, and developments. II - Design p 271 A92-22712
Prediction of low cycle fatigue life of engine cases p 295 A92-23385
Study on the reliability evaluation of engine fuel accessories p 392 A92-24749
Influence of air liquefaction cycle on performance of combined cycle engine p 372 A92-24878
Thermal management systems for high Mach airbreathing propulsion
[AIAA PAPER 92-0515] p 373 A92-26941
CUSAE '91; Proceedings of the 1st China-USSR Seminar on Aero Engines, Nanjing, People's Republic of China, Apr. 15-20, 1991 p 469 A92-29709
On the experimental investigation of air-breathing engine of new schemes p 469 A92-29711
Simulation of vibrational status of gas-turbine engine p 470 A92-29731
Russians say D-30F6 engine used in MiG-31 is highly reliable p 472 A92-32298
Saturn/Lyulka diversifies business to cope with Russian economic crisis p 472 A92-32299
Russia bids to salvage development of Soyuz-powered VTOL fighter p 472 A92-32300
Integration of artificial intelligence and numerical optimization techniques for the design of complex aerospace systems
[AIAA PAPER 92-1189] p 600 A92-33301
Applications of Busemann inlet designs for flight at hypersonic speeds
[AIAA PAPER 92-1210] p 517 A92-33314
Design and analysis of reengine Boeing 727-100 center inlet S duct by a reduced Navier-Stokes code
[AIAA PAPER 92-1221] p 517 A92-33320
The engine inside p 558 A92-36126
Advanced propulsion systems for large subsonic transports p 653 A92-36977
Research and development of turbofan engine for supersonic aircraft p 654 A92-38025
Challenging power-density requirements for future fighter APUs
[SAE PAPER 912177] p 655 A92-40002
Secondary power system preliminary design
[SAE PAPER 912189] p 656 A92-40008
Single lever power management of turboprop engines
[SAE PAPER 912200] p 656 A92-40013
Pressurization effects in kinematic heat engines p 696 A92-40866
Pusher turboprop installation technology for the Embraer CBA-123 vector
[SAE PAPER 911030] p 658 A92-40943
Operational progress of the STOL research aircraft Asuka p 730 A92-43138
Aerodynamic design of an advanced turboprop using Euler codes p 737 A92-43196
Row-by-row off-design performance calculation method for turbines p 737 A92-44514
VSTOL engine design evolution - Growth of the Pegasus engine for Harrier p 860 A92-45306
Current technology propulsion systems meet the STOVL window of opportunity p 860 A92-45307
A USAF assessment of STOVL fighter options p 842 A92-45310
Hot-gas reingestion - Engine response considerations p 860 A92-45317
Suppression of fatigue-inducing cavity acoustic modes in turbofan engines p 925 A92-46809
CIS engines. I - The range revealed p 786 A92-47821
The impact of advanced materials on small turbine engines
[SAE PAPER 911207] p 862 A92-48021
Design and test of an Active Tip Clearance System for centrifugal compressors
[AIAA PAPER 92-3189] p 863 A92-48801
Aero mechanics in the twenty-first century
[AIAA PAPER 92-3194] p 863 A92-48805
A comparative study of scramjet injection strategies for high Mach numbers flows
[AIAA PAPER 92-3287] p 904 A92-48876
Investigation of three-dimensional flow field in a turbine including rotor/stator interaction. I - Design development and performance of the research facility
[AIAA PAPER 92-3325] p 883 A92-48908
Advanced Rotorcraft Transmission program summary
[AIAA PAPER 92-3363] p 905 A92-48936
Boeing Helicopters Advanced Rotorcraft Transmission (ART) Program summary of component tests
[AIAA PAPER 92-3364] p 905 A92-48937
Analysis of a hydrocarbon scramjet with augmented preburning
[AIAA PAPER 92-3425] p 865 A92-48984
Restart of theory of air-breathing engines
[AIAA PAPER 92-3472] p 906 A92-49018
Naval aircraft/engine mission payoff analyses
[AIAA PAPER 92-3473] p 865 A92-49019
Analytical design and demonstration of a low-cost expendable turbine engine combustor
[AIAA PAPER 92-3754] p 867 A92-49112
Generators inside small engines
[AIAA PAPER 92-3755] p 867 A92-49113
Emerging technologies for gas turbine engines - U.A.V. synergies
[AIAA PAPER 92-3757] p 867 A92-49114
Conceptual study of separated core ultra high bypass engine
[AIAA PAPER 92-3775] p 867 A92-49119
Design and off-design point characteristics of Separated Core Ultra High Bypass Engine (SCUBE)
[AIAA PAPER 92-3776] p 867 A92-49120
Application of an unsteady Navier-Stokes solver to transonic turbine design p 935 A92-50273
Simulation analysis of the influence of variation in some selected design and control parameters on the acceleration time of a turbojet engine p 970 A92-52890
The VRT gas turbine combustor - Phase II
[AIAA PAPER 92-3471] p 1067 A92-54035
The study of experimental turboramjets
[AIAA PAPER 92-3720] p 1067 A92-54135
Improvements in teaching aircraft engine design
[AIAA PAPER 92-3758] p 1141 A92-54152
Development of ITS90 small gas turbine engine p 1070 A92-55500
'A new proposal for an old problem' - The right engine for the right helicopter p 1070 A92-56281
V-22 propulsion system design p 1070 A92-56300
Description of a pressure measurement technique for obtaining surface static pressures of a radial turbine
[AIAA PAPER 92-4006] p 1123 A92-56829
Structural tailoring of advanced turboprops (STAT): User's manual
[NASA-CR-187101] p 26 N92-11016
Engine dynamic analysis with general nonlinear finite element codes
[NASA-CR-187222] p 44 N92-11379
Gas turbine engine control
[PATENT-1-274-606] p 130 N92-13069
International aviation (selected article)
[AD-A240987] p 170 N92-13992
Theoretical models for duct acoustic propagation and radiation p 236 N92-14782
Study of the engine bird ingestion experience of the Boeing 737 aircraft
[DOT/FAA/CT-89/16] p 187 N92-15053
Army research concerns in engine sealing p 228 N92-15089
Underwater turbojet engine
[AD-D015017] p 279 N92-15992
Program plans: Aviation safety research
[NIAR-91-30] p 264 N92-17587
Advanced tactical fighter engine
[ETN-92-90840] p 376 N92-18728
AGARD/SMP Review: Damage Tolerance for Engine Structures. 4: Reliability and Quality Assurance
[AGARD-R-773] p 402 N92-19004
Introduction: Needs and approaches to reliability and quality assurance in design and manufacture p 402 N92-19005
Engine Structures Modeling Software System (ESMOSS)
[NASA-CR-187227] p 404 N92-19277
Component-specific modeling --- jet engine hot section components
[NASA-CR-189088] p 377 N92-19726
Materials and process directions for advanced aero-engine design
[PNR-90814] p 378 N92-19938
Use of CFD in the design of a modern multistage aero engine LP turbine design
[PNR-90862] p 472 N92-20179
Currently available fuel gas booster compressor equipment for small gas turbine engines
[PB92-127026] p 499 N92-20265
The 60 years of Bristol engines
[PNR-90845] p 473 N92-20460
Holographic flow visualization in rotating turbomachinery
[PNR-90837] p 500 N92-20491
Application of a water droplet trajectory prediction code to the design of inlet particle separator anti-icing systems
[PNR-90839] p 474 N92-20573
The NASA hypersonic research engine program p 474 N92-21521
Hypersonic airbreathing propulsion/airframe integration p 474 N92-21522
Cryogenic hydrogen-induced air-liquefaction technologies for combined-cycle propulsion applications p 487 N92-21526
H2-fueled high-bypass turbofan p 475 N92-21529
H2 fueled flightweight ramjet construction and test p 475 N92-21531
Scramjet analysis, testing p 475 N92-21532
NASA's hypersonic propulsion program: History and direction p 476 N92-21535
Metal-metal bondline NDE methods
[AD-A244429] p 503 N92-21730
Compressing the compressor
[PNR-90824] p 476 N92-21848
The evolution of the bypass engine
[PNR-90832] p 476 N92-21850
Impact of regulation changes on engine design and certification
[PNR-90789] p 559 N92-22098
Principles and computer simulations of intercooled-turbocharged gas generator/expander engine p 592 N92-22132

Aeropropulsion 1987
[NASA-CP-3049] p 559 N92-22510
Ceramics for engines p 578 N92-22517
Overview of the subsonic propulsion technology session p 560 N92-22531
Small engine technology programs
p 560 N92-22532
Propulsion challenges and opportunities for high-speed transport aircraft p 561 N92-22540
Supersonic throughflow fans for high-speed aircraft
p 561 N92-22541
Effects of turbine cooling assumptions on performance and sizing of high-speed civil transport
[NASA-TM-105610] p 562 N92-23537
A multiblock grid generation technique applied to a jet engine configuration p 692 N92-24428
Description of a pressure measurement technique for obtaining surface static pressures of a radial turbine
[NASA-TM-105643] p 680 N92-24959
Advanced Turbine Technology Applications Project (ATTAP)
[NASA-CR-189142] p 682 N92-25649
Algorithmic development in structures technology
p 684 N92-25924
Computational structural analysis and advanced commercial engines p 660 N92-25933
Military engine computational structures technology
p 660 N92-25934
Development of natural gas rotary engines
[PB92-149665] p 765 N92-26816
VSTOL engine design evolution: Growth of the Pegasus engine for Harrier
[PNR-90805] p 739 N92-27039
ASTOVL engine control
[PNR-90808] p 740 N92-27040
Simultaneous engineering in aero-gas turbine design and manufacture
[PNR-90811] p 740 N92-27043
The changing role of experimentation in aeroengine R and D: The point of view of the research worker
[AD-A246372] p 740 N92-27062
Users manual and modeling improvements for axial turbine design and performance computer code TD2-2
[NASA-CR-189118] p 716 N92-27376
Application of CFD in the design of gas turbine engine components p 741 N92-27461
Feasibility of magnetic bearings for advanced gas turbine engines p 772 N92-27738
Steady and Transient Performance Prediction of Gas Turbine Engines
[AGARD-LS-183] p 868 N92-28458
Overview on basis and use of performance prediction methods p 869 N92-28459
Practical considerations in designing the engine cycle
p 869 N92-28460
Component performance requirements
p 869 N92-28462
Dynamic simulation of compressor and gas turbine performance p 869 N92-28463
Contingency power for a small turboshaft engine by using water injection into turbine cooling air
[NASA-TM-105680] p 871 N92-29661
Users manual for updated computer code for axial-flow compressor conceptual design
[NASA-CR-189171] p 924 N92-30207
Re-engining for real stage 3 compliance
[PNR-90872] p 1072 N92-33748
The Rolls-Royce Trent
[PNR-90875] p 1061 N92-33750
A graphical user-interface for propulsion system analysis
[NASA-TM-105696] p 1134 N92-33894

ENGINE FAILURE
An analytical study of the helicopter flight safety under an engine failure in proximity of ground
p 91 A92-14454
Implanted component faults and their effects on gas turbine engine performance
[ASME PAPER 91-GT-41] p 121 A92-15524
On-line distortion analysis system for inlet-engine testing
[ASME PAPER 91-GT-166] p 136 A92-15601
Stage-by-stage poststall compression system modeling technique p 80 A92-17194
Jet engine fault detection with discrete operating points gas path analysis p 129 A92-17200
Aeroengine sensor failure detection by Bayesian multiple hypothesis testing p 391 A92-24747
Integral minimization of engine fault equations based on least fault principle p 374 A92-27857
Dealing with pilot response in failure case testing
p 549 A92-35952
United 232 - Coping with the 'one-in-a-billion' loss of all flight controls p 530 A92-36349
Analytical condition inspection and extension of time between overhaul of F3-30 engine
[ASME PAPER 91-GT-277] p 653 A92-36888
Optimal measurement and health index selection for gas turbine performance status and fault diagnosis
[ASME PAPER 91-GT-294] p 653 A92-36889
Distributed health management systems technology for future propulsion control systems
[SAE PAPER 912167] p 655 A92-39995
Mathematical modeling of the flight of passenger aircraft in the case of engine failure p 875 A92-47777
Optimal control of helicopters following power failure
[AIAA PAPER 92-4471] p 1076 A92-55231
A simulation model for tail rotor failure
[AIAA PAPER 92-4633] p 1081 A92-55380
The advantages of digital engine control as compared with traditional systems (hydraulic or pneumatic)
p 1070 A92-56338
Smoothing CFM56 engine removal rate at USAir
[AIAA PAPER 92-3928] p 1070 A92-56759
Helicopter rejected takeoff airspace requirements
[SCT-91RR-28] p 116 N92-13058
Program plans: Aviation safety research
[NIAR-91-30] p 264 N92-17587
ETOPS: A developing scene
[PNR-90844] p 473 N92-20459
Statistics on aircraft gas turbine engine rotor failures that occurred in US commercial aviation during 1989
[DOT/FAA/CT-92/5] p 971 N92-30303
Bird ingestion into large turbofan engines
[DOT/FAA/CT-91/17] p 1043 N92-33005
Statistics on aircraft gas turbine engine rotor failures that occurred in US commercial aviation during 1988
[DOT/FAA/CT-91/28] p 1071 N92-33105

ENGINE INLETS
Distortion tolerance of the T800-LHT-800 turboshaft engine p 120 A92-14409
On-line distortion analysis system for inlet-engine testing
[ASME PAPER 91-GT-166] p 136 A92-15601
Analytical investigation of the rules of component matching in turbojet engines
[ASME PAPER 91-GT-170] p 123 A92-15605
Numerical study of branched turboprop inlet ducts using a multiple block grid procedure
[ASME PAPER 91-GT-339] p 76 A92-15703
A global approach in evaluating inlet/engine compatibility
[ASME PAPER 91-GT-402] p 127 A92-15732
Tangential mass addition for shock/boundary-layer interaction control in scramjet inlets p 80 A92-17197
Analysis of an advanced ducted propeller subsonic inlet
[AIAA PAPER 92-0274] p 318 A92-25728
An investigation of the swirl in an S-shaped inlet
p 343 A92-28476
Study of cavity pumping in supersonic internal flow
p 429 A92-30538
Numerical computation of supersonic intakes
p 430 A92-30539
Computation of scramjet inlet flow
p 430 A92-30541
Navier-Stokes simulation of flow through a highly contoured subsonic diffuser p 433 A92-31491
Design analysis of the T-800 inlet particle separator/air oil cooler blower p 579 A92-32556
Applications of Busemann inlet designs for flight at hypersonic speeds
[AIAA PAPER 92-1210] p 517 A92-33314
Structural tailoring/analysis for hypersonic components - Executive system development
[AIAA PAPER 92-2471] p 583 A92-34360
Study of weld offset in longitudinally welded SSME HPFTP inlet
[AIAA PAPER 92-2305] p 586 A92-34525
The development of an engine air particle separator system for the CH-47 helicopter p 545 A92-35736
The computation of three-dimensional flows using unstructured grids p 612 A92-37539
Influence of inlet conditions on the flowfield in a model gas turbine combustor p 672 A92-38866
LDV measurements of the flowfield in a simulated combustor with axial and side inlets p 672 A92-38867
Measurements and simulation of the flow around a poppet valve p 675 A92-40103
A study of three dimensional turbulent boundary layer separation and vortex flow control using the reduced Navier Stokes equations p 621 A92-40105
Surface cooling of scramjet engine inlets using heat pipe, transpiration, and film cooling p 763 A92-44381
Numerical simulation of aerothermal loads in hypersonic engine inlets due to shock impingement
[AIAA PAPER 92-2605] p 792 A92-45482
Coupled numerical simulation of the external and engine inlet flows for the F-18 at large incidence
[AIAA PAPER 92-2621] p 793 A92-45493
Design and analysis of vortex generators on reengined Boeing 727-100QF center inlet S-duct by a reduced Navier-Stokes code
[AIAA PAPER 92-2700] p 800 A92-45542
Interface of an uncoupled boundary layer algorithm with an inviscid core flow algorithm for unsteady supersonic engine inlets
[AIAA PAPER 92-3083] p 823 A92-48730
Internal shock interactions in propulsion/airframe integrated three-dimensional sidewall compression scramjet inlets
[AIAA PAPER 92-3099] p 824 A92-48741
FNS analysis of an axisymmetric scramjet inlet
[AIAA PAPER 92-3100] p 824 A92-48742
Operating characteristics at Mach 4 of an inlet having forward-swept, sidewall-compression surfaces
[AIAA PAPER 92-3101] p 863 A92-48743
Computational analysis of ramjet engine inlet interaction
[AIAA PAPER 92-3102] p 824 A92-48744
Computational icing analysis for aircraft inlets
[AIAA PAPER 92-3178] p 836 A92-48793
BUWICE - An interactive icing program applied to engine inlets
[AIAA PAPER 92-3179] p 922 A92-48794
A new vane swirler as applied to dual-inlet side-dump combustor
[AIAA PAPER 92-3654] p 906 A92-49085
Flow measurements in scramjet inlets
p 1102 A92-53565
Application of computational fluid dynamics to the study of vortex flow control for the management of inlet distortion
[AIAA PAPER 92-3177] p 1020 A92-54013
Results of a perturbation analysis correlating flows entering and exiting an aircraft inlet system
[AIAA PAPER 92-3624] p 1021 A92-54091
Comparison between computational and experimental data for a hypersonic laser propelled vehicle
[AIAA PAPER 92-3808] p 1023 A92-54179
Development and validation of a freejet technique for inlet-engine compatibility testing
[AIAA PAPER 92-3921] p 1033 A92-56752
Vortex generator design for aircraft inlet distortion as a numerical optimization problem p 194 N92-13959
Analysis of an advanced ducted propeller subsonic inlet
[NASA-TM-105393] p 179 N92-14002
Numerical investigations in three-dimensional internal flows
[NASA-CR-189467] p 221 N92-14313
Modification of Jindivik air intake duct with an auxiliary intake static aerodynamic tests
[AD-A243002] p 275 N92-17234
Optimization of tangential mass injection for minimizing flow separation in a scramjet inlet
[AD-A243868] p 376 N92-18867
Application of a water droplet trajectory prediction code to the design of inlet particle separator anti-icing systems
[PNR-90839] p 474 N92-20573
Air intakes for high speed vehicles
[AGARD-AR-270] p 445 N92-20797
Inlets, ducts, and nozzles p 593 N92-22523
Three-dimensional modeling of diesel engine intake flow, combustion and emissions
[NASA-CR-189126] p 658 N92-24539
Grid generation for a complex aircraft configuration
p 649 N92-25714
Hypersonic aerospace vehicle leading edge cooling using heat pipe, transpiration and film cooling techniques
p 780 N92-26733
Interface of an uncoupled boundary layer algorithm with an inviscid core flow algorithm for unsteady supersonic engine inlets
[NASA-TM-105684] p 739 N92-27037
The application of a Navier-Stokes CFD method to civil engine intake flows p 769 N92-27471
Computational modelling of turbulent flow in S-bends
p 769 N92-27480
Numerical investigations in three-dimensional internal flows
[NASA-CR-190498] p 998 N92-30380
Navier-Stokes analysis and experimental data comparison of compressible flow within ducts
[NASA-TM-105796] p 972 N92-30972
Application of computational fluid dynamics to the study of vortex flow control for the management of inlet distortion
[NASA-TM-105672] p 1128 N92-34112

ENGINE MONITORING INSTRUMENTS
Optimizing instrumentation when measuring jet engine blade vibration
[ASME PAPER 91-GT-71] p 148 A92-15540

A procedure for automated gas turbine blade fault identification based on spectral pattern analysis
[ASME PAPER 91-GT-259] p 151 A92-15661
A test bench for evaluating powerplant electrization
p 138 A92-16830
Aeroengine sensor failure detection by Bayesian multiple hypothesis testing p 391 A92-24747
Failure detection of engine sensors with a bank of Kalman filters p 392 A92-24748
An investigation of real-time diagnostic technique for DEEC system --- digital electronic engine control system
p 470 A92-29742
Engine maintenance technology and its development
p 516 A92-35918
The development and integration of an engine monitoring system for the F-14A+/D Super Tomcat
[SAE PAPER 912094] p 654 A92-39951
Distributed health management systems technology for future propulsion control systems
[SAE PAPER 912167] p 655 A92-39995
Cyclic fatigue behavior of silica fiber
p 754 A92-42040
The use of optical sensors and signal processing gas turbine engines p 856 A92-46247
Wind-tunnel compressor stall monitoring using neural networks p 918 A92-46817
Fiber optic speed sensor for advanced gas turbine engine control p 857 A92-48044
In-flight performance diagnostic capability of an adaptive engine model
[AIAA PAPER 92-3746] p 1068 A92-54147
Engine condition monitoring system for B747-400
p 1064 A92-56082
Smoothing CFM56 engine removal rate at USAir
[AIAA PAPER 92-3928] p 1070 A92-56759
Research sensors p 594 N92-22526
Engine performance and health monitoring models using steady state and transient prediction methods
p 870 N92-28467
Laser induced fluorescence detection of gums in jet fuels
[AD-A252685] p 987 N92-30767
Engine monitoring display study
[NASA-CR-4463] p 979 N92-32175

ENGINE NOISE
A low noise propulsion concept for the supersonic transport
[ASME PAPER 91-GT-397] p 127 A92-15727
Noise control used for turbojet engine test bench
p 284 A92-21749
Combat aircraft jet engine noise studies
[ONERA, TP NO. 1991-192] p 415 A92-26353
A survey of the broadband shock associated noise prediction methods
[AIAA PAPER 92-0501] p 415 A92-26930
NASA's quiet side. I p 607 A92-37875
Research on a low-noise engine for a high-speed VTOL aircraft p 737 A92-43239
The engineering prediction for aircraft noise
p 1010 A92-50206
The interaction between a high-frequency gust and a blade row p 1135 A92-54484
Experimental study of noise generation and propagation in a turbofan model p 1136 A92-56169
Combustion and core noise p 55 N92-10607
Design and performance of duct acoustic treatment
p 236 N92-14783
Quiet aircraft design and operational characteristics
p 236 N92-14787
A survey of the broadband shock associated noise prediction methods
[NASA-TM-105365] p 237 N92-14797
An evaluation of some alternative approaches for reducing fan tone noise
[NASA-TM-105356] p 416 N92-18282
MD-80 aft cabin noise control: A case history
p 1137 N92-32950

ENGINE PARTS
Calculation of the hardening factor for gas turbine engine components shot blasted in an ultrasonic field
p 38 A92-10850
Life time prediction for ceramic gas turbine components
[ASME PAPER 91-GT-96] p 122 A92-15560
Impact design methods for ceramic components in gas turbine engines
[ASME PAPER 91-GT-115] p 123 A92-15566
Ceramic component processing development for advanced gas-turbine engines
[ASME PAPER 91-GT-120] p 142 A92-15567
Development of silicon nitride rotors for the ATTAP program at Garrett Ceramic Components --- Advanced Turbine Technology Applications Project
[ASME PAPER 91-GT-154] p 142 A92-15590
Design and analysis of ceramic and CMC components for advanced gas turbines
[ASME PAPER 91-GT-156] p 142 A92-15592
Gas-generator with high-temperature path ceramic components
[ASME PAPER 91-GT-152] p 148 A92-15594
Development and characterization of high strength SiC rotors
[ASME PAPER 91-GT-191] p 149 A92-15617
NDE of advanced turbine engine components and materials by computed tomography
[ASME PAPER 91-GT-287] p 152 A92-15681
The use of NDE as a process development tool for ceramic engine components
[ASME PAPER 91-GT-290] p 152 A92-15682
Garrett GTP50-1 multipurpose small power unit technology demonstrator program
[ASME PAPER 91-GT-328] p 153 A92-15698
Ceramic matrix composites and its application in gas turbine engines
[ASME PAPER 91-GT-338] p 143 A92-15702
Advanced ceramic engine technology for gas turbines
[ASME PAPER 91-GT-368] p 153 A92-15716
Numerical simulation for various flowfields of aero-engine components p 200 A92-17503
Scramjet research at the National Aerospace Laboratory
[AIAA PAPER 91-5076] p 200 A92-17849
Holographic-interferometry methods employed for vibration-strength testing of aviation-engine workpieces
p 219 A92-20771
Development of film riding face seals for a gas turbine engine p 291 A92-21330
Mechanical testing of glass-ceramic matrix composites
[ONERA, TP NO. 1991-182] p 388 A92-26351
Experimental techniques for the assessment of fuel thermal stability
[AIAA PAPER 92-0685] p 389 A92-27052
Analytical condition inspection and extension of time between overhaul of F3-30 engine
[ASME PAPER 91-GT-277] p 653 A92-36888
Advances in aircraft component superplastic forming/diffusion bonding technology
[SAE PAPER 912216] p 674 A92-40018
Advanced balancing using laser machining
[SAE PAPER 912218] p 674 A92-40020
Basic study of adhesive bonding for fiber-composites - Adhesive bonding technologies on jet engine parts
p 764 A92-44733
Study of grinding process and strength for ceramic heat insulated engine
[SME PAPER MR91-177] p 897 A92-45260
Advanced superalloys for turbine blade and vane applications
[ONERA, TP NO. 1992-2] p 893 A92-48578
Manufacturing technology methodology for propulsion system parts
[AIAA PAPER 92-3525] p 906 A92-49048
The role of PM in the design of lightweight aircraft engine components p 991 A92-50137
Performance analysis of idealized scramjet
p 1066 A92-53493
Current repair technologies for jet engine components
p 1016 A92-56085
Smoothing CFM56 engine removal rate at USAir
[AIAA PAPER 92-3928] p 1070 A92-56759
Turbine engine hot-part temperature measurement techniques
[AIAA PAPER 92-3960] p 1122 A92-56788
Advanced nozzle and engine components test facility
[AIAA PAPER 92-3993] p 1099 A92-56816
Engine component instrumentation development facility at NASA Lewis Research Center
[AIAA PAPER 92-3995] p 1099 A92-56818
Description of a pressure measurement technique for obtaining surface static pressures of a radial turbine
[AIAA PAPER 92-4006] p 1123 A92-56829
Verification of NISA 2 and ENDURE fracture mechanics capability
[NRC-ST-621] p 159 N92-13453
Turbine engine diagnostics system study
[DOT/FAA/CT-91/16] p 202 N92-14064
Probabilistic lifing approach for aero engine disks made of powder nickel base alloys containing ceramic defects
p 226 N92-14424
Areas of seal R/D at GE p 228 N92-15094
Aging Aircraft NDI Development and Demonstration Center (AANC): An overview
[DE92-002358] p 241 N92-15962
Ceramic technology for Advanced Heat Engines Project
[DE92-002397] p 289 N92-16128
An analysis of the aircraft engine Component Improvement Program (CIP): A life cycle cost approach
[AD-A243346] p 280 N92-17729
The 3D inelastic analysis methods for hot section components
[NASA-CR-189089] p 402 N92-18971
AGARD/SMP Review: Damage Tolerance for Engine Structures. 4: Reliability and Quality Assurance
[AGARD-R-773] p 402 N92-19004
Engine Structures Modeling Software System (ESMOSS)
[NASA-CR-187227] p 404 N92-19277
Component-specific modeling --- jet engine hot section components
[NASA-CR-189088] p 377 N92-19726
Materials and process directions for advanced aero-engine design
[PNR-90814] p 378 N92-19938
Superplastic applications in aero engines
[PNR-90788] p 473 N92-20436
Fabrication and testing of corrosion resistant coatings --- for turbine engine components
[DE92-003553] p 490 N92-21063
Evaluation of an innovative high-temperature ceramic wafer seal for hypersonic engine applications
p 578 N92-22205
Life prediction technologies for aeronautical propulsion systems p 560 N92-22520
Optical measurement systems p 594 N92-22527
Small engine technology programs
p 560 N92-22532
Coupled multi-disciplinary simulation of composite engine structures in propulsion environment
[NASA-TM-105575] p 596 N92-23267
Description of a pressure measurement technique for obtaining surface static pressures of a radial turbine
[NASA-TM-105643] p 680 N92-24959
The cost of silicon nitride powder: What must it be to compete?
[DE92-008710] p 669 N92-25223
Engine component instrumentation development facility at NASA Lewis Research Center
[NASA-TM-105644] p 665 N92-25449
Advanced Turbine Technology Applications Project (ATTAP)
[NASA-CR-189142] p 682 N92-25649
Powder processing of aero-engine components
[PNR-90813] p 756 N92-27044
The changing role of experimentation in aeroengine R and D: The point of view of the research worker
[AD-A246372] p 740 N92-27062
Ceramic composites: Enabling aerospace materials
[NASA-TM-105599] p 756 N92-27378
Thermally sprayed coating systems for surface protection and clearance control applications in aero engines
[PNR-90802] p 741 N92-27422
An appraisal of cost-effectiveness models used in the Air Force and Navy aircraft engine component improvement programs
[AD-A245910] p 743 N92-28162
Calculation of installation effects within performance computer programs p 869 N92-28465
Turbine aircraft engine operational trending and JT8D static component reliability study
[DOT/FAA/CT-91/10] p 870 N92-28686
Aging aircraft NDI Development and Demonstration Center (AANC): An overview --- nondestructive inspection p 915 N92-30120
Research into improving the durability of the hot section in the aircraft turbine engine
[AD-A250342] p 973 N92-31439
Life prediction and constitutive models for engine hot section anisotropic materials program
[NASA-CR-189222] p 973 N92-31534
Life prediction and constitutive models for engine hot section anisotropic materials program
[NASA-CR-189223] p 1072 N92-33479

ENGINE STARTERS
Research on altitude simulation of starting for a single-spool small turbojet p 969 A92-49836

ENGINE TESTING LABORATORIES
Scramjet research at the National Aerospace Laboratory
[AIAA PAPER 91-5076] p 200 A92-17849
A conceptual study for future engine test facility
[AIAA PAPER 92-3992] p 1099 A92-56815

ENGINE TESTS
Distortion tolerance of the T800-LHT-800 turboshaft engine p 120 A92-14409
Test results of the expander cycle air turbo ramjet for a future space plane
[IAF PAPER 91-271] p 120 A92-14709
Investigation of engine thrust correlation methods for enclosed test cells
[ASME PAPER 91-GT-68] p 121 A92-15538

NASA low-speed centrifugal compressor for 3-D viscous code assessment and fundamental flow physics research
[ASME PAPER 91-GT-140] p 72 A92-15580
Turbine blade tip clearance improvement
[ASME PAPER 91-GT-164] p 123 A92-15599
On-line distortion analysis system for inlet-engine testing
[ASME PAPER 91-GT-166] p 136 A92-15601
Inlet flow angle determination of transonic compressor cascades
[ASME PAPER 91-GT-274] p 75 A92-15671
A universal turboprop engine dynamometer test cell
[ASME PAPER 91-GT-343] p 137 A92-15706
Inlet planar waves - A current perspective
[ASME PAPER 91-GT-400] p 76 A92-15730
Jet engine test system including expert system for diagnosis
[ASME PAPER 91-GT-408] p 137 A92-15737
Scramjet research at the National Aerospace Laboratory
[AIAA PAPER 91-5076] p 200 A92-17849
Determination of liquid water content in the AEDC engine test cells
[AIAA PAPER 92-0165] p 263 A92-23778
Surge-troubleshooting of a twin-spool turbojet engine tested at a high altitude test facility p 375 A92-28459
French research and technology program on advanced hypersonic propulsion
[AIAA PAPER 91-5003] p 471 A92-31683
Analytical condition inspection and extension of time between overhaul of F3-30 engine
[ASME PAPER 91-GT-277] p 653 A92-36888
An approach for evaluation of gas turbine deposition
[ASME PAPER 91-GT-214] p 653 A92-36890
Laser thermal simulation puts jet engines to the test p 663 A92-38129
Single engine testing of the F-14A(PLUS) airplane in the power approach configuration p 645 A92-40036
An experimental investigation of high-aspect-ratio cooling passages
[AIAA PAPER 92-3154] p 890 A92-48780
Engine fan blade low cycle fatigue testing
[AIAA PAPER 92-3478] p 866 A92-49021
Technical tools of test automation for gas-turbine engines based on cluster CAMAC modules with an increased number of channels p 980 A92-51348
Research capabilities of the NASA Langley 8-foot high temperature tunnel p 980 A92-51403
A comparison of the calculated and experimental off-design performance of a radial flow turbine
[AIAA PAPER 92-3069] p 1020 A92-54004
Effects of bleed air extraction of thrust levels on the F404-GE-400 turbofan engine
[AIAA PAPER 92-3092] p 1066 A92-54009
The study of experimental turboramjets
[AIAA PAPER 92-3720] p 1067 A92-54135
Conception of a UHB engine simulator for the essential characteristics of a true-scale engine --- ultrahigh bypass p 1090 A92-54322
Development of local nonintrusive measurements of inlet and exhaust flows for the ground testing of air-breathing engines
[AIAA PAPER 92-3899] p 1122 A92-56735
Test data models to characterize turbine engine operation in altitude test facilities
[AIAA PAPER 92-3917] p 1095 A92-56749
Development and validation of a freejet technique for inlet-engine compatibility testing
[AIAA PAPER 92-3921] p 1033 A92-56752
Thrust stand design principles
[AIAA PAPER 92-3976] p 1098 A92-56802
Turbine engine performance test and evaluation techniques
[AIAA PAPER 92-3977] p 1071 A92-56803
A model study on diffuser pressure recovery in NAL scramjet test facility with simulated hydrogen combustion
[AIAA PAPER 92-3979] p 1071 A92-56805
Small engine components test facility compressor testing cell at NASA Lewis Research Center
[AIAA PAPER 92-3980] p 1098 A92-56806
Engine component instrumentation development facility at NASA Lewis Research Center
[AIAA PAPER 92-3995] p 1099 A92-56818
Application of electronically scanned pressure measurement system for engine simulation tests in the German-Dutch Wind Tunnel
[AIAA PAPER 92-4003] p 1122 A92-56826
Tests results on Air Turbo Ramjet for a future space plane
[IAF PAPER 92-0657] p 1071 A92-57098
Humidity effects on gas turbine performance
[NRC-30241] p 130 N92-11998
Fuel flow measurement in gas turbine testing
[NRC-29808] p 130 N92-12000
A derivation of gross thrust for a sea-level jet engine test cell
[NRC-30165] p 130 N92-12001
Aerospace technology: Technical data and information on foreign test facilities
[GAO/NSIAD-90-71FS] p 139 N92-13076
Seal development activities at Allison Turbine Division p 228 N92-15093
H2 fueled flightweight ramjet construction and test p 475 N92-21531
Scramjet analysis, testing p 475 N92-21532
Hypersonic propulsion research p 561 N92-22543
Engine component instrumentation development facility at NASA Lewis Research Center
[NASA-TM-105644] p 665 N92-25449
Advanced Turbine Technology Applications Project (ATTAP)
[NASA-CR-189142] p 682 N92-25649
Acoustic interactions between an altitude test facility and jet engine plumes: Theory and experiments
[NASA-CR-190423] p 738 N92-26405
VSTOL engine design evolution: Growth of the Pegasus engine for Harrier
[PNR-90805] p 739 N92-27039
The changing role of experimentation in aeroengine R and D: The point of view of the research worker
[AD-A246372] p 740 N92-27062
A comparison of the calculated and experimental off-design performance of a radial flow turbine
[NASA-CR-189207] p 831 N92-29402
Effects of bleed air extraction on thrust levels on the F404-GE-400 turbofan engine
[NASA-TM-104247] p 871 N92-29425
Small engine components test facility compressor testing cell at NASA Lewis Research Center
[NASA-TM-105685] p 982 N92-30508

ENGINEERING DRAWINGS
Standard for aerodynamic decelerator and parachute drawings --- Book
[ISBN 0-930403-94-0] p 634 A92-38000

ENGINEERING MANAGEMENT
Producibility Demonstrator Program - Technological preeminence through concurrent engineering p 146 A92-14449
An alternative source of flight test services
[AIAA PAPER 92-1088] p 515 A92-33254
BA's 777 p 958 A92-51580
Simultaneous engineering in aero-gas turbine design and manufacture
[PNR-90811] p 740 N92-27043
Profile of an effective engineering manager
[AD-A246525] p 781 N92-27528
NASA engineers and the age of Apollo
[NASA-SP-4104] p 929 N92-28344

ENTHALPY
Calculation of the base pressure and enthalpy behind a step in the path of two supersonic streams with allowance for the effect of boundary layers and heat fluxes p 63 A92-13748
An algebraic model for dissipation in supersonic boundary layers
[AIAA PAPER 92-0311] p 320 A92-25759
Enthalpy damping for high Mach number Euler solutions p 330 A92-26402
Development of an electrothermal de-icing/anti-icing model
[AIAA PAPER 92-0526] p 351 A92-26949
Supersonic combustor testing using optical diagnostics and a high enthalpy shock tunnel
[AIAA PAPER 92-0761] p 384 A92-27102
Strain-induced extinction of hydrogen-air counterflow diffusion flames - Effects of steam, CO2, N2, and O2 additives to air
[AIAA PAPER 92-0877] p 487 A92-29639
Test on high enthalpy hypersonic flow using a ballistic range p 747 A92-43097
Laminar heat transfer to blunt cones in high-enthalpy hypervelocity flows p 713 A92-44372
Separated high enthalpy dissociated laminar hypersonic flow behind a step - Pressure measurements p 809 A92-45858
Measurement of shock-wave/boundary-layer interaction in a free-piston shock tunnel p 813 A92-46903
The high enthalpy shock tunnel in Goettingen
[AIAA PAPER 92-3942] p 1104 A92-56772
High enthalpy nozzle flows p 182 N92-15000
High enthalpy testing in the Aachen (Fed. Republic of Germany) shock tunnel TH 2 p 208 N92-15021
Perspectives on hypersonic viscous and nonequilibrium flow research
[NASA-CR-190817] p 1039 N92-33413

ENTRAINMENT
Jet inflow simulation and its downwash effect on lifting surfaces p 9 A92-13200
Analysis of a dusty wall jet
[NASA-CR-189759] p 257 N92-15965

ENTROPY
Influence of the entropy layer on the separation length in hypersonic aerodynamics in the triple-deck framework. II p 63 A92-13815
Laser-initiated conical detonation wave for supersonic combustion. III
[AIAA PAPER 92-3247] p 893 A92-48846
Calculation of hypersonic leeside vortices over blunt delta wings p 84 N92-13004
Inlet technology p 447 N92-21528

ENTRY GUIDANCE (STS)
Space shuttle entry terminal area energy management
[NASA-TM-104744] p 308 N92-19930

ENVIRONMENT EFFECTS
Environmental impact of a future supersonic transport aircraft
[ONERA, TP NO. 1991-132] p 161 A92-16108
Supersonic transport in the 21st century p 308 A92-26793
Designing a methodology for future air travel scenarios p 409 N92-19125
Ozone response to aircraft emissions: Sensitivity studies with two-dimensional models p 409 N92-19126
The environmental impact of commercial aviation: The evolution of exhaust emissions legislation and control technology
[PNR-90847] p 505 N92-20574
Analysis of measured environmental noise levels: An assessment of the effects of airbase operational model variables on predicted noise exposure levels
[AD-A244805] p 485 N92-21720
Paint removal using cryogenic processes
[AD-A247668] p 895 N92-28912
Wind tunnel aerodynamic characteristics of a transport-type airfoil in a simulated heavy rain environment
[NASA-TP-3184] p 948 N92-31532
NASA High Speed Research Program, Emissions Scenarios Committee report of meetings on 26 September 1991 and 9 January 1992
[NASA-CR-190379] p 1004 N92-32147
Fluid effects: Thermoset and thermoplastic matrix composites p 1110 N92-33049
Flight service environmental effects on composite materials and structures p 1110 N92-33054
The impact of air transport on the environment
[PNR-90876] p 1129 N92-33751

ENVIRONMENT MANAGEMENT
Reducing environmental noise impacts: A USAREUR noise management program handbook
[AD-A240797] p 237 N92-14791
Environmentally sound
[PNR-90776] p 506 N92-21743

ENVIRONMENT POLLUTION
Aircraft gas turbine emissions: Their nature, technology for reduction, and a pollution comparison with channel tunnel transport
[ETN-92-91056] p 559 N92-22406
The impact of air transport on the environment
[PNR-90876] p 1129 N92-33751

ENVIRONMENT SIMULATION
Generic helicopter for multiship simulations
[AIAA PAPER 92-4151] p 959 A92-52442
Algorithmic improvements for simulator motion drive
[AIAA PAPER 92-4158] p 1007 A92-52448
Networked simulation of multiple aircraft using Semi-Automated Forces
[AIAA PAPER 92-4170] p 1008 A92-52455
Effect of a simulated glaze ice shape on the aerodynamic performance of a rectangular wing
[AIAA PAPER 92-4042] p 1035 A92-56861
Wind tunnel aerodynamic characteristics of a transport-type airfoil in a simulated heavy rain environment
[NASA-TP-3184] p 948 N92-31532

ENVIRONMENTAL CONTROL
Demonstration of gas liquid separation under the microgravity by aircraft KC-135
[SAE PAPER 912024] p 897 A92-45416
High-altitude lighter-than-air powered platform
[SAE PAPER 912054] p 844 A92-45438
Anodize and prime your aluminum without environmental headaches p 892 A92-47340

ENVIRONMENTAL MONITORING
Lower stratospheric measurement issues workshop report p 409 N92-19127

ENVIRONMENTAL SURVEYS
Reducing environmental noise impacts: A USAREUR noise management program handbook
[AD-A240797] p 237 N92-14791
High speed civil transport p 649 N92-25919

ENVIRONMENTAL TESTS
Designing through test
[AIAA PAPER 91-3822] p 232 A92-17664
The development and test of thermoplastic composite speed brake p 272 A92-24178

Environmental evaluation of repairs to fuselage lap joints p 699 A92-41534
Cost effectiveness of environmental stress screening (ESS) - A case history p 760 A92-42084
Research of environmental spectrum for aircraft structure p 785 A92-47655
Boiling and condensing pumped loop microgravity experiment - Challenges of testing in both aircraft and rocket environments p 992 A92-50611
A study on rotor induced sand and dust environment and its harmfulness to helicopter p 960 A92-53012
A common engineering-to-manufacturing-to-field test strategy to achieve systems readiness beyond the '90s p 931 A92-53111
Environmental fatigue tests with composite materials p 214 N92-14413
Comparison between hot/wet test and RT/dry test on the Seastar horizontal stabilizer and fin p 226 N92-14414
Evaluation of composite components on the Bell 206L and Sikorsky S-76 helicopters p 1107 N92-32575
Residual strength of repaired graphite/epoxy laminates after 5 years of outdoor exposure p 1108 N92-32577
Evaluation of the effects of the environment on the behavior of the primary structures of composite material aircraft in service: Historic and current situation p 1110 N92-33048

EPHEMERIDES
Compensating user position for GPS ephemeris error p 101 A92-16968
GPS orbit determination at the National Geodetic Survey p 1049 N92-33354
Precise GPS ephemerides from DMA and NGS tested by time transfer p 1049 N92-33355

EPOXY MATRIX COMPOSITES
Processing effects and damage tolerance in poly(etheretherketone) composites p 388 A92-26152
Impact damage tolerance of helicopter sandwich structures p 958 A92-51506
Organic Matrix Composite Helicopter Internal/External Cargo Pallet System (OMC INTEX)
[AD-A251127] p 961 N92-30878
A Protection And Detection Surface (PADS) for damage tolerance p 1107 N92-32523
Processing and environmental effects on mechanical properties of composite repairs
[NRC-LTR-ST-1826] p 1109 N92-32791

EPOXY RESINS
Minimum surface treatments for adhesively bonded repairs p 754 A92-42501
A damage tolerance assessment of bonded repairs to CF-18 composite components. Part 1: Adhesive properties
[DREP-TM-88-25-PT-1] p 143 N92-12060

EQUATIONS OF MOTION
Analysis of crash-resistant fuel systems and airframe structure interaction in a crash environment p 105 A92-14369
Control of the landing of a flight vehicle in the grazing-incidence mode p 134 A92-16808
Some considerations on modeling flight vehicles movement p 281 A92-21311
A new method for calculation of helicopter maneuvering flight p 282 A92-23382
Development of a combined fast method for studying the plane motions of rigid bodies in the atmosphere around the center of mass in the presence of perturbations p 304 A92-23563
Characteristics of the phugoid motion of nonmaneuverable aircraft p 480 A92-30190
The equations governing the motion of wing-aileron structural systems constructed from advanced anisotropic composite materials
[AIAA PAPER 92-2469] p 564 A92-34359
General model of isolated helicopter blade for stability investigation p 547 A92-35774
Calculation of rotational derivatives in the case of local interaction between flow and a body surface p 624 A92-40746
Analysis of airship lateral maneuverability
[AIAA PAPER 91-1274] p 743 A92-41212
Stability and inherent precision of two methods for solving motion and ablation equations for fireball-forming bodies in the earth atmosphere p 929 A92-46595
Aircraft stabilization at large angles of attack p 875 A92-47785
A study of supersonic flow over the ogival bodies with attached shock waves at zero incidence p 936 A92-51896
Modal simulation of gearbox vibration with experimental correlation
[AIAA PAPER 92-3494] p 1112 A92-54036
Effect of atmospheric disturbances on airplane response
[AIAA PAPER 92-4340] p 1078 A92-55329
Robust identification of nonlinear aerodynamic model structure
[AIAA PAPER 92-4503] p 1081 A92-55370
CH-53E/AV-8B aircraft sling load recovery system analysis
[AD-A239950] p 21 N92-10022
Numerical simulation of vortex street-edge interaction p 88 N92-13027
A numerical solution of implicit nonlinear equations of motion for rotor blades p 115 N92-13053
A wing rock model for the F-14A aircraft
[AD-A243109] p 275 N92-17300
Performance and stability analysis of the non-linear dynamics of a simple powered lifting hypersonic vehicle flying on a minor circle
[AD-A243933] p 366 N92-19192
Modal simulation of gearbox vibration with experimental correlation
[NASA-TM-105702] p 1002 N92-31485
Flutter analyses using high speed computers. Part 1: Flutter analyses for large aircraft p 1089 N92-34168

EQUATIONS OF STATE
Analysis of hypersonic nozzles including vibrational nonequilibrium and intermolecular force effects
[AIAA PAPER 92-0330] p 322 A92-25777

EQUILIBRIUM EQUATIONS
A unified numerical approach for the analysis of rotating disks including turbine rotors
[AIAA PAPER 92-2303] p 585 A92-34524
Equilibrium solution of the Euler and Navier-Stokes equations around a double ellipsoidal shape with mono- and multi-blocks including real gas effects, part 1 p 227 N92-15030

EQUILIBRIUM FLOW
Multidimensional Euler/Navier-Stokes analysis for hypersonic equilibrium gas
[SAE PAPER 912026] p 790 A92-45418
Computational study of the aerodynamics and control by blowing of asymmetric vortical flows over delta wings
[NASA-CR-187979] p 14 N92-10990

EQUILIBRIUM METHODS
Experimental determination of the center of mass, the principal central axes of inertia and moments of inertia --- aircrafttt models applied to real aircraf p 40 A92-12346
Aerodynamic design tool development for the calculation code of hypersonic flow p 711 A92-43198

EQUIPMENT SPECIFICATIONS
Integrated wiring system
[SAE PAPER 912058] p 897 A92-45440
Cost/benefit analysis of the AH-64 (Apache) helicopter Automated Test Equipment (ATE)
[AD-A252909] p 1101 N92-33398

EQUIVALENCE
A method of failure analysis of complicated structures p 901 A92-47656
Calculation methods on equivalence ratio of multi-propellant for propulsion system p 893 A92-48269

EROSION
Sand erosion behavior of GFRP p 576 A92-32662
Ground surface erosion - British Aerospace test facility and experimental studies p 881 A92-45323

ERROR ANALYSIS
The statistical estimation of navigation errors p 97 A92-16652
New practical method for measurement error determination in radar systems under real traffic conditions p 155 A92-17238
Computational mechanics today p 399 A92-28464
Error characteristics of a vortex panel method in two-dimensional flow p 421 A92-29521
Never make the same mistake twice - Using configuration control and error analysis to improve software quality p 601 A92-33603
Error estimation of INS ground alignment through observability analysis p 639 A92-40226
MLS system error model identification and synthesis p 639 A92-40232
Second order perturbation method of gas turbine performance calculation p 759 A92-41834
Estimation of spaceplane model inertia characteristics p 752 A92-43212
Tracking performance requirements for rotorcraft instrument approaches to reduced minima. Phase 1: Preliminary study
[NRC-32137-PHASE-1] p 102 N92-11988
MLS system error model identification and synthesis p 189 N92-14015
Public-sector aviation issues: Graduate research award papers, 1989 - 1990
[PB91-242271] p 308 N92-19662
Sensor fault detection on board an aircraft with observer and polynomial classifier
[DLR-FB-91-34] p 859 N92-29870
A continuing study of altitude determination deficiencies of the Service Aircraft Instrumentation Package (SAIP)
[AD-A245952] p 968 N92-32051
A Kalman filter integrated navigation design for the IAR Twin Otter Atmospheric Research Aircraft
[NRC-32148] p 1048 N92-32849
A review and discussion of flight management system incidents reported to the aviation safety reporting system
[AD-A252438] p 1043 N92-32941

ERROR CORRECTING CODES
A robust filter configuration for DGPS users p 101 A92-16967
Compensating user position for GPS ephemeris error p 101 A92-16968
Built-in testable error detection and correction p 394 A92-25846
An analysis of the sidewall boundary layer effect in two-dimensional wind tunnel testing p 626 N92-24856

ERROR CORRECTING DEVICES
An analysis of the sidewall boundary layer effect in two-dimensional wind tunnel testing p 626 N92-24856

ERROR DETECTION CODES
Failure detection of engine sensors with a bank of Kalman filters p 392 A92-24748
Failure detection and fault management techniques for flush airdata sensing systems
[AIAA PAPER 92-0263] p 369 A92-25719
Built-in testable error detection and correction p 394 A92-25846

ERROR FUNCTIONS
Estimation of aerodynamic characteristics from flight-test data. I - Multicollinearity in the equation error method p 960 A92-53007

ERRORS
Periodic trim solutions with hp-version finite elements in time p 874 A92-46931
Identification techniques: Frequency domain methods p 273 N92-17158
The effect of droplet sizing uncertainty on ice accretions p 679 N92-24874
Turbine aircraft engine operational trending and JT8D static component reliability study
[DOT/FAA/CT-91/10] p 870 N92-28686
A simplified dynamic model of the T700 turboshaft engine
[NASA-TM-105805] p 1009 N92-30898

ESCAPE CAPSULES
Investigation on opening and ejection of an aircraft canopy by using a solid rocket engine p 358 A92-28489
US Navy revisits escape modules p 849 A92-47975

ESCAPE SYSTEMS
ACES II PLUS ejection seat p 103 A92-13463
Progress report of Scot's Laser Ordnance Initiator System for crew escape p 580 A92-32988
JPATS escape system development p 543 A92-35434
Methods for predicting successful ejection seat canopy penetration p 544 A92-35441
Computational fluid dynamics as a tool for aerodynamic analysis of ejection seats p 519 A92-35444
Development of an emergency underwater escape breathing system for CH124 seaking aircrew
[DCIEM-87-TR-11] p 92 N92-13041
Ingress, emergency egress, and emergency evacuation testing of army aircraft
[AD-A246398] p 724 N92-27750

ESSENTIALLY NON-OSCILLATORY SCHEMES
Numerical experiments on a new class of nonoscillatory schemes
[AIAA PAPER 92-0421] p 341 A92-28193

ESTERS
Vinyl capped addition polyimides
[NASA-CASE-LEW-15027-2] p 579 N92-24053

ESTIMATES
Estimation of airborne performance in landing
[ESDU-91032] p 272 N92-15988
A demonstration of centimeter-level monitoring of polar motion with the Global Positioning System p 639 N92-24302
Current status of computational methods for transonic unsteady aerodynamics and aeroelastic applications p 718 N92-27937

ESTIMATING
Estimation of airborne performance in landing
[ESDU-91032] p 272 N92-15988
The application of statistical estimation techniques to terrain modeling
[AD-A243799] p 409 N92-19231
Estimating the reliability of a system on the basis of sample paths
[AD-A248585] p 774 N92-28171
An investigation of switched reluctance rotor position estimation using neural networks
[AD-A252846] p 1061 N92-33414

ESTIMATORS
A new class of gradient estimators for queueing systems with real-time constraints p 49 A92-11395
Robust wind shear stochastic controller-estimator p 661 A92-39893
ETHERS
Methyl-tert-butyl ether as a component of aviation gasolines p 34 A92-12146
ETHYLENE
Nonflammable hydraulic power system for tactical aircraft. Volume 2: Equipment and systems test and evaluation
[AD-A239805] p 35 N92-10100
EULER EQUATIONS OF MOTION
A spatial marching technique for the inviscid blunt body problem p 4 A92-10691
Implicit flux-split Euler schemes for unsteady aerodynamic analysis involving unstructured dynamic meshes p 5 A92-11057
Three-dimensional space-marching algorithm on unstructured grids p 5 A92-11058
Finite element solutions of the Euler equations for transonic external flows p 5 A92-11063
Euler code evaluation of a transatmospheric vehicle at supersonic speeds p 9 A92-13202
Aeroelastic analysis of wings using the Euler equations with a deforming mesh p 10 A92-13215
Extension of a three-dimensional Euler method for calculating the flowfield around bypass engines with fan and core jet p 62 A92-13690
Unsteady Euler calculations in 2-D internal aerodynamics with introduced vorticity
[ASME PAPER 91-GT-168] p 73 A92-15603
Euler flow predictions for an oscillating cascade using a high resolution wave-split scheme
[ASME PAPER 91-GT-198] p 74 A92-15623
Solution of the compressible Euler equations for steady flows around helicopter rotor blades by an implicit space-centered method
[ONERA, TP NO. 1991-177] p 77 A92-16139
Effect of nose shape on three-dimensional stagnation region streamlines and heating rates
[AIAA PAPER 91-5032] p 171 A92-17822
Aerodynamic sensitivity analysis methods for the compressible Euler equations p 233 A92-19619
Genuinely upwind algorithms for the multidimensional Euler equations p 175 A92-20733
Upwind scheme for solving the Euler equations on unstructured tetrahedral meshes p 175 A92-20735
Unsteady Euler analysis of the flowfield of a propfan at an angle of attack p 242 A92-21070
Steady supersonic and hypersonic flow computations using Eulerian and new Lagrangian formulations
[AIAA PAPER 92-0055] p 249 A92-22170
Mathematical modeling of supersonic flow over a convex-concave formed body based on the Euler and Navier-Stokes equations p 252 A92-23416
Unsteady Euler solution for oscillatory airfoil and oscillating flap
[AIAA PAPER 92-0131] p 252 A92-23751
Prediction of drag at subsonic and transonic speeds using Euler methods
[AIAA PAPER 92-0169] p 255 A92-23780
On marching algorithms for solving stationary problems p 311 A92-24976
LEWICE/E - An Euler based ice accretion code
[AIAA PAPER 92-0037] p 316 A92-25676
Calculation of the carriage loads of tandem stores on a fighter aircraft
[AIAA PAPER 92-0283] p 319 A92-25736
Euler calculations of axisymmetric under-expanded jets by an adaptive-refinement method
[AIAA PAPER 92-0321] p 321 A92-25768
A wave-model-based refinement criterion for adaptive-grid computation of compressible flows
[AIAA PAPER 92-0322] p 321 A92-25769
Unsteady blade pressures on a propfan at takeoff - Euler analysis and flight data
[AIAA PAPER 92-0376] p 372 A92-26234
Quality assessment of two- and three-dimensional unstructured meshes and validation of an upwind Euler flow solver
[AIAA PAPER 92-0444] p 328 A92-26288
Enthalpy damping for high Mach number Euler solutions p 330 A92-26402
Solution of the Euler and Navier-Stokes equations on MIMD distributed memory multiprocessors using cyclic reduction
[AIAA PAPER 92-0561] p 411 A92-26970
Numerical investigation of vortex breakdown on a delta wing p 340 A92-28027
Cartesian Euler method for arbitrary aircraft configurations p 340 A92-28039
Estimation of propulsion-induced effects on transonic flows over a hypersonic configuration
[AIAA PAPER 92-0523] p 341 A92-28197
Euler solutions for an unbladed jet engine configuration
[AIAA PAPER 92-0544] p 398 A92-28201
Improving the convergence rate of the Petrov-Galerkin techniques for the solution of transonic and supersonic flows p 434 A92-31495
Singularity bypass algorithms in the numerical solution of equations of body motion relative to a center of mass in the atmosphere in the presence of disturbances p 437 A92-31857
Calculation of three-dimensional separated flows in the framework of the unsteady Euler equations p 438 A92-31870
Unsteady transonic Euler solutions using finite elements
[AIAA PAPER 92-2504] p 518 A92-34499
Three-dimensional time-marching aeroelastic analyses using an unstructured-grid Euler method
[AIAA PAPER 92-2506] p 542 A92-34500
Finite element Euler calculations of unsteady transonic cascade flows
[AIAA PAPER 92-2120] p 520 A92-35689
Outflow boundary conditions for Euler analysis of flow in turbine scroll p 591 A92-36037
Efficient direct solvers for large-scale computational fluid dynamics problems p 690 A92-37534
A new finite element formulation for computational fluid dynamics. X - The compressible Euler and Navier-Stokes equations p 612 A92-37552
An information system for the numerical simulation of 3D Euler flows around aircraft p 613 A92-37554
A high-resolution Euler solver based on multigrid, semi-coarsening, and defect correction p 671 A92-37868
Solution of Euler equations for fighter forebody-inlet combinations at high angles of attack p 613 A92-38269
Numerical simulation of separation flow on bodies of revolution at high angle of attack using Euler equations p 616 A92-38919
Numerical predictions of transonic viscous flows around aerofoils through an Euler/boundary layer interaction method p 624 A92-40600
Numerical simulation of leading-edge vortex breakdown using an Euler code p 701 A92-41213
Wake effects on the prediction of transonic viscous flows around airfoils p 702 A92-41232
Accurate prediction of drag using Euler methods p 703 A92-41246
Domain-decomposition algorithm applied to multielement airfoil grids p 703 A92-41261
Minimum-drag bodies moving in locality-law media p 779 A92-42732
Numerical analysis of flow through oscillating cascade sections p 713 A92-44513
Computational aerodynamics in aircraft design - Challenges and opportunities for Euler/Navier-Stokes methods
[SAE PAPER 911990] p 788 A92-45392
Multidimensional Euler/Navier-Stokes analysis for hypersonic equilibrium gas
[SAE PAPER 912026] p 790 A92-45418
Practical design optimization of wing/body configurations using the Euler equations
[AIAA PAPER 92-2633] p 795 A92-45505
Shock fitting with a finite volume approximation to the Euler equations
[AIAA PAPER 92-2646] p 796 A92-45513
Investigation of solution operators for the three-dimensional Euler equations
[AIAA PAPER 92-2666] p 797 A92-45522
An unfactored implicit scheme for 3D inviscid transonic flows
[AIAA PAPER 92-2668] p 798 A92-45523
Spatial and temporal adaptive procedures for the unsteady aerodynamic analysis of airfoils using unstructured meshes
[AIAA PAPER 92-2694] p 800 A92-45540
A transonic/supersonic/hypersonic CFD analysis of the entry Space Shuttle Orbiter
[AIAA PAPER 92-2614] p 805 A92-45571
Application of the Euler method EUFLEX to a fighter-type airplane configuration at transonic speed
[AIAA PAPER 92-2620] p 845 A92-45573
A fast, implicit unstructured-mesh Euler method
[AIAA PAPER 92-2693] p 917 A92-45589
A compact higher order Euler solver for unstructured grids with curved boundaries
[AIAA PAPER 92-2696] p 807 A92-45590
An unstructured approach to the design of multiple-element airfoils
[AIAA PAPER 92-2709] p 807 A92-45592
Predicted pressure distribution on a prop-fan blade through Euler analysis p 810 A92-46791
Temporal adaptive Euler/Navier-Stokes algorithm involving unstructured dynamic meshes p 812 A92-46887
Compact higher order characteristic-based Euler solver for unstructured grids p 812 A92-46889
Parallel computing strategies for block multigrid implicit solution of the Euler equations p 812 A92-46894
Taylor series approximation of geometric shape variation for the Euler equations p 899 A92-46916
An Eulerian/Lagrangian method for computing blade/vortex impingement p 814 A92-46952
Initial validation of an unsteady Euler/Navier-Stokes flow solver for helicopter rotor airloads in forward flight p 815 A92-46956
Mesh adaption for 2D transsonic Euler flows on unstructured meshes p 816 A92-47038
Mesh adaptivity with the quadtree method p 816 A92-47041
A finite difference solution of the Euler equations on non-body-fitted Cartesian grids p 818 A92-47153
Application of non-reflecting boundary conditions to three-dimensional Euler equation calculations for thick strut cascades
[AIAA PAPER 92-3045] p 822 A92-48705
Improved artificial dissipation schemes for the Euler equations p 933 A92-49508
The simulation of inviscid, compressible flows using an upwind kinetic method on unstructured grids p 933 A92-49515
Transonic flow calculation of Euler equations by implicit iterating scheme with flux splitting p 934 A92-50215
Comparison of transonic flow models p 936 A92-50325
Solution of Euler equations with unstructured mesh - 3-D case p 941 A92-52973
Unsteady blade pressures on a propfan - Predicted and measured compressibility effects
[AIAA PAPER 92-3774] p 1023 A92-54161
Numerical simulation of supersonic unsteady flow using a panel method p 1030 A92-56048
Improved calculation of transonic potential flow past swept wings p 1031 A92-56179
Sound produced by vortex-airfoil interaction p 1136 A92-56345
Transonic and supersonic Euler computations of vortex-dominated flow fields about a generic fighter
[NASA-TP-3156] p 11 N92-10011
Numerical simulation of vortex breakdown by solving the Euler equations for an incompressible fluid p 41 N92-10163
Numerical simulation of vortex breakdown via 3-D Euler equations p 41 N92-10164
Euler solutions for an unbladed jet engine configuration
[NASA-TM-105332] p 44 N92-11328
Comparison of solution of various Euler solvers and one Navier-Stokes solver for the flow about a sharp-edged cropped delta wing
[AD-B163639L] p 83 N92-12998
Vortical flow simulation by using structured and unstructured grids p 83 N92-12999
Analysis of results of an Euler-equation method applied to leading-edge vortex flow p 84 N92-13000
Experimental and numerical investigation of the vortex flow over a delta wing at transonic speed p 84 N92-13001
Determination of vortex-breakdown criteria by solving the Euler and Navier-Stokes equations p 87 N92-13018
Investigation of vortex breakdown on a delta wing using Euler and Navier-Stokes equations p 87 N92-13019
Unsteady blade pressures on a propfan at takeoff: Euler analysis and flight data
[NASA-CR-189076] p 130 N92-13071
LEWICE/E: An Euler based ice accretion code
[NASA-TM-105389] p 179 N92-14001
Analysis tools of ONERA and DLR for the aerothermodynamics of reentry vehicles p 211 N92-14977
A multiblock flow solver for inviscid hypersonic flows p 181 N92-14986
Steps towards an efficient and accurate method solving the Euler equations around a re-entry configuration at super- and hypersonic speed p 181 N92-14987
Numerical simulations around models in hypersonic wind tunnels p 182 N92-14998
Hypersonic inviscid flow field simulations around reentry vehicles with flap deflection p 184 N92-15025
Equilibrium solution of the Euler and Navier-Stokes equations around a double ellipsoidal shape with mono- and multi-blocks including real gas effects, part 1 p 227 N92-15030
Grid impact on 3D hypersonic flows p 184 N92-15041

Zonal solutions for a double-ellipse in a hypersonic flowfield
[AERO-REPT-9009] p 345 N92-18233
Resolution of the Euler equations applied to a helicopter rotor in forward flight
[ONERA-RSF-2/3731-AY-004A] p 406 N92-19976
Extension of a three dimensional Euler-code for the investigation of the flow field around bypass engines with fan and core jet
[DLR-FB-91-13] p 503 N92-21699
Two-dimensional transonic flow calculation by interaction of Euler and boundary layer equations
[PB92-136449] p 448 N92-21784
Contributions of MBB-FE211 to the 2nd Antibes Workshop on Hypersonic Flows
[MBB-FE211-S-PUB-449] p 524 N92-22179
Case 7.4: Blunt nose delta wing Euler-boundary layer calculation p 525 N92-22184
Improved shock-capturing of Jameson's scheme for the Euler equations
[PB92-148758] p 596 N92-23251
A two-dimensional Euler solution for an unbladed jet engine configuration
[NASA-TM-105329] p 597 N92-23560
A user guide for the EMTAC-MZ CFD code
[NASA-CR-4283] p 678 N92-24242
A scheme for two dimensional Euler and boundary layer interactive solutions p 627 N92-24860
A two-dimensional Euler solution for an unbladed jet engine configuration p 627 N92-24861
Theoretical principles of a Euler method for the calculation of three dimensional flows
[F+W-TF-2012] p 767 N92-27045
On the computation of unsteady turbomachinery flows. Part 1: Euler equations in vibrating cascades
p 768 N92-27460
Unsteady Euler calculations in 3D internal aerodynamics p 768 N92-27470
Evaluation of an unsteady implicit Euler code against two and three-dimensional standard configurations
p 719 N92-27945
Analysis of results of an Euler-equation method applied to leading-edge vortex flow
[NLR-TP-90368-U] p 827 N92-28657
Development and validation of a characteristic boundary condition for a cell-centered Euler method
[NLR-TP-90144-U] p 828 N92-28692
Boundary conditions for Euler equations at internal block faces of multi-block domains using local grid refinement
[NLR-TP-90134-U] p 908 N92-28712
Spatial and temporal adaptive procedures for the unsteady aerodynamic analysis of airfoils using unstructured meshes
[NASA-TM-107635] p 831 N92-29445
Computation of unsteady transonic flows using an implicit centered Euler solver without artificial viscosity
[ESA-TT-1235] p 944 N92-30514
CFD contributions during hypersonic airplane intake design
[MBB/FE213/S/PUB/459] p 944 N92-30676
Euler solver for arbitrary configurations: Further applications p 949 N92-31888
An installed nacelle design code using a multiblock Euler solver. Volume 1: Theory document
[NASA-CR-189652-VOL-1] p 950 N92-32226
An installed nacelle design code using a multiblock Euler solver. Volume 2: User guide
[NASA-CR-189652-VOL-2] p 951 N92-32228

EULER-CAUCHY EQUATIONS
Limitations to the large strain theory
p 219 A92-20356

EULER-LAGRANGE EQUATION
Steady supersonic and hypersonic flow computations using Eulerian and new Lagrangian formulations
[AIAA PAPER 92-0055] p 249 A92-22170
Numerical simulation of droplet deformation in convective flows p 670 A92-36844
Estimation of aircraft inertial characteristics using maximum likelihood estimation p 1084 A92-56057
Numerical simulation of vortex street-edge interaction
p 88 N92-13027
Periodic Euler and Navier-Stokes solutions about oscillating airfoils p 626 N92-24850
A new Lagrangian method for real gases at supersonic speed p 633 N92-25814

EUROPE
Legal capacity of Eurocontrol to ensure smooth aviation in Europe p 167 A92-16134
Harmonisation and integration of air traffic control in Europe p 532 A92-33437
GPS - Can it contribute to European ATC?
p 637 A92-38380
Avionics standardization in Europe
p 199 N92-14050

EUROPEAN AIRBUS
Flying the A340 iron bird p 20 A92-10666
First flight for Airbus A340 p 21 A92-12750
The long-distance Airbus A340 - Europe's largest aircraft p 113 A92-17094
Airbus A340 - The first phase of flight testing
p 269 A92-21011
The TSE 310 troubleshooting expert prototype for the Airbus A-310 commercial aircraft p 307 A92-25180
New Airbus Industrie airliners on course for long-haul era p 308 A92-26792
The cockpit of a modern aircraft - The Airbus A340 considered as an example p 357 A92-26849
Airbus - The family expands p 419 A92-30092
ELS for the A340 --- Electronic Library System
[SAE PAPER 912111] p 651 A92-39963
Assembling the future p 783 A92-44895
Centre for Flight Simulation Berlin Airbus 340 simulator for research and training p 880 A92-45028
Airbus A319 - Completion of the standard fuselage family p 848 A92-47591
A340 handling, cockpit design improve on predecessor A320 p 849 A92-47969
Fatigue testing and tear down operations on Airbus A320 forward fuselage p 360 N92-18579

EUROPEAN SPACE AGENCY
Aerothermodynamic challenges for ESA programmes
p 180 N92-14974

EUROPEAN SPACE PROGRAMS
Aerothermodynamic challenges for ESA programmes
p 180 N92-14974

EUTECTIC ALLOYS
Cold-crucible directional solidification of refractory metal-silicide eutectics p 755 A92-43684

EVACUATING (TRANSPORTATION)
The effect on aircraft evacuations of passenger behaviour and smoke in the cabin p 834 A92-44998
Ingress, emergency egress, and emergency evacuation testing of army aircraft
[AD-A246398] p 724 N92-27750

EVALUATION
Development and evaluation of an onboard aircraft cabin water spray system for postcrash fire protection
[SAE PAPER 912224] p 636 A92-40022
1991-92 AHS Technical Committee highlights - Test and evaluation p 609 A92-40398
Operational evaluation of a tower workstation for clearance delivery p 879 A92-44981
The modelling of turbulence and downbursts for flight simulators
[UTIAS-339] p 161 N92-12373
An evaluation of the Royal Air Force Shorts Tucano Navigation Instruments Trainer: The NAVIT
[ETN-92-90841] p 354 N92-18729
Evaluation of the COMPAS experimental system
p 355 N92-19044
Evaluating the use of satellite communications in the government of Canada p 594 N92-22577
Aviation safety: Changes needed in FAA's service difficulty reporting program
[GAO/RCED-91-24] p 953 N92-31453
Estimation of aircraft attitude by angular rate measurements p 963 N92-31881

EVAPORATION
Microburst modelling and scaling p 915 A92-46262

EVAPORATION RATE
Radiant heat transfer in supersonic three-dimensional and axisymmetric flow of air past evaporating bodies
p 337 A92-27533

EXCITATION
The flip flop nozzle extended to supersonic flows
[AIAA PAPER 92-2724] p 803 A92-45561
Response of structures to galloping excitation: Background and approximate estimation
[ESDU-91010] p 399 N92-18091
Turbine blade tip and seal clearance excitation forces
[NASA-CR-184341] p 973 N92-31910

EXHAUST DIFFUSERS
Experimental study of an adjustable plane supersonic diffusor p 426 A92-30173
Theoretical analysis of a suction diffuser in the porous test section of a wind tunnel p 428 A92-30207
Limit point flow mode analysis of exhaust diffuser and operation characteristics of injector p 968 A92-49830

EXHAUST EMISSION
Applied analytical combustion/emissions research at the NASA Lewis Research Center - A progress report
[AIAA PAPER 92-3338] p 1067 A92-54025
Development of local nonintrusive measurements of inlet and exhaust flows for the ground testing of air-breathing engines
[AIAA PAPER 92-3899] p 1122 A92-56735
High-speed civil transport aircraft emissions
p 408 N92-19122
Natural cycles, gases p 408 N92-19123
Designing a methodology for future air travel scenarios p 409 N92-19125
Ozone response to aircraft emissions: Sensitivity studies with two-dimensional models p 409 N92-19126
Simulation of chemical kinetics in turbulent natural gas combustion
[PB92-123660] p 488 N92-20329
The environmental impact of commercial aviation: The evolution of exhaust emissions legislation and control technology
[PNR-90847] p 505 N92-20574
The environmental challenges for the next supersonic aircraft
[PNR-90782] p 505 N92-20928
Emissions from aircraft: Standards and potential for improvement
[PNR-90768] p 476 N92-21740
Aircraft gas turbine emissions: Their nature, technology for reduction, and a pollution comparison with channel tunnel transport
[ETN-92-91056] p 559 N92-22406
Propulsion challenges and opportunities for high-speed transport aircraft p 561 N92-22540
High speed civil transport p 649 N92-25919
Applied analytical combustion/emissions research at the NASA Lewis Research Center
[NASA-TM-105731] p 890 N92-29343
NASA High Speed Research Program, Emissions Scenarios Committee report of meetings on 26 September 1991 and 9 January 1992
[NASA-CR-190379] p 1004 N92-32147
The impact of air transport on the environment
[PNR-90876] p 1129 N92-33751

EXHAUST FLOW SIMULATION
Single expansion ramp nozzle simulations
[AIAA PAPER 92-0387] p 323 A92-26243
Flow in a ventral nozzle for short takeoff and vertical landing aircraft p 376 A92-28538
Navier-Stokes analysis of helicopter plume flowfield for infrared calculations
[AIAA PAPER 92-0983] p 580 A92-33185
A scramjet nozzle experiment with hypersonic external flow
[AIAA PAPER 92-3289] p 864 A92-48878

EXHAUST GASES
Impact of heterogeneous chemistry on model-calculated ozone change due to high speed civil transport aircraft
p 45 A92-12941
5,000-hour stability tests of metal sheathed thermocouples at respective temperatures of 538 C and 875 C
[ASME PAPER 91-GT-182] p 148 A92-15614
Hydrogen exhaust gas disposition by afterburning
[AIAA PAPER 91-5075] p 200 A92-17848
Hot gas environment around STOVL aircraft in ground proximity. I - Experimental study p 371 A92-24409
Carcinogenic hydrocarbons emission with gas-turbine engines exhaust gases p 504 A92-29726
The numerical method for calculating the flow field, temperature field and radiation fluxfield in the pipe
p 587 A92-35546
Numerical simulation of opposing sonic jets
p 524 A92-36357
A dynamic digital model for the turbojet with pulse-monitored fueller p 654 A92-38267
Configuration effects on the ingestion of hot gas into the engine intake p 842 A92-45315
A simplified reaction mechanism for prediction of NO(x) emissions in the combustion of hydrocarbons
[AIAA PAPER 92-3340] p 894 A92-48919
Degenerate four-wave mixing for measurement of NO2 and smoke concentration in jet engine exhaust
[AIAA PAPER 92-3658] p 1113 A92-54108
Smoothing CFM56 engine removal rate at USAir
[AIAA PAPER 92-3928] p 1070 A92-56759
Designing a methodology for future air travel scenarios p 409 N92-19125
Ozone response to aircraft emissions: Sensitivity studies with two-dimensional models p 409 N92-19126
Hot jet dilutor
[ETN-92-90860] p 366 N92-19225

EXHAUST NOZZLES
Off-design performance prediction of turbofans using gasdynamics
[ASME PAPER 91-GT-389] p 126 A92-15721
Propulsion aspects of hypersonic turbo-ramjet-engines with special emphasis on nozzle/aftbody integration
[ASME PAPER 91-GT-395] p 127 A92-15725
Effect of the blade height of the nozzle ring of axial-flow microturbines on the flow velocity factor and exit angle
p 128 A92-16831
Thrust nozzle test facility at DLR Cologne
[AIAA PAPER 91-5024] p 206 A92-17818
Hypersonic airbreathing propulsion activities for Saenger
[AIAA PAPER 91-5040] p 200 A92-17828

Computational analysis of drag reduction techniques for afterbody/nozzle/empennage configurations
[SAE PAPER 912127] p 618 A92-39974
Hot gas ingestion characteristics and flow visualization of a vectored thrust STOVL concept
p 860 A92-45316
Experimental and analytical study of close-coupled ventral nozzles for ASTOVL aircraft p 861 A92-45325
Commercial turbofan engine exhaust nozzle flow analyses using PAB3D
[AIAA PAPER 92-2701] p 801 A92-45543
Prediction of a high bypass ratio engine exhaust nozzle flowfield
[AIAA PAPER 92-3259] p 864 A92-48855
A study on the impact of shroud geometry on ejector pumping performance
[AIAA PAPER 92-3260] p 864 A92-48856
Scale model test results of a multi-slotted vectoring 2DCD ejector nozzle
[AIAA PAPER 92-3264] p 864 A92-48859
Experience in the operation of a hypersonic nozzle static thrust stand
[AIAA PAPER 92-3292] p 882 A92-48881
Specifying exhaust nozzle contours in real-time using genetic algorithm trained neural networks
[AIAA PAPER 92-3328] p 865 A92-48911
Emerging airframe/propulsion integration technologies at General Electric
[AIAA PAPER 92-3335] p 850 A92-48917
Preliminary dynamic tests of a flight-type ejector
[AIAA PAPER 92-3261] p 1066 A92-54020
Experimental performance of three design factors for ventral nozzles for SSTOVL aircraft
[AIAA PAPER 92-3789] p 1069 A92-54168
Static internal performance of ventral and rear nozzle concepts for short-takeoff and vertical-landing aircraft
[NASA-TP-3103] p 12 N92-10975
Jet noise suppression p 236 N92-14784
Flow studies in close-coupled ventral nozzles for STOVL aircraft
[NASA-TM-102554] p 445 N92-20934
Application of CFD in the design of gas turbine engine components p 741 N92-27461
Experimental performance of three design factors for ventral nozzles for SSTOVL aircraft
[NASA-TM-105697] p 742 N92-27669
Navier-Stokes analysis and experimental data comparison of compressible flow within ducts
[NASA-TM-105796] p 972 N92-30972
Preliminary dynamic tests of a flight-type ejector
[NASA-TM-105814] p 972 N92-30998

EXHAUST SYSTEMS
Gas turbine exhaust system silencing design
p 882 A92-47365
A computational study of advanced exhaust system transition ducts with experimental validation
[AIAA PAPER 92-3794] p 907 A92-49126
Computational study of a supersonic mixer-ejector exhaust system p 969 A92-50252
Internal reversing flow in a tailpipe offtake configuration for SSTOVL aircraft
[AIAA PAPER 92-3790] p 1069 A92-54169
Advanced nozzle and engine components test facility
[AIAA PAPER 92-3993] p 1099 A92-56816
Static internal performance of ventral and rear nozzle concepts for short-takeoff and vertical-landing aircraft
[NASA-TP-3103] p 12 N92-10975
Internal reversing flow in a tailpipe offtake configuration for SSTOVL aircraft
[NASA-TM-105698] p 868 N92-28418

EXPANSION
Numerical simulation of transient hypervelocity flow in an expansion tube
[NASA-CR-189601] p 402 N92-18965
Temperature effects in FFA HYP 500 at M = 7 in a flow with strong expansion
[FFA-TN-1991-27] p 443 N92-20229

EXPENDABLE STAGES (SPACECRAFT)
Turbofan with a small bypass ratio for first stage of a two-stage to-orbit vehicle p 968 A92-49833

EXPERIMENT DESIGN
Using design of experiments to improve product and process integrity p 928 A92-48555
Man-Vehicle Systems Research Facility - Design and operating characteristics
[AIAA PAPER 92-4177] p 982 A92-52458
Design of experiments p 273 N92-17154
Pallet for helicopter testing instrumentation
p 652 N92-25598

EXPERT SYSTEMS
A novel associative memory for high level control functions p 52 A92-11472
Enhanced diagnostic system for autoclaves and bonding presses p 145 A92-14381
Preliminary experience with an expert system providing initial centrifugal compressor sizing for performance prediction and analysis
[ASME PAPER 91-GT-28] p 162 A92-15513
A procedure for automated gas turbine blade fault identification based on spectral pattern analysis
[ASME PAPER 91-GT-259] p 151 A92-15661
Jet engine test system including expert system for diagnosis
[ASME PAPER 91-GT-408] p 137 A92-15737
Model based reasoning in the aerospace domain
[AIAA PAPER 91-3709] p 230 A92-17582
Knowledge maintenance in an evolving system using a deep structure representation
[AIAA PAPER 91-3941] p 231 A92-17605
Radar troubleshooting assistant expert system
[AIAA PAPER 91-3764] p 231 A92-17626
Fault Tree Interpreter --- expert system shell for rule-based expert systems development for control of ATE
[AIAA PAPER 91-3789] p 232 A92-17645
Probabilistic reasoning for intelligent wind shear avoidance p 302 A92-21181
A parallel architecture adapted to onboard multiexpert systems p 276 A92-23040
AI technology and application development on the Shuttle project p 302 A92-23693
Expert system for real-time aircraft monitoring
p 410 A92-24411
The TSE 310 troubleshooting expert prototype for the Airbus A-310 commercial aircraft p 307 A92-25180
From concept to model: Conception and evaluation of an architecture for a distributed system with SAHARA - Some reflections on results of the utilization of SAHARA in the framework of the Electronic Copilot
[ONERA, TP NO. 1991-216] p 411 A92-26368
Application researches on expert system used for structural layout optimization of wings
p 398 A92-27865
Expert knowledge techniques applied to the analysis of electric field mill data p 408 A92-27991
The initial development of an expert system for designing composite material wing structures p 599 A92-32542
A knowledge acquisition approach for an on-board mission planner
[AIAA PAPER 92-1021] p 531 A92-33204
Constraint-based component-modeling for knowledge-based design
[AIAA PAPER 92-1192] p 600 A92-33304
An expert system to aid real world finite element analysis
[AIAA PAPER 92-2488] p 601 A92-34604
Optimal measurement and health index selection for gas turbine performance status and fault diagnosis
[ASME PAPER 91-GT-294] p 653 A92-36889
Lessons learned about information management within the Pilot's Associate program p 916 A92-44909
Specification of adaptive aiding systems - Information requirements for designers p 916 A92-44915
Wind-tunnel compressor stall monitoring using neural networks p 918 A92-46817
An explanation-based-learning approach to knowledge compilation - A Pilot's Associate application
p 920 A92-48220
An artificial intelligence approach for the verification of requirements for aircraft electrical power systems
p 863 A92-48481
The application of multimedia expert systems to the depot level maintenance environment
p 922 A92-48557
Expert systems for the trouble-shooting and the diagnostics of engines
[AIAA PAPER 92-3327] p 923 A92-48910
Artificial intelligence techniques applied to vehicle management system diagnostics p 965 A92-49315
Integrated system to support computer analysis in conceptual aerospace design p 1130 A92-53596
Discrete event fuzzy airport control
p 1046 A92-55973
Flight simulator test of cockpit advisory system
p 1054 A92-56115
Field test of an advanced maintenance-system
p 1016 A92-56221
Feasibility of using a knowledge-based system concept for in-flight primary flight display research
[NASA-TM-4279] p 17 N92-10017
The development of a requirement specification for an experimental active flight control system for a variable stability helicopter: An Ada simulation in JSD
p 135 N92-12466
Heuristic route optimization: A model for force level route planning p 164 N92-12520
A NASA/RAE cooperation in the development of a real-time knowledge based autopilot
p 164 N92-12528
Pilot's associate: Evolution of a functional prototype
p 118 N92-12531
Expert system for the Tornado ground-based check-out system p 118 N92-12536
A knowledge-based assistant for diagnosis in aircraft maintenance p 61 N92-12538
Integrated Communications, Navigation, Identification, Avionics (ICNIA) expert system for fault tolerant avionics
p 118 N92-12539
Engineering Graphical Analysis Tool (EGAT) development program p 164 N92-12542
Flight simulation p 207 N92-13982
Automated problem resolution prototype in automated en route air traffic control p 190 N92-14028
Knowledge based system applications for guidance and control
[AGARD-AR-284] p 205 N92-14065
Architecture for Survivable System Processing (ASSP)
p 220 N92-14210
Getting expert systems off the ground: Lessons learned from integrating model-based diagnostics with prototype flight hardware p 220 N92-14217
Aviation Diagnostics And Maintenance (ADAM) system preliminary concept of operation and functional description
[AD-A242598] p 170 N92-14966
A CLIPS-based tool for aircraft pilot-vehicle interface design p 303 N92-16605
Technical evaluation report on the 52nd Symposium on Software for Guidance and Control
[AGARD-AR-302] p 303 N92-17498
Development of a knowledge base for use in an Expert System Advisor for Aircraft Maintenance Scheduling (ESAAMS)
[AD-A243435] p 305 N92-17687
An investigation of air transportation technology at the Massachusetts Institute of Technology, 1990-1991
p 265 N92-17985
Delfi: Design, development, and applicability of expert systems shells
[ISBN-90-6275-734-0] p 692 N92-25306
A prototype semantic integrity front end expert system for a relational database
[AD-A246084] p 781 N92-26765
Expert system management system
[AD-A247102] p 781 N92-26863
Parallel knowledge based systems architectures for in-flight mission management p 728 N92-27904
Application of knowledge-based systems for diagnosis of aircraft systems
[NLR-TP-90192-U] p 837 N92-28655
Model analysis and expert system development for planning and scheduling teleoperations for aircraft turnaround functions, volume 1
[AD-A251037] p 932 N92-30253
Model analysis and expert system development for planning and scheduling teleoperations for aircraft turnaround functions. Volume 2: Top user's guide
[AD-A251083] p 932 N92-30258
Proceedings of the 53rd Symposium on Air Vehicle Mission Control and Management
[AGARD-AR-310] p 1010 N92-32229
Advanced software development workstation: Effectiveness of constraint-checking --- spaceflight simulation and planning
[NASA-CR-190712] p 1134 N92-32865

EXPLOSIONS
Safety in the sky - Designing bomb-resistant baggage containers p 836 A92-47775
An explosively driven, fast shock tube
[DE92-008437] p 749 N92-26720
Modular simulation of HEI fragments and blast pressure
[AD-A248205] p 910 N92-29191

EXPLOSIVE DECOMPRESSION
Aircraft accident report: Explosive decompression - loss of cargo door in flight, United Airlines Flight 811, Boeing 747-122, N4713U, Honolulu, Hawaii, February 24, 1989
[PB92-910402] p 953 N92-31159

EXPLOSIVES
Airport X-ray screening technology becomes a viable explosives detector p 836 A92-47925

EXPOSURE
Residual strength of repaired graphite/epoxy laminates after 5 years of outdoor exposure p 1108 N92-32577
Fluid effects: Thermoset and thermoplastic matrix composites p 1110 N92-33049

EXTERNAL COMBUSTION ENGINES
The F/A-18 external burning flight test
[AIAA PAPER 91-5050] p 731 A92-44547
Experiments and analysis concerning the use of external burning to reduce aerospace vehicle transonic drag
[NASA-TM-105397] p 279 N92-17546

EXTERNAL STORE SEPARATION
On the aerodynamics/dynamics of store separation from hypersonic aircraft
[AIAA PAPER 92-2722] p 807 A92-45595
The effect of atmospheric turbulence on the external store separation from an aircraft p 934 A92-50233
Separation of external stores: Comparison of results
[F+W-TF-2058] p 732 N92-26944
Aerodynamic interference between stores
[AD-A247207] p 715 N92-27172
EXTERNAL STORES
Control system design for the free drop test of external stores in a wind tunnel
[IAF PAPER ST-91-002] p 207 A92-20650
Interference flows past cylinder-fin-sting-cavity assemblies p 442 A92-32236
Transition of the flutter mode of a two-dimensional section with an external store p 758 A92-41244
Computations of the unsteady flow about a generic wing/pylon/finned-store configuration
[AIAA PAPER 92-4568] p 1027 A92-55377
Computer program for calculating in-flight aircraft-store interface reaction loads
[AD-A245782] p 731 N92-26896
Aerodynamic interference between stores
[AD-A247207] p 715 N92-27172
Pneumatically actuated multiple store launcher
[AD-D015237] p 732 N92-27188
Calculation of unsteady subsonic and supersonic flow about oscillating wings and bodies by new panel methods
[NLR-TP-89119-U] p 827 N92-28659
An investigation into the interface between three closely spaced axi-symmetric bodies at subsonic speed
[CRANFIELD-AERO-9114] p 948 N92-31514
EXTERNAL TANKS
Results of the space shuttle vehicle ascent air data system probe calibration test using a 0.07-scale external tank forebody model (68T) in the AEDC 16-foot transonic wind tunnel (IA-310), volume 1
[NASA-CR-167696] p 286 N92-17167
Results of the space shuttle vehicle ascent air data system probe calibration test using a 0.07-scale external tank forebody model (68T) in the AEDC 16-foot transonic wind tunnel (IA-310), volume 2
[NASA-CR-167697] p 286 N92-17214
EXTERNALLY BLOWN FLAPS
Study of external dynamic flap loads on a 6 percent B-1B model
[ASME PAPER 91-GT-236] p 125 A92-15645
Large-scale wind tunnel studies of a jet-engined powered ejector-lift STOVL aircraft p 842 A92-45313
The FM-007: An advanced jet commuter for HUB to spoke transportation
[NASA-CR-189988] p 461 N92-20267
EXTINCTION
Theories of turbulent combustion in high speed flows
[AD-A253032] p 1111 N92-33624
EXTINGUISHING
Development of fuel neutralizing agents to prevent flashback on aircraft fires
[AD-A242828] p 264 N92-17259
EXTRAPOLATION
Computational fluid dynamics p 177 N92-13979
Numerical simulations around models in hypersonic wind tunnels p 182 N92-14998
EXTREMELY HIGH FREQUENCIES
A Ka-band instrumentation radar with one foot range resolution p 95 A92-16252
Characteristics of a future aeronautical satellite communications system
[AIAA PAPER 92-2058] p 453 A92-29889
A low-power, high-efficiency Ka-band TWTA
p 671 A92-38163

F

F-104 AIRCRAFT
Airdata calibration techniques for measuring atmospheric wind profiles p 856 A92-46792
F-106 AIRCRAFT
Analysis and modeling of lightning strikes to the F106B, CVF580, and C160 aircraft p 186 A92-20129
F-111 AIRCRAFT
Variable-camber systems integration and operational performance of the AFTI/F-111 mission adaptive wing
[NASA-TM-4370] p 570 N92-22194
Reduction and analysis of F-111C flight data
[AD-A250341] p 853 N92-28771
F-117A AIRCRAFT
Flight management system integration on the F-117A
[AIAA PAPER 92-1077] p 563 A92-33246
Pilot activated automatic recovery system on the F-117A
[AIAA PAPER 92-1126] p 563 A92-33278
Flight management system of the F-117A
p 1082 A92-55910
The Lockheed F-117A
[RAND-P-7746-RGS] p 731 N92-26673
F-14 AIRCRAFT
F-14/F110 engine integration p 112 A92-16055
Flow separation patterns over an F-14A aircraft wing
p 174 A92-20205
Controller design for the F-14 pitch axis control problem using the quantitative feedback theory approach
p 478 A92-29128
The development and integration of an engine monitoring system for the F-14A+/D Super Tomcat
[SAE PAPER 912094] p 654 A92-39951
F-14 dual hydraulic failure flying qualities evaluation
p 645 A92-40029
Single engine testing of the F-14A(PLUS) airplane in the power approach configuration p 645 A92-40036
A wing rock model for the F-14A aircraft
[AD-A243109] p 275 N92-17300
A user guide for the EMTAC-MZ CFD code
[NASA-CR-4283] p 678 N92-24242
Implementation of a personal computer based parameter estimation program
[AD-A252914] p 1061 N92-33502
F-15 AIRCRAFT
F-15 STOL/Maneuvering Technology Demonstrator. Phase III - Thrust vectoring, reversing and STOL operation p 112 A92-16054
Performance improvements of an F-15 airplane with an integrated engine-flight control system
p 205 A92-20204
Fabry-Perot fiber-optic sensors in full-scale fatigue testing on an F-15 aircraft p 391 A92-24553
F15E terrain following system development
[AIAA PAPER 92-1079] p 563 A92-33248
Verification and validation of F-15 and S/MTD unique software p 921 A92-48515
Subsonic flight test evaluation of a performance seeking control algorithm on an F-15 airplane
[AIAA PAPER 92-3743] p 878 A92-49109
Subsonic flight test evaluation of a propulsion system parameter estimation process for the F100 engine
[AIAA PAPER 92-3745] p 866 A92-49110
Thrust stand evaluation of engine performance improvement algorithms in an F-15 airplane
[AIAA PAPER 92-3747] p 866 A92-49111
Analysis of the effects of removing nose ballast from the F-15 eagle
[AD-A244044] p 366 N92-19178
Investigation of the influence of rotary aerodynamics on the study of high angle of attack dynamics of the F-15B using bifurcation analysis
[AD-A243969] p 348 N92-19367
Integrated flight propulsion control research results using the NASA F-15 HIDEC Flight Research Facility
[NASA-TM-4394] p 740 N92-27379
Add-on damping treatment for life extension of the F-15 upper-outer wing skin
[AD-A246149] p 746 N92-27577
Aeroelastic calculations for fighter aircraft using the transonic small disturbance equation
p 720 N92-27951
Flight evaluation of an extended engine life mode on an F-15 airplane
[NASA-TM-104240] p 871 N92-29659
Thrust stand evaluation of engine performance improvement algorithms in an F-15 airplane
[NASA-TM-104252] p 971 N92-30518
Subsonic flight test evaluation of a performance seeking control algorithm on an F-15 airplane
[NASA-TM-4400] p 973 N92-31275
Flight testing and simulation of an F-15 airplane using throttles for flight control
[NASA-TM-104255] p 1087 N92-32864
F-16 AIRCRAFT
Application of Active Flexible Wing technology to the Agile Falcon p 729 A92-41233
Prismatic grid generation with an efficient algebraic method for aircraft configurations
[AIAA PAPER 92-2721] p 803 A92-45559
F-16 failure detection isolation and estimation study
p 876 A92-48490
Simple fly-by-wire actuator p 876 A92-48491
Fighter airframe/propulsion integration - A General Dynamics perspective
[AIAA PAPER 92-3332] p 850 A92-48915
The VISTA/F-16 programmable feel system
[AIAA PAPER 92-4172] p 977 A92-52457
An evaluation of four F-16 vertical velocity indicator configurations
[AD-A243629] p 370 N92-18014
Transport delay measurements: Methodology and analysis for the F-16C combat engagement trainer, the display for advanced research and training, and the F-16A limited field of view
[AD-A248519] p 888 N92-29505
F-18 AIRCRAFT
Wind-tunnel studies of F/A-18 tail buffet
p 310 A92-24421
Canadian CF-18 aircraft ejection seat parachute update p 529 A92-32983
Buffet load measurements on an F/A-18 vertical fin at high-angle-of-attack
[AIAA PAPER 92-2127] p 520 A92-35694
National Aerospace Plane flight test - External burning on the F/A-18 p 645 A92-40032
Water tunnels p 880 A92-45266
Coupled numerical simulation of the external and engine inlet flows for the F-18 at large incidence
[AIAA PAPER 92-2621] p 793 A92-45493
Numerical investigation of tail buffet on F-18 aircraft
[AIAA PAPER 92-2673] p 798 A92-45528
Unsteady pressure and load measurements on an F/A-18 vertical fin at high-angle-of-attack
[AIAA PAPER 92-2675] p 798 A92-45529
Dynamic LEX/forebody vortex interaction effects
[AIAA PAPER 92-2732] p 804 A92-45566
Forebody flow control on a full-scale F/A-18 aircraft
[AIAA PAPER 92-2674] p 806 A92-45583
Full-scale high angle-of-attack tests of an F/A-18
[AIAA PAPER 92-2676] p 806 A92-45584
Navier-Stokes predictions for the F-18 wing and fuselage at large incidence p 810 A92-46783
Statistical prediction of maximum buffet loads on the F/A-18 vertical fin p 811 A92-46816
Thrust vectoring characteristics of the F-18 high alpha research vehicle at angles of attack from 0 to 70 deg
[AIAA PAPER 92-3095] p 877 A92-48737
Use of high-fidelity simulation in the development of an F/A-18 active ground collision avoidance system
[AIAA PAPER 92-4140] p 959 A92-52434
Full Navier-Stokes calculations on the installed F/A-18 inlet at a high angle of attack
[AIAA PAPER 92-3175] p 1020 A92-54012
In-flight flow visualization and pressure measurements at low speeds on the NASA F-18 high alpha research vehicle p 85 N92-13009
Some characteristics and effects of the F/A-18 LEX vortices p 88 N92-13025
Formulation of the linear model from the nonlinear simulation for the F18 HARV p 117 N92-13842
Wind tunnel investigation of vortex flows on F/A-18 configuration at subsonic through transonic speed
[NASA-TP-3111] p 179 N92-14968
F/A-18 stabilator: Equivalent set of point forces required for pneumatic bag load case simulation
[AD-A242637] p 206 N92-15073
A parametric approach to spectrum development
p 360 N92-18578
A static investigation of the thrust vectoring system of the F/A-18 high-alpha research vehicle
[NASA-TM-4359] p 633 N92-25967
Use of high-fidelity simulation in the development of an F/A-18 active ground collision avoidance system
p 837 N92-28530
Identification of aerodynamic models for maneuvering aircraft
[NASA-CR-190444] p 852 N92-28720
Tasking and communication flows in the F/A-18D cockpit: Issues, problems, and possible solutions
[AD-A245977] p 853 N92-28802
Parameter identification for nonlinear aerodynamic systems
[NASA-CR-190264] p 830 N92-29329
In-service evaluation of 2090 aluminum-lithium alloy on F/A-18 aircraft
[AD-A248472] p 986 N92-30321
In-flight leading-edge extension vortex flow-field survey measurements on a F-18 aircraft at high angle of attack
[NASA-TM-4398] p 947 N92-31276
Structural assessment of ultralightweight composites
p 1107 N92-32525
The F-18 high alpha research vehicle: A high-angle-of-attack testbed aircraft
[NASA-TM-104253] p 1060 N92-33404
Experience with Ada on the F-18 High Alpha Research Vehicle Flight Test Program
[NASA-TM-104259] p 1062 N92-34039
F-2 AIRCRAFT
Four decades of transonic fighter design
p 193 A92-20203
F-27 AIRCRAFT
F27 aging aircraft programme emphasizes corrosion prevention p 186 A92-20024

F-8 AIRCRAFT
Transonic wind tunnel test of a 14 percent thick oblique wing
[NASA-TM-102230] p 950 N92-32213
FABRICATION
Operational evaluation of recently developed balloon fabrication methods
[AIAA PAPER 91-3670] p 1 A92-11017
The use of NDE as a process development tool for ceramic engine components
[ASME PAPER 91-GT-290] p 152 A92-15682
Fabrication and properties of fiber-reinforced ceramic composites made by directed metal oxidation
p 669 A92-39861
Fabrication test and evaluation of graphite/PMR-15 polyimide for HOPE primary structure
p 1105 A92-53516
Design and testing of high-performance parachutes
[AGARD-AG-319] p 345 N92-18269
Weight, center of gravity and modal test report for NTF fan blade set no. 3
[NASA-CR-189583] p 498 N92-20072
Polymer infiltration studies
[NASA-CR-190204] p 578 N92-22486
Prototype instrumentation and design studies
[AD-A248378] p 736 N92-28004
Design, evaluation and experimental effort toward development of a high strain composite wing for Navy aircraft p 1107 N92-32514
Evaluation of composite components on the Bell 206L and Sikorsky S-76 helicopters p 1107 N92-32575
High temperature aircraft research furnace facilities
[NASA-CR-184384] p 1101 N92-33826
FABRICS
Metal fibers and fabrics as shielding materials for composites, missiles and airframes p 141 A92-14680
Weaving an aircraft p 392 A92-24911
Air cushion vehicle conductive/semiconductive flexible skirt, and method
[AD-D015160] p 400 N92-18187
Performance of uncoated AFRSI blankets during multiple Space Shuttle flights
[NASA-TM-103892] p 890 N92-29104
Polymer blends, volume 1
[AD-A252112] p 987 N92-31419
FABRY-PEROT INTERFEROMETERS
Fabry-Perot fiber-optic sensors in full-scale fatigue testing on an F-15 aircraft p 391 A92-24553
Progress towards fiber optic smart structures at UTIAS
p 368 A92-24781
FACE CENTERED CUBIC LATTICES
A preliminary study of the microstructure-property relationships in cast gamma titanium aluminide alloys
p 487 A92-30596
FACTORIAL DESIGN
An analysis of fixed wing tactical airlifter characteristics using an intra-theater airlift computer model
[AD-A246908] p 732 N92-27719
FACTORIZATION
A new U-D factorization-based fixed-point smoother and application to flight test p 411 A92-27858
PC based flight path reconstruction using UD factorization filtering algorithm
[NAL-PD-FC-9201] p 534 N92-22389
FAILURE
Failure analysis of the Apache mixer pivot support
[AD-A240858] p 116 N92-13061
Detailed analysis and test correlation of a stiffened composite wing panel
[NASA-TM-104154] p 159 N92-13460
Turbine engine diagnostics system study
[DOT/FAA/CT-91/16] p 202 N92-14064
Rotor-to-stator partial rubbing and its effects on rotor dynamic response p 224 N92-14367
Life management approach for USAF aircraft
p 362 N92-18587
Flying an aircraft as a problem-solving process: About the Instrument-Failure-Simulator (IFS) as a test for pilot-candidates
[DLR-FB-91-23] p 455 N92-20902
Statistics on aircraft gas turbine engine rotor failures that occurred in US commercial aviation during 1989
[DOT/FAA/CT-92/5] p 971 N92-30303
Out of plane analysis for composite structures
p 1107 N92-32527
FAILURE ANALYSIS
Fracture analysis on compressor blades
p 37 A92-10672
Probabilistic fatigue methodology for six nines reliability p 145 A92-14342
Determination of the energy absorption of composite structures under combined loadings p 145 A92-14441
Combination of different unsteady quantity measurements for gas turbine blade fault diagnosis
[ASME PAPER 91-GT-201] p 149 A92-15624
Availability of positioning and receiver autonomous integrity monitoring for the global positioning system
p 100 A92-16963
Real-time microfocus radiography for electronic failure analysis p 214 A92-17289
Failure environment analysis tool (FEAT) development status
[AIAA PAPER 91-3803] p 232 A92-17654
Fluid power distribution and control
p 292 A92-21733
Failure detection of engine sensors with a bank of Kalman filters p 392 A92-24748
Failure detection and fault management techniques for flush airdata sensing systems
[AIAA PAPER 92-0263] p 369 A92-25719
Durability analysis using fracture mechanics for avionics integrity p 396 A92-26799
Failure detection and identification for aircraft sensors
p 370 A92-27832
Integral minimization of engine fault equations based on least fault principle p 374 A92-27857
X-ray computed tomography for the aircraft/aerospace industry p 492 A92-28750
Design for validation p 601 A92-33607
TMFSLAM - Design analysis tool for coated structures
[ASME PAPER 91-GT-141] p 690 A92-36895
Reliability analysis of fatigue life of a structural system
p 671 A92-37395
Statistical analysis of field data for aircraft warranties
p 760 A92-42077
Utilizing the fault monitoring system for the A320 aircraft p 700 A92-43157
A method of failure analysis of complicated structures
p 901 A92-47656
A failure analysis for landing gear structural system
p 849 A92-47667
Approximate analysis for failure probability of structural systems p 901 A92-47671
RTOK elimination with TSMM --- Rerurn Tested OK reproduction using time stress measurement module
p 902 A92-48446
F-16 failure detection isolation and estimation study
p 876 A92-48490
Failure model development for an integrally bladed turbine wheel
[AIAA PAPER 92-3420] p 865 A92-48979
Engine fan blade low cycle fatigue testing
[AIAA PAPER 92-3478] p 866 A92-49021
Application of syndrome pattern-matching approach to fault isolation in avionic systems p 1005 A92-49261
JIAWG module fault coverage metrics methodology
p 989 A92-49279
Detection and identification of axial flow compressor instabilities p 969 A92-50504
Failure analysis and reliability improvement of small turbine engine blades p 993 A92-50860
Detailed investigation of causes of avionics field failures p 995 A92-51925
Effect of a deicing device on the induced drag of a lifting airfoil p 959 A92-51947
A full-scale fatigue test and failure analyses research of F-X fighters p 960 A92-53092
The application of math-dynamic models to characterise a range of helicopter rotor system faults
p 1056 A92-56297
Damage tolerance analysis for rotorcraft - What the issues are p 1058 A92-56336
Damage tolerant design of critical aircraft structural components
[AIAA PAPER 92-4041] p 1123 A92-56860
Failure analysis of the Apache mixer pivot support
[AD-A240858] p 116 N92-13061
Optimization of the calculation margins of landing gears under extreme loads. Rupture static tests. Part 1: Program and test implantation
[CEAT-S8-6551-PARTIEL-1-PT-] p 195 N92-14043
Development and evaluation of a finite element model for a fiber composite helicopter fuselage
[MBB-UD-0584-90-PUB] p 196 N92-15066
Rapid repair of integrally stiffened carbon fibre composite structures by bolted aluminium elements
[MBB-FE202-S-PUB-0453-A] p 290 N92-17310
Explicit finite element method for transparency impact analysis
[AD-A243527] p 264 N92-17478
Program plans: Aviation safety research
[NIAR-91-30] p 264 N92-17587
Fatigue management for the A-7P
p 363 N92-18593
Life prediction technologies for aeronautical propulsion systems p 560 N92-22520
Composite fuselage technology (summary of year 2)
[NASA-CR-190434] p 731 N92-26655
Assessment of valve actuator motor rotor degradation by Fourier Analysis of current waveform
[DE92-013233] p 909 N92-28814
Tensile and interlaminar properties of GLARE (trade name) laminates
[AD-A250188] p 895 N92-28921
Performance of fuselage pressure structure
p 913 N92-30109
Fracture mechanics research at NASA related to the aging commercial transport fleet p 913 N92-30110
Preliminary results on the fracture analysis of multi-site cracking of lap joints in aircraft skins
p 913 N92-30111
Current DOT research on the effect of multiple site damage on structural integrity p 913 N92-30112
Advanced techniques in reliability model representation and solution
[NASA-TP-3242] p 1134 N92-33483
Joint study on the computerisation of in-field aero engines vibration diagnosis
[PNR-90799] p 1072 N92-33815
Stability failure of sandwich structures
[MBB-UD-0613-92-PUB] p 1111 N92-33994
FAILURE MODES
Fault tolerant control based on a new accommodation filter p 51 A92-11453
System reliability and risk assessment
[AIAA PAPER 92-2345] p 582 A92-34320
Economic life analysis for replacing components
p 785 A92-47670
Approximate analysis for failure probability of structural systems p 901 A92-47671
Critical digital systems - A fly-by-light consideration
p 974 A92-49324
Failure analysis and reliability improvement of small turbine engine blades p 993 A92-50860
The system reliability analysis and optimization design for wing-box structures p 997 A92-53292
Redundancy design philosophy for catastrophic loss protection p 1119 A92-56202
Life prediction technologies for aeronautical propulsion systems p 560 N92-22520
Assessment of valve actuator motor rotor degradation by Fourier Analysis of current waveform
[DE92-013233] p 909 N92-28814
FCS skewed sensors array: Practical considerations
p 968 N92-31868
The Utilization of Advanced Composites in Military Aircraft
[AGARD-R-785] p 1109 N92-33033
Advanced techniques in reliability model representation and solution
[NASA-TP-3242] p 1134 N92-33483
Stability failure of sandwich structures
[MBB-UD-0613-92-PUB] p 1111 N92-33994
FAIRINGS
Hub and pylon fairing integration for helicopter drag reduction p 107 A92-14391
FALKNER-SKAN EQUATION
Simplified linear stability transition prediction method for separated boundary layers p 812 A92-46883
FALSE ALARMS
Saberliner flight test and results for forward looking detection and avoidance of airborne windshear
p 98 A92-16656
FAN BLADES
H-76B Fantail demonstrator composite fan blade fabrication p 145 A92-14356
The role of tip clearance in high-speed fan stall
[ASME PAPER 91-GT-83] p 69 A92-15550
An unsteady lifting surface theory for ducted fan blades
[ASME PAPER 91-GT-131] p 71 A92-15575
Multi-blade row Navier-Stokes simulations of fan-bypass configurations
[ASME PAPER 91-GT-148] p 73 A92-15586
An analysis of impact resistance of composite fan blade p 293 A92-22523
The selection of bird impact load types --- on turbojet compressor and turbofan fan blades
p 448 A92-29732
Acoustic emission during changes in the aerodynamic load on the surface of a fan blade p 511 A92-30318
Finite elements analysis of flexural edge wave for composite fan blades
[SAE PAPER 912048] p 861 A92-45432
Engine fan blade low cycle fatigue testing
[AIAA PAPER 92-3478] p 866 A92-49021
Weight, center of gravity and modal test report for NTF fan blade set no. 3
[NASA-CR-189583] p 498 N92-20072
Design and performance of controlled-diffusion stator compared with original double-circular-arc stator
[NASA-TP-2852] p 562 N92-22863
Coupled multi-disciplinary simulation of composite engine structures in propulsion environment
[NASA-TM-105575] p 596 N92-23267

FAR FIELDS
Finite element analysis of large wavelength antenna radome problems for leading edge and radar phased arrays p 267 A92-23984
Accelerated convergence to steady state by gradual far-field damping p 610 A92-36835
Helicopter far-field acoustic levels as a function of reduced rotor speeds p 695 A92-39228
Far-field turbulence structure of the tip vortex shed by a single rectangular wing p 620 A92-40084
Direct computation of turbulence and noise
[NASA-CR-187616] p 236 N92-14788
Automated composite ellipsoid modelling for high frequency GTD analysis
[NASA-CR-189853] p 275 N92-17316
Prediction of far-field harmonic noise from propellers
[ESDU-91033] p 416 N92-18074
Measurement of LORAN-C envelope to cycle difference in the far field
[PB92-128909] p 455 N92-21263
FAST FOURIER TRANSFORMATIONS
Enhancement of modal swept sine data by control of exciting forces p 215 A92-17562
A fast conformal mapping algorithm with no FFT p 1007 A92-50471
FASTENERS
Fatigue life estimation of fastener holes without load transfer p 291 A92-21472
Predication of fastening capacity of screwed joint structure with cone assembly p 391 A92-24737
The role of nonmetallic fasteners in aircraft wings and other composite structures p 784 A92-47413
Use of adhesive bonded attachments for a composite aircraft fuel tank p 785 A92-47414
FATIGUE (MATERIALS)
Aerospace Arall - A challenge for the aircraft designer p 33 A92-10232
Calculation of the hardening factor for gas turbine engine components shot blasted in an ultrasonic field p 38 A92-10850
Comparative study of fatigue in various materials and designs under sonic loading p 287 A92-21003
Industry seeks tonic for aging aircraft p 308 A92-28492
Structural airworthiness of aging Boeing jet transports - 747 fuselage fatigue test program
[AIAA PAPER 92-1128] p 537 A92-33280
Contribution of individual load cycles to crack growth under aircraft spectrum loading p 891 A92-45236
Strength evaluation and safety of machine/structure. III - Case examples on strength and safety evaluation of machine/structure 3.2 aircraft (airframe) p 882 A92-47303
Numerical analysis of an engine turbine disk loaded with a large number of thermomechanical cycles
[ONERA, TP NO. 1992-31] p 902 A92-48592
The static and fatigue computation of the propeller blades retention system p 995 A92-51895
Anti-fatigue optimization design by artificial intelligence strategy p 996 A92-53013
Critical appraisal of the McDonnell Douglas closure model for predicting fatigue crack growth
[ARL-STRUC-R-444] p 44 N92-11376
Failure analysis of the Apache mixer pivot support
[AD-A240858] p 116 N92-13061
Fatigue of repaired composite structures p 214 N92-14411
Environmental fatigue tests with composite materials p 214 N92-14413
Comparison between hot/wet test and RT/dry test on the Seastar horizontal stabilizer and fin p 226 N92-14414
Monitoring load experience of individual aircraft
[NLR-TP-90084-U] p 196 N92-15065
Ceramic technology for Advanced Heat Engines Project
[DE92-002397] p 289 N92-16128
Fatigue in single crystal nickel superalloys
[AD-A243453] p 290 N92-17653
Fatigue Management
[AGARD-CP-506] p 360 N92-18571
Fatigue safety factor: Assessment of associated safety level p 401 N92-18573
Aircraft tracking for structural fatigue p 361 N92-18584
Recent fracture mechanics results from NASA research related to the aging commercial transport fleet p 362 N92-18589
Aircraft fatigue management in the Royal Air Force p 363 N92-18591
Tornado structural fatigue life assessment of the German Air Force p 363 N92-18592
Managing airborne assets through loads monitoring p 363 N92-18594
A review of aging aircraft technology: An IAI perspective
[IAITIC-91-1018] p 461 N92-20500
Application of finite element methods to fracture mechanics
[PNR-90770] p 503 N92-21741
Inspection of aircraft engine components using automated eddy current and pattern recognition techniques
[NRC-LTR-ST-1834] p 504 N92-22029
Life prediction technologies for aeronautical propulsion systems p 560 N92-22520
Evaluation of the elevated-temperature mechanical reliability of a HIPed silicon nitride
[DE92-007838] p 579 N92-23223
Towards GLARE: The development of a fatigue insensitive and damage tolerant aircraft material
[ETN-92-91301] p 648 N92-24966
Simulation of 3D non-planar fatigue crack growth in a turbine blade root
[DE92-006859] p 739 N92-26697
Generation of spectra and stress histories for fatigue and damage tolerance analysis of fuselage repairs
[AD-A250390] p 854 N92-29180
Maintaining the safety of an aging fleet of aircraft p 837 N92-30108
Fracture mechanics research at NASA related to the aging commercial transport fleet p 913 N92-30110
Preliminary results on the fracture analysis of multi-site cracking of lap joints in aircraft skins p 913 N92-30111
Aging commuter aeroplanes: Fatigue evaluation and control methods p 915 N92-30132
Fatigue crack growth of small corner defects from blunt notches in an aeroengine alloy
[PNR-90860] p 1111 N92-34019
FATIGUE LIFE
The maintenance economy and economic life of structures p 37 A92-10673
A method of reliability analysis for propeller blades p 25 A92-10968
Light metal materials for aircraft structure p 140 A92-13444
Continuation of the AHS round robin on fatigue reliability and damage tolerance p 59 A92-14341
Probabilistic fatigue methodology for six nines reliability p 145 A92-14342
Safe life reliability - Evaluation of new statistical methods p 104 A92-14343
Flight service evaluation of composite helicopter components p 106 A92-14372
Rotorcraft airframe structural optimization for combined vibration and fatigue constraints p 106 A92-14390
Main concepts of providing the static/fatigue strength of helicopters in the USSR p 110 A92-14455
Fatigue and damage tolerance verification of aircraft structures p 217 A92-19677
Multiaxial load spectra in a cooled gas turbine blade under in-service conditions p 201 A92-19696
Prediction of fatigue crack growth in a Ti-6Al-4V fan disk forging under spectrum loading p 213 A92-19817
Damage tolerance of the fighter aircraft 37 Viggen. I - Analytical assessment. II - Experimental verification p 192 A92-19819
Methodology for the assessment of material quality effects on airframe fatigue durability p 213 A92-19820
Proof test and fatigue crack growth modeling on 2024-T3 aluminum alloy p 213 A92-19828
Fatigue life estimation of fastener holes without load transfer p 291 A92-21472
Ti-6Al-4V forgings with enhanced fatigue characteristics for engine and airframe applications p 288 A92-22757
Prediction of low cycle fatigue life of engine cases p 295 A92-23385
Review of methods for crack growth testing in gas turbine engine disc materials p 296 A92-24193
Study on reliability design of turbine blade p 371 A92-24739
Inclusion size effect on the fatigue crack propagation mechanism and fracture mechanics of a superalloy p 388 A92-24831
A fatigue crack growth threshold p 389 A92-26667
The reinforcing effect of composite patch repairs on metallic aircraft structures p 419 A92-30498
A method for the construction of safe S-N curves p 586 A92-34759
Life prediction of local stress-strain method p 588 A92-35564
Identification of helicopter component loads using multiple regression
[AIAA PAPER 92-2110] p 544 A92-35681
TMFSLAM - *Design analysis tool for coated structures*
[ASME PAPER 91-GT-141] p 690 A92-36895
Reliability analysis of fatigue life of a structural system p 671 A92-37395
Fretting fatigue p 672 A92-38225
Advanced balancing using laser machining
[SAE PAPER 912218] p 674 A92-40020
Shot peening - Theory and applications --- Book
[ISBN 2-907669-18-4] p 676 A92-40400
A comparison of fatigue life prediction methodologies for rotorcraft p 647 A92-40884
Possibility of increasing durability of blades with damages p 761 A92-42654
Bayesian reliability analysis in connection with the evaluation of multiple-site damage p 762 A92-43126
Aircraft reliability and maintainability p 700 A92-43141
Experimental operation of aircraft-engine turbine blade materials p 737 A92-43233
Advances in fatigue lifetime predictive techniques; Proceedings of the Symposium, San Francisco, CA, Apr. 24, 1990
[ASTM STP-1122] p 896 A92-45226
The fatigue scatter factors and reduction factors in the design of aircraft and helicopter's structural lives
[SAE PAPER 911984] p 843 A92-45387
The large scale test control systems designed and built by the Boeing Company to support the 757 and 767 major fatigue tests
[SAE PAPER 911985] p 881 A92-45388
Probability analysis of structure failure for the wings with main and subordinate components p 848 A92-47657
A study on crack initiation method for durability analysis p 901 A92-47663
Aero mechanics in the twenty-first century
[AIAA PAPER 92-3194] p 863 A92-48805
Failure model development for an integrally bladed turbine wheel
[AIAA PAPER 92-3420] p 865 A92-48979
Research on sonic fatigue calculation and test for aircraft panel p 958 A92-50203
Discs low cycle fatigue life predictions for gas turbine engines in CSFR by using fractographic information p 995 A92-51950
From fatigue test life to structure safe life p 997 A92-53099
Fatigue cracking threshold prediction of transport airplanes p 1118 A92-56094
Damage tolerance analysis for rotorcraft - What the issues are p 1058 A92-56336
A review of aeronautical fatigue investigations in Sweden during the period May 1989 to April 1991
[FFA-TN-1991-24] p 158 N92-12313
Bulging of fatigue cracks in a pressurized aircraft fuselage
[LR-655] p 196 N92-14045
Review of investigations on aeronautical fatigue in the Federal Republic of Germany
[ETN-92-90317] p 225 N92-14397
Low cycle fatigue of cast nickel base turbine rotors p 226 N92-14405
Probabilistic lifing approach for aero engine disks made of powder nickel base alloys containing ceramic defects p 226 N92-14424
Airbus Industrie A330/A340: Full scale fatigue test of center fuselage and wing p 226 N92-14425
Numerical simulation of VAWT stochastic aerodynamic loads produced by atmospheric turbulence: VAWT-SAL code
[DE92-000597] p 229 N92-15392
General requirements and techniques for component fatigue life substantiation in Australian service helicopters
[AD-A242881] p 275 N92-17565
Dynamic stall on wind turbine blades
[DE92-001157] p 262 N92-17874
Fatigue Management
[AGARD-CP-506] p 360 N92-18571
The development of fatigue management requirements and techniques p 360 N92-18572
Fatigue safety factor: Assessment of associated safety level p 401 N92-18573
Probabilistic design and fatigue management based on probabilistic fatigue models with reliability updating p 360 N92-18574
Fatigue life behaviour of composite structures p 390 N92-18577
Durability and damage tolerance testing and fatigue life management: A CF-18 experience p 361 N92-18581
The Operational Loads Monitoring System, OLMS p 361 N92-18586
Tornado structural fatigue life assessment of the German Air Force p 363 N92-18592
Fatigue life variability and reliability analysis of a wind turbine blade
[DE92-008673] p 689 N92-25049
Finite element frequency domain solution of nonlinear *panel flutter with temperature effects and fatigue life* analysis p 682 N92-25589

Simulation of 3D non-planar fatigue crack growth in a turbine blade root
[DE92-006859] p 739 N92-26697
The changing role of experimentation in aeroengine R and D: The point of view of the research worker
[AD-A246372] p 740 N92-27062
A sensitivity analysis on component reliability from fatigue life computations
[AD-A247430] p 908 N92-28425
Short cracks and durability analysis of the Fokker 100 wing/fuselage structure
[NLR-TP-90336-U] p 910 N92-29603
Aging aircraft NDI Development and Demonstration Center (AANC): An overview --- nondestructive inspection p 915 N92-30120
Ageing airplane repair assessment program for Airbus A300 p 838 N92-30123
Acoustic fatigue life prediction for nonlinear structures with multiple resonant modes
[NASA-CR-190471] p 1000 N92-30988
Research into improving the durability of the hot section in the aircraft turbine engine
[AD-A250342] p 973 N92-31439
Life prediction and constitutive models for engine hot section anisotropic materials program
[NASA-CR-189222] p 973 N92-31534
Aging fleet: Maintaining airworthiness p 953 N92-31862

FATIGUE TESTING MACHINES
Analysis and modification of a single-mesh gear fatigue rig for use in diagnostic studies
[NASA-TM-105416] p 773 N92-27879

FATIGUE TESTS
The study on the composite-patching repairs for metallic aircraft structures p 36 A92-10285
Reliability of helicopter composite dynamic components p 145 A92-14344
A full scale airframe high cycle fatigue test methodology and its application to the SH-2G helicopter p 105 A92-14345
High temperature low cycle fatigue of single crystal nickel base superalloys p 213 A92-19796
Fracture analysis and crack propagation in pressurized fuselage structures - Experimental and numerical investigations p 217 A92-19812
Fatigue testing of a gas turbine fan disc p 217 A92-19818
Comparative study of fatigue in various materials and designs under sonic loading p 287 A92-21003
Creep-fatigue crack growth in Jethete M152 at 550 C under mixed mode conditions p 288 A92-21490
The FALSTAFF program - A standard spectrum for simulating the service loading of aircraft with prevailing maneuver loads p 284 A92-21922
Fabry-Perot fiber-optic sensors in full-scale fatigue testing on an F-15 aircraft p 391 A92-24553
Acoustic emission monitoring of a ground durability and damage tolerance test --- for aircraft structures p 492 A92-28737
A compound fatigue investigation of plate specimen under low-cycle load superposed on high cycle load p 587 A92-35555
Environmental evaluation of repairs to fuselage lap joints p 699 A92-41534
Cyclic fatigue behavior of silica fiber p 754 A92-42040
Some consideration for evaluation of structural integrity of aging aircraft p 762 A92-43107
The large scale test control systems designed and built by the Boeing Company to support the 757 and 767 major fatigue tests
[SAE PAPER 911985] p 881 A92-45388
Strength evaluation and safety of machine/structure. III - Case examples on strength and safety evaluation of machine/structure 3.2 aircraft (airframe) p 882 A92-47303
Engine fan blade low cycle fatigue testing
[AIAA PAPER 92-3478] p 866 A92-49021
A full-scale fatigue test and failure analyses research of F-X fighters p 960 A92-53092
From fatigue test life to structure safe life p 997 A92-53099
Effects of spectrum variations on fatigue crack growth p 1123 A92-57399
Tutor aft fuselage and empennage full-scale fatigue test: Resolution of horizontal stabilizer installation difficulties
[NRC-LTR-ST-1804] p 114 N92-11990
A review of aeronautical fatigue investigations in Sweden during the period May 1989 to April 1991
[FFA-TN-1991-24] p 158 N92-12313
Review of investigations on aeronautical fatigue in the Federal Republic of Germany
[ETN-92-90317] p 225 N92-14397
Low cycle fatigue of cast nickel base turbine rotors p 226 N92-14405
Fatigue of repaired composite structures p 214 N92-14411
Environmental fatigue tests with composite materials p 214 N92-14413
Comparison between hot/wet test and RT/dry test on the Seastar horizontal stabilizer and fin p 226 N92-14414
Airbus Industrie A330/A340: Full scale fatigue test of center fuselage and wing p 226 N92-14425
Methodology for assessment of skin repairs on Airbus aircraft p 226 N92-14428
F/A-18 stabilator: Equivalent set of point forces required for pneumatic bag load case simulation
[AD-A242637] p 206 N92-15073
Rapid repair of integrally stiffened carbon fibre composite structures by bolted aluminium elements
[MBB-FE202-S-PUB-0453-A] p 290 N92-17310
Fatigue testing and tear down operations on Airbus A320 forward fuselage p 360 N92-18579
Proposal for the new fatigue management system for the AMX p 361 N92-18580
The G-222 aircraft individual tracking programme p 361 N92-18582
High temperature dynamic engine seal technology development
[NASA-TM-105641] p 596 N92-23435
Stress-strain analysis of a (0/90)sub 2 symmetric titanium matrix laminate subjected to a generic hypersonic flight profile
[NASA-TM-107584] p 685 N92-26128
Properties of a TZP/Al2O3 composite after long-term exposure at 1000 C
[AD-A246407] p 757 N92-27752
Inspection of aging aircraft: A manufacturer's perspective p 914 N92-30117
Thermomechanical fatigue behavior of a silicone carbide fiber-reinforced calcium aluminosilicate glass-ceramic matrix composite
[AD-A249870] p 988 N92-31823

FAULT TOLERANCE
Fault tolerant control based on a new accommodation filter p 51 A92-11453
Built-in testable error detection and correction p 394 A92-25846
Evaluation and comparison of triple and quadruple flight control architectures p 745 A92-43884
Fault tolerant EHA architectures --- electro-hydrostatic actuator p 763 A92-43885
Applying advanced digital simulation techniques in designing fault tolerant systems p 921 A92-48489
Application of syndrome pattern-matching approach to fault isolation in avionic systems p 1005 A92-49261
Implementation of non-dedicated redundancy in a fault tolerant multiprocessor testbed --- flight control p 974 A92-49294
Achieving fault tolerance in multichannel control systems --- for avionics p 974 A92-49296
A fault-tolerant network architecture for integrated avionics p 965 A92-49297
Fault tolerant avionics display system p 965 A92-49312
A low maintenance and highly reliable fly-by-light architecture p 975 A92-49325
The concept exploration stage of a dependable avionic system p 1006 A92-49339
Robust flight control systems - A parameter space design p 976 A92-50503
Distributed flight control system using fiber distributed data interface (FDDI) p 976 A92-51004
A fault-tolerant Air Data/Inertial Reference System p 967 A92-51011
Modular techniques for dynamic fault-tree analysis p 1120 A92-56241
Parallel processing applications for gas turbine engine control p 25 N92-11012
Real-time fault diagnosis for propulsion systems
[NASA-TM-105303] p 26 N92-11017
Advanced information processing system: Inter-computer communication services
[NASA-CR-187556] p 53 N92-11706
An independent review of the Multi-Path Redundant Avionics Suite (MPRAS) architecture assessment and characterization report
[NASA-CR-188126] p 163 N92-12440
Integrated Communications, Navigation, Identification, Avionics (ICNIA) expert system for fault tolerant avionics p 118 N92-12539
Behavior-based fault monitoring
[AD-A241254] p 164 N92-13746
Failure detection and fault management techniques for flush airdata sensing systems
[NASA-TM-4335] p 276 N92-17128
Validation of flight critical control systems
[AGARD-AR-274] p 382 N92-20026
Formal design and verification of a reliable computing platform for real-time control. Phase 2: Results
[NASA-TM-104196] p 602 N92-22320
Design of an integrated airframe/propulsion control system architecture
[NASA-CR-182007] p 602 N92-22644
Development of flight testing of a fault tolerant fly-by-light yaw control system p 662 N92-25599
Expert system management system
[AD-A247102] p 781 N92-26863
Use of Markov methods in analysis of fault-tolerant systems with flexible repair policies
[PNR-90801] p 767 N92-27038
Advanced techniques in reliability model representation and solution
[NASA-TP-3242] p 1134 N92-33483
Distributed systems: Interconnection and fault tolerance studies
[AD-A252869] p 1135 N92-33920

FAULT TREES
Fault Tree Interpreter --- expert system shell for rule-based expert systems development for control of ATE
[AIAA PAPER 91-3789] p 232 A92-17645
Developing intelligent automatic test equipment p 922 A92-48569
Modular techniques for dynamic fault-tree analysis p 1120 A92-56241

FAULTS
Implanted component faults and their effects on gas turbine engine performance
[ASME PAPER 91-GT-41] p 121 A92-15524

FEASIBILITY ANALYSIS
Study on international cooperative test facilities for future SST/HST
[AIAA PAPER 92-3945] p 1097 A92-56775
A knowledge-based assistant for diagnosis in aircraft maintenance p 61 N92-12538
Evaluation of triple simultaneous parallel ILS approaches spaced 4300 feet apart, phase 4a
[ACD-340] p 191 N92-14034
Weight evaluation and sensitivity analysis for space plane. Part 2: TSTO
[NAL-TM-602-PT-2] p 287 N92-17754
H2-fueled high-bypass turbofan p 475 N92-21529
Principles and computer simulations of intercooled-turbocharged gas generator/expander engine p 592 N92-22132
An investigation into the feasibility of providing a proximity warning device for search and rescue helicopters
[ETN-92-91057] p 530 N92-22408
FALKE: Winged re-entry vehicle flight control p 667 N92-24454
Radiant energy power source for jet aircraft
[DE92-008726] p 648 N92-24556
Tilt rotors and the Port Authority of New York and New Jersey Airport System
[RAND-R-3971/1-PA-SUMM] p 636 N92-25262
A prototype semantic integrity front end expert system for a relational database
[AD-A246084] p 781 N92-26765
Aerodynamic interference between stores
[AD-A247207] p 715 N92-27172
Feasibility of magnetic bearings for advanced gas turbine engines p 772 N92-27738
The mechanical properties of metal-void composites --- pressurized microvoids
[AD-A246087] p 757 N92-27749
Feasibility study of hypersonic clinometric measurements at R3Ch
[ONERA-RSF-136/1865-AY-728-] p 829 N92-28789
The design of test-section inserts for higher speed aeroacoustic testing in the Ames 80- by 120-foot wind tunnel
[NASA-TM-103915] p 927 N92-28909
European studies to investigate the feasibility of using 1000 ft vertical separation minima above FL 290. Part 1: Overview of organisation, techniques employed, and conclusions
[NLR-TP-91062-U-PT-1] p 841 N92-29605
Model analysis and expert system development for planning and scheduling teleoperations for aircraft turnaround functions, volume 1
[AD-A251037] p 932 N92-30253
Model analysis and expert system development for planning and scheduling teleoperations for aircraft turnaround functions. Volume 2: Top user's guide
[AD-A251083] p 932 N92-30258
Development statistics for the UH-1 Ada feasibility study
[AD-A252404] p 982 N92-30547
Extension of the integral equation formulation of linearized time dependent subsonic flow
[AD-A250654] p 947 N92-31171

Experimental testing of prototype face gears for helicopter transmissions
[NASA-TM-105434] p 1002 N92-31349
Analytical and experimental studies of heat pipe radiation cooling of hypersonic propulsion systems
[DE92-013428] p 973 N92-31817
Laser-initiated conical detonation wave for supersonic combustion, part 3
[AD-A250522] p 989 N92-32076
Vision-based range estimation using helicopter flight data
[NASA-TM-103930] p 1047 N92-32424

FEDERAL BUDGETS
National Aeronautics and Space Administration
p 238 N92-14923
National Aeronautics and Space Administration
p 238 N92-14925
National Aeronautics and Space Administration
p 238 N92-14927
National Aeronautics and Space Administration research and development p 238 N92-15937
The V-22: Can the nation afford to forgo its production?
[AD-A243158] p 242 N92-17477
National Aeronautics and Space Administration
p 417 N92-18309
Departments of Veterans Affairs and Housing and Urban Development, and independent agencies appropriations for 1993, part 6
[GAO-55-636-PT-6] p 1141 N92-32505

FEEDBACK
The jet edge-tone feedback cycle - Linear theory for the operating stages p 392 A92-24758
Maximum likelihood algorithm and its application to parameter identification of closed-loop flight vehicles
p 1008 A92-53023
An algorithm for robust eigenstructure assignment using the linear quadratic regulator
[AD-A244267] p 412 N92-19335

FEEDBACK CONTROL
Real parameter uncertainty and phase information in the robust control of flexible structures
p 32 A92-11345
Experimental active control of a two-dimensional truss
p 47 A92-11346
Robustness of distributed systems with respect to small time delays p 47 A92-11351
A time approach to robustness of LTI systems with structured uncertainty and unmodelled dynamics --- linear time-invariant p 48 A92-11356
Closed-loop identification and iterative controller design p 48 A92-11362
Reduced-order robust controllers - H(infinity)-balanced truncation and optimal projection p 48 A92-11363
Aircraft control under conditions of windshear
p 27 A92-11384
Robust pole assignment using closed loop controllability conditions p 49 A92-11417
Polygon interval arithmetic and design of robust control systems p 49 A92-11418
Design of reliable control systems p 49 A92-11420
H(infinity) control of linear systems with nonzero initial conditions p 50 A92-11430
Design of non-overshooting feedback control systems
p 50 A92-11431
Robust stabilization with positive real uncertainty - Beyond the small gain theorem p 50 A92-11444
Application of quantitative feedback theory (QFT) to flight control problems p 27 A92-11499
An approach to the optimal output feedback initial stabilizing gain problem p 52 A92-11553
Design of the flare control law for longitudinal autopilot using H(infinity) synthesis p 28 A92-11562
Robust autopilot design for aircraft with multiple lateral-axes controls using H(infinity) synthesis
p 28 A92-11563
A two-feedback-loop robust helicopter controller based on eigenspace techniques and H(infinity) synthesis
p 29 A92-11582
Design of localizer capture and track hold for a transport airplane - An H(infinity)/LTR approach
p 52 A92-11583
State feedback for nonlinear continuous-time systems - Stabilization and the creation of invariant subspaces
p 52 A92-11587
Alleviation of whirl-flutter on tilt-rotor aircraft using active controls p 133 A92-14423
Active control for gas turbine combustors
p 128 A92-16585
Closed-loop operation of GPS aided INS
p 100 A92-16954
A geometric approach to regulator and tracker design for an aerospace plane
[AIAA PAPER 91-5054] p 203 A92-17837
Regulation of relaxed static stability aircraft
p 203 A92-18463
Parameter insensitive control utilizing eigenspace methods --- for flutter suppression in aeroelastic vehicles
p 204 A92-18615
Structure/control design synthesis of active flutter suppression system by goal programming
p 204 A92-18621
Nonlinear control of a twin-lift helicopter configuration
p 204 A92-18624
Parametric robust control by quantitative feedback theory p 302 A92-21176
Aircraft flight controls design using output feedback
p 280 A92-21180
Quantitative Feedback Theory (QFT) applied to the design of a rotorcraft flight control system
[AIAA PAPER 92-0044] p 281 A92-22161
Decentralized-feedback pole placement of linear systems p 411 A92-27347
Optimal output feedback for linear time-periodic systems p 412 A92-28142
High-alpha application of variable-gain output feedback control p 380 A92-28152
Reaching conditions in variable structure systems for output feedback control p 506 A92-29037
Linear systems with output constraints - The theory and application of maximal output admissible sets
p 506 A92-29066
Design of compensators for linear parameter-varying feedback systems by the gain scheduling technique
p 507 A92-29101
Integrated flight/propulsion control specifications for systems with two-way coupling p 477 A92-29117
Controller design for the F-14 pitch axis control problem using the quantitative feedback theory approach
p 478 A92-29128
On the Nyquist envelope of an interval plant family
p 507 A92-29132
The implicit function theorem and robust root locus
p 507 A92-29134
A hierarchical data structure and new capabilities of the Robust-Control Toolbox p 507 A92-29155
The generalized normal forms and method of resonance control of nonlinear dynamical systems
p 507 A92-29189
Frequency response specifications and sensitivity functions in quantitative feedback theory
p 508 A92-29280
Aerobrake guidance law synthesis using feedback linearization p 485 A92-29304
Parameter identification of compressor dynamics during closed-loop operation p 508 A92-29313
Compressor modeling and active control of stall/surge
p 508 A92-29315
A Lyapunov based nonlinear control scheme for stabilizing a basic compression system using a close-coupled control valve p 508 A92-29316
On automatic control of aeroelastic vehicles
p 509 A92-29327
Synthesis of robust nonlinear autopilots using differential game theory p 478 A92-29330
Tiltrotor control law design for rotor loads alleviation using modern control techniques p 478 A92-29331
Trajectory shaping by the U-parameter design method
p 479 A92-29361
An integrated, full-range surge control/rotating stall avoidance compressor control system
p 469 A92-29376
Self-compensating carrier aircraft recovery system
p 448 A92-32238
Trajectory control for a low-lift maneuverable reentry vehicle
[AIAA PAPER 92-1146] p 574 A92-33287
The differential algebraic approach in nonlinear dynamical feedback controlled landing maneuvers
p 574 A92-33639
Outline and discussion of the cooling loop of the heating control system in the exposed facility of the Japanese Experiment Module (JEM) p 574 A92-35610
Achievement of rotorcraft handling qualities specifications via feedback control p 568 A92-35747
Active control of helicopter ground and air resonance
p 568 A92-35762
Evaluation of a constant feedback gain for closed loop higher harmonic control p 568 A92-35768
Improvement of helicopter robustness and performance control law using eigenstructure techniques and H-infinity synthesis p 569 A92-35776
Estimation of flying qualities using a leastsquares lower-order equivalent systems technique
p 570 A92-35947
Aircraft control for take-off in windshear
p 660 A92-36990
A Kalman filter mechanization for the baro-inertial vertical channel p 673 A92-39558
Inverse and optimal control for desired outputs
p 661 A92-39894
Analyzing the flared landing task with pitch-rate flight control systems p 661 A92-39905
Robust stabilisation of multivariable feedback systems with desired performance requirement
p 776 A92-42172
Inspection of stability deterioration with an adaptive regulator p 776 A92-43178
Robust discrete controller design for an unmanned research vehicle (URV) using discrete quantitative feedback theory p 877 A92-48495
Compensating for manufacturing and life-cycle variations in aircraft engine control systems
[AIAA PAPER 92-3869] p 868 A92-49139
Vibration control of rotor-bearing system by controlled squeeze-film damper bearings p 990 A92-49579
Optimal discrete-time static output-feedback design - A W-domain approach p 1007 A92-50499
Robust flight control systems - A parameter space design p 976 A92-50503
The research on Pilot Induced Oscillation
p 977 A92-53088
Identification and control of aircraft dynamics using radial basis function neural networks
[AIAA PAPER 92-4393] p 1074 A92-55194
Robust sampled data eigenstructure assignment using the delta operator
[AIAA PAPER 92-4400] p 1075 A92-55200
Design of robust Quantitative Feedback Theory controllers for pitch attitude hold systems
[AIAA PAPER 92-4409] p 1075 A92-55203
Invertibility and trajectory control for nonlinear maneuvers of aircraft
[AIAA PAPER 92-4410] p 1075 A92-55204
An algorithm for robust eigenstructure assignment using the Linear Quadratic Regulator
[AIAA PAPER 92-4478] p 1131 A92-55237
An framework for robust flight control design using constrained optimization
[AIAA PAPER 92-4603] p 1131 A92-55282
Robust control design of an automatic carrier landing system
[AIAA PAPER 92-4619] p 1077 A92-55296
Nonlinear model-following control application to airplane control (1992 AIAA Controls Design Challenge)
[AIAA PAPER 92-4625] p 1077 A92-55302
Quantitative Feedback Theory approach to AIAA Controls Design Challenge
[AIAA PAPER 92-4626] p 1077 A92-55303
Multiple delay model approach applied to the AIAA 1922 Controls Design Challenge
[AIAA PAPER 92-4630] p 1078 A92-55305
A guidance law for hypersonic descent to a point
[AIAA PAPER 92-4303] p 1104 A92-55311
Numerical simulations of flutter and its suppression by active control
[AIAA PAPER 92-4652] p 1082 A92-55396
An identification procedure for a system with a choice of feedback structures p 1132 A92-55426
Robust control system design with multiple model approach p 1083 A92-56029
MIMO state-feedback control system considering phase stability by -90 deg phase-locus method
p 1084 A92-56066
Design of a flight control system using a feedback-error-learning-type neural network
p 1132 A92-56067
Control of large cryogenic tunnels
[AIAA PAPER 92-3930] p 1096 A92-56761
A compensatory algorithm for the slow-down effect on constant-time-separation approaches
[NASA-TM-4285] p 23 N92-10024
An analytical and experimental study to investigate flutter suppression via piezoelectric actuation
[NASA-TM-893240] p 156 N92-12173
Advanced rotorcraft control using parameter optimization
[NASA-CR-189502] p 135 N92-13073
Approximation methods for control of acoustic/structure models with piezoceramic actuators
[NASA-CR-189578] p 234 N92-15658
Development of high angle of attack control laws for an unstable, non-minimum phase aircraft using variations of the quantitative feedback technique
[AD-A243698] p 282 N92-17096
A robust digital flight control system for an unfanned research vehicle using discrete quantitative feedback theory
[AD-A243638] p 283 N92-17748
Technical notes and correspondence: Stochastic robustness of linear time-invariant control systems
p 303 N92-18002
Application of nonlinear QFT to flight control design for high angle of attack maneuvers with thrust vectoring
[AD-A243821] p 381 N92-19241

Ground collision avoidance using a variable incidence altitude measurement system for the A-7 aircraft
[AD-A243880] p 352 N92-19259
Adaptive control of nonlinear systems with applications to the control of flexible robot arms
[AD-A244409] p 413 N92-19397
Aeroelastic behavior of an adaptive lifting surface
p 443 N92-20378
Numerical simulations of wakes, blade-vortex interaction, flutter, and flutter suppression by feedback control p 597 N92-23997
Application of nonlinear feedback control theory to supermaneuverable aircraft
[NASA-CR-190336] p 663 N92-25648
Active noise control: Piezoceramic actuators in fluid/structure interaction models
[NASA-CR-190328] p 685 N92-26125
Stability and performance of notch filter control for unbalance response p 771 N92-27731
Design of bearings for rotor systems based on stability
p 773 N92-27799
Self-adaptive aeropropulsion components-enhancing axial compressor performance
[AD-A246123] p 743 N92-27817
Dynamic control of aerodynamic instabilities in gas turbine engines p 870 N92-28466
Superconducting bearings with levitation control configurations
[NASA-CASE-GSC-13346-1] p 909 N92-29099
Feedback control laws for highly maneuverable aircraft
[NASA-CR-190535] p 879 N92-29654
Practical method's for robust multivariable control
[AD-A248473] p 1009 N92-30322
Nonlinear system design: Adaptive feedback linearization with unmodeled dynamics
[AD-A248484] p 1009 N92-30335
A simplified dynamic model of the T700 turboshaft engine
[NASA-TM-105805] p 1009 N92-30898
Subsonic flight test evaluation of a performance seeking control algorithm on an F-15 airplane
[NASA-TM-4400] p 973 N92-31275
A parameter optimization approach to controller partitioning for integrated flight/propulsion control application
[NASA-TM-105826] p 979 N92-32241
The multiple-function multi-input/multi-output digital controller system for the AFW wind-tunnel model
[NASA-TM-107600] p 1060 N92-32536
Design of helicopter flight control systems for hover and low speed using eigenstructure assignment
p 1061 N92-33952

FEEDFORWARD CONTROL
A system identification model for adaptive nonlinear control p 508 A92-29248
Maneuver load control using optimized feedforward commands
[AIAA PAPER 92-2100] p 567 A92-35671
Identification of aerodynamic coefficients using computational neural networks
[AD-A244711] p 447 N92-21753

FERROELECTRICITY
Ferroelectric memory evaluation and development system p 902 A92-48460

FERROMAGNETIC MATERIALS
Wide gap, permanent magnet biased magnetic bearing system p 773 N92-27794

FIBER COMPOSITES
Applications of advanced composites in a 3/4 air transportable rack p 36 A92-10314
H-76β Fantail demonstrator composite fan blade fabrication p 145 A92-14356
Evaluation of thermoplastic matrix composites for use in energy-absorbing helicopter subfloors
p 141 A92-14374
Bearingless main rotor system composite component fabrication techniques p 110 A92-14453
Some results on metal and composite patch reinforcement of aluminum honeycomb panel
p 216 A92-18830
Current stabilizing of fastened composite joints to improve non-sparking lightning current performance
p 213 A92-20130
Response of symmetrically laminated rectangular plates subjected to heating p 296 A92-24186
Weaving an aircraft p 392 A92-24911
Non-homogeneous bars under tension, pure bending and thermal loads p 495 A92-31198
Measurement of basic material and processing properties affecting injection-pultrusion technology
p 580 A92-32636
Design of advanced composite components for maintainability based on inservice experience
[AIAA PAPER 92-1085] p 537 A92-33251
Ceramics and ceramic matrix composites - Aerospace potential and status
[AIAA PAPER 92-2445] p 577 A92-34474
Fabrication and properties of fiber-reinforced ceramic composites made by directed metal oxidation
p 669 A92-39861
Mechanics of curved fiber composites
p 757 A92-41034
Composite laminated shells under internal pressure
p 758 A92-41296
Basic study of adhesive bonding for fiber-composites - Adhesive bonding technologies on jet engine parts
p 764 A92-44733
Numerical simulation of impact resistance on composite blade p 738 A92-44734
The relationship between tensile and flexural strength of unidirectional composites p 891 A92-45629
Axial alignment of short-fiber titanium aluminide composites by directional solidification
p 892 A92-46838
Wing leading edge design with composites to meet bird strike requirements p 848 A92-47404
Moldless composite aircraft wing structural design modifications p 958 A92-51527
High temperature MMCs for aero-engines - Challenge and potential p 986 A92-52982
Control augmented structural optimization of aeroelasticity tailored fiber composite wings
[AD-A241464] p 135 N92-13075
Development and evaluation of a finite element model for a fiber composite helicopter fuselage
[MBB-UD-0584-90-PUB] p 196 N92-15066
Analysis of aircraft engine blade subject to ice impact
[NASA-TM-105336] p 229 N92-15402
Polymer infiltration studies
[NASA-CR-189773] p 289 N92-17004
Polymer infiltration studies
[NASA-CR-190204] p 578 N92-22486
Vinyl capped addition polyimides
[NASA-CASE-LEW-15027-2] p 579 N92-24053
Tensile and interlaminar properties of GLARE (trade name) laminates
[AD-A250188] p 895 N92-28921
Low-velocity impact loading on fibre reinforced aluminum laminates (ARALL) and other aircraft sheet materials
[ETN-92-91613] p 987 N92-30414
Multidisciplinary optimization of fiber composite aircraft structures
[MBB/FW321/S/PUB/476] p 961 N92-30424
Development of hardness cycles for fiber bound materials, using DSC: From laboratory specimens to complex high duty structural members
[MBB-Z-0409-91-PUB] p 987 N92-30969
Polymer blends, volume 1
[AD-A252112] p 987 N92-31419
Cutting treatment by drilling of fiber bound synthetic materials
[MBB-UD-0609-91-PUB] p 988 N92-31716
Thermomechanical fatigue behavior of a silicone carbide fiber-reinforced calcium aluminosilicate glass-ceramic matrix composite
[AD-A249870] p 988 N92-31823
Eighth DOD/NASA/FAA Conference on Fibrous Composites in Structural Design, part 1
[NASA-CP-3087-PT-1] p 1106 N92-32513
Design, evaluation and experimental effort toward development of a high strain composite wing for Navy aircraft p 1107 N92-32514
Development of thermoplastic components for structural validation p 1107 N92-32522
Damage tolerance certification methodology for composite structures p 1108 N92-32579
Initial postbuckling response of an unsymmetrically laminated rectangular plate p 1108 N92-32586
Jet fuel absorption and dynamic mechanical analysis of carbon fibre composites p 1110 N92-33050
Advanced airframe structural materials: A primer and cost estimating methodology
[AD-A253371] p 1062 N92-34182

FIBER OPTICS
Development and future view of the technology for fly-by-light control system elements p 131 A92-14027
Fabry-Perot fiber-optic sensors in full-scale fatigue testing on an F-15 aircraft p 391 A92-24553
Fiber optic sensors for smart skins applications
p 392 A92-24778
Fiber optics for the National Aero-Space Plane
p 386 A92-24780
Progress towards fiber optic smart structures at UTIAS
p 368 A92-24781
Smart skins and fiber-optic sensors application and issues p 368 A92-24785
Fiber-coupled position sensors for aerospace applications p 370 A92-27776
Optically powered and interrogated rotary position sensor for aircraft engine control applications
p 370 A92-27777
Fibre optic laser anemometry for turbomachinery applications p 397 A92-27783
Coherence multiplexed polarimetric fibre sensor arrays for aerospace applications p 370 A92-27785
A novel avionic sensor for fly-by-light controls
p 650 A92-38128
Fiber optic systems for mobile platforms IV; Proceedings of the Meeting, San Jose, CA, Sept. 18, 1990
[SPIE-1369] p 779 A92-42601
Wavelength-multiplexed fiber-optic position encoder for aircraft control systems p 734 A92-42602
Efficiency of a 5V/5mW power by light power supply for avionics applications p 734 A92-42603
Code Division Multiple Access (CDMA) system candidate for integrated modular avionics
p 725 A92-42604
Development of fly-by-light systems for commercial aircraft p 744 A92-42605
Singlemode fiber optic rotary joint for aircraft applications p 779 A92-42606
A fiber optic temperature sensor for aerospace applications p 761 A92-42607
LDV measurements on a rectangular wing with a simulated glaze ice accretion
[AIAA PAPER 92-2690] p 800 A92-45537
A high-performance LLLTV CCD camera for nighttime pilotage p 855 A92-46227
Fibre optic rotary position sensors for vehicle and propulsion controls p 855 A92-46243
Fiber optic controls for aircraft engines - Issues and implications p 856 A92-46244
Potential for integrated optical circuits in advanced aircraft with fiber optic control and monitoring systems
p 856 A92-46246
Fiber optic and laser sensors VIII; Proceedings of the Meeting, San Jose, CA, Sept. 17-19, 1990
[SPIE-1367] p 901 A92-48026
Fiber-optic position transducers for aircraft controls
p 857 A92-48041
Application of analog fiber optic position sensors to flight control systems p 857 A92-48042
Multi-analog track fiber coupled position sensor
p 857 A92-48043
Wavelength encoded fiber optic angular displacement sensor p 857 A92-48046
Fiber-optic pressure sensor system for gas turbine engine control p 857 A92-48047
Making fly-by-light a reality p 877 A92-48499
Optics in aircraft engines p 926 A92-48500
Absolute fiber optic pressure transducer for aircraft air data measurement p 858 A92-48501
Design issues in a fiber optic sensor system architecture for aircraft engine control
[AIAA PAPER 92-3483] p 866 A92-49023
A low maintenance and highly reliable fly-by-light architecture p 975 A92-49325
Distributed flight control system using fiber distributed data interface (FDDI) p 976 A92-51004
High performance flight simulation at NASA Langley
[AIAA PAPER 92-4179] p 982 A92-52460
Design of a fiber optic image transmission link
[AD-A243686] p 304 N92-17088
Measurement of vortex flow fields
[NASA-CR-189543] p 443 N92-20283
Fiber optics for controls p 570 N92-22529
Advances in Fibre-Optic Technology in Communications and for Guidance and Control
[AGARD-LS-184] p 774 N92-28084
Fiber optic data busses for aircraft
p 736 N92-28093
Multi-channel fiber optic rotary joint for single-mode fiber
[AD-D015273] p 927 N92-29095
Fly-by-light technology development plan
[NASA-CR-181954] p 1086 N92-32778

FIBER ORIENTATION
The relationship between tensile and flexural strength of unidirectional composites p 891 A92-45629
Multidisciplinary optimization of fiber composite aircraft structures
[MBB/FW321/S/PUB/476] p 961 N92-30424
Continuation of tailored composite structures of ordered staple thermoplastic material
[NASA-CR-189671] p 1110 N92-33613

FIBER STRENGTH
Composite strength statistics from fiber strength statistics
[AD-A245616] p 755 N92-26383

FIBER VOLUME FRACTION
The mechanical properties of metal-void composites --- pressurized microvoids
[AD-A246087] p 757 N92-27749

FIBERS
Universal weaving for turbine engine composite preforms
[AD-A237667] p 202 N92-14059
Towards GLARE: The development of a fatigue insensitive and damage tolerant aircraft material
[ETN-92-91301] p 648 N92-24966
FIBONACCI NUMBERS
A fuel-optimal 4D guidance algorithm
p 978 A92-53095
FIELD OF VIEW
Optical design of dual combiner head-up displays
p 414 A92-24628
Extreme wide field-of-view displays and the enclosed cockpit p 965 A92-49313
Computational algorithms for increased control of depth-viewing volume for stereo three-dimensional graphic displays
[NASA-TM-4379] p 1065 N92-34109
FIGHTER AIRCRAFT
Robust controller design for an advanced fighter aircraft p 28 A92-11500
H(infinity) robust control synthesis for a fighter performing a coordinated bank turn p 29 A92-11585
Tomorrow's cockpit displays p 117 A92-13699
Control systems for the next century's fighter engines
[ASME PAPER 91-GT-278] p 125 A92-15674
F-117A flight test program p 112 A92-16061
YF-23A preliminary flight test results
p 112 A92-16063
Heavy metal --- fighter aircraft test rigs
p 207 A92-18100
Damage tolerance of the fighter aircraft 37 Viggen. I - Analytical assessment. II - Experimental verification
p 192 A92-19819
Four decades of transonic fighter design
p 193 A92-20203
Role of dynamic simulation in fighter engine design and development p 277 A92-21080
The FALSTAFF program - A standard spectrum for simulating the service loading of aircraft with prevailing maneuver loads p 284 A92-21922
Combined H(2)/H(infinity) optimal control design applied to an advanced fighter aircraft
[AIAA PAPER 92-0045] p 281 A92-22162
A simple numerical criterion for vortex breakdown
[AIAA PAPER 92-0057] p 250 A92-22172
Forebody vortex control p 251 A92-22517
Agility as a contributor to design balance
p 356 A92-24405
Industry warms to CFD p 392 A92-24908
The stealth master p 307 A92-25175
The evaluation of canard couplings at high angles of attack
[AIAA PAPER 92-0281] p 318 A92-25735
Calculation of the carriage loads of tandem stores on a fighter aircraft
[AIAA PAPER 92-0283] p 319 A92-25736
Low aspect ratio wing code validation experiment
[AIAA PAPER 92-0402] p 324 A92-26255
Combat aircraft jet engine noise studies
[ONERA, TP NO. 1991-192] p 415 A92-26353
2-D and 3-D minimum-time-to-turn flights via parameter optimization
[AIAA PAPER 92-0731] p 379 A92-27083
Automated mission planning - A striking capability
p 412 A92-28494
Design, analysis, and testing of integrally stiffened composite centre fuselage skin for future fighter aircraft
p 535 A92-32554
Ground test facilities for aerothermal and aero-optical evaluation of hypersonic interceptors
[AIAA PAPER 92-1074] p 573 A92-33244
The ATF YF-23 Vehicle Management System
[AIAA PAPER 92-1076] p 563 A92-33245
YF-22A prototype Advanced Tactical Fighter demonstration/validation flight test program overview
[AIAA PAPER 92-1087] p 537 A92-33253
Multidisciplinary design environment development for air vehicle engineering
[AIAA PAPER 92-1113] p 605 A92-33269
High-performance fighter fly-by-wire flight control actuation system --- for YF-23A prototype
[AIAA PAPER 92-1123] p 563 A92-33277
Application of multidisciplinary optimization to conceptual aircraft design at Rockwell International - A status report
[AIAA PAPER 92-1196] p 537 A92-33307
Transonic wind tunnel investigation of limit cycle oscillations on fighter type wings - Update
[AIAA PAPER 92-2125] p 572 A92-35692
Measures of merit for aircraft dynamic maneuvering
p 642 A92-37825
Solution of Euler equations for fighter forebody-inlet combinations at high angles of attack
p 613 A92-38269
Inverse and optimal control for desired outputs
p 661 A92-39894
Agility and high angle of attack - An Air Force research perspective
[SAE PAPER 912145] p 608 A92-39983
Velocity dependence of high angle of attack longitudinal flying qualities criteria
[SAE PAPER 912149] p 662 A92-39985
Future military APU requirements
[SAE PAPER 912176] p 655 A92-40001
Challenging power-density requirements for future fighter APUs
[SAE PAPER 912177] p 655 A92-40002
1991 report to the aerospace profession; SETP Symposium, 35th, Beverly Hills, CA, Sept. 26-28, 1991, Proceedings p 645 A92-40028
Rafale: Program update - Development of a naval version p 645 A92-40035
YF-22A prototype advanced tactical fighter demonstration/validation flight test program overview
p 646 A92-40037
European Fighter Aircraft (EFA) programme status report p 646 A92-40043
Some aspects of advanced aircraft development
p 729 A92-41176
Self reliance in aerospace structures
p 758 A92-41190
Current growth in the aeronautics p 701 A92-41196
Multi-constraint wing optimization p 701 A92-41197
Flow over a twin-tailed aircraft at angle of attack. I - Spatial characteristics p 702 A92-41229
Symmetry breaking in vortex flows on conical bodies
p 703 A92-41278
Auxiliary power units for advanced fighters
p 737 A92-43545
Specification of adaptive aiding systems - Information requirements for designers p 916 A92-44915
A USAF assessment of STOVL fighter options
p 842 A92-45310
Ground surface erosion - British Aerospace test facility and experimental studies p 881 A92-45323
Development of the DDV actuation system on the IDF aircraft
[SAE PAPER 912080] p 844 A92-45455
Dynamically enhanced sustained lift using oscillating leading-edge flaps
[AIAA PAPER 92-2625] p 794 A92-45497
Application of the Euler method EUFLEX to a fighter-type airplane configuration at transonic speed
[AIAA PAPER 92-2620] p 845 A92-45573
Prediction of leading-edge vortex breakdown on a delta wing oscillating in roll
[AIAA PAPER 92-2677] p 807 A92-45585
Aviation, motor, and space designs --- research and development in U.S.S.R. p 784 A92-46202
Prediction of inviscid supersonic/hypersonic aircraft flowfields p 810 A92-46785
Maximizing thrust-vectoring control power and agility metrics p 874 A92-46794
Design load predictions on a fighter-like aircraft wing
p 811 A92-46797
Generation of efficient multiblock grids for Navier-Stokes computations p 919 A92-47081
Dawn of stealth p 785 A92-47757
The Tonopah years p 785 A92-47758
The airplane --- F-117 aircraft p 849 A92-47759
Identifying design requirements using integrated analysis structures p 922 A92-48527
Aerodynamic performance of a full-scale lifting ejector system in a STOVL fighter aircraft
[AIAA PAPER 92-3094] p 824 A92-48738
Computational icing analysis for aircraft inlets
[AIAA PAPER 92-3178] p 836 A92-48793
Fighter airframe/propulsion integration - A General Dynamics perspective
[AIAA PAPER 92-3332] p 850 A92-48915
Fighter airframe/propulsion integration - A McDonnell Aircraft perspective
[AIAA PAPER 92-3333] p 850 A92-48916
A computational study of advanced exhaust system transition ducts with experimental validation
[AIAA PAPER 92-3794] p 907 A92-49126
Artificial intelligence in the helicopter cockpit of the future p 964 A92-49271
Systems commonality - Integrated avionics for the MH-47E and the MH-60K p 966 A92-49331
The army special operations aircraft integrated avionics subsystem - An operational perspective
p 966 A92-49332
Development of active control technology for the next generation of combat aircraft p 975 A92-50008
The effect of atmospheric turbulence on the external store separation from an aircraft p 934 A92-50233
Distributed flight control system using fiber distributed data interface (FDDI) p 976 A92-51004
Dead reckoning for aircraft in distributed interactive simulation
[AIAA PAPER 92-4171] p 1008 A92-52456
A full-scale fatigue test and failure analyses research of F-X fighters p 960 A92-53092
Optimal implicit model-following approach with frequency-shaped weighting and its application to design of flight control system p 977 A92-53094
Results of a perturbation analysis correlating flows entering and exiting an aircraft inlet system
[AIAA PAPER 92-3624] p 1021 A92-54091
In-flight optimization of the total propulsion system
[AIAA PAPER 92-3744] p 1068 A92-54146
Mikoyan's market-buster p 1052 A92-54981
Flight control law synthesis using neural network theory
[AIAA PAPER 92-4390] p 1074 A92-55191
A fuzzy logic based F/A-18 automatic carrier landing system
[AIAA PAPER 92-4392] p 1074 A92-55193
The flow field characteristics about a fighter configuration at high angles of attack
[AIAA PAPER 92-4358] p 1025 A92-55344
Pulsating spanwise blowing on a fighter aircraft
[AIAA PAPER 92-4359] p 1025 A92-55345
Analytical development of an equivalent system mismatch function
[AIAA PAPER 92-4422] p 1080 A92-55346
Understanding and development of a prediction method of transonic limit cycle oscillation characteristics of fighter aircraft
[AIAA PAPER 92-4501] p 1026 A92-55369
Optimization of composite material wing of fighter type aircrafts p 1053 A92-56018
Design of a flight control system using a feedback-error-learning-type neural network
p 1132 A92-56067
Euler/experiment correlation of a generic fighter
p 1031 A92-56164
Development and validation of a freejet technique for inlet-engine compatibility testing
[AIAA PAPER 92-3921] p 1033 A92-56752
Transonic and supersonic Euler computations of vortex-dominated flow fields about a generic fighter
[NASA-TP-3156] p 11 N92-10011
Static internal performance of ventral and rear nozzle concepts for short-takeoff and vertical-landing aircraft
[NASA-TP-3103] p 12 N92-10975
Development of a 1/7th scale fighter UAV for flight research
[AD-A240703] p 23 N92-11008
Application of Eigenstructure Assignment to the control of powered lift combat aircraft
[RAE-TM-FS-1009] p 135 N92-12004
Tool supported software development experiences from the EFA project p 163 N92-12451
Water tunnel flow visualization studies of a canard-configured X-31A-like fighter aircraft model
[AD-A241362] p 90 N92-13037
Evolution of avionic systems architecture, from the 1950's to the present p 198 N92-14047
Avionics technology beyond 2000
p 200 N92-14058
Monitoring load experience of individual aircraft
[NLR-TP-90084-U] p 196 N92-15065
Ferrundi Company supplies 4500 model head up display devices to India's MIG-21 aircraft
[AD-A241044] p 229 N92-15367
Hot-wire surveys in the vortex wake downstream of a three-percent fighter aircraft model at high angles of attack
[AD-A241869] p 259 N92-15975
Aerodynamic development of the X-31 aircraft for the high angle of attack region
[MBB-FE211-S-PUB-452] p 275 N92-17313
Design, analysis, and testing of integrally stiffened composite centre fuselage skin for future fighter aircraft
[MBB-FE2-PUB-S-450] p 359 N92-18333
Durability and damage tolerance testing and fatigue life management: A CF-18 experience p 361 N92-18581
Advanced tactical fighter engine
[ETN-92-90840] p 376 N92-18728
X-31 enhancement of aerodynamics for maneuvering beyond stall p 363 N92-18779
Aerodynamic control of fighter aircraft by manipulation of forebody vortices p 380 N92-18791
Transformation of flightmechanical design requirements for modern fighters into aerodynamic characteristics
p 365 N92-18794
Aeroservoelastic stability of aircraft at high incidence
p 381 N92-18795
Analysis of an advanced fighter aircraft using jet flap techniques and the vortex lattice method
[AD-A244051] p 366 N92-19185

Nonlinear stability and control study of highly maneuverable high performance aircraft, phase 2
[NASA-CR-189911] p 382 N92-19841
Investigation of a semi-empirical method to predict limit cycle oscillations of modern fighter aircraft
[NLR-TP-90087-U] p 481 N92-20475
The evolution of the bypass engine
[PNR-90832] p 476 N92-21850
Aircraft Ship Operations
[AGARD-CP-509] p 464 N92-21951
Integration of flight and carrier landing aid systems for shipboard operations p 456 N92-21958
Revolution at sea: Aircraft options for the year 2030
p 466 N92-21974
The Air Force Manufacturing Technology (MANTECH): Technology transfer methodology as exemplified by the radar transmit/receive module program
p 593 N92-22451
Flow field over the wing of a delta-wing fighter model with vortex control devices at Mach 0.6 to 1.2
[NASA-TM-4296] p 526 N92-22506
Application of analytical and design tools for fighter wing aeroelastic tailoring p 550 N92-23231
Design of a fighter aircraft vertical tail enhanced buffet environment survivability p 551 N92-23235
Mechanical design of a rotary balance system for NASA. Langley Research Center's vertical spin tunnel
p 664 N92-25090
ICAAS piloted simulation evaluation
p 735 N92-27906
Unsteady aerodynamics for aeroelasticity at the Flight Dynamics Directorate p 718 N92-27939
Aeroelastic calculations for fighter aircraft using the transonic small disturbance equation
p 720 N92-27951
Development of a method to predict transonic limit cycle oscillation characteristics of fighter aircraft
p 746 N92-27958
Transonic wind tunnel investigation of limit cycle oscillations on fighter type wings p 721 N92-27959
Development of telemetry for the agility flight test of a radio controlled fighter model
[AD-A248653] p 753 N92-27994
The role of simulation for the study of APIS (piloting support by synthetic imagery) p 885 N92-28544
Application of piloted simulation to high-angle-of-attack flight-dynamics research for fighter aircraft
p 886 N92-28551
Flow visualization studies of a sidestipping, canard-configured X-31A-Like fighter aircraft model
[AD-A245940] p 829 N92-28883
Research and technology, 1991. Langley Research Center
[NASA-TM-4331] p 1013 N92-30733
Nonlinear stability and control study of highly maneuverable high performance aircraft, phase 2
[NASA-CR-190667] p 978 N92-30922
A parameter optimization approach to controller partitioning for integrated flight/propulsion control application
[NASA-TM-105826] p 979 N92-32241
A learning enhanced flight control system for high performance aircraft
[AD-A252520] p 1086 N92-32435
Aspects of compression in aerospace composites: Future requirements p 1109 N92-33036
Rapid development of the X-31 simulation to support flight-testing
[NASA-TM-104256] p 1060 N92-33149
Effect of afterbody geometry on aerodynamic characteristics of isolated nonaxisymmetric afterbodies at transonic Mach numbers
[NASA-TP-3236] p 1041 N92-33706

FILAMENT WINDING
Processing parameters for carbon/PMR-15 composite flat panels p 34 A92-11812
Filament winding of composite isogrid fuselage structures p 784 A92-47405

FILLETS
The aerodynamic effect of fillet radius in a low speed compressor cascade
[NASA-TM-105347] p 202 N92-14063
Algorithms for blending surface generation
[AD-A245686] p 777 N92-26524

FILM BOILING
Boiling heat transfer from an excavated fin
p 498 A92-32523

FILM COOLING
Film cooling research on the endwall of a turbine nozzle guide vane in a short duration annular cascade. I - Experimental technique and results
[ASME PAPER 91-GT-252] p 150 A92-15657
Film cooling research on the endwall of a turbine nozzle guide vane in a short duration annular cascade. II - Analysis and correlation of results
[ASME PAPER 91-GT-253] p 150 A92-15658
The influence of density difference between hot and coolant gas on film cooling by a row of holes - Predictions and experiments
[ASME PAPER 91-GT-255] p 151 A92-15660
Film cooling on a gas turbine rotor blade
[ASME PAPER 91-GT-279] p 152 A92-15675
Two and three dimensional parabolized Navier-Stokes code for scramjet combustor, nozzle, and film cooling analysis
[AIAA PAPER 92-0391] p 372 A92-26247
Experimental investigation of film cooling effectiveness for slots of various exit geometries p 497 A92-32265
Numerical study of coupled heat transfer under conditions of filtering and film cooling of blunt anisotropic bodies p 610 A92-36552
Evaluation of the ATD-GASP for endo-leap applications --- Aerothermal Technology Development of Generalized Aerodynamic Simulation Programs
[AIAA PAPER 92-2771] p 704 A92-41318
Surface cooling of scramjet engine inlets using heat pipe, transpiration, and film cooling p 763 A92-44381
The flow pattern and external heat transfer investigation for gas turbine vanes end surfaces
[AIAA PAPER 92-3071] p 903 A92-48722
Numerical simulation of turbine 'hot spot' alleviation using film cooling
[AIAA PAPER 92-3309] p 904 A92-48896
Numerical simulation of three-dimensional turbulent flows in combustion chambers p 970 A92-53276
Experimental modeling of film-cooled axial turbine tip seals
[AIAA PAPER 92-4058] p 1119 A92-56141
Effects of wake and shock passing on the heat transfer to a film cooled transonic turbine blade
p 156 N92-12201
Studies of gas turbine heat transfer: Airfoil surfaces and end-wall cooling effects
[AD-A244055] p 376 N92-19097
Hypersonic aerospace vehicle leading edge cooling using heat pipe, transpiration and film cooling techniques
p 780 N92-26733

FILM THICKNESS
Nondestructive depth profiling of the protective coating on a turbine blade p 144 A92-13641
The measurement of water film thickness on airfoils in heavy rain conditions using conductance sensors
p 452 N92-21695

FILTRATION
Numerical study of coupled heat transfer under conditions of filtering and film cooling of blunt anisotropic bodies p 610 A92-36552

FINENESS RATIO
An experimental investigation of the effect of fineness ratio on lateral force on a pointed slender body of revolution p 86 N92-13015

FINISHES
Low volatile organic compound paints
[DE91-017984] p 35 N92-11203

FINITE DIFFERENCE THEORY
Finite difference numerical prediction of aerodynamics of an airfoil flying over wavy wall p 64 A92-14033
Turbine cascade calculations through a fractional step Navier-Stokes algorithm
[ASME PAPER 91-GT-55] p 68 A92-15533
Unsteady Euler calculations in 2-D internal aerodynamics with introduced vorticity
[ASME PAPER 91-GT-168] p 73 A92-15603
Nonlinear triggered lightning models for use in finite difference calculations p 230 A92-20128
The use of finite difference electromagnetic analysis in the design and verification of modern aircraft
p 192 A92-20136
Computation of unsteady, laminar, incompressible, viscous flows using the vorticity streamfunction formulation p 245 A92-21979
On an adaptive numerical method for solution of high gradient problems p 410 A92-24905
Study of numerical computation of inviscid flow field about complex configuration of re-entry vehicle
p 313 A92-25041
The study of inverse boundary layer algorithm for transonic flows over aerofoils p 315 A92-25140
Analysis of a 2-D airfoil motion flying in-proximity-to a wavy-wall surface-lifting surface-scheme
p 315 A92-25506
Aeroelastic analysis of swept, anhedral, and tapered tip rotor blades p 316 A92-25577
Integrated numerical methods for hypersonic aircraft cooling systems analysis
[AIAA PAPER 92-0254] p 357 A92-25712
Preconditioned upwind methods to solve incompressible Navier-Stokes equations p 395 A92-26436
Calculation of compressible boundary layer flow about airfoils by a finite element/finite difference method
[AIAA PAPER 92-0524] p 332 A92-26948
An analytical approach to grid sensitivity analysis --- of NACA wing sections
[AIAA PAPER 92-0660] p 334 A92-27031
Structural and aerodynamic analysis of a large-scale advanced propeller blade p 375 A92-28517
Analysis of a 2-D airfoil motion flying in-proximity-to a wavy-wall surface - Finite difference method
p 421 A92-29517
Flux-difference split algorithm for unsteady thin-layer Navier-Stokes solutions p 431 A92-31158
Quick calculation of three-dimensional supersonic flow past nearly axisymmetric bodies p 624 A92-40605
Numerical simulation of aerothermal loads in hypersonic engine inlets due to shock impingement
[AIAA PAPER 92-2605] p 792 A92-45482
Prediction of laminar boundary layer using cubic splines
[AIAA PAPER 92-2702] p 801 A92-45544
Two-stream, supersonic, wake flowfield behind a thick base. I - General features p 813 A92-46895
A finite difference solution of the Euler equations on non-body-fitted Cartesian grids p 818 A92-47153
Calculation of the transonic full-potential flowfield about 3D fuselage p 941 A92-53021
Flowfield of a lifting rotor in hover - A Navier-Stokes simulation p 1024 A92-54906
Motion analysis of 2-dimensional flat plate in ground effect p 1030 A92-56053
Variable impedance journal bearings for rotor-bearing systems p 157 N92-12270
Wall interference calculation in a transonic wind tunnel with discrete slots p 83 N92-12995
Analysis and design of transonic airfoils using streamwise coordinates p 194 N92-13955
Navier-Stokes analysis of turbulent boundary layer and wake for two-dimensional lifting bodies
p 221 N92-14309
A Navier-Stokes solution of Hull-ring wing-thruster interaction p 221 N92-14310
An initial investigation into methods of computing transonic aerodynamic sensitivity coefficients
[NASA-CR-190040] p 348 N92-19545
On a multi-block method for transonic turbulent flows past a wing-fuselage configuration p 632 N92-25569
Precision of the long baseline acoustic navigation system used by Pegasus
[AD-A246598] p 727 N92-26795
Eulerian computational methods
[DE92-008017] p 765 N92-26853
Unsteady Euler calculations in 3D internal aerodynamics p 768 N92-27470
Fundamental studies on droplet interactions in dense sprays
[AD-A246918] p 770 N92-27546
Special Course on Unstructured Grid Methods for Advection Dominated Flows
[AGARD-R-787] p 771 N92-27671
A boundary integral formulation for unsteady transonic potential flows p 719 N92-27942
Transonic aeroelastic computations on wings using Navier-Stokes equations p 721 N92-27957
Validation of three-dimensional incompressible spatial direct numerical simulation code: A comparison with linear stability and parabolic stability equation theories for boundary-layer transition on a flat plate
[NASA-TP-3205] p 943 N92-30295
Finite difference time domain modeling of steady state scattering from jet engines with moving turbine blades
[NASA-CR-190290] p 971 N92-30753
Computation and stability analysis of laminar flow over a blunt cone in hypersonic flow p 1041 N92-33839
Finite difference time domain grid generation from AMC helicopter models
[NASA-TM-107679] p 1128 N92-34017

FINITE ELEMENT METHOD
Stress analysis of a propeller blade
p 38 A92-10963
Stress analysis of a propeller hub p 38 A92-10964
Structural behavior of scientific balloons - Finite element simulation and verification
[AIAA PAPER 91-3668] p 20 A92-11015
Finite element solutions of the Euler equations for transonic external flows p 5 A92-11063
Experimental active control of a two-dimensional truss
p 47 A92-11346
Three-dimensional finite-element analysis of interlaminar stresses in thick composite laminates
p 39 A92-11791
Traditional finite element analysis - Opportunities for parallelism? p 40 A92-12354
Finite element correlation of the U.S. Army/BHTI ACAP composite airframe helicopter p 108 A92-14399
Evaluation of an advanced finite element analysis for rotor blades p 109 A92-14426

Prediction of generalized aerodynamic forces following linearized supersonic theory
[ONERA, TP NO. 1991-114] p 76 A92-16093
Multidisciplinary modeling and simulation of a generic hypersonic vehicle
[AIAA PAPER 91-5015] p 232 A92-17813
Resonance prediction for slotted circular wind tunnel using finite element p 235 A92-18388
Static aeroelastic analysis for generic configuration wing p 174 A92-20201
Flutter analysis of anisotropic panels with patched cracks p 219 A92-20216
Incompressible steady aerodynamics using a standard finite element code p 174 A92-20218
Formation of shocks within axisymmetric nozzles p 176 A92-20760
Finite element vorticity based methods for the solution of the compressible Navier-Stokes equations p 246 A92-21983
Experiences with finite element methods for the velocity-vorticity formulation of three-dimensional, viscous, incompressible flows p 246 A92-21984
Numerical studies of supersonic/hypersonic combustion
[AIAA PAPER 92-0094] p 293 A92-22200
Application of a universe-series code for inviscid flow over complex 3-dimensional configurations
[AIAA PAPER 92-0150] p 253 A92-23765
Reflections off aircraft and the shape optimization of a ridged waveguide p 267 A92-23967
Finite element analysis of large wavelength antenna radome problems for leading edge and radar phased arrays p 267 A92-23984
Finite element method for computing nonisentropic potential transonic flow with shock waves p 312 A92-25009
Recent progress in finite element method and boundary integral equation method for nonviscous transonic flows p 314 A92-25127
Aeroelastic analysis of swept, anhedral, and tapered tip rotor blades p 316 A92-25577
Unsteady incompressible flow computations with quadrilateral elements p 394 A92-26219
Calculation of compressible boundary layer flow about airfoils by a finite element/finite difference method
[AIAA PAPER 92-0524] p 332 A92-26948
A deforming grid variational principle and finite element method for computing unsteady small disturbance flows in cascades
[AIAA PAPER 92-0665] p 335 A92-27036
Finite-element algorithm for chemically reacting hypersonic flow
[AIAA PAPER 92-0754] p 336 A92-27097
Compressible laminar boundary layers for perfect and real gases in equilibrium at Mach numbers to 30
[AIAA PAPER 92-0757] p 336 A92-27099
Three-dimensional buoyancy-induced flow and heat transfer around the wheel outboard of an aircraft p 397 A92-27773
A superelement simplified analysis for the vibration systems of the complex structures p 398 A92-27903
Effect of different force-functions and initial shock pressure on blade response p 374 A92-27913
Models of space-averaged energetics of plates p 398 A92-28031
Finite element Navier-Stokes solver for unstructured grids p 398 A92-28035
The selection of bird impact load types --- on turbojet compressor and turbofan fan blades p 448 A92-29732
Cyclic symmetric contact stress analysis of aeroengine rotor assembly p 470 A92-29733
Determination of the objective-function gradient in the problem of minimizing stress concentration using the finite element method p 494 A92-30170
Generation of loads for finite-element models of large aircraft p 459 A92-30209
A non-linearly stable implicit finite element algorithm for hypersonic aerodynamics p 433 A92-31487
Improving the convergence rate of the Petrov-Galerkin techniques for the solution of transonic and supersonic flows p 434 A92-31495
An efficient finite element method for aircraft de-icing problems
[AIAA PAPER 92-0532] p 459 A92-31670
Reduction of computational models in strength problems p 496 A92-31858
A procedure for calculating the static aeroelasticity characteristics of flight vehicles by the influence coefficient method using three-dimensional finite element schemes p 460 A92-31896
An analysis of impact resistance of composite blades for aircraft engines (Analysis with two dimensional and three dimensional finite elements) p 579 A92-32562
Coupled analysis of independently modeled finite element subdomains
[AIAA PAPER 92-2235] p 581 A92-34289
Coupled Rayleigh-Ritz/finite element structural analysis using penalty function method
[AIAA PAPER 92-2238] p 581 A92-34292
An independent refinement and integration procedure in multiregion finite element analysis
[AIAA PAPER 92-2290] p 582 A92-34307
AIAA/ASME/ASCE/AHS/ASC Structures, Structural Dynamics and Materials Conference, 33rd, Dallas, TX, Apr. 13-15, 1992, Technical Papers. Pt. 2 - Structures II p 582 A92-34332
Torsion and twisting of symmetric composite laminates
[AIAA PAPER 92-2425] p 582 A92-34354
Coupled 2D-3D finite element method for analysis of a skin panel with a discontinuous stiffener
[AIAA PAPER 92-2474] p 583 A92-34363
Reduced basis technique for evaluating the sensitivity coefficients of the nonlinear tire response
[AIAA PAPER 92-2530] p 583 A92-34376
Thermoviscoplastic analysis of engine cowl leading edge subjected to oscillating shock-shock interaction
[AIAA PAPER 92-2537] p 583 A92-34381
Thermoviscoplastic response of thin plates subjected to intense local heating
[AIAA PAPER 92-2538] p 584 A92-34382
The NASA/Industry Design Analysis Methods for Vibrations (DAMVIBS) Program - A government overview --- of rotorcraft technology development using finite element method
[AIAA PAPER 92-2200] p 539 A92-34390
The NASA/Industry Design Analysis Methods for Vibrations (DAMVIBS) Program - Boeing helicopters airframe finite element modeling
[AIAA PAPER 92-2202] p 539 A92-34392
The NASA/Industry Design Analysis Methods for Vibrations (DAMVIBS) Program - Sikorsky Aircraft - Advances toward interacting with the airframe design process
[AIAA PAPER 92-2204] p 540 A92-34394
Joined-wing model vibrations using PC-based modal testing and finite element analysis
[AIAA PAPER 92-2260] p 541 A92-34417
Application of composite rotor blade stability analysis to extension-twist coupled blades
[AIAA PAPER 92-2254] p 564 A92-34479
Convergence of subsonic unsteady aerodynamics evaluated by a finite element concept based on Huygeuns' wave propagation
[AIAA PAPER 92-2502] p 518 A92-34497
Unsteady transonic Euler solutions using finite elements
[AIAA PAPER 92-2504] p 518 A92-34499
Study of weld offset in longitudinally welded SSME HPFTP inlet
[AIAA PAPER 92-2305] p 586 A92-34525
An expert system to aid real world finite element analysis
[AIAA PAPER 92-2488] p 601 A92-34604
Large eddy simulation of unsteady turbulent wake of a circular cylinder using the finite element method p 587 A92-34825
Analysis of tenon and mortise contact problems by boundary element methods p 587 A92-35554
Research on damage tolerance of compressor blade p 588 A92-35556
Finite element Euler calculations of unsteady transonic cascade flows
[AIAA PAPER 92-2120] p 520 A92-35689
Finite element nonlinear panel flutter with arbitrary temperatures in supersonic flow
[AIAA PAPER 92-2129] p 589 A92-35696
Large-amplitude finite element flutter analysis of composite panels in hypersonic flow
[AIAA PAPER 92-2130] p 589 A92-35697
Theoretical and experimental study of a model rotor p 547 A92-35781
A new finite element formulation for computational fluid dynamics. X - The compressible Euler and Navier-Stokes equations p 612 A92-37552
Rigid and flexible joint modelling in multibody dynamics using finite elements p 671 A92-37559
Structural and aerodynamic data transformation using inverse isoparametric mapping p 758 A92-41242
Finite element analysis of tire critical speeds p 762 A92-42949
Numerical approximation of hypersonic shocks in a finite-element method using flux-corrected transport (FCT) p 708 A92-43060
Impact response of composite UHB propeller blades
[SAE PAPER 912046] p 861 A92-45430
Finite elements analysis of flexural edge wave for composite fan blades
[SAE PAPER 912048] p 861 A92-45432
Ritz vectors synthesis versus modal synthesis for fluid-structure interaction modeling p 898 A92-45885
A general purpose nonlinear rigid body mass finite element for application to rotary wing dynamics p 846 A92-46924
Bilinear formulation applied to the stability and response of helicopter rotor blade p 847 A92-46930
Periodic trim solutions with hp-version finite elements in time p 874 A92-46931
Sensitivity of tire response to variations in material and geometric parameters p 900 A92-47128
Numerical analysis of an engine turbine disk loaded with a large number of thermomechanical cycles
[ONERA, TP NO. 1992-31] p 902 A92-48592
Prediction of gas turbine combustor flow by a finite element code
[AIAA PAPER 92-3469] p 906 A92-49016
Combined application of the energy method and the weighted residual method - A new way to construct the finite elements p 991 A92-50239
A general explicit or semi-explicit algorithm for compressible and incompressible flows p 937 A92-52682
The numerical simulation of flow about installed aero engine nacelle using a finite element Euler solver on unstructured meshes p 941 A92-52848
Solution of Euler equations with unstructured mesh - 3-D case p 941 A92-52973
A bi-directional marching finite element algorithm for three-dimensional boundary layer separation flow computations p 942 A92-53288
A penalty-Galerkin finite element method for calculating transonic flow over wings p 943 A92-53386
Finite-element analysis and multibody dynamics issues in rotorcraft dynamic analysis p 1055 A92-56286
A finite element method for shear stresses calculation in composite blade models p 1121 A92-56322
Transverse shear effect on flutter of composite panels p 1122 A92-56607
Recent advances on a finite element algorithm for computational aerodynamics: Transonics-hypersonics
[DE91-018176] p 11 N92-10010
Structural tailoring of advanced turboprops (STAT): User's manual
[NASA-CR-187101] p 26 N92-11016
Engine dynamic analysis with general nonlinear finite element codes
[NASA-CR-187222] p 44 N92-11379
Numerical verification of NISA 2 finite element analysis of the cracked 5th stage compressor disc of J-85 jet engine
[NRC-LTR-ST-1792] p 129 N92-11997
Verification of NISA 2 and ENDURE fracture mechanics capability
[NRC-ST-621] p 159 N92-13453
Preliminary finite element analysis of unloaded and loaded notched composite laminated plates
[NRC-LTR-ST-1806] p 159 N92-13454
Detailed analysis and test correlation of a stiffened composite wing panel
[NASA-TM-104154] p 159 N92-13460
Preservation and utilization of finite element models of USAF aircraft structures
[AD-A241657] p 160 N92-13470
Variational formulation of hybrid problems for fully 3-D transonic flow with shocks in rotor p 176 N92-13953
Field telemetry of blade-rotor coupled torsional vibration at Matuura Power Station Number 1 unit p 222 N92-14348
Determination of rotordynamic coefficients for labyrinth seals and application to rotordynamic design calculations p 223 N92-14360
Flow and temperature computations for space vehicles using adaptive finite element techniques p 181 N92-14990
Development and evaluation of a finite element model for a fiber composite helicopter fuselage
[MBB-UD-0584-90-PUB] p 196 N92-15066
Analysis of aircraft engine blade subject to ice impact
[NASA-TM-105336] p 229 N92-15402
Periodic trim solutions with HP-version finite elements in time
[NASA-CR-189778] p 282 N92-17019
Explicit finite element method for transparency impact analysis
[AD-A243527] p 264 N92-17478
Finite element analysis of ASTOVL fighter structure
[AD-A243724] p 275 N92-17513
An overview: Challenges in wind technology development
[DE92-001190] p 302 N92-17875
Thermal/structural analysis of a transpiration cooled nozzle
[NASA-TM-104184] p 401 N92-18877

Engine Structures Modeling Software System (ESMOSS)
[NASA-CR-187227] p 404 N92-19277
Inhomogeneous turbulence beyond spectral equilibria: Aeronautical applications
[ETN-92-90867] p 404 N92-19349
Finite element analysis of a riveted repair on a curved composite panel
[AD-A243916] p 404 N92-19384
Component-specific modeling --- jet engine hot section components
[NASA-CR-189088] p 377 N92-19726
Application of analysis techniques for low frequency interior noise and vibration of commercial aircraft
[NASA-CR-189555] p 481 N92-20376
A novel approach in formulation of special transition elements: Mesh interface elements
[NASA-CR-189050] p 501 N92-20954
Application of finite element methods to fracture mechanics
[PNR-90770] p 503 N92-21741
Helicopter rotor blade dynamics with bilinear formulation p 463 N92-21856
Methodology for sensitivity analysis, approximate analysis, and design optimization in CFD for multidisciplinary applications --- computational fluid dynamics
[NASA-CR-190201] p 595 N92-22662
Prediction of response of aircraft panels subjected to acoustic and thermal loads
[NASA-CR-190305] p 678 N92-24345
Navier-Stokes simulation of dynamic stall on a rotating airfoil p 626 N92-24853
The NASA/industry Design Analysis Methods for Vibrations (DAMVIBS) Program: A government overview
[NASA-TM-107579] p 680 N92-25267
Development of pre- and post-processor system for structural analysis
[NAL-TM-628] p 681 N92-25403
Finite element frequency domain solution of nonlinear panel flutter with temperature effects and fatigue life analysis p 682 N92-25589
Computational structures technology at Grumman: *Current practice/future needs* *p 684 N92-25930*
Finite element methods for integrated aerodynamic heating analysis
[NASA-CR-190353] p 633 N92-25959
Preliminary structural sizing of a Mach 3.0 high-speed civil transport model
[NASA-CR-189631] p 685 N92-25960
Iterative methods for large scale static analysis of structures on a scalable multiprocessor supercomputer
[NASA-CR-190369] p 692 N92-26018
Application of finite element method to hypersonic nozzle flow computations p 769 N92-27479
Special Course on Unstructured Grid Methods for Advection Dominated Flows
[AGARD-R-787] p 771 N92-27671
Analysis of unsteady aerodynamic and flutter characteristics of an aeroelastic model in transonic flow p 720 N92-27953
Practical architecture of design optimisation software for aircraft structures taking the MBB-Lagrange code as an example p 851 N92-28471
Nonlinear analyses of composite aerospace structures in sonic fatigue
[NASA-CR-190565] p 854 N92-30209
Influence of structural and aerodynamic modeling on flutter analysis and structural optimization
[AD-A248487] p 978 N92-30323
MBB-LAGRANGE: A general structural reliability and optimization structural system
[MBB/FW321/S/PUB/467] p 998 N92-30423
An analytical and experimental investigation of flutter suppression via piezoelectric actuation
[NASA-TM-107653] p 962 N92-31174
Time simulation of flutter with large stiffness changes
[NASA-TM-107650] p 963 N92-32111
Eighth DOD/NASA/FAA Conference on Fibrous Composites in Structural Design, part 1
[NASA-CP-3087-PT-1] p 1106 N92-32513
Vibro-acoustic FE analyses of the Saab 2000 aircraft p 1137 N92-32952
Computational methods for global/local analysis
[NASA-TM-107591] p 1125 N92-33104
Computational aspects of helicopter trim analysis and damping levels from Floquet theory
[NASA-CR-190736] p 1087 N92-33107
Development of 3D electromagnetic modeling tools for airborne vehicles
[NASA-CR-190810] p 1126 N92-33307
Stability failure of sandwich structures
[MBB-UD-0613-92-PUB] p 1111 N92-33994
Effects of constraint on crack growth under aircraft spectrum loading
[NASA-TM-107677] p 1128 N92-34178

FINITE VOLUME METHOD
Three-dimensional calculation of low-frequency unsteady transonic flow in axial turbine stages p 174 A92-19110
Asymmetric separated flows at supersonic speeds p 176 A92-20742
The finite volume approach for the Navier-Stokes equations p 246 A92-21980
Navier-Stokes computations for aerodynamic configurations at high angles of attack p 246 A92-21981
An algorithm for predicting the flow past fuselage-mounted engine arrangements
[AIAA PAPER 92-0151] p 253 A92-23766
A Navier-Stokes solver for stretched triangular grids
[AIAA PAPER 92-0183] p 256 A92-23793
Design of turbomachinery blading in transonic flows by the circulation method p 311 A92-24725
Three-dimensional simulation of slender delta wing rock and divergence
[AIAA PAPER 92-0280] p 318 A92-25734
A nearly-monotone genuinely multidimensional scheme for the Euler equations
[AIAA PAPER 92-0325] p 322 A92-25772
Predictions of compressible viscous flows at all Mach number using pressure correction, collocated primitive variables and non-orthogonal meshes
[AIAA PAPER 92-0426] p 326 A92-26274
Computational mechanics today p 399 A92-28464
Use of finite volume schemes for transition simulation p 432 A92-31185
Interference flows past cylinder-fin-sting-cavity assemblies p 442 A92-32236
Evaluation of a finite volume method for compressible shear layers p 610 A92-36834
Locally implicit hybrid algorithm for steady and unsteady viscous flows p 610 A92-36836
Vortical flow simulation by the solution of the Navier-Stokes equations p 620 A92-40104
Solution of the parabolized Navier-Stokes equations using Osher's upwind scheme p 713 A92-44371
Application of an unstructured Navier-Stokes solver to multi-element airfoils operating at transonic maneuver conditions
[AIAA PAPER 92-2638] p 796 A92-45507
Shock fitting with a finite volume approximation to the Euler equations
[AIAA PAPER 92-2646] p 796 A92-45513
LU-SGS implicit scheme for entry vehicle flow computation and comparison with aerodynamic data
[AIAA PAPER 92-2671] p 798 A92-45526
Prediction of the viscous transonic aerodynamic performance of supercritical aerofoil sections
[AIAA PAPER 92-2653] p 805 A92-45569
Application of the Euler method EUFLEX to a fighter-type airplane configuration at transonic speed
[AIAA PAPER 92-2620] p 845 A92-45573
A compact higher order Euler solver for unstructured grids with curved boundaries
[AIAA PAPER 92-2696] p 807 A92-45590
Compact higher order characteristic-based Euler solver for unstructured grids p 812 A92-46889
3-D numerical grid generation for the transonic flow analysis about multi-bodies p 817 A92-47061
A time marching method in finite volume for transonic diffuser turbulent flows p 819 A92-47690
Characteristics of the Shuttle Orbiter leeside flow during a reentry condition
[AIAA PAPER 92-2951] p 821 A92-47915
Improved artificial dissipation schemes for the Euler equations p 933 A92-49508
The simulation of inviscid, compressible flows using an upwind kinetic method on unstructured grids p 933 A92-49515
Full Navier-Stokes analysis of a three-dimensional scramjet inlet p 934 A92-50272
A finite-volume numerical method to calculate fluid forces and rotordynamic coefficients in seals
[AIAA PAPER 92-3712] p 1113 A92-54132
Approximate Riemann solver for hypervelocity flows p 1117 A92-54934
Euler/experiment correlation of a generic fighter p 1031 A92-56164
Viscous computations of cold air/air flow around scramjet nozzle afterbody
[NASA-CR-4406] p 13 N92-10982
Vortical flow simulation by using structured and unstructured grids p 83 N92-12999
On the simulation of compressible turbulent flows past delta wing, delta wing-body and delta wing-canard p 84 N92-13003
A multiblock flow solver for inviscid hypersonic flows p 181 N92-14986
Use of CFD in the design of a modern multistage aero engine LP turbine design
[PNR-90862] p 472 N92-20179
Inviscid drag prediction for transonic transport wings using a full-potential method
[NLR-TP-89365-U] p 444 N92-20473
An alternative to unstructured grids for computing gas dynamic flows around arbitrarily complex two-dimensional bodies
[NASA-CR-189612] p 447 N92-21465
A high angle of attack inviscid shuttle orbiter computation
[NASA-TM-107606] p 685 N92-25964
Three-dimensional upwind scheme for solving the Euler equations on unstructured tetrahedral grids --- tetrahedral grids p 714 N92-26585
Boundary conditions for Euler equations at internal block faces of multi-block domains using local grid refinement
[NLR-TP-90134-U] p 908 N92-28712
Development of a multigrid transonic potential flow code for cascades
[NASA-CR-190480] p 830 N92-29361
Methods for direct simulation of transition in hypersonic boundary layers 2 p 912 N92-30064
Computation of unsteady transonic flows using an implicit centered Euler solver without artificial viscosity
[ESA-TT-1235] p 944 N92-30514
A general numerical model for wave rotor analysis
[NASA-TM-105740] p 1002 N92-31484
An installed nacelle design code using a multiblock Euler solver. Volume 1: Theory document
[NASA-CR-189652-VOL-1] p 950 N92-32226

FINNED BODIES
Base pressure on an axisymmetric finned body during forced rotation in the autorotation regime p 7 A92-12165
Ultrasonic motor utilizing elastic fin rotor p 215 A92-17414
Measurement of magnus derivatives with an elastically forced oscillation rig p 749 A92-43172
Low-speed wind tunnel testing of the lateral control force for the upper rudder surface of a joined-wing airfoil p 711 A92-43228
Computations of the unsteady flow about a generic wing/pylon/finned-store configuration
[AIAA PAPER 92-4568] *p 1027 A92-55377*
Further studies in filmwise condensation of steam on horizontal finned tubes
[AD-A252705] p 1011 N92-31767

FINS
Numerical investigation of bleed on three-dimensional turbulent interactions due to sharp fins p 5 A92-11062
Two-dimensional effects in a triangular convecting fin p 219 A92-20324
An experimental/computational study of sharp fin induced shock wave/turbulent boundary layer interactions at Mach 5 - Experimental results
[AIAA PAPER 92-0749] p 335 A92-27093
The aerodynamic characteristics of grid fin wings p 427 A92-30201
Boiling heat transfer from an excavated fin p 498 A92-32523
Two-dimensional heat transfer from a rectangular fin with asymmetrical thermal boundary conditions p 498 A92-32524
Aerothermoelastic analysis of a NASP-like vertical fin
[AIAA PAPER 92-2400] p 541 A92-34471
Buffet load measurements on an F/A-18 vertical fin at high-angle-of-attack
[AIAA PAPER 92-2127] p 520 A92-35694
Prediction for the incipient separation of fin-generated three-dimensional shock wave turbulent boundary layer interactions p 615 A92-38909
Unsteady pressure and load measurements on an F/A-18 vertical fin at high-angle-of-attack
[AIAA PAPER 92-2675] p 798 A92-45529
Statistical prediction of maximum buffet loads on the F/A-18 vertical fin p 811 A92-46816
A field repair of advanced helicopter vertical fin structure p 785 A92-47417
The optimization of variable cross-section spines with temperature dependent thermal parameters p 901 A92-48353
The effect of tip convection on the performance and optimum dimensions of cooling fins p 902 A92-48354
The A320 laminar fin programme
[ONERA, TP NO. 1992-23] p 849 A92-48586
Exploratory study of wall pressure fluctuations in a Mach 5, sharp fin-induced turbulent interaction p 935 A92-50304
Optimization of a thermally non-symmetric fin - Preliminary evaluation p 992 A92-50448
A low speed wind tunnel investigation of a joined-wing aircraft with an overhanging fin p 1030 A92-56078
A low speed wind tunnel investigation of the direct side force control of a joined-wing aircraft with overhanging fin p 1084 A92-56079

Assessment of calculation methods for efficiency of straight fins of rectangular profile p 1121 A92-56374
Effect of twin fins on isolated tailplane lift-curve slope
[ESDU-91009] p 80 N92-11969
Contribution of fin and tailplane to sideforce and yawing moment derivatives due to sideslip at supersonic speeds at low angles of attack
[ESDU-91031] p 259 N92-15971
Scale model measurements of fin buffet due to vortex bursting on F/A-18 p 365 N92-18788
Experimental validation of structural optimization methods
[NASA-TM-104203] p 404 N92-19258
First approach to an integrated fin design
p 551 N92-23236
A fin optimisation study p 551 N92-23237
Flowfield in the vicinity of the F/A-18 vertical fin at high-angle-of-attack p 628 N92-24865
Boiling and condensation in microfin tubes
p 682 N92-25660
Further studies in filmwise condensation of steam on horizontal finned tubes
[AD-A252705] p 1011 N92-31767
Contribution of tailplane-mounted twin fins to sideforce, yawing moment, and rolling moment derivatives due to sideslip
[ESDU-92007] p 1086 N92-32487

FIRE CONTROL
Use of high-fidelity simulation in the development of an F/A-18 active ground collision avoidance system
p 837 N92-28530
The rise of active-element phased-array radar
[RAND-P-7747-RGS] p 999 N92-30755
Airborne experimental FLIR program
p 1064 N92-32447

FIRE DAMAGE
Fokker 50 flameouts in icing conditions
p 548 A92-35940

FIRE EXTINGUISHERS
Damping down the fires --- in civil transport aircraft
p 350 A92-25075
Development and evaluation of an onboard aircraft cabin water spray system for postcrash fire protection
[SAE PAPER 912224] p 636 A92-40022
Onboard cabin water spray system under various discharge configurations
[DOT/FAA/CT-TN91/42] p 93 N92-13043
Effectiveness of an onboard water spray system during an oxygen enriched cabin fire
[DOT/FAA/CT-TN91/51] p 264 N92-17149
Development of fuel neutralizing agents to prevent flashback on aircraft fires
[AD-A242828] p 264 N92-17259
Feasibility of systematic recycling of aircraft Halon extinguishing agents
[DOT/FAA/CT-91/21] p 352 N92-18259
Spray nozzle for fire control
[CA-PATENT-APPL-SN-2-011-94] p 1125 N92-32856
Preliminary screening procedures and criteria for replacements for Halons 1211 and 1301
[AD-A252912] p 1126 N92-33501

FIRE FIGHTING
Fire-fighting foams must meet newly-developed ICAO standard p 448 A92-29508
Thermal energy test apparatus
[AD-A243526] p 305 N92-17537
Spray nozzle for fire control
[CA-PATENT-APPL-SN-2-011-94] p 1125 N92-32856

FIRE PREVENTION
Damping down the fires --- in civil transport aircraft
p 350 A92-25075
An evaluation of in-cabin safety features in passenger aircraft
[ETN-92-90656] p 449 N92-20794
Modular simulation of HEI fragments and blast pressure
[AD-A248205] p 910 N92-29191
Preliminary screening procedures and criteria for replacements for Halons 1211 and 1301
[AD-A252912] p 1126 N92-33501

FIRES
Onboard cabin water spray system under various discharge configurations
[DOT/FAA/CT-TN91/42] p 93 N92-13043
Effectiveness of an onboard water spray system during an oxygen enriched cabin fire
[DOT/FAA/CT-TN91/51] p 264 N92-17149
Thermal energy test apparatus
[AD-A243526] p 305 N92-17537
Preliminary screening procedures and criteria for replacements for Halons 1211 and 1301
[AD-A252912] p 1126 N92-33501

FITTINGS
Reduction and analysis of F-111C flight data
[AD-A250341] p 853 N92-28771

FIXED POINTS (MATHEMATICS)
A new U-D factorization-based fixed-point smoother and application to flight test p 411 A92-27858

FIXED WINGS
Future experimental needs in low-speed aerodynamics
[AIAA PAPER 92-0157] p 254 A92-23772
Laboratory evaluation of a sensor for detection of aircraft wing contaminants
[AIAA PAPER 92-0301] p 369 A92-25753
Numerical simulation of flow separation for rotors and fixed wings
[AIAA PAPER 92-0635] p 334 A92-27013
Reevaluation of the motion of an airship
p 731 A92-43243
Assessment of one-dimensional icing forecast model applied to stratiform clouds p 915 A92-46803
Formation flight system design concept
p 954 A92-49255
Networked simulation of multiple aircraft using Semi-Automated Forces
[AIAA PAPER 92-4170] p 1008 A92-52455
Estimation of airborne performance in landing
[ESDU-91032] p 272 N92-15988
SIMNET plan view display user manual
[AD-A244617] p 510 N92-21392
Aircraft Ship Operations
[AGARD-CP-509] p 464 N92-21951
Evaluating fixed wing aircraft in the aircraft carrier environment p 464 N92-21963
The NASA aircraft icing research program
p 549 N92-22534
Comparison of Janus and field test aircraft detection ranges for the line-of-sight forward heavy system
[AD-A246047] p 770 N92-27600
An analysis of fixed wing tactical airlifter characteristics using an intra-theater airlift computer model
[AD-A246908] p 732 N92-27719
Numerical investigation of the effects of icing on fixed and rotary wing aircraft
[NASA-CR-190542] p 1044 N92-34105

FIXTURES
Thrust test fixture
[AD-D015259] p 983 N92-31192

FLAME HOLDERS
Weak extinction limits of large scale flameholders
[ASME PAPER 91-GT-234] p 125 A92-15643
Development and bench test of high-temperature combustion chamber with structural ceramic components
[ASME PAPER 91-GT-315] p 126 A92-15691
A numerical study of isothermal flows of a slit V-gutter
[AIAA PAPER 92-0100] p 293 A92-22203
An investigation on flame stability by fuel permeability in a flame holder made of porous ceramic material
p 375 A92-28435
Experimental investigation on the mechanism of flame stabilization in afterburner with V-gutter flameholder
p 487 A92-29725
An experimental investigation of the swirling combustor for integral liquid fuel ramjet p 557 A92-35541
Studies on the mechanism of ignition and flameholding by plasma jets p 755 A92-42798
Effectiveness of plasma torches for ignition and flameholding in scramjet p 737 A92-44524

FLAME PROPAGATION
Waves and thermodynamics in high Mach number propulsive ducts p 809 A92-46431
Numerical simulations of the transdetonative ram accelerator combusting flow field on a parallel computer
[AIAA PAPER 92-3249] p 894 A92-48848
Turbulent diffusion flame properties behind a backward-facing step p 985 A92-50255
Contribution to the modelling of turbulent combustion in the case of stabilisation by flame-lock
[ESA-TT-1229] p 988 N92-31942

FLAME RETARDANTS
Damping down the fires --- in civil transport aircraft
p 350 A92-25075

FLAME SPECTROSCOPY
Planar fluorescence imaging of a transverse jet in a supersonic crossflow p 755 A92-44501

FLAME STABILITY
An investigation of fuel nozzles for combustion performance p 278 A92-21745
A numerical study of isothermal flows of a slit V-gutter
[AIAA PAPER 92-0100] p 293 A92-22203
An investigation on flame stability by fuel permeability in a flame holder made of porous ceramic material
p 375 A92-28435
Experimental investigation on the mechanism of flame stabilization in afterburner with V-gutter flameholder
p 487 A92-29725
The aviation kerosene burning in the non-uniform air flow p 487 A92-29728
Second moment closure predictions of jet-on-jet impingement flows p 675 A92-40102
Turbulent diffusion flame properties behind a backward-facing step p 985 A92-50255
An experimental analysis of lateral jet injection into confined swirling crossflows p 156 N92-12199
Fractal image compression of Rayleigh, Raman, LIF and LDV data in turbulent reacting flows
[AD-A246960] p 767 N92-27352
Contribution to the modelling of turbulent combustion in the case of stabilisation by flame-lock
[ESA-TT-1229] p 988 N92-31942

FLAME TEMPERATURE
Flame sheet algorithm for use in numerical modeling of ramjet combustion instability p 390 A92-28503

FLAMMABILITY
Flammability, smoke and toxic gas combustion products of composites used in aircraft cabins p 14 A92-10257
A study of the flammability limit of the backward facing step flow combustion
[AIAA PAPER 92-3846] p 895 A92-49136

FLAPPING
On the adequacy of modeling turbulence and related effects on helicopter response p 847 A92-46945
Measurements of blade flapping motion on a wind tunnel model p 1093 A92-56023
The identification of coupled flapping/inflow models for hovering flight p 1058 A92-56335
Flapping inertia for selected rotor blades
[NASA-TM-104125] p 115 N92-13057
Application areas for rotorcraft system identification: Simulation model validation p 274 N92-17164

FLAPS (CONTROL SURFACES)
Unsteady Euler solution for oscillatory airfoil and oscillating flap
[AIAA PAPER 92-0131] p 252 A92-23751
Identification of aerodynamic effectiveness and interference effects of direct-lift-control flaps from flight data
[AIAA PAPER 92-0171] p 271 A92-23782
Prediction of turbulent flow behavior over a slotted flap p 309 A92-24407
Reduction of wing rock amplitudes using leading-edge vortex manipulations
[AIAA PAPER 92-0279] p 379 A92-25733
Application of computational fluid dynamics to pitch/yaw thrust vectoring spherical convergent flap nozzles
p 737 A92-44511
Rejected takeoffs - Causes, problems, and consequences p 835 A92-45052
Computational evaluation of an airfoil with a Gurney flap
[AIAA PAPER 92-2708] p 802 A92-45550
Separation control on high Reynolds number multi-element airfoils
[AIAA PAPER 92-2636] p 806 A92-45575
Periodic trim solutions with hp-version finite elements in time p 874 A92-46931
Flap control simulation p 980 A92-51398
Hypersonic inviscid flow field simulations around reentry vehicles with flap deflection p 184 N92-15025
Identification of the stability and control derivatives of a DLC-flap system for VSRA
[NAL-TR-1116] p 283 N92-17917
A mathematical model of a tilt-wing aircraft for piloted simulation
[NASA-TM-103864] p 368 N92-19847
Evaluation of landing configuration by flight test of the quiet STOL experimental aircraft ASKA
[NAL-TR-1113] p 733 N92-28191
Flow gradient corrections on hot-wire measurements using an X-wire probe
[NLR-TP-90255-U] p 829 N92-28713
Lift and rolling moment due to spoilers on wings with trailing-edge flaps deflected at subsonic speeds
[ESDU-92002-SUPPL] p 1037 N92-32782

FLASH LAMPS
Surfprep flash-lamp depaint system evaluation
p 497 A92-32411

FLAT PLATES
Processing parameters for carbon/PMR-15 composite flat panels p 34 A92-11812
Heat transfer in supersonic flow past a single crater
p 63 A92-13741
Finite difference numerical prediction of aerodynamics of an airfoil flying over wavy wall p 64 A92-14033
The problem of transition from continuum to rarefied gas flows p 251 A92-22519
Numerical simulation of twin-jet impingement on a flat plate coupled with cross-flow p 315 A92-25374
Application of a new K-tau model to near wall turbulent flows p 395 A92-26437
Holographic flowfield density measurements in swept shock wave/boundary-layer interactions
[AIAA PAPER 92-0746] p 335 A92-27092
Incompressible flow past a flat plate aerofoil with leading edge separation bubble p 421 A92-28943

Investigating the feasibility of controlling the laminar-turbulent transition by means of laminarizing plates p 493 A92-30161
Effect of the longitudinal and transverse riblets of a flat plate on laminar-to-turbulent transition p 428 A92-30210
Use of finite volume schemes for transition simulation p 432 A92-31185
The problem of body motion in a medium with resistance p 604 A92-36416
Hypersonic turbulent separated flow past an unswept circular cylinder on a flat plate p 615 A92-38908
Laminar flow control of subsonic boundary layers by suction and heat transfer strips p 617 A92-39338
Bursts and sources of pressure fluctuation in turbulent boundary layers p 619 A92-40055
Evolution of coherent structures during transition in a flat-plate boundary layer p 621 A92-40126
Experimentally supported investigations into the optical performance of multi-aperture window concepts
[AIAA PAPER 92-2781] p 778 A92-41324
The fluid-dynamic measurement of the fling motion of a three-dimensional flat plate p 710 A92-43194
Solution of the parabolized Navier-Stokes equations using Osher's upwind scheme p 713 A92-44371
Experimental development of spanwise vortex models with streamwise decay due to wall interaction
[AIAA PAPER 92-2688] p 799 A92-45535
Viscous flow past a nacelle isolated and in proximity of a flat plate
[AIAA PAPER 92-2723] p 803 A92-45560
The interaction between a plane shear layer and a slender body p 991 A92-49790
Time domain numerical calculations of unsteady vortical flows about a flat plate airfoil p 936 A92-50473
Heat transfer measurements and CFD comparison of swept shock wave/boundary-layer interactions
[AIAA PAPER 92-3665] p 1021 A92-54110
Nonlinear aspects of aerospace structures at high excitation levels flat aluminum beams and plates studied
[AD-A240600] p 44 N92-11383
An assessment and application of turbulence models for hypersonic flows
[NASA-TM-105124] p 82 N92-11984
An experimental analysis of critical factors involved in the breakdown process of leading edge vortex flows p 89 N92-13031
On the instability of boundary layers on heated flat plates
[NASA-CR-187581] p 347 N92-19250
Separation of relaminarised boundary layers
[CUED/A-AERO/TR-16] p 592 N92-22209
Validation of three-dimensional incompressible spatial direct numerical simulation code: A comparison with linear stability and parabolic stability equation theories for boundary-layer transition on a flat plate
[NASA-TP-3205] p 943 N92-30295
Flat plates placed in depleted hypersonic flow
[SESSIA-430/91.960] p 947 N92-31508
Swept shock/boundary layer interaction experiments in support of CFD code validation
[NASA-CR-190583] p 1036 N92-32494
Leading-edge receptivity for blunt-nose bodies
[NASA-CR-190563] p 1036 N92-32648
Vortex flow visualization using colored and fluorescent dyes on flat plate delta wing with leading edge extension
[AD-A251139] p 1036 N92-32651

FLAT SURFACES
A study of the interaction of a normal shock wave with a turbulent boundary layer at Mach numbers between 1.30 and 1.55 p 339 A92-28006
Boundary-layer receptivity due to a wall suction and control of Tollmien-Schlichting waves p 616 A92-39333
Experimental studies of hypersonic shock-wave boundary-layer interactions
[NASA-CR-190731] p 950 N92-32162

FLEXIBILITY
Microwave landing system modeling with application to air traffic control automation p 725 A92-41220
Planning method of skirt systems for small ACVs p 1118 A92-56038
Variable impedance journal bearings for rotor-bearing systems p 157 N92-12270
An analysis of total quality management in Aeronautical Systems Division
[AD-A246661] p 772 N92-27760

FLEXIBLE BODIES
Real parameter uncertainty and phase information in the robust control of flexible structures p 32 A92-11345
Experimental demonstration of active vibration control for flexible structures p 50 A92-11442
Robust stabilization with positive real uncertainty - Beyond the small gain theorem p 50 A92-11444
Control design via TAM and H-infinity approaches - A flexible beam case study p 51 A92-11445
Computer simulation of weapon blast pressures on flexible surfaces p 39 A92-12115
Aeroservoelastic stabilization techniques for hypersonic flight vehicles
[AIAA PAPER 91-5056] p 203 A92-17839
Representation of geometric stiffening in multibody system simulation p 217 A92-19463
Gust effects on a flexible aircraft p 270 A92-22474
Efficient evaluation of the flexibility of tapered I-beams accounting for shear deformations p 295 A92-23269
Transition control of instability waves over an acoustically excited flexible surface p 416 A92-28037
Experimental and theoretical study for nonlinear aeroelastic behavior of a flexible rotor blade
[AIAA PAPER 92-2253] p 584 A92-34410
Inclusion principle for the Rayleigh-Ritz based substructure synthesis p 670 A92-36851
Rigid and flexible joint modelling in multibody dynamics using finite elements p 671 A92-37559
A mathematical model for the hydroelasticity problem concerning the motion of two flexible profiles in an ideal incompressible fluid. I p 712 A92-44127
Finite elements analysis of flexural edge wave for composite fan blades
[SAE PAPER 912048] p 861 A92-45432
Specifying exhaust nozzle contours in real-time using genetic algorithm trained neural networks
[AIAA PAPER 92-3328] p 865 A92-48911
Optimization of longitudinal corrections of helical gears p 990 A92-49578
New literal approximations for the longitudinal dynamic characteristics of flexible flight vehicles
[AIAA PAPER 92-4411] p 1075 A92-55205
The stability of the steady state and bistable response of a flexible rotor supported on squeeze film dampers p 222 N92-14350
Adaptive control of nonlinear systems with applications to the control of flexible robot arms
[AD-A244409] p 413 N92-19397
Extension of the integral equation formulation of linearized time dependent subsonic flow
[AD-A250654] p 947 N92-31171
Mathematical modeling and numerical simulation of the dynamics of flexible structures undergoing large overall motions
[AD-A250202] p 979 N92-31967
The dynamics of flexible multibody systems: A finite segment approach p 1128 N92-34036

FLEXIBLE SPACECRAFT
AIAA Dynamics Specialists Conference, Dallas, TX, Apr. 16, 17, 1992, Technical Papers p 565 A92-35651
Applications of robust control theory - Educational implications
[AIAA PAPER 92-4559] p 1131 A92-55271
On the stability of a dual spin satellite with asymmetric rotor and flexible platform
[ISBN-0-315-54650-6] p 753 N92-27613

FLEXIBLE WINGS
Analysis of flexible-membrane and jet-flapped airfoils using velocity singularities p 10 A92-13216
Application of aeroservoelastic modeling using minimum-state unsteady aerodynamic approximations p 204 A92-18622
Analysis of circular elastic membrane wings p 245 A92-21722
Comments on 'Fuzzy logic for control of roll and moment for a flexible wing aircraft' p 480 A92-30995
FAMUSS - A new aeroservoelastic modeling tool
[AIAA PAPER 92-2395] p 541 A92-34468
Aeroelasticity - Advances and future directions
[AIAA PAPER 92-2446] p 585 A92-34475
A summary of the Active Flexible Wing program
[AIAA PAPER 92-2080] p 565 A92-35652
Simulation and model reduction for the AFW program
[AIAA PAPER 92-2081] p 572 A92-35653
Further investigations of the aeroelastic behavior of the AFW wind-tunnel model using transonic small disturbance theory
[AIAA PAPER 92-2082] p 565 A92-35654
The multiple-function multi-input/multi-output digital controller system for the AFW wind tunnel model
[AIAA PAPER 92-2083] p 565 A92-35655
On-line analysis capabilities developed to support the AFW wind-tunnel tests
[AIAA PAPER 92-2084] p 572 A92-35656
Flutter suppression for the Active Flexible Wing - Control system design and experimental validation
[AIAA PAPER 92-2097] p 566 A92-35666
A flutter suppression system using strain gages applied to Active Flexible Wing Technology - Design and test
[AIAA PAPER 92-2098] p 566 A92-35669
Design and manufacturing of torsional flexible blade models p 547 A92-35780
Application of Active Flexible Wing technology to the Agile Falcon p 729 A92-41233
Optimum structural design of a cantilevered rectangular elastic wing with a gust load alleviation system p 762 A92-43133
Integrated aeroservoelastic wing synthesis by nonlinear programming/approximation concepts p 873 A92-46752
Navier-Stokes computations on swept-tapered wings, including flexibility p 810 A92-46786
Dynamic analysis of rotor flex-structure based on nonlinear anisotropic shell models p 899 A92-46946
Generalized aerodynamics analysis by the boundary element method p 1030 A92-56050
Unsteady shock-vortex interaction on a flexible delta wing p 1030 A92-56157
Investigation of the aeroelastic stability of the AFW wind-tunnel model using CAP-TSD
[NASA-TM-104142] p 81 N92-11977
Further investigations of the aeroelastic behavior of the AFW wind-tunnel model using transonic small disturbance theory
[NASA-TM-107576] p 526 N92-22240
Investigation of the aeroelastic stability of the AFW wind-tunnel model using CAP-TSD p 721 N92-27955
On-line analysis capabilities developed to support the AFW wind-tunnel tests
[NASA-TM-107651] p 961 N92-30752
Design and experimental validation of a flutter suppression controller for the active flexible wing
[NASA-TM-4381] p 979 N92-31240
A summary of the active flexible wing program
[NASA-TM-107655] p 962 N92-31264
The multiple-function multi-input/multi-output digital controller system for the AFW wind-tunnel model
[NASA-TM-107600] p 1060 N92-32536

FLIGHT ALTITUDE
Hunting phenomena of the balloon motions observed over Antarctica
[AIAA PAPER 91-3667] p 14 A92-11014
Added mass of high-altitude balloons
[AIAA PAPER 91-3693] p 16 A92-11034
Effects of variations in head-up display airspeed and altitude representations on basic flight performance p 46 A92-11204
European studies to investigate the feasibility of using 1000 ft vertical separation minima above FL 290. II - Precision radar data analysis and collision risk assessment p 353 A92-24946
A study of altitude-constrained supersonic cruise transport concepts
[AIAA PAPER 92-1027] p 536 A92-33208
Computation of aircraft geometric height under radar surveillance p 639 A92-40239
Who or what saved the day? A comparison of traditional and glass cockpits p 833 A92-44931
Selected models of aircraft navigation space p 839 A92-45373
Oscillations of balloon-flight altitude p 836 A92-46660

FLIGHT CHARACTERISTICS
Derivation of aircraft linear state equations from implicit nonlinear equations p 27 A92-11361
On-line state estimation and parameter identification for flight p 50 A92-11429
Results from a test of a 2/3-scale V-22 rotor and wing in the 40- by 80-Foot Wind Tunnel p 104 A92-14332
Study of theoretical and wind tunnel results on flight performance degradation due to leading edge rime ice accretion
[AIAA PAPER 92-0038] p 262 A92-22158
Influence of flight parameters on air intake internal flow distortions due to gun blast-air interaction p 310 A92-24426
Flight testing a high performance kit built aircraft
[AIAA PAPER 92-1240] p 538 A92-33333
B-2 handling, automation tailored to two-pilot crew p 643 A92-39725
Some practical aspects of viscous drag reduction concepts
[SAE PAPER 912129] p 618 A92-39976
Velocity dependence of high angle of attack longitudinal flying qualities criteria
[SAE PAPER 912149] p 662 A92-39985
F-14 dual hydraulic failure flying qualities evaluation p 645 A92-40029
JAS 39 Gripen flight test report p 645 A92-40030
X-31 flight test update p 645 A92-40034
Single engine testing of the F-14A(PLUS) airplane in the power approach configuration p 645 A92-40036
DC-3 handling qualities flight tests: NACA - 1950 p 646 A92-40042
Selected models of aircraft navigation space p 839 A92-45373
Mathematical modeling of the effect of windshear on the dynamics of a landing aircraft p 875 A92-47784

Aircraft stabilization at large angles of attack
p 875 A92-47785
B-1B excels in conventional role p 786 A92-47971
Summary of the effects of engine throttle response on airplane formation-flying qualities
[AIAA PAPER 92-3318] p 877 A92-48902
Measurement of angle of attack using a five-hole arrow head pitot tube p 941 A92-53009
Continuous flying quality improvement - The measure and the payoff
[AIAA PAPER 92-4327] p 1073 A92-55171
Analytical development of an equivalent system mismatch function
[AIAA PAPER 92-4422] p 1080 A92-55346
Flight test results using a low order equivalent systems technique to estimate flying qualities
[AIAA PAPER 92-4425] p 1080 A92-55349
Application of digital measurement techniques to analysis of range shadowgraphs
[AD-A241554] p 139 N92-13080
Rotorcraft System Identification
[AGARD-LS-178] p 273 N92-17153
Escape strategies for turboprop aircraft in a microburst windshear
[AD-A243090] p 264 N92-17217
Discussion for possibility of some aerodynamic ground effect craft
[NAL-TM-619] p 300 N92-17757
Aircraft tracking optimization of parameters selection
p 361 N92-18585
Manoeuvring Aerodynamics
[AGARD-CP-497] p 363 N92-18778
The effect of wing ice contamination on essential flight characteristics p 449 N92-21681
Evaluating fixed wing aircraft in the aircraft carrier environment p 464 N92-21963
Assessment of flying-quality criteria for air-breathing aerospacecraft
[NASA-CR-4442] p 663 N92-25982
Outlines of parabolic flight p 764 N92-26441
Automated screening of propulsion system test data by neural networks, phase 1
[NASA-CR-184329] p 753 N92-27403
Flight testing of a half-scale remotely piloted vehicle
[AD-A248568] p 733 N92-28123
NPSNET: Flight simulation dynamic modeling using quaternions
[AD-A247484] p 923 N92-28245
Flight simulation and digital flight controls
p 884 N92-28526
Effects of cockpit lateral stick characteristics on handling qualities and pilot dynamics
[NASA-CR-4443] p 878 N92-28584
In-flight simulation studies at the NASA Dryden Flight Research Facility
[NASA-TM-4396] p 853 N92-29110
Technical evaluation report on the Flight Mechanics Panel Symposium on Piloted Simulation Effectiveness
[AGARD-AR-315] p 983 N92-30769
Preliminary subsonic aerodynamic model for simulation studies of the HL-20 lifting body
[NASA-TM-4302] p 978 N92-31175
A background to the handling qualities of aircraft
[ESDU-92006] p 1087 N92-32780
Analysis of the flight performance of the 155 mm M864 base burn projectile
[BRL-TR-3083] p 1041 N92-33699

FLIGHT CONDITIONS
Small balloon ballistic tracing and behavior anomalies
[AIAA PAPER 91-3682] p 15 A92-11026
Flight in a steady wind field p 131 A92-13696
Sensors and systems to enhance aviation safety against weather hazards p 160 A92-14265
Propulsion requirements for high altitude long endurance flight
[ASME PAPER 91-GT-393] p 127 A92-15723
A theoretical analysis utilizing the LEWICE and EPPLER numerical analyses to predict flight performance degradation under icing conditions
[AIAA PAPER 92-0134] p 263 A92-23754
Aeroelastic response and blade loads of a composite rotor in forward flight
[AIAA PAPER 92-2566] p 564 A92-34480
Aircraft accident reports: Brief format US civil and foreign aviation issue number 2 of 1989 accidents
[PB90-916902] p 263 N92-15978
Piloted simulation study of a balloon-assisted deployment of an aircraft at high altitude
[NASA-TM-104245] p 272 N92-15986
Estimation of airborne performance in landing
[ESDU-91032] p 272 N92-15988
Flight in adverse environmental conditions
p 449 N92-21680
Regulations and their changes for certification of civil aircraft in icing conditions p 450 N92-21683
Practical considerations in designing the engine cycle
p 869 N92-28460
Thermal response of rigid and flexible insulations and reflective coating in an aeroconvective heating environment
[NASA-TM-103925] p 852 N92-28721
Helicopter nighttime parking test results - UH-1
[DOT/FAA/CT-TN92/1] p 961 N92-31165
Stagnation-point heat-transfer rate predictions at aeroassist flight conditions
[NASA-TP-3208] p 1001 N92-31281
User's manual for AeroFcn: A FORTRAN program to compute aerodynamic parameters
[NASA-TM-104237] p 1133 N92-32507

FLIGHT CONTROL
Balloon altitude control by valving - A review and comparison of actual flight data and vertical performance analysis results
[AIAA PAPER 91-3669] p 14 A92-11016
The NASA long duration balloon project
[AIAA PAPER 91-3680] p 15 A92-11024
A valve-down technique for small balloons
[AIAA PAPER 91-3681] p 15 A92-11025
Polar patrol balloon
[AIAA PAPER 91-3688] p 15 A92-11031
Manually flown windshear recovery technique
p 27 A92-11386
Dynamic interpolation for linear systems
p 52 A92-11465
Application of quantitative feedback theory (QFT) to flight control problems p 27 A92-11499
Robust controller design for an advanced fighter aircraft p 28 A92-11500
U-parameter design example - Robust flight control for wind-shear protection p 28 A92-11502
VSTOL aircraft flight control system design using H(infinity) controllers and a switching strategy
p 28 A92-11561
Applying mu-synthesis to missile autopilot design
p 28 A92-11564
An assessment of robustness of variable structure control systems for advanced aircraft manoeuvres
p 29 A92-11595
Development and future view of the technology for fly-by-light control system elements p 131 A92-14027
Practical robustness testing for helicopter flight control systems p 132 A92-14340
Development testing of the EH101 Flight Control System p 132 A92-14380
V-22 thrust power management control law development p 132 A92-14405
The flight test pilot's display - A CRT system for test maneuvers p 118 A92-16057
JAS 39 Gripen progress report p 112 A92-16058
Aircraft ground vibration test by means of flight control surfaces
[ONERA, TP NO. 1991-96] p 133 A92-16079
Utilization of a research simulator for the development of new flight control concepts
[ONERA, TP NO. 1991-161] p 137 A92-16128
Delivered with feeling --- computer-based design of flight control system for Boeing 777 p 134 A92-16621
Baro-inertial loop for the USAF Standard RLG INU
p 97 A92-16647
Formal specification and verification of Ada software
[AIAA PAPER 91-3713] p 230 A92-17585
An intelligent pilot vehicle interface for a day/night adverse weather pilotage system (D/NAPS)
[AIAA PAPER 91-3729] p 197 A92-17596
Sensor fusion for synthetic vision
[AIAA PAPER 91-3730] p 197 A92-17597
A review of digital flight control system upsets caused by electromagnetic interference
[AIAA PAPER 91-3765] p 215 A92-17627
Control concept for maneuvering in hypersonic flight
[AIAA PAPER 91-5055] p 203 A92-17838
Aeroservoelastic stabilization techniques for hypersonic flight vehicles
[AIAA PAPER 91-5056] p 203 A92-17839
Performance improvements of an F-15 airplane with an integrated engine-flight control system
p 205 A92-20204
A low-altitude breakthrough system using optimal path terrain following p 205 A92-20483
Synthesis of a helicopter full-authority controller
p 280 A92-21178
Aircraft flight controls design using output feedback
p 280 A92-21180
Observability under recurrent loss of data
p 302 A92-21191
A theory for mechanical flight control linkages
p 269 A92-21312
Quantitative Feedback Theory (QFT) applied to the design of a rotorcraft flight control system
[AIAA PAPER 92-0044] p 281 A92-22161
Integrated flight control law synthesis for an aeroelastic forward-swept wing aircraft
[AIAA PAPER 92-0046] p 281 A92-22163
The Civil Rotorcraft Initiative - An action agenda
p 241 A92-22707
Failure detection and identification for aircraft sensors
p 370 A92-27832
Reliability aspects in computer integrated manufacturing systems p 397 A92-27838
High-alpha application of variable-gain output feedback control p 380 A92-28152
Integrated flight/propulsion control design for a STOVL aircraft using H-infinity control design techniques
p 476 A92-29093
Integrated flight/propulsion control specifications for systems with two-way coupling p 477 A92-29117
IMPAC - An integrated methodology for propulsion and airframe control p 477 A92-29118
A framework for the analysis of airframe/engine interactions and integrated flight/propulsion control
p 478 A92-29120
Hover control of a PVTOL using nonlinear regulator theory p 478 A92-29171
Robust adaptive nonlinear control of high performance aircraft p 478 A92-29188
System identification requirements for high-bandwidth rotorcraft flight control system design
p 479 A92-29332
Application of the delta-operator in MIMO discrete-time adaptive flight control systems p 479 A92-29516
A note on thrust control for jetliner during approach
p 457 A92-29518
Robustness of control systems with nonlinear parametric correction for certain types of perturbations
p 509 A92-30311
Potential role of neural networks and fuzzy logic in flight control design and development
[AIAA PAPER 92-0999] p 600 A92-33191
The ATF YF-23 Vehicle Management System
[AIAA PAPER 92-1076] p 563 A92-33245
Flight management system integration on the F-117A
[AIAA PAPER 92-1077] p 563 A92-33246
Suit study - The impact of VMS in subsystem integration
[AIAA PAPER 92-1078] p 563 A92-33247
F15E terrain following system development
[AIAA PAPER 92-1079] p 563 A92-33248
High-performance fighter fly-by-wire flight control actuation system --- for YF-23A prototype
[AIAA PAPER 92-1123] p 563 A92-33277
PDFIII - A flight control system for EW UAV's
[TABES PAPER 91-315] p 565 A92-34688
Multivariable methods for helicopter flight control law design - A review p 568 A92-35748
Experiences with high authority helicopter flight control
p 568 A92-35757
High-order state space simulation models of helicopter flight mechanics p 569 A92-35777
Eigenstructure assignment for handling qualities in helicopter flight control law design p 570 A92-35786
Flying qualities testing on the modern technology airship p 570 A92-35933
Estimation of flying qualities using a leastsquares lower-order equivalent systems technique
p 570 A92-35947
United 232 - Coping with the 'one-in-a-billion' loss of all flight controls p 530 A92-36349
A novel avionic sensor for fly-by-light controls
p 650 A92-38128
Robust wind shear stochastic controller-estimator
p 661 A92-39893
Design of low-sensitivity modalized observers using left eigenstructure assignment p 661 A92-39908
Robust flight control system design with multiple model approach p 661 A92-39910
On upsets of analog portions of digital flight control systems due to electromagnetic interference
[SAE PAPER 912144] p 651 A92-39982
Agility and high angle of attack - An Air Force research perspective
[SAE PAPER 912145] p 608 A92-39983
Condor - An all electric airplane
[SAE PAPER 912184] p 644 A92-40004
RAE Bedford VAAC research project --- VSTOL aircraft advanced flight control p 662 A92-40039
The Hummingbird experience at Lockheed Georgia
p 646 A92-40041
Modern navigation, guidance, and control processing --- Book
[ISBN 0-13-596230-7] p 639 A92-40199
MLS system error model identification and synthesis
p 639 A92-40232
Development of fly-by-light systems for commercial aircraft p 744 A92-42605
An adaptive flight control for use in connection with helicopter engine failure p 745 A92-43159

Robust flight control system design using a multimodel approach. II p 745 A92-43180
Flight control system design p 776 A92-43181
Model reference adaptive flight control system (MRAFCS) design with consideration of the balance point p 745 A92-43182
A restructurable flight control system design using nonlinear compensation p 745 A92-43184
The acceleration control system design of a flight vehicle using a two-wing control method p 745 A92-43185
Evaluation and comparison of triple and quadruple flight control architectures p 745 A92-43884
Fault tolerant EHA architectures --- electro-hydrostatic actuator p 763 A92-43885
Toward an integrated multimodal approach to flight simulation p 880 A92-45026
Jet-powered V/STOL aircraft - Lessons learned p 841 A92-45304
A progress report on ASTOVL control concept studies under the VAAC programme p 871 A92-45319
Integrated flight/propulsion control for supersonic STOVL aircraft p 872 A92-45320
International Pacific Air and Space Technology Conference and Aircraft Symposium, 29th, Gifu, Japan, Oct. 7-11, 1991, Proceedings
[SAE P-246] p 783 A92-45376
Avionics flight systems for the 21st century
[SAE PAPER 912033] p 784 A92-45421
Functional mock-up tests for flight control system of the NAL QSTOL research aircraft 'ASKA'
[SAE PAPER 912036] p 881 A92-45422
A simulator study of a flight reference display for powered-lift STOL aircraft
[SAE PAPER 912067] p 855 A92-45449
Manual control of vehicles with time-varying dynamics
[SAE PAPER 912078] p 917 A92-45454
A new milestone in automatic aircraft control - Fly-by-light systems transmit commands optoelectronically p 784 A92-45699
Fibre optic rotary position sensors for vehicle and propulsion controls p 855 A92-46243
The method of determinant equations in the applied theory of optimal systems - Systems with 'rigid' constraints and with fixed boundary conditions p 917 A92-46629
Nonlinear inversion flight control for a supermaneuverable aircraft p 873 A92-46751
Two variations of certainty control p 918 A92-46762
Application of analog fiber optic position sensors to flight control systems p 857 A92-48042
Nonlinear control design for slightly nonminimum phase systems - Application to V/STOL aircraft p 876 A92-48160
The propulsive-only flight control problem p 876 A92-48487
F-16 failure detection isolation and estimation study p 876 A92-48490
Variable displacement electro-hydrostatic actuator --- for flight control systems p 876 A92-48492
C-141 and C-130 power-by-wire flight control systems p 876 A92-48493
Electric actuation system duty cycles --- in fly-by-wire/power-by-wire control p 877 A92-48494
Making fly-by-light a reality p 877 A92-48499
Verification and validation of F-15 and S/MTD unique software p 921 A92-48515
Partitioned software support concept for modular embedded computer software p 922 A92-48518
Comparative investigation of multiplane thrust vectoring nozzles
[AIAA PAPER 92-3263] p 864 A92-48858
Digital flight control systems - Some new commercial twists p 974 A92-49264
Implementation of non-dedicated redundancy in a fault tolerant multiprocessor testbed --- flight control p 974 A92-49294
Achieving fault tolerance in multichannel control systems --- for avionics p 974 A92-49296
MLS/RNAV control display unit development p 965 A92-49303
Critical digital systems - A fly-by-light consideration p 974 A92-49324
Carefree handling systems for helicopters p 975 A92-50010
Terminal area traffic management p 955 A92-50122
Predictive control for optimal path terrain following system p 955 A92-50207
The design and simulation of an intelligence flight control system p 976 A92-50237
Aerospace plane guidance using time-scale decomposition and feedback linearization p 984 A92-50498
Robust flight control systems - A parameter space design p 976 A92-50503
Dynamics and control of maneuverable towed flight vehicles p 976 A92-50508
Roll metrics for handling qualities - The landing approach p 976 A92-50520
Distributed flight control system using fiber distributed data interface (FDDI) p 976 A92-51004
Flight control system design using eigenstructure assignment for rolling the aircraft around the velocity vector p 977 A92-51945
Aircraft longitudinal dynamics equations including wind shear effects p 977 A92-51946
Analysis of propulsion system dynamics in the validation of a high-order state space model of the UH-60
[AIAA PAPER 92-4150] p 959 A92-52441
Developmental evaluation of a centrifuge flight simulator as an enhanced maneuverability flying qualities tool
[AIAA PAPER 92-4157] p 982 A92-52447
Piloted evaluation of an integrated propulsion and flight control simulator
[AIAA PAPER 92-4178] p 960 A92-52459
Optimal implicit model-following approach with frequency-shaped weighting and its application to design of flight control system p 977 A92-53094
A reversed-frame normalization design of robust flight control system p 1009 A92-53382
Improvement of atmospheric flight performance of a space vehicle through H infinity-control theory p 1130 A92-53785
Effects of bleed air extraction of thrust levels on the F404-GE-400 turbofan engine
[AIAA PAPER 92-3092] p 1066 A92-54009
Development of the full-envelope Performance Seeking Control algorithm
[AIAA PAPER 92-3748] p 1068 A92-54148
Performance benefits of adaptive in-flight propulsion system optimization
[AIAA PAPER 92-3749] p 1068 A92-54149
Preliminary assessment of the robustness of dynamic inversion based flight control laws
[AIAA PAPER 92-4330] p 1074 A92-55174
Flight control law synthesis using neural network theory
[AIAA PAPER 92-4390] p 1074 A92-55191
Flight-determined stability analysis of multiple-input-multiple-output control systems
[AIAA PAPER 92-4396] p 1074 A92-55196
Robustness of a helicopter flight control system designed using eigenstructure assignment
[AIAA PAPER 92-4469] p 1076 A92-55229
Constrained control allocation
[AIAA PAPER 92-4550] p 1131 A92-55262
Applications of robust control theory - Educational implications
[AIAA PAPER 92-4559] p 1131 A92-55271
Enlisting industry support for a flight controls design lab
[AIAA PAPER 92-4560] p 1141 A92-55272
E-6 flutter investigation and experience
[AIAA PAPER 92-4601] p 1077 A92-55280
An framework for robust flight control design using constrained optimization
[AIAA PAPER 92-4603] p 1131 A92-55282
Automated procedures for aircraft aeroservoelastic compensation
[AIAA PAPER 92-4606] p 1077 A92-55284
Analysis of airframe/engine interactions for a STOVL aircraft with integrated flight/propulsion control
[AIAA PAPER 92-4623] p 1052 A92-55300
Quantitative Feedback Theory approach to AIAA Controls Design Challenge
[AIAA PAPER 92-4626] p 1077 A92-55303
Computer aided evaluation of aircraft handling qualities and flight control system robustness
[AIAA PAPER 92-4423] p 1080 A92-55347
Flight simulator fidelity assessment in a rotorcraft lateral translation maneuver
[AIAA PAPER 92-4424] p 1092 A92-55348
Robust identification of nonlinear aerodynamic model structure
[AIAA PAPER 92-4503] p 1081 A92-55370
C-17 flight control system overview p 1082 A92-55906
On-line identification and control of linearized aircraft dynamics p 1082 A92-55911
Multiaxis control in longitudinal mode of aircraft p 1083 A92-56027
A320 flight control from the pilot's point of view p 1083 A92-56028
Flight control system design using H(infinity) optimal control p 1083 A92-56030
MIMO state-feedback control system considering phase stability by -90 deg phase-locus method p 1084 A92-56066
Design of a flight control system using a feedback-error-learning-type neural network p 1132 A92-56067
Application of restructurable flight control system using nonlinear control to an airliner p 1084 A92-56068
Piloted simulation for the BK117 FBW demonstrator p 1053 A92-56077
An experimental study on variable pressure hydraulic flight control system p 1084 A92-56119
Redundancy design philosophy for catastrophic loss protection p 1119 A92-56202
Field test of an advanced maintenance-system p 1016 A92-56221
Creation of a living specification for an experimental helicopter active flight control system through incremental simulation p 1057 A92-56312
Helicopter nonlinear flight control system development p 1085 A92-56317
A study of helicopter rotor/fuselage response in low-speed manoeuvres - Comparison of theory with flight p 1086 A92-56334
Issues in developing control zones for international space operations p 1141 A92-56602
Development of a 1/7th scale fighter UAV for flight research
[AD-A240703] p 23 N92-11008
New methods in robust control
[AD-A240221] p 29 N92-11018
Initial design study of existing flight control system of RPH and feasibility study of implementing HHC on the SH-60B
[AD-A240522] p 30 N92-11019
Prediction of forces and moments for hypersonic flight vehicle control effectors
[NASA-CR-188954] p 33 N92-11070
Real Time Data System (RTDS) p 140 N92-12025
A methodology for software specification and development based on simulation p 135 N92-12458
Process/object-oriented Ada software design for an experimental helicopter p 164 N92-12461
The development of a requirement specification for an experimental active flight control system for a variable stability helicopter: An Ada simulation in JSD p 135 N92-12466
Development and verification of software for flight safety critical systems p 164 N92-12469
Soviet electronic display systems under research and manufactured for the civil aviation aircraft of the 1990's
[AD-A240933] p 119 N92-13066
DME growth elements and their use with MLS p 189 N92-14018
Knowledge based system applications for guidance and control
[AGARD-AR-284] p 205 N92-14065
Computational aerothermodynamic methods for industrial applications to re-entry and hypersonic cruise problems p 227 N92-15027
Neural network and fuzzy logic technology for naval flight control
[AD-A242650] p 206 N92-15074
Formulation of a strategy for monitoring control integrity in critical digital control systems
[NASA-TM-104158] p 206 N92-15075
Trim drag reduction concepts for horizontal takeoff single-stage-to-Orbit vehicles
[NASA-TM-102687] p 206 N92-15076
Model identification and control system design for the lambda unmanned research vehicle
[AD-A241859] p 299 N92-17024
Identification techniques: Model structure and time domain methods p 273 N92-17157
Industry view on rotorcraft system identification p 274 N92-17163
System identification requirements for high-bandwidth rotorcraft flight control system design p 282 N92-17166
Advanced flight software reconfiguraton p 287 N92-17350
Flight evaluation of curved MLS precision approaches in a twin otter aircraft, phase 2
[AD-A243025] p 268 N92-17568
A robust digital flight control system for an unfanned research vehicle using discrete quantitative feedback theory
[AD-A243638] p 283 N92-17748
GPS interferometric attitude and heading determination: Initial flight test results p 269 N92-17994
Investigation of air transportation technology at Princeton University, 1990-1991 p 266 N92-17995
Technical notes and correspondence: Stochastic robustness of linear time-invariant control systems p 303 N92-18002
Graphics for interactive PC based parameter estimation package
[NAL-PD-FC-9117] p 412 N92-18252
A parametric approach to spectrum development p 360 N92-18578
Manoeuvring Aerodynamics
[AGARD-CP-497] p 363 N92-18778

Linearized aerodynamic and control law models of the X-29A airplane and comparison with flight data
[NASA-TM-4356] p 381 N92-19174
Application of nonlinear QFT to flight control design for high angle of attack maneuvers with thrust vectoring
[AD-A243821] p 381 N92-19241
NASA TSRV essential flight control system requirements via object oriented analysis
[NASA-CR-189573] p 381 N92-19499
Robust control system design with application to high performance helicopters p 382 N92-19621
Validation of flight critical control systems
[AGARD-AR-274] p 382 N92-20026
Control integration concept for hypersonic cruise-turn maneuvers
[NASA-TP-3136] p 481 N92-20195
Design and evaluation of a robust dynamic neurocontroller for a multivariable aircraft control problem
[NASA-TM-105579] p 481 N92-20586
Data processing aspects of the Hermes Flight Control Center p 513 N92-20629
High-speed civil transport flight- and propulsion-control technological issues
[NASA-CR-186015] p 482 N92-21253
The Guardian: Preliminary design of a close air support aircraft
[NASA-CR-189991] p 463 N92-21566
Computer-aided design of flight control systems
[AD-A244657] p 483 N92-21752
Enhanced displays, flight controls, and guidance systems for approach and landing p 456 N92-21957
Approach and landing guidance p 457 N92-21960
Variable-camber systems integration and operational performance of the AFTI/F-111 mission adaptive wing
[NASA-TM-4370] p 570 N92-22194
Formal design and verification of a reliable computing platform for real-time control. Phase 2: Results
[NASA-TM-104196] p 602 N92-22320
Directions in propulsion control p 560 N92-22530
FALKE: Winged re-entry vehicle flight control
p 667 N92-24454
The DLR test aircraft in FZ-BS VFW614/ATTAS, Dornier DO228-101, MBB BO 105-S-3 p 648 N92-25591
ATTAS experimental cockpit and ATMOS for flight control components and systems investigations
p 641 N92-25595
Development of flight testing of a fault tolerant fly-by-light yaw control system p 662 N92-25599
A preliminary look at an optimal multivariable design for propulsion-only flight control of jet-transport aircraft
[NASA-CR-186014] p 663 N92-25734
Assessment of flying-quality criteria for air-breathing aerospacecraft
[NASA-CR-4442] p 663 N92-25982
F-111C flight dynamic model aerodynamic data-base development and verification
[AD-A246356] p 715 N92-26947
Integrated flight propulsion control research results using the NASA F-15 HIDEC Flight Research Facility
[NASA-TM-4394] p 740 N92-27379
Flight-determined benefits of integrated flight-propulsion control systems
[NASA-TM-4393] p 742 N92-27587
Technical evaluation report on the Flight Mechanics Panel Symposium on Flying Qualities
[AGARD-AR-311] p 733 N92-27870
Knowledge-based planning for controlled airspace flight operation as part of a cockpit assistant
p 727 N92-27895
Fuzzy guidance system evaluation
p 778 N92-27903
Parallel knowledge based systems architectures for in-flight mission management p 728 N92-27904
Robust intelligent flight control for hypersonic vehicles
[NASA-CR-185680] p 746 N92-28209
Utility of ground simulation in flight control problem identification, solution development, and verification
p 883 N92-28525
Flight simulation and digital flight controls
p 884 N92-28526
The application of flight simulation models in support of rotorcraft design and development
p 884 N92-28527
Use of high-fidelity simulation in the development of an F/A-18 active ground collision avoidance system
p 837 N92-28530
Use of simulation in the USAF Test Pilot School curriculum p 884 N92-28535
Full mission simulation: A view into the future
p 884 N92-28537
Use of a research simulator for the development of new concepts of flight control p 885 N92-28543
The role of systems simulation for the development and qualification of ATTAS p 886 N92-28548
Effects of cockpit lateral stick characteristics on handling qualities and pilot dynamics
[NASA-CR-4443] p 878 N92-28584
Stability and control flight testing of a half-scale Pioneer remotely piloted vehicle
[AD-A245973] p 879 N92-28801
Rotorcraft In-Flight Simulation Research at NASA Ames Research Center: A Review of the 1980's and plans for the 1990's
[NASA-TM-103873] p 853 N92-28926
In-flight simulation studies at the NASA Dryden Flight Research Facility
[NASA-TM-4396] p 853 N92-29110
Effects of bleed air extraction on thrust levels on the F404-GE-400 turbofan engine
[NASA-TM-104247] p 871 N92-29425
An analytical and experimental investigation of flutter suppression via piezoelectric actuation
[NASA-TM-107653] p 962 N92-31174
Preliminary subsonic aerodynamic model for simulation studies of the HL-20 lifting body
[NASA-TM-4302] p 978 N92-31175
Proceedings of the 53rd Symposium on Air Vehicle Mission Control and Management
[AGARD-AR-310] p 1010 N92-32229
A parameter optimization approach to controller partitioning for integrated flight/propulsion control application
[NASA-TM-105826] p 979 N92-32241
A learning enhanced flight control system for high performance aircraft
[AD-A252520] p 1086 N92-32435
Fly-by-light technology development plan
[NASA-CR-181954] p 1086 N92-32778
Collaborative research on V/STOL control system/cockpit display tradeoffs under the NASA/MOD joint aeronautical program
[NASA-TM-103910] p 1087 N92-32788
An evaluation of decelerating IFR approaches utilizing a helicopter flight simulator
[CTN-92-60348] p 1048 N92-32845
Flight testing and simulation of an F-15 airplane using throttles for flight control
[NASA-TM-104255] p 1087 N92-32864
Investigation of the flight control requirements of a half-scale ducted fan unmanned aerial vehicle
[AD-A252730] p 1087 N92-32988
Rapid development of the X-31 simulation to support flight-testing
[NASA-TM-104256] p 1060 N92-33149
The F-18 high alpha research vehicle: A high-angle-of-attack testbed aircraft
[NASA-TM-104253] p 1060 N92-33404
Advanced techniques in reliability model representation and solution
[NASA-TP-3242] p 1134 N92-33483
A workstation-based evaluation of a far-field route planner for helicopters
[NASA-TM-102882] p 1051 N92-33609
Design of helicopter flight control systems for hover and low speed using eigenstructure assignment
p 1061 N92-33952
Nonlinear dynamic-inversion flight control of supermaneuverable aircraft p 1062 N92-33953
Experience with Ada on the F-18 High Alpha Research Vehicle Flight Test Program
[NASA-TM-104259] p 1062 N92-34039
Piloted evaluation of an integrated propulsion and flight control simulator
[NASA-TM-105797] p 1088 N92-34107

FLIGHT CREWS

Cockpit distractions - Precursors to emergencies
p 16 A92-11178
A model for evaluation and training in aircrew coordination and cockpit resource management
p 46 A92-11191
Operational and economic benefits of area navigation from the perspective of a major air carrier
p 96 A92-16632
Structural design considerations for a Personnel Launch System p 386 A92-24668
Active noise reduction p 603 A92-32980
Inertia reels for aircrew restraint systems
p 529 A92-32982
Progress report of Scot's Laser Ordnance Initiator System for crew escape p 580 A92-32988
Standardization of NATOPS emergency egress procedures --- Naval Air Training and Operating Procedures Standardization Program p 529 A92-32998
U.S. Coast Guard aviation life support and rescue equipment p 529 A92-32999
The law in Australia relating to negligence of aircrew and engineers p 606 A92-33463
B-2 handling, automation tailored to two-pilot crew
p 643 A92-39725
Windscreen departure p 723 A92-42500
Scenario analysis of thigh gap related ejection injuries
p 834 A92-44995
The effectiveness of training programs for preventing aircrew 'error' p 834 A92-44997
Full model simulation of the National Airspace System - Research and training platform p 880 A92-45042
Rejected takeoffs - Causes, problems, and consequences p 835 A92-45052
Aircraft Command in Emergency Situations (ACES)
[SAE PAPER 912039] p 835 A92-45424
Aircraft route optimization using adaptive simulated annealing p 922 A92-48565
Cockpit crew research p 951 A92-51440
Using the simulation modeling method to estimate the reliability of the crew-flight vehicle system
p 1133 A92-57444
An experimental study of organismic principles of the functioning of the crew-transport aircraft system
p 1133 A92-57446
Aircraft accident report: MarkAir, Inc., Boeing 737-2X6C, N670MA, controlled flight into terrain, Unalakleet, Alaska, 2 June 1990
[PB91-910402] p 92 N92-13039
Development of an emergency underwater escape breathing system for CH124 seaking aircrew
[DCIEM-87-TR-11] p 92 N92-13041
The impact of cockpit automation on crew coordination and communication. Volume 1: Overview, LOFT evaluations, error severity, and questionnaire data
[NASA-CR-177587] p 93 N92-13044
The multi-attribute task battery for human operator workload and strategic behavior research
[NASA-TM-104174] p 303 N92-17130
Approach to crew training in support of the USAF Aircraft Structural Integrity Program (ASIP) p 363 N92-18595
A graphical weather system design for the NASA transport systems research vehicle B-737
[NASA-TM-104205] p 556 N92-22504
Workshop on integrated Crew Resource Management (CRM)
[DOT/FAA/RD-92/5] p 781 N92-27518
An analysis of aircrew communication patterns and content
[AD-A246618] p 907 N92-28253
Use of a commercially available flight simulator during aircrew performance testing
[AD-A245922] p 883 N92-28407
Flight crew integration in the maintenance chain of a commercial aircraft (A 320) p 1012 N92-30957
Canadian aircrew sea water survival, 1952-1987
[DCIEM-88-RR-39] p 954 N92-32219
A review and discussion of flight management system incidents reported to the aviation safety reporting system
[AD-A252438] p 1043 N92-32941
Development of rating instruments and procedures for aviation mishap investigation
[AD-A253072] p 1044 N92-33288
Workshop on Aeronautical Decision Making (ADM). Volume 1: Executive summary
[DOT/FAA/RD-92/14-VOL-1] p 1142 N92-33305

FLIGHT ENVELOPES

V-22 flight test aerodynamics p 104 A92-14333
Helicopter control response types for hover and low-speed near-earth tasks in degraded visual conditions
p 132 A92-14338
Value of survivability enhancement techniques
p 59 A92-14349
Problem of the optimal correction of a flight test program for an aircraft system p 113 A92-16809
A geometric approach to regulator and tracker design for an aerospace plane
[AIAA PAPER 91-5054] p 203 A92-17837
Identification of aerodynamic coefficients using computational neural networks
[AIAA PAPER 92-0172] p 255 A92-23783
Full envelope multivariable control of a gas turbine engine p 468 A92-29116
Flight testing a high performance kit built aircraft
[AIAA PAPER 92-1240] p 538 A92-33333
X-29 high angle of attack flight test procedures, results, and lessons learned p 548 A92-35934
Multi-constraint wing optimization p 701 A92-41197
Update of the X-29 high-angle-of-attack program
[SAE PAPER 912006] p 783 A92-45407
Development of the full-envelope Performance Seeking Control algorithm
[AIAA PAPER 92-3748] p 1068 A92-54148
Gain scheduled linear PID autopilot for the AIAA Controls Design Challenge aircraft
[AIAA PAPER 92-4629] p 1078 A92-55304
Evolution and development of hypersonic configurations 1958-1990
[AD-A242768] p 197 N92-15069

Energy height method for flight path optimisation. Addendum A: Numerical method suitable for rapid use on IBM PC compatible computers
[ESDU-91016-ADD] p 272 N92-15987
Linearized aerodynamic and control law models of the X-29A airplane and comparison with flight data
[NASA-TM-4356] p 381 N92-19174
Analysis of the effects of removing nose ballast from the F-15 eagle
[AD-A244044] p 366 N92-19178
Technical evaluation report on the Flight Mechanics Panel Symposium on Flying Qualities
[AGARD-AR-311] p 733 N92-27870

FLIGHT FATIGUE
Fatigue and accidents - A comparison across modes of transport p 17 A92-13025

FLIGHT HAZARDS
Analysis of general aviation accidents during operations under instrument flight rules p 16 A92-11172
Sensors and systems to enhance aviation safety against weather hazards p 160 A92-14265
Flight test investigation of the wake vortices generated by helicopters p 270 A92-21925
Airborne in situ computation of the wind shear hazard index
[AIAA PAPER 92-0291] p 351 A92-25744
Aircraft icing
[ONERA, TP NO. 1991-202] p 351 A92-26359
Aircraft lightning strikes
[ONERA, TP NO. 1991-204] p 351 A92-26361
Understanding and predicting microbursts p 407 A92-27953
A case study of the Claycomo, Missouri microburst on July 30, 1989 p 407 A92-27961
Loss of cabin pressurization in U.S. naval aircraft - 1969-90 p 634 A92-37168
Flying on thin ice p 634 A92-38375
Collision probability estimate method for impact generated low earth orbit space debris clouds
[AAS PAPER 91-369] p 752 A92-43269
Real targets, unreal displays - The inadvertent suppression of critical radar data p 839 A92-44969
Eliminating pilot-caused altitude deviations - A human factors approach p 834 A92-45041
On the possibility of freezing and sticking phenomena in a transport during the ground taxiing and takeoff run and on the preventions of the hazard
[SAE PAPER 912042] p 836 A92-45426
Modified Doppler detects wind shear more reliably p 1015 A92-55099
Escape strategies for turboprop aircraft in microburst windshear p 1084 A92-56151
A study of the airwake aerodynamics over the flight deck of an AOR model ship
[AD-A241008] p 89 N92-13034
Cockpit display of hazardous weather information p 277 N92-17989
Optimal aircraft performance during microburst encounter p 266 N92-17999
Particle trajectory computer program for icing analysis of axisymmetric bodies
[NASA-CR-189134] p 352 N92-19276

FLIGHT INSTRUMENTS
Through the looking glass --- effectiveness of electronic flight instrument systems p 856 A92-46449
Effect of short-term exposure to stereoscopic three-dimensional flight displays on real-world depth perception
[NASA-TP-3117] p 119 N92-13065
Advanced Transport Operating System (ATOPS) color displays software description: MicroVAX system
[NASA-CR-189603] p 556 N92-22395
Advanced Transport Operating System (ATOPS) color displays software description microprocessor system
[NASA-CR-189605] p 556 N92-22645
Force limited vibration testing p 595 N92-22688
A continuing study of altitude determination deficiencies of the Service Aircraft Instrumentation Package (SAIP)
[AD-A245952] p 968 N92-32051
The utility of analog vertical velocity information during instrument flight with a Head-Up Display (HUD)
[AD-A252863] p 1065 N92-33277

FLIGHT LOAD RECORDERS
The development of fatigue management requirements and techniques p 360 N92-18572

FLIGHT MANAGEMENT SYSTEMS
Managing Europe's air traffic system p 19 A92-11876
Feeling normal --- evaluation of advanced control systems for future Boeing 777 p 134 A92-16623
Single lever power management of turboprop engines p 372 A92-25373
Behind the screens --- development of Central Flow Management Unit for air traffic control p 353 A92-25520
Navigation and flight management systems - Thoughts of a user p 354 A92-26848
The cockpit of a modern aircraft - The Airbus A340 considered as an example p 357 A92-26849
A knowledge acquisition approach for an on-board mission planner
[AIAA PAPER 92-1021] p 531 A92-33204
Flight management system integration on the F-117A
[AIAA PAPER 92-1077] p 563 A92-33246
Pilot activated automatic recovery system on the F-117A
[AIAA PAPER 92-1126] p 563 A92-33278
Profile negotiation - A concept for integrating airborne and ground-based automation for managing arrival traffic p 531 A92-33432
Harmonisation and integration of air traffic control in Europe p 532 A92-33437
Flight management system back-up navigation for the A330/A340 aircraft p 975 A92-49326
Map projections and airborne moving map displays p 966 A92-49327
An advanced flight path management system for low-altitude helicopter flight p 975 A92-49330
GPS integration improves mission capabilities of CH-47D aircraft p 966 A92-49340
Terminal area traffic management p 955 A92-50122
Airline industry safety management systems and feedback p 951 A92-51439
A fuel-optimal 4D guidance algorithm p 978 A92-53095
Flight management system of the F-117A p 1082 A92-55910
Background issues for on-line aircraft documentation p 119 N92-13858
Space software is first of all software p 509 N92-20590
Advanced Transport Operating System (ATOPS) control display unit software description
[NASA-CR-189606] p 652 N92-24689
Flight test of avionic and air-traffic control systems
[ETN-92-91063] p 640 N92-25590
Testing of an experimental FMS p 648 N92-25596
On board planning of 4D-trajectories p 728 N92-27897
ICAAS piloted simulation evaluation p 735 N92-27906
A review and discussion of flight management system incidents reported to the aviation safety reporting system
[AD-A252438] p 1043 N92-32941
CTAS: Computer intelligence for air traffic control in the terminal area
[NASA-TM-103959] p 1044 N92-33080

FLIGHT MECHANICS
Flight in a steady wind field p 131 A92-13696
AHS, Annual Forum, 47th, Phoenix, AZ, May 6-8, 1991, Proceedings. Vols. 1 & 2 p 59 A92-14326
Some considerations on modeling flight vehicles movement p 281 A92-21311
Dynamics of an aircraft-towed body during release
[AIAA PAPER 92-0130] p 295 A92-23750
Elements of airplane performance --- Book
[ISBN 90-6275-608-5] p 357 A92-26550
Investigation of extremal field behavior for two-dimensional linear problems in flight mechanics p 509 A92-30130
Dynamics of the three-dimensional angular motions of rotating flight vehicles in the presence of the aerodynamic hysteresis of the moment characteristic p 428 A92-30371
Horizontal flight of an aircraft with periodic thrust reversal p 480 A92-31876
High-order state space simulation models of helicopter flight mechanics p 569 A92-35777
Symptom of payload-induced flight instability p 873 A92-46761
A Mach-scaled powered model for rotor-fuselage interactional aerodynamics and flight mechanics investigations p 847 A92-46960
Mathematical modeling of the flight of passenger aircraft in the case of engine failure p 875 A92-47777
AIAA Atmospheric Flight Mechanics Conference, Hilton Head Island, SC, Aug. 10-12, 1992, Technical Papers. Pts. 1-2 p 1078 A92-55326
Rotorcraft System Identification
[AGARD-LS-178] p 273 N92-17153
SA 330 Puma identification results p 274 N92-17162
Application areas for rotorcraft system identification: Simulation model validation p 274 N92-17164
System identification methods for handling-qualities evaluation p 274 N92-17165
Transformation of flightmechanical design requirements for modern fighters into aerodynamic characteristics p 365 N92-18794
Towards understanding software: 15 years in the SEL p 413 N92-19423
Activities of NRC-CNRC, Institute for Aerospace Research
[CTN-92-60431] p 420 N92-20204
Modeling methods for high-fidelity rotorcraft flight mechanics simulation
[NASA-TM-103842] p 482 N92-21440
Flight in adverse environmental conditions p 449 N92-21680
Aircraft Ship Operations
[AGARD-CP-509] p 464 N92-21951
Technical evaluation report on the Flight Mechanics Panel Symposium on Flying Qualities
[AGARD-AR-311] p 733 N92-27870
Numerical optimization in Germany: A non-exhaustive survey on current activities with emphasis on aeronautics
[MBB/FE211/S/PUB/474] p 932 N92-30675
Activities of the Aeronautical Research Laboratory p 1013 N92-30768
Technical evaluation report on the Flight Mechanics Panel Symposium on Piloted Simulation Effectiveness
[AGARD-AR-315] p 983 N92-30769
Analysis of spacecraft entry into Mars atmosphere p 1105 N92-33763

FLIGHT OPERATIONS
Integration of flight and carrier landing aid systems for shipboard operations
[ONERA, TP NO. 1991-113] p 134 A92-16092
Aircraft accident report: MarkAir, Inc., Boeing 737-2X6C, N670MA, controlled flight into terrain, Unalakleet, Alaska, 2 June 1990
[PB91-910402] p 92 N92-13039
Flight operations for higher harmonic control research
[AD-A242478] p 196 N92-15067
Tactical Rubidium Frequency Standard (TRFS)
[AD-A243934] p 401 N92-18897
Vortex characteristics of C5A/B, C141B and C130E aircraft applicable to ATC terminal flight operations tower fly-by-data
[PB92-114586] p 449 N92-20318
Aircraft Ship Operations
[AGARD-CP-509] p 464 N92-21951
Deck motion criteria for carrier aircraft operations p 464 N92-21952
EH 101 ship interface trials: Flight test programme and preliminary results p 465 N92-21964
Determination of limitations for helicopter ship-borne operations p 465 N92-21965
United Kingdom approach to deriving military ship helicopter operating limits p 465 N92-21966
A review of Australian activity on modelling the helicopter/ship dynamic interface p 465 N92-21967
United States Navy ski jump experience and future applications p 465 N92-21968
Limitations on helicopter operations in the aeronaval environment p 466 N92-21973
Outlines of parabolic flight p 764 N92-26441
Knowledge-based planning for controlled airspace flight operation as part of a cockpit assistant p 727 N92-27895
Aircraft ship operations
[AGARD-AR-312] p 850 N92-28468
The evaluation of simulator effectiveness for the training of high speed, low level, tactical flight operations p 885 N92-28539
Development of new flight procedures for the Microwave Landing System (MLS)
[NLR-TP-91156-U] p 1047 N92-32830
Federal aviation regulations. Part 91: General operating and flight rules
[PB92-197334] p 1017 N92-33176

FLIGHT OPTIMIZATION
A new method for increasing maximum flight endurance p 280 A92-21006
Investigation of extremal field behavior for two-dimensional linear problems in flight mechanics p 509 A92-30130
The analysis and approximate representation of the optimal control law for a maneuverable aircraft p 479 A92-30131
The application of direct transcription to commercial aircraft trajectory optimization
[AIAA PAPER 92-4528] p 1077 A92-55246
Practical input optimization for aircraft parameter estimation experiments p 114 N92-11989

FLIGHT PATHS
Optimal trajectories and guidance trajectories for aircraft flight through windshears p 27 A92-11383
Manually flown windshear recovery technique p 27 A92-11386
Curved landing approaches using ILS and Loran C p 94 A92-13854
Computer aiding for low-altitude helicopter flight p 94 A92-14444

The sonic boom and problems related to supersonic flights of military aircraft
[ONERA, TP NO. 1991-162] p 77 A92-16129
Regulation of relaxed static stability aircraft
p 203 A92-18463
Development of a combined fast method for studying the plane motions of rigid bodies in the atmosphere around the center of mass in the presence of perturbations
p 304 A92-23563
On the skip flight of a spaceplane
p 387 A92-25503
Trajectory shaping by the U-parameter design method
p 479 A92-29361
A second-order control optimization method for nonlinear dynamic systems and its use for calculating optimal aircraft trajectories p 460 A92-31894
Profile negotiation - A concept for integrating airborne and ground-based automation for managing arrival traffic
p 531 A92-33432
Pocono Mountain SAR data analysis for testing slant range to ground range conversion p 587 A92-35142
A noise survey around Oslo Airport Fornebu
p 687 A92-39061
Microwave landing system modeling with application to air traffic control automation p 725 A92-41220
Path angular control of the STOL research aircraft Asuka p 745 A92-43146
Distance and angle measuring method using laser light and rereflection plates p 762 A92-43206
Eliminating pilot-caused altitude deviations - A human factors approach p 834 A92-45041
Reconstruction of flight path in turbulence
p 874 A92-46777
Aircraft route optimization using adaptive simulated annealing p 922 A92-48565
Route planning --- in real-time of avionics systems
p 1006 A92-49317
An advanced flight path management system for low-altitude helicopter flight p 975 A92-49330
Static and dynamic flight-path stability of airplanes
p 977 A92-52043
An efficient algorithm for optimal aircraft trajectories
[AIAA PAPER 92-4412] p 1076 A92-55206
Optimal recovery from microburst wind shear
[AIAA PAPER 92-4338] p 1078 A92-55327
A Lie Bracket solution of the optimal thrust magnitude on a singular arc in atmospheric flight
[AIAA PAPER 92-4345] p 1079 A92-55334
Multiaxis control in longitudinal mode of aircraft
p 1083 A92-56027
A320 flight control from the pilot's point of view
p 1083 A92-56028
Robust control system design with multiple model approach p 1083 A92-56029
Selection of sampling rate for nonlinear flight trajectory controller of aircraft p 1084 A92-56070
Flight evaluation of navigation systems including MLS using NAL Do228 - Outline p 1047 A92-56116
Flight evaluation of navigation systems including MLS using NAL Do228 - Results of MLS
p 1047 A92-56117
Optimization of two stage reusable space transportation systems with rocket and airbreathing propulsion concepts
[IAF PAPER 92-0863] p 1104 A92-57254
A comparison between the consequences of the liberal and non-liberal UK-Europe bilaterals
[TT-9101] p 18 N92-10018
AI for RPVs, Sensor Driven Airborne Replanner (SDAR), for a Robotic Aircraft Sensor Platform (RASP)
p 114 N92-12534
Air-to-air visual acquisition handbook
[ATC-151] p 93 N92-13042
Energy height method for flight path optimisation. Addendum A: Numerical method suitable for rapid use on IBM PC compatible computers
[ESDU-91016-ADD] p 272 N92-15987
Method of guiding an in-flight vehicle to a designed flight path
[AD-D015061] p 268 N92-17707
Optimal aircraft performance during microburst encounter p 266 N92-17999
Graphics for interactive PC based parameter estimation package
[NAL-PD-FC-9117] p 412 N92-18252
COMPAS system concept p 354 N92-19043
Ground collision avoidance using a variable incidence altitude measurement system for the A-7 aircraft
[AD-A243880] p 352 N92-19259
Proportional plus integral control of aircraft for automated maneuvering formation flight
[AD-A243792] p 382 N92-19505
Cockpit weather information needs
p 449 N92-21503
PC based flight path reconstruction using UD factorization filtering algorithm
[NAL-PD-FC-9201] p 534 N92-22389
Global positioning system supported pilot's display
p 534 N92-22436
Ground and satellite supported flight trajectory measurement by example of the avionics flight test system AFES p 641 N92-25600
Board-autonomous flight trajectory measurement by example of an ILS measuring system
p 641 N92-25601
Status of automatic guidance systems for rotorcraft in low altitude flight p 727 N92-27894
An efficient method for three-dimensional route planning with different strategies and constraints
p 728 N92-27901
Optimal trajectories for an unmanned air vehicle
p 963 N92-31880
A workstation-based evaluation of a far-field route planner for helicopters
[NASA-TM-102882] p 1051 N92-33609

FLIGHT PLANS

Aviation meteorology p 685 A92-38383
Empirical foundations and sensitivity testing - Is it enough for the 90's? p 835 A92-45054
Map projections and airborne moving map displays
p 966 A92-49327
Status of automatic guidance systems for rotorcraft in low altitude flight p 727 N92-27894
Knowledge-based planning for controlled airspace flight operation as part of a cockpit assistant
p 727 N92-27895

FLIGHT RECORDERS

Continuation of the AHS round robin on fatigue reliability and damage tolerance p 59 A92-14341
The SAS Flight Analysis and Aircraft Monitoring System p 555 A92-35941
Double Density recording acquisition and playback
p 920 A92-47534
Severe turbulence and maneuvering from airline flight records
[AIAA PAPER 92-4341] p 1078 A92-55330
Aircraft tracking for structural fatigue
p 361 N92-18584

FLIGHT SAFETY

Pre-flight risk assessment in emergency medical service (EMS) helicopters p 16 A92-11171
Cockpit distractions - Precursors to emergencies
p 16 A92-11178
Rates and risk factors for accidents and incidents versus violations for U.S. airmen p 91 A92-14048
Maintenance, Malfunction Information Report system
p 60 A92-14414
An analytical study of the helicopter flight safety under an engine failure in proximity of ground
p 91 A92-14454
Management decisions have an impact on flight safety
p 92 A92-15175
The canard-wing interference and stall safety of light canard aircraft p 111 A92-15341
Flight safety; Proceedings of the Conference, London, England, Nov. 21, 1991 p 92 A92-16050
A synergistic solution to the GPS integrity problem
p 96 A92-16641
Potential impact of GPS and automatic dependent surveillance on air lane separation in the North Atlantic Organized Track System p 99 A92-16935
Analysis of aircraft performance during lateral maneuvering for microburst avoidance
p 205 A92-20207
Probabilistic reasoning for intelligent wind shear avoidance p 302 A92-21181
Report of the working group Future CNS Systems - Applications and impact on the German air transport system p 266 A92-21325
European studies to investigate the feasibility of using 1000 ft vertical separation minima above FL 290. II - Precision radar data analysis and collision risk assessment p 353 A92-24946
Aircraft lightning strikes
[ONERA, TP NO. 1991-204] p 351 A92-26361
Transgressions in a pilot-helicopter system
p 358 A92-27394
Estimating the probability of a safe flight for an aircraft flying under the effect of disturbances
p 479 A92-30132
Safety test on the rolling angles of a winged vehicle in hypersonic speed p 480 A92-30549
New way of flying (1990 Sir Charles Kingsford Smith Lecture) p 515 A92-33461
Canada making many changes in wake of Dryden crash report p 529 A92-33799
The development of an engine air particle separator system for the CH-47 helicopter p 545 A92-35736
The obstacle avoidance radar - A safety mean for low altitude flights in adverse weather conditions
p 554 A92-35743
Why not a safety rating? --- in Australian civil aviation
p 530 A92-36200
Aviation meteorology p 685 A92-38383
Safety at sea and in the air - Taking stock together; Proceedings of the Conference, London, England, Nov. 13-15, 1990
[ISBN 0-903409-78-X] p 634 A92-39301
Engine reliability p 654 A92-39309
Runway incursions and airport surface traffic automation
[SAE PAPER 912123] p 635 A92-39970
Flight operations safety management
[SAE PAPER 912124] p 635 A92-39971
Sikorski (S-76) High Intensity Radiated Fields (HIRF) test
[SAE PAPER 912214] p 652 A92-40017
Visibility in the atmosphere and flight safety --- Russian book
[ISBN 5-286-00416-4] p 775 A92-42785
Aircraft reliability and maintainability
p 700 A92-43141
Aircraft accidents and human factors
p 723 A92-43219
EICAS in an integrated cockpit --- Engine Indication Crew Alerting System p 855 A92-44922
Who or what saved the day? A comparison of traditional and glass cockpits p 833 A92-44931
Judgement training for Alaskan pilots
p 835 A92-45048
ICAO Flight Safety and Human Factors Programme
p 835 A92-45055
Getting test items to measure knowledge at the level of complexity which licensing authorities desire - Another dimension to test validity p 835 A92-45080
A simulator study of a flight reference display for powered-lift STOL aircraft
[SAE PAPER 912067] p 855 A92-45449
Airline industry safety management systems and feedback p 951 A92-51439
The challenge of commercial aircraft survivability
p 931 A92-52022
The advantages of digital engine control as compared with traditional systems (hydraulic or pneumatic)
p 1070 A92-56338
A comparison of airborne wake vortex detection measurements with values predicted from potential theory
[NASA-TP-3125] p 18 N92-10994
Development and verification of software for flight safety critical systems p 164 N92-12469
Winds of change: Domestic air transport since deregulation
[NRC-SR-230] p 92 N92-13040
Heliport VFR airspace design based on helicopter performance
[SCT-90RR-34] p 103 N92-13049
Aircraft accident/incident summary report: Midair collision involving Lycoming Air Services Piper Aerostar PA-60 and Sun Company Aviation Department Bell 412, Merion, Pennsylvania, April 4, 1991
[PB91-910407] p 187 N92-15055
Validation and verification flight test for TCAS-2 logic changes (MOPS Change 6)
[DOT/FAA/CT-TN91/46] p 268 N92-15981
Design of experiments p 273 N92-17154
Alert generation and cockpit presentation for an integrated microburst alerting system
p 265 N92-17988
Aircraft tracking for structural fatigue
p 361 N92-18584
The effect of hoar-frosted wings on the Fokker 50 take-off characteristics p 451 N92-21692
Analysis of helicopter accident risk exposure near heliports, airports, and unimproved sites
[SCT-91RR-13] p 637 N92-26028
European studies to investigate the feasibility of using 1000 ft vertical separation minima above FL 290. Part 1: Overview of organisation, techniques employed, and conclusions
[NLR-TP-91062-U-PT-1] p 841 N92-29605
On the optimization of windshear warning and guidance systems
[NLR-TP-90196-U] p 837 N92-29703
Statistics on aircraft gas turbine engine rotor failures that occurred in US commercial aviation during 1989
[DOT/FAA/CT-92/5] p 971 N92-30303
A cable detection lidar system for helicopters
p 1001 N92-31068
Aviation safety: Changes needed in FAA's service difficulty reporting program
[GAO/RCED-91-24] p 953 N92-31453
Safety study of TCAS 2 for logic version 6.04
[DOT/FAA/RD-92/22] p 1047 N92-32537

Statistics on aircraft gas turbine engine rotor failures that occurred in US commercial aviation during 1988
[DOT/FAA/CT-91/28] p 1071 N92-33105

FLIGHT SIMULATION

Development of an advanced piloted helicopter simulation p 105 A92-14363
Performance and handling qualities criteria for low cost real time rotorcraft simulators - A methodology development p 136 A92-14365
A full mission simulation data system p 162 A92-14367
Description of a tilt wing mathematical model for piloted simulation p 133 A92-14445
Control concept for maneuvering in hypersonic flight
[AIAA PAPER 91-5055] p 203 A92-17838
Verification of flight software by embedding software simulation in simulation of external environment p 232 A92-19084
Flight simulation and its application p 284 A92-22634
Identification of aerodynamic coefficients using computational neural networks
[AIAA PAPER 92-0172] p 255 A92-23783
Flight investigation of variations in rotorcraft control and display dynamics for hover p 379 A92-28151
Engineering development simulation - Test vehicle of the future p 483 A92-29674
Frequency domain testing of helicopter dynamics using automated input signals p 545 A92-35731
The use of inverse simulation for conceptual design p 546 A92-35738
S-76B certification for vertical take-off and landing operations from confined areas p 530 A92-35760
Control and display combinations for blind vertical landings p 661 A92-39903
A review of recent programs and future plans for rotorcraft in-flight simulation at Ames Research Center
[SAE PAPER 912121] p 608 A92-39969
1991-92 AHS Technical Committee highlights - Flight simulation p 609 A92-40394
Simulation as applied to mission planning p 747 A92-41210
Robust flight reconstruction for helicopter simulation and training p 747 A92-41230
Flight evaluations on in-flight simulation of unstable aircraft p 744 A92-43115
Flight simulation of a spaceplane p 752 A92-43190
Toward an integrated multimodal approach to flight simulation p 880 A92-45026
Centre for Flight Simulation Berlin Airbus 340 simulator for research and training p 880 A92-45028
Knowledge-sensitive task manipulation - Acquiring knowledge from pilots flying a motion-based flight simulator p 916 A92-45064
ASTOVL propulsion systems configuration and concept choice p 842 A92-45312
A progress report on ASTOVL control concept studies under the VAAC programme p 871 A92-45319
In-flight simulation of backside operating models using direct lift controller
[SAE PAPER 912069] p 872 A92-45450
Flight model for unmanned simulated helicopters p 874 A92-46776
Establishing a database for flight in the wakes of structures p 810 A92-46782
AIAA/AHS Flight Simulation Technologies Conference, Hilton Head Island, SC, Aug. 24-26, 1992, Technical Papers p 981 A92-52426
Simulation of automatic rotorcraft nap-of-the-earth flight in graphics workstation environment
[AIAA PAPER 92-4131] p 981 A92-52428
Manipulation and management of data collected at the Crew Station Research and Development Facility - A case study
[AIAA PAPER 92-4162] p 1008 A92-52451
Special Rotation Vectors quaternions in three components
[AIAA PAPER 92-4168] p 1008 A92-52454
Man-Vehicle Systems Research Facility - Design and operating characteristics
[AIAA PAPER 92-4177] p 982 A92-52458
High performance flight simulation at NASA Langley
[AIAA PAPER 92-4179] p 982 A92-52460
Space plane navigation simulation p 1103 A92-53603
Pre-flight physical simulation test of HIMES reentry test vehicle p 1103 A92-53640
A data fusion algorithm for multi-sensor microburst hazard assessment
[AIAA PAPER 92-4339] p 1063 A92-55328
ATTAS flight test and simulation results of the advanced gust management system LARS
[AIAA PAPER 92-4343] p 1079 A92-55332
A simulation model for tail rotor failure
[AIAA PAPER 92-4633] p 1081 A92-55380
Synthesis of a MLS automatic landing control law for the NAL experimental research aircraft Do-228 p 1084 A92-56062
Piloted simulation for the BK117 FBW demonstrator p 1053 A92-56077
Flight simulator test of cockpit advisory system p 1054 A92-56115
Escape strategies for turboprop aircraft in microburst windshear p 1084 A92-56151
Flight simulation modeling in support of engine/airframe integration p 1055 A92-56279
A generic harmonic rotor model for helicopter flight simulation p 1086 A92-56333
Mission oriented investigation of handling qualities through simulation p 1059 A92-56353
Ames life science telescience testbed evaluation
[NASA-CR-188856] p 140 N92-12033
Formulation of the linear model from the nonlinear simulation for the F18 HARV p 117 N92-13842
Flight research p 194 N92-13981
Flight simulation p 207 N92-13982
Numerical simulations around models in hypersonic wind tunnels p 182 N92-14998
Review of the European hypersonic wind tunnel performance and simulation requirements p 209 N92-15043
Investigation of advanced aircraft performance measures of merit including new agility metrics
[AD-A242016] p 272 N92-15990
Weight evaluation and sensitivity analysis for space plane. Part 2: TSTO
[NAL-TM-602-PT-2] p 287 N92-17754
Evaluation of the COMPAS experimental system p 355 N92-19044
A mathematical model of a tilt-wing aircraft for piloted simulation
[NASA-TM-103864] p 368 N92-19847
The Flight Simulation Facility at the Wichita State University p 484 N92-21511
Application of technology developed for flight simulation at NASA. Langley Research Center p 573 N92-22437
ATTAS experimental cockpit and ATMOS for flight control components and systems investigations p 641 N92-25595
Microcomputer-based instrument flight simulation: Undergraduate pilot training student attitude assessment
[AD-A245449] p 749 N92-26527
The modelling of turbulence and downbursts for flight simulators
[ISBN-0-315-59945-6] p 749 N92-27645
Knowledge-based planning for controlled airspace flight operation as part of a cockpit assistant p 727 N92-27895
NPSNET: Flight simulation dynamic modeling using quaternions
[AD-A247484] p 923 N92-28245
Piloted Simulation Effectiveness
[AGARD-CP-513] p 786 N92-28522
Opportunities for flight simulation to improve operational effectiveness p 883 N92-28523
Piloted simulation effectiveness development applications and limitations p 883 N92-28524
Utility of ground simulation in flight control problem identification, solution development, and verification p 883 N92-28525
Flight simulation and digital flight controls p 884 N92-28526
The application of flight simulation models in support of rotorcraft design and development p 884 N92-28527
Experience with piloted simulation in the development of helicopters p 884 N92-28528
Validation of simulation systems for aircraft acceptance testing p 852 N92-28531
Aircraft simulation and pilot proficiency: From surrogate flying towards effective training p 884 N92-28532
The use of a dedicated testbed to evaluate simulator training effectiveness p 884 N92-28533
Use of simulation in the USAF Test Pilot School curriculum p 884 N92-28535
AM-X flight simulator from engineering tool to training device p 884 N92-28536
The role of simulation for the study of APIS (piloting support by synthetic imagery) p 885 N92-28544
The use of ground based simulation for handling qualities research: A new assessment p 885 N92-28545
Initial validation of a R/D simulator with large amplitude motion p 886 N92-28546
The use and effectiveness of piloted simulation in transport aircraft research and development p 886 N92-28549
Application of piloted simulation to high-angle-of-attack flight-dynamics research for fighter aircraft p 886 N92-28551
Effective cueing during approach and touchdown: Comparison with flight p 886 N92-28552
Rotorcraft In-Flight Simulation Research at NASA Ames Research Center: A Review of the 1980's and plans for the 1990's
[NASA-TM-103873] p 853 N92-28926
In-flight simulation studies at the NASA Dryden Flight Research Facility
[NASA-TM-4396] p 853 N92-29110
Transport delay measurements: Methodology and analysis for the F-16C combat engagement trainer, the display for advanced research and training, and the F-16A limited field of view
[AD-A248519] p 888 N92-29505
Results of a flight simulator experiment to establish handling quality guidelines for the design of future transport aircraft
[NLR-MP-88044-U] p 854 N92-29616
Assessment of army aviators' ability to perform individual and collective tasks in the aviation networked simulator
[AD-A250293] p 888 N92-29709
Experience with piloted simulation in the development of helicopters
[MBB-UD-0610-91-PUB] p 889 N92-30076
Numerical methods for the simulation of complex multi-body flows with applications for the integrated Space Shuttle vehicle p 945 N92-30741
Technical evaluation report on the Flight Mechanics Panel Symposium on Piloted Simulation Effectiveness
[AGARD-AR-315] p 983 N92-30769
Preliminary subsonic aerodynamic model for simulation studies of the HL-20 lifting body
[NASA-TM-4302] p 978 N92-31175
Proceedings of the 53rd Symposium on Air Vehicle Mission Control and Management
[AGARD-AR-310] p 1010 N92-32229
Collaborative research on V/STOL control system/cockpit display tradeoffs under the NASA/MOD joint aeronautical program
[NASA-TM-103910] p 1087 N92-32788
Development of new flight procedures for the Microwave Landing System (MLS)
[NLR-TP-91156-U] p 1047 N92-32830
Rapid development of the X-31 simulation to support flight-testing
[NASA-TM-104256] p 1060 N92-33149

FLIGHT SIMULATORS

Flying the A340 iron bird p 20 A92-10666
Prediction of helicopter simulator sickness p 46 A92-11473
MIDIS - A microcomputer flight decision simulator p 136 A92-13845
Helicopter modeling requirements for full mission simulation and handling qualities assessment p 105 A92-14364
MiG-29 prototype and development flight tests - General overview and high angle of attack investigation p 113 A92-16064
Utilization of a research simulator for the development of new flight control concepts
[ONERA, TP NO. 1991-161] p 137 A92-16128
Flight simulation and its application p 284 A92-22634
Forward-look wind-shear detection for microburst recovery p 378 A92-24408
A data base for flight in the wake of a ship
[AIAA PAPER 92-0295] p 319 A92-25748
Engineering development simulation - Test vehicle of the future p 483 A92-29674
Two crew stations for dynamic flight simulation p 572 A92-35443
An exploratory investigation into the definition of tracking standards for IFR helicopter approaches to reduced minima p 533 A92-35726
An application of distributed environment in flight simulation p 602 A92-35739
Piloted simulator studies of the HL-20 Lifting Body p 666 A92-40033
Simulation in the Air Force p 747 A92-41209
Software reliability for flight crew training simulators p 747 A92-41221
Robust flight reconstruction for helicopter simulation and training p 747 A92-41230
Study on a flight simulator of time delays p 744 A92-43112
Study on the effective utilization of the current flight simulator p 748 A92-43113
The development of a real time visual flight simulator for tactical operations research and measurement p 880 A92-45027
A simulator study of a flight reference display for powered-lift STOL aircraft
[SAE PAPER 912067] p 855 A92-45449
Analysis of the VISTA longitudinal simulation capability for a cruise flight condition p 876 A92-48488
MLS/RNAV control display unit development p 965 A92-49303

Takeoff Performance Monitoring System display options
[AIAA PAPER 92-4138] p 967 A92-52433
Use of high-fidelity simulation in the development of an F/A-18 active ground collision avoidance system
[AIAA PAPER 92-4140] p 959 A92-52434
Design and performance of the centrifuge-based Dynamic Flight Simulator
[AIAA PAPER 92-4156] p 981 A92-52446
Developmental evaluation of a centrifuge flight simulator as an enhanced maneuverability flying qualities tool
[AIAA PAPER 92-4157] p 982 A92-52447
Simulation software flowdown in the aircraft design process - Problems and solutions
[AIAA PAPER 92-4160] p 1008 A92-52450
Piloted evaluation of an integrated propulsion and flight control simulator
[AIAA PAPER 92-4178] p 960 A92-52459
Design of robust Quantitative Feedback Theory controllers for pitch attitude hold systems
[AIAA PAPER 92-4409] p 1075 A92-55203
Flight simulator fidelity assessment in a rotorcraft lateral translation maneuver
[AIAA PAPER 92-4424] p 1092 A92-55348
Parameter identification of AV-8B wingborne aerodynamics for flight simulator model updates
[AIAA PAPER 92-4506] p 1027 A92-55373
Real-time helicopter simulation using the blade element method p 1132 A92-56278
HEPO mission simulator - Development and usage for NH90 helicopter p 1094 A92-56313
Mission oriented investigation of handling qualities through simulation p 1059 A92-56353
Parameter identification studies on the NASA/Ames Research Center Advanced Concepts Flight Simulator
[NASA-TM-105126] p 31 N92-11024
The modelling of turbulence and downbursts for flight simulators
[UTIAS-339] p 161 N92-12373
A 3-degree-of-freedom flight simulator evaluation of unsteady aerodynamics effects
[AD-A241540] p 139 N92-13079
Implementation of an object-oriented flight simulator D.C. electrical system on a hypercube architecture
[AD-A243700] p 284 N92-17097
An application of the object-oriented paradigm to a flight simulator
[AD-A243624] p 384 N92-18012
An evaluation of the Royal Air Force Shorts Tucano Navigation Instruments Trainer: The NAVIT
[ETN-92-90841] p 354 N92-18729
Development of nonlinear real-time helicopter simulation using a blade element method
[NLR-TP-90115-U] p 381 N92-18893
The application of statistical estimation techniques to terrain modeling
[AD-A243799] p 409 N92-19231
MULTIRAD
[AD-A244211] p 412 N92-19247
The Flight Simulation Facility at the Wichita State University p 484 N92-21511
Description and simulation results of the Italsat AOCS advanced flight simulator p 667 N92-24472
The DLR test aircraft in FZ-BS VFW614/ATTAS, Dornier DO228-101, MBB BO 105-S-3 p 648 N92-25591
The basic measuring technical equipment of the DLR test aircraft p 652 N92-25592
Expert system management system
[AD-A247102] p 781 N92-26863
Development of the Basic Flight Instruction Tutoring System (BFITS)
[AD-A246458] p 751 N92-27836
Use of a commercially available flight simulator during aircrew performance testing
[AD-A245922] p 883 N92-28407
Piloted Simulation Effectiveness
[AGARD-CP-513] p 786 N92-28522
Opportunities for flight simulation to improve operational effectiveness p 883 N92-28523
Piloted simulation effectiveness development applications and limitations p 883 N92-28524
Utility of ground simulation in flight control problem identification, solution development, and verification p 883 N92-28525
Flight simulation and digital flight controls p 884 N92-28526
The application of flight simulation models in support of rotorcraft design and development p 884 N92-28527
Experience with piloted simulation in the development of helicopters p 884 N92-28528
Use of simulation in the USAF Test Pilot School curriculum p 884 N92-28535
AM-X flight simulator from engineering tool to training device p 884 N92-28536
Full mission simulation: A view into the future p 884 N92-28537
The evaluation of simulator effectiveness for the training of high speed, low level, tactical flight operations p 885 N92-28539
Harrier GR MK 5/7 mission simulators for the Royal Air Force p 885 N92-28540
Use of a research simulator for the development of new concepts of flight control p 885 N92-28543
The use of ground based simulation for handling qualities research: A new assessment p 885 N92-28545
Initial validation of a R/D simulator with large amplitude motion p 886 N92-28546
The use and effectiveness of piloted simulation in transport aircraft research and development p 886 N92-28549
An evaluation of IFR approach techniques: Generic helicopter simulation compared with actual flight p 886 N92-28550
Effective cueing during approach and touchdown: Comparison with flight p 886 N92-28552
Rotorcraft In-Flight Simulation Research at NASA Ames Research Center: A Review of the 1980's and plans for the 1990's
[NASA-TM-103873] p 853 N92-28926
Experience with piloted simulation in the development of helicopters
[MBB-UD-0610-91-PUB] p 889 N92-30076
Development statistics for the UH-1 Ada feasibility study
[AD-A252404] p 982 N92-30547
Technical evaluation report on the Flight Mechanics Panel Symposium on Piloted Simulation Effectiveness
[AGARD-AR-315] p 983 N92-30769
Evaluation of microwave landing system approaches in a wide-body transport simulator
[NASA-CR-4450] p 957 N92-30978
An evaluation of decelerating IFR approaches utilizing a helicopter flight simulator
[CTN-92-60348] p 1048 N92-32845
Flight testing and simulation of an F-15 airplane using throttles for flight control
[NASA-TM-104255] p 1087 N92-32864
Advanced software development workstation: Effectiveness of constraint-checking --- spaceflight simulation and planning
[NASA-CR-190712] p 1134 N92-32865
Piloted evaluation of an integrated propulsion and flight control simulator
[NASA-TM-105797] p 1088 N92-34107

FLIGHT STABILITY TESTS

Flight-determined stability analysis of multiple-input-multiple-output control systems
[AIAA PAPER 92-4396] p 1074 A92-55196
Some interesting phenomena from Lavi test flights relating to aircraft stability and control
[IAITIC-91-1017] p 482 N92-20849

FLIGHT STRESS

NASA test flights with increased flight stress indices
[AIAA PAPER 91-3665] p 20 A92-11012

FLIGHT TEST INSTRUMENTS

Society of Flight Test Engineers, Annual Symposium, 21st, Garden Grove, CA, Aug. 6-10, 1990, Proceedings p 516 A92-35926
Calibration of an aircraft control surface using a tri-axial accelerometer package p 555 A92-35942
Development of pitot static flightline testing p 556 A92-35953
Flight test of avionic and air-traffic control systems
[ETN-92-91063] p 640 N92-25590
The basic measuring technical equipment of the DLR test aircraft p 652 N92-25592
Ground installations for the preparation and evaluation of flight tests p 665 N92-25593
Introduction and execution of flight tests at the DLR p 648 N92-25594
Pallet for helicopter testing instrumentation p 652 N92-25598
Ground and satellite supported flight trajectory measurement by example of the avionics flight test system AFES p 641 N92-25600
Potential applications of laser Doppler anemometry for in-flight measurements
[NLR-TP-90163-U] p 859 N92-28654

FLIGHT TEST VEHICLES

Flight test of avionic and air-traffic control systems
[ETN-92-91063] p 640 N92-25590
The DLR test aircraft in FZ-BS VFW614/ATTAS, Dornier DO228-101, MBB BO 105-S-3 p 648 N92-25591
The basic measuring technical equipment of the DLR test aircraft p 652 N92-25592
The role of systems simulation for the development and qualification of ATTAS p 886 N92-28548

FLIGHT TESTS

Aeroassist flight experiment heating-rate sensitivity study p 3 A92-10427
Overpressurized zero pressure balloon system
[AIAA PAPER 91-3671] p 14 A92-11018
First flight for Airbus A340 p 21 A92-12750
Wind-tunnel and flight tests of a delta-wing remotely piloted vehicle p 21 A92-13208
Modal identification in the presence of steady excitation p 131 A92-13693
Development and future view of the technology for fly-by-light control system elements p 131 A92-14027
V-22 flight test aerodynamics p 104 A92-14333
Flying qualities evaluation of the V22 tiltrotor p 131 A92-14334
Handling qualities of the H-76 Fantail Demonstrator p 131 A92-14335
Identification of higher-order helicopter dynamics using linear modeling methods p 131 A92-14336
Forward flight trim calculation and frequency response validation of a high-order helicopter simulation model p 132 A92-14337
Flight testing the handling qualities requirements of ADS-33C - Lessons learned at ATTC p 104 A92-14339
Results of flight tests of the Boeing Sikorsky Fantail demonstrator p 106 A92-14376
Flight testing the avionics system of the V-22 Osprey p 117 A92-14378
Development testing of the EH101 Flight Control System p 132 A92-14380
Flight vibration testing of the V-22 tiltrotor aircraft p 107 A92-14397
Studying dynamic behavior of X380 helicopter equipped with a new 5-blade composite rotor p 108 A92-14398
Design and flight test evaluation of the Fantail antitorque system p 110 A92-14456
Flight test control --- Russian book p 136 A92-15021
1990 report to the aerospace profession; Society of Experimental Test Pilots, Symposium, 34th, Beverly Hills, CA, Sept. 27-29, 1990, Proceedings p 111 A92-16051
X-29 high angle of attack p 111 A92-16052
V-22 flight test p 112 A92-16056
The flight test pilot's display - A CRT system for test maneuvers p 118 A92-16057
JAS 39 Gripen progress report p 112 A92-16058
The NASP Program - An update p 61 A92-16059
F-117A flight test program p 112 A92-16061
YF-23A preliminary flight test results p 112 A92-16063
MiG-29 prototype and development flight tests - General overview and high angle of attack investigation p 113 A92-16064
In-flight demonstration of hybrid GPS/Loran RAIM p 96 A92-16643
Design and flight test of a differential GPS/inertial navigation system for approach/landing guidance p 97 A92-16650
Saberliner flight test and results for forward looking detection and avoidance of airborne windshear p 98 A92-16656
Problem of the optimal correction of a flight test program for an aircraft system p 113 A92-16809
Flight test results of an Ada coded INS/GPS open loop Kalman filter design p 100 A92-16958
Dornier Do 328 - A start in the world market p 113 A92-17093
The value of sub-scale flight tests in the development of NASP vehicles
[AIAA PAPER 91-5048] p 210 A92-17834
Implementation and usage of the RJ program Data Acquisition System Ground Station p 210 A92-19257
An integrated real-time turbine engine flight test system p 201 A92-19275
Design and implementation of a total flight test system p 189 A92-19278
Dornier 328 first flight p 192 A92-19924
Evaluations of X-29 high-AOA regime show promise for future fighters p 192 A92-19925
Flight test of a half-scale unmanned air vehicle p 193 A92-20208
Heat transfer measurements from a smooth NACA 0012 airfoil p 218 A92-20215
Airbus A340 - The first phase of flight testing p 269 A92-21011
Technology for tomorrow - Do 228 with laminar wings p 269 A92-21013
Flight test investigation of the wake vortices generated by helicopters p 270 A92-21925
Shuttle Entry Air Data System - An experimental investigation of calibration for ascent flight
[AIAA PAPER 92-0133] p 286 A92-23753
One view of experimental aerodynamics
[AIAA PAPER 92-0160] p 254 A92-23775
A flight test study to determine aircraft propulsive efficiency and aerodynamic drag using two parameter identification methods and Lock's propeller model
[AIAA PAPER 92-0170] p 271 A92-23781

Identification of aerodynamic effectiveness and interference effects of direct-lift-control flaps from flight data
[AIAA PAPER 92-0171] p 271 A92-23782
Realistic real-time ground testing
[AIAA PAPER 92-0197] p 284 A92-23805
Flight test validation of tow target trajectory predictions
[AIAA PAPER 92-0209] p 271 A92-23814
Expert system for real-time aircraft monitoring
p 410 A92-24411
Correction of sideslip-induced static pressure errors in flight-test measurements p 309 A92-24416
Tilting at targets --- tilt rotor aircraft development
p 357 A92-25074
Prediction of ice accretion on a swept NACA 0012 airfoil and comparisons to flight test results
[AIAA PAPER 92-0043] p 316 A92-25677
Volume spectra in supercooled clouds for several research flights
[AIAA PAPER 92-0167] p 350 A92-25683
Aircraft lightning strikes
[ONERA, TP NO. 1991-204] p 351 A92-26361
A new U-D factorization-based fixed-point smoother and application to flight test p 411 A92-27858
Dornier 328 now in flight testing p 457 A92-29418
Automatic Dependent Surveillance (ADS) Pacific Engineering Trials (PET)
[AIAA PAPER 92-1812] p 453 A92-29760
GPS interferometric attitude and heading determination - Initial flight test results p 454 A92-30023
Boundary-layer-separation control p 440 A92-31886
Russians want U.S. to join scramjet tests
p 472 A92-32296
The U-2A flight test program
[AIAA PAPER 92-1086] p 537 A92-33252
YF-22A prototype Advanced Tactical Fighter demonstration/validation flight test program overview
[AIAA PAPER 92-1087] p 537 A92-33253
An alternative source of flight test services
[AIAA PAPER 92-1088] p 515 A92-33254
System design from mission definition to flight validation
[AIAA PAPER 92-1091] p 605 A92-33256
Sentinel 1000 flight test programme overview and preliminary results
[AIAA PAPER 92-1229] p 538 A92-33326
ES-3A flight test program
[AIAA PAPER 92-1230] p 538 A92-33327
Flight testing a high performance kit built aircraft
[AIAA PAPER 92-1240] p 538 A92-33333
Saab 2000 begins 1,200-hr. test program at Skavsta site p 538 A92-33800
Development and analysis of flight flutter prediction methods
[AIAA PAPER 92-2101] p 588 A92-35672
Frequency domain testing of helicopter dynamics using automated input signals p 545 A92-35731
A piloted comparison of elastic and rigid blade-element rotor models using parallel processing technology
p 546 A92-35751
Helicopter fog flying trials p 530 A92-35759
S-76B certification for vertical take-off and landing operations from confined areas p 530 A92-35760
The V-22 Osprey - A significant flight test challenge
p 546 A92-35766
Rotor aeromechanics research with the RAE research Lynx - The experimental facility and test programme
p 547 A92-35767
The development and testing of an active control of structural response system for the EH101 helicopter
p 569 A92-35775
Society of Flight Test Engineers, Annual Symposium, 21st, Garden Grove, CA, Aug. 6-10, 1990, Proceedings
p 516 A92-35926
Approach flight trials in the Netherlands for the Navstar GPS Joint Program Office International Test Program
p 533 A92-35928
Flight testing a digital terrain following system
p 548 A92-35929
State-of-the-art airborne video recording
p 555 A92-35932
Flying qualities testing on the modern technology airship p 570 A92-35933
X-29 high angle of attack flight test procedures, results, and lessons learned p 548 A92-35934
Helicopter in-flight frequency response test techniques
p 548 A92-35938
Limit cycle oscillation and flight flutter testing
p 570 A92-35939
Fokker 50 flameouts in icing conditions
p 548 A92-35940
C.A.T.C.H. - Computer aided test conductor handbook: A method for reducing cost, time and effort in an aircraft test and certification program p 602 A92-35943
Research flight test of a scaled unmanned air vehicle
p 549 A92-35944
X-29 high angle-of-attack flight test air data comparisons of an inertial navigation system and noseboom probe
p 549 A92-35945
Estimation of flying qualities using a leastsquares lower-order equivalent systems technique
p 570 A92-35947
Flight testing of the Boeing 747-400 Central Maintenance Computer system p 555 A92-35950
A comparison of transition Reynolds number measured in a wind tunnel and in flight p 522 A92-36026
Prospects for a commercial STOL transportation system p 634 A92-38207
A separated algorithm and application to flight test
p 690 A92-38273
Flight test data analysis of a low cost GPS/IMU integrated navigation system p 638 A92-39560
GPS interferometric attitude and heading determination - Flight test results p 650 A92-39561
Development of a pneumatic high-angle-of-attack flush airdata sensing system
[SAE PAPER 912142] p 651 A92-39980
Concorde flight testing - Powerplant and performance flying
[SAE PAPER 912192] p 644 A92-40009
1991 report to the aerospace profession; SETP Symposium, 35th, Beverly Hills, CA, Sept. 26-28, 1991, Proceedings p 645 A92-40028
F-14 dual hydraulic failure flying qualities evaluation
p 645 A92-40029
JAS 39 Gripen flight test report p 645 A92-40030
The Pond Racer preliminary flight test report
p 645 A92-40031
National Aerospace Plane flight test - External burning on the F/A-18 p 645 A92-40032
X-31 flight test update p 645 A92-40034
Single engine testing of the F-14A(PLUS) airplane in the power approach configuration p 645 A92-40036
YF-22A prototype advanced tactical fighter demonstration/validation flight test program overview
p 646 A92-40037
V-22 full scale development testing
p 646 A92-40038
MD-11 status report p 646 A92-40040
The Hummingbird experience at Lockheed Georgia
p 646 A92-40041
DC-3 handling qualities flight tests: NACA - 1950
p 646 A92-40042
1991-92 AHS Technical Committee highlights - Test and evaluation p 609 A92-40398
Identification of the transfer function between turbulence and aircraft p 743 A92-41226
Free-flight trim-angle predictions for the aeroassist flight experiment p 705 A92-41540
A study of aerophysical and dynamic characteristics using an axisymmetric flight test vehicle with a reusable nose section p 707 A92-42684
Flight evaluations on in-flight simulation of unstable aircraft p 744 A92-43115
Navigation experiment on aircraft flight using the GPS-INS navigation system. II - Test results
p 726 A92-43123
STOL research aircraft Asuka flight analysis in connection with the operation of the monitoring system
p 730 A92-43140
Flight test results and upper surface blowing (USB) technology of the STOL research aircraft Asuka
p 730 A92-43142
Flight tests on the structures of the STOL research aircraft Asuka p 730 A92-43143
Aerodynamic drag as determined from flight test data of the STOL research aircraft Asuka
p 709 A92-43145
Study on the maintainability and inspection of the STOL research aircraft Asuka p 700 A92-43148
Evaluation test on the simulator of the liquid crystal flat display. II p 734 A92-43209
A computerized flight inspection system --- for testing of basic air navigation ground facilities
p 726 A92-43881
The F/A-18 external burning flight test
[AIAA PAPER 91-5050] p 731 A92-44547
ASTOVL propulsion systems configuration and concept choice p 842 A92-45312
Radioaltimeter RWL-750 p 855 A92-45374
Update of the X-29 high-angle-of-attack program
[SAE PAPER 912006] p 783 A92-45407
In-flight simulation of backside operating models using direct lift controller
[SAE PAPER 912069] p 872 A92-45450
Concepts for the stability analysis of NLF-experiments on swept wings
[AIAA PAPER 92-2706] p 801 A92-45548
Maximizing thrust-vectoring control power and agility metrics p 874 A92-46794
Frequency domain flight testing and analysis of an OH-58D helicopter p 847 A92-46943
24-bit flight test data recording format
p 900 A92-47528
New Boeing flight test data acquisition systems
p 920 A92-47537
Robust discrete controller design for an unmanned research vehicle (URV) using discrete quantitative feedback theory p 877 A92-48495
Summary of the effects of engine throttle response on airplane formation-flying qualities
[AIAA PAPER 92-3318] p 877 A92-48902
Subsonic flight test evaluation of a performance seeking control algorithm on an F-15 airplane
[AIAA PAPER 92-3743] p 878 A92-49109
Subsonic flight test evaluation of a propulsion system parameter estimation process for the F100 engine
[AIAA PAPER 92-3745] p 866 A92-49110
Engine flight load reliability analysis
p 968 A92-49827
Boiling and condensing pumped loop microgravity experiment - Challenges of testing in both aircraft and rocket environments p 992 A92-50611
Differential GPS/inertial navigation approach/landing flight test results p 956 A92-51009
Comparison of Hemispherical Resonator Gyro and optical Gyros p 993 A92-51014
The use of photogrammetry in aviation equipment flight testing p 994 A92-51649
Takeoff Performance Monitoring System display options
[AIAA PAPER 92-4138] p 967 A92-52433
Estimation of aerodynamic characteristics from flight-test data. I - Multicollinearity in the equation error method p 960 A92-53007
Regional challenge --- flight test of Canadair Regional Jet p 961 A92-53121
Scramjet engine and its flying test bed
p 1066 A92-53492
In-flight performance diagnostic capability of an adaptive engine model
[AIAA PAPER 92-3746] p 1068 A92-54147
Some important factors in turbulence in flight measurement p 1063 A92-54324
Modified Doppler detects wind shear more reliably
p 1015 A92-55099
Gain scheduled linear PID autopilot for the AIAA Controls Design Challenge aircraft
[AIAA PAPER 92-4629] p 1078 A92-55304
ATTAS flight test and simulation results of the advanced gust management system LARS
[AIAA PAPER 92-4343] p 1079 A92-55332
Flight test results using a low order equivalent systems technique to estimate flying qualities
[AIAA PAPER 92-4425] p 1080 A92-55349
A physical approach to the estimation of aerodynamic characteristics from flight data p 1030 A92-56058
Flight test of a flight reference display for powered-lift STOL aircraft p 1064 A92-56059
A calculation method to predict helicopter noise and its verification p 1135 A92-56074
Flight evaluation of navigation systems including MLS using NAL Do228 - Outline p 1047 A92-56116
Flight evaluation of navigation systems including MLS using NAL Do228 - Results of GPS
p 1047 A92-56118
Model flight tests of a spin-resistant trainer configuration p 1054 A92-56158
High angle-of-attack flush airdata sensing system
p 1064 A92-56172
Flight measurements of downwash on the Ball-Bartoe Jetwing powered lift aircraft p 1054 A92-56174
Short takeoff optimization for the XV-15 tiltrotor aircraft p 1056 A92-56302
The achievement of aerodynamic goals on the EH101 project through the 'single site' concept
p 1058 A92-56342
Correlation of flight, tunnel and prediction data on a helicopter main rotor p 1059 A92-56350
Integrated test and evaluation for hypervelocity systems
[AIAA PAPER 92-3901] p 1017 A92-56736
Feasibility of using a knowledge-based system concept for in-flight primary flight display research
[NASA-TM-4279] p 17 N92-10017
Rotorcraft system identification
[AGARD-AR-280] p 22 N92-11001
Developmental flight testing of a half scale unmanned air vehicle
[AD-A240347] p 22 N92-11002
Development of a 1/7th scale fighter UAV for flight research
[AD-A240703] p 23 N92-11008
Practical input optimization for aircraft parameter estimation experiments p 114 N92-11989

Development of a pneumatic high-angle-of-attack flush airdata sensing (HI-FADS) system
[NASA-TM-104241] p 118 N92-11994
Resonance and control response tests using a control stimulation drive
[MBB-UD-0586-90-PUB] p 134 N92-12003
AI for RPVs, Sensor Driven Airborne Replanner (SDAR), for a Robotic Aircraft Sensor Platform (RASP)
p 114 N92-12534
Air-to-air visual acquisition handbook
[ATC-151] p 93 N92-13042
Helicopter physical and performance data
[SCT-91RR-27] p 116 N92-13060
Flight research p 194 N92-13981
Aerothermodynamic configuration of first generation aerospace planes (of Buran-type) and first flight results
p 211 N92-14975
FALKE and COBRA technology development in aerodynamics and aerothermodynamics
p 183 N92-15017
Development of an analytical method to predict helicopter main rotor performance in icing conditions
[NASA-CR-189110] p 258 N92-15967
Prediction of ice accretion on a swept NACA 0012 airfoil and comparisons to flight test results
[NASA-TM-105368] p 258 N92-15968
Validation and verification flight test for TCAS-2 logic changes (MOPS Change 6)
[DOT/FAA/CT-TN91/46] p 268 N92-15981
Joint Federal Aviation Administration (FAA)/Civil Aviation Authority (CAA) Microwave Landing System (MLS) Area Navigation (RNAV) flight evaluations
[DOT/FAA/CT-TN91/17] p 268 N92-15983
Model identification and control system design for the lambda unmanned research vehicle
[AD-A241859] p 299 N92-17024
Design of experiments p 273 N92-17154
Instrumentation and data processing
p 273 N92-17155
Assessment of rotorcraft system identification as applied to the AH-64 p 274 N92-17160
BO 105 identification results p 274 N92-17161
System identification methods for handling-qualities evaluation p 274 N92-17165
Flight evaluation of curved MLS precision approaches in a twin otter aircraft, phase 2
[AD-A243025] p 268 N92-17568
Example of statistical techniques applied to cruise performance guarantees (Student's t distribution)
[ESDU-91018] p 276 N92-17843
Identification of the stability and control derivatives of a DLC-flap system for VSRA
[NAL-TR-1116] p 283 N92-17917
Model parameter identification techniques for flight flutter testing
[AERO-REPT-9105] p 380 N92-18294
A preliminary flight test on a basic performance of the flight research airplane Do 228: Velocity vs glide path angle
[NAL-TM-613] p 359 N92-18482
Manoeuvring Aerodynamics
[AGARD-CP-497] p 363 N92-18778
X-31: Discussion of steady state and rotary derivatives
p 365 N92-18789
Use of stepwise regression techniques and kinematic compatibility for the analysis of EAP flight data
p 365 N92-18790
CH-46 and OH-58 transmission stress wave analysis
[AD-A244321] p 365 N92-18826
Investigation of the influence of rotary aerodynamics on the study of high angle of attack dynamics of the F-15B using bifurcation analysis
[AD-A243969] p 348 N92-19367
Tiltrotor research aircraft composite blade repairs: Lessons learned
[NASA-TM-103875] p 367 N92-19563
Vortex characteristics of C5A/B, C141B and C130E aircraft applicable to ATC terminal flight operations tower fly-by-data
[PB92-114586] p 449 N92-20318
Postflight aerothermodynamic analysis of Pegasus(tm) using computational fluid dynamic techniques
[NASA-CR-186017] p 445 N92-21188
Helicopter/ship analytic dynamic interface
p 464 N92-21962
Evaluating fixed wing aircraft in the aircraft carrier environment p 464 N92-21963
EH 101 ship interface trials: Flight test programme and preliminary results p 465 N92-21964
Determination of limitations for helicopter ship-borne operations p 465 N92-21965
United Kingdom approach to deriving military ship helicopter operating limits p 465 N92-21966
United States Navy ski jump experience and future applications p 465 N92-21968
Comparison of the performance of a microwave landing system elevation station with the instrument landing system end-fire glide slope at Yeager Airport, Charleston, West Virginia
[DOT/FAA/CT-TN91/22] p 534 N92-22210
Overview of NASA PTA propfan flight test program
p 561 N92-22536
Flight test of ARINC 741 configuration low gain SATCOM system on Boeing 747-400 aircraft p 677 N92-24097
Evaluating the velocity accuracy of an integrated GPS/INS system: Flight test results
[DE92-007519] p 640 N92-25470
Flight test of avionic and air-traffic control systems
[ETN-92-91063] p 640 N92-25590
Ground installations for the preparation and evaluation of flight tests p 665 N92-25593
Introduction and execution of flight tests at the DLR
p 648 N92-25594
Development of flight testing of a fault tolerant fly-by-light yaw control system p 662 N92-25599
Ground and satellite supported flight trajectory measurement by example of the avionics flight test system AFES p 641 N92-25600
Evaluation of a tritium runway lighting system
[DOT/FAA/CT-TN92/15] p 665 N92-25733
Separation of external stores: Comparison of results
[F+W-TF-2058] p 732 N92-26944
Integrated flight propulsion control research results using the NASA F-15 HIDEC Flight Research Facility
[NASA-TM-4394] p 740 N92-27379
Development of telemetry for the agility flight test of a radio controlled fighter model
[AD-A248653] p 753 N92-27994
Flight testing of a half-scale remotely piloted vehicle
[AD-A248568] p 733 N92-28123
Evaluation of high lift devices of the quiet STOL experimental aircraft ASKA
[NAL-TR-1102] p 733 N92-28153
Note on flight measured control effectiveness of the quiet STOL experimental aircraft ASKA
[NAL-TR-1103] p 746 N92-28154
Evaluation of landing configuration by flight test of the quiet STOL experimental aircraft ASKA
[NAL-TR-1113] p 733 N92-28191
Operational noise data for OH-58D Army helicopters
[AD-A246822] p 926 N92-28292
Aircraft ship operations
[AGARD-AR-312] p 850 N92-28468
Use of high-fidelity simulation in the development of an F/A-18 active ground collision avoidance system
p 837 N92-28530
Validation of simulation systems for aircraft acceptance testing p 852 N92-28531
Use of simulation in the USAF Test Pilot School curriculum p 884 N92-28535
An evaluation of IFR approach techniques: Generic helicopter simulation compared with actual flight
p 886 N92-28550
S-76B certification for vertical take-off and landing operations from confined areas
[NLR-TP-90286-U] p 852 N92-28714
Reduction and analysis of F-111C flight data
[AD-A250341] p 853 N92-28771
Stability and control flight testing of a half-scale Pioneer remotely piloted vehicle
[AD-A245973] p 879 N92-28801
Aerodynamic characteristics obtained from alpha sweep test of the quiet STOL experimental aircraft ASKA
[NAL-TR-1112] p 853 N92-28901
A rotorcraft flight database for validation of vision-based ranging algorithms
[NASA-TM-103906] p 841 N92-29103
Flight evaluation of an extended engine life mode on an F-15 airplane
[NASA-TM-104240] p 871 N92-29659
Joint computational and experimental aerodynamics research on a hypersonic vehicle
[DE92-013439] p 943 N92-30367
Organic Matrix Composite Helicopter Internal/External Cargo Pallet System (OMC INTEX)
[AD-A251127] p 961 N92-30878
Helicopter nighttime parking test results - UH-1
[DOT/FAA/CT-TN92/1] p 961 N92-31165
Overview of the NASA Dryden Flight Research Facility aeronautical flight projects
[NASA-TM-104254] p 962 N92-31261
Subsonic flight test evaluation of a performance seeking control algorithm on an F-15 airplane
[NASA-TM-4400] p 973 N92-31275
In-flight leading-edge extension vortex flow-field survey measurements on a F-18 aircraft at high angle of attack
[NASA-TM-4398] p 947 N92-31276
System overview of the NASA Dryden Integrated Test Facility
[NASA-TM-104250] p 984 N92-32201
Vision-based range estimation using helicopter flight data
[NASA-TM-103930] p 1047 N92-32424
A learning enhanced flight control system for high performance aircraft
[AD-A252520] p 1086 N92-32435
Evaluation of composite components on the Bell 206L and Sikorsky S-76 helicopters p 1107 N92-32575
Fly-by-light technology development plan
[NASA-CR-181954] p 1086 N92-32778
An evaluation of decelerating IFR approaches utilizing a helicopter flight simulator
[CTN-92-60348] p 1048 N92-32845
The use of Kalman filtering techniques to improve the accuracy of flight test data
[NRC-32139] p 1064 N92-32850
The design and development of a portable, DSP micro-processor based, high-accuracy data acquisition system
[NRC-32146] p 1134 N92-32851
Flight testing and simulation of an F-15 airplane using throttles for flight control
[NASA-TM-104255] p 1087 N92-32864
The development of an airborne information management system for flight test
[NASA-TM-104251] p 1065 N92-32866
MD-80 aft cabin noise control: A case history
p 1137 N92-32950
Advanced Study for Active Noise Control in Aircraft (ASANCA)
[AIAA PAPER 92-2092] p 1137 N92-32956
Pilots noise exposure during a Boeing 747-400 round trip: Ambient noise and acoustic-head recording and analysis of data p 1137 N92-32960
Flight service environmental effects on composite materials and structures p 1110 N92-33054
Rapid development of the X-31 simulation to support flight-testing
[NASA-TM-104256] p 1060 N92-33149
The F-18 high alpha research vehicle: A high-angle-of-attack testbed aircraft
[NASA-TM-104253] p 1060 N92-33404
Implementation of a personal computer based parameter estimation program
[AD-A252914] p 1061 N92-33502
On the calculation of the response of helicopters to control inputs
[NASA-CR-190812] p 1088 N92-33536
Lateral spread of sonic boom measurements from US Air Force boomfile flight tests p 1140 N92-33883
Experience with Ada on the F-18 High Alpha Research Vehicle Flight Test Program
[NASA-TM-104259] p 1062 N92-34039
Piloted evaluation of an integrated propulsion and flight control simulator
[NASA-TM-105797] p 1088 N92-34107
Flight flutter testing p 1089 N92-34163

FLIGHT TIME

The NASA long duration balloon project
[AIAA PAPER 91-3680] p 15 A92-11024
Optimal thermal management system for HALE UAV --- High Altitude Long Endurance Unmanned Air Vehicles
[ASME PAPER 91-GT-396] p 111 A92-15726
Liquid cooled turbocharged propulsion system for HALE application
[ASME PAPER 91-GT-399] p 127 A92-15729
A new method for increasing maximum flight endurance p 280 A92-21006
Low Reynolds number, long endurance aircraft design
[AIAA PAPER 92-1263] p 538 A92-33343
Time-to-go estimation from infrared images
p 840 A92-48308

FLIGHT TRAINING

Centre for Flight Simulation Berlin Airbus 340 simulator for research and training p 880 A92-45028
The Tonopah years p 785 A92-47758
The impact of cockpit automation on crew coordination and communication. Volume 1: Overview, LOFT evaluations, error severity, and questionnaire data
[NASA-CR-177587] p 93 N92-13044
Aircraft accident/incident summary report: Midair collision involving Lycoming Air Services Piper Aerostar PA-60 and Sun Company Aviation Department Bell 412, Merion, Pennsylvania, April 4, 1991
[PB91-910407] p 187 N92-15055
Simulator data integrity program: Process standard development
[AD-A242207] p 386 N92-19642
Workshop on integrated Crew Resource Management (CRM)
[DOT/FAA/RD-92/5] p 781 N92-27518
Piloted Simulation Effectiveness
[AGARD-CP-513] p 786 N92-28522
Opportunities for flight simulation to improve operational effectiveness p 883 N92-28523

Piloted simulation effectiveness development applications and limitations p 883 N92-28524
Utility of ground simulation in flight control problem identification, solution development, and verification p 883 N92-28525
Aircraft simulation and pilot proficiency: From surrogate flying towards effective training p 884 N92-28532
Transport delay measurements: Methodology and analysis for the F-16C combat engagement trainer, the display for advanced research and training, and the F-16A limited field of view
[AD-A248519] p 888 N92-29505
Technical evaluation report on the Flight Mechanics Panel Symposium on Piloted Simulation Effectiveness
[AGARD-AR-315] p 983 N92-30769

FLIGHT VEHICLES
Control of the landing of a flight vehicle in the grazing-incidence mode p 134 A92-16808
Some considerations on modeling flight vehicles movement p 281 A92-21311
Effect of adaptive material properties on static aeroelastic control
[AIAA PAPER 92-2526] p 539 A92-34373
Flight-vehicle materials, structures, and dynamics - Assessment and future directions. Vol. 3 - Ceramics and ceramic-matrix composites --- Book
[ISBN 0-7918-0661-8] p 668 A92-39852
Advanced experimental design applied to damage tolerance of composite materials p 993 A92-51505
Maximum likelihood algorithm and its application to parameter identification of closed-loop flight vehicles p 1008 A92-53023
An integrated development of the equations of motion for elastic hypersonic flight vehicles
[AIAA PAPER 92-4605] p 1077 A92-55283
Parameter identification of unsteady aerodynamic forces for elastic vehicles
[AIAA PAPER 92-4505] p 1027 A92-55372

FLIR DETECTORS
Infra-red offers new landing aid competition p 198 A92-18937
Airborne experimental FLIR program p 1064 N92-32447

FLOAT ZONES
Development of a new generation of high-temperature composite materials p 578 N92-22515

FLOORS
Experimental and analytical study of the effects of floor location on response of composite fuselage frames
[AIAA PAPER 92-2473] p 539 A92-34362

FLOQUET THEOREM
Computational aspects of helicopter trim analysis and damping levels from Floquet theory p 875 A92-46933
Secondary instability of high-speed flows and the influence of wall cooling and suction
[NASA-CR-4427] p 406 N92-19844
Computational aspects of helicopter trim analysis and damping levels from Floquet theory
[NASA-CR-190736] p 1087 N92-33107

FLOW CHAMBERS
Automation of the measurement process in the N2 wind tunnel with the SPITA N-3 system p 30 A92-12347
A quiet-flow Ludwieg tube for experimental study of high speed boundary layer transition
[AIAA PAPER 91-5026] p 207 A92-17819

FLOW CHARACTERISTICS
Flow analysis and design of three-dimensional wind tunnel contractions p 5 A92-11067
Evolution of three-dimensional flows during the interaction between conical shock waves and a turbulent boundary layer p 7 A92-12169
An analysis of the flow-pattern at the exit of a single-stage turbine p 10 A92-13234
A basis for ice formation design p 146 A92-14556
Realization of a large-scale turbulence field in a small wind tunnel p 67 A92-15487
Detection of flow state in an unsteady separating flow p 219 A92-20741
Calculation of the parameters of separated flow behind a plane rounded body in the path of two supersonic flows p 244 A92-21624
Flow characteristic and flow control of high aspect ratio and highly curved S-bend diffuser p 245 A92-21743
Introduction to three dimensional boundary layers p 245 A92-21977
Flow visualization and wake analysis for complex three-dimensional bluff bodies at subcritical through critical Reynolds numbers
[AIAA PAPER 92-0155] p 253 A92-23770
Characterization of a two-phase flow field downstream of a 3x-scale gas turbine co-axial, counter-swirling, combustor dome swirl cup
[AIAA PAPER 92-0229] p 393 A92-25693
Experimental and computational investigation of wind tunnel effects on airfoil flow fields
[AIAA PAPER 92-0672] p 431 A92-30624
Flow near the trailing edge of an airfoil p 431 A92-31151
A supplement to the second-order shock-expansion method p 437 A92-31861
Change of flow about an elongated rectangular cylinder in a range of Reynolds numbers of 200 to 0.7 x 10 exp 4 p 522 A92-35997
Computation of saddle point of attachment p 703 A92-41276
Buffeting characteristics of a transonic airfoil p 711 A92-43202
Flow and acoustic features of a supersonic tapered nozzle p 712 A92-44328
Limit point flow mode analysis of exhaust diffuser and operation characteristics of injector p 968 A92-49830
Method of large particles in arbitrary curvilinear orthogonal coordinates for the solution of problems of hydro and aerodynamics p 937 A92-52035
Flow characterization in the NASA Ames 16-inch Shock Tunnel
[AIAA PAPER 92-3810] p 1090 A92-54180
The flow field characteristics about a fighter configuration at high angles of attack
[AIAA PAPER 92-4358] p 1025 A92-55344
Surface heat transfer and flow properties of vortex arrays induced artificially and from centrifugal instabilities p 1121 A92-56371
Numerical prediction of the flow characteristics in an arc wind tunnel
[AIAA PAPER 92-4016] p 1100 A92-56838
Study of detached turbulent flow in an air intake by means of high speed tomography and laser velocimetry
[REPT-90/55] p 157 N92-12216
Excrescence drag magnification factors at the drag-rise condition for aerofoils with a specified form of upper-surface pressure distribution
[ESDU-91029] p 259 N92-15973
Manoeuvring Aerodynamics
[AGARD-CP-497] p 363 N92-18778
Forebody vortex control aeromechanics p 380 N92-18792
Inlet technology p 447 N92-21528
Separation of relaminarised boundary layers
[CUED/A-AERO/TR-16] p 592 N92-22209
Boundary Layers in Turbomachines
[VKI-LS-1991-06] p 658 N92-24336
Fundamental aspects of boundary layers and transition in turbomachines p 658 N92-24337
Laminar-turbulent transition process in the presence of simulated wall roughness p 626 N92-24858
On the coupling of Euler/boundary-layer equations p 627 N92-24859
Direct simulation of high-speed mixing layers
[NASA-TP-3186] p 945 N92-30909
Research on aero-thermodynamic distortion induced structural dynamic response of multistage compressor blading
[AD-A250865] p 974 N92-32059
Vaporizing particle velocimeter
[NASA-CASE-LAR-14685-1] p 1042 N92-34172

FLOW CHARTS
The computer analysis of the prediction of aircraft electrical power supply system reliability p 690 A92-37950

FLOW COEFFICIENTS
A shock and an expansion wave in transonic flow p 440 A92-31961
Total losses in turbulent flows inside conical diffusers p 819 A92-47782
Evaluation of rotordynamic coefficients of look-through labyrinths by means of a three volume bulk flow model p 223 N92-14356

FLOW DEFLECTION
Surface flow patterns on an ogive-cylinder at incidence p 176 A92-20762
Aerodynamic characteristics of curved delta wings in the case of subsonic separated flow p 712 A92-44121
Experimental and analytical study of close-coupled ventral nozzles for ASTOVL aircraft p 861 A92-45325

FLOW DISTORTION
Distortion tolerance of the T800-LHT-800 turboshaft engine p 120 A92-14409
Estimation of the maximum instantaneous distortion --- of inlet pressure in aircraft engines p 242 A92-21051
Preliminary investigation of inlet dynamic distortion and it's passive control p 245 A92-21742
Aerodynamics of loaded cascades in subsonic flows subject to unsteady three-dimensional vortical disturbances
[AIAA PAPER 92-0146] p 253 A92-23762
Influence of flight parameters on air intake internal flow distortions due to gun blast-air interaction p 310 A92-24426
Singular perturbation theory of hypersonic flow over blunt bodies p 313 A92-25048
The effect of successive distortions of the boundary layer in a supersonic flow
[AIAA PAPER 92-0309] p 320 A92-25757
Investigation on vortex control technique of flow separation in diffuser p 338 A92-27828
Surge-troubleshooting of a twin-spool turbojet engine tested at a high altitude test facility p 375 A92-28459
An experimental investigation of the inlet exit flow field improved by aerodynamic grid p 343 A92-28477
Helical-perturbation device for cylinder-wing vortex generators p 432 A92-31167
The experimental investigation on the diffuser flow distortion p 519 A92-35543
Separated flow over the protuberances in hypersonic flow p 615 A92-38907
The effects of unsteady perturbation on vortex breakdown p 672 A92-38922
Flow and shape correction problems for thin profiles in incompressible stream p 707 A92-42736
Improved method for estimation of the maximum instantaneous distortion values
[AIAA PAPER 92-3623] p 826 A92-49076
Processing of axisymmetric flow interferograms with density profile bends or discontinuities p 993 A92-51316
An acceptance process for the evaluation of inlet distortion
[AIAA PAPER 92-3918] p 1032 A92-56750
Effects of inlet distortion on the development of secondary flows in a subsonic axial inlet compressor rotor p 89 N92-13030
An experimental study of a turbulent wing-body junction and wake flow
[AD-A243388] p 260 N92-17222
Modification of Jindivik air intake duct with an auxiliary intake static aerodynamic tests
[AD-A243002] p 275 N92-17234
Self-adaptive aeropropulsion components-enhancing axial compressor performance
[AD-A246123] p 743 N92-27817
Inlet distortion effects in aircraft propulsion system integration p 869 N92-28464
Application of computational fluid dynamics to the study of vortex flow control for the management of inlet distortion
[NASA-TM-105672] p 1128 N92-34112

FLOW DISTRIBUTION
Prediction of high-resolution flowfields for rotorcraft aeroacoustics p 53 A92-11053
Topology of steady flows of low viscosity fluids p 38 A92-11219
Impeller flow field measurement and analysis
[ASME PAPER 90-GT-146] p 38 A92-11288
Analysis of flexible-membrane and jet-flapped airfoils using velocity singularities p 10 A92-13216
Heat transfer in supersonic flow past a single crater p 63 A92-13741
Wing tip vortex calculations with an unstructured adaptive-grid Euler solver p 64 A92-14330
Rim sealing of rotor-stator wheelspaces in the absence of external flow
[ASME PAPER 91-GT-33] p 147 A92-15517
Three-dimensional flow and mixing in a axial flow compressor with different rotor tip clearances
[ASME PAPER 91-GT-89] p 70 A92-15554
Unsteady viscous flow in a high speed core compressor
[ASME PAPER 91-GT-91] p 70 A92-15555
Wind tunnel wall effects in a linear oscillating cascade
[ASME PAPER 91-GT-133] p 72 A92-15576
NASA low-speed centrifugal compressor for 3-D viscous code assessment and fundamental flow physics research
[ASME PAPER 91-GT-140] p 72 A92-15580
Gas turbine main shaft internal flow and heat transfer
[ASME PAPER 91-GT-165] p 123 A92-15600
A direct optimization procedure for spanwise work distribution in non-free vortex turbine stages
[ASME PAPER 91-GT-204] p 124 A92-15626
Numerical prediction of wakes in cascades and compressor rotors including the effects of mixing. I - Cascade wakes including the effects of incidence and freestream turbulence
[ASME PAPER 91-GT-225] p 74 A92-15638
Design and performance of advanced blading for a high-speed HP compressor
[ASME PAPER 91-GT-374] p 76 A92-15718
Turbulent flow calculations using unstructured and adaptive meshes p 153 A92-15823
Three-dimensional singularity of flow structure in an underexpanded supersonic jet p 78 A92-16679
Supersonic reacting internal flowfields p 155 A92-16989
CFD application to 2D/3D flow fields in Scramjet engine p 170 A92-17501

Numerical simulation for various flowfields of aero-engine components p 200 A92-17503
Three dimensional hypersonic inlets - Low speed performance
[AIAA PAPER 91-5021] p 171 A92-17817
LDV measurements and investigation of flow field through radial turbine guide vanes p 217 A92-19618
Evaluation of Euler solvers for transonic wing-fuselage geometries p 174 A92-20214
Incompressible steady aerodynamics using a standard finite element code p 174 A92-20218
Newton's method solver for high-speed viscous separated flowfields p 176 A92-20736
Instabilities of flows over bodies at large incidence p 176 A92-20738
Unsteady Euler analysis of the flowfield of a propfan at an angle of attack p 242 A92-21070
Research on supersonic combustion
[AIAA PAPER 92-0001] p 278 A92-22126
Doppler global velocimeter measurements of the vortical flow above a thin delta wing
[AIAA PAPER 92-0005] p 292 A92-22130
An experimental study of pneumatic vortex flow control on high angle of attack forebody model
[AIAA PAPER 92-0018] p 247 A92-22140
Forebody vortex flow control on the F-16C using tangential slot and jet nozzle blowing
[AIAA PAPER 92-0019] p 247 A92-22141
Effect of turbulence modeling on dynamic stall of a NACA0012 airfoil
[AIAA PAPER 92-0027] p 248 A92-22149
Simulation of wind tunnel flowfields
[AIAA PAPER 92-0034] p 249 A92-22155
A simple numerical criterion for vortex breakdown
[AIAA PAPER 92-0057] p 250 A92-22172
Experimental investigation of a supersonic combustion flowfield employing staged transverse injection behind a rearward-facing step
[AIAA PAPER 92-0090] p 292 A92-22196
Application of a universe-series code for inviscid flow over complex 3-dimensional configurations
[AIAA PAPER 92-0150] p 253 A92-23765
An algorithm for predicting the flow past fuselage-mounted engine arrangements
[AIAA PAPER 92-0151] p 253 A92-23766
A study on vortex flow control of inlet distortion in the re-engined 727-100 center inlet duct using computational fluid dynamics
[AIAA PAPER 92-0152] p 253 A92-23767
One view of experimental aerodynamics
[AIAA PAPER 92-0160] p 254 A92-23775
Organized structure in a Mach 5/Mach 3 turbulent shear layer
[AIAA PAPER 92-0180] p 256 A92-23790
Establishment and characterization of a reproducible vortex for use in studying nonsteady two-dimensional phenomena p 310 A92-24428
Flow analysis of rectangular wind tunnel contraction p 312 A92-25001
An experimental study of the flow past spheres at transonic speeds and high Reynolds numbers p 312 A92-25002
Analysis of transonic flow past an axisymmetric convex corner p 312 A92-25015
Pressure wave propagation studies for oscillating cascades
[AIAA PAPER 92-0145] p 316 A92-25682
Aerodynamic effects on fuel spray structure - Experiment and theory
[AIAA PAPER 92-0227] p 317 A92-25691
Pitch-up motions of delta wings
[AIAA PAPER 92-0278] p 318 A92-25732
The evaluation of canard couplings at high angles of attack
[AIAA PAPER 92-0281] p 318 A92-25735
Calculation of the carriage loads of tandem stores on a fighter aircraft
[AIAA PAPER 92-0283] p 319 A92-25736
Prediction of average downwash gradient for canard configurations
[AIAA PAPER 92-0284] p 319 A92-25737
Low-to-high altitude predictions of three-dimensional ablative reentry flowfields
[AIAA PAPER 92-0366] p 394 A92-26227
Flow field measurement and visualization using projected smoke trails
[AIAA PAPER 92-0384] p 323 A92-26241
Cross-flow separation on a prolate spheroid at angles of attack
[AIAA PAPER 92-0428] p 326 A92-26276
Screech noise source structure of a supersonic rectangular jet
[AIAA PAPER 92-0503] p 331 A92-26932
Holographic flowfield density measurements in swept shock wave/boundary-layer interactions
[AIAA PAPER 92-0746] p 335 A92-27092
A new calculating method for the flowfield in turbomachinery - The study on the application of the vorticity-velocity equations for the numerical solution of the flowfield in turbomachinery p 338 A92-27803
Turbulence model effects on separated flow about a prolate spheroid p 340 A92-28036
Flowfield simulation about the SOFIA Airborne Observatory
[AIAA PAPER 92-0656] p 342 A92-28217
Numerical simulation of two incoming streams in a dual-combustion ramjet combustor p 375 A92-28419
Flow pattern characterization and heat transfer behavior in a boiling two-phase flow in an inclined pipe p 493 A92-29722
Experimental investigation on combustor with double co-axial swirlers p 469 A92-29729
A study of the base pressure behind circular steps p 426 A92-30196
Asymptotic solution of the problem of ideal-fluid flow past the vertices of bodies and wings p 427 A92-30199
Study on nozzle flow diffusion p 429 A92-30531
Stability of a nonorthogonal stagnation flow to three-dimensional disturbances p 495 A92-31194
Simulation of hypersonic flows on unstructured grids p 434 A92-31496
Navier-Stokes computations of a viscous optimized waverider
[AIAA PAPER 92-0305] p 435 A92-31653
Combined effect of nose bluntness and angle of attack on slender bodies in viscous hypersonic flows
[AIAA PAPER 92-0755] p 436 A92-31680
Flowpath optimization for hypersonic vehicles
[AIAA PAPER 91-5043] p 437 A92-31688
An exact solution to edge effect problem for a finite-span wing in supersonic flow p 441 A92-31962
Computation of near-wake, aerobrake flowfields p 441 A92-32181
Effects of shock wave precursors ahead of hypersonic entry vehicles p 441 A92-32182
Numerical analysis of three-dimensional unsteady turbulent flows in a turbine stage p 443 A92-32501
Navier-Stokes analysis of helicopter plume flowfield for infrared calculations
[AIAA PAPER 92-0983] p 580 A92-33185
Complete Euler-solution for a rotor in hover and a propeller in forward flight p 520 A92-35755
Measurements of a rotor flowfield and the effects on a fuselage in forward flight p 521 A92-35787
An inverse inviscid method for the design of quasi-three dimensional turbomachinery cascades p 523 A92-36033
International Symposium on Engineering Turbulence Modelling and Measurements, Dubrovnik, Yugoslavia, Sept. 24-24, 1990, Selected Papers p 672 A92-38851
Effect of controlled longitudinal vortex arrays on the development of a turbulent boundary layer p 614 A92-38856
Flow regimes of the cove regions between a slat and wing and between a wing and flap of a multielement airfoil p 614 A92-38858
Influence of inlet conditions on the flowfield in a model gas turbine combustor p 672 A92-38866
LDV measurements of the flowfield in a simulated combustor with axial and side inlets p 672 A92-38867
Measurement and analysis of the flow field above a wing/body configuration p 616 A92-38917
Numerical simulation of interaction between vortexes and shocks in jet flow field p 616 A92-38925
Passive control of supersonic cavity flowfields
[SAE PAPER 912153] p 619 A92-39988
Compressibility effects on the growth and structure of homogeneous turbulent shear flow p 675 A92-40052
Second moment closure predictions of jet-on-jet impingement flows p 675 A92-40102
Measurements and simulation of the flow around a poppet valve p 675 A92-40103
The natural and forced formation of spot-like Lambda-structures caused by vortex dislocations in a wake p 621 A92-40111
Scrutinizing k-epsilon EVM and ASM by means of LES and wind tunnel for flowfield around cube --- Eddy Viscosity Model, Algebraic Stress Model, Large Eddy Simulation p 621 A92-40119
Evolution of coherent structures during transition in a flat-plate boundary layer p 621 A92-40126
Influence of suction through a slot on a turbulent boundary layer p 622 A92-40127
Effect of tabs on the evolution of an axisymmetric jet p 656 A92-40151
Effect of acoustic excitation on stalled flows over an airfoil p 703 A92-41267
Navier-Stokes simulation for cone-derived waverider p 703 A92-41271
Symmetry breaking in vortex flows on conical bodies p 703 A92-41278
Evaluation of the ATD-GASP for endo-leap applications --- Aerothermal Technology Development of Generalized Aerodynamic Simulation Programs
[AIAA PAPER 92-2771] p 704 A92-41318
Experimental technique of measuring fuel concentration in non-uniform flowfield p 734 A92-41928
Study of the flow field and molecular radiation heating around a reentry vehicle p 711 A92-43227
The inviscid stability of supersonic flow past heated or cooled axisymmetric bodies p 712 A92-44363
Integrated electric density and scaling law for hypersonic blunt-body wakes p 714 A92-44865
Simultaneous imaging and interferometric turbule visualization in a high-velocity mixing/shear layer p 896 A92-45130
Prediction and measurement of jet flowfield features for ASTOVL aircraft p 787 A92-45318
The experimental and computational study of jet impingement flowfields with reference to VSTOL aircraft performance p 787 A92-45324
Experimental and analytical study of close-coupled ventral nozzles for ASTOVL aircraft p 861 A92-45325
Computational fluid dynamics applications in airplane cabin ventilation system design
[SAE PAPER 911992] p 788 A92-45394
Flow field around thick delta wing with rounded leading edge
[SAE PAPER 912009] p 789 A92-45409
Experimental investigation of the flowfield of an oscillating airfoil
[AIAA PAPER 92-2622] p 793 A92-45494
Measurements of the velocity and vorticity fields around a pitching airfoil
[AIAA PAPER 92-2626] p 794 A92-45498
Numerical study on a supersonic open cavity flow with geometric modification of aft bulkhead
[AIAA PAPER 92-2627] p 794 A92-45499
Static and dynamic flow field development about a porous suction surface wing
[AIAA PAPER 92-2628] p 795 A92-45500
A nonlinear relaxation/quasi-Newton algorithm for the compressible Navier-Stokes equations
[AIAA PAPER 92-2643] p 796 A92-45510
Navier-Stokes analysis and experimental data comparison of compressible flow in a diffusing S-duct
[AIAA PAPER 92-2699] p 800 A92-45541
The flip flop nozzle extended to supersonic flows
[AIAA PAPER 92-2724] p 803 A92-45561
Computation of turbulent flow about cone-derived waverider
[AIAA PAPER 92-2726] p 804 A92-45562
Surface and flow field measurements in a symmetric crossing shock wave/turbulent boundary layer flow
[AIAA PAPER 92-2634] p 806 A92-45574
Comparison of two flux splitting schemes for calculation of ogive-cylinder at M = 3.5 and alpha = 18 deg
[AIAA PAPER 92-2667] p 806 A92-45582
On the aerodynamics/dynamics of store separation from hypersonic aircraft
[AIAA PAPER 92-2722] p 807 A92-45595
Effect of flow rate on loss mechanisms in a backswept centrifugal impeller p 897 A92-45606
Navier-Stokes predictions for the F-18 wing and fuselage at large incidence p 810 A92-46783
Prediction of inviscid supersonic/hypersonic aircraft flowfields p 810 A92-46785
Flight deck aerodynamics of a nonaviation ship p 810 A92-46790
The application of particle image velocimetry (PIV) in a short-duration transonic annular turbine cascade
[ASME PAPER 91-GT-221] p 899 A92-46825
Interaction between crossing oblique shocks and a turbulent boundary layer p 812 A92-46882
Joint computational/experimental aerodynamics research on hypersonic vehicle. II - Computational results p 812 A92-46891
Interaction between a rotor tip vortex and a separated flowfield p 814 A92-46947
Efficient high-resolution rotor wake calculations using flow field reconstruction p 814 A92-46951
Grid sensitivity in low Reynolds number hypersonic continuum flows p 817 A92-47057
Multi-block grid generation around wing-body-engine-pylon configurations p 817 A92-47060
Simple diagnosis for the quality of generated grid systems p 919 A92-47069
Enhancements to viscous-shock-layer technique
[AIAA PAPER 92-2897] p 820 A92-47873
Comparison between two 3D-NS-codes and experiment on a turbine stator
[AIAA PAPER 92-3042] p 822 A92-48703
Internal shock interactions in propulsion/airframe integrated three-dimensional sidewall compression scramjet inlets
[AIAA PAPER 92-3099] p 824 A92-48741

The influence of spray angle on the continuous- and discrete-phase flowfield downstream of an engine combustor swirl cup
[AIAA PAPER 92-3231] p 863 A92-48832
Numerical simulations of the transdetonative ram accelerator combusting flow field on a parallel computer
[AIAA PAPER 92-3249] p 894 A92-48848
Investigation of three-dimensional flow field in a turbine including rotor/stator interaction. II - Three-dimensional flow field at the exit of the nozzle
[AIAA PAPER 92-3326] p 826 A92-48909
Numerical study of secondary separation in glancing shock/turbulent boundary layer interactions
[AIAA PAPER 92-3666] p 907 A92-49087
An inviscid/viscous coupling approach for vortex flow field calculations p 933 A92-49510
Three-dimensional relaxation effect on quasi-3D flow in a blade row with spanwise loading distribution
p 936 A92-51593
Mixing for multi-stage axial-flow compressors
p 996 A92-53015
Calculation of the transonic full-potential flowfield about 3D fuselage p 941 A92-53021
Numerical simulation of three-dimensional turbulent flows in combustion chambers p 970 A92-53276
Flow measurements in scramjet inlets
p 1102 A92-53565
Full Navier-Stokes analysis of a two-dimensional mixer/ejector nozzle for noise suppression
[AIAA PAPER 92-3570] p 1067 A92-54059
Structure of crossing-shock wave/turbulent boundary-layer interactions
[AIAA PAPER 92-3670] p 1022 A92-54113
Comparison of turbulence models for powered-lift flow fields
[AIAA PAPER 92-3674] p 1022 A92-54117
Numerical study of the 3-D flowfield for a supersonic jet exiting into a hypersonic stream from a conical surface
[AIAA PAPER 92-3675] p 1022 A92-54118
Use of an approximate similarity principle for the thermal scaling of a full-scale thrust augmenting ejector
[AIAA PAPER 92-3792] p 1069 A92-54171
Signal processing schemes for Doppler global velocimetry p 1115 A92-54338
Efficient methods for inviscid non-equilibrium hypersonic flow fields p 1024 A92-54571
Flowfield of a lifting rotor in hover - A Navier-Stokes simulation p 1024 A92-54906
Approximate Riemann solver for hypervelocity flows
p 1117 A92-54934
The flow field characteristics about a fighter configuration at high angles of attack
[AIAA PAPER 92-4358] p 1025 A92-55344
Three-dimensional shock wave-turbulent boundary layer interaction induced by blunt body and protuberance
p 1029 A92-56009
Experimental results for a hypersonic nozzle/afterbody flow field
[AIAA PAPER 92-3915] p 1032 A92-56747
Flow quality studies of the NASA Lewis Research Center 8- by 6-foot supersonic/9- by 15-foot Low Speed Wind Tunnel
[AIAA PAPER 92-3916] p 1095 A92-56748
Engine component instrumentation development facility at NASA Lewis Research Center
[AIAA PAPER 92-3995] p 1099 A92-56818
Numerical prediction of the flow characteristics in an arc wind tunnel
[AIAA PAPER 92-4016] p 1100 A92-56838
Study on supersonic combustion in a hypersonic flight
[IAF PAPER 92-0661] p 1106 A92-57101
Mass flux similarity for slotted transonic-wind-tunnel walls
[NASA-TM-4281] p 11 N92-10006
A computational and experimental investigation of a three-dimensional hypersonic scramjet inlet flow field
p 11 N92-10007
Transonic and supersonic Euler computations of vortex-dominated flow fields about a generic fighter
[NASA-TP-3156] p 11 N92-10011
Downwash measurements on a pitching canard-wing configuration
[AD-A239956] p 12 N92-10016
Numerical simulation of vortex breakdown by solving the Euler equations for an incompressible fluid
p 41 N92-10163
Numerical simulation of vortex breakdown via 3-D Euler equations p 41 N92-10164
Turbomachinery noise p 54 N92-10601
Jet noise classical theory and experiments
p 54 N92-10602
Jet noise generated by large-scale coherent motion
p 55 N92-10604
Results from computational analysis of a mixed compression supersonic inlet
[NASA-TM-104475] p 12 N92-10976
Viscous computations of cold air/air flow around scramjet nozzle afterbody
[NASA-CR-4406] p 13 N92-10982
Computational study of the aerodynamics and control by blowing of asymmetric vortical flows over delta wings
[NASA-CR-187979] p 14 N92-10990
A comparison of airborne wake vortex detection measurements with values predicted from potential theory
[NASA-TP-3125] p 18 N92-10994
Numerical simulation of the reactive flow in advanced (HSR) combustors using KIVA-2
[NASA-CR-188996] p 26 N92-11014
Prediction of forces and moments for hypersonic flight vehicle control effectors
[NASA-CR-188954] p 33 N92-11070
Flow visualization and flow field measurements of a 1/12 scale tilt rotor aircraft in hover
[NASA-CR-189456] p 82 N92-11983
A comparative analysis of XV-15 tiltrotor hover test data and WOPWOP predictions incorporating the fountain effect
[NASA-CR-189455] p 114 N92-11992
An experimental and computational investigation of an annular reverse-flow combustor
[UTIAS-338] p 129 N92-11996
CARS temperature measurements in a hypersonic propulsion test facility p 140 N92-12049
An experimental analysis of lateral jet injection into confined swirling crossflows p 156 N92-12199
Heat transfer and instrumentation studies on rotating turbine blades in a transient facility p 156 N92-12203
Blade surface pressure measurements on the rotor of a model turbine stage in a transient flow facility
p 157 N92-12206
Wind tunnel investigation of the interaction and breakdown characteristics of slender wing vortices at subsonic, transonic, and supersonic speeds
[NASA-TP-3114] p 82 N92-12994
Experimental and numerical investigation of the vortex flow over a delta wing at transonic speed
p 84 N92-13001
On the footprints of three-dimensional separated vortex flows around blunt bodies: Attempts of defining and analyzing complex flow structures p 84 N92-13005
Physics of vortical flow p 86 N92-13016
Breaking down the delta wing vortex: The role of vorticity in the breakdown process p 86 N92-13017
Numerical simulation of vortex flows past impulsively started wings p 88 N92-13028
Numerical investigation of unsteady supersonic cavity flowfield with passive control p 88 N92-13029
An experimental analysis of critical factors involved in the breakdown process of leading edge vortex flows
p 89 N92-13031
Oscillating shock impingement on low-angle gas injection into a supersonic flow p 89 N92-13032
Flow modification over a backward facing step
[AD-A241351] p 158 N92-13406
Supercritical blade design on stream surfaces of revolution with an inverse method p 220 N92-13950
Variational formulation of hybrid problems for fully 3-D transonic flow with shocks in rotor p 176 N92-13953
Analysis and design of transonic airfoils using streamwise coordinates p 194 N92-13955
Research on inverse methods and optimization in Italy
p 202 N92-13956
An inverse method for the aerodynamic design of three-dimensional aircraft engine nacelles
p 194 N92-13958
Airfoil optimization with efficient gradient calculations
p 177 N92-13960
Design optimization of transonic airfoils
p 177 N92-13961
A study on vortex flow control on inlet distortion in the re-engined 727-100 center inlet duct using computational fluid dynamics
[NASA-TM-105321] p 179 N92-13998
The aerodynamic effect of fillet radius in a low speed compressor cascade
[NASA-TM-105347] p 202 N92-14063
Evaluation of rotordynamic coefficients of look-through labyrinths by means of a three volume bulk flow model
p 223 N92-14356
Direct computation of turbulence and noise
[NASA-CR-187616] p 236 N92-14788
Hypersonic flow past delta wing flow simulated by Navier-Stokes solutions p 180 N92-14981
Simulation requirements for RCS plume: Flowfield interaction modelling on a winged reentry vehicle
p 181 N92-14985
Steps towards an efficient and accurate method solving the Euler equations around a re-entry configuration at super- and hypersonic speed p 181 N92-14987
Base pressure measurements on a cone at hypersonic Mach numbers: A contribution to aerothermodynamics for space vehicles p 181 N92-14992
Flow over a delta wing at hypersonic speeds
p 181 N92-14993
Experimental study of hypersonic shock wave boundary layer interactions by means of infrared technique
p 182 N92-14994
Experimental investigation of transverse jet effects related to hypersonic space vehicles
p 182 N92-14995
Numerical simulations around models in hypersonic wind tunnels p 182 N92-14998
SIMOUN and Scirocco wind tunnel nozzle viscous flow study p 208 N92-14999
High enthalpy nozzle flows p 182 N92-15000
Short time force measurement system
p 208 N92-15001
Infrared measurements of aerodynamic heating in hypersonic wind tunnel p 208 N92-15002
Verification and application of the NSFLEX method for hypersonic flow conditions p 182 N92-15005
Influence of chemical modeling on the solution of hypersonic shock layers p 183 N92-15016
Hypersonic inviscid flow field simulations around reentry vehicles with flap deflection p 184 N92-15025
Progress with multigrid schemes for hypersonic flow problems
[NASA-CR-189579] p 185 N92-15047
Experimental research of the aerodynamics of nozzles and plumes at hypersonic speeds
[NASA-CR-187316] p 185 N92-15048
Control of unsteady separated flow associated with the dynamic pitching of airfoils
[NASA-CR-189758] p 258 N92-15966
Computation of the hydrodynamic forces and moments on a body of revolution with and without appendages
[AD-A243033] p 298 N92-16978
An experimental investigation of leading edge vortical flow about a delta wing during wing rock
[AD-A243363] p 260 N92-17114
An experimental study of a turbulent wing-body junction and wake flow
[AD-A243388] p 260 N92-17222
Wind loads on a mirage III O aircraft mounted above a ground plane
[AD-A243004] p 275 N92-17266
Flow visualization and wake analysis for standard and modified configurations of the AN/ALQ-78 antenna pod
[AD-A243552] p 260 N92-17339
Viscous three-dimensional calculations of transonic fan performance
[NASA-TM-103800] p 242 N92-17346
Results of measured temperature distribution on an adiabatic wing model with radiation thermometer
[NAL-TM-610] p 261 N92-17755
Boundary-layer transition and heat transfer on slender delta wings
[AERO-REPT-8904] p 262 N92-17849
Hi-alpha forebody design. Part 2: Determination of body shapes for positive directional stability
[NASA-CR-189850] p 359 N92-18038
Marching with the parabolized Navier-Stokes equations. Problem 1: Numerical study of hypersonic viscous cone flow
[AERO-REPT-9007] p 344 N92-18231
Marching with the parabolized Navier-Stokes equations. Problem 2: Hypersonic viscous flow over a flat plate
[AERO-REPT-9008] p 345 N92-18232
Zonal solutions for a double-ellipse in a hypersonic flowfield
[AERO-REPT-9009] p 345 N92-18233
An improved method for simulating supersonic flow past a wedge shaped body
[NAL-TR-1097] p 345 N92-18239
Calculation of hypersonic non-equilibrium viscous flow using second order boundary layer theory
[MBB-FE122-S-PUB-434] p 345 N92-18316
Towards the computation of turbulent hypersonic flows
[AERO-REPT-9106] p 345 N92-18318
Rotorwash computer model: User's guide
[DOT/FAA/RD-90/25] p 346 N92-18345
An approach to flow field measurement by Laser 2-Focus velocimeter (L2F) in gust wind tunnel
[NAL-TM-617] p 346 N92-18484
Aerodynamic and flowfield hysteresis of slender wing aircraft undergoing large-amplitude motions
p 364 N92-18780
Forebody vortex control aeromechanics
p 380 N92-18792

A user's guide to the Langley 16- by 24-inch water tunnel
[NASA-TM-104200] p 385 N92-18956
Numerical solution of three-dimensional unsteady viscous flows
[AD-A244274] p 403 N92-19052
Asymptotic theory of transonic wind tunnel wall interference
[AD-A244075] p 403 N92-19080
Effect of nonuniform entrance flow profile on hypersonic nozzle pitching moment
[AD-A244050] p 377 N92-19184
Operating ranges of meteorological wind tunnels for the simulation of convective boundary layer phenomena
[AD-A244153] p 409 N92-19195
Modelling of chemical and physical effects with respect to flows around reentry bodies
[MBB-FE-211/S/PUB/0465/A] p 347 N92-19296
A comparative study of numerical versus analytical waverider solutions
[AD-A244183] p 347 N92-19304
Unsteady-flow-field predictions for oscillating cascades
[NASA-TM-105283] p 348 N92-19437
Active control of the flow past a cylinder executing rotary motions p 349 N92-19623
Secondary instability of high-speed flows and the influence of wall cooling and suction
[NASA-CR-4427] p 406 N92-19844
Hypersonic wakes
[ETN-92-91082] p 349 N92-19925
Recent results from data analysis of dynamic stall on wind turbine blades
[DE92-001200] p 505 N92-20245
Measurement of vortex flow fields
[NASA-CR-189543] p 443 N92-20283
MATGRID: A program for generation of C-H and C-O topology grids around wing/body configurations. Mathematical definition document
[FFA-TN-1990-19] p 444 N92-20468
Development of a steady potential solver for use with linearized, unsteady aerodynamic analyses
[NASA-TM-105288] p 473 N92-20525
Unsteady-pressure and dynamic-deflection measurements on an aeroelastic supercritical wing
[NASA-TM-4278] p 445 N92-20654
Timing analysis of parallel algorithms on a MIMD multiprocessor
[ITN-92-85153] p 510 N92-20905
Flow studies in close-coupled ventral nozzles for STOVL aircraft
[NASA-TM-102554] p 445 N92-20934
A quantitative study of unsteady compressible flow on an oscillating airfoil
[AD-A244572] p 445 N92-21012
Blade-mounted trailing edge flap control for BVI noise reduction
[NASA-CR-4426] p 512 N92-21173
Flowfield analysis of modern helicopter rotors in hover by Navier-Stokes method
[AD-A245011] p 446 N92-21333
Current status of computational methods for transonic unsteady aerodynamics and aeroelastic applications
[NASA-TM-104191] p 446 N92-21432
Flow analysis and design optimization methods for nozzle afterbody of a hypersonic vehicle
[NASA-CR-4431] p 446 N92-21456
Active flow control for twenty-first century high-performance aircraft with applications to land and sea vehicles p 447 N92-21504
Extension of a three dimensional Euler-code for the investigation of the flow field around bypass engines with fan and core jet
[DLR-FB-91-13] p 503 N92-21699
Three-dimensional simulations of hypersonic flows
[MBB-UK-0155-89-PUB] p 447 N92-21703
An investigation of the energy loss and near wake flow field of trailing edge injection p 456 N92-21839
The aerodynamics of ship superstructures
p 503 N92-21953
Measurement of the flow distribution over the flight deck of an aircraft carrier p 504 N92-21955
A new method for simulating atmospheric turbulence for rotorcraft applications p 464 N92-21956
Flow field over the wing of a delta-wing fighter model with vortex control devices at Mach 0.6 to 1.2
[NASA-TM-4296] p 526 N92-22506
Inlets, ducts, and nozzles p 593 N92-22523
PAN AIR: A computer program for predicting subsonic or supersonic linear potential flows about arbitrary configurations using a higher order panel method. Volume 2: User's manual (version 3.0)
[NASA-CR-3252] p 527 N92-22865
Grid generation and flow solution method for Euler equations on unstructured grids
[NASA-TM-4295] p 528 N92-23533
Computations of unsteady multistage turbomachinery flows p 562 N92-23671
Numerical simulations of wakes, blade-vortex interaction, flutter, and flutter suppression by feedback control p 597 N92-23997
Development and application of computational aerothermodynamics flowfield computer codes
[NASA-CR-190294] p 624 N92-24229
A user guide for the EMTAC-MZ CFD code
[NASA-CR-4283] p 678 N92-24242
NASA aerodynamics program
[NASA-TM-4368] p 609 N92-24678
A study of viscous interaction effects on hypersonic waveriders
[NASA-CR-189587] p 625 N92-24680
Navier-Stokes simulation of dynamic stall on a rotating airfoil p 626 N92-24853
Flowfield in the vicinity of the F/A-18 vertical fin at high-angle-of-attack p 628 N92-24865
The natural flow wing-design concept
[NASA-TP-3193] p 631 N92-25202
Study of the NAL's 0.1 x 0.1 m magnetic suspension and balance system
[NAL-TM-623] p 665 N92-25365
A compressible Navier-Stokes solver with two-equation and Reynolds stress turbulence closure models
[NASA-CR-4440] p 681 N92-25376
Engine component instrumentation development facility at NASA Lewis Research Center
[NASA-TM-105644] p 665 N92-25449
An experimental investigation of the surface flow and wake dynamics associated with transverse flow over wavy cylinders p 681 N92-25547
On a multi-block method for transonic turbulent flows past a wing-fuselage configuration p 632 N92-25569
TIGER: Turbomachinery interactive grid generation
p 659 N92-25718
Computational Fluid Dynamics --- numerical methods and algorithm development
[NASA-CP-10078] p 660 N92-25808
Study of shock-induced combustion using an implicit TVD scheme p 669 N92-25816
A comparison of predicted and measured inlet distortion flows in a subsonic axial inlet flow compressor rotor
[NASA-TM-105427] p 633 N92-26104
Simulation of a rotorcraft in turbulent flows
[AD-A245742] p 650 N92-26155
Performance prediction and design of maximum thrust planar supersonic nozzles using a flux-difference-splitting technique p 738 N92-26480
CFD mixing analysis of jets injected from straight and slanted slots into confined crossflow in rectangular ducts
[NASA-TM-105699] p 738 N92-26561
An experimental investigation of a 2-D scramjet inlet at flow Mach numbers of 8 to 25 and stagnation temperatures of 800 to 4,100 K p 739 N92-26586
Use of an approximate similarity principle for the thermal scaling of a full-scale thrust augmenting ejector
[NASA-TM-105724] p 739 N92-26613
Observation and measurements of flow structures in the stagnation region of a wing-body junction
p 714 N92-26616
High lift aircraft
[AD-D015215] p 732 N92-27185
Computational method to predict thermodynamic, transport, and flow properties for the modified Langley 8-foot high-temperature tunnel
[NASA-TM-4374] p 767 N92-27193
Fractal image compression of Rayleigh, Raman, LIF and LDV data in turbulent reacting flows
[AD-A246960] p 767 N92-27352
Experimental investigation of the unsteady pressure field around an oscillating blade
[MITT-90-01] p 768 N92-27407
On the computation of unsteady turbomachinery flows. Part 1: Euler equations in vibrating cascades
p 768 N92-27460
Application of CFD in the design of gas turbine engine components p 741 N92-27461
Computation and visualization of specific flow phenomena in turbomachinery application
p 741 N92-27463
An integrated CFD system for 3D turbomachinery applications p 741 N92-27464
Viscous three-dimensional calculations of transonic fan performance p 768 N92-27467
Navier-Stokes analysis of turbine blade heat transfer and performance p 768 N92-27468
Steady and unsteady 3D flow computation through a transonic turbine stage p 742 N92-27469
The 3-D Navier-Stokes flow and temperature field computation for a forced mixer nozzle
p 770 N92-27482
Fundamental studies on droplet interactions in dense sprays
[AD-A246918] p 770 N92-27546
Propulsion simulator for magnetically suspended wind tunnel models p 750 N92-27801
Present status of the MIT/NASA Langley 6-inch MSBS p 750 N92-27802
A study of juncture flow in the NASA Langley 0.3-meter transonic cryogenic tunnel
[NASA-CR-190430] p 773 N92-27880
Experimental investigation of turbulence behavior in shock wave/turbulent boundary layer interactions
[AD-A247792] p 774 N92-27886
Transonic Unsteady Aerodynamics and Aeroelasticity
[AGARD-CP-507] p 718 N92-27936
Current status of computational methods for transonic unsteady aerodynamics and aeroelastic applications
p 718 N92-27937
Unstructured-grid methods development for unsteady aerodynamic and aeroelastic analyses
p 718 N92-27938
Computation of the unsteady transonic 2D cascade flow by an Euler algorithm with interactive grid generation
p 719 N92-27944
Numerical simulation of shock-stall flutter of an airfoil using the Navier-Stokes equations p 746 N92-27956
Full Navier-Stokes analysis of a two-dimensional mixer/ejector nozzle for noise suppression
[NASA-TM-105715] p 868 N92-28419
Calculation of unsteady transonic flows with mild separation by viscous-inviscid interaction
[NASA-TP-3197] p 827 N92-28477
Comparison of LDA and LTA applications for propeller tests in wind tunnels
[NLR-MP-88031-U] p 827 N92-28658
Flow quality studies of the NASA Lewis Research Center 8- by 6-foot supersonic/9- by 15-foot low speed wind tunnel
[NASA-TM-105417] p 887 N92-28673
Flow gradient corrections on hot-wire measurements using an X-wire probe
[NLR-TP-90255-U] p 829 N92-28713
Natural flow wing
[NASA-CASE-LAR-14281-1] p 829 N92-28729
Flow visualization studies of a sideslipping, canard-configured X-31A-Like fighter aircraft model
[AD-A245940] p 829 N92-28883
Computation of three-dimensional effects on two dimensional wings
[NASA-CR-190576] p 832 N92-29691
Explicit Navier-Stokes computation of turbomachinery flows
[AD-A248458] p 911 N92-29933
Experimental investigation of the flowfield of an oscillating airfoil
[NASA-TM-105675] p 833 N92-30182
Ultra high bypass Nacelle aerodynamics inlet flow-through high angle of attack distortion test
[NASA-CR-189149] p 943 N92-30298
Joint computational and experimental aerodynamics research on a hypersonic vehicle
[DE92-013439] p 943 N92-30367
MATGRID, a program for generation of C-H and C-O topology grids around wing/body configurations: Software description document
[FFA-TN-1990-20] p 945 N92-30713
Application of the Chimera overlapped grid scheme to simulation of Space Shuttle ascent flows
p 945 N92-30742
Numerical calculations of two-dimensional single and multi-material flow fields with CCICE
[DE92-015778] p 1000 N92-30903
Navier-Stokes analysis and experimental data comparison of compressible flow within ducts
[NASA-TM-105796] p 972 N92-30972
NASA. Lewis Research Center supersonic throughflow fan program
[NASA-TM-103248] p 972 N92-31250
In-flight leading-edge extension vortex flow-field survey measurements on a F-18 aircraft at high angle of attack
[NASA-TM-4398] p 947 N92-31276
NAS (Numerical Aerodynamic Simulation Program) technical summaries, March 1989 - February 1990
[NASA-TM-107960] p 1013 N92-31852
The three-dimensional stability of the Foeppl vortices
p 949 N92-31889
A computational examination of directional stability for smooth and chined forebodies at high-alpha
[NASA-CR-4465] p 950 N92-32114
Control of unsteady separated flow associated with the dynamic stall of airfoils
[NASA-CR-190688] p 950 N92-32177
An installed nacelle design code using a multiblock Euler solver. Volume 2: User guide
[NASA-CR-189652-VOL-2] p 951 N92-32228
An examination of several high resolution schemes applied to complex problems in high speed flows
[AD-A250814] p 1124 N92-32632

New concepts for multi-block grid generation for flow domains around complex aerodynamic configurations
[NLR-TP-91046-U] p 1037 N92-32730
An experimental study of the flow over a sharp-edged delta wing at subsonic and transonic speeds
[NLR-TP-91117-U] p 1037 N92-32732
Integration of wall interference assessment and wall adaptation
[NLR-TP-91119-U] p 1101 N92-32734
Dynamic interactions between hypersonic vehicle aerodynamics and propulsion system performance
[NASA-CR-190638] p 1038 N92-33304
A nozzle internal performance prediction method
[NASA-TP-3221] p 1040 N92-33625
Static and dynamic flow visualization studies of two double-delta wing models at high angles of attack
[AD-A252878] p 1040 N92-33678
An approximate viscous shock layer technique for calculating chemically reacting hypersonic flows about blunt-nosed bodies p 1041 N92-33837
Influence of the swirl producing construction in the flow and reaction field of turbulent diffusion flames
[ETN-92-92103] p 1127 N92-33916
Investigation of advancing front method for generating unstructured grid
[NASA-CR-190902] p 1128 N92-34043

FLOW EQUATIONS

On thermal-stress gas flows p 37 A92-10657
Finite element solutions of the Euler equations for transonic external flows p 5 A92-11063
An integrated airloads-inflow model for use in rotor aeroelasticity and control analysis p 64 A92-14328
Heat transfer in rotating serpentine passages with trips normal to the flow
[ASME PAPER 91-GT-265] p 151 A92-15663
Inviscid drag prediction for transonic transport wings using a full-potential method p 174 A92-20212
An investigation on detached shock waves ahead of bodies of revolution at transonic speeds
p 251 A92-23381
Unsteady airfoil flow solutions on moving zonal grids
[AIAA PAPER 92-0543] p 342 A92-28200
Quick calculation of three-dimensional supersonic flow past nearly axisymmetric bodies p 624 A92-40605
Recent progress in computational vortex-flow aerodynamics p 84 N92-13002
Design of 3-dimensional complex airplane configurations with specified pressure distribution via optimization
p 194 N92-13948
The research progress on Hodograph Method of aerodynamic design at Tsinghua University
p 177 N92-13974
Behaviour and modelling of the aerothermodynamics of ballistic entry vehicles in the high altitude flow regimes
p 184 N92-15031
Application of analysis techniques for low frequency interior noise and vibration of commercial aircraft
[NASA-CR-189555] p 481 N92-20376
Development of a steady potential solver for use with linearized, unsteady aerodynamic analyses
[NASA-TM-105288] p 473 N92-20525
Boundary layer flow in axial compressors (theoretical part)
[ETN-92-91006] p 501 N92-21232
Boundary layer flow in axial compressors (theoretical part)
[ETN-92-91007] p 501 N92-21233
Modeling of linear isentropic flow systems
p 593 N92-22495
Pressure-based high-order TVD methodology for dynamic stall control
[AD-A247056] p 774 N92-27918
Unstructured-grid methods development for unsteady aerodynamic and aeroelastic analyses
p 718 N92-27938
Computation of viscous phenomena in unsteady transonic flow p 720 N92-27949
Transonic aeroelastic computations on wings using Navier-Stokes equations p 721 N92-27957
Calculation of unsteady transonic flows with mild separation by viscous-inviscid interaction
[NASA-TP-3197] p 827 N92-28477
Explicit Navier-Stokes computation of turbomachinery flows
[AD-A249284] p 909 N92-28879
Progress in unstructured-grid methods development for unsteady aerodynamic applications
[NASA-TM-107643] p 944 N92-30393
Modeling and numerical simulation of vortex flow in aerodynamics
[NLR-TP-91154-U] p 1037 N92-32673

FLOW GEOMETRY

Simple turbulence models for supersonic flows - Bodies at incidence and compression corners p 5 A92-11059
Probe shapes for streamwise momentum and cross-stream turbulence intensity p 9 A92-13210
Heat transfer in supersonic flow past a single crater
p 63 A92-13741
Two-phase flow correlations in air/oil systems of aero engines
[ASME PAPER 91-GT-54] p 121 A92-15532
The effect of blade tip geometry on the tip leakage flow in axial turbine cascades
[ASME PAPER 91-GT-135] p 72 A92-15577
Numerical study of branched turboprop inlet ducts using a multiple block grid procedure
[ASME PAPER 91-GT-339] p 76 A92-15703
Isothermal modeling of gas turbine combustors - Computational study p 129 A92-17203
Control of hypersonic aerodynamic forces with surface blowing p 172 A92-18363
Compressibility effects in thin channels with injection
p 216 A92-18369
Stratified flow around an axisymmetric body at small angle of attack p 172 A92-18385
Surface flow patterns on an ogive-cylinder at incidence p 176 A92-20762
Studies of the effects of curvature on dilution jet mixing p 290 A92-21079
Mathematical modeling of supersonic flow over a convex-concave formed body based on the Euler and Navier-Stokes equations p 252 A92-23416
Flow analysis of rectangular wind tunnel contraction
p 312 A92-25001
An experimental study of the flow past spheres at transonic speeds and high Reynolds numbers
p 312 A92-25002
Numerical simulation of 2-D separated flows caused by suddenly change of the body section
p 312 A92-25004
Analysis of transonic flow past an axisymmetric convex corner p 312 A92-25015
Effect of upstream disturbance on flow asymmetry
[AIAA PAPER 92-0408] p 325 A92-26261
Some thoughts on conical flow asymmetry
[AIAA PAPER 92-0427] p 326 A92-26275
A comparative study of turbulence models for overset grids
[AIAA PAPER 92-0437] p 327 A92-26284
The dimensional reconstruction of vortex cross-section images p 339 A92-27833
Numerical simulation of the flow around rectangular cylinder p 339 A92-27851
Swirl effects on confined flows in axisymmetric geometries p 399 A92-28513
Numerical computation of compressible flow around an object of complex shape p 429 A92-30517
Structure of supersonic turbulent flow past a swept compression corner p 431 A92-31155
Orthogonal grids around difficult bodies
p 432 A92-31160
Asymptotic defect boundary-layer theory applied to hypersonic flows p 610 A92-36839
A study of flow patterns and behaviours of 3D separated flow on a simplified Shuttle model p 615 A92-38906
Scrutinizing k-epsilon EVM and ASM by means of LES and wind tunnel for flowfield around cube --- Eddy Viscosity Model, Algebraic Stress Model, Large Eddy Simulation
p 621 A92-40119
Transition to turbulence in curved channel flow
p 621 A92-40125
Experimental and numerical investigation of a turbulent boundary layer over riblets p 622 A92-40128
Curvature effects for three-dimensional compressible boundary-layer stability p 701 A92-41207
Flow and acoustic features of a supersonic tapered nozzle p 712 A92-44328
Viscous simulation method for unsteady flows past multicomponent configurations p 714 A92-44671
Experimental investigation of vortex dynamics on delta wings
[AIAA PAPER 92-2731] p 804 A92-45565
Taylor series approximation of geometric shape variation for the Euler equations p 899 A92-46916
Basic experiments on the directivity of the sound radiation emitted by a turboshaft engine
[ONERA, TP NO. 1992-36] p 926 A92-48597
Effects of a leading-edge fillet on the flow past an appendage-body junction p 935 A92-50301
A new look at surface flow visualization to provide insight into complex fluid dynamic behavior
p 1090 A92-54307
The vortical structure in the wake during dynamic stall
[AIAA PAPER 92-4496] p 1026 A92-55364
Flight measurements of downwash on the Ball-Bartoe Jetwing powered lift aircraft p 1054 A92-56174
An experimental study of a turbulent wing-body junction and wake flow
[AD-A243388] p 260 N92-17222
Boundary layer flow in axial compressors (theoretical part)
[ETN-92-91006] p 501 N92-21232
Presentation of a computational code for 3-D compressible flow in complex channels and cavities
p 769 N92-27475

FLOW MEASUREMENT

Impeller flow field measurement and analysis
[ASME PAPER 90-GT-146] p 38 A92-11288
Prospects of turbulence research by means of testing bodies in motion p 30 A92-12194
Automation of the measurement process in the N2 wind tunnel with the SPITA N-3 system p 30 A92-12347
Boundary-layer and wake measurements on a swept, circulation-control wing p 9 A92-13205
Airfoil boundary layer measurements at low Re in an accelerating flow from a nonzero velocity
p 62 A92-13673
Isothermal flow fields in a research combustor for lean blowout studies
[ASME PAPER 91-GT-37] p 121 A92-15520
Optimizing instrumentation when measuring jet engine blade vibration
[ASME PAPER 91-GT-71] p 148 A92-15540
NASA low-speed centrifugal compressor for 3-D viscous code assessment and fundamental flow physics research
[ASME PAPER 91-GT-140] p 72 A92-15580
Inlet flow angle determination of transonic compressor cascades
[ASME PAPER 91-GT-274] p 75 A92-15671
Aerodynamic measuring techniques for transonic and supersonic flow in cascades and turbomachines
[ONERA, TP NO. 1991-170] p 137 A92-16135
Measurements of the flow around a lifting-wing/body junction p 175 A92-20726
Modeling the ventilated wind tunnel wall
[AIAA PAPER 92-0035] p 249 A92-22156
A large-scale axial flow compressor facility and dynamic measurement techniques for rotor flow study
p 382 A92-24729
3D LDA measurement in an axial fan rotor
p 391 A92-24730
The LDV measurement of three-component velocity of complex vortex flow in the wind tunnel
p 393 A92-25109
Flow field measurement and visualization using projected smoke trails
[AIAA PAPER 92-0384] p 323 A92-26241
Laser measurements of unsteady flow field in a radial turbine guide vanes
[AIAA PAPER 92-0394] p 395 A92-26249
Measurements of the inflow to a vibrating rotor blade
[AIAA PAPER 92-0634] p 333 A92-27012
Fibre optic laser anemometry for turbomachinery applications p 397 A92-27783
Studying method of measuring flow-field between stages in axial-flow compressor p 423 A92-29720
Testing capabilities at AEDC for development of hypersonic vehicles
[AIAA PAPER 91-5027] p 483 A92-31686
Applications of hot-film anemometers in hypersonic shear layers
[AIAA PAPER 91-5028] p 436 A92-31687
A method for measuring high-subsonic two-dimensional periodic flow field using a single-hole high-response cylindrical pressure probe p 588 A92-35567
Visualization and measurement of helicopter rotor flow using projected smoke filaments and digital image processing p 520 A92-35728
An improved analysis method for cross-wire signals obtained in supersonic flow p 614 A92-38456
A sensitive fast-response probe to measure turbulence and heat flux from any airplane p 775 A92-42097
Test on high enthalpy hypersonic flow using a ballistic range p 747 A92-43097
The fluid-dynamic measurement of the fling motion of a three-dimensional flat plate p 710 A92-43194
On the measurement of subsonic flow around an appended body of revolution at cryogenic conditions in the NTF p 880 A92-45265
Surface and flow field measurements in a symmetric crossing shock wave/turbulent boundary layer flow
[AIAA PAPER 92-2634] p 806 A92-45574
Measurements of the unsteady vortex flow over a wing-body at angle of attack
[AIAA PAPER 92-2729] p 808 A92-45598
Measurement of shock-wave/boundary-layer interaction in a free-piston shock tunnel p 813 A92-46903
Measurement of scalar flowfield at exit of combustor sector using Raman diagnostics
[AIAA PAPER 92-3350] p 894 A92-48927
All-Union Conference on Optical Methods of Flow Research, 1st, Novosibirsk, Russia, Apr. 1991, Proceedings p 993 A92-51311
Measurement of turbulent boundary layer in transonic flow p 941 A92-53010
Hot-wire measurements in turbulent transonic flows
p 941 A92-53078

Flow measurements in scramjet inlets
p 1102 A92-53565
ICIASF '91 - International Congress on Instrumentation in Aerospace Simulation Facilities, 14th, Rockville, MD, Oct. 27-31, 1991, Record
[ISBN 0-0783-0123-4] p 1114 A92-54301
Detecting 3-D, turbulent separation regions using unsteady computerized thermographic technique
p 1023 A92-54308
Nonintrusive measurements in fluid dynamic flows from Mach .0005 to 14 p 1090 A92-54311
Rayleigh imaging and flow tagging in ground test facilities p 1115 A92-54330
A simple three component velocity measurement method using a rotated split-film sensor
p 1115 A92-54333
A laser fluorescence anemometer system for the Langley 16- by 24-inch water tunnel
p 1092 A92-54347
Flight measurements of downwash on the Ball-Bartoe Jetwing powered lift aircraft p 1054 A92-56174
Development of local nonintrusive measurements of inlet and exhaust flows for the ground testing of air-breathing engines
[AIAA PAPER 92-3899] p 1122 A92-56735
Flow quality studies of the NASA Lewis Research Center 8- by 6-foot supersonic/9- by 15-foot Low Speed Wind Tunnel
[AIAA PAPER 92-3916] p 1095 A92-56748
The SR3 low density wind tunnel - Facility capabilities and research development
[AIAA PAPER 92-3972] p 1098 A92-56798
Advanced nozzle and engine components test facility
[AIAA PAPER 92-3993] p 1099 A92-56816
Reflection type skin friction meter
[NASA-CASE-LAR-14520-1-SB] p 11 N92-10008
Fuel flow measurement in gas turbine testing
[NRC-29808] p 130 N92-12000
Effects of inlet distortion on the development of secondary flows in a subsonic axial inlet compressor rotor p 89 N92-13030
An experimental analysis of critical factors involved in the breakdown process of leading edge vortex flows
p 89 N92-13031
A new technique for temperature and specie concentration measurements in unseeded supersonic and hypersonic gas flows
[AD-A241536] p 158 N92-13409
Constant-temperature anemometry measurements in hypersonic boundary layers p 90 N92-13861
An experimental investigation of leading edge vortical flow about a delta wing during wing rock
[AD-A243363] p 260 N92-17114
High accuracy fuel flowmeter. Phase 2C and 3: The mass flowrate calibration of high accuracy fuel flowmeters
[NASA-CR-187108] p 406 N92-19775
Measurement of vortex flow fields
[NASA-CR-189543] p 443 N92-20283
Pressure and velocity measurements about an airfoil during a parallel blade-vortex interaction
p 446 N92-21429
Radial inflow turbine study
[AD-A246938] p 743 N92-28073
Flow quality studies of the NASA Lewis Research Center 8- by 6-foot supersonic/9- by 15-foot low speed wind tunnel
[NASA-TM-105417] p 887 N92-28673
Flow gradient corrections on hot-wire measurements using an X-wire probe
[NLR-TP-90255-U] p 829 N92-28713
Evaluation of measured-boundary-condition methods for 3D subsonic wall interference
[NLR-TR-88072-U] p 832 N92-29884
Three-dimensional laser window formation
[NASA-RP-1280] p 984 N92-30307
Method of measuring cross-flow vortices by use of an array of hot-film sensors
[NASA-CASE-LAR-14824-1-SB] p 998 N92-30390
Radial inflow turbine study
[AD-A252783] p 1127 N92-33538

FLOW REGULATORS
Passive control of supersonic cavity flowfields
[SAE PAPER 912153] p 619 A92-39988
Automatic control of test parameters for intake measurements in a low-speed wind tunnel
p 1091 A92-54341

FLOW RESISTANCE
End plate interference effects on the aerodynamics of a circular cylinder in uniform flow p 313 A92-25097
An experimental study of transonic flow of a gas past wedges p 424 A92-30153
The problem of body motion in a medium with resistance p 604 A92-36416
Comment on 'Modification of the van Driest damping function to include the effects on surface roughness'
p 758 A92-41297

FLOW STABILITY
Inviscid spatial stability of a three-dimensional compressible mixing layer p 39 A92-11816
The dynamic character of the wake of an axisymmetric body at an angle of attack
[AIAA PAPER 91-3268] p 8 A92-12741
On the interaction between first- and second-mode waves in a supersonic boundary layer
p 78 A92-16462
Stability of a viscous compressible shear layer with a temperature drop p 79 A92-16684
Three-dimensional linear stability approach to transition on wings and bodies of revolution at incidence
p 172 A92-18361
Instabilities of flows over bodies at large incidence
p 176 A92-20738
The effects of suction on the nonlinear stability of the three-dimensional boundary layer above a rotating disc
p 393 A92-25366
Three-dimensional structure of a curved wake
[AIAA PAPER 92-0541] p 341 A92-28199
Secondary instability mechanisms in compressible, axisymmetric boundary layers
[AIAA PAPER 92-0743] p 343 A92-28224
Helical-perturbation device for cylinder-wing vortex generators p 432 A92-31167
Stability of a nonorthogonal stagnation flow to three-dimensional disturbances p 495 A92-31194
Secondary instability of high-speed flows and the influence of wall cooling and suction
p 435 A92-31640
Numerical studies of transverse curvature effects on transonic flow stability p 524 A92-36186
Reactive mixing layer between pressure reflecting boundaries p 656 A92-40144
Modern developments in shear flow control with swirl
p 703 A92-41265
Stability of plane nonorthogonal stagnation flow
p 704 A92-41291
Concepts for the stability analysis of NLF-experiments on swept wings
[AIAA PAPER 92-2706] p 801 A92-45548
Nonlinear development and secondary instability of large-amplitude Goertler vortices in hypersonic boundary layers p 942 A92-53080
Mixed flow compressor surge margin gain using a manifolded diffuser system
[AIAA PAPER 92-3753] p 1068 A92-54151
Control of forebody vortices by suction at the nose of the RAE high incidence research model
p 87 N92-13022
Numerical investigation of unsteady supersonic cavity flowfield with passive control p 88 N92-13029
Experimental investigations of exciting forces caused by flow in labyrinth seals p 223 N92-14354
Secondary instability of high-speed flows and the influence of wall cooling and suction
[NASA-CR-4427] p 406 N92-19844
Active flow control for twenty-first century high-performance aircraft with applications to land and sea vehicles p 447 N92-21504
Distributed acoustic receptivity in laminar flow control configurations
[NASA-CR-4438] p 765 N92-26680
Three dimensional boundary layer transition on a yawed cylinder p 766 N92-26909
Turbulent mixing in supersonic jets
p 715 N92-27054
Methods for direct simulation of transition in hypersonic boundary layers 2 p 912 N92-30064
Stability and transition of hypersonic boundary-layer flows
[AD-A250279] p 948 N92-31555
The three-dimensional stability of the Foeppl vortices
p 949 N92-31889
Turbine blade tip and seal clearance excitation forces
[NASA-CR-184341] p 973 N92-31910
Contribution to the modelling of turbulent combustion in the case of stabilisation by flame-lock
[ESA-TT-1229] p 988 N92-31942
Perspectives on hypersonic viscous and nonequilibrium flow research
[NASA-CR-190817] p 1039 N92-33413
Computation and stability analysis of laminar flow over a blunt cone in hypersonic flow p 1041 N92-33839

FLOW THEORY
The effect of steady aerodynamic loading on the flutter stability of turbomachinery blading
[ASME PAPER 91-GT-130] p 71 A92-15574
Effect of suction on the stability of supersonic boundary layers. I - Second-mode waves. II - First-mode waves
p 174 A92-19611
Turbomachinery unsteady load predictions with nonuniform inflow p 611 A92-36972
On the effect of external flow and shear-layer thickness on the expansion cells of under-expanded supersonic circular jets p 969 A92-50478
Boundary layer flow in axial compressors (theoretical part)
[ETN-92-91006] p 501 N92-21232
Boundary layer flow in axial compressors (theoretical part)
[ETN-92-91007] p 501 N92-21233
Boundary layer flow in axial compressors (theoretical part)
[ETN-92-91008] p 502 N92-21234

FLOW VELOCITY
Asymptotics of the upper branch of the neutral curve at subsonic and transonic external flow velocities
p 79 A92-16705
Synthesis of wing profiles from chord velocity diagrams using quasi-solutions for inverse boundary value problems p 80 A92-16815
A model of gasdynamic loads on an oscillating nozzle shell p 80 A92-16817
Effect of the blade height of the nozzle ring of axial-flow microturbines on the flow velocity factor and exit angle
p 128 A92-16831
Newton's method solver for high-speed viscous separated flowfields p 176 A92-20736
Simple method of supersonic flow visualization using smoke p 219 A92-20764
A boundary integral formulation for the kinetic field in aerodynamics. I - Mathematical analysis
p 243 A92-21504
Development and application of a particle image velocimeter for high-speed flows
[AIAA PAPER 92-0004] p 292 A92-22129
Establishment and characterization of a reproducible vortex for use in studying nonsteady two-dimensional phenomena p 310 A92-24428
On velocity profile models for predicting end wall boundary layers and their blade force defects in axial compressor cascades p 311 A92-24877
An experimental study of a turbulent wing-body junction and wake flow
[AIAA PAPER 92-0434] p 327 A92-26281
Measurements of the inflow to a vibrating rotor blade
[AIAA PAPER 92-0634] p 333 A92-27012
A new calculating method for the flowfield in turbomachinery - The study on the application of the vorticity-velocity equations for the numerical solution of the flowfield in turbomachinery p 338 A92-27803
A general nonlinear dynamical analysis of a second-order, one-dimensional, theoretical compression system model p 509 A92-29374
An experimental study of tone-like noise in the flow past a wing at low flow velocities p 425 A92-30160
Experimental study of the characteristics of boundary-layer development on an airfoil
p 425 A92-30171
Three-dimensional flow computation for two interacting, moving droplets
[AIAA PAPER 92-0343] p 496 A92-31655
An experimental study of the noise of flow past a wing at low velocities p 603 A92-33771
The Berlin oil channel for drag reduction research
p 571 A92-34219
The numerical method for calculating the flow field, temperature field and radiation fluxfield in the pipe
p 587 A92-35546
An improved analysis method for cross-wire signals obtained in supersonic flow p 614 A92-38456
Experiments on turbulent flow due to an enclosed rotating disk p 615 A92-38863
Prediction of three-dimensional turbulent boundary layers using a second-moment closure
p 675 A92-40080
Calculation of three-dimensional turbulent flow in wind tunnel entry section p 708 A92-43055
Instantaneous visualization of surface flows
p 763 A92-44327
Quantification of canard and wing interactions using spatial correlation velocimetry
[AIAA PAPER 92-2687] p 807 A92-45588
Viscous high-speed flow computations by adaptive mesh embedding techniques p 808 A92-45839
The application of particle image velocimetry (PIV) in a short-duration transonic annular turbine cascade
[ASME PAPER 91-GT-221] p 899 A92-46825
Laser velocimetry measurements in an MHD aerodynamic duct
[AIAA PAPER 92-2986] p 899 A92-46996
Effect of the grid system on heat transfer computations for high speed flows p 900 A92-47071
Expansion tube experiments for the investigation of ram-accelerator-related combustion and gasdynamic problems
[AIAA PAPER 92-3246] p 904 A92-48845

Flowpath and sensitivity analyses of high speed propulsion systems
[AIAA PAPER 92-3806] p 1069 A92-54178
A simple three component velocity measurement method using a rotated split-film sensor
p 1115 A92-54333
An analysis of boundary layer for droplet aerodynamic stripped in high speed gas flow p 1116 A92-54563
Propulsive lift noise p 55 N92-10606
An experimental and computational investigation of an annular reverse-flow combustor
[UTIAS-338] p 129 N92-11996
Aerodynamic coefficients of a symmetrical airfoil in an oscillating flow
[AD-A241073] p 89 N92-13035
Supercritical blade design on stream surfaces of revolution with an inverse method p 220 N92-13950
Application of program LAURA to perfect gas shock tube flows: A parametric study
[NASA-TM-104190] p 298 N92-17002
Laser based, non-intrusive measurement system for analysis of jet engine flows
[AD-A242398] p 279 N92-17011
An approach to flow field measurement by Laser 2-Focus velocimeter (L2F) in gust wind tunnel
[NAL-TM-617] p 346 N92-18484
A user's guide to the Langley 16- by 24-inch water tunnel
[NASA-TM-104200] p 385 N92-18956
Operating ranges of meteorological wind tunnels for the simulation of convective boundary layer phenomena
[AD-A244153] p 409 N92-19195
Unsteady-flow-field predictions for oscillating cascades
[NASA-TM-105283] p 348 N92-19437
Computer code for preliminary sizing analysis of axial-flow turbines
[NASA-CR-4430] p 473 N92-20196
A laser velocimeter investigation of the normal shockwave boundary layer interaction
p 500 N92-20485
Laser velocimetry measurements of oscillating airfoil dynamic stall flow field
[AD-A244546] p 502 N92-21297
Multi-colored layers for visualizing aerodynamic flow effects
[NASA-CASE-LAR-13742-1] p 447 N92-21588
Experimental evaluation of a flat wake theory for predicting rotor inflow-wake velocities
[NASA-TM-4334] p 630 N92-24882
A comparison of predicted and measured inlet distortion flows in a subsonic axial inlet flow compressor rotor
[NASA-TM-105427] p 633 N92-26104
Flow gradient corrections on hot-wire measurements using an X-wire probe
[NLR-TP-90255-U] p 829 N92-28713
Unsteady response of the leading-edge vortices on a pitching delta wing p 1041 N92-33851
Vaporizing particle velocimeter
[NASA-CASE-LAR-14685-1] p 1042 N92-34172

FLOW VISUALIZATION

Surface flow visualization of rotating propeller
p 4 A92-10959
Disturbance of transonic wind tunnel flow by a slot in the tunnel wall p 135 A92-13675
Simple method of supersonic flow visualization using smoke p 219 A92-20764
Flow visualization and wake analysis for complex three-dimensional bluff bodies at subcritical through critical Reynolds numbers
[AIAA PAPER 92-0155] p 253 A92-23770
Experimental necessities for subsonic transport configuration development
[AIAA PAPER 92-0158] p 254 A92-23773
What we need in experimental aerodynamics - One engineering educator's view
[AIAA PAPER 92-0161] p 241 A92-23776
Flow over an all-body hypersonic aircraft - Experiment and computation p 310 A92-24651
Vortex modeling for rotor aerodynamics - The 1991 Alexander A. Nikolsky Lecture p 315 A92-25576
Unsteady wing surface pressures in the wake of a propeller
[AIAA PAPER 92-0277] p 318 A92-25731
A three-dimensional supersonic turbulent boundary layer generated by an isentropic compression
[AIAA PAPER 92-0310] p 320 A92-25758
Flow visualization image analysis of high-rate roll experiments on a delta wing
[AIAA PAPER 92-0317] p 321 A92-25764
The anchored and loose vortex systems of finite wings
[AIAA PAPER 92-0318] p 321 A92-25765
Flow field measurement and visualization using projected smoke trails
[AIAA PAPER 92-0384] p 323 A92-26241
Flow visualization of a prop-fan leading-edge vortex
[AIAA PAPER 92-0386] p 323 A92-26242
Experimental investigation of a three-dimensional bluff-body wake
[AIAA PAPER 92-0429] p 326 A92-26277
Influence of wing shapes on the surface pressure fluctuations of a wing-body junction
[AIAA PAPER 92-0433] p 327 A92-26280
Flow past a sphere - Topological transitions of the vorticity field p 330 A92-26410
Flowfield visualization of crossing shock-wave/boundary-layer interactions
[AIAA PAPER 92-0750] p 335 A92-27094
The dimensional reconstruction of vortex cross-section images p 339 A92-27833
Helium bubble flow visualization of the spanwise separation on a NACA 0012 with simulated glaze ice
[AIAA PAPER 92-0413] p 341 A92-28192
Observation and testing on supersonic multiphase flow p 429 A92-30502
Aerodynamic performances of spoiler motion
p 429 A92-30526
Study on two-dimensional jet mixing with a vertical supersonic flow p 429 A92-30530
Experimental investigations of the vortex flow on delta wings at high incidence p 432 A92-31172
Experimental study of a low Reynolds number tandem airfoil configuration p 442 A92-32241
Three-dimensional flow visualization of shock wave using double-pulsed holographic interferometry. II - Flow visualization for three-dimensional shock structures in rotating aeroengine fan blade rows p 497 A92-32507
Preliminary design of an intermittent smoke flow visualization system
[AIAA PAPER 92-1028] p 580 A92-33209
Visualization and measurement of helicopter rotor flow using projected smoke filaments and digital image processing p 520 A92-35728
On the influence of blade-vortex-interactions on vortex structure p 521 A92-35783
Change of flow about an elongated rectangular cylinder in a range of Reynolds numbers of 200 to 0.7 x 10 exp 4 p 522 A92-35997
LDV measurements of the flowfield in a simulated combustor with axial and side inlets p 672 A92-38867
A study of flow patterns and behaviours of 3D separated flow on a simplified Shuttle model p 615 A92-38906
A flow visualization experiment on the unsteady flow around two-dimensional airfoil p 615 A92-38913
A new method for visualization and measurement of turbulent flow patterns p 619 A92-40063
The combined wake of an array of oscillating ribbons
p 623 A92-40180
Effect of tunnel walls on vortex breakdown location over delta wings p 703 A92-41279
Flow around two square cylinders in staggered arrangements p 761 A92-42797
Transonic visualization test for the airframe shape improvement of a spaceplane p 752 A92-43200
Buffeting characteristics of a transonic airfoil
p 711 A92-43202
Aerodynamic characteristics of a hypersonic aircraft
p 711 A92-43226
Instantaneous visualization of surface flows
p 763 A92-44327
Simultaneous imaging and interferometric turbule visualization in a high-velocity mixing/shear layer
p 896 A92-45130
Water tunnels p 880 A92-45266
Hot gas ingestion characteristics and flow visualization of a vectored thrust STOVL concept
p 860 A92-45316
Experimental investigation of the flowfield of an oscillating airfoil
[AIAA PAPER 92-2622] p 793 A92-45494
Dynamically enhanced sustained lift using oscillating leading-edge flaps
[AIAA PAPER 92-2625] p 794 A92-45497
Static and dynamic flow field development about a porous suction surface wing
[AIAA PAPER 92-2628] p 795 A92-45500
Experimental development of spanwise vortex models with streamwise decay due to wall interaction
[AIAA PAPER 92-2688] p 799 A92-45535
The flip flop nozzle extended to supersonic flows
[AIAA PAPER 92-2724] p 803 A92-45561
Visualization of stopping flow over airfoils
[AIAA PAPER 92-2730] p 804 A92-45564
Exploratory investigation of a spanwise blowing concept for tip-stall control on cranked-arrow wings
[AIAA PAPER 92-2637] p 806 A92-45576
Quantification of canard and wing interactions using spatial correlation velocimetry
[AIAA PAPER 92-2687] p 807 A92-45588
Streamlines, vorticity lines, and vortices around three-dimensional bodies p 808 A92-45845
Experimental study of vortex flows over delta wings in wing-rock motion p 810 A92-46787
Pitch rate/sideslip effects on leading-edge extension vortices of an F/A-18 aircraft model
p 874 A92-46810
Joint computational/experimental aerodynamics research on a hypersonic vehicle. I - Experimental results p 812 A92-46890
Flow visualisation of a small diameter rotor operating at high rotational speeds with blades at small pitch angles p 814 A92-46949
New concepts for multi-block grid generation for flow domains around complex aerodynamic configurations
p 817 A92-47079
Full field flow visualization and computer-aided velocity measurements in a bank of cylinders in a wind tunnel
p 991 A92-50040
Effects of a leading-edge fillet on the flow past an appendage-body junction p 935 A92-50301
Experimental and numerical investigation of a supersonic free jet impinging on a perpendicular surface
p 1018 A92-53555
Experimental investigation of an ejector-powered free-jet facility
[AIAA PAPER 92-3569] p 1090 A92-54058
Supersonic flow mixing and combustion using RAMP nozzle
[AIAA PAPER 92-3840] p 1113 A92-54198
A new look at surface flow visualization to provide insight into complex fluid dynamic behavior
p 1090 A92-54307
Rayleigh imaging and flow tagging in ground test facilities p 1115 A92-54330
BGK1 airfoil oilflow tests in the NAL two-dimensional wind tunnel. II p 1029 A92-56044
Holographic and PLIF measurements of free-flight hypervelocity flows in the AEDC Range G facility
[AIAA PAPER 92-3935] p 1122 A92-56765
Advanced nozzle and engine components test facility
[AIAA PAPER 92-3993] p 1099 A92-56816
Experimental investigation of the effects of blowing on bursting of strake vortices
[AD-A240256] p 13 N92-10985
Theoretical study (Lagrangian modeling) of turbulent particulate dispersion
[ETN-91-99909] p 42 N92-11287
Hydrodynamic flow visualization around an oscillating vane. Extension of study to the case of higher incidences and amplitudes and the starting off phase from permanent regime
[ONERA-RT-56/1369-AN] p 43 N92-11312
Nonstationary flight aerodynamics in a turbulent environment
[ETN-91-90102] p 82 N92-11980
Flow visualization and flow field measurements of a 1/12 scale tilt rotor aircraft in hover
[NASA-CR-189456] p 82 N92-11983
In-flight flow visualization and pressure measurements at low speeds on the NASA F-18 high alpha research vehicle p 85 N92-13009
Vortex formation over a close-coupled canard-wing-body configuration in unsymmetrical flow p 85 N92-13010
An experimental investigation of the effect of fineness ratio on lateral force on a pointed slender body of revolution p 86 N92-13015
Water tunnel flow visualization studies of a canard-configured X-31A-like fighter aircraft model
[AD-A241362] p 90 N92-13037
Flow over a delta wing at hypersonic speeds
p 181 N92-14993
Infrared measurements of aerodynamic heating in hypersonic wind tunnel p 208 N92-15002
Hot-wire surveys in the vortex wake downstream of a three-percent fighter aircraft model at high angles of attack
[AD-A241869] p 259 N92-15975
Flow around two circular cylinders arranged perpendicular to each other
[PB91-238279] p 297 N92-16225
Flow visualization and wake analysis for standard and modified configurations of the AN/ALQ-78 antenna pod
[AD-A243552] p 260 N92-17339
The effect of freestream turbulence on the vortical flow over a delta wing p 261 N92-17681
Results of measured temperature distribution on an adiabatic wing model with radiation thermometer
[NAL-TM-610] p 261 N92-17755
Analysis of unsteady force, pressure, and flow-visualization data for a pitching straked wing model at high angles of attack p 364 N92-18784
Wind tunnel force measurements and visualization on a 60-deg delta wing in oscillation, stepwise motion, and gusts p 364 N92-18786
Scale model measurements of fin buffet due to vortex bursting on F/A-18 p 365 N92-18788

A user's guide to the Langley 16- by 24-inch water tunnel
[NASA-TM-104200] p 385 N92-18956
Studies of gas turbine heat transfer: Airfoil surfaces and end-wall cooling effects
[AD-A244055] p 376 N92-19097
Study of optical techniques for the Ames unitary wind tunnels. Part 1: Schlieren
[NASA-CR-189951] p 385 N92-19218
WP 4b compressible flow simulation: Information System for flow simulation based on the Navier-Stokes equation (ISNaS). Requirements grid generation for the ISNaS compressible flow solver
[NLR-TR-88103-U] p 405 N92-19490
Calculations of hot gas ingestion for a STOVL aircraft model
[NASA-TM-105437] p 350 N92-19993
Holographic flow visualization in rotating turbomachinery
[PNR-90837] p 500 N92-20491
Flow studies in close-coupled ventral nozzles for STOVL aircraft
[NASA-TM-102554] p 445 N92-20934
Multi-colored layers for visualizing aerodynamic flow effects
[NASA-CASE-LAR-13742-1] p 447 N92-21588
Three-dimensional simulations of hypersonic flows
[MBB-UK-0155-89-PUB] p 447 N92-21703
Contributions of MBB-FE211 to the 2nd Antibes Workshop on Hypersonic Flows
[MBB-FE211-S-PUB-449] p 524 N92-22179
Study of optical techniques for the Ames unitary wind tunnels. Part 2: Light sheet and vapor screen
[NASA-CR-190217] p 573 N92-22195
Wind-tunnel investigation of aerodynamic and stability characteristics of a forward swept wing X-29 model
p 627 N92-24862
Flow visualization using computer animation
p 629 N92-24870
Visualisation in water of vortex flow over sharp-edged canard configurations
[ARL-FLIGHT-MECH-R-189] p 632 N92-25410
A low-speed wind tunnel study of vortex interaction control techniques on a chine-forebody/delta-wing configuration
[NASA-CR-189616] p 632 N92-25510
An experimental investigation of the surface flow and wake dynamics associated with transverse flow over wavy cylinders p 681 N92-25547
Helium bubble flow visualization of the spanwise separation on a NACA 0012 with simulated glaze ice
[NASA-TM-105742] p 714 N92-26612
Observation and measurements of flow structures in the stagnation region of a wing-body junction
p 714 N92-26616
Computation and visualization of specific flow phenomena in turbomachinery application
p 741 N92-27463
An integrated CFD system for 3D turbomachinery applications p 741 N92-27464
Visualization of boundary-layer development on turbomachine blades with liquid crystals
[NASA-CR-190433] p 742 N92-27519
Special Course on Unstructured Grid Methods for Advection Dominated Flows
[AGARD-R-787] p 771 N92-27671
Flow visualization studies of a sideslipping, canard-configured X-31A-Like fighter aircraft model
[AD-A245940] p 829 N92-28883
An experimental study of the relationship between velocity and pressure fluctuations in a wing-body junction
[AD-A249628] p 946 N92-31122
In-flight leading-edge extension vortex flow-field survey measurements on a F-18 aircraft at high angle of attack
[NASA-TM-4398] p 947 N92-31276
Active control of the separation region on a two-dimensional airfoil
[AD-A249739] p 948 N92-31622
Vortex flow visualization using colored and fluorescent dyes on flat plate delta wing with leading edge extension
[AD-A251139] p 1036 N92-32651
An experimental study of the flow over a sharp-edged delta wing at subsonic and transonic speeds
[NLR-TP-91117-U] p 1037 N92-32732
Static and dynamic flow visualization studies of two double-delta wing models at high angles of attack
[AD-A252878] p 1040 N92-33678

FLOWMETERS
Crossed beam correlation modeling and experimental techniques for measuring density fluctuations in hypersonic flows
[AIAA PAPER 92-2779] p 758 A92-41323
Instantaneous visualization of surface flows
p 763 A92-44327
Processing of axisymmetric flow interferograms with density profile bends or discontinuities
p 993 A92-51316
High accuracy fuel flowmeter. Phase 2C and 3: The mass flowrate calibration of high accuracy fuel flowmeters
[NASA-CR-187108] p 406 N92-19775

FLUID BOUNDARIES
Extrapolation procedures for the time-dependent Navier-Stokes equations p 704 A92-41289

FLUID DYNAMICS
Three-dimensional adaptive grid generation with applications in nonlinear fluid dynamics
[AIAA PAPER 92-0661] p 397 A92-27032
Numerical investigation of vortex breakdown on a delta wing p 340 A92-28027
Computational mechanics today p 399 A92-28464
The Second Goldstein Lecture: Modern developments in fluid dynamics - An addendum p 442 A92-32323
Image processing in the undergraduate fluid dynamics laboratory
[AIAA PAPER 92-4020] p 1141 A92-56842
Technical evaluation report, AGARD Fluid Dynamics Panel Symposium on Effects of Adverse Weather on Aerodynamics
[NASA-TM-105192] p 2 N92-10002
Asymmetric vortex flow over circular cones
p 86 N92-13014
Physics of vortical flow p 86 N92-13016
Breaking down the delta wing vortex: The role of vorticity in the breakdown process p 86 N92-13017
Investigation of vortex breakdown on a delta wing using Euler and Navier-Stokes equations p 87 N92-13019
Effects of inlet distortion on the development of secondary flows in a subsonic axial inlet compressor rotor p 89 N92-13030
Unsteady flows in rotor-stator cascades
[AD-A241593] p 158 N92-13410
An inverse method with regularity condition for transonic airfoil design p 177 N92-13969
Analytical/numerical matching and periodic inversion: Two advances in free wake analysis
p 178 N92-13994
Redesign of flight space shuttle main engine nozzle G-15 seal area based on the thermal analysis and flow models p 212 N92-15877
Flow around two circular cylinders arranged perpendicular to each other
[PB91-238279] p 297 N92-16225
Analysis of Euler's and stress tensor methods for calculating power consumption of high speed centrifugal fans and turbocompressors
[DE92-728396] p 298 N92-16325
A weakly nonlinear theory for wave-vortex interactions in curved channel flow
[NASA-TP-3158] p 347 N92-19175
An inviscid stability analysis of unbounded supersonic mixing layer flows p 443 N92-20332
JPRS report: Science and technology. Central Eurasia: Engineering and equipment
[JPRS-UEQ-92-002] p 592 N92-22298
Panel methods for aerodynamic analysis and design
p 552 N92-23955
An experimental investigation of the surface flow and wake dynamics associated with transverse flow over wavy cylinders p 681 N92-25547
Experimental methods to determine heat exchanger performances p 682 N92-25667
Special Course on Skin Friction Drag Reduction
[AGARD-R-786] p 717 N92-27706
Validation of three-dimensional incompressible spatial direct numerical simulation code: A comparison with linear stability and parabolic stability equation theories for boundary-layer transition on a flat plate
[NASA-TP-3205] p 943 N92-30295
High speed transition prediction
[NASA-CR-190836] p 1039 N92-33424

FLUID FILLED SHELLS
Acoustic scattering by a disk or annulus linking two concentric cylindrical shells. I - Theory and results for heavy exterior fluid loading. II - Results for heavy exterior fluid loading on both shells p 696 A92-40588

FLUID FILMS
Development of film riding face seals for a gas turbine engine p 291 A92-21330
Interfacial instability between a liquid film and the surrounding compressible gas
[AIAA PAPER 92-0461] p 395 A92-26302
Flow of a viscous twisted fluid film on the surface of a blunt body in supersonic flow of a gas
p 424 A92-30146
A study of flow of a fluid film on the surface of a plate in the case of slot injection p 496 A92-31892
Seal development activities at Allison Turbine Division
p 228 N92-15093
The measurement of water film thickness on airfoils in heavy rain conditions using conductance sensors
p 452 N92-21695

FLUID FILTERS
Filter debris analysis: A concrete approach to wear diagnosis
[DREP-TM-88-20] p 222 N92-14345

FLUID FLOW
Self-induced flow in a stepped rotating tube
[ASME PAPER 91-GT-276] p 152 A92-15673
Reflection type skin friction meter
[NASA-CASE-LAR-14520-1-SB] p 11 N92-10008
Steady flow of a fluid-solid mixture in a circular cylinder
[DE91-018698] p 41 N92-10174
Industrial code development p 227 N92-15083
Development of a CFD code for analysis of fluid dynamic forces in seals p 228 N92-15084
Redesign of flight space shuttle main engine nozzle G-15 seal area based on the thermal analysis and flow models p 212 N92-15877
Engine panel seals for hypersonic engine applications: High temperature leakage assessments and flow modelling
[NASA-TM-105260] p 298 N92-16336
Studies of gas turbine heat transfer: Airfoil surfaces and *end-wall cooling effects*
[AD-A244055] p 376 N92-19097
Multi-colored layers for visualizing aerodynamic flow effects
[NASA-CASE-LAR-13742-1] p 447 N92-21588
Aerodynamic effects of de/anti-icing fluids and description of a facility and test technique for their assessment p 452 N92-21697
Inlets, ducts, and nozzles p 593 N92-22523
Methodology for sensitivity analysis, approximate analysis, and design optimization in CFD for multidisciplinary applications --- computational fluid dynamics
[NASA-CR-190201] p 595 N92-22662
Flow visualization using computer animation
p 629 N92-24870
An experimental investigation of the surface flow and wake dynamics associated with transverse flow over wavy cylinders p 681 N92-25547
Computation and visualization of specific flow phenomena in turbomachinery application
p 741 N92-27463
Progress in unstructured-grid methods development for unsteady aerodynamic applications
[NASA-TM-107643] p 944 N92-30393
Numerical calculations of two-dimensional single and multi-material flow fields with CCICE
[DE92-015778] p 1000 N92-30903
CFD methods development considerations for unsteady aerodynamic analysis
[NASA-TM-107644] p 947 N92-31239

FLUID INJECTION
Numerical simulation of slot injection into a turbulent supersonic stream
[AIAA PAPER 92-0827] p 421 A92-29595
A study of flow of a fluid film on the surface of a plate in the case of slot injection p 496 A92-31892
Structure and penetration of a transverse fluid jet injected at supercritical pressure in supersonic flow
[AIAA PAPER 92-3652] p 1113 A92-54105
Numerical simulation of slot injection into a turbulent supersonic stream p 1024 A92-54914

FLUID JETS
CFD analysis of jet mixing in low NO(x) flametube combustors
[ASME PAPER 91-GT-217] p 124 A92-15634
Supersonic jet mixing enhancement by 'delta-tabs'
[AIAA PAPER 92-3548] p 826 A92-49063
Supersonic jet mixing enhancement by delta-tabs
[NASA-TM-105664] p 630 N92-24958
Near-injector structure of non-evaporating pressure-atomized sprays at various ambient densities
p 681 N92-25571

FLUID MECHANICS
Evaluation of an adaptive unstructured remeshing technique for integrated fluid-thermal-structural analysis
p 37 A92-10445
Unique high-alpha roll dynamics of a sharp-edged 65 deg delta wing
[AIAA PAPER 92-0276] p 318 A92-25730
Research on aircraft engines p 558 A92-35912
On the mechanics of 3-D turbulent boundary layers
p 620 A92-40068
Biennial Fluid Dynamics Symposium on Advanced Problems and Methods in Fluid Mechanics, 19th, Kozubnik, Poland, Sept. 3-8, 1989, Selected Papers
p 761 A92-42529
Flow induction by pressure forces
[AIAA PAPER 92-3571] p 1067 A92-54060

Institute for experimental fluid mechanics: Results for 1990
[IB-222-90-A-46] p 400 N92-18244
Development of an integrated BEM approach for hot fluid structure interaction: BEST-FSI: Boundary Element Solution Technique for Fluid Structure Interaction
[NASA-CR-189202] p 574 N92-22211
The future challenge for aeropropulsion
[NASA-TM-105613] p 658 N92-25164
Development of a quiet supersonic wind tunnel with a cryogenic adaptive nozzle
[NASA-CR-188055] p 751 N92-27976
Axisymmetric bluff-body flow: A vortex solver for thin shells
[DE92-016748] p 1003 N92-31933
Active control of compressor surge and stall
[AD-A252771] p 1126 N92-33498

FLUID POWER
Fluid power distribution and control
p 292 A92-21733
Fluid power conversion p 357 A92-25372
Nonflammable hydraulic power system for tactical aircraft. Volume 2: Equipment and systems test and evaluation
[AD-A239805] p 35 N92-10100

FLUID-SOLID INTERACTIONS
Self-oscillatory interaction of an underexpanded jet with an obstacle in the presence of a supersonic wake
p 79 A92-16681
Feedback mechanism of self-oscillations in the case of an underexpanded supersonic jet impinging on a plane obstacle p 79 A92-16682
An interactive boundary-layer approach to multielement airfoils at high lift
[AIAA PAPER 92-0404] p 324 A92-26257
The problem of body motion in a medium with resistance p 604 A92-36416
Experimental investigation of supersonic flow over two cavities in tandem p 610 A92-36830
Numerical predictions of transonic viscous flows around aerofoils through an Euler/boundary layer interaction method p 624 A92-40600
A mathematical model for the hydroelasticity problem concerning the motion of two flexible profiles in an ideal incompressible fluid. I p 712 A92-44127
Ritz vectors synthesis versus modal synthesis for fluid-structure interaction modeling p 898 A92-45885
Method of large particles in arbitrary curvilinear orthogonal coordinates for the solution of problems of hydro and aerodynamics p 937 A92-52035
The interaction between a high-frequency gust and a blade row p 1135 A92-54484
Development of an integrated BEM approach for hot fluid structure interaction: BEST-FSI: Boundary Element Solution Technique for Fluid Structure Interaction
[NASA-CR-189202] p 574 N92-22211
The Utilization of Advanced Composites in Military Aircraft
[AGARD-R-785] p 1109 N92-33033
Jet fuel absorption and dynamic mechanical analysis of carbon fibre composites p 1110 N92-33050

FLUTTER
On-line adaptive control of unstable aircraft wing flutter p 27 A92-11374
Alleviation of whirl-flutter on tilt-rotor aircraft using active controls p 133 A92-14423
Comparison of theory and experiment for nonlinear flutter and stall response of a helicopter blade
p 65 A92-14428
Optical measurements of unducted fan flutter
[ASME PAPER 91-GT-19] p 147 A92-15510
The effect of steady aerodynamic loading on the flutter stability of turbomachinery blading
[ASME PAPER 91-GT-130] p 71 A92-15574
A parametric study of the aeroelastic stability of a binary wing-with-engine nacelle flutter system in incompressible flow p 270 A92-22472
Concerning a basic assumption for aeroelasticity in turbomachinery p 373 A92-26920
Chaotic and nonlinear dynamic response of aerosurfaces with structural nonlinearities
[AIAA PAPER 92-2547] p 518 A92-34517
Trends of research on cascade flutter
p 558 A92-35914
A numerical study of control surface buzz using computational fluid dynamic methods
[AIAA PAPER 92-2654] p 806 A92-45578
Experimental investigation on flutter characteristics of composite torsion-box p 996 A92-53055
Numerical simulations of flutter and its suppression by active control
[AIAA PAPER 92-4652] p 1082 A92-55396
An analytical and experimental study to investigate flutter suppression via piezoelectric actuation
[NASA-TM-893240] p 156 N92-12173
The benchmark aeroelastic models program: Description and highlights of initial results
[NASA-TM-104180] p 185 N92-15049
Response of structures to galloping excitation: Background and approximate estimation
[ESDU-91010] p 399 N92-18091
Model parameter identification techniques for flight flutter testing
[AERO-REPT-9105] p 380 N92-18294
NACA0012 benchmark model experimental flutter results with unsteady pressure distributions
[NASA-TM-107581] p 526 N92-22507
Determining structural performance
p 560 N92-22519
Transonic Unsteady Aerodynamics and Aeroelasticity
[AGARD-CP-507] p 718 N92-27936
A time-linearization approach for unsteady transonic flows p 719 N92-27941
Aeroelastic calculations for fighter aircraft using the transonic small disturbance equation
p 720 N92-27951
Computation of flutter boundaries in the time and frequency domain p 720 N92-27952
Analysis of unsteady aerodynamic and flutter characteristics of an aeroelastic model in transonic flow
p 720 N92-27953
Direct coupling of fluid structure in transonic aeroelasticity p 721 N92-27954
Investigation of the aeroelastic stability of the AFW wind-tunnel model using CAP-TSD p 721 N92-27955
Numerical simulation of shock-stall flutter of an airfoil using the Navier-Stokes equations p 746 N92-27956
The benchmark aeroelastic models program: Description and highlights of initial results
p 721 N92-27960
A gust generation method for full configuration aircraft tests in a low speed wind tunnel. Part 1: Design and preliminary experiments
[NAL-TR-1115-PT-1] p 722 N92-28192
Buffet test in the National Transonic Facility
[NASA-CR-189595] p 888 N92-29352
CFD methods development considerations for unsteady aerodynamic analysis
[NASA-TM-107644] p 947 N92-31239
Design and experimental validation of a flutter suppression controller for the active flexible wing
[NASA-TM-4381] p 979 N92-31240
Flutter suppression digital control law design and testing for the AFW wind-tunnel model
[NASA-TM-107652] p 962 N92-31350
Time simulation of flutter with large stiffness changes
[NASA-TM-107650] p 963 N92-32111
The multiple-function multi-input/multi-output digital controller system for the AFW wind-tunnel model
[NASA-TM-107600] p 1060 N92-32536
Introduction to Flutter of Winged Aircraft, volume 2
[VKI-LS-1992-01-VOL-2] p 1088 N92-34161
Flight flutter testing p 1089 N92-34163
Flutter models: Their design, manufacture, and ground testing p 1089 N92-34164
Flutter in the transonic flight regime
p 1089 N92-34167
Flutter analyses using high speed computers. Part 1: Flutter analyses for large aircraft p 1089 N92-34168
Flutter analyses using high speed computers. Part 2: Aerodynamic procedures p 1089 N92-34169

FLUTTER ANALYSIS
Aeroelastic stability analysis of aerial propellers
p 24 A92-10955
Aeroelastic analysis of wings using the Euler equations with a deforming mesh p 10 A92-13215
Aeroelastic tailoring of aeronautical composite wing structures p 146 A92-15343
Computational study of stall flutter in linear cascades
[ASME PAPER 91-GT-5] p 67 A92-15503
Cascade flutter analysis with transient response aerodynamics p 154 A92-15972
Resonance prediction for slotted circular wind tunnel using finite element p 235 A92-18388
Flutter analysis of anisotropic panels with patched cracks p 219 A92-20216
Nonlinear stall flutter and divergence analysis of cantilevered graphite/epoxy wings p 219 A92-20746
Time domain flutter analysis of cascades using a full-potential solver p 176 A92-20747
Transonic aeroelasticity analysis using state-space unsteady aerodynamic modeling p 310 A92-24422
Open-loop model reduction and parameter perturbation for active flutter suppression system
p 379 A92-24879
The measurement of flutter derivatives using mechanical admittance p 393 A92-25014
A study of active flutter suppression for a wing/store system p 379 A92-27826
A numerical method for analyzing the nonlinear flutter of wings at high angles of attack p 338 A92-27827
Aeroelastic analysis of advanced propellers using an efficient Euler solver
[AIAA PAPER 92-0488] p 341 A92-28194
The mean power of forces and moments in unsteady aerodynamics p 421 A92-28949
Problems of strength and aeroelasticity of present-day propfans p 471 A92-30133
Low-speed flutter characteristics of some simple low-aspect-ratio delta-wing models p 460 A92-32247
Experimental and theoretical study for nonlinear aeroelastic behavior of a flexible rotor blade
[AIAA PAPER 92-2253] p 584 A92-34410
Time simulation of flutter with large stiffness changes
[AIAA PAPER 92-2394] p 585 A92-34467
Aeroelasticity - Advances and future directions
[AIAA PAPER 92-2446] p 585 A92-34475
Analysis of cascades using a two dimensional Euler aeroelastic solver
[AIAA PAPER 92-2370] p 556 A92-34598
Flutter suppression for the Active Flexible Wing - Control system design and experimental validation
[AIAA PAPER 92-2097] p 566 A92-35666
Flutter suppression digital control law design and testing for the AFW wind tunnel model
[AIAA PAPER 92-2095] p 566 A92-35668
Development and analysis of flight flutter prediction methods
[AIAA PAPER 92-2101] p 588 A92-35672
An experimental and analytical investigation of wing flutter on a trail rotor V/STOL aircraft
[AIAA PAPER 92-2112] p 544 A92-35682
A numerical classical flutter analysis of advanced propellers
[AIAA PAPER 92-2118] p 557 A92-35687
An investigation of cascade flutter using a two-dimensional full-potential solver
[AIAA PAPER 92-2119] p 558 A92-35688
Limit cycle oscillation and flight flutter testing
p 570 A92-35939
Comparison of two flutter analysis methods for elastic aircraft p 660 A92-37394
Aeroservoelasticity p 642 A92-37577
Modern aerodynamic flutter analysis --- Book
p 676 A92-40898
Coalescence of aeroelastic modes in flutter analysis
p 758 A92-41241
Structural and aerodynamic data transformation using inverse isoparametric mapping p 758 A92-41242
Transition of the flutter mode of a two-dimensional section with an external store p 758 A92-41244
Step response of incompressible unsteady aerodynamic modeling p 744 A92-43131
Response characteristics of a wing in supersonic flow near flutter boundary
[SAE PAPER 911999] p 789 A92-45401
Preliminary study of algorithm for real-time flutter monitoring
[SAE PAPER 912001] p 897 A92-45403
Whirl-flutter stability of a pusher configuration in nonuniform flow p 845 A92-46813
FREPS - A forced response prediction system for turbomachinery blade rows
[AIAA PAPER 92-3072] p 1130 A92-54006
E-6 flutter investigation and experience
[AIAA PAPER 92-4601] p 1077 A92-55280
Flutter analysis and wind tunnel test with respect to a low-aspect-ratio wing with free-rotational control surface
p 1052 A92-56014
An example of whirl flutter analysis
p 1052 A92-56015
Propeller-nacelle whirl flutter analysis and wind tunnel test p 1052 A92-56016
Whirl flutter analysis and application to aircraft design
p 1053 A92-56017
Research on aeroelastic tailoring at NAL
p 1053 A92-56019
Synthesis of gust load alleviation with flutter margin augmentation p 1082 A92-56021
Multidisciplinary optimization of aeroservoelastic systems using reduced-size models
p 1054 A92-56176
Flutter and stall response of a helicopter blade with structural nonlinearity p 1055 A92-56178
Helicopter tail rotor stall flutter p 1056 A92-56290
Aeroelasticity of a coaxial helicopter rotor
p 1057 A92-56309
Transverse shear effect on flutter of composite panels
p 1122 A92-56607
Investigation of the aeroelastic stability of the AFW wind-tunnel model using CAP-TSD
[NASA-TM-104142] p 81 N92-11977
Planform curvature effects on flutter characteristics of a wing with 56 deg leading-edge sweep and panel aspect ratio of 1.14
[NASA-TP-3116] p 115 N92-13054

Flutter suppression via piezoelectric actuation
[NASA-TM-104120] p 197 N92-15070
Model parameter identification techniques for flight flutter testing
[AERO-REPT-9105] p 380 N92-18294
Semi-empirical model for prediction of unsteady forces on an airfoil with application to flutter
[NASA-TM-105414] p 346 N92-18760
Investigation of a semi-empirical method to predict limit cycle oscillations of modern fighter aircraft
[NLR-TP-90087-U] p 481 N92-20475
Current status of computational methods for transonic unsteady aerodynamics and aeroelastic applications
[NASA-TM-104191] p 446 N92-21432
Further investigations of the aeroelastic behavior of the AFW wind-tunnel model using transonic small disturbance theory
[NASA-TM-107576] p 526 N92-22240
Sensitivity analysis of dynamic aeroelastic responses p 571 N92-23229
Multidisciplinary optimization studies using ASTROS p 571 N92-23234
Simultaneous stress and flutter optimization for the wing of a transport aircraft equipped with four engines p 571 N92-23238
Nonliner aspects of transonic aeroelasticity p 628 N92-24864
Prediction and analysis of wing flutter at transonic speeds p 662 N92-25555
A time-linearization approach for unsteady transonic flows p 719 N92-27941
Transonic aeroelastic calculations in both the time and frequency domains p 720 N92-27950
Analysis of unsteady aerodynamic and flutter characteristics of an aeroelastic model in transonic flow p 720 N92-27953
Investigation of the aeroelastic stability of the AFW wind-tunnel model using CAP-TSD p 721 N92-27955
Influence of structural and aerodynamic modeling on flutter analysis and structural optimization
[AD-A248487] p 978 N92-30323
On-line analysis capabilities developed to support the AFW wind-tunnel tests
[NASA-TM-107651] p 961 N92-30752
An analytical and experimental investigation of flutter suppression via piezoelectric actuation
[NASA-TM-107653] p 962 N92-31174
Flutter suppression digital control law design and testing for the AFW wind-tunnel model
[NASA-TM-107652] p 962 N92-31350
Pressure measurements on a rectangular wing with a NACA0012 airfoil during conventional flutter
[NASA-TM-104211] p 1042 N92-34147
Introduction to Flutter of Winged Aircraft, volume 2
[VKI-LS-1992-01-VOL-2] p 1088 N92-34161
Elementary flutter analysis p 1088 N92-34162
Flight flutter testing p 1089 N92-34163
Flutter models: Their design, manufacture, and ground testing p 1089 N92-34164
Unsteady wind tunnel tests p 1089 N92-34166
Flutter in the transonic flight regime p 1089 N92-34167
Flutter analyses using high speed computers. Part 1: Flutter analyses for large aircraft p 1089 N92-34168
Flutter analyses using high speed computers. Part 2: Aerodynamic procedures p 1089 N92-34169

FLUX (RATE)
Prototype instrumentation and design studies
[AD-A248378] p 736 N92-28004

FLUX VECTOR SPLITTING
Implicit flux-split Euler schemes for unsteady aerodynamic analysis involving unstructured dynamic meshes p 5 A92-11057
Genuinely upwind algorithms for the multidimensional Euler equations p 175 A92-20733
Euler calculations of axisymmetric under-expanded jets by an adaptive-refinement method
[AIAA PAPER 92-0321] p 321 A92-25768
Transient behavior of supersonic flow through inlets p 340 A92-28043
Flux-difference split algorithm for unsteady thin-layer Navier-Stokes solutions p 431 A92-31158
Implicit solutions of three-dimensional viscous hypersonic flows p 434 A92-31549
An improved PNS scheme for predicting complex three-dimensional hypersonic flows
[AIAA PAPER 92-0753] p 436 A92-31679
Newton's method solver for the axisymmetric Navier-Stokes equations p 703 A92-41269
Upwind schemes for Navier-Stokes computations at subsonic through hypersonic speeds p 708 A92-43071
A nonlinear relaxation/quasi-Newton algorithm for the compressible Navier-Stokes equations
[AIAA PAPER 92-2643] p 796 A92-45510
LU-SGS implicit scheme for entry vehicle flow computation and comparison with aerodynamic data
[AIAA PAPER 92-2671] p 798 A92-45526
Comparison of two flux splitting schemes for calculation of ogive-cylinder at M = 3.5 and alpha = 18 deg
[AIAA PAPER 92-2667] p 806 A92-45582
Effect of the grid system on heat transfer computations for high speed flows p 900 A92-47071
The simulation of inviscid, compressible flows using an upwind kinetic method on unstructured grids p 933 A92-49515
Transonic flow calculation of Euler equations by implicit iterating scheme with flux splitting p 934 A92-50215
Three-dimensional multigrid algorithm for the Euler and the thin-layer Navier-Stokes equations
[PB92-134329] p 602 N92-22216
Development of a new flux splitting scheme p 596 N92-23352
Development of new flux splitting schemes --- computational fluid dynamics algorithms p 682 N92-25809
An examination of several high resolution schemes applied to complex problems in high speed flows
[AD-A250814] p 1124 N92-32632

FLY BY WIRE CONTROL
First flight for Airbus A340 p 21 A92-12750
Integrated flight/propulsion control for flight critical applications - A propulsion system perspective
[ASME PAPER 91-GT-284] p 125 A92-15679
V-22 flight test p 112 A92-16056
F-117A flight test program p 112 A92-16061
Delivered with feeling --- computer-based design of flight control system for Boeing 777 p 134 A92-16621
Feeling normal --- evaluation of advanced control systems for future Boeing 777 p 134 A92-16623
High-performance fighter fly-by-wire flight control actuation system --- for YF-23A prototype
[AIAA PAPER 92-1123] p 563 A92-33277
Preliminary evaluation of new control laws on the experimental fly-by-wire Dauphin helicopter p 568 A92-35756
Aeroservoelasticity p 642 A92-37577
On upsets of analog portions of digital flight control systems due to electromagnetic interference
[SAE PAPER 912144] p 651 A92-39982
Simple fly-by-wire actuator p 876 A92-48491
C-141 and C-130 power-by-wire flight control systems p 876 A92-48493
Electric actuation system duty cycles --- in fly-by-wire/power-by-wire control p 877 A92-48494
Making fly-by-light a reality p 877 A92-48499
Testing and analysis of a 'smart' interface to connect two complex avionics bus systems without significant modification to the software of either system p 964 A92-49254
A low maintenance and highly reliable fly-by-light architecture p 975 A92-49325
Automatic production test equipment (APTE) for the B-2 p 997 A92-53107
A simulator evaluation of various manual control concepts for fly-by-wire transport aircraft
[AIAA PAPER 92-4328] p 1073 A92-55172
A320 flight control from the pilot's point of view p 1083 A92-56028
Piloted simulation for the BK117 FBW demonstrator p 1053 A92-56077
HEPO mission simulator - Development and usage for NH90 helicopter p 1094 A92-56313
Some interesting phenomena from Lavi test flights relating to aircraft stability and control
[IAITIC-91-1017] p 482 N92-20849
Results of a flight simulator experiment to establish handling quality guidelines for the design of future transport aircraft
[NLR-MP-88044-U] p 854 N92-29616
FCS skewed sensors array: Practical considerations p 968 N92-31868

FLYING PERSONNEL
Full model simulation of the National Airspace System - Research and training platform p 880 A92-45042
Test plan for the international aircraft operator information system
[DOT/FAA/CT-91/18] p 781 N92-26830

FLYING PLATFORMS
Stratospheric lighter-than-air powered platform p 110 A92-15334
AI for RPVs, Sensor Driven Airborne Replanner (SDAR), for a Robotic Aircraft Sensor Platform (RASP) p 114 N92-12534

FLYWHEELS
Active magnetic bearings give systems a lift p 901 A92-48201

FOAMS
Fire-fighting foams must meet newly-developed ICAO standard p 448 A92-29508

FOG
Helicopter fog flying trials p 530 A92-35759
Trial of a slant visual range measuring device p 1000 N92-31043

FOG DISPERSAL
Modeling the effect of helicopter downwash on warm fog p 775 A92-44081
Use of the TMS-65 heating equipment at airports to create fog-dispersal zones above the runway to facilitate takeoff p 775 A92-44084

FOKKER AIRCRAFT
Fokker 50 flameouts in icing conditions p 548 A92-35940
The effect of hoar-frosted wings on the Fokker 50 take-off characteristics p 451 N92-21692
Active synchrophasing of propeller unbalance p 1138 N92-32963
Activities report of the National Aerospace Laboratory
[ETN-92-92053] p 1143 N92-33694

FOLDING STRUCTURES
Nonlinear landing gear behavior at touchdown p 192 A92-19606

FOOTPRINTS
On the footprints of three-dimensional separated vortex flows around blunt bodies: Attempts of defining and analyzing complex flow structures p 84 N92-13005

FORCE DISTRIBUTION
Force measurement on rotating, ablating models using an air bearing balance p 483 A92-31174
An experimental analysis of lateral jet injection into confined swirling crossflows p 156 N92-12199
A study in dynamic control of a super maneuver with neural networks p 463 N92-21510
Force limited vibration testing p 595 N92-22688
Normal force of low aspect ratio wing-body combinations up to high angles of attack at supersonic speeds
[ESDU-91042] p 553 N92-24009
Unsteady transonic aerodynamics of pointed bodies of revolution in supersonic freestream p 719 N92-27946
Force measurements on AGARD calibration model-B at transonic speeds in the NAL two-dimensional wind tunnel
[NAL-TM-639] p 722 N92-28190

FORCED CONVECTION
Heat transfer in the entrance region of semicircular ducts with internal fins p 497 A92-32264
Numerical simulation of droplet deformation in convective flows p 670 A92-36844

FORCED VIBRATION
Euler flow predictions for an oscillating cascade using a high resolution wave-split scheme
[ASME PAPER 91-GT-198] p 74 A92-15623
Recent advancements in turbomachinery forced response analyses
[AIAA PAPER 92-0012] p 278 A92-22136
Forced vibration of rectangular laminated plates with material damping p 294 A92-23167
Experimental and theoretical study for nonlinear aeroelastic behavior of a flexible rotor blade
[AIAA PAPER 92-2253] p 584 A92-34410
Calculation of fuel sloshing and its coupling vibration with a tank p 991 A92-50204
The influences of forced oscillations toward vortex-breakdown p 934 A92-50210
Fourier functional analysis for unsteady aerodynamic modeling p 935 A92-50313
Vibration tests of long plate structural model
[NAL-TM-625] p 400 N92-18485
Identification of aerodynamic models for maneuvering aircraft
[NASA-CR-190039] p 348 N92-19359
Prediction of response of aircraft panels subjected to acoustic and thermal loads
[NASA-CR-190305] p 678 N92-24345

FOREBODIES
An experimental study of pneumatic vortex flow control on high angle of attack forebody model
[AIAA PAPER 92-0018] p 247 A92-22140
Forebody vortex flow control on the F-16C using tangential slot and jet nozzle blowing
[AIAA PAPER 92-0019] p 247 A92-22141
Computational investigation of slot blowing for fuselage forebody flow control
[AIAA PAPER 92-0020] p 248 A92-22142
Aircraft control at high-alpha by tangential blowing
[AIAA PAPER 92-0021] p 281 A92-22143
A computational study on directional stability of chine-shaped forebodies at high-alpha
[AIAA PAPER 92-0030] p 249 A92-22152
Forebody vortex control p 251 A92-22517
Measurements of lateral aerodynamics characteristics of forebodies at high angle of attack in subsonic and transonic flows
[AIAA PAPER 92-0174] p 255 A92-23785
Approach to side force alleviation through modification of the pointed forebody geometry p 309 A92-24418

Solution of Euler equations for fighter forebody-inlet combinations at high angles of attack
p 613 A92-38269
Prediction of vortex shedding from forebodies with chines p 702 A92-41228
Prediction of shock pattern dynamics at hypersonic angle of attack maneuvers of endo-KEW missile forebodies
[AIAA PAPER 92-2768] p 704 A92-41317
The effects of nozzle exit geometry on forebody vortex control using blowing
[AIAA PAPER 92-2603] p 792 A92-45480
Analysis of a pneumatic forebody flow control concept about a full aircraft geometry
[AIAA PAPER 92-2678] p 799 A92-45530
Alleviation of side force on tangent-ogive forebodies using passive porosity
[AIAA PAPER 92-2711] p 802 A92-45552
Forebody vortex control for suppressing wing rock on a highly-swept wing configuration
[AIAA PAPER 92-2716] p 803 A92-45555
Computation of turbulent flow about cone-derived waverider
[AIAA PAPER 92-2726] p 804 A92-45562
Dynamic LEX/forebody vortex interaction effects
[AIAA PAPER 92-2732] p 804 A92-45566
Forebody flow control on a full-scale F/A-18 aircraft
[AIAA PAPER 92-2674] p 806 A92-45583
Full-scale high angle-of-attack tests of an F/A-18
[AIAA PAPER 92-2676] p 806 A92-45584
Forebody vortex control using small, rotatable strakes
p 811 A92-46798
Effect of a nose-boom on forebody vortex flow
p 812 A92-46818
Reduction of the side force on pointed forebodies through add-on tip devices p 1024 A92-54918
Vortical flow control on a wing-body combination using tangential blowing
[AIAA PAPER 92-4430] p 1081 A92-55354
Assessment of passive porosity with free and fixed separation on a tangent ogive forebody
[AIAA PAPER 92-4494] p 1081 A92-55363
Vortex control: Further encounters p 87 N92-13020
Control of forebody vortices by suction at the nose of the RAE high incidence research model
p 87 N92-13022
Wind tunnel investigation of vortex flows on F/A-18 configuration at subsonic through transonic speed
[NASA-TP-3111] p 179 N92-14968
Results of the space shuttle vehicle ascent air data system probe calibration test using a 0.07-scale external tank forebody model (68T) in the AEDC 16-foot transonic wind tunnel (IA-310), volume 1
[NASA-CR-167696] p 286 N92-17167
Results of the space shuttle vehicle ascent air data system probe calibration test using a 0.07-scale external tank forebody model (68T) in the AEDC 16-foot transonic wind tunnel (IA-310), volume 2
[NASA-CR-167697] p 286 N92-17214
Hi-alpha forebody design. Part 1: Methodology base and initial parametrics
[NASA-CR-189849] p 358 N92-18024
Hi-alpha forebody design. Part 2: Determination of body shapes for positive directional stability
[NASA-CR-189850] p 359 N92-18038
Aerodynamic control of fighter aircraft by manipulation of forebody vortices p 380 N92-18791
Forebody vortex control aeromechanics
p 380 N92-18792
Dynamic wind tunnel tests on control of forebody vortices with suction p 380 N92-18793
Simulation of real-gas effects on pressure distributions for aeroassist flight experiment vehicle and comparison with prediction
[NASA-TP-3157] p 501 N92-20677
A low-speed wind tunnel study of vortex interaction control techniques on a chine-forebody/delta-wing configuration
[NASA-CR-189616] p 632 N92-25510
High-alpha vortex decoupling investigations on a chine forebody/Delta wing configuration at transonic Mach numbers
[NASA-CR-189642] p 715 N92-26651
A computational examination of directional stability for smooth and chined forebodies at high-alpha
[NASA-CR-4465] p 950 N92-32114
Prediction and control of asymmetric vortical flows around slender bodies using Navier-Stokes equations
p 1127 N92-33968

FORECASTING
Prediction of helicopter simulator sickness
p 46 A92-11473
FAA aviation forecasts
[AD-A250412] p 837 N92-29182
Developing robust support structures for high-technology subsystems: The AH-64 Apache helicopter
[AD-A252773] p 1017 N92-33499

FORGING
Ti-6Al-4V forgings with enhanced fatigue characteristics for engine and airframe applications p 288 A92-22757

FORMAT
24-bit flight test data recording format
p 900 A92-47528
Design considerations for IAP charts: Approach course track and communication frequencies
[AD-A241482] p 103 N92-13051
Advanced Transport Operating System (ATOPS) control display unit software description
[NASA-CR-189606] p 652 N92-24689
Engine monitoring display study
[NASA-CR-4463] p 979 N92-32175

FORMATIONS
Proportional plus integral control of aircraft for automated maneuvering formation flight
[AD-A243792] p 382 N92-19505

FORMING TECHNIQUES
Cost effective solutions for titanium sheet metal forming p 293 A92-22785
Process control challenges during the manufacture of large superplastically formed/diffusion bonded structure
[SAE PAPER 912195] p 674 A92-40012
Advances in aircraft component superplastic forming/diffusion bonding technology
[SAE PAPER 912216] p 674 A92-40018
Super plastic forming technology applied to aeroengine and space equipment p 764 A92-44732
Examples of advanced near-net shape manufacturing techniques for aerospace
[MBB-Z-0399-91-PUB] p 1125 N92-32742

FOUR-WAVE MIXING
Degenerate four-wave mixing for measurement of NO2 and smoke concentration in jet engine exhaust
[AIAA PAPER 92-3658] p 1113 A92-54108

FOURIER ANALYSIS
Numerical simulations of the structure of supersonic shear layers p 3 A92-10574
Periodic trim solutions with hp-version finite elements in time p 874 A92-46931
Fourier functional analysis for unsteady aerodynamic modeling p 935 A92-50313
Identification of aerodynamic models for maneuvering aircraft
[NASA-CR-190039] p 348 N92-19359
Identification of aerodynamic models for maneuvering aircraft
[NASA-CR-190444] p 852 N92-28720

FOURIER SERIES
Design of turbomachinery blading in transonic flows by the circulation method p 311 A92-24725
Effect of viscous drag on optimum spanwise lift distribution
[AIAA PAPER 92-0287] p 319 A92-25740
Validation of three-dimensional incompressible spatial direct numerical simulation code: A comparison with linear stability and parabolic stability equation theories for boundary-layer transition on a flat plate
[NASA-TP-3205] p 943 N92-30295

FRACTALS
Using fractal dimension for target detection in clutter
p 410 A92-24423
Feature extraction from two-dimensional images using fractal analysis p 496 A92-32130
Multifractal analysis of a lobed mixer flowfield utilizing the proper orthogonal decomposition
p 611 A92-36840
Studies in chaos using stochastic methods
[AD-A246919] p 780 N92-27171
Fractal image compression of Rayleigh, Raman, LIF and LDV data in turbulent reacting flows
[AD-A246960] p 767 N92-27352

FRACTOGRAPHY
Fracture analysis on compressor blades
p 37 A92-10672
Discs low cycle fatigue life predictions for gas turbine engines in CSFR by using fractographic information
p 995 A92-51950

FRACTURE MECHANICS
Applied fracture mechanics research in the aerospace field p 37 A92-10375
Fracture analysis on compressor blades
p 37 A92-10672
Fracture behaviour of high-temperature polymer composites p 34 A92-11993
High temperature multiaxial creep testing of Nimonic 115 p 141 A92-15202
Prediction of long-term creep rupture properties for an aluminium alloy for airframe applications
p 141 A92-15206
Mechanical and fracture behaviour of Ti-6Al-2Sn-4Zr-2Mo-0.1Si alloys p 288 A92-22755
Development and design with advanced materials --- Book
[ISBN 0-444-88706-7] p 296 A92-24176
Inclusion size effect on the fatigue crack propagation mechanism and fracture mechanics of a superalloy
p 388 A92-24831
Creep fracture mechanisms in single crystal superalloys p 388 A92-25031
Simulation of arbitrary crack propagation in three-dimensions p 393 A92-25535
Processing effects and damage tolerance in poly(etheretherketone) composites p 388 A92-26152
Durability analysis using fracture mechanics for avionics integrity p 396 A92-26799
Methods for predicting successful ejection seat canopy penetration p 544 A92-35441
Research on damage tolerance of compressor blade
p 588 A92-35556
Fracture mechanics approach to creep growth in welded IN738LC gas turbine blades
[ASME PAPER 91-GT-119] p 670 A92-36893
A method to determine propagation direction of compressive fracture in carbon-fibre composites
p 672 A92-38770
Mechanics of curved fiber composites
p 757 A92-41034
Advances in fatigue lifetime predictive techniques; Proceedings of the Symposium, San Francisco, CA, Apr. 24, 1990
[ASTM STP-1122] p 896 A92-45226
Probability analysis of structure failure for the wings with main and subordinate components p 848 A92-47657
Durability analysis for a main bulkhead subjected to load on the body of an aircraft p 848 A92-47664
Solution of stress intensity factor by weight function for small surface cracks in plates p 998 A92-53332
Damage tolerant design of critical aircraft structural components
[AIAA PAPER 92-4041] p 1123 A92-56860
Critical appraisal of the McDonnell Douglas closure model for predicting fatigue crack growth
[ARL-STRUC-R-444] p 44 N92-11376
Numerical verification of NISA 2 finite element analysis of the cracked 5th stage compressor disc of J-85 jet engine
[NRC-LTR-ST-1792] p 129 N92-11997
Failure analysis of the Apache mixer pivot support
[AD-A240858] p 116 N92-13061
Verification of NISA 2 and ENDURE fracture mechanics capability
[NRC-ST-621] p 159 N92-13453
Review of investigations on aeronautical fatigue in the Federal Republic of Germany
[ETN-92-90317] p 225 N92-14397
Recent fracture mechanics results from NASA research related to the aging commercial transport fleet
p 362 N92-18589
Application of finite element methods to fracture mechanics
[PNR-90770] p 503 N92-21741
Simulation of 3D non-planar fatigue crack growth in a turbine blade root
[DE92-006859] p 739 N92-26697
Tear straps in airplane fuselage
[AD-A248543] p 854 N92-29511
Fracture mechanics research at NASA related to the aging commercial transport fleet p 913 N92-30110
Preliminary results on the fracture analysis of multi-site cracking of lap joints in aircraft skins
p 913 N92-30111

FRACTURE STRENGTH
Applied fracture mechanics research in the aerospace field p 37 A92-10375
Fracture analysis and crack propagation in pressurized fuselage structures - Experimental and numerical investigations p 217 A92-19812
Composite strengthening of Nb-Ti base alloys
p 577 A92-36380
Effects of T-tabs and large deflections in double cantilever beam specimen tests p 673 A92-39009
The hardness and toughness of HIPed silicon nitride
p 668 A92-39682
Technique for estimating the strength of gas turbine guide vanes with stress raisers p 761 A92-42653

FRACTURES (MATERIALS)
Fatigue in single crystal nickel superalloys
[AD-A243453] p 290 N92-17653

FRACTURING
Preliminary results on the fracture analysis of multi-site cracking of lap joints in aircraft skins
p 913 N92-30111

FRAGMENTS
Statistics on aircraft gas turbine engine rotor failures that occurred in US commercial aviation during 1989
[DOT/FAA/CT-92/5] p 971 N92-30303
FRAMES
Thrust test fixture
[AD-D015259] p 983 N92-31192
FRAMES (DATA PROCESSING)
Modern techniques for monitoring airborne telemetry
p 857 A92-47560
A reversed-frame normalization design of robust flight control system p 1009 A92-53382
FRANCE
Recent progress in inverse methods in France
p 201 N92-13938
FREE FALL
Prospects of turbulence research by means of testing bodies in motion p 30 A92-12194
FREE FLIGHT
Free-flight trim-angle predictions for the aeroassist flight experiment p 705 A92-41540
Hang-glider response to atmospheric inputs
p 874 A92-46765
FALKE and COBRA technology development in aerodynamics and aerothermodynamics
p 183 N92-15017
Wind-tunnel static and free-flight investigation of high-angle-of-attack stability and control characteristics of a model of the EA-6B airplane
[NASA-TP-3194] p 631 N92-25276
FREE FLOW
Effect of riblets on turbulence in the wake of an airfoil
p 5 A92-11051
Poststall airfoil response to a periodic freestream
p 10 A92-13218
Wave motions in a three-dimensional boundary layer
p 244 A92-21629
Computations of multispecies mixing between scramjet nozzle flow and hypersonic freestream
p 376 A92-28534
Analysis of effects of freestream turbulence on cascade performance p 422 A92-29716
Freestream capturing for moving coordinates in three dimensions p 432 A92-31186
Boundary-layer receptivity of sound with roughness
p 604 A92-36006
A comparison of transition Reynolds number measured in a wind tunnel and in flight p 522 A92-36026
Numerical simulation of opposing sonic jets
p 524 A92-36357
Boundary-layer receptivity due to a wall suction and control of Tollmien-Schlichting waves
p 616 A92-39333
Critical Mach number estimates for dense gases
p 933 A92-49498
Aerodynamic characteristics of a standard corrugated body in a free-molecular flow p 940 A92-52818
Measurement of the freestream density for re-entry vehicles - A design study p 940 A92-52821
Increased heat transfer to elliptical leading edges due to spanwise variations in the freestream momentum - Numerical and experimental results
[AIAA PAPER 92-3070] p 1020 A92-54005
Assessment of compressibility corrections to the k-epsilon model in high-speed shear layers
p 1024 A92-54905
An experimental study of the flow over a sharp-edged delta wing at subsonic and transonic speeds
p 85 N92-13011
High enthalpy testing in the Aachen (Fed. Republic of Germany) shock tunnel TH 2 p 208 N92-15021
Flow around two circular cylinders arranged *perpendicular to each other*
[PB91-238279] p 297 N92-16225
The effect of freestream turbulence on the vortical flow over a delta wing p 261 N92-17681
On the instability of boundary layers on heated flat plates
[NASA-CR-187581] p 347 N92-19250
Unsteady transonic aerodynamics of pointed bodies of revolution in supersonic freestream p 719 N92-27946
Swept shock/boundary layer interaction experiments in support of CFD code validation
[NASA-CR-190583] p 1036 N92-32494
An examination of several high resolution schemes applied to complex problems in high speed flows
[AD-A250814] p 1124 N92-32632
Leading-edge receptivity for blunt-nose bodies
[NASA-CR-190563] p 1036 N92-32648
Prediction and control of asymmetric vortical flows *around slender bodies using Navier-Stokes equations*
p 1127 N92-33968
FREE JETS
Development of a freejet capability for evaluating inlet-engine compatibility
[ASME PAPER 91-GT-401] p 137 A92-15731
Numerical simulation of total temperature separation in jets
[AIAA PAPER 92-0535] p 396 A92-26952
Experimental and numerical investigation of a supersonic free jet impinging on a perpendicular surface
p 1018 A92-53555
Experimental investigation of an ejector-powered free-jet facility
[AIAA PAPER 92-3569] p 1090 A92-54058
The design of a subsonic low-noise, low-turbulence wind tunnel for acoustic measurements
[AIAA PAPER 92-3883] p 1094 A92-56726
An acceptance process for the evaluation of inlet distortion
[AIAA PAPER 92-3918] p 1032 A92-56750
Development and validation of a freejet technique for inlet-engine compatibility testing
[AIAA PAPER 92-3921] p 1033 A92-56752
Rarefaction wave eliminator design study
[AD-A244401] p 484 N92-20455
FREE MOLECULAR FLOW
Effects of gas-surface interaction models on aerodynamic characteristics p 244 A92-21718
Temperature and initial curvature effects in low-density panel flutter
[AIAA PAPER 92-2128] p 589 A92-35695
Behaviour and modelling of the aerothermodynamics of *ballistic entry vehicles in the high altitude flow regimes*
p 184 N92-15031
Applicability of bridging methods to hypersonic rarefied flow aerodynamics of reentry vehicles
p 184 N92-15032
FREE RADICALS
Free-radicals aided combustion with scramjet applications
[IAF PAPER 92-0659] p 1106 A92-57100
FREE VIBRATION
Time simulation of flutter with large stiffness changes
[AIAA PAPER 92-2394] p 585 A92-34467
Free vibration analysis of branched blades by the integrating matrix method p 847 A92-47122
Estimation of aircraft inertial characteristics using maximum likelihood estimation p 1084 A92-56057
Safety provision against 'ground resonance' free vibration of a coaxial helicopter p 1056 A92-56289
Prediction of response of aircraft panels subjected to acoustic and thermal loads
[NASA-CR-190305] p 678 N92-24345
FREE WING AIRCRAFT
Direct simulation of high-speed mixing layers
[NASA-TP-3186] p 945 N92-30909
FREE-PISTON ENGINES
Lower-end dynamic characteristics of a magnetically coupled free-piston Stirling engine/compressor system
p 992 A92-50795
The G-range impulse facility - A high-performance free-piston shock tunnel
[AIAA PAPER 92-3946] p 1097 A92-56774
FREEZING
On the possibility of freezing and sticking phenomena in a transport during the ground taxiing and takeoff run and on the preventions of the hazard
[SAE PAPER 912042] p 836 A92-45426
Investigation on freezing and sticking phenomena of slush on airplane surfaces when taxiing on the ground and the succeeding take-off run phase
[NAL-TR-1026] p 352 N92-18182
FRENCH SPACE PROGRAM
French research and technology program on advanced hypersonic propulsion
[AIAA PAPER 91-5003] p 471 A92-31683
FREQUENCIES
Susceptibility of a parallelogram type skin friction balance to rotational motion
[AD-A241348] p 139 N92-13078
Identification techniques: Frequency domain methods
p 273 N92-17158
Analysis of EMP response of structures using frequency domain electromagnetic interaction codes
[AD-A245758] p 765 N92-26592
JTIDS electromagnetic compatibility in the 960-1215 MHz band
[AD-A247834] p 773 N92-27864
Effect of guard band reduction on marker beacon receiver performance
[DOT/FAA/CT-TN92/18] p 1002 N92-31617
FREQUENCY ANALYZERS
Parameter identification for nonlinear aerodynamic systems
[NASA-CR-188985] p 53 N92-10347
FREQUENCY ASSIGNMENT
The Aeronautical Mobile Satellite Service (AMSS). II - Frequency spectrum requirements for the Aeronautical Mobile Satellite Service p 94 A92-13852
World Administrative Radio Conference ends favourably for air transport sector p 956 A92-52650
Spectrum sharing between AMSS(R) and MSS
p 677 N92-24165
FREQUENCY CONTROL
JTIDS electromagnetic compatibility in the 960-1215 MHz band
[AD-A247834] p 773 N92-27864
FREQUENCY DISTRIBUTION
JTIDS electromagnetic compatibility in the 960-1215 MHz band
[AD-A247834] p 773 N92-27864
A preliminary study in the use of phase demodulation techniques for the analysis of gear vibration data
[NRC-32083] p 1002 N92-31469
FREQUENCY RANGES
The Aeronautical Mobile Satellite Service (AMSS). II - Frequency spectrum requirements for the Aeronautical Mobile Satellite Service p 94 A92-13852
Analysis of EMP response of structures using frequency domain electromagnetic interaction codes
[AD-A245758] p 765 N92-26592
On the calculation of the response of helicopters to control inputs
[NASA-CR-190812] p 1088 N92-33536
FREQUENCY RESPONSE
Polygon interval arithmetic and design of robust control systems p 49 A92-11418
Frequency response specifications and sensitivity functions in quantitative feedback theory
p 508 A92-29280
FAMUSS - A new aeroservoelastic modeling tool
[AIAA PAPER 92-2395] p 541 A92-34468
Aircraft aeroservoelastic compensation using constrained optimization
[AIAA PAPER 92-2399] p 564 A92-34470
Frequency domain testing of helicopter dynamics using automated input signals p 545 A92-35731
A frequency domain theory for structural identification
p 590 A92-35745
Helicopter in-flight frequency response test techniques
p 548 A92-35938
Ritz vectors synthesis versus modal synthesis for fluid-structure interaction modeling p 898 A92-45885
Frequency domain flight testing and analysis of an OH-58D helicopter p 847 A92-46943
System identification requirements for high-bandwidth *rotorcraft flight control system design*
p 282 N92-17166
Analysis and modification of a single-mesh gear fatigue rig for use in diagnostic studies
[NASA-TM-105416] p 773 N92-27879
FREQUENCY STANDARDS
Do we really need 57 ways of rating aircraft noise?
p 688 A92-39065
Tactical Rubidium Frequency Standard (TRFS)
[AD-A243934] p 401 N92-18897
The need for GPS standardization
p 1049 N92-33351
FRETTING CORROSION
Improving the properties of titanium alloys by ion implantation p 289 A92-22771
Fretting fatigue p 672 A92-38225
FRICTION
Runway drainage characteristics related to tire friction *performance*
[SAE PAPER 912156] p 664 A92-39991
Rotor-to-stator partial rubbing and its effects on rotor dynamic response p 224 N92-14367
Industrial code development p 227 N92-15083
Tribology needs for future space and aeronautical systems
[NASA-TM-104525] p 214 N92-15191
Multi-colored layers for visualizing aerodynamic flow *effects*
[NASA-CASE-LAR-13742-1] p 447 N92-21588
FRICTION DRAG
Turbulent friction drag reduction: Boundary layer manipulators
[CERT-RSF-DERAT-62/5004-31] p 43 N92-11309
FRICTION FACTOR
Proceedings of Damping 1991, volume 3
[AD-A241313] p 225 N92-14386
FRICTION MEASUREMENT
A method for the optical measurement of surface friction in supersonic flow p 337 A92-27537
Skin-friction gauge for use in hypervelocity impulse facilities p 398 A92-28063
Skin friction measurements in 3-D boundary layers
p 1092 A92-54351
Reflection type skin friction meter
[NASA-CASE-LAR-14520-1-SB] p 11 N92-10008
Susceptibility of a parallelogram type skin friction balance to rotational motion
[AD-A241348] p 139 N92-13078
FRICTION REDUCTION
Technology for tomorrow - Do 228 with laminar wings
p 269 A92-21013

Special Course on Skin Friction Drag Reduction
[AGARD-R-786] p 717 N92-27706
Basic concepts on boundary layers
p 717 N92-27707

FRICTION WELDING
Inertia-friction welding of an advanced rapidly solidified titanium alloy p 212 A92-18898

FRONTS (METEOROLOGY)
The 1990 Airport Surveillance Radar Wind Shear Processor (ASR-WSP) operational test at Orlando International Airport
[AD-A239852] p 18 N92-10019
On the relation between cumulus cloud lines and surface shear lines p 410 N92-19667
A comparison of the performance of two gust front detection algorithms using a length-based scoring technique
[AD-A250862] p 1004 N92-32103

FROST
Aerodynamic characteristics of hoar frost roughness
p 808 A92-45829
Effects of frost on wing aerodynamics and take-off performance p 450 N92-21687
The effect of hoar-frosted wings on the Fokker 50 take-off characteristics p 451 N92-21692
Performance degradation due to hoar frost on lifting surfaces p 628 N92-24866
Performance of insulated pavements at Newton Fields, Jackman, Maine
[CRREL-92-9] p 1101 N92-32903

FROZEN EQUILIBRIUM FLOW
Application of finite element method to hypersonic nozzle flow computations p 769 N92-27479

FUEL COMBUSTION
H2/air subsystem combustion kinetics in aerospaceplane powerplants
[IAF PAPER 91-276] p 25 A92-12600
Weak extinction limits of large scale flameholders
[ASME PAPER 91-GT-234] p 125 A92-15643
Lean blowout in a research combustor at simulated low pressures
[ASME PAPER 91-GT-359] p 137 A92-15713
An experimental investigation of the combustion of a hydrogen jet injected parallel in a supersonic air stream
[AIAA PAPER 91-5102] p 212 A92-17861
Aerodynamic effects on fuel spray structure - Experiment and theory
[AIAA PAPER 92-0227] p 317 A92-25691
An experimental investigation of the swirling combustor for integral liquid fuel ramjet p 557 A92-35541
Experimental investigation of liquid carbonhydrogen fuel combustion in channel at supersonic velocities
[AIAA PAPER 92-3429] p 894 A92-48986
Free-radicals aided combustion with scramjet applications
[IAF PAPER 92-0659] p 1106 A92-57100
An analytical and computational investigation of shock-induced vortical flows with applications to supersonic combustion p 405 N92-19538
NASA's rotary engine technology enablement program: 1983-1991
[NASA-TM-105562] p 378 N92-20033
Simulation of chemical kinetics in turbulent natural gas combustion
[PB92-123660] p 488 N92-20329
Transport phenomena and interfacial kinetics in multiphase combustion systems
[AD-A244849] p 489 N92-20695
Turbocharged pressurized combustion system
[PB92-142579] p 756 N92-26521
Collection of papers of the 31st Israel Annual Conference on Aviation and Astronautics
[ITN-92-85124] p 932 N92-31861

FUEL CONSUMPTION
Propulsion requirements for high altitude long endurance flight
[ASME PAPER 91-GT-393] p 127 A92-15723
Maximum mass allowance to justify passenger-carrying aircraft modification p 113 A92-16802
A new method for increasing maximum flight endurance p 280 A92-21006
High density fuel qualification for a gas turbine engine
[AIAA PAPER 92-0684] p 389 A92-27051
On the experimental investigation of air-breathing engine of new schemes p 469 A92-29711
Improving the efficiency of passenger aircraft during the landing approach p 460 A92-31893
A second-order control optimization method for nonlinear dynamic systems and its use for calculating optimal aircraft trajectories p 460 A92-31894
Optimum cruise lift coefficient in initial design of jet aircraft p 845 A92-46806
High speed rotorcraft propulsion concepts to control power/speed characteristics
[AIAA PAPER 92-3367] p 865 A92-48940
Turboshaft/turboprop cycle sensitivity analysis
[AIAA PAPER 92-3476] p 865 A92-49020
A fuel-optimal 4D guidance algorithm
p 978 A92-53095
Performance improvements and fuel cost savings due to leading edge modification of a vintage delta wing jet fighter
[FFA-TN-1991-22] p 114 N92-11993
Trim drag reduction concepts for horizontal takeoff single-stage-to-Orbit vehicles
[NASA-TM-102687] p 206 N92-15076
Rotary engine performance limits predicted by a zero-dimensional model
[NASA-CR-189129] p 474 N92-20650
Propulsion challenges and opportunities for high-speed transport aircraft p 561 N92-22540
Flight-determined benefits of integrated flight-propulsion control systems
[NASA-TM-4393] p 742 N92-27587
Drag reduction: An industrial challenge
p 717 N92-27708
Practical considerations in designing the engine cycle
p 869 N92-28460
Subsonic flight test evaluation of a performance seeking control algorithm on an F-15 airplane
[NASA-TM-4400] p 973 N92-31275

FUEL CONTAMINATION
Static tests for the evaluation of fuel additives
[AIAA PAPER 92-0686] p 389 A92-27053
Microbiological spoilage of aviation turbine fuel. II - Evaluation of a suitable biocide p 891 A92-45600
Flow contamination and flow quality in arc heaters used for hypersonic testing
[AIAA PAPER 92-4028] p 1100 A92-56850

FUEL CONTROL
An approach for evaluation of gas turbine deposition
[ASME PAPER 91-GT-214] p 653 A92-36890
Solid-fuel ramjet fuel regression rate/thrust modulation
p 666 A92-36966
The numerical simulation of the main fuel control unit of gas turbine engines
[AIAA PAPER 92-3760] p 867 A92-49115

FUEL CORROSION
Transport phenomena and interfacial kinetics in multiphase combustion systems
[AD-A244849] p 489 N92-20695

FUEL FLOW
Deposition during vaporization of jet fuel in a heated tube
[AIAA PAPER 92-0687] p 390 A92-27054
Experimental technique of measuring fuel concentration in non-uniform flowfield p 734 A92-41928
Fault diagnostics on jet engine starting
p 1116 A92-54345
Fuel flow measurement in gas turbine testing
[NRC-29808] p 130 N92-12000
Safety considerations in testing a fuel-rich aeropropulsion gas generator
[NASA-TM-105258] p 279 N92-17061
An analytical and computational investigation of shock-induced vortical flows with applications to supersonic combustion p 405 N92-19538
High accuracy fuel flowmeter. Phase 2C and 3: The mass flowrate calibration of high accuracy fuel flowmeters
[NASA-CR-187108] p 406 N92-19775
Subsonic flight test evaluation of a performance seeking control algorithm on an F-15 airplane
[NASA-TM-4400] p 973 N92-31275

FUEL FLOW REGULATORS
Application of a double actuator electronic fuel control unit on a small gas turbine engine
[SAE PAPER 912160] p 655 A92-39993

FUEL INJECTION
Fuel injection in hypersonic airbreathing engine
[IAF PAPER 91-273] p 120 A92-14710
Development of an innovative high-temperature gas turbine fuel nozzle
[ASME PAPER 91-GT-36] p 121 A92-15519
The role of primary jet injection on mixing in gas turbine combustion p 128 A92-16584
Experimental investigation of a supersonic combustion flowfield employing staged transverse injection behind a rearward-facing step
[AIAA PAPER 92-0090] p 292 A92-22196
A systematic experimental and computational investigation of a class of contoured wall fuel injectors
[AIAA PAPER 92-0625] p 374 A92-27007
A numerical method for simulating the fluid-dynamic and heat-transfer changes in a jet engine injector feed-arm due to fouling
[AIAA PAPER 92-0768] p 374 A92-27108
A numerical study of secondary fuel injection techniques for active control of combustion instability in a ramjet
[AIAA PAPER 92-0777] p 374 A92-27114
An investigation on the characteristics of combustor with oblique air jet p 375 A92-28434
Experimental investigation on the structure of flow field and the total pressure loss in an atomizing channel injector p 375 A92-28436
Evaluation of parallel injector configurations for Mach 2 combustion p 376 A92-28533
Solid-fuel ramjet fuel regression rate/thrust modulation
p 666 A92-36966
Mixing and combustion effects in a sliding-wedge ram accelerator with hydrogen injection
[AIAA PAPER 92-3251] p 890 A92-48849
A comparative study of scramjet injection strategies for high Mach numbers flows
[AIAA PAPER 92-3287] p 904 A92-48876
Computational and experimental investigation of annulus heat transfer with swirl
[AIAA PAPER 92-4060] p 1119 A92-56143
NASA's rotary engine technology enablement program: 1983-1991
[NASA-TM-105562] p 378 N92-20033

FUEL PUMPS
Investigation and application of compressor loading technique p 469 A92-29718
Nonlinear rotordynamics analysis --- Space Shuttle Main Engine turbopumps
[NASA-CR-184263] p 221 N92-14344
Qualification test report. Fuel pump test stand 3C3965G05
[AD-A242929] p 280 N92-17552

FUEL SPRAYS
Aerating fuel nozzle design influences on airflow features p 129 A92-17176
Aerodynamic effects on fuel spray structure - Experiment and theory
[AIAA PAPER 92-0227] p 317 A92-25691
Experimental techniques for the assessment of fuel thermal stability
[AIAA PAPER 92-0685] p 389 A92-27052
Experimental investigation on the structure of flow field and the total pressure loss in an atomizing channel injector p 375 A92-28436
Particle dispersion in highly swirling, turbulent flows
p 675 A92-40093
The influence of spray angle on the continuous- and discrete-phase flowfield downstream of an engine combustor swirl cup
[AIAA PAPER 92-3231] p 863 A92-48832
A numerical study of two-phase flow in gas turbine combustors
[AIAA PAPER 92-3468] p 905 A92-49015

FUEL SYSTEMS
Analysis of crash-resistant fuel systems and airframe structure interaction in a crash environment
p 105 A92-14369
Model based reasoning in the aerospace domain
[AIAA PAPER 91-3709] p 230 A92-17582
An investigation of fuel nozzles for combustion performance p 278 A92-21745
A dynamic digital model for the turbojet with pulse-monitored fueller p 654 A92-38267
Properties of aircraft fuels and related materials
[AD-A240650] p 35 N92-11213
H2-fueled high-bypass turbofan p 475 N92-21529
Laser induced fluorescence detection of gums in jet fuels
[AD-A252685] p 987 N92-30767

FUEL TANKS
Use of adhesive bonded attachments for a composite aircraft fuel tank p 785 A92-47414
Calculation of fuel sloshing and its coupling vibration with a tank p 991 A92-50204
Integral wing/fuel box p 958 A92-51569
Non-curing fuel and water resistant sealant compositions p 985 A92-51906
Separation of external stores: Comparison of results
[F+W-TF-2058] p 732 N92-26944

FUEL TESTS
High temperature, thermally stable JP fuels - An overview
[AIAA PAPER 92-0683] p 389 A92-27050
High density fuel qualification for a gas turbine engine
[AIAA PAPER 92-0684] p 389 A92-27051
Static tests for the evaluation of fuel additives
[AIAA PAPER 92-0686] p 389 A92-27053
Effects of chemical equilibrium on turbine engine performance for various fuels and combustor temperatures
[NASA-TM-105399] p 562 N92-23254
Advanced thermally stable, jet fuels development program annual report. Volume 1: Model and experiment system development
[AD-A249625] p 988 N92-31462

FUEL-AIR RATIO
H2/air subsystem combustion kinetics in aerospaceplane powerplants
[IAF PAPER 91-276] p 25 A92-12600

Lean low NO(x) combustion concept evaluation
p 143 A92-16583
A test bench for evaluating powerplant electrization
p 138 A92-16830
Effects of sidewall disturbances on the supersonic mixing layer p 290 A92-21085
Laser diagnostics for velocity measurements in supersonic combusting environments
[AIAA PAPER 92-0008] p 288 A92-22133
Premixed, turbulent combustion of axisymmetric sudden expansion flows p 397 A92-27770
Calculation methods on equivalence ratio of multi-propellant for propulsion system
p 893 A92-48269
Computational and experimental studies of flow in multi-lobed forced mixers
[AIAA PAPER 92-3568] p 1112 A92-54057
Experiments and analysis concerning the use of external burning to reduce aerospace vehicle transonic drag
[NASA-TM-105397] p 279 N92-17546
NASA's rotary engine technology enablement program: 1983-1991
[NASA-TM-105562] p 378 N92-20033

FULL SCALE TESTS
A full scale airframe high cycle fatigue test methodology and its application to the SH-2G helicopter
p 105 A92-14345
On-line distortion analysis system for inlet-engine testing
[ASME PAPER 91-GT-166] p 136 A92-15601
An iodine hypersonic wind tunnel for the study of nonequilibrium reacting flows
[AIAA PAPER 92-0566] p 383 A92-26974
V-22 full scale development testing
p 646 A92-40038
Large-scale wind tunnel studies of a jet-engined powered ejector-lift STOVL aircraft p 842 A92-45313
The large scale test control systems designed and built by the Boeing Company to support the 757 and 767 major fatigue tests
[SAE PAPER 911985] p 881 A92-45388
Dynamic LEX/forebody vortex interaction effects
[AIAA PAPER 92-2732] p 804 A92-45566
Forebody flow control on a full-scale F/A-18 aircraft
[AIAA PAPER 92-2674] p 806 A92-45583
Full-scale high angle-of-attack tests of an F/A-18
[AIAA PAPER 92-2676] p 806 A92-45584
A full-scale fatigue test and failure analyses research of F-X fighters p 960 A92-53092
Experimental investigation of an ejector-powered free-jet facility
[AIAA PAPER 92-3569] p 1090 A92-54058
Helicopter rotor testing using scaled model
p 1093 A92-56076
Tutor aft fuselage and empennage full-scale fatigue test: Resolution of horizontal stabilizer installation difficulties
[NRC-LTR-ST-1804] p 114 N92-11990
Annular seals of high energy centrifugal pumps: Presentation of full scale measurement
p 224 N92-14362
Acoustic interactions between an altitude test facility and jet engine plumes: Theory and experiments
[NASA-CR-190423] p 738 N92-26405
Aging aircraft NDI Development and Demonstration Center (AANC): An overview --- nondestructive inspection p 915 N92-30120

FUNCTION SPACE
Trajectory fitting in function space with application to analytic modeling of surfaces
[NASA-TP-3232] p 945 N92-30747

FUNCTIONAL ANALYSIS
Fourier functional analysis for unsteady aerodynamic modeling p 935 A92-50313
An exploration of function analysis and function allocation in the commercial flight domain
[NASA-CR-4374] p 368 N92-19871
Identification of aerodynamic models for maneuvering aircraft
[NASA-CR-190444] p 852 N92-28720
Development statistics for the UH-1 Ada feasibility study
[AD-A252404] p 982 N92-30547

FUNCTIONAL DESIGN SPECIFICATIONS
Characteristics of a future aeronautical satellite communications system
[AIAA PAPER 92-2058] p 453 A92-29889
Helmet-mounted image intensification analysis
p 554 A92-35454
Advanced information processing system: Inter-computer communication services
[NASA-CR-187556] p 53 N92-11706
System requirements specification for SMART structures mode p 777 N92-27830
Some longitudinal handling qualities design guidelines for active control technology transport aircraft
[NLR-TP-90129-U] p 878 N92-28652
Design specifications for the Advanced Instructional Design Advisor (AIDA), volume 2
[AD-A248202] p 923 N92-29188
Application of VME-technology on an airborne data link processor unit
[NLR-MP-88040-U] p 841 N92-29615
A multivariable control concept for a gas turbine engine
[ETN-92-92104] p 1072 N92-33645

FUNGICIDES
Evaluation of the fungicide properties of antifreeze additives for jet fuels p 141 A92-15070

FURNACES
High temperature aircraft research furnace facilities
[NASA-CR-184384] p 1101 N92-33826

FUSELAGES
Computation of three-dimensional turbulent vortical flows on bodies at high incidence p 9 A92-13203
Automated composite lay-up p 146 A92-14450
Weathering test of AFRP composites for the application of helicopter fuselage --- Aramide Fiber Reinforced Plastic p 142 A92-15309
Design is the name of the game - Comparison of the F5D Skylancer to the F4D Skyray p 167 A92-16062
Computer-aided equipment layout for the fuselage of maneuverable aircraft p 113 A92-16833
Fracture analysis and crack propagation in pressurized fuselage structures - Experimental and numerical investigations p 217 A92-19812
Proof test and fatigue crack growth modeling on 2024-T3 aluminum alloy p 213 A92-19828
Numerical solution of the boundary-layer equations for a general aviation fuselage p 174 A92-20211
Computational investigation of slot blowing for fuselage forebody flow control
[AIAA PAPER 92-0020] p 248 A92-22142
An algorithm for predicting the flow past fuselage-mounted engine arrangements
[AIAA PAPER 92-0151] p 253 A92-23766
Experimental and theoretical studies on helicopter rotor fuselage interaction
[ONERA, TP NO. 1991-197] p 329 A92-26356
Aerodynamic characteristics of the combination of a wing with a cambered middle surface with a fuselage
p 439 A92-31880
Characteristics of transonic flow past a configuration comprising a wing and a fuselage with a large midsection ratio p 439 A92-31882
Effect of the fuselage midsection ratio on the character of wing-fuselage aerodynamic interference
p 439 A92-31883
Design, analysis, and testing of integrally stiffened composite centre fuselage skin for future fighter aircraft
p 535 A92-32554
Structural airworthiness of aging Boeing jet transports - 747 fuselage fatigue test program
[AIAA PAPER 92-1128] p 537 A92-33280
RCS of four fuselage-like scatterers at HF frequencies
p 533 A92-33632
Experimental and analytical study of the effects of floor location on response of composite fuselage frames
[AIAA PAPER 92-2473] p 539 A92-34362
Aeroelastic response of helicopters with flexible fuselage modeling
[AIAA PAPER 92-2567] p 564 A92-34481
Coupled rotor-fuselage dynamics and aeroelasticity in turning flight
[AIAA PAPER 92-2109] p 544 A92-35680
A study of coupled rotor-fuselage vibration with higher harmonic control using a symbolic computing facility
p 569 A92-35770
Measurements of a rotor flowfield and the effects on a fuselage in forward flight p 521 A92-35787
High alpha aerodynamic control by tangential fuselage blowing p 611 A92-36848
Evaluation of sound transmission into aircraft fuselages by a reciprocity technique p 694 A92-39086
Propeller sound excitation on an aircraft fuselage using a loudspeaker ring p 643 A92-39087
Noise inside aircraft fuselages subjected to airborne excitation p 643 A92-39089
High gain airborne antenna for satellite communications p 639 A92-40188
Design optimization of natural laminar flow bodies in compressible flow p 701 A92-41219
Environmental evaluation of repairs to fuselage lap joints p 699 A92-41534
Study on calculating the subsonic and supersonic aerodynamic characteristics of slender wing-body combinations at large angles of attack
p 706 A92-41926
Navier-Stokes predictions for the F-18 wing and fuselage at large incidence p 810 A92-46783
The unsteady interaction of a 3-dimensional vortex filament with a cylinder p 813 A92-46934
A study of rotor wake development and wake/body interactions in hover p 813 A92-46935
Single block mesh generation for a fuselage plus two lifting surfaces p 817 A92-47054
Filament winding of composite isogrid fuselage structures p 784 A92-47405
Design and test of aircraft aft fuselage structure using postbuckled shear panels p 848 A92-47406
Calculation of the transonic full-potential flowfield about 3D fuselage p 941 A92-53021
Mechanical model of landing impact of three dimensional fuselage landing gear p 960 A92-53090
Coupled rotor-fuselage vibration reduction with multiple frequency blade pitch control p 1085 A92-56315
Analysis of helicopter rotor-fuselage interference with time averaged pressure distribution
p 1032 A92-56331
A study of helicopter rotor/fuselage response in low-speed manoeuvres - Comparison of theory with flight p 1086 A92-56334
Tutor aft fuselage and empennage full-scale fatigue test: Resolution of horizontal stabilizer installation difficulties
[NRC-LTR-ST-1804] p 114 N92-11990
Onboard cabin water spray system under various discharge configurations
[DOT/FAA/CT-TN91/42] p 93 N92-13043
Measurements of fuselage skin strains and displacements near a longitudinal lap joint in a pressurized aircraft
[NASA-TM-104163] p 159 N92-13455
Definition of the unsteady vortex flow over a wing/body configuration
[NASA-CR-180083] p 178 N92-13995
The two-bay crack problem in fuselages built in GLARE and ARALL
[LR-653] p 196 N92-14044
Bulging of fatigue cracks in a pressurized aircraft fuselage
[LR-655] p 196 N92-14045
Airbus Industrie A330/A340: Full scale fatigue test of center fuselage and wing p 226 N92-14425
Development and evaluation of a finite element model for a fiber composite helicopter fuselage
[MBB-UD-0584-90-PUB] p 196 N92-15066
An experimental study of a turbulent wing-body junction and wake flow
[AD-A243388] p 260 N92-17222
Rapid repair of integrally stiffened carbon fibre composite structures by bolted aluminium elements
[MBB-FE202-S-PUB-0453-A] p 290 N92-17310
Design, analysis, and testing of integrally stiffened composite centre fuselage skin for future fighter aircraft
[MBB-FE2-PUB-S-450] p 359 N92-18333
Fatigue testing and tear down operations on Airbus A320 forward fuselage p 360 N92-18579
Recent fracture mechanics results from NASA research related to the aging commercial transport fleet
p 362 N92-18589
Airplane crashes on the runway. Fine modeling of the behavior after burning of a frame submitted to linear crushing
[IMFL-90-64] p 353 N92-19350
A numerical study of fuselage scattering effects on rotor noise p 511 N92-20428
A three-dimensional, compressible, laminar boundary-layer method for general fuselages. Volume 2: User's manual
[NASA-CR-4292-VOL-2] p 678 N92-24344
A three-dimensional, compressible, laminar boundary-layer method for general fuselages. Volume 1: Numerical method
[NASA-CR-4292-VOL-1] p 679 N92-24547
Composite fuselage technology (summary of year 2)
[NASA-CR-190434] p 731 N92-26655
Surface generation and editing operations applied to structural support of aerospace vehicle fuselages
p 777 N92-27831
Generation of spectra and stress histories for fatigue and damage tolerance analysis of fuselage repairs
[AD-A250390] p 854 N92-29180
Tear straps in airplane fuselage
[AD-A248543] p 854 N92-29511
Performance of fuselage pressure structure
p 913 N92-30109
Damaged stiffened shell research at NASA. Langley Research Center p 914 N92-30115
Ageing airplane repair assessment program for Airbus A300 p 838 N92-30123
Two-dimensional aerodynamic characteristics of several polygon-shaped cross-sectional models applicable to helicopter fuselages
[NASA-TP-3233] p 944 N92-30394
The Dornier 328 Acoustic Test Cell (ATC) for interior noise tests and selected test results
[AIAA PAPER 92-2164] p 1137 N92-32951

Active control of sound transmission through stiff lightweight composite fuselage constructions
p 1137 N92-32957
CFRP stiffened panels under compression
p 1109 N92-33044

FUSION (MELTING)
Notes on the use of fusible temperature indicators to bound the temperature of hot graphite in the NAVSWC hypervelocity wind tunnel facility p 1090 A92-54315

FUZZY SETS
Comments on 'Fuzzy logic for control of roll and moment for a flexible wing aircraft' p 480 A92-30995

FUZZY SYSTEMS
Using new aggregation operators in rule-based intelligent control p 51 A92-11456
Fuzzy controller design and stability analysis for an aircraft model p 478 A92-29124
Potential role of neural networks and fuzzy logic in flight control design and development
[AIAA PAPER 92-0999] p 600 A92-33191
A fuzzy logic based F/A-18 automatic carrier landing system
[AIAA PAPER 92-4392] p 1074 A92-55193
Discrete event fuzzy airport control
p 1046 A92-55973
An autorotation-entry control for a helicopter with a fuzzy controller p 1083 A92-56032
Application of fuzzy control to aircraft guidance
p 1083 A92-56033
Neural network and fuzzy logic technology for naval flight control
[AD-A242650] p 206 N92-15074
Fuzzy guidance system evaluation
p 778 N92-27903

G

G-222 AIRCRAFT
The G-222 aircraft individual tracking programme
p 361 N92-18582

GALERKIN METHOD
Finite-element algorithm for chemically reacting hypersonic flow
[AIAA PAPER 92-0754] p 336 A92-27097
A non-linearly stable implicit finite element algorithm for hypersonic aerodynamics p 433 A92-31487
Improving the convergence rate of the Petrov-Galerkin techniques for the solution of transonic and supersonic flows p 434 A92-31495
Reduced basis technique for evaluating the sensitivity coefficients of the nonlinear tire response
[AIAA PAPER 92-2530] p 583 A92-34376
Mesh adaption for 2D transsonic Euler flows on unstructured meshes p 816 A92-47038
A penalty-Galerkin finite element method for calculating transonic flow over wings p 943 A92-53386
Development of 3D electromagnetic modeling tools for airborne vehicles
[NASA-CR-190810] p 1126 N92-33307

GAME THEORY
Synthesis of robust nonlinear autopilots using differential game theory p 478 A92-29330
Three-dimensional game for two aircraft
p 744 A92-43129

GAS ATOMIZATION
Factors influencing the effective spray cone angle of pressure-swirl atomizers p 295 A92-23300

GAS BEARINGS
A gas operated bearing damper for turbomachinery
[ASME PAPER 91-GT-249] p 150 A92-15654

GAS COMPOSITION
Rotational coherent anti-Stokes Raman spectroscopy measurements in a rotating cavity with axial throughflow of cooling air - Oxygen concentration measurements
p 990 A92-49574
A concentration probe for the study of mixing in supersonic shear flows p 991 A92-50039

GAS DENSITY
Prandtl-Meyer function for dense gases
p 415 A92-26441
Critical Mach number estimates for dense gases
p 933 A92-49498
Near-injector structure of non-evaporating pressure-atomized sprays at various ambient densities
p 681 N92-25571

GAS DISSOCIATION
Rate parameters for coupled vibration-dissociation in a generalized SSH approximation --- Schwarz, Slawsky, and Herzfeld p 235 A92-20301
Effects of oxygen dissociation on hypervelocity combustion experiments
[AIAA PAPER 92-3964] p 1098 A92-56791

GAS DYNAMICS
Biennial Fluid Dynamics Symposium on Advanced Problems and Methods in Fluid Mechanics, 19th, Kozubnik, Poland, Sept. 3-8, 1989, Selected Papers
p 37 A92-10654
Shock wave reflection close to the leading edge of a wedge p 37 A92-10660
Fundamentals of applied aerogasdynamics. I - Aerodynamics of wings (profiles), airframes, and their combinations --- Russian book p 64 A92-14280
Off-design performance prediction of turbofans using gasdynamics
[ASME PAPER 91-GT-389] p 126 A92-15721
Asymptotics of the upper branch of the neutral curve at subsonic and transonic external flow velocities
p 79 A92-16705
A model of gasdynamic loads on an oscillating nozzle shell p 80 A92-16817
On marching algorithms for solving stationary problems p 311 A92-24976
Gasdynamic calculation of an impulse wind tunnel with a two-section plenum p 493 A92-30147
Effect of turbulent mixing on the characteristics of a turbofan-engine nozzle p 493 A92-30162
A high-resolution Euler solver based on multigrid, semi-coarsening, and defect correction
p 671 A92-37868
A numerical study of flow of a viscous gas in a Laval nozzle in the narrow channel approximation
p 706 A92-42680
Aerodynamics of two-shock bodies derived by the gasdynamic design method p 707 A92-42683
Smooth solutions for transonic gasdynamic equations --- Russian book
[ISBN 5-02-029345-8] p 809 A92-46626
Expansion tube experiments for the investigation of ram-accelerator-related combustion and gasdynamic problems
[AIAA PAPER 92-3246] p 904 A92-48845
Transonic flows of Bethe-Zel'dovich-Thompson fluids
p 935 A92-50293
All-Union Conference on Optical Methods of Flow Research, 1st, Novosibirsk, Russia, Apr. 1991, Proceedings p 993 A92-51311
The study of experimental turboramjets
[AIAA PAPER 92-3720] p 1067 A92-54135
TSNIIMASH capabilities for aerogasdynamical and thermal testing of hypersonic vehicles
[AIAA PAPER 92-3962] p 1097 A92-56789
Experimental simulation and diagnostics of high-enthalpy real-gas flows
[AD-A241286] p 166 N92-13822
Nonstationary gasdynamics p 220 N92-13985
Parallelization of a Direct Simulation Monte Carlo (DSMC) code for fluid dynamics p 227 N92-15033
A hierarchy for modeling high speed propulsion systems
[NASA-CR-186984] p 387 N92-19934
Improved large perturbation propulsion models for control system design (1988-1989) and large perturbation models of high velocity propulsion systems (1989-1990) and reduced order propulsion models for control system design (1990-1991)
[NASA-CR-190148] p 593 N92-22491
A hierarchy for modeling high speed propulsion systems p 559 N92-22492
Swept shock/boundary layer interaction experiments in support of CFD code validation
[NASA-CR-190583] p 1036 N92-32494
Perspectives on hypersonic viscous and nonequilibrium flow research
[NASA-CR-190817] p 1039 N92-33413

GAS EXPANSION
Limit point flow mode analysis of exhaust diffuser and operation characteristics of injector p 968 A92-49830
Multicomponent gas sorption Joule-Thomson refrigeration
[NASA-CASE-NPO-17569-1-CU] p 228 N92-15203

GAS FLOW
On thermal-stress gas flows p 37 A92-10657
Calculation of flow of a radiating gas in axisymmetric nozzles of specified shape p 7 A92-12179
Calculation of gas combustion regimes in a counterflow vortex chamber p 34 A92-12209
Thermal details in a rotor-stator cavity at engine conditions with a mainstream
[ASME PAPER 91-GT-275] p 151 A92-15672
Stability of a viscous compressible shear layer with a temperature drop p 79 A92-16684
A hot-wire anemometer in compressible subsonic flow
p 244 A92-21623
The problem of transition from continuum to rarefied gas flows p 251 A92-22519
Preliminary laser induced fluorescence measurements in several facilities in preparation for application to studies in the high enthalpy shock tunnel Goettingen (HEG)
[AIAA PAPER 92-0143] p 284 A92-23761
Application of the LAURA code for slender-vehicle aerothermodynamics p 310 A92-24652
Numerical modelling for gas duct in tuboannular combustor p 371 A92-24738
Application of special series for studying nonstationary transonic gas flows p 311 A92-24904
On marching algorithms for solving stationary problems p 311 A92-24976
Hypersonic rarefied flow past spheres including wake structure
[AIAA PAPER 92-0495] p 329 A92-26325
An engineering aerodynamic heating method for hypersonic flow
[AIAA PAPER 92-0499] p 329 A92-26327
Boundary singularities in steady potential compressible flow through plane two-dimensional channels
p 336 A92-27384
Hypersonic flow of a viscous gas past sharp elliptical cones at angles of attack and slip p 336 A92-27531
Calculation of heat transfer and friction for a blunt body in the path of supersonic flow of a chemically equilibrium air-xenon mixture p 336 A92-27532
Calculation of three-dimensional flow past blunt cones near the plane of symmetry for different flow regimes in the shock layer and in the presence of gas injection from the surface p 337 A92-27593
Bodies of revolution with minimal wave drag at transonic gas flow velocities p 424 A92-30135
Flow of a viscous twisted fluid film on the surface of a blunt body in supersonic flow of a gas
p 424 A92-30146
An experimental study of transonic flow of a gas past wedges p 424 A92-30153
Effect of viscosity on the drag of slender axisymmetric bodies in hypersonic flow p 425 A92-30154
The lift-drag ratio of a slender cone in viscous hypersonic gas flow p 425 A92-30172
The effect of the angle-of-attack on laminar-turbulent boundary transition near the lower surface of triangular plates in a supersonic gas flow p 426 A92-30180
Theoretical analysis of a suction diffuser in the porous test section of a wind tunnel p 428 A92-30207
The total drag of a body in the flow of a viscous heat-conducting gas p 439 A92-31873
The numerical method for calculating the flow field, temperature field and radiation fluxfield in the pipe
p 587 A92-35546
Motion of a sphere in a gas - Numerical solution of the linearized Boltzmann equation p 591 A92-36194
Vibrational relaxation effects in hypersonic flows of a viscous gas p 609 A92-36550
Oblique shock wave with sweep p 613 A92-38370
Engineering aerodynamic heating method for hypersonic flow p 705 A92-41539
A two-stage-diaphragm free-piston shock tube for a strong shock wave p 748 A92-43098
Thermal radiation effects on a shocked particle-laden gas p 780 A92-44377
High Reynolds number flows using liquid and gaseous helium
[ISBN 0-387-97475-X] p 897 A92-45261
Multidimensional Euler/Navier-Stokes analysis for hypersonic equilibrium gas
[SAE PAPER 912026] p 790 A92-45418
Numerical simulations of hypersonic real-gas flows over space vehicles
[SAE PAPER 912045] p 791 A92-45429
Analysis of thermo-chemical nonequilibrium models for carbon dioxide flows
[AIAA PAPER 92-2852] p 892 A92-47835
Lower upper implicit total variation diminishing solution of viscous hypersonic flows p 935 A92-50302
Flow of a rarefied gas past a two-dimensional body of an arbitrary shape at small Mach numbers
p 937 A92-52726
Kinetic theory model for the flow of a simple gas from a three-dimensional axisymmetric nozzle
p 937 A92-52730
Rarefied gas flow around a disc with different angles of attack p 938 A92-52753
Approximate aerodynamic analysis for complicated bodies in rarefied gas flows p 938 A92-52754
Enhancements and applications of DSMC for hypersonic rarefied flows p 939 A92-52761
Rarefied gas numerical wind tunnel
p 995 A92-52763
Aerodynamics of complex shape bodies within a wide range of supersonic flows of rarefied gases
p 939 A92-52767
Monte Carlo simulation of the hypersonic mon- and diatomic gas flow past a disk at an angle of attack
p 939 A92-52770

Numerical and experimental investigations of rarefied gas flows through nozzles and composite systems
p 940 A92-52797
Rarefied gas numerical wind tunnel
p 1017 A92-53552
An analysis of boundary layer for droplet aerodynamic stripped in high speed gas flow p 1116 A92-54563
Further calculations of the performance of turbofan engines incorporating a wave rotor
[AD-A240867] p 131 N92-13072
A new technique for temperature and specie concentration measurements in unseeded supersonic and hypersonic gas flows
[AD-A241536] p 158 N92-13409
Experimental simulation and diagnostics of high-enthalpy real-gas flows
[AD-A241286] p 166 N92-13822
Seal related development activities at EG/G
p 228 N92-15095
An alternative to unstructured grids for computing gas dynamic flows around arbitrarily complex two-dimensional bodies
[NASA-CR-189612] p 447 N92-21465
Development of an integrated BEM approach for hot fluid structure interaction: BEST-FSI: Boundary Element Solution Technique for Fluid Structure Interaction
[NASA-CR-189202] p 574 N92-22211
A three-dimensional, compressible, laminar boundary-layer method for general fuselages. Volume 2: User's manual
[NASA-CR-4292-VOL-2] p 678 N92-24344

GAS GENERATORS
Gas-generator with high-temperature path ceramic components
[ASME PAPER 91-GT-152] p 148 A92-15594
Detonation duct gas generator demonstration program
[AIAA PAPER 92-3174] p 1066 A92-54011
Safety considerations in testing a fuel-rich aeropropulsion gas generator
[NASA-TM-105258] p 279 N92-17061
Analysis of the flight performance of the 155 mm M864 base burn projectile
[BRL-TR-3083] p 1041 N92-33699

GAS INJECTION
Experimental and theoretical study of the improvement of the aerodynamic characteristics of supersonic flow past bodies with surface injection of a gas jet with particles
p 8 A92-12204
The influence of density difference between hot and coolant gas on film cooling by a row of holes - Predictions and experiments
[ASME PAPER 91-GT-255] p 151 A92-15660
The dynamics and control of fluctuating pressure loads in the reattachment region of a supersonic free shear layer
[AIAA PAPER 92-0178] p 255 A92-23788
Navier-Stokes computation of hypersonic near wakes with foreign gas injection
[AIAA PAPER 92-0838] p 422 A92-29604
Cooling of a sharp nose by extraneous gas injection into the viscous shock layer p 426 A92-30188
Unsteady hypersonic boundary layers for slender axisymmetric bodies with large injection rates
p 524 A92-36100
LDA measurements in a Mach 2 flow over a rearward facing step with staged transverse injection
[AIAA PAPER 92-2692] p 800 A92-45539
Limit point flow mode analysis of exhaust diffuser and operation characteristics of injector p 968 A92-49830
Mixing studies of helium in air at high supersonic speeds p 935 A92-50310
Simulation research on the dynamic characteristics of steam-injected gas turbine p 971 A92-53389
Numerical study on the secondary jet into a supersonic flow p 1018 A92-53556
Active control of asymmetric vortical flows around cones using injection and heating
[AIAA PAPER 92-4426] p 1025 A92-55350
Numerical simulation of the reactive flow in advanced (HSR) combustors using KIVA-2
[NASA-CR-188996] p 26 N92-11014
Oscillating shock impingement on low-angle gas injection into a supersonic flow p 89 N92-13032

GAS IONIZATION
Direct simulation of re-entry flows with ionization
p 713 A92-44367

GAS JETS
Experimental and theoretical study of the improvement of the aerodynamic characteristics of supersonic flow past bodies with surface injection of a gas jet with particles
p 8 A92-12204
Changing the structure and improving the aerodynamic characteristics of supersonic flow past bodies through ejection of a gas jet with particles p 78 A92-16680
An experimental investigation of the combustion of a hydrogen jet injected parallel in a supersonic air stream
[AIAA PAPER 91-5102] p 212 A92-17861
An analytical and computational investigation of shock-induced vortical flows
[AIAA PAPER 92-0316] p 321 A92-25763
A numerical investigation of hydrogen combustion in Mach 2 flow
[AIAA PAPER 92-0341] p 388 A92-25787
Experiments to evaluate hot-jet simulation capabilities in Cryogenic Wind-Tunnel testing
[AIAA PAPER 92-0567] p 384 A92-26975
Oscillating shock impingement on low-angle gas injection into a supersonic flow p 89 N92-13032
An analytical and computational investigation of shock-induced vortical flows with applications to supersonic combustion p 405 N92-19538
Turbulent mixing in supersonic jets
p 715 N92-27054
Dynamic response of induced pressures, suckdown, and temperatures for two tandem jet STOVL configurations
[NASA-TM-103934] p 1039 N92-33581

GAS LUBRICANTS
Development of high performance compressor discharge seal
[AIAA PAPER 92-3714] p 907 A92-49096

GAS MIXTURES
Laser diagnostics for velocity measurements in supersonic combusting environments
[AIAA PAPER 92-0008] p 288 A92-22133
Calculation of heat transfer and friction for a blunt body in the path of supersonic flow of a chemically equilibrium air-xenon mixture p 336 A92-27532
Cooling of a sharp nose by extraneous gas injection into the viscous shock layer p 426 A92-30188
Calculation methods on equivalence ratio of multi-propellant for propulsion system
p 893 A92-48269
Mixing studies of helium in air at high supersonic speeds p 935 A92-50310
Experimental and computational investigation of scaling phenomena in a large caliber ram accelerator
[AIAA PAPER 92-3245] p 1103 A92-54019
Linear acoustics in gas mixtures with rate processes
p 238 N92-15013
Multicomponent gas sorption Joule-Thomson refrigeration
[NASA-CASE-NPO-17569-1-CU] p 228 N92-15203
Experimental investigation of nozzle/plume aerodynamics at hypersonic speeds
[NASA-CR-190074] p 664 N92-25162

GAS PRESSURE
Effect of Eulerian inertia forces on the stressed state of the rotating components of aircraft turbomachines
p 128 A92-16828
Further calculations of the performance of turbofan engines incorporating a wave rotor
[AD-A240867] p 131 N92-13072
Evaluation of an innovative high-temperature ceramic wafer seal for hypersonic engine applications
p 578 N92-22205
Pneumatically actuated multiple store launcher
[AD-D015237] p 732 N92-27188
Second-order shock-expansion theory extended to include real gas effects
[AD-A247191] p 831 N92-29539

GAS STREAMS
A direct-problem calculation method for gas turbines with bowed and twisted blades p 519 A92-35571

GAS TEMPERATURE
The numerical method for calculating the flow field, temperature field and radiation fluxfield in the pipe
p 587 A92-35546
Microgravity nucleation and particle coagulation experiments support
[NASA-CR-190159] p 502 N92-21385

GAS TUNGSTEN ARC WELDING
High temperature aircraft research furnace facilities
[NASA-CR-184384] p 1101 N92-33826

GAS TURBINE ENGINES
Calculation of the hardening factor for gas turbine engine components shot blasted in an ultrasonic field
p 38 A92-10850
Compressor coating effects on gas turbine engine performance p 25 A92-11282
Developing undergraduate gas turbine and turbomachinery courses
[AIAA PAPER 91-2509] p 56 A92-12700
A method for determining the parameters of mathematical generalizations of experimental data on convective heat transfer p 41 A92-12803
The role of laminar-turbulent transition in gas turbine engines p 120 A92-14868
Intermetallic and ceramic matrix composites for 815 to 1370 C (1500 to 2500 F) gas turbine engine applications
p 141 A92-15128
Development of an innovative high-temperature gas turbine fuel nozzle
[ASME PAPER 91-GT-36] p 121 A92-15519
Implanted component faults and their effects on gas turbine engine performance
[ASME PAPER 91-GT-41] p 121 A92-15524
Investigation of engine thrust correlation methods for enclosed test cells
[ASME PAPER 91-GT-68] p 121 A92-15538
Nickel base alloy GTD-222 - A new gas turbine nozzle alloy
[ASME PAPER 91-GT-73] p 142 A92-15542
Future trends in turboshaft engines up to 5000 horsepower class
[ASME PAPER 91-GT-74] p 122 A92-15543
Life time prediction for ceramic gas turbine components
[ASME PAPER 91-GT-96] p 122 A92-15560
Impact design methods for ceramic components in gas turbine engines
[ASME PAPER 91-GT-115] p 123 A92-15566
Ceramic component processing development for advanced gas-turbine engines
[ASME PAPER 91-GT-120] p 142 A92-15567
NASA low-speed centrifugal compressor for 3-D viscous code assessment and fundamental flow physics research
[ASME PAPER 91-GT-140] p 72 A92-15580
Development of silicon nitride rotors for the ATTAP program at Garrett Ceramic Components --- Advanced Turbine Technology Applications Project
[ASME PAPER 91-GT-154] p 142 A92-15590
Design and analysis of ceramic and CMC components for advanced gas turbines
[ASME PAPER 91-GT-156] p 142 A92-15592
Gas-generator with high-temperature path ceramic components
[ASME PAPER 91-GT-152] p 148 A92-15594
The impact load on containment rings during a multiple blade shed in aircraft gas turbine engines
[ASME PAPER 91-GT-163] p 123 A92-15598
Gas turbine main shaft internal flow and heat transfer
[ASME PAPER 91-GT-165] p 123 A92-15600
5,000-hour stability tests of metal sheathed thermocouples at respective temperatures of 538 C and 875 C
[ASME PAPER 91-GT-182] p 148 A92-15614
Development and characterization of high strength SiC rotors
[ASME PAPER 91-GT-191] p 149 A92-15617
Combination of different unsteady quantity measurements for gas turbine blade fault diagnosis
[ASME PAPER 91-GT-201] p 149 A92-15624
A direct optimization procedure for spanwise work distribution in non-free vortex turbine stages
[ASME PAPER 91-GT-204] p 124 A92-15626
High temperature erosion resistance of coatings for gas turbine
[ASME PAPER 91-GT-213] p 143 A92-15632
Real-time estimation of gas turbine engine damage using a control based Kalman filter algorithm
[ASME PAPER 91-GT-216] p 124 A92-15633
A chambered porous damper for rotor vibration control. II - Imbalance response and bladeloss simulation
[ASME PAPER 91-GT-243] p 149 A92-15648
A procedure for automated gas turbine blade fault identification based on spectral pattern analysis
[ASME PAPER 91-GT-259] p 151 A92-15661
Discharge coefficients of cooling holes with radiused and chamfered inlets
[ASME PAPER 91-GT-269] p 151 A92-15667
Thermal details in a rotor-stator cavity at engine conditions with a mainstream
[ASME PAPER 91-GT-275] p 151 A92-15672
Film cooling on a gas turbine rotor blade
[ASME PAPER 91-GT-279] p 152 A92-15675
Performance characteristics of brush seals for limited-life engines
[ASME PAPER 91-GT-281] p 152 A92-15676
The use of NDE as a process development tool for ceramic engine components
[ASME PAPER 91-GT-290] p 152 A92-15682
Development of T-100 multipurpose small power unit
[ASME PAPER 91-GT-327] p 153 A92-15697
Garrett GTP50-1 multipurpose small power unit technology demonstrator program
[ASME PAPER 91-GT-328] p 153 A92-15698
Ceramic matrix composites and its application in gas turbine engines
[ASME PAPER 91-GT-338] p 143 A92-15702
Advanced ceramic engine technology for gas turbines
[ASME PAPER 91-GT-368] p 153 A92-15716
A simple model to simulate subsonic intakes and propelling nozzles of aircraft gas turbine engines
[ASME PAPER 91-GT-392] p 153 A92-15722

Development of a freejet capability for evaluating inlet-engine compatibility
[ASME PAPER 91-GT-401] p 137 A92-15731
Lean low NO(x) combustion concept evaluation
p 143 A92-16583
The role of primary jet injection on mixing in gas turbine combustion p 128 A92-16584
Active control for gas turbine combustors
p 128 A92-16585
A method for determining the optimal composition of the measured parameters in diagnosing gas turbine engines p 128 A92-16819
Isothermal modeling of gas turbine combustors - Computational study p 129 A92-17203
A probabilistic method for monitoring the remaining life of aircraft gas turbine engine components using the temperature limit criterion p 201 A92-18292
Fatigue testing of a gas turbine fan disc
p 217 A92-19818
Development of film riding face seals for a gas turbine engine p 291 A92-21330
Noise control used for turbojet engine test bench
p 284 A92-21749
Mechanical and fracture behaviour of Ti-6Al-2Sn-4Zr-2Mo-0.1Si alloys p 288 A92-22755
Review of methods for crack growth testing in gas turbine engine disc materials p 296 A92-24193
On the prediction of unsteady forces on gas turbine blades. I - Description of the approach. II - Analysis of the results p 311 A92-24724
Strategies for optimal design of gas turbine disks
p 371 A92-24741
The jet screen ignition scheme and its experimental verification p 388 A92-24744
Triple contra-rotating turbine and its basic analysis
p 371 A92-24745
Characterization of a two-phase flow field downstream of a 3x-scale gas turbine co-axial, counter-swirling, combustor dome swirl cup
[AIAA PAPER 92-0229] p 393 A92-25693
A new unsteady mixing model to predict NO(x) production during rapid mixing in a dual-stage combustor
[AIAA PAPER 92-0233] p 372 A92-25696
The effect of blade solidity on the aerodynamic loss of a transonic turbine cascade
[AIAA PAPER 92-0393] p 323 A92-26248
Laser measurements of unsteady flow field in a radial turbine guide vanes
[AIAA PAPER 92-0394] p 395 A92-26249
CARS temperature measurements and validation of a computing code on a gas-turbine combustor
[ONERA, TP NO. 1991-224] p 373 A92-26376
High density fuel qualification for a gas turbine engine
[AIAA PAPER 92-0684] p 389 A92-27051
Advanced materials for aircraft engine applications
p 390 A92-28251
High-temperature powder-lubricated dampers for gas turbine engines p 399 A92-28528
Unsteady analysis of hot streak migration in a turbine stage p 399 A92-28537
Full envelope multivariable control of a gas turbine engine p 468 A92-29116
A Lyapunov based nonlinear control scheme for stabilizing a basic compression system using a close-coupled control valve p 508 A92-29316
Model development for active surge control/rotating stall avoidance in aircraft gas turbine engines
p 468 A92-29375
Brazing method helps repair aircraft gas-turbine nozzles p 492 A92-29504
CUSAE '91; Proceedings of the 1st China-USSR Seminar on Aero Engines, Nanjing, People's Republic of China, Apr. 15-20, 1991 p 469 A92-29709
Carcinogenic hydrocarbons emission with gas-turbine engines exhaust gases p 504 A92-29726
Experimental investigation on combustor with double co-axial swirlers p 469 A92-29729
Simulation of vibrational status of gas-turbine engine
p 470 A92-29731
Cyclic symmetric contact stress analysis of aeroengine rotor assembly p 470 A92-29733
Investigations of the laws of surge and rotating stall forecast in aeronautical engine p 470 A92-29739
On modelling of aero-gas turbine engine for real-time digital simulator --- of engine control system
p 471 A92-29743
The effect of air-compressor adjustment by means of air-bleed on the reserve of its stable operation
p 471 A92-29973
Calculations of the dilution system in an annular gas turbine combustor p 494 A92-31164
Three-dimensional flow visualization of shock wave using double-pulsed holographic interferometry. II - Flow visualization for three-dimensional shock structures in rotating aeroengine fan blade rows p 497 A92-32507
Stress concentration effects of oblique holes in aspirated-cooled turbine engine liners
[AIAA PAPER 92-1130] p 581 A92-33282
Research on aircraft engines p 558 A92-35912
Combustion research and design technology of aircraft engines p 558 A92-35915
Development trends of recent aircraft engines
p 558 A92-35919
A method for determining equivalent stresses in aviation gas turbine engine blades p 559 A92-36421
Optimal measurement and health index selection for gas turbine performance status and fault diagnosis
[ASME PAPER 91-GT-294] p 653 A92-36889
An approach for evaluation of gas turbine deposition
[ASME PAPER 91-GT-214] p 653 A92-36890
An investigation in the variance in particle surface interactions and their effects in gas turbines
[ASME PAPER 91-GT-380] p 653 A92-36891
Fracture mechanics approach to creep growth in welded IN738LC gas turbine blades
[ASME PAPER 91-GT-119] p 670 A92-36893
Blade repair with adaptive vision tracking
[ASME PAPER 91-GT-208] p 607 A92-36897
Evaluation of NO(x) mechanisms for lean, premixed combustion
[ASME PAPER 91-GT-257] p 668 A92-36900
Influence of inlet conditions on the flowfield in a model gas turbine combustor p 672 A92-38866
Design considerations for a generic E.V.M. --- Engine Vibration Monitoring
[SAE PAPER 912095] p 651 A92-39952
Application of a double actuator electronic fuel control unit on a small gas turbine engine
[SAE PAPER 912160] p 655 A92-39993
Challenging power-density requirements for future fighter APUs
[SAE PAPER 912177] p 655 A92-40002
Advanced balancing using laser machining
[SAE PAPER 912218] p 674 A92-40020
Simulation of turbulent velocity profiles appearing on rotating and stationary parts of subsonic compressors and turbines p 676 A92-40172
Vibration analysis of gas turbines by an intelligent knowledge-based system p 656 A92-40548
A method for estimating the efficiency of gas turbine blade cooling systems p 657 A92-40606
Plotting the universal characteristic of a compressor in low-rpm and autorotation regimes p 657 A92-40607
Heat transfer on a cylindrical surface in the cavities of gas turbine engine rotors p 657 A92-40609
Low-frequency vibrations of the shutters of the variable Laval nozzle of gas turbine engines p 657 A92-40610
A method for estimating the technological and economic efficiency of measures enhancing the reliability of aviation gas turbine engines p 657 A92-40621
Second order perturbation method of gas turbine performance calculation p 759 A92-41834
Technique for estimating the strength of gas turbine guide vanes with stress raisers p 761 A92-42653
Possibility of increasing durability of blades with damages p 761 A92-42654
Row-by-row off-design performance calculation method for turbines p 737 A92-44514
Viscous flow analysis of advanced particle separators
p 737 A92-44517
Auxiliary power units for current and future aircraft
[SAE PAPER 912059] p 862 A92-45441
The use of optical sensors and signal processing gas turbine engines p 856 A92-46247
Gas turbine exhaust system silencing design
p 882 A92-47365
Basic analysis of counter-rotating turbines
p 862 A92-47692
Concept of a one-dimensional model of the dynamic behavior of a gas turbine p 862 A92-47791
The impact of advanced materials on small turbine engines
[SAE PAPER 911207] p 862 A92-48021
Fiber-optic pressure sensor system for gas turbine engine control p 857 A92-48047
Active magnetic bearings give systems a lift
p 901 A92-48201
The flow pattern and external heat transfer investigation for gas turbine vanes end surfaces
[AIAA PAPER 92-3071] p 903 A92-48722
Mixing in the dome region of a staged gas turbine combustor
[AIAA PAPER 92-3089] p 903 A92-48734
Experimental study of cross-stream mixing in a rectangular duct
[AIAA PAPER 92-3090] p 903 A92-48735
Design and test of an Active Tip Clearance System for centrifugal compressors
[AIAA PAPER 92-3189] p 863 A92-48801
Simple effective thickness model for circular brush seals
[AIAA PAPER 92-3192] p 903 A92-48803
Aero mechanics in the twenty-first century
[AIAA PAPER 92-3194] p 863 A92-48805
The influence of spray angle on the continuous- and discrete-phase flowfield downstream of an engine combustor swirl cup
[AIAA PAPER 92-3231] p 863 A92-48832
Numerical simulation of turbine 'hot spot' alleviation using film cooling
[AIAA PAPER 92-3309] p 904 A92-48896
Expert systems for the trouble-shooting and the diagnostics of engines
[AIAA PAPER 92-3327] p 923 A92-48910
An eight month gearbox development program
[AIAA PAPER 92-3368] p 850 A92-48941
A distributed vaporization time-lag model for gas turbine combustor dynamics
[AIAA PAPER 92-3465] p 865 A92-49014
A numerical study of two-phase flow in gas turbine combustors
[AIAA PAPER 92-3468] p 905 A92-49015
Prediction of gas turbine combustor flow by a finite element code
[AIAA PAPER 92-3469] p 906 A92-49016
Experimental pyrometer system for a gas turbine engine
[AIAA PAPER 92-3482] p 859 A92-49022
Manufacturing technology methodology for propulsion system parts
[AIAA PAPER 92-3525] p 906 A92-49048
Flexible manufacturing in repair of gas turbine engine components
[AIAA PAPER 92-3524] p 786 A92-49049
Development of high performance compressor discharge seal
[AIAA PAPER 92-3714] p 907 A92-49096
Emerging technologies for gas turbine engines - U.A.V. synergies
[AIAA PAPER 92-3757] p 867 A92-49114
The numerical simulation of the main fuel control unit of gas turbine engines
[AIAA PAPER 92-3760] p 867 A92-49115
Engine aircraft systems integration course
[AIAA PAPER 92-3762] p 928 A92-49117
Effect of thermodynamic parameters on performance and cost of turbine engines p 969 A92-49834
General performance characteristics of real heat engine p 1011 A92-50401
Technical tools of test automation for gas-turbine engines based on cluster CAMAC modules with an increased number of channels p 980 A92-51348
Discs low cycle fatigue life predictions for gas turbine engines in CSFR by using fractographic information
p 995 A92-51950
Simulation research on the dynamic characteristics of steam-injected gas turbine p 971 A92-53389
High-temperature metal matrix composite
p 1105 A92-53878
Applied analytical combustion/emissions research at the NASA Lewis Research Center - A progress report
[AIAA PAPER 92-3338] p 1067 A92-54025
The VRT gas turbine combustor - Phase II
[AIAA PAPER 92-3471] p 1067 A92-54035
In-flight performance diagnostic capability of an adaptive engine model
[AIAA PAPER 92-3746] p 1068 A92-54147
Improvements in teaching aircraft engine design
[AIAA PAPER 92-3758] p 1141 A92-54152
CIS engines - The range revealed. II
p 1069 A92-54546
Development of ITS90 small gas turbine engine
p 1070 A92-55500
State-of-the-art materials for future gas turbine engines p 1070 A92-56122
Computational and experimental investigation of annulus heat transfer with swirl
[AIAA PAPER 92-4060] p 1119 A92-56143
Small engine components test facility compressor testing cell at NASA Lewis Research Center
[AIAA PAPER 92-3980] p 1098 A92-56806
Combustion and core noise p 55 N92-10607
Parallel processing applications for gas turbine engine control p 25 N92-11012
Engine dynamic analysis with general nonlinear finite element codes
[NASA-CR-187222] p 44 N92-11379
An experimental and computational investigation of an annular reverse-flow combustor
[UTIAS-338] p 129 N92-11996
Humidity effects on gas turbine performance
[NRC-30241] p 130 N92-11998
Fuel flow measurement in gas turbine testing
[NRC-29808] p 130 N92-12000

An experimental analysis of lateral jet injection into confined swirling crossflows p 156 N92-12199
Heat transfer and instrumentation studies on rotating turbine blades in a transient facility p 156 N92-12203
Blade surface pressure measurements on the rotor of a model turbine stage in a transient flow facility p 157 N92-12206
Gas turbine engine control
[PATENT-1-274-606] p 130 N92-13069
Rolling element bearing member
[PATENT-1-271-213] p 158 N92-13434
High temperature static strain gage development
[NASA-CR-189044] p 195 N92-14037
Rub induced rotor/stator vibration analysis on CF700 engine
[NRC-TR-ENG-007] p 202 N92-14060
Army research concerns in engine sealing p 228 N92-15089
Programs at Wright-Patterson Air Force Base p 228 N92-15092
Seal development activities at Allison Turbine Division p 228 N92-15093
Seal related development activities at EG/G p 228 N92-15095
Ceramic technology for Advanced Heat Engines Project
[DE92-002397] p 289 N92-16128
Safety considerations in testing a fuel-rich aeropropulsion gas generator
[NASA-TM-105258] p 279 N92-17061
Proceedings of the USAF Structural Integrity Program Conference
[AD-A242943] p 279 N92-17204
Local extinction mechanisms in non-premixed turbulent combustion
[AD-A242027] p 290 N92-17682
Fiber-sensor design for turbine engines
[DE92-003539] p 376 N92-18230
The 3D inelastic analysis methods for hot section components
[NASA-CR-189089] p 402 N92-18971
Engine Structures Modeling Software System (ESMOSS)
[NASA-CR-187227] p 404 N92-19277
Heat transfer in rotating serpentine passages with trips skewed to the flow
[NASA-TM-105581] p 499 N92-20235
Currently available fuel gas booster compressor equipment for small gas turbine engines
[PB92-127026] p 499 N92-20265
The environmental impact of commercial aviation: The evolution of exhaust emissions legislation and control technology
[PNR-90847] p 505 N92-20574
Transport phenomena and interfacial kinetics in multiphase combustion systems
[AD-A244849] p 489 N92-20695
Metal-metal bondline NDE methods
[AD-A244429] p 503 N92-21730
Emissions from aircraft: Standards and potential for improvement
[PNR-90768] p 476 N92-21740
Principles and computer simulations of intercooled-turbocharged gas generator/expander engine p 592 N92-22132
Development of an integrated BEM approach for hot fluid structure interaction: BEST-FSI: Boundary Element Solution Technique for Fluid Structure Interaction
[NASA-CR-189202] p 574 N92-22211
JPRS report: Science and technology. USSR: Engineering and equipment
[JPRS-UEQ-92-001] p 592 N92-22296
Aircraft gas turbine emissions: Their nature, technology for reduction, and a pollution comparison with channel tunnel transport
[ETN-92-91056] p 559 N92-22406
Ceramics for engines p 578 N92-22517
Aeropropulsion structures p 559 N92-22518
Life prediction technologies for aeronautical propulsion systems p 560 N92-22520
Overview of the subsonic propulsion technology session p 560 N92-22531
Small engine technology programs p 560 N92-22532
Advanced Turbine Technology Applications Project (ATTAP)
[NASA-CR-189142] p 682 N92-25649
Algorithmic development in structures technology p 684 N92-25924
Aircraft photovoltaic power-generating system p 775 N92-26581
Heavy duty transport research needs assessment
[DE92-010622] p 767 N92-27394
Application of CFD in the design of gas turbine engine components p 741 N92-27461
Experimental study of cross-stream mixing in a rectangular duct
[NASA-TM-105694] p 742 N92-27652
Feasibility of magnetic bearings for advanced gas turbine engines p 772 N92-27738
Lubricant evaluation and performance 2
[AD-A247464] p 895 N92-28398
Steady and Transient Performance Prediction of Gas Turbine Engines
[AGARD-LS-183] p 868 N92-28458
Practical considerations in designing the engine cycle p 869 N92-28460
Steady and transient performance calculation method for prediction, analysis, and identification p 869 N92-28461
Component performance requirements p 869 N92-28462
Dynamic simulation of compressor and gas turbine performance p 869 N92-28463
Calculation of installation effects within performance computer programs p 869 N92-28465
Dynamic control of aerodynamic instabilities in gas turbine engines p 870 N92-28466
Engine performance and health monitoring models using steady state and transient prediction methods p 870 N92-28467
Turbine aircraft engine operational trending and JT8D static component reliability study
[DOT/FAA/CT-91/10] p 870 N92-28686
Applied analytical combustion/emissions research at the NASA Lewis Research Center
[NASA-TM-105731] p 890 N92-29343
Fatigue in single crystal nickel superalloys
[AD-A248190] p 896 N92-29408
Flight evaluation of an extended engine life mode on an F-15 airplane
[NASA-TM-104240] p 871 N92-29659
Statistics on aircraft gas turbine engine rotor failures that occurred in US commercial aviation during 1989
[DOT/FAA/CT-92/5] p 971 N92-30303
Small engine components test facility compressor testing cell at NASA Lewis Research Center
[NASA-TM-105685] p 982 N92-30508
A new unsteady mixing model to predict NO(x) production during rapid mixing in a dual-stage combustor
[NASA-CR-189155] p 971 N92-30569
Research into improving the durability of the hot section in the aircraft turbine engine
[AD-A250342] p 973 N92-31439
A general numerical model for wave rotor analysis
[NASA-TM-105740] p 1002 N92-31484
Life prediction and constitutive models for engine hot section anisotropic materials program
[NASA-CR-189222] p 973 N92-31534
Statistics on aircraft gas turbine engine rotor failures that occurred in US commercial aviation during 1988
[DOT/FAA/CT-91/28] p 1071 N92-33105
Life prediction and constitutive models for engine hot section anisotropic materials program
[NASA-CR-189223] p 1072 N92-33479
Current nondestructive inspection methods for aging aircraft
[DOT/FAA/CT-91/5] p 1126 N92-33480
A multivariable control concept for a gas turbine engine
[ETN-92-92104] p 1072 N92-33645
A graphical user-interface for propulsion system analysis
[NASA-TM-105696] p 1134 N92-33894
Cooled high-temperature radial turbine program 2
[NASA-CR-189122] p 1073 N92-34236

GAS TURBINES

Power performance of a nonisentropic Brayton cycle p 54 A92-11281
An analysis of the flow-pattern at the exit of a single-stage turbine p 10 A92-13234
Estimation of the size of separation zone in a turbine stage under small load p 10 A92-13235
The performance evaluation of aeroderivative gas turbines p 119 A92-13296
Thermal barrier coatings for gas turbine use p 142 A92-15245
Computation of flow past a turbine blade with and without tip clearance
[ASME PAPER 91-GT-56] p 68 A92-15534
Reliability analysis of a structural ceramic combustion chamber
[ASME PAPER 91-GT-155] p 123 A92-15591
One-dimensional, stage-by-stage, axial compressor performance model
[ASME PAPER 91-GT-192] p 124 A92-15618
CFD analysis of jet mixing in low NO(x) flametube combustors
[ASME PAPER 91-GT-217] p 124 A92-15634
The design and testing of a radial flow turbine for aerodynamic research
[ASME PAPER 91-GT-220] p 124 A92-15636
Lean blowout in a research combustor at simulated low pressures
[ASME PAPER 91-GT-359] p 137 A92-15713
An improved computation for gas-turbine combustion chamber flow p 375 A92-28479
A direct-problem calculation method for gas turbines with bowed and twisted blades p 519 A92-35571
Secondary power system preliminary design
[SAE PAPER 912189] p 656 A92-40008
Auxiliary power units for advanced fighters p 737 A92-43545
Aircraft engines and gas turbines (2nd revised and enlarged edition) --- Book
[ISBN 0-262-11162-4] p 970 A92-53336
Detonation duct gas generator demonstration program
[AIAA PAPER 92-3174] p 1066 A92-54011
Contractors Meeting in Propulsion
[AD-A240057] p 33 N92-10062
Combustion and core noise p 55 N92-10607
Radial inflow turbine study
[AD-A240169] p 26 N92-11015
The effects of Reynolds number, rotor incidence angle and surface roughness on the heat transfer distribution in a large-scale turbine rotor passage
[NASA-CR-184260] p 42 N92-11297
Effects of wake and shock passing on the heat transfer to a film cooled transonic turbine blade p 156 N92-12201
Recent progress in inverse methods in France p 201 N92-13938
Seal related development activities at EG/G p 228 N92-15095
Studies of gas turbine heat transfer: Airfoil surfaces and end-wall cooling effects
[AD-A244055] p 376 N92-19097
An investigation of the energy loss and near wake flow field of trailing edge injection p 456 N92-21839
Dynamic simulation of a solid fuelled gas turbine system p 592 N92-22315
Turbine drive system of the high pressure LOX turbopump test facility
[DE92-783191] p 680 N92-25342
Turbocharged pressurized combustion system
[PB92-142579] p 756 N92-26521
A parametric numerical study of mixing in a cylindrical duct
[NASA-TM-105695] p 738 N92-26553
CFD mixing analysis of jets injected from straight and slanted slots into confined crossflow in rectangular ducts
[NASA-TM-105699] p 738 N92-26561
Simultaneous engineering in aero-gas turbine design and manufacture
[PNR-90811] p 740 N92-27043
The changing role of experimentation in aeroengine R and D: The point of view of the research worker
[AD-A246372] p 740 N92-27062
Aerothermodynamics of nozzle flows for advanced hypersonic propulsion systems p 769 N92-27478
Modelling the vaporiser and primary zone flows for a modern gas turbine combustion chamber p 742 N92-27484
Radial inflow turbine study
[AD-A246938] p 743 N92-28073
Overview on basis and use of performance prediction methods p 869 N92-28459
Fatigue in single crystal nickel superalloys
[AD-A250068] p 987 N92-31360
Radial inflow turbine study
[AD-A252783] p 1127 N92-33538

GAS VISCOSITY

Gas turbine exhaust system silencing design p 882 A92-47365

GAS-LIQUID INTERACTIONS

An analysis of boundary layer for droplet aerodynamic stripped in high speed gas flow p 1116 A92-54563

GAS-SOLID INTERACTIONS

Effects of gas-surface interaction models on aerodynamic characteristics p 244 A92-21718
Local interaction theory --- Russian book
[ISBN 5-288-00516-8] p 779 A92-42778
Monte Carlo study of vibrational relaxation processes p 940 A92-52777

GASEOUS FUELS

Safety considerations in testing a fuel-rich aeropropulsion gas generator
[NASA-TM-105258] p 279 N92-17061

GASES

Atmospheric pressure flow reactor: Gas phase chemical kinetics under tropospheric conditions without wall effects
[NASA-CASE-MSC-21384-1] p 297 N92-16243

GASOLINE
Methyl-tert-butyl ether as a component of aviation gasolines p 34 A92-12146
GAW-2 AIRFOIL
Experimental studies of a two-element airfoil with large separation
[AIAA PAPER 92-0267] p 317 A92-25723
GEAR
Composite gearbox housing p 110 A92-14448
GEAR TEETH
Optimization of longitudinal corrections of helical gears p 990 A92-49578
Monitoring fatigue cracks in gears
p 1116 A92-54496
Single screw mechanism with gaterotor housing at intermediate pressure
[AD-D015140] p 400 N92-18120
Gear tooth stress measurements of two helicopter planetary stages
[NASA-TM-105651] p 764 N92-26555
A preliminary study in the use of phase demodulation techniques for the analysis of gear vibration data
[NRC-32083] p 1002 N92-31469
GEARS
Tiger MGB - High reliability low weight --- military helicopter Main Gear Box p 109 A92-14418
Manufacturing techniques - Split torque path helicopter transmission p 110 A92-14452
Recent manufacturing advances for spiral bevel gears
[SAE PAPER 912229] p 674 A92-40024
Advanced Rotorcraft Transmission program summary
[AIAA PAPER 92-3363] p 905 A92-48936
An eight month gearbox development program
[AIAA PAPER 92-3368] p 850 A92-48941
Design criteria and analysis of the dynamic behavior of high speed, heavily loaded and precision epicyclic gears for aircraft use
[AIAA PAPER 92-3491] p 906 A92-49028
Analytical evaluation of resonant response of spiral bevel gears in the RAH-66 helicopter Fantail transmission
[AIAA PAPER 92-3495] p 906 A92-49031
Modal simulation of gearbox vibration with experimental correlation
[AIAA PAPER 92-3494] p 1112 A92-54036
Flat belt continuously variable high speed drive
[DE92-008952] p 680 N92-25054
Full-scale transmission testing to evaluate advanced lubricants
[NASA-TM-105668] p 764 N92-26560
Analysis and modification of a single-mesh gear fatigue rig for use in diagnostic studies
[NASA-TM-105416] p 773 N92-27879
Application of face-gear drives in helicopter transmissions
[NASA-TM-105655] p 908 N92-28434
Dynamics of a split torque helicopter transmission
[NASA-TM-105681] p 910 N92-29136
Development of a full-scale transmission testing procedure to evaluate advanced lubricants
[NASA-TP-3265] p 998 N92-30396
Experimental testing of prototype face gears for helicopter transmissions
[NASA-TM-105434] p 1002 N92-31349
Modal simulation of gearbox vibration with experimental correlation
[NASA-TM-105702] p 1002 N92-31485
GENERAL AVIATION AIRCRAFT
Operational and economic benefits of area navigation from the perspective of a major air carrier
p 96 A92-16632
System-identification of airplanes using the 'estimation before modelling' technique p 269 A92-21007
Pratt & Whitney PW300 for general aviation
p 277 A92-21012
Analysis of junction flowfields using the incompressible Navier-Stokes equations
[AIAA PAPER 92-0519] p 331 A92-26944
Evaluation of the aerodynamic effects of commuter class (type 1-1/2) anti-icing fluids on small general aviation airplanes
[AIAA PAPER 92-0643] p 459 A92-31675
Development of a multi-computer in-flight data acquisition and analysis system for general aviation aircraft
[AIAA PAPER 92-1037] p 553 A92-33218
Analysis of accidents during instrument approaches
p 529 A92-34253
Personal air transport: State of the art
[PB91-204768] p 18 N92-10991
Corrosion and your aircraft
[NRC-30465] p 114 N92-11991
Soviet electronic display systems under research and manufactured for the civil aviation aircraft of the 1990's
[AD-A240933] p 119 N92-13066
General aviation activity and avionics survey, calendar year 1989
[PB91-179234] p 169 N92-13926
FAA statistical handbook of aviation: Calendar year 1989
[PB91-202051] p 170 N92-13927
Aircraft accident reports: Brief format US civil and foreign aviation issue number 3 of 1989 accidents
[PB90-916903] p 263 N92-15979
Effect of crash pulse shape on seat stroke requirements for limiting loads on occupants of aircraft
[NASA-TP-3126] p 399 N92-18053
Particle trajectory computer program for icing analysis of axisymmetric bodies
[NASA-CR-189134] p 352 N92-19276
Preliminary design studies of an advanced general aviation aircraft
[NASA-CR-190024] p 461 N92-20064
Small engine technology programs
p 560 N92-22532
Low cost, electronically steered phased array for general aviation p 677 N92-24099
Studies in general aviation aerodynamics
[NASA-CR-190431] p 827 N92-28511
FAA aviation forecasts
[AD-A250412] p 837 N92-29182
Effect of guard band reduction on marker beacon receiver performance
[DOT/FAA/CT-TN92/18] p 1002 N92-31617
GEODETIC SURVEYS
Global satellite navigation using both GPS and GLONASS p 99 A92-16938
GPS orbit determination at the National Geodetic Survey p 1049 N92-33354
Precise GPS ephemerides from DMA and NGS tested by time transfer p 1049 N92-33355
GEODYNAMICS
A demonstration of centimeter-level monitoring of polar motion with the Global Positioning System
p 639 N92-24302
GEOGRAPHIC INFORMATION SYSTEMS
Prototyping the IRDS: An airport application
[PB92-112580] p 484 N92-20448
GEOIDS
Selected models of aircraft navigation space
p 839 A92-45373
GEOMETRIC DILUTION OF PRECISION
Kinematic GPS for differential positioning - Resolving integer ambiguities on the fly p 19 A92-10472
Availability of positioning and receiver autonomous integrity monitoring for the global positioning system
p 100 A92-16963
Possible utilization of GPS in precision approach maneuvers p 637 A92-37075
Flight evaluation of navigation systems including MLS using NAL Do228 - Results of GPS
p 1047 A92-56118
GEOMETRICAL ACOUSTICS
Wave equations and computational models for sonic boom propagation through a turbulent atmosphere
p 1139 N92-33877
Simulations of sonic boom ray tube area fluctuations for propagation through atmospheric turbulence including caustics via a Monte Carlo method
p 1139 N92-33878
GEOMETRICAL THEORY OF DIFFRACTION
SATCOM antenna siting study on P-3C aircraft, volume 1
[NASA-CR-189514] p 221 N92-14262
SATCOM antenna siting study on P-3C aircraft, volume 2
[NASA-CR-189515] p 221 N92-14263
Automated composite ellipsoid modelling for high frequency GTD analysis
[NASA-CR-189853] p 275 N92-17316
GEOMETRY
VORVISC: A vortex lattice method with viscous and compressibility corrections for full aircraft configurations including propulsion p 626 N92-24857
Variable geometry sailplanes Minisigma
p 629 N92-24877
GEOPOTENTIAL
User's manual for AeroFcn: A FORTRAN program to compute aerodynamic parameters
[NASA-TM-104237] p 1133 N92-32507
GEOSYNCHRONOUS ORBITS
Aircraft navigation using Global Positioning System improved with geostationary satellites
p 99 A92-16934
GERMAN SPACE PROGRAM
Saenger and the German Hypersonics Technology Programme - Status report 1991
[IAF PAPER 91-198] p 32 A92-12570
The German Hypersonics Technology Programme - Status report 1992
[IAF PAPER 92-0867] p 1105 A92-57258
DLR-News: Announcements of the German Research Institute for Aeronautics and Astronautics
p 698 N92-26086
GERMANY
Air transport research in Germany
p 241 A92-21014
German-GUS cooperation in civil aviation
p 785 A92-47592
DLR-news: Announcements of the German Research Institute for Aeronautics and Astronautics
p 698 N92-25413
DLR research reports and communications
[ETN-92-91391] p 929 N92-29218
GLASS
Three-dimensional laser window formation
[NASA-RP-1280] p 984 N92-30307
GLASS FIBER REINFORCED PLASTICS
Sand erosion behavior of GFRP p 576 A92-32662
Fabrication and mechanical properties of an optically transparent glass fiber/polymer matrix composite
p 891 A92-45630
Development of aircraft bonded structure and the NDI method p 1016 A92-56100
Computed tomography (CT) as a nondestructive test method used for composite helicopter components
p 1121 A92-56276
Computed Tomography (CT) as a nondestructive test method used for composite helicopter components
[MBB-UD-0603-91-PUB] p 910 N92-29873
Processing and environmental effects on mechanical properties of composite repairs
[NRC-LTR-ST-1826] p 1109 N92-32791
GLASS FIBERS
Tiltrotor research aircraft composite blade repairs: Lessons learned
[NASA-TM-103875] p 367 N92-19563
Towards GLARE: The development of a fatigue insensitive and damage tolerant aircraft material
[ETN-92-91301] p 648 N92-24966
GLASS TRANSITION TEMPERATURE
Addition curing thermosets endcapped with 4-amino (2.2) paracyclophane p 577 A92-33918
The effect of physical aging on the creep response of a thermoplastic composite
[AD-A243600] p 290 N92-17932
GLAZES
LDV measurements on a rectangular wing with a simulated glaze ice accretion
[AIAA PAPER 92-2690] p 800 A92-45537
Experimental ice shape and performance characteristics for a multi-element airfoil in the NASA Lewis Icing Research Tunnel
[NASA-TM-105380] p 261 N92-17347
Results of a low power ice protection system test and a new method of imaging data analysis
[NASA-TM-105745] p 828 N92-28696
GLIDE PATHS
New siting techniques for the ILS glide slope
p 188 A92-17422
An exploratory investigation into the definition of tracking standards for IFR helicopter approaches to reduced minima p 533 A92-35726
A compensatory algorithm for the slow-down effect on constant-time-separation approaches
[NASA-TM-4285] p 23 N92-10024
A preliminary flight test on a basic performance of the flight research airplane Do 228: Velocity vs glide path angle
[NAL-TM-613] p 359 N92-18482
Space shuttle entry terminal area energy management
[NASA-TM-104744] p 308 N92-19930
Comparison of the performance of a microwave landing system elevation station with the instrument landing system end-fire glide slope at Yeager Airport, Charleston, West Virginia
[DOT/FAA/CT-TN91/22] p 534 N92-22210
MLS mathematical modeling study of Philadelphia International Airport runway 27L
[DOT/FAA/CT-TN91/54] p 573 N92-22503
ILS mathematical modeling study of an ILS localizer and glide slope proposed for runway 32R, Moffett Field Airport, California
[DOT/FAA/CT-TN92/28] p 1048 N92-33308
GLIDERS
The 'White Pelican' project - Design and construction of the world's largest paper airplane
p 931 A92-51400
A guidance law for hypersonic descent to a point
[AIAA PAPER 92-4303] p 1104 A92-55311
Review of aerodynamic design in the Netherlands
p 193 N92-13929
Piloted simulation study of a balloon-assisted deployment of an aircraft at high altitude
[NASA-TM-104245] p 272 N92-15986

Simulation of the flow on a space glider. Stagnation point calculation using the 2D Navier-Stokes equations including chemical effects p 624 N92-24393
Variable geometry sailplanes Minisigma p 629 N92-24877
Measurements in the inhomogeneous convective boundary layer using three powered gliders p 775 N92-26350
Further wind tunnel investigation of the SM701 airfoil with aileron and turbulators [NASA-CR-190702] p 1038 N92-33063

GLOBAL POSITIONING SYSTEM
Kinematic GPS for differential positioning - Resolving integer ambiguities on the fly p 19 A92-10472
GPS-INS integration requirements for robust NOE helicopter navigation p 94 A92-14404
Institute of Navigation, National Technical Meeting, 47th, Phoenix, AZ, Jan. 22-24, 1991, Proceedings p 95 A92-16626
Integrating GPS with ranging transponders p 95 A92-16627
RAIM - Will it meet the RTCA GPS minimum operational performance standards? --- Receiver Autonomous Integrity Monitoring p 96 A92-16635
The DOT/DOD Federal Radionavigation Plan p 96 A92-16637
A synergistic solution to the GPS integrity problem p 96 A92-16641
In-flight demonstration of hybrid GPS/Loran RAIM p 96 A92-16643
Graceful degradation of GPS/INS performance with fewer than four satellites p 97 A92-16644
Stellar inertial navigation growing with the times upgrading of the LN-20 integrated inertial navigation system p 97 A92-16646
GPS for precision approaches p 139 A92-16648
Precision approach using GPS and GLONASS p 97 A92-16649
Design and flight test of a differential GPS/inertial navigation system for approach/landing guidance p 97 A92-16650
The statistical estimation of navigation errors p 97 A92-16652
A proposal for a dynamic test platform for inertial units and/or GPS p 138 A92-16653
The 1990 Federal Radionavigation Plan and its impact on the Omega Navigation System p 98 A92-16658
Omega/VLF now and into the 21st century p 98 A92-16659
Omega - GPS integration platform p 98 A92-16660
Digital technology applied to airborne receivers p 98 A92-16927
Aircraft navigation using Global Positioning System improved with geostationary satellites p 99 A92-16934
Potential impact of GPS and automatic dependent surveillance on air lane separation in the North Atlantic Organized Track System p 99 A92-16935
Global satellite navigation using both GPS and GLONASS p 99 A92-16938
SATZAP - A novel approach to GPS integrity p 99 A92-16947
Implementation of a RAIM monitor in a GPS receiver and an integrated GPS/IRS p 99 A92-16948
GPS availability. I - Availability of service achievable for different categories of civil users. II - Evaluation of state probabilities for 21-satellite and 24-satellite constellations p 99 A92-16949
Integrated use of GPS and GLONASS in civil aviation navigation. I - Coverage and data models p 99 A92-16950
Comparison of fixed and variable threshold RAIM algorithms p 100 A92-16951
Probability distributions that are important when assessing barometric aiding to GPS p 100 A92-16952
That all-important interface p 100 A92-16953
Closed-loop operation of GPS aided INS p 100 A92-16954
INS alignment using GPS Phase III user equipment computed corrections p 100 A92-16955
Flight test results of an Ada coded INS/GPS open loop Kalman filter design p 100 A92-16958
Availability of positioning and receiver autonomous integrity monitoring for the global positioning system p 100 A92-16963
Wide area differential GPS p 101 A92-16966
A robust filter configuration for DGPS users p 101 A92-16967
Compensating user position for GPS ephemeris error p 101 A92-16968
Results of a test program for the use of differential GPS for approach guidance p 101 A92-16969
Integrated navigation for approach guidance using differential GPS p 101 A92-16970
Concepts for replacing shipboard TACAN with differential GPS p 101 A92-16971
Transition of GPS user equipment testing from Yuma Proving Ground to Holloman AFB p 138 A92-16972
Flight test of a GPS-aided low-cost inertial navigation system programmed in Ada p 101 A92-16973
Integrated GPS/INS for the National Aerospace Plane p 102 A92-16975
A digital P-code GPS receiver embedded in the AN/APN-217(V)5 Doppler Navigator p 102 A92-16976
Use of distance-measuring equipment (DME) for correcting errors in position, velocity, and wind measurements from aircraft inertial navigation systems p 188 A92-18172
Navsat - A civil complement to GPS and Glonass [IAF PAPER 91-490] p 188 A92-18505
GPS integrated system application in aircraft approach landing p 266 A92-21466
The LISA 6000 - A highly integrated IRS/GPS navigation system p 267 A92-22088
GPS interferometric attitude and heading determination - Initial flight test results p 454 A92-30023
A consistency test of airborne GPS using multiple monitor stations p 454 A92-30651
Kalman filter mechanization for INS airstart p 574 A92-33602
Approach flight trials in the Netherlands for the Navstar GPS Joint Program Office International Test Program p 533 A92-35928
Possible utilization of GPS in precision approach maneuvers p 637 A92-37075
GPS - Can it contribute to European ATC? p 637 A92-38380
Analysis of stand-alone differential GPS for precision approach p 638 A92-38381
GPS/GLONASS user systems in Sweden p 638 A92-38384
Flight test data analysis of a low cost GPS/IMU integrated navigation system p 638 A92-39560
GPS interferometric attitude and heading determination - Flight test results p 650 A92-39561
Receiver autonomous integrity monitoring (RAIM) - Techniques, performance and potential p 638 A92-39567
A system for precise real-time differential GPS positioning in the decimeter range p 638 A92-39569
The evolution of military GPS technology into the Navcore V receiver engine p 651 A92-39570
Navigation experiment on an aircraft using the GPS-INS navigation system. I - Introduction to the system p 726 A92-43122
Navigation experiment on aircraft flight using the GPS-INS navigation system. II - Test results p 726 A92-43123
Global Positioning System telecommand link p 839 A92-47566
Computer-Controlled Navigation System/General Positioning System (CCNS/GPS) - A guidance, positioning, and management system for remote sensing flights p 840 A92-47630
Construction of a real-time DGPS experimental system p 840 A92-47631
Formation flight system design concept p 954 A92-49255
GPS integration improves mission capabilities of CH-47D aircraft p 966 A92-49340
GLONASS data analysis - Interim results p 955 A92-49382
On the calculation of repeatable accuracy, with special reference to GPS p 955 A92-49383
Architectures and GPS/INS integration - Impact on mission accomplishment p 967 A92-51003
Differential GPS/inertial navigation approach/landing flight test results p 956 A92-51009
Receiver Autonomous Integrity Monitoring (RAIM) capability for sole-means GPS navigation in the oceanic phase of flight p 956 A92-51012
GPS tests during approach at Singapore and Roissy p 956 A92-53240
Flight evaluation of navigation systems including MLS using NAL Do228 - Results of GPS p 1047 A92-56118
Investigation of air transportation technology at Ohio University, 1990-1991 p 265 N92-17990
GPS interferometric attitude and heading determination: Initial flight test results p 269 N92-17994
GPS/INS integration for improved aircraft attitude estimates [AD-A243947] p 356 N92-19604
Global positioning system supported pilot's display p 534 N92-22436
NASA's GPS tracking system for Aristoteles p 576 N92-23919
A demonstration of centimeter-level monitoring of polar motion with the Global Positioning System p 639 N92-24302
Current activities and future plans for GPS applications p 640 N92-24735
Evaluating the velocity accuracy of an integrated GPS/INS system: Flight test results [DE92-007519] p 640 N92-25470
An adaptive correction technique for Differential Global Positioning System p 726 N92-26623
Buffered serial data card [AD-A246435] p 727 N92-26948
NAL Dornier 228-200 flight research airplane: Present status and outline of the installed equipment [NAL-TM-637] p 732 N92-27429
Dredging research program: Global positioning system bibliography [AD-A248954] p 729 N92-28079
Global positioning system runway incursion program static ground tests [DOT/FAA/CT-TN91/44] p 957 N92-31838
Decision-making guide for the proposed Coast Guard differential global positioning system [AD-A246046] p 957 N92-32054
The need for GPS standardization p 1049 N92-33351
US Coast Guard GPS Information Center (GPSIC) and its function within the Civil GPS Service (CGS) p 1049 N92-33352
Evaluation of GPS/UTC steering performance p 1049 N92-33353
GPS orbit determination at the National Geodetic Survey p 1049 N92-33354
Precise GPS ephemerides from DMA and NGS tested by time transfer p 1049 N92-33355
Comparison of two-way satellite time transfer and GPS common-view time transfer between OCA and TUG p 1050 N92-33356
Comparison of GLONASS and GPS time transfers between two west European time laboratories and VNIIFTRI p 1050 N92-33381
Calibration of GPS antennas [ETN-92-92034] p 1051 N92-33693

GLOW DISCHARGES
An experimental investigation of large scale instabilities in a low Reynolds number two-stream supersonic shear layer [AIAA PAPER 92-0177] p 255 A92-23787

GLYCEROLS
Particle image velocimetry [AD-A246638] p 750 N92-27753

GOAL THEORY
Structure/control design synthesis of active flutter suppression system by goal programming p 204 A92-18621

GOERTLER INSTABILITY
Three-dimensional singularity of flow structure in an underexpanded supersonic jet p 78 A92-16679
The inviscid compressible Goertler problem in three-dimensional boundary layers p 809 A92-46441
Nonlinear development and secondary instability of large-amplitude Goertler vortices in hypersonic boundary layers p 942 A92-53080

GOGGLES
Helicopter NVG testing in the United Kingdom p 112 A92-16053

GOODNESS OF FIT
An exploratory application of neural networks to the sortie generation forecasting problem [AD-A246626] p 778 N92-27980

GORES
Operational evaluation of recently developed balloon fabrication methods [AIAA PAPER 91-3670] p 1 A92-11017

GOVERNMENT PROCUREMENT
A revolution in air transport - Acquiring the C-141 Starlifter p 607 A92-38101

GOVERNMENT/INDUSTRY RELATIONS
German airports - Capacity crisis p 61 A92-17097
An airlifter for the long haul p 358 A92-28493
Winds of change: Domestic air transport since deregulation [NRC-SR-230] p 92 N92-13040
The NASA/industry design analysis methods for vibrations (DAMVIBS) program: Accomplishments and contributions [NASA-TM-104192] p 299 N92-17034

GRADIENTS
A comparison of two closely-related approaches to aerodynamic design optimization p 193 N92-13933
A novel approach in formulation of special transition elements: Mesh interface elements [NASA-CR-189050] p 501 N92-20954
Observations on computational methodologies for use in large-scale, gradient-based, multidisciplinary design incorporating advanced CFD codes [NASA-TM-104206] p 630 N92-24956

GRAIN SIZE
Improving sample introduction for total wear metal determination by atomic emission spectroscopy
p 389 A92-26850

GRAPH THEORY
Failure environment analysis tool (FEAT) development status
[AIAA PAPER 91-3803] p 232 A92-17654

GRAPHIC ARTS
Design considerations for IAP charts: Approach course track and communication frequencies
[AD-A241482] p 103 N92-13051
Computational algorithms for increased control of depth-viewing volume for stereo three-dimensional graphic displays
[NASA-TM-4379] p 1065 N92-34109

GRAPHITE
Simulation of high heat flux levels with graphite heating and arc lamps p 980 A92-51402
Notes on the use of fusible temperature indicators to bound the temperature of hot graphite in the NAVSWC hypervelocity wind tunnel facility p 1090 A92-54315

GRAPHITE-EPOXY COMPOSITES
Advanced thermoplastic nose landing gear door development p 20 A92-10275
The study on the composite-patching repairs for metallic aircraft structures p 36 A92-10285
Fracture behaviour of high-temperature polymer composites p 34 A92-11993
Laser-based ultrasonics on GR/epoxy composite - Interferometric detection p 144 A92-13554
Mechanics of curved fiber composites
p 140 A92-14346
Flight service evaluation of composite helicopter components p 106 A92-14372
Experimental and theoretical analysis of composite I-beams with elastic couplings p 216 A92-18377
Nonlinear stall flutter and divergence analysis of cantilevered graphite/epoxy wings p 219 A92-20746
Weight estimating guide for advanced composites
p 289 A92-23418
Thermal imaging of graphite/epoxy composite samples with fabricated defects p 491 A92-28655
The reinforcing effect of composite patch repairs on metallic aircraft structures p 419 A92-30498
Torsion and twisting of symmetric composite laminates
[AIAA PAPER 92-2425] p 582 A92-34354
Experimental and analytical study of the effects of floor location on response of composite fuselage frames
[AIAA PAPER 92-2473] p 539 A92-34362
Mechanics of curved fiber composites
p 757 A92-41034
Buckling, postbuckling and crippling of thin walled composite airframe structures under compression
p 899 A92-46940
A damage tolerance assessment of bonded repairs to CF-18 composite components. Part 1: Adhesive properties
[DREP-TM-88-25-PT-1] p 143 N92-12060
Review of investigations on aeronautical fatigue in the Federal Republic of Germany
[ETN-92-90317] p 225 N92-14397
Environmental fatigue tests with composite materials
p 214 N92-14413
Finite element analysis of a riveted repair on a curved composite panel
[AD-A243916] p 404 N92-19384
Manufacturing development of pultruded composite panels
[NASA-CR-181780] p 578 N92-22637
A preliminary study on damage detection using piezoelectric film
[AD-A246350] p 733 N92-28118
A Protection And Detection Surface (PADS) for damage tolerance p 1107 N92-32523
Global/local methods research using the CSM testbed
p 1107 N92-32528
Residual strength of repaired graphite/epoxy laminates after 5 years of outdoor exposure p 1108 N92-32577
Initial postbuckling response of an unsymmetrically laminated rectangular plate p 1108 N92-32586
Advanced airframe structural materials: A primer and cost estimating methodology
[AD-A253371] p 1062 N92-34182

GRAPHS (CHARTS)
A formal definition of the object-oriented paradigm for requirements analysis
[AD-A246814] p 729 N92-28132

GRAVIMETERS
A study of the precision characteristics of a gyroscopic gravimeter p 581 A92-33778

GRAVITATIONAL EFFECTS
Baro-inertial loop for the USAF Standard RLG INU
p 97 A92-16647
Experimental results and numerical modeling of solidification during aircraft high-g arcs
[AIAA PAPER 92-0843] p 493 A92-29609
Convective flow analysis on the KC-135 aircraft
[AIAA PAPER 92-0844] p 493 A92-29610
Process modeling KC-135 aircraft
[NASA-CR-184278] p 359 N92-18347

GRAZING INCIDENCE
Control of the landing of a flight vehicle in the grazing-incidence mode p 134 A92-16808

GREAT CIRCLES
Traveling on the curved earth p 19 A92-10474

GREEN'S FUNCTIONS
Prediction of separation point in compressible turbulent boundary layers by Green's lag-entrainment method
p 700 A92-41178
Application of a wall pressure method in a wind tunnel test section with adjustable longitudinal slots
p 1091 A92-54336
An outline of a numerical scheme for calculating two-dimensional time linearised transonic flow using the Green's function method
[AD-A246349] p 764 N92-26258

GRID GENERATION (MATHEMATICS)
Evaluation of an adaptive unstructured remeshing technique for integrated fluid-thermal-structural analysis
p 37 A92-10445
Three-dimensional space-marching algorithm on unstructured grids p 5 A92-11058
Finite difference numerical prediction of aerodynamics of an airfoil flying over wavy wall p 64 A92-14033
Numerical study of branched turboprop inlet ducts using a multiple block grid procedure
[ASME PAPER 91-GT-339] p 76 A92-15703
Turbulent flow calculations using unstructured and adaptive meshes p 153 A92-15823
Three-dimensional solution-adaptive grid generation on composite configurations p 172 A92-18352
CFD helps the Air Force fly right p 169 A92-20146
The finite volume approach for the Navier-Stokes equations p 246 A92-21980
Adaptation methods for viscous flows
p 246 A92-21982
A Navier-Stokes solver for stretched triangular grids
[AIAA PAPER 92-0183] p 256 A92-23793
Computations of the flow past bodies and wings using Euler equations p 312 A92-25038
Numerical simulation of inviscid flow over a complicated body using an overlapping grid technique
p 313 A92-25043
Automatic grid generation for iced airfoil flowfield predictions
[AIAA PAPER 92-0415] p 326 A92-26266
The NASA Computational Aerosciences Program - Toward teraFLOPS computing
[AIAA PAPER 92-0558] p 411 A92-26968
An analytical approach to grid sensitivity analysis --- of NACA wing sections
[AIAA PAPER 92-0660] p 334 A92-27031
Three-dimensional adaptive grid generation with applications in nonlinear fluid dynamics
[AIAA PAPER 92-0661] p 397 A92-27032
Embedded meshes of controllable quality synthesised from elementary geometric features
[AIAA PAPER 92-0663] p 411 A92-27034
Algebraic turbulence modeling for adaptive unstructured grids p 398 A92-28033
Euler solutions for an unbladed jet engine configuration
[AIAA PAPER 92-0544] p 398 A92-28201
Inviscid and viscous transonic flows in cascades using an implicit upwind algorithm p 344 A92-28522
Optimized control of structured grids
p 429 A92-30520
The unstructured upwind method p 429 A92-30522
Multi-block airfoil profile of grid formation
p 429 A92-30523
Orthogonal grids around difficult bodies
p 432 A92-31160
Solution-adaptive grid procedure for the parabolized Navier-Stokes equations p 432 A92-31163
A new adaptive algorithm for turbulent flows
p 434 A92-31547
Numerical simulations of the flow through cascades with tip clearance p 523 A92-36038
Two- and three-dimensional grid generation by an algebraic homotopy procedure p 611 A92-36861
The computation of three-dimensional flows using unstructured grids p 612 A92-37539
Solution of Euler equations for fighter forebody-inlet combinations at high angles of attack
p 613 A92-38269
Panel method control in 3-D hyperbolic grid generation
p 617 A92-39940
Parallel grid generation/optimization using block-domain decomposition p 776 A92-41199
Flow establishment in a generic scramjet combustor
p 737 A92-44525
Three-dimensional orthogonal-to-surface structured grid generation with transonic Navier-Stokes flow solutions for a commercial transport configuration
[AIAA PAPER 92-2616] p 793 A92-45490
An adaptive grid method for computing the high speed 3D viscous flow about a re-entry vehicle
[AIAA PAPER 92-2685] p 799 A92-45534
Computational evaluation of an airfoil with a Gurney flap
[AIAA PAPER 92-2708] p 802 A92-45550
Surface grid generation in a parameter space
[AIAA PAPER 92-2717] p 803 A92-45556
A new automatic grid generation environment for CFD applications
[AIAA PAPER 92-2720] p 803 A92-45558
Prismatic grid generation with an efficient algebraic method for aircraft configurations
[AIAA PAPER 92-2721] p 803 A92-45559
Temporal adaptive Euler/Navier-Stokes algorithm involving unstructured dynamic meshes
p 812 A92-46887
Compact higher order characteristic-based Euler solver for unstructured grids p 812 A92-46889
Numerical grid generation in computational fluid dynamics and related fields; Proceedings of the 3rd International Conference, Universidad Politecnica de Cataluna, Barcelona, Spain, June 3-7, 1991
[ISBN 0-444-88948-5] p 918 A92-47035
Unstructured and adaptive mesh generation for high Reynolds number viscous flows p 816 A92-47042
Anisotropic control of mesh generation based upon a Voronoi type method p 918 A92-47043
Grid adaptation to multiple functions for applied aerodynamic analysis p 817 A92-47045
Adaptive parallel meshes with complex geometry
p 918 A92-47050
Gridding strategies and associated results for winged entry vehicles p 918 A92-47051
An unstructured mesh generation algorithm for three-dimensional aeronautical configurations
p 918 A92-47053
Single block mesh generation for a fuselage plus two lifting surfaces p 817 A92-47054
Grid generation and compressible flow computations about a high-speed civil transport configuration
p 919 A92-47055
Multi-block grid generation around wing-body-engine-pylon configurations
p 817 A92-47060
3-D numerical grid generation for the transonic flow analysis about multi-bodies p 817 A92-47061
Interactive algebraic mesh generation for twin jet transport aircraft p 817 A92-47064
Interactive generation of structured/unstructured surface meshes using adaptivity p 919 A92-47066
Simple diagnosis for the quality of generated grid systems p 919 A92-47069
Patch-independent structured multiblock grids for CFD computations p 919 A92-47078
New concepts for multi-block grid generation for flow domains around complex aerodynamic configurations
p 817 A92-47079
Generation of efficient multiblock grids for Navier-Stokes computations p 919 A92-47081
A geometry-integrated approach to multiblock grid generation p 919 A92-47083
The construction, application and interpretation of three-dimensional hybrid meshes p 919 A92-47089
Generation of unstructured grids within a hybrid multi-block environment p 818 A92-47090
Orthogonal grids for multiple airfoils
p 818 A92-47096
Prediction of a high bypass ratio engine exhaust nozzle flowfield
[AIAA PAPER 92-3259] p 864 A92-48855
Investigation of three-dimensional flow field in a turbine including rotor/stator interaction. I - Design development and performance of the research facility
[AIAA PAPER 92-3325] p 883 A92-48908
A finite element method for shear stresses calculation in composite blade models p 1121 A92-56322
Computational study of the aerodynamics and control by blowing of asymmetric vortical flows over delta wings
[NASA-CR-187979] p 14 N92-10990
Euler solutions for an unbladed jet engine configuration
[NASA-TM-105332] p 44 N92-11328
Flow and temperature computations for space vehicles using adaptive finite element techniques
p 181 N92-14990
Equilibrium solution of the Euler and Navier-Stokes equations around a double ellipsoidal shape with mono- and multi-blocks including real gas effects, part 1
p 227 N92-15030

Grid impact on 3D hypersonic flows
p 184 N92-15041
WP 4b compressible flow simulation: Information System for flow simulation based on the Navier-Stokes equation (ISNaS). Requirements grid generation for the ISNaS compressible flow solver
[NLR-TR-88103-U] p 405 N92-19490
MATGRID: A program for generation of C-H and C-O topology grids around wing/body configurations. Mathematical definition document
[FFA-TN-1990-19] p 444 N92-20468
Quality assessment of two- and three-dimensional unstructured meshes and validation of an upwind Euler flow solver
[NASA-TM-104215] p 444 N92-20480
A novel approach in formulation of special transition elements: Mesh interface elements
[NASA-CR-189050] p 501 N92-20954
Boundary layer flow in axial compressors (theoretical part)
[ETN-92-91007] p 501 N92-21233
Boundary layer flow in axial compressors (theoretical part)
[ETN-92-91008] p 502 N92-21234
An alternative to unstructured grids for computing gas dynamic flows around arbitrarily complex two-dimensional bodies
[NASA-CR-189612] p 447 N92-21465
Grid generation and flow solution method for Euler equations on unstructured grids
[NASA-TM-4295] p 528 N92-23533
A two-dimensional Euler solution for an unbladed jet engine configuration
[NASA-TM-105329] p 597 N92-23560
Interactive solution-adaptive grid generation procedure
[NASA-TM-105432] p 528 N92-23563
Software Surface Modeling and Grid Generation Steering Committee
[NASA-CP-3143] p 691 N92-24397
Geometry acquisition and grid generation: Recent experiences with complex aircraft configurations
p 691 N92-24400
Domain modeling and grid generation for multi-block structured grids with application to aerodynamic and hydrodynamic configurations p 691 N92-24411
An interactive multi-block grid generation system
p 691 N92-24419
A multiblock grid generation technique applied to a jet engine configuration p 692 N92-24428
A study of transonic aerodynamic analysis methods for use with a hypersonic aircraft synthesis code
[NASA-CR-189854] p 625 N92-24803
Workshop on Grid Generation and Related Areas
[NASA-CP-10089] p 659 N92-25712
Grid management p 632 N92-25713
Grid generation for a complex aircraft configuration
p 649 N92-25714
TCGRID: A three dimensional C-grid generator for turbomachinery p 659 N92-25716
An interactive grid generation technique for turbomachinery p 659 N92-25717
TIGER: Turbomachinery interactive grid generation
p 659 N92-25718
TIGGERC: Turbomachinery interactive grid generator energy distributor and restart code p 659 N92-25719
Multiblock grid generation for jet engine configurations
p 659 N92-25720
Cartesian based grid generation/adaptive mesh refinement p 682 N92-25722
Grid generation research at OSU p 633 N92-25723
Integrating aerodynamic surface modeling for computational fluid dynamics with computer aided structural analysis, design, and manufacturing
p 682 N92-25727
A new Lagrangian method for real gases at supersonic speed p 633 N92-25814
Progress in integrated analysis with adaptive unstructured meshing p 683 N92-25914
An integrated CFD system for 3D turbomachinery applications p 741 N92-27464
A frontal approach for node generation in Delaunay triangulations p 771 N92-27680
Computation of the unsteady transonic 2D cascade flow by an Euler algorithm with interactive grid generation
p 719 N92-27944
Hyperbolic grid generation with BEM source terms
[NLR-TP-90334-U] p 923 N92-28635
Development of a multigrid transonic potential flow code for cascades
[NASA-CR-190480] p 830 N92-29361
Hyperbolic grid generation control by panel methods
[NLR-TP-91061-U] p 924 N92-29604
NASA Workshop on future directions in surface modeling and grid generation
[NASA-CP-10092] p 831 N92-29625
MATGRID, a program for generation of C-H and C-O topology grids around wing/body configurations: Software description document
[FFA-TN-1990-20] p 945 N92-30713
Numerical methods for the simulation of complex multi-body flows with applications for the integrated Space Shuttle vehicle
[NASA-CR-190045] p 945 N92-30740
Application of the Chimera overlapped grid scheme to simulation of Space Shuttle ascent flows
p 945 N92-30742
Trajectory fitting in function space with application to analytic modeling of surfaces
[NASA-TP-3232] p 945 N92-30747
Delaunay triangulation and computational fluid dynamics meshes
[NASA-TM-107663] p 1010 N92-30907
Hypersonic code efficiency and validation studies
[NASA-CR-190680] p 948 N92-31533
An installed nacelle design code using a multiblock Euler solver. Volume 1: Theory document
[NASA-CR-189652-VOL-1] p 950 N92-32226
An installed nacelle design code using a multiblock Euler solver. Volume 2: User guide
[NASA-CR-189652-VOL-2] p 951 N92-32228
New concepts for multi-block grid generation for flow domains around complex aerodynamic configurations
[NLR-TP-91046-U] p 1037 N92-32730
Finite difference time domain grid generation from AMC helicopter models
[NASA-TM-107679] p 1128 N92-34017

GRIDS
An experimental investigation of the inlet exit flow field improved by aerodynamic grid p 343 A92-28477

GRINDING
Study of grinding process and strength for ceramic heat insulated engine
[SME PAPER MR91-177] p 897 A92-45260

GRINDING MACHINES
Recent manufacturing advances for spiral bevel gears
[SAE PAPER 912229] p 674 A92-40024

GROOVES
Experiment of static and dynamic characteristics of spiral grooved seals p 223 N92-14361

GROOVING
Grooved runway surface texture before and after rubber removal p 1093 A92-56111

GROUND BASED CONTROL
A simulator and performance criteria for evaluation of ground and space-based ATC surveillance
p 96 A92-16639
Computation of aircraft geometric height under radar surveillance p 639 A92-40239
Application of fuzzy control to aircraft guidance
p 1083 A92-56033
Ames life science telescience testbed evaluation
[NASA-CR-188856] p 140 N92-12033
Data Multiplexing Network (DMN) phase 3 equipment Operational Test and Evaluation (OT and E)/integration test report
[DOT/FAA/CT-TN91/50] p 221 N92-14270
Controller response to conflict resolution advisory prototype
[PB92-190032] p 1050 N92-33596

GROUND CREWS
Approach to crew training in support of the USAF Aircraft Structural Integrity Program (ASIP) p 363 N92-18595
Human factors evaluation of the work environment of operators engaged in the inspection and repair of aging aircraft
[AD-A246445] p 724 N92-27914
Flight crew integration in the maintenance chain of a commercial aircraft (A 320) p 1012 N92-30957

GROUND EFFECT (AERODYNAMICS)
Hot gas environment around STOVL aircraft in ground proximity. I - Experimental study p 371 A92-24409
A review of impinging jets in cross-flows - Experimentation and computation
[AIAA PAPER 92-0633] p 333 A92-27011
Optimization of bluff body for minimum drag in ground proximity p 431 A92-31154
Analysis of slender bodies of revolution with curved-ground effect and waving-water effect
p 524 A92-36151
Recent research into the aerodynamics of ASTOVL aircraft in ground environment p 623 A92-40549
A USAF assessment of STOVL fighter options
p 842 A92-45310
Recent developments at the Shoeburyness STOVL test facility p 881 A92-45314
Hot-gas reingestion - Engine response considerations
p 860 A92-45317
The experimental and computational study of jet impingement flowfields with reference to VSTOL aircraft performance p 787 A92-45324
Motion analysis of 2-dimensional flat plate in ground effect p 1030 A92-56053
Rotorwash computer model: User's guide
[DOT/FAA/RD-90/25] p 346 N92-18345
Recent developments at the Shoeburyness (England) STOVL Test Facility
[PNR-90806] p 572 N92-22096
Viscous effects on a vortex wake in ground effect
[NASA-CR-190400] p 907 N92-28361
On the anomalies in single-jet hover suckdown data
[NASA-TM-102261] p 1038 N92-33306
On the estimation of jet-induced fountain lift and additional suckdown in hover for two-jet configurations
[NASA-TM-102268] p 1040 N92-33618

GROUND EFFECT MACHINES
PAR-WIG performance prediction during acceleration from water-borne to air-borne p 291 A92-21721
The maneuver performance and control of a hovercraft p 763 A92-43240
Gust response and cross wind performance of a hovercraft with vertical wings p 1118 A92-56034
On the maneuvering tests of an ACV model
p 1118 A92-56035
Configuration of flexible-skirts for an ACV and its CAD
p 1118 A92-56036
Planning method of skirt systems for small ACVs
p 1118 A92-56038
A potential flow theory of two-dimensional bifurcated curtain jets. II p 1118 A92-56039
Three-dimensional numerical analysis of impinging circular jet - Discrete vortex method
p 1029 A92-56040
Discussion for possibility of some aerodynamic ground effect craft
[NAL-TM-619] p 300 N92-17757
Air cushion vehicle conductive/semiconductive flexible skirt, and method
[AD-D015160] p 400 N92-18187
Pitch-heave dynamics models for an air cushion vehicle
[ISBN-0-315-51095-1] p 716 N92-27624

GROUND HANDLING
Enhancement of ground handling through optimum selection/use of Ground Support Equipment (GSE)
[SAE PAPER 911973] p 881 A92-45380
Testing concept of a movement area guidance
p 641 N92-25597

GROUND RESONANCE
Dynamics of helicopters in ground resonance with and without blade dissimilarities
[AIAA PAPER 92-2108] p 544 A92-35679
Active control of helicopter ground and air resonance
p 568 A92-35762
A study on mechanical model of the helicopter 'ground resonance' p 955 A92-50214
Safety provision against 'ground resonance' free vibration of a coaxial helicopter p 1056 A92-56289

GROUND STATIONS
The Aeronautical Mobile Satellite Service (AMSS). II - Frequency spectrum requirements for the Aeronautical Mobile Satellite Service p 94 A92-13852
Implementation and usage of the RJ program Data Acquisition System Ground Station p 210 A92-19257
A consistency test of airborne GPS using multiple monitor stations p 454 A92-30651
Error estimation of INS ground alignment through observability analysis p 639 A92-40226
Remote telemetry concepts p 882 A92-47562
Gulf Range Drone Control Upgrade System Mobile Control System p 882 A92-47567
Aircraft satellite communication systems
p 1046 A92-56091
NASA's GPS tracking system for Aristoteles
p 576 N92-23919
An aircraft Earth station for general aviation
p 678 N92-24194
Current activities and future plans for GPS applications p 640 N92-24735
GPS orbit determination at the National Geodetic Survey p 1049 N92-33354
LORAN-C data reduction at the US Naval Observatory
p 1050 N92-33358

GROUND SUPPORT EQUIPMENT
A study of a ground support equipment (GSE) network
p 748 A92-43158
Enhancement of ground handling through optimum selection/use of Ground Support Equipment (GSE)
[SAE PAPER 911973] p 881 A92-45380
Data Multiplexing Network (DMN) phase 3 equipment Operational Test and Evaluation (OT and E)/integration test report
[DOT/FAA/CT-TN91/50] p 221 N92-14270
Introduction and execution of flight tests at the DLR
p 648 N92-25594

GROUND SUPPORT SYSTEMS
A computerized flight inspection system --- for testing of basic air navigation ground facilities
p 726 A92-43881
Ground installations for the preparation and evaluation of flight tests p 665 N92-25593
Preparation for a new plane (A 320): Experience reviewed p 1010 N92-30954
GROUND TESTS
Aircraft ground vibration test by means of flight control surfaces
[ONERA, TP NO. 1991-96] p 133 A92-16079
Transition of GPS user equipment testing from Yuma Proving Ground to Holloman AFB p 138 A92-16972
ASNT and aerospace - What about the next 50 years?
p 215 A92-17293
Conducting the NASP ground test program
[AIAA PAPER 91-5029] p 209 A92-17820
Realistic real-time ground testing
[AIAA PAPER 92-0197] p 284 A92-23805
Ground test facilities for aerothermal and aero-optical evaluation of hypersonic interceptors
[AIAA PAPER 92-1074] p 573 A92-33244
The development and testing of an active control of structural response system for the EH101 helicopter
p 569 A92-35775
Advances in aircraft modal identification
[ONERA, TP NO. 1992-47] p 877 A92-48608
High temperature ground vibration test techniques
p 980 A92-51404
Development of local nonintrusive measurements of inlet and exhaust flows for the ground testing of air-breathing engines
[AIAA PAPER 92-3899] p 1122 A92-56735
Turbine engine hot-part temperature measurement techniques
[AIAA PAPER 92-3960] p 1122 A92-56788
A multi-diagnostic approach to testing V/STOL craft
[AIAA PAPER 92-4008] p 1099 A92-56831
Aerodynamics laboratory education at Purdue University - Ground testing facilities
[AIAA PAPER 92-4018] p 1100 A92-56840
Resonance and control response tests using a control stimulation drive
[MBB-UD-0586-90-PUB] p 134 N92-12003
Aircraft ground test and subscale model results of axial thrust loss caused by thrust vectoring using turning vanes
[NASA-TM-4341] p 273 N92-17071
Preparation of the ice certification of the Dornier 328 regional airliner by numerical simulation and by ground test p 451 N92-21693
Evaluating fixed wing aircraft in the aircraft carrier environment p 464 N92-21963
The effect of droplet sizing uncertainty on ice accretions p 679 N92-24874
Experimental aerodynamic facilities of the Aerodynamics Research and Concepts Assistance Branch
[AD-A247489] p 883 N92-28248
Resonance and control response tests using a control simulation device
[MBB-UD-0608-91-PUB] p 978 N92-30439
Compact range test applications, phase 2
[AD-A248790] p 999 N92-30583
Global positioning system runway incursion program static ground tests
[DOT/FAA/CT-TN91/44] p 957 N92-31838
Evaluation of composite components on the Bell 206L and Sikorsky S-76 helicopters p 1107 N92-32575
MD-80 aft cabin noise control: A case history
p 1137 N92-32950
Advanced Study for Active Noise Control in Aircraft (ASANCA)
[AIAA PAPER 92-2092] p 1137 N92-32956
Flight service environmental effects on composite materials and structures p 1110 N92-33054
GROUND-AIR-GROUND COMMUNICATION
The Aeronautical Mobile Satellite Service (AMSS). I - Architecture of the AMSS system p 93 A92-13851
The Aeronautical Mobile Satellite Service (AMSS). II - Frequency spectrum requirements for the Aeronautical Mobile Satellite Service p 94 A92-13852
A European perspective on the co-operative air traffic management concept p 531 A92-33427
FANS technology and the future of air traffic services
p 532 A92-33436
Data Link integration in commercial transport operations p 839 A92-44919
Feasibility study on a microwave-powered unmanned aerial vehicle for the communication relay utilization
[SAE PAPER 912052] p 843 A92-45436
Flight deck benefits of integrated data link communication
[NASA-TP-3219] p 456 N92-21459
Inmarsat aeronautical mobile satellite system: Internetworking issues p 677 N92-24098
GROUP DYNAMICS
A model for evaluation and training in aircrew coordination and cockpit resource management
p 46 A92-11191
Tasking and communication flows in the F/A-18D cockpit: Issues, problems, and possible solutions
[AD-A245977] p 853 N92-28802
GUIDANCE (MOTION)
Modern navigation, guidance, and control processing --- Book
[ISBN 0-13-596230-7] p 639 A92-40199
Ideal proportional navigation p 976 A92-50497
AIAA Guidance, Navigation and Control Conference, Hilton Head Island, SC, Aug. 10-12, 1992, Technical Papers. Pts. 1-3 p 1130 A92-55151
Knowledge based system applications for guidance and control
[AGARD-AR-284] p 205 N92-14065
Artificial Neural Network Approaches in Guidance and Control
[AGARD-LS-179] p 234 N92-14673
Introduction to neural computing and categories of neural network applications to guidance, navigation and control p 234 N92-14674
Flight evaluation of curved MLS precision approaches in a twin otter aircraft, phase 2
[AD-A243025] p 268 N92-17568
NASA TSRV essential flight control system requirements via object oriented analysis
[NASA-CR-189573] p 381 N92-19499
Proportional plus integral control of aircraft for automated maneuvering formation flight
[AD-A243792] p 382 N92-19505
GUIDANCE SENSORS
Talons 95 GHz radar sensor for autonomous landing guidance p 1063 A92-55908
FCS skewed sensors array: Practical considerations
p 968 N92-31868
GUIDE VANES
Application of compound leaned blades to controlling secondary flow p 5 A92-10975
The influence of blade leaning on the performance of an integrated OGV-diffuser system
[ASME PAPER 91-GT-104] p 122 A92-15561
Film cooling research on the endwall of a turbine nozzle guide vane in a short duration annular cascade. I - Experimental technique and results
[ASME PAPER 91-GT-252] p 150 A92-15657
Film cooling research on the endwall of a turbine nozzle guide vane in a short duration annular cascade. II - Analysis and correlation of results
[ASME PAPER 91-GT-253] p 150 A92-15658
LDV measurements and investigation of flow field through radial turbine guide vanes p 217 A92-19618
Laser measurements of unsteady flow field in a radial turbine guide vanes
[AIAA PAPER 92-0394] p 395 A92-26249
Technique for estimating the strength of gas turbine guide vanes with stress raisers p 761 A92-42653
Effects of wake and shock passing on the heat transfer to a film cooled transonic turbine blade
p 156 N92-12201
Predictions and measurements of 3D viscous flow in a transonic turbine nozzle guide vane row
p 741 N92-27466
GUMS (SUBSTANCES)
Laser induced fluorescence detection of gums in jet fuels
[AD-A252685] p 987 N92-30767
GUNFIRE
Influence of flight parameters on air intake internal flow distortions due to gun blast-air interaction
p 310 A92-24426
GUST ALLEVIATORS
Rolling Maneuver Load Alleviation using active controls
[AIAA PAPER 92-2099] p 566 A92-35670
Analysis and wind tunnel test of low aspect wing gust load alleviation p 1053 A92-56020
Synthesis of gust load alleviation with flutter margin augmentation p 1082 A92-56021
Optimization of aeroelastic system with active control
p 1083 A92-56022
Rolling maneuver load alleviation using active controls
[NASA-TM-107654] p 962 N92-31351
GUST LOADS
International standardisation of regulations for gust loading calculations p 270 A92-22473
Gust effects on a flexible aircraft p 270 A92-22474
An experiment on the weight vs control relations of subsonic airplanes p 357 A92-25502
New complex pole and gust response approximations for integrated aeroservoelastic synthesis
[AIAA PAPER 92-2377] p 565 A92-34547
Determining design gust loads for nonlinear aircraft similarity between methods based on matched filter theory and on stochastic simulation
[AIAA PAPER 92-2369] p 518 A92-34597
A general gust and maneuver load analysis method to account for the effects of active control saturation and nonlinear aerodynamics
[AIAA PAPER 92-2126] p 567 A92-35693
Gust load alleviation control design for the accuracy of an aeroelastic active control model
p 745 A92-43134
ACT wind tunnel experiment on gust load alleviation. II - Wind tunnel test with active support facility
p 745 A92-43135
System for generating sequences of phased gust or taxi loadings p 845 A92-46800
The interaction between a high-frequency gust and a blade row p 1135 A92-54484
Effect of atmospheric disturbances on airplane response
[AIAA PAPER 92-4340] p 1078 A92-55329
Stability, control and gust response characteristics of an ultralight freewing airplane
[AIAA PAPER 92-4342] p 1079 A92-55331
ATTAS flight test and simulation results of the advanced *gust management system LARS*
[AIAA PAPER 92-4343] p 1079 A92-55332
Gust response and cross wind performance of a hovercraft with vertical wings p 1118 A92-56034
Maximized gust loads for a nonlinear airplane using matched filter theory and constrained optimization
[NASA-TM-104138] p 23 N92-11010
An approach to flow field measurement by Laser 2-Focus velocimeter (L2F) in gust wind tunnel
[NAL-TM-617] p 346 N92-18484
Static aeroelastic analysis of ACT wind tunnel model aircraft
[NAL-TM-624] p 632 N92-25366
Response of helicopters to gusts
[NLR-TP-90159-U] p 879 N92-28653
Short cracks and durability analysis of the Fokker 100 wing/fuselage structure
[NLR-TP-90336-U] p 910 N92-29603
GUSTS
Surface-layer gusts for aircraft operation
p 774 A92-42095
Airfoil wake and linear theory gust response including sub and superresonant flow conditions
[AIAA PAPER 92-3074] p 823 A92-48724
The 1990 Airport Surveillance Radar Wind Shear Processor (ASR-WSP) operational test at Orlando International Airport
[AD-A239852] p 18 N92-10019
Thermographic gust wind tunnel measurements
[ONERA-RF-31/3409-PY] p 81 N92-11972
Loading and vibration reduction through active aerodynamic control
[AD-A242321] p 283 N92-17243
A pressure measurement method using Electronically Scanner Pressure sensors (ESP) installed in a gust wind tunnel
[NAL-TM-638] p 749 N92-27428
A gust generation method for full configuration aircraft tests in a low speed wind tunnel. Part 1: Design and preliminary experiments
[NAL-TR-1115-PT-1] p 722 N92-28192
Upgrading the data processing section of the NAL Gust Wind Tunnel data processing system
[NAL-TM-635] p 888 N92-28833
A comparison of the performance of two gust front detection algorithms using a length-based scoring technique
[AD-A250862] p 1004 N92-32103
Implementation of a personal computer based parameter estimation program
[AD-A252914] p 1061 N92-33502
GYROCOMPASSES
The effect of gyro nonorthogonality error on gyrocompassing p 1045 A92-55955
GYROSCOPIC STABILITY
A study of the precision characteristics of a gyroscopic gravimeter p 581 A92-33778
Wideband control of gyro/accelerometer multisensors in a strapdown guidance system p 856 A92-46736
A simplified method for predicting the stability of aerodynamically excited turbomachinery
p 224 N92-14364

H

H-53 HELICOPTER
Identification of higher-order helicopter dynamics using linear modeling methods p 131 A92-14336

The H-53E Super Stallion - A cost-effective solution to multi-service medium/heavy lift requirements
p 647 A92-40388
On the calculation of the response of helicopters to control inputs
[NASA-CR-190812] p 1088 N92-33536

H-60 HELICOPTER
Control design of a UH-60 rotorcraft via CLTR and direct optimization
[AIAA PAPER 92-4470] p 1076 A92-55230

HALF CONES
Evolution of three-dimensional flows during the interaction between conical shock waves and a turbulent boundary layer p 7 A92-12169

HALOGENS
Preliminary screening procedures and criteria for replacements for Halons 1211 and 1301
[AD-A252912] p 1126 N92-33501

HAMILTONIAN FUNCTIONS
A dynamic stiffness technique for the vibration analysis of stiffened shell structures p 1123 A92-56866
A numerical solution of implicit nonlinear equations of motion for rotor blades p 115 N92-13053

HANDBOOKS
FAA statistical handbook of aviation: Calendar year 1989
[PB91-202051] p 170 N92-13927
General maintenance handbook for airway facilities
[PB92-147586] p 640 N92-25518

HANG GLIDERS
Dynamics of hang-gliders p 204 A92-18608
Hang-glider response to atmospheric inputs
p 874 A92-46765
Wing design for hanggliders having minimum induced drag p 811 A92-46814

HANGARS
ILS mathematical modeling study of an ILS localizer and glide slope proposed for runway 32R, Moffett Field Airport, California
[DOT/FAA/CT-TN92/28] p 1048 N92-33308

HANKEL FUNCTIONS
Approximate truncated balanced realizations for infinite dimensional systems p 602 N92-22493

HARDENING (MATERIALS)
Calculation of the hardening factor for gas turbine engine components shot blasted in an ultrasonic field
p 38 A92-10850
Possibility of increasing durability of blades with damages p 761 A92-42654

HARDNESS
The hardness and toughness of HIPed silicon nitride
p 668 A92-39682
Development of hardness cycles for fiber bound materials, using DSC: From laboratory specimens to complex high duty structural members
[MBB-Z-0409-91-PUB] p 987 N92-30969

HARDWARE
Enhanced autopilot design through hardware-in-the-loop simulation p 204 A92-19103
Instrumented blade experiments using a light autogiro
p 555 A92-35773
A microprocessor-based automation test system for the experiment of the multi-stage compressor
p 997 A92-53100
Test and integration concept for complex helicopter avionic systems p 1064 A92-56292
Architecture for Survivable System Processing (ASSP)
p 220 N92-14210

HARMONIC CONTROL
Analysis of open loop higher harmonic control at high airspeeds on a modern four-bladed articulated rotor
[AIAA PAPER 92-2450] p 542 A92-34477
Evaluation of a constant feedback gain for closed loop higher harmonic control p 568 A92-35768
A study of coupled rotor-fuselage vibration with higher harmonic control using a symbolic computing facility
p 569 A92-35770
Rotor blade-vortex interaction noise reduction and vibration using higher harmonic control
p 604 A92-35778
Effects of higher harmonic control on rotor performance and control loads p 729 A92-41218
Multiharmonic control response of a rotor blade during forward flight (Test) p 744 A92-43120
Multiharmonic control response of a rotor blade during forward flight (Analysis) p 744 A92-43121
BVI impulsive noise reduction by higher harmonic pitch control - Results of a scaled model rotor experiment in the DNW p 1136 A92-56344
Analysis of open loop higher harmonic control at high airspeeds on a modern four-bladed articulated rotor
[NASA-TM-103876] p 21 N92-11000
Initial design study of existing flight control system of RPH and feasibility study of implementing HHC on the SH-60B
[AD-A240522] p 30 N92-11019
Flight operations for higher harmonic control research
[AD-A242478] p 196 N92-15067
Baseline vibration measurements of remotely piloted helicopters for higher harmonic control research
[AD-A244669] p 482 N92-21360
Analysis of rotor vibratory loads using higher harmonic pitch control
[NASA-CR-189591] p 696 N92-24251
Comparison of three controllers applied to helicopter vibration
[NASA-TM-102192] p 878 N92-28457

HARMONIC EXCITATION
Computation of flutter boundaries in the time and frequency domain p 720 N92-27952

HARMONIC MOTION
Euler flow predictions for an oscillating cascade using a high resolution wave-split scheme
[ASME PAPER 91-GT-198] p 74 A92-15623
Identification of aerodynamic models for maneuvering aircraft
[NASA-CR-190039] p 348 N92-19359

HARMONIC OSCILLATION
Wind tunnel wall effects in a linear oscillating cascade
[ASME PAPER 91-GT-133] p 72 A92-15576
Low-frequency vibrations of the shutters of the variable Laval nozzle of gas turbine engines p 657 A92-40610
Wind tunnel force measurements and visualization on a 60-deg delta wing in oscillation, stepwise motion, and gusts p 364 N92-18786
Active control of the flow past a cylinder executing rotary motions p 349 N92-19623
Computation of the unsteady transonic 2D cascade flow by an Euler algorithm with interactive grid generation
p 719 N92-27944

HARMONICS
A generic harmonic rotor model for helicopter flight simulation p 1086 A92-56333
Suppression of radiating harmonics Electro-Impulse Deicing (EIDI) systems
[DOT/FAA/CT-TN90/33] p 405 N92-19764
Optimizing tuning masses for helicopter rotor blade vibration reduction including computed airloads and comparison with test data
[NASA-TM-104194] p 367 N92-19846
Application of analysis techniques for low frequency interior noise and vibration of commercial aircraft
[NASA-CR-189555] p 481 N92-20376
Modeling methods for high-fidelity rotorcraft flight mechanics simulation
[NASA-TM-103842] p 482 N92-21440
Comparison of Euler and full potential methods for unsteady transonic flow calculations
p 719 N92-27943
Computation of the unsteady transonic 2D cascade flow by an Euler algorithm with interactive grid generation
p 719 N92-27944

HARRIER AIRCRAFT
Control and display combinations for blind vertical landings p 661 A92-39903
Harrier international programme p 841 A92-45305
VSTOL engine design evolution - Growth of the Pegasus engine for Harrier p 860 A92-45306
ASTOVL engine control p 860 A92-45321
CH-53E/AV-8B aircraft sling load recovery system analysis
[AD-A239950] p 21 N92-10022
VSTOL engine design evolution: Growth of the Pegasus engine for Harrier
[PNR-90805] p 739 N92-27039
Harrier GR MK 5/7 mission simulators for the Royal Air Force p 885 N92-28540
Collaborative research on V/STOL control system/cockpit display tradeoffs under the NASA/MOD joint aeronautical program
[NASA-TM-103910] p 1087 N92-32788

HAWK MISSILE
Four decades of transonic fighter design
p 193 A92-20203

HAZARDS
Alert generation and cockpit presentation for an integrated microburst alerting system
p 265 N92-17988
Pilot noise exposure during a Boeing 747-400 round trip: Judgement of noise and analysis in respect to hearing impairment of pilots p 1138 N92-32961

HEAD (ANATOMY)
Evaluation of head impact kinematics for passengers seated behind interior walls
[AD-A252651] p 952 N92-30551

HEAD MOVEMENT
Adaptive suppression of biodynamic interference in helmet-mounted displays and head teleoperation
p 197 A92-18611

HEAD-UP DISPLAYS
Effects of variations in head-up display airspeed and altitude representations on basic flight performance
p 46 A92-11204
Infra-red offers new landing aid competition
p 198 A92-18937
Optical design of dual combiner head-up displays
p 414 A92-24628
EVS could expand all-weather landing capability of airliners p 556 A92-36125
Enhanced vision system option on future aircraft
[SAE PAPER 912204] p 651 A92-40014
The standardization of military head-up display symbology p 855 A92-44929
Ferrundi Company supplies 4500 model head up display devices to India's MIG-21 aircraft
[AD-A241044] p 229 N92-15367
MULTIRAD
[AD-A244211] p 412 N92-19247
The utility of analog vertical velocity information during instrument flight with a Head-Up Display (HUD)
[AD-A252863] p 1065 N92-33277

HEARING
Aircraft noise and the elderly p 689 A92-39236
Reference mode effect on the auditory display of aircraft bank angle
[AD-A247825] p 728 N92-27916
Exposures from headset interference tones
[AD-A247175] p 1136 N92-32697

HEAT AFFECTED ZONE
A simplified method for thermal analysis of a cowl leading edge subject to intense local shock-wave-interference heating
[NASA-TP-3167] p 679 N92-24797

HEAT EXCHANGERS
Thermal management of air-breathing propulsion systems
[AIAA PAPER 92-0514] p 373 A92-26940
Heat transfer in the entrance region of semicircular ducts with internal fins p 497 A92-32264
Embedded longitudinal vortex arrays, velocity and temperature fields, loss and heat transfer augmentation
p 621 A92-40121
Assessment of calculation methods for efficiency of straight fins of rectangular profile p 1121 A92-56374
Cryogenic hydrogen-induced air-liquefaction technologies for combined-cycle propulsion applications
p 487 N92-21526
Experimental methods to determine heat exchanger performances p 682 N92-25667
Solid-vapor adsorption refrigeration system development
[PB92-164383] p 771 N92-27715
Study of potassium turbine electric generator system
p 1129 N92-33794

HEAT FLUX
Calculation of the base pressure and enthalpy behind a step in the path of two supersonic streams with allowance for the effect of boundary layers and heat fluxes
p 63 A92-13748
A heat flow peak on the upwind surface of a blunt-leading-edge delta wing p 438 A92-31862
A circumferential non-uniform effect model for multistage axial-flow compressor throughflow p 588 A92-35572
Stagnation point heat flux in hypersonic high enthalpy flow p 613 A92-38373
A sensitive fast-response probe to measure turbulence and heat flux from any airplane p 775 A92-42097
Effect of the grid system on heat transfer computations for high speed flows p 900 A92-47071
Simulation of high heat flux levels with graphite heating and arc lamps p 980 A92-51402
Thermal management of high heat flux electronic components in space and aircraft systems, phase 1
[AD-A239982] p 41 N92-10157
On the footprints of three-dimensional separated vortex flows around blunt bodies: Attempts of defining and analyzing complex flow structures p 84 N92-13005
Heat flux sensor research and development: The cool film calorimeter
[NASA-CR-189789] p 298 N92-17006
Thermal energy test apparatus
[AD-A243526] p 305 N92-17537
Research sensors p 594 N92-22526
Turbulent heat flux measurements in a transitional boundary layer
[NASA-TM-105623] p 716 N92-27377

HEAT GENERATION
Performance of a hybrid cylindrical roller bearing
p 995 A92-51845

HEAT MEASUREMENT
Thermal measurement test in a shock wind tunnel
p 748 A92-43104
Computer-based areal surface temperature and local heat transfer measurements with thermochromic liquid crystals (TLC) p 763 A92-44326

Research sensors p 594 N92-22526
Thermal mechanical analysis of sprag clutches
[NASA-CR-190686] p 1128 N92-34207

HEAT OF COMBUSTION
Ignition delays, heats of combustion, and reaction rates of aluminum alkyl derivatives used as ignition and combustion enhancers for supersonic combustors
[AIAA PAPER 92-3841] p 894 A92-49134
Three-dimensional modeling of diesel engine intake flow, combustion and emissions
[NASA-CR-189126] p 658 N92-24539

HEAT PIPES
Flexible heat pipe cold plates for aircraft thermal control
[SAE PAPER 912105] p 674 A92-39959
Heat pipe and surface mass transfer cooling of hypersonic vehicle structures p 763 A92-44380
Surface cooling of scramjet engine inlets using heat pipe, transpiration, and film cooling p 763 A92-44381
Analytical and experimental studies of heat pipe radiation cooling of hypersonic propulsion systems
[AIAA PAPER 92-3809] p 867 A92-49128
Hypersonic aerospace vehicle leading edge cooling using heat pipe, transpiration and film cooling techniques p 780 N92-26733
Analytical and experimental studies of heat pipe radiation cooling of hypersonic propulsion systems
[DE92-013428] p 973 N92-31817

HEAT PUMPS
Reduction of torque pulsation of Stirling engine-compressor system p 992 A92-50785
Lower-end dynamic characteristics of a magnetically coupled free-piston Stirling engine/compressor system p 992 A92-50795
Benchmark performance analysis of an ECM-modulated air-to-air heat pump with a reciprocating compressor
[DE92-004478] p 500 N92-20341
Thermoacoustic refrigeration p 595 N92-22720
Proof of concept of a magnetically coupled Stirling engine-driven heat pump
[DE92-017129] p 1129 N92-33271

HEAT RADIATORS
Study of potassium turbine electric generator system p 1129 N92-33794

HEAT RESISTANT ALLOYS
High temperature multiaxial creep testing of Nimonic 115 p 141 A92-15202
High temperature erosion resistance of coatings for gas turbine
[ASME PAPER 91-GT-213] p 143 A92-15632
Crack initiation and the short-to-long crack growth transition in a Ni-base superalloy p 213 A92-19767
High temperature low cycle fatigue of single crystal nickel base superalloys p 213 A92-19796
Protective coatings of thermal barrier type p 214 A92-20349
Applications of IMI 834 in aeroengines - A collaborative IMI/MTU programme p 288 A92-22754
Influence of long time exposure at elevated temperatures in air on mechanical properties of the high temperature titanium alloy IMI 834 p 289 A92-22767
A viscoplastic theory for anisotropic materials
[ONERA, TP NO. 1992-90] p 391 A92-24721
Inclusion size effect on the fatigue crack propagation mechanism and fracture mechanics of a superalloy p 388 A92-24831
Creep fracture mechanisms in single crystal superalloys p 388 A92-25031
Brazing method helps repair aircraft gas-turbine nozzles p 492 A92-29504
Structural materials for NASP
[AIAA PAPER 91-5101] p 486 A92-31698
Research and development of aircraft engine materials p 577 A92-35916
Fracture mechanics approach to creep growth in welded IN738LC gas turbine blades
[ASME PAPER 91-GT-119] p 670 A92-36893
Development of intermetallic materials for aerospace systems p 754 A92-41874
Modeling the heat treatment of superalloys p 755 A92-43679
Elevated temperature crack growth in aircraft engine materials p 891 A92-45234
Advanced superalloys for turbine blade and vane applications
[ONERA, TP NO. 1992-2] p 893 A92-48578
Aluminides modified by palladium - Protection of new parts by local finishing
[ONERA, TP NO. 1992-49] p 893 A92-48610
Manufacturing technology methodology for propulsion system parts
[AIAA PAPER 92-3525] p 906 A92-49048
High-temperature metal matrix composite p 1105 A92-53878
Thermoviscoplastic response of Ti-15-3 under various loading conditions
[NASA-CR-187621] p 45 N92-11391
Development and characterization of Powder Metallurgy (PM) 2XXX series Al alloy products and Metal Matrix Composite (MMC) 2XXX Al/SiC materials for high temperature aircraft structural applications
[NASA-CR-187631] p 390 N92-19290
Present and future trends in turbine blade material and manufacturing technology
[PNR-90825] p 488 N92-20164
Fatigue in single crystal nickel superalloys
[AD-A244815] p 489 N92-21015
The search for new materials
[PNR-90777] p 490 N92-21744
Evaluation and qualification of diffusion braze repair techniques for superalloy gas turbine components
[NRC-LTR-ST-1839] p 504 N92-22028
High speed civil transport p 649 N92-25919
Fatigue in single crystal nickel superalloys
[AD-A248190] p 896 N92-29408
Fatigue in single crystal nickel superalloys
[AD-A250068] p 987 N92-31360
Fatigue in single crystal nickel superalloys
[AD-A252492] p 988 N92-32066
Fatigue crack growth of small corner defects from blunt notches in an aeroengine alloy
[PNR-90860] p 1111 N92-34019

HEAT SHIELDING
Analyses of heat isolation property for metallic multiwall thermal protection system p 40 A92-12422
Thermal deformation of a polymer heat shield material on the descent trajectory p 754 A92-42655
Ablation and temperature sensors for flight measurements in reentry body heat shields p 227 N92-15004

HEAT SINKS
The optimization of variable cross-section spines with temperature dependent thermal parameters p 901 A92-48353
High performance heat sink for surface mount applications --- in avionics system design p 989 A92-49275
Progressive avionics packaging technologies p 989 A92-49276
Next generation power electronics for space and aircraft. II - Packaging p 992 A92-50553
Application of advanced composites in SEM-E heatsinks for the thermal management of avionics p 986 A92-51922
Cryogenic hydrogen-induced air-liquefaction technologies for combined-cycle propulsion applications p 487 N92-21526

HEAT TRANSFER
Power performance of a nonisentropic Brayton cycle p 54 A92-11281
Analyses of heat isolation property for metallic multiwall thermal protection system p 40 A92-12422
The role of laminar-turbulent transition in gas turbine engines p 120 A92-14868
Influence of three-dimensional effects on hydrodynamics and heat transfer in subsonic flow of a viscous compressible gas in the initial section of a rectangular duct p 66 A92-15031
Aerodynamics and heat transfer investigations on a high Reynolds number turbine cascade
[ASME PAPER 91-GT-157] p 148 A92-15593
Comparison of time-resolved turbine rotor blade heat transfer measurements and numerical calculations
[ASME PAPER 91-GT-268] p 151 A92-15666
New applications of liquid-crystal thermography in rotating turbomachinery heat transfer research
[ASME PAPER 91-GT-354] p 153 A92-15710
Optimal thermal management system for HALE UAV --- High Altitude Long Endurance Unmanned Air Vehicles
[ASME PAPER 91-GT-396] p 111 A92-15726
Development of an electrothermal de-icing/anti-icing model
[AIAA PAPER 92-0526] p 351 A92-26949
Numerical analysis of a thermal deicer
[AIAA PAPER 92-0527] p 357 A92-26950
A numerical method for simulating the fluid-dynamic and heat-transfer changes in a jet engine injector feed-arm due to fouling
[AIAA PAPER 92-0768] p 374 A92-27108
Further developments in three-dimensional simulation of electrothermal deicing systems
[AIAA PAPER 92-0528] p 459 A92-31668
Heat transfer effects on aerodynamics and implications for wind-tunnel tests p 497 A92-32240
Forced-injection quenching of a hot-tube under microgravity p 590 A92-35977
Compressible turbulent boundary layers with heat addition by homogeneous condensation p 611 A92-36843
Laminar flow control of subsonic boundary layers by suction and heat transfer strips p 617 A92-39338
Heat transfer on a cylindrical surface in the cavities of gas turbine engine rotors p 657 A92-40609
Heat transfer in a channel with built-in wing-type vortex generators p 757 A92-41082
Heat pipe and surface mass transfer cooling of hypersonic vehicle structures p 763 A92-44380
Fuel regression mechanism in a solid fuel ramjet p 860 A92-44898
Experimental and numerical studies of radiation emission from high-temperature air behind 10 km/s shock waves
[SAE PAPER 912025] p 790 A92-45417
Multiple shock-shock interference on a cylindrical leading edge p 813 A92-46899
Grid sensitivity in low Reynolds number hypersonic continuum flows p 817 A92-47057
Effect of the grid system on heat transfer computations for high speed flows p 900 A92-47071
Segmental heat transfer in a pin fin channel with ejection holes p 900 A92-47267
Low density heat transfer phenomena
[AIAA PAPER 92-2899] p 820 A92-47875
The optimization of variable cross-section spines with temperature dependent thermal parameters p 901 A92-48353
Vane-blade interaction in a transonic turbine. II - Heat transfer
[AIAA PAPER 92-3324] p 904 A92-48907
Optimization of a thermally non-symmetric fin - Preliminary evaluation p 992 A92-50448
Three-dimensional Navier-Stokes heat transfer predictions for turbine blade rows
[AIAA PAPER 92-3068] p 1020 A92-54003
Increased heat transfer to elliptical leading edges due to spanwise variations in the freestream momentum - Numerical and experimental results
[AIAA PAPER 92-3070] p 1020 A92-54005
Heat transfer measurements and CFD comparison of swept shock wave/boundary-layer interactions
[AIAA PAPER 92-3665] p 1021 A92-54110
Problems and solutions for transition detection in cryogenic wind tunnels by infrared imaging p 1090 A92-54319
Computational and experimental investigation of annulus heat transfer with swirl
[AIAA PAPER 92-4060] p 1119 A92-56143
Surface heat transfer and flow properties of vortex arrays induced artificially and from centrifugal instabilities p 1121 A92-56371
TSNIIMASH capabilities for aerogasdynamical and thermal testing of hypersonic vehicles
[AIAA PAPER 92-3962] p 1097 A92-56789
Transonic turbine blade cascade testing facility
[AIAA PAPER 92-4034] p 1101 A92-56856
The effects of Reynolds number, rotor incidence angle and surface roughness on the heat transfer distribution in a large-scale turbine rotor passage
[NASA-CR-184260] p 42 N92-11297
Effects of wake and shock passing on the heat transfer to a film cooled transonic turbine blade p 156 N92-12201
The effect of a type 3 and type 4 shock/shock interaction on heat transfer in the stagnation region p 160 N92-13867
Recent progress in inverse methods in France p 201 N92-13938
Boundary-layer transition and heat transfer on slender delta wings
[AERO-REPT-8904] p 262 N92-17849
Investigation on freezing and sticking phenomena of slush on airplane surfaces when taxiing on the ground and the succeeding take-off run phase
[NAL-TR-1026] p 352 N92-18182
Studies of gas turbine heat transfer: Airfoil surfaces and end-wall cooling effects
[AD-A244055] p 376 N92-19097
Heat transfer in rotating serpentine passages with trips skewed to the flow
[NASA-TM-105581] p 499 N92-20235
Postflight aerothermodynamic analysis of Pegasus(tm) using computational fluid dynamic techniques
[NASA-CR-186017] p 445 N92-21188
Development of an integrated BEM approach for hot fluid structure interaction: BEST-FSI: Boundary Element Solution Technique for Fluid Structure Interaction
[NASA-CR-189202] p 574 N92-22211
Heat transfer characteristics of hypersonic waveriders with an emphasis on the leading edge effects
[NASA-CR-189586] p 525 N92-22215
Improved large perturbation propulsion models for control system design (1988-1989) and large perturbation models of high velocity propulsion systems (1989-1990) and reduced order propulsion models for control system design (1990-1991)
[NASA-CR-190148] p 593 N92-22491

Boiling and condensation in microfin tubes
p 682 N92-25660
Transonic turbine blade cascade testing facility
[NASA-TM-105646] p 667 N92-26129
Navier-Stokes analysis of turbine blade heat transfer and performance p 768 N92-27468
Practical considerations in designing the engine cycle
p 869 N92-28460
Second-order shock-expansion theory extended to include real gas effects
[AD-A247191] p 831 N92-29539
Effect of walls on the supersonic reacting mixing layer
p 912 N92-30065
Flat plates placed in depleted hypersonic flow
[SESSIA-430/91.960] p 947 N92-31508
Further studies in filmwise condensation of steam on horizontal finned tubes
[AD-A252705] p 1011 N92-31767
Turbine disk cavity aerodynamics and heat transfer
p 1124 N92-32265
Swept shock/boundary layer interaction experiments in support of CFD code validation
[NASA-CR-190583] p 1036 N92-32494

HEAT TRANSFER COEFFICIENTS
Gas turbine main shaft internal flow and heat transfer
[ASME PAPER 91-GT-165] p 123 A92-15600
Heat transfer measurements from a smooth NACA 0012 airfoil p 218 A92-20215
Roughness effects on heat transfer from a NACA 0012 airfoil p 219 A92-20217
Measurement of convective heat-transfer coefficients on a wind tunnel model by passive and stimulated infrared thermography p 291 A92-21450
Development of a three-dimensional icing code - Comparison with experimental shapes
[AIAA PAPER 92-0041] p 262 A92-22159
Measurement of convective heat-transfer coefficients in wind tunnels using passive and stimulated infrared thermography p 390 A92-24430
Mechanisms resulting in accreted ice roughness
[AIAA PAPER 92-0297] p 351 A92-25750
Flow pattern characterization and heat transfer behavior in a boiling two-phase flow in an inclined pipe
p 493 A92-29722
A heat flow peak on the upwind surface of a blunt-leading-edge delta wing p 438 A92-31862
Boiling heat transfer from an excavated fin
p 498 A92-32523
Turbine blade heat transfer prediction using coupled turbulent Prandtl number and transition models
[SAE PAPER 912152] p 674 A92-39987
Local heat transfer in the perforation channels of turbine nozzle vanes p 657 A92-40615
A thin metal model for aerodynamic heating tests of shock wave interaction p 709 A92-43103
Computer-based areal surface temperature and local heat transfer measurements with thermochromic liquid crystals (TLC) p 763 A92-44326
The flow pattern and external heat transfer investigation for gas turbine vanes end surfaces
[AIAA PAPER 92-3071] p 903 A92-48722
The mechanism of liquid-cooling of vane in high-temperature turbine p 969 A92-49841
The effect of angle of incidence and Reynolds number on heat transfer in a linear turbine cascade
[AD-A243900] p 377 N92-19328
Heat transfer in rotating serpentine passages with trips skewed to the flow
[NASA-TM-105581] p 499 N92-20235
Further studies in filmwise condensation of steam on horizontal finned tubes
[AD-A252705] p 1011 N92-31767

HEAT TRANSMISSION
Comparative analysis of the lift-drag ratio and heat flows toward the surface of wave riders of different configurations p 7 A92-12173
Second-order shock-expansion theory extended to include real gas effects
[AD-A247191] p 831 N92-29539

HEAT TREATMENT
Modeling the heat treatment of superalloys
p 755 A92-43679
Rotor support for the STME oxygen turbopump
[AIAA PAPER 92-3282] p 904 A92-48872

HEATERS
Further developments in three-dimensional simulation of electrothermal deicing systems
[AIAA PAPER 92-0528] p 459 A92-31668

HEATING
On the instability of boundary layers on heated flat plates
[NASA-CR-187581] p 347 N92-19250
In situ measurement of particle formation in heated jet fuels: A new application of photon correlation spectroscopy
[DE92-003641] p 488 N92-20132

HEATING EQUIPMENT
Use of the TMS-65 heating equipment at airports to create fog-dispersal zones above the runway to facilitate takeoff p 775 A92-44084

HEAVING
Measurement of derivatives due to acceleration in heave and sideslip p 364 N92-18785
Pitch-heave dynamics models for an air cushion vehicle
[ISBN-0-315-51095-1] p 716 N92-27624
Performance of insulated pavements at Newton Fields, Jackman, Maine
[CRREL-92-9] p 1101 N92-32903

HEAVY LIFT AIRSHIPS
C-17 flight control system overview
p 1082 A92-55906

HEAVY LIFT HELICOPTERS
The H-53E Super Stallion - A cost-effective solution to multi-service medium/heavy lift requirements
p 647 A92-40388

HELICAL FLOW
Flow about cylinders with helical surface protrusions
[AIAA PAPER 92-0540] p 332 A92-26957
Helical-perturbation device for cylinder-wing vortex generators p 432 A92-31167

HELICES
Experiment of static and dynamic characteristics of spiral grooved seals p 223 N92-14361

HELICOPTER CONTROL
Robust stabilization of a helicopter model
p 28 A92-11501
A two-feedback-loop robust helicopter controller based on eigenspace techniques and H(infinity) synthesis
p 29 A92-11582
Helicopter control response types for hover and low-speed near-earth tasks in degraded visual conditions
p 132 A92-14338
Flight testing the handling qualities requirements of ADS-33C - Lessons learned at ATTC
p 104 A92-14339
Practical robustness testing for helicopter flight control systems p 132 A92-14340
Development testing of the EH101 Flight Control System p 132 A92-14380
Enhanced energy maneuverability for attack helicopters using continuous, variable (C-V) rotor speed control
p 132 A92-14421
Nonlinear control of a twin-lift helicopter configuration
p 204 A92-18624
Helicopter air resonance modeling and suppression using active control p 204 A92-18625
Time-periodic control of a multi-blade helicopter
p 204 A92-18626
Synthesis of a helicopter full-authority controller
p 280 A92-21178
Quantitative Feedback Theory (QFT) applied to the design of a rotorcraft flight control system
[AIAA PAPER 92-0044] p 281 A92-22161
A new method for calculation of helicopter maneuvering flight p 282 A92-23382
Yaw dynamics of a coaxial rotor helicopter
p 378 A92-24427
Dynamics of helicopter tip-over during taxiing
p 479 A92-30149
Analysis of open loop higher harmonic control at high airspeeds on a modern four-bladed articulated rotor
[AIAA PAPER 92-2450] p 542 A92-34477
Frequency domain testing of helicopter dynamics using automated input signals p 545 A92-35731
Full authority active control system design for a high performance helicopter p 567 A92-35732
The use of inverse simulation for conceptual design
p 546 A92-35738
Achievement of rotorcraft handling qualities specifications via feedback control p 568 A92-35747
Multivariable methods for helicopter flight control law design - A review p 568 A92-35748
Command following control law design by linear quadratic optimisation p 568 A92-35749
Preliminary evaluation of new control laws on the experimental fly-by-wire Dauphin helicopter
p 568 A92-35756
Experiences with high authority helicopter flight control
p 568 A92-35757
A study of coupled rotor-fuselage vibration with higher harmonic control using a symbolic computing facility
p 569 A92-35770
Improvement of helicopter robustness and performance control law using eigenstructure techniques and H-infinity synthesis p 569 A92-35776
An evaluation of a simple PID controller designed using optimal control theory when applied to helicopter stabilisation p 569 A92-35785
Eigenstructure assignment for handling qualities in helicopter flight control law design p 570 A92-35786
Measurements of a rotor flowfield and the effects on a fuselage in forward flight p 521 A92-35787
Helicopter in-flight frequency response test techniques
p 548 A92-35938
Pulse response method for vibration reduction in periodic dynamic systems p 661 A92-39909
A review of recent programs and future plans for rotorcraft in-flight simulation at Ames Research Center
[SAE PAPER 912121] p 608 A92-39969
Effects of higher harmonic control on rotor performance and control loads p 729 A92-41218
Chaotic stall response of helicopter rotor in forward flight p 730 A92-43046
Study on the lower aspect view of a helicopter simulator p 748 A92-43110
Multiharmonic control response of a rotor blade during forward flight (Test) p 744 A92-43120
Multiharmonic control response of a rotor blade during forward flight (Analysis) p 744 A92-43121
Study of the flight control of remotely piloted helicopters p 745 A92-43183
Research on a helicopter information control system
p 735 A92-43220
Civil development and certification of a helicopter automatic approach and hover system on the Sikorsky S-76
[SAE PAPER 911975] p 872 A92-45382
A new milestone in automatic aircraft control - Fly-by-light systems transmit commands optoelectronically
p 784 A92-45699
Modeling of the control systems of rotary wing aircraft (Review) p 875 A92-47783
A new method of helicopter rotor blade motion control
p 875 A92-47786
An ultrareliable integrated digital computer for helicopters p 964 A92-49273
Carefree handling systems for helicopters
p 975 A92-50010
Generic helicopter for multiship simulations
[AIAA PAPER 92-4151] p 959 A92-52442
Experimental investigation of in-flight oscillation on helicopters and its prevention p 977 A92-53089
Vision-based stereo ranging as an optimal control problem
[AIAA PAPER 92-4418] p 1045 A92-55211
Robustness of a helicopter flight control system designed using eigenstructure assignment
[AIAA PAPER 92-4469] p 1076 A92-55229
Control design of a UH-60 rotorcraft via CLTR and direct optimization
[AIAA PAPER 92-4470] p 1076 A92-55230
Optimal control of helicopters following power failure
[AIAA PAPER 92-4471] p 1076 A92-55231
Concepts for pilot interaction with an automated NOE obstacle-avoidance system
[AIAA PAPER 92-4472] p 1076 A92-55232
A simulation model for tail rotor failure
[AIAA PAPER 92-4633] p 1081 A92-55380
Optimization approach for helicopter maneuverability with a point mass model p 1083 A92-56025
An investigation of the automation of emergency landings for helicopters p 1083 A92-56026
An autorotation-entry control for a helicopter with a fuzzy controller p 1083 A92-56032
Flight simulation modeling in support of engine/airframe integration p 1055 A92-56279
Trimming rotor blades with periodically deflecting trailing edge flaps p 1085 A92-56283
The solution of the helicopter flight dynamics tasks by the methods of optimal control theory
p 1085 A92-56284
A module-level testing environment for safety-critical software systems p 1132 A92-56293
Modern helicopter technologies at MBB and the application in future programmes p 1016 A92-56304
Creation of a living specification for an experimental helicopter active flight control system through incremental simulation p 1057 A92-56312
Helicopter nonlinear flight control system development
p 1085 A92-56317
Experimental investigation of helicopter coupled rotor/body control p 1086 A92-56318
A high speed edgewise rotor using circulation control only in the reversed flow area p 1059 A92-56347
Mission oriented investigation of handling qualities through simulation p 1059 A92-56353
Analysis of open loop higher harmonic control at high airspeeds on a modern four-bladed articulated rotor
[NASA-TM-103876] p 21 N92-11000
Rotorcraft system identification
[AGARD-AR-280] p 22 N92-11001
Initial design study of existing flight control system of RPH and feasibility study of implementing HHC on the SH-60B
[AD-A240522] p 30 N92-11019

Resonance and control response tests using a control stimulation drive
[MBB-UD-0586-90-PUB] p 134 N92-12003
Application of Eigenstructure Assignment to the control of powered lift combat aircraft
[RAE-TM-FS-1009] p 135 N92-12004
The development of a requirement specification for an experimental active flight control system for a variable stability helicopter: An Ada simulation in JSD
p 135 N92-12466
A numerical solution of implicit nonlinear equations of motion for rotor blades p 115 N92-13053
Flight research p 194 N92-13981
Instrumentation and data processing
p 273 N92-17155
System identification requirements for high-bandwidth rotorcraft flight control system design
p 282 N92-17166
Development of nonlinear real-time helicopter simulation using a blade element method
[NLR-TP-90115-U] p 381 N92-18893
Double loop control law strategy and applications to helicopter
[CERT-2/7724-DERA] p 381 N92-19295
EH 101 ship interface trials: Flight test programme and preliminary results p 465 N92-21964
Determination of limitations for helicopter ship-borne operations p 465 N92-21965
Helicopter handling: Experience and new developments p 465 N92-21969
Control of a helicopter engine in low altitude flight
p 562 N92-23122
Helicopter low-speed yaw control
[NASA-CASE-LAR-14219-1] p 879 N92-30025
Resonance and control response tests using a control simulation device
[MBB-UD-0608-91-PUB] p 978 N92-30439
Computational aspects of helicopter trim analysis and damping levels from Floquet theory
[NASA-CR-190736] p 1087 N92-33107
On the calculation of the response of helicopters to control inputs
[NASA-CR-190812] p 1088 N92-33536
A workstation-based evaluation of a far-field route planner for helicopters
[NASA-TM-102882] p 1051 N92-33609
Design of helicopter flight control systems for hover and low speed using eigenstructure assignment
p 1061 N92-33952

HELICOPTER DESIGN

Technology developments applied to the AH-1W SuperCobra
[AIAA PAPER 91-3071] p 21 A92-11607
Comanche - The armed scout p 103 A92-13291
LH wind tunnel testing - Key to advanced aerodynamic design p 104 A92-14331
Handling qualities of the H-76 Fantail Demonstrator
p 131 A92-14335
Continuation of the AHS round robin on fatigue reliability and damage tolerance p 59 A92-14341
Reliability of helicopter composite dynamic components p 145 A92-14344
A full scale airframe high cycle fatigue test methodology and its application to the SH-2G helicopter
p 105 A92-14345
Expanding U.S.M.C. roles for the AH-1W SuperCobra
p 59 A92-14347
Rotorcraft Maneuverability and Agility Survivability Sensitivity Analysis (RMASSA) p 161 A92-14351
The helicopter air-to-air value-driven engagement model (HAVDEM) - Prototype development
p 105 A92-14353
The design and manufacture of an advanced thermoplastic horizontal stabilator for the AH-64A
p 59 A92-14354
Development of an advanced piloted helicopter simulation p 105 A92-14363
Helicopter modeling requirements for full mission simulation and handling qualities assessment
p 105 A92-14364
Evaluation of thermoplastic matrix composites for use in energy-absorbing helicopter subfloors
p 141 A92-14374
Design optimization of rotor blades for improved performance and vibration p 106 A92-14389
Hub and pylon fairing integration for helicopter drag reduction p 107 A92-14391
Closing the loop on helicopter crashworthiness design requirements p 107 A92-14392
Structural optimization and Mach scale test validation of a low vibration rotor p 107 A92-14395
Experimental investigation of helicopter vibration reduction using rotor blade aeroelastic tailoring
p 107 A92-14396
Studying dynamic behavior of X380 helicopter equipped with a new 5-blade composite rotor p 108 A92-14398
Finite element correlation of the U.S. Army/BHTI ACAP composite airframe helicopter p 108 A92-14399
The practical application of new technology to the civil rotorcraft need p 108 A92-14410
Rotor blade preservation - Getting the most service life with lowest operational costs p 108 A92-14412
Crash-resistant rotorcraft preliminary design optimization p 109 A92-14417
Lifting line predictions for a swept tip rotor blade
p 65 A92-14424
Certifying composite helicopter structures
p 110 A92-14443
P120 programme - First results of the pre-development phase p 60 A92-14447
Composite gearbox housing p 110 A92-14448
An analytical study of the helicopter flight safety under an engine failure in proximity of ground
p 91 A92-14454
Design and flight test evaluation of the Fantail antitorque system p 110 A92-14456
Helicopter NVG testing in the United Kingdom
p 112 A92-16053
EH101 helicopter development p 112 A92-16060
Numerical optimization of helicopter rotor blade airfoils using unsteady aerodynamic calculations
[ONERA, TP NO. 1991-187] p 78 A92-16141
RAH-66 Comanche - A cut above the rest
p 61 A92-16675
Status of the NH90 European Helicopter Program
p 113 A92-16676
Helicopter/heliport operations - Environmental implications p 241 A92-22708
Relating economics to design parameters through a criterion function p 271 A92-22709
McDonnell Douglas' new light twin helicopter - The MDX p 271 A92-22710
Rotor revolutions in the Far East - Helicopters in China, Mongolia, and Siberia p 241 A92-22711
Cold-cycle pressure-jet helicopters - Ventures, designs, and developments. II - Design p 271 A92-22712
Review on the abatement of helicopter noise
p 406 A92-25501
Experimental and theoretical studies on helicopter rotor fuselage interaction
[ONERA, TP NO. 1991-197] p 329 A92-26356
Sikorsky S-92 - Bold bid for future
p 457 A92-29557
Composites usage on the RAH-66 Comanche
p 457 A92-29669
Bell's OH-58D proves its reliability
p 458 A92-29670
Tiger development status --- Franco-German antitank helicopter p 458 A92-29672
Integrated multidisciplinary rotorcraft optimization research at the NASA Langley Research Center
p 419 A92-29673
Engineering development simulation - Test vehicle of the future p 483 A92-29674
Cold-cycle pressure-jet helicopters: Ventures, designs, and developments. III - Costs and developments
p 458 A92-29675
Cold-cycle pressure-jet helicopters: Ventures, designs, and developments. I - Ventures p 459 A92-31325
Impact of structural optimization with aeroelastic/multidisciplinary constraints on helicopter rotor design
[AIAA PAPER 92-1001] p 535 A92-33193
Low-speed cruise aerodynamics of the stopped rotor/disk rotorcraft concept
[AIAA PAPER 92-1067] p 517 A92-33240
Damage tolerant structural design using neural networks
[AIAA PAPER 92-1097] p 581 A92-33261
The NASA/Industry Design Analysis Methods for Vibrations (DAMVIBS) Program - Bell Helicopter Textron accomplishments
[AIAA PAPER 92-2201] p 539 A92-34391
The NASA/Industry Design Analysis Methods for Vibrations (DAMVIBS) program - McDonnell Douglas Helicopter Company achievements
[AIAA PAPER 92-2203] p 540 A92-34393
Comparison between imposed-periodicity and marching-in-time solutions of helicopter rotor blade steady-state response problem
[AIAA PAPER 92-2256] p 540 A92-34411
A new aeroelastic model for composite rotor blades with straight and swept tips
[AIAA PAPER 92-2259] p 541 A92-34414
A study on the feasibility of using adaptive structures in the attenuation of vibration characteristics of rotary wings
[AIAA PAPER 92-2452] p 541 A92-34415
Fully integrated aerodynamic/dynamic optimization of helicopter rotor blades
[AIAA PAPER 92-2374] p 542 A92-34544
Optimizing tuning masses for helicopter rotor blade vibration reduction including computed airloads and comparison with test data
[AIAA PAPER 92-2376] p 542 A92-34546
Smart structures for helicopters p 516 A92-35727
Noise level reduction inside helicopter cabins
p 545 A92-35733
The development of a new light, single engine helicopter family p 545 A92-35734
Acoustic results of the Boeing model 360 whirl tower test p 603 A92-35741
Experimenting a new composite rotor on an Aerospatiale Dauphin helicopter p 546 A92-35744
A frequency domain theory for structural identification
p 590 A92-35745
Crashworthiness of truncated composite cones under side loads p 590 A92-35746
EUROFAR airframe aerodynamic design
p 546 A92-35750
A survey of composite structure technology at the Aerospatiale Helicopter Division p 546 A92-35754
The helicopter commuter - A perspective on regular passenger transportation by rotary wing
p 634 A92-38208
A review of recent programs and future plans for rotorcraft in-flight simulation at Ames Research Center
[SAE PAPER 912121] p 608 A92-39969
1991-92 AHS Technical Committee highlights - Acoustics p 696 A92-40390
1991-92 AHS Technical Committee highlights - Aerodynamics p 623 A92-40391
1991-92 AHS Technical Committee highlights - Aircraft design p 608 A92-40392
1991-92 AHS Technical Committee highlights - Dynamics p 647 A92-40393
1991-92 AHS Technical Committee highlights - Flight simulation p 609 A92-40394
Software package for preliminary design of helicopter
p 775 A92-41195
Helicopter aeroelastic stability and response - Current topics and future trends p 730 A92-43100
Optimization of blade structure to reduce rotor vibration p 730 A92-43118
A perspective on helicopter noise p 780 A92-43160
The fatigue scatter factors and reduction factors in the design of aircraft and helicopter's structural lives
[SAE PAPER 911984] p 843 A92-45387
Sensitivity analysis of discrete periodic systems with applications to helicopter rotor dynamics
p 846 A92-46884
An aeroelastic analysis with a generalized dynamic wake p 847 A92-46932
Design of helicopter composite structures for crashworthiness p 848 A92-47408
Research and studies on quiet helicopters
[ONERA, TP NO. 1992-59] p 926 A92-48618
Advanced Rotorcraft Transmission program summary
[AIAA PAPER 92-3363] p 905 A92-48936
Boeing Helicopters Advanced Rotorcraft Transmission (ART) Program summary of component tests
[AIAA PAPER 92-3364] p 905 A92-48937
Analytical evaluation of resonant response of spiral bevel gears in the RAH-66 helicopter Fantail transmission
[AIAA PAPER 92-3495] p 906 A92-49031
Impact damage tolerance of helicopter sandwich structures p 958 A92-51506
Progress towards quieter civil helicopters
p 1011 A92-52847
A numerical study of the radiation characteristic of an elliptical exhaust jet p 970 A92-53258
Summary highlights of the Advanced Rotorcraft Transmission (ART) program
[AIAA PAPER 92-3362] p 1051 A92-54026
DAMVIBS looks at rotorcraft vibration
p 1052 A92-55128
Measurements of blade flapping motion on a wind tunnel model p 1093 A92-56023
Efficiency and accuracy in helicopter hovering performance calculation p 1053 A92-56072
Repair procedures for advanced composites for helicopters p 1016 A92-56277
Safety provision against 'ground resonance' free vibration of a coaxial helicopter p 1056 A92-56289
Test and integration concept for complex helicopter avionic systems p 1064 A92-56292
The application of math-dynamic models to characterise a range of helicopter rotor system faults
p 1056 A92-56297
Organization and technical status of the NH90 European helicopter programme p 1016 A92-56306
Lynx - A 50 year product? p 1056 A92-56307
Aeroelasticity of a coaxial helicopter rotor
p 1057 A92-56309
Influence of cross section variations on the structural behaviour of composite rotor blades
p 1121 A92-56320

Composite blades for helicopter main and tail rotors developed by Mil Design Bureau p 1057 A92-56325
Current European research activities in helicopter interactional aerodynamics p 1058 A92-56330
Current European rotorcraft research activities on development of advanced CFD methods for the design of rotor blades (BRITE/EURAM 'DACRO' project) p 1032 A92-56332
Damage tolerance analysis for rotorcraft - What the issues are p 1058 A92-56336
Design method of a helicopter cockpit p 1058 A92-56337
First level release of 2GCHAS for comprehensive helicopter analysis p 1133 A92-56339
Development of a conceptual design method for rotary-wing aircraft using digital computers p 1058 A92-56340
The compound helicopter - A concept revisited p 1058 A92-56341
The achievement of aerodynamic goals on the EH101 project through the 'single site' concept p 1058 A92-56342
AS 332 MKII - Development and certification p 1059 A92-56343
A high speed edgewise rotor using circulation control only in the reversed flow area p 1059 A92-56347
Integration of dynamic, aerodynamic, and structural optimization of helicopter rotor blades
[NASA-CR-189018] p 195 N92-14038
Development and evaluation of a finite element model for a fiber composite helicopter fuselage
[MBB-UD-0584-90-PUB] p 196 N92-15066
Design of experiments p 273 N92-17154
BO 105 identification results p 274 N92-17161
Industry view on rotorcraft system identification p 274 N92-17163
Hot jet dilutor
[ETN-92-90860] p 366 N92-19225
Double loop control law strategy and applications to helicopter
[CERT-2/7724-DERA] p 381 N92-19295
A study of the aeroelastic behaviour of helicopter rotor blades featuring swept tips p 367 N92-19701
Blade-vortex noise on a helicopter main rotor. Study of the strong two dimensional incompressible interaction
[ONERA-RT-96/5094-PY] p 511 N92-20388
Fully integrated aerodynamic/dynamic optimization of helicopter rotor blades
[NASA-TM-104226] p 461 N92-20417
Prediction of helicopter noise: Adaptation of noise load calculations to the blade-vortex interaction
[ONERA-RS-97/5094-PY] p 513 N92-21736
Effect of blade planform variation on the forward-flight performance of small-scale rotors
[NASA-TM-4345] p 630 N92-24885
Application of face-gear drives in helicopter transmissions
[NASA-TM-105655] p 908 N92-28434
The application of flight simulation models in support of rotorcraft design and development p 884 N92-28527
Repair procedures for advanced composites for helicopters
[MBB-UD-0606-91-PUB] p 787 N92-29874
Organic Matrix Composite Helicopter Internal/External Cargo Pallet System (OMC INTEX)
[AD-A251127] p 961 N92-30878
Advanced electromagnetic methods for aerospace vehicles
[NASA-CR-190650] p 1001 N92-31156
Experimental testing of prototype face gears for helicopter transmissions
[NASA-TM-105434] p 1002 N92-31349
Evaluation of composite components on the Bell 206L and Sikorsky S-76 helicopters p 1107 N92-32575

HELICOPTER ENGINES

Full-scale investigation of aerodynamic interactions between a rotor and fuselage p 105 A92-14361
Stage 2 noise certification of the Sikorsky S-76A and S-76C helicopters p 91 A92-14388
Optimization of a light helicopter with Arrius power plants p 120 A92-14408
Tiger MGB - High reliability low weight --- military helicopter Main Gear Box p 109 A92-14418
Manufacturing techniques - Split torque path helicopter transmission p 110 A92-14452
Development of a lubrication system for the T800-LHT-800 turboshaft engine
[ASME PAPER 91-GT-398] p 127 A92-15728
Cold-cycle pressure-jet helicopters - Ventures, designs, and developments. II - Design p 271 A92-22712
Modification of the radiated sound directivity due to ground reflections - Application to static tests of helicopter turboshaft engines
[ONERA, TP NO. 1991-210] p 415 A92-26362
Cold-cycle pressure-jet helicopters: Ventures, designs, and developments. III - Costs and developments p 458 A92-29675
Engine air particle separator panels for helicopter engine protection p 545 A92-35735
Navigation preparations for passenger helicopters p 723 A92-43155
An adaptive flight control for use in connection with helicopter engine failure p 745 A92-43159
Using helicopters for the erection of power transmission lines p 723 A92-43162
The 1991 Cierva Lecture - Aberdeen and its influence on the evolution of the commercial IFR twin engined helicopter p 723 A92-43446
Basic experiments on the directivity of the sound radiation emitted by a turboshaft engine
[ONERA, TP NO. 1992-36] p 926 A92-48597
Acoustic spinning-mode analysis by iterative threshold method applied to a helicopter turboshaft engine
[ONERA, TP NO. 1992-41] p 926 A92-48602
Advanced Rotorcraft Transmission (ART) - Component test results
[AIAA PAPER 92-3366] p 905 A92-48939
'A new proposal for an old problem' - The right engine for the right helicopter p 1070 A92-56281
Lynx - A 50 year product? p 1056 A92-56307
Low temperature environment operations of turboengines (design and user's problems) p 450 N92-21682
Control of a helicopter engine in low altitude flight p 562 N92-23122
A simplified dynamic model of the T700 turboshaft engine
[NASA-TM-105805] p 1009 N92-30898

HELICOPTER PERFORMANCE

An anthropometric evaluation of the TH-57 Jetranger helicopter p 46 A92-11164
Pre-flight risk assessment in emergency medical service (EMS) helicopters p 16 A92-11171
Technology developments applied to the AH-1W SuperCobra
[AIAA PAPER 91-3071] p 21 A92-11607
AHS, Annual Forum, 47th, Phoenix, AZ, May 6-8, 1991, Proceedings. Vols. 1 & 2 p 59 A92-14326
Frequency-domain identification of BO 105 derivative models with rotor degrees of freedom p 104 A92-14327
Forward flight trim calculation and frequency response validation of a high-order helicopter simulation model p 132 A92-14337
Probabilistic fatigue methodology for six nines reliability p 145 A92-14342
A full mission simulation data system p 162 A92-14367
A computer programme for the certification of helicopter vertical take-off and landing operations and an application to the S-76B helicopter p 106 A92-14379
Committees, their importance to the structures of the Helicopter Association International p 59 A92-14411
A holistic approach to support p 60 A92-14413
Spares support of your Rotary-Wing Jenny p 60 A92-14435
Main concepts of providing the static/fatigue strength of helicopters in the USSR p 110 A92-14455
1990 report to the aerospace profession; Society of Experimental Test Pilots, Symposium, 34th, Beverly Hills, CA, Sept. 27-29, 1990, Proceedings p 111 A92-16051
Formulation of a simplified model of rotor-horizontal stabilizer interactions and comparison with experimental measurements
[ONERA, TP NO. 1991-157] p 77 A92-16125
The response of a helicopter to windshear p 269 A92-21470
Development of an analytical method to predict helicopter main rotor performance in icing conditions
[AIAA PAPER 92-0418] p 326 A92-26268
Transgressions in a pilot-helicopter system p 358 A92-27394
A theoretical study on helicopter alert time without maintenance p 358 A92-27836
Identification of helicopter component loads using multiple regression
[AIAA PAPER 92-2110] p 544 A92-35681
Helicopter fog flying trials p 530 A92-35759
Inertial reference units with integrated air speed determination for helicopters p 554 A92-35764
Generalized higher harmonic control - Ten years of Aerospatiale experience p 569 A92-35769
LAH main rotor model test at the DNW p 547 A92-35771
The development and testing of an active control of structural response system for the EH101 helicopter p 569 A92-35775
A study of aircraft surface coating technology p 700 A92-43147
Navigation preparations for passenger helicopters p 723 A92-43155
A helicopter transportation system p 723 A92-43161
Helicopters for public services, including rescue, fire fighting, and medical emergency p 723 A92-43163
Using helicopters for coastal alert p 723 A92-43164
Flight model for unmanned simulated helicopters p 874 A92-46776
Establishing a database for flight in the wakes of structures p 810 A92-46782
Flight deck aerodynamics of a nonaviation ship p 810 A92-46790
Aeromechanical stability of hingeless helicopter rotors in forward flight p 874 A92-46923
Relative energy concepts in helicopter dynamics p 846 A92-46925
Chaotic dynamic behavior in a simplified rotor blade lag model p 846 A92-46926
Computational aspects of helicopter trim analysis and damping levels from Floquet theory p 875 A92-46933
Frequency domain flight testing and analysis of an OH-58D helicopter p 847 A92-46943
On the adequacy of modeling turbulence and related effects on helicopter response p 847 A92-46945
A Mach-scaled powered model for rotor-fuselage interactional aerodynamics and flight mechanics investigations p 847 A92-46960
Advanced Rotorcraft Transmission (ART) Program summary
[AIAA PAPER 92-3365] p 905 A92-48938
Advanced Rotorcraft Transmission (ART) - Component test results
[AIAA PAPER 92-3366] p 905 A92-48939
Optimal control of helicopters following power failure
[AIAA PAPER 92-4471] p 1076 A92-55231
Efficiency and accuracy in helicopter hovering performance calculation p 1053 A92-56072
Piloted simulation for the BK117 FBW demonstrator p 1053 A92-56077
Automatic function testing in the aircraft production p 1015 A92-56083
The solution of the helicopter flight dynamics tasks by the methods of optimal control theory p 1085 A92-56284
The computation and validation of hovering rotor performance p 1055 A92-56285
CH-53E/AV-8B aircraft sling load recovery system analysis
[AD-A239950] p 21 N92-10022
Concept evaluation of the UH-60 externally mounted rescue hoist
[AD-A240545] p 22 N92-11004
Heliport VFR airspace design based on helicopter performance
[SCT-90RR-34] p 103 N92-13049
Helicopter rejected takeoff airspace requirements
[SCT-91RR-28] p 116 N92-13058
Rotorcraft acceleration and climb performance model
[SCT-90RR-30] p 116 N92-13059
Helicopter physical and performance data
[SCT-91RR-27] p 116 N92-13060
Flight research p 194 N92-13981
Operational survey: VFR heliport approaches and departures
[SCT-91RR-26] p 190 N92-14033
Development of an analytical method to predict helicopter main rotor performance in icing conditions
[NASA-CR-189110] p 258 N92-15967
BO 105 identification results p 274 N92-17161
SA 330 Puma identification results p 274 N92-17162
Industry view on rotorcraft system identification p 274 N92-17163
Rotorwash computer model: User's guide
[DOT/FAA/RD-90/25] p 346 N92-18345
Robust control system design with application to high performance helicopters p 382 N92-19621
A study of the aeroelastic behaviour of helicopter rotor blades featuring swept tips p 367 N92-19701
Advanced electromagnetic methods for aerospace vehicles
[NASA-CR-188630] p 488 N92-20193
Fully integrated aerodynamic/dynamic optimization of helicopter rotor blades
[NASA-TM-104226] p 461 N92-20417
Baseline vibration measurements of remotely piloted helicopters for higher harmonic control research
[AD-A244669] p 482 N92-21360
A review of icing research at the Royal Aerospace Establishment p 451 N92-21689
Helicopter rotor blade dynamics with bilinear formulation p 463 N92-21856
The aerodynamics of ship superstructures p 503 N92-21953

EH 101 ship interface trials: Flight test programme and preliminary results p 465 N92-21964
Determination of limitations for helicopter ship-borne operations p 465 N92-21965
United Kingdom approach to deriving military ship helicopter operating limits p 465 N92-21966
A review of Australian activity on modelling the helicopter/ship dynamic interface p 465 N92-21967
Helicopter handling: Experience and new developments p 465 N92-21969
Control of a helicopter engine in low altitude flight p 562 N92-23122
Effect of blade planform variation on the forward-flight performance of small-scale rotors
[NASA-TM-4345] p 630 N92-24885
Advanced Rotorcraft Transmission (ART) program summary
[NASA-TM-105665] p 680 N92-24984
Pallet for helicopter testing instrumentation p 652 N92-25598

HELICOPTER PROPELLER DRIVE
Advanced Rotorcraft Transmission (ART) Program summary
[AIAA PAPER 92-3365] p 905 A92-48938
Modal simulation of gearbox vibration with experimental correlation
[AIAA PAPER 92-3494] p 1112 A92-54036
Path identification in structural acoustics p 1059 A92-56346
CH-46 and OH-58 transmission stress wave analysis
[AD-A244321] p 365 N92-18826
Rotorcraft transmissions p 560 N92-22533
Advanced Rotorcraft Transmission (ART) program summary
[NASA-TM-105665] p 680 N92-24984
Full-scale transmission testing to evaluate advanced lubricants
[NASA-TM-105668] p 764 N92-26560
Application of face-gear drives in helicopter transmissions
[NASA-TM-105655] p 908 N92-28434
Dynamics of a split torque helicopter transmission
[NASA-TM-105681] p 910 N92-29136
Development of a full-scale transmission testing procedure to evaluate advanced lubricants
[NASA-TP-3265] p 998 N92-30396
Experimental testing of prototype face gears for helicopter transmissions
[NASA-TM-105434] p 1002 N92-31349
Modal simulation of gearbox vibration with experimental correlation
[NASA-TM-105702] p 1002 N92-31485

HELICOPTER TAIL ROTORS
Flight service evaluation of composite helicopter components p 106 A92-14372
Design and flight test evaluation of the Fantail antitorque system p 110 A92-14456
A simulation model for tail rotor failure
[AIAA PAPER 92-4633] p 1081 A92-55380
A calculation method to predict helicopter noise and its verification p 1135 A92-56074
Computed tomography (CT) as a nondestructive test method used for composite helicopter components p 1121 A92-56276
Helicopter tail rotor stall flutter p 1056 A92-56290
A semi empirical method for the analytical representation of stationary measured profile coefficients for applications of rotary wing aerodynamics
[ETN-92-91491] p 832 N92-29741
Computed Tomography (CT) as a nondestructive test method used for composite helicopter components
[MBB-UD-0603-91-PUB] p 910 N92-29873

HELICOPTER WAKES
Analysis of unsteady pressures induced on a body by a rotor p 10 A92-13212
Flight test investigation of the wake vortices generated by helicopters p 270 A92-21925
Navier-Stokes analysis of helicopter plume flowfield for infrared calculations
[AIAA PAPER 92-0983] p 580 A92-33185
The effects of inner wake modelling on blade airloads p 521 A92-35784
Extension and validation of an unsteady wake model for rotors p 702 A92-41224
Free wake analyses of a hovering rotor using panel method
[SAE PAPER 912004] p 789 A92-45405
A study of rotor wake development and wake/body interactions in hover p 813 A92-46935
A unified procedure for solving rotor flowfield, performance and interference p 814 A92-46950
Efficient high-resolution rotor wake calculations using flow field reconstruction p 814 A92-46951
Experimental and computational studies of hovering rotor flows p 815 A92-46954
Initial validation of an unsteady Euler/Navier-Stokes flow solver for helicopter rotor airloads in forward flight p 815 A92-46956
A new integral equation for potential compressible aerodynamics of rotors in forward flight p 815 A92-46958
Aerodynamic parametric studies and sensitivity analysis for rotor blades in axial flight p 816 A92-46959
The computation and validation of hovering rotor performance p 1055 A92-56285
The application of experimental data to blade wake interaction noise prediction
[NASA-CR-189461] p 237 N92-14789
Flowfield analysis of modern helicopter rotors in hover by Navier-Stokes method
[AD-A245011] p 446 N92-21333
Experimental evaluation of a flat wake theory for predicting rotor inflow-wake velocities
[NASA-TM-4334] p 630 N92-24882
Simulation of a rotorcraft in turbulent flows
[AD-A245742] p 650 N92-26155

HELICOPTERS
Prediction of helicopter simulator sickness p 46 A92-11473
A neural network for the identification of measured helicopter noise p 162 A92-14387
Concurrent engineering at Boeing Helicopters p 162 A92-14393
Functionally integrated aircraft instrumentation for the next generation commercial helicopter p 117 A92-14402
Automatic link establishment - The key to reliable helicopter NOE communications p 94 A92-14403
Ongoing development of a computer jobstream to predict helicopter main rotor performance in icing conditions p 65 A92-14407
The Eurofar vehicle overview p 108 A92-14416
Variation in hover aeromechanical stability trends with bearingless main rotor design p 109 A92-14425
Dynamics of helicopters with dissimilar blades p 133 A92-14427
How to support the 'little guy' --- helicopter maintenance p 60 A92-14437
Computer aiding for low-altitude helicopter flight p 94 A92-14444
Weathering test of AFRP composites for the application of helicopter fuselage --- Aramide Fiber Reinforced Plastic p 142 A92-15309
Fatal occupational injury related to helicopters in the United States 1980-1985 p 186 A92-20720
An optical microphone for the detection of hidden helicopters
[AIAA PAPER 92-0377] p 395 A92-26235
Identification of helicopter noise using a neural network p 416 A92-28032
Active vibration control using fixed order dynamic compensation with frequency shaped cost functionals p 508 A92-29324
Interactive graphics method for removal of helicopter motions from laser profile data p 598 A92-35109
An exploratory investigation into the definition of tracking standards for IFR helicopter approaches to reduced minima p 533 A92-35726
An application of distributed environment in flight simulation p 602 A92-35739
Heterodyne techniques in the I.R. bandwidth for laser obstacle detection p 533 A92-35740
Innovation in the laser warning sensor field p 554 A92-35742
The obstacle avoidance radar - A safety mean for low altitude flights in adverse weather conditions p 554 A92-35743
Transmission vibration monitoring - A single board computer architecture p 554 A92-35765
Temporal change of noisiness of helicopter noise p 689 A92-39103
Temporal change of timbre of helicopter noise p 694 A92-39104
Helicopter far-field acoustic levels as a function of reduced rotor speeds p 695 A92-39228
1991-92 AHS Technical Committee highlights - Manufacturing and product assurance p 609 A92-40396
Robust flight reconstruction for helicopter simulation and training p 747 A92-41230
Adequacy of modeling turbulence and related effects on helicopter response p 730 A92-41263
Aviation, motor, and space designs --- research and development in U.S.S.R. p 784 A92-46202
Experimental investigation of the parallel vortex-airfoil interaction at transonic speeds p 813 A92-46901
A field repair of advanced helicopter vertical fin structure p 785 A92-47417
An advanced flight path management system for low-altitude helicopter flight p 975 A92-49330
Progress towards quieter civil helicopters p 1011 A92-52847
A study on rotor induced sand and dust environment and its harmfulness to helicopter p 960 A92-53012
Real-time helicopter simulation using the blade element method p 1132 A92-56278
Dynamics of helicopters with dissimilar blades in forward flight p 1056 A92-56288
Laser-radar based obstacle avoidance system for helicopters p 1064 A92-56295
Modern helicopter technologies at MBB and the application in future programmes p 1016 A92-56304
HEPO mission simulator - Development and usage for NH90 helicopter p 1094 A92-56313
Research on measurement and control of helicopter rotor response using blade-mounted accelerometers 1990-91 p 1057 A92-56316
Aluminium-lithium alloys - Application on helicopters p 1106 A92-56326
Analysis of helicopter rotor-fuselage interference with time averaged pressure distribution p 1032 A92-56331
CH-53E/AV-8B aircraft sling load recovery system analysis
[AD-A239950] p 21 N92-10022
Guidelines for integrating helicopter assets into emergency planning
[SCT-91RR-18] p 18 N92-10993
Process/object-oriented Ada software design for an experimental helicopter p 164 N92-12461
The development of a requirement specification for an experimental active flight control system for a variable stability helicopter: An Ada simulation in JSD p 135 N92-12466
Heliport VFR airspace design based on helicopter performance
[SCT-90RR-34] p 103 N92-13049
Helicopter rejected takeoff airspace requirements
[SCT-91RR-28] p 116 N92-13058
Helicopter physical and performance data
[SCT-91RR-27] p 116 N92-13060
New York Downtown Manhattan (Wall Street) Heliport: Operations analysis
[DOT/FAA/RD-91/12] p 139 N92-13077
Flow modification over a backward facing step
[AD-A241351] p 158 N92-13406
Operational survey: VFR heliport approaches and departures
[SCT-91RR-26] p 190 N92-14033
Integration of dynamic, aerodynamic, and structural optimization of helicopter rotor blades
[NASA-CR-189018] p 195 N92-14038
Experiences at Langley Research Center in the application of optimization techniques to helicopter airframes for vibration reduction
[NASA-TM-104193] p 299 N92-17033
The NASA/industry design analysis methods for vibrations (DAMVIBS) program: Accomplishments and contributions
[NASA-TM-104192] p 299 N92-17034
Design of experiments p 273 N92-17154
Instrumentation and data processing p 273 N92-17155
Identification techniques: Model structure and time domain methods p 273 N92-17157
Automated composite ellipsoid modelling for high frequency GTD analysis
[NASA-CR-189853] p 275 N92-17316
Human response to helicopter noise: A test of A-weighting
[AD-A243719] p 304 N92-17506
General requirements and techniques for component fatigue life substantiation in Australian service helicopters
[AD-A242881] p 275 N92-17565
An investigation of air transportation technology at the Massachusetts Institute of Technology, 1990-1991 p 265 N92-17985
Experimental investigation of passive infrared ice detection for helicopter applications p 265 N92-17986
Particle trajectory computer program for icing analysis of axisymmetric bodies
[NASA-CR-189134] p 352 N92-19276
Tiltrotor research aircraft composite blade repairs: Lessons learned
[NASA-TM-103875] p 367 N92-19563
Optimizing tuning masses for helicopter rotor blade vibration reduction including computed airloads and comparison with test data
[NASA-TM-104194] p 367 N92-19846
FAA vertical flight research, engineering, and development bibliography, 1962 - 1991
[FAA/ARD-30] p 462 N92-21210
A review of icing research at the Royal Aerospace Establishment p 451 N92-21689

Determination of limitations for helicopter ship-borne operations p 465 N92-21965
Limitations on helicopter operations in the aeronaval environment p 466 N92-21973
Helicopter active rotor control p 570 N92-22157
An investigation into the feasibility of providing a proximity warning device for search and rescue helicopters
[ETN-92-91057] p 530 N92-22408
Rotorcraft transmissions p 560 N92-22533
Development of a helicopter-borne 8-channel ranging scatterometer
[PB92-141977] p 599 N92-23441
Experimental evaluation of a flat wake theory for predicting rotor inflow-wake velocities
[NASA-TM-4334] p 630 N92-24882
Effect of blade planform variation on the forward-flight performance of small-scale rotors
[NASA-TM-4345] p 630 N92-24885
A report on enhancements for existing and future helicopters supporting operations of the Canadian oil and gas industry
[CTN-91-60126] p 636 N92-25350
Analysis of helicopter accident risk exposure near heliports, airports, and unimproved sites
[SCT-91RR-13] p 637 N92-26028
Comparison of Janus and field test aircraft detection ranges for the line-of-sight forward heavy system
[AD-A246047] p 770 N92-27600
Steady-state acoustical noise measurements in aviation systems
[AD-A247831] p 780 N92-27924
Composite profiles of helicopter mishaps at heliports and airports
[AD-A248887] p 724 N92-28052
An analysis of aircrew communication patterns and content
[AD-A246618] p 907 N92-28253
Passive acoustic range estimation of helicopters
[AD-A248033] p 926 N92-28302
A sensitivity analysis on component reliability from fatigue life computations
[AD-A247430] p 908 N92-28425
Comparison of three controllers applied to helicopter vibration
[NASA-TM-102192] p 878 N92-28457
Aircraft ship operations
[AGARD-AR-312] p 850 N92-28468
Experience with piloted simulation in the development of helicopters p 884 N92-28528
Full mission simulation: A view into the future
p 884 N92-28537
An evaluation of IFR approach techniques: Generic helicopter simulation compared with actual flight
p 886 N92-28550
Response of helicopters to gusts
[NLR-TP-90159-U] p 879 N92-28653
LAH-main rotor model test at the DNW
[NLR-TP-90305-U] p 852 N92-28687
S-76B certification for vertical take-off and landing operations from confined areas
[NLR-TP-90286-U] p 852 N92-28714
A rotorcraft flight database for validation of vision-based ranging algorithms
[NASA-TM-103906] p 841 N92-29103
Improving the LAMP Mk 3 SH-60B HF communication system
[AD-A245970] p 910 N92-29344
Helicopter low-speed yaw control
[NASA-CASE-LAR-14219-1] p 879 N92-30025
Experience with piloted simulation in the development of helicopters
[MBB-UD-0610-91-PUB] p 889 N92-30076
Two-dimensional aerodynamic characteristics of several polygon-shaped cross-sectional models applicable to helicopter fuselages
[NASA-TP-3233] p 944 N92-30394
A cable detection lidar system for helicopters
p 1001 N92-31068
A simulation model of a single rotor helicopter
p 979 N92-31865
Report of the aviation safety review of Department of Energy helicopter operations
[DE92-016346] p 954 N92-31928
Vision-based range estimation using helicopter flight data
[NASA-TM-103930] p 1047 N92-32424
Evaluation of composite components on the Bell 206L and Sikorsky S-76 helicopters p 1107 N92-32575
An evaluation of decelerating IFR approaches utilizing a helicopter flight simulator
[CTN-92-60348] p 1048 N92-32845
Flight service environmental effects on composite materials and structures p 1110 N92-33054
Building vibrations induced by noise from rotorcraft and propeller aircraft flyovers
[NASA-TM-104170] p 1138 N92-33160
Development of rating instruments and procedures for aviation mishap investigation
[AD-A253072] p 1044 N92-33288
Workshop on Aeronautical Decision Making (ADM). Volume 1: Executive summary
[DOT/FAA/RD-92/14-VOL-1] p 1142 N92-33305
On the calculation of the response of helicopters to control inputs
[NASA-CR-190812] p 1088 N92-33536
A workstation-based evaluation of a far-field route planner for helicopters
[NASA-TM-102882] p 1051 N92-33609
Finite difference time domain grid generation from AMC helicopter models
[NASA-TM-107679] p 1128 N92-34017
Experimental study of performance degradation of a rotating system in the NASA Lewis RC icing tunnel
[NASA-CR-190684] p 1102 N92-34141
Thermal mechanical analysis of sprag clutches
[NASA-CR-190686] p 1128 N92-34207

HELIOTRONS
Shafranov shift in low-aspect-ratio heliotron/torsatron CHS
[NIFS-110] p 1138 N92-33743

HELIPORTS
Helicopter/heliport operations - Environmental implications p 241 A92-22708
Review on the abatement of helicopter noise
p 406 A92-25501
Heliport VFR airspace design based on helicopter performance
[SCT-90RR-34] p 103 N92-13049
New York Downtown Manhattan (Wall Street) Heliport: Operations analysis
[DOT/FAA/RD-91/12] p 139 N92-13077
Operational survey: VFR heliport approaches and departures
[SCT-91RR-26] p 190 N92-14033
FAA vertical flight research, engineering, and development bibliography, 1962 - 1991
[FAA/ARD-30] p 462 N92-21210
Analysis of helicopter accident risk exposure near heliports, airports, and unimproved sites
[SCT-91RR-13] p 637 N92-26028
Composite profiles of helicopter mishaps at heliports and airports
[AD-A248887] p 724 N92-28052
Helicopter nighttime parking test results - UH-1
[DOT/FAA/CT-TN92/1] p 961 N92-31165

HELIUM
Helium bubble flow visualization of the spanwise separation on a NACA 0012 with simulated glaze ice
[AIAA PAPER 92-0413] p 341 A92-28192
Remarks on high-Reynolds-number turbulence experiments and facilities p 881 A92-45267
Power economy in high-speed wind tunnels by choice of working fluid and temperature p 881 A92-45275
Mixing studies of helium in air at high supersonic speeds p 935 A92-50310
Oscillating shock impingement on low-angle gas injection into a supersonic flow p 89 N92-13032
Brush seal leakage performance with gaseous working fluids at static and low rotor speed conditions
[NASA-TM-105400] p 297 N92-16265
Numerical simulation of transient hypervelocity flow in an expansion tube
[NASA-CR-189601] p 402 N92-18965
Helium bubble flow visualization of the spanwise separation on a NACA 0012 with simulated glaze ice
[NASA-TM-105742] p 714 N92-26612

HELIUM-NEON LASERS
Particle image velocimetry
[AD-A246638] p 750 N92-27753

HELMET MOUNTED DISPLAYS
Expanding U.S.M.C. roles for the AH-1W SuperCobra
p 59 A92-14347
Adaptive suppression of biodynamic interference in helmet-mounted displays and head teleoperation
p 197 A92-18611
A new method for orientation calculation of the electromagnetic helmet-mounted sighting unit
p 370 A92-27837
Helmet-mounted image intensification analysis
p 554 A92-35454
The evaluation of simulator effectiveness for the training of high speed, low level, tactical flight operations
p 885 N92-28539

HELMETS
International aviation (selected article)
[AD-A240987] p 170 N92-13992

HELMHOLTZ RESONATORS
Improvement in transmission loss of aircraft double wall with resonators p 1011 A92-53091
Development and testing of cabin sidewall acoustic resonators for the reduction of cabin tone levels in propfan-powered aircraft
[NASA-CR-4388] p 166 N92-13757
Evaluation of the applicability of Helmholtz resonators for low frequency acoustic liners
[PB92-138544] p 605 N92-23588

HEMISPHERE CYLINDER BODIES
The dynamic character of the wake of an axisymmetric body at an angle of attack
[AIAA PAPER 91-3268] p 8 A92-12741
Separation patterns and flow structures about a hemisphere-cylinder at high incidences
[AIAA PAPER 92-2712] p 807 A92-45593

HERMES MANNED SPACEPLANE
Structures and materials technologies for hypersonic vehicles - Lessons from Hermes experience
[AIAA PAPER 91-5098] p 486 A92-31697
Materials and structures for Hermes
p 666 A92-38213
Is the avionics system of the Hermes Spaceplane centralized or decentralized? p 984 A92-49258
Computation of aerodynamic coefficients on Hermes-Ariane5 configuration p 184 N92-15040
Review of the European hypersonic wind tunnel performance and simulation requirements
p 209 N92-15043
Data processing aspects of the Hermes Flight Control Center p 513 N92-20629

HEURISTIC METHODS
Case-based reasoning - Taming the similarity heuristic --- for development of solutions to real world problems
p 47 A92-11153
Heuristic route optimization: A model for force level route planning p 164 N92-12520

HIERARCHIES
Aircraft optimization by a system approach: Achievements and trends
[NASA-TM-107622] p 650 N92-25995
A modeling strategy for large-scale optimization based on analysis and visualization principles
[AD-A246570] p 777 N92-26620

HIGH ACCELERATION
An explosively driven, fast shock tube
[DE92-008437] p 749 N92-26720

HIGH ALTITUDE
Added mass of high-altitude balloons
[AIAA PAPER 91-3693] p 16 A92-11034
The concept of an unmanned flying vehicle at high altitude p 731 A92-43242
Design and wind tunnel test of low-Reynolds-number airfoil p 1029 A92-56047
Behaviour and modelling of the aerothermodynamics of ballistic entry vehicles in the high altitude flow regimes
p 184 N92-15031
High altitude solar power platform --- aircraft design analysis
[NASA-TM-103578] p 506 N92-21546
SHARP: Subsonic High Altitude Research Platform
[NASA-CR-190004] p 648 N92-25263
A preliminary design and analysis of an advanced heat-rejection system for an extreme altitude advanced variable cycle diesel engine installed in a high-altitude advanced research platform
[NASA-CR-186021] p 871 N92-29427

HIGH ALTITUDE BALLOONS
High-altitude lighter-than-air powered platform
[SAE PAPER 912054] p 844 A92-45438
Piloted simulation study of a balloon-assisted deployment of an aircraft at high altitude
[NASA-TM-104245] p 272 N92-15986

HIGH ALTITUDE ENVIRONMENTS
International aviation (selected article)
[AD-A240987] p 170 N92-13992

HIGH ALTITUDE TESTS
Liquid cooled turbocharged propulsion system for HALE application
[ASME PAPER 91-GT-399] p 127 A92-15729
Surge-troubleshooting of a twin-spool turbojet engine tested at a high altitude test facility p 375 A92-28459

HIGH ASPECT RATIO
Flow characteristic and flow control of high aspect ratio and highly curved S-bend diffuser p 245 A92-21743
An experimental investigation of high-aspect-ratio cooling passages
[AIAA PAPER 92-3154] p 890 A92-48780
Vortex control: Further encounters p 87 N92-13020

HIGH CURRENT
Mechanisms of high-current pulses in lightning and long-spark stepped leaders p 1116 A92-54678

HIGH DEFINITION TELEVISION
DARPA high resolution display technologies
p 218 A92-19977

HIGH FREQUENCIES
High-frequency techniques for antenna analysis
p 494 A92-31071

Antennas on complex platforms p 494 A92-31084
RCS of four fuselage-like scatterers at HF frequencies p 533 A92-33632
New methods to determine the transmission loss of partitions using sound intensity measurements p 924 A92-45879
A sophisticated, multi-channel data acquisition and processing system for high frequency noise research [NASA-CR-189137] p 696 N92-24688
An evaluation of superresolution methods for tactical radio direction finding [AD-A246316] p 726 N92-26291

HIGH GAIN
High gain airborne antenna for satellite communications p 639 A92-40188
A high gain antenna system for airborne satellite communication applications p 677 N92-24096

HIGH IMPULSE
An explosively driven, fast shock tube [DE92-008437] p 749 N92-26720

HIGH PRESSURE
Screech noise source structure of a supersonic rectangular jet [AIAA PAPER 92-0503] p 331 A92-26932
Gasdynamic calculation of an impulse wind tunnel with a two-section plenum p 493 A92-30147
Cut progression during dynamometer testing of foreign object damaged type VII extra high pressure aircraft tires [SAE PAPER 912155] p 644 A92-39990
Paint removal using cryogenic processes [AD-A247668] p 895 N92-28912

HIGH PRESSURE OXYGEN
Test results for rotordynamic coefficients of the SSME HPOTP turbine interstage seal with two swirl brakes p 223 N92-14357
Dynamic characteristics and stability analysis of space shuttle main engine oxygen pump p 224 N92-14366

HIGH RESOLUTION
Euler flow predictions for an oscillating cascade using a high resolution wave-split scheme [ASME PAPER 91-GT-198] p 74 A92-15623
A high-resolution Euler solver based on multigrid, semi-coarsening, and defect correction p 671 A92-37868
High-altitude lighter-than-air powered platform [SAE PAPER 912054] p 844 A92-45438
An evaluation of superresolution methods for tactical radio direction finding [AD-A246316] p 726 N92-26291

HIGH REYNOLDS NUMBER
Aerodynamics and heat transfer investigations on a high Reynolds number turbine cascade [ASME PAPER 91-GT-157] p 148 A92-15593
Base pressure measurements on a cone at Mach numbers from M sub infinity = 5 to 7 p 173 A92-18770
Computation of transonic flow over an airfoil at large Reynolds numbers p 252 A92-23414
Operation and design considerations for unsteady data acquisition with PC-based systems in high Reynolds number hypersonic flowfields [AIAA PAPER 92-0204] p 284 A92-23810
An experimental study of the flow past spheres at transonic speeds and high Reynolds numbers p 312 A92-25002
Experimental studies of a two-element airfoil with large separation [AIAA PAPER 92-0267] p 317 A92-25723
An algebraic model for dissipation in supersonic boundary layers [AIAA PAPER 92-0311] p 320 A92-25759
Experimental investigation of the perpendicular rotor blade-vortex interaction at transonic speeds p 340 A92-28047
Change of flow about an elongated rectangular cylinder in a range of Reynolds numbers of 200 to 0.7 x 10 exp 4 p 522 A92-35997
Behavior of asymmetric unstable modes of a trailing line vortex near the upper neutral curve p 617 A92-39340
Recent airfoil tests in NAL 2D high Reynolds number wind tunnel p 748 A92-43171
High Reynolds number flows using liquid and gaseous helium [ISBN 0-387-97475-X] p 897 A92-45261
High-Reynolds-number test requirements in low-speed aerodynamics p 787 A92-45263
Remarks on high-Reynolds-number turbulence experiments and facilities p 881 A92-45267
Separation control on high Reynolds number multi-element airfoils [AIAA PAPER 92-2636] p 806 A92-45575
Unstructured and adaptive mesh generation for high Reynolds number viscous flows p 816 A92-47042
Development of an efficient analysis for high Reynolds number inviscid/viscid interactions in cascades [AIAA PAPER 92-3073] p 823 A92-48723
High Reynolds number testing in support of transport airplane development [AIAA PAPER 92-3982] p 1099 A92-56807
High-lift testing at high Reynolds numbers [AIAA PAPER 92-3986] p 1033 A92-56810
An approach for increasing aeroelastic divergence dynamic pressure of wind-tunnel models [AIAA PAPER 92-4002] p 1099 A92-56825
The BCAC/IAR collaborative research program to investigate the sidewall boundary layer effects in the IAR/NRC 2-D High Reynolds Number Test Facility [NRC-HSA-434] p 81 N92-11976
Laminar-flow secondary separation on a slender wing p 85 N92-13006
Navier-Stokes calculation of transonic flow past the NTF 65 deg delta wing p 91 N92-13868
The installation of the AVRO 9 by 7 foot low-speed wind tunnel at the University of Manchester (England) [AERO-REPT-9005] p 385 N92-18341
The adverse aerodynamic impact of very small leading-edge ice (roughness) buildups on wings and tails p 451 N92-21691
Measurements of fluctuating pressure in a rectangular cavity in transonic flow at high Reynolds numbers [NASA-TM-4363] p 633 N92-25752
A preliminary experimental investigation of local isotropy in high-Reynolds-number turbulence p 912 N92-30042
High Reynolds number test of the Boeing TR77 airfoil in the Langley 0.3-meter transonic cryogenic tunnel [NASA-TM-4189] p 947 N92-31246

HIGH SPEED
Thermodynamic structural analysis of high speed propulsion systems [IAF PAPER 91-278] p 120 A92-14711
Unsteady viscous flow in a high speed core compressor [ASME PAPER 91-GT-91] p 70 A92-15555
The numerical simulation of a high-speed axial flow compressor [ASME PAPER 91-GT-272] p 75 A92-15669
On the nonlinear stability of a high-speed, axisymmetric boundary layer p 78 A92-16457
The high speed challenge for rotary wing aircraft [SAE PAPER 911974] p 842 A92-45381
Flow visualisation of a small diameter rotor operating at high rotational speeds with blades at small pitch angles p 814 A92-46949
Design criteria and analysis of the dynamic behavior of high speed, heavily loaded and precision epicyclic gears for aircraft use [AIAA PAPER 92-3491] p 906 A92-49028
Evaluation of two high-speed runway exits [DOT/FAA/CT-TN91/36] p 31 N92-11021
Study of detached turbulent flow in an air intake by means of high speed tomography and laser velocimetry [REPT-90/55] p 157 N92-12216
Technology needs for high speed rotorcraft (3) [NASA-CR-177592] p 195 N92-14039
An introduction to high speed aircraft noise prediction [NASA-CR-189582] p 416 N92-19672
Improved large perturbation propulsion models for control system design (1988-1989) and large perturbation models of high velocity propulsion systems (1989-1990) and reduced order propulsion models for control system design (1990-1991) [NASA-CR-190148] p 593 N92-22491
A hierarchy for modeling high speed propulsion systems p 559 N92-22492
Modeling of linear isentropic flow systems p 593 N92-22495
High speed transport cruise drag --- scaling laws using Navier-Stokes equations [NASA-CR-190248] p 527 N92-23103
Flat belt continuously variable high speed drive [DE92-008952] p 680 N92-25054
High speed civil transport p 649 N92-25919
Structural analysis for preliminary design of High Speed Civil Transport (HSCT) p 684 N92-25926
Application of integrated structural analysis to the high speed civil transport p 684 N92-25927
Preliminary structural sizing of a Mach 3.0 high-speed civil transport model [NASA-CR-189631] p 685 N92-25960
Professor Jesse W. Beams and the first practical magnetic suspension p 771 N92-27723
Low power magnetic bearing design for high speed rotating machinery p 772 N92-27739
Evaluation of outdoor-to-indoor response to minimized sonic booms [NASA-CR-189643] p 927 N92-28556
High speed research system study. Advanced flight deck configuration effects [NASA-CR-189650] p 967 N92-30965
Design and analysis issues of integrated control systems for high-speed civil transports [NASA-CR-186022] p 979 N92-31656
An examination of several high resolution schemes applied to complex problems in high speed flows [AD-A250814] p 1124 N92-32632
High speed transition prediction [NASA-CR-190836] p 1039 N92-33424

HIGH SPEED CAMERAS
Development of an electronic high speed camera system for the quantitative analysis of unsteady flows [MPIS-100/1991] p 300 N92-17344

HIGH TEMPERATURE
Sound transmission through a high-temperature acoustic probe tube p 415 A92-26406
High temperature static strain gage development [NASA-CR-189044] p 195 N92-14037
Ultra-high temperature (greater than 2000 C) testing capability at Oak Ridge National Laboratory for carbon materials in air, inert gas and vacuum [DE92-004445] p 385 N92-18069
Evaluation of an innovative high-temperature ceramic wafer seal for hypersonic engine applications p 578 N92-22205
High-temperature polymer matrix composites p 578 N92-22513
Creep and fatigue research efforts on advanced materials p 593 N92-22514
Small engine technology programs p 560 N92-22532
Aircraft engine hot section technology: An overview of the HOST Project p 561 N92-22535
Effects of chemical equilibrium on turbine engine performance for various fuels and combustor temperatures [NASA-TM-105399] p 562 N92-23254
High temperature dynamic engine seal technology development [NASA-TM-105641] p 596 N92-23435
High-temperature miniaturized turbine engine lubrication system simulator [AD-A249259] p 868 N92-28294
Apparatus for elevated temperature compression or tension testing of specimens [NASA-CASE-LAR-14775-1] p 912 N92-30099
Electro optical system to measure strains at high temperature [NASA-CR-190450] p 1127 N92-33696

HIGH TEMPERATURE AIR
Experimental and numerical studies of radiation emission from high-temperature air behind 10 km/s shock waves [SAE PAPER 912025] p 790 A92-45417
Numerical study on the secondary jet into a supersonic flow p 1018 A92-53556

HIGH TEMPERATURE ENVIRONMENTS
Fracture behaviour of high-temperature polymer composites p 34 A92-11993
Response of symmetrically laminated rectangular plates subjected to heating p 296 A92-24186
High-temperature powder-lubricated dampers for gas turbine engines p 399 A92-28528
Laser thermal simulation puts jet engines to the test p 663 A92-38129
Effect of sustained high temperature exposure on the mechanical properties of Nicalon/Al2O3 composites p 668 A92-39672
Monolithic ceramics p 668 A92-39854
Elevated temperature crack growth in aircraft engine materials p 891 A92-45234
The mechanism of liquid-cooling of vane in high-temperature turbine p 969 A92-49841
The Langley 15-inch Mach 6 High Temperature Tunnel [AIAA PAPER 92-3938] p 1096 A92-56768
Life prediction and constitutive models for engine hot section anisotropic materials program [NASA-CR-189223] p 1072 N92-33479
Cooled high-temperature radial turbine program 2 [NASA-CR-189122] p 1073 N92-34236

HIGH TEMPERATURE FLUIDS
High temperature, thermally stable JP fuels - An overview [AIAA PAPER 92-0683] p 389 A92-27050
Thermally regenerative fuel cells [AD-A242900] p 300 N92-17629
Lubricant evaluation and performance 2 [AD-A247464] p 895 N92-28398

HIGH TEMPERATURE GASES
Development and bench test of high-temperature combustion chamber with structural ceramic components [ASME PAPER 91-GT-315] p 126 A92-15691
Hot gas environment around STOVL aircraft in ground proximity. II - Numerical study p 371 A92-24403
Hot gas environment around STOVL aircraft in ground proximity. I - Experimental study p 371 A92-24409

Turbine disk temperatures resulting from the hot mainstream at engine conditions
[AIAA PAPER 92-0398] p 373 A92-26252
A dynamic digital model for the turbojet with pulse-monitored fueller p 654 A92-38267
Use of the TMS-65 heating equipment at airports to create fog-dispersal zones above the runway to facilitate takeoff p 775 A92-44084
Configuration effects on the ingestion of hot gas into the engine intake p 842 A92-45315
Hot gas ingestion characteristics and flow visualization of a vectored thrust STOVL concept p 860 A92-45316
Hot-gas reingestion - Engine response considerations p 860 A92-45317
Redesign of flight space shuttle main engine nozzle G-15 seal area based on the thermal analysis and flow models p 212 N92-15877
Calculations of hot gas ingestion for a STOVL aircraft model
[NASA-TM-105437] p 350 N92-19993
Development of an integrated BEM approach for hot fluid structure interaction: BEST-FSI: Boundary Element Solution Technique for Fluid Structure Interaction
[NASA-CR-189202] p 574 N92-22211
TVD finite-difference solutions of nonequilibrium vibrationally relaxing and chemically reacting gaseous flows p 626 N92-24854
Hot-gas reingestion engine response considerations
[PNR-90810] p 740 N92-27042
Contingency power for a small turboshaft engine by using water injection into turbine cooling air
[NASA-TM-105680] p 871 N92-29661
Dynamic response of induced pressures, suckdown, and temperatures for two tandem jet STOVL configurations
[NASA-TM-103934] p 1039 N92-33581

HIGH TEMPERATURE LUBRICANTS
Development and tribological properties of new cyclotriphosphazene high temperature lubricants for aircraft gas turbine engines p 287 A92-21327
Lubricant evaluation and performance 2
[AD-A247464] p 895 N92-28398
Liquid lubricants for advanced aircraft engines
[NASA-TM-104531] p 1109 N92-32863

HIGH TEMPERATURE RESEARCH
Experimental simulation and diagnostics of high-enthalpy real-gas flows
[AD-A241286] p 166 N92-13822
Electro optical system to measure strains at high temperature
[NASA-CR-190450] p 1127 N92-33696
High temperature aircraft research furnace facilities
[NASA-CR-184384] p 1101 N92-33826

HIGH TEMPERATURE SUPERCONDUCTORS
Levitation of YBa2Cu3O(7-x) superconductor in a variable magnetic field p 771 N92-27735
Characterization of superconducting magnetic bearings (dynamic stiffness and damping coefficient in axial direction) p 772 N92-27737
Magnetic suspension using high temperature superconducting cores p 772 N92-27789
Superconducting bearings with levitation control configurations
[NASA-CASE-GSC-13346-1] p 909 N92-29099

HIGH TEMPERATURE TESTS
High temperature multiaxial creep testing of Nimonic 115 p 141 A92-15202
Development of an innovative high-temperature gas turbine fuel nozzle
[ASME PAPER 91-GT-36] p 121 A92-15519
The basics of powder lubrication in high-temperature powder-lubricated dampers
[ASME PAPER 91-GT-248] p 150 A92-15653
Influence of long time exposure at elevated temperatures in air on mechanical properties of the high temperature titanium alloy IMI 834 p 289 A92-22767
Review of methods for crack growth testing in gas turbine engine disc materials p 296 A92-24193
A viscoplastic theory for anisotropic materials
[ONERA, TP NO. 1992-90] p 391 A92-24721
Mechanical testing of glass-ceramic matrix composites
[ONERA, TP NO. 1991-182] p 388 A92-26351
Static tests for the evaluation of fuel additives
[AIAA PAPER 92-0686] p 389 A92-27053
Structural testing technology at high temperature; Proceedings of the Conference, Dayton, OH, Nov. 4-6, 1991
[ISBN 0-912053-34-8] p 980 A92-51401
Research capabilities of the NASA Langley 8-foot high temperature tunnel p 980 A92-51403
High temperature ground vibration test techniques p 980 A92-51404
Acoustic testing at elevated temperatures p 981 A92-51405
A history of high-temperature testing at WPAFB p 981 A92-51406
A historical overview of high-temperature structural testing at the NASA Dryden Flight Research Facility p 981 A92-51407
Thermal-structural panel buckling tests p 993 A92-51409
High temperature MMCs for aero-engines - Challenge and potential p 986 A92-52982
High enthalpy wind tunnel for erosion testing of advanced materials
[AIAA PAPER 92-3888] p 1094 A92-56729
High-temperature durability considerations for HSCT combustor
[NASA-TP-3162] p 289 N92-17070
Ultra-high temperature (greater than 2000 C) testing capability at Oak Ridge National Laboratory for carbon materials in air, inert gas and vacuum
[DE92-004445] p 385 N92-18069
NLR experience with high velocity burner rig testing, 1979-1989
[NLR-TP-89152-U] p 385 N92-18415
High temperature strain gage technology for hypersonic aircraft development applications
[NASA-CR-189101] p 592 N92-22239
Properties of a TZP/Al2O3 composite after long-term exposure at 1000 C
[AD-A246407] p 757 N92-27752
Thermomechanical fatigue behavior of a silicone carbide fiber-reinforced calcium aluminosilicate glass-ceramic matrix composite
[AD-A249870] p 988 N92-31823

HIGH VOLTAGES
Study of simulated lightning discharge effects on wires of a rotorcraft
[ONERA, TP NO. 1991-173] p 92 A92-16137
The formation and structure of plasma wakes behind large high-voltage space platforms in ionosphere
[AIAA PAPER 92-0577] p 407 A92-26984
The use of high voltage direct current in aircraft electrical systems - A Navy perspective
[SAE PAPER 912173] p 655 A92-39998
Repetitive High Energy Pulsed Power (RHEPP) temperature monitoring system utilizing Luxtron fluoroptic sensors and thermocouples technical reference manual
[DE92-013461] p 999 N92-30893

HIGHLY MANEUVERABLE AIRCRAFT
Computer-aided equipment layout for the fuselage of maneuverable aircraft p 113 A92-16833
Roll-performance criteria for high augmented aircraft p 204 A92-18623
Nonlinear aircraft tracking filter utilizing control variable estimation p 302 A92-21179
Robust adaptive nonlinear control of high performance aircraft p 478 A92-29188
Nonlinear inversion flight control for a supermaneuverable aircraft p 873 A92-46751
Force production mechanisms of a tangential jet on bodies at high alpha
[AIAA PAPER 92-4648] p 1082 A92-55393
Aerodynamic development of the X-31 aircraft for the high angle of attack region
[MBB-FE211-S-PUB-452] p 275 N92-17313
Nonlinear stability and control study of highly maneuverable high performance aircraft, phase 2
[NASA-CR-189911] p 382 N92-19841
Feedback control laws for highly maneuverable aircraft
[NASA-CR-190535] p 879 N92-29654
Nonlinear stability and control study of highly maneuverable high performance aircraft, phase 2
[NASA-CR-190667] p 978 N92-30922

HIGHWAYS
Bibliography of technical reports, 1980 - 1990
[PB92-110691] p 417 N92-18814

HILSCH TUBES
An investigation of two cooling technologies as applied to a distributed propulsion control architecture
[ASME PAPER 91-GT-341] p 111 A92-15705

HISTORIES
Lighter than air - An illustrated history of the airship (Revised edition) --- Book p 418 A92-25680
36th Roy Chadwick Lecture - Manufacturing breakout 1941-1991: Development in aerospace industry manufacturing techniques p 419 A92-28941
Test facilities and instrumentation for research in rarefied gas dynamics - An historical perspective
[AIAA PAPER 92-3969] p 1098 A92-56795
Study of alternatives: Dayton's Aviation heritage, Ohio
[PB91-202275] p 2 N92-10972
Eighty years of aerospace technique through ATMA bulletins
[ETN-91-90097] p 57 N92-11963
Evolution of avionic systems architecture, from the 1950's to the present p 198 N92-14047
Historical perspective on the evolution of avionics standards p 198 N92-14049
The evolution of the bypass engine
[PNR-90832] p 476 N92-21850
NASA engineers and the age of Apollo
[NASA-SP-4104] p 929 N92-28344

HODOGRAPHS
Extended mapping and characteristics techniques for inverse aerodynamic design p 194 N92-13949
Design of transonic compressor cascades using hodograph method p 202 N92-13973
The research progress on Hodograph Method of aerodynamic design at Tsinghua University p 177 N92-13974

HOLE GEOMETRY (MECHANICS)
Stress concentration effects of oblique holes in aspirated-cooled turbine engine liners
[AIAA PAPER 92-1130] p 581 A92-33282

HOLES (MECHANICS)
Minimization of the number of cooling holes in internally cooled turbine blades
[ASME PAPER 91-GT-52] p 121 A92-15530
Fatigue life estimation of fastener holes without load transfer p 291 A92-21472
Dynamic wind tunnel tests on control of forebody vortices with suction p 380 N92-18793

HOLOGRAPHIC INTERFEROMETRY
Holographic-interferometry methods employed for vibration-strength testing of aviation-engine workpieces p 219 A92-20771
Measurement of a three-dimensional hypersonic density field
[AIAA PAPER 92-0383] p 323 A92-26240
Holographic flowfield density measurements in swept shock wave/boundary-layer interactions
[AIAA PAPER 92-0746] p 335 A92-27092
Three-dimensional flow visualization of shock wave using double-pulsed holographic interferometry. II - Flow visualization for three-dimensional shock structures in rotating aeroengine fan blade rows p 497 A92-32507
Comparison of interferometric measurements with 3-D Euler computations for circular cones in supersonic flow
[AIAA PAPER 92-2691] p 800 A92-45538
Holographic and PLIF measurements of free-flight hypervelocity flows in the AEDC Range G facility
[AIAA PAPER 92-3935] p 1122 A92-56765
Electro optical system to measure strains at high temperature
[NASA-CR-190450] p 1127 N92-33696

HOLOGRAPHY
Holographic and PLIF measurements of free-flight hypervelocity flows in the AEDC Range G facility
[AIAA PAPER 92-3935] p 1122 A92-56765
Limitations of a holographic 3-D pixel projector for cockpit displays
[AD-A241295] p 119 N92-13067
Holographic flow visualization in rotating turbomachinery
[PNR-90837] p 500 N92-20491
Concept design phase expendable holographic sensor to measure ocean small angle optical scattering
[AD-A245067] p 501 N92-20997
Electro optical system to measure strains at high temperature
[NASA-CR-190450] p 1127 N92-33696

HOMING DEVICES
Ground test facilities for aerothermal and aero-optical evaluation of hypersonic interceptors
[AIAA PAPER 92-1074] p 573 A92-33244
Binary optic-corrected conformal windows for optical seekers
[AIAA PAPER 92-2802] p 779 A92-41340
Multiple aperture window and seeker concepts for endo KEW applications
[AIAA PAPER 92-2806] p 752 A92-41344
Ideal proportional navigation p 976 A92-50497
A radar signal processing ASIC and a VME interface circuit p 859 N92-28380

HOMOGENEOUS TURBULENCE
Compressibility effects on the growth and structure of homogeneous turbulent shear flow p 675 A92-40052
Simulation and modeling of homogeneous compressible turbulence under isotropic mean compression p 622 A92-40134
Non-linear interactions in homogeneous turbulence with and without background rotation p 912 N92-30044

HOMOTOPY THEORY
Two- and three-dimensional grid generation by an algebraic homotopy procedure p 611 A92-36861

HONEYCOMB CORES
Combined compressive and shear buckling analysis of hypersonic aircraft sandwich panels
[AIAA PAPER 92-2487] p 586 A92-34603
Performance of aluminum honeycomb panels with structural defects and core anomalies. II - Specimen description and test results p 591 A92-36156

Tiltrotor research aircraft composite blade repairs: Lessons learned
[NASA-TM-103875] p 367 N92-19563

HONEYCOMB STRUCTURES
Some results on metal and composite patch reinforcement of aluminum honeycomb panel
p 216 A92-18830
Design and testing leading to certification of the Airbus A340 nose landing gear doors p 272 A92-24192
The aerodynamic characteristics of grid fin wings
p 427 A92-30201
Development of aircraft bonded structure and the NDI method p 1016 A92-56100
Flow quality studies of the NASA Lewis Research Center 8- by 6-foot supersonic/9- by 15-foot Low Speed Wind Tunnel
[AIAA PAPER 92-3916] p 1095 A92-56748
Flow quality studies of the NASA Lewis Research Center 8- by 6-foot supersonic/9- by 15-foot low speed wind tunnel
[NASA-TM-105417] p 887 N92-28673
Detection of honeycomb damage using hexagonal grid discontinuities
[DREP-89-9] p 1109 N92-32846
Active control of sound transmission through stiff lightweight composite fuselage constructions
p 1137 N92-32957

HOOKS
Evaluation of grounding and mooring points for Army aircraft
[AD-A250749] p 953 N92-31193

HORIZONTAL FLIGHT
Control surfaces correlation in DSFC maneuvers --- Direct Side-Force Control p 281 A92-21307
Horizontal flight of an aircraft with periodic thrust reversal p 480 A92-31876
Optimization of constant altitude-constant airspeed flight of turbojet aircraft p 845 A92-46815
Optimal trajectories for an unmanned air-vehicle in the horizontal plane
[AIAA PAPER 92-4344] p 1079 A92-55333
Trim drag reduction concepts for horizontal takeoff single-stage-to-Orbit vehicles
[NASA-TM-102687] p 206 N92-15076
Fully integrated aerodynamic/dynamic optimization of helicopter rotor blades
[NASA-TM-104226] p 461 N92-20417
Effect of blade planform variation on the forward-flight performance of small-scale rotors
[NASA-TM-4345] p 630 N92-24885
Investigation of the flight control requirements of a half-scale ducted fan unmanned aerial vehicle
[AD-A252730] p 1087 N92-32988

HORIZONTAL ORIENTATION
Flow modification over a backward facing step
[AD-A241351] p 158 N92-13406

HORIZONTAL SPACECRAFT LANDING
Space shuttle entry terminal area energy management
[NASA-TM-104744] p 308 N92-19930

HORIZONTAL TAIL SURFACES
Automation of composite material structure installation
p 700 A92-43248
Analysis and testing of a composite sandwich shell horizontal tail p 755 A92-44617
An improved wall correction method for the longitudinal stability p 978 A92-53388
Contribution of fin and tailplane to sideforce and yawing moment derivatives due to sideslip at supersonic speeds at low angles of attack
[ESDU-91031] p 259 N92-15971
Investigation on freezing and sticking phenomena of slush on airplane surfaces when taxiing on the ground and the succeeding take-off run phase
[NAL-TR-1026] p 352 N92-18182
Contribution of tailplane-mounted twin fins to sideforce, yawing moment, and rolling moment derivatives due to sideslip
[ESDU-92007] p 1086 N92-32487

HORSESHOE VORTICES
Suppression of the wing-body junction vortex by body surface suction p 309 A92-24417
An experimental study of a turbulent wing-body junction and wake flow
[AIAA PAPER 92-0434] p 327 A92-26281
A review of impinging jets in cross-flows - Experimentation and computation
[AIAA PAPER 92-0633] p 333 A92-27011
Turbulent flow in the wake of an idealized wing-body junction
[AIAA PAPER 92-0282] p 435 A92-31652
Effects of attack angle on leg portion of the horseshoe vortex around the idealized wing p 623 A92-40177
Investigation of three-dimensional flow field in a turbine including rotor/stator interaction. II - Three-dimensional flow field at the exit of the nozzle
[AIAA PAPER 92-3326] p 826 A92-48909
Navier-Stokes computations of horseshoe vortex flows
p 990 A92-49516

HOT CORROSION
Thermal barrier coatings for gas turbine use
p 142 A92-15245
High temperature erosion resistance of coatings for gas turbine
[ASME PAPER 91-GT-213] p 143 A92-15632
Cyclic hot corrosion of Haynes 230 alloy
p 754 A92-41091
NLR experience with high velocity burner rig testing, 1979-1989
[NLR-TP-89152-U] p 385 N92-18415

HOT ISOSTATIC PRESSING
Development and characterization of high strength SiC rotors
[ASME PAPER 91-GT-191] p 149 A92-15617
The hardness and toughness of HIPed silicon nitride
p 668 A92-39682
The role of PM in the design of lightweight aircraft engine components p 991 A92-50137
Titanium alloy casting for aerospace
p 1106 A92-56103
Evaluation of the elevated-temperature mechanical reliability of a HIPed silicon nitride
[DE92-007838] p 579 N92-23223

HOT SURFACES
Effect of nose shape on three-dimensional stagnation region streamlines and heating rates
[AIAA PAPER 91-5032] p 171 A92-17822
Experimental investigation of the reflection of a shock wave on a heated surface in presence of a turbulent boundary layer p 1023 A92-54569

HOT WORKING
Cost effective solutions for titanium sheet metal forming p 293 A92-22785

HOT-FILM ANEMOMETERS
Applications of hot-film anemometers in hypersonic shear layers
[AIAA PAPER 91-5028] p 436 A92-31687
A concentration probe for the study of mixing in supersonic shear flows p 991 A92-50039
Crossflow vortex and transition measurements by use of multielement hot films p 935 A92-50307
Shock detection on airfoils by means of piezo foil- and hot film arrays p 1115 A92-54334
Investigations of blade row interaction and boundary layer transition phenomena in a multistage aero engine low-pressure turbine by measurements with hot-film probes and surface-mounted hot-film gauges
p 658 N92-24338

HOT-WIRE ANEMOMETERS
Stall inception in axial flow compressors
[ASME PAPER 91-GT-86] p 69 A92-15551
A hot-wire anemometer in compressible subsonic flow
p 244 A92-21623
An assessment of particle velocimetry potential in hypersonic flow
[AIAA PAPER 92-0010] p 247 A92-22135
A data base for flight in the wake of a ship
[AIAA PAPER 92-0295] p 319 A92-25748
On hypersonic boundary-layer stability
[AIAA PAPER 92-0737] p 335 A92-27088
Hot-wire measurements in turbulent transonic flows
p 941 A92-53078
The use of silicon microsensors in smart skins for aerodynamic research p 1116 A92-54348
Measurements of turbulence in hypersonic flow
p 1092 A92-56005
Characteristics of a boundary layer in a leading edge vortex p 86 N92-13012
Flow gradient corrections on hot-wire measurements using an X-wire probe
[NLR-TP-90255-U] p 829 N92-28713

HOT-WIRE FLOWMETERS
Hot-wire surveys in the vortex wake downstream of a three-percent fighter aircraft model at high angles of attack
[AD-A241869] p 259 N92-15975

HOUSINGS
Composite gearbox housing p 110 A92-14448
Single screw mechanism with gaterotor housing at intermediate pressure
[AD-D015140] p 400 N92-18120

HOVERCRAFT GROUND EFFECT MACHINES
Aircraft design experience p 110 A92-15326

HOVERING
Solution of the compressible Euler equations for steady flows around helicopter rotor blades by an implicit space-centered method
[ONERA, TP NO. 1991-177] p 77 A92-16139
Aerodynamic and acoustic calculations of transonic nonlifting hovering rotors
[ONERA, TP NO. 1991-178] p 77 A92-16140
Hover evaluation of an integrated pneumatic lift/reaction-drive rotor system
[AIAA PAPER 92-0630] p 333 A92-27010
Flight investigation of variations in rotorcraft control and display dynamics for hover p 379 A92-28151
Acoustic characteristics and dynamic structural loading of an ASTOVL aircraft in hover
[AIAA PAPER 92-0370] p 416 A92-28190
Hover control of a PVTOL using nonlinear regulator theory p 478 A92-29171
Complete Euler-solution for a rotor in hover and a propeller in forward flight p 520 A92-35755
Navier-Stokes analysis of blade tip shape in hover
p 521 A92-35758
Civil development and certification of a helicopter automatic approach and hover system on the Sikorsky S-76
[SAE PAPER 911975] p 872 A92-45382
Ducted fan VTOL for working platform
[SAE PAPER 911995] p 843 A92-45397
Free wake analyses of a hovering rotor using panel method
[SAE PAPER 912004] p 789 A92-45405
Navier-Stokes computation of wing leading edge tangential blowing for a tilt rotor in hover
[AIAA PAPER 92-2608] p 805 A92-45568
Sensitivity analysis of discrete periodic systems with applications to helicopter rotor dynamics
p 846 A92-46884
A study of rotor wake development and wake/body interactions in hover p 813 A92-46935
Experimental and computational studies of hovering rotor flows p 815 A92-46954
Flowfield of a lifting rotor in hover - A Navier-Stokes simulation p 1024 A92-54906
Efficiency and accuracy in helicopter hovering performance calculation p 1053 A92-56072
Response of helicopter blades to a sharp collective increase p 1084 A92-56282
The computation and validation of hovering rotor performance p 1055 A92-56285
A time-dependent tip loss formula for rotor blade dynamic analysis p 1057 A92-56310
The identification of coupled flapping/inflow models for hovering flight p 1058 A92-56335
Flow visualization and flow field measurements of a 1/12 scale tilt rotor aircraft in hover
[NASA-CR-189456] p 82 N92-11983
A comparative analysis of XV-15 tiltrotor hover test data and WOPWOP predictions incorporating the fountain effect
[NASA-CR-189455] p 114 N92-11992
A numerical solution of implicit nonlinear equations of motion for rotor blades p 115 N92-13053
Flight operations for higher harmonic control research
[AD-A242478] p 196 N92-15067
Rotorwash computer model: User's guide
[DOT/FAA/RD-90/25] p 346 N92-18345
Fully integrated aerodynamic/dynamic optimization of helicopter rotor blades
[NASA-TM-104226] p 461 N92-20417
Flowfield analysis of modern helicopter rotors in hover by Navier-Stokes method
[AD-A245011] p 446 N92-21333
Wing force and surface pressure data from a hover test of a 0.658-scale V-22 rotor and wing
[NASA-TM-102244] p 550 N92-22864
On the anomalies in single-jet hover suckdown data
[NASA-TM-102261] p 1038 N92-33306
On the calculation of the response of helicopters to control inputs
[NASA-CR-190812] p 1088 N92-33536
On the estimation of jet-induced fountain lift and additional suckdown in hover for two-jet configurations
[NASA-TM-102268] p 1040 N92-33618
Design of helicopter flight control systems for hover and low speed using eigenstructure assignment
p 1061 N92-33952

HOVERING STABILITY
Results from a test of a 2/3-scale V-22 rotor and wing in the 40- by 80-Foot Wind Tunnel p 104 A92-14332
Identification of higher-order helicopter dynamics using linear modeling methods p 131 A92-14336
Helicopter control response types for hover and low-speed near-earth tasks in degraded visual conditions
p 132 A92-14338
Aerodynamic design of a Coanda induced force and thruster anti-torque system p 109 A92-14419
A re-examination of the aerodynamics of hovering rotors including the presence of the fuselage
p 66 A92-14446
Modeling rotor dynamics with rotor speed degree of freedom for drive train torsional stability analysis
p 547 A92-35779
AV-8B V/STOL performance analysis
p 549 A92-35948

Control and display combinations for blind vertical landings p 661 A92-39903
An experimental study of the sensitivity of helicopter rotor blade tracking to root pitch adjustment in hover
[NASA-TM-4313] p 61 N92-12989

HTPB PROPELLANTS
Solid fuel ramjet infrared signature
[AD-A246299] p 753 N92-26362

HUBS
Stress analysis of a propeller hub p 38 A92-10964
Digital simulation and experimental modal analysis of dynamic characteristics of a propeller hub
p 38 A92-10965
Hub and pylon fairing integration for helicopter drag reduction p 107 A92-14391
Blade root torsional dampers to reduce hub loads
[AIAA PAPER 92-2449] p 541 A92-34476
Prediction of dynamic hub load of a rotor executing multiple sinusoidal blade pitch variations
p 846 A92-46921
Measurement of acoustic properties of the composite materials constituting the main rotor hub of the Agusta-Westland helicopter EH-101 (civil version)
p 1010 A92-49475
The static and fatigue computation of the propeller blades retention system p 995 A92-51895
Design and testing of a composite hingeless hub for rotary-wing aircraft p 1053 A92-56075

HUGONIOT EQUATION OF STATE
Theoretical and experimental investigation of the thermodynamics of the thermally choked ram accelerator p 604 N92-22137

HULLS (STRUCTURES)
Calculation of the exerting force necessary to form the aircraft hull plate in the symmetry plate bender with three rolls and the feeding value of the centre roll
p 998 A92-53297

HUMAN BEHAVIOR
Dealing with pilot response in failure case testing
p 549 A92-35952
Effects of military training route noise on human annoyance p 689 A92-39237
The effect on aircraft evacuations of passenger behaviour and smoke in the cabin p 834 A92-44998

HUMAN CENTRIFUGES
Two crew stations for dynamic flight simulation
p 572 A92-35443
Design and performance of the centrifuge-based Dynamic Flight Simulator
[AIAA PAPER 92-4156] p 981 A92-52446
Developmental evaluation of a centrifuge flight simulator as an enhanced maneuverability flying qualities tool
[AIAA PAPER 92-4157] p 982 A92-52447

HUMAN FACTORS ENGINEERING
An anthropometric evaluation of the TH-57 Jetranger helicopter p 46 A92-11164
Requirements for an aircraft mishap analysis system
p 16 A92-11170
Organizational context for aircraft maintenance and inspection p 2 A92-11181
Prediction of helicopter simulator sickness
p 46 A92-11473
Data-link communication between controllers and pilots - A review and synthesis of the simulation literature
p 94 A92-14045
Active noise reduction p 603 A92-32980
Computational fluid dynamics as a tool for aerodynamic analysis of ejection seats p 519 A92-35444
Dealing with pilot response in failure case testing
p 549 A92-35952
Enhanced vision system option on future aircraft
[SAE PAPER 912204] p 651 A92-40014
British Airways Airbus A320 pilots' autothrust survey
[SAE PAPER 912225] p 636 A92-40023
EICAS in an integrated cockpit --- Engine Indication Crew Alerting System p 855 A92-44922
Electronic presentation of instrument approach information p 855 A92-44923
Perspective versus plan view air traffic control (ATC) displays - Survey and empirical results
p 896 A92-44967
Real-time control tower simulation for evaluation of airport surface traffic automation p 879 A92-44976
The development of an intelligent human factors data base as an aid for the investigation of aircraft accidents
p 928 A92-44994
Airline deregulation - Impact on human factors
p 834 A92-44999
Organizational factors in human factors accident investigation p 834 A92-45000
Eliminating pilot-caused altitude deviations - A human factors approach p 834 A92-45041
Empirical foundations and sensitivity testing - Is it enough for the 90's? p 835 A92-45054
ICAO Flight Safety and Human Factors Programme
p 835 A92-45055
Mandatory psychological testing of pilots as a requirement for licensing in Norway?
p 835 A92-45081
Generic helicopter for multiship simulations
[AIAA PAPER 92-4151] p 959 A92-52442
Man-Vehicle Systems Research Facility - Design and operating characteristics
[AIAA PAPER 92-4177] p 982 A92-52458
Flight simulator test of cockpit advisory system
p 1054 A92-56115
Parameter identification studies on the NASA/Ames Research Center Advanced Concepts Flight Simulator
[NASA-TM-105126] p 31 N92-11024
The impact of cockpit automation on crew coordination and communication. Volume 1: Overview, LOFT evaluations, error severity, and questionnaire data
[NASA-CR-177587] p 93 N92-13044
Design considerations for IAP charts: Approach course track and communication frequencies
[AD-A241482] p 103 N92-13051
Effect of short-term exposure to stereoscopic three-dimensional flight displays on real-world depth perception
[NASA-TP-3117] p 119 N92-13065
Soviet electronic display systems under research and manufactured for the civil aviation aircraft of the 1990's
[AD-A240933] p 119 N92-13066
Limitations of a holographic 3-D pixel projector for cockpit displays
[AD-A241295] p 119 N92-13067
Evolution of avionic systems architecture, from the 1950's to the present p 198 N92-14047
The COMPAS system in the ATC environment
[DLR-MITT-91-08] p 354 N92-19041
The role of planning systems in future air traffic management p 355 N92-19050
Status of automatic guidance systems for rotorcraft in low altitude flight p 727 N92-27894
Human factors evaluation of the work environment of operators engaged in the inspection and repair of aging aircraft
[AD-A246445] p 724 N92-27914
Human factors issues in the use of artificial intelligence in air traffic control. October 1990 Workshop
[NASA-CR-190925] p 1051 N92-34203

HUMAN PERFORMANCE
How to promote error tolerance in complex systems in the context of ships and aircraft p 673 A92-39308
Learning from aircraft accidents and incidents
p 635 A92-39310
Passenger knowledge of airline safety information
[CRANFIELD-AERO-9111] p 187 N92-15054
Cooperative planning in aviation contexts
p 456 N92-21509
Workshop on integrated Crew Resource Management (CRM)
[DOT/FAA/RD-92/5] p 781 N92-27518
An analysis of aircrew communication patterns and content
[AD-A246618] p 907 N92-28253
Introduction to cognitive processes of expert pilots
[DOT/FAA/RD-92/12] p 952 N92-30980

HUMAN REACTIONS
Dealing with pilot response in failure case testing
p 549 A92-35952
A new simulator for assessing subjective effects of sonic booms
[NASA-TM-104150] p 56 N92-11759
Passenger knowledge of airline safety information
[CRANFIELD-AERO-9111] p 187 N92-15054
Evaluation of human response to structural vibrations induced by sonic booms
[NASA-CR-189584] p 697 N92-26130
Application of magnitude estimation scaling to the assessment of subjective loudness response to simulated sonic booms
[NASA-TM-107657] p 1138 N92-33719

HUMAN RESOURCES
An analysis of total quality management in Aeronautical Systems Division
[AD-A246661] p 772 N92-27760

HUMAN TOLERANCES
Aircraft noise and the elderly p 689 A92-39236
Exposures from headset interference tones
[AD-A247175] p 1136 N92-32697
Application of magnitude estimation scaling to the assessment of subjective loudness response to simulated sonic booms
[NASA-TM-107657] p 1138 N92-33719

HUMIDITY
Humidity effects on gas turbine performance
[NRC-30241] p 130 N92-11998
Comparison between hot/wet test and RT/dry test on the Seastar horizontal stabilizer and fin
p 226 N92-14414

HUMIDITY MEASUREMENT
Use of relative humidity sensors for planes measurement p 467 A92-32080
An airborne cryogenic frost-point hygrometer
p 467 A92-32090

HURRICANES
A new aircraft universal lightweight digital dropsonde
p 467 A92-32089

HUYGENS PRINCIPLE
Convergence of subsonic unsteady aerodynamics evaluated by a finite element concept based on Huygeuns' wave propagation
[AIAA PAPER 92-2502] p 518 A92-34497

HYBRID NAVIGATION SYSTEMS
Flight test of a GPS-aided low-cost inertial navigation system programmed in Ada p 101 A92-16973
Navigation experiment on an aircraft using the GPS-INS navigation system. I - Introduction to the system
p 726 A92-43122

HYDRAULIC CONTROL
Hydraulic pumps - The key to power generation
p 215 A92-17348
An experimental study on variable pressure hydraulic flight control system p 1084 A92-56119

HYDRAULIC EQUIPMENT
Hydraulic pumps - The key to power generation
p 215 A92-17348
Fluid power conversion p 357 A92-25372
Aircraft hydraulic systems (3rd revised and enlarged edition) --- Book
[ISBN 0-89464-562-5] p 642 A92-38316
Space Shuttle Orbiter auxiliary power unit status
[SAE PAPER 912060] p 889 A92-45442
Development of the DDV actuation system on the IDF aircraft
[SAE PAPER 912080] p 844 A92-45455
Simple fly-by-wire actuator p 876 A92-48491
An experimental study on variable pressure hydraulic flight control system p 1084 A92-56119
Nonflammable hydraulic power system for tactical aircraft. Volume 2: Equipment and systems test and evaluation
[AD-A239805] p 35 N92-10100
Hydraulic actuator system for rotor control
p 224 N92-14363
A survey of instabilities within centrifugal pumps and concepts for improving the flow range of pumps in rocket engines
[NASA-TM-105439] p 387 N92-18280

HYDRAULIC FLUIDS
Fluid power distribution and control
p 292 A92-21733

HYDRAULIC JETS
Precision drilling of ceramic-coated components with abrasive-waterjets
[ASME PAPER 91-GT-232] p 149 A92-15641
Take it all off - with water --- High-pressure waterjet stripping of protective coatings p 516 A92-34775
Waterjets for removing engine coatings
p 516 A92-35575

HYDRAULIC TEST TUNNELS
Effects of ambient turbulence on the decay of a trailing vortex wake p 442 A92-32245
A laser fluorescence anemometer system for the Langley 16- by 24-inch water tunnel
p 1092 A92-54347
Aerodynamics laboratory education at Purdue University - Ground testing facilities
[AIAA PAPER 92-4018] p 1100 A92-56840
A user's guide to the Langley 16- by 24-inch water tunnel
[NASA-TM-104200] p 385 N92-18956
Pressure measurements in high speed water tunnels
[DE92-004891] p 386 N92-19978
Measurement of vortex flow fields
[NASA-CR-189543] p 443 N92-20283
Observation and measurements of flow structures in the stagnation region of a wing-body junction
p 714 N92-26616
Static and dynamic flow visualization studies of two double-delta wing models at high angles of attack
[AD-A252878] p 1040 N92-33678

HYDRAZINES
Poly 1, 2, 4-triazoles via aromatic nucleophilic displacement
[NASA-CASE-LAR-14440-1] p 35 N92-10066

HYDROCARBON COMBUSTION
Laser diagnostics for velocity measurements in supersonic combusting environments
[AIAA PAPER 92-0008] p 288 A92-22133
Hydrocarbon-fueled scramjet combustor investigation
p 376 A92-28535
Carcinogenic hydrocarbons emission with gas-turbine engines exhaust gases p 504 A92-29726
The aviation kerosene burning in the non-uniform air flow p 487 A92-29728

A simplified reaction mechanism for prediction of NO(x) emissions in the combustion of hydrocarbons
[AIAA PAPER 92-3340] p 894 A92-48919
Experimental investigation of liquid carbonhydrogen fuel combustion in channel at supersonic velocities
[AIAA PAPER 92-3429] p 894 A92-48986

HYDROCARBON FUELS
Methyl-tert-butyl ether as a component of aviation gasolines p 34 A92-12146
Isothermal flow fields in a research combustor for lean blowout studies
[ASME PAPER 91-GT-37] p 121 A92-15520
A test bench for evaluating powerplant electrization p 138 A92-16830
Hydrocarbon-fueled scramjet combustor investigation p 376 A92-28535
Enhancing the performance characteristics of engine fuels by means of surfactant additives p 892 A92-46631
Analysis of a hydrocarbon scramjet with augmented preburning
[AIAA PAPER 92-3425] p 865 A92-48984

HYDRODYNAMIC EQUATIONS
Effect of inertia forces on the characteristics of a long hydrodynamic vibration damper in the mixed flow regime p 154 A92-16811
Method of large particles in arbitrary curvilinear orthogonal coordinates for the solution of problems of hydro and aerodynamics p 937 A92-52035

HYDRODYNAMIC RAM EFFECT
PAR-WIG performance prediction during acceleration from water-borne to air-borne p 291 A92-21721
High spatial resolution measurements of ram accelerator gas dynamic phenomena
[AIAA PAPER 92-3244] p 903 A92-48844
Progress towards the development of transient ram accelerator simulation as part of the U.S. Air Force Armament Directorate Research Program
[AIAA PAPER 92-3248] p 904 A92-48847
The External Propulsion Accelerator - Scramjet thrust without interaction with accelerator barrel
[AIAA PAPER 92-3717] p 866 A92-49098

HYDRODYNAMICS
Heat transfer in the entrance region of semicircular ducts with internal fins p 497 A92-32264
A Navier-Stokes solution of Hull-ring wing-thruster interaction p 221 N92-14310
Computation of the hydrodynamic forces and moments on a body of revolution with and without appendages
[AD-A243033] p 298 N92-16978
Basic hydrodynamics
[AD-A243513] p 300 N92-17387
Deck motion criteria for carrier aircraft operations p 464 N92-21952
Domain modeling and grid generation for multi-block structured grids with application to aerodynamic and hydrodynamic configurations p 691 N92-24411
An explosively driven, fast shock tube
[DE92-008437] p 749 N92-26720
Numerical calculations of two-dimensional single and multi-material flow fields with CCICE
[DE92-015778] p 1000 N92-30903
On the origin and acoustical behaviour of cloud cavitation
[ISBN-90-9004317-9] p 1125 N92-33066
Improved articulated fin/wing control system statement of government interests
[AD-D015268] p 1088 N92-34131

HYDROELASTICITY
Nonstationary aerohydroelasticity of spherical bodies --- Russian book
[ISBN 5-02-014006-6] p 670 A92-36611
A mathematical model for the hydroelasticity problem concerning the motion of two flexible profiles in an ideal incompressible fluid. I p 712 A92-44127

HYDROGEN
A numerical investigation of hydrogen combustion in Mach 2 flow
[AIAA PAPER 92-0341] p 388 A92-25787
Numerical study on the secondary jet into a supersonic flow p 1018 A92-53556
H-N2 interaction energies, transport cross sections, and collision integrals p 1135 A92-54660
Experiments and analysis concerning the use of external burning to reduce aerospace vehicle transonic drag
[NASA-TM-105397] p 279 N92-17546
Preliminary screening procedures and criteria for replacements for Halons 1211 and 1301
[AD-A252912] p 1126 N92-33501

HYDROGEN ENGINES
Strain-induced extinction of hydrogen-air counterflow diffusion flames - Effects of steam, CO2, N2, and O2 additives to air
[AIAA PAPER 92-0877] p 487 A92-29639
Interaction between chemical reaction and turbulence *in supersonic nonpremixed H2-air combustion* p 1117 A92-54931
H2-fueled high-bypass turbofan p 475 N92-21529
H2 fueled flightweight ramjet construction and test p 475 N92-21531

HYDROGEN FUELS
H2/air subsystem combustion kinetics in aerospaceplane powerplants
[IAF PAPER 91-276] p 25 A92-12600
Thermodynamic behaviour of hydrogen-powered hypersonic ramjets flying along ideal trajectories
[IAF PAPER 91-277] p 25 A92-12601
Slush hydrogen (SLH2) technology development for application to the National Aerospace Plane (NASP) p 144 A92-13432
Hydrogen exhaust gas disposition by afterburning
[AIAA PAPER 91-5075] p 200 A92-17848
An experimental investigation of the combustion of a hydrogen jet injected parallel in a supersonic air stream
[AIAA PAPER 91-5102] p 212 A92-17861
Simultaneous coherent anti-Stokes Raman spectroscopy measurements in hydrogen-fueled supersonic combustion p 287 A92-21052
An experimental study of supersonic H2 combustion and heat transfer in a circular duct p 388 A92-25997
Thermal management of propulsion systems in hypersonic vehicles
[AIAA PAPER 92-0516] p 373 A92-26942
On the experimental investigation of air-breathing engine of new schemes p 469 A92-29711
National Aerospace Plane flight test - External burning on the F/A-18 p 645 A92-40032
Turbofan with a small bypass ratio for first stage of a two-stage to-orbit vehicle p 968 A92-49833
A model study on diffuser pressure recovery in NAL scramjet test facility with simulated hydrogen combustion
[AIAA PAPER 92-3979] p 1071 A92-56805

HYDROGEN OXYGEN ENGINES
Hypersonic mixing and combustion studies in the hypulse facility p 737 A92-44526
Experiments on the structure of an annular compressible *reacting shear layer* p 969 A92-50311
Supercharged ejector ramjet p 475 N92-21527

HYDROMECHANICS
An aircraft controller and its development p 558 A92-35917

HYDROPLANING
Runway drainage characteristics related to tire friction performance
[SAE PAPER 912156] p 664 A92-39991

HYDROSTATICS
Fault tolerant EHA architectures --- electro-hydrostatic actuator p 763 A92-43885
Variable displacement electro-hydrostatic actuator --- for flight control systems p 876 A92-48492
Development of high performance compressor discharge seal
[AIAA PAPER 92-3714] p 907 A92-49096

HYDROXYL RADICALS
Evaluation of OH laser-induced fluorescence techniques for supersonic combustion diagnostics
[AIAA PAPER 92-0508] p 396 A92-26935
KrF laser-induced OH fluorescence imaging in a supersonic combustion tunnel
[AIAA PAPER 92-3346] p 905 A92-48923

HYGROMETERS
Use of relative humidity sensors for planes measurement p 467 A92-32080
An airborne cryogenic frost-point hygrometer p 467 A92-32090
The DLR Lyman-alpha hygrometer p 467 A92-32091

HYPERBARIC CHAMBERS
High pressure hypervelocity electrothermal wind tunnel performance study and subscale tests
[AIAA PAPER 92-0329] p 383 A92-25776

HYPERBOLIC DIFFERENTIAL EQUATIONS
Concerning the functional solution of transonic flows p 243 A92-21318
Computation of unsteady transonic flows using an implicit centered Euler solver without artificial viscosity
[ESA-TT-1235] p 944 N92-30514

HYPERBOLIC FUNCTIONS
Panel method control in 3-D hyperbolic grid generation p 617 A92-39940
Hyperbolic grid generation with BEM source terms
[NLR-TP-90334-U] p 923 N92-28635
Hyperbolic grid generation control by panel methods
[NLR-TP-91061-U] p 924 N92-29604

HYPERBOLIC SYSTEMS
The accuracy and coverage of Loran-C and of the Decca Navigator System - and the fallacy of fixed errors p 353 A92-24944

HYPERCUBE MULTIPROCESSORS
Implementation of an object-oriented flight simulator D.C. electrical system on a hypercube architecture
[AD-A243700] p 284 N92-17097
Iterative methods for large scale static analysis of structures on a scalable multiprocessor supercomputer
[NASA-CR-190369] p 692 N92-26018

HYPERSONIC AIRCRAFT
Thermodynamic behaviour of hydrogen-powered hypersonic ramjets flying along ideal trajectories
[IAF PAPER 91-277] p 25 A92-12601
Application of waverider-based configurations to hypersonic vehicle design
[AIAA PAPER 91-3304] p 32 A92-12742
Thermal management of hypersonic aircraft using noncryogenic fuels
[SAE PAPER 911443] p 270 A92-21839
On the threshold - The outlook for supersonic and hypersonic aircraft p 356 A92-24402
Rapid prediction of high-alpha unsteady aerodynamics of slender-wing aircraft p 309 A92-24412
Flow over an all-body hypersonic aircraft - Experiment and computation p 310 A92-24651
Integrated numerical methods for hypersonic aircraft cooling systems analysis
[AIAA PAPER 92-0254] p 357 A92-25712
Estimation of propulsion-induced effects on transonic flows over a hypersonic configuration
[AIAA PAPER 92-0523] p 341 A92-28197
Robust control law development for a hypersonic cruise aircraft p 478 A92-29127
Measurement on hypersonic dynamic stable coefficients of a winged vehicle p 430 A92-30550
Navier-Stokes computations of a viscous optimized waverider
[AIAA PAPER 92-0305] p 435 A92-31653
French research and technology program on advanced hypersonic propulsion
[AIAA PAPER 91-5003] p 471 A92-31683
Low-speed flutter characteristics of some simple low-aspect-ratio delta-wing models p 460 A92-32247
Ground test facilities for aerothermal and aero-optical *evaluation of hypersonic interceptors*
[AIAA PAPER 92-1074] p 573 A92-33244
Overview and major characteristics of future aeronautical and space systems
[AIAA PAPER 92-2441] p 585 A92-34472
Accelerators and decelerators for large hypersonic aircraft p 665 A92-36952
Thermal management for a Mach 5 cruise aircraft using endothermic fuel p 736 A92-41225
Aerodynamic characteristics of a hypersonic aircraft p 711 A92-43226
On the aerodynamics/dynamics of store separation from hypersonic aircraft
[AIAA PAPER 92-2722] p 807 A92-45595
Prediction of inviscid supersonic/hypersonic aircraft flowfields p 810 A92-46785
Japan pushes high speed research p 1015 A92-53434
Current status of R&D on materials for super/hypersonic transports p 1106 A92-56002
Study on international cooperative test facilities for future SST/HST
[AIAA PAPER 92-3945] p 1097 A92-56775
A conceptual study for future engine test facility
[AIAA PAPER 92-3992] p 1099 A92-56815
A study of transonic aerodynamic analysis methods for use with a hypersonic aircraft synthesis code
[NASA-CR-189854] p 625 N92-24803
Trajectory optimization for hypersonic aircraft guidance p 728 N92-27898

HYPERSONIC BOUNDARY LAYER
A systematic experimental and computational investigation of a class of contoured wall fuel injectors
[AIAA PAPER 92-0625] p 374 A92-27007
On hypersonic boundary-layer stability
[AIAA PAPER 92-0737] p 335 A92-27088
Compressible laminar boundary layers for perfect and real gases in equilibrium at Mach numbers to 30
[AIAA PAPER 92-0757] p 336 A92-27099
Secondary instability of high-speed flows and the influence of wall cooling and suction p 435 A92-31640
Supersonic and hypersonic boundary-layer transition induced by discrete trips p 522 A92-36023
Unsteady hypersonic boundary layers for slender axisymmetric bodies with large injection rates p 524 A92-36100
Asymptotic defect boundary-layer theory applied to hypersonic flows p 610 A92-36839
Analysis of turbulence models for hypersonic boundary layers p 623 A92-40182
Models of turbulence in a hypersonic boundary layer p 705 A92-41817

Measurement of shock-wave/boundary-layer interaction in a free-piston shock tunnel p 813 A92-46903
Nonlinear development and secondary instability of large-amplitude Goertler vortices in hypersonic boundary layers p 942 A92-53080
Constant-temperature anemometry measurements in hypersonic boundary layers p 90 N92-13861
Experimental study of hypersonic shock wave boundary layer interactions by means of infrared technique p 182 N92-14994
Calculation of hypersonic non-equilibrium viscous flow using second order boundary layer theory
[MBB-FE122-S-PUB-434] p 345 N92-18316
Secondary instability of high-speed flows and the influence of wall cooling and suction
[NASA-CR-4427] p 406 N92-19844
Hypersonic wakes
[ETN-92-91082] p 349 N92-19925
Contributions of MBB-FE211 to the 2nd Antibes Workshop on Hypersonic Flows
[MBB-FE211-S-PUB-449] p 524 N92-22179
Methods for direct simulation of transition in hypersonic boundary layers 2 p 912 N92-30064
Stability and transition of hypersonic boundary-layer flows
[AD-A250279] p 948 N92-31555
Experimental studies of hypersonic shock-wave boundary-layer interactions
[NASA-CR-190731] p 950 N92-32162

HYPERSONIC COMBUSTION

Effects of unsteady shock impingement on high-speed gaseous mixing
[AIAA PAPER 91-5091] p 172 A92-17857
Numerical studies of supersonic/hypersonic combustion
[AIAA PAPER 92-0094] p 293 A92-22200
Investigation of hypersonic ramjet propulsion cycles using a ram accelerator test facility
[IAF PAPER 91-275] p 278 A92-22482
Experiments on shear layer mixing at hypervelocity conditions
[AIAA PAPER 92-0628] p 396 A92-27009
Hypersonic mixing and combustion studies in the hypulse facility p 737 A92-44526
Instrumentation key to NASP combustor tests p 1092 A92-55100
Shock enhancement and control of hypersonic combustion
[AD-A248558] p 896 N92-29580

HYPERSONIC FLIGHT

Saenger and the German Hypersonics Technology Programme - Status report 1991
[IAF PAPER 91-198] p 32 A92-12570
Test results of the expander cycle air turbo ramjet for a future space plane
[IAF PAPER 91-271] p 120 A92-14709
Propulsion aspects of hypersonic turbo-ramjet-engines with special emphasis on nozzle/aftbody integration
[ASME PAPER 91-GT-395] p 127 A92-15725
The NASP Program - An update p 61 A92-16059
Integrated GPS/INS for the National Aerospace Plane p 102 A92-16975
Three dimensional hypersonic inlets - Low speed performance
[AIAA PAPER 91-5021] p 171 A92-17817
Numerical and experimental study of jet impingement or interaction effects at hypersonic and supersonic speeds
[AIAA PAPER 91-5038] p 171 A92-17826
The value of sub-scale flight tests in the development of NASP vehicles
[AIAA PAPER 91-5048] p 210 A92-17834
Control concept for maneuvering in hypersonic flight
[AIAA PAPER 91-5055] p 203 A92-17838
Hypersonic materials p 212 A92-18002
Control of hypersonic aerodynamic forces with surface blowing p 172 A92-18363
Some Aspects of uncertainty in computational fluid dynamics results p 233 A92-19609
Research on supersonic combustion
[AIAA PAPER 92-0001] p 278 A92-22126
Spaceplane system studies p 285 A92-22632
Fiber optics for the National Aero-Space Plane p 386 A92-24780
Pitching derivatives of wing in supersonic and hypersonic stream - Method for local flow piston theory p 312 A92-25012
Design and modeling issues for integrated airframe/propulsion control of hypersonic flight vehicles p 477 A92-29115
Numerical computation and experimental study of shock wave reflection p 430 A92-30542
Safety test on the rolling angles of a winged vehicle in hypersonic speed p 480 A92-30549
Approximate analysis of aerodynamic heating at hypersonic speed p 430 A92-30551
French research and technology program on advanced hypersonic propulsion
[AIAA PAPER 91-5003] p 471 A92-31683
Aero-propulsive effects on configuration shaping
[AIAA PAPER 91-5064] p 459 A92-31691
Applications of Busemann inlet designs for flight at hypersonic speeds
[AIAA PAPER 92-1210] p 517 A92-33314
Structural tailoring/analysis for hypersonic components - Executive system development
[AIAA PAPER 92-2471] p 583 A92-34360
Temperature and initial curvature effects in low-density panel flutter
[AIAA PAPER 92-2128] p 589 A92-35695
Characteristic-based algorithms for flows in thermochemical nonequilibrium p 670 A92-36846
Control strategy for maximizing reconnaissance range of hypersonic cruise vehicles p 729 A92-41222
A time-integrated image model for aero-optic analysis
[AIAA PAPER 92-2793] p 779 A92-41332
The beginnings of the hypersonic and the renewal of the supersonic ramjet p 782 A92-41824
Numerical analysis of RCS jet in hypersonic flights
[SAE PAPER 912063] p 791 A92-45445
Aerospace plane hydrogen scramjet boosting
[SAE PAPER 912071] p 891 A92-45451
Propulsion system performance and integration for high Mach air breathing flight p 862 A92-46429
Hypersonic plasma predictions at nonzero angle of attack
[AIAA PAPER 92-3027] p 925 A92-47028
Analytical and experimental studies of heat pipe radiation cooling of hypersonic propulsion systems
[AIAA PAPER 92-3809] p 867 A92-49128
Some thermodynamical aspects in the optimization of supersonic combustors p 1065 A92-53486
Performance analysis of idealized scramjet p 1066 A92-53493
Radiative heat transfer from nonequilibrium shock layer to a hypersonic reentry body p 1019 A92-53579
Concepts of flight experiments for HOPE development p 1103 A92-53635
Aerodynamic studies on space plane configuration at hypersonic speed p 1019 A92-53641
Lateral control of spaceplane at hypersonic flight p 1104 A92-56069
Integrated test and evaluation for hypervelocity systems
[AIAA PAPER 92-3901] p 1017 A92-56736
The trisonic wind tunnel Muenchen and its involvement in the German SAeNGER-programme
[AIAA PAPER 92-4019] p 1100 A92-56841
Study on supersonic combustion in a hypersonic flight
[IAF PAPER 92-0661] p 1106 A92-57101
Technologies for the National Aero-Space Plane
[IAF PAPER 92-0868] p 1105 A92-57259
CARS temperature measurements in a hypersonic propulsion test facility p 140 N92-12049
FALKE and COBRA technology development in aerodynamics and aerothermodynamics p 183 N92-15017
Computational aerothermodynamic methods for industrial applications to re-entry and hypersonic cruise problems p 227 N92-15027
Evolution and development of hypersonic configurations 1958-1990
[AD-A242768] p 197 N92-15069
Control integration concept for hypersonic cruise-turn maneuvers
[NASA-TP-3136] p 481 N92-20195
The NASA hypersonic research engine program p 474 N92-21521
Hypersonic airbreathing propulsion/airframe integration p 474 N92-21522
Inlet technology p 447 N92-21528
High speed airbreathing propulsion in Europe p 575 N92-22277
Hypersonic propulsion research p 561 N92-22543
Design challenges for the National Aero-Space Plane p 551 N92-23822
Stretched skin concept for the entry aerodynamic decelerator system of planetary probes p 576 N92-23836
Turbulence modeling for hypersonic flight
[NASA-CR-190313] p 630 N92-24898
Study of shock-induced combustion using an implicit TVD scheme p 669 N92-25816
Aerothermodynamics of nozzle flows for advanced hypersonic propulsion systems p 769 N92-27478
Application of finite element method to hypersonic nozzle flow computations p 769 N92-27479
An analysis of combustion studies in shock expansion tunnels and reflected shock tunnels
[NASA-TP-3224] p 895 N92-28374
Aerothermodynamics and propulsion integration in the Saenger technology programme
[MBB-FE-202-S-PUB-0469-A] p 831 N92-29649
Analytical and experimental studies of heat pipe radiation cooling of hypersonic propulsion systems
[DE92-013428] p 973 N92-31817
Dynamic interactions between hypersonic vehicle aerodynamics and propulsion system performance
[NASA-CR-190638] p 1038 N92-33304
Perspectives on hypersonic viscous and nonequilibrium flow research
[NASA-CR-190817] p 1039 N92-33413
Thermal-structural test facilities at NASA Dryden
[NASA-TM-104249] p 1062 N92-34202

HYPERSONIC FLOW

A unified nonequilibrium model for hypersonic flows p 3 A92-10575
A spatial marching technique for the inviscid blunt body problem p 4 A92-10691
Simple turbulence models for supersonic flows - Bodies at incidence and compression corners p 5 A92-11059
Influence of the entropy layer on the separation length in hypersonic aerodynamics in the triple-deck framework. II p 63 A92-13815
Three-dimensional thin-layer and space-marching Navier-Stokes computations using an implicit MUSCL approach - Comparison with experiments and Euler computations
[ONERA, TP NO. 1991-131] p 77 A92-16107
Similarity solutions for supersonic axisymmetric flows p 173 A92-18387
Hypersonic flows over slender circular cones at small angles of attack p 173 A92-19068
Rate parameters for coupled vibration-dissociation in a generalized SSH approximation --- Schwarz, Slawsky, and Herzfeld p 235 A92-20301
Flat-ended circular cylinder in hypersonic rarefied flow p 174 A92-20304
Engineering calculations of three-dimensional inviscid hypersonic flowfields p 175 A92-20378
Nonequilibrium hypersonic inviscid steady flows p 176 A92-20737
Turbulent boundary-layer characteristics over a flat-plate/wedge configuration at Mach 6 p 176 A92-20761
Effects of gas-surface interaction models on aerodynamic characteristics p 244 A92-21718
An assessment of particle velocimetry potential in hypersonic flow
[AIAA PAPER 92-0010] p 247 A92-22135
Steady supersonic and hypersonic flow computations using Eulerian and new Lagrangian formulations
[AIAA PAPER 92-0055] p 249 A92-22170
Computational aerodynamic simulation on HOPE p 251 A92-22635
Simulation of supersonic and hypersonic flows p 251 A92-22790
Operation and design considerations for unsteady data acquisition with PC-based systems in high Reynolds number hypersonic flowfields
[AIAA PAPER 92-0204] p 284 A92-23810
HOPE looks to CFD for help --- NASDA's H-II Orbiting Plane p 386 A92-24910
Space-marching calculations of hypersonic inviscid flowfield p 313 A92-25040
Singular perturbation theory of hypersonic flow over blunt bodies p 313 A92-25048
Numerical simulation and analysis for hypersonic flow with separation over blunt cone at angle of attack p 314 A92-25126
An efficient Euler solver for predominantly supersonic flows with embedded subsonic pockets
[AIAA PAPER 92-0323] p 322 A92-25770
Initial operation of the UTA shock tunnel
[AIAA PAPER 92-0331] p 383 A92-25778
Hypersonic flow simulations using DSMC (direct simulation Monte Carlo) p 323 A92-26216
Hypersonic rarefied flow past spheres including wake structure
[AIAA PAPER 92-0495] p 329 A92-26325
An approximate viscous shock layer technique for calculating nonequilibrium hypersonic flows about blunt-nosed bodies
[AIAA PAPER 92-0498] p 329 A92-26326
An engineering aerodynamic heating method for hypersonic flow
[AIAA PAPER 92-0499] p 329 A92-26327
Plasmadynamic effects in thermochemical nonequilibrium aerobrake flows
[AIAA PAPER 92-0573] p 333 A92-26980
Effects of nose bluntness and angle of attack on slender bodies in hypersonic flows
[AIAA PAPER 92-0638] p 334 A92-27016
Finite-element algorithm for chemically reacting hypersonic flow
[AIAA PAPER 92-0754] p 336 A92-27097

Computation of laminar flow over a long slender axisymmetric blunted cone in hypersonic flow
[AIAA PAPER 92-0756] p 336 A92-27098
Hypersonic flow of a viscous gas past sharp elliptical cones at angles of attack and slip p 336 A92-27531
Oscillating two-dimensional hypersonic airfoils at small angles of attack p 340 A92-28042
Full Navier-Stokes analysis of a three-dimensional hypersonic mixed compression inlet p 343 A92-28501
Computations of multispecies mixing between scramjet nozzle flow and hypersonic freestream p 376 A92-28534
The effect of wing twist optimized in the framework of the plane cross section hypothesis on the aerodynamic characteristics of a wing-body combination at hypersonic speeds p 424 A92-30129
Effect of viscosity on the drag of slender axisymmetric bodies in hypersonic flow p 425 A92-30154
The lift-drag ratio of a slender cone in viscous hypersonic gas flow p 425 A92-30172
Aerodynamic characteristics of slender sharp-leading-edge delta wings with air scooping through the air intake at hypersonic velocities. I p 427 A92-30206
Study on effectiveness of the front wedge shape in hypersonic flow p 430 A92-30552
Solution-adaptive grid procedure for the parabolized Navier-Stokes equations p 432 A92-31163
On hypersonic flow over two-dimensional aerofoils p 433 A92-31425
A non-linearly stable implicit finite element algorithm for hypersonic aerodynamics p 433 A92-31487
Implicit solutions of three-dimensional viscous hypersonic flows p 434 A92-31549
An improved PNS scheme for predicting complex three-dimensional hypersonic flows
[AIAA PAPER 92-0753] p 436 A92-31679
Combined effect of nose bluntness and angle of attack on slender bodies in viscous hypersonic flows
[AIAA PAPER 92-0755] p 436 A92-31680
Applications of hot-film anemometers in hypersonic shear layers
[AIAA PAPER 91-5028] p 436 A92-31687
Liquid crystal coatings for surface shear-stress visualization in hypersonic flows p 496 A92-32177
Computation of near-wake, aerobrake flowfields p 441 A92-32181
Structural tailoring/analysis for hypersonic components - Executive system development
[AIAA PAPER 92-2471] p 583 A92-34360
Simulation of 3-D shear flows around a nozzle-afterbody at high speeds p 519 A92-34826
Large-amplitude finite element flutter analysis of composite panels in hypersonic flow
[AIAA PAPER 92-2130] p 589 A92-35697
Vibrational relaxation effects in hypersonic flows of a viscous gas p 609 A92-36550
Experimental study of a two-dimensional scramjet inset, M(freestream) = 10.1-25.1 p 611 A92-36974
Numerical simulation of hypersonic viscous flow for the design of H-II orbiting plane (HOPE) p 612 A92-37549
An exploration of chemically reacting viscous hypersonic flow p 612 A92-37550
Non-equilibrium hypersonic flow simulations using the second-order boundary layer equations p 612 A92-37551
Stagnation point heat flux in hypersonic high enthalpy flow p 613 A92-38373
Separated flow over the protuberances in hypersonic flow p 615 A92-38907
Hypersonic turbulent separated flow past an unswept circular cylinder on a flat plate p 615 A92-38908
Hypersonic shock-wave turbulent-boundary-layer interaction flows p 703 A92-41264
Navier-Stokes cavity solutions based on second-order turbulence modeling
[AIAA PAPER 92-2765] p 704 A92-41314
Evaluation of the ATD-GASP for endo-leap applications --- Aerothermal Technology Development of Generalized Aerodynamic Simulation Programs
[AIAA PAPER 92-2771] p 704 A92-41318
Visualization and analysis of hypersonic flows and comparison to experimental data
[AIAA PAPER 92-2774] p 704 A92-41320
Adaptive mesh for turbulent hypersonic flow
[AIAA PAPER 92-2776] p 704 A92-41322
Crossed beam correlation modeling and experimental techniques for measuring density fluctuations in hypersonic flows
[AIAA PAPER 92-2779] p 758 A92-41323
Aero-optical testing in the NSWC Hypervelocity Tunnel No. 9
[AIAA PAPER 92-2797] p 747 A92-41336
Hybrid Navier-Stokes/Monte Carlo method for reacting flow calculations p 705 A92-41537
Plasmadynamic effects in thermochemical nonequilibrium aerobrake flows p 705 A92-41538
Engineering aerodynamic heating method for hypersonic flow p 705 A92-41539
Local bridging to predict aerodynamic coefficients in hypersonic, rarefied flow p 705 A92-41541
Optimum hypersonic wings and wave riders p 706 A92-42531
Flow of a rarefied gas over a cylinder at angle of sideslip p 708 A92-42738
Gasdynamic design --- Russian book
[ISBN 5-02-029715-1] p 708 A92-42777
Upwind schemes for Navier-Stokes computations at subsonic through hypersonic speeds p 708 A92-43071
Three-dimensional visualizations of the aerodynamic characteristics of delta wings for the transition from subsonic to supersonic leading edges in supersonic-hypersonic flow p 709 A92-43073
Test on high enthalpy hypersonic flow using a ballistic range p 747 A92-43097
Study on small stalker tube performance and numerical calculation p 748 A92-43099
Aerodynamic heating measurement in hypersonic flow p 709 A92-43102
A thin metal model for aerodynamic heating tests of shock wave interaction p 709 A92-43103
Thermal measurement test in a shock wind tunnel p 748 A92-43104
Direct simulation of hypersonic rarefied flows about atmospheric re-entry vehicles p 710 A92-43169
Numerical simulation of unsteady hypersonic viscous flows in shock tunnel p 710 A92-43170
Aerodynamic design tool development for the calculation code of hypersonic flow p 711 A92-43198
Solution of the parabolized Navier-Stokes equations using Osher's upwind scheme p 713 A92-44371
Multidimensional Euler/Navier-Stokes analysis for hypersonic equilibrium gas
[SAE PAPER 912026] p 790 A92-45418
Aerodynamic heating in three-dimensional shock wave turbulent boundary layer interaction induced by sweptback sharp fins in hypersonic flows
[SAE PAPER 912044] p 791 A92-45428
Numerical simulations of hypersonic real-gas flows over space vehicles
[SAE PAPER 912045] p 791 A92-45429
LU-SGS implicit scheme for entry vehicle flow computation and comparison with aerodynamic data
[AIAA PAPER 92-2671] p 798 A92-45526
Computations of hypersonic flows around a three-dimensional concave/convex body
[AIAA PAPER 92-2606] p 805 A92-45570
Aerothermodynamics of a 1.6-meter-diameter sphere in hypersonic rarefied flow p 808 A92-45840
Separated high enthalpy dissociated laminar hypersonic flow behind a step - Pressure measurements p 809 A92-45858
Hypersonic rarefied flow about a delta wing - direct simulation and comparison with experiment p 812 A92-46892
Grid sensitivity in low Reynolds number hypersonic continuum flows p 817 A92-47057
Calculation of hypersonic, viscous, non-equilibrium flows around reentry bodies using a coupled boundary layer/Euler method
[AIAA PAPER 92-2856] p 819 A92-47839
Computation of hypersonic flowfields in thermal and chemical nonequilibrium
[AIAA PAPER 92-2874] p 819 A92-47856
Computation of 3-D hypersonic flows in chemical non-equilibrium including transport phenomena
[AIAA PAPER 92-2876] p 820 A92-47858
Laminar hypersonic flow over a compression using the HANA code
[AIAA PAPER 92-2896] p 820 A92-47872
Numerical and experimental investigation of rarefied compression corner flow
[AIAA PAPER 92-2900] p 820 A92-47876
Solution of the Burnett equations for hypersonic flows near the continuum limit
[AIAA PAPER 92-2922] p 821 A92-47894
A scramjet nozzle experiment with hypersonic external flow
[AIAA PAPER 92-3289] p 864 A92-48878
Similarity relations for calculating three-dimensional chemically nonequilibrium viscous flows p 827 A92-49188
Lower upper implicit total variation diminishing solution of viscous hypersonic flows p 935 A92-50302
Exploratory study of wall pressure fluctuations in a Mach 5, sharp fin-induced turbulent interaction p 935 A92-50304
Application of a solution adaptive grid scheme to complex three-dimensional flows p 935 A92-50309
Mixing studies of helium in air at high supersonic speeds p 935 A92-50310
Hypersonic flow calculations around a 3D delta wing at low Knudsen numbers p 937 A92-52734
Heat transfer to a delta wing and two waverider wings in rarefied hypersonic flow p 937 A92-52748
One-dimensional kinetic model for flows near a stagnation point of a highly cooled body in hypersonic rarefied streams p 938 A92-52751
Influence of internal molecular degrees of freedom on the hypersonic rarefied gas flow about a conical body p 938 A92-52752
Approximate aerodynamic analysis for complicated bodies in rarefied gas flows p 938 A92-52754
Experiments on separation at a compression corner in rarefied hypersonic flows p 938 A92-52755
Hypersonic merged layer blunt body flows with wakes p 939 A92-52757
Enhancements and applications of DSMC for hypersonic rarefied flows p 939 A92-52761
Force and heat transfer on a disc in rarefied flow p 939 A92-52764
DSMC simulation of hypersonic flows past 2-dimensional bodies p 939 A92-52772
Application of the DSMC method to hypersonic flow about a delta wing p 940 A92-52775
Supersonic flow past pointed-nose thin airfoils p 940 A92-52844
Hypersonic flows with air chemistry over a reentry vehicle at high altitudes p 1017 A92-53549
Calculations for aerodynamic characteristics of HOPE type vehicle in subsonic and hypersonic flow p 1018 A92-53560
Thermally and chemically nonequilibrium hypersonic flow in three-dimensional geometry p 1019 A92-53580
Numerical study of the 3-D flowfield for a supersonic jet exiting into a hypersonic stream from a conical surface
[AIAA PAPER 92-3675] p 1022 A92-54118
A fine-wire thermocouple probe for measurement of stagnation temperatures in real gas hypersonic flows of nitrogen p 1114 A92-54317
Efficient methods for inviscid non-equilibrium hypersonic flow fields p 1024 A92-54571
Application of a parallel direct simulation Monte Carlo method to hypersonic rarefied flows p 1024 A92-54916
Measurements of turbulence in hypersonic flow p 1092 A92-56005
A code validation strategy and facility for nonequilibrium, reacting flows
[AIAA PAPER 92-3970] p 1098 A92-56796
The SR3 low density wind tunnel - Facility capabilities and research development
[AIAA PAPER 92-3972] p 1098 A92-56798
Computational and numerical analysis of hypersonic nozzle flows with comparisons to wind tunnel calibration data
[AIAA PAPER 92-4011] p 1033 A92-56834
Hypersonic shock tunnel testing for undergraduate laboratory instruction
[AIAA PAPER 92-4021] p 1100 A92-56843
A database of aerothermal measurements in hypersonic flow for CFD validation
[AIAA PAPER 92-4023] p 1034 A92-56845
CFD validation experiments for hypersonic flows
[AIAA PAPER 92-4024] p 1034 A92-56846
Flow contamination and flow quality in arc heaters used for hypersonic testing
[AIAA PAPER 92-4028] p 1100 A92-56850
Numerical simulation of unsteady flow in a hypersonic shock tunnel facility
[AIAA PAPER 92-4029] p 1034 A92-56851
Numerical simulation of hypersonic viscous flow for the design of H-2 orbiting plane (HOPE-2)
[NAL-TR-1093] p 11 N92-10009
Recent advances on a finite element algorithm for computational aerodynamics: Transonics-hypersonics
[DE91-018176] p 11 N92-10010
Prediction of forces and moments for hypersonic flight vehicle control effectors
[NASA-CR-188954] p 33 N92-11070
Studies of aerothermal loads generated in regions of shock/shock interaction in hypersonic flow
[NASA-CR-181893] p 43 N92-11319
An assessment and application of turbulence models for hypersonic flows
[NASA-TM-105124] p 82 N92-11984
Calculation of hypersonic leeside vortices over blunt delta wings p 84 N92-13004
A new technique for temperature and specie concentration measurements in unseeded supersonic and hypersonic gas flows
[AD-A241536] p 158 N92-13409

Numerical investigations in three-dimensional internal flows
[NASA-CR-189467] p 221 N92-14313
Aerothermodynamics for Space Vehicles
[ESA-SP-318] p 180 N92-14973
Hypersonic flow past delta wing flow simulated by Navier-Stokes solutions p 180 N92-14981
A multiblock flow solver for inviscid hypersonic flows p 181 N92-14986
Flow and temperature computations for space vehicles using adaptive finite element techniques p 181 N92-14990
Base pressure measurements on a cone at hypersonic Mach numbers: A contribution to aerothermodynamics for space vehicles p 181 N92-14992
Heat transfer measurements in ONERA supersonic and hypersonic wind tunnels using passive and active infrared thermography p 208 N92-15003
Verification and application of the NSFLEX method for hypersonic flow conditions p 182 N92-15005
Hypersonic aerothermodynamic computations using a point-implicit TVD method p 183 N92-15006
Hypersonic viscous shock layer in thermochemical nonequilibrium p 183 N92-15014
Influence of chemical modeling on the solution of hypersonic shock layers p 183 N92-15016
Hypersonic inviscid flow field simulations around reentry vehicles with flap deflection p 184 N92-15025
Behaviour and modelling of the aerothermodynamics of ballistic entry vehicles in the high altitude flow regimes p 184 N92-15031
Applicability of bridging methods to hypersonic rarefied flow aerodynamics of reentry vehicles p 184 N92-15032
Transitional flows around re-entry bodies p 184 N92-15035
Grid impact on 3D hypersonic flows p 184 N92-15041
Progress with multigrid schemes for hypersonic flow problems
[NASA-CR-189579] p 185 N92-15047
Experimental research of the aerodynamics of nozzles and plumes at hypersonic speeds
[NASA-CR-187316] p 185 N92-15048
Marching with the parabolized Navier-Stokes equations. Problem 1: Numerical study of hypersonic viscous cone flow
[AERO-REPT-9007] p 344 N92-18231
Marching with the parabolized Navier-Stokes equations. Problem 2: Hypersonic viscous flow over a flat plate
[AERO-REPT-9008] p 345 N92-18232
Zonal solutions for a double-ellipse in a hypersonic flowfield
[AERO-REPT-9009] p 345 N92-18233
Calculation of hypersonic non-equilibrium viscous flow using second order boundary layer theory
[MBB-FE122-S-PUB-434] p 345 N92-18316
Towards the computation of turbulent hypersonic flows
[AERO-REPT-9106] p 345 N92-18318
Reaction speed constant for the reactions between N + O2 and between O + N2
[ETN-92-90861] p 347 N92-19252
Modelling of chemical and physical effects with respect to flows around reentry bodies
[MBB-FE-211/S/PUB/0465/A] p 347 N92-19296
A comparative study of numerical versus analytical waverider solutions
[AD-A244183] p 347 N92-19304
Temperature effects in FFA HYP 500 at M = 7 in a flow with strong expansion
[FFA-TN-1991-27] p 443 N92-20229
Flow analysis and design optimization methods for nozzle afterbody of a hypersonic vehicle
[NASA-CR-4431] p 446 N92-21456
Three-dimensional simulations of hypersonic flows
[MBB-UK-0155-89-PUB] p 447 N92-21703
Contributions of MBB-FE211 to the 2nd Antibes Workshop on Hypersonic Flows
[MBB-FE211-S-PUB-449] p 524 N92-22179
Numerical simulation of transient hypervelocity flow in an expansion tube
[NASA-CR-189615] p 592 N92-22228
Hypersonic laminar flow computations over a blunt leading edged delta wing at three different chord Reynolds numbers
[FFA-TN-1991-40] p 528 N92-23168
Development of a new flux splitting scheme p 596 N92-23352
A user guide for the EMTAC-MZ CFD code
[NASA-CR-4283] p 678 N92-24242
A study of viscous interaction effects on hypersonic waveriders
[NASA-CR-189587] p 625 N92-24680
An engineering method for interactive inviscid-boundary layers in three-dimensional hypersonic flows
[NASA-TM-107838] p 632 N92-25279
Joint computational and experimental aerodynamics research on a reentry vehicle
[DE91-017315] p 667 N92-25315
Development of new flux splitting schemes --- computational fluid dynamics algorithms p 682 N92-25809
A high angle of attack inviscid shuttle orbiter computation
[NASA-TM-107606] p 685 N92-25964
An experimental investigation of a 2-D scramjet inlet at flow Mach numbers of 8 to 25 and stagnation temperatures of 800 to 4,100 K p 739 N92-26586
CFD contributions during hypersonic airplane intake design p 769 N92-27472
Special Course on Unstructured Grid Methods for Advection Dominated Flows
[AGARD-R-787] p 771 N92-27671
Feasibility study of hypersonic clinometric measurements at R3Ch
[ONERA-RSF-136/1865-AY-728-] p 829 N92-28789
Hypersonic flow past radiation-cooled surfaces
[MBB-FE-202-S-PUB-0468-A] p 832 N92-29713
Joint computational and experimental aerodynamics research on a hypersonic vehicle
[DE92-013439] p 943 N92-30367
CFD contributions during hypersonic airplane intake design
[MBB/FE213/S/PUB/459] p 944 N92-30676
Development of a 3-D upwind PNS code for chemically reacting hypersonic flowfields
[NASA-CR-190182] p 946 N92-30977
Stagnation-point heat-transfer rate predictions at aeroassist flight conditions
[NASA-TP-3208] p 1001 N92-31281
Flat plates placed in depleted hypersonic flow
[SESSIA-430/91.960] p 947 N92-31508
Hypersonic code efficiency and validation studies
[NASA-CR-190680] p 948 N92-31533
Stability and transition of hypersonic boundary-layer flows
[AD-A250279] p 948 N92-31555
Low density real gas flows about hypersonic vehicles
[AD-A250048] p 949 N92-31777
Perspectives on hypersonic viscous and nonequilibrium flow research
[NASA-CR-190817] p 1039 N92-33413
An approximate viscous shock layer technique for calculating chemically reacting hypersonic flows about blunt-nosed bodies p 1041 N92-33837
Computation and stability analysis of laminar flow over a blunt cone in hypersonic flow p 1041 N92-33839

HYPERSONIC FORCES
Aerodynamic characteristics of a blunt delta wing with air bleed through an intake at supersonic and hypersonic velocities. II p 437 A92-31855

HYPERSONIC HEAT TRANSFER
Application of the STAPAT II code to hypersonic vehicle aerothermodynamics
[AIAA PAPER 91-5035] p 209 A92-17824
Hypersonic flow past radiation-cooled surfaces
[MBB-FE-202-S-PUB-0468-A] p 832 N92-29713
Stagnation-point heat-transfer rate predictions at aeroassist flight conditions
[NASA-TP-3208] p 1001 N92-31281

HYPERSONIC INLETS
Tangential mass addition for shock/boundary-layer interaction control in scramjet inlets p 80 A92-17197
Three dimensional hypersonic inlets - Low speed performance
[AIAA PAPER 91-5021] p 171 A92-17817
Numerical and experimental investigation of airframe-integrated inlet for high velocities p 243 A92-21072
Three-dimensional viscous analysis of a Mach 5 inlet and comparison with experimental data p 344 A92-28526
Multiple shock-shock interference on a cylindrical leading edge p 813 A92-46899
Comparative study of turbulence models in predicting hypersonic inlet flows
[AIAA PAPER 92-3098] p 824 A92-48740
Comparison between computational and experimental data for a hypersonic laser propelled vehicle
[AIAA PAPER 92-3808] p 1023 A92-54179
A computational and experimental investigation of a three-dimensional hypersonic scramjet inlet flow field p 11 N92-10007
Air intakes for high speed vehicles
[AGARD-AR-270] p 445 N92-20797
Comparative study of turbulence models in predicting hypersonic inlet flows
[NASA-TM-105720] p 722 N92-28102
CFD contributions during hypersonic airplane intake design
[MBB/FE213/S/PUB/459] p 944 N92-30676

HYPERSONIC NOZZLES
Mach 4 and Mach 8 axisymmetric nozzles for a high-enthalpy shock tunnel p 78 A92-16668
Thrust nozzle test facility at DLR Cologne
[AIAA PAPER 91-5024] p 206 A92-17818
Analysis of hypersonic nozzles including vibrational nonequilibrium and intermolecular force effects
[AIAA PAPER 92-0330] p 322 A92-25777
Aerodynamic design of axisymmetric hypersonic wind-tunnel nozzles using least-squares/parabolized Navier-Stokes procedure
[AIAA PAPER 92-0332] p 322 A92-25779
Computations of multispecies mixing between scramjet nozzle flow and hypersonic freestream p 376 A92-28534
Experience in the operation of a hypersonic nozzle static thrust stand
[AIAA PAPER 92-3292] p 882 A92-48881
Unsteady shock propagation in a steady flow nozzle expansion p 1023 A92-54489
Experimental results for a hypersonic nozzle/afterbody flow field
[AIAA PAPER 92-3915] p 1032 A92-56747
Computational and numerical analysis of hypersonic nozzle flows with comparisons to wind tunnel calibration data
[AIAA PAPER 92-4011] p 1033 A92-56834
Hypersonic wind tunnel nozzle study
[AIAA PAPER 92-4012] p 1033 A92-56835
Boundary layer study on nozzle wall at hypersonic velocities
[AIAA PAPER 92-4013] p 1034 A92-56836
Effect of nonuniform entrance flow profile on hypersonic nozzle pitching moment
[AD-A244050] p 377 N92-19184
Initial calibration of the HEAT-H2 arc-heated wind tunnel
[AD-A245072] p 484 N92-20898
Application of finite element method to hypersonic nozzle flow computations p 769 N92-27479

HYPERSONIC REENTRY
Low-to-high altitude predictions of three-dimensional ablative reentry flowfields
[AIAA PAPER 92-0366] p 394 A92-26227
Monte Carlo simulation of reentry flows with ionization
[AIAA PAPER 92-0493] p 328 A92-26323
Calculation of real-gas effects on blunt-body trim angles p 432 A92-31169
Simulation of hypersonic flows on unstructured grids p 434 A92-31496
Effects of shock wave precursors ahead of hypersonic entry vehicles p 441 A92-32182
Earth atmospheric entry studies for manned Mars missions p 442 A92-32251
Asymptotic defect boundary-layer theory applied to hypersonic flows p 610 A92-36839
An exploration of chemically reacting viscous hypersonic flow p 612 A92-37550
Non-equilibrium hypersonic flow simulations using the second-order boundary layer equations p 612 A92-37551
Stagnation point heat flux in hypersonic high enthalpy flow p 613 A92-38373
A transonic/supersonic/hypersonic CFD analysis of the entry Space Shuttle Orbiter
[AIAA PAPER 92-2614] p 805 A92-45571
Aerothermodynamics of a 1.6-meter-diameter sphere in hypersonic rarefied flow p 808 A92-45840
Steps towards an efficient and accurate method solving the Euler equations around a re-entry configuration at super- and hypersonic speed p 181 N92-14987
Verification and application of the NSFLEX method for hypersonic flow conditions p 182 N92-15005
Reaction speed constant for the reactions between N + O2 and between O + N2
[ETN-92-90861] p 347 N92-19252
Modelling of chemical and physical effects with respect to flows around reentry bodies
[MBB-FE-211/S/PUB/0465/A] p 347 N92-19296
Design of orbital re-entry experiment vehicle and outline of the experiment p 667 N92-25374
Analysis of spacecraft entry into Mars atmosphere p 1105 N92-33763

HYPERSONIC SHOCK
Numerical approximation of hypersonic shocks in a finite-element method using flux-corrected transport (FCT) p 708 A92-43060
Measurement of shock-wave/boundary-layer interaction in a free-piston shock tunnel p 813 A92-46903
Three-dimensional calculation of radiative field in hypersonic air shock layers p 1023 A92-54498

HYPERSONIC SPEED
Center of pressure calculations for a bent-axis vehicle
[AIAA PAPER 92-0168] p 254 A92-23779
Aerodynamic characteristics of a hypersonic viscous optimized waverider at high altitudes
[AIAA PAPER 92-0306] p 320 A92-25755
In-flight evaluation of Mach number at hypersonic speeds p 624 A92-40599
An investigation of passive control methods for shock-induced separation at hypersonic speeds
[AIAA PAPER 92-2725] p 808 A92-45596
Aerodynamically blunt and sharp bodies
[AIAA PAPER 92-2727] p 808 A92-45597
Thrust/speed effects on long-term dynamics of aerospace planes p 889 A92-46766
Conceptual design of scramjet engine
p 1065 A92-53490
Key design considerations for scramjet powered space plane p 1066 A92-53491
Flow characterization in the NASA Ames 16-inch Shock Tunnel
[AIAA PAPER 92-3810] p 1090 A92-54180
New 1.27-m leg of the National Aerospace Laboratory hypersonic wind tunnel p 1092 A92-56003
History of EPOS air-launched spaceplane project
p 211 N92-14103
Flow over a delta wing at hypersonic speeds
p 181 N92-14993
Experimental research of the aerodynamics of nozzles and plumes at hypersonic speeds
[NASA-CR-187316] p 185 N92-15048
Center of pressure calculations for a bent-axis vehicle
[DE92-005186] p 498 N92-20143
Simulation of real-gas effects on pressure distributions for aeroassist flight experiment vehicle and comparison with prediction
[NASA-TP-3157] p 501 N92-20677
Heat transfer characteristics of hypersonic waveriders with an emphasis on the leading edge effects
[NASA-CR-189586] p 525 N92-22215
Experimental investigation of nozzle/plume aerodynamics at hypersonic speeds
[NASA-CR-190074] p 664 N92-25162
Assessment of flying-quality criteria for air-breathing aerospacecraft
[NASA-CR-4442] p 663 N92-25982
Experimental studies of hypersonic shock-wave boundary-layer interactions
[NASA-CR-190731] p 950 N92-32162

HYPERSONIC TEST APPARATUS
Research capabilities of the NASA Langley 8-foot high temperature tunnel p 980 A92-51403
Laser-driven hypersonic air-breathing propulsion simulator
[AIAA PAPER 92-3922] p 1095 A92-56753
Hypersonic aerodynamic/aerothermodynamic testing capabilities at Langley Research Center
[AIAA PAPER 92-3937] p 1096 A92-56767

HYPERSONIC VEHICLES
Recombination-dominated nonequilibrium heat transfer to arbitrarily catalytic hypersonic vehicles
p 2 A92-10426
Saenger and the German Hypersonics Technology Programme - Status report 1991
[IAF PAPER 91-198] p 32 A92-12570
Fuel injection in hypersonic airbreathing engine
[IAF PAPER 91-273] p 120 A92-14710
Supersonic reacting internal flowfields
p 155 A92-16989
Solving the structures problem for hypersonic vehicles
p 209 A92-17349
CFD application to 2D/3D flow fields in Scramjet engine p 170 A92-17501
'Spaceplanes' R&D status of Japan
[AIAA PAPER 91-5002] p 209 A92-17802
Multidisciplinary modeling and simulation of a generic hypersonic vehicle
[AIAA PAPER 91-5015] p 232 A92-17813
Application of the STAPAT II code to hypersonic vehicle aerothermodynamics
[AIAA PAPER 91-5035] p 209 A92-17824
Hypersonic airbreathing propulsion activities for Saenger
[AIAA PAPER 91-5040] p 200 A92-17828
Aeroservoelastic stabilization techniques for hypersonic flight vehicles
[AIAA PAPER 91-5056] p 203 A92-17839
Dynamics and control of hypersonic vehicles - The integration challenge for the 1990's
[AIAA PAPER 91-5057] p 203 A92-17840
Engineering method for calculating surface pressures and heating rates on vehicles with embedded shocks
[AIAA PAPER 91-5060] p 171 A92-17842
Analysis of cooling systems for hypersonic aircraft
[AIAA PAPER 91-5063] p 216 A92-17843
Potential hypersonic vehicles applications
[AIAA PAPER 91-5086] p 169 A92-17854
Automated trajectory synthesis for hypersonic vehicles using energy management and variational calculus techniques p 210 A92-19061
Application of the LAURA code for slender-vehicle aerothermodynamics p 310 A92-24652
Hypersonic waveriders - Effects of chemically reacting flow and viscous interaction
[AIAA PAPER 92-0302] p 320 A92-25754
A hypersonic waverider test vehicle - The logical next step
[AIAA PAPER 92-0308] p 387 A92-25756
A ballistic investigation of the aerodynamic characteristics of a blunt vehicle at hypersonic speeds in carbon dioxide and air
[AIAA PAPER 92-0328] p 322 A92-25775
Shock interference prediction using direct simulation Monte Carlo
[AIAA PAPER 92-0492] p 328 A92-26322
Thermal management of propulsion systems in hypersonic vehicles
[AIAA PAPER 92-0516] p 373 A92-26942
Computational studies of a superdetonative ram accelerator mode p 399 A92-28529
Design and modeling issues for integrated airframe/propulsion control of hypersonic flight vehicles
p 477 A92-29115
Thermal control for hypersonic vehicle propulsion
p 468 A92-29356
Design considerations for nozzles of hypersonic airbreathing propulsion
[AIAA PAPER 91-5019] p 471 A92-31685
Testing capabilities at AEDC for development of hypersonic vehicles
[AIAA PAPER 91-5027] p 483 A92-31686
Flowpath optimization for hypersonic vehicles
[AIAA PAPER 91-5043] p 437 A92-31688
Engineering method for aero-propulsive characteristics at hypersonic Mach numbers
[AIAA PAPER 91-5061] p 437 A92-31690
Aero-propulsive effects on configuration shaping
[AIAA PAPER 91-5064] p 459 A92-31691
Energy-heading transients in atmospheric flight guidance for airbreathing hypersonic vehicles
[AIAA PAPER 91-5065] p 480 A92-31692
Structures and materials technologies for hypersonic vehicles - Lessons from Hermes experience
[AIAA PAPER 91-5098] p 486 A92-31697
Possibility of reducing the wave drag of a hypersonic flight vehicle (wave rider) p 438 A92-31863
Effects of shock wave precursors ahead of hypersonic entry vehicles p 441 A92-32182
Axial compression corner flow with shock impingement p 441 A92-32196
Preliminary sizing methodology for hypersonic vehicles
p 460 A92-32233
Design tradeoffs on engine-integrated hypersonic vehicles
[AIAA PAPER 92-1205] p 537 A92-33313
Applications of Busemann inlet designs for flight at hypersonic speeds
[AIAA PAPER 92-1210] p 517 A92-33314
Combined compressive and shear buckling analysis of hypersonic aircraft sandwich panels
[AIAA PAPER 92-2487] p 586 A92-34603
Air data measurement for hypersonic vehicles
[SAE PAPER 912143] p 651 A92-39981
The effects of viscosity and diffusion on a supersonic mixing layer p 622 A92-40143
Experimentally supported investigations into the optical performance of multi-aperture window concepts
[AIAA PAPER 92-2781] p 778 A92-41324
A validated code to predict the performance of onboard broadband optical seekers through a turbulent transonic flow
[AIAA PAPER 92-2792] p 778 A92-41331
Heat pipe and surface mass transfer cooling of hypersonic vehicle structures p 763 A92-44380
Numerical simulations of hypersonic real-gas flows over space vehicles
[SAE PAPER 912045] p 791 A92-45429
Numerical simulation of aerothermal loads in hypersonic engine inlets due to shock impingement
[AIAA PAPER 92-2605] p 792 A92-45482
Aerodynamic shape optimization of hypersonic configurations including viscous effects
[AIAA PAPER 92-2635] p 795 A92-45506
High-speed flight propulsion systems --- Book
[ISBN 1-56347-011-X] p 862 A92-46426
Introduction --- propulsion system performance for hypersonic vehicles p 862 A92-46427
Energy analysis of high-speed flight systems
p 925 A92-46430
Joint computational/experimental aerodynamics research on a hypersonic vehicle. I - Experimental results p 812 A92-46890
Joint computational/experimental aerodynamics research on hypersonic vehicle. II - Computational results p 812 A92-46891
Low density heat transfer phenomena
[AIAA PAPER 92-2899] p 820 A92-47875
Heat transfer characteristics of hypersonic waveriders with an emphasis on leading edge effects
[AIAA PAPER 92-2920] p 821 A92-47892
Analysis of a hydrocarbon scramjet with augmented preburning
[AIAA PAPER 92-3425] p 865 A92-48984
Utility management system for hypersonic vehicles
p 964 A92-49252
High temperature ground vibration test techniques
p 980 A92-51404
A history of high-temperature testing at WPAFB
p 981 A92-51406
The study of experimental turboramjets
[AIAA PAPER 92-3720] p 1067 A92-54135
Getting up to speed in hypersonic structures
p 1117 A92-55127
Dynamics and control of hypersonic aeropropulsive/aeroelastic vehicles
[AIAA PAPER 92-4326] p 1073 A92-55170
An integrated development of the equations of motion for elastic hypersonic flight vehicles
[AIAA PAPER 92-4605] p 1077 A92-55283
Optimal launch trajectory of a hypersonic research vehicle
[AIAA PAPER 92-4302] p 1103 A92-55310
A guidance law for hypersonic descent to a point
[AIAA PAPER 92-4303] p 1104 A92-55311
PAYCOS, a multidisciplinary sizing code for hypersonic vehicles
[AIAA PAPER 92-4564] p 1132 A92-55376
Application of advanced multidisciplinary analysis and optimization methods to vehicle design synthesis
p 1054 A92-56160
The G-range impulse facility - A high-performance free-piston shock tunnel
[AIAA PAPER 92-3946] p 1097 A92-56774
TSNIIMASH capabilities for aerogasdynamical and thermal testing of hypersonic vehicles
[AIAA PAPER 92-3962] p 1097 A92-56789
CFD validation experiments for hypersonic flows
[AIAA PAPER 92-4024] p 1034 A92-56846
An integrated analytical aeropropulsive/aeroelastic model for the dynamic analysis of hypersonic vehicles
[AIAA PAPER 92-4567] p 1035 A92-57034
Combined exo/endoatmospheric transport alternatives
[IAF PAPER 92-0663] p 1104 A92-57102
The German Hypersonics Technology Programme - Status report 1992
[IAF PAPER 92-0867] p 1105 A92-57258
Viscous computations of cold air/air flow around scramjet nozzle afterbody
[NASA-CR-4406] p 13 N92-10982
Prediction of forces and moments for hypersonic flight vehicle control effectors
[NASA-CR-188954] p 33 N92-11070
Aerodynamic shape optimization of arbitrary hypersonic vehicles p 194 N92-13954
Numerical investigations in three-dimensional internal flows
[NASA-CR-189467] p 221 N92-14313
Interference heating near fin/body junctions on hypersonic vehicles p 182 N92-14996
Parallelization of a Direct Simulation Monte Carlo (DSMC) code for fluid dynamics p 227 N92-15033
Evolution and development of hypersonic configurations 1958-1990
[AD-A242768] p 197 N92-15069
Trim drag reduction concepts for horizontal takeoff single-stage-to-Orbit vehicles
[NASA-TM-102687] p 206 N92-15076
Optimization of tangential mass injection for minimizing flow separation in a scramjet inlet
[AD-A243868] p 376 N92-18867
Performance and stability analysis of the non-linear dynamics of a simple powered lifting hypersonic vehicle flying on a minor circle
[AD-A243933] p 366 N92-19192
Secondary instability of high-speed flows and the influence of wall cooling and suction
[NASA-CR-4427] p 406 N92-19844
Control integration concept for hypersonic cruise-turn maneuvers
[NASA-TP-3136] p 481 N92-20195
Conceptual design of two-stage-to-orbit hybrid launch vehicle
[NASA-CR-190006] p 486 N92-20666

Flow analysis and design optimization methods for nozzle afterbody of a hypersonic vehicle
[NASA-CR-4431] p 446 N92-21456
Aeronautical research in the United States: Challenges for the 1990's p 420 N92-21502
Hypersonic airbreathing propulsion/airframe integration p 474 N92-21522
H2 fueled flightweight ramjet construction and test p 475 N92-21531
Scramjet analysis, testing p 475 N92-21532
System controls challenges of hypersonic combined-cycle engine powered vehicles p 475 N92-21533
Hypersonic configurations in slow speed flight p 624 N92-24394
A study of viscous interaction effects on hypersonic waveriders
[NASA-CR-189587] p 625 N92-24680
Progress in integrated analysis with adaptive unstructured meshing p 683 N92-25914
An experimental investigation of a 2-D scramjet inlet at flow Mach numbers of 8 to 25 and stagnation temperatures of 800 to 4,100 K p 739 N92-26586
Hypersonic aerospace vehicle leading edge cooling using heat pipe, transpiration and film cooling techniques p 780 N92-26733
Computational method to predict thermodynamic, transport, and flow properties for the modified Langley 8-foot high-temperature tunnel
[NASA-TM-4374] p 767 N92-27193
CFD contributions during hypersonic airplane intake design p 769 N92-27472
Trajectory optimization for hypersonic aircraft guidance p 728 N92-27898
Robust intelligent flight control for hypersonic vehicles
[NASA-CR-185680] p 746 N92-28209
Acquisition of an aerothermodynamic data base by means of a winged experimental reentry vehicle
[MBB/FE202/S/PUB/461] p 787 N92-30232
Joint computational and experimental aerodynamics research on a hypersonic vehicle
[DE92-013439] p 943 N92-30367
Navier-Stokes computations of a viscous optimized waverider
[NASA-CR-189658] p 944 N92-30392
CFD contributions during hypersonic airplane intake design
[MBB/FE213/S/PUB/459] p 944 N92-30676
Research and technology, 1991. Langley Research Center
[NASA-TM-4331] p 1013 N92-30733
Development of a 3-D upwind PNS code for chemically reacting hypersonic flowfields
[NASA-CR-190182] p 946 N92-30977
Low density real gas flows about hypersonic vehicles
[AD-A250048] p 949 N92-31777
Analytical and experimental studies of heat pipe radiation cooling of hypersonic propulsion systems
[DE92-013428] p 973 N92-31817
Dynamic interactions between hypersonic vehicle aerodynamics and propulsion system performance
[NASA-CR-190638] p 1038 N92-33304

HYPERSONIC WAKES
Navier-Stokes computation of hypersonic near wakes with foreign gas injection
[AIAA PAPER 92-0838] p 422 A92-29604
Integrated electric density and scaling law for hypersonic blunt-body wakes p 714 A92-44865
Hypersonic wakes
[ETN-92-91082] p 349 N92-19925

HYPERSONIC WIND TUNNELS
Investigation of hypersonic ramjet propulsion cycles using a ram accelerator test facility
[IAF PAPER 91-275] p 278 A92-22482
Measurement of a three-dimensional hypersonic density field
[AIAA PAPER 92-0383] p 323 A92-26240
Single expansion ramp nozzle simulations
[AIAA PAPER 92-0387] p 323 A92-26243
An iodine hypersonic wind tunnel for the study of nonequilibrium reacting flows
[AIAA PAPER 92-0566] p 383 A92-26974
Hypersonic testing technology of HOPE (H-II orbiting plane) p 747 A92-43096
Research on hypersonic wind tunnel methods in the 90's p 748 A92-43105
Joint computational/experimental aerodynamics research on a hypersonic vehicle. I - Experimental results p 812 A92-46890
Numerical and experimental investigation of rarefied compression corner flow
[AIAA PAPER 92-2900] p 820 A92-47876
New hypersonic test methods developed at ONERA - The R5 and F4 wind tunnels
[ONERA, TP NO. 1992-39] p 882 A92-48600
Least-squares/parabolized Navier-Stokes procedure for optimizing hypersonic wind-tunnel nozzles p 980 A92-50270
Aerodynamic heating characteristics of space planes tested by NAL hypersonic wind tunnel p 1017 A92-53547
Nonintrusive measurements in fluid dynamic flows from Mach .0005 to 14 p 1090 A92-54311
Quantitative heat transfer measurements in hypersonic wind tunnels by means of infrared thermography p 1115 A92-54321
New 1.27-m leg of the National Aerospace Laboratory hypersonic wind tunnel p 1092 A92-56003
A hypersonic wind tunnel test of a mixed-compression air inlet model p 1028 A92-56007
Aerothermodynamic test of spaceplane by thin-skin method p 1093 A92-56043
Future requirements for hypersonic aerodynamic and aerothermodynamic facilities
[AIAA PAPER 92-3903] p 1094 A92-56738
Supersonic and hypersonic quiet tunnel technology at NASA Langley
[AIAA PAPER 92-3908] p 1094 A92-56743
Experimental results for a hypersonic nozzle/afterbody flow field
[AIAA PAPER 92-3915] p 1032 A92-56747
Hypersonic aerodynamic/aerothermodynamic testing capabilities at Langley Research Center
[AIAA PAPER 92-3937] p 1096 A92-56767
The Langley 15-inch Mach 6 High Temperature Tunnel
[AIAA PAPER 92-3938] p 1096 A92-56768
Test description and preliminary pitot-pressure surveys for Langley Test Technique Demonstrator at Mach 6
[AIAA PAPER 92-3940] p 1096 A92-56770
A code validation strategy and facility for nonequilibrium, reacting flows
[AIAA PAPER 92-3970] p 1098 A92-56796
Rarefied gas research at Berkeley - Current studies and future potentials
[AIAA PAPER 92-3971] p 1098 A92-56797
CAN-DO, CFD-based Aerodynamic Nozzle Design and Optimization program for supersonic/hypersonic wind tunnels
[AIAA PAPER 92-4009] p 1033 A92-56832
Hypersonic wind tunnel nozzle study
[AIAA PAPER 92-4012] p 1033 A92-56835
Numerical simulations around models in hypersonic wind tunnels p 182 N92-14998
Infrared measurements of aerodynamic heating in hypersonic wind tunnel p 208 N92-15002
Review of the European hypersonic wind tunnel performance and simulation requirements p 209 N92-15043
Ultra High Speed Numerical Wind Tunnel (UHSNWT) initiative at National Aerospace Laboratory numerical simulator - second generation
[NAL-TR-1108] p 384 N92-18037
Laser-spectroscopic measurement techniques for hypersonic, turbulent wind tunnel flows
[NASA-TM-103928] p 405 N92-19596
Initial calibration of the HEAT-H2 arc-heated wind tunnel
[AD-A245072] p 484 N92-20898
Instrumentation requirements for laminar flow research in the NLR high speed wind tunnel HST
[NLR-TP-89158-U] p 887 N92-28669
Pilot-pressure probe for measuring pressure in a hypersonic wind tunnel
[NASA-CASE-LAR-14232-1] p 1102 N92-34213

HYPERSONICS
Optimization of the three-dimensional shape of lifting bodies of small aspect ratio at hypersonic velocities p 244 A92-21602
Thrust/speed effects on long-term dynamics of aerospace planes p 889 A92-46766
Recent advances on a finite element algorithm for computational aerodynamics: Transonics-hypersonics
[DE91-018176] p 11 N92-10010
Numerical investigations in three-dimensional internal flows
[NASA-CR-189467] p 221 N92-14313
Flow analysis and design optimization methods for nozzle afterbody of a hypersonic vehicle
[NASA-CR-4431] p 446 N92-21456
Inlet technology p 447 N92-21528
Evaluation of an innovative high-temperature ceramic wafer seal for hypersonic engine applications p 578 N92-22205
Heat transfer characteristics of hypersonic waveriders with an emphasis on the leading edge effects
[NASA-CR-189586] p 525 N92-22215
Hypersonic code efficiency and validation studies
[NASA-CR-190680] p 948 N92-31533
Experimental studies of hypersonic shock-wave boundary-layer interactions
[NASA-CR-190731] p 950 N92-32162

HYPERVELOCITY
Multiple aperture window and seeker concepts for endo KEW applications
[AIAA PAPER 92-2806] p 752 A92-41344

HYPERVELOCITY FLOW
Improved nonequilibrium viscous shock-layer scheme for hypersonic blunt-body flowfields p 310 A92-24653
Skin-friction gauge for use in hypervelocity impulse facilities p 398 A92-28063
Direct numerical simulation of laminar breakdown in high-speed, axisymmetric boundary layers
[AIAA PAPER 92-0742] p 343 A92-28223
Navier-Stokes computation of hypersonic near wakes with foreign gas injection
[AIAA PAPER 92-0838] p 422 A92-29604
Diagonal implicit scheme for computing flows with finite rate chemistry p 488 A92-32253
Laminar heat transfer to blunt cones in high-enthalpy hypervelocity flows p 713 A92-44372
A comparative study of scramjet injection strategies for high Mach numbers flows
[AIAA PAPER 92-3287] p 904 A92-48876
Nonintrusive measurements in fluid dynamic flows from Mach .0005 to 14 p 1090 A92-54311
Approximate Riemann solver for hypervelocity flows p 1117 A92-54934
Holographic and PLIF measurements of free-flight hypervelocity flows in the AEDC Range G facility
[AIAA PAPER 92-3935] p 1122 A92-56765
The high enthalpy shock tunnel in Goettingen
[AIAA PAPER 92-3942] p 1104 A92-56772
Millisecond aerodynamic force measurement with side-jet model in the ISL shock tunnel
[AIAA PAPER 92-3963] p 1097 A92-56790
Effects of oxygen dissociation on hypervelocity combustion experiments
[AIAA PAPER 92-3964] p 1098 A92-56791
Numerical simulation of transient hypervelocity flow in an expansion tube
[NASA-CR-189601] p 402 N92-18965
Numerical simulation of transient hypervelocity flow in an expansion tube
[NASA-CR-189615] p 592 N92-22228

HYPERVELOCITY GUNS
Experimental and computational investigation of scaling phenomena in a large caliber ram accelerator
[AIAA PAPER 92-3245] p 1103 A92-54019

HYPERVELOCITY IMPACT
Collision probability estimate method for impact generated low earth orbit space debris clouds
[AAS PAPER 91-369] p 752 A92-43269

HYPERVELOCITY PROJECTILES
Two variations of certainty control p 918 A92-46762
Experimental and computational investigation of scaling phenomena in a large caliber ram accelerator
[AIAA PAPER 92-3245] p 1103 A92-54019
Holographic and PLIF measurements of free-flight hypervelocity flows in the AEDC Range G facility
[AIAA PAPER 92-3935] p 1122 A92-56765

HYPERVELOCITY WIND TUNNELS
Drag balance for hypervelocity impulse facilities p 207 A92-18375
High pressure hypervelocity electrothermal wind tunnel performance study and subscale tests
[AIAA PAPER 92-0329] p 383 A92-25776
Aero-optical testing in the NSWC Hypervelocity Tunnel No. 9
[AIAA PAPER 92-2797] p 747 A92-41336
Notes on the use of fusible temperature indicators to bound the temperature of hot graphite in the NAVSWC hypervelocity wind tunnel facility p 1090 A92-54315
A new system for recording unstable aerodynamic phenomena in NAVSWC Hypervelocity Wind Tunnel No. 9 p 1091 A92-54325
Hypervelocity Wind Tunnel 9 control system p 1092 A92-54343
Hypersonic aerodynamic/aerothermodynamic testing capabilities at Langley Research Center
[AIAA PAPER 92-3937] p 1096 A92-56767
Boundary layer study on nozzle wall at hypersonic velocities
[AIAA PAPER 92-4013] p 1034 A92-56836

HYPOTHERMIA
U.S. Coast Guard aviation life support and rescue equipment p 529 A92-32999

HYSTERESIS
Heat induced transient behaviours of axial compressors p 469 A92-29721
An experimental investigation of leading edge vortical flow about a delta wing during wing rock
[AD-A243363] p 260 N92-17114

Aerodynamic and flowfield hysteresis of slender wing aircraft undergoing large-amplitude motions
p 364 N92-18780

I

I BEAMS
Experimental and theoretical analysis of composite I-beams with elastic couplings p 216 A92-18377

ICE
LEWICE/E - An Euler based ice accretion code
[AIAA PAPER 92-0037] p 316 A92-25676
Prediction of ice accretion on a swept NACA 0012 airfoil and comparisons to flight test results
[AIAA PAPER 92-0043] p 316 A92-25677
A turbulence model for iced airfoils and its validation
[AIAA PAPER 92-0417] p 326 A92-26267
Results of an icing test on a NACA 0012 airfoil in the NASA Lewis Icing Research Tunnel
[AIAA PAPER 92-0647] p 334 A92-27021
Influence of air velocity on the habit of ice crystal growth from the vapor p 668 A92-38111
LEWICE/E: An Euler based ice accretion code
[NASA-TM-105389] p 179 N92-14001
Results of an icing test on a NACA 0012 airfoil in the NASA Lewis Icing Research Tunnel
[NASA-TM-105374] p 185 N92-15051
A turbulence model for iced airfoils and its validation
[NASA-TM-105373] p 186 N92-15052
Analysis of aircraft engine blade subject to ice impact
[NASA-TM-105336] p 229 N92-15402
Prediction of ice accretion on a swept NACA 0012 airfoil and comparisons to flight test results
[NASA-TM-105368] p 258 N92-15968
Experimental ice shape and performance characteristics for a multi-element airfoil in the NASA Lewis Icing Research Tunnel
[NASA-TM-105380] p 261 N92-17347
Deterministic multi-zone ice accretion modeling
p 265 N92-17987
Effects of Adverse Weather on Aerodynamics
[AGARD-CP-496] p 449 N92-21679
The effect of wing ice contamination on essential flight characteristics p 449 N92-21681
Low temperature environment operations of turboengines (design and user's problems)
p 450 N92-21682
Simulation of iced wing aerodynamics
p 450 N92-21686
The effect of hoar-frosted wings on the Fokker 50 take-off characteristics p 451 N92-21692
Experimental and computational ice shapes and resulting drag increase for a NACA 0012 airfoil
[NASA-TM-105743] p 828 N92-28674
Feasibility of measuring transverse electric noise at VLF and LF on an ice cap
[AD-A252280] p 1129 N92-33220
Experimental study of performance degradation of a rotating system in the NASA Lewis RC icing tunnel
[NASA-CR-190684] p 1102 N92-34141
Analysis of iced wings
[NASA-TM-105773] p 1042 N92-34144

ICE CLOUDS
Feature extraction from two-dimensional images using fractal analysis p 496 A92-32130
Remote measurements of supercooled integrated liquid water during WISP/FAA aircraft icing program
p 915 A92-46788
Predicting droplet impingement on yawed wings
p 1043 A92-56180

ICE FORMATION
Adhesive shear strength of impact ice --- inside wind tunnel p 30 A92-11068
Advanced ice protection systems test in the NASA Lewis Icing Research Tunnel p 108 A92-14406
Ongoing development of a computer jobstream to predict helicopter main rotor performance in icing conditions p 65 A92-14407
A basis for ice formation design p 146 A92-14556
Study of theoretical and wind tunnel results on flight performance degradation due to leading edge rime ice accretion
[AIAA PAPER 92-0038] p 262 A92-22158
Development of a three-dimensional icing code - Comparison with experimental shapes
[AIAA PAPER 92-0041] p 262 A92-22159
Industrial measurement of microphysical parameters - Application to natural and simulated icing clouds --- for aircraft icing p 262 A92-23302
Determination of liquid water content in the AEDC engine test cells
[AIAA PAPER 92-0165] p 263 A92-23778
LEWICE/E - An Euler based ice accretion code
[AIAA PAPER 92-0037] p 316 A92-25676
Prediction of ice accretion on a swept NACA 0012 airfoil and comparisons to flight test results
[AIAA PAPER 92-0043] p 316 A92-25677
Ice property/structure variations across the glaze/rime transition
[AIAA PAPER 92-0296] p 351 A92-25749
Mechanisms resulting in accreted ice roughness
[AIAA PAPER 92-0297] p 351 A92-25750
Proposal for a 3-D, vectorized, adaptable, algorithm for modeling the randomness, unsteadiness, and microphysical properties of ice accretion
[AIAA PAPER 92-0299] p 351 A92-25751
Laboratory evaluation of a sensor for detection of aircraft wing contaminants
[AIAA PAPER 92-0301] p 369 A92-25753
Numerical investigation of performance degradation of wings and rotors due to icing
[AIAA PAPER 92-0412] p 325 A92-26264
Finite wing aerodynamics with simulated glaze ice
[AIAA PAPER 92-0414] p 325 A92-26265
Automatic grid generation for iced airfoil flowfield predictions
[AIAA PAPER 92-0415] p 326 A92-26266
Development of an analytical method to predict helicopter main rotor performance in icing conditions
[AIAA PAPER 92-0418] p 326 A92-26268
Numerical analysis of a thermal deicer
[AIAA PAPER 92-0527] p 357 A92-26950
Results of an icing test on a NACA 0012 airfoil in the NASA Lewis Icing Research Tunnel
[AIAA PAPER 92-0647] p 334 A92-27021
Comparison of two-dimensional and three-dimensional droplet trajectory calculations in the vicinity of finite wings
[AIAA PAPER 92-0645] p 342 A92-28215
Analysis of iced wings
[AIAA PAPER 92-0416] p 423 A92-29972
EIPOS for ice-formation control on aircraft in flight - An alternative technique p 647 A92-40545
LDV measurements on a rectangular wing with a simulated glaze ice accretion
[AIAA PAPER 92-2690] p 800 A92-45537
Remote measurements of supercooled integrated liquid water during WISP/FAA aircraft icing program
p 915 A92-46788
Assessment of one-dimensional icing forecast model applied to stratiform clouds p 915 A92-46803
Computational icing analysis for aircraft inlets
[AIAA PAPER 92-3178] p 836 A92-48793
Effect of a simulated glaze ice shape on the aerodynamic performance of a rectangular wing
[AIAA PAPER 92-4042] p 1035 A92-56861
Technical evaluation report, AGARD Fluid Dynamics Panel Symposium on Effects of Adverse Weather on Aerodynamics
[NASA-TM-105192] p 2 N92-10002
LEWICE/E: An Euler based ice accretion code
[NASA-TM-105389] p 179 N92-14001
Results of an icing test on a NACA 0012 airfoil in the NASA Lewis Icing Research Tunnel
[NASA-TM-105374] p 185 N92-15051
Development of an analytical method to predict helicopter main rotor performance in icing conditions
[NASA-CR-189110] p 258 N92-15967
Prediction of ice accretion on a swept NACA 0012 airfoil and comparisons to flight test results
[NASA-TM-105368] p 258 N92-15968
An investigation of air transportation technology at the Massachusetts Institute of Technology, 1990-1991
p 265 N92-17985
Experimental investigation of passive infrared ice detection for helicopter applications p 265 N92-17986
Deterministic multi-zone ice accretion modeling
p 265 N92-17987
Technical evaluation report on the Fluid Dynamics Panel Specialists' Meeting on Effects of Adverse Weather on Aerodynamics
[AGARD-AR-306] p 352 N92-18242
Freezing precipitation on lifting surfaces
[NRC-32124] p 448 N92-20156
Application of a water droplet trajectory prediction code to the design of inlet particle separator anti-icing systems
[PNR-90839] p 474 N92-20573
Effects of Adverse Weather on Aerodynamics
[AGARD-CP-496] p 449 N92-21679
Low temperature environment operations of turboengines (design and user's problems)
p 450 N92-21682
Regulations and their changes for certification of civil aircraft in icing conditions p 450 N92-21683
Icing simulation: A survey of computer models and experimental facilities p 450 N92-21684
Method for calculating the three-dimensional water concentration coefficients and its industrial applications
p 502 N92-21685
Model rotor icing tests in the NASA. Lewis Icing Research Tunnel p 450 N92-21688
The effect of hoar-frosted wings on the Fokker 50 take-off characteristics p 451 N92-21692
Wind tunnel investigation of the aerodynamic effects of aircraft ground deicing/anti-icing fluids and criteria for aerodynamic acceptance p 452 N92-21698
The NASA aircraft icing research program
p 549 N92-22534
Comparison of two-dimensional and three-dimensional droplet trajectory calculations in the vicinity of finite wings
[NASA-TM-105617] p 596 N92-23154
The effect of droplet sizing uncertainty on ice accretions p 679 N92-24874
Helium bubble flow visualization of the spanwise separation on a NACA 0012 with simulated glaze ice
[NASA-TM-105742] p 714 N92-26612
Experimental and computational ice shapes and resulting drag increase for a NACA 0012 airfoil
[NASA-TM-105743] p 828 N92-28674
Results of a low power ice protection system test and a new method of imaging data analysis
[NASA-TM-105745] p 828 N92-28696
Lewis icing research tunnel test of the aerodynamic effects of aircraft ground deicing/anti-icing fluids
[NASA-TP-3238] p 952 N92-30395
The icing of the elevator of the DLR icing research aircraft of Do 28 type
[DLR-MITT-91-12] p 953 N92-31813
Analysis of three icing test flights reaching the aircraft-referred icing degree of severe
[ESA-TT-1254] p 954 N92-31943
Numerical investigation of the effects of icing on fixed and rotary wing aircraft
[NASA-CR-190542] p 1044 N92-34105
Experimental study of performance degradation of a rotating system in the NASA Lewis RC icing tunnel
[NASA-CR-190684] p 1102 N92-34141
Analysis of iced wings
[NASA-TM-105773] p 1042 N92-34144

ICE PREVENTION
Effect of antiicer on propeller performance
p 25 A92-10969
Advanced ice protection systems test in the NASA Lewis Icing Research Tunnel p 108 A92-14406
Heat transfer measurements from a smooth NACA 0012 airfoil p 218 A92-20215
Examination of a numerical icing-severity scale
[AIAA PAPER 92-0164] p 263 A92-23777
Improvements to expulsive separation ice protection blankets
[AIAA PAPER 92-0533] p 358 A92-26951
Experimental and numerical investigation of anti-icing phenomena on a NACA 0012 assembly
[AIAA PAPER 92-0531] p 459 A92-31669
Technical evaluation report, AGARD Fluid Dynamics Panel Symposium on Effects of Adverse Weather on Aerodynamics
[NASA-TM-105192] p 2 N92-10002
Numerical simulation of an aircraft anti-icing system incorporating a rivulet model for the runback water
p 448 N92-20303
Effects of Adverse Weather on Aerodynamics
[AGARD-CP-496] p 449 N92-21679
Icing simulation: A survey of computer models and experimental facilities p 450 N92-21684
A review of icing research at the Royal Aerospace Establishment p 451 N92-21689
Preparation of the ice certification of the Dornier 328 regional airliner by numerical simulation and by ground test p 451 N92-21693
The NASA aircraft icing research program
p 549 N92-22534
NASA's aircraft icing technology program
[NASA-TM-104518] p 527 N92-23105
Results of a low power ice protection system test and a new method of imaging data analysis
[NASA-TM-105745] p 828 N92-28696

ICE REPORTING
Experimental investigation of passive infrared ice detection for helicopter applications p 265 N92-17986

IDEAL FLUIDS
A variational method for solving the problem of motion of a profile of complex geometry in a fluid
p 397 A92-27482
Asymptotic solution of the problem of ideal-fluid flow past the vertices of bodies and wings
p 427 A92-30199
Combined method for the solution of plane direct problems of flow past bodies with jets
p 427 A92-30200
A mathematical model for the hydroelasticity problem concerning the motion of two flexible profiles in an ideal incompressible fluid. I p 712 A92-44127

A potential flow theory of two-dimensional bifurcated curtain jets. II p 1118 A92-56039

IDEAL GAS

Application of the LAURA code for slender-vehicle aerothermodynamics p 310 A92-24652

Prandtl-Meyer function for dense gases p 415 A92-26441

Compressible laminar boundary layers for perfect and real gases in equilibrium at Mach numbers to 30 [AIAA PAPER 92-0757] p 336 A92-27099

Boundary singularities in steady potential compressible flow through plane two-dimensional channels p 336 A92-27384

Development of a method for calculating the effect of the propeller slipstream on transonic flow over the wing p 424 A92-30144

Oblique shock wave with sweep p 613 A92-38370

Comparison between computational and experimental data for a hypersonic laser propelled vehicle [AIAA PAPER 92-3808] p 1023 A92-54179

Application of program LAURA to perfect gas shock tube flows: A parametric study [NASA-TM-104190] p 298 N92-17002

Interferograms, schlieren, and shadowgraphs constructed from real- and ideal-gas, two- and three-dimensional computed flowfields [NASA-CR-190054] p 446 N92-21356

Numerical simulation of transient hypervelocity flow in an expansion tube [NASA-CR-189615] p 592 N92-22228

TVD finite-difference solutions of nonequilibrium vibrationally relaxing and chemically reacting gaseous flows p 626 N92-24854

An engineering method for interactive inviscid-boundary layers in three-dimensional hypersonic flows [NASA-TM-107838] p 632 N92-25279

A new Lagrangian method for real gases at supersonic speed p 633 N92-25814

Development of a 3-D upwind PNS code for chemically reacting hypersonic flowfields [NASA-CR-190182] p 946 N92-30977

IDENTIFYING

Reference mode effect on the auditory display of aircraft bank angle [AD-A247825] p 728 N92-27916

IFF SYSTEMS (IDENTIFICATION)

Integrated Communications, Navigation, Identification, Avionics (ICNIA) expert system for fault tolerant avionics p 118 N92-12539

IGNITION

The jet screen ignition scheme and its experimental verification p 388 A92-24744

Effectiveness of plasma torches for ignition and flameholding in scramjet p 737 A92-44524

Experimental investigation of liquid carbonhydrogen fuel combustion in channel at supersonic velocities [AIAA PAPER 92-3429] p 894 A92-48986

Development of fuel neutralizing agents to prevent flashback on aircraft fires [AD-A242828] p 264 N92-17259

Three-dimensional modeling of diesel engine intake flow, combustion and emissions [NASA-CR-189126] p 658 N92-24539

Experimental investigation of nozzle/plume aerodynamics at hypersonic speeds [NASA-CR-190074] p 664 N92-25162

IGNITION LIMITS

Studies on the mechanism of ignition and flameholding by plasma jets p 755 A92-42798

Ignition delays, heats of combustion, and reaction rates of aluminum alkyl derivatives used as ignition and combustion enhancers for supersonic combustors [AIAA PAPER 92-3841] p 894 A92-49134

IGNITION TEMPERATURE

Research on altitude simulation of starting for a single-spool small turbojet p 969 A92-49836

ILLUMINATING

Aircraft accident report: Northwest Airlines, Inc., Flights 1482 and 299. Runway incursion and collision, Detroit Metropolitan/Wayne County Airport, Romulus, Michigan, December 3, 1990 [PB91-910405] p 187 N92-14006

Comparative evaluation of internally and externally lighted taxiway guidance signs [DOT/FAA/CT-TN92/2] p 573 N92-22237

Airport smart power lighting system [DOT/FAA/CT-TN91/12] p 573 N92-22966

ILYUSHIN AIRCRAFT

From the history of Soviet aviation - Aircraft of the Il'iushin design bureau (2nd revised and enlarged edition) --- Russian book p 61 A92-15022

IMAGE ANALYSIS

Flow visualization image analysis of high-rate roll experiments on a delta wing [AIAA PAPER 92-0317] p 321 A92-25764

Neutron radiography with SNRS p 492 A92-28747

Feature extraction from two-dimensional images using fractal analysis p 496 A92-32130

Pocono Mountain SAR data analysis for testing slant range to ground range conversion p 587 A92-35142

Close-range photogrammetry meets machine vision; Proceedings of the Meeting, Zurich, Switzerland, Sept. 3-7, 1990 [SPIE-1395] p 994 A92-51626

Inertial navigation sensor integrated motion analysis for autonomous vehicle navigation p 995 A92-52470

Image processing in the undergraduate fluid dynamics laboratory [AIAA PAPER 92-4020] p 1141 A92-56842

Passive range estimation for rotorcraft low-altitude flight [NASA-TM-103897] p 2 N92-10003

Image-based ranging and guidance for rotorcraft [NASA-CR-184829] p 191 N92-14036

Analysis of objects in binary images [NASA-CR-4420] p 234 N92-14598

IMAGE ENHANCEMENT

Helmet-mounted image intensification analysis p 554 A92-35454

The C-17 Multifunction Display - A building block for avionic systems p 1063 A92-55907

IMAGE MOTION COMPENSATION

Adaptive airborne MTI with two-dimensional motion compensation p 102 A92-17240

Numerical calculation of modulation transfer functions for low frequency mechanical vibrations p 235 A92-19982

IMAGE PROCESSING

Numerical calculation of modulation transfer functions for low frequency mechanical vibrations p 235 A92-19982

Reconfigurable Mobile System - Ground, sea and air applications p 218 A92-19986

Interactive graphics method for removal of helicopter motions from laser profile data p 598 A92-35109

Pocono Mountain SAR data analysis for testing slant range to ground range conversion p 587 A92-35142

Visualization and measurement of helicopter rotor flow using projected smoke filaments and digital image processing p 520 A92-35728

A new method for visualization and measurement of turbulent flow patterns p 619 A92-40063

Vibration analysis of gas turbines by an intelligent knowledge-based system p 656 A92-40548

Close-range photogrammetry meets machine vision; Proceedings of the Meeting, Zurich, Switzerland, Sept. 3-7, 1990 [SPIE-1395] p 994 A92-51626

Quantitative heat transfer measurements in hypersonic wind tunnels by means of infrared thermography p 1115 A92-54321

Analysis of image-based navigation system for rotorcraft low-altitude flight p 1046 A92-55968

Image processing in the undergraduate fluid dynamics laboratory [AIAA PAPER 92-4020] p 1141 A92-56842

Application of digital measurement techniques to analysis of range shadowgraphs [AD-A241554] p 139 N92-13080

Image-supported navigation for testing instrument landing systems p 189 N92-14012

Analysis of objects in binary images [NASA-CR-4420] p 234 N92-14598

Design of a fiber optic image transmission link [AD-A243686] p 304 N92-17088

Development of an electronic high speed camera system for the quantitative analysis of unsteady flows [MPIS-100/1991] p 300 N92-17344

Bistatic image processing for a 32 x 19 inch model aircraft using scattered fields obtained in the OSU-ESL compact range [NASA-CR-189932] p 499 N92-20197

Approach and landing assisted by onboard image processing p 457 N92-21959

Fractal image compression of Rayleigh, Raman, LIF and LDV data in turbulent reacting flows [AD-A246960] p 767 N92-27352

Results of a low power ice protection system test and a new method of imaging data analysis [NASA-TM-105745] p 828 N92-28696

Binary optical filters for scale invariant pattern recognition [NASA-TM-103902] p 853 N92-28910

Digital analysis of wind tunnel imagery to measure fluid thickness [NASA-CR-189234] p 983 N92-31252

Detection of honeycomb damage using hexagonal grid discontinuities [DREP-89-9] p 1109 N92-32846

IMAGE RECONSTRUCTION

The dimensional reconstruction of vortex cross-section images p 339 A92-27833

Inverse problems and imaging (Pitman research notes in mathematics series Number 245) [AD-A240333] p 53 N92-11737

IMAGE ROTATION

Multi-channel fiber optic rotary joint for single-mode fiber [AD-D015273] p 927 N92-29095

IMAGE VELOCITY SENSORS

Development and application of a particle image velocimeter for high-speed flows [AIAA PAPER 92-0004] p 292 A92-22129

Particle image velocimetry measurements of the aerodynamics of a wind turbine p 1115 A92-54337

IMAGERY

The role of simulation for the study of APIS (piloting support by synthetic imagery) p 885 N92-28544

A rotorcraft flight database for validation of vision-based ranging algorithms [NASA-TM-103906] p 841 N92-29103

Digital analysis of wind tunnel imagery to measure fluid thickness [NASA-CR-189234] p 983 N92-31252

IMAGING RADAR

Estimation of the P-3/SAR L-, C- and X-band antenna directivity in range direction based on corner reflector measurements within the absolute SAR calibration p 587 A92-35055

94 GHz MMW imaging radar system [SAE PAPER 912208] p 651 A92-40015

IMAGING SPECTROMETERS

The application of high spectral and spatial resolution imaging spectrometers for locating downed aircraft p 598 A92-35132

The imaging spectrometer p 599 N92-23387

IMAGING TECHNIQUES

Stationary neutron radiography system p 144 A92-13589

Eddy current imaging of aircraft using real time image signal processing p 144 A92-13594

Evaluation of OH laser-induced fluorescence techniques for supersonic combustion diagnostics [AIAA PAPER 92-0508] p 396 A92-26935

Mechanical design of an airborne imaging microwave radiometer p 554 A92-35276

Planar fluorescence imaging of a transverse jet in a supersonic crossflow p 755 A92-44501

Simultaneous imaging and interferometric turbule visualization in a high-velocity mixing/shear layer p 896 A92-45130

Bistatic scattering on a monostatic radar range p 849 A92-48408

KrF laser-induced OH fluorescence imaging in a supersonic combustion tunnel [AIAA PAPER 92-3346] p 905 A92-48923

Full field flow visualization and computer-aided velocity measurements in a bank of cylinders in a wind tunnel p 991 A92-50040

Physical model of the swept shock wave/boundary-layer interaction flowfield p 935 A92-50312

Inverse problems and imaging (Pitman research notes in mathematics series Number 245) [AD-A240333] p 53 N92-11737

AI for RPVs, Sensor Driven Airborne Replanner (SDAR), for a Robotic Aircraft Sensor Platform (RASP) p 114 N92-12534

Analysis of objects in binary images [NASA-CR-4420] p 234 N92-14598

Large area QNDE inspection for airframe integrity p 362 N92-18588

Development of an electromagnetic microscope for eddy current evaluation of materials [AD-A242007] p 406 N92-19873

The imaging radar system p 599 N92-23391

Particle image velocimetry [AD-A246638] p 750 N92-27753

Results of a low power ice protection system test and a new method of imaging data analysis [NASA-TM-105745] p 828 N92-28696

IMPACT DAMAGE

Processing effects and damage tolerance in poly(etheretherketone) composites p 388 A92-26152

Experimental research on blade containment p 557 A92-35561

Collision probability estimate method for impact generated low earth orbit space debris clouds [AAS PAPER 91-369] p 752 A92-43269

Advanced experimental design applied to damage tolerance of composite materials p 993 A92-51505

Impact damage tolerance of helicopter sandwich structures p 958 A92-51506

Development of composite structures with enhanced damage tolerance p 985 A92-51555

Damage tolerance and durability design of composite aircraft structures p 996 A92-53067

An impact dynamics investigation on some problems in bird strike on windshields of high-speed aircrafts
p 986 A92-53330
Analysis of aircraft engine blade subject to ice impact
[NASA-TM-105336] p 229 N92-15402
Foreign object damage to tires operating in a wartime environment
[AD-A247195] p 724 N92-27682
Damage tolerance certification methodology for composite structures p 1108 N92-32579
CFRP stiffened panels under compression
p 1109 N92-33044

IMPACT LOADS
The impact load on containment rings during a multiple blade shed in aircraft gas turbine engines
[ASME PAPER 91-GT-163] p 123 A92-15598
An analysis of impact resistance of composite fan blade p 293 A92-22523
Effect of some load factors of bird impact on blade response p 371 A92-24740
The selection of bird impact load types --- on turbojet compressor and turbofan fan blades
p 448 A92-29732
Bird impact analysis of aircraft windshield transparency p 958 A92-50236
Study of dynamic strength on composite wing
p 996 A92-53071
Mechanical model of landing impact of three dimensional fuselage landing gear p 960 A92-53090
Dual mode shock absorber and method
[PATENT-1-265-541] p 115 N92-13055
Application of MSC/DYNA to shock and impact problems in aircraft industry
[MBB-UD-0593-91-PUB] p 225 N92-14382
Analysis of aircraft engine blade subject to ice impact
[NASA-TM-105336] p 229 N92-15402
Explicit finite element method for transparency impact analysis
[AD-A243527] p 264 N92-17478
Structural dynamics division research and technology accomplishments for F.Y. 1991 and plans for F.Y. 1992
[NASA-TM-104188] p 261 N92-17509

IMPACT RESISTANCE
Advanced ceramic engine technology for gas turbines
[ASME PAPER 91-GT-368] p 153 A92-15716
An analysis of impact resistance of composite fan blade p 293 A92-22523
An analysis of impact resistance of composite blades for turbo-fan engines p 294 A92-23109
An analysis of impact resistance of composite blades for aircraft engines (Analysis with two dimensional and three dimensional finite elements) p 579 A92-32562
Numerical simulation of impact resistance on composite blade p 738 A92-44734
An analysis of the effect of centrifugal force on the impact resistance of composite fan blades for turbo-fan engines
[SAE PAPER 912047] p 861 A92-45431

IMPACT STRENGTH
Canadian CF-18 aircraft ejection seat parachute update p 529 A92-32983

IMPACT TESTS
Impact design methods for ceramic components in gas turbine engines
[ASME PAPER 91-GT-115] p 123 A92-15566
Impact response of composite UHB propeller blades
[SAE PAPER 912046] p 861 A92-45430
Advanced experimental design applied to damage tolerance of composite materials p 993 A92-51505
A study of dynamic response to bird impact on arc windshields of aircrafts p 952 A92-53340
Drop test: Cessna Golden Eagle 421B
[DOT/FAA/CT-TN91/32] p 837 N92-28900
Low-velocity impact loading on fibre reinforced aluminum laminates (ARALL) and other aircraft sheet materials
[ETN-92-91613] p 987 N92-30414
Evaluation of head impact kinematics for passengers seated behind interior walls
[AD-A252651] p 952 N92-30551
Design, evaluation and experimental effort toward development of a high strain composite wing for Navy aircraft p 1107 N92-32514

IMPEDANCE MATCHING
Decoupling of antennas using periodic structures
p 725 A92-42634

IMPELLERS
Investigation of the flow at the exit of an unshrouded centrifugal impeller and comparison with the 'classical' jet-wake theory
[ASME PAPER 90-GT-124] p 6 A92-11287
Impeller flow field measurement and analysis
[ASME PAPER 90-GT-146] p 38 A92-11288
An analysis method and applications for 3-D viscous internal flows with complex geometry
p 143 A92-13299
Dynamic analysis technique of rotating centrifugal impeller
[ASME PAPER 91-GT-50] p 148 A92-15528
An improved method for aerodynamic design of centrifugal impeller blades
[ASME PAPER 91-GT-76] p 69 A92-15545
A calculation procedure for three-dimensional turbulent flow in a centrifugal impeller with any blade geometry
[ASME PAPER 91-GT-171] p 73 A92-15606
Performance predictions for centrifugal compressor impellers p 759 A92-41836
Study of a new airfoil used in reversible axial fans
p 177 N92-13970
Thrust test fixture
[AD-D015259] p 983 N92-31192
Effects of curvature and rotation on turbulence in the NASA low-speed centrifugal compressor impeller
p 1124 N92-32292

IMPINGEMENT
Shock interference prediction using direct simulation Monte Carlo
[AIAA PAPER 92-0492] p 328 A92-26322
Oscillating shock impingement on low-angle gas injection into a supersonic flow p 89 N92-13032
Optimization of tangential mass injection for minimizing flow separation in a scramjet inlet
[AD-A243868] p 376 N92-18867

IMPLOSIONS
An explosively driven, fast shock tube
[DE92-008437] p 749 N92-26720

IMPROVEMENT
Avionics modernization/upgrades in the late 1990s
p 199 N92-14055
Accomplishments under the Airport Improvement Program, FY 1991
[AD-A253046] p 1101 N92-33434

IN SITU MEASUREMENT
In situ measurement of particle formation in heated jet fuels: A new application of photon correlation spectroscopy
[DE92-003641] p 488 N92-20132

IN-FLIGHT MONITORING
Expert system for real-time aircraft monitoring
p 410 A92-24411
Atmospheric analysis for airdata calibration on research aircraft
[AIAA PAPER 92-0293] p 369 A92-25746
Airflow effects about PMS probes on the DLR Falcon --- Particle Measuring System for atmospheric research aircraft p 467 A92-32060
Development of a multi-computer in-flight data acquisition and analysis system for general aviation aircraft
[AIAA PAPER 92-1037] p 553 A92-33218
Tail rotor aerodynamic features recorded in flight
p 546 A92-35752
Transmission vibration monitoring - A single board computer architecture p 554 A92-35765
Predicted and measured in-flight wing deformations of a forward-swept-wing aircraft p 548 A92-35936
Helicopter in-flight frequency response test techniques
p 548 A92-35938
The SAS Flight Analysis and Aircraft Monitoring System p 555 A92-35941
EIPOS for ice-formation control on aircraft in flight - An alternative technique p 647 A92-40545
In-flight evaluation of Mach number at hypersonic speeds p 624 A92-40599
Navigation preparations for passenger helicopters
p 723 A92-43155
Using helicopters for coastal alert p 723 A92-43164
Real time presentation for RAFALE in-flight tests
p 882 A92-47522
Experimental investigation of in-flight oscillation on helicopters and its prevention p 977 A92-53089
In-flight optimization of the total propulsion system
[AIAA PAPER 92-3744] p 1068 A92-54146
In-flight performance diagnostic capability of an adaptive engine model
[AIAA PAPER 92-3746] p 1068 A92-54147
A comparison of airborne wake vortex detection measurements with values predicted from potential theory
[NASA-TP-3125] p 18 N92-10994
Proposal for the new fatigue management system for the AMX p 361 N92-18580
Arrangements and methods for the survey of aircraft radio components and systems p 652 N92-25603
High speed research system study. Advanced flight deck configuration effects
[NASA-CR-189650] p 967 N92-30965

INCENDIARY AMMUNITION
Modular simulation of HEI fragments and blast pressure
[AD-A248205] p 910 N92-29191

INCIDENCE
Hydrodynamic flow visualization around an oscillating vane. Extension of study to the case of higher incidences and amplitudes and the starting off phase from permanent regime
[ONERA-RT-56/1369-AN] p 43 N92-11312
An experimental investigation of the effect of fineness ratio on lateral force on a pointed slender body of revolution p 86 N92-13015
Ground collision avoidance using a variable incidence altitude measurement system for the A-7 aircraft
[AD-A243880] p 352 N92-19259
The effect of angle of incidence and Reynolds number on heat transfer in a linear turbine cascade
[AD-A243900] p 377 N92-19328

INCLUSIONS
Inclusion size effect on the fatigue crack propagation mechanism and fracture mechanics of a superalloy
p 388 A92-24831

INCOMPRESSIBLE BOUNDARY LAYER
A numerical calculation of three dimensional incompressible laminar, transition and turbulent boundary layers p 393 A92-25138
Numerical methods in the theory of boundary layer interaction with nonviscous flow p 426 A92-30185
Simplified linear stability transition prediction method for separated boundary layers p 812 A92-46883
An experimental investigation of the separating/reattaching flow over a backstep
[NASA-CR-190426] p 716 N92-27399
The calculation of incompressible separated turbulent boundary layers p 1003 N92-31886

INCOMPRESSIBLE FLOW
Unsteady incompressible viscous flow past an airfoil
p 3 A92-10662
Flow analysis and design of three-dimensional wind tunnel contractions p 5 A92-11067
Optimal boundary control of nonsteady incompressible flow with an application to viscous drag reduction
p 39 A92-11344
Axisymmetric potential flow calculations. II - Design mode p 8 A92-12399
Numerical solution of steady incompressible viscous flows over airfoils p 8 A92-12649
Analysis of flexible-membrane and jet-flapped airfoils using velocity singularities p 10 A92-13216
An analysis method and applications for 3-D viscous internal flows with complex geometry
p 143 A92-13299
Step response of unsteady aerodynamics acting on a plane swept wing in incompressible flow for finite state modeling p 63 A92-14031
Three dimensional analysis of a rotor in forward flight
p 64 A92-14329
Influence of three-dimensional effects on hydrodynamics and heat transfer in subsonic flow of a viscous compressible gas in the initial section of a rectangular duct p 66 A92-15031
Computation of the potential flow through cascades using the conformal mapping and the singularity method
p 66 A92-15356
A calculation procedure for three-dimensional turbulent flow in a centrifugal impeller with any blade geometry
[ASME PAPER 91-GT-171] p 73 A92-15606
Experimental investigation of coannular jet flow with swirl along a centerbody p 172 A92-18367
Incompressible steady aerodynamics using a standard finite element code p 174 A92-20218
Computation of unsteady, laminar, incompressible, viscous flows using the vorticity streamfunction formulation p 245 A92-21979
Experiences with finite element methods for the velocity-vorticity formulation of three-dimensional, viscous, incompressible flows p 246 A92-21984
Two-dimensional, incompressible aerofoil design and analysis p 247 A92-21987
A parametric study of the aeroelastic stability of a binary wing-with-engine nacelle flutter system in incompressible flow p 270 A92-22472
Analysis of a 2-D airfoil motion flying in-proximity-to a wavy-wall surface-lifting surface-scheme
p 315 A92-25506
Prediction of average downwash gradient for canard configurations
[AIAA PAPER 92-0284] p 319 A92-25737
Unsteady incompressible flow computations with quadrilateral elements p 394 A92-26219
Efficient simulation of incompressible viscous flow over single and multi-element airfoils
[AIAA PAPER 92-0405] p 324 A92-26258
An experimental study of a turbulent wing-body junction and wake flow
[AIAA PAPER 92-0434] p 327 A92-26281
Preconditioned upwind methods to solve incompressible Navier-Stokes equations p 395 A92-26436

Analysis of junction flowfields using the incompressible Navier-Stokes equations
[AIAA PAPER 92-0519] p 331 A92-26944
Incompressible flow past a flat plate aerofoil with leading edge separation bubble p 421 A92-28943
Calculation of the aerodynamic characteristics of bodies of revolution in incompressible flow by the vortex surface method p 428 A92-30375
Subsonic flow past a thin airfoil in a channel with porous walls p 438 A92-31867
Inverse solution of 3D incompressible turbulent boundary layer with separated bubbles p 522 A92-35992
Multipoint inverse airfoil design method based on conformal mapping p 610 A92-36827
Bifurcation analysis of airfoils in incompressible flow p 623 A92-40580
Flow and shape correction problems for thin profiles in incompressible stream p 707 A92-42736
Step response of incompressible unsteady aerodynamic modeling p 744 A92-43131
Multi-point inverse design of an infinite cascade of airfoils
[AIAA PAPER 92-2650] p 797 A92-45517
Prediction of laminar boundary layer using cubic splines
[AIAA PAPER 92-2702] p 801 A92-45544
Applied Computational Aerodynamics - Case studies
[AIAA PAPER 92-2661] p 845 A92-45580
Separation patterns and flow structures about a hemisphere-cylinder at high incidences
[AIAA PAPER 92-2712] p 807 A92-45593
Numerical method for predicting transition in three-dimensional flows by spatial amplification theory p 812 A92-46886
Establishing two-dimensional flow in a large-scale planar turbine cascade
[AIAA PAPER 92-3066] p 823 A92-48720
Pulse jet one-way valve performance
[AIAA PAPER 92-3169] p 863 A92-48790
Design and optimization of airfoils in non-stalling incompressible flow with a prescribed range of the angle of attack p 933 A92-49556
A general explicit or semi-explicit algorithm for compressible and incompressible flows p 937 A92-52682
Unsteady flows in rotor-stator cascades
[AD-A241593] p 158 N92-13410
An inverse method with regularity condition for transonic airfoil design p 177 N92-13969
Analysis of a dusty wall jet
[NASA-CR-189759] p 257 N92-15965
An experimental study of a turbulent wing-body junction and wake flow
[AD-A243388] p 260 N92-17222
Semi-empirical model for prediction of unsteady forces on an airfoil with application to flutter
[NASA-TM-105414] p 346 N92-18760
Numerical solution of three-dimensional unsteady viscous flows
[AD-A244274] p 403 N92-19052
Special Course on Unstructured Grid Methods for Advection Dominated Flows
[AGARD-R-787] p 771 N92-27671
A method for computing the 3-dimensional flow about wings with leading-edge vortex separation. Part 2: Description of computer program VORSEP
[NLR-TR-86006-U] p 833 N92-29916
Validation of three-dimensional incompressible spatial direct numerical simulation code: A comparison with linear stability and parabolic stability equation theories for boundary-layer transition on a flat plate
[NASA-TP-3205] p 943 N92-30295
Numerical calculations of two-dimensional single and multi-material flow fields with CCICE
[DE92-015778] p 1000 N92-30903

INCOMPRESSIBLE FLUIDS
Added mass of high-altitude balloons
[AIAA PAPER 91-3693] p 16 A92-11034
Synthesis of wing profiles from chord velocity diagrams using quasi-solutions for inverse boundary value problems p 80 A92-16815
A variational method for solving the problem of motion of a profile of complex geometry in a fluid p 397 A92-27482
Numerical modeling of self-oscillations for a small-aspect-ratio delta wing using measurements of roll motion at large angles of attack p 424 A92-30138
Breakdown of an axisymmetric laminar wake p 424 A92-30145
Combined method for the solution of plane direct problems of flow past bodies with jets p 427 A92-30200
A mathematical model for the hydroelasticity problem concerning the motion of two flexible profiles in an ideal incompressible fluid. I p 712 A92-44127
Numerical simulation of vortex breakdown by solving the Euler equations for an incompressible fluid p 41 N92-10163
Laminar-flow secondary separation on a slender wing p 85 N92-13006

INCONEL (TRADEMARK)
Thermo-mechanical fatigue crack growth in aircraft engine materials p 213 A92-19799

INDEPENDENT VARIABLES
The application of parameter optimisation techniques to linear optimal control system design p 302 A92-23038

INDEXES (DOCUMENTATION)
Magnetic suspension and balance systems: A comprehensive, annotated bibliography
[NASA-TM-4318] p 32 N92-11030
Bibliography of technical reports, 1980 - 1990
[PB92-110691] p 417 N92-18814
Research, services, and facilities (National Institute of Standards and Technology)
[PB92-109172] p 485 N92-21870
Aeronautical Engineering Group publications, 1950 - present
[AERO-REPT-8907] p 910 N92-29683

INDUCED DRAG
Minimum induced drag of a wing in a circular open wind tunnel p 251 A92-22521
Optimization of a lifting surface for minimum induced drag p 437 A92-31853
Non linear induced drag study of generically cambered closely coupled dual wings
[SAE PAPER 912126] p 618 A92-39973
Wing design for hanggliders having minimum induced drag p 811 A92-46814
Induced drag of a wing in a circular wind tunnel p 936 A92-50327
Effect of a deicing device on the induced drag of a lifting airfoil p 959 A92-51947
Remarks on the relation between lift induced drag and vortex drag p 941 A92-53079
Aerodynamic calculation of an elliptic ring wing
[AIAA PAPER 91-0068] p 1035 A92-57035
Analysis and design of planar and non-planar wings for induced drag minimization
[NASA-CR-189509] p 179 N92-13999
A theoretical investigation of the induced drag of wing of finite aspect ratio
[CUED/A-AERO/TR-17(1991)] p 525 N92-22193
Applications of a direct/iterative design method to complex transonic configurations
[NASA-TP-3234] p 1039 N92-33484

INDUCTION MOTORS
Analysis of a 37 kW cage-induction motor
[PB92-142116] p 597 N92-23496
Electromechanical systems with transient high power response operating from a resonant AC link
[NASA-TM-105716] p 870 N92-28985

INDUSTRIAL MANAGEMENT
Organizational context for aircraft maintenance and inspection p 2 A92-11181
Flight crew integration in the maintenance chain of a commercial aircraft (A 320) p 1012 N92-30957

INDUSTRIAL SAFETY
Report of the aviation safety review of Department of Energy helicopter operations
[DE92-016346] p 954 N92-31928

INDUSTRIES
Research, services, and facilities (National Institute of Standards and Technology)
[PB92-109172] p 485 N92-21870
Symposium on Marketing for Technological Products
[MBB-UE-0014-90-PUB] p 606 N92-23928

INELASTIC STRESS
The 3D inelastic analysis methods for hot section components
[NASA-CR-189089] p 402 N92-18971
Airframe life prediction p 649 N92-25931

INERTIA
Effect of Eulerian inertia forces on the stressed state of the rotating components of aircraft turbomachines p 128 A92-16828
Flapping inertia for selected rotor blades
[NASA-TM-104125] p 115 N92-13057

INERTIAL GUIDANCE
Transition of GPS user equipment testing from Yuma Proving Ground to Holloman AFB p 138 A92-16972

INERTIAL NAVIGATION
Observability analysis of piece-wise constant systems with application to inertial navigation p 49 A92-11391
GPS-INS integration requirements for robust NOE helicopter navigation p 94 A92-14404
Graceful degradation of GPS/INS performance with fewer than four satellites p 97 A92-16644
Stellar inertial navigation growing with the times upgrading of the LN-20 integrated inertial navigation system p 97 A92-16646
Design and flight test of a differential GPS/inertial navigation system for approach/landing guidance p 97 A92-16650
Digital technology applied to airborne receivers p 98 A92-16927
Closed-loop operation of GPS aided INS p 100 A92-16954
INS alignment using GPS Phase III user equipment computed corrections p 100 A92-16955
Flight test results of an Ada coded INS/GPS open loop Kalman filter design p 100 A92-16958
Flight test of a GPS-aided low-cost inertial navigation system programmed in Ada p 101 A92-16973
Integrated GPS/INS for the National Aerospace Plane p 102 A92-16975
Use of distance-measuring equipment (DME) for correcting errors in position, velocity, and wind measurements from aircraft inertial navigation systems p 188 A92-18172
Retrofit provides navigation enhancement for older aircraft p 198 A92-20025
GPS integrated system application in aircraft approach landing p 266 A92-21466
The study of constant value thresholds of FDI in strapdown inertial navigation p 267 A92-22087
LOS rate estimation in inertial navigation using landmarks p 453 A92-29360
Navigation - Land, sea, air, and space --- Book
[ISBN 0-87942-257-2] p 496 A92-31778
The design and operational characteristics of a heated radome for air motion measurement p 467 A92-32064
Kalman filter mechanization for INS airstart p 574 A92-33602
X-29 high angle-of-attack flight test air data comparisons of an inertial navigation system and noseboom probe p 549 A92-35945
AV-8B V/STOL performance analysis p 549 A92-35948
A Kalman filter mechanization for the baro-inertial vertical channel p 673 A92-39558
Error estimation of INS ground alignment through observability analysis p 639 A92-40226
Data processing in navigation complexes --- Russian book
[ISBN 5-217-01060-6] p 725 A92-42789
Navigation experiment on an aircraft using the GPS-INS navigation system. I - Introduction to the system p 726 A92-43122
Navigation experiment on aircraft flight using the GPS-INS navigation system. II - Test results p 726 A92-43123
An integrated navigation system manager using federated Kalman filtering p 858 A92-48477
Formation flight system design concept p 954 A92-49255
Inertial navigation sensor integrated motion analysis for obstacle detection p 954 A92-49272
Architectures and GPS/INS integration - Impact on mission accomplishment p 967 A92-51003
Differential GPS/inertial navigation approach/landing flight test results p 956 A92-51009
Inertial navigation sensor integrated motion analysis for autonomous vehicle navigation p 995 A92-52470
Locally linear neural networks for aerospace navigation systems p 103 N92-12530
Testing of the high accuracy inertial navigation system in the Shuttle Avionics Integration Lab p 210 N92-14087
Investigation of air transportation technology at Ohio University, 1990-1991 p 265 N92-17990
Enhanced displays, flight controls, and guidance systems for approach and landing p 456 N92-21957
NAL Dornier 228-200 flight research airplane: Present status and outline of the installed equipment
[NAL-TM-637] p 732 N92-27429
A Kalman filter integrated navigation design for the IAR Twin Otter Atmospheric Research Aircraft
[NRC-32148] p 1048 N92-32849
The use of Kalman filtering techniques to improve the accuracy of flight test data
[NRC-32139] p 1064 N92-32850

INERTIAL PLATFORMS
A proposal for a dynamic test platform for inertial units and/or GPS p 138 A92-16653
Integrated navigation for approach guidance using differential GPS p 101 A92-16970
Flight test data analysis of a low cost GPS/IMU integrated navigation system p 638 A92-39560
Motion errors in an airborne synthetic aperture radar system p 840 A92-48416
Comparison of Hemispherical Resonator Gyro and optical Gyros p 993 A92-51014
The effect of gyro nonorthogonality error on gyrocompassing p 1045 A92-55955
Evaluation of a IMU with optical fiber gyros in dynamic windtunnel tests p 1104 A92-56121

INERTIAL REFERENCE SYSTEMS
The LISA 6000 - A highly integrated IRS/GPS navigation system p 267 A92-22088
Analysis of stand-alone differential GPS for precision approach p 638 A92-38381
A fault-tolerant Air Data/Inertial Reference System p 967 A92-51011
Ground and satellite supported flight trajectory measurement by example of the avionics flight test system AFES p 641 N92-25600
Board-autonomous flight trajectory measurement by example of an ILS measuring system p 641 N92-25601

INFILTRATION
Polymer infiltration studies [NASA-CR-189773] p 289 N92-17004
Polymer infiltration studies [NASA-CR-190204] p 578 N92-22486

INFINITE SPAN WINGS
Experimental investigation of the coefficients of the normal-force derivatives for rectangular wings with translational oscillations p 423 A92-30127
Lift characteristics of an infinite-span cylindrical wing of a thick symmetric profile at low subsonic velocities p 440 A92-31897

INFLATABLE STRUCTURES
Inflatable traversing probe seal p 595 N92-22692

INFLATING
An air-launched balloon system for a 230 lb gross inflation [AIAA PAPER 91-3689] p 16 A92-11032

INFLUENCE COEFFICIENT
Cascade flutter analysis with transient response aerodynamics p 154 A92-15972

INFORMATION DISSEMINATION
NASA/DOD Aerospace Knowledge Diffusion Research Project. Paper 13: The information-seeking habits and practices of engineers [NASA-TM-107931] p 782 N92-28114
Aviation safety: Changes needed in FAA's service difficulty reporting program [GAO/RCED-91-24] p 953 N92-31453
US Coast Guard GPS Information Center (GPSIC) and its function within the Civil GPS Service (CGS) p 1049 N92-33352

INFORMATION MANAGEMENT
ELS pilot evaluation --- Electronic Library System [SAE PAPER 912107] p 691 A92-39960
Multidimensional ELS user interface --- Electronic Library System [SAE PAPER 912108] p 691 A92-39961
ELS for the A340 --- Electronic Library System [SAE PAPER 912111] p 651 A92-39963
Lessons learned about information management within the Pilot's Associate program p 916 A92-44909
EICAS in an integrated cockpit --- Engine Indication Crew Alerting System p 855 A92-44922
Electronic presentation of instrument approach information p 855 A92-44923
Managing simulator wiring information and deriving system continuity p 964 A92-49287
Feasibility of using a knowledge-based system concept for in-flight primary flight display research [NASA-TM-4279] p 17 N92-10017
Background issues for on-line aircraft documentation p 119 N92-13858
Information Management Engineering (IME) laboratory: A database development facility [AD-A243191] p 305 N92-17369
Prototyping the IRDS: An airport application [PB92-112580] p 484 N92-20448
National airspace data interchange network analysis [AD-A247345] p 727 N92-27217
The development of an airborne information management system for flight test [NASA-TM-104251] p 1065 N92-32866
An international aerospace information system: A cooperative opportunity [NASA-TM-108171] p 1142 N92-33237

INFORMATION PROCESSING (BIOLOGY)
Passenger knowledge of airline safety information [CRANFIELD-AERO-9111] p 187 N92-15054

INFORMATION RETRIEVAL
Background issues for on-line aircraft documentation p 119 N92-13858
Towards coherent hypermedia navigation by pragmatic dialogue modeling [PB92-114735] p 455 N92-20818

INFORMATION SYSTEMS
That all-important interface p 100 A92-16953
An information system for the numerical simulation of 3D Euler flows around aircraft p 613 A92-37554
ELS pilot evaluation --- Electronic Library System [SAE PAPER 912107] p 691 A92-39960
Multidimensional ELS user interface --- Electronic Library System [SAE PAPER 912108] p 691 A92-39961
ELS for the A340 --- Electronic Library System [SAE PAPER 912111] p 651 A92-39963
MassInfo - An intelligent mass properties information system p 928 A92-47628
A development of hypermedia type database system for instruction of aircraft conceptual design p 1132 A92-56113
A systematic formulation, as an approach to air traffic [MBB-Z-0371-91-PUB] p 19 N92-10996
Advanced information processing system: Inter-computer communication services [NASA-CR-187556] p 53 N92-11706
Historical perspective on the evolution of avionics standards p 198 N92-14049
Architecture for Survivable System Processing (ASSP) p 220 N92-14210
Towards coherent hypermedia navigation by pragmatic dialogue modeling [PB92-114735] p 455 N92-20818
Test plan for the international aircraft operator information system [DOT/FAA/CT-91/18] p 781 N92-26830
NASA/DOD Aerospace Knowledge Diffusion Research Project. Paper 13: The information-seeking habits and practices of engineers [NASA-TM-107931] p 782 N92-28114
NASA/DOD Aerospace Knowledge Diffusion Research Project. Paper 14: An analysis of the technical communications practices reported by Israeli and US aerospace engineers and scientists [NASA-TM-107924] p 782 N92-28183
An international aerospace information system: A cooperative opportunity [NASA-TM-108171] p 1142 N92-33237
US Coast Guard GPS Information Center (GPSIC) and its function within the Civil GPS Service (CGS) p 1049 N92-33352
LORAN-C data reduction at the US Naval Observatory p 1050 N92-33358

INFORMATION TRANSFER
Identification of high-level functional/system requirements for future civil transports [NASA-CR-189561] p 276 N92-15991
Cockpit display of hazardous weather information p 277 N92-17989

INFRARED DETECTORS
An investigation of air transportation technology at the Massachusetts Institute of Technology, 1990-1991 p 265 N92-17985
Experimental investigation of passive infrared ice detection for helicopter applications p 265 N92-17986

INFRARED IMAGERY
Thermal imaging of afterburning plumes p 129 A92-17179
Shuttle Infrared Leeside Temperature Sensing (SILTS) experiment - STS-35 and STS-40 preliminary results [AIAA PAPER 92-0126] p 286 A92-23746
Measurement of convective heat-transfer coefficients in wind tunnels using passive and stimulated infrared thermography p 390 A92-24430
Twenty-five years of aerodynamic research with infrared imaging p 497 A92-32232
Time-to-go estimation from infrared images p 840 A92-48308
Problems and solutions for transition detection in cryogenic wind tunnels by infrared imaging p 1090 A92-54319
Application of infrared thermography to thermal flux measurement in wind tunnels [AAAF-NT-89-12] p 31 N92-11020
Thermographic gust wind tunnel measurements [ONERA-RF-31/3409-PY] p 81 N92-11972
Experimental study of hypersonic shock wave boundary layer interactions by means of infrared technique p 182 N92-14994
Design of a fiber optic image transmission link [AD-A243686] p 304 N92-17088

INFRARED INSPECTION
Thermal imaging of graphite/epoxy composite samples with fabricated defects p 491 A92-28655

INFRARED LASERS
Heterodyne techniques in the I.R. bandwidth for laser obstacle detection p 533 A92-35740

INFRARED PHOTOGRAPHY
Heat transfer measurements in ONERA supersonic and hypersonic wind tunnels using passive and active infrared thermography p 208 N92-15003

INFRARED RADAR
Simplified signal processing for an airborne CO2 Doppler lidar p 1000 N92-31023

INFRARED RADIOMETERS
Quantitative heat transfer measurements in hypersonic wind tunnels by means of infrared thermography p 1115 A92-54321

INFRARED SCANNERS
Infrared measurements of aerodynamic heating in hypersonic wind tunnel p 208 N92-15002

INFRARED SIGNATURES
Controlling radar signature p 967 A92-52018
Hot jet dilutor [ETN-92-90860] p 366 N92-19225
Solid fuel ramjet infrared signature [AD-A246299] p 753 N92-26362

INFRARED SUPPRESSION
A numerical study of the radiation characteristic of an elliptical exhaust jet p 970 A92-53258
Hot jet dilutor [ETN-92-90860] p 366 N92-19225

INFRARED TRACKING
Windshear detection p 652 A92-40883

INFRARED WINDOWS
Experimentally supported investigations into the optical performance of multi-aperture window concepts [AIAA PAPER 92-2781] p 778 A92-41324

INGESTION (ENGINES)
Hot gas environment around STOVL aircraft in ground proximity. I - Experimental study p 371 A92-24409
Calculations of hot gas ingestion for a STOVL aircraft model [AIAA PAPER 92-0385] p 374 A92-28191
Engine air particle separator panels for helicopter engine protection p 545 A92-35735
The development of an engine air particle separator system for the CH-47 helicopter p 545 A92-35736
Configuration effects on the ingestion of hot gas into the engine intake p 842 A92-45315
Hot gas ingestion characteristics and flow visualization of a vectored thrust STOVL concept p 860 A92-45316
Hot-gas reingestion - Engine response considerations p 860 A92-45317
Study of the engine bird ingestion experience of the Boeing 737 aircraft [DOT/FAA/CT-89/16] p 187 N92-15053
Hot-gas reingestion engine response considerations [PNR-90810] p 740 N92-27042
Bird ingestion into large turbofan engines [DOT/FAA/CT-91/17] p 1043 N92-33005

INHOMOGENEITY
Inhomogeneous turbulence beyond spectral equilibria: Aeronautical applications [ETN-92-90867] p 404 N92-19349
Measurements in the inhomogeneous convective boundary layer using three powered gliders p 775 N92-26350

INITIATORS (EXPLOSIVES)
Progress report of Scot's Laser Ordnance Initiator System for crew escape p 580 A92-32988
Laser ordnance initiation system p 577 A92-35465

INJECTION
A study of the diffusion of slot-injected drag-reducing polymer solution in a turbulent boundary layer modified by large-eddy breakup devices [AD-A243411] p 344 N92-18007
Optimization of tangential mass injection for minimizing flow separation in a scramjet inlet [AD-A243868] p 376 N92-18867
An investigation of the energy loss and near wake flow field of trailing edge injection p 456 N92-21839

INJECTION MOLDING
Development and characterization of high strength SiC rotors [ASME PAPER 91-GT-191] p 149 A92-15617
RTM: Cost-effective processing of composite structures p 578 N92-22678

INJECTORS
Near-injector structure of non-evaporating pressure-atomized sprays at various ambient densities p 681 N92-25571
The FML compressor as a drive system for the LFSWT: A narrative p 751 N92-27978

INJURIES
Aircraft accident report: Unstabilized approach and loss of control NPA, Inc. dba United Express Flight 2415, British Aerospace BA-3101, N41OUE, Tri-Cities Airport, Pasco, Washington, December 26, 1989 [PB91-910406] p 453 N92-21873
Risk to hearing from overflight noise of military aircraft [ISVR-TR-194] p 604 N92-22241
Evaluation of head impact kinematics for passengers seated behind interior walls [AD-A252651] p 952 N92-30551

INLET AIRFRAME CONFIGURATIONS
Numerical and experimental investigation of airframe-integrated inlet for high velocities p 243 A92-21072

Solution of Euler equations for fighter forebody-inlet combinations at high angles of attack
p 613 A92-38269
Air intakes for high speed vehicles
[AGARD-AR-270] p 445 N92-20797
Grid generation for a complex aircraft configuration
p 649 N92-25714

INLET FLOW
Distortion tolerance of the T800-LHT-800 turboshaft engine p 120 A92-14409
Effects of stator wakes and spanwise nonuniform inlet conditions on the rotor flow of an axial turbine stage
[ASME PAPER 91-GT-93] p 70 A92-15557
Discharge coefficients of cooling holes with radiused and chamfered inlets
[ASME PAPER 91-GT-269] p 151 A92-15667
Inlet flow angle determination of transonic compressor cascades
[ASME PAPER 91-GT-274] p 75 A92-15671
A low noise propulsion concept for the supersonic transport
[ASME PAPER 91-GT-397] p 127 A92-15727
Inlet planar waves - A current perspective
[ASME PAPER 91-GT-400] p 76 A92-15730
Development of a freejet capability for evaluating inlet-engine compatibility
[ASME PAPER 91-GT-401] p 137 A92-15731
Inviscid analysis of a dual mode scramjet inlet
p 80 A92-17198
Supersonic inlet flow computation
p 171 A92-17502
LDV measurements and investigation of flow field through radial turbine guide vanes p 217 A92-19618
Estimation of the maximum instantaneous distortion --- of inlet pressure in aircraft engines p 242 A92-21051
Numerical investigation of supersonic mixed-compression inlet using an implicit upwind scheme p 243 A92-21073
Method for the prediction of supersonic compressor blade performance p 277 A92-21078
Preliminary investigation of inlet dynamic distortion and it's passive control p 245 A92-21742
Flow characteristic and flow control of high aspect ratio and highly curved S-bend diffuser p 245 A92-21743
Modeling supersonic inlet boundary layer bleed roughness
[AIAA PAPER 92-0269] p 317 A92-25725
Three-dimensional simulation of a translating strut inlet
[AIAA PAPER 92-0270] p 317 A92-25726
Evaluation of two flow analyses for subsonic diffuser design
[AIAA PAPER 92-0273] p 317 A92-25727
An efficient Euler solver for predominantly supersonic flows with embedded subsonic pockets
[AIAA PAPER 92-0323] p 322 A92-25770
The unsteady flow characteristics of an S-shaped inlet at high incidence p 339 A92-27905
Transient behavior of supersonic flow through inlets
p 340 A92-28043
Leading edge sweep effects in generic three-dimensional sidewall compression scramjet inlets
[AIAA PAPER 92-0674] p 343 A92-28218
Numerical simulation of two incoming streams in a dual-combustion ramjet combustor p 375 A92-28419
An investigation of the swirl in an S-shaped inlet
p 343 A92-28476
An experimental investigation of the inlet exit flow field improved by aerodynamic grid p 343 A92-28477
Three-dimensional viscous analysis of a Mach 5 inlet and comparison with experimental data
p 344 A92-28526
Iterative algorithms for solving problems of the shaping of three-dimensional ducts p 428 A92-30212
Computation of scramjet inlet flow
p 430 A92-30541
A study on the rotating stall of centrifugal compressors. II - Effect of vaneless diffuser inlet shape on rotating stall p 497 A92-32508
Applications of Busemann inlet designs for flight at hypersonic speeds
[AIAA PAPER 92-1210] p 517 A92-33314
An inverse inviscid method for the design of quasi-three dimensional turbomachinery cascades
p 523 A92-36033
Numerical study of the effects of reverse sweep on scramjet inlet performance p 611 A92-36979
Measurements and simulation of the flow around a poppet valve p 675 A92-40103
A study of three dimensional turbulent boundary layer separation and vortex flow control using the reduced Navier Stokes equations p 621 A92-40105
Calculation of three-dimensional turbulent flow in wind tunnel entry section p 708 A92-43055
Subcritical flow studies on two-dimensional external compression supersonic inlets p 713 A92-44518
Numerical investigation of supersonic inlet with realistic bleed and bypass systems p 713 A92-44519
Bleed-boundary conditions for numerically simulated mixed-compression supersonic inlet flow
p 713 A92-44520
Coupled numerical simulation of the external and engine inlet flows for the F-18 at large incidence
[AIAA PAPER 92-2621] p 793 A92-45493
LDA measurements in a Mach 2 flow over a rearward facing step with staged transverse injection
[AIAA PAPER 92-2692] p 800 A92-45539
Numerical simulations using a dynamic solution-adaptive grid algorithm, with applications to unsteady internal flows
[AIAA PAPER 92-2719] p 803 A92-45557
Comparative study of turbulence models in predicting hypersonic inlet flows
[AIAA PAPER 92-3098] p 824 A92-48740
Computational analysis of ramjet engine inlet interaction
[AIAA PAPER 92-3102] p 824 A92-48744
A Navier-Stokes analysis of a controlled-diffusion compressor cascade at increasing inlet-flow angles
[AIAA PAPER 92-3313] p 825 A92-48899
Full Navier-Stokes calculations on the installed F/A-18 inlet at a high angle of attack
[AIAA PAPER 92-3175] p 1020 A92-54012
Results of a perturbation analysis correlating flows entering and exiting an aircraft inlet system
[AIAA PAPER 92-3624] p 1021 A92-54091
Mach 3 wind tunnel test of mixed compression supersonic inlet
[AIAA PAPER 92-3625] p 1021 A92-54092
Thermal paints for shock/boundary layer interaction in inlet flows
[AIAA PAPER 92-3626] p 1113 A92-54093
Methodology for calculating aerodynamic sensitivity derivatives p 1024 A92-54911
A hypersonic wind tunnel test of a mixed-compression air inlet model p 1028 A92-56007
Development of local nonintrusive measurements of inlet and exhaust flows for the ground testing of air-breathing engines
[AIAA PAPER 92-3899] p 1122 A92-56735
A computational and experimental investigation of a three-dimensional hypersonic scramjet inlet flow field
p 11 N92-10007
Radial inflow turbine study
[AD-A240169] p 26 N92-11015
Effects of inlet distortion on the development of secondary flows in a subsonic axial inlet compressor rotor p 89 N92-13030
Numerical investigations in three-dimensional internal flows
[NASA-CR-189467] p 221 N92-14313
Inlet technology p 447 N92-21528
Control of a helicopter engine in low altitude flight
p 562 N92-23122
Supersonic flow in compression stages and inlets
p 625 N92-24395
A comparison of predicted and measured inlet distortion flows in a subsonic axial inlet flow compressor rotor
[NASA-TM-105427] p 633 N92-26104
An experimental investigation of a 2-D scramjet inlet at flow Mach numbers of 8 to 25 and stagnation temperatures of 800 to 4,100 K p 739 N92-26586
Comparative study of turbulence models in predicting hypersonic inlet flows
[NASA-TM-105720] p 722 N92-28102
Inlet distortion effects in aircraft propulsion system integration p 869 N92-28464
Ultra high bypass Nacelle aerodynamics inlet flow-through high angle of attack distortion test
[NASA-CR-189149] p 943 N92-30298
Application of computational fluid dynamics to the study of vortex flow control for the management of inlet distortion
[NASA-TM-105672] p 1128 N92-34112

INLET NOZZLES
Development of an innovative high-temperature gas turbine fuel nozzle
[ASME PAPER 91-GT-36] p 121 A92-15519
Full Navier-Stokes analysis of a three-dimensional hypersonic mixed compression inlet p 343 A92-28501
Design and analysis of reengine Boeing 727-100 center inlet S duct by a reduced Navier-Stokes code
[AIAA PAPER 92-1221] p 517 A92-33320
NASA's hypersonic propulsion program: History and direction p 476 N92-21535

INLET PRESSURE
Estimation of the maximum instantaneous distortion --- of inlet pressure in aircraft engines p 242 A92-21051
Experimental investigation of terminal shock sensors for mixed-compression inlets p 276 A92-21074
A random vortex method for prediction of maximum instantaneous inlet total pressure distortion
p 311 A92-24731
Results of a perturbation analysis correlating flows entering and exiting an aircraft inlet system
[AIAA PAPER 92-3624] p 1021 A92-54091
An acceptance process for the evaluation of inlet distortion
[AIAA PAPER 92-3918] p 1032 A92-56750
Experimental investigations of exciting forces caused by flow in labyrinth seals p 223 N92-14354
Modification of Jindivik air intake duct with an auxiliary intake static aerodynamic tests
[AD-A243002] p 275 N92-17234
Experimental investigation of trailing edge crenulation effects on losses in a compressor cascade
[AD-A243902] p 377 N92-19329
Calculation of installation effects within performance computer programs p 869 N92-28465

INLET TEMPERATURE
Development of the full-envelope Performance Seeking Control algorithm
[AIAA PAPER 92-3748] p 1068 A92-54148
Cooled high-temperature radial turbine program 2
[NASA-CR-189122] p 1073 N92-34236

INPUT/OUTPUT ROUTINES
Estimation of flying qualities using a leastsquares lower-order equivalent systems technique
p 570 A92-35947
Application of nonlinear QFT to flight control design for high angle of attack maneuvers with thrust vectoring
[AD-A243821] p 381 N92-19241

INSERTS
The design of test-section inserts for higher speed aeroacoustic testing in the Ames 80- by 120-foot wind tunnel
[NASA-TM-103915] p 927 N92-28909

INSPECTION
Enhanced visual technique for rapid inspection of aircraft structures p 214 A92-17290
Inspection of composite structures
p 676 A92-40882
Space Shuttle airframe inspection trend-analysis report p 759 A92-42052
Maintenance scheduling for critical parts of aircraft
p 699 A92-42054
A concept for the revisions of structural inspection schedules p 226 N92-14431
The Operational Loads Monitoring System, OLMS
p 361 N92-18586
Life management approach for USAF aircraft
p 362 N92-18587
Large area QNDE inspection for airframe integrity
p 362 N92-18588
Recent fracture mechanics results from NASA research related to the aging commercial transport fleet
p 362 N92-18589
Approach to crew training in support of the USAF Aircraft Structural Integrity Program (ASIP) p 363 N92-18595
Tiltrotor research aircraft composite blade repairs: Lessons learned
[NASA-TM-103875] p 367 N92-19563
Advisory Circular: Corrosion control for aircraft
[FAA-AC-43-4A] p 420 N92-21834
Methodology for the determination of criticality codes and recertification intervals for Tank Mounted Air Compressors (TMAC) and Base Mounted Air Compressors (BMAC)
[NASA-CR-189268] p 770 N92-27649
Human factors evaluation of the work environment of operators engaged in the inspection and repair of aging aircraft
[AD-A246445] p 724 N92-27914
Turbine aircraft engine operational trending and JT8D static component reliability study
[DOT/FAA/CT-91/10] p 870 N92-28686
Federal Aviation Administration aging aircraft nondestructive inspection research plan
p 914 N92-30116
Inspection of aging aircraft: A manufacturer's perspective p 914 N92-30117
NDE research efforts at the FAA Center for Aviation Systems Reliability p 914 N92-30119
Aging aircraft NDI Development and Demonstration Center (AANC): An overview --- nondestructive inspection p 915 N92-30120
Nondestructive inspection perspectives
p 915 N92-30121
Ageing airplane repair assessment program for Airbus A300 p 838 N92-30123
Survey of French activities concerning structural airworthiness and aging aircraft p 838 N92-30130
Aging commuter aeroplanes: Fatigue evaluation and control methods p 915 N92-30132

Current nondestructive inspection methods for aging aircraft
[DOT/FAA/CT-91/5] p 1126 N92-33480
Inspection of fabricated fuselage panels using electronic shearography
[DOT/FAA/CT-TN92/26] p 1127 N92-33627

INSTRUCTION SETS (COMPUTERS)
Behavior-based fault monitoring
[AD-A241254] p 164 N92-13746

INSTRUCTORS
A training program for airline line instructors
p 835 A92-45044

INSTRUMENT APPROACH
Curved landing approaches using ILS and Loran C
p 94 A92-13854
From Russia and beyond --- equipment and areas of coverage for Loran navigation outside NAS
p 96 A92-16638
Analysis of accidents during instrument approaches
p 529 A92-34253
An exploratory investigation into the definition of tracking standards for IFR helicopter approaches to reduced minima p 533 A92-35726
Electronic presentation of instrument approach information p 855 A92-44923
Design considerations for IAP charts: Approach course track and communication frequencies
[AD-A241482] p 103 N92-13051
Loran-C performance assurance assessment program
[NASA-CR-190469] p 840 N92-28718

INSTRUMENT COMPENSATION
Baro-inertial loop for the USAF Standard RLG INU
p 97 A92-16647
Acceptance of two identical radars in the absence of a precision reference p 533 A92-35931
Calibration of an aircraft control surface using a tri-axial accelerometer package p 555 A92-35942
IsoDoppler and mocomp corrections improve MTI radar p 898 A92-45774
Computational and numerical analysis of hypersonic nozzle flows with comparisons to wind tunnel calibration data
[AIAA PAPER 92-4011] p 1033 A92-56834

INSTRUMENT ERRORS
Radiometric properties of the NS001 Thematic Mapper Simulator aircraft multispectral scanner
p 155 A92-17110
Failure detection and fault management techniques for flush airdata sensing systems
[AIAA PAPER 92-0263] p 369 A92-25719
A study of the precision characteristics of a gyroscopic gravimeter p 581 A92-33778
Radioaltimeter RWL-750 p 855 A92-45374
Reconstruction of flight path in turbulence
p 874 A92-46777
The effect of gyro nonorthogonality error on gyrocompassing p 1045 A92-55955
Development of an uncertainty methodology for multiple-channel instrumentation systems
[AIAA PAPER 92-3953] p 1133 A92-56781
C-29A aircraft altimeter errors
[AD-A240486] p 23 N92-11011
CDI sensitivity and crosstrack error on nonprecision approaches
[AD-A243981] p 356 N92-19391
Estimation of cable-mounted model inertia characteristics for dynamic wind-tunnel test
[NAL-TM-641] p 722 N92-28152
A continuing study of altitude determination deficiencies of the Service Aircraft Instrumentation Package (SAIP)
[AD-A245952] p 968 N92-32051
A Kalman filter integrated navigation design for the IAR Twin Otter Atmospheric Research Aircraft
[NRC-32148] p 1048 N92-32849

INSTRUMENT FLIGHT RULES
Analysis of general aviation accidents during operations under instrument flight rules p 16 A92-11172
The 1991 Cierva Lecture - Aberdeen and its influence on the evolution of the commercial IFR twin engined helicopter p 723 A92-43446
Operational evaluation of a tower workstation for clearance delivery p 879 A92-44981
Rotorcraft low altitude IFR benefit/cost analysis: Operations analysis
[SCT-90RR-44] p 191 N92-15061
JPL's Real-Time Weather Processor project (RWP) metrics and observations at system completion
p 413 N92-19428
Rotorcraft terminal ATC route standards
[SCT-90RR-33] p 641 N92-26101
Knowledge-based planning for controlled airspace flight operation as part of a cockpit assistant
p 727 N92-27895
An evaluation of decelerating IFR approaches utilizing a helicopter flight simulator
[CTN-92-60348] p 1048 N92-32845
Federal aviation regulations. Part 91: General operating and flight rules
[PB92-197334] p 1017 N92-33176
Aircraft accident/incident summary report: Controlled flight into terrain Bruno's Inc., Beechjet, N25BR, Rome, Georgia, 11 December 1991
[PB92-910404] p 1044 N92-34081

INSTRUMENT LANDING SYSTEMS
Curved landing approaches using ILS and Loran C
p 94 A92-13854
Integrated navigation for approach guidance using differential GPS p 101 A92-16970
New siting techniques for the ILS glide slope
p 188 A92-17422
Possible utilization of GPS in precision approach maneuvers p 637 A92-37075
Microwave landing system modeling with application to air traffic control automation p 725 A92-41220
The appropriate concern for possible aberrations in landing guidance signals p 839 A92-44932
Simulation of triple simultaneous parallel ILS approaches p 880 A92-45025
A DSP-based microwave landing system (MLS) post-IF processor p 955 A92-49306
Image-supported navigation for testing instrument landing systems p 189 N92-14012
Evaluation of triple simultaneous parallel ILS approaches spaced 4300 feet apart, phase 4a
[ACD-340] p 191 N92-14034
Microwave landing system autoland system analysis
[NASA-CR-189551] p 191 N92-15060
An evaluation of four F-16 vertical velocity indicator configurations
[AD-A243629] p 370 N92-18014
Evaluation of triple simultaneous parallel ILS approaches spaced 5000 feet apart, phase 4.b
[DOT/FAA/CT-91/31] p 456 N92-21404
Comparison of the performance of a microwave landing system elevation station with the instrument landing system end-fire glide slope at Yeager Airport, Charleston, West Virginia
[DOT/FAA/CT-TN91/22] p 534 N92-22210
Board-autonomous flight trajectory measurement by example of an ILS measuring system
p 641 N92-25601
Effect of guard band reduction on marker beacon receiver performance
[DOT/FAA/CT-TN92/18] p 1002 N92-31617
Aircraft accident report: L'Express Airlines, Inc., Flight 508, Beech C99, N7217L weather encounter and crash near Birmingham, Alabama, July 10, 1991
[PB92-910401] p 1043 N92-32455
ILS mathematical modeling study of an ILS localizer and glide slope proposed for runway 32R, Moffett Field Airport, California
[DOT/FAA/CT-TN92/28] p 1048 N92-33308

INSTRUMENT ORIENTATION
A new method for orientation calculation of the electromagnetic helmet-mounted sighting unit
p 370 A92-27837

INSTRUMENT PACKAGES
Modern techniques for monitoring airborne telemetry
p 857 A92-47560
Development of an uncertainty methodology for multiple-channel instrumentation systems
[AIAA PAPER 92-3953] p 1133 A92-56781
Prototype instrumentation and design studies
[AD-A248378] p 736 N92-28004

INSULATED STRUCTURES
Effect of the wake flow on the soundproofing of aircraft structures p 166 A92-16824

INSULATION
Performance of uncoated AFRSI blankets during multiple Space Shuttle flights
[NASA-TM-103892] p 890 N92-29104

INTAKE SYSTEMS
A study on vortex flow control of inlet distortion in the re-engined 727-100 center inlet duct using computational fluid dynamics
[AIAA PAPER 92-0152] p 253 A92-23767
Design and calculation of performance of a subsonic inlet duct p 343 A92-28478
A study on vortex flow control on inlet distortion in the re-engined 727-100 center inlet duct using computational fluid dynamics
[NASA-TM-105321] p 179 N92-13998
Numerical investigations in three-dimensional internal flows
[NASA-CR-190498] p 998 N92-30380

INTEGRAL EQUATIONS
A boundary element method for the potential, compressible aerodynamics of bodies in arbitrary motion
p 314 A92-25098
Slenderness approximations in RCS estimation - The simplest 2-D case p 533 A92-33622
Integral equation methods for linear and nonlinear aerodynamics p 617 A92-39949
Approximate truncated balanced realizations for infinite dimensional systems p 602 N92-22493
Extension of the integral equation formulation of linearized time dependent subsonic flow
[AD-A250654] p 947 N92-31171

INTEGRATED CIRCUITS
VHDL design and simulation for airborne graphics generation requirements --- VLSI hardware description language p 902 A92-48465
The use of silicon microsensors in smart skins for aerodynamic research p 1116 A92-54348
Ultra High Speed Numerical Wind Tunnel (UHSNWT) initiative at National Aerospace Laboratory numerical simulator - second generation
[NAL-TR-1108] p 384 N92-18037
Applications of silicon hybrid multi-chip modules to avionics p 859 N92-28379

INTEGRATED MISSION CONTROL CENTER
FAA air traffic activity: FY 1990. Addendum
[AD-A241484] p 93 N92-13046
Controller response to conflict resolution advisory prototype
[PB92-190032] p 1050 N92-33596

INTEGRATED OPTICS
Potential for integrated optical circuits in advanced aircraft with fiber optic control and monitoring systems
p 856 A92-46246
Integrated optic components for advanced turbine engine control systems p 925 A92-46248

INTEGRITY
Receiver autonomous integrity monitoring (RAIM) - Techniques, performance and potential
p 638 A92-39567

INTERACTIONAL AERODYNAMICS
Triple-deck structure p 3 A92-10690
Two-phase flows at supersonic velocities
p 4 A92-10907
Emergence of coherent patterns of vortex stretching during reconnection - A scattering paradigm
p 38 A92-11041
Correlation of separation shock motion with pressure fluctuations in the incoming boundary layer
p 5 A92-11061
Numerical investigation of bleed on three-dimensional turbulent interactions due to sharp fins
p 5 A92-11062
Flight in a steady wind field p 131 A92-13696
Experimental studies of the interaction of converging axisymmetric shock waves with sharp and blunt cones in supersonic flow p 63 A92-13749
Influence of the entropy layer on the separation length in hypersonic aerodynamics in the triple-deck framework. II p 63 A92-13815
Fundamentals of applied aerogasdynamics. I - Aerodynamics of wings (profiles), airframes, and their combinations --- Russian book p 64 A92-14280
V-22 pilot-in-the-loop aeroelastic stability analysis
p 133 A92-14422
A re-examination of the aerodynamics of hovering rotors including the presence of the fuselage
p 66 A92-14446
Flow unsteadiness by weak normal shock wave/turbulent boundary layer interaction in internal flow
p 67 A92-15359
The influence of shock waves on the viscous flow field of axial compressors
[ASME PAPER 91-GT-173] p 73 A92-15608
Study of external dynamic flap loads on a 6 percent B-1B model
[ASME PAPER 91-GT-236] p 125 A92-15645
Inlet planar waves - A current perspective
[ASME PAPER 91-GT-400] p 76 A92-15730
Detailed analysis of wing-nacelle interaction for commercial transport aircraft
[ONERA, TP NO. 1991-152] p 77 A92-16122
Formulation of a simplified model of rotor-horizontal stabilizer interactions and comparison with experimental measurements
[ONERA, TP NO. 1991-157] p 77 A92-16125
Supersonic stator-rotor interaction in a turbine stage
[ONERA, TP NO. 1991-166] p 77 A92-16133
Theoretical study and prediction of BVI noise including close interactions
[ONERA, TP NO. 1991-174] p 165 A92-16138
On the interaction between first- and second-mode waves in a supersonic boundary layer
p 78 A92-16462
Self-oscillatory interaction of an underexpanded jet with an obstacle in the presence of a supersonic wake
p 79 A92-16681
Feedback mechanism of self-oscillations in the case of an underexpanded supersonic jet impinging on a plane obstacle p 79 A92-16682

Confined normal-shock/turbulent-boundary-layer interaction followed by an adverse pressure gradient
p 172 A92-18365
Helicopter air resonance modeling and suppression using active control p 204 A92-18625
CFD helps the Air Force fly right p 169 A92-20146
Direct-inverse transonic wing-design method in curvilinear coordinates including viscous interaction
p 193 A92-20202
Three-dimensional thermal structural analysis of a swept cowl leading edge subjected to skewed shock-shock interference heating p 174 A92-20306
Formation of shocks within axisymmetric nozzles
p 176 A92-20760
Analysis of circular elastic membrane wings
p 245 A92-21722
Preliminary investigation of inlet dynamic distortion and it's passive control p 245 A92-21742
Computational methods in viscous aerodynamics --- Book p 245 A92-21976
The finite volume approach for the Navier-Stokes equations p 246 A92-21980
Finite element vorticity based methods for the solution of the compressible Navier-Stokes equations
p 246 A92-21983
A fast viscous correction method for transonic aerodynamics p 247 A92-21986
Effect of turbulence modeling on dynamic stall of a NACA0012 airfoil
[AIAA PAPER 92-0027] p 248 A92-22149
Shock-boundary layer interaction control with low-profile vortex generators and passive cavity
[AIAA PAPER 92-0064] p 250 A92-22178
The Baldwin-Lomax model for separated and wake flows using the entropy envelope concept
[AIAA PAPER 92-0148] p 253 A92-23764
An algorithm for predicting the flow past fuselage-mounted engine arrangements
[AIAA PAPER 92-0151] p 253 A92-23766
Efficient panel method for vortex sheet roll-up
p 309 A92-24404
Prediction of turbulent flow behavior over a slotted flap p 309 A92-24407
Suppression of the wing-body junction vortex by body surface suction p 309 A92-24417
A simplified method for simulating steady, unsteady flow around canard wing configuration p 311 A92-24876
The rolling-up and interaction of the leading-edge and trailing-edge vortex sheets of a delta wing
p 314 A92-25101
A numerical method for solving the circulation control airfoil with wall jet p 314 A92-25103
An approach to the design of wings - The role of mathematics, physics and economics
[AIAA PAPER 92-0286] p 319 A92-25739
Hypersonic waveriders - Effects of chemically reacting flow and viscous interaction
[AIAA PAPER 92-0302] p 320 A92-25754
The effect of successive distortions of the boundary layer in a supersonic flow
[AIAA PAPER 92-0309] p 320 A92-25757
Turbulence amplification through a shock wave
[AIAA PAPER 92-0313] p 320 A92-25761
An analytical and computational investigation of shock-induced vortical flows
[AIAA PAPER 92-0316] p 321 A92-25763
A simplified model for the interaction of a rotor tip vortex with an airframe
[AIAA PAPER 92-0320] p 321 A92-25767
Turbulence modeling for high speed flows
[AIAA PAPER 92-0436] p 327 A92-26283
Quality assessment of two- and three-dimensional unstructured meshes and validation of an upwind Euler flow solver
[AIAA PAPER 92-0444] p 328 A92-26288
Experimental and theoretical studies on helicopter rotor fuselage interaction
[ONERA, TP NO. 1991-197] p 329 A92-26356
Crossing shock wave turbulent boundary layer interactions - Variable angle and shock generator length geometry effects at Mach 3
[AIAA PAPER 92-0636] p 334 A92-27014
An experimental/computational study of sharp fin induced shock wave/turbulent boundary layer interactions at Mach 5 - Experimental results
[AIAA PAPER 92-0749] p 335 A92-27093
A study on the superconvergence of Multhopp's discretization in vortex-lattice methods
p 336 A92-27381
Effect of rarefaction on the nonstationary interaction of a supersonic underexpanded jet with a perpendicular obstacle p 337 A92-27594
Determination of duty factors from experimental data in local interaction theory p 338 A92-27645
The computation of transonic viscous flow
p 338 A92-27831
Experimental investigation of the perpendicular rotor blade-vortex interaction at transonic speeds
p 340 A92-28047
Unsteady aerodynamic interaction effects on turbomachinery blade life and performance
[AIAA PAPER 92-0149] p 341 A92-28186
Investigation of oblique shock/boundary-layer bleed interaction p 344 A92-28524
Multiple normal shock wave/turbulent boundary-layer interactions p 344 A92-28527
Analysis of a 2-D airfoil motion flying in-proximity-to a wavy-wall surface - Finite difference method
p 421 A92-29517
Generalized expression of chorochronic periodicity in turbomachinery blade-row interaction
p 423 A92-30000
An asymptotic transonic theory and optimal porosity of wind tunnel walls at M greater than about 1
p 425 A92-30159
Numerical methods in the theory of boundary layer interaction with nonviscous flow p 426 A92-30185
A method for calculating the separated flow past a circular cone, taking viscous-inviscid interaction into account p 427 A92-30203
Numerical determination of the regions of existence of two types of shock-wave interaction p 428 A92-30211
Flow near the trailing edge of an airfoil
p 431 A92-31151
Structure of supersonic turbulent flow past a swept compression corner p 431 A92-31155
Experimental investigations of the vortex flow on delta wings at high incidence p 432 A92-31172
Cylinder-induced shock-wave boundary-layer interaction p 433 A92-31188
Numerical investigation of the high-speed conical flow past a sharp fin p 433 A92-31468
Effects of sweepback on unsteady separation in Mach 5 compression ramp interactions
[AIAA PAPER 92-0430] p 435 A92-31663
A preliminary study of the turbulent structures associated with unsteady separation shock motion in a Mach 5 compression ramp interaction
[AIAA PAPER 92-0744] p 436 A92-31677
Unsteady separation in sharp fin-induced shock wave/turbulent boundary layer interaction at Mach 5
[AIAA PAPER 92-0748] p 436 A92-31678
A supplement to the second-order shock-expansion method p 437 A92-31861
Interaction of jets ejected from two-dimensional nozzles with a curved surface p 438 A92-31869
Effect of the fuselage midsection ratio on the character of wing-fuselage aerodynamic interference
p 439 A92-31883
Aerodynamic effect of compression shocks on an oscillating aileron in transonic flow p 440 A92-31898
Evaluation of a Navier-Stokes prediction of a jet in a crossflow p 441 A92-32235
Role of shock dynamics in transonic flutter
[AIAA PAPER 92-2121] p 520 A92-35690
A new method for transonic static aeroelasticity problems
[AIAA PAPER 92-2123] p 589 A92-35691
Experimental design of a supersonic shock wave/vortex interaction at Mach 3 p 521 A92-35988
Separated and cavitation flows - Principal properties and computational models --- Russian book
[ISBN 5-02-014005-8] p 610 A92-36600
Reynolds stress budget in the outwash jet arising from colliding curved wall jets p 614 A92-38860
Separated flow over the protuberances in hypersonic flow p 615 A92-38907
Hypersonic turbulent separated flow past an unswept circular cylinder on a flat plate p 615 A92-38908
Prediction for the incipient separation of fin-generated three-dimensional shock wave turbulent boundary layer interactions p 615 A92-38909
Delay of wing vortex bursting by using favorable interaction of vortices p 615 A92-38910
Experimental investigation on reducing fluctuating pressures of launch vehicles by passive shock-wave/boundary-layer control p 616 A92-38916
Measurement and analysis of the flow field above a wing/body configuration p 616 A92-38917
Numerical simulation of interaction between vortexes and shocks in jet flow field p 616 A92-38925
Knowledge-based nonlinear boundary integral models of compressible viscous flows over arbitrary bodies - Taking CFD back to basics p 617 A92-39941
An experimental evaluation of some turbulence models from a three-dimensional turbulent boundary layer around a wing-body junction p 620 A92-40087
Effects of attack angle on leg portion of the horseshoe vortex around the idealized wing p 623 A92-40177
Wake effects on the prediction of transonic viscous flows around airfoils p 702 A92-41232
Coalescence of aeroelastic modes in flutter analysis
p 758 A92-41241
Hypersonic shock-wave turbulent-boundary-layer interaction flows p 703 A92-41264
Stability of plane nonorthogonal stagnation flow
p 704 A92-41291
Aerodynamics of two-shock bodies derived by the gasdynamic design method p 707 A92-42683
A study of aerophysical and dynamic characteristics using an axisymmetric flight test vehicle with a reusable nose section p 707 A92-42684
Susceptibility of a supersonic boundary layer to acoustic perturbations p 707 A92-42730
Local interaction theory --- Russian book
[ISBN 5-288-00516-8] p 779 A92-42778
Aerodynamic heating measurement in hypersonic flow
p 709 A92-43102
A thin metal model for aerodynamic heating tests of shock wave interaction p 709 A92-43103
Research on hypersonic wind tunnel methods in the 90's p 748 A92-43105
An economic approach to accurate wing design
[SAE PAPER 912008] p 789 A92-45408
Aerodynamic characteristics near the tip of a finite wing by a panel method
[SAE PAPER 912020] p 790 A92-45413
Aerodynamic heating in three-dimensional shock wave turbulent boundary layer interaction induced by sweptback sharp fins in hypersonic flows
[SAE PAPER 912044] p 791 A92-45428
Boundary-layer measurements during a parallel blade-vortex interaction
[AIAA PAPER 92-2623] p 794 A92-45495
Airfoil pressure measurements during oblique shock wave-vortex interaction in a Mach 3 stream
[AIAA PAPER 92-2631] p 795 A92-45503
Experimental development of spanwise vortex models with streamwise decay due to wall interaction
[AIAA PAPER 92-2688] p 799 A92-45535
Vortex-in-cell analysis of wing wake roll-up
[AIAA PAPER 92-2703] p 801 A92-45545
Quantification of canard and wing interactions using spatial correlation velocimetry
[AIAA PAPER 92-2687] p 807 A92-45588
Effect of a fan of rarefaction waves on the development of disturbances in a supersonic boundary layer
p 809 A92-46519
Self-induced roll oscillations of low-aspect-ratio rectangular wings p 874 A92-46802
Comment on 'Canard-wing interaction in unsteady supersonic flow' p 812 A92-46820
Two-stream, supersonic, wake flowfield behind a thick base. I - General features p 813 A92-46895
Multiple shock-shock interference on a cylindrical leading edge p 813 A92-46899
Measurement of shock-wave/boundary-layer interaction in a free-piston shock tunnel p 813 A92-46903
Interaction between a rotor tip vortex and a separated flowfield p 814 A92-46947
A Mach-scaled powered model for rotor-fuselage interactional aerodynamics and flight mechanics investigations p 847 A92-46960
The calculation of three-dimensional compressible boundary layer stability on swept wings
p 818 A92-47684
An improved multiple line-vortex method for simulation of separated vortices of slender wings
p 819 A92-47694
Aerodynamic sensitivities for subsonic lifting-surface
p 819 A92-47695
Calculation of fully three-dimensional separated flows with an unsteady viscous-inviscid interaction method
[ONERA, TP NO. 1992-1] p 821 A92-48577
Computational analysis of ramjet engine inlet interaction
[AIAA PAPER 92-3102] p 824 A92-48744
Vane-blade interaction in a transonic turbine. I - Aerodynamics
[AIAA PAPER 92-3323] p 825 A92-48906
Physical model of the swept shock wave/boundary-layer interaction flowfield p 935 A92-50312
A direct viscous-inviscid interaction method for the flow calculation around airfoils p 936 A92-52028
Development of a real-time simulation of a ship-correlated airwake model interfaced with a rotorcraft dynamic model
[AIAA PAPER 92-4149] p 1007 A92-52440
Flow of a rarefied gas past a two-dimensional body of an arbitrary shape at small Mach numbers
p 937 A92-52726
Hypersonic flow calculations around a 3D delta wing at low Knudsen numbers p 937 A92-52734
Heat transfer to a delta wing and two waverider wings in rarefied hypersonic flow p 937 A92-52748

Thermal and chemical nonequilibrium viscous shock layer flows over a blunt body at high altitudes
p 938 A92-52749
Influence of atmospheric rarefaction on aerodynamic characteristics of flying vehicles p 938 A92-52750
One-dimensional kinetic model for flows near a stagnation point of a highly cooled body in hypersonic rarefied streams p 938 A92-52751
Influence of internal molecular degrees of freedom on the hypersonic rarefied gas flow about a conical body
p 938 A92-52752
Rarefied gas flow around a disc with different angles of attack p 938 A92-52753
Approximate aerodynamic analysis for complicated bodies in rarefied gas flows p 938 A92-52754
Experiments on separation at a compression corner in rarefied hypersonic flows p 938 A92-52755
Hypersonic merged layer blunt body flows with wakes
p 939 A92-52757
Enhancements and applications of DSMC for hypersonic rarefied flows p 939 A92-52761
Force and heat transfer on a disc in rarefied flow
p 939 A92-52764
Direct simulation of vortex shedding in dilute gas flows past bluff bodies p 939 A92-52766
Aerodynamics of complex shape bodies within a wide range of supersonic flows of rarefied gases
p 939 A92-52767
Monte Carlo simulation of the hypersonic mon- and diatomic gas flow past a disk at an angle of attack
p 939 A92-52770
DSMC simulation of hypersonic flows past 2-dimensional bodies p 939 A92-52772
Application of the DSMC method to hypersonic flow about a delta wing p 940 A92-52775
Aerodynamic characteristics of a standard corrugated body in a free-molecular flow p 940 A92-52818
Measurement of the freestream density for re-entry vehicles - A design study p 940 A92-52821
The application of a theoretical blade sailing model to predict the behaviour of articulated helicopter rotors
p 960 A92-52849
Calculation of the transonic full-potential flowfield about 3D fuselage p 941 A92-53021
The relation among the general unsteady aerodynamic coefficients of a wing in subsonic and supersonic speed
p 941 A92-53022
Experimental investigation on turbulent phenomena in three-dimensional shock wave/turbulent boundary layer interaction induced by blunt fin p 1018 A92-53557
Interaction between a body flying at a supersonic velocity and a point explosion p 1019 A92-53867
Experimental study on three-dimensional shock wave-turbulent boundary layer interaction induced by protuberance p 1019 A92-53997
Thermal paints for shock/boundary layer interaction in inlet flows
[AIAA PAPER 92-3626] p 1113 A92-54093
An experimental examination of the effects of incoming boundary layer modifications on the dynamics of a turbulent compression corner interaction
[AIAA PAPER 92-3667] p 1022 A92-54111
A laser fluorescence anemometer system for the Langley 16- by 24-inch water tunnel
p 1092 A92-54347
The interaction between a high-frequency gust and a blade row p 1135 A92-54484
Active control of asymmetric vortical flows around cones using injection and heating
[AIAA PAPER 92-4426] p 1025 A92-55350
Navier-Stokes prediction of large-amplitude delta-wing roll oscillations characterizing wing rock
[AIAA PAPER 92-4428] p 1080 A92-55352
Vortical flow control on a wing-body combination using tangential blowing
[AIAA PAPER 92-4430] p 1081 A92-55354
Tow-tank study of nonlinear aerodynamics of a 2-D airfoil
[AIAA PAPER 92-4499] p 1026 A92-55367
Robust identification of nonlinear aerodynamic model structure
[AIAA PAPER 92-4503] p 1081 A92-55370
Approximate aerodynamic analysis of jet interaction
[AIAA PAPER 92-4640] p 1027 A92-55387
Force production mechanisms of a tangential jet on bodies at high alpha
[AIAA PAPER 92-4648] p 1082 A92-55393
Unsteady shock-vortex interaction on a flexible delta wing p 1030 A92-56157
Euler/experiment correlation of a generic fighter
p 1031 A92-56164
Trimming rotor blades with periodically deflecting trailing edge flaps p 1085 A92-56283
Current European research activities in helicopter interactional aerodynamics p 1058 A92-56330
Wind tunnel blockage effects on slender wings undergoing large amplitude motions
[AIAA PAPER 92-3926] p 1096 A92-56757
A multi-diagnostic approach to testing V/STOL craft
[AIAA PAPER 92-4008] p 1099 A92-56831
Numerical modeling of transonic juncture flow
[AIAA PAPER 92-4036] p 1035 A92-56858
Increasing the accuracy of the Godunov scheme for calculating steady-state supersonic gas flows by solving the generalized Riemann problem p 1035 A92-57499
Airframe noise p 55 N92-10605
Experimental investigation of the effects of blowing on bursting of strake vortices
[AD-A240256] p 13 N92-10985
Studies of aerothermal loads generated in regions of shock/shock interaction in hypersonic flow
[NASA-CR-181893] p 43 N92-11319
Flow visualization and flow field measurements of a 1/12 scale tilt rotor aircraft in hover
[NASA-CR-189456] p 82 N92-11983
An experimental investigation of vortex flaps on a canard combat-aircraft configuration p 87 N92-13023
Effect of solidity and inclination on propeller-nacelle force coefficients
[NASA-TM-4316] p 90 N92-13038
Wind tunnel investigation of vortex flows on F/A-18 configuration at subsonic through transonic speed
[NASA-TP-3111] p 179 N92-14968
Simulation requirements for RCS plume: Flowfield interaction modelling on a winged reentry vehicle
p 181 N92-14985
Experimental investigation of transverse jet effects related to hypersonic space vehicles
p 182 N92-14995
Contribution of fin and tailplane to sideforce and yawing moment derivatives due to sideslip at supersonic speeds at low angles of attack
[ESDU-91031] p 259 N92-15971
Installation effects of wing-mounted turbofan nacelle-pylons on a 1/17-scale, twin-engine, low-wing transport model
[NASA-TP-3168] p 346 N92-19002
Integrated aerodynamic-structural-control wing design
p 349 N92-19698
Flowfield analysis of modern helicopter rotors in hover by Navier-Stokes method
[AD-A245011] p 446 N92-21333
A new method for simulating atmospheric turbulence for rotorcraft applications p 464 N92-21956
Inlets, ducts, and nozzles p 593 N92-22523
A study of viscous interaction effects on hypersonic waveriders
[NASA-CR-189587] p 625 N92-24680
Experimental evaluation of a flat wake theory for predicting rotor inflow-wake velocities
[NASA-TM-4334] p 630 N92-24882
Subsonic investigations of vortex interaction control for enhanced high-alpha aerodynamics of a chine forebody/Delta wing configuration
[NASA-CR-189641] p 715 N92-26652
Further development of the CANAERO computer code to include propulsor modelling
[DREA-CR-90-425] p 1038 N92-32811
Effect of afterbody geometry on aerodynamic characteristics of isolated nonaxisymmetric afterbodies at transonic Mach numbers
[NASA-TP-3236] p 1041 N92-33706

INTERACTIONS
Non-linear interactions in homogeneous turbulence with and without background rotation p 912 N92-30044

INTERACTIVE CONTROL
Networked simulation of multiple aircraft using Semi-Automated Forces
[AIAA PAPER 92-4170] p 1008 A92-52455
An interactive multi-block grid generation system
p 691 N92-24419

INTERCEPTION
A method of passive range determination using only two bearing measurements
[AD-D015182] p 455 N92-20834

INTERCEPTORS
Transient aerodynamics of a high dynamic pressure shroud separation for a ground-based interceptor missile
[AIAA PAPER 92-2820] p 705 A92-41348
Two variations of certainty control
p 918 A92-46762

INTERFACE STABILITY
Interfacial instability between a liquid film and the surrounding compressible gas
[AIAA PAPER 92-0461] p 395 A92-26302
Interlaminar fracture characteristics of bonding concepts for thermoplastic primary structures p 758 A92-41282

INTERFACES
A CLIPS-based tool for aircraft pilot-vehicle interface design p 303 N92-16605
MULTIRAD
[AD-A244211] p 412 N92-19247

INTERFACIAL TENSION
Numerical simulation of droplet deformation in convective flows p 670 A92-36844
Fundamental studies on Marangoni convection related to Bridgman crystal growth p 1111 A92-53758
Flow induction by pressure forces
[AIAA PAPER 92-3571] p 1067 A92-54060
Stokes flows in superposed immiscible liquids with horizontal heating
[IAF PAPER 92-0909] p 1123 A92-57288

INTERFERENCE
Exposures from headset interference tones
[AD-A247175] p 1136 N92-32697

INTERFERENCE DRAG
Aircraft drag reduction p 717 N92-27709
Applications of a direct/iterative design method to complex transonic configurations
[NASA-TP-3234] p 1039 N92-33484

INTERFERENCE IMMUNITY
Distributed flight control system using fiber distributed data interface (FDDI) p 976 A92-51004

INTERFEROMETERS
Simultaneous imaging and interferometric turbule visualization in a high-velocity mixing/shear layer
p 896 A92-45130
Combined VISAR and flash x ray testing techniques
[DE92-004732] p 385 N92-18290
Study of optical techniques for the Ames unitary wind tunnels. Part 3: Angle of attack
[NASA-CR-190541] p 888 N92-29655
Electro optical system to measure strains at high temperature
[NASA-CR-190450] p 1127 N92-33696

INTERFEROMETRY
GPS interferometric attitude and heading determination - Initial flight test results p 454 A92-30023
GPS interferometric attitude and heading determination - Flight test results p 650 A92-39561
GPS interferometric attitude and heading determination: Initial flight test results p 269 N92-17994
A quantitative study of unsteady compressible flow on an oscillating airfoil
[AD-A244572] p 445 N92-21012
Interferograms, schlieren, and shadowgraphs constructed from real- and ideal-gas, two- and three-dimensional computed flowfields
[NASA-CR-190054] p 446 N92-21356

INTERLAMINAR STRESS
Composite beam analysis linear analysis of naturally curved and twisted anisotropic beams
[AD-A252652] p 999 N92-30766

INTERMETALLICS
Intermetallic and ceramic matrix composites for 815 to 1370 C (1500 to 2500 F) gas turbine engine applications
p 141 A92-15128
Thermo-mechanical fatigue crack growth in aircraft engine materials p 213 A92-19799
A preliminary study of the microstructure-property relationships in cast gamma titanium aluminide alloys
p 487 A92-30596
Manufacture of XD gamma titanium aluminide airfoils via investment casting and machining
p 494 A92-30603
Development of intermetallic materials for aerospace systems p 754 A92-41874
Axial alignment of short-fiber titanium aluminide composites by directional solidification
p 892 A92-46838
Development of a new generation of high-temperature composite materials p 578 N92-22515

INTERNAL COMBUSTION ENGINES
Development of natural gas rotary engines
[PB92-149665] p 765 N92-26816

INTERNAL COMPRESSION INLETS
Experimental study of the swirling flow in the internal volute of a centrifugal compressor
[ASME PAPER 91-GT-7] p 67 A92-15505
Numerical study of the effects of reverse sweep on scramjet inlet performance p 611 A92-36979

INTERNAL PRESSURE
Composite laminated shells under internal pressure
p 758 A92-41296

INTERNATIONAL COOPERATION
International survey of scientific ballooning support organizations
[AIAA PAPER 91-3677] p 1 A92-11022
China-Soviet long duration balloon flight project
[AIAA PAPER 91-3678] p 1 A92-11036
Legal capacity of Eurocontrol to ensure smooth aviation in Europe p 167 A92-16134
Status of the NH90 European Helicopter Program
p 113 A92-16676

Integrated use of GPS and GLONASS in civil aviation navigation. I - Coverage and data models
p 99 A92-16950
Soviet CFD - An international perspective
p 233 A92-20150
Pratt & Whitney PW300 for general aviation
p 277 A92-21012
International standardisation of regulations for gust loading calculations p 270 A92-22473
Russians want U.S. to join scramjet tests
p 472 A92-32296
GE, Snecma consider venture to develop uprated Perm PS-90 p 472 A92-32297
A European perspective on the co-operative air traffic management concept p 531 A92-33427
Perspectives on the cooperative air traffic management concept - Far East/Pacific point of view
p 606 A92-33428
CATMAC - A way to integrate ground ATC and airborne systems p 531 A92-33429
European ATC integration faces dual challenges
p 534 A92-36076
Internationalization of telemetry systems
p 920 A92-47535
German-GUS cooperation in civil aviation
p 785 A92-47592
Study on international cooperative test facilities for future SST/HST
[AIAA PAPER 92-3945] p 1097 A92-56775
System considerations, projected requirements and applications for aeronautical mobile satellite communications for air traffic services
p 677 N92-24163
Preparation for a new plane (A 320): Experience reviewed p 1010 N92-30954
An international aerospace information system: A cooperative opportunity
[NASA-TM-108171] p 1142 N92-33237

INTERNATIONAL LAW
Opening closed skies - The prospects for further liberalization of trade in international air transport services p 697 A92-39244
Joint Aviation Authorities: Development of an international standard for safety regulation - The first steps are being taken by the JAA p 781 A92-43548

INTERNATIONAL TRADE
Aerospace technology: Technical data and information on foreign test facilities
[GAO/NSIAD-90-71FS] p 139 N92-13076

INTERPLANETARY DUST
JPRS report: Science and technology. Central Eurasia: Space
[JPRS-USP-92-002] p 575 N92-23705

INTERPOLATION
Computational fluid dynamics p 177 N92-13979
The application of statistical estimation techniques to terrain modeling
[AD-A243799] p 409 N92-19231
An analytical approach to grid sensitivity analysis for NACA four-digit wing sections
[NASA-CR-190251] p 631 N92-25175
An interactive grid generation technique for turbomachinery p 659 N92-25717
A surface definition code for turbine blade surfaces
[DE92-010574] p 1004 N92-31498
Global/local methods research using the CSM testbed
p 1107 N92-32528

INTERPROCESSOR COMMUNICATION
Putting ten pounds of avionics in a one pound package (Can we do it again?)
[AIAA PAPER 91-3766] p 197 A92-17628
Testing and analysis of a 'smart' interface to connect two complex avionics bus systems without significant modification to the software of either system
p 964 A92-49254
Timing analysis of parallel algorithms on a MIMD multiprocessor
[ITN-92-85153] p 510 N92-20905
Application of VME-technology on an airborne data link processor unit
[NLR-MP-88040-U] p 841 N92-29615

INVARIANCE
A time approach to robustness of LTI systems with structured uncertainty and unmodelled dynamics --- linear time-invariant p 48 A92-11356
Binary optical filters for scale invariant pattern recognition
[NASA-TM-103902] p 853 N92-28910

INVENTORIES
Developing robust support structures for high-technology subsystems: The AH-64 Apache helicopter
[AD-A252773] p 1017 N92-33499

INVENTORY CONTROLS
Aviation Diagnostics And Maintenance (ADAM) system preliminary concept of operation and functional description
[AD-A242598] p 170 N92-14966

INVERSE KINEMATICS
Inverse control problems: Mathematical preliminaries, system theoretical approaches, and their applications to aircraft dynamics
[LR-665] p 923 N92-28581

INVERSIONS
Inverse problems and imaging (Pitman research notes in mathematics series Number 245)
[AD-A240333] p 53 N92-11737
Analytical/numerical matching and periodic inversion: Two advances in free wake analysis
p 178 N92-13994
Nonlinear dynamic-inversion flight control of supermaneuverable aircraft p 1062 N92-33953

INVERTED CONVERTERS (DC TO AC)
Testing and evaluation of the Vanner electrical inverters, models 24-1500 and SP 00112
[AD-A241914] p 299 N92-17216

INVESTMENT CASTING
Manufacturing technology methodology for propulsion system parts
[AIAA PAPER 92-3525] p 906 A92-49048

INVESTMENTS
Aviation system: Capital investment plan
p 636 N92-25297

INVISCID FLOW
A spatial marching technique for the inviscid blunt body problem p 4 A92-10691
Topology of steady flows of low viscosity fluids
p 38 A92-11219
Secondary separation from a slender wing
p 62 A92-13448
Transonic and supersonic inviscid computations in cascades using adaptive unstructured meshes
[ASME PAPER 91-GT-312] p 75 A92-15689
Inviscid analysis of a dual mode scramjet inlet
p 80 A92-17198
Analysis of spiraling vortical flows around slender delta wings moving in an inviscid medium p 173 A92-18900
CFD helps the Air Force fly right p 169 A92-20146
Inviscid drag prediction for transonic transport wings using a full-potential method p 174 A92-20212
Engineering calculations of three-dimensional inviscid hypersonic flowfields p 175 A92-20378
Nonequilibrium hypersonic inviscid steady flows
p 176 A92-20737
Application of a universe-series code for inviscid flow over complex 3-dimensional configurations
[AIAA PAPER 92-0150] p 253 A92-23765
Space-marching calculations of hypersonic inviscid flowfield p 313 A92-25040
Study of numerical computation of inviscid flow field about complex configuration of re-entry vehicle
p 313 A92-25041
Numerical simulation of inviscid flow over a complicated body using an overlapping grid technique
p 313 A92-25043
Recent progress in finite element method and boundary integral equation method for nonviscous transonic flows
p 314 A92-25127
Analysis of a 2-D airfoil motion flying in-proximity-to a wavy-wall surface-lifting surface-scheme
p 315 A92-25506
Multidomain spectral solutions of high-speed flows over blunt cones
[AIAA PAPER 92-0324] p 322 A92-25771
A turbulence model for iced airfoils and its validation
[AIAA PAPER 92-0417] p 326 A92-26267
An engineering aerodynamic heating method for hypersonic flow
[AIAA PAPER 92-0499] p 329 A92-26327
An unsteady Euler scheme for the analysis of ducted propellers
[AIAA PAPER 92-0522] p 332 A92-26947
Numerical experiments on a new class of nonoscillatory schemes
[AIAA PAPER 92-0421] p 341 A92-28193
Inviscid and viscous transonic flows in cascades using an implicit upwind algorithm p 344 A92-28522
Computations of a transonic flow about an airfoil in a wind tunnel with porous walls p 423 A92-30128
Numerical methods in the theory of boundary layer interaction with nonviscous flow p 426 A92-30185
A method for calculating the separated flow past a circular cone, taking viscous-inviscid interaction into account p 427 A92-30203
A numerical solution of inviscid transonic flow using the Boltzmann equation p 443 A92-32504
An inverse inviscid method for the design of quasi-three dimensional turbomachinery cascades
p 523 A92-36033
Inviscid and viscous quasi-three-dimensional flow solutions in a transonic turbine cascade
p 523 A92-36035
Spectral solution of inviscid supersonic flows over wedges and axisymmetric cones p 524 A92-36359
Spatial adaptation of unstructured meshes for unsteady aerodynamic flow computations p 610 A92-36838
A high-resolution Euler solver based on multigrid, semi-coarsening, and defect correction
p 671 A92-37868
Oblique shock wave with sweep p 613 A92-38370
The numerical simulation of transonic inviscid flow over oscillating airfoils p 616 A92-38918
Behavior of asymmetric unstable modes of a trailing line vortex near the upper neutral curve p 617 A92-39340
CFD calculations of closely coupled scissor wings - Inviscid, viscous, and vortex lattice with rollup results
[SAE PAPER 912150] p 619 A92-39986
Engineering aerodynamic heating method for hypersonic flow p 705 A92-41539
The inviscid stability of supersonic flow past heated or cooled axisymmetric bodies p 712 A92-44363
Solution of the parabolized Navier-Stokes equations using Osher's upwind scheme p 713 A92-44371
An unfactored implicit scheme for 3D inviscid transonic flows
[AIAA PAPER 92-2668] p 798 A92-45523
Comparison of interferometric measurements with 3-D Euler computations for circular cones in supersonic flow
[AIAA PAPER 92-2691] p 800 A92-45538
Transonic unsteady inviscid and viscous flow's simulation around 2-D moving bodies
[AIAA PAPER 92-2704] p 801 A92-45546
Numerical simulations using a dynamic solution-adaptive grid algorithm, with applications to unsteady internal flows
[AIAA PAPER 92-2719] p 803 A92-45557
Calculation of potential flow around airfoils using a discrete vortex method p 808 A92-45827
The inviscid compressible Goertler problem in three-dimensional boundary layers p 809 A92-46441
Prediction of inviscid supersonic/hypersonic aircraft flowfields p 810 A92-46785
Simulation of transonic flow over twin-jet transport aircraft p 811 A92-46793
Some exact and numerical results for plane steady sheared flow of an incompressible inviscid fluid
p 821 A92-48019
Development of an efficient analysis for high Reynolds number inviscid/viscid interactions in cascades
[AIAA PAPER 92-3073] p 823 A92-48723
A fast, uncoupled, compressible, two-dimensional, unsteady boundary layer algorithm with separation for engine inlets
[AIAA PAPER 92-3082] p 823 A92-48729
Interface of an uncoupled boundary layer algorithm with an inviscid core flow algorithm for unsteady supersonic engine inlets
[AIAA PAPER 92-3083] p 823 A92-48730
The simulation of inviscid, compressible flows using an upwind kinetic method on unstructured grids
p 933 A92-49515
A complete boundary integral formulation for steady compressible inviscid flows governed by nonlinear equations p 934 A92-50211
A direct viscous-inviscid interaction method for the flow calculation around airfoils p 936 A92-52028
Brownian-motion limited aerodynamic focusing of heavy molecules p 995 A92-52722
Supersonic flow past pointed-nose thin airfoils
p 940 A92-52844
The numerical simulation of flow about installed aero engine nacelle using a finite element Euler solver on unstructured meshes p 941 A92-52848
Solution of Euler equations with unstructured mesh - 3-D case p 941 A92-52973
Discussion of improved transonic potential method
p 942 A92-53290
A numerical investigation of axial flow compressor casing treatment p 942 A92-53381
The behaviour of the pressure temperature and density in an inviscid unsteady transonic axisymmetric flow with shock waves p 1018 A92-53553
A comparison of the calculated and experimental off-design performance of a radial flow turbine
[AIAA PAPER 92-3069] p 1020 A92-54004
Efficient methods for inviscid non-equilibrium hypersonic flow fields p 1024 A92-54571
Methodology for calculating aerodynamic sensitivity derivatives p 1024 A92-54911
A multiblock flow solver for inviscid hypersonic flows
p 181 N92-14986
Hypersonic inviscid flow field simulations around reentry vehicles with flap deflection p 184 N92-15025
A turbulence model for iced airfoils and its validation
[NASA-TM-105373] p 186 N92-15052

Supersonic propulsion simulation by incorporating component models in the large perturbation inlet (LAPIN) computer code
[NASA-TM-105193] p 279 N92-15993
Application of program LAURA to perfect gas shock tube flows: A parametric study
[NASA-TM-104190] p 298 N92-17002
Zonal solutions for a double-ellipse in a hypersonic flowfield
[AERO-REPT-9009] p 345 N92-18233
A comparative study of numerical versus analytical waverider solutions
[AD-A244183] p 347 N92-19304
An inviscid stability analysis of unbounded supersonic mixing layer flows p 443 N92-20332
Inviscid drag prediction for transonic transport wings using a full-potential method
[NLR-TP-89365-U] p 444 N92-20473
Development of a steady potential solver for use with linearized, unsteady aerodynamic analyses
[NASA-TM-105288] p 473 N92-20525
Three-dimensional simulations of hypersonic flows
[MBB-UK-0155-89-PUB] p 447 N92-21703
A theoretical investigation of the induced drag of wing of finite aspect ratio
[CUED/A-AERO/TR-17(1991)] p 525 N92-22193
Three-dimensional multigrid algorithm for the Euler and the thin-layer Navier-Stokes equations
[PB92-134329] p 602 N92-22216
Modeling of linear isentropic flow systems
p 593 N92-22495
Improved shock-capturing of Jameson's scheme for the Euler equations
[PB92-148758] p 596 N92-23251
Computations of unsteady multistage turbomachinery flows p 562 N92-23671
Numerical simulations of wakes, blade-vortex interaction, flutter, and flutter suppression by feedback control p 597 N92-23997
Periodic Euler and Navier-Stokes solutions about oscillating airfoils p 626 N92-24850
TVD finite-difference solutions of nonequilibrium vibrationally relaxing and chemically reacting gaseous flows p 626 N92-24854
On the coupling of Euler/boundary-layer equations
p 627 N92-24859
An engineering method for interactive inviscid-boundary layers in three-dimensional hypersonic flows
[NASA-TM-107838] p 632 N92-25279
A high angle of attack inviscid shuttle orbiter computation
[NASA-TM-107606] p 685 N92-25964
Performance prediction and design of maximum thrust planar supersonic nozzles using a flux-difference-splitting technique p 738 N92-26480
Cross-flow instabilities and pressure gradients in boundary layers p 767 N92-26922
Interface of an uncoupled boundary layer algorithm with an inviscid core flow algorithm for unsteady supersonic engine inlets
[NASA-TM-105684] p 739 N92-27037
Aerodynamic interference between stores
[AD-A247207] p 715 N92-27172
A fast, uncoupled, compressible, two-dimensional, unsteady boundary layer algorithm with separation for engine inlets
[NASA-TM-105686] p 770 N92-27653
NLR inviscid transonic unsteady loads prediction methods in aeroelasticity p 720 N92-27947
Development of an unsteady three-dimensional viscous-inviscid interaction numerical method for the calculation of airfoils vibration
[ONERA-RSF-7/3617-AY-022A] p 830 N92-29206
A comparison of the calculated and experimental off-design performance of a radial flow turbine
[NASA-CR-189207] p 831 N92-29402
A computational investigation of airfoil stall flutter
[AD-A247302] p 947 N92-31300
Investigation of advancing front method for generating unstructured grid
[NASA-CR-190902] p 1128 N92-34043
Analysis of iced wings
[NASA-TM-105773] p 1042 N92-34144

IODINE
An iodine hypersonic wind tunnel for the study of nonequilibrium reacting flows
[AIAA PAPER 92-0566] p 383 A92-26974

ION BEAMS
Report on the workshop on Ion Implantation and Ion Beam Assisted Deposition
[AD-A250561] p 927 N92-28923

ION CURRENTS
Ionospheric plasma flow over large high-voltage space platforms. I - Ion-plasma-time scale interactions of a plate at zero angle of attack. II - The formation and structure of plasma wake p 779 A92-41359

ION IMPACT
The formation and structure of plasma wakes behind large high-voltage space platforms in ionosphere
[AIAA PAPER 92-0577] p 407 A92-26984

ION IMPLANTATION
Improving the properties of titanium alloys by ion implantation p 289 A92-22771
Report on the workshop on Ion Implantation and Ion Beam Assisted Deposition
[AD-A250561] p 927 N92-28923

ION PROBES
Prototype instrumentation and design studies
[AD-A248378] p 736 N92-28004

IONIZATION
Hypersonic plasma predictions at nonzero angle of attack
[AIAA PAPER 92-3027] p 925 A92-47028

IONIZING RADIATION
Effects of ionizing and nonionizing radiation on aircraft
p 295 A92-23301
Criteria for the operation of federally-owned secondary calibration laboratories (ionizing radiation)
[PB92-112481] p 485 N92-21777

IONOSPHERIC SOUNDING
A ionospheric-sounding experiment from an aircraft
p 160 A92-13809

IONS
Prototype instrumentation and design studies
[AD-A248378] p 736 N92-28004

IPAD
Development of pre- and post-processor system for structural analysis
[NAL-TM-628] p 681 N92-25403

IRON ALLOYS
Diffusion bonding a creep-resistant Fe-ODS alloy
p 1117 A92-54868

IRRADIATION
Criteria for the operation of federally-owned secondary calibration laboratories (ionizing radiation)
[PB92-112481] p 485 N92-21777

ISENTROPIC PROCESSES
A computational study of flow past bodies and heat transfer for isentropic compression flows
p 425 A92-30158
Modeling of linear isentropic flow systems
p 593 N92-22495

ISOLATION
Active thermal isolation for temperature responsive sensors
[NASA-CASE-LAR-14612-1] p 911 N92-29954

ISOLATORS
Active thermal isolation for temperature responsive sensors
[NASA-CASE-LAR-14612-1] p 911 N92-29954

ISOPARAMETRIC FINITE ELEMENTS
Structural and aerodynamic data transformation using inverse isoparametric mapping p 758 A92-41242

ISOTHERMAL FLOW
Isothermal flow fields in a research combustor for lean blowout studies
[ASME PAPER 91-GT-37] p 121 A92-15520
Isothermal modeling of gas turbine combustors - Computational study p 129 A92-17203
A numerical study of isothermal flows of a slit V-gutter
[AIAA PAPER 92-0100] p 293 A92-22203
Similarity in supersonic mixing layers
p 611 A92-36842

ISOTHERMAL PROCESSES
Isothermal aging of IM7/8320 and IM7/5260
[NASA-TM-107666] p 1110 N92-33423

ISOTROPIC TURBULENCE
Simulation and modeling of homogeneous compressible turbulence under isotropic mean compression
p 622 A92-40134
Some problems on atmospheric turbulence spectrum and aircraft response p 975 A92-50235
The modelling of turbulence and downbursts for flight simulators
[UTIAS-339] p 161 N92-12373
A preliminary experimental investigation of local isotropy in high-Reynolds-number turbulence
p 912 N92-30042

ITERATION
Aerodynamic aircraft design methods and their notable applications: Survey of the activity in Japan
p 193 N92-13930
Efficient and robust design optimization of transonic airfoils p 528 N92-23717

ITERATIVE SOLUTION
Closed-loop identification and iterative controller design p 48 A92-11362
Similarity transformations for compressor blading
[ASME PAPER 91-GT-123] p 70 A92-15568
Numerical methods in the theory of boundary layer interaction with nonviscous flow p 426 A92-30185
Acoustic spinning-mode analysis by iterative threshold method applied to a helicopter turboshaft engine
[ONERA, TP NO. 1992-41] p 926 A92-48602
Navier-Stokes computations of horseshoe vortex flows
p 990 A92-49516
Transonic flow calculation of Euler equations by implicit iterating scheme with flux splitting p 934 A92-50215
Efficient iterative methods for the transonic small disturbance equation p 1025 A92-54933
An incremental strategy for calculating consistent discrete CFD sensitivity derivatives
[NASA-TM-104207] p 625 N92-24681
Iterative methods for large scale static analysis of structures on a scalable multiprocessor supercomputer
[NASA-CR-190369] p 692 N92-26018

J

J-85 ENGINE
Numerical verification of NISA 2 finite element analysis of the cracked 5th stage compressor disc of J-85 jet engine
[NRC-LTR-ST-1792] p 129 N92-11997

JAPAN
Aerospace plane technology: Research and development efforts in Japan and Australia
[AD-A241641] p 62 N92-12991
Aerodynamic aircraft design methods and their notable applications: Survey of the activity in Japan
p 193 N92-13930

JAPANESE SPACE PROGRAM
Japan pushes high speed research
p 1015 A92-53434
Concepts of flight experiments for HOPE development
p 1103 A92-53635

JAPANESE SPACECRAFT
'Spaceplanes' R&D status of Japan
[AIAA PAPER 91-5002] p 209 A92-17802
HOPE looks to CFD for help --- NASDA's H-II Orbiting Plane p 386 A92-24910
Outline and discussion of the cooling loop of the heating control system in the exposed facility of the Japanese Experiment Module (JEM) p 574 A92-35610
Numerical simulation of hypersonic viscous flow for the design of H-II orbiting plane (HOPE)
p 612 A92-37549
Experiments on aeronautical satellite communications using ETS-V satellite p 639 A92-40187
Engineering and technology Japanese aircraft/spacecraft p 699 A92-41781
Calculations for aerodynamic characteristics of HOPE type vehicle in subsonic and hypersonic flow
p 1018 A92-53560
Design of orbital re-entry experiment vehicle and outline of the experiment p 667 N92-25374
Study of potassium turbine electric generator system
p 1129 N92-33794

JET AIRCRAFT
Implementation and usage of the RJ program Data Acquisition System Ground Station p 210 A92-19257
Beriev Be-42 - A unique jet-propelled seaplane
p 269 A92-21010
A note on thrust control for jetliner during approach
p 457 A92-29518
Cold-cycle pressure-jet helicopters: Ventures, designs, and developments. III - Costs and developments
p 458 A92-29675
Ageing airliner census - Still flying safely
p 634 A92-38374
The landing equipment of a high-tech aircraft
p 730 A92-43149
Jet-powered V/STOL aircraft - Lessons learned
p 841 A92-45304
Aircraft Command in Emergency Situations (ACES)
[SAE PAPER 912039] p 835 A92-45424
Recent CFD applications on jet transport configurations
[AIAA PAPER 92-2658] p 844 A92-45519
Effect of throat contouring on two-dimensional converging-diverging nozzles using URS method
[AIAA PAPER 92-2659] p 797 A92-45520
Optimum cruise lift coefficient in initial design of jet aircraft p 845 A92-46806
Optimization of constant altitude-constant airspeed flight of turbojet aircraft p 845 A92-46815
Interactive algebraic mesh generation for twin jet transport aircraft p 817 A92-47064
Steels for aerospace applications p 986 A92-52983
Ferrundi Company supplies 4500 model head up display devices to India's MIG-21 aircraft
[AD-A241044] p 229 N92-15367
Window cooling for high speed flight
[AD-D015145] p 344 N92-18193
Structural airworthiness of aging Boeing jet transports
p 362 N92-18590

Natural cycles, gases p 408 N92-19123
Analysis of an advanced fighter aircraft using jet flap techniques and the vortex lattice method
[AD-A244051] p 366 N92-19185
Scorpion: Close Air Support (CAS) aircraft
[NASA-CR-189974] p 462 N92-20664
Radiant energy power source for jet aircraft
[DE92-008726] p 648 N92-24556
Aircraft photovoltaic power-generating system
p 775 N92-26581
Effective cueing during approach and touchdown: Comparison with flight p 886 N92-28552
On the estimation of jet-induced fountain lift and additional suckdown in hover for two-jet configurations
[NASA-TM-102268] p 1040 N92-33618

JET AIRCRAFT NOISE
The sonic boom and problems related to supersonic flights of military aircraft
[ONERA, TP NO. 1991-162] p 77 A92-16129
NASA research program directed at reducing supersonic transport noise p 61 A92-16150
Combat aircraft jet engine noise studies
[ONERA, TP NO. 1991-192] p 415 A92-26353
Broadband shock associated noise from supersonic jets measured by a ground observer
[AIAA PAPER 92-0502] p 416 A92-26931
Structure-borne noise transmission in the Propfan Test Assessment aircraft p 778 A92-41240
Silent solutions --- noise suppression for Stage 3 corporate fleets p 970 A92-53120
Full Navier-Stokes analysis of a two-dimensional mixer/ejector nozzle for noise suppression
[AIAA PAPER 92-3570] p 1067 A92-54059
Broadband shock associated noise from supersonic jets measured by a ground observer p 1135 A92-54909
Jet noise classical theory and experiments
p 54 N92-10602
Noise from turbulent shear flows p 55 N92-10603
Jet noise generated by large-scale coherent motion
p 55 N92-10604
Aeroacoustics of flight vehicles: Theory and practice. Volume 2: Noise control
[NASA-RP-1258-VOL-2] p 235 N92-14779
Jet noise suppression p 236 N92-14784
Quiet aircraft design and operational characteristics
p 236 N92-14787
Direct computation of turbulence and noise
[NASA-CR-187616] p 236 N92-14788
An introduction to high speed aircraft noise prediction
[NASA-CR-189582] p 416 N92-19672
A sophisticated, multi-channel data acquisition and processing system for high frequency noise research
[NASA-CR-189137] p 696 N92-24688
Full Navier-Stokes analysis of a two-dimensional mixer/ejector nozzle for noise suppression
[NASA-TM-105715] p 868 N92-28419
Jet aircraft noise at high subsonic flight Mach numbers
[DLR-FB-91-28] p 928 N92-29997
Acoustic loads prediction on jet aircraft
p 1136 N92-32949
MD-80 aft cabin noise control: A case history
p 1137 N92-32950
Pilots noise exposure during a Boeing 747-400 round trip: Ambient noise and acoustic-head recording and analysis of data p 1137 N92-32960
Pilot noise exposure during a Boeing 747-400 round trip: Judgement of noise and analysis in respect to hearing impairment of pilots p 1138 N92-32961

JET BOUNDARIES
Numerical simulation of opposing sonic jets
p 524 A92-36357

JET CONTROL
Experimental investigation of transverse jet effects related to hypersonic space vehicles
p 182 N92-14995

JET ENGINE FUELS
Evaluation of the fungicide properties of antifreeze additives for jet fuels p 141 A92-15070
Thermal management of hypersonic aircraft using noncryogenic fuels
[SAE PAPER 911443] p 270 A92-21839
High temperature, thermally stable JP fuels - An overview
[AIAA PAPER 92-0683] p 389 A92-27050
High density fuel qualification for a gas turbine engine
[AIAA PAPER 92-0684] p 389 A92-27051
Static tests for the evaluation of fuel additives
[AIAA PAPER 92-0686] p 389 A92-27053
Deposition during vaporization of jet fuel in a heated tube
[AIAA PAPER 92-0687] p 390 A92-27054
Performance of hybrid ball bearings in oil and jet fuel
p 900 A92-47176
Safety considerations in testing a fuel-rich aeropropulsion gas generator
[NASA-TM-105258] p 279 N92-17061
In situ measurement of particle formation in heated jet fuels: A new application of photon correlation spectroscopy
[DE92-003641] p 488 N92-20132
Monitoring jet fuel degradation using quartz crystal microbalances
[DE92-004730] p 489 N92-20858
Laser induced fluorescence detection of gums in jet fuels
[AD-A252685] p 987 N92-30767
Advanced thermally stable jet fuel development program. Volume 2: Compositional factors affecting thermal degradation of jet fuels
[AD-A252656] p 987 N92-31399
Advanced thermally stable, jet fuels development program annual report. Volume 1: Model and experiment system development
[AD-A249625] p 988 N92-31462
Jet fuel absorption and dynamic mechanical analysis of carbon fibre composites p 1110 N92-33050

JET ENGINES
P&W F119 - Vectored thrust for the F-22
p 25 A92-13219
Extension of a three-dimensional Euler method for calculating the flowfield around bypass engines with fan and core jet p 62 A92-13690
Optimizing instrumentation when measuring jet engine blade vibration
[ASME PAPER 91-GT-71] p 148 A92-15540
Interactive engine system dynamics analysis
[ASME PAPER 91-GT-193] p 124 A92-15619
The selective bleed variable cycle engine --- aircraft propulsion
[ASME PAPER 91-GT-388] p 126 A92-15720
Jet engine test system including expert system for diagnosis
[ASME PAPER 91-GT-408] p 137 A92-15737
Size and critical supersaturation for condensation of jet engine exhaust particles p 161 A92-15884
Jet engine fault detection with discrete operating points gas path analysis p 129 A92-17200
Simulation of radar clutter and jet engine modulation using digital quadrature modulator p 216 A92-19091
Influence of long time exposure at elevated temperatures in air on mechanical properties of the high temperature titanium alloy IMI 834 p 289 A92-22767
A study on vortex flow control of inlet distortion in the re-engined 727-100 center inlet duct using computational fluid dynamics
[AIAA PAPER 92-0152] p 253 A92-23767
UV laser spectroscopic measurements in jet engine combustion exit flows
[AIAA PAPER 92-0513] p 396 A92-26939
A numerical method for simulating the fluid-dynamic and heat-transfer changes in a jet engine injector feed-arm due to fouling
[AIAA PAPER 92-0768] p 374 A92-27108
Integral minimization of engine fault equations based on least fault principle p 374 A92-27857
Euler solutions for an unbladed jet engine configuration
[AIAA PAPER 92-0544] p 398 A92-28201
Rule based identifier for unknown systems
p 509 A92-31430
Experimental investigation of film cooling effectiveness for slots of various exit geometries p 497 A92-32265
Energy analysis of aeroengine and its significance
p 557 A92-35569
Waterjets for removing engine coatings
p 516 A92-35575
Technical history of aircraft engines
p 558 A92-35911
Laser thermal simulation puts jet engines to the test
p 663 A92-38129
Experimental operation of aircraft-engine turbine blade materials p 737 A92-43233
Basic study of adhesive bonding for fiber-composites - Adhesive bonding technologies on jet engine parts
p 764 A92-44733
Hot-gas reingestion - Engine response considerations
p 860 A92-45317
Numerical analysis of RCS jet in hypersonic flights
[SAE PAPER 912063] p 791 A92-45445
Derivation of ABCD system matrices from nonlinear dynamic simulation of jet engines
[AIAA PAPER 92-3319] p 923 A92-48903
Degenerate four-wave mixing for measurement of NO2 and smoke concentration in jet engine exhaust
[AIAA PAPER 92-3658] p 1113 A92-54108
Fault diagnostics on jet engine starting
p 1116 A92-54345
Current repair technologies for jet engine components
p 1016 A92-56085
Jet noise classical theory and experiments
p 54 N92-10602
Euler solutions for an unbladed jet engine configuration
[NASA-TM-105332] p 44 N92-11328
A derivation of gross thrust for a sea-level jet engine test cell
[NRC-30165] p 130 N92-12001
Verification of NISA 2 and ENDURE fracture mechanics capability
[NRC-ST-621] p 159 N92-13453
Recent progress in inverse methods in France
p 201 N92-13938
A study on vortex flow control on inlet distortion in the re-engined 727-100 center inlet duct using computational fluid dynamics
[NASA-TM-105321] p 179 N92-13998
Stability of intershaft squeeze film dampers
p 222 N92-14351
Laser based, non-intrusive measurement system for analysis of jet engine flows
[AD-A242398] p 279 N92-17011
Air intakes for high speed vehicles
[AGARD-AR-270] p 445 N92-20797
Extension of a three dimensional Euler-code for the investigation of the flow field around bypass engines with fan and core jet
[DLR-FB-91-13] p 503 N92-21699
The evolution of the bypass engine
[PNR-90832] p 476 N92-21850
Evaluation of an innovative high-temperature ceramic wafer seal for hypersonic engine applications
p 578 N92-22205
Directions in propulsion control p 560 N92-22530
A two-dimensional Euler solution for an unbladed jet engine configuration
[NASA-TM-105329] p 597 N92-23560
A multiblock grid generation technique applied to a jet engine configuration p 692 N92-24428
A two-dimensional Euler solution for an unbladed jet engine configuration p 627 N92-24861
Multiblock grid generation for jet engine configurations
p 659 N92-25720
Acoustic interactions between an altitude test facility and jet engine plumes: Theory and experiments
[NASA-CR-190423] p 738 N92-26405
Aircraft photovoltaic power-generating system
p 775 N92-26581
Use of Markov methods in analysis of fault-tolerant systems with flexible repair policies
[PNR-90801] p 767 N92-27038
Finite difference time domain modeling of steady state scattering from jet engines with moving turbine blades
[NASA-CR-190290] p 971 N92-30753
Engine monitoring display study
[NASA-CR-4463] p 979 N92-32175

JET EXHAUST
Size and critical supersaturation for condensation of jet engine exhaust particles p 161 A92-15884
A numerical study of the radiation characteristic of an elliptical exhaust jet p 970 A92-53258
Direct computation of turbulence and noise
[NASA-CR-187616] p 236 N92-14788

JET FLAPS
Analysis of flexible-membrane and jet-flapped airfoils using velocity singularities p 10 A92-13216
Analysis of an advanced fighter aircraft using jet flap techniques and the vortex lattice method
[AD-A244051] p 366 N92-19185

JET FLOW
Investigation of the flow at the exit of an unshrouded centrifugal impeller and comparison with the 'classical' jet-wake theory
[ASME PAPER 90-GT-124] p 6 A92-11287
Jet inflow simulation and its downwash effect on lifting surfaces p 9 A92-13200
Probe systems for static pressure and cross-stream turbulence intensity p 10 A92-13211
The role of primary jet injection on mixing in gas turbine combustion p 128 A92-16584
Three-dimensional singularity of flow structure in an underexpanded supersonic jet p 78 A92-16679
Experimental investigation of coannular jet flow with swirl along a centerbody p 172 A92-18367
X-29 forebody jet blowing
[AIAA PAPER 92-0017] p 247 A92-22139
The jet screen ignition scheme and its experimental verification p 388 A92-24744
The jet edge-tone feedback cycle - Linear theory for the operating stages p 392 A92-24758
Euler calculations of axisymmetric under-expanded jets by an adaptive-refinement method
[AIAA PAPER 92-0321] p 321 A92-25768
Single expansion ramp nozzle simulations
[AIAA PAPER 92-0387] p 323 A92-26243

The effects of blowing on delta wing vortices during dynamic pitching at high angles of attack
[AIAA PAPER 92-0407] p 325 A92-26260
Combined method for the solution of plane direct problems of flow past bodies with jets
p 427 A92-30200
Flow past a highly curved wing with tangential jet ejection p 438 A92-31868
Interaction of jets ejected from two-dimensional nozzles with a curved surface p 438 A92-31869
Evaluation of a Navier-Stokes prediction of a jet in a crossflow p 441 A92-32235
Numerical simulation of opposing sonic jets
p 524 A92-36357
An experimental and numerical study of confined axisymmetric jet with a bluff body p 621 A92-40106
Effect of tabs on the evolution of an axisymmetric jet
p 656 A92-40151
Prediction and measurement of jet flowfield features for ASTOVL aircraft p 787 A92-45318
The effects of nozzle exit geometry on forebody vortex control using blowing
[AIAA PAPER 92-2603] p 792 A92-45480
Simulation of transonic flow over twin-jet transport aircraft p 811 A92-46793
Direct evaluation of aeroacoustic theory in a jet
p 1010 A92-50296
Structure and penetration of a transverse fluid jet injected at supercritical pressure in supersonic flow
[AIAA PAPER 92-3652] p 1113 A92-54105
Experimental observations of instability modes in a rectangular jet p 1135 A92-54908
Approximate aerodynamic analysis of jet interaction
[AIAA PAPER 92-4640] p 1027 A92-55387
Force production mechanisms of a tangential jet on bodies at high alpha
[AIAA PAPER 92-4648] p 1082 A92-55393
A potential flow theory of two-dimensional bifurcated curtain jets. II p 1118 A92-56039
Experimental investigation of the effects of blowing on bursting of strake vortices
[AD-A240256] p 13 N92-10985
Experimental investigation of transverse jet effects related to hypersonic space vehicles
p 182 N92-14995
Laser based, non-intrusive measurement system for analysis of jet engine flows
[AD-A242398] p 279 N92-17011
Simulation of chemical kinetics in turbulent natural gas combustion
[PB92-123660] p 488 N92-20329
Extension of a three dimensional Euler-code for the investigation of the flow field around bypass engines with fan and core jet
[DLR-FB-91-13] p 503 N92-21699
Effect of collector configuration on test section turbulence levels in an open-jet wind tunnel
[NASA-TM-4333] p 750 N92-27670
Propulsion simulator for magnetically suspended wind tunnel models p 750 N92-27801
A new unsteady mixing model to predict NO(x) production during rapid mixing in a dual-stage combustor
[NASA-CR-189155] p 971 N92-30569
Numerical simulation of turbulence at the back of the airplane
[ETN-92-91664] p 1037 N92-32769
On the anomalies in single-jet hover suckdown data
[NASA-TM-102261] p 1038 N92-33306

JET IMPINGEMENT
Numerical and experimental study of jet impingement or interaction effects at hypersonic and supersonic speeds
[AIAA PAPER 91-5038] p 171 A92-17826
Effects of unsteady shock impingement on high-speed gaseous mixing
[AIAA PAPER 91-5091] p 172 A92-17857
Computation of normal impinging jets in cross-flow and comparison with experiment p 250 A92-22446
Numerical simulation of twin-jet impingement on a flat plate coupled with cross-flow p 315 A92-25374
A review of impinging jets in cross-flows - Experimentation and computation
[AIAA PAPER 92-0633] p 333 A92-27011
Reynolds stress budget in the outwash jet arising from colliding curved wall jets p 614 A92-38860
Turbulent energy budgets in impinging zones
p 620 A92-40081
Second moment closure predictions of jet-on-jet impingement flows p 675 A92-40102
Recent research into the aerodynamics of ASTOVL aircraft in ground environment p 623 A92-40549
The experimental and computational study of jet impingement flowfields with reference to VSTOL aircraft performance p 787 A92-45324
Numerical simulation of a supersonic jet impingement on a ground
[SAE PAPER 912014] p 789 A92-45412
Shock interaction induced by two hemisphere-cylinders
[SAE PAPER 912043] p 790 A92-45427
Numerical analysis of RCS jet in hypersonic flights
[SAE PAPER 912063] p 791 A92-45445
Experimental and numerical investigation of a supersonic free jet impinging on a perpendicular surface
p 1018 A92-53555
Three-dimensional numerical analysis of impinging circular jet - Discrete vortex method
p 1029 A92-56040
On the anomalies in single-jet hover suckdown data
[NASA-TM-102261] p 1038 N92-33306

JET MIXING FLOW
Probe shapes for streamwise momentum and cross-stream turbulence intensity p 9 A92-13210
CFD analysis of jet mixing in low NO(x) flametube combustors
[ASME PAPER 91-GT-217] p 124 A92-15634
The application of high pressure ejectors to reaction control systems p 128 A92-16666
Enhanced mixing of supersonic jets
p 80 A92-17195
Effects of unsteady shock impingement on high-speed gaseous mixing
[AIAA PAPER 91-5091] p 172 A92-17857
Studies of the effects of curvature on dilution jet mixing p 290 A92-21079
A computational investigation of mixing and reacting flows in supersonic combustors
[AIAA PAPER 92-0626] p 278 A92-23817
An analytical and computational investigation of shock-induced vortical flows
[AIAA PAPER 92-0316] p 321 A92-25763
Computation of supersonic jet mixing noise for an axisymmetric CD nozzle using k-epsilon turbulence model
[AIAA PAPER 92-0500] p 414 A92-26328
Numerical investigation of a transverse jet for supersonic aerodynamic control
[AIAA PAPER 92-0639] p 334 A92-27017
Study on two-dimensional jet mixing with a vertical supersonic flow p 429 A92-30530
Effect of tabs on the evolution of an axisymmetric jet
p 656 A92-40151
Planar fluorescence imaging of a transverse jet in a supersonic crossflow p 755 A92-44501
Experimental study of cross-stream mixing in a rectangular duct
[AIAA PAPER 92-3090] p 903 A92-48735
The enhancement of mixing in high-speed heated jets using a counterflowing nozzle
[AIAA PAPER 92-3262] p 825 A92-48857
Supersonic jet mixing enhancement by 'delta-tabs'
[AIAA PAPER 92-3548] p 826 A92-49063
Mach 3 wind tunnel test of mixed compression supersonic inlet
[AIAA PAPER 92-3625] p 1021 A92-54092
Acoustic control of combustor primary zone air-jet mixing
[AIAA PAPER 92-3651] p 1067 A92-54104
Supersonic flow mixing and combustion using RAMP nozzle
[AIAA PAPER 92-3840] p 1113 A92-54198
Viscous computations of cold air/air flow around scramjet nozzle afterbody
[NASA-CR-4406] p 13 N92-10982
Numerical simulation of the reactive flow in advanced (HSR) combustors using KIVA-2
[NASA-CR-188996] p 26 N92-11014
Jet noise suppression p 236 N92-14784
Computation of supersonic jet mixing noise for an axisymmetric CD nozzle using k-epsilon turbulence model
[NASA-TM-105338] p 237 N92-14795
Supersonic jet mixing enhancement by delta-tabs
[NASA-TM-105664] p 630 N92-24958
A parametric numerical study of mixing in a cylindrical duct
[NASA-TM-105695] p 738 N92-26553
CFD mixing analysis of jets injected from straight and slanted slots into confined crossflow in rectangular ducts
[NASA-TM-105699] p 738 N92-26561
Experimental study of cross-stream mixing in a rectangular duct
[NASA-TM-105694] p 742 N92-27652
Acoustic loads prediction on jet aircraft
p 1136 N92-32949

JET NOZZLES
A model of gasdynamic loads on an oscillating nozzle shell p 80 A92-16817
Forebody vortex flow control on the F-16C using tangential slot and jet nozzle blowing
[AIAA PAPER 92-0019] p 247 A92-22141
Restoration of aircraft engine nozzle block blades by vacuum arc brazing with controlled current
p 471 A92-30381
Flow past a highly curved wing with tangential jet ejection p 438 A92-31868
Interaction of jets ejected from two-dimensional nozzles with a curved surface p 438 A92-31869
A method for determining the internal force characteristics of a model in external supersonic flow
p 706 A92-42682
Full Navier-Stokes analysis of a two-dimensional mixer/ejector nozzle for noise suppression
[AIAA PAPER 92-3570] p 1067 A92-54059
Full Navier-Stokes analysis of a two-dimensional mixer/ejector nozzle for noise suppression
[NASA-TM-105715] p 868 N92-28419

JET PROPULSION
Review of propulsion applications and numerical simulations of the pulsed detonation engine concept
p 129 A92-17177
Cold-cycle pressure-jet helicopters: Ventures, designs, and developments. I - Ventures p 459 A92-31325
Mechanics and thermodynamics of propulsion (2nd revised and enlarged edition) --- Book
[ISBN 0-201-14659-2] p 672 A92-38275
Flow induction by pressure forces
[AIAA PAPER 92-3571] p 1067 A92-54060
Powder processing of aero-engine components
[PNR-90813] p 756 N92-27044

JET STREAMS (METEOROLOGY)
Severe turbulence with a low-level jet ahead of a squall line p 407 A92-27939

JET THRUST
Thrust stand evaluation of engine performance improvement algorithms in an F-15 airplane
[AIAA PAPER 92-3747] p 866 A92-49111
Lateral control of spaceplane at hypersonic flight
p 1104 A92-56069
Experimental investigation of transverse jet effects related to hypersonic space vehicles
p 182 N92-14995

JINDIVIK TARGET AIRCRAFT
Modification of Jindivik air intake duct with an auxiliary intake static aerodynamic tests
[AD-A243002] p 275 N92-17234

JOINED WINGS
An approach to the low-speed longitudinal aerodynamic characteristics of the joined wing configuration
p 339 A92-27909
Joined-wing model vibrations using PC-based modal testing and finite element analysis
[AIAA PAPER 92-2260] p 541 A92-34417
Downwash for joined-wing airframe with control surface deflections p 702 A92-41235
Low-speed wind tunnel testing of the lateral control force for the upper rudder surface of a joined-wing airfoil
p 711 A92-43228
Low-speed wind tunnel testing of a joined-wing airfoil
p 711 A92-43229
Effectiveness of aircraft aerodynamic performance on each part of a joined wing p 712 A92-43230
A low speed wind tunnel investigation of a joined-wing aircraft with an overhanging fin p 1030 A92-56078
A low speed wind tunnel investigation of the direct side force control of a joined-wing aircraft with overhanging fin p 1084 A92-56079

JOINTS (JUNCTIONS)
Current stabilizing of fastened composite joints to improve non-sparking lightning current performance
p 213 A92-20130
Predication of fastening capacity of screwed joint structure with cone assembly p 391 A92-24737
Rigid and flexible joint modelling in multibody dynamics using finite elements p 671 A92-37559
Composite material stub-blade wing joint
p 763 A92-44618
A damage tolerance assessment of bonded repairs to CF-18 composite components. Part 1: Adhesive properties
[DREP-TM-88-25-PT-1] p 143 N92-12060
Preliminary evaluation of adhesion strength measurement devices for ceramic/titanium matrix composite bonds
[NASA-TM-105803] p 932 N92-31267
Out of plane analysis for composite structures
p 1107 N92-32527

JOULE-THOMSON EFFECT
Evaluation of metal hydride compressors for applications in Joule-Thomson cryocoolers p 296 A92-23835
Multicomponent gas sorption Joule-Thomson refrigeration
[NASA-CASE-NPO-17569-1-CU] p 228 N92-15203

JOURNAL BEARINGS
Vibration control of rotor-bearing system by controlled squeeze-film damper bearings p 990 A92-49579
Variable impedance journal bearings for rotor-bearing systems p 157 N92-12270
Determination of rotordynamic coefficients for labyrinth seals and application to rotordynamic design calculations p 223 N92-14360
Annular seals of high energy centrifugal pumps: Presentation of full scale measurement p 224 N92-14362
Effect of eccentricity on the static and dynamic performance of a turbulent hybrid bearing p 225 N92-14373
JP-4 JET FUEL
The effect of jet fuel exposure on advanced aerospace composites. Part 1: Thermal and chemical analysis [AD-A246559] p 756 N92-27531
Fluid effects: Thermoset and thermoplastic matrix composites p 1110 N92-33049
JP-5 JET FUEL
The VRT gas turbine combustor - Phase II [AIAA PAPER 92-3471] p 1067 A92-54035
JUDGMENTS
Annoyance caused by aircraft en route noise [NASA-TP-3165] p 512 N92-20479

K

K-EPSILON TURBULENCE MODEL
Prediction of wake in a curved duct p 3 A92-10487
Turbulence modelling for secondary flow prediction in a turbine cascade [ASME PAPER 91-GT-57] p 68 A92-15535
Three-dimensional Navier-Stokes computation of turbomachinery flows using an explicit numerical procedure and a coupled k-epsilon turbulence model [ASME PAPER 91-GT-146] p 72 A92-15584
Explicit Navier-Stokes computation of cascade flows using the k-epsilon turbulence model p 175 A92-20727
Evaluation of a bounded high-resolution scheme for combustor flow computations p 201 A92-20734
Control of turbulent flow on a backward-facing step [AIAA PAPER 92-0066] p 250 A92-22179
Navier-Stokes computation of airfoil in stall using algebraic Reynolds-stress model [AIAA PAPER 92-0195] p 257 A92-23803
Evaluation of two flow analyses for subsonic diffuser design [AIAA PAPER 92-0273] p 317 A92-25727
Computation of supersonic jet mixing noise for an axisymmetric CD nozzle using k-epsilon turbulence model [AIAA PAPER 92-0500] p 414 A92-26328
Navier-Stokes computations for turbulent transonic projectile with a two layer model combining the ASM model of turbulence and the k-epsilon model near the wall [AIAA PAPER 92-0518] p 331 A92-26943
Finite element Navier-Stokes solver for unstructured grids p 398 A92-28035
Calculations of the dilution system in an annular gas turbine combustor p 494 A92-31164
Performance of turbulence models to predict supersonic boundary layer flows p 613 A92-37553
Scrutinizing k-epsilon EVM and ASM by means of LES and wind tunnel for flowfield around cube --- Eddy Viscosity Model, Algebraic Stress Model, Large Eddy Simulation p 621 A92-40119
Hypersonic shock-wave turbulent-boundary-layer interaction flows p 703 A92-41264
Predictions of a turbulent backward-facing-step flow with a cubic pressure-strain model [AIAA PAPER 92-2647] p 796 A92-45514
Navier-Stokes analysis and experimental data comparison of compressible flow in a diffusing S-duct [AIAA PAPER 92-2699] p 800 A92-45541
Development and application of a zonal k-epsilon turbulence model for complex 3-D flowfields [AIAA PAPER 92-3176] p 903 A92-48792
Assessment of compressibility corrections to the k-epsilon model in high-speed shear layers p 1024 A92-54905
Computation of supersonic jet mixing noise for an axisymmetric CD nozzle using k-epsilon turbulence model [NASA-TM-105338] p 237 N92-14795
Wall functions for the kappa-epsilon turbulence model in generalized nonorthogonal curvilinear coordinates [NASA-CR-190368] p 685 N92-25962
The 3-D Navier-Stokes flow and temperature field computation for a forced mixer nozzle p 770 N92-27482
Modelling the vaporiser and primary zone flows for a modern gas turbine combustion chamber p 742 N92-27484
Numerical simulation of turbomachinery flows with advanced turbulence models p 1124 N92-32270
Navier-Stokes analysis and experimental data comparison of compressible flow in a diffusing S-duct [NASA-TM-105683] p 1072 N92-33746
KALMAN FILTERS
Observability analysis of piece-wise constant systems with application to inertial navigation p 49 A92-11391
Real-time estimation of gas turbine engine damage using a control based Kalman filter algorithm [ASME PAPER 91-GT-216] p 124 A92-15633
Closed-loop operation of GPS aided INS p 100 A92-16954
INS alignment using GPS Phase III user equipment computed corrections p 100 A92-16955
Flight test results of an Ada coded INS/GPS open loop Kalman filter design p 100 A92-16958
Flight test of a GPS-aided low-cost inertial navigation system programmed in Ada p 101 A92-16973
An alternative derivation of the modified gain function of Song and Speyer p 232 A92-18464
Autonomously aided strapdown attitude reference system p 204 A92-18610
GPS integrated system application in aircraft approach landing p 266 A92-21466
The study of constant value thresholds of FDI in strapdown inertial navigation p 267 A92-22087
Failure detection of engine sensors with a bank of Kalman filters p 392 A92-24748
A new U-D factorization-based fixed-point smoother and application to flight test p 411 A92-27858
A consistency test of airborne GPS using multiple monitor stations p 454 A92-30651
Kalman filter mechanization for INS airstart p 574 A92-33602
A Kalman filter mechanization for the baro-inertial vertical channel p 673 A92-39558
Pulse response method for vibration reduction in periodic dynamic systems p 661 A92-39909
Design and implementation of a generic Kalman filter in Ada p 858 A92-48475
An integrated navigation system manager using federated Kalman filtering p 858 A92-48477
Location and tracking technique in a multistatic system established by multiple bistatic systems p 840 A92-48480
Integration of radar altimeter, precision navigation, and digital terrain data for low-altitude flight [AIAA PAPER 92-4420] p 1063 A92-55212
A data fusion algorithm for multi-sensor microburst hazard assessment [AIAA PAPER 92-4339] p 1063 A92-55328
Passive range estimation for rotorcraft low-altitude flight [NASA-TM-103897] p 2 N92-10003
Formulation of a strategy for monitoring control integrity in critical digital control systems [NASA-TM-104158] p 206 N92-15075
GPS/INS integration for improved aircraft attitude estimates [AD-A243947] p 356 N92-19604
Evaluating the velocity accuracy of an integrated GPS/INS system: Flight test results [DE92-007519] p 640 N92-25470
An adaptive correction technique for Differential Global Positioning System p 726 N92-26623
Vision-based range estimation using helicopter flight data [NASA-TM-103930] p 1047 N92-32424
The use of Kalman filtering techniques to improve the accuracy of flight test data [NRC-32139] p 1064 N92-32850
KALMAN-SCHMIDT FILTERING
A Kalman filter integrated navigation design for the IAR Twin Otter Atmospheric Research Aircraft [NRC-32148] p 1048 N92-32849
The use of Kalman filtering techniques to improve the accuracy of flight test data [NRC-32139] p 1064 N92-32850
KARMAN VORTEX STREET
A DFW microburst model based on DL-191 data p 17 A92-11380
KELVIN-HELMHOLTZ INSTABILITY
Relationship between the instability waves and noise of high-speed jets p 924 A92-45835
Computation of a Kelvin-Helmholtz instability for delta wing vortex flows [AD-A244320] p 346 N92-18825
KERNEL FUNCTIONS
Kernel function occurring in supersonic unsteady potential flow p 6 A92-11080
A new method for solving the kernel equations of transonic flows - An auxiliary kernel method p 410 A92-25108
Approximate truncated balanced realizations for infinite dimensional systems p 602 N92-22493
KEROSENE
The aviation kerosene burning in the non-uniform air flow p 487 A92-29728
The mechanism of liquid-cooling of vane in high-temperature turbine p 969 A92-49841
KEVLAR (TRADEMARK)
LDF thermoplastic composites technology p 34 A92-13243
Design and testing of high-performance parachutes [AGARD-AG-319] p 345 N92-18269
A Protection And Detection Surface (PADS) for damage tolerance p 1107 N92-32523
KINEMATIC EQUATIONS
A new method for calculation of helicopter maneuvering flight p 282 A92-23382
An integrated development of the equations of motion for elastic hypersonic flight vehicles [AIAA PAPER 92-4605] p 1077 A92-55283
KINEMATICS
Advanced stress analysis methods applicable to turbine engine structures [NASA-CR-187235] p 44 N92-11378
SA 330 Puma identification results p 274 N92-17162
Use of stepwise regression techniques and kinematic compatibility for the analysis of EAP flight data p 365 N92-18790
Quaternion and Euler angles in kinematics [NAL-TM-636] p 909 N92-28836
KINETIC ENERGY
A unified nonequilibrium model for hypersonic flows p 3 A92-10575
Energy attenuation for crashworthy seating systems - Past, present, and possible future development p 544 A92-35452
Turbulent energy budgets in impinging zones p 620 A92-40081
The relationship between mode localization and energy transmission parameters in the vibration of coupled structures p 925 A92-45921
Relative energy concepts in helicopter dynamics p 846 A92-46925
Further studies of kinetic energy methods in high speed ramjet cycle analysis [AIAA PAPER 92-3805] p 1069 A92-54177
Synthesis of gust load alleviation with flutter margin augmentation p 1082 A92-56021
SERI advanced wind turbine blades [DE92-001216] p 598 N92-22971
An experimental investigation of the separating/reattaching flow over a backstep [NASA-CR-190426] p 716 N92-27399
KINETIC EQUATIONS
A boundary integral formulation for the kinetic field in aerodynamics. II - Applications to unsteady 2D flows p 339 A92-28005
One-dimensional kinetic model for flows near a stagnation point of a highly cooled body in hypersonic rarefied streams p 938 A92-52751
KINETIC THEORY
Kinetic theory model for the flow of a simple gas from a three-dimensional axisymmetric nozzle p 937 A92-52730
KINETICS
Aerothermodynamic radiation studies [NASA-CR-185666] p 284 N92-15998
A new unsteady mixing model to predict NO(x) production during rapid mixing in a dual-stage combustor [NASA-CR-189155] p 971 N92-30569
KLYSTRONS
Experimental studies of compact toroids [DE92-003469] p 512 N92-21046
KNOWLEDGE
Research into the development of a knowledge acquisition taxonomy [NASA-CR-189939] p 778 N92-28150
KNOWLEDGE BASES (ARTIFICIAL INTELLIGENCE)
Radar troubleshooting assistant expert system [AIAA PAPER 91-3764] p 231 A92-17626
A parallel architecture adapted to onboard multiexpert systems p 276 A92-23040
The TSE 310 troubleshooting expert prototype for the Airbus A-310 commercial aircraft p 307 A92-25180
Multisensor data fusion and decision support for airborne target identification p 454 A92-31063
Knowledge-based nonlinear boundary integral models of compressible viscous flows over arbitrary bodies - Taking CFD back to basics p 617 A92-39941
Vibration analysis of gas turbines by an intelligent knowledge-based system p 656 A92-40548

The importance of implicit and explicit knowledge in a pilot's associate system p 858 A92-48567
Artificial intelligence in the helicopter cockpit of the future p 964 A92-49271
Artificial intelligence techniques applied to vehicle management system diagnostics p 965 A92-49315
A NASA/RAE cooperation in the development of a real-time knowledge based autopilot p 164 N92-12528
Adaptive tactical navigation program p 102 N92-12529
Pilot's associate: Evolution of a functional prototype p 118 N92-12531
Industrial code development p 227 N92-15083
Development of a knowledge base for use in an Expert System Advisor for Aircraft Maintenance Scheduling (ESAAMS)
[AD-A243435] p 305 N92-17687
Towards coherent hypermedia navigation by pragmatic dialogue modeling
[PB92-114735] p 455 N92-20818
Knowledge-based planning for controlled airspace flight operation as part of a cockpit assistant p 727 N92-27895
Parallel knowledge based systems architectures for in-flight mission management p 728 N92-27904
Application of knowledge-based systems for diagnosis of aircraft systems
[NLR-TP-90192-U] p 837 N92-28655

KNOWLEDGE REPRESENTATION
Knowledge maintenance in an evolving system using a deep structure representation
[AIAA PAPER 91-3941] p 231 A92-17605
Probabilistic reasoning for intelligent wind shear avoidance p 302 A92-21181
A knowledge acquisition approach for an on-board mission planner
[AIAA PAPER 92-1021] p 531 A92-33204
Knowledge-sensitive task manipulation - Acquiring knowledge from pilots flying a motion-based flight simulator p 916 A92-45064
Getting test items to measure knowledge at the level of complexity which licensing authorities desire - Another dimension to test validity p 835 A92-45080
An explanation-based-learning approach to knowledge compilation - A Pilot's Associate application p 920 A92-48220
Identifying design requirements using integrated analysis structures p 922 A92-48527
The importance of implicit and explicit knowledge in a pilot's associate system p 858 A92-48567
Discrete event fuzzy airport control p 1046 A92-55973
Constraint propagation through electromagnetic interaction topologies
[NRC-31761] p 155 N92-12154
A CLIPS-based tool for aircraft pilot-vehicle interface design p 303 N92-16605
The role of planning systems in future air traffic management p 355 N92-19050
Delfi: Design, development, and applicability of expert systems shells
[ISBN-90-6275-734-0] p 692 N92-25306
Knowledge-based planning for controlled airspace flight operation as part of a cockpit assistant p 727 N92-27895

KNUDSEN FLOW
On thermal-stress gas flows p 37 A92-10657
Low density heat transfer phenomena
[AIAA PAPER 92-2899] p 820 A92-47875
Hypersonic flow calculations around a 3D delta wing at low Knudsen numbers p 937 A92-52734

KOLMOGOROFF THEORY
Examination of energy spectra moments in a developing turbulent flow
[NIAR-91-28] p 399 N92-18116
Non-linear interactions in homogeneous turbulence with and without background rotation p 912 N92-30044

KRYPTON FLUORIDE LASERS
UV laser spectroscopic measurements in jet engine combustion exit flows
[AIAA PAPER 92-0513] p 396 A92-26939
KrF laser-induced OH fluorescence imaging in a supersonic combustion tunnel
[AIAA PAPER 92-3346] p 905 A92-48923

KURTOSIS
Volume spectra in supercooled clouds for several research flights
[AIAA PAPER 92-0167] p 350 A92-25683

KUTTA-JOUKOWSKI CONDITION
A note on the Kutta condition in Glauert's solution of the thin aerofoil problem p 613 A92-37933
Analysis and design of planar and non-planar wings for induced drag minimization
[NASA-CR-189509] p 179 N92-13999

L

L-1011 AIRCRAFT
A DFW microburst model based on DL-191 data p 17 A92-11380

LABORATORIES
Development and integration of modern laboratories in aerospace education
[AIAA PAPER 92-4022] p 1141 A92-56844
Impact of a process improvement program in a production software environment: Are we any better? p 413 N92-19422
Towards understanding software: 15 years in the SEL p 413 N92-19423
Activities of NRC-CNRC, Institute for Aerospace Research
[CTN-92-60431] p 420 N92-20204
Research, services, and facilities (National Institute of Standards and Technology)
[PB92-109172] p 485 N92-21870

LABYRINTH SEALS
Development of high performance compressor discharge seal
[AIAA PAPER 92-3714] p 907 A92-49096
Experimental investigations of exciting forces caused by flow in labyrinth seals p 223 N92-14354
Evaluation of rotordynamic coefficients of look-through labyrinths by means of a three volume bulk flow model p 223 N92-14356
Determination of rotordynamic coefficients for labyrinth seals and application to rotordynamic design calculations p 223 N92-14360
Development of a CFD code for analysis of fluid dynamic forces in seals p 228 N92-15084
Turbine blade tip and seal clearance excitation forces
[NASA-CR-184341] p 973 N92-31910

LAGRANGE COORDINATES
An Eulerian/Lagrangian method for computing blade/vortex impingement p 814 A92-46952

LAGRANGE MULTIPLIERS
Minimum-drag bodies moving in locality-law media p 779 A92-42732

LAKES
Aerodynamic roughness measured in the field and simulated in a wind tunnel
[NASA-CR-4422] p 347 N92-19354

LAMINAR BOUNDARY LAYER
Comparative studies of flow around a wing profile in two wind tunnels p 7 A92-12170
Fundamentals of applied aerogasdynamics. II - Viscous flow past bodies. Control devices --- Russian book p 64 A92-14281
Effect of suction on the stability of supersonic boundary layers. I - Second-mode waves. II - First-mode waves p 174 A92-19611
Control of laminar boundary layer separation p 393 A92-24980
A numerical calculation of three dimensional incompressible laminar, transition and turbulent boundary layers p 393 A92-25138
Design of a hybrid laminar flow control nacelle
[AIAA PAPER 92-0400] p 373 A92-26253
Compressible laminar boundary layers for perfect and real gases in equilibrium at Mach numbers to 30
[AIAA PAPER 92-0757] p 336 A92-27099
Transition control of instability waves over an acoustically excited flexible surface p 416 A92-28037
Three-dimensional structure of a curved wake
[AIAA PAPER 92-0541] p 341 A92-28199
Direct numerical simulation of laminar breakdown in high-speed, axisymmetric boundary layers
[AIAA PAPER 92-0742] p 343 A92-28223
Investigation of oblique shock/boundary-layer bleed interaction p 344 A92-28524
Control of the development of boundary layer disturbances p 423 A92-30126
Investigating the feasibility of controlling the laminar-turbulent transition by means of laminarizing plates p 493 A92-30161
Experimental study of the characteristics of boundary-layer development on an airfoil p 425 A92-30171
The effect of the angle-of-attack on laminar-turbulent boundary transition near the lower surface of triangular plates in a supersonic gas flow p 426 A92-30180
Asymptotic form of the lower branch of the neutral curve in a transonic boundary layer p 427 A92-30204
A method of boundary layer laminarization on an oscillating wing p 441 A92-31969
Studies on laminar boundary-layer receptivity to freestream turbulence near a leading edge p 591 A92-36007
Supersonic and hypersonic boundary-layer transition induced by discrete trips p 522 A92-36023
Determination of physicochemical constant in the wake of a body from ballistic experiments p 609 A92-36549
Laminar flow control of subsonic boundary layers by suction and heat transfer strips p 617 A92-39338
Analysis for the application of hybrid laminar flow control to a long-range subsonic transport aircraft
[SAE PAPER 912113] p 617 A92-39964
Application of laminar flow control to high-bypass-ratio turbofan engine nacelles
[SAE PAPER 912114] p 618 A92-39965
Application of linear stability theory in laminar flow design
[SAE PAPER 912116] p 618 A92-39967
Prediction of laminar boundary layer using cubic splines
[AIAA PAPER 92-2702] p 801 A92-45544
Gortler instability and supersonic quiet nozzle design p 813 A92-46902
The design and testing of an airfoil with hybrid laminar flow control
[ONERA, TP NO. 1992-22] p 822 A92-48585
Enhancement of laminar boundary layer heat transfer by a vortex generator p 1118 A92-55453
Basic hydrodynamics
[AD-A243513] p 300 N92-17387
The NASA Langley laminar-flow-control experiment on a swept, supercritical airfoil: Evaluation of initial perforated configuration
[NASA-TM-4309] p 525 N92-22196
A three-dimensional, compressible, laminar boundary-layer method for general fuselages. Volume 2: User's manual
[NASA-CR-4292-VOL-2] p 678 N92-24344
A three-dimensional, compressible, laminar boundary-layer method for general fuselages. Volume 1: Numerical method
[NASA-CR-4292-VOL-1] p 679 N92-24547
Distributed acoustic receptivity in laminar flow control configurations
[NASA-CR-4438] p 765 N92-26680
Aircraft drag reduction p 717 N92-27709
Turbulent spot generation and growth rates in a transonic boundary layer
[AD-A250221] p 909 N92-29118
Method of reducing drag in aerodynamic systems
[NASA-CASE-LEW-14791-1] p 1043 N92-34243

LAMINAR FLOW
Calculation of gas combustion regimes in a counterflow vortex chamber p 34 A92-12209
The role of laminar-turbulent transition in gas turbine engines p 120 A92-14868
Self-induced flow in a stepped rotating tube
[ASME PAPER 91-GT-276] p 152 A92-15673
A discrete vortex study of stationary flow past three-dimensional lifting systems at subsonic and supersonic velocities p 79 A92-16813
A quiet-flow Ludwieg tube for experimental study of high speed boundary layer transition
[AIAA PAPER 91-5026] p 207 A92-17819
Effect of nose shape on three-dimensional stagnation region streamlines and heating rates
[AIAA PAPER 91-5032] p 171 A92-17822
Introduction to three dimensional boundary layers p 245 A92-21977
Computation of unsteady, laminar, incompressible, viscous flows using the vorticity streamfunction formulation p 245 A92-21979
Implementation of Vigneron's streamwise pressure gradient approximation in the PNS equations
[AIAA PAPER 92-0189] p 256 A92-23798
Multigrid Navier-Stokes calculations for three dimensional cascades
[AIAA PAPER 92-0190] p 256 A92-23799
Problems of laminar-turbulent transition control in a boundary layer p 312 A92-24979
Design of a hybrid laminar flow control nacelle
[AIAA PAPER 92-0400] p 373 A92-26253
Calculation of compressible boundary layer flow about airfoils by a finite element/finite difference method
[AIAA PAPER 92-0524] p 332 A92-26948
Computation of laminar flow over a long slender axisymmetric blunted cone in hypersonic flow
[AIAA PAPER 92-0756] p 336 A92-27098
Numerical investigation of laminar separated trailing-edge flows p 339 A92-28026
Breakdown of an axisymmetric laminar wake p 424 A92-30145
Investigation of the effect of an ultrasonic acoustic field on boundary layer separation on an airfoil p 511 A92-30205
Effect of the longitudinal and transverse riblets of a flat plate on laminar-to-turbulent transition p 428 A92-30210
Numerical analysis on laminar flow control of transonic airfoils p 430 A92-30557
Computational studies of transonic flow past a swept wing and the boundary layer characteristics p 438 A92-31872

The effects of wall suction on laminar-turbulent transition in three-dimensional flow p 522 A92-36021
Evaluation of a finite volume method for compressible shear layers p 610 A92-36834
Behavior of asymmetric unstable modes of a trailing line vortex near the upper neutral curve p 617 A92-39340
Application of laminar flow control to high-bypass-ratio turbofan engine nacelles
[SAE PAPER 912114] p 618 A92-39965
Application of laminar flow control to the High Speed Civil Transport - The NASA Supersonic Laminar Flow Control Program
[SAE PAPER 912115] p 643 A92-39966
Design optimization of natural laminar flow bodies in compressible flow p 701 A92-41219
Navier-Stokes simulation for cone-derived waverider p 703 A92-41271
The flow over a backward-facing step under controlled perturbation - Laminar separation p 705 A92-41653
A new approach for the calculation of transitional flows
[AIAA PAPER 92-2669] p 798 A92-45524
Concepts for the stability analysis of NLF-experiments on swept wings
[AIAA PAPER 92-2706] p 801 A92-45548
Turbulent drag reduction by laminar sublayer thickening
[AIAA PAPER 92-2707] p 801 A92-45549
Separated high enthalpy dissociated laminar hypersonic flow behind a step - Pressure measurements p 809 A92-45858
Laminar hypersonic flow over a compression using the HANA code
[AIAA PAPER 92-2896] p 820 A92-47872
High subsonic wind tunnel test of a two-dimensional hybrid-laminar-flow-control airfoil with slotted surface p 1029 A92-56045
Resolution of the Navier-Stokes equations applied to the computation of the laminar flow around a two dimensional wing profile
[CERT-RT-65/5604-35] p 43 N92-11307
On the footprints of three-dimensional separated vortex flows around blunt bodies: Attempts of defining and analyzing complex flow structures p 84 N92-13005
Laminar-flow secondary separation on a slender wing p 85 N92-13006
Atmospheric pressure flow reactor: Gas phase chemical kinetics under tropospheric conditions without wall effects
[NASA-CASE-MSC-21384-1] p 297 N92-16243
Deterministic multi-zone ice accretion modeling p 265 N92-17987
Numerical simulation of transient hypervelocity flow in an expansion tube
[NASA-CR-189601] p 402 N92-18965
Hypersonic wakes
[ETN-92-91082] p 349 N92-19925
The NASA Langley laminar-flow-control experiment on a swept, supercritical airfoil: Evaluation of initial perforated configuration
[NASA-TM-4309] p 525 N92-22196
Numerical simulation of transient hypervelocity flow in an expansion tube
[NASA-CR-189615] p 592 N92-22228
Hypersonic laminar flow computations over a blunt leading edged delta wing at three different chord Reynolds numbers
[FFA-TN-1991-40] p 528 N92-23168
An engineering method for interactive inviscid-boundary layers in three-dimensional hypersonic flows
[NASA-TM-107838] p 632 N92-25279
Reynolds number dependence of the drag coefficient for laminar flow through fine-scale screens
[DE92-002930] p 765 N92-26698
Special Course on Skin Friction Drag Reduction
[AGARD-R-786] p 717 N92-27706
Basic concepts on boundary layers p 717 N92-27707
Laminar-turbulent transition: Fundamentals p 717 N92-27710
Development of a quiet supersonic wind tunnel with a cryogenic adaptive nozzle
[NASA-CR-188055] p 751 N92-27976
Development of a quiet supersonic wind tunnel with a cryogenic adaptive nozzle p 751 N92-27977
The FML compressor as a drive system for the LFSWT: A narrative p 751 N92-27978
Instrumentation requirements for laminar flow research in the NLR high speed wind tunnel HST
[NLR-TP-89158-U] p 887 N92-28669
Active thermal isolation for temperature responsive sensors
[NASA-CASE-LAR-14612-1] p 911 N92-29954
Further wind tunnel investigation of the SM701 airfoil with aileron and turbulators
[NASA-CR-190702] p 1038 N92-33063
Computation and stability analysis of laminar flow over a blunt cone in hypersonic flow p 1041 N92-33839

LAMINAR FLOW AIRFOILS
Technology for tomorrow - Do 228 with laminar wings p 269 A92-21013
Application of linear stability theory in laminar flow design
[SAE PAPER 912116] p 618 A92-39967
Laminar separation bubbles and airfoil design at low Reynolds numbers
[AIAA PAPER 92-2735] p 797 A92-45515
Effect of a bulge on the subharmonic instability of subsonic boundary layers p 898 A92-45833
The design and testing of an airfoil with hybrid laminar flow control
[ONERA, TP NO. 1992-22] p 822 A92-48585
The A320 laminar fin programme
[ONERA, TP NO. 1992-23] p 849 A92-48586
The FM-007: An advanced jet commuter for HUB to spoke transportation
[NASA-CR-189988] p 461 N92-20267
The windtunnel as a tool for laminar flow research
[NLR-TP-90145-U] p 887 N92-28661
Instrumentation requirements for laminar flow research in the NLR high speed wind tunnel HST
[NLR-TP-89158-U] p 887 N92-28669

LAMINAR HEAT TRANSFER
Heat transfer in the entrance region of semicircular ducts with internal fins p 497 A92-32264
Laminar heat transfer to blunt cones in high-enthalpy hypervelocity flows p 713 A92-44372

LAMINAR MIXING
Supersonic combustion studies p 211 N92-14984

LAMINAR WAKES
Breakdown of an axisymmetric laminar wake p 424 A92-30145

LAMINATES
BMI/bis (allylphenoxyphthalimide)-copolymers - A new family of resins for advanced composites with improved thermal oxidative stability p 33 A92-10213
Aerospace Arall - A challenge for the aircraft designer p 33 A92-10232
Forced vibration of rectangular laminated plates with material damping p 294 A92-23167
Response of symmetrically laminated rectangular plates subjected to heating p 296 A92-24186
Numerical comparison of experimentally measured ultrasound through a multilayered specimen p 510 A92-28682
Integrated aeroelastic control optimization of laminated composite lifting surfaces p 481 A92-32248
Analytical shape sensitivities and approximations of modal response of generally laminated tapered skew plates
[AIAA PAPER 92-2391] p 585 A92-34465
The evolution from bonded F27 aircraft to Arall structures p 699 A92-41177
Interlaminar fracture characteristics of bonding concepts for thermoplastic primary structures p 758 A92-41282
Composite laminated shells under internal pressure p 758 A92-41296
Acoustic transmission through a 2-D orthotropic multi-layered infinite cylindrical shell p 780 A92-44197
Impact response of composite UHB propeller blades
[SAE PAPER 912046] p 861 A92-45430
An analysis of the effect of centrifugal force on the impact resistance of composite fan blades for turbo-fan engines
[SAE PAPER 912047] p 861 A92-45431
Linear analysis of naturally curved and twisted anisotropic beam p 899 A92-46936
Dynamic analysis of rotor flex-structure based on nonlinear anisotropic shell models p 899 A92-46946
Sensitivity of tire response to variations in material and geometric parameters p 900 A92-47128
Safety factor and reliability for composite laminates p 996 A92-53070
Mechanical properties of laminate aluminum matrix composites p 1106 A92-56102
Repair procedures for advanced composites for helicopters p 1016 A92-56277
Preliminary finite element analysis of unloaded and loaded notched composite laminated plates
[NRC-LTR-ST-1806] p 159 N92-13454
The two-bay crack problem in fuselages built in GLARE and ARALL
[LR-653] p 196 N92-14044
Bulging of fatigue cracks in a pressurized aircraft fuselage
[LR-655] p 196 N92-14045
Fatigue of repaired composite structures p 214 N92-14411
Development and evaluation of a finite element model for a fiber composite helicopter fuselage
[MBB-UD-0584-90-PUB] p 196 N92-15066
Analysis of aircraft engine blade subject to ice impact
[NASA-TM-105336] p 229 N92-15402
Explicit finite element method for transparency impact analysis
[AD-A243527] p 264 N92-17478
Aeroelastic behavior of an adaptive lifting surface p 443 N92-20378
Prediction of response of aircraft panels subjected to acoustic and thermal loads
[NASA-CR-190305] p 678 N92-24345
Stress-strain analysis of a (0/90)sub 2 symmetric titanium matrix laminate subjected to a generic hypersonic flight profile
[NASA-TM-107584] p 685 N92-26128
A preliminary study on damage detection using piezoelectric film
[AD-A246350] p 733 N92-28118
Tensile and interlaminar properties of GLARE (trade name) laminates
[AD-A250188] p 895 N92-28921
Repair procedures for advanced composites for helicopters
[MBB-UD-0606-91-PUB] p 787 N92-29874
Low-velocity impact loading on fibre reinforced aluminum laminates (ARALL) and other aircraft sheet materials
[ETN-92-91613] p 987 N92-30414
Composite beam analysis linear analysis of naturally curved and twisted anisotropic beams
[AD-A252652] p 999 N92-30766
Cutting treatment by drilling of fiber bound synthetic materials
[MBB-UD-0609-91-PUB] p 988 N92-31716
A Protection And Detection Surface (PADS) for damage tolerance p 1107 N92-32523
Out of plane analysis for composite structures p 1107 N92-32527
Global/local methods research using the CSM testbed p 1107 N92-32528
Residual strength of repaired graphite/epoxy laminates after 5 years of outdoor exposure p 1108 N92-32577
Damage tolerance certification methodology for composite structures p 1108 N92-32579
Initial postbuckling response of an unsymmetrically laminated rectangular plate p 1108 N92-32586
CFRP stiffened panels under compression p 1109 N92-33044
Global/local interlaminar stress analysis of a grid-stiffened composite panel
[NASA-CR-190822] p 1125 N92-33139
Isothermal aging of IM7/8320 and IM7/5260
[NASA-TM-107666] p 1110 N92-33423
Continuation of tailored composite structures of ordered staple thermoplastic material
[NASA-CR-189671] p 1110 N92-33613

LAND MOBILE SATELLITE SERVICE
The Aeronautical Mobile Satellite Service (AMSS). I - Architecture of the AMSS system p 93 A92-13851

LAND USE
NATO CCMS aircraft noise study on receiver technology p 686 A92-39050
DANSIM applications - Development of airport noise reduction strategies and environmental policy p 687 A92-39057

LANDING AIDS
The new airport aeronautic meteorological codes p 160 A92-13855
JAS 39 Gripen progress report p 112 A92-16058
Integration of flight and carrier landing aid systems for shipboard operations
[ONERA, TP NO. 1991-113] p 134 A92-16092
Infra-red offers new landing aid competition p 198 A92-18937
New specifications proposed for taxiing guidance signs p 483 A92-29505
Improving the efficiency of passenger aircraft during the landing approach p 460 A92-31893
EVS could expand all-weather landing capability of airliners p 556 A92-36125
Shuttle autoland status summary
[AIAA PAPER 92-1273] p 666 A92-38478
Enhanced vision system option on future aircraft
[SAE PAPER 912204] p 651 A92-40014
The appropriate concern for possible aberrations in landing guidance signals p 839 A92-44932
Autonomous landing - Functional requirements p 840 A92-48470
Robust control design of an automatic carrier landing system
[AIAA PAPER 92-4619] p 1077 A92-55296
Neural network and fuzzy logic technology for naval flight control
[AD-A242650] p 206 N92-15074
An evaluation of four F-16 vertical velocity indicator configurations
[AD-A243629] p 370 N92-18014
Enhanced displays, flight controls, and guidance systems for approach and landing p 456 N92-21957

Integration of flight and carrier landing aid systems for shipboard operations p 456 N92-21958
Approach and landing assisted by onboard image processing p 457 N92-21959
Approach and landing guidance p 457 N92-21960
Limitations on helicopter operations in the aeronaval environment p 466 N92-21973

LANDING GEAR
Advanced thermoplastic nose landing gear door development p 20 A92-10275
Dynamic behavior analysis for landing-gear with different types of dual-chamber shock-struts p 111 A92-15342
A study of the nonlinear stress-strain state of spring-type landing gear p 154 A92-16825
Nonlinear landing gear behavior at touchdown p 192 A92-19606
Aircraft landing-induced tire spinup p 193 A92-20209
Design and testing leading to certification of the Airbus A340 nose landing gear doors p 272 A92-24192
Yaw dynamics of a coaxial rotor helicopter p 378 A92-24427
The stability analysis of the nonlinear shimmy p 358 A92-27902
Reduced basis technique for evaluating the sensitivity coefficients of the nonlinear tire response
[AIAA PAPER 92-2530] p 583 A92-34376
Determination of tire-wheel interface loads for aircraft wheels
[AIAA PAPER 92-2482] p 543 A92-34599
Vibration of gear system with web structure p 588 A92-35573
Dynamic response of landing gears on rough repaired runway
[SAE PAPER 912154] p 644 A92-39989
Testing of a titanium matrix composite landing gear
[SAE PAPER 912175] p 644 A92-40000
Quality management of landing gear with pulling support system p 762 A92-43156
Sensitivity of tire response to variations in material and geometric parameters p 900 A92-47128
A failure analysis for landing gear structural system p 849 A92-47667
Optimization of longitudinal corrections of helical gears p 990 A92-49578
On travelling wave vibration of high-speed duplex helical gears p 990 A92-49580
Shimmy of nose undercarriage wheels p 959 A92-51948
Mechanical model of landing impact of three dimensional fuselage landing gear p 960 A92-53090
Structural design and testing results of composite landing gear components p 1057 A92-56328
Optimization of the calculation margins of landing gears under extreme loads. Rupture static tests. Part 1: Program and test implantation
[CEAT-S8-6551-PARTIEL-1-PT-] p 195 N92-14043
Dynamic performance of an aircraft on its landing gear: Test and evaluation on a dihedral p 466 N92-21970
An assessment of the B-747's capability to operate on rough surfaces
[AD-A250134] p 963 N92-31793
Landing gear mechanism including runway-roughness restrictor assembly
[CA-PATENT-1-257-618] p 1061 N92-33585

LANDING INSTRUMENTS
The landing equipment of a high-tech aircraft p 730 A92-43149

LANDING LOADS
Testing of a titanium matrix composite landing gear
[SAE PAPER 912175] p 644 A92-40000
The landing equipment of a high-tech aircraft p 730 A92-43149
Mechanical model of landing impact of three dimensional fuselage landing gear p 960 A92-53090
Dual mode shock absorber and method
[PATENT-1-265-541] p 115 N92-13055
Structural dynamics division research and technology accomplishments for F.Y. 1991 and plans for F.Y. 1992
[NASA-TM-104188] p 261 N92-17509
An assessment of the B-747's capability to operate on rough surfaces
[AD-A250134] p 963 N92-31793

LANDING RADAR
Talons 95 GHz radar sensor for autonomous landing guidance p 1063 A92-55908

LANDING SIMULATION
Control of the landing of a flight vehicle in the grazing-incidence mode p 134 A92-16808
Analyzing the flared landing task with pitch-rate flight control systems p 661 A92-39905
Simulation of triple simultaneous parallel ILS approaches p 880 A92-45025
Mechanical model of landing impact of three dimensional fuselage landing gear p 960 A92-53090

LANDING SITES
New siting techniques for the ILS glide slope p 188 A92-17422

LANDING SPEED
Aircraft landing-induced tire spinup p 193 A92-20209
Accelerators and decelerators for large hypersonic aircraft p 665 A92-36952

LANDMARKS
Study of alternatives: Dayton's Aviation heritage, Ohio
[PB91-202275] p 2 N92-10972

LAP JOINTS
Environmental evaluation of repairs to fuselage lap joints p 699 A92-41534
Stress field sensitivity of a composite patch repair as a result of varying patch thickness p 763 A92-44630
Measurements of fuselage skin strains and displacements near a longitudinal lap joint in a pressurized aircraft
[NASA-TM-104163] p 159 N92-13455
Large area QNDE inspection for airframe integrity p 362 N92-18588
Preliminary results on the fracture analysis of multi-site cracking of lap joints in aircraft skins p 913 N92-30111
Thermal QNDE detection of airframe disbonds p 914 N92-30118

LARGE SPACE STRUCTURES
Experimental demonstration of active vibration control for flexible structures p 50 A92-11442
Active vibration control of smart structural materials p 673 A92-39281
Experimental validation of structural optimization methods
[NASA-TM-104203] p 404 N92-19258

LASER ANEMOMETERS
3D LDA measurement in an axial fan rotor p 391 A92-24730
Laser velocimetry seed particles within compressible, vortical flows p 395 A92-26413
LDA measurements in a Mach 2 flow over a rearward facing step with staged transverse injection
[AIAA PAPER 92-2692] p 800 A92-45539
A laser fluorescence anemometer system for the Langley 16- by 24-inch water tunnel p 1092 A92-54347
Measurement of vortex flow fields
[NASA-CR-189543] p 443 N92-20283
Radial inflow turbine study
[AD-A246938] p 743 N92-28073
Potential applications of laser Doppler anemometry for in-flight measurements
[NLR-TP-90163-U] p 859 N92-28654
Comparison of LDA and LTA applications for propeller tests in wind tunnels
[NLR-MP-88031-U] p 827 N92-28658
Laser anemometer measurements and computations in an annular cascade of high turning core turbine vanes
[NASA-TP-3252] p 830 N92-28980
A 4-spot time-of-flight anemometer for small centrifugal compressor velocity measurements
[NASA-TM-105717] p 909 N92-29105
Theoretical simulation of a 2 micron airborne solid state laser anemometer p 1000 N92-31059

LASER APPLICATIONS
Laser-initiated conical detonation wave for supersonic combustion. II
[AIAA PAPER 92-0088] p 292 A92-22195
Flowfield visualization of crossing shock-wave/boundary-layer interactions
[AIAA PAPER 92-0750] p 335 A92-27094
Progress report of Scot's Laser Ordnance Initiator System for crew escape p 580 A92-32988
Laser ordnance initiation system p 577 A92-35465
Heterodyne techniques in the I.R. bandwidth for laser obstacle detection p 533 A92-35740
Distance and angle measuring method using laser light and rereflection plates p 762 A92-43206
Measurement of position and attitude using laser and retro-reflectors p 1047 A92-56120
Laser based, non-intrusive measurement system for analysis of jet engine flows
[AD-A242398] p 279 N92-17011
Welding technology transfer task/laser based weld joint tracking system for compressor girth welds p 593 N92-22426
Optical measurement systems p 594 N92-22527
The fibre optic three dimensional laser two focus velocimeter for the low-speed windtunnel. Part 1: Two-dimensional measurement evaluations
[NAL-TM-627] p 665 N92-25402
Study of optical techniques for the Ames unitary wind tunnels. Part 3: Angle of attack
[NASA-CR-190541] p 888 N92-29655
Three-dimensional laser window formation
[NASA-RP-1280] p 984 N92-30307
Inspection of fabricated fuselage panels using electronic shearography
[DOT/FAA/CT-TN92/26] p 1127 N92-33627

LASER BEAMS
Characteristics of the energy analysis of optical radar in the case of nonstationary irradiation of flying objects p 454 A92-31955
Innovation in the laser warning sensor field p 554 A92-35742

LASER CUTTING
Successful transfer of technology from a research and development laboratory to an Aerospatiale production unit p 931 A92-51808

LASER DOPPLER VELOCIMETERS
Helicopter local blade circulation calculations for a model rotor in forward flight using laser velocimeter measurements p 65 A92-14362
LDV measurements of a mixed-flow impeller at design and near stall
[ASME PAPER 91-GT-310] p 153 A92-15688
LDV measurements and investigation of flow field through radial turbine guide vanes p 217 A92-19618
Doppler global velocimeter measurements of the vortical flow above a thin delta wing
[AIAA PAPER 92-0005] p 292 A92-22130
Laser diagnostics for velocity measurements in supersonic combusting environments
[AIAA PAPER 92-0008] p 288 A92-22133
Experimental measurement of the vortex development downstream of a lobed forced mixer
[ASME PAPER 90-GT-27] p 295 A92-23299
Leading edge velocity field of an oscillating airfoil in compressible dynamic stall
[AIAA PAPER 92-0193] p 257 A92-23802
3D LDA measurement in an axial fan rotor p 391 A92-24730
The LDV measurement of three-component velocity of complex vortex flow in the wind tunnel p 393 A92-25109
An optical microphone for the detection of hidden helicopters
[AIAA PAPER 92-0377] p 395 A92-26235
Laser measurements of unsteady flow field in a radial turbine guide vanes
[AIAA PAPER 92-0394] p 395 A92-26249
Finite wing aerodynamics with simulated glaze ice
[AIAA PAPER 92-0414] p 325 A92-26265
Experimental investigation of a three-dimensional bluff-body wake
[AIAA PAPER 92-0429] p 326 A92-26277
Measurements of the inflow to a vibrating rotor blade
[AIAA PAPER 92-0634] p 333 A92-27012
Fibre optic laser anemometry for turbomachinery applications p 397 A92-27783
LDV measurements of the velocity field in an underexpanded supersonic jet (Ma = 1.5)
[AIAA PAPER 92-0504] p 341 A92-28196
Semiconductor laser Doppler anemometer for applications in aerodynamic research p 495 A92-31173
An investigation in the variance in particle surface interactions and their effects in gas turbines
[ASME PAPER 91-GT-380] p 653 A92-36891
LDV measurements of the flowfield in a simulated combustor with axial and side inlets p 672 A92-38867
LDV measurements in the unsteady tip-vortex behind an oscillating rectangular wing p 620 A92-40085
Swirl number effects on confined flows in a model of a dump combustor p 896 A92-45202
LDV measurements in the three-dimensional near wake of a stationary and oscillating rectangular wind
[AIAA PAPER 92-2689] p 799 A92-45536
LDV measurements on a rectangular wing with a simulated glaze ice accretion
[AIAA PAPER 92-2690] p 800 A92-45537
Laser velocimetry measurements in an MHD aerodynamic duct
[AIAA PAPER 92-2986] p 899 A92-46996
Nonintrusive measurements in fluid dynamic flows from Mach .0005 to 14 p 1090 A92-54311
Comparison of frequency domain and time domain laser velocimeter signal processors p 1114 A92-54314
Signal processing schemes for Doppler global velocimetry p 1115 A92-54338
Investigation of a plate-ramp-configuration by means of laser Doppler anemometry at Mach 2.95
[AIAA PAPER 92-3956] p 1097 A92-56784
Experimental investigation of the effects of blowing on bursting of strake vortices
[AD-A240256] p 13 N92-10985
An experimental analysis of lateral jet injection into confined swirling crossflows p 156 N92-12199
Study of detached turbulent flow in an air intake by means of high speed tomography and laser velocimetry
[REPT-90/55] p 157 N92-12216

An evaluation of preliminary Doppler global velocimetry measurements p 90 N92-13849
A study of the diffusion of slot-injected drag-reducing polymer solution in a turbulent boundary layer modified by large-eddy breakup devices
[AD-A243411] p 344 N92-18007
Examination of energy spectra moments in a developing turbulent flow
[NIAR-91-28] p 399 N92-18116
An approach to flow field measurement by Laser 2-Focus velocimeter (L2F) in gust wind tunnel
[NAL-TM-617] p 346 N92-18484
A laser velocimeter investigation of the normal shockwave boundary layer interaction
p 500 N92-20485
Particle image velocimetry
[AD-A246638] p 750 N92-27753
Potential applications of laser Doppler anemometry for in-flight measurements
[NLR-TP-90163-U] p 859 N92-28654
Comparison of LDA and LTA applications for propeller tests in wind tunnels
[NLR-MP-88031-U] p 827 N92-28658
Vaporizing particle velocimeter
[NASA-CASE-LAR-14685-1] p 1042 N92-34172

LASER GUIDANCE
Differential GPS/inertial navigation approach/landing flight test results p 956 A92-51009

LASER GYROSCOPES
Retrofit provides navigation enhancement for older aircraft p 198 A92-20025
Bias of an optical passive ring-resonator gyro caused by the misalignment of the polarization axis in the polarization-maintaining fiber resonator
p 652 A92-40262
Investigation of the dynamic behaviour and the frequency response of the GG 1342 laser gyro
[ESA-TT-1236] p 595 N92-22641

LASER HEATING
Laser-initiated conical detonation wave for supersonic combustion p 375 A92-28531
Laser thermal simulation puts jet engines to the test
p 663 A92-38129
Laser-initiated conical detonation wave for supersonic combustion. III
[AIAA PAPER 92-3247] p 893 A92-48846
Laser-driven hypersonic air-breathing propulsion simulator
[AIAA PAPER 92-3922] p 1095 A92-56753

LASER INDUCED FLUORESCENCE
Preliminary laser induced fluorescence measurements in several facilities in preparation for application to studies in the high enthalpy shock tunnel Goettingen (HEG)
[AIAA PAPER 92-0143] p 284 A92-23761
Evaluation of OH laser-induced fluorescence techniques for supersonic combustion diagnostics
[AIAA PAPER 92-0508] p 396 A92-26935
Planar fluorescence imaging of a transverse jet in a supersonic crossflow p 755 A92-44501
KrF laser-induced OH fluorescence imaging in a supersonic combustion tunnel
[AIAA PAPER 92-3346] p 905 A92-48923
A laser fluorescence anemometer system for the Langley 16- by 24-inch water tunnel
p 1092 A92-54347
Holographic and PLIF measurements of free-flight hypervelocity flows in the AEDC Range G facility
[AIAA PAPER 92-3935] p 1122 A92-56765
A study of the diffusion of slot-injected drag-reducing polymer solution in a turbulent boundary layer modified by large-eddy breakup devices
[AD-A243411] p 344 N92-18007
Laser-spectroscopic measurement techniques for hypersonic, turbulent wind tunnel flows
[NASA-TM-103928] p 405 N92-19596
Measurement of vortex flow fields
[NASA-CR-189543] p 443 N92-20283
Laser induced fluorescence detection of gums in jet fuels
[AD-A252685] p 987 N92-30767

LASER INTERFEROMETRY
Laser-based ultrasonics on GR/epoxy composite - Interferometric detection p 144 A92-13554
A method for the optical measurement of surface friction in supersonic flow p 337 A92-27537

LASER OUTPUTS
Characteristics of the energy analysis of optical radar in the case of nonstationary irradiation of flying objects
p 454 A92-31955
One joule output from a diode-array-pumped Nd:YAG laser with side-pumped rod geometry
p 671 A92-37188

LASER POWER BEAMING
Efficiency of a 5V/5mW power by light power supply for avionics applications p 734 A92-42603

LASER PROPULSION
Contractors Meeting in Propulsion
[AD-A240057] p 33 N92-10062

LASER PUMPING
One joule output from a diode-array-pumped Nd:YAG laser with side-pumped rod geometry
p 671 A92-37188
Degenerate four-wave mixing for measurement of NO2 and smoke concentration in jet engine exhaust
[AIAA PAPER 92-3658] p 1113 A92-54108

LASER RANGE FINDERS
Innovation in the laser warning sensor field
p 554 A92-35742
A novel avionic sensor for fly-by-light controls
p 650 A92-38128

LASER SPECTROSCOPY
UV laser spectroscopic measurements in jet engine combustion exit flows
[AIAA PAPER 92-0513] p 396 A92-26939
Composition monitoring of electron beam melting processes using diode lasers
[DE92-009527] p 669 N92-25259

LASER WELDING
Successful transfer of technology from a research and development laboratory to an Aerospatiale production unit p 931 A92-51808
Welding technology transfer task/laser based weld joint tracking system for compressor girth welds
p 593 N92-22426

LASER WINDOWS
Three-dimensional laser window formation
[NASA-RP-1280] p 984 N92-30307

LASERS
Wind tunnel investigation of the interaction and breakdown characteristics of slender wing vortices at subsonic, transonic, and supersonic speeds
[NASA-TP-3114] p 82 N92-12994

LATERAL CONTROL
Robust autopilot design for aircraft with multiple lateral-axes controls using H(infinity) synthesis
p 28 A92-11563
An assessment of robustness of variable structure control systems for advanced aircraft manoeuvres
p 29 A92-11595
Identification of higher-order helicopter dynamics using linear modeling methods p 131 A92-14336
Analysis of aircraft performance during lateral maneuvering for microburst avoidance
p 205 A92-20207
Computational investigation of slot blowing for fuselage forebody flow control
[AIAA PAPER 92-0020] p 248 A92-22142
Comments on 'Fuzzy logic for control of roll and moment for a flexible wing aircraft' p 480 A92-30995
Inverse and optimal control for desired outputs
p 661 A92-39894
Analysis of airship lateral maneuverability
[AIAA PAPER 91-1274] p 743 A92-41212
Low-speed wind tunnel testing of the lateral control force for the upper rudder surface of a joined-wing airfoil
p 711 A92-43228
Low-speed wind tunnel testing of a joined-wing airfoil
p 711 A92-43229
A LEX blowing technique for post-stall lateral control of trapezoidal wings
[AIAA PAPER 92-2714] p 802 A92-45553
Gain scheduled linear PID autopilot for the AIAA Controls Design Challenge aircraft
[AIAA PAPER 92-4629] p 1078 A92-55304
Lateral control of spaceplane at hypersonic flight
p 1104 A92-56069
The effect of wing ice contamination on essential flight characteristics p 449 N92-21681
Progress of magnetic suspension and balance systems for wind tunnels in the USSR p 751 N92-27803
Initial validation of a R/D simulator with large amplitude motion p 886 N92-28546
Effects of cockpit lateral stick characteristics on handling qualities and pilot dynamics
[NASA-CR-4443] p 878 N92-28584
On-line analysis capabilities developed to support the AFW wind-tunnel tests
[NASA-TM-107651] p 961 N92-30752
Rolling maneuver load alleviation using active controls
[NASA-TM-107654] p 962 N92-31351

LATERAL OSCILLATION
Model oscillations at high angle of attack in a low speed wind tunnel test
[IAF PAPER ST-91-001] p 175 A92-20649

LATERAL STABILITY
Analysis of the stability of the lateral motion of aircraft
p 480 A92-30191
Estimation of spaceplane lateral-directional stability and control derivatives from dynamic wind tunnel test
[SAE PAPER 911979] p 872 A92-45384
Thrust vectoring for lateral-directional stability
[NASA-CR-186016] p 482 N92-21357

LATTICES (MATHEMATICS)
A study on the superconvergence of Multhopp's discretization in vortex-lattice methods
p 336 A92-27381
Flutter analyses using high speed computers. Part 2: Aerodynamic procedures p 1089 N92-34169

LAUNCH VEHICLE CONFIGURATIONS
Numerical simulation of inviscid flow over a complicated body using an overlapping grid technique
p 313 A92-25043

LAUNCH VEHICLES
Structural design considerations for a Personnel Launch System p 386 A92-24668
Experimental investigation on reducing fluctuating pressures of launch vehicles by passive shock-wave/boundary-layer control p 616 A92-38916
Distributed health management systems technology for future propulsion control systems
[SAE PAPER 912167] p 655 A92-39995
Trends in propulsion technology p 757 A92-41186
Conceptual design of two-stage-to-orbit hybrid launch vehicle
[NASA-CR-190006] p 486 N92-20666

LAUNCHERS
Pneumatically actuated multiple store launcher
[AD-D015237] p 732 N92-27188
Fuzzy guidance system evaluation
p 778 N92-27903

LAUNCHING
Kestrel balloon launch system
[AIAA PAPER 91-3684] p 15 A92-11027
Dynamic performance of an aircraft on its landing gear: Test and evaluation on a dihedral p 466 N92-21970

LAUNCHING BASES
Expert knowledge techniques applied to the analysis of electric field mill data p 408 A92-27991

LAY-UP
Automated composite lay-up p 146 A92-14450
Bearingless main rotor system composite component fabrication techniques p 110 A92-14453
Design analysis of the T-800 inlet particle separator/air oil cooler blower p 579 A92-32556
Finite element analysis of a riveted repair on a curved composite panel
[AD-A243916] p 404 N92-19384
Composite fuselage technology (summary of year 2)
[NASA-CR-190434] p 731 N92-26655

LEAD (METAL)
Analysis of the effects of removing nose ballast from the F-15 eagle
[AD-A244044] p 366 N92-19178

LEADERSHIP
Research and technology, 1991. Langley Research Center
[NASA-TM-4331] p 1013 N92-30733

LEADING EDGE FLAPS
Interference of high-mounted propfan nacelles with an unswept wing and ways to attenuate it
p 460 A92-31881
Dynamically enhanced sustained lift using oscillating leading-edge flaps
[AIAA PAPER 92-2625] p 794 A92-45497
Effects of leading and trailing edge flaps on the aerodynamics of airfoil/vortex interactions
p 815 A92-46957
Experimental studies of vortex flaps and vortex plates. Part 1: 0.53 m span 60 deg delta wing
[CRANFIELD-AERO-9113-PT-1] p 349 N92-19679

LEADING EDGE SLATS
Flow regimes of the cove regions between a slat and wing and between a wing and flap of a multielement airfoil p 614 A92-38858

LEADING EDGE SWEEP
Maximum lift of wings with trailing-edge flaps at low speeds
[ESDU-91014] p 81 N92-11970
Planform curvature effects on flutter characteristics of a wing with 56 deg leading-edge sweep and panel aspect ratio of 1.14
[NASA-TP-3116] p 115 N92-13054

LEADING EDGES
Shock wave reflection close to the leading edge of a wedge p 37 A92-10660
The just attached shock-wave at the leading edge of a profile p 3 A92-10663
An analysis of pitch and plunge effects on unsteady airfoil behavior p 65 A92-14359
Three-dimensional thermal structural analysis of a swept cowl leading edge subjected to skewed shock-shock interference heating p 174 A92-20306
Forebody vortex flow control on the F-16C using tangential slot and jet nozzle blowing
[AIAA PAPER 92-0019] p 247 A92-22141

Study of theoretical and wind tunnel results on flight performance degradation due to leading edge rime ice accretion
[AIAA PAPER 92-0038] p 262 A92-22158
On the calculation of the compressible boundary layer on a nonplanar delta wing with supersonic leading edges
p 252 A92-23409
Effect of leading-edge cross-sectional geometry on slender wing unsteady aerodynamics
[AIAA PAPER 92-0173] p 255 A92-23784
Leading edge velocity field of an oscillating airfoil in compressible dynamic stall
[AIAA PAPER 92-0193] p 257 A92-23802
The rolling-up and interaction of the leading-edge and trailing-edge vortex sheets of a delta wing
p 314 A92-25101
Unsteady wing surface pressures in the wake of a propeller
[AIAA PAPER 92-0277] p 318 A92-25731
Reduction of wing rock amplitudes using leading-edge vortex manipulations
[AIAA PAPER 92-0279] p 379 A92-25733
Flow visualization of a prop-fan leading-edge vortex
[AIAA PAPER 92-0386] p 323 A92-26242
Computational study of the aerodynamics and control by blowing of asymmetric vortical flows over delta wings
[AIAA PAPER 92-0410] p 325 A92-26263
Leading edge sweep effects in generic three-dimensional sidewall compression scramjet inlets
[AIAA PAPER 92-0674] p 343 A92-28218
Analysis of iced wings
[AIAA PAPER 92-0416] p 423 A92-29972
Calculation of the rolling moment for a wing with a supersonic leading edge in the presence of sideslip
p 426 A92-30186
Lifting surface design using the principle of passive control of elastic characteristics p 480 A92-31865
Computational studies of the aerodynamic characteristics of delta wings with a subsonic leading edge p 439 A92-31874
Computational study of incipient leading-edge separation on a supersonic delta wing
p 442 A92-32237
Thermoviscoplastic analysis of engine cowl leading edge subjected to oscillating shock-shock interaction
[AIAA PAPER 92-2537] p 583 A92-34381
Studies on laminar boundary-layer receptivity to freestream turbulence near a leading edge
p 591 A92-36007
The numerical simulation of separation control using moving surface effect p 616 A92-38924
Measurements in a leading-edge separation bubble due to a simulated airfoil ice accretion p 723 A92-41262
The acceleration control system design of a flight vehicle using a two-wing control method p 745 A92-43185
Flow field around thick delta wing with rounded leading edge
[SAE PAPER 912009] p 789 A92-45409
Computational study of transition front on a swept wing leading-edge model
[AIAA PAPER 92-2630] p 795 A92-45502
The subsonic and transonic flow around the leading edge of a thin airfoil with a parabolic nose
[AIAA PAPER 92-2649] p 797 A92-45516
Analysis of a pneumatic forebody flow control concept about a full aircraft geometry
[AIAA PAPER 92-2678] p 799 A92-45530
A LEX blowing technique for post-stall lateral control of trapezoidal wings
[AIAA PAPER 92-2714] p 802 A92-45553
An experimental investigation of the effect of leading-edge extensions on directional stability and the effectiveness of forebody nose strakes
[AIAA PAPER 92-2715] p 802 A92-45554
Experimental investigation of vortex dynamics on delta wings
[AIAA PAPER 92-2731] p 804 A92-45565
Navier-Stokes computation of wing leading edge tangential blowing for a tilt rotor in hover
[AIAA PAPER 92-2608] p 805 A92-45568
Prediction of leading-edge vortex breakdown on a delta wing oscillating in roll
[AIAA PAPER 92-2677] p 807 A92-45585
Nonuniform motion of leading-edge vortex breakdown on ramp pitching delta wings p 808 A92-45828
Experimental study of vortex flows over delta wings in wing-rock motion p 810 A92-46787
Pitch rate/sideslip effects on leading-edge extension vortices of an F/A-18 aircraft model
p 874 A92-46810
Multiple shock-shock interference on a cylindrical leading edge p 813 A92-46899
Wing leading edge design with composites to meet bird strike requirements p 848 A92-47404
Heat transfer characteristics of hypersonic waveriders with an emphasis on leading edge effects
[AIAA PAPER 92-2920] p 821 A92-47892
Effects of a leading-edge fillet on the flow past an appendage-body junction p 935 A92-50301
Effect of wing tip vortices on a trailing aircraft
p 935 A92-50303
Induction bonding procedures for graphite reinforced thermoplastic assemblies p 994 A92-51545
Increased heat transfer to elliptical leading edges due to spanwise variations in the freestream momentum - Numerical and experimental results
[AIAA PAPER 92-3070] p 1020 A92-54005
Analysis of the onset of dynamic stall
p 1024 A92-54919
Pulsating spanwise blowing on a fighter aircraft
[AIAA PAPER 92-4359] p 1025 A92-55345
Model flight tests of a spin-resistant trainer configuration p 1054 A92-56158
Forcing level effects of internal acoustic excitation on the improvement of airfoil performance
p 1136 A92-56162
Predicting droplet impingement on yawed wings
p 1043 A92-56180
Experimental unsteady pressures on an oscillating cascade with supersonic leading edge locus
[AIAA PAPER 92-4035] p 1035 A92-56857
Numerical investigation of the effect of leading edge geometry on dynamic stall of airfoils
[AD-A239949] p 12 N92-10015
Performance improvements and fuel cost savings due to leading edge modification of a vintage delta wing jet fighter
[FFA-TN-1991-22] p 114 N92-11993
Wind tunnel investigation of the interaction and breakdown characteristics of slender wing vortices at subsonic, transonic, and supersonic speeds
[NASA-TP-3114] p 82 N92-12994
Modeling and numerical simulation of vortex flow in aerodynamics
[AD-B163670L] p 83 N92-12997
Characteristics of a boundary layer in a leading edge vortex p 86 N92-13012
Vortex control: Further encounters p 87 N92-13020
Some characteristics and effects of the F/A-18 LEX vortices p 88 N92-13025
Numerical simulation of vortex street-edge interaction
p 88 N92-13027
An experimental analysis of critical factors involved in the breakdown process of leading edge vortex flows
p 89 N92-13031
Navier-Stokes calculation of transonic flow past the NTF 65 deg delta wing p 91 N92-13868
Supercritical blade design on stream surfaces of revolution with an inverse method p 220 N92-13950
Definition of the unsteady vortex flow over a wing/body configuration
[NASA-CR-180083] p 178 N92-13995
Wind tunnel investigation of vortex flows on F/A-18 configuration at subsonic through transonic speed
[NASA-TP-3111] p 179 N92-14968
Numerical simulation of swept-wing flows
[NASA-CR-189457] p 180 N92-14969
Simplified method for the prediction of aerofoil excrescence drag magnification factor for turbulent boundary layers at subcritical Mach numbers
[ESDU-91028] p 259 N92-15972
Heat flux sensor research and development: The cool film calorimeter
[NASA-CR-189789] p 298 N92-17006
An experimental investigation of leading edge vortical flow about a delta wing during wing rock
[AD-A243363] p 260 N92-17114
Computation of a Kelvin-Helmholtz instability for delta wing vortex flows
[AD-A244320] p 346 N92-18825
Influence of airfoil geometry on delta wing leading-edge vortices and vortex-induced aerodynamics at supersonic speeds
[NASA-TP-3105] p 350 N92-20038
Blade-mounted trailing edge flap control for BVI noise reduction
[NASA-CR-4426] p 512 N92-21173
The effect of wing ice contamination on essential flight characteristics p 449 N92-21681
Effects of frost on wing aerodynamics and take-off performance p 450 N92-21687
Wind tunnel investigation of a wing-propeller model performance degradation due to distributed upper-surface roughness and leading edge shape modification
p 451 N92-21690
The adverse aerodynamic impact of very small leading-edge ice (roughness) buildups on wings and tails
p 451 N92-21691
The effect of hoar-frosted wings on the Fokker 50 take-off characteristics p 451 N92-21692
Heat transfer characteristics of hypersonic waveriders with an emphasis on the leading edge effects
[NASA-CR-189586] p 525 N92-22215
Hypersonic laminar flow computations over a blunt leading edged delta wing at three different chord Reynolds numbers
[FFA-TN-1991-40] p 528 N92-23168
A simplified method for thermal analysis of a cowl leading edge subject to intense local shock-wave-interference heating
[NASA-TP-3167] p 679 N92-24797
The natural flow wing-design concept
[NASA-TP-3193] p 631 N92-25202
Hypersonic aerospace vehicle leading edge cooling using heat pipe, transpiration and film cooling techniques
p 780 N92-26733
Study of the leading-edge vortex dynamics in the unsteady flow over an airfoil
[AD-A247532] p 829 N92-28865
A method for computing the 3-dimensional flow about wings with leading-edge vortex separation. Part 2: Description of computer program VORSEP
[NLR-TR-86006-U] p 833 N92-29916
In-flight leading-edge extension vortex flow-field survey measurements on a F-18 aircraft at high angle of attack
[NASA-TM-4398] p 947 N92-31276
Vortex flow visualization using colored and fluorescent dyes on flat plate delta wing with leading edge extension
[AD-A251139] p 1036 N92-32651
Unsteady response of the leading-edge vortices on a pitching delta wing p 1041 N92-33851

LEAKAGE
Pressure oscillation in the leakage annulus between a shrouded impeller and its housing due to impeller-discharge-pressure disturbances
p 580 A92-32942
Simple effective thickness model for circular brush seals
[AIAA PAPER 92-3192] p 903 A92-48803
Effects of material choices on brush seal performance
p 1116 A92-54650
Army research concerns in engine sealing
p 228 N92-15089
Seal development activities at Allison Turbine Division
p 228 N92-15093
Redesign of flight space shuttle main engine nozzle G-15 seal area based on the thermal analysis and flow models p 212 N92-15877
Brush seal leakage performance with gaseous working fluids at static and low rotor speed conditions
[NASA-TM-105400] p 297 N92-16265
Engine panel seals for hypersonic engine applications: High temperature leakage assessments and flow modelling
[NASA-TM-105260] p 298 N92-16336
Evaluation of an innovative high-temperature ceramic wafer seal for hypersonic engine applications
p 578 N92-22205
Inflatable traversing probe seal p 595 N92-22692
Turbine blade tip and seal clearance excitation forces
[NASA-CR-184341] p 973 N92-31910

LEARNING
Learning from aircraft accidents and incidents
p 635 A92-39310
Project of an adaptive multiaxial autopilot with learning pilot control
[ETN-92-90592] p 205 N92-15072

LEARNING THEORY
Designing a better engineer p 606 A92-34771

LEASING
Registration of aircraft in the aircraft registrar using the 'Leasing Decree' of the Federal Minister of Transport of February 12, 1991 p 56 A92-11215

LEAST SQUARES METHOD
On the overdetermined celestial fix p 19 A92-10475
Aerodynamic design of axisymmetric hypersonic wind-tunnel nozzles using least-squares/parabolized Navier-Stokes procedure
[AIAA PAPER 92-0332] p 322 A92-25779
Estimation of flying qualities using a leastsquares lower-order equivalent systems technique
p 570 A92-35947
Least-squares/parabolized Navier-Stokes procedure for optimizing hypersonic wind-tunnel nozzles
p 980 A92-50270
Application of recursive partially unknown system identification to aerodynamic coefficients estimation
[AIAA PAPER 92-4504] p 1081 A92-55371

LEGAL LIABILITY
Legal problems in aircraft towing using the PTS procedure p 56 A92-11214
Registration of aircraft in the aircraft registrar using the 'Leasing Decree' of the Federal Minister of Transport of February 12, 1991 p 56 A92-11215
No end to incidents in airspace? III
p 262 A92-23172

The law in Australia relating to negligence of aircrew and engineers p 606 A92-33463
Aviation products liability and navigation - Recent developments and future directions p 697 A92-39563
Navigation charts on trial - How safe is safe? p 1012 A92-49380
Annals of air and space law. Vol. 16 p 1012 A92-51450

LEGENDRE FUNCTIONS
Minimum-drag bodies moving in locality-law media p 779 A92-42732

LENSES
Study of optical techniques for the Ames unitary wind tunnels. Part 2: Light sheet and vapor screen [NASA-CR-190217] p 573 N92-22195

LEVITATION
Materials processing in low gravity [NASA-CR-184280] p 499 N92-20198
Levitation of YBa2Cu3O(7-x) superconductor in a variable magnetic field p 771 N92-27735
Cryogenic test rig with an aerodynamic magnetically levitated carriage p 750 N92-27792
Superconducting bearings with levitation control configurations [NASA-CASE-GSC-13346-1] p 909 N92-29099

LIAPUNOV FUNCTIONS
Model-reference adaptive control for systems with D matrices p 506 A92-29052
Fuzzy controller design and stability analysis for an aircraft model p 478 A92-29124
Lyapunov exponents for systems described by differential equations with discontinuous right-hand sides p 507 A92-29237
A Lyapunov based nonlinear control scheme for stabilizing a basic compression system using a close-coupled control valve p 508 A92-29316
Comparison of six robustness tests evaluating missile autopilot robustness to uncertain aerodynamics p 873 A92-46737
Stability of an adaptive controller for aircraft. I - Analysis via Liapunov theory p 976 A92-51940

LIBRARIES
Background issues for on-line aircraft documentation p 119 N92-13858
NASA/DOD Aerospace Knowledge Diffusion Research Project. Paper 14: An analysis of the technical communications practices reported by Israeli and US aerospace engineers and scientists [NASA-TM-107924] p 782 N92-28183

LICENSING
Mandatory psychological testing of pilots as a requirement for licensing in Norway? p 835 A92-45081

LIFE (DURABILITY)
Thermal barrier coating life prediction model development [ASME PAPER 91-GT-40] p 147 A92-15523
Performance characteristics of brush seals for limited-life engines [ASME PAPER 91-GT-281] p 152 A92-15676
Evolving partnership for NDE in materials engineering and extended life cycle performance p 490 A92-28556
A study on crack initiation method for durability analysis p 901 A92-47663
Durability analysis for a main bulkhead subjected to load on the body of an aircraft p 848 A92-47664
Economic life analysis for replacing components p 785 A92-47670
Areas of seal R/D at GE p 228 N92-15094
Life prediction technologies for aeronautical propulsion systems p 560 N92-22520
Airframe life prediction p 649 N92-25931
Military engine computational structures technology p 660 N92-25934
The use of load enhancement factors in the certification of composite aircraft structures [NLR-TP-90068-U] p 852 N92-28649
Subsonic flight test evaluation of a performance seeking control algorithm on an F-15 airplane [NASA-TM-4400] p 973 N92-31275
Life prediction and constitutive models for engine hot section anisotropic materials program [NASA-CR-189222] p 973 N92-31534
Cost/benefit analysis of the AH-64 (Apache) helicopter Automated Test Equipment (ATE) [AD-A252909] p 1101 N92-33398
Life prediction and constitutive models for engine hot section anisotropic materials program [NASA-CR-189223] p 1072 N92-33479

LIFE CYCLE COSTS
The maintenance economy and economic life of structures p 37 A92-10673
Composite gearbox housing p 110 A92-14448
The C-17 - Modern airlift technology [AIAA PAPER 92-1262] p 538 A92-33342
VSTOL engine design evolution - Growth of the Pegasus engine for Harrier p 860 A92-45306
The concept exploration stage of a dependable avionic system p 1006 A92-49339
Effect of thermodynamic parameters on performance and cost of turbine engines p 969 A92-49834
Research on aircraft life cycle cost reduction p 1012 A92-49835
A fault-tolerant Air Data/Inertial Reference System p 967 A92-51011
Aviation Diagnostics And Maintenance (ADAM) system preliminary concept of operation and functional description [AD-A242598] p 170 N92-14966
An analysis of the aircraft engine Component Improvement Program (CIP): A life cycle cost approach [AD-A243346] p 280 N92-17729
Manufacturing process control as a damage tolerance concept p 403 N92-19006
Scorpion: Close Air Support (CAS) aircraft [NASA-CR-189974] p 462 N92-20664
An appraisal of cost-effectiveness models used in the Air Force and Navy aircraft engine component improvement programs [AD-A245910] p 743 N92-28162
Life cycle costs of the C-130 electrical power system upgrade [AD-A246759] p 786 N92-28348
Cost/benefit analysis of the AH-64 (Apache) helicopter Automated Test Equipment (ATE) [AD-A252909] p 1101 N92-33398

LIFE SCIENCES
Ames life science telescience testbed evaluation [NASA-CR-188856] p 140 N92-12033

LIFE SUPPORT SYSTEMS
U.S. Coast Guard aviation life support and rescue equipment p 529 A92-32999

LIFT
Efficient lifting line method for computing performance of propeller p 24 A92-10956
Design of the flare control law for longitudinal autopilot using H(infinity) synthesis p 28 A92-11562
Pressure on a cylinder with a screen in transverse flow p 6 A92-12164
Vibration of a wing of finite span in subsonic flow at small distances from a solid boundary p 9 A92-12808
Lift development of delta wings undergoing constant acceleration from rest p 9 A92-13209
A 3-D separation model for arbitrary planforms p 65 A92-14360
Review of the physics of enhancing vortex lift by unsteady excitation p 66 A92-15344
A lifting line theory for supersonic flow applications [AIAA PAPER 91-5058] p 171 A92-17841
Control surfaces correlation in DLC maneuvers p 280 A92-21301
Identification of aerodynamic effectiveness and interference effects of direct-lift-control flaps from flight data [AIAA PAPER 92-0171] p 271 A92-23782
Controlling unsteady lift using unsteady trailing-edge flap motions [AIAA PAPER 92-0275] p 318 A92-25729
Investigation on effects on enhancing lift by acoustic excitation p 693 A92-38923
Unsteady aerodynamic loading produced by a sinusoidally oscillating delta wing p 701 A92-41223
In-flight simulation of backside operating models using direct lift controller [SAE PAPER 912069] p 872 A92-45450
Dynamically enhanced sustained lift using oscillating leading-edge flaps [AIAA PAPER 92-2625] p 794 A92-45497
Vortex trapping on a 60 degree delta wing [AIAA PAPER 92-2639] p 796 A92-45508
A LEX blowing technique for post-stall lateral control of trapezoidal wings [AIAA PAPER 92-2714] p 802 A92-45553
Time-average loading on a two-dimensional airfoil in a large amplitude motion p 811 A92-46805
Optimum cruise lift coefficient in initial design of jet aircraft p 845 A92-46806
Wing design for hanggliders having minimum induced drag p 811 A92-46814
Aerodynamic parametric studies and sensitivity analysis for rotor blades in axial flight p 816 A92-46959
Estimation of lift and drag characteristics of an aircraft from flight data p 959 A92-51942
Remarks on the relation between lift induced drag and vortex drag p 941 A92-53079
Use of an approximate similarity principle for the thermal scaling of a full-scale thrust augmenting ejector [AIAA PAPER 92-3792] p 1069 A92-54171
Flight test of a flight reference display for powered-lift STOL aircraft p 1064 A92-56059
Two-fence concept for efficient trapping of vortices on airfoils p 1031 A92-56165
High Reynolds number testing in support of transport airplane development [AIAA PAPER 92-3982] p 1099 A92-56807
High-lift testing at high Reynolds numbers [AIAA PAPER 92-3986] p 1033 A92-56810
Downwash measurements on a pitching canard-wing configuration [AD-A239956] p 12 N92-10016
Propulsive lift noise p 55 N92-10606
Model representation in the PANCOR wall interference assessment code [NASA-TM-104152] p 31 N92-11022
Effect of twin fins on isolated tailplane lift-curve slope [ESDU-91009] p 80 N92-11969
Maximum lift of wings with trailing-edge flaps at low speeds [ESDU-91014] p 81 N92-11970
A unified viscous theory of lift and drag of 2-D thin airfoils and 3-D thin wings [NASA-CR-4414] p 178 N92-13997
A method of estimating a flow breakdown boundary for aerofoils and swept wings in transonic flows [ESDU-91021] p 258 N92-15970
Excrescence drag magnification factors at the drag-rise condition for aerofoils with a specified form of upper-surface pressure distribution [ESDU-91029] p 259 N92-15973
An experimental study of a sting-mounted circulation control wing [AD-A243912] p 346 N92-18895
Pressure and velocity measurements about an airfoil during a parallel blade-vortex interaction p 446 N92-21429
Serrated trailing edges for improving lift and drag characteristics of lifting surfaces [NASA-CASE-LAR-13870-1-CU] p 463 N92-21587
A summary of NASA research on effects of heavy rain on airfoils p 452 N92-21694
Experimental investigation of heavy rainfall effect on a 2-D high lift airfoil p 452 N92-21696
Aerodynamic effects of de/anti-icing fluids and description of a facility and test technique for their assessment p 452 N92-21697
Performance degradation due to hoar frost on lifting surfaces p 628 N92-24866
Use of an approximate similarity principle for the thermal scaling of a full-scale thrust augmenting ejector [NASA-TM-105724] p 739 N92-26613
High lift aircraft [AD-D015215] p 732 N92-27185
Computation of the unsteady transonic 2D cascade flow by an Euler algorithm with interactive grid generation p 719 N92-27944
Evaluation of high lift devices of the quiet STOL experimental aircraft ASKA [NAL-TR-1102] p 733 N92-28153
Force measurements on AGARD calibration model-B at transonic speeds in the NAL two-dimensional wind tunnel [NAL-TM-639] p 722 N92-28190
Experimental investigation of the flowfield of an oscillating airfoil [NASA-TM-105675] p 833 N92-30182
Lift and rolling moment due to spoilers on wings with trailing-edge flaps deflected at subsonic speeds [ESDU-92002-SUPPL] p 1037 N92-32782
On the estimation of jet-induced fountain lift and additional suckdown in hover for two-jet configurations [NASA-TM-102268] p 1040 N92-33618

LIFT AUGMENTATION
Nonlinear control of a twin-lift helicopter configuration p 204 A92-18624
Aerodynamic characteristics of a propeller powered high lift semispan wing [AIAA PAPER 92-0388] p 323 A92-26244
Drag reduction of bluff bodies through momentum injection p 702 A92-41231
Large-scale wind tunnel studies of a jet-engined powered ejector-lift STOVL aircraft p 842 A92-45313

LIFT DEVICES
Aerodynamic characteristics of a propeller powered high lift semispan wing [AIAA PAPER 92-0388] p 323 A92-26244
Lifting surface design using the principle of passive control of elastic characteristics p 480 A92-31865
Optimum hypersonic wings and wave riders p 706 A92-42531
Single block mesh generation for a fuselage plus two lifting surfaces p 817 A92-47054
Serrated trailing edges for improving lift and drag characteristics of lifting surfaces [NASA-CASE-LAR-13870-1-CU] p 463 N92-21587

Constrained spanload optimization for minimum drag of multi-lifting-surface configurations
[NLR-TP-89126-U] p 828 N92-28660

LIFT DRAG RATIO
Nonstationary forces on a wing airfoil
p 4 A92-10825
An experimental study of subsonic separated flow over parawings p 4 A92-10901
Comparative analysis of the lift-drag ratio and heat flows toward the surface of wave riders of different configurations p 7 A92-12173
Experimental investigation on the effect of crescent planform on lift and drag p 9 A92-13206
Grid studies for thin-layer Navier-Stokes computations of airfoil flowfields
[AIAA PAPER 92-0184] p 256 A92-23794
Hypersonic waveriders - Effects of chemically reacting flow and viscous interaction
[AIAA PAPER 92-0302] p 320 A92-25754
A hypersonic waverider test vehicle - The logical next step
[AIAA PAPER 92-0308] p 387 A92-25756
The lift-drag ratio of a slender cone in viscous hypersonic gas flow p 425 A92-30172
A parametric study of the lift-drag ratio of blunt cones
p 437 A92-31860
Possibility of reducing the wave drag of a hypersonic flight vehicle (wave rider) p 438 A92-31863
Determination of the mass-flow-rate characteristics of porous panels p 439 A92-31875
Accurate prediction of drag using Euler methods
p 703 A92-41246
Earth aerobraking strategies for manned return from Mars p 752 A92-41535
Experimental and numerical study of aerodynamic characteristics for second generation SST
[SAE PAPER 912056] p 844 A92-45439
Unsteady Navier-Stokes simulations of supersonic flow over a three-dimensional cavity
[AIAA PAPER 92-2632] p 795 A92-45504
Effect of a deicing device on the induced drag of a lifting airfoil p 959 A92-51947
An aerodynamical analysis of 'seesaw' type rotor for autogyro p 937 A92-52034
Grid studies for thin-layer Navier-Stokes computations of airfoil flowfields p 1025 A92-54935
Experiences with optimizing airfoil shapes for maximum lift over drag p 90 N92-13838
On a global aerodynamic optimization of a civil transport aircraft p 193 N92-13931
Excrescence drag magnification factors at the drag-rise condition for aerofoils with a specified form of upper-surface pressure distribution
[ESDU-91029] p 259 N92-15973
Experimental studies of vortex flaps and vortex plates. Part 1: 0.53 m span 60 deg delta wing
[CRANFIELD-AERO-9113-PT-1] p 349 N92-19679
Manx: Close air support aircraft preliminary design
[NASA-CR-189992] p 463 N92-21565
Variable geometry sailplanes Minisigma
p 629 N92-24877
Aircraft drag reduction p 717 N92-27709

LIFT FANS
An unsteady lifting surface theory for ducted fan blades
[ASME PAPER 91-GT-131] p 71 A92-15575

LIFTING BODIES
Jet inflow simulation and its downwash effect on lifting surfaces p 9 A92-13200
Finite difference numerical prediction of aerodynamics of an airfoil flying over wavy wall p 64 A92-14033
Unsteady lifting surface theory for a rotating transonic cascade of swept blades
[ASME PAPER 91-GT-178] p 73 A92-15610
Measurements of the flow around a lifting-wing/body junction p 175 A92-20726
Optimization of the three-dimensional shape of lifting bodies of small aspect ratio at hypersonic velocities
p 244 A92-21602
PAR-WIG performance prediction during acceleration from water-borne to air-borne p 291 A92-21721
An experimental system to investigate subsonic aeroelastic behavior of lifting surfaces
[AIAA PAPER 92-0061] p 250 A92-22176
Structural design considerations for a Personnel Launch System p 386 A92-24668
Analysis of a 2-D airfoil motion flying in-proximity-to a wavy-wall surface-lifting surface-scheme
p 315 A92-25506
Maximum lift prediction for multielement wings
[AIAA PAPER 92-0401] p 324 A92-26254
An interactive boundary-layer approach to multielement airfoils at high lift
[AIAA PAPER 92-0404] p 324 A92-26257
Numerical and experimental analysis of vortex sheets behind lifting surfaces
[AIAA PAPER 92-0409] p 325 A92-26262
An improved PNS scheme for predicting complex three-dimensional hypersonic flows
[AIAA PAPER 92-0753] p 436 A92-31679
Integrated aeroelastic control optimization of laminated composite lifting surfaces p 481 A92-32248
An aerodynamic design study of a series of lifting bodies at angles of attack from 10 to 53 degrees at Mach numbers from 2.30 to 4.62 p 442 A92-32500
Piloted simulator studies of the HL-20 Lifting Body
p 666 A92-40033
Aerodynamics of lifting configurations --- Russian book
p 712 A92-44125
Gridding strategies and associated results for winged entry vehicles p 918 A92-47051
Analysis of motion of airfoil flying over wavy-wall surface (lifting surface method) p 818 A92-47100
Aerodynamic sensitivities for subsonic lifting-surface
p 819 A92-47695
Aerodynamic performance of a full-scale lifting ejector system in a STOVL fighter aircraft
[AIAA PAPER 92-3094] p 824 A92-48738
Small two-dimensional surface excrescences on aircraft wings approaching separation p 1031 A92-56170
Predicted aerodynamic characteristics for HL-20 lifting-body using the aerodynamic preliminary analysis system (APAS)
[AIAA PAPER 92-3941] p 1033 A92-56771
Navier-Stokes analysis of turbulent boundary layer and wake for two-dimensional lifting bodies
p 221 N92-14309
Evolution and development of hypersonic configurations 1958-1990
[AD-A242768] p 197 N92-15069
Performance and stability analysis of the non-linear dynamics of a simple powered lifting hypersonic vehicle flying on a minor circle
[AD-A243933] p 366 N92-19192
Serrated trailing edges for improving lift and drag characteristics of lifting surfaces
[NASA-CASE-LAR-13870-1-CU] p 463 N92-21587
The adverse aerodynamic impact of very small leading-edge ice (roughness) buildups on wings and tails
p 451 N92-21691
In-flight simulation studies at the NASA Dryden Flight Research Facility
[NASA-TM-4396] p 853 N92-29110
Aerodynamic centre of wing-body combinations
[ESDU-92024] p 1036 N92-32479

LIFTING REENTRY VEHICLES
Weight evaluation and sensitivity analysis for space plane. Part 2: TSTO
[NAL-TM-602-PT-2] p 287 N92-17754
Rarefied-flow aerodynamics
[NASA-CR-190452] p 715 N92-27191
Preliminary subsonic aerodynamic model for simulation studies of the HL-20 lifting body
[NASA-TM-4302] p 978 N92-31175

LIFTING ROTORS
Lifting line predictions for a swept tip rotor blade
p 65 A92-14424
Flowfield of a lifting rotor in hover - A Navier-Stokes simulation p 1024 A92-54906
Helicopter main-rotor speed effects: A comparison of predicted ranges of detection from the aural detection program ICHIN and the electronic detection program ARCAS
[NASA-TM-104134] p 166 N92-12598
A simulation model of a single rotor helicopter
p 979 N92-31865

LIGHT AIRCRAFT
Stratospheric lighter-than-air powered platform
p 110 A92-15334
Fair weather convection and light aircraft accidents
[IAF PAPER ST-91-004] p 186 A92-20651
The application of high spectral and spatial resolution imaging spectrometers for locating downed aircraft
p 598 A92-35132
The role of PM in the design of lightweight aircraft engine components p 991 A92-50137
Dynamic flying investigations on 1/13.5 NALLA model (Longitudinal Results)
[NAL-PD-FC-9113] p 359 N92-18073

LIGHT BEAMS
Transmission of thin light beams through turbulent mixing layers
[AIAA PAPER 92-0658] p 396 A92-27029
Crossed beam correlation modeling and experimental techniques for measuring density fluctuations in hypersonic flows
[AIAA PAPER 92-2779] p 758 A92-41323

LIGHT EMITTING DIODES
Terrain following of arbitrary surfaces using a high intensity LED proximity sensor
[DE92-007161] p 455 N92-21201

LIGHT GAS GUNS
Nonstationary gasdynamics p 220 N92-13985

LIGHT HELICOPTERS
Comanche - The armed scout p 103 A92-13291
LH wind tunnel testing - Key to advanced aerodynamic design p 104 A92-14331
Helicopter modeling requirements for full mission simulation and handling qualities assessment
p 105 A92-14364
A full mission simulation data system
p 162 A92-14367
Results of flight tests of the Boeing Sikorsky Fantail demonstrator p 106 A92-14376
Optimization of a light helicopter with Arrius power plants p 120 A92-14408
Tiger MGB - High reliability low weight --- military helicopter Main Gear Box p 109 A92-14418
P120 programme - First results of the pre-development phase p 60 A92-14447
Flight safety; Proceedings of the Conference, London, England, Nov. 21, 1991 p 92 A92-16050
The development of a new light, single engine helicopter family p 545 A92-35734
Self reliance in aerospace structures
p 758 A92-41190

LIGHT SCATTERING
In situ measurement of particle formation in heated jet fuels: A new application of photon correlation spectroscopy
[DE92-003641] p 488 N92-20132
Concept design phase expendable holographic sensor to measure ocean small angle optical scattering
[AD-A245067] p 501 N92-20997
Optical measurement systems p 594 N92-22527

LIGHT SOURCES
The acoustic flashlight
[MBB-Z-0359-90-PUB] p 239 N92-15938
Study of optical techniques for the Ames unitary wind tunnels. Part 1: Schlieren
[NASA-CR-189951] p 385 N92-19218

LIGHT TRANSMISSION
Transmission of thin light beams through turbulent mixing layers
[AIAA PAPER 92-0658] p 396 A92-27029

LIGHTING EQUIPMENT
Comparative evaluation of internally and externally lighted taxiway guidance signs
[DOT/FAA/CT-TN92/2] p 573 N92-22237

LIGHTNING
Lightning standards for aircraft protection
p 91 A92-14688
Lightning activity in microburst producing storm cells
[ONERA, TP NO. 1991-98] p 161 A92-16080
Study of simulated lightning discharge effects on wires of a rotorcraft
[ONERA, TP NO. 1991-173] p 92 A92-16137
Analysis technique for lightning attachment zoning of aircraft p 186 A92-20126
Nonlinear triggered lightning models for use in finite difference calculations p 230 A92-20128
Analysis and modeling of lightning strikes to the F106B, CVF580, and C160 aircraft p 186 A92-20129
Current stabilizing of fastened composite joints to improve non-sparking lightning current performance
p 213 A92-20130
Aircraft lightning strikes
[ONERA, TP NO. 1991-204] p 351 A92-26361
Aircraft-triggered lightning - Processes following strike initiation that affect aircraft p 836 A92-46784
Mechanisms of high-current pulses in lightning and long-spark stepped leaders p 1116 A92-54678
Lightning protection requirements for aircraft: A proposed specification
[RAE-TM-FS(F)-632-REV-ISSUE] p 187 N92-14007
Lightning strike tests of composite connectors
[AD-A252281] p 1044 N92-33249

LIGHTNING SUPPRESSION
Lightning protection for the Dornier 328
p 113 A92-17253
Whole aircraft lightning indirect effects evaluation using low level injection techniques p 192 A92-20134
The use of finite difference electromagnetic analysis in the design and verification of modern aircraft
p 192 A92-20136

LINE OF SIGHT
LOS rate estimation in inertial navigation using landmarks p 453 A92-29360
Comparison of Janus and field test aircraft detection ranges for the line-of-sight forward heavy system
[AD-A246047] p 770 N92-27600

LINEAR ARRAYS
Wall pressure wavenumber-frequency spectrum beneath a turbulent boundary layer measured with transducer arrays calibrated with an acoustical method
[ONERA, TP NO. 1991-212] p 329 A92-26364
New systolic array for all-nearest-neighbours problem
p 776 A92-41419

LINEAR EQUATIONS
Derivation of aircraft linear state equations from implicit nonlinear equations p 27 A92-11361
Investigation of extremal field behavior for two-dimensional linear problems in flight mechanics
p 509 A92-30130
Application of linearization analysis to aircraft dynamics p 661 A92-39902
A parallel-vector algorithm for rapid structural analysis on high-performance computers
[NASA-TM-102614] p 595 N92-22649

LINEAR FILTERS
PC based flight path reconstruction using UD factorization filtering algorithm
[NAL-PD-FC-9201] p 534 N92-22389

LINEAR PROGRAMMING
A low-altitude breakthrough system using optimal path terrain following p 205 A92-20483
A constraint satisfaction approach to operative management of aircraft routing p 350 A92-25181

LINEAR QUADRATIC GAUSSIAN CONTROL
Real parameter uncertainty and phase information in the robust control of flexible structures
p 32 A92-11345
On-line adaptive control of unstable aircraft wing flutter p 27 A92-11374
Parameter insensitive control utilizing eigenspace methods --- for flutter suppression in aeroelastic vehicles
p 204 A92-18615
Application of stochastic robustness to aircraft control systems p 204 A92-18620
Structure/control design synthesis of active flutter suppression system by goal programming
p 204 A92-18621
Combined H(2)/H(infinity) optimal control design applied to an advanced fighter aircraft
[AIAA PAPER 92-0045] p 281 A92-22162
Loop shaping in mixed H2 and H-infinity optimal control p 507 A92-29177
Tiltrotor control law design for rotor loads alleviation using modern control techniques p 478 A92-29331
Flight control system design p 776 A92-43181
Wideband control of gyro/accelerometer multisensors in a strapdown guidance system p 856 A92-46736
Linear quadratic minimax controllers
p 917 A92-46748
Optimal implicit model-following approach with frequency-shaped weighting and its application to design of flight control system p 977 A92-53094
Quantitative Feedback Theory approach to AIAA Controls Design Challenge
[AIAA PAPER 92-4626] p 1077 A92-55303

LINEAR QUADRATIC REGULATOR
Study of the discrete singularly perturbed linear-quadratic control problem by a bilinear transformation p 163 A92-16072
The application of parameter optimisation techniques to linear optimal control system design
p 302 A92-23038
Command following control law design by linear quadratic optimisation p 568 A92-35749
Robust flight control system design with multiple model approach p 661 A92-39910
Negative state weighting in the linear quadratic regulator for aircraft control p 1007 A92-50513
An algorithm for robust eigenstructure assignment using the Linear Quadratic Regulator
[AIAA PAPER 92-4478] p 1131 A92-55237
Gain scheduled linear PID autopilot for the AIAA Controls Design Challenge aircraft
[AIAA PAPER 92-4629] p 1078 A92-55304
Synthesis of gust load alleviation with flutter margin augmentation p 1082 A92-56021
Robust control system design with multiple model approach p 1083 A92-56029
Approximation methods for control of acoustic/structure models with piezoceramic actuators
[NASA-CR-189578] p 234 N92-15658
Multiple input sliding mode control for autonomous diving and steering of underwater vehicles
[AD-A241935] p 283 N92-17442
An algorithm for robust eigenstructure assignment using the linear quadratic regulator
[AD-A244267] p 412 N92-19335
A multi-loop guidance scheme using singular perturbation and linear quadratic regulator techniques simultaneously p 481 N92-20148

LINEAR RECEIVERS
Probability of cycle jumps in Omega receivers and other phase locked loop applications
[PB92-128891] p 455 N92-21279

LINEAR SYSTEMS
Robustness of distributed systems with respect to small time delays p 47 A92-11351
A time approach to robustness of LTI systems with structured uncertainty and unmodelled dynamics --- linear time-invariant p 48 A92-11356
Observability analysis of piece-wise constant systems with application to inertial navigation p 49 A92-11391
Robust pole assignment using closed loop controllability conditions p 49 A92-11417
Design of reliable control systems p 49 A92-11420
H(infinity) control of linear systems with nonzero initial conditions p 50 A92-11430
Fault tolerant control based on a new accommodation filter p 51 A92-11453
A design of continuous-time model reference adaptive control based on a function estimation of periodically time varying linear system p 51 A92-11454
Optimal rejection of bounded persistent disturbances in periodic systems p 51 A92-11464
Dynamic interpolation for linear systems
p 52 A92-11465
Equivalence of optimal control problems and the use of parameterization methods p 52 A92-11466
Decentralized-feedback pole placement of linear systems p 411 A92-27347
Optimal output feedback for linear time-periodic systems p 412 A92-28142
Linear systems with output constraints - The theory and application of maximal output admissible sets
p 506 A92-29066
Parameter identification of linear systems based on smoothing p 873 A92-46742
Robustness characteristics of fast-sampling digital PI controllers for high-performance aircraft with impaired control surfaces p 877 A92-48496
Parameter identification for nonlinear aerodynamic systems
[NASA-CR-188985] p 53 N92-10347
Technical notes and correspondence: Stochastic robustness of linear time-invariant control systems
p 303 N92-18002
A methodology for computing uncertainty bounds of multivariable systems based on sector stability theory concepts
[NASA-TP-3166] p 482 N92-21410
Modeling of linear isentropic flow systems
p 593 N92-22495

LINEAR TRANSFORMATIONS
Computational algorithms for increased control of depth-viewing volume for stereo three-dimensional graphic displays
[NASA-TM-4379] p 1065 N92-34109

LINEARIZATION
Aerobrake guidance law synthesis using feedback linearization p 485 A92-29304
Nonlinear system design: Adaptive feedback linearization with unmodeled dynamics
[AD-A248484] p 1009 N92-30335

LININGS
High-temperature combustor and seal for a water piston propulsor
[AD-A242493] p 229 N92-15385
High-temperature durability considerations for HSCT combustor
[NASA-TP-3162] p 289 N92-17070
Evaluation of the applicability of Helmholtz resonators for low frequency acoustic liners
[PB92-138544] p 605 N92-23588

LINKAGES
A theory for mechanical flight control linkages
p 269 A92-21312

LIQUEFACTION
Cryogenic hydrogen-induced air-liquefaction technologies for combined-cycle propulsion applications
p 487 N92-21526

LIQUID AIR
Cryogenic hydrogen-induced air-liquefaction technologies for combined-cycle propulsion applications
p 487 N92-21526

LIQUID AIR CYCLE ENGINES
Advanced SCRAM-LACE system concept for single-stage-to-orbit space plane
[IAF PAPER 91-272] p 32 A92-12599
Influence of air liquefaction cycle on performance of combined cycle engine p 372 A92-24878
Cryogenic hydrogen-induced air-liquefaction technologies for combined-cycle propulsion applications
p 487 N92-21526

LIQUID BEARINGS
The stability of the steady state and bistable response of a flexible rotor supported on squeeze film dampers
p 222 N92-14350
The application of a cylindrical-spherical floating ring bearing as a device to control stability of turbogenerators p 224 N92-14371
Effect of eccentricity on the static and dynamic performance of a turbulent hybrid bearing
p 225 N92-14373

LIQUID COOLING
Liquid cooled turbocharged propulsion system for HALE application
[ASME PAPER 91-GT-399] p 127 A92-15729
Outline and discussion of the cooling loop of the heating control system in the exposed facility of the Japanese Experiment Module (JEM) p 574 A92-35610
Liquid flow-through cooling for avionics applications
p 902 A92-48448
Liquid cooled approaches for high density avionics
p 989 A92-49274
The mechanism of liquid-cooling of vane in high-temperature turbine p 969 A92-49841

LIQUID CRYSTALS
New applications of liquid-crystal thermography in rotating turbomachinery heat transfer research
[ASME PAPER 91-GT-354] p 153 A92-15710
Liquid crystal coatings for surface shear-stress visualization in hypersonic flows p 496 A92-32177
C-130 glass cockpit system development program
[AIAA PAPER 92-1050] p 553 A92-33230
Development of the D-size liquid crystal flat panel display for aircraft p 734 A92-43208
Evaluation test on the simulator of the liquid crystal flat display. II p 734 A92-43209
Current status and future tasks of a cockpit liquid crystal display p 735 A92-43222
Demonstration performance of an aircraft liquid crystal display p 735 A92-43224
Computer-based areal surface temperature and local heat transfer measurements with thermochromic liquid crystals (TLC) p 763 A92-44326
Visualization of boundary-layer development on turbomachine blades with liquid crystals
[NASA-CR-190433] p 742 N92-27519

LIQUID FILLED SHELLS
Calculation of fuel sloshing and its coupling vibration with a tank p 991 A92-50204

LIQUID FLOW
A study of flow of a fluid film on the surface of a plate in the case of slot injection p 496 A92-31892
High Reynolds number flows using liquid and gaseous helium
[ISBN 0-387-97475-X] p 897 A92-45261
Liquid flow-through cooling for avionics applications
p 902 A92-48448

LIQUID FUELS
One-dimensional analysis of liquid-fueled combustion instability p 143 A92-17188
Self reliance in aerospace structures
p 758 A92-41190

LIQUID HELIUM
High Reynolds number flows using liquid and gaseous helium
[ISBN 0-387-97475-X] p 897 A92-45261
High-Reynolds-number test requirements in low-speed aerodynamics p 787 A92-45263
Water tunnels p 880 A92-45266
Magnetic suspension using high temperature superconducting cores p 772 N92-27789

LIQUID INJECTION
Factors influencing the effective spray cone angle of pressure-swirl atomizers p 295 A92-23300
Forced-injection quenching of a hot-tube under microgravity p 590 A92-35977

LIQUID NITROGEN
Structure and penetration of a transverse fluid jet injected at supercritical pressure in supersonic flow
[AIAA PAPER 92-3652] p 1113 A92-54105
Magnetic suspension using high temperature superconducting cores p 772 N92-27789

LIQUID OXYGEN
Rotor support for the STME oxygen turbopump
[AIAA PAPER 92-3282] p 904 A92-48872
Turbine drive system of the high pressure LOX turbopump test facility
[DE92-783191] p 680 N92-25342

LIQUID PHASES
Determination of liquid water content in the AEDC engine test cells
[AIAA PAPER 92-0165] p 263 A92-23778
Metal matrix composite fabrication processes for high performance aerospace structures p 760 A92-42145

LIQUID PROPELLANT ROCKET ENGINES
One-dimensional analysis of liquid-fueled combustion instability p 143 A92-17188

Calculation methods on equivalence ratio of multi-propellant for propulsion system
p 893 A92-48269

LIQUID ROCKET PROPELLANTS
Experimental investigation of liquid carbonhydrogen fuel combustion in channel at supersonic velocities
[AIAA PAPER 92-3429] p 894 A92-48986

LIQUID SLOSHING
Calculation of fuel sloshing and its coupling vibration with a tank p 991 A92-50204

LIQUID SURFACES
Modeling the effect of helicopter downwash on warm fog p 775 A92-44081

LIQUID-LIQUID INTERFACES
Calculating the steady-state nonlinear aerodynamic characteristics of thin wings near the interface between two fluids p 426 A92-30181
Stokes flows in superposed immiscible liquids with horizontal heating
[IAF PAPER 92-0909] p 1123 A92-57288

LIQUID-SOLID INTERFACES
Experimental study of convection effects around the phase charge interface p 1111 A92-53755
Method and apparatus for acoustic plate mode liquid-solid phase transition detection
[DE92-003778] p 401 N92-18705

LIQUID-VAPOR INTERFACES
Flow pattern characterization and heat transfer behavior in a boiling two-phase flow in an inclined pipe
p 493 A92-29722

LOAD CARRYING CAPACITY
The development and test of thermoplastic composite speed brake p 272 A92-24178
Evaluation of methods for estimating store carriage loads
[AIAA PAPER 92-0675] p 379 A92-27043

LOAD DISTRIBUTION (FORCES)
Effect of some load factors of bird impact on blade response p 371 A92-24740
Crashworthiness of truncated composite cones under side loads p 590 A92-35746
A study on crack initiation method for durability analysis p 901 A92-47663
Durability analysis for a main bulkhead subjected to load on the body of an aircraft p 848 A92-47664
Optimization of longitudinal corrections of helical gears p 990 A92-49578
Three-dimensional relaxation effect on quasi-3D flow in a blade row with spanwise loading distribution
p 936 A92-51593
The static and fatigue computation of the propeller blades retention system p 995 A92-51895
Force production mechanisms of a tangential jet on bodies at high alpha
[AIAA PAPER 92-4648] p 1082 A92-55393
Effects of spectrum variations on fatigue crack growth
p 1123 A92-57399
Experimental study of an independently deflected wingtip mounted on a semispan wing
[NASA-TM-102842] p 13 N92-10983
Gear tooth stress measurements of two helicopter planetary stages
[NASA-TM-105651] p 764 N92-26555

LOAD TESTING MACHINES
Apparatus for elevated temperature compression or tension testing of specimens
[NASA-CASE-LAR-14775-1] p 912 N92-30099

LOAD TESTS
Certifying composite helicopter structures
p 110 A92-14443
Experimental and theoretical analysis of composite I-beams with elastic couplings p 216 A92-18377
Multiaxial load spectra in a cooled gas turbine blade under in-service conditions p 201 A92-19696
Prediction of fatigue crack growth in a Ti-6Al-4V fan disk forging under spectrum loading p 213 A92-19817
Design and testing leading to certification of the Airbus A340 nose landing gear doors p 272 A92-24192
Design, analysis, testing, and certification of composite primary structure for the Piaggio P-180 Avanti
p 535 A92-32553
Effects of T-tabs and large deflections in double cantilever beam specimen tests p 673 A92-39009
Testing of a titanium matrix composite landing gear
[SAE PAPER 912175] p 644 A92-40000
Dynamic stall on wind turbine blades
[DE92-001157] p 262 N92-17874
CH-46 and OH-58 transmission stress wave analysis
[AD-A244321] p 365 N92-18826
The use of load enhancement factors in the certification of composite aircraft structures
[NLR-TP-90068-U] p 852 N92-28649
Combined load test apparatus for flat panels
[NASA-CASE-LAR-14698-1] p 911 N92-30028
Apparatus for elevated temperature compression or tension testing of specimens
[NASA-CASE-LAR-14775-1] p 912 N92-30099

LOADING MOMENTS
Short time force measurement system
p 208 N92-15001

LOADING OPERATIONS
Enhancement of ground handling through optimum selection/use of Ground Support Equipment (GSE)
[SAE PAPER 911973] p 881 A92-45380

LOADING RATE
A viscoplastic model for single crystals
p 391 A92-24717
A compound fatigue investigation of plate specimen under low-cycle load superposed on high cycle load
p 587 A92-35555

LOADS (FORCES)
Dual strain gage balance system for measuring light loads
[NASA-CASE-LAR-14419-1] p 42 N92-10185
Critical appraisal of the McDonnell Douglas closure model for predicting fatigue crack growth
[ARL-STRUC-R-444] p 44 N92-11376
On the limitations of Froude's actuator disc concept
[ETN-91-90136] p 81 N92-11973
F/A-18 stabilator: Equivalent set of point forces required for pneumatic bag load case simulation
[AD-A242637] p 206 N92-15073
Industrial code development p 227 N92-15083
Effect of crash pulse shape on seat stroke requirements for limiting loads on occupants of aircraft
[NASA-TP-3126] p 399 N92-18053
Aircraft tracking optimization of parameters selection
p 361 N92-18585
The Operational Loads Monitoring System, OLMS
p 361 N92-18586
Life management approach for USAF aircraft
p 362 N92-18587
Managing airborne assets through loads monitoring
p 363 N92-18594
Aircraft engine hot section technology: An overview of the HOST Project p 561 N92-22535
Combined load test apparatus for flat panels
[NASA-CASE-LAR-14698-1] p 911 N92-30028
Landing gear mechanism including runway-roughness restrictor assembly
[CA-PATENT-1-257-618] p 1061 N92-33585

LOCAL AREA NETWORKS
Airborne/shipborne PSK telemetry data link
p 839 A92-47511
Networked simulation of multiple aircraft using Semi-Automated Forces
[AIAA PAPER 92-4170] p 1008 A92-52455
MULTIRAD
[AD-A244211] p 412 N92-19247
Identification of aerodynamic models for maneuvering aircraft
[NASA-CR-190444] p 852 N92-28720

LOCKHEED AIRCRAFT
The stealth master p 307 A92-25175
YF-22A prototype Advanced Tactical Fighter demonstration/validation flight test program overview
[AIAA PAPER 92-1087] p 537 A92-33253
Dawn of stealth p 785 A92-47757
The Tonopah years p 785 A92-47758
The airplane --- F-117 aircraft p 849 A92-47759

LOFTING
Algorithms for blending surface generation
[AD-A245686] p 777 N92-26524

LOGIC DESIGN
Neural network and fuzzy logic technology for naval flight control
[AD-A242650] p 206 N92-15074
Safety study of TCAS 2 for logic version 6.04
[DOT/FAA/RD-92/22] p 1047 N92-32537

LOGIC PROGRAMMING
Parameter identification studies on the NASA/Ames Research Center Advanced Concepts Flight Simulator
[NASA-TM-105126] p 31 N92-11024

LOGISTICS
Integration of supportability elements into the conceptual design process
[AIAA PAPER 92-1194] p 600 A92-33306
A development-memory approach for enhancing avionics software logistics p 119 N92-12540
A review of aging aircraft technology: An IAI perspective
[IAITIC-91-1018] p 461 N92-20500
Revolution at sea: Aircraft options for the year 2030
p 466 N92-21974
Developing robust support structures for high-technology subsystems: The AH-64 Apache helicopter
[AD-A252773] p 1017 N92-33499

LOGISTICS MANAGEMENT
Preparation for a new plane (A 320): Experience reviewed p 1010 N92-30954
Flight crew integration in the maintenance chain of a commercial aircraft (A 320) p 1012 N92-30957

LONGERONS
Surface generation and editing operations applied to structural support of aerospace vehicle fuselages
p 777 N92-27831

LONGITUDE MEASUREMENT
Measurements of longitudinal static aerodynamic coefficients with cable mount system
p 1093 A92-56013

LONGITUDINAL CONTROL
Identification of higher-order helicopter dynamics using linear modeling methods p 131 A92-14336
Optimization of the aerodynamic balance and parameters of the horizontal tail surfaces of the three-surface aircraft configuration with allowance for the capabilities of the stability and control augmentation system p 134 A92-16803
Use of neural networks in control of high alpha maneuvers
[AIAA PAPER 92-0048] p 282 A92-22164
Lyapunov exponents for systems described by differential equations with discontinuous right-hand sides
p 507 A92-29237
Velocity dependence of high angle of attack longitudinal flying qualities criteria
[SAE PAPER 912149] p 662 A92-39985
X-29 H-infinity controller synthesis
p 873 A92-46749
Analysis of the VISTA longitudinal simulation capability for a cruise flight condition p 876 A92-48488
Some problems on atmospheric turbulence spectrum and aircraft response p 975 A92-50235
Gain scheduled linear PID autopilot for the AIAA Controls Design Challenge aircraft
[AIAA PAPER 92-4629] p 1078 A92-55304
Multiaxis control in longitudinal mode of aircraft
p 1083 A92-56027
Robust control system design with multiple model approach p 1083 A92-56029
Flight control system design using H(infinity) optimal control p 1083 A92-56030
The effect of wing ice contamination on essential flight characteristics p 449 N92-21681
Some longitudinal handling qualities design guidelines for active control technology transport aircraft
[NLR-TP-90129-U] p 878 N92-28652

LONGITUDINAL STABILITY
Evaluation method of longitudinal static stability of tailless airplane p 282 A92-22520
An approach to the low-speed longitudinal aerodynamic characteristics of the joined wing configuration
p 339 A92-27909
Comment on 'Effect of thrust/speed dependence on long-period dynamics in supersonic flight'
p 643 A92-39913
Estimation of spaceplane longitudinal stability and control derivatives from dynamic wind tunnel test
p 752 A92-43211
Aircraft longitudinal dynamics equations including wind shear effects p 977 A92-51946
An improved wall correction method for the longitudinal stability p 978 A92-53388
Stability and dynamic coupling of elastic vehicles with unsteady aerodynamic forces considered
p 1102 A92-53545
Multiple delay model approach applied to the AIAA 1922 Controls Design Challenge
[AIAA PAPER 92-4630] p 1078 A92-55305
Flight testing of a half-scale remotely piloted vehicle
[AD-A248568] p 733 N92-28123

LOOP ANTENNAS
Transfer function between airborne VLF transmit and receive loop antenna p 1045 A92-54754

LORAN
The FAA Loran program status and expectations
p 95 A92-16629
From Russia and beyond --- equipment and areas of coverage for Loran navigation outside NAS
p 96 A92-16638
The statistical estimation of navigation errors
p 97 A92-16652
Omega/VLF now and into the 21st century
p 98 A92-16659
The status of Loran's implementation in the National Airspace System (NAS) p 638 A92-39565
A Kalman filter integrated navigation design for the IAR Twin Otter Atmospheric Research Aircraft
[NRC-32148] p 1048 N92-32849

LORAN C
Curved landing approaches using ILS and Loran C
p 94 A92-13854

The future of Loran-C navigation, instrument approaches and flight following for air traffic management
p 95 A92-16630
Strategic vs tactical air traffic control utilizing ADS and earth reference area NAV p 96 A92-16631
Loran time difference correction factors - Valid information or blue smoke and mirrors?
p 96 A92-16633
The DOT/DOD Federal Radionavigation Plan
p 96 A92-16637
In-flight demonstration of hybrid GPS/Loran RAIM
p 96 A92-16643
The 1990 Federal Radionavigation Plan and its impact on the Omega Navigation System p 98 A92-16658
The accuracy and coverage of Loran-C and of the Decca Navigator System - and the fallacy of fixed errors
p 353 A92-24944
Measurement of LORAN-C envelope to cycle difference in the far field
[PB92-128909] p 455 N92-21263
Loran-C performance assurance assessment program
[NASA-CR-190469] p 840 N92-28718
LORAN-C data reduction at the US Naval Observatory
p 1050 N92-33358

LORENTZ FORCE
Research activities on CFD at the Ship Research Institute p 766 N92-26908

LOSSES
Experimental investigation into the effects of riblets on compressor cascade performance
[AD-A243881] p 377 N92-19235
Examination of the main error factors with regards to secondary losses in compression and turbine cascades by variations of the blade picture ratio
[ETN-92-91493] p 871 N92-29927
An improved compressor performance prediction model
[PNR-90873] p 1072 N92-33749

LOSSY MEDIA
Analysis of lossy composite terminating structures
[NASA-CR-189901] p 404 N92-19217

LOUDNESS
A loudness calculation procedure applied to shaped sonic booms
[NASA-TP-3134] p 56 N92-11765
Application of magnitude estimation scaling to the assessment of subjective loudness response to simulated sonic booms
[NASA-TM-107657] p 1138 N92-33719
The effect of turbulence on the loudness of minimized sonic boom signatures p 1139 N92-33880
Subjective loudness response to simulated sonic booms p 1140 N92-33885

LOUDSPEAKERS
Propeller sound excitation on an aircraft fuselage using a loudspeaker ring p 643 A92-39087
Thermoacoustic refrigeration p 595 N92-22720
A lightweight loudspeaker for aircraft communications and active noise control p 1125 N92-32964

LOW ALTITUDE
Stochastic prediction techniques for wind shear hazard assessment p 48 A92-11381
Computer aiding for low-altitude helicopter flight
p 94 A92-14444
A multidimensional terrain model for low altitude tracking scenarios p 205 A92-19107
Predicting summer microburst hazard from thunderstorm day statistics p 407 A92-27960
Aerothermal ablation behavior of selected candidate external insulation materials
[AIAA PAPER 92-3056] p 893 A92-48714
An advanced flight path management system for low-altitude helicopter flight p 975 A92-49330
Stochastic prediction techniques for wind shear hazard assessment p 1007 A92-50505
Analysis of image-based navigation system for rotorcraft low-altitude flight p 1046 A92-55968
Passive range estimation for rotorcraft low-altitude flight
[NASA-TM-103897] p 2 N92-10003
Rotorcraft low altitude IFR benefit/cost analysis: Operations analysis
[SCT-90RR-44] p 191 N92-15061
Trajectory analysis of the G-11 family of clustered parachutes to determine minimum altitude
[AD-A243375] p 261 N92-17404
Spectrum modal analysis for the detection of low-altitude windshear with airborne Doppler radar
[NASA-CR-4457] p 953 N92-31549

LOW ASPECT RATIO
Optimization of the three-dimensional shape of lifting bodies of small aspect ratio at hypersonic velocities
p 244 A92-21602
3D Navier-Stokes analysis for a tip leakage flow in a low aspect ratio turbine
[AIAA PAPER 92-0395] p 278 A92-23816
Experimental observations of instability modes in a rectangular jet p 1135 A92-54908
On simple aerodynamic sensitivity derivatives for use in interdisciplinary optimization
[NASA-TM-104145] p 82 N92-11985
The effect of rounding the leading edges on the characteristics of separated flow past delta wings of low aspect ratio
[RAE-LIB-TRANS-2164] p 257 N92-15964
Normal force of low aspect ratio wing-body combinations up to high angles of attack at supersonic speeds
[ESDU-91042] p 553 N92-24009
A critical evaluation of a three-dimensional Navier-Stokes method as a tool to calculate transonic flows inside a low-aspect-ratio compressor
p 768 N92-27459
Formation and sustainment of a very low aspect ratio tokamak using coaxial helicity injection: Helicity Injected Torus (HIT) experiment
[DE92-014311] p 1136 N92-32595
Shafranov shift in low-aspect-ratio heliotron/torsatron CHS
[NIFS-110] p 1138 N92-33743

LOW ASPECT RATIO WINGS
Modeling of the vortex structure at delta wings of low aspect ratio by the discrete vortex method
p 7 A92-12203
Low aspect ratio wing code validation experiment
[AIAA PAPER 92-0402] p 324 A92-26255
Boundary layer on slender wings of small aspect ratio
p 441 A92-31963
Low-speed flutter characteristics of some simple low-aspect-ratio delta-wing models p 460 A92-32247
A model of a deformable aeroplane with a wing of low aspect ratio and movable control surfaces for studying natural vibrations p 744 A92-41528
Self-induced roll oscillations of low-aspect-ratio rectangular wings p 874 A92-46802
Flutter analysis and wind tunnel test with respect to a low-aspect-ratio wing with free-rotational control surface
p 1052 A92-56014
Analysis and wind tunnel test of low aspect wing gust load alleviation p 1053 A92-56020
Aeroelastic effects of spoiler surfaces on a low-aspect-ratio rectangular wing p 1030 A92-56154
Numerical modeling of transonic juncture flow
[AIAA PAPER 92-4036] p 1035 A92-56858
Nonequilibrium turbulence modeling effects on transonic vortical flows about delta wings p 85 N92-13007
The effects of winglets on low aspect ratio wings at supersonic Mach numbers
[NASA-CR-4407] p 178 N92-13996
Studies in general aviation aerodynamics
[NASA-CR-190431] p 827 N92-28511

LOW CARBON STEELS
Rolling element bearing member
[PATENT-1-271-213] p 158 N92-13434

LOW COST
Analytical design and demonstration of a low-cost expendable turbine engine combustor
[AIAA PAPER 92-3754] p 867 A92-49112
Low cost HIRF troubleshooting and verification method for digital avionics systems p 990 A92-49304
An aircraft Earth station for general aviation
p 678 N92-24194

LOW DENSITY FLOW
Solution of the Burnett equations for hypersonic flows near the continuum limit
[AIAA PAPER 92-2922] p 821 A92-47894
Direct simulation of low-density flow over airfoils
p 1030 A92-56159

LOW FREQUENCIES
Mechanical noise from large wind turbines - Experiences from Swedish prototypes p 686 A92-39046
Feasibility of measuring transverse electric noise at VLF and LF on an ice cap
[AD-A252280] p 1129 N92-33220

LOW GRAVITY MANUFACTURING
Modifications to the rapid melt/rapid quench and transparent polymer video furnaces for the KC-135
[NASA-CR-184215] p 157 N92-12231

LOW NOISE
Interior noise reduction program for the Dornier 328
p 114 A92-17254
Noise from turbine generators - Noise control, propagation, and assessment p 686 A92-39044
Research on a low-noise engine for a high-speed VTOL aircraft p 737 A92-43239
The design of a subsonic low-noise, low-turbulence wind tunnel for acoustic measurements
[AIAA PAPER 92-3883] p 1094 A92-56726

LOW PASS FILTERS
An adaptive correction technique for Differential Global Positioning System p 726 N92-26623

LOW PRESSURE
Aerothermodynamic radiation studies
[NASA-CR-185666] p 284 N92-15998
Investigations of blade row interaction and boundary layer transition phenomena in a multistage aero engine low-pressure turbine by measurements with hot-film probes and surface-mounted hot-film gauges
p 658 N92-24338

LOW REYNOLDS NUMBER
Airfoil boundary layer measurements at low Re in an accelerating flow from a nonzero velocity
p 62 A92-13673
An experimental investigation of large scale instabilities in a low Reynolds number two-stream supersonic shear layer
[AIAA PAPER 92-0177] p 255 A92-23787
Experimental study of a low Reynolds number tandem airfoil configuration p 442 A92-32241
Low Reynolds number, long endurance aircraft design
[AIAA PAPER 92-1263] p 538 A92-33343
Subsonic and transonic low-Reynolds-number airfoils with reduced pitching moments p 701 A92-41211
Design - Analysis and experimental verification of a propeller working in the low Reynolds number range
p 710 A92-43174
Laminar separation bubbles and airfoil design at low Reynolds numbers
[AIAA PAPER 92-2735] p 797 A92-45515
Unsteady aerodynamics of a Wortmann wing at low Reynolds numbers p 810 A92-46778
Grid sensitivity in low Reynolds number hypersonic continuum flows p 817 A92-47057
Design and wind tunnel test of low-Reynolds-number airfoil p 1029 A92-56047
A quiet-flow Ludwieg tube for experimental study of high speed boundary layer transition
[AIAA PAPER 92-3885] p 1094 A92-56727
Numerical simulation of turbomachinery flows with advanced turbulence models p 1124 N92-32270

LOW SPEED
NASA low-speed centrifugal compressor for 3-D viscous code assessment and fundamental flow physics research
[ASME PAPER 91-GT-140] p 72 A92-15580
NACA 0015 wing pressure and trailing vortex measurements
[NASA-TP-3151] p 13 N92-10981
A low-speed wind tunnel study of vortex interaction control techniques on a chine-forebody/delta-wing configuration
[NASA-CR-189616] p 632 N92-25510
Observation and measurements of flow structures in the stagnation region of a wing-body junction
p 714 N92-26616
Helicopter low-speed yaw control
[NASA-CASE-LAR-14219-1] p 879 N92-30025
Effects of curvature and rotation on turbulence in the NASA low-speed centrifugal compressor impeller
p 1124 N92-32292

LOW SPEED STABILITY
Hypersonic configurations in slow speed flight
p 624 N92-24394

LOW SPEED WIND TUNNELS
An experiment on unsteady flow over an oscillating airfoil
[ASME PAPER 91-GT-181] p 73 A92-15613
Model oscillations at high angle of attack in a low speed wind tunnel test
[IAF PAPER ST-91-001] p 175 A92-20649
A theoretical analysis utilizing the LEWICE and EPPLER numerical analyses to predict flight performance degradation under icing conditions
[AIAA PAPER 92-0134] p 263 A92-23754
Flow visualization and wake analysis for complex three-dimensional bluff bodies at subcritical through critical Reynolds numbers
[AIAA PAPER 92-0155] p 253 A92-23770
Future experimental needs in low-speed aerodynamics
[AIAA PAPER 92-0157] p 254 A92-23772
Flow analysis of rectangular wind tunnel contraction
p 312 A92-25001
Tests of models equipped with a turbofan powered simulator in the ONERA F1 low-speed pressurized wind tunnel
[ONERA, TP NO. 1991-219] p 383 A92-26371
Flow about cylinders with helical surface protrusions
[AIAA PAPER 92-0540] p 332 A92-26957
An approach to the low-speed longitudinal aerodynamic characteristics of the joined wing configuration
p 339 A92-27909
Motion estimation for cable-mount dynamic wind-tunnel test p 749 A92-43210
High-Reynolds-number test requirements in low-speed aerodynamics p 787 A92-45263

A LEX blowing technique for post-stall lateral control of trapezoidal wings
[AIAA PAPER 92-2714] p 802 A92-45553
An experimental investigation of the effect of leading-edge extensions on directional stability and the effectiveness of forebody nose strakes
[AIAA PAPER 92-2715] p 802 A92-45554
The effect of afterbody devices on drag reduction
p 942 A92-53097
Automatic control of test parameters for intake measurements in a low-speed wind tunnel
p 1091 A92-54341
Effects of the roll angle on cruciform wing-body configurations at high incidences
[AIAA PAPER 92-4356] p 1079 A92-55342
Low-speed wind tunnel testing for the high-speed propeller at high shaft angle of attack
p 1030 A92-56054
Noise test of high-speed counterrotation propeller in low-speed wind tunnel p 1135 A92-56055
A low speed wind tunnel investigation of a joined-wing aircraft with an overhanging fin p 1030 A92-56078
A low speed wind tunnel investigation of the direct side force control of a joined-wing aircraft with overhanging fin p 1084 A92-56079
Flow quality studies of the NASA Lewis Research Center 8- by 6-foot supersonic/9- by 15-foot Low Speed Wind Tunnel
[AIAA PAPER 92-3916] p 1095 A92-56748
An overview of the planned aerospace test facilities at Capua, Italy
[AIAA PAPER 92-3944] p 1097 A92-56773
The installation of the AVRO 9 by 7 foot low-speed wind tunnel at the University of Manchester (England)
[AERO-REPT-9005] p 385 N92-18341
Characterization of unsteady aerodynamic phenomena at high angles p 364 N92-18787
Propeller noise research at NRC p 628 N92-24863
The fibre optic three dimensional laser two focus velocimeter for the low-speed windtunnel. Part 1: Two-dimensional measurement evaluations
[NAL-TM-627] p 665 N92-25402
A gust generation method for full configuration aircraft tests in a low speed wind tunnel. Part 1: Design and preliminary experiments
[NAL-TR-1115-PT-1] p 722 N92-28192
Flow quality studies of the NASA Lewis Research Center 8- by 6-foot supersonic/9- by 15-foot low speed wind tunnel
[NASA-TM-105417] p 887 N92-28673

LOW TEMPERATURE
Viscosity characteristics of synthetic aviation oils at low temperatures p 1105 A92-53875

LOW TEMPERATURE ENVIRONMENTS
On thermal-stress gas flows p 37 A92-10657
Low temperature environment operations of turboengines (design and user's problems)
p 450 N92-21682

LOW TURBULENCE
The design of a subsonic low-noise, low-turbulence wind tunnel for acoustic measurements
[AIAA PAPER 92-3883] p 1094 A92-56726

LOW VISIBILITY
Helicopter fog flying trials p 530 A92-35759
Surface painted taxiway markings at Seattle-Tacoma International Airport
[DOT/FAA/CT-TN91/49] p 32 N92-11029
An investigation into the feasibility of providing a proximity warning device for search and rescue helicopters
[ETN-92-91057] p 530 N92-22408

LUBRICANT TESTS
Development of a full-scale transmission testing procedure to evaluate advanced lubricants
[NASA-TP-3265] p 998 N92-30396
Liquid lubricants for advanced aircraft engines
[NASA-TM-104531] p 1109 N92-32863

LUBRICANTS
Full-scale transmission testing to evaluate advanced lubricants
[NASA-TM-105668] p 764 N92-26560
High-temperature miniaturized turbine engine lubrication system simulator
[AD-A249259] p 868 N92-28294

LUBRICATING OILS
Development of a lubrication system for the T800-LHT-800 turboshaft engine
[ASME PAPER 91-GT-398] p 127 A92-15728
Performance of hybrid ball bearings in oil and jet fuel
p 900 A92-47176
Performance of a hybrid cylindrical roller bearing
p 995 A92-51845
Viscosity characteristics of synthetic aviation oils at low temperatures p 1105 A92-53875
Filter debris analysis: A concrete approach to wear diagnosis
[DREP-TM-88-20] p 222 N92-14345
Full-scale transmission testing to evaluate advanced lubricants
[NASA-TM-105668] p 764 N92-26560
Development of a full-scale transmission testing procedure to evaluate advanced lubricants
[NASA-TP-3265] p 998 N92-30396
Liquid lubricants for advanced aircraft engines
[NASA-TM-104531] p 1109 N92-32863

LUBRICATION
Programs at Wright-Patterson Air Force Base
p 228 N92-15092
Tribology needs for future space and aeronautical systems
[NASA-TM-104525] p 214 N92-15191
High-temperature miniaturized turbine engine lubrication system simulator
[AD-A249259] p 868 N92-28294
Development of a full-scale transmission testing procedure to evaluate advanced lubricants
[NASA-TP-3265] p 998 N92-30396

LUBRICATION SYSTEMS
Tiger MGB - High reliability low weight --- military helicopter Main Gear Box p 109 A92-14418
The basics of powder lubrication in high-temperature powder-lubricated dampers
[ASME PAPER 91-GT-248] p 150 A92-15653
Development of a lubrication system for the T800-LHT-800 turboshaft engine
[ASME PAPER 91-GT-398] p 127 A92-15728
High-temperature miniaturized turbine engine lubrication system simulator
[AD-A249259] p 868 N92-28294
Liquid lubricants for advanced aircraft engines
[NASA-TM-104531] p 1109 N92-32863

LUMINAIRES
Examination of aircraft warning and caution lights after shock testing
[NLR-TP-89284-U] p 952 N92-30474

LUMPED PARAMETER SYSTEMS
Two-parameter bifurcation analysis of axial flow compressor dynamics p 421 A92-29355
A hierarchy for modeling high speed propulsion systems
[NASA-CR-186984] p 387 N92-19934
Improved large perturbation propulsion models for control system design (1988-1989) and large perturbation models of high velocity propulsion systems (1989-1990) and reduced order propulsion models for control system design (1990-1991)
[NASA-CR-190148] p 593 N92-22491
A hierarchy for modeling high speed propulsion systems p 559 N92-22492

LYMAN ALPHA RADIATION
The DLR Lyman-alpha hygrometer
p 467 A92-32091

M

MACH CONES
Base pressure measurements on a cone at Mach numbers from M sub infinity = 5 to 7
p 173 A92-18770

MACH NUMBER
A numerical procedure of three-dimensional design problem in turbomachinery
[ASME PAPER 91-GT-144] p 72 A92-15583
Large chord turbine cascade testing at engine Mach and Reynolds number p 173 A92-18771
Wedge-induced turbulent boundary-layer separation on a roughened surface at Mach 6.0 p 175 A92-20379
Predictions of compressible viscous flows at all Mach number using pressure correction, collocated primitive variables and non-orthogonal meshes
[AIAA PAPER 92-0426] p 326 A92-26274
Interfacial instability between a liquid film and the surrounding compressible gas
[AIAA PAPER 92-0461] p 395 A92-26302
Full Navier-Stokes analysis of a three-dimensional hypersonic mixed compression inlet p 343 A92-28501
Three-dimensional viscous analysis of a Mach 5 inlet and comparison with experimental data
p 344 A92-28526
Comparison of heating calculations with experimental data on a modified Shuttle Orbiter p 441 A92-32184
Computational study of incipient leading-edge separation on a supersonic delta wing
p 442 A92-32237
A method for measuring high-subsonic two-dimensional periodic flow field using a single-hole high-response cylindrical pressure probe p 588 A92-35567
Numerical studies of transverse curvature effects on transonic flow stability p 524 A92-36186
A note on the Kutta condition in Glauert's solution of the thin aerofoil problem p 613 A92-37933
Concorde flight testing - Powerplant and performance flying
[SAE PAPER 912192] p 644 A92-40009
Effect of tabs on the evolution of an axisymmetric jet
p 656 A92-40151
In-flight evaluation of Mach number at hypersonic speeds p 624 A92-40599
Numerical approximation of hypersonic shocks in a finite-element method using flux-corrected transport (FCT) p 708 A92-43060
LDA measurements in a Mach 2 flow over a rearward facing step with staged transverse injection
[AIAA PAPER 92-2692] p 800 A92-45539
Propulsion system performance and integration for high Mach air breathing flight p 862 A92-46429
Waves and thermodynamics in high Mach number propulsive ducts p 809 A92-46431
Calculation of the aerodynamic derivatives of aircraft in the supersonic region using the Mach box method
p 875 A92-47779
Critical Mach number estimates for dense gases
p 933 A92-49498
Turbofan with a small bypass ratio for first stage of a two-stage to-orbit vehicle p 968 A92-49833
Direct evaluation of aeroacoustic theory in a jet
p 1010 A92-50296
Mixing studies of helium in air at high supersonic speeds p 935 A92-50310
Flow of a rarefied gas past a two-dimensional body of an arbitrary shape at small Mach numbers
p 937 A92-52726
Conceptual design of scramjet engine
p 1065 A92-53490
Aerodynamic heating characteristics of space planes tested by NAL hypersonic wind tunnel
p 1017 A92-53547
Mach 3 wind tunnel test of mixed compression supersonic inlet
[AIAA PAPER 92-3625] p 1021 A92-54092
Direct simulation of low-density flow over airfoils
p 1030 A92-56159
An approach for increasing aeroelastic divergence dynamic pressure of wind-tunnel models
[AIAA PAPER 92-4002] p 1099 A92-56825
The measurement of plate vibration and sound radiation from a turbulent boundary layer manipulator
[AD-A240127] p 42 N92-10206
Some characteristics and effects of the F/A-18 LEX vortices p 88 N92-13025
The effects of winglets on low aspect ratio wings at supersonic Mach numbers
[NASA-CR-4407] p 178 N92-13996
Numerical investigations in three-dimensional internal flows
[NASA-CR-189467] p 221 N92-14313
A method of estimating a flow breakdown boundary for aerofoils and swept wings in transonic flows
[ESDU-91021] p 258 N92-15970
Simplified method for the prediction of aerofoil excrescence drag magnification factor for turbulent boundary layers at subcritical Mach numbers
[ESDU-91028] p 259 N92-15972
Piloted simulation study of a balloon-assisted deployment of an aircraft at high altitude
[NASA-TM-104245] p 272 N92-15986
Detailed noise measurements on the SR-7A propeller: Tone behavior with helical tip Mach number
[NASA-TM-105206] p 304 N92-16705
Hydrogen fueled subsonic-ram-combustor model tests for an air-turbo-ram engine
[NAL-TR-1064T] p 280 N92-17855
A laser velocimeter investigation of the normal shockwave boundary layer interaction
p 500 N92-20485
Experimental study of a generic high-speed civil transport: Tabulated data
[NASA-TM-104216] p 525 N92-22232
NASA thrusts in high-speed aeropropulsion research and development: An overview p 561 N92-22538
Longitudinal and lateral-directional aerodynamic characteristics of a wing-cone configuration at Mach numbers from 2.5 to 4.5
[NASA-TM-4337] p 630 N92-24977
Production of periodical Mach number variations in high subsonic flow in a blow down wind tunnel, and its influence on profile measurements
[ETN-92-91492] p 833 N92-29889
Transonic wind tunnel test of a 14 percent thick oblique wing
[NASA-TM-102230] p 950 N92-32213
Numerical simulation of turbulence at the back of the airplane
[ETN-92-91664] p 1037 N92-32769

Experimental study of a generic high-speed civil transport
[NASA-TM-4382] p 1040 N92-33631
Lateral spread of sonic boom measurements from US Air Force boomfile flight tests p 1140 N92-33883
Parametric investigation of single-expansion-ramp nozzles at Mach numbers from 0.60 to 1.20
[NASA-TP-3240] p 1042 N92-34193

MACH REFLECTION
Numerical simulations of shock reflections by a TVD scheme p 1018 A92-53558

MACHINE LEARNING
Classification of radar clutter using neural networks p 145 A92-14252
Damage tolerant structural design using neural networks
[AIAA PAPER 92-1097] p 581 A92-33261
An explanation-based-learning approach to knowledge compilation - A Pilot's Associate application p 920 A92-48220
Design of a flight control system using a feedback-error-learning-type neural network p 1132 A92-56067
Neural networks for aircraft system identification p 303 N92-17998
A learning enhanced flight control system for high performance aircraft
[AD-A252520] p 1086 N92-32435

MACHINE TOOLS
RTM - Simultaneous design and tooling reduces cost and lead time p 994 A92-51537

MACHINERY
Determination of rotordynamic coefficients for labyrinth seals and application to rotordynamic design calculations p 223 N92-14360

MACHINING
Advanced balancing using laser machining
[SAE PAPER 912218] p 674 A92-40020
Investigation of a method for determining machining stress in polymethylmethacrylate (PMMA) of airplane canopies p 986 A92-53096

MAGNETIC ANOMALIES
Design and construction of a Helmholtz coil magnetic test cell
[AD-A249944] p 983 N92-30849

MAGNETIC BEARINGS
Magnetic bearing design and control optimization for a four-stage centrifugal compressor p 900 A92-47188
Active magnetic bearings give systems a lift p 901 A92-48201
Performance tests of a cryogenic hybrid magnetic bearing for turbopumps
[NASA-TM-105627] p 473 N92-20523
Stability and performance of notch filter control for unbalance response p 771 N92-27731
Characterization of superconducting magnetic bearings (dynamic stiffness and damping coefficient in axial direction) p 772 N92-27737
Feasibility of magnetic bearings for advanced gas turbine engines p 772 N92-27738
Low power magnetic bearing design for high speed rotating machinery p 772 N92-27739
Progress of magnetic suspension systems and magnetic bearings in the USSR p 772 N92-27740
International Symposium on Magnetic Suspension Technology, part 2
[NASA-CP-3152-PT-2] p 753 N92-27788
Wide gap, permanent magnet biased magnetic bearing system p 773 N92-27794
Design of bearings for rotor systems based on stability p 773 N92-27799
An evaluation of some strategies for vibration control of flexible rotors p 773 N92-27800
Superconducting bearings with levitation control configurations
[NASA-CASE-GSC-13346-1] p 909 N92-29099

MAGNETIC COILS
Magnetic particle testing of turbine blades mounted on the turbine rotor shaft p 898 A92-46498
Design and construction of a Helmholtz coil magnetic test cell
[AD-A249944] p 983 N92-30849

MAGNETIC EFFECTS
Proof of concept of a magnetically coupled Stirling engine-driven heat pump
[DE92-017129] p 1129 N92-33271

MAGNETIC FIELD CONFIGURATIONS
Nondestructive testing developments in the aircraft industry p 214 A92-17288

MAGNETIC FIELDS
Levitation of YBa2Cu3O(7-x) superconductor in a variable magnetic field p 771 N92-27735
Design and construction of a Helmholtz coil magnetic test cell
[AD-A249944] p 983 N92-30849

MAGNETIC FLUX
Development of an electromagnetic microscope for eddy current evaluation of materials
[AD-A242007] p 406 N92-19873

MAGNETIC LEVITATION VEHICLES
New Ways: Tiltrotor aircraft and magnetically levitated vehicles
[OTA-SET-507] p 238 N92-14933

MAGNETIC MEASUREMENT
Design and construction of a Helmholtz coil magnetic test cell
[AD-A249944] p 983 N92-30849

MAGNETIC RESONANCE
Large area QNDE inspection for airframe integrity p 362 N92-18588

MAGNETIC STORMS
JPRS report: Science and technology. Central Eurasia: Space
[JPRS-USP-92-002] p 575 N92-23705

MAGNETIC SUSPENSION
An electromagnetic suspension system for aerodynamic studies p 483 A92-30409
Further developments relating to the NASA Langley Research Center 13-inch magnetic suspension and balance system
[NASA-CR-188995] p 31 N92-11023
Magnetic suspension and balance systems: A comprehensive, annotated bibliography
[NASA-TM-4318] p 32 N92-11030
Study of the NAL's 0.1 x 0.1 m magnetic suspension and balance system
[NAL-TM-623] p 665 N92-25365
Professor Jesse W. Beams and the first practical magnetic suspension p 771 N92-27723
Low power magnetic bearing design for high speed rotating machinery p 772 N92-27739
Progress of magnetic suspension systems and magnetic bearings in the USSR p 772 N92-27740
International Symposium on Magnetic Suspension Technology, part 2
[NASA-CP-3152-PT-2] p 753 N92-27788
Magnetic suspension using high temperature superconducting cores p 772 N92-27789
Cryogenic test rig with an aerodynamic magnetically levitated carriage p 750 N92-27792
Wide gap, permanent magnet biased magnetic bearing system p 773 N92-27794
Propulsion simulator for magnetically suspended wind tunnel models p 750 N92-27801
Present status of the MIT/NASA Langley 6-inch MSBS p 750 N92-27802
Progress of magnetic suspension and balance systems for wind tunnels in the USSR p 751 N92-27803
Wind tunnel magnetic Suspension Systems at the University of Southampton, England p 751 N92-27804
Dynamics and control of a five degree-of-freedom magnetic suspension system
[NASA-CR-191259] p 1102 N92-34222

MAGNETIZATION
Nondestructive testing developments in the aircraft industry p 214 A92-17288

MAGNETOHYDRODYNAMIC FLOW
Magnetohydrodynamic boundary layer flow over a rotating disk p 304 A92-21338
The formation and structure of plasma wakes behind large high-voltage space platforms in ionosphere
[AIAA PAPER 92-0577] p 407 A92-26984
Ionospheric plasma flow over large high-voltage space platforms. I - Ion-plasma-time scale interactions of a plate at zero angle of attack. II - The formation and structure of plasma wake p 779 A92-41359
Laser velocimetry measurements in an MHD aerodynamic duct
[AIAA PAPER 92-2986] p 899 A92-46996
Hypersonic plasma predictions at nonzero angle of attack
[AIAA PAPER 92-3027] p 925 A92-47028
Shafranov shift in low-aspect-ratio heliotron/torsatron CHS
[NIFS-110] p 1138 N92-33743

MAGNETOHYDRODYNAMICS
Shafranov shift in low-aspect-ratio heliotron/torsatron CHS
[NIFS-110] p 1138 N92-33743

MAGNETOMETERS
Autonomously aided strapdown attitude reference system p 204 A92-18610

MAGNETOPLASMADYNAMICS
IRS organigram p 33 N92-10053

MAGNIFICATION
Simplified method for the prediction of aerofoil excrescence drag magnification factor for turbulent boundary layers at subcritical Mach numbers
[ESDU-91028] p 259 N92-15972

MAGNUS EFFECT
Measurement of magnus derivatives with an elastically forced oscillation rig p 749 A92-43172
Transonic Navier-Stokes computations for a spinning body of revolution
[AD-A241015] p 180 N92-14972

MAINTAINABILITY
The V-22 Osprey - Preparing for fleet operations p 458 A92-29671
Design of advanced composite components for maintainability based on inservice experience
[AIAA PAPER 92-1085] p 537 A92-33251
Annual Reliability and Maintainability Symposium, Orlando, FL, Jan. 29-31, 1991, Proceedings
[ISBN 0-87942-661-6] p 759 A92-42051
Annual Reliability and Maintainability Symposium, Las Vegas, NV, Jan. 21-23, 1992, Proceedings
[ISBN 0-7803-0521-3] p 1119 A92-56201
Improving reliability and maintainability through process management p 1141 A92-56212
Solutions to supportability concerns related to reduced-signature aircraft p 1055 A92-56220
Field test of an advanced maintenance-system p 1016 A92-56221
A testability-dependent maintainability-prediction technique p 1120 A92-56222
Engineering reliability and maintainability review - A regimen for discovering production deficiencies p 1120 A92-56254
RAMREQ: A computerized tool for the definition of RAM (Reliability, Availability, Maintainability) requirements of complex systems p 412 N92-18647

MAINTENANCE
The study on the composite-patching repairs for metallic aircraft structures p 36 A92-10285
Transmission overhaul and component replacement predictions using Weibull and renewal theory p 155 A92-17201
Optimal maintenance program of damage tolerance structure p 785 A92-47660
Expert systems for the trouble-shooting and the diagnostics of engines
[AIAA PAPER 92-3327] p 923 A92-48910
Flexible manufacturing in repair of gas turbine engine components
[AIAA PAPER 92-3524] p 786 A92-49049
A low maintenance and highly reliable fly-by-light architecture p 975 A92-49325
Effective maintenance practices to manage system aging p 1119 A92-56215
A testability-dependent maintainability-prediction technique p 1120 A92-56222
Repair procedures for advanced composites for helicopters p 1016 A92-56277
Aviation Diagnostics And Maintenance (ADAM) system preliminary concept of operation and functional description
[AD-A242598] p 170 N92-14966
National Airspace System maintenance and support operational concept
[DOT/FAA/SE-92/1] p 308 N92-18969
Tiltrotor research aircraft composite blade repairs: Lessons learned
[NASA-TM-103875] p 367 N92-19563
Evaluation and qualification of diffusion braze repair techniques for superalloy gas turbine components
[NRC-LTR-ST-1839] p 504 N92-22028
General maintenance handbook for airway facilities
[PB92-147586] p 640 N92-25518
A prototype semantic integrity front end expert system for a relational database
[AD-A246084] p 781 N92-26765
Flight-determined benefits of integrated flight-propulsion control systems
[NASA-TM-4393] p 742 N92-27587
Turbine aircraft engine operational trending and JT8D static component reliability study
[DOT/FAA/CT-91/10] p 870 N92-28686
Diffuser casing upgrade for an advanced turbofan
[NLR-TP-90097-U] p 870 N92-28711
A methodology for the evaluation of runway roughness for repair
[AD-A250407] p 887 N92-28772
Design specifications for the Advanced Instructional Design Advisor (AIDA), volume 2
[AD-A248202] p 923 N92-29188
Repair procedures for advanced composites for helicopters
[MBB-UD-0606-91-PUB] p 787 N92-29874
Ageing airplane repair assessment program for Airbus A300 p 838 N92-30123
Communication: An important element of maintenance and repair p 838 N92-30124
Processing and environmental effects on mechanical properties of composite repairs
[NRC-LTR-ST-1826] p 1109 N92-32791

Criteria for use of seal coats on airport pavements
[DOT/FAA/RD-92/18] p 1102 N92-34247

MAINTENANCE TRAINING
Advanced technology for aviation maintenance training - An industry status report and development plan
p 47 A92-11180

MALFUNCTIONS
Receiver Autonomous Integrity Monitoring (RAIM) capability for sole-means GPS navigation in the oceanic phase of flight p 956 A92-51012

MAN ENVIRONMENT INTERACTIONS
Aircraft-triggered lightning - Processes following strike initiation that affect aircraft p 836 A92-46784

MAN MACHINE SYSTEMS
Utilization of a research simulator for the development of new flight control concepts
[ONERA, TP NO. 1991-161] p 137 A92-16128
An intelligent pilot vehicle interface for a day/night adverse weather pilotage system (D/NAPS)
[AIAA PAPER 91-3729] p 197 A92-17596
Sensor fusion for synthetic vision
[AIAA PAPER 91-3730] p 197 A92-17597
Estimation of the optimal load characteristics of aircraft control levers p 479 A92-30150
Display trends in aircraft cockpits p 734 A92-43217
A study of the pilot's associate system
p 745 A92-43218
Advanced display system for an aircraft payload
p 735 A92-43221
Digital mapping display technology
p 735 A92-43225
Specification of adaptive aiding systems - Information requirements for designers p 916 A92-44915
Mode S data link pilot-system interface - A blessing in de skies or a beast of burden? p 839 A92-44920
Organizational factors in human factors accident investigation p 834 A92-45000
Knowledge-sensitive task manipulation - Acquiring knowledge from pilots flying a motion-based flight simulator p 916 A92-45064
Manual control of vehicles with time-varying dynamics
[SAE PAPER 912078] p 917 A92-45454
Extreme wide field-of-view displays and the enclosed cockpit p 965 A92-49313
Man-Vehicle Systems Research Facility - Design and operating characteristics
[AIAA PAPER 92-4177] p 982 A92-52458
The research on Pilot Induced Oscillation
p 977 A92-53088
Concepts for pilot interaction with an automated NOE obstacle-avoidance system
[AIAA PAPER 92-4472] p 1076 A92-55232
HEPO mission simulator - Development and usage for NH90 helicopter p 1094 A92-56313
Using the simulation modeling method to estimate the reliability of the crew-flight vehicle system
p 1133 A92-57444
An approach to the organization of an adaptive man-machine system for flight vehicle control
p 1133 A92-57445
An experimental study of organismic principles of the functioning of the crew-transport aircraft system
p 1133 A92-57446
A CLIPS-based tool for aircraft pilot-vehicle interface design p 303 N92-16605
An application of the object-oriented paradigm to a flight simulator
[AD-A243624] p 384 N92-18012
Design principles of automation aids for ATC approach control p 354 N92-19042
The role of simulation for the study of APIS (piloting support by synthetic imagery) p 885 N92-28544
NARSIM: A real-time simulator for air traffic control research
[NLR-TP-90147-U] p 888 N92-29204
Controller response to conflict resolution advisory prototype
[PB92-190032] p 1050 N92-33596

MAN-COMPUTER INTERFACE
Concept for future cockpits p 118 A92-16148
Implementation of a RAIM monitor in a GPS receiver and an integrated GPS/IRS p 99 A92-16948
An intelligent pilot vehicle interface for a day/night adverse weather pilotage system (D/NAPS)
[AIAA PAPER 91-3729] p 197 A92-17596
Multidimensional ELS user interface --- Electronic Library System
[SAE PAPER 912108] p 691 A92-39961
Data Link integration in commercial transport operations p 839 A92-44919
Internationalization of telemetry systems
p 920 A92-47535
MassInfo - An intelligent mass properties information system p 928 A92-47628
BUWICE - An interactive icing program applied to engine inlets
[AIAA PAPER 92-3179] p 922 A92-48794
The VISTA/F-16 programmable feel system
[AIAA PAPER 92-4172] p 977 A92-52457
Evolution of avionic systems architecture, from the 1950's to the present p 198 N92-14047
AGSSS: The Airborne Graphics Software Support System; an Ada/PHIGS-based display editor for the rapid development of cockpit display software systems
[AD-A243224] p 277 N92-17221
Information Management Engineering (IME) laboratory: A database development facility
[AD-A243191] p 305 N92-17369
The COMPAS system in the ATC environment
[DLR-MITT-91-08] p 354 N92-19041
COMPAS system concept p 354 N92-19043
Evaluation of the COMPAS experimental system
p 355 N92-19044
Steps toward acceptance p 355 N92-19046
Towards coherent hypermedia navigation by pragmatic dialogue modeling
[PB92-114735] p 455 N92-20818
Naval Postgraduate School aircraft synthesis program (user's manual)
[AD-A246198] p 777 N92-26458
Status of automatic guidance systems for rotorcraft in low altitude flight p 727 N92-27894
Knowledge-based planning for controlled airspace flight operation as part of a cockpit assistant
p 727 N92-27895
Parallel knowledge based systems architectures for in-flight mission management p 728 N92-27904
Implementation and operational experience with a new arrival traffic management system at the Frankfurt ATC-Center p 728 N92-27905
Advanced software development workstation: Effectiveness of constraint-checking --- spaceflight simulation and planning
[NASA-CR-190712] p 1134 N92-32865
A graphical user-interface for propulsion system analysis
[NASA-TM-105696] p 1134 N92-33894

MANAGEMENT
Total quality treatment for science and technology --- in USAF p 697 A92-36950
Structural risk assessment in the Israel Air Force for fleet management p 836 A92-46779

MANAGEMENT ANALYSIS
Behind the screens --- development of Central Flow Management Unit for air traffic control
p 353 A92-25520
A study on the marginal analysis method for the airline yield management p 951 A92-53018
Preparation for a new plane (A 320): Experience reviewed p 1010 N92-30954

MANAGEMENT INFORMATION SYSTEMS
Development of a flight information system using the structured method
[AD-A248207] p 859 N92-29222
The development of an airborne information management system for flight test
[NASA-TM-104251] p 1065 N92-32866

MANAGEMENT METHODS
An overview of systems engineering management methods and processes
[AIAA PAPER 92-1539] p 690 A92-38636
Implementing total quality management at the intermediate level of aircraft maintenance
[AD-A241768] p 62 N92-12992
The development of fatigue management requirements and techniques p 360 N92-18572
Aircraft fatigue management in the Royal Air Force
p 363 N92-18591
Managing airborne assets through loads monitoring
p 363 N92-18594
General maintenance handbook for airway facilities
[PB92-147586] p 640 N92-25518
Report of the aviation safety review of Department of Energy helicopter operations
[DE92-016346] p 954 N92-31928

MANAGEMENT PLANNING
CATMAC - A way to integrate ground ATC and airborne systems p 531 A92-33429
Information Management Engineering (IME) laboratory: A database development facility
[AD-A243191] p 305 N92-17369
An efficient method for three-dimensional route planning with different strategies and constraints
p 728 N92-27901
DoD key technologies plan
[AD-A253692] p 1142 N92-33238

MANAGEMENT SYSTEMS
Transition to cooperative ATM system requires commitment --- Air Traffic Management
p 267 A92-23297
Thermal management systems for high Mach airbreathing propulsion
[AIAA PAPER 92-0515] p 373 A92-26941
The ATF YF-23 Vehicle Management System
[AIAA PAPER 92-1076] p 563 A92-33245
Suit study - The impact of VMS in subsystem integration
[AIAA PAPER 92-1078] p 563 A92-33247
Integrated flight control systems - Architectural considerations for future aircraft concepts
p 872 A92-45322
Utility management system for hypersonic vehicles
p 964 A92-49252
Proposal for the new fatigue management system for the AMX p 361 N92-18580
The role of planning systems in future air traffic management p 355 N92-19050
Expert system management system
[AD-A247102] p 781 N92-26863
An analysis of total quality management in Aeronautical Systems Division
[AD-A246661] p 772 N92-27760
GNAS Maintenance Control Center (GMCC) Design Qualification Test and Evaluation (DQT/E) test procedures
[DOT/FAA/CT-TN91/40] p 983 N92-30976
GNAS Maintenance Control Center (GMCC) Design Qualification Test and Evaluation (DQT/E) test report
[DOT/FAA/CT-TN91/39] p 932 N92-31615

MANEUVERABILITY
Results of flight tests of the Boeing Sikorsky Fantail demonstrator p 106 A92-14376
Analysis of airship lateral maneuverability
[AIAA PAPER 91-1274] p 743 A92-41212
Maximizing thrust-vectoring control power and agility metrics p 874 A92-46794
Optimization approach for helicopter maneuverability with a point mass model p 1083 A92-56025
On the maneuvering tests of an ACV model
p 1118 A92-56035
Developmental flight testing of a half scale unmanned air vehicle
[AD-A240347] p 22 N92-11002
Development of a 1/7th scale fighter UAV for flight research
[AD-A240703] p 23 N92-11008
Investigation of advanced aircraft performance measures of merit including new agility metrics
[AD-A242016] p 272 N92-15990
Industry view on rotorcraft system identification
p 274 N92-17163
Prediction of aerodynamic phenomena limiting aircraft manoeuvrability p 364 N92-18781
Forebody vortex control aeromechanics
p 380 N92-18792
Analysis of the effects of removing nose ballast from the F-15 eagle
[AD-A244044] p 366 N92-19178
The SnoDog: Preliminary design of a close air support aircraft
[NASA-CR-189990] p 462 N92-21489
Manx: Close air support aircraft preliminary design
[NASA-CR-189992] p 463 N92-21565
A-2000: Close air support aircraft design team
[NASA-CR-190022] p 463 N92-21567
Flight-determined benefits of integrated flight-propulsion control systems
[NASA-TM-4393] p 742 N92-27587
Technical evaluation report on the Flight Mechanics Panel Symposium on Flying Qualities
[AGARD-AR-311] p 733 N92-27870
Study of the leading-edge vortex dynamics in the unsteady flow over an airfoil
[AD-A247532] p 829 N92-28865
Rapid development of the X-31 simulation to support flight-testing
[NASA-TM-104256] p 1060 N92-33149
Nonlinear dynamic-inversion flight control of supermaneuverable aircraft p 1062 N92-33953

MANEUVERABLE REENTRY BODIES
Trajectory control for a low-lift maneuverable reentry vehicle
[AIAA PAPER 92-1146] p 574 A92-33287

MANEUVERS
The use of ground based simulation for handling qualities research: A new assessment p 885 N92-28545

MANIFOLDS
Mixed flow compressor surge margin gain using a manifolded diffuser system
[AIAA PAPER 92-3753] p 1068 A92-54151

MANIPULATORS
Flow quality studies of the NASA Lewis Research Center 8- by 6-foot supersonic/9- by 15-foot Low Speed Wind Tunnel
[AIAA PAPER 92-3916] p 1095 A92-56748

Flow quality studies of the NASA Lewis Research Center 8- by 6-foot supersonic/9- by 15-foot low speed wind tunnel
[NASA-TM-105417] p 887 N92-28673

MANNED MARS MISSIONS
A six-degree-of-freedom guidance and control analysis of Mars aerocapture
[AIAA PAPER 92-0736] p 486 A92-31676
Thermal protection analysis of Mars-earth return vehicles p 497 A92-32183
Earth aerobraking strategies for manned return from Mars p 752 A92-41535

MANNED REENTRY
Earth atmospheric entry studies for manned Mars missions p 442 A92-32251

MANNED SPACE FLIGHT
Crew transportation for the 1990s. I - Commercializing manned flight with today's propulsion p 889 A92-46726
SHARP: Subsonic High Altitude Research Platform
[NASA-CR-190004] p 648 N92-25263

MANUAL CONTROL
Estimation of the optimal load characteristics of aircraft control levers p 479 A92-30150
Nonstationary manual control. III p 776 A92-43187
Manual control of vehicles with time-varying dynamics
[SAE PAPER 912078] p 917 A92-45454
A simulator evaluation of various manual control concepts for fly-by-wire transport aircraft
[AIAA PAPER 92-4328] p 1073 A92-55172
Multiaxis control in longitudinal mode of aircraft p 1083 A92-56027
An approach to the organization of an adaptive man-machine system for flight vehicle control p 1133 A92-57445
Flight testing and simulation of an F-15 airplane using throttles for flight control
[NASA-TM-104255] p 1087 N92-32864
Human factors issues in the use of artificial intelligence in air traffic control. October 1990 Workshop
[NASA-CR-190925] p 1051 N92-34203

MANUALS
Standardization of NATOPS emergency egress procedures --- Naval Air Training and Operating Procedures Standardization Program p 529 A92-32998

MANUFACTURING
36th Roy Chadwick Lecture - Manufacturing breakout 1941-1991: Development in aerospace industry manufacturing techniques p 419 A92-28941
An overview of systems engineering management methods and processes
[AIAA PAPER 92-1539] p 690 A92-38636
1991-92 AHS Technical Committee highlights - Manufacturing and product assurance p 609 A92-40396
Composites in manufacturing - Case studies
[ISBN 0-87263-406-X] p 784 A92-47403
Development of an automatic drilling system. II p 1118 A92-56107
International aviation (selected article)
[AD-A240986] p 170 N92-13991
B-2 program: Trends in manufacturing
[AD-A242141] p 242 N92-15963
Manufacturing process control as a damage tolerance concept p 403 N92-19006
Materials and process directions for advanced aero-engine design
[PNR-90814] p 378 N92-19938
Superplastic applications in aero engines
[PNR-90788] p 473 N92-20436
Research, services, and facilities (National Institute of Standards and Technology)
[PB92-109172] p 485 N92-21870
Welding technology transfer task/laser based weld joint tracking system for compressor girth welds p 593 N92-22426
The Air Force Manufacturing Technology (MANTECH): Technology transfer methodology as exemplified by the radar transmit/receive module program p 593 N92-22451
Manufacturing development of pultruded composite panels
[NASA-CR-181780] p 578 N92-22637
Simultaneous engineering in aero-gas turbine design and manufacture
[PNR-90811] p 740 N92-27043
A manufacturer's approach to ensure long term structural integrity p 838 N92-30133
Flutter models: Their design, manufacture, and ground testing p 1089 N92-34164

MANY BODY PROBLEM
A multibody analog of the dual-spin problem p 49 A92-11426

MAP MATCHING GUIDANCE
Talons 95 GHz radar sensor for autonomous landing guidance p 1063 A92-55908

MAPPING
Extended mapping and characteristics techniques for inverse aerodynamic design p 194 N92-13949

MAPS
An efficient method for three-dimensional route planning with different strategies and constraints p 728 N92-27901

MARANGONI CONVECTION
Fundamental studies on Marangoni convection related to Bridgman crystal growth p 1111 A92-53758

MARINE PROPULSION
Algorithms for blending surface generation
[AD-A245686] p 777 N92-26524

MARINE TECHNOLOGY
Underwater turbojet engine
[AD-D015017] p 279 N92-15992

MARINE TRANSPORTATION
Electronic systems in transportation
[TP-9983] p 189 N92-14009

MARITIME SATELLITES
Using satellite communication for aircraft Automatic Dependent Surveillance p 725 A92-42486
Evaluation report of an experimental Satcom operation by a Japan Airline's B747 passenger plane p 1046 A92-56092

MARKERS
Surface painted taxiway markings at Seattle-Tacoma International Airport
[DOT/FAA/CT-TN91/49] p 32 N92-11029
Effect of guard band reduction on marker beacon receiver performance
[DOT/FAA/CT-TN92/18] p 1002 N92-31617

MARKET RESEARCH
Dornier Do 328 - A start in the world market p 113 A92-17093
Using design of experiments to improve product and process integrity p 928 A92-48555
Aerospace technology: Technical data and information on foreign test facilities
[GAO/NSIAD-90-71FS] p 139 N92-13076
New York Downtown Manhattan (Wall Street) Heliport: Operations analysis
[DOT/FAA/RD-91/12] p 139 N92-13077

MARKETING
Symposium on Marketing for Technological Products
[MBB-UE-0014-90-PUB] p 606 N92-23928

MARKOV PROCESSES
Availability of positioning and receiver autonomous integrity monitoring for the global positioning system p 100 A92-16963
Use of Markov methods in analysis of fault-tolerant systems with flexible repair policies
[PNR-90801] p 767 N92-27038

MARS (PLANET)
Analysis of spacecraft entry into Mars atmosphere p 1105 N92-33763

MARS ATMOSPHERE
Monte Carlo simulation of entry in the Martian atmosphere
[AIAA PAPER 92-0494] p 329 A92-26324
Flowpath and sensitivity analyses of high speed propulsion systems
[AIAA PAPER 92-3806] p 1069 A92-54178
Analysis of spacecraft entry into Mars atmosphere p 1105 N92-33763

MARS LANDING
Analysis of spacecraft entry into Mars atmosphere p 1105 N92-33763

MARS PROBES
Analysis of spacecraft entry into Mars atmosphere p 1105 N92-33763

MASS
A general purpose nonlinear rigid body mass finite element for application to rotary wing dynamics p 846 A92-46924

MASS DISTRIBUTION
Maximum mass allowance to justify passenger-carrying aircraft modification p 113 A92-16802
Computational analysis of inertial effects on the stability of an ACES-II ejection seat p 543 A92-35436
Wing mass formula for subsonic aircraft p 845 A92-46812
Wing mass formula for twin fuselage aircraft p 1054 A92-56171
Computational structures technology at Grumman: Current practice/future needs p 684 N92-25930

MASS FLOW
Determination of the mass-flow-rate characteristics of porous panels p 439 A92-31875
Extension and validation of an unsteady wake model for rotors p 702 A92-41224
Experimental study of cross-stream mixing in a rectangular duct
[AIAA PAPER 92-3090] p 903 A92-48735
A parametric numerical study of mixing in a cylindrical duct
[NASA-TM-105695] p 738 N92-26553
Experimental study of cross-stream mixing in a rectangular duct
[NASA-TM-105694] p 742 N92-27652
Analysis of the flight performance of the 155 mm M864 base burn projectile
[BRL-TR-3083] p 1041 N92-33699
Cooled high-temperature radial turbine program 2
[NASA-CR-189122] p 1073 N92-34236

MASS FLOW RATE
Notes on the cause of parachute critical velocity
[AD-A244417] p 347 N92-19085
High accuracy fuel flowmeter. Phase 2C and 3: The mass flowrate calibration of high accuracy fuel flowmeters
[NASA-CR-187108] p 406 N92-19775

MASS SPECTROSCOPY
Rarefied gas research at Berkeley - Current studies and future potentials
[AIAA PAPER 92-3971] p 1098 A92-56797

MASS TRANSFER
Fundamentals of applied aerogasdynamics. II - Viscous flow past bodies. Control devices --- Russian book p 64 A92-14281
Numerical study of coupled heat transfer under conditions of filtering and film cooling of blunt anisotropic bodies p 610 A92-36552
Heat pipe and surface mass transfer cooling of hypersonic vehicle structures p 763 A92-44380
Presentation of a computational code for 3-D compressible flow in complex channels and cavities p 769 N92-27475

MASSIVELY PARALLEL PROCESSORS
Optical computing at NASA Ames Research Center
[AIAA PAPER 91-3779] p 231 A92-17637
Aircraft optimization by a system approach: Achievements and trends
[NASA-TM-107622] p 650 N92-25995

MATCHED FILTERS
Determining design gust loads for nonlinear aircraft similarity between methods based on matched filter theory and on stochastic simulation
[AIAA PAPER 92-2369] p 518 A92-34597
Maximized gust loads for a nonlinear airplane using matched filter theory and constrained optimization
[NASA-TM-104138] p 23 N92-11010

MATERIALS HANDLING
Organic Matrix Composite Helicopter Internal/External Cargo Pallet System (OMC INTEX)
[AD-A251127] p 961 N92-30878
Fire bombing and fire bombers
[CA-PATENT-1-268-164] p 1061 N92-33582

MATERIALS SCIENCE
Advanced materials for aircraft engine applications p 390 A92-28251
International SAMPE Electronics Conference, 5th, Los Angeles, CA, June 18-20, 1991, Proceedings
[ISBN 0-938994-58-1] p 985 A92-51901

MATERIALS TESTS
New insulation constructions for aerospace wiring applications. Volume 1: Testing and evaluation
[AD-A240638] p 22 N92-11006
Evaluation of the effects of the environment on the behavior of the primary structures of composite material aircraft in service: Historic and current situation p 1110 N92-33048
Fluid effects: Thermoset and thermoplastic matrix composites p 1110 N92-33049
Jet fuel absorption and dynamic mechanical analysis of carbon fibre composites p 1110 N92-33050
Flight service environmental effects on composite materials and structures p 1110 N92-33054

MATHEMATICAL MODELS
Slush hydrogen (SLH2) technology development for application to the National Aerospace Plane (NASP) p 144 A92-13432
Helicopter modeling requirements for full mission simulation and handling qualities assessment p 105 A92-14364
Analysis of crash-resistant fuel systems and airframe structure interaction in a crash environment p 105 A92-14369
Description of a tilt wing mathematical model for piloted simulation p 133 A92-14445
Thermal barrier coating life prediction model development
[ASME PAPER 91-GT-40] p 147 A92-15523
Modelling of unsteady transitional boundary layers
[ASME PAPER 91-GT-282] p 152 A92-15677
Turbulent flow calculations using unstructured and adaptive meshes p 153 A92-15823
Problem of the optimal correction of a flight test program for an aircraft system p 113 A92-16809

A method for determining the optimal composition of the measured parameters in diagnosing gas turbine engines p 128 A92-16819
Mathematical modeling of supersonic flow over a convex-concave formed body based on the Euler and Navier-Stokes equations p 252 A92-23416
A simplified method of transient mathematical model for non-augmentation engine p 372 A92-24750
Aerobrake guidance law synthesis using feedback linearization p 485 A92-29304
A general nonlinear dynamical analysis of a second-order, one-dimensional, theoretical compression system model p 509 A92-29374
Simulation of vibrational status of gas-turbine engine p 470 A92-29731
An investigation of real-time diagnostic technique for DEEC system --- digital electronic engine control system p 470 A92-29742
Simulation of hypersonic flows on unstructured grids p 434 A92-31496
Mathematical modeling of nonstationary viscous flow over a solid angle of finite span p 440 A92-31890
Computational structures technology
[AIAA PAPER 92-2442] p 585 A92-34473
An estimate of the influence of the compressor stability margin on the pick-up time of a turbojet engine p 654 A92-37423
Distribution of maximum levels of aircraft noise around their mean value p 693 A92-39062
A model of the operation of the pulsejet engine and a study of its characteristics p 657 A92-40608
Maintenance scheduling for critical parts of aircraft p 699 A92-42054
Selected models of aircraft navigation space p 839 A92-45373
Aircraft stabilization at large angles of attack p 875 A92-47785
Characterization of thermal performance of wheel outboard of an aircraft p 849 A92-48352
Location and tracking technique in a multistatic system established by multiple bistatic systems p 840 A92-48480
DYNamic Turbine Engine Compressor Code (DYNTECC) - Theory and capabilities
[AIAA PAPER 92-3190] p 923 A92-48802
Numerical investigation of surge and rotating stall in multistage axial compressors
[AIAA PAPER 92-3193] p 825 A92-48804
The use of math-dynamic models to aid the development of integrated health and usage monitoring systems p 1006 A92-50013
Fourier functional analysis for unsteady aerodynamic modeling p 935 A92-50313
On central-difference and upwind schemes p 1007 A92-50466
The research on Pilot Induced Oscillation p 977 A92-53088
Simulation research on the dynamic characteristics of steam-injected gas turbine p 971 A92-53389
Modal simulation of gearbox vibration with experimental correlation
[AIAA PAPER 92-3494] p 1112 A92-54036
Multidisciplinary optimization of aeroservoelastic systems using reduced-size models p 1054 A92-56176
The G-range impulse facility - A high-performance free-piston shock tunnel
[AIAA PAPER 92-3946] p 1097 A92-56774
Jet noise generated by large-scale coherent motion p 55 N92-10604
Airframe noise p 55 N92-10605
Sonic boom p 55 N92-10608
Rotorcraft system identification
[AGARD-AR-280] p 22 N92-11001
Numerical simulation of the reactive flow in advanced (HSR) combustors using KIVA-2
[NASA-CR-188996] p 26 N92-11014
Effects of elevated temperature on the viscoplastic modeling of graphite/polymeric composites
[NASA-TM-104160] p 35 N92-11149
Theoretical study (Lagrangian modeling) of turbulent particulate dispersion
[ETN-91-99909] p 42 N92-11287
Critical appraisal of the McDonnell Douglas closure model for predicting fatigue crack growth
[ARL-STRUC-R-444] p 44 N92-11376
Advanced stress analysis methods applicable to turbine engine structures
[NASA-CR-187235] p 44 N92-11378
Nonlinear aspects of aerospace structures at high excitation levels flat aluminum beams and plates studied
[AD-A240600] p 44 N92-11383
On the limitations of Froude's actuator disc concept
[ETN-91-90136] p 81 N92-11973
Practical input optimization for aircraft parameter estimation experiments p 114 N92-11989
Modeling and numerical simulation of vortex flow in aerodynamics
[AD-B163670L] p 83 N92-12997
The effect of a type 3 and type 4 shock/shock interaction on heat transfer in the stagnation region p 160 N92-13867
Extended mapping and characteristics techniques for inverse aerodynamic design p 194 N92-13949
MLS system error model identification and synthesis p 189 N92-14015
Theoretical models for duct acoustic propagation and radiation p 236 N92-14782
Simulation requirements for RCS plume: Flowfield interaction modelling on a winged reentry vehicle p 181 N92-14985
Hypersonic viscous shock layer in thermochemical nonequilibrium p 183 N92-15014
Influence of chemical modeling on the solution of hypersonic shock layers p 183 N92-15016
Flutter suppression via piezoelectric actuation
[NASA-TM-104120] p 197 N92-15070
Approximation methods for control of acoustic/structure models with piezoceramic actuators
[NASA-CR-189578] p 234 N92-15658
Development of high angle of attack control laws for an unstable, non-minimum phase aircraft using variations of the quantitative feedback technique
[AD-A243698] p 282 N92-17096
Rotorcraft System Identification
[AGARD-LS-178] p 273 N92-17153
Instrumentation and data processing p 273 N92-17155
Modelling aspects and robustness issues in rotorcraft system identification p 274 N92-17159
Automated composite ellipsoid modelling for high frequency GTD analysis
[NASA-CR-189853] p 275 N92-17316
Aircraft aerodynamics and stability and control during air-to-air refueling
[AERO-REPT-9017] p 380 N92-18321
Rotorwash computer model: User's guide
[DOT/FAA/RD-90/25] p 346 N92-18345
A preliminary flight test on a basic performance of the flight research airplane Do 228: Velocity vs glide path angle
[NAL-TM-613] p 359 N92-18482
Investigation of the effects of aeroelastic deformations on the radar cross section of aircraft
[AD-A243889] p 402 N92-18940
Parametric bicubic spline and CAD tools for complex targets shape modelling in physical optics radar cross section prediction p 403 N92-19151
Thermal nonequilibrium effects on turbine cascade aerodynamics
[AD-A244049] p 404 N92-19183
Simple models for the description of turbulence in the atmospheric boundary layer
[DLR-FB-90-17] p 410 N92-19292
A comparative study of numerical versus analytical waverider solutions
[AD-A244183] p 347 N92-19304
Inhomogeneous turbulence beyond spectral equilibria: Aeronautical applications
[ETN-92-90867] p 404 N92-19349
Airplane crashes on the runway. Fine modeling of the behavior after burning of a frame submitted to linear crushing
[IMFL-90-64] p 353 N92-19350
Dynamical systems analysis of an aerodynamic decelerator's behavior during the initial opening process
[AD-A244194] p 348 N92-19394
Reuse metrics and measurement: A framework p 413 N92-19432
A guide for the consideration of composite material impacts on airframe costs
[AD-A243928] p 417 N92-19466
Estimating the probability of vertical overlap from the paired aircraft data obtained in the European vertical data collection using the program DGLDiF
[NLR-TR-88108-U] p 356 N92-19491
An analytical and computational investigation of shock-induced vortical flows with applications to supersonic combustion p 405 N92-19538
A mathematical model of a tilt-wing aircraft for piloted simulation
[NASA-TM-103864] p 368 N92-19847
A hierarchy for modeling high speed propulsion systems
[NASA-CR-186984] p 387 N92-19934
Runway exit designs for capacity improvement demonstrations. Phase 2: Computer model development
[NASA-CR-190166] p 484 N92-21162
Measurement of LORAN-C envelope to cycle difference in the far field
[PB92-128909] p 455 N92-21263
Probability of cycle jumps in Omega receivers and other phase locked loop applications
[PB92-128891] p 455 N92-21279
Modelling methods for high-fidelity rotorcraft flight mechanics simulation
[NASA-TM-103842] p 482 N92-21440
Method for calculating the three-dimensional water concentration coefficients and its industrial applications p 502 N92-21685
A review of icing research at the Royal Aerospace Establishment p 451 N92-21689
A new method for simulating atmospheric turbulence for rotorcraft applications p 464 N92-21956
Theoretical and experimental investigation of the thermodynamics of the thermally choked ram accelerator p 604 N92-22137
A theoretical investigation of the induced drag of wing of finite aspect ratio
[CUED/A-AERO/TR-17(1991)] p 525 N92-22193
Dynamic simulation of a solid fuelled gas turbine system p 592 N92-22315
A hierarchy for modeling high speed propulsion systems p 559 N92-22492
Approximate truncated balanced realizations for infinite dimensional systems p 602 N92-22493
Modeling of linear isentropic flow systems p 593 N92-22495
MLS mathematical modeling study of Philadelphia International Airport runway 27L
[DOT/FAA/CT-TN91/54] p 573 N92-22503
Time-optimal reorientation maneuvers of an aircraft p 549 N92-22605
A two-stroke diesel engine simulation program
[NASA-CR-185155] p 562 N92-22647
Three-dimensional time-marching aeroelastic analyses using an unstructured-grid Euler method
[NASA-TM-107567] p 527 N92-23116
Comparison of two-dimensional and three-dimensional droplet trajectory calculations in the vicinity of finite wings
[NASA-TM-105617] p 596 N92-23154
Hypersonic laminar flow computations over a blunt leading edged delta wing at three different chord Reynolds numbers
[FFA-TN-1991-40] p 528 N92-23168
Sensitivity analysis of dynamic aeroelastic responses p 571 N92-23229
Application of analytical and design tools for fighter wing aeroelastic tailoring p 550 N92-23231
The structural optimization system OPTSYS: Current status and applications p 550 N92-23232
Multidisciplinary optimization studies using ASTROS p 571 N92-23234
Design of a fighter aircraft vertical tail enhanced buffet environment survivability p 551 N92-23235
A fin optimisation study p 551 N92-23237
Simultaneous stress and flutter optimization for the wing of a transport aircraft equipped with four engines p 571 N92-23238
Structural optimization of aircraft practice and trends p 551 N92-23239
Coupled multi-disciplinary simulation of composite engine structures in propulsion environment
[NASA-TM-105575] p 596 N92-23267
Analysis of a 37 kW cage-induction motor
[PB92-142116] p 597 N92-23496
A two-dimensional Euler solution for an unbladed jet engine configuration
[NASA-TM-105329] p 597 N92-23560
Computational procedures for preliminary design p 552 N92-23952
Panel methods for aerodynamic analysis and design p 552 N92-23955
Adaptive active flutter suppression of wings in subsonic and transonic flight regimes p 553 N92-24010
Boundary Layers in Turbomachines
[VKI-LS-1991-06] p 658 N92-24336
Aspects of unsteady blade-surface boundary layers and transition in axial turbomachines p 658 N92-24340
Software Surface Modeling and Grid Generation Steering Committee
[NASA-CP-3143] p 691 N92-24397
Dynamics of aerospace shuttles p 667 N92-24760
Navier-Stokes simulation of dynamic stall on a rotating airfoil p 626 N92-24853
A two-dimensional Euler solution for an unbladed jet engine configuration p 627 N92-24861
Vibroacoustic simulation of an airplane structure p 629 N92-24871
Nonunique solutions in unsteady transonic flow p 629 N92-24872
MLS and DME/P multipath simulation model user's manual. Volume 1: Operating instructions
[DOT/FAA/CT-TN91/47] p 640 N92-24888

Fatigue life variability and reliability analysis of a wind turbine blade
[DE92-008673] p 689 N92-25049
The NASA/industry Design Analysis Methods for Vibrations (DAMVIBS) Program: A government overview
[NASA-TM-107579] p 680 N92-25267
Static aeroelastic analysis of ACT wind tunnel model aircraft
[NAL-TM-624] p 632 N92-25366
Prediction and analysis of wing flutter at transonic speeds p 662 N92-25555
Application of nonlinear feedback control theory to supermaneuverable aircraft
[NASA-CR-190336] p 663 N92-25648
Activities for numerical propulsion systems simulation program p 692 N92-25726
Computational Fluid Dynamics --- numerical methods and algorithm development
[NASA-CP-10078] p 660 N92-25808
Computational structures technology at Grumman: Current practice/future needs p 684 N92-25930
Finite element methods for integrated aerodynamic heating analysis
[NASA-CR-190353] p 633 N92-25959
Trajectory optimization for the National Aerospace Plane
[NASA-CR-190355] p 650 N92-26017
Iterative methods for large scale static analysis of structures on a scalable multiprocessor supercomputer
[NASA-CR-190369] p 692 N92-26018
Simulation of a rotorcraft in turbulent flows
[AD-A245742] p 650 N92-26155
Composite strength statistics from fiber strength statistics
[AD-A245616] p 755 N92-26383
Acoustic interactions between an altitude test facility and jet engine plumes: Theory and experiments
[NASA-CR-190423] p 738 N92-26405
Analysis of EMP response of structures using frequency domain electromagnetic interaction codes
[AD-A245758] p 765 N92-26592
A modeling strategy for large-scale optimization based on analysis and visualization principles
[AD-A246570] p 777 N92-26620
The changing role of experimentation in aeroengine R and D: The point of view of the research worker
[AD-A246372] p 740 N92-27062
Users manual and modeling improvements for axial turbine design and performance computer code TD2-2
[NASA-CR-189118] p 716 N92-27376
The coherent flamelet model for propulsion applications p 756 N92-27486
Three dimensional calculations of reactive flows within aircraft combustion chambers including some combustion models p 770 N92-27490
Modeling of heavy-gas effects on airfoil flows
[NASA-CR-190357] p 716 N92-27558
Basic concepts on boundary layers
p 717 N92-27707
Turbulent skin-friction drag reduction by active and passive means, part 1 p 718 N92-27714
Investigation of the aeroelastic stability of the AFW wind-tunnel model using CAP-TSD p 721 N92-27955
An appraisal of cost-effectiveness models used in the Air Force and Navy aircraft engine component improvement programs
[AD-A245910] p 743 N92-28162
Calculation of unsteady transonic flows with mild separation by viscous-inviscid interaction
[NASA-TP-3197] p 827 N92-28477
Inverse control problems: Mathematical preliminaries, system theoretical approaches, and their applications to aircraft dynamics
[LR-665] p 923 N92-28581
Experimental validation of a line-duct acoustics model including flow
[NLR-TP-90223-U] p 927 N92-28695
Calculation of support interferences on the aerodynamic coefficients for a wind tunnel calibration model
[ESA-TT-1247] p 830 N92-29159
Boundary layer induced noise in aircraft
[CUED/A-AERO/TR-18] p 927 N92-29201
Development of a multigrid transonic potential flow code for cascades
[NASA-CR-190480] p 830 N92-29361
Tear straps in airplane fuselage
[AD-A248543] p 854 N92-29511
A semi empirical method for the analytical representation of stationary measured profile coefficients for applications of rotary wing aerodynamics
[ETN-92-91491] p 832 N92-29741
Modeling and analysis methodology for aeroelastically tailored chordwise deformable wings
[NASA-CR-189620] p 961 N92-30304
Low-velocity impact loading on fibre reinforced aluminum laminates (ARALL) and other aircraft sheet materials
[ETN-92-91613] p 987 N92-30414
Numerical optimization in Germany: A non-exhaustive survey on current activities with emphasis on aeronautics
[MBB/FE211/S/PUB/474] p 932 N92-30675
Trajectory fitting in function space with application to analytic modeling of surfaces
[NASA-TP-3232] p 945 N92-30747
Finite difference time domain modeling of steady state scattering from jet engines with moving turbine blades
[NASA-CR-190290] p 971 N92-30753
Composite beam analysis linear analysis of naturally curved and twisted anisotropic beams
[AD-A252652] p 999 N92-30766
Preliminary subsonic aerodynamic model for simulation studies of the HL-20 lifting body
[NASA-TM-4302] p 978 N92-31175
A general numerical model for wave rotor analysis
[NASA-TM-105740] p 1002 N92-31484
Modal simulation of gearbox vibration with experimental correlation
[NASA-TM-105702] p 1002 N92-31485
Life prediction and constitutive models for engine hot section anisotropic materials program
[NASA-CR-189222] p 973 N92-31534
Low density real gas flows about hypersonic vehicles
[AD-A250048] p 949 N92-31777
Integrated computer systems in aircraft design and manufacture: Difficulties and implications
p 1010 N92-31864
A simulation model of a single rotor helicopter
p 979 N92-31865
Contribution to the modelling of turbulent combustion in the case of stabilisation by flame-lock
[ESA-TT-1229] p 988 N92-31942
Mathematical modeling and numerical simulation of the dynamics of flexible structures undergoing large overall motions
[AD-A250202] p 979 N92-31967
A continuing study of altitude determination deficiencies of the Service Aircraft Instrumentation Package (SAIP)
[AD-A245952] p 968 N92-32051
Eighth DOD/NASA/FAA Conference on Fibrous Composites in Structural Design, part 1
[NASA-CP-3087-PT-1] p 1106 N92-32513
Modeling and numerical simulation of vortex flow in aerodynamics
[NLR-TP-91154-U] p 1037 N92-32673
Vibro-acoustic FE analyses of the Saab 2000 aircraft
p 1137 N92-32952
Active control of sound transmission through stiff lightweight composite fuselage constructions
p 1137 N92-32957
On the origin and acoustical behaviour of cloud cavitation
[ISBN-90-9004317-9] p 1125 N92-33066
Ideal efficiency of propellers based on Theodorsen's theory: A review and computer study, with extended plus simplified charts
[UTIAS-TN-271] p 1071 N92-33102
ILS mathematical modeling study of an ILS localizer and glide slope proposed for runway 32R, Moffett Field Airport, California
[DOT/FAA/CT-TN92/28] p 1048 N92-33308
Advanced techniques in reliability model representation and solution
[NASA-TP-3242] p 1134 N92-33483
Active control of compressor surge and stall
[AD-A252771] p 1126 N92-33498
Simulation model of a twin-tail, high performance airplane
[NASA-TM-107601] p 1088 N92-33537
A numerical model for sonic boom propagation through an inhomogeneous, windy atmosphere
p 1138 N92-33876
Wave equations and computational models for sonic boom propagation through a turbulent atmosphere
p 1139 N92-33877
Design of helicopter flight control systems for hover and low speed using eigenstructure assignment
p 1061 N92-33952
Finite difference time domain grid generation from AMC helicopter models
[NASA-TM-107679] p 1128 N92-34017
Effects of constraint on crack growth under aircraft spectrum loading
[NASA-TM-107677] p 1128 N92-34178

MATHEMATICAL PROGRAMMING
Equivalence of optimal control problems and the use of parameterization methods p 52 A92-11466
Impact of structural optimization with aeroelastic/multidisciplinary constraints on helicopter rotor design
[AIAA PAPER 92-1001] p 535 A92-33193
The structural optimization system OPTSYS: Current status and applications p 550 N92-23232
Mathematical optimization: A powerful tool for aircraft design p 851 N92-28474

MATRICES (MATHEMATICS)
Diagonal implicit scheme for computing flows with finite rate chemistry p 488 A92-32253
Efficient direct solvers for large-scale computational fluid dynamics problems p 690 A92-37534
CSM solutions of rotating blade dynamics using integrating matrices
[NASA-CR-190577] p 1003 N92-31619

MATRIX MATERIALS
New thermoplastic composites for aircraft structures and interiors p 34 A92-10271
Poly 1, 2, 4-triazoles via aromatic nucleophilic displacement
[NASA-CASE-LAR-14440-1] p 35 N92-10066
The search for new materials
[PNR-90777] p 490 N92-21744
Stress-strain analysis of a (0/90)sub 2 symmetric titanium matrix laminate subjected to a generic hypersonic flight profile
[NASA-TM-107584] p 685 N92-26128

MATRIX METHODS
Free vibration analysis of branched blades by the integrating matrix method p 847 A92-47122

MAXIMUM ENTROPY METHOD
The Baldwin-Lomax model for separated and wake flows using the entropy envelope concept
[AIAA PAPER 92-0148] p 253 A92-23764

MAXIMUM LIKELIHOOD ESTIMATES
System-identification of airplanes using the 'estimation before modelling' technique p 269 A92-21007
Parameter identification of linear systems based on smoothing p 873 A92-46742
Detection and imaging of moving objects with synthetic aperture radar. I - Optimal detection and parameter estimation theory p 955 A92-50033
Maximum likelihood algorithm and its application to parameter identification of closed-loop flight vehicles
p 1008 A92-53023
Estimation of aircraft inertial characteristics using maximum likelihood estimation p 1084 A92-56057
STS-40 descent BET products: Development and results
[NASA-CR-189570] p 286 N92-16012
Graphics for interactive PC based parameter estimation package
[NAL-PD-FC-9117] p 412 N92-18252
Implementation of a personal computer based parameter estimation program
[AD-A252914] p 1061 N92-33502

MAXWELL EQUATION
Nonlinear triggered lightning models for use in finite difference calculations p 230 A92-20128
Finite difference time domain modeling of steady state scattering from jet engines with moving turbine blades
[NASA-CR-190290] p 971 N92-30753

MCDONNELL AIRCRAFT
Fighter airframe/propulsion integration - A McDonnell Aircraft perspective
[AIAA PAPER 92-3333] p 850 A92-48916

MCDONNELL DOUGLAS AIRCRAFT
McDonnell Douglas' new light twin helicopter - The MDX p 271 A92-22710
An airlifter for the long haul p 358 A92-28493
The NASA/Industry Design Analysis Methods for Vibrations (DAMVIBS) program - McDonnell Douglas Helicopter Company achievements
[AIAA PAPER 92-2203] p 540 A92-34393
Artificial intelligence techniques applied to vehicle management system diagnostics p 965 A92-49315

MEASUREMENT
Measurements in the inhomogeneous convective boundary layer using three powered gliders
p 775 N92-26350

MEASURING INSTRUMENTS
Skin-friction gauge for use in hypervelocity impulse facilities p 398 A92-28063
Flow quality studies of the NASA Lewis Research Center 8- by 6-foot supersonic/9- by 15-foot Low Speed Wind Tunnel
[AIAA PAPER 92-3916] p 1095 A92-56748
Reflection type skin friction meter
[NASA-CASE-LAR-14520-1-SB] p 11 N92-10008
Heat transfer and instrumentation studies on rotating turbine blades in a transient facility p 156 N92-12203
Susceptibility of a parallelogram type skin friction balance to rotational motion
[AD-A241348] p 139 N92-13078
Evaluation of electrolytic tilt sensors for measuring model angle of attack in wind tunnel tests
[NASA-TM-4315] p 297 N92-16283

Model incidence measurement using SAAB ELOPTOPOS system
[NLR-TP-89182-U] p 385 N92-18416
Research sensors p 594 N92-22526
Inflatable traversing probe seal p 595 N92-22692
The effect of droplet sizing uncertainty on ice accretions p 679 N92-24874
The basic measuring technical equipment of the DLR test aircraft p 652 N92-25592
A simple and low cost system to measure delay times in pneumatic systems
[NLR-TP-90174-U] p 859 N92-28644
Flow quality studies of the NASA Lewis Research Center 8- by 6-foot supersonic/9- by 15-foot low speed wind tunnel
[NASA-TM-105417] p 887 N92-28673
Sensor fault detection on board an aircraft with observer and polynomial classifier
[DLR-FB-91-34] p 859 N92-29870
Method of measuring cross-flow vortices by use of an array of hot-film sensors
[NASA-CASE-LAR-14824-1-SB] p 998 N92-30390
FCS skewed sensors array: Practical considerations
p 968 N92-31868

MECHANICAL DEVICES
Single screw mechanism with gaterotor housing at intermediate pressure
[AD-D015140] p 400 N92-18120

MECHANICAL DRIVES
An eight month gearbox development program
[AIAA PAPER 92-3368] p 850 A92-48941
Preliminary analysis of baseline vibration data from Allison T56-A-14LFE engine and reduction gearbox
[NRC-31578] p 130 N92-11999

MECHANICAL ENGINEERING
Computational mechanics today p 399 A92-28464
Chaotic motion in mechanical and engineering systems p 695 A92-39480
Mechanics Pan-America 1991; Pan-American Congress of Applied Mechanics, 2nd (PACAM II), Universidad Tecnica, Valparaiso, Chile, Jan. 2-5, 1991, Selected and Revised Proceedings p 673 A92-39930
Repair procedures for advanced composites for helicopters p 1016 A92-56277
Compressing the compressor
[PNR-90824] p 476 N92-21848
AFRAPT Program at Texas A and M University research for advanced aircraft engine structures
[AD-A247040] p 743 N92-28076
Repair procedures for advanced composites for helicopters
[MBB-UD-0606-91-PUB] p 787 N92-29874
United States Air Force summer research program 1991. Volume 1: Program management report
[AD-A248763] p 1142 N92-32338

MECHANICAL IMPEDANCE
Variable impedance journal bearings for rotor-bearing systems p 157 N92-12270

MECHANICAL MEASUREMENT
Short time force measurement system
p 208 N92-15001

MECHANICAL OSCILLATORS
Chaotic motion in mechanical and engineering systems p 695 A92-39480

MECHANICAL PROPERTIES
Aerospace Arall - A challenge for the aircraft designer
p 33 A92-10232
Inertia-friction welding of an advanced rapidly solidified titanium alloy p 212 A92-18898
Holographic-interferometry methods employed for vibration-strength testing of aviation-engine workpieces
p 219 A92-20771
Mechanical and fracture behaviour of Ti-6Al-2Sn-4Zr-2Mo-0.1Si alloys p 288 A92-22755
The beta-CEZ - A high performance titanium alloy for aerospace engines p 289 A92-22760
Influence of long time exposure at elevated temperatures in air on mechanical properties of the high temperature titanium alloy IMI 834 p 289 A92-22767
Development and design with advanced materials --- Book
[ISBN 0-444-88706-7] p 296 A92-24176
Design and testing leading to certification of the Airbus A340 nose landing gear doors p 272 A92-24192
Ice property/structure variations across the glaze/rime transition
[AIAA PAPER 92-0296] p 351 A92-25749
Mechanical testing of glass-ceramic matrix composites
[ONERA, TP NO. 1991-182] p 388 A92-26351
Numerical comparison of experimentally measured ultrasound through a multilayered specimen
p 510 A92-28682
A critical appraisal of thermomechanical processing of structural titanium alloys p 488 A92-30611
Effects of T-tabs and large deflections in double cantilever beam specimen tests p 673 A92-39009
Effect of sustained high temperature exposure on the mechanical properties of Nicalon/Al2O3 composites
p 668 A92-39672
Monolithic ceramics p 668 A92-39854
Fabrication and properties of fiber-reinforced ceramic composites made by directed metal oxidation
p 669 A92-39861
Modeling the heat treatment of superalloys
p 755 A92-43679
Al-Li alloys find their niche p 755 A92-43685
Fabrication and mechanical properties of an optically transparent glass fiber/polymer matrix composite
p 891 A92-45630
Advanced superalloys for turbine blade and vane applications
[ONERA, TP NO. 1992-2] p 893 A92-48578
Addressing the challenge of aircraft component design and manufacture from metal matrix composites
p 985 A92-50007
New thermoplastic polyimide composite for supersonic aircraft structures p 985 A92-51512
Induction bonding procedures for graphite reinforced thermoplastic assemblies p 994 A92-51545
Development of composite structures with enhanced damage tolerance p 985 A92-51555
Mechanical properties of laminate aluminum matrix composites p 1106 A92-56102
Titanium alloy casting for aerospace
p 1106 A92-56103
Present status of Al-Li alloys p 1106 A92-56105
State-of-the-art materials for future gas turbine engines p 1070 A92-56122
Aluminium-lithium alloys - Application on helicopters
p 1106 A92-56326
Behavior of aircraft tire coupons under various loading conditions
[AD-A241416] p 116 N92-13063
Optimization of the calculation margins of landing gears under extreme loads. Rupture static tests. Part 1: Program and test implantation
[CEAT-S8-6551-PARTIEL-1-PT-] p 195 N92-14043
Evaluation of the elevated-temperature mechanical reliability of a HIPed silicon nitride
[DE92-007838] p 579 N92-23223
Light thermal structures and materials for high speed flight p 649 N92-25922
Composite strength statistics from fiber strength statistics
[AD-A245616] p 755 N92-26383
The effect of jet fuel exposure on advanced aerospace composites. Part 1: Thermal and chemical analysis
[AD-A246559] p 756 N92-27531
The mechanical properties of metal-void composites --- pressurized microvoids
[AD-A246087] p 757 N92-27749
Mechanical behavior and processing of aluminum metal matrix composites
[AD-A249918] p 987 N92-30874
Thermomechanical fatigue behavior of a silicone carbide fiber-reinforced calcium aluminosilicate glass-ceramic matrix composite
[AD-A249870] p 988 N92-31823
Eighth DOD/NASA/FAA Conference on Fibrous Composites in Structural Design, part 1
[NASA-CP-3087-PT-1] p 1106 N92-32513
Fluid effects: Thermoset and thermoplastic matrix composites p 1110 N92-33049
Jet fuel absorption and dynamic mechanical analysis of carbon fibre composites p 1110 N92-33050

MECHANICAL SHOCK
Application of MSC/DYNA to shock and impact problems in aircraft industry
[MBB-UD-0593-91-PUB] p 225 N92-14382

MEDICAL EQUIPMENT
Testing and evaluation of the Vanner electrical inverters, models 24-1500 and SP 00112
[AD-A241914] p 299 N92-17216

MEDICAL PERSONNEL
Testing and evaluation of the Vanner electrical inverters, models 24-1500 and SP 00112
[AD-A241914] p 299 N92-17216

MEDICAL SERVICES
Pre-flight risk assessment in emergency medical service (EMS) helicopters p 16 A92-11171

MELTING
Modifications to the rapid melt/rapid quench and transparent polymer video furnaces for the KC-135
[NASA-CR-184215] p 157 N92-12231
Composition monitoring of electron beam melting processes using diode lasers
[DE92-009527] p 669 N92-25259

MELTING POINTS
Wind tunnel investigation of the aerodynamic effects of aircraft ground deicing/anti-icing fluids and criteria for aerodynamic acceptance p 452 N92-21698

MEMBRANE STRUCTURES
Analysis of circular elastic membrane wings
p 245 A92-21722
Measurements of fuselage skin strains and displacements near a longitudinal lap joint in a pressurized aircraft
[NASA-TM-104163] p 159 N92-13455

MEMORY
Controller memory enhancement: Field facility concepts and techniques
[DOT/FAA/CT-TN92/7] p 640 N92-24799

MEMORY (COMPUTERS)
A novel associative memory for high level control functions p 52 A92-11472
Global memory in the Pave Pace architecture
p 920 A92-48447
The importance of implicit and explicit knowledge in a pilot's associate system p 858 A92-48567

MENTAL PERFORMANCE
Automated planning with special relevance to associate systems technology and mission planning
[AD-A241924] p 303 N92-17438
The role of planning systems in future air traffic management p 355 N92-19050

MERIDIONAL FLOW
An inverse inviscid method for the design of quasi-three dimensional turbomachinery cascades
p 523 A92-36033
A multiblock grid generation technique applied to a jet engine configuration p 692 N92-24428

MESOSCALE PHENOMENA
Mesoscale dynamics of cold fronts - Structures described by dropsoundings in Fronts 87
p 230 A92-18902
High altitude airborne remote sensing mission using the advanced microwave precipitation radiometer (AMPR)
p 574 A92-34893

MESSAGE PROCESSING
Implementing data link across the Pacific
[SAE PAPER 912235] p 638 A92-40027
Expert system management system
[AD-A247102] p 781 N92-26863

METAL BONDING
Characterization of diffusion bonds using an acoustic microscope p 491 A92-28686

METAL FATIGUE
Short fatigue crack growth from blunt notches in an aero-engine alloy p 212 A92-19760
Crack initiation and the short-to-long crack growth transition in a Ni-base superalloy p 213 A92-19767
High temperature low cycle fatigue of single crystal nickel base superalloys p 213 A92-19796
Thermo-mechanical fatigue crack growth in aircraft engine materials p 213 A92-19799
Comparative study of fatigue in various materials and designs under sonic loading p 287 A92-21003
Fatigue life estimation of fastener holes without load transfer p 291 A92-21472
Creep-fatigue crack growth in Jethete M152 at 550 C under mixed mode conditions p 288 A92-21490
Inclusion size effect on the fatigue crack propagation mechanism and fracture mechanics of a superalloy
p 388 A92-24831
A fatigue crack growth threshold p 389 A92-26667
The problem of aging aircraft - Is mandatory retirement the answer? p 308 A92-27448
Reliability centered maintenance for metallic airframes based on a stochastic crack growth approach
p 897 A92-45242
Monitoring fatigue cracks in gears
p 1116 A92-54496
Low cycle fatigue of cast nickel base turbine rotors
p 226 N92-14405
Fatigue in single crystal nickel superalloys
[AD-A243453] p 290 N92-17653
Fatigue in single crystal nickel superalloys
[AD-A244815] p 489 N92-21015
Durability and damage tolerance of aluminum castings
[AD-A245237] p 490 N92-21159
Aging fleet: Maintaining airworthiness
p 953 N92-31862
Fatigue in single crystal nickel superalloys
[AD-A252492] p 988 N92-32066

METAL FIBERS
Metal fibers and fabrics as shielding materials for composites, missiles and airframes p 141 A92-14680

METAL FOILS
Observational study of pool boiling under microgravity
p 757 A92-41060

METAL HYDRIDES
Evaluation of metal hydride compressors for applications in Joule-Thomson cryocoolers p 296 A92-23835

METAL MATRIX COMPOSITES
Applications of advanced composites in a 3/4 air transportable rack p 36 A92-10314

The microstructural stability of TiC reinforced rapidly solidified Al-Fe-V-Si composite structures
p 141 A92-15169
Hypersonic materials p 212 A92-18002
Current stabilizing of fastened composite joints to improve non-sparking lightning current performance
p 213 A92-20130
The compatibility and tradeoffs of titanium and composites p 288 A92-22758
Ultrasonic NDE for ceramic- and metal-matrix composite material characterization p 491 A92-28690
Flight vehicles of the future p 419 A92-31525
Composite strengthening of Nb-Ti base alloys
p 577 A92-36380
Testing of a titanium matrix composite landing gear
[SAE PAPER 912175] p 644 A92-40000
Metal matrix composite fabrication processes for high performance aerospace structures p 760 A92-42145
Cold-crucible directional solidification of refractory metal-silicide eutectics p 755 A92-43684
Axial alignment of short-fiber titanium aluminide composites by directional solidification
p 892 A92-46838
Addressing the challenge of aircraft component design and manufacture from metal matrix composites
p 985 A92-50007
Application of resin and metal matrix composites to advanced avionics enclosure p 985 A92-51921
High temperature MMCs for aero-engines - Challenge and potential p 986 A92-52982
High-temperature metal matrix composite
p 1105 A92-53878
Mechanical properties of laminate aluminum matrix composites p 1106 A92-56102
Thermoviscoplastic response of Ti-15-3 under various loading conditions
[NASA-CR-187621] p 45 N92-11391
Development and characterization of Powder Metallurgy (PM) 2XXX series Al alloy products and Metal Matrix Composite (MMC) 2XXX Al/SiC materials for high temperature aircraft structural applications
[NASA-CR-187631] p 390 N92-19290
The mechanical properties of metal-void composites --- pressurized microvoids
[AD-A246087] p 757 N92-27749
Mechanical behavior and processing of aluminum metal matrix composites
[AD-A249918] p 987 N92-30874
Preliminary evaluation of adhesion strength measurement devices for ceramic/titanium matrix composite bonds
[NASA-TM-105803] p 932 N92-31267

METAL OXIDES
Fabrication and properties of fiber-reinforced ceramic composites made by directed metal oxidation
p 669 A92-39861
Microgravity nucleation and particle coagulation experiments support
[NASA-CR-189899] p 502 N92-21433

METAL PARTICLES
Improving sample introduction for total wear metal determination by atomic emission spectroscopy
p 389 A92-26850

METAL PLATES
Aerodynamic characteristics of hoar frost roughness
p 808 A92-45829
The ASU Transition Research Facility
[AIAA PAPER 92-3910] p 1094 A92-56744
Nonlinear aspects of aerospace structures at high excitation levels flat aluminum beams and plates studied
[AD-A240600] p 44 N92-11383
Surface residual stress analysis of metals and alloys
[AD-A248372] p 895 N92-28426

METAL POWDER
Probabilistic lifing approach for aero engine disks made of powder nickel base alloys containing ceramic defects
p 226 N92-14424
Development and characterization of Powder Metallurgy (PM) 2XXX series Al alloy products and Metal Matrix Composite (MMC) 2XXX Al/SiC materials for high temperature aircraft structural applications
[NASA-CR-187631] p 390 N92-19290
Powder processing of aero-engine components
[PNR-90813] p 756 N92-27044

METAL PROPELLANTS
Solid fuel ramjet infrared signature
[AD-A246299] p 753 N92-26362

METAL SHEETS
Analyses of heat isolation property for metallic multiwall thermal protection system p 40 A92-12422
Cost effective solutions for titanium sheet metal forming p 293 A92-22785
Active control of airborne noise transmitted through a ribbed panel p 695 A92-39111
EIPOS for ice-formation control on aircraft in flight - An alternative technique p 647 A92-40545
Development of an automatic metal sheet working machine for interior structure p 700 A92-43247
Effects of constraint on crack growth under aircraft spectrum loading
[NASA-TM-107677] p 1128 N92-34178

METAL SURFACES
5,000-hour stability tests of metal sheathed thermocouples at respective temperatures of 538 C and 875 C
[ASME PAPER 91-GT-182] p 148 A92-15614
Thin bondline measurement of adhesively bonded metallic aircraft structures using an ultrasonic analyzer
p 491 A92-28684
The reinforcing effect of composite patch repairs on metallic aircraft structures p 419 A92-30498

METAL VAPORS
Microgravity nucleation and particle coagulation experiments support
[NASA-CR-189899] p 502 N92-21433

METAL-METAL BONDING
The study on the composite-patching repairs for metallic aircraft structures p 36 A92-10285
Metal-metal bondline NDE methods
[AD-A244429] p 503 N92-21730

METAL-WATER REACTIONS
Corrosion prevention field test utilizing water displacement compounds p 110 A92-14436

METALLIZING
Mechanical behavior and processing of aluminum metal matrix composites
[AD-A249918] p 987 N92-30874

METALS
Overview of mechanics of materials branch activities in the computational structures area
p 684 N92-25917
Surface residual stress analysis of metals and alloys
[AD-A248372] p 895 N92-28426

METEOROLOGICAL INSTRUMENTS
The design and operational characteristics of a heated radome for air motion measurement p 467 A92-32064
Use of relative humidity sensors for planes measurement p 467 A92-32080
An airborne Doppler lidar for meteorological research
p 467 A92-32082
A new aircraft universal lightweight digital dropsonde
p 467 A92-32089
Design and preliminary tests of a new airborne thermometer p 468 A92-32097

METEOROLOGICAL PARAMETERS
Sensors and systems to enhance aviation safety against weather hazards p 160 A92-14265
Fair weather convection and light aircraft accidents
[IAF PAPER ST-91-004] p 186 A92-20651
Atmospheric analysis for airdata calibration on research aircraft
[AIAA PAPER 92-0293] p 369 A92-25746
The DLR Lyman-alpha hygrometer
p 467 A92-32091
Simple models for the description of turbulence in the atmospheric boundary layer
[DLR-FB-90-17] p 410 N92-19292
A graphical weather system design for the NASA transport systems research vehicle B-737
[NASA-TM-104205] p 556 N92-22504
Analysis of sonic boom data to quantify distortions of shock profiles p 1139 N92-33879

METEOROLOGICAL RADAR
Characteristics of thunderstorm-generated low altitude wind shear - A survey based on nationwide terminal Doppler weather radar testbed measurements
p 45 A92-11378
Polish radar technology. III - Weather channel for primary surveillance radar p 40 A92-12291
The future of Loran-C navigation, instrument approaches and flight following for air traffic management
p 95 A92-16630
Saberliner flight test and results for forward looking detection and avoidance of airborne windshear
p 98 A92-16656
Predicting summer microburst hazard from thunderstorm day statistics p 407 A92-27960
A case study of the Claycomo, Missouri microburst on July 30, 1989 p 407 A92-27961
A prototype microburst prediction product for the Terminal Doppler Weather Radar p 408 A92-27962
Aspect angle dependence of outflow strength in Denver microbursts - Spatial and temporal variations
p 408 A92-27963
Enclosing shapes for single-Doppler radar features
p 494 A92-30476
The 1990 Airport Surveillance Radar Wind Shear Processor (ASR-WSP) operational test at Orlando International Airport
[AD-A239852] p 18 N92-10019
Terminal Doppler weather radar test bed operation, Orlando: January-June 1990
[AD-A242890] p 301 N92-17028
Radar multipath study for rain-on-radome experiments at the Aircraft Landing Dynamics Facility
[NASA-TM-101657] p 680 N92-25137
Simplified signal processing for an airborne CO2 Doppler lidar p 1000 N92-31023
A study of atmospheric optical scattering parameters at 1.5 and 2 micron region for solid state Doppler lidar applications p 1001 N92-31067
A comparison of the performance of two gust front detection algorithms using a length-based scoring technique
[AD-A250862] p 1004 N92-32103
Airport Surveillance Radar (ASR-9) wind shear processor: 1991 test at Orlando, Florida
[AD-A252246] p 1124 N92-32686

METEOROLOGICAL RESEARCH AIRCRAFT
Airflow effects about PMS probes on the DLR Falcon --- Particle Measuring System for atmospheric research aircraft p 467 A92-32060
Modifications to and data correction methods for some radiometers used on aircraft p 467 A92-32062
The DLR Lyman-alpha hygrometer
p 467 A92-32091

METEOROLOGICAL SERVICES
The new airport aeronautic meteorological codes
p 160 A92-13855
Shear progress --- wind shear handling and recognition technologies for aviation p 609 A92-40880
Pilot's Automated Weather Support System (PAWSS) concepts demonstration project. Phase 1: Pilot's weather information requirements and implications for weather data systems design
[NASA-CR-188228] p 46 N92-11593
JPL's Real-Time Weather Processor project (RWP) metrics and observations at system completion
p 413 N92-19428
A graphical weather system design for the NASA transport systems research vehicle B-737
[NASA-TM-104205] p 556 N92-22504

METEOROLOGY
Operating ranges of meteorological wind tunnels for the simulation of convective boundary layer phenomena
[AD-A244153] p 409 N92-19195

METHOD OF CHARACTERISTICS
Quasi-three-dimensional characteristics method for a supersonic compressor rotor
[ASME PAPER 91-GT-81] p 69 A92-15549
Extended mapping and characteristics techniques for inverse aerodynamic design p 194 N92-13949

METHODOLOGY
A methodology for the analysis and modeling of thrust vectoring usage
[AIAA PAPER 92-0389] p 357 A92-26245
Development of an uncertainty methodology for multiple-channel instrumentation systems
[AIAA PAPER 92-3953] p 1133 A92-56781

METROLOGY
Comparison of GLONASS and GPS time transfers between two west European time laboratories and VNIIFTRI p 1050 N92-33381

MICROBALANCES
Monitoring jet fuel degradation using quartz crystal microbalances
[DE92-004730] p 489 N92-20858

MICROBURSTS (METEOROLOGY)
Characteristics of thunderstorm-generated low altitude wind shear - A survey based on nationwide terminal Doppler weather radar testbed measurements
p 45 A92-11378
Evaluation of a technique to quantify microburst windshear hazard potential to aircraft p 17 A92-11379
A DFW microburst model based on DL-191 data
p 17 A92-11380
Windshear detection and avoidance - Airborne systems survey p 17 A92-11382
Lightning activity in microburst producing storm cells
[ONERA, TP NO. 1991-98] p 161 A92-16080
Analysis of aircraft performance during lateral maneuvering for microburst avoidance
p 205 A92-20207
Forward-look wind-shear detection for microburst recovery p 378 A92-24408
Experimental evaluation of candidate graphical microburst alert displays
[AIAA PAPER 92-0292] p 369 A92-25745
Target pitch angle for the microburst escape maneuver
[AIAA PAPER 92-0730] p 379 A92-27082
Understanding and predicting microbursts
p 407 A92-27953
Three-dimensional simulation of the Denver 11 July Storm of 1988 - An intense microburst event
p 407 A92-27958

Predicting summer microburst hazard from thunderstorm day statistics p 407 A92-27960
A case study of the Claycomo, Missouri microburst on July 30, 1989 p 407 A92-27961
A prototype microburst prediction product for the Terminal Doppler Weather Radar p 408 A92-27962
Aspect angle dependence of outflow strength in Denver microbursts - Spatial and temporal variations p 408 A92-27963
Enclosing shapes for single-Doppler radar features p 494 A92-30476
Windshear detection p 652 A92-40883
Microburst modelling and scaling p 915 A92-46262
Thrust laws for microburst wind shear penetration p 873 A92-46750
Optimal recovery from microburst wind shear
[AIAA PAPER 92-4338] p 1078 A92-55327
A data fusion algorithm for multi-sensor microburst hazard assessment
[AIAA PAPER 92-4339] p 1063 A92-55328
Escape strategies for turboprop aircraft in microburst windshear p 1084 A92-56151
Escape strategies for turboprop aircraft in a microburst windshear
[AD-A243090] p 264 N92-17217
An investigation of air transportation technology at the Massachusetts Institute of Technology, 1990-1991 p 265 N92-17985
Alert generation and cockpit presentation for an integrated microburst alerting system p 265 N92-17988
Cockpit display of hazardous weather information p 277 N92-17989
Target pitch angle for the microburst escape maneuver p 266 N92-17996
Optimal aircraft performance during microburst encounter p 266 N92-17999
Experimental evaluation of candidate graphical microburst alert displays
[NASA-CR-189633] p 735 N92-27424
The modelling of turbulence and downbursts for flight simulators
[ISBN-0-315-59945-6] p 749 N92-27645

MICROCOMPUTERS
EDMS: Microcomputer pollution model for civilian airports and Air Force bases, (user's guide)
[AD-A240528] p 45 N92-11578
The NASA Langley Research Center 0.3-meter transonic cryogenic tunnel microcomputer controller source code
[NASA-CR-189556] p 209 N92-15077
Microcomputer-based instrument flight simulation: Undergraduate pilot training student attitude assessment
[AD-A245449] p 749 N92-26527

MICROCRACKS
Fatigue in single crystal nickel superalloys
[AD-A244815] p 489 N92-21015
Metal-metal bondline NDE methods
[AD-A244429] p 503 N92-21730
High-temperature polymer matrix composites p 578 N92-22513

MICROGRAVITY APPLICATIONS
Demonstration of gas liquid separation under the microgravity by aircraft KC-135
[SAE PAPER 912024] p 897 A92-45416

MICROORGANISMS
Microbiological spoilage of aviation turbine fuel. II - Evaluation of a suitable biocide p 891 A92-45600

MICROPHONES
An optical microphone for the detection of hidden helicopters
[AIAA PAPER 92-0377] p 395 A92-26235
The acoustic flashlight
[MBB-Z-0359-90-PUB] p 239 N92-15938

MICROPROCESSORS
An application of distributed environment in flight simulation p 602 A92-35739
A microprocessor-based automation test system for the experiment of the multi-stage compressor p 997 A92-53100
Advanced Transport Operating System (ATOPS) color displays software description microprocessor system
[NASA-CR-189605] p 556 N92-22645
The design and development of a portable, DSP micro-processor based, high-accuracy data acquisition system
[NRC-32146] p 1134 N92-32851
The development of an airborne information management system for flight test
[NASA-TM-104251] p 1065 N92-32866

MICROSTRIP ANTENNAS
A parallel-series-fed microstrip array with high efficiency and low cross-polarization p 496 A92-31630
Advanced electromagnetic methods for aerospace vehicles
[NASA-CR-188630] p 488 N92-20193

MICROSTRUCTURE
The microstructural stability of TiC reinforced rapidly solidified Al-Fe-V-Si composite structures p 141 A92-15169
Protective coatings of thermal barrier type p 214 A92-20349
A technique for quantitatively measuring microstructurally induced ultrasonic noise p 510 A92-28720
Experimental results and numerical modeling of solidification during aircraft high-g arcs
[AIAA PAPER 92-0843] p 493 A92-29609
A preliminary study of the microstructure-property relationships in cast gamma titanium aluminide alloys p 487 A92-30596
Investigation of the structural inhomogeneity of a titanium alloy p 893 A92-47958
Durability and damage tolerance of aluminum castings
[AD-A245237] p 490 N92-21159
Creep and fatigue research efforts on advanced materials p 593 N92-22514
Aeropropulsion structures p 559 N92-22518

MICROWAVE ANTENNAS
Estimation of the P-3/SAR L-, C- and X-band antenna directivity in range direction based on corner reflector measurements within the absolute SAR calibration p 587 A92-35055

MICROWAVE COUPLING
Radiation and coupling between antennas mounted on a complex metallic structure p 760 A92-42315

MICROWAVE EQUIPMENT
Mobile Microwave Landing System (MMLS): Operational requirements for setup accuracy
[AD-A241844] p 103 N92-13052
Recommended system concept p 599 N92-23383

MICROWAVE FREQUENCIES
Bistatic scattering on a monostatic radar range p 849 A92-48408

MICROWAVE IMAGERY
Global and high resolution radar cross section measurements and two-dimensional microwave images of a scaled aircraft model from the type Airbus A 310
[DLR-MITT-91-10] p 911 N92-29877

MICROWAVE LANDING SYSTEMS
Polish radar technology. II - Adaptive radar AVIA CM p 39 A92-12290
Growing need to replace ILS can best be met by MLS p 534 A92-36124
MLS system error model identification and synthesis p 639 A92-40232
Microwave landing system modeling with application to air traffic control automation p 725 A92-41220
A DSP-based microwave landing system (MLS) post-IF processor p 955 A92-49306
Synthesis of a MLS automatic landing control law for the NAL experimental research aircraft Do-228 p 1084 A92-56062
Flight evaluation of navigation systems including MLS using NAL Do228 - Outline p 1047 A92-56116
Flight evaluation of navigation systems including MLS using NAL Do228 - Results of MLS p 1047 A92-56117
Flight evaluation of navigation systems including MLS using NAL Do228 - Results of GPS p 1047 A92-56118
Mobile Microwave Landing System (MMLS): Operational requirements for setup accuracy
[AD-A241844] p 103 N92-13052
Electronic systems in transportation
[TP-9983] p 189 N92-14009
MLS system error model identification and synthesis p 189 N92-14015
DME growth elements and their use with MLS p 189 N92-14018
A strategy for exploiting the full potential of MLS based terminal procedures in Canada p 190 N92-14025
The problem of multiple solutions in area navigation and computed centerline operations with the microwave landing system
[AD-A242757] p 191 N92-15058
Microwave landing system autoland system analysis
[NASA-CR-189551] p 191 N92-15060
Joint Federal Aviation Administration (FAA)/Civil Aviation Authority (CAA) Microwave Landing System (MLS) Area Navigation (RNAV) flight evaluations
[DOT/FAA/CT-TN91/17] p 268 N92-15983
Flight evaluation of curved MLS precision approaches in a twin otter aircraft, phase 2
[AD-A243025] p 268 N92-17568
Evaluation of advanced microwave landing system procedures in the New York terminal area
[DOT/FAA/ND-91/1] p 354 N92-18967
Activities of NRC-CNRC, Institute for Aerospace Research, Flight Research Lab.
[CTN-92-60432] p 420 N92-20205
Attributes of winged manned space vehicles and their relationship to ground site characteristics and facilities p 487 N92-20776
Comparison of the performance of a microwave landing system elevation station with the instrument landing system end-fire glide slope at Yeager Airport, Charleston, West Virginia
[DOT/FAA/CT-TN91/22] p 534 N92-22210
MLS mathematical modeling study of Philadelphia International Airport runway 27L
[DOT/FAA/CT-TN91/54] p 573 N92-22503
MLS and DME/P multipath simulation model user's manual. Volume 1: Operating instructions
[DOT/FAA/CT-TN91/47] p 640 N92-24888
Nationwide system delay study of the microwave landing system in the New York terminal area, volume 1
[DOT/FAA/CT-TN91/59-VOL-1] p 640 N92-25098
NAL Dornier 228-200 flight research airplane: Present status and outline of the installed equipment
[NAL-TM-637] p 732 N92-27429
Evaluation of microwave landing system approaches in a wide-body transport simulator
[NASA-CR-4450] p 957 N92-30978
Development of new flight procedures for the Microwave Landing System (MLS)
[NLR-TP-91156-U] p 1047 N92-32830

MICROWAVE POWER BEAMING
Power beaming - Energy transmission at 35 GHz and higher frequencies --- for terrestrial and space applications with rectennas
[AIAA PAPER 92-2027] p 471 A92-29944

MICROWAVE RADIOMETERS
Retrieval of total precipitable water over high latitude regions using radiometric measurements near 90 and 183 GHz p 505 A92-32129
High altitude airborne remote sensing mission using the advanced microwave precipitation radiometer (AMPR) p 574 A92-34893
Mechanical design of an airborne imaging microwave radiometer p 554 A92-35276
Microwave temperature profiler for clear air turbulence prediction
[NASA-CASE-NPO-18115-1-CU] p 916 N92-29148

MICROWAVE SCANNING BEAM LANDING SYSTEM
Global positioning system supported pilot's display p 534 N92-22436

MICROWAVE SCATTERING
X-band side-looking airborne radar for remote sensing p 554 A92-34976

MICROWAVES
The design of broadband radar absorbing surfaces
[AD-A240521] p 42 N92-11235
Television Microwave Link (TML) Operational Test and Evaluation (OT/E)/integration test report
[DOT/FAA/CT-TN91/57] p 500 N92-20653

MIDAIR COLLISIONS
Midair collision - The links in a chain p 951 A92-52645
Air-to-air visual acquisition handbook
[ATC-151] p 93 N92-13042
Aircraft accident/incident summary report: Midair collision involving Lycoming Air Services Piper Aerostar PA-60 and Sun Company Aviation Department Bell 412, Merion, Pennsylvania, April 4, 1991
[PB91-910407] p 187 N92-15055
UK airmisses involving commercial air transport: September - December 1990
[ETN-92-91050] p 452 N92-21746
Safety study of TCAS 2 for logic version 6.04
[DOT/FAA/RD-92/22] p 1047 N92-32537

MIDCOURSE GUIDANCE
Space shuttle entry terminal area energy management
[NASA-TM-104744] p 308 N92-19930

MIG AIRCRAFT
MiG-29 prototype and development flight tests - General overview and high angle of attack investigation p 113 A92-16064
Russians say D-30F6 engine used in MiG-31 is highly reliable p 472 A92-32298
Mikoyan's market-buster p 1052 A92-54981

MILITARY AIR FACILITIES
Effects of military training route noise on human annoyance p 689 A92-39237
The Tonopah years p 785 A92-47758
A neural network based postattack damage assessment system p 922 A92-48520
EDMS: Microcomputer pollution model for civilian airports and Air Force bases, (user's guide)
[AD-A240528] p 45 N92-11578
Analysis of measured environmental noise levels: An assessment of the effects of airbase operational model variables on predicted noise exposure levels
[AD-A244805] p 485 N92-21720
An exploratory application of neural networks to the sortie generation forecasting problem
[AD-A246626] p 778 N92-27980

MILITARY AIRCRAFT
A review of rigid body response on sting supported models at high angles of incidence p 66 A92-15345
An investigation of two cooling technologies as applied to a distributed propulsion control architecture
[ASME PAPER 91-GT-341] p 111 A92-15705
Status of the NH90 European Helicopter Program p 113 A92-16676
Clever cockpits p 241 A92-21700
Interference flows past cylinder-fin-sting-cavity assemblies p 442 A92-32236
Recent advances in restraint technology p 535 A92-32979
Composite cylinder blast overpressure testing p 529 A92-32984
Agile responsive effective support - Design and testing of the ARES concept demonstrator aircraft
[AIAA PAPER 92-1038] p 536 A92-33219
The Mission Computer/Electronic Display Subsystem for the United States Air Force C-17A transport aircraft
[AIAA PAPER 92-1244] p 553 A92-33337
Damage tolerance and repair experience of composite structures
[AIAA PAPER 92-1256] p 515 A92-33339
The C-17 - Modern airlift technology
[AIAA PAPER 92-1262] p 538 A92-33342
A revolution in air transport - Acquiring the C-141 Starlifter p 607 A92-38101
Production technologies and aircraft design p 608 A92-38220
Noise from military airfields in the United Kingdom p 686 A92-39052
Comparison of aircraft noise indices for noise zoning at military airfields p 687 A92-39056
Rafale: Program update - Development of a naval version p 645 A92-40035
International Powered Lift Conference, London, England, Aug, 29-31, 1990, Proceedings
[ISBN 0-903409-68-2] p 783 A92-45302
An overview of US Navy and Marine Corps V/STOL p 783 A92-45303
Current technology propulsion systems meet the STOVL window of opportunity p 860 A92-45307
Low cost HIRF troubleshooting and verification method for digital avionics systems p 990 A92-49304
The role of stealth in naval aviation and joint/combined operations
[AD-A240595] p 22 N92-11005
Implementing total quality management at the intermediate level of aircraft maintenance
[AD-A241768] p 62 N92-12992
Development of a knowledge base for use in an Expert System Advisor for Aircraft Maintenance Scheduling (ESAAMS)
[AD-A243435] p 305 N92-17687
The SnoDog: Preliminary design of a close air support aircraft
[NASA-CR-189990] p 462 N92-21489
Aeronautical research in the United States: Challenges for the 1990's p 420 N92-21502
Sonic booms produced by US Air Force and US Navy aircraft: Measured data
[AD-A244804] p 512 N92-21719
Overview of computational structural methods for modern military aircraft p 684 N92-25928
A prototype semantic integrity front end expert system for a relational database
[AD-A246084] p 781 N92-26765
Ingress, emergency egress, and emergency evacuation testing of army aircraft
[AD-A246398] p 724 N92-27750
Evaluation of grounding and mooring points for Army aircraft
[AD-A250749] p 953 N92-31193
The Utilization of Advanced Composites in Military Aircraft
[AGARD-R-785] p 1109 N92-33033

MILITARY AVIATION
Anglo-American avionics p 307 A92-25575
Military and civil software standards and guidelines for guidance and control p 163 N92-12452

MILITARY HELICOPTERS
Technology developments applied to the AH-1W SuperCobra
[AIAA PAPER 91-3071] p 21 A92-11607
Value of survivability enhancement techniques p 59 A92-14349
Helicopter local blade circulation calculations for a model rotor in forward flight using laser velocimeter measurements p 65 A92-14362
GPS-INS integration requirements for robust NOE helicopter navigation p 94 A92-14404
Tiger MGB - High reliability low weight --- military helicopter Main Gear Box p 109 A92-14418
Day/Night Adverse weather Pilotage System (D/NAPS) p 94 A92-14429
Certifying composite helicopter structures p 110 A92-14443
P120 programme - First results of the pre-development phase p 60 A92-14447
Composite electromagnetic pulse threat p 146 A92-14689
Development of a lubrication system for the T800-LHT-800 turboshaft engine
[ASME PAPER 91-GT-398] p 127 A92-15728
EH101 helicopter development p 112 A92-16060
RAH-66 Comanche - A cut above the rest p 61 A92-16675
A new method for calculation of helicopter maneuvering flight p 282 A92-23382
Composites usage on the RAH-66 Comanche p 457 A92-29669
Tiger development status --- Franco-German antitank helicopter p 458 A92-29672
Inertia reels for aircrew restraint systems p 529 A92-32982
High-order state space simulation models of helicopter flight mechanics p 569 A92-35777
1991-92 AHS Technical Committee highlights - Aircraft design p 608 A92-40392
Some issues on modeling atmospheric turbulence experienced by helicopter rotor blades p 647 A92-40885
Advanced Rotorcraft Transmission program summary
[AIAA PAPER 92-3363] p 905 A92-48936
Boeing Helicopters Advanced Rotorcraft Transmission (ART) Program summary of component tests
[AIAA PAPER 92-3364] p 905 A92-48937
Advanced Rotorcraft Transmission (ART) - Component test results
[AIAA PAPER 92-3366] p 905 A92-48939
Formation flight system design concept p 954 A92-49255
GPS integration improves mission capabilities of CH-47D aircraft p 966 A92-49340
Generic helicopter for multiship simulations
[AIAA PAPER 92-4151] p 959 A92-52442
Response of helicopter blades to a sharp collective increase p 1084 A92-56282
Lynx - A 50 year product? p 1056 A92-56307
AS 332 MKII - Development and certification p 1059 A92-56343
A study of the airwake aerodynamics over the flight deck of an AOR model ship
[AD-A241008] p 89 N92-13034
Analytical modeling of SH-2F helicopter shipboard operation p 464 N92-21961
Helicopter/ship analytic dynamic interface p 464 N92-21962
EH 101 ship interface trials: Flight test programme and preliminary results p 465 N92-21964
United Kingdom approach to deriving military ship helicopter operating limits p 465 N92-21966
Helicopter handling: Experience and new developments p 465 N92-21969
A modeling strategy for large-scale optimization based on analysis and visualization principles
[AD-A246570] p 777 N92-26620
Report on the workshop on Ion Implantation and Ion Beam Assisted Deposition
[AD-A250561] p 927 N92-28923
Resonance and control response tests using a control simulation device
[MBB-UD-0608-91-PUB] p 978 N92-30439

MILITARY OPERATIONS
Effectiveness of V-22 tiltrotors in support of land combat operations p 60 A92-14442
The H-53E Super Stallion - A cost-effective solution to multi-service medium/heavy lift requirements p 647 A92-40388
The development of a real time visual flight simulator for tactical operations research and measurement p 880 A92-45027
The role of stealth in naval aviation and joint/combined operations
[AD-A240595] p 22 N92-11005
Reducing environmental noise impacts: A USAREUR noise management program handbook
[AD-A240797] p 237 N92-14791
Approach and landing guidance p 457 N92-21960
United Kingdom approach to deriving military ship helicopter operating limits p 465 N92-21966
Opportunities for flight simulation to improve operational effectiveness p 883 N92-28523

MILITARY TECHNOLOGY
Clever cockpits p 241 A92-21700
Opportunities for advanced speech processing in military computer-based systems p 293 A92-22299
Anglo-American avionics p 307 A92-25575
The evolution of military GPS technology into the Navcore V receiver engine p 651 A92-39570
Requirements for high flux cooling of future avionics systems
[SAE PAPER 912104] p 673 A92-39958
Tiltrotor UAV - The next generation unmanned system p 646 A92-40384
Sikorsky Aircraft UAV program p 646 A92-40385
An analysis tool for UAV effectiveness evaluation p 608 A92-40386
Conceptual design and analysis of a special operations transport p 646 A92-40387
Some aspects of advanced aircraft development p 729 A92-41176
Integrated test and evaluation for hypervelocity systems
[AIAA PAPER 92-3901] p 1017 A92-56736
The role of stealth in naval aviation and joint/combined operations
[AD-A240595] p 22 N92-11005
Avionics technology beyond 2000 p 200 N92-14058
Pulsed field system for detecting the presence of a target in a subsurface environment
[AD-D015074] p 296 N92-16174
Revolution at sea: Aircraft options for the year 2030 p 466 N92-21974
When should we start high-rate production of the B-2? An analysis based on flight test results
[RAND/P-7757] p 697 N92-25204
Advances in Fibre-Optic Technology in Communications and for Guidance and Control
[AGARD-LS-184] p 774 N92-28084
The rise of active-element phased-array radar
[RAND-P-7747-RGS] p 999 N92-30755

MILLIMETER WAVES
A Ka-band instrumentation radar with one foot range resolution p 95 A92-16252
Power beaming - Energy transmission at 35 GHz and higher frequencies --- for terrestrial and space applications with rectennas
[AIAA PAPER 92-2027] p 471 A92-29944
A low-power, high-efficiency Ka-band TWTA p 671 A92-38163
Laser-radar based obstacle avoidance system for helicopters p 1064 A92-56295

MIMD (COMPUTERS)
Solution of the Euler and Navier-Stokes equations on MIMD distributed memory multiprocessors using cyclic reduction
[AIAA PAPER 92-0561] p 411 A92-26970
Future directions in computing and CFD
[AIAA PAPER 92-2734] p 917 A92-45489
Timing analysis of parallel algorithms on a MIMD multiprocessor
[ITN-92-85153] p 510 N92-20905

MIMO (CONTROL SYSTEMS)
A time approach to robustness of LTI systems with structured uncertainty and unmodelled dynamics --- linear time-invariant p 48 A92-11356
A horizon-recursive form for predictors and their computation p 50 A92-11427
Practical robustness testing for helicopter flight control systems p 132 A92-14340
Design of compensators for linear parameter-varying feedback systems by the gain scheduling technique p 507 A92-29101
Controller design for the F-14 pitch axis control problem using the quantitative feedback theory approach p 478 A92-29128
Application of the delta-operator in MIMO discrete-time adaptive flight control systems p 479 A92-29516
Rule based identifier for unknown systems p 509 A92-31430
The multiple-function multi-input/multi-output digital controller system for the AFW wind tunnel model
[AIAA PAPER 92-2083] p 565 A92-35655
Eigenstructure assignment for handling qualities in helicopter flight control law design p 570 A92-35786
The development of multiple-input models for airborne noise prediction p 695 A92-39243
Robust discrete controller design for an unmanned research vehicle (URV) using discrete quantitative feedback theory p 877 A92-48495
Compensating for manufacturing and life-cycle variations in aircraft engine control systems
[AIAA PAPER 92-3869] p 868 A92-49139
Flight-determined stability analysis of multiple-input-multiple-output control systems
[AIAA PAPER 92-4396] p 1074 A92-55196
MIMO state-feedback control system considering phase stability by -90 deg phase-locus method p 1084 A92-56066
A robust digital flight control system for an unfanned research vehicle using discrete quantitative feedback theory
[AD-A243638] p 283 N92-17748

A methodology for computing uncertainty bounds of multivariable systems based on sector stability theory concepts
[NASA-TP-3166] p 482 N92-21410
Multifunction tests of a frequency domain based flutter suppression system
[NASA-TM-107615] p 662 N92-25607
Dynamics and control of a five degree-of-freedom magnetic suspension system
[NASA-CR-191259] p 1102 N92-34222

MINIATURIZATION
Tactical Rubidium Frequency Standard (TRFS)
[AD-A243934] p 401 N92-18897
High-temperature miniaturized turbine engine lubrication system simulator
[AD-A249259] p 868 N92-28294

MINIMAX TECHNIQUE
Linear quadratic minimax controllers
p 917 A92-46748

MINIMUM DRAG
Optimization of a lifting surface for minimum induced drag p 437 A92-31853
Wing design for hanggliders having minimum induced drag p 811 A92-46814
Optimal design of wing shape by use of neural-network p 1054 A92-56112
Analysis and design of planar and non-planar wings for induced drag minimization
[NASA-CR-189509] p 179 N92-13999
Constrained spanload optimization for minimum drag of multi-lifting-surface configurations
[NLR-TP-89126-U] p 828 N92-28660

MINING
JPRS report: Science and technology. USSR: Engineering and equipment
[JPRS-UEQ-91-010] p 593 N92-22397

MINOR CIRCLE TURNING FLIGHT
2-D and 3-D minimum-time-to-turn flights via parameter optimization
[AIAA PAPER 92-0731] p 379 A92-27083

MIRAGE AIRCRAFT
Mirage 2000-5 - Dassault's delta described
p 113 A92-16622
Wind loads on a mirage III O aircraft mounted above a ground plane
[AD-A243004] p 275 N92-17266
Aircraft tracking optimization of parameters selection
p 361 N92-18585
Dynamic performance of an aircraft on its landing gear: Test and evaluation on a dihedral p 466 N92-21970

MIRRORS
Study of optical techniques for the Ames unitary wind tunnels. Part 1: Schlieren
[NASA-CR-189951] p 385 N92-19218

MISALIGNMENT
Bias of an optical passive ring-resonator gyro caused by the misalignment of the polarization axis in the polarization-maintaining fiber resonator
p 652 A92-40262
The effects of manufacturing tolerances on the vibration of aero-engine rotor-damper assemblies
p 222 N92-14349
Analysis and modification of a single-mesh gear fatigue rig for use in diagnostic studies
[NASA-TM-105416] p 773 N92-27879

MISSILE BODIES
Basic experiment on a supersonic vortex flow around a missile body p 705 A92-41545

MISSILE CONFIGURATIONS
Rapid synthesis for evaluating missile maneuverability parameters
[AIAA PAPER 92-2615] p 873 A92-45488
Non-slender shapes of minimum drag
p 937 A92-52029
Dynamic wind tunnel tests on control of forebody vortices with suction p 380 N92-18793

MISSILE CONTROL
Applying mu-synthesis to missile autopilot design
p 28 A92-11564
Enhanced autopilot design through hardware-in-the-loop simulation p 204 A92-19103
A study of active flutter suppression for a wing/store system p 379 A92-27826
On the adaptive control of missile autopilots
p 477 A92-29102
Wideband control of gyro/accelerometer multisensors in a strapdown guidance system p 856 A92-46736
Avionics software reusability observations and recommendations p 921 A92-48502
Collection of papers of the 31st Israel Annual Conference on Aviation and Astronautics
[ITN-92-85124] p 932 N92-31861

MISSILE DESIGN
Future experimental needs in high-alpha vehicle dynamics
[AIAA PAPER 92-0159] p 254 A92-23774
A correlation study of the wing-body interference factor for high angles of attack p 700 A92-41179
The beginnings of the hypersonic and the renewal of the supersonic ramjet p 782 A92-41824
Rapid synthesis for evaluating missile maneuverability parameters
[AIAA PAPER 92-2615] p 873 A92-45488

MISSILE DETECTION
Controlling radar signature p 967 A92-52018

MISSILE RANGES
Preliminary results from the White Sands Missile Range sonic boom propagation experiment
p 1140 N92-33884

MISSILE SYSTEMS
Prediction of shock pattern dynamics at hypersonic angle of attack maneuvers of endo-KEW missile forebodies
[AIAA PAPER 92-2768] p 704 A92-41317

MISSILE TRACKING
Design considerations for a modern telemetry processing and display system p 882 A92-47584

MISSILE TRAJECTORIES
A calculating method of the kill probability attack area for AAM p 975 A92-50212

MISSILES
Metal fibers and fabrics as shielding materials for composites, missiles and airframes p 141 A92-14680
Binary optic-corrected conformal windows for optical seekers
[AIAA PAPER 92-2802] p 779 A92-41340
New ramjet configurations p 736 A92-41822
Ablation performance characterization of thermal protection materials using a Mach 4.4 Sled Test
[AIAA PAPER 92-3055] p 893 A92-48713
Aerothermal ablation behavior of selected candidate external insulation materials
[AIAA PAPER 92-3056] p 893 A92-48714
The use and misuse of aircraft and missile RCS statistics
[AD-A239892] p 41 N92-10141

MISSION ADAPTIVE WINGS
Effect of adaptive material properties on static aeroelastic control
[AIAA PAPER 92-2526] p 539 A92-34373
Variable-camber systems integration and operational performance of the AFTI/F-111 mission adaptive wing
[NASA-TM-4370] p 570 N92-22194
Variable geometry sailplanes Minisigma
p 629 N92-24877

MISSION PLANNING
Computer aiding for low-altitude helicopter flight
p 94 A92-14444
Automated mission planning - A striking capability
p 412 A92-28494
A knowledge acquisition approach for an on-board mission planner
[AIAA PAPER 92-1021] p 531 A92-33204
Generalities on the ramjet p 736 A92-41819
Issues in developing control zones for international space operations p 1141 A92-56602
Heuristic route optimization: A model for force level route planning p 164 N92-12520
Monitoring operational concept
[DOT/FAA/SE-91/3] p 268 N92-15980
Advanced flight software reconfiguraton
p 287 N92-17350
Automated planning with special relevance to associate systems technology and mission planning
[AD-A241924] p 303 N92-17438
Helicopter handling: Experience and new developments p 465 N92-21969
SHARP: Subsonic High Altitude Research Platform
[NASA-CR-190004] p 648 N92-25263
Proceedings of the 53rd Symposium on Air Vehicle Mission Control and Management
[AGARD-AR-310] p 1010 N92-32229
Advanced software development workstation: Effectiveness of constraint-checking --- spaceflight simulation and planning
[NASA-CR-190712] p 1134 N92-32865

MIXERS
Multifractal analysis of a lobed mixer flowfield utilizing the proper orthogonal decomposition
p 611 A92-36840
Failure analysis of the Apache mixer pivot support
[AD-A240858] p 116 N92-13061

MIXING
Numerical prediction of wakes in cascades and compressor rotors including the effects of mixing. II - Rotor passage flow and wakes including the effects of spanwise mixing
[ASME PAPER 91-GT-222] p 74 A92-15639
The 8th Symposium on Turbulent Shear Flows. Volume 1: Sessions 1-18
[AD-A243809] p 402 N92-18933
An analytical and computational investigation of shock-induced vortical flows with applications to supersonic combustion p 405 N92-19538
A new unsteady mixing model to predict NO(x) production during rapid mixing in a dual-stage combustor
[NASA-CR-189155] p 971 N92-30569

MIXING LAYERS (FLUIDS)
Numerical simulations of the structure of supersonic shear layers p 3 A92-10574
Inviscid spatial stability of a three-dimensional compressible mixing layer p 39 A92-11816
Effects of sidewall disturbances on the supersonic mixing layer p 290 A92-21085
Transition to turbulence in confined, compressible mixing layers. I - 3D numerical simulations with excitation of random, broadband white noise
[AIAA PAPER 92-0553] p 332 A92-26964
Experiments on shear layer mixing at hypervelocity conditions
[AIAA PAPER 92-0628] p 396 A92-27009
Transmission of thin light beams through turbulent mixing layers
[AIAA PAPER 92-0658] p 396 A92-27029
Computations of multispecies mixing between scramjet nozzle flow and hypersonic freestream
p 376 A92-28534
Two- and three-dimensional effects in the supersonic mixing layer p 432 A92-31165
Similarity in supersonic mixing layers
p 611 A92-36842
Evolution of three-dimensionality in stable and unstable curved mixing layers p 619 A92-40059
Direct simulation of a supersonic reacting mixing-layer
p 676 A92-40132
The effects of viscosity and diffusion on a supersonic mixing layer p 622 A92-40143
Reactive mixing layer between pressure reflecting boundaries p 656 A92-40144
Simultaneous imaging and interferometric turbule visualization in a high-velocity mixing/shear layer
p 896 A92-45130
Supersonic jet mixing enhancement by 'delta-tabs'
[AIAA PAPER 92-3548] p 826 A92-49063
Experiments on the enhancement of compressible mixing via streamwise vorticity. I - Optical measurements
[AIAA PAPER 92-3549] p 906 A92-49064
Computational study of a supersonic mixer-ejector exhaust system p 969 A92-50252
Mixing for multi-stage axial-flow compressors
p 996 A92-53015
High-speed cinematography of supersonic mixing layers
[AIAA PAPER 92-3545] p 1112 A92-54044
Mixed flow compressor surge margin gain using a manifolded diffuser system
[AIAA PAPER 92-3753] p 1068 A92-54151
Effect of streamwise pressure gradient on the supersonic mixing layer p 1025 A92-54936
Jet noise generated by large-scale coherent motion
p 55 N92-10604
An inviscid stability analysis of unbounded supersonic mixing layer flows p 443 N92-20332
Supersonic jet mixing enhancement by delta-tabs
[NASA-TM-105664] p 630 N92-24958
Near-injector structure of non-evaporating pressure-atomized sprays at various ambient densities
p 681 N92-25571
Effect of walls on the supersonic reacting mixing layer
p 912 N92-30065
Turbulent reacting flows and supersonic combustion
[AD-A251065] p 986 N92-30256
Direct simulation of high-speed mixing layers
[NASA-TP-3186] p 945 N92-30909

MIXING LENGTH FLOW THEORY
Turbulence modelling for secondary flow prediction in a turbine cascade
[ASME PAPER 91-GT-57] p 68 A92-15535
Mixing and combustion effects in a sliding-wedge ram accelerator with hydrogen injection
[AIAA PAPER 92-3251] p 890 A92-48849
The application of a Navier-Stokes CFD method to civil engine intake flows p 769 N92-27471
Turbulence modeling: Survey of activities in Belgium and the Netherlands, and appraisal of the status and a view on the prospects
[NLR-TP-90184-U] p 908 N92-28694
Effects of curvature and rotation on turbulence in the NASA low-speed centrifugal compressor impeller
p 1124 N92-32292

MIXTURES
Criteria for use of seal coats on airport pavements
[DOT/FAA/RD-92/18] p 1102 N92-34247

MOBILE COMMUNICATION SYSTEMS
The Aeronautical Mobile Satellite Service (AMSS). I - Architecture of the AMSS system p 93 A92-13851

The Aeronautical Mobile Satellite Service (AMSS). II - Frequency spectrum requirements for the Aeronautical Mobile Satellite Service p 94 A92-13852
ETS-V/EMSS mobile satellite communication experiments p 395 A92-26776
Gulf Range Drone Control Upgrade System Mobile Control System p 882 A92-47567
Capacity as a consideration for providing aeronautical mobile satellite air traffic services in the U.S. domestic *airspace* p 956 A92-51007
Inmarsat aeronautical mobile satellite system: Internetworking issues p 677 N92-24098
System considerations, projected requirements and applications for aeronautical mobile satellite *communications for air traffic services* p 677 N92-24163
Aeronautical mobile satellite service: Air traffic control *applications* p 677 N92-24164
Spectrum sharing between AMSS(R) and MSS p 677 N92-24165
Proceedings of the Workshop on Advanced Network and Technology Concepts for Mobile, Micro, and Personal Communications
[NASA-CR-190459] p 1000 N92-30923

MODAL RESPONSE
Digital simulation and experimental modal analysis of dynamic characteristics of a propeller hub p 38 A92-10965
Dynamic characterization and identification of nonlinear systems application to aeronautical structures p 39 A92-11830
Traditional finite element analysis - Opportunities for parallelism? p 40 A92-12354
On the choice of appropriate bases for nonlinear dynamic modal analysis p 847 A92-46927
Acoustic spinning-mode analysis by iterative threshold *method applied to a helicopter turboshaft engine*
[ONERA, TP NO. 1992-41] p 926 A92-48602
Advances in aircraft modal identification
[ONERA, TP NO. 1992-47] p 877 A92-48608
Linear stability of supersonic cone boundary layers p 1024 A92-54910
Aeroelastic modal characteristics of mistuned blade assemblies - Mode localization and loss of eigenstructure p 1117 A92-54921
Multi-disciplinary optimization of aeroservoelastic systems
[NASA-CR-188983] p 44 N92-11377
Flight flutter testing p 1089 N92-34163

MODEL REFERENCE ADAPTIVE CONTROL
A design of continuous-time model reference adaptive control based on a function estimation of periodically time varying linear system p 51 A92-11454
New robust adaptive control system using multiple *regularization parameters* p 51 A92-11455
Robustness analysis of a model reference adaptive control system p 412 A92-27859
Model-reference adaptive control for systems with D matrices p 506 A92-29052
Application of the delta-operator in MIMO discrete-time *adaptive flight control systems* p 479 A92-29516
Self-compensating carrier aircraft recovery system p 448 A92-32238
Model reference adaptive flight control system (MRAFCS) design with consideration of the balance point p 745 A92-43182
Optimal implicit model-following approach with frequency-shaped weighting and its application to design of flight control system p 977 A92-53094
Application of neural network to adaptive control theory for super-augmented aircraft
[AD-A246596] p 745 N92-27505

MODELS
Dual strain gage balance system for measuring light loads
[NASA-CASE-LAR-14419-1] p 42 N92-10185
Comparison of a two-dimensional adaptive-wall technique with analytical wall interference correction techniques
[NASA-TP-3132] p 444 N92-20494

MODEMS
Programmable channelized digital radio/modem p 955 A92-49291

MODULARITY
Modular avionics - A commercial perspective p 858 A92-48427
Avionics standardization in Europe p 199 N92-14050
Recommended system concept p 599 N92-23383

MODULATION
Secondary instability of high-speed flows and the influence of wall cooling and suction
[NASA-CR-4427] p 406 N92-19844

MODULATION TRANSFER FUNCTION
Numerical calculation of modulation transfer functions for low frequency mechanical vibrations p 235 A92-19982
Modulation transfer function degradation in segmented windows p 733 A92-41431
Concept design phase expendable holographic sensor to measure ocean small angle optical scattering
[AD-A245067] p 501 N92-20997

MODULATORS
Simulation of radar clutter and jet engine modulation using digital quadrature modulator p 216 A92-19091

MODULES
Mixed approach towards modular avionics conflicting requirements p 199 N92-14051
Data reduction formulas for the 16-foot transonic tunnel: NASA Langley Research Center, revision 2
[NASA-TM-107646] p 984 N92-31900

MODULUS OF ELASTICITY
Mechanics of curved fiber composites p 140 A92-14346
Mechanics of curved fiber composites p 757 A92-41034

MOISTURE CONTENT
An advanced neutron radiography system p 492 A92-28748
A comparison of measured and modeled broadband fluxes from aircraft data during the ICE '89 field experiment p 1003 A92-49771
Progress report on analysis of differential attenuation radar data obtained during WISP-91
[PB92-133800] p 503 N92-21828
The icing of the wing upper side and bottom side of the icing research aircraft of the DLR p 724 N92-26349

MOISTURE RESISTANCE
Non-curing fuel and water resistant sealant compositions p 985 A92-51906

MOLECULAR FLOW
Low density heat transfer phenomena
[AIAA PAPER 92-2899] p 820 A92-47875
Brownian-motion limited aerodynamic focusing of heavy molecules p 995 A92-52722
Monte Carlo study of vibrational relaxation processes p 940 A92-52777
Numerical and experimental investigations of rarefied gas flows through nozzles and composite systems p 940 A92-52797
Aerodynamic characteristics of a standard corrugated body in a free-molecular flow p 940 A92-52818

MOLECULAR RELAXATION
A unified nonequilibrium model for hypersonic flows p 3 A92-10575
Vibrational relaxation effects in hypersonic flows of a viscous gas p 609 A92-36550
The effect of molecular relaxation processes in air on the rise time of sonic booms p 898 A92-45883
Monte Carlo study of vibrational relaxation processes p 940 A92-52777
Thermal nonequilibrium effects on turbine cascade aerodynamics
[AD-A244049] p 404 N92-19183
Nonlinear acoustic propagation of shock waves through the atmosphere with molecular relaxation p 511 N92-20360
A numerical model for sonic boom propagation through an inhomogeneous, windy atmosphere p 1138 N92-33876
Analysis of sonic boom data to quantify distortions of shock profiles p 1139 N92-33879
Model experiment to study the effect of turbulence on *risetime and waveform of N waves* p 1139 N92-33881

MOLECULAR ROTATION
Influence of internal molecular degrees of freedom on the hypersonic rarefied gas flow about a conical body p 938 A92-52752

MOLECULAR WEIGHT
Vinyl capped addition polyimides
[NASA-CASE-LEW-15027-2] p 579 N92-24053

MOLYBDENUM ALLOYS
Rolling element bearing member
[PATENT-1-271-213] p 158 N92-13434

MOMENT DISTRIBUTION
Measurement of magnus derivatives with an elastically forced oscillation rig p 749 A92-43172
Computation of the unsteady transonic 2D cascade flow by an Euler algorithm with interactive grid generation p 719 N92-27944

MOMENTS
Prediction of forces and moments for hypersonic flight vehicle control effectors
[NASA-CR-188954] p 33 N92-11070
Computation of the hydrodynamic forces and moments on a body of revolution with and without appendages
[AD-A243033] p 298 N92-16978

MOMENTS OF INERTIA
Experimental determination of the center of mass, the principal central axes of inertia and moments of inertia --- aircrafttt models applied to real aircraf p 40 A92-12346
Effect of inertia forces on the characteristics of a long hydrodynamic vibration damper in the mixed flow regime p 154 A92-16811
A new approach to determining control surface's *moments of inertia with test-twice vibrations approach* p 379 A92-27914
Computational analysis of inertial effects on the stability of an ACES-II ejection seat p 543 A92-35436
An estimate of the influence of the compressor stability *margin on the pick-up time of a turbojet engine* p 654 A92-37423
Estimation of spaceplane model inertia characteristics p 752 A92-43212
Estimation of aircraft inertial characteristics using maximum likelihood estimation p 1084 A92-56057

MOMENTUM THEORY
Design - Analysis and experimental verification of a propeller working in the low Reynolds number range p 710 A92-43174

MOMENTUM TRANSFER
Rarefied gas research at Berkeley - Current studies and future potentials
[AIAA PAPER 92-3971] p 1098 A92-56797

MONATOMIC GASES
Flow of a rarefied gas over a cylinder at angle of sideslip p 708 A92-42738

MONITORS
Application of smart structures to aircraft health *monitoring* p 20 A92-11123
Behavior-based fault monitoring
[AD-A241254] p 164 N92-13746
Turbine engine diagnostics system study
[DOT/FAA/CT-91/16] p 202 N92-14064
The Operational Loads Monitoring System, OLMS p 361 N92-18586
Repetitive High Energy Pulsed Power (RHEPP) temperature monitoring system utilizing Luxtron fluoroptic sensors and thermocouples technical reference manual
[DE92-013461] p 999 N92-30893
Engine monitoring display study
[NASA-CR-4463] p 979 N92-32175

MONOMERS
Poly 1, 2, 4-triazoles via aromatic nucleophilic displacement
[NASA-CASE-LAR-14440-1] p 35 N92-10066

MONOPOLE ANTENNAS
High-frequency techniques for antenna analysis p 494 A92-31071

MONOPULSE RADAR
Analysis and design optimization of monopulse receivers *for secondary surveillance radar* p 40 A92-12299
Monopulse secondary surveillance radar and the mode-S surveillance system p 956 A92-53239

MONOTECTIC ALLOYS
The effectiveness of Coriolis dampening of convection during aircraft high-g arcs p 581 A92-33847

MONOTONE FUNCTIONS
Three-dimensional thin-layer and space-marching Navier-Stokes computations using an implicit MUSCL approach - Comparison with experiments and Euler computations
[ONERA, TP NO. 1991-131] p 77 A92-16107
A nearly-monotone genuinely multidimensional scheme for the Euler equations
[AIAA PAPER 92-0325] p 322 A92-25772

MONTE CARLO METHOD
On the accuracy of an aircraft-borne ambient electric-field measuring system p 186 A92-20127
Hypersonic flow simulations using DSMC (direct simulation Monte Carlo) p 323 A92-26216
Shock interference prediction using direct simulation Monte Carlo
[AIAA PAPER 92-0492] p 328 A92-26322
Monte Carlo simulation of reentry flows with ionization
[AIAA PAPER 92-0493] p 328 A92-26323
Monte Carlo simulation of entry in the Martian atmosphere
[AIAA PAPER 92-0494] p 329 A92-26324
Computation of aircraft geometric height under radar surveillance p 639 A92-40239
Hybrid Navier-Stokes/Monte Carlo method for reacting flow calculations p 705 A92-41537
Flow of a rarefied gas over a cylinder at angle of sideslip p 708 A92-42738
Direct simulation of hypersonic rarefied flows about atmospheric re-entry vehicles p 710 A92-43169
Comparison of six robustness tests evaluating missile autopilot robustness to uncertain aerodynamics p 873 A92-46737

Hypersonic rarefied flow about a delta wing - direct simulation and comparison with experiment
p 812 A92-46892
Numerical and experimental investigation of rarefied compression corner flow
[AIAA PAPER 92-2900] p 820 A92-47876
Enhancements and applications of DSMC for hypersonic rarefied flows p 939 A92-52761
Direct simulation of vortex shedding in dilute gas flows past bluff bodies p 939 A92-52766
Monte Carlo simulation of the hypersonic mon- and diatomic gas flow past a disk at an angle of attack
p 939 A92-52770
DSMC simulation of hypersonic flows past 2-dimensional bodies p 939 A92-52772
Application of the DSMC method to hypersonic flow about a delta wing p 940 A92-52775
Monte Carlo study of vibrational relaxation processes
p 940 A92-52777
Application of a parallel direct simulation Monte Carlo method to hypersonic rarefied flows
p 1024 A92-54916
Direct simulation of low-density flow over airfoils
p 1030 A92-56159
Parallelization of a Direct Simulation Monte Carlo (DSMC) code for fluid dynamics p 227 N92-15033
Transitional flows around re-entry bodies
p 184 N92-15035
Technical notes and correspondence: Stochastic robustness of linear time-invariant control systems
p 303 N92-18002
Simulations of sonic boom ray tube area fluctuations for propagation through atmospheric turbulence including caustics via a Monte Carlo method
p 1139 N92-33878

MOORING
Evaluation of grounding and mooring points for Army aircraft
[AD-A250749] p 953 N92-31193

MORPHOLOGY
Fatigue crack initiation and small crack growth in several airframe alloys p 212 A92-19754

MOTION
Deck motion criteria for carrier aircraft operations
p 464 N92-21952

MOTION SICKNESS
Prediction of helicopter simulator sickness
p 46 A92-11473
Flight simulation p 207 N92-13982

MOTION SIMULATION
Knowledge-sensitive task manipulation - Acquiring knowledge from pilots flying a motion-based flight simulator p 916 A92-45064
Use of high-fidelity simulation in the development of an F/A-18 active ground collision avoidance system
[AIAA PAPER 92-4140] p 959 A92-52434
Flight simulation p 207 N92-13982
Helicopter/ship analytic dynamic interface
p 464 N92-21962
The basic research simulator programme and the industrial and aerospace community: Opportunities for cooperative research
[LR-662] p 887 N92-28579
Mathematical modeling and numerical simulation of the dynamics of flexible structures undergoing large overall motions
[AD-A250202] p 979 N92-31967

MOTION SIMULATORS
Adaptive simulator motion software with supervisory control p 412 A92-28136
Design and performance of the centrifuge-based Dynamic Flight Simulator
[AIAA PAPER 92-4156] p 981 A92-52446

MOTION STABILITY
Development of a combined fast method for studying the plane motions of rigid bodies in the atmosphere around the center of mass in the presence of perturbations
p 304 A92-23563
Analysis of the stability of the lateral motion of aircraft
p 480 A92-30191
Oscillations of balloon-flight altitude
p 836 A92-46660
Symptom of payload-induced flight instability
p 873 A92-46761
Multiple delay model approach applied to the AIAA 1922 Controls Design Challenge
[AIAA PAPER 92-4630] p 1078 A92-55305
Thrust test fixture
[AD-D015259] p 983 N92-31192

MOUNTAINS
Aircraft accident/incident summary report: Controlled flight into terrain Bruno's Inc., Beechjet, N25BR, Rome, Georgia, 11 December 1991
[PB92-910404] p 1044 N92-34081

MOVING TARGET INDICATORS
Polish radar technology. V - Adaptive MTI filters for uniform and staggered sampling p 40 A92-12293
Adaptive airborne MTI with two-dimensional motion compensation p 102 A92-17240
IsoDoppler and mocomp corrections improve MTI radar p 898 A92-45774
Detection and imaging of moving objects with synthetic aperture radar. I - Optimal detection and parameter estimation theory p 955 A92-50033
Modeling radar clutter
[AD-A240965] p 158 N92-13351
Low-noise oscillators for airborne radar applications
[AD-A242264] p 300 N92-17258
The application of lattice-structure adaptive filters to clutter-suppression for scanning radar
p 403 N92-19154

MRCA AIRCRAFT
Expert system for the Tornado ground-based check-out system p 118 N92-12536
Aircraft fatigue management in the Royal Air Force
p 363 N92-18591
Tornado structural fatigue life assessment of the German Air Force p 363 N92-18592
The evaluation of simulator effectiveness for the training of high speed, low level, tactical flight operations
p 885 N92-28539
Airborne experimental FLIR program
p 1064 N92-32447

MTBF
Transmission overhaul and component replacement predictions using Weibull and renewal theory
p 155 A92-17201
The study of constant value thresholds of FDI in strapdown inertial navigation p 267 A92-22087

MUFFLERS
Theoretical and experimental methods in acoustics of ducts and mufflers - A critical review
p 693 A92-39068

MULLITES
Fabrication and testing of corrosion resistant coatings --- for turbine engine components
[DE92-003553] p 490 N92-21063

MULTIGRID METHODS
Multigrid Navier-Stokes calculations for three dimensional cascades
[AIAA PAPER 92-0190] p 256 A92-23799
Embedded meshes of controllable quality synthesised from elementary geometric features
[AIAA PAPER 92-0663] p 411 A92-27034
Euler solutions for an unbladed jet engine configuration
[AIAA PAPER 92-0544] p 398 A92-28201
Viscous supersonic flow computations over a delta-rectangular wing with slanting surfaces
p 441 A92-32178
A high-resolution Euler solver based on multigrid, semi-coarsening, and defect correction
p 671 A92-37868
A fast, implicit unstructured-mesh Euler method
[AIAA PAPER 92-2693] p 917 A92-45589
Parallel computing strategies for block multigrid implicit solution of the Euler equations p 812 A92-46894
Patch-independent structured multiblock grids for CFD computations p 919 A92-47078
Generation of unstructured grids within a hybrid multi-block environment p 818 A92-47090
On multiple grid method p 1006 A92-49585
Evaluation of a multigrid-based Navier-Stokes solver for aerothermodynamic computations
[AIAA PAPER 92-4563] p 1027 A92-55375
Euler solutions for an unbladed jet engine configuration
[NASA-TM-105332] p 44 N92-11328
Inverse airfoil design procedure using a multigrid Navier-Stokes method p 193 N92-13932
Progress with multigrid schemes for hypersonic flow problems
[NASA-CR-189579] p 185 N92-15047
Three-dimensional multigrid algorithm for the Euler and the thin-layer Navier-Stokes equations
[PB92-134329] p 602 N92-22216
Improved shock-capturing of Jameson's scheme for the Euler equations
[PB92-148758] p 596 N92-23251
An interactive multi-block grid generation system
p 691 N92-24419
On a multi-block method for transonic turbulent flows past a wing-fuselage configuration p 632 N92-25569
Workshop on Grid Generation and Related Areas
[NASA-CP-10089] p 659 N92-25712
Grid generation for a complex aircraft configuration
p 649 N92-25714
Multiblock grid generation for jet engine configurations
p 659 N92-25720
An installed nacelle design code using a multiblock Euler solver. Volume 1: Theory document
[NASA-CR-189652-VOL-1] p 950 N92-32226
An installed nacelle design code using a multiblock Euler solver. Volume 2: User guide
[NASA-CR-189652-VOL-2] p 951 N92-32228
New concepts for multi-block grid generation for flow domains around complex aerodynamic configurations
[NLR-TP-91046-U] p 1037 N92-32730

MULTILAYER INSULATION
Effect of the wake flow on the soundproofing of aircraft structures p 166 A92-16824

MULTIPATH TRANSMISSION
Microwave landing system modeling with application to air traffic control automation p 725 A92-41220
Radar multipath study for rain-on-radome experiments at the Aircraft Landing Dynamics Facility
[NASA-TM-101657] p 680 N92-25137

MULTIPHASE FLOW
Observation and testing on supersonic multiphase flow p 429 A92-30502
Performance of a high-pressure-ratio centrifugal compressor influenced by distribution of tip clearance of the mixed-flow impeller p 498 A92-32509

MULTIPLEXING
MIL-STD-1553 data bus/PCM multiplexer system
p 188 A92-19211
Coherence multiplexed polarimetric fibre sensor arrays for aerospace applications p 370 A92-27785

MULTIPROCESSING (COMPUTERS)
Solution of the Euler and Navier-Stokes equations on MIMD distributed memory multiprocessors using cyclic reduction
[AIAA PAPER 92-0561] p 411 A92-26970
Software safety analysis in heterogeneous multiprocessor control systems p 776 A92-42073
Implementation of non-dedicated redundancy in a fault tolerant multiprocessor testbed --- flight control
p 974 A92-49294
Operating principles for integrated sensor processing
p 966 A92-49336
Parallel processing applications for gas turbine engine control p 25 N92-11012
Timing analysis of parallel algorithms on a MIMD multiprocessor
[ITN-92-85153] p 510 N92-20905
Iterative methods for large scale static analysis of structures on a scalable multiprocessor supercomputer
[NASA-CR-190369] p 692 N92-26018
Expert system management system
[AD-A247102] p 781 N92-26863
A model of the ADA avionics real-time system: An example of the benefits of the hardware/software codesign approach in development of real-time systems
[AD-A248893] p 967 N92-30524

MULTISENSOR APPLICATIONS
Sensor fusion for synthetic vision
[AIAA PAPER 91-3730] p 197 A92-17597
Multisensor data fusion and decision support for airborne target identification p 454 A92-31063
An integrated navigation system manager using federated Kalman filtering p 858 A92-48477
Inertial navigation sensor integrated motion analysis for obstacle detection p 954 A92-49272
Recommended system concept p 599 N92-23383
Method of measuring cross-flow vortices by use of an array of hot-film sensors
[NASA-CASE-LAR-14824-1-SB] p 998 N92-30390

MULTISPECTRAL BAND SCANNERS
Radiometric properties of the NS001 Thematic Mapper Simulator aircraft multispectral scanner
p 155 A92-17110
Automated thematic processing of aircraft scanner data gathered over pasture territory in Turkmenia
p 406 A92-25330
A high resolution multispectral video system
p 587 A92-35479

MULTISPECTRAL RADAR
Estimation of the P-3/SAR L-, C- and X-band antenna directivity in range direction based on corner reflector measurements within the absolute SAR calibration
p 587 A92-35055
Recommended system concept p 599 N92-23383

MULTISTAGE ROCKET VEHICLES
Optimization of two stage reusable space transportation systems with rocket and airbreathing propulsion concepts
[IAF PAPER 92-0863] p 1104 A92-57254
High speed airbreathing propulsion in Europe
p 575 N92-22277

MULTIVARIABLE CONTROL
Polygon interval arithmetic and design of robust control systems p 49 A92-11418
Full envelope multivariable control of a gas turbine engine p 468 A92-29116

A hierarchical data structure and new capabilities of the Robust-Control Toolbox p 507 A92-29155
Loop shaping in mixed H2 and H-infinity optimal control p 507 A92-29177
Rule based identifier for unknown systems p 509 A92-31430
Multivariable methods for helicopter flight control law design - A review p 568 A92-35748
An evaluation of a simple PID controller designed using optimal control theory when applied to helicopter stabilisation p 569 A92-35785
Robust stabilisation of multivariable feedback systems with desired performance requirement p 776 A92-42172
Design and evaluation of a robust dynamic neurocontroller for a multivariable aircraft control problem
[NASA-TM-105579] p 481 N92-20586
A methodology for computing uncertainty bounds of multivariable systems based on sector stability theory concepts
[NASA-TP-3166] p 482 N92-21410
Practical method's for robust multivariable control
[AD-A248473] p 1009 N92-30322

MULTIVARIATE STATISTICAL ANALYSIS
Studies in chaos using stochastic methods
[AD-A246919] p 780 N92-27171
Estimating the reliability of a system on the basis of sample paths
[AD-A248585] p 774 N92-28171
Full mission simulation: A view into the future p 884 N92-28537

N

NACELLES
Computational fluid dynamics based three-dimensional turbofan inlet/fan cowl analysis system p 243 A92-21075
A parametric study of the aeroelastic stability of a binary wing-with-engine nacelle flutter system in incompressible flow p 270 A92-22472
Design of a hybrid laminar flow control nacelle
[AIAA PAPER 92-0400] p 373 A92-26253
Application of laminar flow control to high-bypass-ratio turbofan engine nacelles
[SAE PAPER 912114] p 618 A92-39965
Scale model test of an isolated turbofan nacelle with riblets
[SAE PAPER 912128] p 618 A92-39975
Viscous flow past a nacelle isolated and in proximity *of a flat plate*
[AIAA PAPER 92-2723] p 803 A92-45560
Investigations of propulsion integration interference effects on a transport aircraft configuration
[AIAA PAPER 92-3097] p 849 A92-48739
The numerical simulation of flow about installed aero engine nacelle using a finite element Euler solver on unstructured meshes p 941 A92-52848
Propeller-nacelle whirl flutter analysis and wind tunnel test p 1052 A92-56016
Whirl flutter analysis and application to aircraft design p 1053 A92-56017
Effect of solidity and inclination on propeller-nacelle force coefficients
[NASA-TM-4316] p 90 N92-13038
An inverse method for the aerodynamic design of three-dimensional aircraft engine nacelles p 194 N92-13958
Ultra high bypass Nacelle aerodynamics inlet flow-through high angle of attack distortion test
[NASA-CR-189149] p 943 N92-30298
Analytical and experimental studies of heat pipe radiation cooling of hypersonic propulsion systems
[DE92-013428] p 973 N92-31817
An installed nacelle design code using a multiblock Euler solver. Volume 1: Theory document
[NASA-CR-189652-VOL-1] p 950 N92-32226
An installed nacelle design code using a multiblock Euler solver. Volume 2: User guide
[NASA-CR-189652-VOL-2] p 951 N92-32228
Applications of a direct/iterative design method to complex transonic configurations
[NASA-TP-3234] p 1039 N92-33484

NAP-OF-THE-EARTH NAVIGATION
Automatic link establishment - The key to reliable helicopter NOE communications p 94 A92-14403
GPS-INS integration requirements for robust NOE helicopter navigation p 94 A92-14404
Heterodyne techniques in the I.R. bandwidth for laser obstacle detection p 533 A92-35740
The obstacle avoidance radar - A safety mean for low altitude flights in adverse weather conditions p 554 A92-35743
Study on the lower aspect view of a helicopter simulator p 748 A92-43110
A high-performance LLLTV CCD camera for nighttime pilotage p 855 A92-46227
Inertial navigation sensor integrated motion analysis for obstacle detection p 954 A92-49272
An ultrareliable integrated digital computer for helicopters p 964 A92-49273
Simulation of automatic rotorcraft nap-of-the-earth flight in graphics workstation environment
[AIAA PAPER 92-4131] p 981 A92-52428
Vision-based obstacle detection for rotorcraft flight p 967 A92-52465
Vision-based stereo ranging as an optimal control problem
[AIAA PAPER 92-4418] p 1045 A92-55211
Concepts for pilot interaction with an automated NOE obstacle-avoidance system
[AIAA PAPER 92-4472] p 1076 A92-55232
Analysis of image-based navigation system for rotorcraft low-altitude flight p 1046 A92-55968
Passive range estimation for rotorcraft low-altitude flight
[NASA-TM-103897] p 2 N92-10003
Image-based ranging and guidance for rotorcraft
[NASA-CR-184829] p 191 N92-14036
Status of automatic guidance systems for rotorcraft in low altitude flight p 727 N92-27894
A workstation-based evaluation of a far-field route planner for helicopters
[NASA-TM-102882] p 1051 N92-33609

NAPHTHALENE
Multi-colored layers for visualizing aerodynamic flow *effects*
[NASA-CASE-LAR-13742-1] p 447 N92-21588

NARROWBAND
Programmable channelized digital radio/modem p 955 A92-49291
Integrating a radar/ESM antenna suite with the S-70 helicopter --- Electronic Surveillance Measures p 957 A92-49333

NASA PROGRAMS
NASA research program directed at reducing supersonic *transport noise* p 61 A92-16150
On the threshold - The outlook for supersonic and hypersonic aircraft p 356 A92-24402
IMPAC - An integrated methodology for propulsion and airframe control p 477 A92-29118
The NASA/Industry Design Analysis Methods for Vibrations (DAMVIBS) Program - A government overview --- of rotorcraft technology development using finite element method
[AIAA PAPER 92-2200] p 539 A92-34390
The NASA/Industry Design Analysis Methods for Vibrations (DAMVIBS) Program - Bell Helicopter Textron accomplishments
[AIAA PAPER 92-2201] p 539 A92-34391
The NASA/Industry Design Analysis Methods for Vibrations (DAMVIBS) Program - Boeing helicopters airframe finite element modeling
[AIAA PAPER 92-2202] p 539 A92-34392
The NASA/Industry Design Analysis Methods for Vibrations (DAMVIBS) program - McDonnell Douglas Helicopter Company achievements
[AIAA PAPER 92-2203] p 540 A92-34393
The NASA/Industry Design Analysis Methods for *Vibrations (DAMVIBS) Program - Sikorsky Aircraft* - Advances toward interacting with the airframe design process
[AIAA PAPER 92-2204] p 540 A92-34394
National Aeronautics and Space Administration p 238 N92-14923
National Aeronautics and Space Administration p 238 N92-14925
National Aeronautics and Space Administration p 238 N92-14927
Structural Dynamics Branch research and accomplishments for FY 1990
[NASA-TM-103747] p 230 N92-15406
National Aeronautics and Space Administration research and development p 238 N92-15937
National Aeronautics and Space Administration p 417 N92-18309
Alpha Group: The Behemoth Apteryx. Final design proposal
[NASA-CR-190026] p 462 N92-20951
NASA's aircraft icing technology program
[NASA-TM-104518] p 527 N92-23105
The future challenge for aeropropulsion
[NASA-TM-105613] p 658 N92-25164
Constraint-based scheduling
[NASA-TM-107873] p 692 N92-25190
National Aeronautics and Space Administration Authorization Act, 1993
[S-2558-IS] p 698 N92-25606
NASA Workshop on future directions in surface modeling and grid generation
[NASA-CP-10092] p 831 N92-29625
Research and technology, 1991. Langley Research Center
[NASA-TM-4331] p 1013 N92-30733
System overview of the NASA Dryden Integrated Test Facility
[NASA-TM-104250] p 984 N92-32201
Departments of Veterans Affairs and Housing and Urban Development, and independent agencies appropriations for 1993, part 6
[GAO-55-636-PT-6] p 1141 N92-32505
NASA authorization, 1993, volume 1
[GPO-55-260-VOL-1] p 1142 N92-33147

NASTRAN
Traditional finite element analysis - Opportunities for *parallelism?* p 40 A92-12354
Static aeroelastic analysis for generic configuration wing p 174 A92-20201
Incompressible steady aerodynamics using a standard finite element code p 174 A92-20218
Structural and aerodynamic analysis of a large-scale advanced propeller blade p 375 A92-28517
An expert system to aid real world finite element analysis
[AIAA PAPER 92-2488] p 601 A92-34604
FREPS - A forced response prediction system for turbomachinery blade rows
[AIAA PAPER 92-3072] p 1130 A92-54006

NATIONAL AEROSPACE PLANE PROGRAM
NASP - Expanding space launch opportunities p 33 A92-13247
Slush hydrogen (SLH2) technology development for application to the National Aerospace Plane (NASP) p 144 A92-13432
The NASP Program - An update p 61 A92-16059
Integrated GPS/INS for the National Aerospace Plane p 102 A92-16975
Conducting the NASP ground test program
[AIAA PAPER 91-5029] p 209 A92-17820
A configuration development strategy for the NASP
[AIAA PAPER 91-5044] p 210 A92-17830
The value of sub-scale flight tests in the development of NASP vehicles
[AIAA PAPER 91-5048] p 210 A92-17834
Operational design factors for NASP derived vehicles
[AIAA PAPER 91-5081] p 210 A92-17851
Thermal control for hypersonic vehicle propulsion p 468 A92-29356
Structural materials for NASP
[AIAA PAPER 91-5101] p 486 A92-31698
Aerothermoelastic analysis of a NASP-like vertical fin
[AIAA PAPER 92-2400] p 541 A92-34471
The National Aerospace Plane program and the APL role p 666 A92-37375
NASP - A status report
[AIAA PAPER 92-1417] p 666 A92-38569
National Aerospace Plane flight test - External burning on the F/A-18 p 645 A92-40032
The F/A-18 external burning flight test
[AIAA PAPER 91-5050] p 731 A92-44547
Some thermodynamical aspects in the optimization of supersonic combustors p 1065 A92-53486
Instrumentation key to NASP combustor tests p 1092 A92-55100
The Langley 15-inch Mach 6 High Temperature *Tunnel*
[AIAA PAPER 92-3938] p 1096 A92-56768
An integrated analytical aeropropulsive/aeroelastic model for the dynamic analysis of hypersonic vehicles
[AIAA PAPER 92-4567] p 1035 A92-57034
Technologies for the National Aero-Space Plane
[IAF PAPER 92-0868] p 1105 A92-57259
Experimental simulation and diagnostics of high-enthalpy real-gas flows
[AD-A241286] p 166 N92-13822
Rapid near-optimal aerospace plane trajectory generation and guidance
[NASA-CR-189469] p 205 N92-14066
NASP X-30 Propulsion technology status p 475 N92-21534
High temperature dynamic engine seal technology development
[NASA-TM-105641] p 596 N92-23435
Design challenges for the National Aero-Space Plane p 551 N92-23822
Structures technology applications for the National AeroSpace Plane p 649 N92-25920
Assessment of flying-quality criteria for air-breathing aerospacecraft
[NASA-CR-4442] p 663 N92-25982
Trajectory optimization for the National Aerospace Plane
[NASA-CR-190355] p 650 N92-26017

An experimental investigation of a 2-D scramjet inlet at flow Mach numbers of 8 to 25 and stagnation temperatures of 800 to 4,100 K p 739 N92-26586
Development of a 3-D upwind PNS code for chemically reacting hypersonic flowfields
[NASA-CR-190182] p 946 N92-30977
Thermal-structural test facilities at NASA Dryden
[NASA-TM-104249] p 1062 N92-34202

NATIONAL AIRSPACE SYSTEM
The FAA Loran program status and expectations
p 95 A92-16629
Strategic vs tactical air traffic control utilizing ADS and earth reference area NAV p 96 A92-16631
Loran time difference correction factors - Valid information or blue smoke and mirrors?
p 96 A92-16633
From Russia and beyond --- equipment and areas of coverage for Loran navigation outside NAS
p 96 A92-16638
GPS for precision approaches p 139 A92-16648
The status of Loran's implementation in the National Airspace System (NAS) p 638 A92-39565
FAA air traffic activity: FY 1990. Addendum
[AD-A241484] p 93 N92-13046
Data Multiplexing Network (DMN) phase 3 equipment Operational Test and Evaluation (OT and E)/integration test report
[DOT/FAA/CT-TN91/50] p 221 N92-14270
Rotorcraft low altitude IFR benefit/cost analysis: Operations analysis
[SCT-90RR-44] p 191 N92-15061
Monitoring operational concept
[DOT/FAA/SE-91/3] p 268 N92-15980
Identification of high-level functional/system requirements for future civil transports
[NASA-CR-189561] p 276 N92-15991
Joint University Program for Air Transportation Research, 1990-1991
[NASA-CP-3131] p 242 N92-17984
High Capacity Voice Recorder (HCVR) Operational Test and Evaluation (OT and E)/integration test plan
[DOT/FAA/CT-TN91/55] p 402 N92-18959
National Airspace System maintenance and support operational concept
[DOT/FAA/SE-92/1] p 308 N92-18969
JPL's Real-Time Weather Processor project (RWP) metrics and observations at system completion
p 413 N92-19428
National airspace system: System effectiveness operational concept NAS-SR-138
[DOT/FAA/SE-92/2] p 535 N92-23096
Nationwide system delay study of the microwave landing system in the New York terminal area, volume 1
[DOT/FAA/CT-TN91/59-VOL-1] p 640 N92-25098
General maintenance handbook for airway facilities
[PB92-147586] p 640 N92-25518
Rotorcraft terminal ATC route standards
[SCT-90RR-33] p 641 N92-26101
GNAS Maintenance Control Center (GMCC) Design Qualification Test and Evaluation (DQT/E) test procedures
[DOT/FAA/CT-TN91/40] p 983 N92-30976
National airspace system. Air defense and law enforcement surveillance operational concept NAS-SR-135
[DOT/FAA/SE-92/3] p 953 N92-31211
GNAS Maintenance Control Center (GMCC) Design Qualification Test and Evaluation (DQT/E) test report
[DOT/FAA/CT-TN91/39] p 932 N92-31615
A review and discussion of flight management system incidents reported to the aviation safety reporting system
[AD-A252438] p 1043 N92-32941
Impacts of technology on the capacity needs of the US national airspace system
[NASA-CR-4470] p 1045 N92-34192

NATIONAL AVIATION SYSTEM
The FAA Loran program status and expectations
p 95 A92-16629
Aviation system: Capital investment plan
p 636 N92-25297

NATIONAL PARKS
Study of alternatives: Dayton's Aviation heritage, Ohio
[PB91-202275] p 2 N92-10972

NATURAL GAS
Turbocharged pressurized combustion system
[PB92-142579] p 756 N92-26521
Development of natural gas rotary engines
[PB92-149665] p 765 N92-26816

NATURAL LANGUAGE (COMPUTERS)
Internationalization of telemetry systems
p 920 A92-47535

NAVIER-STOKES EQUATION
A semi-elliptic analysis for 2-D viscous flows through cascade configurations p 3 A92-10688
Triple-deck structure p 3 A92-10690
Viscous flow solutions for slender bodies of revolution at incidence p 4 A92-10692
Computational investigation of circular-to-rectangular transition ducts
[AIAA PAPER 91-3342] p 6 A92-11605
Turbine cascade calculations through a fractional step Navier-Stokes algorithm
[ASME PAPER 91-GT-55] p 68 A92-15533
Three-dimensional Navier-Stokes computation of turbomachinery flows using an explicit numerical procedure and a coupled k-epsilon turbulence model
[ASME PAPER 91-GT-146] p 72 A92-15584
Unsteady Navier-Stokes simulation of transonic cascade flow using an unfactored implicit upwind relaxation scheme with inner iterations
[ASME PAPER 91-GT-223] p 74 A92-15637
Deterministic blade row interactions in a centrifugal compressor stage
[ASME PAPER 91-GT-273] p 75 A92-15670
Thermal details in a rotor-stator cavity at engine conditions with a mainstream
[ASME PAPER 91-GT-275] p 151 A92-15672
Transonic cascade flow prediction using the Navier-Stokes equations
[ASME PAPER 91-GT-313] p 76 A92-15690
Three-dimensional thin-layer and space-marching Navier-Stokes computations using an implicit MUSCL approach - Comparison with experiments and Euler computations
[ONERA, TP NO. 1991-131] p 77 A92-16107
On the nonlinear stability of a high-speed, axisymmetric boundary layer p 78 A92-16457
Eigenvalue calculation procedure for an Euler/Navier-Stokes solver with application to flows over airfoils p 170 A92-17429
Flow separation patterns over an F-14A aircraft wing
p 174 A92-20205
Explicit Navier-Stokes computation of cascade flows using the k-epsilon turbulence model
p 175 A92-20727
Asymmetric separated flows at supersonic speeds
p 176 A92-20742
Navier-Stokes computations for aerodynamic configurations at high angles of attack
p 246 A92-21981
Finite element vorticity based methods for the solution of the compressible Navier-Stokes equations
p 246 A92-21983
Navier-Stokes code development for transonic flow simulations p 246 A92-21985
A fast viscous correction method for transonic aerodynamics p 247 A92-21986
An efficient upwind relaxation-sweeping algorithm for three-dimensional Navier-Stokes equations
[AIAA PAPER 92-0023] p 248 A92-22145
Effect of turbulence modeling on dynamic stall of a NACA0012 airfoil
[AIAA PAPER 92-0027] p 248 A92-22149
Computational vorticity capturing - Application to helicopter rotor flows
[AIAA PAPER 92-0056] p 250 A92-22171
Mathematical modeling of supersonic flow over a convex-concave formed body based on the Euler and Navier-Stokes equations p 252 A92-23416
A Navier-Stokes solver for stretched triangular grids
[AIAA PAPER 92-0183] p 256 A92-23793
Grid studies for thin-layer Navier-Stokes computations of airfoil flowfields
[AIAA PAPER 92-0184] p 256 A92-23794
Implementation of Vigneron's streamwise pressure gradient approximation in the PNS equations
[AIAA PAPER 92-0189] p 256 A92-23798
Multigrid Navier-Stokes calculations for three dimensional cascades
[AIAA PAPER 92-0190] p 256 A92-23799
Navier-Stokes computation of airfoil in stall using algebraic Reynolds-stress model
[AIAA PAPER 92-0195] p 257 A92-23803
Study of role of unsteady separation in formation of dynamic stall vortex
[AIAA PAPER 92-0196] p 257 A92-23804
3D Navier-Stokes analysis for a tip leakage flow in a low aspect ratio turbine
[AIAA PAPER 92-0395] p 278 A92-23816
Navier-Stokes calculations of inboard stall delay due to rotation p 309 A92-24410
Comparison of two Navier-Stokes codes for attached transonic wing flows p 309 A92-24414
Application of the LAURA code for slender-vehicle aerothermodynamics p 310 A92-24652
Multizonal Navier-Stokes solutions for the multibody Space Shuttle configuration p 310 A92-24667
Numerical simulation of twin-jet impingement on a flat plate coupled with cross-flow p 315 A92-25374
Modeling supersonic inlet boundary layer bleed roughness
[AIAA PAPER 92-0269] p 317 A92-25725
Three-dimensional simulation of a translating strut inlet
[AIAA PAPER 92-0270] p 317 A92-25726
Evaluation of two flow analyses for subsonic diffuser design
[AIAA PAPER 92-0273] p 317 A92-25727
Analysis of an advanced ducted propeller subsonic inlet
[AIAA PAPER 92-0274] p 318 A92-25728
Non-planar wing design by Navier-Stokes inverse computation
[AIAA PAPER 92-0285] p 319 A92-25738
Aerodynamic design of axisymmetric hypersonic wind-tunnel nozzles using least-squares/parabolized Navier-Stokes procedure
[AIAA PAPER 92-0332] p 322 A92-25779
Unsteady incompressible flow computations with quadrilateral elements p 394 A92-26219
Turbine disk temperatures resulting from the hot mainstream at engine conditions
[AIAA PAPER 92-0398] p 373 A92-26252
Computational analysis of high-speed ejection seats
[AIAA PAPER 92-0403] p 324 A92-26256
Shock interference prediction using direct simulation Monte Carlo
[AIAA PAPER 92-0492] p 328 A92-26322
Hypersonic rarefied flow past spheres including wake structure
[AIAA PAPER 92-0495] p 329 A92-26325
Validation of a 3D Navier-Stokes code on experimental compressor bladings
[ONERA, TP NO. 1991-229] p 330 A92-26381
New nonequilibrium turbulence model for calculating flows over airfoils p 330 A92-26403
Preconditioned upwind methods to solve incompressible Navier-Stokes equations p 395 A92-26436
Navier-Stokes computations for turbulent transonic projectile with a two layer model combining the ASM model of turbulence and the k-epsilon model near the wall
[AIAA PAPER 92-0518] p 331 A92-26943
Solution of the Euler and Navier-Stokes equations on MIMD distributed memory multiprocessors using cyclic reduction
[AIAA PAPER 92-0561] p 411 A92-26970
Numerical simulation of flow separation for rotors and fixed wings
[AIAA PAPER 92-0635] p 334 A92-27013
Loss prediction of annular cascade flow based upon S1/S2 stream surface Navier-Stokes analysis
p 338 A92-27802
Numerical investigation of vortex breakdown on a delta wing p 340 A92-28027
Finite element Navier-Stokes solver for unstructured grids p 398 A92-28035
Estimation of propulsion-induced effects on transonic flows over a hypersonic configuration
[AIAA PAPER 92-0523] p 341 A92-28197
Unsteady airfoil flow solutions on moving zonal grids
[AIAA PAPER 92-0543] p 342 A92-28200
Effective treatments of the singular line boundary problem for three dimensional grids
[AIAA PAPER 92-0545] p 342 A92-28202
Full Navier-Stokes analysis of a three-dimensional hypersonic mixed compression inlet p 343 A92-28501
Navier-Stokes solution of transonic cascade flows using nonperiodic C-type grids p 344 A92-28523
Investigation of oblique shock/boundary-layer bleed interaction p 344 A92-28524
Unsteady analysis of hot streak migration in a turbine stage p 399 A92-28537
Applications of an implicit, upwind Navier-Stokes code, CRAFT, to steady/unsteady reacting, multi-phase flowfields
[AIAA PAPER 92-0837] p 422 A92-29603
Navier-Stokes computation of hypersonic near wakes with foreign gas injection
[AIAA PAPER 92-0838] p 422 A92-29604
Flux-difference split algorithm for unsteady thin-layer Navier-Stokes solutions p 431 A92-31158
Solution-adaptive grid procedure for the parabolized Navier-Stokes equations p 432 A92-31163
Use of finite volume schemes for transition simulation
p 432 A92-31185
Numerical investigation of the high-speed conical flow past a sharp fin p 433 A92-31468
A non-linearly stable implicit finite element algorithm for hypersonic aerodynamics p 433 A92-31487
Navier-Stokes simulation of flow through a highly contoured subsonic diffuser p 433 A92-31491
A new adaptive algorithm for turbulent flows
p 434 A92-31547
Implicit solutions of three-dimensional viscous hypersonic flows p 434 A92-31549

Navier-Stokes computations of a viscous optimized waverider
[AIAA PAPER 92-0305] p 435 A92-31653
Evaluation of a Navier-Stokes prediction of a jet in a crossflow p 441 A92-32235
Interference flows past cylinder-fin-sting-cavity assemblies p 442 A92-32236
Navier-Stokes study of supersonic cavity flowfield with passive control p 442 A92-32239
Navier-Stokes methods to predict circulation control airfoil performance p 442 A92-32243
Numerical studies of supersonic flow over a compression corner p 442 A92-32324
Navier-Stokes analysis of helicopter plume flowfield for infrared calculations
[AIAA PAPER 92-0983] p 580 A92-33185
Design and analysis of reengine Boeing 727-100 center inlet S duct by a reduced Navier-Stokes code
[AIAA PAPER 92-1221] p 517 A92-33320
Unsteady aerodynamic characteristics of a dual-element airfoil
[AIAA PAPER 92-2508] p 518 A92-34501
Aerobrake aerothermodynamic environment predictions in support of the Aeroassist Flight Experiment
[TABES PAPER 91-278] p 519 A92-34683
Navier-Stokes analysis of blade tip shape in hover p 521 A92-35758
Unsteady Navier-Stokes simulation of turbulent flows through a supersonic compressor cascade p 523 A92-36036
Numerical simulations of the flow through cascades with tip clearance p 523 A92-36038
High alpha aerodynamic control by tangential fuselage blowing p 611 A92-36848
Efficient direct solvers for large-scale computational fluid dynamics problems p 690 A92-37534
A new finite element formulation for computational fluid dynamics. X - The compressible Euler and Navier-Stokes equations p 612 A92-37552
Vortical flow simulation by the solution of the Navier-Stokes equations p 620 A92-40104
A study of three dimensional turbulent boundary layer separation and vortex flow control using the reduced Navier Stokes equations p 621 A92-40105
Heat transfer in a channel with built-in wing-type vortex generators p 757 A92-41082
Transonic Navier-Stokes computations for an oscillating wing using zonal grids p 701 A92-41217
Numerical study of vortex-dominated flows for wings at high incidence and sideslip p 702 A92-41227
Newton's method solver for the axisymmetric Navier-Stokes equations p 703 A92-41269
Navier-Stokes simulation for cone-derived waverider p 703 A92-41271
Extrapolation procedures for the time-dependent Navier-Stokes equations p 704 A92-41289
Navier-Stokes cavity solutions based on second-order turbulence modeling
[AIAA PAPER 92-2765] p 704 A92-41314
Prediction of shock pattern dynamics at hypersonic angle of attack maneuvers of endo-KEW missile forebodies
[AIAA PAPER 92-2768] p 704 A92-41317
Adaptive mesh for turbulent hypersonic flow
[AIAA PAPER 92-2776] p 704 A92-41322
Navier-Stokes computations for pointed, spherical, and flat tipped shell at Mach 3 p 705 A92-41536
Hybrid Navier-Stokes/Monte Carlo method for reacting flow calculations p 705 A92-41537
Similarity solutions for viscous vortex cores p 759 A92-41658
Flow analysis for axial compressor including secondary flow effects p 759 A92-41835
Upwind schemes for Navier-Stokes computations at subsonic through hypersonic speeds p 708 A92-43071
Aerodynamic design of a nonplanar airfoil by an inverse method with Navier-Stokes equations p 711 A92-43197
Solution of the parabolized Navier-Stokes equations using Osher's upwind scheme p 713 A92-44371
Numerical analysis of flow through oscillating cascade sections p 713 A92-44513
Navier-Stokes solutions of transonic nozzle flow with shock-induced flow separations p 713 A92-44515
Viscous simulation method for unsteady flows past multicomponent configurations p 714 A92-44671
Experimental and analytical study of close-coupled ventral nozzles for ASTOVL aircraft p 861 A92-45325
Computational aerodynamics in aircraft design - Challenges and opportunities for Euler/Navier-Stokes methods
[SAE PAPER 911990] p 788 A92-45392
Recent applications of the FNS zonal Method to complex flow problems
[SAE PAPER 912003] p 789 A92-45404
Multidimensional Euler/Navier-Stokes analysis for hypersonic equilibrium gas
[SAE PAPER 912026] p 790 A92-45418
Critical effects of downstream boundary conditions on vortex breakdown
[AIAA PAPER 92-2601] p 792 A92-45478
Effect of canard deflection on close-coupled canard-wing-body aerodynamics
[AIAA PAPER 92-2602] p 792 A92-45479
Navier-Stokes and Euler solutions for an unmanned aerial vehicle
[AIAA PAPER 92-2609] p 792 A92-45483
Three-dimensional orthogonal-to-surface structured grid generation with transonic Navier-Stokes flow solutions for a commercial transport configuration
[AIAA PAPER 92-2616] p 793 A92-45490
Computational study of transition front on a swept wing leading-edge model
[AIAA PAPER 92-2630] p 795 A92-45502
Unsteady Navier-Stokes simulations of supersonic flow over a three-dimensional cavity
[AIAA PAPER 92-2632] p 795 A92-45504
Application of an unstructured Navier-Stokes solver to multi-element airfoils operating at transonic maneuver conditions
[AIAA PAPER 92-2638] p 796 A92-45507
A nonlinear relaxation/quasi-Newton algorithm for the compressible Navier-Stokes equations
[AIAA PAPER 92-2643] p 796 A92-45510
Transonic airfoil and wing design using Navier-Stokes codes
[AIAA PAPER 92-2651] p 797 A92-45518
Effect of throat contouring on two-dimensional converging-diverging nozzles using URS method
[AIAA PAPER 92-2659] p 797 A92-45520
Numerical investigation of tail buffet on F-18 aircraft
[AIAA PAPER 92-2673] p 798 A92-45528
Calculation of high speed base flows
[AIAA PAPER 92-2679] p 799 A92-45531
Spatial and temporal adaptive procedures for the unsteady aerodynamic analysis of airfoils using unstructured meshes
[AIAA PAPER 92-2694] p 800 A92-45540
Navier-Stokes analysis and experimental data comparison of compressible flow in a diffusing S-duct
[AIAA PAPER 92-2699] p 800 A92-45541
Design and analysis of vortex generators on reengined Boeing 727-100QF center inlet S-duct by a reduced Navier-Stokes code
[AIAA PAPER 92-2700] p 800 A92-45542
Commercial turbofan engine exhaust nozzle flow analyses using PAB3D
[AIAA PAPER 92-2701] p 801 A92-45543
Computational evaluation of an airfoil with a Gurney flap
[AIAA PAPER 92-2708] p 802 A92-45550
Compressible Navier-Stokes solutions for a suction boundary control airfoil
[AIAA PAPER 92-2710] p 802 A92-45551
Time accurate computation of unsteady transonic flows around an airfoil with oscillating flap on dynamic grid
[AIAA PAPER 92-2733] p 805 A92-45567
Navier-Stokes computation of wing leading edge tangential blowing for a tilt rotor in hover
[AIAA PAPER 92-2608] p 805 A92-45568
Comparison of two flux splitting schemes for calculation of ogive-cylinder at M = 3.5 and alpha = 18 deg
[AIAA PAPER 92-2667] p 806 A92-45582
Separation patterns and flow structures about a hemisphere-cylinder at high incidences
[AIAA PAPER 92-2712] p 807 A92-45593
Navier-Stokes predictions for the F-18 wing and fuselage at large incidence p 810 A92-46783
Navier-Stokes computations on swept-tapered wings, including flexibility p 810 A92-46786
Temporal adaptive Euler/Navier-Stokes algorithm involving unstructured dynamic meshes p 812 A92-46887
Joint computational/experimental aerodynamics research on hypersonic vehicle. II - Computational results p 812 A92-46891
Numerical simulation of multizone two-dimensional transonic flows using the full Navier-Stokes equations p 815 A92-46955
Initial validation of an unsteady Euler/Navier-Stokes flow solver for helicopter rotor airloads in forward flight p 815 A92-46956
Grid adaptation to multiple functions for applied aerodynamic analysis p 817 A92-47045
Simple diagnosis for the quality of generated grid systems p 919 A92-47069
Generation of efficient multiblock grids for Navier-Stokes computations p 919 A92-47081
Numerical experiments on unsteady shock reflection processes using the thin-layer Navier-Stokes equations p 818 A92-47155
Numerical and experimental investigation of rarefied compression corner flow
[AIAA PAPER 92-2900] p 820 A92-47876
Solution of the Burnett equations for hypersonic flows near the continuum limit
[AIAA PAPER 92-2922] p 821 A92-47894
Some exact and numerical results for plane steady sheared flow of an incompressible inviscid fluid p 821 A92-48019
Numerical computations of transonic flows through cascades
[AIAA PAPER 92-3041] p 822 A92-48702
Comparison between two 3D-NS-codes and experiment on a turbine stator
[AIAA PAPER 92-3042] p 822 A92-48703
A higher-order accurate Navier-Stokes solver for transonic and supersonic flows in turbomachinery
[AIAA PAPER 92-3044] p 822 A92-48704
FNS analysis of an axisymmetric scramjet inlet
[AIAA PAPER 92-3100] p 824 A92-48742
Computational analysis of ramjet engine inlet interaction
[AIAA PAPER 92-3102] p 824 A92-48744
Prediction of a high bypass ratio engine exhaust nozzle flowfield
[AIAA PAPER 92-3259] p 864 A92-48855
Numerical simulation of turbine 'hot spot' alleviation using film cooling
[AIAA PAPER 92-3309] p 904 A92-48896
Navier-Stokes investigation of a transonic centrifugal compressor stage using an algebraic Reynolds stress model
[AIAA PAPER 92-3311] p 825 A92-48897
A Navier-Stokes analysis of a controlled-diffusion compressor cascade at increasing inlet-flow angles
[AIAA PAPER 92-3313] p 825 A92-48899
Vane-blade interaction in a transonic turbine. II - Heat transfer
[AIAA PAPER 92-3324] p 904 A92-48907
A computational study of advanced exhaust system transition ducts with experimental validation
[AIAA PAPER 92-3794] p 907 A92-49126
Navier-Stokes computations of horseshoe vortex flows p 990 A92-49516
Least-squares/parabolized Navier-Stokes procedure for optimizing hypersonic wind-tunnel nozzles p 980 A92-50270
Full Navier-Stokes analysis of a three-dimensional scramjet inlet p 934 A92-50272
Application of an unsteady Navier-Stokes solver to transonic turbine design p 935 A92-50273
On the application of parabolized Navier-Stokes equations to flow field simulations p 936 A92-51943
Finite analytic numerical solution of Navier-Stokes equations p 996 A92-53011
Navier-Stokes simulation for the winged space vehicle 'HOPE' at subsonic, transonic, and supersonic regimes p 1018 A92-53559
Three-dimensional Navier-Stokes heat transfer predictions for turbine blade rows
[AIAA PAPER 92-3068] p 1020 A92-54003
Increased heat transfer to elliptical leading edges due to spanwise variations in the freestream momentum - Numerical and experimental results
[AIAA PAPER 92-3070] p 1020 A92-54005
Full Navier-Stokes calculations on the installed F/A-18 inlet at a high angle of attack
[AIAA PAPER 92-3175] p 1020 A92-54012
Application of computational fluid dynamics to the study of vortex flow control for the management of inlet distortion
[AIAA PAPER 92-3177] p 1020 A92-54013
Navier-Stokes analysis of three-dimensional unsteady flows inside turbine stages
[AIAA PAPER 92-3211] p 1021 A92-54016
The enhancement of the mixing and combustion processes in supersonic flow applied to scramjet engine
[AIAA PAPER 92-3428] p 1112 A92-54029
Full Navier-Stokes analysis of a two-dimensional mixer/ejector nozzle for noise suppression
[AIAA PAPER 92-3570] p 1067 A92-54059
A finite-volume numerical method to calculate fluid forces and rotordynamic coefficients in seals
[AIAA PAPER 92-3712] p 1113 A92-54132
Assessment of compressibility corrections to the k-epsilon model in high-speed shear layers p 1024 A92-54905
Flowfield of a lifting rotor in hover - A Navier-Stokes simulation p 1024 A92-54906
Approximate Riemann solver for hypervelocity flows p 1117 A92-54934
Grid studies for thin-layer Navier-Stokes computations of airfoil flowfields p 1025 A92-54935
Navier-Stokes prediction of large-amplitude delta-wing roll oscillations characterizing wing rock
[AIAA PAPER 92-4428] p 1080 A92-55352

Navier-Stokes computations for oscillating control surfaces
[AIAA PAPER 92-4431] p 1026 A92-55355
Evaluation of a multigrid-based Navier-Stokes solver for aerothermodynamic computations
[AIAA PAPER 92-4563] p 1027 A92-55375
Wind tunnel test of M = 2.5 mixed compression inlet
p 1028 A92-56008
Navier-Stokes simulation of a close-coupled canard-wing-body configuration p 1031 A92-56163
Application of computational fluid dynamics to sonic boom near- and mid-field prediction
p 1031 A92-56173
Improved calculation of transonic potential flow past swept wings p 1031 A92-56179
Hypersonic wind tunnel nozzle study
[AIAA PAPER 92-4012] p 1033 A92-56835
Boundary layer study on nozzle wall at hypersonic velocities
[AIAA PAPER 92-4013] p 1034 A92-56836
Numerical prediction of the flow characteristics in an arc wind tunnel
[AIAA PAPER 92-4016] p 1100 A92-56838
Numerical simulation of hypersonic viscous flow for the design of H-2 orbiting plane (HOPE-2)
[NAL-TR-1093] p 11 N92-10009
Numerical investigation of the effect of leading edge geometry on dynamic stall of airfoils
[AD-A239949] p 12 N92-10015
Viscous computations of cold air/air flow around scramjet nozzle afterbody
[NASA-CR-4406] p 13 N92-10982
Resolution of the Navier-Stokes equations applied to the computation of the laminar flow around a two dimensional wing profile
[CERT-RT-65/5604-35] p 43 N92-11307
Resolution of Navier-Stokes equations around profiles: Drag evolution
[ONERA-RTS-86/1685-AY-156A] p 43 N92-11310
An assessment and application of turbulence models for hypersonic flows
[NASA-TM-105124] p 82 N92-11984
Comparison of solution of various Euler solvers and one Navier-Stokes solver for the flow about a sharp-edged cropped delta wing
[AD-B163639L] p 83 N92-12998
Recent progress in computational vortex-flow aerodynamics p 84 N92-13002
On the simulation of compressible turbulent flows past delta wing, delta wing-body and delta wing-canard
p 84 N92-13003
Determination of vortex-breakdown criteria by solving the Euler and Navier-Stokes equations
p 87 N92-13018
Investigation of vortex breakdown on a delta wing using Euler and Navier-Stokes equations p 87 N92-13019
Numerical simulation of vortex street-edge interaction
p 88 N92-13027
Numerical investigation of unsteady supersonic cavity flowfield with passive control p 88 N92-13029
Experiences with optimizing airfoil shapes for maximum lift over drag p 90 N92-13838
Navier-Stokes calculation of transonic flow past the NTF 65 deg delta wing p 91 N92-13868
Inverse airfoil design procedure using a multigrid Navier-Stokes method p 193 N92-13932
Analysis of an advanced ducted propeller subsonic inlet
[NASA-TM-105393] p 179 N92-14002
Navier-Stokes analysis of turbulent boundary layer and wake for two-dimensional lifting bodies
p 221 N92-14309
A Navier-Stokes solution of Hull-ring wing-thruster interaction p 221 N92-14310
Transonic Navier-Stokes computations for a spinning body of revolution
[AD-A241015] p 180 N92-14972
Analysis tools of ONERA and DLR for the aerothermodynamics of reentry vehicles
p 211 N92-14977
Hypersonic flow past delta wing flow simulated by Navier-Stokes solutions p 180 N92-14981
Flow and temperature computations for space vehicles using adaptive finite element techniques
p 181 N92-14990
SIMOUN and Scirocco wind tunnel nozzle viscous flow study p 208 N92-14999
Verification and application of the NSFLEX method for hypersonic flow conditions p 182 N92-15005
Hypersonic aerothermodynamic computations using a point-implicit TVD method p 183 N92-15006
Viscous shock-layer equations for the calculation of reentry aerothermodynamics p 183 N92-15008
Equilibrium solution of the Euler and Navier-Stokes equations around a double ellipsoidal shape with mono- and multi-blocks including real gas effects, part 1
p 227 N92-15030
Seal development activities at Allison Turbine Division
p 228 N92-15093
Use of Navier-Stokes analysis in section design
[AD-A242074] p 299 N92-17168
Marching with the parabolized Navier-Stokes equations. Problem 1: Numerical study of hypersonic viscous cone flow
[AERO-REPT-9007] p 344 N92-18231
Marching with the parabolized Navier-Stokes equations. Problem 2: Hypersonic viscous flow over a flat plate
[AERO-REPT-9008] p 345 N92-18232
WP 4b compressible flow simulation: Information System for flow simulation based on the Navier-Stokes equation (ISNaS). Requirements grid generation for the ISNaS compressible flow solver
[NLR-TR-88103-U] p 405 N92-19490
Use of CFD in the design of a modern multistage aero engine LP turbine design
[PNR-90862] p 472 N92-20179
Flowfield analysis of modern helicopter rotors in hover by Navier-Stokes method
[AD-A245011] p 446 N92-21333
Current status of computational methods for transonic unsteady aerodynamics and aeroelastic applications
[NASA-TM-104191] p 446 N92-21432
Contributions of MBB-FE211 to the 2nd Antibes Workshop on Hypersonic Flows
[MBB-FE211-S-PUB-449] p 524 N92-22179
Cases 6.1 and 6.8 double ellipsoid: Navier-Stokes calculation p 525 N92-22181
Case 7.4 delta wing: Navier-Stokes calculation
p 525 N92-22182
Three-dimensional multigrid algorithm for the Euler and the thin-layer Navier-Stokes equations
[PB92-134329] p 602 N92-22216
Numerical simulation of transient hypervelocity flow in an expansion tube
[NASA-CR-189615] p 592 N92-22228
Inlets, ducts, and nozzles p 593 N92-22523
Methodology for sensitivity analysis, approximate analysis, and design optimization in CFD for multidisciplinary applications --- computational fluid dynamics
[NASA-CR-190201] p 595 N92-22662
Simulation of the flow on a space glider. Stagnation point calculation using the 2D Navier-Stokes equations including chemical effects p 624 N92-24393
On constructing three-dimensional overlapping grids with CMPGRD p 691 N92-24424
An incremental strategy for calculating consistent discrete CFD sensitivity derivatives
[NASA-TM-104207] p 625 N92-24681
Periodic Euler and Navier-Stokes solutions about oscillating airfoils p 626 N92-24850
Navier-Stokes simulation of dynamic stall on a rotating airfoil p 626 N92-24853
Automated grid generation for high-lift configurations
p 628 N92-24869
Boundary layer computations using a generalized formulation p 679 N92-24873
Algorithm and code development for unsteady three-dimensional Navier-Stokes equations
[NASA-CR-190077] p 692 N92-25264
Joint computational and experimental aerodynamics research on a reentry vehicle
[DE91-017315] p 667 N92-25315
A compressible Navier-Stokes solver with two-equation and Reynolds stress turbulence closure models
[NASA-CR-4440] p 681 N92-25376
On a multi-block method for transonic turbulent flows past a wing-fuselage configuration p 632 N92-25569
Cartesian based grid generation/adaptive mesh refinement p 682 N92-25722
Wall functions for the kappa-epsilon turbulence model in generalized nonorthogonal curvilinear coordinates
[NASA-CR-190368] p 685 N92-25962
A critical evaluation of a three-dimensional Navier-Stokes method as a tool to calculate transonic flows inside a low-aspect-ratio compressor
p 768 N92-27459
Navier-Stokes analysis of turbine blade heat transfer and performance p 768 N92-27468
The application of a Navier-Stokes CFD method to civil engine intake flows p 769 N92-27471
The 3-D Navier-Stokes flow and temperature field computation for a forced mixer nozzle
p 770 N92-27482
Fundamental studies on droplet interactions in dense sprays
[AD-A246918] p 770 N92-27546
A study of juncture flow in the NASA Langley 0.3-meter transonic cryogenic tunnel
[NASA-CR-190430] p 773 N92-27880
Current status of computational methods for transonic unsteady aerodynamics and aeroelastic applications
p 718 N92-27937
Computations of unsteady flows around airfoil sections by explicit and implicit methods solving the Euler and Navier-Stokes equations p 720 N92-27948
Numerical simulation of shock-stall flutter of an airfoil using the Navier-Stokes equations p 746 N92-27956
Transonic aeroelastic computations on wings using Navier-Stokes equations p 721 N92-27957
Viscous effects on a vortex wake in ground effect
[NASA-CR-190400] p 907 N92-28361
Full Navier-Stokes analysis of a two-dimensional mixer/ejector nozzle for noise suppression
[NASA-TM-105715] p 868 N92-28419
Explicit Navier-Stokes computation of turbomachinery flows
[AD-A249284] p 909 N92-28879
Joint computational and experimental aerodynamics research on a hypersonic vehicle
[DE92-013439] p 943 N92-30367
Numerical investigations in three-dimensional internal flows
[NASA-CR-190498] p 998 N92-30380
Navier-Stokes computations of a viscous optimized waverider
[NASA-CR-189658] p 944 N92-30392
A gridless Euler/Navier-Stokes solution algorithm for complex two-dimensional applications
[NASA-TM-107631] p 944 N92-30570
Navier-Stokes analysis and experimental data comparison of compressible flow within ducts
[NASA-TM-105796] p 972 N92-30972
Stagnation-point heat-transfer rate predictions at aeroassist flight conditions
[NASA-TP-3208] p 1001 N92-31281
A computational investigation of airfoil stall flutter
[AD-A247302] p 947 N92-31300
Hypersonic code efficiency and validation studies
[NASA-CR-190680] p 948 N92-31533
Low density real gas flows about hypersonic vehicles
[AD-A250048] p 949 N92-31777
The calculation of incompressible separated turbulent boundary layers p 1003 N92-31886
Three-dimensional compressible turbulent computations for a nondiffusing S-duct
[NASA-CR-4391] p 951 N92-32240
A critical evaluation of a three-dimensional Navier-Stokes CFD as a tool to design supersonic turbine stages p 1124 N92-32268
Numerical simulation of turbomachinery flows with advanced turbulence models p 1124 N92-32270
Research on some centered implicit methods for calculating transonic flows by solving Navier-Stokes equations
[ONERA-RSF-24/1408-AY-150A] p 1037 N92-32773
High speed transition prediction
[NASA-CR-190836] p 1039 N92-33424
A nozzle internal performance prediction method
[NASA-TP-3221] p 1040 N92-33625
Navier-Stokes analysis and experimental data comparison of compressible flow in a diffusing S-duct
[NASA-TM-105683] p 1072 N92-33746
An approximate viscous shock layer technique for calculating chemically reacting hypersonic flows about blunt-nosed bodies p 1041 N92-33837
Computation and stability analysis of laminar flow over a blunt cone in hypersonic flow p 1041 N92-33839
Prediction and control of asymmetric vortical flows around slender bodies using Navier-Stokes equations
p 1127 N92-33968
Numerical investigation of the effects of icing on fixed and rotary wing aircraft
[NASA-CR-190542] p 1044 N92-34105

NAVIGATION

Modern navigation, guidance, and control processing --- Book
[ISBN 0-13-596230-7] p 639 A92-40199
Space plane navigation simulation
p 1103 A92-53603
AIAA Guidance, Navigation and Control Conference, Hilton Head Island, SC, Aug. 10-12, 1992, Technical Papers. Pts. 1-3 p 1130 A92-55151
Knowledge based system applications for guidance and control
[AGARD-AR-284] p 205 N92-14065
Artificial Neural Network Approaches in Guidance and Control
[AGARD-LS-179] p 234 N92-14673
Introduction to neural computing and categories of neural network applications to guidance, navigation and control p 234 N92-14674

Joint University Program for Air Transportation Research, 1990-1991
[NASA-CP-3131] p 242 N92-17984
A method of passive range determination using only two bearing measurements
[AD-D015182] p 455 N92-20834
Measurement of LORAN-C envelope to cycle difference in the far field
[PB92-128909] p 455 N92-21263
Trajectory optimization for hypersonic aircraft guidance p 728 N92-27898
Airborne experimental FLIR program
p 1064 N92-32447
Comparison of GLONASS and GPS time transfers between two west European time laboratories and VNIIFTRI p 1050 N92-33381

NAVIGATION AIDS
Institute of Navigation, National Technical Meeting, 47th, Phoenix, AZ, Jan. 22-24, 1991, Proceedings
p 95 A92-16626
The FAA Loran program status and expectations
p 95 A92-16629
Loran time difference correction factors - Valid information or blue smoke and mirrors?
p 96 A92-16633
Transition of GPS user equipment testing from Yuma Proving Ground to Holloman AFB p 138 A92-16972
Navsat - A civil complement to GPS and Glonass
[IAF PAPER 91-490] p 188 A92-18505
The accuracy and coverage of Loran-C and of the Decca Navigator System - and the fallacy of fixed errors
p 353 A92-24944
Navigation and flight management systems - Thoughts of a user p 354 A92-26848
The cockpit of a modern aircraft - The Airbus A340 considered as an example p 357 A92-26849
Possible utilization of GPS in precision approach maneuvers p 637 A92-37075
Flight test data analysis of a low cost GPS/IMU integrated navigation system p 638 A92-39560
A system for precise real-time differential GPS positioning in the decimeter range p 638 A92-39569
The Automatic Dependent Surveillance (ADS) system
p 724 A92-41208
NAECON 91; Proceedings of the IEEE National Aerospace and Electronics Conference, Dayton, OH, May 20-24, 1991. Vols. 1-3
[ISBN 0-7803-0084-X] p 786 A92-48426
Rapid systems integration of navigation avionics
p 858 A92-48473
An integrated navigation system manager using federated Kalman filtering p 858 A92-48477
A new development in embedded computer performance measurement p 921 A92-48506
Verification and validation testing of the pilot's associate p 966 A92-49318
Flight management system back-up navigation for the A330/A340 aircraft p 975 A92-49326
Navigation charts on trial - How safe is safe?
p 1012 A92-49380
On the calculation of repeatable accuracy, with special reference to GPS p 955 A92-49383
Vision-based obstacle detection for rotorcraft flight
p 967 A92-52465
Analysis of image-based navigation system for rotorcraft low-altitude flight p 1046 A92-55968
Flight evaluation of navigation systems including MLS using NAL Do228 - Outline p 1047 A92-56116
Flight evaluation of navigation systems including MLS using NAL Do228 - Results of MLS
p 1047 A92-56117
Flight evaluation of navigation systems including MLS using NAL Do228 - Results of GPS
p 1047 A92-56118
Adaptive tactical navigation program
p 102 N92-12529
Integrated Communications, Navigation, Identification, Avionics (ICNIA) expert system for fault tolerant avionics
p 118 N92-12539
Visual approach data collection at San Francisco International Airport (SFO)
[DOT/FAA/CT-90/23] p 354 N92-18112
Cockpit weather information needs
p 449 N92-21503
Future developments in aeronautical satellite communications p 678 N92-24167
The navigation data logger for a suitcase navigation system
[AD-A245997] p 727 N92-26756
Precision of the long baseline acoustic navigation system used by Pegasus
[AD-A246598] p 727 N92-26795
Loran-C performance assurance assessment program
[NASA-CR-190469] p 840 N92-28718
Global positioning system runway incursion program static ground tests
[DOT/FAA/CT-TN91/44] p 957 N92-31838
Decision-making guide for the proposed Coast Guard differential global positioning system
[AD-A246046] p 957 N92-32054
US Coast Guard GPS Information Center (GPSIC) and its function within the Civil GPS Service (CGS)
p 1049 N92-33352
A workstation-based evaluation of a far-field route planner for helicopters
[NASA-TM-102882] p 1051 N92-33609
Integrated Russian VLF/Omega receiver design
[PB92-193390] p 1051 N92-33809

NAVIGATION INSTRUMENTS
SATZAP - A novel approach to GPS integrity
p 99 A92-16947
Integrated navigation for approach guidance using differential GPS p 101 A92-16970
The LISA 6000 - A highly integrated IRS/GPS navigation system p 267 A92-22088
Aviation products liability and navigation - Recent developments and future directions p 697 A92-39563
Engineering Graphical Analysis Tool (EGAT) development program p 164 N92-12542
GPS interferometric attitude and heading determination: Initial flight test results p 269 N92-17994
An evaluation of the Royal Air Force Shorts Tucano Navigation Instruments Trainer: The NAVIT
[ETN-92-90841] p 354 N92-18729
Evaluating the velocity accuracy of an integrated GPS/INS system: Flight test results
[DE92-007519] p 640 N92-25470
Techniques for autonomous navigation
[DE92-013458] p 957 N92-31746

NAVIGATION SATELLITES
Global satellite navigation using both GPS and GLONASS p 99 A92-16938
Navsat - A civil complement to GPS and Glonass
[IAF PAPER 91-490] p 188 A92-18505
Simulation as applied to mission planning
p 747 A92-41210
An adaptive correction technique for Differential Global Positioning System p 726 N92-26623
US Coast Guard GPS Information Center (GPSIC) and its function within the Civil GPS Service (CGS)
p 1049 N92-33352
GPS orbit determination at the National Geodetic Survey p 1049 N92-33354
Comparison of two-way satellite time transfer and GPS common-view time transfer between OCA and TUG
p 1050 N92-33356
Comparison of GLONASS and GPS time transfers between two west European time laboratories and VNIIFTRI p 1050 N92-33381

NAVSTAR SATELLITES
Aircraft navigation using Global Positioning System improved with geostationary satellites
p 99 A92-16934
SATZAP - A novel approach to GPS integrity
p 99 A92-16947
Approach flight trials in the Netherlands for the Navstar GPS Joint Program Office International Test Program
p 533 A92-35928

NAVY
US Navy revisits escape modules p 849 A92-47975
Revolution at sea: Aircraft options for the year 2030
p 466 N92-21974

NEAR WAKES
Navier-Stokes computation of hypersonic near wakes with foreign gas injection
[AIAA PAPER 92-0838] p 422 A92-29604
The aviation kerosene burning in the non-uniform air flow p 487 A92-29728
Computation of near-wake, aerobrake flowfields
p 441 A92-32181
Large eddy simulation of unsteady turbulent wake of a circular cylinder using the finite element method
p 587 A92-34825
Phase-averaged turbulence statistics in a near wake with an asymmetric vortex shedding p 620 A92-40086
An experimental and numerical study of confined axisymmetric jet with a bluff body p 621 A92-40106
LDV measurements in the three-dimensional near wake of a stationary and oscillating rectangular wind
[AIAA PAPER 92-2689] p 799 A92-45536
The vortical structure in the wake during dynamic stall
[AIAA PAPER 92-4496] p 1026 A92-55364
A comparison of airborne wake vortex detection measurements with values predicted from potential theory
[NASA-TP-3125] p 18 N92-10994
Use of Navier-Stokes analysis in section design
[AD-A242074] p 299 N92-17168
An investigation of the energy loss and near wake flow field of trailing edge injection p 456 N92-21839
Analysis of rotor vibratory loads using higher harmonic pitch control
[NASA-CR-189591] p 696 N92-24251

NEODYMIUM LASERS
Laser-based ultrasonics on GR/epoxy composite - Interferometric detection p 144 A92-13554
One joule output from a diode-array-pumped Nd:YAG laser with side-pumped rod geometry
p 671 A92-37188
Advanced balancing using laser machining
[SAE PAPER 912218] p 674 A92-40020
Fiber-sensor design for turbine engines
[DE92-003539] p 376 N92-18230

NETHERLANDS
Review of aerodynamic design in the Netherlands
p 193 N92-13929

NETWORK ANALYSIS
National airspace data interchange network analysis
[AD-A247345] p 727 N92-27217

NETWORK CONTROL
Neural network and fuzzy logic technology for naval flight control
[AD-A242650] p 206 N92-15074
Application of neural network to adaptive control theory for super-augmented aircraft
[AD-A246596] p 745 N92-27505

NEUMANN PROBLEM
Numerical methods in elastoacoustics in the nonmodal domain
[ONERA, TP NO. 1991-232] p 415 A92-26383

NEURAL NETS
A novel associative memory for high level control functions p 52 A92-11472
Classification of radar clutter using neural networks
p 145 A92-14252
A neural network for the identification of measured helicopter noise p 162 A92-14387
The application of neural networks to drone control
p 205 A92-19273
A multi-layer neural network classifier for radar clutter
p 291 A92-21691
Use of neural networks in control of high alpha maneuvers
[AIAA PAPER 92-0048] p 282 A92-22164
Identification of aerodynamic coefficients using computational neural networks
[AIAA PAPER 92-0172] p 255 A92-23783
Identification of helicopter noise using a neural network p 416 A92-28032
A system identification model for adaptive nonlinear control p 508 A92-29248
Potential role of neural networks and fuzzy logic in flight control design and development
[AIAA PAPER 92-0999] p 600 A92-33191
Damage tolerant structural design using neural networks
[AIAA PAPER 92-1097] p 581 A92-33261
Wind-tunnel compressor stall monitoring using neural networks p 918 A92-46817
A neural network based postattack damage assessment system p 922 A92-48520
Specifying exhaust nozzle contours in real-time using genetic algorithm trained neural networks
[AIAA PAPER 92-3328] p 865 A92-48911
Flight control law synthesis using neural network theory
[AIAA PAPER 92-4390] p 1074 A92-55191
Neural networks for feedback linearization in aircraft control
[AIAA PAPER 92-4391] p 1074 A92-55192
Identification and control of aircraft dynamics using radial basis function neural networks
[AIAA PAPER 92-4393] p 1074 A92-55194
Design of a flight control system using a feedback-error-learning-type neural network
p 1132 A92-56067
Optimal design of wing shape by use of neural-network p 1054 A92-56112
Robotic non-destructive inspection of aircraft, phase 1
[AD-A240777] p 44 N92-11367
Locally linear neural networks for aerospace navigation systems p 103 N92-12530
Comparison of polynomial approximations and artificial neural nets for response surfaces in engineering optimization p 165 N92-13835
The use of artificial neural networks in experimental data acquisition and aerodynamic design p 90 N92-13848
Artificial Neural Network Approaches in Guidance and Control
[AGARD-LS-179] p 234 N92-14673
Introduction to neural computing and categories of neural network applications to guidance, navigation and control p 234 N92-14674
Processing complexity of two approaches to object detection and recognition p 234 N92-14677

Neural network and fuzzy logic technology for naval flight control
[AD-A242650] p 206 N92-15074
Neural networks for aircraft system identification
p 303 N92-17998
A connectionist approach to autonomous robotic navigation p 454 N92-20356
Design and evaluation of a robust dynamic neurocontroller for a multivariable aircraft control problem
[NASA-TM-105579] p 481 N92-20586
A study in dynamic control of a super maneuver with neural networks p 463 N92-21510
Identification of aerodynamic coefficients using computational neural networks
[AD-A244711] p 447 N92-21753
Automated screening of propulsion system test data by neural networks, phase 1
[NASA-CR-184329] p 753 N92-27403
Application of neural network to adaptive control theory for super-augmented aircraft
[AD-A246596] p 745 N92-27505
An exploratory application of neural networks to the sortie generation forecasting problem
[AD-A246626] p 778 N92-27980
An investigation of switched reluctance rotor position estimation using neural networks
[AD-A252846] p 1061 N92-33414

NEUTRAL BEAMS
Formation and sustainment of a very low aspect ratio tokamak using coaxial helicity injection: Helicity Injected Torus (HIT) experiment
[DE92-014311] p 1136 N92-32595

NEUTRON RADIOGRAPHY
Stationary neutron radiography system
p 144 A92-13589
Neutron radiography with SNRS p 492 A92-28747
An advanced neutron radiography system
p 492 A92-28748

NEW YORK CITY (NY)
New York Downtown Manhattan (Wall Street) Heliport: Operations analysis
[DOT/FAA/RD-91/12] p 139 N92-13077

NEWS MEDIA
Aerobureau - Strategic television airmobile reports via satellite p 218 A92-19988

NEWTON METHODS
Newton's method solver for high-speed viscous separated flowfields p 176 A92-20736
Newton's method solver for the axisymmetric Navier-Stokes equations p 703 A92-41269
Multi-point inverse design of an infinite cascade of airfoils
[AIAA PAPER 92-2650] p 797 A92-45517
Development of a steady potential solver for use with linearized, unsteady aerodynamic analyses
[NASA-TM-105288] p 473 N92-20525
Evaluation of an unsteady implicit Euler code against two and three-dimensional standard configurations
p 719 N92-27945

NEWTONIAN FLUIDS
Non-slender shapes of minimum drag
p 937 A92-52029
Wind tunnel investigation of the aerodynamic effects of aircraft ground deicing/anti-icing fluids and criteria for aerodynamic acceptance p 452 N92-21698
Lewis icing research tunnel test of the aerodynamic effects of aircraft ground deicing/anti-icing fluids
[NASA-TP-3238] p 952 N92-30395

NICKEL ALLOYS
High temperature multiaxial creep testing of Nimonic 115 p 141 A92-15202
Corrosion damage and regeneration of aluminide coatings on aircraft turbine blades p 142 A92-15244
Nickel base alloy GTD-222 - A new gas turbine nozzle alloy
[ASME PAPER 91-GT-73] p 142 A92-15542
Short fatigue crack growth from blunt notches in an aero-engine alloy p 212 A92-19760
High temperature low cycle fatigue of single crystal nickel base superalloys p 213 A92-19796
A viscoplastic theory for anisotropic materials
[ONERA, TP NO. 1992-90] p 391 A92-24721
Brazing method helps repair aircraft gas-turbine nozzles p 492 A92-29504
Fracture mechanics approach to creep growth in welded IN738LC gas turbine blades
[ASME PAPER 91-GT-119] p 670 A92-36893
Development of intermetallic materials for aerospace systems p 754 A92-41874
Technique for estimating the strength of gas turbine guide vanes with stress raisers p 761 A92-42653
Aluminides modified by palladium - Protection of new parts by local finishing
[ONERA, TP NO. 1992-49] p 893 A92-48610
Joining a Ni-based creep-resistant (ODS) alloy by brazing p 1116 A92-54867
Rolling element bearing member
[PATENT-1-271-213] p 158 N92-13434
Low cycle fatigue of cast nickel base turbine rotors
p 226 N92-14405
Probabilistic lifing approach for aero engine disks made of powder nickel base alloys containing ceramic defects
p 226 N92-14424
Fatigue in single crystal nickel superalloys
[AD-A243453] p 290 N92-17653
Fatigue in single crystal nickel superalloys
[AD-A244815] p 489 N92-21015
Evaluation and qualification of diffusion braze repair techniques for superalloy gas turbine components
[NRC-LTR-ST-1839] p 504 N92-22028
Fatigue in single crystal nickel superalloys
[AD-A248190] p 896 N92-29408
Fatigue in single crystal nickel superalloys
[AD-A252492] p 988 N92-32066

NICKEL HYDROGEN BATTERIES
Nickel hydrogen common pressure vessel battery development p 598 N92-22770

NIGHT
Helicopter nighttime parking test results - UH-1
[DOT/FAA/CT-TN92/1] p 961 N92-31165

NIGHT FLIGHTS (AIRCRAFT)
A re-analysis of the causes of Boeing 727 'black hole landing' crashes p 833 A92-44985
A high-performance LLLTV CCD camera for nighttime pilotage p 855 A92-46227

NIGHT VISION
Expanding U.S.M.C. roles for the AH-1W SuperCobra
p 59 A92-14347
Helicopter NVG testing in the United Kingdom
p 112 A92-16053
Helmet-mounted image intensification analysis
p 554 A92-35454
A high-performance LLLTV CCD camera for nighttime pilotage p 855 A92-46227
Evaluation of a tritium runway lighting system
[DOT/FAA/CT-TN92/15] p 665 N92-25733

NIOBIUM ALLOYS
Composite strengthening of Nb-Ti base alloys
p 577 A92-36380

NITRIC OXIDE
Evaluation of NO(x) mechanisms for lean, premixed combustion
[ASME PAPER 91-GT-257] p 668 A92-36900
Effects of oxygen dissociation on hypervelocity combustion experiments
[AIAA PAPER 92-3964] p 1098 A92-56791
Simulation of chemical kinetics in turbulent natural gas combustion
[PB92-123660] p 488 N92-20329

NITROGEN
Rate parameters for coupled vibration-dissociation in a generalized SSH approximation --- Schwarz, Slawsky, and Herzfeld p 235 A92-20301
A fine-wire thermocouple probe for measurement of stagnation temperatures in real gas hypersonic flows of nitrogen p 1114 A92-54317
H-N2 interaction energies, transport cross sections, and collision integrals p 1135 A92-54660

NITROGEN DIOXIDE
Degenerate four-wave mixing for measurement of NO2 and smoke concentration in jet engine exhaust
[AIAA PAPER 92-3658] p 1113 A92-54108

NITROGEN OXIDES
CFD analysis of jet mixing in low NO(x) flametube combustors
[ASME PAPER 91-GT-217] p 124 A92-15634
Environmental impact of a future supersonic transport aircraft
[ONERA, TP NO. 1991-132] p 161 A92-16108
Studies on the effect of high-flying air-traffic on the atmosphere
[IAF PAPER 91-737] p 301 A92-22495
A simplified reaction mechanism for prediction of NO(x) emissions in the combustion of hydrocarbons
[AIAA PAPER 92-3340] p 894 A92-48919
Emissions from aircraft: Standards and potential for improvement
[PNR-90768] p 476 N92-21740

NITROLYSIS
Reaction speed constant for the reactions between N + O2 and between O + N2
[ETN-92-90861] p 347 N92-19252

NOISE (SOUND)
Turbomachinery noise p 54 N92-10601
Prediction of helicopter noise: Adaptation of noise load calculations to the blade-vortex interaction
[ONERA-RS-97/5094-PY] p 513 N92-21736
Experimental study of the mechanism of sound generation by rotating stall in centrifugal turbomachines
p 605 N92-23726

NOISE GENERATORS
Screech noise source structure of a supersonic rectangular jet
[AIAA PAPER 92-0503] p 331 A92-26932
Experimental study of the equivalent sound source center of the propeller rotating noise
p 1011 A92-53257
Aeroacoustics of flight vehicles: Theory and practice. Volume 1: Noise sources
[NASA-RP-1258-VOL-1] p 54 N92-10598
Jet noise generated by large-scale coherent motion
p 55 N92-10604
Combustion and core noise p 55 N92-10607
Sonic boom p 55 N92-10608
Boundary layer induced noise in aircraft
[CUED/A-AERO/TR-18] p 927 N92-29201

NOISE INTENSITY
Screech noise source structure of a supersonic rectangular jet
[AIAA PAPER 92-0503] p 331 A92-26932
Active noise reduction p 603 A92-32980
Noise level reduction inside helicopter cabins
p 545 A92-35733
A survey of active control in aircraft cabins
p 643 A92-39084
Trading number of operations versus loudness of aircraft p 688 A92-39102
Temporal change of noisiness of helicopter noise
p 689 A92-39103
Effects of military training route noise on human annoyance p 689 A92-39237
Annoyance from aircraft overflights in wilderness
p 689 A92-39239
Relating the annoyance of aircraft overflights to their audibility by outdoor recreationists p 689 A92-39240
Analysis of measured environmental noise levels: An assessment of the effects of airbase operational model variables on predicted noise exposure levels
[AD-A244805] p 485 N92-21720
Interior noise prediction methodology: ATDAC theory and validation
[NASA-CR-187626] p 697 N92-25368
Operational noise data for OH-58D Army helicopters
[AD-A246822] p 926 N92-28292
Aviation noise: Costs of phasing out noisy aircraft
[GAO/RCED-91-128] p 1011 N92-31454
Pilot noise exposure during a Boeing 747-400 round trip: Judgement of noise and analysis in respect to hearing impairment of pilots p 1138 N92-32961
Building vibrations induced by noise from rotorcraft and propeller aircraft flyovers
[NASA-TM-104170] p 1138 N92-33160
Application of magnitude estimation scaling to the assessment of subjective loudness response to simulated sonic booms
[NASA-TM-107657] p 1138 N92-33719
Advanced subsonic transport approach noise: The relative contribution of airframe noise
[NASA-TM-104112] p 1140 N92-34148

NOISE MEASUREMENT
A neural network for the identification of measured helicopter noise p 162 A92-14387
Review on the abatement of helicopter noise
p 406 A92-25501
A technique for quantitatively measuring microstructurally induced ultrasonic noise
p 510 A92-28720
Noise generated by wind turbines p 686 A92-39045
Mechanical noise from large wind turbines - Experiences from Swedish prototypes p 686 A92-39046
Aircraft noise - The calculation of the noise exposure by aircraft in the Netherlands p 687 A92-39054
A noise survey around Oslo Airport Fornebu
p 687 A92-39061
Do we really need 57 ways of rating aircraft noise?
p 688 A92-39065
Azimuthal noise characteristics of contra-rotating propellers - Results of a wind tunnel model test
p 693 A92-39066
A mobile system for measuring airport noise
p 688 A92-39099
Temporal change of noisiness of helicopter noise
p 689 A92-39103
New methods to determine the transmission loss of partitions using sound intensity measurements
p 924 A92-45879
Flyover-noise measurement and prediction
p 236 N92-14786
Detailed noise measurements on the SR-7A propeller: Tone behavior with helical tip Mach number
[NASA-TM-105206] p 304 N92-16705
Sonic booms produced by US Air Force and US Navy aircraft: Measured data
[AD-A244804] p 512 N92-21719

Analysis of measured environmental noise levels: An assessment of the effects of airbase operational model variables on predicted noise exposure levels
[AD-A244805] p 485 N92-21720
Propeller noise research at NRC p 628 N92-24863
Steady-state acoustical noise measurements in aviation systems
[AD-A247831] p 780 N92-27924
Operational noise data for OH-58D Army helicopters
[AD-A246822] p 926 N92-28292
Fourth Aircraft Interior Noise Workshop
[NASA-CP-10103] p 1136 N92-32948
Use of SEA to predict structure-borne noise in aircraft
p 1137 N92-32955
Advanced Study for Active Noise Control in Aircraft (ASANCA)
[AIAA PAPER 92-2092] p 1137 N92-32956
Pilots noise exposure during a Boeing 747-400 round trip: Ambient noise and acoustic-head recording and analysis of data p 1137 N92-32960
Pilot noise exposure during a Boeing 747-400 round trip: Judgement of noise and analysis in respect to hearing impairment of pilots p 1138 N92-32961
Feasibility of measuring transverse electric noise at VLF and LF on an ice cap
[AD-A252280] p 1129 N92-33220
Implementation of a personal computer based parameter estimation program
[AD-A252914] p 1061 N92-33502

NOISE POLLUTION
Helicopter/heliport operations - Environmental implications p 241 A92-22708
The price of success - Mitigation and litigation in airport growth p 417 A92-27450
Noise from turbine generators - Noise control, propagation, and assessment p 686 A92-39044
Noise generated by wind turbines p 686 A92-39045
NATO CCMS aircraft noise study on receiver technology p 686 A92-39050
Noisemap 6.0 - The USAF microcomputer program for airport noise analysis p 686 A92-39051
Noise from military airfields in the United Kingdom
p 686 A92-39052
Do we really need 57 ways of rating aircraft noise?
p 688 A92-39065
A mobile system for measuring airport noise
p 688 A92-39099
NSBIT program - Development of assessment system for aircraft noise and research on human impacts due to aircraft noise p 688 A92-39100
A model for the effects of aircraft overflight noise on the reproductive success of raptorial birds
p 688 A92-39101
Trading number of operations versus loudness of aircraft p 688 A92-39102
Some experiences with community response to low levels of aircraft noise p 689 A92-39235
Effects of military training route noise on human annoyance p 689 A92-39237
Annoyance from aircraft overflights in wilderness
p 689 A92-39239
Relating the annoyance of aircraft overflights to their audibility by outdoor recreationists p 689 A92-39240
Research and studies on quiet helicopters
[ONERA, TP NO. 1992-59] p 926 A92-48618
Sonic boom p 55 N92-10608
Flyover-noise measurement and prediction
p 236 N92-14786
Reducing environmental noise impacts: A USAREUR noise management program handbook
[AD-A240797] p 237 N92-14791
The atmospheric effects of stratospheric aircraft: A first program report
[NASA-RP-1272] p 408 N92-19121
The environmental challenges for the next supersonic aircraft
[PNR-90782] p 505 N92-20928
Environmentally sound
[PNR-90776] p 506 N92-21743
High speed civil transport p 649 N92-25919

NOISE PREDICTION
Prediction of high-resolution flowfields for rotorcraft aeroacoustics p 53 A92-11053
Development of a shock noise prediction code for high-speed helicopters - The subsonically moving shock
p 165 A92-14384
Acoustic predictions using measured pressures from a model rotor in the DNW p 165 A92-14385
Computation of the BVI noise for the BO105 Model Rotor in forward flight and comparison with wind tunnel tests
p 165 A92-14386
Propeller and propfan noise p 54 N92-10599
Prediction of noise field of a propfan at angle of attack
[NASA-CR-189047] p 166 N92-13759
Aeroacoustics of flight vehicles: Theory and practice. Volume 2: Noise control
[NASA-RP-1258-VOL-2] p 235 N92-14779
The application of experimental data to blade wake interaction noise prediction
[NASA-CR-189461] p 237 N92-14789
Prediction of far-field harmonic noise from propellers
[ESDU-91033] p 416 N92-18074
Fourth Aircraft Interior Noise Workshop
[NASA-CP-10103] p 1136 N92-32948

NOISE PREDICTION (AIRCRAFT)
Acoustic isolation of layers p 54 A92-12345
Theoretical study and prediction of BVI noise including close interactions
[ONERA, TP NO. 1991-174] p 165 A92-16138
Importance of an accurate prediction of shock curvature for high-speed rotor noise p 414 A92-25578
A survey of the broadband shock associated noise prediction methods
[AIAA PAPER 92-0501] p 415 A92-26930
Broadband shock associated noise from supersonic jets measured by a ground observer
[AIAA PAPER 92-0502] p 416 A92-26931
NASA's quiet side. I p 607 A92-37875
Noise from military airfields in the United Kingdom
p 686 A92-39052
Comparison of aircraft noise indices for noise zoning at military airfields p 687 A92-39056
DANSIM applications - Development of airport noise reduction strategies and environmental policy
p 687 A92-39057
Calculation of aircraft noise contours taking into account the lateral flight track dispersion p 687 A92-39059
Advanced method for single event aircraft noise analysis p 693 A92-39060
Propeller aircraft interior noise - Physical background and possible treatments p 642 A92-39082
Propeller sound excitation on an aircraft fuselage using a loudspeaker ring p 643 A92-39087
Noise inside aircraft fuselages subjected to airborne excitation p 643 A92-39089
NSBIT program - Development of assessment system for aircraft noise and research on human impacts due to aircraft noise p 688 A92-39100
Active control of structurally-coupled sound fields generated by localized force inputs p 694 A92-39106
Helicopter far-field acoustic levels as a function of reduced rotor speeds p 695 A92-39228
A review of computational/experimental methodology developments in aeroacoustics p 695 A92-39241
The development of multiple-input models for airborne noise prediction p 695 A92-39243
High-speed propeller noise prediction - A multidisciplinary approach p 924 A92-45831
Noise of two high-speed model counter-rotation propellers at takeoff/approach conditions
p 925 A92-46799
Basic experiments on the directivity of the sound radiation emitted by a turboshaft engine
[ONERA, TP NO. 1992-36] p 926 A92-48597
Research and studies on quiet helicopters
[ONERA, TP NO. 1992-59] p 926 A92-48618
The engineering prediction for aircraft noise
p 1010 A92-50206
Broadband shock associated noise from supersonic jets measured by a ground observer p 1135 A92-54909
A calculation method to predict helicopter noise and its verification p 1135 A92-56074
Path identification in structural acoustics
p 1059 A92-56346
Helicopter main-rotor speed effects: A comparison of predicted ranges of detection from the aural detection program ICHIN and the electronic detection program ARCAS
[NASA-TM-104134] p 166 N92-12598
Flyover-noise measurement and prediction
p 236 N92-14786
Quiet aircraft design and operational characteristics
p 236 N92-14787
A survey of the broadband shock associated noise prediction methods
[NASA-TM-105365] p 237 N92-14797
The solution of a singular integral equation arising from a lifting surface theory for rotating blades
p 260 N92-17303
An introduction to high speed aircraft noise prediction
[NASA-CR-189582] p 416 N92-19672
Analysis of measured environmental noise levels: An assessment of the effects of airbase operational model variables on predicted noise exposure levels
[AD-A244805] p 485 N92-21720
Interior noise prediction methodology: ATDAC theory and validation
[NASA-CR-187626] p 697 N92-25368
Jet aircraft noise at high subsonic flight Mach numbers
[DLR-FB-91-28] p 928 N92-29997
High speed turboprop aeroacoustic study (counterrotation). Volume 2: Computer programs
[NASA-CR-185242] p 1011 N92-31248
Acoustic loads prediction on jet aircraft
p 1136 N92-32949
MD-80 aft cabin noise control: A case history
p 1137 N92-32950
Vibro-acoustic FE analyses of the Saab 2000 aircraft
p 1137 N92-32952
Use of SEA to predict structure-borne noise in aircraft
p 1137 N92-32955
Advanced Study for Active Noise Control in Aircraft (ASANCA)
[AIAA PAPER 92-2092] p 1137 N92-32956
Advanced subsonic transport approach noise: The relative contribution of airframe noise
[NASA-TM-104112] p 1140 N92-34148

NOISE PROPAGATION
Determination of aircraft noise levels while the engine is running on the ground - An approach from the point of urbanization and architecture p 688 A92-39064
Study model for the reduction of noise through double wall cylindrical shells - Comparison with experimentation
p 694 A92-39088
Structure-borne noise transmission in the Propfan Test Assessment aircraft p 778 A92-41240
Path identification in structural acoustics
p 1059 A92-56346
Aeroacoustics of flight vehicles: Theory and practice. Volume 2: Noise control
[NASA-RP-1258-VOL-2] p 235 N92-14779
Theoretical models for duct acoustic propagation and radiation p 236 N92-14782
Interior noise p 236 N92-14785
Flyover-noise measurement and prediction
p 236 N92-14786
Use of SEA to predict structure-borne noise in aircraft
p 1137 N92-32955

NOISE REDUCTION
Acoustic isolation of layers p 54 A92-12345
A low noise propulsion concept for the supersonic transport
[ASME PAPER 91-GT-397] p 127 A92-15727
NASA research program directed at reducing supersonic transport noise p 61 A92-16150
Dornier Do 328 - A start in the world market
p 113 A92-17093
Interior noise reduction program for the Dornier 328
p 114 A92-17254
Cabin structural vibration and noise for transport aircraft p 192 A92-17876
Noise control used for turbojet engine test bench
p 284 A92-21749
Helicopter/heliport operations - Environmental implications p 241 A92-22708
Review on the abatement of helicopter noise
p 406 A92-25501
Combat aircraft jet engine noise studies
[ONERA, TP NO. 1991-192] p 415 A92-26353
The price of success - Mitigation and litigation in airport growth p 417 A92-27450
Improved noise rejection in automatic carrier landing systems p 380 A92-28154
Reducing the background noise level in the test section of a wind tunnel for transonic flow velocities
p 511 A92-30143
Active noise reduction p 603 A92-32980
Noise level reduction inside helicopter cabins
p 545 A92-35733
Generalized higher harmonic control - Ten years of Aerospatiale experience p 569 A92-35769
Rotor blade-vortex interaction noise reduction and vibration using higher harmonic control
p 604 A92-35778
The quiet STOL research aircraft ASUKA
p 642 A92-38206
Noise from turbine generators - Noise control, propagation, and assessment p 686 A92-39044
NATO CCMS aircraft noise study on receiver technology p 686 A92-39050
DANSIM applications - Development of airport noise reduction strategies and environmental policy
p 687 A92-39057
Theoretical and experimental methods in acoustics of ducts and mufflers - A critical review
p 693 A92-39068
Propeller aircraft interior noise - Physical background and possible treatments p 642 A92-39082
Summary of Dornier 328 interior noise control study
p 643 A92-39083
Study model for the reduction of noise through double wall cylindrical shells - Comparison with experimentation
p 694 A92-39088

Noise inside aircraft fuselages subjected to airborne excitation p 643 A92-39089
Trading number of operations versus loudness of aircraft p 688 A92-39102
Active control of structurally-coupled sound fields generated by localized force inputs p 694 A92-39106
Active control of airborne noise transmitted through a ribbed panel p 695 A92-39111
NOISE-CON 90; Proceedings of the 10th National Conference on Noise Control Engineering, University of Texas, Austin, Oct. 15-17, 1990
[ISBN 0-931784-21-2] p 695 A92-39226
Loudness of shaped sonic booms p 695 A92-39238
Noise abatement procedures vs. safety
[SAE PAPER 912137] p 635 A92-39977
1991-92 AHS Technical Committee highlights - Acoustics p 696 A92-40390
A perspective on helicopter noise p 780 A92-43160
New methods to determine the transmission loss of partitions using sound intensity measurements p 924 A92-45879
Solutions of acoustic field problems using parallel computers p 925 A92-45929
Gas turbine exhaust system silencing design p 882 A92-47365
Research and studies on quiet helicopters
[ONERA, TP NO. 1992-59] p 926 A92-48618
Advanced Rotorcraft Transmission (ART) Program summary
[AIAA PAPER 92-3365] p 905 A92-48938
Progress towards quieter civil helicopters p 1011 A92-52847
Silent solutions --- noise suppression for Stage 3 corporate fleets p 970 A92-53120
Summary highlights of the Advanced Rotorcraft Transmission (ART) program
[AIAA PAPER 92-3362] p 1051 A92-54026
Full Navier-Stokes analysis of a two-dimensional mixer/ejector nozzle for noise suppression
[AIAA PAPER 92-3570] p 1067 A92-54059
Experimental study of noise generation and propagation in a turbofan model p 1136 A92-56169
BVI impulsive noise reduction by higher harmonic pitch control - Results of a scaled model rotor experiment in the DNW p 1136 A92-56344
A quiet-flow Ludwieg tube for experimental study of high speed boundary layer transition
[AIAA PAPER 92-3885] p 1094 A92-56727
Aeroacoustics of flight vehicles: Theory and practice. Volume 1: Noise sources
[NASA-RP-1258-VOL-1] p 54 N92-10598
Propeller and propfan noise p 54 N92-10599
Rotor noise p 54 N92-10600
Jet noise classical theory and experiments p 54 N92-10602
Airframe noise p 55 N92-10605
Sonic boom p 55 N92-10608
Helicopter main-rotor speed effects: A comparison of predicted ranges of detection from the aural detection program ICHIN and the electronic detection program ARCAS
[NASA-TM-104134] p 166 N92-12598
Development and testing of cabin sidewall acoustic resonators for the reduction of cabin tone levels in propfan-powered aircraft
[NASA-CR-4388] p 166 N92-13757
Aeroacoustics of flight vehicles: Theory and practice. Volume 2: Noise control
[NASA-RP-1258-VOL-2] p 235 N92-14779
Design and performance of duct acoustic treatment p 236 N92-14783
Jet noise suppression p 236 N92-14784
Interior noise p 236 N92-14785
Direct computation of turbulence and noise
[NASA-CR-187616] p 236 N92-14788
Reducing environmental noise impacts: A USAREUR noise management program handbook
[AD-A240797] p 237 N92-14791
Propeller-driven-small airplane noise certification
[LR-650] p 237 N92-14798
Approximation methods for control of acoustic/structure models with piezoceramic actuators
[NASA-CR-189578] p 234 N92-15658
An evaluation of some alternative approaches for reducing fan tone noise
[NASA-TM-105356] p 416 N92-18282
Re-engining appears to offer best payback for young: Chapter 2 compliant aircraft
[PNR-90848] p 378 N92-19939
The impact of aircraft noise control technology
[PNR-90846] p 512 N92-20461
Analysis of rotor vibratory loads using higher harmonic pitch control
[NASA-CR-189591] p 696 N92-24251
Advanced Rotorcraft Transmission (ART) program summary
[NASA-TM-105665] p 680 N92-24984
Active noise control: Piezoceramic actuators in fluid/structure interaction models
[NASA-CR-190328] p 685 N92-26125
Full Navier-Stokes analysis of a two-dimensional mixer/ejector nozzle for noise suppression
[NASA-TM-105715] p 868 N92-28419
Jet aircraft noise at high subsonic flight Mach numbers
[DLR-FB-91-28] p 928 N92-29997
Aviation noise: Costs of phasing out noisy aircraft
[GAO/RCED-91-128] p 1011 N92-31454
Fourth Aircraft Interior Noise Workshop
[NASA-CP-10103] p 1136 N92-32948
MD-80 aft cabin noise control: A case history p 1137 N92-32950
The Dornier 328 Acoustic Test Cell (ATC) for interior noise tests and selected test results
[AIAA PAPER 92-2164] p 1137 N92-32951
Vibro-acoustic FE analyses of the Saab 2000 aircraft p 1137 N92-32952
Advanced Study for Active Noise Control in Aircraft (ASANCA)
[AIAA PAPER 92-2092] p 1137 N92-32956
Active control of interior noise in a large scale cylinder using piezoelectric actuators p 1137 N92-32958
Pilots noise exposure during a Boeing 747-400 round trip: Ambient noise and acoustic-head recording and analysis of data p 1137 N92-32960
Pilot noise exposure during a Boeing 747-400 round trip: Judgement of noise and analysis in respect to hearing impairment of pilots p 1138 N92-32961
Active vibrations and noise control for turboprop application research program activities p 1138 N92-32962
Active synchrophasing of propeller unbalance p 1138 N92-32963
A lightweight loudspeaker for aircraft communications and active noise control p 1125 N92-32964
Re-engining for real stage 3 compliance
[PNR-90872] p 1072 N92-33748
Impacts of technology on the capacity needs of the US national airspace system
[NASA-CR-4470] p 1045 N92-34192

NOISE SPECTRA

Noise generated by wind turbines p 686 A92-39045
Mechanical noise from large wind turbines - Experiences from Swedish prototypes p 686 A92-39046
Advanced method for single event aircraft noise analysis p 693 A92-39060
Sonic fatigue analysis and anti-sonic fatigue design of aircraft structure p 848 A92-47666
Development of an annoyance model based upon elementary auditory sensations for steady-state aircraft interior noise containing tonal components
[NASA-TM-104147] p 166 N92-13758
Direct computation of turbulence and noise
[NASA-CR-187616] p 236 N92-14788
An introduction to high speed aircraft noise prediction
[NASA-CR-189582] p 416 N92-19672
Operational noise data for OH-58D Army helicopters
[AD-A246822] p 926 N92-28292

NOISE THRESHOLD

Helicopter main-rotor speed effects: A comparison of predicted ranges of detection from the aural detection program ICHIN and the electronic detection program ARCAS
[NASA-TM-104134] p 166 N92-12598

NOISE TOLERANCE

NSBIT program - Development of assessment system for aircraft noise and research on human impacts due to aircraft noise p 688 A92-39100
A model for the effects of aircraft overflight noise on the reproductive success of raptorial birds p 688 A92-39101
Some experiences with community response to low levels of aircraft noise p 689 A92-39235
Aircraft noise and the elderly p 689 A92-39236
Effects of military training route noise on human annoyance p 689 A92-39237
Human response to aircraft noise p 236 N92-14780
Human response to helicopter noise: A test of A-weighting
[AD-A243719] p 304 N92-17506
Application of magnitude estimation scaling to the assessment of subjective loudness response to simulated sonic booms
[NASA-TM-107657] p 1138 N92-33719

NONADIABATIC CONDITIONS

Nonadiabatic and three-dimensional effects in compressible turbulent boundary layers p 431 A92-31156

NONCONSERVATIVE FORCES

Experimental investigations of exciting forces caused by flow in labyrinth seals p 223 N92-14354

NONDESTRUCTIVE TESTS

X-ray computed tomography of composites p 36 A92-10143
The INFO-ROC technique - A method for comparing and optimizing inspection systems p 144 A92-13563
Inspection of compressor discs by ultrasonic leaky waves using an automated C-scan system p 144 A92-13584
Stationary neutron radiography system p 144 A92-13589
Eddy current imaging of aircraft using real time image signal processing p 144 A92-13594
Damage assessment for composite smart structures p 140 A92-13601
Nondestructive depth profiling of the protective coating on a turbine blade p 144 A92-13641
The aging aircraft fleet - A challenge for nondestructive inspection p 145 A92-13657
Combination of different unsteady quantity measurements for gas turbine blade fault diagnosis
[ASME PAPER 91-GT-201] p 149 A92-15624
NDE of advanced turbine engine components and materials by computed tomography
[ASME PAPER 91-GT-287] p 152 A92-15681
The use of NDE as a process development tool for ceramic engine components
[ASME PAPER 91-GT-290] p 152 A92-15682
Nondestructive testing developments in the aircraft industry p 214 A92-17288
Real-time microfocus radiography for electronic failure analysis p 214 A92-17289
Enhanced visual technique for rapid inspection of aircraft structures p 214 A92-17290
Rapid ultrasonic scanning of aircraft structures p 215 A92-17292
ASNT and aerospace - What about the next 50 years? p 215 A92-17293
National research program for nondestructive inspection of aging aircraft p 169 A92-17294
Historical development of eddy current testing in aircraft maintenance p 292 A92-21900
Ultimate strength prediction of ASTM D - 3039 tensile specimens from acoustic emission amplitude data
[AIAA PAPER 92-0258] p 394 A92-25716
Evolving partnership for NDE in materials engineering and extended life cycle performance p 490 A92-28556
New developments in the computer simulation of X-ray nondestructive evaluation process p 490 A92-28588
A new method to estimate the effective geometric focal length and radius of ultrasonic focused probes p 490 A92-28633
Thermal imaging of graphite/epoxy composite samples with fabricated defects p 491 A92-28655
Smart structures - A damage detection concept p 491 A92-28672
Numerical comparison of experimentally measured ultrasound through a multilayered specimen p 510 A92-28682
Characterization of diffusion bonds using an acoustic microscope p 491 A92-28686
Ultrasonic NDE for ceramic- and metal-matrix composite material characterization p 491 A92-28690
X-ray computed tomographic inspection of castings p 492 A92-28725
Acoustic emission monitoring of a ground durability and damage tolerance test --- for aircraft structures p 492 A92-28737
Nortec 30 Eddyscan - Portable flaw imaging for aging aircraft p 492 A92-28745
Neutron radiography with SNRS p 492 A92-28747
An advanced neutron radiography system p 492 A92-28748
X-ray computed tomography for the aircraft/aerospace industry p 492 A92-28750
Seeing beneath the surface with NDE p 671 A92-36948
Materials and structures for Hermes p 666 A92-38213
Inspection of composite structures p 676 A92-40882
Repair operation on a composite material structure p 700 A92-43153
Magnetic particle testing of turbine blades mounted on the turbine rotor shaft p 898 A92-46498
Application of X-ray image radiography system for aircraft p 1118 A92-56084
Development of aircraft bonded structure and the NDI method p 1016 A92-56100
Computed tomography (CT) as a nondestructive test method used for composite helicopter components p 1121 A92-56276

Repair procedures for advanced composites for helicopters p 1016 A92-56277
Robotic non-destructive inspection of aircraft, phase 1
[AD-A240777] p 44 N92-11367
Aging Aircraft NDI Development and Demonstration Center (AANC): An overview
[DE92-002358] p 241 N92-15962
Laser based, non-intrusive measurement system for analysis of jet engine flows
[AD-A242398] p 279 N92-17011
Large area QNDE inspection for airframe integrity p 362 N92-18588
Development of an electromagnetic microscope for eddy current evaluation of materials
[AD-A242007] p 406 N92-19873
Computered tomography: Experimental data acquisition and parallelization of reconstruction algorithm
[DE92-005151] p 499 N92-20301
Metal-metal bondline NDE methods
[AD-A244429] p 503 N92-21730
Inspection of aircraft engine components using automated eddy current and pattern recognition techniques
[NRC-LTR-ST-1834] p 504 N92-22029
A preliminary study on damage detection using piezoelectric film
[AD-A246350] p 733 N92-28118
Diffuser casing upgrade for an advanced turbofan
[NLR-TP-90097-U] p 870 N92-28711
Computed Tomography (CT) as a nondestructive test method used for composite helicopter components
[MBB-UD-0603-91-PUB] p 910 N92-29873
Repair procedures for advanced composites for helicopters
[MBB-UD-0606-91-PUB] p 787 N92-29874
The 1991 International Conference on Aging Aircraft and Structural Airworthiness
[NASA-CP-3160] p 912 N92-30106
Federal Aviation Administration aging aircraft nondestructive inspection research plan p 914 N92-30116
Inspection of aging aircraft: A manufacturer's perspective p 914 N92-30117
Thermal QNDE detection of airframe disbonds p 914 N92-30118
NDE research efforts at the FAA Center for Aviation Systems Reliability p 914 N92-30119
Aging aircraft NDI Development and Demonstration Center (AANC): An overview --- nondestructive inspection p 915 N92-30120
Nondestructive inspection perspectives p 915 N92-30121
Current and future developments in civil aircraft non-destructive evaluation from an operator's point of view p 787 N92-30122
Ageing airplane repair assessment program for Airbus A300 p 838 N92-30123
Transport Canada aging aircraft activities p 838 N92-30131
Current nondestructive inspection methods for aging aircraft
[DOT/FAA/CT-91/5] p 1126 N92-33480
Inspection of fabricated fuselage panels using electronic shearography
[DOT/FAA/CT-TN92/26] p 1127 N92-33627

NONEQUILIBRIUM CONDITIONS
Thermochemical nonequilibrium and radiative interactions in supersonic hydrogen-air combustion
[AIAA PAPER 92-0340] p 394 A92-25786
Analysis of thermo-chemical nonequilibrium models for carbon dioxide flows
[AIAA PAPER 92-2852] p 892 A92-47835
Numerical simulation of thermochemical non-equilibrium viscous flows around reentry bodies p 227 N92-15029

NONEQUILIBRIUM FLOW
Nonequilibrium hypersonic inviscid steady flows p 176 A92-20737
Nonequilibrium algebraic turbulence modeling considerations for transonic airfoils and wings
[AIAA PAPER 92-0026] p 248 A92-22148
Improved nonequilibrium viscous shock-layer scheme for hypersonic blunt-body flowfields p 310 A92-24653
Analysis of hypersonic nozzles including vibrational nonequilibrium and intermolecular force effects
[AIAA PAPER 92-0330] p 322 A92-25777
An approximate viscous shock layer technique for calculating nonequilibrium hypersonic flows about blunt-nosed bodies
[AIAA PAPER 92-0498] p 329 A92-26326
New nonequilibrium turbulence model for calculating flows over airfoils p 330 A92-26403
An iodine hypersonic wind tunnel for the study of nonequilibrium reacting flows
[AIAA PAPER 92-0566] p 383 A92-26974
Plasmadynamic effects in thermochemical nonequilibrium aerobrake flows
[AIAA PAPER 92-0573] p 333 A92-26980
Calculation of real-gas effects on blunt-body trim angles p 432 A92-31169
Determination of physicochemical constant in the wake of a body from ballistic experiments p 609 A92-36549
Vibrational relaxation effects in hypersonic flows of a viscous gas p 609 A92-36550
Non-equilibrium hypersonic flow simulations using the second-order boundary layer equations p 612 A92-37551
Plasmadynamic effects in thermochemical nonequilibrium aerobrake flows p 705 A92-41538
Hypersonic plasma predictions at nonzero angle of attack
[AIAA PAPER 92-3027] p 925 A92-47028
Calculation of hypersonic, viscous, non-equilibrium flows around reentry bodies using a coupled boundary layer/Euler method
[AIAA PAPER 92-2856] p 819 A92-47839
Computation of hypersonic flowfields in thermal and chemical nonequilibrium
[AIAA PAPER 92-2874] p 819 A92-47856
Computation of 3-D hypersonic flows in chemical non-equilibrium including transport phenomena
[AIAA PAPER 92-2876] p 820 A92-47858
Numerical simulation of chemical and thermal nonequilibrium flows behind compression shocks
[AIAA PAPER 92-2879] p 820 A92-47860
Similarity relations for calculating three-dimensional chemically nonequilibrium viscous flows p 827 A92-49188
Thermal and chemical nonequilibrium viscous shock layer flows over a blunt body at high altitudes p 938 A92-52749
Thermally and chemically nonequilibrium hypersonic flow in three-dimensional geometry p 1019 A92-53580
A code validation strategy and facility for nonequilibrium, reacting flows
[AIAA PAPER 92-3970] p 1098 A92-56796
Aerodynamic heating on AFE due to nonequilibrium flow with variable entropy at boundary layer edge p 183 N92-15020
Numerical simulation of thermochemical non-equilibrium viscous flows around reentry bodies p 227 N92-15029
Thermal nonequilibrium effects on turbine cascade aerodynamics
[AD-A244049] p 404 N92-19183
Modelling of chemical and physical effects with respect to flows around reentry bodies
[MBB-FE-211/S/PUB/0465/A] p 347 N92-19296
Perspectives on hypersonic viscous and nonequilibrium flow research
[NASA-CR-190817] p 1039 N92-33413

NONEQUILIBRIUM RADIATION
Aerothermodynamic radiation studies
[NASA-CR-185666] p 284 N92-15998

NONEQUILIBRIUM THERMODYNAMICS
A unified nonequilibrium model for hypersonic flows p 3 A92-10575
Characteristic-based algorithms for flows in thermochemical nonequilibrium p 670 A92-36846
Thermochemical nonequilibrium flow computations of flow around the aeroassist flight experiment p 713 A92-44368
Linear acoustics in gas mixtures with rate processes p 238 N92-15013
Hypersonic viscous shock layer in thermochemical nonequilibrium p 183 N92-15014
Aerothermodynamic radiation studies
[NASA-CR-185666] p 284 N92-15998

NONISENTROPICITY
Finite element method for computing nonisentropic potential transonic flow with shock waves p 312 A92-25009

NONISOTHERMAL PROCESSES
On thermal-stress gas flows p 37 A92-10657

NONLINEAR EQUATIONS
Gain-scheduled control of nonlinear partial differential equations p 47 A92-11347
Derivation of aircraft linear state equations from implicit nonlinear equations p 27 A92-11361
Nonlinear control of a twin-lift helicopter configuration p 204 A92-18624
A Lyapunov based nonlinear control scheme for stabilizing a basic compression system using a close-coupled control valve p 508 A92-29316
A second-order control optimization method for nonlinear dynamic systems and its use for calculating optimal aircraft trajectories p 460 A92-31894
Nonlinear control law with application to high angle-of-attack flight p 661 A92-39904
A restructurable flight control system design using nonlinear compensation p 745 A92-43184
A complete boundary integral formulation for steady compressible inviscid flows governed by nonlinear equations p 934 A92-50211
Nonlinear dynamic stability characteristics of recovery bodies p 977 A92-52041
Application of restructurable flight control system using nonlinear control to an airliner p 1084 A92-56068
A numerical solution of implicit nonlinear equations of motion for rotor blades p 115 N92-13053
Critical problems of computational aeroacoustics p 167 N92-13857
Periodic trim solutions with HP-version finite elements in time
[NASA-CR-189778] p 282 N92-17019
Performance and stability analysis of the non-linear dynamics of a simple powered lifting hypersonic vehicle flying on a minor circle
[AD-A243933] p 366 N92-19192
User's manual for AeroFcn: A FORTRAN program to compute aerodynamic parameters
[NASA-TM-104237] p 1133 N92-32507

NONLINEAR FEEDBACK
Gain-scheduled control of nonlinear partial differential equations p 47 A92-11347
Retrospective essay on nonlinearities in aircraft flight control p 204 A92-18601
Nonlinear model-following control application to airplane control (1992 AIAA Controls Design Challenge)
[AIAA PAPER 92-4625] p 1077 A92-55302
Application of nonlinear QFT to flight control design for high angle of attack maneuvers with thrust vectoring
[AD-A243821] p 381 N92-19241
Application of nonlinear feedback control theory to supermaneuverable aircraft
[NASA-CR-190336] p 663 N92-25648

NONLINEAR FILTERS
Nonlinear aircraft tracking filter utilizing control variable estimation p 302 A92-21179

NONLINEAR PROGRAMMING
Simple formulae for optimal solidity of two-dimensional compressor cascades based on diffusion concept
[ASME PAPER 91-GT-308] p 126 A92-15687
Integrated aeroservoelastic wing synthesis by nonlinear programming/approximation concepts p 873 A92-46752
A general approach to optimal real-time guidance of dynamic systems based on nonlinear programming
[AIAA PAPER 92-4378] p 1131 A92-55182

NONLINEAR SYSTEMS
State feedback for nonlinear continuous-time systems - Stabilization and the creation of invariant subspaces p 52 A92-11587
Dynamic characterization and identification of nonlinear systems application to aeronautical structures p 39 A92-11830
Regulation of relaxed static stability aircraft p 203 A92-18463
Identification of aerodynamic effectiveness and interference effects of direct-lift-control flaps from flight data
[AIAA PAPER 92-0171] p 271 A92-23782
Robust adaptive nonlinear control of high performance aircraft p 478 A92-29188
The generalized normal forms and method of resonance control of nonlinear dynamical systems p 507 A92-29189
A system identification model for adaptive nonlinear control p 508 A92-29248
Synthesis of robust nonlinear autopilots using differential game theory p 478 A92-29330
Robustness of control systems with nonlinear parametric correction for certain types of perturbations p 509 A92-30311
Determining design gust loads for nonlinear aircraft similarity between methods based on matched filter theory and on stochastic simulation
[AIAA PAPER 92-2369] p 518 A92-34597
A general gust and maneuver load analysis method to account for the effects of active control saturation and nonlinear aerodynamics
[AIAA PAPER 92-2126] p 567 A92-35693
On the choice of appropriate bases for nonlinear dynamic modal analysis p 847 A92-46927
Nonlinear control design for slightly nonminimum phase systems - Application to V/STOL aircraft p 876 A92-48160
Preliminary assessment of the robustness of dynamic inversion based flight control laws
[AIAA PAPER 92-4330] p 1074 A92-55174
G-Field Control of nonlinear systems
[AIAA PAPER 92-4555] p 1131 A92-55267
Helicopter nonlinear flight control system development p 1085 A92-56317

Parameter identification for nonlinear aerodynamic systems
[NASA-CR-188985] p 53 N92-10347
An aircraft model for the AIAA controls design challenge
[NASA-CR-186019] p 117 N92-13064
Formulation of the linear model from the nonlinear simulation for the F18 HARV p 117 N92-13842
Nonlinear rotordynamics analysis --- Space Shuttle Main Engine turbopumps
[NASA-CR-184263] p 221 N92-14344
The 3D inelastic analysis methods for hot section components
[NASA-CR-189089] p 402 N92-18971
Adaptive control of nonlinear systems with applications to the control of flexible robot arms
[AD-A244409] p 413 N92-19397
Nonlinear stability and control study of highly maneuverable high performance aircraft, phase 2
[NASA-CR-189911] p 382 N92-19841
Identification of aerodynamic coefficients using computational neural networks
[AD-A244711] p 447 N92-21753
Helicopter rotor blade dynamics with bilinear formulation p 463 N92-21856
A hierarchy for modeling high speed propulsion systems p 559 N92-22492
Advanced techniques in current signature analysis
[DE92-007680] p 679 N92-24892
Studies in chaos using stochastic methods
[AD-A246919] p 780 N92-27171
Parameter identification for nonlinear aerodynamic systems
[NASA-CR-190264] p 830 N92-29329
Nonlinear system design: Adaptive feedback linearization with unmodeled dynamics
[AD-A248484] p 1009 N92-30335
Acoustic fatigue life prediction for nonlinear structures with multiple resonant modes
[NASA-CR-190471] p 1000 N92-30988
Thermal mechanical analysis of sprag clutches
[NASA-CR-190686] p 1128 N92-34207

NONLINEARITY
Optical measurements of unducted fan flutter
[ASME PAPER 91-GT-19] p 147 A92-15510
On the nonlinear stability of a high-speed, axisymmetric boundary layer p 78 A92-16457
Three-dimensional adaptive grid generation with applications in nonlinear fluid dynamics
[AIAA PAPER 92-0661] p 397 A92-27032
Effects of T-tabs and large deflections in double cantilever beam specimen tests p 673 A92-39009
Engine dynamic analysis with general nonlinear finite element codes
[NASA-CR-187222] p 44 N92-11379
Nonlinear aspects of aerospace structures at high excitation levels flat aluminum beams and plates studied
[AD-A240600] p 44 N92-11383
Detailed analysis and test correlation of a stiffened composite wing panel
[NASA-TM-104154] p 159 N92-13460
Identification techniques: Frequency domain methods p 273 N92-17158
Non-linear airloads hypersurface representation: A time domain perspective p 346 N92-18783
A weakly nonlinear theory for wave-vortex interactions in curved channel flow
[NASA-TP-3158] p 347 N92-19175
Application of nonlinear QFT to flight control design for high angle of attack maneuvers with thrust vectoring
[AD-A243821] p 381 N92-19241
Nonliner aspects of transonic aeroelasticity p 628 N92-24864
Recent applications of linear and nonlinear unsteady aerodynamics for aeroelastic analysis p 718 N92-27940
Nonlinear normal and axial force indicial responses for a two dimensional airfoil
[AD-A247196] p 830 N92-28888
Non-linear interactions in homogeneous turbulence with and without background rotation p 912 N92-30044
Nonlinear analyses of composite aerospace structures in sonic fatigue
[NASA-CR-190565] p 854 N92-30209
Nonlinear stability and control study of highly maneuverable high performance aircraft, phase 2
[NASA-CR-190667] p 978 N92-30922
Nonlinear aerodynamics and the design of wing tips
[NASA-CR-190649] p 946 N92-31157
Preliminary subsonic aerodynamic model for simulation studies of the HL-20 lifting body
[NASA-TM-4302] p 978 N92-31175
Nonlinear dynamic-inversion flight control of supermaneuverable aircraft p 1062 N92-33953

NONUNIFORM FLOW
The aviation kerosene burning in the non-uniform air flow p 487 A92-29728
A circumferential non-uniform effect model for multistage axial-flow compressor throughflow p 588 A92-35572
Turbomachinery unsteady load predictions with nonuniform inflow p 611 A92-36972
Experimental technique of measuring fuel concentration in non-uniform flowfield p 734 A92-41928
Nonstationary viscous shock layer in supersonic motion over an inhomogeneity p 708 A92-42737
Whirl-flutter stability of a pusher configuration in nonuniform flow p 845 A92-46813
Effect of nonuniform entrance flow profile on hypersonic nozzle pitching moment
[AD-A244050] p 377 N92-19184
Inhomogeneous turbulence beyond spectral equilibria: Aeronautical applications
[ETN-92-90867] p 404 N92-19349

NORMAL DENSITY FUNCTIONS
Potential impact of GPS and automatic dependent surveillance on air lane separation in the North Atlantic Organized Track System p 99 A92-16935
MLS system error model identification and synthesis p 639 A92-40232
Example of statistical techniques applied to autoland touchdown dispersion (confidence intervals for normal and skew distributions)
[ESDU-91019] p 268 N92-17844
Statistical methods applicable to analysis of aircraft performance data
[ESDU-91017] p 359 N92-18096

NORMAL SHOCK WAVES
Flow unsteadiness by weak normal shock wave/turbulent boundary layer interaction in internal flow p 67 A92-15359
Confined normal-shock/turbulent-boundary-layer interaction followed by an adverse pressure gradient p 172 A92-18365
Experimental investigation of terminal shock sensors for mixed-compression inlets p 276 A92-21074
Experimental investigation of normal-shock/turbulent-boundary-layer interactions with and without mass removal p 330 A92-26411
A study of the interaction of a normal shock wave with a turbulent boundary layer at Mach numbers between 1.30 and 1.55 p 339 A92-28006
Multiple normal shock wave/turbulent boundary-layer interactions p 344 A92-28527
Solution of the Burnett equations for hypersonic flows near the continuum limit
[AIAA PAPER 92-2922] p 821 A92-47894

NOSE CONES
Effects of nose bluntness and angle of attack on slender bodies in hypersonic flows
[AIAA PAPER 92-0638] p 334 A92-27016
Combined effect of nose bluntness and angle of attack on slender bodies in viscous hypersonic flows
[AIAA PAPER 92-0755] p 436 A92-31680

NOSE FINS
Experimental investigation on turbulent phenomena in three-dimensional shock wave/turbulent boundary layer interaction induced by blunt fin p 1018 A92-53557

NOSE TIPS
Effects of tip Reynolds number and tip asymmetry on vortex wakes of axisymmetric bodies at various angles of attack
[AIAA PAPER 92-0406] p 324 A92-26259
Navier-Stokes computations for pointed, spherical, and flat tipped shell at Mach 3 p 705 A92-41536
Effect of a nose-boom on forebody vortex flow p 812 A92-46818

NOSE WHEELS
Shimmy of nose undercarriage wheels p 959 A92-51948

NOSES (FOREBODIES)
Fickle effect of nose microasymmetry on the high-alpha aerodynamics p 10 A92-13217
A method of calculation for the radius of curvature of the attached shock waves in front of a sharp-nosed axi-symmetrical body placed in a uniform stream p 243 A92-21319
Forebody vortex control with miniature, rotatable nose-boom strakes
[AIAA PAPER 92-0022] p 281 A92-22144
A study of flow past bodies of revolution with a *Riabushinskii generatrix* p 252 A92-23502
Study on effectiveness of the front wedge shape in hypersonic flow p 430 A92-30552
An experimental investigation of the effect of leading-edge extensions on directional stability and the effectiveness of forebody nose strakes
[AIAA PAPER 92-2715] p 802 A92-45554
Decoupled predictions of radiative heating in air using a particle simulation method
[AIAA PAPER 92-2971] p 816 A92-46986
Failure detection and fault management techniques for flush airdata sensing systems
[NASA-TM-4335] p 276 N92-17128
Analysis of the effects of removing nose ballast from the F-15 eagle
[AD-A244044] p 366 N92-19178
High speed research system study. Advanced flight deck configuration effects
[NASA-CR-189650] p 967 N92-30965

NOTCH SENSITIVITY
Failure analysis of the Apache mixer pivot support
[AD-A240858] p 116 N92-13061

NOTCH STRENGTH
Preliminary finite element analysis of unloaded and loaded notched composite laminated plates
[NRC-LTR-ST-1806] p 159 N92-13454

NOTCH TESTS
Short fatigue crack growth from blunt notches in an aero-engine alloy p 212 A92-19760
A comparison of fatigue life prediction methodologies for rotorcraft p 647 A92-40884

NOTCHES
Fatigue crack growth of small corner defects from blunt notches in an aeroengine alloy
[PNR-90860] p 1111 N92-34019

NOZZLE DESIGN
Computation of vectoring nozzle performance p 10 A92-13213
Development of an innovative high-temperature gas turbine fuel nozzle
[ASME PAPER 91-GT-36] p 121 A92-15519
Aerating fuel nozzle design influences on airflow features p 129 A92-17176
A quiet-flow Ludwieg tube for experimental study of high speed boundary layer transition
[AIAA PAPER 91-5026] p 207 A92-17819
Aerodynamic design of axisymmetric hypersonic wind-tunnel nozzles using least-squares/parabolized Navier-Stokes procedure
[AIAA PAPER 92-0332] p 322 A92-25779
Computation of supersonic jet mixing noise for an axisymmetric CD nozzle using k-epsilon turbulence model
[AIAA PAPER 92-0500] p 414 A92-26328
Laser-initiated conical detonation wave for supersonic combustion p 375 A92-28531
Supersonic nozzle mixer ejector p 376 A92-28536
Design considerations for nozzles of hypersonic airbreathing propulsion
[AIAA PAPER 91-5019] p 471 A92-31685
Commercial airplane air distribution system development through the use of computational fluid dynamics
[AIAA PAPER 92-0987] p 535 A92-33182
Nozzle design using generalized one-dimensional flow p 714 A92-44531
Effect of throat contouring on two-dimensional converging-diverging nozzles using URS method
[AIAA PAPER 92-2659] p 797 A92-45520
Comparative investigation of multiplane thrust vectoring nozzles
[AIAA PAPER 92-3263] p 864 A92-48858
CAN-DO, CFD-based Aerodynamic Nozzle Design and Optimization program for supersonic/hypersonic wind tunnels
[AIAA PAPER 92-4009] p 1033 A92-56832
Hypersonic wind tunnel nozzle study
[AIAA PAPER 92-4012] p 1033 A92-56835
Viscous computations of cold air/air flow around scramjet nozzle afterbody
[NASA-CR-4406] p 13 N92-10982
Computation of supersonic jet mixing noise for an axisymmetric CD nozzle using k-epsilon turbulence model
[NASA-TM-105338] p 237 N92-14795
Performance prediction and design of maximum thrust planar supersonic nozzles using a flux-difference-splitting technique p 738 N92-26480
Development of a quiet supersonic wind tunnel with a cryogenic adaptive nozzle p 751 N92-27977
A nozzle internal performance prediction method
[NASA-TP-3221] p 1040 N92-33625
Parametric investigation of single-expansion-ramp nozzles at Mach numbers from 0.60 to 1.20
[NASA-TP-3240] p 1042 N92-34193

NOZZLE EFFICIENCY
Nickel base alloy GTD-222 - A new gas turbine nozzle alloy
[ASME PAPER 91-GT-73] p 142 A92-15542
Film cooling research on the endwall of a turbine nozzle guide vane in a short duration annular cascade. I - Experimental technique and results
[ASME PAPER 91-GT-252] p 150 A92-15657
Film cooling research on the endwall of a turbine nozzle guide vane in a short duration annular cascade. II - Analysis and correlation of results
[ASME PAPER 91-GT-253] p 150 A92-15658

Experimental and analytical study of close-coupled ventral nozzles for ASTOVL aircraft p 861 A92-45325
A static investigation of the thrust vectoring system of the F/A-18 high-alpha research vehicle
[NASA-TM-4359] p 633 N92-25967
A nozzle internal performance prediction method
[NASA-TP-3221] p 1040 N92-33625

NOZZLE FLOW
Calculation of flow of a radiating gas in axisymmetric nozzles of specified shape p 7 A92-12179
An analysis of the flow-pattern at the exit of a single-stage turbine p 10 A92-13234
Mach 4 and Mach 8 axisymmetric nozzles for a high-enthalpy shock tunnel p 78 A92-16668
Aerating fuel nozzle design influences on airflow features p 129 A92-17176
Enhanced mixing of supersonic jets p 80 A92-17195
LDV measurements and investigation of flow field through radial turbine guide vanes p 217 A92-19618
An investigation of fuel nozzles for combustion performance p 278 A92-21745
Single expansion ramp nozzle simulations
[AIAA PAPER 92-0387] p 323 A92-26243
Two and three dimensional parabolized Navier-Stokes code for scramjet combustor, nozzle, and film cooling analysis
[AIAA PAPER 92-0391] p 372 A92-26247
Numerical investigation of unsteady transonic nozzle flows p 331 A92-26443
Computations of multispecies mixing between scramjet nozzle flow and hypersonic freestream p 376 A92-28534
Flow in a ventral nozzle for short takeoff and vertical landing aircraft p 376 A92-28538
Effect of turbulent mixing on the characteristics of a turbofan-engine nozzle p 493 A92-30162
Study on nozzle flow diffusion p 429 A92-30531
Numerical simulation of supersonic nozzle flow p 430 A92-30540
Design considerations for nozzles of hypersonic airbreathing propulsion
[AIAA PAPER 91-5019] p 471 A92-31685
Applications of hot-film anemometers in hypersonic shear layers
[AIAA PAPER 91-5028] p 436 A92-31687
Effect of tabs on the evolution of an axisymmetric jet p 656 A92-40151
Application of computational fluid dynamics to pitch/yaw thrust vectoring spherical convergent flap nozzles p 737 A92-44511
Navier-Stokes solutions of transonic nozzle flow with shock-induced flow separations p 713 A92-44515
Nozzle design using generalized one-dimensional flow p 714 A92-44531
Oscillation of oblique shock waves generated in a two dimensional asymmetric nozzle
[SAE PAPER 912061] p 791 A92-45443
Commercial turbofan engine exhaust nozzle flow analyses using PAB3D
[AIAA PAPER 92-2701] p 801 A92-45543
The flip flop nozzle extended to supersonic flows
[AIAA PAPER 92-2724] p 803 A92-45561
Prediction of a high bypass ratio engine exhaust nozzle flowfield
[AIAA PAPER 92-3259] p 864 A92-48855
The enhancement of mixing in high-speed heated jets using a counterflowing nozzle
[AIAA PAPER 92-3262] p 825 A92-48857
A scramjet nozzle experiment with hypersonic external flow
[AIAA PAPER 92-3289] p 864 A92-48878
Experimental validation of scramjet nozzle performance
[AIAA PAPER 92-3290] p 864 A92-48879
Investigation of three-dimensional flow field in a turbine including rotor/stator interaction. II - Three-dimensional flow field at the exit of the nozzle
[AIAA PAPER 92-3326] p 826 A92-48909
Least-squares/parabolized Navier-Stokes procedure for optimizing hypersonic wind-tunnel nozzles p 980 A92-50270
Kinetic theory model for the flow of a simple gas from a three-dimensional axisymmetric nozzle p 937 A92-52730
Numerical and experimental investigations of rarefied gas flows through nozzles and composite systems p 940 A92-52797
Pulsation characteristics of one-phase and two-phase steam flows in Laval nozzles under off-design conditions p 1019 A92-53882
Preliminary dynamic tests of a flight-type ejector
[AIAA PAPER 92-3261] p 1066 A92-54020
An advanced scramjet propulsion concept for a 350 MG SSTO space plane - External nozzle performance
[AIAA PAPER 92-3719] p 1067 A92-54134
Methodology for calculating aerodynamic sensitivity derivatives p 1024 A92-54911
Computational and numerical analysis of hypersonic nozzle flows with comparisons to wind tunnel calibration data
[AIAA PAPER 92-4011] p 1033 A92-56834
Flow contamination and flow quality in arc heaters used for hypersonic testing
[AIAA PAPER 92-4028] p 1100 A92-56850
Viscous computations of cold air/air flow around scramjet nozzle afterbody
[NASA-CR-4406] p 13 N92-10982
Numerical simulations around models in hypersonic wind tunnels p 182 N92-14998
SIMOUN and Scirocco wind tunnel nozzle viscous flow study p 208 N92-14999
High enthalpy nozzle flows p 182 N92-15000
Experimental research of the aerodynamics of nozzles and plumes at hypersonic speeds
[NASA-CR-187316] p 185 N92-15048
Aircraft ground test and subscale model results of axial thrust loss caused by thrust vectoring using turning vanes
[NASA-TM-4341] p 273 N92-17071
Thrust vector control of an overexpanded supersonic nozzle using pin insertion and rotating airfoils
[AD-A243891] p 387 N92-18942
Effect of nonuniform entrance flow profile on hypersonic nozzle pitching moment
[AD-A244050] p 377 N92-19184
Interferograms, schlieren, and shadowgraphs constructed from real- and ideal-gas, two- and three-dimensional computed flowfields
[NASA-CR-190054] p 446 N92-21356
An incremental strategy for calculating consistent discrete CFD sensitivity derivatives
[NASA-TM-104207] p 625 N92-24681
Experimental investigation of nozzle/plume aerodynamics at hypersonic speeds
[NASA-CR-190074] p 664 N92-25162
Predictions and measurements of 3D viscous flow in a transonic turbine nozzle guide vane row p 741 N92-27466
Aerothermodynamics of nozzle flows for advanced hypersonic propulsion systems p 769 N92-27478
Application of finite element method to hypersonic nozzle flow computations p 769 N92-27479
The 3-D Navier-Stokes flow and temperature field computation for a forced mixer nozzle p 770 N92-27482
Preliminary dynamic tests of a flight-type ejector
[NASA-TM-105814] p 972 N92-30998
Dynamic interactions between hypersonic vehicle aerodynamics and propulsion system performance
[NASA-CR-190638] p 1038 N92-33304
A nozzle internal performance prediction method
[NASA-TP-3221] p 1040 N92-33625
Parametric investigation of single-expansion-ramp nozzles at Mach numbers from 0.60 to 1.20
[NASA-TP-3240] p 1042 N92-34193

NOZZLE GEOMETRY
A simple model to simulate subsonic intakes and propelling nozzles of aircraft gas turbine engines
[ASME PAPER 91-GT-392] p 153 A92-15722
Effect of the blade height of the nozzle ring of axial-flow microturbines on the flow velocity factor and exit angle p 128 A92-16831
A comparison of cooling methods for the airframe nozzle of a single-stage-to-orbit aircraft
[AIAA PAPER 91-5036] p 210 A92-17825
Formation of shocks within axisymmetric nozzles p 176 A92-20760
Broadband shock associated noise from supersonic jets measured by a ground observer
[AIAA PAPER 92-0502] p 416 A92-26931
LDV measurements of the velocity field in an underexpanded supersonic jet (Ma = 1.5)
[AIAA PAPER 92-0504] p 341 A92-28196
Low-frequency vibrations of the shutters of the variable Laval nozzle of gas turbine engines p 657 A92-40610
The effects of nozzle exit geometry on forebody vortex control using blowing
[AIAA PAPER 92-2603] p 792 A92-45480
The flip flop nozzle extended to supersonic flows
[AIAA PAPER 92-2724] p 803 A92-45561
Taylor series approximation of geometric shape variation for the Euler equations p 899 A92-46916
Ablative control mechanism in nozzle thermo-protection
[AIAA PAPER 92-3054] p 889 A92-48712
A study on the impact of shroud geometry on ejector pumping performance
[AIAA PAPER 92-3260] p 864 A92-48856
Specifying exhaust nozzle contours in real-time using genetic algorithm trained neural networks
[AIAA PAPER 92-3328] p 865 A92-48911
Least-squares/parabolized Navier-Stokes procedure for optimizing hypersonic wind-tunnel nozzles p 980 A92-50270
The behaviour of the pressure temperature and density in an inviscid unsteady transonic axisymmetric flow with shock waves p 1018 A92-53553
Broadband shock associated noise from supersonic jets measured by a ground observer p 1135 A92-54909
A static investigation of the thrust vectoring system of the F/A-18 high-alpha research vehicle
[NASA-TM-4359] p 633 N92-25967
Dynamic interactions between hypersonic vehicle aerodynamics and propulsion system performance
[NASA-CR-190638] p 1038 N92-33304

NOZZLE THRUST COEFFICIENTS
A nozzle internal performance prediction method
[NASA-TP-3221] p 1040 N92-33625

NOZZLE WALLS
Gortler instability and supersonic quiet nozzle design p 813 A92-46902
Aerothermodynamics of nozzle flows for advanced hypersonic propulsion systems p 769 N92-27478

NOZZLES
Simulation of 3-D shear flows around a nozzle-afterbody at high speeds p 519 A92-34826
Thermal/structural analysis of a transpiration cooled nozzle
[NASA-TM-104184] p 401 N92-18877
Inlets, ducts, and nozzles p 593 N92-22523

NUCLEAR DEVICES
Experimental studies of compact toroids
[DE92-003469] p 512 N92-21046

NUCLEAR ENERGY
Risk management - Expanding horizons in nuclear power and other industries --- Book
[ISBN 1-56032-231-4] p 993 A92-51438

NUCLEAR EXPLOSION EFFECT
Effects of ionizing and nonionizing radiation on aircraft p 295 A92-23301

NUCLEAR RADIATION
JPRS report: Science and technology. USSR: Engineering and equipment
[JPRS-UEQ-91-010] p 593 N92-22397

NUCLEAR REACTORS
JPRS report: Science and technology. USSR: Engineering and equipment
[JPRS-UEQ-92-001] p 592 N92-22296

NUCLEATE BOILING
Conjugate conduction/convection/nucleate-boiling heat transfer with a high-speed boundary layer
[AIAA PAPER 91-5033] p 215 A92-17823

NUCLEATION
Microgravity nucleation and particle coagulation experiments support
[NASA-CR-190159] p 502 N92-21385
Microgravity nucleation and particle coagulation experiments support
[NASA-CR-189899] p 502 N92-21433

NUCLEI (NUCLEAR PHYSICS)
System of cryogenic security of the superconducting accelerator of relativistic nuclei-nuclotron
[DE91-643289] p 304 N92-16789

NUCLIDES
Surface activation of Concorde by Be-7 p 605 N92-23295

NUMERICAL ANALYSIS
Numerical modeling technique for field-to-cable coupling through advanced composite material p 146 A92-14684
Numerical analysis of airflow in aircraft cabins
[SAE PAPER 911441] p 245 A92-21837
Numerical analysis of techniques for efficient generation of vorticity in supersonic flows
[AIAA PAPER 92-0828] p 422 A92-29596
Time marching integral equation method for unsteady transonic flows around airfoils p 433 A92-31489
Experimental and numerical investigation of anti-icing phenomena on a NACA 0012 assembly
[AIAA PAPER 92-0531] p 459 A92-31669
Boundary-layer receptivity due to a wall suction and control of Tollmien-Schlichting waves p 616 A92-39333
Numerical analysis of flow through oscillating cascade sections p 713 A92-44513
Three-dimensional numerical analysis of impinging circular jet - Discrete vortex method p 1029 A92-56040
Numerical investigation of the effect of leading edge geometry on dynamic stall of airfoils
[AD-A239949] p 12 N92-10015
Introduction to Special Course on Engineering Methods in Aerodynamic Analysis and Design of Aircraft p 552 N92-23951
Aerodynamic design and analysis of a light aircraft propeller p 629 N92-24876

Computational Fluid Dynamics --- numerical methods and algorithm development
[NASA-CP-10078] p 660 N92-25808
Analysis and design technology for high-speed aircraft structures p 684 N92-25918
Algorithms for blending surface generation
[AD-A245686] p 777 N92-26524
Study of turbulence structure through numerical simulations: The perspective of drag and reduction
p 717 N92-27713
Numerical calculations of two-dimensional single and multi-material flow fields with CCICE
[DE92-015778] p 1000 N92-30903
Ideal efficiency of propellers based on Theodorsen's theory: A review and computer study, with extended plus simplified charts
[UTIAS-TN-271] p 1071 N92-33102
Computational aspects of helicopter trim analysis and damping levels from Floquet theory
[NASA-CR-190736] p 1087 N92-33107

NUMERICAL CONTROL
Development testing of the EH101 Flight Control System p 132 A92-14380
Numerical investigation of a transverse jet for supersonic aerodynamic control
[AIAA PAPER 92-0639] p 334 A92-27017
The multiple-function multi-input/multi-output digital controller system for the AFW wind tunnel model
[AIAA PAPER 92-2083] p 565 A92-35655
Flutter suppression digital control law design and testing for the AFW wind tunnel model
[AIAA PAPER 92-2095] p 566 A92-35668
Robustness characteristics of fast-sampling digital controllers for active flutter suppression
[AIAA PAPER 92-2104] p 567 A92-35675
Design of adaptive fast-sampling digital controllers for active flutter suppression
[AIAA PAPER 92-2105] p 567 A92-35676
On-line performance evaluation of multiloop digital control systems p 873 A92-46739
Computer-Controlled Navigation System/General Positioning System (CCNS/GPS) - A guidance, positioning, and management system for remote sensing flights
p 840 A92-47630
Flexible manufacturing in repair of gas turbine engine components
[AIAA PAPER 92-3524] p 786 A92-49049
Optimal discrete-time static output-feedback design - A W-domain approach p 1007 A92-50499
Terrain following of arbitrary surfaces using a high intensity LED proximity sensor
[DE92-007161] p 455 N92-21201
From IGES to STEP
[REPT-3.1.6] p 603 N92-23881
Flutter suppression digital control law design and testing for the AFW wind-tunnel model
[NASA-TM-107652] p 962 N92-31350
Techniques for autonomous navigation
[DE92-013458] p 957 N92-31746
Integrated computer systems in aircraft design and manufacture: Difficulties and implications
p 1010 N92-31864
Air traffic control: FAA's advanced automation system contract
[GAO/IMTEC-91-25] p 1048 N92-32861

NUMERICAL DIFFERENTIATION
A study of a version of the boundary conditions of a two-dimensional spline in surface and line modeling
p 163 A92-16826

NUMERICAL FLOW VISUALIZATION
Emergence of coherent patterns of vortex stretching during reconnection - A scattering paradigm
p 38 A92-11041
Computation of three-dimensional turbulent vortical flows on bodies at high incidence p 9 A92-13203
The numerical simulation of a high-speed axial flow compressor
[ASME PAPER 91-GT-272] p 75 A92-15669
A numerical study of isothermal flows of a slit V-gutter
[AIAA PAPER 92-0100] p 293 A92-22203
A study of the interaction of a normal shock wave with a turbulent boundary layer at Mach numbers between 1.30 and 1.55 p 339 A92-28006
Numerical simulation of leading-edge vortex breakdown using an Euler code p 701 A92-41213
Visualization and analysis of hypersonic flows and comparison to experimental data
[AIAA PAPER 92-2774] p 704 A92-41320
Three-dimensional visualizations of the aerodynamic characteristics of delta wings for the transition from subsonic to supersonic leading edges in supersonic-hypersonic flow p 709 A92-43073
Experimental and numerical investigations on separated flows around pitching airfoils p 710 A92-43166
Numerical investigation of supersonic inlet with realistic bleed and bypass systems p 713 A92-44519
Aerothermodynamics of a 1.6-meter-diameter sphere in hypersonic rarefied flow p 808 A92-45840
Mesh adaption for 2D transsonic Euler flows on unstructured meshes p 816 A92-47038
The construction, application and interpretation of three-dimensional hybrid meshes p 919 A92-47089
Numerical prediction of the flow characteristics in an arc wind tunnel
[AIAA PAPER 92-4016] p 1100 A92-56838
Proceedings of the Seminar on Investigation and Control of Boundary-Layer Transition
[NAL-SP-11] p 400 N92-18483
Construction of a numerical optimization method for the definition of hypersupported profiles
[ONERA-RSF-43/1736-AY-146A] p 908 N92-28788
Development of an unsteady three-dimensional viscous-inviscid interaction numerical method for the calculation of airfoils vibration
[ONERA-RSF-7/3617-AY-022A] p 830 N92-29206

NUMERICAL INTEGRATION
A pressure-drag-determination method for aerodynamic-interference problems p 425 A92-30157
CSM solutions of rotating blade dynamics using integrating matrices
[NASA-CR-190577] p 1003 N92-31619

NYQUIST DIAGRAM
On the Nyquist envelope of an interval plant family
p 507 A92-29132

O

OBJECT-ORIENTED PROGRAMMING
A development of computer support system for wing design p 162 A92-15332
Modular techniques for dynamic fault-tree analysis
p 1120 A92-56241
Implementation of an object-oriented flight simulator D.C. electrical system on a hypercube architecture
[AD-A243700] p 284 N92-17097
An application of the object-oriented paradigm to a flight simulator
[AD-A243624] p 384 N92-18012
Accurate, productive aerodynamic simulation on patched mesh systems
[AD-A243977] p 405 N92-19386
NASA TSRV essential flight control system requirements via object oriented analysis
[NASA-CR-189573] p 381 N92-19499
A formal definition of the object-oriented paradigm for requirements analysis
[AD-A246814] p 729 N92-28132

OBLIQUE SHOCK WAVES
Experiments on shock/vortex interactions
[AIAA PAPER 92-0315] p 320 A92-25762
Flowfield visualization of crossing shock-wave/boundary-layer interactions
[AIAA PAPER 92-0750] p 335 A92-27094
Axial compression corner flow with shock impingement p 441 A92-32196
Oblique shock wave with sweep p 613 A92-38370
Oscillation of oblique shock waves generated in a two dimensional asymmetric nozzle
[SAE PAPER 912061] p 791 A92-45443
Airfoil pressure measurements during oblique shock wave-vortex interaction in a Mach 3 stream
[AIAA PAPER 92-2631] p 795 A92-45503
Detailed numerical analysis of standing oblique detonation p 1111 A92-53550

OBLIQUE WINGS
Transonic wind tunnel test of a 14 percent thick oblique wing
[NASA-TM-102230] p 950 N92-32213

OBSERVABILITY (SYSTEMS)
Observability analysis of piece-wise constant systems with application to inertial navigation p 49 A92-11391
Observability under recurrent loss of data
p 302 A92-21191
Meeting VSTOL aircraft performance requirements using scheduled H(infinity) controllers p 477 A92-29094
Design of low-sensitivity modalized observers using left eigenstructure assignment p 661 A92-39908

OBSERVATION
Sensor fault detection on board an aircraft with observer and polynomial classifier
[DLR-FB-91-34] p 859 N92-29870

OBSTACLE AVOIDANCE
Inertial navigation sensor integrated motion analysis for obstacle detection p 954 A92-49272
Vision-based obstacle detection for rotorcraft flight
p 967 A92-52465
Inertial navigation sensor integrated motion analysis for autonomous vehicle navigation p 995 A92-52470
Concepts for pilot interaction with an automated NOE obstacle-avoidance system
[AIAA PAPER 92-4472] p 1076 A92-55232
Analysis of image-based navigation system for rotorcraft low-altitude flight p 1046 A92-55968
Laser-radar based obstacle avoidance system for helicopters p 1064 A92-56295
Passive range estimation for rotorcraft low-altitude flight
[NASA-TM-103897] p 2 N92-10003
A connectionist approach to autonomous robotic navigation p 454 N92-20356

OCCUPATIONAL DISEASES
Fatal occupational injury related to helicopters in the United States 1980-1985 p 186 A92-20720

OCEAN BOTTOM
Precision of the long baseline acoustic navigation system used by Pegasus
[AD-A246598] p 727 N92-26795

OCEAN CURRENTS
Precision of the long baseline acoustic navigation system used by Pegasus
[AD-A246598] p 727 N92-26795

OCEAN SURFACE
Comparison of aircraft synthetic aperture radar and buoy spectra during NORCSEX '88 p 597 A92-34878
Relating the microwave radar cross section to the sea surface stress - Physics and algorithms
p 597 A92-35028

OFF-ON CONTROL
Lyapunov exponents for systems described by differential equations with discontinuous right-hand sides
p 507 A92-29237

OGIVES
Surface flow patterns on an ogive-cylinder at incidence p 176 A92-20762
Binary optic-corrected conformal windows for optical seekers
[AIAA PAPER 92-2802] p 779 A92-41340
Alleviation of side force on tangent-ogive forebodies using passive porosity
[AIAA PAPER 92-2711] p 802 A92-45552
Comparison of two flux splitting schemes for calculation of ogive-cylinder at M = 3.5 and alpha = 18 deg
[AIAA PAPER 92-2667] p 806 A92-45582
Asymmetric turbulent vortical flows over slender bodies p 935 A92-50314
A study of supersonic flow over the ogival bodies with attached shock waves at zero incidence
p 936 A92-51896

OH-58 HELICOPTER
Flight testing the handling qualities requirements of ADS-33C - Lessons learned at ATTC
p 104 A92-14339
Bell's OH-58D proves its reliability
p 458 A92-29670
Frequency domain flight testing and analysis of an OH-58D helicopter p 847 A92-46943
CH-46 and OH-58 transmission stress wave analysis
[AD-A244321] p 365 N92-18826
Gear tooth stress measurements of two helicopter planetary stages
[NASA-TM-105651] p 764 N92-26555
Operational noise data for OH-58D Army helicopters
[AD-A246822] p 926 N92-28292

OHIO
Study of alternatives: Dayton's Aviation heritage, Ohio
[PB91-202275] p 2 N92-10972

OIL EXPLORATION
A report on enhancements for existing and future helicopters supporting operations of the Canadian oil and gas industry
[CTN-91-60126] p 636 N92-25350

OILS
The Berlin oil channel for drag reduction research
p 571 A92-34219
Reflection type skin friction meter
[NASA-CASE-LAR-14520-1-SB] p 11 N92-10008
Stability of intershaft squeeze film dampers
p 222 N92-14351

OMEGA NAVIGATION SYSTEM
The DOT/DOD Federal Radionavigation Plan
p 96 A92-16637
The 1990 Federal Radionavigation Plan and its impact on the Omega Navigation System p 98 A92-16658
Omega/VLF now and into the 21st century
p 98 A92-16659
Omega - GPS integration platform p 98 A92-16660
Probability of cycle jumps in Omega receivers and other phase locked loop applications
[PB92-128891] p 455 N92-21279
Integrated Russian VLF/Omega receiver design
[PB92-193390] p 1051 N92-33809

ON-LINE PROGRAMMING
Delfi: Design, development, and applicability of expert systems shells
[ISBN-90-6275-734-0] p 692 N92-25306

ON-LINE SYSTEMS
On-line adaptive control of unstable aircraft wing flutter p 27 A92-11374
A new study on a class of discrete event dynamic systems p 48 A92-11377
Comparison of elastic and rigid blade-element rotor models using parallel processing technology for piloted simulations
[SAE PAPER 912120] p 608 A92-39968
Hypervelocity Wind Tunnel 9 control system p 1092 A92-54343
Neural networks for feedback linearization in aircraft control
[AIAA PAPER 92-4391] p 1074 A92-55192
On-line identification and control of linearized aircraft dynamics p 1082 A92-55911
Background issues for on-line aircraft documentation p 119 N92-13858
Improvement of data processing system for gust wind tunnel data acquisition part: System conversion from off-line to on-line processing
[NAL-TM-611] p 285 N92-17756
Structured Hypermedia Application Development Model (SHADM): A structured model for technical documentation application design
[AD-A244268] p 417 N92-19336
Delfi: Design, development, and applicability of expert systems shells
[ISBN-90-6275-734-0] p 692 N92-25306
An interactive grid generation technique for turbomachinery p 659 N92-25717
TIGER: Turbomachinery interactive grid generation p 659 N92-25718
TIGGERC: Turbomachinery interactive grid generator energy distributor and restart code p 659 N92-25719
NASA/DOD Aerospace Knowledge Diffusion Research Project. Paper 14: An analysis of the technical communications practices reported by Israeli and US aerospace engineers and scientists
[NASA-TM-107924] p 782 N92-28183
On-line analysis capabilities developed to support the AFW wind-tunnel tests
[NASA-TM-107651] p 961 N92-30752

ONBOARD DATA PROCESSING
Distributed artificial intelligence approach to air traffic control p 161 A92-13436
On-board data acquisition system for Embraer's CBA123 p 198 A92-19251
A parallel architecture adapted to onboard multiexpert systems p 276 A92-23040
A knowledge acquisition approach for an on-board mission planner
[AIAA PAPER 92-1021] p 531 A92-33204
New Boeing flight test data acquisition systems p 920 A92-47537
Airborne Data Acquisition and Relay System p 839 A92-47574
The development of fatigue management requirements and techniques p 360 N92-18572
Space software is first of all software p 509 N92-20590
Approach and landing assisted by onboard image processing p 457 N92-21959
Quick-look system p 599 N92-23393
Trajectory optimization for hypersonic aircraft guidance p 728 N92-27898

ONBOARD EQUIPMENT
Development and evaluation of an onboard aircraft cabin water spray system for postcrash fire protection
[SAE PAPER 912224] p 636 A92-40022
A validated code to predict the performance of onboard broadband optical seekers through a turbulent transonic flow
[AIAA PAPER 92-2792] p 778 A92-41331
Operation of the on-board measuring system of the STOL research aircraft Asuka p 734 A92-43139
Next generation power electronics for space and aircraft. II - Packaging p 992 A92-50553
Some important factors in turbulence in flight measurement p 1063 A92-54324
Soviet electronic display systems under research and manufactured for the civil aviation aircraft of the 1990's
[AD-A240933] p 119 N92-13066
Introduction and execution of flight tests at the DLR p 648 N92-25594
Board-autonomous flight trajectory measurement by example of an ILS measuring system p 641 N92-25601
On board planning of 4D-trajectories p 728 N92-27897
Potential applications of laser Doppler anemometry for in-flight measurements
[NLR-TP-90163-U] p 859 N92-28654
Loran-C performance assurance assessment program
[NASA-CR-190469] p 840 N92-28718

ONE DIMENSIONAL FLOW
Nozzle design using generalized one-dimensional flow p 714 A92-44531
Modeling of heavy-gas effects on airfoil flows
[NASA-CR-190357] p 716 N92-27558

OPERATING COSTS
Rotor blade preservation - Getting the most service life with lowest operational costs p 108 A92-14412
Maintenance, Malfunction Information Report system p 60 A92-14414
How to support the 'little guy' --- helicopter maintenance p 60 A92-14437
Malfunction/discrepancy reporting p 60 A92-14438
Operational and economic benefits of area navigation from the perspective of a major air carrier p 96 A92-16632
Airlines could reap big saving with new Pratt common core p 736 A92-42400
Kappa Group: The initial guess. A proposal in response to a commercial air transportation study
[NASA-CR-189981] p 366 N92-19374
Allocation and recovery of federal airport and airway costs, 1991
[AD-A249436] p 983 N92-30777

OPERATING SYSTEMS (COMPUTERS)
NASA TSRV essential flight control system requirements via object oriented analysis
[NASA-CR-189573] p 381 N92-19499
Timing analysis of parallel algorithms on a MIMD multiprocessor
[ITN-92-85153] p 510 N92-20905
Advanced Transport Operating System (ATOPS) control display unit software description
[NASA-CR-189606] p 652 N92-24689
A model of the ADA avionics real-time system: An example of the benefits of the hardware/software codesign approach in development of real-time systems
[AD-A248893] p 967 N92-30524
Distributed systems: Interconnection and fault tolerance studies
[AD-A252869] p 1135 N92-33920

OPERATING TEMPERATURE
High temperature MMCs for aero-engines - Challenge and potential p 986 A92-52982
Notes on the use of fusible temperature indicators to bound the temperature of hot graphite in the NAVSWC hypervelocity wind tunnel facility p 1090 A92-54315
Calculation of installation effects within performance computer programs p 869 N92-28465

OPERATIONAL PROBLEMS
A review of Australian activity on modelling the helicopter/ship dynamic interface p 465 N92-21967
Advanced thermally stable, jet fuels development program annual report. Volume 1: Model and experiment system development
[AD-A249625] p 988 N92-31462
Simulation test and evaluation of TCAS 2 logic version 6.04
[DOT/FAA/RD-92/23] p 1048 N92-33098

OPERATIONS
New York Downtown Manhattan (Wall Street) Heliport: Operations analysis
[DOT/FAA/RD-91/12] p 139 N92-13077

OPERATOR PERFORMANCE
Perspective versus plan view air traffic control (ATC) displays - Survey and empirical results p 896 A92-44967
The multi-attribute task battery for human operator workload and strategic behavior research
[NASA-TM-104174] p 303 N92-17130
Controller memory enhancement: Field facility concepts and techniques
[DOT/FAA/CT-TN92/7] p 640 N92-24799

OPERATORS (MATHEMATICS)
Using new aggregation operators in rule-based intelligent control p 51 A92-11456

OPTICAL COMMUNICATION
Intra-flight laser data links - Technology focus p 725 A92-41472
Fiber optic controls for aircraft engines - Issues and implications p 856 A92-46244
Advances in Fibre-Optic Technology in Communications and for Guidance and Control
[AGARD-LS-184] p 774 N92-28084
Fiber optic data busses for aircraft p 736 N92-28093

OPTICAL COMPUTERS
Optical computing at NASA Ames Research Center
[AIAA PAPER 91-3779] p 231 A92-17637

OPTICAL CORRECTION PROCEDURE
Binary optic-corrected conformal windows for optical seekers
[AIAA PAPER 92-2802] p 779 A92-41340

OPTICAL CORRELATORS
Optical computing at NASA Ames Research Center
[AIAA PAPER 91-3779] p 231 A92-17637

OPTICAL DATA PROCESSING
Development and future view of the technology for fly-by-light control system elements p 131 A92-14027
Optical computing at NASA Ames Research Center
[AIAA PAPER 91-3779] p 231 A92-17637

OPTICAL EQUIPMENT
Reliability growth of coolers for advanced optical systems and instruments p 294 A92-22879
JPRS report: Science and technology. Central Eurasia: Engineering and equipment
[JPRS-UEQ-92-002] p 592 N92-22298

OPTICAL FIBERS
The detection of damage and the measurement of strain within composites by means of embedded optical fiber sensors p 491 A92-28669
Cyclic fatigue behavior of silica fiber p 754 A92-42040
Evaluation of a IMU with optical fiber gyros in dynamic windtunnel tests p 1104 A92-56121
Development of digital/optical rotary position transducer
[NAL-TR-1106] p 29 N92-10028
Fiber-sensor design for turbine engines
[DE92-003539] p 376 N92-18230
The fibre optic three dimensional laser two focus velocimeter for the low-speed windtunnel. Part 1: Two-dimensional measurement evaluations
[NAL-TM-627] p 665 N92-25402
Fiber optic data busses for aircraft p 736 N92-28093

OPTICAL FILTERS
Binary optical filters for scale invariant pattern recognition
[NASA-TM-103902] p 853 N92-28910

OPTICAL GYROSCOPES
Fiber optic and laser sensors VIII; Proceedings of the Meeting, San Jose, CA, Sept. 17-19, 1990
[SPIE-1367] p 901 A92-48026
Comparison of Hemispherical Resonator Gyro and optical Gyros p 993 A92-51014
Evaluation of a IMU with optical fiber gyros in dynamic windtunnel tests p 1104 A92-56121

OPTICAL MEASUREMENT
Optical measurements of unducted fan flutter
[ASME PAPER 91-GT-19] p 147 A92-15510
Ground test facilities for aerothermal and aero-optical evaluation of hypersonic interceptors
[AIAA PAPER 92-1074] p 573 A92-33244
Experiments on the enhancement of compressible mixing via streamwise vorticity. I - Optical measurements
[AIAA PAPER 92-3549] p 906 A92-49064
Aircraft lidar sensitivity study for measuring water vapor
[AD-A240549] p 42 N92-11237
The role of crack growth in defect assessment
[PNR-90798] p 501 N92-20909
Study of optical techniques for the Ames unitary wind tunnels. Part 2: Light sheet and vapor screen
[NASA-CR-190217] p 573 N92-22195
Optical measurement systems p 594 N92-22527
Three-dimensional laser window formation
[NASA-RP-1280] p 984 N92-30307

OPTICAL MEASURING INSTRUMENTS
Fabry-Perot fiber-optic sensors in full-scale fatigue testing on an F-15 aircraft p 391 A92-24553
Optical velocity sensor for air data applications p 368 A92-24575
Fiber optic sensors for smart skins applications p 392 A92-24778
Smart skins and fiber-optic sensors application and issues p 368 A92-24785
The detection of damage and the measurement of strain within composites by means of embedded optical fiber sensors p 491 A92-28669
A validated code to predict the performance of onboard broadband optical seekers through a turbulent transonic flow
[AIAA PAPER 92-2792] p 778 A92-41331
Development of an instrument for measuring runway roughness p 748 A92-43124
The use of optical sensors and signal processing gas turbine engines p 856 A92-46247
Fiber optic and laser sensors VIII; Proceedings of the Meeting, San Jose, CA, Sept. 17-19, 1990
[SPIE-1367] p 901 A92-48026
Wavelength encoded fiber optic angular displacement sensor p 857 A92-48046
All-Union Conference on Optical Methods of Flow Research, 1st, Novosibirsk, Russia, Apr. 1991, Proceedings p 993 A92-51311
ICIASF '91 - International Congress on Instrumentation in Aerospace Simulation Facilities, 14th, Rockville, MD, Oct. 27-31, 1991, Record
[ISBN 0-0783-0123-4] p 1114 A92-54301

Aerodynamic assessment of an optical pressure measurement system (OPMS) by comparison with conventional pressure measurements in a high speed wind tunnel p 1114 A92-54304
Ablation and temperature sensors for flight measurements in reentry body heat shields p 227 N92-15004
Study of optical techniques for the Ames unitary wind tunnels. Part 2: Light sheet and vapor screen [NASA-CR-190217] p 573 N92-22195
Study of optical techniques for the Ames unitary wind tunnels. Part 3: Angle of attack [NASA-CR-190541] p 888 N92-29655

OPTICAL PATHS
Aircraft lidar sensitivity study for measuring water vapor [AD-A240549] p 42 N92-11237
Multi-channel fiber optic rotary joint for single-mode fiber [AD-D015273] p 927 N92-29095

OPTICAL POLARIZATION
Bias of an optical passive ring-resonator gyro caused by the misalignment of the polarization axis in the polarization-maintaining fiber resonator p 652 A92-40262

OPTICAL PROPERTIES
Experimentally supported investigations into the optical performance of multi-aperture window concepts [AIAA PAPER 92-2781] p 778 A92-41324
A time-integrated image model for aero-optic analysis [AIAA PAPER 92-2793] p 779 A92-41332
Measured and calculated optical property profiles in the mixed layer and free troposphere p 1129 A92-54630
Concept design phase expendable holographic sensor to measure ocean small angle optical scattering [AD-A245067] p 501 N92-20997

OPTICAL RADAR
Several results of lidar measurements of the characteristics of oblique visibility at an airfield p 45 A92-12844
Selection of the time parameters of the probing pulse during the nonstationary irradiation of flight vehicles p 454 A92-31951
Characteristics of the energy analysis of optical radar in the case of nonstationary irradiation of flying objects p 454 A92-31955
An airborne Doppler lidar for meteorological research p 467 A92-32082
Heterodyne techniques in the I.R. bandwidth for laser obstacle detection p 533 A92-35740
Innovation in the laser warning sensor field p 554 A92-35742
Measured and calculated optical property profiles in the mixed layer and free troposphere p 1129 A92-54630
Laser-radar based obstacle avoidance system for helicopters p 1064 A92-56295
Time Resolved Lidar Fluorosensor operating from helicopter p 1121 A92-56296
Aircraft lidar sensitivity study for measuring water vapor [AD-A240549] p 42 N92-11237
Simplified signal processing for an airborne CO2 Doppler lidar p 1000 N92-31023
Trial of a slant visual range measuring device p 1000 N92-31043
Theoretical simulation of a 2 micron airborne solid state laser anemometer p 1000 N92-31059
A study of atmospheric optical scattering parameters at 1.5 and 2 micron region for solid state Doppler lidar applications p 1001 N92-31067
A cable detection lidar system for helicopters p 1001 N92-31068

OPTICAL REFLECTION
Reflection type skin friction meter [NASA-CASE-LAR-14520-1-SB] p 11 N92-10008

OPTICAL RESONATORS
Comparison of Hemispherical Resonator Gyro and optical Gyros p 993 A92-51014

OPTICAL SCANNERS
Study of optical techniques for the Ames unitary wind tunnels. Part 3: Angle of attack [NASA-CR-190541] p 888 N92-29655

OPTICAL SLANT RANGE
Trial of a slant visual range measuring device p 1000 N92-31043

OPTICAL THICKNESS
Modulation transfer function degradation in segmented windows p 733 A92-41431

OPTICAL TRACKING
A time-integrated image model for aero-optic analysis [AIAA PAPER 92-2793] p 779 A92-41332
Welding technology transfer task/laser based weld joint tracking system for compressor girth welds p 593 N92-22426

OPTIMAL CONTROL
Static aeroelastic control using strain actuated adaptive structures p 26 A92-11122
Optimal boundary control of nonsteady incompressible flow with an application to viscous drag reduction p 39 A92-11344
Stochastic ordering properties and optimal routing control for a class of finite capacity queueing systems p 48 A92-11375
Optimal stabilization of discrete event systems p 48 A92-11376
H(infinity) control of linear systems with nonzero initial conditions p 50 A92-11430
Equivalence of optimal control problems and the use of parameterization methods p 52 A92-11466
A method of centers based on barrier functions for solving optimal control problems with continuum state and control constraints p 52 A92-11467
An approach to the optimal output feedback initial stabilizing gain problem p 52 A92-11553
VSTOL aircraft flight control system design using H(infinity) controllers and a switching strategy p 28 A92-11561
H(infinity) robust control synthesis for a fighter performing a coordinated bank turn p 29 A92-11585
Computer aiding for low-altitude helicopter flight p 94 A92-14444
Study of the discrete singularly perturbed linear-quadratic control problem by a bilinear transformation p 163 A92-16072
Optimal control problems with maximum functional p 232 A92-18616
A new method for increasing maximum flight endurance p 280 A92-21006
Aircraft flight controls design using output feedback p 280 A92-21180
Combined H(2)/H(infinity) optimal control design applied to an advanced fighter aircraft [AIAA PAPER 92-0045] p 281 A92-22162
The application of parameter optimisation techniques to linear optimal control system design p 302 A92-23038
Open-loop model reduction and parameter perturbation for active flutter suppression system p 379 A92-24879
Optimal output feedback for linear time-periodic systems p 412 A92-28142
Loop shaping in mixed H2 and H-infinity optimal control p 507 A92-29177
Frequency response specifications and sensitivity functions in quantitative feedback theory p 508 A92-29280
Robust optimal control with a worst case time domain performance criterion p 509 A92-29368
The analysis and approximate representation of the optimal control law for a maneuverable aircraft p 479 A92-30131
Estimation of the optimal load characteristics of aircraft control levers p 479 A92-30150
Integrated aeroelastic control optimization of laminated composite lifting surfaces p 481 A92-32248
Full authority active control system design for a high performance helicopter p 567 A92-35732
An evaluation of a simple PID controller designed using optimal control theory when applied to helicopter stabilisation p 569 A92-35785
Inverse and optimal control for desired outputs p 661 A92-39894
Control strategy for maximizing reconnaissance range of hypersonic cruise vehicles p 729 A92-41222
Parallel solver for trajectory optimization search directions p 777 A92-43399
The method of determinant equations in the applied theory of optimal systems - Systems with 'rigid' constraints and with fixed boundary conditions p 917 A92-46629
Two variations of certainty control p 918 A92-46762
Magnetic bearing design and control optimization for a four-stage centrifugal compressor p 900 A92-47188
Subsonic flight test evaluation of a performance seeking control algorithm on an F-15 airplane [AIAA PAPER 92-3743] p 878 A92-49109
Subsonic flight test evaluation of a propulsion system parameter estimation process for the F100 engine [AIAA PAPER 92-3745] p 866 A92-49110
Three-dimensional optimal reentry trajectory and aerodynamic heating history of the Space Shuttle p 984 A92-49582
Predictive control for optimal path terrain following system p 955 A92-50207
Conditions of optimality in problems of generalized control. II - Sufficient conditions of optimality p 1007 A92-51328
Improvement of atmospheric flight performance of a space vehicle through H infinity-control theory p 1130 A92-53785
A general approach to optimal real-time guidance of dynamic systems based on nonlinear programming [AIAA PAPER 92-4378] p 1131 A92-55182
An efficient algorithm for optimal aircraft trajectories [AIAA PAPER 92-4412] p 1076 A92-55206
Vision-based stereo ranging as an optimal control problem [AIAA PAPER 92-4418] p 1045 A92-55211
Optimal control of helicopters following power failure [AIAA PAPER 92-4471] p 1076 A92-55231
The application of direct transcription to commercial aircraft trajectory optimization [AIAA PAPER 92-4528] p 1077 A92-55246
A robust gain scheduler interpolated into multiple models by membership functions [AIAA PAPER 92-4553] p 1131 A92-55265
Robust control design of an automatic carrier landing system [AIAA PAPER 92-4619] p 1077 A92-55296
A Lie Bracket solution of the optimal thrust magnitude on a singular arc in atmospheric flight [AIAA PAPER 92-4345] p 1079 A92-55334
Optimization approach for helicopter maneuverability with a point mass model p 1083 A92-56025
An investigation of the automation of emergency landings for helicopters p 1083 A92-56026
Flight control system design using H(infinity) optimal control p 1083 A92-56030
The solution of the helicopter flight dynamics tasks by the methods of optimal control theory p 1085 A92-56284
Optimal control of tiltrotor aircraft following power failure p 1085 A92-56303
Research on inverse, hybrid and optimization problems in engineering sciences with emphasis on turbomachine aerodynamics: Review of Chinese advances p 201 N92-13939
Optimal aircraft performance during microburst encounter p 266 N92-17999
Directions in propulsion control p 560 N92-22530
Time-optimal reorientation maneuvers of an aircraft p 549 N92-22605
Sensor compatibility/optimal sensor combinations p 599 N92-23403
A modeling strategy for large-scale optimization based on analysis and visualization principles [AD-A246570] p 777 N92-26620
Feedback control laws for highly maneuverable aircraft [NASA-CR-190535] p 879 N92-29654

OPTIMIZATION
Aerodynamic design of propeller by numerical optimization p 24 A92-10957
Control theory for optimum design of aerodynamic shapes p 6 A92-11328
Optimal rejection of bounded persistent disturbances in periodic systems p 51 A92-11464
Analysis and design optimization of monopulse receivers for secondary surveillance radar p 40 A92-12299
The INFO-ROC technique - A method for comparing and optimizing inspection systems p 144 A92-13563
Design optimization of rotor blades for improved performance and vibration p 106 A92-14389
Rotorcraft airframe structural optimization for combined vibration and fatigue constraints p 106 A92-14390
Optimization of a light helicopter with Arrius power plants p 120 A92-14408
Crash-resistant rotorcraft preliminary design optimization p 109 A92-14417
Minimization of the number of cooling holes in internally cooled turbine blades [ASME PAPER 91-GT-52] p 121 A92-15530
Subsonic propulsion system installation analysis and optimization [ASME PAPER 91-GT-167] p 111 A92-15602
A direct optimization procedure for spanwise work distribution in non-free vortex turbine stages [ASME PAPER 91-GT-204] p 124 A92-15626
Simple formulae for optimal solidity of two-dimensional compressor cascades based on diffusion concept [ASME PAPER 91-GT-308] p 126 A92-15687
Preliminary design of axial compressors using artificial intelligence and numerical optimization techniques [ASME PAPER 91-GT-334] p 126 A92-15699
Numerical optimization of helicopter rotor blade airfoils using unsteady aerodynamic calculations [ONERA, TP NO. 1991-187] p 78 A92-16141
Optimization of the three-dimensional shape of lifting bodies of small aspect ratio at hypersonic velocities p 244 A92-21602
Aerodynamic design and optimization in one shot [AIAA PAPER 92-0025] p 248 A92-22147
Strategies for optimal design of gas turbine disks p 371 A92-24741
Optimization of multistage axial-flow compressor vane setting p 371 A92-24746

Application of the multiplier penalty function method to the optimum design of wing configurations of aerospace vehicle p 356 A92-25013
A comparison of optimization-based approaches for a model computational aerodynamics design problem p 316 A92-25636
Optimum design of helicopter rotor blades with multidisciplinary couplings
[AIAA PAPER 92-0214] p 357 A92-25687
Shape-sensitivity analysis and design optimization of linear, thermoelastic solids p 395 A92-26433
Integral minimization of engine fault equations based on least fault principle p 374 A92-27857
Application researches on expert system used for structural layout optimization of wings p 398 A92-27865
Aerodynamic design optimization using sensitivity analysis and computational fluid dynamics p 340 A92-28044
A new method to estimate the effective geometric focal length and radius of ultrasonic focused probes p 490 A92-28633
Integrated multidisciplinary rotorcraft optimization research at the NASA Langley Research Center p 419 A92-29673
The effect of wing twist optimized in the framework of the plane cross section hypothesis on the aerodynamic characteristics of a wing-body combination at hypersonic speeds p 424 A92-30129
Determination of the objective-function gradient in the problem of minimizing stress concentration using the finite element method p 494 A92-30170
Optimization of bluff body for minimum drag in ground proximity p 431 A92-31154
Navier-Stokes computations of a viscous optimized waverider
[AIAA PAPER 92-0305] p 435 A92-31653
Flowpath optimization for hypersonic vehicles
[AIAA PAPER 91-5043] p 437 A92-31688
Aero-propulsive effects on configuration shaping
[AIAA PAPER 91-5064] p 459 A92-31691
Optimization of a lifting surface for minimum induced drag p 437 A92-31853
Reduction of computational models in strength problems p 496 A92-31858
Dynamics of an optimized rotor blade at off-design flight conditions p 461 A92-32250
Approximate closed-form buckling solutions for the optimization of aircraft structures p 579 A92-32578
Impact of structural optimization with aeroelastic/multidisciplinary constraints on helicopter rotor design
[AIAA PAPER 92-1001] p 535 A92-33193
Multidisciplinary design optimization of a large transport aircraft wing
[AIAA PAPER 92-1002] p 536 A92-33194
Concepts for a future aircraft design environment
[AIAA PAPER 92-1188] p 600 A92-33300
Integration of artificial intelligence and numerical optimization techniques for the design of complex aerospace systems
[AIAA PAPER 92-1189] p 600 A92-33301
An interactive system for aircraft design and optimization
[AIAA PAPER 92-1190] p 600 A92-33302
Application of multidisciplinary optimization to conceptual aircraft design at Rockwell International - A status report
[AIAA PAPER 92-1196] p 537 A92-33307
Structural optimization at Aerospatiale Aircraft
[AIAA PAPER 92-2371] p 601 A92-34542
A design optimization procedure for high-speed prop-rotors
[AIAA PAPER 92-2375] p 542 A92-34545
Improved coordination in non-hierarchic system optimization
[AIAA PAPER 92-2497] p 601 A92-34554
Space Shuttle shell structure waffle panel optimization
[AIAA PAPER 92-2359] p 586 A92-34591
Aeroelastic optimization of an advanced geometry helicopter rotor
[AIAA PAPER 92-2360] p 543 A92-34592
A structural design and optimization tool for ducted rotor/wing blades
[AIAA PAPER 92-2361] p 543 A92-34593
Exploratory design studies of actively controlled wings using integrated multidisciplinary synthesis p 641 A92-36828
Aerodynamic analysis and modification design of NPU airfoils p 613 A92-38270
Control system optimization using genetic algorithms p 661 A92-39900
Design of low-sensitivity modalized observers using left eigenstructure assignment p 661 A92-39908
Optimum dimensions of convective-radiative spines using a temperature correlated profile p 676 A92-40869
Multi-constraint wing optimization p 701 A92-41197
Control strategy for maximizing reconnaissance range of hypersonic cruise vehicles p 729 A92-41222
Optimum hypersonic wings and wave riders p 706 A92-42531
The design of fully-optimized configurations by using the iterative optimum-optimorum theory --- shape of delta wings of minimum drag p 709 A92-43072
The impact of CFD on the airplane design process - Today and tomorrow
[SAE PAPER 911989] p 788 A92-45391
Practical design optimization of wing/body configurations using the Euler equations
[AIAA PAPER 92-2633] p 795 A92-45505
Aerodynamic shape optimization of hypersonic configurations including viscous effects
[AIAA PAPER 92-2635] p 795 A92-45506
Minimizing supersonic wave drag with physical constraints at design and off-design Mach numbers p 811 A92-46808
Wing design for hanggliders having minimum induced drag p 811 A92-46814
Optimization of constant altitude-constant airspeed flight of turbojet aircraft p 845 A92-46815
An aeroelastic analysis with a generalized dynamic wake p 847 A92-46932
The optimization of variable cross-section spines with temperature dependent thermal parameters p 901 A92-48353
Thrust stand evaluation of engine performance improvement algorithms in an F-15 airplane
[AIAA PAPER 92-3747] p 866 A92-49111
Design and optimization of airfoils in non-stalling incompressible flow with a prescribed range of the angle of attack p 933 A92-49556
Optimization of a thermally non-symmetric fin - Preliminary evaluation p 992 A92-50448
Aerospace plane guidance using time-scale decomposition and feedback linearization p 984 A92-50498
Anti-fatigue optimization design by artificial intelligence strategy p 996 A92-53013
Structural optimization and vibration control of composite rotor blades p 960 A92-53056
The system reliability analysis and optimization design for wing-box structures p 997 A92-53292
In-flight optimization of the total propulsion system
[AIAA PAPER 92-3744] p 1068 A92-54146
Experimental investigation of the stability of a clearance-excited rotor system with optimal parameters p 1114 A92-54223
Control design of a UH-60 rotorcraft via CLTR and direct optimization
[AIAA PAPER 92-4470] p 1076 A92-55230
Intelligent control law tuning for AIAA Controls Design Challenge
[AIAA PAPER 92-4631] p 1132 A92-55306
On-line identification and control of linearized aircraft dynamics p 1082 A92-55911
Optimization of composite material wing of fighter type aircrafts p 1053 A92-56018
Research on aeroelastic tailoring at NAL p 1053 A92-56019
Optimization of aeroelastic system with active control p 1083 A92-56022
Structural optimization of a cantilevered beam subject to combined static loadings p 1118 A92-56024
Sensitivity analysis for structural optimization of helicopter rotor blades p 1053 A92-56073
Optimal design of wing shape by use of neural-network p 1054 A92-56112
Application of advanced multidisciplinary analysis and optimization methods to vehicle design synthesis p 1054 A92-56160
Multidisciplinary optimization of aeroservoelastic systems using reduced-size models p 1054 A92-56176
Demonstration of structural optimization applied to wind-tunnel model design p 1119 A92-56181
Short takeoff optimization for the XV-15 tiltrotor aircraft p 1056 A92-56302
CAN-DO, CFD-based Aerodynamic Nozzle Design and Optimization program for supersonic/hypersonic wind tunnels
[AIAA PAPER 92-4009] p 1033 A92-56832
Maximized gust loads for a nonlinear airplane using matched filter theory and constrained optimization
[NASA-TM-104138] p 23 N92-11010
Structural tailoring of advanced turboprops (STAT): User's manual
[NASA-CR-187101] p 26 N92-11016
Multi-disciplinary optimization of aeroservoelastic systems
[NASA-CR-188983] p 44 N92-11377
On simple aerodynamic sensitivity derivatives for use in interdisciplinary optimization
[NASA-TM-104145] p 82 N92-11985
Optimal design of nonlinear shell structures
[FFA-TN-1991-18] p 157 N92-12312
Heuristic route optimization: A model for force level route planning p 164 N92-12520
Advanced rotorcraft control using parameter optimization
[NASA-CR-189502] p 135 N92-13073
Control augmented structural optimization of aeroelasticity tailored fiber composite wings
[AD-A241464] p 135 N92-13075
Comparison of polynomial approximations and artificial neural nets for response surfaces in engineering optimization p 165 N92-13835
Third International Conference on Inverse Design Concepts and Optimization in Engineering Sciences (ICIDES-3)
[NASA-CR-188125] p 170 N92-13928
On a global aerodynamic optimization of a civil transport aircraft p 193 N92-13931
A comparison of two closely-related approaches to aerodynamic design optimization p 193 N92-13933
Research on inverse, hybrid and optimization problems in engineering sciences with emphasis on turbomachine aerodynamics: Review of Chinese advances p 201 N92-13939
Design of 3-dimensional complex airplane configurations with specified pressure distribution via optimization p 194 N92-13948
Application of direct inverse analogy method (DIVA) and viscous design optimization techniques p 176 N92-13951
Aerodynamic shape optimization of arbitrary hypersonic vehicles p 194 N92-13954
Research on inverse methods and optimization in Italy p 202 N92-13956
Vortex generator design for aircraft inlet distortion as a numerical optimization problem p 194 N92-13959
Airfoil optimization with efficient gradient calculations p 177 N92-13960
Design optimization of transonic airfoils p 177 N92-13961
Integration of dynamic, aerodynamic, and structural optimization of helicopter rotor blades
[NASA-CR-189018] p 195 N92-14038
Optimization of the calculation margins of landing gears under extreme loads. Rupture static tests. Part 1: Program and test implantation
[CEAT-S8-6551-PARTIEL-1-PT-] p 195 N92-14043
Avionics standardization in Europe p 199 N92-14050
Experiences at Langley Research Center in the application of optimization techniques to helicopter airframes for vibration reduction
[NASA-TM-104193] p 299 N92-17033
Aircraft tracking optimization of parameters selection p 361 N92-18585
Evaluation of the COMPAS experimental system p 355 N92-19044
Experimental validation of structural optimization methods
[NASA-TM-104203] p 404 N92-19258
Robust control system design with application to high performance helicopters p 382 N92-19621
Optimizing tuning masses for helicopter rotor blade vibration reduction including computed airloads and comparison with test data
[NASA-TM-104194] p 367 N92-19846
MATGRID: A program for generation of C-H and C-O topology grids around wing/body configurations. Mathematical definition document
[FFA-TN-1990-19] p 444 N92-20468
Optimization of composite sandwich cover panels subjected to compressive loadings
[NASA-TP-3173] p 489 N92-20679
Flow analysis and design optimization methods for nozzle afterbody of a hypersonic vehicle
[NASA-CR-4431] p 446 N92-21456
Methodology for sensitivity analysis, approximate analysis, and design optimization in CFD for multidisciplinary applications --- computational fluid dynamics
[NASA-CR-190201] p 595 N92-22662
Integrated Design Analysis and Optimisation of Aircraft Structures
[AGARD-R-784] p 550 N92-23227
A system approach to aircraft optimization p 550 N92-23228
Application of multidisciplinary optimization methods to the design of a supersonic transport p 550 N92-23230

Application of an automated multidisciplinary analysis and optimisation system to the design of aircraft structures p 551 N92-23233
Multidisciplinary optimization studies using ASTROS p 571 N92-23234
A fin optimisation study p 551 N92-23237
Structural optimization of aircraft practice and trends p 551 N92-23239
Efficient and robust design optimization of transonic airfoils p 528 N92-23717
Large scale optimization using ASTROS: An overview p 649 N92-25921
Application of integrated structural analysis to the high speed civil transport p 684 N92-25927
Aircraft optimization by a system approach: Achievements and trends
[NASA-TM-107622] p 650 N92-25995
Trajectory optimization for the National Aerospace Plane
[NASA-CR-190355] p 650 N92-26017
Rarefied-flow aerodynamics
[NASA-CR-190452] p 715 N92-27191
Integrated Design Analysis and Optimisation of Aircraft Structures
[AGARD-LS-186] p 851 N92-28469
Fundamentals of structural optimisation p 851 N92-28470
Practical architecture of design optimisation software for aircraft structures taking the MBB-Lagrange code as an example p 851 N92-28471
Structural optimization of aircraft p 851 N92-28472
Multidisciplinary design and optimization
[AGARD-PAPER-2] p 851 N92-28473
Mathematical optimization: A powerful tool for aircraft design p 851 N92-28474
Constrained spanload optimization for minimum drag of multi-lifting-surface configurations
[NLR-TP-89126-U] p 828 N92-28660
Construction of a numerical optimization method for the definition of hypersupported profiles
[ONERA-RSF-43/1736-AY-146A] p 908 N92-28788
Concurrent engineering in design of aircraft structures
[MBB-FE-2-S-PUB-472] p 854 N92-29650
Aerodynamic design optimization using sensitivity analysis and computational fluid dynamics
[NASA-CASE-LAR-14815-1-CU] p 910 N92-29830
MBB-LAGRANGE: A general structural reliability and optimization structural system
[MBB/FW321/S/PUB/467] p 998 N92-30423
Multidisciplinary optimization of fiber composite aircraft structures
[MBB/FW321/S/PUB/476] p 961 N92-30424
Numerical optimization in Germany: A non-exhaustive survey on current activities with emphasis on aeronautics
[MBB/FE211/S/PUB/474] p 932 N92-30675
Nonlinear aerodynamics and the design of wing tips
[NASA-CR-190649] p 946 N92-31157
ASTOVL combat aircraft design synthesis and optimization
[CRANFIELD-AERO-9201] p 963 N92-31515

OPTOELECTRONIC DEVICES
Optical velocity sensor for air data applications p 368 A92-24575
A new milestone in automatic aircraft control - Fly-by-light systems transmit commands optoelectronically p 784 A92-45699
Potential for integrated optical circuits in advanced aircraft with fiber optic control and monitoring systems p 856 A92-46246
Fiber-optic position transducers for aircraft controls p 857 A92-48041
Multi-analog track fiber coupled position sensor p 857 A92-48043
Fiber optic speed sensor for advanced gas turbine engine control p 857 A92-48044
Fiber-optic pressure sensor system for gas turbine engine control p 857 A92-48047
Electro optical system to measure strains at high temperature
[NASA-CR-190450] p 1127 N92-33696

ORBIT CALCULATION
Current activities and future plans for GPS applications p 640 N92-24735
GPS orbit determination at the National Geodetic Survey p 1049 N92-33354

ORBIT PERTURBATION
Simulation of GRM drag compensation system --- Geopotential Research Mission p 285 A92-21023

ORBIT TRANSFER VEHICLES
Study of the flow field and molecular radiation heating around a reentry vehicle p 711 A92-43227
Simulation of real-gas effects on pressure distributions for aeroassist flight experiment vehicle and comparison with prediction
[NASA-TP-3157] p 501 N92-20677
Thermal response of rigid and flexible insulations and reflective coating in an aeroconvective heating environment
[NASA-TM-103925] p 852 N92-28721

ORBITAL LAUNCHING
Conceptual design of two-stage-to-orbit hybrid launch vehicle
[NASA-CR-190006] p 486 N92-20666

ORBITAL MANEUVERS
An alternative concept for aeroassisted orbit transfers
[AD-A243409] p 287 N92-17325

ORBITAL POSITION ESTIMATION
Integrating GPS with ranging transponders p 95 A92-16627

ORDNANCE
Laser ordnance initiation system p 577 A92-35465

ORGANIC COMPOUNDS
Low VOC primer for structural bonding --- volatile organic compound p 892 A92-47338
Low volatile organic compound paints
[DE91-017984] p 35 N92-11203

ORGANIC MATERIALS
High temperature thermoplastic and polyimide processing using CARE-MOLD wash-out tooling p 36 A92-10259

ORGANIZATIONS
Committees, their importance to the structures of the Helicopter Association International p 59 A92-14411
Monitoring operational concept
[DOT/FAA/SE-91/3] p 268 N92-15980
An analysis of total quality management in Aeronautical Systems Division
[AD-A246661] p 772 N92-27760

ORGANIZING
Preparation for a new plane (A 320): Experience reviewed p 1010 N92-30954
Flight crew integration in the maintenance chain of a commercial aircraft (A 320) p 1012 N92-30957

ORIFICES
A parametric numerical study of mixing in a cylindrical duct
[NASA-TM-105695] p 738 N92-26553

OROGRAPHY
The 1988 Australian Winter Storms Experiment - Case study: 6 August 1988 p 301 A92-23009

ORR-SOMMERFELD EQUATIONS
Numerical method for predicting transition in three-dimensional flows by spatial amplification theory p 812 A92-46886

ORTHOGONALITY
Orthogonal grids for multiple airfoils p 818 A92-47096

ORTHOTROPIC PLATES
Nonlinear flutter of orthotropic composite panel under aerodynamic heating
[AIAA PAPER 92-2132] p 589 A92-35699

ORTHOTROPIC SHELLS
Acoustic transmission through a 2-D orthotropic multi-layered infinite cylindrical shell p 780 A92-44197

OSCILLATING FLOW
Oscillation of nearly circular shock waves p 146 A92-15358
A model of gasdynamic loads on an oscillating nozzle shell p 80 A92-16817
The jet edge-tone feedback cycle - Linear theory for the operating stages p 392 A92-24758
Pressure wave propagation studies for oscillating cascades
[AIAA PAPER 92-0145] p 316 A92-25682
Characteristics of the mechanism of separated flow pulsation ahead of a spike-tipped cylinder in supersonic flow p 337 A92-27597
The numerical simulation of transonic inviscid flow over oscillating airfoils p 616 A92-38918
The combined wake of an array of oscillating ribbons p 623 A92-40180
Oscillation of oblique shock waves generated in a two dimensional asymmetric nozzle
[SAE PAPER 912061] p 791 A92-45443
The flip flop nozzle extended to supersonic flows
[AIAA PAPER 92-2724] p 803 A92-45561
Numerical solutions of unsteady oscillating flows past an airfoil
[AIAA PAPER 92-3212] p 825 A92-48817
The influences of forced oscillations toward vortex-breakdown p 934 A92-50210
Pulsation characteristics of one-phase and two-phase steam flows in Laval nozzles under off-design conditions p 1019 A92-53882
Downwash measurements on a pitching canard-wing configuration
[AD-A239956] p 12 N92-10016
Oscillating shock impingement on low-angle gas injection into a supersonic flow p 89 N92-13032
Aerodynamic coefficients of a symmetrical airfoil in an oscillating flow
[AD-A241073] p 89 N92-13035
Non-linear airloads hypersurface representation: A time domain perspective p 346 N92-18783
Unsteady-flow-field predictions for oscillating cascades
[NASA-TM-105283] p 348 N92-19437
A quantitative study of unsteady compressible flow on an oscillating airfoil
[AD-A244572] p 445 N92-21012
Periodic Euler and Navier-Stokes solutions about oscillating airfoils p 626 N92-24850
Comparison of Euler and full potential methods for unsteady transonic flow calculations p 719 N92-27943
NLR inviscid transonic unsteady loads prediction methods in aeroelasticity p 720 N92-27947
Transonic aeroelastic computations on wings using Navier-Stokes equations p 721 N92-27957
Experimental investigation of the flowfield of an oscillating airfoil
[NASA-TM-105675] p 833 N92-30182

OSCILLATION DAMPERS
Experimental investigation on blade loss transient response of rotor with flexible damped support p 557 A92-35551
A wing rock model for the F-14A aircraft
[AD-A243109] p 275 N92-17300

OSCILLATIONS
Prediction of dynamic hub load of a rotor executing multiple sinusoidal blade pitch variations p 846 A92-46921
Oscillations of an anisotropic rotor on an elastic anisotropic support p 1057 A92-56311
Multiple roll attractors of a delta wing at high incidence p 88 N92-13026
Identification of dynamic characteristics of flexible rotors as dynamic inverse problem p 220 N92-13962
Control of unsteady separated flow associated with the dynamic pitching of airfoils
[NASA-CR-189758] p 258 N92-15966
An experimental investigation of leading edge vortical flow about a delta wing during wing rock
[AD-A243363] p 260 N92-17114
Aeroservoelastic stability of aircraft at high incidence p 381 N92-18795
Investigation of a semi-empirical method to predict limit cycle oscillations of modern fighter aircraft
[NLR-TP-90087-U] p 481 N92-20475
Algorithm and code development for unsteady three-dimensional Navier-Stokes equations
[NASA-CR-190077] p 692 N92-25264
Turbine drive system of the high pressure LOX turbopump test facility
[DE92-783191] p 680 N92-25342
Experimental investigation of the unsteady pressure field around an oscillating blade
[MITT-90-01] p 768 N92-27407
Comparison of Euler and full potential methods for unsteady transonic flow calculations p 719 N92-27943
Evaluation of an unsteady implicit Euler code against two and three-dimensional standard configurations p 719 N92-27945
Unsteady transonic aerodynamics of pointed bodies of revolution in supersonic freestream p 719 N92-27946
Development of a method to predict transonic limit cycle oscillation characteristics of fighter aircraft p 746 N92-27958
Transonic wind tunnel investigation of limit cycle oscillations on fighter type wings p 721 N92-27959
A review of scale effects on surfaces in unsteady motion p 722 N92-27962
Organized turbulent structures and their induced wall pressure fluctuations p 949 N92-31853
Exploratory experimental investigation of a wave propeller
[AD-A252175] p 949 N92-32062
Time simulation of flutter with large stiffness changes
[NASA-TM-107650] p 963 N92-32111

OSCILLATORS
Low-noise oscillators for airborne radar applications
[AD-A242264] p 300 N92-17258
Response of structures to galloping excitation: Background and approximate estimation
[ESDU-91010] p 399 N92-18091

OUTLET FLOW
Investigation of the flow at the exit of an unshrouded centrifugal impeller and comparison with the 'classical' jet-wake theory
[ASME PAPER 90-GT-124] p 6 A92-11287
The influence of blade leaning on the performance of an integrated OGV-diffuser system
[ASME PAPER 91-GT-104] p 122 A92-15561

UV laser spectroscopic measurements in jet engine combustion exit flows
[AIAA PAPER 92-0513] p 396 A92-26939
A review of impinging jets in cross-flows - Experimentation and computation
[AIAA PAPER 92-0633] p 333 A92-27011
The unsteady flow characteristics of an S-shaped inlet at high incidence p 339 A92-27905
Outflow boundary conditions for Euler analysis of flow in turbine scroll p 591 A92-36037
Outflow boundary conditions using Duhamel's equation p 813 A92-46913
Hydrogen fueled subsonic-ram-combustor model tests for an air-turbo-ram engine
[NAL-TR-1064T] p 280 N92-17855

OVERPRESSURE
Investigation and application of compressor loading technique p 469 A92-29718
Composite cylinder blast overpressure testing p 529 A92-32984
Application of computational fluid dynamics to sonic boom near- and mid-field prediction p 1031 A92-56173
Sonic boom p 55 N92-10608
Sonic booms produced by US Air Force and US Navy aircraft: Measured data
[AD-A244804] p 512 N92-21719
Lateral spread of sonic boom measurements from US Air Force boomfile flight tests p 1140 N92-33883
Preliminary results from the White Sands Missile Range sonic boom propagation experiment p 1140 N92-33884
Subjective loudness response to simulated sonic booms p 1140 N92-33885

OXIDATION
Effect of sustained high temperature exposure on the mechanical properties of Nicalon/Al2O3 composites p 668 A92-39672
Fabrication and properties of fiber-reinforced ceramic composites made by directed metal oxidation p 669 A92-39861
NLR experience with high velocity burner rig testing, 1979-1989
[NLR-TP-89152-U] p 385 N92-18415
Advisory Circular: Corrosion control for aircraft
[FAA-AC-43-4A] p 420 N92-21834

OXIDATION RESISTANCE
BMI/bis (allylphenoxyphthalimide)-copolymers - A new family of resins for advanced composites with improved thermal oxidative stability p 33 A92-10213
Thermal oxidation stability of aviation turbine fuels --- Book
[ISBN 0-8031-1248-3] p 669 A92-40409
Joining a Ni-based creep-resistant (ODS) alloy by brazing p 1116 A92-54867
Large thin composite thermostructural parts p 576 N92-23821
Liquid lubricants for advanced aircraft engines
[NASA-TM-104531] p 1109 N92-32863

OXYGEN
Rotational coherent anti-Stokes Raman spectroscopy measurements in a rotating cavity with axial throughflow of cooling air - Oxygen concentration measurements p 990 A92-49574
Effectiveness of an onboard water spray system during an oxygen enriched cabin fire
[DOT/FAA/CT-TN91/51] p 264 N92-17149
Preliminary screening procedures and criteria for replacements for Halons 1211 and 1301
[AD-A252912] p 1126 N92-33501
A numerical model for sonic boom propagation through an inhomogeneous, windy atmosphere p 1138 N92-33876

OXYGEN ATOMS
Effects of oxygen dissociation on hypervelocity combustion experiments
[AIAA PAPER 92-3964] p 1098 A92-56791

OZONE
A preliminary design and analysis of an advanced heat-rejection system for an extreme altitude advanced variable cycle diesel engine installed in a high-altitude advanced research platform
[NASA-CR-186021] p 871 N92-29427

OZONE DEPLETION
Impact of heterogeneous chemistry on model-calculated ozone change due to high speed civil transport aircraft p 45 A92-12941
Environmental impact of a future supersonic transport aircraft
[ONERA, TP NO. 1991-132] p 161 A92-16108
The atmospheric effects of stratospheric aircraft: A first program report
[NASA-RP-1272] p 408 N92-19121
Ozone response to aircraft emissions: Sensitivity studies with two-dimensional models p 409 N92-19126

OZONOMETRY
Digital ozonesondes - Examples of results from the EMEFS experiments of 1988 and 1990 p 468 A92-32140

OZONOSPHERE
SHARP: Subsonic High Altitude Research Platform
[NASA-CR-190004] p 648 N92-25263

P

P-3 AIRCRAFT
SATCOM antenna siting study on P-3C aircraft, volume 2
[NASA-CR-189515] p 221 N92-14263

PACIFIC ISLANDS
A view from the Pacific Basin --- air traffic p 532 A92-33440

PACKET TRANSMISSION
24-bit flight test data recording format p 900 A92-47528

PACKETS (COMMUNICATION)
Future developments in aeronautical satellite communications p 678 N92-24167

PACKINGS (SEALS)
Rotor-to-stator partial rubbing and its effects on rotor dynamic response p 224 N92-14367

PADE APPROXIMATION
Aeroservoelasticity p 642 A92-37577

PAINTS
Aerodynamic applications of pressure-sensitive paint
[AIAA PAPER 92-0264] p 394 A92-25720
Paint under pressure p 399 A92-28495
Surfprep flash-lamp depaint system evaluation p 497 A92-32411
Thermal paints for shock/boundary layer interaction in inlet flows
[AIAA PAPER 92-3626] p 1113 A92-54093
Low volatile organic compound paints
[DE91-017984] p 35 N92-11203
Paint removal using cryogenic processes
[AD-A247668] p 895 N92-28912

PALLADIUM ALLOYS
Aluminides modified by palladium - Protection of new parts by local finishing
[ONERA, TP NO. 1992-49] p 893 A92-48610
High temperature strain gage technology for hypersonic aircraft development applications
[NASA-CR-189101] p 592 N92-22239

PALMGREN-MINER RULE
A comparison of fatigue life prediction methodologies for rotorcraft p 647 A92-40884

PANEL FLUTTER
Optimization of the flutter load by material orientation p 146 A92-15222
Linear panel flutter of an elliptic cylindrical shell p 291 A92-21216
Temperature and initial curvature effects in low-density panel flutter
[AIAA PAPER 92-2128] p 589 A92-35695
Finite element nonlinear panel flutter with arbitrary temperatures in supersonic flow
[AIAA PAPER 92-2129] p 589 A92-35696
Large-amplitude finite element flutter analysis of composite panels in hypersonic flow
[AIAA PAPER 92-2130] p 589 A92-35697
Nonlinear flutter of orthotropic composite panel under aerodynamic heating
[AIAA PAPER 92-2132] p 589 A92-35699
Finite element frequency domain solution of nonlinear panel flutter with temperature effects and fatigue life analysis p 682 N92-25589

PANEL METHOD (FLUID DYNAMICS)
A re-examination of the aerodynamics of hovering rotors including the presence of the fuselage p 66 A92-14446
Application of holomorphic vectors theory in three-dimensional potential flow problem p 292 A92-21923
Parallel algorithms for panel methods --- in fluid dynamics p 293 A92-22346
Aerodynamic characteristics of a wing near its tip using panel method p 251 A92-22524
Efficient panel method for vortex sheet roll-up p 309 A92-24404
Maximum lift prediction for multielement wings
[AIAA PAPER 92-0401] p 324 A92-26254
Numerical and experimental analysis of vortex sheets behind lifting surfaces
[AIAA PAPER 92-0409] p 325 A92-26262
A turbulence model for iced airfoils and its validation
[AIAA PAPER 92-0417] p 326 A92-26267
Theoretical and experimental studies of helicopter rotor/fuselage interaction
[ONERA, TP NO. 1991-198] p 329 A92-26357
Zonal flow analysis method for two-dimensional airfoils p 330 A92-26435
Theoretical study on the unsteady aerodynamic characteristics of an oscillating cascade with tip clearance (In the case of loaded cascade) p 331 A92-26797
Effect of airfoil (trailing-edge) thickness on the numerical solution of panel methods based on the Dirichlet boundary condition p 340 A92-28041
Error characteristics of a vortex panel method in two-dimensional flow p 421 A92-29521
Panel method control in 3-D hyperbolic grid generation p 617 A92-39940
Unsteady airloading panel method for propfans p 780 A92-44512
Free wake analyses of a hovering rotor using panel method
[SAE PAPER 912004] p 789 A92-45405
Aerodynamic characteristics near the tip of a finite wing by a panel method
[SAE PAPER 912020] p 790 A92-45413
Thin-airfoil correction for panel methods p 811 A92-46811
Aerodynamic analysis of the Pioneer unmanned air vehicle
[AIAA PAPER 92-4635] p 1027 A92-55382
Three-dimensional numerical analysis of impinging circular jet - Discrete vortex method p 1029 A92-56040
Numerical simulation of supersonic unsteady flow using a panel method p 1030 A92-56048
Generalized aerodynamics analysis by the boundary element method p 1030 A92-56050
Analysis of the main wing lift distribution of the STOL research aircraft Asuka p 1053 A92-56051
Prediction of forces and moments for hypersonic flight vehicle control effectors
[NASA-CR-188954] p 33 N92-11070
Design of 3-dimensional complex airplane configurations with specified pressure distribution via optimization p 194 N92-13948
Analysis and design of planar and non-planar wings for induced drag minimization
[NASA-CR-189509] p 179 N92-13999
Analysis tools of ONERA and DLR for the aerothermodynamics of reentry vehicles p 211 N92-14977
A turbulence model for iced airfoils and its validation
[NASA-TM-105373] p 186 N92-15052
Use of Navier-Stokes analysis in section design
[AD-A242074] p 299 N92-17168
CAR 88: A method to calculate subsonic and supersonic, steady and unsteady, potential flow about complex configurations
[NLR-TR-88154-U] p 400 N92-18221
Thrust vectoring for lateral-directional stability
[NASA-CR-186016] p 482 N92-21357
Effects of frost on wing aerodynamics and take-off performance p 450 N92-21687
Modernized MBB panel code: User's guide including background theory
[PB92-136431] p 526 N92-22233
PAN AIR: A computer program for predicting subsonic or supersonic linear potential flows about arbitrary configurations using a higher order panel method. Volume 1: Theory document (version 3.0)
[NASA-CR-3251] p 526 N92-22648
PAN AIR: A computer program for predicting subsonic or supersonic linear potential flows about arbitrary configurations using a higher order panel method. Volume 2: User's manual (version 3.0)
[NASA-CR-3252] p 527 N92-22865
Panel methods for aerodynamic analysis and design p 552 N92-23955
VORVISC: A vortex lattice method with viscous and compressibility corrections for full aircraft configurations including propulsion p 626 N92-24857
Calculation of unsteady subsonic and supersonic flow about oscillating wings and bodies by new panel methods
[NLR-TP-89119-U] p 827 N92-28659
Hyperbolic grid generation control by panel methods
[NLR-TP-91061-U] p 924 N92-29604
A method for computing the 3-dimensional flow about wings with leading-edge vortex separation. Part 2: Description of computer program VORSEP
[NLR-TR-86006-U] p 833 N92-29916
Potential flow theory and operation guide for the panel code PMARC
[NASA-TM-102851] p 1036 N92-32422
Further development of the CANAERO computer code to include propulsor modelling
[DREA-CR-90-425] p 1038 N92-32811

PANELS
Stability of stiffened panels with allowance for plasticity under nonstationary heating and loading p 493 A92-30152

Coupled 2D-3D finite element method for analysis of a skin panel with a discontinuous stiffener
[AIAA PAPER 92-2474] p 583 A92-34363
Space Shuttle shell structure waffle panel optimization
[AIAA PAPER 92-2359] p 586 A92-34591
Combined compressive and shear buckling analysis of hypersonic aircraft sandwich panels
[AIAA PAPER 92-2487] p 586 A92-34603
Performance of aluminum honeycomb panels with structural defects and core anomalies. II - Specimen description and test results p 591 A92-36156
Design and test of aircraft aft fuselage structure using postbuckled shear panels p 848 A92-47406
Design and performance of duct acoustic treatment p 236 N92-14783
The influence of a retarding rocket on parameter limits for reentry trajectories p 211 N92-15037
Engine panel seals for hypersonic engine applications: High temperature leakage assessments and flow modelling
[NASA-TM-105260] p 298 N92-16336
Rapid repair of integrally stiffened carbon fibre composite structures by bolted aluminium elements
[MBB-FE202-S-PUB-0453-A] p 290 N92-17310
Finite element analysis of a riveted repair on a curved composite panel
[AD-A243916] p 404 N92-19384
Manufacturing development of pultruded composite panels
[NASA-CR-181780] p 578 N92-22637
Prediction of response of aircraft panels subjected to acoustic and thermal loads
[NASA-CR-190305] p 678 N92-24345
Combined load test apparatus for flat panels
[NASA-CASE-LAR-14698-1] p 911 N92-30028
Global/local methods research using the CSM testbed p 1107 N92-32528
Inspection of fabricated fuselage panels using electronic shearography
[DOT/FAA/CT-TN92/26] p 1127 N92-33627

PAPER (MATERIAL)
The 'White Pelican' project - Design and construction of the world's largest paper airplane p 931 A92-51400

PAPERS
A modern view of Theodore Theodorsen --- Book
[ISBN 0-930403-85-1] p 307 A92-26250

PARABOLIC DIFFERENTIAL EQUATIONS
Implementation of Vigneron's streamwise pressure gradient approximation in the PNS equations
[AIAA PAPER 92-0189] p 256 A92-23798
Solution-adaptive grid procedure for the parabolized Navier-Stokes equations p 432 A92-31163
Marching with the parabolized Navier-Stokes equations. Problem 1: Numerical study of hypersonic viscous cone flow
[AERO-REPT-9007] p 344 N92-18231
Marching with the parabolized Navier-Stokes equations. Problem 2: Hypersonic viscous flow over a flat plate
[AERO-REPT-9008] p 345 N92-18232

PARABOLIC FLIGHT
Observational study of pool boiling under microgravity p 757 A92-41060
Process modeling KC-135 aircraft
[NASA-CR-184278] p 359 N92-18347
Outlines of parabolic flight p 764 N92-26441

PARABOLIC REFLECTORS
Mid-range UV communications --- ultraviolet radiation
[AD-D015213] p 770 N92-27615
Antenna pattern measurement facilities
[AD-A248964] p 982 N92-30329

PARACHUTE DESCENT
Landing spacecraft gently on earth - The Soviet parachute systems p 33 A92-13227
Parachute canopy control simulation - A solution for aircrew emergency training p 572 A92-35428
Notes on the cause of parachute critical velocity
[AD-A244417] p 347 N92-19085

PARACHUTE FABRICS
Canadian CF-18 aircraft ejection seat parachute update p 529 A92-32983
Selection of opening model for parachute scaling studies
[AD-A250882] p 943 N92-30239

PARACHUTES
Evolution of ejection systems --- Russian book p 262 A92-21684
Standard for aerodynamic decelerator and parachute drawings --- Book
[ISBN 0-930403-94-0] p 634 A92-38000
Improved measurement of the dynamic loads acting on rotating parachutes p 702 A92-41236
The influence of a retarding rocket on parameter limits for reentry trajectories p 211 N92-15037
Trajectory analysis of the G-11 family of clustered parachutes to determine minimum altitude
[AD-A243375] p 261 N92-17404
Notes on the cause of parachute critical velocity
[AD-A244417] p 347 N92-19085
Selection of opening model for parachute scaling studies
[AD-A250882] p 943 N92-30239
Effects of the abrasiveness of test and training site soils on parachute life
[AD-A252389] p 1038 N92-32900

PARALLEL COMPUTERS
Current growth in the aeronautics p 701 A92-41196
Parallel grid generation/optimization using block-domain decomposition p 776 A92-41199
Solutions of acoustic field problems using parallel computers p 925 A92-45929
The Office of Naval Research initiative on ultradependable multicomputers and electronic systems p 1005 A92-49278
Implementation of an object-oriented flight simulator D.C. electrical system on a hypercube architecture
[AD-A243700] p 284 N92-17097

PARALLEL FLOW
The problem of body motion in a medium with resistance p 604 A92-36416
Linear stability of supersonic cone boundary layers p 1024 A92-54910
Pressure and velocity measurements about an airfoil during a parallel blade-vortex interaction p 446 N92-21429

PARALLEL PLATES
Compressibility effects in thin channels with injection p 216 A92-18369
The jet edge-tone feedback cycle - Linear theory for the operating stages p 392 A92-24758

PARALLEL PROCESSING (COMPUTERS)
Stochastic ordering properties and optimal routing control for a class of finite capacity queueing systems p 48 A92-11375
Traditional finite element analysis - Opportunities for parallelism? p 40 A92-12354
Parallel computation of aerodynamic influence coefficients for aeroelastic analysis on a transputer network p 53 A92-12367
Study of the discrete singularly perturbed linear-quadratic control problem by a bilinear transformation p 163 A92-16072
A processor-in-the-loop simulation using an XANALOG computer p 232 A92-19094
Parallel algorithms for panel methods --- in fluid dynamics p 293 A92-22346
A parallel architecture adapted to onboard multiexpert systems p 276 A92-23040
On modelling of aero-gas turbine engine for real-time digital simulator --- of engine control system p 471 A92-29743
Improved coordination in non-hierarchic system optimization
[AIAA PAPER 92-2497] p 601 A92-34554
A piloted comparison of elastic and rigid blade-element rotor models using parallel processing technology p 546 A92-35751
Comparison of elastic and rigid blade-element rotor models using parallel processing technology for piloted simulations
[SAE PAPER 912120] p 608 A92-39968
Parallel solver for trajectory optimization search directions p 777 A92-43399
Future directions in computing and CFD
[AIAA PAPER 92-2734] p 917 A92-45489
Parallel computing strategies for block multigrid implicit solution of the Euler equations p 812 A92-46894
Application of a parallel direct simulation Monte Carlo method to hypersonic rarefied flows p 1024 A92-54916
Modular techniques for dynamic fault-tree analysis p 1120 A92-56241
Parallel processing applications for gas turbine engine control p 25 N92-11012
A multiblock flow solver for inviscid hypersonic flows p 181 N92-14986
Parallelization of a Direct Simulation Monte Carlo (DSMC) code for fluid dynamics p 227 N92-15033
Timing analysis of parallel algorithms on a MIMD multiprocessor
[ITN-92-85153] p 510 N92-20905
A parallel-vector algorithm for rapid structural analysis on high-performance computers
[NASA-TM-102614] p 595 N92-22649
Application of neural network to adaptive control theory for super-augmented aircraft
[AD-A246596] p 745 N92-27505
ICAAS piloted simulation evaluation p 735 N92-27906
Real-time processing of radar return on a parallel computer
[NASA-CR-4456] p 1043 N92-32606
Advanced techniques in reliability model representation and solution
[NASA-TP-3242] p 1134 N92-33483

PARAMETER IDENTIFICATION
On-line state estimation and parameter identification for flight p 50 A92-11429
A method for determining the optimal composition of the measured parameters in diagnosing gas turbine engines p 128 A92-16819
A flight test study to determine aircraft propulsive efficiency and aerodynamic drag using two parameter identification methods and Lock's propeller model
[AIAA PAPER 92-0170] p 271 A92-23781
Using fractal dimension for target detection in clutter p 410 A92-24423
Parameter identification of compressor dynamics during closed-loop operation p 508 A92-29313
LOS rate estimation in inertial navigation using landmarks p 453 A92-29360
Nonlinear damping estimation from rotor stability data using time and frequency domain techniques p 641 A92-36855
Spaceplane longitudinal aerodynamic parameter estimation by cable-mount dynamic wind-tunnel test
[SAE PAPER 911980] p 788 A92-45385
Parameter identification of linear systems based on smoothing p 873 A92-46742
Aerodynamic parametric studies and sensitivity analysis for rotor blades in axial flight p 816 A92-46959
Subsonic flight test evaluation of a propulsion system parameter estimation process for the F100 engine
[AIAA PAPER 92-3745] p 866 A92-49110
Detection and identification of axial flow compressor instabilities p 969 A92-50504
Maximum likelihood algorithm and its application to parameter identification of closed-loop flight vehicles p 1008 A92-53023
Parameter estimation of an augmented airplane with unsteady aerodynamics modelling p 1073 A92-53546
Parameter identification of unsteady aerodynamic forces for elastic vehicles
[AIAA PAPER 92-4505] p 1027 A92-55372
Parameter identification of AV-8B wingborne aerodynamics for flight simulator model updates
[AIAA PAPER 92-4506] p 1027 A92-55373
On-line identification and control of linearized aircraft dynamics p 1082 A92-55911
Application of restructurable flight control system using nonlinear control to an airliner p 1084 A92-56068
Aerodynamic model identification of a spaceplane model from a cable-mount dynamic wind-tunnel test p 1093 A92-56114
The identification of coupled flapping/inflow models for hovering flight p 1058 A92-56335
Parameter identification for nonlinear aerodynamic systems
[NASA-CR-188985] p 53 N92-10347
Parameter identification studies on the NASA/Ames Research Center Advanced Concepts Flight Simulator
[NASA-TM-105126] p 31 N92-11024
Graphics for interactive PC based parameter estimation package
[NAL-PD-FC-9117] p 412 N92-18252
Model parameter identification techniques for flight flutter testing
[AERO-REPT-9105] p 380 N92-18294
Use of stepwise regression techniques and kinematic compatibility for the analysis of EAP flight data p 365 N92-18790
Blade-vortex noise on a helicopter main rotor. Study of the strong two dimensional incompressible interaction
[ONERA-RT-96/5094-PY] p 511 N92-20388
Parameter identification for nonlinear aerodynamic systems
[NASA-CR-190264] p 830 N92-29329
The design and development of a portable, DSP micro-processor based, high-accuracy data acquisition system
[NRC-32146] p 1134 N92-32851
Elementary flutter analysis p 1088 N92-34162

PARAMETERIZATION
A parametric study of airbreathing Pulsed Detonation Engine
[AIAA PAPER 92-0392] p 471 A92-31660
Measures of merit for aircraft dynamic maneuvering p 642 A92-37825
Estimation of lift and drag characteristics of an aircraft from flight data p 959 A92-51942
Advanced rotorcraft control using parameter optimization
[NASA-CR-189502] p 135 N92-13073

An analytical approach to grid sensitivity analysis for NACA four-digit wing sections
[NASA-CR-190251] p 631 N92-25175
Fundamentals of structural optimisation
p 851 N92-28470
Ageing airplane repair assessment program for Airbus A300 p 838 N92-30123

PARAWINGS
An experimental study of subsonic separated flow over parawings p 4 A92-10901

PARTIAL DIFFERENTIAL EQUATIONS
Gain-scheduled control of nonlinear partial differential equations p 47 A92-11347
Modeling of linear isentropic flow systems
p 593 N92-22495
On constructing three-dimensional overlapping grids with CMPGRD p 691 N92-24424
PDES application protocol suite for composites (PAS-C). Functional needs report for the PAS-C program
[AD-A247886] p 1108 N92-32629

PARTICLE INTERACTIONS
An investigation in the variance in particle surface interactions and their effects in gas turbines
[ASME PAPER 91-GT-380] p 653 A92-36891
Microgravity nucleation and particle coagulation experiments support
[NASA-CR-189899] p 502 N92-21433

PARTICLE LADEN JETS
Effect of carbon particles and mixing on afterburning of exhaust plumes
[AIAA PAPER 92-0767] p 387 A92-27107
Thermal radiation effects on a shocked particle-laden gas p 780 A92-44377

PARTICLE MOTION
An assessment of particle velocimetry potential in hypersonic flow
[AIAA PAPER 92-0010] p 247 A92-22135
Laser velocimetry seed particles within compressible, vortical flows p 395 A92-26413
Motion of a sphere in a gas - Numerical solution of the linearized Boltzmann equation p 591 A92-36194
Theoretical study (Lagrangian modeling) of turbulent particulate dispersion
[ETN-91-99909] p 42 N92-11287
Vaporizing particle velocimeter
[NASA-CASE-LAR-14685-1] p 1042 N92-34172

PARTICLE SIZE DISTRIBUTION
Size and critical supersaturation for condensation of jet engine exhaust particles p 161 A92-15884
Improving sample introduction for total wear metal determination by atomic emission spectroscopy
p 389 A92-26850
Airflow effects about PMS probes on the DLR Falcon --- Particle Measuring System for atmospheric research aircraft p 467 A92-32060
Measured and calculated optical property profiles in the mixed layer and free troposphere p 1129 A92-54630
In situ measurement of particle formation in heated jet fuels: A new application of photon correlation spectroscopy
[DE92-003641] p 488 N92-20132

PARTICLE THEORY
Transport phenomena and interfacial kinetics in multiphase combustion systems
[AD-A244849] p 489 N92-20695

PARTICLE TRAJECTORIES
Coating effect on particle trajectories and turbine blade erosion p 653 A92-36892
Viscous flow analysis of advanced particle separators
p 737 A92-44517
Particle trajectory computer program for icing analysis of axisymmetric bodies
[NASA-CR-189134] p 352 N92-19276
Application of a water droplet trajectory prediction code to the design of inlet particle separator anti-icing systems
[PNR-90839] p 474 N92-20573

PARTICLES
In situ measurement of particle formation in heated jet fuels: A new application of photon correlation spectroscopy
[DE92-003641] p 488 N92-20132
Microgravity nucleation and particle coagulation experiments support
[NASA-CR-190159] p 502 N92-21385

PARTITIONS (MATHEMATICS)
Decentralized hierarchical partitioning of centralized integrated controllers --- for flight propulsion in STOVLs
p 477 A92-29119

PASSENGER AIRCRAFT
Dornier Do.328 special - Examining the high-speed commuter p 21 A92-11882
Maximum mass allowance to justify passenger-carrying aircraft modification p 113 A92-16802
Implementation and usage of the RJ program Data Acquisition System Ground Station p 210 A92-19257
Aging aircraft programme entails major effort and expense p 169 A92-20023
Improving the efficiency of passenger aircraft during the landing approach p 460 A92-31893
An aircraft manufacturer's perspective
p 515 A92-33430
Saab 2000 begins 1,200-hr. test program at Skavsta site p 538 A92-33800
The helicopter commuter - A perspective on regular passenger transportation by rotary wing
p 634 A92-38208
High speed civil transport electrical power system technology requirements
[SAE PAPER 912185] p 655 A92-40005
Pusher turboprop installation technology for the Embraer CBA-123 vector
[SAE PAPER 911030] p 658 A92-40943
Navigation preparations for passenger helicopters
p 723 A92-43155
A helicopter transportation system
p 723 A92-43161
WIG transportation efficiency considering the influence of no-load situation p 781 A92-43241
Small and cost-effective airship for transportation
p 731 A92-43244
Aviation, motor, and space designs --- research and development in U.S.S.R. p 784 A92-46202
Mathematical modeling of the flight of passenger aircraft in the case of engine failure p 875 A92-47777
Regional challenge --- flight test of Canadair Regional Jet p 961 A92-53121
777 - The airlines' higher-order technology airplane
p 1052 A92-55104
A note on thrust control for jetliner during approach
p 1053 A92-56061
Application of restructurable flight control system using nonlinear control to an airliner p 1084 A92-56068
Evaluation report of an experimental Satcom operation by a Japan Airline's B747 passenger plane
p 1046 A92-56092
Development of aircraft bonded structure and the NDI method p 1016 A92-56100
Kappa Group: The initial guess. A proposal in response to a commercial air transportation study
[NASA-CR-189981] p 366 N92-19374
An evaluation of in-cabin safety features in passenger aircraft
[ETN-92-90656] p 449 N92-20794
Aeronautical research in the United States: Challenges for the 1990's p 420 N92-21502
Experimental study of a generic high-speed civil transport: Tabulated data
[NASA-TM-104216] p 525 N92-22232
Gamma Group-The Pale Horse: A proposal in response to a commercial air transportation study ort study
[NASA-CR-190019] p 731 N92-26435
Aging commuter aeroplanes: Fatigue evaluation and control methods p 915 N92-30132

PASSENGERS
Airport activity statistics of certificated route air carriers: Calendar year 1990
[AD-A241483] p 93 N92-13045
Development of an annoyance model based upon elementary auditory sensations for steady-state aircraft interior noise containing tonal components
[NASA-TM-104147] p 166 N92-13758
Passenger knowledge of airline safety information
[CRANFIELD-AERO-9111] p 187 N92-15054

PATTERN RECOGNITION
Optical computing at NASA Ames Research Center
[AIAA PAPER 91-3779] p 231 A92-17637
Analysis of objects in binary images
[NASA-CR-4420] p 234 N92-14598
Processing complexity of two approaches to object detection and recognition p 234 N92-14677
Inspection of aircraft engine components using automated eddy current and pattern recognition techniques
[NRC-LTR-ST-1834] p 504 N92-22029
Binary optical filters for scale invariant pattern *recognition*
[NASA-TM-103902] p 853 N92-28910

PAVEMENTS
Alternate/modified binders for asphalt airfield pavements
[AD-A242829] p 285 N92-17260
A methodology for the evaluation of runway roughness for repair
[AD-A250407] p 887 N92-28772
Performance of insulated pavements at Newton Fields, Jackman, Maine
[CRREL-92-9] p 1101 N92-32903
Criteria for use of seal coats on airport pavements
[DOT/FAA/RD-92/18] p 1102 N92-34247

PAYLOADS
NASA test flights with increased flight stress indices
[AIAA PAPER 91-3665] p 20 A92-11012
Symptom of payload-induced flight instability
p 873 A92-46761
Structural considerations for aircraft payload Modification: P-3C zero fuel weight increase
[AD-A242690] p 196 N92-15068
SHARP: Subsonic High Altitude Research Platform
[NASA-CR-190004] p 648 N92-25263

PCM TELEMETRY
An alternative method for acquiring avionic bus data in a class I PCM telemetry system p 217 A92-19202
MIL-STD-1553 data bus/PCM multiplexer system
p 188 A92-19211
Compression techniques for video telemetry
p 188 A92-19214
A state-of-the-art data acquisition system
p 217 A92-19231
Design and implementation of a total flight test system
p 189 A92-19278
High rate PCM data receiving, recording and relying
p 189 A92-19279
Real time presentation for RAFALE in-flight tests
p 882 A92-47522
24-bit flight test data recording format
p 900 A92-47528
Modern techniques for monitoring airborne telemetry
p 857 A92-47560
Remote telemetry concepts p 882 A92-47562
Design considerations for a modern telemetry processing and display system p 882 A92-47584

PEEK
Manufacture of a primary flight structure using thermoplastics p 1 A92-10197
The development and test of thermoplastic composite speed brake p 272 A92-24178
Processing effects and damage tolerance in poly(etheretherketone) composites p 388 A92-26152

PEELING
Behavior of aircraft tire coupons under various loading conditions
[AD-A241416] p 116 N92-13063

PENALTY FUNCTION
Application of the multiplier penalty function method to the optimum design of wing configurations of aerospace vehicle p 356 A92-25013
Coupled Rayleigh-Ritz/finite element structural analysis using penalty function method
[AIAA PAPER 92-2238] p 581 A92-34292
A penalty-Galerkin finite element method for calculating transonic flow over wings p 943 A92-53386
Airfoil optimization with efficient gradient calculations
p 177 N92-13960

PERCEPTUAL ERRORS
Reference mode effect on the auditory display of aircraft bank angle
[AD-A247825] p 728 N92-27916

PERFORATED PLATES
New method for boundary layer thickness control on ground plate in wind tunnel p 383 A92-25110
Determination of the mass-flow-rate characteristics of porous panels p 439 A92-31875
Local heat transfer in the perforation channels of turbine nozzle vanes p 657 A92-40615
Preliminary finite element analysis of unloaded and loaded notched composite laminated plates
[NRC-LTR-ST-1806] p 159 N92-13454

PERFORMANCE
The design of test-section inserts for higher speed aeroacoustic testing in the Ames 80- by 120-foot wind tunnel
[NASA-TM-103915] p 927 N92-28909

PERFORMANCE PREDICTION
Efficient lifting line method for computing performance of propeller p 24 A92-10956
Aerodynamic design of propeller by numerical optimization p 24 A92-10957
Power performance of a nonisentropic Brayton cycle
p 54 A92-11281
Ongoing development of a computer jobstream to predict helicopter main rotor performance in icing conditions p 65 A92-14407
Preliminary experience with an expert system providing initial centrifugal compressor sizing for performance prediction and analysis
[ASME PAPER 91-GT-28] p 162 A92-15513
One-dimensional, stage-by-stage, axial compressor performance model
[ASME PAPER 91-GT-192] p 124 A92-15618
Off-design performance prediction of turbofans using gasdynamics
[ASME PAPER 91-GT-389] p 126 A92-15721
Jet engine test system including expert system for diagnosis
[ASME PAPER 91-GT-408] p 137 A92-15737

Prediction of generalized aerodynamic forces following linearized supersonic theory
[ONERA, TP NO. 1991-114] p 76 A92-16093
Diffuser efficiency estimation parameters
p 79 A92-16814
PAR-WIG performance prediction during acceleration from water-borne to air-borne p 291 A92-21721
Maximum lift prediction for multielement wings
[AIAA PAPER 92-0401] p 324 A92-26254
Computational analysis of high-speed ejection seats
[AIAA PAPER 92-0403] p 324 A92-26256
Development of an analytical method to predict helicopter main rotor performance in icing conditions
[AIAA PAPER 92-0418] p 326 A92-26268
Predictions of compressible viscous flows at all Mach number using pressure correction, collocated primitive variables and non-orthogonal meshes
[AIAA PAPER 92-0426] p 326 A92-26274
Design and calculation of performance of a subsonic inlet duct p 343 A92-28478
Calculation of combustion efficiency of dump combustor in ramjet engine p 375 A92-28480
Robust optimal control with a worst case time domain performance criterion p 509 A92-29368
Effects of bleed and power extraction on the operating line of engines p 469 A92-29717
Investigations of the laws of surge and rotating stall forecast in aeronautical engine p 470 A92-29739
Navier-Stokes methods to predict circulation control airfoil performance p 442 A92-32243
Aircraft performance --- Book
[ISBN 0-521-36264-4] p 538 A92-33919
Effect of adaptive material properties on static aeroelastic control
[AIAA PAPER 92-2526] p 539 A92-34373
Life prediction of local stress-strain method
p 588 A92-35564
Statistical analysis and prediction of aeroengine deterioration p 557 A92-35570
Handling and performance considerations when conducting air-to-air refuelling of large aircraft by the probe and drogue system p 548 A92-35937
Performance of turbulence models to predict supersonic boundary layer flows p 613 A92-37553
Quantification of aircraft carbon brake wear using regression analysis and periodic wave forms
[SAE PAPER 912174] p 644 A92-39999
An analysis tool for UAV effectiveness evaluation
p 608 A92-40386
A validated code to predict the performance of onboard broadband optical seekers through a turbulent transonic flow
[AIAA PAPER 92-2792] p 778 A92-41331
Finite element analysis of tire critical speeds
p 762 A92-42949
Row-by-row off-design performance calculation method for turbines p 737 A92-44514
Indicial method calculating dynamic stall on a vertical axis wind turbine p 714 A92-44528
An experimental investigation on aft bypass supersonic inlet performance at high angle of attack and yaw
p 862 A92-48268
Characterization of thermal performance of wheel outboard of an aircraft p 849 A92-48352
The effect of tip convection on the performance and optimum dimensions of cooling fins p 902 A92-48354
Systems simulation of an advanced avionics COMSEC unit p 921 A92-48485
A testability-dependent maintainability-prediction technique p 1120 A92-56222
Tohoku University low-turbulence wind tunnel
[AIAA PAPER 92-3913] p 1095 A92-56746
Performance evaluation of a transonic wind tunnel compressor
[AIAA PAPER 92-3927] p 1096 A92-56758
Predicted aerodynamic characteristics for HL-20 lifting-body using the aerodynamic preliminary analysis system (APAS)
[AIAA PAPER 92-3941] p 1033 A92-56771
Air-to-air visual acquisition handbook
[ATC-151] p 93 N92-13042
Further calculations of the performance of turbofan engines incorporating a wave rotor
[AD-A240867] p 131 N92-13072
Nonstationary gasdynamics p 220 N92-13985
The effects of winglets on low aspect ratio wings at supersonic Mach numbers
[NASA-CR-4407] p 178 N92-13996
Design and performance of duct acoustic treatment
p 236 N92-14783
Discussion for possibility of some aerodynamic ground effect craft
[NAL-TM-619] p 300 N92-17757
A study of the aeroelastic behaviour of helicopter rotor blades featuring swept tips p 367 N92-19701
Component-specific modeling --- jet engine hot section components
[NASA-CR-189088] p 377 N92-19726
Rotary engine performance limits predicted by a zero-dimensional model
[NASA-CR-189129] p 474 N92-20650
Cooperative planning in aviation contexts
p 456 N92-21509
A review of icing research at the Royal Aerospace Establishment p 451 N92-21689
Principles and computer simulations of intercooled-turbocharged gas generator/expander engine p 592 N92-22132
Heat transfer characteristics of hypersonic waveriders with an emphasis on the leading edge effects
[NASA-CR-189586] p 525 N92-22215
Three-dimensional compressible turbulent computations for a diffusing S-duct
[NASA-CR-4392] p 526 N92-22249
Design of an integrated airframe/propulsion control system architecture
[NASA-CR-182004] p 602 N92-22643
Measured and predicted rotor performance for the SERI advanced wind turbine blades
[DE92-001215] p 598 N92-23119
Effects of chemical equilibrium on turbine engine performance for various fuels and combustor temperatures
[NASA-TM-105399] p 562 N92-23254
Special Course on Engineering Methods in Aerodynamic Analysis and Design of Aircraft
[AGARD-R-783] p 552 N92-23950
Introduction to Special Course on Engineering Methods in Aerodynamic Analysis and Design of Aircraft
p 552 N92-23951
Survey of experimental techniques for performance prediction p 552 N92-23954
Aircraft drag analysis methods p 552 N92-23957
Nationwide system delay study of the microwave landing system in the New York terminal area, volume 1
[DOT/FAA/CT-TN91/59-VOL-1] p 640 N92-25098
Performance prediction and design of maximum thrust planar supersonic nozzles using a flux-difference-splitting technique p 738 N92-26480
Users manual and modeling improvements for axial turbine design and performance computer code TD2-2
[NASA-CR-189118] p 716 N92-27376
Steady and Transient Performance Prediction of Gas Turbine Engines
[AGARD-LS-183] p 868 N92-28458
Overview on basis and use of performance prediction methods p 869 N92-28459
Steady and transient performance calculation method for prediction, analysis, and identification
p 869 N92-28461
Component performance requirements
p 869 N92-28462
Dynamic simulation of compressor and gas turbine performance p 869 N92-28463
Calculation of installation effects within performance computer programs p 869 N92-28465
Thrust stand evaluation of engine performance improvement algorithms in an F-15 airplane
[NASA-TM-104252] p 971 N92-30518
Acoustic fatigue life prediction for nonlinear structures with multiple resonant modes
[NASA-CR-190471] p 1000 N92-30988
Preliminary subsonic aerodynamic model for simulation studies of the HL-20 lifting body
[NASA-TM-4302] p 978 N92-31175
Wind tunnel aerodynamic characteristics of a transport-type airfoil in a simulated heavy rain environment
[NASA-TP-3184] p 948 N92-31532
Ski jump takeoff performance predictions for a mixed-flow, remote-lift STOVL aircraft
[NASA-TM-103866] p 1060 N92-32887
Simulation model of a twin-tail, high performance airplane
[NASA-TM-107601] p 1088 N92-33537
A nozzle internal performance prediction method
[NASA-TP-3221] p 1040 N92-33625
An improved compressor performance prediction model
[PNR-90873] p 1072 N92-33749
Finite difference time domain grid generation from AMC helicopter models
[NASA-TM-107679] p 1128 N92-34017

PERFORMANCE TESTS

Compressor coating effects on gas turbine engine performance p 25 A92-11282
Mind that restyle --- failure analysis of aircraft composite structures p 91 A92-13700
The design and testing of a radial flow turbine for aerodynamic research
[ASME PAPER 91-GT-220] p 124 A92-15636
Performance characteristics of brush seals for limited-life engines
[ASME PAPER 91-GT-281] p 152 A92-15676
Development of T-100 multipurpose small power unit
[ASME PAPER 91-GT-327] p 153 A92-15697
Helicopter NVG testing in the United Kingdom
p 112 A92-16053
Lean low NO(x) combustion concept evaluation
p 143 A92-16583
Mach 4 and Mach 8 axisymmetric nozzles for a high-enthalpy shock tunnel p 78 A92-16668
Resonant cryogenic chopper --- for infrared and submillimeter radiometers p 294 A92-22796
Optimization of multistage axial-flow compressor vane setting p 371 A92-24746
High pressure hypervelocity electrothermal wind tunnel performance study and subscale tests
[AIAA PAPER 92-0329] p 383 A92-25776
Initial operation of the UTA shock tunnel
[AIAA PAPER 92-0331] p 383 A92-25778
Numerical investigation of performance degradation of wings and rotors due to icing
[AIAA PAPER 92-0412] p 325 A92-26264
High density fuel qualification for a gas turbine engine
[AIAA PAPER 92-0684] p 389 A92-27051
Design and calculation of performance of a subsonic inlet duct p 343 A92-28478
Materials and structures for Hermes
p 666 A92-38213
26 x 6.6 radial-belted aircraft tire performance
[SAE PAPER 912157] p 644 A92-39992
1991-92 AHS Technical Committee highlights - Dynamics p 647 A92-40393
Analysis and testing of a composite sandwich shell horizontal tail p 755 A92-44617
Performance of hybrid ball bearings in oil and jet fuel
p 900 A92-47176
Construction of a real-time DGPS experimental system
p 840 A92-47631
Robust discrete controller design for an unmanned research vehicle (URV) using discrete quantitative feedback theory p 877 A92-48495
A study on the impact of shroud geometry on ejector pumping performance
[AIAA PAPER 92-3260] p 864 A92-48856
Experimental validation of scramjet nozzle performance
[AIAA PAPER 92-3290] p 864 A92-48879
Effect of thermodynamic parameters on performance and cost of turbine engines p 969 A92-49834
General performance characteristics of real heat engine p 1011 A92-50401
Performance of a hybrid cylindrical roller bearing
p 995 A92-51845
Design and performance of the centrifuge-based Dynamic Flight Simulator
[AIAA PAPER 92-4156] p 981 A92-52446
High performance flight simulation at NASA Langley
[AIAA PAPER 92-4179] p 982 A92-52460
Pre-flight physical simulation test of HIMES reentry test vehicle p 1103 A92-53640
A comparison of the calculated and experimental off-design performance of a radial flow turbine
[AIAA PAPER 92-3069] p 1020 A92-54004
Internal reversing flow in a tailpipe offtake configuration for SSTOVL aircraft
[AIAA PAPER 92-3790] p 1069 A92-54169
Evaluation of electrolytic tilt sensors for wind tunnel model angle-of-attack (AOA) measurements
p 1116 A92-54344
Effects of material choices on brush seal performance
p 1116 A92-54650
Performance data of the new free-piston shock tunnel at GALCIT
[AIAA PAPER 92-3943] p 1033 A92-56776
Description of a pressure measurement technique for obtaining surface static pressures of a radial turbine
[AIAA PAPER 92-4006] p 1123 A92-56829
Effect of a simulated glaze ice shape on the aerodynamic performance of a rectangular wing
[AIAA PAPER 92-4042] p 1035 A92-56861
New insulation constructions for aerospace wiring applications. Volume 1: Testing and evaluation
[AD-A240638] p 22 N92-11006
Tracking performance requirements for rotorcraft instrument approaches to reduced minima. Phase 1: Preliminary study
[NRC-32137-PHASE-1] p 102 N92-11988
Performance improvements and fuel cost savings due to leading edge modification of a vintage delta wing jet fighter
[FFA-TN-1991-22] p 114 N92-11993
Humidity effects on gas turbine performance
[NRC-30241] p 130 N92-11998

Review of the European hypersonic wind tunnel performance and simulation requirements
p 209 N92-15043
Validation and verification flight test for TCAS-2 logic changes (MOPS Change 6)
[DOT/FAA/CT-TN91/46] p 268 N92-15981
Qualification test report. Fuel pump test stand 3C3965G05
[AD-A242929] p 280 N92-17552
Flight evaluation of curved MLS precision approaches in a twin otter aircraft, phase 2
[AD-A243025] p 268 N92-17568
Design and testing of high-performance parachutes
[AGARD-AG-319] p 345 N92-18269
Tactical Rubidium Frequency Standard (TRFS)
[AD-A243934] p 401 N92-18897
Performance and stability analysis of the non-linear dynamics of a simple powered lifting hypersonic vehicle flying on a minor circle
[AD-A243933] p 366 N92-19192
Benchmark performance analysis of an ECM-modulated air-to-air heat pump with a reciprocating compressor
[DE92-004478] p 500 N92-20341
Comparison of the performance of a microwave landing system elevation station with the instrument landing system end-fire glide slope at Yeager Airport, Charleston, West Virginia
[DOT/FAA/CT-TN91/22] p 534 N92-22210
Comparative evaluation of internally and externally lighted taxiway guidance signs
[DOT/FAA/CT-TN92/2] p 573 N92-22237
High temperature strain gage technology for hypersonic aircraft development applications
[NASA-CR-189101] p 592 N92-22239
Static performance of a cruciform nozzle with multiaxis thrust-vectoring and reverse-thrust capabilities
[NASA-TP-3188] p 527 N92-23095
Effect of blade planform variation on the forward-flight performance of small-scale rotors
[NASA-TM-4345] p 630 N92-24885
Description of a pressure measurement technique for obtaining surface static pressures of a radial turbine
[NASA-TM-105643] p 680 N92-24959
Flat belt continuously variable high speed drive
[DE92-008952] p 680 N92-25054
Pallet for helicopter testing instrumentation
p 652 N92-25598
Experimental methods to determine heat exchanger performances p 682 N92-25667
Application of S1BYL2 to the AGARD WG18 compressor test cases p 768 N92-27452
Development of the Basic Flight Instruction Tutoring System (BFITS)
[AD-A246458] p 751 N92-27836
JTIDS electromagnetic compatibility in the 960-1215 MHz band
[AD-A247834] p 773 N92-27864
Internal reversing flow in a tailpipe offtake configuration for SSTOVL aircraft
[NASA-TM-105698] p 868 N92-28418
LAH-main rotor model test at the DNW
[NLR-TP-90305-U] p 852 N92-28687
Tasking and communication flows in the F/A-18D cockpit: Issues, problems, and possible solutions
[AD-A245977] p 853 N92-28802
A comparison of the calculated and experimental off-design performance of a radial flow turbine
[NASA-CR-189207] p 831 N92-29402
Compact range test applications, phase 2
[AD-A248790] p 999 N92-30583
GNAS Maintenance Control Center (GMCC) Design Qualification Test and Evaluation (DQT/E) test procedures
[DOT/FAA/CT-TN91/40] p 983 N92-30976
A study of atmospheric optical scattering parameters at 1.5 and 2 micron region for solid state Doppler lidar applications p 1001 N92-31067
Evaluation of grounding and mooring points for Army aircraft
[AD-A250749] p 953 N92-31193
Experimental testing of prototype face gears for helicopter transmissions
[NASA-TM-105434] p 1002 N92-31349
GNAS Maintenance Control Center (GMCC) Design Qualification Test and Evaluation (DQT/E) test report
[DOT/FAA/CT-TN91/39] p 932 N92-31615
FCS skewed sensors array: Practical considerations
p 968 N92-31868
Supportability evaluation of thermoplastic and thermoset composites p 1108 N92-32576
Residual strength of repaired graphite/epoxy laminates after 5 years of outdoor exposure p 1108 N92-32577
Simulation test and evaluation of TCAS 2 logic version 6.04
[DOT/FAA/RD-92/23] p 1048 N92-33098
Rapid development of the X-31 simulation to support flight-testing
[NASA-TM-104256] p 1060 N92-33149

PERIODIC VARIATIONS
Effect of model cooling on periodic transonic flow
p 813 A92-46900
Production of periodical Mach number variations in high subsonic flow in a blow down wind tunnel, and its influence on profile measurements
[ETN-92-91492] p 833 N92-29889

PERIPHERAL EQUIPMENT (COMPUTERS)
Upgrading the data processing section of the NAL Gust Wind Tunnel data processing system
[NAL-TM-635] p 888 N92-28833

PERMANENT MAGNETS
Counterrotating brushless DC permanent magnet motor
[DE92-003825] p 401 N92-18550
Performance tests of a cryogenic hybrid magnetic bearing for turbopumps
[NASA-TM-105627] p 473 N92-20523
Wide gap, permanent magnet biased magnetic bearing system p 773 N92-27794

PERMEABILITY
An investigation on flame stability by fuel permeability in a flame holder made of porous ceramic material
p 375 A92-28435

PERMITTIVITY
The design of broadband radar absorbing surfaces
[AD-A240521] p 42 N92-11235
Radar multipath study for rain-on-radome experiments at the Aircraft Landing Dynamics Facility
[NASA-TM-101657] p 680 N92-25137

PERSONAL COMPUTERS
Operation and design considerations for unsteady data acquisition with PC-based systems in high Reynolds number hypersonic flowfields
[AIAA PAPER 92-0204] p 284 A92-23810
Ferroelectric memory evaluation and development system p 902 A92-48460
Implementation of a personal computer based parameter estimation program
[AD-A252914] p 1061 N92-33502

PERSONNEL
Monitoring operational concept
[DOT/FAA/SE-91/3] p 268 N92-15980
Ingress, emergency egress, and emergency evacuation testing of army aircraft
[AD-A246398] p 724 N92-27750
An analysis of total quality management in Aeronautical Systems Division
[AD-A246661] p 772 N92-27760
NASA engineers and the age of Apollo
[NASA-SP-4104] p 929 N92-28344

PERSONNEL DEVELOPMENT
Approach to crew training in support of the USAF Aircraft Structural Integrity Program (ASIP) p 363 N92-18595

PERSONNEL MANAGEMENT
Organizational context for aircraft maintenance and inspection p 2 A92-11181
Management decisions have an impact on flight safety
p 92 A92-15175
An alternative source of flight test services
[AIAA PAPER 92-1088] p 515 A92-33254
Test plan for the international aircraft operator information system
[DOT/FAA/CT-91/18] p 781 N92-26830
Workshop on integrated Crew Resource Management (CRM)
[DOT/FAA/RD-92/5] p 781 N92-27518
Profile of an effective engineering manager
[AD-A246525] p 781 N92-27528
Flight crew integration in the maintenance chain of a commercial aircraft (A 320) p 1012 N92-30957

PERTURBATION
Robustness of control systems with nonlinear parametric correction for certain types of perturbations
p 509 A92-30311
Results of a perturbation analysis correlating flows entering and exiting an aircraft inlet system
[AIAA PAPER 92-3624] p 1021 A92-54091
Numerical simulation of transient hypervelocity flow in an expansion tube
[NASA-CR-189601] p 402 N92-18965
A multi-loop guidance scheme using singular perturbation and linear quadratic regulator techniques simultaneously p 481 N92-20148
Improved large perturbation propulsion models for control system design (1988-1989) and large perturbation models of high velocity propulsion systems (1989-1990) and reduced order propulsion models for control system design (1990-1991)
[NASA-CR-190148] p 593 N92-22491
A boundary integral formulation for unsteady transonic potential flows p 719 N92-27942
Unsteady transonic aerodynamics of pointed bodies of revolution in supersonic freestream p 719 N92-27946
Computation of viscous phenomena in unsteady transonic flow p 720 N92-27949
Transonic aeroelastic calculations in both the time and frequency domains p 720 N92-27950
Computation of flutter boundaries in the time and frequency domain p 720 N92-27952
Analysis of unsteady aerodynamic and flutter characteristics of an aeroelastic model in transonic flow
p 720 N92-27953
Direct coupling of fluid structure in transonic aeroelasticity p 721 N92-27954
Investigation of the aeroelastic stability of the AFW wind-tunnel model using CAP-TSD p 721 N92-27955

PERTURBATION THEORY
Singular perturbation theory of hypersonic flow over blunt bodies p 313 A92-25048
Synthesis of optimal digital systems for the stabilization of stochastically perturbed unstable dynamic systems
p 601 A92-33754
Compressible turbulent boundary layers with heat addition by homogeneous condensation
p 611 A92-36843
The flow over a backward-facing step under controlled perturbation - Laminar separation p 705 A92-41653
Second order perturbation method of gas turbine performance calculation p 759 A92-41834
Aeroelastic modal characteristics of mistuned blade assemblies - Mode localization and loss of eigenstructure p 1117 A92-54921
Selection of sampling rate for nonlinear flight trajectory controller of aircraft p 1084 A92-56070
Comments on frequency swept rotating input perturbation techniques and identification of the fluid force models in rotor/bearing/seal systems and fluid handling machines p 224 N92-14370
Thrust vectoring for lateral-directional stability
[NASA-CR-186016] p 482 N92-21357
Turbulent mixing in supersonic jets
p 715 N92-27054

PHASE DEVIATION
MIMO state-feedback control system considering phase stability by -90 deg phase-locus method
p 1084 A92-56066

PHASE ERROR
Motion errors in an airborne synthetic aperture radar system p 840 A92-48416

PHASE LOCKED SYSTEMS
Probability of cycle jumps in Omega receivers and other phase locked loop applications
[PB92-128891] p 455 N92-21279

PHASE MODULATION
A preliminary study in the use of phase demodulation techniques for the analysis of gear vibration data
[NRC-32083] p 1002 N92-31469

PHASE SEPARATION (MATERIALS)
Demonstration of gas liquid separation under the microgravity by aircraft KC-135
[SAE PAPER 912024] p 897 A92-45416

PHASE SHIFT
Invariant boundary conditions for cascade flows
p 498 N92-20147

PHASE TRANSFORMATIONS
Numerical analysis of a thermal deicer
[AIAA PAPER 92-0527] p 357 A92-26950
An efficient finite element method for aircraft de-icing problems
[AIAA PAPER 92-0532] p 459 A92-31670
Experimental study of convection effects around the phase charge interface p 1111 A92-53755
Method and apparatus for acoustic plate mode liquid-solid phase transition detection
[DE92-003778] p 401 N92-18705

PHASED ARRAYS
ETS-V/EMSS mobile satellite communication experiments p 395 A92-26776
High gain airborne antenna for satellite communications p 639 A92-40188
Beam scanning error of phased array antenna
p 676 A92-40189
Single slotted array achieves multimode performance
p 726 A92-44428
The Air Force Manufacturing Technology (MANTECH): Technology transfer methodology as exemplified by the radar transmit/receive module program
p 593 N92-22451
A high gain antenna system for airborne satellite communication applications p 677 N92-24096
Low cost, electronically steered phased array for general aviation p 677 N92-24099
The rise of active-element phased-array radar
[RAND-P-7747-RGS] p 999 N92-30755

PHENOLIC EPOXY RESINS
BMI/bis (allylphenoxyphthalimide)-copolymers - A new family of resins for advanced composites with improved thermal oxidative stability p 33 A92-10213
PHOSPHAZENE
Development and tribological properties of new cyclotriphosphazene high temperature lubricants for aircraft gas turbine engines p 287 A92-21327
PHOTODIODES
Semiconductor laser Doppler anemometer for applications in aerodynamic research p 495 A92-31173
Study of optical techniques for the Ames unitary wind tunnels. Part 3: Angle of attack
[NASA-CR-190541] p 888 N92-29655
PHOTOELASTIC ANALYSIS
Analysis of tenon and mortise contact problems by boundary element methods p 587 A92-35554
Photoelastic coating study of CT-114 coupon joint test specimen for horizontal stabilizer rear attachment fitting to vertical stabilizer rear spar
[NRC-LTR-ST-1689] p 489 N92-21018
PHOTOELECTRICITY
Fault diagnostics on jet engine starting p 1116 A92-54345
PHOTOGRAMMETRY
Dimensional characterization of a large aircraft structure by photogrammetry p 607 A92-37061
Close-range photogrammetry meets machine vision; Proceedings of the Meeting, Zurich, Switzerland, Sept. 3-7, 1990
[SPIE-1395] p 994 A92-51626
The use of photogrammetry in aviation equipment flight testing p 994 A92-51649
PHOTOLUMINESCENCE
Aerodynamic applications of pressure-sensitive paint
[AIAA PAPER 92-0264] p 394 A92-25720
PHOTOMETRY
Visual photometric experiment data processing system
[AD-A248657] p 729 N92-27964
PHOTONS
In situ measurement of particle formation in heated jet fuels: A new application of photon correlation spectroscopy
[DE92-003641] p 488 N92-20132
Mid-range UV communications --- ultraviolet radiation
[AD-D015213] p 770 N92-27615
PHOTOSTRESSES
Liquid crystal coatings for surface shear-stress visualization in hypersonic flows p 496 A92-32177
PHOTOVOLTAIC CELLS
Analysis, development, and integration of the mechanical components of a vehicle powered by photo-voltaic cells
[TABES PAPER 91-503] p 606 A92-34692
Radiant energy power source for jet aircraft
[DE92-008726] p 648 N92-24556
Aircraft photovoltaic power-generating system p 775 N92-26581
PHOTOVOLTAIC CONVERSION
Aircraft photovoltaic power-generating system p 775 N92-26581
PHYSICAL CHEMISTRY
DLR-News: Announcements of the German Research Institute for Aeronautics and Astronautics p 698 N92-26086
PHYSICAL OPTICS
Parametric bicubic spline and CAD tools for complex targets shape modelling in physical optics radar cross section prediction p 403 N92-19151
Remote sensing of trapping layer base height using ATIS transmissions
[AD-A250074] p 1004 N92-31362
PHYSICAL PROPERTIES
Viscosity characteristics of synthetic aviation oils at low temperatures p 1105 A92-53875
The mechanical properties of metal-void composites --- pressurized microvoids
[AD-A246087] p 757 N92-27749
PHYSICS
DLR-News: Announcements of the German Research Institute for Aeronautics and Astronautics p 698 N92-26086
PHYSIOLOGICAL EFFECTS
Flight simulation p 207 N92-13982
Human response to aircraft noise p 236 N92-14780
Risk to hearing from overflight noise of military aircraft
[ISVR-TR-194] p 604 N92-22241
PHYSIOLOGICAL TESTS
Ames life science telescience testbed evaluation
[NASA-CR-188856] p 140 N92-12033
PIERCING
Cut progression during dynamometer testing of foreign object damaged type VII extra high pressure aircraft tires
[SAE PAPER 912155] p 644 A92-39990
PIEZOELECTRIC CERAMICS
Ultrasonic motor utilizing elastic fin rotor p 215 A92-17414
Effect of adaptive material properties on static aeroelastic control
[AIAA PAPER 92-2526] p 539 A92-34373
An analytical and experimental investigation of flutter suppression via piezoelectric actuation
[AIAA PAPER 92-2106] p 567 A92-35677
Approximation methods for control of acoustic/structure models with piezoceramic actuators
[NASA-CR-189578] p 234 N92-15658
Active noise control: Piezoceramic actuators in fluid/structure interaction models
[NASA-CR-190328] p 685 N92-26125
PIEZOELECTRIC CRYSTALS
Laser ordnance initiation system p 577 A92-35465
PIEZOELECTRIC TRANSDUCERS
Active control of sound transmission through elastic plates using piezoelectric actuators p 53 A92-11052
A piezoelectric droplet generator for use in wind tunnels p 291 A92-21374
Skin-friction gauge for use in hypervelocity impulse facilities p 398 A92-28063
PIEZOELECTRICITY
An analytical and experimental study to investigate flutter suppression via piezoelectric actuation
[NASA-TM-893240] p 156 N92-12173
Flutter suppression via piezoelectric actuation
[NASA-TM-104120] p 197 N92-15070
Aeroelastic behavior of an adaptive lifting surface p 443 N92-20378
A preliminary study on damage detection using piezoelectric film
[AD-A246350] p 733 N92-28118
An analytical and experimental investigation of flutter suppression via piezoelectric actuation
[NASA-TM-107653] p 962 N92-31174
Active control of interior noise in a large scale cylinder using piezoelectric actuators p 1137 N92-32958
PILOT ERROR
Analysis of general aviation accidents during operations under instrument flight rules p 16 A92-11172
Fatigue and accidents - A comparison across modes of transport p 17 A92-13025
How to promote error tolerance in complex systems in the context of ships and aircraft p 673 A92-39308
The effectiveness of training programs for preventing aircrew 'error' p 834 A92-44997
Eliminating pilot-caused altitude deviations - A human factors approach p 834 A92-45041
Rejected takeoffs - Causes, problems, and consequences p 835 A92-45052
ICAO Flight Safety and Human Factors Programme p 835 A92-45055
Human factors and simulation p 951 A92-53236
Introduction to cognitive processes of expert pilots
[DOT/FAA/RD-92/12] p 952 N92-30980
A review and discussion of flight management system incidents reported to the aviation safety reporting system
[AD-A252438] p 1043 N92-32941
PILOT INDUCED OSCILLATION
Characteristics of the phugoid motion of nonmaneuverable aircraft p 480 A92-30190
Study on a flight simulator of time delays p 744 A92-43112
The research on Pilot Induced Oscillation p 977 A92-53088
Experimental investigation of in-flight oscillation on helicopters and its prevention p 977 A92-53089
PILOT PERFORMANCE
A model for evaluation and training in aircrew coordination and cockpit resource management p 46 A92-11191
Effects of variations in head-up display airspeed and altitude representations on basic flight performance p 46 A92-11204
Prediction of helicopter simulator sickness p 46 A92-11473
Fatigue and accidents - A comparison across modes of transport p 17 A92-13025
Data-link communication between controllers and pilots - A review and synthesis of the simulation literature p 94 A92-14045
V-22 pilot-in-the-loop aeroelastic stability analysis p 133 A92-14422
An analytical study of the helicopter flight safety under an engine failure in proximity of ground p 91 A92-14454
Adaptive simulator motion software with supervisory control p 412 A92-28136
Dealing with pilot response in failure case testing p 549 A92-35952
B-2 handling, automation tailored to two-pilot crew p 643 A92-39725
The standardization of military head-up display symbology p 855 A92-44929
Toward an integrated multimodal approach to flight simulation p 880 A92-45026
Getting test items to measure knowledge at the level of complexity which licensing authorities desire - Another dimension to test validity p 835 A92-45080
The importance of implicit and explicit knowledge in a pilot's associate system p 858 A92-48567
An investigation of the automation of emergency landings for helicopters p 1083 A92-56026
The impact of cockpit automation on crew coordination and communication. Volume 1: Overview, LOFT evaluations, error severity, and questionnaire data
[NASA-CR-177587] p 93 N92-13044
Design considerations for IAP charts: Approach course track and communication frequencies
[AD-A241482] p 103 N92-13051
Effect of short-term exposure to stereoscopic three-dimensional flight displays on real-world depth perception
[NASA-TP-3117] p 119 N92-13065
Limitations of a holographic 3-D pixel projector for cockpit displays
[AD-A241295] p 119 N92-13067
System identification methods for handling-qualities evaluation p 274 N92-17165
Development of the Basic Flight Instruction Tutoring System (BFITS)
[AD-A246458] p 751 N92-27836
Use of a commercially available flight simulator during aircrew performance testing
[AD-A245922] p 883 N92-28407
Helicopter nighttime parking test results - UH-1
[DOT/FAA/CT-TN92/1] p 961 N92-31165
Workshop on Aeronautical Decision Making (ADM). Volume 1: Executive summary
[DOT/FAA/RD-92/14-VOL-1] p 1142 N92-33305
Aircraft accident/incident summary report: Controlled flight into terrain Bruno's Inc., Beechjet, N25BR, Rome, Georgia, 11 December 1991
[PB92-910404] p 1044 N92-34081
PILOT SELECTION
Mandatory psychological testing of pilots as a requirement for licensing in Norway? p 835 A92-45081
PILOT TRAINING
MIDIS - A microcomputer flight decision simulator p 136 A92-13845
Rates and risk factors for accidents and incidents versus violations for U.S. airmen p 91 A92-14048
YF-23A preliminary flight test results p 112 A92-16063
Standardization of NATOPS emergency egress procedures --- Naval Air Training and Operating Procedures Standardization Program p 529 A92-32998
Parachute canopy control simulation - A solution for aircrew emergency training p 572 A92-35428
JPATS escape system development p 543 A92-35434
Simulation in the Air Force p 747 A92-41209
Software reliability for flight crew training simulators p 747 A92-41221
Stop, look and learn from accident investigation p 834 A92-44996
The effectiveness of training programs for preventing aircrew 'error' p 834 A92-44997
Centre for Flight Simulation Berlin Airbus 340 simulator for research and training p 880 A92-45028
A training program for airline line instructors p 835 A92-45044
Judgement training for Alaskan pilots p 835 A92-45048
Shipboard mission training effectiveness of the Naval Air Warfare Center's V-22 Government Test Pilot Trainer
[AIAA PAPER 92-4130] p 959 A92-52427
Algorithmic improvements for simulator motion drive
[AIAA PAPER 92-4158] p 1007 A92-52448
Human factors and simulation p 951 A92-53236
The advantages of digital engine control as compared with traditional systems (hydraulic or pneumatic) p 1070 A92-56338
The impact of cockpit automation on crew coordination and communication. Volume 1: Overview, LOFT evaluations, error severity, and questionnaire data
[NASA-CR-177587] p 93 N92-13044
An evaluation of the Royal Air Force Shorts Tucano Navigation Instruments Trainer: The NAVIT
[ETN-92-90841] p 354 N92-18729
Flying an aircraft as a problem-solving process: About the Instrument-Failure-Simulator (IFS) as a test for pilot-candidates
[DLR-FB-91-23] p 455 N92-20902
Ship airwake measurement and modeling options for rotorcraft applications p 503 N92-21954

Microcomputer-based instrument flight simulation: Undergraduate pilot training student attitude assessment
[AD-A245449] p 749 N92-26527
Experimental evaluation of candidate graphical microburst alert displays
[NASA-CR-189633] p 735 N92-27424
The modelling of turbulence and downbursts for flight simulators
[ISBN-0-315-59945-6] p 749 N92-27645
Development of the Basic Flight Instruction Tutoring System (BFITS)
[AD-A246458] p 751 N92-27836
Use of a commercially available flight simulator during aircrew performance testing
[AD-A245922] p 883 N92-28407
Piloted Simulation Effectiveness
[AGARD-CP-513] p 786 N92-28522
Opportunities for flight simulation to improve operational effectiveness p 883 N92-28523
Utility of ground simulation in flight control problem identification, solution development, and verification
p 883 N92-28525
Experience with piloted simulation in the development of helicopters p 884 N92-28528
Harrier GR MK 5/7 mission simulators for the Royal Air Force p 885 N92-28540
Experience with piloted simulation in the development of helicopters
[MBB-UD-0610-91-PUB] p 889 N92-30076
Technical evaluation report on the Flight Mechanics Panel Symposium on Piloted Simulation Effectiveness
[AGARD-AR-315] p 983 N92-30769
Introduction to cognitive processes of expert pilots
[DOT/FAA/RD-92/12] p 952 N92-30980

PILOTLESS AIRCRAFT
Optimal thermal management system for HALE UAV --- High Altitude Long Endurance Unmanned Air Vehicles
[ASME PAPER 91-GT-396] p 111 A92-15726
Liquid cooled turbocharged propulsion system for HALE application
[ASME PAPER 91-GT-399] p 127 A92-15729
Propulsion system evaluation for an unmanned high altitude long endurance RPV
[ASME PAPER 91-GT-409] p 128 A92-15738
Flight test of a half-scale unmanned air vehicle
p 193 A92-20208
Research flight test of a scaled unmanned air vehicle
p 549 A92-35944
Condor - An all electric airplane
[SAE PAPER 912184] p 644 A92-40004
Tiltrotor UAV - The next generation unmanned system
p 646 A92-40384
Sikorsky Aircraft UAV program p 646 A92-40385
An analysis tool for UAV effectiveness evaluation
p 608 A92-40386
Study of the flight control of remotely piloted helicopters p 745 A92-43183
The concept of an unmanned flying vehicle at high altitude p 731 A92-43242
Navier-Stokes and Euler solutions for an unmanned aerial vehicle
[AIAA PAPER 92-2609] p 792 A92-45483
Airborne Data Acquisition and Relay System
p 839 A92-47574
Robust discrete controller design for an unmanned research vehicle (URV) using discrete quantitative feedback theory p 877 A92-48495
Emerging technologies for gas turbine engines - U.A.V. synergies
[AIAA PAPER 92-3757] p 867 A92-49114
Aerodynamic analysis of the Pioneer unmanned air vehicle
[AIAA PAPER 92-4635] p 1027 A92-55382
Piloted simulation study of a balloon-assisted deployment of an aircraft at high altitude
[NASA-TM-104245] p 272 N92-15986

PILOTS (PERSONNEL)
Microcomputer-based instrument flight simulation: Undergraduate pilot training student attitude assessment
[AD-A245449] p 749 N92-26527
Pilots noise exposure during a Boeing 747-400 round trip: Ambient noise and acoustic-head recording and analysis of data p 1137 N92-32960
Pilot noise exposure during a Boeing 747-400 round trip: Judgement of noise and analysis in respect to hearing impairment of pilots p 1138 N92-32961

PINS
Thrust vector control of an overexpanded supersonic nozzle using pin insertion and rotating airfoils
[AD-A243891] p 387 N92-18942

PIONEER SPACE PROBES
Developmental flight testing of a half scale unmanned air vehicle
[AD-A240347] p 22 N92-11002

PIPE FLOW
Deposition during vaporization of jet fuel in a heated tube
[AIAA PAPER 92-0687] p 390 A92-27054
Flow pattern characterization and heat transfer behavior in a boiling two-phase flow in an inclined pipe
p 493 A92-29722
The numerical method for calculating the flow field, temperature field and radiation fluxfield in the pipe
p 587 A92-35546
Steady flow of a fluid-solid mixture in a circular cylinder
[DE91-018698] p 41 N92-10174
Application of riblet surface to pipe flow
p 766 N92-26915

PIPELINES
Application of riblet surface to pipe flow
p 766 N92-26915

PIPES (TUBES)
Self-induced flow in a stepped rotating tube
[ASME PAPER 91-GT-276] p 152 A92-15673
Sound generation by a stenosis in a pipe
p 415 A92-26405
Forced-injection quenching of a hot-tube under microgravity p 590 A92-35977
Boiling and condensation in microfin tubes
p 682 N92-25660

PISTON ENGINES
Pressurization effects in kinematic heat engines
p 696 A92-40866
Study of grinding process and strength for ceramic heat insulated engine
[SME PAPER MR91-177] p 897 A92-45260
Restart of theory of air-breathing engines
[AIAA PAPER 92-3472] p 906 A92-49018
CIS engines - The range revealed. II
p 1069 A92-54546
Combustion and core noise p 55 N92-10607
Principles and computer simulations of intercooled-turbocharged gas generator/expander engine p 592 N92-22132
Proof of concept of a magnetically coupled Stirling engine-driven heat pump
[DE92-017129] p 1129 N92-33271

PISTON THEORY
Pitching derivatives of wing in supersonic and hypersonic stream - Method for local flow piston theory
p 312 A92-25012
On simple aerodynamic sensitivity derivatives for use in interdisciplinary optimization
[NASA-TM-104145] p 82 N92-11985

PITCH
Exposures from headset interference tones
[AD-A247175] p 1136 N92-32697

PITCH (INCLINATION)
An analysis of pitch and plunge effects on unsteady airfoil behavior p 65 A92-14359
Description of a tilt wing mathematical model for piloted simulation p 133 A92-14445
Design and analysis of a high pitch to chord ratio cascade representative of ducted propfans
[ASME PAPER 91-GT-335] p 126 A92-15700
Target pitch angle for the microburst escape maneuver
[AIAA PAPER 92-0730] p 379 A92-27082
Controller design for the F-14 pitch axis control problem using the quantitative feedback theory approach
p 478 A92-29128
Trajectory shaping by the U-parameter design method
p 479 A92-29361
Characteristics of the phugoid motion of nonmaneuverable aircraft p 480 A92-30190
Robustness of control systems with nonlinear parametric correction for certain types of perturbations
p 509 A92-30311
Generalized higher harmonic control - Ten years of Aerospatiale experience p 569 A92-35769
Analyzing the flared landing task with pitch-rate flight control systems p 661 A92-39905
Measurements of the velocity and vorticity fields around a pitching airfoil
[AIAA PAPER 92-2626] p 794 A92-45498
Unsteady crossflow on a delta wing using particle image velocimetry p 811 A92-46804
Pitch rate/sideslip effects on leading-edge extension vortices of an F/A-18 aircraft model
p 874 A92-46810
Prediction of dynamic hub load of a rotor executing multiple sinusoidal blade pitch variations
p 846 A92-46921
Flow visualisation of a small diameter rotor operating at high rotational speeds with blades at small pitch angles p 814 A92-46949
Static and dynamic flight-path stability of airplanes
p 977 A92-52043
Calibration of hemispherical-head flow angularity probes
[AIAA PAPER 92-4005] p 1122 A92-56828
An experimental study of the sensitivity of helicopter rotor blade tracking to root pitch adjustment in hover
[NASA-TM-4313] p 61 N92-12989
Steady and unsteady aerodynamics of a pitching straked wing model at high angles of attack p 87 N92-13024
Water tunnel flow visualization studies of a canard-configured X-31A-like fighter aircraft model
[AD-A241362] p 90 N92-13037
Target pitch angle for the microburst escape maneuver p 266 N92-17996
Eddy current transducing system
[DE91-018924] p 401 N92-18515
Pitch-heave dynamics models for an air cushion vehicle
[ISBN-0-315-51095-1] p 716 N92-27624
Stability and control flight testing of a half-scale Pioneer remotely piloted vehicle
[AD-A245973] p 879 N92-28801
Nonlinear normal and axial force indicial responses for a two dimensional airfoil
[AD-A247196] p 830 N92-28888
An investigation into the interface between three closely spaced axi-symmetric bodies at subsonic speed
[CRANFIELD-AERO-9114] p 948 N92-31514
Unsteady response of the leading-edge vortices on a pitching delta wing p 1041 N92-33851

PITCHING MOMENTS
Pitching derivatives of wing in supersonic and hypersonic stream - Method for local flow piston theory
p 312 A92-25012
Oscillating two-dimensional hypersonic airfoils at small angles of attack p 340 A92-28042
The mean power of forces and moments in unsteady aerodynamics p 421 A92-28949
Experiment on pitching moments of separated flow around airfoil profiles p 429 A92-30527
Unsteady flow past an airfoil pitching at a constant rate p 610 A92-36826
Comment on 'Effect of thrust/speed dependence on long-period dynamics in supersonic flight'
p 643 A92-39913
Subsonic and transonic low-Reynolds-number airfoils with reduced pitching moments p 701 A92-41211
Aircraft spoiler effects under wind shear
[AIAA PAPER 92-2642] p 796 A92-45509
An advanced scramjet propulsion concept for a 350 MG SSTO space plane - External nozzle performance
[AIAA PAPER 92-3719] p 1067 A92-54134
Dynamics of helicopters with dissimilar blades in forward flight p 1056 A92-56288
Experimental study of an independently deflected wingtip mounted on a semispan wing
[NASA-TM-102842] p 13 N92-10983
Transonic Navier-Stokes computations for a spinning body of revolution
[AD-A241015] p 180 N92-14972
Grid impact on 3D hypersonic flows
p 184 N92-15041
Dynamic stall on wind turbine blades
[DE92-001157] p 262 N92-17874
Wind tunnel force measurements and visualization on a 60-deg delta wing in oscillation, stepwise motion, and gusts p 364 N92-18786
An experimental study of a sting-mounted circulation control wing
[AD-A243912] p 346 N92-18895
Effect of nonuniform entrance flow profile on hypersonic nozzle pitching moment
[AD-A244050] p 377 N92-19184
Experimental investigation of heavy rainfall effect on a 2-D high lift airfoil p 452 N92-21696
High Reynolds number test of the Boeing TR77 airfoil in the Langley 0.3-meter transonic cryogenic tunnel
[NASA-TM-4189] p 947 N92-31246
On the estimation of jet-induced fountain lift and additional suckdown in hover for two-jet configurations
[NASA-TM-102268] p 1040 N92-33618
A nozzle internal performance prediction method
[NASA-TP-3221] p 1040 N92-33625

PITOT TUBES
X-29 high angle-of-attack flight test air data comparisons of an inertial navigation system and noseboom probe
p 549 A92-35945
Development of pitot static flightline testing
p 556 A92-35953
Measurement of angle of attack using a five-hole arrow head pitot tube p 941 A92-53009
Comparison between computational and experimental data for a hypersonic laser propelled vehicle
[AIAA PAPER 92-3808] p 1023 A92-54179
Test description and preliminary pitot-pressure surveys for Langley Test Technique Demonstrator at Mach 6
[AIAA PAPER 92-3940] p 1096 A92-56770

Millisecond aerodynamic force measurement with side-jet model in the ISL shock tunnel
[AIAA PAPER 92-3963] p 1097 A92-56790
Boundary layer study on nozzle wall at hypersonic velocities
[AIAA PAPER 92-4013] p 1034 A92-56836
Pilot-pressure probe for measuring pressure in a hypersonic wind tunnel
[NASA-CASE-LAR-14232-1] p 1102 N92-34213

PITTING
Failure analysis of the Apache mixer pivot support
[AD-A240858] p 116 N92-13061
Full-scale transmission testing to evaluate advanced lubricants
[NASA-TM-105668] p 764 N92-26560

PIVOTS
Failure analysis of the Apache mixer pivot support
[AD-A240858] p 116 N92-13061
Reduction and analysis of F-111C flight data
[AD-A250341] p 853 N92-28771

PIXELS
Limitations of a holographic 3-D pixel projector for cockpit displays
[AD-A241295] p 119 N92-13067

PLAN POSITION INDICATORS
Polish radar technology. III - Weather channel for primary surveillance radar p 40 A92-12291

PLANAR STRUCTURES
A variational method for solving the problem of motion of a profile of complex geometry in a fluid
p 397 A92-27482

PLANE STRAIN
Torsion and twisting of symmetric composite laminates
[AIAA PAPER 92-2425] p 582 A92-34354

PLANE WAVES
Inlet planar waves - A current perspective
[ASME PAPER 91-GT-400] p 76 A92-15730
Acoustic transmission through a 2-D orthotropic multi-layered infinite cylindrical shell p 780 A92-44197

PLANETARY BOUNDARY LAYER
Steady state risetimes of shock waves in the atmosphere p 1140 N92-33882

PLANETARY GEOLOGY
Aerodynamic roughness measured in the field and simulated in a wind tunnel
[NASA-CR-4422] p 347 N92-19354

PLANETARY SURFACES
The differential algebraic approach in nonlinear dynamical feedback controlled landing maneuvers
p 574 A92-33639

PLANETARY SYSTEMS
JPRS report: Science and technology. Central Eurasia: Space
[JPRS-USP-92-002] p 575 N92-23705

PLANFORMS
Determination of aerodynamic sensitivity coefficients based on the three-dimensional full potential equation
[AIAA PAPER 92-2670] p 798 A92-45525
Planform curvature effects on flutter characteristics of a wing with 56 deg leading-edge sweep and panel aspect ratio of 1.14
[NASA-TP-3116] p 115 N92-13054
Effect of blade planform variation on the forward-flight performance of small-scale rotors
[NASA-TM-4345] p 630 N92-24885

PLANNING
A cognitive temporal model for the planning in aircraft maintenance p 307 A92-25178
COMPAS system concept p 354 N92-19043
Evaluation of the COMPAS operational system
p 355 N92-19047
Extension of the Frankfurt COMPAS for general application p 355 N92-19048
The impact of COMPAS on the future Cooperative Air Traffic Management Concept (CATMAC)
p 355 N92-19049
The role of planning systems in future air traffic management p 355 N92-19050

PLANT DESIGN
Small engine components test facility compressor testing cell at NASA Lewis Research Center
[AIAA PAPER 92-3980] p 1098 A92-56806
Transonic turbine blade cascade testing facility
[AIAA PAPER 92-4034] p 1101 A92-56856
Transonic turbine blade cascade testing facility
[NASA-TM-105646] p 667 N92-26129
Small engine components test facility compressor testing cell at NASA Lewis Research Center
[NASA-TM-105685] p 982 N92-30508

PLASMA ACCELERATION
Research activities on CFD at the Ship Research Institute p 766 N92-26908

PLASMA CONTROL
Scoping studies for small steady-state tokamaks for divertor testing
[DE92-000740] p 238 N92-15761
Formation and sustainment of a very low aspect ratio tokamak using coaxial helicity injection: Helicity Injected Torus (HIT) experiment
[DE92-014311] p 1136 N92-32595

PLASMA DIAGNOSTICS
Formation and sustainment of a very low aspect ratio tokamak using coaxial helicity injection: Helicity Injected Torus (HIT) experiment
[DE92-014311] p 1136 N92-32595

PLASMA DYNAMICS
Plasmadynamic effects in thermochemical nonequilibrium aerobrake flows
[AIAA PAPER 92-0573] p 333 A92-26980
Plasmadynamic effects in thermochemical nonequilibrium aerobrake flows p 705 A92-41538

PLASMA EQUILIBRIUM
Shafranov shift in low-aspect-ratio heliotron/torsatron CHS
[NIFS-110] p 1138 N92-33743

PLASMA GENERATORS
Materials and structures for Hermes
p 666 A92-38213
The IRS plasma wind tunnels for the investigation of thermal protection materials for reentry vehicles
p 208 N92-15009

PLASMA HEATING
Scoping studies for small steady-state tokamaks for divertor testing
[DE92-000740] p 238 N92-15761
Experimental studies of compact toroids
[DE92-003469] p 512 N92-21046

PLASMA INTERACTIONS
Scoping studies for small steady-state tokamaks for divertor testing
[DE92-000740] p 238 N92-15761

PLASMA JET WIND TUNNELS
High enthalpy wind tunnel for erosion testing of advanced materials
[AIAA PAPER 92-3888] p 1094 A92-56729
An overview of the planned aerospace test facilities at Capua, Italy
[AIAA PAPER 92-3944] p 1097 A92-56773
Hydrodynamic flow visualization around an oscillating vane. Extension of study to the case of higher incidences and amplitudes and the starting off phase from permanent regime
[ONERA-RT-56/1369-AN] p 43 N92-11312
The IRS plasma wind tunnels for the investigation of thermal protection materials for reentry vehicles
p 208 N92-15009

PLASMA JETS
Studies on the mechanism of ignition and flameholding by plasma jets p 755 A92-42798
Thermal response of rigid and flexible insulations and reflective coating in an aeroconvective heating environment
[NASA-TM-103925] p 852 N92-28721
High temperature aircraft research furnace facilities
[NASA-CR-184384] p 1101 N92-33826

PLASMA PRESSURE
Shafranov shift in low-aspect-ratio heliotron/torsatron CHS
[NIFS-110] p 1138 N92-33743

PLASMA PROPULSION
IRS organigram p 33 N92-10053

PLASMA SPRAYING
Thermally sprayed coating systems for surface protection and clearance control applications in aero engines p 488 A92-32394
Thermally sprayed coating systems for surface protection and clearance control applications in aero engines
[PNR-90802] p 741 N92-27422

PLASMA TORCHES
Effectiveness of plasma torches for ignition and flameholding in scramjet p 737 A92-44524

PLASMA-PARTICLE INTERACTIONS
Ionospheric plasma flow over large high-voltage space platforms. I - Ion-plasma-time scale interactions of a plate at zero angle of attack. II - The formation and structure of plasma wake p 779 A92-41359

PLASTIC AIRCRAFT STRUCTURES
The design and manufacture of an advanced thermoplastic horizontal stabilator for the AH-64A
p 59 A92-14354
Aeroelastic tailoring of aeronautical composite wing structures p 146 A92-15343
A method to determine propagation direction of compressive fracture in carbon-fibre composites
p 672 A92-38770
Interlaminar fracture characteristics of bonding concepts for thermoplastic primary structures p 758 A92-41282
Composite makers sense changes
p 754 A92-42345
Thermal fiber-reinforced-plastic composite technology for aircraft structures p 755 A92-43237
Impact response of composite UHB propeller blades
[SAE PAPER 912046] p 861 A92-45430
Finite elements analysis of flexural edge wave for composite fan blades
[SAE PAPER 912048] p 861 A92-45432
Structural concept of main wings of high altitude unmanned aerial vehicle and basic properties of thermoplastic composites as candidate material
[SAE PAPER 912053] p 843 A92-45437
Fabrication and mechanical properties of an optically transparent glass fiber/polymer matrix composite
p 891 A92-45630
Induction bonding procedures for graphite reinforced thermoplastic assemblies p 994 A92-51545
Detailed analysis and test correlation of a stiffened composite wing panel p 1121 A92-56324
The use of load enhancement factors in the certification of composite aircraft structures
[NLR-TP-90068-U] p 852 N92-28649

PLASTIC DEFORMATION
Stability of stiffened panels with allowance for plasticity under nonstationary heating and loading
p 493 A92-30152
Thermal deformation of a polymer heat shield material on the descent trajectory p 754 A92-42655

PLASTIC FLOW
Light thermal structures and materials for high speed flight p 649 N92-25922

PLASTIC PROPERTIES
Cost effective close tolerance plastic master models
p 958 A92-51538

PLATE THEORY
An independent refinement and integration procedure in multiregion finite element analysis
[AIAA PAPER 92-2290] p 582 A92-34307
Solution of stress intensity factor by weight function for small surface cracks in plates p 998 A92-53332
Transverse shear effect on flutter of composite panels
p 1122 A92-56607
An analytical and experimental study to investigate flutter suppression via piezoelectric actuation
[NASA-TM-893240] p 156 N92-12173

PLATES (STRUCTURAL MEMBERS)
Coupled analysis of independently modeled finite element subdomains
[AIAA PAPER 92-2235] p 581 A92-34289
A compound fatigue investigation of plate specimen under low-cycle load superposed on high cycle load
p 587 A92-35555
Calculation of the exerting force necessary to form the aircraft hull plate in the symmetry plate bender with three rolls and the feeding value of the centre roll
p 998 A92-53297
Investigation of a plate-ramp-configuration by means of laser Doppler anemometry at Mach 2.95
[AIAA PAPER 92-3956] p 1097 A92-56784
An analytical and experimental study to investigate flutter suppression via piezoelectric actuation
[NASA-TM-893240] p 156 N92-12173
Combined VISAR and flash x ray testing techniques
[DE92-004732] p 385 N92-18290
Vibration tests of long plate structural model
[NAL-TM-625] p 400 N92-18485
Experimental studies of vortex flaps and vortex plates. Part 1: 0.53 m span 60 deg delta wing
[CRANFIELD-AERO-9113-PT-1] p 349 N92-19679
Nonlinear analyses of composite aerospace structures in sonic fatigue
[NASA-CR-190565] p 854 N92-30209
An analytical and experimental investigation of flutter suppression via piezoelectric actuation
[NASA-TM-107653] p 962 N92-31174

PLUG NOZZLES
Design considerations for nozzles of hypersonic airbreathing propulsion
[AIAA PAPER 91-5019] p 471 A92-31685
Application of finite element method to hypersonic nozzle flow computations p 769 N92-27479

PLUMES
Thermal imaging of afterburning plumes
p 129 A92-17179
Single expansion ramp nozzle simulations
[AIAA PAPER 92-0387] p 323 A92-26243
Navier-Stokes analysis of helicopter plume flowfield for infrared calculations
[AIAA PAPER 92-0983] p 580 A92-33185
Experimental research of the aerodynamics of nozzles and plumes at hypersonic speeds
[NASA-CR-187316] p 185 N92-15048
Comparison of jet plume shape predictions and plume influence on sonic boom signature
[NASA-TP-3172] p 631 N92-25133

Experimental investigation of nozzle/plume aerodynamics at hypersonic speeds
[NASA-CR-190074] p 664 N92-25162
Acoustic interactions between an altitude test facility and jet engine plumes: Theory and experiments
[NASA-CR-190423] p 738 N92-26405

PLY ORIENTATION
Integrated aeroelastic control optimization of laminated composite lifting surfaces p 481 A92-32248

PNEUMATIC CIRCUITS
A simple and low cost system to measure delay times in pneumatic systems
[NLR-TP-90174-U] p 859 N92-28644

PNEUMATIC CONTROL
An experimental study of pneumatic vortex flow control on high angle of attack forebody model
[AIAA PAPER 92-0018] p 247 A92-22140
Analysis of a pneumatic forebody flow control concept about a full aircraft geometry
[AIAA PAPER 92-2678] p 799 A92-45530
Effects of bleed air extraction of thrust levels on the F404-GE-400 turbofan engine
[AIAA PAPER 92-3092] p 1066 A92-54009
Aerodynamic control of fighter aircraft by manipulation of forebody vortices p 380 N92-18791
Forebody vortex control aeromechanics p 380 N92-18792
Effects of bleed air extraction on thrust levels on the F404-GE-400 turbofan engine
[NASA-TM-104247] p 871 N92-29425

PNEUMATIC EQUIPMENT
Pneumatic distortion compensation for aircraft surface pressure sensing devices p 218 A92-20206
Advanced pneumatic impulse ice protection system (PIIP) for aircraft p 845 A92-46807
Low energy ice protection for helicopters p 1059 A92-56348
F/A-18 stabilator: Equivalent set of point forces required for pneumatic bag load case simulation
[AD-A242637] p 206 N92-15073
Pneumatically actuated multiple store launcher
[AD-D015237] p 732 N92-27188

PNEUMATICS
Advanced ice protection systems test in the NASA Lewis Icing Research Tunnel p 108 A92-14406
Development of a pneumatic high-angle-of-attack flush airdata sensing system
[SAE PAPER 912142] p 651 A92-39980
Development of a pneumatic high-angle-of-attack flush airdata sensing (HI-FADS) system
[NASA-TM-104241] p 118 N92-11994

PODS (EXTERNAL STORES)
Flow visualization and wake analysis for standard and modified configurations of the AN/ALQ-78 antenna pod
[AD-A243552] p 260 N92-17339

POINT SOURCES
Discrete modes and continuous spectra in supersonic boundary layers p 809 A92-46264

POLAR METEOROLOGY
Retrieval of total precipitable water over high latitude regions using radiometric measurements near 90 and 183 GHz p 505 A92-32129

POLAR WANDERING (GEOLOGY)
A demonstration of centimeter-level monitoring of polar motion with the Global Positioning System p 639 N92-24302

POLARIMETERS
Development of a 3-D remote sensing radar p 597 A92-34908

POLARIMETRY
Coherence multiplexed polarimetric fibre sensor arrays for aerospace applications p 370 A92-27785

POLARIZATION (WAVES)
Global and high resolution radar cross section measurements and two-dimensional microwave images of a scaled aircraft model from the type Airbus A 310
[DLR-MITT-91-10] p 911 N92-29877

POLARIZED LIGHT
Bias of an optical passive ring-resonator gyro caused by the misalignment of the polarization axis in the polarization-maintaining fiber resonator p 652 A92-40262

POLICIES
A review of UK aviation policy
[TT-9107] p 61 N92-12988
New Ways: Tiltrotor aircraft and magnetically levitated vehicles
[OTA-SET-507] p 238 N92-14933
The impact of aircraft noise control technology
[PNR-90846] p 512 N92-20461
Tilt rotors and the Port Authority of New York and New Jersey Airport System
[RAND-R-3971/1-PA-SUMM] p 636 N92-25262
The FAA aging airplane program plan for transport aircraft p 838 N92-30128

POLLUTION CONTROL
CARS temperature measurements and validation of a computing code on a gas-turbine combustor
[ONERA, TP NO. 1991-224] p 373 A92-26376
Low VOC primer for structural bonding --- volatile organic compound p 892 A92-47338
Non-chromated anodize process for corrosion resistance and adhesive bonding p 892 A92-47341
Applied analytical combustion/emissions research at the NASA Lewis Research Center - A progress report
[AIAA PAPER 92-3338] p 1067 A92-54025
Low volatile organic compound paints
[DE91-017984] p 35 N92-11203
Emissions from aircraft: Standards and potential for improvement
[PNR-90768] p 476 N92-21740
Applied analytical combustion/emissions research at the NASA Lewis Research Center
[NASA-TM-105731] p 890 N92-29343

POLLUTION MONITORING
Time Resolved Lidar Fluorosensor operating from helicopter p 1121 A92-56296
A small light-weight rotor platform for ground observation and pollution control p 1057 A92-56329

POLLUTION TRANSPORT
Natural cycles, gases p 408 N92-19123
Aircraft gas turbine emissions: Their nature, technology for reduction, and a pollution comparison with channel tunnel transport
[ETN-92-91056] p 559 N92-22406

POLYCRYSTALS
Properties of a TZP/Al2O3 composite after long-term exposure at 1000 C
[AD-A246407] p 757 N92-27752

POLYETHER RESINS
Thermal properties of high performance thermoplastic composites based on poly(ether ketone ketone) (PEKK) p 34 A92-10238

POLYETHYLENES
Recent developments in the use of thin-film polyethylene balloons for meteorological applications p 16 A92-11033

POLYGONS
Two-dimensional aerodynamic characteristics of several polygon-shaped cross-sectional models applicable to helicopter fuselages
[NASA-TP-3233] p 944 N92-30394

POLYIMIDE RESINS
Processing parameters for carbon/PMR-15 composite flat panels p 34 A92-11812
Addition curing thermosets endcapped with 4-amino (2,2) paracyclophane p 577 A92-33918
New thermoplastic polyimide composite for supersonic aircraft structures p 985 A92-51512
Fabrication test and evaluation of graphite/PMR-15 polyimide for HOPE primary structure p 1105 A92-53516
Vinyl capped addition polyimides
[NASA-CASE-LEW-15027-2] p 579 N92-24053

POLYMER BLENDS
Polymer infiltration studies
[NASA-CR-190204] p 578 N92-22486

POLYMER CHEMISTRY
Polymer blends, volume 1
[AD-A252112] p 987 N92-31419

POLYMER MATRIX COMPOSITES
X-ray computed tomography of composites p 36 A92-10143
Manufacture of a primary flight structure using thermoplastics p 1 A92-10197
New thermoplastic composites for aircraft structures and interiors p 34 A92-10271
Fracture behaviour of high-temperature polymer composites p 34 A92-11993
Evaluation of thermoplastic matrix composites for use in energy-absorbing helicopter subfloors p 141 A92-14374
Processing effects and damage tolerance in poly(etheretherketone) composites p 388 A92-26152
An analysis of impact resistance of composite blades for aircraft engines (Analysis with two dimensional and three dimensional finite elements) p 579 A92-32562
Addition curing thermosets endcapped with 4-amino (2,2) paracyclophane p 577 A92-33918
Thermal deformation of a polymer heat shield material on the descent trajectory p 754 A92-42655
Fabrication and mechanical properties of an optically transparent glass fiber/polymer matrix composite p 891 A92-45630
Effects of elevated temperature on the viscoplastic modeling of graphite/polymeric composites
[NASA-TM-104160] p 35 N92-11149
High-temperature polymer matrix composites p 578 N92-22513
Advanced airframe structural materials: A primer and cost estimating methodology
[AD-A253371] p 1062 N92-34182

POLYMERIC FILMS
Recent developments in the use of thin-film polyethylene balloons for meteorological applications p 16 A92-11033
Interlaminar fracture characteristics of bonding concepts for thermoplastic primary structures p 758 A92-41282
A study of aircraft surface coating technology p 700 A92-43147

POLYMETHYL METHACRYLATE
Investigation of a method for determining machining stress in polymethylmethacrylate (PMMA) of airplane canopies p 986 A92-53096
Solid fuel ramjet infrared signature
[AD-A246299] p 753 N92-26362

POLYNOMIALS
Compact higher order characteristic-based Euler solver for unstructured grids p 812 A92-46889
Comparison of polynomial approximations and artificial neural nets for response surfaces in engineering optimization p 165 N92-13835
Sensor fault detection on board an aircraft with observer and polynomial classifier
[DLR-FB-91-34] p 859 N92-29870

POLYSTYRENE
Performance of insulated pavements at Newton Fields, Jackman, Maine
[CRREL-92-9] p 1101 N92-32903

POROSITY
Alleviation of side force on tangent-ogive forebodies using passive porosity
[AIAA PAPER 92-2711] p 802 A92-45552
Effect of porosity in transpiration cooling system p 1112 A92-53786
Assessment of passive porosity with free and fixed separation on a tangent ogive forebody
[AIAA PAPER 92-4494] p 1081 A92-55363

POROUS BOUNDARY LAYER CONTROL
Shock-boundary layer interaction control with low-profile vortex generators and passive cavity
[AIAA PAPER 92-0064] p 250 A92-22178
New method for boundary layer thickness control on ground plate in wind tunnel p 383 A92-25110
Computations of a transonic flow about an airfoil in a wind tunnel with porous walls p 423 A92-30128
Theoretical analysis of a suction diffuser in the porous test section of a wind tunnel p 428 A92-30207
Subsonic flow past a thin airfoil in a channel with porous walls p 438 A92-31867
Determination of the mass-flow-rate characteristics of porous panels p 439 A92-31875
Consideration of the effect of viscosity in the problem of porous-wall induction p 440 A92-31887
Experimental investigation on reducing fluctuating pressures of launch vehicles by passive shock-wave/boundary-layer control p 616 A92-38916
High subsonic wind tunnel test of a two-dimensional hybrid-laminar-flow-control airfoil with slotted surface p 1029 A92-56045

POROUS MATERIALS
A chambered porous damper for rotor vibration control. II - Imbalance response and bladeless simulation
[ASME PAPER 91-GT-243] p 149 A92-15648
A chambered porous damper for rotor vibration control. I - Concept development
[ASME PAPER 91-GT-244] p 150 A92-15649
An investigation on flame stability by fuel permeability in a flame holder made of porous ceramic material p 375 A92-28435
Flow modification over a backward facing step
[AD-A241351] p 158 N92-13406

POROUS WALLS
Theoretical analysis of the effect of the porous walls of a wind tunnel on transonic flow past bodies of cone-cylinder type p 427 A92-30202
Static and dynamic flow field development about a porous suction surface wing
[AIAA PAPER 92-2628] p 795 A92-45500

POSITION (LOCATION)
GPS availability. I - Availability of service achievable for different categories of civil users. II - Evaluation of state probabilities for 21-satellite and 24-satellite constellations p 99 A92-16949
SATCOM antenna siting study on P-3C aircraft, volume 2
[NASA-CR-189515] p 221 N92-14263
Joint Federal Aviation Administration (FAA)/Civil Aviation Authority (CAA) Microwave Landing System (MLS) Area Navigation (RNAV) flight evaluations
[DOT/FAA/CT-TN91/17] p 268 N92-15983
Proportional plus integral control of aircraft for automated maneuvering formation flight
[AD-A243792] p 382 N92-19505

US Coast Guard GPS Information Center (GPSIC) and its function within the Civil GPS Service (CGS) p 1049 N92-33352
Evaluation of GPS/UTC steering performance p 1049 N92-33353
Precise GPS ephemerides from DMA and NGS tested by time transfer p 1049 N92-33355

POSITION ERRORS
On the overdetermined celestial fix p 19 A92-10475
Comparison of fixed and variable threshold RAIM algorithms p 100 A92-16951
Probability distributions that are important when assessing barometric aiding to GPS p 100 A92-16952
Wide area differential GPS p 101 A92-16966
Results of a test program for the use of differential GPS for approach guidance p 101 A92-16969
Use of distance-measuring equipment (DME) for correcting errors in position, velocity, and wind measurements from aircraft inertial navigation systems p 188 A92-18172
The accuracy and coverage of Loran-C and of the Decca Navigator System - and the fallacy of fixed errors p 353 A92-24944
An exploratory investigation into the definition of tracking standards for IFR helicopter approaches to reduced minima p 533 A92-35726
On the calculation of repeatable accuracy, with special reference to GPS p 955 A92-49383
Receiver Autonomous Integrity Monitoring (RAIM) capability for sole-means GPS navigation in the oceanic phase of flight p 956 A92-51012
A Kalman filter integrated navigation design for the IAR Twin Otter Atmospheric Research Aircraft
[NRC-32148] p 1048 N92-32849

POSITION INDICATORS
Digital technology applied to airborne receivers p 98 A92-16927
Wavelength-multiplexed fiber-optic position encoder for aircraft control systems p 734 A92-42602
An airborne multimode radar display processor p 965 A92-49308
Reflection type skin friction meter
[NASA-CASE-LAR-14520-1-SB] p 11 N92-10008
Study of optical techniques for the Ames unitary wind tunnels. Part 3: Angle of attack
[NASA-CR-190541] p 888 N92-29655
Techniques for autonomous navigation
[DE92-013458] p 957 N92-31746
An investigation of switched reluctance rotor position estimation using neural networks
[AD-A252846] p 1061 N92-33414
Radar clutter classification
[ISBN-0-315-57981-1] p 1126 N92-33440

POSITION SENSING
Fiber-coupled position sensors for aerospace applications p 370 A92-27776
Optically powered and interrogated rotary position sensor for aircraft engine control applications p 370 A92-27777
A novel avionic sensor for fly-by-light controls p 650 A92-38128
Fibre optic rotary position sensors for vehicle and propulsion controls p 855 A92-46243
Fiber-optic position transducers for aircraft controls p 857 A92-48041
Application of analog fiber optic position sensors to flight control systems p 857 A92-48042
Multi-analog track fiber coupled position sensor p 857 A92-48043
Evaluation of electrolytic tilt sensors for wind tunnel model angle-of-attack (AOA) measurements p 1116 A92-54344
On improvements of three-dimensional position measuring system for dynamic wind tunnel testing p 1093 A92-56012
Measurement of position and attitude using laser and retro-reflectors p 1047 A92-56120
Development of digital/optical rotary position transducer
[NAL-TR-1106] p 29 N92-10028
Further developments relating to the NASA Langley Research Center 13-inch magnetic suspension and balance system
[NASA-CR-188995] p 31 N92-11023
Progress of magnetic suspension and balance systems for wind tunnels in the USSR p 751 N92-27803

POSITIONING
Kinematic GPS for differential positioning - Resolving integer ambiguities on the fly p 19 A92-10472
A demonstration of centimeter-level monitoring of polar motion with the Global Positioning System p 639 N92-24302
An adaptive correction technique for Differential Global Positioning System p 726 N92-26623

POSITIVE FEEDBACK
Baro-inertial loop for the USAF Standard RLG INU p 97 A92-16647

POSTFLIGHT ANALYSIS
Navigation preparations for passenger helicopters p 723 A92-43155
STS-40 descent BET products: Development and results
[NASA-CR-189570] p 286 N92-16012
Postflight aerothermodynamic analysis of Pegasus(tm) using computational fluid dynamic techniques
[NASA-CR-186017] p 445 N92-21188

POTENTIAL FLOW
Flow analysis and design of three-dimensional wind tunnel contractions p 5 A92-11067
Kernel function occurring in supersonic unsteady potential flow p 6 A92-11080
Axisymmetric potential flow calculations. II - Design mode p 8 A92-12399
Analysis of flexible-membrane and jet-flapped airfoils using velocity singularities p 10 A92-13216
Computation of the potential flow through cascades using the conformal mapping and the singularity method p 66 A92-15356
Complex variable boundary element method for external potential flows p 172 A92-18353
Inviscid drag prediction for transonic transport wings using a full-potential method p 174 A92-20212
Time domain flutter analysis of cascades using a full-potential solver p 176 A92-20747
An improvement of the double-point method for unsteady subsonic flow p 243 A92-21315
Concerning the functional solution of transonic flows p 243 A92-21318
Application of holomorphic vectors theory in three-dimensional potential flow problem p 292 A92-21923
Aerodynamic design and optimization in one shot
[AIAA PAPER 92-0025] p 248 A92-22147
Development of a three-dimensional icing code - Comparison with experimental shapes
[AIAA PAPER 92-0041] p 262 A92-22159
Parallel algorithms for panel methods --- in fluid dynamics p 293 A92-22346
An AF3 algorithm for the calculation of transonic nonconservative full potential flow around axisymmetric inlet cowls p 251 A92-23380
Efficient panel method for vortex sheet roll-up p 309 A92-24404
Finite element method for computing nonisentropic potential transonic flow with shock waves p 312 A92-25009
Zonal flow analysis method for two-dimensional airfoils p 330 A92-26435
Obtaining the velocity field required for the calculation of propeller unsteady forces using 'traditional' approximate methods and CFD
[AIAA PAPER 92-0520] p 331 A92-26945
Boundary singularities in steady potential compressible flow through plane two-dimensional channels p 336 A92-27384
Study on nozzle flow diffusion p 429 A92-30531
Consideration of the effect of viscosity in the problem of porous-wall induction p 440 A92-31887
Mathematical modeling of nonstationary viscous flow over a solid angle of finite span p 440 A92-31890
Numerical computation of improved transonic potential method p 441 A92-32234
Multipoint inverse airfoil design method based on conformal mapping p 610 A92-36827
Performance predictions for centrifugal compressor impellers p 759 A92-41836
Calculation of potential flow around airfoils using a discrete vortex method p 808 A92-45827
A new integral equation for potential compressible aerodynamics of rotors in forward flight p 815 A92-46958
Discussion of improved transonic potential method p 942 A92-53290
A potential flow theory of two-dimensional bifurcated curtain jets. II p 1118 A92-56039
Improved calculation of transonic potential flow past swept wings p 1031 A92-56179
Unsteady flows in rotor-stator cascades
[AD-A241593] p 158 N92-13410
CAR 88: A method to calculate subsonic and supersonic, steady and unsteady, potential flow about complex configurations
[NLR-TR-88154-U] p 400 N92-18221
Inviscid drag prediction for transonic transport wings using a full-potential method
[NLR-TP-89365-U] p 444 N92-20473
Development of a steady potential solver for use with linearized, unsteady aerodynamic analyses
[NASA-TM-105288] p 473 N92-20525
PAN AIR: A computer program for predicting subsonic or supersonic linear potential flows about arbitrary configurations using a higher order panel method. Volume 1: Theory document (version 3.0)
[NASA-CR-3251] p 526 N92-22648
PAN AIR: A computer program for predicting subsonic or supersonic linear potential flows about arbitrary configurations using a higher order panel method. Volume 2: User's manual (version 3.0)
[NASA-CR-3252] p 527 N92-22865
A boundary integral formulation for unsteady transonic potential flows p 719 N92-27942
Viscous effects on a vortex wake in ground effect
[NASA-CR-190400] p 907 N92-28361
Wave drag determination in the transonic full-potential flow code MATRICS
[NLR-TP-90062-U] p 828 N92-28709
Development of a multigrid transonic potential flow code for cascades
[NASA-CR-190480] p 830 N92-29361
The three-dimensional stability of the Foeppl vortices p 949 N92-31889
Potential flow theory and operation guide for the panel code PMARC
[NASA-TM-102851] p 1036 N92-32422

POTENTIAL THEORY
Cascade flutter analysis with transient response aerodynamics p 154 A92-15972
Recent applications of linear and nonlinear unsteady aerodynamics for aeroelastic analysis p 718 N92-27940

POWDER (PARTICLES)
The basics of powder lubrication in high-temperature powder-lubricated dampers
[ASME PAPER 91-GT-248] p 150 A92-15653
The cost of silicon nitride powder: What must it be to compete?
[DE92-008710] p 669 N92-25223

POWDER METALLURGY
The role of PM in the design of lightweight aircraft engine components p 991 A92-50137
Probabilistic lifing approach for aero engine disks made of powder nickel base alloys containing ceramic defects p 226 N92-14424
Development and characterization of Powder Metallurgy (PM) 2XXX series Al alloy products and Metal Matrix Composite (MMC) 2XXX Al/SiC materials for high temperature aircraft structural applications
[NASA-CR-187631] p 390 N92-19290
Development of a new generation of high-temperature composite materials p 578 N92-22515
Powder processing of aero-engine components
[PNR-90813] p 756 N92-27044

POWER AMPLIFIERS
One joule output from a diode-array-pumped Nd:YAG laser with side-pumped rod geometry p 671 A92-37188

POWER CONDITIONING
Power beaming - Energy transmission at 35 GHz and higher frequencies --- for terrestrial and space applications with rectennas
[AIAA PAPER 92-2027] p 471 A92-29944
A criterion for estimating the economic and operational efficiency of the power distribution systems of commercial aircraft p 657 A92-40611

POWER CONVERTERS
Optically powered and interrogated rotary position sensor for aircraft engine control applications p 370 A92-27777
Next generation power electronics for space and aircraft. II - Packaging p 992 A92-50553

POWER EFFICIENCY
Energy analysis of high-speed flight systems p 925 A92-46430
Analysis of Euler's and stress tensor methods for calculating power consumption of high speed centrifugal fans and turbocompressors
[DE92-728396] p 298 N92-16325
Calculation of local power consumptions and efficiencies of centrifugal fans and turbocompressors
[DE92-728402] p 298 N92-16326

POWER SERIES
Flexure-torsion behavior of sheat-deformable beams with applications to aircraft wing sections
[AIAA PAPER 92-2467] p 582 A92-34357

POWER SPECTRA
Combination of different unsteady quantity measurements for gas turbine blade fault diagnosis
[ASME PAPER 91-GT-201] p 149 A92-15624
Power spectrum of ring modes of pressure fluctuations at the surface of a cylinder in axial flow p 603 A92-33770
Flowfield in the vicinity of the F/A-18 vertical fin at high-angle-of-attack p 628 N92-24865

POWER TRANSMISSION
Using helicopters for the erection of power transmission lines p 723 A92-43162
Proof of concept of a magnetically coupled Stirling engine-driven heat pump
[DE92-017129] p 1129 N92-33271
POWERED LIFT AIRCRAFT
Hover evaluation of an integrated pneumatic lift/reaction-drive rotor system
[AIAA PAPER 92-0630] p 333 A92-27010
NASA's quiet side. I p 607 A92-37875
Harrier international programme p 841 A92-45305
VSTOL engine design evolution - Growth of the Pegasus engine for Harrier p 860 A92-45306
A USAF assessment of STOVL fighter options p 842 A92-45310
Evolution of ASTOVL aircraft design p 842 A92-45311
Comparison of turbulence models for powered-lift flow fields
[AIAA PAPER 92-3674] p 1022 A92-54117
Experimental performance of three design factors for ventral nozzles for SSTOVL aircraft
[AIAA PAPER 92-3789] p 1069 A92-54168
Internal reversing flow in a tailpipe offtake configuration for SSTOVL aircraft
[AIAA PAPER 92-3790] p 1069 A92-54169
Flight measurements of downwash on the Ball-Bartoe Jetwing powered lift aircraft p 1054 A92-56174
Experimental performance of three design factors for ventral nozzles for SSTOVL aircraft
[NASA-TM-105697] p 742 N92-27669
Evaluation of landing configuration by flight test of the quiet STOL experimental aircraft ASKA
[NAL-TR-1113] p 733 N92-28191
Internal reversing flow in a tailpipe offtake configuration for SSTOVL aircraft
[NASA-TM-105698] p 868 N92-28418
Aerodynamic characteristics obtained from alpha sweep test of the quiet STOL experimental aircraft ASKA
[NAL-TR-1112] p 853 N92-28901
POWERED MODELS
Tests of models equipped with a turbofan powered simulator in the ONERA F1 low-speed pressurized wind tunnel
[ONERA, TP NO. 1991-219] p 383 A92-26371
A Mach-scaled powered model for rotor-fuselage interactional aerodynamics and flight mechanics investigations p 847 A92-46960
PRANDTL NUMBER
Turbine blade heat transfer prediction using coupled turbulent Prandtl number and transition models
[SAE PAPER 912152] p 674 A92-39987
PRANDTL-MEYER EXPANSION
Prandtl-Meyer function for dense gases p 415 A92-26441
PREBURNERS
Analysis of a hydrocarbon scramjet with augmented preburning
[AIAA PAPER 92-3425] p 865 A92-48984
PRECIPITATION (METEOROLOGY)
Precipitation development in Colorado Front Range snowstorms - 15 November 1987 case study p 301 A92-23008
The 1988 Australian Winter Storms Experiment - Case study: 6 August 1988 p 301 A92-23009
High altitude airborne remote sensing mission using the advanced microwave precipitation radiometer (AMPR) p 574 A92-34893
Microburst modelling and scaling p 915 A92-46262
PRECIPITATION HARDENING
Joining a Ni-based creep-resistant (ODS) alloy by brazing p 1116 A92-54867
Diffusion bonding a creep-resistant Fe-ODS alloy p 1117 A92-54868
PRECIPITATION PARTICLE MEASUREMENT
Retrieval of total precipitable water over high latitude regions using radiometric measurements near 90 and 183 GHz p 505 A92-32129
Feature extraction from two-dimensional images using fractal analysis p 496 A92-32130
PRECISION
The effect of droplet sizing uncertainty on ice accretions p 679 N92-24874
Precision of the long baseline acoustic navigation system used by Pegasus
[AD-A246598] p 727 N92-26795
Estimation of aircraft attitude by angular rate measurements p 963 N92-31881
PREDICTION ANALYSIS TECHNIQUES
Stochastic prediction techniques for wind shear hazard assessment p 48 A92-11381
Life time prediction for ceramic gas turbine components
[ASME PAPER 91-GT-96] p 122 A92-15560
A survey of the broadband shock associated noise prediction methods
[AIAA PAPER 92-0501] p 415 A92-26930
Computational fluid dynamics and aircraft design p 457 A92-28875
Analysis of open loop higher harmonic control at high airspeeds on a modern four-bladed articulated rotor
[AIAA PAPER 92-2450] p 542 A92-34477
Development and analysis of flight flutter prediction methods
[AIAA PAPER 92-2101] p 588 A92-35672
The computer analysis of the prediction of aircraft electrical power supply system reliability p 690 A92-37950
A comparison of fatigue life prediction methodologies for rotorcraft p 647 A92-40884
Prediction of separation point in compressible turbulent boundary layers by Green's lag-entrainment method p 700 A92-41178
Prediction of vortex shedding from forebodies with chines p 702 A92-41228
Advances in fatigue lifetime predictive techniques; Proceedings of the Symposium, San Francisco, CA, Apr. 24, 1990
[ASTM STP-1122] p 896 A92-45226
Stochastic prediction techniques for wind shear hazard assessment p 1007 A92-50505
Three-dimensional Navier-Stokes heat transfer predictions for turbine blade rows
[AIAA PAPER 92-3068] p 1020 A92-54003
Understanding and development of a prediction method of transonic limit cycle oscillation characteristics of fighter aircraft
[AIAA PAPER 92-4501] p 1026 A92-55369
Development of unsteady aerodynamic analyses for turbomachinery aeroelastic and aeroacoustic applications
[NASA-CR-4405] p 12 N92-10979
Analysis of open loop higher harmonic control at high airspeeds on a modern four-bladed articulated rotor
[NASA-TM-103876] p 21 N92-11000
Studies of aerothermal loads generated in regions of shock/shock interaction in hypersonic flow
[NASA-CR-181893] p 43 N92-11319
Numerical simulation of vortex flows past impulsively started wings p 88 N92-13028
Prediction of noise field of a propfan at angle of attack
[NASA-CR-189047] p 166 N92-13759
The effect of a type 3 and type 4 shock/shock interaction on heat transfer in the stagnation region p 160 N92-13867
Design and performance of duct acoustic treatment p 236 N92-14783
The application of experimental data to blade wake interaction noise prediction
[NASA-CR-189461] p 237 N92-14789
A survey of the broadband shock associated noise prediction methods
[NASA-TM-105365] p 237 N92-14797
Aerodynamic heating on AFE due to nonequilibrium flow with variable entropy at boundary layer edge p 183 N92-15020
Seal development activities at Allison Turbine Division p 228 N92-15093
STS-40 descent BET products: Development and results
[NASA-CR-189570] p 286 N92-16012
Design of a fiber optic image transmission link
[AD-A243686] p 304 N92-17088
Program plans: Aviation safety research
[NIAR-91-30] p 264 N92-17587
Fatigue management for the A-7P p 363 N92-18593
Prediction of aerodynamic phenomena limiting aircraft manoeuvrability p 364 N92-18781
An analytical and computational investigation of shock-induced vortical flows with applications to supersonic combustion p 405 N92-19538
The NREL teetering hub rotor code: Final results and conclusions
[DE92-001187] p 410 N92-19633
An introduction to high speed aircraft noise prediction
[NASA-CR-189582] p 416 N92-19672
A study of the aeroelastic behaviour of helicopter rotor blades featuring swept tips p 367 N92-19701
Blade-vortex noise on a helicopter main rotor. Study of the strong two dimensional incompressible interaction
[ONERA-RT-96/5094-PY] p 511 N92-20388
Investigation of a semi-empirical method to predict limit cycle oscillations of modern fighter aircraft
[NLR-TP-90087-U] p 481 N92-20475
Application of a water droplet trajectory prediction code to the design of inlet particle separator anti-icing systems
[PNR-90839] p 474 N92-20573
Rotary engine performance limits predicted by a zero-dimensional model
[NASA-CR-189129] p 474 N92-20650
A review of icing research at the Royal Aerospace Establishment p 451 N92-21689
Preparation of the ice certification of the Dornier 328 regional airliner by numerical simulation and by ground test p 451 N92-21693
Prediction of helicopter noise: Adaptation of noise load calculations to the blade-vortex interaction
[ONERA-RS-97/5094-PY] p 513 N92-21736
Integration of flight and carrier landing aid systems for shipboard operations p 456 N92-21958
Life prediction technologies for aeronautical propulsion systems p 560 N92-22520
Experimental evaluation of a flat wake theory for predicting rotor inflow-wake velocities
[NASA-TM-4334] p 630 N92-24882
Structural analysis for preliminary design of High Speed Civil Transport (HSCT) p 684 N92-25926
Transonic Unsteady Aerodynamics and Aeroelasticity
[AGARD-CP-507] p 718 N92-27936
NLR inviscid transonic unsteady loads prediction methods in aeroelasticity p 720 N92-27947
Development of a method to predict transonic limit cycle oscillation characteristics of fighter aircraft p 746 N92-27958
Steady and Transient Performance Prediction of Gas Turbine Engines
[AGARD-LS-183] p 868 N92-28458
Overview on basis and use of performance prediction methods p 869 N92-28459
Engine performance and health monitoring models using steady state and transient prediction methods p 870 N92-28467
Experimental and computational ice shapes and resulting drag increase for a NACA 0012 airfoil
[NASA-TM-105743] p 828 N92-28674
Fracture mechanics research at NASA related to the aging commercial transport fleet p 913 N92-30110
Joint computational and experimental aerodynamics research on a hypersonic vehicle
[DE92-013439] p 943 N92-30367
A new unsteady mixing model to predict NO(x) production during rapid mixing in a dual-stage combustor
[NASA-CR-189155] p 971 N92-30569
Numerical methods for the simulation of complex multi-body flows with applications for the integrated Space Shuttle vehicle p 945 N92-30741
Life prediction and constitutive models for engine hot section anisotropic materials program
[NASA-CR-189222] p 973 N92-31534
Leading-edge receptivity for blunt-nose bodies
[NASA-CR-190563] p 1036 N92-32648
Integration of wall interference assessment and wall adaptation
[NLR-TP-91119-U] p 1101 N92-32734
Life prediction and constitutive models for engine hot section anisotropic materials program
[NASA-CR-189223] p 1072 N92-33479
Dynamic response of induced pressures, suckdown, and temperatures for two tandem jet STOVL configurations
[NASA-TM-103934] p 1039 N92-33581
An improved compressor performance prediction model
[PNR-90873] p 1072 N92-33749
Prediction and control of asymmetric vortical flows around slender bodies using Navier-Stokes equations p 1127 N92-33968
PREDICTIONS
Prediction of ice accretion on a swept NACA 0012 airfoil and comparisons to flight test results
[AIAA PAPER 92-0043] p 316 A92-25677
Critical appraisal of the McDonnell Douglas closure model for predicting fatigue crack growth
[ARL-STRUC-R-444] p 44 N92-11376
Turbine engine diagnostics system study
[DOT/FAA/CT-91/16] p 202 N92-14064
A simplified method for predicting the stability of aerodynamically excited turbomachinery p 224 N92-14364
Prediction of ice accretion on a swept NACA 0012 airfoil and comparisons to flight test results
[NASA-TM-105368] p 258 N92-15968
Simplified method for the prediction of aerofoil excrescence drag magnification factor for turbulent boundary layers at subcritical Mach numbers
[ESDU-91028] p 259 N92-15972
Statistical methods applicable to analysis of aircraft performance data
[ESDU-91017] p 359 N92-18096
Comparison of jet plume shape predictions and plume influence on sonic boom signature
[NASA-TP-3172] p 631 N92-25133

Overview of mechanics of materials branch activities in the computational structures area
p 684 N92-25917
Analysis of unsteady aerodynamic and flutter characteristics of an aeroelastic model in transonic flow
p 720 N92-27953
Microwave temperature profiler for clear air turbulence prediction
[NASA-CASE-NPO-18115-1-CU] p 916 N92-29148
High speed transition prediction
[NASA-CR-190836] p 1039 N92-33424

PREDICTOR-CORRECTOR METHODS
An improved approach for the computation of transonic/supersonic flows with applications to aerospace configurations
[AIAA PAPER 92-2613] p 793 A92-45487
Enhancements to viscous-shock-layer technique
[AIAA PAPER 92-2897] p 820 A92-47873

PREFLIGHT ANALYSIS
Pre-flight physical simulation test of HIMES reentry test vehicle p 1103 A92-53640

PREFORMS
Universal weaving for turbine engine composite preforms
[AD-A237667] p 202 N92-14059
RTM: Cost-effective processing of composite structures p 578 N92-22678

PREMIXED FLAMES
Thermochemical nonequilibrium and radiative interactions in supersonic hydrogen-air combustion
[AIAA PAPER 92-0340] p 394 A92-25786
Premixed, turbulent combustion of axisymmetric sudden expansion flows p 397 A92-27770
Evaluation of NO(x) mechanisms for lean, premixed combustion
[ASME PAPER 91-GT-257] p 668 A92-36900
The coherent flamelet model for propulsion applications p 756 N92-27486

PREMIXING
Experimental investigation of nozzle/plume aerodynamics at hypersonic speeds
[NASA-CR-190074] p 664 N92-25162

PREPROCESSING
Development of pre- and post-processor system for structural analysis
[NAL-TM-628] p 681 N92-25403

PRESSURE
Unsteady-pressure and dynamic-deflection measurements on an aeroelastic supercritical wing
[NASA-TM-4278] p 445 N92-20654

PRESSURE CHAMBERS
Gasdynamic calculation of an impulse wind tunnel with a two-section plenum p 493 A92-30147

PRESSURE DEPENDENCE
User's manual for AeroFcn: A FORTRAN program to compute aerodynamic parameters
[NASA-TM-104237] p 1133 N92-32507

PRESSURE DISTRIBUTION
Analysis of unsteady pressures induced on a body by a rotor p 10 A92-13212
Experimental investigation on gas-particle flow in cascades p 62 A92-13300
An experiment on unsteady flow over an oscillating airfoil
[ASME PAPER 91-GT-181] p 73 A92-15613
Effect of nose shape on three-dimensional stagnation region streamlines and heating rates
[AIAA PAPER 91-5032] p 171 A92-17822
Engineering method for calculating surface pressures and heating rates on vehicles with embedded shocks
[AIAA PAPER 91-5060] p 171 A92-17842
Large chord turbine cascade testing at engine Mach and Reynolds number p 173 A92-18771
Evaluation of Euler solvers for transonic wing-fuselage geometries p 174 A92-20214
Inverse solution uniqueness and domain of existence for supersonic space marching applications
[AIAA PAPER 92-0028] p 248 A92-22150
Correction of sideslip-induced static pressure errors in flight-test measurements p 309 A92-24416
Measurements of the pressure and velocity distribution in low-speed turbomachinery by means of high-frequency pressure transducers p 391 A92-24723
A random vortex method for prediction of maximum instantaneous inlet total pressure distortion
p 311 A92-24731
A comparative study of turbulence models for overset grids
[AIAA PAPER 92-0437] p 327 A92-26284
Screech noise source structure of a supersonic rectangular jet
[AIAA PAPER 92-0503] p 331 A92-26932
A supplement to the second-order shock-expansion method p 437 A92-31861
Interaction of jets ejected from two-dimensional nozzles with a curved surface p 438 A92-31869
NACA 0012 benchmark model experimental flutter results with unsteady pressure distributions
[AIAA PAPER 92-2396] p 517 A92-34469
Convergence of subsonic unsteady aerodynamics evaluated by a finite element concept based on Huygeuns' wave propagation
[AIAA PAPER 92-2502] p 518 A92-34497
Determination of tire-wheel interface loads for aircraft wheels
[AIAA PAPER 92-2482] p 543 A92-34599
An analytical evaluation of the aerodynamic forces acting on a circular cylinder in a uniform shear flow
p 522 A92-35995
Plotting the universal characteristic of a compressor in low-rpm and autorotation regimes p 657 A92-40607
Study on small stalker tube performance and numerical calculation p 748 A92-43099
Scale effects on the flow past the mated Space Shuttle configuration
[AIAA PAPER 92-2680] p 799 A92-45532
Alleviation of side force on tangent-ogive forebodies using passive porosity
[AIAA PAPER 92-2711] p 802 A92-45552
Experimental investigation of vortex dynamics on delta wings
[AIAA PAPER 92-2731] p 804 A92-45565
An unstructured approach to the design of multiple-element airfoils
[AIAA PAPER 92-2709] p 807 A92-45592
Separation patterns and flow structures about a hemisphere-cylinder at high incidences
[AIAA PAPER 92-2712] p 807 A92-45593
Separated high enthalpy dissociated laminar hypersonic flow behind a step - Pressure measurements
p 809 A92-45858
Experimental performance of three design factors for ventral nozzles for SSTOVL aircraft
[AIAA PAPER 92-3789] p 1069 A92-54168
Use of an approximate similarity principle for the thermal scaling of a full-scale thrust augmenting ejector
[AIAA PAPER 92-3792] p 1069 A92-54171
Aerodynamic assessment of an optical pressure measurement system (OPMS) by comparison with conventional pressure measurements in a high speed wind tunnel p 1114 A92-54304
Preliminary airfoil testing experience in the NDA cryogenic wind tunnel p 1091 A92-54326
Evaluation of sidewall interference in the NAL two-dimensional transonic wind tunnel
p 1092 A92-56011
Planning method of skirt systems for small ACVs
p 1118 A92-56038
A potential flow theory of two-dimensional bifurcated curtain jets. II p 1118 A92-56039
Analysis of the main wing lift distribution of the STOL research aircraft Asuka p 1053 A92-56051
Analysis of helicopter rotor-fuselage interference with time averaged pressure distribution
p 1032 A92-56331
An approach for increasing aeroelastic divergence dynamic pressure of wind-tunnel models
[AIAA PAPER 92-4002] p 1099 A92-56825
Transonic and supersonic Euler computations of vortex-dominated flow fields about a generic fighter
[NASA-TP-3156] p 11 N92-10011
Blade surface pressure measurements on the rotor of a model turbine stage in a transient flow facility
p 157 N92-12206
Vortex formation over a close-coupled canard-wing-body configuration in unsymmetrical flow p 85 N92-13010
An experimental study of the flow over a sharp-edged delta wing at subsonic and transonic speeds
p 85 N92-13011
Aerodynamic coefficients of a symmetrical airfoil in an oscillating flow
[AD-A241073] p 89 N92-13035
Inverse airfoil design procedure using a multigrid Navier-Stokes method p 193 N92-13932
Design of 3-dimensional complex airplane configurations with specified pressure distribution via optimization
p 194 N92-13948
An inverse method for the aerodynamic design of three-dimensional aircraft engine nacelles
p 194 N92-13958
An inverse method with regularity condition for transonic airfoil design p 177 N92-13969
Definition of the unsteady vortex flow over a wing/body configuration
[NASA-CR-180083] p 178 N92-13995
Experimental investigations of exciting forces caused by flow in labyrinth seals p 223 N92-14354
Transonic Navier-Stokes computations for a spinning body of revolution
[AD-A241015] p 180 N92-14972
A method of estimating a flow breakdown boundary for aerofoils and swept wings in transonic flows
[ESDU-91021] p 258 N92-15970
Simplified method for the prediction of aerofoil excrescence drag magnification factor for turbulent boundary layers at subcritical Mach numbers
[ESDU-91028] p 259 N92-15972
Excrescence drag magnification factors at the drag-rise condition for aerofoils with a specified form of upper-surface pressure distribution
[ESDU-91029] p 259 N92-15973
Failure detection and fault management techniques for flush airdata sensing systems
[NASA-TM-4335] p 276 N92-17128
Surface pressure measurements on the wing of a wind tunnel model during steady rotation
[AD-A243047] p 260 N92-17281
Marching with the parabolized Navier-Stokes equations. Problem 2: Hypersonic viscous flow over a flat plate
[AERO-REPT-9008] p 345 N92-18232
Analysis of unsteady force, pressure, and flow-visualization data for a pitching straked wing model at high angles of attack p 364 N92-18784
Use of CFD in the design of a modern multistage aero engine LP turbine design
[PNR-90862] p 472 N92-20179
Simulation of real-gas effects on pressure distributions for aeroassist flight experiment vehicle and comparison with prediction
[NASA-TP-3157] p 501 N92-20677
Evaluation of NACA0012 airfoil test results in the NAL two-dimensional transonic wind tunnel
[NAL-TR-1109T] p 445 N92-21287
NACA0012 benchmark model experimental flutter results with unsteady pressure distributions
[NASA-TM-107581] p 526 N92-22507
Wing force and surface pressure data from a hover test of a 0.658-scale V-22 rotor and wing
[NASA-TM-102244] p 550 N92-22864
Development of wall pressure measuring apparatus for an existing transonic wind tunnel test section
[NAL-TM-565] p 573 N92-23778
Flowfield in the vicinity of the F/A-18 vertical fin at high-angle-of-attack p 628 N92-24865
Use of an approximate similarity principle for the thermal scaling of a full-scale thrust augmenting ejector
[NASA-TM-105724] p 739 N92-26613
Subsonic investigations of vortex interaction control for enhanced high-alpha aerodynamics of a chine forebody/Delta wing configuration
[NASA-CR-189641] p 715 N92-26652
Experimental investigation of the unsteady pressure field around an oscillating blade
[MITT-90-01] p 768 N92-27407
Experimental performance of three design factors for ventral nozzles for SSTOVL aircraft
[NASA-TM-105697] p 742 N92-27669
A study of juncture flow in the NASA Langley 0.3-meter transonic cryogenic tunnel
[NASA-CR-190430] p 773 N92-27880
A time-linearization approach for unsteady transonic flows p 719 N92-27941
Comparison of Euler and full potential methods for unsteady transonic flow calculations
p 719 N92-27943
Analysis of unsteady aerodynamic and flutter characteristics of an aeroelastic model in transonic flow
p 720 N92-27953
Numerical simulation of shock-stall flutter of an airfoil using the Navier-Stokes equations p 746 N92-27956
NACA0012 airfoil data corrected for sidewall boundary-layer effects in the NAL two-dimensional transonic wind tunnel
[NAL-TM-640T] p 722 N92-28151
Calculation of installation effects within performance computer programs p 869 N92-28465
Combined load test apparatus for flat panels
[NASA-CASE-LAR-14698-1] p 911 N92-30028
Exploratory experimental investigation of a wave propeller
[AD-A252175] p 949 N92-32062
Three-dimensional compressible turbulent computations for a nondiffusing S-duct
[NASA-CR-4391] p 951 N92-32240
Computations of unsteady multistage compressor flows in a workstation environment
[NASA-TM-103839] p 1071 N92-32452
Unsteady wind tunnel tests p 1089 N92-34166

PRESSURE DRAG
A pressure-drag-determination method for aerodynamic-interference problems p 425 A92-30157
Aerodynamic coefficients of a symmetrical airfoil in an oscillating flow
[AD-A241073] p 89 N92-13035

A theoretical investigation of the induced drag of wing of finite aspect ratio
[CUED/A-AERO/TR-17(1991)] p 525 N92-22193
An experimental investigation of the surface flow and wake dynamics associated with transverse flow over wavy cylinders p 681 N92-25547
Automatic design of transonic airfoils to reduce the shock induced pressure drag p 949 N92-31863

PRESSURE DROP
Two-phase flow correlations in air/oil systems of aero engines
[ASME PAPER 91-GT-54] p 121 A92-15532
Analysis and prediction of transonic turbine blade losses
[ASME PAPER 91-GT-183] p 73 A92-15615
The effect of blade solidity on the aerodynamic loss of a transonic turbine cascade
[AIAA PAPER 92-0393] p 323 A92-26248
Prediction of the pressure loss coefficient of wind tunnel *turbulence reducing screens*
[AIAA PAPER 92-0568] p 384 A92-26976
Loss prediction of annular cascade flow based upon S1/S2 stream surface Navier-Stokes analysis p 338 A92-27802
Loss of cabin pressurization in U.S. naval aircraft - 1969-90 p 634 A92-37168

PRESSURE EFFECTS
Fatigue due to noise-induced pressure
[ASME PAPER 91-GT-150] p 148 A92-15588
Design of wing profiles with tangential suction or injection p 624 A92-40602
Simulation of iced wing aerodynamics p 450 N92-21686
Building vibrations induced by noise from rotorcraft and propeller aircraft flyovers
[NASA-TM-104170] p 1138 N92-33160

PRESSURE GRADIENTS
Pressure on a cylinder with a screen in transverse flow p 6 A92-12164
Stall inception in axial flow compressors
[ASME PAPER 91-GT-86] p 69 A92-15551
Confined normal-shock/turbulent-boundary-layer interaction followed by an adverse pressure gradient p 172 A92-18365
Implementation of Vigneron's streamwise pressure gradient approximation in the PNS equations
[AIAA PAPER 92-0189] p 256 A92-23798
Flight studies of the riblet effect on drag variation p 438 A92-31871
Bursts and sources of pressure fluctuation in turbulent boundary layers p 619 A92-40055
On the mechanics of 3-D turbulent boundary layers p 620 A92-40068
A model of the operation of the pulsejet engine and a study of its characteristics p 657 A92-40608
Effect of streamwise pressure gradient on the supersonic mixing layer p 1025 A92-54936
Experimental investigation into the effects of riblets on compressor cascade performance
[AD-A243881] p 377 N92-19235
Separation of relaminarised boundary layers
[CUED/A-AERO/TR-16] p 592 N92-22209
NACA0012 airfoil data corrected for sidewall *boundary-layer effects in the NAL two-dimensional* transonic wind tunnel
[NAL-TM-640T] p 722 N92-28151
Structure of three-dimensional turbulent boundary layers p 999 N92-30654

PRESSURE HEADS
The aerodynamic effect of fillet radius in a low speed *compressor cascade*
[NASA-TM-105347] p 202 N92-14063

PRESSURE MEASUREMENT
A small five-hole spherical pressure probe for compressor experiments p 38 A92-10970
Base pressure on an axisymmetric finned body during forced rotation in the autorotation regime p 7 A92-12165
Probe shapes for streamwise momentum and cross-stream turbulence intensity p 9 A92-13210
Probe systems for static pressure and cross-stream turbulence intensity p 10 A92-13211
Acoustic predictions using measured pressures from a *model rotor in the DNW* p 165 A92-14385
Unsteady blade-surface pressures on a large-scale advanced propeller - Prediction and data p 80 A92-17178
Base pressure measurements on a cone at Mach numbers from M sub infinity = 5 to 7 p 173 A92-18770
Pneumatic distortion compensation for aircraft surface pressure sensing devices p 218 A92-20206
A random vortex method for prediction of maximum instantaneous inlet total pressure distortion p 311 A92-24731
Failure detection and fault management techniques for flush airdata sensing systems
[AIAA PAPER 92-0263] p 369 A92-25719
Aerodynamic applications of pressure-sensitive paint
[AIAA PAPER 92-0264] p 394 A92-25720
Unsteady wing surface pressures in the wake of a propeller
[AIAA PAPER 92-0277] p 318 A92-25731
Pitch-up motions of delta wings
[AIAA PAPER 92-0278] p 318 A92-25732
A study of the base pressure behind circular steps p 426 A92-30196
Low profile microsensor for aerodynamic pressure measurement p 555 A92-35949
Flow around two square cylinders in staggered arrangements p 761 A92-42797
Static and dynamic flow field development about a porous suction surface wing
[AIAA PAPER 92-2628] p 795 A92-45500
Airfoil pressure measurements during oblique shock wave-vortex interaction in a Mach 3 stream
[AIAA PAPER 92-2631] p 795 A92-45503
Unsteady pressure and load measurements on an F/A-18 vertical fin at high-angle-of-attack
[AIAA PAPER 92-2675] p 798 A92-45529
ICIASF '91 - International Congress on Instrumentation *in Aerospace Simulation Facilities, 14th, Rockville, MD,* Oct. 27-31, 1991, Record
[ISBN 0-0783-0123-4] p 1114 A92-54301
Aerodynamic assessment of an optical pressure measurement system (OPMS) by comparison with conventional pressure measurements in a high speed wind tunnel p 1114 A92-54304
Application of a wall pressure method in a wind tunnel test section with adjustable longitudinal slots p 1091 A92-54336
The wind tunnel test 'system' of 1995 - Cost effective experimentation through a fusion of related technologies p 1091 A92-54342
Three-dimensional shock wave-turbulent boundary layer interaction induced by blunt body and protuberance p 1029 A92-56009
An experimental study on variable pressure hydraulic flight control system p 1084 A92-56119
Test description and preliminary pitot-pressure surveys for Langley Test Technique Demonstrator at Mach 6
[AIAA PAPER 92-3940] p 1096 A92-56770
Application of electronically scanned pressure measurement system for engine simulation tests in the German-Dutch Wind Tunnel
[AIAA PAPER 92-4003] p 1122 A92-56826
Description of a pressure measurement technique for obtaining surface static pressures of a radial turbine
[AIAA PAPER 92-4006] p 1123 A92-56829
NACA 0015 wing pressure and trailing vortex measurements
[NASA-TP-3151] p 13 N92-10981
Blade surface pressure measurements on the rotor of a model turbine stage in a transient flow facility p 157 N92-12206
Wall interference calculation in a transonic wind tunnel with discrete slots p 83 N92-12995
In-flight flow visualization and pressure measurements *at low speeds on the NASA F-18 high alpha research* vehicle p 85 N92-13009
Base pressure measurements on a cone at hypersonic Mach numbers: A contribution to aerothermodynamics for space vehicles p 181 N92-14992
Flow over a delta wing at hypersonic speeds p 181 N92-14993
The benchmark aeroelastic models program: Description and highlights of initial results
[NASA-TM-104180] p 185 N92-15049
A comparison of spanwise aerodynamic loads estimated from measured bending moments versus direct pressure measurements on horizontal axis wind turbine blades
[DE92-001158] p 301 N92-16458
Stagnation and dynamic pressure limits for the S1 wind tunnel
[AD-A242989] p 285 N92-17297
Flow visualization and wake analysis for standard and modified configurations of the AN/ALQ-78 antenna pod
[AD-A243552] p 260 N92-17339
Scale model measurements of fin buffet due to vortex bursting on F/A-18 p 365 N92-18788
Pressure measurements in high speed water tunnels
[DE92-004891] p 386 N92-19978
A laser velocimeter investigation of the normal shockwave boundary layer interaction p 500 N92-20485
Pressure and velocity measurements about an airfoil during a parallel blade-vortex interaction p 446 N92-21429
Sonic booms produced by US Air Force and US Navy aircraft: Measured data
[AD-A244804] p 512 N92-21719
The problem of static pressure measurement in turbomachinery annuli using traversable instrumentation
[PNR-90791] p 591 N92-22099
Development of wall pressure measuring apparatus for an existing transonic wind tunnel test section
[NAL-TM-565] p 573 N92-23778
Description of a pressure measurement technique for obtaining surface static pressures of a radial turbine
[NASA-TM-105643] p 680 N92-24959
A pressure measurement method using Electronically Scanner Pressure sensors (ESP) installed in a gust wind tunnel
[NAL-TM-638] p 749 N92-27428
The benchmark aeroelastic models program: Description and highlights of initial results p 721 N92-27960
A review of scale effects on surfaces in unsteady motion p 722 N92-27962
Study of the leading-edge vortex dynamics in the *unsteady flow over an airfoil*
[AD-A247532] p 829 N92-28865
An experimental study of the relationship between velocity and pressure fluctuations in a wing-body junction
[AD-A249628] p 946 N92-31122
Active control of the separation region on a two-dimensional airfoil
[AD-A249739] p 948 N92-31622
Pressure measurements on a rectangular wing with a NACA0012 airfoil during conventional flutter
[NASA-TM-104211] p 1042 N92-34147
Unsteady wind tunnel tests p 1089 N92-34166
Pilot-pressure probe for measuring pressure in a hypersonic wind tunnel
[NASA-CASE-LAR-14232-1] p 1102 N92-34213

PRESSURE OSCILLATIONS
Inlet planar waves - A current perspective
[ASME PAPER 91-GT-400] p 76 A92-15730
Low-frequency pressure oscillations in a model ramjet combustor p 154 A92-16026
Unsteady blade-surface pressures on a large-scale advanced propeller - Prediction and data p 80 A92-17178
A calculating method of shock wave oscillating frequency due to turbulent shear layer fluctuations in supersonic flow p 251 A92-22720
Influence of wing shapes on the surface pressure fluctuations of a wing-body junction
[AIAA PAPER 92-0433] p 327 A92-26280
Unsteady pressure field and vorticity production over a pitching airfoil p 330 A92-26416
Resonance of circular shock waves p 395 A92-26795
Premixed, turbulent combustion of axisymmetric sudden expansion flows p 397 A92-27770
Compressor modeling and active control of stall/surge p 508 A92-29315
Experimental study of a two-dimensional random frequency generator p 483 A92-29712
Transverse correlation of the spectral components of pressure fluctuations on a plate ahead of a step p 426 A92-30187
Investigation of the aerodynamic features of flows past *models using thin-film capacitance-type sensors of* pressure oscillations p 440 A92-31884
Pressure oscillation in the leakage annulus between a shrouded impeller and its housing due to impeller-discharge-pressure disturbances p 580 A92-32942
Power spectrum of ring modes of pressure fluctuations *at the surface of a cylinder in axial flow* p 603 A92-33770
Response of plate-like structures to correlated random pressure fluctuations
[AIAA PAPER 92-2378] p 584 A92-34452
Aerodynamic coefficients of a symmetrical airfoil in an oscillating flow
[AD-A241073] p 89 N92-13035
Experimental study of the wall pressure fluctuations under a turbulent boundary layer downstream of tandem *aerofoil external manipulators*
[REPT-207-90-78] p 500 N92-20497
An experimental study of the relationship between velocity and pressure fluctuations in a wing-body junction
[AD-A249628] p 946 N92-31122
Organized turbulent structures and their induced wall pressure fluctuations p 949 N92-31853

PRESSURE PULSES
Pulsating spanwise blowing on a fighter aircraft
[AIAA PAPER 92-4359] p 1025 A92-55345

PRESSURE RATIO
Preliminary experience with an expert system providing initial centrifugal compressor sizing for performance prediction and analysis
[ASME PAPER 91-GT-28] p 162 A92-15513

Analytical investigation of the rules of component matching in turbojet engines
[ASME PAPER 91-GT-170] p 123 A92-15605
Performance of a high-pressure-ratio centrifugal compressor influenced by distribution of tip clearance of the mixed-flow impeller p 498 A92-32509
A refined analytical method for designing high pressure ratio centrifugal impellers p 591 A92-36032
Turboshaft/turboprop cycle sensitivity analysis
[AIAA PAPER 92-3476] p 865 A92-49020
Further calculations of the performance of turbofan engines incorporating a wave rotor
[AD-A240867] p 131 N92-13072
Aircraft ground test and subscale model results of axial thrust loss caused by thrust vectoring using turning vanes
[NASA-TM-4341] p 273 N92-17071
Viscous three-dimensional calculations of transonic fan performance
[NASA-TM-103800] p 242 N92-17346
Computer code for preliminary sizing analysis of axial-flow turbines
[NASA-CR-4430] p 473 N92-20196
Flow studies in close-coupled ventral nozzles for STOVL aircraft
[NASA-TM-102554] p 445 N92-20934

PRESSURE RECOVERY
Diffuser efficiency estimation parameters p 79 A92-16814
Results of a perturbation analysis correlating flows entering and exiting an aircraft inlet system
[AIAA PAPER 92-3624] p 1021 A92-54091
Wind tunnel test of M = 2.5 mixed compression inlet p 1028 A92-56008
A model study on diffuser pressure recovery in NAL scramjet test facility with simulated hydrogen combustion
[AIAA PAPER 92-3979] p 1071 A92-56805

PRESSURE REDUCTION
Measurements and correlation of two-phase pressure drop under microgravity conditions p 37 A92-10435
The selective bleed variable cycle engine --- aircraft propulsion
[ASME PAPER 91-GT-388] p 126 A92-15720
Experimental investigation on the structure of flow field and the total pressure loss in an atomizing channel injector p 375 A92-28436
Investigation of oblique shock/boundary-layer bleed interaction p 344 A92-28524
Effects of bleed and power extraction on the operating line of engines p 469 A92-29717
Experimental investigation on reducing fluctuating pressures of launch vehicles by passive shock-wave/boundary-layer control p 616 A92-38916
Bleed-boundary conditions for numerically simulated mixed-compression supersonic inlet flow p 713 A92-44520
Spectrogram diagnosis of aircraft disasters
[SAE PAPER 912041] p 836 A92-45425
An experimental investigation of high-aspect-ratio cooling passages
[AIAA PAPER 92-3154] p 890 A92-48780
Effects of bleed air extraction of thrust levels on the F404-GE-400 turbofan engine
[AIAA PAPER 92-3092] p 1066 A92-54009
Prediction of the pressure loss coefficient of wind tunnel turbulence reducing screens
[AIAA PAPER 92-4043] p 1035 A92-56862
Vortex generator design for aircraft inlet distortion as a numerical optimization problem p 194 N92-13959
Effects of bleed air extraction on thrust levels on the F404-GE-400 turbofan engine
[NASA-TM-104247] p 871 N92-29425

PRESSURE SENSORS
A small five-hole spherical pressure probe for compressor experiments p 38 A92-10970
Probe systems for static pressure and cross-stream turbulence intensity p 10 A92-13211
Pneumatic distortion compensation for aircraft surface pressure sensing devices p 218 A92-20206
Experimental investigation of terminal shock sensors for mixed-compression inlets p 276 A92-21074
Measurements of the pressure and velocity distribution in low-speed turbomachinery by means of high-frequency pressure transducers p 391 A92-24723
Comprehensive helicopter rotor instrumentation - A retrofit approach using miniature transducers
[AIAA PAPER 92-0268] p 369 A92-25724
Wall pressure wavenumber-frequency spectrum beneath a turbulent boundary layer measured with transducer arrays calibrated with an acoustical method
[ONERA, TP NO. 1991-212] p 329 A92-26364
Paint under pressure p 399 A92-28495
Studying method of measuring flow-field between stages in axial-flow compressor p 423 A92-29720
Investigation of the aerodynamic features of flows past models using thin-film capacitance-type sensors of pressure oscillations p 440 A92-31884
Power spectrum of ring modes of pressure fluctuations at the surface of a cylinder in axial flow p 603 A92-33770
A method for measuring high-subsonic two-dimensional periodic flow field using a single-hole high-response cylindrical pressure probe p 588 A92-35567
Low profile microsensor for aerodynamic pressure measurement p 555 A92-35949
Development of pitot static flightline testing p 556 A92-35953
Development of a pneumatic high-angle-of-attack flush airdata sensing system
[SAE PAPER 912142] p 651 A92-39980
Fiber-optic pressure sensor system for gas turbine engine control p 857 A92-48047
Absolute fiber optic pressure transducer for aircraft air data measurement p 858 A92-48501
Aerodynamic assessment of an optical pressure measurement system (OPMS) by comparison with conventional pressure measurements in a high speed wind tunnel p 1114 A92-54304
Hypervelocity Wind Tunnel 9 control system p 1092 A92-54343
Skin friction measurements in 3-D boundary layers p 1092 A92-54351
Advanced nozzle and engine components test facility
[AIAA PAPER 92-3993] p 1099 A92-56816
Calibration of hemispherical-head flow angularity probes
[AIAA PAPER 92-4005] p 1122 A92-56828
Development of a pneumatic high-angle-of-attack flush airdata sensing (HI-FADS) system
[NASA-TM-104241] p 118 N92-11994
Failure detection and fault management techniques for flush airdata sensing systems
[NASA-TM-4335] p 276 N92-17128
Thrust vector control of an overexpanded supersonic nozzle using pin insertion and rotating airfoils
[AD-A243891] p 387 N92-18942
The problem of static pressure measurement in turbomachinery annuli using traversable instrumentation
[PNR-90791] p 591 N92-22099
A pressure measurement method using Electronically Scanner Pressure sensors (ESP) installed in a gust wind tunnel
[NAL-TM-638] p 749 N92-27428
A continuing study of altitude determination deficiencies of the Service Aircraft Instrumentation Package (SAIP)
[AD-A245952] p 968 N92-32051
Pilot-pressure probe for measuring pressure in a hypersonic wind tunnel
[NASA-CASE-LAR-14232-1] p 1102 N92-34213

PRESSURE VESSELS
Inflatable traversing probe seal p 595 N92-22692
Nickel hydrogen common pressure vessel battery development p 598 N92-22770
Turbocharged pressurized combustion system
[PB92-142579] p 756 N92-26521
Methodology for the determination of criticality codes and recertification intervals for Tank Mounted Air Compressors (TMAC) and Base Mounted Air Compressors (BMAC)
[NASA-CR-189268] p 770 N92-27649
Replacement of the NAL high pressure air storage system
[NAL-TM-634] p 888 N92-28835

PRESSURIZED CABINS
Fracture analysis and crack propagation in pressurized fuselage structures - Experimental and numerical investigations p 217 A92-19812
Proof test and fatigue crack growth modeling on 2024-T3 aluminum alloy p 213 A92-19828
Loss of cabin pressurization in U.S. naval aircraft - 1969-90 p 634 A92-37168
Aerospace pressurization system design
[SAE AIR 1168/7] p 849 A92-48022

PRESSURIZING
Pressurization effects in kinematic heat engines p 696 A92-40866

PRIMERS (COATINGS)
Low VOC primer for structural bonding --- volatile organic compound p 892 A92-47338
Anodize and prime your aluminum without environmental headaches p 892 A92-47340

PROBABILITY DENSITY FUNCTIONS
Improved method for estimation of the maximum instantaneous distortion values
[AIAA PAPER 92-3623] p 826 A92-49076
An assumed joint-Beta PDF approach for supersonic turbulent combustion
[AIAA PAPER 92-3844] p 1113 A92-54199
Modeling of the reactant conversion rate in a turbulent shear flow p 829 N92-28820

PROBABILITY DISTRIBUTION FUNCTIONS
Volume spectra in supercooled clouds for several research flights
[AIAA PAPER 92-0167] p 350 A92-25683
Probabilistic design and fatigue management based on probabilistic fatigue models with reliability updating p 360 N92-18574

PROBABILITY THEORY
Some Aspects of uncertainty in computational fluid dynamics results p 233 A92-19609
Analysis of the efficiency of some structural-inspection strategies in aircraft maintenance p 419 A92-30141
System reliability and risk assessment
[AIAA PAPER 92-2345] p 582 A92-34320
Computational structures technology
[AIAA PAPER 92-2442] p 585 A92-34473
Probability analysis of structure failure for the wings with main and subordinate components p 848 A92-47657
Approximate analysis for failure probability of structural systems p 901 A92-47671
A calculating method of the kill probability attack area for AAM p 975 A92-50212
Development of an uncertainty methodology for multiple-channel instrumentation systems
[AIAA PAPER 92-3953] p 1133 A92-56781
Example of statistical techniques applied to autoland touchdown dispersion (confidence intervals for normal and skew distributions)
[ESDU-91019] p 268 N92-17844
Statistical methods applicable to analysis of aircraft performance data
[ESDU-91017] p 359 N92-18096
Probabilistic design and fatigue management based on probabilistic fatigue models with reliability updating p 360 N92-18574
Aging aircraft structural damage analysis p 360 N92-18575
A probabilistic procedure for aircraft fleet management p 360 N92-18576
Estimating the probability of vertical overlap from the paired aircraft data obtained in the European vertical data collection using the program DGLDiF
[NLR-TR-88108-U] p 356 N92-19491
Analysis of measured environmental noise levels: An assessment of the effects of airbase operational model variables on predicted noise exposure levels
[AD-A244805] p 485 N92-21720
Composite strength statistics from fiber strength statistics
[AD-A245616] p 755 N92-26383
A comparison of the performance of two gust front detection algorithms using a length-based scoring technique
[AD-A250862] p 1004 N92-32103

PROBLEM SOLVING
Case-based reasoning - Taming the similarity heuristic --- for development of solutions to real world problems p 47 A92-11153
Automated problem resolution prototype in automated en route air traffic control p 190 N92-14028
Flying an aircraft as a problem-solving process: About the Instrument-Failure-Simulator (IFS) as a test for pilot-candidates
[DLR-FB-91-23] p 455 N92-20902
Nonunique solutions in unsteady transonic flow p 629 N92-24872
Research into the development of a knowledge acquisition taxonomy
[NASA-CR-189939] p 778 N92-28150

PROCEDURES
NASA reliability preferred practices for design and test
[NASA-TM-4322] p 157 N92-12286
A proposed composite repair methodology for primary structure
[NRC-LTR-ST-1658] p 115 N92-13056

PROCESS CONTROL (INDUSTRY)
The use of CT for dimensional measurements of green and sintered ceramic components p 490 A92-28592
An overview of systems engineering management methods and processes
[AIAA PAPER 92-1539] p 690 A92-38636
Process control challenges during the manufacture of large superplastically formed/diffusion bonded structure
[SAE PAPER 912195] p 674 A92-40012
Composite makers sense changes p 754 A92-42345
Integrated wiring system
[SAE PAPER 912058] p 897 A92-45440
Improving reliability and maintainability through process management p 1141 A92-56212
Introduction: Needs and approaches to reliability and quality assurance in design and manufacture p 402 N92-19005
Impact of a process improvement program in a production software environment: Are we any better? p 413 N92-19422

The Air Force Manufacturing Technology (MANTECH): Technology transfer methodology as exemplified by the radar transmit/receive module program
p 593 N92-22451

PROCUREMENT
An airlifter for the long haul p 358 A92-28493
Preliminary screening procedures and criteria for replacements for Halons 1211 and 1301
[AD-A252912] p 1126 N92-33501

PROCUREMENT MANAGEMENT
Spares support of your Rotary-Wing Jenny
p 60 A92-14435

PRODUCT DEVELOPMENT
The background and the development of the TAL-WAR (Rose) shape blimp with the articulated thruster
[AIAA PAPER 91-3692] p 17 A92-12749
P&W F119 - Vectored thrust for the F-22
p 25 A92-13219
Will hydraulic systems meet tomorrow's aircraft power requirements? p 21 A92-13246
NASP - Expanding space launch opportunities
p 33 A92-13247
Concurrent engineering at Boeing Helicopters
p 162 A92-14393
P120 programme - First results of the pre-development phase p 60 A92-14447
NASA research program directed at reducing supersonic transport noise p 61 A92-16150
Technology in the lives of an aircraft designer
[AIAA PAPER 91-3069] p 192 A92-20000
Resonant cryogenic chopper --- for infrared and submillimeter radiometers p 294 A92-22796
Development of a sensor for the detection of aircraft wing contaminants
[AIAA PAPER 92-0300] p 369 A92-25752
Advanced materials for aircraft engine applications
p 390 A92-28251
An airlifter for the long haul p 358 A92-28493
The V-22 Osprey - Preparing for fleet operations
p 458 A92-29671
Cold-cycle pressure-jet helicopters: Ventures, designs, and developments. I - Ventures p 459 A92-31325
Perspectives in aerospace design --- Book
[ISBN 1-56347-010-1] p 459 A92-31606
GE, Snecma consider venture to develop uprated Perm PS-90 p 472 A92-32297
Saturn/Lyulka diversifies business to cope with Russian economic crisis p 472 A92-32299
Russia bids to salvage development of Soyuz-powered VTOL fighter p 472 A92-32300
Development of an advanced composite material on vertical stabilizer of F-X aircraft p 579 A92-32555
Systems engineering as applied to the Boeing 777
[AIAA PAPER 92-1010] p 515 A92-33198
YF-22A prototype Advanced Tactical Fighter demonstration/validation flight test program overview
[AIAA PAPER 92-1087] p 537 A92-33253
Multidisciplinary design environment development for air vehicle engineering
[AIAA PAPER 92-1113] p 605 A92-33269
Structural design for durability - Lessons learned from service and test data
[AIAA PAPER 92-1129] p 537 A92-33281
Saab 2000 begins 1,200-hr. test program at Skavsta site p 538 A92-33800
Development trends of recent aircraft engines
p 558 A92-35919
EVS could expand all-weather landing capability of airliners p 556 A92-36125
The engine inside p 558 A92-36126
The Delta Clipper dream p 574 A92-36127
The development and integration of an engine monitoring system for the F-14A+/D Super Tomcat
[SAE PAPER 912094] p 654 A92-39951
ELS pilot evaluation --- Electronic Library System
[SAE PAPER 912107] p 691 A92-39960
Development and evaluation of an onboard aircraft cabin water spray system for postcrash fire protection
[SAE PAPER 912224] p 636 A92-40022
Tiltrotor UAV - The next generation unmanned system
p 646 A92-40384
Sikorsky Aircraft UAV program p 646 A92-40385
Conceptual design and analysis of a special operations transport p 646 A92-40387
1991-92 AHS Technical Committee highlights - Aerodynamics p 623 A92-40391
1991-92 AHS Technical Committee highlights - Aircraft design p 608 A92-40392
1991-92 AHS Technical Committee highlights - Dynamics p 647 A92-40393
1991-92 AHS Technical Committee highlights - Flight simulation p 609 A92-40394
1991-92 AHS Technical Committee highlights - Test and evaluation p 609 A92-40398
Airbus A319 - Completion of the standard fuselage family p 848 A92-47591
German-GUS cooperation in civil aviation
p 785 A92-47592
Dawn of stealth p 785 A92-47757
An eight month gearbox development program
[AIAA PAPER 92-3368] p 850 A92-48941
Addressing the challenge of aircraft component design and manufacture from metal matrix composites
p 985 A92-50007
British Aerospace Hawk into the 1990s
p 957 A92-50009
RTM - Simultaneous design and tooling reduces cost and lead time p 994 A92-51537
777 shaping up p 959 A92-52300
A common engineering-to-manufacturing-to-field test strategy to achieve systems readiness beyond the '90s
p 931 A92-53111
Improving designer productivity
[AIAA PAPER 92-1187] p 1130 A92-54285
Turning up the heat on aircraft structures --- design and analysis for high-temperature conditions
p 1052 A92-55131
Designing to cost effectiveness - Enhancing quality
p 1119 A92-56209
Engineering reliability and maintainability review - A regimen for discovering production deficiencies
p 1120 A92-56254
Design and development of test rigs for main rotor and main rotor transmission of a helicopter in the 6-ton-class
p 1093 A92-56280
'A new proposal for an old problem' - The right engine for the right helicopter p 1070 A92-56281
AS 332 MKII - Development and certification
p 1059 A92-56343
Impact of a process improvement program in a production software environment: Are we any better?
p 413 N92-19422
Towards understanding software: 15 years in the SEL
p 413 N92-19423
The 60 years of Bristol engines
[PNR-90845] p 473 N92-20460
Piloted Simulation Effectiveness
[AGARD-CP-513] p 786 N92-28522
Flight simulation and digital flight controls
p 884 N92-28526
The application of flight simulation models in support of rotorcraft design and development
p 884 N92-28527
Experience with piloted simulation in the development of helicopters p 884 N92-28528
Technical evaluation report on the Flight Mechanics Panel Symposium on Piloted Simulation Effectiveness
[AGARD-AR-315] p 983 N92-30769
Preparation for a new plane (A 320): Experience reviewed p 1010 N92-30954
The 1991 Federal Aviation Administration plan for research, engineering and development
p 1142 N92-32453
SATWG networked quality function deployment
p 1134 N92-33339

PRODUCTION ENGINEERING
A holistic approach to support p 60 A92-14413
Automated composite lay-up p 146 A92-14450
Development of an automatic drilling system. II
p 1118 A92-56107
From IGES to STEP
[REPT-3.1.6] p 603 N92-23881
Symposium on Marketing for Technological Products
[MBB-UE-0014-90-PUB] p 606 N92-23928

PRODUCTION MANAGEMENT
Aviation Diagnostics And Maintenance (ADAM) system preliminary concept of operation and functional description
[AD-A242598] p 170 N92-14966
B-2 program: Trends in manufacturing
[AD-A242141] p 242 N92-15963

PRODUCTIVITY
Improving designer productivity
[AIAA PAPER 92-1187] p 1130 A92-54285
Improving designer productivity --- artificial intelligence
[NASA-TM-103929] p 854 N92-29417

PROGRAM VERIFICATION (COMPUTERS)
Formal specification and verification of Ada software
[AIAA PAPER 91-3713] p 230 A92-17585
Cleanroom - An alternative software development process p 233 A92-19386
Low aspect ratio wing code validation experiment
[AIAA PAPER 92-0402] p 324 A92-26255
Verification and validation of F-15 and S/MTD unique software p 921 A92-48515
Numerical simulation of hypersonic viscous flow for the design of H-2 orbiting plane (HOPE-2)
[NAL-TR-1093] p 11 N92-10009
Numerical verification of NISA 2 finite element analysis of the cracked 5th stage compressor disc of J-85 jet engine
[NRC-LTR-ST-1792] p 129 N92-11997
Development and verification of software for flight safety critical systems p 164 N92-12469
Verification of NISA 2 and ENDURE fracture mechanics capability
[NRC-ST-621] p 159 N92-13453
Hypersonic aerothermodynamic computations using a point-implicit TVD method p 183 N92-15006
Validation of flight critical control systems
[AGARD-AR-274] p 382 N92-20026
Formal design and verification of a reliable computing platform for real-time control. Phase 2: Results
[NASA-TM-104196] p 602 N92-22320
Design of an integrated airframe/propulsion control system architecture
[NASA-CR-182007] p 602 N92-22644
Validation of a CANARI code by the computation of three dimensional turbulent flow in turbine valve
p 741 N92-27462
Simulation test and evaluation of TCAS 2 logic version 6.04
[DOT/FAA/RD-92/23] p 1048 N92-33098

PROGRAMMING LANGUAGES
Test Engineering Language for Avionic Systems
p 554 A92-35763
Avionics systems development: Technological trends, conflicts, and cost issues in a changing European environment p 199 N92-14054
Development of a flight information system using the structured method
[AD-A248207] p 859 N92-29222

PROGRESS
Recent progress in inverse methods in France
p 201 N92-13938
Activities of NRC-CNRC, Institute for Aerospace Research, Flight Research Lab.
[CTN-92-60432] p 420 N92-20205

PROJECT MANAGEMENT
An eight month gearbox development program
[AIAA PAPER 92-3368] p 850 A92-48941
Avionics systems engineering education
p 1012 A92-49269
High Intensity Radiated Fields (HIRF) project plan
[DOT/FAA/CT-TN91/1] p 297 N92-16181
Computational procedures for preliminary design
p 552 N92-23952
National Aeronautics and Space Administration Authorization Act, 1993
[S-2558-IS] p 698 N92-25606
United States Air Force summer research program 1991. Volume 1: Program management report
[AD-A248763] p 1142 N92-32338
DoD key technologies plan
[AD-A253692] p 1142 N92-33238

PROJECT PLANNING
The German Hypersonics Technology Programme - Status report 1992
[IAF PAPER 92-0867] p 1105 A92-57258
Study of alternatives: Dayton's Aviation heritage, Ohio
[PB91-202275] p 2 N92-10972
Program plan: National aging aircraft research program
[DOT/FAA/CT-88/32-1] p 18 N92-10992
Avionics technology beyond 2000
p 200 N92-14058
Identification of high-level functional/system requirements for future civil transports
[NASA-CR-189561] p 276 N92-15991
High Intensity Radiated Fields (HIRF) project plan
[DOT/FAA/CT-TN91/1] p 297 N92-16181
Aviation system: Capital investment plan
p 636 N92-25297
Design of orbital re-entry experiment vehicle and outline of the experiment p 667 N92-25374
CSM activities at the NASA Langley Research Center
p 683 N92-25916
The FAA aging airplane program plan for transport aircraft p 838 N92-30128
High-speed civil transport issues and technology program
[NASA-CR-186020] p 962 N92-31208

PROJECTILES
Application of digital measurement techniques to analysis of range shadowgraphs
[AD-A241554] p 139 N92-13080
Transonic Navier-Stokes computations for a spinning body of revolution
[AD-A241015] p 180 N92-14972
Analysis of the flight performance of the 155 mm M864 base burn projectile
[BRL-TR-3083] p 1041 N92-33699

PROJECTORS
Limitations of a holographic 3-D pixel projector for cockpit displays
[AD-A241295] p 119 N92-13067

PROLATE SPHEROIDS
Viscous flow solutions for slender bodies of revolution at incidence p 4 A92-10692
Cross-flow separation on a prolate spheroid at angles of attack
[AIAA PAPER 92-0428] p 326 A92-26276
Turbulence model effects on separated flow about a prolate spheroid p 340 A92-28036
Linear stability of three-dimensional boundary layers over axisymmetric bodies at incidence
p 431 A92-31157

PROP-FAN TECHNOLOGY
Time-dependent aerodynamic analysis of ducted and unducted propfans at angle of attack
[ASME PAPER 91-GT-190] p 74 A92-15616
Design and analysis of a high pitch to chord ratio cascade representative of ducted propfans
[ASME PAPER 91-GT-335] p 126 A92-15700
Unsteady Euler analysis of the flowfield of a propfan at an angle of attack p 242 A92-21070
Prediction of periodic loadings on single rotation propfan with off-axis inflow p 277 A92-21071
Unsteady blade pressures on a propfan at takeoff - Euler analysis and flight data
[AIAA PAPER 92-0376] p 372 A92-26234
Flow visualization of a prop-fan leading-edge vortex
[AIAA PAPER 92-0386] p 323 A92-26242
Aerodynamic computations of high-speed transonic propellers
[ONERA, TP NO. 1991-218] p 330 A92-26370
Unsteady flowfield simulation of ducted prop-fan configurations
[AIAA PAPER 92-0521] p 332 A92-26946
Aeroelastic analysis of advanced propellers using an efficient Euler solver
[AIAA PAPER 92-0488] p 341 A92-28194
Problems of strength and aeroelasticity of present-day propfans p 471 A92-30133
Interference of high-mounted propfan nacelles with an unswept wing and ways to attenuate it
p 460 A92-31881
A numerical classical flutter analysis of advanced propellers
[AIAA PAPER 92-2118] p 557 A92-35687
Azimuthal noise characteristics of contra-rotating propellers - Results of a wind tunnel model test
p 693 A92-39066
Structure-borne noise transmission in the Propfan Test Assessment aircraft p 778 A92-41240
Dynamic response and aeroelastic analysis of a propeller blade of a prop-fan engine p 762 A92-43109
Unsteady airloading panel method for propfans
p 780 A92-44512
Predicted pressure distribution on a prop-fan blade through Euler analysis p 810 A92-46791
German-GUS cooperation in civil aviation
p 785 A92-47592
Numerical flow simulation and analysis of a shrouded propfan rotor
[AIAA PAPER 92-3773] p 826 A92-49118
Wind tunnel performance results of swirl recovery vanes as tested with an advanced high speed propeller
[AIAA PAPER 92-3770] p 1068 A92-54159
Numerical calculations of propfan/swirl recovery vane flow field
[AIAA PAPER 92-3771] p 1022 A92-54160
Unsteady blade pressures on a propfan - Predicted and measured compressibility effects
[AIAA PAPER 92-3774] p 1023 A92-54161
Propeller and propfan noise p 54 N92-10599
Unsteady blade pressures on a propfan at takeoff: Euler analysis and flight data
[NASA-CR-189076] p 130 N92-13071
Development and testing of cabin sidewall acoustic resonators for the reduction of cabin tone levels in propfan-powered aircraft
[NASA-CR-4388] p 166 N92-13757
Prediction of noise field of a propfan at angle of attack
[NASA-CR-189047] p 166 N92-13759
Annoyance caused by aircraft en route noise
[NASA-TP-3165] p 512 N92-20479
Overview of NASA PTA propfan flight test program
p 561 N92-22536
Computational structural analysis and advanced commercial engines p 660 N92-25933

PROPAGATION MODES
Reflections off aircraft and the shape optimization of a ridged waveguide p 267 A92-23967
Three-dimensional-mode resonance in far wakes
p 898 A92-46252
Experimental validation of a line-duct acoustics model including flow
[NLR-TP-90223-U] p 927 N92-28695

PROPELLANT ADDITIVES
Microbiological spoilage of aviation turbine fuel. II - Evaluation of a suitable biocide p 891 A92-45600
Enhancing the performance characteristics of engine fuels by means of surfactant additives
p 892 A92-46631

PROPELLANT CHEMISTRY
Advanced thermally stable jet fuel development program. Volume 2: Compositional factors affecting thermal degradation of jet fuels
[AD-A252656] p 987 N92-31399

PROPELLANT COMBUSTION
Experimental and computational investigation of scaling phenomena in a large caliber ram accelerator
[AIAA PAPER 92-3245] p 1103 A92-54019
Nonstationary gasdynamics p 220 N92-13985
Experiments and analysis concerning the use of external burning to reduce aerospace vehicle transonic drag
[NASA-TM-105397] p 279 N92-17546

PROPELLANT DECOMPOSITION
A numerical method for simulating the fluid-dynamic and heat-transfer changes in a jet engine injector feed-arm due to fouling
[AIAA PAPER 92-0768] p 374 A92-27108

PROPELLANT PROPERTIES
Enhancing the performance characteristics of engine fuels by means of surfactant additives
p 892 A92-46631
Properties of aircraft fuels and related materials
[AD-A240650] p 35 N92-11213

PROPELLANT TANKS
Self reliance in aerospace structures
p 758 A92-41190

PROPELLANTS
Theoretical and experimental investigation of the thermodynamics of the thermally choked ram accelerator p 604 N92-22137

PROPELLER BLADES
Surface flow visualization of rotating propeller
p 4 A92-10959
Stress analysis of a propeller blade
p 38 A92-10963
Vibration characteristic analysis of a propeller blade
p 38 A92-10967
A method of reliability analysis for propeller blades
p 25 A92-10968
Unsteady blade-surface pressures on a large-scale advanced propeller - Prediction and data
p 80 A92-17178
Structural and aerodynamic analysis of a large-scale advanced propeller blade p 375 A92-28517
Complete Euler-solution for a rotor in hover and a propeller in forward flight p 520 A92-35755
Aeroelastic tailoring analysis for advanced turbo propellers with composite blades p 558 A92-36358
Structure-borne noise transmission in the Propfan Test Assessment aircraft p 778 A92-41240
Dynamic response and aeroelastic analysis of a propeller blade of a prop-fan engine p 762 A92-43109
Design - Analysis and experimental verification of a propeller working in the low Reynolds number range
p 710 A92-43174
Whirl-flutter stability of a pusher configuration in nonuniform flow p 845 A92-46813
The static and fatigue computation of the propeller blades retention system p 995 A92-51895
An example of whirl flutter analysis
p 1052 A92-56015
Whirl flutter analysis and application to aircraft design
p 1053 A92-56017
Study of a new airfoil used in reversible axial fans
p 177 N92-13970
Analysis of aircraft engine blade subject to ice impact
[NASA-TM-105336] p 229 N92-15402
Detailed noise measurements on the SR-7A propeller: Tone behavior with helical tip Mach number
[NASA-TM-105206] p 304 N92-16705
The solution of a singular integral equation arising from a lifting surface theory for rotating blades
p 260 N92-17303
Prediction of far-field harmonic noise from propellers
[ESDU-91033] p 416 N92-18074
Resolution of the Euler equations applied to a helicopter rotor in forward flight
[ONERA-RSF-2/3731-AY-004A] p 406 N92-19976
Propeller noise research at NRC p 628 N92-24863
Aerodynamic design and analysis of a light aircraft propeller p 629 N92-24876
Algorithms for blending surface generation
[AD-A245686] p 777 N92-26524
Active synchrophasing of propeller unbalance
p 1138 N92-32963

PROPELLER DRIVE
System-identification of airplanes using the 'estimation before modelling' technique p 269 A92-21007
PAR-WIG performance prediction during acceleration from water-borne to air-borne p 291 A92-21721
Aerodynamic characteristics of a propeller powered high lift semispan wing
[AIAA PAPER 92-0388] p 323 A92-26244
Propeller aircraft interior noise - Physical background and possible treatments p 642 A92-39082
A review of computational/experimental methodology developments in aeroacoustics p 695 A92-39241
The Pond Racer preliminary flight test report
p 645 A92-40031
Low-speed wind tunnel testing for the high-speed propeller at high shaft angle of attack
p 1030 A92-56054
Propeller-driven-small airplane noise certification
[LR-650] p 237 N92-14798
Ideal efficiency of propellers based on Theodorsen's theory: A review and computer study, with extended plus simplified charts
[UTIAS-TN-271] p 1071 N92-33102

PROPELLER EFFICIENCY
Efficient lifting line method for computing performance of propeller p 24 A92-10956
Aeroacoustical modification of a propeller
p 24 A92-10961
Experimental characteristics comparison between two scale-model propellers p 24 A92-10962
Effect of antiicer on propeller performance
p 25 A92-10969
A quick automatic method for computing performance of nonducted propeller with constant-revolutional-speed
p 393 A92-25505
A pressure-drag-determination method for aerodynamic-interference problems p 425 A92-30157
A numerical classical flutter analysis of advanced propellers
[AIAA PAPER 92-2118] p 557 A92-35687
Research flight test of a scaled unmanned air vehicle
p 549 A92-35944
A review of computational/experimental methodology developments in aeroacoustics p 695 A92-39241
Pusher turboprop installation technology for the Embraer CBA-123 vector
[SAE PAPER 911030] p 658 A92-40943
Design - Analysis and experimental verification of a propeller working in the low Reynolds number range
p 710 A92-43174
Wind tunnel test for a high speed propeller with coaxial contrarotation p 737 A92-43195
Propeller-nacelle whirl flutter analysis and wind tunnel test p 1052 A92-56016
Aerodynamic design and analysis of a light aircraft propeller p 629 N92-24876
Ideal efficiency of propellers based on Theodorsen's theory: A review and computer study, with extended plus simplified charts
[UTIAS-TN-271] p 1071 N92-33102

PROPELLER FANS
Prediction of periodic loadings on single rotation propfan with off-axis inflow p 277 A92-21071
Unsteady blade pressures on a propfan at takeoff - Euler analysis and flight data
[AIAA PAPER 92-0376] p 372 A92-26234
Propeller and propfan noise p 54 N92-10599
Unsteady blade pressures on a propfan at takeoff: Euler analysis and flight data
[NASA-CR-189076] p 130 N92-13071
Development and testing of cabin sidewall acoustic resonators for the reduction of cabin tone levels in propfan-powered aircraft
[NASA-CR-4388] p 166 N92-13757
Prediction of noise field of a propfan at angle of attack
[NASA-CR-189047] p 166 N92-13759
Analysis of aircraft engine blade subject to ice impact
[NASA-TM-105336] p 229 N92-15402
Overview of NASA PTA propfan flight test program
p 561 N92-22536

PROPELLER NOISE
Aeroacoustical modification of a propeller
p 24 A92-10961
Experimental characteristics comparison between two scale-model propellers p 24 A92-10962
Obtaining the velocity field required for the calculation of propeller unsteady forces using 'traditional' approximate methods and CFD
[AIAA PAPER 92-0520] p 331 A92-26945
Propeller aircraft interior noise - Physical background and possible treatments p 642 A92-39082
A survey of active control in aircraft cabins
p 643 A92-39084
Coupled propeller contributions to aircraft noise and vibration p 694 A92-39085
Propeller sound excitation on an aircraft fuselage using a loudspeaker ring p 643 A92-39087
Structure-borne noise transmission in the Propfan Test Assessment aircraft p 778 A92-41240
High-speed propeller noise prediction - A multidisciplinary approach p 924 A92-45831

Noise test of high-speed counterrotation propeller in low-speed wind tunnel p 1135 A92-56055
Propeller and propfan noise p 54 N92-10599
Annoyance caused by advanced turboprop aircraft flyover noise: Comparison of different propeller configurations
[NASA-TP-3104] p 56 N92-11758
Development and testing of cabin sidewall acoustic resonators for the reduction of cabin tone levels in propfan-powered aircraft
[NASA-CR-4388] p 166 N92-13757
Prediction of noise field of a propfan at angle of attack
[NASA-CR-189047] p 166 N92-13759
Detailed noise measurements on the SR-7A propeller: Tone behavior with helical tip Mach number
[NASA-TM-105206] p 304 N92-16705
Prediction of far-field harmonic noise from propellers
[ESDU-91033] p 416 N92-18074
High speed turboprop aeroacoustic study (counterrotation). Volume 2: Computer programs
[NASA-CR-185242] p 1011 N92-31248
Vibro-acoustic FE analyses of the Saab 2000 aircraft
p 1137 N92-32952
Building vibrations induced by noise from rotorcraft and propeller aircraft flyovers
[NASA-TM-104170] p 1138 N92-33160

PROPELLER SLIPSTREAMS
Unsteady wing surface pressures in the wake of a propeller
[AIAA PAPER 92-0277] p 318 A92-25731
Development of a method for calculating the effect of the propeller slipstream on transonic flow over the wing
p 424 A92-30144
Further development of the CANAERO computer code to include propulsor modelling
[DREA-CR-90-425] p 1038 N92-32811

PROPELLERS
Aeroelastic stability analysis of aerial propellers
p 24 A92-10955
Aerodynamic design of propeller by numerical optimization p 24 A92-10957
Aerodynamic modification of a propeller
p 4 A92-10958
Stress analysis of a propeller hub p 38 A92-10964
Digital simulation and experimental modal analysis of dynamic characteristics of a propeller hub
p 38 A92-10965
An unsteady Euler scheme for the analysis of ducted propellers
[AIAA PAPER 92-0522] p 332 A92-26947
Aeroelastic analysis of advanced propellers using an efficient Euler solver
[AIAA PAPER 92-0488] p 341 A92-28194
Experimental study of the equivalent sound source center of the propeller rotating noise
p 1011 A92-53257
Wind tunnel performance results of swirl recovery vanes as tested with an advanced high speed propeller
[AIAA PAPER 92-3770] p 1068 A92-54159
Propeller and propfan noise p 54 N92-10599
Annoyance caused by advanced turboprop aircraft flyover noise: Comparison of different propeller configurations
[NASA-TP-3104] p 56 N92-11758
Aerodynamics p 202 N92-13977
A Navier-Stokes solution of Hull-ring wing-thruster interaction p 221 N92-14310
Calibration data for improved correction of UVW propeller anemometers
[DE92-002935] p 297 N92-16281
The solution of a singular integral equation arising from a lifting surface theory for rotating blades
p 260 N92-17303
Prediction of far-field harmonic noise from propellers
[ESDU-91033] p 416 N92-18074
Application of analysis techniques for low frequency interior noise and vibration of commercial aircraft
[NASA-CR-189555] p 481 N92-20376
Wind tunnel investigation of a wing-propeller model performance degradation due to distributed upper-surface roughness and leading edge shape modification
p 451 N92-21690
Comparison of LDA and LTA applications for propeller tests in wind tunnels
[NLR-MP-88031-U] p 827 N92-28658
Thrust test fixture
[AD-D015259] p 983 N92-31192
Exploratory experimental investigation of a wave propeller
[AD-A252175] p 949 N92-32062
Further development of the CANAERO computer code to include propulsor modelling
[DREA-CR-90-425] p 1038 N92-32811
On the origin and acoustical behaviour of cloud cavitation
[ISBN-90-9004317-9] p 1125 N92-33066

PROPORTIONAL CONTROL
Real-time simulation and adaptive PID control of QSK-06A control for gas turbine p 470 A92-29740
An evaluation of a simple PID controller designed using optimal control theory when applied to helicopter stabilisation p 569 A92-35785
Robust flight control system design with multiple model approach p 661 A92-39910
Robustness characteristics of fast-sampling digital PI controllers for high-performance aircraft with impaired control surfaces p 877 A92-48496
Proportional plus integral control of aircraft for automated maneuvering formation flight
[AD-A243792] p 382 N92-19505

PROPULSION
Supersonic reacting internal flowfields
p 155 A92-16989
The mean power of forces and moments in unsteady aerodynamics p 421 A92-28949
Cryogenic hydrogen-induced air-liquefaction technologies for combined-cycle propulsion applications
p 487 N92-21526
Low temperature environment operations of turboengines (design and user's problems)
p 450 N92-21682
Directions in propulsion control p 560 N92-22530
Overview of the subsonic propulsion technology session p 560 N92-22531
Workshop on Engineering Turbulence Modeling
[NASA-CP-10088] p 678 N92-24514
Some comments on turbulence modeling from an industrial perspective p 678 N92-24531
The future challenge for aeropropulsion
[NASA-TM-105613] p 658 N92-25164
Integrated flight propulsion control research results using the NASA F-15 HIDEC Flight Research Facility
[NASA-TM-4394] p 740 N92-27379
Thrust stand evaluation of engine performance improvement algorithms in an F-15 airplane
[NASA-TM-104252] p 971 N92-30518
Activities of the Aeronautical Research Laboratory
p 1013 N92-30768
Trends in aeropropulsion research and their impact on engineering education
[NASA-TM-105682] p 972 N92-31172
A parameter optimization approach to controller partitioning for integrated flight/propulsion control application
[NASA-TM-105826] p 979 N92-32241
DoD key technologies plan
[AD-A253692] p 1142 N92-33238
Perspectives on hypersonic viscous and nonequilibrium flow research
[NASA-CR-190817] p 1039 N92-33413

PROPULSION SYSTEM CONFIGURATIONS
Renewed interest in pulsed engines may be linked to 'black' aircraft p 24 A92-10600
Advanced SCRAM-LACE system concept for single-stage-to-orbit space plane
[IAF PAPER 91-272] p 32 A92-12599
Subsonic propulsion system installation analysis and optimization
[ASME PAPER 91-GT-167] p 111 A92-15602
Propulsion aspects of hypersonic turbo-ramjet-engines with special emphasis on nozzle/aftbody integration
[ASME PAPER 91-GT-395] p 127 A92-15725
Propulsion system evaluation for an unmanned high altitude long endurance RPV
[ASME PAPER 91-GT-409] p 128 A92-15738
Hypersonic airbreathing propulsion activities for Saenger
[AIAA PAPER 91-5040] p 200 A92-17828
Potential hypersonic vehicles applications
[AIAA PAPER 91-5086] p 169 A92-17854
Study on the reliability evaluation of engine fuel accessories p 392 A92-24749
Flow in a ventral nozzle for short takeoff and vertical landing aircraft p 376 A92-28538
IMPAC - An integrated methodology for propulsion and airframe control p 477 A92-29118
Engineering method for aero-propulsive characteristics at hypersonic Mach numbers
[AIAA PAPER 91-5061] p 437 A92-31690
Advanced propulsion systems for large subsonic transports p 653 A92-36977
NASP - A status report
[AIAA PAPER 92-1417] p 666 A92-38569
Trends in propulsion technology p 757 A92-41186
Thermal management for a Mach 5 cruise aircraft using endothermic fuel p 736 A92-41225
Generalities on the ramjet p 736 A92-41819
New ramjet configurations p 736 A92-41822
The F/A-18.external burning flight test
[AIAA PAPER 91-5050] p 731 A92-44547
Current technology propulsion systems meet the STOVL window of opportunity p 860 A92-45307
ASTOVL propulsion systems configuration and concept choice p 842 A92-45312
ASTOVL engine control p 860 A92-45321
Fiber optic controls for aircraft engines - Issues and implications p 856 A92-46244
High speed rotorcraft propulsion concepts to control power/speed characteristics
[AIAA PAPER 92-3367] p 865 A92-48940
A new vane swirler as applied to dual-inlet side-dump combustor
[AIAA PAPER 92-3654] p 906 A92-49085
The External Propulsion Accelerator - Scramjet thrust without interaction with accelerator barrel
[AIAA PAPER 92-3717] p 866 A92-49098
The VRT gas turbine combustor - Phase II
[AIAA PAPER 92-3471] p 1067 A92-54035
V-22 propulsion system design p 1070 A92-56300
Test data models to characterize turbine engine operation in altitude test facilities
[AIAA PAPER 92-3917] p 1095 A92-56749
Static internal performance of ventral and rear nozzle concepts for short-takeoff and vertical-landing aircraft
[NASA-TP-3103] p 12 N92-10975
High-temperature combustor and seal for a water piston propulsor
[AD-A242493] p 229 N92-15385
Scorpion: Close Air Support (CAS) aircraft
[NASA-CR-189974] p 462 N92-20664
NASA advanced aeronautics design solar powered remotely piloted vehicle
[NASA-CR-190007] p 462 N92-20665
Pioneering scramjet developments by Antonio Ferri
p 474 N92-21519
Advanced ramjet concepts program
p 474 N92-21520
Airbreathing combined cycle engine systems
p 475 N92-21523
Supercharged ejector ramjet p 475 N92-21527
System controls challenges of hypersonic combined-cycle engine powered vehicles
p 475 N92-21533
NASP X-30 Propulsion technology status
p 475 N92-21534
NASA's hypersonic propulsion program: History and direction p 476 N92-21535
Some implications for advanced STOVL operation from invincible class ships p 466 N92-21971
JPRS report: Science and technology. USSR: Engineering and equipment
[JPRS-UEQ-92-001] p 592 N92-22296
Improved large perturbation propulsion models for control system design (1988-1989) and large perturbation models of high velocity propulsion systems (1989-1990) and reduced order propulsion models for control system design (1990-1991)
[NASA-CR-190148] p 593 N92-22491
A hierarchy for modeling high speed propulsion systems p 559 N92-22492
Aeropropulsion 1987
[NASA-CP-3049] p 559 N92-22510
Impact and promise of NASA aeropropulsion technology p 559 N92-22511
Rotorcraft transmissions p 560 N92-22533
NASA thrusts in high-speed aeropropulsion research and development: An overview p 561 N92-22538
Supersonic STOVL propulsion technology program: An overview p 561 N92-22539
Two stage to orbit design
[NASA-CR-189994] p 575 N92-22625
Design of an integrated airframe/propulsion control system architecture
[NASA-CR-182007] p 602 N92-22644
Configuration development --- preliminary aircraft design p 552 N92-23953
The future challenge for aeropropulsion
[NASA-TM-105613] p 658 N92-25164
Activities for numerical propulsion systems simulation program p 692 N92-25726
Study of shock-induced combustion using an implicit TVD scheme p 669 N92-25816
Computational Structures Technology for Airframes and Propulsion Systems
[NASA-CP-3142] p 683 N92-25911
Computational structures technology and UVA Center for CST p 683 N92-25912
Computer codes developed and under development at Lewis p 692 N92-25913
A brief overview of computational structures technology related activities at NASA Lewis Research Center
p 683 N92-25915
ASTOVL propulsion systems: Configuration and concept choice
[PNR-90809] p 740 N92-27041
Integrated flight propulsion control research results using the NASA F-15 HIDEC Flight Research Facility
[NASA-TM-4394] p 740 N92-27379

Aerothermodynamics of nozzle flows for advanced hypersonic propulsion systems p 769 N92-27478
Application of finite element method to hypersonic nozzle flow computations p 769 N92-27479
Flight-determined benefits of integrated flight-propulsion control systems
[NASA-TM-4393] p 742 N92-27587
A preliminary design and analysis of an advanced heat-rejection system for an extreme altitude advanced variable cycle diesel engine installed in a high-altitude advanced research platform
[NASA-CR-186021] p 871 N92-29427
Flight evaluation of an extended engine life mode on an F-15 airplane
[NASA-TM-104240] p 871 N92-29659
Supersonic Throughflow Fan Test Facility at NASA. Lewis Research Center
[NASA-TP-3038] p 983 N92-31640
Analytical and experimental studies of heat pipe radiation cooling of hypersonic propulsion systems
[DE92-013428] p 973 N92-31817
Dynamic interactions between hypersonic vehicle aerodynamics and propulsion system performance
[NASA-CR-190638] p 1038 N92-33304
A graphical user-interface for propulsion system analysis
[NASA-TM-105696] p 1134 N92-33894

PROPULSION SYSTEM PERFORMANCE
Numerical simulation of the actuation system for the ALDF's propulsion control valve --- Aircraft Landing Dynamics Facility p 41 A92-13204
The performance evaluation of aeroderivative gas turbines p 119 A92-13296
Implanted component faults and their effects on gas turbine engine performance
[ASME PAPER 91-GT-41] p 121 A92-15524
An investigation of two cooling technologies as applied to a distributed propulsion control architecture
[ASME PAPER 91-GT-341] p 111 A92-15705
Propulsion requirements for high altitude long endurance flight
[ASME PAPER 91-GT-393] p 127 A92-15723
Propulsion system evaluation for an unmanned high altitude long endurance RPV
[ASME PAPER 91-GT-409] p 128 A92-15738
F-15 STOL/Maneuvering Technology Demonstrator. Phase III - Thrust vectoring, reversing and STOL operation p 112 A92-16054
Supersonic reacting internal flowfields p 155 A92-16989
Engineering model for analysis of scramjet combustor performance with finite-rate chemistry p 129 A92-17202
An investigation of fuel nozzles for combustion performance p 278 A92-21745
Cold-cycle pressure-jet helicopters - Ventures, designs, and developments. II - Design p 271 A92-22712
Thermal management of propulsion systems in hypersonic vehicles
[AIAA PAPER 92-0516] p 373 A92-26942
Design and modeling issues for integrated airframe/propulsion control of hypersonic flight vehicles p 477 A92-29115
Integrated flight/propulsion control specifications for systems with two-way coupling p 477 A92-29117
IMPAC - An integrated methodology for propulsion and airframe control p 477 A92-29118
Thermal control for hypersonic vehicle propulsion p 468 A92-29356
Flowpath optimization for hypersonic vehicles
[AIAA PAPER 91-5043] p 437 A92-31688
Engineering method for aero-propulsive characteristics at hypersonic Mach numbers
[AIAA PAPER 91-5061] p 437 A92-31690
Russians want U.S. to join scramjet tests p 472 A92-32296
Russia bids to salvage development of Soyuz-powered VTOL fighter p 472 A92-32300
Experimental investigation on performances of two-dimensional inlet at supersonic speed p 519 A92-35544
Numerical study of the effects of reverse sweep on scramjet inlet performance p 611 A92-36979
Mechanics and thermodynamics of propulsion (2nd revised and enlarged edition) --- Book
[ISBN 0-201-14659-2] p 672 A92-38275
Distributed health management systems technology for future propulsion control systems
[SAE PAPER 912167] p 655 A92-39995
Generalities on the ramjet p 736 A92-41819
New ramjet configurations p 736 A92-41822
ASTOVL flexibility in the 21st century p 783 A92-45309
High-speed flight propulsion systems --- Book
[ISBN 1-56347-011-X] p 862 A92-46426
Introduction --- propulsion system performance for hypersonic vehicles p 862 A92-46427
Propulsion system performance and integration for high Mach air breathing flight p 862 A92-46429
Energy analysis of high-speed flight systems p 925 A92-46430
Calculation methods on equivalence ratio of multi-propellant for propulsion system p 893 A92-48269
Prediction of a high bypass ratio engine exhaust nozzle flowfield
[AIAA PAPER 92-3259] p 864 A92-48855
High speed rotorcraft propulsion concepts to control power/speed characteristics
[AIAA PAPER 92-3367] p 865 A92-48940
Design issues in a fiber optic sensor system architecture for aircraft engine control
[AIAA PAPER 92-3483] p 866 A92-49023
Subsonic flight test evaluation of a performance seeking control algorithm on an F-15 airplane
[AIAA PAPER 92-3743] p 878 A92-49109
Subsonic flight test evaluation of a propulsion system parameter estimation process for the F100 engine
[AIAA PAPER 92-3745] p 866 A92-49110
Thrust stand evaluation of engine performance improvement algorithms in an F-15 airplane
[AIAA PAPER 92-3747] p 866 A92-49111
Analytical design and demonstration of a low-cost expendable turbine engine combustor
[AIAA PAPER 92-3754] p 867 A92-49112
Some readily quantifiable aspects of scramjet engine performance p 969 A92-50278
Research capabilities of the NASA Langley 8-foot high temperature tunnel p 980 A92-51403
Some thermodynamical aspects in the optimization of supersonic combustors p 1065 A92-53486
Performance analysis of idealized scramjet p 1066 A92-53493
In-flight optimization of the total propulsion system
[AIAA PAPER 92-3744] p 1068 A92-54146
Development of the full-envelope Performance Seeking Control algorithm
[AIAA PAPER 92-3748] p 1068 A92-54148
Performance benefits of adaptive in-flight propulsion system optimization
[AIAA PAPER 92-3749] p 1068 A92-54149
Further studies of kinetic energy methods in high speed ramjet cycle analysis
[AIAA PAPER 92-3805] p 1069 A92-54177
Flowpath and sensitivity analyses of high speed propulsion systems
[AIAA PAPER 92-3806] p 1069 A92-54178
Propulsion system performance resulting from an Integrated Flight/Propulsion Control design
[AIAA PAPER 92-4602] p 1069 A92-55281
Analysis of airframe/engine interactions for a STOVL aircraft with integrated flight/propulsion control
[AIAA PAPER 92-4623] p 1052 A92-55300
Thrust stand design principles
[AIAA PAPER 92-3976] p 1098 A92-56802
Turbine engine performance test and evaluation techniques
[AIAA PAPER 92-3977] p 1071 A92-56803
Tests results on Air Turbo Ramjet for a future space plane
[IAF PAPER 92-0657] p 1071 A92-57098
Airbreathing engine selection criteria for SSTO propulsion system
[IAF PAPER 92-0658] p 1071 A92-57099
Real-time fault diagnosis for propulsion systems
[NASA-TM-105303] p 26 N92-11017
Properties of aircraft fuels and related materials
[AD-A240650] p 35 N92-11213
Engine dynamic analysis with general nonlinear finite element codes
[NASA-CR-187222] p 44 N92-11379
A derivation of gross thrust for a sea-level jet engine test cell
[NRC-30165] p 130 N92-12001
High-temperature combustor and seal for a water piston propulsor
[AD-A242493] p 229 N92-15385
Design of a turbofan powered regional transport aircraft
[NASA-CR-190130] p 461 N92-20280
Scorpion: Close Air Support (CAS) aircraft
[NASA-CR-189974] p 462 N92-20664
Pioneering scramjet developments by Antonio Ferri p 474 N92-21519
Advanced ramjet concepts program p 474 N92-21520
The NASA hypersonic research engine program p 474 N92-21521
Airbreathing combined cycle engine systems p 475 N92-21523
Inlet technology p 447 N92-21528
Scramjet analysis, testing p 475 N92-21532
System controls challenges of hypersonic combined-cycle engine powered vehicles p 475 N92-21533
NASP X-30 Propulsion technology status p 475 N92-21534
NASA's hypersonic propulsion program: History and direction p 476 N92-21535
Modeling of linear isentropic flow systems p 593 N92-22495
Aeropropulsion 1987
[NASA-CP-3049] p 559 N92-22510
Impact and promise of NASA aeropropulsion technology p 559 N92-22511
Determining structural performance p 560 N92-22519
Optical measurement systems p 594 N92-22527
Directions in propulsion control p 560 N92-22530
NASA thrusts in high-speed aeropropulsion research and development: An overview p 561 N92-22538
Supersonic STOVL propulsion technology program: An overview p 561 N92-22539
Hypersonic propulsion research p 561 N92-22543
The future challenge for aeropropulsion
[NASA-TM-105613] p 658 N92-25164
Activities for numerical propulsion systems simulation program p 692 N92-25726
Study of shock-induced combustion using an implicit TVD scheme p 669 N92-25816
ASTOVL propulsion systems: Configuration and concept choice
[PNR-90809] p 740 N92-27041
Automated screening of propulsion system test data by neural networks, phase 1
[NASA-CR-184329] p 753 N92-27403
CFD contributions during hypersonic airplane intake design p 769 N92-27472
The coherent flamelet model for propulsion applications p 756 N92-27486
Component performance requirements p 869 N92-28462
Inlet distortion effects in aircraft propulsion system integration p 869 N92-28464
Engine performance and health monitoring models using steady state and transient prediction methods p 870 N92-28467
Flight evaluation of an extended engine life mode on an F-15 airplane
[NASA-TM-104240] p 871 N92-29659
Subsonic flight test evaluation of a performance seeking control algorithm on an F-15 airplane
[NASA-TM-4400] p 973 N92-31275
Supersonic Throughflow Fan Test Facility at NASA. Lewis Research Center
[NASA-TP-3038] p 983 N92-31640
Analytical and experimental studies of heat pipe radiation cooling of hypersonic propulsion systems
[DE92-013428] p 973 N92-31817
Dynamic interactions between hypersonic vehicle aerodynamics and propulsion system performance
[NASA-CR-190638] p 1038 N92-33304
A graphical user-interface for propulsion system analysis
[NASA-TM-105696] p 1134 N92-33894
Parametric investigation of single-expansion-ramp nozzles at Mach numbers from 0.60 to 1.20
[NASA-TP-3240] p 1042 N92-34193

PROPULSIVE EFFICIENCY
A flight test study to determine aircraft propulsive efficiency and aerodynamic drag using two parameter identification methods and Lock's propeller model
[AIAA PAPER 92-0170] p 271 A92-23781
A quick automatic method for computing performance of ducted-propeller p 736 A92-42800
Technology needs for high speed rotorcraft (3)
[NASA-CR-177592] p 195 N92-14039

PROTECTION
Lightning protection requirements for aircraft: A proposed specification
[RAE-TM-FS(F)-632-REV-ISSUE] p 187 N92-14007
A Protection And Detection Surface (PADS) for damage tolerance p 1107 N92-32523

PROTECTIVE CLOTHING
Active noise reduction p 603 A92-32980
International aviation (selected article)
[AD-A240987] p 170 N92-13992
Thermal energy test apparatus
[AD-A243526] p 305 N92-17537

PROTECTIVE COATINGS
Nondestructive depth profiling of the protective coating on a turbine blade p 144 A92-13641
Corrosion prevention field test utilizing water displacement compounds p 110 A92-14436
High temperature erosion resistance of coatings for gas turbine
[ASME PAPER 91-GT-213] p 143 A92-15632

PVD coatings for aircraft turbine blades
p 216 A92-17950
Protective coatings of thermal barrier type
p 214 A92-20349
Sound produced by an aerodynamic source adjacent to a partly coated, finite elastic plate
p 414 A92-25365
Thermally sprayed coating systems for surface protection and clearance control applications in aero engines p 488 A92-32394
Take it all off - with water --- High-pressure waterjet stripping of protective coatings p 516 A92-34775
Removing aircraft surface coatings
p 516 A92-35574
Waterjets for removing engine coatings
p 516 A92-35575
Coating effect on particle trajectories and turbine blade erosion p 653 A92-36892
TMFSLAM - Design analysis tool for coated structures
[ASME PAPER 91-GT-141] p 690 A92-36895
A study of aircraft surface coating technology
p 700 A92-43147
Low VOC primer for structural bonding --- volatile organic compound p 892 A92-47338
Aluminides modified by palladium - Protection of new parts by local finishing
[ONERA, TP NO. 1992-49] p 893 A92-48610
Ablation performance characterization of thermal protection materials using a Mach 4.4 Sled Test
[AIAA PAPER 92-3055] p 893 A92-48713
High-temperature combustor and seal for a water piston propulsor
[AD-A242493] p 229 N92-15385
Fabrication and testing of corrosion resistant coatings --- for turbine engine components
[DE92-003553] p 490 N92-21063
Thermally sprayed coating systems for surface protection and clearance control applications in aero engines
[PNR-90802] p 741 N92-27422
Life prediction and constitutive models for engine hot section anisotropic materials program
[NASA-CR-189222] p 973 N92-31534

PROTOCOL (COMPUTERS)
RTOK elimination with TSMM --- Rerun Tested OK reproduction using time stress measurement module
p 902 A92-48446
A fault-tolerant network architecture for integrated avionics p 965 A92-49297
Application of VME-technology on an airborne data link processor unit
[NLR-MP-88040-U] p 841 N92-29615

PROTOTYPES
The helicopter air-to-air value-driven engagement model (HAVDEM) - Prototype development
p 105 A92-14353
Cold-cycle pressure-jet helicopters: Ventures, designs, and developments. I - Ventures p 459 A92-31325
Flexible manufacturing in repair of gas turbine engine components
[AIAA PAPER 92-3524] p 786 A92-49049
Design and testing of high-performance parachutes
[AGARD-AG-319] p 345 N92-18269
A prototype semantic integrity front end expert system for a relational database
[AD-A246084] p 781 N92-26765
Resonance and control response tests using a control simulation device
[MBB-UD-0608-91-PUB] p 978 N92-30439

PROVING
Design for validation p 601 A92-33607
VORVISC: A vortex lattice method with viscous and compressibility corrections for full aircraft configurations including propulsion p 626 N92-24857
Experimental validation of a line-duct acoustics model including flow
[NLR-TP-90223-U] p 927 N92-28695

PSYCHOACOUSTICS
NSBIT program - Development of assessment system for aircraft noise and research on human impacts due to aircraft noise p 688 A92-39100
Temporal change of timbre of helicopter noise
p 694 A92-39104
Some experiences with community response to low levels of aircraft noise p 689 A92-39235
Aircraft noise and the elderly p 689 A92-39236
Effects of military training route noise on human annoyance p 689 A92-39237
Annoyance from aircraft overflights in wilderness
p 689 A92-39239
Relating the annoyance of aircraft overflights to their audibility by outdoor recreationists p 689 A92-39240
Annoyance caused by advanced turboprop aircraft flyover noise: Comparison of different propeller configurations
[NASA-TP-3104] p 56 N92-11758

PSYCHOLOGICAL TESTS
Mandatory psychological testing of pilots as a requirement for licensing in Norway?
p 835 A92-45081

PUBLIC LAW
Navigation charts on trial - How safe is safe?
p 1012 A92-49380

PULLEYS
Flat belt continuously variable high speed drive
[DE92-008952] p 680 N92-25054

PULSE CODE MODULATION
A new 1553 all-bus instrumentation monitor
p 198 A92-19252
The basic measuring technical equipment of the DLR test aircraft p 652 N92-25592
Ground installations for the preparation and evaluation of flight tests p 665 N92-25593

PULSE COMMUNICATION
High rate PCM data receiving, recording and relying
p 189 A92-19279
Programmable channelized digital radio/modem
p 955 A92-49291
Flight deck benefits of integrated data link communication
[NASA-TP-3219] p 456 N92-21459
Technical feasibility of digital three-dimensional cellular communications for air traffic control applications. Volume 1: Introduction and summary
[AD-A244573] p 534 N92-22104
Technical feasibility of digital three-dimensional cellular communications for air traffic control applications. Volume 2: Example system design details
[AD-A244574] p 534 N92-22105
Technical feasibility of digital three-dimensional cellular communications for air traffic control applications. Volume 3: Ground network architecture
[AD-A244575] p 534 N92-22106

PULSE DOPPLER RADAR
Spectrum modal analysis for the detection of low-altitude windshear with airborne Doppler radar
[NASA-CR-4457] p 953 N92-31549
Real-time processing of radar return on a parallel computer
[NASA-CR-4456] p 1043 N92-32606

PULSE DURATION
Characteristics of the energy analysis of optical radar in the case of nonstationary irradiation of flying objects
p 454 A92-31955

PULSE GENERATORS
Comparison of R2SPG waveforms with simulated EMP --- Repetitive Random Square-wave Pulse Generator
p 760 A92-42317

PULSE REPETITION RATE
Selection of the time parameters of the probing pulse during the nonstationary irradiation of flight vehicles
p 454 A92-31951

PULSED JET ENGINES
Review of propulsion applications and numerical simulations of the pulsed detonation engine concept
p 129 A92-17177
A parametric study of airbreathing Pulsed Detonation Engine
[AIAA PAPER 92-0392] p 471 A92-31660
Pulse jet one-way valve performance
[AIAA PAPER 92-3169] p 863 A92-48790

PULSED LASERS
Development and application of a particle image velocimeter for high-speed flows
[AIAA PAPER 92-0004] p 292 A92-22129
Laser-initiated conical detonation wave for supersonic combustion. II
[AIAA PAPER 92-0088] p 292 A92-22195
Laser-initiated conical detonation wave for supersonic combustion, part 3
[AD-A250522] p 989 N92-32076

PULSED RADIATION
Active control of pulsed flow for low frequency noises attenuation p 694 A92-39109

PULSEJET ENGINES
A model of the operation of the pulsejet engine and a study of its characteristics p 657 A92-40608

PULTRUSION
Measurement of basic material and processing properties affecting injection-pultrusion technology
p 580 A92-32636
Manufacturing development of pultruded composite panels
[NASA-CR-181780] p 578 N92-22637

PUMP IMPELLERS
Pressure oscillation in the leakage annulus between a shrouded impeller and its housing due to impeller-discharge-pressure disturbances
p 580 A92-32942
Experimental study of the mechanism of sound generation by rotating stall in centrifugal turbomachines
p 605 N92-23726

PUMP SEALS
Test results for rotordynamic coefficients of the SSME HPOTP turbine interstage seal with two swirl brakes
p 223 N92-14357
Dynamic characteristics and stability analysis of space shuttle main engine oxygen pump p 224 N92-14366

PUMPS
Hydraulic pumps - The key to power generation
p 215 A92-17348
Variable displacement electro-hydrostatic actuator --- for flight control systems p 876 A92-48492

PUNCHED CARDS
Buffered serial data card
[AD-A246435] p 727 N92-26948

PURSUIT TRACKING
Aircraft evasive maneuvers against flying objects
p 744 A92-43128

PYLON MOUNTING
Experimental study of pylon geometries for transport aircraft
[AIAA PAPER 92-0153] p 271 A92-23768
Computations of the unsteady flow about a generic wing/pylon/finned-store configuration
[AIAA PAPER 92-4568] p 1027 A92-55377

PYLONS
Hub and pylon fairing integration for helicopter drag reduction p 107 A92-14391

PYROLYSIS
In situ measurement of particle formation in heated jet fuels: A new application of photon correlation spectroscopy
[DE92-003641] p 488 N92-20132

PYROMETERS
Experimental pyrometer system for a gas turbine engine
[AIAA PAPER 92-3482] p 859 A92-49022

Q

Q SWITCHED LASERS
One joule output from a diode-array-pumped Nd:YAG laser with side-pumped rod geometry
p 671 A92-37188

QUADRATIC PROGRAMMING
An algorithm for robust eigenstructure assignment using the linear quadratic regulator
[AD-A244267] p 412 N92-19335
Simultaneous stress and flutter optimization for the wing of a transport aircraft equipped with four engines
p 571 N92-23238

QUADRATURE PHASE SHIFT KEYING
ETS-V/EMSS mobile satellite communication experiments p 395 A92-26776

QUADRUPOLES
Critical problems of computational aeroacoustics
p 167 N92-13857

QUALIFICATIONS
Diffuser casing upgrade for an advanced turbofan
[NLR-TP-90097-U] p 870 N92-28711

QUALITATIVE ANALYSIS
Advanced nozzle and engine components test facility
[AIAA PAPER 92-3993] p 1099 A92-56816

QUALITY CONTROL
The use of NDE as a process development tool for ceramic engine components
[ASME PAPER 91-GT-290] p 152 A92-15682
Methodology for the assessment of material quality effects on airframe fatigue durability p 213 A92-19820
Embedded meshes of controllable quality synthesised from elementary geometric features
[AIAA PAPER 92-0663] p 411 A92-27034
1991-92 AHS Technical Committee highlights - Manufacturing and product assurance
p 609 A92-40396
Quality management of landing gear with pulling support system p 762 A92-43156
Joint Aviation Authorities: Development of an international standard for safety regulation - The first steps are being taken by the JAA p 781 A92-43548
Designing to cost effectiveness - Enhancing quality
p 1119 A92-56209
Electronics/avionics integrity - Definition, measurement and improvement p 1120 A92-56252
Engineering reliability and maintainability review - A regimen for discovering production deficiencies
p 1120 A92-56254
Implementing total quality management at the intermediate level of aircraft maintenance
[AD-A241768] p 62 N92-12992
Mechanical qualification tests for materials used in the fabrication of aircraft parts
[CEAT-M5-5443/01] p 195 N92-14042

Aviation Diagnostics And Maintenance (ADAM) system preliminary concept of operation and functional description
[AD-A242598] p 170 N92-14966
Introduction: Needs and approaches to reliability and quality assurance in design and manufacture
p 402 N92-19005
Reuse metrics and measurement: A framework
p 413 N92-19432
Criteria for the operation of federally-owned secondary calibration laboratories (ionizing radiation)
[PB92-112481] p 485 N92-21777
An analysis of total quality management in Aeronautical Systems Division
[AD-A246661] p 772 N92-27760
A manufacturer's approach to ensure long term structural integrity p 838 N92-30133
The 1991 Federal Aviation Administration plan for research, engineering and development
p 1142 N92-32453
SATWG networked quality function deployment
p 1134 N92-33339

QUANTITATIVE ANALYSIS
Escape strategies for turboprop aircraft in a microburst windshear
[AD-A243090] p 264 N92-17217

QUARTZ CRYSTALS
Monitoring jet fuel degradation using quartz crystal microbalances
[DE92-004730] p 489 N92-20858

QUATERNIONS
Special Rotation Vectors quaternions in three components
[AIAA PAPER 92-4168] p 1008 A92-52454
NPSNET: Flight simulation dynamic modeling using quaternions
[AD-A247484] p 923 N92-28245
Quaternion and Euler angles in kinematics
[NAL-TM-636] p 909 N92-28836

QUENCHING (COOLING)
Forced-injection quenching of a hot-tube under microgravity p 590 A92-35977
Modifications to the rapid melt/rapid quench and transparent polymer video furnaces for the KC-135
[NASA-CR-184215] p 157 N92-12231

QUERY LANGUAGES
The designer-FEM model interface based on the data base management concept p 163 A92-16832

QUEUEING THEORY
Stochastic ordering properties and optimal routing control for a class of finite capacity queueing systems
p 48 A92-11375
A new study on a class of discrete event dynamic systems p 48 A92-11377
A new class of gradient estimators for queueing systems with real-time constraints p 49 A92-11395

R

RACKS (FRAMES)
Applications of advanced composites in a 3/4 air transportable rack p 36 A92-10314
Liquid flow-through cooling for avionics applications
p 902 A92-48448

RADAR
Radar troubleshooting assistant expert system
[AIAA PAPER 91-3764] p 231 A92-17626
Avionics modernization/upgrades in the late 1990s
p 199 N92-14055
Terminal Doppler weather radar test bed operation, Orlando: January-June 1990
[AD-A242890] p 301 N92-17028
An investigation into the feasibility of providing a proximity warning device for search and rescue helicopters
[ETN-92-91057] p 530 N92-22408

RADAR ABSORBERS
The design of broadband radar absorbing surfaces
[AD-A240521] p 42 N92-11235
B-2 program: Trends in manufacturing
[AD-A242141] p 242 N92-15963

RADAR ANTENNAS
Multiple phase centre DPCA for airborne radar --- Displaced Phase Centre Antenna p 95 A92-16257
A parallel-series-fed microstrip array with high efficiency and low cross-polarization p 496 A92-31630
Estimation of the P-3/SAR L-, C- and X-band antenna directivity in range direction based on corner reflector measurements within the absolute SAR calibration
p 587 A92-35055
Acceptance of two identical radars in the absence of a precision reference p 533 A92-35931
Singlemode fiber optic rotary joint for aircraft applications p 779 A92-42606
Integrating a radar/ESM antenna suite with the S-70 helicopter --- Electronic Surveillance Measures
p 957 A92-49333
The B-2 radar p 956 A92-53102

RADAR APPROACH CONTROL
Simulation of triple simultaneous parallel ILS approaches p 880 A92-45025
Autonomous landing - Functional requirements
p 840 A92-48470
State and time granularity in system description: An example
[REPT-91-040] p 603 N92-22673

RADAR ATTENUATION
Progress report on analysis of differential attenuation radar data obtained during WISP-91
[PB92-133800] p 503 N92-21828

RADAR BEACONS
Solid-State Radar Beacon Decoder (SSRBD) Operational Test and Evaluation (OT/E) integration test plan
[DOT/FAA/CT-TN91/30] p 19 N92-10020

RADAR CLUTTER MAPS
Using fractal dimension for target detection in clutter
p 410 A92-24423

RADAR CROSS SECTIONS
Precision analysis on static measurement of radar cross section p 370 A92-27906
Slenderness approximations in RCS estimation - The simplest 2-D case p 533 A92-33622
RCS of four fuselage-like scatterers at HF frequencies
p 533 A92-33632
Relating the microwave radar cross section to the sea surface stress - Physics and algorithms
p 597 A92-35028
Scattering mechanism and RCS reduction of antennas
p 726 A92-44850
The use and misuse of aircraft and missile RCS statistics
[AD-A239892] p 41 N92-10141
Investigation of the effects of aeroelastic deformations on the radar cross section of aircraft
[AD-A243889] p 402 N92-18940
Parametric bicubic spline and CAD tools for complex targets shape modelling in physical optics radar cross section prediction p 403 N92-19151
An investigation into the feasibility of providing a proximity warning device for search and rescue helicopters
[ETN-92-91057] p 530 N92-22408
Global and high resolution radar cross section measurements and two-dimensional microwave images of a scaled aircraft model from the type Airbus A 310
[DLR-MITT-91-10] p 911 N92-29877

RADAR DATA
European studies to investigate the feasibility of using 1000 ft vertical separation minima above FL 290. II - Precision radar data analysis and collision risk assessment p 353 A92-24946
Real targets, unreal displays - The inadvertent suppression of critical radar data p 839 A92-44969

RADAR DETECTION
Polish radar technology. V - Adaptive MTI filters for uniform and staggered sampling p 40 A92-12293
Analysis and design optimization of monopulse receivers for secondary surveillance radar p 40 A92-12299
Radar Detection Analysis of Rotor Systems (RADARS)
p 117 A92-14350
Using fractal dimension for target detection in clutter
p 410 A92-24423
Heterodyne techniques in the I.R. bandwidth for laser obstacle detection p 533 A92-35740
The obstacle avoidance radar - A safety mean for low altitude flights in adverse weather conditions
p 554 A92-35743
Detection and imaging of moving objects with synthetic aperture radar. I - Optimal detection and parameter estimation theory p 955 A92-50033
The use and misuse of aircraft and missile RCS statistics
[AD-A239892] p 41 N92-10141
Parametric bicubic spline and CAD tools for complex targets shape modelling in physical optics radar cross section prediction p 403 N92-19151
The application of lattice-structure adaptive filters to clutter-suppression for scanning radar
p 403 N92-19154
Use of target spectrum for detection enhancement and identification p 404 N92-19155
The Lockheed F-117A
[RAND-P-7746-RGS] p 731 N92-26673

RADAR ECHOES
Adaptive airborne MTI with two-dimensional motion compensation p 102 A92-17240
Precision analysis on static measurement of radar cross section p 370 A92-27906
Enclosing shapes for single-Doppler radar features
p 494 A92-30476
Detection and imaging of moving objects with synthetic aperture radar. I - Optimal detection and parameter estimation theory p 955 A92-50033
Use of target spectrum for detection enhancement and identification p 404 N92-19155

RADAR EQUIPMENT
Polish radar technology. II - Adaptive radar AVIA CM
p 39 A92-12290
Advanced ASDE provides new eyes and ears for controllers p 453 A92-29506
The 1990 Airport Surveillance Radar Wind Shear Processor (ASR-WSP) operational test at Orlando International Airport
[AD-A239852] p 18 N92-10019
The use and misuse of aircraft and missile RCS statistics
[AD-A239892] p 41 N92-10141
Low-noise oscillators for airborne radar applications
[AD-A242264] p 300 N92-17258
The Air Force Manufacturing Technology (MANTECH): Technology transfer methodology as exemplified by the radar transmit/receive module program
p 593 N92-22451
Airport Surveillance Radar (ASR-9) wind shear processor: 1991 test at Orlando, Florida
[AD-A252246] p 1124 N92-32686

RADAR IMAGERY
Comparison of aircraft synthetic aperture radar and buoy spectra during NORCSEX '88 p 597 A92-34878
Development of a 3-D remote sensing radar
p 597 A92-34908
An airborne multimode radar display processor
p 965 A92-49308
Detection and imaging of moving objects with synthetic aperture radar. I - Optimal detection and parameter estimation theory p 955 A92-50033
The application of imaging sensors to aircraft landings in adverse weather p 1045 A92-54902
Talons 95 GHz radar sensor for autonomous landing guidance p 1063 A92-55908
Low-noise oscillators for airborne radar applications
[AD-A242264] p 300 N92-17258
GPS/INS integration for improved aircraft attitude estimates
[AD-A243947] p 356 N92-19604
Bistatic image processing for a 32 x 19 inch model aircraft using scattered fields obtained in the OSU-ESL compact range
[NASA-CR-189932] p 499 N92-20197
Progress report on analysis of differential attenuation radar data obtained during WISP-91
[PB92-133800] p 503 N92-21828
The imaging radar system p 599 N92-23391

RADAR MEASUREMENT
Characteristics of thunderstorm-generated low altitude wind shear - A survey based on nationwide terminal Doppler weather radar testbed measurements
p 45 A92-11378
New practical method for measurement error determination in radar systems under real traffic conditions p 155 A92-17238
Talons 95 GHz radar sensor for autonomous landing guidance p 1063 A92-55908
Time Resolved Lidar Fluorosensor operating from helicopter p 1121 A92-56296
Aircraft lidar sensitivity study for measuring water vapor
[AD-A240549] p 42 N92-11237

RADAR NAVIGATION
Inertial navigation sensor integrated motion analysis for obstacle detection p 954 A92-49272
GPS/INS integration for improved aircraft attitude estimates
[AD-A243947] p 356 N92-19604
NAL Dornier 228-200 flight research airplane: Present status and outline of the installed equipment
[NAL-TM-637] p 732 N92-27429

RADAR RANGE
A Ka-band instrumentation radar with one foot range resolution p 95 A92-16252
Computation of aircraft geometric height under radar surveillance p 639 A92-40239
Bistatic scattering on a monostatic radar range
p 849 A92-48408

RADAR RECEIVERS
Classification of radar clutter using neural networks
p 145 A92-14252
Multiple phase centre DPCA for airborne radar --- Displaced Phase Centre Antenna p 95 A92-16257

RADAR RESOLUTION
A Ka-band instrumentation radar with one foot range resolution p 95 A92-16252

RADAR SCATTERING
RCS of four fuselage-like scatterers at HF frequencies p 533 A92-33632
Bistatic scattering on a monostatic radar range p 849 A92-48408
Parametric bicubic spline and CAD tools for complex targets shape modelling in physical optics radar cross section prediction p 403 N92-19151
Development of a helicopter-borne 8-channel ranging scatterometer
[PB92-141977] p 599 N92-23441
RADAR SIGNATURES
Radar Detection Analysis of Rotor Systems (RADARS) p 117 A92-14350
Controlling radar signature p 967 A92-52018
Modeling radar clutter
[AD-A240965] p 158 N92-13351
Use of target spectrum for detection enhancement and identification p 404 N92-19155
Global and high resolution radar cross section measurements and two-dimensional microwave images of a scaled aircraft model from the type Airbus A 310
[DLR-MITT-91-10] p 911 N92-29877
RADAR TARGETS
Precision analysis on static measurement of radar cross section p 370 A92-27906
Multisensor data fusion and decision support for airborne target identification p 454 A92-31063
Selection of the time parameters of the probing pulse during the nonstationary irradiation of flight vehicles p 454 A92-31951
X-band side-looking airborne radar for remote sensing p 554 A92-34976
IsoDoppler and mocomp corrections improve MTI radar p 898 A92-45774
Location and tracking technique in a multistatic system established by multiple bistatic systems p 840 A92-48480
Modeling radar clutter
[AD-A240965] p 158 N92-13351
The application of lattice-structure adaptive filters to clutter-suppression for scanning radar p 403 N92-19154
Use of target spectrum for detection enhancement and identification p 404 N92-19155
GPS/INS integration for improved aircraft attitude estimates
[AD-A243947] p 356 N92-19604
Development of a helicopter-borne 8-channel ranging scatterometer
[PB92-141977] p 599 N92-23441
RADAR TRACKING
Several results of lidar measurements of the characteristics of oblique visibility at an airfield p 45 A92-12844
Acceptance of two identical radars in the absence of a precision reference p 533 A92-35931
A fuzzy logic based F/A-18 automatic carrier landing system
[AIAA PAPER 92-4392] p 1074 A92-55193
The rise of active-element phased-array radar
[RAND-P-7747-RGS] p 999 N92-30755
RADIAL FLOW
Oscillation of nearly circular shock waves p 146 A92-15358
Performance of radial clearance rim seals in upstream and downstream rotor-stator wheelspaces
[ASME PAPER 91-GT-32] p 147 A92-15516
The design and testing of a radial flow turbine for aerodynamic research
[ASME PAPER 91-GT-220] p 124 A92-15636
Laser measurements of unsteady flow field in a radial turbine guide vanes
[AIAA PAPER 92-0394] p 395 A92-26249
Resonance of circular shock waves p 395 A92-26795
A comparison of the calculated and experimental off-design performance of a radial flow turbine
[AIAA PAPER 92-3069] p 1020 A92-54004
Radial inflow turbine study
[AD-A240169] p 26 N92-11015
A comparison of the calculated and experimental off-design performance of a radial flow turbine
[NASA-CR-189207] p 831 N92-29402
Radial inflow turbine study
[AD-A252783] p 1127 N92-33538
RADIANT COOLING
Effect of model cooling on periodic transonic flow p 813 A92-46900
Analytical and experimental studies of heat pipe radiation cooling of hypersonic propulsion systems
[AIAA PAPER 92-3809] p 867 A92-49128
Hypersonic flow past radiation-cooled surfaces
[MBB-FE-202-S-PUB-0468-A] p 832 N92-29713
Analytical and experimental studies of heat pipe radiation cooling of hypersonic propulsion systems
[DE92-013428] p 973 N92-31817
RADIANT FLUX DENSITY
Surfprep flash-lamp depaint system evaluation p 497 A92-32411
The numerical method for calculating the flow field, temperature field and radiation fluxfield in the pipe p 587 A92-35546
A comparison of measured and modeled broadband fluxes from aircraft data during the ICE '89 field experiment p 1003 A92-49771
Radiant energy power source for jet aircraft
[DE92-008726] p 648 N92-24556
Aircraft photovoltaic power-generating system p 775 N92-26581
RADIANT HEATING
Effect of porosity in transpiration cooling system p 1112 A92-53786
RADIATION BELTS
JPRS report: Science and technology. Central Eurasia: Space
[JPRS-USP-92-002] p 575 N92-23705
RADIATION DISTRIBUTION
A parametric analysis of radiative structure in aerobrake shock layers
[AIAA PAPER 92-2970] p 816 A92-46985
RADIATION EFFECTS
Effects of ionizing and nonionizing radiation on aircraft p 295 A92-23301
Sikorski (S-76) High Intensity Radiated Fields (HIRF) test
[SAE PAPER 912214] p 652 A92-40017
RADIATION HARDENING
Composite electromagnetic pulse threat p 146 A92-14689
High Intensity Radiated Fields (HIRF) project plan
[DOT/FAA/CT-TN91/1] p 297 N92-16181
RADIATION MEASUREMENT
A comparison of measured and modeled broadband fluxes from aircraft data during the ICE '89 field experiment p 1003 A92-49771
Aerothermodynamic radiation studies
[NASA-CR-185666] p 284 N92-15998
RADIATION PYROMETERS
Results of measured temperature distribution on an adiabatic wing model with radiation thermometer
[NAL-TM-610] p 261 N92-17755
RADIATION SPECTRA
Calculation of flow of a radiating gas in axisymmetric nozzles of specified shape p 7 A92-12179
RADIATIVE HEAT TRANSFER
Radiant heat transfer in supersonic three-dimensional and axisymmetric flow of air past evaporating bodies p 337 A92-27533
Optimum dimensions of convective-radiative spines using a temperature correlated profile p 676 A92-40869
A parametric analysis of radiative structure in aerobrake shock layers
[AIAA PAPER 92-2970] p 816 A92-46985
Decoupled predictions of radiative heating in air using a particle simulation method
[AIAA PAPER 92-2971] p 816 A92-46986
Heat transfer characteristics of hypersonic waveriders with an emphasis on leading edge effects
[AIAA PAPER 92-2920] p 821 A92-47892
Analytical and experimental studies of heat pipe radiation cooling of hypersonic propulsion systems
[AIAA PAPER 92-3809] p 867 A92-49128
Radiative heat transfer from nonequilibrium shock layer to a hypersonic reentry body p 1019 A92-53579
Simulation of chemical kinetics in turbulent natural gas combustion
[PB92-123660] p 488 N92-20329
Stagnation-point heat-transfer rate predictions at aeroassist flight conditions
[NASA-TP-3208] p 1001 N92-31281
RADIATIVE TRANSFER
Three-dimensional calculation of radiative field in hypersonic air shock layers p 1023 A92-54498
RADIO ALTIMETERS
Development of a 3-D remote sensing radar p 597 A92-34908
Flight testing a digital terrain following system p 548 A92-35929
Radioaltimeter RWL-750 p 855 A92-45374
Integration of radar altimeter, precision navigation, and digital terrain data for low-altitude flight
[AIAA PAPER 92-4420] p 1063 A92-55212
RADIO COMMUNICATION
Automatic link establishment - The key to reliable helicopter NOE communications p 94 A92-14403
ARINC and commercial aircraft avionics. I p 353 A92-25655
Data Link integration in commercial transport operations p 839 A92-44919
Remote telemetry concepts p 882 A92-47562
Programmable channelized digital radio/modem p 955 A92-49291
History of aeronautical satellite communications p 1046 A92-56088
Technical feasibility of digital three-dimensional cellular communications for air traffic control applications. Volume 1: Introduction and summary
[AD-A244573] p 534 N92-22104
Technical feasibility of digital three-dimensional cellular communications for air traffic control applications. Volume 2: Example system design details
[AD-A244574] p 534 N92-22105
Technical feasibility of digital three-dimensional cellular communications for air traffic control applications. Volume 3: Ground network architecture
[AD-A244575] p 534 N92-22106
National airspace data interchange network analysis
[AD-A247345] p 727 N92-27217
RADIO CONTROL
The maneuver performance and control of a *hovercraft p 763 A92-43240*
RADIO DIRECTION FINDERS
An evaluation of superresolution methods for tactical *radio direction finding*
[AD-A246316] p 726 N92-26291
RADIO FREQUENCIES
Terminal Doppler weather radar test bed operation, Orlando: January-June 1990
[AD-A242890] p 301 N92-17028
Improving the LAMP Mk 3 SH-60B HF communication system
[AD-A245970] p 910 N92-29344
Integrated Russian VLF/Omega receiver design
[PB92-193390] p 1051 N92-33809
RADIO FREQUENCY HEATING
Experimental studies of compact toroids
[DE92-003469] p 512 N92-21046
RADIO FREQUENCY INTERFERENCE
RFI effects analysis of an airport-installed HF transmitter on aircraft COMM/NAV receivers p 725 A92-42313
An investigation of the desensitizing effects by high power HF broadcast transmitters on HF airborne receivers p 726 A92-43937
RADIO NAVIGATION
The DOT/DOD Federal Radionavigation Plan p 96 A92-16637
From Russia and beyond --- equipment and areas of coverage for Loran navigation outside NAS p 96 A92-16638
A synergistic solution to the GPS integrity problem p 96 A92-16641
A prelude to interoperability - Comments on the lack of Federal Radionavigation Plan procedures for assessing the potential of a candidate system to fit into the mix of domestic radionavigation systems p 97 A92-16651
The 1990 Federal Radionavigation Plan and its impact on the Omega Navigation System p 98 A92-16658
Processing and displaying radio navigation data --- Russian book p 266 A92-21683
Navigation - Land, sea, air, and space --- Book
[ISBN 0-87942-257-2] p 496 A92-31778
RFI effects analysis of an airport-installed HF transmitter on aircraft COMM/NAV receivers p 725 A92-42313
Data processing in navigation complexes --- Russian book
[ISBN 5-217-01060-6] p 725 A92-42789
Selected models of aircraft navigation space p 839 A92-45373
Probability of cycle jumps in Omega receivers and other phase locked loop applications
[PB92-128891] p 455 N92-21279
Arrangements and methods for the survey of aircraft *radio components and systems p 652 N92-25603*
RADIO RECEIVERS
RAIM - Will it meet the RTCA GPS minimum operational performance standards? --- Receiver Autonomous Integrity Monitoring p 96 A92-16635
In-flight demonstration of hybrid GPS/Loran RAIM p 96 A92-16643
Omega - GPS integration platform p 98 A92-16660
Implementation of a RAIM monitor in a GPS receiver and an integrated GPS/IRS p 99 A92-16948
Comparison of fixed and variable threshold RAIM algorithms p 100 A92-16951
A digital P-code GPS receiver embedded in the AN/APN-217(V)5 Doppler Navigator p 102 A92-16976
Receiver autonomous integrity monitoring (RAIM) - Techniques, performance and potential p 638 A92-39567
The evolution of military GPS technology into the Navcore V receiver engine p 651 A92-39570

An investigation of the desensitizing effects by high power HF broadcast transmitters on HF airborne receivers p 726 A92-43937
GPS tests during approach at Singapore and Roissy p 956 A92-53240
Integrated Russian VLF/Omega receiver design
[PB92-193390] p 1051 N92-33809

RADIO RELAY SYSTEMS
Feasibility study on a microwave-powered unmanned aerial vehicle for the communication relay utilization
[SAE PAPER 912052] p 843 A92-45436

RADIO TELEMETRY
Development of telemetry for the agility flight test of a radio controlled fighter model
[AD-A248653] p 753 N92-27994

RADIO TRANSMISSION
Remote sensing of trapping layer base height using ATIS transmissions
[AD-A250074] p 1004 N92-31362

RADIO TRANSMITTERS
RFI effects analysis of an airport-installed HF transmitter on aircraft COMM/NAV receivers p 725 A92-42313
An investigation of the desensitizing effects by high power HF broadcast transmitters on HF airborne receivers p 726 A92-43937

RADIOGRAPHY
Real-time microfocus radiography for electronic failure analysis p 214 A92-17289
Application of X-ray image radiography system for aircraft p 1118 A92-56084
Large area QNDE inspection for airframe integrity p 362 N92-18588
Detection of honeycomb damage using hexagonal grid discontinuities
[DREP-89-9] p 1109 N92-32846

RADIOMETERS
Modifications to and data correction methods for some radiometers used on aircraft p 467 A92-32062
Visual photometric experiment data processing system
[AD-A248657] p 729 N92-27964

RADIOMETRIC CORRECTION
Radiometric properties of the NS001 Thematic Mapper Simulator aircraft multispectral scanner p 155 A92-17110
Modifications to and data correction methods for some radiometers used on aircraft p 467 A92-32062

RADIOSONDES
Digital ozonesondes - Examples of results from the EMEFS experiments of 1988 and 1990 p 468 A92-32140
A comparison of measured and modeled broadband fluxes from aircraft data during the ICE '89 field experiment p 1003 A92-49771

RADOMES
Finite element analysis of large wavelength antenna radome problems for leading edge and radar phased arrays p 267 A92-23984
The design and operational characteristics of a heated *radome for air motion measurement* p 467 A92-32064
Flow visualization and wake analysis for standard and modified configurations of the AN/ALQ-78 antenna pod
[AD-A243552] p 260 N92-17339

RAIL TRANSPORTATION
Electronic systems in transportation
[TP-9983] p 189 N92-14009
Bibliography of technical reports, 1980 - 1990
[PB92-110691] p 417 N92-18814
Aircraft gas turbine emissions: Their nature, technology for reduction, and a pollution comparison with channel tunnel transport
[ETN-92-91056] p 559 N92-22406
Aerodynamic drag on the bullet trains p 766 N92-26911

RAIN
A summary of NASA research on effects of heavy rain on airfoils p 452 N92-21694
The measurement of water film thickness on airfoils in heavy rain conditions using conductance sensors p 452 N92-21695
Experimental investigation of heavy rainfall effect on a 2-D high lift airfoil p 452 N92-21696
Radar multipath study for rain-on-radome experiments at the Aircraft Landing Dynamics Facility
[NASA-TM-101657] p 680 N92-25137
Wind tunnel aerodynamic characteristics of a transport-type airfoil in a simulated heavy rain environment
[NASA-TP-3184] p 948 N92-31532

RAIN GAGES
Observation and comparison of rainfall measured at a high sample rate p 505 A92-32073

RAMAN SPECTRA
Measurement of scalar flowfield at exit of combustor sector using Raman diagnostics
[AIAA PAPER 92-3350] p 894 A92-48927
Laser-spectroscopic measurement techniques for hypersonic, turbulent wind tunnel flows
[NASA-TM-103928] p 405 N92-19596

RAMAN SPECTROSCOPY
CARS temperature/multi-species measurement strategies for high speed airbreathing and rocket propulsion testing p 154 A92-16615
Simultaneous coherent anti-Stokes Raman spectroscopy measurements in hydrogen-fueled supersonic combustion p 287 A92-21052
CARS temperature measurements and validation of a computing code on a gas-turbine combustor
[ONERA, TP NO. 1991-224] p 373 A92-26376
Rotational coherent anti-Stokes Raman spectroscopy measurements in a rotating cavity with axial throughflow of cooling air - Oxygen concentration measurements p 990 A92-49574
CARS temperature measurements in a hypersonic propulsion test facility p 140 N92-12049
Fractal image compression of Rayleigh, Raman, LIF and LDV data in turbulent reacting flows
[AD-A246960] p 767 N92-27352

RAMJET ENGINES
Numerical simulations of unsteady reactive flows in a combustion chamber p 39 A92-11761
Thermodynamic behaviour of hydrogen-powered hypersonic ramjets flying along ideal trajectories
[IAF PAPER 91-277] p 25 A92-12601
Fuel injection in hypersonic airbreathing engine
[IAF PAPER 91-273] p 120 A92-14710
Low-frequency pressure oscillations in a model ramjet combustor p 154 A92-16026
CARS temperature/multi-species measurement strategies for high speed airbreathing and rocket propulsion testing p 154 A92-16615
One-dimensional analysis of liquid-fueled combustion instability p 143 A92-17188
Thrust nozzle test facility at DLR Cologne
[AIAA PAPER 91-5024] p 206 A92-17818
Hypersonic airbreathing propulsion activities for Saenger
[AIAA PAPER 91-5040] p 200 A92-17828
Investigation of hypersonic ramjet propulsion cycles using a ram accelerator test facility
[IAF PAPER 91-275] p 278 A92-22482
Influence of air liquefaction cycle on performance of combined cycle engine p 372 A92-24878
A numerical study of secondary fuel injection techniques for active control of combustion instability in a ramjet
[AIAA PAPER 92-0777] p 374 A92-27114
Premixed, turbulent combustion of axisymmetric sudden expansion flows p 397 A92-27770
Numerical simulation of two incoming streams in a dual-combustion ramjet combustor p 375 A92-28419
Calculation of combustion efficiency of dump combustor in ramjet engine p 375 A92-28460
Flame sheet algorithm for use in numerical modeling of ramjet combustion instability p 390 A92-28503
Computational studies of a superdetonative ram accelerator mode p 399 A92-28529
Experimental investigation on the mechanism of flame stabilization in afterburner with V-gutter flameholder p 487 A92-29725
Wide-range combustion chamber of ramjet
[AIAA PAPER 91-5094] p 472 A92-31696
Applications of Busemann inlet designs for flight at hypersonic speeds
[AIAA PAPER 92-1210] p 517 A92-33314
An experimental investigation of the swirling combustor for integral liquid fuel ramjet p 557 A92-35541
Experimental investigation on performances of two-dimensional inlet at supersonic speed p 519 A92-35544
Perspective on future aircraft engines p 558 A92-35921
Swirl and fuel composition effects on boron combustion in solid-fuel ramjets p 668 A92-36964
Similarity and scale effects in solid-fuel ramjet combustors p 666 A92-36965
Solid-fuel ramjet fuel regression rate/thrust modulation p 666 A92-36966
Generalities on the ramjet p 736 A92-41819
The turbo-ramjet Griffon p 782 A92-41820
New ramjet configurations p 736 A92-41822
Fuel regression mechanism in a solid fuel ramjet p 860 A92-44898
High spatial resolution measurements of ram accelerator gas dynamic phenomena
[AIAA PAPER 92-3244] p 903 A92-48844
Expansion tube experiments for the investigation of ram-accelerator-related combustion and gasdynamic problems
[AIAA PAPER 92-3246] p 904 A92-48845
Progress towards the development of transient ram accelerator simulation as part of the U.S. Air Force Armament Directorate Research Program
[AIAA PAPER 92-3248] p 904 A92-48847
Numerical simulations of the transdetonative ram accelerator combusting flow field on a parallel computer
[AIAA PAPER 92-3249] p 894 A92-48848
Mixing and combustion effects in a sliding-wedge ram accelerator with hydrogen injection
[AIAA PAPER 92-3251] p 890 A92-48849
Combustion of solid fueled ramjet. I
[AIAA PAPER 92-3727] p 894 A92-49105
Combustion of solid fueled ramjet. II
[AIAA PAPER 92-3728] p 894 A92-49106
A study of the flammability limit of the backward facing step flow combustion
[AIAA PAPER 92-3846] p 895 A92-49136
Development study on air turbo-ramjet engine for space plane p 1065 A92-53487
A preliminary study of a supersonic wind tunnel for a ram jet test facility p 1089 A92-53564
Turbulent combustion modelling in a side dump ramjet combustor
[AIAA PAPER 92-3599] p 1112 A92-54075
Ceramic regenerator program
[NASA-CR-189053] p 225 N92-14374
Engine panel seals for hypersonic engine applications: High temperature leakage assessments and flow modelling
[NASA-TM-105260] p 298 N92-16336
Hydrogen fueled subsonic-ram-combustor model tests for an air-turbo-ram engine
[NAL-TR-1064T] p 280 N92-17855
A hierarchy for modeling high speed propulsion systems
[NASA-CR-186984] p 387 N92-19934
Transport phenomena and interfacial kinetics in multiphase combustion systems
[AD-A244849] p 489 N92-20695
Advanced ramjet concepts program p 474 N92-21520
Supercharged ejector ramjet p 475 N92-21527
H2 fueled flightweight ramjet construction and test p 475 N92-21531
Symposium on High Speed Airbreathing Propulsion: The Solid Fuel Combustion Chamber and Beyond
[ETN-92-90685] p 575 N92-22268
A hierarchy for modeling high speed propulsion systems p 559 N92-22492
NASA thrusts in high-speed aeropropulsion research and development: An overview p 561 N92-22538
Solid fuel ramjet infrared signature
[AD-A246299] p 753 N92-26362
Collection of papers of the 31st Israel Annual Conference on Aviation and Astronautics
[ITN-92-85124] p 932 N92-31861

RAMPS (STRUCTURES)
EH101 helicopter development p 112 A92-16060
Single expansion ramp nozzle simulations
[AIAA PAPER 92-0387] p 323 A92-26243
Investigation of a plate-ramp-configuration by means of laser Doppler anemometry at Mach 2.95
[AIAA PAPER 92-3956] p 1097 A92-56784
United States Navy ski jump experience and future applications p 465 N92-21968

RANDOM ACCESS
Aircraft satellite communication systems p 1046 A92-56091

RANDOM ACCESS MEMORY
Ferroelectric memory evaluation and development system p 902 A92-48460

RANDOM ERRORS
On the calculation of repeatable accuracy, with special reference to GPS p 955 A92-49383

RANDOM LOADS
Numerical simulation of VAWT stochastic aerodynamic loads produced by atmospheric turbulence: VAWT-SAL code
[DE92-000597] p 229 N92-15392

RANDOM NOISE
Probability of cycle jumps in Omega receivers and other phase locked loop applications
[PB92-128891] p 455 N92-21279
Comparison of three controllers applied to helicopter vibration
[NASA-TM-102192] p 878 N92-28457

RANDOM PROCESSES
Proposal for a 3-D, vectorized, adaptable, algorithm for modeling the randomness, unsteadiness, and microphysical properties of ice accretion
[AIAA PAPER 92-0299] p 351 A92-25751
Rarefaction wave eliminator design study
[AD-A244401] p 484 N92-20455

RANDOM VIBRATION
Modal identification in the presence of steady excitation p 131 A92-13693

Experimental study of a two-dimensional random frequency generator p 483 A92-29712
Response of plate-like structures to correlated random pressure fluctuations
[AIAA PAPER 92-2378] p 584 A92-34452

RANGE (EXTREMES)
Passive acoustic range estimation of helicopters
[AD-A248033] p 926 N92-28302

RANGE ERRORS
Receiver Autonomous Integrity Monitoring (RAIM) capability for sole-means GPS navigation in the oceanic phase of flight p 956 A92-51012

RANGEFINDING
Synthesis of the algorithm of a spatial-temporal discriminator and the potential accuracy of the velocity meter p 41 A92-12828
Compensating user position for GPS ephemeris error p 101 A92-16968
Vision-based stereo ranging as an optimal control problem
[AIAA PAPER 92-4418] p 1045 A92-55211
Passive range estimation for rotorcraft low-altitude flight
[NASA-TM-103897] p 2 N92-10003
Image-based ranging and guidance for rotorcraft
[NASA-CR-184829] p 191 N92-14036
A method of passive range determination using only two bearing measurements
[AD-D015182] p 455 N92-20834
Development of a helicopter-borne 8-channel ranging scatterometer
[PB92-141977] p 599 N92-23441
Passive acoustic range estimation of helicopters
[AD-A248033] p 926 N92-28302
A rotorcraft flight database for validation of vision-based ranging algorithms
[NASA-TM-103906] p 841 N92-29103
Compact range test applications, phase 2
[AD-A248790] p 999 N92-30583
Vision-based range estimation using helicopter flight data
[NASA-TM-103930] p 1047 N92-32424

RANKINE CYCLE
General performance characteristics of real heat engine p 1011 A92-50401
Small engine technology programs p 560 N92-22532
Study of potassium turbine electric generator system p 1129 N92-33794

RANKINE-HUGONIOT RELATION
Computation and stability analysis of laminar flow over a blunt cone in hypersonic flow p 1041 N92-33839

RAPID QUENCHING (METALLURGY)
The microstructural stability of TiC reinforced rapidly solidified Al-Fe-V-Si composite structures p 141 A92-15169
Inertia-friction welding of an advanced rapidly solidified titanium alloy p 212 A92-18898
Research and development of aircraft engine materials p 577 A92-35916

RAPID TRANSIT SYSTEMS
Preliminary structural sizing of a Mach 3.0 high-speed civil transport model
[NASA-CR-189631] p 685 N92-25960
Aerodynamic drag on the bullet trains p 766 N92-26911
NASA High Speed Research Program, Emissions Scenarios Committee report of meetings on 26 September 1991 and 9 January 1992
[NASA-CR-190379] p 1004 N92-32147

RARE GASES
Thermoacoustic refrigeration p 595 N92-22720

RAREFIED GAS DYNAMICS
Flat-ended circular cylinder in hypersonic rarefied flow p 174 A92-20304
Effects of gas-surface interaction models on aerodynamic characteristics p 244 A92-21718
Hypersonic flow simulations using DSMC (direct simulation Monte Carlo) p 323 A92-26216
Monte Carlo simulation of reentry flows with ionization
[AIAA PAPER 92-0493] p 328 A92-26323
Hypersonic rarefied flow past spheres including wake structure
[AIAA PAPER 92-0495] p 329 A92-26325
Effect of rarefaction on the nonstationary interaction of a supersonic underexpanded jet with a perpendicular obstacle p 337 A92-27594
Local bridging to predict aerodynamic coefficients in hypersonic, rarefied flow p 705 A92-41541
Flow of a rarefied gas over a cylinder at angle of sideslip p 708 A92-42738
Direct simulation of hypersonic rarefied flows about atmospheric re-entry vehicles p 710 A92-43169
Direct simulation of re-entry flows with ionization p 713 A92-44367
Aerothermodynamics of a 1.6-meter-diameter sphere in hypersonic rarefied flow p 808 A92-45840
Hypersonic rarefied flow about a delta wing - direct simulation and comparison with experiment p 812 A92-46892
Numerical and experimental investigation of rarefied compression corner flow
[AIAA PAPER 92-2900] p 820 A92-47876
Flow of a rarefied gas past a two-dimensional body of an arbitrary shape at small Mach numbers p 937 A92-52726
Hypersonic flow calculations around a 3D delta wing at low Knudsen numbers p 937 A92-52734
Heat transfer to a delta wing and two waverider wings in rarefied hypersonic flow p 937 A92-52748
Influence of atmospheric rarefaction on aerodynamic characteristics of flying vehicles p 938 A92-52750
One-dimensional kinetic model for flows near a stagnation point of a highly cooled body in hypersonic rarefied streams p 938 A92-52751
Influence of internal molecular degrees of freedom on the hypersonic rarefied gas flow about a conical body p 938 A92-52752
Rarefied gas flow around a disc with different angles of attack p 938 A92-52753
Approximate aerodynamic analysis for complicated bodies in rarefied gas flows p 938 A92-52754
Experiments on separation at a compression corner in rarefied hypersonic flows p 938 A92-52755
Enhancements and applications of DSMC for hypersonic rarefied flows p 939 A92-52761
Rarefied gas numerical wind tunnel p 995 A92-52763
Force and heat transfer on a disc in rarefied flow p 939 A92-52764
Direct simulation of vortex shedding in dilute gas flows past bluff bodies p 939 A92-52766
Aerodynamics of complex shape bodies within a wide range of supersonic flows of rarefied gases p 939 A92-52767
DSMC simulation of hypersonic flows past 2-dimensional bodies p 939 A92-52772
Application of the DSMC method to hypersonic flow about a delta wing p 940 A92-52775
Numerical and experimental investigations of rarefied gas flows through nozzles and composite systems p 940 A92-52797
Application of a parallel direct simulation Monte Carlo method to hypersonic rarefied flows p 1024 A92-54916
Test facilities and instrumentation for research in rarefied gas dynamics - An historical perspective
[AIAA PAPER 92-3969] p 1098 A92-56795
A new technique for temperature and specie concentration measurements in unseeded supersonic and hypersonic gas flows
[AD-A241536] p 158 N92-13409
Transitional flows around re-entry bodies p 184 N92-15035
Institute for experimental fluid mechanics: Results for 1990
[IB-222-90-A-46] p 400 N92-18244
Rarefied-flow aerodynamics
[NASA-CR-190452] p 715 N92-27191

RAREFIED GASES
The problem of transition from continuum to rarefied gas flows p 251 A92-22519
CFD state-of-the-art in the U.S.S.R p 495 A92-31486
Rarefied gas numerical wind tunnel p 1017 A92-53552
Rarefied gas research at Berkeley - Current studies and future potentials
[AIAA PAPER 92-3971] p 1098 A92-56797
Applicability of bridging methods to hypersonic rarefied flow aerodynamics of reentry vehicles p 184 N92-15032
Low density real gas flows about hypersonic vehicles
[AD-A250048] p 949 N92-31777

RASTER SCANNING
The C-17 Multifunction Display - A building block for avionic systems p 1063 A92-55907

RATINGS
Profile of an effective engineering manager
[AD-A246525] p 781 N92-27528
Assessment of army aviators' ability to perform individual and collective tasks in the aviation networked simulator
[AD-A250293] p 888 N92-29709

RAY TRACING
Finite element analysis of large wavelength antenna radome problems for leading edge and radar phased arrays p 267 A92-23984

RAYLEIGH SCATTERING
Rayleigh imaging and flow tagging in ground test facilities p 1115 A92-54330
Shock enhancement and control of hypersonic combustion
[AD-A248558] p 896 N92-29580

RAYLEIGH-RITZ METHOD
Coupled Rayleigh-Ritz/finite element structural analysis using penalty function method
[AIAA PAPER 92-2238] p 581 A92-34292
A Rayleigh-Ritz design methodology for cutouts in composite structures
[AIAA PAPER 92-2278] p 582 A92-34297
Combined compressive and shear buckling analysis of hypersonic aircraft sandwich panels
[AIAA PAPER 92-2487] p 586 A92-34603
The use of Stodola modes in rotor-blade aeroelastic studies p 590 A92-35729
Inclusion principle for the Rayleigh-Ritz based substructure synthesis p 670 A92-36851
On the three-dimensional vibration analysis of simultaneously skewed and twisted cantilevered parallelepipeds p 759 A92-41801
Continuation of tailored composite structures of ordered staple thermoplastic material
[NASA-CR-189671] p 1110 N92-33613

REACTING FLOW
Numerical simulations of unsteady reactive flows in a combustion chamber p 39 A92-11761
Thermal details in a rotor-stator cavity at engine conditions with a mainstream
[ASME PAPER 91-GT-275] p 151 A92-15672
Three-dimensional calculations of reactive flows in aircraft combustion chambers performed using two combustion models
[ONERA, TP NO. 1991-110] p 154 A92-16089
A computational investigation of mixing and reacting flows in supersonic combustors
[AIAA PAPER 92-0626] p 278 A92-23817
Hypersonic waveriders - Effects of chemically reacting flow and viscous interaction
[AIAA PAPER 92-0302] p 320 A92-25754
A numerical investigation of hydrogen combustion in Mach 2 flow
[AIAA PAPER 92-0341] p 388 A92-25787
An iodine hypersonic wind tunnel for the study of nonequilibrium reacting flows
[AIAA PAPER 92-0566] p 383 A92-26974
Finite-element algorithm for chemically reacting hypersonic flow
[AIAA PAPER 92-0754] p 336 A92-27097
Similarity and scale effects in solid-fuel ramjet combustors p 666 A92-36965
An exploration of chemically reacting viscous hypersonic flow p 612 A92-37550
Direct simulation of a supersonic reacting mixing-layer p 676 A92-40132
Reactive mixing layer between pressure reflecting boundaries p 656 A92-40144
Hybrid Navier-Stokes/Monte Carlo method for reacting flow calculations p 705 A92-41537
Hypersonic plasma predictions at nonzero angle of attack
[AIAA PAPER 92-3027] p 925 A92-47028
Computation of hypersonic flowfields in thermal and chemical nonequilibrium
[AIAA PAPER 92-2874] p 819 A92-47856
Progress towards the development of transient ram accelerator simulation as part of the U.S. Air Force Armament Directorate Research Program
[AIAA PAPER 92-3248] p 904 A92-48847
A simplified reaction mechanism for prediction of NO(x) emissions in the combustion of hydrocarbons
[AIAA PAPER 92-3340] p 894 A92-48919
Detailed numerical analysis of standing oblique detonation p 1111 A92-53550
Efficient methods for inviscid non-equilibrium hypersonic flow fields p 1024 A92-54571
A code validation strategy and facility for nonequilibrium, reacting flows
[AIAA PAPER 92-3970] p 1098 A92-56796
CARS temperature measurements in a hypersonic propulsion test facility p 140 N92-12049
Interferograms, schlieren, and shadowgraphs constructed from real- and ideal-gas, two- and three-dimensional computed flowfields
[NASA-CR-190054] p 446 N92-21356
Fractal image compression of Rayleigh, Raman, LIF and LDV data in turbulent reacting flows
[AD-A246960] p 767 N92-27352
Three dimensional calculations of reactive flows within aircraft combustion chambers including some combustion models p 770 N92-27490
Modeling of the reactant conversion rate in a turbulent shear flow p 829 N92-28820
Turbulent reacting flows and supersonic combustion
[AD-A251065] p 986 N92-30256

Development of a 3-D upwind PNS code for chemically reacting hypersonic flowfields
[NASA-CR-190182] p 946 N92-30977
Stagnation-point heat-transfer rate predictions at aeroassist flight conditions
[NASA-TP-3208] p 1001 N92-31281
An approximate viscous shock layer technique for calculating chemically reacting hypersonic flows about blunt-nosed bodies p 1041 N92-33837

REACTION CONTROL
The application of high pressure ejectors to reaction control systems p 128 A92-16666
A shock tunnel experiment on aerodynamic interference induced by RCS jet p 1029 A92-56042

REACTION KINETICS
H2/air subsystem combustion kinetics in aerospaceplane powerplants
[IAF PAPER 91-276] p 25 A92-12600
Engineering model for analysis of scramjet combustor performance with finite-rate chemistry
p 129 A92-17202
Rate parameters for coupled vibration-dissociation in a generalized SSH approximation --- Schwarz, Slawsky, and Herzfeld p 235 A92-20301
Diagonal implicit scheme for computing flows with finite rate chemistry p 488 A92-32253
Evaluation of NO(x) mechanisms for lean, premixed combustion
[ASME PAPER 91-GT-257] p 668 A92-36900
An exploration of chemically reacting viscous hypersonic flow p 612 A92-37550
Fuel regression mechanism in a solid fuel ramjet
p 860 A92-44898
A simplified reaction mechanism for prediction of NO(x) emissions in the combustion of hydrocarbons
[AIAA PAPER 92-3340] p 894 A92-48919
Experimental and computational investigation of scaling phenomena in a large caliber ram accelerator
[AIAA PAPER 92-3245] p 1103 A92-54019
Flow contamination and flow quality in arc heaters used for hypersonic testing
[AIAA PAPER 92-4028] p 1100 A92-56850
Linear acoustics in gas mixtures with rate processes
p 238 N92-15013
Hypersonic viscous shock layer in thermochemical nonequilibrium p 183 N92-15014
Influence of chemical modeling on the solution of hypersonic shock layers p 183 N92-15016
Numerical simulation of thermochemical non-equilibrium viscous flows around reentry bodies
p 227 N92-15029
Reaction speed constant for the reactions between N + O2 and between O + N2
[ETN-92-90861] p 347 N92-19252
Simulation of chemical kinetics in turbulent natural gas combustion
[PB92-123660] p 488 N92-20329
The coherent flamelet model for propulsion applications p 756 N92-27486
An analysis of combustion studies in shock expansion tunnels and reflected shock tunnels
[NASA-TP-3224] p 895 N92-28374
Influence of the swirl producing construction in the flow and reaction field of turbulent diffusion flames
[ETN-92-92103] p 1127 N92-33916

READING
Design considerations for IAP charts: Approach course track and communication frequencies
[AD-A241482] p 103 N92-13051

READOUT
The utility of analog vertical velocity information during instrument flight with a Head-Up Display (HUD)
[AD-A252863] p 1065 N92-33277

REAL GASES
Compressible laminar boundary layers for perfect and real gases in equilibrium at Mach numbers to 30
[AIAA PAPER 92-0757] p 336 A92-27099
Calculation of real-gas effects on blunt-body trim angles p 432 A92-31169
Numerical simulations of hypersonic real-gas flows over space vehicles
[SAE PAPER 912045] p 791 A92-45429
A fine-wire thermocouple probe for measurement of stagnation temperatures in real gas hypersonic flows of nitrogen p 1114 A92-54317
Experimental simulation and diagnostics of high-enthalpy real-gas flows
[AD-A241286] p 166 N92-13822
Equilibrium solution of the Euler and Navier-Stokes equations around a double ellipsoidal shape with mono- and multi-blocks including real gas effects, part 1
p 227 N92-15030
Simulation of real-gas effects on pressure distributions for aeroassist flight experiment vehicle and comparison with prediction
[NASA-TP-3157] p 501 N92-20677
Interferograms, schlieren, and shadowgraphs constructed from real- and ideal-gas, two- and three-dimensional computed flowfields
[NASA-CR-190054] p 446 N92-21356
Computational Fluid Dynamics --- numerical methods and algorithm development
[NASA-CP-10078] p 660 N92-25808
A new Lagrangian method for real gases at supersonic speed p 633 N92-25814
Modeling of heavy-gas effects on airfoil flows
[NASA-CR-190357] p 716 N92-27558
Second-order shock-expansion theory extended to include real gas effects
[AD-A247191] p 831 N92-29539
Low density real gas flows about hypersonic vehicles
[AD-A250048] p 949 N92-31777

REAL TIME OPERATION
A new class of gradient estimators for queueing systems with real-time constraints p 49 A92-11395
On-line state estimation and parameter identification for flight p 50 A92-11429
A novel associative memory for high level control functions p 52 A92-11472
Real-time estimation of gas turbine engine damage using a control based Kalman filter algorithm
[ASME PAPER 91-GT-216] p 124 A92-15633
Real-time microfocus radiography for electronic failure analysis p 214 A92-17289
Case for real-time systems development - Quo vadis?
[AIAA PAPER 91-3726] p 231 A92-17594
A processor-in-the-loop simulation using an XANALOG computer p 232 A92-19094
A new 1553 all-bus instrumentation monitor
p 198 A92-19252
An integrated real-time turbine engine flight test system p 201 A92-19275
Reconfigurable Mobile System - Ground, sea and air applications p 218 A92-19986
Realistic real-time ground testing
[AIAA PAPER 92-0197] p 284 A92-23805
Expert system for real-time aircraft monitoring
p 410 A92-24411
A simplified method of transient mathematical model for non-augmentation engine p 372 A92-24750
Real-time decision aiding - Aircraft guidance for wind shear avoidance
[AIAA PAPER 92-0290] p 350 A92-25743
Smart structures - A damage detection concept
p 491 A92-28672
A new approach to the real-time simulation of control systems with discontinuities p 508 A92-29291
Real-time simulation and adaptive PID control of QSK-06A control for gas turbine p 470 A92-29740
An investigation of real-time diagnostic technique for DEEC system --- digital electronic engine control system
p 470 A92-29742
On modelling of aero-gas turbine engine for real-time digital simulator --- of engine control system
p 471 A92-29743
A real-time rain-flow method of cycle counting and its program design for aeroengine service loads
p 557 A92-35560
A system for precise real-time differential GPS positioning in the decimeter range p 638 A92-39569
Microwave landing system modeling with application to air traffic control automation p 725 A92-41220
STOL research aircraft Asuka flight analysis in connection with the operation of the monitoring system
p 730 A92-43140
Parallel solver for trajectory optimization search directions p 777 A92-43399
Real-time control tower simulation for evaluation of airport surface traffic automation p 879 A92-44976
Simulation of triple simultaneous parallel ILS approaches p 880 A92-45025
The development of a real time visual flight simulator for tactical operations research and measurement
p 880 A92-45027
Construction of a real-time DGPS experimental system
p 840 A92-47631
A simplified real-time engine model for developing aeroengine control system
[AIAA PAPER 92-3321] p 864 A92-48904
Specifying exhaust nozzle contours in real-time using genetic algorithm trained neural networks
[AIAA PAPER 92-3328] p 865 A92-48911
The Office of Naval Research initiative on ultradependable multicomputers and electronic systems
p 1005 A92-49278
An integrated analysis and simulation tool for avionics system development p 1005 A92-49289
A fault-tolerant network architecture for integrated avionics p 965 A92-49297
Artificial intelligence techniques applied to vehicle management system diagnostics p 965 A92-49315
Route planning --- in real-time of avionics systems
p 1006 A92-49317
Verification and validation testing of the pilot's associate p 966 A92-49318
JTIDS relative navigation and data registration
p 955 A92-51006
Development of a real-time simulation of a ship-correlated airwake model interfaced with a rotorcraft dynamic model
[AIAA PAPER 92-4149] p 1007 A92-52440
High performance flight simulation at NASA Langley
[AIAA PAPER 92-4179] p 982 A92-52460
Recent developments in data acquisition and control systems at the Aircraft Research Association Limited
p 1091 A92-54323
Signal processing schemes for Doppler global velocimetry p 1115 A92-54338
Fault diagnostics on jet engine starting
p 1116 A92-54345
A general approach to optimal real-time guidance of dynamic systems based on nonlinear programming
[AIAA PAPER 92-4378] p 1131 A92-55182
Real-time helicopter simulation using the blade element method p 1132 A92-56278
A simulation study of tiltrotor vertical takeoff procedures *using conventional and variable diameter rotor systems*
p 1056 A92-56301
HEPO mission simulator - Development and usage for NH90 helicopter p 1094 A92-56313
Feasibility of using a knowledge-based system concept for in-flight primary flight display research
[NASA-TM-4279] p 17 N92-10017
Real-time fault diagnosis for propulsion systems
[NASA-TM-105303] p 26 N92-11017
Real Time Data System (RTDS) p 140 N92-12025
Ames life science telescience testbed evaluation
[NASA-CR-188856] p 140 N92-12033
Process/object-oriented Ada software design for an experimental helicopter p 164 N92-12461
A NASA/RAE cooperation in the development of a real-time knowledge based autopilot
p 164 N92-12528
AI for RPVs, Sensor Driven Airborne Replanner (SDAR), for a Robotic Aircraft Sensor Platform (RASP)
p 114 N92-12534
Engineering Graphical Analysis Tool (EGAT) development program p 164 N92-12542
Background issues for on-line aircraft documentation
p 119 N92-13858
Image-based ranging and guidance for rotorcraft
[NASA-CR-184829] p 191 N92-14036
Rapid near-optimal aerospace plane trajectory generation and guidance
[NASA-CR-189469] p 205 N92-14066
Technical evaluation report on the 52nd Symposium on Software for Guidance and Control
[AGARD-AR-302] p 303 N92-17498
Development of nonlinear real-time helicopter simulation using a blade element method
[NLR-TP-90115-U] p 381 N92-18893
JPL's Real-Time Weather Processor project (RWP) metrics and observations at system completion
p 413 N92-19428
Cockpit weather information needs
p 449 N92-21503
Application of technology developed for flight simulation at NASA. Langley Research Center p 573 N92-22437
State and time granularity in system description: An example
[REPT-91-040] p 603 N92-22673
NASA's GPS tracking system for Aristoteles
p 576 N92-23919
Delfi: Design, development, and applicability of expert systems shells
[ISBN-90-6275-734-0] p 692 N92-25306
Expert system management system
[AD-A247102] p 781 N92-26863
Status of automatic guidance systems for rotorcraft in low altitude flight p 727 N92-27894
Trajectory optimization for hypersonic aircraft guidance p 728 N92-27898
Parallel knowledge based systems architectures for in-flight mission management p 728 N92-27904
Robust intelligent flight control for hypersonic vehicles
[NASA-CR-185680] p 746 N92-28209
NPSNET: Flight simulation dynamic modeling using quaternions
[AD-A247484] p 923 N92-28245
A radar signal processing ASIC and a VME interface circuit p 859 N92-28380
The role of simulation for the study of APIS (piloting support by synthetic imagery) p 885 N92-28544
NARSIM: A real-time simulator for air traffic control research
[NLR-TP-90147-U] p 888 N92-29204

A model of the ADA avionics real-time system: An example of the benefits of the hardware/software codesign approach in development of real-time systems
[AD-A248893] p 967 N92-30524
On-line analysis capabilities developed to support the AFW wind-tunnel tests
[NASA-TM-107651] p 961 N92-30752
Repetitive High Energy Pulsed Power (RHEPP) temperature monitoring system utilizing Luxtron fluoroptic sensors and thermocouples technical reference manual
[DE92-013461] p 999 N92-30893
System overview of the NASA Dryden Integrated Test Facility
[NASA-TM-104250] p 984 N92-32201
The multiple-function multi-input/multi-output digital controller system for the AFW wind-tunnel model
[NASA-TM-107600] p 1060 N92-32536
Real-time processing of radar return on a parallel computer
[NASA-CR-4456] p 1043 N92-32606
The development of an airborne information management system for flight test
[NASA-TM-104251] p 1065 N92-32866
Rapid development of the X-31 simulation to support flight-testing
[NASA-TM-104256] p 1060 N92-33149
Distributed systems: Interconnection and fault tolerance studies
[AD-A252869] p 1135 N92-33920
Piloted evaluation of an integrated propulsion and flight control simulator
[NASA-TM-105797] p 1088 N92-34107

REATTACHED FLOW
The just attached shock-wave at the leading edge of a profile p 3 A92-10663
The dynamics and control of fluctuating pressure loads in the reattachment region of a supersonic free shear layer
[AIAA PAPER 92-0178] p 255 A92-23788
Computation of saddle point of attachment p 703 A92-41276
Supersonic flow over an axisymmetric backward-facing step p 705 A92-41542
Predictions of a turbulent backward-facing-step flow with a cubic pressure-strain model
[AIAA PAPER 92-2647] p 796 A92-45514
A numerical study of the stability of the swept attachment line boundary layer
[AERO-REPT-9103] p 345 N92-18293
Visualization of boundary-layer development on turbomachine blades with liquid crystals
[NASA-CR-190433] p 742 N92-27519
The calculation of incompressible separated turbulent boundary layers p 1003 N92-31886

RECEIVERS
GPS interferometric attitude and heading determination: Initial flight test results p 269 N92-17994
Measurement of LORAN-C envelope to cycle difference in the far field
[PB92-128909] p 455 N92-21263
The Air Force Manufacturing Technology (MANTECH): Technology transfer methodology as exemplified by the radar transmit/receive module program p 593 N92-22451
Effect of guard band reduction on marker beacon receiver performance
[DOT/FAA/CT-TN92/18] p 1002 N92-31617

RECIPROCATION
Benchmark performance analysis of an ECM-modulated air-to-air heat pump with a reciprocating compressor
[DE92-004478] p 500 N92-20341

RECIPROCITY THEOREM
Evaluation of sound transmission into aircraft fuselages by a reciprocity technique p 694 A92-39086

RECIRCULATIVE FLUID FLOW
Isothermal modeling of gas turbine combustors - Computational study p 129 A92-17203
Numerical simulation of interaction of diffusion flame with vortex pair in a recirculation zone p 390 A92-28433
Flow visualization and flow field measurements of a 1/12 scale tilt rotor aircraft in hover
[NASA-CR-189456] p 82 N92-11983

RECOGNITION
Sensor fault detection on board an aircraft with observer and polynomial classifier
[DLR-FB-91-34] p 859 N92-29870

RECOMMENDATIONS
A report on enhancements for existing and future helicopters supporting operations of the Canadian oil and gas industry
[CTN-91-60126] p 636 N92-25350
Aviation safety: Changes needed in FAA's service difficulty reporting program
[GAO/RCED-91-24] p 953 N92-31453
Canadian aircrew sea water survival, 1952-1987
[DCIEM-88-RR-39] p 954 N92-32219

RECONNAISSANCE
The rise of active-element phased-array radar
[RAND-P-7747-RGS] p 999 N92-30755

RECONNAISSANCE AIRCRAFT
RAH-66 Comanche - A cut above the rest p 61 A92-16675
ES-3A flight test program
[AIAA PAPER 92-1230] p 538 A92-33327
An analysis tool for UAV effectiveness evaluation p 608 A92-40386
Control strategy for maximizing reconnaissance range of hypersonic cruise vehicles p 729 A92-41222
Using satellite communication for aircraft Automatic Dependent Surveillance p 725 A92-42486
Avionics systems development: Technological trends, conflicts, and cost issues in a changing European environment p 199 N92-14054
Reduction and analysis of F-111C flight data
[AD-A250341] p 853 N92-28771

RECONSTRUCTION
Reconstruction of flight path in turbulence p 874 A92-46777
Efficient high-resolution rotor wake calculations using flow field reconstruction p 814 A92-46951

RECORDING HEADS
Double Density recording acquisition and playback p 920 A92-47534

RECOVERABILITY
Conceptual design of two-stage-to-orbit hybrid launch vehicle
[NASA-CR-190006] p 486 N92-20666

RECOVERABLE SPACECRAFT
Attributes of winged manned space vehicles and their relationship to ground site characteristics and facilities p 487 N92-20776

RECOVERY PARACHUTES
Landing spacecraft gently on earth - The Soviet parachute systems p 33 A92-13227
Parachute canopy control simulation - A solution for aircrew emergency training p 572 A92-35428

RECTANGULAR PANELS
Processing parameters for carbon/PMR-15 composite flat panels p 34 A92-11812
Application of a local panel buckling constraint within automated multidisciplinary structural analysis and design
[AIAA PAPER 92-1116] p 537 A92-33271
Research on sonic fatigue calculation and test for aircraft panel p 958 A92-50203

RECTANGULAR PLANFORMS
Dynamic characteristics of a Benchmark models program supercritical wing
[AIAA PAPER 92-2368] p 571 A92-34596

RECTANGULAR PLATES
Forced vibration of rectangular laminated plates with material damping p 294 A92-23167
Response of symmetrically laminated rectangular plates subjected to heating p 296 A92-24186
Initial postbuckling response of an unsymmetrically laminated rectangular plate p 1108 N92-32586

RECTANGULAR WAVEGUIDES
Reflections off aircraft and the shape optimization of a ridged waveguide p 267 A92-23967

RECTANGULAR WIND TUNNELS
Flow analysis and design of three-dimensional wind tunnel contractions p 5 A92-11067
Flow analysis of rectangular wind tunnel contraction p 312 A92-25001

RECTANGULAR WINGS
Wing tip vortex calculations with an unstructured adaptive-grid Euler solver p 64 A92-14330
Nonlinear stall flutter and divergence analysis of cantilevered graphite/epoxy wings p 219 A92-20746
Aerodynamic characteristics of a wing near its tip using panel method p 251 A92-22524
Effect of viscous drag on optimum spanwise lift distribution
[AIAA PAPER 92-0287] p 319 A92-25740
Experimental investigation of the coefficients of the normal-force derivatives for rectangular wings with translational oscillations p 423 A92-30127
An approximate method for calculating flow past solid wings of small aspect ratio based on a nonlinear theory of a continuous vortex surface p 428 A92-30373
Flow past a highly curved wing with tangential jet ejection p 438 A92-31868
Viscous supersonic flow computations over a delta-rectangular wing with slanting surfaces p 441 A92-32178
Optimum structural design of a cantilevered rectangular elastic wing with a gust load alleviation system p 762 A92-43133
Aerodynamic characteristics near the tip of a finite wing by a panel method
[SAE PAPER 912020] p 790 A92-45413
LDV measurements in the three-dimensional near wake of a stationary and oscillating rectangular wind
[AIAA PAPER 92-2689] p 799 A92-45536
LDV measurements on a rectangular wing with a simulated glaze ice accretion
[AIAA PAPER 92-2690] p 800 A92-45537
Self-induced roll oscillations of low-aspect-ratio rectangular wings p 874 A92-46802
Computation of vortex wake flows and control of their effects on trailing wings
[AIAA PAPER 92-4429] p 1025 A92-55353
Aeroelastic effects of spoiler surfaces on a low-aspect-ratio rectangular wing p 1030 A92-56154
Effect of a simulated glaze ice shape on the aerodynamic performance of a rectangular wing
[AIAA PAPER 92-4042] p 1035 A92-56861
Unsteady aerodynamic calculations for general configurations by the double-point method
[NAL-TR-1101T] p 12 N92-10980
Experimental study of a vortex subjected to imposed strain
[NASA-CR-189757] p 258 N92-15969
An experimental study of a sting-mounted circulation control wing
[AD-A243912] p 346 N92-18895
Normal force of low aspect ratio wing-body combinations up to high angles of attack at supersonic speeds
[ESDU-91042] p 553 N92-24009
Pressure measurements on a rectangular wing with a NACA0012 airfoil during conventional flutter
[NASA-TM-104211] p 1042 N92-34147

RECTENNAS
Power beaming - Energy transmission at 35 GHz and higher frequencies --- for terrestrial and space applications with rectennas
[AIAA PAPER 92-2027] p 471 A92-29944

RECURSIVE FUNCTIONS
A horizon-recursive form for predictors and their computation p 50 A92-11427
Application of recursive partially unknown system identification to aerodynamic coefficients estimation
[AIAA PAPER 92-4504] p 1081 A92-55371

RECYCLING
Feasibility of systematic recycling of aircraft Halon extinguishing agents
[DOT/FAA/CT-91/21] p 352 N92-18259

REDUCED GRAVITY
Measurements and correlation of two-phase pressure drop under microgravity conditions p 37 A92-10435
The effectiveness of Coriolis dampening of convection during aircraft high-g arcs p 581 A92-33847
Forced-injection quenching of a hot-tube under microgravity p 590 A92-35977
Observational study of pool boiling under microgravity p 757 A92-41060
Boiling and condensing pumped loop microgravity experiment - Challenges of testing in both aircraft and rocket environments p 992 A92-50611
Experimental study of convection effects around the phase charge interface p 1111 A92-53755
Fundamental studies on Marangoni convection related to Bridgman crystal growth p 1111 A92-53758
Process modeling KC-135 aircraft
[NASA-CR-184278] p 359 N92-18347
Materials processing in low gravity
[NASA-CR-184280] p 499 N92-20198
Activities of NRC-CNRC, Institute for Aerospace Research, Flight Research Lab.
[CTN-92-60432] p 420 N92-20205
Microgravity nucleation and particle coagulation experiments support
[NASA-CR-190159] p 502 N92-21385
Microgravity nucleation and particle coagulation experiments support
[NASA-CR-189899] p 502 N92-21433
Outlines of parabolic flight p 764 N92-26441

REDUCED ORDER FILTERS
Reduced-order robust controllers - H(infinity)-balanced truncation and optimal projection p 48 A92-11363
Synthesis of a helicopter full-authority controller p 280 A92-21178
Open-loop model reduction and parameter perturbation for active flutter suppression system p 379 A92-24879

REDUNDANCY
Implementation of non-dedicated redundancy in a fault tolerant multiprocessor testbed --- flight control p 974 A92-49294
Redundancy design philosophy for catastrophic loss protection p 1119 A92-56202
Real-time fault diagnosis for propulsion systems
[NASA-TM-105303] p 26 N92-11017
An independent review of the Multi-Path Redundant Avionics Suite (MPRAS) architecture assessment and characterization report
[NASA-CR-188126] p 163 N92-12440

FCS skewed sensors array: Practical considerations
p 968 N92-31868
REDUNDANT COMPONENTS
Failure detection and identification for aircraft sensors
p 370 A92-27832
REELS
Inertia reels for aircrew restraint systems
p 529 A92-32982
REENTRY
Calculation of hypersonic, viscous, non-equilibrium flows around reentry bodies using a coupled boundary layer/Euler method
[AIAA PAPER 92-2856] p 819 A92-47839
Large thin composite thermostructural parts
p 576 N92-23821
Stretched skin concept for the entry aerodynamic decelerator system of planetary probes
p 576 N92-23836
Dynamics of aerospace shuttles p 667 N92-24760
REENTRY EFFECTS
Viscous shock-layer equations for the calculation of reentry aerothermodynamics p 183 N92-15008
Computational aerothermodynamic methods for industrial applications to re-entry and hypersonic cruise problems p 227 N92-15027
Reaction speed constant for the reactions between N + O2 and between O + N2
[ETN-92-90861] p 347 N92-19252
REENTRY GUIDANCE
FALKE: Winged re-entry vehicle flight control
p 667 N92-24454
REENTRY PHYSICS
Hypersonic flow simulations using DSMC (direct simulation Monte Carlo) p 323 A92-26216
REENTRY SHIELDING
Thermal protection analysis of Mars-earth return vehicles p 497 A92-32183
The IRS plasma wind tunnels for the investigation of thermal protection materials for reentry vehicles
p 208 N92-15009
REENTRY TRAJECTORIES
An efficient calculation method of subsonic aerodynamic characteristics for a Space Shuttle orbiter in the reentry attitude p 252 A92-23383
A transonic/supersonic/hypersonic CFD analysis of the entry Space Shuttle Orbiter
[AIAA PAPER 92-2614] p 805 A92-45571
Similarity relations for calculating three-dimensional chemically nonequilibrium viscous flows
p 827 A92-49188
Three-dimensional optimal reentry trajectory and aerodynamic heating history of the Space Shuttle
p 984 A92-49582
Optimal launch trajectory of a hypersonic research vehicle
[AIAA PAPER 92-4302] p 1103 A92-55310
The influence of a retarding rocket on parameter limits for reentry trajectories p 211 N92-15037
REENTRY VEHICLES
Potential hypersonic vehicles applications
[AIAA PAPER 91-5086] p 169 A92-17854
Study of numerical computation of inviscid flow field about complex configuration of re-entry vehicle
p 313 A92-25041
Measurement of a three-dimensional hypersonic density field
[AIAA PAPER 92-0383] p 323 A92-26240
Navier-Stokes computation of hypersonic near wakes with foreign gas injection
[AIAA PAPER 92-0838] p 422 A92-29604
Acquisition of an aerothermodynamic data base by means of a winged experimental reentry vehicle
p 486 A92-30685
Direct simulation of hypersonic rarefied flows about atmospheric re-entry vehicles p 710 A92-43169
Study of the flow field and molecular radiation heating around a reentry vehicle p 711 A92-43227
Experimental and numerical studies of radiation emission from high-temperature air behind 10 km/s shock waves
[SAE PAPER 912025] p 790 A92-45417
Multidimensional Euler/Navier-Stokes analysis for hypersonic equilibrium gas
[SAE PAPER 912026] p 790 A92-45418
Calculation of high speed base flows
[AIAA PAPER 92-2679] p 799 A92-45531
An adaptive grid method for computing the high speed 3D viscous flow about a re-entry vehicle
[AIAA PAPER 92-2685] p 799 A92-45534
Gridding strategies and associated results for winged entry vehicles p 918 A92-47051
Measurement of the freestream density for re-entry vehicles - A design study p 940 A92-52821
Hypersonic flows with air chemistry over a reentry vehicle at high altitudes p 1017 A92-53549
Radiative heat transfer from nonequilibrium shock layer to a hypersonic reentry body p 1019 A92-53579
Pre-flight physical simulation test of HIMES reentry test vehicle p 1103 A92-53640
HOPE re-entry experimental vehicle
p 1103 A92-55098
A shock tunnel experiment on aerodynamic interference induced by RCS jet p 1029 A92-56042
Numerical simulation of hypersonic viscous flow for the design of H-2 orbiting plane (HOPE-2)
[NAL-TR-1093] p 11 N92-10009
Aerothermodynamics for Space Vehicles
[ESA-SP-318] p 180 N92-14973
Analysis tools of ONERA and DLR for the aerothermodynamics of reentry vehicles
p 211 N92-14977
Aerothermodynamic development of the CARINA re-entry vehicle: CFD analyses and experimental tests
p 211 N92-14980
Simulation requirements for RCS plume: Flowfield interaction modelling on a winged reentry vehicle
p 181 N92-14985
Steps towards an efficient and accurate method solving the Euler equations around a re-entry configuration at super- and hypersonic speed p 181 N92-14987
Flow and temperature computations for space vehicles using adaptive finite element techniques
p 181 N92-14990
Ablation and temperature sensors for flight measurements in reentry body heat shields
p 227 N92-15004
The IRS plasma wind tunnels for the investigation of thermal protection materials for reentry vehicles
p 208 N92-15009
Hypersonic inviscid flow field simulations around reentry vehicles with flap deflection p 184 N92-15025
Numerical simulation of thermochemical non-equilibrium viscous flows around reentry bodies
p 227 N92-15029
Behaviour and modelling of the aerothermodynamics of ballistic entry vehicles in the high altitude flow regimes
p 184 N92-15031
Applicability of bridging methods to hypersonic rarefied flow aerodynamics of reentry vehicles
p 184 N92-15032
Transitional flows around re-entry bodies
p 184 N92-15035
FALKE: Winged re-entry vehicle flight control
p 667 N92-24454
Joint computational and experimental aerodynamics research on a reentry vehicle
[DE91-017315] p 667 N92-25315
Design of orbital re-entry experiment vehicle and outline of the experiment p 667 N92-25374
Acquisition of an aerothermodynamic data base by means of a winged experimental reentry vehicle
[MBB/FE202/S/PUB/461] p 787 N92-30232
REFLECTANCE
The design of broadband radar absorbing surfaces
[AD-A240521] p 42 N92-11235
REFLECTION
Thermal response of rigid and flexible insulations and reflective coating in an aeroconvective heating environment
[NASA-TM-103925] p 852 N92-28721
REFLECTOR ANTENNAS
High-frequency techniques for antenna analysis
p 494 A92-31071
REFRACTED WAVES
Numerical determination of the regions of existence of two types of shock-wave interaction p 428 A92-30211
REFRACTORY COATINGS
PVD coatings for aircraft turbine blades
p 216 A92-17950
REFRACTORY MATERIALS
Intermetallic and ceramic matrix composites for 815 to 1370 C (1500 to 2500 F) gas turbine engine applications
p 141 A92-15128
Ceramic matrix composites and its application in gas turbine engines
[ASME PAPER 91-GT-338] p 143 A92-15702
Hypersonic materials p 212 A92-18002
Materials and structures for Hermes
p 666 A92-38213
High temperature MMCs for aero-engines - Challenge and potential p 986 A92-52982
High enthalpy wind tunnel for erosion testing of advanced materials
[AIAA PAPER 92-3888] p 1094 A92-56729
High-temperature durability considerations for HSCT combustor
[NASA-TP-3162] p 289 N92-17070
Alternate/modified binders for asphalt airfield pavements
[AD-A242829] p 285 N92-17260
Fatigue in single crystal nickel superalloys
[AD-A244815] p 489 N92-21015
Development of a new generation of high-temperature composite materials p 578 N92-22515
Powder processing of aero-engine components
[PNR-90813] p 756 N92-27044
REFRACTORY METAL ALLOYS
Cold-crucible directional solidification of refractory metal-silicide eutectics p 755 A92-43684
REFRACTORY METALS
Microgravity nucleation and particle coagulation experiments support
[NASA-CR-189899] p 502 N92-21433
REFRIGERANTS
Feasibility of systematic recycling of aircraft Halon extinguishing agents
[DOT/FAA/CT-91/21] p 352 N92-18259
REFRIGERATING
Thermoacoustic refrigeration p 595 N92-22720
Solid-vapor adsorption refrigeration system development
[PB92-164383] p 771 N92-27715
REFRIGERATING MACHINERY
Evolutionary upgrade and application of the C-130H simple-cycle refrigeration system
[SAE PAPER 911439] p 270 A92-21836
Solid-vapor adsorption refrigeration system development
[PB92-164383] p 771 N92-27715
REFRIGERATORS
Computer simulation model for Lucas Stirling refrigerators p 296 A92-23837
Multicomponent gas sorption Joule-Thomson refrigeration
[NASA-CASE-NPO-17569-1-CU] p 228 N92-15203
Three-stage sorption type cryogenic refrigeration system and method employing heat regeneration
[NASA-CASE-NPO-18366-1-CU] p 300 N92-17674
Thermoacoustic refrigeration p 595 N92-22720
REGENERATION (ENGINEERING)
Corrosion damage and regeneration of aluminide coatings on aircraft turbine blades p 142 A92-15244
REGENERATIVE COOLING
Thermal control for hypersonic vehicle propulsion
p 468 A92-29356
Three-stage sorption type cryogenic refrigeration system and method employing heat regeneration
[NASA-CASE-NPO-18366-1-CU] p 300 N92-17674
REGENERATIVE FUEL CELLS
Thermally regenerative fuel cells
[AD-A242900] p 300 N92-17629
REGENERATORS
Ceramic regenerator program
[NASA-CR-189053] p 225 N92-14374
REGIONAL PLANNING
Interdependencies of aircraft-/airport-noise and urban- and regional-planning standards p 688 A92-39063
REGIONS
Issues in developing control zones for international space operations p 1141 A92-56602
REGRESSION ANALYSIS
Use of distance-measuring equipment (DME) for correcting errors in position, velocity, and wind measurements from aircraft inertial navigation systems
p 188 A92-18172
Identification of helicopter component loads using multiple regression
[AIAA PAPER 92-2110] p 544 A92-35681
Nonparametric methods of regression analysis in problems related to the processing of aerodynamic balance calibration tests p 602 A92-36417
Quantification of aircraft carbon brake wear using regression analysis and periodic wave forms
[SAE PAPER 912174] p 644 A92-39999
An analysis of fixed wing tactical airlifter characteristics using an intra-theater airlift computer model
[AD-A246908] p 732 N92-27719
REGULARITY
An inverse method with regularity condition for transonic airfoil design p 177 N92-13969
REGULATIONS
Flammability, smoke and toxic gas combustion products of composites used in aircraft cabins p 14 A92-10257
Why not a safety rating? --- in Australian civil aviation
p 530 A92-36200
Airline deregulation - Impact on human factors
p 834 A92-44999
A strategy for exploiting the full potential of MLS based terminal procedures in Canada p 190 N92-14025
ETOPS: A developing scene
[PNR-90844] p 473 N92-20459
The environmental impact of commercial aviation: The evolution of exhaust emissions legislation and control technology
[PNR-90847] p 505 N92-20574
The environmental challenges for the next supersonic aircraft
[PNR-90782] p 505 N92-20928

Regulations and their changes for certification of civil aircraft in icing conditions p 450 N92-21683
Impact of regulation changes on engine design and certification
[PNR-90789] p 559 N92-22098
Aeronautical mobile satellite service: An overview
p 594 N92-22573
Evaluation of a tritium runway lighting system
[DOT/FAA/CT-TN92/15] p 665 N92-25733
Aviation noise: Costs of phasing out noisy aircraft
[GAO/RCED-91-128] p 1011 N92-31454
Report of the aviation safety review of Department of Energy helicopter operations
[DE92-016346] p 954 N92-31928
Federal aviation regulations. Part 91: General operating and flight rules
[PB92-197334] p 1017 N92-33176

REGULATORS
Hover control of a PVTOL using nonlinear regulator theory p 478 A92-29171

REINFORCED PLASTICS
Interlaminar fracture characteristics of bonding concepts for thermoplastic primary structures p 758 A92-41282

REINFORCED PLATES
Optimization of the flutter load by material orientation
p 146 A92-15222
Some results on metal and composite patch reinforcement of aluminum honeycomb panel
p 216 A92-18830
Stability of stiffened panels with allowance for plasticity under nonstationary heating and loading
p 493 A92-30152
Analytical shape sensitivities and approximations of modal response of generally laminated tapered skew plates
[AIAA PAPER 92-2391] p 585 A92-34465

REINFORCED SHELLS
Composite laminated shells under internal pressure
p 758 A92-41296
A dynamic stiffness technique for the vibration analysis of stiffened shell structures p 1123 A92-56866
Damaged stiffened shell research at NASA. Langley Research Center p 914 N92-30115

REINFORCEMENT (STRUCTURES)
Mechanical behavior and processing of aluminum metal matrix composites
[AD-A249918] p 987 N92-30874

REINFORCING FIBERS
Mechanics of curved fiber composites
p 140 A92-14346
Manufacturing development of pultruded composite panels
[NASA-CR-181780] p 578 N92-22637

REISSNER THEORY
Nonlinear flutter of orthotropic composite panel under aerodynamic heating
[AIAA PAPER 92-2132] p 589 A92-35699

RELAXATION (MECHANICS)
Three-dimensional relaxation effect on quasi-3D flow in a blade row with spanwise loading distribution
p 936 A92-51593

RELAXATION METHOD (MATHEMATICS)
Inviscid and viscous transonic flows in cascades using an implicit upwind algorithm p 344 A92-28522
Implicit solutions of three-dimensional viscous hypersonic flows p 434 A92-31549
Boundary layer computations using a generalized formulation p 679 N92-24873

RELIABILITY
Integration of supportability elements into the conceptual design process
[AIAA PAPER 92-1194] p 600 A92-33306
Annual Reliability and Maintainability Symposium, Orlando, FL, Jan. 29-31, 1991, Proceedings
[ISBN 0-87942-661-6] p 759 A92-42051
Annual Reliability and Maintainability Symposium, Las Vegas, NV, Jan. 21-23, 1992, Proceedings
[ISBN 0-7803-0521-3] p 1119 A92-56201
Improving reliability and maintainability through process management p 1141 A92-56212
Field test of an advanced maintenance-system
p 1016 A92-56221
NASA reliability preferred practices for design and test
[NASA-TM-4322] p 157 N92-12286
Avionics reliability, durability, and integrity: Can they be independent of application? p 200 N92-14056
Fatigue safety factor: Assessment of associated safety level p 401 N92-18573
An adaptive correction technique for Differential Global Positioning System p 726 N92-26623
Turbine aircraft engine operational trending and JT8D static component reliability study
[DOT/FAA/CT-91/10] p 870 N92-28686
Concurrent engineering in design of aircraft structures
[MBB-FE-2-S-PUB-472] p 854 N92-29650
Communication: An important element of maintenance and repair p 838 N92-30124
Aging commuter aeroplanes: Fatigue evaluation and control methods p 915 N92-30132
A manufacturer's approach to ensure long term structural integrity p 838 N92-30133

RELIABILITY ANALYSIS
A method of reliability analysis for propeller blades
p 25 A92-10968
Reliability analysis of a structural ceramic combustion chamber
[ASME PAPER 91-GT-155] p 123 A92-15591
Transmission overhaul and component replacement predictions using Weibull and renewal theory
p 155 A92-17201
Operational design factors for NASP derived vehicles
[AIAA PAPER 91-5081] p 210 A92-17851
Reliability growth of coolers for advanced optical systems and instruments p 294 A92-22879
Study on reliability design of turbine blade
p 371 A92-24739
Study on the reliability evaluation of engine fuel accessories p 392 A92-24749
Durability analysis using fracture mechanics for avionics integrity p 396 A92-26799
Reliability aspects in computer integrated manufacturing systems p 397 A92-27838
Evolving partnership for NDE in materials engineering and extended life cycle performance
p 490 A92-28556
The V-22 Osprey - Preparing for fleet operations
p 458 A92-29671
Electronic control of a turbine power unit
p 470 A92-29741
Design for validation p 601 A92-33607
System reliability and risk assessment
[AIAA PAPER 92-2345] p 582 A92-34320
State-of-the-art airborne video recording
p 555 A92-35932
Flying qualities testing on the modern technology airship p 570 A92-35933
Reliability analysis of fatigue life of a structural system
p 671 A92-37395
The computer analysis of the prediction of aircraft electrical power supply system reliability
p 690 A92-37950
A method for estimating the technological and economic efficiency of measures enhancing the reliability of aviation gas turbine engines p 657 A92-40621
A comparison of fatigue life prediction methodologies for rotorcraft p 647 A92-40884
Cyclic fatigue behavior of silica fiber
p 754 A92-42040
Statistical analysis of field data for aircraft warranties
p 760 A92-42077
Design-for-reliability through durability analysis
p 760 A92-42086
Probability analysis of structure failure for the wings with main and subordinate components p 848 A92-47657
A failure analysis for landing gear structural system
p 849 A92-47667
Engine flight load reliability analysis
p 968 A92-49827
Safety factor and reliability for composite laminates
p 996 A92-53070
The system reliability analysis and optimization design for wing-box structures p 997 A92-53292
Change and reliability of the DC-9-81 digital flight guidance system p 1084 A92-56086
Electronics/avionics integrity - Definition, measurement and improvement p 1120 A92-56252
Smoothing CFM56 engine removal rate at USAir
[AIAA PAPER 92-3928] p 1070 A92-56759
Using the simulation modeling method to estimate the reliability of the crew-flight vehicle system
p 1133 A92-57444
Constraint propagation through electromagnetic interaction topologies
[NRC-31761] p 155 N92-12154
Development of a calibrated software reliability model for flight and supporting ground software for avionic systems p 234 N92-15870
Fatigue safety factor: Assessment of associated safety level p 401 N92-18573
Tornado structural fatigue life assessment of the German Air Force p 363 N92-18592
Fatigue management for the A-7P
p 363 N92-18593
RAMREQ: A computerized tool for the definition of RAM (Reliability, Availability, Maintainability) requirements of complex systems p 412 N92-18647
Fatigue life variability and reliability analysis of a wind turbine blade
[DE92-008673] p 689 N92-25049
Use of Markov methods in analysis of fault-tolerant systems with flexible repair policies
[PNR-90801] p 767 N92-27038
Estimating the reliability of a system on the basis of sample paths
[AD-A248585] p 774 N92-28171
A sensitivity analysis on component reliability from fatigue life computations
[AD-A247430] p 908 N92-28425
Damage tolerance certification methodology for composite structures p 1108 N92-32579
Analysis of data from a DO-178A software development process p 1134 N92-32880
Advanced techniques in reliability model representation and solution
[NASA-TP-3242] p 1134 N92-33483

RELIABILITY ENGINEERING
Design of reliable control systems p 49 A92-11420
The V-22 Osprey - Preparing for fleet operations
p 458 A92-29671
AIAA/ASME/ASCE/AHS/ASC Structures, Structural Dynamics and Materials Conference, 33rd, Dallas, TX, Apr. 13-15, 1992, Technical Papers. Pt. 2 - Structures II
p 582 A92-34332
Zonal analysis - The final step in system safety assessment p 760 A92-42071
Cost effectiveness of environmental stress screening (ESS) - A case history p 760 A92-42084
Advanced Rotorcraft Transmission (ART) - Component test results
[AIAA PAPER 92-3366] p 905 A92-48939
Testability of the PAALS auto-align sensor system --- Precision Accelerometer Alignment and Leveling System
p 965 A92-49310
A new resonant link aircraft power generating system
p 970 A92-50528
Failure analysis and reliability improvement of small turbine engine blades p 993 A92-50860
Redundancy design philosophy for catastrophic loss protection p 1119 A92-56202
Designing to cost effectiveness - Enhancing quality
p 1119 A92-56209
Modular techniques for dynamic fault-tree analysis
p 1120 A92-56241
Engineering reliability and maintainability review - A regimen for discovering production deficiencies
p 1120 A92-56254
HiRel - Reliability/availability integrated workstation tool p 1120 A92-56257
Thrust stand design principles
[AIAA PAPER 92-3976] p 1098 A92-56802
AGARD/SMP Review: Damage Tolerance for Engine Structures. 4: Reliability and Quality Assurance
[AGARD-R-773] p 402 N92-19004
Introduction: Needs and approaches to reliability and quality assurance in design and manufacture
p 402 N92-19005
Manufacturing process control as a damage tolerance concept p 403 N92-19006
Composite strength statistics from fiber strength statistics
[AD-A245616] p 755 N92-26383
MBB-LAGRANGE: A general structural reliability and optimization structural system
[MBB/FW321/S/PUB/467] p 998 N92-30423

REMOTE CONTROL
CARS temperature/multi-species measurement strategies for high speed airbreathing and rocket propulsion testing p 154 A92-16615
Ames life science telescience testbed evaluation
[NASA-CR-188856] p 140 N92-12033
Experimental investigation of passive infrared ice detection for helicopter applications p 265 N92-17986
Airport smart power lighting system
[DOT/FAA/CT-TN91/12] p 573 N92-22966

REMOTE SENSING
Aerobureau - Strategic television airmobile reports via satellite p 218 A92-19988
A consistency test of airborne GPS using multiple monitor stations p 454 A92-30651
Development of a 3-D remote sensing radar
p 597 A92-34908
X-band side-looking airborne radar for remote sensing
p 554 A92-34976
Relating the microwave radar cross section to the sea surface stress - Physics and algorithms
p 597 A92-35028
The application of high spectral and spatial resolution imaging spectrometers for locating downed aircraft
p 598 A92-35132
Time Resolved Lidar Fluorosensor operating from helicopter p 1121 A92-56296
High altitude solar power platform --- aircraft design analysis
[NASA-TM-103578] p 506 N92-21546
Recommended system concept p 599 N92-23383

Remote sensing of trapping layer base height using ATIS transmissions
[AD-A250074] p 1004 N92-31362

REMOTE SENSORS
Preconsiderations on aircraft integration
p 599 N92-23402
Sensor compatibility/optimal sensor combinations
p 599 N92-23403

REMOTELY PILOTED VEHICLES
The background and the development of the TAL-WAR (Rose) shape blimp with the articulated thruster
[AIAA PAPER 91-3692] p 17 A92-12749
Wind-tunnel and flight tests of a delta-wing remotely piloted vehicle p 21 A92-13208
Propulsion system evaluation for an unmanned high altitude long endurance RPV
[ASME PAPER 91-GT-409] p 128 A92-15738
Flight test of a half-scale unmanned air vehicle
p 193 A92-20208
Condor, an all-electric airplane p 269 A92-21734
System design from mission definition to flight validation
[AIAA PAPER 92-1091] p 605 A92-33256
Analysis of the aerodynamic characteristics of a simple remotely piloted research vehicle (RPRV)
p 710 A92-43191
Ducted fan VTOL for working platform
[SAE PAPER 911995] p 843 A92-45397
Feasibility study on a microwave-powered unmanned aerial vehicle for the communication relay utilization
[SAE PAPER 912052] p 843 A92-45436
Structural concept of main wings of high altitude unmanned aerial vehicle and basic properties of thermoplastic composites as candidate material
[SAE PAPER 912053] p 843 A92-45437
Unsteady aerodynamics of a Wortmann wing at low Reynolds numbers p 810 A92-46778
Aerodynamic analysis of the Pioneer unmanned air vehicle
[AIAA PAPER 92-4635] p 1027 A92-55382
Development of a 1/7th scale fighter UAV for flight research
[AD-A240703] p 23 N92-11008
Initial design study of existing flight control system of RPH and feasibility study of implementing HHC on the SH-60B
[AD-A240522] p 30 N92-11019
Piloted simulation study of a balloon-assisted deployment of an aircraft at high altitude
[NASA-TM-104245] p 272 N92-15986
NASA advanced aeronautics design solar powered remotely piloted vehicle
[NASA-CR-190007] p 462 N92-20665
Baseline vibration measurements of remotely piloted helicopters for higher harmonic control research
[AD-A244669] p 482 N92-21360
Gamma Group-The Pale Horse: A proposal in response to a commercial air transportation study ort study
[NASA-CR-190019] p 731 N92-26435
A wind tunnel study of the pioneer remotely piloted vehicle
[AD-A247028] p 732 N92-27335
Development of telemetry for the agility flight test of a radio controlled fighter model
[AD-A248653] p 753 N92-27994
Flight testing of a half-scale remotely piloted vehicle
[AD-A248568] p 733 N92-28123
Stability and control flight testing of a half-scale Pioneer remotely piloted vehicle
[AD-A245973] p 879 N92-28801
A preliminary design and analysis of an advanced heat-rejection system for an extreme altitude advanced variable cycle diesel engine installed in a high-altitude advanced research platform
[NASA-CR-186021] p 871 N92-29427
Thrust test fixture
[AD-D015259] p 983 N92-31192
Optimal trajectories for an unmanned air vehicle
p 963 N92-31880

REMOVAL
Removing aircraft surface coatings
p 516 A92-35574
Waterjets for removing engine coatings
p 516 A92-35575
Paint removal using cryogenic processes
[AD-A247668] p 895 N92-28912

RENDEZVOUS
Formation flight system design concept
p 954 A92-49255

RENDEZVOUS TRAJECTORIES
Time-to-go estimation from infrared images
p 840 A92-48308

RENORMALIZATION GROUP METHODS
Renormalization group based algebraic turbulence model for three-dimensional turbomachinery flows
p 703 A92-41268
A turbulence model based on RNG for quasi-three-dimensional cascade flows --- renormalization group methods
[AIAA PAPER 92-3312] p 825 A92-48898

REPLACING
Bearing servicing tool
[NASA-CASE-MSC-21881-1] p 912 N92-30082

REPORT GENERATORS
An integrated analysis and simulation tool for avionics system development p 1005 A92-49289

REPORTS
Malfunction/discrepancy reporting p 60 A92-14438
DLR research reports and communications
[ETN-92-91391] p 929 N92-29218

REPRODUCTION (BIOLOGY)
A model for the effects of aircraft overflight noise on the reproductive success of raptorial birds
p 688 A92-39101

REQUIREMENTS
Guidelines for integrating helicopter assets into emergency planning
[SCT-91RR-18] p 18 N92-10993
A proposed composite repair methodology for primary structure
[NRC-LTR-ST-1658] p 115 N92-13056
Lightning protection requirements for aircraft: A proposed specification
[RAE-TM-FS(F)-632-REV-ISSUE] p 187 N92-14007
Review of the European hypersonic wind tunnel performance and simulation requirements
p 209 N92-15043
General requirements and techniques for component fatigue life substantiation in Australian service helicopters
[AD-A242881] p 275 N92-17565
Saenger: The reference concept and its technological requirements - aerothermodynamics
[MBB-FE-202-S-PUB-0463-A] p 890 N92-29629
Aerothermodynamic challenges of the Saenger space-transportation system
[MBB-FE-202-S-PUB-0462-A] p 890 N92-29680
Fly-by-light technology development plan
[NASA-CR-181954] p 1086 N92-32778

RESCUE OPERATIONS
U.S. Coast Guard aviation life support and rescue equipment p 529 A92-32999
Piloted simulator studies of the HL-20 Lifting Body
p 666 A92-40033
Helicopters for public services, including rescue, fire fighting, and medical emergency p 723 A92-43163
Guidelines for integrating helicopter assets into emergency planning
[SCT-91RR-18] p 18 N92-10993
Concept evaluation of the UH-60 externally mounted rescue hoist
[AD-A240545] p 22 N92-11004

RESEARCH
Investigation of air transportation technology at Princeton University, 1990-1991 p 266 N92-17995
Aeronautical Engineering Group publications, 1950 - present
[AERO-REPT-8907] p 910 N92-29683
United States Air Force summer research program 1991. Volume 1: Program management report
[AD-A248763] p 1142 N92-32338

RESEARCH AIRCRAFT
Twenty years of airborne research at the University of Washington p 161 A92-14925
Air transport research in Germany p 61 A92-17095
On the accuracy of an aircraft-borne ambient electric-field measuring system p 186 A92-20127
Identification of aerodynamic effectiveness and interference effects of direct-lift-control flaps from flight data
[AIAA PAPER 92-0171] p 271 A92-23782
Atmospheric analysis for airdata calibration on research aircraft
[AIAA PAPER 92-0293] p 369 A92-25746
Agile responsive effective support - Design and testing of the ARES concept demonstrator aircraft
[AIAA PAPER 92-1038] p 536 A92-33219
The quiet STOL research aircraft ASUKA
p 642 A92-38206
The progress of a STOL project p 699 A92-43137
STOL research aircraft Asuka flight analysis in connection with the operation of the monitoring system
p 730 A92-43140
Flight test results and upper surface blowing (USB) technology of the STOL research aircraft Asuka
p 730 A92-43142
Flight tests on the structures of the STOL research aircraft Asuka p 730 A92-43143
The main wing boundary layer separation pattern of STOL research aircraft Asuka p 709 A92-43144
Aerodynamic drag as determined from flight test data of the STOL research aircraft Asuka
p 709 A92-43145
Path angular control of the STOL research aircraft Asuka p 745 A92-43146
Study on the maintainability and inspection of the STOL research aircraft Asuka p 700 A92-43148
Analysis of the aerodynamic characteristics of a simple remotely piloted research vehicle (RPRV)
p 710 A92-43191
Aerodynamic development of boundary layer control system for NAL QSTOL research aircraft 'ASKA'
[SAE PAPER 912010] p 843 A92-45410
Synthesis of a MLS automatic landing control law for the NAL experimental research aircraft Do-228
p 1084 A92-56062
Development of a 1/7th scale fighter UAV for flight research
[AD-A240703] p 23 N92-11008
Aerodynamic development of the X-31 aircraft for the high angle of attack region
[MBB-FE211-S-PUB-452] p 275 N92-17313
X-31 enhancement of aerodynamics for maneuvering beyond stall p 363 N92-18779
Activities of NRC-CNRC, Institute for Aerospace Research, Flight Research Lab.
[CTN-92-60432] p 420 N92-20205
Agreements/subagreements applicable to Wallops, 12 Nov. 1991 p 575 N92-22598
Pallet for helicopter testing instrumentation
p 652 N92-25598
The icing of the wing upper side and bottom side of the icing research aircraft of the DLR
p 724 N92-26349
NAL Dornier 228-200 flight research airplane: Present status and outline of the installed equipment
[NAL-TM-637] p 732 N92-27429
Evaluation of landing configuration by flight test of the quiet STOL experimental aircraft ASKA
[NAL-TR-1113] p 733 N92-28191
Aerodynamic characteristics obtained from alpha sweep test of the quiet STOL experimental aircraft ASKA
[NAL-TR-1112] p 853 N92-28901
Feedback control laws for highly maneuverable aircraft
[NASA-CR-190535] p 879 N92-29654
Flight evaluation of an extended engine life mode on an F-15 airplane
[NASA-TM-104240] p 871 N92-29659
Overview of the NASA Dryden Flight Research Facility aeronautical flight projects
[NASA-TM-104254] p 962 N92-31261
System overview of the NASA Dryden Integrated Test Facility
[NASA-TM-104250] p 984 N92-32201
Transonic wind tunnel test of a 14 percent thick oblique wing
[NASA-TM-102230] p 950 N92-32213
Collaborative research on V/STOL control system/cockpit display tradeoffs under the NASA/MOD joint aeronautical program
[NASA-TM-103910] p 1087 N92-32788
Rapid development of the X-31 simulation to support flight-testing
[NASA-TM-104256] p 1060 N92-33149

RESEARCH AND DEVELOPMENT
The design and testing of a radial flow turbine for aerodynamic research
[ASME PAPER 91-GT-220] p 124 A92-15636
'Spaceplanes' R&D status of Japan
[AIAA PAPER 91-5002] p 209 A92-17802
Soviet CFD - An international perspective
p 233 A92-20150
Pratt & Whitney PW300 for general aviation
p 277 A92-21012
Air transport research in Germany
p 241 A92-21014
Europe presents a united CFD front
p 392 A92-24909
Integrated multidisciplinary rotorcraft optimization research at the NASA Langley Research Center
p 419 A92-29673
Preliminary results from the High Speed Airframe Integration Research project
[AIAA PAPER 92-1004] p 536 A92-33196
Technical history of aircraft engines
p 558 A92-35911
Combustion research and design technology of aircraft engines p 558 A92-35915
Research and development of aircraft engine materials p 577 A92-35916
Research and development of turbofan engine for supersonic aircraft p 654 A92-38025
Agility and high angle of attack - An Air Force research perspective
[SAE PAPER 912145] p 608 A92-39983

1991-92 AHS Technical Committee highlights - Handling qualities p 662 A92-40395
1991-92 AHS Technical Committee highlights - Structures and materials p 609 A92-40397
Putting the control back in air traffic control - An enhanced Universal Development Simulation System p 916 A92-44982
Emerging technology in the Soviet Union: Selected papers with analysis
[ISBN 1-55831-117-1] p 929 A92-46201
Aviation, motor, and space designs --- research and development in U.S.S.R. p 784 A92-46202
The impact of advanced materials on small turbine engines
[SAE PAPER 911207] p 862 A92-48021
Simple fly-by-wire actuator p 876 A92-48491
C-141 and C-130 power-by-wire flight control systems p 876 A92-48493
Optics in aircraft engines p 926 A92-48500
Avionics software reusability observations and recommendations p 921 A92-48502
Japan pushes high speed research p 1015 A92-53434
Organization and technical status of the NH90 European helicopter programme p 1016 A92-56306
The SR3 low density wind tunnel - Facility capabilities and research development
[AIAA PAPER 92-3972] p 1098 A92-56798
A conceptual study for future engine test facility
[AIAA PAPER 92-3992] p 1099 A92-56815
Eighty years of aerospace technique through ATMA bulletins
[ETN-91-90097] p 57 N92-11963
JPRS report: Science and technology. USSR: Space
[JPRS-USP-91-007] p 211 N92-14101
National Aeronautics and Space Administration p 238 N92-14925
Seal development activities at Allison Turbine Division p 228 N92-15093
Areas of seal R/D at GE p 228 N92-15094
Activities of NRC-CNRC, Institute for Aerospace Research
[CTN-92-60431] p 420 N92-20204
Activities of NRC-CNRC, Institute for Aerospace Research, Flight Research Lab.
[CTN-92-60432] p 420 N92-20205
Research, services, and facilities (National Institute of Standards and Technology)
[PB92-109172] p 485 N92-21870
Impact and promise of NASA aeropropulsion technology p 559 N92-22511
Report on aerospace structures and structural materials R and D in Europe
[PB92-123553] p 550 N92-22785
NASA's aircraft icing technology program
[NASA-TM-104518] p 527 N92-23105
Radiant energy power source for jet aircraft
[DE92-008726] p 648 N92-24556
Computational Fluid Dynamics --- numerical methods and algorithm development
[NASA-CP-10078] p 660 N92-25808
Algorithmic development in structures technology p 684 N92-25924
Overview of computational structural methods for modern military aircraft p 684 N92-25928
Research and technology, 1991. Langley Research Center
[NASA-TM-4331] p 1013 N92-30733
Trends in aeropropulsion research and their impact on engineering education
[NASA-TM-105682] p 972 N92-31172
Departments of Veterans Affairs and Housing and Urban Development, and independent agencies appropriations for 1993, part 6
[GAO-55-636-PT-6] p 1141 N92-32505
Research and technology, 1990
[NASA-TM-107967] p 1143 N92-33948

RESEARCH FACILITIES

Rotor aeromechanics research with the RAE research Lynx - The experimental facility and test programme p 547 A92-35767
Investigation of three-dimensional flow field in a turbine including rotor/stator interaction. I - Design development and performance of the research facility
[AIAA PAPER 92-3325] p 883 A92-48908
A historical overview of high-temperature structural testing at the NASA Dryden Flight Research Facility p 981 A92-51407
Man-Vehicle Systems Research Facility - Design and operating characteristics
[AIAA PAPER 92-4177] p 982 A92-52458
Future requirements for hypersonic aerodynamic and aerothermodynamic facilities
[AIAA PAPER 92-3903] p 1094 A92-56738
The ASU Transition Research Facility
[AIAA PAPER 92-3910] p 1094 A92-56744
Test facilities and instrumentation for research in rarefied gas dynamics - An historical perspective
[AIAA PAPER 92-3969] p 1098 A92-56795
Aerospace technology: Technical data and information on foreign test facilities
[GAO/NSIAD-90-71FS] p 139 N92-13076
Experimental simulation and diagnostics of high-enthalpy real-gas flows
[AD-A241286] p 166 N92-13822
Aerothermodynamic challenges for ESA programmes p 180 N92-14974
Structural Dynamics Branch research and accomplishments for FY 1990
[NASA-TM-103747] p 230 N92-15406
The Goldstein Engineering Research Laboratory
[AERO-REPT-8906] p 308 N92-18322
Activities of NRC-CNRC, Institute for Aerospace Research
[CTN-92-60431] p 420 N92-20204
Activities of NRC-CNRC, Institute for Aerospace Research, Flight Research Lab.
[CTN-92-60432] p 420 N92-20205
Icing simulation: A survey of computer models and experimental facilities p 450 N92-21684
Criteria for the operation of federally-owned secondary calibration laboratories (ionizing radiation)
[PB92-112481] p 485 N92-21777
Research, services, and facilities (National Institute of Standards and Technology)
[PB92-109172] p 485 N92-21870
DLR-news: Announcements of the German Research Institute for Aeronautics and Astronautics p 698 N92-25413
Integrated flight propulsion control research results using the NASA F-15 HIDEC Flight Research Facility
[NASA-TM-4394] p 740 N92-27379
Experimental aerodynamic facilities of the Aerodynamics Research and Concepts Assistance Branch
[AD-A247489] p 883 N92-28248
Expand turbulence laboratory facilities to meet new DOD research interest
[AD-A248581] p 883 N92-28388
Use of a research simulator for the development of new concepts of flight control p 885 N92-28543
The basic research simulator programme and the industrial and aerospace community: Opportunities for cooperative research
[LR-662] p 887 N92-28579
Research and technology, 1991. Langley Research Center
[NASA-TM-4331] p 1013 N92-30733
Activities of the Aeronautical Research Laboratory p 1013 N92-30768
Overview of the NASA Dryden Flight Research Facility aeronautical flight projects
[NASA-TM-104254] p 962 N92-31261
System overview of the NASA Dryden Integrated Test Facility
[NASA-TM-104250] p 984 N92-32201
High temperature aircraft research furnace facilities
[NASA-CR-184384] p 1101 N92-33826
Research and technology, 1990
[NASA-TM-107967] p 1143 N92-33948

RESEARCH MANAGEMENT

An independent review of the Multi-Path Redundant Avionics Suite (MPRAS) architecture assessment and characterization report
[NASA-CR-188126] p 163 N92-12440
DoD key technologies plan
[AD-A253692] p 1142 N92-33238

RESEARCH PROJECTS

Review of aerodynamic design in the Netherlands p 193 N92-13929
Report on aerospace structures and structural materials R and D in Europe
[PB92-123553] p 550 N92-22785
DLR-news: Announcements of the German Research Institute for Aeronautics and Astronautics p 698 N92-25413
DLR research reports and communications
[ETN-92-91391] p 929 N92-29218

RESEARCH VEHICLES

Conducting the NASP ground test program
[AIAA PAPER 91-5029] p 209 A92-17820
Acquisition of an aerothermodynamic data base by means of a winged experimental reentry vehicle p 486 A92-30685
Nonlinear control law with application to high angle-of-attack flight p 661 A92-39904
A review of recent programs and future plans for rotorcraft in-flight simulation at Ames Research Center
[SAE PAPER 912121] p 608 A92-39969
Controls for agility research in the NASA High-Alpha Technology Program
[SAE PAPER 912148] p 661 A92-39984
Numerical investigations in three-dimensional internal flows
[NASA-CR-189467] p 221 N92-14313
Model identification and control system design for the lambda unmanned research vehicle
[AD-A241859] p 299 N92-17024
A robust digital flight control system for an unfanned research vehicle using discrete quantitative feedback theory
[AD-A243638] p 283 N92-17748
Joint computational and experimental aerodynamics research on a reentry vehicle
[DE91-017315] p 667 N92-25315
A static investigation of the thrust vectoring system of the F/A-18 high-alpha research vehicle
[NASA-TM-4359] p 633 N92-25967
Rotorcraft In-Flight Simulation Research at NASA Ames Research Center: A Review of the 1980's and plans for the 1990's
[NASA-TM-103873] p 853 N92-28926
Joint computational and experimental aerodynamics research on a hypersonic vehicle
[DE92-013439] p 943 N92-30367
The F-18 high alpha research vehicle: A high-angle-of-attack testbed aircraft
[NASA-TM-104253] p 1060 N92-33404
Experience with Ada on the F-18 High Alpha Research Vehicle Flight Test Program
[NASA-TM-104259] p 1062 N92-34039

RESIDENTIAL ENERGY

Benchmark performance analysis of an ECM-modulated air-to-air heat pump with a reciprocating compressor
[DE92-004478] p 500 N92-20341

RESIDUAL STRENGTH

Bulging of fatigue cracks in a pressurized aircraft fuselage
[LR-655] p 196 N92-14045
Damaged stiffened shell research at NASA. Langley Research Center p 914 N92-30115
Residual strength of repaired graphite/epoxy laminates after 5 years of outdoor exposure p 1108 N92-32577

RESIDUAL STRESS

Shot peening - Theory and applications --- Book
[ISBN 2-907669-18-4] p 676 A92-40400
Investigation of a method for determining machining stress in polymethylmethacrylate (PMMA) of airplane canopies p 986 A92-53096
Surface residual stress analysis of metals and alloys
[AD-A248372] p 895 N92-28426

RESILIENCE

Mechanical qualification tests for materials used in the fabrication of aircraft parts
[CEAT-M5-5443/01] p 195 N92-14042

RESIN MATRIX COMPOSITES

BMI/bis (allylphenoxyphthalimide)-copolymers - A new family of resins for advanced composites with improved thermal oxidative stability p 33 A92-10213
Applications of advanced composites in a 3/4 air transportable rack p 36 A92-10314
The design and manufacture of an advanced thermoplastic horizontal stabilator for the AH-64A p 59 A92-14354
The development and test of thermoplastic composite speed brake p 272 A92-24178
Measurement of basic material and processing properties affecting injection-pultrusion technology p 580 A92-32636
Thermal fiber-reinforced-plastic composite technology for aircraft structures p 755 A92-43237
Basic study of adhesive bonding for fiber-composites - Adhesive bonding technologies on jet engine parts p 764 A92-44733
New thermoplastic polyimide composite for supersonic aircraft structures p 985 A92-51512
Application of resin and metal matrix composites to advanced avionics enclosure p 985 A92-51921
Poly 1, 2, 4-triazoles via aromatic nucleophilic displacement
[NASA-CASE-LAR-14440-1] p 35 N92-10066
Advanced airframe structural materials: A primer and cost estimating methodology
[AD-A253371] p 1062 N92-34182

RESIN TRANSFER MOLDING

Resin transfer molding of a complex composite aircraft structure p 784 A92-47410
RTM - Simultaneous design and tooling reduces cost and lead time p 994 A92-51537

RESINS

Polymer infiltration studies
[NASA-CR-189773] p 289 N92-17004
Polymer infiltration studies
[NASA-CR-190204] p 578 N92-22486
High-temperature polymer matrix composites p 578 N92-22513
RTM: Cost-effective processing of composite structures p 578 N92-22678

RESISTANCE HEATING
Further developments in three-dimensional simulation of electrothermal deicing systems
[AIAA PAPER 92-0528] p 459 A92-31668
An efficient finite element method for aircraft de-icing problems
[AIAA PAPER 92-0532] p 459 A92-31670
Improved articulated fin/wing control system statement of government interests
[AD-D015268] p 1088 N92-34131
RESOLUTION
A two-dimensional Euler solution for an unbladed jet engine configuration p 627 N92-24861
RESONANCE
Resonance of circular shock waves
p 395 A92-26795
Field telemetry of blade-rotor coupled torsional vibration at Matuura Power Station Number 1 unit
p 222 N92-14348
The effects of manufacturing tolerances on the vibration of aero-engine rotor-damper assemblies
p 222 N92-14349
RESONANCE FLUORESCENCE
A new technique for temperature and specie concentration measurements in unseeded supersonic and hypersonic gas flows
[AD-A241536] p 158 N92-13409
RESONANCE TESTING
Resonance and control response tests using a control stimulation drive
[MBB-UD-0586-90-PUB] p 134 N92-12003
Resonance and control response tests using a control simulation device
[MBB-UD-0608-91-PUB] p 978 N92-30439
RESONANT FREQUENCIES
Evaluation of an advanced finite element analysis for rotor blades p 109 A92-14426
Resonance prediction for slotted circular wind tunnel using finite element p 235 A92-18388
Evaluation of shear layer cavity resonance mechanisms by numerical simulation
[AIAA PAPER 92-0555] p 333 A92-26965
Analytical shape sensitivities and approximations of modal response of generally laminated tapered skew plates
[AIAA PAPER 92-2391] p 585 A92-34465
Coupled vibrations of turbomachine blades
p 738 A92-44545
Analytical evaluation of resonant response of spiral bevel gears in the RAH-66 helicopter Fantail transmission
[AIAA PAPER 92-3495] p 906 A92-49031
Improvement in transmission loss of aircraft double wall with resonators p 1011 A92-53091
Aircraft ride quality controller design using new robust root clustering theory for linear uncertain systems
[AIAA PAPER 92-4399] p 1075 A92-55199
Flapping inertia for selected rotor blades
[NASA-TM-104125] p 115 N92-13057
Development and testing of cabin sidewall acoustic resonators for the reduction of cabin tone levels in propfan-powered aircraft
[NASA-CR-4388] p 166 N92-13757
Structural dynamics and vibrations of damped, aircraft-type structures
[NASA-CR-4424] p 499 N92-20194
Monitoring jet fuel degradation using quartz crystal microbalances
[DE92-004730] p 489 N92-20858
A fin optimisation study p 551 N92-23237
Characterization of superconducting magnetic bearings (dynamic stiffness and damping coefficient in axial direction) p 772 N92-27737
RESONANT VIBRATION
Detuning from the natural resonances of the blade in the computer-aided design of blade rows for axial-flow compressors p 80 A92-16818
Experimental investigation of supersonic flow over two cavities in tandem p 610 A92-36830
A model of a deformable aeroplane with a wing of low aspect ratio and movable control surfaces for studying natural vibrations p 744 A92-41528
Free vibration analysis of branched blades by the integrating matrix method p 847 A92-47122
On travelling wave vibration of high-speed duplex helical gears p 990 A92-49580
Add-on damping treatment for life extension of the F-15 upper-outer wing skin
[AD-A246149] p 746 N92-27577
RESONATORS
Acoustic sources in a tripped flow past a resonator tube p 778 A92-41266
RESOURCES MANAGEMENT
Workshop on integrated Crew Resource Management (CRM)
[DOT/FAA/RD-92/5] p 781 N92-27518
RESPONSE TIME (COMPUTERS)
National airspace system: System effectiveness operational concept NAS-SR-138
[DOT/FAA/SE-92/2] p 535 N92-23096
RESPONSES
Comparison of polynomial approximations and artificial neural nets for response surfaces in engineering optimization p 165 N92-13835
RESTORATION
The 12-foot pressure wind tunnel restoration project model support systems p 664 N92-25091
RETENTION (PSYCHOLOGY)
Controller memory enhancement: Field facility concepts and techniques
[DOT/FAA/CT-TN92/7] p 640 N92-24799
RETIREMENT FOR CAUSE
Discs low cycle fatigue life predictions for gas turbine engines in CSFR by using fractographic information
p 995 A92-51950
Life management approach for USAF aircraft
p 362 N92-18587
RETROFITTING
Comprehensive helicopter rotor instrumentation - A retrofit approach using miniature transducers
[AIAA PAPER 92-0268] p 369 A92-25724
Ferrundi Company supplies 4500 model head up display devices to India's MIG-21 aircraft
[AD-A241044] p 229 N92-15367
Assessment of cockpit interface concepts for data link retrofit
[NASA-CR-187615] p 268 N92-17512
RETROREFLECTION
Measurement of position and attitude using laser and retro-reflectors p 1047 A92-56120
RETROROCKET ENGINES
The influence of a retarding rocket on parameter limits for reentry trajectories p 211 N92-15037
RETURN TO EARTH SPACE FLIGHT
Thermal protection analysis of Mars-earth return vehicles p 497 A92-32183
Earth aerobraking strategies for manned return from Mars p 752 A92-41535
REUSABLE SPACECRAFT
Conceptual design of two-stage-to-orbit hybrid launch vehicle
[NASA-CR-190006] p 486 N92-20666
REVERSE ENGINEERING
Integrating aerodynamic surface modeling for computational fluid dynamics with computer aided structural analysis, design, and manufacturing
p 682 N92-25727
REVERSED FLOW
Internal reversing flow in a tailpipe offtake configuration for SSTOVL aircraft
[AIAA PAPER 92-3790] p 1069 A92-54169
A high speed edgewise rotor using circulation control only in the reversed flow area p 1059 A92-56347
An experimental and computational investigation of an annular reverse-flow combustor
[UTIAS-338] p 129 N92-11996
Internal reversing flow in a tailpipe offtake configuration for SSTOVL aircraft
[NASA-TM-105698] p 868 N92-28418
REVERSING
Study of a new airfoil used in reversible axial fans
p 177 N92-13970
REYNOLDS EQUATION
Numerical investigation of tail buffet on F-18 aircraft
[AIAA PAPER 92-2673] p 798 A92-45528
Comparative study of turbulence models in predicting hypersonic inlet flows
[AIAA PAPER 92-3098] p 824 A92-48740
The application of a Navier-Stokes CFD method to civil engine intake flows p 769 N92-27471
Comparative study of turbulence models in predicting hypersonic inlet flows
[NASA-TM-105720] p 722 N92-28102
REYNOLDS NUMBER
Experimental investigation on the effect of crescent planform on lift and drag p 9 A92-13206
Large chord turbine cascade testing at engine Mach and Reynolds number p 173 A92-18771
Flow visualization and wake analysis for complex three-dimensional bluff bodies at subcritical through critical Reynolds numbers
[AIAA PAPER 92-0155] p 253 A92-23770
Effects of tip Reynolds number and tip asymmetry on vortex wakes of axisymmetric bodies at various angles of attack
[AIAA PAPER 92-0406] p 324 A92-26259
Effect of compressibility on the value of the acceptable roughness Reynolds number p 427 A92-30197
A comparison of transition Reynolds number measured in a wind tunnel and in flight p 522 A92-36026
The flow over a backward-facing step under controlled perturbation - Laminar separation p 705 A92-41653
Dynamic LEX/forebody vortex interaction effects
[AIAA PAPER 92-2732] p 804 A92-45566
Calibration-related pseudo-Reynolds number trends in transonic wind tunnels p 882 A92-46780
A review of scale effects in unsteady aerodynamics
p 934 A92-50121
Increased heat transfer to elliptical leading edges due to spanwise variations in the freestream momentum - Numerical and experimental results
[AIAA PAPER 92-3070] p 1020 A92-54005
Computational and experimental studies of flow in multi-lobed forced mixers
[AIAA PAPER 92-3568] p 1112 A92-54057
Some characteristics and effects of the F/A-18 LEX vortices p 88 N92-13025
A numerical study of the stability of the swept attachment line boundary layer
[AERO-REPT-9103] p 345 N92-18293
The effect of angle of incidence and Reynolds number on heat transfer in a linear turbine cascade
[AD-A243900] p 377 N92-19328
Comparison of a two-dimensional adaptive-wall technique with analytical wall interference correction techniques
[NASA-TP-3132] p 444 N92-20494
Hypersonic laminar flow computations over a blunt leading edged delta wing at three different chord Reynolds numbers
[FFA-TN-1991-40] p 528 N92-23168
Longitudinal and lateral-directional aerodynamic characteristics of a wing-cone configuration at Mach numbers from 2.5 to 4.5
[NASA-TM-4337] p 630 N92-24977
Wall functions for the kappa-epsilon turbulence model in generalized nonorthogonal curvilinear coordinates
[NASA-CR-190368] p 685 N92-25962
Reynolds number dependence of the drag coefficient for laminar flow through fine-scale screens
[DE92-002930] p 765 N92-26698
The eddy structures in bounded shear flows
p 717 N92-27712
A review of scale effects on surfaces in unsteady motion p 722 N92-27962
Transonic wind tunnel test of a 14 percent thick oblique wing
[NASA-TM-102230] p 950 N92-32213
REYNOLDS STRESS
Deterministic blade row interactions in a centrifugal compressor stage
[ASME PAPER 91-GT-273] p 75 A92-15670
Studies of the effects of curvature on dilution jet mixing p 290 A92-21079
Navier-Stokes computation of airfoil in stall using algebraic Reynolds-stress model
[AIAA PAPER 92-0195] p 257 A92-23803
Experimental investigation of a three-dimensional bluff-body wake
[AIAA PAPER 92-0429] p 326 A92-26277
Navier-Stokes computations for turbulent transonic projectile with a two layer model combining the ASM model of turbulence and the k-epsilon model near the wall
[AIAA PAPER 92-0518] p 331 A92-26943
Three-dimensional structure of a curved wake
[AIAA PAPER 92-0541] p 341 A92-28199
Direct numerical simulation of laminar breakdown in high-speed, axisymmetric boundary layers
[AIAA PAPER 92-0742] p 343 A92-28223
Turbulent flow in the wake of an idealized wing-body junction
[AIAA PAPER 92-0282] p 435 A92-31652
Inverse solution of 3D incompressible turbulent boundary layer with separated bubbles
p 522 A92-35992
Reynolds stress budget in the outwash jet arising from colliding curved wall jets p 614 A92-38860
Reynolds stress distribution downstream of a turbine cascade p 614 A92-38861
Experiments on turbulent flow due to an enclosed rotating disk p 615 A92-38863
Navier-Stokes investigation of a transonic centrifugal compressor stage using an algebraic Reynolds stress model
[AIAA PAPER 92-3311] p 825 A92-48897
Comparison of turbulence models for powered-lift flow fields
[AIAA PAPER 92-3674] p 1022 A92-54117
Constant-temperature anemometry measurements in hypersonic boundary layers p 90 N92-13861
A compressible Navier-Stokes solver with two-equation and Reynolds stress turbulence closure models
[NASA-CR-4440] p 681 N92-25376
Numerical simulation of turbomachinery flows with advanced turbulence models p 1124 N92-32270

RHEOLOGY
Lewis icing research tunnel test of the aerodynamic effects of aircraft ground deicing/anti-icing fluids
[NASA-TP-3238] p 952 N92-30395
RIBLETS
Effect of riblets on turbulence in the wake of an airfoil
p 5 A92-11051
Scale model test of an isolated turbofan nacelle with riblets
[SAE PAPER 912128] p 618 A92-39975
Experimental and numerical investigation of a turbulent boundary layer over riblets p 622 A92-40128
Experimental investigation into the effects of riblets on compressor cascade performance
[AD-A243881] p 377 N92-19235
Application of riblet surface to pipe flow
p 766 N92-26915
RICCATI EQUATION
Study of the discrete singularly perturbed linear-quadratic control problem by a bilinear transformation p 163 A92-16072
RIDING QUALITY
Aircraft ride quality controller design using new robust root clustering theory for linear uncertain systems
[AIAA PAPER 92-4399] p 1075 A92-55199
RIEMANN MANIFOLD
Mesh adaption for 2D transsonic Euler flows on unstructured meshes p 816 A92-47038
Anisotropic control of mesh generation based upon a Voronoi type method p 918 A92-47043
RIGGING
NLR experience with high velocity burner rig testing, 1979-1989
[NLR-TP-89152-U] p 385 N92-18415
RIGID ROTOR HELICOPTERS
A piloted comparison of elastic and rigid blade-element rotor models using parallel processing technology
p 546 A92-35751
RIGID ROTORS
Frequency-domain identification of BO 105 derivative models with rotor degrees of freedom
p 104 A92-14327
Dynamics of helicopters with dissimilar blades
p 133 A92-14427
A torque-free flexible model gyro p 495 A92-31552
Aeroelastic optimization of an advanced geometry helicopter rotor
[AIAA PAPER 92-2360] p 543 A92-34592
Comparison of elastic and rigid blade-element rotor models using parallel processing technology for piloted simulations
[SAE PAPER 912120] p 608 A92-39968
Aeromechanical stability of hingeless helicopter rotors in forward flight p 874 A92-46923
Design and testing of a composite hingeless hub for rotary-wing aircraft p 1053 A92-56075
Stability and performance of notch filter control for *unbalance response* p 771 N92-27731
RIGID STRUCTURES
A multibody analog of the dual-spin problem
p 49 A92-11426
Development of a combined fast method for studying the plane motions of rigid bodies in the atmosphere around the center of mass in the presence of perturbations
p 304 A92-23563
On automatic control of aeroelastic vehicles
p 509 A92-29327
Orthogonal grids around difficult bodies
p 432 A92-31160
Rigid and flexible joint modelling in multibody dynamics using finite elements p 671 A92-37559
A general purpose nonlinear rigid body mass finite element for application to rotary wing dynamics
p 846 A92-46924
Static aeroelastic analysis of ACT wind tunnel model aircraft
[NAL-TM-624] p 632 N92-25366
Quaternion and Euler angles in kinematics
[NAL-TM-636] p 909 N92-28836
RIGID WINGS
Wing design for hanggliders having minimum induced drag p 811 A92-46814
The benchmark aeroelastic models program: Description and highlights of initial results
[NASA-TM-104180] p 185 N92-15049
NACA0012 benchmark model experimental flutter results with unsteady pressure distributions
[NASA-TM-107581] p 526 N92-22507
Transonic aeroelastic computations on wings using Navier-Stokes equations p 721 N92-27957
Pressure measurements on a rectangular wing with a NACA0012 airfoil during conventional flutter
[NASA-TM-104211] p 1042 N92-34147
RIGIDITY
A method of failure analysis of complicated structures
p 901 A92-47656
RIMS
Performance of radial clearance rim seals in upstream and downstream rotor-stator wheelspaces
[ASME PAPER 91-GT-32] p 147 A92-15516
Rim sealing of rotor-stator wheelspaces in the absence of external flow
[ASME PAPER 91-GT-33] p 147 A92-15517
RING LASERS
Bias of an optical passive ring-resonator gyro caused by the misalignment of the polarization axis in the polarization-maintaining fiber resonator
p 652 A92-40262
Comparison of Hemispherical Resonator Gyro and *optical Gyros* p 993 A92-51014
RING STRUCTURES
The impact load on containment rings during a multiple blade shed in aircraft gas turbine engines
[ASME PAPER 91-GT-163] p 123 A92-15598
RING WINGS
Aerodynamic calculation of an elliptic ring wing
[AIAA PAPER 91-0068] p 1035 A92-57035
A Navier-Stokes solution of Hull-ring wing-thruster interaction p 221 N92-14310
RISK
Pre-flight risk assessment in emergency medical service (EMS) helicopters p 16 A92-11171
Structural risk assessment in the Israel Air Force for fleet management p 836 A92-46779
Risk management - Expanding horizons in nuclear power and other industries --- Book
[ISBN 1-56032-231-4] p 993 A92-51438
Cockpit crew research p 951 A92-51440
When should we start high-rate production of the B-2? An analysis based on flight test results
[RAND/P-7757] p 697 N92-25204
Analysis of helicopter accident risk exposure near heliports, airports, and unimproved sites
[SCT-91RR-13] p 637 N92-26028
RIVETED JOINTS
Bayesian reliability analysis in connection with the evaluation of multiple-site damage p 762 A92-43126
Finite element analysis of a riveted repair on a curved composite panel
[AD-A243916] p 404 N92-19384
Photoelastic coating study of CT-114 coupon joint test specimen for horizontal stabilizer rear attachment fitting to vertical stabilizer rear spar
[NRC-LTR-ST-1689] p 489 N92-21018
RIVETS
Recent fracture mechanics results from NASA research related to the aging commercial transport fleet
p 362 N92-18589
ROBOT ARMS
Adaptive control of nonlinear systems with applications to the control of flexible robot arms
[AD-A244409] p 413 N92-19397
ROBOT CONTROL
Adaptive control of nonlinear systems with applications to the control of flexible robot arms
[AD-A244409] p 413 N92-19397
Techniques for autonomous navigation
[DE92-013458] p 957 N92-31746
ROBOT DYNAMICS
Representation of geometric stiffening in multibody system simulation p 217 A92-19463
Robotics application in aerospace manufacturing
p 671 A92-38216
Chaotic motion in mechanical and engineering systems p 695 A92-39480
Techniques for autonomous navigation
[DE92-013458] p 957 N92-31746
ROBOTICS
Automated composite lay-up p 146 A92-14450
Robotic non-destructive inspection of aircraft, phase 1
[AD-A240777] p 44 N92-11367
AI for RPVs, Sensor Driven Airborne Replanner (SDAR), for a Robotic Aircraft Sensor Platform (RASP)
p 114 N92-12534
A connectionist approach to autonomous robotic navigation p 454 N92-20356
ROBOTS
Terrain following of arbitrary surfaces using a high intensity LED proximity sensor
[DE92-007161] p 455 N92-21201
ROBUSTNESS (MATHEMATICS)
Real parameter uncertainty and phase information in the robust control of flexible structures
p 32 A92-11345
Robustness of distributed systems with respect to small time delays p 47 A92-11351
A time approach to robustness of LTI systems with *structured uncertainty and unmodelled dynamics --- linear* time-invariant p 48 A92-11356
Reduced-order robust controllers - H(infinity)-balanced truncation and optimal projection p 48 A92-11363
Robust pole assignment using closed loop controllability conditions p 49 A92-11417
Polygon interval arithmetic and design of robust control systems p 49 A92-11418
Robust stabilization with positive real uncertainty - Beyond the small gain theorem p 50 A92-11444
Control design via TAM and H-infinity approaches - A flexible beam case study p 51 A92-11445
New robust adaptive control system using multiple *regularization parameters* p 51 A92-11455
Optimal rejection of bounded persistent disturbances in periodic systems p 51 A92-11464
Robust controller design for an advanced fighter aircraft p 28 A92-11500
Robust stabilization of a helicopter model
p 28 A92-11501
Robust autopilot design for aircraft with multiple lateral-axes controls using H(infinity) synthesis
p 28 A92-11563
A two-feedback-loop robust helicopter controller based on eigenspace techniques and H(infinity) synthesis
p 29 A92-11582
H(infinity) robust control synthesis for a fighter performing a coordinated bank turn p 29 A92-11585
An assessment of robustness of variable structure control systems for advanced aircraft manoeuvres
p 29 A92-11595
A robust filter configuration for DGPS users
p 101 A92-16967
Application of stochastic robustness to aircraft control systems p 204 A92-18620
Parametric robust control by quantitative feedback theory p 302 A92-21176
Robustness analysis of a model reference adaptive control system p 412 A92-27859
Integrated flight/propulsion control design for a STOVL aircraft using H-infinity control design techniques
p 476 A92-29093
Robust control law development for a hypersonic cruise aircraft p 478 A92-29127
The implicit function theorem and robust root locus
p 507 A92-29134
A hierarchical data structure and new capabilities of the Robust-Control Toolbox p 507 A92-29155
Synthesis of robust nonlinear autopilots using differential game theory p 478 A92-29330
Robust optimal control with a worst case time domain performance criterion p 509 A92-29368
Robustness of control systems with nonlinear parametric correction for certain types of perturbations
p 509 A92-30311
Robustness characteristics of fast-sampling digital controllers for active flutter suppression
[AIAA PAPER 92-2104] p 567 A92-35675
Improvement of helicopter robustness and performance control law using eigenstructure techniques and H-infinity synthesis p 569 A92-35776
Robust frequency design of linear stationary systems in aeroautoelastics p 690 A92-37791
Robust wind shear stochastic controller-estimator
p 661 A92-39893
Robust flight control system design with multiple model approach p 661 A92-39910
Robust stabilisation of multivariable feedback systems with desired performance requirement
p 776 A92-42172
Robust flight control system design using a multimodel approach. II p 745 A92-43180
Prismatic grid generation with an efficient algebraic method for aircraft configurations
[AIAA PAPER 92-2721] p 803 A92-45559
Comparison of six robustness tests evaluating missile autopilot robustness to uncertain aerodynamics
p 873 A92-46737
Robust discrete controller design for an unmanned research vehicle (URV) using discrete quantitative feedback theory p 877 A92-48495
Robustness characteristics of fast-sampling digital PI controllers for high-performance aircraft with impaired control surfaces p 877 A92-48496
Compensating for manufacturing and life-cycle variations in aircraft engine control systems
[AIAA PAPER 92-3869] p 868 A92-49139
A reversed-frame normalization design of robust flight control system p 1009 A92-53382
Robust dynamic inversion control laws for aircraft control
[AIAA PAPER 92-4329] p 1073 A92-55173
Preliminary assessment of the robustness of dynamic inversion based flight control laws
[AIAA PAPER 92-4330] p 1074 A92-55174
Flight-determined stability analysis of multiple-input-multiple-output control systems
[AIAA PAPER 92-4396] p 1074 A92-55196

Aircraft ride quality controller design using new robust root clustering theory for linear uncertain systems
[AIAA PAPER 92-4399] p 1075 A92-55199
Robust sampled data eigenstructure assignment using the delta operator
[AIAA PAPER 92-4400] p 1075 A92-55200
Design of robust Quantitative Feedback Theory controllers for pitch attitude hold systems
[AIAA PAPER 92-4409] p 1075 A92-55203
Robustness of a helicopter flight control system designed using eigenstructure assignment
[AIAA PAPER 92-4469] p 1076 A92-55229
An algorithm for robust eigenstructure assignment using the Linear Quadratic Regulator
[AIAA PAPER 92-4478] p 1131 A92-55237
The application of direct transcription to commercial aircraft trajectory optimization
[AIAA PAPER 92-4528] p 1077 A92-55246
A robust gain scheduler interpolated into multiple models by membership functions
[AIAA PAPER 92-4553] p 1131 A92-55265
Applications of robust control theory - Educational implications
[AIAA PAPER 92-4559] p 1131 A92-55271
An framework for robust flight control design using constrained optimization
[AIAA PAPER 92-4603] p 1131 A92-55282
Robust control design of an automatic carrier landing system
[AIAA PAPER 92-4619] p 1077 A92-55296
Computer aided evaluation of aircraft handling qualities and flight control system robustness
[AIAA PAPER 92-4423] p 1080 A92-55347
Robust identification of nonlinear aerodynamic model structure
[AIAA PAPER 92-4503] p 1081 A92-55370
Robust control system design with multiple model approach p 1083 A92-56029
Flight control system design using H(infinity) optimal control p 1083 A92-56030
Modelling aspects and robustness issues in rotorcraft system identification p 274 N92-17159
Technical notes and correspondence: Stochastic robustness of linear time-invariant control systems p 303 N92-18002
Robust control system design with application to high performance helicopters p 382 N92-19621
Design and evaluation of a robust dynamic neurocontroller for a multivariable aircraft control problem
[NASA-TM-105579] p 481 N92-20586
Estimation of aircraft attitude by angular rate measurements p 963 N92-31881
A learning enhanced flight control system for high performance aircraft
[AD-A252520] p 1086 N92-32435

ROCKET ENGINE CONTROL
Real-time fault diagnosis for propulsion systems
[NASA-TM-105303] p 26 N92-11017

ROCKET ENGINE DESIGN
Trends in propulsion technology p 757 A92-41186
Development study on air turbo-ramjet engine for space plane p 1065 A92-53487
Conceptual design of scramjet engine p 1065 A92-53490
Key design considerations for scramjet powered space plane p 1066 A92-53491
A survey of instabilities within centrifugal pumps and concepts for improving the flow range of pumps in rocket engines
[NASA-TM-105439] p 387 N92-18280

ROCKET ENGINES
CARS temperature/multi-species measurement strategies for high speed airbreathing and rocket propulsion testing p 154 A92-16615
Ceramics and ceramic matrix composites - Aerospace potential and status
[AIAA PAPER 92-2445] p 577 A92-34474
Technical history of aircraft engines p 558 A92-35911
Mechanics and thermodynamics of propulsion (2nd revised and enlarged edition) --- Book
[ISBN 0-201-14659-2] p 672 A92-38275
Monolithic ceramics p 668 A92-39854
Introduction --- propulsion system performance for hypersonic vehicles p 862 A92-46427
Propulsion systems from takeoff to high-speed flight p 889 A92-46428
An experimental investigation of high-aspect-ratio cooling passages
[AIAA PAPER 92-3154] p 890 A92-48780
A survey of instabilities within centrifugal pumps and concepts for improving the flow range of pumps in rocket engines
[NASA-TM-105439] p 387 N92-18280

ROCKET EXHAUST
Effect of carbon particles and mixing on afterburning of exhaust plumes
[AIAA PAPER 92-0767] p 387 A92-27107

ROCKET FIRING
Scramjet engine and its flying test bed p 1066 A92-53492

ROCKET LAUNCHERS
Aerodynamic study of H-II Orbiting Plane, HOPE p 1103 A92-53639

ROCKET TEST FACILITIES
Scramjet engine and its flying test bed p 1066 A92-53492
Performance analysis of idealized scramjet p 1066 A92-53493

RODS
Combined load test apparatus for flat panels
[NASA-CASE-LAR-14698-1] p 911 N92-30028

ROLL
The calculation of the static elastic aerodynamic distribution for the rolling maneuver aircraft p 379 A92-25010
Unique high-alpha roll dynamics of a sharp-edged 65 deg delta wing
[AIAA PAPER 92-0276] p 318 A92-25730
Reduction of wing rock amplitudes using leading-edge vortex manipulations
[AIAA PAPER 92-0279] p 379 A92-25733
Flow visualization image analysis of high-rate roll experiments on a delta wing
[AIAA PAPER 92-0317] p 321 A92-25764
Prediction of leading-edge vortex breakdown on a delta wing oscillating in roll
[AIAA PAPER 92-2677] p 807 A92-45585
Flight control system design using eigenstructure assignment for rolling the aircraft around the velocity vector p 977 A92-51945
Robust dynamic inversion control laws for aircraft control
[AIAA PAPER 92-4329] p 1073 A92-55173
An experimental investigation of the effect of fineness ratio on lateral force on a pointed slender body of revolution p 86 N92-13015
Model identification and control system design for the lambda unmanned research vehicle
[AD-A241859] p 299 N92-17024
A summary of the active flexible wing program
[NASA-TM-107655] p 962 N92-31264
Rolling maneuver load alleviation using active controls
[NASA-TM-107654] p 962 N92-31351
A background to the handling qualities of aircraft
[ESDU-92006] p 1087 N92-32780

ROLL FORMING
Calculation of the exerting force necessary to form the aircraft hull plate in the symmetry plate bender with three rolls and the feeding value of the centre roll p 998 A92-53297

ROLLER BEARINGS
Quasi-static analysis of roller bearing p 391 A92-24732
Performance of a hybrid cylindrical roller bearing p 995 A92-51845

ROLLING MOMENTS
Roll-performance criteria for high augmented aircraft p 204 A92-18623
Calculation of the rolling moment for a wing with a supersonic leading edge in the presence of sideslip p 426 A92-30186
Safety test on the rolling angles of a winged vehicle in hypersonic speed p 480 A92-30549
Self-induced roll oscillations of low-aspect-ratio rectangular wings p 874 A92-46802
Effects of the roll angle on cruciform wing-body configurations at high incidences
[AIAA PAPER 92-4356] p 1079 A92-55342
Steady and unsteady aerodynamics of a pitching straked wing model at high angles of attack p 87 N92-13024
Multiple roll attractors of a delta wing at high incidence p 88 N92-13026
An experimental investigation of leading edge vortical flow about a delta wing during wing rock
[AD-A243363] p 260 N92-17114
Non-linear airloads hypersurface representation: A time domain perspective p 346 N92-18783
Contribution of tailplane-mounted twin fins to sideforce, yawing moment, and rolling moment derivatives due to sideslip
[ESDU-92007] p 1086 N92-32487
Lift and rolling moment due to spoilers on wings with trailing-edge flaps deflected at subsonic speeds
[ESDU-92002-SUPPL] p 1037 N92-32782
A nozzle internal performance prediction method
[NASA-TP-3221] p 1040 N92-33625

ROOT-MEAN-SQUARE ERRORS
A data base for flight in the wake of a ship
[AIAA PAPER 92-0295] p 319 A92-25748

ROTARY ENGINES
NASA's rotary engine technology enablement program: 1983-1991
[NASA-TM-105562] p 378 N92-20033
Rotary engine performance limits predicted by a zero-dimensional model
[NASA-CR-189129] p 474 N92-20650
Small engine technology programs p 560 N92-22532
Development of natural gas rotary engines
[PB92-149665] p 765 N92-26816

ROTARY GYROSCOPES
A torque-free flexible model gyro p 495 A92-31552
A study of the precision characteristics of a gyroscopic gravimeter p 581 A92-33778

ROTARY STABILITY
Variation in hover aeromechanical stability trends with bearingless main rotor design p 109 A92-14425
Aeroelastic optimization of an advanced geometry helicopter rotor
[AIAA PAPER 92-2360] p 543 A92-34592
Nonlinear damping estimation from rotor stability data using time and frequency domain techniques p 641 A92-36855
Aeromechanical stability of hingeless helicopter rotors in forward flight p 874 A92-46923
Bilinear formulation applied to the stability and response of helicopter rotor blade p 847 A92-46930
Experimental investigation of the stability of a clearance-excited rotor system with optimal parameters p 1114 A92-54223
Nonlinear rotordynamics analysis --- Space Shuttle Main Engine turbopumps
[NASA-CR-184263] p 221 N92-14344
The stability of the steady state and bistable response of a flexible rotor supported on squeeze film dampers p 222 N92-14350
Experiment of static and dynamic characteristics of spiral grooved seals p 223 N92-14361
A simplified method for predicting the stability of aerodynamically excited turbomachinery p 224 N92-14364
Comments on frequency swept rotating input perturbation techniques and identification of the fluid force models in rotor/bearing/seal systems and fluid handling machines p 224 N92-14370
The application of a cylindrical-spherical floating ring bearing as a device to control stability of turbogenerators p 224 N92-14371
Effect of eccentricity on the static and dynamic performance of a turbulent hybrid bearing p 225 N92-14373
Application areas for rotorcraft system identification: Simulation model validation p 274 N92-17164
Mechanical design of a rotary balance system for NASA. Langley Research Center's vertical spin tunnel p 664 N92-25090
Self-adaptive aeropropulsion components-enhancing axial compressor performance
[AD-A246123] p 743 N92-27817
Explicit Navier-Stokes computation of turbomachinery flows
[AD-A249284] p 909 N92-28879
Explicit Navier-Stokes computation of turbomachinery flows
[AD-A248458] p 911 N92-29933

ROTARY WING AIRCRAFT
Prediction of high-resolution flowfields for rotorcraft aeroacoustics p 53 A92-11053
AHS, Annual Forum, 47th, Phoenix, AZ, May 6-8, 1991, Proceedings. Vols. 1 & 2 p 59 A92-14326
Wing tip vortex calculations with an unstructured adaptive-grid Euler solver p 64 A92-14330
Development of a reclined crashworthy crewseat for rotorcraft p 105 A92-14370
Recent rotorcraft aeroelastic testing in the Langley Transonic Dynamics Tunnel p 136 A92-14377
Rotorcraft airframe structural optimization for combined vibration and fatigue constraints p 106 A92-14390
The practical application of new technology to the civil rotorcraft need p 108 A92-14410
High speed rotorcraft - Comparison of leading concepts and technology needs p 108 A92-14415
A multibody approach to modeling tilt-wing rotorcraft dynamics
[AIAA PAPER 92-0487] p 328 A92-26318
System identification requirements for high-bandwidth rotorcraft flight control system design p 479 A92-29332
A structural design and optimization tool for ducted rotor/wing blades
[AIAA PAPER 92-2361] p 543 A92-34593
Rotary-wing aeroservoelastic problems
[AIAA PAPER 92-2107] p 567 A92-35678
An experimental investigation of the oblique blade-vortex interaction p 712 A92-43447

International Pacific Air and Space Technology Conference and Aircraft Symposium, 29th, Gifu, Japan, Oct. 7-11, 1991, Proceedings
[SAE P-246] p 783 A92-45376
The high speed challenge for rotary wing aircraft
[SAE PAPER 911974] p 842 A92-45381
Prediction of rotor unsteady airloads using vortex filament theory
[AIAA PAPER 92-2610] p 792 A92-45484
Periodic trim solutions with hp-version finite elements in time p 874 A92-46931
Advanced Rotorcraft Transmission (ART) Program summary
[AIAA PAPER 92-3365] p 905 A92-48938
High speed rotorcraft propulsion concepts to control power/speed characteristics
[AIAA PAPER 92-3367] p 865 A92-48940
Networked simulation of multiple aircraft using Semi-Automated Forces
[AIAA PAPER 92-4170] p 1008 A92-52455
Vision-based obstacle detection for rotorcraft flight p 967 A92-52465
Inertial navigation sensor integrated motion analysis for autonomous vehicle navigation p 995 A92-52470
Summary highlights of the Advanced Rotorcraft Transmission (ART) program
[AIAA PAPER 92-3362] p 1051 A92-54026
Rotary wing structural dynamics and aeroelasticity --- Book
[ISBN 1-56347-031-4] p 1052 A92-54550
Design and testing of a composite hingeless hub for rotary-wing aircraft p 1053 A92-56075
Finite-element analysis and multibody dynamics issues in rotorcraft dynamic analysis p 1055 A92-56286
A small light-weight rotor platform for ground observation and pollution control p 1057 A92-56329
Current European rotorcraft research activities on development of advanced CFD methods for the design of rotor blades (BRITE/EURAM 'DACRO' project) p 1032 A92-56332
Development of a conceptual design method for rotary-wing aircraft using digital computers p 1058 A92-56340
Passive range estimation for rotorcraft low-altitude flight
[NASA-TM-103897] p 2 N92-10003
Rotor noise p 54 N92-10600
Rotorcraft system identification
[AGARD-AR-280] p 22 N92-11001
Tracking performance requirements for rotorcraft instrument approaches to reduced minima. Phase 1: Preliminary study
[NRC-32137-PHASE-1] p 102 N92-11988
Rotorcraft acceleration and climb performance model
[SCT-90RR-30] p 116 N92-13059
Advanced rotorcraft control using parameter optimization
[NASA-CR-189502] p 135 N92-13073
Technical activities of the configuration aeroelasticity branch
[NASA-TM-104146] p 159 N92-13458
Image-based ranging and guidance for rotorcraft
[NASA-CR-184829] p 191 N92-14036
Technology needs for high speed rotorcraft (3)
[NASA-CR-177592] p 195 N92-14039
Rotorcraft low altitude IFR benefit/cost analysis: Operations analysis
[SCT-90RR-44] p 191 N92-15061
Rotorcraft System Identification
[AGARD-LS-178] p 273 N92-17153
Modelling aspects and robustness issues in rotorcraft system identification p 274 N92-17159
Assessment of rotorcraft system identification as applied to the AH-64 p 274 N92-17160
BO 105 identification results p 274 N92-17161
Industry view on rotorcraft system identification p 274 N92-17163
Application areas for rotorcraft system identification: Simulation model validation p 274 N92-17164
System identification methods for handling-qualities evaluation p 274 N92-17165
SIMNET plan view display user manual
[AD-A244617] p 510 N92-21392
Ship airwake measurement and modeling options for rotorcraft applications p 503 N92-21954
A new method for simulating atmospheric turbulence for rotorcraft applications p 464 N92-21956
Small engine technology programs p 560 N92-22532
Rotorcraft transmissions p 560 N92-22533
NASA aerodynamics program
[NASA-TM-4368] p 609 N92-24678
Advanced Rotorcraft Transmission (ART) program summary
[NASA-TM-105665] p 680 N92-24984
The NASA/industry Design Analysis Methods for Vibrations (DAMVIBS) Program: A government overview
[NASA-TM-107579] p 680 N92-25267
Rotorcraft terminal ATC route standards
[SCT-90RR-33] p 641 N92-26101
Status of automatic guidance systems for rotorcraft in low altitude flight p 727 N92-27894
The application of flight simulation models in support of rotorcraft design and development p 884 N92-28527
Rotorcraft In-Flight Simulation Research at NASA Ames Research Center: A Review of the 1980's and plans for the 1990's
[NASA-TM-103873] p 853 N92-28926
Contingency power for a small turboshaft engine by using water injection into turbine cooling air
[NASA-TM-105680] p 871 N92-29661
Building vibrations induced by noise from rotorcraft and propeller aircraft flyovers
[NASA-TM-104170] p 1138 N92-33160
The dynamics of flexible multibody systems: A finite segment approach p 1128 N92-34036

ROTARY WINGS

Frequency-domain identification of BO 105 derivative models with rotor degrees of freedom p 104 A92-14327
Three dimensional analysis of a rotor in forward flight p 64 A92-14329
Radar Detection Analysis of Rotor Systems (RADARS) p 117 A92-14350
Helicopter local blade circulation calculations for a model rotor in forward flight using laser velocimeter measurements p 65 A92-14362
Development of a shock noise prediction code for high-speed helicopters - The subsonically moving shock p 165 A92-14384
Computation of the BVI noise for the BO105 Model Rotor in forward flight and comparison with wind tunnel tests p 165 A92-14386
Design optimization of rotor blades for improved performance and vibration p 106 A92-14389
Analysis of rotor blade dynamics using experimental UH-60A airloads obtained at the DNW p 107 A92-14394
Structural optimization and Mach scale test validation of a low vibration rotor p 107 A92-14395
Ongoing development of a computer jobstream to predict helicopter main rotor performance in icing conditions p 65 A92-14407
Rotor blade preservation - Getting the most service life with lowest operational costs p 108 A92-14412
Bearingless main rotor system composite component fabrication techniques p 110 A92-14453
Transient aerodynamic behaviours associated with stepwise incidence variation of airfoils p 66 A92-15327
Solution of the compressible Euler equations for steady flows around helicopter rotor blades by an implicit space-centered method
[ONERA, TP NO. 1991-177] p 77 A92-16139
Aerodynamic and acoustic calculations of transonic nonlifting hovering rotors
[ONERA, TP NO. 1991-178] p 77 A92-16140
Numerical optimization of helicopter rotor blade airfoils using unsteady aerodynamic calculations
[ONERA, TP NO. 1991-187] p 78 A92-16141
Time-periodic control of a multi-blade helicopter p 204 A92-18626
Experimental investigation of periodically excited rotating composite rotor blades p 218 A92-20213
Computational vorticity capturing - Application to helicopter rotor flows
[AIAA PAPER 92-0056] p 250 A92-22171
Yaw dynamics of a coaxial rotor helicopter p 378 A92-24427
Aeroelastic analysis of swept, anhedral, and tapered tip rotor blades p 316 A92-25577
Importance of an accurate prediction of shock curvature for high-speed rotor noise p 414 A92-25578
Optimum design of helicopter rotor blades with multidisciplinary couplings
[AIAA PAPER 92-0214] p 357 A92-25687
Comprehensive helicopter rotor instrumentation - A retrofit approach using miniature transducers
[AIAA PAPER 92-0268] p 369 A92-25724
Laboratory evaluation of a sensor for detection of aircraft wing contaminants
[AIAA PAPER 92-0301] p 369 A92-25753
A simplified model for the interaction of a rotor tip vortex with an airframe
[AIAA PAPER 92-0320] p 321 A92-25767
Numerical investigation of performance degradation of wings and rotors due to icing
[AIAA PAPER 92-0412] p 325 A92-26264
Development of an analytical method to predict helicopter main rotor performance in icing conditions
[AIAA PAPER 92-0418] p 326 A92-26268
Experimental and theoretical studies on helicopter rotor fuselage interaction
[ONERA, TP NO. 1991-197] p 329 A92-26356
Theoretical and experimental studies of helicopter rotor/fuselage interaction
[ONERA, TP NO. 1991-198] p 329 A92-26357
Numerical simulation of flow separation for rotors and fixed wings
[AIAA PAPER 92-0635] p 334 A92-27013
Integrated multidisciplinary rotorcraft optimization research at the NASA Langley Research Center p 419 A92-29673
Numerical analysis of helicopter rotor blades p 430 A92-30558
Non-homogeneous bars under tension, pure bending and thermal loads p 495 A92-31198
Impact of structural optimization with aeroelastic/multidisciplinary constraints on helicopter rotor design
[AIAA PAPER 92-1001] p 535 A92-33193
A study on the feasibility of using adaptive structures in the attenuation of vibration characteristics of rotary wings
[AIAA PAPER 92-2452] p 541 A92-34415
Blade root torsional dampers to reduce hub loads
[AIAA PAPER 92-2449] p 541 A92-34476
Analysis of open loop higher harmonic control at high airspeeds on a modern four-bladed articulated rotor
[AIAA PAPER 92-2450] p 542 A92-34477
Vibration reduction in helicopter rotors using an active control surface located on the blade
[AIAA PAPER 92-2451] p 564 A92-34478
Aeroelastic response of helicopters with flexible fuselage *modeling*
[AIAA PAPER 92-2567] p 564 A92-34481
Fully integrated aerodynamic/dynamic optimization of helicopter rotor blades
[AIAA PAPER 92-2374] p 542 A92-34544
Optimizing tuning masses for helicopter rotor blade vibration reduction including computed airloads and comparison with test data
[AIAA PAPER 92-2376] p 542 A92-34546
Aeroelastic optimization of an advanced geometry helicopter rotor
[AIAA PAPER 92-2360] p 543 A92-34592
Dynamics of helicopters in ground resonance with and without blade dissimilarities
[AIAA PAPER 92-2108] p 544 A92-35679
Visualization and measurement of helicopter rotor flow using projected smoke filaments and digital image processing p 520 A92-35728
Acoustic results of the Boeing model 360 whirl tower test p 603 A92-35741
Experimenting a new composite rotor on an Aerospatiale Dauphin helicopter p 546 A92-35744
Calculation of pitch-link loads in deep stall using state-of-the-art methodology p 520 A92-35753
Navier-Stokes analysis of blade tip shape in hover p 521 A92-35758
Evaluation of a constant feedback gain for closed loop *higher harmonic control* p 568 A92-35768
Generalized higher harmonic control - Ten years of Aerospatiale experience p 569 A92-35769
LAH main rotor model test at the DNW p 547 A92-35771
Design and manufacturing of torsional flexible blade models p 547 A92-35780
Measurements of a rotor flowfield and the effects on a fuselage in forward flight p 521 A92-35787
Nonlinear damping estimation from rotor stability data using time and frequency domain techniques p 641 A92-36855
Recent manufacturing advances for spiral bevel gears
[SAE PAPER 912229] p 674 A92-40024
Effects of higher harmonic control on rotor performance and control loads p 729 A92-41218
Chaotic stall response of helicopter rotor in forward flight p 730 A92-43046
Analysis of the aerodynamic performance of rotors with the boundary element method p 709 A92-43119
Modeling the effect of helicopter downwash on warm fog p 775 A92-44081
Free wake analyses of a hovering rotor using panel method
[SAE PAPER 912004] p 789 A92-45405
Impact response of composite UHB propeller blades
[SAE PAPER 912046] p 861 A92-45430
Assessment of one-dimensional icing forecast model applied to stratiform clouds p 915 A92-46803
Sensitivity analysis of discrete periodic systems with *applications to helicopter rotor dynamics* p 846 A92-46884

Prediction of dynamic hub load of a rotor executing multiple sinusoidal blade pitch variations p 846 A92-46921
Chaotic oscillation in helicopter blade stall response p 846 A92-46922
Aeromechanical stability of hingeless helicopter rotors in forward flight p 874 A92-46923
A general purpose nonlinear rigid body mass finite element for application to rotary wing dynamics p 846 A92-46924
Chaotic dynamic behavior in a simplified rotor blade lag model p 846 A92-46926
On the choice of appropriate bases for nonlinear dynamic modal analysis p 847 A92-46927
Bilinear formulation applied to the stability and response of helicopter rotor blade p 847 A92-46930
An aeroelastic analysis with a generalized dynamic wake p 847 A92-46932
The unsteady interaction of a 3-dimensional vortex filament with a cylinder p 813 A92-46934
A study of rotor wake development and wake/body interactions in hover p 813 A92-46935
Linear analysis of naturally curved and twisted anisotropic beam p 899 A92-46936
On the adequacy of modeling turbulence and related effects on helicopter response p 847 A92-46945
Dynamic analysis of rotor flex-structure based on nonlinear anisotropic shell models p 899 A92-46946
Experimental and numerical study of flow around helicopter rotor blade tips p 814 A92-46948
An Eulerian/Lagrangian method for computing blade/vortex impingement p 814 A92-46952
Aerodynamic parametric studies and sensitivity analysis for rotor blades in axial flight p 816 A92-46959
Free vibration analysis of branched blades by the integrating matrix method p 847 A92-47122
Research on helicopter rotors - Progress in aerodynamics, aeroelasticity and acoustics
[ONERA, TP NO. 1992-27] p 849 A92-48589
Influence of geometrical parameters on helicopter rotor high speed impulsive noise
[ONERA, TP NO. 1992-40] p 926 A92-48601
The use of math-dynamic models to aid the development of integrated health and usage monitoring systems p 1006 A92-50013
A study on mechanical model of the helicopter 'ground resonance' p 955 A92-50214
Helicopter rotor blade aeroelasticity in forward flight with an implicit structural formulation p 958 A92-50315
The application of a theoretical blade sailing model to predict the behaviour of articulated helicopter rotors p 960 A92-52849
Rotary wing structural dynamics and aeroelasticity --- Book
[ISBN 1-56347-031-4] p 1052 A92-54550
Sensitivity analysis for structural optimization of helicopter rotor blades p 1053 A92-56073
A calculation method to predict helicopter noise and its verification p 1135 A92-56074
Helicopter rotor testing using scaled model p 1093 A92-56076
Flutter and stall response of a helicopter blade with structural nonlinearity p 1055 A92-56178
Design and development of test rigs for main rotor and main rotor transmission of a helicopter in the 6-ton-class p 1093 A92-56280
Response of helicopter blades to a sharp collective increase p 1084 A92-56282
Simulation of helicopter see-saw rotor motion p 1055 A92-56287
Dynamics of helicopters with dissimilar blades in forward flight p 1056 A92-56288
The application of math-dynamic models to characterise a range of helicopter rotor system faults p 1056 A92-56297
Modern helicopter technologies at MBB and the application in future programmes p 1016 A92-56304
Aeroelasticity of a coaxial helicopter rotor p 1057 A92-56309
Influence of cross section variations on the structural behaviour of composite rotor blades p 1121 A92-56320
A finite element method for shear stresses calculation in composite blade models p 1121 A92-56322
A generic harmonic rotor model for helicopter flight simulation p 1086 A92-56333
A study of helicopter rotor/fuselage response in low-speed manoeuvres - Comparison of theory with flight p 1086 A92-56334
Low energy ice protection for helicopters p 1059 A92-56348
Aerodynamic features of a coaxial rotor helicopter p 1032 A92-56349
Correlation of flight, tunnel and prediction data on a helicopter main rotor p 1059 A92-56350
Measurements of the dynamic stall vortex convection speed p 1032 A92-56351
Experimental study of an independently deflected wingtip mounted on a semispan wing
[NASA-TM-102842] p 13 N92-10983
Analysis of open loop higher harmonic control at high airspeeds on a modern four-bladed articulated rotor
[NASA-TM-103876] p 21 N92-11000
A numerical solution of implicit nonlinear equations of motion for rotor blades p 115 N92-13053
Flapping inertia for selected rotor blades
[NASA-TM-104125] p 115 N92-13057
Integration of dynamic, aerodynamic, and structural optimization of helicopter rotor blades
[NASA-CR-189018] p 195 N92-14038
Development of an analytical method to predict helicopter main rotor performance in icing conditions
[NASA-CR-189110] p 258 N92-15967
Periodic trim solutions with HP-version finite elements in time
[NASA-CR-189778] p 282 N92-17019
The solution of a singular integral equation arising from a lifting surface theory for rotating blades p 260 N92-17303
Development of nonlinear real-time helicopter simulation using a blade element method
[NLR-TP-90115-U] p 381 N92-18893
Experimental validation of structural optimization methods
[NASA-TM-104203] p 404 N92-19258
A study of the aeroelastic behaviour of helicopter rotor blades featuring swept tips p 367 N92-19701
Optimizing tuning masses for helicopter rotor blade vibration reduction including computed airloads and comparison with test data
[NASA-TM-104194] p 367 N92-19846
Resolution of the Euler equations applied to a helicopter rotor in forward flight
[ONERA-RSF-2/3731-AY-004A] p 406 N92-19976
Fully integrated aerodynamic/dynamic optimization of helicopter rotor blades
[NASA-TM-104226] p 461 N92-20417
Modeling methods for high-fidelity rotorcraft flight mechanics simulation
[NASA-TM-103842] p 482 N92-21440
A review of icing research at the Royal Aerospace Establishment p 451 N92-21689
Helicopter rotor blade dynamics with bilinear formulation p 463 N92-21856
Helicopter active rotor control p 570 N92-22157
The NASA aircraft icing research program p 549 N92-22534
Experimental evaluation of a flat wake theory for predicting rotor inflow-wake velocities
[NASA-TM-4334] p 630 N92-24882
Effect of blade planform variation on the forward-flight performance of small-scale rotors
[NASA-TM-4345] p 630 N92-24885
A semi empirical method for the analytical representation of stationary measured profile coefficients for applications of rotary wing aerodynamics
[ETN-92-91491] p 832 N92-29741
Development of a full-scale transmission testing procedure to evaluate advanced lubricants
[NASA-TP-3265] p 998 N92-30396
Composite beam analysis linear analysis of naturally curved and twisted anisotropic beams
[AD-A252652] p 999 N92-30766
Development of hardness cycles for fiber bound materials, using DSC: From laboratory specimens to complex high duty structural members
[MBB-Z-0409-91-PUB] p 987 N92-30969
A demonstration of passive blade twist control using extension-twist coupling
[NASA-TM-107642] p 1001 N92-31155
Numerical investigation of the effects of icing on fixed and rotary wing aircraft
[NASA-CR-190542] p 1044 N92-34105

ROTATING BODIES

Surface flow visualization of rotating propeller p 4 A92-10959
Base pressure on an axisymmetric finned body during forced rotation in the autorotation regime p 7 A92-12165
Unsteady lifting surface theory for a rotating transonic cascade of swept blades
[ASME PAPER 91-GT-178] p 73 A92-15610
Effect of Eulerian inertia forces on the stressed state of the rotating components of aircraft turbomachines p 128 A92-16828
Vibration characteristics of pretwisted aerofoil cross-section blade packets under rotating conditions p 219 A92-20756
Theoretical and experimental study of a model rotor p 547 A92-35781
Improved measurement of the dynamic loads acting on rotating parachutes p 702 A92-41236
Singlemode fiber optic rotary joint for aircraft applications p 779 A92-42606
Navier-Stokes simulation of dynamic stall on a rotating airfoil p 626 N92-24853
Professor Jesse W. Beams and the first practical magnetic suspension p 771 N92-27723
CSM solutions of rotating blade dynamics using integrating matrices
[NASA-CR-190577] p 1003 N92-31619
The dynamics of flexible multibody systems: A finite segment approach p 1128 N92-34036

ROTATING CYLINDERS

Prospects of turbulence research by means of testing bodies in motion p 30 A92-12194

ROTATING DISKS

Inspection of compressor discs by ultrasonic leaky waves using an automated C-scan system p 144 A92-13584
Dynamic analysis technique of rotating centrifugal impeller
[ASME PAPER 91-GT-50] p 148 A92-15528
Magnetohydrodynamic boundary layer flow over a rotating disk p 304 A92-21338
The effects of suction on the nonlinear stability of the three-dimensional boundary layer above a rotating disc p 393 A92-25366
Turbine disk temperatures resulting from the hot mainstream at engine conditions
[AIAA PAPER 92-0398] p 373 A92-26252
A torque-free flexible model gyro p 495 A92-31552
A unified numerical approach for the analysis of rotating disks including turbine rotors
[AIAA PAPER 92-2303] p 585 A92-34524
A new method for calculating burst speed of aeroengine disks
[ASME PAPER 91-GT-121] p 670 A92-36899
Experiments on turbulent flow due to an enclosed rotating disk p 615 A92-38863
Rotational coherent anti-Stokes Raman spectroscopy measurements in a rotating cavity with axial throughflow of cooling air - Oxygen concentration measurements p 990 A92-49574
Discs low cycle fatigue life predictions for gas turbine engines in CSFR by using fractographic information p 995 A92-51950
Numerical verification of NISA 2 finite element analysis of the cracked 5th stage compressor disc of J-85 jet engine
[NRC-LTR-ST-1792] p 129 N92-11997

ROTATING FLUIDS

Aerodynamic design of a Coanda induced force and thruster anti-torque system p 109 A92-14419
Self-induced flow in a stepped rotating tube
[ASME PAPER 91-GT-276] p 152 A92-15673
A boundary integral formulation for the kinetic field in aerodynamics. I - Mathematical analysis p 243 A92-21504
Simulation of turbulent velocity profiles appearing on rotating and stationary parts of subsonic compressors and turbines p 676 A92-40172
Flow induction by pressure forces
[AIAA PAPER 92-3571] p 1067 A92-54060

ROTATING GENERATORS

A new resonant link aircraft power generating system p 970 A92-50528

ROTATING MIRRORS

Professor Jesse W. Beams and the first practical magnetic suspension p 771 N92-27723

ROTATING SHAFTS

Active magnetic bearings give systems a lift p 901 A92-48201
Stability of intershaft squeeze film dampers p 222 N92-14351
Experimental investigations of exciting forces caused by flow in labyrinth seals p 223 N92-14354
Hydraulic actuator system for rotor control p 224 N92-14363
Rotor-to-stator partial rubbing and its effects on rotor dynamic response p 224 N92-14367
Comments on frequency swept rotating input perturbation techniques and identification of the fluid force models in rotor/bearing/seal systems and fluid handling machines p 224 N92-14370
The application of a cylindrical-spherical floating ring bearing as a device to control stability of turbogenerators p 224 N92-14371
Programs at Wright-Patterson Air Force Base p 228 N92-15092

ROTATING SPHERES

Motion of a sphere in a gas - Numerical solution of the linearized Boltzmann equation p 591 A92-36194

ROTATING STALLS

Stall inception in axial flow compressors
[ASME PAPER 91-GT-86] p 69 A92-15551

Active suppression of rotating stall and surge in axial compressors
[ASME PAPER 91-GT-87] p 122 A92-15552
Active control of rotating stall in a low speed axial compressor
[ASME PAPER 91-GT-88] p 122 A92-15553
LDV measurements of a mixed-flow impeller at design and near stall
[ASME PAPER 91-GT-310] p 153 A92-15688
Stage-by-stage poststall compression system modeling technique p 80 A92-17194
An aeroacoustic model about the rotating stall of a compressor p 416 A92-27855
Parameter identification of compressor dynamics during closed-loop operation p 508 A92-29313
Compressor modeling and active control of stall/surge p 508 A92-29315
Two-parameter bifurcation analysis of axial flow compressor dynamics p 421 A92-29355
Model development for active surge control/rotating stall avoidance in aircraft gas turbine engines p 468 A92-29375
An integrated, full-range surge control/rotating stall *avoidance compressor control system* p 469 A92-29376
Heat induced transient behaviours of axial compressors p 469 A92-29721
A study of surge control using fuel pulse cutoff for dual spool turbo-jet engine p 470 A92-29737
Investigations of the laws of surge and rotating stall forecast in aeronautical engine p 470 A92-29739
Relationship between the rotating stall and vibrations of a blade row p 496 A92-31988
A study on the rotating stall of centrifugal compressors. II - Effect of vaneless diffuser inlet shape on rotating stall p 497 A92-32508
Current topics connected with rotating stall p 521 A92-35913
Unsteady flow within centrifugal compressor channels under rotating stall and surge
[ASME PAPER 91-GT-85] p 670 A92-36901
Wind-tunnel compressor stall monitoring using neural networks p 918 A92-46817
Numerical investigation of surge and rotating stall in multistage axial compressors
[AIAA PAPER 92-3193] p 825 A92-48804
A theoretical study of sensor-actuator schemes for rotating stall control
[AIAA PAPER 92-3486] p 878 A92-49025
Experimental study of the mechanism of sound generation by rotating stall in centrifugal turbomachines p 605 N92-23726
Dynamic control of aerodynamic instabilities in gas turbine engines p 870 N92-28466
Active control of compressor surge and stall
[AD-A252771] p 1126 N92-33498

ROTATION
Heat transfer and instrumentation studies on rotating turbine blades in a transient facility p 156 N92-12203
Identification of dynamic characteristics of flexible rotors as dynamic inverse problem p 220 N92-13962
Turbine engine diagnostics system study
[DOT/FAA/CT-91/16] p 202 N92-14064
Surface pressure measurements on the wing of a wind tunnel model during steady rotation
[AD-A243047] p 260 N92-17281
Helicopter active rotor control p 570 N92-22157
Investigation of the dynamic behaviour and the frequency response of the GG 1342 laser gyro
[ESA-TT-1236] p 595 N92-22641
Analysis and modification of a single-mesh gear fatigue rig for use in diagnostic studies
[NASA-TM-105416] p 773 N92-27879
Non-linear interactions in homogeneous turbulence with *and without background rotation* p 912 N92-30044
Effects of curvature and rotation on turbulence in the NASA low-speed centrifugal compressor impeller p 1124 N92-32292

ROTATIONAL SPECTRA
Rotational coherent anti-Stokes Raman spectroscopy measurements in a rotating cavity with axial throughflow of cooling air - Oxygen concentration measurements p 990 A92-49574

ROTOR AERODYNAMICS
Prediction of high-resolution flowfields for rotorcraft aeroacoustics p 53 A92-11053
Design and testing of a controlled diffusion airfoil cascade for industrial axial flow compressor application
[ASME PAPER 90-GT-140] p 6 A92-11286
Analysis of unsteady pressures induced on a body by a rotor p 10 A92-13212
An integrated airloads-inflow model for use in rotor aeroelasticity and control analysis p 64 A92-14328
Three dimensional analysis of a rotor in forward flight p 64 A92-14329
Wing tip vortex calculations with an unstructured adaptive-grid Euler solver p 64 A92-14330
Results from a test of a 2/3-scale V-22 rotor and wing in the 40- by 80-Foot Wind Tunnel p 104 A92-14332
Identification of higher-order helicopter dynamics using linear modeling methods p 131 A92-14336
Forward flight trim calculation and frequency response *validation of a high-order helicopter simulation model* p 132 A92-14337
Fundamental research in helicopter rotor blade-vortex interaction modeling p 65 A92-14358
Comparison of theory and experiment for nonlinear flutter and stall response of a helicopter blade p 65 A92-14428
A re-examination of the aerodynamics of hovering rotors including the presence of the fuselage p 66 A92-14446
An Axial Turbobrake
[ASME PAPER 91-GT-1] p 147 A92-15501
Wave engine aerothermodynamic design
[ASME PAPER 91-GT-4] p 120 A92-15502
Computational study of stall flutter in linear cascades
[ASME PAPER 91-GT-5] p 67 A92-15503
Experimental study of the swirling flow in the internal volute of a centrifugal compressor
[ASME PAPER 91-GT-7] p 67 A92-15505
Stator averaged, rotor blade-to-blade near wall flow in a multistage axial compressor with tip clearance variation
[ASME PAPER 91-GT-30] p 67 A92-15514
Surge dynamics in a free-spool centrifugal compressor system
[ASME PAPER 91-GT-31] p 68 A92-15515
Performance of radial clearance rim seals in upstream and downstream rotor-stator wheelspaces
[ASME PAPER 91-GT-32] p 147 A92-15516
Rim sealing of rotor-stator wheelspaces in the absence of external flow
[ASME PAPER 91-GT-33] p 147 A92-15517
A viscous flow study of shock-boundary layer interaction, radial transport, and wake development in a transonic compressor
[ASME PAPER 91-GT-69] p 68 A92-15539
An improved method for aerodynamic design of centrifugal impeller blades
[ASME PAPER 91-GT-76] p 69 A92-15545
A 3D FEM variational aerodynamic calculation and performance analysis of a leaned turbine stator cascade
[ASME PAPER 91-GT-79] p 69 A92-15548
Quasi-three-dimensional characteristics method for a supersonic compressor rotor
[ASME PAPER 91-GT-81] p 69 A92-15549
The role of tip clearance in high-speed fan stall
[ASME PAPER 91-GT-83] p 69 A92-15550
Effects of stator wakes and spanwise nonuniform inlet conditions on the rotor flow of an axial turbine stage
[ASME PAPER 91-GT-93] p 70 A92-15557
The influence of blade leaning on the performance of an integrated OGV-diffuser system
[ASME PAPER 91-GT-104] p 122 A92-15561
Similarity transformations for compressor blading
[ASME PAPER 91-GT-123] p 70 A92-15568
Effects of simulated rotation on tip leakage in a planar cascade of turbine blades. I - Tip gap flow
[ASME PAPER 91-GT-127] p 71 A92-15572
Effects of simulated rotation on tip leakage in a planar cascade of turbine blades. II - Downstream flow field and *blade loading*
[ASME PAPER 91-GT-128] p 71 A92-15573
Numerical prediction of wakes in cascades and compressor rotors including the effects of mixing. I - *Cascade wakes including the effects of incidence and* freestream turbulence
[ASME PAPER 91-GT-225] p 74 A92-15638
Performance improvements of compressor cascades by *controlling the profile and sidewall boundary layers*
[ASME PAPER 91-GT-260] p 75 A92-15662
Validation of a numerical method for unsteady flow calculations
[ASME PAPER 91-GT-271] p 151 A92-15668
Formulation of a simplified model of rotor-horizontal stabilizer interactions and comparison with experimental measurements
[ONERA, TP NO. 1991-157] p 77 A92-16125
Supersonic stator-rotor interaction in a turbine stage
[ONERA, TP NO. 1991-166] p 77 A92-16133
Numerical optimization of helicopter rotor blade airfoils using unsteady aerodynamic calculations
[ONERA, TP NO. 1991-187] p 78 A92-16141
Helicopter air resonance modeling and suppression using active control p 204 A92-18625
Time-periodic control of a multi-blade helicopter p 204 A92-18626
Weak coupling between an unsteady 3D full potential code and an unsteady turbulent boundary layer code - Application to a helicopter rotor in forward flight
[AIAA PAPER 92-0029] p 249 A92-22151
Measurements of the pressure and velocity distribution in low-speed turbomachinery by means of high-frequency pressure transducers p 391 A92-24723
A large-scale axial flow compressor facility and dynamic measurement techniques for rotor flow study p 382 A92-24729
A quick automatic method for computing performance of nonducted propeller with constant-revolutional-speed p 393 A92-25505
Vortex modeling for rotor aerodynamics - The 1991 Alexander A. Nikolsky Lecture p 315 A92-25576
Optimum design of helicopter rotor blades with multidisciplinary couplings
[AIAA PAPER 92-0214] p 357 A92-25687
An experimental and analytical study of the interaction *of a vortex with an airframe*
[AIAA PAPER 92-0319] p 321 A92-25766
Unsteady flowfield simulation of ducted prop-fan configurations
[AIAA PAPER 92-0521] p 332 A92-26946
Measurements of the inflow to a vibrating rotor blade
[AIAA PAPER 92-0634] p 333 A92-27012
Experimental investigation of the perpendicular rotor blade-vortex interaction at transonic speeds p 340 A92-28047
Numerical analysis of helicopter rotor blades p 430 A92-30558
Freestream capturing for moving coordinates in three dimensions p 432 A92-31186
Dynamics of an optimized rotor blade at off-design flight conditions p 461 A92-32250
Comparison between imposed-periodicity and marching-in-time solutions of helicopter rotor blade steady-state response problem
[AIAA PAPER 92-2256] p 540 A92-34411
Nonlinear large amplitude aeroelastic behavior of composite rotor blades at large static deflection
[AIAA PAPER 92-2257] p 540 A92-34412
Analytical aeroelastic stability considerations and conversion loads for an XV-15 tilt-rotor in a wind tunnel simulation
[AIAA PAPER 92-2258] p 540 A92-34413
Dynamics of helicopters in ground resonance with and without blade dissimilarities
[AIAA PAPER 92-2108] p 544 A92-35679
Coupled rotor-fuselage dynamics and aeroelasticity in turning flight
[AIAA PAPER 92-2109] p 544 A92-35680
Complete Euler-solution for a rotor in hover and a propeller in forward flight p 520 A92-35755
Rotor aeromechanics research with the RAE research Lynx - The experimental facility and test programme p 547 A92-35767
Bearingless rotor aeromechanical stability measurements and correlations using nonlinear aerodynamics p 547 A92-35772
General model of isolated helicopter blade for stability investigation p 547 A92-35774
Theoretical model to calculate aerodynamic interference effects between rotor and wing of tiltrotors p 521 A92-35788
Comparison of elastic and rigid blade-element rotor models using parallel processing technology for piloted simulations
[SAE PAPER 912120] p 608 A92-39968
Design and development of a compressible dynamic stall facility p 747 A92-41215
Extension and validation of an unsteady wake model for rotors p 702 A92-41224
Analysis of the aerodynamic performance of rotors with *the boundary element method* p 709 A92-43119
Sensitivity analysis of discrete periodic systems with applications to helicopter rotor dynamics p 846 A92-46884
Experimental and numerical study of flow around helicopter rotor blade tips p 814 A92-46948
Flow visualisation of a small diameter rotor operating at high rotational speeds with blades at small pitch *angles* p 814 A92-46949
A unified procedure for solving rotor flowfield, performance and interference p 814 A92-46950
Efficient high-resolution rotor wake calculations using *flow field reconstruction* p 814 A92-46951
An Eulerian/Lagrangian method for computing blade/vortex impingement p 814 A92-46952
Three-dimensional blade vortex interactions p 815 A92-46953
Experimental and computational studies of hovering rotor flows p 815 A92-46954
Initial validation of an unsteady Euler/Navier-Stokes flow solver for helicopter rotor airloads in forward flight p 815 A92-46956

Effects of leading and trailing edge flaps on the aerodynamics of airfoil/vortex interactions
p 815 A92-46957
A new integral equation for potential compressible aerodynamics of rotors in forward flight
p 815 A92-46958
Research on helicopter rotors - Progress in aerodynamics, aeroelasticity and acoustics
[ONERA, TP NO. 1992-27] p 849 A92-48589
A turbulence model based on RNG for quasi-three-dimensional cascade flows --- renormalization group methods
[AIAA PAPER 92-3312] p 825 A92-48898
Numerical flow simulation and analysis of a shrouded propfan rotor
[AIAA PAPER 92-3773] p 826 A92-49118
The use of math-dynamic models to aid the development of integrated health and usage monitoring systems
p 1006 A92-50013
A finite-volume numerical method to calculate fluid forces and rotordynamic coefficients in seals
[AIAA PAPER 92-3712] p 1113 A92-54132
Experimental investigation of the stability of a clearance-excited rotor system with optimal parameters
p 1114 A92-54223
Comparison of frequency domain and time domain laser velocimeter signal processors p 1114 A92-54314
Particle image velocimetry measurements of the aerodynamics of a wind turbine p 1115 A92-54337
Helicopter rotor testing using scaled model
p 1093 A92-56076
Dynamic analysis of rotor blades with root retention design variations p 1054 A92-56156
The computation and validation of hovering rotor performance p 1055 A92-56285
Finite-element analysis and multibody dynamics issues in rotorcraft dynamic analysis p 1055 A92-56286
The application of math-dynamic models to characterise a range of helicopter rotor system faults
p 1056 A92-56297
Blade instability of horizontally stoppable rotors
p 1085 A92-56308
A time-dependent tip loss formula for rotor blade dynamic analysis p 1057 A92-56310
Smart structures in the active control of blade vortex interaction p 1085 A92-56314
Current European research activities in helicopter interactional aerodynamics p 1058 A92-56330
A generic harmonic rotor model for helicopter flight simulation p 1086 A92-56333
BVI impulsive noise reduction by higher harmonic pitch control - Results of a scaled model rotor experiment in the DNW p 1136 A92-56344
Aerodynamic features of a coaxial rotor helicopter
p 1032 A92-56349
Correlation of flight, tunnel and prediction data on a helicopter main rotor p 1059 A92-56350
Measurements of the dynamic stall vortex convection speed p 1032 A92-56351
Rotor noise p 54 N92-10600
Radial inflow turbine study
[AD-A240169] p 26 N92-11015
Analytical/numerical matching and periodic inversion: Two advances in free wake analysis
p 178 N92-13994
Rotorcraft System Identification
[AGARD-LS-178] p 273 N92-17153
Application areas for rotorcraft system identification: Simulation model validation p 274 N92-17164
Development of nonlinear real-time helicopter simulation using a blade element method
[NLR-TP-90115-U] p 381 N92-18893
Investigation of the influence of rotary aerodynamics on the study of high angle of attack dynamics of the F-15B using bifurcation analysis
[AD-A243969] p 348 N92-19367
A numerical study of fuselage scattering effects on rotor noise p 511 N92-20428
Model rotor icing tests in the NASA. Lewis Icing Research Tunnel p 450 N92-21688
LAH-main rotor model test at the DNW
[NLR-TP-90305-U] p 852 N92-28687
A general numerical model for wave rotor analysis
[NASA-TM-105740] p 1002 N92-31484
Radial inflow turbine study
[AD-A252783] p 1127 N92-33538

ROTOR BLADES

Three dimensional analysis of a rotor in forward flight
p 64 A92-14329
LH wind tunnel testing - Key to advanced aerodynamic design p 104 A92-14331
Forward flight trim calculation and frequency response validation of a high-order helicopter simulation model
p 132 A92-14337
Helicopter local blade circulation calculations for a model rotor in forward flight using laser velocimeter measurements p 65 A92-14362
A new method for simulating atmospheric turbulence for rotorcraft applications p 162 A92-14368
Design optimization of rotor blades for improved performance and vibration p 106 A92-14389
Analysis of rotor blade dynamics using experimental UH-60A airloads obtained at the DNW
p 107 A92-14394
Experimental investigation of helicopter vibration reduction using rotor blade aeroelastic tailoring
p 107 A92-14396
Studying dynamic behavior of X380 helicopter equipped with a new 5-blade composite rotor p 108 A92-14398
Rotor blade preservation - Getting the most service life with lowest operational costs p 108 A92-14412
Aerodynamic design of a Coanda induced force and thruster anti-torque system p 109 A92-14419
Lifting line predictions for a swept tip rotor blade
p 65 A92-14424
Evaluation of an advanced finite element analysis for rotor blades p 109 A92-14426
Comparison of theory and experiment for nonlinear flutter and stall response of a helicopter blade
p 65 A92-14428
Design method for subsonic and transonic cascade with prescribed Mach number distribution
[ASME PAPER 91-GT-18] p 67 A92-15509
Unsteady lifting surface theory for a rotating transonic cascade of swept blades
[ASME PAPER 91-GT-178] p 73 A92-15610
Comparison of time-resolved turbine rotor blade heat transfer measurements and numerical calculations
[ASME PAPER 91-GT-268] p 151 A92-15666
High-speed impulsive noise and aerodynamic results for rectangular and swept rotor blade tip tests in S1-Modane wind tunnel
[ONERA, TP NO. 1991-124] p 76 A92-16102
Experimental investigation of periodically excited rotating composite rotor blades p 218 A92-20213
Time domain flutter analysis of cascades using a full-potential solver p 176 A92-20747
Optimum design of helicopter rotor blades with multidisciplinary couplings
[AIAA PAPER 92-0214] p 357 A92-25687
Numerical investigation of performance degradation of wings and rotors due to icing
[AIAA PAPER 92-0412] p 325 A92-26264
Measurements of the inflow to a vibrating rotor blade
[AIAA PAPER 92-0634] p 333 A92-27012
Numerical simulation of flow separation for rotors and fixed wings
[AIAA PAPER 92-0635] p 334 A92-27013
The unresolved unsteady flow in multistage compressor blade rows p 421 A92-29472
Non-homogeneous bars under tension, pure bending and thermal loads p 495 A92-31198
Dynamics of an optimized rotor blade at off-design flight conditions p 461 A92-32250
Low-speed cruise aerodynamics of the stopped rotor/disk rotorcraft concept
[AIAA PAPER 92-1067] p 517 A92-33240
A demonstration of passive blade twist control using extension-twist coupling
[AIAA PAPER 92-2468] p 539 A92-34358
Blade root torsional dampers to reduce hub loads
[AIAA PAPER 92-2449] p 541 A92-34476
Vibration reduction in helicopter rotors using an active control surface located on the blade
[AIAA PAPER 92-2451] p 564 A92-34478
Application of composite rotor blade stability analysis to extension-twist coupled blades
[AIAA PAPER 92-2254] p 564 A92-34479
Aeroelastic response and blade loads of a composite rotor in forward flight
[AIAA PAPER 92-2566] p 564 A92-34480
Fully integrated aerodynamic/dynamic optimization of helicopter rotor blades
[AIAA PAPER 92-2374] p 542 A92-34544
Optimizing tuning masses for helicopter rotor blade vibration reduction including computed airloads and comparison with test data
[AIAA PAPER 92-2376] p 542 A92-34546
Aeroelastic optimization of an advanced geometry helicopter rotor
[AIAA PAPER 92-2360] p 543 A92-34592
A structural design and optimization tool for ducted rotor/wing blades
[AIAA PAPER 92-2361] p 543 A92-34593
The use of Stodola modes in rotor-blade aeroelastic studies p 590 A92-35729
Tail rotor aerodynamic features recorded in flight
p 546 A92-35752
Instrumented blade experiments using a light autogiro
p 555 A92-35773
General model of isolated helicopter blade for stability investigation p 547 A92-35774
Rotor blade-vortex interaction noise reduction and vibration using higher harmonic control
p 604 A92-35778
Modeling rotor dynamics with rotor speed degree of freedom for drive train torsional stability analysis
p 547 A92-35779
Theoretical and experimental study of a model rotor
p 547 A92-35781
The effects of inner wake modelling on blade airloads
p 521 A92-35784
Comparison of elastic and rigid blade-element rotor models using parallel processing technology for piloted simulations
[SAE PAPER 912120] p 608 A92-39968
Some issues on modeling atmospheric turbulence experienced by helicopter rotor blades
p 647 A92-40885
Effects of higher harmonic control on rotor performance and control loads p 729 A92-41218
Transonic aeroelasticity analysis for rotor blades
p 758 A92-41238
Chaotic stall response of helicopter rotor in forward flight p 730 A92-43046
Helicopter aeroelastic stability and response - Current topics and future trends p 730 A92-43100
Optimization of blade structure to reduce rotor vibration p 730 A92-43118
Multiharmonic control response of a rotor blade during forward flight (Test) p 744 A92-43120
Multiharmonic control response of a rotor blade during forward flight (Analysis) p 744 A92-43121
Prediction of rotor unsteady airloads using vortex filament theory
[AIAA PAPER 92-2610] p 792 A92-45484
The relationship between tensile and flexural strength of unidirectional composites p 891 A92-45629
Approach for analysis and design of composite rotor blades p 899 A92-46801
Free vibration analysis of branched blades by the integrating matrix method p 847 A92-47122
A new method of helicopter rotor blade motion control
p 875 A92-47786
The application of a theoretical blade sailing model to predict the behaviour of articulated helicopter rotors
p 960 A92-52849
The interaction between a high-frequency gust and a blade row p 1135 A92-54484
Measurements of blade flapping motion on a wind tunnel model p 1093 A92-56023
Structural optimization of a cantilevered beam subject to combined static loadings p 1118 A92-56024
Sensitivity analysis for structural optimization of helicopter rotor blades p 1053 A92-56073
Dynamic analysis of rotor blades with root retention design variations p 1054 A92-56156
Helicopter tail rotor stall flutter p 1056 A92-56290
Blade instability of horizontally stoppable rotors
p 1085 A92-56308
A time-dependent tip loss formula for rotor blade dynamic analysis p 1057 A92-56310
Oscillations of an anisotropic rotor on an elastic anisotropic support p 1057 A92-56311
Coupled rotor-fuselage vibration reduction with multiple frequency blade pitch control p 1085 A92-56315
Current European rotorcraft research activities on development of advanced CFD methods for the design of rotor blades (BRITE/EURAM 'DACRO' project)
p 1032 A92-56332
A study of helicopter rotor/fuselage response in low-speed manoeuvres - Comparison of theory with flight p 1086 A92-56334
Low energy ice protection for helicopters
p 1059 A92-56348
Numerical simulation of unsteady rotor wakes
p 1032 A92-56352
Effect of blade planform variation on the forward-flight performance of small-scale rotors
[NASA-TM-4345] p 630 N92-24885
LAH-main rotor model test at the DNW
[NLR-TP-90305-U] p 852 N92-28687
A demonstration of passive blade twist control using extension-twist coupling
[NASA-TM-107642] p 1001 N92-31155
CSM solutions of rotating blade dynamics using integrating matrices
[NASA-CR-190577] p 1003 N92-31619
Experimental study of performance degradation of a rotating system in the NASA Lewis RC icing tunnel
[NASA-CR-190684] p 1102 N92-34141

ROTOR BLADES (TURBOMACHINERY)

Optimizing instrumentation when measuring jet engine blade vibration
[ASME PAPER 91-GT-71] p 148 A92-15540

A numerical procedure of three-dimensional design problem in turbomachinery
[ASME PAPER 91-GT-144] p 72 A92-15583
Experiments on the blade loss transient response of rotor with flexible damped support
[ASME PAPER 91-GT-149] p 148 A92-15587
Film cooling on a gas turbine rotor blade
[ASME PAPER 91-GT-279] p 152 A92-15675
Blade row interaction in a multistage low-pressure turbine
[ASME PAPER 91-GT-283] p 125 A92-15678
Solution of the problem of three-dimensional flow past the blade rows of turbomachines with allowance for viscosity effects p 244 A92-21618
Navier-Stokes calculations of inboard stall delay due to rotation p 309 A92-24410
Dynamic analysis of annular cascade shrouded blades p 397 A92-27856
Experimental and theoretical study for nonlinear aeroelastic behavior of a flexible rotor blade
[AIAA PAPER 92-2253] p 584 A92-34410
Comparison between imposed-periodicity and marching-in-time solutions of helicopter rotor blade steady-state response problem
[AIAA PAPER 92-2256] p 540 A92-34411
Nonlinear large amplitude aeroelastic behavior of composite rotor blades at large static deflection
[AIAA PAPER 92-2257] p 540 A92-34412
A new aeroelastic model for composite rotor blades with straight and swept tips
[AIAA PAPER 92-2259] p 541 A92-34414
A study on the feasibility of using adaptive structures in the attenuation of vibration characteristics of rotary wings
[AIAA PAPER 92-2452] p 541 A92-34415
Experimental investigation on blade loss transient response of rotor with flexible damped support p 557 A92-35551
Dynamics of helicopters in ground resonance with and without blade dissimilarities
[AIAA PAPER 92-2108] p 544 A92-35679
A refined analytical method for designing high pressure ratio centrifugal impellers p 591 A92-36032
Turbomachinery unsteady load predictions with nonuniform inflow p 611 A92-36972
Vibration analysis of gas turbines by an intelligent knowledge-based system p 656 A92-40548
Segmental heat transfer in a pin fin channel with ejection holes p 900 A92-47267
Structural optimization and vibration control of composite rotor blades p 960 A92-53056
Real-time helicopter simulation using the blade element method p 1132 A92-56278
Trimming rotor blades with periodically deflecting trailing edge flaps p 1085 A92-56283
Research on measurement and control of helicopter rotor response using blade-mounted accelerometers 1990-91 p 1057 A92-56316
Composite blades for helicopter main and tail rotors developed by Mil Design Bureau p 1057 A92-56325
An experimental study of the sensitivity of helicopter rotor blade tracking to root pitch adjustment in hover
[NASA-TM-4313] p 61 N92-12989
Recent progress in inverse methods in France p 201 N92-13938
Rub induced rotor/stator vibration analysis on CF700 engine
[NRC-TR-ENG-007] p 202 N92-14060
Low cycle fatigue of cast nickel base turbine rotors p 226 N92-14405
Heat transfer in rotating serpentine passages with trips skewed to the flow
[NASA-TM-105581] p 499 N92-20235
Aspects of unsteady blade-surface boundary layers and transition in axial turbomachines p 658 N92-24340
Statistics on aircraft gas turbine engine rotor failures that occurred in US commercial aviation during 1988
[DOT/FAA/CT-91/28] p 1071 N92-33105

ROTOR BODY INTERACTIONS

Analysis of unsteady pressures induced on a body by a rotor p 10 A92-13212
Full-scale investigation of aerodynamic interactions between a rotor and fuselage p 105 A92-14361
A re-examination of the aerodynamics of hovering rotors including the presence of the fuselage p 66 A92-14446
Formulation of a simplified model of rotor-horizontal stabilizer interactions and comparison with experimental measurements
[ONERA, TP NO. 1991-157] p 77 A92-16125
Supersonic stator-rotor interaction in a turbine stage
[ONERA, TP NO. 1991-166] p 77 A92-16133
Helicopter air resonance modeling and suppression using active control p 204 A92-18625
Experimental and theoretical studies on helicopter rotor fuselage interaction
[ONERA, TP NO. 1991-197] p 329 A92-26356
Theoretical and experimental studies of helicopter rotor/fuselage interaction
[ONERA, TP NO. 1991-198] p 329 A92-26357
Aeroelastic response of helicopters with flexible fuselage modeling
[AIAA PAPER 92-2567] p 564 A92-34481
Experimental investigation on blade loss transient response of rotor with flexible damped support p 557 A92-35551
Tail rotor aerodynamic features recorded in flight p 546 A92-35752
Active control of helicopter ground and air resonance p 568 A92-35762
A study of coupled rotor-fuselage vibration with higher harmonic control using a symbolic computing facility p 569 A92-35770
High-order state space simulation models of helicopter flight mechanics p 569 A92-35777
Modeling rotor dynamics with rotor speed degree of freedom for drive train torsional stability analysis p 547 A92-35779
Theoretical model to calculate aerodynamic interference effects between rotor and wing of tiltrotors p 521 A92-35788
Sensitivity analysis of discrete periodic systems with applications to helicopter rotor dynamics p 846 A92-46884
The unsteady interaction of a 3-dimensional vortex filament with a cylinder p 813 A92-46934
A study of rotor wake development and wake/body interactions in hover p 813 A92-46935
Interaction between a rotor tip vortex and a separated flowfield p 814 A92-46947
A unified procedure for solving rotor flowfield, performance and interference p 814 A92-46950
A Mach-scaled powered model for rotor-fuselage interactional aerodynamics and flight mechanics investigations p 847 A92-46960
Vibration control of rotor-bearing system by controlled squeeze-film damper bearings p 990 A92-49579
Response of helicopter blades to a sharp collective increase p 1084 A92-56282
Coupled rotor-fuselage vibration reduction with multiple frequency blade pitch control p 1085 A92-56315
Experimental investigation of helicopter coupled rotor/body control p 1086 A92-56318
Current European research activities in helicopter interactional aerodynamics p 1058 A92-56330
Analysis of helicopter rotor-fuselage interference with time averaged pressure distribution p 1032 A92-56331
A study of helicopter rotor/fuselage response in low-speed manoeuvres - Comparison of theory with flight p 1086 A92-56334
Approximations for inclusion of rotor lag dynamics in helicopter flight dynamics models p 1060 A92-56354
Rotorcraft System Identification
[AGARD-LS-178] p 273 N92-17153

ROTOR DYNAMICS

Advanced multi-squeeze film dampers for rotor vibration control p 36 A92-10102
Analysis of rotor blade dynamics using experimental UH-60A airloads obtained at the DNW p 107 A92-14394
Structural optimization and Mach scale test validation of a low vibration rotor p 107 A92-14395
Experimental investigation of helicopter vibration reduction using rotor blade aeroelastic tailoring p 107 A92-14396
Studying dynamic behavior of X380 helicopter equipped with a new 5-blade composite rotor p 108 A92-14398
Dynamic response of a variable-speed rotor during rapid shaft tilt p 132 A92-14400
Variation in hover aeromechanical stability trends with bearingless main rotor design p 109 A92-14425
Dynamics of helicopters with dissimilar blades p 133 A92-14427
Dynamic analysis technique of rotating centrifugal impeller
[ASME PAPER 91-GT-50] p 148 A92-15528
Experiments on the blade loss transient response of rotor with flexible damped support
[ASME PAPER 91-GT-149] p 148 A92-15587
Rotordynamic evaluation of an advanced multi-squeeze film damper - Imbalance response and bladeloss simulation
[ASME PAPER 91-GT-242] p 149 A92-15647
A chambered porous damper for rotor vibration control. II - Imbalance response and bladeloss simulation
[ASME PAPER 91-GT-243] p 149 A92-15648
A chambered porous damper for rotor vibration control. I - Concept development
[ASME PAPER 91-GT-244] p 150 A92-15649
The basics of powder lubrication in high-temperature powder-lubricated dampers
[ASME PAPER 91-GT-248] p 150 A92-15653
A gas operated bearing damper for turbomachinery
[ASME PAPER 91-GT-249] p 150 A92-15654
The response of a helicopter to windshear p 269 A92-21470
Cyclic symmetric contact stress analysis of aeroengine rotor assembly p 470 A92-29733
Some rotordynamic problems in small turbo-engines p 470 A92-29736
A demonstration of passive blade twist control using extension-twist coupling
[AIAA PAPER 92-2468] p 539 A92-34358
Tail rotor aerodynamic features recorded in flight p 546 A92-35752
Instrumented blade experiments using a light autogiro p 555 A92-35773
Modeling rotor dynamics with rotor speed degree of freedom for drive train torsional stability analysis p 547 A92-35779
Measurements of a rotor flowfield and the effects on a fuselage in forward flight p 521 A92-35787
Prediction of dynamic hub load of a rotor executing multiple sinusoidal blade pitch variations p 846 A92-46921
A general purpose nonlinear rigid body mass finite element for application to rotary wing dynamics p 846 A92-46924
Chaotic dynamic behavior in a simplified rotor blade lag model p 846 A92-46926
On the choice of appropriate bases for nonlinear dynamic modal analysis p 847 A92-46927
Bilinear formulation applied to the stability and response of helicopter rotor blade p 847 A92-46930
Vibration control of rotor-bearing system by controlled squeeze-film damper bearings p 990 A92-49579
A study on rotor induced sand and dust environment and its harmfulness to helicopter p 960 A92-53012
Structural optimization and vibration control of composite rotor blades p 960 A92-53056
Transient response of the rotor-support system of aeroengines p 997 A92-53293
Aeroelasticity of a coaxial helicopter rotor p 1057 A92-56309
Oscillations of an anisotropic rotor on an elastic anisotropic support p 1057 A92-56311
Research on measurement and control of helicopter rotor response using blade-mounted accelerometers 1990-91 p 1057 A92-56316
The identification of coupled flapping/inflow models for hovering flight p 1058 A92-56335
A high speed edgewise rotor using circulation control only in the reversed flow area p 1059 A92-56347
Approximations for inclusion of rotor lag dynamics in helicopter flight dynamics models p 1060 A92-56354
Flapping inertia for selected rotor blades
[NASA-TM-104125] p 115 N92-13057
Technical activities of the configuration aeroelasticity branch
[NASA-TM-104146] p 159 N92-13458
Limit cycle vibrations in turbomachinery
[NASA-TP-3181] p 211 N92-14108
Nonlinear rotordynamics analysis --- Space Shuttle Main Engine turbopumps
[NASA-CR-184263] p 221 N92-14344
Rotordynamic Instability Problems in High-Performance Turbomachinery, 1990
[NASA-CP-3122] p 222 N92-14346
The stability of the steady state and bistable response of a flexible rotor supported on squeeze film dampers p 222 N92-14350
Evaluation of rotordynamic coefficients of look-through labyrinths by means of a three volume bulk flow model p 223 N92-14356
Determination of rotordynamic coefficients for labyrinth seals and application to rotordynamic design calculations p 223 N92-14360
Annular seals of high energy centrifugal pumps: Presentation of full scale measurement p 224 N92-14362
A simplified method for predicting the stability of aerodynamically excited turbomachinery p 224 N92-14364
Rotor-to-stator partial rubbing and its effects on rotor dynamic response p 224 N92-14367
Comments on frequency swept rotating input perturbation techniques and identification of the fluid force models in rotor/bearing/seal systems and fluid handling machines p 224 N92-14370
The application of a cylindrical-spherical floating ring bearing as a device to control stability of turbogenerators p 224 N92-14371
Helicopter rotor blade dynamics with bilinear formulation p 463 N92-21856

AFRAPT Program at Texas A and M University research for advanced aircraft engine structures
[AD-A247040] p 743 N92-28076
CSM solutions of rotating blade dynamics using integrating matrices
[NASA-CR-190577] p 1003 N92-31619
A simulation model of a single rotor helicopter
p 979 N92-31865
Joint study on the computerisation of in-field aero engines vibration diagnosis
[PNR-90799] p 1072 N92-33815

ROTOR LIFT
Hover evaluation of an integrated pneumatic lift/reaction-drive rotor system
[AIAA PAPER 92-0630] p 333 A92-27010
Experimental study of an independently deflected wingtip mounted on a semispan wing
[NASA-TM-102842] p 13 N92-10983
A simulation model of a single rotor helicopter
p 979 N92-31865

ROTOR SPEED
Dynamic response of a variable-speed rotor during rapid shaft tilt p 132 A92-14400
Enhanced energy maneuverability for attack helicopters using continuous, variable (C-V) rotor speed control
p 132 A92-14421
A design optimization procedure for high-speed prop-rotors
[AIAA PAPER 92-2375] p 542 A92-34545
Experimental investigation on blade loss transient response of rotor with flexible damped support
p 557 A92-35551
A new method for calculating burst speed of aeroengine disks
[ASME PAPER 91-GT-121] p 670 A92-36899
Helicopter far-field acoustic levels as a function of reduced rotor speeds p 695 A92-39228
Flow visualisation of a small diameter rotor operating at high rotational speeds with blades at small pitch angles p 814 A92-46949
An aerodynamical analysis of 'seesaw' type rotor for autogyro p 937 A92-52034
Noise test of high-speed counterrotation propeller in low-speed wind tunnel p 1135 A92-56055
Helicopter main-rotor speed effects: A comparison of predicted ranges of detection from the aural detection program ICHIN and the electronic detection program ARCAS
[NASA-TM-104134] p 166 N92-12598
Brush seal leakage performance with gaseous working fluids at static and low rotor speed conditions
[NASA-TM-105400] p 297 N92-16265
Model rotor icing tests in the NASA. Lewis Icing Research Tunnel p 450 N92-21688
Control of a helicopter engine in low altitude flight
p 562 N92-23122
Explicit Navier-Stokes computation of turbomachinery flows
[AD-A249284] p 909 N92-28879
Turbulence-induced loads on a teetered rotor
p 1042 N92-34029

ROTORCRAFT AIRCRAFT
Probabilistic fatigue methodology for six nines reliability p 145 A92-14342
Safe life reliability - Evaluation of new statistical methods p 104 A92-14343
Rotorcraft Maneuverability and Agility Survivability Sensitivity Analysis (RMASSA) p 161 A92-14351
Performance and handling qualities criteria for low cost real time rotorcraft simulators - A methodology development p 136 A92-14365
A new method for simulating atmospheric turbulence for rotorcraft applications p 162 A92-14368
Enhanced diagnostic system for autoclaves and bonding presses p 145 A92-14381
Crash-resistant rotorcraft preliminary design optimization p 109 A92-14417
Determination of the energy absorption of composite structures under combined loadings p 145 A92-14441
Study of simulated lightning discharge effects on wires of a rotorcraft
[ONERA, TP NO. 1991-173] p 92 A92-16137
The Civil Rotorcraft Initiative - An action agenda
p 241 A92-22707
Relating economics to design parameters through a criterion function p 271 A92-22709
Rotor revolutions in the Far East - Helicopters in China, Mongolia, and Siberia p 241 A92-22711
Flight investigation of variations in rotorcraft control and display dynamics for hover p 379 A92-28151
Integrated multidisciplinary rotorcraft optimization research at the NASA Langley Research Center
p 419 A92-29673
Low-speed cruise aerodynamics of the stopped rotor/disk rotorcraft concept
[AIAA PAPER 92-1067] p 517 A92-33240
Damage tolerance and repair experience of composite structures
[AIAA PAPER 92-1256] p 515 A92-33339
The NASA/Industry Design Analysis Methods for Vibrations (DAMVIBS) Program - A government overview --- of rotorcraft technology development using finite element method
[AIAA PAPER 92-2200] p 539 A92-34390
Overview and major characteristics of future aeronautical and space systems
[AIAA PAPER 92-2441] p 585 A92-34472
A design optimization procedure for high-speed prop-rotors
[AIAA PAPER 92-2375] p 542 A92-34545
Structural testing of commercial rotorcraft seats - An overview p 544 A92-35437
Achievement of rotorcraft handling qualities specifications via feedback control p 568 A92-35747
Comparison of elastic and rigid blade-element rotor models using parallel processing technology for piloted simulations
[SAE PAPER 912120] p 608 A92-39968
A review of recent programs and future plans for rotorcraft in-flight simulation at Ames Research Center
[SAE PAPER 912121] p 608 A92-39969
1991-92 AHS Technical Committee highlights - Acoustics p 696 A92-40390
1991-92 AHS Technical Committee highlights - Aircraft design p 608 A92-40392
1991-92 AHS Technical Committee highlights - Flight simulation p 609 A92-40394
1991-92 AHS Technical Committee highlights - Handling qualities p 662 A92-40395
1991-92 AHS Technical Committee highlights - Structures and materials p 609 A92-40397
1991-92 AHS Technical Committee highlights - Test and evaluation p 609 A92-40398
A comparison of fatigue life prediction methodologies for rotorcraft p 647 A92-40884
Navier-Stokes and Euler solutions for an unmanned aerial vehicle
[AIAA PAPER 92-2609] p 792 A92-45483
Boundary-layer measurements during a parallel blade-vortex interaction
[AIAA PAPER 92-2623] p 794 A92-45495
AHS International Specialists' Meeting on Rotorcraft Basic Research, Georgia Institute of Technology, Atlanta, Mar. 25-27, 1991, Proceedings p 846 A92-46919
Modeling of the control systems of rotary wing aircraft (Review) p 875 A92-47783
Testing and analysis of a 'smart' interface to connect two complex avionics bus systems without significant modification to the software of either system
p 964 A92-49254
Inertial navigation sensor integrated motion analysis for obstacle detection p 954 A92-49272
Simulation of automatic rotorcraft nap-of-the-earth flight in graphics workstation environment
[AIAA PAPER 92-4131] p 981 A92-52428
Development of a real-time simulation of a ship-correlated airwake model interfaced with a rotorcraft dynamic model
[AIAA PAPER 92-4149] p 1007 A92-52440
Summary highlights of the Advanced Rotorcraft Transmission (ART) program
[AIAA PAPER 92-3362] p 1051 A92-54026
Flight simulator fidelity assessment in a rotorcraft lateral translation maneuver
[AIAA PAPER 92-4424] p 1092 A92-55348
Analysis of image-based navigation system for rotorcraft low-altitude flight p 1046 A92-55968
Technology exploitation for in-service support of future rotorcraft p 1016 A92-56327
Damage tolerance analysis for rotorcraft - What the issues are p 1058 A92-56336
First level release of 2GCHAS for comprehensive helicopter analysis p 1133 A92-56339
Approximations for inclusion of rotor lag dynamics in helicopter flight dynamics models p 1060 A92-56354
Analytical/numerical matching and periodic inversion: Two advances in free wake analysis
p 178 N92-13994
SA 330 Puma identification results
p 274 N92-17162

ROTORS
Optical measurements of unducted fan flutter
[ASME PAPER 91-GT-19] p 147 A92-15510
Experimental and analytical investigation of hybrid squeeze film dampers
[ASME PAPER 91-GT-250] p 150 A92-15655
Ultrasonic motor utilizing elastic fin rotor
p 215 A92-17414
Rotor support for the STME oxygen turbopump
[AIAA PAPER 92-3282] p 904 A92-48872
Measurement of acoustic properties of the composite materials constituting the main rotor hub of the Agusta-Westland helicopter EH-101 (civil version)
p 1010 A92-49475
Description of a pressure measurement technique for obtaining surface static pressures of a radial turbine
[AIAA PAPER 92-4006] p 1123 A92-56829
The effects of Reynolds number, rotor incidence angle and surface roughness on the heat transfer distribution in a large-scale turbine rotor passage
[NASA-CR-184260] p 42 N92-11297
On the limitations of Froude's actuator disc concept
[ETN-91-90136] p 81 N92-11973
Variable impedance journal bearings for rotor-bearing systems p 157 N92-12270
Unsteady flows in rotor-stator cascades
[AD-A241593] p 158 N92-13410
Variational formulation of hybrid problems for fully 3-D transonic flow with shocks in rotor p 176 N92-13953
Identification of dynamic characteristics of flexible rotors as dynamic inverse problem p 220 N92-13962
Integration of dynamic, aerodynamic, and structural optimization of helicopter rotor blades
[NASA-CR-189018] p 195 N92-14038
Limit cycle vibrations in turbomachinery
[NASA-TP-3181] p 211 N92-14108
Field telemetry of blade-rotor coupled torsional vibration at Matuura Power Station Number 1 unit
p 222 N92-14348
The effects of manufacturing tolerances on the vibration of aero-engine rotor-damper assemblies
p 222 N92-14349
The stability of the steady state and bistable response of a flexible rotor supported on squeeze film dampers
p 222 N92-14350
Experimental investigations of exciting forces caused by flow in labyrinth seals p 223 N92-14354
Experiment of static and dynamic characteristics of spiral grooved seals p 223 N92-14361
Hydraulic actuator system for rotor control
p 224 N92-14363
Rotor-to-stator partial rubbing and its effects on rotor dynamic response p 224 N92-14367
Comments on frequency swept rotating input perturbation techniques and identification of the fluid force models in rotor/bearing/seal systems and fluid handling machines p 224 N92-14370
Flight operations for higher harmonic control research
[AD-A242478] p 196 N92-15067
Development of a CFD code for analysis of fluid dynamic forces in seals p 228 N92-15084
High-temperature combustor and seal for a water piston propulsor
[AD-A242493] p 229 N92-15385
Numerical simulation of VAWT stochastic aerodynamic loads produced by atmospheric turbulence: VAWT-SAL code
[DE92-000597] p 229 N92-15392
Viscous three-dimensional calculations of transonic fan performance
[NASA-TM-103800] p 242 N92-17346
Single screw mechanism with gaterotor housing at intermediate pressure
[AD-D015140] p 400 N92-18120
The NREL teetering hub rotor code: Final results and conclusions
[DE92-001187] p 410 N92-19633
A numerical study of fuselage scattering effects on rotor noise p 511 N92-20428
Modeling methods for high-fidelity rotorcraft flight mechanics simulation
[NASA-TM-103842] p 482 N92-21440
Metal-metal bondline NDE methods
[AD-A244429] p 503 N92-21730
Helicopter active rotor control p 570 N92-22157
Measured and predicted rotor performance for the SERI advanced wind turbine blades
[DE92-001215] p 598 N92-23119
Analysis of a 37 kW cage-induction motor
[PB92-142116] p 597 N92-23496
Computations of unsteady multistage turbomachinery flows p 562 N92-23671
Analysis of rotor vibratory loads using higher harmonic pitch control
[NASA-CR-189591] p 696 N92-24251
Description of a pressure measurement technique for obtaining surface static pressures of a radial turbine
[NASA-TM-105643] p 680 N92-24959
Viscous three-dimensional calculations of transonic fan performance p 768 N92-27467
Feasibility of magnetic bearings for advanced gas turbine engines p 772 N92-27738
Low power magnetic bearing design for high speed rotating machinery p 772 N92-27739
Wide gap, permanent magnet biased magnetic bearing system p 773 N92-27794

Design of bearings for rotor systems based on stability
p 773 N92-27799
An evaluation of some strategies for vibration control of flexible rotors p 773 N92-27800
Assessment of valve actuator motor rotor degradation by Fourier Analysis of current waveform
[DE92-013233] p 909 N92-28814
Multi-channel fiber optic rotary joint for single-mode fiber
[AD-D015273] p 927 N92-29095
Superconducting bearings with levitation control configurations
[NASA-CASE-GSC-13346-1] p 909 N92-29099
Statistics on aircraft gas turbine engine rotor failures that occurred in US commercial aviation during 1989
[DOT/FAA/CT-92/5] p 971 N92-30303
Yaw dynamics of horizontal axis wind turbines
[DE92-001245] p 1004 N92-30837
A general numerical model for wave rotor analysis
[NASA-TM-105740] p 1002 N92-31484
An investigation of switched reluctance rotor position estimation using neural networks
[AD-A252846] p 1061 N92-33414
Cooled high-temperature radial turbine program 2
[NASA-CR-189122] p 1073 N92-34236

ROUTES
A constraint satisfaction approach to operative management of aircraft routing p 350 A92-25181
Route planning --- in real-time of avionics systems
p 1006 A92-49317
Heuristic route optimization: A model for force level route planning p 164 N92-12520
FAA air traffic activity: FY 1990. Addendum
[AD-A241484] p 93 N92-13046
Rotorcraft terminal ATC route standards
[SCT-90RR-33] p 641 N92-26101
On board planning of 4D-trajectories
p 728 N92-27897
An efficient method for three-dimensional route planning with different strategies and constraints
p 728 N92-27901

RUBBER
Behavior of aircraft tire coupons under various loading conditions
[AD-A241416] p 116 N92-13063

RUBIDIUM
Tactical Rubidium Frequency Standard (TRFS)
[AD-A243934] p 401 N92-18897

RUDDERS
Mind that restyle --- failure analysis of aircraft composite structures p 91 A92-13700
747-400 upper rudder control system
p 731 A92-43546
A numerical study of control surface buzz using computational fluid dynamic methods
[AIAA PAPER 92-2654] p 806 A92-45578
E-6 flutter investigation and experience
[AIAA PAPER 92-4601] p 1077 A92-55280
A preliminary look at an optimal multivariable design for propulsion-only flight control of jet-transport aircraft
[NASA-CR-186014] p 663 N92-25734

RUN TIME (COMPUTERS)
Computations of unsteady multistage compressor flows in a workstation environment
[NASA-TM-103839] p 1071 N92-32452

RUNGE-KUTTA METHOD
Calculation of 3D flow field in a single transonic compressor stage p 422 A92-29719
Use of finite volume schemes for transition simulation
p 432 A92-31185
A non-linearly stable implicit finite element algorithm for hypersonic aerodynamics p 433 A92-31487
Bifurcation analysis of airfoils in incompressible flow
p 623 A92-40580
Numerical simulations using a dynamic solution-adaptive grid algorithm, with applications to unsteady internal flows
[AIAA PAPER 92-2719] p 803 A92-45557
A finite difference solution of the Euler equations on non-body-fitted Cartesian grids p 818 A92-47153
Zonal solutions for a double-ellipse in a hypersonic flowfield
[AERO-REPT-9009] p 345 N92-18233
Improved shock-capturing of Jameson's scheme for the Euler equations
[PB92-148758] p 596 N92-23251
Three-dimensional upwind scheme for solving the Euler equations on unstructured tetrahedral grids --- tetrahedral grids p 714 N92-26585
Computations of unsteady flows around airfoil sections by explicit and implicit methods solving the Euler and Navier-Stokes equations p 720 N92-27948
Validation of three-dimensional incompressible spatial direct numerical simulation code: A comparison with linear stability and parabolic stability equation theories for boundary-layer transition on a flat plate
[NASA-TP-3205] p 943 N92-30295

RUNWAY CONDITIONS
Aircraft landing-induced tire spinup
p 193 A92-20209
Dynamic response of landing gears on rough repaired runway
[SAE PAPER 912154] p 644 A92-39989
Runway drainage characteristics related to tire friction performance
[SAE PAPER 912156] p 664 A92-39991
Development of an instrument for measuring runway roughness p 748 A92-43124
A proposed method for evaluating runway roughness
p 748 A92-43125
ASTOVL flexibility in the 21st century
p 783 A92-45309
Ground surface erosion - British Aerospace test facility and experimental studies p 881 A92-45323
A neural network based postattack damage assessment system p 922 A92-48520
Grooved runway surface texture before and after rubber removal p 1093 A92-56111
Criteria for use of seal coats on airport pavements
[DOT/FAA/RD-92/18] p 1102 N92-34247

RUNWAY LIGHTS
New specifications proposed for taxiing guidance signs p 483 A92-29505
Evaluation of two high-speed runway exits
[DOT/FAA/CT-TN91/36] p 31 N92-11021
Attributes of winged manned space vehicles and their relationship to ground site characteristics and facilities
p 487 N92-20776
Evaluation of a tritium runway lighting system
[DOT/FAA/CT-TN92/15] p 665 N92-25733

RUNWAYS
An electronically scanned precision runway monitor
p 98 A92-16654
New siting techniques for the ILS glide slope
p 188 A92-17422
DANSIM applications - Development of airport noise reduction strategies and environmental policy
p 687 A92-39057
Computation of aircraft noise exposure using digitized topography data p 687 A92-39058
Runway incursions and airport surface traffic automation
[SAE PAPER 912123] p 635 A92-39970
Use of the TMS-65 heating equipment at airports to create fog-dispersal zones above the runway to facilitate takeoff p 775 A92-44084
Evaluation of two high-speed runway exits
[DOT/FAA/CT-TN91/36] p 31 N92-11021
Prototype runway hold-short lighting system
[DOT/FAA/CT-TN91/43] p 31 N92-11028
Surface painted taxiway markings at Seattle-Tacoma International Airport
[DOT/FAA/CT-TN91/49] p 32 N92-11029
Electronic systems in transportation
[TP-9983] p 189 N92-14009
Joint Federal Aviation Administration (FAA)/Civil Aviation Authority (CAA) Microwave Landing System (MLS) Area Navigation (RNAV) flight evaluations
[DOT/FAA/CT-TN91/17] p 268 N92-15983
Runway exit designs for capacity improvement demonstrations. Phase 2: Computer model development
[NASA-CR-190166] p 484 N92-21162
A methodology for the evaluation of runway roughness for repair
[AD-A250407] p 887 N92-28772
An assessment of the B-747's capability to operate on rough surfaces
[AD-A250134] p 963 N92-31793
Global positioning system runway incursion program static ground tests
[DOT/FAA/CT-TN91/44] p 957 N92-31838
Performance of insulated pavements at Newton Fields, Jackman, Maine
[CRREL-92-9] p 1101 N92-32903
ILS mathematical modeling study of an ILS localizer and glide slope proposed for runway 32R, Moffett Field Airport, California
[DOT/FAA/CT-TN92/28] p 1048 N92-33308
Criteria for use of seal coats on airport pavements
[DOT/FAA/RD-92/18] p 1102 N92-34247

S

S CURVES
An investigation of the swirl in an S-shaped inlet
p 343 A92-28476
A new approach to swirl control in an S-duct
p 422 A92-29710
New method of swirl control in a diffusing S-duct
p 809 A92-45859

S-N DIAGRAMS
A method for the construction of safe S-N curves
p 586 A92-34759

S-3 AIRCRAFT
ES-3A flight test program
[AIAA PAPER 92-1230] p 538 A92-33327

SAAB AIRCRAFT
Saab 2000 begins 1,200-hr. test program at Skavsta site p 538 A92-33800
A manufacturer's approach to ensure long term structural integrity p 838 N92-30133
Vibro-acoustic FE analyses of the Saab 2000 aircraft
p 1137 N92-32952

SADDLE POINTS
Computation of saddle point of attachment
p 703 A92-41276

SAFETY
Software safety analysis in heterogeneous multiprocessor control systems p 776 A92-42073
Buffet test in the National Transonic Facility
[NASA-CR-189595] p 888 N92-29352

SAFETY DEVICES
Development and evaluation of an onboard aircraft cabin water spray system for postcrash fire protection
[SAE PAPER 912224] p 636 A92-40022
Development of an emergency underwater escape breathing system for CH124 seaking aircrew
[DCIEM-87-TR-11] p 92 N92-13041
Onboard cabin water spray system under various discharge configurations
[DOT/FAA/CT-TN91/42] p 93 N92-13043
An evaluation of in-cabin safety features in passenger aircraft
[ETN-92-90656] p 449 N92-20794
A report on enhancements for existing and future helicopters supporting operations of the Canadian oil and gas industry
[CTN-91-60126] p 636 N92-25350
A cable detection lidar system for helicopters
p 1001 N92-31068

SAFETY FACTORS
New way of flying (1990 Sir Charles Kingsford Smith Lecture) p 515 A92-33461
Helmet-mounted image intensification analysis
p 554 A92-35454
Noise abatement procedures vs. safety
[SAE PAPER 912137] p 635 A92-39977
The appropriate concern for possible aberrations in landing guidance signals p 839 A92-44932
Safety vs. economy, system-theoretic approach to the problem analysis p 916 A92-45002
Safety factor and reliability for composite laminates
p 996 A92-53070
Safety provision against 'ground resonance' free vibration of a coaxial helicopter p 1056 A92-56289
A module-level testing environment for safety-critical software systems p 1132 A92-56293
Aircraft accident report: Northwest Airlines, Inc., Flights 1482 and 299. Runway incursion and collision, Detroit Metropolitan/Wayne County Airport, Romulus, Michigan, December 3, 1990
[PB91-910405] p 187 N92-14006
Passenger knowledge of airline safety information
[CRANFIELD-AERO-9111] p 187 N92-15054
Discussion for possibility of some aerodynamic ground effect craft
[NAL-TM-619] p 300 N92-17757
Fatigue safety factor: Assessment of associated safety level p 401 N92-18573
Safety study of TCAS 2 for logic version 6.04
[DOT/FAA/RD-92/22] p 1047 N92-32537

SAFETY MANAGEMENT
Why not a safety rating? --- in Australian civil aviation
p 530 A92-36200
Safety at sea and in the air - Taking stock together; Proceedings of the Conference, London, England, Nov. 13-15, 1990
[ISBN 0-903409-78-X] p 634 A92-39301
How to promote error tolerance in complex systems in the context of ships and aircraft p 673 A92-39308
Flight operations safety management
[SAE PAPER 912124] p 635 A92-39971
Risk management - Expanding horizons in nuclear power and other industries --- Book
[ISBN 1-56032-231-4] p 993 A92-51438
Airline industry safety management systems and feedback p 951 A92-51439
Cockpit crew research p 951 A92-51440
Program plan: National aging aircraft research program
[DOT/FAA/CT-88/32-1] p 18 N92-10992

Maintaining the safety of an aging fleet of aircraft
p 837 N92-30108

SAINT VENANT PRINCIPLE
Flexure-torsion behavior of sheat-deformable beams with applications to aircraft wing sections
[AIAA PAPER 92-2467] p 582 A92-34357

SAMPLED DATA SYSTEMS
A microprocessor-based automation test system for the experiment of the multi-stage compressor
p 997 A92-53100
A new system for recording unstable aerodynamic phenomena in NAVSWC Hypervelocity Wind Tunnel No. 9 p 1091 A92-54325

SANDS
A study on rotor induced sand and dust environment and its harmfulness to helicopter p 960 A92-53012

SANDWICH STRUCTURES
Combined compressive and shear buckling analysis of hypersonic aircraft sandwich panels
[AIAA PAPER 92-2487] p 586 A92-34603
Technological excellence in honeycomb sandwich and composite structures for aerospace applications
p 757 A92-41180
Analysis and testing of a composite sandwich shell horizontal tail p 755 A92-44617
Design and use of aramid fiber in aircraft structures
p 784 A92-47407
Impact damage tolerance of helicopter sandwich structures p 958 A92-51506
Optimization of composite sandwich cover panels subjected to compressive loadings
[NASA-TP-3173] p 489 N92-20679
A Protection And Detection Surface (PADS) for damage tolerance p 1107 N92-32523
Stability failure of sandwich structures
[MBB-UD-0613-92-PUB] p 1111 N92-33994

SATELLITE ANTENNAS
Experiments on aeronautical satellite communications using ETS-V p 395 A92-26779
Calibration of GPS antennas
[ETN-92-92034] p 1051 N92-33693

SATELLITE ATTITUDE CONTROL
A multibody analog of the dual-spin problem
p 49 A92-11426

SATELLITE COMMUNICATION
The Aeronautical Mobile Satellite Service (AMSS). II - Frequency spectrum requirements for the Aeronautical Mobile Satellite Service p 94 A92-13852
Potential impact of FANS - Far-reaching and positive --- Future Air Navigation Systems p 267 A92-23296
ETS-V/EMSS mobile satellite communication experiments p 395 A92-26776
Experiments on aeronautical satellite communications using ETS-V p 395 A92-26779
High gain airborne antenna for satellite communications p 354 A92-26780
Automatic Dependent Surveillance (ADS) Pacific Engineering Trials (PET)
[AIAA PAPER 92-1812] p 453 A92-29760
Characteristics of a future aeronautical satellite communications system
[AIAA PAPER 92-2058] p 453 A92-29889
ACTS aeronautical experiments
[AIAA PAPER 92-2042] p 485 A92-29956
Experiments on aeronautical satellite communications using ETS-V satellite p 639 A92-40187
High gain airborne antenna for satellite communications p 639 A92-40188
Beam scanning error of phased array antenna
p 676 A92-40189
Using satellite communication for aircraft Automatic Dependent Surveillance p 725 A92-42486
History of aeronautical satellite communications
p 1046 A92-56088
Aeronautical satellite communications system
p 1046 A92-56089
Aircraft satellite communication systems
p 1046 A92-56091
Evaluation report of an experimental Satcom operation by a Japan Airline's B747 passenger plane
p 1046 A92-56092
An experimental program concerning a satellite data link for oceanic ATC p 1046 A92-56093
A TMS320-based modem for the aeronautical-satellite core data service p 594 N92-22562
Design considerations for general aviation mobile satellite terminals p 594 N92-22572
Aeronautical mobile satellite service: An overview
p 594 N92-22573
Evaluating the use of satellite communications in the government of Canada p 594 N92-22577
A high gain antenna system for airborne satellite communication applications p 677 N92-24096
Inmarsat aeronautical mobile satellite system: Internetworking issues p 677 N92-24098
Low cost, electronically steered phased array for general aviation p 677 N92-24099
System considerations, projected requirements and applications for aeronautical mobile satellite communications for air traffic services
p 677 N92-24163
Aeronautical mobile satellite service: Air traffic control applications p 677 N92-24164
Spectrum sharing between AMSS(R) and MSS
p 677 N92-24165
Future developments in aeronautical satellite communications p 678 N92-24167
An aircraft Earth station for general aviation
p 678 N92-24194
Decision-making guide for the proposed Coast Guard differential global positioning system
[AD-A246046] p 957 N92-32054

SATELLITE CONTROL
Receiver Autonomous Integrity Monitoring (RAIM) capability for sole-means GPS navigation in the oceanic phase of flight p 956 A92-51012

SATELLITE DESIGN
Quaternion and Euler angles in kinematics
[NAL-TM-636] p 909 N92-28836

SATELLITE INSTRUMENTS
Aeronautical satellite system test and implementation
p 676 N92-24095

SATELLITE NAVIGATION SYSTEMS
The Aeronautical Mobile Satellite Service (AMSS). I - Architecture of the AMSS system p 93 A92-13851
The Aeronautical Mobile Satellite Service (AMSS). II - Frequency spectrum requirements for the Aeronautical Mobile Satellite Service p 94 A92-13852
RAIM - Will it meet the RTCA GPS minimum operational performance standards? --- Receiver Autonomous Integrity Monitoring p 96 A92-16635
A synergistic solution to the GPS integrity problem
p 96 A92-16641
In-flight demonstration of hybrid GPS/Loran RAIM
p 96 A92-16643
Precision approach using GPS and GLONASS
p 97 A92-16649
The 1990 Federal Radionavigation Plan and its impact on the Omega Navigation System p 98 A92-16658
Omega/VLF now and into the 21st century
p 98 A92-16659
SATZAP - A novel approach to GPS integrity
p 99 A92-16947
Probability distributions that are important when assessing barometric aiding to GPS p 100 A92-16952
That all-important interface p 100 A92-16953
GPS interferometric attitude and heading determination - Initial flight test results p 454 A92-30023
Growing need to replace ILS can best be met by MLS
p 534 A92-36124
Analysis of stand-alone differential GPS for precision approach p 638 A92-38381
GPS/GLONASS user systems in Sweden
p 638 A92-38384
Data processing in navigation complexes --- Russian book
[ISBN 5-217-01060-6] p 725 A92-42789
GLONASS data analysis - Interim results
p 955 A92-49382
NASA's GPS tracking system for Aristoteles
p 576 N92-23919

SATELLITE NETWORKS
Global satellite navigation using both GPS and GLONASS p 99 A92-16938
GPS availability. I - Availability of service achievable for different categories of civil users. II - Evaluation of state probabilities for 21-satellite and 24-satellite constellations p 99 A92-16949
Low earth orbit satellite concepts for air traffic control applications
[AIAA PAPER 92-1927] p 453 A92-29856
Using satellite communication for aircraft Automatic Dependent Surveillance p 725 A92-42486
Aeronautical satellite system test and implementation
p 676 N92-24095
Inmarsat aeronautical mobile satellite system: Internetworking issues p 677 N92-24098

SATELLITE ORBITS
Simulation of GRM drag compensation system --- Geopotential Research Mission p 285 A92-21023

SATELLITE TELEVISION
Aerobureau - Strategic television airmobile reports via satellite p 218 A92-19988

SATELLITE TRACKING
Navsat - A civil complement to GPS and Glonass
[IAF PAPER 91-490] p 188 A92-18505
NASA's GPS tracking system for Aristoteles
p 576 N92-23919

SCALARS
Modeling of the reactant conversion rate in a turbulent shear flow p 829 N92-28820

SCALE EFFECT
The Second Goldstein Lecture: Modern developments in fluid dynamics - An addendum p 442 A92-32323
Similarity and scale effects in solid-fuel ramjet combustors p 666 A92-36965
Scale effects on the flow past the mated Space Shuttle configuration
[AIAA PAPER 92-2680] p 799 A92-45532
A review of scale effects in unsteady aerodynamics
p 934 A92-50121
A review of scale effects on surfaces in unsteady motion p 722 N92-27962

SCALE MODELS
Recent rotorcraft aeroelastic testing in the Langley Transonic Dynamics Tunnel p 136 A92-14377
Flight test of a half-scale unmanned air vehicle
p 193 A92-20208
LAH main rotor model test at the DNW
p 547 A92-35771
Research flight test of a scaled unmanned air vehicle
p 549 A92-35944
Scale model test of an isolated turbofan nacelle with riblets
[SAE PAPER 912128] p 618 A92-39975
An automated workstation for the half-scale testing of the flight vehicle stabilization circuit p 664 A92-40622
A method for determining the internal force characteristics of a model in external supersonic flow
p 706 A92-42682
Maximizing thrust-vectoring control power and agility metrics p 874 A92-46794
A Mach-scaled powered model for rotor-fuselage interactional aerodynamics and flight mechanics investigations p 847 A92-46960
Scale model test results of a multi-slotted vectoring 2DCD ejector nozzle
[AIAA PAPER 92-3264] p 864 A92-48859
Experimental investigation of an ejector-powered free-jet facility
[AIAA PAPER 92-3569] p 1090 A92-54058
On the maneuvering tests of an ACV model
p 1118 A92-56035
Helicopter rotor testing using scaled model
p 1093 A92-56076
Experimental study of noise generation and propagation in a turbofan model p 1136 A92-56169
Demonstration of structural optimization applied to wind-tunnel model design p 1119 A92-56181
BVI impulsive noise reduction by higher harmonic pitch control - Results of a scaled model rotor experiment in the DNW p 1136 A92-56344
Design of a variable contraction for a full-scale automotive wind tunnel
[AIAA PAPER 92-3929] p 1096 A92-56760
Developmental flight testing of a half scale unmanned air vehicle
[AD-A240347] p 22 N92-11002
Control aspects of the transition from transversal to transonic flow, step effects
[ETN-91-90106] p 82 N92-11981
Scale model measurements of fin buffet due to vortex bursting on F/A-18 p 365 N92-18788
Forebody vortex control aeromechanics
p 380 N92-18792
Survey of experimental techniques for performance prediction p 552 N92-23954
Flowfield in the vicinity of the F/A-18 vertical fin at high-angle-of-attack p 628 N92-24865
Wind tunnel aerodynamic characteristics of a transport-type airfoil in a simulated heavy rain environment
[NASA-TP-3184] p 948 N92-31532
Transonic wind tunnel test of a 14 percent thick oblique wing
[NASA-TM-102230] p 950 N92-32213

SCALING
Experimental and computational investigation of scaling phenomena in a large caliber ram accelerator
[AIAA PAPER 92-3245] p 1103 A92-54019

SCALING LAWS
Integrated electric density and scaling law for hypersonic blunt-body wakes p 714 A92-44865
Dynamical scaling of a model unsteady separating flow p 1117 A92-54932
High speed transport cruise drag --- scaling laws using Navier-Stokes equations
[NASA-CR-190248] p 527 N92-23103
Selection of opening model for parachute scaling studies
[AD-A250882] p 943 N92-30239

SCALLOPING
Prediction of ice accretion on a swept NACA 0012 airfoil and comparisons to flight test results
[AIAA PAPER 92-0043] p 316 A92-25677

Prediction of ice accretion on a swept NACA 0012 airfoil and comparisons to flight test results
[NASA-TM-105368] p 258 N92-15968
SCANNERS
Nortec 30 Eddyscan - Portable flaw imaging for aging aircraft p 492 A92-28745
SCANNING
Study of optical techniques for the Ames unitary wind tunnels. Part 2: Light sheet and vapor screen
[NASA-CR-190217] p 573 N92-22195
SCARFING
Processing and environmental effects on mechanical properties of composite repairs
[NRC-LTR-ST-1826] p 1109 N92-32791
SCATTERING
Microwave landing system modeling with application to air traffic control automation p 725 A92-41220
Investigation of the effects of aeroelastic deformations on the radar cross section of aircraft
[AD-A243889] p 402 N92-18940
Mid-range UV communications --- ultraviolet radiation
[AD-D015213] p 770 N92-27615
Development of 3D electromagnetic modeling tools for airborne vehicles
[NASA-CR-190810] p 1126 N92-33307
SCATTEROMETERS
Concept design phase expendable holographic sensor to measure ocean small angle optical scattering
[AD-A245067] p 501 N92-20997
Development of a helicopter-borne 8-channel ranging scatterometer
[PB92-141977] p 599 N92-23441
SCENE ANALYSIS
Time-to-go estimation from infrared images
p 840 A92-48308
SCHEDULING
Meeting VSTOL aircraft performance requirements using scheduled H(infinity) controllers p 477 A92-29094
Design of compensators for linear parameter-varying feedback systems by the gain scheduling technique
p 507 A92-29101
Maintenance scheduling for critical parts of aircraft
p 699 A92-42054
Process/object-oriented Ada software design for an experimental helicopter p 164 N92-12461
Development of a knowledge base for use in an Expert System Advisor for Aircraft Maintenance Scheduling (ESAAMS)
[AD-A243435] p 305 N92-17687
Constraint-based scheduling
[NASA-TM-107873] p 692 N92-25190
Delfi: Design, development, and applicability of expert systems shells
[ISBN-90-6275-734-0] p 692 N92-25306
Model analysis and expert system development for planning and scheduling teleoperations for aircraft turnaround functions, volume 1
[AD-A251037] p 932 N92-30253
Model analysis and expert system development for planning and scheduling teleoperations for aircraft turnaround functions. Volume 2: Top user's guide
[AD-A251083] p 932 N92-30258
Analysis of delay reducing and fuel saving sequencing and spacing algorithms for arrival traffic
[NASA-TM-103880] p 1044 N92-33194
SCHLIEREN PHOTOGRAPHY
Experimental design of a supersonic shock wave/vortex interaction at Mach 3 p 521 A92-35988
Study of optical techniques for the Ames unitary wind tunnels. Part 1: Schlieren
[NASA-CR-189951] p 385 N92-19218
Interferograms, schlieren, and shadowgraphs constructed from real- and ideal-gas, two- and three-dimensional computed flowfields
[NASA-CR-190054] p 446 N92-21356
An experimental study of the flow over a sharp-edged delta wing at subsonic and transonic speeds
[NLR-TP-91117-U] p 1037 N92-32732
SCHULER TUNING
The LISA 6000 - A highly integrated IRS/GPS navigation system p 267 A92-22088
SCIENTIFIC SATELLITES
NASA's GPS tracking system for Aristoteles
p 576 N92-23919
SCIENTISTS
NASA/DOD Aerospace Knowledge Diffusion Research Project. Paper 13: The information-seeking habits and practices of engineers
[NASA-TM-107931] p 782 N92-28114
NASA engineers and the age of Apollo
[NASA-SP-4104] p 929 N92-28344
SCORING
A comparison of the performance of two gust front detection algorithms using a length-based scoring technique
[AD-A250862] p 1004 N92-32103
SCREENS
Prediction of the pressure loss coefficient of wind tunnel turbulence reducing screens
[AIAA PAPER 92-0568] p 384 A92-26976
Prediction of the pressure loss coefficient of wind tunnel turbulence reducing screens
[AIAA PAPER 92-4043] p 1035 A92-56862
Reynolds number dependence of the drag coefficient for laminar flow through fine-scale screens
[DE92-002930] p 765 N92-26698
SCREWS
Single screw mechanism with gaterotor housing at intermediate pressure
[AD-D015140] p 400 N92-18120
SEA BREEZE
Boundary-layer transition across a stratocumulus cloud edge in a coastal zone p 45 A92-10489
SEA ICE
Interactive graphics method for removal of helicopter motions from laser profile data p 598 A92-35109
SEA LAUNCHING
United Kingdom approach to deriving military ship helicopter operating limits p 465 N92-21966
A review of Australian activity on modelling the helicopter/ship dynamic interface p 465 N92-21967
SEA STATES
Integration of flight and carrier landing aid systems for shipboard operations
[ONERA, TP NO. 1991-113] p 134 A92-16092
Determination of limitations for helicopter ship-borne operations p 465 N92-21965
SEA TRUTH
Relating the microwave radar cross section to the sea surface stress - Physics and algorithms
p 597 A92-35028
SEA WATER
Concept design phase expendable holographic sensor to measure ocean small angle optical scattering
[AD-A245067] p 501 N92-20997
SEALERS
Non-curing fuel and water resistant sealant compositions p 985 A92-51906
Criteria for use of seal coats on airport pavements
[DOT/FAA/RD-92/18] p 1102 N92-34247
SEALING
Army research concerns in engine sealing
p 228 N92-15089
Areas of seal R/D at GE p 228 N92-15094
Seal related development activities at EG/G
p 228 N92-15095
Redesign of flight space shuttle main engine nozzle G-15 seal area based on the thermal analysis and flow models p 212 N92-15877
Evaluation of an innovative high-temperature ceramic wafer seal for hypersonic engine applications
p 578 N92-22205
SEALS (STOPPERS)
Performance of radial clearance rim seals in upstream and downstream rotor-stator wheelspaces
[ASME PAPER 91-GT-32] p 147 A92-15516
Rim sealing of rotor-stator wheelspaces in the absence of external flow
[ASME PAPER 91-GT-33] p 147 A92-15517
Development of film riding face seals for a gas turbine engine p 291 A92-21330
A finite-volume numerical method to calculate fluid forces and rotordynamic coefficients in seals
[AIAA PAPER 92-3712] p 1113 A92-54132
Experiment of static and dynamic characteristics of spiral grooved seals p 223 N92-14361
Annular seals of high energy centrifugal pumps: Presentation of full scale measurement
p 224 N92-14362
Industrial code development p 227 N92-15083
Army research concerns in engine sealing
p 228 N92-15089
Programs at Wright-Patterson Air Force Base
p 228 N92-15092
Areas of seal R/D at GE p 228 N92-15094
Seal related development activities at EG/G
p 228 N92-15095
High-temperature combustor and seal for a water piston propulsor
[AD-A242493] p 229 N92-15385
Engine panel seals for hypersonic engine applications: High temperature leakage assessments and flow modelling
[NASA-TM-105260] p 298 N92-16336
Inflatable traversing probe seal p 595 N92-22692
High temperature dynamic engine seal technology development
[NASA-TM-105641] p 596 N92-23435
SEAPLANES
Beriev Be-42 - A unique jet-propelled seaplane
p 269 A92-21010
SEARCH PROFILES
Parallel solver for trajectory optimization search directions p 777 A92-43399
SEAT BELTS
Evaluation of head impact kinematics for passengers seated behind interior walls
[AD-A252651] p 952 N92-30551
SEATS
Development of a reclined crashworthy crewseat for rotorcraft p 105 A92-14370
Structural testing of commercial rotorcraft seats - An overview p 544 A92-35437
Energy attenuation for crashworthy seating systems - Past, present, and possible future development
p 544 A92-35452
Effect of crash pulse shape on seat stroke requirements for limiting loads on occupants of aircraft
[NASA-TP-3126] p 399 N92-18053
Evaluation of head impact kinematics for passengers seated behind interior walls
[AD-A252651] p 952 N92-30551
SECONDARY FLOW
Application of compound leaned blades to controlling secondary flow p 5 A92-10975
Convective transport phenomena on the suction surface of a turbine blade including the influence of secondary flows near the endwall
[ASME PAPER 91-GT-35] p 147 A92-15518
Turbulence modelling for secondary flow prediction in a turbine cascade
[ASME PAPER 91-GT-57] p 68 A92-15535
3-D loss prediction based on secondary flow and blade shear layer interaction
[ASME PAPER 91-GT-59] p 68 A92-15536
The influence of shock waves on the viscous flow field of axial compressors
[ASME PAPER 91-GT-173] p 73 A92-15608
Experimental measurement of the vortex development downstream of a lobed forced mixer
[ASME PAPER 90-GT-27] p 295 A92-23299
Secondary instability mechanisms in compressible, axisymmetric boundary layers
[AIAA PAPER 92-0743] p 343 A92-28224
Secondary instabilities in compressible boundary layers p 435 A92-31639
Secondary instability of high-speed flows and the influence of wall cooling and suction
p 435 A92-31640
Turbulent flow in the wake of an idealized wing-body junction
[AIAA PAPER 92-0282] p 435 A92-31652
Multifractal analysis of a lobed mixer flowfield utilizing the proper orthogonal decomposition
p 611 A92-36840
Flow analysis for axial compressor including secondary flow effects p 759 A92-41835
Secondary flow investigation inside the passage of a compressor cascade p 706 A92-42124
Effect of flow rate on loss mechanisms in a backswept centrifugal impeller p 897 A92-45606
Wake mixing and performance measurements in a linear compressor cascade with crenulated trailing edges
[AIAA PAPER 92-3188] p 824 A92-48800
A study on the impact of shroud geometry on ejector pumping performance
[AIAA PAPER 92-3260] p 864 A92-48856
Numerical study on the secondary jet into a supersonic flow p 1018 A92-53556
Application of computational fluid dynamics to the study of vortex flow control for the management of inlet distortion
[AIAA PAPER 92-3177] p 1020 A92-54013
Flow induction by pressure forces
[AIAA PAPER 92-3571] p 1067 A92-54060
An experimental study of the flow over a sharp-edged delta wing at subsonic and transonic speeds
p 85 N92-13011
Army research concerns in engine sealing
p 228 N92-15089
Areas of seal R/D at GE p 228 N92-15094
An experimental study of a turbulent wing-body junction and wake flow
[AD-A243388] p 260 N92-17222
Viscous three-dimensional calculations of transonic fan performance p 768 N92-27467
Examination of the main error factors with regards to secondary losses in compression and turbine cascades by variations of the blade picture ratio
[ETN-92-91493] p 871 N92-29927
Application of computational fluid dynamics to the study of vortex flow control for the management of inlet distortion
[NASA-TM-105672] p 1128 N92-34112
SECONDARY RADAR
The European ATC challenge p 19 A92-11877

Analysis and design optimization of monopulse receivers for secondary surveillance radar p 40 A92-12299
Quantitative estimation of secondary surveillance radar information p 353 A92-24943
Monopulse secondary surveillance radar and the mode-S surveillance system p 956 A92-53239

SECURITY
System of cryogenic security of the superconducting accelerator of relativistic nuclei-nuclotron
[DE91-643289] p 304 N92-16789

SEDIMENT TRANSPORT
Aerodynamic roughness measured in the field and simulated in a wind tunnel
[NASA-CR-4422] p 347 N92-19354

SELECTION
Airbreathing engine selection criteria for SSTO propulsion system
[IAF PAPER 92-0658] p 1071 A92-57099

SELF ALIGNMENT
Predication of fastening capacity of screwed joint structure with cone assembly p 391 A92-24737

SELF CONSISTENT FIELDS
H-N2 interaction energies, transport cross sections, and collision integrals p 1135 A92-54660

SELF EXCITATION
Separation-induced self-excited structural oscillations
[AIAA PAPER 92-0486] p 328 A92-26317

SELF OSCILLATION
Self-oscillatory interaction of an underexpanded jet with an obstacle in the presence of a supersonic wake
p 79 A92-16681
Feedback mechanism of self-oscillations in the case of an underexpanded supersonic jet impinging on a plane obstacle p 79 A92-16682
Numerical modeling of self-oscillations for a small-aspect-ratio delta wing using measurements of roll motion at large angles of attack p 424 A92-30138
Stochastic self-induced roll oscillations of slender delta wing at high angles of attack
[AIAA PAPER 92-4498] p 1081 A92-55366

SELF TESTS
Smart structures - A damage detection concept
p 491 A92-28672
Utility management system for hypersonic vehicles
p 964 A92-49252

SEMANTICS
A prototype semantic integrity front end expert system for a relational database
[AD-A246084] p 781 N92-26765

SEMICONDUCTOR DEVICES
Optically powered and interrogated rotary position sensor for aircraft engine control applications
p 370 A92-27777

SEMICONDUCTOR LASERS
Optical velocity sensor for air data applications
p 368 A92-24575
Efficiency of a 5V/5mW power by light power supply for avionics applications p 734 A92-42603
Composition monitoring of electron beam melting processes using diode lasers
[DE92-009527] p 669 N92-25259

SEMICONDUCTORS (MATERIALS)
Next generation power electronics for space and aircraft. II - Packaging p 992 A92-50553

SEMIEMPIRICAL EQUATIONS
Rapid synthesis for evaluating missile maneuverability parameters
[AIAA PAPER 92-2615] p 873 A92-45488
A semi empirical method for the analytical representation of stationary measured profile coefficients for applications of rotary wing aerodynamics
[ETN-92-91491] p 832 N92-29741

SEMISPAN MODELS
Aerodynamic characteristics of a propeller powered high lift semispan wing
[AIAA PAPER 92-0388] p 323 A92-26244
NACA 0015 wing pressure and trailing vortex measurements
[NASA-TP-3151] p 13 N92-10981
Experimental study of an independently deflected wingtip mounted on a semispan wing
[NASA-TM-102842] p 13 N92-10983

SENSITIVITY
Aerodynamic sensitivity analysis methods for the compressible Euler equations p 233 A92-19619
An analytical approach to grid sensitivity analysis --- of NACA wing sections
[AIAA PAPER 92-0660] p 334 A92-27031
Aeroelastic optimization of an advanced geometry helicopter rotor
[AIAA PAPER 92-2360] p 543 A92-34592
Determination of aerodynamic sensitivity coefficients based on the three-dimensional full potential equation
[AIAA PAPER 92-2670] p 798 A92-45525
Sensitivity analysis of discrete periodic systems with applications to helicopter rotor dynamics
p 846 A92-46884
Sensitivity of tire response to variations in material and geometric parameters p 900 A92-47128
On simple aerodynamic sensitivity derivatives for use in interdisciplinary optimization
[NASA-TM-104145] p 82 N92-11985
An experimental study of the sensitivity of helicopter rotor blade tracking to root pitch adjustment in hover
[NASA-TM-4313] p 61 N92-12989
Methodology for sensitivity analysis, approximate analysis, and design optimization in CFD for multidisciplinary applications --- computational fluid dynamics
[NASA-CR-190201] p 595 N92-22662
Integrated Design Analysis and Optimisation of Aircraft Structures
[AGARD-R-784] p 550 N92-23227
A system approach to aircraft optimization
p 550 N92-23228
Sensitivity analysis of dynamic aeroelastic responses
p 571 N92-23229
An incremental strategy for calculating consistent discrete CFD sensitivity derivatives
[NASA-TM-104207] p 625 N92-24681
An analytical approach to grid sensitivity analysis for NACA four-digit wing sections
[NASA-CR-190251] p 631 N92-25175
A sensitivity analysis on component reliability from fatigue life computations
[AD-A247430] p 908 N92-28425
Determination of aerodynamic sensitivity coefficients for wings in transonic flow
[NASA-CR-190570] p 832 N92-29657

SENSORS
Development of a sensor for the detection of aircraft wing contaminants
[AIAA PAPER 92-0300] p 369 A92-25752
Failure detection and identification for aircraft sensors
p 370 A92-27832
Design issues in a fiber optic sensor system architecture for aircraft engine control
[AIAA PAPER 92-3483] p 866 A92-49023
A theoretical study of sensor-actuator schemes for rotating stall control
[AIAA PAPER 92-3486] p 878 A92-49025
Research sensors p 594 N92-22526

SENSORY PERCEPTION
Reference mode effect on the auditory display of aircraft bank angle
[AD-A247825] p 728 N92-27916

SEPARATED FLOW
An experimental study of subsonic separated flow over parawings p 4 A92-10901
Pressure on a cylinder with a screen in transverse flow p 6 A92-12164
A numerical simulation of separated flows around bodies p 8 A92-12423
Computation of three-dimensional turbulent vortical flows on bodies at high incidence p 9 A92-13203
Estimation of the size of separation zone in a turbine stage under small load p 10 A92-13235
Secondary separation from a slender wing
p 62 A92-13448
A 3-D separation model for arbitrary planforms
p 65 A92-14360
A review of rigid body response on sting supported models at high angles of incidence p 66 A92-15345
Numerical prediction of subsonic turbulent flows over slender bodies at high incidence p 172 A92-18358
Flow separation patterns over an F-14A aircraft wing
p 174 A92-20205
Newton's method solver for high-speed viscous separated flowfields p 176 A92-20736
Asymmetric separated flows at supersonic speeds
p 176 A92-20742
Development and application of a particle image velocimeter for high-speed flows
[AIAA PAPER 92-0004] p 292 A92-22129
Compressor blade row unsteady aerodynamic response to attached and separated flow forcing functions
[AIAA PAPER 92-0147] p 253 A92-23763
The Baldwin-Lomax model for separated and wake flows using the entropy envelope concept
[AIAA PAPER 92-0148] p 253 A92-23764
Experimental necessities for subsonic transport configuration development
[AIAA PAPER 92-0158] p 254 A92-23773
The dynamics and control of fluctuating pressure loads in the reattachment region of a supersonic free shear layer
[AIAA PAPER 92-0178] p 255 A92-23788
Compressibility effects on the dynamic stall of a three-dimensional wing
[AIAA PAPER 92-0191] p 256 A92-23800
Effects of trailing-edge flap on buffet characteristics of a supercritical airfoil p 378 A92-24413
Control of laminar boundary layer separation
p 393 A92-24980
Numerical simulation of 2-D separated flows caused by suddenly change of the body section
p 312 A92-25004
Numerical simulation of supersonic separated flow over blunt cones at high angles of attack p 313 A92-25039
Multiple line-vortex model of vortex flows around body of revolution at high angles of attack up to 60 degrees
p 314 A92-25104
Numerical simulation and analysis for hypersonic flow with separation over blunt cone at angle of attack
p 314 A92-25126
The study of inverse boundary layer algorithm for transonic flows over aerofoils p 315 A92-25140
Cross-flow separation on a prolate spheroid at angles of attack
[AIAA PAPER 92-0428] p 326 A92-26276
Separation-induced self-excited structural oscillations
[AIAA PAPER 92-0486] p 328 A92-26317
Flow past a sphere - Topological transitions of the vorticity field p 330 A92-26410
Numerical simulation of flow separation for rotors and fixed wings
[AIAA PAPER 92-0635] p 334 A92-27013
Ground facility interference on aircraft configurations with separated flow
[AIAA PAPER 92-0673] p 384 A92-27042
Numerical analysis of shock-induced separation alleviation using vortex generators
[AIAA PAPER 92-0751] p 335 A92-27095
Characteristics of the mechanism of separated flow pulsation ahead of a spike-tipped cylinder in supersonic flow p 337 A92-27597
Investigation on vortex control technique of flow separation in diffuser p 338 A92-27828
Separation control by vortex generators in subsonic diffuser p 338 A92-27829
Helium bubble flow visualization of the spanwise separation on a NACA 0012 with simulated glaze ice
[AIAA PAPER 92-0413] p 341 A92-28192
A method for calculating the separated flow past a circular cone, taking viscous-inviscid interaction into account p 427 A92-30203
Calculation of the aerodynamic characteristics of bodies of revolution in incompressible flow by the vortex surface method p 428 A92-30375
Experiment on pitching moments of separated flow around airfoil profiles p 429 A92-30527
Stability of a nonorthogonal stagnation flow to three-dimensional disturbances p 495 A92-31194
A preliminary study of the turbulent structures associated with unsteady separation shock motion in a Mach 5 compression ramp interaction
[AIAA PAPER 92-0744] p 436 A92-31677
Calculation of three-dimensional separated flows in the framework of the unsteady Euler equations
p 438 A92-31870
Some characteristics of transonic flow past an airfoil in the case of developed separation
p 440 A92-31885
Heat transfer effects on aerodynamics and implications for wind-tunnel tests p 497 A92-32240
Rotor aeromechanics research with the RAE research Lynx - The experimental facility and test programme
p 547 A92-35767
Active control of the hydraulic forces of a body by a splitter plate p 591 A92-36351
Structure of the separated flow region in a dihedral corner in front of an obstacle in supersonic flow
p 524 A92-36420
Separated and cavitation flows - Principal properties and computational models --- Russian book
[ISBN 5-02-014005-8] p 610 A92-36600
A study of flow patterns and behaviours of 3D separated flow on a simplified Shuttle model p 615 A92-38906
Separated flow over the protuberances in hypersonic flow p 615 A92-38907
Hypersonic turbulent separated flow past an unswept circular cylinder on a flat plate p 615 A92-38908
Numerical simulation of separation flow on bodies of revolution at high angle of attack using Euler equations
p 616 A92-38919
Prediction of separation point in compressible turbulent boundary layers by Green's lag-entrainment method
p 700 A92-41178
Acoustic sources in a tripped flow past a resonator tube p 778 A92-41266
Effect of acoustic excitation on stalled flows over an airfoil p 703 A92-41267
The flow over a backward-facing step under controlled perturbation - Laminar separation p 705 A92-41653
The main wing boundary layer separation pattern of STOL research aircraft Asuka p 709 A92-43144

Experimental and numerical investigations on separated flows around pitching airfoils p 710 A92-43166
Numerical simulations of separated flows around oscillating airfoil for dynamic stall phenomena
[SAE PAPER 911991] p 788 A92-45393
Turbulent drag reduction by laminar sublayer thickening
[AIAA PAPER 92-2707] p 801 A92-45549
Active control of vortex structures in a separating flow over an airfoil
[AIAA PAPER 92-2728] p 804 A92-45563
A numerical study of control surface buzz using computational fluid dynamic methods
[AIAA PAPER 92-2654] p 806 A92-45578
Separation patterns and flow structures about a hemisphere-cylinder at high incidences
[AIAA PAPER 92-2712] p 807 A92-45593
Separated high enthalpy dissociated laminar hypersonic flow behind a step - Pressure measurements
p 809 A92-45858
Simplified linear stability transition prediction method for separated boundary layers p 812 A92-46883
Joint computational/experimental aerodynamics research on a hypersonic vehicle. I - Experimental results p 812 A92-46890
Two-stream, supersonic, wake flowfield behind a thick base. I - General features p 813 A92-46895
Computation of turbulent, separated, unswept compression ramp interactions p 813 A92-46897
Interaction between a rotor tip vortex and a separated flowfield p 814 A92-46947
An improved multiple line-vortex method for simulation of separated vortices of slender wings
p 819 A92-47694
Calculation of fully three-dimensional separated flows with an unsteady viscous-inviscid interaction method
[ONERA, TP NO. 1992-1] p 821 A92-48577
Pulse jet one-way valve performance
[AIAA PAPER 92-3169] p 863 A92-48790
Application of submerged vortex generators for separation control of a subsonic diffuser
p 933 A92-49832
A review of scale effects in unsteady aerodynamics
p 934 A92-50121
Exploratory study of wall pressure fluctuations in a Mach 5, sharp fin-induced turbulent interaction
p 935 A92-50304
A direct viscous-inviscid interaction method for the flow calculation around airfoils p 936 A92-52028
Experiments on separation at a compression corner in rarefied hypersonic flows p 938 A92-52755
Detecting 3-D, turbulent separation regions using unsteady computerized thermographic technique
p 1023 A92-54308
Dynamical scaling of a model unsteady separating flow p 1117 A92-54932
Assessment of passive porosity with free and fixed separation on a tangent ogive forebody
[AIAA PAPER 92-4494] p 1081 A92-55363
State-space representation of aerodynamic characteristics of an aircraft at high angels of attack
[AIAA PAPER 92-4651] p 1028 A92-55395
Numerical investigation of the effect of leading edge geometry on dynamic stall of airfoils
[AD-A239949] p 12 N92-10015
Vortex Flow Aerodynamics
[AGARD-CP-494] p 83 N92-12996
Modeling and numerical simulation of vortex flow in aerodynamics
[AD-B163670L] p 83 N92-12997
Recent progress in computational vortex-flow aerodynamics p 84 N92-13002
Calculation of hypersonic leeside vortices over blunt delta wings p 84 N92-13004
On the footprints of three-dimensional separated vortex flows around blunt bodies: Attempts of defining and analyzing complex flow structures p 84 N92-13005
Laminar-flow secondary separation on a slender wing
p 85 N92-13006
Nonequilibrium turbulence modeling effects on transonic vortical flows about delta wings p 85 N92-13007
Review of aircraft dynamic loads due to flow separation p 85 N92-13008
Physics of vortical flow p 86 N92-13016
A Navier-Stokes solution of Hull-ring wing-thruster interaction p 221 N92-14310
The effect of rounding the leading edges on the characteristics of separated flow past delta wings of low aspect ratio
[RAE-LIB-TRANS-2164] p 257 N92-15964
Control of unsteady separated flow associated with the dynamic pitching of airfoils
[NASA-CR-189758] p 258 N92-15966
Computation of the hydrodynamic forces and moments on a body of revolution with and without appendages
[AD-A243033] p 298 N92-16978
Optimization of tangential mass injection for minimizing flow separation in a scramjet inlet
[AD-A243868] p 376 N92-18867
Laser velocimetry measurements of oscillating airfoil dynamic stall flow field
[AD-A244546] p 502 N92-21297
Current status of computational methods for transonic unsteady aerodynamics and aeroelastic applications
[NASA-TM-104191] p 446 N92-21432
Two-dimensional transonic flow calculation by interaction of Euler and boundary layer equations
[PB92-136449] p 448 N92-21784
Hypersonic laminar flow computations over a blunt leading edged delta wing at three different chord Reynolds numbers
[FFA-TN-1991-40] p 528 N92-23168
High angle of attack: Aerodynamics
p 528 N92-23956
Helium bubble flow visualization of the spanwise separation on a NACA 0012 with simulated glaze ice
[NASA-TM-105742] p 714 N92-26612
An experimental investigation of the separating/reattaching flow over a backstep
[NASA-CR-190426] p 716 N92-27399
Visualization of boundary-layer development on turbomachine blades with liquid crystals
[NASA-CR-190433] p 742 N92-27519
Current status of computational methods for transonic unsteady aerodynamics and aeroelastic applications
p 718 N92-27937
A review of scale effects on surfaces in unsteady motion p 722 N92-27962
Inlet distortion effects in aircraft propulsion system integration p 869 N92-28464
A method for computing the 3-dimensional flow about wings with leading-edge vortex separation. Part 2: Description of computer program VORSEP
[NLR-TR-86006-U] p 833 N92-29916
Vortex flow aerodynamics
[AGARD-AR-299] p 946 N92-30947
A computational investigation of airfoil stall flutter
[AD-A247302] p 947 N92-31300
Control of unsteady separated flow associated with the dynamic stall of airfoils
[NASA-CR-190688] p 950 N92-32177
A critical evaluation of a three-dimensional Navier-Stokes CFD as a tool to design supersonic turbine stages p 1124 N92-32268
Numerical investigation of the effects of icing on fixed and rotary wing aircraft
[NASA-CR-190542] p 1044 N92-34105

SEPARATORS
Design analysis of the T-800 inlet particle separator/air oil cooler blower p 579 A92-32556
Viscous flow analysis of advanced particle separators
p 737 A92-44517

SEQUENCING
A cognitive temporal model for the planning in aircraft maintenance p 307 A92-25178
System for generating sequences of phased gust or taxi loadings p 845 A92-46800

SEQUENTIAL COMPUTERS
State and time granularity in system description: An example
[REPT-91-040] p 603 N92-22673

SEQUENTIAL CONTROL
Helicopter active rotor control p 570 N92-22157
Turbine drive system of the high pressure LOX turbopump test facility
[DE92-783191] p 680 N92-25342

SERIES EXPANSION
Determination of duty factors from experimental data in local interaction theory p 338 A92-27645

SERVICE LIFE
Application of smart structures to aircraft health monitoring p 20 A92-11123
Rotor blade preservation - Getting the most service life with lowest operational costs p 108 A92-14412
Stratospheric lighter-than-air powered platform
p 110 A92-15334
Life time prediction for ceramic gas turbine components
[ASME PAPER 91-GT-96] p 122 A92-15560
A global approach in evaluating inlet/engine compatibility
[ASME PAPER 91-GT-402] p 127 A92-15732
Transmission overhaul and component replacement predictions using Weibull and renewal theory
p 155 A92-17201
National research program for nondestructive inspection of aging aircraft p 169 A92-17294
A probabilistic method for monitoring the remaining life of aircraft gas turbine engine components using the temperature limit criterion p 201 A92-18292
Multiaxial load spectra in a cooled gas turbine blade under in-service conditions p 201 A92-19696
Durability analysis using fracture mechanics for avionics integrity p 396 A92-26799
The problem of aging aircraft - Is mandatory retirement the answer? p 308 A92-27448
A theoretical study on helicopter alert time without maintenance p 358 A92-27836
Unsteady aerodynamic interaction effects on turbomachinery blade life and performance
[AIAA PAPER 92-0149] p 341 A92-28186
Evolving partnership for NDE in materials engineering and extended life cycle performance
p 490 A92-28556
Analysis of the efficiency of some structural-inspection strategies in aircraft maintenance p 419 A92-30141
Structural design for durability - Lessons learned from service and test data
[AIAA PAPER 92-1129] p 537 A92-33281
Ageing airliner census - Still flying safely
p 634 A92-38374
Aging aircraft and structural airworthiness
[SAE PAPER 912212] p 635 A92-40016
A method for estimating the technological and economic efficiency of measures enhancing the reliability of aviation gas turbine engines p 657 A92-40621
Some consideration for evaluation of structural integrity of aging aircraft p 762 A92-43107
Electric actuation system duty cycles --- in fly-by-wire/power-by-wire control p 877 A92-48494
Aging aircraft and airworthiness p 931 A92-51399
Effective maintenance practices to manage system aging p 1119 A92-56215
Program plan: National aging aircraft research program
[DOT/FAA/CT-88/32-1] p 18 N92-10992
Monitoring load experience of individual aircraft
[NLR-TP-90084-U] p 196 N92-15065
Flight operations for higher harmonic control research
[AD-A242478] p 196 N92-15067
Aging Aircraft NDI Development and Demonstration Center (AANC): An overview
[DE92-002358] p 241 N92-15962
Durability and damage tolerance testing and fatigue life management: A CF-18 experience p 361 N92-18581
The G-222 aircraft individual tracking programme
p 361 N92-18582
Structural airworthiness of aging Boeing jet transports
p 362 N92-18590
Managing airborne assets through loads monitoring
p 363 N92-18594
AGARD/SMP Review: Damage Tolerance for Engine Structures. 4: Reliability and Quality Assurance
[AGARD-R-773] p 402 N92-19004
A review of aging aircraft technology: An IAI perspective
[IAITIC-91-1018] p 461 N92-20500
Fatigue life variability and reliability analysis of a wind turbine blade
[DE92-008673] p 689 N92-25049
Research into improving the durability of the hot section in the aircraft turbine engine
[AD-A250342] p 973 N92-31439
Aging fleet: Maintaining airworthiness
p 953 N92-31862
Supportability evaluation of thermoplastic and thermoset composites p 1108 N92-32576
Residual strength of repaired graphite/epoxy laminates after 5 years of outdoor exposure p 1108 N92-32577
PDES application protocol suite for composites (PAS-C). Functional needs report for the PAS-C program
[AD-A247886] p 1108 N92-32629
Effects of the abrasiveness of test and training site soils on parachute life
[AD-A252389] p 1038 N92-32900

SERVOCONTROL
Aircraft aeroservoelastic compensation using constrained optimization
[AIAA PAPER 92-2399] p 564 A92-34470
Aeroelasticity - Advances and future directions
[AIAA PAPER 92-2446] p 585 A92-34475
Aeroservoelasticity p 642 A92-37577
An analytical and experimental investigation of flutter suppression via piezoelectric actuation
[NASA-TM-107653] p 962 N92-31174

SERVOMECHANISMS
Retrospective essay on nonlinearities in aircraft flight control p 204 A92-18601
On the characteristics of servo actuators attached to a model spaceplane for dynamic wind-tunnel test
p 762 A92-43213
Hydraulic actuator system for rotor control
p 224 N92-14363
Evaluation of electrolytic tilt sensors for measuring model angle of attack in wind tunnel tests
[NASA-TM-4315] p 297 N92-16283

Variable-camber systems integration and operational performance of the AFTI/F-111 mission adaptive wing
[NASA-TM-4370] p 570 N92-22194
An analytical and experimental investigation of flutter suppression via piezoelectric actuation
[NASA-TM-107653] p 962 N92-31174

SET THEORY
A formal definition of the object-oriented paradigm for requirements analysis
[AD-A246814] p 729 N92-28132

SHADOWGRAPH PHOTOGRAPHY
High-speed cinematography of supersonic mixing layers
[AIAA PAPER 92-3545] p 1112 A92-54044
Application of digital measurement techniques to analysis of range shadowgraphs
[AD-A241554] p 139 N92-13080

SHAFTS (MACHINE ELEMENTS)
Gas turbine main shaft internal flow and heat transfer
[ASME PAPER 91-GT-165] p 123 A92-15600
Quasi-static analysis of roller bearing
p 391 A92-24732
Magnetic particle testing of turbine blades mounted on the turbine rotor shaft p 898 A92-46498
Analysis and modification of a single-mesh gear fatigue rig for use in diagnostic studies
[NASA-TM-105416] p 773 N92-27879
Application of face-gear drives in helicopter transmissions
[NASA-TM-105655] p 908 N92-28434

SHAPE CONTROL
Control theory for optimum design of aerodynamic shapes p 6 A92-11328
Shape optimization of three-dimensional structures with adaptive meshing
[AIAA PAPER 92-2434] p 586 A92-34548

SHAPE MEMORY ALLOYS
Improved articulated fin/wing control system statement of government interests
[AD-D015268] p 1088 N92-34131

SHAPES
Results of an icing test on a NACA 0012 airfoil in the NASA Lewis Icing Research Tunnel
[AIAA PAPER 92-0647] p 334 A92-27021
Adaptive parallel meshes with complex geometry
p 918 A92-47050
Aerodynamic characteristics of a standard corrugated body in a free-molecular flow p 940 A92-52818
Results of an Icing test on a NACA 0012 airfoil in the NASA Lewis Icing Research Tunnel
[NASA-TM-105374] p 185 N92-15051
Experimental ice shape and performance characteristics for a multi-element airfoil in the NASA Lewis Icing Research Tunnel
[NASA-TM-105380] p 261 N92-17347
Hi-alpha forebody design. Part 1: Methodology base and initial parametrics
[NASA-CR-189849] p 358 N92-18024
Hi-alpha forebody design. Part 2: Determination of body shapes for positive directional stability
[NASA-CR-189850] p 359 N92-18038
Effect of crash pulse shape on seat stroke requirements for limiting loads on occupants of aircraft
[NASA-TP-3126] p 399 N92-18053
Comparison of jet plume shape predictions and plume influence on sonic boom signature
[NASA-TP-3172] p 631 N92-25133
Experimental and computational ice shapes and resulting drag increase for a NACA 0012 airfoil
[NASA-TM-105743] p 828 N92-28674
A semi empirical method for the analytical representation of stationary measured profile coefficients for applications of rotary wing aerodynamics
[ETN-92-91491] p 832 N92-29741
Examples of advanced near-net shape manufacturing techniques for aerospace
[MBB-Z-0399-91-PUB] p 1125 N92-32742
Development of 3D electromagnetic modeling tools for airborne vehicles
[NASA-CR-190810] p 1126 N92-33307

SHARP LEADING EDGES
Incompressible flow past a flat plate aerofoil with leading edge separation bubble p 421 A92-28943
Aerodynamic characteristics of slender sharp-leading-edge delta wings with air scooping through the air intake at hypersonic velocities. I
p 427 A92-30206
On hypersonic flow over two-dimensional aerofoils
p 433 A92-31425
Numerical simulation of leading-edge vortex breakdown using an Euler code p 701 A92-41213
Numerical investigation into high-angle-of-attack leading-edge vortex flow
[AIAA PAPER 92-2600] p 791 A92-45477
Aerodynamically blunt and sharp bodies
[AIAA PAPER 92-2727] p 808 A92-45597
Perfect compressible two dimensional boundary layer strong fluid coupling in the case of sharp leading edge profiles. Unsteady case of isolated profiles and steady case of blade grids
[ONERA-RT-43/1621-RY-006-R] p 43 N92-11311
Comparison of solution of various Euler solvers and one Navier-Stokes solver for the flow about a sharp-edged cropped delta wing
[AD-B163639L] p 83 N92-12998
Analysis of results of an Euler-equation method applied to leading-edge vortex flow p 84 N92-13000
Experimental and numerical investigation of the vortex flow over a delta wing at transonic speed
p 84 N92-13001
Visualisation in water of vortex flow over sharp-edged canard configurations
[ARL-FLIGHT-MECH-R-189] p 632 N92-25410
Analysis of results of an Euler-equation method applied to leading-edge vortex flow
[NLR-TP-90368-U] p 827 N92-28657
An experimental study of the flow over a sharp-edged delta wing at subsonic and transonic speeds
[NLR-TP-91117-U] p 1037 N92-32732
Strong coupling between inviscid fluid and boundary layer of sharp leading edges: Two-dimensional stationary and turbulent cases for isolated profiles and guard vanes
[ONERA-RT-44/1621-RY-016-R] p 1125 N92-32776

SHEAR FLOW
Vortex-induced energy separation in shear flows
[AIAA PAPER 92-0192] p 257 A92-23801
Simulation of 3-D shear flows around a nozzle-afterbody at high speeds p 519 A92-34826
An analytical evaluation of the aerodynamic forces acting on a circular cylinder in a uniform shear flow
p 522 A92-35995
An improved analysis method for cross-wire signals obtained in supersonic flow p 614 A92-38456
The effect of a velocity gradient on the aerodynamic forces of a circular cylinder with tangential blowing
p 614 A92-38859
Symposium on Turbulent Shear Flows, 8th, Technical University of Munich, Federal Republic of Germany, Sept. 9-11, 1991, Proceedings. Vols. 1 & 2
p 675 A92-40051
Compressibility effects on the growth and structure of homogeneous turbulent shear flow p 675 A92-40052
A new method for visualization and measurement of turbulent flow patterns p 619 A92-40063
Turbulent energy budgets in impinging zones
p 620 A92-40081
Modern developments in shear flow control with swirl
p 703 A92-41265
Some exact and numerical results for plane steady sheared flow of an incompressible inviscid fluid
p 821 A92-48019
The interaction between a plane shear layer and a slender body p 991 A92-49790
A concentration probe for the study of mixing in supersonic shear flows p 991 A92-50039
Assessment of compressibility corrections to the k-epsilon model in high-speed shear layers
p 1024 A92-54905
Noise from turbulent shear flows p 55 N92-10603
Computation of a Kelvin-Helmholtz instability for delta wing vortex flows
[AD-A244320] p 346 N92-18825
The 8th Symposium on Turbulent Shear Flows. Volume 1: Sessions 1-18
[AD-A243809] p 402 N92-18933
The eddy structures in bounded shear flows
p 717 N92-27712
Modeling of the reactant conversion rate in a turbulent shear flow p 829 N92-28820

SHEAR LAYERS
Numerical simulations of the structure of supersonic shear layers p 3 A92-10574
Numerical simulations of unsteady reactive flows in a combustion chamber p 39 A92-11761
3-D loss prediction based on secondary flow and blade shear layer interaction
[ASME PAPER 91-GT-59] p 68 A92-15536
Stability of a viscous compressible shear layer with a temperature drop p 79 A92-16684
The finite volume approach for the Navier-Stokes equations p 246 A92-21980
A calculating method of shock wave oscillating frequency due to turbulent shear layer fluctuations in supersonic flow p 251 A92-22720
An experimental investigation of large scale instabilities in a low Reynolds number two-stream supersonic shear layer
[AIAA PAPER 92-0177] p 255 A92-23787
The dynamics and control of fluctuating pressure loads in the reattachment region of a supersonic free shear layer
[AIAA PAPER 92-0178] p 255 A92-23788
Organized structure in a Mach 5/Mach 3 turbulent shear layer
[AIAA PAPER 92-0180] p 256 A92-23790
Evaluation of shear layer cavity resonance mechanisms by numerical simulation
[AIAA PAPER 92-0555] p 333 A92-26965
Experiments on shear layer mixing at hypervelocity conditions
[AIAA PAPER 92-0628] p 396 A92-27009
Algebraic turbulence modeling for adaptive unstructured grids p 398 A92-28033
Flowfield simulation about the SOFIA Airborne Observatory
[AIAA PAPER 92-0656] p 342 A92-28217
Flame sheet algorithm for use in numerical modeling of ramjet combustion instability p 390 A92-28503
Numerical simulation of three-dimensional supersonic free shear layers p 431 A92-31152
Applications of hot-film anemometers in hypersonic shear layers
[AIAA PAPER 91-5028] p 436 A92-31687
Evaluation of a finite volume method for compressible shear layers p 610 A92-36834
Similarity in supersonic mixing layers
p 611 A92-36842
Particle dispersion in highly swirling, turbulent flows
p 675 A92-40093
Direct simulation of a supersonic reacting mixing-layer
p 676 A92-40132
The interaction between a plane shear layer and a slender body p 991 A92-49790
Effects of vortex generators on the growth of a compressible shear layer
[AIAA PAPER 90-1979] p 934 A92-50269
Experiments on the structure of an annular compressible reacting shear layer p 969 A92-50311
On the effect of external flow and shear-layer thickness on the expansion cells of under-expanded supersonic circular jets p 969 A92-50478
Supersonic flow mixing and combustion using RAMP nozzle
[AIAA PAPER 92-3840] p 1113 A92-54198
A laser fluorescence anemometer system for the Langley 16- by 24-inch water tunnel
p 1092 A92-54347
Contractors Meeting in Propulsion
[AD-A240057] p 33 N92-10062
Calculation of hypersonic leeside vortices over blunt delta wings p 84 N92-13004
Computation of a Kelvin-Helmholtz instability for delta wing vortex flows
[AD-A244320] p 346 N92-18825
The 8th Symposium on Turbulent Shear Flows. Volume 1: Sessions 1-18
[AD-A243809] p 402 N92-18933
Inlets, ducts, and nozzles p 593 N92-22523
Turbulent mixing in supersonic jets
p 715 N92-27054
The eddy structures in bounded shear flows
p 717 N92-27712
Effect of walls on the supersonic reacting mixing layer
p 912 N92-30065
High speed transition prediction
[NASA-CR-190836] p 1039 N92-33424

SHEAR PROPERTIES
Nondestructive testing developments in the aircraft industry p 214 A92-17288
KGR-1 thick adherend specimen evaluation for the determination of adhesive mechanical properties
p 994 A92-51513

SHEAR STRAIN
Efficient evaluation of the flexibility of tapered I-beams accounting for shear deformations p 295 A92-23269
Flexure-torsion behavior of sheat-deformable beams with applications to aircraft wing sections
[AIAA PAPER 92-2467] p 582 A92-34357
A new method for calculating burst speed of aeroengine disks
[ASME PAPER 91-GT-121] p 670 A92-36899
Transverse shear effect on flutter of composite panels
p 1122 A92-56607

SHEAR STRENGTH
Adhesive shear strength of impact ice --- inside wind tunnel p 30 A92-11068
Combined compressive and shear buckling analysis of hypersonic aircraft sandwich panels
[AIAA PAPER 92-2487] p 586 A92-34603
The evaluation of non-tank surface treatments for aluminium bonding repairs p 761 A92-42502
Tensile and interlaminar properties of GLARE (trade name) laminates
[AD-A250188] p 895 N92-28921

Processing and environmental effects on mechanical properties of composite repairs
[NRC-LTR-ST-1826] p 1109 N92-32791

SHEAR STRESS
Aerodynamic characteristics of a hypersonic viscous optimized waverider at high altitudes
[AIAA PAPER 92-0306] p 320 A92-25755
Three-dimensional structure of a curved wake
[AIAA PAPER 92-0541] p 341 A92-28199
Liquid crystal coatings for surface shear-stress visualization in hypersonic flows p 496 A92-32177
An experimental and numerical study of confined axisymmetric jet with a bluff body p 621 A92-40106
Predictions of a turbulent backward-facing-step flow with a cubic pressure-strain model
[AIAA PAPER 92-2647] p 796 A92-45514
A new approach for the calculation of transitional flows
[AIAA PAPER 92-2669] p 798 A92-45524
Shock detection on airfoils by means of piezo foil- and hot film arrays p 1115 A92-54334
A finite element method for shear stresses calculation in composite blade models p 1121 A92-56322
Analysis of a dusty wall jet
[NASA-CR-189759] p 257 N92-15965
An experimental investigation of the separating/reattaching flow over a backstep
[NASA-CR-190426] p 716 N92-27399
Active thermal isolation for temperature responsive sensors
[NASA-CASE-LAR-14612-1] p 911 N92-29954

SHELL THEORY
Vibration characteristic analysis of a propeller blade p 38 A92-10967
Acoustic scattering by a disk or annulus linking two concentric cylindrical shells. I - Theory and results for heavy exterior fluid loading. II - Results for heavy exterior fluid loading on both shells p 696 A92-40588
Analysis and testing of a composite sandwich shell horizontal tail p 755 A92-44617

SHELLS (STRUCTURAL FORMS)
Coupled analysis of independently modeled finite element subdomains
[AIAA PAPER 92-2235] p 581 A92-34289
Space Shuttle shell structure waffle panel optimization
[AIAA PAPER 92-2359] p 586 A92-34591
Optimal design of nonlinear shell structures
[FFA-TN-1991-18] p 157 N92-12312
Explicit finite element method for transparency impact analysis
[AD-A243527] p 264 N92-17478

SHIP HULLS
Deck motion criteria for carrier aircraft operations p 464 N92-21952

SHIPS
Safety at sea and in the air - Taking stock together; Proceedings of the Conference, London, England, Nov. 13-15, 1990
[ISBN 0-903409-78-X] p 634 A92-39301
How to promote error tolerance in complex systems in the context of ships and aircraft p 673 A92-39308
Flight deck aerodynamics of a nonaviation ship p 810 A92-46790
Aircraft Ship Operations
[AGARD-CP-509] p 464 N92-21951
The aerodynamics of ship superstructures p 503 N92-21953
United Kingdom approach to deriving military ship helicopter operating limits p 465 N92-21966
Limitations on helicopter operations in the aeronaval environment p 466 N92-21973

SHOCK ABSORBERS
Dynamic behavior analysis for landing-gear with different types of dual-chamber shock-struts p 111 A92-15342
Nonlinear landing gear behavior at touchdown p 192 A92-19606
Dual mode shock absorber and method
[PATENT-1-265-541] p 115 N92-13055

SHOCK DISCONTINUITY
Development of new flux splitting schemes --- computational fluid dynamics algorithms p 682 N92-25809

SHOCK HEATING
Experimental and numerical studies of radiation emission from high-temperature air behind 10 km/s shock waves
[SAE PAPER 912025] p 790 A92-45417
Examination of ultraviolet radiation theory for bow shock rocket experiments
[AIAA PAPER 92-2871] p 901 A92-47853

SHOCK LAYERS
A viscous flow study of shock-boundary layer interaction, radial transport, and wake development in a transonic compressor
[ASME PAPER 91-GT-69] p 68 A92-15539
Self-oscillatory interaction of an underexpanded jet with an obstacle in the presence of a supersonic wake p 79 A92-16681
Control of hypersonic aerodynamic forces with surface blowing p 172 A92-18363
Axisymmetric analogy for three-dimensional viscous flow problems p 244 A92-21617
Improved nonequilibrium viscous shock-layer scheme for hypersonic blunt-body flowfields p 310 A92-24653
An approximate viscous shock layer technique for calculating nonequilibrium hypersonic flows about blunt-nosed bodies
[AIAA PAPER 92-0498] p 329 A92-26326
Calculation of three-dimensional flow past blunt cones near the plane of symmetry for different flow regimes in the shock layer and in the presence of gas injection from the surface p 337 A92-27593
Cooling of a sharp nose by extraneous gas injection into the viscous shock layer p 426 A92-30188
Nonstationary viscous shock layer in supersonic motion over an inhomogeneity p 708 A92-42737
Similarity and resistance in near-sonic flows for given heat conduction p 708 A92-43065
A parametric analysis of radiative structure in aerobrake shock layers
[AIAA PAPER 92-2970] p 816 A92-46985
Enhancements to viscous-shock-layer technique
[AIAA PAPER 92-2897] p 820 A92-47873
Thermal and chemical nonequilibrium viscous shock layer flows over a blunt body at high altitudes p 938 A92-52749
Hypersonic flows with air chemistry over a reentry vehicle at high altitudes p 1017 A92-53549
Radiative heat transfer from nonequilibrium shock layer to a hypersonic reentry body p 1019 A92-53579
Three-dimensional calculation of radiative field in hypersonic air shock layers p 1023 A92-54498
Viscous shock-layer equations for the calculation of reentry aerothermodynamics p 183 N92-15008
Hypersonic viscous shock layer in thermochemical nonequilibrium p 183 N92-15014
Influence of chemical modeling on the solution of hypersonic shock layers p 183 N92-15016
A laser velocimeter investigation of the normal shockwave boundary layer interaction p 500 N92-20485
Development of new flux splitting schemes --- computational fluid dynamics algorithms p 682 N92-25809
Stagnation-point heat-transfer rate predictions at aeroassist flight conditions
[NASA-TP-3208] p 1001 N92-31281
The structure and control of three-dimensional shock wave turbulent boundary layer interactions
[AD-A250209] p 1003 N92-31824
An approximate viscous shock layer technique for calculating chemically reacting hypersonic flows about blunt-nosed bodies p 1041 N92-33837

SHOCK LOADS
Numerical simulation of transient hypervelocity flow in an expansion tube
[NASA-CR-189601] p 402 N92-18965
An explosively driven, fast shock tube
[DE92-008437] p 749 N92-26720

SHOCK SIMULATORS
Rarefaction wave eliminator design study
[AD-A244401] p 484 N92-20455

SHOCK TESTS
Examination of aircraft warning and caution lights after shock testing
[NLR-TP-89284-U] p 952 N92-30474

SHOCK TUBES
Simulation of supersonic and hypersonic flows p 251 A92-22790
Some aerodynamic mechanisms of impulsive noise during blade-vortex-interaction p 604 A92-35782
A two-stage-diaphragm free-piston shock tube for a strong shock wave p 748 A92-43098
Study on small stalker tube performance and numerical calculation p 748 A92-43099
The DAM vertical shock-tube p 880 A92-45096
Expansion tube experiments for the investigation of ram-accelerator-related combustion and gasdynamic problems
[AIAA PAPER 92-3246] p 904 A92-48845
Unsteady shock propagation in a steady flow nozzle expansion p 1023 A92-54489
Double piston shock-wave valve p 1117 A92-54938
A quiet-flow Ludwieg tube for experimental study of high speed boundary layer transition
[AIAA PAPER 92-3885] p 1094 A92-56727
The high enthalpy shock tunnel in Goettingen
[AIAA PAPER 92-3942] p 1104 A92-56772
TSNIIMASH capabilities for aerogasdynamical and thermal testing of hypersonic vehicles
[AIAA PAPER 92-3962] p 1097 A92-56789
Study on supersonic combustion in a hypersonic flight
[IAF PAPER 92-0661] p 1106 A92-57101
Nonstationary gasdynamics p 220 N92-13985
Aerothermodynamic radiation studies
[NASA-CR-185666] p 284 N92-15998
Application of program LAURA to perfect gas shock tube flows: A parametric study
[NASA-TM-104190] p 298 N92-17002
Numerical simulation of transient hypervelocity flow in an expansion tube
[NASA-CR-189601] p 402 N92-18965
Rarefaction wave eliminator design study
[AD-A244401] p 484 N92-20455
An explosively driven, fast shock tube
[DE92-008437] p 749 N92-26720
Shock enhancement and control of hypersonic combustion
[AD-A248558] p 896 N92-29580

SHOCK TUNNELS
Mach 4 and Mach 8 axisymmetric nozzles for a high-enthalpy shock tunnel p 78 A92-16668
Drag balance for hypervelocity impulse facilities p 207 A92-18375
Preliminary laser induced fluorescence measurements in several facilities in preparation for application to studies in the high enthalpy shock tunnel Goettingen (HEG)
[AIAA PAPER 92-0143] p 284 A92-23761
Reactivation and upgrade of the NASA Ames 16-Inch Shock Tunnel - Status report
[AIAA PAPER 92-0327] p 383 A92-25774
Initial operation of the UTA shock tunnel
[AIAA PAPER 92-0331] p 383 A92-25778
Supersonic combustor testing using optical diagnostics and a high enthalpy shock tunnel
[AIAA PAPER 92-0761] p 384 A92-27102
Experimental study of a two-dimensional scramjet inset, M(freestream) = 10.1-25.1 p 611 A92-36974
Experimental studies on aerodynamic heating and thermal protection in hypersonic flight p 709 A92-43101
Thermal measurement test in a shock wind tunnel p 748 A92-43104
Numerical simulation of unsteady hypersonic viscous flows in shock tunnel p 710 A92-43170
Hypersonic mixing and combustion studies in the hypulse facility p 737 A92-44526
Vane-blade interaction in a transonic turbine. II - Heat transfer
[AIAA PAPER 92-3324] p 904 A92-48907
Three-dimensional Navier-Stokes heat transfer predictions for turbine blade rows
[AIAA PAPER 92-3068] p 1020 A92-54003
Comparison between computational and experimental data for a hypersonic laser propelled vehicle
[AIAA PAPER 92-3808] p 1023 A92-54179
Flow characterization in the NASA Ames 16-inch Shock Tunnel
[AIAA PAPER 92-3810] p 1090 A92-54180
Instrumentation key to NASP combustor tests p 1092 A92-55100
A shock tunnel experiment on aerodynamic interference induced by RCS jet p 1029 A92-56042
The high enthalpy shock tunnel in Goettingen
[AIAA PAPER 92-3942] p 1104 A92-56772
The G-range impulse facility - A high-performance free-piston shock tunnel
[AIAA PAPER 92-3946] p 1097 A92-56774
Performance data of the new free-piston shock tunnel at GALCIT
[AIAA PAPER 92-3943] p 1033 A92-56776
Millisecond aerodynamic force measurement with side-jet model in the ISL shock tunnel
[AIAA PAPER 92-3963] p 1097 A92-56790
Effects of oxygen dissociation on hypervelocity combustion experiments
[AIAA PAPER 92-3964] p 1098 A92-56791
Hypersonic shock tunnel testing for undergraduate laboratory instruction
[AIAA PAPER 92-4021] p 1100 A92-56843
Numerical simulation of unsteady flow in a hypersonic shock tunnel facility
[AIAA PAPER 92-4029] p 1034 A92-56851
Aerospace technology: Technical data and information on foreign test facilities
[GAO/NSIAD-90-71FS] p 139 N92-13076
High enthalpy testing in the Aachen (Fed. Republic of Germany) shock tunnel TH 2 p 208 N92-15021
Experimental investigation of nozzle/plume aerodynamics at hypersonic speeds
[NASA-CR-190074] p 664 N92-25162
An analysis of combustion studies in shock expansion tunnels and reflected shock tunnels
[NASA-TP-3224] p 895 N92-28374

SHOCK WAVE GENERATORS
Crossing shock wave turbulent boundary layer interactions - Variable angle and shock generator length geometry effects at Mach 3
[AIAA PAPER 92-0636] p 334 A92-27014
SHOCK WAVE INTERACTION
Shock wave reflection close to the leading edge of a wedge p 37 A92-10660
Two-phase flows at supersonic velocities p 4 A92-10907
Correlation of separation shock motion with pressure fluctuations in the incoming boundary layer p 5 A92-11061
Numerical investigation of bleed on three-dimensional turbulent interactions due to sharp fins p 5 A92-11062
A study on the interaction between a bow shock wave generated by a blunt body and a turbulent boundary layer p 8 A92-12424
Experimental studies of the interaction of converging axisymmetric shock waves with sharp and blunt cones in supersonic flow p 63 A92-13749
Development of a shock noise prediction code for high-speed helicopters - The subsonically moving shock p 165 A92-14384
Oscillation of nearly circular shock waves p 146 A92-15358
Flow unsteadiness by weak normal shock wave/turbulent boundary layer interaction in internal flow p 67 A92-15359
An investigation of a strong shock-wave turbulent boundary layer interaction in a supersonic compressor cascade
[ASME PAPER 91-GT-92] p 70 A92-15556
The influence of shock waves on the viscous flow field of axial compressors
[ASME PAPER 91-GT-173] p 73 A92-15608
Tangential mass addition for shock/boundary-layer interaction control in scramjet inlets p 80 A92-17197
Confined normal-shock/turbulent-boundary-layer interaction followed by an adverse pressure gradient p 172 A92-18365
Three-dimensional thermal structural analysis of a swept cowl leading edge subjected to skewed shock-shock interference heating p 174 A92-20306
Formation of shocks within axisymmetric nozzles p 176 A92-20760
Preliminary investigation of inlet dynamic distortion and it's passive control p 245 A92-21742
A fast viscous correction method for transonic aerodynamics p 247 A92-21986
Shock-boundary layer interaction control with low-profile vortex generators and passive cavity
[AIAA PAPER 92-0064] p 250 A92-22178
A calculating method of shock wave oscillating frequency due to turbulent shear layer fluctuations in supersonic flow p 251 A92-22720
Space-marching calculations of hypersonic inviscid flowfield p 313 A92-25040
Turbulence amplification through a shock wave
[AIAA PAPER 92-0313] p 320 A92-25761
Experiments on shock/vortex interactions
[AIAA PAPER 92-0315] p 320 A92-25762
An analytical and computational investigation of shock-induced vortical flows
[AIAA PAPER 92-0316] p 321 A92-25763
Turbulence modeling for high speed flows
[AIAA PAPER 92-0436] p 327 A92-26283
Shock interference prediction using direct simulation Monte Carlo
[AIAA PAPER 92-0492] p 328 A92-26322
Experimental investigation of normal-shock/turbulent-boundary-layer interactions with and without mass removal p 330 A92-26411
Crossing shock wave turbulent boundary layer interactions - Variable angle and shock generator length geometry effects at Mach 3
[AIAA PAPER 92-0636] p 334 A92-27014
Holographic flowfield density measurements in swept shock wave/boundary-layer interactions
[AIAA PAPER 92-0746] p 335 A92-27092
An experimental/computational study of sharp fin induced shock wave/turbulent boundary layer interactions at Mach 5 - Experimental results
[AIAA PAPER 92-0749] p 335 A92-27093
Flowfield visualization of crossing shock-wave/boundary-layer interactions
[AIAA PAPER 92-0750] p 335 A92-27094
Numerical analysis of shock-induced separation alleviation using vortex generators
[AIAA PAPER 92-0751] p 335 A92-27095
Effect of rarefaction on the nonstationary interaction of a supersonic underexpanded jet with a perpendicular obstacle p 337 A92-27594
A study of the interaction of a normal shock wave with a turbulent boundary layer at Mach numbers between 1.30 and 1.55 p 339 A92-28006
Investigation of oblique shock/boundary-layer bleed interaction p 344 A92-28524
Multiple normal shock wave/turbulent boundary-layer interactions p 344 A92-28527
Control of strong shock-turbulent boundary layer interaction in rectangular channels p 422 A92-29714
Assessment of three models of turbulence in a shock-boundary layer interaction of a heated wall p 423 A92-29999
Effect of shock waves on the critical rate of bending-torsional flutter of an airfoil p 494 A92-30208
Numerical determination of the regions of existence of two types of shock-wave interaction p 428 A92-30211
Structure of supersonic turbulent flow past a swept compression corner p 431 A92-31155
Cylinder-induced shock-wave boundary-layer interaction p 433 A92-31188
Effects of sweepback on unsteady separation in Mach 5 compression ramp interactions
[AIAA PAPER 92-0430] p 435 A92-31663
A preliminary study of the turbulent structures associated with unsteady separation shock motion in a Mach 5 compression ramp interaction
[AIAA PAPER 92-0744] p 436 A92-31677
Unsteady separation in sharp fin-induced shock wave/turbulent boundary layer interaction at Mach 5
[AIAA PAPER 92-0748] p 436 A92-31678
A supplement to the second-order shock-expansion method p 437 A92-31861
Experimental investigation of the air bypass effect in the shock-wave region on the aerodynamic characteristics of a wing profile p 439 A92-31877
Aerodynamic effect of compression shocks on an oscillating aileron in transonic flow p 440 A92-31898
Effects of shock wave precursors ahead of hypersonic entry vehicles p 441 A92-32182
Three-dimensional flow visualization of shock wave using double-pulsed holographic interferometry. II - Flow visualization for three-dimensional shock structures in rotating aeroengine fan blade rows p 497 A92-32507
Thermoviscoplastic analysis of engine cowl leading edge subjected to oscillating shock-shock interaction
[AIAA PAPER 92-2537] p 583 A92-34381
Thermoviscoplastic response of thin plates subjected to intense local heating
[AIAA PAPER 92-2538] p 584 A92-34382
The experimental investigation on the diffuser flow distortion p 519 A92-35543
Role of shock dynamics in transonic flutter
[AIAA PAPER 92-2121] p 520 A92-35690
Experimental design of a supersonic shock wave/vortex interaction at Mach 3 p 521 A92-35988
Computational methods for shock waves in three-dimensional supersonic flow p 611 A92-37537
Stagnation point heat flux in hypersonic high enthalpy flow p 613 A92-38373
Separated flow over the protuberances in hypersonic flow p 615 A92-38907
Prediction for the incipient separation of fin-generated three-dimensional shock wave turbulent boundary layer interactions p 615 A92-38909
Experimental investigation on reducing fluctuating pressures of launch vehicles by passive shock-wave/boundary-layer control p 616 A92-38916
Numerical simulation of interaction between vortexes and shocks in jet flow field p 616 A92-38925
Hypersonic shock-wave turbulent-boundary-layer interaction flows p 703 A92-41264
A two-stage-diaphragm free-piston shock tube for a strong shock wave p 748 A92-43098
Study on small stalker tube performance and numerical calculation p 748 A92-43099
Aerodynamic heating measurement in hypersonic flow p 709 A92-43102
A thin metal model for aerodynamic heating tests of shock wave interaction p 709 A92-43103
BGK airfoil oil flow test in a two-dimensional transonic wind tunnel p 711 A92-43201
Navier-Stokes solutions of transonic nozzle flow with shock-induced flow separations p 713 A92-44515
Experimental and numerical studies of radiation emission from high-temperature air behind 10 km/s shock waves
[SAE PAPER 912025] p 790 A92-45417
Shock interaction induced by two hemisphere-cylinders
[SAE PAPER 912043] p 790 A92-45427
Aerodynamic heating in three-dimensional shock wave turbulent boundary layer interaction induced by sweptback sharp fins in hypersonic flows
[SAE PAPER 912044] p 791 A92-45428
Airfoil pressure measurements during oblique shock wave-vortex interaction in a Mach 3 stream
[AIAA PAPER 92-2631] p 795 A92-45503
Surface and flow field measurements in a symmetric crossing shock wave/turbulent boundary layer flow
[AIAA PAPER 92-2634] p 806 A92-45574
A numerical study of control surface buzz using computational fluid dynamic methods
[AIAA PAPER 92-2654] p 806 A92-45578
Interaction between crossing oblique shocks and a turbulent boundary layer p 812 A92-46882
Computation of turbulent, separated, unswept compression ramp interactions p 813 A92-46897
Multiple shock-shock interference on a cylindrical leading edge p 813 A92-46899
Measurement of shock-wave/boundary-layer interaction in a free-piston shock tunnel p 813 A92-46903
Numerical simulation of chemical and thermal nonequilibrium flows behind compression shocks
[AIAA PAPER 92-2879] p 820 A92-47860
Experience with the Johnson-King turbulence model in a transonic turbine cascade flow solver p 821 A92-48207
Internal shock interactions in propulsion/airframe integrated three-dimensional sidewall compression scramjet inlets
[AIAA PAPER 92-3099] p 824 A92-48741
Numerical simulation of a confined transonic normal shock wave/turbulent boundary layer interaction
[AIAA PAPER 92-3668] p 826 A92-49088
Exploratory study of wall pressure fluctuations in a Mach 5, sharp fin-induced turbulent interaction p 935 A92-50304
Physical model of the swept shock wave/boundary-layer interaction flowfield p 935 A92-50312
Three-dimensional wings and waveriders with attached shock waves p 936 A92-50322
Experiments on separation at a compression corner in rarefied hypersonic flows p 938 A92-52755
The behaviour of the pressure temperature and density in an inviscid unsteady transonic axisymmetric flow with shock waves p 1018 A92-53553
Experimental investigation on turbulent phenomena in three-dimensional shock wave/turbulent boundary layer interaction induced by blunt fin p 1018 A92-53557
Numerical simulations of shock reflections by a TVD scheme p 1018 A92-53558
Interaction between a body flying at a supersonic velocity and a point explosion p 1019 A92-53867
Experimental study on three-dimensional shock wave-turbulent boundary layer interaction induced by protuberance p 1019 A92-53997
Thermal paints for shock/boundary layer interaction in inlet flows
[AIAA PAPER 92-3626] p 1113 A92-54093
Heat transfer measurements and CFD comparison of swept shock wave/boundary-layer interactions
[AIAA PAPER 92-3665] p 1021 A92-54110
An experimental examination of the effects of incoming boundary layer modifications on the dynamics of a turbulent compression corner interaction
[AIAA PAPER 92-3667] p 1022 A92-54111
Structure of crossing-shock wave/turbulent boundary-layer interactions
[AIAA PAPER 92-3670] p 1022 A92-54113
Experimental investigation of the reflection of a shock wave on a heated surface in presence of a turbulent boundary layer p 1023 A92-54569
Three-dimensional shock wave-turbulent boundary layer interaction induced by blunt body and protuberance p 1029 A92-56009
On the structure of unsteady shock induced separation of the transonic airfoil in the NAL two-dimensional wind tunnel p 1029 A92-56010
Unsteady shock-vortex interaction on a flexible delta wing p 1030 A92-56157
Studies of aerothermal loads generated in regions of shock/shock interaction in hypersonic flow
[NASA-CR-181893] p 43 N92-11319
The effect of a type 3 and type 4 shock/shock interaction on heat transfer in the stagnation region p 160 N92-13867
Preliminary investigation of the shock-boundary layer interaction in a simulated fan passage
[AD-A242656] p 185 N92-15045
An analytical and computational investigation of shock-induced vortical flows with applications to supersonic combustion p 405 N92-19538
A laser velocimeter investigation of the normal shockwave boundary layer interaction p 500 N92-20485
Inlets, ducts, and nozzles p 593 N92-22523
Development of a new flux splitting scheme p 596 N92-23352
The structure and control of three-dimensional shock wave turbulent boundary layer interactions
[AD-A250209] p 1003 N92-31824

Experimental studies of hypersonic shock-wave boundary-layer interactions
[NASA-CR-190731] p 950 N92-32162

SHOCK WAVE PROFILES
The just attached shock-wave at the leading edge of a profile p 3 A92-10663
Experimental studies of the interaction of converging axisymmetric shock waves with sharp and blunt cones in supersonic flow p 63 A92-13749
Oscillation of nearly circular shock waves p 146 A92-15358
An investigation on detached shock waves ahead of bodies of revolution at transonic speeds p 251 A92-23381
Numerical determination of the regions of existence of two types of shock-wave interaction p 428 A92-30211
Numerical computation and experimental study of shock wave reflection p 430 A92-30542
Evaluation of outdoor-to-indoor response to minimized sonic booms
[NASA-CR-189643] p 927 N92-28556
Analysis of sonic boom data to quantify distortions of shock profiles p 1139 N92-33879
The effect of turbulence on the loudness of minimized sonic boom signatures p 1139 N92-33880
Lateral spread of sonic boom measurements from US Air Force boomfile flight tests p 1140 N92-33883
Subjective loudness response to simulated sonic booms p 1140 N92-33885

SHOCK WAVE PROPAGATION
Influences of wind tunnel parameters on airfoil characteristics at high subsonic speeds p 173 A92-18769
Time marching integral equation method for the solutions of unsteady transonic flows p 314 A92-25129
Resonance of circular shock waves p 395 A92-26795
A shock and an expansion wave in transonic flow p 440 A92-31961
Oblique shock wave with sweep p 613 A92-38370
Thermal radiation effects on a shocked particle-laden gas p 780 A92-44377
Oscillation of oblique shock waves generated in a two dimensional asymmetric nozzle
[SAE PAPER 912061] p 791 A92-45443
The effect of molecular relaxation processes in air on the rise time of sonic booms p 898 A92-45883
Unsteady shock propagation in a steady flow nozzle expansion p 1023 A92-54489
Nonlinear acoustic propagation of shock waves through the atmosphere with molecular relaxation p 511 N92-20360
High-Speed Research: Sonic Boom, volume 1
[NASA-CP-3172] p 1061 N92-33874
A numerical model for sonic boom propagation through an inhomogeneous, windy atmosphere p 1138 N92-33876
Wave equations and computational models for sonic boom propagation through a turbulent atmosphere p 1139 N92-33877
Simulations of sonic boom ray tube area fluctuations for propagation through atmospheric turbulence including caustics via a Monte Carlo method p 1139 N92-33878
Analysis of sonic boom data to quantify distortions of shock profiles p 1139 N92-33879
Model experiment to study the effect of turbulence on risetime and waveform of N waves p 1139 N92-33881
Steady state risetimes of shock waves in the atmosphere p 1140 N92-33882
Lateral spread of sonic boom measurements from US Air Force boomfile flight tests p 1140 N92-33883
Preliminary results from the White Sands Missile Range sonic boom propagation experiment p 1140 N92-33884
Subjective loudness response to simulated sonic booms p 1140 N92-33885

SHOCK WAVES
Evolution of three-dimensional flows during the interaction between conical shock waves and a turbulent boundary layer p 7 A92-12169
Engineering method for calculating surface pressures and heating rates on vehicles with embedded shocks
[AIAA PAPER 91-5060] p 171 A92-17842
Effects of unsteady shock impingement on high-speed *gaseous mixing*
[AIAA PAPER 91-5091] p 172 A92-17857
Similarity solutions for supersonic axisymmetric flows p 173 A92-18387
Broadband shock-associated noise from supersonic jets in flight p 235 A92-18683
A method of calculation for the radius of curvature of the attached shock waves in front of a sharp-nosed axi-symmetrical body placed in a uniform stream p 243 A92-21319
Effect of supersonic diffuser geometry on operation conditions p 310 A92-24599
On one method of constructing adaptive difference grids *in aerodynamics problems* p 311 A92-24902
Finite element method for computing nonisentropic potential transonic flow with shock waves p 312 A92-25009
Pitching derivatives of wing in supersonic and hypersonic stream - Method for local flow piston theory p 312 A92-25012
The lateral shock wave family on the surface of a cone-cylinder in transonic flowfield p 315 A92-25136
Importance of an accurate prediction of shock curvature for high-speed rotor noise p 414 A92-25578
A numerical study of the effects of geometry on the performance of a supersonic combustor
[AIAA PAPER 92-0624] p 342 A92-28213
Leading edge sweep effects in generic three-dimensional sidewall compression scramjet inlets
[AIAA PAPER 92-0674] p 343 A92-28218
Experimental study of a two-dimensional random frequency generator p 483 A92-29712
Shock fitting with a finite volume approximation to the Euler equations
[AIAA PAPER 92-2646] p 796 A92-45513
An investigation of passive control methods for shock-induced separation at hypersonic speeds
[AIAA PAPER 92-2725] p 808 A92-45596
Examination of ultraviolet radiation theory for bow shock rocket experiments
[AIAA PAPER 92-2871] p 901 A92-47853
Transonic flows of Bethe-Zel'dovich-Thompson fluids p 935 A92-50293
A study of supersonic flow over the ogival bodies with attached shock waves at zero incidence p 936 A92-51896
A double chaotic attractor in transonic flow p 1019 A92-53561
Shock detection on airfoils by means of piezo foil- and hot film arrays p 1115 A92-54334
Experimental investigation of the reflection of a shock wave on a heated surface in presence of a turbulent boundary layer p 1023 A92-54569
Double piston shock-wave valve p 1117 A92-54938
A hypersonic wind tunnel test of a mixed-compression air inlet model p 1028 A92-56007
Aerothermodynamic test of spaceplane by thin-skin method p 1093 A92-56043
The research of reducing 3-D low supersonic shock wave reflection in a 2-D transonic flexible walls adaptive wind tunnel
[AIAA PAPER 92-3924] p 1095 A92-56755
Sonic boom p 55 N92-10608
Effects of wake and shock passing on the heat transfer to a film cooled transonic turbine blade p 156 N92-12201
Calculation of hypersonic leeside vortices over blunt delta wings p 84 N92-13004
Experimental study of hypersonic shock wave boundary layer interactions by means of infrared technique p 182 N92-14994
Aerothermodynamic radiation studies
[NASA-CR-185666] p 284 N92-15998
An improved method for simulating supersonic flow past a wedge shaped body
[NAL-TR-1097] p 345 N92-18239
Propagation of shock waves through clouds
[AERO-REPT-9104] p 400 N92-18317
Three-dimensional simulations of hypersonic flows
[MBB-UK-0155-89-PUB] p 447 N92-21703
Improved shock-capturing of Jameson's scheme for the Euler equations
[PB92-148758] p 596 N92-23251
A simplified method for thermal analysis of a cowl leading edge subject to intense local shock-wave-interference heating
[NASA-TP-3167] p 679 N92-24797
Experimental investigation of turbulence behavior in shock wave/turbulent boundary layer interactions
[AD-A247792] p 774 N92-27886
Second-order shock-expansion theory extended to include real gas effects
[AD-A247191] p 831 N92-29539
Automatic design of transonic airfoils to reduce the shock *induced pressure drag* p 949 N92-31863
Experimental studies of hypersonic shock-wave boundary-layer interactions
[NASA-CR-190731] p 950 N92-32162
Swept shock/boundary layer interaction experiments in support of CFD code validation
[NASA-CR-190583] p 1036 N92-32494
An examination of several high resolution schemes applied to complex problems in high speed flows
[AD-A250814] p 1124 N92-32632

SHORT CIRCUITS
New insulation constructions for aerospace wiring applications. Volume 2: The 270 VDC arc tracking testing *with power controllers*
[AD-A240639] p 23 N92-11007

SHORT CRACKS
Short fatigue crack growth from blunt notches in an aero-engine alloy p 212 A92-19760
Crack initiation and the short-to-long crack growth transition in a Ni-base superalloy p 213 A92-19767
Review of methods for crack growth testing in gas turbine engine disc materials p 296 A92-24193
Solution of stress intensity factor by weight function for small surface cracks in plates p 998 A92-53332
Short cracks and durability analysis of the Fokker 100 wing/fuselage structure
[NLR-TP-90336-U] p 910 N92-29603
Inspection of fabricated fuselage panels using electronic shearography
[DOT/FAA/CT-TN92/26] p 1127 N92-33627

SHORT HAUL AIRCRAFT
NASA's quiet side. I p 607 A92-37875
Tilt rotors and the Port Authority of New York and New *Jersey Airport System*
[RAND-R-3971/1-PA-SUMM] p 636 N92-25262

SHORT TAKEOFF AIRCRAFT
Aircraft design experience p 110 A92-15326
F-15 STOL/Maneuvering Technology Demonstrator. Phase III - Thrust vectoring, reversing and STOL operation p 112 A92-16054
Advancing airlift avionics - C-17 avionics suite
[AIAA PAPER 92-1243] p 553 A92-33336
Technical history of aircraft engines p 558 A92-35911
The quiet STOL research aircraft ASUKA p 642 A92-38206
Prospects for a commercial STOL transportation system p 634 A92-38207
RAE Bedford VAAC research project --- VSTOL aircraft advanced flight control p 662 A92-40039
The progress of a STOL project p 699 A92-43137
Operational progress of the STOL research aircraft Asuka p 730 A92-43138
Operation of the on-board measuring system of the STOL research aircraft Asuka p 734 A92-43139
STOL research aircraft Asuka flight analysis in connection with the operation of the monitoring system p 730 A92-43140
Flight test results and upper surface blowing (USB) technology of the STOL research aircraft Asuka p 730 A92-43142
Flight tests on the structures of the STOL research aircraft Asuka p 730 A92-43143
The main wing boundary layer separation pattern of STOL research aircraft Asuka p 709 A92-43144
Aerodynamic drag as determined from flight test data of the STOL research aircraft Asuka p 709 A92-43145
Path angular control of the STOL research aircraft Asuka p 745 A92-43146
Study on the maintainability and inspection of the STOL research aircraft Asuka p 700 A92-43148
An adaptive flight control for use in connection with helicopter engine failure p 745 A92-43159
Wind tunnel investigation of an improved upper surface blown flap transport semi-span model
[SAE PAPER 911993] p 789 A92-45395
Results and lessons learned from the STOL and Maneuver Demonstration Program
[SAE PAPER 912005] p 843 A92-45406
Aerodynamic development of boundary layer control system for NAL QSTOL research aircraft 'ASKA'
[SAE PAPER 912010] p 843 A92-45410
Functional mock-up tests for flight control system of the NAL QSTOL research aircraft 'ASKA'
[SAE PAPER 912036] p 881 A92-45422
A simulator study of a flight reference display for powered-lift STOL aircraft
[SAE PAPER 912067] p 855 A92-45449
Nonlinear control design for slightly nonminimum phase systems - Application to V/STOL aircraft p 876 A92-48160
Verification and validation of F-15 and S/MTD unique software p 921 A92-48515
Experimental performance of three design factors for ventral nozzles for SSTOVL aircraft
[AIAA PAPER 92-3789] p 1069 A92-54168
Internal reversing flow in a tailpipe offtake configuration for SSTOVL aircraft
[AIAA PAPER 92-3790] p 1069 A92-54169
Analysis of airframe/engine interactions for a STOVL aircraft with integrated flight/propulsion control
[AIAA PAPER 92-4623] p 1052 A92-55300
Analysis of the main wing lift distribution of the STOL research aircraft Asuka p 1053 A92-56051

Flight test of a flight reference display for powered-lift STOL aircraft p 1064 A92-56059
Flight simulator test of cockpit advisory system p 1054 A92-56115
Short takeoff optimization for the XV-15 tiltrotor aircraft p 1056 A92-56302
Static internal performance of ventral and rear nozzle concepts for short-takeoff and vertical-landing aircraft [NASA-TP-3103] p 12 N92-10975
Finite element analysis of ASTOVL fighter structure [AD-A243724] p 275 N92-17513
The FM-007: An advanced jet commuter for HUB to spoke transportation [NASA-CR-189988] p 461 N92-20267
Experimental performance of three design factors for ventral nozzles for SSTOVL aircraft [NASA-TM-105697] p 742 N92-27669
Evaluation of high lift devices of the quiet STOL experimental aircraft ASKA [NAL-TR-1102] p 733 N92-28153
Evaluation of landing configuration by flight test of the quiet STOL experimental aircraft ASKA [NAL-TR-1113] p 733 N92-28191
Internal reversing flow in a tailpipe offtake configuration for SSTOVL aircraft [NASA-TM-105698] p 868 N92-28418
Aerodynamic characteristics obtained from alpha sweep test of the quiet STOL experimental aircraft ASKA [NAL-TR-1112] p 853 N92-28901
ASTOVL combat aircraft design synthesis and optimization [CRANFIELD-AERO-9201] p 963 N92-31515

SHOT PEENING
Shot peening - Theory and applications --- Book [ISBN 2-907669-18-4] p 676 A92-40400

SHROUDED NOZZLES
Flow and acoustic features of a supersonic tapered nozzle p 712 A92-44328
A study on the impact of shroud geometry on ejector pumping performance [AIAA PAPER 92-3260] p 864 A92-48856

SHROUDED PROPELLERS
Design and flight test evaluation of the Fantail antitorque system p 110 A92-14456
Analysis of an advanced ducted propeller subsonic inlet [AIAA PAPER 92-0274] p 318 A92-25728
Pressure oscillation in the leakage annulus between a shrouded impeller and its housing due to impeller-discharge-pressure disturbances p 580 A92-32942
A quick automatic method for computing performance of ducted-propeller p 736 A92-42800
Analysis of an advanced ducted propeller subsonic inlet [NASA-TM-105393] p 179 N92-14002
TIGER: Turbomachinery interactive grid generation p 659 N92-25718

SHROUDED TURBINES
Dynamic analysis of annular cascade shrouded blades p 397 A92-27856
Experimental modeling of film-cooled axial turbine tip seals [AIAA PAPER 92-4058] p 1119 A92-56141
Turbine blade tip and seal clearance excitation forces [NASA-CR-184341] p 973 N92-31910

SHROUDS
Transient aerodynamics of a high dynamic pressure shroud separation for a ground-based interceptor missile [AIAA PAPER 92-2820] p 705 A92-41348
Effects of curvature and rotation on turbulence in the NASA low-speed centrifugal compressor impeller p 1124 N92-32292

SHUTTERS
Low-frequency vibrations of the shutters of the variable Laval nozzle of gas turbine engines p 657 A92-40610

SIDE INLETS
Hypersonic propulsion research p 561 N92-22543

SIDE-LOOKING RADAR
X-band side-looking airborne radar for remote sensing p 554 A92-34976
The imaging radar system p 599 N92-23391

SIDESLIP
Correction of sideslip-induced static pressure errors in flight-test measurements p 309 A92-24416
Evaluation of methods for estimating store carriage loads [AIAA PAPER 92-0675] p 379 A92-27043
Calculation of the rolling moment for a wing with a supersonic leading edge in the presence of sideslip p 426 A92-30186
Development of a pneumatic high-angle-of-attack flush airdata sensing system [SAE PAPER 912142] p 651 A92-39980
Numerical study of vortex-dominated flows for wings at high incidence and sideslip p 702 A92-41227
Development of a pneumatic high-angle-of-attack flush airdata sensing (HI-FADS) system [NASA-TM-104241] p 118 N92-11994
Computer programs for the calculation of dual sting pitch and roll angles required for an articulated sting to obtain angles of attack and sideslip on wind-tunnel models [NASA-TM-104161] p 138 N92-12007
Contribution of fin and tailplane to sideforce and yawing moment derivatives due to sideslip at supersonic speeds at low angles of attack [ESDU-91031] p 259 N92-15971
Failure detection and fault management techniques for flush airdata sensing systems [NASA-TM-4335] p 276 N92-17128
Measurement of derivatives due to acceleration in heave and sideslip p 364 N92-18785
Flow visualization studies of a sideslipping, canard-configured X-31A-Like fighter aircraft model [AD-A245940] p 829 N92-28883
Contribution of tailplane-mounted twin fins to sideforce, yawing moment, and rolling moment derivatives due to sideslip [ESDU-92007] p 1086 N92-32487

SIGNAL ANALYSIS
Quick-look system p 599 N92-23393

SIGNAL DETECTORS
Passive acoustic range estimation of helicopters [AD-A248033] p 926 N92-28302

SIGNAL FADING
Experiments on aeronautical satellite communications using ETS-V p 395 A92-26779

SIGNAL MEASUREMENT
Compact range test applications, phase 2 [AD-A248790] p 999 N92-30583
Remote sensing of trapping layer base height using ATIS transmissions [AD-A250074] p 1004 N92-31362

SIGNAL PROCESSING
Application of smart structures to aircraft health monitoring p 20 A92-11123
Eddy current imaging of aircraft using real time image signal processing p 144 A92-13594
Simulation of radar clutter and jet engine modulation using digital quadrature modulator p 216 A92-19091
MIL-STD-1553 data bus/PCM multiplexer system p 188 A92-19211
A state-of-the-art data acquisition system p 217 A92-19231
Processing and displaying radio navigation data --- Russian book p 266 A92-21683
X-band side-looking airborne radar for remote sensing p 554 A92-34976
Transmission vibration monitoring - A single board computer architecture p 554 A92-35765
MLS system error model identification and synthesis p 639 A92-40232
The use of optical sensors and signal processing gas turbine engines p 856 A92-46247
Remote telemetry concepts p 882 A92-47562
Design considerations for a modern telemetry processing and display system p 882 A92-47584
NAECON 91; Proceedings of the IEEE National Aerospace and Electronics Conference, Dayton, OH, May 20-24, 1991. Vols. 1-3 [ISBN 0-7803-0084-X] p 786 A92-48426
Programmable channelized digital radio/modem p 955 A92-49291
Operating principles for integrated sensor processing p 966 A92-49336
Comparison of frequency domain and time domain laser velocimeter signal processors p 1114 A92-54314
Signal processing schemes for Doppler global velocimetry p 1115 A92-54338
The use of silicon microsensors in smart skins for aerodynamic research p 1116 A92-54348
Nonlinear aspects of aerospace structures at high excitation levels flat aluminum beams and plates studied [AD-A240600] p 44 N92-11383
A TMS320-based modem for the aeronautical-satellite core data service p 594 N92-22562
Design considerations for general aviation mobile satellite terminals p 594 N92-22572
Advanced techniques in current signature analysis [DE92-007680] p 679 N92-24892
A radar signal processing ASIC and a VME interface circuit p 859 N92-28380
Simplified signal processing for an airborne CO2 Doppler lidar p 1000 N92-31023
Real-time processing of radar return on a parallel computer [NASA-CR-4456] p 1043 N92-32606
Airport Surveillance Radar (ASR-9) wind shear processor: 1991 test at Orlando, Florida [AD-A252246] p 1124 N92-32686
The design and development of a portable, DSP micro-processor based, high-accuracy data acquisition system [NRC-32146] p 1134 N92-32851
Distributed systems: Interconnection and fault tolerance studies [AD-A252869] p 1135 N92-33920

SIGNAL RECEPTION
The Air Force Manufacturing Technology (MANTECH): Technology transfer methodology as exemplified by the radar transmit/receive module program p 593 N92-22451

SIGNAL TO NOISE RATIOS
Closed-loop operation of GPS aided INS p 100 A92-16954
Helicopter main-rotor speed effects: A comparison of predicted ranges of detection from the aural detection program ICHIN and the electronic detection program ARCAS [NASA-TM-104134] p 166 N92-12598
Modeling radar clutter [AD-A240965] p 158 N92-13351

SIGNAL TRANSMISSION
Selection of the time parameters of the probing pulse during the nonstationary irradiation of flight vehicles p 454 A92-31951

SIGNATURE ANALYSIS
Radar Detection Analysis of Rotor Systems (RADARS) p 117 A92-14350
Blockage correction in three-dimensional wind tunnel testing based on the wall signature method [AIAA PAPER 92-3925] p 1095 A92-56756
Rub induced rotor/stator vibration analysis on CF700 engine [NRC-TR-ENG-007] p 202 N92-14060
Advanced techniques in current signature analysis [DE92-007680] p 679 N92-24892
Evaluation of outdoor-to-indoor response to minimized sonic booms [NASA-CR-189643] p 927 N92-28556

SIGNATURES
Behavior-based fault monitoring [AD-A241254] p 164 N92-13746
A wall interference assessment/correction system [NASA-CR-189785] p 259 N92-15974
A summary of XB-70 sonic boom signature data [NASA-CR-189630] p 696 N92-24800
Comparison of jet plume shape predictions and plume influence on sonic boom signature [NASA-TP-3172] p 631 N92-25133
Evaluation of outdoor-to-indoor response to minimized sonic booms [NASA-CR-189643] p 927 N92-28556
The effect of turbulence on the loudness of minimized sonic boom signatures p 1139 N92-33880
Lateral spread of sonic boom measurements from US Air Force boomfile flight tests p 1140 N92-33883
Subjective loudness response to simulated sonic booms p 1140 N92-33885

SIKORSKY AIRCRAFT
Comanche - The armed scout p 103 A92-13291
H-76B Fantail demonstrator composite fan blade fabrication p 145 A92-14356
A full mission simulation data system p 162 A92-14367
Results of flight tests of the Boeing Sikorsky Fantail demonstrator p 106 A92-14376
Stage 2 noise certification of the Sikorsky S-76A and S-76C helicopters p 91 A92-14388
Sikorsky S-92 - Bold bid for future p 457 A92-29557
The NASA/Industry Design Analysis Methods for Vibrations (DAMVIBS) Program - Sikorsky Aircraft - Advances toward interacting with the airframe design process [AIAA PAPER 92-2204] p 540 A92-34394
Analysis of open loop higher harmonic control at high airspeeds on a modern four-bladed articulated rotor [AIAA PAPER 92-2450] p 542 A92-34477
Sikorski (S-76) High Intensity Radiated Fields (HIRF) test [SAE PAPER 912214] p 652 A92-40017
Sikorsky Aircraft UAV program p 646 A92-40385
Civil development and certification of a helicopter automatic approach and hover system on the Sikorsky S-76 [SAE PAPER 911975] p 872 A92-45382
Analysis of open loop higher harmonic control at high airspeeds on a modern four-bladed articulated rotor [NASA-TM-103876] p 21 N92-11000
Model rotor icing tests in the NASA. Lewis Icing Research Tunnel p 450 N92-21688
Evaluation of composite components on the Bell 206L and Sikorsky S-76 helicopters p 1107 N92-32575

SILANES
Minimum surface treatments for adhesively bonded repairs p 754 A92-42501
SILENCE
Inter-noise 90; Proceedings of the International Conference on Noise Control Engineering, Goteborg, Sweden, Aug. 13-15, 1990. Vols. 1 & 2
[ISBN 91-7848-224-0] p 693 A92-39042
SILICIDES
Cold-crucible directional solidification of refractory metal-silicide eutectics p 755 A92-43684
SILICON
Applications of silicon hybrid multi-chip modules to avionics p 859 N92-28379
SILICON CARBIDES
Development and characterization of high strength SiC rotors
[ASME PAPER 91-GT-191] p 149 A92-15617
Mechanical testing of glass-ceramic matrix composites
[ONERA, TP NO. 1991-182] p 388 A92-26351
The hardness and toughness of HIPed silicon nitride p 668 A92-39682
Ceramic technology for Advanced Heat Engines Project
[DE92-002397] p 289 N92-16128
Fabrication and testing of corrosion resistant coatings --- for turbine engine components
[DE92-003553] p 490 N92-21063
Development of a new generation of high-temperature composite materials p 578 N92-22515
Stress-strain analysis of a (0/90)sub 2 symmetric titanium matrix laminate subjected to a generic hypersonic flight profile
[NASA-TM-107584] p 685 N92-26128
Thermomechanical fatigue behavior of a silicone carbide fiber-reinforced calcium aluminosilicate glass-ceramic matrix composite
[AD-A249870] p 988 N92-31823
SILICON NITRIDES
Development of silicon nitride rotors for the ATTAP program at Garrett Ceramic Components --- Advanced Turbine Technology Applications Project
[ASME PAPER 91-GT-154] p 142 A92-15590
Reliability analysis of a structural ceramic combustion chamber
[ASME PAPER 91-GT-155] p 123 A92-15591
The hardness and toughness of HIPed silicon nitride p 668 A92-39682
Ceramic regenerator program
[NASA-CR-189053] p 225 N92-14374
Fabrication and testing of corrosion resistant coatings --- for turbine engine components
[DE92-003553] p 490 N92-21063
Evaluation of the elevated-temperature mechanical reliability of a HIPed silicon nitride
[DE92-007838] p 579 N92-23223
The cost of silicon nitride powder: What must it be to compete?
[DE92-008710] p 669 N92-25223
SILICON OXIDES
Cyclic fatigue behavior of silica fiber p 754 A92-42040
SIMD (COMPUTERS)
Future directions in computing and CFD
[AIAA PAPER 92-2734] p 917 A92-45489
SIMILARITY THEOREM
Surface-layer gusts for aircraft operation p 774 A92-42095
Similarity and resistance in near-sonic flows for given heat conduction p 708 A92-43065
Similarity relations for calculating three-dimensional chemically nonequilibrium viscous flows p 827 A92-49188
Use of an approximate similarity principle for the thermal scaling of a full-scale thrust augmenting ejector
[AIAA PAPER 92-3792] p 1069 A92-54171
Use of an approximate similarity principle for the thermal scaling of a full-scale thrust augmenting ejector
[NASA-TM-105724] p 739 N92-26613
SIMULATION
The simulation of three-dimensional viscous flow in turbomachinery geometries using a solution-adaptive unstructured mesh methodology
[ASME PAPER 91-GT-124] p 71 A92-15569
Materials and structures for Hermes p 666 A92-38213
Modal simulation of gearbox vibration with experimental correlation
[AIAA PAPER 92-3494] p 1112 A92-54036
Flowfield of a lifting rotor in hover - A Navier-Stokes simulation p 1024 A92-54906
The modelling of turbulence and downbursts for flight simulators
[UTIAS-339] p 161 N92-12373
Atmospheric pressure flow reactor: Gas phase chemical kinetics under tropospheric conditions without wall effects
[NASA-CASE-MSC-21384-1] p 297 N92-16243
Numerical simulation of transient hypervelocity flow in an expansion tube
[NASA-CR-189601] p 402 N92-18965
Evaluation of advanced microwave landing system procedures in the New York terminal area
[DOT/FAA/ND-91/1] p 354 N92-18967
Development of a wind chamber for model testing of tornado forces on structures
[PB92-104165] p 386 N92-19940
Simulation of real-gas effects on pressure distributions for aeroassist flight experiment vehicle and comparison with prediction
[NASA-TP-3157] p 501 N92-20677
Modeling methods for high-fidelity rotorcraft flight mechanics simulation
[NASA-TM-103842] p 482 N92-21440
Vibroacoustic simulation of an airplane structure p 629 N92-24871
Nationwide system delay study of the microwave landing system in the New York terminal area, volume 1
[DOT/FAA/CT-TN91/59-VOL-1] p 640 N92-25098
Full mission simulation: A view into the future p 884 N92-28537
A model of the ADA avionics real-time system: An example of the benefits of the hardware/software codesign approach in development of real-time systems
[AD-A248893] p 967 N92-30524
Modal simulation of gearbox vibration with experimental correlation
[NASA-TM-105702] p 1002 N92-31485
A simulation model of a single rotor helicopter p 979 N92-31865
Time simulation of flutter with large stiffness changes
[NASA-TM-107650] p 963 N92-32111
Ski jump takeoff performance predictions for a mixed-flow, remote-lift STOVL aircraft
[NASA-TM-103866] p 1060 N92-32887
SIMULATORS
Managing simulator wiring information and deriving system continuity p 964 A92-49287
Conception of a UHB engine simulator for the essential characteristics of a true-scale engine --- ultrahigh bypass p 1090 A92-54322
A new simulator for assessing subjective effects of sonic booms
[NASA-TM-104150] p 56 N92-11759
Atmospheric pressure flow reactor: Gas phase chemical kinetics under tropospheric conditions without wall effects
[NASA-CASE-MSC-21384-1] p 297 N92-16243
Propulsion simulator for magnetically suspended wind tunnel models p 750 N92-27801
High-temperature miniaturized turbine engine lubrication system simulator
[AD-A249259] p 868 N92-28294
Full mission simulation: A view into the future p 884 N92-28537
Use of a virtual cockpit for the development of a future transport aircraft p 886 N92-28547
The role of systems simulation for the development and qualification of ATTAS p 886 N92-28548
The basic research simulator programme and the industrial and aerospace community: Opportunities for cooperative research
[LR-662] p 887 N92-28579
NARSIM: A real-time simulator for air traffic control research
[NLR-TP-90147-U] p 888 N92-29204
SINE WAVES
Vibration tests of long plate structural model
[NAL-TM-625] p 400 N92-18485
SINGLE CHANNEL PER CARRIER TRANSMISSION
Evaluating the use of satellite communications in the government of Canada p 594 N92-22577
SINGLE CRYSTALS
High temperature low cycle fatigue of single crystal nickel base superalloys p 213 A92-19796
A viscoplastic model for single crystals p 391 A92-24717
A viscoplastic theory for anisotropic materials
[ONERA, TP NO. 1992-90] p 391 A92-24721
Creep fracture mechanisms in single crystal superalloys p 388 A92-25031
Advanced superalloys for turbine blade and vane applications
[ONERA, TP NO. 1992-2] p 893 A92-48578
Fatigue in single crystal nickel superalloys
[AD-A243453] p 290 N92-17653
Present and future trends in turbine blade material and manufacturing technology
[PNR-90825] p 488 N92-20164
Fatigue in single crystal nickel superalloys
[AD-A244815] p 489 N92-21015
Creep and fatigue research efforts on advanced materials p 593 N92-22514
Fatigue in single crystal nickel superalloys
[AD-A248190] p 896 N92-29408
Fatigue in single crystal nickel superalloys
[AD-A250068] p 987 N92-31360
Fatigue in single crystal nickel superalloys
[AD-A252492] p 988 N92-32066
Life prediction and constitutive models for engine hot section anisotropic materials program
[NASA-CR-189223] p 1072 N92-33479
SINGLE ENGINE AIRCRAFT
The development of a new light, single engine helicopter family p 545 A92-35734
Single engine testing of the F-14A(PLUS) airplane in the power approach configuration p 645 A92-40036
SINGLE EVENT UPSETS
Formulation of a strategy for monitoring control integrity in critical digital control systems
[NASA-TM-104158] p 206 N92-15075
SINGLE STAGE TO ORBIT VEHICLES
Advanced SCRAM-LACE system concept for single-stage-to-orbit space plane
[IAF PAPER 91-272] p 32 A92-12599
Integrated GPS/INS for the National Aerospace Plane p 102 A92-16975
Solving the structures problem for hypersonic vehicles p 209 A92-17349
A comparison of cooling methods for the airframe nozzle of a single-stage-to-orbit aircraft
[AIAA PAPER 91-5036] p 210 A92-17825
Operational design factors for NASP derived vehicles
[AIAA PAPER 91-5081] p 210 A92-17851
Spaceplane system studies p 285 A92-22632
Fiber optics for the National Aero-Space Plane p 386 A92-24780
The Delta Clipper dream p 574 A92-36127
NASP - A status report
[AIAA PAPER 92-1417] p 666 A92-38569
Experimental studies on aerodynamic characteristics of SSTO vehicle at low subsonic speeds
[SAE PAPER 911981] p 788 A92-45386
Crew transportation for the 1990s. I - Commercializing manned flight with today's propulsion p 889 A92-46726
Aerospace plane guidance using time-scale decomposition and feedback linearization p 984 A92-50498
Key design considerations for scramjet powered space plane p 1066 A92-53491
Aerodynamic studies on space plane configuration at hypersonic speed p 1019 A92-53641
An advanced scramjet propulsion concept for a 350 MG SSTO space plane - External nozzle performance
[AIAA PAPER 92-3719] p 1067 A92-54134
Airbreathing engine selection criteria for SSTO propulsion system
[IAF PAPER 92-0658] p 1071 A92-57099
Trim drag reduction concepts for horizontal takeoff single-stage-to-Orbit vehicles
[NASA-TM-102687] p 206 N92-15076
System controls challenges of hypersonic combined-cycle engine powered vehicles p 475 N92-21533
High speed airbreathing propulsion in Europe p 575 N92-22277
Design challenges for the National Aero-Space Plane p 551 N92-23822
Robust intelligent flight control for hypersonic vehicles
[NASA-CR-185680] p 746 N92-28209
SINGLE-PHASE FLOW
Transonic flows of Bethe-Zel'dovich-Thompson fluids p 935 A92-50293
Pulsation characteristics of one-phase and two-phase steam flows in Laval nozzles under off-design conditions p 1019 A92-53882
SINGULAR INTEGRAL EQUATIONS
The solution of a singular integral equation arising from a lifting surface theory for rotating blades p 260 N92-17303
SINGULARITY (MATHEMATICS)
Study of the discrete singularly perturbed linear-quadratic control problem by a bilinear transformation p 163 A92-16072
Singularity bypass algorithms in the numerical solution of equations of body motion relative to a center of mass in the atmosphere in the presence of disturbances p 437 A92-31857
A Lie Bracket solution of the optimal thrust magnitude on a singular arc in atmospheric flight
[AIAA PAPER 92-4345] p 1079 A92-55334
Non-linear airloads hypersurface representation: A time domain perspective p 346 N92-18783

On constructing three-dimensional overlapping grids with CMPGRD p 691 N92-24424

SINTERING

The use of CT for dimensional measurements of green and sintered ceramic components p 490 A92-28592

SISO (CONTROL SYSTEMS)

A horizon-recursive form for predictors and their computation p 50 A92-11427

Design of non-overshooting feedback control systems p 50 A92-11431

Dynamic interpolation for linear systems p 52 A92-11465

A two-feedback-loop robust helicopter controller based on eigenspace techniques and H(infinity) synthesis p 29 A92-11582

Practical robustness testing for helicopter flight control systems p 132 A92-14340

Rule based identifier for unknown systems p 509 A92-31430

A robust digital flight control system for an unfanned research vehicle using discrete quantitative feedback theory [AD-A243638] p 283 N92-17748

Adaptive control of nonlinear systems with applications to the control of flexible robot arms [AD-A244409] p 413 N92-19397

Flutter suppression digital control law design and testing for the AFW wind-tunnel model [NASA-TM-107652] p 962 N92-31350

SIZE DETERMINATION

Preliminary sizing methodology for hypersonic vehicles p 460 A92-32233

SIZING (SHAPING)

PAYCOS, a multidisciplinary sizing code for hypersonic vehicles [AIAA PAPER 92-4564] p 1132 A92-55376

SKID LANDINGS

Control of the landing of a flight vehicle in the grazing-incidence mode p 134 A92-16808

Aircraft landing-induced tire spinup p 193 A92-20209

SKIN (STRUCTURAL MEMBER)

Development of an improved model for runback water on aircraft surfaces [AIAA PAPER 92-0042] p 270 A92-22160

Fiber optic sensors for smart skins applications p 392 A92-24778

Smart skins and fiber-optic sensors application and issues p 368 A92-24785

Acoustic emission monitoring of a ground durability and damage tolerance test --- for aircraft structures p 492 A92-28737

Nortec 30 Eddyscan - Portable flaw imaging for aging aircraft p 492 A92-28745

Design, analysis, and testing of integrally stiffened composite centre fuselage skin for future fighter aircraft p 535 A92-32554

Coupled 2D-3D finite element method for analysis of a skin panel with a discontinuous stiffener [AIAA PAPER 92-2474] p 583 A92-34363

Experimental investigation on flutter characteristics of composite torsion-box p 996 A92-53055

The use of silicon microsensors in smart skins for aerodynamic research p 1116 A92-54348

Aerothermodynamic test of spaceplane by thin-skin method p 1093 A92-56043

Measurements of fuselage skin strains and displacements near a longitudinal lap joint in a pressurized aircraft [NASA-TM-104163] p 159 N92-13455

Methodology for assessment of skin repairs on Airbus aircraft p 226 N92-14428

Design, analysis, and testing of integrally stiffened composite centre fuselage skin for future fighter aircraft [MBB-FE2-PUB-S-450] p 359 N92-18333

Stretched skin concept for the entry aerodynamic decelerator system of planetary probes p 576 N92-23836

Generation of spectra and stress histories for fatigue and damage tolerance analysis of fuselage repairs [AD-A250390] p 854 N92-29180

Preliminary results on the fracture analysis of multi-site cracking of lap joints in aircraft skins p 913 N92-30111

Ageing airplane repair assessment program for Airbus A300 p 838 N92-30123

SKIN FRICTION

Skin-friction gauge for use in hypervelocity impulse facilities p 398 A92-28063

Skin friction measurements in 3-D boundary layers p 1092 A92-54351

Physics of vortical flows p 1031 A92-56166

Reflection type skin friction meter [NASA-CASE-LAR-14520-1-SB] p 11 N92-10008

Susceptibility of a parallelogram type skin friction balance to rotational motion [AD-A241348] p 139 N92-13078

Separation of relaminarised boundary layers [CUED/A-AERO/TR-16] p 592 N92-22209

Special Course on Skin Friction Drag Reduction [AGARD-R-786] p 717 N92-27706

Basic concepts on boundary layers p 717 N92-27707

Aircraft drag reduction p 717 N92-27709

Boundary layer transition: Prediction, application to drag reduction p 717 N92-27711

Turbulent skin-friction drag reduction by active and passive means, part 1 p 718 N92-27714

Active thermal isolation for temperature responsive sensors [NASA-CASE-LAR-14612-1] p 911 N92-29954

SKIRTS

Configuration of flexible-skirts for an ACV and its CAD p 1118 A92-56036

Planning method of skirt systems for small ACVs p 1118 A92-56038

Air cushion vehicle conductive/semiconductive flexible skirt, and method [AD-D015160] p 400 N92-18187

SKIS

United States Navy ski jump experience and future applications p 465 N92-21968

SLENDER BODIES

Viscous flow solutions for slender bodies of revolution at incidence p 4 A92-10692

Fickle effect of nose microasymmetry on the high-alpha aerodynamics p 10 A92-13217

On the sensitivity of transonic flow p 315 A92-25132

Some thoughts on conical flow asymmetry [AIAA PAPER 92-0427] p 326 A92-26275

Flow about cylinders with helical surface protrusions [AIAA PAPER 92-0540] p 332 A92-26957

Effects of nose bluntness and angle of attack on slender bodies in hypersonic flows [AIAA PAPER 92-0638] p 334 A92-27016

Numerical simulation of vortex unsteadiness on a slender body at high incidence p 340 A92-28062

Unsteady hypersonic boundary layers for slender axisymmetric bodies with large injection rates p 524 A92-36100

Analysis of slender bodies of revolution with curved-ground effect and waving-water effect p 524 A92-36151

A correlation study of the wing-body interference factor for high angles of attack p 700 A92-41179

The interaction between a plane shear layer and a slender body p 991 A92-49790

Asymmetric turbulent vortical flows over slender bodies p 935 A92-50314

Asymmetric vortex flow over circular cones p 86 N92-13014

An experimental investigation of the effect of fineness ratio on lateral force on a pointed slender body of revolution p 86 N92-13015

Prediction and control of asymmetric vortical flows around slender bodies using Navier-Stokes equations p 1127 N92-33968

SLENDER CONES

Hypersonic flows over slender circular cones at small angles of attack p 173 A92-19068

Application of the LAURA code for slender-vehicle aerothermodynamics p 310 A92-24652

Hypersonic flow of a viscous gas past sharp elliptical cones at angles of attack and slip p 336 A92-27531

The lift-drag ratio of a slender cone in viscous hypersonic gas flow p 425 A92-30172

A method for calculating the separated flow past a circular cone, taking viscous-inviscid interaction into account p 427 A92-30203

Combined effect of nose bluntness and angle of attack on slender bodies in viscous hypersonic flows [AIAA PAPER 92-0755] p 436 A92-31680

Approximate Riemann solver for hypervelocity flows p 1117 A92-54934

SLENDER WINGS

Secondary separation from a slender wing p 62 A92-13448

Design is the name of the game - Comparison of the F5D Skylancer to the F4D Skyray p 167 A92-16062

Analysis of spiraling vortical flows around slender delta wings moving in an inviscid medium p 173 A92-18900

Effect of leading-edge cross-sectional geometry on slender wing unsteady aerodynamics [AIAA PAPER 92-0173] p 255 A92-23784

Rapid prediction of high-alpha unsteady aerodynamics of slender-wing aircraft p 309 A92-24412

Numerical modeling of self-oscillations for a small-aspect-ratio delta wing using measurements of roll motion at large angles of attack p 424 A92-30138

Aerodynamic characteristics of slender sharp-leading-edge delta wings with air scooping through the air intake at hypersonic velocities. I p 427 A92-30206

Experimental investigations of the vortex flow on delta wings at high incidence p 432 A92-31172

Effect of the fuselage midsection ratio on the character of wing-fuselage aerodynamic interference p 439 A92-31883

An exact solution to edge effect problem for a finite-span wing in supersonic flow p 441 A92-31962

Boundary layer on slender wings of small aspect ratio p 441 A92-31963

New, unusual and nonclassical behavior of thin-walled composite structures p 580 A92-32746

A calculation of influence of vortex breakdown on aerodynamic characteristics for slender wings p 616 A92-38920

A mathematical model for the hydroelasticity problem concerning the motion of two flexible profiles in an ideal incompressible fluid. I p 712 A92-44127

An improved multiple line-vortex method for simulation of separated vortices of slender wings p 819 A92-47694

A discrete vortex model for predicting wing rock of slender wings [AIAA PAPER 92-4497] p 1026 A92-55365

Stochastic self-induced roll oscillations of slender delta wing at high angles of attack [AIAA PAPER 92-4498] p 1081 A92-55366

Wind tunnel blockage effects on slender wings undergoing large amplitude motions [AIAA PAPER 92-3926] p 1096 A92-56757

Wind tunnel investigation of the interaction and breakdown characteristics of slender wing vortices at subsonic, transonic, and supersonic speeds [NASA-TP-3114] p 82 N92-12994

Laminar-flow secondary separation on a slender wing p 85 N92-13006

Boundary-layer transition and heat transfer on slender delta wings [AERO-REPT-8904] p 262 N92-17849

Aerodynamic and flowfield hysteresis of slender wing aircraft undergoing large-amplitude motions p 364 N92-18780

The natural flow wing-design concept [NASA-TP-3193] p 631 N92-25202

A method for computing the 3-dimensional flow about wings with leading-edge vortex separation. Part 2: Description of computer program VORSEP [NLR-TR-86006-U] p 833 N92-29916

SLIDING

An assessment of robustness of variable structure control systems for advanced aircraft manoeuvres p 29 A92-11595

Multiple input sliding mode control for autonomous diving and steering of underwater vehicles [AD-A241935] p 283 N92-17442

SLIP CASTING

Ceramic component processing development for advanced gas-turbine engines [ASME PAPER 91-GT-120] p 142 A92-15567

SLOT ANTENNAS

Single slotted array achieves multimode performance p 726 A92-44428

Advanced electromagnetic methods for aerospace vehicles [NASA-CR-188630] p 488 N92-20193

SLOTS

Numerical simulation of slot injection into a turbulent supersonic stream [AIAA PAPER 92-0827] p 421 A92-29595

Experimental investigation of film cooling effectiveness for slots of various exit geometries p 497 A92-32265

Boundary-layer receptivity due to a wall suction and control of Tollmien-Schlichting waves p 616 A92-39333

Influence of suction through a slot on a turbulent boundary layer p 622 A92-40127

Numerical simulation of slot injection into a turbulent supersonic stream p 1024 A92-54914

Wall interference calculation in a transonic wind tunnel with discrete slots p 83 N92-12995

A study of the diffusion of slot-injected drag-reducing polymer solution in a turbulent boundary layer modified by large-eddy breakup devices [AD-A243411] p 344 N92-18007

CFD mixing analysis of jets injected from straight and slanted slots into confined crossflow in rectangular ducts [NASA-TM-105699] p 738 N92-26561

SLOTTED WIND TUNNELS

Disturbance of transonic wind tunnel flow by a slot in the tunnel wall p 135 A92-13675

High speed wind tunnel wall interference research progress at Nanjing Aeronautical Institute p 136 A92-15338

Resonance prediction for slotted circular wind tunnel using finite element p 235 A92-18388
Wall interference calculation in a transonic test section including simulation of discrete slots
[AIAA PAPER 92-0032] p 249 A92-22153
Discussion on sidewall suction in two-dimensional wind tunnel p 997 A92-53263
Mass flux similarity for slotted transonic-wind-tunnel walls
[NASA-TM-4281] p 11 N92-10006
Model representation in the PANCOR wall interference assessment code
[NASA-TM-104152] p 31 N92-11022

SLURRIES
Steady flow of a fluid-solid mixture in a circular cylinder
[DE91-018698] p 41 N92-10174

SLURRY PROPELLANTS
Transport phenomena and interfacial kinetics in multiphase combustion systems
[AD-A244849] p 489 N92-20695

SLUSH
Slush hydrogen (SLH2) technology development for application to the National Aerospace Plane (NASP) p 144 A92-13432
Investigation on freezing and sticking phenomena of *slush on airplane surfaces when taxiing on the ground* and the succeeding take-off run phase
[NAL-TR-1026] p 352 N92-18182

SLUSH HYDROGEN
Cryogenic hydrogen-induced air-liquefaction *technologies for combined-cycle propulsion applications* p 487 N92-21526

SMALL PERTURBATION FLOW
Stability of a viscous compressible shear layer with a temperature drop p 79 A92-16684
A deforming grid variational principle and finite element method for computing unsteady small disturbance flows in cascades
[AIAA PAPER 92-0665] p 335 A92-27036
Further investigations of the aeroelastic behavior of the AFW wind-tunnel model using transonic small disturbance theory
[AIAA PAPER 92-2082] p 565 A92-35654
Optimum hypersonic wings and wave riders p 706 A92-42531
Transonic flows of Bethe-Zel'dovich-Thompson fluids p 935 A92-50293
Discussion of improved transonic potential method p 942 A92-53290
Efficient iterative methods for the transonic small disturbance equation p 1025 A92-54933
Three dimensional numerical method for resolving small transonic perturbations in unstructured mesh
[ONERA-RT-56/3064-RY-006-R] p 13 N92-10989

SMART STRUCTURES
Application of smart structures to aircraft health monitoring p 20 A92-11123
Damage assessment for composite smart structures p 140 A92-13601
Fiber optic sensors for smart skins applications p 392 A92-24778
Progress towards fiber optic smart structures at UTIAS p 368 A92-24781
Smart skins and fiber-optic sensors application and issues p 368 A92-24785
Smart structures - A damage detection concept p 491 A92-28672
Smart structures for helicopters p 516 A92-35727
International Aerospace Symposium 90, Nagoya, Japan, Nov. 26, 27, 1990, Proceedings p 607 A92-38201
Active vibration control of smart structural materials p 673 A92-39281
Basic design concepts for smart actuators for aerospace plane control p 752 A92-41193
The use of silicon microsensors in smart skins for aerodynamic research p 1116 A92-54348
Smart structures in the active control of blade vortex interaction p 1085 A92-56314
System requirements specification for SMART structures mode p 777 N92-27830
Active vibrations and noise control for turboprop application research program activities p 1138 N92-32962

SMOKE
The effect on aircraft evacuations of passenger behaviour and smoke in the cabin p 834 A92-44998
Degenerate four-wave mixing for measurement of NO2 and smoke concentration in jet engine exhaust
[AIAA PAPER 92-3658] p 1113 A92-54108

SMOKE ABATEMENT
Damping down the fires --- in civil transport aircraft p 350 A92-25075

SMOKE DETECTORS
Aircraft Command in Emergency Situations (ACES)
[SAE PAPER 912039] p 835 A92-45424

SMOKE TRAILS
Simple method of supersonic flow visualization using smoke p 219 A92-20764
Flow field measurement and visualization using projected smoke trails
[AIAA PAPER 92-0384] p 323 A92-26241
Preliminary design of an intermittent smoke flow visualization system
[AIAA PAPER 92-1028] p 580 A92-33209
Visualization and measurement of helicopter rotor flow using projected smoke filaments and digital image processing p 520 A92-35728
Hot-wire surveys in the vortex wake downstream of a three-percent fighter aircraft model at high angles of attack
[AD-A241869] p 259 N92-15975

SMOOTHING
Trajectory fitting in function space with application to analytic modeling of surfaces
[NASA-TP-3232] p 945 N92-30747

SNOW
Freezing precipitation on lifting surfaces
[NRC-32124] p 448 N92-20156

SNOWSTORMS
Precipitation development in Colorado Front Range snowstorms - 15 November 1987 case study p 301 A92-23008

SOFIA (AIRBORNE OBSERVATORY)
Flowfield simulation about the SOFIA Airborne Observatory
[AIAA PAPER 92-0656] p 342 A92-28217

SOFT LANDING
The differential algebraic approach in nonlinear dynamical feedback controlled landing maneuvers p 574 A92-33639

SOFTWARE ENGINEERING
Distributed artificial intelligence approach to air traffic control p 161 A92-13436
Case for real-time systems development - Quo vadis?
[AIAA PAPER 91-3726] p 231 A92-17594
Advanced avionics system development environment
[AIAA PAPER 91-3944] p 231 A92-17608
Applications of an automated programming system
[AIAA PAPER 91-3767] p 231 A92-17629
Designing through test
[AIAA PAPER 91-3822] p 232 A92-17664
Verification of flight software by embedding software simulation in simulation of external environment p 232 A92-19084
A processor-in-the-loop simulation using an XANALOG computer p 232 A92-19094
Cleanroom - An alternative software development process p 233 A92-19386
Aerospace software engineering in the United Kingdom p 233 A92-19405
Aerospace software in Sweden p 233 A92-19406
AI technology and application development on the Shuttle project p 302 A92-23693
From concept to model: Conception and evaluation of an architecture for a distributed system with SAHARA - Some reflections on results of the utilization of SAHARA in the framework of the Electronic Copilot
[ONERA, TP NO. 1991-216] p 411 A92-26368
Never make the same mistake twice - Using configuration control and error analysis to improve software quality p 601 A92-33603
Software safety analysis in heterogeneous multiprocessor control systems p 776 A92-42073
Avionics software reusability observations and recommendations p 921 A92-48502
Application of syndrome pattern-matching approach to fault isolation in avionic systems p 1005 A92-49261
Avionics systems engineering education p 1012 A92-49269
The Catalyst software engineering environment --- in avionics p 1005 A92-49300
Computer software in civil aircraft p 1006 A92-49302
The data flow simulator, a tool for system simulation --- in digital avionics p 1006 A92-49329
Tool supported software development experiences from the EFA project p 163 N92-12451
Process/object-oriented Ada software design for an experimental helicopter p 164 N92-12461
Development and verification of software for flight safety critical systems p 164 N92-12469
Avionics software evolution p 199 N92-14052
Avionics systems development: Technological trends, conflicts, and cost issues in a changing European environment p 199 N92-14054
Avionics technology beyond 2000 p 200 N92-14058
Architecture for Survivable System Processing (ASSP) p 220 N92-14210
Advanced flight software reconfiguraton p 287 N92-17350
Software Engineering Laboratory (SEL) Ada performance study report
[NASA-TM-105510] p 412 N92-18125
Impact of a process improvement program in a production software environment: Are we any better? p 413 N92-19422
Towards understanding software: 15 years in the SEL p 413 N92-19423
Reuse metrics and measurement: A framework p 413 N92-19432
Prototyping the IRDS: An airport application
[PB92-112580] p 484 N92-20448
Space software is first of all software p 509 N92-20590
The proposed revision to RTCA DO178A and its influence on system design
[PNR-90821] p 510 N92-21847
Software Surface Modeling and Grid Generation Steering Committee
[NASA-CP-3143] p 691 N92-24397
Research into the development of a knowledge acquisition taxonomy
[NASA-CR-189939] p 778 N92-28150
Analysis of data from a DO-178A software development process p 1134 N92-32880

SOFTWARE REUSE
Avionics software reusability observations and recommendations p 921 A92-48502

SOFTWARE TOOLS
The European ATC challenge p 19 A92-11877
Preliminary design of axial compressors using artificial *intelligence and numerical optimization techniques*
[ASME PAPER 91-GT-334] p 126 A92-15699
Case for real-time systems development - Quo vadis?
[AIAA PAPER 91-3726] p 231 A92-17594
Knowledge maintenance in an evolving system using a deep structure representation
[AIAA PAPER 91-3941] p 231 A92-17605
Advanced avionics system development environment
[AIAA PAPER 91-3944] p 231 A92-17608
Fault Tree Interpreter --- expert system shell for rule-based expert systems development for control of ATE
[AIAA PAPER 91-3789] p 232 A92-17645
Failure environment analysis tool (FEAT) development status
[AIAA PAPER 91-3803] p 232 A92-17654
One view of experimental aerodynamics
[AIAA PAPER 92-0160] p 254 A92-23775
Atmospheric disturbance model for aircraft and space capable vehicles
[AIAA PAPER 92-0294] p 407 A92-25747
The NASA Computational Aerosciences Program - Toward teraFLOPS computing
[AIAA PAPER 92-0558] p 411 A92-26968
The Software Factory, version 5.0
[AIAA PAPER 92-0590] p 411 A92-26992
Adaptive simulator motion software with supervisory control p 412 A92-28136
Concepts for a future aircraft design environment
[AIAA PAPER 92-1188] p 600 A92-33300
A structural design and optimization tool for ducted rotor/wing blades
[AIAA PAPER 92-2361] p 543 A92-34593
ARINC and the avionics of commercial aircraft. II p 637 A92-37072
Iberia's Aeronautical Mapping Application (ACAI) p 637 A92-37073
Software reliability for flight crew training simulators p 747 A92-41221
Interactive generation of structured/unstructured surface meshes using adaptivity p 919 A92-47066
Design and implementation of a generic Kalman filter in Ada p 858 A92-48475
Expert Avionics Code Modification p 921 A92-48513
Partitioned software support concept for modular embedded computer software p 922 A92-48518
Testing and analysis of a 'smart' interface to connect two complex avionics bus systems without significant modification to the software of either system p 964 A92-49254
A new approach to embedded computer performance measurement --- in avionics p 1005 A92-49288
Implementation of non-dedicated redundancy in a fault tolerant multiprocessor testbed --- flight control p 974 A92-49294
Computer software in civil aircraft p 1006 A92-49302
Verification and validation testing of the pilot's associate p 966 A92-49318
Operating principles for integrated sensor processing p 966 A92-49336
The B-2 radar p 956 A92-53102

FREPS - A forced response prediction system for turbomachinery blade rows
[AIAA PAPER 92-3072] p 1130 A92-54006
Multidisciplinary optimization of aeroservoelastic systems using reduced-size models
p 1054 A92-56176
HiRel - Reliability/availability integrated workstation tool p 1120 A92-56257
Test and integration concept for complex helicopter avionic systems p 1064 A92-56292
First level release of 2GCHAS for comprehensive helicopter analysis p 1133 A92-56339
Tool supported software development experiences from the EFA project p 163 N92-12451
Automated problem resolution prototype in automated en route air traffic control p 190 N92-14028
Mixed approach towards modular avionics conflicting requirements p 199 N92-14051
Avionics software evolution p 199 N92-14052
Architecture for Survivable System Processing (ASSP)
p 220 N92-14210
Getting expert systems off the ground: Lessons learned from integrating model-based diagnostics with prototype flight hardware p 220 N92-14217
An application of the object-oriented paradigm to a flight simulator
[AD-A243624] p 384 N92-18012
RAMREQ: A computerized tool for the definition of RAM (Reliability, Availability, Maintainability) requirements of complex systems p 412 N92-18647
Development of nonlinear real-time helicopter simulation using a blade element method
[NLR-TP-90115-U] p 381 N92-18893
Accurate, productive aerodynamic simulation on patched mesh systems
[AD-A243977] p 405 N92-19386
Prototyping the IRDS: An airport application
[PB92-112580] p 484 N92-20448
Advanced Transport Operating System (ATOPS) color displays software description: MicroVAX system
[NASA-CR-189603] p 556 N92-22395
High angle of attack: Aerodynamics
p 528 N92-23956
Description and simulation results of the Italsat AOCS advanced flight simulator p 667 N92-24472
Current activities and future plans for GPS applications p 640 N92-24735
System requirements specification for SMART structures mode p 777 N92-27830
Surface generation and editing operations applied to structural support of aerospace vehicle fuselages
p 777 N92-27831
MBB-LAGRANGE: A general structural reliability and optimization structural system
[MBB/FW321/S/PUB/467] p 998 N92-30423
MATGRID, a program for generation of C-H and C-O topology grids around wing/body configurations: Software description document
[FFA-TN-1990-20] p 945 N92-30713
On-line analysis capabilities developed to support the AFW wind-tunnel tests
[NASA-TM-107651] p 961 N92-30752
Rapid development of the X-31 simulation to support flight-testing
[NASA-TM-104256] p 1060 N92-33149
Advanced techniques in reliability model representation and solution
[NASA-TP-3242] p 1134 N92-33483

SOIL MECHANICS
Evaluation of grounding and mooring points for Army aircraft
[AD-A250749] p 953 N92-31193

SOILS
Effects of the abrasiveness of test and training site soils on parachute life
[AD-A252389] p 1038 N92-32900

SOLAR CELLS
New-type of ultralight flexible a-Si solar cell and its application on an airplane p 970 A92-53181
NASA advanced aeronautics design solar powered remotely piloted vehicle
[NASA-CR-190007] p 462 N92-20665

SOLAR ELECTRIC PROPULSION
Stratospheric lighter-than-air powered platform
p 110 A92-15334
Analysis, development, and integration of the mechanical components of a vehicle powered by photo-voltaic cells
[TABES PAPER 91-503] p 606 A92-34692

SOLAR ENERGY
High altitude solar power platform --- aircraft design analysis
[NASA-TM-103578] p 506 N92-21546

SOLAR GENERATORS
High-altitude lighter-than-air powered platform
[SAE PAPER 912054] p 844 A92-45438
Study of potassium turbine electric generator system
p 1129 N92-33794

SOLAR POWERED AIRCRAFT
New-type of ultralight flexible a-Si solar cell and its application on an airplane p 970 A92-53181

SOLAR PROPULSION
NASA advanced aeronautics design solar powered remotely piloted vehicle
[NASA-CR-190007] p 462 N92-20665

SOLAR SAILS
JPRS report: Science and technology. Central Eurasia: Space
[JPRS-USP-92-002] p 575 N92-23705

SOLID LUBRICANTS
High-temperature powder-lubricated dampers for gas turbine engines p 399 A92-28528

SOLID MECHANICS
Shape-sensitivity analysis and design optimization of linear, thermoelastic solids p 395 A92-26433
Mechanics Pan-America 1991; Pan-American Congress of Applied Mechanics, 2nd (PACAM II), Universidad Tecnica, Valparaiso, Chile, Jan. 2-5, 1991, Selected and Revised Proceedings p 673 A92-39930
Development of an integrated BEM approach for hot fluid structure interaction: BEST-FSI: Boundary Element Solution Technique for Fluid Structure Interaction
[NASA-CR-189202] p 574 N92-22211

SOLID PHASES
Metal matrix composite fabrication processes for high performance aerospace structures p 760 A92-42145

SOLID PROPELLANT COMBUSTION
Swirl and fuel composition effects on boron combustion in solid-fuel ramjets p 668 A92-36964
Similarity and scale effects in solid-fuel ramjet combustors p 666 A92-36965
Solid-fuel ramjet fuel regression rate/thrust modulation
p 666 A92-36966
Wind tunnel study of aerodynamic characteristics of base combustion p 666 A92-36967
Fuel regression mechanism in a solid fuel ramjet
p 860 A92-44898
Combustion of solid fueled ramjet. I
[AIAA PAPER 92-3727] p 894 A92-49105
Symposium on High Speed Airbreathing Propulsion: The Solid Fuel Combustion Chamber and Beyond
[ETN-92-90685] p 575 N92-22268

SOLID PROPELLANT ROCKET ENGINES
Investigation on opening and ejection of an aircraft canopy by using a solid rocket engine
p 358 A92-28489
Combustion of solid fueled ramjet. II
[AIAA PAPER 92-3728] p 894 A92-49106
Optimal launch trajectory of a hypersonic research vehicle
[AIAA PAPER 92-4302] p 1103 A92-55310

SOLID STATE
Solid-State Radar Beacon Decoder (SSRBD) Operational Test and Evaluation (OT/E) integration test plan
[DOT/FAA/CT-TN91/30] p 19 N92-10020

SOLID STATE LASERS
A study of atmospheric optical scattering parameters at 1.5 and 2 micron region for solid state Doppler lidar applications p 1001 N92-31067

SOLID SURFACES
Analysis of motion of airfoil flying over wavy-wall surface (lifting surface method) p 818 A92-47100
Experimental and numerical investigation of a supersonic free jet impinging on a perpendicular surface
p 1018 A92-53555
Grid generation and flow solution method for Euler equations on unstructured grids
[NASA-TM-4295] p 528 N92-23533

SOLIDIFICATION
Research and development of aircraft engine materials p 577 A92-35916
Modifications to the rapid melt/rapid quench and transparent polymer video furnaces for the KC-135
[NASA-CR-184215] p 157 N92-12231

SOLIDS
Eulerian computational methods
[DE92-008017] p 765 N92-26853
Solid-vapor adsorption refrigeration system development
[PB92-164383] p 771 N92-27715

SOLIDS FLOW
Steady flow of a fluid-solid mixture in a circular cylinder
[DE91-018698] p 41 N92-10174

SONAR
Precision of the long baseline acoustic navigation system used by Pegasus
[AD-A246598] p 727 N92-26795

SONIC ANEMOMETERS
Measured and predicted rotor performance for the SERI advanced wind turbine blades
[DE92-001215] p 598 N92-23119

SONIC BOOMS
Environmental impact of a future supersonic transport aircraft
[ONERA, TP NO. 1991-132] p 161 A92-16108
The sonic boom and problems related to supersonic flights of military aircraft
[ONERA, TP NO. 1991-162] p 77 A92-16129
NSBIT program - Development of assessment system for aircraft noise and research on human impacts due to aircraft noise p 688 A92-39100
Loudness of shaped sonic booms
p 695 A92-39238
The effect of molecular relaxation processes in air on the rise time of sonic booms p 898 A92-45883
Application of computational fluid dynamics to sonic boom near- and mid-field prediction
p 1031 A92-56173
Sonic boom p 55 N92-10608
A new simulator for assessing subjective effects of sonic booms
[NASA-TM-104150] p 56 N92-11759
A loudness calculation procedure applied to shaped sonic booms
[NASA-TP-3134] p 56 N92-11765
Propagation of shock waves through clouds
[AERO-REPT-9104] p 400 N92-18317
The atmospheric effects of stratospheric aircraft: A first program report
[NASA-RP-1272] p 408 N92-19121
Nonlinear acoustic propagation of shock waves through the atmosphere with molecular relaxation
p 511 N92-20360
Sonic booms produced by US Air Force and US Navy aircraft: Measured data
[AD-A244804] p 512 N92-21719
A summary of XB-70 sonic boom signature data
[NASA-CR-189630] p 696 N92-24800
Comparison of jet plume shape predictions and plume influence on sonic boom signature
[NASA-TP-3172] p 631 N92-25133
Evaluation of human response to structural vibrations induced by sonic booms
[NASA-CR-189584] p 697 N92-26130
Evaluation of outdoor-to-indoor response to minimized sonic booms
[NASA-CR-189643] p 927 N92-28556
Application of magnitude estimation scaling to the assessment of subjective loudness response to simulated sonic booms
[NASA-TM-107657] p 1138 N92-33719
High-Speed Research: Sonic Boom, volume 1
[NASA-CP-3172] p 1061 N92-33874
A numerical model for sonic boom propagation through an inhomogeneous, windy atmosphere
p 1138 N92-33876
Wave equations and computational models for sonic boom propagation through a turbulent atmosphere
p 1139 N92-33877
Simulations of sonic boom ray tube area fluctuations for propagation through atmospheric turbulence including caustics via a Monte Carlo method
p 1139 N92-33878
Analysis of sonic boom data to quantify distortions of shock profiles p 1139 N92-33879
The effect of turbulence on the loudness of minimized sonic boom signatures p 1139 N92-33880
Model experiment to study the effect of turbulence on risetime and waveform of N waves
p 1139 N92-33881
Steady state risetimes of shock waves in the atmosphere p 1140 N92-33882
Lateral spread of sonic boom measurements from US Air Force boomfile flight tests p 1140 N92-33883
Preliminary results from the White Sands Missile Range sonic boom propagation experiment
p 1140 N92-33884
Subjective loudness response to simulated sonic booms p 1140 N92-33885

SORBENTS
Multicomponent gas sorption Joule-Thomson refrigeration
[NASA-CASE-NPO-17569-1-CU] p 228 N92-15203

SORPTION
Multicomponent gas sorption Joule-Thomson refrigeration
[NASA-CASE-NPO-17569-1-CU] p 228 N92-15203
Three-stage sorption type cryogenic refrigeration system and method employing heat regeneration
[NASA-CASE-NPO-18366-1-CU] p 300 N92-17674

SOUND FIELDS
Screech noise source structure of a supersonic rectangular jet
[AIAA PAPER 92-0503] p 331 A92-26932
NATO CCMS aircraft noise study on receiver technology p 686 A92-39050
Noise from military airfields in the United Kingdom p 686 A92-39052
Solutions of acoustic field problems using parallel computers p 925 A92-45929
Direct evaluation of aeroacoustic theory in a jet p 1010 A92-50296
Prediction of noise field of a propfan at angle of attack
[NASA-CR-189047] p 166 N92-13759
Critical problems of computational aeroacoustics p 167 N92-13857
Theoretical models for duct acoustic propagation and radiation p 236 N92-14782
The acoustic flashlight
[MBB-Z-0359-90-PUB] p 239 N92-15938
Measurements of fluctuating pressure in a rectangular cavity in transonic flow at high Reynolds numbers
[NASA-TM-4363] p 633 N92-25752
A lightweight loudspeaker for aircraft communications and active noise control p 1125 N92-32964

SOUND GENERATORS
Sound produced by an aerodynamic source adjacent to a partly coated, finite elastic plate p 414 A92-25365
Direct computation of the sound from a compressible co-rotating vortex pair
[AIAA PAPER 92-0374] p 414 A92-26232
Sound generation by a stenosis in a pipe p 415 A92-26405
Sound produced by vortex-airfoil interaction p 1136 A92-56345
Noise from turbulent shear flows p 55 N92-10603
Development and testing of cabin sidewall acoustic resonators for the reduction of cabin tone levels in propfan-powered aircraft
[NASA-CR-4388] p 166 N92-13757
The acoustic flashlight
[MBB-Z-0359-90-PUB] p 239 N92-15938
Experimental study of the mechanism of sound generation by rotating stall in centrifugal turbomachines p 605 N92-23726

SOUND INTENSITY
New methods to determine the transmission loss of partitions using sound intensity measurements p 924 A92-45879
The measurement of plate vibration and sound radiation from a turbulent boundary layer manipulator
[AD-A240127] p 42 N92-10206

SOUND PRESSURE
High-speed impulsive noise and aerodynamic results for rectangular and swept rotor blade tip tests in S1-Modane wind tunnel
[ONERA, TP NO. 1991-124] p 76 A92-16102
Screech noise source structure of a supersonic rectangular jet
[AIAA PAPER 92-0503] p 331 A92-26932
Azimuthal noise characteristics of contra-rotating propellers - Results of a wind tunnel model test p 693 A92-39066
Acoustic testing at elevated temperatures p 981 A92-51405
Approximation methods for control of acoustic/structure models with piezoceramic actuators
[NASA-CR-189578] p 234 N92-15658
Active noise control: Piezoceramic actuators in fluid/structure interaction models
[NASA-CR-190328] p 685 N92-26125
Exposures from headset interference tones
[AD-A247175] p 1136 N92-32697
Building vibrations induced by noise from rotorcraft and propeller aircraft flyovers
[NASA-TM-104170] p 1138 N92-33160

SOUND PROPAGATION
Computation of aircraft noise exposure using digitized topography data p 687 A92-39058
Active control of structurally-coupled sound fields generated by localized force inputs p 694 A92-39106
Active control of airborne noise transmitted through a ribbed panel p 695 A92-39111

SOUND TRANSMISSION
Active control of sound transmission through elastic plates using piezoelectric actuators p 53 A92-11052
Acoustic isolation of layers p 54 A92-12345
Effect of the wake flow on the soundproofing of aircraft structures p 166 A92-16824
Sound transmission through a high-temperature acoustic probe tube p 415 A92-26406
Evaluation of sound transmission into aircraft fuselages by a reciprocity technique p 694 A92-39086
Acoustic transmission through a 2-D orthotropic multi-layered infinite cylindrical shell p 780 A92-44197
New methods to determine the transmission loss of partitions using sound intensity measurements p 924 A92-45879
Active control of sound transmission through stiff lightweight composite fuselage constructions p 1137 N92-32957
Pilot noise exposure during a Boeing 747-400 round trip: Judgement of noise and analysis in respect to hearing impairment of pilots p 1138 N92-32961

SOUND WAVES
Fatigue due to noise-induced pressure
[ASME PAPER 91-GT-150] p 148 A92-15588
Comparative study of fatigue in various materials and designs under sonic loading p 287 A92-21003
A wave-model-based refinement criterion for adaptive-grid computation of compressible flows
[AIAA PAPER 92-0322] p 321 A92-25769
Modification of the radiated sound directivity due to ground reflections - Application to static tests of helicopter turboshaft engines
[ONERA, TP NO. 1991-210] p 415 A92-26362
Experimental study of the effects of atmospheric turbulence on sound propagation over the ground
[ONERA, TP NO. 1991-211] p 415 A92-26363
Transition control of instability waves over an acoustically excited flexible surface p 416 A92-28037
Acoustic results of the Boeing model 360 whirl tower test p 603 A92-35741
Some aerodynamic mechanisms of impulsive noise during blade-vortex-interaction p 604 A92-35782
Boundary-layer receptivity of sound with roughness p 604 A92-36006
Susceptibility of a supersonic boundary layer to acoustic perturbations p 707 A92-42730
International Congress on Recent Developments in Air- and Structure-Borne Sound and Vibration, Auburn University, AL, Mar. 6-8, 1990, Proceedings. Vols. 1 & 2 p 924 A92-45876
The measurement of plate vibration and sound radiation from a turbulent boundary layer manipulator
[AD-A240127] p 42 N92-10206
Jet noise classical theory and experiments p 54 N92-10602
Propulsive lift noise p 55 N92-10606
Method and apparatus for acoustic plate mode liquid-solid phase transition detection
[DE92-003778] p 401 N92-18705
A numerical study of fuselage scattering effects on rotor noise p 511 N92-20428
Evaluation of the applicability of Helmholtz resonators for low frequency acoustic liners
[PB92-138544] p 605 N92-23588
Distributed acoustic receptivity in laminar flow control configurations
[NASA-CR-4438] p 765 N92-26680
Exposures from headset interference tones
[AD-A247175] p 1136 N92-32697

SOUNDING
Wing tip turbine: Analysis of the results of S2MA sounding of marginal vortex of the A320, technical summary
[ONERA-RTS-21/4365-AY-056A] p 23 N92-11009

SPACE DEBRIS
Collision probability estimate method for impact generated low earth orbit space debris clouds
[AAS PAPER 91-369] p 752 A92-43269

SPACE EXPLORATION
Analysis of spacecraft entry into Mars atmosphere p 1105 N92-33763

SPACE FLIGHT
Improvement of atmospheric flight performance of a space vehicle through H infinity-control theory p 1130 A92-53785
Ames life science telescience testbed evaluation
[NASA-CR-188856] p 140 N92-12033
Research and technology, 1991
[NASA-TM-105320] p 516 N92-22659

SPACE LAW
Annals of air and space law. Vol. 16 p 1012 A92-51450

SPACE MISSIONS
Issues in developing control zones for international space operations p 1141 A92-56602
STS-41 Space Shuttle mission report
[NASA-TM-105479] p 286 N92-16973

SPACE NAVIGATION
GPS availability. I - Availability of service achievable for different categories of civil users. II - Evaluation of state probabilities for 21-satellite and 24-satellite constellations p 99 A92-16949
Navigation - Land, sea, air, and space --- Book
[ISBN 0-87942-257-2] p 496 A92-31778
JTIDS relative navigation and data registration p 955 A92-51006
FALKE: Winged re-entry vehicle flight control p 667 N92-24454
DLR research reports and communications
[ETN-92-91391] p 929 N92-29218

SPACE PERCEPTION
Perspective versus plan view air traffic control (ATC) displays - Survey and empirical results p 896 A92-44967
A re-analysis of the causes of Boeing 727 'black hole landing' crashes p 833 A92-44985
An aircraft landing accident caused by visually induced spatial disorientation p 834 A92-44993
Effect of short-term exposure to stereoscopic three-dimensional flight displays on real-world depth perception
[NASA-TP-3117] p 119 N92-13065

SPACE PLATFORMS
The formation and structure of plasma wakes behind large high-voltage space platforms in ionosphere
[AIAA PAPER 92-0577] p 407 A92-26984
Ionospheric plasma flow over large high-voltage space platforms. I - Ion-plasma-time scale interactions of a plate at zero angle of attack. II - The formation and structure of plasma wake p 779 A92-41359
On the stability of a dual spin satellite with asymmetric rotor and flexible platform
[ISBN-0-315-54650-6] p 753 N92-27613

SPACE PROCESSING
Convective flow analysis on the KC-135 aircraft
[AIAA PAPER 92-0844] p 493 A92-29610
Modifications to the rapid melt/rapid quench and transparent polymer video furnaces for the KC-135
[NASA-CR-184215] p 157 N92-12231

SPACE PROGRAMS
International survey of scientific ballooning support organizations
[AIAA PAPER 91-3677] p 1 A92-11022

SPACE SHUTTLE ASCENT STAGE
Shuttle Entry Air Data System - An experimental investigation of calibration for ascent flight
[AIAA PAPER 92-0133] p 286 A92-23753

SPACE SHUTTLE BOOSTERS
Numerical methods for the simulation of complex multi-body flows with applications for the integrated Space Shuttle vehicle p 945 N92-30741

SPACE SHUTTLE MAIN ENGINE
Aerodynamics and heat transfer investigations on a high Reynolds number turbine cascade
[ASME PAPER 91-GT-157] p 148 A92-15593
Pressure oscillation in the leakage annulus between a shrouded impeller and its housing due to impeller-discharge-pressure disturbances p 580 A92-32942
Study of weld offset in longitudinally welded SSME HPFTP inlet
[AIAA PAPER 92-2305] p 586 A92-34525
Rotor support for the STME oxygen turbopump
[AIAA PAPER 92-3282] p 904 A92-48872
Limit cycle vibrations in turbomachinery
[NASA-TP-3181] p 211 N92-14108
Nonlinear rotordynamics analysis --- Space Shuttle Main Engine turbopumps
[NASA-CR-184263] p 221 N92-14344
Test results for rotordynamic coefficients of the SSME HPOTP turbine interstage seal with two swirl brakes p 223 N92-14357
Dynamic characteristics and stability analysis of space shuttle main engine oxygen pump p 224 N92-14366
Airfoil Vibration Dampers program
[NASA-CR-184276] p 225 N92-14391
Redesign of flight space shuttle main engine nozzle G-15 seal area based on the thermal analysis and flow models p 212 N92-15877

SPACE SHUTTLE ORBITERS
An efficient calculation method of subsonic aerodynamic characteristics for a Space Shuttle orbiter in the reentry attitude p 252 A92-23383
Space-marching calculations of hypersonic inviscid flowfield p 313 A92-25040
Comparison of heating calculations with experimental data on a modified Shuttle Orbiter p 441 A92-32184
Shuttle autoland status summary
[AIAA PAPER 92-1273] p 666 A92-38478
Space Shuttle airframe inspection trend-analysis report p 759 A92-42052
Space Shuttle Orbiter auxiliary power unit status
[SAE PAPER 912060] p 889 A92-45442
A transonic/supersonic/hypersonic CFD analysis of the entry Space Shuttle Orbiter
[AIAA PAPER 92-2614] p 805 A92-45571
Characteristics of the Shuttle Orbiter leeside flow during a reentry condition
[AIAA PAPER 92-2951] p 821 A92-47915
Aerothermodynamic calculations for the Space Shuttle Orbiter
[AIAA PAPER 92-2953] p 821 A92-47917

Testing of the high accuracy inertial navigation system in the Shuttle Avionics Integration Lab
p 210 N92-14087
Space shuttle entry terminal area energy management
[NASA-TM-104744] p 308 N92-19930
Attributes of winged manned space vehicles and their relationship to ground site characteristics and facilities
p 487 N92-20776
A high angle of attack inviscid shuttle orbiter computation
[NASA-TM-107606] p 685 N92-25964

SPACE SHUTTLE PAYLOADS
Thermochemical nonequilibrium flow computations of flow around the aeroassist flight experiment
p 713 A92-44368

SPACE SHUTTLES
AI technology and application development on the Shuttle project p 302 A92-23693
Multizonal Navier-Stokes solutions for the multibody Space Shuttle configuration p 310 A92-24667
Never make the same mistake twice - Using configuration control and error analysis to improve software quality p 601 A92-33603
Space Shuttle shell structure waffle panel optimization
[AIAA PAPER 92-2359] p 586 A92-34591
A study of flow patterns and behaviours of 3D separated flow on a simplified Shuttle model p 615 A92-38906
Scale effects on the flow past the mated Space Shuttle configuration
[AIAA PAPER 92-2680] p 799 A92-45532
Three-dimensional optimal reentry trajectory and aerodynamic heating history of the Space Shuttle
p 984 A92-49582
STS-40 descent BET products: Development and results
[NASA-CR-189570] p 286 N92-16012
Results of the space shuttle vehicle ascent air data system probe calibration test using a 0.07-scale external tank forebody model (68T) in the AEDC 16-foot transonic wind tunnel (IA-310), volume 1
[NASA-CR-167696] p 286 N92-17167
Results of the space shuttle vehicle ascent air data system probe calibration test using a 0.07-scale external tank forebody model (68T) in the AEDC 16-foot transonic wind tunnel (IA-310), volume 2
[NASA-CR-167697] p 286 N92-17214
Two stage to orbit design
[NASA-CR-189994] p 575 N92-22625
Dynamics of aerospace shuttles p 667 N92-24760
In-flight simulation studies at the NASA Dryden Flight Research Facility
[NASA-TM-4396] p 853 N92-29110
Numerical methods for the simulation of complex multi-body flows with applications for the integrated Space Shuttle vehicle
[NASA-CR-190045] p 945 N92-30740
Numerical methods for the simulation of complex multi-body flows with applications for the integrated Space Shuttle vehicle p 945 N92-30741
Application of the Chimera overlapped grid scheme to simulation of Space Shuttle ascent flows
p 945 N92-30742

SPACE STATION FREEDOM
Structural design considerations for a Personnel Launch System p 386 A92-24668
Issues in developing control zones for international space operations p 1141 A92-56602
Advanced flight software reconfiguraton
p 287 N92-17350

SPACE STATIONS
Structural design considerations for a Personnel Launch System p 386 A92-24668
Issues in developing control zones for international space operations p 1141 A92-56602
Ames life science telescience testbed evaluation
[NASA-CR-188856] p 140 N92-12033

SPACE TRANSPORTATION
Saenger and the German Hypersonics Technology Programme - Status report 1991
[IAF PAPER 91-198] p 32 A92-12570
Structural design considerations for a Personnel Launch System p 386 A92-24668
An aerodynamic design study of a series of lifting bodies at angles of attack from 10 to 53 degrees at Mach numbers from 2.30 to 4.62 p 442 A92-32500
NASP - A status report
[AIAA PAPER 92-1417] p 666 A92-38569
Crew transportation for the 1990s. I - Commercializing manned flight with today's propulsion
p 889 A92-46726
IRS organigram p 33 N92-10053
Aerothermodynamics for United States advanced programs p 184 N92-15039
Saenger: The reference concept and its technological requirements - aerothermodynamics
[MBB-FE-202-S-PUB-0463-A] p 890 N92-29629
Technology programme: Aerothermodynamics and propulsion integration. Numerical and experimental aerothermodynamics
[MBB-FE-202-S-PUB-0464-A] p 831 N92-29648
Aerothermodynamics and propulsion integration in the Saenger technology programme
[MBB-FE-202-S-PUB-0469-A] p 831 N92-29649
Aerothermodynamic challenges of the Saenger space-transportation system
[MBB-FE-202-S-PUB-0462-A] p 890 N92-29680
Research and technology, 1991. Langley Research Center
[NASA-TM-4331] p 1013 N92-30733

SPACE TRANSPORTATION SYSTEM
Thermodynamic behaviour of hydrogen-powered hypersonic ramjets flying along ideal trajectories
[IAF PAPER 91-277] p 25 A92-12601
'Spaceplanes' R&D status of Japan
[AIAA PAPER 91-5002] p 209 A92-17802
Shuttle Entry Air Data System - An experimental investigation of calibration for ascent flight
[AIAA PAPER 92-0133] p 286 A92-23753
Optimization of two stage reusable space transportation systems with rocket and airbreathing propulsion concepts
[IAF PAPER 92-0863] p 1104 A92-57254
National Aeronautics and Space Administration
p 238 N92-14923
Aerothermodynamic challenges of the Saenger space-transportation system p 184 N92-15042

SPACE TRANSPORTATION SYSTEM FLIGHTS
STS-41 Space Shuttle mission report
[NASA-TM-105479] p 286 N92-16973
Performance of uncoated AFRSI blankets during multiple Space Shuttle flights
[NASA-TM-103892] p 890 N92-29104

SPACE WEAPONS
Experimentally supported investigations into the optical performance of multi-aperture window concepts
[AIAA PAPER 92-2781] p 778 A92-41324
Multiple aperture window and seeker concepts for endo KEW applications
[AIAA PAPER 92-2806] p 752 A92-41344
Transient aerodynamics of a high dynamic pressure shroud separation for a ground-based interceptor missile
[AIAA PAPER 92-2820] p 705 A92-41348

SPACEBORNE EXPERIMENTS
Shuttle Infrared Leeside Temperature Sensing (SILTS) experiment - STS-35 and STS-40 preliminary results
[AIAA PAPER 92-0126] p 286 A92-23746
Experiments on aeronautical satellite communications using ETS-V p 395 A92-26779
ACTS aeronautical experiments
[AIAA PAPER 92-2042] p 485 A92-29956

SPACECRAFT CHARGING
Ionospheric plasma flow over large high-voltage space platforms. I - Ion-plasma-time scale interactions of a plate at zero angle of attack. II - The formation and structure of plasma wake p 779 A92-41359
Direct simulation of re-entry flows with ionization
p 713 A92-44367

SPACECRAFT COMPONENTS
Tribology needs for future space and aeronautical systems
[NASA-TM-104525] p 214 N92-15191

SPACECRAFT CONFIGURATIONS
Multizonal Navier-Stokes solutions for the multibody Space Shuttle configuration p 310 A92-24667
Study of numerical computation of inviscid flow field about complex configuration of re-entry vehicle
p 313 A92-25041
A ballistic investigation of the aerodynamic characteristics of a blunt vehicle at hypersonic speeds in carbon dioxide and air
[AIAA PAPER 92-0328] p 322 A92-25775
Scale effects on the flow past the mated Space Shuttle configuration
[AIAA PAPER 92-2680] p 799 A92-45532
Aerodynamics of complex shape bodies within a wide range of supersonic flows of rarefied gases
p 939 A92-52767
Numerical simulation of hypersonic viscous flow for the design of H-2 orbiting plane (HOPE-2)
[NAL-TR-1093] p 11 N92-10009
Hypersonic configurations in slow speed flight
p 624 N92-24394

SPACECRAFT CONSTRUCTION MATERIALS
High temperature thermoplastic and polyimide processing using CARE-MOLD wash-out tooling
p 36 A92-10259
Solving the structures problem for hypersonic vehicles
p 209 A92-17349
Flight vehicles of the future p 419 A92-31525
Structures and materials technologies for hypersonic vehicles - Lessons from Hermes experience
[AIAA PAPER 91-5098] p 486 A92-31697
Structural materials for NASP
[AIAA PAPER 91-5101] p 486 A92-31698
Flight-vehicle materials, structures, and dynamics - Assessment and future directions. Vol. 3 - Ceramics and ceramic-matrix composites --- Book
[ISBN 0-7918-0661-8] p 668 A92-39852
Metal matrix composite fabrication processes for high performance aerospace structures p 760 A92-42145
Thermoviscoplastic response of Ti-15-3 under various loading conditions
[NASA-CR-187621] p 45 N92-11391
The IRS plasma wind tunnels for the investigation of thermal protection materials for reentry vehicles
p 208 N92-15009
Report on aerospace structures and structural materials R and D in Europe
[PB92-123553] p 550 N92-22785
Large thin composite thermostructural parts
p 576 N92-23821
Design challenges for the National Aero-Space Plane
p 551 N92-23822
The effect of jet fuel exposure on advanced aerospace composites. Part 1: Thermal and chemical analysis
[AD-A246559] p 756 N92-27531

SPACECRAFT CONTROL
Dynamics and control of hypersonic vehicles - The integration challenge for the 1990's
[AIAA PAPER 91-5057] p 203 A92-17840
Simulation of GRM drag compensation system --- Geopotential Research Mission p 285 A92-21023
A six-degree-of-freedom guidance and control analysis of Mars aerocapture
[AIAA PAPER 92-0736] p 486 A92-31676
A design of strongly stabilizing controller
[SAE PAPER 912081] p 917 A92-45456
Dynamics and control of hypersonic aeropropulsive/aeroelastic vehicles
[AIAA PAPER 92-4326] p 1073 A92-55170
Simulation requirements for RCS plume: Flowfield interaction modelling on a winged reentry vehicle
p 181 N92-14985
Advanced flight software reconfiguraton
p 287 N92-17350
Technical notes and correspondence: Stochastic robustness of linear time-invariant control systems
p 303 N92-18002
FALKE: Winged re-entry vehicle flight control
p 667 N92-24454
Description and simulation results of the Italsat AOCS advanced flight simulator p 667 N92-24472
Robust intelligent flight control for hypersonic vehicles
[NASA-CR-185680] p 746 N92-28209

SPACECRAFT DESIGN
Saenger and the German Hypersonics Technology Programme - Status report 1991
[IAF PAPER 91-198] p 32 A92-12570
The value of sub-scale flight tests in the development of NASP vehicles
[AIAA PAPER 91-5048] p 210 A92-17834
Dynamics and control of hypersonic vehicles - The integration challenge for the 1990's
[AIAA PAPER 91-5057] p 203 A92-17840
HOPE looks to CFD for help --- NASDA's H-II Orbiting Plane p 386 A92-24910
Acquisition of an aerothermodynamic data base by means of a winged experimental reentry vehicle
p 486 A92-30685
Simulation of hypersonic flows on unstructured grids
p 434 A92-31496
An aerodynamic design study of a series of lifting bodies at angles of attack from 10 to 53 degrees at Mach numbers from 2.30 to 4.62 p 442 A92-32500
The Delta Clipper dream p 574 A92-36127
The National Aerospace Plane program and the APL role p 666 A92-37375
On the application of parabolized Navier-Stokes equations to flow field simulations p 936 A92-51943
Spaceplane aerodynamic heating and thermal protection design method p 1102 A92-53578
Integrated system to support computer analysis in conceptual aerospace design p 1130 A92-53596
Optimization of a 2D scramjet-vehicle using CFD and simplified approximate flow analysis techniques
[AIAA PAPER 92-3673] p 1022 A92-54116
Prediction of forces and moments for hypersonic flight vehicle control effectors
[NASA-CR-188954] p 33 N92-11070
NASA reliability preferred practices for design and test
[NASA-TM-4322] p 157 N92-12286
Aerothermodynamics for United States advanced programs p 184 N92-15039
Evolution and development of hypersonic configurations 1958-1990
[AD-A242768] p 197 N92-15069
Scramjet analysis, testing p 475 N92-21532

System controls challenges of hypersonic combined-cycle engine powered vehicles
p 475 N92-21533
Conceptional design to heat-resistant airframe of HOPE p 575 N92-23820
Large thin composite thermostructural parts
p 576 N92-23821
Design challenges for the National Aero-Space Plane
p 551 N92-23822
Design of orbital re-entry experiment vehicle and outline of the experiment p 667 N92-25374
Computational Structures Technology for Airframes and Propulsion Systems
[NASA-CP-3142] p 683 N92-25911
Computational structures technology and UVA Center for CST p 683 N92-25912
Computer codes developed and under development at Lewis p 692 N92-25913
CSM activities at the NASA Langley Research Center
p 683 N92-25916
Rarefied-flow aerodynamics
[NASA-CR-190452] p 715 N92-27191
System requirements specification for SMART structures mode p 777 N92-27830
Surface generation and editing operations applied to structural support of aerospace vehicle fuselages
p 777 N92-27831

SPACECRAFT ELECTRONIC EQUIPMENT
Effects of ionizing and nonionizing radiation on aircraft
p 295 A92-23301
Next generation power electronics for space and aircraft. II - Packaging p 992 A92-50553

SPACECRAFT EQUIPMENT
Space Cryogenics Workshop, 10th, Cleveland, OH, June 18-20, 1991, Proceedings p 295 A92-23826
Force limited vibration testing p 595 N92-22688
Prototype instrumentation and design studies
[AD-A248378] p 736 N92-28004

SPACECRAFT GUIDANCE
Aerobrake guidance law synthesis using feedback linearization p 485 A92-29304
A six-degree-of-freedom guidance and control analysis of Mars aerocapture
[AIAA PAPER 92-0736] p 486 A92-31676
Trajectory control for a low-lift maneuverable reentry vehicle
[AIAA PAPER 92-1146] p 574 A92-33287
Aerospace plane guidance using time-scale decomposition and feedback linearization
p 984 A92-50498
A guidance law for hypersonic descent to a point
[AIAA PAPER 92-4303] p 1104 A92-55311
Testing of the high accuracy inertial navigation system in the Shuttle Avionics Integration Lab
p 210 N92-14087

SPACECRAFT LANDING
Landing spacecraft gently on earth - The Soviet parachute systems p 33 A92-13227
The differential algebraic approach in nonlinear dynamical feedback controlled landing maneuvers
p 574 A92-33639
Shuttle autoland status summary
[AIAA PAPER 92-1273] p 666 A92-38478
Attributes of winged manned space vehicles and their relationship to ground site characteristics and facilities
p 487 N92-20776

SPACECRAFT LAUNCHING
Expert knowledge techniques applied to the analysis of electric field mill data p 408 A92-27991

SPACECRAFT MAINTENANCE
Space Shuttle airframe inspection trend-analysis report p 759 A92-42052

SPACECRAFT MANEUVERS
Center of pressure calculations for a bent-axis vehicle
[AIAA PAPER 92-0168] p 254 A92-23779
Aerobrake guidance law synthesis using feedback linearization p 485 A92-29304
Aerobang - A new synergetic plane-change maneuver
[AAS PAPER 91-418] p 753 A92-43356
Rapid synthesis for evaluating missile maneuverability parameters
[AIAA PAPER 92-2615] p 873 A92-45488
An alternative concept for aeroassisted orbit transfers
[AD-A243409] p 287 N92-17325
Center of pressure calculations for a bent-axis vehicle
[DE92-005186] p 498 N92-20143

SPACECRAFT MODULES
Outline and discussion of the cooling loop of the heating control system in the exposed facility of the Japanese Experiment Module (JEM) p 574 A92-35610

SPACECRAFT MOTION
Simulation of GRM drag compensation system --- Geopotential Research Mission p 285 A92-21023

SPACECRAFT PERFORMANCE
Laboratory simulation of aerothermodynamic phenomena - A review
[AIAA PAPER 92-4025] p 1104 A92-56847

SPACECRAFT POWER SUPPLIES
Integration of artificial intelligence and numerical optimization techniques for the design of complex aerospace systems
[AIAA PAPER 92-1189] p 600 A92-33301

SPACECRAFT PROPULSION
Spaceplane system studies p 285 A92-22632
Mechanics and thermodynamics of propulsion (2nd revised and enlarged edition) --- Book
[ISBN 0-201-14659-2] p 672 A92-38275
Aerothermodynamics for Space Vehicles
[ESA-SP-318] p 180 N92-14973
Aerothermodynamic challenges of the Saenger space-transportation system p 184 N92-15042
A survey of instabilities within centrifugal pumps and concepts for improving the flow range of pumps in rocket engines
[NASA-TM-105439] p 387 N92-18280
H2 fueled flightweight ramjet construction and test
p 475 N92-21531
Scramjet analysis, testing p 475 N92-21532
System controls challenges of hypersonic combined-cycle engine powered vehicles
p 475 N92-21533
Symposium on High Speed Airbreathing Propulsion: The Solid Fuel Combustion Chamber and Beyond
[ETN-92-90685] p 575 N92-22268
High speed airbreathing propulsion in Europe
p 575 N92-22277
Saenger: The reference concept and its technological requirements - aerothermodynamics
[MBB-FE-202-S-PUB-0463-A] p 890 N92-29629
Technology programme: Aerothermodynamics and propulsion integration. Numerical and experimental aerothermodynamics
[MBB-FE-202-S-PUB-0464-A] p 831 N92-29648
Aerothermodynamics and propulsion integration in the Saenger technology programme
[MBB-FE-202-S-PUB-0469-A] p 831 N92-29649

SPACECRAFT REENTRY
Effects of shock wave precursors ahead of hypersonic entry vehicles p 441 A92-32182
Characteristics of the Shuttle Orbiter leeside flow during a reentry condition
[AIAA PAPER 92-2951] p 821 A92-47915
New hypersonic test methods developed at ONERA - The R5 and F4 wind tunnels
[ONERA, TP NO. 1992-39] p 882 A92-48600
Thermally and chemically nonequilibrium hypersonic flow in three-dimensional geometry
p 1019 A92-53580
Design of orbital re-entry experiment vehicle and outline of the experiment p 667 N92-25374
Analysis of spacecraft entry into Mars atmosphere
p 1105 N92-33763

SPACECRAFT SHIELDING
Thermal deformation of a polymer heat shield material on the descent trajectory p 754 A92-42655
The IRS plasma wind tunnels for the investigation of thermal protection materials for reentry vehicles
p 208 N92-15009

SPACECRAFT STABILITY
Developmental flight testing of a half scale unmanned air vehicle
[AD-A240347] p 22 N92-11002
On the stability of a dual spin satellite with asymmetric rotor and flexible platform
[ISBN-0-315-54650-6] p 753 N92-27613

SPACECRAFT STRUCTURES
Enhancement of modal swept sine data by control of exciting forces p 215 A92-17562
Computational structures technology
[AIAA PAPER 92-2442] p 585 A92-34473
Space Shuttle shell structure waffle panel optimization
[AIAA PAPER 92-2359] p 586 A92-34591
International Congress on Recent Developments in Air- and Structure-Borne Sound and Vibration, Auburn University, AL, Mar. 6-8, 1990, Proceedings. Vols. 1 & 2
p 924 A92-45876
Large thin composite thermostructural parts
p 576 N92-23821
Computational Structures Technology for Airframes and Propulsion Systems
[NASA-CP-3142] p 683 N92-25911
Computational structures technology and UVA Center for CST p 683 N92-25912
Computer codes developed and under development at Lewis p 692 N92-25913
A brief overview of computational structures technology related activities at NASA Lewis Research Center
p 683 N92-25915
CSM activities at the NASA Langley Research Center
p 683 N92-25916
Research and technology, 1991. Langley Research Center
[NASA-TM-4331] p 1013 N92-30733

SPACECRAFT TEMPERATURE
Shuttle Infrared Leeside Temperature Sensing (SILTS) experiment - STS-35 and STS-40 preliminary results
[AIAA PAPER 92-0126] p 286 A92-23746

SPACECRAFT TRAJECTORIES
Automated trajectory synthesis for hypersonic vehicles using energy management and variational calculus techniques p 210 A92-19061
On the skip flight of a spaceplane
p 387 A92-25503
Influence of atmospheric rarefaction on aerodynamic characteristics of flying vehicles p 938 A92-52750
The influence of a retarding rocket on parameter limits for reentry trajectories p 211 N92-15037
STS-40 descent BET products: Development and results
[NASA-CR-189570] p 286 N92-16012

SPACECREWS
Crew transportation for the 1990s. I - Commercializing manned flight with today's propulsion
p 889 A92-46726

SPANWISE BLOWING
An efficient upwind relaxation-sweeping algorithm for three-dimensional Navier-Stokes equations
[AIAA PAPER 92-0023] p 248 A92-22145
Navier-Stokes computation of wing leading edge tangential blowing for a tilt rotor in hover
[AIAA PAPER 92-2608] p 805 A92-45568
Exploratory investigation of a spanwise blowing concept for tip-stall control on cranked-arrow wings
[AIAA PAPER 92-2637] p 806 A92-45576
Assessment of potential aerodynamic benefits from spanwise blowing at the wing tip
[NASA-TM-107847] p 631 N92-25261

SPARE PARTS
Spares support of your Rotary-Wing Jenny
p 60 A92-14435

SPARK IGNITION
Current stabilizing of fastened composite joints to improve non-sparking lightning current performance
p 213 A92-20130

SPATIAL DISTRIBUTION
Effect of some load factors of bird impact on blade response p 371 A92-24740
Reference mode effect on the auditory display of aircraft bank angle
[AD-A247825] p 728 N92-27916

SPATIAL MARCHING
A spatial marching technique for the inviscid blunt body problem p 4 A92-10691
Three-dimensional space-marching algorithm on unstructured grids p 5 A92-11058
Three-dimensional thin-layer and space-marching Navier-Stokes computations using an implicit MUSCL approach - Comparison with experiments and Euler computations
[ONERA, TP NO. 1991-131] p 77 A92-16107
Conjugate conduction/convection/nucleate-boiling heat transfer with a high-speed boundary layer
[AIAA PAPER 91-5033] p 215 A92-17823
Inverse solution uniqueness and domain of existence for supersonic space marching applications
[AIAA PAPER 92-0028] p 248 A92-22150
Semi-inverse marching characteristics scheme for supersonic flows p 432 A92-31187
Prediction of inviscid supersonic/hypersonic aircraft flowfields p 810 A92-46785
Grid adaptation to multiple functions for applied aerodynamic analysis p 817 A92-47045
Marching with the parabolized Navier-Stokes equations. Problem 1: Numerical study of hypersonic viscous cone flow
[AERO-REPT-9007] p 344 N92-18231
Marching with the parabolized Navier-Stokes equations. Problem 2: Hypersonic viscous flow over a flat plate
[AERO-REPT-9008] p 345 N92-18232

SPATIAL RESOLUTION
Synthesis of the algorithm of a spatial-temporal discriminator and the potential accuracy of the velocity meter p 41 A92-12828
The application of high spectral and spatial resolution imaging spectrometers for locating downed aircraft
p 598 A92-35132
High spatial resolution measurements of ram accelerator gas dynamic phenomena
[AIAA PAPER 92-3244] p 903 A92-48844
Processing complexity of two approaches to object detection and recognition p 234 N92-14677

SPECIFIC HEAT
Users manual and modeling improvements for axial turbine design and performance computer code TD2-2
[NASA-CR-189118] p 716 N92-27376
SPECIFIC IMPULSE
Propulsion systems from takeoff to high-speed flight
p 889 A92-46428
Propulsion system performance and integration for high Mach air breathing flight p 862 A92-46429
Turbofan with a small bypass ratio for first stage of a two-stage to-orbit vehicle p 968 A92-49833
Conceptual design of scramjet engine
p 1065 A92-53490
Experiments and analysis concerning the use of external burning to reduce aerospace vehicle transonic drag
[NASA-TM-105397] p 279 N92-17546
SPECIFICATIONS
A methodology for software specification and development based on simulation p 135 N92-12458
Common avionics baseline: The product of the joint integrated avionics working group p 199 N92-14053
SPECIMEN GEOMETRY
KGR-1 thick adherend specimen evaluation for the determination of adhesive mechanical properties
p 994 A92-51513
SPECIMENS
Development of hardness cycles for fiber bound materials, using DSC: From laboratory specimens to complex high duty structural members
[MBB-Z-0409-91-PUB] p 987 N92-30969
SPECTRA
A parametric approach to spectrum development
p 360 N92-18578
SPECTRAL BANDS
Comparison of aircraft synthetic aperture radar and buoy spectra during NORCSEX '88 p 597 A92-34878
SPECTRAL CORRELATION
Transverse correlation of the spectral components of pressure fluctuations on a plate ahead of a step
p 426 A92-30187
SPECTRAL METHODS
Spectral solution of inviscid supersonic flows over wedges and axisymmetric cones p 524 A92-36359
Discrete modes and continuous spectra in supersonic boundary layers p 809 A92-46264
Experimental study of the equivalent sound source center of the propeller rotating noise
p 1011 A92-53257
Effects of spectrum variations on fatigue crack growth
p 1123 A92-57399
Inhomogeneous turbulence beyond spectral equilibria: Aeronautical applications
[ETN-92-90867] p 404 N92-19349
SPECTRAL RECONNAISSANCE
The imaging spectrometer p 599 N92-23387
SPECTRAL RESOLUTION
The application of high spectral and spatial resolution imaging spectrometers for locating downed aircraft
p 598 A92-35132
SPECTRAL SIGNATURES
A procedure for automated gas turbine blade fault identification based on spectral pattern analysis
[ASME PAPER 91-GT-259] p 151 A92-15661
Preliminary analysis of baseline vibration data from Allison T56-A-14LFE engine and reduction gearbox
[NRC-31578] p 130 N92-11999
SPECTROGRAMS
Spectrogram diagnosis of aircraft disasters
[SAE PAPER 912041] p 836 A92-45425
SPECTROSCOPY
In situ measurement of particle formation in heated jet fuels: A new application of photon correlation spectroscopy
[DE92-003641] p 488 N92-20132
SPECTRUM ANALYSIS
Preliminary analysis of baseline vibration data from Allison T56-A-14LFE engine and reduction gearbox
[NRC-31578] p 130 N92-11999
A sophisticated, multi-channel data acquisition and processing system for high frequency noise research
[NASA-CR-189137] p 696 N92-24688
Generation of spectra and stress histories for fatigue and damage tolerance analysis of fuselage repairs
[AD-A250390] p 854 N92-29180
A preliminary experimental investigation of local isotropy in high-Reynolds-number turbulence
p 912 N92-30042
Spectrum modal analysis for the detection of low-altitude windshear with airborne Doppler radar
[NASA-CR-4457] p 953 N92-31549
SPEED CONTROL
Multiaxis control in longitudinal mode of aircraft
p 1083 A92-56027
A note on thrust control for jetliner during approach
p 1053 A92-56061
Evaluation of advanced microwave landing system procedures in the New York terminal area
[DOT/FAA/ND-91/1] p 354 N92-18967
SPEED INDICATORS
Estimation of aircraft attitude by angular rate measurements p 963 N92-31881
SPHERES
An experimental study of the flow past spheres at transonic speeds and high Reynolds numbers
p 312 A92-25002
Hypersonic rarefied flow past spheres including wake structure
[AIAA PAPER 92-0495] p 329 A92-26325
Flow past a sphere - Topological transitions of the vorticity field p 330 A92-26410
SPHERICAL CAPS
Shock interaction induced by two hemisphere-cylinders
[SAE PAPER 912043] p 790 A92-45427
SPHERICAL COORDINATES
Direct-inverse transonic wing-design method in curvilinear coordinates including viscous interaction
p 193 A92-20202
Method of large particles in arbitrary curvilinear orthogonal coordinates for the solution of problems of hydro and aerodynamics p 937 A92-52035
Boundary layer flow in axial compressors (theoretical part)
[ETN-92-91008] p 502 N92-21234
Wall functions for the kappa-epsilon turbulence model in generalized nonorthogonal curvilinear coordinates
[NASA-CR-190368] p 685 N92-25962
SPHERICAL SHELLS
Nonstationary aerohydroelasticity of spherical bodies --- Russian book
[ISBN 5-02-014006-6] p 670 A92-36611
SPHEROMAKS
Experimental studies of compact toroids
[DE92-003469] p 512 N92-21046
SPILLING
Criteria for use of seal coats on airport pavements
[DOT/FAA/RD-92/18] p 1102 N92-34247
SPIN STABILIZATION
A multibody analog of the dual-spin problem
p 49 A92-11426
Model flight tests of a spin-resistant trainer configuration p 1054 A92-56158
On the stability of a dual spin satellite with asymmetric rotor and flexible platform
[ISBN-0-315-54650-6] p 753 N92-27613
SPIN TESTS
Analysis of the flight performance of the 155 mm M864 base burn projectile
[BRL-TR-3083] p 1041 N92-33699
SPLINE FUNCTIONS
A study of a version of the boundary conditions of a two-dimensional spline in surface and line modeling
p 163 A92-16826
Prediction of laminar boundary layer using cubic splines
[AIAA PAPER 92-2702] p 801 A92-45544
Parametric bicubic spline and CAD tools for complex targets shape modelling in physical optics radar cross section prediction p 403 N92-19151
PAN AIR: A computer program for predicting subsonic or supersonic linear potential flows about arbitrary configurations using a higher order panel method. Volume 1: Theory document (version 3.0)
[NASA-CR-3251] p 526 N92-22648
SPLIT FLAPS
Active control of the hydraulic forces of a body by a splitter plate p 591 A92-36351
Construction of a numerical optimization method for the definition of hypersupported profiles
[ONERA-RSF-43/1736-AY-146A] p 908 N92-28788
SPOILER SLOT AILERONS
Computer simulation of an unsteady flow around an airfoil with a spoiler p 710 A92-43167
SPOILERS
Aerodynamic performances of spoiler motion
p 429 A92-30526
Aeroelastic effects of spoiler surfaces on a low-aspect-ratio rectangular wing p 1030 A92-56154
Experimental investigation of transverse jet effects related to hypersonic space vehicles
p 182 N92-14995
Note on flight measured control effectiveness of the quiet STOL experimental aircraft ASKA
[NAL-TR-1103] p 746 N92-28154
Lift and rolling moment due to spoilers on wings with trailing-edge flaps deflected at subsonic speeds
[ESDU-92002-SUPPL] p 1037 N92-32782
SPRAY CHARACTERISTICS
Aerating fuel nozzle design influences on airflow features p 129 A92-17176
Factors influencing the effective spray cone angle of pressure-swirl atomizers p 295 A92-23300
The effect of droplet sizing uncertainty on ice accretions p 679 N92-24874
Spray nozzle for fire control
[CA-PATENT-APPL-SN-2-011-94] p 1125 N92-32856
SPRAY NOZZLES
Experimental investigation on the structure of flow field and the total pressure loss in an atomizing channel injector p 375 A92-28436
Spray nozzle for fire control
[CA-PATENT-APPL-SN-2-011-94] p 1125 N92-32856
SPRAYED COATINGS
Thermal barrier coatings for gas turbine use
p 142 A92-15245
SPRAYERS
Development and evaluation of an onboard aircraft cabin water spray system for postcrash fire protection
[SAE PAPER 912224] p 636 A92-40022
Onboard cabin water spray system under various discharge configurations
[DOT/FAA/CT-TN91/42] p 93 N92-13043
Effectiveness of an onboard water spray system during an oxygen enriched cabin fire
[DOT/FAA/CT-TN91/51] p 264 N92-17149
Fundamental studies on droplet interactions in dense sprays
[AD-A246918] p 770 N92-27546
SPRAYING
Interfacial instability between a liquid film and the surrounding compressible gas
[AIAA PAPER 92-0461] p 395 A92-26302
Current repair technologies for jet engine components
p 1016 A92-56085
SPREAD SPECTRUM TRANSMISSION
A robust filter configuration for DGPS users
p 101 A92-16967
Global Positioning System telecommand link
p 839 A92-47566
Programmable channelized digital radio/modem
p 955 A92-49291
SPRINGS (ELASTIC)
A study of the nonlinear stress-strain state of spring-type landing gear p 154 A92-16825
SPUTTERING
High temperature static strain gage development
[NASA-CR-189044] p 195 N92-14037
SQUALLS
Severe turbulence with a low-level jet ahead of a squall line p 407 A92-27939
SQUEEZE FILMS
Advanced multi-squeeze film dampers for rotor vibration control p 36 A92-10102
Experiments on the blade loss transient response of rotor with flexible damped support
[ASME PAPER 91-GT-149] p 148 A92-15587
Rotordynamic evaluation of an advanced multi-squeeze film damper - Imbalance response and bladeless simulation
[ASME PAPER 91-GT-242] p 149 A92-15647
A chambered porous damper for rotor vibration control. I - Concept development
[ASME PAPER 91-GT-244] p 150 A92-15649
Experimental and analytical investigation of hybrid squeeze film dampers
[ASME PAPER 91-GT-250] p 150 A92-15655
Experimental investigation on blade loss transient response of rotor with flexible damped support
p 557 A92-35551
Vibration control of rotor-bearing system by controlled squeeze-film damper bearings p 990 A92-49579
Transient response of the rotor-support system of aeroengines p 997 A92-53293
The effects of manufacturing tolerances on the vibration of aero-engine rotor-damper assemblies
p 222 N92-14349
The stability of the steady state and bistable response of a flexible rotor supported on squeeze film dampers
p 222 N92-14350
Stability of intershaft squeeze film dampers
p 222 N92-14351
SQUID (DETECTORS)
Development of an electromagnetic microscope for eddy current evaluation of materials
[AD-A242007] p 406 N92-19873
STABILITY
On the nonlinear stability of a high-speed, axisymmetric boundary layer p 78 A92-16457
Stabilized square parachute
[AD-D015014] p 90 N92-13036
On the instability of boundary layers on heated flat plates
[NASA-CR-187581] p 347 N92-19250
Nonlinear stability and control study of highly maneuverable high performance aircraft, phase 2
[NASA-CR-189911] p 382 N92-19841

An inviscid stability analysis of unbounded supersonic mixing layer flows p 443 N92-20332
Unsteady transonic aerodynamics of pointed bodies of revolution in supersonic freestream p 719 N92-27946

STABILITY AUGMENTATION
Roll-performance criteria for high augmented aircraft p 204 A92-18623
Robust flight control systems - A parameter space design p 976 A92-50503
Roll metrics for handling qualities - The landing approach p 976 A92-50520
C-17 flight control system overview p 1082 A92-55906
Flight-determined benefits of integrated flight-propulsion control systems
[NASA-TM-4393] p 742 N92-27587
Practical method's for robust multivariable control
[AD-A248473] p 1009 N92-30322

STABILITY DERIVATIVES
Comments on 'Fuzzy logic for control of roll and moment for a flexible wing aircraft' p 480 A92-30995
Calculation of rotational derivatives in the case of local interaction between flow and a body surface p 624 A92-40746
Estimation of spaceplane longitudinal stability and control derivatives from dynamic wind tunnel test p 752 A92-43211
Estimation of spaceplane lateral-directional stability and control derivatives from dynamic wind tunnel test
[SAE PAPER 911979] p 872 A92-45384
Symptom of payload-induced flight instability p 873 A92-46761
Calculation of the aerodynamic derivatives of aircraft in the supersonic region using the Mach box method p 875 A92-47779
Dynamic derivative data for high angle of attack simulation
[AIAA PAPER 92-4355] p 1079 A92-55341
Experimental study of an independently deflected wingtip mounted on a semispan wing
[NASA-TM-102842] p 13 N92-10983
On simple aerodynamic sensitivity derivatives for use in interdisciplinary optimization
[NASA-TM-104145] p 82 N92-11985
Short time force measurement system p 208 N92-15001
Identification of the stability and control derivatives of a DLC-flap system for VSRA
[NAL-TR-1116] p 283 N92-17917
Measurement of derivatives due to acceleration in heave and sideslip p 364 N92-18785
Dynamic wind tunnel tests on control of forebody vortices with suction p 380 N92-18793
Performance and stability analysis of the non-linear dynamics of a simple powered lifting hypersonic vehicle flying on a minor circle
[AD-A243933] p 366 N92-19192
A review of scale effects on surfaces in unsteady motion p 722 N92-27962
Simulation model of a twin-tail, high performance airplane
[NASA-TM-107601] p 1088 N92-33537

STABILITY TESTS
Computational analysis of inertial effects on the stability of an ACES-II ejection seat p 543 A92-35436
China's first variable stability aircraft: The BW-1-Gets its pre-acceptance flight tests
[AD-A240941] p 116 N92-13062
Performance and stability analysis of the non-linear dynamics of a simple powered lifting hypersonic vehicle flying on a minor circle
[AD-A243933] p 366 N92-19192
Nonlinear stability and control study of highly maneuverable high performance aircraft, phase 2
[NASA-CR-189911] p 382 N92-19841
Wind-tunnel investigation of aerodynamic and stability characteristics of a forward swept wing X-29 model p 627 N92-24862
Mechanical design of a rotary balance system for NASA. Langley Research Center's vertical spin tunnel p 664 N92-25090
Stability and control flight testing of a half-scale Pioneer remotely piloted vehicle
[AD-A245973] p 879 N92-28801
Nonlinear stability and control study of highly maneuverable high performance aircraft, phase 2
[NASA-CR-190667] p 978 N92-30922
Computation and stability analysis of laminar flow over a blunt cone in hypersonic flow p 1041 N92-33839

STABILIZATION
Aeroservoelastic stabilization techniques for hypersonic flight vehicles
[AIAA PAPER 91-5056] p 203 A92-17839
Active control of compressor surge and stall
[AD-A252771] p 1126 N92-33498

STABILIZERS (FLUID DYNAMICS)
The design and manufacture of an advanced thermoplastic horizontal stabilator for the AH-64A p 59 A92-14354
Formulation of a simplified model of rotor-horizontal stabilizer interactions and comparison with experimental measurements
[ONERA, TP NO. 1991-157] p 77 A92-16125
Selection of efficient primary-structure/force configurations for aircraft lifting surfaces subjected to displacement constraints p 458 A92-30140
Development of an advanced composite material on vertical stabilizer of F-X aircraft p 579 A92-32555
Flow over a twin-tailed aircraft at angle of attack. II - Temporal characteristics p 810 A92-46781
Tutor aft fuselage and empennage full-scale fatigue test: Resolution of horizontal stabilizer installation difficulties
[NRC-LTR-ST-1804] p 114 N92-11990
F/A-18 stabilator: Equivalent set of point forces required for pneumatic bag load case simulation
[AD-A242637] p 206 N92-15073
Longitudinal and lateral-directional aerodynamic characteristics of a wing-cone configuration at Mach numbers from 2.5 to 4.5
[NASA-TM-4337] p 630 N92-24977

STABLE OSCILLATIONS
A wing rock model for the F-14A aircraft
[AD-A243109] p 275 N92-17300

STACKS
Nickel hydrogen common pressure vessel battery development p 598 N92-22770

STAGE SEPARATION
A method for estimating the minimum distance between two flight vehicles during their separation p 486 A92-30139

STAGNATION FLOW
Stability of a nonorthogonal stagnation flow to three-dimensional disturbances p 495 A92-31194
Turbulent energy budgets in impinging zones p 620 A92-40081
Stability of plane nonorthogonal stagnation flow p 704 A92-41291

STAGNATION POINT
Recombination-dominated nonequilibrium heat transfer to arbitrarily catalytic hypersonic vehicles p 2 A92-10426
Influence of wing shapes on the surface pressure fluctuations of a wing-body junction
[AIAA PAPER 92-0433] p 327 A92-26280
Stability of a nonorthogonal stagnation flow to three-dimensional disturbances p 495 A92-31194
Earth atmospheric entry studies for manned Mars missions p 442 A92-32251
Multipoint inverse airfoil design method based on conformal mapping p 610 A92-36827
Stagnation point heat flux in hypersonic high enthalpy flow p 613 A92-38373
Earth aerobraking strategies for manned return from Mars p 752 A92-41535
Decoupled predictions of radiative heating in air using a particle simulation method
[AIAA PAPER 92-2971] p 816 A92-46986
One-dimensional kinetic model for flows near a stagnation point of a highly cooled body in hypersonic rarefied streams p 938 A92-52751
The high enthalpy shock tunnel in Goettingen
[AIAA PAPER 92-3942] p 1104 A92-56772
The effect of a type 3 and type 4 shock/shock interaction on heat transfer in the stagnation region p 160 N92-13867
Cases 6.1 and 6.8 double ellipsoid: Navier-Stokes calculation p 525 N92-22181
Simulation of the flow on a space glider. Stagnation point calculation using the 2D Navier-Stokes equations including chemical effects p 624 N92-24393
Observation and measurements of flow structures in the stagnation region of a wing-body junction p 714 N92-26616
Stagnation-point heat-transfer rate predictions at aeroassist flight conditions
[NASA-TP-3208] p 1001 N92-31281

STAGNATION PRESSURE
The effect of blade tip geometry on the tip leakage flow in axial turbine cascades
[ASME PAPER 91-GT-135] p 72 A92-15577
Combustion of solid fueled ramjet. II
[AIAA PAPER 92-3728] p 894 A92-49106
Structure of crossing-shock wave/turbulent boundary-layer interactions
[AIAA PAPER 92-3670] p 1022 A92-54113
The G-range impulse facility - A high-performance free-piston shock tunnel
[AIAA PAPER 92-3946] p 1097 A92-56774
Stagnation and dynamic pressure limits for the S1 wind tunnel
[AD-A242989] p 285 N92-17297

STAGNATION TEMPERATURE
A fine-wire thermocouple probe for measurement of stagnation temperatures in real gas hypersonic flows of nitrogen p 1114 A92-54317
High enthalpy testing in the Aachen (Fed. Republic of Germany) shock tunnel TH 2 p 208 N92-15021
Temperature effects in FFA HYP 500 at M = 7 in a flow with strong expansion
[FFA-TN-1991-27] p 443 N92-20229
An experimental investigation of a 2-D scramjet inlet at flow Mach numbers of 8 to 25 and stagnation temperatures of 800 to 4,100 K p 739 N92-26586
Turbine disk cavity aerodynamics and heat transfer p 1124 N92-32265

STAINLESS STEELS
Stainless steel welding shines through on wind tunnel project p 1123 A92-57039

STALLING
The F-18 high alpha research vehicle: A high-angle-of-attack testbed aircraft
[NASA-TM-104253] p 1060 N92-33404

STANDARD DEVIATION
Example of statistical techniques applied to autoland touchdown dispersion (confidence intervals for normal and skew distributions)
[ESDU-91019] p 268 N92-17844
Variability of standard aircraft performance parameters
[ESDU-91020] p 276 N92-17847

STANDARDIZATION
International standardisation of regulations for gust loading calculations p 270 A92-22473
Standardization of NATOPS emergency egress procedures --- Naval Air Training and Operating Procedures Standardization Program p 529 A92-32998
International standardization p 533 A92-33441
Avionics standardization in the USAF: 1980 to 1990 p 198 N92-14048
Historical perspective on the evolution of avionics standards p 198 N92-14049
Avionics standardization in Europe p 199 N92-14050
Common avionics baseline: The product of the joint integrated avionics working group p 199 N92-14053
Research, services, and facilities (National Institute of Standards and Technology)
[PB92-109172] p 485 N92-21870
Core avionics and standardization
[AD-A248326] p 735 N92-27925
Avionic data bus integration technology
[DOT/FAA/CT-91/19] p 736 N92-27973
PDES application protocol suite for composites (PAS-C). Functional needs report for the PAS-C program
[AD-A247886] p 1108 N92-32629
The need for GPS standardization p 1049 N92-33351

STANDARDS
Standard for aerodynamic decelerator and parachute drawings --- Book
[ISBN 0-930403-94-0] p 634 A92-38000
Interdependencies of aircraft-/airport-noise and urban- and regional-planning standards p 688 A92-39063
Joint Aviation Authorities: Development of an international standard for safety regulation - The first steps are being taken by the JAA p 781 A92-43548
Internationalization of telemetry systems p 920 A92-47535
Capacity as a consideration for providing aeronautical mobile satellite air traffic services in the U.S. domestic airspace p 956 A92-51007
Military and civil software standards and guidelines for guidance and control p 163 N92-12452
Historical perspective on the evolution of avionics standards p 198 N92-14049
Common avionics baseline: The product of the joint integrated avionics working group p 199 N92-14053
Propeller-driven-small airplane noise certification
[LR-650] p 237 N92-14798
Re-engining appears to offer best payback for young: Chapter 2 compliant aircraft
[PNR-90848] p 378 N92-19939
Criteria for the operation of federally-owned secondary calibration laboratories (ionizing radiation)
[PB92-112481] p 485 N92-21777
Research, services, and facilities (National Institute of Standards and Technology)
[PB92-109172] p 485 N92-21870
A TMS320-based modem for the aeronautical-satellite core data service p 594 N92-22562
Aeronautical mobile satellite service: An overview p 594 N92-22573
From IGES to STEP
[REPT-3.1.6] p 603 N92-23881
System considerations, projected requirements and applications for aeronautical mobile satellite communications for air traffic services p 677 N92-24163

STAR TRACKERS
Visual photometric experiment data processing system
[AD-A248657] p 729 N92-27964
STARS
Visual photometric experiment data processing system
[AD-A248657] p 729 N92-27964
STARTING
Fault diagnostics on jet engine starting
p 1116 A92-54345
STATE ESTIMATION
Observability analysis of piece-wise constant systems with application to inertial navigation p 49 A92-11391
On-line state estimation and parameter identification for flight p 50 A92-11429
An alternative derivation of the modified gain function of Song and Speyer p 232 A92-18464
Transonic aeroelasticity analysis using state-space unsteady aerodynamic modeling p 310 A92-24422
Robust flight reconstruction for helicopter simulation and training p 747 A92-41230
Estimation of aircraft inertial characteristics using maximum likelihood estimation p 1084 A92-56057
A physical approach to the estimation of aerodynamic characteristics from flight data p 1030 A92-56058
STATE VECTORS
Derivation of aircraft linear state equations from implicit nonlinear equations p 27 A92-11361
A study on the stability of aircraft at high angles-of-attack and state vector propagation sensitivity
p 978 A92-53394
STATIC AERODYNAMIC CHARACTERISTICS
Measurements of longitudinal static aerodynamic coefficients with cable mount system
p 1093 A92-56013
STATIC CHARACTERISTICS
Static aeroelastic analysis for generic configuration wing p 174 A92-20201
Experiment of static and dynamic characteristics of spiral grooved seals p 223 N92-14361
STATIC DEFORMATION
Nonlinear large amplitude aeroelastic behavior of composite rotor blades at large static deflection
[AIAA PAPER 92-2257] p 540 A92-34412
Static aeroelastic analysis of ACT wind tunnel model aircraft
[NAL-TM-624] p 632 N92-25366
STATIC ELECTRICITY
Nonlinear triggered lightning models for use in finite difference calculations p 230 A92-20128
Analysis and modeling of lightning strikes to the F106B, CVF580, and C160 aircraft p 186 A92-20129
Air cushion vehicle conductive/semiconductive flexible skirt, and method
[AD-D015160] p 400 N92-18187
STATIC LOADS
Structural optimization of a cantilevered beam subject to combined static loadings p 1118 A92-56024
Computational structures technology engine/airframe coupling p 649 N92-25935
STATIC PRESSURE
Probe systems for static pressure and cross-stream turbulence intensity p 10 A92-13211
Three-dimensional singularity of flow structure in an underexpanded supersonic jet p 78 A92-16679
Correction of sideslip-induced static pressure errors in flight-test measurements p 309 A92-24416
The unsteady flow characteristics of an S-shaped inlet at high incidence p 339 A92-27905
Paint under pressure p 399 A92-28495
A computational study of flow past bodies and heat transfer for isentropic compression flows
p 425 A92-30158
Study on nozzle flow diffusion p 429 A92-30531
Structure of a boundary layer on the lower surface of a wing in flight and in a wind tunnel p 440 A92-31899
Description of a pressure measurement technique for obtaining surface static pressures of a radial turbine
[AIAA PAPER 92-4006] p 1123 A92-56829
Aerodynamic coefficients of a symmetrical airfoil in an oscillating flow
[AD-A241073] p 89 N92-13035
A wall interference assessment/correction system
[NASA-CR-189785] p 259 N92-15974
Experimental investigation into the effects of riblets on compressor cascade performance
[AD-A243881] p 377 N92-19235
The problem of static pressure measurement in turbomachinery annuli using traversable instrumentation
[PNR-90791] p 591 N92-22099
Development of wall pressure measuring apparatus for an existing transonic wind tunnel test section
[NAL-TM-565] p 573 N92-23778
Description of a pressure measurement technique for obtaining surface static pressures of a radial turbine
[NASA-TM-105643] p 680 N92-24959
STATIC STABILITY
Main concepts of providing the static/fatigue strength of helicopters in the USSR p 110 A92-14455
Regulation of relaxed static stability aircraft
p 203 A92-18463
Evaluation method of longitudinal static stability of tailless airplane p 282 A92-22520
A procedure for calculating the static aeroelasticity characteristics of flight vehicles by the influence coefficient method using three-dimensional finite element schemes
p 460 A92-31896
Static and dynamic flight-path stability of airplanes
p 977 A92-52043
Flight testing of a half-scale remotely piloted vehicle
[AD-A248568] p 733 N92-28123
Stability and control flight testing of a half-scale Pioneer remotely piloted vehicle
[AD-A245973] p 879 N92-28801
Calculation of support interferences on the aerodynamic coefficients for a wind tunnel calibration model
[ESA-TT-1247] p 830 N92-29159
STATIC TESTS
Modification of the radiated sound directivity due to ground reflections - Application to static tests of helicopter turboshaft engines
[ONERA, TP NO. 1991-210] p 415 A92-26362
Static tests for the evaluation of fuel additives
[AIAA PAPER 92-0686] p 389 A92-27053
Structural testing of commercial rotorcraft seats - An overview p 544 A92-35437
Development of pitot static flightline testing
p 556 A92-35953
Strength evaluation and safety of machine/structure. III - Case examples on strength and safety evaluation of machine/structure 3.2 aircraft (airframe)
p 882 A92-47303
Scale model test results of a multi-slotted vectoring 2DCD ejector nozzle
[AIAA PAPER 92-3264] p 864 A92-48859
Methodology for assessment of skin repairs on Airbus aircraft p 226 N92-14428
Modification of Jindivik air intake duct with an auxiliary intake static aerodynamic tests
[AD-A243002] p 275 N92-17234
Proposal for the new fatigue management system for the AMX p 361 N92-18580
Wind-tunnel static and free-flight investigation of high-angle-of-attack stability and control characteristics of a model of the EA-6B airplane
[NASA-TP-3194] p 631 N92-25276
A static investigation of the thrust vectoring system of the F/A-18 high-alpha research vehicle
[NASA-TM-4359] p 633 N92-25967
Properties of a TZP/Al2O3 composite after long-term exposure at 1000 C
[AD-A246407] p 757 N92-27752
Global positioning system runway incursion program static ground tests
[DOT/FAA/CT-TN91/44] p 957 N92-31838
STATIC THRUST
Experience in the operation of a hypersonic nozzle static thrust stand
[AIAA PAPER 92-3292] p 882 A92-48881
STATICS
Water tunnel flow visualization studies of a canard-configured X-31A-like fighter aircraft model
[AD-A241362] p 90 N92-13037
STATISTICAL ANALYSIS
Safe life reliability - Evaluation of new statistical methods p 104 A92-14343
The statistical estimation of navigation errors
p 97 A92-16652
Statistical analysis and prediction of aeroengine deterioration p 557 A92-35570
Review of aviation record p 634 A92-39302
Statistical analysis of field data for aircraft warranties
p 760 A92-42077
Aircraft accidents and human factors
p 723 A92-43219
Statistical prediction of maximum buffet loads on the F/A-18 vertical fin p 811 A92-46816
Development of an uncertainty methodology for multiple-channel instrumentation systems
[AIAA PAPER 92-3953] p 1133 A92-56781
Airport activity statistics of certificated route air carriers: Calendar year 1990
[AD-A241483] p 93 N92-13045
Study of the engine bird ingestion experience of the Boeing 737 aircraft
[DOT/FAA/CT-89/16] p 187 N92-15053
Example of statistical techniques applied to cruise performance guarantees (Student's t distribution)
[ESDU-91018] p 276 N92-17843
Example of statistical techniques applied to autoland touchdown dispersion (confidence intervals for normal and skew distributions)
[ESDU-91019] p 268 N92-17844
Statistical methods applicable to analysis of aircraft performance data
[ESDU-91017] p 359 N92-18096
A probabilistic procedure for aircraft fleet management
p 360 N92-18576
The application of statistical estimation techniques to terrain modeling
[AD-A243799] p 409 N92-19231
Application of analysis techniques for low frequency interior noise and vibration of commercial aircraft
[NASA-CR-189555] p 481 N92-20376
Flowfield in the vicinity of the F/A-18 vertical fin at high-angle-of-attack p 628 N92-24865
Atmospheric turbulence spectra and correlation functions
[NLR-TP-89217-U] p 915 N92-28689
Statistics on aircraft gas turbine engine rotor failures that occurred in US commercial aviation during 1989
[DOT/FAA/CT-92/5] p 971 N92-30303
Development statistics for the UH-1 Ada feasibility study
[AD-A252404] p 982 N92-30547
Use of SEA to predict structure-borne noise in aircraft
p 1137 N92-32955
Experimental study of performance degradation of a rotating system in the NASA Lewis RC icing tunnel
[NASA-CR-190684] p 1102 N92-34141
Engine bird ingestion experience of the Boeing 737 aircraft: Expanded data base
[DOT/FAA/CT-91/32] p 1045 N92-34151
STATISTICAL DISTRIBUTIONS
Distribution of maximum levels of aircraft noise around their mean value p 693 A92-39062
Example of statistical techniques applied to cruise performance guarantees (Student's t distribution)
[ESDU-91018] p 276 N92-17843
STATISTICAL TESTS
Example of statistical techniques applied to autoland touchdown dispersion (confidence intervals for normal and skew distributions)
[ESDU-91019] p 268 N92-17844
STATISTICAL WEATHER FORECASTING
Predicting summer microburst hazard from thunderstorm day statistics p 407 A92-27960
STATISTICS
General aviation activity and avionics survey, calendar year 1989
[PB91-179234] p 169 N92-13926
FAA statistical handbook of aviation: Calendar year 1989
[PB91-202051] p 170 N92-13927
STATOR BLADES
Stator averaged, rotor blade-to-blade near wall flow in a multistage axial compressor with tip clearance variation
[ASME PAPER 91-GT-30] p 67 A92-15514
Performance of radial clearance rim seals in upstream and downstream rotor-stator wheelspaces
[ASME PAPER 91-GT-32] p 147 A92-15516
Rim sealing of rotor-stator wheelspaces in the absence of external flow
[ASME PAPER 91-GT-33] p 147 A92-15517
A 3D FEM variational aerodynamic calculation and performance analysis of a leaned turbine stator cascade
[ASME PAPER 91-GT-79] p 69 A92-15548
Vibration analysis of gas turbines by an intelligent knowledge-based system p 656 A92-40548
Vane-blade interaction in a transonic turbine. II - Heat transfer
[AIAA PAPER 92-3324] p 904 A92-48907
Unsteady flows in rotor-stator cascades
[AD-A241593] p 158 N92-13410
Experimental investigation of trailing edge crenulation effects on losses in a compressor cascade
[AD-A243902] p 377 N92-19329
Design and performance of controlled-diffusion stator compared with original double-circular-arc stator
[NASA-TP-2852] p 562 N92-22863
STATORS
Effects of stator wakes and spanwise nonuniform inlet conditions on the rotor flow of an axial turbine stage
[ASME PAPER 91-GT-93] p 70 A92-15557
Supersonic stator-rotor interaction in a turbine stage
[ONERA, TP NO. 1991-166] p 77 A92-16133
Comparison between two 3D-NS-codes and experiment on a turbine stator
[AIAA PAPER 92-3042] p 822 A92-48703
Airfoil wake and linear theory gust response including sub and superresonant flow conditions
[AIAA PAPER 92-3074] p 823 A92-48724

Rub induced rotor/stator vibration analysis on CF700 engine
[NRC-TR-ENG-007] p 202 N92-14060
Rotor-to-stator partial rubbing and its effects on rotor dynamic response p 224 N92-14367
Design and performance of controlled-diffusion stator compared with original double-circular-arc stator
[NASA-TP-2852] p 562 N92-22863
Computations of unsteady multistage turbomachinery flows p 562 N92-23671
Characterization of superconducting magnetic bearings (dynamic stiffness and damping coefficient in axial direction) p 772 N92-27737
Investigation of the flight control requirements of a half-scale ducted fan unmanned aerial vehicle
[AD-A252730] p 1087 N92-32988
An investigation of switched reluctance rotor position estimation using neural networks
[AD-A252846] p 1061 N92-33414

STEADY FLOW
Computation of steady and unsteady control surface loads in transonic flow p 5 A92-11066
Topology of steady flows of low viscosity fluids p 38 A92-11219
Numerical solution of steady incompressible viscous flows over airfoils p 8 A92-12649
Three dimensional analysis of a rotor in forward flight p 64 A92-14329
A calculation procedure for three-dimensional turbulent flow in a centrifugal impeller with any blade geometry
[ASME PAPER 91-GT-171] p 73 A92-15606
Solution of the compressible Euler equations for steady flows around helicopter rotor blades by an implicit space-centered method
[ONERA, TP NO. 1991-177] p 77 A92-16139
Prediction of steady and unsteady asymmetric vortical flows around circular cones p 172 A92-18372
Numerical calculation of subsonic and supersonic aerodynamic loads around complex configuration vehicle p 175 A92-20488
Nonequilibrium hypersonic inviscid steady flows p 176 A92-20737
Steady supersonic and hypersonic flow computations using Eulerian and new Lagrangian formulations
[AIAA PAPER 92-0055] p 249 A92-22170
A simplified method for simulating steady, unsteady flow around canard wing configuration p 311 A92-24876
Multidomain spectral solutions of high-speed flows over *blunt cones*
[AIAA PAPER 92-0324] p 322 A92-25771
Prandtl-Meyer function for dense gases p 415 A92-26441
Solution of the Euler and Navier-Stokes equations on MIMD distributed memory multiprocessors using cyclic reduction
[AIAA PAPER 92-0561] p 411 A92-26970
Boundary singularities in steady potential compressible flow through plane two-dimensional channels p 336 A92-27384
Numerical experiments on a new class of nonoscillatory schemes
[AIAA PAPER 92-0421] p 341 A92-28193
Heat transfer effects on aerodynamics and implications for wind-tunnel tests p 497 A92-32240
Complete Euler-solution for a rotor in hover and a propeller in forward flight p 520 A92-35755
Locally implicit hybrid algorithm for steady and unsteady viscous flows p 610 A92-36836
Measurements and simulation of the flow around a poppet valve p 675 A92-40103
Prediction of vortex shedding from forebodies with chines p 702 A92-41228
Subcritical flow studies on two-dimensional external compression supersonic inlets p 713 A92-44518
A nonlinear relaxation/quasi-Newton algorithm for the compressible Navier-Stokes equations
[AIAA PAPER 92-2643] p 796 A92-45510
Visualization of stopping flow over airfoils
[AIAA PAPER 92-2730] p 804 A92-45564
Some exact and numerical results for plane steady sheared flow of an incompressible inviscid fluid p 821 A92-48019
Pulse jet one-way valve performance
[AIAA PAPER 92-3169] p 863 A92-48790
A complete boundary integral formulation for steady *compressible inviscid flows governed by nonlinear* equations p 934 A92-50211
Supersonic flow past pointed-nose thin airfoils p 940 A92-52844
Solution of Euler equations with unstructured mesh - 3-D case p 941 A92-52973
Unsteady shock propagation in a steady flow nozzle expansion p 1023 A92-54489
Efficient iterative methods for the transonic small disturbance equation p 1025 A92-54933
Increasing the accuracy of the Godunov scheme for calculating steady-state supersonic gas flows by solving the generalized Riemann problem p 1035 A92-57499
Steady flow of a fluid-solid mixture in a circular cylinder
[DE91-018698] p 41 N92-10174
Flow around two circular cylinders arranged perpendicular to each other
[PB91-238279] p 297 N92-16225
Application of program LAURA to perfect gas shock tube flows: A parametric study
[NASA-TM-104190] p 298 N92-17002
CAR 88: A method to calculate subsonic and supersonic, steady and unsteady, potential flow about complex configurations
[NLR-TR-88154-U] p 400 N92-18221
Active control of the flow past a cylinder executing rotary motions p 349 N92-19623
Development of a steady potential solver for use with linearized, unsteady aerodynamic analyses
[NASA-TM-105288] p 473 N92-20525
Unsteady-pressure and dynamic-deflection measurements on an aeroelastic supercritical wing
[NASA-TM-4278] p 445 N92-20654
Prediction and analysis of wing flutter at transonic speeds p 662 N92-25555
An outline of a numerical scheme for calculating two-dimensional time linearised transonic flow using the Green's function method
[AD-A246349] p 764 N92-26258
Steady and unsteady 3D flow computation through a transonic turbine stage p 742 N92-27469
A computational investigation of airfoil stall flutter
[AD-A247302] p 947 N92-31300

STEADY STATE
Accelerated convergence to steady state by gradual far-field damping p 610 A92-36835
A fast, implicit unstructured-mesh Euler method
[AIAA PAPER 92-2693] p 917 A92-45589
Scoping studies for small steady-state tokamaks for divertor testing
[DE92-000740] p 238 N92-15761
Engine performance and health monitoring models using steady state and transient prediction methods p 870 N92-28467
Finite difference time domain modeling of steady state scattering from jet engines with moving turbine blades
[NASA-CR-190290] p 971 N92-30753
Steady state risetimes of shock waves in the atmosphere p 1140 N92-33882

STEAM FLOW
Two-phase flows at supersonic velocities p 4 A92-10907
Estimation of the size of separation zone in a turbine stage under small load p 10 A92-13235
Pulsation characteristics of one-phase and two-phase steam flows in Laval nozzles under off-design conditions p 1019 A92-53882

STEAM TURBINES
General performance characteristics of real heat engine p 1011 A92-50401
Field telemetry of blade-rotor coupled torsional vibration at Matuura Power Station Number 1 unit p 222 N92-14348

STEELS
Steels for aerospace applications p 986 A92-52983
Surface residual stress analysis of metals and alloys
[AD-A248372] p 895 N92-28426

STEEPEST DESCENT METHOD
Airfoil optimization with efficient gradient calculations p 177 N92-13960

STEERABLE ANTENNAS
The B-2 radar p 956 A92-53102
Electronically steerable antenna for aircraft p 229 N92-15272
DRES unmanned aerial vehicle data link research
[AD-A244272] p 365 N92-19030
A high gain antenna system for airborne satellite communication applications p 677 N92-24096
Low cost, electronically steered phased array for general aviation p 677 N92-24099

STEERING
Multiple input sliding mode control for autonomous diving and steering of underwater vehicles
[AD-A241935] p 283 N92-17442
Evaluation of GPS/UTC steering performance p 1049 N92-33353

STELLAR EVOLUTION
JPRS report: Science and technology. Central Eurasia: Space
[JPRS-USP-92-002] p 575 N92-23705

STEREOSCOPIC VISION
Vision-based stereo ranging as an optimal control problem
[AIAA PAPER 92-4418] p 1045 A92-55211
Effect of short-term exposure to stereoscopic three-dimensional flight displays on real-world depth perception
[NASA-TP-3117] p 119 N92-13065

STEREOSCOPY
Computational algorithms for increased control of depth-viewing volume for stereo three-dimensional graphic displays
[NASA-TM-4379] p 1065 N92-34109

STIFFENING
Representation of geometric stiffening in multibody system simulation p 217 A92-19463
Coupled 2D-3D finite element method for analysis of a skin panel with a discontinuous stiffener
[AIAA PAPER 92-2474] p 583 A92-34363

STIFFNESS
Gust effects on a flexible aircraft p 270 A92-22474
Design, analysis, and testing of integrally stiffened composite centre fuselage skin for future fighter aircraft p 535 A92-32554
Variable impedance journal bearings for rotor-bearing systems p 157 N92-12270
An experimental study of the sensitivity of helicopter rotor blade tracking to root pitch adjustment in hover
[NASA-TM-4313] p 61 N92-12989
Industrial code development p 227 N92-15083
Design, analysis, and testing of integrally stiffened composite centre fuselage skin for future fighter aircraft
[MBB-FE2-PUB-S-450] p 359 N92-18333
Performance tests of a cryogenic hybrid magnetic bearing for turbopumps
[NASA-TM-105627] p 473 N92-20523
In-service evaluation of 2090 aluminum-lithium alloy on F/A-18 aircraft
[AD-A248472] p 986 N92-30321
Time simulation of flutter with large stiffness changes
[NASA-TM-107650] p 963 N92-32111

STIFFNESS MATRIX
Mechanics of curved fiber composites p 140 A92-14346
Application of composite rotor blade stability analysis to extension-twist coupled blades
[AIAA PAPER 92-2254] p 564 A92-34479
A dynamic stiffness technique for the vibration analysis of stiffened shell structures p 1123 A92-56866

STIRLING CYCLE
Computer simulation model for Lucas Stirling refrigerators p 296 A92-23837
Heavy duty transport research needs assessment
[DE92-010622] p 767 N92-27394

STIRLING ENGINES
Pressurization effects in kinematic heat engines p 696 A92-40866
Reduction of torque pulsation of Stirling engine-compressor system p 992 A92-50785
Lower-end dynamic characteristics of a magnetically coupled free-piston Stirling engine/compressor system p 992 A92-50795
Proof of concept of a magnetically coupled Stirling engine-driven heat pump
[DE92-017129] p 1129 N92-33271

STOCHASTIC PROCESSES
Stochastic ordering properties and optimal routing control for a class of finite capacity queueing systems p 48 A92-11375
Stochastic prediction techniques for wind shear hazard assessment p 48 A92-11381
Application of stochastic robustness to aircraft control systems p 204 A92-18620
A stochastic regulator for integrated communication and control systems. I - Formulation of control law. II - Numerical analysis and simulation p 233 A92-19605
Estimating the probability of a safe flight for an aircraft flying under the effect of disturbances p 479 A92-30132
Synthesis of optimal digital systems for the stabilization *of stochastically perturbed unstable dynamic systems* p 601 A92-33754
Determining design gust loads for nonlinear aircraft similarity between methods based on matched filter theory and on stochastic simulation
[AIAA PAPER 92-2369] p 518 A92-34597
Robust frequency design of linear stationary systems in aeroautoelastics p 690 A92-37791
Robust wind shear stochastic controller-estimator p 661 A92-39893
Reliability centered maintenance for metallic airframes based on a stochastic crack growth approach p 897 A92-45242
Stochastic prediction techniques for wind shear hazard assessment p 1007 A92-50505
Numerical simulation of VAWT stochastic aerodynamic loads produced by atmospheric turbulence: VAWT-SAL code
[DE92-000597] p 229 N92-15392

Technical notes and correspondence: Stochastic robustness of linear time-invariant control systems p 303 N92-18002
Studies in chaos using stochastic methods [AD-A246919] p 780 N92-27171

STOKES FLOW
Stokes flows in superposed immiscible liquids with horizontal heating [IAF PAPER 92-0909] p 1123 A92-57288

STORAGE TANKS
Replacement of the NAL high pressure air storage system [NAL-TM-634] p 888 N92-28835

STORMS
The 1990 Airport Surveillance Radar Wind Shear Processor (ASR-WSP) operational test at Orlando International Airport [AD-A239852] p 18 N92-10019

STORMS (METEOROLOGY)
Lightning activity in microburst producing storm cells [ONERA, TP NO. 1991-98] p 161 A92-16080
The 1988 Australian Winter Storms Experiment - Case study: 6 August 1988 p 301 A92-23009
Three-dimensional simulation of the Denver 11 July Storm of 1988 - An intense microburst event p 407 A92-27958

STOVL AIRCRAFT
The selective bleed variable cycle engine --- aircraft propulsion [ASME PAPER 91-GT-388] p 126 A92-15720
Hot gas environment around STOVL aircraft in ground proximity. II - Numerical study p 371 A92-24403
Acoustic characteristics and dynamic structural loading of an ASTOVL aircraft in hover [AIAA PAPER 92-0370] p 416 A92-28190
Calculations of hot gas ingestion for a STOVL aircraft model [AIAA PAPER 92-0385] p 374 A92-28191
Integrated flight/propulsion control specifications for systems with two-way coupling p 477 A92-29117
Decentralized hierarchical partitioning of centralized integrated controllers --- for flight propulsion in STOVLs p 477 A92-29119
Recent research into the aerodynamics of ASTOVL aircraft in ground environment p 623 A92-40549
International Powered Lift Conference, London, England, Aug, 29-31, 1990, Proceedings [ISBN 0-903409-68-2] p 783 A92-45302
Current technology propulsion systems meet the STOVL window of opportunity p 860 A92-45307
ASTOVL flexibility in the 21st century p 783 A92-45309
A USAF assessment of STOVL fighter options p 842 A92-45310
ASTOVL propulsion systems configuration and concept choice p 842 A92-45312
Large-scale wind tunnel studies of a jet-engined powered ejector-lift STOVL aircraft p 842 A92-45313
Hot gas ingestion characteristics and flow visualization of a vectored thrust STOVL concept p 860 A92-45316
Hot-gas reingestion - Engine response considerations p 860 A92-45317
Prediction and measurement of jet flowfield features for ASTOVL aircraft p 787 A92-45318
A progress report on ASTOVL control concept studies under the VAAC programme p 871 A92-45319
Integrated flight/propulsion control for supersonic STOVL aircraft p 872 A92-45320
ASTOVL engine control p 860 A92-45321
Integrated flight control systems - Architectural considerations for future aircraft concepts p 872 A92-45322
Ground surface erosion - British Aerospace test facility and experimental studies p 881 A92-45323
Aerodynamic performance of a full-scale lifting ejector system in a STOVL fighter aircraft [AIAA PAPER 92-3094] p 824 A92-48738
Preliminary dynamic tests of a flight-type ejector [AIAA PAPER 92-3261] p 1066 A92-54020
Propulsion system performance resulting from an Integrated Flight/Propulsion Control design [AIAA PAPER 92-4602] p 1069 A92-55281
Calculations of hot gas ingestion for a STOVL aircraft model [NASA-TM-105437] p 350 N92-19993
Supersonic STOVL propulsion technology program: An overview p 561 N92-22539
Preliminary dynamic tests of a flight-type ejector [NASA-TM-105814] p 972 N92-30998
Ski jump takeoff performance predictions for a mixed-flow, remote-lift STOVL aircraft [NASA-TM-103866] p 1060 N92-32887
Dynamic response of induced pressures, suckdown, and temperatures for two tandem jet STOVL configurations [NASA-TM-103934] p 1039 N92-33581

STRAIN DISTRIBUTION
Static aeroelastic control using strain actuated adaptive structures p 26 A92-11122
Experimental and analytical study of the effects of floor location on response of composite fuselage frames [AIAA PAPER 92-2473] p 539 A92-34362
Experimental study of a vortex subjected to imposed strain [NASA-CR-189757] p 258 N92-15969

STRAIN ENERGY RELEASE RATE
Effects of T-tabs and large deflections in double cantilever beam specimen tests p 673 A92-39009

STRAIN GAGE BALANCES
The cryogenic balance design and balance calibration methods [AIAA PAPER 92-4001] p 1122 A92-56824
Dual strain gage balance system for measuring light loads [NASA-CASE-LAR-14419-1] p 42 N92-10185
Studies in general aviation aerodynamics [NASA-CR-190431] p 827 N92-28511

STRAIN GAGES
Force measurement on rotating, ablating models using an air bearing balance p 483 A92-31174
A flutter suppression system using strain gages applied to Active Flexible Wing Technology - Design and test [AIAA PAPER 92-2098] p 566 A92-35669
High temperature static strain gage development [NASA-CR-189044] p 195 N92-14037
A comparison of spanwise aerodynamic loads estimated from measured bending moments versus direct pressure measurements on horizontal axis wind turbine blades [DE92-001158] p 301 N92-16458
Proposal for the new fatigue management system for the AMX p 361 N92-18580
Aircraft tracking for structural fatigue p 361 N92-18584
The Operational Loads Monitoring System, OLMS p 361 N92-18586
High temperature strain gage technology for hypersonic aircraft development applications [NASA-CR-189101] p 592 N92-22239

STRAIN MEASUREMENT
Fabry-Perot fiber-optic sensors in full-scale fatigue testing on an F-15 aircraft p 391 A92-24553
The detection of damage and the measurement of strain within composites by means of embedded optical fiber sensors p 491 A92-28669
Smart structures - A damage detection concept p 491 A92-28672
The Operational Loads Monitoring System, OLMS p 361 N92-18586
High temperature strain gage technology for hypersonic aircraft development applications [NASA-CR-189101] p 592 N92-22239
Research sensors p 594 N92-22526
Electro optical system to measure strains at high temperature [NASA-CR-190450] p 1127 N92-33696

STRAIN RATE
Limitations to the large strain theory p 219 A92-20356

STRAKES
Forebody vortex control with miniature, rotatable nose-boom strakes [AIAA PAPER 92-0022] p 281 A92-22144
A numerical investigation of vortex flow control through small geometry modifications at the strake/wing junction of a cropped double-delta wing [AIAA PAPER 92-0411] p 435 A92-31661
An experimental investigation of the effect of leading-edge extensions on directional stability and the effectiveness of forebody nose strakes [AIAA PAPER 92-2715] p 802 A92-45554
Forebody vortex control using small, rotatable strakes p 811 A92-46798
Experimental investigation of the effects of blowing on bursting of strake vortices [AD-A240256] p 13 N92-10985
Steady and unsteady aerodynamics of a pitching straked wing model at high angles of attack p 87 N92-13024
Analysis of unsteady force, pressure, and flow-visualization data for a pitching straked wing model at high angles of attack p 364 N92-18784
Helicopter low-speed yaw control [NASA-CASE-LAR-14219-1] p 879 N92-30025

STRANGE ATTRACTORS
A double chaotic attractor in transonic flow p 1019 A92-53561

STRAPDOWN INERTIAL GUIDANCE
The study of constant value thresholds of FDI in strapdown inertial navigation p 267 A92-22087
Navigation and flight management systems - Thoughts of a user p 354 A92-26848
Inertial reference units with integrated air speed determination for helicopters p 554 A92-35764
Flight test data analysis of a low cost GPS/IMU integrated navigation system p 638 A92-39560
Wideband control of gyro/accelerometer multisensors in a strapdown guidance system p 856 A92-46736

STRAPS
Tear straps in airplane fuselage [AD-A248543] p 854 N92-29511

STRATIFIED FLOW
Stratified flow around an axisymmetric body at small angle of attack p 172 A92-18385

STRATOCUMULUS CLOUDS
Boundary-layer transition across a stratocumulus cloud edge in a coastal zone p 45 A92-10489
Assessment of one-dimensional icing forecast model applied to stratiform clouds p 915 A92-46803

STRATOSPHERE
Stratospheric electrodynamics from superpressure balloons - A technical challenge for small payload environments [AIAA PAPER 91-3674] p 14 A92-11019
Stratospheric lighter-than-air powered platform p 110 A92-15334
Studies on the effect of high-flying air-traffic on the atmosphere [IAF PAPER 91-737] p 301 A92-22495
The atmospheric effects of stratospheric aircraft: A first program report [NASA-RP-1272] p 408 N92-19121
High-speed civil transport aircraft emissions p 408 N92-19122
Natural cycles, gases p 408 N92-19123
Lower stratospheric measurement issues workshop report p 409 N92-19127

STREAM FUNCTIONS (FLUIDS)
Triple-deck structure p 3 A92-10690
Probe shapes for streamwise momentum and cross-stream turbulence intensity p 9 A92-13210
Calculation of the base pressure and enthalpy behind a step in the path of two supersonic streams with allowance for the effect of boundary layers and heat fluxes p 63 A92-13748
A numerical procedure of three-dimensional design problem in turbomachinery [ASME PAPER 91-GT-144] p 72 A92-15583
Control of hypersonic aerodynamic forces with surface blowing p 172 A92-18363
Computation of unsteady, laminar, incompressible, viscous flows using the vorticity streamfunction formulation p 245 A92-21979
Finite element vorticity based methods for the solution of the compressible Navier-Stokes equations p 246 A92-21983
Three-dimensional compressible flows in turbo-machinery solved by the pseudostream function formulation p 338 A92-27801
The structure and development of streamwise vortex arrays embedded in a turbulent boundary layer [AIAA PAPER 92-0551] p 342 A92-28204
Nonadiabatic and three-dimensional effects in compressible turbulent boundary layers p 431 A92-31156
Evolution of three-dimensionality in stable and unstable curved mixing layers p 619 A92-40059
Experiments on the enhancement of compressible mixing via streamwise vorticity. I - Optical measurements [AIAA PAPER 92-3549] p 906 A92-49064
Pseudostream function formulation - A method of solving three-dimensional aerodynamic analysis and design problems in turbomachinery p 996 A92-52981
Effect of streamwise pressure gradient on the supersonic mixing layer p 1025 A92-54936

STREAMLINED BODIES
Streamlines, vorticity lines, and vortices around three-dimensional bodies p 808 A92-45845

STREAMLINING
A simplified model for aerodynamic flows around streamlined models p 63 A92-13816

STREAMS
Experimental study of cross-stream mixing in a rectangular duct [AIAA PAPER 92-3090] p 903 A92-48735
Experimental study of cross-stream mixing in a rectangular duct [NASA-TM-105694] p 742 N92-27652

STRESS (PHYSIOLOGY)
Controller memory enhancement: Field facility concepts and techniques [DOT/FAA/CT-TN92/7] p 640 N92-24799

STRESS ANALYSIS
Stress analysis of a propeller blade p 38 A92-10963
Stress analysis of a propeller hub p 38 A92-10964
A method of reliability analysis for propeller blades p 25 A92-10968

Three-dimensional finite-element analysis of interlaminar stresses in thick composite laminates
p 39 A92-11791
Efficient evaluation of the flexibility of tapered I-beams accounting for shear deformations p 295 A92-23269
Quasi-static analysis of roller bearing
p 391 A92-24732
Effect of some load factors of bird impact on blade response p 371 A92-24740
Cyclic symmetric contact stress analysis of aeroengine rotor assembly p 470 A92-29733
A Rayleigh-Ritz design methodology for cutouts in composite structures
[AIAA PAPER 92-2278] p 582 A92-34297
Study of weld offset in longitudinally welded SSME HPFTP inlet
[AIAA PAPER 92-2305] p 586 A92-34525
A method for determining equivalent stresses in aviation gas turbine engine blades p 559 A92-36421
Linear analysis of naturally curved and twisted anisotropic beam p 899 A92-46936
Advanced stress analysis methods applicable to turbine engine structures
[NASA-CR-187235] p 44 N92-11378
An experimental and computational investigation of an annular reverse-flow combustor
[UTIAS-338] p 129 N92-11996
Numerical verification of NISA 2 finite element analysis of the cracked 5th stage compressor disc of J-85 jet engine
[NRC-LTR-ST-1792] p 129 N92-11997
A review of aeronautical fatigue investigations in Sweden during the period May 1989 to April 1991
[FFA-TN-1991-24] p 158 N92-12313
Detailed analysis and test correlation of a stiffened composite wing panel
[NASA-TM-104154] p 159 N92-13460
Analysis of Euler's and stress tensor methods for calculating power consumption of high speed centrifugal fans and turbocompressors
[DE92-728396] p 298 N92-16325
CH-46 and OH-58 transmission stress wave analysis
[AD-A244321] p 365 N92-18826
The 3D inelastic analysis methods for hot section components
[NASA-CR-189089] p 402 N92-18971
Component-specific modeling --- jet engine hot section components
[NASA-CR-189088] p 377 N92-19726
Application of finite element methods to fracture mechanics
[PNR-90770] p 503 N92-21741
Simultaneous stress and flutter optimization for the wing of a transport aircraft equipped with four engines
p 571 N92-23238
Estimation of cable-mounted model inertia characteristics for dynamic wind-tunnel test
[NAL-TM-641] p 722 N92-28152
Surface residual stress analysis of metals and alloys
[AD-A248372] p 895 N92-28426
Generation of spectra and stress histories for fatigue and damage tolerance analysis of fuselage repairs
[AD-A250390] p 854 N92-29180
Global/local methods research using the CSM testbed
p 1107 N92-32528
Computational methods for global/local analysis
[NASA-TM-107591] p 1125 N92-33104
Global/local interlaminar stress analysis of a grid-stiffened composite panel
[NASA-CR-190822] p 1125 N92-33139
Effects of constraint on crack growth under aircraft spectrum loading
[NASA-TM-107677] p 1128 N92-34178

STRESS CONCENTRATION
Determination of the objective-function gradient in the problem of minimizing stress concentration using the finite element method p 494 A92-30170
Stress concentration effects of oblique holes in aspirated-cooled turbine engine liners
[AIAA PAPER 92-1130] p 581 A92-33282
Technique for estimating the strength of gas turbine guide vanes with stress raisers p 761 A92-42653
Failure analysis of the Apache mixer pivot support
[AD-A240858] p 116 N92-13061
Gear tooth stress measurements of two helicopter planetary stages
[NASA-TM-105651] p 764 N92-26555

STRESS CORROSION CRACKING
Failure analysis of the Apache mixer pivot support
[AD-A240858] p 116 N92-13061

STRESS DISTRIBUTION
Stress concentration effects of oblique holes in aspirated-cooled turbine engine liners
[AIAA PAPER 92-1130] p 581 A92-33282
A unified numerical approach for the analysis of rotating disks including turbine rotors
[AIAA PAPER 92-2303] p 585 A92-34524
Reynolds stress budget in the outwash jet arising from colliding curved wall jets p 614 A92-38860
Reynolds stress distribution downstream of a turbine cascade p 614 A92-38861
Stress field sensitivity of a composite patch repair as a result of varying patch thickness p 763 A92-44630
Preliminary finite element analysis of unloaded and loaded notched composite laminated plates
[NRC-LTR-ST-1806] p 159 N92-13454
Finite element frequency domain solution of nonlinear panel flutter with temperature effects and fatigue life analysis p 682 N92-25589
Computational structures technology at Grumman: Current practice/future needs p 684 N92-25930
Gear tooth stress measurements of two helicopter planetary stages
[NASA-TM-105651] p 764 N92-26555
Combined load test apparatus for flat panels
[NASA-CASE-LAR-14698-1] p 911 N92-30028
Damaged stiffened shell research at NASA. Langley Research Center p 914 N92-30115

STRESS INTENSITY FACTORS
A study of the nonlinear stress-strain state of spring-type landing gear p 154 A92-16825
Fatigue crack initiation and small crack growth in several airframe alloys p 212 A92-19754
A fatigue crack growth threshold p 389 A92-26667
Research on damage tolerance of compressor blade
p 588 A92-35556
Solution of stress intensity factor by weight function for small surface cracks in plates p 998 A92-53332
Application of finite element methods to fracture mechanics
[PNR-90770] p 503 N92-21741
Towards GLARE: The development of a fatigue insensitive and damage tolerant aircraft material
[ETN-92-91301] p 648 N92-24966
Effects of constraint on crack growth under aircraft spectrum loading
[NASA-TM-107677] p 1128 N92-34178

STRESS MEASUREMENT
RTOK elimination with TSMM --- Rerurn Tested OK reproduction using time stress measurement module
p 902 A92-48446
The Operational Loads Monitoring System, OLMS
p 361 N92-18586
Gear tooth stress measurements of two helicopter planetary stages
[NASA-TM-105651] p 764 N92-26555

STRESS RELAXATION
Effects of elevated temperature on the viscoplastic modeling of graphite/polymeric composites
[NASA-TM-104160] p 35 N92-11149
Light thermal structures and materials for high speed flight p 649 N92-25922
Experimental investigation of turbulence behavior in shock wave/turbulent boundary layer interactions
[AD-A247792] p 774 N92-27886

STRESS TENSORS
Limitations to the large strain theory
p 219 A92-20356
Analysis of Euler's and stress tensor methods for calculating power consumption of high speed centrifugal fans and turbocompressors
[DE92-728396] p 298 N92-16325

STRESS WAVES
Relationship between the rotating stall and vibrations of a blade row p 496 A92-31988
CH-46 and OH-58 transmission stress wave analysis
[AD-A244321] p 365 N92-18826

STRESS-STRAIN DIAGRAMS
Life prediction of local stress-strain method
p 588 A92-35564

STRESS-STRAIN RELATIONSHIPS
Mechanics of curved fiber composites
p 140 A92-14346
A study of the nonlinear stress-strain state of spring-type landing gear p 154 A92-16825
Limitations to the large strain theory
p 219 A92-20356
Fatigue life estimation of fastener holes without load transfer p 291 A92-21472
Prediction of low cycle fatigue life of engine cases
p 295 A92-23385
Mechanics of curved fiber composites
p 757 A92-41034
Helicopter rotor blade aeroelasticity in forward flight with an implicit structural formulation p 958 A92-50315
Effects of elevated temperature on the viscoplastic modeling of graphite/polymeric composites
[NASA-TM-104160] p 35 N92-11149
Review of investigations on aeronautical fatigue in the Federal Republic of Germany
[ETN-92-90317] p 225 N92-14397
Computational structures technology at Grumman: Current practice/future needs p 684 N92-25930
Stress-strain analysis of a (0/90)sub 2 symmetric titanium matrix laminate subjected to a generic hypersonic flight profile
[NASA-TM-107584] p 685 N92-26128

STRESSES
Measurements of fuselage skin strains and displacements near a longitudinal lap joint in a pressurized aircraft
[NASA-TM-104163] p 159 N92-13455
Stretched skin concept for the entry aerodynamic decelerator system of planetary probes
p 576 N92-23836
Experimental investigation of turbulence behavior in shock wave/turbulent boundary layer interactions
[AD-A247792] p 774 N92-27886

STRETCH FORMING
Continuation of tailored composite structures of ordered staple thermoplastic material
[NASA-CR-189671] p 1110 N92-33613

STRINGERS
Stringer subsystem automation p 700 A92-43246
Measurements of fuselage skin strains and displacements near a longitudinal lap joint in a pressurized aircraft
[NASA-TM-104163] p 159 N92-13455
Fatigue of repaired composite structures
p 214 N92-14411

STRIPPING
Take it all off - with water --- High-pressure waterjet stripping of protective coatings p 516 A92-34775

STRUCTURAL ANALYSIS
Evaluation of an adaptive unstructured remeshing technique for integrated fluid-thermal-structural analysis
p 37 A92-10445
Vibration characteristic analysis of a propeller blade
p 38 A92-10967
Structural behavior of scientific balloons - Finite element simulation and verification
[AIAA PAPER 91-3668] p 20 A92-11015
Overpressurized zero pressure balloon system
[AIAA PAPER 91-3671] p 14 A92-11018
Application of smart structures to aircraft health monitoring p 20 A92-11123
Traditional finite element analysis - Opportunities for parallelism? p 40 A92-12354
Thermodynamic structural analysis of high speed propulsion systems
[IAF PAPER 91-278] p 120 A92-14711
Static aeroelastic analysis for generic configuration wing p 174 A92-20201
Static aeroelastic tailoring of composite aircraft swept wings modelled as thin-walled beam structures
p 294 A92-23114
Efficient evaluation of the flexibility of tapered I-beams accounting for shear deformations p 295 A92-23269
Application researches on expert system used for structural layout optimization of wings
p 398 A92-27865
Design, analysis, testing, and certification of composite primary structure for the Piaggio P-180 Avanti
p 535 A92-32553
Coupled Rayleigh-Ritz/finite element structural analysis using penalty function method
[AIAA PAPER 92-2238] p 581 A92-34292
An independent refinement and integration procedure in multiregion finite element analysis
[AIAA PAPER 92-2290] p 582 A92-34307
AIAA/ASME/ASCE/AHS/ASC Structures, Structural Dynamics and Materials Conference, 33rd, Dallas, TX, Apr. 13-15, 1992, Technical Papers. Pt. 2 - Structures II
p 582 A92-34332
Reduced basis technique for evaluating the sensitivity coefficients of the nonlinear tire response
[AIAA PAPER 92-2530] p 583 A92-34376
Combined compressive and shear buckling analysis of hypersonic aircraft sandwich panels
[AIAA PAPER 92-2487] p 586 A92-34603
An expert system to aid real world finite element analysis
[AIAA PAPER 92-2488] p 601 A92-34604
Behavior of thin-walled beams made of advanced composite materials and incorporating non-classical effects p 673 A92-39944
Sensitivity analysis for structural optimization of helicopter rotor blades p 1053 A92-56073
Fatigue cracking threshold prediction of transport airplanes p 1118 A92-56094
Detailed analysis and test correlation of a stiffened composite wing panel p 1121 A92-56324

A review of aeronautical fatigue investigations in Sweden during the period May 1989 to April 1991
[FFA-TN-1991-24] p 158 N92-12313
Detailed analysis and test correlation of a stiffened composite wing panel
[NASA-TM-104154] p 159 N92-13460
Structural considerations for aircraft payload Modification: P-3C zero fuel weight increase
[AD-A242690] p 196 N92-15068
Industrial code development p 227 N92-15083
Finite element analysis of ASTOVL fighter structure
[AD-A243724] p 275 N92-17513
Design and testing of high-performance parachutes
[AGARD-AG-319] p 345 N92-18269
Aging aircraft structural damage analysis
p 360 N92-18575
Thermal/structural analysis of a transpiration cooled nozzle
[NASA-TM-104184] p 401 N92-18877
Investigation of the effects of aeroelastic deformations on the radar cross section of aircraft
[AD-A243889] p 402 N92-18940
The 3D inelastic analysis methods for hot section components
[NASA-CR-189089] p 402 N92-18971
Integrated aerodynamic-structural-control wing design
p 349 N92-19698
Component-specific modeling --- jet engine hot section components
[NASA-CR-189088] p 377 N92-19726
Development of a wind chamber for model testing of tornado forces on structures
[PB92-104165] p 386 N92-19940
A novel approach in formulation of special transition elements: Mesh interface elements
[NASA-CR-189050] p 501 N92-20954
Aeropropulsion structures p 559 N92-22518
Manufacturing development of pultruded composite panels
[NASA-CR-181780] p 578 N92-22637
A parallel-vector algorithm for rapid structural analysis on high-performance computers
[NASA-TM-102614] p 595 N92-22649
Research and technology, 1991
[NASA-TM-105320] p 516 N92-22659
Integrated Design Analysis and Optimisation of Aircraft Structures
[AGARD-R-784] p 550 N92-23227
The structural optimization system OPTSYS: Current status and applications p 550 N92-23232
Application of an automated multidisciplinary analysis and optimisation system to the design of aircraft structures p 551 N92-23233
Design of a fighter aircraft vertical tail enhanced buffet environment survivability p 551 N92-23235
First approach to an integrated fin design
p 551 N92-23236
A fin optimisation study p 551 N92-23237
Structural optimization of aircraft practice and trends
p 551 N92-23239
Coupled multi-disciplinary simulation of composite engine structures in propulsion environment
[NASA-TM-105575] p 596 N92-23267
The future challenge for aeropropulsion
[NASA-TM-105613] p 658 N92-25164
Integrating aerodynamic surface modeling for computational fluid dynamics with computer aided structural analysis, design, and manufacturing
p 682 N92-25727
Computational Structures Technology for Airframes and Propulsion Systems
[NASA-CP-3142] p 683 N92-25911
Computational structures technology and UVA Center for CST p 683 N92-25912
Computer codes developed and under development at Lewis p 692 N92-25913
Progress in integrated analysis with adaptive unstructured meshing p 683 N92-25914
A brief overview of computational structures technology related activities at NASA Lewis Research Center
p 683 N92-25915
CSM activities at the NASA Langley Research Center
p 683 N92-25916
Algorithmic development in structures technology
p 684 N92-25924
Structural analysis for preliminary design of High Speed Civil Transport (HSCT) p 684 N92-25926
Application of integrated structural analysis to the high speed civil transport p 684 N92-25927
Overview of computational structural methods for modern military aircraft p 684 N92-25928
Computational structural analysis and advanced commercial engines p 660 N92-25933
Military engine computational structures technology
p 660 N92-25934
Finite element methods for integrated aerodynamic heating analysis
[NASA-CR-190353] p 633 N92-25959
Preliminary structural sizing of a Mach 3.0 high-speed civil transport model
[NASA-CR-189631] p 685 N92-25960
Iterative methods for large scale static analysis of structures on a scalable multiprocessor supercomputer
[NASA-CR-190369] p 692 N92-26018
Analysis of EMP response of structures using frequency domain electromagnetic interaction codes
[AD-A245758] p 765 N92-26592
Surface generation and editing operations applied to structural support of aerospace vehicle fuselages
p 777 N92-27831
Unsteady aerodynamics for aeroelasticity at the Flight Dynamics Directorate p 718 N92-27939
Integrated Design Analysis and Optimisation of Aircraft Structures
[AGARD-LS-186] p 851 N92-28469
Fundamentals of structural optimisation
p 851 N92-28470
Structural optimization of aircraft p 851 N92-28472
Multidisciplinary design and optimization
[AGARD-PAPER-2] p 851 N92-28473
Damaged stiffened shell research at NASA. Langley Research Center p 914 N92-30115
Nonlinear analyses of composite aerospace structures in sonic fatigue
[NASA-CR-190565] p 854 N92-30209
Multidisciplinary optimization of fiber composite aircraft structures
[MBB/FW321/S/PUB/476] p 961 N92-30424
Research into improving the durability of the hot section in the aircraft turbine engine
[AD-A250342] p 973 N92-31439
Structural assessment of ultralightweight composites
p 1107 N92-32525
Global/local methods research using the CSM testbed
p 1107 N92-32528
Initial postbuckling response of an unsymmetrically laminated rectangular plate p 1108 N92-32586
Computational methods for global/local analysis
[NASA-TM-107591] p 1125 N92-33104

STRUCTURAL DESIGN

Manned orbital balloon flight - Available techniques
[AIAA PAPER 91-3675] p 15 A92-11020
Design of a trans-global manned balloon system with relevance to scientific ballooning
[AIAA PAPER 91-3687] p 15 A92-11030
Dynamic behavior analysis for landing-gear with different types of dual-chamber shock-struts p 111 A92-15342
Design and analysis of ceramic and CMC components for advanced gas turbines
[ASME PAPER 91-GT-156] p 142 A92-15592
One-dimensional, stage-by-stage, axial compressor performance model
[ASME PAPER 91-GT-192] p 124 A92-15618
Design of a small axial compressor for high efficiency over a wide operating range
[ASME PAPER 91-GT-195] p 124 A92-15620
Operation and design considerations for unsteady data acquisition with PC-based systems in high Reynolds number hypersonic flowfields
[AIAA PAPER 92-0204] p 284 A92-23810
Structural design considerations for a Personnel Launch System p 386 A92-24668
Optimum design of helicopter rotor blades with multidisciplinary couplings
[AIAA PAPER 92-0214] p 357 A92-25687
Application researches on expert system used for structural layout optimization of wings
p 398 A92-27865
A superelement simplified analysis for the vibration systems of the complex structures p 398 A92-27903
Design and calculation of performance of a subsonic inlet duct p 343 A92-28478
The initial development of an expert system for designing composite material wing structures p 599 A92-32542
Design, analysis, testing, and certification of composite primary structure for the Piaggio P-180 Avanti
p 535 A92-32553
Development of an advanced composite material on vertical stabilizer of F-X aircraft p 579 A92-32555
Approximate closed-form buckling solutions for the optimization of aircraft structures p 579 A92-32578
New, unusual and nonclassical behavior of thin-walled composite structures p 580 A92-32746
Multidisciplinary design optimization of a large transport aircraft wing
[AIAA PAPER 92-1002] p 536 A92-33194
Damage tolerant structural design using neural networks
[AIAA PAPER 92-1097] p 581 A92-33261
Application of a local panel buckling constraint within automated multidisciplinary structural analysis and design
[AIAA PAPER 92-1116] p 537 A92-33271
Structural design for durability - Lessons learned from service and test data
[AIAA PAPER 92-1129] p 537 A92-33281
A Rayleigh-Ritz design methodology for cutouts in composite structures
[AIAA PAPER 92-2278] p 582 A92-34297
Structural tailoring/analysis for hypersonic components - Executive system development
[AIAA PAPER 92-2471] p 583 A92-34360
Improved coordination in non-hierarchic system optimization
[AIAA PAPER 92-2497] p 601 A92-34554
A structural design and optimization tool for ducted rotor/wing blades
[AIAA PAPER 92-2361] p 543 A92-34593
Mechanical design of an airborne imaging microwave radiometer p 554 A92-35276
Vibration of gear system with web structure
p 588 A92-35573
Multifunction tests of a frequency domain based flutter suppression system
[AIAA PAPER 92-2096] p 566 A92-35667
Thermal structures and materials for high-speed flight; Collection of Papers of the 1st Thermal Structures Conference, University of Virginia, Charlottesville, Nov. 13-15, 1990
[ISBN 1-56347-017-9] p 590 A92-35847
Arbitrary blade section design based on viscous considerations - Background information
p 523 A92-36029
Arbitrary blade section design based on viscous considerations - Blade optimization p 523 A92-36030
A refined analytical method for designing high pressure ratio centrifugal impellers p 591 A92-36032
Aeroelastic tailoring analysis for advanced turbo propellers with composite blades p 558 A92-36358
Composite materials for aerospace applications
p 577 A92-36377
Aircraft structural design p 643 A92-39304
Basic design concepts for smart actuators for aerospace plane control p 752 A92-41193
Application of Active Flexible Wing technology to the Agile Falcon p 729 A92-41233
Composite laminated shells under internal pressure
p 758 A92-41296
The fatigue scatter factors and reduction factors in the design of aircraft and helicopter's structural lives
[SAE PAPER 911984] p 843 A92-45387
Aero-structural integrated design of forward swept wing
[SAE PAPER 912021] p 790 A92-45414
Integrated aeroservoelastic wing synthesis by nonlinear programming/approximation concepts
p 873 A92-46752
Approach for analysis and design of composite rotor blades p 899 A92-46801
Magnetic bearing design and control optimization for a four-stage centrifugal compressor p 900 A92-47188
Design and use of aramid fiber in aircraft structures
p 784 A92-47407
Design of helicopter composite structures for crashworthiness p 848 A92-47408
A failure analysis for landing gear structural system
p 849 A92-47667
Moldless composite aircraft wing structural design modifications p 958 A92-51527
Manufacturing cost model for composites
p 1012 A92-51565
Design and performance of the centrifuge-based Dynamic Flight Simulator
[AIAA PAPER 92-4156] p 981 A92-52446
Anti-fatigue optimization design by artificial intelligence strategy p 996 A92-53013
Structural optimization and vibration control of composite rotor blades p 960 A92-53056
Damage tolerance and durability design of composite aircraft structures p 996 A92-53067
Design variables and constraint derivatives in aeroelastic tailoring p 997 A92-53074
Turning up the heat on aircraft structures --- design and analysis for high-temperature conditions
p 1052 A92-55131
Wing mass formula for twin fuselage aircraft
p 1054 A92-56171
Multidisciplinary optimization of aeroservoelastic systems using reduced-size models
p 1054 A92-56176
Demonstration of structural optimization applied to wind-tunnel model design p 1119 A92-56181
Structural design and testing results of composite landing gear components p 1057 A92-56328

The cryogenic balance design and balance calibration methods
[AIAA PAPER 92-4001] p 1122 A92-56824
Optimal design of nonlinear shell structures
[FFA-TN-1991-18] p 157 N92-12312
Fatigue testing and tear down operations on Airbus A320 forward fuselage p 360 N92-18579
Experimental validation of structural optimization methods
[NASA-TM-104203] p 404 N92-19258
Engine Structures Modeling Software System (ESMOSS)
[NASA-CR-187227] p 404 N92-19277
Optimization of composite sandwich cover panels subjected to compressive loadings
[NASA-TP-3173] p 489 N92-20679
The aerodynamics of ship superstructures
p 503 N92-21953
Multidisciplinary optimization studies using ASTROS
p 571 N92-23234
Design of a fighter aircraft vertical tail enhanced buffet environment survivability p 551 N92-23235
First approach to an integrated fin design
p 551 N92-23236
Simultaneous stress and flutter optimization for the wing of a transport aircraft equipped with four engines
p 571 N92-23238
Conceptional design to heat-resistant airframe of HOPE p 575 N92-23820
Design challenges for the National Aero-Space Plane
p 551 N92-23822
Development of pre- and post-processor system for structural analysis
[NAL-TM-628] p 681 N92-25403
Computational Structures Technology for Airframes and Propulsion Systems
[NASA-CP-3142] p 683 N92-25911
Structures technology applications for the National AeroSpace Plane p 649 N92-25920
Large scale optimization using ASTROS: An overview
p 649 N92-25921
Composite fuselage technology (summary of year 2)
[NASA-CR-190434] p 731 N92-26655
Surface generation and editing operations applied to *structural support of aerospace vehicle fuselages*
p 777 N92-27831
A preliminary study on damage detection using piezoelectric film
[AD-A246350] p 733 N92-28118
Multidisciplinary design and optimization
[AGARD-PAPER-2] p 851 N92-28473
Mathematical optimization: A powerful tool for aircraft design p 851 N92-28474
Concurrent engineering in design of aircraft structures
[MBB-FE-2-S-PUB-472] p 854 N92-29650
Modeling and analysis methodology for aeroelastically tailored chordwise deformable wings
[NASA-CR-189620] p 961 N92-30304
MBB-LAGRANGE: A general structural reliability and optimization structural system
[MBB/FW321/S/PUB/467] p 998 N92-30423
Multidisciplinary optimization of fiber composite aircraft structures
[MBB/FW321/S/PUB/476] p 961 N92-30424
Composite beam analysis linear analysis of naturally curved and twisted anisotropic beams
[AD-A252652] p 999 N92-30766
Mechanical behavior and processing of aluminum metal matrix composites
[AD-A249918] p 987 N92-30874
Vortex flow aerodynamics
[AGARD-AR-299] p 946 N92-30947
Eighth DOD/NASA/FAA Conference on Fibrous Composites in Structural Design, part 1
[NASA-CP-3087-PT-1] p 1106 N92-32513
Evaluation of composite components on the Bell 206L and Sikorsky S-76 helicopters p 1107 N92-32575

STRUCTURAL DESIGN CRITERIA
Optimization of the flutter load by material orientation
p 146 A92-15222
International standardisation of regulations for gust loading calculations p 270 A92-22473
Evaluation of methods for estimating store carriage loads
[AIAA PAPER 92-0675] p 379 A92-27043
Selection of efficient primary-structure/force configurations for aircraft lifting surfaces subjected to displacement constraints p 458 A92-30140
The NASA/Industry Design Analysis Methods for Vibrations (DAMVIBS) Program - A government overview --- of rotorcraft technology development using finite element method
[AIAA PAPER 92-2200] p 539 A92-34390
Response of plate-like structures to correlated random pressure fluctuations
[AIAA PAPER 92-2378] p 584 A92-34452
AIAA/ASME/ASCE/AHS/ASC Structures, Structural Dynamics and Materials Conference, 33rd, Dallas, TX, Apr. 13-15, 1992, Technical Papers. Pt. 5 - Design engineering/design optimization, materials, work-in-progress p 585 A92-34522
Fully integrated aerodynamic/dynamic optimization of helicopter rotor blades
[AIAA PAPER 92-2374] p 542 A92-34544
Shape optimization of three-dimensional structures with *adaptive meshing*
[AIAA PAPER 92-2434] p 586 A92-34548
Composite material repairs to metallic airframe components p 699 A92-41237
Optimum structural design of a cantilevered rectangular elastic wing with a gust load alleviation system
p 762 A92-43133
Wing leading edge design with composites to meet bird strike requirements p 848 A92-47404
Design and test of aircraft aft fuselage structure using postbuckled shear panels p 848 A92-47406
Variable impedance journal bearings for rotor-bearing systems p 157 N92-12270
Short cracks and durability analysis of the Fokker 100 *wing/fuselage structure*
[NLR-TP-90336-U] p 910 N92-29603
Global/local interlaminar stress analysis of a grid-stiffened composite panel
[NASA-CR-190822] p 1125 N92-33139
The Rolls-Royce Trent
[PNR-90875] p 1061 N92-33750

STRUCTURAL ENGINEERING
The maintenance economy and economic life of structures p 37 A92-10673
Structural testing technology at high temperature; Proceedings of the Conference, Dayton, OH, Nov. 4-6, 1991
[ISBN 0-912053-34-8] p 980 A92-51401
Simulation of high heat flux levels with graphite heating and arc lamps p 980 A92-51402
A history of high-temperature testing at WPAFB
p 981 A92-51406
A historical overview of high-temperature structural testing at the NASA Dryden Flight Research Facility
p 981 A92-51407
Repair procedures for advanced composites for helicopters p 1016 A92-56277
Computational structures technology and UVA Center for CST p 683 N92-25912
A brief overview of computational structures technology related activities at NASA Lewis Research Center
p 683 N92-25915
Structures technology applications for the National AeroSpace Plane p 649 N92-25920
Algorithmic development in structures technology
p 684 N92-25924
A methodology for the evaluation of runway roughness for repair
[AD-A250407] p 887 N92-28772
Concurrent engineering in design of aircraft structures
[MBB-FE-2-S-PUB-472] p 854 N92-29650
Repair procedures for advanced composites for helicopters
[MBB-UD-0606-91-PUB] p 787 N92-29874
Aeroelasticity of bluff bodies p 1089 N92-34165

STRUCTURAL FAILURE
NASA test flights with increased flight stress indices
[AIAA PAPER 91-3665] p 20 A92-11012
Mind that restyle --- failure analysis of aircraft composite structures p 91 A92-13700
Reliability analysis of a structural ceramic combustion chamber
[ASME PAPER 91-GT-155] p 123 A92-15591
A method to determine propagation direction of compressive fracture in carbon-fibre composites
p 672 A92-38770
Structural risk assessment in the Israel Air Force for fleet management p 836 A92-46779
A method of failure analysis of complicated structures
p 901 A92-47656
Probability analysis of structure failure for the wings with main and subordinate components p 848 A92-47657
Approximate analysis for failure probability of structural systems p 901 A92-47671
The use of math-dynamic models to aid the development of integrated health and usage monitoring systems
p 1006 A92-50013
Developmental flight testing of a half scale unmanned air vehicle
[AD-A240347] p 22 N92-11002
Proceedings of the USAF Structural Integrity Program Conference
[AD-A242943] p 279 N92-17204
A probabilistic procedure for aircraft fleet management
p 360 N92-18576
Life management approach for USAF aircraft
p 362 N92-18587
Recent fracture mechanics results from NASA research related to the aging commercial transport fleet
p 362 N92-18589
Structural airworthiness of aging Boeing jet transports
p 362 N92-18590
Aircraft fatigue management in the Royal Air Force
p 363 N92-18591
Fatigue management for the A-7P
p 363 N92-18593
Managing airborne assets through loads monitoring
p 363 N92-18594
Approach to crew training in support of the USAF Aircraft Structural Integrity Program (ASIP) p 363 N92-18595
Airplane crashes on the runway. Fine modeling of the behavior after burning of a frame submitted to linear crushing
[IMFL-90-64] p 353 N92-19350
Overview of mechanics of materials branch activities in the computational structures area
p 684 N92-25917
Composite fuselage technology (summary of year 2)
[NASA-CR-190434] p 731 N92-26655
Turbine aircraft engine operational trending and JT8D *static component reliability study*
[DOT/FAA/CT-91/10] p 870 N92-28686
A methodology for the evaluation of runway roughness for repair
[AD-A250407] p 887 N92-28772
Structural integrity of future aging airplanes
p 913 N92-30107
Maintaining the safety of an aging fleet of aircraft
p 837 N92-30108
Performance of fuselage pressure structure
p 913 N92-30109
Fracture mechanics research at NASA related to the aging commercial transport fleet p 913 N92-30110
Current DOT research on the effect of multiple site *damage on structural integrity* p 913 N92-30112
Damage tolerance for commuter aircraft
p 914 N92-30114
Thermal QNDE detection of airframe disbonds
p 914 N92-30118
A manufacturer's approach to ensure long term structural integrity p 838 N92-30133
Design, evaluation and experimental effort toward development of a high strain composite wing for Navy aircraft p 1107 N92-32514

STRUCTURAL MEMBERS
Photoelastic coating study of CT-114 coupon joint test specimen for horizontal stabilizer rear attachment fitting to vertical stabilizer rear spar
[NRC-LTR-ST-1689] p 489 N92-21018
Development of hardness cycles for fiber bound materials, using DSC: From laboratory specimens to complex high duty structural members
[MBB-Z-0409-91-PUB] p 987 N92-30969

STRUCTURAL RELIABILITY
Structural airworthiness of aging Boeing jet transports - 747 fuselage fatigue test program
[AIAA PAPER 92-1128] p 537 A92-33280
Reliability analysis of fatigue life of a structural system
p 671 A92-37395
Reliability centered maintenance for metallic airframes based on a stochastic crack growth approach
p 897 A92-45242
Optimal maintenance program of damage tolerance structure p 785 A92-47660
A failure analysis for landing gear structural system
p 849 A92-47667
Safety factor and reliability for composite laminates
p 996 A92-53070
From fatigue test life to structure safe life
p 997 A92-53099
A concept for the revisions of structural inspection schedules p 226 N92-14431
Proceedings of the USAF Structural Integrity Program Conference
[AD-A242943] p 279 N92-17204
Probabilistic design and fatigue management based on *probabilistic fatigue models with reliability updating*
p 360 N92-18574
Aging aircraft structural damage analysis
p 360 N92-18575
Tornado structural fatigue life assessment of the German Air Force p 363 N92-18592
A review of aging aircraft technology: An IAI perspective
[IAITIC-91-1018] p 461 N92-20500
Current DOT research on the effect of multiple site *damage on structural integrity* p 913 N92-30112

STRUCTURAL STABILITY
Optimization of the flutter load by material orientation
p 146 A92-15222
The torsional stability of a compressor cascade
[ASME PAPER 91-GT-180] p 123 A92-15612

The stability analysis of the nonlinear shimmy
p 358 A92-27902
Stability of stiffened panels with allowance for plasticity under nonstationary heating and loading
p 493 A92-30152
Reduction of computational models in strength problems p 496 A92-31858
AIAA/ASME/ASCE/AHS/ASC Structures, Structural Dynamics and Materials Conference, 33rd, Dallas, TX, Apr. 13-15, 1992, Technical Papers. Pt. 2 - Structures II
p 582 A92-34332
Comparison between imposed-periodicity and marching-in-time solutions of helicopter rotor blade steady-state response problem
[AIAA PAPER 92-2256] p 540 A92-34411
Analytical aeroelastic stability considerations and conversion loads for an XV-15 tilt-rotor in a wind tunnel simulation
[AIAA PAPER 92-2258] p 540 A92-34413
A new aeroelastic model for composite rotor blades with straight and swept tips
[AIAA PAPER 92-2259] p 541 A92-34414
Application of composite rotor blade stability analysis to extension-twist coupled blades
[AIAA PAPER 92-2254] p 564 A92-34479
General model of isolated helicopter blade for stability investigation p 547 A92-35774
Helicopter aeroelastic stability and response - Current topics and future trends p 730 A92-43100
Flight tests on the structures of the STOL research aircraft Asuka p 730 A92-43143
Stability of intershaft squeeze film dampers
p 222 N92-14351
Evaluating fixed wing aircraft in the aircraft carrier environment p 464 N92-21963
Stability failure of sandwich structures
[MBB-UD-0613-92-PUB] p 1111 N92-33994

STRUCTURAL STRAIN
The development of fatigue management requirements and techniques p 360 N92-18572

STRUCTURAL VIBRATION
Advanced multi-squeeze film dampers for rotor vibration control p 36 A92-10102
Robustness of distributed systems with respect to small time delays p 47 A92-11351
Experimental demonstration of active vibration control for flexible structures p 50 A92-11442
Dynamic characterization and identification of nonlinear systems application to aeronautical structures
p 39 A92-11830
Fundamental research in helicopter rotor blade-vortex interaction modeling p 65 A92-14358
Design optimization of rotor blades for improved performance and vibration p 106 A92-14389
Rotorcraft airframe structural optimization for combined vibration and fatigue constraints p 106 A92-14390
Analysis of rotor blade dynamics using experimental UH-60A airloads obtained at the DNW
p 107 A92-14394
Structural optimization and Mach scale test validation of a low vibration rotor p 107 A92-14395
Interactive engine system dynamics analysis
[ASME PAPER 91-GT-193] p 124 A92-15619
A chambered porous damper for rotor vibration control. II - Imbalance response and bladeless simulation
[ASME PAPER 91-GT-243] p 149 A92-15648
Vibration characteristics of pretwisted aerofoil cross-section blade packets under rotating conditions
p 219 A92-20756
Comparative study of fatigue in various materials and designs under sonic loading p 287 A92-21003
An analysis of impact resistance of composite blades for turbo-fan engines p 294 A92-23109
Separation-induced self-excited structural oscillations
[AIAA PAPER 92-0486] p 328 A92-26317
A superelement simplified analysis for the vibration systems of the complex structures p 398 A92-27903
Models of space-averaged energetics of plates
p 398 A92-28031
An investigation of the swirl in an S-shaped inlet
p 343 A92-28476
Active vibration control using fixed order dynamic compensation with frequency shaped cost functionals
p 508 A92-29324
Simulation of vibrational status of gas-turbine engine
p 470 A92-29731
Relationship between the rotating stall and vibrations of a blade row p 496 A92-31988
Impact of structural optimization with aeroelastic/multidisciplinary constraints on helicopter rotor design
[AIAA PAPER 92-1001] p 535 A92-33193
The NASA/Industry Design Analysis Methods for Vibrations (DAMVIBS) Program - A government overview --- of rotorcraft technology development using finite element method
[AIAA PAPER 92-2200] p 539 A92-34390
The NASA/Industry Design Analysis Methods for Vibrations (DAMVIBS) Program - Bell Helicopter Textron accomplishments
[AIAA PAPER 92-2201] p 539 A92-34391
The NASA/Industry Design Analysis Methods for Vibrations (DAMVIBS) Program - Boeing helicopters airframe finite element modeling
[AIAA PAPER 92-2202] p 539 A92-34392
Optimizing tuning masses for helicopter rotor blade vibration reduction including computed airloads and comparison with test data
[AIAA PAPER 92-2376] p 542 A92-34546
Vibration of gear system with web structure
p 588 A92-35573
Smart structures for helicopters p 516 A92-35727
A frequency domain theory for structural identification
p 590 A92-35745
Active control of helicopter ground and air resonance
p 568 A92-35762
Transmission vibration monitoring - A single board computer architecture p 554 A92-35765
A study of coupled rotor-fuselage vibration with higher harmonic control using a symbolic computing facility
p 569 A92-35770
The development and testing of an active control of structural response system for the EH101 helicopter
p 569 A92-35775
Coupled propeller contributions to aircraft noise and vibration p 694 A92-39085
Pulse response method for vibration reduction in periodic dynamic systems p 661 A92-39909
Bifurcation analysis of airfoils in incompressible flow
p 623 A92-40580
Acoustic scattering by a disk or annulus linking two concentric cylindrical shells. I - Theory and results for heavy exterior fluid loading. II - Results for heavy exterior fluid loading on both shells p 696 A92-40588
Effects of higher harmonic control on rotor performance and control loads p 729 A92-41218
Adequacy of modeling turbulence and related effects on helicopter response p 730 A92-41263
A model of a deformable aeroplane with a wing of low aspect ratio and movable control surfaces for studying natural vibrations p 744 A92-41528
On the three-dimensional vibration analysis of simultaneously skewed and twisted cantilevered parallelepipeds p 759 A92-41801
Acoustic transmission through a 2-D orthotropic multi-layered infinite cylindrical shell p 780 A92-44197
The relationship between mode localization and energy transmission parameters in the vibration of coupled structures p 925 A92-45921
Sonic fatigue analysis and anti-sonic fatigue design of aircraft structure p 848 A92-47666
Aero mechanics in the twenty-first century
[AIAA PAPER 92-3194] p 863 A92-48805
On travelling wave vibration of high-speed duplex helical gears p 990 A92-49580
H-infinity synthesis using a bilinear pole shifting transform p 1007 A92-50490
Failure analysis and reliability improvement of small turbine engine blades p 993 A92-50860
Shimmy of nose undercarriage wheels
p 959 A92-51948
Monitoring fatigue cracks in gears
p 1116 A92-54496
DAMVIBS looks at rotorcraft vibration
p 1052 A92-55128
Safety provision against 'ground resonance' free vibration of a coaxial helicopter p 1056 A92-56289
The application of math-dynamic models to characterise a range of helicopter rotor system faults
p 1056 A92-56297
Coupled rotor-fuselage vibration reduction with multiple frequency blade pitch control p 1085 A92-56315
Path identification in structural acoustics
p 1059 A92-56346
Rotordynamic Instability Problems in High-Performance Turbomachinery, 1990
[NASA-CP-3122] p 222 N92-14346
Proceedings of Damping 1991, volume 3
[AD-A241313] p 225 N92-14386
The NASA/industry design analysis methods for vibrations (DAMVIBS) program: Accomplishments and contributions
[NASA-TM-104192] p 299 N92-17034
Loading and vibration reduction through active aerodynamic control
[AD-A242321] p 283 N92-17243
Response of structures to galloping excitation: Background and approximate estimation
[ESDU-91010] p 399 N92-18091
Experimental validation of structural optimization methods
[NASA-TM-104203] p 404 N92-19258
Baseline vibration measurements of remotely piloted helicopters for higher harmonic control research
[AD-A244669] p 482 N92-21360
Determining structural performance
p 560 N92-22519
Vibroacoustic simulation of an airplane structure
p 629 N92-24871
The NASA/industry Design Analysis Methods for Vibrations (DAMVIBS) Program: A government overview
[NASA-TM-107579] p 680 N92-25267
Evaluation of human response to structural vibrations induced by sonic booms
[NASA-CR-189584] p 697 N92-26130
AFRAPT Program at Texas A and M University research for advanced aircraft engine structures
[AD-A247040] p 743 N92-28076
Acoustic fatigue life prediction for nonlinear structures with multiple resonant modes
[NASA-CR-190471] p 1000 N92-30988
Building vibrations induced by noise from rotorcraft and propeller aircraft flyovers
[NASA-TM-104170] p 1138 N92-33160

STRUCTURAL WEIGHT
Weight estimating guide for advanced composites
p 289 A92-23418
An experiment on the weight vs control relations of subsonic airplanes p 357 A92-25502
Application of a local panel buckling constraint within automated multidisciplinary structural analysis and design
[AIAA PAPER 92-1116] p 537 A92-33271
Technological excellence in honeycomb sandwich and composite structures for aerospace applications
p 757 A92-41180
The relationship between the weight and flight characteristics of a transonic aircraft
p 731 A92-43189
MassInfo - An intelligent mass properties information system p 928 A92-47628
The effect of composite material allowable changes on VTOL airframe weights p 848 A92-47629
Structural considerations for aircraft payload Modification: P-3C zero fuel weight increase
[AD-A242690] p 196 N92-15068
Manx: Close air support aircraft preliminary design
[NASA-CR-189992] p 463 N92-21565

STRUTS
Application of non-reflecting boundary conditions to three-dimensional Euler equation calculations for thick strut cascades
[AIAA PAPER 92-3045] p 822 A92-48705

STUDENTS
Alpha Group: The Behemoth Apteryx. Final design proposal
[NASA-CR-190026] p 462 N92-20951
AFRAPT Program at Texas A and M University research for advanced aircraft engine structures
[AD-A247040] p 743 N92-28076
United States Air Force summer research program 1991. Volume 1: Program management report
[AD-A248763] p 1142 N92-32338

SUBCRITICAL FLOW
Subcritical flow studies on two-dimensional external compression supersonic inlets p 713 A92-44518
Prediction of the viscous transonic aerodynamic performance of supercritical aerofoil sections
[AIAA PAPER 92-2653] p 805 A92-45569
Simplified method for the prediction of aerofoil excrescence drag magnification factor for turbulent boundary layers at subcritical Mach numbers
[ESDU-91028] p 259 N92-15972

SUBJECTS
Magnetic suspension and balance systems: A comprehensive, annotated bibliography
[NASA-TM-4318] p 32 N92-11030

SUBMERGED BODIES
Heat transfer to a cylinder submerged in a rectangular cavity in supersonic flow --- to simulate electrical cables routed through Space Shuttle Solid Rocket Booster External Tank
[AIAA PAPER 92-2949] p 901 A92-47913
Application of submerged vortex generators for separation control of a subsonic diffuser
p 933 A92-49832
Thrust test fixture
[AD-D015259] p 983 N92-31192

SUBMERGING
Added mass of high-altitude balloons
[AIAA PAPER 91-3693] p 16 A92-11034

SUBROUTINES
Advanced Transport Operating System (ATOPS) control display unit software description
[NASA-CR-189606] p 652 N92-24689
SUBSONIC AIRCRAFT
Subsonic propulsion system installation analysis and optimization
[ASME PAPER 91-GT-167] p 111 A92-15602
Future experimental needs in low-speed aerodynamics
[AIAA PAPER 92-0157] p 254 A92-23772
Experimental necessities for subsonic transport configuration development
[AIAA PAPER 92-0158] p 254 A92-23773
An experiment on the weight vs control relations of subsonic airplanes p 357 A92-25502
Aerodynamic wing-nacelle integration
p 458 A92-30134
Approximate determination of the effect of deviations of wing and tail geometry from design parameters on the drag coefficient of subsonic aircraft p 460 A92-31878
Advanced propulsion systems for large subsonic transports p 653 A92-36977
Analysis for the application of hybrid laminar flow control to a long-range subsonic transport aircraft
[SAE PAPER 912113] p 617 A92-39964
Study on calculating the subsonic and supersonic aerodynamic characteristics of slender wing-body combinations at large angles of attack
p 706 A92-41926
The impact of CFD on the airplane design process - Today and tomorrow
[SAE PAPER 911989] p 788 A92-45391
Wing mass formula for subsonic aircraft
p 845 A92-46812
Design and off-design point characteristics of Separated Core Ultra High Bypass Engine (SCUBE)
[AIAA PAPER 92-3776] p 867 A92-49120
Nonlinear dynamic stability characteristics of recovery bodies p 977 A92-52041
High angle-of-attack flush airdata sensing system
p 1064 A92-56172
High Reynolds number testing in support of transport airplane development
[AIAA PAPER 92-3982] p 1099 A92-56807
Aeronautical research in the United States: Challenges for the 1990's p 420 N92-21502
SUBSONIC FLOW
An experimental study of subsonic separated flow over parawings p 4 A92-10901
Subsonic axisymmetric viscoelastic flow past thin tapered bodies of revolution p 6 A92-12134
Vibration of a wing of finite span in subsonic flow at small distances from a solid boundary p 9 A92-12808
Influence of three-dimensional effects on hydrodynamics and heat transfer in subsonic flow of a viscous compressible gas in the initial section of a rectangular duct p 66 A92-15031
Design method for subsonic and transonic cascade with prescribed Mach number distribution
[ASME PAPER 91-GT-18] p 67 A92-15509
An unsteady lifting surface theory for ducted fan blades
[ASME PAPER 91-GT-131] p 71 A92-15575
Wind tunnel wall effects in a linear oscillating cascade
[ASME PAPER 91-GT-133] p 72 A92-15576
A simple model to simulate subsonic intakes and propelling nozzles of aircraft gas turbine engines
[ASME PAPER 91-GT-392] p 153 A92-15722
Asymptotics of the upper branch of the neutral curve at subsonic and transonic external flow velocities
p 79 A92-16705
A discrete vortex study of stationary flow past three-dimensional lifting systems at subsonic and supersonic velocities p 79 A92-16813
Numerical prediction of subsonic turbulent flows over slender bodies at high incidence p 172 A92-18358
Numerical study on using sulfur hexafluoride as a wind tunnel test gas p 216 A92-18373
Influences of wind tunnel parameters on airfoil characteristics at high subsonic speeds
p 173 A92-18769
Numerical calculation of subsonic and supersonic aerodynamic loads around complex configuration vehicle
p 175 A92-20488
Genuinely upwind algorithms for the multidimensional Euler equations p 175 A92-20733
An improvement of the double-point method for unsteady subsonic flow p 243 A92-21315
Solution of the problem of three-dimensional flow past *the blade rows of turbomachines with allowance for* viscosity effects p 244 A92-21618
A hot-wire anemometer in compressible subsonic flow
p 244 A92-21623
Wave motions in a three-dimensional boundary layer
p 244 A92-21629
Aerodynamic design and optimization in one shot
[AIAA PAPER 92-0025] p 248 A92-22147
An experimental system to investigate subsonic aeroelastic behavior of lifting surfaces
[AIAA PAPER 92-0061] p 250 A92-22176
Computation of normal impinging jets in cross-flow and comparison with experiment p 250 A92-22446
Aerodynamics of loaded cascades in subsonic flows subject to unsteady three-dimensional vortical disturbances
[AIAA PAPER 92-0146] p 253 A92-23762
Prediction of drag at subsonic and transonic speeds using Euler methods
[AIAA PAPER 92-0169] p 255 A92-23780
Measurements of lateral aerodynamics characteristics of forebodies at high angle of attack in subsonic and transonic flows
[AIAA PAPER 92-0174] p 255 A92-23785
Numerical simulations of flow fields over aircrafts
p 313 A92-25042
Construction of aerodynamic profiles
p 315 A92-25299
An efficient Euler solver for predominantly supersonic flows with embedded subsonic pockets
[AIAA PAPER 92-0323] p 322 A92-25770
Experimental results on a wall interference correction method with interface measurements
[AIAA PAPER 92-0570] p 333 A92-26978
Separation control by vortex generators in subsonic diffuser p 338 A92-27829
Design and calculation of performance of a subsonic inlet duct p 343 A92-28478
High angle of attack aerodynamics - Subsonic, transonic, and supersonic flows --- Book
[ISBN 0-387-97672-8] p 431 A92-30850
Navier-Stokes simulation of flow through a highly contoured subsonic diffuser p 433 A92-31491
A numerical investigation of vortex flow control through small geometry modifications at the strake/wing junction of a cropped double-delta wing
[AIAA PAPER 92-0411] p 435 A92-31661
Subsonic flow past a thin airfoil in a channel with porous *walls* p 438 A92-31867
Computational studies of the aerodynamic characteristics of delta wings with a subsonic leading edge p 439 A92-31874
Analytical study on plate edge noise. I - Trailing edge noise caused by vorticity waves p 511 A92-32502
A method for measuring high-subsonic two-dimensional periodic flow field using a single-hole high-response cylindrical pressure probe p 588 A92-35567
Arbitrary blade section design based on viscous considerations - Blade optimization p 523 A92-36030
Laminar flow control of subsonic boundary layers by suction and heat transfer strips p 617 A92-39338
Compressibility effects in turbulent far wakes
p 622 A92-40140
Simulation of turbulent velocity profiles appearing on rotating and stationary parts of subsonic compressors and turbines p 676 A92-40172
Subsonic and transonic low-Reynolds-number airfoils with reduced pitching moments p 701 A92-41211
Design optimization of natural laminar flow bodies in compressible flow p 701 A92-41219
Extrapolation procedures for the time-dependent Navier-Stokes equations p 704 A92-41289
Upwind schemes for Navier-Stokes computations at subsonic through hypersonic speeds
p 708 A92-43071
Aerodynamic characteristics of curved delta wings in the case of subsonic separated flow
p 712 A92-44121
On the measurement of subsonic flow around an appended body of revolution at cryogenic conditions in the NTF p 880 A92-45265
Numerical investigation into high-angle-of-attack leading-edge vortex flow
[AIAA PAPER 92-2600] p 791 A92-45477
Two-point optimization of complete three-dimensional *airplane configuration*
[AIAA PAPER 92-2618] p 844 A92-45491
The subsonic and transonic flow around the leading edge of a thin airfoil with a parabolic nose
[AIAA PAPER 92-2649] p 797 A92-45516
Investigation of solution operators for the three-dimensional Euler equations
[AIAA PAPER 92-2666] p 797 A92-45522
Calculation of high speed base flows
[AIAA PAPER 92-2679] p 799 A92-45531
Effect of a bulge on the subharmonic instability of subsonic boundary layers p 898 A92-45833
Aerodynamic sensitivities for subsonic lifting-surface
p 819 A92-47695
Total losses in turbulent flows inside conical diffusers
p 819 A92-47782
Asymmetric turbulent vortical flows over slender bodies p 935 A92-50314
On the effect of external flow and shear-layer thickness on the expansion cells of under-expanded supersonic circular jets p 969 A92-50478
The relation among the general unsteady aerodynamic coefficients of a wing in subsonic and supersonic speed
p 941 A92-53022
Navier-Stokes simulation for the winged space vehicle 'HOPE' at subsonic, transonic, and supersonic regimes
p 1018 A92-53559
Calculations for aerodynamic characteristics of HOPE type vehicle in subsonic and hypersonic flow
p 1018 A92-53560
An experimental investigation of the flow in a diffusing S-duct
[AIAA PAPER 92-3622] p 1021 A92-54090
The SR3 low density wind tunnel - Facility capabilities and research development
[AIAA PAPER 92-3972] p 1098 A92-56798
Effects of external influences in subsonic delta wing vortices
[AIAA PAPER 92-4033] p 1034 A92-56855
Phenomenological modeling of the wake produced by a straight two dimensional base in subsonic flow
[REPT-90/59] p 82 N92-11982
An experimental study of the flow over a sharp-edged delta wing at subsonic and transonic speeds
p 85 N92-13011
Research on inverse methods and optimization in Italy
p 202 N92-13956
CAR 88: A method to calculate subsonic and supersonic, steady and unsteady, potential flow about complex configurations
[NLR-TR-88154-U] p 400 N92-18221
Institute for experimental fluid mechanics: Results for 1990
[IB-222-90-A-46] p 400 N92-18244
An initial investigation into methods of computing transonic aerodynamic sensitivity coefficients
[NASA-CR-190040] p 348 N92-19545
Invariant boundary conditions for cascade flows
p 498 N92-20147
Numerical simulation of vortical flow over a delta wing at subsonic and transonic speeds
[NLR-TP-90029-U] p 444 N92-20498
A quantitative study of unsteady compressible flow on an oscillating airfoil
[AD-A244572] p 445 N92-21012
Three-dimensional compressible turbulent computations for a diffusing S-duct
[NASA-CR-4392] p 526 N92-22249
NACA0012 benchmark model experimental flutter results with unsteady pressure distributions
[NASA-TM-107581] p 526 N92-22507
PAN AIR: A computer program for predicting subsonic or supersonic linear potential flows about arbitrary configurations using a higher order panel method. Volume 1: Theory document (version 3.0)
[NASA-CR-3251] p 526 N92-22648
PAN AIR: A computer program for predicting subsonic or supersonic linear potential flows about arbitrary configurations using a higher order panel method. Volume 2: User's manual (version 3.0)
[NASA-CR-3252] p 527 N92-22865
Adaptive active flutter suppression of wings in subsonic and transonic flight regimes p 553 N92-24010
A user guide for the EMTAC-MZ CFD code
[NASA-CR-4283] p 678 N92-24242
Assessment of potential aerodynamic benefits from spanwise blowing at the wing tip
[NASA-TM-107847] p 631 N92-25261
Measurements of fluctuating pressure in a rectangular cavity in transonic flow at high Reynolds numbers
[NASA-TM-4363] p 633 N92-25752
A comparison of predicted and measured inlet distortion flows in a subsonic axial inlet flow compressor rotor
[NASA-TM-105427] p 633 N92-26104
An outline of a numerical scheme for calculating two-dimensional time linearised transonic flow using the Green's function method
[AD-A246349] p 764 N92-26258
Subsonic investigations of vortex interaction control for enhanced high-alpha aerodynamics of a chine forebody/Delta wing configuration
[NASA-CR-189641] p 715 N92-26652
Unsteady Euler calculations in 3D internal aerodynamics p 768 N92-27470
Evaluation of measured-boundary-condition methods for *3D subsonic wall interference*
[NLR-TR-88072-U] p 832 N92-29884
Production of periodical Mach number variations in high subsonic flow in a blow down wind tunnel, and its influence on profile measurements
[ETN-92-91492] p 833 N92-29889

Extension of the integral equation formulation of linearized time dependent subsonic flow
[AD-A250654] p 947 N92-31171
An experimental study of the flow over a sharp-edged delta wing at subsonic and transonic speeds
[NLR-TP-91117-U] p 1037 N92-32732
High speed transition prediction
[NASA-CR-190836] p 1039 N92-33424

SUBSONIC FLUTTER
Modern aerodynamic flutter analysis --- Book
p 676 A92-40898
E-6 flutter investigation and experience
[AIAA PAPER 92-4601] p 1077 A92-55280
A computational investigation of airfoil stall flutter
[AD-A247302] p 947 N92-31300

SUBSONIC SPEED
Development of a shock noise prediction code for high-speed helicopters - The subsonically moving shock
p 165 A92-14384
An efficient calculation method of subsonic aerodynamic characteristics for a Space Shuttle orbiter in the reentry attitude p 252 A92-23383
Evaluation of two flow analyses for subsonic diffuser design
[AIAA PAPER 92-0273] p 317 A92-25727
Lift characteristics of an infinite-span cylindrical wing of a thick symmetric profile at low subsonic velocities
p 440 A92-31897
Experimental studies on aerodynamic characteristics of SSTO vehicle at low subsonic speeds
[SAE PAPER 911981] p 788 A92-45386
Comparison between two 3D-NS-codes and experiment on a turbine stator
[AIAA PAPER 92-3042] p 822 A92-48703
Development of high performance compressor discharge seal
[AIAA PAPER 92-3714] p 907 A92-49096
Subsonic flight test evaluation of a performance seeking control algorithm on an F-15 airplane
[AIAA PAPER 92-3743] p 878 A92-49109
Application of submerged vortex generators for separation control of a subsonic diffuser
p 933 A92-49832
Flow field over the wing of a delta-wing fighter model with vortex control devices at Mach 0.6 to 1.2
[NASA-TM-4296] p 526 N92-22506
Overview of the subsonic propulsion technology session p 560 N92-22531
Boundary layer transition: Prediction, application to drag reduction p 717 N92-27711
Present status of the MIT/NASA Langley 6-inch MSBS p 750 N92-27802
Jet aircraft noise at high subsonic flight Mach numbers
[DLR-FB-91-28] p 928 N92-29997
Preliminary subsonic aerodynamic model for simulation studies of the HL-20 lifting body
[NASA-TM-4302] p 978 N92-31175
An investigation into the interface between three closely spaced axi-symmetric bodies at subsonic speed
[CRANFIELD-AERO-9114] p 948 N92-31514
Advanced subsonic transport approach noise: The relative contribution of airframe noise
[NASA-TM-104112] p 1140 N92-34148

SUBSONIC WIND TUNNELS
Experimental investigation on the effect of crescent planform on lift and drag p 9 A92-13206
Recent development of wind-tunnel test techniques at ONERA
[ONERA, TP NO. 1991-135] p 137 A92-16110
Determination of the mass-flow-rate characteristics of porous panels p 439 A92-31875
Some problems on the sidewall interference in two-dimensional subsonic and transonic wind tunnel testing p 747 A92-41929
Turbulent diffusion flame properties behind a backward-facing step p 985 A92-50255
Assessment of passive porosity with free and fixed separation on a tangent ogive forebody
[AIAA PAPER 92-4494] p 1081 A92-55363
High subsonic wind tunnel test of a two-dimensional hybrid-laminar-flow-control airfoil with slotted surface
p 1029 A92-56045
The design of a subsonic low-noise, low-turbulence wind tunnel for acoustic measurements
[AIAA PAPER 92-3883] p 1094 A92-56726
Subsonic wind tunnel testing handbook
[AD-A240263] p 13 N92-10986
Effect of collector configuration on test section turbulence levels in an open-jet wind tunnel
[NASA-TM-4333] p 750 N92-27670
Calculation of support interferences on the aerodynamic coefficients for a wind tunnel calibration model
[ESA-TT-1247] p 830 N92-29159

SUBSTRATES
Removing aircraft surface coatings
p 516 A92-35574

SUBSTRUCTURES
Inclusion principle for the Rayleigh-Ritz based substructure synthesis p 670 A92-36851

SUCTION
Supersonic boundary-layer stability analysis on an aircraft wing p 9 A92-13207
Convective transport phenomena on the suction surface of a turbine blade including the influence of secondary flows near the endwall
[ASME PAPER 91-GT-35] p 147 A92-15518
Film cooling on a gas turbine rotor blade
[ASME PAPER 91-GT-279] p 152 A92-15675
Effect of suction on the stability of supersonic boundary layers. I - Second-mode waves. II - First-mode waves
p 174 A92-19611
Suppression of the wing-body junction vortex by body surface suction p 309 A92-24417
The effects of suction on the nonlinear stability of the three-dimensional boundary layer above a rotating disc
p 393 A92-25366
Theoretical analysis of a suction diffuser in the porous test section of a wind tunnel p 428 A92-30207
The effects of wall suction on laminar-turbulent transition in three-dimensional flow p 522 A92-36021
Boundary-layer receptivity due to a wall suction and control of Tollmien-Schlichting waves
p 616 A92-39333
Laminar flow control of subsonic boundary layers by suction and heat transfer strips p 617 A92-39338
Influence of suction through a slot on a turbulent boundary layer p 622 A92-40127
Design of wing profiles with tangential suction or injection p 624 A92-40602
Study on calculating the subsonic and supersonic aerodynamic characteristics of slender wing-body combinations at large angles of attack
p 706 A92-41926
Compressible Navier-Stokes solutions for a suction boundary control airfoil
[AIAA PAPER 92-2710] p 802 A92-45551
Discussion on sidewall suction in two-dimensional wind tunnel p 997 A92-53263
Experimental evaluation of a 50-percent thick airfoil with blowing and suction boundary layer control
[AIAA PAPER 92-4500] p 1026 A92-55368
Characteristics of a boundary layer in a leading edge vortex p 86 N92-13012
Control of forebody vortices by suction at the nose of the RAE high incidence research model
p 87 N92-13022
Dynamic wind tunnel tests on control of forebody vortices with suction p 380 N92-18793
Experimental investigation into the effects of riblets on compressor cascade performance
[AD-A243881] p 377 N92-19235
Secondary instability of high-speed flows and the influence of wall cooling and suction
[NASA-CR-4427] p 406 N92-19844
Calculations of hot gas ingestion for a STOVL aircraft model
[NASA-TM-105437] p 350 N92-19993

SULFUR FLUORIDES
Numerical study on using sulfur hexafluoride as a wind tunnel test gas p 216 A92-18373

SULFURIC ACID
Non-chromated anodize process for corrosion resistance and adhesive bonding p 892 A92-47341

SUPERCHARGERS
Surge dynamics in a free-spool centrifugal compressor system
[ASME PAPER 91-GT-31] p 68 A92-15515
Rotary engine performance limits predicted by a zero-dimensional model
[NASA-CR-189129] p 474 N92-20650
Supercharged ejector ramjet p 475 N92-21527
Principles and computer simulations of intercooled-turbocharged gas generator/expander engine p 592 N92-22132
Small engine technology programs
p 560 N92-22532
Turbocharged pressurized combustion system
[PB92-142579] p 756 N92-26521
Radial inflow turbine study
[AD-A252783] p 1127 N92-33538

SUPERCOMPUTERS
Traditional finite element analysis - Opportunities for parallelism? p 40 A92-12354
Aerospace - Collected translations of selected papers
p 608 A92-38266
Application of technology developed for flight simulation at NASA. Langley Research Center p 573 N92-22437
NAS (Numerical Aerodynamic Simulation Program) technical summaries, March 1989 - February 1990
[NASA-TM-107960] p 1013 N92-31852

SUPERCONDUCTING FILMS
Magnetic suspension using high temperature superconducting cores p 772 N92-27789

SUPERCONDUCTING MAGNETS
Characterization of superconducting magnetic bearings (dynamic stiffness and damping coefficient in axial direction) p 772 N92-27737
International Symposium on Magnetic Suspension Technology, part 2
[NASA-CP-3152-PT-2] p 753 N92-27788
Superconducting bearings with levitation control configurations
[NASA-CASE-GSC-13346-1] p 909 N92-29099

SUPERCONDUCTIVITY
Development of an electromagnetic microscope for eddy current evaluation of materials
[AD-A242007] p 406 N92-19873
Characterization of superconducting magnetic bearings (dynamic stiffness and damping coefficient in axial direction) p 772 N92-27737
International Symposium on Magnetic Suspension Technology, part 2
[NASA-CP-3152-PT-2] p 753 N92-27788
Cryogenic test rig with an aerodynamic magnetically levitated carriage p 750 N92-27792
Superconducting bearings with levitation control configurations
[NASA-CASE-GSC-13346-1] p 909 N92-29099

SUPERCOOLING
Volume spectra in supercooled clouds for several research flights
[AIAA PAPER 92-0167] p 350 A92-25683
Remote measurements of supercooled integrated liquid water during WISP/FAA aircraft icing program
p 915 A92-46788

SUPERCRITICAL AIRFOILS
Effects of trailing-edge flap on buffet characteristics of a supercritical airfoil p 378 A92-24413
Experimental study of the characteristics of boundary-layer development on an airfoil
p 425 A92-30171
Investigation of the aerodynamic features of flows past models using thin-film capacitance-type sensors of pressure oscillations p 440 A92-31884
Some characteristics of transonic flow past an airfoil in the case of developed separation
p 440 A92-31885
Comparison of Euler and full potential methods for unsteady transonic flow calculations
p 719 N92-27943
Development and validation of a characteristic boundary condition for a cell-centered Euler method
[NLR-TP-90144-U] p 828 N92-28692

SUPERCRITICAL FLOW
Analysis of transonic flow over plane compressor cascades using the large-particle method
p 79 A92-16812
Prediction of the viscous transonic aerodynamic performance of supercritical aerofoil sections
[AIAA PAPER 92-2653] p 805 A92-45569
A compact higher order Euler solver for unstructured grids with curved boundaries
[AIAA PAPER 92-2696] p 807 A92-45590
Supercritical blade design on stream surfaces of revolution with an inverse method p 220 N92-13950

SUPERCRITICAL PRESSURES
Structure and penetration of a transverse fluid jet injected at supercritical pressure in supersonic flow
[AIAA PAPER 92-3652] p 1113 A92-54105

SUPERCRITICAL WINGS
Interference effects of very high bypass ratio nacelle installations on a low-wing transport
[ASME PAPER 91-GT-241] p 75 A92-15646
Investigation of the effect of an ultrasonic acoustic field on boundary layer separation on an airfoil
p 511 A92-30205
Flux-difference split algorithm for unsteady thin-layer Navier-Stokes solutions p 431 A92-31158
Experimental investigation of the air bypass effect in the shock-wave region on the aerodynamic characteristics of a wing profile p 439 A92-31877
Experimental investigation of the optimal deflection of a single-slotted flap with different degrees of extension on a modern supercritical profile p 439 A92-31879
Dynamic characteristics of a Benchmark models program supercritical wing
[AIAA PAPER 92-2368] p 571 A92-34596
Installation effects of wing-mounted turbofan nacelle-pylons on a 1/17-scale, twin-engine, low-wing transport model
[NASA-TP-3168] p 346 N92-19002

Inviscid drag prediction for transonic transport wings using a full-potential method
[NLR-TP-89365-U] p 444 N92-20473
Unsteady-pressure and dynamic-deflection measurements on an aeroelastic supercritical wing
[NASA-TM-4278] p 445 N92-20654
The SnoDog: Preliminary design of a close air support aircraft
[NASA-CR-189990] p 462 N92-21489
The NASA Langley laminar-flow-control experiment on a swept, supercritical airfoil: Evaluation of initial perforated configuration
[NASA-TM-4309] p 525 N92-22196

SUPERPLASTICITY
Process control challenges during the manufacture of large superplastically formed/diffusion bonded structure
[SAE PAPER 912195] p 674 A92-40012
Advances in aircraft component superplastic forming/diffusion bonding technology
[SAE PAPER 912216] p 674 A92-40018
Super plastic forming technology applied to aeroengine and space equipment p 764 A92-44732
Superplastic applications in aero engines
[PNR-90788] p 473 N92-20436

SUPERPRESSURE BALLOONS
Stratospheric electrodynamics from superpressure balloons - A technical challenge for small payload environments
[AIAA PAPER 91-3674] p 14 A92-11019
Manned orbital balloon flight - Available techniques
[AIAA PAPER 91-3675] p 15 A92-11020

SUPERSATURATION
Size and critical supersaturation for condensation of jet engine exhaust particles p 161 A92-15884
Influence of air velocity on the habit of ice crystal growth from the vapor p 668 A92-38111
Microgravity nucleation and particle coagulation experiments support
[NASA-CR-190159] p 502 N92-21385

SUPERSONIC AIRCRAFT
The selective bleed variable cycle engine --- aircraft propulsion
[ASME PAPER 91-GT-388] p 126 A92-15720
Four decades of transonic fighter design p 193 A92-20203
On the threshold - The outlook for supersonic and hypersonic aircraft p 356 A92-24402
Variable-complexity aerodynamic optimization of an HSCT wing using structural wing-weight equations
[AIAA PAPER 92-0212] p 317 A92-25685
Cooling of a sharp nose by extraneous gas injection into the viscous shock layer p 426 A92-30188
Progress report of Scot's Laser Ordnance Initiator System for crew escape p 580 A92-32988
Preliminary results from the High Speed Airframe Integration Research project
[AIAA PAPER 92-1004] p 536 A92-33196
YF-22A prototype Advanced Tactical Fighter demonstration/validation flight test program overview
[AIAA PAPER 92-1087] p 537 A92-33253
Comparison of two flutter analysis methods for elastic aircraft p 660 A92-37394
Research and development of turbofan engine for supersonic aircraft p 654 A92-38025
Loudness of shaped sonic booms p 695 A92-39238
A review of computational/experimental methodology developments in aeroacoustics p 695 A92-39241
High speed civil transport electrical power system technology requirements
[SAE PAPER 912185] p 655 A92-40005
Aerodynamic characteristics of a high-speed composite airfoil p 712 A92-43231
Large-scale wind tunnel studies of a jet-engined powered ejector-lift STOVL aircraft p 842 A92-45313
Integrated flight/propulsion control for supersonic STOVL aircraft p 872 A92-45320
Results and lessons learned from the STOL and Maneuver Demonstration Program
[SAE PAPER 912005] p 843 A92-45406
Computational study of transition front on a swept wing leading-edge model
[AIAA PAPER 92-2630] p 795 A92-45502
Determination of aerodynamic sensitivity coefficients based on the three-dimensional full potential equation
[AIAA PAPER 92-2670] p 798 A92-45525
Viscous flow past a nacelle isolated and in proximity of a flat plate
[AIAA PAPER 92-2723] p 803 A92-45560
Aviation, motor, and space designs --- research and development in U.S.S.R. p 784 A92-46202
Prediction of inviscid supersonic/hypersonic aircraft flowfields p 810 A92-46785
New thermoplastic polyimide composite for supersonic aircraft structures p 985 A92-51512
A full-scale fatigue test and failure analyses research of F-X fighters p 960 A92-53092
Study on international cooperative test facilities for future SST/HST
[AIAA PAPER 92-3945] p 1097 A92-56775
High-speed civil transport aircraft emissions p 408 N92-19122
Nonlinear stability and control study of highly maneuverable high performance aircraft, phase 2
[NASA-CR-189911] p 382 N92-19841
The environmental challenges for the next supersonic aircraft
[PNR-90782] p 505 N92-20928
Aeronautical research in the United States: Challenges for the 1990's p 420 N92-21502
Polymer infiltration studies
[NASA-CR-190204] p 578 N92-22486
Fiber optics for controls p 570 N92-22529
Mechanical design of a rotary balance system for NASA. Langley Research Center's vertical spin tunnel p 664 N92-25090
Determination of aerodynamic sensitivity coefficients for wings in transonic flow
[NASA-CR-190570] p 832 N92-29657
A method for designing blended wing-body configurations for low wave drag
[NASA-TP-3261] p 1036 N92-32480
Supportability evaluation of thermoplastic and thermoset composites p 1108 N92-32576
Survey and analysis of research on supersonic drag-due-to-lift minimization with recommendations for wing design
[NASA-TP-3202] p 1040 N92-33656
Lateral spread of sonic boom measurements from US Air Force boomfile flight tests p 1140 N92-33883

SUPERSONIC AIRFOILS
Calculation of the rolling moment for a wing with a supersonic leading edge in the presence of sideslip p 426 A92-30186
Numerical analysis on laminar flow control of transonic airfoils p 430 A92-30557
Unsteady separation in sharp fin-induced shock wave/turbulent boundary layer interaction at Mach 5
[AIAA PAPER 92-0748] p 436 A92-31678
Analytical and experimental studies of the aerodynamic characteristics of a delta wing at a slip angle at high supersonic velocities p 437 A92-31854
Aerodynamic characteristics of a blunt delta wing with air bleed through an intake at supersonic and hypersonic velocities. II p 437 A92-31855

SUPERSONIC BOUNDARY LAYERS
Supersonic boundary-layer stability analysis on an aircraft wing p 9 A92-13207
Calculation of the base pressure and enthalpy behind a step in the path of two supersonic streams with allowance for the effect of boundary layers and heat fluxes p 63 A92-13748
On the interaction between first- and second-mode waves in a supersonic boundary layer p 78 A92-16462
Effect of suction on the stability of supersonic boundary layers. I - Second-mode waves. II - First-mode waves p 174 A92-19611
Modeling supersonic inlet boundary layer bleed roughness
[AIAA PAPER 92-0269] p 317 A92-25725
A three-dimensional supersonic turbulent boundary layer generated by an isentropic compression
[AIAA PAPER 92-0310] p 320 A92-25758
An algebraic model for dissipation in supersonic boundary layers
[AIAA PAPER 92-0311] p 320 A92-25759
Evolution of perturbations in a supersonic boundary layer p 337 A92-27596
Control of strong shock-turbulent boundary layer interaction in rectangular channels p 422 A92-29714
Structure of supersonic turbulent flow past a swept compression corner p 431 A92-31155
Secondary instability of high-speed flows and the influence of wall cooling and suction p 435 A92-31640
Boundary layer on slender wings of small aspect ratio p 441 A92-31963
Supersonic and hypersonic boundary-layer transition induced by discrete trips p 522 A92-36023
Performance of turbulence models to predict supersonic boundary layer flows p 613 A92-37553
Application of linear stability theory in laminar flow design
[SAE PAPER 912116] p 618 A92-39967
Susceptibility of a supersonic boundary layer to acoustic perturbations p 707 A92-42730
Computational study of transition front on a swept wing leading-edge model
[AIAA PAPER 92-2630] p 795 A92-45502
Discrete modes and continuous spectra in supersonic boundary layers p 809 A92-46264
Effect of a fan of rarefaction waves on the development of disturbances in a supersonic boundary layer p 809 A92-46519
Lower upper implicit total variation diminishing solution of viscous hypersonic flows p 935 A92-50302
Linear stability of supersonic cone boundary layers p 1024 A92-54910
Supersonic combustion studies p 211 N92-14984
Secondary instability of high-speed flows and the influence of wall cooling and suction
[NASA-CR-4427] p 406 N92-19844

SUPERSONIC COMBUSTION
H2/air subsystem combustion kinetics in aerospaceplane powerplants
[IAF PAPER 91-276] p 25 A92-12600
Supersonic reacting internal flowfields p 155 A92-16989
An experimental investigation of the combustion of a hydrogen jet injected parallel in a supersonic air stream
[AIAA PAPER 91-5102] p 212 A92-17861
Compressibility effects in thin channels with injection p 216 A92-18369
Simultaneous coherent anti-Stokes Raman spectroscopy measurements in hydrogen-fueled supersonic combustion p 287 A92-21052
Laser diagnostics for velocity measurements in supersonic combusting environments
[AIAA PAPER 92-0008] p 288 A92-22133
Laser-initiated conical detonation wave for supersonic combustion. II
[AIAA PAPER 92-0088] p 292 A92-22195
Experimental investigation of a supersonic combustion flowfield employing staged transverse injection behind a rearward-facing step
[AIAA PAPER 92-0090] p 292 A92-22196
Numerical studies of supersonic/hypersonic combustion
[AIAA PAPER 92-0094] p 293 A92-22200
Thermochemical nonequilibrium and radiative interactions in supersonic hydrogen-air combustion
[AIAA PAPER 92-0340] p 394 A92-25786
A numerical investigation of hydrogen combustion in Mach 2 flow
[AIAA PAPER 92-0341] p 388 A92-25787
An experimental study of supersonic H2 combustion and heat transfer in a circular duct p 388 A92-25997
Interfacial instability between a liquid film and the surrounding compressible gas
[AIAA PAPER 92-0461] p 395 A92-26302
Evaluation of OH laser-induced fluorescence techniques for supersonic combustion diagnostics
[AIAA PAPER 92-0508] p 396 A92-26935
Experiments on shear layer mixing at hypervelocity conditions
[AIAA PAPER 92-0628] p 396 A92-27009
A numerical study of the effects of geometry on the performance of a supersonic combustor
[AIAA PAPER 92-0624] p 342 A92-28213
Laser-initiated conical detonation wave for supersonic combustion p 375 A92-28531
Strain-induced extinction of hydrogen-air counterflow diffusion flames - Effects of steam, CO2, N2, and O2 additives to air
[AIAA PAPER 92-0877] p 487 A92-29639
Experimental design of a supersonic shock wave/vortex interaction at Mach 3 p 521 A92-35988
Direct simulation of a supersonic reacting mixing-layer p 676 A92-40132
Planar fluorescence imaging of a transverse jet in a supersonic crossflow p 755 A92-44501
Waves and thermodynamics in high Mach number propulsive ducts p 809 A92-46431
Laser-initiated conical detonation wave for supersonic combustion. III
[AIAA PAPER 92-3247] p 893 A92-48846
KrF laser-induced OH fluorescence imaging in a supersonic combustion tunnel
[AIAA PAPER 92-3346] p 905 A92-48923
Experimental investigation of liquid carbonhydrogen fuel combustion in channel at supersonic velocities
[AIAA PAPER 92-3429] p 894 A92-48986
Ignition delays, heats of combustion, and reaction rates of aluminum alkyl derivatives used as ignition and combustion enhancers for supersonic combustors
[AIAA PAPER 92-3841] p 894 A92-49134
Experiments on the structure of an annular compressible reacting shear layer p 969 A92-50311
Supersonic flow mixing and combustion using RAMP nozzle
[AIAA PAPER 92-3840] p 1113 A92-54198
An assumed joint-Beta PDF approach for supersonic turbulent combustion
[AIAA PAPER 92-3844] p 1113 A92-54199

Interaction between chemical reaction and turbulence in supersonic nonpremixed H2-air combustion
p 1117 A92-54931
Free-radicals aided combustion with scramjet applications
[IAF PAPER 92-0659] p 1106 A92-57100
Study on supersonic combustion in a hypersonic flight
[IAF PAPER 92-0661] p 1106 A92-57101
Supersonic combustion studies p 211 N92-14984
An analytical and computational investigation of shock-induced vortical flows with applications to supersonic combustion p 405 N92-19538
NASA's hypersonic propulsion program: History and direction p 476 N92-21535
NASA thrusts in high-speed aeropropulsion research and development: An overview p 561 N92-22538
Study of shock-induced combustion using an implicit TVD scheme p 669 N92-25816
Turbulent reacting flows and supersonic combustion
[AD-A251065] p 986 N92-30256
Laser-initiated conical detonation wave for supersonic combustion, part 3
[AD-A250522] p 989 N92-32076
Theories of turbulent combustion in high speed flows
[AD-A253032] p 1111 N92-33624

SUPERSONIC COMBUSTION RAMJET ENGINES

Advanced SCRAM-LACE system concept for single-stage-to-orbit space plane
[IAF PAPER 91-272] p 32 A92-12599
Fuel injection in hypersonic airbreathing engine
[IAF PAPER 91-273] p 120 A92-14710
Supersonic reacting internal flowfields
p 155 A92-16989
Tangential mass addition for shock/boundary-layer interaction control in scramjet inlets p 80 A92-17197
Inviscid analysis of a dual mode scramjet inlet
p 80 A92-17198
Engineering model for analysis of scramjet combustor performance with finite-rate chemistry
p 129 A92-17202
CFD application to 2D/3D flow fields in Scramjet engine p 170 A92-17501
Scramjet research at the National Aerospace Laboratory
[AIAA PAPER 91-5076] p 200 A92-17849
An experimental investigation of the combustion of a hydrogen jet injected parallel in a supersonic air stream
[AIAA PAPER 91-5102] p 212 A92-17861
Research on supersonic combustion
[AIAA PAPER 92-0001] p 278 A92-22126
An experimental investigation of large scale instabilities in a low Reynolds number two-stream supersonic shear layer
[AIAA PAPER 92-0177] p 255 A92-23787
A computational investigation of mixing and reacting flows in supersonic combustors
[AIAA PAPER 92-0626] p 278 A92-23817
Three-dimensional simulation of a translating strut inlet
[AIAA PAPER 92-0270] p 317 A92-25726
Two and three dimensional parabolized Navier-Stokes code for scramjet combustor, nozzle, and film cooling analysis
[AIAA PAPER 92-0391] p 372 A92-26247
Thermal management systems for high Mach airbreathing propulsion
[AIAA PAPER 92-0515] p 373 A92-26941
A systematic experimental and computational investigation of a class of contoured wall fuel injectors
[AIAA PAPER 92-0625] p 374 A92-27007
Supersonic combustor testing using optical diagnostics and a high enthalpy shock tunnel
[AIAA PAPER 92-0761] p 384 A92-27102
Leading edge sweep effects in generic three-dimensional sidewall compression scramjet inlets
[AIAA PAPER 92-0674] p 343 A92-28218
Full Navier-Stokes analysis of a three-dimensional hypersonic mixed compression inlet p 343 A92-28501
Evaluation of parallel injector configurations for Mach 2 combustion p 376 A92-28533
Computations of multispecies mixing between scramjet nozzle flow and hypersonic freestream
p 376 A92-28534
Hydrocarbon-fueled scramjet combustor investigation
p 376 A92-28535
Computation of scramjet inlet flow
p 430 A92-30541
Numerical simulation of three-dimensional supersonic free shear layers p 431 A92-31152
French research and technology program on advanced hypersonic propulsion
[AIAA PAPER 91-5003] p 471 A92-31683
A computational exploration of the importance of three-dimensionality, boundary layer development, and flow chemistry to the prediction of scramjet nozzle performance
[AIAA PAPER 91-5059] p 472 A92-31689
Russians want U.S. to join scramjet tests
p 472 A92-32296
Design tradeoffs on engine-integrated hypersonic vehicles
[AIAA PAPER 92-1205] p 537 A92-33313
Perspective on future aircraft engines
p 558 A92-35921
Experimental study of a two-dimensional scramjet inset, M(freestream) = 10.1-25.1 p 611 A92-36974
Numerical study of the effects of reverse sweep on scramjet inlet performance p 611 A92-36979
The thermodynamic approach in the study of large systems - Application to high-velocity airbreathing propulsion p 654 A92-37824
The beginnings of the hypersonic and the renewal of the supersonic ramjet p 782 A92-41824
Surface cooling of scramjet engine inlets using heat pipe, transpiration, and film cooling p 763 A92-44381
Effectiveness of plasma torches for ignition and flameholding in scramjet p 737 A92-44524
Flow establishment in a generic scramjet combustor
p 737 A92-44525
Aerospace plane hydrogen scramjet boosting
[SAE PAPER 912071] p 891 A92-45451
Internal shock interactions in propulsion/airframe integrated three-dimensional sidewall compression scramjet inlets
[AIAA PAPER 92-3099] p 824 A92-48741
FNS analysis of an axisymmetric scramjet inlet
[AIAA PAPER 92-3100] p 824 A92-48742
Operating characteristics at Mach 4 of an inlet having forward-swept, sidewall-compression surfaces
[AIAA PAPER 92-3101] p 863 A92-48743
Computational analysis of ramjet engine inlet interaction
[AIAA PAPER 92-3102] p 824 A92-48744
A comparative study of scramjet injection strategies for high Mach numbers flows
[AIAA PAPER 92-3287] p 904 A92-48876
A scramjet nozzle experiment with hypersonic external flow
[AIAA PAPER 92-3289] p 864 A92-48878
Experimental validation of scramjet nozzle performance
[AIAA PAPER 92-3290] p 864 A92-48879
Analysis of a hydrocarbon scramjet with augmented preburning
[AIAA PAPER 92-3425] p 865 A92-48984
Experimental investigation of liquid carbonhydrogen fuel combustion in channel at supersonic velocities
[AIAA PAPER 92-3429] p 894 A92-48986
The External Propulsion Accelerator - Scramjet thrust without interaction with accelerator barrel
[AIAA PAPER 92-3717] p 866 A92-49098
Full Navier-Stokes analysis of a three-dimensional scramjet inlet p 934 A92-50272
Some readily quantifiable aspects of scramjet engine performance p 969 A92-50278
Some thermodynamical aspects in the optimization of supersonic combustors p 1065 A92-53486
Conceptual design of scramjet engine
p 1065 A92-53490
Key design considerations for scramjet powered space plane p 1066 A92-53491
Scramjet engine and its flying test bed
p 1066 A92-53492
Performance analysis of idealized scramjet
p 1066 A92-53493
Detailed numerical analysis of standing oblique detonation p 1111 A92-53550
Flow measurements in scramjet inlets
p 1102 A92-53565
The enhancement of the mixing and combustion processes in supersonic flow applied to scramjet engine
[AIAA PAPER 92-3428] p 1112 A92-54029
Optimization of a 2D scramjet-vehicle using CFD and simplified approximate flow analysis techniques
[AIAA PAPER 92-3673] p 1022 A92-54116
An advanced scramjet propulsion concept for a 350 MG SSTO space plane - External nozzle performance
[AIAA PAPER 92-3719] p 1067 A92-54134
Further studies of kinetic energy methods in high speed ramjet cycle analysis
[AIAA PAPER 92-3805] p 1069 A92-54177
Dynamics and control of hypersonic aeropropulsive/aeroelastic vehicles
[AIAA PAPER 92-4326] p 1073 A92-55170
A clean air continuous flow propulsion facility
[AIAA PAPER 92-3912] p 1094 A92-56745
Test description and preliminary pitot-pressure surveys for Langley Test Technique Demonstrator at Mach 6
[AIAA PAPER 92-3940] p 1096 A92-56770
A model study on diffuser pressure recovery in NAL scramjet test facility with simulated hydrogen combustion
[AIAA PAPER 92-3979] p 1071 A92-56805
Free-radicals aided combustion with scramjet applications
[IAF PAPER 92-0659] p 1106 A92-57100
A computational and experimental investigation of a three-dimensional hypersonic scramjet inlet flow field
p 11 N92-10007
Contractors Meeting in Propulsion
[AD-A240057] p 33 N92-10062
Viscous computations of cold air/air flow around scramjet nozzle afterbody
[NASA-CR-4406] p 13 N92-10982
Experimental simulation and diagnostics of high-enthalpy real-gas flows
[AD-A241286] p 166 N92-13822
Supersonic combustion studies p 211 N92-14984
Optimization of tangential mass injection for minimizing flow separation in a scramjet inlet
[AD-A243868] p 376 N92-18867
A hierarchy for modeling high speed propulsion systems
[NASA-CR-186984] p 387 N92-19934
Pioneering scramjet developments by Antonio Ferri
p 474 N92-21519
Advanced ramjet concepts program
p 474 N92-21520
The NASA hypersonic research engine program
p 474 N92-21521
Scramjet analysis, testing p 475 N92-21532
NASP X-30 Propulsion technology status
p 475 N92-21534
Improved large perturbation propulsion models for control system design (1988-1989) and large perturbation models of high velocity propulsion systems (1989-1990) and reduced order propulsion models for control system design (1990-1991)
[NASA-CR-190148] p 593 N92-22491
A hierarchy for modeling high speed propulsion systems p 559 N92-22492
Hypersonic propulsion research p 561 N92-22543
Two stage to orbit design
[NASA-CR-189994] p 575 N92-22625
High temperature dynamic engine seal technology development
[NASA-TM-105641] p 596 N92-23435
Study of shock-induced combustion using an implicit TVD scheme p 669 N92-25816
An experimental investigation of a 2-D scramjet inlet at flow Mach numbers of 8 to 25 and stagnation temperatures of 800 to 4,100 K p 739 N92-26586
Hypersonic aerospace vehicle leading edge cooling using heat pipe, transpiration and film cooling techniques
p 780 N92-26733
Dynamic interactions between hypersonic vehicle aerodynamics and propulsion system performance
[NASA-CR-190638] p 1038 N92-33304
Perspectives on hypersonic viscous and nonequilibrium flow research
[NASA-CR-190817] p 1039 N92-33413

SUPERSONIC COMMERCIAL AIR TRANSPORT

Lower stratospheric measurement issues workshop report p 409 N92-19127

SUPERSONIC COMPRESSORS

Quasi-three-dimensional characteristics method for a supersonic compressor rotor
[ASME PAPER 91-GT-81] p 69 A92-15549
An investigation of a strong shock-wave turbulent boundary layer interaction in a supersonic compressor cascade
[ASME PAPER 91-GT-92] p 70 A92-15556
The influence of shock waves on the viscous flow field of axial compressors
[ASME PAPER 91-GT-173] p 73 A92-15608
Method for the prediction of supersonic compressor blade performance p 277 A92-21078
Unsteady Navier-Stokes simulation of turbulent flows through a supersonic compressor cascade
p 523 A92-36036
Supersonic flow in compression stages and inlets
p 625 N92-24395
NASA. Lewis Research Center supersonic throughflow fan program
[NASA-TM-103248] p 972 N92-31250

SUPERSONIC DIFFUSERS

Diffuser efficiency estimation parameters
p 79 A92-16814
Effect of supersonic diffuser geometry on operation conditions p 310 A92-24599
Experimental study of a two-dimensional random frequency generator p 483 A92-29712

Experimental study of an adjustable plane supersonic diffusor p 426 A92-30173
A time marching method in finite volume for transonic diffuser turbulent flows p 819 A92-47690
A model study on diffuser pressure recovery in NAL scramjet test facility with simulated hydrogen combustion
[AIAA PAPER 92-3979] p 1071 A92-56805

SUPERSONIC DRAG
Minimizing supersonic wave drag with physical constraints at design and off-design Mach numbers p 811 A92-46808
Survey and analysis of research on supersonic drag-due-to-lift minimization with recommendations for wing design
[NASA-TP-3202] p 1040 N92-33656

SUPERSONIC FLIGHT
Design is the name of the game - Comparison of the F5D Skylancer to the F4D Skyray p 167 A92-16062
YF-23A preliminary flight test results p 112 A92-16063
Prediction of generalized aerodynamic forces following linearized supersonic theory
[ONERA, TP NO. 1991-114] p 76 A92-16093
The sonic boom and problems related to supersonic flights of military aircraft
[ONERA, TP NO. 1991-162] p 77 A92-16129
Numerical and experimental study of jet impingement or interaction effects at hypersonic and supersonic speeds
[AIAA PAPER 91-5038] p 171 A92-17826
Broadband shock-associated noise from supersonic jets in flight p 235 A92-18683
Pitching derivatives of wing in supersonic and hypersonic stream - Method for local flow piston theory p 312 A92-25012
Computational study of incipient leading-edge separation on a supersonic delta wing p 442 A92-32237
An aerodynamic design study of a series of lifting bodies at angles of attack from 10 to 53 degrees at Mach numbers from 2.30 to 4.62 p 442 A92-32500
Comment on 'Effect of thrust/speed dependence on long-period dynamics in supersonic flight' p 643 A92-39913
In-flight evaluation of Mach number at hypersonic speeds p 624 A92-40599
The turbo-ramjet Griffon p 782 A92-41820
Study on calculating the subsonic and supersonic aerodynamic characteristics of slender wing-body combinations at large angles of attack p 706 A92-41926
Evolution of ASTOVL aircraft design p 842 A92-45311
ASTOVL propulsion systems configuration and concept choice p 842 A92-45312
Waves and thermodynamics in high Mach number propulsive ducts p 809 A92-46431
The trisonic wind tunnel Muenchen and its involvement in the German SAeNGER-programme
[AIAA PAPER 92-4019] p 1100 A92-56841
Sonic boom p 55 N92-10608
FALKE and COBRA technology development in aerodynamics and aerothermodynamics p 183 N92-15017
Supersonic propulsion simulation by incorporating component models in the large perturbation inlet (LAPIN) computer code
[NASA-TM-105193] p 279 N92-15993
Advanced tactical fighter engine
[ETN-92-90840] p 376 N92-18728
Sonic booms produced by US Air Force and US Navy aircraft: Measured data
[AD-A244804] p 512 N92-21719
Supersonic STOVL propulsion technology program: An overview p 561 N92-22539
Supersonic throughflow fans for high-speed aircraft p 561 N92-22541
A summary of XB-70 sonic boom signature data
[NASA-CR-189630] p 696 N92-24800
ASTOVL engine control
[PNR-90808] p 740 N92-27040

SUPERSONIC FLOW
Numerical simulations of the structure of supersonic shear layers p 3 A92-10574
Triple-deck structure p 3 A92-10690
Two-phase flows at supersonic velocities p 4 A92-10907
Simple turbulence models for supersonic flows - Bodies at incidence and compression corners p 5 A92-11059
Kernel function occurring in supersonic unsteady potential flow p 6 A92-11080
Evolution of three-dimensional flows during the interaction between conical shock waves and a turbulent boundary layer p 7 A92-12169
Experimental and theoretical study of the improvement of the aerodynamic characteristics of supersonic flow past bodies with surface injection of a gas jet with particles p 8 A92-12204
Heat transfer in supersonic flow past a single crater p 63 A92-13741
Calculation of the base pressure and enthalpy behind a step in the path of two supersonic streams with allowance for the effect of boundary layers and heat fluxes p 63 A92-13748
Experimental studies of the interaction of converging axisymmetric shock waves with sharp and blunt cones in supersonic flow p 63 A92-13749
Fundamentals of applied aerogasdynamics. I - Aerodynamics of wings (profiles), airframes, and their combinations --- Russian book p 64 A92-14280
Oscillation of nearly circular shock waves p 146 A92-15358
Transonic and supersonic inviscid computations in cascades using adaptive unstructured meshes
[ASME PAPER 91-GT-312] p 75 A92-15689
Three-dimensional thin-layer and space-marching Navier-Stokes computations using an implicit MUSCL approach - Comparison with experiments and Euler computations
[ONERA, TP NO. 1991-131] p 77 A92-16107
Aerodynamic measuring techniques for transonic and supersonic flow in cascades and turbomachines
[ONERA, TP NO. 1991-170] p 137 A92-16135
CARS temperature/multi-species measurement strategies for high speed airbreathing and rocket propulsion testing p 154 A92-16615
Three-dimensional singularity of flow structure in an underexpanded supersonic jet p 78 A92-16679
Changing the structure and improving the aerodynamic characteristics of supersonic flow past bodies through ejection of a gas jet with particles p 78 A92-16680
A discrete vortex study of stationary flow past three-dimensional lifting systems at subsonic and supersonic velocities p 79 A92-16813
Supersonic reacting internal flowfields p 155 A92-16989
A lifting line theory for supersonic flow applications
[AIAA PAPER 91-5058] p 171 A92-17841
Prediction of steady and unsteady asymmetric vortical flows around circular cones p 172 A92-18372
Similarity solutions for supersonic axisymmetric flows p 173 A92-18387
Noise-driven flow p 173 A92-18680
Numerical calculation of subsonic and supersonic aerodynamic loads around complex configuration vehicle p 175 A92-20488
Genuinely upwind algorithms for the multidimensional Euler equations p 175 A92-20733
Newton's method solver for high-speed viscous separated flowfields p 176 A92-20736
Asymmetric separated flows at supersonic speeds p 176 A92-20742
Simple method of supersonic flow visualization using smoke p 219 A92-20764
Effects of sidewall disturbances on the supersonic mixing layer p 290 A92-21085
Linear panel flutter of an elliptic cylindrical shell p 291 A92-21216
Axisymmetric analogy for three-dimensional viscous flow problems p 244 A92-21617
Calculation of the parameters of separated flow behind a plane rounded body in the path of two supersonic flows p 244 A92-21624
Wave motions in a three-dimensional boundary layer p 244 A92-21629
Inverse solution uniqueness and domain of existence for supersonic space marching applications
[AIAA PAPER 92-0028] p 248 A92-22150
Steady supersonic and hypersonic flow computations using Eulerian and new Lagrangian formulations
[AIAA PAPER 92-0055] p 249 A92-22170
The problem of transition from continuum to rarefied gas flows p 251 A92-22519
A calculating method of shock wave oscillating frequency due to turbulent shear layer fluctuations in supersonic flow p 251 A92-22720
Simulation of supersonic and hypersonic flows p 251 A92-22790
On the calculation of the compressible boundary layer on a nonplanar delta wing with supersonic leading edges p 252 A92-23409
Mathematical modeling of supersonic flow over a convex-concave formed body based on the Euler and Navier-Stokes equations p 252 A92-23416
The Baldwin-Lomax model for separated and wake flows using the entropy envelope concept
[AIAA PAPER 92-0148] p 253 A92-23764
An experimental investigation of large scale instabilities in a low Reynolds number two-stream supersonic shear layer
[AIAA PAPER 92-0177] p 255 A92-23787
The dynamics and control of fluctuating pressure loads in the reattachment region of a supersonic free shear layer
[AIAA PAPER 92-0178] p 255 A92-23788
Organized structure in a Mach 5/Mach 3 turbulent shear layer
[AIAA PAPER 92-0180] p 256 A92-23790
Implementation of Vigneron's streamwise pressure gradient approximation in the PNS equations
[AIAA PAPER 92-0189] p 256 A92-23798
Effect of supersonic diffuser geometry on operation conditions p 310 A92-24599
On marching algorithms for solving stationary problems p 311 A92-24976
Numerical simulation of supersonic separated flow over blunt cones at high angles of attack p 313 A92-25039
Numerical simulations of flow fields over aircrafts p 313 A92-25042
Numerical simulation of inviscid flow over a complicated body using an overlapping grid technique p 313 A92-25043
A boundary element method for the potential, compressible aerodynamics of bodies in arbitrary motion p 314 A92-25098
The effect of successive distortions of the boundary layer in a supersonic flow
[AIAA PAPER 92-0309] p 320 A92-25757
Experiments on shock/vortex interactions
[AIAA PAPER 92-0315] p 320 A92-25762
An efficient Euler solver for predominantly supersonic flows with embedded subsonic pockets
[AIAA PAPER 92-0323] p 322 A92-25770
Multidomain spectral solutions of high-speed flows over blunt cones
[AIAA PAPER 92-0324] p 322 A92-25771
A nearly-monotone genuinely multidimensional scheme for the Euler equations
[AIAA PAPER 92-0325] p 322 A92-25772
Thermochemical nonequilibrium and radiative interactions in supersonic hydrogen-air combustion
[AIAA PAPER 92-0340] p 394 A92-25786
Enthalpy damping for high Mach number Euler solutions p 330 A92-26402
Experimental investigation of normal-shock/turbulent-boundary-layer interactions with and without mass removal p 330 A92-26411
Base pressure in supersonic flow - Further thoughts about a theory p 331 A92-26442
Resonance of circular shock waves p 395 A92-26795
Crossing shock wave turbulent boundary layer interactions - Variable angle and shock generator length geometry effects at Mach 3
[AIAA PAPER 92-0636] p 334 A92-27014
Numerical investigation of a transverse jet for supersonic aerodynamic control
[AIAA PAPER 92-0639] p 334 A92-27017
Calculation of heat transfer and friction for a blunt body in the path of supersonic flow of a chemically equilibrium air-xenon mixture p 336 A92-27532
Radiant heat transfer in supersonic three-dimensional and axisymmetric flow of air past evaporating bodies p 337 A92-27533
A method for the optical measurement of surface friction in supersonic flow p 337 A92-27537
Characteristics of the mechanism of separated flow pulsation ahead of a spike-tipped cylinder in supersonic flow p 337 A92-27597
A study of the interaction of a normal shock wave with a turbulent boundary layer at Mach numbers between 1.30 and 1.55 p 339 A92-28006
Numerical investigation of laminar separated trailing-edge flows p 339 A92-28026
An investigation of the swirl in an S-shaped inlet p 343 A92-28476
An experimental investigation of the inlet exit flow field improved by aerodynamic grid p 343 A92-28477
Inviscid and viscous transonic flows in cascades using an implicit upwind algorithm p 344 A92-28522
Numerical simulation of slot injection into a turbulent supersonic stream
[AIAA PAPER 92-0827] p 421 A92-29595
Numerical analysis of techniques for efficient generation of vorticity in supersonic flows
[AIAA PAPER 92-0828] p 422 A92-29596
Assessment of three models of turbulence in a shock-boundary layer interaction of a heated wall p 423 A92-29999
Flow of a viscous twisted fluid film on the surface of a blunt body in supersonic flow of a gas p 424 A92-30146

The effect of the angle-of-attack on laminar-turbulent boundary transition near the lower surface of triangular plates in a supersonic gas flow p 426 A92-30180
Numerical methods in the theory of boundary layer interaction with nonviscous flow p 426 A92-30185
Transverse correlation of the spectral components of pressure fluctuations on a plate ahead of a step p 426 A92-30187
Iterative algorithms for solving problems of the shaping of three-dimensional ducts p 428 A92-30212
Observation and testing on supersonic multiphase flow p 429 A92-30502
Study on two-dimensional jet mixing with a vertical supersonic flow p 429 A92-30530
Study of cavity pumping in supersonic internal flow p 429 A92-30538
Numerical simulation of supersonic nozzle flow p 430 A92-30540
High angle of attack aerodynamics - Subsonic, transonic, and supersonic flows --- Book
[ISBN 0-387-97672-8] p 431 A92-30850
Numerical simulation of three-dimensional supersonic free shear layers p 431 A92-31152
Two- and three-dimensional effects in the supersonic mixing layer p 432 A92-31165
Semi-inverse marching characteristics scheme for supersonic flows p 432 A92-31187
Numerical investigation of the high-speed conical flow past a sharp fin p 433 A92-31468
Numerical simulation of three-dimensional supersonic flow around aerodynamic configurations p 434 A92-31492
Improving the convergence rate of the Petrov-Galerkin techniques for the solution of transonic and supersonic flows p 434 A92-31495
Secondary instabilities in compressible boundary layers p 435 A92-31639
A preliminary study of the turbulent structures associated with unsteady separation shock motion in a Mach 5 compression ramp interaction
[AIAA PAPER 92-0744] p 436 A92-31677
A parametric study of the lift-drag ratio of blunt cones p 437 A92-31860
A supplement to the second-order shock-expansion method p 437 A92-31861
Computational studies of the aerodynamic characteristics of delta wings with a subsonic leading edge p 439 A92-31874
A study of flow of a fluid film on the surface of a plate in the case of slot injection p 496 A92-31892
An exact solution to edge effect problem for a finite-span wing in supersonic flow p 441 A92-31962
Viscous supersonic flow computations over a delta-rectangular wing with slanting surfaces p 441 A92-32178
Navier-Stokes study of supersonic cavity flowfield with passive control p 442 A92-32239
Numerical studies of supersonic flow over a compression corner p 442 A92-32324
Subcritical flutter characteristics of a swept-back wing in a turbulent supersonic flow - Comparison between analysis and experiment
[AIAA PAPER 92-2393] p 517 A92-34466
Simulation of 3-D shear flows around a nozzle-afterbody at high speeds p 519 A92-34826
Finite element nonlinear panel flutter with arbitrary temperatures in supersonic flow
[AIAA PAPER 92-2129] p 589 A92-35696
Numerical simulation of opposing sonic jets p 524 A92-36357
Spectral solution of inviscid supersonic flows over wedges and axisymmetric cones p 524 A92-36359
Structure of the separated flow region in a dihedral corner in front of an obstacle in supersonic flow p 524 A92-36420
Experimental investigation of supersonic flow over two cavities in tandem p 610 A92-36830
Similarity in supersonic mixing layers p 611 A92-36842
Computational methods for shock waves in three-dimensional supersonic flow p 611 A92-37537
An improved analysis method for cross-wire signals obtained in supersonic flow p 614 A92-38456
Application of laminar flow control to the High Speed Civil Transport - The NASA Supersonic Laminar Flow Control Program
[SAE PAPER 912115] p 643 A92-39966
Passive control of supersonic cavity flowfields
[SAE PAPER 912153] p 619 A92-39988
Direct simulation of a supersonic reacting mixing-layer p 676 A92-40132
Compressibility effects in turbulent far wakes p 622 A92-40140
The effects of viscosity and diffusion on a supersonic mixing layer p 622 A92-40143
Reactive mixing layer between pressure reflecting boundaries p 656 A92-40144
The calculation of a compressible boundary layer past a pointed body and a delta wing p 622 A92-40173
Quick calculation of three-dimensional supersonic flow past nearly axisymmetric bodies p 624 A92-40605
Newton's method solver for the axisymmetric Navier-Stokes equations p 703 A92-41269
Navier-Stokes computations for pointed, spherical, and flat tipped shell at Mach 3 p 705 A92-41536
Supersonic flow over an axisymmetric backward-facing step p 705 A92-41542
Basic experiment on a supersonic vortex flow around a missile body p 705 A92-41545
A method for determining the internal force characteristics of a model in external supersonic flow p 706 A92-42682
Nonstationary viscous shock layer in supersonic motion over an inhomogeneity p 708 A92-42737
Three-dimensional visualizations of the aerodynamic characteristics of delta wings for the transition from subsonic to supersonic leading edges in supersonic-hypersonic flow p 709 A92-43073
The inviscid stability of supersonic flow past heated or cooled axisymmetric bodies p 712 A92-44363
Solution of the parabolized Navier-Stokes equations using Osher's upwind scheme p 713 A92-44371
Response characteristics of a wing in supersonic flow near flutter boundary
[SAE PAPER 911999] p 789 A92-45401
An improved approach for the computation of transonic/supersonic flows with applications to aerospace configurations
[AIAA PAPER 92-2613] p 793 A92-45487
Numerical study on a supersonic open cavity flow with geometric modification of aft bulkhead
[AIAA PAPER 92-2627] p 794 A92-45499
Unsteady Navier-Stokes simulations of supersonic flow over a three-dimensional cavity
[AIAA PAPER 92-2632] p 795 A92-45504
Investigation of solution operators for the three-dimensional Euler equations
[AIAA PAPER 92-2666] p 797 A92-45522
Comparison of interferometric measurements with 3-D Euler computations for circular cones in supersonic flow
[AIAA PAPER 92-2691] p 800 A92-45538
LDA measurements in a Mach 2 flow over a rearward facing step with staged transverse injection
[AIAA PAPER 92-2692] p 800 A92-45539
A transonic/supersonic/hypersonic CFD analysis of the entry Space Shuttle Orbiter
[AIAA PAPER 92-2614] p 805 A92-45571
Comment on 'Canard-wing interaction in unsteady supersonic flow' p 812 A92-46820
Two-stream, supersonic, wake flowfield behind a thick base. I - General features p 813 A92-46895
Calculation of the aerodynamic derivatives of aircraft in the supersonic region using the Mach box method p 875 A92-47779
Heat transfer to a cylinder submerged in a rectangular cavity in supersonic flow --- to simulate electrical cables routed through Space Shuttle Solid Rocket Booster External Tank
[AIAA PAPER 92-2949] p 901 A92-47913
A higher-order accurate Navier-Stokes solver for transonic and supersonic flows in turbomachinery
[AIAA PAPER 92-3044] p 822 A92-48704
A concentration probe for the study of mixing in supersonic shear flows p 991 A92-50039
Computational study of a supersonic mixer-ejector exhaust system p 969 A92-50252
Full Navier-Stokes analysis of a three-dimensional scramjet inlet p 934 A92-50272
Processing of axisymmetric flow interferograms with density profile bends or discontinuities p 993 A92-51316
A study of supersonic flow over the ogival bodies with attached shock waves at zero incidence p 936 A92-51896
A general explicit or semi-explicit algorithm for compressible and incompressible flows p 937 A92-52682
Aerodynamics of complex shape bodies within a wide range of supersonic flows of rarefied gases p 939 A92-52767
Supersonic flow past pointed-nose thin airfoils p 940 A92-52844
The relation among the general unsteady aerodynamic coefficients of a wing in subsonic and supersonic speed p 941 A92-53022
Numerical study on the secondary jet into a supersonic flow p 1018 A92-53556
Navier-Stokes simulation for the winged space vehicle 'HOPE' at subsonic, transonic, and supersonic regimes p 1018 A92-53559
The enhancement of the mixing and combustion processes in supersonic flow applied to scramjet engine
[AIAA PAPER 92-3428] p 1112 A92-54029
High-speed cinematography of supersonic mixing layers
[AIAA PAPER 92-3545] p 1112 A92-54044
Structure and penetration of a transverse fluid jet injected at supercritical pressure in supersonic flow
[AIAA PAPER 92-3652] p 1113 A92-54105
Supersonic flow mixing and combustion using RAMP nozzle
[AIAA PAPER 92-3840] p 1113 A92-54198
A new look at surface flow visualization to provide insight into complex fluid dynamic behavior p 1090 A92-54307
Nonintrusive measurements in fluid dynamic flows from Mach .0005 to 14 p 1090 A92-54311
Numerical simulation of slot injection into a turbulent supersonic stream p 1024 A92-54914
Effect of streamwise pressure gradient on the supersonic mixing layer p 1025 A92-54936
Numerical simulation of supersonic unsteady flow using a panel method p 1030 A92-56048
Euler/experiment correlation of a generic fighter p 1031 A92-56164
The research of reducing 3-D low supersonic shock wave reflection in a 2-D transonic flexible walls adaptive wind tunnel
[AIAA PAPER 92-3924] p 1095 A92-56755
Investigation of a plate-ramp-configuration by means of laser Doppler anemometry at Mach 2.95
[AIAA PAPER 92-3956] p 1097 A92-56784
The SR3 low density wind tunnel - Facility capabilities and research development
[AIAA PAPER 92-3972] p 1098 A92-56798
Experimental unsteady pressures on an oscillating cascade with supersonic leading edge locus
[AIAA PAPER 92-4035] p 1035 A92-56857
Increasing the accuracy of the Godunov scheme for calculating steady-state supersonic gas flows by solving the generalized Riemann problem p 1035 A92-57499
Recent advances on a finite element algorithm for computational aerodynamics: Transonics-hypersonics
[DE91-018176] p 11 N92-10010
Noise from turbulent shear flows p 55 N92-10603
Unsteady aerodynamic calculations for general configurations by the double-point method
[NAL-TR-1101T] p 12 N92-10980
CARS temperature measurements in a hypersonic propulsion test facility p 140 N92-12049
Numerical investigation of unsteady supersonic cavity flowfield with passive control p 88 N92-13029
Oscillating shock impingement on low-angle gas injection into a supersonic flow p 89 N92-13032
A new technique for temperature and specie concentration measurements in unseeded supersonic and hypersonic gas flows
[AD-A241536] p 158 N92-13409
Constant-temperature anemometry measurements in hypersonic boundary layers p 90 N92-13861
The effects of winglets on low aspect ratio wings at supersonic Mach numbers
[NASA-CR-4407] p 178 N92-13996
Steps towards an efficient and accurate method solving the Euler equations around a re-entry configuration at super- and hypersonic speed p 181 N92-14987
Heat transfer measurements in ONERA supersonic and hypersonic wind tunnels using passive and active infrared thermography p 208 N92-15003
Computation of aerodynamic coefficients on Hermes-Ariane5 configuration p 184 N92-15040
CAR 88: A method to calculate subsonic and supersonic, steady and unsteady, potential flow about complex configurations
[NLR-TR-88154-U] p 400 N92-18221
Marching with the parabolized Navier-Stokes equations. Problem 1: Numerical study of hypersonic viscous cone flow
[AERO-REPT-9007] p 344 N92-18231
An improved method for simulating supersonic flow past a wedge shaped body
[NAL-TR-1097] p 345 N92-18239
Thrust vector control of an overexpanded supersonic nozzle using pin insertion and rotating airfoils
[AD-A243891] p 387 N92-18942
An inviscid stability analysis of unbounded supersonic mixing layer flows p 443 N92-20332
A quantitative study of unsteady compressible flow on an oscillating airfoil
[AD-A244572] p 445 N92-21012
Theoretical and experimental investigation of the thermodynamics of the thermally choked ram accelerator p 604 N92-22137
Supersonic throughflow fans for high-speed aircraft p 561 N92-22541

PAN AIR: A computer program for predicting subsonic or supersonic linear potential flows about arbitrary configurations using a higher order panel method. Volume 1: Theory document (version 3.0)
[NASA-CR-3251] p 526 N92-22648
PAN AIR: A computer program for predicting subsonic or supersonic linear potential flows about arbitrary configurations using a higher order panel method. Volume 2: User's manual (version 3.0)
[NASA-CR-3252] p 527 N92-22865
Development of a new flux splitting scheme
p 596 N92-23352
Development of wall pressure measuring apparatus for an existing transonic wind tunnel test section
[NAL-TM-565] p 573 N92-23778
A user guide for the EMTAC-MZ CFD code
[NASA-CR-4283] p 678 N92-24242
Supersonic flow in compression stages and inlets
p 625 N92-24395
The natural flow wing-design concept
[NASA-TP-3193] p 631 N92-25202
Development of new flux splitting schemes --- computational fluid dynamics algorithms
p 682 N92-25809
Performance prediction and design of maximum thrust planar supersonic nozzles using a flux-difference-splitting technique p 738 N92-26480
Development of a quiet supersonic wind tunnel with a cryogenic adaptive nozzle p 751 N92-27977
Effect of walls on the supersonic reacting mixing layer
p 912 N92-30065
Turbulent reacting flows and supersonic combustion
[AD-A251065] p 986 N92-30256
NASA. Lewis Research Center supersonic throughflow fan program
[NASA-TM-103248] p 972 N92-31250
Hypersonic code efficiency and validation studies
[NASA-CR-190680] p 948 N92-31533
Stability and transition of hypersonic boundary-layer flows
[AD-A250279] p 948 N92-31555
Supersonic Throughflow Fan Test Facility at NASA. Lewis Research Center
[NASA-TP-3038] p 983 N92-31640
Euler solver for arbitrary configurations: Further applications p 949 N92-31888
Laser-initiated conical detonation wave for supersonic combustion, part 3
[AD-A250522] p 989 N92-32076
Dynamic interactions between hypersonic vehicle aerodynamics and propulsion system performance
[NASA-CR-190638] p 1038 N92-33304
Prediction and control of asymmetric vortical flows around slender bodies using Navier-Stokes equations
p 1127 N92-33968

SUPERSONIC FLUTTER
Optimization of the flutter load by material orientation
p 146 A92-15222
Subcritical flutter characteristics of a swept-back wing in a turbulent supersonic flow - Comparison between analysis and experiment
[AIAA PAPER 92-2393] p 517 A92-34466
Aerothermoelastic analysis of a NASP-like vertical fin
[AIAA PAPER 92-2400] p 541 A92-34471
Finite element nonlinear panel flutter with arbitrary temperatures in supersonic flow
[AIAA PAPER 92-2129] p 589 A92-35696
Transverse shear effect on flutter of composite panels
p 1122 A92-56607

SUPERSONIC HEAT TRANSFER
A heat flow peak on the upwind surface of a blunt-leading-edge delta wing p 438 A92-31862

SUPERSONIC INLETS
Inviscid analysis of a dual mode scramjet inlet
p 80 A92-17198
Supersonic inlet flow computation
p 171 A92-17502
Numerical investigation of supersonic mixed-compression inlet using an implicit upwind scheme p 243 A92-21073
Experimental investigation of terminal shock sensors for mixed-compression inlets p 276 A92-21074
Method for the prediction of supersonic compressor blade performance p 277 A92-21078
An AF3 algorithm for the calculation of transonic nonconservative full potential flow around axisymmetric inlet cowls p 251 A92-23380
Transient behavior of supersonic flow through inlets
p 340 A92-28043
Control of strong shock-turbulent boundary layer interaction in rectangular channels p 422 A92-29714
Numerical computation of supersonic intakes
p 430 A92-30539
Experimental investigation on performances of two-dimensional inlet at supersonic speed
p 519 A92-35544
Experimental study of the aerodynamic characteristics at Mach 3 of an air-intake model p 711 A92-43204
Wind tunnel test of a supersonic air intake
p 711 A92-43205
Subcritical flow studies on two-dimensional external compression supersonic inlets p 713 A92-44518
Numerical investigation of supersonic inlet with realistic bleed and bypass systems p 713 A92-44519
Bleed-boundary conditions for numerically simulated mixed-compression supersonic inlet flow
p 713 A92-44520
An experimental investigation on aft bypass supersonic inlet performance at high angle of attack and yaw
p 862 A92-48268
A fast, uncoupled, compressible, two-dimensional, unsteady boundary layer algorithm with separation for engine inlets
[AIAA PAPER 92-3082] p 823 A92-48729
Interface of an uncoupled boundary layer algorithm with an inviscid core flow algorithm for unsteady supersonic engine inlets
[AIAA PAPER 92-3083] p 823 A92-48730
Numerical simulation of a confined transonic normal shock wave/turbulent boundary layer interaction
[AIAA PAPER 92-3668] p 826 A92-49088
Results from computational analysis of a mixed compression supersonic inlet
[NASA-TM-104475] p 12 N92-10976
Supersonic propulsion simulation by incorporating component models in the large perturbation inlet (LAPIN) computer code
[NASA-TM-105193] p 279 N92-15993
Air intakes for high speed vehicles
[AGARD-AR-270] p 445 N92-20797
Modeling of linear isentropic flow systems
p 593 N92-22495
Propulsion challenges and opportunities for high-speed transport aircraft p 561 N92-22540
Interactive solution-adaptive grid generation procedure
[NASA-TM-105432] p 528 N92-23563
Interface of an uncoupled boundary layer algorithm with an inviscid core flow algorithm for unsteady supersonic engine inlets
[NASA-TM-105684] p 739 N92-27037
A fast, uncoupled, compressible, two-dimensional, unsteady boundary layer algorithm with separation for engine inlets
[NASA-TM-105686] p 770 N92-27653
NASA. Lewis Research Center supersonic throughflow fan program
[NASA-TM-103248] p 972 N92-31250

SUPERSONIC JET FLOW
Self-oscillatory interaction of an underexpanded jet with an obstacle in the presence of a supersonic wake
p 79 A92-16681
Feedback mechanism of self-oscillations in the case of an underexpanded supersonic jet impinging on a plane obstacle p 79 A92-16682
Enhanced mixing of supersonic jets
p 80 A92-17195
Broadband shock-associated noise from supersonic jets in flight p 235 A92-18683
Computation of supersonic jet mixing noise for an axisymmetric CD nozzle using k-epsilon turbulence model
[AIAA PAPER 92-0500] p 414 A92-26328
A survey of the broadband shock associated noise prediction methods
[AIAA PAPER 92-0501] p 415 A92-26930
Broadband shock associated noise from supersonic jets measured by a ground observer
[AIAA PAPER 92-0502] p 416 A92-26931
Screech noise source structure of a supersonic rectangular jet
[AIAA PAPER 92-0503] p 331 A92-26932
Effect of rarefaction on the nonstationary interaction of a supersonic underexpanded jet with a perpendicular obstacle p 337 A92-27594
LDV measurements of the velocity field in an underexpanded supersonic jet (Ma = 1.5)
[AIAA PAPER 92-0504] p 341 A92-28196
Numerical simulation of interaction between vortexes and shocks in jet flow field p 616 A92-38925
Flow and acoustic features of a supersonic tapered nozzle p 712 A92-44328
Numerical simulation of a supersonic jet impingement on a ground
[SAE PAPER 912014] p 789 A92-45412
The flip flop nozzle extended to supersonic flows
[AIAA PAPER 92-2724] p 803 A92-45561
Relationship between the instability waves and noise of high-speed jets p 924 A92-45835
The enhancement of mixing in high-speed heated jets using a counterflowing nozzle
[AIAA PAPER 92-3262] p 825 A92-48857
Supersonic jet mixing enhancement by 'delta-tabs'
[AIAA PAPER 92-3548] p 826 A92-49063
Experiments on the structure of an annular compressible reacting shear layer p 969 A92-50311
On the effect of external flow and shear-layer thickness on the expansion cells of under-expanded supersonic circular jets p 969 A92-50478
Experimental and numerical investigation of a supersonic free jet impinging on a perpendicular surface
p 1018 A92-53555
Numerical study of the 3-D flowfield for a supersonic jet exiting into a hypersonic stream from a conical surface
[AIAA PAPER 92-3675] p 1022 A92-54118
Broadband shock associated noise from supersonic jets measured by a ground observer p 1135 A92-54909
Jet noise generated by large-scale coherent motion
p 55 N92-10604
Computation of supersonic jet mixing noise for an axisymmetric CD nozzle using k-epsilon turbulence model
[NASA-TM-105338] p 237 N92-14795
A survey of the broadband shock associated noise prediction methods
[NASA-TM-105365] p 237 N92-14797
Supersonic jet mixing enhancement by delta-tabs
[NASA-TM-105664] p 630 N92-24958
Acoustic interactions between an altitude test facility and jet engine plumes: Theory and experiments
[NASA-CR-190423] p 738 N92-26405
Turbulent mixing in supersonic jets
p 715 N92-27054

SUPERSONIC NOZZLES
Mach 4 and Mach 8 axisymmetric nozzles for a high-enthalpy shock tunnel p 78 A92-16668
Formation of shocks within axisymmetric nozzles
p 176 A92-20760
Supersonic nozzle mixer ejector p 376 A92-28536
Numerical simulation of supersonic nozzle flow
p 430 A92-30540
A computational exploration of the importance of three-dimensionality, boundary layer development, and flow chemistry to the prediction of scramjet nozzle performance
[AIAA PAPER 91-5059] p 472 A92-31689
Issues associated with long duration high enthalpy scramjet combustor testing p 472 A92-31700
A time-integrated image model for aero-optic analysis
[AIAA PAPER 92-2793] p 779 A92-41332
Flow and acoustic features of a supersonic tapered nozzle p 712 A92-44328
Gortler instability and supersonic quiet nozzle design
p 813 A92-46902
Experimental validation of scramjet nozzle performance
[AIAA PAPER 92-3290] p 864 A92-48879
Supersonic flow mixing and combustion using RAMP nozzle
[AIAA PAPER 92-3840] p 1113 A92-54198
Thrust vector control of an overexpanded supersonic nozzle using pin insertion and rotating airfoils
[AD-A243891] p 387 N92-18942
Performance prediction and design of maximum thrust planar supersonic nozzles using a flux-difference-splitting technique p 738 N92-26480

SUPERSONIC SPEED
Euler code evaluation of a transatmospheric vehicle at supersonic speeds p 9 A92-13202
Center of pressure calculations for a bent-axis vehicle
[AIAA PAPER 92-0168] p 254 A92-23779
The flip flop nozzle extended to supersonic flows
[AIAA PAPER 92-2724] p 803 A92-45561
Aerodynamically blunt and sharp bodies
[AIAA PAPER 92-2727] p 808 A92-45597
Aerothermal ablation behavior of selected candidate external insulation materials
[AIAA PAPER 92-3056] p 893 A92-48714
Interaction between a body flying at a supersonic velocity and a point explosion p 1019 A92-53867
Application of computational fluid dynamics to sonic boom near- and mid-field prediction
p 1031 A92-56173
Contribution of fin and tailplane to sideforce and yawing moment derivatives due to sideslip at supersonic speeds at low angles of attack
[ESDU-91031] p 259 N92-15971
Detailed noise measurements on the SR-7A propeller: Tone behavior with helical tip Mach number
[NASA-TM-105206] p 304 N92-16705
Influence of airfoil geometry on delta wing leading-edge vortices and vortex-induced aerodynamics at supersonic speeds
[NASA-TP-3105] p 350 N92-20038
Center of pressure calculations for a bent-axis vehicle
[DE92-005186] p 498 N92-20143

Effects of turbine cooling assumptions on performance and sizing of high-speed civil transport
[NASA-TM-105610] p 562 N92-23537
Normal force of low aspect ratio wing-body combinations up to high angles of attack at supersonic speeds
[ESDU-91042] p 553 N92-24009
Longitudinal and lateral-directional aerodynamic characteristics of a wing-cone configuration at Mach numbers from 2.5 to 4.5
[NASA-TM-4337] p 630 N92-24977
A compressible Navier-Stokes solver with two-equation and Reynolds stress turbulence closure models
[NASA-CR-4440] p 681 N92-25376
A new Lagrangian method for real gases at supersonic speed p 633 N92-25814
Navier-Stokes computations of a viscous optimized waverider
[NASA-CR-189658] p 944 N92-30392
Supersonic Throughflow Fan Test Facility at NASA. Lewis Research Center
[NASA-TP-3038] p 983 N92-31640

SUPERSONIC TEST APPARATUS
Development of wall pressure measuring apparatus for an existing transonic wind tunnel test section
[NAL-TM-565] p 573 N92-23778
Supersonic Throughflow Fan Test Facility at NASA. Lewis Research Center
[NASA-TP-3038] p 983 N92-31640

SUPERSONIC TRANSPORTS
A propulsion perspective of the next generation supersonic transport
[ASME PAPER 91-GT-385] p 126 A92-15719
A low noise propulsion concept for the supersonic transport
[ASME PAPER 91-GT-397] p 127 A92-15727
Environmental impact of a future supersonic transport aircraft
[ONERA, TP NO. 1991-132] p 161 A92-16108
NASA research program directed at reducing supersonic transport noise p 61 A92-16150
A new unsteady mixing model to predict NO(x) production during rapid mixing in a dual-stage combustor
[AIAA PAPER 92-0233] p 372 A92-25696
Supersonic transport in the 21st century p 308 A92-26793
Numerical computation of supersonic intakes p 430 A92-30539
A study of altitude-constrained supersonic cruise transport concepts
[AIAA PAPER 92-1027] p 536 A92-33208
Application of laminar flow control to the High Speed Civil Transport - The NASA Supersonic Laminar Flow Control Program
[SAE PAPER 912115] p 643 A92-39966
Concorde, fifteen years on the front line
[SAE PAPER 912193] p 644 A92-40010
The effectiveness of the warp shape airfoil of a supersonic transport p 711 A92-43203
Experimental and numerical study of aerodynamic characteristics for second generation SST
[SAE PAPER 912056] p 844 A92-45439
Effects of wing planform on HSCT off-design aerodynamics --- High Speed Civil Transport
[AIAA PAPER 92-2629] p 844 A92-45501
Introduction --- propulsion system performance for hypersonic vehicles p 862 A92-46427
Experimental investigation of an ejector-powered free-jet facility
[AIAA PAPER 92-3569] p 1090 A92-54058
Full Navier-Stokes analysis of a two-dimensional mixer/ejector nozzle for noise suppression
[AIAA PAPER 92-3570] p 1067 A92-54059
Roles of wind tunnel tests and CFD analyses in the design of energy-efficient SST
[AIAA PAPER 92-3923] p 1133 A92-56754
A loudness calculation procedure applied to shaped sonic booms
[NASA-TP-3134] p 56 N92-11765
Designing a methodology for future air travel scenarios p 409 N92-19125
Ozone response to aircraft emissions: Sensitivity studies with two-dimensional models p 409 N92-19126
High-speed civil transport flight- and propulsion-control technological issues
[NASA-CR-186015] p 482 N92-21253
Experimental study of a generic high-speed civil transport: Tabulated data
[NASA-TM-104216] p 525 N92-22232
Propulsion challenges and opportunities for high-speed transport aircraft p 561 N92-22540
Application of multidisciplinary optimization methods to the design of a supersonic transport p 550 N92-23230
Computational Structures Technology for Airframes and Propulsion Systems
[NASA-CP-3142] p 683 N92-25911
Structural analysis for preliminary design of High Speed Civil Transport (HSCT) p 684 N92-25926
Full Navier-Stokes analysis of a two-dimensional mixer/ejector nozzle for noise suppression
[NASA-TM-105715] p 868 N92-28419
Integrating aerodynamics and structures in the minimum weight design of a supersonic transport wing
[NASA-TM-107586] p 850 N92-28435
Evaluation of outdoor-to-indoor response to minimized sonic booms
[NASA-CR-189643] p 927 N92-28556
Methods for direct simulation of transition in hypersonic boundary layers 2 p 912 N92-30064
A new unsteady mixing model to predict NO(x) production during rapid mixing in a dual-stage combustor
[NASA-CR-189155] p 971 N92-30569
High-speed civil transport issues and technology program
[NASA-CR-186020] p 962 N92-31208
NASA. Lewis Research Center supersonic throughflow fan program
[NASA-TM-103248] p 972 N92-31250
Design and analysis issues of integrated control systems for high-speed civil transports
[NASA-CR-186022] p 979 N92-31656
Isothermal aging of IM7/8320 and IM7/5260
[NASA-TM-107666] p 1110 N92-33423
Experimental study of a generic high-speed civil transport
[NASA-TM-4382] p 1040 N92-33631

SUPERSONIC TURBINES
Supersonic stator-rotor interaction in a turbine stage
[ONERA, TP NO. 1991-166] p 77 A92-16133
Calculation of three-dimensional transonic turbine cascade flow p 344 A92-28519
Inviscid and viscous quasi-three-dimensional flow solutions in a transonic turbine cascade p 523 A92-36035
The application of particle image velocimetry (PIV) in a short-duration transonic annular turbine cascade
[ASME PAPER 91-GT-221] p 899 A92-46825
Experience with the Johnson-King turbulence model in a transonic turbine cascade flow solver p 821 A92-48207
Vane-blade interaction in a transonic turbine. I - Aerodynamics
[AIAA PAPER 92-3323] p 825 A92-48906
The research progress on Hodograph Method of aerodynamic design at Tsinghua University p 177 N92-13974
Predictions and measurements of 3D viscous flow in a transonic turbine nozzle guide vane row p 741 N92-27466
Steady and unsteady 3D flow computation through a transonic turbine stage p 742 N92-27469
Supersonic Throughflow Fan Test Facility at NASA. Lewis Research Center
[NASA-TP-3038] p 983 N92-31640
A critical evaluation of a three-dimensional Navier-Stokes CFD as a tool to design supersonic turbine stages p 1124 N92-32268

SUPERSONIC WAKES
Self-oscillatory interaction of an underexpanded jet with an obstacle in the presence of a supersonic wake p 79 A92-16681
Sonic eddy - A model for compressible turbulence p 176 A92-20739

SUPERSONIC WIND TUNNELS
A quiet-flow Ludwieg tube for experimental study of high speed boundary layer transition
[AIAA PAPER 91-5026] p 207 A92-17819
A heat flow peak on the upwind surface of a blunt-leading-edge delta wing p 438 A92-31862
Gortler instability and supersonic quiet nozzle design p 813 A92-46902
Operating characteristics at Mach 4 of an inlet having forward-swept, sidewall-compression surfaces
[AIAA PAPER 92-3101] p 863 A92-48743
Research capabilities of the NASA Langley 8-foot high temperature tunnel p 980 A92-51403
A preliminary study of a supersonic wind tunnel for a ram jet test facility p 1089 A92-53564
High-speed cinematography of supersonic mixing layers
[AIAA PAPER 92-3545] p 1112 A92-54044
Mach 3 wind tunnel test of mixed compression supersonic inlet
[AIAA PAPER 92-3625] p 1021 A92-54092
Structure of crossing-shock wave/turbulent boundary-layer interactions
[AIAA PAPER 92-3670] p 1022 A92-54113
A new look at surface flow visualization to provide insight into complex fluid dynamic behavior p 1090 A92-54307
Rayleigh imaging and flow tagging in ground test facilities p 1115 A92-54330
Double piston shock-wave valve p 1117 A92-54938
Supersonic wind tunnel test of airintake/airframe integrated models p 1028 A92-56006
Supersonic and hypersonic quiet tunnel technology at NASA Langley
[AIAA PAPER 92-3908] p 1094 A92-56743
Roles of wind tunnel tests and CFD analyses in the design of energy-efficient SST
[AIAA PAPER 92-3923] p 1133 A92-56754
CAN-DO, CFD-based Aerodynamic Nozzle Design and Optimization program for supersonic/hypersonic wind tunnels
[AIAA PAPER 92-4009] p 1033 A92-56832
Experimental unsteady pressures on an oscillating cascade with supersonic leading edge locus
[AIAA PAPER 92-4035] p 1035 A92-56857
Study of optical techniques for the Ames unitary wind tunnels. Part 2: Light sheet and vapor screen
[NASA-CR-190217] p 573 N92-22195
Study of the NAL's 0.1 x 0.1 m magnetic suspension and balance system
[NAL-TM-623] p 665 N92-25365
Development of a quiet supersonic wind tunnel with a cryogenic adaptive nozzle
[NASA-CR-188055] p 751 N92-27976
Development of a quiet supersonic wind tunnel with a cryogenic adaptive nozzle p 751 N92-27977
The FML compressor as a drive system for the LFSWT: A narrative p 751 N92-27978
Air ejector experiments using the two-dimensional supersonic cascade tunnel: Zero secondary flow performance
[NAL-TM-632] p 887 N92-28829
Shock enhancement and control of hypersonic combustion
[AD-A248558] p 896 N92-29580
Supersonic Throughflow Fan Test Facility at NASA. Lewis Research Center
[NASA-TP-3038] p 983 N92-31640

SUPPORT INTERFERENCE
Calculation of support interferences on the aerodynamic coefficients for a wind tunnel calibration model
[ESA-TT-1247] p 830 N92-29159

SUPPORT SYSTEMS
Standardizing operational flight data handling p 1009 A92-53109
Pilot's Automated Weather Support System (PAWSS) concepts demonstration project. Phase 1: Pilot's weather information requirements and implications for weather data systems design
[NASA-CR-188228] p 46 N92-11593
AGSSS: The Airborne Graphics Software Support System; an Ada/PHIGS-based display editor for the rapid development of cockpit display software systems
[AD-A243224] p 277 N92-17221
National Airspace System maintenance and support operational concept
[DOT/FAA/SE-92/1] p 308 N92-18969
The COMPAS system in the ATC environment
[DLR-MITT-91-08] p 354 N92-19041
Design principles of automation aids for ATC approach control p 354 N92-19042
The role of planning systems in future air traffic management p 355 N92-19050
The 12-foot pressure wind tunnel restoration project model support systems p 664 N92-25091
Overview of mechanics of materials branch activities in the computational structures area p 684 N92-25917
The role of simulation for the study of APIS (piloting support by synthetic imagery) p 885 N92-28544
Tasking and communication flows in the F/A-18D cockpit: Issues, problems, and possible solutions
[AD-A245977] p 853 N92-28802
Developing robust support structures for high-technology subsystems: The AH-64 Apache helicopter
[AD-A252773] p 1017 N92-33499

SUPPORTS
Study of the NAL's 0.1 x 0.1 m magnetic suspension and balance system
[NAL-TM-623] p 665 N92-25365

SURFACE COOLING
Heat pipe and surface mass transfer cooling of hypersonic vehicle structures p 763 A92-44380
Surface cooling of scramjet engine inlets using heat pipe, transpiration, and film cooling p 763 A92-44381
Thermal management of high heat flux electronic components in space and aircraft systems, phase 1
[AD-A239982] p 41 N92-10157
Window cooling for high speed flight
[AD-D015145] p 344 N92-18193

SURFACE CRACKS
Historical development of eddy current testing in aircraft maintenance p 292 A92-21900

Magnetic particle testing of turbine blades mounted on the turbine rotor shaft p 898 A92-46498
Solution of stress intensity factor by weight function for small surface cracks in plates p 998 A92-53332
A preliminary study on damage detection using piezoelectric film
[AD-A246350] p 733 N92-28118

SURFACE DEFECTS
Enhanced visual technique for rapid inspection of aircraft structures p 214 A92-17290
Failure analysis of the Apache mixer pivot support
[AD-A240858] p 116 N92-13061

SURFACE FINISHING
The design of broadband radar absorbing surfaces
[AD-A240521] p 42 N92-11235

SURFACE GEOMETRY
A study of a version of the boundary conditions of a two-dimensional spline in surface and line modeling
p 163 A92-16826
Calculation of the parameters of separated flow behind a plane rounded body in the path of two supersonic flows p 244 A92-21624
Determination of the objective-function gradient in the problem of minimizing stress concentration using the finite element method p 494 A92-30170
Interaction of jets ejected from two-dimensional nozzles with a curved surface p 438 A92-31869
Surface grid generation in a parameter space
[AIAA PAPER 92-2717] p 803 A92-45556

SURFACE LAYERS
Modelling of unsteady transitional boundary layers
[ASME PAPER 91-GT-282] p 152 A92-15677
Surface-layer gusts for aircraft operation
p 774 A92-42095

SURFACE NAVIGATION
Traveling on the curved earth p 19 A92-10474
Navigation - Land, sea, air, and space --- Book
[ISBN 0-87942-257-2] p 496 A92-31778
Terrain following of arbitrary surfaces using a high intensity LED proximity sensor
[DE92-007161] p 455 N92-21201

SURFACE PROPERTIES
Improving the properties of titanium alloys by ion implantation p 289 A92-22771
Software Surface Modeling and Grid Generation Steering Committee
[NASA-CP-3143] p 691 N92-24397
Grid generation research at OSU p 633 N92-25723
A surface definition code for turbine blade surfaces
[DE92-010574] p 1004 N92-31498

SURFACE ROUGHNESS
Wedge-induced turbulent boundary-layer separation on a roughened surface at Mach 6.0 p 175 A92-20379
Prediction of ice accretion on a swept NACA 0012 airfoil and comparisons to flight test results
[AIAA PAPER 92-0043] p 316 A92-25677
Modeling supersonic inlet boundary layer bleed roughness
[AIAA PAPER 92-0269] p 317 A92-25725
Mechanisms resulting in accreted ice roughness
[AIAA PAPER 92-0297] p 351 A92-25750
A method of boundary layer laminarization on an oscillating wing p 441 A92-31969
Development of an instrument for measuring runway roughness p 748 A92-43124
A proposed method for evaluating runway roughness
p 748 A92-43125
Grooved runway surface texture before and after rubber removal p 1093 A92-56111
Prediction of ice accretion on a swept NACA 0012 airfoil and comparisons to flight test results
[NASA-TM-105368] p 258 N92-15968
Deterministic multi-zone ice accretion modeling
p 265 N92-17987
Aerodynamic roughness measured in the field and simulated in a wind tunnel
[NASA-CR-4422] p 347 N92-19354
The effect of wing ice contamination on essential flight characteristics p 449 N92-21681
Effects of frost on wing aerodynamics and take-off performance p 450 N92-21687
Wind tunnel investigation of a wing-propeller model performance degradation due to distributed upper-surface roughness and leading edge shape modification
p 451 N92-21690
The adverse aerodynamic impact of very small leading-edge ice (roughness) buildups on wings and tails
p 451 N92-21691
Laminar-turbulent transition process in the presence of simulated wall roughness p 626 N92-24858
Performance degradation due to hoar frost on lifting surfaces p 628 N92-24866
Flow around an isolated surface roughness in the laminar boundary layer p 766 N92-26913
A methodology for the evaluation of runway roughness for repair
[AD-A250407] p 887 N92-28772
An assessment of the B-747's capability to operate on rough surfaces
[AD-A250134] p 963 N92-31793
The icing of the elevator of the DLR icing research aircraft of Do 28 type
[DLR-MITT-91-12] p 953 N92-31813
Numerical investigation of the effects of icing on fixed and rotary wing aircraft
[NASA-CR-190542] p 1044 N92-34105

SURFACE ROUGHNESS EFFECTS
Roughness effects on heat transfer from a NACA 0012 airfoil p 219 A92-20217
Effect of compressibility on the value of the acceptable roughness Reynolds number p 427 A92-30197
Effect of the longitudinal and transverse riblets of a flat plate on laminar-to-turbulent transition
p 428 A92-30210
Flight studies of the riblet effect on drag variation
p 438 A92-31871
Boundary-layer receptivity of sound with roughness
p 604 A92-36006
Dynamic response of landing gears on rough repaired runway
[SAE PAPER 912154] p 644 A92-39989
Comment on 'Modification of the van Driest damping function to include the effects on surface roughness'
p 758 A92-41297
Aerodynamic characteristics of hoar frost roughness
p 808 A92-45829
Aerodynamic roughness measured in the field and simulated in a wind tunnel
[NASA-CR-4422] p 347 N92-19354

SURFACE TEMPERATURE
Turbine disk temperatures resulting from the hot mainstream at engine conditions
[AIAA PAPER 92-0398] p 373 A92-26252
Aerodynamic design tool development for the calculation code of hypersonic flow p 711 A92-43198
Computer-based areal surface temperature and local heat transfer measurements with thermochromic liquid crystals (TLC) p 763 A92-44326
High temperature ground vibration test techniques
p 980 A92-51404
Second-order shock-expansion theory extended to include real gas effects
[AD-A247191] p 831 N92-29539
Hypersonic flow past radiation-cooled surfaces
[MBB-FE-202-S-PUB-0468-A] p 832 N92-29713
Swept shock/boundary layer interaction experiments in support of CFD code validation
[NASA-CR-190583] p 1036 N92-32494

SURFACE TO AIR MISSILES
Propulsion systems from takeoff to high-speed flight
p 889 A92-46428
Ideal proportional navigation p 976 A92-50497

SURFACE TREATMENT
Surfprep flash-lamp depaint system evaluation
p 497 A92-32411
Removing aircraft surface coatings
p 516 A92-35574
Minimum surface treatments for adhesively bonded repairs p 754 A92-42501
The evaluation of non-tank surface treatments for aluminium bonding repairs p 761 A92-42502
Anodize and prime your aluminum without environmental headaches p 892 A92-47340

SURFACE VEHICLES
Discussion for possibility of some aerodynamic ground effect craft
[NAL-TM-619] p 300 N92-17757

SURFACE WATER
Numerical simulation of an aircraft anti-icing system incorporating a rivulet model for the runback water
p 448 N92-20303

SURFACE WAVES
Diffracted and head waves associated with waves on nonseparable surfaces
[NASA-TP-3169] p 444 N92-20545

SURFACES
Comparison of polynomial approximations and artificial neural nets for response surfaces in engineering optimization p 165 N92-13835
Workshop on Grid Generation and Related Areas
[NASA-CP-10089] p 659 N92-25712

SURFACTANTS
Enhancing the performance characteristics of engine fuels by means of surfactant additives
p 892 A92-46631

SURGES
Active suppression of rotating stall and surge in axial compressors
[ASME PAPER 91-GT-87] p 122 A92-15552
Whole aircraft lightning indirect effects evaluation using low level injection techniques p 192 A92-20134
Compressor modeling and active control of stall/surge
p 508 A92-29315
Model development for active surge control/rotating stall avoidance in aircraft gas turbine engines
p 468 A92-29375
Investigation and application of compressor loading technique p 469 A92-29718
Heat induced transient behaviours of axial compressors p 469 A92-29721
A study of surge control using fuel pulse cutoff for dual spool turbo-jet engine p 470 A92-29737
Investigations of the laws of surge and rotating stall forecast in aeronautical engine p 470 A92-29739
Unsteady flow within centrifugal compressor channels under rotating stall and surge
[ASME PAPER 91-GT-85] p 670 A92-36901
Numerical investigation of surge and rotating stall in multistage axial compressors
[AIAA PAPER 92-3193] p 825 A92-48804
Dynamic control of aerodynamic instabilities in gas turbine engines p 870 N92-28466

SURVEILLANCE
Using helicopters for coastal alert p 723 A92-43164
National airspace system. Air defense and law enforcement surveillance operational concept NAS-SR-135
[DOT/FAA/SE-92/3] p 953 N92-31211
DoD key technologies plan
[AD-A253692] p 1142 N92-33238

SURVEILLANCE RADAR
A simulator and performance criteria for evaluation of ground and space-based ATC surveillance
p 96 A92-16639
An electronically scanned precision runway monitor
p 98 A92-16654
A multi-layer neural network classifier for radar clutter
p 291 A92-21691
Computation of aircraft geometric height under radar surveillance p 639 A92-40239
A new aspect of future air navigation systems - How Secondary Surveillance Radar Mode S could protect civil aviation p 1012 A92-51424
The 1990 Airport Surveillance Radar Wind Shear Processor (ASR-WSP) operational test at Orlando International Airport
[AD-A239852] p 18 N92-10019
The application of lattice-structure adaptive filters to clutter-suppression for scanning radar
p 403 N92-19154
The rise of active-element phased-array radar
[RAND-P-7747-RGS] p 999 N92-30755
Airport Surveillance Radar (ASR-9) wind shear processor: 1991 test at Orlando, Florida
[AD-A252246] p 1124 N92-32686

SURVEYS
General aviation activity and avionics survey, calendar year 1989
[PB91-179234] p 169 N92-13926
Scramjet analysis, testing p 475 N92-21532
Icing simulation: A survey of computer models and experimental facilities p 450 N92-21684
Profile of an effective engineering manager
[AD-A246525] p 781 N92-27528
Survey and analysis of research on supersonic drag-due-to-lift minimization with recommendations for wing design
[NASA-TP-3202] p 1040 N92-33656

SURVIVAL
Canadian aircrew sea water survival, 1952-1987
[DCIEM-88-RR-39] p 954 N92-32219

SURVIVAL EQUIPMENT
U.S. Coast Guard aviation life support and rescue equipment p 529 A92-32999
Learning from aircraft accidents and incidents
p 635 A92-39310

SUSPENSION SYSTEMS (VEHICLES)
The structural optimization system OPTSYS: Current status and applications p 550 N92-23232

SWEAT COOLING
Evaluation of the ATD-GASP for endo-leap applications --- Aerothermal Technology Development of Generalized Aerodynamic Simulation Programs
[AIAA PAPER 92-2771] p 704 A92-41318
Surface cooling of scramjet engine inlets using heat pipe, transpiration, and film cooling p 763 A92-44381
Effect of porosity in transpiration cooling system
p 1112 A92-53786
Thermal/structural analysis of a transpiration cooled nozzle
[NASA-TM-104184] p 401 N92-18877
Hypersonic aerospace vehicle leading edge cooling using heat pipe, transpiration and film cooling techniques
p 780 N92-26733

SWEEP EFFECT
Enhancement of modal swept sine data by control of exciting forces p 215 A92-17562
Leading edge sweep effects in generic three-dimensional sidewall compression scramjet inlets
[AIAA PAPER 92-0674] p 343 A92-28218
Operating characteristics at Mach 4 of an inlet having forward-swept, sidewall-compression surfaces
[AIAA PAPER 92-3101] p 863 A92-48743
SWEEP FREQUENCY
Whole aircraft lightning indirect effects evaluation using low level injection techniques p 192 A92-20134
SWEEPBACK
Effects of sweepback on unsteady separation in Mach 5 compression ramp interactions
[AIAA PAPER 92-0430] p 435 A92-31663
SWEPT FORWARD WINGS
On vortex interference for canard configuration
p 64 A92-14071
Integrated flight control law synthesis for an aeroelastic forward-swept wing aircraft
[AIAA PAPER 92-0046] p 281 A92-22163
Parametric studies for tiltrotor aeroelastic stability in high-speed flight
[AIAA PAPER 92-2568] p 565 A92-34482
Predicted and measured in-flight wing deformations of a forward-swept-wing aircraft p 548 A92-35936
Research on aeroelastic tailoring at NAL
p 1053 A92-56019
Manx: Close air support aircraft preliminary design
[NASA-CR-189992] p 463 N92-21565
Numerical simulation of shock-stall flutter of an airfoil using the Navier-Stokes equations p 746 N92-27956
SWEPT WINGS
Boundary-layer and wake measurements on a swept, circulation-control wing p 9 A92-13205
Step response of unsteady aerodynamics acting on a plane swept wing in incompressible flow for finite state modeling p 63 A92-14031
A 3-D separation model for arbitrary planforms
p 65 A92-14360
Three-dimensional linear stability approach to transition on wings and bodies of revolution at incidence
p 172 A92-18361
Three-dimensional thermal structural analysis of a swept cowl leading edge subjected to skewed shock-shock interference heating p 174 A92-20306
Calculation methods of three-dimensional boundary layers p 245 A92-21978
X-29 forebody jet blowing
[AIAA PAPER 92-0017] p 247 A92-22139
Static aeroelastic tailoring of composite aircraft swept wings modelled as thin-walled beam structures
p 294 A92-23114
Prediction of ice accretion on a swept NACA 0012 airfoil and comparisons to flight test results
[AIAA PAPER 92-0043] p 316 A92-25677
Design of a hybrid laminar flow control nacelle
[AIAA PAPER 92-0400] p 373 A92-26253
Development of a method for calculating the effect of the propeller slipstream on transonic flow over the wing
p 424 A92-30144
An inverse method for the design of transonic wings
[AIAA PAPER 92-1025] p 517 A92-33206
Effect of adaptive material properties on static aeroelastic control
[AIAA PAPER 92-2526] p 539 A92-34373
Analytical shape sensitivities and approximations of modal response of generally laminated tapered skew plates
[AIAA PAPER 92-2391] p 585 A92-34465
Prediction of three-dimensional turbulent boundary layers using a second-moment closure
p 675 A92-40080
Aero-structural integrated design of forward swept wing
[SAE PAPER 912021] p 790 A92-45414
Computational study of transition front on a swept wing leading-edge model
[AIAA PAPER 92-2630] p 795 A92-45502
Laminar separation bubbles and airfoil design at low Reynolds numbers
[AIAA PAPER 92-2735] p 797 A92-45515
Prediction of laminar boundary layer using cubic splines
[AIAA PAPER 92-2702] p 801 A92-45544
Concepts for the stability analysis of NLF-experiments on swept wings
[AIAA PAPER 92-2706] p 801 A92-45548
Forebody vortex control for suppressing wing rock on a highly-swept wing configuration
[AIAA PAPER 92-2716] p 803 A92-45555
Flow over a twin-tailed aircraft at angle of attack. II - Temporal characteristics p 810 A92-46781
Navier-Stokes computations on swept-tapered wings, including flexibility p 810 A92-46786
The calculation of three-dimensional compressible boundary layer stability on swept wings
p 818 A92-47684
Crossflow vortex and transition measurements by use of multielement hot films p 935 A92-50307
High angle-of-attack control enhancement on a forward swept wing aircraft
[AIAA PAPER 92-4427] p 1080 A92-55351
Improved calculation of transonic potential flow past swept wings p 1031 A92-56179
Characteristics of a boundary layer in a leading edge vortex p 86 N92-13012
An experimental investigation of vortex flaps on a canard combat-aircraft configuration p 87 N92-13023
Planform curvature effects on flutter characteristics of a wing with 56 deg leading-edge sweep and panel aspect ratio of 1.14
[NASA-TP-3116] p 115 N92-13054
An evaluation of preliminary Doppler global velocimetry measurements p 90 N92-13849
Numerical simulation of swept-wing flows
[NASA-CR-189457] p 180 N92-14969
Prediction of ice accretion on a swept NACA 0012 airfoil and comparisons to flight test results
[NASA-TM-105368] p 258 N92-15968
A method of estimating a flow breakdown boundary for aerofoils and swept wings in transonic flows
[ESDU-91021] p 258 N92-15970
A numerical study of the stability of the swept attachment line boundary layer
[AERO-REPT-9103] p 345 N92-18293
Aerodynamic and flowfield hysteresis of slender wing aircraft undergoing large-amplitude motions
p 364 N92-18780
Resolution of the Euler equations applied to a helicopter rotor in forward flight
[ONERA-RSF-2/3731-AY-004A] p 406 N92-19976
The NASA Langley laminar-flow-control experiment on a swept, supercritical airfoil: Evaluation of initial perforated configuration
[NASA-TM-4309] p 525 N92-22196
The natural flow wing-design concept
[NASA-TP-3193] p 631 N92-25202
Assessment of potential aerodynamic benefits from spanwise blowing at the wing tip
[NASA-TM-107847] p 631 N92-25261
Visualisation in water of vortex flow over sharp-edged canard configurations
[ARL-FLIGHT-MECH-R-189] p 632 N92-25410
Boundary layer transition: Prediction, application to drag reduction p 717 N92-27711
Comparison of Euler and full potential methods for unsteady transonic flow calculations
p 719 N92-27943
Natural flow wing
[NASA-CASE-LAR-14281-1] p 829 N92-28729
Analysis of iced wings
[NASA-TM-105773] p 1042 N92-34144
SWEPTBACK TAIL SURFACES
Extending a transonic small disturbance code to treat swept vertical surfaces
[AIAA PAPER 92-2503] p 518 A92-34498
Effect of twin fins on isolated tailplane lift-curve slope
[ESDU-91009] p 80 N92-11969
SWEPTBACK WINGS
Subcritical flutter characteristics of a swept-back wing in a turbulent supersonic flow - Comparison between analysis and experiment
[AIAA PAPER 92-2393] p 517 A92-34466
Instantaneous visualization of surface flows
p 763 A92-44327
Aerodynamic heating in three-dimensional shock wave turbulent boundary layer interaction induced by sweptback sharp fins in hypersonic flows
[SAE PAPER 912044] p 791 A92-45428
Research on aeroelastic tailoring at NAL
p 1053 A92-56019
Three dimensional boundary layer transition on a yawed cylinder p 766 N92-26909
Cross-flow instabilities and pressure gradients in boundary layers p 767 N92-26922
SWIMMING
Canadian aircrew sea water survival, 1952-1987
[DCIEM-88-RR-39] p 954 N92-32219
SWIRLING
Experimental study of the swirling flow in the internal volute of a centrifugal compressor
[ASME PAPER 91-GT-7] p 67 A92-15505
Experimental investigation of coannular jet flow with swirl along a centerbody p 172 A92-18367
Factors influencing the effective spray cone angle of pressure-swirl atomizers p 295 A92-23300
Characterization of a two-phase flow field downstream of a 3x-scale gas turbine co-axial, counter-swirling, combustor dome swirl cup
[AIAA PAPER 92-0229] p 393 A92-25693
An investigation of the swirl in an S-shaped inlet
p 343 A92-28476
Swirl effects on confined flows in axisymmetric geometries p 399 A92-28513
A new approach to swirl control in an S-duct
p 422 A92-29710
Experimental investigation on combustor with double co-axial swirlers p 469 A92-29729
An experimental investigation of the swirling combustor for integral liquid fuel ramjet p 557 A92-35541
Swirl and fuel composition effects on boron combustion in solid-fuel ramjets p 668 A92-36964
Solid-fuel ramjet fuel regression rate/thrust modulation
p 666 A92-36966
Particle dispersion in highly swirling, turbulent flows
p 675 A92-40093
Modern developments in shear flow control with swirl
p 703 A92-41265
Swirl number effects on confined flows in a model of a dump combustor p 896 A92-45202
New method of swirl control in a diffusing S-duct
p 809 A92-45859
A new vane swirler as applied to dual-inlet side-dump combustor
[AIAA PAPER 92-3654] p 906 A92-49085
Wind tunnel performance results of swirl recovery vanes as tested with an advanced high speed propeller
[AIAA PAPER 92-3770] p 1068 A92-54159
Numerical calculations of propfan/swirl recovery vane flow field
[AIAA PAPER 92-3771] p 1022 A92-54160
Computational and experimental investigation of annulus heat transfer with swirl
[AIAA PAPER 92-4060] p 1119 A92-56143
An experimental analysis of lateral jet injection into confined swirling crossflows p 156 N92-12199
Influence of the swirl producing construction in the flow and reaction field of turbulent diffusion flames
[ETN-92-92103] p 1127 N92-33916
SWITCHING THEORY
Lyapunov exponents for systems described by differential equations with discontinuous right-hand sides
p 507 A92-29237
SYMBOLS
The standardization of military head-up display symbology p 855 A92-44929
Comparative evaluation of internally and externally lighted taxiway guidance signs
[DOT/FAA/CT-TN92/2] p 573 N92-22237
SYMMETRY
Aerodynamic coefficients of a symmetrical airfoil in an oscillating flow
[AD-A241073] p 89 N92-13035
SYNCHRONISM
Achieving fault tolerance in multichannel control systems --- for avionics p 974 A92-49296
SYNCHRONOUS SATELLITES
Ranging and positioning experiments for aircraft using Engineering Test Satellite V p 102 A92-17242
Beam scanning error of phased array antenna
p 676 A92-40189
SYNCHROPHASING
The Dornier 328 Acoustic Test Cell (ATC) for interior noise tests and selected test results
[AIAA PAPER 92-2164] p 1137 N92-32951
Active synchrophasing of propeller unbalance
p 1138 N92-32963
SYNCHROTRONS
System of cryogenic security of the superconducting accelerator of relativistic nuclei-nuclotron
[DE91-643289] p 304 N92-16789
SYNOPTIC METEOROLOGY
Severe turbulence with a low-level jet ahead of a squall line p 407 A92-27939
SYNTHESIS (CHEMISTRY)
Addition curing thermosets endcapped with 4-amino (2.2) paracyclophane p 577 A92-33918
SYNTHETIC APERTURE RADAR
Comparison of aircraft synthetic aperture radar and buoy spectra during NORCSEX '88 p 597 A92-34878
Development of a 3-D remote sensing radar
p 597 A92-34908
Estimation of the P-3/SAR L-, C- and X-band antenna directivity in range direction based on corner reflector measurements within the absolute SAR calibration
p 587 A92-35055
Pocono Mountain SAR data analysis for testing slant range to ground range conversion p 587 A92-35142
Airborne/shipborne PSK telemetry data link
p 839 A92-47511
Motion errors in an airborne synthetic aperture radar system p 840 A92-48416
Detection and imaging of moving objects with synthetic aperture radar. I - Optimal detection and parameter estimation theory p 955 A92-50033

Bistatic image processing for a 32 x 19 inch model aircraft using scattered fields obtained in the OSU-ESL compact range
[NASA-CR-189932] p 499 N92-20197
The imaging radar system p 599 N92-23391

SYSTEM EFFECTIVENESS
National airspace system: System effectiveness operational concept NAS-SR-138
[DOT/FAA/SE-92/2] p 535 N92-23096

SYSTEM FAILURES
The propulsive-only flight control problem
p 876 A92-48487
F-16 failure detection isolation and estimation study
p 876 A92-48490
JIAWG module fault coverage metrics methodology
p 989 A92-49279
Detection and identification of axial flow compressor instabilities p 969 A92-50504
Detailed investigation of causes of avionics field failures p 995 A92-51925
Development of a calibrated software reliability model for flight and supporting ground software for avionic systems p 234 N92-15870

SYSTEM IDENTIFICATION
Closed-loop identification and iterative controller design p 48 A92-11362
Dynamic characterization and identification of nonlinear systems application to aeronautical structures
p 39 A92-11830
Frequency-domain identification of BO 105 derivative models with rotor degrees of freedom
p 104 A92-14327
System-identification of airplanes using the 'estimation before modelling' technique p 269 A92-21007
A system identification model for adaptive nonlinear control p 508 A92-29248
System identification requirements for high-bandwidth rotorcraft flight control system design
p 479 A92-29332
Rule based identifier for unknown systems
p 509 A92-31430
Improved coordination in non-hierarchic system optimization
[AIAA PAPER 92-2497] p 601 A92-34554
A frequency domain theory for structural identification
p 590 A92-35745
Robust identification of nonlinear aerodynamic model structure
[AIAA PAPER 92-4503] p 1081 A92-55370
Application of recursive partially unknown system identification to aerodynamic coefficients estimation
[AIAA PAPER 92-4504] p 1081 A92-55371
An identification procedure for a system with a choice of feedback structures p 1132 A92-55426
Parameter identification for nonlinear aerodynamic systems
[NASA-CR-188985] p 53 N92-10347
Rotorcraft system identification
[AGARD-AR-280] p 22 N92-11001
Identification of dynamic characteristics of flexible rotors as dynamic inverse problem p 220 N92-13962
Rotorcraft System Identification
[AGARD-LS-178] p 273 N92-17153
Design of experiments p 273 N92-17154
Instrumentation and data processing
p 273 N92-17155
Identification techniques: Model structure and time domain methods p 273 N92-17157
Identification techniques: Frequency domain methods
p 273 N92-17158
Modelling aspects and robustness issues in rotorcraft system identification p 274 N92-17159
Assessment of rotorcraft system identification as applied to the AH-64 p 274 N92-17160
BO 105 identification results p 274 N92-17161
SA 330 Puma identification results
p 274 N92-17162
Industry view on rotorcraft system identification
p 274 N92-17163
Application areas for rotorcraft system identification: Simulation model validation p 274 N92-17164
System identification methods for handling-qualities evaluation p 274 N92-17165
System identification requirements for high-bandwidth rotorcraft flight control system design
p 282 N92-17166
Neural networks for aircraft system identification
p 303 N92-17998
Model parameter identification techniques for flight flutter testing
[AERO-REPT-9105] p 380 N92-18294
The role of systems simulation for the development and qualification of ATTAS p 886 N92-28548
A simplified dynamic model of the T700 turboshaft engine
[NASA-TM-105805] p 1009 N92-30898

SYSTEMS ANALYSIS
A new study on a class of discrete event dynamic systems p 48 A92-11377
A general nonlinear dynamical analysis of a second-order, one-dimensional, theoretical compression system model p 509 A92-29374
Zonal analysis - The final step in system safety assessment p 760 A92-42071
Avionics systems engineering education
p 1012 A92-49269
Towards coherent hypermedia navigation by pragmatic dialogue modeling
[PB92-114735] p 455 N92-20818
A system approach to aircraft optimization
p 550 N92-23228
Nationwide system delay study of the microwave landing system in the New York terminal area, volume 1
[DOT/FAA/CT-TN91/59-VOL-1] p 640 N92-25098
Aircraft optimization by a system approach: Achievements and trends
[NASA-TM-107622] p 650 N92-25995
Fuzzy guidance system evaluation
p 778 N92-27903
A graphical user-interface for propulsion system analysis
[NASA-TM-105696] p 1134 N92-33894

SYSTEMS COMPATIBILITY
Constraint propagation through electromagnetic interaction topologies
[NRC-31761] p 155 N92-12154
Airport smart power lighting system
[DOT/FAA/CT-TN91/12] p 573 N92-22966

SYSTEMS ENGINEERING
Aerothermodynamic systems engineering and design
[SAE AIR 1168/3] p 36 A92-10039
Navy Aircrew Common Ejection Seat (NACES) program summary p 104 A92-13465
Thermodynamic structural analysis of high speed propulsion systems
[IAF PAPER 91-278] p 120 A92-14711
Case for real-time systems development - Quo vadis?
[AIAA PAPER 91-3726] p 231 A92-17594
Radar troubleshooting assistant expert system
[AIAA PAPER 91-3764] p 231 A92-17626
Enhanced autopilot design through hardware-in-the-loop simulation p 204 A92-19103
Some Aspects of uncertainty in computational fluid dynamics results p 233 A92-19609
Systems engineering as applied to the Boeing 777
[AIAA PAPER 92-1010] p 515 A92-33198
F15E terrain following system development
[AIAA PAPER 92-1079] p 563 A92-33248
System design from mission definition to flight validation
[AIAA PAPER 92-1091] p 605 A92-33256
Pilot activated automatic recovery system on the F-117A
[AIAA PAPER 92-1126] p 563 A92-33278
An interactive system for aircraft design and optimization
[AIAA PAPER 92-1190] p 600 A92-33302
Integration of supportability elements into the conceptual design process
[AIAA PAPER 92-1194] p 600 A92-33306
Design for validation p 601 A92-33607
Test Engineering Language for Avionic Systems
p 554 A92-35763
The thermodynamic approach in the study of large systems - Application to high-velocity airbreathing propulsion p 654 A92-37824
An overview of systems engineering management methods and processes
[AIAA PAPER 92-1539] p 690 A92-38636
British Airways Airbus A320 pilots' autothrust survey
[SAE PAPER 912225] p 636 A92-40023
Design-for-reliability through durability analysis
p 760 A92-42086
A computerized flight inspection system --- for testing of basic air navigation ground facilities
p 726 A92-43881
Applying advanced digital simulation techniques in designing fault tolerant systems p 921 A92-48489
Emerging airframe/propulsion integration technologies at General Electric
[AIAA PAPER 92-3335] p 850 A92-48917
Engine aircraft systems integration course
[AIAA PAPER 92-3762] p 928 A92-49117
Application of syndrome pattern-matching approach to fault isolation in avionic systems p 1005 A92-49261
Avionics systems engineering education
p 1012 A92-49269
A new approach to embedded computer performance measurement --- in avionics p 1005 A92-49288
The Catalyst software engineering environment --- in avionics p 1005 A92-49300
Improving designer productivity
[AIAA PAPER 92-1187] p 1130 A92-54285
Enlisting industry support for a flight controls design lab
[AIAA PAPER 92-4560] p 1141 A92-55272
Designing to cost effectiveness - Enhancing quality
p 1119 A92-56209
Helicopter nonlinear flight control system development
p 1085 A92-56317
A systematic formulation, as an approach to air traffic
[MBB-Z-0371-91-PUB] p 19 N92-10996
Calibration of the Naval Postgraduate School 3.5' x 5.0' academic wind tunnel
[AD-A240614] p 31 N92-11025
NASA reliability preferred practices for design and test
[NASA-TM-4322] p 157 N92-12286
Avionics systems development: Technological trends, conflicts, and cost issues in a changing European environment p 199 N92-14054
Avionics reliability, durability, and integrity: Can they be independent of application? p 200 N92-14056
RAMREQ: A computerized tool for the definition of RAM (Reliability, Availability, Maintainability) requirements of complex systems p 412 N92-18647
Experiences developed in transfering the experimental COMPAS system to an operational prototype version
p 355 N92-19045
Cooperative planning in aviation contexts
p 456 N92-21509
The proposed revision to RTCA DO178A and its influence on system design
[PNR-90821] p 510 N92-21847
A system approach to aircraft optimization
p 550 N92-23228
Sensor compatibility/optimal sensor combinations
p 599 N92-23403
ICAAS piloted simulation evaluation
p 735 N92-27906
Integrated Design Analysis and Optimisation of Aircraft Structures
[AGARD-LS-186] p 851 N92-28469
Multidisciplinary design and optimization
[AGARD-PAPER-2] p 851 N92-28473
Design specifications for the Advanced Instructional Design Advisor (AIDA), volume 2
[AD-A248202] p 923 N92-29188
Development of a flight information system using the structured method
[AD-A248207] p 859 N92-29222
Model analysis and expert system development for planning and scheduling teleoperations for aircraft turnaround functions. Volume 2: Top user's guide
[AD-A251083] p 932 N92-30258
A model of the ADA avionics real-time system: An example of the benefits of the hardware/software codesign approach in development of real-time systems
[AD-A248893] p 967 N92-30524
Advanced thermally stable, jet fuels development program annual report. Volume 1: Model and experiment system development
[AD-A249625] p 988 N92-31462
The 1991 Federal Aviation Administration plan for research, engineering and development
p 1142 N92-32453

SYSTEMS INTEGRATION
Navy Aircrew Common Ejection Seat (NACES) program summary p 104 A92-13465
Propulsion aspects of hypersonic turbo-ramjet-engines with special emphasis on nozzle/aftbody integration
[ASME PAPER 91-GT-395] p 127 A92-15725
Integration of flight and carrier landing aid systems for shipboard operations
[ONERA, TP NO. 1991-113] p 134 A92-16092
Stellar inertial navigation growing with the times upgrading of the LN-20 integrated inertial navigation system p 97 A92-16646
Implementation of a RAIM monitor in a GPS receiver and an integrated GPS/IRS p 99 A92-16948
Availability of positioning and receiver autonomous integrity monitoring for the global positioning system
p 100 A92-16963
Integrated navigation for approach guidance using differential GPS p 101 A92-16970
A digital P-code GPS receiver embedded in the AN/APN-217(V)5 Doppler Navigator
p 102 A92-16976
Performance improvements of an F-15 airplane with an integrated engine-flight control system
p 205 A92-20204
Observability under recurrent loss of data
p 302 A92-21191
Integrated flight control law synthesis for an aeroelastic forward-swept wing aircraft
[AIAA PAPER 92-0046] p 281 A92-22163
IMPAC - An integrated methodology for propulsion and airframe control p 477 A92-29118

Decentralized hierarchical partitioning of centralized integrated controllers --- for flight propulsion in STOVLs
p 477 A92-29119
The ATF YF-23 Vehicle Management System
[AIAA PAPER 92-1076] p 563 A92-33245
Flight management system integration on the F-117A
[AIAA PAPER 92-1077] p 563 A92-33246
Suit study - The impact of VMS in subsystem integration
[AIAA PAPER 92-1078] p 563 A92-33247
Integration of artificial intelligence and numerical optimization techniques for the design of complex aerospace systems
[AIAA PAPER 92-1189] p 600 A92-33301
CATMAC - A way to integrate ground ATC and airborne systems p 531 A92-33429
Profile negotiation - A concept for integrating airborne and ground-based automation for managing arrival traffic
p 531 A92-33432
The development and integration of an engine monitoring system for the F-14A+/D Super Tomcat
[SAE PAPER 912094] p 654 A92-39951
Code Division Multiple Access (CDMA) system candidate for integrated modular avionics
p 725 A92-42604
Integrated flight/propulsion control for supersonic STOVL aircraft p 872 A92-45320
Aero-structural integrated design of forward swept wing
[SAE PAPER 912021] p 790 A92-45414
A geometry-integrated approach to multiblock grid generation p 919 A92-47083
Modern techniques for monitoring airborne telemetry
p 857 A92-47560
Modular avionics - A commercial perspective
p 858 A92-48427
Rapid systems integration of navigation avionics
p 858 A92-48473
Using design of experiments to improve product and process integrity p 928 A92-48555
Utility management system for hypersonic vehicles
p 964 A92-49252
Formation flight system design concept
p 954 A92-49255
Is the avionics system of the Hermes Spaceplane centralized or decentralized? p 984 A92-49258
Digital flight control systems - Some new commercial twists p 974 A92-49264
A fault-tolerant network architecture for integrated avionics p 965 A92-49297
The Catalyst software engineering environment --- in avionics p 1005 A92-49300
Artificial intelligence techniques applied to vehicle management system diagnostics p 965 A92-49315
Systems commonality - Integrated avionics for the MH-47E and the MH-60K p 966 A92-49331
The army special operations aircraft integrated avionics subsystem - An operational perspective
p 966 A92-49332
Integrating a radar/ESM antenna suite with the S-70 helicopter --- Electronic Surveillance Measures
p 957 A92-49333
Operating principles for integrated sensor processing
p 966 A92-49336
GPS integration improves mission capabilities of CH-47D aircraft p 966 A92-49340
Architectures and GPS/INS integration - Impact on mission accomplishment p 967 A92-51003
Integral wing/fuel box p 958 A92-51569
Piloted evaluation of an integrated propulsion and flight control simulator
[AIAA PAPER 92-4178] p 960 A92-52459
Development of data base system in CIEM project
p 1009 A92-53093
Integrated system to support computer analysis in conceptual aerospace design p 1130 A92-53596
Test and integration concept for complex helicopter avionic systems p 1064 A92-56292
Integrated test and evaluation for hypervelocity systems
[AIAA PAPER 92-3901] p 1017 A92-56736
Solid-State Radar Beacon Decoder (SSRBD) Operational Test and Evaluation (OT/E) integration test plan
[DOT/FAA/CT-TN91/30] p 19 N92-10020
Avionics technology beyond 2000
p 200 N92-14058
Data Multiplexing Network (DMN) phase 3 equipment Operational Test and Evaluation (OT and E)/integration test report
[DOT/FAA/CT-TN91/50] p 221 N92-14270
Extension of the Frankfurt COMPAS for general application p 355 N92-19048
The impact of COMPAS on the future Cooperative Air Traffic Management Concept (CATMAC)
p 355 N92-19049
MULTIRAD
[AD-A244211] p 412 N92-19247
Revolution at sea: Aircraft options for the year 2030
p 466 N92-21974
Variable-camber systems integration and operational performance of the AFTI/F-111 mission adaptive wing
[NASA-TM-4370] p 570 N92-22194
Fiber optics for controls p 570 N92-22529
A system approach to aircraft optimization
p 550 N92-23228
Application of multidisciplinary optimization methods to the design of a supersonic transport
p 550 N92-23230
Application of an automated multidisciplinary analysis and optimisation system to the design of aircraft structures p 551 N92-23233
First approach to an integrated fin design
p 551 N92-23236
Structural optimization of aircraft practice and trends
p 551 N92-23239
Preconsiderations on aircraft integration
p 599 N92-23402
Assessment of flying-quality criteria for air-breathing aerospacecraft
[NASA-CR-4442] p 663 N92-25982
Computer program for calculating in-flight aircraft-store interface reaction loads
[AD-A245782] p 731 N92-26896
Inlet distortion effects in aircraft propulsion system integration p 869 N92-28464
Design and analysis issues of integrated control systems for high-speed civil transports
[NASA-CR-186022] p 979 N92-31656
System overview of the NASA Dryden Integrated Test Facility
[NASA-TM-104250] p 984 N92-32201
Design and evaluation of an advanced air-ground data-link system for air traffic control
[NASA-TM-103899] p 1050 N92-33407

SYSTEMS MANAGEMENT
Failure detection and fault management techniques for flush airdata sensing systems
[AIAA PAPER 92-0263] p 369 A92-25719
Integrated wiring system
[SAE PAPER 912058] p 897 A92-45440
Managing airborne assets through loads monitoring
p 363 N92-18594

SYSTEMS SIMULATION
A new approach to the real-time simulation of control systems with discontinuities p 508 A92-29291
Steady state and quasi-transient analysis of aircraft hydraulic system with network theory
p 642 A92-37391
Putting the control back in air traffic control - An enhanced Universal Development Simulation System
p 916 A92-44982
Analysis of the VISTA longitudinal simulation capability for a cruise flight condition p 876 A92-48488
F-16 failure detection isolation and estimation study
p 876 A92-48490
The data flow simulator, a tool for system simulation --- in digital avionics p 1006 A92-49329
The use of math-dynamic models to aid the development of integrated health and usage monitoring systems
p 1006 A92-50013
Testing of an experimental FMS p 648 N92-25596
Activities for numerical propulsion systems simulation program p 692 N92-25726
Harrier GR MK 5/7 mission simulators for the Royal Air Force p 885 N92-28540
The role of systems simulation for the development and qualification of ATTAS p 886 N92-28548

SYSTEMS STABILITY
Optimal stabilization of discrete event systems
p 48 A92-11376
Robust stabilization with positive real uncertainty - Beyond the small gain theorem p 50 A92-11444
An approach to the optimal output feedback initial stabilizing gain problem p 52 A92-11553
State feedback for nonlinear continuous-time systems - Stabilization and the creation of invariant subspaces
p 52 A92-11587
Synthesis of optimal digital systems for the stabilization of stochastically perturbed unstable dynamic systems
p 601 A92-33754
Detection and identification of axial flow compressor instabilities p 969 A92-50504
A survey of instabilities within centrifugal pumps and concepts for improving the flow range of pumps in rocket engines
[NASA-TM-105439] p 387 N92-18280
A methodology for computing uncertainty bounds of multivariable systems based on sector stability theory concepts
[NASA-TP-3166] p 482 N92-21410
Stability and performance of notch filter control for unbalance response p 771 N92-27731
Design of bearings for rotor systems based on stability
p 773 N92-27799

SYSTOLIC ARRAYS
New systolic array for all-nearest-neighbours problem
p 776 A92-41419

T

T-37 AIRCRAFT
Implementation of a personal computer based parameter estimation program
[AD-A252914] p 1061 N92-33502

T-38 AIRCRAFT
Using fractal dimension for target detection in clutter
p 410 A92-24423

T-39 AIRCRAFT
Saberliner flight test and results for forward looking detection and avoidance of airborne windshear
p 98 A92-16656

TABLES (DATA)
General aviation activity and avionics survey, calendar year 1989
[PB91-179234] p 169 N92-13926
FAA statistical handbook of aviation: Calendar year 1989
[PB91-202051] p 170 N92-13927
Experimental study of a generic high-speed civil transport: Tabulated data
[NASA-TM-104216] p 525 N92-22232

TABS (CONTROL SURFACES)
Effects of T-tabs and large deflections in double cantilever beam specimen tests p 673 A92-39009
Effect of tabs on the evolution of an axisymmetric jet
p 656 A92-40151
Supersonic jet mixing enhancement by 'delta-tabs'
[AIAA PAPER 92-3548] p 826 A92-49063
Supersonic jet mixing enhancement by delta-tabs
[NASA-TM-105664] p 630 N92-24958

TACAN
Concepts for replacing shipboard TACAN with differential GPS p 101 A92-16971
JTIDS electromagnetic compatibility in the 960-1215 MHz band
[AD-A247834] p 773 N92-27864

TACTICS
Revolution at sea: Aircraft options for the year 2030
p 466 N92-21974

TAIL ASSEMBLIES
Handling qualities of the H-76 Fantail Demonstrator
p 131 A92-14335
Effect of the wake flow on the soundproofing of aircraft structures p 166 A92-16824
Computational analysis of drag reduction techniques for afterbody/nozzle/empennage configurations
[SAE PAPER 912127] p 618 A92-39974
The maneuver performance and control of a hovercraft p 763 A92-43240
Numerical investigation of tail buffet on F-18 aircraft
[AIAA PAPER 92-2673] p 798 A92-45528
Unsteady pressure and load measurements on an F/A-18 vertical fin at high-angle-of-attack
[AIAA PAPER 92-2675] p 798 A92-45529
Flow over a twin-tailed aircraft at angle of attack. II - Temporal characteristics p 810 A92-46781
Investigation of the tail buffeting of the C-101
p 942 A92-53253
Effect of twin fins on isolated tailplane lift-curve slope
[ESDU-91009] p 80 N92-11969
Tutor aft fuselage and empennage full-scale fatigue test: Resolution of horizontal stabilizer installation difficulties
[NRC-LTR-ST-1804] p 114 N92-11990
F/A-18 stabilator: Equivalent set of point forces required for pneumatic bag load case simulation
[AD-A242637] p 206 N92-15073
The adverse aerodynamic impact of very small leading-edge ice (roughness) buildups on wings and tails
p 451 N92-21691
Design of a fighter aircraft vertical tail enhanced buffet environment survivability p 551 N92-23235
Composite strength statistics from fiber strength statistics
[AD-A245616] p 755 N92-26383

TAIL ROTORS
Handling qualities of the H-76 Fantail Demonstrator
p 131 A92-14335
Tail rotor aerodynamic features recorded in flight
p 546 A92-35752
Composite blades for helicopter main and tail rotors developed by Mil Design Bureau p 1057 A92-56325
Model rotor icing tests in the NASA. Lewis Icing Research Tunnel p 450 N92-21688

TAIL SURFACES
Aerodynamic balance range of aircraft of different configurations p 134 A92-16801
Optimization of the aerodynamic balance and parameters of the horizontal tail surfaces of the three-surface aircraft configuration with allowance for the capabilities of the stability and control augmentation system p 134 A92-16803
Investigation on freezing and sticking phenomena of slush on airplane surfaces when taxiing on the ground and the succeeding take-off run phase
[NAL-TR-1026] p 352 N92-18182
TAILLESS AIRCRAFT
Evaluation method of longitudinal static stability of tailless airplane p 282 A92-22520
Cold-cycle pressure-jet helicopters: Ventures, designs, and developments. III - Costs and developments p 458 A92-29675
TAKEOFF
Optimal trajectories and guidance trajectories for aircraft flight through windshears p 27 A92-11383
Aircraft control under conditions of windshear p 27 A92-11384
Aircraft control in a downburst on takeoff and landing p 27 A92-11385
Unsteady blade pressures on a propfan at takeoff - Euler analysis and flight data
[AIAA PAPER 92-0376] p 372 A92-26234
Aircraft control for take-off in windshear p 660 A92-36990
Aircraft noise - The calculation of the noise exposure by aircraft in the Netherlands p 687 A92-39054
Noise abatement procedures vs. safety
[SAE PAPER 912137] p 635 A92-39977
V-22 full scale development testing p 646 A92-40038
Microwave landing system modeling with application to air traffic control automation p 725 A92-41220
Operational evaluation of a tower workstation for clearance delivery p 879 A92-44981
Rejected takeoffs - Causes, problems, and consequences p 835 A92-45052
On the possibility of freezing and sticking phenomena in a transport during the ground taxiing and takeoff run and on the preventions of the hazard
[SAE PAPER 912042] p 836 A92-45426
Takeoff Performance Monitoring System display options
[AIAA PAPER 92-4138] p 967 A92-52433
Optimal control of tiltrotor aircraft following power failure p 1085 A92-56303
Helicopter rejected takeoff airspace requirements
[SCT-91RR-28] p 116 N92-13058
Rotorcraft acceleration and climb performance model
[SCT-90RR-30] p 116 N92-13059
Unsteady blade pressures on a propfan at takeoff: Euler analysis and flight data
[NASA-CR-189076] p 130 N92-13071
Variability of standard aircraft performance parameters
[ESDU-91020] p 276 N92-17847
Investigation on freezing and sticking phenomena of slush on airplane surfaces when taxiing on the ground and the succeeding take-off run phase
[NAL-TR-1026] p 352 N92-18182
Annoyance caused by aircraft en route noise
[NASA-TP-3165] p 512 N92-20479
Effects of frost on wing aerodynamics and take-off performance p 450 N92-21687
The effect of hoar-frosted wings on the Fokker 50 take-off characteristics p 451 N92-21692
A summary of NASA research on effects of heavy rain on airfoils p 452 N92-21694
Aerodynamic effects of de/anti-icing fluids and description of a facility and test technique for their assessment p 452 N92-21697
Integration of flight and carrier landing aid systems for shipboard operations p 456 N92-21958
Evaluating fixed wing aircraft in the aircraft carrier environment p 464 N92-21963
United States Navy ski jump experience and future applications p 465 N92-21968
Some implications for advanced STOVL operation from invincible class ships p 466 N92-21971
Aircraft accident report: Runway collision of USAir Flight 1493, Boeing 737 and Skywest Flight 5569 Fairchild Metroliner, Los Angeles International Airport, Los Angeles, CA, February 1, 1991
[PB91-910409] p 530 N92-23596
Aircraft accident report: Ryan International Airlines DC-9-15, N565PC, loss of control on takeoff, Cleveland-Hopkins International Airport, Cleveland, Ohio, February 17, 1991
[PB91-910410] p 530 N92-23597
Ski jump takeoff performance predictions for a mixed-flow, remote-lift STOVL aircraft
[NASA-TM-103866] p 1060 N92-32887
TAKEOFF RUNS
Investigation on freezing and sticking phenomena of slush on airplane surfaces when taxiing on the ground and the succeeding take-off run phase
[NAL-TR-1026] p 352 N92-18182
Freezing precipitation on lifting surfaces
[NRC-32124] p 448 N92-20156
An assessment of the B-747's capability to operate on rough surfaces
[AD-A250134] p 963 N92-31793
TANDEM WING AIRCRAFT
Experimental study of a low Reynolds number tandem airfoil configuration p 442 A92-32241
TANKER AIRCRAFT
The aerodynamic interference between a flapped tanker aircraft and a receiver aircraft during air-to-air refuelling p 29 A92-13199
A review of aging aircraft technology: An IAI perspective
[IAITIC-91-1018] p 461 N92-20500
TANKS (COMBAT VEHICLES)
SIMNET plan view display user manual
[AD-A244617] p 510 N92-21392
TANKS (CONTAINERS)
Demonstration of gas liquid separation under the microgravity by aircraft KC-135
[SAE PAPER 912024] p 897 A92-45416
Fire bombing and fire bombers
[CA-PATENT-1-268-164] p 1061 N92-33582
TANTALUM OXIDES
Fabrication and testing of corrosion resistant coatings --- for turbine engine components
[DE92-003553] p 490 N92-21063
TAPE RECORDERS
Advanced method for single event aircraft noise analysis p 693 A92-39060
TARGET ACQUISITION
Expanding U.S.M.C. roles for the AH-1W SuperCobra p 59 A92-14347
Identifying design requirements using integrated analysis structures p 922 A92-48527
JTIDS relative navigation and data registration p 955 A92-51006
Pulsed field system for detecting the presence of a target in a subsurface environment
[AD-D015074] p 296 N92-16174
Method of guiding an in-flight vehicle to a designed flight path
[AD-D015061] p 268 N92-17707
The application of lattice-structure adaptive filters to clutter-suppression for scanning radar p 403 N92-19154
Use of target spectrum for detection enhancement and identification p 404 N92-19155
TARGET RECOGNITION
Radar Detection Analysis of Rotor Systems (RADARS) p 117 A92-14350
Multisensor data fusion and decision support for airborne target identification p 454 A92-31063
Study on an induction method for a flying object, taking accelerating targets into account p 744 A92-43127
Use of target spectrum for detection enhancement and identification p 404 N92-19155
TARGETS
Flight test validation of tow target trajectory predictions
[AIAA PAPER 92-0209] p 271 A92-23814
Development of 3D electromagnetic modeling tools for airborne vehicles
[NASA-CR-190810] p 1126 N92-33307
TARS
Criteria for use of seal coats on airport pavements
[DOT/FAA/RD-92/18] p 1102 N92-34247
TASK COMPLEXITY
Knowledge-sensitive task manipulation - Acquiring knowledge from pilots flying a motion-based flight simulator p 916 A92-45064
The multi-attribute task battery for human operator workload and strategic behavior research
[NASA-TM-104174] p 303 N92-17130
TAXIING
New specifications proposed for taxiing guidance signs p 483 A92-29505
On the possibility of freezing and sticking phenomena in a transport during the ground taxiing and takeoff run and on the preventions of the hazard
[SAE PAPER 912042] p 836 A92-45426
Evaluation of two high-speed runway exits
[DOT/FAA/CT-TN91/36] p 31 N92-11021
Surface painted taxiway markings at Seattle-Tacoma International Airport
[DOT/FAA/CT-TN91/49] p 32 N92-11029
Investigation on freezing and sticking phenomena of slush on airplane surfaces when taxiing on the ground and the succeeding take-off run phase
[NAL-TR-1026] p 352 N92-18182
Runway exit designs for capacity improvement demonstrations. Phase 2: Computer model development
[NASA-CR-190166] p 484 N92-21162
Testing concept of a movement area guidance p 641 N92-25597
TAXONOMY
Research into the development of a knowledge acquisition taxonomy
[NASA-CR-189939] p 778 N92-28150
TAYLOR INSTABILITY
CFD state-of-the-art in the U.S.S.R p 495 A92-31486
The DAM vertical shock-tube p 880 A92-45096
TAYLOR SERIES
A fast three-dimensional vortex method for unsteady wake calculations
[AIAA PAPER 92-2624] p 794 A92-45496
Taylor series approximation of geometric shape variation for the Euler equations p 899 A92-46916
TECHNOLOGICAL FORECASTING
Tomorrow's cockpit displays p 117 A92-13699
High speed rotorcraft - Comparison of leading concepts and technology needs p 108 A92-14415
Composite gearbox housing p 110 A92-14448
Producibility Demonstrator Program - Technological preeminence through concurrent engineering p 146 A92-14449
Future trends in turboshaft engines up to 5000 horsepower class
[ASME PAPER 91-GT-74] p 122 A92-15543
Control systems for the next century's fighter engines
[ASME PAPER 91-GT-278] p 125 A92-15674
A propulsion perspective of the next generation supersonic transport
[ASME PAPER 91-GT-385] p 126 A92-15719
Omega/VLF now and into the 21st century p 98 A92-16659
Future experimental needs to support applied aerodynamics - A transonic perspective
[AIAA PAPER 92-0156] p 254 A92-23771
Future experimental needs in high-alpha vehicle dynamics
[AIAA PAPER 92-0159] p 254 A92-23774
Supersonic transport in the 21st century p 308 A92-26793
Flight vehicles of the future p 419 A92-31525
Overview and major characteristics of future aeronautical and space systems
[AIAA PAPER 92-2441] p 585 A92-34472
Aeroelasticity - Advances and future directions
[AIAA PAPER 92-2446] p 585 A92-34475
Energy attenuation for crashworthy seating systems - Past, present, and possible future development p 544 A92-35452
Future military APU requirements
[SAE PAPER 912176] p 655 A92-40001
Enhanced vision system option on future aircraft
[SAE PAPER 912204] p 651 A92-40014
International Conference on Aerospace Trends...2001 - From Aeroplane to Aerospace Plane, Thiruvananthapuram, India, June 27, 28, 1991, Proceedings p 751 A92-41184
Trends in propulsion technology p 757 A92-41186
ASTOVL flexibility in the 21st century p 783 A92-45309
British Aerospace Hawk into the 1990s p 957 A92-50009
Air transports in the 21st century p 1015 A92-55103
International aviation (selected article)
[AD-A240986] p 170 N92-13991
Automated planning with special relevance to associate systems technology and mission planning
[AD-A241924] p 303 N92-17438
Revolution at sea: Aircraft options for the year 2030 p 466 N92-21974
TECHNOLOGIES
Composites in manufacturing - Case studies
[ISBN 0-87263-406-X] p 784 A92-47403
The impact of aircraft noise control technology
[PNR-90846] p 512 N92-20461
Symposium on Marketing for Technological Products
[MBB-UE-0014-90-PUB] p 606 N92-23928
DoD key technologies plan
[AD-A253692] p 1142 N92-33238
TECHNOLOGY ASSESSMENT
LDF thermoplastic composites technology p 34 A92-13243
Historical development of eddy current testing in aircraft maintenance p 292 A92-21900
High costs force avionics links p 276 A92-22000
Anglo-American avionics p 307 A92-25575
Productivity and quality in the Modane and Fauga wind tunnels - Prospects for the 90s
[ONERA, TP NO. 1991-203] p 383 A92-26360

Navigation and flight management systems - Thoughts of a user p 354 A92-26848
The cockpit of a modern aircraft - The Airbus A340 considered as an example p 357 A92-26849
Advanced materials for aircraft engine applications p 390 A92-28251
Potential role of neural networks and fuzzy logic in flight control design and development
[AIAA PAPER 92-0999] p 600 A92-33191
Why composites wait in the wings p 577 A92-35475
A survey of composite structure technology at the Aerospatiale Helicopter Division p 546 A92-35754
International Aerospace Symposium 90, Nagoya, Japan, Nov. 26, 27, 1990, Proceedings p 607 A92-38201
GPS - Can it contribute to European ATC? p 637 A92-38380
GPS/GLONASS user systems in Sweden p 638 A92-38384
NASP - A status report
[AIAA PAPER 92-1417] p 666 A92-38569
Controls for agility research in the NASA High-Alpha Technology Program
[SAE PAPER 912148] p 661 A92-39984
The use of high voltage direct current in aircraft electrical systems - A Navy perspective
[SAE PAPER 912173] p 655 A92-39998
Advanced power generation systems for more electric aircraft
[SAE PAPER 912186] p 656 A92-40006
Advances in aircraft component superplastic forming/diffusion bonding technology
[SAE PAPER 912216] p 674 A92-40018
1991-92 AHS Technical Committee highlights - Aerodynamics p 623 A92-40391
Shear progress --- wind shear handling and recognition technologies for aviation p 609 A92-40880
Simulation as applied to mission planning p 747 A92-41210
Study on the effective utilization of the current flight simulator p 748 A92-43113
AIAA/AHS Flight Simulation Technologies Conference, Hilton Head Island, SC, Aug. 24-26, 1992, Technical Papers p 981 A92-52426
Getting up to speed in hypersonic structures p 1117 A92-55127
New materials drive high-performance aircraft p 1105 A92-55134
State-of-the-art materials for future gas turbine engines p 1070 A92-56122
New aircraft technologies - Challenges for dependability p 1120 A92-56225
Modern helicopter technologies at MBB and the application in future programmes p 1016 A92-56304
The role of stealth in naval aviation and joint/combined operations
[AD-A240595] p 22 N92-11005
Eighty years of aerospace technique through ATMA bulletins
[ETN-91-90097] p 57 N92-11963
An independent review of the Multi-Path Redundant Avionics Suite (MPRAS) architecture assessment and characterization report
[NASA-CR-188126] p 163 N92-12440
Aerospace plane technology: Research and development efforts in Japan and Australia
[AD-A241641] p 62 N92-12991
International aviation (selected article)
[AD-A240986] p 170 N92-13991
New Ways: Tiltrotor aircraft and magnetically levitated vehicles
[OTA-SET-507] p 238 N92-14933
Present and future trends in turbine blade material and manufacturing technology
[PNR-90825] p 488 N92-20164
The status of the US VAWT program
[DE92-002931] p 505 N92-21040
A historical overview of tiltrotor aeroelastic research at Langley Research Center
[NASA-TM-107578] p 502 N92-21460
NASP X-30 Propulsion technology status p 475 N92-21534
High altitude solar power platform --- aircraft design analysis
[NASA-TM-103578] p 506 N92-21546
Technical feasibility of digital three-dimensional cellular communications for air traffic control applications. Volume 1: Introduction and summary
[AD-A244573] p 534 N92-22104
Technical feasibility of digital three-dimensional cellular communications for air traffic control applications. Volume 2: Example system design details
[AD-A244574] p 534 N92-22105
Technical feasibility of digital three-dimensional cellular communications for air traffic control applications. Volume 3: Ground network architecture
[AD-A244575] p 534 N92-22106
Study of optical techniques for the Ames unitary wind tunnels. Part 2: Light sheet and vapor screen
[NASA-CR-190217] p 573 N92-22195
High temperature dynamic engine seal technology development
[NASA-TM-105641] p 596 N92-23435
When should we start high-rate production of the B-2? An analysis based on flight test results
[RAND/P-7757] p 697 N92-25204
Wind energy program overview
[DE91-002178] p 689 N92-25498
Ceramic composites: Enabling aerospace materials
[NASA-TM-105599] p 756 N92-27378
Feasibility of magnetic bearings for advanced gas turbine engines p 772 N92-27738
Progress of magnetic suspension systems and magnetic bearings in the USSR p 772 N92-27740
Technical evaluation report on the Flight Mechanics Panel Symposium on Flying Qualities
[AGARD-AR-311] p 733 N92-27870
Fiber optic data busses for aircraft p 736 N92-28093
Piloted simulation effectiveness development applications and limitations p 883 N92-28524
Saenger: The reference concept and its technological requirements - aerothermodynamics
[MBB-FE-202-S-PUB-0463-A] p 890 N92-29629
Nondestructive inspection perspectives p 915 N92-30121
Current and future developments in civil aircraft non-destructive evaluation from an operator's point of view p 787 N92-30122
The Eurofar program: An European overview on advanced VTOL civil transportation system
[MBB-UD-0611-91-PUB] p 952 N92-30418
Numerical optimization in Germany: A non-exhaustive survey on current activities with emphasis on aeronautics
[MBB/FE211/S/PUB/474] p 932 N92-30675
Technical evaluation report on the Flight Mechanics Panel Symposium on Piloted Simulation Effectiveness
[AGARD-AR-315] p 983 N92-30769
Advanced electromagnetic methods for aerospace vehicles
[NASA-CR-190650] p 1001 N92-31156
Trends in aeropropulsion research and their impact on engineering education
[NASA-TM-105682] p 972 N92-31172
The 1991 Federal Aviation Administration plan for research, engineering and development p 1142 N92-32453
Examples of advanced near-net shape manufacturing techniques for aerospace
[MBB-Z-0399-91-PUB] p 1125 N92-32742
Fly-by-light technology development plan
[NASA-CR-181954] p 1086 N92-32778
Study objectives: Will commercial avionics do the job? Improvements needed? p 1065 N92-33340

TECHNOLOGY TRANSFER
Successful transfer of technology from a research and development laboratory to an Aerospatiale production unit p 931 A92-51808
Welding technology transfer task/laser based weld joint tracking system for compressor girth welds p 593 N92-22426
The Air Force Manufacturing Technology (MANTECH): Technology transfer methodology as exemplified by the radar transmit/receive module program p 593 N92-22451
Wind energy program overview
[DE91-002178] p 689 N92-25498
NASA/DOD Aerospace Knowledge Diffusion Research Project. Paper 13: The information-seeking habits and practices of engineers
[NASA-TM-107931] p 782 N92-28114
Communication: An important element of maintenance and repair p 838 N92-30124
An international aerospace information system: A cooperative opportunity
[NASA-TM-108171] p 1142 N92-33237

TECHNOLOGY UTILIZATION
Technology in the lives of an aircraft designer
[AIAA PAPER 91-3069] p 192 A92-20000
Opportunities for advanced speech processing in military computer-based systems p 293 A92-22299
New Airbus Industrie airliners on course for long-haul era p 308 A92-26792
Airfield construction (3rd revised and enlarged edition) --- Russian book
[ISBN 5-277-01070-X] p 670 A92-36606
Development of active control technology for the next generation of combat aircraft p 975 A92-50008
Use of high-fidelity simulation in the development of an F/A-18 active ground collision avoidance system
[AIAA PAPER 92-4140] p 959 A92-52434
JPRS report: Science and technology. USSR: Space
[JPRS-USP-91-007] p 211 N92-14101
Ceramic composites: Enabling aerospace materials
[NASA-TM-105599] p 756 N92-27378

TEETERING
The NREL teetering hub rotor code: Final results and conclusions
[DE92-001187] p 410 N92-19633
Model rotor icing tests in the NASA. Lewis Icing Research Tunnel p 450 N92-21688

TEFLON (TRADEMARK)
Design and testing of high-performance parachutes
[AGARD-AG-319] p 345 N92-18269

TELECOMMUNICATION
Airborne/shipborne PSK telemetry data link p 839 A92-47511
Capacity as a consideration for providing aeronautical mobile satellite air traffic services in the U.S. domestic airspace p 956 A92-51007
Advances in Fibre-Optic Technology in Communications and for Guidance and Control
[AGARD-LS-184] p 774 N92-28084
Tasking and communication flows in the F/A-18D cockpit: Issues, problems, and possible solutions
[AD-A245977] p 853 N92-28802
Proceedings of the Workshop on Advanced Network and Technology Concepts for Mobile, Micro, and Personal Communications
[NASA-CR-190459] p 1000 N92-30923

TELEMETRY
Telemetry antenna patterns for single and multi-element arrays p 188 A92-19216
A new 1553 all-bus instrumentation monitor p 198 A92-19252
Implementation and usage of the RJ program Data Acquisition System Ground Station p 210 A92-19257
An integrated real-time turbine engine flight test system p 201 A92-19275
Internationalization of telemetry systems p 920 A92-47535
Airborne Data Acquisition and Relay System p 839 A92-47574
Further developments relating to the NASA Langley Research Center 13-inch magnetic suspension and balance system
[NASA-CR-188995] p 31 N92-11023
Ground installations for the preparation and evaluation of flight tests p 665 N92-25593
Flight testing of a half-scale remotely piloted vehicle
[AD-A248568] p 733 N92-28123
Stability and control flight testing of a half-scale Pioneer remotely piloted vehicle
[AD-A245973] p 879 N92-28801

TELEOPERATORS
Adaptive suppression of biodynamic interference in helmet-mounted displays and head teleoperation p 197 A92-18611
Model analysis and expert system development for planning and scheduling teleoperations for aircraft turnaround functions, volume 1
[AD-A251037] p 932 N92-30253
Model analysis and expert system development for planning and scheduling teleoperations for aircraft turnaround functions. Volume 2: Top user's guide
[AD-A251083] p 932 N92-30258

TELEVISION CAMERAS
Salvaging the wreckage - Multidistrict litigation and aviation p 697 A92-39245
A high-performance LLLTV CCD camera for nighttime pilotage p 855 A92-46227

TELEVISION SYSTEMS
Television Microwave Link (TML) Operational Test and Evaluation (OT/E)/integration test report
[DOT/FAA/CT-TN91/57] p 500 N92-20653

TEMPERATURE
The icing of the wing upper side and bottom side of the icing research aircraft of the DLR p 724 N92-26349

TEMPERATURE CONTROL
A comparison of cooling methods for the airframe nozzle of a single-stage-to-orbit aircraft
[AIAA PAPER 91-5036] p 210 A92-17825
A probabilistic method for monitoring the remaining life of aircraft gas turbine engine components using the temperature limit criterion p 201 A92-18292
Evolutionary upgrade and application of the C-130H simple-cycle refrigeration system
[SAE PAPER 911439] p 270 A92-21836
Thermal management of hypersonic aircraft using noncryogenic fuels
[SAE PAPER 911443] p 270 A92-21839

Thermal management of air-breathing propulsion systems
[AIAA PAPER 92-0514] p 373 A92-26940
Thermal management systems for high Mach airbreathing propulsion
[AIAA PAPER 92-0515] p 373 A92-26941
Thermal management of propulsion systems in hypersonic vehicles
[AIAA PAPER 92-0516] p 373 A92-26942
Thermal control for hypersonic vehicle propulsion
p 468 A92-29356
Outline and discussion of the cooling loop of the heating control system in the exposed facility of the Japanese Experiment Module (JEM) p 574 A92-35610
Requirements for high flux cooling of future avionics systems
[SAE PAPER 912104] p 673 A92-39958
Flexible heat pipe cold plates for aircraft thermal control
[SAE PAPER 912105] p 674 A92-39959
Application of advanced composites in SEM-E heatsinks for the thermal management of avionics
p 986 A92-51922
A clean air continuous flow propulsion facility
[AIAA PAPER 92-3912] p 1094 A92-56745
Thermal management of high heat flux electronic components in space and aircraft systems, phase 1
[AD-A239982] p 41 N92-10157
Active thermal isolation for temperature responsive sensors
[NASA-CASE-LAR-14612-1] p 911 N92-29954
Subsonic flight test evaluation of a performance seeking control algorithm on an F-15 airplane
[NASA-TM-4400] p 973 N92-31275

TEMPERATURE DEPENDENCE
The optimization of variable cross-section spines with temperature dependent thermal parameters
p 901 A92-48353
Use of an approximate similarity principle for the thermal scaling of a full-scale thrust augmenting ejector
[AIAA PAPER 92-3792] p 1069 A92-54171
Pressure measurements in high speed water tunnels
[DE92-004891] p 386 N92-19978
Use of an approximate similarity principle for the thermal scaling of a full-scale thrust augmenting ejector
[NASA-TM-105724] p 739 N92-26613

TEMPERATURE DISTRIBUTION
Embedded longitudinal vortex arrays, velocity and temperature fields, loss and heat transfer augmentation
p 621 A92-40121
Local heat transfer in the perforation channels of turbine nozzle vanes p 657 A92-40615
Optimum dimensions of convective-radiative spines using a temperature correlated profile
p 676 A92-40869
Experimental technique of measuring fuel concentration in non-uniform flowfield p 734 A92-41928
New 1.27-m leg of the National Aerospace Laboratory hypersonic wind tunnel p 1092 A92-56003
Application of infrared thermography to thermal flux measurement in wind tunnels
[AAAF-NT-89-12] p 31 N92-11020
Results of measured temperature distribution on an adiabatic wing model with radiation thermometer
[NAL-TM-610] p 261 N92-17755
Numerical simulation of an aircraft anti-icing system incorporating a rivulet model for the runback water
p 448 N92-20303
Light thermal structures and materials for high speed flight p 649 N92-25922
The 3-D Navier-Stokes flow and temperature field computation for a forced mixer nozzle
p 770 N92-27482

TEMPERATURE EFFECTS
Analyses of heat isolation property for metallic multiwall thermal protection system p 40 A92-12422
Experiments to evaluate hot-jet simulation capabilities in Cryogenic Wind-Tunnel testing
[AIAA PAPER 92-0567] p 384 A92-26975
Heat induced transient behaviours of axial compressors p 469 A92-29721
Temperature and initial curvature effects in low-density panel flutter
[AIAA PAPER 92-2128] p 589 A92-35695
Finite element nonlinear panel flutter with arbitrary temperatures in supersonic flow
[AIAA PAPER 92-2129] p 589 A92-35696
Effect of sustained high temperature exposure on the mechanical properties of Nicalon/Al2O3 composites
p 668 A92-39672
The cryogenic balance design and balance calibration methods
[AIAA PAPER 92-4001] p 1122 A92-56824
A damage tolerance assessment of bonded repairs to CF-18 composite components. Part 1: Adhesive properties
[DREP-TM-88-25-PT-1] p 143 N92-12060
Ultra-high temperature (greater than 2000 C) testing capability at Oak Ridge National Laboratory for carbon materials in air, inert gas and vacuum
[DE92-004445] p 385 N92-18069
Thermal nonequilibrium effects on turbine cascade aerodynamics
[AD-A244049] p 404 N92-19183
On the instability of boundary layers on heated flat plates
[NASA-CR-187581] p 347 N92-19250
Temperature effects in FFA HYP 500 at M = 7 in a flow with strong expansion
[FFA-TN-1991-27] p 443 N92-20229
Evaluation of an innovative high-temperature ceramic wafer seal for hypersonic engine applications
p 578 N92-22205
Finite element frequency domain solution of nonlinear panel flutter with temperature effects and fatigue life analysis p 682 N92-25589
Advanced Turbine Technology Applications Project (ATTAP)
[NASA-CR-189142] p 682 N92-25649
Hot-gas reingestion engine response considerations
[PNR-90810] p 740 N92-27042
Experimental and computational ice shapes and resulting drag increase for a NACA 0012 airfoil
[NASA-TM-105743] p 828 N92-28674
Thermal response of rigid and flexible insulations and reflective coating in an aeroconvective heating environment
[NASA-TM-103925] p 852 N92-28721
Effect of walls on the supersonic reacting mixing layer
p 912 N92-30065
Performance of insulated pavements at Newton Fields, Jackman, Maine
[CRREL-92-9] p 1101 N92-32903
Isothermal aging of IM7/8320 and IM7/5260
[NASA-TM-107666] p 1110 N92-33423
Electro optical system to measure strains at high temperature
[NASA-CR-190450] p 1127 N92-33696

TEMPERATURE GRADIENTS
On thermal-stress gas flows p 37 A92-10657
Stability of a viscous compressible shear layer with a temperature drop p 79 A92-16684
Airframe life prediction p 649 N92-25931

TEMPERATURE MEASUREMENT
CARS temperature/multi-species measurement strategies for high speed airbreathing and rocket propulsion testing p 154 A92-16615
Shuttle Infrared Leeside Temperature Sensing (SILTS) experiment - STS-35 and STS-40 preliminary results
[AIAA PAPER 92-0126] p 286 A92-23746
Preliminary laser induced fluorescence measurements in several facilities in preparation for application to studies in the high enthalpy shock tunnel Goettingen (HEG)
[AIAA PAPER 92-0143] p 284 A92-23761
Measurement of convective heat-transfer coefficients in wind tunnels using passive and stimulated infrared thermography p 390 A92-24430
A new thermometric instrument for airborne measurements in clouds p 368 A92-24918
CARS temperature measurements and validation of a computing code on a gas-turbine combustor
[ONERA, TP NO. 1991-224] p 373 A92-26376
Design and preliminary tests of a new airborne thermometer p 468 A92-32097
A fiber optic temperature sensor for aerospace applications p 761 A92-42607
Acoustic control of combustor primary zone air-jet mixing
[AIAA PAPER 92-3651] p 1067 A92-54104
A fine-wire thermocouple probe for measurement of stagnation temperatures in real gas hypersonic flows of nitrogen p 1114 A92-54317
Turbine engine hot-part temperature measurement techniques
[AIAA PAPER 92-3960] p 1122 A92-56788
Boundary layer study on nozzle wall at hypersonic velocities
[AIAA PAPER 92-4013] p 1034 A92-56836
Application of infrared thermography to thermal flux measurement in wind tunnels
[AAAF-NT-89-12] p 31 N92-11020
CARS temperature measurements in a hypersonic propulsion test facility p 140 N92-12049
Heat transfer measurements in ONERA supersonic and hypersonic wind tunnels using passive and active infrared thermography p 208 N92-15003
Results of measured temperature distribution on an adiabatic wing model with radiation thermometer
[NAL-TM-610] p 261 N92-17755
Experimental investigation of passive infrared ice detection for helicopter applications p 265 N92-17986
Ultra-high temperature (greater than 2000 C) testing capability at Oak Ridge National Laboratory for carbon materials in air, inert gas and vacuum
[DE92-004445] p 385 N92-18069
Fiber-sensor design for turbine engines
[DE92-003539] p 376 N92-18230
Laser-spectroscopic measurement techniques for hypersonic, turbulent wind tunnel flows
[NASA-TM-103928] p 405 N92-19596
Lubricant evaluation and performance 2
[AD-A247464] p 895 N92-28398
Repetitive High Energy Pulsed Power (RHEPP) temperature monitoring system utilizing Luxtron fluoroptic sensors and thermocouples technical reference manual
[DE92-013461] p 999 N92-30893
Feasibility of measuring transverse electric noise at VLF and LF on an ice cap
[AD-A252280] p 1129 N92-33220

TEMPERATURE MEASURING INSTRUMENTS
Notes on the use of fusible temperature indicators to bound the temperature of hot graphite in the NAVSWC hypervelocity wind tunnel facility p 1090 A92-54315
Ablation and temperature sensors for flight measurements in reentry body heat shields
p 227 N92-15004

TEMPERATURE PROFILES
An investigation on the characteristics of combustor with oblique air jet p 375 A92-28434
Structural features of a heated round turbulent jet in a cross-flow p 676 A92-40148
A study of aerophysical and dynamic characteristics using an axisymmetric flight test vehicle with a reusable nose section p 707 A92-42684
A comparison of measured and modeled broadband fluxes from aircraft data during the ICE '89 field experiment p 1003 A92-49771
Microwave temperature profiler for clear air turbulence prediction
[NASA-CASE-NPO-18115-1-CU] p 916 N92-29148

TEMPERATURE SENSORS
Shuttle Infrared Leeside Temperature Sensing (SILTS) experiment - STS-35 and STS-40 preliminary results
[AIAA PAPER 92-0126] p 286 A92-23746
A fiber optic temperature sensor for aerospace applications p 761 A92-42607
Research sensors p 594 N92-22526
Active thermal isolation for temperature responsive sensors
[NASA-CASE-LAR-14612-1] p 911 N92-29954

TEMPORAL DISTRIBUTION
Temporal change of timbre of helicopter noise
p 694 A92-39104

TEMPORAL RESOLUTION
Synthesis of the algorithm of a spatial-temporal discriminator and the potential accuracy of the velocity meter p 41 A92-12828

TENSILE PROPERTIES
Tensile and interlaminar properties of GLARE (trade name) laminates
[AD-A250188] p 895 N92-28921

TENSILE STRENGTH
Ultimate strength prediction of ASTM D - 3039 tensile specimens from acoustic emission amplitude data
[AIAA PAPER 92-0258] p 394 A92-25716
A demonstration of passive blade twist control using extension-twist coupling
[AIAA PAPER 92-2468] p 539 A92-34358
The relationship between tensile and flexural strength of unidirectional composites p 891 A92-45629
Processing and environmental effects on mechanical properties of composite repairs
[NRC-LTR-ST-1826] p 1109 N92-32791

TENSILE STRESS
Non-homogeneous bars under tension, pure bending and thermal loads p 495 A92-31198

TENSILE TESTS
A viscoplastic model for single crystals
p 391 A92-24717
Thermomechanical fatigue behavior of a silicone carbide fiber-reinforced calcium aluminosilicate glass-ceramic matrix composite
[AD-A249870] p 988 N92-31823

TENSION
Apparatus for elevated temperature compression or tension testing of specimens
[NASA-CASE-LAR-14775-1] p 912 N92-30099

TERMINAL AREA ENERGY MANAGEMENT
Space shuttle entry terminal area energy management
[NASA-TM-104744] p 308 N92-19930

TERMINAL FACILITIES
Airport terminals p 283 A92-21125
Terminal area traffic management
p 955 A92-50122

Television Microwave Link (TML) Operational Test and Evaluation (OT/E)/integration test report
[DOT/FAA/CT-TN91/57] p 500 N92-20653
FAA aviation forecasts
[AD-A250412] p 837 N92-29182
Accomplishments under the Airport Improvement Program, FY 1991
[AD-A253046] p 1101 N92-33434

TERMINAL GUIDANCE
Method of guiding an in-flight vehicle to a designed flight path
[AD-D015061] p 268 N92-17707
Evaluation of advanced microwave landing system procedures in the New York terminal area
[DOT/FAA/ND-91/1] p 354 N92-18967
Integration of flight and carrier landing aid systems for shipboard operations p 456 N92-21958
Approach and landing guidance p 457 N92-21960
CTAS: Computer intelligence for air traffic control in the terminal area
[NASA-TM-103959] p 1044 N92-33080

TERMINAL VELOCITY
Stability and inherent precision of two methods for solving motion and ablation equations for fireball-forming bodies in the earth atmosphere p 929 A92-46595

TERMINOLOGY
PDES application protocol suite for composites (PAS-C). Functional needs report for the PAS-C program
[AD-A247886] p 1108 N92-32629

TERRAIN
A multidimensional terrain model for low altitude tracking scenarios p 205 A92-19107
Pocono Mountain SAR data analysis for testing slant range to ground range conversion p 587 A92-35142
The application of statistical estimation techniques to terrain modeling
[AD-A243799] p 409 N92-19231
Terrain following of arbitrary surfaces using a high intensity LED proximity sensor
[DE92-007161] p 455 N92-21201
An efficient method for three-dimensional route planning with different strategies and constraints
p 728 N92-27901
Aircraft accident/incident summary report: Controlled flight into terrain Bruno's Inc., Beechjet, N25BR, Rome, Georgia, 11 December 1991
[PB92-910404] p 1044 N92-34081

TERRAIN ANALYSIS
Automated thematic processing of aircraft scanner data gathered over pasture territory in Turkmenia
p 406 A92-25330
Design and implementation of a generic Kalman filter in Ada p 858 A92-48475
The application of statistical estimation techniques to terrain modeling
[AD-A243799] p 409 N92-19231

TERRAIN FOLLOWING AIRCRAFT
A low-altitude breakthrough system using optimal path terrain following p 205 A92-20483
Robust optimal control with a worst case time domain performance criterion p 509 A92-29368
F15E terrain following system development
[AIAA PAPER 92-1079] p 563 A92-33248
Flight testing a digital terrain following system
p 548 A92-35929
An ultrareliable integrated digital computer for helicopters p 964 A92-49273
Predictive control for optimal path terrain following system p 955 A92-50207
Integration of radar altimeter, precision navigation, and digital terrain data for low-altitude flight
[AIAA PAPER 92-4420] p 1063 A92-55212
Laser-radar based obstacle avoidance system for helicopters p 1064 A92-56295
A-2000: Close air support aircraft design team
[NASA-CR-190022] p 463 N92-21567

TEST CHAMBERS
Calibration of the Naval Postgraduate School 3.5' x 5.0' academic wind tunnel
[AD-A240614] p 31 N92-11025
Experimental investigation of heavy rainfall effect on a 2-D high lift airfoil p 452 N92-21696
Effect of collector configuration on test section turbulence levels in an open-jet wind tunnel
[NASA-TM-4333] p 750 N92-27670
The FML compressor as a drive system for the LFSWT: A narrative p 751 N92-27978
The design of test-section inserts for higher speed aeroacoustic testing in the Ames 80- by 120-foot wind tunnel
[NASA-TM-103915] p 927 N92-28909

TEST EQUIPMENT
Mach 4 and Mach 8 axisymmetric nozzles for a high-enthalpy shock tunnel p 78 A92-16668
Noise control used for turbojet engine test bench
p 284 A92-21749
An automated workstation for the half-scale testing of the flight vehicle stabilization circuit p 664 A92-40622
Ames life science telescience testbed evaluation
[NASA-CR-188856] p 140 N92-12033
Thermal energy test apparatus
[AD-A243526] p 305 N92-17537
NLR experience with high velocity burner rig testing, 1979-1989
[NLR-TP-89152-U] p 385 N92-18415
Design and construction of a Helmholtz coil magnetic test cell
[AD-A249944] p 983 N92-30849
System overview of the NASA Dryden Integrated Test Facility
[NASA-TM-104250] p 984 N92-32201

TEST FACILITIES
Experimental demonstration of active vibration control for flexible structures p 50 A92-11442
Helicopter modeling requirements for full mission simulation and handling qualities assessment
p 105 A92-14364
Investigation of engine thrust correlation methods for enclosed test cells
[ASME PAPER 91-GT-68] p 121 A92-15538
NASA low-speed centrifugal compressor for 3-D viscous code assessment and fundamental flow physics research
[ASME PAPER 91-GT-140] p 72 A92-15580
A universal turboprop engine dynamometer test cell
[ASME PAPER 91-GT-343] p 137 A92-15706
Using uncertainty analysis in the debugging and qualification of a turbulent heat transfer test facility
p 138 A92-17224
'Spaceplanes' R&D status of Japan
[AIAA PAPER 91-5002] p 209 A92-17802
Thrust nozzle test facility at DLR Cologne
[AIAA PAPER 91-5024] p 206 A92-17818
Conducting the NASP ground test program
[AIAA PAPER 91-5029] p 209 A92-17820
Heavy metal --- fighter aircraft test rigs
p 207 A92-18100
Design and implementation of a total flight test system
p 189 A92-19278
Experimental investigation of periodically excited rotating composite rotor blades p 218 A92-20213
Rotor revolutions in the Far East - Helicopters in China, Mongolia, and Siberia p 241 A92-22711
A large-scale axial flow compressor facility and dynamic measurement techniques for rotor flow study
p 382 A92-24729
Supersonic combustor testing using optical diagnostics and a high enthalpy shock tunnel
[AIAA PAPER 92-0761] p 384 A92-27102
Ground test facilities for aerothermal and aero-optical evaluation of hypersonic interceptors
[AIAA PAPER 92-1074] p 573 A92-33244
1991-92 AHS Technical Committee highlights - Flight simulation p 609 A92-40394
Stringer subsystem automation p 700 A92-43246
Hypersonic mixing and combustion studies in the hypulse facility p 737 A92-44526
Water tunnels p 880 A92-45266
Remarks on high-Reynolds-number turbulence experiments and facilities p 881 A92-45267
Recent developments at the Shoeburyness STOVL test facility p 881 A92-45314
Ground surface erosion - British Aerospace test facility and experimental studies p 881 A92-45323
Making fly-by-light a reality p 877 A92-48499
Structural testing technology at high temperature; Proceedings of the Conference, Dayton, OH, Nov. 4-6, 1991
[ISBN 0-912053-34-8] p 980 A92-51401
Simulation of high heat flux levels with graphite heating and arc lamps p 980 A92-51402
Acoustic testing at elevated temperatures
p 981 A92-51405
A history of high-temperature testing at WPAFB
p 981 A92-51406
A preliminary study of a supersonic wind tunnel for a ram jet test facility p 1089 A92-53564
V-22 propulsion system design p 1070 A92-56300
Supersonic and hypersonic quiet tunnel technology at NASA Langley
[AIAA PAPER 92-3908] p 1094 A92-56743
A clean air continuous flow propulsion facility
[AIAA PAPER 92-3912] p 1094 A92-56745
An overview of the planned aerospace test facilities at Capua, Italy
[AIAA PAPER 92-3944] p 1097 A92-56773
Study on international cooperative test facilities for future SST/HST
[AIAA PAPER 92-3945] p 1097 A92-56775
TSNIIMASH capabilities for aerogasdynamical and thermal testing of hypersonic vehicles
[AIAA PAPER 92-3962] p 1097 A92-56789
Test facilities and instrumentation for research in rarefied gas dynamics - An historical perspective
[AIAA PAPER 92-3969] p 1098 A92-56795
A code validation strategy and facility for nonequilibrium, reacting flows
[AIAA PAPER 92-3970] p 1098 A92-56796
Thrust stand design principles
[AIAA PAPER 92-3976] p 1098 A92-56802
Turbine engine performance test and evaluation techniques
[AIAA PAPER 92-3977] p 1071 A92-56803
Small engine components test facility compressor testing cell at NASA Lewis Research Center
[AIAA PAPER 92-3980] p 1098 A92-56806
Comparison of recent results from different wind tunnel facilities along with comparisons of measured flight results and wind tunnel based predictions
[AIAA PAPER 92-3985] p 1060 A92-56809
Advanced nozzle and engine components test facility
[AIAA PAPER 92-3993] p 1099 A92-56816
Engine component instrumentation development facility at NASA Lewis Research Center
[AIAA PAPER 92-3995] p 1099 A92-56818
Calibration of hemispherical-head flow angularity probes
[AIAA PAPER 92-4005] p 1122 A92-56828
Aerodynamics laboratory education at Purdue University - Ground testing facilities
[AIAA PAPER 92-4018] p 1100 A92-56840
The trisonic wind tunnel Muenchen and its involvement in the German SAeNGER-programme
[AIAA PAPER 92-4019] p 1100 A92-56841
Laboratory simulation of aerothermodynamic phenomena - A review
[AIAA PAPER 92-4025] p 1104 A92-56847
Transonic turbine blade cascade testing facility
[AIAA PAPER 92-4034] p 1101 A92-56856
Fuel flow measurement in gas turbine testing
[NRC-29808] p 130 N92-12000
A derivation of gross thrust for a sea-level jet engine test cell
[NRC-30165] p 130 N92-12001
Aerospace technology: Technical data and information on foreign test facilities
[GAO/NSIAD-90-71FS] p 139 N92-13076
Image-supported navigation for testing instrument landing systems p 189 N92-14012
Review of the European hypersonic wind tunnel performance and simulation requirements
p 209 N92-15043
Safety considerations in testing a fuel-rich aeropropulsion gas generator
[NASA-TM-105258] p 279 N92-17061
Ultra-high temperature (greater than 2000 C) testing capability at Oak Ridge National Laboratory for carbon materials in air, inert gas and vacuum
[DE92-004445] p 385 N92-18069
The Goldstein Engineering Research Laboratory
[AERO-REPT-8906] p 308 N92-18322
Numerical simulation of transient hypervelocity flow in an expansion tube
[NASA-CR-189601] p 402 N92-18965
Activities of NRC-CNRC, Institute for Aerospace Research
[CTN-92-60431] p 420 N92-20204
Recent developments at the Shoeburyness (England) STOVL Test Facility
[PNR-90806] p 572 N92-22096
Symposium on High Speed Airbreathing Propulsion: The Solid Fuel Combustion Chamber and Beyond
[ETN-92-90685] p 575 N92-22268
Propeller noise research at NRC p 628 N92-24863
Engine component instrumentation development facility at NASA Lewis Research Center
[NASA-TM-105644] p 665 N92-25449
Introduction and execution of flight tests at the DLR
p 648 N92-25594
Experimental methods to determine heat exchanger performances p 682 N92-25667
Transonic turbine blade cascade testing facility
[NASA-TM-105646] p 667 N92-26129
Acoustic interactions between an altitude test facility and jet engine plumes: Theory and experiments
[NASA-CR-190423] p 738 N92-26405
Computational method to predict thermodynamic, transport, and flow properties for the modified Langley 8-foot high-temperature tunnel
[NASA-TM-4374] p 767 N92-27193
Cryogenic test rig with an aerodynamic magnetically levitated carriage p 750 N92-27792
Antenna pattern measurement facilities
[AD-A248964] p 982 N92-30329
Small engine components test facility compressor testing cell at NASA Lewis Research Center
[NASA-TM-105685] p 982 N92-30508

Compact range test applications, phase 2
[AD-A248790] p 999 N92-30583
Turbine blade tip and seal clearance excitation forces
[NASA-CR-184341] p 973 N92-31910
System overview of the NASA Dryden Integrated Test Facility
[NASA-TM-104250] p 984 N92-32201
Thermal-structural test facilities at NASA Dryden
[NASA-TM-104249] p 1062 N92-34202

TEST FIRING
High spatial resolution measurements of ram accelerator gas dynamic phenomena
[AIAA PAPER 92-3244] p 903 A92-48844
Scramjet engine and its flying test bed
p 1066 A92-53492

TEST PILOTS
Use of simulation in the USAF Test Pilot School curriculum p 884 N92-28535

TEST RANGES
Remote telemetry concepts p 882 A92-47562
Antenna pattern measurement facilities
[AD-A248964] p 982 N92-30329

TEST STANDS
A test bench for evaluating powerplant electrization
p 138 A92-16830
Statistical analysis and prediction of aeroengine deterioration p 557 A92-35570
270-Vdc/hydrid 115-Vac electric power generating system technology demonstrator evolution to a dual-channel, more electric aircraft technology development testbed
[SAE PAPER 912183] p 655 A92-40003
Experience in the operation of a hypersonic nozzle static thrust stand
[AIAA PAPER 92-3292] p 882 A92-48881
Implementation of non-dedicated redundancy in a fault tolerant multiprocessor testbed --- flight control
p 974 A92-49294
Technical tools of test automation for gas-turbine engines based on cluster CAMAC modules with an increased number of channels p 980 A92-51348
Scramjet engine and its flying test bed
p 1066 A92-53492
Design and development of test rigs for main rotor and main rotor transmission of a helicopter in the 6-ton-class
p 1093 A92-56280
Development of an uncertainty methodology for multiple-channel instrumentation systems
[AIAA PAPER 92-3953] p 1133 A92-56781
Qualification test report. Fuel pump test stand 3C3965G05
[AD-A242929] p 280 N92-17552
Development of a full-scale transmission testing procedure to evaluate advanced lubricants
[NASA-TP-3265] p 998 N92-30396
Thrust stand evaluation of engine performance improvement algorithms in an F-15 airplane
[NASA-TM-104252] p 971 N92-30518

TEST VEHICLES
A hypersonic waverider test vehicle - The logical next step
[AIAA PAPER 92-0308] p 387 A92-25756
Engineering development simulation - Test vehicle of the future p 483 A92-29674
The German Hypersonics Technology Programme - Status report 1992
[IAF PAPER 92-0867] p 1105 A92-57258
Design of orbital re-entry experiment vehicle and outline of the experiment p 667 N92-25374

TESTING TIME
Problem of the optimal correction of a flight test program for an aircraft system p 113 A92-16809

TETHERED BALLOONS
Determination of balloon drag
[AIAA PAPER 91-3666] p 5 A92-11013

TETRAHEDRONS
Three-dimensional upwind scheme for solving the Euler equations on unstructured tetrahedral grids --- tetrahedral grids p 714 N92-26585

TEXTILES
Polymer infiltration studies
[NASA-CR-189773] p 289 N92-17004
RTM: Cost-effective processing of composite structures p 578 N92-22678

THEMATIC MAPPERS (LANDSAT)
Radiometric properties of the NS001 Thematic Mapper Simulator aircraft multispectral scanner
p 155 A92-17110

THEMATIC MAPPING
Automated thematic processing of aircraft scanner data gathered over pasture territory in Turkmenia
p 406 A92-25330

THEODORSEN TRANSFORMATION
Ideal efficiency of propellers based on Theodorsen's theory: A review and computer study, with extended plus simplified charts
[UTIAS-TN-271] p 1071 N92-33102

THEOREM PROVING
Uniqueness of solutions of the generalized Tricomi problem arising in the theory of the Laval nozzle
p 428 A92-30319

THEOREMS
On the limitations of Froude's actuator disc concept
[ETN-91-90136] p 81 N92-11973

THERMAL ANALYSIS
Hunting phenomena of the balloon motions observed over Antarctica
[AIAA PAPER 91-3667] p 14 A92-11014
Analyses of heat isolation property for metallic multiwall thermal protection system p 40 A92-12422
Application of the STAPAT II code to hypersonic vehicle aerothermodynamics
[AIAA PAPER 91-5035] p 209 A92-17824
Analysis of cooling systems for hypersonic aircraft
[AIAA PAPER 91-5063] p 216 A92-17843
Integrated numerical methods for hypersonic aircraft cooling systems analysis
[AIAA PAPER 92-0254] p 357 A92-25712
Thermal structures - Four decades of progress
p 729 A92-41239
The optimization of variable cross-section spines with temperature dependent thermal parameters
p 901 A92-48353
The effect of tip convection on the performance and optimum dimensions of cooling fins p 902 A92-48354
Redesign of flight space shuttle main engine nozzle G-15 seal area based on the thermal analysis and flow models p 212 N92-15877
Thermal/structural analysis of a transpiration cooled nozzle
[NASA-TM-104184] p 401 N92-18877
A simplified method for thermal analysis of a cowl leading edge subject to intense local shock-wave-interference heating
[NASA-TP-3167] p 679 N92-24797
Progress in integrated analysis with adaptive unstructured meshing p 683 N92-25914
Analysis and design technology for high-speed aircraft structures p 684 N92-25918
Finite element methods for integrated aerodynamic heating analysis
[NASA-CR-190353] p 633 N92-25959
The effect of jet fuel exposure on advanced aerospace composites. Part 1: Thermal and chemical analysis
[AD-A246559] p 756 N92-27531
Lubricant evaluation and performance 2
[AD-A247464] p 895 N92-28398
Thermal response of rigid and flexible insulations and reflective coating in an aeroconvective heating environment
[NASA-TM-103925] p 852 N92-28721
Research into improving the durability of the hot section in the aircraft turbine engine
[AD-A250342] p 973 N92-31439
Thermal mechanical analysis of sprag clutches
[NASA-CR-190686] p 1128 N92-34207

THERMAL BOUNDARY LAYER
Development of a three-dimensional icing code - Comparison with experimental shapes
[AIAA PAPER 92-0041] p 262 A92-22159
Thermal structures - Four decades of progress
p 729 A92-41239

THERMAL CONDUCTIVITY
The total drag of a body in the flow of a viscous heat-conducting gas p 439 A92-31873
High performance heat sink for surface mount applications --- in avionics system design
p 989 A92-49275

THERMAL CONTROL COATINGS
Thermal barrier coatings for gas turbine use
p 142 A92-15245
Thermal barrier coating life prediction model development
[ASME PAPER 91-GT-40] p 147 A92-15523
Protective coatings of thermal barrier type
p 214 A92-20349

THERMAL CYCLING TESTS
High temperature low cycle fatigue of single crystal nickel base superalloys p 213 A92-19796
Ceramics for engines p 578 N92-22517
Stress-strain analysis of a (0/90)sub 2 symmetric titanium matrix laminate subjected to a generic hypersonic flight profile
[NASA-TM-107584] p 685 N92-26128
Criteria for use of seal coats on airport pavements
[DOT/FAA/RD-92/18] p 1102 N92-34247

THERMAL DEGRADATION
Deposition during vaporization of jet fuel in a heated tube
[AIAA PAPER 92-0687] p 390 A92-27054
A numerical method for simulating the fluid-dynamic and heat-transfer changes in a jet engine injector feed-arm due to fouling
[AIAA PAPER 92-0768] p 374 A92-27108
Advanced thermally stable jet fuel development program. Volume 2: Compositional factors affecting thermal degradation of jet fuels
[AD-A252656] p 987 N92-31399

THERMAL EMISSION
Experimentally supported investigations into the optical performance of multi-aperture window concepts
[AIAA PAPER 92-2781] p 778 A92-41324

THERMAL ENERGY
Studies on the mechanism of ignition and flameholding by plasma jets p 755 A92-42798

THERMAL ENVIRONMENTS
Hypersonic airbreathing propulsion/airframe integration p 474 N92-21522
Performance of uncoated AFRSI blankets during multiple Space Shuttle flights
[NASA-TM-103892] p 890 N92-29104
Thermal-structural test facilities at NASA Dryden
[NASA-TM-104249] p 1062 N92-34202

THERMAL EXPANSION
Non-homogeneous bars under tension, pure bending and thermal loads p 495 A92-31198
High performance heat sink for surface mount applications --- in avionics system design
p 989 A92-49275
Next-generation avionics packaging and cooling 'test results from a prototype system' p 989 A92-49277

THERMAL FATIGUE
Applied fracture mechanics research in the aerospace field p 37 A92-10375
High temperature low cycle fatigue of single crystal nickel base superalloys p 213 A92-19796
Thermo-mechanical fatigue crack growth in aircraft engine materials p 213 A92-19799
Creep-fatigue crack growth in Jethete M152 at 550 C under mixed mode conditions p 288 A92-21490
Elevated temperature crack growth in aircraft engine materials p 891 A92-45234
Fatigue in single crystal nickel superalloys
[AD-A244815] p 489 N92-21015
Properties of a TZP/Al2O3 composite after long-term exposure at 1000 C
[AD-A246407] p 757 N92-27752
Fatigue in single crystal nickel superalloys
[AD-A250068] p 987 N92-31360
Fatigue in single crystal nickel superalloys
[AD-A252492] p 988 N92-32066
Life prediction and constitutive models for engine hot section anisotropic materials program
[NASA-CR-189223] p 1072 N92-33479

THERMAL INSULATION
Study of grinding process and strength for ceramic heat insulated engine
[SME PAPER MR91-177] p 897 A92-45260
Thermal response of rigid and flexible insulations and reflective coating in an aeroconvective heating environment
[NASA-TM-103925] p 852 N92-28721
Performance of insulated pavements at Newton Fields, Jackman, Maine
[CRREL-92-9] p 1101 N92-32903

THERMAL PROTECTION
Evaluation of an adaptive unstructured remeshing technique for integrated fluid-thermal-structural analysis
p 37 A92-10445
Analyses of heat isolation property for metallic multiwall thermal protection system p 40 A92-12422
Cooling of a sharp nose by extraneous gas injection into the viscous shock layer p 426 A92-30188
A study of flow of a fluid film on the surface of a plate in the case of slot injection p 496 A92-31892
Thermal protection analysis of Mars-earth return vehicles p 497 A92-32183
Numerical study of coupled heat transfer under conditions of filtering and film cooling of blunt anisotropic bodies p 610 A92-36552
Materials and structures for Hermes
p 666 A92-38213
Experimental studies on aerodynamic heating and thermal protection in hypersonic flight
p 709 A92-43101
Ablative control mechanism in nozzle thermo-protection
[AIAA PAPER 92-3054] p 889 A92-48712
Ablation performance characterization of thermal protection materials using a Mach 4.4 Sled Test
[AIAA PAPER 92-3055] p 893 A92-48713

Aerothermal ablation behavior of selected candidate external insulation materials
[AIAA PAPER 92-3056] p 893 A92-48714
Spaceplane aerodynamic heating and thermal protection design method p 1102 A92-53578
Effect of porosity in transpiration cooling system p 1112 A92-53786
The IRS plasma wind tunnels for the investigation of thermal protection materials for reentry vehicles p 208 N92-15009
Aerodynamic heating on AFE due to nonequilibrium flow with variable entropy at boundary layer edge p 183 N92-15020
Computational aerothermodynamic methods for industrial applications to re-entry and hypersonic cruise problems p 227 N92-15027
Thermal energy test apparatus
[AD-A243526] p 305 N92-17537
Postflight aerothermodynamic analysis of Pegasus(tm) using computational fluid dynamic techniques
[NASA-CR-186017] p 445 N92-21188
Progress in integrated analysis with adaptive unstructured meshing p 683 N92-25914
Thermally sprayed coating systems for surface protection and clearance control applications in aero engines
[PNR-90802] p 741 N92-27422
Thermal response of rigid and flexible insulations and reflective coating in an aeroconvective heating environment
[NASA-TM-103925] p 852 N92-28721

THERMAL RADIATION
Measurement of convective heat-transfer coefficients in wind tunnels using passive and stimulated infrared thermography p 390 A92-24430
Thermal radiation effects on a shocked particle-laden gas p 780 A92-44377

THERMAL RESISTANCE
Development and characterization of high strength SiC rotors
[ASME PAPER 91-GT-191] p 149 A92-15617
High temperature erosion resistance of coatings for gas turbine
[ASME PAPER 91-GT-213] p 143 A92-15632
Influence of long time exposure at elevated temperatures in air on mechanical properties of the high temperature titanium alloy IMI 834 p 289 A92-22767
Thermal fiber-reinforced-plastic composite technology for aircraft structures p 755 A92-43237
Conceptional design to heat-resistant airframe of HOPE p 575 N92-23820
Large thin composite thermostructural parts p 576 N92-23821
Further studies in filmwise condensation of steam on horizontal finned tubes
[AD-A252705] p 1011 N92-31767

THERMAL SHOCK
Paint removal using cryogenic processes
[AD-A247668] p 895 N92-28912

THERMAL SIMULATION
Laser thermal simulation puts jet engines to the test p 663 A92-38129
Thermal-structural test facilities at NASA Dryden
[NASA-TM-104249] p 1062 N92-34202

THERMAL STABILITY
BMI/bis (allylphenoxyphthalimide)-copolymers - A new family of resins for advanced composites with improved thermal oxidative stability p 33 A92-10213
The microstructural stability of TiC reinforced rapidly solidified Al-Fe-V-Si composite structures p 141 A92-15169
Nickel base alloy GTD-222 - A new gas turbine nozzle alloy
[ASME PAPER 91-GT-73] p 142 A92-15542
Development of silicon nitride rotors for the ATTAP program at Garrett Ceramic Components --- Advanced Turbine Technology Applications Project
[ASME PAPER 91-GT-154] p 142 A92-15590
Gas-generator with high-temperature path ceramic components
[ASME PAPER 91-GT-152] p 148 A92-15594
5,000-hour stability tests of metal sheathed thermocouples at respective temperatures of 538 C and 875 C
[ASME PAPER 91-GT-182] p 148 A92-15614
High temperature, thermally stable JP fuels - An overview
[AIAA PAPER 92-0683] p 389 A92-27050
Experimental techniques for the assessment of fuel thermal stability
[AIAA PAPER 92-0685] p 389 A92-27052
A preliminary study of the microstructure-property relationships in cast gamma titanium aluminide alloys p 487 A92-30596
Ceramics and ceramic matrix composites - Aerospace potential and status
[AIAA PAPER 92-2445] p 577 A92-34474
Thermal oxidation stability of aviation turbine fuels --- Book
[ISBN 0-8031-1248-3] p 669 A92-40409
High-temperature metal matrix composite p 1105 A92-53878
High-temperature durability considerations for HSCT combustor
[NASA-TP-3162] p 289 N92-17070
Vinyl capped addition polyimides
[NASA-CASE-LEW-15027-2] p 579 N92-24053
Advanced thermally stable jet fuel development program. Volume 2: Compositional factors affecting thermal degradation of jet fuels
[AD-A252656] p 987 N92-31399
Advanced thermally stable, jet fuels development program annual report. Volume 1: Model and experiment system development
[AD-A249625] p 988 N92-31462
Liquid lubricants for advanced aircraft engines
[NASA-TM-104531] p 1109 N92-32863

THERMAL STRESSES
Thermal management of hypersonic aircraft using noncryogenic fuels
[SAE PAPER 911443] p 270 A92-21839
Response of symmetrically laminated rectangular plates subjected to heating p 296 A92-24186
Non-homogeneous bars under tension, pure bending and thermal loads p 495 A92-31198
Design for the relief of thermal stresses in a large high-speed wing
[AIAA PAPER 92-1082] p 536 A92-33250
Aerothermoelastic analysis of a NASP-like vertical fin
[AIAA PAPER 92-2400] p 541 A92-34471
TMFSLAM - Design analysis tool for coated structures
[ASME PAPER 91-GT-141] p 690 A92-36895
Local heat transfer in the perforation channels of turbine nozzle vanes p 657 A92-40615
Numerical analysis of an engine turbine disk loaded with a large number of thermomechanical cycles
[ONERA, TP NO. 1992-31] p 902 A92-48592
Turning up the heat on aircraft structures --- design and analysis for high-temperature conditions p 1052 A92-55131
Studies of aerothermal loads generated in regions of shock/shock interaction in hypersonic flow
[NASA-CR-181893] p 43 N92-11319
Aeropropulsion structures p 559 N92-22518
Finite element frequency domain solution of nonlinear panel flutter with temperature effects and fatigue life analysis p 682 N92-25589
Progress in integrated analysis with adaptive unstructured meshing p 683 N92-25914
Research into improving the durability of the hot section in the aircraft turbine engine
[AD-A250342] p 973 N92-31439

THERMOCHEMICAL PROPERTIES
Fundamental studies on droplet interactions in dense sprays
[AD-A246918] p 770 N92-27546

THERMOCHEMISTRY
Thermochemical nonequilibrium and radiative interactions in supersonic hydrogen-air combustion
[AIAA PAPER 92-0340] p 394 A92-25786
Analysis of thermo-chemical nonequilibrium models for carbon dioxide flows
[AIAA PAPER 92-2852] p 892 A92-47835

THERMOCHROMATIC MATERIALS
Computer-based areal surface temperature and local heat transfer measurements with thermochromic liquid crystals (TLC) p 763 A92-44326

THERMOCOUPLES
5,000-hour stability tests of metal sheathed thermocouples at respective temperatures of 538 C and 875 C
[ASME PAPER 91-GT-182] p 148 A92-15614
A fine-wire thermocouple probe for measurement of stagnation temperatures in real gas hypersonic flows of nitrogen p 1114 A92-54317
Microgravity nucleation and particle coagulation experiments support
[NASA-CR-190159] p 502 N92-21385
Repetitive High Energy Pulsed Power (RHEPP) temperature monitoring system utilizing Luxtron fluoroptic sensors and thermocouples technical reference manual
[DE92-013461] p 999 N92-30893

THERMODYNAMIC CYCLES
Monolithic ceramics p 668 A92-39854
Turboshaft/turboprop cycle sensitivity analysis
[AIAA PAPER 92-3476] p 865 A92-49020
Some thermodynamical aspects in the optimization of supersonic combustors p 1065 A92-53486
Component-specific modeling --- jet engine hot section components
[NASA-CR-189088] p 377 N92-19726
Small engine technology programs p 560 N92-22532
A two-stroke diesel engine simulation program
[NASA-CR-185155] p 562 N92-22647
Practical considerations in designing the engine cycle p 869 N92-28460

THERMODYNAMIC EFFICIENCY
A model of gasdynamic loads on an oscillating nozzle shell p 80 A92-16817
Restart of theory of air-breathing engines
[AIAA PAPER 92-3472] p 906 A92-49018

THERMODYNAMIC EQUILIBRIUM
Linear acoustics in gas mixtures with rate processes p 238 N92-15013
Hypersonic viscous shock layer in thermochemical nonequilibrium p 183 N92-15014

THERMODYNAMIC PROPERTIES
Thermal properties of high performance thermoplastic composites based on poly(ether ketone ketone) (PEKK) p 34 A92-10238
Thermodynamic behaviour of hydrogen-powered hypersonic ramjets flying along ideal trajectories
[IAF PAPER 91-277] p 25 A92-12601
Heat transfer characteristics of hypersonic waveriders with an emphasis on leading edge effects
[AIAA PAPER 92-2920] p 821 A92-47892
Characterization of thermal performance of wheel outboard of an aircraft p 849 A92-48352
Effect of thermodynamic parameters on performance and cost of turbine engines p 969 A92-49834
Heat transfer and instrumentation studies on rotating turbine blades in a transient facility p 156 N92-12203
Theoretical and experimental investigation of the thermodynamics of the thermally choked ram accelerator p 604 N92-22137
Experimental methods to determine heat exchanger performances p 682 N92-25667
Computational method to predict thermodynamic, transport, and flow properties for the modified Langley 8-foot high-temperature tunnel
[NASA-TM-4374] p 767 N92-27193

THERMODYNAMICS
Thermodynamic structural analysis of high speed propulsion systems
[IAF PAPER 91-278] p 120 A92-14711
The thermodynamic approach in the study of large systems - Application to high-velocity airbreathing propulsion p 654 A92-37824
Mechanics and thermodynamics of propulsion (2nd revised and enlarged edition) --- Book
[ISBN 0-201-14659-2] p 672 A92-38275
On the instability of boundary layers on heated flat plates
[NASA-CR-187581] p 347 N92-19250
Theoretical and experimental investigation of the thermodynamics of the thermally choked ram accelerator p 604 N92-22137
Aircraft engine hot section technology: An overview of the HOST Project p 561 N92-22535
TVD finite-difference solutions of nonequilibrium vibrationally relaxing and chemically reacting gaseous flows p 626 N92-24854
DLR-News: Announcements of the German Research Institute for Aeronautics and Astronautics p 698 N92-26086
Modeling of heavy-gas effects on airfoil flows
[NASA-CR-190357] p 716 N92-27558
Steady and transient performance calculation method for prediction, analysis, and identification p 869 N92-28461
Thermomechanical fatigue behavior of a silicone carbide fiber-reinforced calcium aluminosilicate glass-ceramic matrix composite
[AD-A249870] p 988 N92-31823

THERMOELASTICITY
Shape-sensitivity analysis and design optimization of linear, thermoelastic solids p 395 A92-26433
High temperature ground vibration test techniques p 980 A92-51404
Industrial code development p 227 N92-15083

THERMOELECTRIC COOLING
An investigation of two cooling technologies as applied to a distributed propulsion control architecture
[ASME PAPER 91-GT-341] p 111 A92-15705

THERMOELECTRIC POWER GENERATION
General performance characteristics of real heat engine p 1011 A92-50401
Thermally regenerative fuel cells
[AD-A242900] p 300 N92-17629

THERMOELECTRICITY
Development of an electrothermal de-icing/anti-icing model
[AIAA PAPER 92-0526] p 351 A92-26949

Experimental and numerical investigation of anti-icing phenomena on a NACA 0012 assembly
[AIAA PAPER 92-0531] p 459 A92-31669

THERMOGRAPHY
New applications of liquid-crystal thermography in rotating turbomachinery heat transfer research
[ASME PAPER 91-GT-354] p 153 A92-15710
Measurement of convective heat-transfer coefficients on a wind tunnel model by passive and stimulated infrared thermography p 291 A92-21450
Measurement of convective heat-transfer coefficients in wind tunnels using passive and stimulated infrared thermography p 390 A92-24430
Indirect measurements of convective flow by IR thermography
[ONERA, TP NO. 1992-46] p 902 A92-48607
Detecting 3-D, turbulent separation regions using unsteady computerized thermographic technique p 1023 A92-54308
Quantitative heat transfer measurements in hypersonic wind tunnels by means of infrared thermography p 1115 A92-54321
Application of infrared thermography to thermal flux measurement in wind tunnels
[AAAF-NT-89-12] p 31 N92-11020
Thermographic gust wind tunnel measurements
[ONERA-RF-31/3409-PY] p 81 N92-11972
Experimental study of hypersonic shock wave boundary layer interactions by means of infrared technique p 182 N92-14994
Heat transfer measurements in ONERA supersonic and hypersonic wind tunnels using passive and active infrared thermography p 208 N92-15003
Thermal QNDE detection of airframe disbonds p 914 N92-30118

THERMOMECHANICAL TREATMENT
A critical appraisal of thermomechanical processing of structural titanium alloys p 488 A92-30611

THERMOMETERS
Design and preliminary tests of a new airborne thermometer p 468 A92-32097

THERMOPLASTIC RESINS
Manufacture of a primary flight structure using thermoplastics p 1 A92-10197
Thermal properties of high performance thermoplastic composites based on poly(ether ketone ketone) (PEKK) p 34 A92-10238
High temperature thermoplastic and polyimide processing using CARE-MOLD wash-out tooling p 36 A92-10259
New thermoplastic composites for aircraft structures and interiors p 34 A92-10271
Advanced thermoplastic nose landing gear door development p 20 A92-10275
LDF thermoplastic composites technology p 34 A92-13243
The development and test of thermoplastic composite speed brake p 272 A92-24178
Interlaminar fracture characteristics of bonding concepts for thermoplastic primary structures p 758 A92-41282
Structural concept of main wings of high altitude unmanned aerial vehicle and basic properties of thermoplastic composites as candidate material
[SAE PAPER 912053] p 843 A92-45437
New thermoplastic polyimide composite for supersonic aircraft structures p 985 A92-51512
Induction bonding procedures for graphite reinforced thermoplastic assemblies p 994 A92-51545
Supportability evaluation of thermoplastic and thermoset composites p 1108 N92-32576
Fluid effects: Thermoset and thermoplastic matrix composites p 1110 N92-33049
Jet fuel absorption and dynamic mechanical analysis of carbon fibre composites p 1110 N92-33050
Isothermal aging of IM7/8320 and IM7/5260
[NASA-TM-107666] p 1110 N92-33423

THERMOPLASTICITY
Evaluation of thermoplastic matrix composites for use in energy-absorbing helicopter subfloors p 141 A92-14374
Thermoviscoplastic analysis of engine cowl leading edge subjected to oscillating shock-shock interaction
[AIAA PAPER 92-2537] p 583 A92-34381
Thermoviscoplastic response of thin plates subjected to intense local heating
[AIAA PAPER 92-2538] p 584 A92-34382
Thermoviscoplastic response of Ti-15-3 under various loading conditions
[NASA-CR-187621] p 45 N92-11391
The effect of physical aging on the creep response of a thermoplastic composite
[AD-A243600] p 290 N92-17932
Development of thermoplastic components for structural validation p 1107 N92-32522
Continuation of tailored composite structures of ordered staple thermoplastic material
[NASA-CR-189671] p 1110 N92-33613

THERMOSETTING RESINS
Flight service evaluation of composite helicopter components p 106 A92-14372
Enhanced diagnostic system for autoclaves and bonding presses p 145 A92-14381
Addition curing thermosets endcapped with 4-amino (2.2) paracyclophane p 577 A92-33918
Supportability evaluation of thermoplastic and thermoset composites p 1108 N92-32576
CFRP stiffened panels under compression p 1109 N92-33044
Isothermal aging of IM7/8320 and IM7/5260
[NASA-TM-107666] p 1110 N92-33423

THICK PLATES
Three-dimensional finite-element analysis of interlaminar stresses in thick composite laminates p 39 A92-11791

THICKNESS
Simple effective thickness model for circular brush seals
[AIAA PAPER 92-3192] p 903 A92-48803
Digital analysis of wind tunnel imagery to measure fluid thickness
[NASA-CR-189234] p 983 N92-31252

THICKNESS RATIO
Effect of airfoil (trailing-edge) thickness on the numerical solution of panel methods based on the Dirichlet boundary condition p 340 A92-28041

THIGH
Scenario analysis of thigh gap related ejection injuries p 834 A92-44995

THIN AIRFOILS
An integrated airloads-inflow model for use in rotor aeroelasticity and control analysis p 64 A92-14328
Numerical prediction of subsonic turbulent flows over slender bodies at high incidence p 172 A92-18358
Incompressible flow past a flat plate aerofoil with leading edge separation bubble p 421 A92-28943
Effect of shock waves on the critical rate of bending-torsional flutter of an airfoil p 494 A92-30208
On hypersonic flow over two-dimensional aerofoils p 433 A92-31425
Subsonic flow past a thin airfoil in a channel with porous walls p 438 A92-31867
A note on the Kutta condition in Glauert's solution of the thin aerofoil problem p 613 A92-37933
Flow and shape correction problems for thin profiles in incompressible stream p 707 A92-42736
The subsonic and transonic flow around the leading edge of a thin airfoil with a parabolic nose
[AIAA PAPER 92-2649] p 797 A92-45516
Thin-airfoil correction for panel methods p 811 A92-46811
Supersonic flow past pointed-nose thin airfoils p 940 A92-52844
Flutter and stall response of a helicopter blade with structural nonlinearity p 1055 A92-56178
A unified viscous theory of lift and drag of 2-D thin airfoils and 3-D thin wings
[NASA-CR-4414] p 178 N92-13997

THIN BODIES
Subsonic axisymmetric viscoelastic flow past thin tapered bodies of revolution p 6 A92-12134
Analysis of motion of airfoil flying over wavy-wall surface (lifting surface method) p 818 A92-47100

THIN FILMS
Reflection type skin friction meter
[NASA-CASE-LAR-14520-1-SB] p 11 N92-10008
High temperature static strain gage development
[NASA-CR-189044] p 195 N92-14037
Heat flux sensor research and development: The cool film calorimeter
[NASA-CR-189789] p 298 N92-17006
Research sensors p 594 N92-22526

THIN PLATES
Thermoviscoplastic response of thin plates subjected to intense local heating
[AIAA PAPER 92-2538] p 584 A92-34382
The interaction between a plane shear layer and a slender body p 991 A92-49790

THIN WALLED SHELLS
Acoustic isolation of layers p 54 A92-12345
Behavior of thin-walled beams made of advanced composite materials and incorporating non-classical effects p 673 A92-39944
Diffracted and head waves associated with waves on nonseparable surfaces
[NASA-TP-3169] p 444 N92-20545

THIN WALLS
New, unusual and nonclassical behavior of thin-walled composite structures p 580 A92-32746
Buckling, postbuckling and crippling of thin walled composite airframe structures under compression p 899 A92-46940
The role of PM in the design of lightweight aircraft engine components p 991 A92-50137

THIN WINGS
Vibration of a wing of finite span in subsonic flow at small distances from a solid boundary p 9 A92-12808
Calculating the steady-state nonlinear aerodynamic characteristics of thin wings near the interface between two fluids p 426 A92-30181
A unified viscous theory of lift and drag of 2-D thin airfoils and 3-D thin wings
[NASA-CR-4414] p 178 N92-13997

THREAT EVALUATION
Optimal control problems with maximum functional p 232 A92-18616
Adaptive tactical navigation program p 102 N92-12529

THREE DIMENSIONAL BODIES
Three-dimensional finite-element analysis of interlaminar stresses in thick composite laminates p 39 A92-11791
Incompressible steady aerodynamics using a standard finite element code p 174 A92-20218
Inverse solution uniqueness and domain of existence for supersonic space marching applications
[AIAA PAPER 92-0028] p 248 A92-22150
Compressibility effects on the dynamic stall of a three-dimensional wing
[AIAA PAPER 92-0191] p 256 A92-23800
Simulation of arbitrary crack propagation in three-dimensions p 393 A92-25535
Iterative algorithms for solving problems of the shaping of three-dimensional ducts p 428 A92-30212
Shape optimization of three-dimensional structures with adaptive meshing
[AIAA PAPER 92-2434] p 586 A92-34548
Prismatic grid generation with an efficient algebraic method for aircraft configurations
[AIAA PAPER 92-2721] p 803 A92-45559
Computations of hypersonic flows around a three-dimensional concave/convex body
[AIAA PAPER 92-2606] p 805 A92-45570
Three-dimensional wings and waveriders with attached shock waves p 936 A92-50322
Rarefied gas numerical wind tunnel p 1017 A92-53552
Three-dimensional calculation of radiative field in hypersonic air shock layers p 1023 A92-54498
Advanced stress analysis methods applicable to turbine engine structures
[NASA-CR-187235] p 44 N92-11378
A walk through the planned CS building
[NASA-CR-189963] p 386 N92-19675
Three-dimensional laser window formation
[NASA-RP-1280] p 984 N92-30307

THREE DIMENSIONAL BOUNDARY LAYER
Effect of nose shape on three-dimensional stagnation region streamlines and heating rates
[AIAA PAPER 91-5032] p 171 A92-17822
Numerical solution of the boundary-layer equations for a general aviation fuselage p 174 A92-20211
Wave motions in a three-dimensional boundary layer p 244 A92-21629
Introduction to three dimensional boundary layers p 245 A92-21977
Calculation methods of three-dimensional boundary layers p 245 A92-21978
Weak coupling between an unsteady 3D full potential code and an unsteady turbulent boundary layer code - Application to a helicopter rotor in forward flight
[AIAA PAPER 92-0029] p 249 A92-22151
A numerical calculation of three dimensional incompressible laminar, transition and turbulent boundary layers p 393 A92-25138
The effects of suction on the nonlinear stability of the three-dimensional boundary layer above a rotating disc p 393 A92-25366
A three-dimensional supersonic turbulent boundary layer generated by an isentropic compression
[AIAA PAPER 92-0310] p 320 A92-25758
Nonadiabatic and three-dimensional effects in compressible turbulent boundary layers p 431 A92-31156
Linear stability of three-dimensional boundary layers over axisymmetric bodies at incidence p 431 A92-31157
Computational studies of transonic flow past a swept wing and the boundary layer characteristics p 438 A92-31872
Boundary layer on slender wings of small aspect ratio p 441 A92-31963
Inverse solution of 3D incompressible turbulent boundary layer with separated bubbles p 522 A92-35992

The effects of wall suction on laminar-turbulent transition in three-dimensional flow p 522 A92-36021
Prediction for the incipient separation of fin-generated three-dimensional shock wave turbulent boundary layer interactions p 615 A92-38909
On the mechanics of 3-D turbulent boundary layers p 620 A92-40068
Prediction of three-dimensional turbulent boundary layers using a second-moment closure p 675 A92-40080
An experimental evaluation of some turbulence models from a three-dimensional turbulent boundary layer around a wing-body junction p 620 A92-40087
A study of three dimensional turbulent boundary layer separation and vortex flow control using the reduced Navier Stokes equations p 621 A92-40105
The calculation of a compressible boundary layer past a pointed body and a delta wing p 622 A92-40173
Curvature effects for three-dimensional compressible boundary-layer stability p 701 A92-41207
Aerodynamic heating in three-dimensional shock wave turbulent boundary layer interaction induced by sweptback sharp fins in hypersonic flows
[SAE PAPER 912044] p 791 A92-45428
Concepts for the stability analysis of NLF-experiments on swept wings
[AIAA PAPER 92-2706] p 801 A92-45548
The inviscid compressible Goertler problem in three-dimensional boundary layers p 809 A92-46441
The calculation of three-dimensional compressible boundary layer stability on swept wings p 818 A92-47684
Experimental investigation on turbulent phenomena in three-dimensional shock wave/turbulent boundary layer interaction induced by blunt fin p 1018 A92-53557
Experimental study on three-dimensional shock wave-turbulent boundary layer interaction induced by protuberance p 1019 A92-53997
Skin friction measurements in 3-D boundary layers p 1092 A92-54351
Proceedings of the Seminar on Investigation and Control of Boundary-Layer Transition
[NAL-SP-11] p 400 N92-18483
A three-dimensional, compressible, laminar boundary-layer method for general fuselages. Volume 2: User's manual
[NASA-CR-4292-VOL-2] p 678 N92-24344
A three-dimensional, compressible, laminar boundary-layer method for general fuselages. Volume 1: Numerical method
[NASA-CR-4292-VOL-1] p 679 N92-24547
The fibre optic three dimensional laser two focus velocimeter for the low-speed windtunnel. Part 1: Two-dimensional measurement evaluations
[NAL-TM-627] p 665 N92-25402
Three dimensional boundary layer transition on a yawed cylinder p 766 N92-26909
Cross-flow instabilities and pressure gradients in boundary layers p 767 N92-26922
Structure of three-dimensional turbulent boundary layers p 999 N92-30654
The structure and control of three-dimensional shock wave turbulent boundary layer interactions
[AD-A250209] p 1003 N92-31824

THREE DIMENSIONAL COMPOSITES

Coupled 2D-3D finite element method for analysis of a skin panel with a discontinuous stiffener
[AIAA PAPER 92-2474] p 583 A92-34363

THREE DIMENSIONAL FLOW

Three-dimensional space-marching algorithm on unstructured grids p 5 A92-11058
Numerical investigation of bleed on three-dimensional turbulent interactions due to sharp fins p 5 A92-11062
Flow analysis and design of three-dimensional wind tunnel contractions p 5 A92-11067
Impeller flow field measurement and analysis
[ASME PAPER 90-GT-146] p 38 A92-11288
Computational investigation of circular-to-rectangular transition ducts
[AIAA PAPER 91-3342] p 6 A92-11605
Inviscid spatial stability of a three-dimensional compressible mixing layer p 39 A92-11816
Evolution of three-dimensional flows during the interaction between conical shock waves and a turbulent boundary layer p 7 A92-12169
An efficient method for calculating three-dimensional transonic flow past air intakes p 7 A92-12178
An analysis method and applications for 3-D viscous internal flows with complex geometry p 143 A92-13299
Extension of a three-dimensional Euler method for calculating the flowfield around bypass engines with fan and core jet p 62 A92-13690
Influence of three-dimensional effects on hydrodynamics and heat transfer in subsonic flow of a viscous compressible gas in the initial section of a rectangular duct p 66 A92-15031
3-D loss prediction based on secondary flow and blade shear layer interaction
[ASME PAPER 91-GT-59] p 68 A92-15536
Computation of 3D flow phenomena in axial flow compressor blade rows
[ASME PAPER 91-GT-78] p 69 A92-15547
A 3D FEM variational aerodynamic calculation and performance analysis of a leaned turbine stator cascade
[ASME PAPER 91-GT-79] p 69 A92-15548
Quasi-three-dimensional characteristics method for a supersonic compressor rotor
[ASME PAPER 91-GT-81] p 69 A92-15549
Three-dimensional flow and mixing in a axial flow compressor with different rotor tip clearances
[ASME PAPER 91-GT-89] p 70 A92-15554
Three dimensional flow in a linear compressor cascade at design conditions
[ASME PAPER 91-GT-114] p 70 A92-15565
The simulation of three-dimensional viscous flow in turbomachinery geometries using a solution-adaptive unstructured mesh methodology
[ASME PAPER 91-GT-124] p 71 A92-15569
Three-dimensional Navier-Stokes computation of turbomachinery flows using an explicit numerical procedure and a coupled k-epsilon turbulence model
[ASME PAPER 91-GT-146] p 72 A92-15584
Multi-blade row Navier-Stokes simulations of fan-bypass configurations
[ASME PAPER 91-GT-148] p 73 A92-15586
A calculation procedure for three-dimensional turbulent flow in a centrifugal impeller with any blade geometry
[ASME PAPER 91-GT-171] p 73 A92-15606
Deterministic blade row interactions in a centrifugal compressor stage
[ASME PAPER 91-GT-273] p 75 A92-15670
LDV measurements of a mixed-flow impeller at design and near stall
[ASME PAPER 91-GT-310] p 153 A92-15688
Numerical study of branched turboprop inlet ducts using a multiple block grid procedure
[ASME PAPER 91-GT-339] p 76 A92-15703
Three-dimensional calculations of reactive flows in aircraft combustion chambers performed using two combustion models
[ONERA, TP NO. 1991-110] p 154 A92-16089
Three-dimensional thin-layer and space-marching Navier-Stokes computations using an implicit MUSCL approach - Comparison with experiments and Euler computations
[ONERA, TP NO. 1991-131] p 77 A92-16107
Euler flow analysis of turbine powered simulator and fanjet engine p 80 A92-17196
CFD application to 2D/3D flow fields in Scramjet engine p 170 A92-17501
Three-dimensional solution-adaptive grid generation on composite configurations p 172 A92-18352
Three-dimensional calculation of low-frequency unsteady transonic flow in axial turbine stages p 174 A92-19110
Three-dimensional thermal structural analysis of a swept cowl leading edge subjected to skewed shock-shock interference heating p 174 A92-20306
Engineering calculations of three-dimensional inviscid hypersonic flowfields p 175 A92-20378
Evaluation of a bounded high-resolution scheme for combustor flow computations p 201 A92-20734
Upwind scheme for solving the Euler equations on unstructured tetrahedral meshes p 175 A92-20735
Studies of the effects of curvature on dilution jet mixing p 290 A92-21079
A boundary integral formulation for the kinetic field in aerodynamics. I - Mathematical analysis p 243 A92-21504
Axisymmetric analogy for three-dimensional viscous flow problems p 244 A92-21617
Solution of the problem of three-dimensional flow past the blade rows of turbomachines with allowance for viscosity effects p 244 A92-21618
Numerical analysis of airflow in aircraft cabins
[SAE PAPER 911441] p 245 A92-21837
Application of holomorphic vectors theory in three-dimensional potential flow problem p 292 A92-21923
Experiences with finite element methods for the velocity-vorticity formulation of three-dimensional, viscous, incompressible flows p 246 A92-21984
Doppler global velocimeter measurements of the vortical flow above a thin delta wing
[AIAA PAPER 92-0005] p 292 A92-22130
Aerodynamics of loaded cascades in subsonic flows subject to unsteady three-dimensional vortical disturbances
[AIAA PAPER 92-0146] p 253 A92-23762
Application of a universe-series code for inviscid flow over complex 3-dimensional configurations
[AIAA PAPER 92-0150] p 253 A92-23765
Multigrid Navier-Stokes calculations for three dimensional cascades
[AIAA PAPER 92-0190] p 256 A92-23799
3D Navier-Stokes analysis for a tip leakage flow in a low aspect ratio turbine
[AIAA PAPER 92-0395] p 278 A92-23816
Comparison of two Navier-Stokes codes for attached transonic wing flows p 309 A92-24414
3D LDA measurement in an axial fan rotor p 391 A92-24730
The LDV measurement of three-component velocity of complex vortex flow in the wind tunnel p 393 A92-25109
Three-dimensional simulation of slender delta wing rock and divergence
[AIAA PAPER 92-0280] p 318 A92-25734
An approach to the design of wings - The role of mathematics, physics and economics
[AIAA PAPER 92-0286] p 319 A92-25739
An experimental and analytical study of the interaction of a vortex with an airframe
[AIAA PAPER 92-0319] p 321 A92-25766
Low-to-high altitude predictions of three-dimensional ablative reentry flowfields
[AIAA PAPER 92-0366] p 394 A92-26227
Measurement of a three-dimensional hypersonic density field
[AIAA PAPER 92-0383] p 323 A92-26240
Numerical and experimental analysis of vortex sheets behind lifting surfaces
[AIAA PAPER 92-0409] p 325 A92-26262
Experimental investigation of a three-dimensional bluff-body wake
[AIAA PAPER 92-0429] p 326 A92-26277
Validation of a 3D Navier-Stokes code on experimental compressor bladings
[ONERA, TP NO. 1991-229] p 330 A92-26381
Flow past a sphere - Topological transitions of the vorticity field p 330 A92-26410
Preconditioned upwind methods to solve incompressible Navier-Stokes equations p 395 A92-26436
Analysis of junction flowfields using the incompressible Navier-Stokes equations
[AIAA PAPER 92-0519] p 331 A92-26944
An unsteady Euler scheme for the analysis of ducted propellers
[AIAA PAPER 92-0522] p 332 A92-26947
Transition to turbulence in confined, compressible mixing layers. I - 3D numerical simulations with excitation of random, broadband white noise
[AIAA PAPER 92-0553] p 332 A92-26964
Three-dimensional buoyancy-induced flow and heat transfer around the wheel outboard of an aircraft p 397 A92-27773
Three-dimensional compressible flows in turbo-machinery solved by the pseudostream function formulation p 338 A92-27801
Aeroelastic analysis of advanced propellers using an efficient Euler solver
[AIAA PAPER 92-0488] p 341 A92-28194
Three-dimensional structure of a curved wake
[AIAA PAPER 92-0541] p 341 A92-28199
Effective treatments of the singular line boundary problem for three dimensional grids
[AIAA PAPER 92-0545] p 342 A92-28202
Full Navier-Stokes analysis of a three-dimensional hypersonic mixed compression inlet p 343 A92-28501
Calculation of three-dimensional transonic turbine cascade flow p 344 A92-28519
Three-dimensional viscous analysis of a Mach 5 inlet and comparison with experimental data p 344 A92-28526
Calculation of 3D flow field in a single transonic compressor stage p 422 A92-29719
Numerical simulation of three-dimensional supersonic free shear layers p 431 A92-31152
Solution-adaptive grid procedure for the parabolized Navier-Stokes equations p 432 A92-31163
Two- and three-dimensional effects in the supersonic mixing layer p 432 A92-31165
Numerical simulation of three-dimensional supersonic flow around aerodynamic configurations p 434 A92-31492
Implicit solutions of three-dimensional viscous hypersonic flows p 434 A92-31549
Three-dimensional flow computation for two interacting, moving droplets
[AIAA PAPER 92-0343] p 496 A92-31655

An improved PNS scheme for predicting complex three-dimensional hypersonic flows
[AIAA PAPER 92-0753] p 436 A92-31679
Calculation of three-dimensional separated flows in the framework of the unsteady Euler equations
p 438 A92-31870
Computation of near-wake, aerobrake flowfields
p 441 A92-32181
Interference flows past cylinder-fin-sting-cavity assemblies p 442 A92-32236
Numerical analysis of three-dimensional unsteady turbulent flows in a turbine stage p 443 A92-32501
Three-dimensional flow visualization of shock wave using double-pulsed holographic interferometry. II - Flow visualization for three-dimensional shock structures in rotating aeroengine fan blade rows p 497 A92-32507
An inverse method for the design of transonic wings
[AIAA PAPER 92-1025] p 517 A92-33206
Simulation of 3-D shear flows around a nozzle-afterbody at high speeds p 519 A92-34826
The effects of wall suction on laminar-turbulent transition in three-dimensional flow p 522 A92-36021
Inviscid and viscous quasi-three-dimensional flow solutions in a transonic turbine cascade
p 523 A92-36035
Numerical simulations of the flow through cascades with tip clearance p 523 A92-36038
High alpha aerodynamic control by tangential fuselage blowing p 611 A92-36848
Coating effect on particle trajectories and turbine blade erosion p 653 A92-36892
Efficient direct solvers for large-scale computational fluid dynamics problems p 690 A92-37534
Computational methods for shock waves in three-dimensional supersonic flow p 611 A92-37537
The computation of three-dimensional flows using unstructured grids p 612 A92-37539
An information system for the numerical simulation of 3D Euler flows around aircraft p 613 A92-37554
A study of flow patterns and behaviours of 3D separated flow on a simplified Shuttle model p 615 A92-38906
Mixed volume boundary element approach for aerodynamics p 617 A92-39934
Three-dimensional vortical structure of a large-scale coherent vortex in a turbulent boundary layer
p 619 A92-40056
Evolution of three-dimensionality in stable and unstable curved mixing layers p 619 A92-40059
The natural and forced formation of spot-like Lambda-structures caused by vortex dislocations in a wake p 621 A92-40111
Scrutinizing k-epsilon EVM and ASM by means of LES and wind tunnel for flowfield around cube --- Eddy Viscosity Model, Algebraic Stress Model, Large Eddy Simulation
p 621 A92-40119
Quick calculation of three-dimensional supersonic flow past nearly axisymmetric bodies p 624 A92-40605
Numerical study of vortex-dominated flows for wings at high incidence and sideslip p 702 A92-41227
Renormalization group based algebraic turbulence model for three-dimensional turbomachinery flows
p 703 A92-41268
Navier-Stokes simulation for cone-derived waverider
p 703 A92-41271
Secondary flow investigation inside the passage of a compressor cascade p 706 A92-42124
Calculation of three-dimensional turbulent flow in wind tunnel entry section p 708 A92-43055
Three-dimensional visualizations of the aerodynamic characteristics of delta wings for the transition from subsonic to supersonic leading edges in supersonic-hypersonic flow p 709 A92-43073
The fluid-dynamic measurement of the fling motion of a three-dimensional flat plate p 710 A92-43194
An experimental investigation of the oblique blade-vortex interaction p 712 A92-43447
Thermochemical nonequilibrium flow computations of flow around the aeroassist flight experiment
p 713 A92-44368
Application of computational fluid dynamics to pitch/yaw thrust vectoring spherical convergent flap nozzles
p 737 A92-44511
Viscous simulation method for unsteady flows past multicomponent configurations p 714 A92-44671
An economic approach to accurate wing design
[SAE PAPER 912008] p 789 A92-45408
Aerodynamic characteristics near the tip of a finite wing by a panel method
[SAE PAPER 912020] p 790 A92-45413
Navier-Stokes and Euler solutions for an unmanned aerial vehicle
[AIAA PAPER 92-2609] p 792 A92-45483
The design of a system of codes for industrial calculations of flows around aircraft and other complex aerodynamic configurations
[AIAA PAPER 92-2619] p 917 A92-45492
A fast three-dimensional vortex method for unsteady wake calculations
[AIAA PAPER 92-2624] p 794 A92-45496
Effect of throat contouring on two-dimensional converging-diverging nozzles using URS method
[AIAA PAPER 92-2659] p 797 A92-45520
Investigation of solution operators for the three-dimensional Euler equations
[AIAA PAPER 92-2666] p 797 A92-45522
An unfactored implicit scheme for 3D inviscid transonic flows
[AIAA PAPER 92-2668] p 798 A92-45523
An adaptive grid method for computing the high speed 3D viscous flow about a re-entry vehicle
[AIAA PAPER 92-2685] p 799 A92-45534
LDV measurements in the three-dimensional near wake of a stationary and oscillating rectangular wind
[AIAA PAPER 92-2689] p 799 A92-45536
Comparison of interferometric measurements with 3-D Euler computations for circular cones in supersonic flow
[AIAA PAPER 92-2691] p 800 A92-45538
Computation of turbulent flow about cone-derived waverider
[AIAA PAPER 92-2726] p 804 A92-45562
Effect of flow rate on loss mechanisms in a backswept centrifugal impeller p 897 A92-45606
Interaction between crossing oblique shocks and a *turbulent boundary layer p 812 A92-46882*
Numerical method for predicting transition in three-dimensional flows by spatial amplification theory
p 812 A92-46886
Parallel computing strategies for block multigrid implicit solution of the Euler equations p 812 A92-46894
Three-dimensional blade vortex interactions
p 815 A92-46953
Grid adaptation to multiple functions for applied aerodynamic analysis p 817 A92-47045
Computation of 3-D hypersonic flows in chemical non-equilibrium including transport phenomena
[AIAA PAPER 92-2876] p 820 A92-47858
Calculation of fully three-dimensional separated flows with an unsteady viscous-inviscid interaction method
[ONERA, TP NO. 1992-1] p 821 A92-48577
Separation and vortex formation in turbulent flows
[ONERA, TP NO. 1992-7] p 822 A92-48579
Application of non-reflecting boundary conditions to three-dimensional Euler equation calculations for thick strut cascades
[AIAA PAPER 92-3045] p 822 A92-48705
Internal shock interactions in propulsion/airframe integrated three-dimensional sidewall compression scramjet inlets
[AIAA PAPER 92-3099] p 824 A92-48741
Development and application of a zonal k-epsilon turbulence model for complex 3-D flowfields
[AIAA PAPER 92-3176] p 903 A92-48792
Navier-Stokes investigation of a transonic centrifugal compressor stage using an algebraic Reynolds stress model
[AIAA PAPER 92-3311] p 825 A92-48897
A turbulence model based on RNG for quasi-three-dimensional cascade flows --- renormalization group methods
[AIAA PAPER 92-3312] p 825 A92-48898
Investigation of three-dimensional flow field in a turbine including rotor/stator interaction. I - Design development and performance of the research facility
[AIAA PAPER 92-3325] p 883 A92-48908
Investigation of three-dimensional flow field in a turbine including rotor/stator interaction. II - Three-dimensional flow field at the exit of the nozzle
[AIAA PAPER 92-3326] p 826 A92-48909
Similarity relations for calculating three-dimensional chemically nonequilibrium viscous flows
p 827 A92-49188
Application of submerged vortex generators for separation control of a subsonic diffuser
p 933 A92-49832
The influences of forced oscillations toward vortex-breakdown p 934 A92-50210
Numerical investigation of axial flow compressor casing treatment p 934 A92-50216
Application of a solution adaptive grid scheme to complex three-dimensional flows p 935 A92-50309
Three-dimensional relaxation effect on quasi-3D flow in a blade row with spanwise loading distribution
p 936 A92-51593
Kinetic theory model for the flow of a simple gas from a three-dimensional axisymmetric nozzle
p 937 A92-52730
Pseudostream function formulation - A method of solving three-dimensional aerodynamic analysis and design problems in turbomachinery p 996 A92-52981
A bi-directional marching finite element algorithm for three-dimensional boundary layer separation flow computations p 942 A92-53288
A numerical investigation of axial flow compressor casing treatment p 942 A92-53381
Navier-Stokes analysis of three-dimensional unsteady flows inside turbine stages
[AIAA PAPER 92-3211] p 1021 A92-54016
High-speed cinematography of supersonic mixing layers
[AIAA PAPER 92-3545] p 1112 A92-54044
Numerical calculations of propfan/swirl recovery vane flow field
[AIAA PAPER 92-3771] p 1022 A92-54160
Detecting 3-D, turbulent separation regions using unsteady computerized thermographic technique
p 1023 A92-54308
Flowfield of a lifting rotor in hover - A Navier-Stokes simulation p 1024 A92-54906
Three-dimensional shock wave-turbulent boundary layer interaction induced by blunt body and protuberance
p 1029 A92-56009
Physics of vortical flows p 1031 A92-56166
Improved calculation of transonic potential flow past swept wings p 1031 A92-56179
A time-dependent tip loss formula for rotor blade dynamic analysis p 1057 A92-56310
The research of reducing 3-D low supersonic shock wave reflection in a 2-D transonic flexible walls adaptive wind tunnel
[AIAA PAPER 92-3924] p 1095 A92-56755
Blockage correction in three-dimensional wind tunnel testing based on the wall signature method
[AIAA PAPER 92-3925] p 1095 A92-56756
A computational and experimental investigation of a three-dimensional hypersonic scramjet inlet flow field
p 11 N92-10007
Numerical simulation of vortex breakdown via 3-D Euler equations p 41 N92-10164
The effects of Reynolds number, rotor incidence angle and surface roughness on the heat transfer distribution in a large-scale turbine rotor passage
[NASA-CR-184260] p 42 N92-11297
Turbulent friction drag reduction: Boundary layer manipulators
[CERT-RSF-DERAT-62/5004-31] p 43 N92-11309
Physics of vortical flow p 86 N92-13016
Variational formulation of hybrid problems for fully 3-D *transonic flow with shocks in rotor p 176 N92-13953*
Numerical investigations in three-dimensional internal flows
[NASA-CR-189467] p 221 N92-14313
Transonic Navier-Stokes computations for a spinning body of revolution
[AD-A241015] p 180 N92-14972
Grid impact on 3D hypersonic flows
p 184 N92-15041
Viscous three-dimensional calculations of transonic fan performance
[NASA-TM-103800] p 242 N92-17346
Basic hydrodynamics
[AD-A243513] p 300 N92-17387
Computation of a Kelvin-Helmholtz instability for delta wing vortex flows
[AD-A244320] p 346 N92-18825
Numerical solution of three-dimensional unsteady viscous flows
[AD-A244274] p 403 N92-19052
Resolution of the Euler equations applied to a helicopter rotor in forward flight
[ONERA-RSF-2/3731-AY-004A] p 406 N92-19976
Flowfield analysis of modern helicopter rotors in hover by Navier-Stokes method
[AD-A245011] p 446 N92-21333
Extension of a three dimensional Euler-code for the investigation of the flow field around bypass engines with fan and core jet
[DLR-FB-91-13] p 503 N92-21699
Three-dimensional simulations of hypersonic flows
[MBB-UK-0155-89-PUB] p 447 N92-21703
Three-dimensional compressible turbulent computations for a diffusing S-duct
[NASA-CR-4392] p 526 N92-22249
An engineering method for interactive inviscid-boundary layers in three-dimensional hypersonic flows
[NASA-TM-107838] p 632 N92-25279
Grid generation research at OSU p 633 N92-25723
Reynolds number dependence of the drag coefficient for laminar flow through fine-scale screens
[DE92-002930] p 765 N92-26698
Theoretical principles of a Euler method for the calculation of three dimensional flows
[F+W-TF-2012] p 767 N92-27045
A critical evaluation of a three-dimensional Navier-Stokes method as a tool to calculate transonic flows inside a low-aspect-ratio compressor
p 768 N92-27459

Validation of a CANARI code by the computation of three dimensional turbulent flow in turbine valve
p 741 N92-27462
Computation and visualization of specific flow phenomena in turbomachinery application
p 741 N92-27463
Predictions and measurements of 3D viscous flow in a transonic turbine nozzle guide vane row
p 741 N92-27466
Viscous three-dimensional calculations of transonic fan performance p 768 N92-27467
The 3-D Navier-Stokes flow and temperature field computation for a forced mixer nozzle
p 770 N92-27482
Three dimensional calculations of reactive flows within aircraft combustion chambers including some combustion models p 770 N92-27490
Calculation of unsteady transonic flows with mild separation by viscous-inviscid interaction
[NASA-TP-3197] p 827 N92-28477
Development and validation of a characteristic boundary condition for a cell-centered Euler method
[NLR-TP-90144-U] p 828 N92-28692
Development of an unsteady three-dimensional viscous-inviscid interaction numerical method for the calculation of airfoils vibration
[ONERA-RSF-7/3617-AY-022A] p 830 N92-29206
Development of a multigrid transonic potential flow code for cascades
[NASA-CR-190480] p 830 N92-29361
Evaluation of measured-boundary-condition methods for 3D subsonic wall interference
[NLR-TR-88072-U] p 832 N92-29884
A method for computing the 3-dimensional flow about wings with leading-edge vortex separation. Part 2: Description of computer program VORSEP
[NLR-TR-86006-U] p 833 N92-29916
Explicit Navier-Stokes computation of turbomachinery flows
[AD-A248458] p 911 N92-29933
Numerical investigations in three-dimensional internal flows
[NASA-CR-190498] p 998 N92-30380
Development of a 3-D upwind PNS code for chemically reacting hypersonic flowfields
[NASA-CR-190182] p 946 N92-30977
An experimental study of the relationship between velocity and pressure fluctuations in a wing-body junction
[AD-A249628] p 946 N92-31122
The three-dimensional stability of the Foeppl vortices
p 949 N92-31889
Three-dimensional compressible turbulent computations for a nondiffusing S-duct
[NASA-CR-4391] p 951 N92-32240
A critical evaluation of a three-dimensional Navier-Stokes CFD as a tool to design supersonic turbine stages p 1124 N92-32268
Numerical simulation of turbulence at the back of the airplane
[ETN-92-91664] p 1037 N92-32769
Shafranov shift in low-aspect-ratio heliotron/torsatron CHS
[NIFS-110] p 1138 N92-33743

THREE DIMENSIONAL MODELS

Aeroelastic analysis of wings using the Euler equations with a deforming mesh p 10 A92-13215
Three dimensional analysis of a rotor in forward flight
p 64 A92-14329
A 3-D separation model for arbitrary planforms
p 65 A92-14360
A numerical procedure of three-dimensional design problem in turbomachinery
[ASME PAPER 91-GT-144] p 72 A92-15583
Three dimensional hypersonic inlets - Low speed performance
[AIAA PAPER 91-5021] p 171 A92-17817
Three-dimensional linear stability approach to transition on wings and bodies of revolution at incidence
p 172 A92-18361
Studies of the effects of curvature on dilution jet mixing p 290 A92-21079
An efficient upwind relaxation-sweeping algorithm for three-dimensional Navier-Stokes equations
[AIAA PAPER 92-0023] p 248 A92-22145
Weak coupling between an unsteady 3D full potential code and an unsteady turbulent boundary layer code - Application to a helicopter rotor in forward flight
[AIAA PAPER 92-0029] p 249 A92-22151
Development of a three-dimensional icing code - Comparison with experimental shapes
[AIAA PAPER 92-0041] p 262 A92-22159
Computational aerodynamic simulation on HOPE
p 251 A92-22635
Three-dimensional simulation of a translating strut inlet
[AIAA PAPER 92-0270] p 317 A92-25726
Non-planar wing design by Navier-Stokes inverse computation
[AIAA PAPER 92-0285] p 319 A92-25738
Proposal for a 3-D, vectorized, adaptable, algorithm for modeling the randomness, unsteadiness, and microphysical properties of ice accretion
[AIAA PAPER 92-0299] p 351 A92-25751
Two and three dimensional parabolized Navier-Stokes code for scramjet combustor, nozzle, and film cooling analysis
[AIAA PAPER 92-0391] p 372 A92-26247
Quality assessment of two- and three-dimensional unstructured meshes and validation of an upwind Euler flow solver
[AIAA PAPER 92-0444] p 328 A92-26288
Laser velocimetry seed particles within compressible, vortical flows p 395 A92-26413
Three-dimensional adaptive grid generation with applications in nonlinear fluid dynamics
[AIAA PAPER 92-0661] p 397 A92-27032
Three-dimensional simulation of the Denver 11 July Storm of 1988 - An intense microburst event
p 407 A92-27958
Cartesian Euler method for arbitrary aircraft configurations p 340 A92-28039
Comparison of two-dimensional and three-dimensional droplet trajectory calculations in the vicinity of finite wings
[AIAA PAPER 92-0645] p 342 A92-28215
A computational exploration of the importance of three-dimensionality, boundary layer development, and flow chemistry to the prediction of scramjet nozzle performance
[AIAA PAPER 91-5059] p 472 A92-31689
Torsion and twisting of symmetric composite laminates
[AIAA PAPER 92-2425] p 582 A92-34354
A numerical classical flutter analysis of advanced propellers
[AIAA PAPER 92-2118] p 557 A92-35687
Two- and three-dimensional grid generation by an algebraic homotopy procedure p 611 A92-36861
Two-point optimization of complete three-dimensional airplane configuration
[AIAA PAPER 92-2618] p 844 A92-45491
Transonic airfoil and wing design using Navier-Stokes codes
[AIAA PAPER 92-2651] p 797 A92-45518
Three-dimensional-mode resonance in far wakes
p 898 A92-46252
An unstructured mesh generation algorithm for three-dimensional aeronautical configurations
p 918 A92-47053
Full Navier-Stokes analysis of a three-dimensional scramjet inlet p 934 A92-50272
A numerical study of the radiation characteristic of an elliptical exhaust jet p 970 A92-53258
Numerical simulation of three-dimensional turbulent flows in combustion chambers p 970 A92-53276
Three-dimensional Navier-Stokes heat transfer predictions for turbine blade rows
[AIAA PAPER 92-3068] p 1020 A92-54003
Modal simulation of gearbox vibration with experimental correlation
[AIAA PAPER 92-3494] p 1112 A92-54036
Numerical study of the 3-D flowfield for a supersonic jet exiting into a hypersonic stream from a conical surface
[AIAA PAPER 92-3675] p 1022 A92-54118
A unified viscous theory of lift and drag of 2-D thin airfoils and 3-D thin wings
[NASA-CR-4414] p 178 N92-13997
Viscous shock-layer equations for the calculation of reentry aerothermodynamics p 183 N92-15008
Hypersonic inviscid flow field simulations around reentry vehicles with flap deflection p 184 N92-15025
A walk through the planned CS building
[NASA-CR-189963] p 386 N92-19675
Quality assessment of two- and three-dimensional unstructured meshes and validation of an upwind Euler flow solver
[NASA-TM-104215] p 444 N92-20480
Three-dimensional compressible turbulent computations for a diffusing S-duct
[NASA-CR-4392] p 526 N92-22249
Three-dimensional time-marching aeroelastic analyses using an unstructured-grid Euler method
[NASA-TM-107567] p 527 N92-23116
Comparison of two-dimensional and three-dimensional droplet trajectory calculations in the vicinity of finite wings
[NASA-TM-105617] p 596 N92-23154
Coupled multi-disciplinary simulation of composite engine structures in propulsion environment
[NASA-TM-105575] p 596 N92-23267
Computational procedures for preliminary design
p 552 N92-23952
Three-dimensional modeling of diesel engine intake flow, combustion and emissions
[NASA-CR-189126] p 658 N92-24539
Turbulence modeling for hypersonic flight
[NASA-CR-190313] p 630 N92-24898
CAD product data exchange: Conversions for curves and surfaces
[ISBN-90-6275-723-9] p 648 N92-24964
TCGRID: A three dimensional C-grid generator for turbomachinery p 659 N92-25716
An interactive grid generation technique for turbomachinery p 659 N92-25717
Computational structures technology engine/airframe coupling p 649 N92-25935
Finite element methods for integrated aerodynamic heating analysis
[NASA-CR-190353] p 633 N92-25959
Simulation of 3D non-planar fatigue crack growth in a turbine blade root
[DE92-006859] p 739 N92-26697
A critical evaluation of a three-dimensional Navier-Stokes method as a tool to calculate transonic flows inside a low-aspect-ratio compressor
p 768 N92-27459
Steady and unsteady 3D flow computation through a transonic turbine stage p 742 N92-27469
Force measurements on AGARD calibration model-B at transonic speeds in the NAL two-dimensional wind tunnel
[NAL-TM-639] p 722 N92-28190
NPSNET: Flight simulation dynamic modeling using quaternions
[AD-A247484] p 923 N92-28245
Modal simulation of gearbox vibration with experimental correlation
[NASA-TM-105702] p 1002 N92-31485
Euler solver for arbitrary configurations: Further applications p 949 N92-31888
Potential flow theory and operation guide for the panel code PMARC
[NASA-TM-102851] p 1036 N92-32422
Shafranov shift in low-aspect-ratio heliotron/torsatron CHS
[NIFS-110] p 1138 N92-33743
Numerical investigation of the effects of icing on fixed and rotary wing aircraft
[NASA-CR-190542] p 1044 N92-34105

THREE DIMENSIONAL MOTION

The avoidance of collisions for Newtonian bodies with hidden variables p 353 A92-24945
Three-dimensional optimal reentry trajectory and aerodynamic heating history of the Space Shuttle
p 984 A92-49582

THRESHOLDS (PERCEPTION)

Risk to hearing from overflight noise of military aircraft
[ISVR-TR-194] p 604 N92-22241

THROATS

Initial calibration of the HEAT-H2 arc-heated wind tunnel
[AD-A245072] p 484 N92-20898

THROTTLING

A general nonlinear dynamical analysis of a second-order, one-dimensional, theoretical compression system model p 509 A92-29374
The propulsive-only flight control problem
p 876 A92-48487
Summary of the effects of engine throttle response on airplane formation-flying qualities
[AIAA PAPER 92-3318] p 877 A92-48902
Flight testing and simulation of an F-15 airplane using throttles for flight control
[NASA-TM-104255] p 1087 N92-32864

THRUST

Thrust/speed effects on long-term dynamics of aerospace planes p 889 A92-46766
Effects of bleed air extraction of thrust levels on the F404-GE-400 turbofan engine
[AIAA PAPER 92-3092] p 1066 A92-54009
Preliminary dynamic tests of a flight-type ejector
[AIAA PAPER 92-3261] p 1066 A92-54020
Effect of nonuniform entrance flow profile on hypersonic nozzle pitching moment
[AD-A244050] p 377 N92-19184
Performance prediction and design of maximum thrust planar supersonic nozzles using a flux-difference-splitting technique p 738 N92-26480
Effects of bleed air extraction on thrust levels on the F404-GE-400 turbofan engine
[NASA-TM-104247] p 871 N92-29425
Preliminary dynamic tests of a flight-type ejector
[NASA-TM-105814] p 972 N92-30998

Thrust test fixture
[AD-D015259] p 983 N92-31192
Investigation of the flight control requirements of a half-scale ducted fan unmanned aerial vehicle
[AD-A252730] p 1087 N92-32988
Ideal efficiency of propellers based on Theodorsen's theory: A review and computer study, with extended plus simplified charts
[UTIAS-TN-271] p 1071 N92-33102

THRUST AUGMENTATION
F-14/F110 engine integration p 112 A92-16055
The application of high pressure ejectors to reaction control systems p 128 A92-16666
Comment on 'Effect of thrust/speed dependence on long-period dynamics in supersonic flight' p 643 A92-39913
Use of an approximate similarity principle for the thermal scaling of a full-scale thrust augmenting ejector
[AIAA PAPER 92-3792] p 1069 A92-54171
The compound helicopter - A concept revisited p 1058 A92-56341
Use of an approximate similarity principle for the thermal scaling of a full-scale thrust augmenting ejector
[NASA-TM-105724] p 739 N92-26613

THRUST BEARINGS
Low power magnetic bearing design for high speed rotating machinery p 772 N92-27739

THRUST CHAMBER PRESSURE
An experimental investigation of high-aspect-ratio cooling passages
[AIAA PAPER 92-3154] p 890 A92-48780

THRUST CHAMBERS
An experimental investigation of high-aspect-ratio cooling passages
[AIAA PAPER 92-3154] p 890 A92-48780

THRUST CONTROL
V-22 thrust power management control law development p 132 A92-14405
A note on thrust control for jetliner during approach p 457 A92-29518
An estimate of the influence of the compressor stability margin on the thrust of a turbojet engine p 654 A92-37424
Fighter airframe/propulsion integration - A McDonnell Aircraft perspective
[AIAA PAPER 92-3333] p 850 A92-48916
Performance benefits of adaptive in-flight propulsion system optimization
[AIAA PAPER 92-3749] p 1068 A92-54149
A note on thrust control for jetliner during approach p 1053 A92-56061
Application of Eigenstructure Assignment to the control of powered lift combat aircraft
[RAE-TM-FS-1009] p 135 N92-12004
Gas turbine engine control
[PATENT-1-274-606] p 130 N92-13069
Simulation requirements for RCS plume: Flowfield interaction modelling on a winged reentry vehicle p 181 N92-14985
Experimental investigation of transverse jet effects related to hypersonic space vehicles p 182 N92-14995
ASTOVL engine control
[PNR-90808] p 740 N92-27040
Subsonic flight test evaluation of a performance seeking control algorithm on an F-15 airplane
[NASA-TM-4400] p 973 N92-31275

THRUST DISTRIBUTION
Aerodynamic design of a Coanda induced force and thruster anti-torque system p 109 A92-14419

THRUST LOADS
Effect of solidity and inclination on propeller-nacelle force coefficients
[NASA-TM-4316] p 90 N92-13038
Thrust stand evaluation of engine performance improvement algorithms in an F-15 airplane
[NASA-TM-104252] p 971 N92-30518

THRUST MEASUREMENT
Investigation of engine thrust correlation methods for enclosed test cells
[ASME PAPER 91-GT-68] p 121 A92-15538
Thrust stand evaluation of engine performance improvement algorithms in an F-15 airplane
[AIAA PAPER 92-3747] p 866 A92-49111
Thrust stand design principles
[AIAA PAPER 92-3976] p 1098 A92-56802
A derivation of gross thrust for a sea-level jet engine test cell
[NRC-30165] p 130 N92-12001

THRUST REVERSAL
F-15 STOL/Maneuvering Technology Demonstrator. Phase III - Thrust vectoring, reversing and STOL operation p 112 A92-16054
Horizontal flight of an aircraft with periodic thrust reversal p 480 A92-31876
Static performance of a cruciform nozzle with multiaxis thrust-vectoring and reverse-thrust capabilities
[NASA-TP-3188] p 527 N92-23095

THRUST VECTOR CONTROL
Computation of vectoring nozzle performance p 10 A92-13213
F-15 STOL/Maneuvering Technology Demonstrator. Phase III - Thrust vectoring, reversing and STOL operation p 112 A92-16054
A methodology for the analysis and modeling of thrust vectoring usage
[AIAA PAPER 92-0389] p 357 A92-26245
Effect of thrust vectoring on level-turn performance p 729 A92-41243
Application of computational fluid dynamics to pitch/yaw thrust vectoring spherical convergent flap nozzles p 737 A92-44511
Harrier international programme p 841 A92-45305
Maximizing thrust-vectoring control power and agility metrics p 874 A92-46794
Thrust vectoring characteristics of the F-18 high alpha research vehicle at angles of attack from 0 to 70 deg
[AIAA PAPER 92-3095] p 877 A92-48737
Comparative investigation of multiplane thrust vectoring nozzles
[AIAA PAPER 92-3263] p 864 A92-48858
Specifying exhaust nozzle contours in real-time using genetic algorithm trained neural networks
[AIAA PAPER 92-3328] p 865 A92-48911
Fighter airframe/propulsion integration - A General Dynamics perspective
[AIAA PAPER 92-3332] p 850 A92-48915
Emerging airframe/propulsion integration technologies at General Electric
[AIAA PAPER 92-3335] p 850 A92-48917
Optimal launch trajectory of a hypersonic research vehicle
[AIAA PAPER 92-4302] p 1103 A92-55310
Aircraft ground test and subscale model results of axial thrust loss caused by thrust vectoring using turning vanes
[NASA-TM-4341] p 273 N92-17071
X-31 enhancement of aerodynamics for maneuvering beyond stall p 363 N92-18779
Thrust vector control of an overexpanded supersonic nozzle using pin insertion and rotating airfoils
[AD-A243891] p 387 N92-18942
Application of nonlinear QFT to flight control design for high angle of attack maneuvers with thrust vectoring
[AD-A243821] p 381 N92-19241
A multi-loop guidance scheme using singular perturbation and linear quadratic regulator techniques simultaneously p 481 N92-20148
Thrust vectoring for lateral-directional stability
[NASA-CR-186016] p 482 N92-21357
Time-optimal reorientation maneuvers of an aircraft p 549 N92-22605
Static performance of a cruciform nozzle with multiaxis thrust-vectoring and reverse-thrust capabilities
[NASA-TP-3188] p 527 N92-23095
A static investigation of the thrust vectoring system of the F/A-18 high-alpha research vehicle
[NASA-TM-4359] p 633 N92-25967
Hot-gas reingestion engine response considerations
[PNR-90810] p 740 N92-27042
Flight-determined benefits of integrated flight-propulsion control systems
[NASA-TM-4393] p 742 N92-27587
Fuzzy guidance system evaluation p 778 N92-27903
Ski jump takeoff performance predictions for a mixed-flow, remote-lift STOVL aircraft
[NASA-TM-103866] p 1060 N92-32887
The F-18 high alpha research vehicle: A high-angle-of-attack testbed aircraft
[NASA-TM-104253] p 1060 N92-33404
Nonlinear dynamic-inversion flight control of supermaneuverable aircraft p 1062 N92-33953

THRUST-WEIGHT RATIO
Fracture behaviour of high-temperature polymer composites p 34 A92-11993
Use of the thrust-weight diagram versus transport cargo in the initial dimensioning of passenger-transport aircraft p 642 A92-37074
Airlines could reap big saving with new Pratt common core p 736 A92-42400

THUNDERSTORMS
Characteristics of thunderstorm-generated low altitude wind shear - A survey based on nationwide terminal Doppler weather radar testbed measurements p 45 A92-11378
Severe turbulence with a low-level jet ahead of a squall line p 407 A92-27939
Understanding and predicting microbursts p 407 A92-27953
Predicting summer microburst hazard from thunderstorm day statistics p 407 A92-27960
A case study of the Claycomo, Missouri microburst on July 30, 1989 p 407 A92-27961
High altitude airborne remote sensing mission using the advanced microwave precipitation radiometer (AMPR) p 574 A92-34893
Airport Surveillance Radar (ASR-9) wind shear processor: 1991 test at Orlando, Florida
[AD-A252246] p 1124 N92-32686

TILT ROTOR AIRCRAFT
V-22 flight test aerodynamics p 104 A92-14333
Flying qualities evaluation of the V22 tiltrotor p 131 A92-14334
Flight vibration testing of the V-22 tiltrotor aircraft p 107 A92-14397
V-22 thrust power management control law development p 132 A92-14405
The Eurofar vehicle overview p 108 A92-14416
V-22 Osprey tiltrotor blade fold/wing stow system design and testing p 109 A92-14420
Alleviation of whirl-flutter on tilt-rotor aircraft using active controls p 133 A92-14423
Tilting at targets --- tilt rotor aircraft development p 357 A92-25074
A multibody approach to modeling tilt-wing rotorcraft dynamics
[AIAA PAPER 92-0487] p 328 A92-26318
Tiltrotor control law design for rotor loads alleviation using modern control techniques p 478 A92-29331
Conceptual design and analysis of a special operations transport
[AIAA PAPER 92-1066] p 536 A92-33239
A demonstration of passive blade twist control using extension-twist coupling
[AIAA PAPER 92-2468] p 539 A92-34358
Parametric studies for tiltrotor aeroelastic stability in high-speed flight
[AIAA PAPER 92-2568] p 565 A92-34482
The V-22 Osprey - A significant flight test challenge p 546 A92-35766
Theoretical model to calculate aerodynamic interference effects between rotor and wing of tiltrotors p 521 A92-35788
The helicopter commuter - A perspective on regular passenger transportation by rotary wing p 634 A92-38208
Tiltrotor UAV - The next generation unmanned system p 646 A92-40384
Conceptual design and analysis of a special operations transport p 646 A92-40387
Aeroelasticity and the Tiltrotor VTOL aircraft p 647 A92-40389
1991-92 AHS Technical Committee highlights - Dynamics p 647 A92-40393
The high speed challenge for rotary wing aircraft
[SAE PAPER 911974] p 842 A92-45381
High speed VSTOL on the horizon - The answer to congestion?
[SAE PAPER 911976] p 843 A92-45383
Navier-Stokes computation of wing leading edge tangential blowing for a tilt rotor in hover
[AIAA PAPER 92-2608] p 805 A92-45568
Approach for analysis and design of composite rotor blades p 899 A92-46801
Shipboard mission training effectiveness of the Naval Air Warfare Center's V-22 Government Test Pilot Trainer
[AIAA PAPER 92-4130] p 959 A92-52427
Summary highlights of the Advanced Rotorcraft Transmission (ART) program
[AIAA PAPER 92-3362] p 1051 A92-54026
Research needs for a commercial passenger tiltrotor p 1056 A92-56298
The Eurofar program - An European overview on advanced VTOL civil transportation system p 1016 A92-56299
V-22 propulsion system design p 1070 A92-56300
A simulation study of tiltrotor vertical takeoff procedures using conventional and variable diameter rotor systems p 1056 A92-56301
Short takeoff optimization for the XV-15 tiltrotor aircraft p 1056 A92-56302
Optimal control of tiltrotor aircraft following power failure p 1085 A92-56303
Development of a conceptual design method for rotary-wing aircraft using digital computers p 1058 A92-56340
Flow visualization and flow field measurements of a 1/12 scale tilt rotor aircraft in hover
[NASA-CR-189456] p 82 N92-11983
New Ways: Tiltrotor aircraft and magnetically levitated vehicles
[OTA-SET-507] p 238 N92-14933
FAA vertical flight research, engineering, and development bibliography, 1962 - 1991
[FAA/ARD-30] p 462 N92-21210

The V-22 tilt rotor: A comparison with existing Coast Guard aircraft
[AD-A245843] p 650 N92-26039
The Eurofar program: An European overview on advanced VTOL civil transportation system
[MBB-UD-0611-91-PUB] p 952 N92-30418
Impacts of technology on the capacity needs of the US national airspace system
[NASA-CR-4470] p 1045 N92-34192

TILT ROTOR RESEARCH AIRCRAFT PROGRAM
A historical overview of tiltrotor aeroelastic research at Langley Research Center
[NASA-TM-107578] p 502 N92-21460

TILT WING AIRCRAFT
Description of a tilt wing mathematical model for piloted simulation p 133 A92-14445
A multibody approach to modeling tilt-wing rotorcraft dynamics
[AIAA PAPER 92-0487] p 328 A92-26318
Conceptual design and analysis of a special operations transport
[AIAA PAPER 92-1066] p 536 A92-33239
Conceptual design and analysis of a special operations transport p 646 A92-40387
High speed VSTOL on the horizon - The answer to congestion?
[SAE PAPER 911976] p 843 A92-45383
Flap control simulation p 980 A92-51398
A mathematical model of a tilt-wing aircraft for piloted simulation
[NASA-TM-103864] p 368 N92-19847

TILTING ROTORS
Dynamic response of a variable-speed rotor during rapid shaft tilt p 132 A92-14400
High speed rotorcraft - Comparison of leading concepts and technology needs p 108 A92-14415
The V-22: Can the nation afford to forgo its production?
[AD-A243158] p 242 N92-17477
Wing force and surface pressure data from a hover test of a 0.658-scale V-22 rotor and wing
[NASA-TM-102244] p 550 N92-22864

TIME
Comparison of GLONASS and GPS time transfers between two west European time laboratories and VNIIFTRI p 1050 N92-33381

TIME DEPENDENCE
Observability analysis of piece-wise constant systems with application to inertial navigation p 49 A92-11391
A new class of gradient estimators for queueing systems with real-time constraints p 49 A92-11395
Nonlinear damping estimation from rotor stability data using time and frequency domain techniques p 641 A92-36855
Application of technology developed for flight simulation at NASA. Langley Research Center p 573 N92-22437
Improving designer productivity --- artificial intelligence
[NASA-TM-103929] p 854 N92-29417
Progress in unstructured-grid methods development for unsteady aerodynamic applications
[NASA-TM-107643] p 944 N92-30393
Finite difference time domain modeling of steady state scattering from jet engines with moving turbine blades
[NASA-CR-190290] p 971 N92-30753
Extension of the integral equation formulation of linearized time dependent subsonic flow
[AD-A250654] p 947 N92-31171
Dynamic response of induced pressures, suckdown, and temperatures for two tandem jet STOVL configurations
[NASA-TM-103934] p 1039 N92-33581
Investigation of advancing front method for generating unstructured grid
[NASA-CR-190902] p 1128 N92-34043

TIME DIVISION MULTIPLE ACCESS
Evaluating the use of satellite communications in the government of Canada p 594 N92-22577

TIME DIVISION MULTIPLEXING
Common airborne instrumentation system (CAIS) --- time-division multiplexed data acquisition system p 856 A92-47538
Data Multiplexing Network (DMN) phase 3 equipment Operational Test and Evaluation (OT and E)/integration test report
[DOT/FAA/CT-TN91/50] p 221 N92-14270

TIME LAG
Robustness of distributed systems with respect to small time delays p 47 A92-11351
Consideration of the time lag of engine processes in the problem of VTOL aircraft control synthesis p 134 A92-16807
Study on a flight simulator of time delays p 744 A92-43112
A distributed vaporization time-lag model for gas turbine combustor dynamics
[AIAA PAPER 92-3465] p 865 A92-49014
Ignition delays, heats of combustion, and reaction rates of aluminum alkyl derivatives used as ignition and combustion enhancers for supersonic combustors
[AIAA PAPER 92-3841] p 894 A92-49134
Approximations for inclusion of rotor lag dynamics in helicopter flight dynamics models p 1060 A92-56354
A simple and low cost system to measure delay times in pneumatic systems
[NLR-TP-90174-U] p 859 N92-28644
Transport delay measurements: Methodology and analysis for the F-16C combat engagement trainer, the display for advanced research and training, and the F-16A limited field of view
[AD-A248519] p 888 N92-29505

TIME MARCHING
Cascade flutter analysis with transient response aerodynamics p 154 A92-15972
Time marching integral equation method for the solutions of unsteady transonic flows p 314 A92-25129
Analysis of an advanced ducted propeller subsonic inlet
[AIAA PAPER 92-0274] p 318 A92-25728
Comparison between imposed-periodicity and marching-in-time solutions of helicopter rotor blade steady-state response problem
[AIAA PAPER 92-2256] p 540 A92-34411
Three-dimensional time-marching aeroelastic analyses using an unstructured-grid Euler method
[AIAA PAPER 92-2506] p 542 A92-34500
Temporal adaptive Euler/Navier-Stokes algorithm involving unstructured dynamic meshes p 812 A92-46887
A time marching method in finite volume for transonic diffuser turbulent flows p 819 A92-47690
Evaluation of a multigrid-based Navier-Stokes solver for aerothermodynamic computations
[AIAA PAPER 92-4563] p 1027 A92-55375
Analysis of an advanced ducted propeller subsonic inlet
[NASA-TM-105393] p 179 N92-14002
Periodic trim solutions with HP-version finite elements in time
[NASA-CR-189778] p 282 N92-17019
Three-dimensional time-marching aeroelastic analyses using an unstructured-grid Euler method
[NASA-TM-107567] p 527 N92-23116
Three-dimensional upwind scheme for solving the Euler equations on unstructured tetrahedral grids --- tetrahedral grids p 714 N92-26585
The application of a Navier-Stokes CFD method to civil engine intake flows p 769 N92-27471

TIME MEASUREMENT
The need for GPS standardization p 1049 N92-33351
Evaluation of GPS/UTC steering performance p 1049 N92-33353
Precise GPS ephemerides from DMA and NGS tested by time transfer p 1049 N92-33355
Comparison of two-way satellite time transfer and GPS common-view time transfer between OCA and TUG p 1050 N92-33356
LORAN-C data reduction at the US Naval Observatory p 1050 N92-33358

TIME OPTIMAL CONTROL
Time-periodic control of a multi-blade helicopter p 204 A92-18626
2-D and 3-D minimum-time-to-turn flights via parameter optimization
[AIAA PAPER 92-0731] p 379 A92-27083
Thrust laws for microburst wind shear penetration p 873 A92-46750
Optimal discrete-time static output-feedback design - A W-domain approach p 1007 A92-50499
Optimal trajectories for an unmanned air vehicle p 963 N92-31880

TIME RESPONSE
Loran time difference correction factors - Valid information or blue smoke and mirrors? p 96 A92-16633
The effect of molecular relaxation processes in air on the rise time of sonic booms p 898 A92-45883
Flight test results using a low order equivalent systems technique to estimate flying qualities
[AIAA PAPER 92-4425] p 1080 A92-55349

TIME SERIES ANALYSIS
Digital time series analysis for flutter test data
[AIAA PAPER 92-2103] p 589 A92-35674

TIME SIGNALS
Evaluation of GPS/UTC steering performance p 1049 N92-33353
Precise GPS ephemerides from DMA and NGS tested by time transfer p 1049 N92-33355
Comparison of two-way satellite time transfer and GPS common-view time transfer between OCA and TUG p 1050 N92-33356

TIME TEMPERATURE PARAMETER
Lubricant evaluation and performance 2
[AD-A247464] p 895 N92-28398

TIP SPEED
Detailed noise measurements on the SR-7A propeller: Tone behavior with helical tip Mach number
[NASA-TM-105206] p 304 N92-16705
Model rotor icing tests in the NASA. Lewis Icing Research Tunnel p 450 N92-21688
Overview of NASA PTA propfan flight test program p 561 N92-22536

TIRES
Sensitivity of tire response to variations in material and geometric parameters p 900 A92-47128

TITANIUM
Stress-strain analysis of a (0/90)sub 2 symmetric titanium matrix laminate subjected to a generic hypersonic flight profile
[NASA-TM-107584] p 685 N92-26128
Preliminary evaluation of adhesion strength measurement devices for ceramic/titanium matrix composite bonds
[NASA-TM-105803] p 932 N92-31267

TITANIUM ALLOYS
Light metal materials for aircraft structure p 140 A92-13444
A study of the nonlinear stress-strain state of spring-type landing gear p 154 A92-16825
Inertia-friction welding of an advanced rapidly solidified titanium alloy p 212 A92-18898
Prediction of fatigue crack growth in a Ti-6Al-4V fan disk forging under spectrum loading p 213 A92-19817
Applications of IMI 834 in aeroengines - A collaborative IMI/MTU programme p 288 A92-22754
Mechanical and fracture behaviour of Ti-6Al-2Sn-4Zr-2Mo-0.1Si alloys p 288 A92-22755
Ti-6Al-4V forgings with enhanced fatigue characteristics for engine and airframe applications p 288 A92-22757
The compatibility and tradeoffs of titanium and composites p 288 A92-22758
The beta-CEZ - A high performance titanium alloy for aerospace engines p 289 A92-22760
Improving the properties of titanium alloys by ion implantation p 289 A92-22771
Cost effective solutions for titanium sheet metal forming p 293 A92-22785
A technique for quantitatively measuring microstructurally induced ultrasonic noise p 510 A92-28720
A preliminary study of the microstructure-property relationships in cast gamma titanium aluminide alloys p 487 A92-30596
Manufacture of XD gamma titanium aluminide airfoils via investment casting and machining p 494 A92-30603
A critical appraisal of thermomechanical processing of structural titanium alloys p 488 A92-30611
Composite strengthening of Nb-Ti base alloys p 577 A92-36380
Robotics application in aerospace manufacturing p 671 A92-38216
Testing of a titanium matrix composite landing gear
[SAE PAPER 912175] p 644 A92-40000
New titanium applications on the Boeing 777 airplane p 754 A92-41119
Development of intermetallic materials for aerospace systems p 754 A92-41874
Possibility of increasing durability of blades with damages p 761 A92-42654
Super plastic forming technology applied to aeroengine and space equipment p 764 A92-44732
Axial alignment of short-fiber titanium aluminide composites by directional solidification p 892 A92-46838
Investigation of the structural inhomogeneity of a titanium alloy p 893 A92-47958
Titanium alloy casting for aerospace p 1106 A92-56103
Thermoviscoplastic response of Ti-15-3 under various loading conditions
[NASA-CR-187621] p 45 N92-11391
Composition monitoring of electron beam melting processes using diode lasers
[DE92-009527] p 669 N92-25259
Surface residual stress analysis of metals and alloys
[AD-A248372] p 895 N92-28426

TITANIUM CARBIDES
The microstructural stability of TiC reinforced rapidly solidified Al-Fe-V-Si composite structures p 141 A92-15169

TITANIUM COMPOUNDS
Thermo-mechanical fatigue crack growth in aircraft engine materials p 213 A92-19799

TOKAMAK DEVICES
Scoping studies for small steady-state tokamaks for divertor testing
[DE92-000740] p 238 N92-15761
Formation and sustainment of a very low aspect ratio tokamak using coaxial helicity injection: Helicity Injected Torus (HIT) experiment
[DE92-014311] p 1136 N92-32595
TOLERANCES (MECHANICS)
Fatigue and damage tolerance verification of aircraft structures p 217 A92-19677
Damage tolerance and repair experience of composite structures
[AIAA PAPER 92-1256] p 515 A92-33339
Research on damage tolerance of compressor blade p 588 A92-35556
Optimal maintenance program of damage tolerance structure p 785 A92-47660
Advanced experimental design applied to damage tolerance of composite materials p 993 A92-51505
Impact damage tolerance of helicopter sandwich structures p 958 A92-51506
Development of composite structures with enhanced damage tolerance p 985 A92-51555
Durability and damage tolerance testing and fatigue life management: A CF-18 experience p 361 N92-18581
Aircraft tracking optimization of parameters selection p 361 N92-18585
The Operational Loads Monitoring System, OLMS p 361 N92-18586
Fatigue management for the A-7P p 363 N92-18593
Thermal/structural analysis of a transpiration cooled nozzle
[NASA-TM-104184] p 401 N92-18877
AGARD/SMP Review: Damage Tolerance for Engine Structures. 4: Reliability and Quality Assurance
[AGARD-R-773] p 402 N92-19004
Introduction: Needs and approaches to reliability and quality assurance in design and manufacture p 402 N92-19005
Manufacturing process control as a damage tolerance concept p 403 N92-19006
Durability and damage tolerance of aluminum castings
[AD-A245237] p 490 N92-21159
Overview of mechanics of materials branch activities in the computational structures area p 684 N92-25917
Composite fuselage technology (summary of year 2)
[NASA-CR-190434] p 731 N92-26655
Generation of spectra and stress histories for fatigue and damage tolerance analysis of fuselage repairs
[AD-A250390] p 854 N92-29180
Aging commuter aeroplanes: Fatigue evaluation and control methods p 915 N92-30132
A Protection And Detection Surface (PADS) for damage tolerance p 1107 N92-32523
Damage tolerance certification methodology for composite structures p 1108 N92-32579
TOLLMIEN-SCHLICHTING WAVES
Secondary instability of high-speed flows and the influence of wall cooling and suction p 435 A92-31640
A method of boundary layer laminarization on an oscillating wing p 441 A92-31969
Boundary-layer receptivity of sound with roughness p 604 A92-36006
Studies on laminar boundary-layer receptivity to freestream turbulence near a leading edge p 591 A92-36007
Boundary-layer receptivity due to a wall suction and control of Tollmien-Schlichting waves p 616 A92-39333
A new approach for the calculation of transitional flows
[AIAA PAPER 92-2669] p 798 A92-45524
Numerical simulation of swept-wing flows
[NASA-CR-189457] p 180 N92-14969
A weakly nonlinear theory for wave-vortex interactions in curved channel flow
[NASA-TP-3158] p 347 N92-19175
TOMOGRAPHY
Inverse problems and imaging (Pitman research notes in mathematics series Number 245)
[AD-A240333] p 53 N92-11737
TOOLING
High temperature thermoplastic and polyimide processing using CARE-MOLD wash-out tooling p 36 A92-10259
Tooling for C-17 composite parts p 900 A92-47412
TOOLS
Bearing servicing tool
[NASA-CASE-MSC-21881-1] p 912 N92-30082
TOPOGRAPHY
Computation of aircraft noise exposure using digitized topography data p 687 A92-39058
TOPOLOGY
Topology of steady flows of low viscosity fluids p 38 A92-11219
TORNADOES
Development of a wind chamber for model testing of tornado forces on structures
[PB92-104165] p 386 N92-19940
TOROIDAL PLASMAS
Scoping studies for small steady-state tokamaks for divertor testing
[DE92-000740] p 238 N92-15761
Experimental studies of compact toroids
[DE92-003469] p 512 N92-21046
Formation and sustainment of a very low aspect ratio tokamak using coaxial helicity injection: Helicity Injected Torus (HIT) experiment
[DE92-014311] p 1136 N92-32595
TOROIDS
Spray nozzle for fire control
[CA-PATENT-APPL-SN-2-011-94] p 1125 N92-32856
TORQUE
A torque-free flexible model gyro p 495 A92-31552
Reduction of torque pulsation of Stirling engine-compressor system p 992 A92-50785
Dynamics of helicopters with dissimilar blades in forward flight p 1056 A92-56288
Dynamics of a split torque helicopter transmission
[NASA-TM-105681] p 910 N92-29136
Thermal mechanical analysis of sprag clutches
[NASA-CR-190686] p 1128 N92-34207
TORSION
An experimental study of the sensitivity of helicopter rotor blade tracking to root pitch adjustment in hover
[NASA-TM-4313] p 61 N92-12989
Field telemetry of blade-rotor coupled torsional vibration at Matuura Power Station Number 1 unit p 222 N92-14348
Elementary flutter analysis p 1088 N92-34162
Thermal mechanical analysis of sprag clutches
[NASA-CR-190686] p 1128 N92-34207
TORSIONAL STRESS
Comparison of theory and experiment for nonlinear flutter and stall response of a helicopter blade p 65 A92-14428
Torsion and twisting of symmetric composite laminates
[AIAA PAPER 92-2425] p 582 A92-34354
Flexure-torsion behavior of sheat-deformable beams with applications to aircraft wing sections
[AIAA PAPER 92-2467] p 582 A92-34357
Blade root torsional dampers to reduce hub loads
[AIAA PAPER 92-2449] p 541 A92-34476
Design and manufacturing of torsional flexible blade models p 547 A92-35780
Behavior of thin-walled beams made of advanced composite materials and incorporating non-classical effects p 673 A92-39944
TORSIONAL VIBRATION
The torsional stability of a compressor cascade
[ASME PAPER 91-GT-180] p 123 A92-15612
Effect of shock waves on the critical rate of bending-torsional flutter of an airfoil p 494 A92-30208
The use of Stodola modes in rotor-blade aeroelastic studies p 590 A92-35729
Modeling rotor dynamics with rotor speed degree of freedom for drive train torsional stability analysis p 547 A92-35779
Helicopter tail rotor stall flutter p 1056 A92-56290
Field telemetry of blade-rotor coupled torsional vibration at Matuura Power Station Number 1 unit p 222 N92-14348
TORUSES
Formation and sustainment of a very low aspect ratio tokamak using coaxial helicity injection: Helicity Injected Torus (HIT) experiment
[DE92-014311] p 1136 N92-32595
TOTAL QUALITY MANAGEMENT
Improving reliability and maintainability through process management p 1141 A92-56212
An analysis of total quality management in Aeronautical Systems Division
[AD-A246661] p 772 N92-27760
TOUCHDOWN
Nonlinear landing gear behavior at touchdown p 192 A92-19606
Example of statistical techniques applied to autoland touchdown dispersion (confidence intervals for normal and skew distributions)
[ESDU-91019] p 268 N92-17844
Attributes of winged manned space vehicles and their relationship to ground site characteristics and facilities p 487 N92-20776
Effective cueing during approach and touchdown: Comparison with flight p 886 N92-28552
TOUGHNESS
Mechanical qualification tests for materials used in the fabrication of aircraft parts
[CEAT-M5-5443/01] p 195 N92-14042
TOWED BODIES
Dynamics of an aircraft-towed body during release
[AIAA PAPER 92-0130] p 295 A92-23750
Flight test validation of tow target trajectory predictions
[AIAA PAPER 92-0209] p 271 A92-23814
Handling and performance considerations when conducting air-to-air refuelling of large aircraft by the probe and drogue system p 548 A92-35937
Dynamics and control of maneuverable towed flight vehicles p 976 A92-50508
TOWING
Legal problems in aircraft towing using the PTS procedure p 56 A92-11214
TOXIC HAZARDS
Flammability, smoke and toxic gas combustion products of composites used in aircraft cabins p 14 A92-10257
TOXICITY
Preliminary screening procedures and criteria for replacements for Halons 1211 and 1301
[AD-A252912] p 1126 N92-33501
TRACE ELEMENTS
Airborne tests of flux measurement by the relaxed eddy accumulation technique p 504 A92-32052
High-speed civil transport aircraft emissions p 408 N92-19122
TRACKING (POSITION)
The Automatic Dependent Surveillance (ADS) system p 724 A92-41208
Location and tracking technique in a multistatic system established by multiple bistatic systems p 840 A92-48480
Predictive control for optimal path terrain following system p 955 A92-50207
JTIDS relative navigation and data registration p 955 A92-51006
Pulsed field system for detecting the presence of a target in a subsurface environment
[AD-D015074] p 296 N92-16174
Flight evaluation of curved MLS precision approaches in a twin otter aircraft, phase 2
[AD-A243025] p 268 N92-17568
Aircraft tracking for structural fatigue p 361 N92-18584
Aircraft tracking optimization of parameters selection p 361 N92-18585
CDI sensitivity and crosstrack error on nonprecision approaches
[AD-A243981] p 356 N92-19391
Passive acoustic range estimation of helicopters
[AD-A248033] p 926 N92-28302
Development of new flight procedures for the Microwave Landing System (MLS)
[NLR-TP-91156-U] p 1047 N92-32830
TRACKING FILTERS
New practical method for measurement error determination in radar systems under real traffic conditions p 155 A92-17238
Nonlinear aircraft tracking filter utilizing control variable estimation p 302 A92-21179
TRACKING PROBLEM
Design of localizer capture and track hold for a transport airplane - An H(infinity)/LTR approach p 52 A92-11583
A multidimensional terrain model for low altitude tracking scenarios p 205 A92-19107
Tracking performance requirements for rotorcraft instrument approaches to reduced minima. Phase 1: Preliminary study
[NRC-32137-PHASE-1] p 102 N92-11988
TRACTION
Determination of tire-wheel interface loads for aircraft wheels
[AIAA PAPER 92-2482] p 543 A92-34599
TRADEOFFS
Characteristics of a future aeronautical satellite communications system
[AIAA PAPER 92-2058] p 453 A92-29889
Design tradeoffs on engine-integrated hypersonic vehicles
[AIAA PAPER 92-1205] p 537 A92-33313
TRAFFIC
Bibliography of technical reports, 1980 - 1990
[PB92-110691] p 417 N92-18814
TRAFFIC CONTROL
Runway exit designs for capacity improvement demonstrations. Phase 2: Computer model development
[NASA-CR-190166] p 484 N92-21162
TRAILING EDGE FLAPS
Effects of trailing-edge flap on buffet characteristics of a supercritical airfoil p 378 A92-24413

Interference of high-mounted propfan nacelles with an unswept wing and ways to attenuate it
p 460 A92-31881
Flow regimes of the cove regions between a slat and wing and between a wing and flap of a multielement airfoil p 614 A92-38858
Active control of blade vortex interaction
p 814 A92-46944
Effects of leading and trailing edge flaps on the aerodynamics of airfoil/vortex interactions
p 815 A92-46957
Trimming rotor blades with periodically deflecting trailing edge flaps p 1085 A92-56283
Maximum lift of wings with trailing-edge flaps at low speeds
[ESDU-91014] p 81 N92-11970
Flow over a delta wing at hypersonic speeds
p 181 N92-14993
Blade-mounted trailing edge flap control for BVI noise reduction
[NASA-CR-4426] p 512 N92-21173
Evaluation of an unsteady implicit Euler code against two and three-dimensional standard configurations
p 719 N92-27945
Lift and rolling moment due to spoilers on wings with trailing-edge flaps deflected at subsonic speeds
[ESDU-92002-SUPPL] p 1037 N92-32782

TRAILING EDGES
Calculation of the parameters of separated flow behind a plane rounded body in the path of two supersonic flows p 244 A92-21624
Navier-Stokes analysis of blunt trailing edge airfoils
[AIAA PAPER 92-0024] p 248 A92-22146
The rolling-up and interaction of the leading-edge and trailing-edge vortex sheets of a delta wing
p 314 A92-25101
Controlling unsteady lift using unsteady trailing-edge flap motions
[AIAA PAPER 92-0275] p 318 A92-25729
Numerical investigation of laminar separated trailing-edge flows p 339 A92-28026
Effect of airfoil (trailing-edge) thickness on the numerical solution of panel methods based on the Dirichlet boundary condition p 340 A92-28041
Flow near the trailing edge of an airfoil
p 431 A92-31151
Helical-perturbation device for cylinder-wing vortex generators p 432 A92-31167
Analytical study on plate edge noise. I - Trailing edge noise caused by vorticity waves p 511 A92-32502
Secondary flow investigation inside the passage of a compressor cascade p 706 A92-42124
The acceleration control system design of a flight vehicle using a two-wing control method p 745 A92-43185
Wake mixing and performance measurements in a linear compressor cascade with crenulated trailing edges
[AIAA PAPER 92-3188] p 824 A92-48800
Computation of vortex wake flows and control of their effects on trailing wings
[AIAA PAPER 92-4429] p 1025 A92-55353
NACA 0015 wing pressure and trailing vortex measurements
[NASA-TP-3151] p 13 N92-10981
Application of direct inverse analogy method (DIVA) and viscous design optimization techniques
p 176 N92-13951
Navier-Stokes analysis of turbulent boundary layer and wake for two-dimensional lifting bodies
p 221 N92-14309
Use of Navier-Stokes analysis in section design
[AD-A242074] p 299 N92-17168
Thermal nonequilibrium effects on turbine cascade aerodynamics
[AD-A244049] p 404 N92-19183
Experimental investigation of trailing edge crenulation effects on losses in a compressor cascade
[AD-A243902] p 377 N92-19329
Serrated trailing edges for improving lift and drag characteristics of lifting surfaces
[NASA-CASE-LAR-13870-1-CU] p 463 N92-21587
An investigation of the energy loss and near wake flow field of trailing edge injection p 456 N92-21839
Case 7.4 delta wing: Navier-Stokes calculation
p 525 N92-22182
Development of a method to predict transonic limit cycle oscillation characteristics of fighter aircraft
p 746 N92-27958
Computation of three-dimensional effects on two dimensional wings
[NASA-CR-190576] p 832 N92-29691
Improved articulated fin/wing control system statement of government interests
[AD-D015268] p 1088 N92-34131

TRAINING AIRCRAFT
An anthropometric evaluation of the TH-57 Jetranger helicopter p 46 A92-11164
Analytical condition inspection and extension of time between overhaul of F3-30 engine
[ASME PAPER 91-GT-277] p 653 A92-36888
British Aerospace Hawk into the 1990s
p 957 A92-50009
Investigation of the tail buffeting of the C-101
p 942 A92-53253
Model flight tests of a spin-resistant trainer configuration p 1054 A92-56158
An evaluation of the Royal Air Force Shorts Tucano Navigation Instruments Trainer: The NAVIT
[ETN-92-90841] p 354 N92-18729
Parametric effects of some aircraft components on high-alpha aerodynamic characteristics
p 364 N92-18782

TRAINING ANALYSIS
Approach to crew training in support of the USAF Aircraft Structural Integrity Program (ASIP) p 363 N92-18595
Development of the Basic Flight Instruction Tutoring System (BFITS)
[AD-A246458] p 751 N92-27836
Assessment of army aviators' ability to perform individual and collective tasks in the aviation networked simulator
[AD-A250293] p 888 N92-29709

TRAINING DEVICES
Software reliability for flight crew training simulators
p 747 A92-41221
The modelling of turbulence and downbursts for flight simulators
[UTIAS-339] p 161 N92-12373
An evaluation of the Royal Air Force Shorts Tucano Navigation Instruments Trainer: The NAVIT
[ETN-92-90841] p 354 N92-18729
Ship airwake measurement and modeling options for rotorcraft applications p 503 N92-21954
Development of the Basic Flight Instruction Tutoring System (BFITS)
[AD-A246458] p 751 N92-27836
Piloted Simulation Effectiveness
[AGARD-CP-513] p 786 N92-28522
AM-X flight simulator from engineering tool to training device p 884 N92-28536
Transport delay measurements: Methodology and analysis for the F-16C combat engagement trainer, the display for advanced research and training, and the F-16A limited field of view
[AD-A248519] p 888 N92-29505

TRAINING EVALUATION
Advanced training systems for the next decade and beyond
[AIAA PAPER 92-1626] p 690 A92-38699
Shipboard mission training effectiveness of the Naval Air Warfare Center's V-22 Government Test Pilot Trainer
[AIAA PAPER 92-4130] p 959 A92-52427
Developmental evaluation of a centrifuge flight simulator as an enhanced maneuverability flying qualities tool
[AIAA PAPER 92-4157] p 982 A92-52447
Piloted evaluation of an integrated propulsion and flight control simulator
[AIAA PAPER 92-4178] p 960 A92-52459
The multi-attribute task battery for human operator workload and strategic behavior research
[NASA-TM-104174] p 303 N92-17130
Microcomputer-based instrument flight simulation: Undergraduate pilot training student attitude assessment
[AD-A245449] p 749 N92-26527
Workshop on integrated Crew Resource Management (CRM)
[DOT/FAA/RD-92/5] p 781 N92-27518
Development of the Basic Flight Instruction Tutoring System (BFITS)
[AD-A246458] p 751 N92-27836

TRAINING SIMULATORS
Full model simulation of the National Airspace System - Research and training platform p 880 A92-45042
Dead reckoning for aircraft in distributed interactive simulation
[AIAA PAPER 92-4171] p 1008 A92-52456
Simulator data integrity program: Process standard development
[AD-A242207] p 386 N92-19642
Flying an aircraft as a problem-solving process: About the Instrument-Failure-Simulator (IFS) as a test for pilot-candidates
[DLR-FB-91-23] p 455 N92-20902
SIMNET plan view display user manual
[AD-A244617] p 510 N92-21392
Piloted simulation effectiveness development applications and limitations p 883 N92-28524
Experience with piloted simulation in the development of helicopters p 884 N92-28528
Validation of simulation systems for aircraft acceptance testing p 852 N92-28531
Aircraft simulation and pilot proficiency: From surrogate flying towards effective training p 884 N92-28532
The use of a dedicated testbed to evaluate simulator training effectiveness p 884 N92-28533
AM-X flight simulator from engineering tool to training device p 884 N92-28536
The evaluation of simulator effectiveness for the training of high speed, low level, tactical flight operations
p 885 N92-28539
Harrier GR MK 5/7 mission simulators for the Royal Air Force p 885 N92-28540
Results of a flight simulator experiment to establish handling quality guidelines for the design of future transport aircraft
[NLR-MP-88044-U] p 854 N92-29616
Assessment of army aviators' ability to perform individual and collective tasks in the aviation networked simulator
[AD-A250293] p 888 N92-29709

TRAJECTORIES
An alternative concept for aeroassisted orbit transfers
[AD-A243409] p 287 N92-17325
Trajectory analysis of the G-11 family of clustered parachutes to determine minimum altitude
[AD-A243375] p 261 N92-17404
On board planning of 4D-trajectories
p 728 N92-27897
Trajectory optimization for hypersonic aircraft guidance p 728 N92-27898
Trajectory fitting in function space with application to analytic modeling of surfaces
[NASA-TP-3232] p 945 N92-30747
Analysis of the flight performance of the 155 mm M864 base burn projectile
[BRL-TR-3083] p 1041 N92-33699

TRAJECTORY ANALYSIS
Aeroassist flight experiment heating-rate sensitivity study p 3 A92-10427
Small balloon ballistic tracing and behavior anomalies
[AIAA PAPER 91-3682] p 15 A92-11026
Flight test validation of tow target trajectory predictions
[AIAA PAPER 92-0209] p 271 A92-23814
STS-40 descent BET products: Development and results
[NASA-CR-189570] p 286 N92-16012
Trajectory analysis of the G-11 family of clustered parachutes to determine minimum altitude
[AD-A243375] p 261 N92-17404
Graphics for interactive PC based parameter estimation package
[NAL-PD-FC-9117] p 412 N92-18252
Application of a water droplet trajectory prediction code to the design of inlet particle separator anti-icing systems
[PNR-90839] p 474 N92-20573

TRAJECTORY CONTROL
Dynamic interpolation for linear systems
p 52 A92-11465
Results of a test program for the use of differential GPS for approach guidance p 101 A92-16969
Optimal control problems with maximum functional
p 232 A92-18616
Trajectory control for a low-lift maneuverable reentry vehicle
[AIAA PAPER 92-1146] p 574 A92-33287
The differential algebraic approach in nonlinear dynamical feedback controlled landing maneuvers
p 574 A92-33639
Invertibility and trajectory control for nonlinear maneuvers of aircraft
[AIAA PAPER 92-4410] p 1075 A92-55204
Selection of sampling rate for nonlinear flight trajectory controller of aircraft p 1084 A92-56070
Rapid near-optimal aerospace plane trajectory generation and guidance
[NASA-CR-189469] p 205 N92-14066
Proportional plus integral control of aircraft for automated maneuvering formation flight
[AD-A243792] p 382 N92-19505
A multi-loop guidance scheme using singular perturbation and linear quadratic regulator techniques simultaneously p 481 N92-20148
Trajectory optimization for hypersonic aircraft guidance p 728 N92-27898
A workstation-based evaluation of a far-field route planner for helicopters
[NASA-TM-102882] p 1051 N92-33609

TRAJECTORY MEASUREMENT
Comparison of two-dimensional and three-dimensional droplet trajectory calculations in the vicinity of finite wings
[AIAA PAPER 92-0645] p 342 A92-28215
Comparison of two-dimensional and three-dimensional droplet trajectory calculations in the vicinity of finite wings
[NASA-TM-105617] p 596 N92-23154

Board-autonomous flight trajectory measurement by example of an ILS measuring system
p 641 N92-25601

TRAJECTORY OPTIMIZATION
Optimal stabilization of discrete event systems
p 48 A92-11376
Optimal trajectories and guidance trajectories for aircraft flight through windshears p 27 A92-11383
Thermodynamic behaviour of hydrogen-powered hypersonic ramjets flying along ideal trajectories
[IAF PAPER 91-277] p 25 A92-12601
Automated trajectory synthesis for hypersonic vehicles using energy management and variational calculus techniques p 210 A92-19061
A low-altitude breakthrough system using optimal path terrain following p 205 A92-20483
On the skip flight of a spaceplane
p 387 A92-25503
Target pitch angle for the microburst escape maneuver
[AIAA PAPER 92-0730] p 379 A92-27082
Trajectory shaping by the U-parameter design method
p 479 A92-29361
Energy-heading transients in atmospheric flight guidance for airbreathing hypersonic vehicles
[AIAA PAPER 91-5065] p 480 A92-31692
A second-order control optimization method for nonlinear dynamic systems and its use for calculating optimal aircraft trajectories p 460 A92-31894
Estimation of overall drag coefficient of an aerospace plane p 700 A92-41188
Parallel solver for trajectory optimization search directions p 777 A92-43399
Thrust laws for microburst wind shear penetration
p 873 A92-46750
Aircraft route optimization using adaptive simulated annealing p 922 A92-48565
Three-dimensional optimal reentry trajectory and aerodynamic heating history of the Space Shuttle
p 984 A92-49582
Terminal area traffic management
p 955 A92-50122
A fuel-optimal 4D guidance algorithm
p 978 A92-53095
An efficient algorithm for optimal aircraft trajectories
[AIAA PAPER 92-4412] p 1076 A92-55206
The application of direct transcription to commercial aircraft trajectory optimization
[AIAA PAPER 92-4528] p 1077 A92-55246
Optimal launch trajectory of a hypersonic research vehicle
[AIAA PAPER 92-4302] p 1103 A92-55310
Optimal recovery from microburst wind shear
[AIAA PAPER 92-4338] p 1078 A92-55327
Optimal trajectories for an unmanned air-vehicle in the horizontal plane
[AIAA PAPER 92-4344] p 1079 A92-55333
Rapid near-optimal aerospace plane trajectory generation and guidance
[NASA-CR-189469] p 205 N92-14066
Energy height method for flight path optimisation. Addendum A: Numerical method suitable for rapid use on IBM PC compatible computers
[ESDU-91016-ADD] p 272 N92-15987
Optimal aircraft performance during microburst encounter p 266 N92-17999
Trajectory optimization for the National Aerospace Plane
[NASA-CR-190355] p 650 N92-26017
Trajectory optimization for hypersonic aircraft guidance p 728 N92-27898
Optimal trajectories for an unmanned air vehicle
p 963 N92-31880
Proceedings of the 53rd Symposium on Air Vehicle Mission Control and Management
[AGARD-AR-310] p 1010 N92-32229

TRAJECTORY PLANNING
A calculating method of the kill probability attack area for AAM p 975 A92-50212
Cockpit weather information needs
p 449 N92-21503
Status of automatic guidance systems for rotorcraft in low altitude flight p 727 N92-27894
Knowledge-based planning for controlled airspace flight operation as part of a cockpit assistant
p 727 N92-27895
An efficient method for three-dimensional route planning with different strategies and constraints
p 728 N92-27901
Robust intelligent flight control for hypersonic vehicles
[NASA-CR-185680] p 746 N92-28209
A workstation-based evaluation of a far-field route planner for helicopters
[NASA-TM-102882] p 1051 N92-33609

TRANSATMOSPHERIC VEHICLES
Euler code evaluation of a transatmospheric vehicle at supersonic speeds p 9 A92-13202
Hypersonic flow simulations using DSMC (direct simulation Monte Carlo) p 323 A92-26216
Conceptual design of two-stage-to-orbit hybrid launch vehicle
[NASA-CR-190006] p 486 N92-20666

TRANSDUCERS
Fiber-optic position transducers for aircraft controls
p 857 A92-48041
Development of digital/optical rotary position transducer
[NAL-TR-1106] p 29 N92-10028
Thrust test fixture
[AD-D015259] p 983 N92-31192

TRANSFER FUNCTIONS
Robust pole assignment using closed loop controllability conditions p 49 A92-11417
Robust stabilization with positive real uncertainty - Beyond the small gain theorem p 50 A92-11444
On the Nyquist envelope of an interval plant family
p 507 A92-29132
Tiltrotor control law design for rotor loads alleviation using modern control techniques p 478 A92-29331
Trajectory shaping by the U-parameter design method
p 479 A92-29361
Application of the delta-operator in MIMO discrete-time adaptive flight control systems p 479 A92-29516
Identification of the transfer function between turbulence and aircraft p 743 A92-41226
Transfer function between airborne VLF transmit and receive loop antenna p 1045 A92-54754
MIMO state-feedback control system considering phase stability by -90 deg phase-locus method
p 1084 A92-56066
Parameter identification for nonlinear aerodynamic systems
[NASA-CR-188985] p 53 N92-10347
Approximate truncated balanced realizations for infinite dimensional systems p 602 N92-22493
Design of bearings for rotor systems based on stability
p 773 N92-27799

TRANSFER OF TRAINING
Development and integration of modern laboratories in aerospace education
[AIAA PAPER 92-4022] p 1141 A92-56844
The use of a dedicated testbed to evaluate simulator training effectiveness p 884 N92-28533
AM-X flight simulator from engineering tool to training device p 884 N92-28536
Assessment of army aviators' ability to perform individual and collective tasks in the aviation networked simulator
[AD-A250293] p 888 N92-29709

TRANSFER ORBITS
Aerobang - A new synergetic plane-change maneuver
[AAS PAPER 91-418] p 753 A92-43356
An alternative concept for aeroassisted orbit transfers
[AD-A243409] p 287 N92-17325

TRANSFORMATIONS (MATHEMATICS)
Decentralized-feedback pole placement of linear systems p 411 A92-27347
H-infinity synthesis using a bilinear pole shifting transform p 1007 A92-50490
Mass flux similarity for slotted transonic-wind-tunnel walls
[NASA-TM-4281] p 11 N92-10006

TRANSIENT HEATING
Stability of stiffened panels with allowance for plasticity under nonstationary heating and loading
p 493 A92-30152
Thermoviscoplastic response of thin plates subjected to intense local heating
[AIAA PAPER 92-2538] p 584 A92-34382

TRANSIENT LOADS
Dual mode shock absorber and method
[PATENT-1-265-541] p 115 N92-13055

TRANSIENT RESPONSE
Experiments on the blade loss transient response of rotor with flexible damped support
[ASME PAPER 91-GT-149] p 148 A92-15587
Nonlinear transient analysis of composite ATP blade model p 294 A92-23111
Effect of different force-functions and initial shock pressure on blade response p 374 A92-27913
Improved noise rejection in automatic carrier landing systems p 380 A92-28154
Heat induced transient behaviours of axial compressors p 469 A92-29721
The selection of bird impact load types --- on turbojet compressor and turbofan fan blades
p 448 A92-29732
Experimental investigation on blade loss transient response of rotor with flexible damped support
p 557 A92-35551
Nonlinear damping estimation from rotor stability data using time and frequency domain techniques
p 641 A92-36855
Steady state and quasi-transient analysis of aircraft hydraulic system with network theory
p 642 A92-37391
Optimal implicit model-following approach with frequency-shaped weighting and its application to design of flight control system p 977 A92-53094
Transient response of the rotor-support system of aeroengines p 997 A92-53293
Preliminary dynamic tests of a flight-type ejector
[AIAA PAPER 92-3261] p 1066 A92-54020
Electromechanical systems with transient high power response operating from a resonant AC link
[NASA-TM-105716] p 870 N92-28985
Nonlinear stability and control study of highly maneuverable high performance aircraft, phase 2
[NASA-CR-190667] p 978 N92-30922
Preliminary dynamic tests of a flight-type ejector
[NASA-TM-105814] p 972 N92-30998

TRANSITION FLOW
Computational investigation of circular-to-rectangular transition ducts
[AIAA PAPER 91-3342] p 6 A92-11605
Three-dimensional linear stability approach to transition on wings and bodies of revolution at incidence
p 172 A92-18361
Effects of gas-surface interaction models on aerodynamic characteristics p 244 A92-21718
Transition to turbulence in confined, compressible mixing layers. I - 3D numerical simulations with excitation of random, broadband white noise
[AIAA PAPER 92-0553] p 332 A92-26964
Use of finite volume schemes for transition simulation
p 432 A92-31185
The effects of wall suction on laminar-turbulent transition in three-dimensional flow p 522 A92-36021
Effect of controlled longitudinal vortex arrays on the development of a turbulent boundary layer
p 614 A92-38856
The natural and forced formation of spot-like Lambda-structures caused by vortex dislocations in a wake p 621 A92-40111
Transition to turbulence in curved channel flow
p 621 A92-40125
A new approach for the calculation of transitional flows
[AIAA PAPER 92-2669] p 798 A92-45524
Numerical method for predicting transition in three-dimensional flows by spatial amplification theory
p 812 A92-46886
Computational aerothermodynamic methods for industrial applications to re-entry and hypersonic cruise problems p 227 N92-15027
Applicability of bridging methods to hypersonic rarefied flow aerodynamics of reentry vehicles
p 184 N92-15032
Transitional flows around re-entry bodies
p 184 N92-15035
Hypersonic wakes
[ETN-92-91082] p 349 N92-19925
Aspects of unsteady blade-surface boundary layers and transition in axial turbomachines p 658 N92-24340
Laminar-turbulent transition process in the presence of simulated wall roughness p 626 N92-24858
Distributed acoustic receptivity in laminar flow control configurations
[NASA-CR-4438] p 765 N92-26680
Stability and transition of hypersonic boundary-layer flows
[AD-A250279] p 948 N92-31555

TRANSITION POINTS
Results of measured temperature distribution on an adiabatic wing model with radiation thermometer
[NAL-TM-610] p 261 N92-17755

TRANSLATIONAL MOTION
Analysis of slender bodies of revolution with curved-ground effect and waving-water effect
p 524 A92-36151
Motion of a sphere in a gas - Numerical solution of the linearized Boltzmann equation p 591 A92-36194

TRANSMISSION
The Air Force Manufacturing Technology (MANTECH): Technology transfer methodology as exemplified by the radar transmit/receive module program
p 593 N92-22451

TRANSMISSION EFFICIENCY
Mid-range UV communications --- ultraviolet radiation
[AD-D015213] p 770 N92-27615

TRANSMISSION LINES
Comparison of R2SPG waveforms with simulated EMP --- Repetitive Random Square-wave Pulse Generator
p 760 A92-42317
Efficiency of a 5V/5mW power by light power supply for avionics applications p 734 A92-42603

Methods for determining atmospheric correction for radio-rangefinder measurements of inclined trajectories
p 775 A92-44070
Suppression of radiating harmonics Electro-Impulse Deicing (EIDI) systems
[DOT/FAA/CT-TN90/33] p 405 N92-19764
A cable detection lidar system for helicopters
p 1001 N92-31068

TRANSMISSION LOSS
Observability under recurrent loss of data
p 302 A92-21191
Laboratory testing of a high transmission loss aircraft cabin structure p 663 A92-39229
Gas turbine exhaust system silencing design
p 882 A92-47365
Improvement in transmission loss of aircraft double wall with resonators p 1011 A92-53091

TRANSMISSIONS (MACHINE ELEMENTS)
Manufacturing techniques - Split torque path helicopter transmission p 110 A92-14452
Transmission overhaul and component replacement predictions using Weibull and renewal theory
p 155 A92-17201
Transmission vibration monitoring - A single board computer architecture p 554 A92-35765
Recent manufacturing advances for spiral bevel gears
[SAE PAPER 912229] p 674 A92-40024
Advanced Rotorcraft Transmission program summary
[AIAA PAPER 92-3363] p 905 A92-48936
Boeing Helicopters Advanced Rotorcraft Transmission (ART) Program summary of component tests
[AIAA PAPER 92-3364] p 905 A92-48937
Advanced Rotorcraft Transmission (ART) Program summary
[AIAA PAPER 92-3365] p 905 A92-48938
Advanced Rotorcraft Transmission (ART) - Component test results
[AIAA PAPER 92-3366] p 905 A92-48939
Analytical evaluation of resonant response of spiral bevel gears in the RAH-66 helicopter Fantail transmission
[AIAA PAPER 92-3495] p 906 A92-49031
Summary highlights of the Advanced Rotorcraft Transmission (ART) program
[AIAA PAPER 92-3362] p 1051 A92-54026
Modal simulation of gearbox vibration with experimental correlation
[AIAA PAPER 92-3494] p 1112 A92-54036
Design and development of test rigs for main rotor and main rotor transmission of a helicopter in the 6-ton-class
p 1093 A92-56280
CH-46 and OH-58 transmission stress wave analysis
[AD-A244321] p 365 N92-18826
Rotorcraft transmissions p 560 N92-22533
Advanced Rotorcraft Transmission (ART) program summary
[NASA-TM-105665] p 680 N92-24984
Flat belt continuously variable high speed drive
[DE92-008952] p 680 N92-25054
Gear tooth stress measurements of two helicopter planetary stages
[NASA-TM-105651] p 764 N92-26555
Full-scale transmission testing to evaluate advanced lubricants
[NASA-TM-105668] p 764 N92-26560
Analysis and modification of a single-mesh gear fatigue rig for use in diagnostic studies
[NASA-TM-105416] p 773 N92-27879
Application of face-gear drives in helicopter transmissions
[NASA-TM-105655] p 908 N92-28434
Dynamics of a split torque helicopter transmission
[NASA-TM-105681] p 910 N92-29136
Development of a full-scale transmission testing procedure to evaluate advanced lubricants
[NASA-TP-3265] p 998 N92-30396
Experimental testing of prototype face gears for helicopter transmissions
[NASA-TM-105434] p 1002 N92-31349
Modal simulation of gearbox vibration with experimental correlation
[NASA-TM-105702] p 1002 N92-31485

TRANSMISSOMETERS
Visibility measurements for the Automated Surface Observing System (ASOS) p 468 A92-32095
Trial of a slant visual range measuring device
p 1000 N92-31043

TRANSMITTERS
The Air Force Manufacturing Technology (MANTECH): Technology transfer methodology as exemplified by the radar transmit/receive module program
p 593 N92-22451
Mid-range UV communications --- ultraviolet radiation
[AD-D015213] p 770 N92-27615

TRANSOCEANIC FLIGHT
Design of a trans-global manned balloon system with relevance to scientific ballooning
[AIAA PAPER 91-3687] p 15 A92-11030
China-Soviet long duration balloon flight project
[AIAA PAPER 91-3678] p 1 A92-11036
The technological revolution in oceanic air traffic control p 531 A92-33431
Halfway around the world is far enough
p 516 A92-33462
Experiments on aeronautical satellite communications using ETS-V satellite p 639 A92-40187
Receiver Autonomous Integrity Monitoring (RAIM) capability for sole-means GPS navigation in the oceanic phase of flight p 956 A92-51012

TRANSONIC COMPRESSORS
A viscous flow study of shock-boundary layer interaction, radial transport, and wake development in a transonic compressor
[ASME PAPER 91-GT-69] p 68 A92-15539
Validation of a numerical method for unsteady flow calculations
[ASME PAPER 91-GT-271] p 151 A92-15668
Inlet flow angle determination of transonic compressor cascades
[ASME PAPER 91-GT-274] p 75 A92-15671
Analysis of transonic flow over plane compressor cascades using the large-particle method
p 79 A92-16812
Calculation of 3D flow field in a single transonic compressor stage p 422 A92-29719
Wind-tunnel compressor stall monitoring using neural networks p 918 A92-46817
Design of transonic compressor cascades using hodograph method p 202 N92-13973
The research progress on Hodograph Method of aerodynamic design at Tsinghua University
p 177 N92-13974
A critical evaluation of a three-dimensional Navier-Stokes method as a tool to calculate transonic flows inside a low-aspect-ratio compressor
p 768 N92-27459
On the computation of unsteady turbomachinery flows. Part 1: Euler equations in vibrating cascades
p 768 N92-27460
Application of CFD in the design of gas turbine engine components p 741 N92-27461
Numerical simulation of turbomachinery flows with advanced turbulence models p 1124 N92-32270

TRANSONIC FLIGHT
Aerodynamic and acoustic calculations of transonic nonlifting hovering rotors
[ONERA, TP NO. 1991-178] p 77 A92-16140
An investigation on detached shock waves ahead of bodies of revolution at transonic speeds
p 251 A92-23381
Aerodynamic computations of high-speed transonic propellers
[ONERA, TP NO. 1991-218] p 330 A92-26370
An inverse method for the design of transonic wings
[AIAA PAPER 92-1025] p 517 A92-33206
Aero-structural integrated design of forward swept wing
[SAE PAPER 912021] p 790 A92-45414
FALKE and COBRA technology development in aerodynamics and aerothermodynamics
p 183 N92-15017
Inviscid drag prediction for transonic transport wings using a full-potential method
[NLR-TP-89365-U] p 444 N92-20473
Adaptive active flutter suppression of wings in subsonic and transonic flight regimes p 553 N92-24010
An experimental study of the flow over a sharp-edged delta wing at subsonic and transonic speeds
[NLR-TP-91117-U] p 1037 N92-32732
Flutter in the transonic flight regime
p 1089 N92-34167

TRANSONIC FLOW
The just attached shock-wave at the leading edge of a profile p 3 A92-10663
Finite element solutions of the Euler equations for transonic external flows p 5 A92-11063
Computation of steady and unsteady control surface loads in transonic flow p 5 A92-11066
An efficient method for calculating three-dimensional transonic flow past air intakes p 7 A92-12178
Solution of the Reynolds-averaged Navier-Stokes equations for transonic aerofoil flows p 9 A92-13198
Two-dimensional adaptive-wall tests in the NASA Ames two- by two-foot transonic wind tunnel
p 30 A92-13201
Wall interference assessment/correction for transonic airfoil data p 30 A92-13214
Disturbance of transonic wind tunnel flow by a slot in the tunnel wall p 135 A92-13675
Design method for subsonic and transonic cascade with prescribed Mach number distribution
[ASME PAPER 91-GT-18] p 67 A92-15509
Inviscid-viscous coupled solution for unsteady flows through vibrating blades. II - Computational results
[ASME PAPER 91-GT-126] p 71 A92-15571
Analysis and prediction of transonic turbine blade losses
[ASME PAPER 91-GT-183] p 73 A92-15615
Euler flow predictions for an oscillating cascade using a high resolution wave-split scheme
[ASME PAPER 91-GT-198] p 74 A92-15623
Unsteady Navier-Stokes simulation of transonic cascade flow using an unfactored implicit upwind relaxation scheme with inner iterations
[ASME PAPER 91-GT-223] p 74 A92-15637
Transonic and supersonic inviscid computations in cascades using adaptive unstructured meshes
[ASME PAPER 91-GT-312] p 75 A92-15689
Transonic cascade flow prediction using the Navier-Stokes equations
[ASME PAPER 91-GT-313] p 76 A92-15690
Aerodynamic measuring techniques for transonic and supersonic flow in cascades and turbomachines
[ONERA, TP NO. 1991-170] p 137 A92-16135
Asymptotics of the upper branch of the neutral curve at subsonic and transonic external flow velocities
p 79 A92-16705
Analysis of transonic flow over plane compressor cascades using the large-particle method
p 79 A92-16812
Euler flow analysis of turbine powered simulator and fanjet engine p 80 A92-17196
Numerical study on using sulfur hexafluoride as a wind tunnel test gas p 216 A92-18373
Three-dimensional calculation of low-frequency unsteady transonic flow in axial turbine stages
p 174 A92-19110
Direct-inverse transonic wing-design method in curvilinear coordinates including viscous interaction
p 193 A92-20202
Inviscid drag prediction for transonic transport wings using a full-potential method p 174 A92-20212
Evaluation of Euler solvers for transonic wing-fuselage geometries p 174 A92-20214
Sonic eddy - A model for compressible turbulence
p 176 A92-20739
Concerning the functional solution of transonic flows
p 243 A92-21318
Navier-Stokes code development for transonic flow simulations p 246 A92-21985
A fast viscous correction method for transonic aerodynamics p 247 A92-21986
Development and application of a particle image velocimeter for high-speed flows
[AIAA PAPER 92-0004] p 292 A92-22129
Nonequilibrium algebraic turbulence modeling considerations for transonic airfoils and wings
[AIAA PAPER 92-0026] p 248 A92-22148
An AF3 algorithm for the calculation of transonic nonconservative full potential flow around axisymmetric inlet cowls p 251 A92-23380
Computation of transonic flow over an airfoil at large Reynolds numbers p 252 A92-23414
The Baldwin-Lomax model for separated and wake flows using the entropy envelope concept
[AIAA PAPER 92-0148] p 253 A92-23764
An algorithm for predicting the flow past fuselage-mounted engine arrangements
[AIAA PAPER 92-0151] p 253 A92-23766
Prediction of drag at subsonic and transonic speeds using Euler methods
[AIAA PAPER 92-0169] p 255 A92-23780
Measurements of lateral aerodynamics characteristics of forebodies at high angle of attack in subsonic and transonic flows
[AIAA PAPER 92-0174] p 255 A92-23785
Comparison of two Navier-Stokes codes for attached transonic wing flows p 309 A92-24414
Design of turbomachinery blading in transonic flows by the circulation method p 311 A92-24725
Application of special series for studying nonstationary transonic gas flows p 311 A92-24904
Finite element method for computing nonisentropic potential transonic flow with shock waves
p 312 A92-25009
Analysis of transonic flow past an axisymmetric convex corner p 312 A92-25015
Numerical simulations of flow fields over aircrafts
p 313 A92-25042
A numerical method for unsteady transonic flow about wings with control surface p 314 A92-25107
A new method for solving the kernel equations of transonic flows - An auxiliary kernel method
p 410 A92-25108

Recent progress in finite element method and boundary integral equation method for nonviscous transonic flows p 314 A92-25127
Time marching integral equation method for the solutions of unsteady transonic flows p 314 A92-25129
On the sensitivity of transonic flow p 315 A92-25132
The lateral shock wave family on the surface of a cone-cylinder in transonic flowfield p 315 A92-25136
The study of inverse boundary layer algorithm for transonic flows over aerofoils p 315 A92-25140
Experimental studies of a two-element airfoil with large separation
[AIAA PAPER 92-0267] p 317 A92-25723
Calculation of the carriage loads of tandem stores on a fighter aircraft
[AIAA PAPER 92-0283] p 319 A92-25736
Non-planar wing design by Navier-Stokes inverse computation
[AIAA PAPER 92-0285] p 319 A92-25738
An approach to the design of wings - The role of mathematics, physics and economics
[AIAA PAPER 92-0286] p 319 A92-25739
An efficient Euler solver for predominantly supersonic flows with embedded subsonic pockets
[AIAA PAPER 92-0323] p 322 A92-25770
The effect of blade solidity on the aerodynamic loss of a transonic turbine cascade
[AIAA PAPER 92-0393] p 323 A92-26248
Low aspect ratio wing code validation experiment
[AIAA PAPER 92-0402] p 324 A92-26255
Numerical investigation of unsteady transonic nozzle flows p 331 A92-26443
Multibody interference at transonic Mach numbers
[AIAA PAPER 92-0651] p 334 A92-27023
Boundary singularities in steady potential compressible flow through plane two-dimensional channels p 336 A92-27384
The computation of transonic viscous flow p 338 A92-27831
Estimation of propulsion-induced effects on transonic flows over a hypersonic configuration
[AIAA PAPER 92-0523] p 341 A92-28197
Calculation of three-dimensional transonic turbine cascade flow p 344 A92-28519
Navier-Stokes solution of transonic cascade flows using nonperiodic C-type grids p 344 A92-28523
Computations of a transonic flow about an airfoil in a wind tunnel with porous walls p 423 A92-30128
Bodies of revolution with minimal wave drag at transonic gas flow velocities p 424 A92-30135
Reducing the background noise level in the test section of a wind tunnel for transonic flow velocities p 511 A92-30143
Development of a method for calculating the effect of the propeller slipstream on transonic flow over the wing p 424 A92-30144
An experimental study of transonic flow of a gas past wedges p 424 A92-30153
An asymptotic transonic theory and optimal porosity of wind tunnel walls at M greater than about 1 p 425 A92-30159
Theoretical analysis of the effect of the porous walls of a wind tunnel on transonic flow past bodies of cone-cylinder type p 427 A92-30202
Asymptotic form of the lower branch of the neutral curve in a transonic boundary layer p 427 A92-30204
High angle of attack aerodynamics - Subsonic, transonic, and supersonic flows --- Book
[ISBN 0-387-97672-8] p 431 A92-30850
Time marching integral equation method for unsteady transonic flows around airfoils p 433 A92-31489
Improving the convergence rate of the Petrov-Galerkin techniques for the solution of transonic and supersonic flows p 434 A92-31495
Calculation of three-dimensional separated flows in the framework of the unsteady Euler equations p 438 A92-31870
Computational studies of transonic flow past a swept wing and the boundary layer characteristics p 438 A92-31872
Characteristics of transonic flow past a configuration comprising a wing and a fuselage with a large midsection ratio p 439 A92-31882
Some characteristics of transonic flow past an airfoil in the case of developed separation p 440 A92-31885
Aerodynamic effect of compression shocks on an oscillating aileron in transonic flow p 440 A92-31898
A shock and an expansion wave in transonic flow p 440 A92-31961
Numerical computation of improved transonic potential method p 441 A92-32234
A numerical solution of inviscid transonic flow using the Boltzmann equation p 443 A92-32504
Three-dimensional flow visualization of shock wave using double-pulsed holographic interferometry. II - Flow visualization for three-dimensional shock structures in rotating aeroengine fan blade rows p 497 A92-32507
Unsteady transonic Euler solutions using finite elements
[AIAA PAPER 92-2504] p 518 A92-34499
A direct-problem calculation method for gas turbines with bowed and twisted blades p 519 A92-35571
An investigation of cascade flutter using a two-dimensional full-potential solver
[AIAA PAPER 92-2119] p 558 A92-35688
Finite element Euler calculations of unsteady transonic cascade flows
[AIAA PAPER 92-2120] p 520 A92-35689
A new method for transonic static aeroelasticity problems
[AIAA PAPER 92-2123] p 589 A92-35691
Trends of research on cascade flutter p 558 A92-35914
Numerical studies of transverse curvature effects on transonic flow stability p 524 A92-36186
Compressible turbulent boundary layers with heat addition by homogeneous condensation p 611 A92-36843
The numerical simulation of transonic inviscid flow over oscillating airfoils p 616 A92-38918
Numerical predictions of transonic viscous flows around aerofoils through an Euler/boundary layer interaction method p 624 A92-40600
Subsonic and transonic low-Reynolds-number airfoils with reduced pitching moments p 701 A92-41211
Transonic Navier-Stokes computations for an oscillating wing using zonal grids p 701 A92-41217
Transonic aeroelasticity analysis for rotor blades p 758 A92-41238
A validated code to predict the performance of onboard broadband optical seekers through a turbulent transonic flow
[AIAA PAPER 92-2792] p 778 A92-41331
Similarity and resistance in near-sonic flows for given heat conduction p 708 A92-43065
Calculation of transonic flow in turbomachine cascades p 708 A92-43067
Transonic visualization test for the airframe shape improvement of a spaceplane p 752 A92-43200
Buffeting characteristics of a transonic airfoil p 711 A92-43202
Navier-Stokes solutions of transonic nozzle flow with shock-induced flow separations p 713 A92-44515
Prediction and measurement of jet flowfield features for ASTOVL aircraft p 787 A92-45318
An economic approach to accurate wing design
[SAE PAPER 912008] p 789 A92-45408
Effect of canard deflection on close-coupled canard-wing-body aerodynamics
[AIAA PAPER 92-2602] p 792 A92-45479
An improved approach for the computation of transonic/supersonic flows with applications to aerospace configurations
[AIAA PAPER 92-2613] p 793 A92-45487
Three-dimensional orthogonal-to-surface structured grid generation with transonic Navier-Stokes flow solutions for a commercial transport configuration
[AIAA PAPER 92-2616] p 793 A92-45490
Application of an unstructured Navier-Stokes solver to multi-element airfoils operating at transonic maneuver conditions
[AIAA PAPER 92-2638] p 796 A92-45507
The subsonic and transonic flow around the leading edge of a thin airfoil with a parabolic nose
[AIAA PAPER 92-2649] p 797 A92-45516
Transonic airfoil and wing design using Navier-Stokes codes
[AIAA PAPER 92-2651] p 797 A92-45518
Recent CFD applications on jet transport configurations
[AIAA PAPER 92-2658] p 844 A92-45519
Investigation of solution operators for the three-dimensional Euler equations
[AIAA PAPER 92-2666] p 797 A92-45522
An unfactored implicit scheme for 3D inviscid transonic flows
[AIAA PAPER 92-2668] p 798 A92-45523
Transonic unsteady inviscid and viscous flow's simulation around 2-D moving bodies
[AIAA PAPER 92-2704] p 801 A92-45546
Time accurate computation of unsteady transonic flows around an airfoil with oscillating flap on dynamic grid
[AIAA PAPER 92-2733] p 805 A92-45567
Prediction of the viscous transonic aerodynamic performance of supercritical aerofoil sections
[AIAA PAPER 92-2653] p 805 A92-45569
Transonic calculations for wings with deflected control surfaces
[AIAA PAPER 92-2617] p 805 A92-45572
Smooth solutions for transonic gasdynamic equations --- Russian book
[ISBN 5-02-029345-8] p 809 A92-46626
Simulation of transonic flow over twin-jet transport aircraft p 811 A92-46793
Design load predictions on a fighter-like aircraft wing p 811 A92-46797
The application of particle image velocimetry (PIV) in a short-duration transonic annular turbine cascade
[ASME PAPER 91-GT-221] p 899 A92-46825
Compact higher order characteristic-based Euler solver for unstructured grids p 812 A92-46889
Effect of model cooling on periodic transonic flow p 813 A92-46900
Numerical simulation of multizone two-dimensional transonic flows using the full Navier-Stokes equations p 815 A92-46955
Mesh adaption for 2D transsonic Euler flows on unstructured meshes p 816 A92-47038
Mesh adaptivity with the quadtree method p 816 A92-47041
3-D numerical grid generation for the transonic flow analysis about multi-bodies p 817 A92-47061
A finite difference solution of the Euler equations on non-body-fitted Cartesian grids p 818 A92-47153
Numerical computations of transonic flows through cascades
[AIAA PAPER 92-3041] p 822 A92-48702
A higher-order accurate Navier-Stokes solver for transonic and supersonic flows in turbomachinery
[AIAA PAPER 92-3044] p 822 A92-48704
Navier-Stokes investigation of a transonic centrifugal compressor stage using an algebraic Reynolds stress model
[AIAA PAPER 92-3311] p 825 A92-48897
Critical Mach number estimates for dense gases p 933 A92-49498
Transonic flow calculation of Euler equations by implicit iterating scheme with flux splitting p 934 A92-50215
Transonic flows of Bethe-Zel'dovich-Thompson fluids p 935 A92-50293
Comparison of transonic flow models p 936 A92-50325
A general explicit or semi-explicit algorithm for compressible and incompressible flows p 937 A92-52682
Solution of Euler equations with unstructured mesh - 3-D case p 941 A92-52973
Measurement of turbulent boundary layer in transonic flow p 941 A92-53010
Calculation of the transonic full-potential flowfield about 3D fuselage p 941 A92-53021
Hot-wire measurements in turbulent transonic flows p 941 A92-53078
A penalty-Galerkin finite element method for calculating transonic flow over wings p 943 A92-53386
The behaviour of the pressure temperature and density in an inviscid unsteady transonic axisymmetric flow with shock waves p 1018 A92-53553
Navier-Stokes simulation for the winged space vehicle 'HOPE' at subsonic, transonic, and supersonic regimes p 1018 A92-53559
A double chaotic attractor in transonic flow p 1019 A92-53561
Nonintrusive measurements in fluid dynamic flows from Mach .0005 to 14 p 1090 A92-54311
Efficient iterative methods for the transonic small disturbance equation p 1025 A92-54933
Navier-Stokes computations for oscillating control surfaces
[AIAA PAPER 92-4431] p 1026 A92-55355
Understanding and development of a prediction method of transonic limit cycle oscillation characteristics of fighter aircraft
[AIAA PAPER 92-4501] p 1026 A92-55369
Unsteady shock-vortex interaction on a flexible delta wing p 1030 A92-56157
Navier-Stokes simulation of a close-coupled canard-wing-body configuration p 1031 A92-56163
Euler/experiment correlation of a generic fighter p 1031 A92-56164
Improved calculation of transonic potential flow past swept wings p 1031 A92-56179
Numerical modeling of transonic juncture flow
[AIAA PAPER 92-4036] p 1035 A92-56858
Recent advances on a finite element algorithm for computational aerodynamics: Transonics-hypersonics
[DE91-018176] p 11 N92-10010
Three dimensional numerical method for resolving small transonic perturbations in unstructured mesh
[ONERA-RT-56/3064-RY-006-R] p 13 N92-10989
Control aspects of the transition from transversal to transonic flow, step effects
[ETN-91-90106] p 82 N92-11981
Vortical flow simulation by using structured and unstructured grids p 83 N92-12999

Nonequilibrium turbulence modeling effects on transonic vortical flows about delta wings p 85 N92-13007
An experimental study of the flow over a sharp-edged delta wing at subsonic and transonic speeds p 85 N92-13011
Navier-Stokes calculation of transonic flow past the NTF 65 deg delta wing p 91 N92-13868
Aerodynamic aircraft design methods and their notable applications: Survey of the activity in Japan p 193 N92-13930
A comparison of two closely-related approaches to aerodynamic design optimization p 193 N92-13933
Variational formulation of hybrid problems for fully 3-D transonic flow with shocks in rotor p 176 N92-13953
Analysis and design of transonic airfoils using streamwise coordinates p 194 N92-13955
Research on inverse methods and optimization in Italy p 202 N92-13956
Design optimization of transonic airfoils p 177 N92-13961
An inverse method with regularity condition for transonic airfoil design p 177 N92-13969
The research progress on Hodograph Method of aerodynamic design at Tsinghua University p 177 N92-13974
Transonic Navier-Stokes computations for a spinning body of revolution
[AD-A241015] p 180 N92-14972
Preliminary investigation of the shock-boundary layer interaction in a simulated fan passage
[AD-A242656] p 185 N92-15045
A method of estimating a flow breakdown boundary for aerofoils and swept wings in transonic flows
[ESDU-91021] p 258 N92-15970
Experiments and analysis concerning the use of external burning to reduce aerospace vehicle transonic drag
[NASA-TM-105397] p 279 N92-17546
Results of measured temperature distribution on an adiabatic wing model with radiation thermometer
[NAL-TM-610] p 261 N92-17755
Thermal nonequilibrium effects on turbine cascade aerodynamics
[AD-A244049] p 404 N92-19183
An initial investigation into methods of computing transonic aerodynamic sensitivity coefficients
[NASA-CR-190040] p 348 N92-19545
Drag prediction using computation methods
[ONERA-RSF-82/1685-AY-154-4] p 349 N92-19682
Quality assessment of two- and three-dimensional unstructured meshes and validation of an upwind Euler flow solver
[NASA-TM-104215] p 444 N92-20480
Numerical simulation of vortical flow over a delta wing at subsonic and transonic speeds
[NLR-TP-90029-U] p 444 N92-20498
Current status of computational methods for transonic unsteady aerodynamics and aeroelastic applications
[NASA-TM-104191] p 446 N92-21432
Two-dimensional transonic flow calculation by interaction of Euler and boundary layer equations
[PB92-136449] p 448 N92-21784
The NASA Langley laminar-flow-control experiment on a swept, supercritical airfoil: Evaluation of initial perforated configuration
[NASA-TM-4309] p 525 N92-22196
Efficient and robust design optimization of transonic airfoils p 528 N92-23717
Adaptive active flutter suppression of wings in subsonic and transonic flight regimes p 553 N92-24010
A user guide for the EMTAC-MZ CFD code
[NASA-CR-4283] p 678 N92-24242
An incremental strategy for calculating consistent discrete CFD sensitivity derivatives
[NASA-TM-104207] p 625 N92-24681
A scheme for two dimensional Euler and boundary layer interactive solutions p 627 N92-24860
Nonunique solutions in unsteady transonic flow p 629 N92-24872
Algorithm and code development for unsteady three-dimensional Navier-Stokes equations
[NASA-CR-190077] p 692 N92-25264
On a multi-block method for transonic turbulent flows past a wing-fuselage configuration p 632 N92-25569
Measurements of fluctuating pressure in a rectangular cavity in transonic flow at high Reynolds numbers
[NASA-TM-4363] p 633 N92-25752
Development of new flux splitting schemes --- computational fluid dynamics algorithms p 682 N92-25809
An outline of a numerical scheme for calculating two-dimensional time linearised transonic flow using the Green's function method
[AD-A246349] p 764 N92-26258
A critical evaluation of a three-dimensional Navier-Stokes method as a tool to calculate transonic flows inside a low-aspect-ratio compressor p 768 N92-27459
Predictions and measurements of 3D viscous flow in a transonic turbine nozzle guide vane row p 741 N92-27466
Modeling of heavy-gas effects on airfoil flows
[NASA-CR-190357] p 716 N92-27558
Special Course on Unstructured Grid Methods for Advection Dominated Flows
[AGARD-R-787] p 771 N92-27671
Transonic Unsteady Aerodynamics and Aeroelasticity
[AGARD-CP-507] p 718 N92-27936
Current status of computational methods for transonic unsteady aerodynamics and aeroelastic applications p 718 N92-27937
Unsteady aerodynamics for aeroelasticity at the Flight Dynamics Directorate p 718 N92-27939
A time-linearization approach for unsteady transonic flows p 719 N92-27941
A boundary integral formulation for unsteady transonic potential flows p 719 N92-27942
Computation of the unsteady transonic 2D cascade flow by an Euler algorithm with interactive grid generation p 719 N92-27944
Evaluation of an unsteady implicit Euler code against two and three-dimensional standard configurations p 719 N92-27945
Unsteady transonic aerodynamics of pointed bodies of revolution in supersonic freestream p 719 N92-27946
NLR inviscid transonic unsteady loads prediction methods in aeroelasticity p 720 N92-27947
Computation of viscous phenomena in unsteady transonic flow p 720 N92-27949
Transonic aeroelastic calculations in both the time and frequency domains p 720 N92-27950
Analysis of unsteady aerodynamic and flutter characteristics of an aeroelastic model in transonic flow p 720 N92-27953
Transonic aeroelastic computations on wings using Navier-Stokes equations p 721 N92-27957
Further investigation of the effect of model cooling on periodic transonic flow p 721 N92-27961
NACA0012 airfoil data corrected for sidewall boundary-layer effects in the NAL two-dimensional transonic wind tunnel
[NAL-TM-640T] p 722 N92-28151
Force measurements on AGARD calibration model-B at transonic speeds in the NAL two-dimensional wind tunnel
[NAL-TM-639] p 722 N92-28190
Calculation of unsteady transonic flows with mild separation by viscous-inviscid interaction
[NASA-TP-3197] p 827 N92-28477
Analysis of results of an Euler-equation method applied to leading-edge vortex flow
[NLR-TP-90368-U] p 827 N92-28657
Wave drag determination in the transonic full-potential flow code MATRICS
[NLR-TP-90062-U] p 828 N92-28709
Explicit Navier-Stokes computation of turbomachinery flows
[AD-A249284] p 909 N92-28879
Turbulent spot generation and growth rates in a transonic boundary layer
[AD-A250221] p 909 N92-29118
Development of a multigrid transonic potential flow code for cascades
[NASA-CR-190480] p 830 N92-29361
Determination of aerodynamic sensitivity coefficients for wings in transonic flow
[NASA-CR-190570] p 832 N92-29657
Progress in unstructured-grid methods development for unsteady aerodynamic applications
[NASA-TM-107643] p 944 N92-30393
Computation of unsteady transonic flows using an implicit centered Euler solver without artificial viscosity
[ESA-TT-1235] p 944 N92-30514
A gridless Euler/Navier-Stokes solution algorithm for complex two-dimensional applications
[NASA-TM-107631] p 944 N92-30570
Implicit upwind-Euler solution algorithms for unstructured-grid applications
[NASA-TM-107645] p 945 N92-30691
Application of the Chimera overlapped grid scheme to simulation of Space Shuttle ascent flows p 945 N92-30742
Automatic design of transonic airfoils to reduce the shock induced pressure drag p 949 N92-31863
An examination of several high resolution schemes applied to complex problems in high speed flows
[AD-A250814] p 1124 N92-32632
Research on some centered implicit methods for calculating transonic flows by solving Navier-Stokes equations
[ONERA-RSF-24/1408-AY-150A] p 1037 N92-32773
Flutter in the transonic flight regime p 1089 N92-34167

TRANSONIC FLUTTER

The position of the unsteady flow computation in the compressor and turbine design and analysis process
[AIAA PAPER 92-0015] p 278 A92-22137
Effect of shock waves on the critical rate of bending-torsional flutter of an airfoil p 494 A92-30208
NACA 0012 benchmark model experimental flutter results with unsteady pressure distributions
[AIAA PAPER 92-2396] p 517 A92-34469
Further investigations of the aeroelastic behavior of the AFW wind-tunnel model using transonic small disturbance theory
[AIAA PAPER 92-2082] p 565 A92-35654
Multifunction tests of a frequency domain based flutter suppression system
[AIAA PAPER 92-2096] p 566 A92-35667
A flutter suppression system using strain gages applied to Active Flexible Wing Technology - Design and test
[AIAA PAPER 92-2098] p 566 A92-35669
New time-domain technique for flutter boundary identification
[AIAA PAPER 92-2102] p 588 A92-35673
Finite element Euler calculations of unsteady transonic cascade flows
[AIAA PAPER 92-2120] p 520 A92-35689
Role of shock dynamics in transonic flutter
[AIAA PAPER 92-2121] p 520 A92-35690
Transonic wind tunnel tests of flutter suppression equipment (Wing response data processing) p 748 A92-43136
Aeroelastic effects of spoiler surfaces on a low-aspect-ratio rectangular wing p 1030 A92-56154
Planform curvature effects on flutter characteristics of a wing with 56 deg leading-edge sweep and panel aspect ratio of 1.14
[NASA-TP-3116] p 115 N92-13054
Technical activities of the configuration aeroelasticity branch
[NASA-TM-104146] p 159 N92-13458
Current status of computational methods for transonic unsteady aerodynamics and aeroelastic applications
[NASA-TM-104191] p 446 N92-21432
Nonliner aspects of transonic aeroelasticity p 628 N92-24864
Prediction and analysis of wing flutter at transonic speeds p 662 N92-25555
Current status of computational methods for transonic unsteady aerodynamics and aeroelastic applications p 718 N92-27937
NLR inviscid transonic unsteady loads prediction methods in aeroelasticity p 720 N92-27947
Pressure measurements on a rectangular wing with a NACA0012 airfoil during conventional flutter
[NASA-TM-104211] p 1042 N92-34147

TRANSONIC NOZZLES

Numerical investigation of unsteady transonic nozzle flows p 331 A92-26443
Navier-Stokes solutions of transonic nozzle flow with shock-induced flow separations p 713 A92-44515

TRANSONIC SPEED

An experimental study of the flow past spheres at transonic speeds and high Reynolds numbers p 312 A92-25002
The relationship between the weight and flight characteristics of a transonic aircraft p 731 A92-43189
Application of the Euler method EUFLEX to a fighter-type airplane configuration at transonic speed
[AIAA PAPER 92-2620] p 845 A92-45573
Experimental investigation of the parallel vortex-airfoil interaction at transonic speeds p 813 A92-46901
Discussion of improved transonic potential method p 942 A92-53290
Investigation of the aeroelastic stability of the AFW wind-tunnel model using CAP-TSD
[NASA-TM-104142] p 81 N92-11977
Further investigations of the aeroelastic behavior of the AFW wind-tunnel model using transonic small disturbance theory
[NASA-TM-107576] p 526 N92-22240
Flow field over the wing of a delta-wing fighter model with vortex control devices at Mach 0.6 to 1.2
[NASA-TM-4296] p 526 N92-22506
Prediction and analysis of wing flutter at transonic speeds p 662 N92-25555
Measurements of fluctuating pressure in a rectangular cavity in transonic flow at high Reynolds numbers
[NASA-TM-4363] p 633 N92-25752

High-alpha vortex decoupling investigations on a chine forebody/Delta wing configuration at transonic Mach numbers
[NASA-CR-189642] p 715 N92-26651
Boundary layer transition: Prediction, application to drag reduction p 717 N92-27711
Development of a method to predict transonic limit cycle oscillation characteristics of fighter aircraft
p 746 N92-27958

TRANSONIC WIND TUNNELS
Automation of the measurement process in the N2 wind tunnel with the SPITA N-3 system p 30 A92-12347
Two-dimensional adaptive-wall tests in the NASA Ames two- by two-foot transonic wind tunnel
p 30 A92-13201
Recent rotorcraft aeroelastic testing in the Langley Transonic Dynamics Tunnel p 136 A92-14377
Study on transonic cascade performance by use of newly built facility p 136 A92-15328
High speed wind tunnel wall interference research progress at Nanjing Aeronautical Institute
p 136 A92-15338
Influences of wind tunnel parameters on airfoil characteristics at high subsonic speeds
p 173 A92-18769
Wall interference calculation in a transonic test section including simulation of discrete slots
[AIAA PAPER 92-0032] p 249 A92-22153
Modeling the ventilated wind tunnel wall
[AIAA PAPER 92-0035] p 249 A92-22156
Wind tunnel boundary interference prediction and correction
[AIAA PAPER 92-0036] p 249 A92-22157
Experimental study of pylon geometries for transport aircraft
[AIAA PAPER 92-0153] p 271 A92-23768
Future experimental needs to support applied aerodynamics - A transonic perspective
[AIAA PAPER 92-0156] p 254 A92-23771
Experimental necessities for subsonic transport configuration development
[AIAA PAPER 92-0158] p 254 A92-23773
Experiments to evaluate hot-jet simulation capabilities in Cryogenic Wind-Tunnel testing
[AIAA PAPER 92-0567] p 384 A92-26975
The dimensional reconstruction of vortex cross-section images p 339 A92-27833
Experimental investigation of the perpendicular rotor blade-vortex interaction at transonic speeds
p 340 A92-28047
Reducing the background noise level in the test section of a wind tunnel for transonic flow velocities
p 511 A92-30143
Theoretical analysis of the effect of the porous walls of a wind tunnel on transonic flow past bodies of cone-cylinder type p 427 A92-30202
The Bauer-Garabedian-Korn airfoil test in a two-dimensional wind tunnel p 429 A92-30532
Experimental investigation of the air bypass effect in the shock-wave region on the aerodynamic characteristics of a wing profile p 439 A92-31877
Investigation of the aerodynamic features of flows past models using thin-film capacitance-type sensors of pressure oscillations p 440 A92-31884
Further investigations of the aeroelastic behavior of the AFW wind-tunnel model using transonic small disturbance theory
[AIAA PAPER 92-2082] p 565 A92-35654
Transonic wind tunnel investigation of limit cycle oscillations on fighter type wings - Update
[AIAA PAPER 92-2125] p 572 A92-35692
Experimental investigation on reducing fluctuating pressures of launch vehicles by passive shock-wave/boundary-layer control p 616 A92-38916
Some problems on the sidewall interference in two-dimensional subsonic and transonic wind tunnel testing p 747 A92-41929
Transonic wind tunnel tests of flutter suppression equipment (Wing response data processing)
p 748 A92-43136
Wing test at the cryogenic wind tunnel of the National Defense Academy p 749 A92-43199
BGK airfoil oil flow test in a two-dimensional transonic wind tunnel p 711 A92-43201
On the measurement of subsonic flow around an appended body of revolution at cryogenic conditions in the NTF p 880 A92-45265
Calibration-related pseudo-Reynolds number trends in transonic wind tunnels p 882 A92-46780
The numerical simulation of flow about installed aero engine nacelle using a finite element Euler solver on unstructured meshes p 941 A92-52848
Aerodynamic assessment of an optical pressure measurement system (OPMS) by comparison with conventional pressure measurements in a high speed wind tunnel p 1114 A92-54304
Recent developments in data acquisition and control systems at the Aircraft Research Association Limited
p 1091 A92-54323
Shock detection on airfoils by means of piezo foil- and hot film arrays p 1115 A92-54334
Application of a wall pressure method in a wind tunnel test section with adjustable longitudinal slots
p 1091 A92-54336
On the structure of unsteady shock induced separation of the transonic airfoil in the NAL two-dimensional wind tunnel p 1029 A92-56010
Evaluation of sidewall interference in the NAL two-dimensional transonic wind tunnel
p 1092 A92-56011
The research of reducing 3-D low supersonic shock wave reflection in a 2-D transonic flexible walls adaptive wind tunnel
[AIAA PAPER 92-3924] p 1095 A92-56755
Performance evaluation of a transonic wind tunnel compressor
[AIAA PAPER 92-3927] p 1096 A92-56758
An overview of the planned aerospace test facilities at Capua, Italy
[AIAA PAPER 92-3944] p 1097 A92-56773
The cryogenic balance design and balance calibration methods
[AIAA PAPER 92-4001] p 1122 A92-56824
Transonic turbine blade cascade testing facility
[AIAA PAPER 92-4034] p 1101 A92-56856
Stainless steel welding shines through on wind tunnel project p 1123 A92-57039
Model representation in the PANCOR wall interference assessment code
[NASA-TM-104152] p 31 N92-11022
Technical activities of the configuration aeroelasticity branch
[NASA-TM-104146] p 159 N92-13458
The NASA Langley Research Center 0.3-meter transonic cryogenic tunnel microcomputer controller source code
[NASA-CR-189556] p 209 N92-15077
Results of the space shuttle vehicle ascent air data system probe calibration test using a 0.07-scale external tank forebody model (68T) in the AEDC 16-foot transonic wind tunnel (IA-310), volume 1
[NASA-CR-167696] p 286 N92-17167
Stagnation and dynamic pressure limits for the S1 wind tunnel
[AD-A242989] p 285 N92-17297
User guide for WIACX: A transonic wind-tunnel wall interference assessment and correction procedure for the NTF
[NASA-TM-104168] p 261 N92-17547
Results of measured temperature distribution on an adiabatic wing model with radiation thermometer
[NAL-TM-610] p 261 N92-17755
Asymptotic theory of transonic wind tunnel wall interference
[AD-A244075] p 403 N92-19080
Weight, center of gravity and modal test report for NTF fan blade set no. 3
[NASA-CR-189583] p 498 N92-20072
Comparison of a two-dimensional adaptive-wall technique with analytical wall interference correction techniques
[NASA-TP-3132] p 444 N92-20494
Evaluation of NACA0012 airfoil test results in the NAL two-dimensional transonic wind tunnel
[NAL-TR-1109T] p 445 N92-21287
Study of optical techniques for the Ames unitary wind tunnels. Part 2: Light sheet and vapor screen
[NASA-CR-190217] p 573 N92-22195
Development of wall pressure measuring apparatus for an existing transonic wind tunnel test section
[NAL-TM-565] p 573 N92-23778
Transonic turbine blade cascade testing facility
[NASA-TM-105646] p 667 N92-26129
A study of juncture flow in the NASA Langley 0.3-meter transonic cryogenic tunnel
[NASA-CR-190430] p 773 N92-27880
Transonic wind tunnel investigation of limit cycle oscillations on fighter type wings p 721 N92-27959
Force measurements on AGARD calibration model-B at transonic speeds in the NAL two-dimensional wind tunnel
[NAL-TM-639] p 722 N92-28190
The windtunnel as a tool for laminar flow research
[NLR-TP-90145-U] p 887 N92-28661
Replacement of the NAL high pressure air storage system
[NAL-TM-634] p 888 N92-28835
Buffet test in the National Transonic Facility
[NASA-CR-189595] p 888 N92-29352
High Reynolds number test of the Boeing TR77 airfoil in the Langley 0.3-meter transonic cryogenic tunnel
[NASA-TM-4189] p 947 N92-31246
Data reduction formulas for the 16-foot transonic tunnel: NASA Langley Research Center, revision 2
[NASA-TM-107646] p 984 N92-31900
Transonic wind tunnel test of a 14 percent thick oblique wing
[NASA-TM-102230] p 950 N92-32213

TRANSPARENCE
Fabrication and mechanical properties of an optically transparent glass fiber/polymer matrix composite
p 891 A92-45630
Bird impact analysis of aircraft windshield transparency p 958 A92-50236

TRANSPONDERS
Integrating GPS with ranging transponders
p 95 A92-16627
The problem of multiple solutions in area navigation and computed centerline operations with the microwave landing system
[AD-A242757] p 191 N92-15058

TRANSPORT AIRCRAFT
Design of the flare control law for longitudinal autopilot using H(infinity) synthesis p 28 A92-11562
Design of localizer capture and track hold for a transport airplane - An H(infinity)/LTR approach
p 52 A92-11583
Impact of heterogeneous chemistry on model-calculated ozone change due to high speed civil transport aircraft
p 45 A92-12941
The Eurofar vehicle overview p 108 A92-14416
Subsonic propulsion system installation analysis and optimization
[ASME PAPER 91-GT-167] p 111 A92-15602
Interference effects of very high bypass ratio nacelle installations on a low-wing transport
[ASME PAPER 91-GT-241] p 75 A92-15646
Detailed analysis of wing-nacelle interaction for commercial transport aircraft
[ONERA, TP NO. 1991-152] p 77 A92-16122
Air transport research in Germany p 61 A92-17095
Cabin structural vibration and noise for transport aircraft p 192 A92-17876
Dornier 328 first flight p 192 A92-19924
Experimental study of pylon geometries for transport aircraft
[AIAA PAPER 92-0153] p 271 A92-23768
Future experimental needs in low-speed aerodynamics
[AIAA PAPER 92-0157] p 254 A92-23772
Identification of aerodynamic coefficients using computational neural networks
[AIAA PAPER 92-0172] p 255 A92-23783
The use of variable camber to reduce drag, weight and costs of transport aircraft p 313 A92-25096
Fleet modernization - One approach
p 307 A92-25371
Variable-complexity aerodynamic optimization of an HSCT wing using structural wing-weight equations
[AIAA PAPER 92-0212] p 317 A92-25685
Supersonic transport in the 21st century
p 308 A92-26793
Navigation and flight management systems - Thoughts of a user p 354 A92-26848
Trends in the selection of airliners
p 417 A92-28183
An airlifter for the long haul p 358 A92-28493
Effect of the fuselage midsection ratio on the character of wing-fuselage aerodynamic interference
p 439 A92-31883
Multidisciplinary design optimization of a large transport aircraft wing
[AIAA PAPER 92-1002] p 536 A92-33194
Conceptual design and analysis of a special operations transport
[AIAA PAPER 92-1066] p 536 A92-33239
Study of materials and structures for the High-Speed Civil Transport
[AIAA PAPER 92-1080] p 536 A92-33249
Design for the relief of thermal stresses in a large high-speed wing
[AIAA PAPER 92-1082] p 536 A92-33250
Advancing airlift avionics - C-17 avionics suite
[AIAA PAPER 92-1243] p 553 A92-33336
The Mission Computer/Electronic Display Subsystem for the United States Air Force C-17A transport aircraft
[AIAA PAPER 92-1244] p 553 A92-33337
The C-17 - Modern airlift technology
[AIAA PAPER 92-1262] p 538 A92-33342
Design for validation p 601 A92-33607
Mass-transporter p 543 A92-34650
Advanced propulsion systems for large subsonic transports p 653 A92-36977
Dimensional characterization of a large aircraft structure by photogrammetry p 607 A92-37061
Use of the thrust-weight diagram versus transport cargo in the initial dimensioning of passenger-transport aircraft
p 642 A92-37074
Review of aviation record p 634 A92-39302

Engine reliability p 654 A92-39309
Panel method control in 3-D hyperbolic grid generation p 617 A92-39940
Analysis for the application of hybrid laminar flow control to a long-range subsonic transport aircraft
[SAE PAPER 912113] p 617 A92-39964
MD-11 status report p 646 A92-40040
Conceptual design and analysis of a special operations transport p 646 A92-40387
Numerical investigation of supersonic inlet with realistic bleed and bypass systems p 713 A92-44519
Data Link integration in commercial transport operations p 839 A92-44919
High speed VSTOL on the horizon - The answer to congestion?
[SAE PAPER 911976] p 843 A92-45383
The impact of CFD on the airplane design process - Today and tomorrow
[SAE PAPER 911989] p 788 A92-45391
Wind tunnel investigation of an improved upper surface blown flap transport semi-span model
[SAE PAPER 911993] p 789 A92-45395
Avionics flight systems for the 21st century
[SAE PAPER 912033] p 784 A92-45421
Functional mock-up tests for flight control system of the NAL QSTOL research aircraft 'ASKA'
[SAE PAPER 912036] p 881 A92-45422
On the possibility of freezing and sticking phenomena in a transport during the ground taxiing and takeoff run and on the preventions of the hazard
[SAE PAPER 912042] p 836 A92-45426
Three-dimensional orthogonal-to-surface structured grid generation with transonic Navier-Stokes flow solutions for a commercial transport configuration
[AIAA PAPER 92-2616] p 793 A92-45490
The design of a system of codes for industrial calculations of flows around aircraft and other complex aerodynamic configurations
[AIAA PAPER 92-2619] p 917 A92-45492
Recent CFD applications on jet transport configurations
[AIAA PAPER 92-2658] p 844 A92-45519
Simulation of transonic flow over twin-jet transport aircraft p 811 A92-46793
Grid generation and compressible flow computations about a high-speed civil transport configuration p 919 A92-47055
Interactive algebraic mesh generation for twin jet transport aircraft p 817 A92-47064
Electric actuation system duty cycles --- in fly-by-wire/power-by-wire control p 877 A92-48494
Trends in commercial aircraft design - What evolution factors and what approach?
[ONERA, TP NO. 1992-25] p 786 A92-48587
Investigations of propulsion integration interference effects on a transport aircraft configuration
[AIAA PAPER 92-3097] p 849 A92-48739
A low maintenance and highly reliable fly-by-light architecture p 975 A92-49325
Applied analytical combustion/emissions research at the NASA Lewis Research Center - A progress report
[AIAA PAPER 92-3338] p 1067 A92-54025
Continuous flying quality improvement - The measure and the payoff
[AIAA PAPER 92-4327] p 1073 A92-55171
A simulator evaluation of various manual control concepts for fly-by-wire transport aircraft
[AIAA PAPER 92-4328] p 1073 A92-55172
Optimal recovery from microburst wind shear
[AIAA PAPER 92-4338] p 1078 A92-55327
Fatigue cracking threshold prediction of transport airplanes p 1118 A92-56094
The Eurofar program - An European overview on advanced VTOL civil transportation system p 1016 A92-56299
Study on international cooperative test facilities for future SST/HST
[AIAA PAPER 92-3945] p 1097 A92-56775
High Reynolds number testing in support of transport airplane development
[AIAA PAPER 92-3982] p 1099 A92-56807
Combined exo/endoatmospheric transport alternatives
[IAF PAPER 92-0663] p 1104 A92-57102
An experimental study of organismic principles of the functioning of the crew-transport aircraft system p 1133 A92-57446
Wing tip turbine: Analysis of the results of S2MA sounding of marginal vortex of the A320, technical summary
[ONERA-RTS-21/4365-AY-056A] p 23 N92-11009
On a global aerodynamic optimization of a civil transport aircraft p 193 N92-13931
Aging Aircraft NDI Development and Demonstration Center (AANC): An overview
[DE92-002358] p 241 N92-15962
Estimation of airborne performance in landing
[ESDU-91032] p 272 N92-15988
Identification of high-level functional/system requirements for future civil transports
[NASA-CR-189561] p 276 N92-15991
The G-222 aircraft individual tracking programme p 361 N92-18582
The Operational Loads Monitoring System, OLMS p 361 N92-18586
Recent fracture mechanics results from NASA research related to the aging commercial transport fleet p 362 N92-18589
Structural airworthiness of aging Boeing jet transports p 362 N92-18590
The atmospheric effects of stratospheric aircraft: A first program report
[NASA-RP-1272] p 408 N92-19121
High-speed civil transport aircraft emissions p 408 N92-19122
Design of a turbofan powered regional transport aircraft
[NASA-CR-190130] p 461 N92-20280
Aeronautical research in the United States: Challenges for the 1990's p 420 N92-21502
Advanced Transport Operating System (ATOPS) color displays software description microprocessor system
[NASA-CR-189605] p 556 N92-22645
High speed transport cruise drag --- scaling laws using Navier-Stokes equations
[NASA-CR-190248] p 527 N92-23103
Simultaneous stress and flutter optimization for the wing of a transport aircraft equipped with four engines p 571 N92-23238
Effects of turbine cooling assumptions on performance and sizing of high-speed civil transport
[NASA-TM-105610] p 562 N92-23537
Structural analysis for preliminary design of High Speed Civil Transport (HSCT) p 684 N92-25926
Application of integrated structural analysis to the high speed civil transport p 684 N92-25927
Preliminary structural sizing of a Mach 3.0 high-speed civil transport model
[NASA-CR-189631] p 685 N92-25960
Drag reduction: An industrial challenge p 717 N92-27708
An analysis of fixed wing tactical airlifter characteristics using an intra-theater airlift computer model
[AD-A246908] p 732 N92-27719
Use of a virtual cockpit for the development of a future transport aircraft p 886 N92-28547
The use and effectiveness of piloted simulation in transport aircraft research and development p 886 N92-28549
Hyperbolic grid generation with BEM source terms
[NLR-TP-90334-U] p 923 N92-28635
Some longitudinal handling qualities design guidelines for active control technology transport aircraft
[NLR-TP-90129-U] p 878 N92-28652
Applied analytical combustion/emissions research at the NASA Lewis Research Center
[NASA-TM-105731] p 890 N92-29343
Hyperbolic grid generation control by panel methods
[NLR-TP-91061-U] p 924 N92-29604
Results of a flight simulator experiment to establish handling quality guidelines for the design of future transport aircraft
[NLR-MP-88044-U] p 854 N92-29616
Fracture mechanics research at NASA related to the aging commercial transport fleet p 913 N92-30110
Status of the FAA flight loads monitoring program p 914 N92-30113
Aging aircraft NDI Development and Demonstration Center (AANC): An overview --- nondestructive inspection p 915 N92-30120
The FAA aging airplane program plan for transport aircraft p 838 N92-30128
Transport Canada aging aircraft activities p 838 N92-30131
Research and technology, 1991. Langley Research Center
[NASA-TM-4331] p 1013 N92-30733
Evaluation of microwave landing system approaches in a wide-body transport simulator
[NASA-CR-4450] p 957 N92-30978
Current nondestructive inspection methods for aging aircraft
[DOT/FAA/CT-91/5] p 1126 N92-33480
Applications of a direct/iterative design method to complex transonic configurations
[NASA-TP-3234] p 1039 N92-33484
Advanced subsonic transport approach noise: The relative contribution of airframe noise
[NASA-TM-104112] p 1140 N92-34148
Flutter analyses using high speed computers. Part 1: Flutter analyses for large aircraft p 1089 N92-34168

TRANSPORT PROPERTIES
A one-equation turbulence model for aerodynamic flows
[AIAA PAPER 92-0439] p 327 A92-26285
Propagation of shock waves through clouds
[AERO-REPT-9104] p 400 N92-18317
Transport phenomena and interfacial kinetics in multiphase combustion systems
[AD-A244849] p 489 N92-20695
Computational method to predict thermodynamic, transport, and flow properties for the modified Langley 8-foot high-temperature tunnel
[NASA-TM-4374] p 767 N92-27193
An experimental investigation of the separating/reattaching flow over a backstep
[NASA-CR-190426] p 716 N92-27399

TRANSPORT THEORY
Isothermal modeling of gas turbine combustors - Computational study p 129 A92-17203
Particle dispersion in highly swirling, turbulent flows p 675 A92-40093
Models of turbulence in a hypersonic boundary layer p 705 A92-41817

TRANSPORT VEHICLES
NASA TSRV essential flight control system requirements via object oriented analysis
[NASA-CR-189573] p 381 N92-19499

TRANSPORTATION
Heavy duty transport research needs assessment
[DE92-010622] p 767 N92-27394
Air traffic control: FAA's advanced automation system contract
[GAO/IMTEC-91-25] p 1048 N92-32861

TRANSPORTATION NETWORKS
Electronic systems in transportation
[TP-9983] p 189 N92-14009

TRANSPUTERS
Parallel computation of aerodynamic influence coefficients for aeroelastic analysis on a transputer network p 53 A92-12367
An application of distributed environment in flight simulation p 602 A92-35739
Parallel processing applications for gas turbine engine control p 25 N92-11012
Real-time processing of radar return on a parallel computer
[NASA-CR-4456] p 1043 N92-32606

TRANSVERSE OSCILLATION
Pressure on a cylinder with a screen in transverse flow p 6 A92-12164

TRANSVERSE WAVES
Detonation duct gas generator demonstration program
[AIAA PAPER 92-3174] p 1066 A92-54011
Cross-flow instabilities and pressure gradients in boundary layers p 767 N92-26922

TRAPEZOIDAL WINGS
A LEX blowing technique for post-stall lateral control of trapezoidal wings
[AIAA PAPER 92-2714] p 802 A92-45553

TRAPPED VORTICES
Investigation on vortex control technique of flow separation in diffuser p 338 A92-27828
Vortex trapping on a 60 degree delta wing
[AIAA PAPER 92-2639] p 796 A92-45508
Two-fence concept for efficient trapping of vortices on airfoils p 1031 A92-56165

TRAVELING WAVE AMPLIFIERS
A low-power, high-efficiency Ka-band TWTA p 671 A92-38163

TRAVELING WAVE TUBES
A low-power, high-efficiency Ka-band TWTA p 671 A92-38163

TRAVELING WAVES
Noise-driven flow p 173 A92-18680
Reflections off aircraft and the shape optimization of a ridged waveguide p 267 A92-23967
On travelling wave vibration of high-speed duplex helical gears p 990 A92-49580

TREES (MATHEMATICS)
Euler calculations of axisymmetric under-expanded jets by an adaptive-refinement method
[AIAA PAPER 92-0321] p 321 A92-25768
Mesh adaptivity with the quadtree method p 816 A92-47041

TREND ANALYSIS
Trends in the selection of airliners p 417 A92-28183
Opening closed skies - The prospects for further liberalization of trade in international air transport services p 697 A92-39244
Space Shuttle airframe inspection trend-analysis report p 759 A92-42052
Regional airline and equipment review - Evolution, trends, and future prospects p 1015 A92-55102

TRENDS
New York Downtown Manhattan (Wall Street) Heliport: Operations analysis
[DOT/FAA/RD-91/12] p 139 N92-13077
Materials and process directions for advanced aero-engine design
[PNR-90814] p 378 N92-19938
TRIANGULATION
A Navier-Stokes solver for stretched triangular grids
[AIAA PAPER 92-0183] p 256 A92-23793
Adaptive parallel meshes with complex geometry
p 918 A92-47050
Grid generation and flow solution method for Euler equations on unstructured grids
[NASA-TM-4295] p 528 N92-23533
A frontal approach for node generation in Delaunay triangulations p 771 N92-27680
Delaunay triangulation and computational fluid dynamics meshes
[NASA-TM-107663] p 1010 N92-30907
TRIBOLOGY
Development and tribological properties of new cyclotriphosphazene high temperature lubricants for aircraft gas turbine engines p 287 A92-21327
Seal related development activities at EG/G
p 228 N92-15095
Tribology needs for future space and aeronautical systems
[NASA-TM-104525] p 214 N92-15191
High-temperature miniaturized turbine engine lubrication system simulator
[AD-A249259] p 868 N92-28294
TRISONIC WIND TUNNELS
Wind-tunnel studies of F/A-18 tail buffet
p 310 A92-24421
TRITIUM
Evaluation of a tritium runway lighting system
[DOT/FAA/CT-TN92/15] p 665 N92-25733
TROPOSPHERE
Digital ozonesondes - Examples of results from the EMEFS experiments of 1988 and 1990
p 468 A92-32140
Measured and calculated optical property profiles in the mixed layer and free troposphere p 1129 A92-54630
Atmospheric pressure flow reactor: Gas phase chemical kinetics under tropospheric conditions without wall effects
[NASA-CASE-MSC-21384-1] p 297 N92-16243
TRUSSES
Experimental active control of a two-dimensional truss
p 47 A92-11346
Selection of efficient primary-structure/force configurations for aircraft lifting surfaces subjected to displacement constraints p 458 A92-30140
TUNABLE LASERS
Evaluation of OH laser-induced fluorescence techniques for supersonic combustion diagnostics
[AIAA PAPER 92-0508] p 396 A92-26935
TUNGSTEN ALLOYS
Cyclic hot corrosion of Haynes 230 alloy
p 754 A92-41091
High-temperature metal matrix composite
p 1105 A92-53878
TUNING
Intelligent control law tuning for AIAA Controls Design Challenge
[AIAA PAPER 92-4631] p 1132 A92-55306
Optimizing tuning masses for helicopter rotor blade vibration reduction including computed airloads and comparison with test data
[NASA-TM-104194] p 367 N92-19846
TURBINE BLADES
Two-phase flows at supersonic velocities
p 4 A92-10907
An analysis of the flow-pattern at the exit of a single-stage turbine p 10 A92-13234
Nondestructive depth profiling of the protective coating on a turbine blade p 144 A92-13641
Corrosion damage and regeneration of aluminide coatings on aircraft turbine blades p 142 A92-15244
Convective transport phenomena on the suction surface of a turbine blade including the influence of secondary flows near the endwall
[ASME PAPER 91-GT-35] p 147 A92-15518
Minimization of the number of cooling holes in internally cooled turbine blades
[ASME PAPER 91-GT-52] p 121 A92-15530
Turbine cascade calculations through a fractional step Navier-Stokes algorithm
[ASME PAPER 91-GT-55] p 68 A92-15533
Computation of flow past a turbine blade with and without tip clearance
[ASME PAPER 91-GT-56] p 68 A92-15534
A 3D FEM variational aerodynamic calculation and performance analysis of a leaned turbine stator cascade
[ASME PAPER 91-GT-79] p 69 A92-15548
Inviscid-viscous coupled solution for unsteady flows through vibrating blades. II - Computational results
[ASME PAPER 91-GT-126] p 71 A92-15571
Effects of simulated rotation on tip leakage in a planar cascade of turbine blades. I - Tip gap flow
[ASME PAPER 91-GT-127] p 71 A92-15572
Effects of simulated rotation on tip leakage in a planar cascade of turbine blades. II - Downstream flow field and blade loading
[ASME PAPER 91-GT-128] p 71 A92-15573
The impact load on containment rings during a multiple blade shed in aircraft gas turbine engines
[ASME PAPER 91-GT-163] p 123 A92-15598
Turbine blade tip clearance improvement
[ASME PAPER 91-GT-164] p 123 A92-15599
Analysis and prediction of transonic turbine blade losses
[ASME PAPER 91-GT-183] p 73 A92-15615
Combination of different unsteady quantity measurements for gas turbine blade fault diagnosis
[ASME PAPER 91-GT-201] p 149 A92-15624
The influence of density difference between hot and coolant gas on film cooling by a row of holes - Predictions and experiments
[ASME PAPER 91-GT-255] p 151 A92-15660
A procedure for automated gas turbine blade fault identification based on spectral pattern analysis
[ASME PAPER 91-GT-259] p 151 A92-15661
Heat transfer in rotating serpentine passages with trips normal to the flow
[ASME PAPER 91-GT-265] p 151 A92-15663
Comparison of time-resolved turbine rotor blade heat transfer measurements and numerical calculations
[ASME PAPER 91-GT-268] p 151 A92-15666
Modelling of unsteady transitional boundary layers
[ASME PAPER 91-GT-282] p 152 A92-15677
Blade row interaction in a multistage low-pressure turbine
[ASME PAPER 91-GT-283] p 125 A92-15678
Design and analysis of a high pitch to chord ratio cascade representative of ducted propfans
[ASME PAPER 91-GT-335] p 126 A92-15700
Effect of the blade height of the nozzle ring of axial-flow microturbines on the flow velocity factor and exit angle
p 128 A92-16831
PVD coatings for aircraft turbine blades
p 216 A92-17950
Large chord turbine cascade testing at engine Mach and Reynolds number p 173 A92-18771
Multiaxial load spectra in a cooled gas turbine blade under in-service conditions p 201 A92-19696
Vibration characteristics of pretwisted aerofoil cross-section blade packets under rotating conditions
p 219 A92-20756
Recent advancements in turbomachinery forced response analyses
[AIAA PAPER 92-0012] p 278 A92-22136
The position of the unsteady flow computation in the compressor and turbine design and analysis process
[AIAA PAPER 92-0015] p 278 A92-22137
An analysis of impact resistance of composite blades for turbo-fan engines p 294 A92-23109
Nonlinear transient analysis of composite ATP blade model p 294 A92-23111
Unsteady aerodynamic methods for turbomachinery aeroelastic and aeroacoustic applications
[AIAA PAPER 92-0011] p 252 A92-23730
3D Navier-Stokes analysis for a tip leakage flow in a low aspect ratio turbine
[AIAA PAPER 92-0395] p 278 A92-23816
On the prediction of unsteady forces on gas turbine blades. I - Description of the approach. II - Analysis of the results p 311 A92-24724
Design of turbomachinery blading in transonic flows by the circulation method p 311 A92-24725
Study on reliability design of turbine blade
p 371 A92-24739
Triple contra-rotating turbine and its basic analysis
p 371 A92-24745
Optimization of multistage axial-flow compressor vane setting p 371 A92-24746
The effect of blade solidity on the aerodynamic loss of a transonic turbine cascade
[AIAA PAPER 92-0393] p 323 A92-26248
Effect of different force-functions and initial shock pressure on blade response p 374 A92-27913
Restoration of aircraft engine nozzle block blades by vacuum arc brazing with controlled current
p 471 A92-30381
A compound fatigue investigation of plate specimen under low-cycle load superposed on high cycle load
p 587 A92-35555
A direct-problem calculation method for gas turbines with bowed and twisted blades p 519 A92-35571
Research and development of aircraft engine materials p 577 A92-35916
Arbitrary blade section design based on viscous considerations - Blade optimization p 523 A92-36030
An inverse inviscid method for the design of quasi-three dimensional turbomachinery cascades
p 523 A92-36033
Inviscid and viscous quasi-three-dimensional flow solutions in a transonic turbine cascade
p 523 A92-36035
A method for determining equivalent stresses in aviation gas turbine engine blades p 559 A92-36421
An investigation in the variance in particle surface interactions and their effects in gas turbines
[ASME PAPER 91-GT-380] p 653 A92-36891
Coating effect on particle trajectories and turbine blade erosion p 653 A92-36892
Fracture mechanics approach to creep growth in welded IN738LC gas turbine blades
[ASME PAPER 91-GT-119] p 670 A92-36893
Blade repair with adaptive vision tracking
[ASME PAPER 91-GT-208] p 607 A92-36897
Reynolds stress distribution downstream of a turbine cascade p 614 A92-38861
Turbine blade heat transfer prediction using coupled turbulent Prandtl number and transition models
[SAE PAPER 912152] p 674 A92-39987
A method for estimating the efficiency of gas turbine blade cooling systems p 657 A92-40606
Experimental operation of aircraft-engine turbine blade materials p 737 A92-43233
An analysis of the effect of centrifugal force on the impact resistance of composite fan blades for turbo-fan engines
[SAE PAPER 912047] p 861 A92-45431
Magnetic particle testing of turbine blades mounted on the turbine rotor shaft p 898 A92-46498
Advanced superalloys for turbine blade and vane applications
[ONERA, TP NO. 1992-2] p 893 A92-48578
Vane-blade interaction in a transonic turbine. II - Heat transfer
[AIAA PAPER 92-3324] p 904 A92-48907
Failure model development for an integrally bladed turbine wheel
[AIAA PAPER 92-3420] p 865 A92-48979
Flexible manufacturing in repair of gas turbine engine components
[AIAA PAPER 92-3524] p 786 A92-49049
Transonic flows of Bethe-Zel'dovich-Thompson fluids
p 935 A92-50293
Failure analysis and reliability improvement of small turbine engine blades p 993 A92-50860
Three-dimensional relaxation effect on quasi-3D flow in a blade row with spanwise loading distribution
p 936 A92-51593
Three-dimensional Navier-Stokes heat transfer predictions for turbine blade rows
[AIAA PAPER 92-3068] p 1020 A92-54003
FREPS - A forced response prediction system for turbomachinery blade rows
[AIAA PAPER 92-3072] p 1130 A92-54006
Unsteady blade pressures on a propfan - Predicted and measured compressibility effects
[AIAA PAPER 92-3774] p 1023 A92-54161
State-of-the-art materials for future gas turbine engines p 1070 A92-56122
Transonic turbine blade cascade testing facility
[AIAA PAPER 92-4034] p 1101 A92-56856
Structural tailoring of advanced turboprops (STAT): User's manual
[NASA-CR-187101] p 26 N92-11016
Effects of wake and shock passing on the heat transfer to a film cooled transonic turbine blade
p 156 N92-12201
Heat transfer and instrumentation studies on rotating turbine blades in a transient facility p 156 N92-12203
Blade surface pressure measurements on the rotor of a model turbine stage in a transient flow facility
p 157 N92-12206
Airfoil Vibration Dampers program
[NASA-CR-184276] p 225 N92-14391
A comparison of spanwise aerodynamic loads estimated from measured bending moments versus direct pressure measurements on horizontal axis wind turbine blades
[DE92-001158] p 301 N92-16458
Dynamic stall on wind turbine blades
[DE92-001157] p 262 N92-17874
Fiber-sensor design for turbine engines
[DE92-003539] p 376 N92-18230
Eddy current transducing system
[DE91-018924] p 401 N92-18515
Thermal nonequilibrium effects on turbine cascade aerodynamics
[AD-A244049] p 404 N92-19183
Experimental validation of structural optimization methods
[NASA-TM-104203] p 404 N92-19258

The effect of angle of incidence and Reynolds number on heat transfer in a linear turbine cascade
[AD-A243900] p 377 N92-19328
The NREL teetering hub rotor code: Final results and conclusions
[DE92-001187] p 410 N92-19633
Present and future trends in turbine blade material and manufacturing technology
[PNR-90825] p 488 N92-20164
Recent results from data analysis of dynamic stall on wind turbine blades
[DE92-001200] p 505 N92-20245
Transport phenomena and interfacial kinetics in multiphase combustion systems
[AD-A244849] p 489 N92-20695
An investigation of the energy loss and near wake flow field of trailing edge injection p 456 N92-21839
Evaluation and qualification of diffusion braze repair techniques for superalloy gas turbine components
[NRC-LTR-ST-1839] p 504 N92-22028
Creep and fatigue research efforts on advanced materials p 593 N92-22514
SERI advanced wind turbine blades
[DE92-001216] p 598 N92-22971
Measured and predicted rotor performance for the SERI advanced wind turbine blades
[DE92-001215] p 598 N92-23119
Investigations of blade row interaction and boundary layer transition phenomena in a multistage aero engine low-pressure turbine by measurements with hot-film probes and surface-mounted hot-film gauges
p 658 N92-24338
Fatigue life variability and reliability analysis of a wind turbine blade
[DE92-008673] p 689 N92-25049
An interactive grid generation technique for turbomachinery p 659 N92-25717
Transonic turbine blade cascade testing facility
[NASA-TM-105646] p 667 N92-26129
Simulation of 3D non-planar fatigue crack growth in a turbine blade root
[DE92-006859] p 739 N92-26697
An integrated CFD system for 3D turbomachinery applications p 741 N92-27464
Navier-Stokes analysis of turbine blade heat transfer and performance p 768 N92-27468
Visualization of boundary-layer development on turbomachine blades with liquid crystals
[NASA-CR-190433] p 742 N92-27519
Laser anemometer measurements and computations in an annular cascade of high turning core turbine vanes
[NASA-TP-3252] p 830 N92-28980
Fatigue in single crystal nickel superalloys
[AD-A248190] p 896 N92-29408
Examination of the main error factors with regards to secondary losses in compression and turbine cascades by variations of the blade picture ratio
[ETN-92-91493] p 871 N92-29927
Finite difference time domain modeling of steady state scattering from jet engines with moving turbine blades
[NASA-CR-190290] p 971 N92-30753
Yaw dynamics of horizontal axis wind turbines
[DE92-001245] p 1004 N92-30837
Fatigue in single crystal nickel superalloys
[AD-A250068] p 987 N92-31360
A surface definition code for turbine blade surfaces
[DE92-010574] p 1004 N92-31498
Turbine blade tip and seal clearance excitation forces
[NASA-CR-184341] p 973 N92-31910
Fatigue in single crystal nickel superalloys
[AD-A252492] p 988 N92-32066
A critical evaluation of a three-dimensional Navier-Stokes CFD as a tool to design supersonic turbine stages p 1124 N92-32268
The dynamics of flexible multibody systems: A finite segment approach p 1128 N92-34036

TURBINE ENGINES
Thermal barrier coating life prediction model development
[ASME PAPER 91-GT-40] p 147 A92-15523
On-line distortion analysis system for inlet-engine testing
[ASME PAPER 91-GT-166] p 136 A92-15601
Film cooling research on the endwall of a turbine nozzle guide vane in a short duration annular cascade. I - Experimental technique and results
[ASME PAPER 91-GT-252] p 150 A92-15657
Film cooling research on the endwall of a turbine nozzle guide vane in a short duration annular cascade. II - Analysis and correlation of results
[ASME PAPER 91-GT-253] p 150 A92-15658
NDE of advanced turbine engine components and materials by computed tomography
[ASME PAPER 91-GT-287] p 152 A92-15681
An integrated real-time turbine engine flight test system p 201 A92-19275
LDV measurements and investigation of flow field through radial turbine guide vanes p 217 A92-19618
Development and tribological properties of new cyclotriphosphazene high temperature lubricants for aircraft gas turbine engines p 287 A92-21327
Electronic control of a turbine power unit
p 470 A92-29741
Experimental investigation of film cooling effectiveness for slots of various exit geometries p 497 A92-32265
A unified numerical approach for the analysis of rotating disks including turbine rotors
[AIAA PAPER 92-2303] p 585 A92-34524
A compound fatigue investigation of plate specimen under low-cycle load superposed on high cycle load
p 587 A92-35555
Thermal oxidation stability of aviation turbine fuels --- Book
[ISBN 0-8031-1248-3] p 669 A92-40409
A fiber optic temperature sensor for aerospace applications p 761 A92-42607
Study of grinding process and strength for ceramic heat insulated engine
[SME PAPER MR91-177] p 897 A92-45260
Integrated optic components for advanced turbine engine control systems p 925 A92-46248
Fiber optic speed sensor for advanced gas turbine engine control p 857 A92-48044
Indirect measurements of convective flow by IR thermography
[ONERA, TP NO. 1992-46] p 902 A92-48607
Comparison between two 3D-NS-codes and experiment on a turbine stator
[AIAA PAPER 92-3042] p 822 A92-48703
DYNamic Turbine Engine Compressor Code (DYNTECC) - Theory and capabilities
[AIAA PAPER 92-3190] p 923 A92-48802
Naval aircraft/engine mission payoff analyses
[AIAA PAPER 92-3473] p 865 A92-49019
Intelligent Engine Control (IEC)
[AIAA PAPER 92-3484] p 866 A92-49024
Application of an unsteady Navier-Stokes solver to transonic turbine design p 935 A92-50273
Performance of a hybrid cylindrical roller bearing
p 995 A92-51845
Development study on air turbo-ramjet engine for space plane p 1065 A92-53487
Turbine engine hot-part temperature measurement techniques
[AIAA PAPER 92-3960] p 1122 A92-56788
Turbine engine performance test and evaluation techniques
[AIAA PAPER 92-3977] p 1071 A92-56803
Engine component instrumentation development facility at NASA Lewis Research Center
[AIAA PAPER 92-3995] p 1099 A92-56818
Wing tip turbine: Analysis of the results of S2MA sounding of marginal vortex of the A320, technical summary
[ONERA-RTS-21/4365-AY-056A] p 23 N92-11009
Advanced stress analysis methods applicable to turbine engine structures
[NASA-CR-187235] p 44 N92-11378
Technology needs for high speed rotorcraft (3)
[NASA-CR-177592] p 195 N92-14039
Universal weaving for turbine engine composite preforms
[AD-A237667] p 202 N92-14059
Turbine engine diagnostics system study
[DOT/FAA/CT-91/16] p 202 N92-14064
Institute for experimental fluid mechanics: Results for 1990
[IB-222-90-A-46] p 400 N92-18244
Present and future trends in turbine blade material and manufacturing technology
[PNR-90825] p 488 N92-20164
Use of CFD in the design of a modern multistage aero engine LP turbine design
[PNR-90862] p 472 N92-20179
Fabrication and testing of corrosion resistant coatings --- for turbine engine components
[DE92-003553] p 490 N92-21063
Research sensors p 594 N92-22526
Aircraft engine hot section technology: An overview of the HOST Project p 561 N92-22535
Engine component instrumentation development facility at NASA Lewis Research Center
[NASA-TM-105644] p 665 N92-25449
Military engine computational structures technology
p 660 N92-25934
Ceramic composites: Enabling aerospace materials
[NASA-TM-105599] p 756 N92-27378
High-temperature miniaturized turbine engine lubrication system simulator
[AD-A249259] p 868 N92-28294
Contingency power for a small turboshaft engine by using water injection into turbine cooling air
[NASA-TM-105680] p 871 N92-29661
A simplified dynamic model of the T700 turboshaft engine
[NASA-TM-105805] p 1009 N92-30898
Study of potassium turbine electric generator system
p 1129 N92-33794

TURBINE EXHAUST NOZZLES
Nickel base alloy GTD-222 - A new gas turbine nozzle alloy
[ASME PAPER 91-GT-73] p 142 A92-15542
Brazing method helps repair aircraft gas-turbine nozzles p 492 A92-29504

TURBINE INSTRUMENTS
An Axial Turbobrake
[ASME PAPER 91-GT-1] p 147 A92-15501
High accuracy fuel flowmeter. Phase 2C and 3: The mass flowrate calibration of high accuracy fuel flowmeters
[NASA-CR-187108] p 406 N92-19775

TURBINE PUMPS
Rotor support for the STME oxygen turbopump
[AIAA PAPER 92-3282] p 904 A92-48872
Investigation of three-dimensional flow field in a turbine including rotor/stator interaction. II - Three-dimensional flow field at the exit of the nozzle
[AIAA PAPER 92-3326] p 826 A92-48909
The effects of Reynolds number, rotor incidence angle and surface roughness on the heat transfer distribution in a large-scale turbine rotor passage
[NASA-CR-184260] p 42 N92-11297
Limit cycle vibrations in turbomachinery
[NASA-TP-3181] p 211 N92-14108
Nonlinear rotordynamics analysis --- Space Shuttle Main Engine turbopumps
[NASA-CR-184263] p 221 N92-14344
Test results for rotordynamic coefficients of the SSME HPOTP turbine interstage seal with two swirl brakes
p 223 N92-14357
Dynamic characteristics and stability analysis of space shuttle main engine oxygen pump p 224 N92-14366
Airfoil Vibration Dampers program
[NASA-CR-184276] p 225 N92-14391
A survey of instabilities within centrifugal pumps and concepts for improving the flow range of pumps in rocket engines
[NASA-TM-105439] p 387 N92-18280
Determining structural performance
p 560 N92-22519
Turbine drive system of the high pressure LOX turbopump test facility
[DE92-783191] p 680 N92-25342
Turbine disk cavity aerodynamics and heat transfer
p 1124 N92-32265

TURBINE WHEELS
Performance of radial clearance rim seals in upstream and downstream rotor-stator wheelspaces
[ASME PAPER 91-GT-32] p 147 A92-15516
Rim sealing of rotor-stator wheelspaces in the absence of external flow
[ASME PAPER 91-GT-33] p 147 A92-15517
Development of silicon nitride rotors for the ATTAP program at Garrett Ceramic Components --- Advanced Turbine Technology Applications Project
[ASME PAPER 91-GT-154] p 142 A92-15590
Prediction of fatigue crack growth in a Ti-6Al-4V fan disk forging under spectrum loading p 213 A92-19817
Fatigue testing of a gas turbine fan disc
p 217 A92-19818
Review of methods for crack growth testing in gas turbine engine disc materials p 296 A92-24193
Strategies for optimal design of gas turbine disks
p 371 A92-24741
Turbine disk temperatures resulting from the hot mainstream at engine conditions
[AIAA PAPER 92-0398] p 373 A92-26252
Outflow boundary conditions for Euler analysis of flow in turbine scroll p 591 A92-36037
Heat transfer on a cylindrical surface in the cavities of gas turbine engine rotors p 657 A92-40609
Magnetic particle testing of turbine blades mounted on the turbine rotor shaft p 898 A92-46498
Numerical analysis of an engine turbine disk loaded with a large number of thermomechanical cycles
[ONERA, TP NO. 1992-31] p 902 A92-48592
Failure model development for an integrally bladed turbine wheel
[AIAA PAPER 92-3420] p 865 A92-48979
Discs low cycle fatigue life predictions for gas turbine engines in CSFR by using fractographic information
p 995 A92-51950
Transient response of the rotor-support system of aeroengines p 997 A92-53293
Aeroelastic modal characteristics of mistuned blade assemblies - Mode localization and loss of eigenstructure p 1117 A92-54921

Test results for rotordynamic coefficients of the SSME HPOTP turbine interstage seal with two swirl brakes
p 223 N92-14357
Radial inflow turbine study
[AD-A246938] p 743 N92-28073
Turbine disk cavity aerodynamics and heat transfer
p 1124 N92-32265
Cooled high-temperature radial turbine program 2
[NASA-CR-189122] p 1073 N92-34236

TURBINES

Aerodynamics and heat transfer investigations on a high Reynolds number turbine cascade
[ASME PAPER 91-GT-157] p 148 A92-15593
Full field flow visualization and computer-aided velocity measurements in a bank of cylinders in a wind tunnel
p 991 A92-50040
A comparison of the calculated and experimental off-design performance of a radial flow turbine
[AIAA PAPER 92-3069] p 1020 A92-54004
Description of a pressure measurement technique for obtaining surface static pressures of a radial turbine
[AIAA PAPER 92-4006] p 1123 A92-56829
Effects of turbine cooling assumptions on performance and sizing of high-speed civil transport
[NASA-TM-105610] p 562 N92-23537
Description of a pressure measurement technique for obtaining surface static pressures of a radial turbine
[NASA-TM-105643] p 680 N92-24959
Validation of a CANARI code by the computation of three dimensional turbulent flow in turbine valve
p 741 N92-27462
Computation of the unsteady transonic 2D cascade flow by an Euler algorithm with interactive grid generation
p 719 N92-27944
A comparison of the calculated and experimental off-design performance of a radial flow turbine
[NASA-CR-189207] p 831 N92-29402
Method of reducing drag in aerodynamic systems
[NASA-CASE-LEW-14791-1] p 1043 N92-34243

TURBOCOMPRESSORS

Design and testing of a controlled diffusion airfoil cascade for industrial axial flow compressor application
[ASME PAPER 90-GT-140] p 6 A92-11286
Stator averaged, rotor blade-to-blade near wall flow in a multistage axial compressor with tip clearance variation
[ASME PAPER 91-GT-30] p 67 A92-15514
Surge dynamics in a free-spool centrifugal compressor system
[ASME PAPER 91-GT-31] p 68 A92-15515
Computation of 3D flow phenomena in axial flow compressor blade rows
[ASME PAPER 91-GT-78] p 69 A92-15547
Stall inception in axial flow compressors
[ASME PAPER 91-GT-86] p 69 A92-15551
Active suppression of rotating stall and surge in axial compressors
[ASME PAPER 91-GT-87] p 122 A92-15552
Active control of rotating stall in a low speed axial compressor
[ASME PAPER 91-GT-88] p 122 A92-15553
Three-dimensional flow and mixing in a axial flow compressor with different rotor tip clearances
[ASME PAPER 91-GT-89] p 70 A92-15554
Unsteady viscous flow in a high speed core compressor
[ASME PAPER 91-GT-91] p 70 A92-15555
Similarity transformations for compressor blading
[ASME PAPER 91-GT-123] p 70 A92-15568
Gas-generator with high-temperature path ceramic components
[ASME PAPER 91-GT-152] p 148 A92-15594
The influence of shock waves on the viscous flow field of axial compressors
[ASME PAPER 91-GT-173] p 73 A92-15608
One-dimensional, stage-by-stage, axial compressor performance model
[ASME PAPER 91-GT-192] p 124 A92-15618
Design of a small axial compressor for high efficiency over a wide operating range
[ASME PAPER 91-GT-195] p 124 A92-15620
The numerical simulation of a high-speed axial flow compressor
[ASME PAPER 91-GT-272] p 75 A92-15669
Simple formulae for optimal solidity of two-dimensional compressor cascades based on diffusion concept
[ASME PAPER 91-GT-308] p 126 A92-15687
Preliminary design of axial compressors using artificial intelligence and numerical optimization techniques
[ASME PAPER 91-GT-334] p 126 A92-15699
Computations of unsteady multistage compressor flows in a workstation environment
[ASME PAPER 91-GT-336] p 163 A92-15701
Design and performance of advanced blading for a high-speed HP compressor
[ASME PAPER 91-GT-374] p 76 A92-15718
Active stabilization of multistage axial-compressor aerodynamic system instabilities
[ASME PAPER 91-GT-403] p 76 A92-15733
Analysis of transonic flow over plane compressor cascades using the large-particle method
p 79 A92-16812
Detuning from the natural resonances of the blade in the computer-aided design of blade rows for axial-flow compressors p 80 A92-16818
Stage-by-stage poststall compression system modeling technique p 80 A92-17194
A large-scale axial flow compressor facility and dynamic measurement techniques for rotor flow study
p 382 A92-24729
Optimization of multistage axial-flow compressor vane setting p 371 A92-24746
On velocity profile models for predicting end wall boundary layers and their blade force defects in axial compressor cascades p 311 A92-24877
Fibre optic laser anemometry for turbomachinery applications p 397 A92-27783
An aeroacoustic model about the rotating stall of a compressor p 416 A92-27855
Dynamic analysis of annular cascade shrouded blades
p 397 A92-27856
Parameter identification of compressor dynamics during closed-loop operation p 508 A92-29313
Compressor modeling and active control of stall/surge
p 508 A92-29315
Two-parameter bifurcation analysis of axial flow compressor dynamics p 421 A92-29355
A general nonlinear dynamical analysis of a second-order, one-dimensional, theoretical compression system model p 509 A92-29374
An integrated, full-range surge control/rotating stall avoidance compressor control system
p 469 A92-29376
Investigation and application of compressor loading technique p 469 A92-29718
Studying method of measuring flow-field between stages in axial-flow compressor p 423 A92-29720
Heat induced transient behaviours of axial compressors p 469 A92-29721
Some rotordynamic problems in small turbo-engines
p 470 A92-29736
Investigations of the laws of surge and rotating stall forecast in aeronautical engine p 470 A92-29739
The effect of air-compressor adjustment by means of air-bleed on the reserve of its stable operation
p 471 A92-29973
A circumferential non-uniform effect model for multistage axial-flow compressor throughflow p 588 A92-35572
New model for predicting end wall boundary layer in an axial cascade p 611 A92-37389
Plotting the universal characteristic of a compressor in low-rpm and autorotation regimes p 657 A92-40607
Flow analysis for axial compressor including secondary flow effects p 759 A92-41835
A new method for predicting the end wall boundary layers and the blade force defects inside the passage of axial compressor cascades p 819 A92-47691
Advanced CFD simulation and testing of compressor blading in the multistage environment
[AIAA PAPER 92-3040] p 822 A92-48701
Wake mixing and performance measurements in a linear compressor cascade with crenulated trailing edges
[AIAA PAPER 92-3188] p 824 A92-48800
DYNamic Turbine Engine Compressor Code (DYNTECC) - Theory and capabilities
[AIAA PAPER 92-3190] p 923 A92-48802
Numerical investigation of surge and rotating stall in multistage axial compressors
[AIAA PAPER 92-3193] p 825 A92-48804
A theoretical study of sensor-actuator schemes for rotating stall control
[AIAA PAPER 92-3486] p 878 A92-49025
Numerical investigation of axial flow compressor casing treatment p 934 A92-50216
Detection and identification of axial flow compressor instabilities p 969 A92-50504
Mixing for multi-stage axial-flow compressors
p 996 A92-53015
A microprocessor-based automation test system for the experiment of the multi-stage compressor
p 997 A92-53100
A numerical investigation of axial flow compressor casing treatment p 942 A92-53381
Mixed flow compressor surge margin gain using a manifolded diffuser system
[AIAA PAPER 92-3753] p 1068 A92-54151
Radial inflow turbine study
[AD-A240169] p 26 N92-11015
Analysis of Euler's and stress tensor methods for calculating power consumption of high speed centrifugal fans and turbocompressors
[DE92-728396] p 298 N92-16325
Calculation of local power consumptions and efficiencies of centrifugal fans and turbocompressors
[DE92-728402] p 298 N92-16326
Experimental investigation of trailing edge crenulation effects on losses in a compressor cascade
[AD-A243902] p 377 N92-19329
Rotary engine performance limits predicted by a zero-dimensional model
[NASA-CR-189129] p 474 N92-20650
The role of crack growth in defect assessment
[PNR-90798] p 501 N92-20909
Boundary layer flow in axial compressors (theoretical part)
[ETN-92-91006] p 501 N92-21232
Boundary layer flow in axial compressors (theoretical part)
[ETN-92-91007] p 501 N92-21233
Boundary layer flow in axial compressors (theoretical part)
[ETN-92-91008] p 502 N92-21234
Compressing the compressor
[PNR-90824] p 476 N92-21848
Principles and computer simulations of intercooled-turbocharged gas generator/expander engine p 592 N92-22132
Investigations of blade row interaction and boundary layer transition phenomena in a multistage aero engine low-pressure turbine by measurements with hot-film probes and surface-mounted hot-film gauges
p 658 N92-24338
Aspects of unsteady blade-surface boundary layers and transition in axial turbomachines p 658 N92-24340
A comparison of predicted and measured inlet distortion flows in a subsonic axial inlet flow compressor rotor
[NASA-TM-105427] p 633 N92-26104
Turbocharged pressurized combustion system
[PB92-142579] p 756 N92-26521
Application of S1BYL2 to the AGARD WG18 compressor test cases p 768 N92-27452
Self-adaptive aeropropulsion components-enhancing axial compressor performance
[AD-A246123] p 743 N92-27817
Dynamic simulation of compressor and gas turbine performance p 869 N92-28463
Users manual for updated computer code for axial-flow compressor conceptual design
[NASA-CR-189171] p 924 N92-30207
Research on aero-thermodynamic distortion induced structural dynamic response of multistage compressor blading
[AD-A250865] p 974 N92-32059
Computations of unsteady multistage compressor flows in a workstation environment
[NASA-TM-103839] p 1071 N92-32452
Active control of compressor surge and stall
[AD-A252771] p 1126 N92-33498
Radial inflow turbine study
[AD-A252783] p 1127 N92-33538

TURBOFAN AIRCRAFT

Annoyance caused by advanced turboprop aircraft flyover noise: Comparison of different propeller configurations
[NASA-TP-3104] p 56 N92-11758
Development of an annoyance model based upon elementary auditory sensations for steady-state aircraft interior noise containing tonal components
[NASA-TM-104147] p 166 N92-13758
Design of a turbofan powered regional transport aircraft
[NASA-CR-190130] p 461 N92-20280
Annoyance caused by aircraft en route noise
[NASA-TP-3165] p 512 N92-20479

TURBOFAN ENGINES

The performance evaluation of aeroderivative gas turbines p 119 A92-13296
Investigation of engine thrust correlation methods for enclosed test cells
[ASME PAPER 91-GT-68] p 121 A92-15538
Off-design performance prediction of turbofans using gasdynamics
[ASME PAPER 91-GT-389] p 126 A92-15721
F-14/F110 engine integration p 112 A92-16055
Euler flow analysis of turbine powered simulator and fanjet engine p 80 A92-17196
Jet engine fault detection with discrete operating points gas path analysis p 129 A92-17200
Pratt & Whitney PW300 for general aviation
p 277 A92-21012
Computational fluid dynamics based three-dimensional turbofan inlet/fan cowl analysis system
p 243 A92-21075
An analysis of impact resistance of composite blades for turbo-fan engines p 294 A92-23109

Tests of models equipped with a turbofan powered simulator in the ONERA F1 low-speed pressurized wind tunnel
[ONERA, TP NO. 1991-219] p 383 A92-26371
Effects of bleed and power extraction on the operating line of engines p 469 A92-29717
Experimental investigation on the mechanism of flame stabilization in afterburner with V-gutter flameholder p 487 A92-29725
Effect of turbulent mixing on the characteristics of a turbofan-engine nozzle p 493 A92-30162
GE, Snecma consider venture to develop uprated Perm PS-90 p 472 A92-32297
Saturn/Lyulka diversifies business to cope with Russian economic crisis p 472 A92-32299
Analytical condition inspection and extension of time between overhaul of F3-30 engine
[ASME PAPER 91-GT-277] p 653 A92-36888
NASA's quiet side. I p 607 A92-37875
Research and development of turbofan engine for supersonic aircraft p 654 A92-38025
Application of laminar flow control to high-bypass-ratio turbofan engine nacelles
[SAE PAPER 912114] p 618 A92-39965
Scale model test of an isolated turbofan nacelle with riblets
[SAE PAPER 912128] p 618 A92-39975
Research on a low-noise engine for a high-speed VTOL aircraft p 737 A92-43239
An analysis of the effect of centrifugal force on the impact resistance of composite fan blades for turbo-fan engines
[SAE PAPER 912047] p 861 A92-45431
High speed aerodynamics of upper surface blowing aircraft configurations
[AIAA PAPER 92-2611] p 793 A92-45485
Commercial turbofan engine exhaust nozzle flow analyses using PAB3D
[AIAA PAPER 92-2701] p 801 A92-45543
Suppression of fatigue-inducing cavity acoustic modes in turbofan engines p 925 A92-46809
Engine fan blade low cycle fatigue testing
[AIAA PAPER 92-3478] p 866 A92-49021
Thrust stand evaluation of engine performance improvement algorithms in an F-15 airplane
[AIAA PAPER 92-3747] p 866 A92-49111
Design and off-design point characteristics of Separated Core Ultra High Bypass Engine (SCUBE)
[AIAA PAPER 92-3776] p 867 A92-49120
Turbofan with a small bypass ratio for first stage of a two-stage to-orbit vehicle p 968 A92-49833
Technical tools of test automation for gas-turbine engines based on cluster CAMAC modules with an increased number of channels p 980 A92-51348
Effects of bleed air extraction of thrust levels on the F404-GE-400 turbofan engine
[AIAA PAPER 92-3092] p 1066 A92-54009
Performance benefits of adaptive in-flight propulsion system optimization
[AIAA PAPER 92-3749] p 1068 A92-54149
CIS engines - The range revealed. II p 1069 A92-54546
Experimental study of noise generation and propagation in a turbofan model p 1136 A92-56169
Test data models to characterize turbine engine operation in altitude test facilities
[AIAA PAPER 92-3917] p 1095 A92-56749
Application of electronically scanned pressure measurement system for engine simulation tests in the German-Dutch Wind Tunnel
[AIAA PAPER 92-4003] p 1122 A92-56826
Turbomachinery noise p 54 N92-10601
Further calculations of the performance of turbofan engines incorporating a wave rotor
[AD-A240867] p 131 N92-13072
International aviation (selected article)
[AD-A240987] p 170 N92-13992
Theoretical models for duct acoustic propagation and radiation p 236 N92-14782
Design and performance of duct acoustic treatment p 236 N92-14783
An evaluation of some alternative approaches for reducing fan tone noise
[NASA-TM-105356] p 416 N92-18282
Installation effects of wing-mounted turbofan nacelle-pylons on a 1/17-scale, twin-engine, low-wing transport model
[NASA-TP-3168] p 346 N92-19002
The SnoDog: Preliminary design of a close air support aircraft
[NASA-CR-189990] p 462 N92-21489
H2-fueled high-bypass turbofan p 475 N92-21529
Effects of chemical equilibrium on turbine engine performance for various fuels and combustor temperatures
[NASA-TM-105399] p 562 N92-23254
Computational structural analysis and advanced commercial engines p 660 N92-25933
Diffuser casing upgrade for an advanced turbofan
[NLR-TP-90097-U] p 870 N92-28711
Effects of bleed air extraction on thrust levels on the F404-GE-400 turbofan engine
[NASA-TM-104247] p 871 N92-29425
Thrust stand evaluation of engine performance improvement algorithms in an F-15 airplane
[NASA-TM-104252] p 971 N92-30518
Subsonic flight test evaluation of a performance seeking control algorithm on an F-15 airplane
[NASA-TM-4400] p 973 N92-31275
Bird ingestion into large turbofan engines
[DOT/FAA/CT-91/17] p 1043 N92-33005
Engine bird ingestion experience of the Boeing 737 aircraft: Expanded data base
[DOT/FAA/CT-91/32] p 1045 N92-34151

TURBOFANS

Study of a new airfoil used in reversible axial fans p 177 N92-13970
An evaluation of some alternative approaches for reducing fan tone noise
[NASA-TM-105356] p 416 N92-18282
Advanced tactical fighter engine
[ETN-92-90840] p 376 N92-18728
Installation effects of wing-mounted turbofan nacelle-pylons on a 1/17-scale, twin-engine, low-wing transport model
[NASA-TP-3168] p 346 N92-19002
Re-engining appears to offer best payback for young: Chapter 2 compliant aircraft
[PNR-90848] p 378 N92-19939
Determining structural performance p 560 N92-22519
The future challenge for aeropropulsion
[NASA-TM-105613] p 658 N92-25164
Computational structural analysis and advanced commercial engines p 660 N92-25933
Steady and transient performance calculation method for prediction, analysis, and identification p 869 N92-28461
Component performance requirements p 869 N92-28462
Supersonic Throughflow Fan Test Facility at NASA. Lewis Research Center
[NASA-TP-3038] p 983 N92-31640

TURBOGENERATORS

The application of a cylindrical-spherical floating ring bearing as a device to control stability of turbogenerators p 224 N92-14371

TURBOJET ENGINE CONTROL

An integrated, full-range surge control/rotating stall avoidance compressor control system p 469 A92-29376
A multivariable control concept for a gas turbine engine
[ETN-92-92104] p 1072 N92-33645

TURBOJET ENGINES

Fracture analysis on compressor blades p 37 A92-10672
Fatigue due to noise-induced pressure
[ASME PAPER 91-GT-150] p 148 A92-15588
Analytical investigation of the rules of component matching in turbojet engines
[ASME PAPER 91-GT-170] p 123 A92-15605
Noise control used for turbojet engine test bench p 284 A92-21749
A numerical study of isothermal flows of a slit V-gutter
[AIAA PAPER 92-0100] p 293 A92-22203
Combat aircraft jet engine noise studies
[ONERA, TP NO. 1991-192] p 415 A92-26353
Thermal management of propulsion systems in hypersonic vehicles
[AIAA PAPER 92-0516] p 373 A92-26942
Surge-troubleshooting of a twin-spool turbojet engine tested at a high altitude test facility p 375 A92-28459
Effects of bleed and power extraction on the operating line of engines p 469 A92-29717
Some rotordynamic problems in small turbo-engines p 470 A92-29736
A study of surge control using fuel pulse cutoff for dual spool turbo-jet engine p 470 A92-29737
Russians say D-30F6 engine used in MiG-31 is highly reliable p 472 A92-32298
An estimate of the influence of the compressor stability margin on the pick-up time of a turbojet engine p 654 A92-37423
An estimate of the influence of the compressor stability margin on the thrust of a turbojet engine p 654 A92-37424
Aerospace - Collected translations of selected papers p 608 A92-38266
A dynamic digital model for the turbojet with pulse-monitored fueller p 654 A92-38267
The turbo-ramjet Griffon p 782 A92-41820
Study on two variable control plan for twin spool turbojet engine p 862 A92-47697
Analytical design and demonstration of a low-cost expendable turbine engine combustor
[AIAA PAPER 92-3754] p 867 A92-49112
Conceptual study of separated core ultra high bypass engine
[AIAA PAPER 92-3775] p 867 A92-49119
Engine flight load reliability analysis p 968 A92-49827
Research on altitude simulation of starting for a single-spool small turbojet p 969 A92-49836
Simulation analysis of the influence of variation in some selected design and control parameters on the acceleration time of a turbojet engine p 970 A92-52890
Underwater turbojet engine
[AD-D015017] p 279 N92-15992
Advanced tactical fighter engine
[ETN-92-90840] p 376 N92-18728
Component-specific modeling --- jet engine hot section components
[NASA-CR-189088] p 377 N92-19726
Computational structural analysis and advanced commercial engines p 660 N92-25933
Liquid lubricants for advanced aircraft engines
[NASA-TM-104531] p 1109 N92-32863

TURBOMACHINE BLADES

Application of compound leaned blades to controlling secondary flow p 5 A92-10975
Aerodynamic damping of blade vibrations in turbomachines --- Russian book p 200 A92-18198
Effect of some load factors of bird impact on blade response p 371 A92-24740
Unsteady aerodynamic interaction effects on turbomachinery blade life and performance
[AIAA PAPER 92-0149] p 341 A92-28186
Generalized expression of chorochronic periodicity in turbomachinery blade-row interaction p 423 A92-30000
Relationship between the rotating stall and vibrations of a blade row p 496 A92-31988
An analysis of impact resistance of composite blades for aircraft engines (Analysis with two dimensional and three dimensional finite elements) p 579 A92-32562
Numerical simulations in turbomachinery; Proceedings of the Symposium, ASME and JSME Joint Fluids Engineering Conference, 1st, Portland, OR, June 23-27, 1991
[ISBN 0-7918-0714-2] p 522 A92-36028
Arbitrary blade section design based on viscous considerations - Background information p 523 A92-36029
Adequacy of modeling turbulence and related effects on helicopter response p 730 A92-41263
Calculation of transonic flow in turbomachine cascades p 708 A92-43067
Coupled vibrations of turbomachine blades p 738 A92-44545
Numerical simulation of impact resistance on composite blade p 738 A92-44734
A new method for predicting the end wall boundary layers and the blade force defects inside the passage of axial compressor cascades p 819 A92-47691
Vane-blade interaction in a transonic turbine. I - Aerodynamics
[AIAA PAPER 92-3323] p 825 A92-48906
Navier-Stokes analysis of three-dimensional unsteady flows inside turbine stages
[AIAA PAPER 92-3211] p 1021 A92-54016
Numerical calculations of propfan/swirl recovery vane flow field
[AIAA PAPER 92-3771] p 1022 A92-54160
Turbomachinery noise p 54 N92-10601
Computation of the unsteady transonic 2D cascade flow by an Euler algorithm with interactive grid generation p 719 N92-27944
Explicit Navier-Stokes computation of turbomachinery flows
[AD-A248458] p 911 N92-29933

TURBOMACHINERY

Developing undergraduate gas turbine and turbomachinery courses
[AIAA PAPER 91-2509] p 56 A92-12700
Preliminary experience with an expert system providing initial centrifugal compressor sizing for performance prediction and analysis
[ASME PAPER 91-GT-28] p 162 A92-15513
The simulation of three-dimensional viscous flow in turbomachinery geometries using a solution-adaptive unstructured mesh methodology
[ASME PAPER 91-GT-124] p 71 A92-15569
The effect of steady aerodynamic loading on the flutter stability of turbomachinery blading
[ASME PAPER 91-GT-130] p 71 A92-15574

Three-dimensional Navier-Stokes computation of turbomachinery flows using an explicit numerical procedure and a coupled k-epsilon turbulence model
[ASME PAPER 91-GT-146] p 72 A92-15584
A gas operated bearing damper for turbomachinery
[ASME PAPER 91-GT-249] p 150 A92-15654
New applications of liquid-crystal thermography in rotating turbomachinery heat transfer research
[ASME PAPER 91-GT-354] p 153 A92-15710
Aerodynamic measuring techniques for transonic and supersonic flow in cascades and turbomachines
[ONERA, TP NO. 1991-170] p 137 A92-16135
Effect of Eulerian inertia forces on the stressed state of the rotating components of aircraft turbomachines
p 128 A92-16828
Concerning a basic assumption for aeroelasticity in turbomachinery p 373 A92-26920
Fibre optic laser anemometry for turbomachinery applications p 397 A92-27783
Three-dimensional compressible flows in turbo-machinery solved by the pseudostream function formulation p 338 A92-27801
A new calculating method for the flowfield in turbomachinery - The study on the application of the vorticity-velocity equations for the numerical solution of the flowfield in turbomachinery p 338 A92-27803
An inverse inviscid method for the design of quasi-three dimensional turbomachinery cascades
p 523 A92-36033
A higher-order accurate Navier-Stokes solver for transonic and supersonic flows in turbomachinery
[AIAA PAPER 92-3044] p 822 A92-48704
Development of an efficient analysis for high Reynolds number inviscid/viscid interactions in cascades
[AIAA PAPER 92-3073] p 823 A92-48723
Pseudostream function formulation - A method of solving three-dimensional aerodynamic analysis and design problems in turbomachinery p 996 A92-52981
Turbomachinery noise p 54 N92-10601
Development of unsteady aerodynamic analyses for turbomachinery aeroelastic and aeroacoustic applications
[NASA-CR-4405] p 12 N92-10979
Research on inverse, hybrid and optimization problems in engineering sciences with emphasis on turbomachine aerodynamics: Review of Chinese advances
p 201 N92-13939
Research on inverse methods and optimization in Italy
p 202 N92-13956
Limit cycle vibrations in turbomachinery
[NASA-TP-3181] p 211 N92-14108
Rotordynamic Instability Problems in High-Performance Turbomachinery, 1990
[NASA-CP-3122] p 222 N92-14346
A simplified method for predicting the stability of aerodynamically excited turbomachinery
p 224 N92-14364
Comments on frequency swept rotating input perturbation techniques and identification of the fluid force models in rotor/bearing/seal systems and fluid handling machines p 224 N92-14370
Basic hydrodynamics
[AD-A243513] p 300 N92-17387
Holographic flow visualization in rotating turbomachinery
[PNR-90837] p 500 N92-20491
The problem of static pressure measurement in turbomachinery annuli using traversable instrumentation
[PNR-90791] p 591 N92-22099
Computations of unsteady multistage turbomachinery flows p 562 N92-23671
Experimental study of the mechanism of sound generation by rotating stall in centrifugal turbomachines
p 605 N92-23726
Boundary Layers in Turbomachines
[VKI-LS-1991-06] p 658 N92-24336
Fundamental aspects of boundary layers and transition in turbomachines p 658 N92-24337
TCGRID: A three dimensional C-grid generator for turbomachinery p 659 N92-25716
An interactive grid generation technique for turbomachinery p 659 N92-25717
TIGER: Turbomachinery interactive grid generation
p 659 N92-25718
TIGGERC: Turbomachinery interactive grid generator energy distributor and restart code p 659 N92-25719
On the computation of unsteady turbomachinery flows. Part 1: Euler equations in vibrating cascades
p 768 N92-27460
Computation and visualization of specific flow phenomena in turbomachinery application
p 741 N92-27463
Presentation of a computational code for 3-D compressible flow in complex channels and cavities
p 769 N92-27475
Visualization of boundary-layer development on turbomachine blades with liquid crystals
[NASA-CR-190433] p 742 N92-27519
Low power magnetic bearing design for high speed rotating machinery p 772 N92-27739
Progress of magnetic suspension systems and magnetic bearings in the USSR p 772 N92-27740
Laser anemometer measurements and computations in an annular cascade of high turning core turbine vanes
[NASA-TP-3252] p 830 N92-28980

TURBOPROP AIRCRAFT
On-board data acquisition system for Embraer's CBA123 p 198 A92-19251
F27 aging aircraft programme emphasizes corrosion prevention p 186 A92-20024
Active control of structurally-coupled sound fields generated by localized force inputs p 694 A92-39106
Noise of two high-speed model counter-rotation propellers at takeoff/approach conditions
p 925 A92-46799
Escape strategies for turboprop aircraft in microburst windshear p 1084 A92-56151
Annoyance caused by advanced turboprop aircraft flyover noise: Comparison of different propeller configurations
[NASA-TP-3104] p 56 N92-11758
Escape strategies for turboprop aircraft in a microburst windshear
[AD-A243090] p 264 N92-17217
Application of analysis techniques for low frequency interior noise and vibration of commercial aircraft
[NASA-CR-189555] p 481 N92-20376
Annoyance caused by aircraft en route noise
[NASA-TP-3165] p 512 N92-20479
Interior noise prediction methodology: ATDAC theory and validation
[NASA-CR-187626] p 697 N92-25368
Active vibrations and noise control for turboprop application research program activities
p 1138 N92-32962

TURBOPROP ENGINES
Compressor coating effects on gas turbine engine performance p 25 A92-11282
Numerical study of branched turboprop inlet ducts using a multiple block grid procedure
[ASME PAPER 91-GT-339] p 76 A92-15703
A universal turboprop engine dynamometer test cell
[ASME PAPER 91-GT-343] p 137 A92-15706
Cold-cycle pressure-jet helicopters - Ventures, designs, and developments. II - Design p 271 A92-22712
Nonlinear transient analysis of composite ATP blade model p 294 A92-23111
Single lever power management of turboprop engines
p 372 A92-25373
Aerodynamic characteristics of a propeller powered high lift semispan wing
[AIAA PAPER 92-0388] p 323 A92-26244
Real-time simulation and adaptive PID control of QSK-06A control for gas turbine p 470 A92-29740
Problems of strength and aeroelasticity of present-day propfans p 471 A92-30133
Single lever power management of turboprop engines
[SAE PAPER 912200] p 656 A92-40013
Pusher turboprop installation technology for the Embraer CBA-123 vector
[SAE PAPER 911030] p 658 A92-40943
Aerodynamic design of an advanced turboprop using Euler codes p 737 A92-43196
Finite elements analysis of flexural edge wave for composite fan blades
[SAE PAPER 912048] p 861 A92-45432
Turboshaft/turboprop cycle sensitivity analysis
[AIAA PAPER 92-3476] p 865 A92-49020
Structural tailoring of advanced turboprops (STAT): User's manual
[NASA-CR-187101] p 26 N92-11016
Preliminary analysis of baseline vibration data from Allison T56-A-14LFE engine and reduction gearbox
[NRC-31578] p 130 N92-11999
The Langley turbo-prop commuter design: A complete project description
[NASA-CR-189987] p 463 N92-21540
Low temperature environment operations of turboengines (design and user's problems)
p 450 N92-21682
Determining structural performance
p 560 N92-22519
High speed turboprop aeroacoustic study (counterrotation). Volume 2: Computer programs
[NASA-CR-185242] p 1011 N92-31248

TURBORAMJET ENGINES
Test results of the expander cycle air turbo ramjet for a future space plane
[IAF PAPER 91-271] p 120 A92-14709
Propulsion aspects of hypersonic turbo-ramjet-engines with special emphasis on nozzle/aftbody integration
[ASME PAPER 91-GT-395] p 127 A92-15725
The study of experimental turboramjets
[AIAA PAPER 92-3720] p 1067 A92-54135
Tests results on Air Turbo Ramjet for a future space plane
[IAF PAPER 92-0657] p 1071 A92-57098
Airbreathing combined cycle engine systems
p 475 N92-21523

TURBOROCKET ENGINES
Airbreathing combined cycle engine systems
p 475 N92-21523

TURBOSHAFTS
The performance evaluation of aeroderivative gas turbines p 119 A92-13296
Optimization of a light helicopter with Arrius power plants p 120 A92-14408
Distortion tolerance of the T800-LHT-800 turboshaft engine p 120 A92-14409
Future trends in turboshaft engines up to 5000 horsepower class
[ASME PAPER 91-GT-74] p 122 A92-15543
Development of a lubrication system for the T800-LHT-800 turboshaft engine
[ASME PAPER 91-GT-398] p 127 A92-15728
Modification of the radiated sound directivity due to ground reflections - Application to static tests of helicopter turboshaft engines
[ONERA, TP NO. 1991-210] p 415 A92-26362
Investigation and application of compressor loading technique p 469 A92-29718
Some rotordynamic problems in small turbo-engines
p 470 A92-29736
High speed rotorcraft propulsion concepts to control power/speed characteristics
[AIAA PAPER 92-3367] p 865 A92-48940
Turboshaft/turboprop cycle sensitivity analysis
[AIAA PAPER 92-3476] p 865 A92-49020
Contingency power for a small turboshaft engine by using water injection into turbine cooling air
[NASA-TM-105680] p 871 N92-29661
A simplified dynamic model of the T700 turboshaft *engine*
[NASA-TM-105805] p 1009 N92-30898

TURBULENCE
Far-field turbulence structure of the tip vortex shed by a single rectangular wing p 620 A92-40084
The low-turbulence wind tunnel at Tohoku University
p 623 A92-40598
Identification of the transfer function between turbulence and aircraft p 743 A92-41226
Numerical investigation of the effect of leading edge geometry on dynamic stall of airfoils
[AD-A239949] p 12 N92-10015
The application of experimental data to blade wake interaction noise prediction
[NASA-CR-189461] p 237 N92-14789
Experimental study of a vortex subjected to imposed strain
[NASA-CR-189757] p 258 N92-15969
Atmospheric pressure flow reactor: Gas phase chemical kinetics under tropospheric conditions without wall effects
[NASA-CASE-MSC-21384-1] p 297 N92-16243
An overview: Challenges in wind technology development
[DE92-001190] p 302 N92-17875
Examination of energy spectra moments in a developing turbulent flow
[NIAR-91-28] p 399 N92-18116
Separation of relaminarised boundary layers
[CUED/A-AERO/TR-16] p 592 N92-22209
Workshop on Engineering Turbulence Modeling
[NASA-CP-10088] p 678 N92-24514
Near-injector structure of non-evaporating pressure-atomized sprays at various ambient densities
p 681 N92-25571
Measurements in the inhomogeneous convective boundary layer using three powered gliders
p 775 N92-26350
Reynolds number dependence of the drag coefficient for laminar flow through fine-scale screens
[DE92-002930] p 765 N92-26698
An experimental investigation of the separating/reattaching flow over a backstep
[NASA-CR-190426] p 716 N92-27399
Effect of collector configuration on test section turbulence levels in an open-jet wind tunnel
[NASA-TM-4333] p 750 N92-27670
Study of turbulence structure through numerical simulations: The perspective of drag and reduction
p 717 N92-27713
Particle image velocimetry
[AD-A246638] p 750 N92-27753

Expand turbulence laboratory facilities to meet new DOD research interest
[AD-A248581] p 883 N92-28388
Laser anemometer measurements and computations in an annular cascade of high turning core turbine vanes
[NASA-TP-3252] p 830 N92-28980
Methods for direct simulation of transition in hypersonic boundary layers 2 p 912 N92-30064
Direct simulation of high-speed mixing layers
[NASA-TP-3186] p 945 N92-30909
Evaluation of microwave landing system approaches in a wide-body transport simulator
[NASA-CR-4450] p 957 N92-30978
Organized turbulent structures and their induced wall pressure fluctuations p 949 N92-31853
Effects of curvature and rotation on turbulence in the NASA low-speed centrifugal compressor impeller
p 1124 N92-32292
Swept shock/boundary layer interaction experiments in support of CFD code validation
[NASA-CR-190583] p 1036 N92-32494
Perspectives on hypersonic viscous and nonequilibrium flow research
[NASA-CR-190817] p 1039 N92-33413
High speed transition prediction
[NASA-CR-190836] p 1039 N92-33424
Influence of the swirl producing construction in the flow and reaction field of turbulent diffusion flames
[ETN-92-92103] p 1127 N92-33916

TURBULENCE EFFECTS

An improved computation for gas-turbine combustion chamber flow p 375 A92-28479
Experimental study of a two-dimensional random frequency generator p 483 A92-29712
Analysis of effects of freestream turbulence on cascade performance p 422 A92-29716
Effects of ambient turbulence on the decay of a trailing vortex wake p 442 A92-32245
An experimental study of the noise of flow past a wing at low velocities p 603 A92-33771
A time-integrated image model for aero-optic analysis
[AIAA PAPER 92-2793] p 779 A92-41332
Hang-glider response to atmospheric inputs
p 874 A92-46765
Reconstruction of flight path in turbulence
p 874 A92-46777
Unsteady aerodynamics of a Wortmann wing at low Reynolds numbers p 810 A92-46778
Establishing a database for flight in the wakes of structures p 810 A92-46782
On the adequacy of modeling turbulence and related effects on helicopter response p 847 A92-46945
Motion errors in an airborne synthetic aperture radar system p 840 A92-48416
Some important factors in turbulence in flight measurement p 1063 A92-54324
Noise from turbulent shear flows p 55 N92-10603
Jet noise generated by large-scale coherent motion
p 55 N92-10604
Propulsive lift noise p 55 N92-10606
Review of aircraft dynamic loads due to flow separation p 85 N92-13008
Direct computation of turbulence and noise
[NASA-CR-187616] p 236 N92-14788
The effect of freestream turbulence on the vortical flow over a delta wing p 261 N92-17681
Turbulent skin-friction drag reduction by active and passive means, part 1 p 718 N92-27714
Viscous effects on a vortex wake in ground effect
[NASA-CR-190400] p 907 N92-28361
High-Speed Research: Sonic Boom, volume 1
[NASA-CP-3172] p 1061 N92-33874
Wave equations and computational models for sonic boom propagation through a turbulent atmosphere
p 1139 N92-33877
The effect of turbulence on the loudness of minimized sonic boom signatures p 1139 N92-33880
Model experiment to study the effect of turbulence on risetime and waveform of N waves
p 1139 N92-33881
Turbulence-induced loads on a teetered rotor
p 1042 N92-34029

TURBULENCE METERS

A sensitive fast-response probe to measure turbulence and heat flux from any airplane p 775 A92-42097
The ASU Transition Research Facility
[AIAA PAPER 92-3910] p 1094 A92-56744

TURBULENCE MODELS

Emergence of coherent patterns of vortex stretching during reconnection - A scattering paradigm
p 38 A92-11041
Simple turbulence models for supersonic flows - Bodies at incidence and compression corners p 5 A92-11059
Solution of the Reynolds-averaged Navier-Stokes equations for transonic aerofoil flows p 9 A92-13198
Turbine cascade calculations through a fractional step Navier-Stokes algorithm
[ASME PAPER 91-GT-55] p 68 A92-15533
Turbulence modelling for secondary flow prediction in a turbine cascade
[ASME PAPER 91-GT-57] p 68 A92-15535
Algebraic turbulence modeling for unstructured and adaptive meshes p 216 A92-18362
Sonic eddy - A model for compressible turbulence
p 176 A92-20739
Studies of the effects of curvature on dilution jet mixing p 290 A92-21079
Calculation methods of three-dimensional boundary layers p 245 A92-21978
An assessment of particle velocimetry potential in hypersonic flow
[AIAA PAPER 92-0010] p 247 A92-22135
Recent advancements in turbomachinery forced response analyses
[AIAA PAPER 92-0012] p 278 A92-22136
Navier-Stokes analysis of blunt trailing edge airfoils
[AIAA PAPER 92-0024] p 248 A92-22146
Nonequilibrium algebraic turbulence modeling considerations for transonic airfoils and wings
[AIAA PAPER 92-0026] p 248 A92-22148
Effect of turbulence modeling on dynamic stall of a NACA0012 airfoil
[AIAA PAPER 92-0027] p 248 A92-22149
The Baldwin-Lomax model for separated and wake flows using the entropy envelope concept
[AIAA PAPER 92-0148] p 253 A92-23764
Modeling supersonic inlet boundary layer bleed roughness
[AIAA PAPER 92-0269] p 317 A92-25725
Calculation of the carriage loads of tandem stores on a fighter aircraft
[AIAA PAPER 92-0283] p 319 A92-25736
Turbulence amplification through a shock wave
[AIAA PAPER 92-0313] p 320 A92-25761
A turbulence model for iced airfoils and its validation
[AIAA PAPER 92-0417] p 326 A92-26267
Turbulence modeling for high speed flows
[AIAA PAPER 92-0436] p 327 A92-26283
A comparative study of turbulence models for overset grids
[AIAA PAPER 92-0437] p 327 A92-26284
A one-equation turbulence model for aerodynamic flows
[AIAA PAPER 92-0439] p 327 A92-26285
New nonequilibrium turbulence model for calculating flows over airfoils p 330 A92-26403
Application of a new K-tau model to near wall turbulent flows p 395 A92-26437
Algebraic turbulence modeling for adaptive unstructured grids p 398 A92-28033
Turbulence model effects on separated flow about a prolate spheroid p 340 A92-28036
Navier-Stokes solution of transonic cascade flows using nonperiodic C-type grids p 344 A92-28523
Applications of an implicit, upwind Navier-Stokes code, CRAFT, to steady/unsteady reacting, multi-phase flowfields
[AIAA PAPER 92-0837] p 422 A92-29603
Assessment of three models of turbulence in a shock-boundary layer interaction of a heated wall
p 423 A92-29999
Determination of the mean duration of normal acceleration loads at the center of mass of aircraft during a flight in a turbulent atmosphere p 480 A92-30192
Navier-Stokes methods to predict circulation control airfoil performance p 442 A92-32243
Numerical studies of supersonic flow over a compression corner p 442 A92-32324
International Symposium on Engineering Turbulence Modelling and Measurements, Dubrovnik, Yugoslavia, Sept. 24-24, 1990, Selected Papers p 672 A92-38851
Influence of inlet conditions on the flowfield in a model gas turbine combustor p 672 A92-38866
Turbine blade heat transfer prediction using coupled turbulent Prandtl number and transition models
[SAE PAPER 912152] p 674 A92-39987
Prediction of three-dimensional turbulent boundary layers using a second-moment closure
p 675 A92-40080
Phase-averaged turbulence statistics in a near wake with an asymmetric vortex shedding p 620 A92-40086
An experimental evaluation of some turbulence models from a three-dimensional turbulent boundary layer around a wing-body junction p 620 A92-40087
Second moment closure predictions of jet-on-jet impingement flows p 675 A92-40102
Vortical flow simulation by the solution of the Navier-Stokes equations p 620 A92-40104
Simulation and modeling of homogeneous compressible turbulence under isotropic mean compression
p 622 A92-40134
Analysis of turbulence models for hypersonic boundary layers p 623 A92-40182
Adequacy of modeling turbulence and related effects on helicopter response p 730 A92-41263
Renormalization group based algebraic turbulence model for three-dimensional turbomachinery flows
p 703 A92-41268
Navier-Stokes cavity solutions based on second-order turbulence modeling
[AIAA PAPER 92-2765] p 704 A92-41314
Models of turbulence in a hypersonic boundary layer
p 705 A92-41817
The DAM vertical shock-tube p 880 A92-45096
Computational evaluation of an airfoil with a Gurney flap
[AIAA PAPER 92-2708] p 802 A92-45550
Computation of turbulent, separated, unswept compression ramp interactions p 813 A92-46897
On the adequacy of modeling turbulence and related effects on helicopter response p 847 A92-46945
Experience with the Johnson-King turbulence model in a transonic turbine cascade flow solver
p 821 A92-48207
Comparative study of turbulence models in predicting hypersonic inlet flows
[AIAA PAPER 92-3098] p 824 A92-48740
FNS analysis of an axisymmetric scramjet inlet
[AIAA PAPER 92-3100] p 824 A92-48742
A turbulence model based on RNG for quasi-three-dimensional cascade flows --- renormalization group methods
[AIAA PAPER 92-3312] p 825 A92-48898
Numerical study of secondary separation in glancing shock/turbulent boundary layer interactions
[AIAA PAPER 92-3666] p 907 A92-49087
The enhancement of the mixing and combustion processes in supersonic flow applied to scramjet engine
[AIAA PAPER 92-3428] p 1112 A92-54029
Comparison of turbulence models for powered-lift flow fields
[AIAA PAPER 92-3674] p 1022 A92-54117
Comparative numerical study of two turbulence models for airfoil static and dynamic stall
[AIAA PAPER 92-4649] p 1028 A92-55394
Computational study of the aerodynamics and control by blowing of asymmetric vortical flows over delta wings
[NASA-CR-187979] p 14 N92-10990
The effects of Reynolds number, rotor incidence angle and surface roughness on the heat transfer distribution in a large-scale turbine rotor passage
[NASA-CR-184260] p 42 N92-11297
An assessment and application of turbulence models for hypersonic flows
[NASA-TM-105124] p 82 N92-11984
Nonequilibrium turbulence modeling effects on transonic vortical flows about delta wings p 85 N92-13007
Navier-Stokes analysis of turbulent boundary layer and wake for two-dimensional lifting bodies
p 221 N92-14309
Determination of rotordynamic coefficients for labyrinth seals and application to rotordynamic design calculations p 223 N92-14360
A turbulence model for iced airfoils and its validation
[NASA-TM-105373] p 186 N92-15052
Viscous three-dimensional calculations of transonic fan performance
[NASA-TM-103800] p 242 N92-17346
Hi-alpha forebody design. Part 2: Determination of body shapes for positive directional stability
[NASA-CR-189850] p 359 N92-18038
Towards the computation of turbulent hypersonic flows
[AERO-REPT-9106] p 345 N92-18318
Methodology for sensitivity analysis, approximate analysis, and design optimization in CFD for multidisciplinary applications --- computational fluid dynamics
[NASA-CR-190201] p 595 N92-22662
Workshop on Engineering Turbulence Modeling
[NASA-CP-10088] p 678 N92-24514
Some comments on turbulence modeling from an industrial perspective p 678 N92-24531
Turbulence modeling for hypersonic flight
[NASA-CR-190313] p 630 N92-24898
A compressible Navier-Stokes solver with two-equation and Reynolds stress turbulence closure models
[NASA-CR-4440] p 681 N92-25376
An integrated CFD system for 3D turbomachinery applications p 741 N92-27464
Predictions and measurements of 3D viscous flow in a transonic turbine nozzle guide vane row
p 741 N92-27466
Viscous three-dimensional calculations of transonic fan performance p 768 N92-27467

A study of juncture flow in the NASA Langley 0.3-meter transonic cryogenic tunnel
[NASA-CR-190430] p 773 N92-27880
Comparative study of turbulence models in predicting hypersonic inlet flows
[NASA-TM-105720] p 722 N92-28102
Turbulence modeling: Survey of activities in Belgium and the Netherlands, and appraisal of the status and a view on the prospects
[NLR-TP-90184-U] p 908 N92-28694
Computation of three-dimensional effects on two dimensional wings
[NASA-CR-190576] p 832 N92-29691
Application of the Chimera overlapped grid scheme to simulation of Space Shuttle ascent flows
p 945 N92-30742
A computational investigation of airfoil stall flutter
[AD-A247302] p 947 N92-31300
NAS (Numerical Aerodynamic Simulation Program) technical summaries, March 1989 - February 1990
[NASA-TM-107960] p 1013 N92-31852
A computational examination of directional stability for smooth and chined forebodies at high-alpha
[NASA-CR-4465] p 950 N92-32114
Turbulence-induced loads on a teetered rotor
p 1042 N92-34029

TURBULENT BOUNDARY LAYER

Correlation of separation shock motion with pressure fluctuations in the incoming boundary layer
p 5 A92-11061
Numerical investigation of bleed on three-dimensional turbulent interactions due to sharp fins
p 5 A92-11062
Pressure on a cylinder with a screen in transverse flow p 6 A92-12164
Evolution of three-dimensional flows during the interaction between conical shock waves and a turbulent boundary layer p 7 A92-12169
A study on the interaction between a bow shock wave generated by a blunt body and a turbulent boundary layer p 8 A92-12424
Fundamentals of applied aerogasdynamics. II - Viscous flow past bodies. Control devices --- Russian book
p 64 A92-14281
Flow unsteadiness by weak normal shock wave/turbulent boundary layer interaction in internal flow
p 67 A92-15359
An investigation of a strong shock-wave turbulent boundary layer interaction in a supersonic compressor cascade
[ASME PAPER 91-GT-92] p 70 A92-15556
Confined normal-shock/turbulent-boundary-layer interaction followed by an adverse pressure gradient
p 172 A92-18365
Wedge-induced turbulent boundary-layer separation on a roughened surface at Mach 6.0 p 175 A92-20379
Turbulent boundary-layer characteristics over a flat-plate/wedge configuration at Mach 6
p 176 A92-20761
The experimental approach to the LEBU on turbulent drag reduction p 243 A92-21469
A fast viscous correction method for transonic aerodynamics p 247 A92-21986
Nonequilibrium algebraic turbulence modeling considerations for transonic airfoils and wings
[AIAA PAPER 92-0026] p 248 A92-22148
Weak coupling between an unsteady 3D full potential code and an unsteady turbulent boundary layer code - Application to a helicopter rotor in forward flight
[AIAA PAPER 92-0029] p 249 A92-22151
Shock-boundary layer interaction control with low-profile vortex generators and passive cavity
[AIAA PAPER 92-0064] p 250 A92-22178
A calculating method of shock wave oscillating frequency due to turbulent shear layer fluctuations in supersonic flow p 251 A92-22720
Effect of supersonic diffuser geometry on operation conditions p 310 A92-24599
A numerical calculation of three dimensional incompressible laminar, transition and turbulent boundary layers p 393 A92-25138
A three-dimensional supersonic turbulent boundary layer generated by an isentropic compression
[AIAA PAPER 92-0310] p 320 A92-25758
An algebraic model for dissipation in supersonic boundary layers
[AIAA PAPER 92-0311] p 320 A92-25759
Wall pressure wavenumber-frequency spectrum beneath a turbulent boundary layer measured with transducer arrays calibrated with an acoustical method
[ONERA, TP NO. 1991-212] p 329 A92-26364
Experimental investigation of normal-shock/turbulent-boundary-layer interactions with and without mass removal p 330 A92-26411
Crossing shock wave turbulent boundary layer interactions - Variable angle and shock generator length geometry effects at Mach 3
[AIAA PAPER 92-0636] p 334 A92-27014
Holographic flowfield density measurements in swept shock wave/boundary-layer interactions
[AIAA PAPER 92-0746] p 335 A92-27092
An experimental/computational study of sharp fin induced shock wave/turbulent boundary layer interactions at Mach 5 - Experimental results
[AIAA PAPER 92-0749] p 335 A92-27093
Flowfield visualization of crossing shock-wave/boundary-layer interactions
[AIAA PAPER 92-0750] p 335 A92-27094
Evolution of perturbations in a supersonic boundary layer p 337 A92-27596
A study of the interaction of a normal shock wave with a turbulent boundary layer at Mach numbers between 1.30 and 1.55 p 339 A92-28006
The structure and development of streamwise vortex arrays embedded in a turbulent boundary layer
[AIAA PAPER 92-0551] p 342 A92-28204
Multiple normal shock wave/turbulent boundary-layer interactions p 344 A92-28527
Control of strong shock-turbulent boundary layer interaction in rectangular channels p 422 A92-29714
Investigating the feasibility of controlling the laminar-turbulent transition by means of laminarizing plates p 493 A92-30161
Experimental study of the characteristics of boundary-layer development on an airfoil
p 425 A92-30171
The effect of the angle-of-attack on laminar-turbulent boundary transition near the lower surface of triangular plates in a supersonic gas flow p 426 A92-30180
Effect of compressibility on the value of the acceptable roughness Reynolds number p 427 A92-30197
Structure of supersonic turbulent flow past a swept compression corner p 431 A92-31155
Nonadiabatic and three-dimensional effects in compressible turbulent boundary layers
p 431 A92-31156
Semiconductor laser Doppler anemometer for applications in aerodynamic research
p 495 A92-31173
Cylinder-induced shock-wave boundary-layer interaction p 433 A92-31188
Effects of sweepback on unsteady separation in Mach 5 compression ramp interactions
[AIAA PAPER 92-0430] p 435 A92-31663
A preliminary study of the turbulent structures associated with unsteady separation shock motion in a Mach 5 compression ramp interaction
[AIAA PAPER 92-0744] p 436 A92-31677
Unsteady separation in sharp fin-induced shock wave/turbulent boundary layer interaction at Mach 5
[AIAA PAPER 92-0748] p 436 A92-31678
Flight studies of the riblet effect on drag variation
p 438 A92-31871
Consideration of the effect of viscosity in the problem of porous-wall induction p 440 A92-31887
Structure of a boundary layer on the lower surface of a wing in flight and in a wind tunnel p 440 A92-31899
Response of plate-like structures to correlated random pressure fluctuations
[AIAA PAPER 92-2378] p 584 A92-34452
Inverse solution of 3D incompressible turbulent boundary layer with separated bubbles
p 522 A92-35992
Supersonic and hypersonic boundary-layer transition induced by discrete trips p 522 A92-36023
Structure of the separated flow region in a dihedral corner in front of an obstacle in supersonic flow
p 524 A92-36420
Compressible turbulent boundary layers with heat addition by homogeneous condensation
p 611 A92-36843
Effect of controlled longitudinal vortex arrays on the development of a turbulent boundary layer
p 614 A92-38856
Experiments on turbulent flow due to an enclosed rotating disk p 615 A92-38863
Prediction for the incipient separation of fin-generated three-dimensional shock wave turbulent boundary layer interactions p 615 A92-38909
Bursts and sources of pressure fluctuation in turbulent boundary layers p 619 A92-40055
Three-dimensional vortical structure of a large-scale coherent vortex in a turbulent boundary layer
p 619 A92-40056
On the mechanics of 3-D turbulent boundary layers
p 620 A92-40068
Prediction of three-dimensional turbulent boundary layers using a second-moment closure
p 675 A92-40080
An experimental evaluation of some turbulence models from a three-dimensional turbulent boundary layer around a wing-body junction p 620 A92-40087
A study of three dimensional turbulent boundary layer separation and vortex flow control using the reduced Navier Stokes equations p 621 A92-40105
Influence of suction through a slot on a turbulent boundary layer p 622 A92-40127
Experimental and numerical investigation of a turbulent boundary layer over riblets p 622 A92-40128
Effects of attack angle on leg portion of the horseshoe vortex around the idealized wing p 623 A92-40177
Prediction of separation point in compressible turbulent boundary layers by Green's lag-entrainment method
p 700 A92-41178
Hypersonic shock-wave turbulent-boundary-layer interaction flows p 703 A92-41264
A study of aerophysical and dynamic characteristics using an axisymmetric flight test vehicle with a reusable nose section p 707 A92-42684
Turbulent drag reduction by laminar sublayer thickening
[AIAA PAPER 92-2707] p 801 A92-45549
Surface and flow field measurements in a symmetric crossing shock wave/turbulent boundary layer flow
[AIAA PAPER 92-2634] p 806 A92-45574
Interaction between crossing oblique shocks and a turbulent boundary layer p 812 A92-46882
Total losses in turbulent flows inside conical diffusers
p 819 A92-47782
Supersonic jet mixing enhancement by 'delta-tabs'
[AIAA PAPER 92-3548] p 826 A92-49063
Numerical study of secondary separation in glancing shock/turbulent boundary layer interactions
[AIAA PAPER 92-3666] p 907 A92-49087
Numerical simulation of a confined transonic normal shock wave/turbulent boundary layer interaction
[AIAA PAPER 92-3668] p 826 A92-49088
Effects of a leading-edge fillet on the flow past an appendage-body junction p 935 A92-50301
Exploratory study of wall pressure fluctuations in a Mach 5, sharp fin-induced turbulent interaction
p 935 A92-50304
Physical model of the swept shock wave/boundary-layer interaction flowfield p 935 A92-50312
Measurement of turbulent boundary layer in transonic flow p 941 A92-53010
Experimental investigation on turbulent phenomena in three-dimensional shock wave/turbulent boundary layer interaction induced by blunt fin p 1018 A92-53557
Experimental study on three-dimensional shock wave-turbulent boundary layer interaction induced by protuberance p 1019 A92-53997
Thermal paints for shock/boundary layer interaction in inlet flows
[AIAA PAPER 92-3626] p 1113 A92-54093
Heat transfer measurements and CFD comparison of swept shock wave/boundary-layer interactions
[AIAA PAPER 92-3665] p 1021 A92-54110
An experimental examination of the effects of incoming boundary layer modifications on the dynamics of a turbulent compression corner interaction
[AIAA PAPER 92-3667] p 1022 A92-54111
Structure of crossing-shock wave/turbulent boundary-layer interactions
[AIAA PAPER 92-3670] p 1022 A92-54113
Experimental investigation of the reflection of a shock wave on a heated surface in presence of a turbulent boundary layer p 1023 A92-54569
Three-dimensional shock wave-turbulent boundary layer interaction induced by blunt body and protuberance
p 1029 A92-56009
Surface heat transfer and flow properties of vortex arrays induced artificially and from centrifugal instabilities
p 1121 A92-56371
A quiet-flow Ludwieg tube for experimental study of high speed boundary layer transition
[AIAA PAPER 92-3885] p 1094 A92-56727
The measurement of plate vibration and sound radiation from a turbulent boundary layer manipulator
[AD-A240127] p 42 N92-10206
Results from computational analysis of a mixed compression supersonic inlet
[NASA-TM-104475] p 12 N92-10976
Turbulent friction drag reduction: Boundary layer manipulators
[CERT-RSF-DERAT-62/5004-31] p 43 N92-11309
Constant-temperature anemometry measurements in hypersonic boundary layers p 90 N92-13861
Navier-Stokes analysis of turbulent boundary layer and wake for two-dimensional lifting bodies
p 221 N92-14309
Preliminary investigation of the shock-boundary layer interaction in a simulated fan passage
[AD-A242656] p 185 N92-15045

Simplified method for the prediction of aerofoil excrescence drag magnification factor for turbulent boundary layers at subcritical Mach numbers
[ESDU-91028] p 259 N92-15972
An experimental study of a turbulent wing-body junction and wake flow
[AD-A243388] p 260 N92-17222
Basic hydrodynamics
[AD-A243513] p 300 N92-17387
The effect of freestream turbulence on the vortical flow over a delta wing p 261 N92-17681
Deterministic multi-zone ice accretion modeling
p 265 N92-17987
A study of the diffusion of slot-injected drag-reducing polymer solution in a turbulent boundary layer modified by large-eddy breakup devices
[AD-A243411] p 344 N92-18007
Towards the computation of turbulent hypersonic flows
[AERO-REPT-9106] p 345 N92-18318
Proceedings of the Seminar on Investigation and Control of Boundary-Layer Transition
[NAL-SP-11] p 400 N92-18483
Operating ranges of meteorological wind tunnels for the simulation of convective boundary layer phenomena
[AD-A244153] p 409 N92-19195
Experimental investigation of trailing edge crenulation effects on losses in a compressor cascade
[AD-A243902] p 377 N92-19329
Laser-spectroscopic measurement techniques for hypersonic, turbulent wind tunnel flows
[NASA-TM-103928] p 405 N92-19596
A laser velocimeter investigation of the normal shockwave boundary layer interaction
p 500 N92-20485
Experimental study of the wall pressure fluctuations under a turbulent boundary layer downstream of tandem aerofoil external manipulators
[REPT-207-90-78] p 500 N92-20497
Supersonic jet mixing enhancement by delta-tabs
[NASA-TM-105664] p 630 N92-24958
Turbulent heat flux measurements in a transitional boundary layer
[NASA-TM-105623] p 716 N92-27377
An experimental investigation of the separating/reattaching flow over a backstep
[NASA-CR-190426] p 716 N92-27399
Visualization of boundary-layer development on turbomachine blades with liquid crystals
[NASA-CR-190433] p 742 N92-27519
Basic concepts on boundary layers
p 717 N92-27707
Laminar-turbulent transition: Fundamentals
p 717 N92-27710
Study of turbulence structure through numerical simulations: The perspective of drag and reduction
p 717 N92-27713
Turbulent skin-friction drag reduction by active and passive means, part 1 p 718 N92-27714
Experimental investigation of turbulence behavior in shock wave/turbulent boundary layer interactions
[AD-A247792] p 774 N92-27886
Computation of viscous phenomena in unsteady transonic flow p 720 N92-27949
Turbulence modeling: Survey of activities in Belgium and the Netherlands, and appraisal of the status and a view on the prospects
[NLR-TP-90184-U] p 908 N92-28694
Turbulent spot generation and growth rates in a transonic boundary layer
[AD-A250221] p 909 N92-29118
Structure of three-dimensional turbulent boundary layers p 999 N92-30654
An experimental study of the relationship between velocity and pressure fluctuations in a wing-body junction
[AD-A249628] p 946 N92-31122
The structure and control of three-dimensional shock wave turbulent boundary layer interactions
[AD-A250209] p 1003 N92-31824
Organized turbulent structures and their induced wall pressure fluctuations p 949 N92-31853
The calculation of incompressible separated turbulent boundary layers p 1003 N92-31886
Acoustic loads prediction on jet aircraft
p 1136 N92-32949
Simulations of sonic boom ray tube area fluctuations for propagation through atmospheric turbulence including caustics via a Monte Carlo method
p 1139 N92-33878
Analysis of sonic boom data to quantify distortions of shock profiles p 1139 N92-33879

TURBULENT COMBUSTION
Turbulent combustion modelling in a side dump ramjet combustor
[AIAA PAPER 92-3599] p 1112 A92-54075
An assumed joint-Beta PDF approach for supersonic turbulent combustion
[AIAA PAPER 92-3844] p 1113 A92-54199

TURBULENT DIFFUSION
A circumferential non-uniform effect model for multistage axial-flow compressor throughflow p 588 A92-35572
Turbulent diffusion flame properties behind a backward-facing step p 985 A92-50255
An experimental investigation of the flow in a diffusing S-duct
[AIAA PAPER 92-3622] p 1021 A92-54090
Numerical simulation of unsteady rotor wakes
p 1032 A92-56352
Analysis of a dusty wall jet
[NASA-CR-189759] p 257 N92-15965
Local extinction mechanisms in non-premixed turbulent combustion
[AD-A242027] p 290 N92-17682
Theories of turbulent combustion in high speed flows
[AD-A253032] p 1111 N92-33624

TURBULENT FLOW
Prediction of wake in a curved duct p 3 A92-10487
Nonstationary forces on a wing airfoil
p 4 A92-10825
Comparative studies of flow around a wing profile in two wind tunnels p 7 A92-12170
Prospects of turbulence research by means of testing bodies in motion p 30 A92-12194
Solution of the Reynolds-averaged Navier-Stokes equations for transonic aerofoil flows p 9 A92-13198
Probe shapes for streamwise momentum and cross-stream turbulence intensity p 9 A92-13210
Probe systems for static pressure and cross-stream turbulence intensity p 10 A92-13211
The role of laminar-turbulent transition in gas turbine engines p 120 A92-14868
Realization of a large-scale turbulence field in a small wind tunnel p 67 A92-15487
A calculation procedure for three-dimensional turbulent flow in a centrifugal impeller with any blade geometry
[ASME PAPER 91-GT-171] p 73 A92-15606
Thermal details in a rotor-stator cavity at engine conditions with a mainstream
[ASME PAPER 91-GT-275] p 151 A92-15672
Turbulent flow calculations using unstructured and adaptive meshes p 153 A92-15823
Numerical prediction of subsonic turbulent flows over slender bodies at high incidence p 172 A92-18358
Numerical study on using sulfur hexafluoride as a wind tunnel test gas p 216 A92-18373
A perspective on aerospace CFD p 169 A92-20145
CFD helps the Air Force fly right p 169 A92-20146
The experimental approach to the LEBU on turbulent drag reduction p 243 A92-21469
Control of turbulent flow on a backward-facing step
[AIAA PAPER 92-0066] p 250 A92-22179
Numerical studies of supersonic/hypersonic combustion
[AIAA PAPER 92-0094] p 293 A92-22200
Organized structure in a Mach 5/Mach 3 turbulent shear layer
[AIAA PAPER 92-0180] p 256 A92-23790
Multigrid Navier-Stokes calculations for three dimensional cascades
[AIAA PAPER 92-0190] p 256 A92-23799
Prediction of turbulent flow behavior over a slotted flap p 309 A92-24407
Problems of laminar-turbulent transition control in a boundary layer p 312 A92-24979
Turbulence amplification through a shock wave
[AIAA PAPER 92-0313] p 320 A92-25761
Efficient simulation of incompressible viscous flow over single and multi-element airfoils
[AIAA PAPER 92-0405] p 324 A92-26258
An experimental study of a turbulent wing-body junction and wake flow
[AIAA PAPER 92-0434] p 327 A92-26281
A one-equation turbulence model for aerodynamic flows
[AIAA PAPER 92-0439] p 327 A92-26285
New nonequilibrium turbulence model for calculating flows over airfoils p 330 A92-26403
Application of a new K-tau model to near wall turbulent flows p 395 A92-26437
Transition to turbulence in confined, compressible mixing layers. I - 3D numerical simulations with excitation of random, broadband white noise
[AIAA PAPER 92-0553] p 332 A92-26964
Prediction of the pressure loss coefficient of wind tunnel turbulence reducing screens
[AIAA PAPER 92-0568] p 384 A92-26976
A method for the optical measurement of surface friction in supersonic flow p 337 A92-27537
Premixed, turbulent combustion of axisymmetric sudden expansion flows p 397 A92-27770
Algebraic turbulence modeling for adaptive unstructured grids p 398 A92-28033
An improved computation for gas-turbine combustion chamber flow p 375 A92-28479
Swirl effects on confined flows in axisymmetric geometries p 399 A92-28513
Numerical simulation of slot injection into a turbulent supersonic stream
[AIAA PAPER 92-0827] p 421 A92-29595
Analysis of effects of freestream turbulence on cascade performance p 422 A92-29716
Effect of the longitudinal and transverse riblets of a flat plate on laminar-to-turbulent transition
p 428 A92-30210
CFD state-of-the-art in the U.S.S.R
p 495 A92-31486
A new adaptive algorithm for turbulent flows
p 434 A92-31547
Turbulent flow in the wake of an idealized wing-body junction
[AIAA PAPER 92-0282] p 435 A92-31652
Computational studies of transonic flow past a swept wing and the boundary layer characteristics
p 438 A92-31872
Numerical analysis of three-dimensional unsteady turbulent flows in a turbine stage p 443 A92-32501
Power spectrum of ring modes of pressure fluctuations at the surface of a cylinder in axial flow
p 603 A92-33770
The Berlin oil channel for drag reduction research
p 571 A92-34219
Subcritical flutter characteristics of a swept-back wing in a turbulent supersonic flow - Comparison between analysis and experiment
[AIAA PAPER 92-2393] p 517 A92-34466
Simulation of 3-D shear flows around a nozzle-afterbody at high speeds p 519 A92-34826
Studies on laminar boundary-layer receptivity to freestream turbulence near a leading edge
p 591 A92-36007
The effects of wall suction on laminar-turbulent transition in three-dimensional flow p 522 A92-36021
Unsteady Navier-Stokes simulation of turbulent flows through a supersonic compressor cascade
p 523 A92-36036
Separated and cavitation flows - Principal properties and computational models --- Russian book
[ISBN 5-02-014005-8] p 610 A92-36600
Multifractal analysis of a lobed mixer flowfield utilizing the proper orthogonal decomposition
p 611 A92-36840
Similarity in supersonic mixing layers
p 611 A92-36842
An improved analysis method for cross-wire signals obtained in supersonic flow p 614 A92-38456
International Symposium on Engineering Turbulence Modelling and Measurements, Dubrovnik, Yugoslavia, Sept. 24-24; 1990, Selected Papers p 672 A92-38851
Flow regimes of the cove regions between a slat and wing and between a wing and flap of a multielement airfoil p 614 A92-38858
Reynolds stress distribution downstream of a turbine cascade p 614 A92-38861
Experiments on turbulent flow due to an enclosed rotating disk p 615 A92-38863
LDV measurements of the flowfield in a simulated combustor with axial and side inlets p 672 A92-38867
Hypersonic turbulent separated flow past an unswept circular cylinder on a flat plate p 615 A92-38908
Symposium on Turbulent Shear Flows, 8th, Technical University of Munich, Federal Republic of Germany, Sept. 9-11, 1991, Proceedings. Vols. 1 & 2
p 675 A92-40051
Compressibility effects on the growth and structure of homogeneous turbulent shear flow p 675 A92-40052
A new method for visualization and measurement of turbulent flow patterns p 619 A92-40063
Turbulent energy budgets in impinging zones
p 620 A92-40081
Particle dispersion in highly swirling, turbulent flows
p 675 A92-40093
Measurements and simulation of the flow around a poppet valve p 675 A92-40103
An experimental and numerical study of confined axisymmetric jet with a bluff body p 621 A92-40106
Transition to turbulence in curved channel flow
p 621 A92-40125
Evolution of coherent structures during transition in a flat-plate boundary layer p 621 A92-40126
Influence of suction through a slot on a turbulent boundary layer p 622 A92-40127
Reactive mixing layer between pressure reflecting boundaries p 656 A92-40144
Simulation of turbulent velocity profiles appearing on rotating and stationary parts of subsonic compressors and turbines p 676 A92-40172

Data analysis for unsteady turbulence measurements over airfoils p 701 A92-41214
Adaptive mesh for turbulent hypersonic flow
[AIAA PAPER 92-2776] p 704 A92-41322
A validated code to predict the performance of onboard broadband optical seekers through a turbulent transonic flow
[AIAA PAPER 92-2792] p 778 A92-41331
The flow over a backward-facing step under controlled perturbation - Laminar separation p 705 A92-41653
Calculation of three-dimensional turbulent flow in wind tunnel entry section p 708 A92-43055
Calculation of transonic flow in turbomachine cascades p 708 A92-43067
Simultaneous imaging and interferometric turbule visualization in a high-velocity mixing/shear layer p 896 A92-45130
High Reynolds number flows using liquid and gaseous helium
[ISBN 0-387-97475-X] p 897 A92-45261
Remarks on high-Reynolds-number turbulence experiments and facilities p 881 A92-45267
Response characteristics of a wing in supersonic flow near flutter boundary
[SAE PAPER 911999] p 789 A92-45401
A new approach for the calculation of transitional flows
[AIAA PAPER 92-2669] p 798 A92-45524
Calculation of high speed base flows
[AIAA PAPER 92-2679] p 799 A92-45531
Turbulent drag reduction by laminar sublayer thickening
[AIAA PAPER 92-2707] p 801 A92-45549
Computation of turbulent flow about cone-derived waverider
[AIAA PAPER 92-2726] p 804 A92-45562
Interaction between crossing oblique shocks and a turbulent boundary layer p 812 A92-46882
Computation of turbulent, separated, unswept compression ramp interactions p 813 A92-46897
Segmental heat transfer in a pin fin channel with ejection holes p 900 A92-47267
A time marching method in finite volume for transonic diffuser turbulent flows p 819 A92-47690
Calculation of fully three-dimensional separated flows with an unsteady viscous-inviscid interaction method
[ONERA, TP NO. 1992-1] p 821 A92-48577
Separation and vortex formation in turbulent flows
[ONERA, TP NO. 1992-7] p 822 A92-48579
Development and application of a zonal k-epsilon turbulence model for complex 3-D flowfields
[AIAA PAPER 92-3176] p 903 A92-48792
Wake mixing and performance measurements in a linear compressor cascade with crenulated trailing edges
[AIAA PAPER 92-3188] p 824 A92-48800
A numerical study of two-phase flow in gas turbine combustors
[AIAA PAPER 92-3468] p 905 A92-49015
A study of the flammability limit of the backward facing step flow combustion
[AIAA PAPER 92-3846] p 895 A92-49136
Navier-Stokes computations of horseshoe vortex flows p 990 A92-49516
Effects of vortex generators on the growth of a compressible shear layer
[AIAA PAPER 90-1979] p 934 A92-50269
Finite analytic numerical solution of Navier-Stokes equations p 996 A92-53011
Hot-wire measurements in turbulent transonic flows p 941 A92-53078
Numerical simulation of three-dimensional turbulent flows in combustion chambers p 970 A92-53276
Turbulent combustion modelling in a side dump ramjet combustor
[AIAA PAPER 92-3599] p 1112 A92-54075
Detecting 3-D, turbulent separation regions using unsteady computerized thermographic technique p 1023 A92-54308
Numerical simulation of slot injection into a turbulent supersonic stream p 1024 A92-54914
Measurements of turbulence in hypersonic flow p 1092 A92-56005
Tohoku University low-turbulence wind tunnel
[AIAA PAPER 92-3913] p 1095 A92-56746
Prediction of the pressure loss coefficient of wind tunnel turbulence reducing screens
[AIAA PAPER 92-4043] p 1035 A92-56862
Noise from turbulent shear flows p 55 N92-10603
Propulsive lift noise p 55 N92-10606
Theoretical study (Lagrangian modeling) of turbulent particulate dispersion
[ETN-91-99909] p 42 N92-11287
An assessment and application of turbulence models for hypersonic flows
[NASA-TM-105124] p 82 N92-11984
An experimental and computational investigation of an annular reverse-flow combustor
[UTIAS-338] p 129 N92-11996
Study of detached turbulent flow in an air intake by means of high speed tomography and laser velocimetry
[REPT-90/55] p 157 N92-12216
On the simulation of compressible turbulent flows past delta wing, delta wing-body and delta wing-canard p 84 N92-13003
Numerical investigation of unsteady supersonic cavity flowfield with passive control p 88 N92-13029
Navier-Stokes analysis of turbulent boundary layer and wake for two-dimensional lifting bodies p 221 N92-14309
Evaluation of rotordynamic coefficients of look-through labyrinths by means of a three volume bulk flow model p 223 N92-14356
Dynamic characteristics and stability analysis of space shuttle main engine oxygen pump p 224 N92-14366
Effect of eccentricity on the static and dynamic performance of a turbulent hybrid bearing p 225 N92-14373
Base pressure measurements on a cone at hypersonic Mach numbers: A contribution to aerothermodynamics for space vehicles p 181 N92-14992
Use of Navier-Stokes analysis in section design
[AD-A242074] p 299 N92-17168
An experimental study of a turbulent wing-body junction and wake flow
[AD-A243388] p 260 N92-17222
Local extinction mechanisms in non-premixed turbulent combustion
[AD-A242027] p 290 N92-17682
Deterministic multi-zone ice accretion modeling p 265 N92-17987
Examination of energy spectra moments in a developing turbulent flow
[NIAR-91-28] p 399 N92-18116
Towards the computation of turbulent hypersonic flows
[AERO-REPT-9106] p 345 N92-18318
The 8th Symposium on Turbulent Shear Flows. Volume 1: Sessions 1-18
[AD-A243809] p 402 N92-18933
Numerical solution of three-dimensional unsteady viscous flows
[AD-A244274] p 403 N92-19052
Inhomogeneous turbulence beyond spectral equilibria: Aeronautical applications
[ETN-92-90867] p 404 N92-19349
Laser-spectroscopic measurement techniques for hypersonic, turbulent wind tunnel flows
[NASA-TM-103928] p 405 N92-19596
Calculations of hot gas ingestion for a STOVL aircraft model
[NASA-TM-105437] p 350 N92-19993
A new method for simulating atmospheric turbulence for rotorcraft applications p 464 N92-21956
Three-dimensional multigrid algorithm for the Euler and the thin-layer Navier-Stokes equations
[PB92-134329] p 602 N92-22216
Three-dimensional compressible turbulent computations for a diffusing S-duct
[NASA-CR-4392] p 526 N92-22249
Boundary Layers in Turbomachines
[VKI-LS-1991-06] p 658 N92-24336
Fundamental aspects of boundary layers and transition in turbomachines p 658 N92-24337
Investigations of blade row interaction and boundary layer transition phenomena in a multistage aero engine low-pressure turbine by measurements with hot-film probes and surface-mounted hot-film gauges p 658 N92-24338
A compressible Navier-Stokes solver with two-equation and Reynolds stress turbulence closure models
[NASA-CR-4440] p 681 N92-25376
On a multi-block method for transonic turbulent flows past a wing-fuselage configuration p 632 N92-25569
Simulation of a rotorcraft in turbulent flows
[AD-A245742] p 650 N92-26155
Fractal image compression of Rayleigh, Raman, LIF and LDV data in turbulent reacting flows
[AD-A246960] p 767 N92-27352
Turbulent heat flux measurements in a transitional boundary layer
[NASA-TM-105623] p 716 N92-27377
Validation of a CANARI code by the computation of three dimensional turbulent flow in turbine valve p 741 N92-27462
Computational modelling of turbulent flow in S-bends p 769 N92-27480
Modelling the vaporiser and primary zone flows for a modern gas turbine combustion chamber p 742 N92-27484
The coherent flamelet model for propulsion applications p 756 N92-27486
Laminar-turbulent transition: Fundamentals p 717 N92-27710
Study of turbulence structure through numerical simulations: The perspective of drag and reduction p 717 N92-27713
Turbulent skin-friction drag reduction by active and passive means, part 1 p 718 N92-27714
Self-adaptive aeropropulsion components-enhancing axial compressor performance
[AD-A246123] p 743 N92-27817
Flow gradient corrections on hot-wire measurements using an X-wire probe
[NLR-TP-90255-U] p 829 N92-28713
Modeling of the reactant conversion rate in a turbulent shear flow p 829 N92-28820
Laser anemometer measurements and computations in an annular cascade of high turning core turbine vanes
[NASA-TP-3252] p 830 N92-28980
Explicit Navier-Stokes computation of turbomachinery flows
[AD-A248458] p 911 N92-29933
Active thermal isolation for temperature responsive sensors
[NASA-CASE-LAR-14612-1] p 911 N92-29954
Turbulent reacting flows and supersonic combustion
[AD-A251065] p 986 N92-30256
Structure of three-dimensional turbulent boundary layers p 999 N92-30654
Organized turbulent structures and their induced wall pressure fluctuations p 949 N92-31853
Contribution to the modelling of turbulent combustion in the case of stabilisation by flame-lock
[ESA-TT-1229] p 988 N92-31942
Experimental studies of hypersonic shock-wave boundary-layer interactions
[NASA-CR-190731] p 950 N92-32162
Three-dimensional compressible turbulent computations for a nondiffusing S-duct
[NASA-CR-4391] p 951 N92-32240
Numerical simulation of turbulence at the back of the airplane
[ETN-92-91664] p 1037 N92-32769
Further wind tunnel investigation of the SM701 airfoil with aileron and turbulators
[NASA-CR-190702] p 1038 N92-33063
Theories of turbulent combustion in high speed flows
[AD-A253032] p 1111 N92-33624

TURBULENT HEAT TRANSFER

Using uncertainty analysis in the debugging and qualification of a turbulent heat transfer test facility p 138 A92-17224
Embedded longitudinal vortex arrays, velocity and temperature fields, loss and heat transfer augmentation p 621 A92-40121
Heat transfer and instrumentation studies on rotating turbine blades in a transient facility p 156 N92-12203
The effect of angle of incidence and Reynolds number on heat transfer in a linear turbine cascade
[AD-A243900] p 377 N92-19328
Turbulent heat flux measurements in a transitional boundary layer
[NASA-TM-105623] p 716 N92-27377
Turbulent spot generation and growth rates in a transonic boundary layer
[AD-A250221] p 909 N92-29118

TURBULENT JETS

Jet inflow simulation and its downwash effect on lifting surfaces p 9 A92-13200
Structural features of a heated round turbulent jet in a cross-flow p 676 A92-40148
Modern developments in shear flow control with swirl p 703 A92-41265
Eigenfunction analysis of turbulent mixing phenomena p 898 A92-45826
A numerical study of the radiation characteristic of an elliptical exhaust jet p 970 A92-53258
Interaction between chemical reaction and turbulence in supersonic nonpremixed H2-air combustion p 1117 A92-54931
Analysis of a dusty wall jet
[NASA-CR-189759] p 257 N92-15965

TURBULENT MIXING

Numerical prediction of wakes in cascades and compressor rotors including the effects of mixing. I - Cascade wakes including the effects of incidence and freestream turbulence
[ASME PAPER 91-GT-225] p 74 A92-15638
Compressibility effects in thin channels with injection p 216 A92-18369
Experimental measurement of the vortex development downstream of a lobed forced mixer
[ASME PAPER 90-GT-27] p 295 A92-23299
A new unsteady mixing model to predict NO(x) production during rapid mixing in a dual-stage combustor
[AIAA PAPER 92-0233] p 372 A92-25696

Computation of supersonic jet mixing noise for an axisymmetric CD nozzle using k-epsilon turbulence model
[AIAA PAPER 92-0500] p 414 A92-26328
Experiments on shear layer mixing at hypervelocity conditions
[AIAA PAPER 92-0628] p 396 A92-27009
Transmission of thin light beams through turbulent mixing layers
[AIAA PAPER 92-0658] p 396 A92-27029
Effect of turbulent mixing on the characteristics of a turbofan-engine nozzle p 493 A92-30162
Two- and three-dimensional effects in the supersonic mixing layer p 432 A92-31165
The experimental investigation on the diffuser flow distortion p 519 A92-35543
Evolution of three-dimensionality in stable and unstable curved mixing layers p 619 A92-40059
The DAM vertical shock-tube p 880 A92-45096
Eigenfunction analysis of turbulent mixing phenomena p 898 A92-45826
Mixing in the dome region of a staged gas turbine combustor
[AIAA PAPER 92-3089] p 903 A92-48734
A concentration probe for the study of mixing in supersonic shear flows p 991 A92-50039
The enhancement of the mixing and combustion processes in supersonic flow applied to scramjet engine
[AIAA PAPER 92-3428] p 1112 A92-54029
Computational and experimental studies of flow in multi-lobed forced mixers
[AIAA PAPER 92-3568] p 1112 A92-54057
Jet noise suppression p 236 N92-14784
Computation of supersonic jet mixing noise for an axisymmetric CD nozzle using k-epsilon turbulence model
[NASA-TM-105338] p 237 N92-14795
Supersonic combustion studies p 211 N92-14984
Simulation of chemical kinetics in turbulent natural gas combustion
[PB92-123660] p 488 N92-20329
Turbulent mixing in supersonic jets p 715 N92-27054

TURBULENT WAKES
Prediction of wake in a curved duct p 3 A92-10487
Effect of riblets on turbulence in the wake of an airfoil p 5 A92-11051
Poststall airfoil response to a periodic freestream p 10 A92-13218
A viscous flow study of shock-boundary layer interaction, radial transport, and wake development in a transonic compressor
[ASME PAPER 91-GT-69] p 68 A92-15539
Effects of stator wakes and spanwise nonuniform inlet conditions on the rotor flow of an axial turbine stage
[ASME PAPER 91-GT-93] p 70 A92-15557
Numerical prediction of wakes in cascades and compressor rotors including the effects of mixing. II - Rotor passage flow and wakes including the effects of spanwise mixing
[ASME PAPER 91-GT-222] p 74 A92-15639
Stratified flow around an axisymmetric body at small angle of attack p 172 A92-18385
Flight test investigation of the wake vortices generated by helicopters p 270 A92-21925
Experimental investigation of a three-dimensional bluff-body wake
[AIAA PAPER 92-0429] p 326 A92-26277
Three-dimensional structure of a curved wake
[AIAA PAPER 92-0541] p 341 A92-28199
A new approach to swirl control in an S-duct p 422 A92-29710
Experimental investigation on combustor with double co-axial swirlers p 469 A92-29729
Large eddy simulation of unsteady turbulent wake of a circular cylinder using the finite element method p 587 A92-34825
Active control of the hydraulic forces of a body by a splitter plate p 591 A92-36351
Phase-averaged turbulence statistics in a near wake with an asymmetric vortex shedding p 620 A92-40086
The natural and forced formation of spot-like Lambda-structures caused by vortex dislocations in a wake p 621 A92-40111
Compressibility effects in turbulent far wakes p 622 A92-40140
Vortex interaction in the wake behind an oscillating airfoil p 623 A92-40175
Wake effects on the prediction of transonic viscous flows around airfoils p 702 A92-41232
An aerodynamic hypothesis for the wing aeroelasticity problem p 761 A92-42665
High-Reynolds-number test requirements in low-speed aerodynamics p 787 A92-45263
New method of swirl control in a diffusing S-duct p 809 A92-45859
Effect of wing tip vortices on a trailing aircraft p 935 A92-50303
Asymmetric turbulent vortical flows over slender bodies p 935 A92-50314
Development of a real-time simulation of a ship-correlated airwake model interfaced with a rotorcraft dynamic model
[AIAA PAPER 92-4149] p 1007 A92-52440
Blockage correction in three-dimensional wind tunnel testing based on the wall signature method
[AIAA PAPER 92-3925] p 1095 A92-56756
Turbulent friction drag reduction: Boundary layer manipulators
[CERT-RSF-DERAT-62/5004-31] p 43 N92-11309
Phenomenological modeling of the wake produced by a straight two dimensional base in subsonic flow
[REPT-90/59] p 82 N92-11982
Hot-wire surveys in the vortex wake downstream of a three-percent fighter aircraft model at high angles of attack
[AD-A241869] p 259 N92-15975
Use of Navier-Stokes analysis in section design
[AD-A242074] p 299 N92-17168
An experimental study of a turbulent wing-body junction and wake flow
[AD-A243388] p 260 N92-17222
Experimental investigation of trailing edge crenulation effects on losses in a compressor cascade
[AD-A243902] p 377 N92-19329
Explicit Navier-Stokes computation of turbomachinery flows
[AD-A248458] p 911 N92-29933

TURNING FLIGHT
H(infinity) robust control synthesis for a fighter performing a coordinated bank turn p 29 A92-11585
2-D and 3-D minimum-time-to-turn flights via parameter optimization
[AIAA PAPER 92-0731] p 379 A92-27083
Coupled rotor-fuselage dynamics and aeroelasticity in turning flight
[AIAA PAPER 92-2109] p 544 A92-35680
Effect of thrust vectoring on level-turn performance p 729 A92-41243

TVD SCHEMES
Space-marching calculations of hypersonic inviscid flowfield p 313 A92-25040
Navier-Stokes computations for turbulent transonic projectile with a two layer model combining the ASM model of turbulence and the k-epsilon model near the wall
[AIAA PAPER 92-0518] p 331 A92-26943
Prediction of shock pattern dynamics at hypersonic angle of attack maneuvers of endo-KEW missile forebodies
[AIAA PAPER 92-2768] p 704 A92-41317
Aerodynamic design of an advanced turboprop using Euler codes p 737 A92-43196
Numerical study on a supersonic open cavity flow with geometric modification of aft bulkhead
[AIAA PAPER 92-2627] p 794 A92-45499
LU-SGS implicit scheme for entry vehicle flow computation and comparison with aerodynamic data
[AIAA PAPER 92-2671] p 798 A92-45526
Computations of hypersonic flows around a three-dimensional concave/convex body
[AIAA PAPER 92-2606] p 805 A92-45570
Predicted pressure distribution on a prop-fan blade through Euler analysis p 810 A92-46791
Numerical experiments on unsteady shock reflection processes using the thin-layer Navier-Stokes equations p 818 A92-47155
Development and application of a zonal k-epsilon turbulence model for complex 3-D flowfields
[AIAA PAPER 92-3176] p 903 A92-48792
Improved artificial dissipation schemes for the Euler equations p 933 A92-49508
Full Navier-Stokes analysis of a three-dimensional scramjet inlet p 934 A92-50272
Lower upper implicit total variation diminishing solution of viscous hypersonic flows p 935 A92-50302
On central-difference and upwind schemes p 1007 A92-50466
Numerical simulations of shock reflections by a TVD scheme p 1018 A92-53558
Hypersonic aerothermodynamic computations using a point-implicit TVD method p 183 N92-15006
Study of shock-induced combustion using an implicit TVD scheme p 669 N92-25816
Pressure-based high-order TVD methodology for dynamic stall control
[AD-A247056] p 774 N92-27918
Development of a 3-D upwind PNS code for chemically reacting hypersonic flowfields
[NASA-CR-190182] p 946 N92-30977

TWISTED WINGS
A demonstration of passive blade twist control using extension-twist coupling
[AIAA PAPER 92-2468] p 539 A92-34358
A demonstration of passive blade twist control using extension-twist coupling
[NASA-TM-107642] p 1001 N92-31155
Survey and analysis of research on supersonic drag-due-to-lift minimization with recommendations for wing design
[NASA-TP-3202] p 1040 N92-33656

TWISTING
On the behavior of pretwisted beams with irregular cross-sections p 495 A92-31564
Torsion and twisting of symmetric composite laminates
[AIAA PAPER 92-2425] p 582 A92-34354
On the three-dimensional vibration analysis of simultaneously skewed and twisted cantilevered parallelepipeds p 759 A92-41801
Linear analysis of naturally curved and twisted anisotropic beam p 899 A92-46936

TWO DIMENSIONAL BODIES
Two-dimensional effects in a triangular convecting fin p 219 A92-20324
Unsteady pressure field and vorticity production over a pitching airfoil p 330 A92-26416
Analysis of tenon and mortise contact problems by boundary element methods p 587 A92-35554
A flow visualization experiment on the unsteady flow around two-dimensional airfoil p 615 A92-38913
Phase-averaged turbulence statistics in a near wake with an asymmetric vortex shedding p 620 A92-40086
Transonic unsteady inviscid and viscous flow's simulation around 2-D moving bodies
[AIAA PAPER 92-2704] p 801 A92-45546
Time-average loading on a two-dimensional airfoil in a large amplitude motion p 811 A92-46805
Analysis of motion of airfoil flying over wavy-wall surface (lifting surface method) p 818 A92-47100
Flow of a rarefied gas past a two-dimensional body of an arbitrary shape at small Mach numbers p 937 A92-52726
DSMC simulation of hypersonic flows past 2-dimensional bodies p 939 A92-52772
Tow-tank study of nonlinear aerodynamics of a 2-D airfoil
[AIAA PAPER 92-4499] p 1026 A92-55367
Navier-Stokes analysis of turbulent boundary layer and wake for two-dimensional lifting bodies p 221 N92-14309
An alternative to unstructured grids for computing gas dynamic flows around arbitrarily complex two-dimensional bodies
[NASA-CR-189612] p 447 N92-21465
Construction of a numerical optimization method for the definition of hypersupported profiles
[ONERA-RSF-43/1736-AY-146A] p 908 N92-28788

TWO DIMENSIONAL BOUNDARY LAYER
Effect of suction on the stability of supersonic boundary layers. I - Second-mode waves. II - First-mode waves p 174 A92-19611
Effects of attack angle on leg portion of the horseshoe vortex around the idealized wing p 623 A92-40177
Simplified linear stability transition prediction method for separated boundary layers p 812 A92-46883
A fast, uncoupled, compressible, two-dimensional, unsteady boundary layer algorithm with separation for engine inlets
[AIAA PAPER 92-3082] p 823 A92-48729
Perfect compressible two dimensional boundary layer strong fluid coupling in the case of sharp leading edge profiles. Unsteady case of isolated profiles and steady case of blade grids
[ONERA-RT-43/1621-RY-006-R] p 43 N92-11311
Proceedings of the Seminar on Investigation and Control of Boundary-Layer Transition
[NAL-SP-11] p 400 N92-18483
A fast, uncoupled, compressible, two-dimensional, unsteady boundary layer algorithm with separation for engine inlets
[NASA-TM-105686] p 770 N92-27653

TWO DIMENSIONAL FLOW
A semi-elliptic analysis for 2-D viscous flows through cascade configurations p 3 A92-10688
Unsteady Euler calculations in 2-D internal aerodynamics with introduced vorticity
[ASME PAPER 91-GT-168] p 73 A92-15603
Simple formulae for optimal solidity of two-dimensional compressor cascades based on diffusion concept
[ASME PAPER 91-GT-308] p 126 A92-15687
Supersonic stator-rotor interaction in a turbine stage
[ONERA, TP NO. 1991-166] p 77 A92-16133
CFD application to 2D/3D flow fields in Scramjet engine p 170 A92-17501
Aerodynamic sensitivity analysis methods for the compressible Euler equations p 233 A92-19619
Concerning the functional solution of transonic flows p 243 A92-21318

Two-dimensional, incompressible aerofoil design and analysis p 247 A92-21987
Establishment and characterization of a reproducible vortex for use in studying nonsteady two-dimensional phenomena p 310 A92-24428
On one method of constructing adaptive difference grids *in aerodynamics problems* p 311 A92-24902
On marching algorithms for solving stationary problems p 311 A92-24976
Numerical simulation of 2-D separated flows caused by suddenly change of the body section p 312 A92-25004
Controlling unsteady lift using unsteady trailing-edge flap motions
[AIAA PAPER 92-0275] p 318 A92-25729
Turbulence modeling for high speed flows
[AIAA PAPER 92-0436] p 327 A92-26283
Zonal flow analysis method for two-dimensional airfoils p 330 A92-26435
Base pressure in supersonic flow - Further thoughts about a theory p 331 A92-26442
Experimental results on a wall interference correction method with interface measurements
[AIAA PAPER 92-0570] p 333 A92-26978
A study on the superconvergence of Multhopp's discretization in vortex-lattice methods p 336 A92-27381
A boundary integral formulation for the kinetic field in aerodynamics. II - Applications to unsteady 2D flows p 339 A92-28005
Numerical experiments on a new class of nonoscillatory schemes
[AIAA PAPER 92-0421] p 341 A92-28193
Calculation of three-dimensional transonic turbine cascade flow p 344 A92-28519
Error characteristics of a vortex panel method in two-dimensional flow p 421 A92-29521
Transverse correlation of the spectral components of pressure fluctuations on a plate ahead of a step p 426 A92-30187
The Bauer-Garabedian-Korn airfoil test in a two-dimensional wind tunnel p 429 A92-30532
Two- and three-dimensional effects in the supersonic mixing layer p 432 A92-31165
On hypersonic flow over two-dimensional aerofoils p 433 A92-31425
Time marching integral equation method for unsteady transonic flows around airfoils p 433 A92-31489
Two-dimensional heat transfer from a rectangular fin with asymmetrical thermal boundary conditions p 498 A92-32524
Analysis of cascades using a two dimensional Euler aeroelastic solver
[AIAA PAPER 92-2370] p 556 A92-34598
Experimental investigation on performances of two-dimensional inlet at supersonic speed p 519 A92-35544
A method for measuring high-subsonic two-dimensional periodic flow field using a single-hole high-response cylindrical pressure probe p 588 A92-35567
Outflow boundary conditions for Euler analysis of flow in turbine scroll p 591 A92-36037
Experimental study of a two-dimensional scramjet inset, M(freestream) = 10.1-25.1 p 611 A92-36974
Some problems on the sidewall interference in two-dimensional subsonic and transonic wind tunnel testing p 747 A92-41929
Secondary flow investigation inside the passage of a compressor cascade p 706 A92-42124
Measurements of the velocity and vorticity fields around a pitching airfoil
[AIAA PAPER 92-2626] p 794 A92-45498
A nonlinear relaxation/quasi-Newton algorithm for the compressible Navier-Stokes equations
[AIAA PAPER 92-2643] p 796 A92-45510
Predictions of a turbulent backward-facing-step flow with a cubic pressure-strain model
[AIAA PAPER 92-2647] p 796 A92-45514
Computational evaluation of an airfoil with a Gurney flap
[AIAA PAPER 92-2708] p 802 A92-45550
Compressible Navier-Stokes solutions for a suction boundary control airfoil
[AIAA PAPER 92-2710] p 802 A92-45551
Numerical simulation of multizone two-dimensional transonic flows using the full Navier-Stokes equations p 815 A92-46955
Mesh adaptivity with the quadtree method p 816 A92-47041
Solution of the Burnett equations for hypersonic flows near the continuum limit
[AIAA PAPER 92-2922] p 821 A92-47894
Establishing two-dimensional flow in a large-scale planar turbine cascade
[AIAA PAPER 92-3066] p 823 A92-48720
Prediction of gas turbine combustor flow by a finite element code
[AIAA PAPER 92-3469] p 906 A92-49016
Lower upper implicit total variation diminishing solution of viscous hypersonic flows p 935 A92-50302
Brownian-motion limited aerodynamic focusing of heavy molecules p 995 A92-52722
Discussion on sidewall suction in two-dimensional wind tunnel p 997 A92-53263
Methodology for calculating aerodynamic sensitivity derivatives p 1024 A92-54911
Evaluation of sidewall interference in the NAL two-dimensional transonic wind tunnel p 1092 A92-56011
BGK1 airfoil oilflow tests in the NAL two-dimensional wind tunnel. II p 1029 A92-56044
Small two-dimensional surface excrescences on aircraft wings approaching separation p 1031 A92-56170
Resolution of the Navier-Stokes equations applied to the computation of the laminar flow around a two dimensional wing profile
[CERT-RT-65/5604-35] p 43 N92-11307
Resolution of Navier-Stokes equations around profiles: Drag evolution
[ONERA-RTS-86/1685-AY-156A] p 43 N92-11310
Two-dimensional transonic flow calculation by interaction of Euler and boundary layer equations
[PB92-136449] p 448 N92-21784
Static performance of a cruciform nozzle with multiaxis thrust-vectoring and reverse-thrust capabilities
[NASA-TP-3188] p 527 N92-23095
Improved shock-capturing of Jameson's scheme for the Euler equations
[PB92-148758] p 596 N92-23251
TVD finite-difference solutions of nonequilibrium vibrationally relaxing and chemically reacting gaseous flows p 626 N92-24854
The fibre optic three dimensional laser two focus velocimeter for the low-speed windtunnel. Part 1: Two-dimensional measurement evaluations
[NAL-TM-627] p 665 N92-25402
Grid generation research at OSU p 633 N92-25723
An outline of a numerical scheme for calculating two-dimensional time linearised transonic flow using the Green's function method
[AD-A246349] p 764 N92-26258
Modeling of heavy-gas effects on airfoil flows
[NASA-CR-190357] p 716 N92-27558
NACA0012 airfoil data corrected for sidewall boundary-layer effects in the NAL two-dimensional transonic wind tunnel
[NAL-TM-640T] p 722 N92-28151
Force measurements on AGARD calibration model-B at transonic speeds in the NAL two-dimensional wind tunnel
[NAL-TM-639] p 722 N92-28190
Explicit Navier-Stokes computation of turbomachinery flows
[AD-A249284] p 909 N92-28879
Spatial and temporal adaptive procedures for the unsteady aerodynamic analysis of airfoils using unstructured meshes
[NASA-TM-107635] p 831 N92-29445
A gridless Euler/Navier-Stokes solution algorithm for complex two-dimensional applications
[NASA-TM-107631] p 944 N92-30570
Structure of three-dimensional turbulent boundary layers p 999 N92-30654
Numerical calculations of two-dimensional single and multi-material flow fields with CCICE
[DE92-015778] p 1000 N92-30903
Automatic design of transonic airfoils to reduce the shock induced pressure drag p 949 N92-31863

TWO DIMENSIONAL JETS

Study on two-dimensional jet mixing with a vertical supersonic flow p 429 A92-30530
Numerical study on the secondary jet into a supersonic flow p 1018 A92-53556
Numerical simulation of turbulence at the back of the airplane
[ETN-92-91664] p 1037 N92-32769

TWO DIMENSIONAL MODELS

Fundamental research in helicopter rotor blade-vortex interaction modeling p 65 A92-14358
Turbulent flow calculations using unstructured and adaptive meshes p 153 A92-15823
Low-frequency pressure oscillations in a model ramjet combustor p 154 A92-16026
A multidimensional terrain model for low altitude tracking scenarios p 205 A92-19107
A wave-model-based refinement criterion for adaptive-grid computation of compressible flows
[AIAA PAPER 92-0322] p 321 A92-25769
A nearly-monotone genuinely multidimensional scheme for the Euler equations
[AIAA PAPER 92-0325] p 322 A92-25772
Two and three dimensional parabolized Navier-Stokes code for scramjet combustor, nozzle, and film cooling analysis
[AIAA PAPER 92-0391] p 372 A92-26247
Quality assessment of two- and three-dimensional unstructured meshes and validation of an upwind Euler *flow solver*
[AIAA PAPER 92-0444] p 328 A92-26288
Development of an electrothermal de-icing/anti-icing model
[AIAA PAPER 92-0526] p 351 A92-26949
Comparison of two-dimensional and three-dimensional droplet trajectory calculations in the vicinity of finite wings
[AIAA PAPER 92-0645] p 342 A92-28215
The unstructured upwind method p 429 A92-30522
Horizontal flight of an aircraft with periodic thrust reversal p 480 A92-31876
Slenderness approximations in RCS estimation - The *simplest 2-D case* p 533 A92-33622
An investigation of cascade flutter using a *two-dimensional full-potential solver*
[AIAA PAPER 92-2119] p 558 A92-35688
Two- and three-dimensional grid generation by an algebraic homotopy procedure p 611 A92-36861
Transonic airfoil and wing design using Navier-Stokes codes
[AIAA PAPER 92-2651] p 797 A92-45518
Optimization of a 2D scramjet-vehicle using CFD and simplified approximate flow analysis techniques
[AIAA PAPER 92-3673] p 1022 A92-54116
Drag computation by vortex methods p 1031 A92-56161
Predicting droplet impingement on yawed wings p 1043 A92-56180
The BCAC/IAR collaborative research program to investigate the sidewall boundary layer effects in the IAR/NRC 2-D High Reynolds Number Test Facility
[NRC-HSA-434] p 81 N92-11976
Phenomenological modeling of the wake produced by a straight two dimensional base in subsonic flow
[REPT-90/59] p 82 N92-11982
A unified viscous theory of lift and drag of 2-D thin airfoils and 3-D thin wings
[NASA-CR-4414] p 178 N92-13997
Ozone response to aircraft emissions: Sensitivity studies with two-dimensional models p 409 N92-19126
Quality assessment of two- and three-dimensional unstructured meshes and validation of an upwind Euler *flow solver*
[NASA-TM-104215] p 444 N92-20480
A two-dimensional Euler solution for an unbladed jet engine configuration
[NASA-TM-105329] p 597 N92-23560
Interactive solution-adaptive grid generation procedure
[NASA-TM-105432] p 528 N92-23563
Numerical simulations of wakes, blade-vortex interaction, flutter, and flutter suppression by feedback control p 597 N92-23997
Air ejector experiments using the two-dimensional supersonic cascade tunnel: Zero secondary flow performance
[NAL-TM-632] p 887 N92-28829
A gridless Euler/Navier-Stokes solution algorithm for complex two-dimensional applications
[NASA-TM-107631] p 944 N92-30570
Research on some centered implicit methods for calculating transonic flows by solving Navier-Stokes equations
[ONERA-RSF-24/1408-AY-150A] p 1037 N92-32773
Numerical investigation of the effects of icing on fixed and rotary wing aircraft
[NASA-CR-190542] p 1044 N92-34105

TWO FLUID MODELS

Two-phase flow correlations in air/oil systems of aero engines
[ASME PAPER 91-GT-54] p 121 A92-15532
The DAM vertical shock-tube p 880 A92-45096

TWO PHASE FLOW

Measurements and correlation of two-phase pressure drop under microgravity conditions p 37 A92-10435
Two-phase flows at supersonic velocities p 4 A92-10907
Experimental and theoretical study of the improvement of the aerodynamic characteristics of supersonic flow past bodies with surface injection of a gas jet with particles p 8 A92-12204
Two-phase flow correlations in air/oil systems of aero engines
[ASME PAPER 91-GT-54] p 121 A92-15532
Changing the structure and improving the aerodynamic characteristics of supersonic flow past bodies through ejection of a gas jet with particles p 78 A92-16680
Analysis of transonic flow over plane compressor cascades using the large-particle method p 79 A92-16812

Characterization of a two-phase flow field downstream of a 3x-scale gas turbine co-axial, counter-swirling, combustor dome swirl cup
[AIAA PAPER 92-0229] p 393 A92-25693
Effect of carbon particles and mixing on afterburning of exhaust plumes
[AIAA PAPER 92-0767] p 387 A92-27107
Flow pattern characterization and heat transfer behavior in a boiling two-phase flow in an inclined pipe
p 493 A92-29722
Three-dimensional flow computation for two interacting, moving droplets
[AIAA PAPER 92-0343] p 496 A92-31655
Particle dispersion in highly swirling, turbulent flows
p 675 A92-40093
Aerodynamic drag of a cylinder in two-phase flow
p 707 A92-42735
Demonstration of gas liquid separation under the microgravity by aircraft KC-135
[SAE PAPER 912024] p 897 A92-45416
A numerical study of two-phase flow in gas turbine combustors
[AIAA PAPER 92-3468] p 905 A92-49015
Boiling and condensing pumped loop microgravity experiment - Challenges of testing in both aircraft and rocket environments p 992 A92-50611
Pulsation characteristics of one-phase and two-phase steam flows in Laval nozzles under off-design conditions
p 1019 A92-53882
Steady flow of a fluid-solid mixture in a circular cylinder
[DE91-018698] p 41 N92-10174
Theoretical study (Lagrangian modeling) of turbulent particulate dispersion
[ETN-91-99909] p 42 N92-11287
Propagation of shock waves through clouds
[AERO-REPT-9104] p 400 N92-18317
The 8th Symposium on Turbulent Shear Flows. Volume 1: Sessions 1-18
[AD-A243809] p 402 N92-18933
Pressure measurements in high speed water tunnels
[DE92-004891] p 386 N92-19978

TWO STAGE PLASMA ENGINES
Aerothermodynamic challenges of the Saenger space-transportation system p 184 N92-15042

TWO STAGE TURBINES
A direct optimization procedure for spanwise work distribution in non-free vortex turbine stages
[ASME PAPER 91-GT-204] p 124 A92-15626
Some rotordynamic problems in small turbo-engines
p 470 A92-29736

U

U.S.S.R.
Soviet aerospace in turmoil --- miltary to civil production conversion p 2 A92-13220
Soviet CFD - An international perspective
p 233 A92-20150
Emerging technology in the Soviet Union: Selected papers with analysis
[ISBN 1-55831-117-1] p 929 A92-46201
German-GUS cooperation in civil aviation
p 785 A92-47592
CIS engines. I - The range revealed
p 786 A92-47821
Russian realities --- changes in aviation industry infrastructure p 932 A92-53250
JPRS report: Science and technology. USSR: Space
[JPRS-USP-91-007] p 211 N92-14101
JPRS report: Science and technology. USSR: Engineering and equipment
[JPRS-UEQ-92-001] p 592 N92-22296
JPRS report: Science and technology. Central Eurasia: Engineering and equipment
[JPRS-UEQ-92-002] p 592 N92-22298
JPRS report: Science and technology. USSR: Engineering and equipment
[JPRS-UEQ-91-010] p 593 N92-22397
Progress of magnetic suspension systems and magnetic bearings in the USSR p 772 N92-27740

U-2 AIRCRAFT
The U-2A flight test program
[AIAA PAPER 92-1086] p 537 A92-33252

UH-1 HELICOPTER
Importance of an accurate prediction of shock curvature for high-speed rotor noise p 414 A92-25578
Development statistics for the UH-1 Ada feasibility study
[AD-A252404] p 982 N92-30547
Helicopter nighttime parking test results - UH-1
[DOT/FAA/CT-TN92/1] p 961 N92-31165

UH-60A HELICOPTER
Analysis of propulsion system dynamics in the validation of a high-order state space model of the UH-60
[AIAA PAPER 92-4150] p 959 A92-52441
Concept evaluation of the UH-60 externally mounted rescue hoist
[AD-A240545] p 22 N92-11004
Rotorcraft In-Flight Simulation Research at NASA Ames Research Center: A Review of the 1980's and plans for the 1990's
[NASA-TM-103873] p 853 N92-28926

ULTRAHIGH FREQUENCIES
Polish radar technology. II - Adaptive radar AVIA CM
p 39 A92-12290
Experiments on aeronautical satellite communications using ETS-V satellite p 639 A92-40187
An evaluation of superresolution methods for tactical radio direction finding
[AD-A246316] p 726 N92-26291

ULTRAHIGH VACUUM
Ultra-high temperature (greater than 2000 C) testing capability at Oak Ridge National Laboratory for carbon materials in air, inert gas and vacuum
[DE92-004445] p 385 N92-18069

ULTRALIGHT AIRCRAFT
Stability, control and gust response characteristics of an ultralight freewing airplane
[AIAA PAPER 92-4342] p 1079 A92-55331

ULTRASONIC FLAW DETECTION
Laser-based ultrasonics on GR/epoxy composite - Interferometric detection p 144 A92-13554
Inspection of compressor discs by ultrasonic leaky waves using an automated C-scan system
p 144 A92-13584
A technique for quantitatively measuring microstructurally induced ultrasonic noise
p 510 A92-28720
Inspection of composite structures
p 676 A92-40882
Measurement of acoustic properties of the composite materials constituting the main rotor hub of the Agusta-Westland helicopter EH-101 (civil version)
p 1010 A92-49475

ULTRASONIC MACHINING
Calculation of the hardening factor for gas turbine engine components shot blasted in an ultrasonic field
p 38 A92-10850

ULTRASONIC RADIATION
Investigation of the effect of an ultrasonic acoustic field on boundary layer separation on an airfoil
p 511 A92-30205

ULTRASONIC SCANNERS
Rapid ultrasonic scanning of aircraft structures
p 215 A92-17292

ULTRASONIC TESTS
Rapid ultrasonic scanning of aircraft structures
p 215 A92-17292
A new method to estimate the effective geometric focal length and radius of ultrasonic focused probes
p 490 A92-28633
Numerical comparison of experimentally measured ultrasound through a multilayered specimen
p 510 A92-28682
Thin bondline measurement of adhesively bonded metallic aircraft structures using an ultrasonic analyzer
p 491 A92-28684
Ultrasonic NDE for ceramic- and metal-matrix composite material characterization p 491 A92-28690
Nondestructive inspection perspectives
p 915 N92-30121

ULTRASONIC WAVE TRANSDUCERS
Nondestructive depth profiling of the protective coating on a turbine blade p 144 A92-13641
A new method to estimate the effective geometric focal length and radius of ultrasonic focused probes
p 490 A92-28633

ULTRASONICS
Ultrasonic motor utilizing elastic fin rotor
p 215 A92-17414
Large area QNDE inspection for airframe integrity
p 362 N92-18588

ULTRAVIOLET LASERS
UV laser spectroscopic measurements in jet engine combustion exit flows
[AIAA PAPER 92-0513] p 396 A92-26939

ULTRAVIOLET RADIATION
Examination of ultraviolet radiation theory for bow shock rocket experiments
[AIAA PAPER 92-2871] p 901 A92-47853
Mid-range UV communications --- ultraviolet radiation
[AD-D015213] p 770 N92-27615

UNDERCARRIAGES
A review of Australian activity on modelling the helicopter/ship dynamic interface p 465 N92-21967

UNDERWATER ACOUSTICS
Precision of the long baseline acoustic navigation system used by Pegasus
[AD-A246598] p 727 N92-26795
On the origin and acoustical behaviour of cloud cavitation
[ISBN-90-9004317-9] p 1125 N92-33066

UNDERWATER BREATHING APPARATUS
Development of an emergency underwater escape breathing system for CH124 seaking aircrew
[DCIEM-87-TR-11] p 92 N92-13041

UNDERWATER PROPULSION
Underwater turbojet engine
[AD-D015017] p 279 N92-15992

UNDERWATER STRUCTURES
Pulsed field system for detecting the presence of a target in a subsurface environment
[AD-D015074] p 296 N92-16174

UNDERWATER VEHICLES
Multiple input sliding mode control for autonomous diving and steering of underwater vehicles
[AD-A241935] p 283 N92-17442
Counterrotating brushless DC permanent magnet motor
[DE92-003825] p 401 N92-18550

UNIFORM FLOW
A method of calculation for the radius of curvature of the attached shock waves in front of a sharp-nosed axi-symmetrical body placed in a uniform stream
p 243 A92-21319
End plate interference effects on the aerodynamics of a circular cylinder in uniform flow p 313 A92-25097
The combined wake of an array of oscillating ribbons
p 623 A92-40180
Outflow boundary conditions using Duhamel's equation p 813 A92-46913
Excrescence drag magnification factors at the drag-rise condition for aerofoils with a specified form of upper-surface pressure distribution
[ESDU-91029] p 259 N92-15973
Flow around two circular cylinders arranged perpendicular to each other
[PB91-238279] p 297 N92-16225
Active control of the flow past a cylinder executing rotary motions p 349 N92-19623
Numerical investigations in three-dimensional internal flows
[NASA-CR-190498] p 998 N92-30380

UNIQUENESS
Inverse solution uniqueness and domain of existence for supersonic space marching applications
[AIAA PAPER 92-0028] p 248 A92-22150

UNITED KINGDOM
A review of UK aviation policy
[TT-9107] p 61 N92-12988
Aircraft fatigue management in the Royal Air Force
p 363 N92-18591

UNITED STATES
General aviation activity and avionics survey, calendar year 1989
[PB91-179234] p 169 N92-13926
Aerothermodynamics for United States advanced programs p 184 N92-15039
The status of the US VAWT program
[DE92-002931] p 505 N92-21040
Research and technology, 1991. Langley Research Center
[NASA-TM-4331] p 1013 N92-30733

UNIVERSAL TIME
Evaluation of GPS/UTC steering performance
p 1049 N92-33353

UNIVERSITIES
Facing the crisis in aircraft design education
p 606 A92-34770
Designing a better engineer p 606 A92-34771
Enlisting industry support for a flight controls design lab
[AIAA PAPER 92-4560] p 1141 A92-55272
Development and integration of modern laboratories in aerospace education
[AIAA PAPER 92-4022] p 1141 A92-56844
United States Air Force summer research program 1991. Volume 1: Program management report
[AD-A248763] p 1142 N92-32338

UNIVERSITY PROGRAM
Developing undergraduate gas turbine and turbomachinery courses
[AIAA PAPER 91-2509] p 56 A92-12700
System design from mission definition to flight validation
[AIAA PAPER 92-1091] p 605 A92-33256
The use of large teams in conceptual aircraft design
[AIAA PAPER 92-1092] p 605 A92-33257
Avionics systems engineering education
p 1012 A92-49269

Joint University Program for Air Transportation Research, 1990-1991
[NASA-CP-3131] p 242 N92-17984
An investigation of air transportation technology at the Massachusetts Institute of Technology, 1990-1991
p 265 N92-17985
Investigation of air transportation technology at Ohio University, 1990-1991 p 265 N92-17990
Alpha Group: The Behemoth Apteryx. Final design proposal
[NASA-CR-190026] p 462 N92-20951
Grid generation research at OSU p 633 N92-25723

UNIX (OPERATING SYSTEM)
An integrated analysis and simulation tool for avionics system development p 1005 A92-49289
An installed nacelle design code using a multiblock Euler solver. Volume 2: User guide
[NASA-CR-189652-VOL-2] p 951 N92-32228

UNMANNED SPACECRAFT
PDFIII - A flight control system for EW UAV's
[TABES PAPER 91-315] p 565 A92-34688

UNSTEADY AERODYNAMICS
Biennial Fluid Dynamics Symposium on Advanced Problems and Methods in Fluid Mechanics, 19th, Kozubnik, Poland, Sept. 3-8, 1989, Selected Papers
p 37 A92-10654
Unsteady incompressible viscous flow past an airfoil
p 3 A92-10662
Implicit flux-split Euler schemes for unsteady aerodynamic analysis involving unstructured dynamic meshes p 5 A92-11057
Computation of steady and unsteady control surface loads in transonic flow p 5 A92-11066
Kernel function occurring in supersonic unsteady potential flow p 6 A92-11080
Extensions to the minimum-state aeroelastic modeling method p 20 A92-11081
Analysis of unsteady pressures induced on a body by a rotor p 10 A92-13212
Step response of unsteady aerodynamics acting on a plane swept wing in incompressible flow for finite state modeling p 63 A92-14031
Lifting line predictions for a swept tip rotor blade
p 65 A92-14424
Transient aerodynamic behaviours associated with stepwise incidence variation of airfoils
p 66 A92-15327
Investigation of unsteady excitation effects on aerodynamic properties of airfoils p 66 A92-15335
Review of the physics of enhancing vortex lift by unsteady excitation p 66 A92-15344
Three-dimensional flow and mixing in a axial flow compressor with different rotor tip clearances
[ASME PAPER 91-GT-89] p 70 A92-15554
Inviscid-viscous coupled solution for unsteady flows through vibrating blades. II - Computational results
[ASME PAPER 91-GT-126] p 71 A92-15571
The effect of steady aerodynamic loading on the flutter stability of turbomachinery blading
[ASME PAPER 91-GT-130] p 71 A92-15574
An unsteady lifting surface theory for ducted fan blades
[ASME PAPER 91-GT-131] p 71 A92-15575
Wind tunnel wall effects in a linear oscillating cascade
[ASME PAPER 91-GT-133] p 72 A92-15576
Unsteady Euler calculations in 2-D internal aerodynamics with introduced vorticity
[ASME PAPER 91-GT-168] p 73 A92-15603
Unsteady lifting surface theory for a rotating transonic cascade of swept blades
[ASME PAPER 91-GT-178] p 73 A92-15610
Numerical optimization of helicopter rotor blade airfoils using unsteady aerodynamic calculations
[ONERA, TP NO. 1991-187] p 78 A92-16141
Unsteady blade-surface pressures on a large-scale advanced propeller - Prediction and data
p 80 A92-17178
Prediction of steady and unsteady asymmetric vortical flows around circular cones p 172 A92-18372
Resonance prediction for slotted circular wind tunnel using finite element p 235 A92-18388
Application of aeroservoelastic modeling using minimum-state unsteady aerodynamic approximations
p 204 A92-18622
Helicopter air resonance modeling and suppression using active control p 204 A92-18625
Instabilities of flows over bodies at large incidence
p 176 A92-20738
Detection of flow state in an unsteady separating flow
p 219 A92-20741
Asymmetric separated flows at supersonic speeds
p 176 A92-20742
Time domain flutter analysis of cascades using a full-potential solver p 176 A92-20747
Surface flow patterns on an ogive-cylinder at incidence p 176 A92-20762
A hot-wire anemometer in compressible subsonic flow
p 244 A92-21623
Computational methods in viscous aerodynamics --- Book p 245 A92-21976
Computation of unsteady, laminar, incompressible, viscous flows using the vorticity streamfunction formulation p 245 A92-21979
Navier-Stokes code development for transonic flow simulations p 246 A92-21985
Recent advancements in turbomachinery forced response analyses
[AIAA PAPER 92-0012] p 278 A92-22136
The position of the unsteady flow computation in the compressor and turbine design and analysis process
[AIAA PAPER 92-0015] p 278 A92-22137
Unsteady aerodynamic methods for turbomachinery aeroelastic and aeroacoustic applications
[AIAA PAPER 92-0011] p 252 A92-23730
Unsteady Euler solution for oscillatory airfoil and oscillating flap
[AIAA PAPER 92-0131] p 252 A92-23751
Aerodynamics of loaded cascades in subsonic flows subject to unsteady three-dimensional vortical disturbances
[AIAA PAPER 92-0146] p 253 A92-23762
Compressor blade row unsteady aerodynamic response to attached and separated flow forcing functions
[AIAA PAPER 92-0147] p 253 A92-23763
What we need in experimental aerodynamics - One engineering educator's view
[AIAA PAPER 92-0161] p 241 A92-23776
Effect of leading-edge cross-sectional geometry on slender wing unsteady aerodynamics
[AIAA PAPER 92-0173] p 255 A92-23784
The dynamics and control of fluctuating pressure loads in the reattachment region of a supersonic free shear layer
[AIAA PAPER 92-0178] p 255 A92-23788
Vortex-induced energy separation in shear flows
[AIAA PAPER 92-0192] p 257 A92-23801
Study of role of unsteady separation in formation of dynamic stall vortex
[AIAA PAPER 92-0196] p 257 A92-23804
Rapid prediction of high-alpha unsteady aerodynamics of slender-wing aircraft p 309 A92-24412
Transonic aeroelasticity analysis using state-space unsteady aerodynamic modeling p 310 A92-24422
Influence of flight parameters on air intake internal flow distortions due to gun blast-air interaction
p 310 A92-24426
On the prediction of unsteady forces on gas turbine blades. I - Description of the approach. II - Analysis of the results p 311 A92-24724
A numerical method for unsteady transonic flow about wings with control surface p 314 A92-25107
Pressure wave propagation studies for oscillating cascades
[AIAA PAPER 92-0145] p 316 A92-25682
A new unsteady mixing model to predict NO(x) production during rapid mixing in a dual-stage combustor
[AIAA PAPER 92-0233] p 372 A92-25696
Controlling unsteady lift using unsteady trailing-edge flap motions
[AIAA PAPER 92-0275] p 318 A92-25729
Separation-induced self-excited structural oscillations
[AIAA PAPER 92-0486] p 328 A92-26317
Unsteady circulation control aerodynamics of a circular cylinder with periodic jet blowing p 330 A92-26401
Theoretical study on the unsteady aerodynamic characteristics of an oscillating cascade with tip clearance (In the case of loaded cascade) p 331 A92-26797
Obtaining the velocity field required for the calculation of propeller unsteady forces using 'traditional' approximate methods and CFD
[AIAA PAPER 92-0520] p 331 A92-26945
Evaluation of shear layer cavity resonance mechanisms by numerical simulation
[AIAA PAPER 92-0555] p 333 A92-26965
Characteristics of the mechanism of separated flow pulsation ahead of a spike-tipped cylinder in supersonic flow p 337 A92-27597
Oscillating two-dimensional hypersonic airfoils at small angles of attack p 340 A92-28042
Transient behavior of supersonic flow through inlets
p 340 A92-28043
Numerical simulation of vortex unsteadiness on a slender body at high incidence p 340 A92-28062
Unsteady aerodynamic interaction effects on turbomachinery blade life and performance
[AIAA PAPER 92-0149] p 341 A92-28186
Unsteady airfoil flow solutions on moving zonal grids
[AIAA PAPER 92-0543] p 342 A92-28200
Unsteady analysis of hot streak migration in a turbine stage p 399 A92-28537
The mean power of forces and moments in unsteady aerodynamics p 421 A92-28949
Dynamic stability of elastic vehicles with unsteady aerodynamic force modeling p 509 A92-29326
The unresolved unsteady flow in multistage compressor blade rows p 421 A92-29472
Aerodynamic performances of spoiler motion
p 429 A92-30526
Study on nozzle flow diffusion p 429 A92-30531
Flux-difference split algorithm for unsteady thin-layer Navier-Stokes solutions p 431 A92-31158
High aerodynamic loads on an airfoil submerged in an unsteady stream p 432 A92-31183
Effects of sweepback on unsteady separation in Mach 5 compression ramp interactions
[AIAA PAPER 92-0430] p 435 A92-31663
A preliminary study of the turbulent structures associated with unsteady separation shock motion in a Mach 5 compression ramp interaction
[AIAA PAPER 92-0744] p 436 A92-31677
Unsteady separation in sharp fin-induced shock wave/turbulent boundary layer interaction at Mach 5
[AIAA PAPER 92-0748] p 436 A92-31678
Calculation of three-dimensional separated flows in the framework of the unsteady Euler equations
p 438 A92-31870
Mathematical modeling of nonstationary viscous flow over a solid angle of finite span p 440 A92-31890
Numerical analysis of three-dimensional unsteady turbulent flows in a turbine stage p 443 A92-32501
NACA 0012 benchmark model experimental flutter results with unsteady pressure distributions
[AIAA PAPER 92-2396] p 517 A92-34469
Convergence of subsonic unsteady aerodynamics evaluated by a finite element concept based on Huygeuns' wave propagation
[AIAA PAPER 92-2502] p 518 A92-34497
Unsteady aerodynamic characteristics of a dual-element airfoil
[AIAA PAPER 92-2508] p 518 A92-34501
Analysis of cascades using a two dimensional Euler aeroelastic solver
[AIAA PAPER 92-2370] p 556 A92-34598
An investigation of cascade flutter using a two-dimensional full-potential solver
[AIAA PAPER 92-2119] p 558 A92-35688
Finite element Euler calculations of unsteady transonic cascade flows
[AIAA PAPER 92-2120] p 520 A92-35689
Transonic wind tunnel investigation of limit cycle oscillations on fighter type wings - Update
[AIAA PAPER 92-2125] p 572 A92-35692
Unsteady Navier-Stokes simulation of turbulent flows through a supersonic compressor cascade
p 523 A92-36036
Aeroelastic tailoring analysis for advanced turbo propellers with composite blades p 558 A92-36358
Unsteady flow past an airfoil pitching at a constant rate p 610 A92-36826
Spatial adaptation of unstructured meshes for unsteady aerodynamic flow computations p 610 A92-36838
Turbomachinery unsteady load predictions with nonuniform inflow p 611 A92-36972
A flow visualization experiment on the unsteady flow around two-dimensional airfoil p 615 A92-38913
The effects of unsteady perturbation on vortex breakdown p 672 A92-38922
Mixed volume boundary element approach for aerodynamics p 617 A92-39934
Integral equation methods for linear and nonlinear aerodynamics p 617 A92-39949
LDV measurements in the unsteady tip-vortex behind an oscillating rectangular wing p 620 A92-40085
Vortex interaction in the wake behind an oscillating airfoil p 623 A92-40175
Transonic Navier-Stokes computations for an oscillating wing using zonal grids p 701 A92-41217
Unsteady aerodynamic loading produced by a sinusoidally oscillating delta wing p 701 A92-41223
Extension and validation of an unsteady wake model for rotors p 702 A92-41224
Identification of the transfer function between turbulence and aircraft p 743 A92-41226
Nonstationary viscous shock layer in supersonic motion over an inhomogeneity p 708 A92-42737
Dynamic response and aeroelastic analysis of a propeller blade of a prop-fan engine p 762 A92-43109
Step response of incompressible unsteady aerodynamic modeling p 744 A92-43131
Research on state equations of unsteady aerodynamics p 709 A92-43132
Experimental and numerical investigations on separated flows around pitching airfoils p 710 A92-43166
Numerical simulation of unsteady hypersonic viscous flows in shock tunnel p 710 A92-43170
Unsteady airloading panel method for propfans
p 780 A92-44512

Numerical analysis of flow through oscillating cascade sections p 713 A92-44513
Critical effects of downstream boundary conditions on vortex breakdown
[AIAA PAPER 92-2601] p 792 A92-45478
Prediction of rotor unsteady airloads using vortex filament theory
[AIAA PAPER 92-2610] p 792 A92-45484
A fast three-dimensional vortex method for unsteady wake calculations
[AIAA PAPER 92-2624] p 794 A92-45496
Unsteady Navier-Stokes simulations of supersonic flow over a three-dimensional cavity
[AIAA PAPER 92-2632] p 795 A92-45504
Spatial and temporal adaptive procedures for the unsteady aerodynamic analysis of airfoils using unstructured meshes
[AIAA PAPER 92-2694] p 800 A92-45540
Hang-glider response to atmospheric inputs p 874 A92-46765
Unsteady aerodynamics of a Wortmann wing at low Reynolds numbers p 810 A92-46778
Temporal adaptive Euler/Navier-Stokes algorithm involving unstructured dynamic meshes p 812 A92-46887
The unsteady interaction of a 3-dimensional vortex filament with a cylinder p 813 A92-46934
Numerical experiments on unsteady shock reflection processes using the thin-layer Navier-Stokes equations p 818 A92-47155
The numerical simulation of compressible flow around an airfoil at high angle of attack p 818 A92-47686
Airfoil wake and linear theory gust response including sub and superresonant flow conditions
[AIAA PAPER 92-3074] p 823 A92-48724
A review of scale effects in unsteady aerodynamics p 934 A92-50121
The influences of forced oscillations toward vortex-breakdown p 934 A92-50210
Fourier functional analysis for unsteady aerodynamic modeling p 935 A92-50313
Nonlinear dynamic stability characteristics of recovery bodies p 977 A92-52041
The relation among the general unsteady aerodynamic coefficients of a wing in subsonic and supersonic speed p 941 A92-53022
Stability and dynamic coupling of elastic vehicles with unsteady aerodynamic forces considered p 1102 A92-53545
Parameter estimation of an augmented airplane with unsteady aerodynamics modelling p 1073 A92-53546
Numerical simulations of shock reflections by a TVD scheme p 1018 A92-53558
Pulsation characteristics of one-phase and two-phase steam flows in Laval nozzles under off-design conditions p 1019 A92-53882
Navier-Stokes analysis of three-dimensional unsteady flows inside turbine stages
[AIAA PAPER 92-3211] p 1021 A92-54016
Unsteady blade pressures on a propfan - Predicted and measured compressibility effects
[AIAA PAPER 92-3774] p 1023 A92-54161
Unsteady shock propagation in a steady flow nozzle expansion p 1023 A92-54489
Vortical flow computations on a flexible blended wing-body configuration p 1024 A92-54922
Pulsating spanwise blowing on a fighter aircraft
[AIAA PAPER 92-4359] p 1025 A92-55345
Active control of asymmetric vortical flows around cones using injection and heating
[AIAA PAPER 92-4426] p 1025 A92-55350
Navier-Stokes computations for oscillating control surfaces
[AIAA PAPER 92-4431] p 1026 A92-55355
A discrete vortex model for predicting wing rock of slender wings
[AIAA PAPER 92-4497] p 1026 A92-55365
Stochastic self-induced roll oscillations of slender delta wing at high angles of attack
[AIAA PAPER 92-4498] p 1081 A92-55366
Understanding and development of a prediction method of transonic limit cycle oscillation characteristics of fighter aircraft
[AIAA PAPER 92-4501] p 1026 A92-55369
Parameter identification of unsteady aerodynamic forces for elastic vehicles
[AIAA PAPER 92-4505] p 1027 A92-55372
State-space representation of aerodynamic characteristics of an aircraft at high angels of attack
[AIAA PAPER 92-4651] p 1028 A92-55395
Numerical simulations of flutter and its suppression by active control
[AIAA PAPER 92-4652] p 1082 A92-55396
Computing high-speed flows past an oscillating cylinder near a vertical wall
[AIAA PAPER 92-4653] p 1028 A92-55397
Current European rotorcraft research activities on development of advanced CFD methods for the design of rotor blades (BRITE/EURAM 'DACRO' project) p 1032 A92-56332
Numerical simulation of unsteady rotor wakes p 1032 A92-56352
The ASU Transition Research Facility
[AIAA PAPER 92-3910] p 1094 A92-56744
Experimental unsteady pressures on an oscillating cascade with supersonic leading edge locus
[AIAA PAPER 92-4035] p 1035 A92-56857
Development of unsteady aerodynamic analyses for turbomachinery aeroelastic and aeroacoustic applications
[NASA-CR-4405] p 12 N92-10979
Unsteady aerodynamic calculations for general configurations by the double-point method
[NAL-TR-1101T] p 12 N92-10980
Three dimensional numerical method for resolving small transonic perturbations in unstructured mesh
[ONERA-RT-56/3064-RY-006-R] p 13 N92-10989
Nonstationary flight aerodynamics in a turbulent environment
[ETN-91-90102] p 82 N92-11980
Steady and unsteady aerodynamics of a pitching straked wing model at high angles of attack p 87 N92-13024
Some characteristics and effects of the F/A-18 LEX vortices p 88 N92-13025
Multiple roll attractors of a delta wing at high incidence p 88 N92-13026
Numerical simulation of vortex flows past impulsively started wings p 88 N92-13028
A 3-degree-of-freedom flight simulator evaluation of unsteady aerodynamics effects
[AD-A241540] p 139 N92-13079
FALKE and COBRA technology development in aerodynamics and aerothermodynamics p 183 N92-15017
The benchmark aeroelastic models program: Description and highlights of initial results
[NASA-TM-104180] p 185 N92-15049
Structural dynamics division research and technology accomplishments for F.Y. 1991 and plans for F.Y. 1992
[NASA-TM-104188] p 261 N92-17509
Semi-empirical model for prediction of unsteady forces on an airfoil with application to flutter
[NASA-TM-105414] p 346 N92-18760
Manoeuvring Aerodynamics
[AGARD-CP-497] p 363 N92-18778
Aerodynamic and flowfield hysteresis of slender wing aircraft undergoing large-amplitude motions p 364 N92-18780
Characterization of unsteady aerodynamic phenomena at high angles p 364 N92-18787
Aeroservoelastic stability of aircraft at high incidence p 381 N92-18795
Unsteady-flow-field predictions for oscillating cascades
[NASA-TM-105283] p 348 N92-19437
Quality assessment of two- and three-dimensional unstructured meshes and validation of an upwind Euler flow solver
[NASA-TM-104215] p 444 N92-20480
Development of a steady potential solver for use with linearized, unsteady aerodynamic analyses
[NASA-TM-105288] p 473 N92-20525
Current status of computational methods for transonic unsteady aerodynamics and aeroelastic applications
[NASA-TM-104191] p 446 N92-21432
Wing force and surface pressure data from a hover test of a 0.658-scale V-22 rotor and wing
[NASA-TM-102244] p 550 N92-22864
Periodic Euler and Navier-Stokes solutions about oscillating airfoils p 626 N92-24850
Algorithm and code development for unsteady three-dimensional Navier-Stokes equations
[NASA-CR-190077] p 692 N92-25264
Transonic Unsteady Aerodynamics and Aeroelasticity
[AGARD-CP-507] p 718 N92-27936
Current status of computational methods for transonic unsteady aerodynamics and aeroelastic applications p 718 N92-27937
Unstructured-grid methods development for unsteady aerodynamic and aeroelastic analyses p 718 N92-27938
Unsteady aerodynamics for aeroelasticity at the Flight Dynamics Directorate p 718 N92-27939
Recent applications of linear and nonlinear unsteady aerodynamics for aeroelastic analysis p 718 N92-27940
Evaluation of an unsteady implicit Euler code against two and three-dimensional standard configurations p 719 N92-27945
Unsteady transonic aerodynamics of pointed bodies of revolution in supersonic freestream p 719 N92-27946
NLR inviscid transonic unsteady loads prediction methods in aeroelasticity p 720 N92-27947
Computations of unsteady flows around airfoil sections by explicit and implicit methods solving the Euler and Navier-Stokes equations p 720 N92-27948
Computation of viscous phenomena in unsteady transonic flow p 720 N92-27949
Aeroelastic calculations for fighter aircraft using the transonic small disturbance equation p 720 N92-27951
Computation of flutter boundaries in the time and frequency domain p 720 N92-27952
Analysis of unsteady aerodynamic and flutter characteristics of an aeroelastic model in transonic flow p 720 N92-27953
Numerical simulation of shock-stall flutter of an airfoil using the Navier-Stokes equations p 746 N92-27956
Transonic wind tunnel investigation of limit cycle oscillations on fighter type wings p 721 N92-27959
The benchmark aeroelastic models program: Description and highlights of initial results p 721 N92-27960
A review of scale effects on surfaces in unsteady motion p 722 N92-27962
Study of the leading-edge vortex dynamics in the unsteady flow over an airfoil
[AD-A247532] p 829 N92-28865
Spatial and temporal adaptive procedures for the unsteady aerodynamic analysis of airfoils using unstructured meshes
[NASA-TM-107635] p 831 N92-29445
Experimental investigation of the flowfield of an oscillating airfoil
[NASA-TM-105675] p 833 N92-30182
Progress in unstructured-grid methods development for unsteady aerodynamic applications
[NASA-TM-107643] p 944 N92-30393
Extension of the integral equation formulation of linearized time dependent subsonic flow
[AD-A250654] p 947 N92-31171
CFD methods development considerations for unsteady aerodynamic analysis
[NASA-TM-107644] p 947 N92-31239
Active control of the separation region on a two-dimensional airfoil
[AD-A249739] p 948 N92-31622
Research on aero-thermodynamic distortion induced structural dynamic response of multistage compressor blading
[AD-A250865] p 974 N92-32059
Potential flow theory and operation guide for the panel code PMARC
[NASA-TM-102851] p 1036 N92-32422
Strong coupling between inviscid fluid and boundary layer of sharp leading edges: Two-dimensional stationary and turbulent cases for isolated profiles and guard vanes
[ONERA-RT-44/1621-RY-016-R] p 1125 N92-32776
Introduction to Flutter of Winged Aircraft, volume 2
[VKI-LS-1992-01-VOL-2] p 1088 N92-34161
Elementary flutter analysis p 1088 N92-34162
Unsteady wind tunnel tests p 1089 N92-34166
Flutter in the transonic flight regime p 1089 N92-34167
Flutter analyses using high speed computers. Part 2: Aerodynamic procedures p 1089 N92-34169

UNSTEADY FLOW

Unsteady incompressible viscous flow past an airfoil p 3 A92-10662
Kernel function occurring in supersonic unsteady potential flow p 6 A92-11080
Optimal boundary control of nonsteady incompressible flow with an application to viscous drag reduction p 39 A92-11344
Numerical simulations of unsteady reactive flows in a combustion chamber p 39 A92-11761
Flow unsteadiness by weak normal shock wave/turbulent boundary layer interaction in internal flow p 67 A92-15359
Unsteady viscous flow in a high speed core compressor
[ASME PAPER 91-GT-91] p 70 A92-15555
Inviscid-viscous coupled solution for unsteady flows through vibrating blades. II - Computational results
[ASME PAPER 91-GT-126] p 71 A92-15571
An experiment on unsteady flow over an oscillating airfoil
[ASME PAPER 91-GT-181] p 73 A92-15613
Euler flow predictions for an oscillating cascade using a high resolution wave-split scheme
[ASME PAPER 91-GT-198] p 74 A92-15623
Unsteady Navier-Stokes simulation of transonic cascade flow using an unfactored implicit upwind relaxation scheme with inner iterations
[ASME PAPER 91-GT-223] p 74 A92-15637
Validation of a numerical method for unsteady flow calculations
[ASME PAPER 91-GT-271] p 151 A92-15668

Blade row interaction in a multistage low-pressure turbine
[ASME PAPER 91-GT-283] p 125 A92-15678
Computations of unsteady multistage compressor flows in a workstation environment
[ASME PAPER 91-GT-336] p 163 A92-15701
Noise-driven flow p 173 A92-18680
Three-dimensional calculation of low-frequency unsteady transonic flow in axial turbine stages
p 174 A92-19110
Numerical calculation of subsonic and supersonic aerodynamic loads around complex configuration vehicle
p 175 A92-20488
Unsteady Euler analysis of the flowfield of a propfan at an angle of attack p 242 A92-21070
An improvement of the double-point method for unsteady subsonic flow p 243 A92-21315
Weak coupling between an unsteady 3D full potential code and an unsteady turbulent boundary layer code - Application to a helicopter rotor in forward flight
[AIAA PAPER 92-0029] p 249 A92-22151
Vortex-induced energy separation in shear flows
[AIAA PAPER 92-0192] p 257 A92-23801
Establishment and characterization of a reproducible vortex for use in studying nonsteady two-dimensional phenomena p 310 A92-24428
A simplified method for simulating steady, unsteady flow around canard wing configuration p 311 A92-24876
Application of special series for studying nonstationary transonic gas flows p 311 A92-24904
A new method for solving the kernel equations of transonic flows - An auxiliary kernel method
p 410 A92-25108
Time marching integral equation method for the solutions of unsteady transonic flows p 314 A92-25129
Pressure wave propagation studies for oscillating cascades
[AIAA PAPER 92-0145] p 316 A92-25682
Unsteady incompressible flow computations with quadrilateral elements p 394 A92-26219
Direct computation of the sound from a compressible co-rotating vortex pair
[AIAA PAPER 92-0374] p 414 A92-26232
Unsteady blade pressures on a propfan at takeoff - Euler analysis and flight data
[AIAA PAPER 92-0376] p 372 A92-26234
Laser measurements of unsteady flow field in a radial turbine guide vanes
[AIAA PAPER 92-0394] p 395 A92-26249
Separation-induced self-excited structural oscillations
[AIAA PAPER 92-0486] p 328 A92-26317
Flow past a sphere - Topological transitions of the vorticity field p 330 A92-26410
Numerical investigation of unsteady transonic nozzle flows p 331 A92-26443
Theoretical study on the unsteady aerodynamic characteristics of an oscillating cascade with tip clearance (In the case of loaded cascade) p 331 A92-26797
Concerning a basic assumption for aeroelasticity in turbomachinery p 373 A92-26920
Unsteady flowfield simulation of ducted prop-fan configurations
[AIAA PAPER 92-0521] p 332 A92-26946
An unsteady Euler scheme for the analysis of ducted propellers
[AIAA PAPER 92-0522] p 332 A92-26947
A deforming grid variational principle and finite element method for computing unsteady small disturbance flows in cascades
[AIAA PAPER 92-0665] p 335 A92-27036
The unsteady flow characteristics of an S-shaped inlet at high incidence p 339 A92-27905
A boundary integral formulation for the kinetic field in aerodynamics. II - Applications to unsteady 2D flows
p 339 A92-28005
Numerical simulation of vortex unsteadiness on a slender body at high incidence p 340 A92-28062
Numerical experiments on a new class of nonoscillatory schemes
[AIAA PAPER 92-0421] p 341 A92-28193
Flowfield simulation about the SOFIA Airborne Observatory
[AIAA PAPER 92-0656] p 342 A92-28217
The unresolved unsteady flow in multistage compressor blade rows p 421 A92-29472
Applications of an implicit, upwind Navier-Stokes code, CRAFT, to steady/unsteady reacting, multi-phase flowfields
[AIAA PAPER 92-0837] p 422 A92-29603
Generalized expression of chorochronic periodicity in turbomachinery blade-row interaction
p 423 A92-30000
High aerodynamic loads on an airfoil submerged in an unsteady stream p 432 A92-31183
CFD state-of-the-art in the U.S.S.R
p 495 A92-31486
Time marching integral equation method for unsteady transonic flows around airfoils p 433 A92-31489
Interference flows past cylinder-fin-sting-cavity assemblies p 442 A92-32236
Navier-Stokes study of supersonic cavity flowfield with passive control p 442 A92-32239
Preliminary design of an intermittent smoke flow visualization system
[AIAA PAPER 92-1028] p 580 A92-33209
Unsteady transonic Euler solutions using finite elements
[AIAA PAPER 92-2504] p 518 A92-34499
Large eddy simulation of unsteady turbulent wake of a circular cylinder using the finite element method
p 587 A92-34825
Trends of research on cascade flutter
p 558 A92-35914
Unsteady hypersonic boundary layers for slender axisymmetric bodies with large injection rates
p 524 A92-36100
Unsteady flow past an airfoil pitching at a constant rate p 610 A92-36826
Experimental investigation of supersonic flow over two cavities in tandem p 610 A92-36830
Locally implicit hybrid algorithm for steady and unsteady viscous flows p 610 A92-36836
Spatial adaptation of unstructured meshes for unsteady aerodynamic flow computations p 610 A92-36838
Unsteady flow within centrifugal compressor channels under rotating stall and surge
[ASME PAPER 91-GT-85] p 670 A92-36901
A flow visualization experiment on the unsteady flow around two-dimensional airfoil p 615 A92-38913
Boundary-layer receptivity due to a wall suction and control of Tollmien-Schlichting waves
p 616 A92-39333
Phase-averaged turbulence statistics in a near wake with an asymmetric vortex shedding p 620 A92-40086
Data analysis for unsteady turbulence measurements over airfoils p 701 A92-41214
Wind tunnel wall corrections for unsteady flow applying steady wall adaptation and CFD-techniques
p 706 A92-42533
Computer simulation of an unsteady flow around an airfoil with a spoiler p 710 A92-43167
Flow establishment in a generic scramjet combustor
p 737 A92-44525
Viscous simulation method for unsteady flows past multicomponent configurations p 714 A92-44671
Recent applications of the FNS zonal Method to complex flow problems
[SAE PAPER 912003] p 789 A92-45404
Transonic unsteady inviscid and viscous flow's simulation around 2-D moving bodies
[AIAA PAPER 92-2704] p 801 A92-45546
Numerical simulations using a dynamic solution-adaptive grid algorithm, with applications to unsteady internal flows
[AIAA PAPER 92-2719] p 803 A92-45557
Time accurate computation of unsteady transonic flows around an airfoil with oscillating flap on dynamic grid
[AIAA PAPER 92-2733] p 805 A92-45567
Measurements of the unsteady vortex flow over a wing-body at angle of attack
[AIAA PAPER 92-2729] p 808 A92-45598
Unsteady crossflow on a delta wing using particle image velocimetry p 811 A92-46804
Comment on 'Canard-wing interaction in unsteady supersonic flow' p 812 A92-46820
Initial validation of an unsteady Euler/Navier-Stokes flow solver for helicopter rotor airloads in forward flight
p 815 A92-46956
Calculation of fully three-dimensional separated flows with an unsteady viscous-inviscid interaction method
[ONERA, TP NO. 1992-1] p 821 A92-48577
Numerical solutions of unsteady oscillating flows past an airfoil
[AIAA PAPER 92-3212] p 825 A92-48817
Vane-blade interaction in a transonic turbine. I - Aerodynamics
[AIAA PAPER 92-3323] p 825 A92-48906
Time domain numerical calculations of unsteady vortical flows about a flat plate airfoil p 936 A92-50473
Solution of Euler equations with unstructured mesh - 3-D case p 941 A92-52973
The behaviour of the pressure temperature and density in an inviscid unsteady transonic axisymmetric flow with shock waves p 1018 A92-53553
Navier-Stokes analysis of three-dimensional unsteady flows inside turbine stages
[AIAA PAPER 92-3211] p 1021 A92-54016
Analysis of the onset of dynamic stall
p 1024 A92-54919
Dynamical scaling of a model unsteady separating flow p 1117 A92-54932
Computations of the unsteady flow about a generic wing/pylon/finned-store configuration
[AIAA PAPER 92-4568] p 1027 A92-55377
Computing high-speed flows past an oscillating cylinder near a vertical wall
[AIAA PAPER 92-4653] p 1028 A92-55397
Numerical simulation of supersonic unsteady flow using a panel method p 1030 A92-56048
Generalized aerodynamics analysis by the boundary element method p 1030 A92-56050
Simulation of helicopter see-saw rotor motion
p 1055 A92-56287
Image processing in the undergraduate fluid dynamics laboratory
[AIAA PAPER 92-4020] p 1141 A92-56842
Numerical simulation of unsteady flow in a hypersonic shock tunnel facility
[AIAA PAPER 92-4029] p 1034 A92-56851
Experimental unsteady pressures on an oscillating cascade with supersonic leading edge locus
[AIAA PAPER 92-4035] p 1035 A92-56857
Numerical investigation of the effect of leading edge geometry on dynamic stall of airfoils
[AD-A239949] p 12 N92-10015
Jet noise classical theory and experiments
p 54 N92-10602
Blade surface pressure measurements on the rotor of a model turbine stage in a transient flow facility
p 157 N92-12206
Vortex formation over a close-coupled canard-wing-body configuration in unsymmetrical flow p 85 N92-13010
Numerical investigation of unsteady supersonic cavity flowfield with passive control p 88 N92-13029
Unsteady blade pressures on a propfan at takeoff: Euler analysis and flight data
[NASA-CR-189076] p 130 N92-13071
Unsteady flows in rotor-stator cascades
[AD-A241593] p 158 N92-13410
Definition of the unsteady vortex flow over a wing/body configuration
[NASA-CR-180083] p 178 N92-13995
The benchmark aeroelastic models program: Description and highlights of initial results
[NASA-TM-104180] p 185 N92-15049
Control of unsteady separated flow associated with the dynamic pitching of airfoils
[NASA-CR-189758] p 258 N92-15966
Development of an electronic high speed camera system for the quantitative analysis of unsteady flows
[MPIS-100/1991] p 300 N92-17344
CAR 88: A method to calculate subsonic and supersonic, steady and unsteady, potential flow about complex configurations
[NLR-TR-88154-U] p 400 N92-18221
Analysis of unsteady force, pressure, and flow-visualization data for a pitching straked wing model at high angles of attack p 364 N92-18784
Computation of a Kelvin-Helmholtz instability for delta wing vortex flows
[AD-A244320] p 346 N92-18825
The 8th Symposium on Turbulent Shear Flows. Volume 1: Sessions 1-18
[AD-A243809] p 402 N92-18933
Numerical simulation of transient hypervelocity flow in an expansion tube
[NASA-CR-189601] p 402 N92-18965
Numerical solution of three-dimensional unsteady viscous flows
[AD-A244274] p 403 N92-19052
Unsteady-flow-field predictions for oscillating cascades
[NASA-TM-105283] p 348 N92-19437
Recent results from data analysis of dynamic stall on wind turbine blades
[DE92-001200] p 505 N92-20245
Unsteady-pressure and dynamic-deflection measurements on an aeroelastic supercritical wing
[NASA-TM-4278] p 445 N92-20654
A quantitative study of unsteady compressible flow on an oscillating airfoil
[AD-A244572] p 445 N92-21012
Laser velocimetry measurements of oscillating airfoil dynamic stall flow field
[AD-A244546] p 502 N92-21297
An alternative to unstructured grids for computing gas dynamic flows around arbitrarily complex two-dimensional bodies
[NASA-CR-189612] p 447 N92-21465
Numerical simulation of transient hypervelocity flow in an expansion tube
[NASA-CR-189615] p 592 N92-22228
Computations of unsteady multistage turbomachinery flows p 562 N92-23671
Survey of experimental techniques for performance prediction p 552 N92-23954
Fundamental aspects of boundary layers and transition in turbomachines p 658 N92-24337

Investigations of blade row interaction and boundary layer transition phenomena in a multistage aero engine low-pressure turbine by measurements with hot-film probes and surface-mounted hot-film gauges
p 658 N92-24338
Aspects of unsteady blade-surface boundary layers and transition in axial turbomachines p 658 N92-24340
Nonunique solutions in unsteady transonic flow
p 629 N92-24872
Measurements of fluctuating pressure in a rectangular cavity in transonic flow at high Reynolds numbers
[NASA-TM-4363] p 633 N92-25752
On the computation of unsteady turbomachinery flows. Part 1: Euler equations in vibrating cascades
p 768 N92-27460
Steady and unsteady 3D flow computation through a transonic turbine stage p 742 N92-27469
Unsteady Euler calculations in 3D internal aerodynamics p 768 N92-27470
Transonic Unsteady Aerodynamics and Aeroelasticity
[AGARD-CP-507] p 718 N92-27936
A time-linearization approach for unsteady transonic flows p 719 N92-27941
A boundary integral formulation for unsteady transonic potential flows p 719 N92-27942
Computation of the unsteady transonic 2D cascade flow by an Euler algorithm with interactive grid generation
p 719 N92-27944
Evaluation of an unsteady implicit Euler code against two and three-dimensional standard configurations
p 719 N92-27945
Computations of unsteady flows around airfoil sections by explicit and implicit methods solving the Euler and Navier-Stokes equations p 720 N92-27948
Computation of viscous phenomena in unsteady transonic flow p 720 N92-27949
Analysis of unsteady aerodynamic and flutter characteristics of an aeroelastic model in transonic flow
p 720 N92-27953
The benchmark aeroelastic models program: Description and highlights of initial results
p 721 N92-27960
Calculation of unsteady transonic flows with mild separation by viscous-inviscid interaction
[NASA-TP-3197] p 827 N92-28477
Study of the leading-edge vortex dynamics in the unsteady flow over an airfoil
[AD-A247532] p 829 N92-28865
Development of an unsteady three-dimensional viscous-inviscid interaction numerical method for the calculation of airfoils vibration
[ONERA-RSF-7/3617-AY-022A] p 830 N92-29206
Production of periodical Mach number variations in high subsonic flow in a blow down wind tunnel, and its influence on profile measurements
[ETN-92-91492] p 833 N92-29889
A computational investigation of airfoil stall flutter
[AD-A247302] p 947 N92-31300
Active control of the separation region on a two-dimensional airfoil
[AD-A249739] p 948 N92-31622
Control of unsteady separated flow associated with the dynamic stall of airfoils
[NASA-CR-190688] p 950 N92-32177
Computations of unsteady multistage compressor flows in a workstation environment
[NASA-TM-103839] p 1071 N92-32452
Unsteady response of the leading-edge vortices on a pitching delta wing p 1041 N92-33851
Prediction and control of asymmetric vortical flows around slender bodies using Navier-Stokes equations
p 1127 N92-33968

UNSTEADY STATE
Experimental investigation of the unsteady pressure field around an oscillating blade
[MITT-90-01] p 768 N92-27407

UNSWEPT WINGS
Interference of high-mounted propfan nacelles with an unswept wing and ways to attenuate it
p 460 A92-31881

UPGRADING
Reactivation and upgrade of the NASA Ames 16-Inch Shock Tunnel - Status report
[AIAA PAPER 92-0327] p 383 A92-25774
Mechanical design of a rotary balance system for NASA. Langley Research Center's vertical spin tunnel
p 664 N92-25090
Life cycle costs of the C-130 electrical power system upgrade
[AD-A246759] p 786 N92-28348

UPPER ATMOSPHERE
On the skip flight of a spaceplane
p 387 A92-25503

UPPER SURFACE BLOWING
Flight test results and upper surface blowing (USB) technology of the STOL research aircraft Asuka
p 730 A92-43142
High speed aerodynamics of upper surface blowing aircraft configurations
[AIAA PAPER 92-2611] p 793 A92-45485
Analysis of the main wing lift distribution of the STOL research aircraft Asuka p 1053 A92-56051
Computational study of the aerodynamics and control by blowing of asymmetric vortical flows over delta wings
[NASA-CR-187979] p 14 N92-10990
Aerodynamic aircraft design methods and their notable applications: Survey of the activity in Japan
p 193 N92-13930
Evaluation of high lift devices of the quiet STOL experimental aircraft ASKA
[NAL-TR-1102] p 733 N92-28153
Note on flight measured control effectiveness of the quiet STOL experimental aircraft ASKA
[NAL-TR-1103] p 746 N92-28154
Evaluation of landing configuration by flight test of the quiet STOL experimental aircraft ASKA
[NAL-TR-1113] p 733 N92-28191
Aerodynamic characteristics obtained from alpha sweep test of the quiet STOL experimental aircraft ASKA
[NAL-TR-1112] p 853 N92-28901

UPPER SURFACE BLOWN FLAPS
Wind tunnel investigation of an improved upper surface blown flap transport semi-span model
[SAE PAPER 911993] p 789 A92-45395

UPWASH
A comparative analysis of XV-15 tiltrotor hover test data and WOPWOP predictions incorporating the fountain effect
[NASA-CR-189455] p 114 N92-11992
Rotorwash computer model: User's guide
[DOT/FAA/RD-90/25] p 346 N92-18345

UPWIND SCHEMES (MATHEMATICS)
An improved approach for the computation of transonic/supersonic flows with applications to aerospace configurations
[AIAA PAPER 92-2613] p 793 A92-45487
Effect of throat contouring on two-dimensional converging-diverging nozzles using URS method
[AIAA PAPER 92-2659] p 797 A92-45520
Characteristics of the Shuttle Orbiter leeside flow during a reentry condition
[AIAA PAPER 92-2951] p 821 A92-47915
Improved artificial dissipation schemes for the Euler equations p 933 A92-49508
The simulation of inviscid, compressible flows using an upwind kinetic method on unstructured grids
p 933 A92-49515

URBAN PLANNING
Interdependencies of aircraft-/airport-noise and urban- and regional-planning standards p 688 A92-39063
Determination of aircraft noise levels while the engine is running on the ground - An approach from the point of urbanization and architecture p 688 A92-39064

URBAN TRANSPORTATION
WIG transportation efficiency considering the influence of no-load situation p 781 A92-43241
Bibliography of technical reports, 1980 - 1990
[PB92-110691] p 417 N92-18814

USER MANUALS (COMPUTER PROGRAMS)
C.A.T.C.H. - Computer aided test conductor handbook: A method for reducing cost, time and effort in an aircraft test and certification program p 602 A92-35943
Structural tailoring of advanced turboprops (STAT): User's manual
[NASA-CR-187101] p 26 N92-11016
F/A-18 stabilator: Equivalent set of point forces required for pneumatic bag load case simulation
[AD-A242637] p 206 N92-15073
User guide for WIACX: A transonic wind-tunnel wall interference assessment and correction procedure for the NTF
[NASA-TM-104168] p 261 N92-17547
An introduction to high speed aircraft noise prediction
[NASA-CR-189582] p 416 N92-19672
SIMNET plan view display user manual
[AD-A244617] p 510 N92-21392
Modernized MBB panel code: User's guide including background theory
[PB92-136431] p 526 N92-22233
A three-dimensional, compressible, laminar boundary-layer method for general fuselages. Volume 2: User's manual
[NASA-CR-4292-VOL-2] p 678 N92-24344
MLS and DME/P multipath simulation model user's manual. Volume 1: Operating instructions
[DOT/FAA/CT-TN91/47] p 640 N92-24888
Naval Postgraduate School aircraft synthesis program (user's manual)
[AD-A246198] p 777 N92-26458
Computer program for calculating in-flight aircraft-store interface reaction loads
[AD-A245782] p 731 N92-26896
Users manual and modeling improvements for axial turbine design and performance computer code TD2-2
[NASA-CR-189118] p 716 N92-27376
Users manual for updated computer code for axial-flow compressor conceptual design
[NASA-CR-189171] p 924 N92-30207
An installed nacelle design code using a multiblock Euler solver. Volume 2: User guide
[NASA-CR-189652-VOL-2] p 951 N92-32228
User's manual for AeroFcn: A FORTRAN program to compute aerodynamic parameters
[NASA-TM-104237] p 1133 N92-32507

USER REQUIREMENTS
First level release of 2GCHAS for comprehensive helicopter analysis p 1133 A92-56339
Information Management Engineering (IME) laboratory: A database development facility
[AD-A243191] p 305 N92-17369
Structured Hypermedia Application Development Model (SHADM): A structured model for technical documentation application design
[AD-A244268] p 417 N92-19336
Instrumentation requirements for laminar flow research in the NLR high speed wind tunnel HST
[NLR-TP-89158-U] p 887 N92-28669
Development of a flight information system using the structured method
[AD-A248207] p 859 N92-29222

V

V-22 AIRCRAFT
Advanced thermoplastic nose landing gear door development p 20 A92-10275
Results from a test of a 2/3-scale V-22 rotor and wing in the 40- by 80-Foot Wind Tunnel p 104 A92-14332
V-22 flight test aerodynamics p 104 A92-14333
Flying qualities evaluation of the V22 tiltrotor
p 131 A92-14334
Flight testing the avionics system of the V-22 Osprey
p 117 A92-14378
V-22 thrust power management control law development p 132 A92-14405
V-22 Osprey tiltrotor blade fold/wing stow system design and testing p 109 A92-14420
V-22 pilot-in-the-loop aeroelastic stability analysis
p 133 A92-14422
Effectiveness of V-22 tiltrotors in support of land combat operations p 60 A92-14442
V-22 flight test p 112 A92-16056
Tiltrotor control law design for rotor loads alleviation using modern control techniques p 478 A92-29331
The V-22 Osprey - Preparing for fleet operations
p 458 A92-29671
The V-22 Osprey - A significant flight test challenge
p 546 A92-35766
V-22 full scale development testing
p 646 A92-40038
Military utility of medium speed V/STOL designs
p 841 A92-45308
Shipboard mission training effectiveness of the Naval Air Warfare Center's V-22 Government Test Pilot Trainer
[AIAA PAPER 92-4130] p 959 A92-52427
V-22 propulsion system design p 1070 A92-56300
The V-22: Can the nation afford to forgo its production?
[AD-A243158] p 242 N92-17477
A historical overview of tiltrotor aeroelastic research at Langley Research Center
[NASA-TM-107578] p 502 N92-21460
Development of thermoplastic components for structural validation p 1107 N92-32522

V/STOL AIRCRAFT
The application of high pressure ejectors to reaction control systems p 128 A92-16666
Consideration of the time lag of engine processes in the problem of VTOL aircraft control synthesis
p 134 A92-16807
Hot gas environment around STOVL aircraft in ground proximity. I - Experimental study p 371 A92-24409
Correction of sideslip-induced static pressure errors in flight-test measurements p 309 A92-24416
Flow in a ventral nozzle for short takeoff and vertical landing aircraft p 376 A92-28538
Integrated flight/propulsion control design for a STOVL aircraft using H-infinity control design techniques
p 476 A92-29093
Meeting VSTOL aircraft performance requirements using scheduled H(infinity) controllers p 477 A92-29094
IMPAC - An integrated methodology for propulsion and airframe control p 477 A92-29118

An experimental and analytical investigation of wing flutter on a trail rotor V/STOL aircraft
[AIAA PAPER 92-2112] p 544 A92-35682
The aerodynamic assistant - A tool for V/STOL aircraft conceptual design p 545 A92-35737
The V-22 Osprey - A significant flight test challenge p 546 A92-35766
AV-8B V/STOL performance analysis p 549 A92-35948
RAE Bedford VAAC research project --- VSTOL aircraft advanced flight control p 662 A92-40039
International Powered Lift Conference, London, England, Aug, 29-31, 1990, Proceedings
[ISBN 0-903409-68-2] p 783 A92-45302
An overview of US Navy and Marine Corps V/STOL p 783 A92-45303
Jet-powered V/STOL aircraft - Lessons learned p 841 A92-45304
Harrier international programme p 841 A92-45305
Military utility of medium speed V/STOL designs p 841 A92-45308
Evolution of ASTOVL aircraft design p 842 A92-45311
Recent developments at the Shoeburyness STOVL test facility p 881 A92-45314
Configuration effects on the ingestion of hot gas into the engine intake p 842 A92-45315
The experimental and computational study of jet impingement flowfields with reference to VSTOL aircraft performance p 787 A92-45324
Experimental and analytical study of close-coupled ventral nozzles for ASTOVL aircraft p 861 A92-45325
High speed VSTOL on the horizon - The answer to congestion?
[SAE PAPER 911976] p 843 A92-45383
Aviation, motor, and space designs --- research and development in U.S.S.R. p 784 A92-46202
Shipboard mission training effectiveness of the Naval Air Warfare Center's V-22 Government Test Pilot Trainer
[AIAA PAPER 92-4130] p 959 A92-52427
Reduction of the side force on pointed forebodies through add-on tip devices p 1024 A92-54918
A multi-diagnostic approach to testing V/STOL craft
[AIAA PAPER 92-4008] p 1099 A92-56831
Finite element analysis of ASTOVL fighter structure
[AD-A243724] p 275 N92-17513
United States Navy ski jump experience and future applications p 465 N92-21968
Some implications for advanced STOVL operation from invincible class ships p 466 N92-21971
Recent developments at the Shoeburyness (England) STOVL Test Facility
[PNR-90806] p 572 N92-22096
Directions in propulsion control p 560 N92-22530
Supersonic STOVL propulsion technology program: An overview p 561 N92-22539
VSTOL engine design evolution: Growth of the Pegasus engine for Harrier
[PNR-90805] p 739 N92-27039
ASTOVL engine control
[PNR-90808] p 740 N92-27040
ASTOVL propulsion systems: Configuration and concept choice
[PNR-90809] p 740 N92-27041
Collaborative research on V/STOL control system/cockpit display tradeoffs under the NASA/MOD joint aeronautical program
[NASA-TM-103910] p 1087 N92-32788
On the anomalies in single-jet hover suckdown data
[NASA-TM-102261] p 1038 N92-33306
Dynamic response of induced pressures, suckdown, and temperatures for two tandem jet STOVL configurations
[NASA-TM-103934] p 1039 N92-33581
On the estimation of jet-induced fountain lift and additional suckdown in hover for two-jet configurations
[NASA-TM-102268] p 1040 N92-33618

VACUUM CHAMBERS
Experimental investigation of periodically excited rotating composite rotor blades p 218 A92-20213
Gasdynamic calculation of an impulse wind tunnel with a two-section plenum p 493 A92-30147

VACUUM DEPOSITION
PVD coatings for aircraft turbine blades p 216 A92-17950

VACUUM FURNACES
Modifications to the rapid melt/rapid quench and transparent polymer video furnaces for the KC-135
[NASA-CR-184215] p 157 N92-12231

VALVES
Measurements and simulation of the flow around a poppet valve p 675 A92-40103
Development of the DDV actuation system on the IDF aircraft
[SAE PAPER 912080] p 844 A92-45455
Pulse jet one-way valve performance
[AIAA PAPER 92-3169] p 863 A92-48790
Double piston shock-wave valve p 1117 A92-54938
Hydraulic actuator system for rotor control p 224 N92-14363
Assessment of valve actuator motor rotor degradation by Fourier Analysis of current waveform
[DE92-013233] p 909 N92-28814

VANADIUM ALLOYS
Rolling element bearing member
[PATENT-1-271-213] p 158 N92-13434
Surface residual stress analysis of metals and alloys
[AD-A248372] p 895 N92-28426

VANELESS DIFFUSERS
A study on the rotating stall of centrifugal compressors. II - Effect of vaneless diffuser inlet shape on rotating stall p 497 A92-32508
Unsteady flow within centrifugal compressor channels under rotating stall and surge
[ASME PAPER 91-GT-85] p 670 A92-36901

VANES
Optimization of multistage axial-flow compressor vane setting p 371 A92-24746
Local heat transfer in the perforation channels of turbine nozzle vanes p 657 A92-40615
Advanced superalloys for turbine blade and vane applications
[ONERA, TP NO. 1992-2] p 893 A92-48578
The flow pattern and external heat transfer investigation for gas turbine vanes end surfaces
[AIAA PAPER 92-3071] p 903 A92-48722
Airfoil wake and linear theory gust response including sub and superresonant flow conditions
[AIAA PAPER 92-3074] p 823 A92-48724
Vane-blade interaction in a transonic turbine. I - Aerodynamics
[AIAA PAPER 92-3323] p 825 A92-48906
The mechanism of liquid-cooling of vane in high-temperature turbine p 969 A92-49841
Wind tunnel performance results of swirl recovery vanes as tested with an advanced high speed propeller
[AIAA PAPER 92-3770] p 1068 A92-54159
Numerical calculations of propfan/swirl recovery vane flow field
[AIAA PAPER 92-3771] p 1022 A92-54160
Hydrodynamic flow visualization around an oscillating vane. Extension of study to the case of higher incidences and amplitudes and the starting off phase from permanent regime
[ONERA-RT-56/1369-AN] p 43 N92-11312
High temperature static strain gage development
[NASA-CR-189044] p 195 N92-14037
Ceramic regenerator program
[NASA-CR-189053] p 225 N92-14374
Aircraft ground test and subscale model results of axial thrust loss caused by thrust vectoring using turning vanes
[NASA-TM-4341] p 273 N92-17071
Evaluation and qualification of diffusion braze repair techniques for superalloy gas turbine components
[NRC-LTR-ST-1839] p 504 N92-22028
Laser anemometer measurements and computations in an annular cascade of high turning core turbine vanes
[NASA-TP-3252] p 830 N92-28980
Strong coupling between inviscid fluid and boundary layer of sharp leading edges: Two-dimensional stationary and turbulent cases for isolated profiles and guard vanes
[ONERA-RT-44/1621-RY-016-R] p 1125 N92-32776
Investigation of the flight control requirements of a half-scale ducted fan unmanned aerial vehicle
[AD-A252730] p 1087 N92-32988
Cooled high-temperature radial turbine program 2
[NASA-CR-189122] p 1073 N92-34236

VAPOR DEPOSITION
Thermally sprayed coating systems for surface protection and clearance control applications in aero engines p 488 A92-32394
Fabrication and testing of corrosion resistant coatings --- for turbine engine components
[DE92-003553] p 490 N92-21063

VAPOR PHASES
Atmospheric pressure flow reactor: Gas phase chemical kinetics under tropospheric conditions without wall effects
[NASA-CASE-MSC-21384-1] p 297 N92-16243

VAPORIZERS
Modelling the vaporiser and primary zone flows for a modern gas turbine combustion chamber p 742 N92-27484

VAPORIZING
Deposition during vaporization of jet fuel in a heated tube
[AIAA PAPER 92-0687] p 390 A92-27054
A distributed vaporization time-lag model for gas turbine combustor dynamics
[AIAA PAPER 92-3465] p 865 A92-49014
Fundamental studies on droplet interactions in dense sprays
[AD-A246918] p 770 N92-27546
Vaporizing particle velocimeter
[NASA-CASE-LAR-14685-1] p 1042 N92-34172

VAPORS
Microgravity nucleation and particle coagulation experiments support
[NASA-CR-190159] p 502 N92-21385
Solid-vapor adsorption refrigeration system development
[PB92-164383] p 771 N92-27715
Further studies in filmwise condensation of steam on horizontal finned tubes
[AD-A252705] p 1011 N92-31767

VARIABLE CYCLE ENGINES
The selective bleed variable cycle engine --- aircraft propulsion
[ASME PAPER 91-GT-388] p 126 A92-15720
Effects of turbine cooling assumptions on performance and sizing of high-speed civil transport
[NASA-TM-105610] p 562 N92-23537
A preliminary design and analysis of an advanced heat-rejection system for an extreme altitude advanced variable cycle diesel engine installed in a high-altitude advanced research platform
[NASA-CR-186021] p 871 N92-29427

VARIABLE GEOMETRY STRUCTURES
A geometric approach to regulator and tracker design for an aerospace plane
[AIAA PAPER 91-5054] p 203 A92-17837
Mechanics of curved fiber composites p 757 A92-41034
Methodology for calculating aerodynamic sensitivity derivatives p 1024 A92-54911
An improved model-creation program for EM interaction analysis
[NRC-31764] p 155 N92-12153

VARIABLE STREAM CONTROL ENGINES
A multivariable control concept for a gas turbine engine
[ETN-92-92104] p 1072 N92-33645

VARIABLE SWEEP WINGS
History of EPOS air-launched spaceplane project p 211 N92-14103

VARIABLE THRUST
Effect of thermodynamic parameters on performance and cost of turbine engines p 969 A92-49834

VARIANCE (STATISTICS)
The effect of droplet sizing uncertainty on ice accretions p 679 N92-24874

VARIATIONAL PRINCIPLES
A deforming grid variational principle and finite element method for computing unsteady small disturbance flows in cascades
[AIAA PAPER 92-0665] p 335 A92-27036
A variational method for solving the problem of motion of a profile of complex geometry in a fluid p 397 A92-27482
Lyapunov exponents for systems described by differential equations with discontinuous right-hand sides p 507 A92-29237
Investigation of extremal field behavior for two-dimensional linear problems in flight mechanics p 509 A92-30130
Minimum-drag bodies moving in locality-law media p 779 A92-42732
Finite element analysis of tire critical speeds p 762 A92-42949
Advanced stress analysis methods applicable to turbine engine structures
[NASA-CR-187235] p 44 N92-11378
Variational formulation of hybrid problems for fully 3-D transonic flow with shocks in rotor p 176 N92-13953

VARIATIONS
Examination of the main error factors with regards to secondary losses in compression and turbine cascades by variations of the blade picture ratio
[ETN-92-91493] p 871 N92-29927

VATOL AIRCRAFT
High lift aircraft
[AD-D015215] p 732 N92-27185

VAX COMPUTERS
Advanced Transport Operating System (ATOPS) color displays software description: MicroVAX system
[NASA-CR-189603] p 556 N92-22395

VECTOR ANALYSIS
Traveling on the curved earth p 19 A92-10474

VECTOR PROCESSING (COMPUTERS)
Efficient direct solvers for large-scale computational fluid dynamics problems p 690 A92-37534
Special Rotation Vectors quaternions in three components
[AIAA PAPER 92-4168] p 1008 A92-52454

A parallel-vector algorithm for rapid structural analysis on high-performance computers
[NASA-TM-102614] p 595 N92-22649

VECTORS (MATHEMATICS)
Application of holomorphic vectors theory in three-dimensional potential flow problem
p 292 A92-21923

VEHICLE WHEELS
Determination of tire-wheel interface loads for aircraft wheels
[AIAA PAPER 92-2482] p 543 A92-34599

VELOCITY
Combined VISAR and flash x ray testing techniques
[DE92-004732] p 385 N92-18290
The utility of analog vertical velocity information during instrument flight with a Head-Up Display (HUD)
[AD-A252863] p 1065 N92-33277

VELOCITY COUPLING
Experimental investigation of the effects of blowing on bursting of strake vortices
[AD-A240256] p 13 N92-10985

VELOCITY DISTRIBUTION
Boundary-layer and wake measurements on a swept, circulation-control wing p 9 A92-13205
Synthesis of wing profiles from chord velocity diagrams using quasi-solutions for inverse boundary value problems p 80 A92-16815
Concerning the functional solution of transonic flows
p 243 A92-21318
Measurements of the pressure and velocity distribution in low-speed turbomachinery by means of high-frequency pressure transducers p 391 A92-24723
The LDV measurement of three-component velocity of complex vortex flow in the wind tunnel
p 393 A92-25109
LDV measurements of the velocity field in an underexpanded supersonic jet (Ma = 1.5)
[AIAA PAPER 92-0504] p 341 A92-28196
Low speed aerodynamic performance of a capsule-shaped flying object p 430 A92-30559
On the influence of blade-vortex-interactions on vortex structure p 521 A92-35783
Current topics connected with rotating stall
p 521 A92-35913
The effect of a velocity gradient on the aerodynamic forces of a circular cylinder with tangential blowing
p 614 A92-38859
Embedded longitudinal vortex arrays, velocity and temperature fields, loss and heat transfer augmentation
p 621 A92-40121
Oscillating airfoil velocity field during large amplitude dynamic stall p 622 A92-40171
Some issues on modeling atmospheric turbulence experienced by helicopter rotor blades
p 647 A92-40885
Experimental technique of measuring fuel concentration in non-uniform flowfield p 734 A92-41928
Construction of a wing profile with a flap modeled by a point vortex p 707 A92-42726
Swirl number effects on confined flows in a model of a dump combustor p 896 A92-45202
Boundary-layer measurements during a parallel blade-vortex interaction
[AIAA PAPER 92-2623] p 794 A92-45495
Multi-point inverse design of an infinite cascade of airfoils
[AIAA PAPER 92-2650] p 797 A92-45517
Vortex-in-cell analysis of wing wake roll-up
[AIAA PAPER 92-2703] p 801 A92-45545
Quantification of canard and wing interactions using spatial correlation velocimetry
[AIAA PAPER 92-2687] p 807 A92-45588
Unsteady crossflow on a delta wing using particle image velocimetry p 811 A92-46804
The flow pattern and external heat transfer investigation for gas turbine vanes end surfaces
[AIAA PAPER 92-3071] p 903 A92-48722
Design and optimization of airfoils in non-stalling incompressible flow with a prescribed range of the angle of attack p 933 A92-49556
Time domain numerical calculations of unsteady vortical flows about a flat plate airfoil p 936 A92-50473
Flow visualization and flow field measurements of a 1/12 scale tilt rotor aircraft in hover
[NASA-CR-189456] p 82 N92-11983
Breaking down the delta wing vortex: The role of vorticity in the breakdown process p 86 N92-13017
Supercritical blade design on stream surfaces of revolution with an inverse method p 220 N92-13950
Experimental study of a vortex subjected to imposed strain
[NASA-CR-189757] p 258 N92-15969
Separation of relaminarised boundary layers
[CUED/A-AERO/TR-16] p 592 N92-22209
Wall functions for the kappa-epsilon turbulence model in generalized nonorthogonal curvilinear coordinates
[NASA-CR-190368] p 685 N92-25962
A comparison of predicted and measured inlet distortion flows in a subsonic axial inlet flow compressor rotor
[NASA-TM-105427] p 633 N92-26104
Unsteady Euler calculations in 3D internal aerodynamics p 768 N92-27470
A preliminary experimental investigation of local isotropy in high-Reynolds-number turbulence
p 912 N92-30042
Three-dimensional compressible turbulent computations for a nondiffusing S-duct
[NASA-CR-4391] p 951 N92-32240

VELOCITY ERRORS
Evaluating the velocity accuracy of an integrated GPS/INS system: Flight test results
[DE92-007519] p 640 N92-25470
A Kalman filter integrated navigation design for the IAR Twin Otter Atmospheric Research Aircraft
[NRC-32148] p 1048 N92-32849

VELOCITY MEASUREMENT
Synthesis of the algorithm of a spatial-temporal discriminator and the potential accuracy of the velocity meter p 41 A92-12828
Helicopter local blade circulation calculations for a model rotor in forward flight using laser velocimeter measurements p 65 A92-14362
Doppler global velocimeter measurements of the vortical flow above a thin delta wing
[AIAA PAPER 92-0005] p 292 A92-22130
Laser diagnostics for velocity measurements in supersonic combusting environments
[AIAA PAPER 92-0008] p 288 A92-22133
Optical velocity sensor for air data applications
p 368 A92-24575
Experimental study of the characteristics of boundary-layer development on an airfoil
p 425 A92-30171
Relative accuracy of wind tunnel calibration speeds
p 484 A92-32056
A sensitive fast-response probe to measure turbulence and heat flux from any airplane p 775 A92-42097
Quantification of canard and wing interactions using spatial correlation velocimetry
[AIAA PAPER 92-2687] p 807 A92-45588
The application of particle image velocimetry (PIV) in a short-duration transonic annular turbine cascade
[ASME PAPER 91-GT-221] p 899 A92-46825
Laser velocimetry measurements in an MHD aerodynamic duct
[AIAA PAPER 92-2986] p 899 A92-46996
Full field flow visualization and computer-aided velocity measurements in a bank of cylinders in a wind tunnel
p 991 A92-50040
Measurement of angle of attack using a five-hole arrow head pitot tube p 941 A92-53009
Comparison of frequency domain and time domain laser velocimeter signal processors p 1114 A92-54314
Rayleigh imaging and flow tagging in ground test facilities p 1115 A92-54330
A simple three component velocity measurement method using a rotated split-film sensor
p 1115 A92-54333
NACA 0015 wing pressure and trailing vortex measurements
[NASA-TP-3151] p 13 N92-10981
Characteristics of a boundary layer in a leading edge vortex p 86 N92-13012
A study of the airwake aerodynamics over the flight deck of an AOR model ship
[AD-A241008] p 89 N92-13034
An evaluation of preliminary Doppler global velocimetry measurements p 90 N92-13849
Constant-temperature anemometry measurements in hypersonic boundary layers p 90 N92-13861
Viscous three-dimensional calculations of transonic fan performance
[NASA-TM-103800] p 242 N92-17346
Examination of energy spectra moments in a developing turbulent flow
[NIAR-91-28] p 399 N92-18116
A laser velocimeter investigation of the normal shockwave boundary layer interaction
p 500 N92-20485
A method of passive range determination using only two bearing measurements
[AD-D015182] p 455 N92-20834
Laser velocimetry measurements of oscillating airfoil dynamic stall flow field
[AD-A244546] p 502 N92-21297
Pressure and velocity measurements about an airfoil during a parallel blade-vortex interaction
p 446 N92-21429
The fibre optic three dimensional laser two focus velocimeter for the low-speed windtunnel. Part 1: Two-dimensional measurement evaluations
[NAL-TM-627] p 665 N92-25402
Particle image velocimetry
[AD-A246638] p 750 N92-27753
Study of the leading-edge vortex dynamics in the unsteady flow over an airfoil
[AD-A247532] p 829 N92-28865
A 4-spot time-of-flight anemometer for small centrifugal compressor velocity measurements
[NASA-TM-105717] p 909 N92-29105
Theoretical simulation of a 2 micron airborne solid state laser anemometer p 1000 N92-31059
An experimental study of the relationship between velocity and pressure fluctuations in a wing-body junction
[AD-A249628] p 946 N92-31122
Vaporizing particle velocimeter
[NASA-CASE-LAR-14685-1] p 1042 N92-34172

VENTILATION
Commercial airplane air distribution system development through the use of computational fluid dynamics
[AIAA PAPER 92-0987] p 535 A92-33182
Computational fluid dynamics applications in airplane cabin ventilation system design
[SAE PAPER 911992] p 788 A92-45394
Indirect measurements of convective flow by IR thermography
[ONERA, TP NO. 1992-46] p 902 A92-48607
Study of a new airfoil used in reversible axial fans
p 177 N92-13970

VENTING
Lift and rolling moment due to spoilers on wings with trailing-edge flaps deflected at subsonic speeds
[ESDU-92002-SUPPL] p 1037 N92-32782

VENTURI TUBES
Experimental investigation on combustor with double co-axial swirlers p 469 A92-29729

VERBAL COMMUNICATION
An analysis of aircrew communication patterns and content
[AD-A246618] p 907 N92-28253

VERTICAL AIR CURRENTS
The modelling of turbulence and downbursts for flight simulators
[ISBN-0-315-59945-6] p 749 N92-27645

VERTICAL DISTRIBUTION
The vortical structure in the wake during dynamic stall
[AIAA PAPER 92-4496] p 1026 A92-55364
Feasibility study of hypersonic clinometric measurements at R3Ch
[ONERA-RSF-136/1865-AY-728-] p 829 N92-28789
Antenna pattern measurement facilities
[AD-A248964] p 982 N92-30329

VERTICAL FLIGHT
Balloon altitude control by valving - A review and comparison of actual flight data and vertical performance analysis results
[AIAA PAPER 91-3669] p 14 A92-11016
Future considerations for vertical flight
p 608 A92-40383
Oscillations of balloon-flight altitude
p 836 A92-46660
A Lie Bracket solution of the optimal thrust magnitude on a singular arc in atmospheric flight
[AIAA PAPER 92-4345] p 1079 A92-55334
An evaluation of four F-16 vertical velocity indicator configurations
[AD-A243629] p 370 N92-18014
FAA vertical flight research, engineering, and development bibliography, 1962 - 1991
[FAA/ARD-30] p 462 N92-21210
Investigation of the flight control requirements of a half-scale ducted fan unmanned aerial vehicle
[AD-A252730] p 1087 N92-32988

VERTICAL LANDING
A computer programme for the certification of helicopter vertical take-off and landing operations and an application to the S-76B helicopter p 106 A92-14379
S-76B certification for vertical take-off and landing operations from confined areas p 530 A92-35760
Control and display combinations for blind vertical landings p 661 A92-39903
RAE Bedford VAAC research project --- VSTOL aircraft advanced flight control p 662 A92-40039
Military utility of medium speed V/STOL designs
p 841 A92-45308
Prediction and measurement of jet flowfield features for ASTOVL aircraft p 787 A92-45318
Ground surface erosion - British Aerospace test facility and experimental studies p 881 A92-45323
Experimental performance of three design factors for ventral nozzles for SSTOVL aircraft
[AIAA PAPER 92-3789] p 1069 A92-54168

Internal reversing flow in a tailpipe offtake configuration for SSTOVL aircraft
[AIAA PAPER 92-3790] p 1069 A92-54169
Analysis of airframe/engine interactions for a STOVL aircraft with integrated flight/propulsion control
[AIAA PAPER 92-4623] p 1052 A92-55300
Static internal performance of ventral and rear nozzle concepts for short-takeoff and vertical-landing aircraft
[NASA-TP-3103] p 12 N92-10975
Analytical modeling of SH-2F helicopter shipboard operation p 464 N92-21961
Helicopter/ship analytic dynamic interface p 464 N92-21962
Experimental performance of three design factors for ventral nozzles for SSTOVL aircraft
[NASA-TM-105697] p 742 N92-27669
Internal reversing flow in a tailpipe offtake configuration for SSTOVL aircraft
[NASA-TM-105698] p 868 N92-28418
ASTOVL combat aircraft design synthesis and optimization
[CRANFIELD-AERO-9201] p 963 N92-31515

VERTICAL MOTION
The utility of analog vertical velocity information during instrument flight with a Head-Up Display (HUD)
[AD-A252863] p 1065 N92-33277

VERTICAL MOTION SIMULATORS
Algorithmic improvements for simulator motion drive
[AIAA PAPER 92-4158] p 1007 A92-52448
The use of ground based simulation for handling qualities research: A new assessment p 885 N92-28545

VERTICAL ORIENTATION
Estimating the probability of vertical overlap from the paired aircraft data obtained in the European vertical data collection using the program DGLDiF
[NLR-TR-88108-U] p 356 N92-19491
The status of the US VAWT program
[DE92-002931] p 505 N92-21040

VERTICAL TAKEOFF
A computer programme for the certification of helicopter vertical take-off and landing operations and an application to the S-76B helicopter p 106 A92-14379
Propulsion systems from takeoff to high-speed flight p 889 A92-46428
Analytical modeling of SH-2F helicopter shipboard operation p 464 N92-21961
Helicopter/ship analytic dynamic interface p 464 N92-21962
S-76B certification for vertical take-off and landing operations from confined areas
[NLR-TP-90286-U] p 852 N92-28714

VERTICAL TAKEOFF AIRCRAFT
VSTOL aircraft flight control system design using H(infinity) controllers and a switching strategy p 28 A92-11561
Hover evaluation of an integrated pneumatic lift/reaction-drive rotor system
[AIAA PAPER 92-0630] p 333 A92-27010
Hover control of a PVTOL using nonlinear regulator theory p 478 A92-29171
Russia bids to salvage development of Soyuz-powered VTOL fighter p 472 A92-32300
Conceptual design and analysis of a special operations transport
[AIAA PAPER 92-1066] p 536 A92-33239
S-76B certification for vertical take-off and landing operations from confined areas p 530 A92-35760
Sikorsky Aircraft UAV program p 646 A92-40385
Aeroelasticity and the Tiltrotor VTOL aircraft p 647 A92-40389
Research on a low-noise engine for a high-speed VTOL aircraft p 737 A92-43239
The high speed challenge for rotary wing aircraft
[SAE PAPER 911974] p 842 A92-45381
Ducted fan VTOL for working platform
[SAE PAPER 911995] p 843 A92-45397
The effect of composite material allowable changes on VTOL airframe weights p 848 A92-47629
Nonlinear control design for slightly nonminimum phase systems - Application to V/STOL aircraft p 876 A92-48160
Conceptual study of separated core ultra high bypass engine
[AIAA PAPER 92-3775] p 867 A92-49119
Design and off-design point characteristics of Separated Core Ultra High Bypass Engine (SCUBE)
[AIAA PAPER 92-3776] p 867 A92-49120
Calculations of aerodynamic forces on a wing with thrust using B.E.M p 1030 A92-56049
The Eurofar program - An European overview on advanced VTOL civil transportation system p 1016 A92-56299
A simulation study of tiltrotor vertical takeoff procedures using conventional and variable diameter rotor systems p 1056 A92-56301
Blade instability of horizontally stoppable rotors p 1085 A92-56308
Application of Eigenstructure Assignment to the control of powered lift combat aircraft
[RAE-TM-FS-1009] p 135 N92-12004
Technology needs for high speed rotorcraft (3)
[NASA-CR-177592] p 195 N92-14039
Aircraft ship operations
[AGARD-AR-312] p 850 N92-28468
The Eurofar program: An European overview on advanced VTOL civil transportation system
[MBB-UD-0611-91-PUB] p 952 N92-30418
On the estimation of jet-induced fountain lift and additional suckdown in hover for two-jet configurations
[NASA-TM-102268] p 1040 N92-33618

VERY LARGE SCALE INTEGRATION
Polish radar technology. V - Adaptive MTI filters for uniform and staggered sampling p 40 A92-12293
VHDL design and simulation for airborne graphics generation requirements --- VLSI hardware description language p 902 A92-48465
Applications of silicon hybrid multi-chip modules to avionics p 859 N92-28379

VERY LOW FREQUENCIES
Transfer function between airborne VLF transmit and receive loop antenna p 1045 A92-54754
Feasibility of measuring transverse electric noise at VLF and LF on an ice cap
[AD-A252280] p 1129 N92-33220
Integrated Russian VLF/Omega receiver design
[PB92-193390] p 1051 N92-33809

VHSIC (CIRCUITS)
A model of the ADA avionics real-time system: An example of the benefits of the hardware/software codesign approach in development of real-time systems
[AD-A248893] p 967 N92-30524

VIBRATION
Modal simulation of gearbox vibration with experimental correlation
[AIAA PAPER 92-3494] p 1112 A92-54036
Variable impedance journal bearings for rotor-bearing systems p 157 N92-12270
Integration of dynamic, aerodynamic, and structural optimization of helicopter rotor blades
[NASA-CR-189018] p 195 N92-14038
Limit cycle vibrations in turbomachinery
[NASA-TP-3181] p 211 N92-14108
Field telemetry of blade-rotor coupled torsional vibration at Matuura Power Station Number 1 unit p 222 N92-14348
The effects of manufacturing tolerances on the vibration of aero-engine rotor-damper assemblies p 222 N92-14349
Eddy current transducing system
[DE91-018924] p 401 N92-18515
Fully integrated aerodynamic/dynamic optimization of helicopter rotor blades
[NASA-TM-104226] p 461 N92-20417
Helicopter active rotor control p 570 N92-22157
Control of a helicopter engine in low altitude flight p 562 N92-23122
Analysis of rotor vibratory loads using higher harmonic pitch control
[NASA-CR-189591] p 696 N92-24251
Numerical simulation of shock-stall flutter of an airfoil using the Navier-Stokes equations p 746 N92-27956
Comparison of three controllers applied to helicopter vibration
[NASA-TM-102192] p 878 N92-28457
Modal simulation of gearbox vibration with experimental correlation
[NASA-TM-105702] p 1002 N92-31485
Joint study on the computerisation of in-field aero engines vibration diagnosis
[PNR-90799] p 1072 N92-33815

VIBRATION DAMPING
Advanced multi-squeeze film dampers for rotor vibration control p 36 A92-10102
On-line adaptive control of unstable aircraft wing flutter p 27 A92-11374
Experimental demonstration of active vibration control for flexible structures p 50 A92-11442
Robust stabilization with positive real uncertainty - Beyond the small gain theorem p 50 A92-11444
Electrorheological fluids; Proceedings of the 2nd International Conference, Raleigh, NC, Aug. 7-9, 1989 p 40 A92-12625
Experimental investigation of helicopter vibration reduction using rotor blade aeroelastic tailoring p 107 A92-14396
Flight vibration testing of the V-22 tiltrotor aircraft p 107 A92-14397
Variation in hover aeromechanical stability trends with bearingless main rotor design p 109 A92-14425
A review of rigid body response on sting supported models at high angles of incidence p 66 A92-15345
A chambered porous damper for rotor vibration control. II - Imbalance response and bladeless simulation
[ASME PAPER 91-GT-243] p 149 A92-15648
A chambered porous damper for rotor vibration control. I - Concept development
[ASME PAPER 91-GT-244] p 150 A92-15649
A gas operated bearing damper for turbomachinery
[ASME PAPER 91-GT-249] p 150 A92-15654
Effect of inertia forces on the characteristics of a long hydrodynamic vibration damper in the mixed flow regime p 154 A92-16811
Cabin structural vibration and noise for transport aircraft p 192 A92-17876
Aerodynamic damping of blade vibrations in turbomachines --- Russian book p 200 A92-18198
Parameter insensitive control utilizing eigenspace methods --- for flutter suppression in aeroelastic vehicles p 204 A92-18615
Structure/control design synthesis of active flutter suppression system by goal programming p 204 A92-18621
Time-periodic control of a multi-blade helicopter p 204 A92-18626
Open-loop model reduction and parameter perturbation for active flutter suppression system p 379 A92-24879
Active vibration control using fixed order dynamic compensation with frequency shaped cost functionals p 508 A92-29324
AIAA/ASME/ASCE/AHS/ASC Structures, Structural Dynamics and Materials Conference, 33rd, Dallas, TX, Apr. 13-15, 1992, Technical Papers. Pt. 3 - Structural dynamics I p 584 A92-34389
The NASA/Industry Design Analysis Methods for Vibrations (DAMVIBS) Program - Bell Helicopter Textron accomplishments
[AIAA PAPER 92-2201] p 539 A92-34391
The NASA/Industry Design Analysis Methods for Vibrations (DAMVIBS) program - McDonnell Douglas Helicopter Company achievements
[AIAA PAPER 92-2203] p 540 A92-34393
The NASA/Industry Design Analysis Methods for Vibrations (DAMVIBS) Program - Sikorsky Aircraft - Advances toward interacting with the airframe design process
[AIAA PAPER 92-2204] p 540 A92-34394
Comparison between imposed-periodicity and marching-in-time solutions of helicopter rotor blade steady-state response problem
[AIAA PAPER 92-2256] p 540 A92-34411
A study on the feasibility of using adaptive structures in the attenuation of vibration characteristics of rotary wings
[AIAA PAPER 92-2452] p 541 A92-34415
AIAA/ASME/ASCE/AHS/ASC Structures, Structural Dynamics and Materials Conference, 33rd, Dallas, TX, Apr. 13-15, 1992, Technical Papers. Pt. 4 - Structural dynamics II p 584 A92-34451
Subcritical flutter characteristics of a swept-back wing in a turbulent supersonic flow - Comparison between analysis and experiment
[AIAA PAPER 92-2393] p 517 A92-34466
Aircraft aeroservoelastic compensation using constrained optimization
[AIAA PAPER 92-2399] p 564 A92-34470
Aerothermoelastic analysis of a NASP-like vertical fin
[AIAA PAPER 92-2400] p 541 A92-34471
Blade root torsional dampers to reduce hub loads
[AIAA PAPER 92-2449] p 541 A92-34476
Vibration reduction in helicopter rotors using an active control surface located on the blade
[AIAA PAPER 92-2451] p 564 A92-34478
Application of composite rotor blade stability analysis to extension-twist coupled blades
[AIAA PAPER 92-2254] p 564 A92-34479
Aeroelastic response and blade loads of a composite rotor in forward flight
[AIAA PAPER 92-2566] p 564 A92-34480
Aeroelastic response of helicopters with flexible fuselage modeling
[AIAA PAPER 92-2567] p 564 A92-34481
Parametric studies for tiltrotor aeroelastic stability in high-speed flight
[AIAA PAPER 92-2568] p 565 A92-34482
Optimizing tuning masses for helicopter rotor blade vibration reduction including computed airloads and comparison with test data
[AIAA PAPER 92-2376] p 542 A92-34546
AIAA Dynamics Specialists Conference, Dallas, TX, Apr. 16, 17, 1992, Technical Papers p 565 A92-35651
A summary of the Active Flexible Wing program
[AIAA PAPER 92-2080] p 565 A92-35652
Simulation and model reduction for the AFW program
[AIAA PAPER 92-2081] p 572 A92-35653

The multiple-function multi-input/multi-output digital controller system for the AFW wind tunnel model
[AIAA PAPER 92-2083] p 565 A92-35655
On-line analysis capabilities developed to support the AFW wind-tunnel tests
[AIAA PAPER 92-2084] p 572 A92-35656
Flutter suppression for the Active Flexible Wing - Control system design and experimental validation
[AIAA PAPER 92-2097] p 566 A92-35666
Multifunction tests of a frequency domain based flutter suppression system
[AIAA PAPER 92-2096] p 566 A92-35667
Flutter suppression digital control law design and testing for the AFW wind tunnel model
[AIAA PAPER 92-2095] p 566 A92-35668
A flutter suppression system using strain gages applied to Active Flexible Wing Technology - Design and test
[AIAA PAPER 92-2098] p 566 A92-35669
Rolling Maneuver Load Alleviation using active controls
[AIAA PAPER 92-2099] p 566 A92-35670
Maneuver load control using optimized feedforward commands
[AIAA PAPER 92-2100] p 567 A92-35671
Development and analysis of flight flutter prediction methods
[AIAA PAPER 92-2101] p 588 A92-35672
New time-domain technique for flutter boundary identification
[AIAA PAPER 92-2102] p 588 A92-35673
Digital time series analysis for flutter test data
[AIAA PAPER 92-2103] p 589 A92-35674
Robustness characteristics of fast-sampling digital controllers for active flutter suppression
[AIAA PAPER 92-2104] p 567 A92-35675
Design of adaptive fast-sampling digital controllers for active flutter suppression
[AIAA PAPER 92-2105] p 567 A92-35676
An analytical and experimental investigation of flutter suppression via piezoelectric actuation
[AIAA PAPER 92-2106] p 567 A92-35677
Rotary-wing aeroservoelastic problems
[AIAA PAPER 92-2107] p 567 A92-35678
Dynamics of helicopters in ground resonance with and without blade dissimilarities
[AIAA PAPER 92-2108] p 544 A92-35679
Coupled rotor-fuselage dynamics and aeroelasticity in turning flight
[AIAA PAPER 92-2109] p 544 A92-35680
An experimental and analytical investigation of wing flutter on a trail rotor V/STOL aircraft
[AIAA PAPER 92-2112] p 544 A92-35682
Active control of helicopter ground and air resonance p 568 A92-35762
Evaluation of a constant feedback gain for closed loop higher harmonic control p 568 A92-35768
Generalized higher harmonic control - Ten years of Aerospatiale experience p 569 A92-35769
A study of coupled rotor-fuselage vibration with higher harmonic control using a symbolic computing facility p 569 A92-35770
General model of isolated helicopter blade for stability investigation p 547 A92-35774
The development and testing of an active control of structural response system for the EH101 helicopter p 569 A92-35775
Rotor blade-vortex interaction noise reduction and vibration using higher harmonic control p 604 A92-35778
Modeling rotor dynamics with rotor speed degree of freedom for drive train torsional stability analysis p 547 A92-35779
Limit cycle oscillation and flight flutter testing p 570 A92-35939
Nonlinear damping estimation from rotor stability data using time and frequency domain techniques p 641 A92-36855
Coupled propeller contributions to aircraft noise and vibration p 694 A92-39085
Study model for the reduction of noise through double wall cylindrical shells - Comparison with experimentation p 694 A92-39088
Active control of structurally-coupled sound fields generated by localized force inputs p 694 A92-39106
Active vibration control of smart structural materials p 673 A92-39281
Pulse response method for vibration reduction in periodic dynamic systems p 661 A92-39909
Robust flight control system design with multiple model approach p 661 A92-39910
Helicopter aeroelastic stability and response - Current topics and future trends p 730 A92-43100
Optimization of blade structure to reduce rotor vibration p 730 A92-43118
Multiharmonic control response of a rotor blade during forward flight (Test) p 744 A92-43120
Multiharmonic control response of a rotor blade during forward flight (Analysis) p 744 A92-43121
Step response of incompressible unsteady aerodynamic modeling p 744 A92-43131
Gust load alleviation control design for the accuracy of an aeroelastic active control model p 745 A92-43134
ACT wind tunnel experiment on gust load alleviation. II - Wind tunnel test with active support facility p 745 A92-43135
Transonic wind tunnel tests of flutter suppression equipment (Wing response data processing) p 748 A92-43136
A restructurable flight control system design using nonlinear compensation p 745 A92-43184
Response characteristics of a wing in supersonic flow near flutter boundary
[SAE PAPER 911999] p 789 A92-45401
Preliminary study of algorithm for real-time flutter monitoring
[SAE PAPER 912001] p 897 A92-45403
Forebody vortex control for suppressing wing rock on a highly-swept wing configuration
[AIAA PAPER 92-2716] p 803 A92-45555
International Congress on Recent Developments in Air- and Structure-Borne Sound and Vibration, Auburn University, AL, Mar. 6-8, 1990, Proceedings. Vols. 1 & 2 p 924 A92-45876
Suppression of fatigue-inducing cavity acoustic modes in turbofan engines p 925 A92-46809
A new method of helicopter rotor blade motion control p 875 A92-47786
Vibration control of rotor-bearing system by controlled squeeze-film damper bearings p 990 A92-49579
Reduction of torque pulsation of Stirling engine-compressor system p 992 A92-50785
Structural optimization and vibration control of composite rotor blades p 960 A92-53056
New literal approximations for the longitudinal dynamic characteristics of flexible flight vehicles
[AIAA PAPER 92-4411] p 1075 A92-55205
Numerical simulations of flutter and its suppression by active control
[AIAA PAPER 92-4652] p 1082 A92-55396
Aeroelastic effects of spoiler surfaces on a low-aspect-ratio rectangular wing p 1030 A92-56154
Dynamic analysis of rotor blades with root retention design variations p 1054 A92-56156
Helicopter tail rotor stall flutter p 1056 A92-56290
Modern helicopter technologies at MBB and the application in future programmes p 1016 A92-56304
Coupled rotor-fuselage vibration reduction with multiple frequency blade pitch control p 1085 A92-56315
The compound helicopter - A concept revisited p 1058 A92-56341
A dynamic stiffness technique for the vibration analysis of stiffened shell structures p 1123 A92-56866
An analytical and experimental study to investigate flutter suppression via piezoelectric actuation
[NASA-TM-893240] p 156 N92-12173
Rotordynamic Instability Problems in High-Performance Turbomachinery, 1990
[NASA-CP-3122] p 222 N92-14346
The stability of the steady state and bistable response of a flexible rotor supported on squeeze film dampers p 222 N92-14350
Stability of intershaft squeeze film dampers p 222 N92-14351
Proceedings of Damping 1991, volume 3
[AD-A241313] p 225 N92-14386
Airfoil Vibration Dampers program
[NASA-CR-184276] p 225 N92-14391
Flight operations for higher harmonic control research
[AD-A242478] p 196 N92-15067
Flutter suppression via piezoelectric actuation
[NASA-TM-104120] p 197 N92-15070
Experiences at Langley Research Center in the application of optimization techniques to helicopter airframes for vibration reduction
[NASA-TM-104193] p 299 N92-17033
Loading and vibration reduction through active aerodynamic control
[AD-A242321] p 283 N92-17243
Response of structures to galloping excitation: Background and approximate estimation
[ESDU-91010] p 399 N92-18091
Optimizing tuning masses for helicopter rotor blade vibration reduction including computed airloads and comparison with test data
[NASA-TM-104194] p 367 N92-19846
Structural dynamics and vibrations of damped, aircraft-type structures
[NASA-CR-4424] p 499 N92-20194
Performance tests of a cryogenic hybrid magnetic bearing for turbopumps
[NASA-TM-105627] p 473 N92-20523
Determining structural performance p 560 N92-22519
Numerical simulations of wakes, blade-vortex interaction, flutter, and flutter suppression by feedback control p 597 N92-23997
Adaptive active flutter suppression of wings in subsonic and transonic flight regimes p 553 N92-24010
Multifunction tests of a frequency domain based flutter suppression system
[NASA-TM-107615] p 662 N92-25607
Add-on damping treatment for life extension of the F-15 upper-outer wing skin
[AD-A246149] p 746 N92-27577
Stability and performance of notch filter control for unbalance response p 771 N92-27731
Characterization of superconducting magnetic bearings (dynamic stiffness and damping coefficient in axial direction) p 772 N92-27737
Progress of magnetic suspension systems and magnetic bearings in the USSR p 772 N92-27740
The mechanical properties of metal-void composites --- pressurized microvoids
[AD-A246087] p 757 N92-27749
An evaluation of some strategies for vibration control of flexible rotors p 773 N92-27800
Analysis and modification of a single-mesh gear fatigue rig for use in diagnostic studies
[NASA-TM-105416] p 773 N92-27879
Comparison of three controllers applied to helicopter vibration
[NASA-TM-102192] p 878 N92-28457
An analytical and experimental investigation of flutter suppression via piezoelectric actuation
[NASA-TM-107653] p 962 N92-31174
Design and experimental validation of a flutter suppression controller for the active flexible wing
[NASA-TM-4381] p 979 N92-31240
A summary of the active flexible wing program
[NASA-TM-107655] p 962 N92-31264
Flutter suppression digital control law design and testing for the AFW wind-tunnel model
[NASA-TM-107652] p 962 N92-31350
Rolling maneuver load alleviation using active controls
[NASA-TM-107654] p 962 N92-31351
The multiple-function multi-input/multi-output digital controller system for the AFW wind-tunnel model
[NASA-TM-107600] p 1060 N92-32536
Computational aspects of helicopter trim analysis and damping levels from Floquet theory
[NASA-CR-190736] p 1087 N92-33107

VIBRATION EFFECTS

Adaptive suppression of biodynamic interference in helmet-mounted displays and head teleoperation p 197 A92-18611
Numerical calculation of modulation transfer functions for low frequency mechanical vibrations p 235 A92-19982
Calculation of real-gas effects on blunt-body trim angles p 432 A92-31169
A study of the precision characteristics of a gyroscopic gravimeter p 581 A92-33778
Oscillations of balloon-flight altitude p 836 A92-46660
Preliminary analysis of baseline vibration data from Allison T56-A-14LFE engine and reduction gearbox
[NRC-31578] p 130 N92-11999
High enthalpy nozzle flows p 182 N92-15000
Low-noise oscillators for airborne radar applications
[AD-A242264] p 300 N92-17258
Investigation of the dynamic behaviour and the frequency response of the GG 1342 laser gyro
[ESA-TT-1236] p 595 N92-22641
Force limited vibration testing p 595 N92-22688
Computational structures technology engine/airframe coupling p 649 N92-25935
On the computation of unsteady turbomachinery flows. Part 1: Euler equations in vibrating cascades p 768 N92-27460

VIBRATION ISOLATORS

Advanced multi-squeeze film dampers for rotor vibration control p 36 A92-10102
Experimental and analytical investigation of hybrid squeeze film dampers
[ASME PAPER 91-GT-250] p 150 A92-15655
Effect of inertia forces on the characteristics of a long hydrodynamic vibration damper in the mixed flow regime p 154 A92-16811
Nonlinear landing gear behavior at touchdown p 192 A92-19606
Airfoil Vibration Dampers program
[NASA-CR-184276] p 225 N92-14391
Progress of magnetic suspension systems and magnetic bearings in the USSR p 772 N92-27740
MD-80 aft cabin noise control: A case history p 1137 N92-32950

The Dornier 328 Acoustic Test Cell (ATC) for interior noise tests and selected test results
[AIAA PAPER 92-2164] p 1137 N92-32951
Active control of interior noise in a large scale cylinder using piezoelectric actuators p 1137 N92-32958
Active vibrations and noise control for turboprop application research program activities
p 1138 N92-32962

VIBRATION MEASUREMENT
Studying dynamic behavior of X380 helicopter equipped with a new 5-blade composite rotor p 108 A92-14398
Optimizing instrumentation when measuring jet engine blade vibration
[ASME PAPER 91-GT-71] p 148 A92-15540
Predicted and measured in-flight wing deformations of a forward-swept-wing aircraft p 548 A92-35936
Design considerations for a generic E.V.M. --- Engine Vibration Monitoring
[SAE PAPER 912095] p 651 A92-39952
The use of optical sensors and signal processing gas turbine engines p 856 A92-46247
The measurement of plate vibration and sound radiation from a turbulent boundary layer manipulator
[AD-A240127] p 42 N92-10206
Rub induced rotor/stator vibration analysis on CF700 engine
[NRC-TR-ENG-007] p 202 N92-14060
Field telemetry of blade-rotor coupled torsional vibration at Matuura Power Station Number 1 unit
p 222 N92-14348
Baseline vibration measurements of remotely piloted helicopters for higher harmonic control research
[AD-A244669] p 482 N92-21360
A preliminary study in the use of phase demodulation techniques for the analysis of gear vibration data
[NRC-32083] p 1002 N92-31469
The Dornier 328 Acoustic Test Cell (ATC) for interior noise tests and selected test results
[AIAA PAPER 92-2164] p 1137 N92-32951
Vibro-acoustic FE analyses of the Saab 2000 aircraft
p 1137 N92-32952
Advanced Study for Active Noise Control in Aircraft (ASANCA)
[AIAA PAPER 92-2092] p 1137 N92-32956
Active control of sound transmission through stiff lightweight composite fuselage constructions
p 1137 N92-32957

VIBRATION METERS
Design considerations for a generic E.V.M. --- Engine Vibration Monitoring
[SAE PAPER 912095] p 651 A92-39952

VIBRATION MODE
Modal identification in the presence of steady excitation p 131 A92-13693
A review of rigid body response on sting supported models at high angles of incidence p 66 A92-15345
Optical measurements of unducted fan flutter
[ASME PAPER 91-GT-19] p 147 A92-15510
Detuning from the natural resonances of the blade in the computer-aided design of blade rows for axial-flow compressors p 80 A92-16818
Enhancement of modal swept sine data by control of exciting forces p 215 A92-17562
Resonance of circular shock waves
p 395 A92-26795
A new approach to determining control surface's moments of inertia with test-twice vibrations approach
p 379 A92-27914
AIAA/ASME/ASCE/AHS/ASC Structures, Structural Dynamics and Materials Conference, 33rd, Dallas, TX, Apr. 13-15, 1992, Technical Papers. Pt. 3 - Structural dynamics I p 584 A92-34389
The NASA/Industry Design Analysis Methods for Vibrations (DAMVIBS) program - McDonnell Douglas Helicopter Company achievements
[AIAA PAPER 92-2203] p 540 A92-34393
Joined-wing model vibrations using PC-based modal testing and finite element analysis
[AIAA PAPER 92-2260] p 541 A92-34417
Analytical shape sensitivities and approximations of modal response of generally laminated tapered skew plates
[AIAA PAPER 92-2391] p 585 A92-34465
Time simulation of flutter with large stiffness changes
[AIAA PAPER 92-2394] p 585 A92-34467
Vibration of gear system with web structure
p 588 A92-35573
The use of Stodola modes in rotor-blade aeroelastic studies p 590 A92-35729
Limit cycle oscillation and flight flutter testing
p 570 A92-35939
Inclusion principle for the Rayleigh-Ritz based substructure synthesis p 670 A92-36851
Transition of the flutter mode of a two-dimensional section with an external store p 758 A92-41244
Measurement of magnus derivatives with an elastically forced oscillation rig p 749 A92-43172
Coupled vibrations of turbomachine blades
p 738 A92-44545
Preliminary study of algorithm for real-time flutter monitoring
[SAE PAPER 912001] p 897 A92-45403
Ritz vectors synthesis versus modal synthesis for fluid-structure interaction modeling p 898 A92-45885
The relationship between mode localization and energy transmission parameters in the vibration of coupled structures p 925 A92-45921
On the choice of appropriate bases for nonlinear dynamic modal analysis p 847 A92-46927
Analytical evaluation of resonant response of spiral bevel gears in the RAH-66 helicopter Fantail transmission
[AIAA PAPER 92-3495] p 906 A92-49031
Shimmy of nose undercarriage wheels
p 959 A92-51948
Modal simulation of gearbox vibration with experimental correlation
[AIAA PAPER 92-3494] p 1112 A92-54036
Automated procedures for aircraft aeroservoelastic compensation
[AIAA PAPER 92-4606] p 1077 A92-55284
Flutter analysis and wind tunnel test with respect to a low-aspect-ratio wing with free-rotational control surface
p 1052 A92-56014
An example of whirl flutter analysis
p 1052 A92-56015
Simulation of helicopter see-saw rotor motion
p 1055 A92-56287
Vibration tests of long plate structural model
[NAL-TM-625] p 400 N92-18485
Computational structures technology at Grumman: Current practice/future needs p 684 N92-25930
Add-on damping treatment for life extension of the F-15 upper-outer wing skin
[AD-A246149] p 746 N92-27577
Modal simulation of gearbox vibration with experimental correlation
[NASA-TM-105702] p 1002 N92-31485
Time simulation of flutter with large stiffness changes
[NASA-TM-107650] p 963 N92-32111

VIBRATION TESTS
Modal identification in the presence of steady excitation p 131 A92-13693
Flight vibration testing of the V-22 tiltrotor aircraft
p 107 A92-14397
Finite element correlation of the U.S. Army/BHTI ACAP composite airframe helicopter p 108 A92-14399
Aircraft ground vibration test by means of flight control surfaces
[ONERA, TP NO. 1991-96] p 133 A92-16079
Vibration characteristics of pretwisted aerofoil cross-section blade packets under rotating conditions
p 219 A92-20756
Holographic-interferometry methods employed for vibration-strength testing of aviation-engine workpieces
p 219 A92-20771
The measurement of flutter derivatives using mechanical admittance p 393 A92-25014
Dynamic characteristics of a Benchmark models program supercritical wing
[AIAA PAPER 92-2368] p 571 A92-34596
Digital time series analysis for flutter test data
[AIAA PAPER 92-2103] p 589 A92-35674
An analytical and experimental investigation of flutter suppression via piezoelectric actuation
[AIAA PAPER 92-2106] p 567 A92-35677
Vibration analysis of gas turbines by an intelligent knowledge-based system p 656 A92-40548
Dynamic response and aeroelastic analysis of a propeller blade of a prop-fan engine p 762 A92-43109
Transonic wind tunnel tests of flutter suppression equipment (Wing response data processing)
p 748 A92-43136
High temperature ground vibration test techniques
p 980 A92-51404
Acoustic testing at elevated temperatures
p 981 A92-51405
Monitoring fatigue cracks in gears
p 1116 A92-54496
Susceptibility of a parallelogram type skin friction balance to rotational motion
[AD-A241348] p 139 N92-13078
Vibration tests of long plate structural model
[NAL-TM-625] p 400 N92-18485
Weight, center of gravity and modal test report for NTF fan blade set no. 3
[NASA-CR-189583] p 498 N92-20072
Force limited vibration testing p 595 N92-22688
Evaluation of human response to structural vibrations induced by sonic booms
[NASA-CR-189584] p 697 N92-26130
Flight flutter testing p 1089 N92-34163

VIBRATIONAL SPECTRA
A unified nonequilibrium model for hypersonic flows
p 3 A92-10575
Rate parameters for coupled vibration-dissociation in a generalized SSH approximation --- Schwarz, Slawsky, and Herzfeld p 235 A92-20301
Monte Carlo study of vibrational relaxation processes
p 940 A92-52777

VIBRATIONAL STRESS
The stability analysis of the nonlinear shimmy
p 358 A92-27902

VIBRATORY LOADS
A full scale airframe high cycle fatigue test methodology and its application to the SH-2G helicopter
p 105 A92-14345
Dynamics of an optimized rotor blade at off-design flight conditions p 461 A92-32250
Aeroelastic response and blade loads of a composite rotor in forward flight
[AIAA PAPER 92-2566] p 564 A92-34480
Optimizing tuning masses for helicopter rotor blade vibration reduction including computed airloads and comparison with test data
[NASA-TM-104194] p 367 N92-19846
Analysis of rotor vibratory loads using higher harmonic pitch control
[NASA-CR-189591] p 696 N92-24251
Add-on damping treatment for life extension of the F-15 upper-outer wing skin
[AD-A246149] p 746 N92-27577

VIDEO COMMUNICATION
Compression techniques for video telemetry
p 188 A92-19214

VIDEO DATA
Compression techniques for video telemetry
p 188 A92-19214
The Center/TRACON Automation System (CTAS): A video presentation
[NASA-TM-103887] p 356 N92-20029

VIDEO EQUIPMENT
DARPA high resolution display technologies
p 218 A92-19977
A high resolution multispectral video system
p 587 A92-35479
The fluid-dynamic measurement of the fling motion of a three-dimensional flat plate p 710 A92-43194
On improvements of three-dimensional position measuring system for dynamic wind tunnel testing
p 1093 A92-56012
Modifications to the rapid melt/rapid quench and transparent polymer video furnaces for the KC-135
[NASA-CR-184215] p 157 N92-12231
Image-supported navigation for testing instrument landing systems p 189 N92-14012

VIDEO TAPE RECORDERS
State-of-the-art airborne video recording
p 555 A92-35932

VIEWING
Computational algorithms for increased control of depth-viewing volume for stereo three-dimensional graphic displays
[NASA-TM-4379] p 1065 N92-34109

VISCOELASTIC DAMPING
Forced vibration of rectangular laminated plates with material damping p 294 A92-23167

VISCOELASTICITY
Subsonic axisymmetric viscoelastic flow past thin tapered bodies of revolution p 6 A92-12134
The effect of physical aging on the creep response of a thermoplastic composite
[AD-A243600] p 290 N92-17932

VISCOPLASTICITY
A viscoplastic model for single crystals
p 391 A92-24717
A viscoplastic theory for anisotropic materials
[ONERA, TP NO. 1992-90] p 391 A92-24721
Thermoviscoplastic analysis of engine cowl leading edge subjected to oscillating shock-shock interaction
[AIAA PAPER 92-2537] p 583 A92-34381
Thermoviscoplastic response of thin plates subjected to intense local heating
[AIAA PAPER 92-2538] p 584 A92-34382
Numerical analysis of an engine turbine disk loaded with a large number of thermomechanical cycles
[ONERA, TP NO. 1992-31] p 902 A92-48592
Effects of elevated temperature on the viscoplastic modeling of graphite/polymeric composites
[NASA-TM-104160] p 35 N92-11149
Advanced stress analysis methods applicable to turbine engine structures
[NASA-CR-187235] p 44 N92-11378
Thermoviscoplastic response of Ti-15-3 under various loading conditions
[NASA-CR-187621] p 45 N92-11391
Light thermal structures and materials for high speed flight p 649 N92-25922

VISCOSITY
Grid sensitivity in low Reynolds number hypersonic continuum flows p 817 A92-47057
Three-dimensional multigrid algorithm for the Euler and the thin-layer Navier-Stokes equations
[PB92-134329] p 602 N92-22216
Laminar-turbulent transition: Fundamentals
p 717 N92-27710

VISCOUS DAMPING
Proceedings of Damping 1991, volume 3
[AD-A241313] p 225 N92-14386
Structural dynamics and vibrations of damped, aircraft-type structures
[NASA-CR-4424] p 499 N92-20194

VISCOUS DRAG
Effect of viscous drag on optimum spanwise lift distribution
[AIAA PAPER 92-0287] p 319 A92-25740
Some practical aspects of viscous drag reduction concepts
[SAE PAPER 912129] p 618 A92-39976
Aerodynamic shape optimization of hypersonic configurations including viscous effects
[AIAA PAPER 92-2635] p 795 A92-45506
Drag prediction using computation methods
[ONERA-RSF-82/1685-AY-154-4] p 349 N92-19682
Aircraft drag reduction p 717 N92-27709
Study of turbulence structure through numerical simulations: The perspective of drag and reduction
p 717 N92-27713

VISCOUS FLOW
Unsteady incompressible viscous flow past an airfoil
p 3 A92-10662
A semi-elliptic analysis for 2-D viscous flows through cascade configurations p 3 A92-10688
Viscous flow solutions for slender bodies of revolution at incidence p 4 A92-10692
Subsonic axisymmetric viscoelastic flow past thin tapered bodies of revolution p 6 A92-12134
Numerical solution of steady incompressible viscous flows over airfoils p 8 A92-12649
Solution of the Reynolds-averaged Navier-Stokes equations for transonic aerofoil flows p 9 A92-13198
An analysis method and applications for 3-D viscous internal flows with complex geometry
p 143 A92-13299
Influence of the entropy layer on the separation length in hypersonic aerodynamics in the triple-deck framework. II p 63 A92-13815
Influence of three-dimensional effects on hydrodynamics and heat transfer in subsonic flow of a viscous compressible gas in the initial section of a rectangular duct p 66 A92-15031
A viscous flow study of shock-boundary layer interaction, radial transport, and wake development in a transonic compressor
[ASME PAPER 91-GT-69] p 68 A92-15539
Unsteady viscous flow in a high speed core compressor
[ASME PAPER 91-GT-91] p 70 A92-15555
The simulation of three-dimensional viscous flow in turbomachinery geometries using a solution-adaptive unstructured mesh methodology
[ASME PAPER 91-GT-124] p 71 A92-15569
Inviscid-viscous coupled solution for unsteady flows through vibrating blades. II - Computational results
[ASME PAPER 91-GT-126] p 71 A92-15571
The influence of shock waves on the viscous flow field of axial compressors
[ASME PAPER 91-GT-173] p 73 A92-15608
An experiment on unsteady flow over an oscillating airfoil
[ASME PAPER 91-GT-181] p 73 A92-15613
Analysis and prediction of transonic turbine blade losses
[ASME PAPER 91-GT-183] p 73 A92-15615
Deterministic blade row interactions in a centrifugal compressor stage
[ASME PAPER 91-GT-273] p 75 A92-15670
Newton's method solver for high-speed viscous separated flowfields p 176 A92-20736
Axisymmetric analogy for three-dimensional viscous flow problems p 244 A92-21617
Computational methods in viscous aerodynamics --- Book p 245 A92-21976
Computation of unsteady, laminar, incompressible, viscous flows using the vorticity streamfunction formulation p 245 A92-21979
Adaptation methods for viscous flows
p 246 A92-21982
Finite element vorticity based methods for the solution of the compressible Navier-Stokes equations
p 246 A92-21983
Experiences with finite element methods for the velocity-vorticity formulation of three-dimensional, viscous, incompressible flows p 246 A92-21984
Navier-Stokes code development for transonic flow simulations p 246 A92-21985
A fast viscous correction method for transonic aerodynamics p 247 A92-21986
Two-dimensional, incompressible aerofoil design and analysis p 247 A92-21987
Simulation of supersonic and hypersonic flows
p 251 A92-22790
Improved nonequilibrium viscous shock-layer scheme for hypersonic blunt-body flowfields p 310 A92-24653
Multizonal Navier-Stokes solutions for the multibody Space Shuttle configuration p 310 A92-24667
Hypersonic waveriders - Effects of chemically reacting flow and viscous interaction
[AIAA PAPER 92-0302] p 320 A92-25754
Aerodynamic characteristics of a hypersonic viscous optimized waverider at high altitudes
[AIAA PAPER 92-0306] p 320 A92-25755
Efficient simulation of incompressible viscous flow over single and multi-element airfoils
[AIAA PAPER 92-0405] p 324 A92-26258
A turbulence model for iced airfoils and its validation
[AIAA PAPER 92-0417] p 326 A92-26267
Predictions of compressible viscous flows at all Mach number using pressure correction, collocated primitive variables and non-orthogonal meshes
[AIAA PAPER 92-0426] p 326 A92-26274
A one-equation turbulence model for aerodynamic flows
[AIAA PAPER 92-0439] p 327 A92-26285
An approximate viscous shock layer technique for calculating nonequilibrium hypersonic flows about blunt-nosed bodies
[AIAA PAPER 92-0498] p 329 A92-26326
Preconditioned upwind methods to solve incompressible Navier-Stokes equations p 395 A92-26436
Hypersonic flow of a viscous gas past sharp elliptical cones at angles of attack and slip p 336 A92-27531
The computation of transonic viscous flow
p 338 A92-27831
Numerical simulation of the flow around rectangular cylinder p 339 A92-27851
Numerical investigation of laminar separated trailing-edge flows p 339 A92-28026
Inviscid and viscous transonic flows in cascades using an implicit upwind algorithm p 344 A92-28522
Three-dimensional viscous analysis of a Mach 5 inlet and comparison with experimental data
p 344 A92-28526
Effect of viscosity on the drag of slender axisymmetric bodies in hypersonic flow p 425 A92-30154
The lift-drag ratio of a slender cone in viscous hypersonic gas flow p 425 A92-30172
Cooling of a sharp nose by extraneous gas injection into the viscous shock layer p 426 A92-30188
A method for calculating the separated flow past a circular cone, taking viscous-inviscid interaction into account p 427 A92-30203
A new adaptive algorithm for turbulent flows
p 434 A92-31547
Implicit solutions of three-dimensional viscous hypersonic flows p 434 A92-31549
Combined effect of nose bluntness and angle of attack on slender bodies in viscous hypersonic flows
[AIAA PAPER 92-0755] p 436 A92-31680
A parametric study of the lift-drag ratio of blunt cones
p 437 A92-31860
The total drag of a body in the flow of a viscous heat-conducting gas p 439 A92-31873
Mathematical modeling of nonstationary viscous flow over a solid angle of finite span p 440 A92-31890
Viscous supersonic flow computations over a delta-rectangular wing with slanting surfaces
p 441 A92-32178
Computation of near-wake, aerobrake flowfields
p 441 A92-32181
Arbitrary blade section design based on viscous considerations - Background information
p 523 A92-36029
Arbitrary blade section design based on viscous considerations - Blade optimization p 523 A92-36030
Inviscid and viscous quasi-three-dimensional flow solutions in a transonic turbine cascade
p 523 A92-36035
Vibrational relaxation effects in hypersonic flows of a viscous gas p 609 A92-36550
Locally implicit hybrid algorithm for steady and unsteady viscous flows p 610 A92-36836
Numerical simulation of hypersonic viscous flow for the design of H-II orbiting plane (HOPE)
p 612 A92-37549
An exploration of chemically reacting viscous hypersonic flow p 612 A92-37550
Knowledge-based nonlinear boundary integral models of compressible viscous flows over arbitrary bodies - Taking CFD back to basics p 617 A92-39941
CFD calculations of closely coupled scissor wings - Inviscid, viscous, and vortex lattice with rollup results
[SAE PAPER 912150] p 619 A92-39986
Simulation and modeling of homogeneous compressible turbulence under isotropic mean compression
p 622 A92-40134
The effects of viscosity and diffusion on a supersonic mixing layer p 622 A92-40143
Simulation of turbulent velocity profiles appearing on rotating and stationary parts of subsonic compressors and turbines p 676 A92-40172
Numerical predictions of transonic viscous flows around aerofoils through an Euler/boundary layer interaction method p 624 A92-40600
Similarity solutions for viscous vortex cores
p 759 A92-41658
A numerical study of flow of a viscous gas in a Laval nozzle in the narrow channel approximation
p 706 A92-42680
Nonstationary viscous shock layer in supersonic motion over an inhomogeneity p 708 A92-42737
Flow around two square cylinders in staggered arrangements p 761 A92-42797
Numerical simulation of unsteady hypersonic viscous flows in shock tunnel p 710 A92-43170
Viscous flow analysis of advanced particle separators
p 737 A92-44517
Three-dimensional orthogonal-to-surface structured grid generation with transonic Navier-Stokes flow solutions for a commercial transport configuration
[AIAA PAPER 92-2616] p 793 A92-45490
Application of an unstructured Navier-Stokes solver to multi-element airfoils operating at transonic maneuver conditions
[AIAA PAPER 92-2638] p 796 A92-45507
An adaptive grid method for computing the high speed 3D viscous flow about a re-entry vehicle
[AIAA PAPER 92-2685] p 799 A92-45534
Transonic unsteady inviscid and viscous flow's simulation around 2-D moving bodies
[AIAA PAPER 92-2704] p 801 A92-45546
Viscous flow past a nacelle isolated and in proximity of a flat plate
[AIAA PAPER 92-2723] p 803 A92-45560
Viscous high-speed flow computations by adaptive mesh embedding techniques p 808 A92-45839
Unstructured and adaptive mesh generation for high Reynolds number viscous flows p 816 A92-47042
Calculation of hypersonic, viscous, non-equilibrium flows around reentry bodies using a coupled boundary layer/Euler method
[AIAA PAPER 92-2856] p 819 A92-47839
Enhancements to viscous-shock-layer technique
[AIAA PAPER 92-2897] p 820 A92-47873
Development of an efficient analysis for high Reynolds number inviscid/viscid interactions in cascades
[AIAA PAPER 92-3073] p 823 A92-48723
A fast, uncoupled, compressible, two-dimensional, unsteady boundary layer algorithm with separation for engine inlets
[AIAA PAPER 92-3082] p 823 A92-48729
Lower upper implicit total variation diminishing solution of viscous hypersonic flows p 935 A92-50302
A direct viscous-inviscid interaction method for the flow calculation around airfoils p 936 A92-52028
Thermal and chemical nonequilibrium viscous shock layer flows over a blunt body at high altitudes
p 938 A92-52749
Hypersonic flows with air chemistry over a reentry vehicle at high altitudes p 1017 A92-53549
Flowfield of a lifting rotor in hover - A Navier-Stokes simulation p 1024 A92-54906
Numerical simulation of hypersonic viscous flow for the design of H-2 orbiting plane (HOPE-2)
[NAL-TR-1093] p 11 N92-10009
Viscous computations of cold air/air flow around scramjet nozzle afterbody
[NASA-CR-4406] p 13 N92-10982
The effects of Reynolds number, rotor incidence angle and surface roughness on the heat transfer distribution in a large-scale turbine rotor passage
[NASA-CR-184260] p 42 N92-11297
Physics of vortical flow p 86 N92-13016
Application of direct inverse analogy method (DIVA) and viscous design optimization techniques
p 176 N92-13951
A unified viscous theory of lift and drag of 2-D thin airfoils and 3-D thin wings
[NASA-CR-4414] p 178 N92-13997
SIMOUN and Scirocco wind tunnel nozzle viscous flow study p 208 N92-14999
Verification and application of the NSFLEX method for hypersonic flow conditions p 182 N92-15005
Viscous shock-layer equations for the calculation of reentry aerothermodynamics p 183 N92-15008

Hypersonic viscous shock layer in thermochemical nonequilibrium p 183 N92-15014
Numerical simulation of thermochemical non-equilibrium viscous flows around reentry bodies p 227 N92-15029
Progress with multigrid schemes for hypersonic flow problems
[NASA-CR-189579] p 185 N92-15047
A turbulence model for iced airfoils and its validation
[NASA-TM-105373] p 186 N92-15052
Analysis of Euler's and stress tensor methods for calculating power consumption of high speed centrifugal fans and turbocompressors
[DE92-728396] p 298 N92-16325
Viscous three-dimensional calculations of transonic fan performance
[NASA-TM-103800] p 242 N92-17346
Marching with the parabolized Navier-Stokes equations. Problem 1: Numerical study of hypersonic viscous cone flow
[AERO-REPT-9007] p 344 N92-18231
Marching with the parabolized Navier-Stokes equations. Problem 2: Hypersonic viscous flow over a flat plate
[AERO-REPT-9008] p 345 N92-18232
Calculation of hypersonic non-equilibrium viscous flow using second order boundary layer theory
[MBB-FE122-S-PUB-434] p 345 N92-18316
Numerical solution of three-dimensional unsteady viscous flows
[AD-A244274] p 403 N92-19052
Flowfield analysis of modern helicopter rotors in hover by Navier-Stokes method
[AD-A245011] p 446 N92-21333
Current status of computational methods for transonic unsteady aerodynamics and aeroelastic applications
[NASA-TM-104191] p 446 N92-21432
Three-dimensional multigrid algorithm for the Euler and the thin-layer Navier-Stokes equations
[PB92-134329] p 602 N92-22216
A study of viscous interaction effects on hypersonic waveriders
[NASA-CR-189587] p 625 N92-24680
On the coupling of Euler/boundary-layer equations p 627 N92-24859
Boundary layer computations using a generalized formulation p 679 N92-24873
TIGGERC: Turbomachinery interactive grid generator energy distributor and restart code p 659 N92-25719
Aerodynamic interference between stores
[AD-A247207] p 715 N92-27172
Predictions and measurements of 3D viscous flow in a transonic turbine nozzle guide vane row p 741 N92-27466
Viscous three-dimensional calculations of transonic fan performance p 768 N92-27467
The application of a Navier-Stokes CFD method to civil engine intake flows p 769 N92-27471
A fast, uncoupled, compressible, two-dimensional, unsteady boundary layer algorithm with separation for engine inlets
[NASA-TM-105686] p 770 N92-27653
Current status of computational methods for transonic unsteady aerodynamics and aeroelastic applications p 718 N92-27937
Recent applications of linear and nonlinear unsteady aerodynamics for aeroelastic analysis p 718 N92-27940
Evaluation of an unsteady implicit Euler code against two and three-dimensional standard configurations p 719 N92-27945
Computation of viscous phenomena in unsteady transonic flow p 720 N92-27949
Viscous effects on a vortex wake in ground effect
[NASA-CR-190400] p 907 N92-28361
Calculation of unsteady transonic flows with mild separation by viscous-inviscid interaction
[NASA-TP-3197] p 827 N92-28477
Development of an unsteady three-dimensional viscous-inviscid interaction numerical method for the calculation of airfoils vibration
[ONERA-RSF-7/3617-AY-022A] p 830 N92-29206
Navier-Stokes computations of a viscous optimized waverider
[NASA-CR-189658] p 944 N92-30392
A gridless Euler/Navier-Stokes solution algorithm for complex two-dimensional applications
[NASA-TM-107631] p 944 N92-30570
Stagnation-point heat-transfer rate predictions at aeroassist flight conditions
[NASA-TP-3208] p 1001 N92-31281
Numerical simulation of turbomachinery flows with advanced turbulence models p 1124 N92-32270
Perspectives on hypersonic viscous and nonequilibrium flow research
[NASA-CR-190817] p 1039 N92-33413
An approximate viscous shock layer technique for calculating chemically reacting hypersonic flows about blunt-nosed bodies p 1041 N92-33837
Analysis of iced wings
[NASA-TM-105773] p 1042 N92-34144

VISCOUS FLUIDS
Solution of the problem of three-dimensional flow past the blade rows of turbomachines with allowance for viscosity effects p 244 A92-21618
Breakdown of an axisymmetric laminar wake p 424 A92-30145
Flow of a viscous twisted fluid film on the surface of a blunt body in supersonic flow of a gas p 424 A92-30146
Viscosity characteristics of synthetic aviation oils at low temperatures p 1105 A92-53875
Continuation of tailored composite structures of ordered staple thermoplastic material
[NASA-CR-189671] p 1110 N92-33613

VISIBILITY
Visibility measurements for the Automated Surface Observing System (ASOS) p 468 A92-32095
Visibility in the atmosphere and flight safety --- Russian book
[ISBN 5-286-00416-4] p 775 A92-42785
Global positioning system supported pilot's display p 534 N92-22436
Transport delay measurements: Methodology and analysis for the F-16C combat engagement trainer, the display for advanced research and training, and the F-16A limited field of view
[AD-A248519] p 888 N92-29505
Trial of a slant visual range measuring device p 1000 N92-31043

VISION
Reference mode effect on the auditory display of aircraft bank angle
[AD-A247825] p 728 N92-27916

VISUAL ACUITY
Helicopter control response types for hover and low-speed near-earth tasks in degraded visual conditions p 132 A92-14338

VISUAL AIDS
Identifying design requirements using integrated analysis structures p 922 A92-48527

VISUAL CONTROL
Visual approach data collection at San Francisco International Airport (SFO)
[DOT/FAA/CT-90/23] p 354 N92-18112
Approach and landing assisted by onboard image processing p 457 N92-21959

VISUAL DISCRIMINATION
Investigation of air transportation technology at Ohio University, 1990-1991 p 265 N92-17990

VISUAL FIELDS
Demonstration performance of an aircraft liquid crystal display p 735 A92-43224

VISUAL FLIGHT
Helicopter fog flying trials p 530 A92-35759
EVS could expand all-weather landing capability of airliners p 556 A92-36125
Visual approach data collection at San Francisco International Airport (SFO)
[DOT/FAA/CT-90/23] p 354 N92-18112
Helicopter nighttime parking test results - UH-1
[DOT/FAA/CT-TN92/1] p 961 N92-31165

VISUAL FLIGHT RULES
Analysis of general aviation accidents during operations under instrument flight rules p 16 A92-11172
Analysis of accidents during instrument approaches p 529 A92-34253
Heliport VFR airspace design based on helicopter performance
[SCT-90RR-34] p 103 N92-13049
Operational survey: VFR heliport approaches and departures
[SCT-91RR-26] p 190 N92-14033
Evaluation of a tritium runway lighting system
[DOT/FAA/CT-TN92/15] p 665 N92-25733
Rotorcraft terminal ATC route standards
[SCT-90RR-33] p 641 N92-26101
Federal aviation regulations. Part 91: General operating and flight rules
[PB92-197334] p 1017 N92-33176
Aircraft accident/incident summary report: Controlled flight into terrain Bruno's Inc., Beechjet, N25BR, Rome, Georgia, 11 December 1991
[PB92-910404] p 1044 N92-34081

VISUAL OBSERVATION
Several results of lidar measurements of the characteristics of oblique visibility at an airfield p 45 A92-12844
Vision-based range estimation using helicopter flight data
[NASA-TM-103930] p 1047 N92-32424

VISUAL PERCEPTION
An aircraft landing accident caused by visually induced spatial disorientation p 834 A92-44993
A connectionist approach to autonomous robotic navigation p 454 N92-20356

VISUAL TASKS
The development of a real time visual flight simulator for tactical operations research and measurement p 880 A92-45027

VOICE COMMUNICATION
Opportunities for advanced speech processing in military computer-based systems p 293 A92-22299
Electronically steerable antenna for aircraft p 229 N92-15272
High Capacity Voice Recorder (HCVR) Operational Test and Evaluation (OT and E)/integration test plan
[DOT/FAA/CT-TN91/55] p 402 N92-18959
MULTIRAD
[AD-A244211] p 412 N92-19247
Design considerations for general aviation mobile satellite terminals p 594 N92-22572
Future developments in aeronautical satellite communications p 678 N92-24167
Improving the LAMP Mk 3 SH-60B HF communication system
[AD-A245970] p 910 N92-29344

VOICE DATA PROCESSING
Opportunities for advanced speech processing in military computer-based systems p 293 A92-22299

VOIDS
The mechanical properties of metal-void composites --- pressurized microvoids
[AD-A246087] p 757 N92-27749
On the origin and acoustical behaviour of cloud cavitation
[ISBN-90-9004317-9] p 1125 N92-33066

VOLATILITY
Low volatile organic compound paints
[DE91-017984] p 35 N92-11203

VOLTERRA EQUATIONS
The solution of a singular integral equation arising from a lifting surface theory for rotating blades p 260 N92-17303

VORTEX ALLEVIATION
A new approach to swirl control in an S-duct p 422 A92-29710
New method of swirl control in a diffusing S-duct p 809 A92-45859
On aircraft wake properties and some methods for stimulating decay and breakdown of tip vortices p 87 N92-13021
Subsonic investigations of vortex interaction control for enhanced high-alpha aerodynamics of a chine forebody/Delta wing configuration
[NASA-CR-189641] p 715 N92-26652
Flow visualization studies of a sideslipping, canard-configured X-31A-Like fighter aircraft model
[AD-A245940] p 829 N92-28883

VORTEX AVOIDANCE
A low-speed wind tunnel study of vortex interaction control techniques on a chine-forebody/delta-wing configuration
[NASA-CR-189616] p 632 N92-25510

VORTEX BREAKDOWN
A simple numerical criterion for vortex breakdown
[AIAA PAPER 92-0057] p 250 A92-22172
Experimental measurement of the vortex development downstream of a lobed forced mixer
[ASME PAPER 90-GT-27] p 295 A92-23299
Experiments on shock/vortex interactions
[AIAA PAPER 92-0315] p 320 A92-25762
Numerical investigation of vortex breakdown on a delta wing p 340 A92-28027
Effects of ambient turbulence on the decay of a trailing vortex wake p 442 A92-32245
A calculation of influence of vortex breakdown on aerodynamic characteristics for slender wings p 616 A92-38920
The effects of unsteady perturbation on vortex breakdown p 672 A92-38922
Behavior of asymmetric unstable modes of a trailing line vortex near the upper neutral curve p 617 A92-39340
Numerical simulation of leading-edge vortex breakdown using an Euler code p 701 A92-41213
Modern developments in shear flow control with swirl p 703 A92-41265
Symmetry breaking in vortex flows on conical bodies p 703 A92-41278
Effect of tunnel walls on vortex breakdown location over delta wings p 703 A92-41279
Numerical investigation into high-angle-of-attack leading-edge vortex flow
[AIAA PAPER 92-2600] p 791 A92-45477
Critical effects of downstream boundary conditions on vortex breakdown
[AIAA PAPER 92-2601] p 792 A92-45478

Prediction of leading-edge vortex breakdown on a delta wing oscillating in roll
[AIAA PAPER 92-2677] p 807 A92-45585
Nonuniform motion of leading-edge vortex breakdown on ramp pitching delta wings p 808 A92-45828
State-space representation of aerodynamic characteristics of an aircraft at high angels of attack
[AIAA PAPER 92-4651] p 1028 A92-55395
Numerical simulation of vortex breakdown by solving the Euler equations for an incompressible fluid
p 41 N92-10163
Numerical simulation of vortex breakdown via 3-D Euler equations p 41 N92-10164
Experimental investigation of the effects of blowing on bursting of strake vortices
[AD-A240256] p 13 N92-10985
Vortex Flow Aerodynamics
[AGARD-CP-494] p 83 N92-12996
Experimental and numerical investigation of the vortex flow over a delta wing at transonic speed
p 84 N92-13001
In-flight flow visualization and pressure measurements at low speeds on the NASA F-18 high alpha research vehicle p 85 N92-13009
Physics of vortical flow p 86 N92-13016
Breaking down the delta wing vortex: The role of vorticity in the breakdown process p 86 N92-13017
Determination of vortex-breakdown criteria by solving the Euler and Navier-Stokes equations
p 87 N92-13018
Investigation of vortex breakdown on a delta wing using Euler and Navier-Stokes equations p 87 N92-13019
On aircraft wake properties and some methods for stimulating decay and breakdown of tip vortices
p 87 N92-13021
An experimental analysis of critical factors involved in the breakdown process of leading edge vortex flows
p 89 N92-13031
Wind tunnel investigation of vortex flows on F/A-18 configuration at subsonic through transonic speed
[NASA-TP-3111] p 179 N92-14968
Experimental study of a vortex subjected to imposed strain
[NASA-CR-189757] p 258 N92-15969
Aerodynamic and flowfield hysteresis of slender wing aircraft undergoing large-amplitude motions
p 364 N92-18780
Scale model measurements of fin buffet due to vortex bursting on F/A-18 p 365 N92-18788
Visualisation in water of vortex flow over sharp-edged canard configurations
[ARL-FLIGHT-MECH-R-189] p 632 N92-25410
Trajectories and stability of trailing vortices very near the ground
[NRC-32151] p 716 N92-27344
In-flight leading-edge extension vortex flow-field survey measurements on a F-18 aircraft at high angle of attack
[NASA-TM-4398] p 947 N92-31276
Modeling and numerical simulation of vortex flow in aerodynamics
[NLR-TP-91154-U] p 1037 N92-32673
Static and dynamic flow visualization studies of two double-delta wing models at high angles of attack
[AD-A252878] p 1040 N92-33678
Unsteady response of the leading-edge vortices on a pitching delta wing p 1041 N92-33851

VORTEX FILAMENTS
An experimental and analytical study of the interaction of a vortex with an airframe
[AIAA PAPER 92-0319] p 321 A92-25766
A simplified model for the interaction of a rotor tip vortex with an airframe
[AIAA PAPER 92-0320] p 321 A92-25767
The effects of inner wake modelling on blade airloads
p 521 A92-35784
Prediction of rotor unsteady airloads using vortex filament theory
[AIAA PAPER 92-2610] p 792 A92-45484
The unsteady interaction of a 3-dimensional vortex filament with a cylinder p 813 A92-46934
Analytical/numerical matching and periodic inversion: Two advances in free wake analysis
p 178 N92-13994
The three-dimensional stability of the Foeppl vortices
p 949 N92-31889

VORTEX FLAPS
Vortex control: Further encounters p 87 N92-13020
An experimental investigation of vortex flaps on a canard combat-aircraft configuration p 87 N92-13023
Analysis of an advanced fighter aircraft using jet flap techniques and the vortex lattice method
[AD-A244051] p 366 N92-19185
Experimental studies of vortex flaps and vortex plates. Part 1: 0.53 m span 60 deg delta wing
[CRANFIELD-AERO-9113-PT-1] p 349 N92-19679
Flow field over the wing of a delta-wing fighter model with vortex control devices at Mach 0.6 to 1.2
[NASA-TM-4296] p 526 N92-22506

VORTEX GENERATORS
Shock-boundary layer interaction control with low-profile vortex generators and passive cavity
[AIAA PAPER 92-0064] p 250 A92-22178
A study on vortex flow control of inlet distortion in the re-engined 727-100 center inlet duct using computational fluid dynamics
[AIAA PAPER 92-0152] p 253 A92-23767
Separation control using moving surface effects - A numerical simulation p 309 A92-24419
Establishment and characterization of a reproducible vortex for use in studying nonsteady two-dimensional phenomena p 310 A92-24428
Effects of tip Reynolds number and tip asymmetry on vortex wakes of axisymmetric bodies at various angles of attack
[AIAA PAPER 92-0406] p 324 A92-26259
Unsteady pressure field and vorticity production over a pitching airfoil p 330 A92-26416
Numerical analysis of shock-induced separation alleviation using vortex generators
[AIAA PAPER 92-0751] p 335 A92-27095
Separation control by vortex generators in subsonic diffuser p 338 A92-27829
Helical-perturbation device for cylinder-wing vortex generators p 432 A92-31167
Experimental design of a supersonic shock wave/vortex interaction at Mach 3 p 521 A92-35988
Effect of tabs on the evolution of an axisymmetric jet
p 656 A92-40151
Recent research into the aerodynamics of ASTOVL aircraft in ground environment p 623 A92-40549
Heat transfer in a channel with built-in wing-type vortex generators p 757 A92-41082
Design and analysis of vortex generators on reengined Boeing 727-100QF center inlet S-duct by a reduced Navier-Stokes code
[AIAA PAPER 92-2700] p 800 A92-45542
Active control of vortex structures in a separating flow over an airfoil
[AIAA PAPER 92-2728] p 804 A92-45563
Separation control on high Reynolds number multi-element airfoils
[AIAA PAPER 92-2636] p 806 A92-45575
Pitch rate/sideslip effects on leading-edge extension vortices of an F/A-18 aircraft model
p 874 A92-46810
Supersonic jet mixing enhancement by 'delta-tabs'
[AIAA PAPER 92-3548] p 826 A92-49063
Application of submerged vortex generators for separation control of a subsonic diffuser
p 933 A92-49832
Effects of vortex generators on the growth of a compressible shear layer
[AIAA PAPER 90-1979] p 934 A92-50269
Application of computational fluid dynamics to the study of vortex flow control for the management of inlet distortion
[AIAA PAPER 92-3177] p 1020 A92-54013
Enhancement of laminar boundary layer heat transfer by a vortex generator p 1118 A92-55453
Vortex generator design for aircraft inlet distortion as a numerical optimization problem p 194 N92-13959
A study on vortex flow control on inlet distortion in the re-engined 727-100 center inlet duct using computational fluid dynamics
[NASA-TM-105321] p 179 N92-13998
Preliminary investigation of the shock-boundary layer interaction in a simulated fan passage
[AD-A242656] p 185 N92-15045
Supersonic jet mixing enhancement by delta-tabs
[NASA-TM-105664] p 630 N92-24958
Evaluation of high lift devices of the quiet STOL experimental aircraft ASKA
[NAL-TR-1102] p 733 N92-28153
A gust generation method for full configuration aircraft tests in a low speed wind tunnel. Part 1: Design and preliminary experiments
[NAL-TR-1115-PT-1] p 722 N92-28192
Aerodynamic characteristics obtained from alpha sweep test of the quiet STOL experimental aircraft ASKA
[NAL-TR-1112] p 853 N92-28901
Ultra high bypass Nacelle aerodynamics inlet flow-through high angle of attack distortion test
[NASA-CR-189149] p 943 N92-30298
Application of computational fluid dynamics to the study of vortex flow control for the management of inlet distortion
[NASA-TM-105672] p 1128 N92-34112

VORTEX LATTICE METHOD
Non linear induced drag study of generically cambered closely coupled dual wings
[SAE PAPER 912126] p 618 A92-39973
CFD calculations of closely coupled scissor wings - Inviscid, viscous, and vortex lattice with rollup results
[SAE PAPER 912150] p 619 A92-39986
Development of a high-angle-of-attack stability and control prediction code
[AIAA PAPER 92-4354] p 1079 A92-55340
Optimal design of wing shape by use of neural-network p 1054 A92-56112
Drag computation by vortex methods
p 1031 A92-56161
Analysis of an advanced fighter aircraft using jet flap techniques and the vortex lattice method
[AD-A244051] p 366 N92-19185

VORTEX RINGS
Emergence of coherent patterns of vortex stretching during reconnection - A scattering paradigm
p 38 A92-11041
A DFW microburst model based on DL-191 data
p 17 A92-11380
Direct evaluation of aeroacoustic theory in a jet
p 1010 A92-50296

VORTEX SHEDDING
Modeling of the vortex structure at delta wings of low aspect ratio by the discrete vortex method
p 7 A92-12203
Experimental investigation of coannular jet flow with swirl along a centerbody p 172 A92-18367
The jet edge-tone feedback cycle - Linear theory for the operating stages p 392 A92-24758
Effect of upstream disturbance on flow asymmetry
[AIAA PAPER 92-0408] p 325 A92-26261
Some thoughts on conical flow asymmetry
[AIAA PAPER 92-0427] p 326 A92-26275
Unsteady pressure field and vorticity production over a pitching airfoil p 330 A92-26416
Combustion instability related to vortex shedding in dump combustors and their passive control
p 374 A92-27354
Evaluation of parallel injector configurations for Mach 2 combustion p 376 A92-28533
Unsteady aerodynamic characteristics of a dual-element airfoil
[AIAA PAPER 92-2508] p 518 A92-34501
Investigation on effects on enhancing lift by acoustic excitation p 693 A92-38923
Phase-averaged turbulence statistics in a near wake with an asymmetric vortex shedding p 620 A92-40086
The natural and forced formation of spot-like Lambda-structures caused by vortex dislocations in a wake p 621 A92-40111
The combined wake of an array of oscillating ribbons
p 623 A92-40180
Prediction of vortex shedding from forebodies with chines p 702 A92-41228
Acoustic sources in a tripped flow past a resonator tube p 778 A92-41266
Separation and vortex formation in turbulent flows
[ONERA, TP NO. 1992-7] p 822 A92-48579
Direct simulation of vortex shedding in dilute gas flows past bluff bodies p 939 A92-52766
On the footprints of three-dimensional separated vortex flows around blunt bodies: Attempts of defining and analyzing complex flow structures p 84 N92-13005
Control of unsteady separated flow associated with the dynamic pitching of airfoils
[NASA-CR-189758] p 258 N92-15966
Flow visualization and wake analysis for standard and modified configurations of the AN/ALQ-78 antenna pod
[AD-A243552] p 260 N92-17339
An experimental investigation of the surface flow and wake dynamics associated with transverse flow over wavy cylinders p 681 N92-25547
Prediction and control of asymmetric vortical flows around slender bodies using Navier-Stokes equations
p 1127 N92-33968
Aeroelasticity of bluff bodies p 1089 N92-34165

VORTEX SHEETS
Modeling of the vortex structure at delta wings of low aspect ratio by the discrete vortex method
p 7 A92-12203
Secondary separation from a slender wing
p 62 A92-13448
Computational vorticity capturing - Application to helicopter rotor flows
[AIAA PAPER 92-0056] p 250 A92-22171
Efficient panel method for vortex sheet roll-up
p 309 A92-24404
The rolling-up and interaction of the leading-edge and trailing-edge vortex sheets of a delta wing
p 314 A92-25101
The anchored and loose vortex systems of finite wings
[AIAA PAPER 92-0318] p 321 A92-25765
Numerical and experimental analysis of vortex sheets behind lifting surfaces
[AIAA PAPER 92-0409] p 325 A92-26262

The effects of inner wake modelling on blade airloads p 521 A92-35784
Similarity solutions for viscous vortex cores p 759 A92-41658
On the effect of external flow and shear-layer thickness on the expansion cells of under-expanded supersonic circular jets p 969 A92-50478
Physics of vortical flows p 1031 A92-56166
A theoretical investigation of the induced drag of wing of finite aspect ratio
[CUED/A-AERO/TR-17(1991)] p 525 N92-22193
A method for computing the 3-dimensional flow about wings with leading-edge vortex separation. Part 2: Description of computer program VORSEP
[NLR-TR-86006-U] p 833 N92-29916
Vortex flow visualization using colored and fluorescent dyes on flat plate delta wing with leading edge extension
[AD-A251139] p 1036 N92-32651
Further development of the CANAERO computer code to include propulsor modelling
[DREA-CR-90-425] p 1038 N92-32811

VORTEX STREETS
Effects of ambient turbulence on the decay of a trailing vortex wake p 442 A92-32245
Numerical simulation of vortex street-edge interaction p 88 N92-13027

VORTICES
Topology of steady flows of low viscosity fluids p 38 A92-11219
Calculation of gas combustion regimes in a counterflow vortex chamber p 34 A92-12209
Computation of three-dimensional turbulent vortical flows on bodies at high incidence p 9 A92-13203
Review of the physics of enhancing vortex lift by unsteady excitation p 66 A92-15344
A discrete vortex study of stationary flow past three-dimensional lifting systems at subsonic and supersonic velocities p 79 A92-16813
Analysis of spiraling vortical flows around slender delta wings moving in an inviscid medium p 173 A92-18900
A perspective on aerospace CFD p 169 A92-20145
Instabilities of flows over bodies at large incidence p 176 A92-20738
Sonic eddy - A model for compressible turbulence p 176 A92-20739
A hot-wire anemometer in compressible subsonic flow p 244 A92-21623
An experimental study of pneumatic vortex flow control on high angle of attack forebody model
[AIAA PAPER 92-0018] p 247 A92-22140
Forebody vortex control with miniature, rotatable nose-boom strakes
[AIAA PAPER 92-0022] p 281 A92-22144
An experimental system to investigate subsonic aeroelastic behavior of lifting surfaces
[AIAA PAPER 92-0061] p 250 A92-22176
Forebody vortex control p 251 A92-22517
Aerodynamics of loaded cascades in subsonic flows subject to unsteady three-dimensional vortical disturbances
[AIAA PAPER 92-0146] p 253 A92-23762
A study on vortex flow control of inlet distortion in the re-engined 727-100 center inlet duct using computational fluid dynamics
[AIAA PAPER 92-0152] p 253 A92-23767
Vortex-induced energy separation in shear flows
[AIAA PAPER 92-0192] p 257 A92-23801
Study of role of unsteady separation in formation of dynamic stall vortex
[AIAA PAPER 92-0196] p 257 A92-23804
Multiple line-vortex model of vortex flows around body of revolution at high angles of attack up to 60 degrees p 314 A92-25104
Vortex modeling for rotor aerodynamics - The 1991 Alexander A. Nikolsky Lecture p 315 A92-25576
Pitch-up motions of delta wings
[AIAA PAPER 92-0278] p 318 A92-25732
The evaluation of canard couplings at high angles of attack
[AIAA PAPER 92-0281] p 318 A92-25735
An analytical and computational investigation of shock-induced vortical flows
[AIAA PAPER 92-0316] p 321 A92-25763
Direct computation of the sound from a compressible co-rotating vortex pair
[AIAA PAPER 92-0374] p 414 A92-26232
Flow visualization of a prop-fan leading-edge vortex
[AIAA PAPER 92-0386] p 323 A92-26242
Hypersonic rarefied flow past spheres including wake structure
[AIAA PAPER 92-0495] p 329 A92-26325
Numerical simulation of total temperature separation in jets
[AIAA PAPER 92-0535] p 396 A92-26952
Flow about cylinders with helical surface protrusions
[AIAA PAPER 92-0540] p 332 A92-26957
A study on the superconvergence of Multhopp's discretization in vortex-lattice methods p 336 A92-27381
The dimensional reconstruction of vortex cross-section images p 339 A92-27833
Numerical investigation of vortex breakdown on a delta wing p 340 A92-28027
Numerical simulation of vortex unsteadiness on a slender body at high incidence p 340 A92-28062
Numerical simulation of interaction of diffusion flame with vortex pair in a recirculation zone p 390 A92-28433
Combined method for the solution of plane direct problems of flow past bodies with jets p 427 A92-30200
An approximate method for calculating flow past solid wings of small aspect ratio based on a nonlinear theory of a continuous vortex surface p 428 A92-30373
Calculation of the aerodynamic characteristics of bodies of revolution in incompressible flow by the vortex surface method p 428 A92-30375
Experimental investigations of the vortex flow on delta wings at high incidence p 432 A92-31172
A numerical investigation of vortex flow control through small geometry modifications at the strake/wing junction of a cropped double-delta wing
[AIAA PAPER 92-0411] p 435 A92-31661
Calculation of three-dimensional separated flows in the framework of the unsteady Euler equations p 438 A92-31870
Boundary-layer-separation control p 440 A92-31886
Airborne tests of flux measurement by the relaxed eddy accumulation technique p 504 A92-32052
Analytical study on plate edge noise. I - Trailing edge noise caused by vorticity waves p 511 A92-32502
Preliminary design of an intermittent smoke flow visualization system
[AIAA PAPER 92-1028] p 580 A92-33209
Effect of controlled longitudinal vortex arrays on the development of a turbulent boundary layer p 614 A92-38856
Numerical simulation of interaction between vortexes and shocks in jet flow field p 616 A92-38925
Three-dimensional vortical structure of a large-scale coherent vortex in a turbulent boundary layer p 619 A92-40056
A study of three dimensional turbulent boundary layer separation and vortex flow control using the reduced Navier Stokes equations p 621 A92-40105
The natural and forced formation of spot-like Lambda-structures caused by vortex dislocations in a wake p 621 A92-40111
Embedded longitudinal vortex arrays, velocity and temperature fields, loss and heat transfer augmentation p 621 A92-40121
Effect of tabs on the evolution of an axisymmetric jet p 656 A92-40151
Prediction of vortex shedding from forebodies with chines p 702 A92-41228
Basic experiment on a supersonic vortex flow around a missile body p 705 A92-41545
The effects of nozzle exit geometry on forebody vortex control using blowing
[AIAA PAPER 92-2603] p 792 A92-45480
Experimental investigation of the flowfield of an oscillating airfoil
[AIAA PAPER 92-2622] p 793 A92-45494
Airfoil pressure measurements during oblique shock wave-vortex interaction in a Mach 3 stream
[AIAA PAPER 92-2631] p 795 A92-45503
Visualization of stopping flow over airfoils
[AIAA PAPER 92-2730] p 804 A92-45564
Experimental investigation of vortex dynamics on delta wings
[AIAA PAPER 92-2731] p 804 A92-45565
Forebody flow control on a full-scale F/A-18 aircraft
[AIAA PAPER 92-2674] p 806 A92-45583
Calculation of potential flow around airfoils using a discrete vortex method p 808 A92-45827
Effect of a nose-boom on forebody vortex flow p 812 A92-46818
Experimental investigation of the parallel vortex-airfoil interaction at transonic speeds p 813 A92-46901
An improved multiple line-vortex method for simulation of separated vortices of slender wings p 819 A92-47694
Supersonic jet mixing enhancement by 'delta-tabs'
[AIAA PAPER 92-3548] p 826 A92-49063
An inviscid/viscous coupling approach for vortex flow field calculations p 933 A92-49510
The influences of forced oscillations toward vortex-breakdown p 934 A92-50210
Effect of wing tip vortices on a trailing aircraft p 935 A92-50303
Crossflow vortex and transition measurements by use of multielement hot films p 935 A92-50307
Asymmetric turbulent vortical flows over slender bodies p 935 A92-50314
Time domain numerical calculations of unsteady vortical flows about a flat plate airfoil p 936 A92-50473
Remarks on the relation between lift induced drag and vortex drag p 941 A92-53079
Nonlinear development and secondary instability of large-amplitude Goertler vortices in hypersonic boundary layers p 942 A92-53080
Active control of asymmetric vortical flows around cones using injection and heating
[AIAA PAPER 92-4426] p 1025 A92-55350
Navier-Stokes prediction of large-amplitude delta-wing roll oscillations characterizing wing rock
[AIAA PAPER 92-4428] p 1080 A92-55352
Computation of vortex wake flows and control of their effects on trailing wings
[AIAA PAPER 92-4429] p 1025 A92-55353
Vortical flow control on a wing-body combination using tangential blowing
[AIAA PAPER 92-4430] p 1081 A92-55354
A discrete vortex model for predicting wing rock of slender wings
[AIAA PAPER 92-4497] p 1026 A92-55365
Unsteady shock-vortex interaction on a flexible delta wing p 1030 A92-56157
Measurements of the dynamic stall vortex convection speed p 1032 A92-56351
Surface heat transfer and flow properties of vortex arrays induced artificially and from centrifugal instabilities p 1121 A92-56371
Effects of external influences in subsonic delta wing vortices
[AIAA PAPER 92-4033] p 1034 A92-56855
NACA 0015 wing pressure and trailing vortex measurements
[NASA-TP-3151] p 13 N92-10981
A comparison of airborne wake vortex detection measurements with values predicted from potential theory
[NASA-TP-3125] p 18 N92-10994
Wing tip turbine: Analysis of the results of S2MA sounding of marginal vortex of the A320, technical summary
[ONERA-RTS-21/4365-AY-056A] p 23 N92-11009
An experimental and computational investigation of an annular reverse-flow combustor
[UTIAS-338] p 129 N92-11996
Wind tunnel investigation of the interaction and breakdown characteristics of slender wing vortices at subsonic, transonic, and supersonic speeds
[NASA-TP-3114] p 82 N92-12994
Vortex Flow Aerodynamics
[AGARD-CP-494] p 83 N92-12996
Modeling and numerical simulation of vortex flow in aerodynamics
[AD-B163670L] p 83 N92-12997
Comparison of solution of various Euler solvers and one Navier-Stokes solver for the flow about a sharp-edged cropped delta wing
[AD-B163639L] p 83 N92-12998
Vortical flow simulation by using structured and unstructured grids p 83 N92-12999
Analysis of results of an Euler-equation method applied to leading-edge vortex flow p 84 N92-13000
Experimental and numerical investigation of the vortex flow over a delta wing at transonic speed p 84 N92-13001
Recent progress in computational vortex-flow aerodynamics p 84 N92-13002
On the simulation of compressible turbulent flows past delta wing, delta wing-body and delta wing-canard p 84 N92-13003
Calculation of hypersonic leeside vortices over blunt delta wings p 84 N92-13004
On the footprints of three-dimensional separated vortex flows around blunt bodies: Attempts of defining and analyzing complex flow structures p 84 N92-13005
Nonequilibrium turbulence modeling effects on transonic vortical flows about delta wings p 85 N92-13007
In-flight flow visualization and pressure measurements at low speeds on the NASA F-18 high alpha research vehicle p 85 N92-13009
Vortex formation over a close-coupled canard-wing-body configuration in unsymmetrical flow p 85 N92-13010
An experimental study of the flow over a sharp-edged delta wing at subsonic and transonic speeds p 85 N92-13011
Characteristics of a boundary layer in a leading edge vortex p 86 N92-13012
Asymmetric vortex flow over circular cones p 86 N92-13014
An experimental investigation of the effect of fineness ratio on lateral force on a pointed slender body of revolution p 86 N92-13015

Breaking down the delta wing vortex: The role of vorticity in the breakdown process p 86 N92-13017
Determination of vortex-breakdown criteria by solving the Euler and Navier-Stokes equations p 87 N92-13018
Investigation of vortex breakdown on a delta wing using Euler and Navier-Stokes equations p 87 N92-13019
Vortex control: Further encounters p 87 N92-13020
On aircraft wake properties and some methods for stimulating decay and breakdown of tip vortices p 87 N92-13021
Control of forebody vortices by suction at the nose of the RAE high incidence research model p 87 N92-13022
Some characteristics and effects of the F/A-18 LEX vortices p 88 N92-13025
Multiple roll attractors of a delta wing at high incidence p 88 N92-13026
Numerical simulation of vortex street-edge interaction p 88 N92-13027
Numerical simulation of vortex flows past impulsively started wings p 88 N92-13028
An experimental analysis of critical factors involved in the breakdown process of leading edge vortex flows p 89 N92-13031
Water tunnel flow visualization studies of a canard-configured X-31A-like fighter aircraft model
[AD-A241362] p 90 N92-13037
Unsteady flows in rotor-stator cascades
[AD-A241593] p 158 N92-13410
Analytical/numerical matching and periodic inversion: Two advances in free wake analysis p 178 N92-13994
Definition of the unsteady vortex flow over a wing/body configuration
[NASA-CR-180083] p 178 N92-13995
A study on vortex flow control on inlet distortion in the *re-engined 727-100 center inlet duct using computational* fluid dynamics
[NASA-TM-105321] p 179 N92-13998
The application of experimental data to blade wake interaction noise prediction
[NASA-CR-189461] p 237 N92-14789
Wind tunnel investigation of vortex flows on F/A-18 configuration at subsonic through transonic speed
[NASA-TP-3111] p 179 N92-14968
Experimental study of a vortex subjected to imposed strain
[NASA-CR-189757] p 258 N92-15969
Hot-wire surveys in the vortex wake downstream of a three-percent fighter aircraft model at high angles of attack
[AD-A241869] p 259 N92-15975
An experimental investigation of leading edge vortical flow about a delta wing during wing rock
[AD-A243363] p 260 N92-17114
The effect of freestream turbulence on the vortical flow over a delta wing p 261 N92-17681
Aerodynamic and flowfield hysteresis of slender wing aircraft undergoing large-amplitude motions p 364 N92-18780
Aerodynamic control of fighter aircraft by manipulation of forebody vortices p 380 N92-18791
Forebody vortex control aeromechanics p 380 N92-18792
Dynamic wind tunnel tests on control of forebody vortices with suction p 380 N92-18793
Computation of a Kelvin-Helmholtz instability for delta wing vortex flows
[AD-A244320] p 346 N92-18825
A weakly nonlinear theory for wave-vortex interactions in curved channel flow
[NASA-TP-3158] p 347 N92-19175
Analysis of an advanced fighter aircraft using jet flap techniques and the vortex lattice method
[AD-A244051] p 366 N92-19185
An analytical and computational investigation of shock-induced vortical flows with applications to supersonic combustion p 405 N92-19538
Development of a wind chamber for model testing of tornado forces on structures
[PB92-104165] p 386 N92-19940
Influence of airfoil geometry on delta wing leading-edge vortices and vortex-induced aerodynamics at supersonic speeds
[NASA-TP-3105] p 350 N92-20038
Measurement of vortex flow fields
[NASA-CR-189543] p 443 N92-20283
Vortex characteristics of C5A/B, C141B and C130E aircraft applicable to ATC terminal flight operations tower fly-by-data
[PB92-114586] p 449 N92-20318
Numerical simulation of vortical flow over a delta wing at subsonic and transonic speeds
[NLR-TP-90029-U] p 444 N92-20498
Laser velocimetry measurements of oscillating airfoil dynamic stall flow field
[AD-A244546] p 502 N92-21297
Flowfield analysis of modern helicopter rotors in hover by Navier-Stokes method
[AD-A245011] p 446 N92-21333
Current status of computational methods for transonic unsteady aerodynamics and aeroelastic applications
[NASA-TM-104191] p 446 N92-21432
High angle of attack: Aerodynamics p 528 N92-23956
Flowfield in the vicinity of the F/A-18 vertical fin at high-angle-of-attack p 628 N92-24865
Supersonic jet mixing enhancement by delta-tabs
[NASA-TM-105664] p 630 N92-24958
Visualisation in water of vortex flow over sharp-edged canard configurations
[ARL-FLIGHT-MECH-R-189] p 632 N92-25410
A low-speed wind tunnel study of vortex interaction control techniques on a chine-forebody/delta-wing configuration
[NASA-CR-189616] p 632 N92-25510
An experimental investigation of the surface flow and wake dynamics associated with transverse flow over wavy cylinders p 681 N92-25547
High-alpha vortex decoupling investigations on a chine forebody/Delta wing configuration at transonic Mach numbers
[NASA-CR-189642] p 715 N92-26651
The eddy structures in bounded shear flows p 717 N92-27712
Pressure-based high-order TVD methodology for dynamic stall control
[AD-A247056] p 774 N92-27918
Current status of computational methods for transonic unsteady aerodynamics and aeroelastic applications p 718 N92-27937
Viscous effects on a vortex wake in ground effect
[NASA-CR-190400] p 907 N92-28361
Study of the leading-edge vortex dynamics in the unsteady flow over an airfoil
[AD-A247532] p 829 N92-28865
Explicit Navier-Stokes computation of turbomachinery flows
[AD-A248458] p 911 N92-29933
Method of measuring cross-flow vortices by use of an array of hot-film sensors
[NASA-CASE-LAR-14824-1-SB] p 998 N92-30390
Vortex flow aerodynamics
[AGARD-AR-299] p 946 N92-30947
In-flight leading-edge extension vortex flow-field survey measurements on a F-18 aircraft at high angle of attack
[NASA-TM-4398] p 947 N92-31276
Turbine blade tip and seal clearance excitation forces
[NASA-CR-184341] p 973 N92-31910
Axisymmetric bluff-body flow: A vortex solver for thin shells
[DE92-016748] p 1003 N92-31933
Vortex flow visualization using colored and fluorescent dyes on flat plate delta wing with leading edge extension
[AD-A251139] p 1036 N92-32651
Modeling and numerical simulation of vortex flow in aerodynamics
[NLR-TP-91154-U] p 1037 N92-32673
Unsteady response of the leading-edge vortices on a pitching delta wing p 1041 N92-33851
Prediction and control of asymmetric vortical flows around slender bodies using Navier-Stokes equations p 1127 N92-33968
Application of computational fluid dynamics to the study of vortex flow control for the management of inlet distortion
[NASA-TM-105672] p 1128 N92-34112

VORTICITY
Lift development of delta wings undergoing constant acceleration from rest p 9 A92-13209
On vortex interference for canard configuration p 64 A92-14071
Unsteady Euler calculations in 2-D internal aerodynamics with introduced vorticity
[ASME PAPER 91-GT-168] p 73 A92-15603
Prediction of steady and unsteady asymmetric vortical flows around circular cones p 172 A92-18372
Finite element vorticity based methods for the solution of the compressible Navier-Stokes equations p 246 A92-21983
A study on vortex flow control of inlet distortion in the re-engined 727-100 center inlet duct using computational fluid dynamics
[AIAA PAPER 92-0152] p 253 A92-23767
A random vortex method for prediction of maximum instantaneous inlet total pressure distortion p 311 A92-24731
A simplified method for simulating steady, unsteady flow around canard wing configuration p 311 A92-24876
The measurement of flutter derivatives using mechanical admittance p 393 A92-25014
Flow past a sphere - Topological transitions of the vorticity field p 330 A92-26410
Laser velocimetry seed particles within compressible, vortical flows p 395 A92-26413
A new calculating method for the flowfield in turbomachinery - The study on the application of the vorticity-velocity equations for the numerical solution of the flowfield in turbomachinery p 338 A92-27803
The structure and development of streamwise vortex arrays embedded in a turbulent boundary layer
[AIAA PAPER 92-0551] p 342 A92-28204
Error characteristics of a vortex panel method in two-dimensional flow p 421 A92-29521
Numerical analysis of techniques for efficient generation of vorticity in supersonic flows
[AIAA PAPER 92-0828] p 422 A92-29596
Evaluation of a Navier-Stokes prediction of a jet in a crossflow p 441 A92-32235
Three-dimensional vortical structure of a large-scale coherent vortex in a turbulent boundary layer p 619 A92-40056
A new method for visualization and measurement of turbulent flow patterns p 619 A92-40063
Far-field turbulence structure of the tip vortex shed by a single rectangular wing p 620 A92-40084
Vortical flow simulation by the solution of the Navier-Stokes equations p 620 A92-40104
Numerical study of vortex-dominated flows for wings at high incidence and sideslip p 702 A92-41227
Water tunnels p 880 A92-45266
A fast three-dimensional vortex method for unsteady wake calculations
[AIAA PAPER 92-2624] p 794 A92-45496
Measurements of the velocity and vorticity fields around a pitching airfoil
[AIAA PAPER 92-2626] p 794 A92-45498
Experimental development of spanwise vortex models with streamwise decay due to wall interaction
[AIAA PAPER 92-2688] p 799 A92-45535
Vortex-in-cell analysis of wing wake roll-up
[AIAA PAPER 92-2703] p 801 A92-45545
Separation and vortex formation in turbulent flows
[ONERA, TP NO. 1992-7] p 822 A92-48579
Discussion of improved transonic potential method p 942 A92-53290
Vortical flow computations on a flexible blended wing-body configuration p 1024 A92-54922
Numerical simulation of unsteady rotor wakes p 1032 A92-56352
Breaking down the delta wing vortex: The role of vorticity in the breakdown process p 86 N92-13017
On aircraft wake properties and some methods for stimulating decay and breakdown of tip vortices p 87 N92-13021
Numerical simulation of vortex street-edge interaction p 88 N92-13027
An experimental analysis of critical factors involved in the breakdown process of leading edge vortex flows p 89 N92-13031
Analytical/numerical matching and periodic inversion: Two advances in free wake analysis p 178 N92-13994
A study on vortex flow control on inlet distortion in the re-engined 727-100 center inlet duct using computational fluid dynamics
[NASA-TM-105321] p 179 N92-13998

VORTICITY EQUATIONS
Streamlines, vorticity lines, and vortices around three-dimensional bodies p 808 A92-45845
The interaction between a high-frequency gust and a blade row p 1135 A92-54484

VULNERABILITY
The challenge of commercial aircraft survivability p 931 A92-52022

W

WAFERS
Evaluation of an innovative high-temperature ceramic wafer seal for hypersonic engine applications p 578 N92-22205

WAKES
Investigation of the flow at the exit of an unshrouded centrifugal impeller and comparison with the 'classical' jet-wake theory
[ASME PAPER 90-GT-124] p 6 A92-11287
Boundary-layer and wake measurements on a swept, circulation-control wing p 9 A92-13205
Numerical prediction of wakes in cascades and compressor rotors including the effects of mixing. I - Cascade wakes including the effects of incidence and freestream turbulence
[ASME PAPER 91-GT-225] p 74 A92-15638

Three-dimensional structure of a curved wake
[AIAA PAPER 92-0541] p 341 A92-28199
Navier-Stokes solution of transonic cascade flows using nonperiodic C-type grids p 344 A92-28523
Turbulent flow in the wake of an idealized wing-body junction
[AIAA PAPER 92-0282] p 435 A92-31652
Effects of ambient turbulence on the decay of a trailing vortex wake p 442 A92-32245
The combined wake of an array of oscillating ribbons p 623 A92-40180
Vortex-in-cell analysis of wing wake roll-up
[AIAA PAPER 92-2703] p 801 A92-45545
Three-dimensional-mode resonance in far wakes p 898 A92-46252
Establishing a database for flight in the wakes of structures p 810 A92-46782
An aeroelastic analysis with a generalized dynamic wake p 847 A92-46932
Airfoil wake and linear theory gust response including sub and superresonant flow conditions
[AIAA PAPER 92-3074] p 823 A92-48724
Hypersonic merged layer blunt body flows with wakes p 939 A92-52757
Numerical simulation of unsteady rotor wakes p 1032 A92-56352
A comparison of airborne wake vortex detection measurements with values predicted from potential theory
[NASA-TP-3125] p 18 N92-10994
Effects of wake and shock passing on the heat transfer to a film cooled transonic turbine blade p 156 N92-12201
Modeling and numerical simulation of vortex flow in aerodynamics
[AD-B163670L] p 83 N92-12997
Navier-Stokes analysis of turbulent boundary layer and wake for two-dimensional lifting bodies p 221 N92-14309
Flow visualization and wake analysis for standard and modified configurations of the AN/ALQ-78 antenna pod
[AD-A243552] p 260 N92-17339
Response of structures to galloping excitation: Background and approximate estimation
[ESDU-91010] p 399 N92-18091
Drag prediction using computation methods
[ONERA-RSF-82/1685-AY-154-4] p 349 N92-19682
An investigation of the energy loss and near wake flow field of trailing edge injection p 456 N92-21839
Ship airwake measurement and modeling options for rotorcraft applications p 503 N92-21954
Measurement of the flow distribution over the flight deck of an aircraft carrier p 504 N92-21955
A theoretical investigation of the induced drag of wing of finite aspect ratio
[CUED/A-AERO/TR-17(1991)] p 525 N92-22193
Numerical simulations of wakes, blade-vortex interaction, flutter, and flutter suppression by feedback control p 597 N92-23997
An experimental investigation of the surface flow and wake dynamics associated with transverse flow over wavy cylinders p 681 N92-25547

WALL FLOW
Two-dimensional adaptive-wall tests in the NASA Ames two- by two-foot transonic wind tunnel p 30 A92-13201
Blade defect force investigation in a compressor cascade p 10 A92-13233
Flow unsteadiness by weak normal shock wave/turbulent boundary layer interaction in internal flow p 67 A92-15359
Stator averaged, rotor blade-to-blade near wall flow in a multistage axial compressor with tip clearance variation
[ASME PAPER 91-GT-30] p 67 A92-15514
Convective transport phenomena on the suction surface of a turbine blade including the influence of secondary flows near the endwall
[ASME PAPER 91-GT-35] p 147 A92-15518
Noise-driven flow p 173 A92-18680
Effects of sidewall disturbances on the supersonic mixing layer p 290 A92-21085
On velocity profile models for predicting end wall boundary layers and their blade force defects in axial compressor cascades p 311 A92-24877
Application of a new K-tau model to near wall turbulent flows p 395 A92-26437
A systematic experimental and computational investigation of a class of contoured wall fuel injectors
[AIAA PAPER 92-0625] p 374 A92-27007
Analysis of a 2-D airfoil motion flying in-proximity-to a wavy-wall surface - Finite difference method p 421 A92-29517
A shock and an expansion wave in transonic flow p 440 A92-31961
The effects of wall suction on laminar-turbulent transition in three-dimensional flow p 522 A92-36021
New model for predicting end wall boundary layer in an axial cascade p 611 A92-37389
Performance of turbulence models to predict supersonic boundary layer flows p 613 A92-37553
Embedded longitudinal vortex arrays, velocity and temperature fields, loss and heat transfer augmentation p 621 A92-40121
Wind tunnel wall corrections for unsteady flow applying steady wall adaptation and CFD-techniques p 706 A92-42533
A numerical study of flow of a viscous gas in a Laval nozzle in the narrow channel approximation p 706 A92-42680
A calculation of penetration of the jet issuing normally into a cross flow across a wall boundary layer
[SAE PAPER 912029] p 790 A92-45419
Analysis of motion of airfoil flying over wavy-wall surface (lifting surface method) p 818 A92-47100
A new method for predicting the end wall boundary layers and the blade force defects inside the passage of axial compressor cascades p 819 A92-47691
Discussion on sidewall suction in two-dimensional wind tunnel p 997 A92-53263
Computing high-speed flows past an oscillating cylinder near a vertical wall
[AIAA PAPER 92-4653] p 1028 A92-55397
Model representation in the PANCOR wall interference assessment code
[NASA-TM-104152] p 31 N92-11022
The BCAC/IAR collaborative research program to investigate the sidewall boundary layer effects in the IAR/NRC 2-D High Reynolds Number Test Facility
[NRC-HSA-434] p 81 N92-11976
Wall interference calculation in a transonic wind tunnel with discrete slots p 83 N92-12995
A wall interference assessment/correction system
[NASA-CR-189785] p 259 N92-15974
Atmospheric pressure flow reactor: Gas phase chemical kinetics under tropospheric conditions without wall effects
[NASA-CASE-MSC-21384-1] p 297 N92-16243
User guide for WIACX: A transonic wind-tunnel wall interference assessment and correction procedure for the NTF
[NASA-TM-104168] p 261 N92-17547
Asymptotic theory of transonic wind tunnel wall interference
[AD-A244075] p 403 N92-19080
Operating ranges of meteorological wind tunnels for the simulation of convective boundary layer phenomena
[AD-A244153] p 409 N92-19195
Comparison of a two-dimensional adaptive-wall technique with analytical wall interference correction techniques
[NASA-TP-3132] p 444 N92-20494
An analysis of the sidewall boundary layer effect in two-dimensional wind tunnel testing p 626 N92-24856
Wall functions for the kappa-epsilon turbulence model in generalized nonorthogonal curvilinear coordinates
[NASA-CR-190368] p 685 N92-25962
Theoretical principles of a Euler method for the calculation of three dimensional flows
[F+W-TF-2012] p 767 N92-27045
Computational modelling of turbulent flow in S-bends p 769 N92-27480
Study of turbulence structure through numerical simulations: The perspective of drag and reduction p 717 N92-27713
Evaluation of measured-boundary-condition methods for 3D subsonic wall interference
[NLR-TR-88072-U] p 832 N92-29884
Effect of walls on the supersonic reacting mixing layer p 912 N92-30065
Integration of wall interference assessment and wall adaptation
[NLR-TP-91119-U] p 1101 N92-32734

WALL JETS
A numerical method for solving the circulation control airfoil with wall jet p 314 A92-25103
Unsteady circulation control aerodynamics of a circular cylinder with periodic jet blowing p 330 A92-26401
Reynolds stress budget in the outwash jet arising from colliding curved wall jets p 614 A92-38860
Analysis of a dusty wall jet
[NASA-CR-189759] p 257 N92-15965

WALL PRESSURE
Correlation of separation shock motion with pressure fluctuations in the incoming boundary layer p 5 A92-11061
Calculation of flow of a radiating gas in axisymmetric nozzles of specified shape p 7 A92-12179
Experimental investigation of terminal shock sensors for mixed-compression inlets p 276 A92-21074
Application of the wall pressure method to wall interference corrections for model tests at high angle of attack in high speed wind tunnel p 315 A92-25134
Wall pressure wavenumber-frequency spectrum beneath a turbulent boundary layer measured with transducer arrays calibrated with an acoustical method
[ONERA, TP NO. 1991-212] p 329 A92-26364
Calculation of 3D flow field in a single transonic compressor stage p 422 A92-29719
Comparison between two 3D-NS-codes and experiment on a turbine stator
[AIAA PAPER 92-3042] p 822 A92-48703
Numerical simulation of a confined transonic normal shock wave/turbulent boundary layer interaction
[AIAA PAPER 92-3668] p 826 A92-49088
Exploratory study of wall pressure fluctuations in a Mach 5, sharp fin-induced turbulent interaction p 935 A92-50304
Blockage correction in three-dimensional wind tunnel testing based on the wall signature method
[AIAA PAPER 92-3925] p 1095 A92-56756
Wall interference calculation in a transonic wind tunnel with discrete slots p 83 N92-12995
A wall interference assessment/correction system
[NASA-CR-189785] p 259 N92-15974
Experimental study of the wall pressure fluctuations under a turbulent boundary layer downstream of tandem aerofoil external manipulators
[REPT-207-90-78] p 500 N92-20497
Flat plates placed in depleted hypersonic flow
[SESSIA-430/91.960] p 947 N92-31508
Organized turbulent structures and their induced wall pressure fluctuations p 949 N92-31853

WALL TEMPERATURE
Gas turbine main shaft internal flow and heat transfer
[ASME PAPER 91-GT-165] p 123 A92-15600
Assessment of three models of turbulence in a shock-boundary layer interaction of a heated wall p 423 A92-29999
Secondary instability of high-speed flows and the influence of wall cooling and suction p 435 A92-31640
Forced-injection quenching of a hot-tube under microgravity p 590 A92-35977
The inviscid stability of supersonic flow past heated or cooled axisymmetric bodies p 712 A92-44363
Effect of model cooling on periodic transonic flow p 813 A92-46900
Experimental investigation of the reflection of a shock wave on a heated surface in presence of a turbulent boundary layer p 1023 A92-54569
Numerical simulation of an aircraft anti-icing system incorporating a rivulet model for the runback water p 448 N92-20303
Further investigation of the effect of model cooling on periodic transonic flow p 721 N92-27961

WALLOPS ISLAND
Agreements/subagreements applicable to Wallops, 12 Nov. 1991 p 575 N92-22598

WALLS
Boundary-layer receptivity due to a wall suction and control of Tollmien-Schlichting waves p 616 A92-39333
Comparative study of turbulence models in predicting hypersonic inlet flows
[AIAA PAPER 92-3098] p 824 A92-48740
Engine panel seals for hypersonic engine applications: High temperature leakage assessments and flow modelling
[NASA-TM-105260] p 298 N92-16336
Secondary instability of high-speed flows and the influence of wall cooling and suction
[NASA-CR-4427] p 406 N92-19844
Evaluation of an innovative high-temperature ceramic wafer seal for hypersonic engine applications p 578 N92-22205
Three-dimensional modeling of diesel engine intake flow, combustion and emissions
[NASA-CR-189126] p 658 N92-24539
Particle image velocimetry
[AD-A246638] p 750 N92-27753
Comparative study of turbulence models in predicting hypersonic inlet flows
[NASA-TM-105720] p 722 N92-28102
A preliminary experimental investigation of local isotropy in high-Reynolds-number turbulence p 912 N92-30042

WARFARE
Simulation as applied to mission planning p 747 A92-41210
A neural network based postattack damage assessment system p 922 A92-48520
Controlling radar signature p 967 A92-52018
The role of stealth in naval aviation and joint/combined operations
[AD-A240595] p 22 N92-11005

Revolution at sea: Aircraft options for the year 2030
p 466 N92-21974
Foreign object damage to tires operating in a wartime environment
[AD-A247195] p 724 N92-27682
WARNING SYSTEMS
Windshear detection and avoidance - Airborne systems survey p 17 A92-11382
Innovation in the laser warning sensor field
p 554 A92-35742
EICAS in an integrated cockpit --- Engine Indication Crew Alerting System p 855 A92-44922
Laser-radar based obstacle avoidance system for helicopters p 1064 A92-56295
Validation and verification flight test for TCAS-2 logic changes (MOPS Change 6)
[DOT/FAA/CT-TN91/46] p 268 N92-15981
An investigation of air transportation technology at the Massachusetts Institute of Technology, 1990-1991
p 265 N92-17985
Cockpit display of hazardous weather information
p 277 N92-17989
An investigation into the feasibility of providing a proximity warning device for search and rescue helicopters
[ETN-92-91057] p 530 N92-22408
On the optimization of windshear warning and guidance systems
[NLR-TP-90196-U] p 837 N92-29703
Examination of aircraft warning and caution lights after shock testing
[NLR-TP-89284-U] p 952 N92-30474
A cable detection lidar system for helicopters
p 1001 N92-31068
Engine monitoring display study
[NASA-CR-4463] p 979 N92-32175
Safety study of TCAS 2 for logic version 6.04
[DOT/FAA/RD-92/22] p 1047 N92-32537
Simulation test and evaluation of TCAS 2 logic version 6.04
[DOT/FAA/RD-92/23] p 1048 N92-33098
Aircraft accident/incident summary report: Controlled flight into terrain Bruno's Inc., Beechjet, N25BR, Rome, Georgia, 11 December 1991
[PB92-910404] p 1044 N92-34081
WASHERS (CLEANERS)
The operational status of automated aircraft washing system p 1016 A92-56087
WASPALOY
Fatigue crack growth of small corner defects from blunt notches in an aeroengine alloy
[PNR-90860] p 1111 N92-34019
WASTE ENERGY UTILIZATION
Configuration effects on the ingestion of hot gas into the engine intake p 842 A92-45315
WASTE HEAT
Optimal thermal management system for HALE UAV --- High Altitude Long Endurance Unmanned Air Vehicles
[ASME PAPER 91-GT-396] p 111 A92-15726
WATER
Determination of liquid water content in the AEDC engine test cells
[AIAA PAPER 92-0165] p 263 A92-23778
Aircraft lidar sensitivity study for measuring water vapor
[AD-A240549] p 42 N92-11237
Effectiveness of an onboard water spray system during an oxygen enriched cabin fire
[DOT/FAA/CT-TN91/51] p 264 N92-17149
Pressure measurements in high speed water tunnels
[DE92-004891] p 386 N92-19978
Method for calculating the three-dimensional water concentration coefficients and its industrial applications
p 502 N92-21685
The measurement of water film thickness on airfoils in heavy rain conditions using conductance sensors
p 452 N92-21695
Progress report on analysis of differential attenuation radar data obtained during WISP-91
[PB92-133800] p 503 N92-21828
Fire bombing and fire bombers
[CA-PATENT-1-268-164] p 1061 N92-33582
WATER EROSION
Two-phase flows at supersonic velocities
p 4 A92-10907
WATER FLOW
Development of an improved model for runback water on aircraft surfaces
[AIAA PAPER 92-0042] p 270 A92-22160
Water tunnel flow visualization studies of a canard-configured X-31A-like fighter aircraft model
[AD-A241362] p 90 N92-13037
WATER IMMERSION
Development of an emergency underwater escape breathing system for CH124 seaking aircrew
[DCIEM-87-TR-11] p 92 N92-13041
Canadian aircrew sea water survival, 1952-1987
[DCIEM-88-RR-39] p 954 N92-32219
WATER INJECTION
Contingency power for a small turboshaft engine by using water injection into turbine cooling air
[NASA-TM-105680] p 871 N92-29661
WATER PRESSURE
Take it all off - with water --- High-pressure waterjet stripping of protective coatings p 516 A92-34775
WATER TAKEOFF AND LANDING AIRCRAFT
Aircraft design experience p 110 A92-15326
WATER TEMPERATURE
Numerical simulation of an aircraft anti-icing system incorporating a rivulet model for the runback water
p 448 N92-20303
WATER TUNNEL TESTS
Topology of steady flows of low viscosity fluids
p 38 A92-11219
Water tunnels p 880 A92-45266
Dynamically enhanced sustained lift using oscillating leading-edge flaps
[AIAA PAPER 92-2625] p 794 A92-45497
Experimental study of vortex flows over delta wings in wing-rock motion p 810 A92-46787
Pitch rate/sideslip effects on leading-edge extension vortices of an F/A-18 aircraft model
p 874 A92-46810
On aircraft wake properties and some methods for stimulating decay and breakdown of tip vortices
p 87 N92-13021
Visualisation in water of vortex flow over sharp-edged canard configurations
[ARL-FLIGHT-MECH-R-189] p 632 N92-25410
Observation and measurements of flow structures in the stagnation region of a wing-body junction
p 714 N92-26616
Vortex flow visualization using colored and fluorescent dyes on flat plate delta wing with leading edge extension
[AD-A251139] p 1036 N92-32651
Static and dynamic flow visualization studies of two double-delta wing models at high angles of attack
[AD-A252878] p 1040 N92-33678
WATER VAPOR
Studies on the effect of high-flying air-traffic on the atmosphere
[IAF PAPER 91-737] p 301 A92-22495
Influence of air velocity on the habit of ice crystal growth from the vapor p 668 A92-38111
Aircraft lidar sensitivity study for measuring water vapor
[AD-A240549] p 42 N92-11237
WATER WAVES
Analysis of slender bodies of revolution with curved-ground effect and waving-water effect
p 524 A92-36151
WAVE DIFFRACTION
Diffracted and head waves associated with waves on nonseparable surfaces
[NASA-TP-3169] p 444 N92-20545
WAVE DRAG
Effects of trailing-edge flap on buffet characteristics of a supercritical airfoil p 378 A92-24413
Bodies of revolution with minimal wave drag at transonic gas flow velocities p 424 A92-30135
Possibility of reducing the wave drag of a hypersonic flight vehicle (wave rider) p 438 A92-31863
The total drag of a body in the flow of a viscous heat-conducting gas p 439 A92-31873
Aerodynamic shape optimization of hypersonic configurations including viscous effects
[AIAA PAPER 92-2635] p 795 A92-45506
Minimizing supersonic wave drag with physical constraints at design and off-design Mach numbers
p 811 A92-46808
Comparison of transonic flow models
p 936 A92-50325
Inviscid drag prediction for transonic transport wings using a full-potential method
[NLR-TP-89365-U] p 444 N92-20473
Efficient and robust design optimization of transonic airfoils p 528 N92-23717
Wave drag determination in the transonic full-potential flow code MATRICS
[NLR-TP-90062-U] p 828 N92-28709
A method for designing blended wing-body configurations for low wave drag
[NASA-TP-3261] p 1036 N92-32480
WAVE EQUATIONS
Reflections off aircraft and the shape optimization of a ridged waveguide p 267 A92-23967
An exact solution to edge effect problem for a finite-span wing in supersonic flow p 441 A92-31962
Critical problems of computational aeroacoustics
p 167 N92-13857
Wave equations and computational models for sonic boom propagation through a turbulent atmosphere
p 1139 N92-33877
WAVE GENERATION
Boundary-layer receptivity of sound with roughness
p 604 A92-36006
Studies on laminar boundary-layer receptivity to freestream turbulence near a leading edge
p 591 A92-36007
Oscillation of oblique shock waves generated in a two dimensional asymmetric nozzle
[SAE PAPER 912061] p 791 A92-45443
WAVE INTERACTION
Review of the physics of enhancing vortex lift by unsteady excitation p 66 A92-15344
On the interaction between first- and second-mode waves in a supersonic boundary layer
p 78 A92-16462
Effect of a fan of rarefaction waves on the development of disturbances in a supersonic boundary layer
p 809 A92-46519
Numerical simulation of swept-wing flows
[NASA-CR-189457] p 180 N92-14969
WAVE PACKETS
Generation of several wave packets in the boundary layer of a wing profile p 424 A92-30136
Studies on laminar boundary-layer receptivity to freestream turbulence near a leading edge
p 591 A92-36007
WAVE PROPAGATION
Noise-driven flow p 173 A92-18680
Wave motions in a three-dimensional boundary layer
p 244 A92-21629
Pressure wave propagation studies for oscillating cascades
[AIAA PAPER 92-0145] p 316 A92-25682
Analytical study on plate edge noise. I - Trailing edge noise caused by vorticity waves p 511 A92-32502
Convergence of subsonic unsteady aerodynamics evaluated by a finite element concept based on Huygeuns' wave propagation
[AIAA PAPER 92-2502] p 518 A92-34497
Spectrogram diagnosis of aircraft disasters
[SAE PAPER 912041] p 836 A92-45425
Propagation of shock waves through clouds
[AERO-REPT-9104] p 400 N92-18317
Measurement of LORAN-C envelope to cycle difference in the far field
[PB92-128909] p 455 N92-21263
Eulerian computational methods
[DE92-008017] p 765 N92-26853
Effect of walls on the supersonic reacting mixing layer
p 912 N92-30065
WAVE REFLECTION
Shock wave reflection close to the leading edge of a wedge p 37 A92-10660
Modification of the radiated sound directivity due to ground reflections - Application to static tests of helicopter turboshaft engines
[ONERA, TP NO. 1991-210] p 415 A92-26362
Numerical computation and experimental study of shock wave reflection p 430 A92-30542
Accelerated convergence to steady state by gradual far-field damping p 610 A92-36835
Experimental investigation of the reflection of a shock wave on a heated surface in presence of a turbulent boundary layer p 1023 A92-54569
The research of reducing 3-D low supersonic shock wave reflection in a 2-D transonic flexible walls adaptive wind tunnel
[AIAA PAPER 92-3924] p 1095 A92-56755
Validation of three-dimensional incompressible spatial direct numerical simulation code: A comparison with linear stability and parabolic stability equation theories for boundary-layer transition on a flat plate
[NASA-TP-3205] p 943 N92-30295
WAVE SCATTERING
SATCOM antenna siting study on P-3C aircraft, volume 1
[NASA-CR-189514] p 221 N92-14262
WAVE-PARTICLE INTERACTIONS
Prototype instrumentation and design studies
[AD-A248378] p 736 N92-28004
WAVEFORMS
Quantification of aircraft carbon brake wear using regression analysis and periodic wave forms
[SAE PAPER 912174] p 644 A92-39999
Comparison of R2SPG waveforms with simulated EMP --- Repetitive Random Square-wave Pulse Generator
p 760 A92-42317
Measurement of LORAN-C envelope to cycle difference in the far field
[PB92-128909] p 455 N92-21263
Assessment of valve actuator motor rotor degradation by Fourier Analysis of current waveform
[DE92-013233] p 909 N92-28814

Analysis of sonic boom data to quantify distortions of shock profiles p 1139 N92-33879
Model experiment to study the effect of turbulence on risetime and waveform of N waves p 1139 N92-33881

WAVEGUIDE ANTENNAS
Decoupling of antennas using periodic structures p 725 A92-42634

WAVELENGTH DIVISION MULTIPLEXING
Fiber-coupled position sensors for aerospace applications p 370 A92-27776

WAVERIDERS
Comparative analysis of the lift-drag ratio and heat flows toward the surface of wave riders of different configurations p 7 A92-12173
Application of waverider-based configurations to hypersonic vehicle design
[AIAA PAPER 91-3304] p 32 A92-12742
Hypersonic waveriders - Effects of chemically reacting flow and viscous interaction
[AIAA PAPER 92-0302] p 320 A92-25754
Aerodynamic characteristics of a hypersonic viscous optimized waverider at high altitudes
[AIAA PAPER 92-0306] p 320 A92-25755
A hypersonic waverider test vehicle - The logical next step
[AIAA PAPER 92-0308] p 387 A92-25756
Navier-Stokes computations of a viscous optimized waverider
[AIAA PAPER 92-0305] p 435 A92-31653
Possibility of reducing the wave drag of a hypersonic flight vehicle (wave rider) p 438 A92-31863
Navier-Stokes simulation for cone-derived waverider p 703 A92-41271
Optimum hypersonic wings and wave riders p 706 A92-42531
Heat transfer characteristics of hypersonic waveriders with an emphasis on leading edge effects
[AIAA PAPER 92-2920] p 821 A92-47892
Three-dimensional wings and waveriders with attached shock waves p 936 A92-50322
Heat transfer to a delta wing and two waverider wings in rarefied hypersonic flow p 937 A92-52748
A comparative study of numerical versus analytical waverider solutions
[AD-A244183] p 347 N92-19304
Heat transfer characteristics of hypersonic waveriders with an emphasis on the leading edge effects
[NASA-CR-189586] p 525 N92-22215
A study of viscous interaction effects on hypersonic waveriders
[NASA-CR-189587] p 625 N92-24680
Navier-Stokes computations of a viscous optimized waverider
[NASA-CR-189658] p 944 N92-30392

WEAPON SYSTEM MANAGEMENT
Gulf Range Drone Control Upgrade System Mobile Control System p 882 A92-47567

WEAPON SYSTEMS
Computer simulation of weapon blast pressures on flexible surfaces p 39 A92-12115
Suit study - The impact of VMS in subsystem integration
[AIAA PAPER 92-1078] p 563 A92-33247
Statistical analysis of field data for aircraft warranties p 760 A92-42077
Current technology propulsion systems meet the STOVL window of opportunity p 860 A92-45307
NAECON 91; Proceedings of the IEEE National Aerospace and Electronics Conference, Dayton, OH, May 20-24, 1991. Vols. 1-3
[ISBN 0-7803-0084-X] p 786 A92-48426
Expert Avionics Code Modification p 921 A92-48513
Progressive avionics packaging technologies p 989 A92-49276
Controlling radar signature p 967 A92-52018
Generic helicopter for multiship simulations
[AIAA PAPER 92-4151] p 959 A92-52442
A development-memory approach for enhancing avionics software logistics p 119 N92-12540
Evolution of avionic systems architecture, from the 1950's to the present p 198 N92-14047
Avionics technology beyond 2000 p 200 N92-14058
Simulator data integrity program: Process standard development
[AD-A242207] p 386 N92-19642
Expert system management system
[AD-A247102] p 781 N92-26863
Computer program for calculating in-flight aircraft-store interface reaction loads
[AD-A245782] p 731 N92-26896
Developing robust support structures for high-technology subsystems: The AH-64 Apache helicopter
[AD-A252773] p 1017 N92-33499

WEAPONS DEVELOPMENT
Integration of supportability elements into the conceptual design process
[AIAA PAPER 92-1194] p 600 A92-33306
Avionics technology beyond 2000 p 200 N92-14058

WEAR
Filter debris analysis: A concrete approach to wear diagnosis
[DREP-TM-88-20] p 222 N92-14345
Tribology needs for future space and aeronautical systems
[NASA-TM-104525] p 214 N92-15191
Turbine aircraft engine operational trending and JT8D static component reliability study
[DOT/FAA/CT-91/10] p 870 N92-28686

WEAR RESISTANCE
Improving the properties of titanium alloys by ion implantation p 289 A92-22771
Improving sample introduction for total wear metal determination by atomic emission spectroscopy p 389 A92-26850

WEAR TESTS
Quantification of aircraft carbon brake wear using regression analysis and periodic wave forms
[SAE PAPER 912174] p 644 A92-39999
Effects of material choices on brush seal performance p 1116 A92-54650
Development of a full-scale transmission testing procedure to evaluate advanced lubricants
[NASA-TP-3265] p 998 N92-30396
A preliminary study in the use of phase demodulation techniques for the analysis of gear vibration data
[NRC-32083] p 1002 N92-31469

WEATHER
Technical evaluation report on the Fluid Dynamics Panel Specialists' Meeting on Effects of Adverse Weather on Aerodynamics
[AGARD-AR-306] p 352 N92-18242
JPL's Real-Time Weather Processor project (RWP) metrics and observations at system completion p 413 N92-19428
Cockpit weather information needs p 449 N92-21503
Effects of Adverse Weather on Aerodynamics
[AGARD-CP-496] p 449 N92-21679
Flight in adverse environmental conditions p 449 N92-21680
Integration of flight and carrier landing aid systems for shipboard operations p 456 N92-21958
Aircraft accident/incident summary report: Controlled flight into terrain Bruno's Inc., Beechjet, N25BR, Rome, Georgia, 11 December 1991
[PB92-910404] p 1044 N92-34081

WEATHER FORECASTING
A prototype microburst prediction product for the Terminal Doppler Weather Radar p 408 A92-27962
Expert knowledge techniques applied to the analysis of electric field mill data p 408 A92-27991
Shear progress --- wind shear handling and recognition technologies for aviation p 609 A92-40880
Windshear detection p 652 A92-40883
Pilot's Automated Weather Support System (PAWSS) concepts demonstration project. Phase 1: Pilot's weather information requirements and implications for weather data systems design
[NASA-CR-188228] p 46 N92-11593

WEATHERING
Weathering test of AFRP composites for the application of helicopter fuselage --- Aramide Fiber Reinforced Plastic p 142 A92-15309

WEAVING
Weaving an aircraft p 392 A92-24911
Universal weaving for turbine engine composite preforms
[AD-A237667] p 202 N92-14059

WEBS (SUPPORTS)
Vibration of gear system with web structure p 588 A92-35573

WEDGE FLOW
Shock wave reflection close to the leading edge of a wedge p 37 A92-10660
Wedge-induced turbulent boundary-layer separation on a roughened surface at Mach 6.0 p 175 A92-20379
Turbulent boundary-layer characteristics over a flat-plate/wedge configuration at Mach 6 p 176 A92-20761
Transverse correlation of the spectral components of pressure fluctuations on a plate ahead of a step p 426 A92-30187
Study on effectiveness of the front wedge shape in hypersonic flow p 430 A92-30552
Spectral solution of inviscid supersonic flows over wedges and axisymmetric cones p 524 A92-36359
Development of a CFD code for analysis of fluid dynamic forces in seals p 228 N92-15084

WEDGES
An experimental study of transonic flow of a gas past wedges p 424 A92-30153
An improved method for simulating supersonic flow past a wedge shaped body
[NAL-TR-1097] p 345 N92-18239

WEIBULL DENSITY FUNCTIONS
Reliability analysis of a structural ceramic combustion chamber
[ASME PAPER 91-GT-155] p 123 A92-15591
Transmission overhaul and component replacement predictions using Weibull and renewal theory p 155 A92-17201

WEIGHT ANALYSIS
MassInfo - An intelligent mass properties information system p 928 A92-47628
The effect of composite material allowable changes on VTOL airframe weights p 848 A92-47629
Weight evaluation and sensitivity analysis for space plane. Part 2: TSTO
[NAL-TM-602-PT-2] p 287 N92-17754
Application of integrated structural analysis to the high speed civil transport p 684 N92-25927

WEIGHT INDICATORS
Force measurement on rotating, ablating models using an air bearing balance p 483 A92-31174

WEIGHT REDUCTION
Aeroelastic tailoring of aeronautical composite wing structures p 146 A92-15343
Propulsion requirements for high altitude long endurance flight
[ASME PAPER 91-GT-393] p 127 A92-15723
Weight estimating guide for advanced composites p 289 A92-23418
The use of variable camber to reduce drag, weight and costs of transport aircraft p 313 A92-25096
Lifting surface design using the principle of passive control of elastic characteristics p 480 A92-31865
Space Shuttle shell structure waffle panel optimization
[AIAA PAPER 92-2359] p 586 A92-34591
WIG transportation efficiency considering the influence of no-load situation p 781 A92-43241
Al-Li alloys find their niche p 755 A92-43685
Advanced Rotorcraft Transmission (ART) Program summary
[AIAA PAPER 92-3365] p 905 A92-48938
Aluminium-lithium alloys - Application on helicopters p 1106 A92-56326
Superplastic applications in aero engines
[PNR-90788] p 473 N92-20436
Advanced Rotorcraft Transmission (ART) program summary
[NASA-TM-105665] p 680 N92-24984
Feasibility of magnetic bearings for advanced gas turbine engines p 772 N92-27738
Structural assessment of ultralightweight composites p 1107 N92-32525
Aspects of compression in aerospace composites: Future requirements p 1109 N92-33036

WEIGHTING FUNCTIONS
Negative state weighting in the linear quadratic regulator for aircraft control p 1007 A92-50513
Solution of stress intensity factor by weight function for small surface cracks in plates p 998 A92-53332

WEIGHTLESSNESS
Outlines of parabolic flight p 764 N92-26441

WEIGHTLESSNESS SIMULATION
Convective flow analysis on the KC-135 aircraft
[AIAA PAPER 92-0844] p 493 A92-29610
Process modeling KC-135 aircraft
[NASA-CR-184278] p 359 N92-18347
Microgravity nucleation and particle coagulation experiments support
[NASA-CR-189899] p 502 N92-21433

WELDED JOINTS
Study of weld offset in longitudinally welded SSME HPFTP inlet
[AIAA PAPER 92-2305] p 586 A92-34525
Welding technology transfer task/laser based weld joint tracking system for compressor girth welds p 593 N92-22426

WELDING
Current repair technologies for jet engine components p 1016 A92-56085

WHEEL BRAKES
Quantification of aircraft carbon brake wear using regression analysis and periodic wave forms
[SAE PAPER 912174] p 644 A92-39999
Characterization of thermal performance of wheel outboard of an aircraft p 849 A92-48352

WHIRL TOWERS
Acoustic results of the Boeing model 360 whirl tower test p 603 A92-35741
WHISKER COMPOSITES
Ceramics for engines p 578 N92-22517
WHITE NOISE
Transition to turbulence in confined, compressible mixing layers. I - 3D numerical simulations with excitation of random, broadband white noise
[AIAA PAPER 92-0553] p 332 A92-26964
WIENER HOPF EQUATIONS
A general nonlinear dynamical analysis of a second-order, one-dimensional, theoretical compression system model p 509 A92-29374
Analytical study on plate edge noise. I - Trailing edge noise caused by vorticity waves p 511 A92-32502
WILDERNESS
Annoyance from aircraft overflights in wilderness p 689 A92-39239
Relating the annoyance of aircraft overflights to their audibility by outdoor recreationists p 689 A92-39240
WIND (METEOROLOGY)
Airdata calibration techniques for measuring atmospheric wind profiles p 856 A92-46792
Flight evaluation of curved MLS precision approaches in a twin otter aircraft, phase 2
[AD-A243025] p 268 N92-17568
Analytical modeling of SH-2F helicopter shipboard operation p 464 N92-21961
Evaluation of grounding and mooring points for Army aircraft
[AD-A250749] p 953 N92-31193
WIND DIRECTION
Parachute canopy control simulation - A solution for aircrew emergency training p 572 A92-35428
Calibration data for improved correction of UVW propeller anemometers
[DE92-002935] p 297 N92-16281
Measurement of the flow distribution over the flight deck of an aircraft carrier p 504 N92-21955
Evaluation of microwave landing system approaches in a wide-body transport simulator
[NASA-CR-4450] p 957 N92-30978
WIND EFFECTS
Estimating the probability of a safe flight for an aircraft flying under the effect of disturbances p 479 A92-30132
Aircraft longitudinal dynamics equations including wind shear effects p 977 A92-51946
Severe turbulence and maneuvering from airline flight records
[AIAA PAPER 92-4341] p 1078 A92-55330
Estimation of airborne performance in landing
[ESDU-91032] p 272 N92-15988
Wind loads on a mirage III O aircraft mounted above a ground plane
[AD-A243004] p 275 N92-17266
On the relation between cumulus cloud lines and surface shear lines p 410 N92-19667
Determination of limitations for helicopter ship-borne operations p 465 N92-21965
WIND EROSION
Aerodynamic roughness measured in the field and simulated in a wind tunnel
[NASA-CR-4422] p 347 N92-19354
WIND MEASUREMENT
Stochastic prediction techniques for wind shear hazard assessment p 48 A92-11381
Use of distance-measuring equipment (DME) for correcting errors in position, velocity, and wind measurements from aircraft inertial navigation systems p 188 A92-18172
Aspect angle dependence of outflow strength in Denver microbursts - Spatial and temporal variations p 408 A92-27963
The design and operational characteristics of a heated radome for air motion measurement p 467 A92-32064
Airdata calibration techniques for measuring atmospheric wind profiles p 856 A92-46792
Stochastic prediction techniques for wind shear hazard assessment p 1007 A92-50505
Expand turbulence laboratory facilities to meet new DOD research interest
[AD-A248581] p 883 N92-28388
On the optimization of windshear warning and guidance systems
[NLR-TP-90196-U] p 837 N92-29703
WIND PROFILES
Boundary-layer transition across a stratocumulus cloud edge in a coastal zone p 45 A92-10489
Flight in a steady wind field p 131 A92-13696
Remote measurements of supercooled integrated liquid water during WISP/FAA aircraft icing program p 915 A92-46788
Airdata calibration techniques for measuring atmospheric wind profiles p 856 A92-46792
Effect of a simulated glaze ice shape on the aerodynamic performance of a rectangular wing
[AIAA PAPER 92-4042] p 1035 A92-56861
Aerodynamic roughness measured in the field and simulated in a wind tunnel
[NASA-CR-4422] p 347 N92-19354
WIND SHEAR
Characteristics of thunderstorm-generated low altitude wind shear - A survey based on nationwide terminal Doppler weather radar testbed measurements p 45 A92-11378
Evaluation of a technique to quantify microburst windshear hazard potential to aircraft p 17 A92-11379
Stochastic prediction techniques for wind shear hazard assessment p 48 A92-11381
Windshear detection and avoidance - Airborne systems survey p 17 A92-11382
Optimal trajectories and guidance trajectories for aircraft flight through windshears p 27 A92-11383
Aircraft control under conditions of windshear p 27 A92-11384
Manually flown windshear recovery technique p 27 A92-11386
U-parameter design example - Robust flight control for wind-shear protection p 28 A92-11502
Saberliner flight test and results for forward looking detection and avoidance of airborne windshear p 98 A92-16656
Probabilistic reasoning for intelligent wind shear avoidance p 302 A92-21181
The response of a helicopter to windshear p 269 A92-21470
Forward-look wind-shear detection for microburst recovery p 378 A92-24408
Real-time decision aiding - Aircraft guidance for wind shear avoidance
[AIAA PAPER 92-0290] p 350 A92-25743
Airborne in situ computation of the wind shear hazard index
[AIAA PAPER 92-0291] p 351 A92-25744
Target pitch angle for the microburst escape maneuver
[AIAA PAPER 92-0730] p 379 A92-27082
Understanding and predicting microbursts p 407 A92-27953
Predicting summer microburst hazard from thunderstorm day statistics p 407 A92-27960
Effect of wind shear on airspeed during airplane landing approach p 481 A92-32242
Aircraft control for take-off in windshear p 660 A92-36990
Robust wind shear stochastic controller-estimator p 661 A92-39893
Control system optimization using genetic algorithms p 661 A92-39900
Shear progress --- wind shear handling and recognition technologies for aviation p 609 A92-40880
Windshear detection p 652 A92-40883
Aircraft spoiler effects under wind shear
[AIAA PAPER 92-2642] p 796 A92-45509
Thrust laws for microburst wind shear penetration p 873 A92-46750
Mathematical modeling of the effect of windshear on the dynamics of a landing aircraft p 875 A92-47784
Stochastic prediction techniques for wind shear hazard assessment p 1007 A92-50505
Aircraft longitudinal dynamics equations including wind shear effects p 977 A92-51946
Modified Doppler detects wind shear more reliably p 1015 A92-55099
Optimal recovery from microburst wind shear
[AIAA PAPER 92-4338] p 1078 A92-55327
Escape strategies for turboprop aircraft in microburst windshear p 1084 A92-56151
The 1990 Airport Surveillance Radar Wind Shear Processor (ASR-WSP) operational test at Orlando International Airport
[AD-A239852] p 18 N92-10019
The modelling of turbulence and downbursts for flight simulators
[UTIAS-339] p 161 N92-12373
Escape strategies for turboprop aircraft in a microburst windshear
[AD-A243090] p 264 N92-17217
Alert generation and cockpit presentation for an integrated microburst alerting system p 265 N92-17988
Cockpit display of hazardous weather information p 277 N92-17989
Target pitch angle for the microburst escape maneuver p 266 N92-17996
Optimal aircraft performance during microburst encounter p 266 N92-17999
On the relation between cumulus cloud lines and surface shear lines p 410 N92-19667
Recent results from data analysis of dynamic stall on wind turbine blades
[DE92-001200] p 505 N92-20245
Experimental evaluation of candidate graphical microburst alert displays
[NASA-CR-189633] p 735 N92-27424
The modelling of turbulence and downbursts for flight simulators
[ISBN-0-315-59945-6] p 749 N92-27645
On the optimization of windshear warning and guidance systems
[NLR-TP-90196-U] p 837 N92-29703
Spectrum modal analysis for the detection of low-altitude windshear with airborne Doppler radar
[NASA-CR-4457] p 953 N92-31549
Airport Surveillance Radar (ASR-9) wind shear processor: 1991 test at Orlando, Florida
[AD-A252246] p 1124 N92-32686
WIND TUNNEL APPARATUS
Study on transonic cascade performance by use of newly built facility p 136 A92-15328
Recent development of wind-tunnel test techniques at ONERA
[ONERA, TP NO. 1991-135] p 137 A92-16110
Initial operation of the UTA shock tunnel
[AIAA PAPER 92-0331] p 383 A92-25778
Productivity and quality in the Modane and Fauga wind tunnels - Prospects for the 90s
[ONERA, TP NO. 1991-203] p 383 A92-26360
Force measurement on rotating, ablating models using an air bearing balance p 483 A92-31174
Improved measurement of the dynamic loads acting on rotating parachutes p 702 A92-41236
Research on hypersonic wind tunnel methods in the 90's p 748 A92-43105
Wind tunnel test for a high speed propeller with coaxial contrarotation p 737 A92-43195
High enthalpy wind tunnel for erosion testing of advanced materials
[AIAA PAPER 92-3888] p 1094 A92-56729
Tohoku University low-turbulence wind tunnel
[AIAA PAPER 92-3913] p 1095 A92-56746
Flow quality studies of the NASA Lewis Research Center 8- by 6-foot supersonic/9- by 15-foot Low Speed Wind Tunnel
[AIAA PAPER 92-3916] p 1095 A92-56748
Performance evaluation of a transonic wind tunnel compressor
[AIAA PAPER 92-3927] p 1096 A92-56758
Computer programs for the calculation of dual sting pitch and roll angles required for an articulated sting to obtain angles of attack and sideslip on wind-tunnel models
[NASA-TM-104161] p 138 N92-12007
Susceptibility of a parallelogram type skin friction balance to rotational motion
[AD-A241348] p 139 N92-13078
Evaluation of electrolytic tilt sensors for measuring model angle of attack in wind tunnel tests
[NASA-TM-4315] p 297 N92-16283
Improvement of data processing system for gust wind tunnel data acquisition part: System conversion from off-line to on-line processing
[NAL-TM-611] p 285 N92-17756
Measurement of derivatives due to acceleration in heave and sideslip p 364 N92-18785
Study of the NAL's 0.1 x 0.1 m magnetic suspension and balance system
[NAL-TM-623] p 665 N92-25365
Development of a quiet supersonic wind tunnel with a cryogenic adaptive nozzle p 751 N92-27977
Estimation of cable-mounted model inertia characteristics for dynamic wind-tunnel test
[NAL-TM-641] p 722 N92-28152
Studies in general aviation aerodynamics
[NASA-CR-190431] p 827 N92-28511
Instrumentation requirements for laminar flow research in the NLR high speed wind tunnel HST
[NLR-TP-89158-U] p 887 N92-28669
Flow quality studies of the NASA Lewis Research Center 8- by 6-foot supersonic/9- by 15-foot low speed wind tunnel
[NASA-TM-105417] p 887 N92-28673
Upgrading the data processing section of the NAL Gust Wind Tunnel data processing system
[NAL-TM-635] p 888 N92-28833
The design of test-section inserts for higher speed aeroacoustic testing in the Ames 80- by 120-foot wind tunnel
[NASA-TM-103915] p 927 N92-28909
Study of optical techniques for the Ames unitary wind tunnels. Part 3: Angle of attack
[NASA-CR-190541] p 888 N92-29655
Pilot-pressure probe for measuring pressure in a hypersonic wind tunnel
[NASA-CASE-LAR-14232-1] p 1102 N92-34213

WIND TUNNEL CALIBRATION
Investigation of the diffuser flow quality in an icing research wind tunnel p 382 A92-24406
Relative accuracy of wind tunnel calibration speeds p 484 A92-32056
Calibration-related pseudo-Reynolds number trends in transonic wind tunnels p 882 A92-46780
High enthalpy wind tunnel for erosion testing of advanced materials
[AIAA PAPER 92-3888] p 1094 A92-56729
Calibration of the Naval Postgraduate School 3.5' x 5.0' academic wind tunnel
[AD-A240614] p 31 N92-11025
Results of measured temperature distribution on an adiabatic wing model with radiation thermometer
[NAL-TM-610] p 261 N92-17755
WIND TUNNEL DRIVES
Reactivation and upgrade of the NASA Ames 16-Inch Shock Tunnel - Status report
[AIAA PAPER 92-0327] p 383 A92-25774
An overview of the planned aerospace test facilities at Capua, Italy
[AIAA PAPER 92-3944] p 1097 A92-56773
Supersonic Throughflow Fan Test Facility at NASA. Lewis Research Center
[NASA-TP-3038] p 983 N92-31640
WIND TUNNEL MODELS
A simplified model for aerodynamic flows around streamlined models p 63 A92-13816
A review of rigid body response on sting supported models at high angles of incidence p 66 A92-15345
Recent development of wind-tunnel test techniques at ONERA
[ONERA, TP NO. 1991-135] p 137 A92-16110
Base pressure measurements on a cone at Mach numbers from M sub infinity = 5 to 7 p 173 A92-18770
Measurement of convective heat-transfer coefficients on a wind tunnel model by passive and stimulated infrared thermography p 291 A92-21450
Simulation of wind tunnel flowfields
[AIAA PAPER 92-0034] p 249 A92-22155
Wind-tunnel studies of F/A-18 tail buffet p 310 A92-24421
High pressure hypervelocity electrothermal wind tunnel performance study and subscale tests
[AIAA PAPER 92-0329] p 383 A92-25776
Model attitude measurements at NASA Langley Research Center
[AIAA PAPER 92-0763] p 398 A92-28226
Paint under pressure p 399 A92-28495
An experimental study of transonic flow of a gas past wedges p 424 A92-30153
Simulation and model reduction for the AFW program
[AIAA PAPER 92-2081] p 572 A92-35653
Further investigations of the aeroelastic behavior of the AFW wind-tunnel model using transonic small disturbance theory
[AIAA PAPER 92-2082] p 565 A92-35654
The multiple-function multi-input/multi-output digital controller system for the AFW wind tunnel model
[AIAA PAPER 92-2083] p 565 A92-35655
Flutter suppression for the Active Flexible Wing - Control system design and experimental validation
[AIAA PAPER 92-2097] p 566 A92-35666
A flutter suppression system using strain gages applied to Active Flexible Wing Technology - Design and test
[AIAA PAPER 92-2098] p 566 A92-35669
Azimuthal noise characteristics of contra-rotating propellers - Results of a wind tunnel model test p 693 A92-39066
Subcritical flow studies on two-dimensional external compression supersonic inlets p 713 A92-44518
High speed aerodynamics of upper surface blowing aircraft configurations
[AIAA PAPER 92-2611] p 793 A92-45485
Scale effects on the flow past the mated Space Shuttle configuration
[AIAA PAPER 92-2680] p 799 A92-45532
LDV measurements on a rectangular wing with a simulated glaze ice accretion
[AIAA PAPER 92-2690] p 800 A92-45537
On-line performance evaluation of multiloop digital control systems p 873 A92-46739
Conception of a UHB engine simulator for the essential characteristics of a true-scale engine --- ultrahigh bypass p 1090 A92-54322
Evaluation of electrolytic tilt sensors for wind tunnel model angle-of-attack (AOA) measurements p 1116 A92-54344
Research on aeroelastic tailoring at NAL p 1053 A92-56019
Measurements of blade flapping motion on a wind tunnel model p 1093 A92-56023
Demonstration of structural optimization applied to wind-tunnel model design p 1119 A92-56181
Laser-driven hypersonic air-breathing propulsion simulator
[AIAA PAPER 92-3922] p 1095 A92-56753
An approach for increasing aeroelastic divergence dynamic pressure of wind-tunnel models
[AIAA PAPER 92-4002] p 1099 A92-56825
Buffet test in the National Transonic Facility
[AIAA PAPER 92-4032] p 1100 A92-56854
Downwash measurements on a pitching canard-wing configuration
[AD-A239956] p 12 N92-10016
Model representation in the PANCOR wall interference assessment code
[NASA-TM-104152] p 31 N92-11022
The BCAC/IAR collaborative research program to investigate the sidewall boundary layer effects in the IAR/NRC 2-D High Reynolds Number Test Facility
[NRC-HSA-434] p 81 N92-11976
Computer programs for the calculation of dual sting pitch and roll angles required for an articulated sting to obtain angles of attack and sideslip on wind-tunnel models
[NASA-TM-104161] p 138 N92-12007
Steady and unsteady aerodynamics of a pitching straked wing model at high angles of attack p 87 N92-13024
Planform curvature effects on flutter characteristics of a wing with 56 deg leading-edge sweep and panel aspect ratio of 1.14
[NASA-TP-3116] p 115 N92-13054
Navier-Stokes calculation of transonic flow past the NTF 65 deg delta wing p 91 N92-13868
Preliminary investigation of the shock-boundary layer interaction in a simulated fan passage
[AD-A242656] p 185 N92-15045
Flutter suppression via piezoelectric actuation
[NASA-TM-104120] p 197 N92-15070
Surface pressure measurements on the wing of a wind tunnel model during steady rotation
[AD-A243047] p 260 N92-17281
Model incidence measurement using SAAB ELOPTOPOS system
[NLR-TP-89182-U] p 385 N92-18416
Analysis of unsteady force, pressure, and flow-visualization data for a pitching straked wing model at high angles of attack p 364 N92-18784
Wind tunnel investigation of a wing-propeller model performance degradation due to distributed upper-surface roughness and leading edge shape modification p 451 N92-21690
Further investigations of the aeroelastic behavior of the AFW wind-tunnel model using transonic small disturbance theory
[NASA-TM-107576] p 526 N92-22240
Flow field over the wing of a delta-wing fighter model with vortex control devices at Mach 0.6 to 1.2
[NASA-TM-4296] p 526 N92-22506
NACA0012 benchmark model experimental flutter results with unsteady pressure distributions
[NASA-TM-107581] p 526 N92-22507
The 12-foot pressure wind tunnel restoration project model support systems p 664 N92-25091
Multifunction tests of a frequency domain based flutter suppression system
[NASA-TM-107615] p 662 N92-25607
High-alpha vortex decoupling investigations on a chine forebody/Delta wing configuration at transonic Mach numbers
[NASA-CR-189642] p 715 N92-26651
A wind tunnel study of the pioneer remotely piloted vehicle
[AD-A247028] p 732 N92-27335
A pressure measurement method using Electronically Scanner Pressure sensors (ESP) installed in a gust wind tunnel
[NAL-TM-638] p 749 N92-27428
Propulsion simulator for magnetically suspended wind tunnel models p 750 N92-27801
Present status of the MIT/NASA Langley 6-inch MSBS p 750 N92-27802
Wind tunnel magnetic Suspension Systems at the University of Southampton, England p 751 N92-27804
Investigation of the aeroelastic stability of the AFW wind-tunnel model using CAP-TSD p 721 N92-27955
Estimation of cable-mounted model inertia characteristics for dynamic wind-tunnel test
[NAL-TM-641] p 722 N92-28152
Instrumentation requirements for laminar flow research in the NLR high speed wind tunnel HST
[NLR-TP-89158-U] p 887 N92-28669
LAH-main rotor model test at the DNW
[NLR-TP-90305-U] p 852 N92-28687
An analytical and experimental investigation of flutter suppression via piezoelectric actuation
[NASA-TM-107653] p 962 N92-31174
Time simulation of flutter with large stiffness changes
[NASA-TM-107650] p 963 N92-32111
The multiple-function multi-input/multi-output digital controller system for the AFW wind-tunnel model
[NASA-TM-107600] p 1060 N92-32536
Experimental study of a generic high-speed civil transport
[NASA-TM-4382] p 1040 N92-33631
Effect of afterbody geometry on aerodynamic characteristics of isolated nonaxisymmetric afterbodies at transonic Mach numbers
[NASA-TP-3236] p 1041 N92-33706
WIND TUNNEL NOZZLES
Flow analysis and design of three-dimensional wind tunnel contractions p 5 A92-11067
A quiet-flow Ludwieg tube for experimental study of high speed boundary layer transition
[AIAA PAPER 91-5026] p 207 A92-17819
Aerodynamic design of axisymmetric hypersonic wind-tunnel nozzles using least-squares/parabolized Navier-Stokes procedure
[AIAA PAPER 92-0332] p 322 A92-25779
Experimental study of an adjustable plane supersonic diffusor p 426 A92-30173
Hypersonic aerodynamic/aerothermodynamic testing capabilities at Langley Research Center
[AIAA PAPER 92-3937] p 1096 A92-56767
CAN-DO, CFD-based Aerodynamic Nozzle Design and Optimization program for supersonic/hypersonic wind tunnels
[AIAA PAPER 92-4009] p 1033 A92-56832
SIMOUN and Scirocco wind tunnel nozzle viscous flow study p 208 N92-14999
Effect of collector configuration on test section turbulence levels in an open-jet wind tunnel
[NASA-TM-4333] p 750 N92-27670
WIND TUNNEL STABILITY TESTS
A wing rock model for the F-14A aircraft
[AD-A243109] p 275 N92-17300
A wind tunnel study of the pioneer remotely piloted vehicle
[AD-A247028] p 732 N92-27335
WIND TUNNEL TESTS
Effect of antiicer on propeller performance p 25 A92-10969
Correlation of separation shock motion with pressure fluctuations in the incoming boundary layer p 5 A92-11061
Topology of steady flows of low viscosity fluids p 38 A92-11219
On-line adaptive control of unstable aircraft wing flutter p 27 A92-11374
Comparative studies of flow around a wing profile in two wind tunnels p 7 A92-12170
Prospects of turbulence research by means of testing bodies in motion p 30 A92-12194
Automation of the measurement process in the N2 wind tunnel with the SPITA N-3 system p 30 A92-12347
The dynamic character of the wake of an axisymmetric body at an angle of attack
[AIAA PAPER 91-3268] p 8 A92-12741
Two-dimensional adaptive-wall tests in the NASA Ames two- by two-foot transonic wind tunnel p 30 A92-13201
Experimental investigation on the effect of crescent planform on lift and drag p 9 A92-13206
Wind-tunnel and flight tests of a delta-wing remotely piloted vehicle p 21 A92-13208
Wall interference assessment/correction for transonic airfoil data p 30 A92-13214
LH wind tunnel testing - Key to advanced aerodynamic design p 104 A92-14331
Results from a test of a 2/3-scale V-22 rotor and wing in the 40- by 80-Foot Wind Tunnel p 104 A92-14332
Full-scale investigation of aerodynamic interactions between a rotor and fuselage p 105 A92-14361
Helicopter local blade circulation calculations for a model rotor in forward flight using laser velocimeter measurements p 65 A92-14362
Recent rotorcraft aeroelastic testing in the Langley Transonic Dynamics Tunnel p 136 A92-14377
Acoustic predictions using measured pressures from a model rotor in the DNW p 165 A92-14385
Computation of the BVI noise for the BO105 Model Rotor in forward flight and comparison with wind tunnel tests p 165 A92-14386
Structural optimization and Mach scale test validation of a low vibration rotor p 107 A92-14395
Comparison of theory and experiment for nonlinear flutter and stall response of a helicopter blade p 65 A92-14428
A review of rigid body response on sting supported models at high angles of incidence p 66 A92-15345
Realization of a large-scale turbulence field in a small wind tunnel p 67 A92-15487
MiG-29 prototype and development flight tests - General overview and high angle of attack investigation p 113 A92-16064

Recent development of wind-tunnel test techniques at ONERA
[ONERA, TP NO. 1991-135] p 137 A92-16110
Detailed analysis of wing-nacelle interaction for commercial transport aircraft
[ONERA, TP NO. 1991-152] p 77 A92-16122
The application of high pressure ejectors to reaction control systems p 128 A92-16666
Enhanced mixing of supersonic jets p 80 A92-17195
Euler flow analysis of turbine powered simulator and fanjet engine p 80 A92-17196
Engine air inlet and de-icing system - At -30 C in the icing tunnel of NRC Ottawa p 92 A92-17252
Numerical study on using sulfur hexafluoride as a wind tunnel test gas p 216 A92-18373
Broadband shock-associated noise from supersonic jets in flight p 235 A92-18683
Model oscillations at high angle of attack in a low speed wind tunnel test
[IAF PAPER ST-91-001] p 175 A92-20649
Control system design for the free drop test of external stores in a wind tunnel
[IAF PAPER ST-91-002] p 207 A92-20650
Measurement of convective heat-transfer coefficients on a wind tunnel model by passive and stimulated infrared thermography p 291 A92-21450
The experimental approach to the LEBU on turbulent drag reduction p 243 A92-21469
X-29 forebody jet blowing
[AIAA PAPER 92-0017] p 247 A92-22139
Wall interference calculation in a transonic test section including simulation of discrete slots
[AIAA PAPER 92-0032] p 249 A92-22153
Simulation of wind tunnel flowfields
[AIAA PAPER 92-0034] p 249 A92-22155
Study of theoretical and wind tunnel results on flight performance degradation due to leading edge rime ice accretion
[AIAA PAPER 92-0038] p 262 A92-22158
Minimum induced drag of a wing in a circular open wind tunnel p 251 A92-22521
A study of flow past bodies of revolution with a Riabushinskii generatrix p 252 A92-23502
Dynamics of an aircraft-towed body during release
[AIAA PAPER 92-0130] p 295 A92-23750
A theoretical analysis utilizing the LEWICE and EPPLER numerical analyses to predict flight performance degradation under icing conditions
[AIAA PAPER 92-0134] p 263 A92-23754
Experimental study of pylon geometries for transport aircraft
[AIAA PAPER 92-0153] p 271 A92-23768
One view of experimental aerodynamics
[AIAA PAPER 92-0160] p 254 A92-23775
What we need in experimental aerodynamics - One engineering educator's view
[AIAA PAPER 92-0161] p 241 A92-23776
Measurements of lateral aerodynamics characteristics of forebodies at high angle of attack in subsonic and transonic flows
[AIAA PAPER 92-0174] p 255 A92-23785
Flight test validation of tow target trajectory predictions
[AIAA PAPER 92-0209] p 271 A92-23814
Investigation of the diffuser flow quality in an icing research wind tunnel p 382 A92-24406
Wind-tunnel studies of F/A-18 tail buffet p 310 A92-24421
Flow over an all-body hypersonic aircraft - Experiment and computation p 310 A92-24651
The measurement of flutter derivatives using mechanical admittance p 393 A92-25014
The LDV measurement of three-component velocity of complex vortex flow in the wind tunnel p 393 A92-25109
New method for boundary layer thickness control on ground plate in wind tunnel p 383 A92-25110
Application of the wall pressure method to wall interference corrections for model tests at high angle of attack in high speed wind tunnel p 315 A92-25134
Aerodynamic applications of pressure-sensitive paint
[AIAA PAPER 92-0264] p 394 A92-25720
Pitch-up motions of delta wings
[AIAA PAPER 92-0278] p 318 A92-25732
Mechanisms resulting in accreted ice roughness
[AIAA PAPER 92-0297] p 351 A92-25750
Flow visualization image analysis of high-rate roll experiments on a delta wing
[AIAA PAPER 92-0317] p 321 A92-25764
Finite wing aerodynamics with simulated glaze ice
[AIAA PAPER 92-0414] p 325 A92-26265
Theoretical and experimental studies of helicopter rotor/fuselage interaction
[ONERA, TP NO. 1991-198] p 329 A92-26357
Productivity and quality in the Modane and Fauga wind tunnels - Prospects for the 90s
[ONERA, TP NO. 1991-203] p 383 A92-26360
Wall pressure wavenumber-frequency spectrum beneath a turbulent boundary layer measured with transducer arrays calibrated with an acoustical method
[ONERA, TP NO. 1991-212] p 329 A92-26364
Tests of models equipped with a turbofan powered simulator in the ONERA F1 low-speed pressurized wind tunnel
[ONERA, TP NO. 1991-219] p 383 A92-26371
Flow about cylinders with helical surface protrusions
[AIAA PAPER 92-0540] p 332 A92-26957
Experiments to evaluate hot-jet simulation capabilities in Cryogenic Wind-Tunnel testing
[AIAA PAPER 92-0567] p 384 A92-26975
Prediction of the pressure loss coefficient of wind tunnel turbulence reducing screens
[AIAA PAPER 92-0568] p 384 A92-26976
Experimental results on a wall interference correction method with interface measurements
[AIAA PAPER 92-0570] p 333 A92-26978
Results of an icing test on a NACA 0012 airfoil in the NASA Lewis Icing Research Tunnel
[AIAA PAPER 92-0647] p 334 A92-27021
Ground facility interference on aircraft configurations with separated flow
[AIAA PAPER 92-0673] p 384 A92-27042
On hypersonic boundary-layer stability
[AIAA PAPER 92-0737] p 335 A92-27088
A study of active flutter suppression for a wing/store system p 379 A92-27826
An approach to the low-speed longitudinal aerodynamic characteristics of the joined wing configuration p 339 A92-27909
Experimental investigation of the perpendicular rotor blade-vortex interaction at transonic speeds p 340 A92-28047
Model attitude measurements at NASA Langley Research Center
[AIAA PAPER 92-0763] p 398 A92-28226
Paint under pressure p 399 A92-28495
Computational fluid dynamics and aircraft design p 457 A92-28875
Control of the development of boundary layer disturbances p 423 A92-30126
Computations of a transonic flow about an airfoil in a wind tunnel with porous walls p 423 A92-30128
An asymptotic transonic theory and optimal porosity of wind tunnel walls at M greater than about 1 p 425 A92-30159
A study of the base pressure behind circular steps p 426 A92-30196
Investigation of the effect of an ultrasonic acoustic field on boundary layer separation on an airfoil p 511 A92-30205
Effect of the longitudinal and transverse riblets of a flat plate on laminar-to-turbulent transition p 428 A92-30210
An electromagnetic suspension system for aerodynamic studies p 483 A92-30409
The Bauer-Garabedian-Korn airfoil test in a two-dimensional wind tunnel p 429 A92-30532
Approximate analysis of aerodynamic heating at hypersonic speed p 430 A92-30551
Study on effectiveness of the front wedge shape in hypersonic flow p 430 A92-30552
Experimental and computational investigation of wind tunnel effects on airfoil flow fields
[AIAA PAPER 92-0672] p 431 A92-30624
Two- and three-dimensional effects in the supersonic mixing layer p 432 A92-31165
Force measurement on rotating, ablating models using an air bearing balance p 483 A92-31174
Experimental and numerical investigation of anti-icing phenomena on a NACA 0012 assembly
[AIAA PAPER 92-0531] p 459 A92-31669
Testing capabilities at AEDC for development of hypersonic vehicles
[AIAA PAPER 91-5027] p 483 A92-31686
Applications of hot-film anemometers in hypersonic shear layers
[AIAA PAPER 91-5028] p 436 A92-31687
Lift characteristics of an infinite-span cylindrical wing of a thick symmetric profile at low subsonic velocities p 440 A92-31897
Structure of a boundary layer on the lower surface of a wing in flight and in a wind tunnel p 440 A92-31899
Relative accuracy of wind tunnel calibration speeds p 484 A92-32056
Computational study of incipient leading-edge separation on a supersonic delta wing p 442 A92-32237
Heat transfer effects on aerodynamics and implications for wind-tunnel tests p 497 A92-32240
Experimental study of a low Reynolds number tandem airfoil configuration p 442 A92-32241
The Second Goldstein Lecture: Modern developments in fluid dynamics - An addendum p 442 A92-32323
Low-speed cruise aerodynamics of the stopped rotor/disk rotorcraft concept
[AIAA PAPER 92-1067] p 517 A92-33240
A demonstration of passive blade twist control using extension-twist coupling
[AIAA PAPER 92-2468] p 539 A92-34358
Analytical aeroelastic stability considerations and conversion loads for an XV-15 tilt-rotor in a wind tunnel simulation
[AIAA PAPER 92-2258] p 540 A92-34413
Chaotic and nonlinear dynamic response of aerosurfaces with structural nonlinearities
[AIAA PAPER 92-2547] p 518 A92-34517
Application of analytical and design tools for fighter wing aeroelastic tailoring
[AIAA PAPER 92-2373] p 542 A92-34543
Fully integrated aerodynamic/dynamic optimization of helicopter rotor blades
[AIAA PAPER 92-2374] p 542 A92-34544
Aerobrake aerothermodynamic environment predictions in support of the Aeroassist Flight Experiment
[TABES PAPER 91-278] p 519 A92-34683
On-line analysis capabilities developed to support the AFW wind-tunnel tests
[AIAA PAPER 92-2084] p 572 A92-35656
Flutter suppression digital control law design and testing for the AFW wind tunnel model
[AIAA PAPER 92-2095] p 566 A92-35668
Digital time series analysis for flutter test data
[AIAA PAPER 92-2103] p 589 A92-35674
Transonic wind tunnel investigation of limit cycle oscillations on fighter type wings - Update
[AIAA PAPER 92-2125] p 572 A92-35692
EUROFAR airframe aerodynamic design p 546 A92-35750
Calculation of pitch-link loads in deep stall using state-of-the-art methodology p 520 A92-35753
LAH main rotor model test at the DNW p 547 A92-35771
Bearingless rotor aeromechanical stability measurements and correlations using nonlinear aerodynamics p 547 A92-35772
Design and manufacturing of torsional flexible blade models p 547 A92-35780
Some aerodynamic mechanisms of impulsive noise during blade-vortex-interaction p 604 A92-35782
Measurements of a rotor flowfield and the effects on a fuselage in forward flight p 521 A92-35787
Experimental design of a supersonic shock wave/vortex interaction at Mach 3 p 521 A92-35988
Change of flow about an elongated rectangular cylinder in a range of Reynolds numbers of 200 to 0.7 x 10 exp 4 p 522 A92-35997
A comparison of transition Reynolds number measured in a wind tunnel and in flight p 522 A92-36026
Structure of the separated flow region in a dihedral corner in front of an obstacle in supersonic flow p 524 A92-36420
Experimental investigation of supersonic flow over two cavities in tandem p 610 A92-36830
Multifractal analysis of a lobed mixer flowfield utilizing the proper orthogonal decomposition p 611 A92-36840
Wind tunnel study of aerodynamic characteristics of base combustion p 666 A92-36967
Experimental study of a two-dimensional scramjet inset, M(freestream) = 10.1-25.1 p 611 A92-36974
Effect of controlled longitudinal vortex arrays on the development of a turbulent boundary layer p 614 A92-38856
Flow regimes of the cove regions between a slat and wing and between a wing and flap of a multielement airfoil p 614 A92-38858
Investigation on effects on enhancing lift by acoustic excitation p 693 A92-38923
Azimuthal noise characteristics of contra-rotating propellers - Results of a wind tunnel model test p 693 A92-39066
Scale model test of an isolated turbofan nacelle with riblets
[SAE PAPER 912128] p 618 A92-39975
Some practical aspects of viscous drag reduction concepts
[SAE PAPER 912129] p 618 A92-39976
Vortical flow simulation by the solution of the Navier-Stokes equations p 620 A92-40104
Scrutinizing k-epsilon EVM and ASM by means of LES and wind tunnel for flowfield around cube --- Eddy Viscosity Model, Algebraic Stress Model, Large Eddy Simulation p 621 A92-40119
Design and development of a compressible dynamic stall facility p 747 A92-41215

Drag reduction of bluff bodies through momentum injection p 702 A92-41231
Effect of tunnel walls on vortex breakdown location over delta wings p 703 A92-41279
Aero-optical testing in the NSWC Hypervelocity Tunnel No. 9
[AIAA PAPER 92-2797] p 747 A92-41336
Some problems on the sidewall interference in two-dimensional subsonic and transonic wind tunnel testing p 747 A92-41929
Aerodynamic drag of a cylinder in two-phase flow p 707 A92-42735
Calculation of three-dimensional turbulent flow in wind tunnel entry section p 708 A92-43055
Hypersonic testing technology of HOPE (H-II orbiting plane) p 747 A92-43096
Thermal measurement test in a shock wind tunnel p 748 A92-43104
Research on hypersonic wind tunnel methods in the 90's p 748 A92-43105
ACT wind tunnel experiment on gust load alleviation. II - Wind tunnel test with active support facility p 745 A92-43135
Recent airfoil tests in NAL 2D high Reynolds number wind tunnel p 748 A92-43171
Wind tunnel tests on the motion of a spaceplane simulation for cable mount p 752 A92-43192
Wind tunnel test for a high speed propeller with coaxial contrarotation p 737 A92-43195
Wing test at the cryogenic wind tunnel of the National Defense Academy p 749 A92-43199
BGK airfoil oil flow test in a two-dimensional transonic wind tunnel p 711 A92-43201
Wind tunnel test of a supersonic air intake p 711 A92-43205
Motion estimation for cable-mount dynamic wind-tunnel test p 749 A92-43210
Estimation of spaceplane longitudinal stability and control derivatives from dynamic wind tunnel test p 752 A92-43211
Estimation of spaceplane model inertia characteristics p 752 A92-43212
On the characteristics of servo actuators attached to a model spaceplane for dynamic wind-tunnel test p 762 A92-43213
Aerodynamic characteristics of a hypersonic aircraft p 711 A92-43226
Low-speed wind tunnel testing of the lateral control force for the upper rudder surface of a joined-wing airfoil p 711 A92-43228
Low-speed wind tunnel testing of a joined-wing airfoil p 711 A92-43229
Aerodynamic characteristics of a high-speed composite airfoil p 712 A92-43231
On the measurement of subsonic flow around an appended body of revolution at cryogenic conditions in the NTF p 880 A92-45265
Large-scale wind tunnel studies of a jet-engined powered ejector-lift STOVL aircraft p 842 A92-45313
Estimation of spaceplane lateral-directional stability and control derivatives from dynamic wind tunnel test
[SAE PAPER 911979] p 872 A92-45384
Spaceplane longitudinal aerodynamic parameter estimation by cable-mount dynamic wind-tunnel test
[SAE PAPER 911980] p 788 A92-45385
Experimental studies on aerodynamic characteristics of SSTO vehicle at low subsonic speeds
[SAE PAPER 911981] p 788 A92-45386
Wind tunnel investigation of an improved upper surface blown flap transport semi-span model
[SAE PAPER 911993] p 789 A92-45395
Laminar separation bubbles and airfoil design at low Reynolds numbers
[AIAA PAPER 92-2735] p 797 A92-45515
Analysis of a pneumatic forebody flow control concept about a full aircraft geometry
[AIAA PAPER 92-2678] p 799 A92-45530
Experimental development of spanwise vortex models with streamwise decay due to wall interaction
[AIAA PAPER 92-2688] p 799 A92-45535
Alleviation of side force on tangent-ogive forebodies using passive porosity
[AIAA PAPER 92-2711] p 802 A92-45552
An experimental investigation of the effect of leading-edge extensions on directional stability and the effectiveness of forebody nose strakes
[AIAA PAPER 92-2715] p 802 A92-45554
Forebody vortex control for suppressing wing rock on a highly-swept wing configuration
[AIAA PAPER 92-2716] p 803 A92-45555
Dynamic LEX/forebody vortex interaction effects
[AIAA PAPER 92-2732] p 804 A92-45566
Separation control on high Reynolds number multi-element airfoils
[AIAA PAPER 92-2636] p 806 A92-45575
Exploratory investigation of a spanwise blowing concept for tip-stall control on cranked-arrow wings
[AIAA PAPER 92-2637] p 806 A92-45576
Forebody flow control on a full-scale F/A-18 aircraft
[AIAA PAPER 92-2674] p 806 A92-45583
Full-scale high angle-of-attack tests of an F/A-18
[AIAA PAPER 92-2676] p 806 A92-45584
Separated high enthalpy dissociated laminar hypersonic flow behind a step - Pressure measurements p 809 A92-45858
Joint computational/experimental aerodynamics research on a hypersonic vehicle. I - Experimental results p 812 A92-46890
Two-stream, supersonic, wake flowfield behind a thick base. I - General features p 813 A92-46895
New hypersonic test methods developed at ONERA - The R5 and F4 wind tunnels
[ONERA, TP NO. 1992-39] p 882 A92-48600
Comparative investigation of multiplane thrust vectoring nozzles
[AIAA PAPER 92-3263] p 864 A92-48858
Full field flow visualization and computer-aided velocity measurements in a bank of cylinders in a wind tunnel p 991 A92-50040
Turbulent diffusion flame properties behind a backward-facing step p 985 A92-50255
Effect of wing tip vortices on a trailing aircraft p 935 A92-50303
The application of a theoretical blade sailing model to predict the behaviour of articulated helicopter rotors p 960 A92-52849
The wall interference correction and test data processing methods for airfoil wind tunnel test with endplates p 942 A92-53087
The effect of afterbody devices on drag reduction p 942 A92-53097
Investigation of the tail buffeting of the C-101 p 942 A92-53253
Discussion on sidewall suction in two-dimensional wind tunnel p 997 A92-53263
Rarefied gas numerical wind tunnel p 1017 A92-53552
A preliminary study of a supersonic wind tunnel for a ram jet test facility p 1089 A92-53564
Mach 3 wind tunnel test of mixed compression supersonic inlet
[AIAA PAPER 92-3625] p 1021 A92-54092
Structure of crossing-shock wave/turbulent boundary-layer interactions
[AIAA PAPER 92-3670] p 1022 A92-54113
Wind tunnel performance results of swirl recovery vanes as tested with an advanced high speed propeller
[AIAA PAPER 92-3770] p 1068 A92-54159
Aerodynamic assessment of an optical pressure measurement system (OPMS) by comparison with conventional pressure measurements in a high speed wind tunnel p 1114 A92-54304
Notes on the use of fusible temperature indicators to bound the temperature of hot graphite in the NAVSWC hypervelocity wind tunnel facility p 1090 A92-54315
Application of a wall pressure method in a wind tunnel test section with adjustable longitudinal slots p 1091 A92-54336
The wind tunnel test 'system' of 1995 - Cost effective experimentation through a fusion of related technologies p 1091 A92-54342
Evaluation of electrolytic tilt sensors for wind tunnel model angle-of-attack (AOA) measurements p 1116 A92-54344
Instrumentation key to NASP combustor tests p 1092 A92-55100
Aerodynamic parameters of the X-31 drop model estimated from flight-data at high angles of attack
[AIAA PAPER 92-4357] p 1080 A92-55343
Aerodynamic analysis of the Pioneer unmanned air vehicle
[AIAA PAPER 92-4635] p 1027 A92-55382
Supersonic wind tunnel test of airintake/airframe integrated models p 1028 A92-56006
A hypersonic wind tunnel test of a mixed-compression air inlet model p 1028 A92-56007
Wind tunnel test of M = 2.5 mixed compression inlet p 1028 A92-56008
On the structure of unsteady shock induced separation of the transonic airfoil in the NAL two-dimensional wind tunnel p 1029 A92-56010
On improvements of three-dimensional position measuring system for dynamic wind tunnel testing p 1093 A92-56012
Flutter analysis and wind tunnel test with respect to a low-aspect-ratio wing with free-rotational control surface p 1052 A92-56014
Propeller-nacelle whirl flutter analysis and wind tunnel test p 1052 A92-56016
Whirl flutter analysis and application to aircraft design p 1053 A92-56017
Analysis and wind tunnel test of low aspect wing gust load alleviation p 1053 A92-56020
High subsonic wind tunnel test of a two-dimensional hybrid-laminar-flow-control airfoil with slotted surface p 1029 A92-56045
Design and wind tunnel test of low-Reynolds-number airfoil p 1029 A92-56047
On the effect of canards on NAL spaceplane model (0 order) in low speed area p 1030 A92-56052
Low-speed wind tunnel testing for the high-speed propeller at high shaft angle of attack p 1030 A92-56054
Helicopter rotor testing using scaled model p 1093 A92-56076
A low speed wind tunnel investigation of a joined-wing aircraft with an overhanging fin p 1030 A92-56078
Aerodynamic model identification of a spaceplane model from a cable-mount dynamic wind-tunnel test p 1093 A92-56114
Evaluation of a IMU with optical fiber gyros in dynamic windtunnel tests p 1104 A92-56121
Small two-dimensional surface excrescences on aircraft wings approaching separation p 1031 A92-56170
BVI impulsive noise reduction by higher harmonic pitch control - Results of a scaled model rotor experiment in the DNW p 1136 A92-56344
Correlation of flight, tunnel and prediction data on a helicopter main rotor p 1059 A92-56350
High enthalpy wind tunnel for erosion testing of advanced materials
[AIAA PAPER 92-3888] p 1094 A92-56729
Supersonic and hypersonic quiet tunnel technology at NASA Langley
[AIAA PAPER 92-3908] p 1094 A92-56743
The ASU Transition Research Facility
[AIAA PAPER 92-3910] p 1094 A92-56744
Development and validation of a freejet technique for inlet-engine compatibility testing
[AIAA PAPER 92-3921] p 1033 A92-56752
Laser-driven hypersonic air-breathing propulsion simulator
[AIAA PAPER 92-3922] p 1095 A92-56753
Roles of wind tunnel tests and CFD analyses in the design of energy-efficient SST
[AIAA PAPER 92-3923] p 1133 A92-56754
Blockage correction in three-dimensional wind tunnel testing based on the wall signature method
[AIAA PAPER 92-3925] p 1095 A92-56756
Wind tunnel blockage effects on slender wings undergoing large amplitude motions
[AIAA PAPER 92-3926] p 1096 A92-56757
Control of large cryogenic tunnels
[AIAA PAPER 92-3930] p 1096 A92-56761
Hypersonic aerodynamic/aerothermodynamic testing capabilities at Langley Research Center
[AIAA PAPER 92-3937] p 1096 A92-56767
Performance data of the new free-piston shock tunnel at GALCIT
[AIAA PAPER 92-3943] p 1033 A92-56776
TSNIIMASH capabilities for aerogasdynamical and thermal testing of hypersonic vehicles
[AIAA PAPER 92-3962] p 1097 A92-56789
The SR3 low density wind tunnel - Facility capabilities and research development
[AIAA PAPER 92-3972] p 1098 A92-56798
Comparison of recent results from different wind tunnel facilities along with comparisons of measured flight results and wind tunnel based predictions
[AIAA PAPER 92-3985] p 1060 A92-56809
High-lift testing at high Reynolds numbers
[AIAA PAPER 92-3986] p 1033 A92-56810
Application of electronically scanned pressure measurement system for engine simulation tests in the German-Dutch Wind Tunnel
[AIAA PAPER 92-4003] p 1122 A92-56826
Computational and numerical analysis of hypersonic nozzle flows with comparisons to wind tunnel calibration data
[AIAA PAPER 92-4011] p 1033 A92-56834
Hypersonic wind tunnel nozzle study
[AIAA PAPER 92-4012] p 1033 A92-56835
Numerical prediction of the flow characteristics in an arc wind tunnel
[AIAA PAPER 92-4016] p 1100 A92-56838
Hypersonic shock tunnel testing for undergraduate laboratory instruction
[AIAA PAPER 92-4021] p 1100 A92-56843
Laboratory simulation of aerothermodynamic phenomena - A review
[AIAA PAPER 92-4025] p 1104 A92-56847
Buffet test in the National Transonic Facility
[AIAA PAPER 92-4032] p 1100 A92-56854
Effects of external influences in subsonic delta wing vortices
[AIAA PAPER 92-4033] p 1034 A92-56855

Mass flux similarity for slotted transonic-wind-tunnel walls
[NASA-TM-4281] p 11 N92-10006
Dual strain gage balance system for measuring light loads
[NASA-CASE-LAR-14419-1] p 42 N92-10185
Experimental study of an independently deflected wingtip mounted on a semispan wing
[NASA-TM-102842] p 13 N92-10983
Subsonic wind tunnel testing handbook
[AD-A240263] p 13 N92-10986
Application of infrared thermography to thermal flux measurement in wind tunnels
[AAAF-NT-89-12] p 31 N92-11020
Further developments relating to the NASA Langley Research Center 13-inch magnetic suspension and balance system
[NASA-CR-188995] p 31 N92-11023
Thermographic gust wind tunnel measurements
[ONERA-RF-31/3409-PY] p 81 N92-11972
Wind tunnel tests on A4, A4.1, and A4.2 2-D airfoil models in the IAR 5-ft. wind tunnel: Boeing Commercial Airplane Company and Institute for Aerospace Research collaborative work program
[NRC-IAR-C3] p 81 N92-11975
The BCAC/IAR collaborative research program to investigate the sidewall boundary layer effects in the IAR/NRC 2-D High Reynolds Number Test Facility
[NRC-HSA-434] p 81 N92-11976
Nonstationary flight aerodynamics in a turbulent environment
[ETN-91-90102] p 82 N92-11980
Control aspects of the transition from transversal to transonic flow, step effects
[ETN-91-90106] p 82 N92-11981
Phenomenological modeling of the wake produced by a straight two dimensional base in subsonic flow
[REPT-90/59] p 82 N92-11982
Study of interactions on anemoclinometric sensors
[REPT-90/30] p 138 N92-12006
CARS temperature measurements in a hypersonic propulsion test facility p 140 N92-12049
Wall interference calculation in a transonic wind tunnel with discrete slots p 83 N92-12995
An experimental investigation of the effect of fineness ratio on lateral force on a pointed slender body of revolution p 86 N92-13015
Control of forebody vortices by suction at the nose of the RAE high incidence research model
p 87 N92-13022
An experimental investigation of vortex flaps on a canard combat-aircraft configuration p 87 N92-13023
Steady and unsteady aerodynamics of a pitching straked wing model at high angles of attack p 87 N92-13024
Some characteristics and effects of the F/A-18 LEX vortices p 88 N92-13025
Multiple roll attractors of a delta wing at high incidence p 88 N92-13026
Planform curvature effects on flutter characteristics of a wing with 56 deg leading-edge sweep and panel aspect ratio of 1.14
[NASA-TP-3116] p 115 N92-13054
An evaluation of preliminary Doppler global velocimetry measurements p 90 N92-13849
Navier-Stokes calculation of transonic flow past the NTF 65 deg delta wing p 91 N92-13868
International aviation (selected articles)
[AD-A241119] p 170 N92-13993
Wind tunnel investigation of vortex flows on F/A-18 configuration at subsonic through transonic speed
[NASA-TP-3111] p 179 N92-14968
FALKE and COBRA technology development in aerodynamics and aerothermodynamics
p 183 N92-15017
Preliminary investigation of the shock-boundary layer interaction in a simulated fan passage
[AD-A242656] p 185 N92-15045
Results of an Icing test on a NACA 0012 airfoil in the NASA Lewis Icing Research Tunnel
[NASA-TM-105374] p 185 N92-15051
Flutter suppression via piezoelectric actuation
[NASA-TM-104120] p 197 N92-15070
A wall interference assessment/correction system
[NASA-CR-189785] p 259 N92-15974
Evaluation of electrolytic tilt sensors for measuring model angle of attack in wind tunnel tests
[NASA-TM-4315] p 297 N92-16283
Results of the space shuttle vehicle ascent air data system probe calibration test using a 0.07-scale external tank forebody model (68T) in the AEDC 16-foot transonic wind tunnel (IA-310), volume 2
[NASA-CR-167697] p 286 N92-17214
Surface pressure measurements on the wing of a wind tunnel model during steady rotation
[AD-A243047] p 260 N92-17281
Stagnation and dynamic pressure limits for the S1 wind tunnel
[AD-A242989] p 285 N92-17297
Aerodynamic development of the X-31 aircraft for the high angle of attack region
[MBB-FE211-S-PUB-452] p 275 N92-17313
Flow visualization and wake analysis for standard and modified configurations of the AN/ALQ-78 antenna pod
[AD-A243552] p 260 N92-17339
A preliminary flight test on a basic performance of the flight research airplane Do 228: Velocity vs glide path angle
[NAL-TM-613] p 359 N92-18482
Parametric effects of some aircraft components on high-alpha aerodynamic characteristics
p 364 N92-18782
Characterization of unsteady aerodynamic phenomena at high angles p 364 N92-18787
Scale model measurements of fin buffet due to vortex bursting on F/A-18 p 365 N92-18788
X-31: Discussion of steady state and rotary derivatives
p 365 N92-18789
Use of stepwise regression techniques and kinematic compatibility for the analysis of EAP flight data
p 365 N92-18790
Dynamic wind tunnel tests on control of forebody vortices with suction p 380 N92-18793
Thermal/structural analysis of a transpiration cooled nozzle
[NASA-TM-104184] p 401 N92-18877
An experimental study of a sting-mounted circulation control wing
[AD-A243912] p 346 N92-18895
Aerodynamic roughness measured in the field and simulated in a wind tunnel
[NASA-CR-4422] p 347 N92-19354
Experimental studies of vortex flaps and vortex plates. Part 1: 0.53 m span 60 deg delta wing
[CRANFIELD-AERO-9113-PT-1] p 349 N92-19679
Influence of airfoil geometry on delta wing leading-edge vortices and vortex-induced aerodynamics at supersonic speeds
[NASA-TP-3105] p 350 N92-20038
A laser velocimeter investigation of the normal shockwave boundary layer interaction
p 500 N92-20485
Evaluation of NACA0012 airfoil test results in the NAL two-dimensional transonic wind tunnel
[NAL-TR-1109T] p 445 N92-21287
A historical overview of tiltrotor aeroelastic research at Langley Research Center
[NASA-TM-107578] p 502 N92-21460
Wind tunnel investigation of a wing-propeller model performance degradation due to distributed upper-surface roughness and leading edge shape modification
p 451 N92-21690
Preparation of the ice certification of the Dornier 328 regional airliner by numerical simulation and by ground test p 451 N92-21693
Measurement of the flow distribution over the flight deck of an aircraft carrier p 504 N92-21955
The NASA Langley laminar-flow-control experiment on a swept, supercritical airfoil: Evaluation of initial perforated configuration
[NASA-TM-4309] p 525 N92-22196
Separation of relaminarised boundary layers
[CUED/A-AERO/TR-16] p 592 N92-22209
Experimental study of a generic high-speed civil transport: Tabulated data
[NASA-TM-104216] p 525 N92-22232
Flow field over the wing of a delta-wing fighter model with vortex control devices at Mach 0.6 to 1.2
[NASA-TM-4296] p 526 N92-22506
NACA0012 benchmark model experimental flutter results with unsteady pressure distributions
[NASA-TM-107581] p 526 N92-22507
Wing force and surface pressure data from a hover test of a 0.658-scale V-22 rotor and wing
[NASA-TM-102244] p 550 N92-22864
Static performance of a cruciform nozzle with multiaxis thrust-vectoring and reverse-thrust capabilities
[NASA-TP-3188] p 527 N92-23095
Survey of experimental techniques for performance prediction p 552 N92-23954
A study of transonic aerodynamic analysis methods for use with a hypersonic aircraft synthesis code
[NASA-CR-189854] p 625 N92-24803
Wind-tunnel investigation of aerodynamic and stability characteristics of a forward swept wing X-29 model
p 627 N92-24862
Propeller noise research at NRC p 628 N92-24863
Flowfield in the vicinity of the F/A-18 vertical fin at high-angle-of-attack p 628 N92-24865
Effect of blade planform variation on the forward-flight performance of small-scale rotors
[NASA-TM-4345] p 630 N92-24885
Longitudinal and lateral-directional aerodynamic characteristics of a wing-cone configuration at Mach numbers from 2.5 to 4.5
[NASA-TM-4337] p 630 N92-24977
Assessment of potential aerodynamic benefits from spanwise blowing at the wing tip
[NASA-TM-107847] p 631 N92-25261
Wind-tunnel static and free-flight investigation of high-angle-of-attack stability and control characteristics of a model of the EA-6B airplane
[NASA-TP-3194] p 631 N92-25276
Joint computational and experimental aerodynamics research on a reentry vehicle
[DE91-017315] p 667 N92-25315
Study of the NAL's 0.1 x 0.1 m magnetic suspension and balance system
[NAL-TM-623] p 665 N92-25365
Static aeroelastic analysis of ACT wind tunnel model aircraft
[NAL-TM-624] p 632 N92-25366
A low-speed wind tunnel study of vortex interaction control techniques on a chine-forebody/delta-wing configuration
[NASA-CR-189616] p 632 N92-25510
A static investigation of the thrust vectoring system of the F/A-18 high-alpha research vehicle
[NASA-TM-4359] p 633 N92-25967
High-alpha vortex decoupling investigations on a chine forebody/Delta wing configuration at transonic Mach numbers
[NASA-CR-189642] p 715 N92-26651
Turbulent heat flux measurements in a transitional boundary layer
[NASA-TM-105623] p 716 N92-27377
An experimental investigation of the separating/reattaching flow over a backstep
[NASA-CR-190426] p 716 N92-27399
A pressure measurement method using Electronically Scanner Pressure sensors (ESP) installed in a gust wind tunnel
[NAL-TM-638] p 749 N92-27428
Propulsion simulator for magnetically suspended wind tunnel models p 750 N92-27801
Present status of the MIT/NASA Langley 6-inch MSBS p 750 N92-27802
Estimation of cable-mounted model inertia characteristics for dynamic wind-tunnel test
[NAL-TM-641] p 722 N92-28152
Note on flight measured control effectiveness of the quiet STOL experimental aircraft ASKA
[NAL-TR-1103] p 746 N92-28154
Force measurements on AGARD calibration model-B at transonic speeds in the NAL two-dimensional wind tunnel
[NAL-TM-639] p 722 N92-28190
A gust generation method for full configuration aircraft tests in a low speed wind tunnel. Part 1: Design and preliminary experiments
[NAL-TR-1115-PT-1] p 722 N92-28192
Studies in general aviation aerodynamics
[NASA-CR-190431] p 827 N92-28511
Comparison of LDA and LTA applications for propeller tests in wind tunnels
[NLR-MP-88031-U] p 827 N92-28658
The windtunnel as a tool for laminar flow research
[NLR-TP-90145-U] p 887 N92-28661
LAH-main rotor model test at the DNW
[NLR-TP-90305-U] p 852 N92-28687
Feasibility study of hypersonic clinometric measurements at R3Ch
[ONERA-RSF-136/1865-AY-728-] p 829 N92-28789
Aerodynamic characteristics obtained from alpha sweep test of the quiet STOL experimental aircraft ASKA
[NAL-TR-1112] p 853 N92-28901
Calculation of support interferences on the aerodynamic coefficients for a wind tunnel calibration model
[ESA-TT-1247] p 830 N92-29159
Shock enhancement and control of hypersonic combustion
[AD-A248558] p 896 N92-29580
Evaluation of measured-boundary-condition methods for 3D subsonic wall interference
[NLR-TR-88072-U] p 832 N92-29884
Joint computational and experimental aerodynamics research on a hypersonic vehicle
[DE92-013439] p 943 N92-30367
Two-dimensional aerodynamic characteristics of several polygon-shaped cross-sectional models applicable to helicopter fuselages
[NASA-TP-3233] p 944 N92-30394
Lewis icing research tunnel test of the aerodynamic effects of aircraft ground deicing/anti-icing fluids
[NASA-TP-3238] p 952 N92-30395
On-line analysis capabilities developed to support the AFW wind-tunnel tests
[NASA-TM-107651] p 961 N92-30752

An experimental study of the relationship between velocity and pressure fluctuations in a wing-body junction
[AD-A249628] p 946 N92-31122
A demonstration of passive blade twist control using extension-twist coupling
[NASA-TM-107642] p 1001 N92-31155
An analytical and experimental investigation of flutter suppression via piezoelectric actuation
[NASA-TM-107653] p 962 N92-31174
High Reynolds number test of the Boeing TR77 airfoil in the Langley 0.3-meter transonic cryogenic tunnel
[NASA-TM-4189] p 947 N92-31246
Flutter suppression digital control law design and testing for the AFW wind-tunnel model
[NASA-TM-107652] p 962 N92-31350
Flat plates placed in depleted hypersonic flow
[SESSIA-430/91.960] p 947 N92-31508
Wind tunnel aerodynamic characteristics of a transport-type airfoil in a simulated heavy rain environment
[NASA-TP-3184] p 948 N92-31532
Euler solver for arbitrary configurations: Further applications p 949 N92-31888
Exploratory experimental investigation of a wave propeller
[AD-A252175] p 949 N92-32062
Experimental studies of hypersonic shock-wave boundary-layer interactions
[NASA-CR-190731] p 950 N92-32162
Transonic wind tunnel test of a 14 percent thick oblique wing
[NASA-TM-102230] p 950 N92-32213
The multiple-function multi-input/multi-output digital controller system for the AFW wind-tunnel model
[NASA-TM-107600] p 1060 N92-32536
Integration of wall interference assessment and wall adaptation
[NLR-TP-91119-U] p 1101 N92-32734
Further wind tunnel investigation of the SM701 airfoil with aileron and turbulators
[NASA-CR-190702] p 1038 N92-33063
Implementation of a personal computer based parameter estimation program
[AD-A252914] p 1061 N92-33502
Experimental study of a generic high-speed civil transport
[NASA-TM-4382] p 1040 N92-33631
Effect of afterbody geometry on aerodynamic characteristics of isolated nonaxisymmetric afterbodies at transonic Mach numbers
[NASA-TP-3236] p 1041 N92-33706
Flutter models: Their design, manufacture, and ground testing p 1089 N92-34164
Unsteady wind tunnel tests p 1089 N92-34166
Parametric investigation of single-expansion-ramp nozzles at Mach numbers from 0.60 to 1.20
[NASA-TP-3240] p 1042 N92-34193

WIND TUNNEL WALLS

Adhesive shear strength of impact ice --- inside wind tunnel p 30 A92-11068
Two-dimensional adaptive-wall tests in the NASA Ames two- by two-foot transonic wind tunnel p 30 A92-13201
Wall interference assessment/correction for transonic airfoil data p 30 A92-13214
Disturbance of transonic wind tunnel flow by a slot in the tunnel wall p 135 A92-13675
High speed wind tunnel wall interference research progress at Nanjing Aeronautical Institute p 136 A92-15338
Wind tunnel wall effects in a linear oscillating cascade
[ASME PAPER 91-GT-133] p 72 A92-15576
Wall interference calculation in a transonic test section including simulation of discrete slots
[AIAA PAPER 92-0032] p 249 A92-22153
Modeling the ventilated wind tunnel wall
[AIAA PAPER 92-0035] p 249 A92-22156
Wind tunnel boundary interference prediction and correction
[AIAA PAPER 92-0036] p 249 A92-22157
Application of the wall pressure method to wall interference corrections for model tests at high angle of attack in high speed wind tunnel p 315 A92-25134
Experimental results on a wall interference correction method with interface measurements
[AIAA PAPER 92-0570] p 333 A92-26978
An asymptotic transonic theory and optimal porosity of wind tunnel walls at M greater than about 1 p 425 A92-30159
Theoretical analysis of the effect of the porous walls of a wind tunnel on transonic flow past bodies of cone-cylinder type p 427 A92-30202
Theoretical analysis of a suction diffuser in the porous test section of a wind tunnel p 428 A92-30207
Consideration of the effect of viscosity in the problem of porous-wall induction p 440 A92-31887
Effect of tunnel walls on vortex breakdown location over delta wings p 703 A92-41279
Some problems on the sidewall interference in two-dimensional subsonic and transonic wind tunnel testing p 747 A92-41929
Wind tunnel wall corrections for unsteady flow applying steady wall adaptation and CFD-techniques p 706 A92-42533
The wall interference correction and test data processing methods for airfoil wind tunnel test with endplates p 942 A92-53087
Evaluation of sidewall interference in the NAL two-dimensional transonic wind tunnel p 1092 A92-56011
Tohoku University low-turbulence wind tunnel
[AIAA PAPER 92-3913] p 1095 A92-56746
The research of reducing 3-D low supersonic shock wave reflection in a 2-D transonic flexible walls adaptive wind tunnel
[AIAA PAPER 92-3924] p 1095 A92-56755
Numerical modeling of transonic juncture flow
[AIAA PAPER 92-4036] p 1035 A92-56858
Mass flux similarity for slotted transonic-wind-tunnel walls
[NASA-TM-4281] p 11 N92-10006
Wind tunnel tests on A4, A4.1, and A4.2 2-D airfoil models in the IAR 5-ft. wind tunnel: Boeing Commercial Airplane Company and Institute for Aerospace Research collaborative work program
[NRC-IAR-C3] p 81 N92-11975
A wall interference assessment/correction system
[NASA-CR-189785] p 259 N92-15974
User guide for WIACX: A transonic wind-tunnel wall interference assessment and correction procedure for the NTF
[NASA-TM-104168] p 261 N92-17547
Comparison of a two-dimensional adaptive-wall technique with analytical wall interference correction techniques
[NASA-TP-3132] p 444 N92-20494
Effect of collector configuration on test section turbulence levels in an open-jet wind tunnel
[NASA-TM-4333] p 750 N92-27670
Further investigation of the effect of model cooling on periodic transonic flow p 721 N92-27961
Evaluation of measured-boundary-condition methods for 3D subsonic wall interference
[NLR-TR-88072-U] p 832 N92-29884

WIND TUNNELS

A piezoelectric droplet generator for use in wind tunnels p 291 A92-21374
The low-turbulence wind tunnel at Tohoku University p 623 A92-40598
Induced drag of a wing in a circular wind tunnel p 936 A92-50327
Rarefied gas numerical wind tunnel p 995 A92-52763
A quiet-flow Ludwieg tube for experimental study of high speed boundary layer transition
[AIAA PAPER 92-3885] p 1094 A92-56727
Tohoku University low-turbulence wind tunnel
[AIAA PAPER 92-3913] p 1095 A92-56746
Design of a variable contraction for a full-scale automotive wind tunnel
[AIAA PAPER 92-3929] p 1096 A92-56760
Calibration of hemispherical-head flow angularity probes
[AIAA PAPER 92-4005] p 1122 A92-56828
The wind tunnel, its evolution for aerospace test purposes, perspective for curriculum development
[AIAA PAPER 92-4017] p 1100 A92-56839
Aerodynamics laboratory education at Purdue University - Ground testing facilities
[AIAA PAPER 92-4018] p 1100 A92-56840
The trisonic wind tunnel Muenchen and its involvement in the German SAeNGER-programme
[AIAA PAPER 92-4019] p 1100 A92-56841
Prediction of the pressure loss coefficient of wind tunnel turbulence reducing screens
[AIAA PAPER 92-4043] p 1035 A92-56862
Numerical simulation of hypersonic viscous flow for the design of H-2 orbiting plane (HOPE-2)
[NAL-TR-1093] p 11 N92-10009
Calibration of the Naval Postgraduate School 3.5' x 5.0' academic wind tunnel
[AD-A240614] p 31 N92-11025
Aerospace technology: Technical data and information on foreign test facilities
[GAO/NSIAD-90-71FS] p 139 N92-13076
The IRS plasma wind tunnels for the investigation of thermal protection materials for reentry vehicles p 208 N92-15009
Calibration data for improved correction of UVW propeller anemometers
[DE92-002935] p 297 N92-16281
An experimental investigation of leading edge vortical flow about a delta wing during wing rock
[AD-A243363] p 260 N92-17114
An approach to flow field measurement by Laser 2-Focus velocimeter (L2F) in gust wind tunnel
[NAL-TM-617] p 346 N92-18484
Operating ranges of meteorological wind tunnels for the simulation of convective boundary layer phenomena
[AD-A244153] p 409 N92-19195
Study of optical techniques for the Ames unitary wind tunnels. Part 1: Schlieren
[NASA-CR-189951] p 385 N92-19218
Development of a wind chamber for model testing of tornado forces on structures
[PB92-104165] p 386 N92-19940
Wind tunnel investigation of the aerodynamic effects of aircraft ground deicing/anti-icing fluids and criteria for aerodynamic acceptance p 452 N92-21698
Inflatable traversing probe seal p 595 N92-22692
An analysis of the sidewall boundary layer effect in two-dimensional wind tunnel testing p 626 N92-24856
Laminar-turbulent transition process in the presence of simulated wall roughness p 626 N92-24858
Mechanical design of a rotary balance system for NASA. Langley Research Center's vertical spin tunnel p 664 N92-25090
The 12-foot pressure wind tunnel restoration project model support systems p 664 N92-25091
CFD contributions during hypersonic airplane intake design p 769 N92-27472
Further investigation of the effect of model cooling on periodic transonic flow p 721 N92-27961
Experimental aerodynamic facilities of the Aerodynamics Research and Concepts Assistance Branch
[AD-A247489] p 883 N92-28248
Expand turbulence laboratory facilities to meet new DOD research interest
[AD-A248581] p 883 N92-28388
The design of test-section inserts for higher speed aeroacoustic testing in the Ames 80- by 120-foot wind tunnel
[NASA-TM-103915] p 927 N92-28909
Turbulent spot generation and growth rates in a transonic boundary layer
[AD-A250221] p 909 N92-29118
Buffet test in the National Transonic Facility
[NASA-CR-189595] p 888 N92-29352
Digital analysis of wind tunnel imagery to measure fluid thickness
[NASA-CR-189234] p 983 N92-31252
Further wind tunnel investigation of the SM701 airfoil with aileron and turbulators
[NASA-CR-190702] p 1038 N92-33063

WIND TURBINES

Noise from turbine generators - Noise control, propagation, and assessment p 686 A92-39044
Noise generated by wind turbines p 686 A92-39045
Mechanical noise from large wind turbines - Experiences from Swedish prototypes p 686 A92-39046
Indicial method calculating dynamic stall on a vertical axis wind turbine p 714 A92-44528
Particle image velocimetry measurements of the aerodynamics of a wind turbine p 1115 A92-54337
Numerical simulation of VAWT stochastic aerodynamic loads produced by atmospheric turbulence: VAWT-SAL code
[DE92-000597] p 229 N92-15392
A comparison of spanwise aerodynamic loads estimated from measured bending moments versus direct pressure measurements on horizontal axis wind turbine blades
[DE92-001158] p 301 N92-16458
Dynamic stall on wind turbine blades
[DE92-001157] p 262 N92-17874
An overview: Challenges in wind technology development
[DE92-001190] p 302 N92-17875
The NREL teetering hub rotor code: Final results and conclusions
[DE92-001187] p 410 N92-19633
Recent results from data analysis of dynamic stall on wind turbine blades
[DE92-001200] p 505 N92-20245
The status of the US VAWT program
[DE92-002931] p 505 N92-21040
SERI advanced wind turbine blades
[DE92-001216] p 598 N92-22971
Measured and predicted rotor performance for the SERI advanced wind turbine blades
[DE92-001215] p 598 N92-23119
Fatigue life variability and reliability analysis of a wind turbine blade
[DE92-008673] p 689 N92-25049

Wind energy program overview
[DE91-002178] p 689 N92-25498
Yaw dynamics of horizontal axis wind turbines
[DE92-001245] p 1004 N92-30837
A surface definition code for turbine blade surfaces
[DE92-010574] p 1004 N92-31498
Turbulence-induced loads on a teetered rotor
p 1042 N92-34029

WIND VELOCITY
Fair weather convection and light aircraft accidents
[IAF PAPER ST-91-004] p 186 A92-20651
A case study of the Claycomo, Missouri microburst on July 30, 1989 p 407 A92-27961
Surface-layer gusts for aircraft operation
p 774 A92-42095
Microburst modelling and scaling p 915 A92-46262
The application of a theoretical blade sailing model to predict the behaviour of articulated helicopter rotors
p 960 A92-52849
On the effect of canards on NAL spaceplane model (0 order) in low speed area p 1030 A92-56052
Calibration data for improved correction of UVW propeller anemometers
[DE92-002935] p 297 N92-16281
Wind loads on a mirage III O aircraft mounted above a ground plane
[AD-A243004] p 275 N92-17266
Response of structures to galloping excitation: Background and approximate estimation
[ESDU-91010] p 399 N92-18091
Measurement of the flow distribution over the flight deck of an aircraft carrier p 504 N92-21955
Measured and predicted rotor performance for the SERI advanced wind turbine blades
[DE92-001215] p 598 N92-23119
Spectrum modal analysis for the detection of low-altitude windshear with airborne Doppler radar
[NASA-CR-4457] p 953 N92-31549
A comparison of the performance of two gust front detection algorithms using a length-based scoring technique
[AD-A250862] p 1004 N92-32103

WIND VELOCITY MEASUREMENT
Improved noise rejection in automatic carrier landing systems p 380 A92-28154
Potential applications of laser Doppler anemometry for in-flight measurements
[NLR-TP-90163-U] p 859 N92-28654

WINDING
Analysis of a 37 kW cage-induction motor
[PB92-142116] p 597 N92-23496

WINDOWS (APERTURES)
Binary optic-corrected conformal windows for optical seekers
[AIAA PAPER 92-2802] p 779 A92-41340
Multiple aperture window and seeker concepts for endo KEW applications
[AIAA PAPER 92-2806] p 752 A92-41344
Modulation transfer function degradation in segmented windows p 733 A92-41431
Window cooling for high speed flight
[AD-D015145] p 344 N92-18193

WINDPOWER UTILIZATION
Measured and predicted rotor performance for the SERI advanced wind turbine blades
[DE92-001215] p 598 N92-23119
Wind energy program overview
[DE91-002178] p 689 N92-25498

WINDPOWERED GENERATORS
An overview: Challenges in wind technology development
[DE92-001190] p 302 N92-17875
Measured and predicted rotor performance for the SERI advanced wind turbine blades
[DE92-001215] p 598 N92-23119

WINDS ALOFT
Airdata calibration techniques for measuring atmospheric wind profiles p 856 A92-46792

WINDSHIELDS
Windscreen departure p 723 A92-42500
Bird impact analysis of aircraft windshield transparency p 958 A92-50236
An impact dynamics investigation on some problems in bird strike on windshields of high-speed aircrafts
p 986 A92-53330
A study of dynamic response to bird impact on arc windshields of aircrafts p 952 A92-53340

WING CAMBER
A new method for increasing maximum flight endurance p 280 A92-21006
Non linear induced drag study of generically cambered closely coupled dual wings
[SAE PAPER 912126] p 618 A92-39973
Multi-constraint wing optimization p 701 A92-41197
Variable-camber systems integration and operational performance of the AFTI/F-111 mission adaptive wing
[NASA-TM-4370] p 570 N92-22194

WING FLAPS
The aerodynamic interference between a flapped tanker aircraft and a receiver aircraft during air-to-air refuelling
p 29 A92-13199
Controlling unsteady lift using unsteady trailing-edge flap motions
[AIAA PAPER 92-0275] p 318 A92-25729
Reduction of wing rock amplitudes using leading-edge vortex manipulations
[AIAA PAPER 92-0279] p 379 A92-25733
Experimental investigation of the optimal deflection of a single-slotted flap with different degrees of extension on a modern supercritical profile p 439 A92-31879
Experimental ice shape and performance characteristics for a multi-element airfoil in the NASA Lewis Icing Research Tunnel
[NASA-TM-105380] p 261 N92-17347
A mathematical model of a tilt-wing aircraft for piloted simulation
[NASA-TM-103864] p 368 N92-19847
Variable geometry sailplanes Minisigma
p 629 N92-24877

WING FLOW METHOD TESTS
Delay of wing vortex bursting by using favorable interaction of vortices p 615 A92-38910
Control aspects of the transition from transversal to transonic flow, step effects
[ETN-91-90106] p 82 N92-11981

WING LOADING
A lifting line theory for supersonic flow applications
[AIAA PAPER 91-5058] p 171 A92-17841
Acoustic emission monitoring of a ground durability and damage tolerance test --- for aircraft structures
p 492 A92-28737
Use of the thrust-weight diagram versus transport cargo in the initial dimensioning of passenger-transport aircraft
p 642 A92-37074
Design load predictions on a fighter-like aircraft wing
p 811 A92-46797
Time-average loading on a two-dimensional airfoil in a large amplitude motion p 811 A92-46805
Wing mass formula for subsonic aircraft
p 845 A92-46812
Effects of the roll angle on cruciform wing-body configurations at high incidences
[AIAA PAPER 92-4356] p 1079 A92-55342
Monitoring load experience of individual aircraft
[NLR-TP-90084-U] p 196 N92-15065
Variable geometry sailplanes Minisigma
p 629 N92-24877

WING NACELLE CONFIGURATIONS
Study of external dynamic flap loads on a 6 percent B-1B model
[ASME PAPER 91-GT-236] p 125 A92-15645
Interference effects of very high bypass ratio nacelle installations on a low-wing transport
[ASME PAPER 91-GT-241] p 75 A92-15646
V-22 flight test p 112 A92-16056
Detailed analysis of wing-nacelle interaction for commercial transport aircraft
[ONERA, TP NO. 1991-152] p 77 A92-16122
Aerodynamic wing-nacelle integration
p 458 A92-30134
Interference of high-mounted propfan nacelles with an unswept wing and ways to attenuate it
p 460 A92-31881
Installation effects of wing-mounted turbofan nacelle-pylons on a 1/17-scale, twin-engine, low-wing transport model
[NASA-TP-3168] p 346 N92-19002

WING OSCILLATIONS
On-line adaptive control of unstable aircraft wing flutter p 27 A92-11374
Vibration of a wing of finite span in subsonic flow at small distances from a solid boundary p 9 A92-12808
Aeroelastic analysis of wings using the Euler equations with a deforming mesh p 10 A92-13215
Aeroelastic tailoring of aeronautical composite wing structures p 146 A92-15343
Euler flow predictions for an oscillating cascade using a high resolution wave-split scheme
[ASME PAPER 91-GT-198] p 74 A92-15623
Structure/control design synthesis of active flutter suppression system by goal programming
p 204 A92-18621
Direct-inverse transonic wing-design method in curvilinear coordinates including viscous interaction
p 193 A92-20202
Unique high-alpha roll dynamics of a sharp-edged 65 deg delta wing
[AIAA PAPER 92-0276] p 318 A92-25730
Reduction of wing rock amplitudes using leading-edge vortex manipulations
[AIAA PAPER 92-0279] p 379 A92-25733
Three-dimensional simulation of slender delta wing rock and divergence
[AIAA PAPER 92-0280] p 318 A92-25734
Flow visualization image analysis of high-rate roll experiments on a delta wing
[AIAA PAPER 92-0317] p 321 A92-25764
A study of active flutter suppression for a wing/store system p 379 A92-27826
A numerical method for analyzing the nonlinear flutter of wings at high angles of attack p 338 A92-27827
Experimental investigation of the coefficients of the normal-force derivatives for rectangular wings with translational oscillations p 423 A92-30127
Numerical modeling of self-oscillations for a small-aspect-ratio delta wing using measurements of roll motion at large angles of attack p 424 A92-30138
Aerodynamic effect of compression shocks on an oscillating aileron in transonic flow p 440 A92-31898
A method of boundary layer laminarization on an oscillating wing p 441 A92-31969
Dynamic response to time-dependent excitations of cantilevered aircraft wing structures modelled as thin-walled beams
[AIAA PAPER 92-2213] p 584 A92-34403
Dynamic characteristics of a Benchmark models program supercritical wing
[AIAA PAPER 92-2368] p 571 A92-34596
Design of adaptive fast-sampling digital controllers for active flutter suppression
[AIAA PAPER 92-2105] p 567 A92-35676
An experimental and analytical investigation of wing flutter on a trail rotor V/STOL aircraft
[AIAA PAPER 92-2112] p 544 A92-35682
Transonic wind tunnel investigation of limit cycle oscillations on fighter type wings - Update
[AIAA PAPER 92-2125] p 572 A92-35692
Predicted and measured in-flight wing deformations of a forward-swept-wing aircraft p 548 A92-35936
LDV measurements in the unsteady tip-vortex behind an oscillating rectangular wing p 620 A92-40085
Effects of attack angle on leg portion of the horseshoe vortex around the idealized wing p 623 A92-40177
Transonic Navier-Stokes computations for an oscillating wing using zonal grids p 701 A92-41217
Unsteady aerodynamic loading produced by a sinusoidally oscillating delta wing p 701 A92-41223
Chaotic stall response of helicopter rotor in forward flight p 730 A92-43046
Research on state equations of unsteady aerodynamics p 709 A92-43132
Gust load alleviation control design for the accuracy of an aeroelastic active control model
p 745 A92-43134
ACT wind tunnel experiment on gust load alleviation. II - Wind tunnel test with active support facility
p 745 A92-43135
Transonic wind tunnel tests of flutter suppression equipment (Wing response data processing)
p 748 A92-43136
Response characteristics of a wing in supersonic flow near flutter boundary
[SAE PAPER 911999] p 789 A92-45401
Dynamically enhanced sustained lift using oscillating leading-edge flaps
[AIAA PAPER 92-2625] p 794 A92-45497
LDV measurements in the three-dimensional near wake of a stationary and oscillating rectangular wind
[AIAA PAPER 92-2689] p 799 A92-45536
Forebody vortex control for suppressing wing rock on a highly-swept wing configuration
[AIAA PAPER 92-2716] p 803 A92-45555
Dynamic LEX/forebody vortex interaction effects
[AIAA PAPER 92-2732] p 804 A92-45566
Flow over a twin-tailed aircraft at angle of attack. II - Temporal characteristics p 810 A92-46781
Navier-Stokes computations on swept-tapered wings, including flexibility p 810 A92-46786
Experimental study of vortex flows over delta wings in wing-rock motion p 810 A92-46787
Chaotic oscillation in helicopter blade stall response
p 846 A92-46922
Navier-Stokes prediction of large-amplitude delta-wing roll oscillations characterizing wing rock
[AIAA PAPER 92-4428] p 1080 A92-55352
Navier-Stokes computations for oscillating control surfaces
[AIAA PAPER 92-4431] p 1026 A92-55355
Stochastic self-induced roll oscillations of slender delta wing at high angles of attack
[AIAA PAPER 92-4498] p 1081 A92-55366
Multidisciplinary optimization of aeroservoelastic systems using reduced-size models
p 1054 A92-56176

Nonstationary flight aerodynamics in a turbulent environment
[ETN-91-90102] p 82 N92-11980
Aerodynamic and flowfield hysteresis of slender wing aircraft undergoing large-amplitude motions
p 364 N92-18780
Analysis of unsteady force, pressure, and flow-visualization data for a pitching straked wing model at high angles of attack p 364 N92-18784
Wind tunnel force measurements and visualization on a 60-deg delta wing in oscillation, stepwise motion, and gusts p 364 N92-18786
Three-dimensional time-marching aeroelastic analyses using an unstructured-grid Euler method
[NASA-TM-107567] p 527 N92-23116
Wind-tunnel investigation of aerodynamic and stability characteristics of a forward swept wing X-29 model
p 627 N92-24862
Elementary flutter analysis p 1088 N92-34162

WING PANELS
Flow separation patterns over an F-14A aircraft wing
p 174 A92-20205
Efficient panel method for vortex sheet roll-up
p 309 A92-24404
The initial development of an expert system for designing composite material wing structures p 599 A92-32542
Static and dynamic flow field development about a porous suction surface wing
[AIAA PAPER 92-2628] p 795 A92-45500
Vortex-in-cell analysis of wing wake roll-up
[AIAA PAPER 92-2703] p 801 A92-45545
Exploratory investigation of a spanwise blowing concept for tip-stall control on cranked-arrow wings
[AIAA PAPER 92-2637] p 806 A92-45576
Detailed analysis and test correlation of a stiffened composite wing panel p 1121 A92-56324
Nonstationary flight aerodynamics in a turbulent environment
[ETN-91-90102] p 82 N92-11980
Detailed analysis and test correlation of a stiffened composite wing panel
[NASA-TM-104154] p 159 N92-13460
Optimization of composite sandwich cover panels subjected to compressive loadings
[NASA-TP-3173] p 489 N92-20679
Add-on damping treatment for life extension of the F-15 upper-outer wing skin
[AD-A246149] p 746 N92-27577
Transonic wind tunnel investigation of limit cycle oscillations on fighter type wings p 721 N92-27959
Global/local interlaminar stress analysis of a grid-stiffened composite panel
[NASA-CR-190822] p 1125 N92-33139

WING PLANFORMS
The anchored and loose vortex systems of finite wings
[AIAA PAPER 92-0318] p 321 A92-25765
The feasibility of reducing induced wing drag by using crescent planform wings p 425 A92-30167
Low-speed flutter characteristics of some simple low-aspect-ratio delta-wing models p 460 A92-32247
The maneuver performance and control of a hovercraft p 763 A92-43240
Effects of wing planform on HSCT off-design aerodynamics --- High Speed Civil Transport
[AIAA PAPER 92-2629] p 844 A92-45501
Numerical simulation of vortex flows past impulsively started wings p 88 N92-13028
Analysis and design of planar and non-planar wings for induced drag minimization
[NASA-CR-189509] p 179 N92-13999
Studies in general aviation aerodynamics
[NASA-CR-190431] p 827 N92-28511
Lift and rolling moment due to spoilers on wings with trailing-edge flaps deflected at subsonic speeds
[ESDU-92002-SUPPL] p 1037 N92-32782

WING PROFILES
Nonstationary forces on a wing airfoil
p 4 A92-10825
Static aeroelastic control using strain actuated adaptive structures p 26 A92-11122
Comparative studies of flow around a wing profile in two wind tunnels p 7 A92-12170
Fundamentals of applied aerogasdynamics. I - Aerodynamics of wings (profiles), airframes, and their combinations --- Russian book p 64 A92-14280
A development of computer support system for wing design p 162 A92-15332
A discrete vortex study of stationary flow past three-dimensional lifting systems at subsonic and supersonic velocities p 79 A92-16813
Synthesis of wing profiles from chord velocity diagrams using quasi-solutions for inverse boundary value problems p 80 A92-16815
Inviscid drag prediction for transonic transport wings using a full-potential method p 174 A92-20212
Upwind scheme for solving the Euler equations on unstructured tetrahedral meshes p 175 A92-20735
Analysis of circular elastic membrane wings
p 245 A92-21722
Minimum induced drag of a wing in a circular open wind tunnel p 251 A92-22521
An efficient calculation method of subsonic aerodynamic characteristics for a Space Shuttle orbiter in the reentry attitude p 252 A92-23383
Compressibility effects on the dynamic stall of a three-dimensional wing
[AIAA PAPER 92-0191] p 256 A92-23800
Suppression of the wing-body junction vortex by body surface suction p 309 A92-24417
Application of the multiplier penalty function method to the optimum design of wing configurations of aerospace vehicle p 356 A92-25013
Computations of the flow past bodies and wings using Euler equations p 312 A92-25038
A numerical method for unsteady transonic flow about wings with control surface p 314 A92-25107
Variable-complexity aerodynamic optimization of an HSCT wing using structural wing-weight equations
[AIAA PAPER 92-0212] p 317 A92-25685
The anchored and loose vortex systems of finite wings
[AIAA PAPER 92-0318] p 321 A92-25765
Maximum lift prediction for multielement wings
[AIAA PAPER 92-0401] p 324 A92-26254
Finite wing aerodynamics with simulated glaze ice
[AIAA PAPER 92-0414] p 325 A92-26265
Influence of wing shapes on the surface pressure fluctuations of a wing-body junction
[AIAA PAPER 92-0433] p 327 A92-26280
Quality assessment of two- and three-dimensional unstructured meshes and validation of an upwind Euler flow solver
[AIAA PAPER 92-0444] p 328 A92-26288
Application researches on expert system used for structural layout optimization of wings
p 398 A92-27865
Analysis of iced wings
[AIAA PAPER 92-0416] p 423 A92-29972
The effect of wing twist optimized in the framework of the plane cross section hypothesis on the aerodynamic characteristics of a wing-body combination at hypersonic speeds p 424 A92-30129
Generation of several wave packets in the boundary layer of a wing profile p 424 A92-30136
An experimental study of tone-like noise in the flow past a wing at low flow velocities p 425 A92-30160
Asymptotic solution of the problem of ideal-fluid flow past the vertices of bodies and wings
p 427 A92-30199
The aerodynamic characteristics of grid fin wings
p 427 A92-30201
An approximate method for calculating flow past solid wings of small aspect ratio based on a nonlinear theory of a continuous vortex surface p 428 A92-30373
A numerical investigation of vortex flow control through small geometry modifications at the strake/wing junction of a cropped double-delta wing
[AIAA PAPER 92-0411] p 435 A92-31661
Flight studies of the riblet effect on drag variation
p 438 A92-31871
Experimental investigation of the air bypass effect in the shock-wave region on the aerodynamic characteristics of a wing profile p 439 A92-31877
Boundary-layer-separation control p 440 A92-31886
Lift characteristics of an infinite-span cylindrical wing of a thick symmetric profile at low subsonic velocities
p 440 A92-31897
Structure of a boundary layer on the lower surface of a wing in flight and in a wind tunnel p 440 A92-31899
Observation and comparison of rainfall measured at a high sample rate p 505 A92-32073
Experimental study of a low Reynolds number tandem airfoil configuration p 442 A92-32241
Effects of ambient turbulence on the decay of a trailing vortex wake p 442 A92-32245
Multidisciplinary design optimization of a large transport aircraft wing
[AIAA PAPER 92-1002] p 536 A92-33194
Design for the relief of thermal stresses in a large high-speed wing
[AIAA PAPER 92-1082] p 536 A92-33250
Flexure-torsion behavior of sheat-deformable beams with applications to aircraft wing sections
[AIAA PAPER 92-2467] p 582 A92-34357
Adaptive response control of wing structures carrying heavy tip weights
[AIAA PAPER 92-2527] p 583 A92-34374
EUROFAR airframe aerodynamic design
p 546 A92-35750
Theoretical model to calculate aerodynamic interference effects between rotor and wing of tiltrotors
p 521 A92-35788
Measurement and analysis of the flow field above a wing/body configuration p 616 A92-38917
CFD calculations of closely coupled scissor wings - Inviscid, viscous, and vortex lattice with rollup results
[SAE PAPER 912150] p 619 A92-39986
Design of wing profiles with tangential suction or injection p 624 A92-40602
Accurate prediction of drag using Euler methods
p 703 A92-41246
Study on calculating the subsonic and supersonic aerodynamic characteristics of slender wing-body combinations at large angles of attack
p 706 A92-41926
An aerodynamic hypothesis for the wing aeroelasticity problem p 761 A92-42665
Aerodynamics of two-shock bodies derived by the gasdynamic design method p 707 A92-42683
Construction of a wing profile with a flap modeled by a point vortex p 707 A92-42726
The main wing boundary layer separation pattern of STOL research aircraft Asuka p 709 A92-43144
The fluid-dynamic measurement of the fling motion of a three-dimensional flat plate p 710 A92-43194
An economic approach to accurate wing design
[SAE PAPER 912008] p 789 A92-45408
Transonic airfoil and wing design using Navier-Stokes codes
[AIAA PAPER 92-2651] p 797 A92-45518
Vortex-in-cell analysis of wing wake roll-up
[AIAA PAPER 92-2703] p 801 A92-45545
Wing design for hanggliders having minimum induced drag p 811 A92-46814
Integral wing/fuel box p 958 A92-51569
A penalty-Galerkin finite element method for calculating transonic flow over wings p 943 A92-53386
Optimal design of wing shape by use of neural-network p 1054 A92-56112
Small two-dimensional surface excrescences on aircraft wings approaching separation p 1031 A92-56170
Wing mass formula for twin fuselage aircraft
p 1054 A92-56171
Computational study of the aerodynamics and control by blowing of asymmetric vortical flows over delta wings
[NASA-CR-187979] p 14 N92-10990
Resolution of the Navier-Stokes equations applied to the computation of the laminar flow around a two dimensional wing profile
[CERT-RT-65/5604-35] p 43 N92-11307
Maximum lift of wings with trailing-edge flaps at low speeds
[ESDU-91014] p 81 N92-11970
Control aspects of the transition from transversal to transonic flow, step effects
[ETN-91-90106] p 82 N92-11981
Research on inverse methods and optimization in Italy
p 202 N92-13956
Surface pressure measurements on the wing of a wind tunnel model during steady rotation
[AD-A243047] p 260 N92-17281
Aeroelastic behavior of an adaptive lifting surface
p 443 N92-20378
The Guardian: Preliminary design of a close air support aircraft
[NASA-CR-189991] p 463 N92-21566
Simulation of iced wing aerodynamics
p 450 N92-21686
Effects of frost on wing aerodynamics and take-off performance p 450 N92-21687
Adaptive active flutter suppression of wings in subsonic and transonic flight regimes p 553 N92-24010

WING ROOTS
Composite material stub-blade wing joint
p 763 A92-44618
Dynamic analysis of rotor blades with root retention design variations p 1054 A92-56156

WING SLOTS
Experimental investigation of the optimal deflection of a single-slotted flap with different degrees of extension on a modern supercritical profile p 439 A92-31879

WING SPAN
Comparison of two-dimensional and three-dimensional droplet trajectory calculations in the vicinity of finite wings
[AIAA PAPER 92-0645] p 342 A92-28215
Mathematical modeling of nonstationary viscous flow over a solid angle of finite span p 440 A92-31890
Composite material stub-blade wing joint
p 763 A92-44618

WING TIP VORTICES
The aerodynamic interference between a flapped tanker aircraft and a receiver aircraft during air-to-air refuelling
p 29 A92-13199

Wing tip vortex calculations with an unstructured adaptive-grid Euler solver p 64 A92-14330
Unsteady wing surface pressures in the wake of a propeller
[AIAA PAPER 92-0277] p 318 A92-25731
The anchored and loose vortex systems of finite wings
[AIAA PAPER 92-0318] p 321 A92-25765
The effects of blowing on delta wing vortices during dynamic pitching at high angles of attack
[AIAA PAPER 92-0407] p 325 A92-26260
Computational study of the aerodynamics and control by blowing of asymmetric vortical flows over delta wings
[AIAA PAPER 92-0410] p 325 A92-26263
Numerical analysis of helicopter rotor blades p 430 A92-30558
Visualization and measurement of helicopter rotor flow using projected smoke filaments and digital image processing p 520 A92-35728
Navier-Stokes analysis of blade tip shape in hover p 521 A92-35758
On the influence of blade-vortex-interactions on vortex structure p 521 A92-35783
Far-field turbulence structure of the tip vortex shed by a single rectangular wing p 620 A92-40084
LDV measurements in the unsteady tip-vortex behind an oscillating rectangular wing p 620 A92-40085
Measurements of the unsteady vortex flow over a wing-body at angle of attack
[AIAA PAPER 92-2729] p 808 A92-45598
Flow visualisation of a small diameter rotor operating at high rotational speeds with blades at small pitch angles p 814 A92-46949
Flowfield of a lifting rotor in hover - A Navier-Stokes simulation p 1024 A92-54906
Two-fence concept for efficient trapping of vortices on airfoils p 1031 A92-56165
On aircraft wake properties and some methods for stimulating decay and breakdown of tip vortices p 87 N92-13021
Analysis of results of an Euler-equation method applied to leading-edge vortex flow
[NLR-TP-90368-U] p 827 N92-28657

WING TIPS
Aerodynamic characteristics of a wing near its tip using panel method p 251 A92-22524
Adaptive response control of wing structures carrying heavy tip weights
[AIAA PAPER 92-2527] p 583 A92-34374
Aerodynamic characteristics near the tip of a finite wing by a panel method
[SAE PAPER 912020] p 790 A92-45413
Effect of wing tip vortices on a trailing aircraft p 935 A92-50303
NACA 0015 wing pressure and trailing vortex measurements
[NASA-TP-3151] p 13 N92-10981
Experimental study of an independently deflected wingtip mounted on a semispan wing
[NASA-TM-102842] p 13 N92-10983
Wing tip turbine: Analysis of the results of S2MA sounding of marginal vortex of the A320, technical summary
[ONERA-RTS-21/4365-AY-056A] p 23 N92-11009
Experimental study of a generic high-speed civil transport: Tabulated data
[NASA-TM-104216] p 525 N92-22232
Assessment of potential aerodynamic benefits from spanwise blowing at the wing tip
[NASA-TM-107847] p 631 N92-25261
Nonlinear aerodynamics and the design of wing tips
[NASA-CR-190649] p 946 N92-31157
Experimental study of a generic high-speed civil transport
[NASA-TM-4382] p 1040 N92-33631

WINGED VEHICLES
Measurement on hypersonic dynamic stable coefficients of a winged vehicle p 430 A92-30550
Navier-Stokes simulation for the winged space vehicle 'HOPE' at subsonic, transonic, and supersonic regimes p 1018 A92-53559
Improvement of atmospheric flight performance of a space vehicle through H infinity-control theory p 1130 A92-53785

WINGLETS
The effects of winglets on low aspect ratio wings at supersonic Mach numbers
[NASA-CR-4407] p 178 N92-13996

WINGS
Supersonic boundary-layer stability analysis on an aircraft wing p 9 A92-13207
Multidisciplinary design optimization of a large transport aircraft wing
[AIAA PAPER 92-1002] p 536 A92-33194
Exploratory design studies of actively controlled wings using integrated multidisciplinary synthesis p 641 A92-36828
Flow regimes of the cove regions between a slat and wing and between a wing and flap of a multielement airfoil p 614 A92-38858
Structural concept of main wings of high altitude unmanned aerial vehicle and basic properties of thermoplastic composites as candidate material
[SAE PAPER 912053] p 843 A92-45437
Unsteady aerodynamics of a Wortmann wing at low Reynolds numbers p 810 A92-46778
Navier-Stokes predictions for the F-18 wing and fuselage at large incidence p 810 A92-46783
Wing leading edge design with composites to meet bird strike requirements p 848 A92-47404
The role of nonmetallic fasteners in aircraft wings and other composite structures p 784 A92-47413
Probability analysis of structure failure for the wings with main and subordinate components p 848 A92-47657
Three-dimensional wings and waveriders with attached shock waves p 936 A92-50322
Moldless composite aircraft wing structural design modifications p 958 A92-51527
The relation among the general unsteady aerodynamic coefficients of a wing in subsonic and supersonic speed p 941 A92-53022
Study of dynamic strength on composite wing p 996 A92-53071
The system reliability analysis and optimization design for wing-box structures p 997 A92-53292
Computations of the unsteady flow about a generic wing/pylon/finned-store configuration
[AIAA PAPER 92-4568] p 1027 A92-55377
NACA 0015 wing pressure and trailing vortex measurements
[NASA-TP-3151] p 13 N92-10981
Vortex control: Further encounters p 87 N92-13020
Steady and unsteady aerodynamics of a pitching straked wing model at high angles of attack p 87 N92-13024
Control augmented structural optimization of aeroelasticity tailored fiber composite wings
[AD-A241464] p 135 N92-13075
Review of aerodynamic design in the Netherlands p 193 N92-13929
Aerodynamic aircraft design methods and their notable applications: Survey of the activity in Japan p 193 N92-13930
Application of direct inverse analogy method (DIVA) and viscous design optimization techniques p 176 N92-13951
An inverse method with regularity condition for transonic airfoil design p 177 N92-13969
Definition of the unsteady vortex flow over a wing/body configuration
[NASA-CR-180083] p 178 N92-13995
The effects of winglets on low aspect ratio wings at supersonic Mach numbers
[NASA-CR-4407] p 178 N92-13996
Analysis and design of planar and non-planar wings for induced drag minimization
[NASA-CR-189509] p 179 N92-13999
Airbus Industrie A330/A340: Full scale fatigue test of center fuselage and wing p 226 N92-14425
Wind tunnel investigation of vortex flows on F/A-18 configuration at subsonic through transonic speed
[NASA-TP-3111] p 179 N92-14968
A wing rock model for the F-14A aircraft
[AD-A243109] p 275 N92-17300
Results of measured temperature distribution on an adiabatic wing model with radiation thermometer
[NAL-TM-610] p 261 N92-17755
An initial investigation into methods of computing transonic aerodynamic sensitivity coefficients
[NASA-CR-190040] p 348 N92-19545
Integrated aerodynamic-structural-control wing design p 349 N92-19698
Suppression of radiating harmonics Electro-Impulse Deicing (EIDI) systems
[DOT/FAA/CT-TN90/33] p 405 N92-19764
Freezing precipitation on lifting surfaces
[NRC-32124] p 448 N92-20156
Scorpion: Close Air Support (CAS) aircraft
[NASA-CR-189974] p 462 N92-20664
The effect of wing ice contamination on essential flight characteristics p 449 N92-21681
Wind tunnel investigation of a wing-propeller model performance degradation due to distributed upper-surface roughness and leading edge shape modification p 451 N92-21690
The adverse aerodynamic impact of very small leading-edge ice (roughness) buildups on wings and tails p 451 N92-21691
The effect of hoar-frosted wings on the Fokker 50 take-off characteristics p 451 N92-21692
A theoretical investigation of the induced drag of wing of finite aspect ratio
[CUED/A-AERO/TR-17(1991)] p 525 N92-22193
Three-dimensional multigrid algorithm for the Euler and the thin-layer Navier-Stokes equations
[PB92-134329] p 602 N92-22216
High speed transport cruise drag --- scaling laws using Navier-Stokes equations
[NASA-CR-190248] p 527 N92-23103
Comparison of two-dimensional and three-dimensional droplet trajectory calculations in the vicinity of finite wings
[NASA-TM-105617] p 596 N92-23154
Sensitivity analysis of dynamic aeroelastic responses p 571 N92-23229
Application of multidisciplinary optimization methods to the design of a supersonic transport p 550 N92-23230
Application of analytical and design tools for fighter wing aeroelastic tailoring p 550 N92-23231
The structural optimization system OPTSYS: Current status and applications p 550 N92-23232
Simultaneous stress and flutter optimization for the wing of a transport aircraft equipped with four engines p 571 N92-23238
Performance degradation due to hoar frost on lifting surfaces p 628 N92-24866
An analytical approach to grid sensitivity analysis for NACA four-digit wing sections
[NASA-CR-190251] p 631 N92-25175
Algorithm and code development for unsteady three-dimensional Navier-Stokes equations
[NASA-CR-190077] p 692 N92-25264
The icing of the wing upper side and bottom side of the icing research aircraft of the DLR p 724 N92-26349
Recent applications of linear and nonlinear unsteady aerodynamics for aeroelastic analysis p 718 N92-27940
A time-linearization approach for unsteady transonic flows p 719 N92-27941
Evaluation of an unsteady implicit Euler code against two and three-dimensional standard configurations p 719 N92-27945
Computation of viscous phenomena in unsteady transonic flow p 720 N92-27949
Transonic aeroelastic calculations in both the time and frequency domains p 720 N92-27950
Analysis of unsteady aerodynamic and flutter characteristics of an aeroelastic model in transonic flow p 720 N92-27953
Transonic wind tunnel investigation of limit cycle oscillations on fighter type wings p 721 N92-27959
A review of scale effects on surfaces in unsteady motion p 722 N92-27962
Integrating aerodynamics and structures in the minimum weight design of a supersonic transport wing
[NASA-TM-107586] p 850 N92-28435
Turbulence modeling: Survey of activities in Belgium and the Netherlands, and appraisal of the status and a view on the prospects
[NLR-TP-90184-U] p 908 N92-28694
Reduction and analysis of F-111C flight data
[AD-A250341] p 853 N92-28771
Determination of aerodynamic sensitivity coefficients for wings in transonic flow
[NASA-CR-190570] p 832 N92-29657
Computation of three-dimensional effects on two dimensional wings
[NASA-CR-190576] p 832 N92-29691
Modeling and analysis methodology for aeroelastically tailored chordwise deformable wings
[NASA-CR-189620] p 961 N92-30304
Influence of structural and aerodynamic modeling on flutter analysis and structural optimization
[AD-A248487] p 978 N92-30323
Nonlinear aerodynamics and the design of wing tips
[NASA-CR-190649] p 946 N92-31157
Analysis of three icing test flights reaching the aircraft-referred icing degree of severe
[ESA-TT-1254] p 954 N92-31943
Exploratory experimental investigation of a wave propeller
[AD-A252175] p 949 N92-32062
Aerodynamic centre of wing-body combinations
[ESDU-92024] p 1036 N92-32479
Design, evaluation and experimental effort toward development of a high strain composite wing for Navy aircraft p 1107 N92-32514
Out of plane analysis for composite structures p 1107 N92-32527
Damage tolerance certification methodology for composite structures p 1108 N92-32579
Lift and rolling moment due to spoilers on wings with trailing-edge flaps deflected at subsonic speeds
[ESDU-92002-SUPPL] p 1037 N92-32782

Survey and analysis of research on supersonic drag-due-to-lift minimization with recommendations for wing design
[NASA-TP-3202] p 1040 N92-33656
Investigation of advancing front method for generating unstructured grid
[NASA-CR-190902] p 1128 N92-34043
Improved articulated fin/wing control system statement of government interests
[AD-D015268] p 1088 N92-34131

WIRE
Magnetic suspension using high temperature superconducting cores p 772 N92-27789

WIRING
Zonal analysis - The final step in system safety assessment p 760 A92-42071
Integrated wiring system
[SAE PAPER 912058] p 897 A92-45440
Managing simulator wiring information and deriving system continuity p 964 A92-49287
New insulation constructions for aerospace wiring applications. Volume 1: Testing and evaluation
[AD-A240638] p 22 N92-11006

WOOD
Dynamic simulation of a solid fuelled gas turbine system p 592 N92-22315

WORK
Relative energy concepts in helicopter dynamics p 846 A92-46925

WORKING FLUIDS
An iodine hypersonic wind tunnel for the study of nonequilibrium reacting flows
[AIAA PAPER 92-0566] p 383 A92-26974
Evaluation of the aerodynamic effects of commuter class (type 1-1/2) anti-icing fluids on small general aviation airplanes
[AIAA PAPER 92-0643] p 459 A92-31675
Power economy in high-speed wind tunnels by choice of working fluid and temperature p 881 A92-45275
Concept of a one-dimensional model of the dynamic behavior of a gas turbine p 862 A92-47791
Thermally regenerative fuel cells
[AD-A242900] p 300 N92-17629

WORKLOADS (PSYCHOPHYSIOLOGY)
B-2 handling, automation tailored to two-pilot crew p 643 A92-39725
Integrated flight control systems - Architectural considerations for future aircraft concepts p 872 A92-45322
A consideration on air traffic control processing capability in terminal area p 1047 A92-56110
The advantages of digital engine control as compared with traditional systems (hydraulic or pneumatic) p 1070 A92-56338
Ames life science telescience testbed evaluation
[NASA-CR-188856] p 140 N92-12033
The impact of cockpit automation on crew coordination and communication. Volume 1: Overview, LOFT evaluations, error severity, and questionnaire data
[NASA-CR-177587] p 93 N92-13044
Soviet electronic display systems under research and manufactured for the civil aviation aircraft of the 1990's
[AD-A240933] p 119 N92-13066
The multi-attribute task battery for human operator workload and strategic behavior research
[NASA-TM-104174] p 303 N92-17130
The Flight Simulation Facility at the Wichita State University p 484 N92-21511

WORKSTATIONS
DARPA high resolution display technologies p 218 A92-19977
An automated workstation for the half-scale testing of the flight vehicle stabilization circuit p 664 A92-40622
Operational evaluation of a tower workstation for clearance delivery p 879 A92-44981
Simulation of automatic rotorcraft nap-of-the-earth flight in graphics workstation environment
[AIAA PAPER 92-4131] p 981 A92-52428
Automatic production test equipment (APTE) for the B-2 p 997 A92-53107
Computations of unsteady multistage compressor flows in a workstation environment
[NASA-TM-103839] p 1071 N92-32452

WRECKAGE
Salvaging the wreckage - Multidistrict litigation and aviation p 697 A92-39245

X

X RAY ANALYSIS
X-ray computed tomographic inspection of castings p 492 A92-28725
Nondestructive inspection perspectives p 915 N92-30121

X RAY DETECTORS
Airport X-ray screening technology becomes a viable explosives detector p 836 A92-47925

X RAY IMAGERY
X-ray computed tomography of composites p 36 A92-10143
X-ray computed tomography for the aircraft/aerospace industry p 492 A92-28750
Application of X-ray image radiography system for aircraft p 1118 A92-56084

X RAY INSPECTION
New developments in the computer simulation of X-ray nondestructive evaluation process p 490 A92-28588
X-ray computed tomography for the aircraft/aerospace industry p 492 A92-28750
Airport X-ray screening technology becomes a viable explosives detector p 836 A92-47925
Detection of honeycomb damage using hexagonal grid discontinuities
[DREP-89-9] p 1109 N92-32846

X RAY SCATTERING
New developments in the computer simulation of X-ray nondestructive evaluation process p 490 A92-28588

X RAYS
Combined VISAR and flash x ray testing techniques
[DE92-004732] p 385 N92-18290
Computered tomography: Experimental data acquisition and parallelization of reconstruction algorithm
[DE92-005151] p 499 N92-20301

X-15 AIRCRAFT
A historical overview of high-temperature structural testing at the NASA Dryden Flight Research Facility p 981 A92-51407

X-22 AIRCRAFT
Wing force and surface pressure data from a hover test of a 0.658-scale V-22 rotor and wing
[NASA-TM-102244] p 550 N92-22864

X-29 AIRCRAFT
X-29 high angle of attack p 111 A92-16052
Evaluations of X-29 high-AOA regime show promise for future fighters p 192 A92-19925
X-29 forebody jet blowing
[AIAA PAPER 92-0017] p 247 A92-22139
An experimental study of pneumatic vortex flow control on high angle of attack forebody model
[AIAA PAPER 92-0018] p 247 A92-22140
X-29 high angle of attack flight test procedures, results, and lessons learned p 548 A92-35934
Predicted and measured in-flight wing deformations of a forward-swept-wing aircraft p 548 A92-35936
X-29 high angle-of-attack flight test air data comparisons of an inertial navigation system and noseboom probe p 549 A92-35945
Update of the X-29 high-angle-of-attack program
[SAE PAPER 912006] p 783 A92-45407
X-29 H-infinity controller synthesis p 873 A92-46749
High angle-of-attack control enhancement on a forward swept wing aircraft
[AIAA PAPER 92-4427] p 1080 A92-55351
Development of high angle of attack control laws for an unstable, non-minimum phase aircraft using variations of the quantitative feedback technique
[AD-A243698] p 282 N92-17096
Linearized aerodynamic and control law models of the X-29A airplane and comparison with flight data
[NASA-TM-4356] p 381 N92-19174
Wind-tunnel investigation of aerodynamic and stability characteristics of a forward swept wing X-29 model p 627 N92-24862

X-30 VEHICLE
NASP - Expanding space launch opportunities p 33 A92-13247
Conducting the NASP ground test program
[AIAA PAPER 91-5029] p 209 A92-17820
Dynamics and control of hypersonic vehicles - The integration challenge for the 1990's
[AIAA PAPER 91-5057] p 203 A92-17840
Hydrogen exhaust gas disposition by afterburning
[AIAA PAPER 91-5075] p 200 A92-17848
Hypersonic materials p 212 A92-18002
Fiber optics for the National Aero-Space Plane p 386 A92-24780
Supersonic and hypersonic quiet tunnel technology at NASA Langley
[AIAA PAPER 92-3908] p 1094 A92-56743
Technologies for the National Aero-Space Plane
[IAF PAPER 92-0868] p 1105 A92-57259

XV-15 AIRCRAFT
Analytical aeroelastic stability considerations and conversion loads for an XV-15 tilt-rotor in a wind tunnel simulation
[AIAA PAPER 92-2258] p 540 A92-34413
Short takeoff optimization for the XV-15 tiltrotor aircraft p 1056 A92-56302
A comparative analysis of XV-15 tiltrotor hover test data and WOPWOP predictions incorporating the fountain effect
[NASA-CR-189455] p 114 N92-11992
Tiltrotor research aircraft composite blade repairs: Lessons learned
[NASA-TM-103875] p 367 N92-19563

XV-4 AIRCRAFT
The Hummingbird experience at Lockheed Georgia p 646 A92-40041

Y

YAG LASERS
One joule output from a diode-array-pumped Nd:YAG laser with side-pumped rod geometry p 671 A92-37188
Advanced balancing using laser machining
[SAE PAPER 912218] p 674 A92-40020
Theoretical simulation of a 2 micron airborne solid state laser anemometer p 1000 N92-31059

YAW
747-400 upper rudder control system p 731 A92-43546
An experimental investigation on aft bypass supersonic inlet performance at high angle of attack and yaw p 862 A92-48268
Full Navier-Stokes calculations on the installed F/A-18 inlet at a high angle of attack
[AIAA PAPER 92-3175] p 1020 A92-54012
A simple three component velocity measurement method using a rotated split-film sensor p 1115 A92-54333
On the maneuvering tests of an ACV model p 1118 A92-56035
Predicting droplet impingement on yawed wings p 1043 A92-56180
Calibration of hemispherical-head flow angularity probes
[AIAA PAPER 92-4005] p 1122 A92-56828
Thrust vectoring for lateral-directional stability
[NASA-CR-186016] p 482 N92-21357
Development of flight testing of a fault tolerant fly-by-light yaw control system p 662 N92-25599
Helicopter low-speed yaw control
[NASA-CASE-LAR-14219-1] p 879 N92-30025
Yaw dynamics of horizontal axis wind turbines
[DE92-001245] p 1004 N92-30837
An investigation into the interface between three closely spaced axi-symmetric bodies at subsonic speed
[CRANFIELD-AERO-9114] p 948 N92-31514
Contribution of tailplane-mounted twin fins to sideforce, yawing moment, and rolling moment derivatives due to sideslip
[ESDU-92007] p 1086 N92-32487

YAWING MOMENTS
Yaw dynamics of a coaxial rotor helicopter p 378 A92-24427
Forebody vortex control using small, rotatable strakes p 811 A92-46798
Contribution of fin and tailplane to sideforce and yawing moment derivatives due to sideslip at supersonic speeds at low angles of attack
[ESDU-91031] p 259 N92-15971
Dynamic stall on wind turbine blades
[DE92-001157] p 262 N92-17874
Contribution of tailplane-mounted twin fins to sideforce, yawing moment, and rolling moment derivatives due to sideslip
[ESDU-92007] p 1086 N92-32487
A nozzle internal performance prediction method
[NASA-TP-3221] p 1040 N92-33625

YF-12 AIRCRAFT
A historical overview of high-temperature structural testing at the NASA Dryden Flight Research Facility p 981 A92-51407

YTTRIUM COMPOUNDS
Levitation of YBa2Cu3O(7-x) superconductor in a variable magnetic field p 771 N92-27735

Z

ZERO ANGLE OF ATTACK
Susceptibility of a supersonic boundary layer to acoustic perturbations p 707 A92-42730

ZERO LIFT
A Lie Bracket solution of the optimal thrust magnitude on a singular arc in atmospheric flight
[AIAA PAPER 92-4345] p 1079 A92-55334

ZIPPERS
Inflatable traversing probe seal p 595 N92-22692

ZIRCONIUM OXIDES
Fabrication and testing of corrosion resistant coatings
--- for turbine engine components
[DE92-003553] p 490 N92-21063
Properties of a TZP/Al2O3 composite after long-term exposure at 1000 C
[AD-A246407] p 757 N92-27752
ZODIACAL LIGHT
Visual photometric experiment data processing system
[AD-A248657] p 729 N92-27964

Typical Personal Author Index Listing

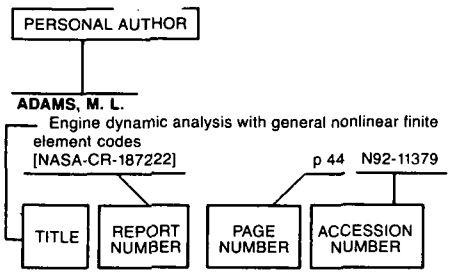

Listings in this index are arranged alphabetically by personal author. The title of the document provides the user with a brief description of the subject matter. The report number helps to indicate the type of document listed (e.g., NASA report, translation, NASA contractor report). The page and accession numbers are located beneath and to the right of the title. Under any one author's name the accession numbers are arranged in sequence.

A

AALFS, DAVID D.
Real-time processing of radar return on a parallel computer
[NASA-CR-4456] p 1043 N92-32606

AANSTOOS, JAMES V.
AGSSS: The Airborne Graphics Software Support System; an Ada/PHIGS-based display editor for the rapid development of cockpit display software systems
[AD-A243224] p 277 N92-17221

ABADIE, G.
Use of relative humidity sensors for planes measurement p 467 A92-32080

ABBAS, G. L.
Fiber-coupled position sensors for aerospace applications p 370 A92-27776
A novel avionic sensor for fly-by-light controls p 650 A92-38128

ABBAS, JEHAD F.
Nonlinear flutter of orthotropic composite panel under aerodynamic heating
[AIAA PAPER 92-2132] p 589 A92-35699

ABBE, BRIAN
ACTS aeronautical experiments
[AIAA PAPER 92-2042] p 485 A92-29956

ABBITT, JOHN D., III
Experimental investigation of a supersonic combustion flowfield employing staged transverse injection behind a rearward-facing step
[AIAA PAPER 92-0090] p 292 A92-22196

ABBOTT, JOHN M.
Inlets, ducts, and nozzles p 593 N92-22523

ABBOTT, TERENCE S.
A compensatory algorithm for the slow-down effect on constant-time-separation approaches
[NASA-TM-4285] p 23 N92-10024

ABBOTT, W.
Prediction and measurement of jet flowfield features for ASTOVL aircraft p 787 A92-45318

ABDEL-FATTAH, A. M.
Modification of Jindivik air intake duct with an auxiliary intake static aerodynamic tests
[AD-A243002] p 275 N92-17234

ABDEL-RAHIM, A.
Computational study of stall flutter in linear cascades
[ASME PAPER 91-GT-5] p 67 A92-15503

ABDELRAHMAN, M. M.
Aircraft spoiler effects under wind shear
[AIAA PAPER 92-2642] p 796 A92-45509

ABDELRAZIK, M. A.
Using satellite communication for aircraft Automatic Dependent Surveillance p 725 A92-42486

ABDOL-HAMID, KHALED S.
Computational investigation of circular-to-rectangular transition ducts
[AIAA PAPER 91-3342] p 6 A92-11605
Computational analysis of drag reduction techniques for afterbody/nozzle/empennage configurations
[SAE PAPER 912127] p 618 A92-39974
Commercial turbofan engine exhaust nozzle flow analyses using PAB3D
[AIAA PAPER 92-2701] p 801 A92-45543
Grid adaptation to multiple functions for applied aerodynamic analysis p 817 A92-47045

ABE, KIYATAKA
Stringer subsystem automation p 700 A92-43246

ABE, S.
Analytical condition inspection and extension of time between overhaul of F3-30 engine
[ASME PAPER 91-GT-277] p 653 A92-36888

ABE, T.
A thin metal model for aerodynamic heating tests of shock wave interaction p 709 A92-43103

ABE, TAKASHI
Effect of streamwise pressure gradient on the supersonic mixing layer p 1025 A92-54936

ABE, YOSHIYUKI
Observational study of pool boiling under microgravity p 757 A92-41060

ABED, EYAD H.
Washout filters in the bifurcation control of high alpha flight dynamics p 476 A92-29061
Two-parameter bifurcation analysis of axial flow compressor dynamics p 421 A92-29355

ABEL, JONATHAN S.
Integrating GPS with ranging transponders p 95 A92-16627

ABERLE, JAMES T.
Advanced electromagnetic methods for aerospace vehicles
[NASA-CR-188630] p 488 N92-20193
Advanced electromagnetic methods for aerospace vehicles
[NASA-CR-190650] p 1001 N92-31156

ABGRALL, R.
Numerical simulations around models in hypersonic wind tunnels p 182 N92-14998

ABHARI, R. S.
Comparison of time-resolved turbine rotor blade heat transfer measurements and numerical calculations
[ASME PAPER 91-GT-268] p 151 A92-15666

ABID, R.
Application of a new K-tau model to near wall turbulent flows p 395 A92-26437

ABOLFADL, MOHAMED A.
Application of CFD in the design of gas turbine engine components p 741 N92-27461

ABOLHASSANI, J. S.
Grid generation and compressible flow computations about a high-speed civil transport configuration p 919 A92-47055

ABOOSAIDI, FRED
Numerical analysis of airflow in aircraft cabins
[SAE PAPER 911441] p 245 A92-21837
Computational fluid dynamics applications in airplane cabin ventilation system design
[SAE PAPER 911992] p 788 A92-45394

ABOU-HAIDAR, N. I.
Computational modelling of turbulent flow in S-bends p 769 N92-27480

ABOUELKHEIR, M.
Row-by-row off-design performance calculation method for turbines p 737 A92-44514

ABRAMIAN, M.
Wind-tunnel investigation of aerodynamic and stability characteristics of a forward swept wing X-29 model p 627 N92-24862

ABRAMS, RICHARD
F-117A flight test program p 112 A92-16061
YF-22A prototype advanced tactical fighter demonstration/validation flight test program overview p 646 A92-40037

ABTAHI, A.
Heat flux sensor research and development: The cool film calorimeter
[NASA-CR-189789] p 298 N92-17006

ABUMERI, G. H.
Analysis of aircraft engine blade subject to ice impact
[NASA-TM-105336] p 229 N92-15402

ACEVEDO, D. A.
Application of a local panel buckling constraint within automated multidisciplinary structural analysis and design
[AIAA PAPER 92-1116] p 537 A92-33271

ACHAR, N. S.
Computational aspects of helicopter trim analysis and damping levels from Floquet theory p 875 A92-46933
Computational aspects of helicopter trim analysis and damping levels from Floquet theory
[NASA-CR-190736] p 1087 N92-33107

ACHARYA, MUKUND
Detection of flow state in an unsteady separating flow p 219 A92-20741
Unsteady pressure field and vorticity production over a pitching airfoil p 330 A92-26416
Dynamical scaling of a model unsteady separating flow p 1117 A92-54932

ACHARYA, SUMANTA
Solution-adaptive grid procedure for the parabolized Navier-Stokes equations p 432 A92-31163

ADAM, P.
Hypersonic shock tunnel testing for undergraduate laboratory instruction
[AIAA PAPER 92-4021] p 1100 A92-56843

ADAM, V.
On board planning of 4D-trajectories p 728 N92-27897

ADAM, VOLKMAR
Testing of an experimental FMS p 648 N92-25596

ADAMCZYK, J. J.
The role of tip clearance in high-speed fan stall
[ASME PAPER 91-GT-83] p 69 A92-15550

ADAMCZYK, JOHN J.
The numerical simulation of a high-speed axial flow compressor
[ASME PAPER 91-GT-272] p 75 A92-15669
Unsteady aerodynamic interaction effects on turbomachinery blade life and performance
[AIAA PAPER 92-0149] p 341 A92-28186

ADAMS, C. D. D.
Stratospheric electrodynamics from superpressure balloons - A technical challenge for small payload environments
[AIAA PAPER 91-3674] p 14 A92-11019

ADAMS, CATHERINE
Guidelines for integrating helicopter assets into emergency planning
[SCT-91RR-18] p 18 N92-10993

ADAMS, CATHERINE A.
Workshop on Aeronautical Decision Making (ADM). Volume 1: Executive summary
[DOT/FAA/RD-92/14-VOL-1] p 1142 N92-33305

ADAMS, FREDERICK C., JR.
Improving the LAMP Mk 3 SH-60B HF communication system
[AD-A245970] p 910 N92-29344

ADAMS, J. D.
Operational design factors for NASP derived vehicles
[AIAA PAPER 91-5081] p 210 A92-17851

ADAMS, M. L.
Engine dynamic analysis with general nonlinear finite element codes
[NASA-CR-187222] p 44 N92-11379

AUTHOR

ADAMS, R. J.
Analysis of helicopter accident risk exposure near heliports, airports, and unimproved sites
[SCT-91RR-13] p 637 N92-26028
Composite profiles of helicopter mishaps at heliports and airports
[AD-A248887] p 724 N92-28052
ADAMS, R. M.
An investigation into the feasibility of providing a proximity warning device for search and rescue helicopters
[ETN-92-91057] p 530 N92-22408
ADAMS, RICHARD J.
Gain scheduled linear PID autopilot for the AIAA Controls Design Challenge aircraft
[AIAA PAPER 92-4629] p 1078 A92-55304
Introduction to cognitive processes of expert pilots
[DOT/FAA/RD-92/12] p 952 N92-30980
Workshop on Aeronautical Decision Making (ADM). Volume 1: Executive summary
[DOT/FAA/RD-92/14-VOL-1] p 1142 N92-33305
ADAMS, STUART
A fault-tolerant network architecture for integrated avionics p 965 A92-49297
ADAMS, WILLIAM M., JR.
Parameter insensitive control utilizing eigenspace methods p 204 A92-18615
Multifunction tests of a frequency domain based flutter suppression system
[AIAA PAPER 92-2096] p 566 A92-35667
Multifunction tests of a frequency domain based flutter suppression system
[NASA-TM-107615] p 662 N92-25607
ADAMSON, T. C., JR.
Control of hypersonic aerodynamic forces with surface blowing p 172 A92-18363
ADDINGTON, GREGORY A.
Static and dynamic flow field development about a porous suction surface wing
[AIAA PAPER 92-2628] p 795 A92-45500
ADDISON, J. S.
Modelling of unsteady transitional boundary layers
[ASME PAPER 91-GT-282] p 152 A92-15677
ADDISON, R. C., JR.
Laser-based ultrasonics on GR/epoxy composite - Interferometric detection p 144 A92-13554
ADDY, A. L.
Two-stream, supersonic, wake flowfield behind a thick base. I - General features p 813 A92-46895
ADDY, HAROLD E., JR.
Investigation of the diffuser flow quality in an icing research wind tunnel p 382 A92-24406
Lewis icing research tunnel test of the aerodynamic effects of aircraft ground deicing/anti-icing fluids
[NASA-TP-3238] p 952 N92-30395
ADELMAN, HOWARD M.
Integrated multidisciplinary rotorcraft optimization research at the NASA Langley Research Center p 419 A92-29673
Fully integrated aerodynamic/dynamic optimization of helicopter rotor blades
[AIAA PAPER 92-2374] p 542 A92-34544
Optimizing tuning masses for helicopter rotor blade vibration reduction including computed airloads and comparison with test data
[AIAA PAPER 92-2376] p 542 A92-34546
Experimental validation of structural optimization methods
[NASA-TM-104203] p 404 N92-19258
Optimizing tuning masses for helicopter rotor blade vibration reduction including computed airloads and comparison with test data
[NASA-TM-104194] p 367 N92-19846
Fully integrated aerodynamic/dynamic optimization of helicopter rotor blades
[NASA-TM-104226] p 461 N92-20417
ADELMANN, JOHN C.
KGR-1 thick adherend specimen evaluation for the determination of adhesive mechanical properties p 994 A92-51513
ADIBHATLA, SHRIDER
Intelligent Engine Control (IEC)
[AIAA PAPER 92-3484] p 866 A92-49024
ADLER, CHARLES O.
Development of a high-angle-of-attack stability and control prediction code
[AIAA PAPER 92-4354] p 1079 A92-55340
ADLER, R. M.
A low noise propulsion concept for the supersonic transport
[ASME PAPER 91-GT-397] p 127 A92-15727
ADOMAITIS, RAYMOND A.
Two-parameter bifurcation analysis of axial flow compressor dynamics p 421 A92-29355
ADRIAN, EDWARD D.
An anthropometric evaluation of the TH-57 Jetranger helicopter p 46 A92-11164
ADRIAN, RONALD J.
The interaction between a plane shear layer and a slender body p 991 A92-49790
ADVANI, S.
Flight simulation p 207 N92-13982
An evaluation of IFR approach techniques: Generic helicopter simulation compared with actual flight p 886 N92-28550
An evaluation of decelerating IFR approaches utilizing a helicopter flight simulator
[CTN-92-60348] p 1048 N92-32845
ADVANI, S. K.
The basic research simulator programme and the industrial and aerospace community: Opportunities for cooperative research
[LR-662] p 887 N92-28579
AESCHLIMAN, D. P.
Liquid crystal coatings for surface shear-stress visualization in hypersonic flows p 496 A92-32177
Joint computational and experimental aerodynamics research on a hypersonic vehicle
[DE92-013439] p 943 N92-30367
AESCHLIMAN, DANIEL P.
Joint computational/experimental aerodynamics research on a hypersonic vehicle. I - Experimental results p 812 A92-46890
Calibration of hemispherical-head flow angularity probes
[AIAA PAPER 92-4005] p 1122 A92-56828
AFFELT, E.
Probabilistic lifing approach for aero engine disks made of powder nickel base alloys containing ceramic defects p 226 N92-14424
AFFES, H.
An experimental and analytical study of the interaction of a vortex with an airframe
[AIAA PAPER 92-0319] p 321 A92-25766
A simplified model for the interaction of a rotor tip vortex with an airframe
[AIAA PAPER 92-0320] p 321 A92-25767
The unsteady interaction of a 3-dimensional vortex filament with a cylinder p 813 A92-46934
AFFOLTER, H.
Separation of external stores: Comparison of results
[F+W-TF-2058] p 732 N92-26944
AFTOSMIS, MICHAEL
An examination of several high resolution schemes applied to complex problems in high speed flows
[AD-A250814] p 1124 N92-32632
AFZALI, H.
Development and verification of software for flight safety critical systems p 164 N92-12469
AGAMATA, BAL N.
A proposal for a dynamic test platform for inertial units and/or GPS p 138 A92-16653
AGAMI, D.
FCS skewed sensors array: Practical considerations p 968 N92-31868
AGAPOV, N. N.
System of cryogenic security of the superconducting accelerator of relativistic nuclei-nuclotron
[DE91-643289] p 304 N92-16789
AGARWAL, NAVAL K.
Effects of a leading-edge fillet on the flow past an appendage-body junction p 935 A92-50301
Crossflow vortex and transition measurements by use of multielement hot films p 935 A92-50307
Method of measuring cross-flow vortices by use of an array of hot-film sensors
[NASA-CASE-LAR-14824-1-SB] p 998 N92-30390
AGARWAL, R. K.
Finite element Navier-Stokes solver for unstructured grids p 398 A92-28035
Solution of the parabolized Navier-Stokes equations using Osher's upwind scheme p 713 A92-44371
A compact higher order Euler solver for unstructured grids with curved boundaries
[AIAA PAPER 92-2696] p 807 A92-45590
Compact higher order characteristic-based Euler solver for unstructured grids p 812 A92-46889
AGARWAL, RAMESH K.
Simulation of wind tunnel flowfields
[AIAA PAPER 92-0034] p 249 A92-22155
AGARWAL, TARUN K.
A parallel-vector algorithm for rapid structural analysis on high-performance computers
[NASA-TM-102614] p 595 N92-22649
AGARWALA, AJAY S.
Redundancy design philosophy for catastrophic loss protection p 1119 A92-56202
AGAWALA, ASHOK
Distributed systems: Interconnection and fault tolerance studies
[AD-A252869] p 1135 N92-33920
AGLAN, H.
Fracture behaviour of high-temperature polymer composites p 34 A92-11993
AGNELLO, MARK
Control systems for the next century's fighter engines
[ASME PAPER 91-GT-278] p 125 A92-15674
AGRAWAL, S.
A simple numerical criterion for vortex breakdown
[AIAA PAPER 92-0057] p 250 A92-22172
Design load predictions on a fighter-like aircraft wing p 811 A92-46797
Investigation of vortex breakdown on a delta wing using Euler and Navier-Stokes equations p 87 N92-13019
AGRAWAL, SHREEKANT
Supersonic boundary-layer stability analysis on an aircraft wing p 9 A92-13207
Evaluation of Euler solvers for transonic wing-fuselage geometries p 174 A92-20214
Numerical investigation of vortex breakdown on a delta wing p 340 A92-28027
A numerical study of control surface buzz using computational fluid dynamic methods
[AIAA PAPER 92-2654] p 806 A92-45578
AGRONIK, ALEKSANDR G.
Evolution of ejection systems p 262 A92-21684
AHERN, JOHN E.
Thermal management of air-breathing propulsion systems
[AIAA PAPER 92-0514] p 373 A92-26940
AHMAD, SURAIYA P.
Radiometric properties of the NS001 Thematic Mapper Simulator aircraft multispectral scanner p 155 A92-17110
AHMED-ZAID, F.
Identification and control of aircraft dynamics using radial basis function neural networks
[AIAA PAPER 92-4393] p 1074 A92-55194
AHMED, A.
Effect of riblets on turbulence in the wake of an airfoil p 5 A92-11051
Experimental investigation of a three-dimensional bluff-body wake
[AIAA PAPER 92-0429] p 326 A92-26277
AHMED, N. A.
Fibre optic laser anemometry for turbomachinery applications p 397 A92-27783
AHMED, S.
New nonequilibrium turbulence model for calculating flows over airfoils p 330 A92-26403
AHMED, S. A.
Premixed, turbulent combustion of axisymmetric sudden expansion flows p 397 A92-27770
Swirl effects on confined flows in axisymmetric geometries p 399 A92-28513
Swirl number effects on confined flows in a model of a dump combustor p 896 A92-45202
AHMED, S. R.
Analysis of helicopter rotor-fuselage interference with time averaged pressure distribution p 1032 A92-56331
AHMED, SAJEER
Control of unsteady separated flow associated with the dynamic pitching of airfoils
[NASA-CR-189758] p 258 N92-15966
AHMED, SYED R.
A Mach-scaled powered model for rotor-fuselage interactional aerodynamics and flight mechanics investigations p 847 A92-46960
AHN, I. S.
A simulator and performance criteria for evaluation of ground and space-based ATC surveillance p 96 A92-16639
AHN, SEUNGKI
Cross-flow separation on a prolate spheroid at angles of attack
[AIAA PAPER 92-0428] p 326 A92-26276
AHOLA, PEKKA J.
X-band side-looking airborne radar for remote sensing p 554 A92-34976
AHUJA, J. S.
Non-slender shapes of minimum drag p 937 A92-52029
AHUJA, K. K.
Acoustic interactions between an altitude test facility and jet engine plumes: Theory and experiments
[NASA-CR-190423] p 738 N92-26405
AHUMADA, A.
Sensor fusion for synthetic vision
[AIAA PAPER 91-3730] p 197 A92-17597
AI, S. H.
Creep fracture mechanisms in single crystal superalloys p 388 A92-25031

AI, XIANFENG
Study on the reliability evaluation of engine fuel accessories p 392 A92-24749
AIBARA, YASUYOSHI
Aerodynamic performances of spoiler motion p 429 A92-30526
AIHARA, Y.
Transient aerodynamic behaviours associated with stepwise incidence variation of airfoils p 66 A92-15327
Measurements of turbulence in hypersonic flow p 1092 A92-56005
AIKEN, EDWIN W.
A review of recent programs and future plans for rotorcraft in-flight simulation at Ames Research Center [SAE PAPER 912121] p 608 A92-39969
Rotorcraft In-Flight Simulation Research at NASA Ames Research Center: A Review of the 1980's and plans for the 1990's [NASA-TM-103873] p 853 N92-28926
AIKIN, A. C.
Natural cycles, gases p 408 N92-19123
AILINGER, KEVIN G.
Low Reynolds number, long endurance aircraft design [AIAA PAPER 92-1263] p 538 A92-33343
AINSCOW, K.
Evolution of ASTOVL aircraft design p 842 A92-45311
Some implications for advanced STOVL operation from invincible class ships p 466 N92-21971
AINSWORTH, R. W.
An Axial Turbobrake [ASME PAPER 91-GT-1] p 147 A92-15501
AITCHESON, KENT ROBERT
Stability and control flight testing of a half-scale Pioneer remotely piloted vehicle [AD-A245973] p 879 N92-28801
AIZAWA, YASUTAKA
A robust gain scheduler interpolated into multiple models by membership functions [AIAA PAPER 92-4553] p 1131 A92-55265
AJDARI, E.
Thermal imaging of afterburning plumes p 129 A92-17179
AKASHI, E.
Transient aerodynamic behaviours associated with stepwise incidence variation of airfoils p 66 A92-15327
AKIMOTO, TOSHIO
Computational aerodynamic simulation on HOPE p 251 A92-22635
Navier-Stokes simulation for the winged space vehicle 'HOPE' at subsonic, transonic, and supersonic regimes p 1018 A92-53559
Calculations for aerodynamic characteristics of HOPE type vehicle in subsonic and hypersonic flow p 1018 A92-53560
Concepts of flight experiments for HOPE development p 1103 A92-53635
Aerodynamic study of H-II Orbiting Plane, HOPE p 1103 A92-53639
HOPE re-entry experimental vehicle p 1103 A92-55098
Numerical simulation of hypersonic viscous flow for the design of H-2 orbiting plane (HOPE-2) [NAL-TR-1093] p 11 N92-10009
Design of orbital re-entry experiment vehicle and outline of the experiment p 667 N92-25374
AKIYAMA, M.
Polar patrol balloon [AIAA PAPER 91-3688] p 15 A92-11031
AKIYOSHI, RYO
Fundamental studies on Marangoni convection related to Bridgman crystal growth p 1111 A92-53758
AL-BAHI, A. M.
Aircraft spoiler effects under wind shear [AIAA PAPER 92-2642] p 796 A92-45509
AL-BAHI, ALI M.
Effect of atmospheric disturbances on airplane response [AIAA PAPER 92-4340] p 1078 A92-55329
AL-KHALIL, KAMEL M.
Development of an improved model for runback water on aircraft surfaces [AIAA PAPER 92-0042] p 270 A92-22160
AL-KHALIL, KAMEL MAHMOUD
Numerical simulation of an aircraft anti-icing system incorporating a rivulet model for the runback water p 448 N92-20303
AL-MAAITAH, A. A.
Effect of suction on the stability of supersonic boundary layers. I - Second-mode waves. II - First-mode waves p 174 A92-19611
AL-SAADI, JASSIM A.
Wall interference calculation in a transonic test section including simulation of discrete slots [AIAA PAPER 92-0032] p 249 A92-22153
Model representation in the PANCOR wall interference assessment code [NASA-TM-104152] p 31 N92-11022
AL-SAADI, JASSIM ABBASS
Wall interference calculation in a transonic wind tunnel with discrete slots p 83 N92-12995
AL-SHARIF, M.
Measurements and correlation of two-phase pressure drop under microgravity conditions p 37 A92-10435
AL-SUNNI, F.
Aircraft flight controls design using output feedback p 280 A92-21180
AL-SUNNI, F. M.
Negative state weighting in the linear quadratic regulator for aircraft control p 1007 A92-50513
AL-ZUBAIDY, SARIM N. J.
A refined analytical method for designing high pressure ratio centrifugal impellers p 591 A92-36032
AL'-DZHANABI, SH. KH.
Pulsation characteristics of one-phase and two-phase steam flows in Laval nozzles under off-design conditions p 1019 A92-53882
ALAKOZ, A. V.
Determination of the mean duration of normal acceleration loads at the center of mass of aircraft during a flight in a turbulent atmosphere p 480 A92-30192
ALAPHILIPPE, M.
Feasibility study of hypersonic clinometric measurements at R3Ch [ONERA-RSF-136/1865-AY-728-] p 829 N92-28789
ALBAKIAN, KIRA
The use of photogrammetry in aviation equipment flight testing p 994 A92-51649
ALBEGOV, R. V.
An experimental study of supersonic H2 combustion and heat transfer in a circular duct p 388 A92-25997
ALBERS, MARTIN
High-speed civil transport aircraft emissions p 408 N92-19122
ALBONE, C. M.
Embedded meshes of controllable quality synthesised from elementary geometric features [AIAA PAPER 92-0663] p 411 A92-27034
ALCORN, CHARLES
Present status of the MIT/NASA Langley 6-inch MSBS p 750 N92-27802
ALDEN, RALPH
C-141 and C-130 power-by-wire flight control systems p 876 A92-48493
ALDER, MARTIN
British Airways Airbus A320 pilots' autothrust survey [SAE PAPER 912225] p 636 A92-40023
ALDERETE, THOMAS S.
1991-92 AHS Technical Committee highlights - Flight simulation p 609 A92-40394
ALEKSANDROV, E. L.
Oscillations of balloon-flight altitude p 836 A92-46660
ALEKSANDROVICH, E. V.
Numerical and experimental investigation of airframe-integrated inlet for high velocities p 243 A92-21072
ALESHIN, N. P.
Relationship between the rotating stall and vibrations of a blade row p 496 A92-31988
ALEXANDER, HAROLD
Research needs for a commercial passenger tiltrotor p 1056 A92-56298
ALEXANDER, MICHAEL G.
Subsonic wind tunnel testing handbook [AD-A240263] p 13 N92-10986
ALEXOPOULOS, G. A.
An assumed joint-Beta PDF approach for supersonic turbulent combustion [AIAA PAPER 92-3844] p 1113 A92-54199
ALFANO, SALVATORE
Two variations of certainty control p 918 A92-46762
ALFREDSSON, P. H.
Transition to turbulence in curved channel flow p 621 A92-40125
ALGER, LINDA S.
Advanced information processing system: Inter-computer communication services [NASA-CR-187556] p 53 N92-11706
ALHUSEIN, MAHMOUD A.
Small two-dimensional surface excrescences on aircraft wings approaching separation p 1031 A92-56170
ALJABARI, SAMER
Prediction of the pressure loss coefficient of wind tunnel turbulence reducing screens [AIAA PAPER 92-0568] p 384 A92-26976
Prediction of the pressure loss coefficient of wind tunnel turbulence reducing screens [AIAA PAPER 92-4043] p 1035 A92-56862
ALLAIRE, P. E.
Professor Jesse W. Beams and the first practical magnetic suspension p 771 N92-27723
Low power magnetic bearing design for high speed rotating machinery p 772 N92-27739
ALLAN, WILLIAM D. E.
Heat transfer and instrumentation studies on rotating turbine blades in a transient facility p 156 N92-12203
ALLARD, D. W.
ETOPS: A developing scene [PNR-90844] p 473 N92-20459
ALLEGRE, J.
The SR3 low density wind tunnel - Facility capabilities and research development [AIAA PAPER 92-3972] p 1098 A92-56798
Experimental investigation of transverse jet effects related to hypersonic space vehicles p 182 N92-14995
Flat plates placed in depleted hypersonic flow [SESSIA-430/91.960] p 947 N92-31508
ALLEN, C. B.
An efficient Euler solver for predominantly supersonic flows with embedded subsonic pockets [AIAA PAPER 92-0323] p 322 A92-25770
ALLEN, CHRIS
Scorpion: Close Air Support (CAS) aircraft [NASA-CR-189974] p 462 N92-20664
ALLEN, DAVID H.
Thermoviscoplastic response of thin plates subjected to intense local heating [AIAA PAPER 92-2538] p 584 A92-34382
ALLEN, G. E.
A low noise propulsion concept for the supersonic transport [ASME PAPER 91-GT-397] p 127 A92-15727
ALLEN, M. G.
Supersonic combustor testing using optical diagnostics and a high enthalpy shock tunnel [AIAA PAPER 92-0761] p 384 A92-27102
ALLEN, R. W.
Parachute canopy control simulation - A solution for aircrew emergency training p 572 A92-35428
ALLEN, SCOTT M.
An alternative concept for aeroassisted orbit transfers [AD-A243409] p 287 N92-17325
ALLEN, T. K.
The LISA 6000 - A highly integrated IRS/GPS navigation system p 267 A92-22088
ALLGOOD, GLENN O.
Prediction of helicopter simulator sickness p 46 A92-11473
ALLMAN, MICHAEL G.
Filament winding of composite isogrid fuselage structures p 784 A92-47405
ALLMARAS, S. R.
A one-equation turbulence model for aerodynamic flows [AIAA PAPER 92-0439] p 327 A92-26285
ALLRED, J. W.
Mechanical design of a rotary balance system for NASA. Langley Research Center's vertical spin tunnel p 664 N92-25090
ALLWOOD, R. J.
Vibration analysis of gas turbines by an intelligent knowledge-based system p 656 A92-40548
ALON, YAIR
94 GHz MMW imaging radar system [SAE PAPER 912208] p 651 A92-40015
ALPERINE, S.
Protective coatings of thermal barrier type p 214 A92-20349
Aluminides modified by palladium - Protection of new parts by local finishing [ONERA, TP NO. 1992-49] p 893 A92-48610
ALTHAUS, JOSEF
Hydraulic actuator system for rotor control p 224 N92-14363
ALTHOFF, SUSAN L.
Effect of blade planform variation on the forward-flight performance of small-scale rotors [NASA-TM-4345] p 630 N92-24885
ALTRICHTER, WAYNE W.
JTIDS relative navigation and data registration p 955 A92-51006
ALVAR, KENNETH
Neutron radiography with SNRS p 492 A92-28747
ALVES, DANIEL F., JR.
Global Positioning System telecommand link p 839 A92-47566
ALVI, F. S.
Physical model of the swept shock wave/boundary-layer interaction flowfield p 935 A92-50312

ALWANG, ROGER
V-22 thrust power management control law development p 132 A92-14405
ALZIARY, T.
Hypersonic wakes
[ETN-92-91082] p 349 N92-19925
ALZIARYDEROQUEFORT, T.
Infrared measurements of aerodynamic heating in hypersonic wind tunnel p 208 N92-15002
AMABILE, P.
Proposal for the new fatigue management system for the AMX p 361 N92-18580
AMANI, G.
Remarks on the relation between lift induced drag and vortex drag p 941 A92-53079
AMANO, K.
Noise test of high-speed counterrotation propeller in low-speed wind tunnel p 1135 A92-56055
AMATO, M.
Numerical predictions of transonic viscous flows around aerofoils through an Euler/boundary layer interaction method p 624 A92-40600
Wake effects on the prediction of transonic viscous flows around airfoils p 702 A92-41232
AMATUCCI, V. A.
Two-stream, supersonic, wake flowfield behind a thick base. I - General features p 813 A92-46895
AMBLE, CURTIS R.
Thrust vector control of an overexpanded supersonic nozzle using pin insertion and rotating airfoils
[AD-A243891] p 387 N92-18942
AMBUR, TODD A.
Measurement of vortex flow fields
[NASA-CR-189543] p 443 N92-20283
AMER, KENNETH B.
Closing the loop on helicopter crashworthiness design requirements p 107 A92-14392
AMES, GREGORY H.
Multi-channel fiber optic rotary joint for single-mode fiber
[AD-D015273] p 927 N92-29095
AMIELH, M.
Hot jet dilutor
[ETN-92-90860] p 366 N92-19225
AMIET, R. K.
Propeller and propfan noise p 54 N92-10599
AMIN, F.
A new method to estimate the effective geometric focal length and radius of ultrasonic focused probes p 490 A92-28633
AMIN, S.
Flow induction by pressure forces
[AIAA PAPER 92-3571] p 1067 A92-54060
AMINPOUR, M. A.
Coupled analysis of independently modeled finite element subdomains
[AIAA PAPER 92-2235] p 581 A92-34289
AMINPOUR, MOHAMMAD A.
Computational methods for global/local analysis
[NASA-TM-107591] p 1125 N92-33104
AMONO, KANICHI
Wind tunnel test for a high speed propeller with coaxial contrarotation p 737 A92-43195
AMUEDO, KURT C.
Hot gas ingestion characteristics and flow visualization of a vectored thrust STOVL concept p 860 A92-45316
AMY, ANNIE
Manx: Close air support aircraft preliminary design
[NASA-CR-189992] p 463 N92-21565
AMZAJERDIAN, FARZIN
A study of atmospheric optical scattering parameters at 1.5 and 2 micron region for solid state Doppler lidar applications p 1001 N92-31067
AN, C.-F.
Analysis and design of transonic airfoils using streamwise coordinates p 194 N92-13955
AN, DONG
The relation among the general unsteady aerodynamic coefficients of a wing in subsonic and supersonic speed p 941 A92-53022
AN, JINWEN
A low-altitude breakthrough system using optimal path terrain following p 205 A92-20483
ANANTHKRISHNAN, N.
Aircraft longitudinal dynamics equations including wind shear effects p 977 A92-51946
ANDERS, S. G.
Supersonic and hypersonic quiet tunnel technology at NASA Langley
[AIAA PAPER 92-3908] p 1094 A92-56743
ANDERSON, BERNHARD H.
A study on vortex flow control of inlet distortion in the re-engined 727-100 center inlet duct using computational fluid dynamics
[AIAA PAPER 92-0152] p 253 A92-23767
Design and analysis of reengine Boeing 727-100 center inlet S duct by a reduced Navier-Stokes code
[AIAA PAPER 92-1221] p 517 A92-33320
A study of three dimensional turbulent boundary layer separation and vortex flow control using the reduced Navier Stokes equations p 621 A92-40105
Design and analysis of vortex generators on reengined Boeing 727-100QF center inlet S-duct by a reduced Navier-Stokes code
[AIAA PAPER 92-2700] p 800 A92-45542
Comparative study of turbulence models in predicting hypersonic inlet flows
[AIAA PAPER 92-3098] p 824 A92-48740
Application of computational fluid dynamics to the study of vortex flow control for the management of inlet distortion
[AIAA PAPER 92-3177] p 1020 A92-54013
Vortex generator design for aircraft inlet distortion as a numerical optimization problem p 194 N92-13959
A study on vortex flow control on inlet distortion in the re-engined 727-100 center inlet duct using computational fluid dynamics
[NASA-TM-105321] p 179 N92-13998
Inlets, ducts, and nozzles p 593 N92-22523
Comparative study of turbulence models in predicting hypersonic inlet flows
[NASA-TM-105720] p 722 N92-28102
Application of computational fluid dynamics to the study of vortex flow control for the management of inlet distortion
[NASA-TM-105672] p 1128 N92-34112
ANDERSON, J. R.
Blade repair with adaptive vision tracking
[ASME PAPER 91-GT-208] p 607 A92-36897
ANDERSON, JOHN A.
Variable displacement electro-hydrostatic actuator p 876 A92-48492
ANDERSON, JOHN D.
Numerical simulation of unsteady hypersonic viscous flows in shock tunnel p 710 A92-43170
ANDERSON, JOHN D., JR.
Hypersonic waveriders - Effects of chemically reacting flow and viscous interaction
[AIAA PAPER 92-0302] p 320 A92-25754
Heat transfer characteristics of hypersonic waveriders with an emphasis on leading edge effects
[AIAA PAPER 92-2920] p 821 A92-47892
Heat transfer characteristics of hypersonic waveriders with an emphasis on the leading edge effects
[NASA-CR-189586] p 525 N92-22215
ANDERSON, KARL F.
Thermal-structural test facilities at NASA Dryden
[NASA-TM-104249] p 1062 N92-34202
ANDERSON, MARK C.
ELS pilot evaluation
[SAE PAPER 912107] p 691 A92-39960
ANDERSON, MARK R.
Three dimensional hypersonic inlets - Low speed performance
[AIAA PAPER 91-5021] p 171 A92-17817
Robust control law development for a hypersonic cruise aircraft p 478 A92-29127
Analytical development of an equivalent system mismatch function
[AIAA PAPER 92-4422] p 1080 A92-55346
ANDERSON, O. L.
Computational study of a supersonic mixer-ejector exhaust system p 969 A92-50252
ANDERSON, ROY E.
Spectrum sharing between AMSS(R) and MSS p 677 N92-24165
ANDERSON, S. D.
High temperature, thermally stable JP fuels - An overview
[AIAA PAPER 92-0683] p 389 A92-27050
ANDERSON, SETH B.
Jet-powered V/STOL aircraft - Lessons learned p 841 A92-45304
ANDERSON, STEVEN D.
Static tests for the evaluation of fuel additives
[AIAA PAPER 92-0686] p 389 A92-27053
ANDERSON, TORGER J.
CARS temperature/multi-species measurement strategies for high speed airbreathing and rocket propulsion testing p 154 A92-16615
Simultaneous coherent anti-Stokes Raman spectroscopy measurements in hydrogen-fueled supersonic combustion p 287 A92-21052
ANDERSON, W. J.
Added mass of high-altitude balloons
[AIAA PAPER 91-3693] p 16 A92-11034
ANDERSON, W. K.
Numerical study on using sulfur hexafluoride as a wind tunnel test gas p 216 A92-18373
ANDERSON, W. KYLE
Grid generation and flow solution method for Euler equations on unstructured grids
[NASA-TM-4295] p 528 N92-23533
ANDERSON, W. L.
High temperature static strain gage development
[NASA-CR-189044] p 195 N92-14037
High temperature strain gage technology for hypersonic aircraft development applications
[NASA-CR-189101] p 592 N92-22239
ANDERSON, WILLIAM
Internationalization of telemetry systems p 920 A92-47535
ANDERSON, WILLIAM J.
Wing mass formula for subsonic aircraft p 845 A92-46812
Wing mass formula for twin fuselage aircraft p 1054 A92-56171
ANDERSON, WILLIAM P.
Fiber optic controls for aircraft engines - Issues and implications p 856 A92-46244
ANDERTON, GARY L.
Alternate/modified binders for asphalt airfield pavements
[AD-A242829] p 285 N92-17260
ANDES, ROBERT C., JR.
Specification of adaptive aiding systems - Information requirements for designers p 916 A92-44915
ANDO, HIROYUKI
Application of automation for structural-composites production p 1119 A92-56109
ANDO, S.
WIG transportation efficiency considering the influence of no-load situation p 781 A92-43241
Reevaluation of the motion of an airship p 731 A92-43243
Small and cost-effective airship for transportation p 731 A92-43244
ANDO, SHIGENORI
Finite difference numerical prediction of aerodynamics of an airfoil flying over wavy wall p 64 A92-14033
PAR-WIG performance prediction during acceleration from water-borne to air-borne p 291 A92-21721
Evaluation method of longitudinal static stability of tailless airplane p 282 A92-22520
A quick automatic method for computing performance of nonducted propeller with constant-revolutional-speed p 393 A92-25505
Analysis of a 2-D airfoil motion flying in-proximity-to a wavy-wall surface-lifting surface-scheme p 315 A92-25506
Analysis of a 2-D airfoil motion flying in-proximity-to a wavy-wall surface - Finite difference method p 421 A92-29517
A quick automatic method for computing performance of ducted-propeller p 736 A92-42800
Analysis of motion of airfoil flying over wavy-wall surface (lifting surface method) p 818 A92-47100
ANDO, YASUKATSU
Vibration tests of long plate structural model
[NAL-TM-625] p 400 N92-18485
Vibration tests and structural modeling of an aircraft model for active control technology experiments
[NAL-TM-626] p 662 N92-25401
ANDO, YASUNORI
CFD application to 2D/3D flow fields in Scramjet engine p 170 A92-17501
Numerical simulation for various flowfields of aero-engine components p 200 A92-17503
ANDRADE, LUIZ
Design of the Boeing 777 electric system p 1070 A92-55902
ANDRE, R.
Analysis of lossy composite terminating structures
[NASA-CR-189901] p 404 N92-19217
ANDREW, M. J.
The use of math-dynamic models to aid the development of integrated health and usage monitoring systems p 1006 A92-50013
ANDREW, MIKE
The application of math-dynamic models to characterise a range of helicopter rotor system faults p 1056 A92-56297
ANDREW, T. L.
Scale model test of an isolated turbofan nacelle with riblets
[SAE PAPER 912128] p 618 A92-39975
ANDREWS, HAROLD
Technical evaluation report on the Flight Mechanics Panel Symposium on Flying Qualities
[AGARD-AR-311] p 733 N92-27870
ANDREWS, J. W.
Air-to-air visual acquisition handbook
[ATC-151] p 93 N92-13042

ANDREWS, ROGER
Rapid systems integration of navigation avionics
p 858 A92-48473
ANDREWS, S. J.
An evaluation of a simple PID controller designed using optimal control theory when applied to helicopter stabilisation p 569 A92-35785
ANFIMOV, N. A.
TSNIIMASH capabilities for aerogasdynamical and thermal testing of hypersonic vehicles
[AIAA PAPER 92-3962] p 1097 A92-56789
ANGEL, R. G. A.
Ground surface erosion - British Aerospace test facility and experimental studies p 881 A92-45323
ANGERER, JAMES R.
Development of an annoyance model based upon elementary auditory sensations for steady-state aircraft interior noise containing tonal components
[NASA-TM-104147] p 166 N92-13758
ANGERMANN, W.
Flight test validation of tow target trajectory predictions
[AIAA PAPER 92-0209] p 271 A92-23814
ANIKIN, V. A.
Aerodynamic features of a coaxial rotor helicopter
p 1032 A92-56349
ANILKUMAR, R.
Estimation of overall drag coefficient of an aerospace plane p 700 A92-41188
ANKUDINOV, A. L.
Cooling of a sharp nose by extraneous gas injection into the viscous shock layer p 426 A92-30188
ANNATI, R. E.
Garrett GTP50-1 multipurpose small power unit technology demonstrator program
[ASME PAPER 91-GT-328] p 153 A92-15698
ANNIS, CHARLES
Fatigue in single crystal nickel superalloys
[AD-A248190] p 896 N92-29408
Fatigue in single crystal nickel superalloys
[AD-A250068] p 987 N92-31360
ANOLL, ROBERT K.
Heliport VFR airspace design based on helicopter performance
[SCT-90RR-34] p 103 N92-13049
Helicopter rejected takeoff airspace requirements
[SCT-91RR-28] p 116 N92-13058
Rotorcraft acceleration and climb performance model
[SCT-90RR-30] p 116 N92-13059
Helicopter physical and performance data
[SCT-91RR-27] p 116 N92-13060
Rotorcraft low altitude IFR benefit/cost analysis: Operations analysis
[SCT-90RR-44] p 191 N92-15061
ANSART, D.
CARS temperature measurements and validation of a computing code on a gas-turbine combustor
[ONERA, TP NO. 1991-224] p 373 A92-26376
ANSELL, HANS
A manufacturer's approach to ensure long term structural integrity p 838 N92-30133
ANSELMET, F.
Influence of suction through a slot on a turbulent boundary layer p 622 A92-40127
Experimental and numerical investigation of a turbulent boundary layer over riblets p 622 A92-40128
ANSLEY, GEORGE
Current nondestructive inspection methods for aging aircraft
[DOT/FAA/CT-91/5] p 1126 N92-33480
ANTAR, B. N.
Forced-injection quenching of a hot-tube under microgravity p 590 A92-35977
ANTCLIFF, R. R.
CARS temperature measurements in a hypersonic propulsion test facility p 140 N92-12049
ANTHAN, DONALD J.
Wavelength-multiplexed fiber-optic position encoder for aircraft control systems p 734 A92-42602
ANTONESCO, MICHEL
Programmable channelized digital radio/modem
p 955 A92-49291
ANTONOV, S. G.
Influence of atmospheric rarefaction on aerodynamic characteristics of flying vehicles p 938 A92-52750
ANTONOV, V. A.
Mathematical modeling of supersonic flow over a convex-concave formed body based on the Euler and Navier-Stokes equations p 252 A92-23416
ANTREASIAN, PETER G.
Simulation of GRM drag compensation system
p 285 A92-21023
ANTSAKLIS, PANOS J.
Optimal stabilization of discrete event systems
p 48 A92-11376
AOKI, SUNAO
Film cooling on a gas turbine rotor blade
[ASME PAPER 91-GT-279] p 152 A92-15675
AOKI, TAKEO
Experiments to evaluate hot-jet simulation capabilities in Cryogenic Wind-Tunnel testing
[AIAA PAPER 92-0567] p 384 A92-26975
AOKI, TOSHIYUKI
Mechanical properties of laminate aluminum matrix composites p 1106 A92-56102
AONO, H.
Flight tests on the structures of the STOL research aircraft Asuka p 730 A92-43143
AOYAMA, G.
Numerical analysis of helicopter rotor blades
p 430 A92-30558
AOYAMA, TAKASHI
Navier-Stokes analysis of blade tip shape in hover
p 521 A92-35758
APICELLA, A.
The G-222 aircraft individual tracking programme
p 361 N92-18582
APKARIAN, P.
A two-feedback-loop robust helicopter controller based on eigenspace techniques and H(infinity) synthesis
p 29 A92-11582
Improvement of helicopter robustness and performance control law using eigenstructure techniques and H-infinity synthesis p 569 A92-35776
APKARIAN, PIERRE
Double loop control law strategy and applications to helicopter
[CERT-2/7724-DERA] p 381 N92-19295
APONSO, BIMAL L.
Identification of higher-order helicopter dynamics using linear modeling methods p 131 A92-14336
Effects of cockpit lateral stick characteristics on handling qualities and pilot dynamics
[NASA-CR-4443] p 878 N92-28584
APONTE, ALFONSO G.
Approach to crew training in support of the USAF Aircraft Structural Integrity Program (ASIP) p 363 N92-18595
APPA, KARI
Recent advances in maneuver loads analysis
p 642 A92-37576
APPLEBY, RUTH
An interactive multi-block grid generation system
p 691 N92-24419
APSHTEIN, E. Z.
Radiant heat transfer in supersonic three-dimensional and axisymmetric flow of air past evaporating bodies
p 337 A92-27533
ARABYAN, ARA
A multibody approach to modeling tilt-wing rotorcraft dynamics
[AIAA PAPER 92-0487] p 328 A92-26318
ARAI, NORIO
Active control of the hydraulic forces of a body by a splitter plate p 591 A92-36351
ARAI, T.
Numerical prediction of the flow characteristics in an arc wind tunnel
[AIAA PAPER 92-4016] p 1100 A92-56838
ARAKI, TAKAHITO
Basic study of adhesive bonding for fiber-composites - Adhesive bonding technologies on jet engine parts
p 764 A92-44733
ARASHI, KAZUO
A study on the interaction between a bow shock wave generated by a blunt body and a turbulent boundary layer p 8 A92-12424
Numerical simulation of a supersonic jet impingement on a ground
[SAE PAPER 912014] p 789 A92-45412
Experimental study on three-dimensional shock wave-turbulent boundary layer interaction induced by protuberance p 1019 A92-53997
Three-dimensional shock wave-turbulent boundary layer interaction induced by blunt body and protuberance
p 1029 A92-56009
ARBUCKLE, P. DOUGLAS
Simulation model of a twin-tail, high performance airplane
[NASA-TM-107601] p 1088 N92-33537
ARCARA, P. C., JR.
Analysis for the application of hybrid laminar flow control to a long-range subsonic transport aircraft
[SAE PAPER 912113] p 617 A92-39964
ARCILLA, A. S.
Numerical grid generation in computational fluid dynamics and related fields; Proceedings of the 3rd International Conference, Universidad Politecnica de Cataluna, Barcelona, Spain, June 3-7, 1991
[ISBN 0-444-88948-5] p 918 A92-47035
ARDONCEAU, P.
Remarks on the relation between lift induced drag and vortex drag p 941 A92-53079
Nonstationary flight aerodynamics in a turbulent environment
[ETN-91-90102] p 82 N92-11980
ARENA, ANDREW S., JR.
A discrete vortex model for predicting wing rock of slender wings
[AIAA PAPER 92-4497] p 1026 A92-55365
Aerodynamic and flowfield hysteresis of slender wing aircraft undergoing large-amplitude motions
p 364 N92-18780
ARGYRIS, JOHN
An exploration of chemically reacting viscous hypersonic flow p 612 A92-37550
ARIELI, R.
Measurements of lateral aerodynamics characteristics of forebodies at high angle of attack in subsonic and transonic flows
[AIAA PAPER 92-0174] p 255 A92-23785
ARIGA, HIRONOBU
Effect of streamwise pressure gradient on the supersonic mixing layer p 1025 A92-54936
ARIMOTO, H.
Shafranov shift in low-aspect-ratio heliotron/torsatron CHS
[NIFS-110] p 1138 N92-33743
ARIN, KEMAL
Current DOT research on the effect of multiple site damage on structural integrity p 913 N92-30112
ARISTOVA, E. IU.
Design of wing profiles with tangential suction or injection p 624 A92-40602
ARKHIPOV, N. I.
Lift characteristics of an infinite-span cylindrical wing of a thick symmetric profile at low subsonic velocities
p 440 A92-31897
ARKHIPOV, V. A.
Calculation of gas combustion regimes in a counterflow vortex chamber p 34 A92-12209
ARKKIO, A.
Analysis of a 37 kW cage-induction motor
[PB92-142116] p 597 N92-23496
ARMANDO, A.
AM-X flight simulator from engineering tool to training device p 884 N92-28536
ARMANIOS, ERIAN A.
Buckling, postbuckling and crippling of thin walled composite airframe structures under compression
p 899 A92-46940
ARMISTEAD, MICHAEL A.
Second-order shock-expansion theory extended to include real gas effects
[AD-A247191] p 831 N92-29539
ARMSTRONG, J. P.
Development of an innovative high-temperature gas turbine fuel nozzle
[ASME PAPER 91-GT-36] p 121 A92-15519
ARMSTRONG, RICHARD
Knowledge maintenance in an evolving system using a deep structure representation
[AIAA PAPER 91-3941] p 231 A92-17605
ARNAL, D.
Three-dimensional linear stability approach to transition on wings and bodies of revolution at incidence
p 172 A92-18361
The effects of wall suction on laminar-turbulent transition in three-dimensional flow p 522 A92-36021
Boundary layer transition: Prediction, application to drag reduction p 717 N92-27711
ARNDT, N.
Blade row interaction in a multistage low-pressure turbine
[ASME PAPER 91-GT-283] p 125 A92-15678
ARNDT, STEPHEN M.
Evaluation of thermoplastic matrix composites for use in energy-absorbing helicopter subfloors
p 141 A92-14374
ARNEGARD, RUTH J.
The multi-attribute task battery for human operator workload and strategic behavior research
[NASA-TM-104174] p 303 N92-17130
ARNEY, A. M.
A review of Australian activity on modelling the helicopter/ship dynamic interface p 465 N92-21967
ARNOLD, RICHARD P.
The FAA Loran program status and expectations
p 95 A92-16629
ARNOLD, U.
Active control of helicopter ground and air resonance
p 568 A92-35762
Blade instability of horizontally stoppable rotors
p 1085 A92-56308

ARNONE, A.
Transonic cascade flow prediction using the Navier-Stokes equations
[ASME PAPER 91-GT-313] p 76 A92-15690
ARNONE, ANDREA
Navier-Stokes solution of transonic cascade flows using nonperiodic C-type grids p 344 A92-28523
AROESTY, JEROME
Tilt rotors and the Port Authority of New York and New Jersey Airport System
[RAND-R-3971/1-PA-SUMM] p 636 N92-25262
ARRIGONI, NICOLA
Joint Aviation Authorities: Development of an international standard for safety regulation - The first steps are being taken by the JAA p 781 A92-43548
ARRINGTON, E. A.
Flow quality studies of the NASA Lewis Research Center 8- by 6-foot supersonic/9- by 15-foot Low Speed Wind Tunnel
[AIAA PAPER 92-3916] p 1095 A92-56748
ARRINGTON, E. ALLEN
Flow quality studies of the NASA Lewis Research Center 8- by 6-foot supersonic/9- by 15-foot low speed wind tunnel
[NASA-TM-105417] p 887 N92-28673
ARTEMKOV, V. S.
Automated thematic processing of aircraft scanner data gathered over pasture territory in Turkmenia p 406 A92-25330
ARTIGUES, C.
International standardisation of regulations for gust loading calculations p 270 A92-22473
ASADA, H.
Bayesian reliability analysis in connection with the evaluation of multiple-site damage p 762 A92-43126
ASADA, HIROO
Some consideration for evaluation of structural integrity of aging aircraft p 762 A92-43107
ASADA, SHOICHIRO
HOPE re-entry experimental vehicle p 1103 A92-55098
ASAI, KEISUKE
Euler flow analysis of turbine powered simulator and fanjet engine p 80 A92-17196
Experiments to evaluate hot-jet simulation capabilities in Cryogenic Wind-Tunnel testing
[AIAA PAPER 92-0567] p 384 A92-26975
ASAY, A. A.
Utility of ground simulation in flight control problem identification, solution development, and verification p 883 N92-28525
ASBURY, M. J. A.
Probability distributions that are important when assessing barometric aiding to GPS p 100 A92-16952
ASBURY, SCOTT C.
Thrust vectoring characteristics of the F-18 high alpha research vehicle at angles of attack from 0 to 70 deg
[AIAA PAPER 92-3095] p 877 A92-48737
Static performance of a cruciform nozzle with multiaxis thrust-vectoring and reverse-thrust capabilities
[NASA-TP-3188] p 527 N92-23095
A static investigation of the thrust vectoring system of the F/A-18 high-alpha research vehicle
[NASA-TM-4359] p 633 N92-25967
ASENSIO, A.
New practical method for measurement error determination in radar systems under real traffic conditions p 155 A92-17238
ASGHAR, A.
Experimental investigations of the vortex flow on delta wings at high incidence p 432 A92-31172
ASH, L. E.
Progress report on analysis of differential attenuation radar data obtained during WISP-91
[PB92-133800] p 503 N92-21828
ASH, ROBERT L.
Helical-perturbation device for cylinder-wing vortex generators p 432 A92-31167
Viscous effects on a vortex wake in ground effect
[NASA-CR-190400] p 907 N92-28361
ASHBAUGH, SCOTT
The SnoDog: Preliminary design of a close air support aircraft
[NASA-CR-189990] p 462 N92-21489
ASHBY, DALE L.
Large-scale wind tunnel studies of a jet-engined powered ejector-lift STOVL aircraft p 842 A92-45313
Potential flow theory and operation guide for the panel code PMARC
[NASA-TM-102851] p 1036 N92-32422
ASHBY, GEORGE C., JR.
Test description and preliminary pitot-pressure surveys for Langley Test Technique Demonstrator at Mach 6
[AIAA PAPER 92-3940] p 1096 A92-56770
Pilot-pressure probe for measuring pressure in a hypersonic wind tunnel
[NASA-CASE-LAR-14232-1] p 1102 N92-34213
ASHBY, R. L.
A USAF assessment of STOVL fighter options p 842 A92-45310
ASHILL, P. R.
Comment on 'Transition effects on airfoil dynamics and implications for subscale tests' p 703 A92-41247
ASHKENAS, IRVING L.
Assessment of flying-quality criteria for air-breathing aerospacecraft
[NASA-CR-4442] p 663 N92-25982
ASHLEY, STEVEN
Safety in the sky - Designing bomb-resistant baggage containers p 836 A92-47775
ASHTON, LARRY J.
Filament winding of composite isogrid fuselage structures p 784 A92-47405
ASHWILL, T. D.
The status of the US VAWT program
[DE92-002931] p 505 N92-21040
Fatigue life variability and reliability analysis of a wind turbine blade
[DE92-008673] p 689 N92-25049
ASO, S.
Numerical simulation of opposing sonic jets p 524 A92-36357
ASO, SHIGERU
A numerical simulation of separated flows around bodies p 8 A92-12423
A study on the interaction between a bow shock wave generated by a blunt body and a turbulent boundary layer p 8 A92-12424
Experiment on pitching moments of separated flow around airfoil profiles p 429 A92-30527
Study on two-dimensional jet mixing with a vertical supersonic flow p 429 A92-30530
Numerical computation and experimental study of shock wave reflection p 430 A92-30542
Aerodynamic heating measurement in hypersonic flow p 709 A92-43102
Experimental and numerical investigations on separated flows around pitching airfoils p 710 A92-43166
Numerical simulations of separated flows around oscillating airfoil for dynamic stall phenomena
[SAE PAPER 911991] p 788 A92-45393
Aerodynamic heating in three-dimensional shock wave turbulent boundary layer interaction induced by sweptback sharp fins in hypersonic flows
[SAE PAPER 912044] p 791 A92-45428
Experimental investigation on turbulent phenomena in three-dimensional shock wave/turbulent boundary layer interaction induced by blunt fin p 1018 A92-53557
Numerical simulations of shock reflections by a TVD scheme p 1018 A92-53558
Experimental study on three-dimensional shock wave-turbulent boundary layer interaction induced by protuberance p 1019 A92-53997
Three-dimensional shock wave-turbulent boundary layer interaction induced by blunt body and protuberance p 1029 A92-56009
ASO, SHIGHERU
Numerical experiments on unsteady shock reflection processes using the thin-layer Navier-Stokes equations p 818 A92-47155
ATALLA, NOUREDDINE
A numerical study of fuselage scattering effects on rotor noise p 511 N92-20428
ATAMANENKO, A. V.
Aerodynamic characteristics of a standard corrugated body in a free-molecular flow p 940 A92-52818
ATASSI, H. M.
Aerodynamics of loaded cascades in subsonic flows subject to unsteady three-dimensional vortical disturbances
[AIAA PAPER 92-0146] p 253 A92-23762
ATENCIO, A., JR.
Flight simulator fidelity assessment in a rotorcraft lateral translation maneuver
[AIAA PAPER 92-4424] p 1092 A92-55348
ATENCIO, ADOLPH, JR.
The use of ground based simulation for handling qualities research: A new assessment p 885 N92-28545
ATHAVALE, M. M.
A finite-volume numerical method to calculate fluid forces and rotordynamic coefficients in seals
[AIAA PAPER 92-3712] p 1113 A92-54132
ATHAVALE, MAHESH M.
Development of a CFD code for analysis of fluid dynamic forces in seals p 228 N92-15084
ATILGAN, ALI R.
New, unusual and nonclassical behavior of thin-walled composite structures p 580 A92-32746
ATKIN, C. J.
A study of the interaction of a normal shock wave with a turbulent boundary layer at Mach numbers between 1.30 and 1.55 p 339 A92-28006
ATKINS, H. L.
Evaluation of a finite volume method for compressible shear layers p 610 A92-36834
ATKINSON, EDWARD
Effects of material choices on brush seal performance p 1116 A92-54650
ATSUMI, MOTOHIRO
Fabrication test and evaluation of graphite/PMR-15 polyimide for HOPE primary structure p 1105 A92-53516
ATTAR, MOSHE
Some interesting phenomena from Lavi test flights relating to aircraft stability and control
[IAITIC-91-1017] p 482 N92-20849
ATTISHA, M. R.
A unique approach to aircraft conflict resolution using artificial intelligence techniques p 190 N92-14029
ATWOOD, CHRISTOPHER A.
Flowfield simulation about the SOFIA Airborne Observatory
[AIAA PAPER 92-0656] p 342 A92-28217
AUCLAIR, RICHARD A.
Information Management Engineering (IME) laboratory: A database development facility
[AD-A243191] p 305 N92-17369
AUDET, N. F.
Thermal energy test apparatus
[AD-A243526] p 305 N92-17537
AUGUST, R.
Structural and aerodynamic analysis of a large-scale advanced propeller blade p 375 A92-28517
AULEHLA, FELIX
Calibration-related pseudo-Reynolds number trends in transonic wind tunnels p 882 A92-46780
AULT, B. A.
Active control for gas turbine combustors p 128 A92-16585
AUPOIX, B.
Asymptotic defect boundary-layer theory applied to hypersonic flows p 610 A92-36839
Analysis of turbulence models for hypersonic boundary layers p 623 A92-40182
Models of turbulence in a hypersonic boundary layer p 705 A92-41817
AUSMAN, J. D.
Application of a local panel buckling constraint within automated multidisciplinary structural analysis and design
[AIAA PAPER 92-1116] p 537 A92-33271
AUSMAN, J. S.
Baro-inertial loop for the USAF Standard RLG INU p 97 A92-16647
A Kalman filter mechanization for the baro-inertial vertical channel p 673 A92-39558
AUSROTAS, RAYMOND A.
Impacts of technology on the capacity needs of the US national airspace system
[NASA-CR-4470] p 1045 N92-34192
AUST, BRIAN
Automatic production test equipment (APTE) for the B-2 p 997 A92-53107
AUSTIN, MICHAEL
Beam scanning error of phased array antenna p 676 A92-40189
AUSTIN, MICHAEL E.
Failure environment analysis tool (FEAT) development status
[AIAA PAPER 91-3803] p 232 A92-17654
AUTRY, M.
A Ka-band instrumentation radar with one foot range resolution p 95 A92-16252
AUWETER-KURTZ, M.
The IRS plasma wind tunnels for the investigation of thermal protection materials for reentry vehicles p 208 N92-15009
AVERY, JOHN G.
Development of thermoplastic components for structural validation p 1107 N92-32522
AVITAL, GAVRIEL
The External Propulsion Accelerator - Scramjet thrust without interaction with accelerator barrel
[AIAA PAPER 92-3717] p 866 A92-49098
AVNI, MICHA
Electronic systems in transportation
[TP-9983] p 189 N92-14009
AVRITCH, STEVEN A.
Achieving fault tolerance in multichannel control systems p 974 A92-49296
AVVA, V. S.
Behavior of aircraft tire coupons under various loading conditions
[AD-A241416] p 116 N92-13063

AWAD, J.
Experimental measurement of the vortex development downstream of a lobed forced mixer
[ASME PAPER 90-GT-27] p 295 A92-23299
AWAMURA, E.
Demonstration performance of an aircraft liquid crystal display p 735 A92-43224
AWBREY, FRANK T.
A model for the effects of aircraft overflight noise on the reproductive success of raptorial birds
p 688 A92-39101
AXELRAD, PENINA
Wide area differential GPS p 101 A92-16966
AYALA, JESSE
Standardizing operational flight data handling
p 1009 A92-53109
AYDER, E.
Experimental study of the swirling flow in the internal volute of a centrifugal compressor
[ASME PAPER 91-GT-7] p 67 A92-15505
AYER, T. C.
Development of an efficient analysis for high Reynolds number inviscid/viscid interactions in cascades
[AIAA PAPER 92-3073] p 823 A92-48723
AYER, TIMOTHY C.
Development of unsteady aerodynamic analyses for turbomachinery aeroelastic and aeroacoustic applications
[NASA-CR-4405] p 12 N92-10979
AYERS, BERT
Forebody vortex control for suppressing wing rock on a highly-swept wing configuration
[AIAA PAPER 92-2716] p 803 A92-45555
AYMERDELACHEVALERIE, D.
Infrared measurements of aerodynamic heating in hypersonic wind tunnel p 208 N92-15002
AYOUB, PETER
Methods for predicting successful ejection seat canopy penetration p 544 A92-35441
Computational fluid dynamics as a tool for aerodynamic analysis of ejection seats p 519 A92-35444
AYRES, J. C.
Application of an automated multidisciplinary analysis and optimisation system to the design of aircraft structures p 551 N92-23233
AYRES, WILLIAM R.
Comparison of R2SPG waveforms with simulated EMP
p 760 A92-42317
AZAM, MISBAHUL
Neural networks for feedback linearization in aircraft control
[AIAA PAPER 92-4391] p 1074 A92-55192
Invertibility and trajectory control for nonlinear maneuvers of aircraft
[AIAA PAPER 92-4410] p 1075 A92-55204
AZIZ, A.
Two-dimensional effects in a triangular convecting fin
p 219 A92-20324
Two-dimensional heat transfer from a rectangular fin with asymmetrical thermal boundary conditions
p 498 A92-32524
AZZAM, H.
The use of math-dynamic models to aid the development of integrated health and usage monitoring systems
p 1006 A92-50013
AZZAM, HESHAM
The application of math-dynamic models to characterise a range of helicopter rotor system faults
p 1056 A92-56297
AZZANO, CHRISTOPHER P.
A preliminary look at an optimal multivariable design for propulsion-only flight control of jet-transport aircraft
[NASA-CR-186014] p 663 N92-25734

B

BAAKLINI, GEORGE Y.
NDE of advanced turbine engine components and materials by computed tomography
[ASME PAPER 91-GT-287] p 152 A92-15681
BABA, ICHIRO
Utilizing the fault monitoring system for the A320 aircraft p 700 A92-43157
BABA, S.
Recent airfoil tests in NAL 2D high Reynolds number wind tunnel p 748 A92-43171
Transonic visualization test for the airframe shape improvement of a spaceplane p 752 A92-43200
Noise test of high-speed counterrotation propeller in low-speed wind tunnel p 1135 A92-56055
BABA, SHIGEO
On the structure of unsteady shock induced separation of the transonic airfoil in the NAL two-dimensional wind tunnel p 1029 A92-56010
BGK1 airfoil oilflow tests in the NAL two-dimensional wind tunnel. II p 1029 A92-56044
Results of measured temperature distribution on an adiabatic wing model with radiation thermometer
[NAL-TM-610] p 261 N92-17755
NACA0012 airfoil data corrected for sidewall boundary-layer effects in the NAL two-dimensional transonic wind tunnel
[NAL-TM-640T] p 722 N92-28151
Force measurements on AGARD calibration model-B at transonic speeds in the NAL two-dimensional wind tunnel
[NAL-TM-639] p 722 N92-28190
Replacement of the NAL high pressure air storage system
[NAL-TM-634] p 888 N92-28835
BABA, Y.
Selection of sampling rate for nonlinear flight trajectory controller of aircraft p 1084 A92-56070
BABA, YORIAKI
Study on an induction method for a flying object, taking accelerating targets into account p 744 A92-43127
BABCHENKO, I. V.
Diffuser efficiency estimation parameters
p 79 A92-16814
Experimental study of an adjustable plane supersonic diffusor p 426 A92-30173
BABCOCK, DALE A.
Thermal/structural analysis of a transpiration cooled nozzle
[NASA-TM-104184] p 401 N92-18877
BABER, BURL B.
High-temperature miniaturized turbine engine lubrication system simulator
[AD-A249259] p 868 N92-28294
BABICH, OLEG A.
Data processing in navigation complexes
[ISBN 5-217-01060-6] p 725 A92-42789
BABIKOV, P. E.
Flow of a viscous twisted fluid film on the surface of a blunt body in supersonic flow of a gas
p 424 A92-30146
A study of flow of a fluid film on the surface of a plate in the case of slot injection p 496 A92-31892
BABIN, ROBERT S.
Engineering reliability and maintainability review - A regimen for discovering production deficiencies
p 1120 A92-56254
BABINSKY, H.
Flow over a delta wing at hypersonic speeds
p 181 N92-14993
BABISH, CHARLES A., III
Application of the STAPAT II code to hypersonic vehicle aerothermodynamics
[AIAA PAPER 91-5035] p 209 A92-17824
BABKIN, V. I.
The feasibility of reducing induced wing drag by using crescent planform wings p 425 A92-30167
BABU, G. L. N.
Smart structures for helicopters p 516 A92-35727
BACH, RALPH E., JR.
Correction of sideslip-induced static pressure errors in flight-test measurements p 309 A92-24416
BACKES, P. G.
Detailed investigation of causes of avionics field failures p 995 A92-51925
BACKMAN, DANIEL G.
Advanced materials for aircraft engine applications
p 390 A92-28251
BACKSTROM, M. G.
The use of finite difference electromagnetic analysis in the design and verification of modern aircraft
p 192 A92-20136
BACON, BARTON
Simulation and model reduction for the AFW program
[AIAA PAPER 92-2081] p 572 A92-35653
BADIAGIN, A. A.
Aerodynamic balance range of aircraft of different configurations p 134 A92-16801
BADINELLI, MARTIN
Effect of guard band reduction on marker beacon receiver performance
[DOT/FAA/CT-TN92/18] p 1002 N92-31617
BADMUS, O. O.
An integrated, full-range surge control/rotating stall avoidance compressor control system
p 469 A92-29376
BAE, GYUNGHYUN
Integrated flight control law synthesis for an aeroelastic forward-swept wing aircraft
[AIAA PAPER 92-0046] p 281 A92-22163
BAEDER, J. D.
Aerodynamic and acoustic calculations of transonic nonlifting hovering rotors
[ONERA, TP NO. 1991-178] p 77 A92-16140
Flowfield of a lifting rotor in hover - A Navier-Stokes simulation p 1024 A92-54906
BAESLACK, W. A., III
Inertia-friction welding of an advanced rapidly solidified titanium alloy p 212 A92-18898
BAGAI, A.
A study of rotor wake development and wake/body interactions in hover p 813 A92-46935
BAGLEY, DANIEL T.
GPS/INS integration for improved aircraft attitude estimates
[AD-A243947] p 356 N92-19604
BAGOT, KEITH W.
Surface painted taxiway markings at Seattle-Tacoma International Airport
[DOT/FAA/CT-TN91/49] p 32 N92-11029
BAI, XUE-SONG
Numerical computation of improved transonic potential method p 441 A92-32234
BAI, XUESONG
Discussion of improved transonic potential method
p 942 A92-53290
BAI, ZHENZHU
The canard-wing interference and stall safety of light canard aircraft p 111 A92-15341
BAIK, KI-YOUNG
Resonance prediction for slotted circular wind tunnel using finite element p 235 A92-18388
BAILEY, F. R.
Future directions in computing and CFD
[AIAA PAPER 92-2734] p 917 A92-45489
BAILEY, J. E.
Robust wind shear stochastic controller-estimator
p 661 A92-39893
Robust flight reconstruction for helicopter simulation and training p 747 A92-41230
BAILEY, J. M.
Counterrotating brushless DC permanent magnet motor
[DE92-003825] p 401 N92-18550
BAILEY, M. D.
High altitude solar power platform
[NASA-TM-103578] p 506 N92-21546
BAILEY, P. J.
The experimental and computational study of jet impingement flowfields with reference to VSTOL aircraft performance p 787 A92-45324
BAILEY, R. S.
High temperature static strain gage development
[NASA-CR-189044] p 195 N92-14037
BAILLEUX, P.
Study of interactions on anemoclinometric sensors
[REPT-90/30] p 138 N92-12006
BAILLIE, S. W.
Tracking performance requirements for rotorcraft instrument approaches to reduced minima. Phase 1: Preliminary study
[NRC-32137-PHASE-1] p 102 N92-11988
BAILLIE, STEWART W.
An exploratory investigation into the definition of tracking standards for IFR helicopter approaches to reduced minima p 533 A92-35726
BAIN, D. B.
CFD mixing analysis of jets injected from straight and slanted slots into confined crossflow in rectangular ducts
[NASA-TM-105699] p 738 N92-26561
BAITIS, ERICH
Analytical modeling of SH-2F helicopter shipboard operation p 464 N92-21961
BAKANAS, STEPHEN
Current nondestructive inspection methods for aging aircraft
[DOT/FAA/CT-91/5] p 1126 N92-33480
BAKER, A. A.
Minimum surface treatments for adhesively bonded repairs p 754 A92-42501
BAKER, A. J.
A non-linearly stable implicit finite element algorithm for hypersonic aerodynamics p 433 A92-31487
Recent advances on a finite element algorithm for computational aerodynamics: Transonics-hypersonics
[DE91-018176] p 11 N92-10010
BAKER, DONALD J.
Evaluation of composite components on the Bell 206L and Sikorsky S-76 helicopters p 1107 N92-32575
Flight service environmental effects on composite materials and structures p 1110 N92-33054
BAKER, J. E.
Terrain following of arbitrary surfaces using a high intensity LED proximity sensor
[DE92-007161] p 455 N92-21201
BAKER, PAUL A.
An alternative source of flight test services
[AIAA PAPER 92-1088] p 515 A92-33254

BAKER, S. J.
Second moment closure predictions of jet-on-jet impingement flows p 675 A92-40102
BAKER, TIMOTHY J.
Single block mesh generation for a fuselage plus two lifting surfaces p 817 A92-47054
BAKHAREV, S. A.
Aerodynamic characteristics of slender sharp-leading-edge delta wings with air scooping through the air intake at hypersonic velocities. I p 427 A92-30206
Aerodynamic characteristics of a blunt delta wing with air bleed through an intake at supersonic and hypersonic velocities. II p 437 A92-31855
BAKHLE, M. A.
Cascade flutter analysis with transient response aerodynamics p 154 A92-15972
BAKHLE, MILIND A.
Time domain flutter analysis of cascades using a full-potential solver p 176 A92-20747
Analysis of cascades using a two dimensional Euler aeroelastic solver
[AIAA PAPER 92-2370] p 556 A92-34598
An investigation of cascade flutter using a two-dimensional full-potential solver
[AIAA PAPER 92-2119] p 558 A92-35688
BAKOS, R. J.
Hypersonic mixing and combustion studies in the hypulse facility p 737 A92-44526
Effects of oxygen dissociation on hypervelocity combustion experiments
[AIAA PAPER 92-3964] p 1098 A92-56791
BAKOS, ROBERT
Experiments on shear layer mixing at hypervelocity conditions
[AIAA PAPER 92-0628] p 396 A92-27009
BAKULEV, V. I.
On the experimental investigation of air-breathing engine of new schemes p 469 A92-29711
BAKUNIN, V. N.
Viscosity characteristics of synthetic aviation oils at low temperatures p 1105 A92-53875
BALABANOV, O. V.
The analysis and approximate representation of the optimal control law for a maneuverable aircraft p 479 A92-30131
BALAGEAS, D.
Application of infrared thermography to thermal flux measurement in wind tunnels
[AAAF-NT-89-12] p 31 N92-11020
BALAGEAS, D. L.
Measurement of convective heat-transfer coefficients on a wind tunnel model by passive and stimulated infrared thermography p 291 A92-21450
Measurement of convective heat-transfer coefficients in wind tunnels using passive and stimulated infrared thermography p 390 A92-24430
Heat transfer measurements in ONERA supersonic and hypersonic wind tunnels using passive and active infrared thermography p 208 N92-15003
Ablation and temperature sensors for flight measurements in reentry body heat shields p 227 N92-15004
BALAKRISHNA, S.
Control of large cryogenic tunnels
[AIAA PAPER 92-3930] p 1096 A92-56761
The NASA Langley Research Center 0.3-meter transonic cryogenic tunnel microcomputer controller source code
[NASA-CR-189556] p 209 N92-15077
Dynamic flying investigations on 1/13.5 NALLA model (Longitudinal Results)
[NAL-PD-FC-9113] p 359 N92-18073
BALAKRISHNAN, G.
Compressibility effects in thin channels with injection p 216 A92-18369
BALAKUMAR, P.
Discrete modes and continuous spectra in supersonic boundary layers p 809 A92-46264
BALANIS, CONSTANTINE A.
Advanced electromagnetic methods for aerospace vehicles
[NASA-CR-188630] p 488 N92-20193
Advanced electromagnetic methods for aerospace vehicles
[NASA-CR-190650] p 1001 N92-31156
BALAS, GARY J.
Robust dynamic inversion control laws for aircraft control
[AIAA PAPER 92-4329] p 1073 A92-55173
Feedback control laws for highly maneuverable aircraft
[NASA-CR-190535] p 879 N92-29654
BALDENKOV, G. N.
Several results of lidar measurements of the characteristics of oblique visibility at an airfield p 45 A92-12844
BALDWIN, DOROTHY M.
Simulation software flowdown in the aircraft design process - Problems and solutions
[AIAA PAPER 92-4160] p 1008 A92-52450
BALDWIN, LARRY J.
Addition curing thermosets endcapped with 4-amino (2.2) paracyclophane p 577 A92-33918
BALENA, F. J.
Development and testing of cabin sidewall acoustic resonators for the reduction of cabin tone levels in propfan-powered aircraft
[NASA-CR-4388] p 166 N92-13757
BALIAKIN, V. B.
Effect of inertia forces on the characteristics of a long hydrodynamic vibration damper in the mixed flow regime p 154 A92-16811
BALL, CALVIN L.
Supersonic throughflow fans for high-speed aircraft p 561 N92-22541
BALL, D. R. J.
Long duration ballooning in Antarctica - An operational perspective
[AIAA PAPER 91-3679] p 15 A92-11023
BALL, N. G.
Propeller noise research at NRC p 628 N92-24863
BALL, W. H.
Inlet planar waves - A current perspective
[ASME PAPER 91-GT-400] p 76 A92-15730
BALLAL, D. R.
Isothermal flow fields in a research combustor for lean blowout studies
[ASME PAPER 91-GT-37] p 121 A92-15520
Lean blowout in a research combustor at simulated low pressures
[ASME PAPER 91-GT-359] p 137 A92-15713
BALLARD, DAN
Artificial intelligence in the helicopter cockpit of the future p 964 A92-49271
BALLMANN, J.
Some aerodynamic mechanisms of impulsive noise during blade-vortex-interaction p 604 A92-35782
BALMA, M.
Radiation and coupling between antennas mounted on a complex metallic structure p 760 A92-42315
BALMFORD, D. E. H.
The compound helicopter - A concept revisited p 1058 A92-56341
BALTSAVIAS, EMMANUEL P.
Close-range photogrammetry meets machine vision; Proceedings of the Meeting, Zurich, Switzerland, Sept. 3-7, 1990
[SPIE-1395] p 994 A92-51626
BALZER, RICHARD
V-22 flight test p 112 A92-16056
BAMBERGER, ERIC N.
Rolling element bearing member
[PATENT-1-271-213] p 158 N92-13434
BANACH, ANTONI S.
Gain-scheduled control of nonlinear partial differential equations p 47 A92-11347
BANAS, CONRAD M.
Laser thermal simulation puts jet engines to the test p 663 A92-38129
BANDA, SIVA S.
Combined H(2)/H(infinity) optimal control design applied to an advanced fighter aircraft
[AIAA PAPER 92-0045] p 281 A92-22162
Loop shaping in mixed H2 and H-infinity optimal control p 507 A92-29177
Gain scheduled linear PID autopilot for the AIAA Controls Design Challenge aircraft
[AIAA PAPER 92-4629] p 1078 A92-55304
BANDO, TOSHIO
Flight test results and upper surface blowing (USB) technology of the STOL research aircraft Asuka p 730 A92-43142
BANDOU, SHUNICHI
Design and testing of a composite hingeless hub for rotary-wing aircraft p 1053 A92-56075
BANDOU, TOSHIO
Evaluation of high lift devices of the quiet STOL experimental aircraft ASKA
[NAL-TR-1102] p 733 N92-28153
Note on flight measured control effectiveness of the quiet STOL experimental aircraft ASKA
[NAL-TR-1103] p 746 N92-28154
Evaluation of landing configuration by flight test of the quiet STOL experimental aircraft ASKA
[NAL-TR-1113] p 733 N92-28191
Aerodynamic characteristics obtained from alpha sweep test of the quiet STOL experimental aircraft ASKA
[NAL-TR-1112] p 853 N92-28901
BANDYOPADHYAY, PROMODE R.
Helical-perturbation device for cylinder-wing vortex generators p 432 A92-31167
Reflection type skin friction meter
[NASA-CASE-LAR-14520-1-SB] p 11 N92-10008
BANERJEE, DEV
Assessment of rotorcraft system identification as applied to the AH-64 p 274 N92-17160
Industry view on rotorcraft system identification p 274 N92-17163
BANERJEE, P. K.
Development of an integrated BEM approach for hot fluid structure interaction: BEST-FSI: Boundary Element Solution Technique for Fluid Structure Interaction
[NASA-CR-189202] p 574 N92-22211
BANGERT, LINDA S.
Effect of afterbody geometry on aerodynamic characteristics of isolated nonaxisymmetric afterbodies at transonic Mach numbers
[NASA-TP-3236] p 1041 N92-33706
BANGUI, F.
Three dimensional numerical method for resolving small transonic perturbations in unstructured mesh
[ONERA-RT-56/3064-RY-006-R] p 13 N92-10989
BANILOWER, HOWARD
Bird ingestion into large turbofan engines
[DOT/FAA/CT-91/17] p 1043 N92-33005
BANISH, M. R.
Experimentally supported investigations into the optical performance of multi-aperture window concepts
[AIAA PAPER 92-2781] p 778 A92-41324
BANISH, MICHELE
A validated code to predict the performance of onboard broadband optical seekers through a turbulent transonic flow
[AIAA PAPER 92-2792] p 778 A92-41331
BANISTER, BRAD
New thermoplastic composites for aircraft structures and interiors p 34 A92-10271
BANKS, DANIEL W.
Assessment of passive porosity with free and fixed separation on a tangent ogive forebody
[AIAA PAPER 92-4494] p 1081 A92-55363
BANKS, H. T.
Approximation methods for control of acoustic/structure models with piezoceramic actuators
[NASA-CR-189578] p 234 N92-15658
Active noise control: Piezoceramic actuators in fluid/structure interaction models
[NASA-CR-190328] p 685 N92-26125
BANKS, SHEILA B.
Pilot's associate: Evolution of a functional prototype p 118 N92-12531
BANNINK, W. J.
Experimental and numerical investigation of the vortex flow over a delta wing at transonic speed p 84 N92-13001
BANNYKH, O. A.
High-temperature metal matrix composite p 1105 A92-53878
BANSAI, I.
Compensating for manufacturing and life-cycle variations in aircraft engine control systems
[AIAA PAPER 92-3869] p 868 A92-49139
BANZHAF, M.
Investigation of the flow at the exit of an unshrouded centrifugal impeller and comparison with the 'classical' jet-wake theory
[ASME PAPER 90-GT-124] p 6 A92-11287
BAO, HESHENG
An impact dynamics investigation on some problems in bird strike on windshields of high-speed aircrafts p 986 A92-53330
BAR-ITZHACK, I. Y.
Observability analysis of piece-wise constant systems with application to inertial navigation p 49 A92-11391
BAR-KANA, IZHAK
On-line identification and control of linearized aircraft dynamics p 1082 A92-55911
BAR-SHALOM, YAAKOV
LOS rate estimation in inertial navigation using landmarks p 453 A92-29360
BARANKIEWICZ, WENDY
Use of an approximate similarity principle for the thermal scaling of a full-scale thrust augmenting ejector
[AIAA PAPER 92-3792] p 1069 A92-54171
BARANKIEWICZ, WENDY S.
Use of an approximate similarity principle for the thermal scaling of a full-scale thrust augmenting ejector
[NASA-TM-105724] p 739 N92-26613
BARANOV, ALEKSANDR M.
Visibility in the atmosphere and flight safety
[ISBN 5-286-00416-4] p 775 A92-42785
BARANOVSKII, S. I.
Wide-range combustion chamber of ramjet
[AIAA PAPER 91-5094] p 472 A92-31696

BARAT, MICHEL
From concept to model: Conception and evaluation of an architecture for a distributed system with SAHARA - Some reflections on results of the utilization of SAHARA in the framework of the Electronic Copilot
[ONERA, TP NO. 1991-216] p 411 A92-26368
BARATA, J. M. M.
Turbulent energy budgets in impinging zones
p 620 A92-40081
BARBAROSSA, S.
Detection and imaging of moving objects with synthetic aperture radar. I - Optimal detection and parameter estimation theory p 955 A92-50033
BARBER, D. J.
Propeller noise research at NRC p 628 N92-24863
BARBER, T. J.
Eigenfunction analysis of turbulent mixing phenomena
p 898 A92-45826
Computational study of a supersonic mixer-ejector exhaust system p 969 A92-50252
BARBER, THOMAS J.
Numerical analysis of shock-induced separation alleviation using vortex generators
[AIAA PAPER 92-0751] p 335 A92-27095
BARBERO, J.
Electronically steerable antenna for aircraft
p 229 N92-15272
BARBIER, BRUNO
Concept for future cockpits p 118 A92-16148
BARBOZA, JANET L.
Heuristic route optimization: A model for force level route planning p 164 N92-12520
BARCLAY, REBECCA O.
NASA/DOD Aerospace Knowledge Diffusion Research Project. Paper 14: An analysis of the technical communications practices reported by Israeli and US aerospace engineers and scientists
[NASA-TM-107924] p 782 N92-28183
BARD, STEVEN
Multicomponent gas sorption Joule-Thomson refrigeration
[NASA-CASE-NPO-17569-1-CU] p 228 N92-15203
Three-stage sorption type cryogenic refrigeration system and method employing heat regeneration
[NASA-CASE-NPO-18366-1-CU] p 300 N92-17674
BARDINA, JORGE E.
Turbulence modeling for hypersonic flight
[NASA-CR-190313] p 630 N92-24898
BARE, E. ANN
Flow field over the wing of a delta-wing fighter model with vortex control devices at Mach 0.6 to 1.2
[NASA-TM-4296] p 526 N92-22506
Parametric investigation of single-expansion-ramp nozzles at Mach numbers from 0.60 to 1.20
[NASA-TP-3240] p 1042 N92-34193
BARFIELD, WOODROW
Perspective versus plan view air traffic control (ATC) displays - Survey and empirical results
p 896 A92-44967
BARGER, RAYMOND L.
Diffracted and head waves associated with waves on nonseparable surfaces
[NASA-TP-3169] p 444 N92-20545
Comparison of jet plume shape predictions and plume influence on sonic boom signature
[NASA-TP-3172] p 631 N92-25133
Trajectory fitting in function space with application to analytic modeling of surfaces
[NASA-TP-3232] p 945 N92-30747
A method for designing blended wing-body configurations for low wave drag
[NASA-TP-3261] p 1036 N92-32480
BARILLOT, P.
Analysis tools of ONERA and DLR for the aerothermodynamics of reentry vehicles
p 211 N92-14977
BARINOV, V. A.
Approximate determination of the effect of deviations of wing and tail geometry from design parameters on the drag coefficient of subsonic aircraft p 460 A92-31878
BARKER, DANIEL K.
Application of analytical and design tools for fighter wing aeroelastic tailoring p 550 N92-23231
BARKER, DANIEL, K.
Application of analytical and design tools for fighter wing aeroelastic tailoring
[AIAA PAPER 92-2373] p 542 A92-34543
BARKER, J. C.
Lynx - A 50 year product? p 1056 A92-56307
BARKEY, D. A.
Design for the relief of thermal stresses in a large high-speed wing
[AIAA PAPER 92-1082] p 536 A92-33250
BARLAS, M. R.
Nonlinear model-following control application to airplane control (1992 AIAA Controls Design Challenge)
[AIAA PAPER 92-4625] p 1077 A92-55302
BARLAS, REMZI
Nonequilibrium turbulence modeling effects on transonic vortical flows about delta wings p 85 N92-13007
BARLOW, JEWEL B.
Integrated flight control law synthesis for an aeroelastic forward-swept wing aircraft
[AIAA PAPER 92-0046] p 281 A92-22163
Stability, control and gust response characteristics of an ultralight freewing airplane
[AIAA PAPER 92-4342] p 1079 A92-55331
The wind tunnel, its evolution for aerospace test purposes, perspective for curriculum development
[AIAA PAPER 92-4017] p 1100 A92-56839
BARLOW, R. S.
Experiments on the structure of an annular compressible reacting shear layer p 969 A92-50311
BARNA, P. STEPHEN
Effect of collector configuration on test section turbulence levels in an open-jet wind tunnel
[NASA-TM-4333] p 750 N92-27670
BARNABO, GEOFFREY A.
A fiber optic temperature sensor for aerospace applications p 761 A92-42607
BARNDT, LUANN
US Coast Guard GPS Information Center (GPSIC) and its function within the Civil GPS Service (CGS)
p 1049 N92-33352
BARNERSSOI, HANS
Development and evaluation of a finite element model for a fiber composite helicopter fuselage
[MBB-UD-0584-90-PUB] p 196 N92-15066
BARNES, A. G.
Technical evaluation report on the Flight Mechanics Panel Symposium on Piloted Simulation Effectiveness
[AGARD-AR-315] p 983 N92-30769
BARNES, J. D.
Preliminary screening procedures and criteria for replacements for Halons 1211 and 1301
[AD-A252912] p 1126 N92-33501
BARNES, JEREMY
The challenge of commercial aircraft survivability
p 931 A92-52022
BARNES, TERENCE J.
Status of the FAA flight loads monitoring program
p 914 N92-30113
BARNES, VALERIE E.
Cockpit distractions - Precursors to emergencies
p 16 A92-11178
BARNETT, M.
Development of an efficient analysis for high Reynolds number inviscid/viscid interactions in cascades
[AIAA PAPER 92-3073] p 823 A92-48723
BARNETT, MARK
Development of unsteady aerodynamic analyses for turbomachinery aeroelastic and aeroacoustic applications
[NASA-CR-4405] p 12 N92-10979
BARNETT, R. M.
A simple numerical criterion for vortex breakdown
[AIAA PAPER 92-0057] p 250 A92-22172
Numerical simulation of leading-edge vortex breakdown using an Euler code p 701 A92-41213
Investigation of vortex breakdown on a delta wing using Euler and Navier-Stokes equations p 87 N92-13019
BARNETT, RAYMOND M.
Numerical investigation of vortex breakdown on a delta wing p 340 A92-28027
BARNEY, DAVE
Cost effective close tolerance plastic master models
p 958 A92-51538
BARNWELL, RICHARD W.
Nonadiabatic and three-dimensional effects in compressible turbulent boundary layers
p 431 A92-31156
BARON, A.
Numerical simulation of unsteady rotor wakes
p 1032 A92-56352
Numerical simulation of vortex flows past impulsively started wings p 88 N92-13028
BARON, J. R.
The finite volume approach for the Navier-Stokes equations p 246 A92-21980
Adaptation methods for viscous flows
p 246 A92-21982
BARON, JUDSON R.
A new adaptive algorithm for turbulent flows
p 434 A92-31547
BARRAL, M.
The advantages of digital engine control as compared with traditional systems (hydraulic or pneumatic)
p 1070 A92-56338
BARRE, S.
Hot-wire measurements in turbulent transonic flows
p 941 A92-53078
BARRERE, M.
The thermodynamic approach in the study of large systems - Application to high-velocity airbreathing propulsion p 654 A92-37824
BARRETT, FRANK J.
Profile of an effective engineering manager
[AD-A246525] p 781 N92-27528
BARRETT, L. E.
Design of bearings for rotor systems based on stability
p 773 N92-27799
BARRETT, R. V.
The evaluation of canard couplings at high angles of attack
[AIAA PAPER 92-0281] p 318 A92-25735
BARRETT, RON
Preliminary design studies of an advanced general aviation aircraft
[NASA-CR-190024] p 461 N92-20064
BARRIE, DOUGLAS
Dornier Do.328 special - Examining the high-speed commuter p 21 A92-11882
Heavy metal p 207 A92-18100
Assembling the future p 783 A92-44895
BARRON, R. M.
Axisymmetric potential flow calculations. II - Design mode p 8 A92-12399
Analysis and design of transonic airfoils using streamwise coordinates p 194 N92-13955
BARTEL, KENT
The SnoDog: Preliminary design of a close air support aircraft
[NASA-CR-189990] p 462 N92-21489
BARTEL, T. J.
Measurement of the freestream density for re-entry vehicles - A design study p 940 A92-52821
BARTELDS, G.
Ageing aircraft research in the Netherlands
p 838 N92-30129
BARTELS, P.
Summary of Dornier 328 interior noise control study
p 643 A92-39083
BARTELS, PETER
Interior noise reduction program for the Dornier 328
p 114 A92-17254
BARTH, C. F.
Advances in aircraft component superplastic forming/diffusion bonding technology
[SAE PAPER 912216] p 674 A92-40018
BARTH, G.-J.
Ground installations for the preparation and evaluation of flight tests p 665 N92-25593
BARTHELEMY, J. P.
Status of the NH90 European Helicopter Program
p 113 A92-16676
Organization and technical status of the NH90 European helicopter programme p 1016 A92-56306
BARTHELEMY, J.-F. M.
Application of multidisciplinary optimization methods to the design of a supersonic transport
p 550 N92-23230
BARTHELEMY, JEAN-FRANCOIS M.
Integrating aerodynamics and structures in the minimum weight design of a supersonic transport wing
[NASA-TM-107586] p 850 N92-28435
BARTLER, TOMASZ
A new method of helicopter rotor blade motion control
p 875 A92-47786
BARTLETT, C. S.
Hydrogen exhaust gas disposition by afterburning
[AIAA PAPER 91-5075] p 200 A92-17848
BARTLETT, C. SCOTT
The effect of droplet sizing uncertainty on ice accretions p 679 N92-24874
BARTLETT, D. W.
Analysis for the application of hybrid laminar flow control to a long-range subsonic transport aircraft
[SAE PAPER 912113] p 617 A92-39964
BARTLETT, FELTON D., JR.
Probabilistic fatigue methodology for six nines reliability p 145 A92-14342
BARTLETT, SCOTT
Determination of liquid water content in the AEDC engine test cells
[AIAA PAPER 92-0165] p 263 A92-23778
BARTO, SAM
Effect of guard band reduction on marker beacon receiver performance
[DOT/FAA/CT-TN92/18] p 1002 N92-31617
BARTOLI, A.
Prediction of aerodynamic phenomena limiting aircraft manoeuvrability p 364 N92-18781

BARTOSH, BRADY J.
Use of a commercially available flight simulator during aircrew performance testing
[AD-A245922] p 883 N92-28407
BARTRAND, TIMOTHY A.
Rotary engine performance limits predicted by a zero-dimensional model
[NASA-CR-189129] p 474 N92-20650
BARUAH, PRANAB K.
PAN AIR: A computer program for predicting subsonic or supersonic linear potential flows about arbitrary configurations using a higher order panel method. Volume 2: User's manual (version 3.0)
[NASA-CR-3252] p 527 N92-22865
BARUZZI, G. S.
Finite element solutions of the Euler equations for transonic external flows p 5 A92-11063
BARWICK, M.
Liquid flow-through cooling for avionics applications
p 902 A92-48448
BARZDO, V. I.
Airfield construction (3rd revised and enlarged edition)
[ISBN 5-277-01070-X] p 670 A92-36606
BASCH, R. E., JR.
Severe turbulence and maneuvering from airline flight records
[AIAA PAPER 92-4341] p 1078 A92-55330
BASHYAM, MANOHAR
Ultrasonic NDE for ceramic- and metal-matrix composite material characterization p 491 A92-28690
BASIULIS, DANA
International SAMPE Electronics Conference, 5th, Los Angeles, CA, June 18-20, 1991, Proceedings
[ISBN 0-938994-58-1] p 985 A92-51901
BASKHARONE, ERIAN
Test results for rotordynamic coefficients of the SSME HPOTP turbine interstage seal with two swirl brakes
p 223 N92-14357
BASON, R.
Loss of cabin pressurization in U.S. naval aircraft - 1969-90 p 634 A92-37168
BASS, HENRY
Steady state risetimes of shock waves in the atmosphere p 1140 N92-33882
BASSANINI, P.
A boundary integral formulation for the kinetic field in aerodynamics. I - Mathematical analysis
p 243 A92-21504
A boundary integral formulation for the kinetic field in aerodynamics. II - Applications to unsteady 2D flows
p 339 A92-28005
BASSI, F.
Transonic and supersonic inviscid computations in cascades using adaptive unstructured meshes
[ASME PAPER 91-GT-312] p 75 A92-15689
Numerical computations of transonic flows through cascades
[AIAA PAPER 92-3041] p 822 A92-48702
BASSLER, STUART
Preliminary design of axial compressors using artificial intelligence and numerical optimization techniques
[ASME PAPER 91-GT-334] p 126 A92-15699
BASSOM, ANDREW P.
The effects of suction on the nonlinear stability of the three-dimensional boundary layer above a rotating disc
p 393 A92-25366
BASTOS-NETTO, DEMETRIO
Some thermodynamical aspects in the optimization of supersonic combustors p 1065 A92-53486
The behaviour of the pressure temperature and density in an inviscid unsteady transonic axisymmetric flow with shock waves p 1018 A92-53553
BASU, B. S.
Prediction of laminar boundary layer using cubic splines
[AIAA PAPER 92-2702] p 801 A92-45544
BATCHO, P.
Direct computation of turbulence and noise
[NASA-CR-187616] p 236 N92-14788
BATES, JIM
Enhanced diagnostic system for autoclaves and bonding presses p 145 A92-14381
BATES, PRESTON R.
Damage tolerance analysis for rotorcraft - What the issues are p 1058 A92-56336
BATES, WILLIAM F., JR.
New materials drive high-performance aircraft
p 1105 A92-55134
BATHURST, RICHARD L.
Wavelength-multiplexed fiber-optic position encoder for aircraft control systems p 734 A92-42602
BATILL, S. M.
Flow about cylinders with helical surface protrusions
[AIAA PAPER 92-0540] p 332 A92-26957
System design from mission definition to flight validation
[AIAA PAPER 92-1091] p 605 A92-33256
Damage tolerant structural design using neural networks
[AIAA PAPER 92-1097] p 581 A92-33261
Digital time series analysis for flutter test data
[AIAA PAPER 92-2103] p 589 A92-35674
The design of a subsonic low-noise, low-turbulence wind tunnel for acoustic measurements
[AIAA PAPER 92-3883] p 1094 A92-56726
BATINA, J. T.
Temporal adaptive Euler/Navier-Stokes algorithm involving unstructured dynamic meshes
p 812 A92-46887
BATINA, JOHN T.
Implicit flux-split Euler schemes for unsteady *aerodynamic analysis involving unstructured dynamic* meshes p 5 A92-11057
Aeroelastic analysis of wings using the Euler equations with a deforming mesh p 10 A92-13215
Quality assessment of two- and three-dimensional unstructured meshes and validation of an upwind Euler flow solver
[AIAA PAPER 92-0444] p 328 A92-26288
A fast implicit upwind solution algorithm for three-dimensional unstructured dynamic meshes
[AIAA PAPER 92-0447] p 328 A92-26291
Three-dimensional time-marching aeroelastic analyses using an unstructured-grid Euler method
[AIAA PAPER 92-2506] p 542 A92-34500
Spatial adaptation of unstructured meshes for unsteady aerodynamic flow computations p 610 A92-36838
Spatial and temporal adaptive procedures for the unsteady aerodynamic analysis of airfoils using unstructured meshes
[AIAA PAPER 92-2694] p 800 A92-45540
A fast implicit upwind solution algorithm for three-dimensional unstructured dynamic meshes
[NASA-TM-104186] p 185 N92-15050
Quality assessment of two- and three-dimensional unstructured meshes and validation of an upwind Euler flow solver
[NASA-TM-104215] p 444 N92-20480
Three-dimensional time-marching aeroelastic analyses using an unstructured-grid Euler method
[NASA-TM-107567] p 527 N92-23116
Unstructured-grid methods development for unsteady aerodynamic and aeroelastic analyses
p 718 N92-27938
Spatial and temporal adaptive procedures for the unsteady aerodynamic analysis of airfoils using unstructured meshes
[NASA-TM-107635] p 831 N92-29445
Progress in unstructured-grid methods development for unsteady aerodynamic applications
[NASA-TM-107643] p 944 N92-30393
A gridless Euler/Navier-Stokes solution algorithm for complex two-dimensional applications
[NASA-TM-107631] p 944 N92-30570
Implicit upwind-Euler solution algorithms for unstructured-grid applications
[NASA-TM-107645] p 945 N92-30691
CFD methods development considerations for unsteady aerodynamic analysis
[NASA-TM-107644] p 947 N92-31239
BATTERTON, PETER G.
Supersonic STOVL propulsion technology program: An overview p 561 N92-22539
BATTRICK, B.
Aerothermodynamics for Space Vehicles
[ESA-SP-318] p 180 N92-14973
BATY, R. S.
Numerical calculations of two-dimensional single and multi-material flow fields with CCICE
[DE92-015778] p 1000 N92-30903
BAUCH, T.
Space Shuttle Orbiter auxiliary power unit status
[SAE PAPER 912060] p 889 A92-45442
BAUCHAU, O. A.
On the choice of appropriate bases for nonlinear dynamic modal analysis p 847 A92-46927
BAUCHAU, OLIVIER
Evaluation of an advanced finite element analysis for rotor blades p 109 A92-14426
BAUCHAU, OLIVIER A.
Dynamic analysis of rotor flex-structure based on nonlinear anisotropic shell models p 899 A92-46946
BAUDOUIN, C.
CARS temperature measurements and validation of a computing code on a gas-turbine combustor
[ONERA, TP NO. 1991-224] p 373 A92-26376
BAUER, JEFFREY
Piloted simulation study of a balloon-assisted deployment of an aircraft at high altitude
[NASA-TM-104245] p 272 N92-15986
BAUER, STEVEN X. S.
Euler code evaluation of a transatmospheric vehicle at supersonic speeds p 9 A92-13202
Alleviation of side force on tangent-ogive forebodies using passive porosity
[AIAA PAPER 92-2711] p 802 A92-45552
Assessment of passive porosity with free and fixed separation on a tangent ogive forebody
[AIAA PAPER 92-4494] p 1081 A92-55363
The natural flow wing-design concept
[NASA-TP-3193] p 631 N92-25202
Natural flow wing
[NASA-CASE-LAR-14281-1] p 829 N92-28729
BAUGHCUM, STEVEN L.
Designing a methodology for future air travel scenarios p 409 N92-19125
BAUGHMAN, J.
Space Shuttle Orbiter auxiliary power unit status
[SAE PAPER 912060] p 889 A92-45442
BAULD, N. R., JR.
Global/local interlaminar stress analysis of a *grid-stiffened composite panel*
[NASA-CR-190822] p 1125 N92-33139
BAULIN, N. N.
Determination of physicochemical constant in the wake of a body from ballistic experiments p 609 A92-36549
BAULLINGER, NORMAN C.
Propulsion system evaluation for an unmanned high altitude long endurance RPV
[ASME PAPER 91-GT-409] p 128 A92-15738
BAUM, J.
Formation of shocks within axisymmetric nozzles
p 176 A92-20760
BAUMANN, C. E.
Improving the convergence rate of the Petrov-Galerkin techniques for the solution of transonic and supersonic flows p 434 A92-31495
BAUMANN, WILLIAM T.
Gain-scheduled control of nonlinear partial differential equations p 47 A92-11347
BAUMBICK, ROBERT
Potential for integrated optical circuits in advanced aircraft with fiber optic control and monitoring systems
p 856 A92-46246
BAUMGARDNER, D.
Airflow effects about PMS probes on the DLR Falcon
p 467 A92-32060
BAUMGARDNER, DARREL
Feature extraction from two-dimensional images using fractal analysis p 496 A92-32130
Meeting Review: Airborne Aerosol Inlet Workshop
[NASA-CR-189814] p 301 N92-17393
BAUMONT, FRANCOISE S.
Comparison of two-way satellite time transfer and GPS common-view time transfer between OCA and TUG
p 1050 N92-33356
BAURLE, R. A.
An assumed joint-Beta PDF approach for supersonic turbulent combustion
[AIAA PAPER 92-3844] p 1113 A92-54199
BAUWENS, LUC
Flame sheet algorithm for use in numerical modeling of ramjet combustion instability p 390 A92-28503
BAVUSO, SALVATORE J.
HiRel - Reliability/availability integrated workstation tool p 1120 A92-56257
BAWCOM, DWIGHT M.
International survey of scientific ballooning support organizations
[AIAA PAPER 91-3677] p 1 A92-11022
BAXTER, M. R.
Weak extinction limits of large scale flameholders
[ASME PAPER 91-GT-234] p 125 A92-15643
BAYAR, K. C.
Numerical simulation of vortex street-edge interaction
p 88 N92-13027
BAYLISS, A.
On the interaction between first- and second-mode waves in a supersonic boundary layer
p 78 A92-16462
BAYLISS, E.
Integrated use of GPS and GLONASS in civil aviation navigation. I - Coverage and data models
p 99 A92-16950
GLONASS data analysis - Interim results
p 955 A92-49382
BAYS-MUCHMORE, B.
Experimental investigation of a three-dimensional *bluff-body wake*
[AIAA PAPER 92-0429] p 326 A92-26277
BAYS-MUCHMORE, BYRAM
An experimental investigation of the surface flow and wake dynamics associated with transverse flow over wavy cylinders p 681 N92-25547

BAYSAL, O.
Interference flows past cylinder-fin-sting-cavity assemblies p 442 A92-32236
BAYSAL, OKTAY
Aerodynamic sensitivity analysis methods for the compressible Euler equations p 233 A92-19619
Aerodynamic design optimization using sensitivity analysis and computational fluid dynamics p 340 A92-28044
Computations of multispecies mixing between scramjet nozzle flow and hypersonic freestream p 376 A92-28534
Simulation of 3-D shear flows around a nozzle-afterbody at high speeds p 519 A92-34826
Viscous simulation method for unsteady flows past multicomponent configurations p 714 A92-44671
Computing high-speed flows past an oscillating cylinder near a vertical wall
[AIAA PAPER 92-4653] p 1028 A92-55397
Viscous computations of cold air/air flow around scramjet nozzle afterbody
[NASA-CR-4406] p 13 N92-10982
Flow analysis and design optimization methods for nozzle afterbody of a hypersonic vehicle
[NASA-CR-4431] p 446 N92-21456
Aerodynamic design optimization using sensitivity analysis and computational fluid dynamics
[NASA-CASE-LAR-14815-1-CU] p 910 N92-29830
BEACH, T. A.
Deterministic blade row interactions in a centrifugal compressor stage
[ASME PAPER 91-GT-273] p 75 A92-15670
BEACH, TIM
An interactive grid generation technique for turbomachinery p 659 N92-25717
BEACKEN, M. J.
Operating principles for integrated sensor processing p 966 A92-49336
BEALE, D. K.
Development of a freejet capability for evaluating inlet-engine compatibility
[ASME PAPER 91-GT-401] p 137 A92-15731
Development and validation of a freejet technique for inlet-engine compatibility testing
[AIAA PAPER 92-3921] p 1033 A92-56752
BEALE, DAVID K.
An acceptance process for the evaluation of inlet distortion
[AIAA PAPER 92-3918] p 1032 A92-56750
BEALS, TODD
SHARP: Subsonic High Altitude Research Platform
[NASA-CR-190004] p 648 N92-25263
BEANS, E. W.
Nozzle design using generalized one-dimensional flow p 714 A92-44531
BEARDEN, DAVID A.
Damage tolerant design of critical aircraft structural components
[AIAA PAPER 92-4041] p 1123 A92-56860
BEAUCHAMP, CHARLES H.
Improved articulated fin/wing control system statement of government interests
[AD-D015268] p 1088 N92-34131
BEAUCHAMP, GARY M.
The design and development of a portable, DSP micro-processor based, high-accuracy data acquisition system
[NRC-32146] p 1134 N92-32851
BEAUFILS, J. Y.
Fatigue testing and tear down operations on Airbus A320 forward fuselage p 360 N92-18579
BEAVERS, F.
Application of advanced composites in SEM-E heatsinks for the thermal management of avionics p 986 A92-51922
BECHERT, D. W.
The Berlin oil channel for drag reduction research p 571 A92-34219
BECHTEL, G. S.
TMFSLAM - Design analysis tool for coated structures
[ASME PAPER 91-GT-141] p 690 A92-36895
BECK, JEFFREY A.
Agility and high angle of attack - An Air Force research perspective
[SAE PAPER 912145] p 608 A92-39983
BECK, W. H.
Preliminary laser induced fluorescence measurements in several facilities in preparation for application to studies in the high enthalpy shock tunnel Goettingen (HEG)
[AIAA PAPER 92-0143] p 284 A92-23761
The high enthalpy shock tunnel in Goettingen
[AIAA PAPER 92-3942] p 1104 A92-56772
BECKER, A.
DME growth elements and their use with MLS p 189 N92-14018
Testing concept of a movement area guidance p 641 N92-25597
BECKER, JUERGEN
Aeroservoelastic stability of aircraft at high incidence p 381 N92-18795
BECKER, K.
Simulation of transonic flow over twin-jet transport aircraft p 811 A92-46793
Interactive algebraic mesh generation for twin jet transport aircraft p 817 A92-47064
BECKER, WAYNE
RTM - Simultaneous design and tooling reduces cost and lead time p 994 A92-51537
BECKETT, PETER
Effective cueing during approach and touchdown: Comparison with flight p 886 N92-28552
BECKWITH, I. E.
Supersonic and hypersonic quiet tunnel technology at NASA Langley
[AIAA PAPER 92-3908] p 1094 A92-56743
BECKWITH, IVAN E.
Gortler instability and supersonic quiet nozzle design p 813 A92-46902
BEDDOES, T. S.
A 3-D separation model for arbitrary planforms p 65 A92-14360
BEDIONES, D.
5,000-hour stability tests of metal sheathed thermocouples at respective temperatures of 538 C and 875 C
[ASME PAPER 91-GT-182] p 148 A92-15614
BEDNAREK, SLAWOMIR
An analysis of the flow-pattern at the exit of a single-stage turbine p 10 A92-13234
BEESTEN, B. M. J.
On the influence of blade-vortex-interactions on vortex structure p 521 A92-35783
BEGGS, JOHN H.
Finite difference time domain modeling of steady state scattering from jet engines with moving turbine blades
[NASA-CR-190290] p 971 N92-30753
BEHEIM, GLENN
Wavelength-multiplexed fiber-optic position encoder for aircraft control systems p 734 A92-42602
BEIGELMAN, Z.
A simulation model of a single rotor helicopter p 979 N92-31865
BEIN, THOMAS W.
Unsteady flows in rotor-stator cascades
[AD-A241593] p 158 N92-13410
BELAN, V. V.
Synthesis of optimal digital systems for the stabilization of stochastically perturbed unstable dynamic systems p 601 A92-33754
BELCASTRO, CELESTE M.
Formulation of a strategy for monitoring control integrity in critical digital control systems
[NASA-TM-104158] p 206 N92-15075
BELCHER, GORDON
Validation of flight critical control systems
[AGARD-AR-274] p 382 N92-20026
BELCHER, P. J.
Automated trajectory synthesis for hypersonic vehicles using energy management and variational calculus techniques p 210 A92-19061
Control strategy for maximizing reconnaissance range of hypersonic cruise vehicles p 729 A92-41222
BELIAEVSKII, LEONID S.
Processing and displaying radio navigation data p 266 A92-21683
BELIAKOV, A. R.
Technique for estimating the strength of gas turbine guide vanes with stress raisers p 761 A92-42653
BELIAKOV, K. V.
A model of the operation of the pulsejet engine and a study of its characteristics p 657 A92-40608
BELIAKOV, ROSTISLAV A.
Some aspects of advanced aircraft development p 729 A92-41176
BELL, R. A.
An inverse method for the aerodynamic design of three-dimensional aircraft engine nacelles p 194 N92-13958
BELL, WAYNE E.
Data Multiplexing Network (DMN) phase 3 equipment Operational Test and Evaluation (OT and E)/integration test report
[DOT/FAA/CT-TN91/50] p 221 N92-14270
High Capacity Voice Recorder (HCVR) Operational Test and Evaluation (OT and E)/integration test plan
[DOT/FAA/CT-TN91/55] p 402 N92-18959
Television Microwave Link (TML) Operational Test and Evaluation (OT/E)/integration test report
[DOT/FAA/CT-TN91/57] p 500 N92-20653
BELLAVIA, DAVID C.
On the anomalies in single-jet hover suckdown data
[NASA-TM-102261] p 1038 N92-33306
On the estimation of jet-induced fountain lift and additional suckdown in hover for two-jet configurations
[NASA-TM-102268] p 1040 N92-33618
BELLE, STEVEN D.
A NASA/RAE cooperation in the development of a real-time knowledge based autopilot p 164 N92-12528
BELLINGER, N. C.
Inspection of compressor discs by ultrasonic leaky waves using an automated C-scan system p 144 A92-13584
Preliminary finite element analysis of unloaded and loaded notched composite laminated plates
[NRC-LTR-ST-1806] p 159 N92-13454
BELLO, M. A.
Research, services, and facilities (National Institute of Standards and Technology)
[PB92-109172] p 485 N92-21870
BELOTSERKOVSKII, O. M.
CFD state-of-the-art in the U.S.S.R p 495 A92-31486
BELOUSOV, A. I.
Effect of inertia forces on the characteristics of a long hydrodynamic vibration damper in the mixed flow regime p 154 A92-16811
BELOV, I. A.
Investigating the feasibility of controlling the laminar-turbulent transition by means of laminarizing plates p 493 A92-30161
Effect of the longitudinal and transverse riblets of a flat plate on laminar-to-turbulent transition p 428 A92-30210
BELTON, PAMELA S.
Experimental study of a generic high-speed civil transport: Tabulated data
[NASA-TM-104216] p 525 N92-22232
Experimental study of a generic high-speed civil transport
[NASA-TM-4382] p 1040 N92-33631
BELTRAN, A. M.
Nickel base alloy GTD-222 - A new gas turbine nozzle alloy
[ASME PAPER 91-GT-73] p 142 A92-15542
BELTRAN, LUIS R.
Advanced nozzle and engine components test facility
[AIAA PAPER 92-3993] p 1099 A92-56816
BELTRAN, MICHAEL R.
Development of fuel neutralizing agents to prevent flashback on aircraft fires
[AD-A242828] p 264 N92-17259
BEN-AROSH, RACHEL
Similarity and scale effects in solid-fuel ramjet combustors p 666 A92-36965
BEN-ASHER, JOSEPH Z.
Optimal trajectories for an unmanned air-vehicle in the horizontal plane
[AIAA PAPER 92-4344] p 1079 A92-55333
Optimal trajectories for an unmanned air vehicle p 963 N92-31880
BENAY, R.
Assessment of three models of turbulence in a shock-boundary layer interaction of a heated wall p 423 A92-29999
BENCHERIFA, B.
Experimental and numerical study of flow around helicopter rotor blade tips p 814 A92-46948
BENCIC, TIMOTHY J.
Hot gas ingestion characteristics and flow visualization of a vectored thrust STOVL concept p 860 A92-45316
BENCIVENGA, VINCENT L.
The status of Loran's implementation in the National Airspace System (NAS) p 638 A92-39565
BENCZE, D. P.
Navier-Stokes simulation of flow through a highly contoured subsonic diffuser p 433 A92-31491
BENDER, B. S.
The compound helicopter - A concept revisited p 1058 A92-56341
BENDER, JAMES
Realistic real-time ground testing
[AIAA PAPER 92-0197] p 284 A92-23805
BENDER, K.
Development of flight testing of a fault tolerant fly-by-light yaw control system p 662 N92-25599
BENDER, THOMAS R.
Fatal occupational injury related to helicopters in the United States 1980-1985 p 186 A92-20720
BENDIKSEN, ODDVAR O.
Unsteady transonic Euler solutions using finite elements
[AIAA PAPER 92-2504] p 518 A92-34499

Finite element Euler calculations of unsteady transonic cascade flows
[AIAA PAPER 92-2120] p 520 A92-35689
Role of shock dynamics in transonic flutter
[AIAA PAPER 92-2121] p 520 A92-35690
BENDOTTI, P.
On the adaptive control of missile autopilots
p 477 A92-29102
BENEKE, D. L.
Development of a wind chamber for model testing of tornado forces on structures
[PB92-104165] p 386 N92-19940
BENENSON, L. S.
Decoupling of antennas using periodic structures
p 725 A92-42634
BENETSCHIK, HANNES
Inviscid and viscous transonic flows in cascades using an implicit upwind algorithm p 344 A92-28522
BENGELINK, RONALD L.
The impact of CFD on the airplane design process - Today and tomorrow
[SAE PAPER 911989] p 788 A92-45391
BENHALILOU, M.
Experimental and numerical investigation of a turbulent boundary layer over riblets p 622 A92-40128
BENHAMOU, PHILIPPE
From concept to model: Conception and evaluation of an architecture for a distributed system with SAHARA - Some reflections on results of the utilization of SAHARA in the framework of the Electronic Copilot
[ONERA, TP NO. 1991-216] p 411 A92-26368
BENNER, ROBERT H.
Suppression of fatigue-inducing cavity acoustic modes in turbofan engines p 925 A92-46809
BENNETT, BRADFORD C.
Hypersonic code efficiency and validation studies
[NASA-CR-190680] p 948 N92-31533
BENNETT, C. T.
Analysis of general aviation accidents during operations under instrument flight rules p 16 A92-11172
Analysis of accidents during instrument approaches
p 529 A92-34253
A re-analysis of the causes of Boeing 727 'black hole landing' crashes p 833 A92-44985
BENNETT, GEORGE
A flight test study to determine aircraft propulsive efficiency and aerodynamic drag using two parameter identification methods and Lock's propeller model
[AIAA PAPER 92-0170] p 271 A92-23781
BENNETT, J.
A preliminary study on damage detection using piezoelectric film
[AD-A246350] p 733 N92-28118
BENNETT, JOHN C.
Computational and experimental investigation of annulus heat transfer with swirl
[AIAA PAPER 92-4060] p 1119 A92-56143
BENNETT, RICHARD L.
Analysis of the effects of removing nose ballast from the F-15 eagle
[AD-A244044] p 366 N92-19178
BENNETT, ROBERT M.
NACA 0012 benchmark model experimental flutter results with unsteady pressure distributions
[AIAA PAPER 92-2396] p 517 A92-34469
Further investigations of the aeroelastic behavior of the AFW wind-tunnel model using transonic small disturbance theory
[AIAA PAPER 92-2082] p 565 A92-35654
Investigation of the aeroelastic stability of the AFW wind-tunnel model using CAP-TSD
[NASA-TM-104142] p 81 N92-11977
The benchmark aeroelastic models program: Description and highlights of initial results
[NASA-TM-104180] p 185 N92-15049
Further investigations of the aeroelastic behavior of the AFW wind-tunnel model using transonic small disturbance theory
[NASA-TM-107576] p 526 N92-22240
NACA0012 benchmark model experimental flutter results with unsteady pressure distributions
[NASA-TM-107581] p 526 N92-22507
Investigation of the aeroelastic stability of the AFW wind-tunnel model using CAP-TSD p 721 N92-27955
The benchmark aeroelastic models program: Description and highlights of initial results
p 721 N92-27960
Pressure measurements on a rectangular wing with a NACA0012 airfoil during conventional flutter
[NASA-TM-104211] p 1042 N92-34147
BENNETT, WILLIAM H.
Regulation of relaxed static stability aircraft
p 203 A92-18463
BENNING, STEPHEN L.
Progressive avionics packaging technologies
p 989 A92-49276
BENOIST, RODNEY
A study of atmospheric optical scattering parameters at 1.5 and 2 micron region for solid state Doppler lidar applications p 1001 N92-31067
BENSEL, L. W.
Evaluation of triple simultaneous parallel ILS approaches spaced 4300 feet apart, phase 4a
[ACD-340] p 191 N92-14034
Evaluation of triple simultaneous parallel ILS approaches spaced 5000 feet apart, phase 4.b
[DOT/FAA/CT-91/31] p 456 N92-21404
BENSER, EARL T.
Air data measurement for hypersonic vehicles
[SAE PAPER 912143] p 651 A92-39981
BENSMAN, D. A.
SATCOM antenna siting study on P-3C aircraft, volume 1
[NASA-CR-189514] p 221 N92-14262
SATCOM antenna siting study on P-3C aircraft, volume 2
[NASA-CR-189515] p 221 N92-14263
BENSON, L. J.
Operational noise data for OH-58D Army helicopters
[AD-A246822] p 926 N92-28292
BENSON, RUSTY A.
Numerical simulations using a dynamic solution-adaptive grid algorithm, with applications to unsteady internal flows
[AIAA PAPER 92-2719] p 803 A92-45557
BENT, JOHN
A training program for airline line instructors
p 835 A92-45044
BENT, NATHANIEL E.
The helicopter air-to-air value-driven engagement model (HAVDEM) - Prototype development
p 105 A92-14353
BENTLY, DONALD E.
Comments on frequency swept rotating input perturbation techniques and identification of the fluid force models in rotor/bearing/seal systems and fluid handling machines p 224 N92-14370
BENTON, CHARLES J.
Development of the Basic Flight Instruction Tutoring System (BFITS)
[AD-A246458] p 751 N92-27836
BENTZIEN, JOACHIM F.
No end to incidents in airspace? III
p 262 A92-23172
BENWAY, R. B.
Liquid cooled turbocharged propulsion system for HALE application
[ASME PAPER 91-GT-399] p 127 A92-15729
BENZ, MARK G.
Composite strengthening of Nb-Ti base alloys
p 577 A92-36380
BERCHTOLD, G.
Concurrent engineering in design of aircraft structures
[MBB-FE-2-S-PUB-472] p 854 N92-29650
BERDUGO, ALBERT
A new 1553 all-bus instrumentation monitor
p 198 A92-19252
BERECZ, IMRE
The role of nonmetallic fasteners in aircraft wings and other composite structures p 784 A92-47413
BERENJI, HAMID R.
Using new aggregation operators in rule-based intelligent control p 51 A92-11456
BERENS, A. P.
Aging aircraft structural damage analysis
p 360 N92-18575
BERESTOV, LEONID M.
Flight test control p 136 A92-15021
BERG, D. E.
The status of the US VAWT program
[DE92-002931] p 505 N92-21040
BERG, JORDAN
Regulation of relaxed static stability aircraft
p 203 A92-18463
BERG, M.
Environmental fatigue tests with composite materials
p 214 N92-14413
BERG, RICHARD L.
Performance of insulated pavements at Newton Fields, Jackman, Maine
[CRREL-92-9] p 1101 N92-32903
BERGEMANN, FRANK
Monte Carlo simulation of the hypersonic mon- and diatomic gas flow past a disk at an angle of attack
p 939 A92-52770
BERGER, HAIM
Modern techniques for monitoring airborne telemetry
p 857 A92-47560
BERGERON, D.
Computational fluid dynamics p 177 N92-13979
Boundary layer computations using a generalized formulation p 679 N92-24873
BERGHOLZ, ROBERT F.
Thermal management systems for high Mach airbreathing propulsion
[AIAA PAPER 92-0515] p 373 A92-26941
BERGLIND, TORSTEN
Generation of efficient multiblock grids for Navier-Stokes computations p 919 A92-47081
BERGMAN, C. M.
A multiblock flow solver for inviscid hypersonic flows
p 181 N92-14986
BERGMANN, A.
Vortex formation over a close-coupled canard-wing-body configuration in unsymmetrical flow p 85 N92-13010
BERGMANN, J. W.
Low cycle fatigue of cast nickel base turbine rotors
p 226 N92-14405
Probabilistic lifing approach for aero engine disks made of powder nickel base alloys containing ceramic defects
p 226 N92-14424
BERIOS, G.
Jet engine fault detection with discrete operating points gas path analysis p 129 A92-17200
BERKOWITZ, BRIAN M.
Experimental ice shape and performance characteristics for a multi-element airfoil in the NASA Lewis Icing Research Tunnel
[NASA-TM-105380] p 261 N92-17347
BERLEMONT, A.
Theoretical study (Lagrangian modeling) of turbulent particulate dispersion
[ETN-91-99909] p 42 N92-11287
BERMAN, C.
Direct computation of turbulence and noise
[NASA-CR-187616] p 236 N92-14788
BERMAN, MORTON B.
Developing robust support structures for high-technology subsystems: The AH-64 Apache helicopter
[AD-A252773] p 1017 N92-33499
BERNARD, DENYS
A cognitive temporal model for the planning in aircraft maintenance p 307 A92-25178
BERNE, C.
Use of relative humidity sensors for planes measurement p 467 A92-32080
BERNELLA, DAVID M.
Terminal Doppler weather radar test bed operation, Orlando: January-June 1990
[AD-A242890] p 301 N92-17028
BERNHARD, R. J.
Models of space-averaged energetics of plates
p 398 A92-28031
BERNHARD, ROBERT J.
The development of multiple-input models for airborne noise prediction p 695 A92-39243
BERNING, SANDRA L.
Adaptive tactical navigation program
p 102 N92-12529
BERNSTEIN, D. S.
Real parameter uncertainty and phase information in the robust control of flexible structures
p 32 A92-11345
BERNSTEIN, DENNIS S.
Robust stabilization with positive real uncertainty - Beyond the small gain theorem p 50 A92-11444
BERRICHE, R.
The hardness and toughness of HIPed silicon nitride
p 668 A92-39682
BERRIER, BOBBY L.
Data reduction formulas for the 16-foot transonic tunnel: NASA Langley Research Center, revision 2
[NASA-TM-107646] p 984 N92-31900
BERRY, BERNARD F.
Noise from military airfields in the United Kingdom
p 686 A92-39052
BERRY, JOHN D.
Flapping inertia for selected rotor blades
[NASA-TM-104125] p 115 N92-13057
BERRY, NORM
New specifications proposed for taxiing guidance signs p 483 A92-29505
BERRY, W.
Aerothermodynamic challenges for ESA programmes
p 180 N92-14974
Grid impact on 3D hypersonic flows
p 184 N92-15041
BERT, C. W.
Forced vibration of rectangular laminated plates with material damping p 294 A92-23167
BERTHIER, J. M.
Certifying composite helicopter structures
p 110 A92-14443
BERTHIER, J.-M.
A survey of composite structure technology at the Aerospatiale Helicopter Division p 546 A92-35754

BERTHOLD, J. W.
Absolute fiber optic pressure transducer for aircraft air data measurement p 858 A92-48501
BERTHOUMIEUX, P.
Application of infrared thermography to thermal flux measurement in wind tunnels
[AAAF-NT-89-12] p 31 N92-11020
BERTIN, D.
A new automatic grid generation environment for CFD applications
[AIAA PAPER 92-2720] p 803 A92-45558
BERTOGLIO, JEAN-PIERRE
Inhomogeneous turbulence beyond spectral equilibria: Aeronautical applications
[ETN-92-90867] p 404 N92-19349
BERTOLAZZI, ANDREW N.
Design and flight test evaluation of the Fantail antitorque system p 110 A92-14456
BERTON, PIERRE
The beginnings of the hypersonic and the renewal of the supersonic ramjet p 782 A92-41824
BERTRAND, DENIS J.
Application of neural network to adaptive control theory for super-augmented aircraft
[AD-A246596] p 745 N92-27505
BERZINS, L. V.
Composition monitoring of electron beam melting processes using diode lasers
[DE92-009527] p 669 N92-25259
BES, CH.
Structural optimization at Aerospatiale Aircraft
[AIAA PAPER 92-2371] p 601 A92-34542
BESHEARS, D. L.
Fiber-sensor design for turbine engines
[DE92-003539] p 376 N92-18230
BESSACINI, ANTHONY F.
A method of passive range determination using only two bearing measurements
[AD-D015182] p 455 N92-20834
BESSENAY, G.
Mechanical testing of glass-ceramic matrix composites
[ONERA, TP NO. 1991-182] p 388 A92-26351
BETHKE, KARL-HEINZ
Global and high resolution radar cross section measurements and two-dimensional microwave images of a scaled aircraft model from the type Airbus A 310
[DLR-MITT-91-10] p 911 N92-29877
BETTNER, J. L.
High speed rotorcraft propulsion concepts to control power/speed characteristics
[AIAA PAPER 92-3367] p 865 A92-48940
BETTS, EDWARD E.
High lift aircraft
[AD-D015215] p 732 N92-27185
BETTS, JOHN T.
The application of direct transcription to commercial aircraft trajectory optimization
[AIAA PAPER 92-4528] p 1077 A92-55246
BETTSCHART, N.
Experimental and theoretical studies on helicopter rotor fuselage interaction
[ONERA, TP NO. 1991-197] p 329 A92-26356
Theoretical and experimental studies of helicopter rotor/fuselage interaction
[ONERA, TP NO. 1991-198] p 329 A92-26357
BEUTH, J. L., JR.
Preliminary results on the fracture analysis of multi-site cracking of lap joints in aircraft skins
p 913 N92-30111
BEVER, GLENN A.
The development of an airborne information management system for flight test
[NASA-TM-104251] p 1065 N92-32866
BEWLAY, B. P.
Cold-crucible directional solidification of refractory metal-silicide eutectics p 755 A92-43684
BEYER, MAUREEN R.
Application of digital measurement techniques to analysis of range shadowgraphs
[AD-A241554] p 139 N92-13080
BEYER, RALF
ATTAS experimental cockpit and ATMOS for flight control components and systems investigations
p 641 N92-25595
BEYER, RICHARD A.
Application of digital measurement techniques to analysis of range shadowgraphs
[AD-A241554] p 139 N92-13080
BEYERS, M. E.
Ground facility interference on aircraft configurations with separated flow
[AIAA PAPER 92-0673] p 384 A92-27042
BEZARD, H.
Numerical optimization of helicopter rotor blade airfoils using unsteady aerodynamic calculations
[ONERA, TP NO. 1991-187] p 78 A92-16141
BEZIAC, G.
Status of the NH90 European Helicopter Program
p 113 A92-16676
Organization and technical status of the NH90 European helicopter programme p 1016 A92-56306
BEZOS, GAUDY M.
A summary of NASA research on effects of heavy rain on airfoils p 452 N92-21694
Wind tunnel aerodynamic characteristics of a transport-type airfoil in a simulated heavy rain environment
[NASA-TP-3184] p 948 N92-31532
BEZVESIL'NAIA, E. N.
A study of the precision characteristics of a gyroscopic gravimeter p 581 A92-33778
BHAGAT, WILBUR W.
Design-for-reliability through durability analysis
p 760 A92-42086
BHANSALI, KIRIT J.
Failure analysis of the Apache mixer pivot support
[AD-A240858] p 116 N92-13061
BHANU, BIR
Inertial navigation sensor integrated motion analysis for obstacle detection p 954 A92-49272
Inertial navigation sensor integrated motion analysis for autonomous vehicle navigation p 995 A92-52470
BHARADVAJ, BALA K.
Computation of steady and unsteady control surface loads in transonic flow p 5 A92-11066
BHAT, M. K.
A low-speed wind tunnel study of vortex interaction control techniques on a chine-forebody/delta-wing configuration
[NASA-CR-189616] p 632 N92-25510
High-alpha vortex decoupling investigations on a chine forebody/Delta wing configuration at transonic Mach numbers
[NASA-CR-189642] p 715 N92-26651
Subsonic investigations of vortex interaction control for enhanced high-alpha aerodynamics of a chine forebody/Delta wing configuration
[NASA-CR-189641] p 715 N92-26652
BHAT, M. V.
Efficient direct solvers for large-scale computational fluid dynamics problems p 690 A92-37534
BHATIA, KUMAR G.
Structural analysis for preliminary design of High Speed Civil Transport (HSCT) p 684 N92-25926
BHATIA, R.
One-dimensional analysis of liquid-fueled combustion instability p 143 A92-17188
BHAVNANI, SUSHIL H.
Analysis, development, and integration of the mechanical components of a vehicle powered by photo-voltaic cells
[TABES PAPER 91-503] p 606 A92-34692
BHINDER, F. S.
A simple model to simulate subsonic intakes and propelling nozzles of aircraft gas turbine engines
[ASME PAPER 91-GT-392] p 153 A92-15722
BHUTTA, BILAL A.
Improved nonequilibrium viscous shock-layer scheme for hypersonic blunt-body flowfields p 310 A92-24653
Low-to-high altitude predictions of three-dimensional ablative reentry flowfields
[AIAA PAPER 92-0366] p 394 A92-26227
An improved PNS scheme for predicting complex three-dimensional hypersonic flows
[AIAA PAPER 92-0753] p 436 A92-31679
BI, NAI-PEI
Analysis of unsteady pressures induced on a body by a rotor p 10 A92-13212
Measurements of a rotor flowfield and the effects on a fuselage in forward flight p 521 A92-35787
BIANCHI, A.
Heterodyne techniques in the I.R. bandwidth for laser obstacle detection p 533 A92-35740
Innovation in the laser warning sensor field
p 554 A92-35742
BIANCHI, ALFREDO
Time Resolved Lidar Fluorosensor operating from helicopter p 1121 A92-56296
BIBER, KASIM
Experimental studies of a two-element airfoil with large separation
[AIAA PAPER 92-0267] p 317 A92-25723
BIBIKOV, V. V.
Detuning from the natural resonances of the blade in the computer-aided design of blade rows for axial-flow compressors p 80 A92-16818
BIBKO, V. N.
Transverse correlation of the spectral components of pressure fluctuations on a plate ahead of a step
p 426 A92-30187
BIDDLE, TEDD B.
Properties of aircraft fuels and related materials
[AD-A240650] p 35 N92-11213
BIDIAN, PETER A.
Achievement of rotorcraft handling qualities specifications via feedback control p 568 A92-35747
BIDWELL, COLIN S.
Comparison of two-dimensional and three-dimensional droplet trajectory calculations in the vicinity of finite wings
[AIAA PAPER 92-0645] p 342 A92-28215
Comparison of two-dimensional and three-dimensional droplet trajectory calculations in the vicinity of finite wings
[NASA-TM-105617] p 596 N92-23154
BIEHL, KEITH J.
Flight test investigation of the wake vortices generated by helicopters p 270 A92-21925
BIELAWA, RICHARD L.
Rotary wing structural dynamics and aeroelasticity
[ISBN 1-56347-031-4] p 1052 A92-54550
BIELER, H.
Concepts for the stability analysis of NLF-experiments on swept wings
[AIAA PAPER 92-2706] p 801 A92-45548
BIELSKI, W. P.
Atmospheric disturbance model for aircraft and space capable vehicles
[AIAA PAPER 92-0294] p 407 A92-25747
BIEN, ZEUNGNAM
Fault tolerant control based on a new accommodation filter p 51 A92-11453
BIESIADNY, THOMAS J.
Contingency power for a small turboshaft engine by using water injection into turbine cooling air
[NASA-TM-105680] p 871 N92-29661
BIETERMAN, M. B.
Analysis of unsteady aerodynamic and flutter characteristics of an aeroelastic model in transonic flow
p 720 N92-27953
BIEZAD, DANIEL J.
The propulsive-only flight control problem
p 876 A92-48487
Enlisting industry support for a flight controls design lab
[AIAA PAPER 92-4560] p 1141 A92-55272
BIGGERS, JAMES C.
Revolution at sea: Aircraft options for the year 2030
p 466 N92-21974
BIGGERS, S. B.
A Protection And Detection Surface (PADS) for damage tolerance p 1107 N92-32523
BIKKER, S.
Application of finite element method to hypersonic nozzle flow computations p 769 N92-27479
BILANGE, THIERRY
EUROFAR airframe aerodynamic design
p 546 A92-35750
BILANIN, ALAN J.
Mechanisms resulting in accreted ice roughness
[AIAA PAPER 92-0297] p 351 A92-25750
BILGEN, E.
An efficient upwind relaxation-sweeping algorithm for three-dimensional Navier-Stokes equations
[AIAA PAPER 92-0023] p 248 A92-22145
Effect of throat contouring on two-dimensional converging-diverging nozzles using URS method
[AIAA PAPER 92-2659] p 797 A92-45520
BILIMORIA, KARL D.
An integrated development of the equations of motion for elastic hypersonic flight vehicles
[AIAA PAPER 92-4605] p 1077 A92-55283
BILL, ROBERT C.
Recent manufacturing advances for spiral bevel gears
[SAE PAPER 912229] p 674 A92-40024
Summary highlights of the Advanced Rotorcraft Transmission (ART) program
[AIAA PAPER 92-3362] p 1051 A92-54026
Army research concerns in engine sealing
p 228 N92-15089
BILLIG, F. S.
Research on supersonic combustion
[AIAA PAPER 92-0001] p 278 A92-22126
Propulsion systems from takeoff to high-speed flight
p 889 A92-46428
BILLMANN, BARRY
Joint Federal Aviation Administration (FAA)/Civil Aviation Authority (CAA) Microwave Landing System (MLS) Area Navigation (RNAV) flight evaluations
[DOT/FAA/CT-TN91/17] p 268 N92-15983
BILLONNET, G.
Comparison between two 3D-NS-codes and experiment on a turbine stator
[AIAA PAPER 92-3042] p 822 A92-48703

BILLONNET, GILLES
Supersonic stator-rotor interaction in a turbine stage
[ONERA, TP NO. 1991-166] p 77 A92-16133
BILLY, N.
Reaction speed constant for the reactions between N + O2 and between O + N2
[ETN-92-90861] p 347 N92-19252
BINGHAM, M. G.
Ceramic component processing development for advanced gas-turbine engines
[ASME PAPER 91-GT-120] p 142 A92-15567
BINKLEY, ROBERT L.
System overview of the NASA Dryden Integrated Test Facility
[NASA-TM-104250] p 984 N92-32201
BIRCH, N.
The numerical simulation of flow about installed aero engine nacelle using a finite element Euler solver on unstructured meshes p 941 A92-52848
BIRCH, N. T.
The application of a Navier-Stokes CFD method to civil engine intake flows p 769 N92-27471
BIRCKELBAW, L. D.
NASA Workshop on future directions in surface modeling and grid generation
[NASA-CP-10092] p 831 N92-29625
BIRCKELBAW, LARRY D.
High speed aerodynamics of upper surface blowing aircraft configurations
[AIAA PAPER 92-2611] p 793 A92-45485
BIRCKELBAW, LOURDES G.
Ski jump takeoff performance predictions for a mixed-flow, remote-lift STOVL aircraft
[NASA-TM-103866] p 1060 N92-32887
BIRD, J.
Humidity effects on gas turbine performance
[NRC-30241] p 130 N92-11998
BIRD, J. W.
Investigation of engine thrust correlation methods for enclosed test cells
[ASME PAPER 91-GT-68] p 121 A92-15538
BIRD, VICTOR J.
Fiber-optic pressure sensor system for gas turbine engine control p 857 A92-48047
BIRDSALL, DAVID L.
Aircraft performance
[ISBN 0-521-36264-4] p 538 A92-33919
BIRDWELL, J. D.
Prediction of helicopter simulator sickness
p 46 A92-11473
BIRKAN, M. A.
Contractors Meeting in Propulsion
[AD-A240057] p 33 N92-10062
BIRON, PAUL J.
A case study of the Claycomo, Missouri microburst on July 30, 1989 p 407 A92-27961
BIRR, JAMES E.
Flight test of a GPS-aided low-cost inertial navigation system programmed in Ada p 101 A92-16973
BIRTCHER, CRAIG R.
Advanced electromagnetic methods for aerospace vehicles
[NASA-CR-188630] p 488 N92-20193
Advanced electromagnetic methods for aerospace vehicles
[NASA-CR-190650] p 1001 N92-31156
BISHOP, LEE R.
The use and misuse of aircraft and missile RCS statistics
[AD-A239892] p 41 N92-10141
BISMARCK-NASR, MAHER N.
Kernel function occurring in supersonic unsteady potential flow p 6 A92-11080
Coalescence of aeroelastic modes in flutter analysis
p 758 A92-41241
BISSINGER, N. C.
CFD contributions during hypersonic airplane intake design p 769 N92-27472
CFD contributions during hypersonic airplane intake design
[MBB/FE213/S/PUB/459] p 944 N92-30676
BISWAS, G.
Heat transfer in a channel with built-in wing-type vortex generators p 757 A92-41082
BITHER, CHERYL A.
A modeling strategy for large-scale optimization based on analysis and visualization principles
[AD-A246570] p 777 N92-26620
BITTEN, R.
Application of multidisciplinary optimization to conceptual aircraft design at Rockwell International - A status report
[AIAA PAPER 92-1196] p 537 A92-33307
BITTNER, R. D.
Flow establishment in a generic scramjet combustor
p 737 A92-44525
A comparative study of scramjet injection strategies for high Mach numbers flows
[AIAA PAPER 92-3287] p 904 A92-48876
BJARKE, LISA J.
Water tunnels p 880 A92-45266
BJORKELO, KENNETH
Effective maintenance practices to manage system aging p 1119 A92-56215
BLACHERE, G.
Certifying composite helicopter structures
p 110 A92-14443
A survey of composite structure technology at the Aerospatiale Helicopter Division p 546 A92-35754
BLACK, JOHN D.
Rotational coherent anti-Stokes Raman spectroscopy measurements in a rotating cavity with axial throughflow of cooling air - Oxygen concentration measurements
p 990 A92-49574
BLACK, KLIFFTON M.
Combined H(2)/H(infinity) optimal control design applied to an advanced fighter aircraft
[AIAA PAPER 92-0045] p 281 A92-22162
BLACK, TERRY M.
Tiltrotor control law design for rotor loads alleviation using modern control techniques p 478 A92-29331
BLACKBURN, CHARLES L.
Preliminary structural sizing of a Mach 3.0 high-speed civil transport model
[NASA-CR-189631] p 685 N92-25960
BLACKBURN, KENNETH E.
Moldless composite aircraft wing structural design modifications p 958 A92-51527
BLACKSTOCK, DAVID T.
Model experiment to study the effect of turbulence on risetime and waveform of N waves
p 1139 N92-33881
BLACKWELDER, RON F.
The eddy structures in bounded shear flows
p 717 N92-27712
BLACKWELL, B. F.
Measurement of the freestream density for re-entry vehicles - A design study p 940 A92-52821
BLACKWELL, J.
A review of Australian activity on modelling the helicopter/ship dynamic interface p 465 N92-21967
BLACODON, D.
Acoustic spinning-mode analysis by iterative threshold method applied to a helicopter turboshaft engine
[ONERA, TP NO. 1992-41] p 926 A92-48602
BLADOS, WALTER R.
An international aerospace information system: A cooperative opportunity
[NASA-TM-108171] p 1142 N92-33237
BLAHA, BERNARD J.
Supersonic STOVL propulsion technology program: An overview p 561 N92-22539
BLAIR, D. S.
Method and apparatus for acoustic plate mode liquid-solid phase transition detection
[DE92-003778] p 401 N92-18705
BLAIR, JERRY T.
Sikorski (S-76) High Intensity Radiated Fields (HIRF) test
[SAE PAPER 912214] p 652 A92-40017
High Intensity Radiated Fields (HIRF) project plan
[DOT/FAA/CT-TN91/1] p 297 N92-16181
BLAIR, M.
Unsteady aerodynamics for aeroelasticity at the Flight Dynamics Directorate p 718 N92-27939
BLAIR, M. F.
New applications of liquid-crystal thermography in rotating turbomachinery heat transfer research
[ASME PAPER 91-GT-354] p 153 A92-15710
The effects of Reynolds number, rotor incidence angle and surface roughness on the heat transfer distribution in a large-scale turbine rotor passage
[NASA-CR-184260] p 42 N92-11297
BLAISDELL, G. A.
Compressibility effects on the growth and structure of homogeneous turbulent shear flow p 675 A92-40052
BLAISE, A.
Acoustic transmission through a 2-D orthotropic multi-layered infinite cylindrical shell p 780 A92-44197
BLAKE, CHRISTOPHER L.
Common avionics baseline: The product of the joint integrated avionics working group p 199 N92-14053
BLAKE, DOUG
Non linear induced drag study of generically cambered closely coupled dual wings
[SAE PAPER 912126] p 618 A92-39973
BLAKE, WILLIAM B.
Development of a high-angle-of-attack stability and control prediction code
[AIAA PAPER 92-4354] p 1079 A92-55340
BLANC
Simulation in the Air Force p 747 A92-41209
BLANCHA, BARRY
Comparison of frequency domain and time domain laser velocimeter signal processors p 1114 A92-54314
BLANCHARD, A.
The design and testing of an airfoil with hybrid laminar flow control
[ONERA, TP NO. 1992-22] p 822 A92-48585
BLAND, R. G.
Low earth orbit satellite concepts for air traffic control applications
[AIAA PAPER 92-1927] p 453 A92-29856
BLANDFORD, C. S.
High speed rotorcraft propulsion concepts to control power/speed characteristics
[AIAA PAPER 92-3367] p 865 A92-48940
BLANKEN, CHRISTOPHER L.
Helicopter control response types for hover and low-speed near-earth tasks in degraded visual conditions
p 132 A92-14338
BLEEKER, O. F.
An aircraft manufacturer's perspective
p 515 A92-33430
BLEWITT, G.
A demonstration of centimeter-level monitoring of polar motion with the Global Positioning System
p 639 N92-24302
BLISS, DONALD B.
Prediction of high-resolution flowfields for rotorcraft aeroacoustics p 53 A92-11053
Eigenvalue calculation procedure for an Euler/Navier-Stokes solver with application to flows over airfoils p 170 A92-17429
Efficient high-resolution rotor wake calculations using flow field reconstruction p 814 A92-46951
Analysis of rotor vibratory loads using higher harmonic pitch control
[NASA-CR-189591] p 696 N92-24251
BLOM, ANDERS F.
Fatigue and damage tolerance verification of aircraft structures p 217 A92-19677
Damage tolerance of the fighter aircraft 37 Viggen. I - Analytical assessment. II - Experimental verification
p 192 A92-19819
A review of aeronautical fatigue investigations in Sweden during the period May 1989 to April 1991
[FFA-TN-1991-24] p 158 N92-12313
BLOOMFIELD, JOHN R.
Knowledge-sensitive task manipulation - Acquiring knowledge from pilots flying a motion-based flight simulator p 916 A92-45064
BLOSCH, EDWIN
Numerical simulation of a confined transonic normal shock wave/turbulent boundary layer interaction
[AIAA PAPER 92-3668] p 826 A92-49088
BLOTTNER, FREDERICK G.
A spatial marching technique for the inviscid blunt body problem p 4 A92-10691
BLOUKE, PETER SCOTT
The FM-007: An advanced jet commuter for HUB to spoke transportation
[NASA-CR-189988] p 461 N92-20267
BLOW, CHRISTOPHER J.
Airport terminals p 283 A92-21125
BLOY, A. W.
The aerodynamic interference between a flapped tanker aircraft and a receiver aircraft during air-to-air refuelling
p 29 A92-13199
BLUEMCKE, E.
Particle dispersion in highly swirling, turbulent flows
p 675 A92-40093
BLYSTONE, J. R.
The aerodynamic assistant - A tool for V/STOL aircraft conceptual design p 545 A92-35737
BLYTH, GRAHAM
Parallel algorithms for panel methods
p 293 A92-22346
BOARD, DAVID B.
CH-46 and OH-58 transmission stress wave analysis
[AD-A244321] p 365 N92-18826
BOATMAN, JOE F.
Measured and calculated optical property profiles in the mixed layer and free troposphere p 1129 A92-54630
BOBBITT, RICHARD B.
Escape strategies for turboprop aircraft in microburst windshear p 1084 A92-56151
Escape strategies for turboprop aircraft in a microburst windshear
[AD-A243090] p 264 N92-17217
BOBKO, KAROL J.
Attributes of winged manned space vehicles and their relationship to ground site characteristics and facilities
p 487 N92-20776
BOBO, STEPHAN N.
Current DOT research on the effect of multiple site damage on structural integrity p 913 N92-30112

BOBO, STEPHEN N.
The aging aircraft fleet - A challenge for nondestructive inspection p 145 A92-13657
BOBROW, J. E.
Active control for gas turbine combustors p 128 A92-16585
BOBYR', E. E.
The feasibility of reducing induced wing drag by using crescent planform wings p 425 A92-30167
BOCHAROV, V. A.
Automated thematic processing of aircraft scanner data gathered over pasture territory in Turkmenia p 406 A92-25330
BOCKELIE, MICHAEL J.
An adaptive grid method for computing the high speed 3D viscous flow about a re-entry vehicle
[AIAA PAPER 92-2685] p 799 A92-45534
BOCKMAN, STUART F.
Lyapunov exponents for systems described by differential equations with discontinuous right-hand sides p 507 A92-29237
BOCVAROV, SPIRO
Time-optimal reorientation maneuvers of an aircraft p 549 N92-22605
BODEN, KARL
Wide gap, permanent magnet biased magnetic bearing system p 773 N92-27794
BODENHORN, CHRIS
An advanced flight path management system for low-altitude helicopter flight p 975 A92-49330
BODHAINE, BARRY A.
Measured and calculated optical property profiles in the mixed layer and free troposphere p 1129 A92-54630
BODONYI, R. J.
Boundary-layer receptivity due to a wall suction and control of Tollmien-Schlichting waves p 616 A92-39333
BOECKING, KLAUS F.
Airborne experimental FLIR program p 1064 N92-32447
BOEHLE, M.
Finite-element algorithm for chemically reacting hypersonic flow
[AIAA PAPER 92-0754] p 336 A92-27097
Numerical approximation of hypersonic shocks in a finite-element method using flux-corrected transport (FCT) p 708 A92-43060
BOELCS, A.
Quasi-three-dimensional characteristics method for a supersonic compressor rotor
[ASME PAPER 91-GT-81] p 69 A92-15549
BOENSCH, FRANK D.
Design challenges for the National Aero-Space Plane p 551 N92-23822
BOER, J. N.
The effect of hoar-frosted wings on the Fokker 50 take-off characteristics p 451 N92-21692
BOERRIGTER, H. L.
Quantitative heat transfer measurements in hypersonic wind tunnels by means of infrared thermography p 1115 A92-54321
BOERSTOEL, J. W.
An information system for the numerical simulation of 3D Euler flows around aircraft p 613 A92-37554
The design of a system of codes for industrial calculations of flows around aircraft and other complex aerodynamic configurations
[AIAA PAPER 92-2619] p 917 A92-45492
New concepts for multi-block grid generation for flow domains around complex aerodynamic configurations p 817 A92-47079
Domain modeling and grid generation for multi-block structured grids with application to aerodynamic and hydrodynamic configurations p 691 N92-24411
Development and validation of a characteristic boundary condition for a cell-centered Euler method
[NLR-TP-90144-U] p 828 N92-28692
New concepts for multi-block grid generation for flow domains around complex aerodynamic configurations
[NLR-TP-91046-U] p 1037 N92-32730
BOESSWETTER, C.
Recommended system concept p 599 N92-23383
Sensor compatibility/optimal sensor combinations p 599 N92-23403
BOETSCH, R.
Fatigue testing and tear down operations on Airbus A320 forward fuselage p 360 N92-18579
BOETTCHER, JAN
Jet aircraft noise at high subsonic flight Mach numbers
[DLR-FB-91-28] p 928 N92-29997
BOETTCHER, ROLF-D.
Applicability of bridging methods to hypersonic rarefied flow aerodynamics of reentry vehicles p 184 N92-15032
BOFFADOSSI, M.
Numerical simulation of unsteady rotor wakes p 1032 A92-56352
Numerical simulation of vortex flows past impulsively started wings p 88 N92-13028
BOGAR, T. J.
Confined normal-shock/turbulent-boundary-layer interaction followed by an adverse pressure gradient p 172 A92-18365
BOGDANOFF, DAVID W.
Reactivation and upgrade of the NASA Ames 16-Inch Shock Tunnel - Status report
[AIAA PAPER 92-0327] p 383 A92-25774
Flow characterization in the NASA Ames 16-inch Shock Tunnel
[AIAA PAPER 92-3810] p 1090 A92-54180
Experimental investigation of nozzle/plume aerodynamics at hypersonic speeds
[NASA-CR-190074] p 664 N92-25162
BOGDONOFF, S. M.
Crossing shock wave turbulent boundary layer interactions - Variable angle and shock generator length geometry effects at Mach 3
[AIAA PAPER 92-0636] p 334 A92-27014
Interaction between crossing oblique shocks and a turbulent boundary layer p 812 A92-46882
BOGDONOFF, SEYMOUR
Structure of supersonic turbulent flow past a swept compression corner p 431 A92-31155
BOGDONOFF, SEYMOUR M.
The structure and control of three-dimensional shock wave turbulent boundary layer interactions
[AD-A250209] p 1003 N92-31824
BOGEN, J. S.
An airborne Doppler lidar for meteorological research p 467 A92-32082
BOGODISTOV, S. S.
Dynamics of the three-dimensional angular motions of rotating flight vehicles in the presence of the aerodynamic hysteresis of the moment characteristic p 428 A92-30371
BOGOMOLOV, A. I.
Consideration of the time lag of engine processes in the problem of VTOL aircraft control synthesis p 134 A92-16807
BOGUSLAEV, V. A.
Possibility of increasing durability of blades with damages p 761 A92-42654
BOGUSLAVSKII, ADOL'F M.
Airfield construction (3rd revised and enlarged edition)
[ISBN 5-277-01070-X] p 670 A92-36606
BOHLMANN, JONATHAN
Application of analytical and design tools for fighter wing aeroelastic tailoring
[AIAA PAPER 92-2373] p 542 A92-34543
BOHLMANN, JONATHAN D.
Static aeroelastic control using strain actuated adaptive structures p 26 A92-11122
Application of analytical and design tools for fighter wing aeroelastic tailoring p 550 N92-23231
BOHN, HANS E.
A noise survey around Oslo Airport Fornebu p 687 A92-39061
BOHNING, RAINER
Compressible turbulent boundary layers with heat addition by homogeneous condensation p 611 A92-36843
BOHON, HERMAN L.
Eighth DOD/NASA/FAA Conference on Fibrous Composites in Structural Design, part 1
[NASA-CP-3087-PT-1] p 1106 N92-32513
BOIKO, L. G.
Analysis of transonic flow over plane compressor cascades using the large-particle method p 79 A92-16812
BOITNOTT, RICHARD L.
Experimental and analytical study of the effects of floor location on response of composite fuselage frames
[AIAA PAPER 92-2473] p 539 A92-34362
BOKSER, V. D.
Experimental study of the characteristics of boundary-layer development on an airfoil p 425 A92-30171
Some characteristics of transonic flow past an airfoil in the case of developed separation p 440 A92-31885
BOL'SHAKOV, M. S.
From the history of Soviet aviation - Aircraft of the Il'iushin design bureau (2nd revised and enlarged edition) p 61 A92-15022
BOLDI, D.
Supportability evaluation of thermoplastic and thermoset composites p 1108 N92-32576
BOLDING, R. M.
On-line adaptive control of unstable aircraft wing flutter p 27 A92-11374
BOLDMAN, DONALD R.
Analysis of an advanced ducted propeller subsonic inlet
[AIAA PAPER 92-0274] p 318 A92-25728
Analysis of an advanced ducted propeller subsonic inlet
[NASA-TM-105393] p 179 N92-14002
BOLDYREV, S. M.
Numerical determination of the regions of existence of two types of shock-wave interaction p 428 A92-30211
BOLMS, H. T.
Conception of a UHB engine simulator for the essential characteristics of a true-scale engine p 1090 A92-54322
BOLONKIN, ALEXANDER
Aviation, motor, and space designs p 784 A92-46202
BOLUKBASI, AKIF O.
Analysis of crash-resistant fuel systems and airframe structure interaction in a crash environment p 105 A92-14369
Crash-resistant rotorcraft preliminary design optimization p 109 A92-14417
BOMAN, BRET L.
Application of the STAPAT II code to hypersonic vehicle aerothermodynamics
[AIAA PAPER 91-5035] p 209 A92-17824
Engineering method for calculating surface pressures and heating rates on vehicles with embedded shocks
[AIAA PAPER 91-5060] p 171 A92-17842
BOMAN, PER-OLOF
Damage tolerance of the fighter aircraft 37 Viggen. I - Analytical assessment. II - Experimental verification p 192 A92-19819
BOMMELAER, G.
Industrial measurement of microphysical parameters - Application to natural and simulated icing clouds p 262 A92-23302
BONATAKI, E.
An inverse inviscid method for the design of quasi-three dimensional turbomachinery cascades p 523 A92-36033
BONCYK, W. C.
Retrieval of total precipitable water over high latitude regions using radiometric measurements near 90 and 183 GHz p 505 A92-32129
BOND, C. D.
Lightning strike tests of composite connectors
[AD-A252281] p 1044 N92-33249
BOND, LEONARD J.
Characterization of diffusion bonds using an acoustic microscope p 491 A92-28686
BOND, N. R.
Modelling the vaporiser and primary zone flows for a modern gas turbine combustion chamber p 742 N92-27484
BOND, THOMAS H.
Advanced ice protection systems test in the NASA Lewis Icing Research Tunnel p 108 A92-14406
Results of an icing test on a NACA 0012 airfoil in the NASA Lewis Icing Research Tunnel
[AIAA PAPER 92-0647] p 334 A92-27021
Results of an Icing test on a NACA 0012 airfoil in the NASA Lewis Icing Research Tunnel
[NASA-TM-105374] p 185 N92-15051
Model rotor icing tests in the NASA. Lewis Icing Research Tunnel p 450 N92-21688
Experimental and computational ice shapes and resulting drag increase for a NACA 0012 airfoil
[NASA-TM-105743] p 828 N92-28674
Results of a low power ice protection system test and a new method of imaging data analysis
[NASA-TM-105745] p 828 N92-28696
BOND, W. E.
Model based reasoning in the aerospace domain
[AIAA PAPER 91-3709] p 230 A92-17582
BONDARENKO, A. B.
Aerodynamic characteristics of the combination of a wing with a cambered middle surface with a fuselage p 439 A92-31880
BONDIE, LILLY
Systems simulation of an advanced avionics COMSEC unit p 921 A92-48485
BONDIOU, A.
Lightning activity in microburst producing storm cells
[ONERA, TP NO. 1991-98] p 161 A92-16080
BONDURANT, DAVID W.
Ferroelectric memory evaluation and development system p 902 A92-48460
BONHAUS, DARYL L.
Comparison of two Navier-Stokes codes for attached transonic wing flows p 309 A92-24414

BONIFACE, J. C.
Solution of the compressible Euler equations for steady flows around helicopter rotor blades by an implicit space-centered method
[ONERA, TP NO. 1991-177] p 77 A92-16139
Resolution of the Euler equations applied to a helicopter rotor in forward flight
[ONERA-RSF-2/3731-AY-004A] p 406 N92-19976
BONNEE, W. J. A.
Examination of aircraft warning and caution lights after shock testing
[NLR-TP-89284-U] p 952 N92-30474
BONNESS, WILLIAM K.
Multibody interference at transonic Mach numbers
[AIAA PAPER 92-0651] p 334 A92-27023
BONNET, C.
Stretched skin concept for the entry aerodynamic decelerator system of planetary probes
p 576 N92-23836
BONNET, J. P.
Compressibility effects in turbulent far wakes
p 622 A92-40140
BOOGERS, J. A. M.
NLR experience with high velocity burner rig testing, 1979-1989
[NLR-TP-89152-U] p 385 N92-18415
BOOLE, P. W.
Controller response to conflict resolution advisory prototype
[PB92-190032] p 1050 N92-33596
BOONE, DAVID
Advanced thermoplastic nose landing gear door development p 20 A92-10275
BOOTH, EARL R., JR.
Rotor blade-vortex interaction noise reduction and vibration using higher harmonic control
p 604 A92-35778
BVI impulsive noise reduction by higher harmonic pitch control - Results of a scaled model rotor experiment in the DNW p 1136 A92-56344
BOOTH, ERIC W.
Software Engineering Laboratory (SEL) Ada performance study report
[NASA-TM-105510] p 412 N92-18125
BOOTH, GUY R.
Implementation of an object-oriented flight simulator D.C. electrical system on a hypercube architecture
[AD-A243700] p 284 N92-17097
BOPPE, CHARLES W.
Aircraft drag analysis methods p 552 N92-23957
BORATAV, O. N.
Emergence of coherent patterns of vortex stretching during reconnection - A scattering paradigm
p 38 A92-11041
BORAY, R. S.
Swirl number effects on confined flows in a model of a dump combustor p 896 A92-45202
BORCHARDT, H.
Trial of a slant visual range measuring device
p 1000 N92-31043
BORCHERS, I. U.
Summary of Dornier 328 interior noise control study
p 643 A92-39083
BORCHERS, INGO U.
Interior noise reduction program for the Dornier 328
p 114 A92-17254
The Dornier 328 Acoustic Test Cell (ATC) for interior noise tests and selected test results
[AIAA PAPER 92-2164] p 1137 N92-32951
Advanced Study for Active Noise Control in Aircraft (ASANCA)
[AIAA PAPER 92-2092] p 1137 N92-32956
BOREK, G. T.
Crossed beam correlation modeling and experimental techniques for measuring density fluctuations in hypersonic flows
[AIAA PAPER 92-2779] p 758 A92-41323
BORER, CHRIS J.
An analysis of the aircraft engine Component Improvement Program (CIP): A life cycle cost approach
[AD-A243346] p 280 N92-17729
BORGER, J.
A simulator evaluation of various manual control concepts for fly-by-wire transport aircraft
[AIAA PAPER 92-4328] p 1073 A92-55172
BORGFORD, M.
A high gain antenna system for airborne satellite communication applications p 677 N92-24096
BORGMAN, DEAN C.
McDonnell Douglas' new light twin helicopter - The MDX p 271 A92-22710
BORHO, ALAN A.
A case study of the Claycomo, Missouri microburst on July 30, 1989 p 407 A92-27961
BORILLO, MARIO
A cognitive temporal model for the planning in aircraft maintenance p 307 A92-25178
BORIS, J. P.
Numerical simulations of unsteady reactive flows in a combustion chamber p 39 A92-11761
BORISOV, SERGEY YU.
Cryogenic test rig with an aerodynamic magnetically levitated carriage p 750 N92-27792
BORLAND, C. J.
Analysis of unsteady aerodynamic and flutter characteristics of an aeroelastic model in transonic flow
p 720 N92-27953
BORME, A.
Turbulent flow in the wake of an idealized wing-body junction
[AIAA PAPER 92-0282] p 435 A92-31652
BORONOW, WALTER
Further developments in three-dimensional simulation of electrothermal deicing systems
[AIAA PAPER 92-0528] p 459 A92-31668
BOROOMAND, TIRDAD
Variable impedance journal bearings for rotor-bearing systems p 157 N92-12270
BOROVOI, V. IA.
Heat transfer in supersonic flow past a single crater
p 63 A92-13741
BOROVSKII, EVGENII E.
Fundamentals of applied aerogasdynamics. I - Aerodynamics of wings (profiles), airframes, and their combinations p 64 A92-14280
BOROWSKI, RICHARD A.
Piloted simulation effectiveness development applications and limitations p 883 N92-28524
BORREL, M.
Three-dimensional thin-layer and space-marching Navier-Stokes computations using an implicit MUSCL approach - Comparison with experiments and Euler computations
[ONERA, TP NO. 1991-131] p 77 A92-16107
BORRELLI, SALVATORE
High enthalpy nozzle flows p 182 N92-15000
BORRI, MARCO
Linear analysis of naturally curved and twisted anisotropic beam p 899 A92-46936
Composite beam analysis linear analysis of naturally curved and twisted anisotropic beams
[AD-A252652] p 999 N92-30766
BORRIELLO, G.
Aerothermodynamic development of the CARINA re-entry vehicle: CFD analyses and experimental tests
p 211 N92-14980
BORSI, M.
Comparison of solution of various Euler solvers and one Navier-Stokes solver for the flow about a sharp-edged cropped delta wing
[AD-B163639L] p 83 N92-12998
Vortical flow simulation by using structured and unstructured grids p 83 N92-12999
BORST, ROBERT G.
E-6 flutter investigation and experience
[AIAA PAPER 92-4601] p 1077 A92-55280
BOS, M. J.
Critical appraisal of the McDonnell Douglas closure model for predicting fatigue crack growth
[ARL-STRUC-R-444] p 44 N92-11376
BOSCHER, D.
Application of infrared thermography to thermal flux measurement in wind tunnels
[AAAF-NT-89-12] p 31 N92-11020
Heat transfer measurements in ONERA supersonic and hypersonic wind tunnels using passive and active infrared thermography p 208 N92-15003
BOSCHER, D. M.
Measurement of convective heat-transfer coefficients on a wind tunnel model by passive and stimulated infrared thermography p 291 A92-21450
Measurement of convective heat-transfer coefficients in wind tunnels using passive and stimulated infrared thermography p 390 A92-24430
BOSCHITSCH, ALEXANDER H.
Analysis of rotor vibratory loads using higher harmonic pitch control
[NASA-CR-189591] p 696 N92-24251
BOSSERT, DAVID E.
Design of robust Quantitative Feedback Theory controllers for pitch attitude hold systems
[AIAA PAPER 92-4409] p 1075 A92-55203
BOSSI, R. H.
X-ray computed tomographic inspection of castings
p 492 A92-28725
X-ray computed tomography for the aircraft/aerospace industry p 492 A92-28750
BOSSI, RICHARD H.
X-ray computed tomography of composites
p 36 A92-10143
BOSSLER, R.
Experimental testing of prototype face gears for helicopter transmissions
[NASA-TM-105434] p 1002 N92-31349
BOSSLER, R. B., JR.
Application of face-gear drives in helicopter transmissions
[NASA-TM-105655] p 908 N92-28434
BOSSLER, ROBERT B., JR.
Advanced Rotorcraft Transmission program summary
[AIAA PAPER 92-3363] p 905 A92-48936
An eight month gearbox development program
[AIAA PAPER 92-3368] p 850 A92-48941
BOSWORTH, JOHN T.
Linearized aerodynamic and control law models of the X-29A airplane and comparison with flight data
[NASA-TM-4356] p 381 N92-19174
BOTHE, HELMUT
The basic measuring technical equipment of the DLR test aircraft p 652 N92-25592
Introduction and execution of flight tests at the DLR
p 648 N92-25594
BOTTARO, ALESSANDRO
Transition to turbulence in curved channel flow
p 621 A92-40125
BOUBEL, D.
Preparation for a new plane (A 320): Experience reviewed p 1010 N92-30954
BOUCHAL, LADISLAV
Shimmy of nose undercarriage wheels
p 959 A92-51948
BOUCHARD, EUGENE E.
Concepts for a future aircraft design environment
[AIAA PAPER 92-1188] p 600 A92-33300
BOUCHARD, J.
GPS availability. I - Availability of service achievable for different categories of civil users. II - Evaluation of state probabilities for 21-satellite and 24-satellite constellations p 99 A92-16949
BOUCHIE, Y.
CARS temperature measurements and validation of a computing code on a gas-turbine combustor
[ONERA, TP NO. 1991-224] p 373 A92-26376
BOUDIER, P.
The coherent flamelet model for propulsion applications p 756 N92-27486
BOUGHTON, J.
An aircraft Earth station for general aviation
p 678 N92-24194
BOULAY, JEAN-LOUIS
Aircraft lightning strikes
[ONERA, TP NO. 1991-204] p 351 A92-26361
BOURAS, B.
Arbitrary blade section design based on viscous considerations - Background information
p 523 A92-36029
Arbitrary blade section design based on viscous considerations - Blade optimization p 523 A92-36030
BOURDAIS, E.
Dynamic performance of an aircraft on its landing gear: Test and evaluation on a dihedral p 466 N92-21970
BOURNES, PATRICK
One joule output from a diode-array-pumped Nd:YAG laser with side-pumped rod geometry
p 671 A92-37188
BOUSLOG, S. A.
Aeroassist flight experiment heating-rate sensitivity study p 3 A92-10427
Aerodynamic heating on AFE due to nonequilibrium flow with variable entropy at boundary layer edge
p 183 N92-15020
BOUSMAN, WILLIAM G.
Lifting line predictions for a swept tip rotor blade
p 65 A92-14424
BOUSQUET, J. M.
Analysis tools of ONERA and DLR for the aerothermodynamics of reentry vehicles
p 211 N92-14977
BOUSSIOS, C.
Active control of compressor surge and stall
[AD-A252771] p 1126 N92-33498
BOUTHIER, O. M.
Models of space-averaged energetics of plates
p 398 A92-28031
BOUWER, G.
Experiences with high authority helicopter flight control
p 568 A92-35757
BOVA, S. W.
Parallel grid generation/optimization using block-domain decomposition p 776 A92-41199
BOWATER, STEPHEN P.
The development of a requirement specification for an experimental active flight control system for a variable stability helicopter: An Ada simulation in JSD
p 135 N92-12466

BOWDITCH, DAVID N.
Impact and promise of NASA aeropropulsion technology p 559 N92-22511
The future challenge for aeropropulsion
[NASA-TM-105613] p 658 N92-25164
BOWEN, BRENT D.
Techfest 18 Proceedings
[NIAR-92-1] p 420 N92-21501
BOWEN, KATHLEEN K.
Experimental and numerical investigation of anti-icing phenomena on a NACA 0012 assembly
[AIAA PAPER 92-0531] p 459 A92-31669
BOWER, M. V.
High altitude solar power platform
[NASA-TM-103578] p 506 N92-21546
BOWLES, ANN E.
A model for the effects of aircraft overflight noise on the reproductive success of raptorial birds
p 688 A92-39101
BOWLES, JEFFREY V.
Analysis of a hydrocarbon scramjet with augmented preburning
[AIAA PAPER 92-3425] p 865 A92-48984
BOWLES, R. L.
Evaluation of a technique to quantify microburst windshear hazard potential to aircraft p 17 A92-11379
BOWLES, ROLAND L.
Windshear detection and avoidance - Airborne systems survey p 17 A92-11382
Airborne in situ computation of the wind shear hazard index
[AIAA PAPER 92-0291] p 351 A92-25744
Three-dimensional simulation of the Denver 11 July Storm of 1988 - An intense microburst event
p 407 A92-27958
BOWLES, T.
Active control of blade vortex interaction
p 814 A92-46944
Smart structures in the active control of blade vortex interaction p 1085 A92-56314
BOWMAN, C. T.
Turbulent reacting flows and supersonic combustion
[AD-A251065] p 986 N92-30256
BOWMAN, H. L.
Flow and acoustic features of a supersonic tapered nozzle p 712 A92-44328
BOWMAN, R. C., JR.
Evaluation of metal hydride compressors for applications in Joule-Thomson cryocoolers p 296 A92-23835
BOWYER, M. R.
Parallel knowledge based systems architectures for in-flight mission management p 728 N92-27904
BOYCE, REX A.
Bearing servicing tool
[NASA-CASE-MSC-21881-1] p 912 N92-30082
BOYD-LEE, A. D.
Crack initiation and the short-to-long crack growth transition in a Ni-base superalloy p 213 A92-19767
BOYD, ANDREW D.
A formal definition of the object-oriented paradigm for requirements analysis
[AD-A246814] p 729 N92-28132
BOYD, IAIN D.
Decoupled predictions of radiative heating in air using a particle simulation method
[AIAA PAPER 92-2971] p 816 A92-46986
Monte Carlo study of vibrational relaxation processes
p 940 A92-52777
BOYD, J. E.
Detection of honeycomb damage using hexagonal grid discontinuities
[DREP-89-9] p 1109 N92-32846
BOYER, ROBERT R.
New titanium applications on the Boeing 777 airplane
p 754 A92-41119
BOYLE, R. J.
Three-dimensional Navier-Stokes heat transfer predictions for turbine blade rows
[AIAA PAPER 92-3068] p 1020 A92-54003
BRAASCH, MICHAEL
GPS interferometric attitude and heading determination - Initial flight test results p 454 A92-30023
GPS interferometric attitude and heading determination: Initial flight test results p 269 N92-17994
BRAASCH, MICHAEL S.
GPS interferometric attitude and heading determination - Flight test results p 650 A92-39561
BRAATEN, MARK E.
Numerical study of branched turboprop inlet ducts using a multiple block grid procedure
[ASME PAPER 91-GT-339] p 76 A92-15703
BRACHIO, BRIAN
Acceptance of two identical radars in the absence of a precision reference p 533 A92-35931
BRACKIN, KYLE
Salvaging the wreckage - Multidistrict litigation and aviation p 697 A92-39245
BRADLEY, GERALD A.
Automatic link establishment - The key to reliable helicopter NOE communications p 94 A92-14403
BRADLEY, JAMES T.
Visibility measurements for the Automated Surface Observing System (ASOS) p 468 A92-32095
BRADLEY, JOHN
Handling and performance considerations when conducting air-to-air refuelling of large aircraft by the probe and drogue system p 548 A92-35937
BRADLEY, M. K.
An iodine hypersonic wind tunnel for the study of nonequilibrium reacting flows
[AIAA PAPER 92-0566] p 383 A92-26974
A code validation strategy and facility for nonequilibrium, reacting flows
[AIAA PAPER 92-3970] p 1098 A92-56796
BRADLEY, R.
The use of inverse simulation for conceptual design
p 546 A92-35738
Creation of a living specification for an experimental helicopter active flight control system through incremental simulation p 1057 A92-56312
The identification of coupled flapping/inflow models for hovering flight p 1058 A92-56335
BRADLEY, ROY
The development of a requirement specification for an experimental active flight control system for a variable stability helicopter: An Ada simulation in JSD
p 135 N92-12466
BRADLEY, SUZANNE
Simulation test and evaluation of TCAS 2 logic version 6.04
[DOT/FAA/RD-92/23] p 1048 N92-33098
BRADSHAW, P.
Bursts and sources of pressure fluctuation in turbulent boundary layers p 619 A92-40055
Structure of three-dimensional turbulent boundary layers p 999 N92-30654
BRADY, EDWARD C.
FANS technology and the future of air traffic services
p 532 A92-33436
BRADY, R. A.
Mixing in the dome region of a staged gas turbine combustor
[AIAA PAPER 92-3089] p 903 A92-48734
BRAEUNLING, W.
Conception of a UHB engine simulator for the essential characteristics of a true-scale engine
p 1090 A92-54322
BRAFF, RONALD
Analysis of stand-alone differential GPS for precision approach p 638 A92-38381
BRAGG, M.
Helium bubble flow visualization of the spanwise separation on a NACA 0012 with simulated glaze ice
[AIAA PAPER 92-0413] p 341 A92-28192
Helium bubble flow visualization of the spanwise separation on a NACA 0012 with simulated glaze ice
[NASA-TM-105742] p 714 N92-26612
BRAGG, M. B.
Finite wing aerodynamics with simulated glaze ice
[AIAA PAPER 92-0414] p 325 A92-26265
Measurements in a leading-edge separation bubble due to a simulated airfoil ice accretion p 723 A92-41262
LDV measurements on a rectangular wing with a simulated glaze ice accretion
[AIAA PAPER 92-2690] p 800 A92-45537
Simulation of iced wing aerodynamics
p 450 N92-21686
BRAGG, MICHAEL B.
Predicting droplet impingement on yawed wings
p 1043 A92-56180
BRAGIN, O. A.
A study of aerophysical and dynamic characteristics using an axisymmetric flight test vehicle with a reusable nose section p 707 A92-42684
BRAHNEY, JAMES H.
Will hydraulic systems meet tomorrow's aircraft power requirements? p 21 A92-13246
Hydraulic pumps - The key to power generation
p 215 A92-17348
Fluid power distribution and control
p 292 A92-21733
Fleet modernization - One approach
p 307 A92-25371
Fluid power conversion p 357 A92-25372
BRAILSFORD, E. N.
In-flight evaluation of Mach number at hypersonic speeds p 624 A92-40599
BRAITHWAITE, W. W.
Integrated computer systems in aircraft design and manufacture: Difficulties and implications
p 1010 N92-31864
BRAMA, TORSTEN
The structural optimization system OPTSYS: Current status and applications p 550 N92-23232
BRAMSKI, STEFAN
Selected models of aircraft navigation space
p 839 A92-45373
BRAMSON, B. D.
The avoidance of collisions for Newtonian bodies with hidden variables p 353 A92-24945
BRANAGAN, LYLE
Dynamic characteristics and stability analysis of space shuttle main engine oxygen pump p 224 N92-14366
BRANDAO, MAURICIO P.
Mixed volume boundary element approach for aerodynamics p 617 A92-39934
BRANDECKER, B.
Methodology for assessment of skin repairs on Airbus aircraft p 226 N92-14428
Ageing airplane repair assessment program for Airbus A300 p 838 N92-30123
BRANDES, EDWARD A.
Severe turbulence with a low-level jet ahead of a squall line p 407 A92-27939
BRANDT, M.
Particle dispersion in highly swirling, turbulent flows
p 675 A92-40093
BRANDT, MADS H.
The SAS Flight Analysis and Aircraft Monitoring System p 555 A92-35941
BRANDT, NILS
CATMAC - A way to integrate ground ATC and airborne systems p 531 A92-33429
BRANDT, RUNE
Separation of relaminarised boundary layers
[CUED/A-AERO/TR-16] p 592 N92-22209
BRANDT, S. A.
An inviscid/viscous coupling approach for vortex flow field calculations p 933 A92-49510
BRANDT, S. B.
Preliminary design of an intermittent smoke flow visualization system
[AIAA PAPER 92-1028] p 580 A92-33209
BRANGIER, FRANCIS
The Aeronautical Mobile Satellite Service (AMSS). I - Architecture of the AMSS system p 93 A92-13851
Monopulse secondary surveillance radar and the mode-S surveillance system p 956 A92-53239
BRANNEN, ELIZABETH
The problem of aging aircraft - Is mandatory retirement the answer? p 308 A92-27448
BRANTLEY, A. S.
Partitioned software support concept for modular embedded computer software p 922 A92-48518
BRASCHE, LISA J. H.
NDE research efforts at the FAA Center for Aviation Systems Reliability p 914 N92-30119
BRASE, LARRY O.
A numerical study of control surface buzz using computational fluid dynamic methods
[AIAA PAPER 92-2654] p 806 A92-45578
BRASSEUR, G.
Ozone response to aircraft emissions: Sensitivity studies with two-dimensional models p 409 N92-19126
BRATTON, THOMAS D.
Solid-State Radar Beacon Decoder (SSRBD) Operational Test and Evaluation (OT/E) integration test plan
[DOT/FAA/CT-TN91/30] p 19 N92-10020
BRAUN, D.
Mission oriented investigation of handling qualities through simulation p 1059 A92-56353
BRAUN, M. J.
Full field flow visualization and computer-aided velocity measurements in a bank of cylinders in a wind tunnel
p 991 A92-50040
BRAUN, ROBERT D.
A six-degree-of-freedom guidance and control analysis of Mars aerocapture
[AIAA PAPER 92-0736] p 486 A92-31676
Computation of near-wake, aerobrake flowfields
p 441 A92-32181
Earth aerobraking strategies for manned return from Mars p 752 A92-41535
BRAUSCH, J. F.
Jet noise suppression p 236 N92-14784
BRAY, D.
Computation of normal impinging jets in cross-flow and comparison with experiment p 250 A92-22446
A review of impinging jets in cross-flows - Experimentation and computation
[AIAA PAPER 92-0633] p 333 A92-27011

Recent research into the aerodynamics of ASTOVL aircraft in ground environment p 623 A92-40549
BRAY, ROBERT M.
Aerodynamic analysis of the Pioneer unmanned air vehicle
[AIAA PAPER 92-4635] p 1027 A92-55382
A wind tunnel study of the pioneer remotely piloted vehicle
[AD-A247028] p 732 N92-27335
BRAZIER, J. PH.
Asymptotic defect boundary-layer theory applied to hypersonic flows p 610 A92-36839
BREAUX, PAUL J.
Standardizing operational flight data handling
p 1009 A92-53109
BREBBIA, C. A.
Computational methods in viscous aerodynamics
p 245 A92-21976
BREEDLOVE, PHILLIP
MIL-STD-1553 data bus/PCM multiplexer system
p 188 A92-19211
BREIDENTHAL, ROBERT E.
Sonic eddy - A model for compressible turbulence
p 176 A92-20739
BREITBACH, E.
A study on the feasibility of using adaptive structures in the attenuation of vibration characteristics of rotary wings
[AIAA PAPER 92-2452] p 541 A92-34415
BREITIGAM, W. V.
BMI/bis (allylphenoxyphthalimide)-copolymers - A new family of resins for advanced composites with improved thermal oxidative stability p 33 A92-10213
BREITLING, THOMAS
Compressible turbulent boundary layers with heat addition by homogeneous condensation
p 611 A92-36843
BRENNAN, JAMES R.
Designing to cost effectiveness - Enhancing quality
p 1119 A92-56209
BRENNAN, M.
Fly-by-light technology development plan
[NASA-CR-181954] p 1086 N92-32778
BRENNEIS, A.
Evaluation of an unsteady implicit Euler code against two and three-dimensional standard configurations
p 719 N92-27945
BRENNEISE, C.
A Ka-band instrumentation radar with one foot range resolution p 95 A92-16252
BRENNER, G.
Numerical simulation of chemical and thermal nonequilibrium flows behind compression shocks
[AIAA PAPER 92-2879] p 820 A92-47860
Analysis tools of ONERA and DLR for the aerothermodynamics of reentry vehicles
p 211 N92-14977
BRENNER, MATS
Implementation of a RAIM monitor in a GPS receiver and an integrated GPS/IRS p 99 A92-16948
BRENTNER, KENNETH S.
1991-92 AHS Technical Committee highlights - Acoustics p 696 A92-40390
BRESCIANI, D.
Radiation and coupling between antennas mounted on a complex metallic structure p 760 A92-42315
BRETTHAUER, BERNWARD
Development of an electronic high speed camera system for the quantitative analysis of unsteady flows
[MPIS-100/1991] p 300 N92-17344
BRETZ, PETER L.
Inclusion size effect on the fatigue crack propagation mechanism and fracture mechanics of a superalloy
p 388 A92-24831
BREUSOVA, R. A.
Computational studies of the aerodynamic characteristics of delta wings with a subsonic leading edge p 439 A92-31874
BREWER, JOHN C.
Current DOT research on the effect of multiple site damage on structural integrity p 913 N92-30112
BRIAN, G. J.
Surface pressure measurements on the wing of a wind tunnel model during steady rotation
[AD-A243047] p 260 N92-17281
BRIANT, VICTORIA B.
Risk management - Expanding horizons in nuclear power and other industries
[ISBN 1-56032-231-4] p 993 A92-51438
BRICE, J. M.
What is an ASIC? p 859 N92-28377
BRIDGES, DAVID H.
Effects of tip Reynolds number and tip asymmetry on vortex wakes of axisymmetric bodies at various angles of attack
[AIAA PAPER 92-0406] p 324 A92-26259
BRIDGES, JAMES
Direct evaluation of aeroacoustic theory in a jet
p 1010 A92-50296
A sophisticated, multi-channel data acquisition and processing system for high frequency noise research
[NASA-CR-189137] p 696 N92-24688
BRIDGES, PHILIP
A flight test study to determine aircraft propulsive efficiency and aerodynamic drag using two parameter identification methods and Lock's propeller model
[AIAA PAPER 92-0170] p 271 A92-23781
BRIDGFORD, N.
Environmental evaluation of repairs to fuselage lap joints p 699 A92-41534
BRIGHT, E.
Ceramic component processing development for advanced gas-turbine engines
[ASME PAPER 91-GT-120] p 142 A92-15567
BRIGHT, MICHELLE M.
Piloted evaluation of an integrated propulsion and flight control simulator
[AIAA PAPER 92-4178] p 960 A92-52459
Piloted evaluation of an integrated propulsion and flight control simulator
[NASA-TM-105797] p 1088 N92-34107
BRILEY, W. R.
Computation of flow past a turbine blade with and without tip clearance
[ASME PAPER 91-GT-56] p 68 A92-15534
BRINDLEY, P. K.
Development of a new generation of high-temperature composite materials p 578 N92-22515
BRINGS, WOLF W.
F27 aging aircraft programme emphasizes corrosion prevention p 186 A92-20024
BRINSON, P. R.
Experimental investigation of helicopter coupled rotor/body control p 1086 A92-56318
BRISKI, MARK S.
Integrated test and evaluation for hypervelocity systems
[AIAA PAPER 92-3901] p 1017 A92-56736
BRISLAWN, K.
Enclosing shapes for single-Doppler radar features
p 494 A92-30476
BRISTOL, BRENT
Effects of material choices on brush seal performance
p 1116 A92-54650
BRITCHER, COLIN P.
Further developments relating to the NASA Langley Research Center 13-inch magnetic suspension and balance system
[NASA-CR-188995] p 31 N92-11023
International Symposium on Magnetic Suspension Technology, part 2
[NASA-CP-3152-PT-2] p 753 N92-27788
Dynamics and control of a five degree-of-freedom magnetic suspension system
[NASA-CR-191259] p 1102 N92-34222
BRITT, VICKI O.
Measurements of fuselage skin strains and displacements near a longitudinal lap joint in a pressurized aircraft
[NASA-TM-104163] p 159 N92-13455
Damaged stiffened shell research at NASA. Langley Research Center p 914 N92-30115
BRITTON, RANDALL K.
Ongoing development of a computer jobstream to predict helicopter main rotor performance in icing conditions p 65 A92-14407
Development of an analytical method to predict helicopter main rotor performance in icing conditions
[AIAA PAPER 92-0418] p 326 A92-26268
Development of an analytical method to predict helicopter main rotor performance in icing conditions
[NASA-CR-189110] p 258 N92-15967
Model rotor icing tests in the NASA. Lewis Icing Research Tunnel p 450 N92-21688
BROADBENT, E. G.
Aero-propulsive effects on configuration shaping
[AIAA PAPER 91-5064] p 459 A92-31691
BROATCH, S. A.
An integrated navigation system manager using federated Kalman filtering p 858 A92-48477
BROBECK, CHRIS
Development of a sensor for the detection of aircraft wing contaminants
[AIAA PAPER 92-0300] p 369 A92-25752
BROCHER, E.
Acoustic sources in a tripped flow past a resonator tube p 778 A92-41266
BROCK, J. S.
The Baldwin-Lomax model for separated and wake flows using the entropy envelope concept
[AIAA PAPER 92-0148] p 253 A92-23764
BROCK, N. J.
A quantitative study of unsteady compressible flow on an oscillating airfoil
[AD-A244572] p 445 N92-21012
BROCK, ROBERT
Advanced thermoplastic nose landing gear door development p 20 A92-10275
BROCKETT, TERRY
Some exact and numerical results for plane steady sheared flow of an incompressible inviscid fluid
p 821 A92-48019
BROCKMAN, R. A.
Finite element analysis of tire critical speeds
p 762 A92-42949
Explicit finite element method for transparency impact analysis
[AD-A243527] p 264 N92-17478
BRODERSEN, ROLF
Self-compensating carrier aircraft recovery system
p 448 A92-32238
BRODERSEN, S.
Measurements of the pressure and velocity distribution in low-speed turbomachinery by means of high-frequency pressure transducers p 391 A92-24723
BROECKER, W.
Fatigue life behaviour of composite structures
p 390 N92-18577
BROEK, DAVID
Generation of spectra and stress histories for fatigue and damage tolerance analysis of fuselage repairs
[AD-A250390] p 854 N92-29180
BROGNIEZ, G.
A comparison of measured and modeled broadband fluxes from aircraft data during the ICE '89 field experiment p 1003 A92-49771
BROKOF, U.
Image-supported navigation for testing instrument landing systems p 189 N92-14012
BROKOPP, RICHARD A.
Small engine components test facility compressor testing cell at NASA Lewis Research Center
[AIAA PAPER 92-3980] p 1098 A92-56806
Small engine components test facility compressor testing cell at NASA Lewis Research Center
[NASA-TM-105685] p 982 N92-30508
BRONKHORST, EUGENE A.
Development of rating instruments and procedures for aviation mishap investigation
[AD-A253072] p 1044 N92-33288
BRONKHORST, TINA M.
Development of rating instruments and procedures for aviation mishap investigation
[AD-A253072] p 1044 N92-33288
BROOKS, A. J.
An Axial Turbobrake
[ASME PAPER 91-GT-1] p 147 A92-15501
BROOKS, C. J.
Canadian aircrew sea water survival, 1952-1987
[DCIEM-88-RR-39] p 954 N92-32219
BROOKS, CUYLER W., JR.
The NASA Langley laminar-flow-control experiment on a swept, supercritical airfoil: Evaluation of initial perforated configuration
[NASA-TM-4309] p 525 N92-22196
BROOKS, L. C.
Experimentally supported investigations into the optical performance of multi-aperture window concepts
[AIAA PAPER 92-2781] p 778 A92-41324
A time-integrated image model for aero-optic analysis
[AIAA PAPER 92-2793] p 779 A92-41332
BROOKS, N. KENT
Loran-C performance assurance assessment program
[NASA-CR-190469] p 840 N92-28718
BROOKS, THOMAS F.
Rotor blade-vortex interaction noise reduction and vibration using higher harmonic control
p 604 A92-35778
BVI impulsive noise reduction by higher harmonic pitch control - Results of a scaled model rotor experiment in the DNW p 1136 A92-56344
BROSIUS, DALE
Resin transfer molding of a complex composite aircraft structure p 784 A92-47410
BROT, ABRAHAM
A review of aging aircraft technology: An IAI perspective
[IAITIC-91-1018] p 461 N92-20500
BROTHERS, C. F.
Noise generated by wind turbines p 686 A92-39045
BROUGHTON, T.
Simultaneous engineering in aero-gas turbine design and manufacture
[PNR-90811] p 740 N92-27043
BROUSSARD, JOHN R.
An approach to the optimal output feedback initial stabilizing gain problem p 52 A92-11553

BROUSSAUD, P.
New hypersonic test methods developed at ONERA - The R5 and F4 wind tunnels
[ONERA, TP NO. 1992-39] p 882 A92-48600
BROUWER, J.
Active control for gas turbine combustors
p 128 A92-16585
BROUWER, W.
Real-time helicopter simulation using the blade element method p 1132 A92-56278
Development of nonlinear real-time helicopter simulation using a blade element method
[NLR-TP-90115-U] p 381 N92-18893
BROWN, ALAN S.
Industry seeks tonic for aging aircraft
p 308 A92-28492
Take it all off - with water p 516 A92-34775
Seeing beneath the surface with NDE
p 671 A92-36948
Composite makers sense changes
p 754 A92-42345
BROWN, ALISON K.
Comparison of fixed and variable threshold RAIM algorithms p 100 A92-16951
BROWN, BERNARD
Fire-fighting foams must meet newly-developed ICAO standard p 448 A92-29508
BROWN, BRADFORD M.
Tiltrotor UAV - The next generation unmanned system
p 646 A92-40384
BROWN, C. J.
Flowpath optimization for hypersonic vehicles
[AIAA PAPER 91-5043] p 437 A92-31688
BROWN, D.
Wind-tunnel studies of F/A-18 tail buffet
p 310 A92-24421
Some characteristics and effects of the F/A-18 LEX vortices p 88 N92-13025
Flowfield in the vicinity of the F/A-18 vertical fin at high-angle-of-attack p 628 N92-24865
BROWN, DANIEL M.
Binary optic-corrected conformal windows for optical seekers
[AIAA PAPER 92-2802] p 779 A92-41340
BROWN, DAVID
Evaluation of outdoor-to-indoor response to minimized sonic booms
[NASA-CR-189643] p 927 N92-28556
BROWN, DON
SATWG networked quality function deployment
p 1134 N92-33339
BROWN, EDWARD N.
The design and operational characteristics of a heated radome for air motion measurement p 467 A92-32064
BROWN, F. W.
Analytical evaluation of resonant response of spiral bevel gears in the RAH-66 helicopter Fantail transmission
[AIAA PAPER 92-3495] p 906 A92-49031
BROWN, GERALD
Determining structural performance
p 560 N92-22519
BROWN, GERALD V.
Performance tests of a cryogenic hybrid magnetic bearing for turbopumps
[NASA-TM-105627] p 473 N92-20523
BROWN, GLENN B.
Using uncertainty analysis in the debugging and qualification of a turbulent heat transfer test facility
p 138 A92-17224
BROWN, HAROLD
Intelligent Engine Control (IEC)
[AIAA PAPER 92-3484] p 866 A92-49024
BROWN, JEFFREY C.
Supersonic Throughflow Fan Test Facility at NASA. Lewis Research Center
[NASA-TP-3038] p 983 N92-31640
BROWN, JEROME D.
Proposal for a low cost close air support aircraft for the year 2000: The Raptor
[NASA-CR-190023] p 367 N92-19496
BROWN, K. W.
Structural tailoring of advanced turboprops (STAT): User's manual
[NASA-CR-187101] p 26 N92-11016
BROWN, R. G.
RAIM - Will it meet the RTCA GPS minimum operational performance standards? p 96 A92-16635
BROWN, RICHARD
Cyclic hot corrosion of Haynes 230 alloy
p 754 A92-41091
BROWN, ROBERT A.
Relating the microwave radar cross section to the sea surface stress - Physics and algorithms
p 597 A92-35028
BROWN, S. R.
Characterization of stainless steel pretreatments for adhesive bonding p 994 A92-51546
BROWN, T. M.
Degenerate four-wave mixing for measurement of NO2 and smoke concentration in jet engine exhaust
[AIAA PAPER 92-3658] p 1113 A92-54108
BROWNE, LINDSEY
Potential flow theory and operation guide for the panel code PMARC
[NASA-TM-102851] p 1036 N92-32422
BROZ, ALFRED L.
National research program for nondestructive inspection of aging aircraft p 169 A92-17294
BRUCKART, JAMES E.
Analysis of changes in the pilot population and general aviation accidents p 187 A92-20722
BRUCKNER, A. P.
Investigation of hypersonic ramjet propulsion cycles using a ram accelerator test facility
[IAF PAPER 91-275] p 278 A92-22482
Computational studies of a superdetonative ram accelerator mode p 399 A92-28529
High spatial resolution measurements of ram accelerator gas dynamic phenomena
[AIAA PAPER 92-3244] p 903 A92-48844
BRUCKNER, ROBERT J.
Engine component instrumentation development facility at NASA Lewis Research Center
[AIAA PAPER 92-3995] p 1099 A92-56818
Engine component instrumentation development facility at NASA Lewis Research Center
[NASA-TM-105644] p 665 N92-25449
BRUECKNER-FOIT, A.
Probabilistic lifing approach for aero engine disks made of powder nickel base alloys containing ceramic defects
p 226 N92-14424
BRUEHL, STEPHAN
The acoustic flashlight
[MBB-Z-0359-90-PUB] p 239 N92-15938
BRUGNOLI, E.
Fracture analysis and crack propagation in pressurized fuselage structures - Experimental and numerical investigations p 217 A92-19812
BRUMBAUGH, RANDAL W.
A NASA/RAE cooperation in the development of a real-time knowledge based autopilot
p 164 N92-12528
An aircraft model for the AIAA controls design challenge
[NASA-CR-186019] p 117 N92-13064
BRUMBY, R. E.
The effect of wing ice contamination on essential flight characteristics p 449 N92-21681
BRUNAIR, R. M.
Study of weld offset in longitudinally welded SSME HPFTP inlet
[AIAA PAPER 92-2305] p 586 A92-34525
BRUNDRETT, E.
Wind-tunnel investigation of aerodynamic and stability characteristics of a forward swept wing X-29 model
p 627 N92-24862
BRUNNER, MICHAEL T.
Use of high-fidelity simulation in the development of an F/A-18 active ground collision avoidance system
[AIAA PAPER 92-4140] p 959 A92-52434
Use of high-fidelity simulation in the development of an F/A-18 active ground collision avoidance system
p 837 N92-28530
BRUNO, JOSEPH
Design, evaluation and experimental effort toward development of a high strain composite wing for Navy aircraft p 1107 N92-32514
BRUNS, J. E.
Three-dimensional compressible turbulent computations for a diffusing S-duct
[NASA-CR-4392] p 526 N92-22249
Three-dimensional compressible turbulent computations for a nondiffusing S-duct
[NASA-CR-4391] p 951 N92-32240
BRUNS, JAMES E.
Full Navier-Stokes calculations on the installed F/A-18 inlet at a high angle of attack
[AIAA PAPER 92-3175] p 1020 A92-54012
BRUNS, JIM
Grid generation for a complex aircraft configuration
p 649 N92-25714
BRY, PIERRE-FRANCOIS
Recent progress in inverse methods in France
p 201 N92-13938
BRYANSTON-CROSS, P. J.
The application of particle image velocimetry (PIV) in a short-duration transonic annular turbine cascade
[ASME PAPER 91-GT-221] p 899 A92-46825
BRYANT, JENNINGS R., JR.
F-14/F110 engine integration p 112 A92-16055
BRYCE, J. D.
Unsteady viscous flow in a high speed core compressor
[ASME PAPER 91-GT-91] p 70 A92-15555
BRYKINA, I. G.
Axisymmetric analogy for three-dimensional viscous flow problems p 244 A92-21617
Similarity relations for calculating three-dimensional chemically nonequilibrium viscous flows
p 827 A92-49188
BRYNESTAD, MARK A.
Investigation of the flight control requirements of a half-scale ducted fan unmanned aerial vehicle
[AD-A252730] p 1087 N92-32988
BRYSON, A. E.
Aircraft control in a downburst on takeoff and landing
p 27 A92-11385
Approach guidance in a downburst
p 873 A92-46741
Parameter identification of linear systems based on smoothing p 873 A92-46742
BRYSON, ARTHUR E.
Inverse and optimal control for desired outputs
p 661 A92-39894
BRYSON, ARTHUR E., JR.
Modeling rotor dynamics with rotor speed degree of freedom for drive train torsional stability analysis
p 547 A92-35779
Linear quadratic minimax controllers
p 917 A92-46748
BUALAT, MARIA G.
Optical computing at NASA Ames Research Center
[AIAA PAPER 91-3779] p 231 A92-17637
BUCCI, A.
CFRP stiffened panels under compression
p 1109 N92-33044
BUCCI, R. J.
Methodology for the assessment of material quality effects on airframe fatigue durability p 213 A92-19820
BUCHHOLZ, J. J.
Flight in a steady wind field p 131 A92-13696
BUCHHOLZ, JOERG J.
Sensor fault detection on board an aircraft with observer and polynomial classifier
[DLR-FB-91-34] p 859 N92-29870
BUCHHOLZ, MARK D.
Vortex trapping on a 60 degree delta wing
[AIAA PAPER 92-2639] p 796 A92-45508
BUCK, ARDEN L.
The DLR Lyman-alpha hygrometer
p 467 A92-32091
BUCKLEY, M. J.
Design sheet - An environment for facilitating flexible trade studies during conceptual design
[AIAA PAPER 92-1191] p 600 A92-33303
BUCKLOW, I. A.
Joining a Ni-based creep-resistant (ODS) alloy by brazing p 1116 A92-54867
Diffusion bonding a creep-resistant Fe-ODS alloy
p 1117 A92-54868
BUCKREUSS, STEFAN
Motion errors in an airborne synthetic aperture radar system p 840 A92-48416
BUECHLER, D. W.
Detailed investigation of causes of avionics field failures p 995 A92-51925
BUENO, MIGUEL A. S.
Possible utilization of GPS in precision approach maneuvers p 637 A92-37075
BUETEFISCH, K.
Review of the European hypersonic wind tunnel performance and simulation requirements
p 209 N92-15043
BUFFINGTON, JAMES M.
Gain scheduled linear PID autopilot for the AIAA Controls Design Challenge aircraft
[AIAA PAPER 92-4629] p 1078 A92-55304
BUFFUM, D. H.
Wind tunnel wall effects in a linear oscillating cascade
[ASME PAPER 91-GT-133] p 72 A92-15576
BUGAJSKI, DANIEL J.
Nonlinear control law with application to high angle-of-attack flight p 661 A92-39904
BUGGEIN, RICHARD C.
Three-dimensional blade vortex interactions
p 815 A92-46953
BUGGELE, ALVIN E.
Engine component instrumentation development facility at NASA Lewis Research Center
[AIAA PAPER 92-3995] p 1099 A92-56818
Engine component instrumentation development facility at NASA Lewis Research Center
[NASA-TM-105644] p 665 N92-25449

BUGGELN, R. C.
Computation of flow past a turbine blade with and without tip clearance
[ASME PAPER 91-GT-56] p 68 A92-15534
BUGGELN, RICHARD C.
Gas turbine main shaft internal flow and heat transfer
[ASME PAPER 91-GT-165] p 123 A92-15600
Hybrid Navier-Stokes/Monte Carlo method for reacting flow calculations p 705 A92-41537
BUIST, JAKOB
On the origin and acoustical behaviour of cloud cavitation
[ISBN-90-9004317-9] p 1125 N92-33066
BUNDICK, W. T.
Controls for agility research in the NASA High-Alpha Technology Program
[SAE PAPER 912148] p 661 A92-39984
BUNIMOVICH, A. I.
Calculation of rotational derivatives in the case of local interaction between flow and a body surface
p 624 A92-40746
BUNING, PIETER G.
A comparative study of turbulence models for overset grids
[AIAA PAPER 92-0437] p 327 A92-26284
Application of the Chimera overlapped grid scheme to simulation of Space Shuttle ascent flows
p 945 N92-30742
BUNNELL, JOHN W.
Algorithmic improvements for simulator motion drive
[AIAA PAPER 92-4158] p 1007 A92-52448
BURCHAM, FRANK W., JR.
Flight-determined benefits of integrated flight-propulsion control systems
[NASA-TM-4393] p 742 N92-27587
Flight testing and simulation of an F-15 airplane using throttles for flight control
[NASA-TM-104255] p 1087 N92-32864
BUREEV, A. V.
Calculation of three-dimensional flow past blunt cones near the plane of symmetry for different flow regimes in the shock layer and in the presence of gas injection from the surface p 337 A92-27593
BURESKE, K.
Ozone response to aircraft emissions: Sensitivity studies with two-dimensional models p 409 N92-19126
BURGGRAF, O. R.
Computation of laminar flow over a long slender axisymmetric blunted cone in hypersonic flow
[AIAA PAPER 92-0756] p 336 A92-27098
BURGGRAF, ODUS R.
Numerical investigation of laminar separated trailing-edge flows p 339 A92-28026
BURGSMUELLER, W.
Application of electronically scanned pressure measurement system for engine simulation tests in the German-Dutch Wind Tunnel
[AIAA PAPER 92-4003] p 1122 A92-56826
BURIEZ, J. C.
A comparison of measured and modeled broadband fluxes from aircraft data during the ICE '89 field experiment p 1003 A92-49771
BURKEN, JOHN J.
Flight-determined stability analysis of multiple-input-multiple-output control systems
[AIAA PAPER 92-4396] p 1074 A92-55196
BURKES, J. M.
Performance of aluminum honeycomb panels with structural defects and core anomalies. II - Specimen description and test results p 591 A92-36156
BURKHALTER, JOHN E.
Downwash for joined-wing airframe with control surface deflections p 702 A92-41235
Downwash measurements on a pitching canard-wing configuration
[AD-A239956] p 12 N92-10016
BURKHARD, ALAN H.
Durability analysis using fracture mechanics for avionics integrity p 396 A92-26799
BURKHARDT, LAURA
Advanced information processing system: Inter-computer communication services
[NASA-CR-187556] p 53 N92-11706
BURLEY, CASEY L.
Acoustic predictions using measured pressures from a model rotor in the DNW p 165 A92-14385
BURMAN, R. G.
Application of a universe-series code for inviscid flow over complex 3-dimensional configurations
[AIAA PAPER 92-0150] p 253 A92-23765
BURNETT, D. W.
A hypersonic waverider test vehicle - The logical next step
[AIAA PAPER 92-0308] p 387 A92-25756
BURNETT, MERIDYTH S.
Perspective versus plan view air traffic control (ATC) displays - Survey and empirical results
p 896 A92-44967
BURNETTE, D.
Developments in airborne surveillance and control systems p 98 A92-16655
BURNHAM, E. A.
High spatial resolution measurements of ram accelerator gas dynamic phenomena
[AIAA PAPER 92-3244] p 903 A92-48844
BURNHAM, RALPH
One joule output from a diode-array-pumped Nd:YAG laser with side-pumped rod geometry
p 671 A92-37188
BURNS, J. G.
Aging aircraft structural damage analysis
p 360 N92-18575
BURNS, J. W.
Weight estimating guide for advanced composites
p 289 A92-23418
BURNS, JOHN
Electric power generating system for the Boeing 777 airplane
[SAE PAPER 912050] p 861 A92-45434
BURNSIDE, W. D.
Bistatic image processing for a 32 x 19 inch model aircraft using scattered fields obtained in the OSU-ESL compact range
[NASA-CR-189932] p 499 N92-20197
BURNSIDE, WALTER D.
Antennas on complex platforms p 494 A92-31084
BUROV, A. V.
Dynamics of aerospace shuttles p 667 N92-24760
BURROWS, C. R.
An evaluation of some strategies for vibration control of flexible rotors p 773 N92-27800
BURROWS, LINDA M.
Electromechanical systems with transient high power response operating from a resonant AC link
[NASA-TM-105716] p 870 N92-28985
BURROWS, S. P.
Design of low-sensitivity modalized observers using left eigenstructure assignment p 661 A92-39908
BURSCH, PAUL
Field test of an advanced maintenance-system
p 1016 A92-56221
BURSEY, ROGER, JR.
Rotor support for the STME oxygen turbopump
[AIAA PAPER 92-3282] p 904 A92-48872
BURSTEIN, N. M.
Assessment of valve actuator motor rotor degradation by Fourier Analysis of current waveform
[DE92-013233] p 909 N92-28814
BURTON, C. D.
Film cooling research on the endwall of a turbine nozzle guide vane in a short duration annular cascade. I - Experimental technique and results
[ASME PAPER 91-GT-252] p 150 A92-15657
Film cooling research on the endwall of a turbine nozzle guide vane in a short duration annular cascade. II - Analysis and correlation of results
[ASME PAPER 91-GT-253] p 150 A92-15658
BURTON, CRAIG
SHARP: Subsonic High Altitude Research Platform
[NASA-CR-190004] p 648 N92-25263
BURTON, RODNEY L.
High pressure hypervelocity electrothermal wind tunnel performance study and subscale tests
[AIAA PAPER 92-0329] p 383 A92-25776
BURTSEV, B. N.
Aeroelasticity of a coaxial helicopter rotor
p 1057 A92-56309
BUSCH-VISHNIAC, ILENE J.
NOISE-CON 90; Proceedings of the 10th National Conference on Noise Control Engineering, University of Texas, Austin, Oct. 15-17, 1990
[ISBN 0-931784-21-2] p 695 A92-39226
BUSCH, HAUKE
Visualization of stopping flow over airfoils
[AIAA PAPER 92-2730] p 804 A92-45564
BUSCHEK, H.
Dynamic interactions between hypersonic vehicle aerodynamics and propulsion system performance
[NASA-CR-190638] p 1038 N92-33304
BUSEN, REINHOLD
The DLR Lyman-alpha hygrometer
p 467 A92-32091
BUSEY, JAMES B.
Air transportation - The global vision
p 532 A92-33434
BUSH, LANCE B.
Structural design considerations for a Personnel Launch System p 386 A92-24668
BUSHMAN, M. A.
In-flight performance diagnostic capability of an adaptive engine model
[AIAA PAPER 92-3746] p 1068 A92-54147
BUSHNELL, D. M.
High-Reynolds-number test requirements in low-speed aerodynamics p 787 A92-45263
Aircraft drag reduction p 717 N92-27709
BUSHNELL, DENNIS M.
Serrated trailing edges for improving lift and drag characteristics of lifting surfaces
[NASA-CASE-LAR-13870-1-CU] p 463 N92-21587
BUSHONG, PHILIP MERTON
A multi-loop guidance scheme using singular perturbation and linear quadratic regulator techniques simultaneously p 481 N92-20148
BUSHWAY, R. R.
Deck motion criteria for carrier aircraft operations
p 464 N92-21952
BUSOVNE, B. J., JR.
Development of silicon nitride rotors for the ATTAP program at Garrett Ceramic Components
[ASME PAPER 91-GT-154] p 142 A92-15590
BUSQUETS, ANTHONY M.
Effect of short-term exposure to stereoscopic three-dimensional flight displays on real-world depth perception
[NASA-TP-3117] p 119 N92-13065
BUSSOLARI, STEVEN R.
Real-time control tower simulation for evaluation of airport surface traffic automation p 879 A92-44976
BUSSOLETTI, J. E.
Analysis of unsteady aerodynamic and flutter characteristics of an aeroelastic model in transonic flow
p 720 N92-27953
BUSSOLETTI, JOHN E.
PAN AIR: A computer program for predicting subsonic or supersonic linear potential flows about arbitrary configurations using a higher order panel method. Volume 2: User's manual (version 3.0)
[NASA-CR-3252] p 527 N92-22865
BUTKUS, LAWRENCE M.
Thermomechanical fatigue behavior of a silicone carbide fiber-reinforced calcium aluminosilicate glass-ceramic matrix composite
[AD-A249870] p 988 N92-31823
BUTLER, BRETT E.
Flight model for unmanned simulated helicopters
p 874 A92-46776
BUTLER, BRYAN
A fault-tolerant network architecture for integrated avionics p 965 A92-49297
BUTLER, CHRISTOPHER P.
Flight testing the handling qualities requirements of ADS-33C - Lessons learned at ATTC
p 104 A92-14339
BUTLER, GEOFF
A NASA/RAE cooperation in the development of a real-time knowledge based autopilot
p 164 N92-12528
BUTLER, P. B.
Thermal radiation effects on a shocked particle-laden gas p 780 A92-44377
BUTLER, RICKY W.
Design for validation p 601 A92-33607
Formal design and verification of a reliable computing platform for real-time control. Phase 2: Results
[NASA-TM-104196] p 602 N92-22320
BUTLER, T. D.
Aerodynamic effects on fuel spray structure - Experiment and theory
[AIAA PAPER 92-0227] p 317 A92-25691
BUTLER, THOMAS W.
Buffet test in the National Transonic Facility
[AIAA PAPER 92-4032] p 1100 A92-56854
Buffet test in the National Transonic Facility
[NASA-CR-189595] p 888 N92-29352
BUTOVSKII, L. S.
Development and bench test of high-temperature combustion chamber with structural ceramic components
[ASME PAPER 91-GT-315] p 126 A92-15691
BUTT, R. I.
Prediction of long-term creep rupture properties for an aluminium alloy for airframe applications
p 141 A92-15206
BUTTERFIELD, C. P.
A comparison of spanwise aerodynamic loads estimated from measured bending moments versus direct pressure measurements on horizontal axis wind turbine blades
[DE92-001158] p 301 N92-16458
Dynamic stall on wind turbine blades
[DE92-001157] p 262 N92-17874
The NREL teetering hub rotor code: Final results and conclusions
[DE92-001187] p 410 N92-19633

Recent results from data analysis of dynamic stall on wind turbine blades
[DE92-001200] p 505 N92-20245
BUTTRAM, GREG
The Langley turbo-prop commuter design: A complete project description
[NASA-CR-189987] p 463 N92-21540
BUTTRILL, CAREY
Simulation and model reduction for the AFW program
[AIAA PAPER 92-2081] p 572 A92-35653
BUTTRILL, CAREY S.
Simulation model of a twin-tail, high performance airplane
[NASA-TM-107601] p 1088 N92-33537
BUTYLIN, I. D.
Flight studies of the riblet effect on drag variation
p 438 A92-31871
Boundary-layer-separation control p 440 A92-31886
BUTZ, JAMES R.
Rarefaction wave eliminator design study
[AD-A244401] p 484 N92-20455
BUXBAUM, O.
Review of investigations on aeronautical fatigue in the Federal Republic of Germany
[ETN-92-90317] p 225 N92-14397
BUYUKATAMAN, K.
Design criteria and analysis of the dynamic behavior of high speed, heavily loaded and precision epicyclic gears for aircraft use
[AIAA PAPER 92-3491] p 906 A92-49028
BYCHKOV, N. M.
Pressure on a cylinder with a screen in transverse flow p 6 A92-12164
BYINGTON, C. S.
Evaluation of parallel injector configurations for Mach 2 combustion p 376 A92-28533
BYRD, G. P.
Evaluation of a technique to quantify microburst windshear hazard potential to aircraft p 17 A92-11379
BYRD, JAMES E.
Influence of airfoil geometry on delta wing leading-edge vortices and vortex-induced aerodynamics at supersonic speeds
[NASA-TP-3105] p 350 N92-20038
BYRD, RITA J.
Improving sample introduction for total wear metal determination by atomic emission spectroscopy
p 389 A92-26850
BYRNE, J.
Short fatigue crack growth from blunt notches in an aero-engine alloy p 212 A92-19760
Fatigue crack growth of small corner defects from blunt notches in an aeroengine alloy
[PNR-90860] p 1111 N92-34019
BYRNE, R. H.
Techniques for autonomous navigation
[DE92-013458] p 957 N92-31746
BYRNES, C. I.
Decentralized-feedback pole placement of linear systems p 411 A92-27347
Hover control of a PVTOL using nonlinear regulator theory p 478 A92-29171
G-Field Control of nonlinear systems
[AIAA PAPER 92-4555] p 1131 A92-55267
BYRNS, EDWARD V., JR.
Active vibration control using fixed order dynamic compensation with frequency shaped cost functionals
p 508 A92-29324
BYROM, TED G.
Thermoviscoplastic response of thin plates subjected to intense local heating
[AIAA PAPER 92-2538] p 584 A92-34382
BYUN, YNGHWAN
Numerical simulation of unsteady hypersonic viscous flows in shock tunnel p 710 A92-43170

C

CABATAN, AILEEN
SHARP: Subsonic High Altitude Research Platform
[NASA-CR-190004] p 648 N92-25263
CABATO, NELLIE L.
Fiber-optic pressure sensor system for gas turbine engine control p 857 A92-48047
CABELL, R. H.
A neural network for the identification of measured helicopter noise p 162 A92-14387
CABELL, RANDOLPH H.
Identification of helicopter noise using a neural network p 416 A92-28032
CABRERA, BRIAN E.
Aviation products liability and navigation - Recent developments and future directions p 697 A92-39563
CACCIOLATI, C.
Study model for the reduction of noise through double wall cylindrical shells - Comparison with experimentation
p 694 A92-39088
CAFARELLI, I.
Theoretical and experimental study of a model rotor
p 547 A92-35781
CAGLAYAN, ALPER K.
An alternative concept for aeroassisted orbit transfers
[AD-A243409] p 287 N92-17325
CAHILL, DAVID M.
Development of an uncertainty methodology for multiple-channel instrumentation systems
[AIAA PAPER 92-3953] p 1133 A92-56781
CAI, HANLONG
Separated flow over the protuberances in hypersonic flow p 615 A92-38907
CAI, JUN-XIAN
Basic analysis of counter-rotating turbines
p 862 A92-47692
CAI, KAIYUAN
Reliability aspects in computer integrated manufacturing systems p 397 A92-27838
CAI, RUIXIAN
Triple contra-rotating turbine and its basic analysis
p 371 A92-24745
Second order perturbation method of gas turbine performance calculation p 759 A92-41834
CAI, TANG G.
Effects of bleed and power extraction on the operating line of engines p 469 A92-29717
CAI, YIN-LIN
Approximate analysis for failure probability of structural systems p 901 A92-47671
CAI, YUANHU
A dynamic digital model for the turbojet with pulse-monitored fueller p 654 A92-38267
CAIN, A. B.
A methodology for the analysis and modeling of thrust vectoring usage
[AIAA PAPER 92-0389] p 357 A92-26245
CAIN, ALAN B.
Evaluation of shear layer cavity resonance mechanisms by numerical simulation
[AIAA PAPER 92-0555] p 333 A92-26965
CAIPEN, TERRY LEE
Invariant boundary conditions for cascade flows
p 498 N92-20147
CALANDRA, VINCENT P.
Applying advanced digital simulation techniques in designing fault tolerant systems p 921 A92-48489
CALAPODAS, NICHOLAS J.
Finite element correlation of the U.S. Army/BHTI ACAP composite airframe helicopter p 108 A92-14399
CALDER, ROBERT B.
Networked simulation of multiple aircraft using Semi-Automated Forces
[AIAA PAPER 92-4170] p 1008 A92-52455
CALDWELL, DONALD
Practical robustness testing for helicopter flight control systems p 132 A92-14340
CALDWELL, RICHARD E.
Zonal analysis - The final step in system safety assessment p 760 A92-42071
CALEDONIA, G. E.
Aerothermodynamic radiation studies
[NASA-CR-185666] p 284 N92-15998
CALIANNO, CARL T.
Stabilized square parachute
[AD-D015014] p 90 N92-13036
CALICO, ROBERT A.
Time-periodic control of a multi-blade helicopter
p 204 A92-18626
CALISE, A. J.
Rapid near-optimal aerospace plane trajectory generation and guidance
[NASA-CR-189469] p 205 N92-14066
CALISE, ANTHONY J.
Optimal output feedback for linear time-periodic systems p 412 A92-28142
Active vibration control using fixed order dynamic compensation with frequency shaped cost functionals
p 508 A92-29324
Neural networks for feedback linearization in aircraft control
[AIAA PAPER 92-4391] p 1074 A92-55192
CALKINS, ROBERT B.
ACES II PLUS ejection seat p 103 A92-13463
CALLAHAN, CYNTHIA B.
Design optimization of rotor blades for improved performance and vibration p 106 A92-14389
CALVERT, JEFFREY F.
Developmental evaluation of a centrifuge flight simulator as an enhanced maneuverability flying qualities tool
[AIAA PAPER 92-4157] p 982 A92-52447
CALVERT, W. J.
Application of S1BYL2 to the AGARD WG18 compressor test cases p 768 N92-27452
CAMARDA, CHARLES J.
A simplified method for thermal analysis of a cowl leading edge subject to intense local shock-wave-interference heating
[NASA-TP-3167] p 679 N92-24797
Analysis and design technology for high-speed aircraft structures p 684 N92-25918
CAMARERO, R.
A Navier-Stokes solver for stretched triangular grids
[AIAA PAPER 92-0183] p 256 A92-23793
Interactive generation of structured/unstructured surface meshes using adaptivity p 919 A92-47066
CAMBIER, JEAN-LUC
Numerical simulation of unsteady flow in a hypersonic shock tunnel facility
[AIAA PAPER 92-4029] p 1034 A92-56851
CAMBIER, LAURENT
Validation of a CANARI code by the computation of three dimensional turbulent flow in turbine valve
p 741 N92-27462
CAMCI, C.
Investigation of three-dimensional flow field in a turbine including rotor/stator interaction. I - Design development and performance of the research facility
[AIAA PAPER 92-3325] p 883 A92-48908
CAMERINO, P.
RAMREQ: A computerized tool for the definition of RAM (Reliability, Availability, Maintainability) requirements of complex systems p 412 N92-18647
CAMP, DAVID W.
STS-41 Space Shuttle mission report
[NASA-TM-105479] p 286 N92-16973
CAMPBELL, B. T.
Thermal paints for shock/boundary layer interaction in inlet flows
[AIAA PAPER 92-3626] p 1113 A92-54093
CAMPBELL, F. J.
Lightning strike tests of composite connectors
[AD-A252281] p 1044 N92-33249
CAMPBELL, J. F.
Vortex flow aerodynamics
[AGARD-AR-299] p 946 N92-30947
CAMPBELL, JOE
Nortec 30 Eddyscan - Portable flaw imaging for aging aircraft p 492 A92-28745
CAMPBELL, R. L.
Transonic airfoil and wing design using Navier-Stokes codes
[AIAA PAPER 92-2651] p 797 A92-45518
CAMPBELL, RICHARD L.
Experimental study of a generic high-speed civil transport: Tabulated data
[NASA-TM-104216] p 525 N92-22232
Applications of a direct/iterative design method to complex transonic configurations
[NASA-TP-3234] p 1039 N92-33484
Experimental study of a generic high-speed civil transport
[NASA-TM-4382] p 1040 N92-33631
CAMPBELL, STEVEN D.
A prototype microburst prediction product for the Terminal Doppler Weather Radar p 408 A92-27962
CAMPBELL, W. H., JR.
Solid-fuel ramjet fuel regression rate/thrust modulation
p 666 A92-36966
CAMPERCHIOLI, WILLIAM P.
Transonic turbine blade cascade testing facility
[AIAA PAPER 92-4034] p 1101 A92-56856
Transonic turbine blade cascade testing facility
[NASA-TM-105646] p 667 N92-26129
CANACCI, V. A.
Full field flow visualization and computer-aided velocity measurements in a bank of cylinders in a wind tunnel
p 991 A92-50040
CANARD-CARUANA, S.
Experimental study of the effects of atmospheric turbulence on sound propagation over the ground
[ONERA, TP NO. 1991-211] p 415 A92-26363
Experimental study of noise generation and propagation in a turbofan model p 1136 A92-56169
CANDEL, S.
A unified nonequilibrium model for hypersonic flows
p 3 A92-10575
Turbulent combustion modelling in a side dump ramjet combustor
[AIAA PAPER 92-3599] p 1112 A92-54075
Hypersonic viscous shock layer in thermochemical nonequilibrium p 183 N92-15014
The coherent flamelet model for propulsion applications p 756 N92-27486

CANDEL, T. M.
Use of the thrust-weight diagram versus transport cargo in the initial dimensioning of passenger-transport aircraft
p 642 A92-37074
CANDLER, GRAHAM V.
Analysis of hypersonic nozzles including vibrational nonequilibrium and intermolecular force effects
[AIAA PAPER 92-0330] p 322 A92-25777
Analysis of thermo-chemical nonequilibrium models for carbon dioxide flows
[AIAA PAPER 92-2852] p 892 A92-47835
Examination of ultraviolet radiation theory for bow shock rocket experiments
[AIAA PAPER 92-2871] p 901 A92-47853
CANDLER, L. W.
High temperature multiaxial creep testing of Nimonic 115 p 141 A92-15202
CANEPA, FRANCO
Knowledge based system applications for guidance and control
[AGARD-AR-284] p 205 N92-14065
CANET, J. MIQUEL
Flow and temperature computations for space vehicles using adaptive finite element techniques
p 181 N92-14990
CANETTA, D.
An application of distributed environment in flight simulation p 602 A92-35739
CANNON, M. E.
A consistency test of airborne GPS using multiple monitor stations p 454 A92-30651
CANT, C. G.
Impact of regulation changes on engine design and certification
[PNR-90789] p 559 N92-22098
CANUPP, PATRICK W.
Analysis of hypersonic nozzles including vibrational nonequilibrium and intermolecular force effects
[AIAA PAPER 92-0330] p 322 A92-25777
CAO, FENGLAN
Experimental research on blade containment
p 557 A92-35561
CAO, HOA V.
Three-dimensional orthogonal-to-surface structured grid generation with transonic Navier-Stokes flow solutions for a commercial transport configuration
[AIAA PAPER 92-2616] p 793 A92-45490
CAO, QIKAI
A study of active flutter suppression for a wing/store system p 379 A92-27826
CAO, X. L.
A new vane swirler as applied to dual-inlet side-dump combustor
[AIAA PAPER 92-3654] p 906 A92-49085
CAO, YIHUA
A new method for calculation of helicopter maneuvering flight p 282 A92-23382
CAPBERN, ALAIN
A cable detection lidar system for helicopters
p 1001 N92-31068
CAPLIN, J.
Measurements of the unsteady vortex flow over a wing-body at angle of attack
[AIAA PAPER 92-2729] p 808 A92-45598
Definition of the unsteady vortex flow over a wing/body configuration
[NASA-CR-180083] p 178 N92-13995
CAPONE, F.
Comparative investigation of multiplane thrust vectoring nozzles
[AIAA PAPER 92-3263] p 864 A92-48858
CAPONE, FRANCIS J.
Study of external dynamic flap loads on a 6 percent B-1B model
[ASME PAPER 91-GT-236] p 125 A92-15645
Thrust vectoring characteristics of the F-18 high alpha research vehicle at angles of attack from 0 to 70 deg
[AIAA PAPER 92-3095] p 877 A92-48737
A static investigation of the thrust vectoring system of the F/A-18 high-alpha research vehicle
[NASA-TM-4359] p 633 N92-25967
Data reduction formulas for the 16-foot transonic tunnel: NASA Langley Research Center, revision 2
[NASA-TM-107646] p 984 N92-31900
Parametric investigation of single-expansion-ramp nozzles at Mach numbers from 0.60 to 1.20
[NASA-TP-3240] p 1042 N92-34193
CAPORICCI, L.
Aircraft navigation using Global Positioning System improved with geostationary satellites
p 99 A92-16934
CAPRIOTTI, D. P.
Evaluation of parallel injector configurations for Mach 2 combustion p 376 A92-28533
CARS temperature measurements in a hypersonic propulsion test facility p 140 N92-12049
CAPUANO, A.
Aerothermodynamic development of the CARINA re-entry vehicle: CFD analyses and experimental tests
p 211 N92-14980
CARADONNA, F. X.
Experimental and computational studies of hovering rotor flows p 815 A92-46954
The computation and validation of hovering rotor performance p 1055 A92-56285
CARAM, J. M.
Effect of riblets on turbulence in the wake of an airfoil
p 5 A92-11051
CARAMASCHI, VITTORIO
The Eurofar vehicle overview p 108 A92-14416
CARAVASOS, NIKOLAOS
Damage tolerance and repair experience of composite structures
[AIAA PAPER 92-1256] p 515 A92-33339
CARBONARO, MARIO
Aerodynamic effects of de/anti-icing fluids and description of a facility and test technique for their assessment p 452 N92-21697
CARDEN, HUEY D.
Effect of crash pulse shape on seat stroke requirements for limiting loads on occupants of aircraft
[NASA-TP-3126] p 399 N92-18053
CARDON, BRADLEY P.
A gas operated bearing damper for turbomachinery
[ASME PAPER 91-GT-249] p 150 A92-15654
CARDONA, A.
Rigid and flexible joint modelling in multibody dynamics using finite elements p 671 A92-37559
CARDONE, G.
Infrared measurements of aerodynamic heating in hypersonic wind tunnel p 208 N92-15002
CARDOSI, K. M.
Controller response to conflict resolution advisory prototype
[PB92-190032] p 1050 N92-33596
CAREL, OLIVIER
The Aeronautical Mobile Satellite Service (AMSS). II - Frequency spectrum requirements for the Aeronautical Mobile Satellite Service p 94 A92-13852
CARESSA, J. P.
Experimental investigation of transverse jet effects related to hypersonic space vehicles
p 182 N92-14995
CAREY, D. M.
Digital time series analysis for flutter test data
[AIAA PAPER 92-2103] p 589 A92-35674
CAREY, G. F.
Parallel grid generation/optimization using block-domain decomposition p 776 A92-41199
CARICO, DEAN
Ship airwake measurement and modeling options for rotorcraft applications p 503 N92-21954
CARIOU, JEAN-PIERRE
Theoretical simulation of a 2 micron airborne solid state laser anemometer p 1000 N92-31059
CARLBERG, JAMES R.
Aviation Diagnostics And Maintenance (ADAM) system preliminary concept of operation and functional description
[AD-A242598] p 170 N92-14966
CARLILE, JULIE A.
An experimental investigation of high-aspect-ratio cooling passages
[AIAA PAPER 92-3154] p 890 A92-48780
Brush seal leakage performance with gaseous working fluids at static and low rotor speed conditions
[NASA-TM-105400] p 297 N92-16265
CARLIN, C. M.
High-speed civil transport flight- and propulsion-control technological issues
[NASA-CR-186015] p 482 N92-21253
CARLOMAGNO, G. M.
Infrared measurements of aerodynamic heating in hypersonic wind tunnel p 208 N92-15002
CARLSON, ANN B.
Shock interference prediction using direct simulation Monte Carlo
[AIAA PAPER 92-0492] p 328 A92-26322
Monte Carlo simulation of reentry flows with ionization
[AIAA PAPER 92-0493] p 328 A92-26323
Direct simulation of re-entry flows with ionization
p 713 A92-44367
CARLSON, HARRY W.
Survey and analysis of research on supersonic drag-due-to-lift minimization with recommendations for wing design
[NASA-TP-3202] p 1040 N92-33656
CARLSON, J. D.
Electrorheological fluids; Proceedings of the 2nd International Conference, Raleigh, NC, Aug. 7-9, 1989
p 40 A92-12625
CARLSON, JOHN R.
Computational investigation of circular-to-rectangular transition ducts
[AIAA PAPER 91-3342] p 6 A92-11605
Commercial turbofan engine exhaust nozzle flow analyses using PAB3D
[AIAA PAPER 92-2701] p 801 A92-45543
Airborne/shipborne PSK telemetry data link
p 839 A92-47511
A nozzle internal performance prediction method
[NASA-TP-3221] p 1040 N92-33625
CARLSON, LELAND A.
Direct-inverse transonic wing-design method in curvilinear coordinates including viscous interaction
p 193 A92-20202
Analysis of junction flowfields using the incompressible Navier-Stokes equations
[AIAA PAPER 92-0519] p 331 A92-26944
Effects of shock wave precursors ahead of hypersonic entry vehicles p 441 A92-32182
Determination of aerodynamic sensitivity coefficients based on the three-dimensional full potential equation
[AIAA PAPER 92-2670] p 798 A92-45525
An initial investigation into methods of computing transonic aerodynamic sensitivity coefficients
[NASA-CR-190040] p 348 N92-19545
Determination of aerodynamic sensitivity coefficients for wings in transonic flow
[NASA-CR-190570] p 832 N92-29657
CARLSON, ROBERT L.
Damage tolerance analysis for rotorcraft - What the issues are p 1058 A92-56336
CARLSSON, INGEMAR
Aerospace software in Sweden p 233 A92-19406
CARMICHAEL, RALPH L.
Transonic wind tunnel test of a 14 percent thick oblique wing
[NASA-TM-102230] p 950 N92-32213
CAROLI, JOSEPH A.
A testability-dependent maintainability-prediction technique p 1120 A92-56222
CARON, P.
Advanced superalloys for turbine blade and vane applications
[ONERA, TP NO. 1992-2] p 893 A92-48578
CARPENTER, A.
Tangential mass addition for shock/boundary-layer interaction control in scramjet inlets p 80 A92-17197
CARPENTER, DON
Model-reference adaptive control for systems with D matrices p 506 A92-29052
CARPENTER, ELISABETH J.
The DOT/DOD Federal Radionavigation Plan
p 96 A92-16637
CARPENTER, M. H.
Direct simulation of high-speed mixing layers
[NASA-TP-3186] p 945 N92-30909
CARPENTER, RONALD S.
Gas turbine engine control
[PATENT-1-274-606] p 130 N92-13069
CARPENTER, THOMAS
Thrust vectoring for lateral-directional stability
[NASA-CR-186016] p 482 N92-21357
CARPENTER, WILLIAM C.
Comparison of polynomial approximations and artificial neural nets for response surfaces in engineering optimization p 165 N92-13835
CARR, H. R.
Joint study on the computerisation of in-field aero engines vibration diagnosis
[PNR-90799] p 1072 N92-33815
CARR, L. W.
Design and development of a compressible dynamic stall facility p 747 A92-41215
A quantitative study of unsteady compressible flow on an oscillating airfoil
[AD-A244572] p 445 N92-21012
CARRANNANTO, PAUL
A-2000: Close air support aircraft design team
[NASA-CR-190022] p 463 N92-21567
CARRAWAY, DEBRA L.
The use of silicon microsensors in smart skins for aerodynamic research p 1116 A92-54348
Active thermal isolation for temperature responsive sensors
[NASA-CASE-LAR-14612-1] p 911 N92-29954
CARREIRO, LOUIS R.
Further studies of kinetic energy methods in high speed ramjet cycle analysis
[AIAA PAPER 92-3805] p 1069 A92-54177
CARRIER, ALAIN
Linear quadratic minimax controllers
p 917 A92-46748
CARRIER, G.
Laser-initiated conical detonation wave for supersonic combustion p 375 A92-28531

CARRIER, G. F.
Laser-initiated conical detonation wave for supersonic combustion. III
[AIAA PAPER 92-3247] p 893 A92-48846
Laser-initiated conical detonation wave for supersonic combustion, part 3
[AD-A250522] p 989 N92-32076
CARRILLO, RENE
Steady and transient performance calculation method for prediction, analysis, and identification
p 869 N92-28461
CARROLL, BRUCE F.
Multiple normal shock wave/turbulent boundary-layer interactions p 344 A92-28527
Numerical simulation of a confined transonic normal shock wave/turbulent boundary layer interaction
[AIAA PAPER 92-3668] p 826 A92-49088
CARROTTE, J. F.
The influence of blade leaning on the performance of an integrated OGV-diffuser system
[ASME PAPER 91-GT-104] p 122 A92-15561
CARRUTHERS, W. D.
Advanced ceramic engine technology for gas turbines
[ASME PAPER 91-GT-368] p 153 A92-15716
CARSON, GEORGE T., JR.
Static internal performance of ventral and rear nozzle concepts for short-takeoff and vertical-landing aircraft
[NASA-TP-3103] p 12 N92-10975
Effect of afterbody geometry on aerodynamic characteristics of isolated nonaxisymmetric afterbodies at transonic Mach numbers
[NASA-TP-3236] p 1041 N92-33706
CARSTENS, V.
Computation of the unsteady transonic 2D cascade flow by an Euler algorithm with interactive grid generation
p 719 N92-27944
CARTER, A. F.
Turbocharged pressurized combustion system
[PB92-142579] p 756 N92-26521
CARTER, ALEXANDER B., III
Use of adhesive bonded attachments for a composite aircraft fuel tank p 785 A92-47414
CARTER, J.
Thin-airfoil correction for panel methods
p 811 A92-46811
CARTER, J. M.
Current stabilizing of fastened composite joints to improve non-sparking lightning current performance
p 213 A92-20130
CARTER, JAMES E.
Industry warms to CFD p 392 A92-24908
CARUSO, CARL
Global positioning system runway incursion program static ground tests
[DOT/FAA/CT-TN91/44] p 957 N92-31838
CARUSO, STEVEN C.
Computational analysis of high-speed ejection seats
[AIAA PAPER 92-0403] p 324 A92-26256
Automatic grid generation for iced airfoil flowfield predictions
[AIAA PAPER 92-0415] p 326 A92-26266
CARVER, D. B.
Initial calibration of the HEAT-H2 arc-heated wind tunnel
[AD-A245072] p 484 N92-20898
CASALIS, G.
The effects of wall suction on laminar-turbulent transition in three-dimensional flow p 522 A92-36021
CASAU
Simulation as applied to mission planning
p 747 A92-41210
CASCIOLA, C. M.
A boundary integral formulation for the kinetic field in aerodynamics. I - Mathematical analysis
p 243 A92-21504
A boundary integral formulation for the kinetic field in aerodynamics. II - Applications to unsteady 2D flows
p 339 A92-28005
CASE, A. M.
Trajectory optimization for hypersonic aircraft guidance p 728 N92-27898
CASE, MICHAEL W.
Use of adhesive bonded attachments for a composite aircraft fuel tank p 785 A92-47414
CASEAU, A.
GPS availability. I - Availability of service achievable for different categories of civil users. II - Evaluation of state probabilities for 21-satellite and 24-satellite constellations p 99 A92-16949
CASEY, R.
Study on small stalker tube performance and numerical calculation p 748 A92-43099
CASHIN, WILLIAM
Tactical Rubidium Frequency Standard (TRFS)
[AD-A243934] p 401 N92-18897
CASHON, JOHN L.
High temperature aircraft research furnace facilities
[NASA-CR-184384] p 1101 N92-33826
CASON, RANDALL W.
Helicopter NVG testing in the United Kingdom
p 112 A92-16053
CASPER, PATRICIA A.
An intelligent pilot vehicle interface for a day/night adverse weather pilotage system (D/NAPS)
[AIAA PAPER 91-3729] p 197 A92-17596
CASSAING, J. J.
Ablation and temperature sensors for flight measurements in reentry body heat shields
p 227 N92-15004
CASSANDRAS, CHRISTOS G.
Stochastic ordering properties and optimal routing control for a class of finite capacity queueing systems
p 48 A92-11375
A new class of gradient estimators for queueing systems with real-time constraints p 49 A92-11395
CASSATT, GARY G.
Advanced thermoplastic nose landing gear door development p 20 A92-10275
Development of thermoplastic components for structural validation p 1107 N92-32522
CASSELL, PETER W.
Structured Hypermedia Application Development Model (SHADM): A structured model for technical documentation application design
[AD-A244268] p 417 N92-19336
CASTILLO, R.
Fracture mechanics approach to creep growth in welded IN738LC gas turbine blades
[ASME PAPER 91-GT-119] p 670 A92-36893
CASTLEBERRY, K. N.
Advanced techniques in current signature analysis
[DE92-007680] p 679 N92-24892
CASTOLDI, P.
AM-X flight simulator from engineering tool to training device p 884 N92-28536
CASTRONUOVA, MAURICE
Current nondestructive inspection methods for aging aircraft
[DOT/FAA/CT-91/5] p 1126 N92-33480
CATENA, V.
High temperature low cycle fatigue of single crystal nickel base superalloys p 213 A92-19796
CATTAFESTA, L. N., III
Experiments on shock/vortex interactions
[AIAA PAPER 92-0315] p 320 A92-25762
CATTANEO, GILBERT
Regulations and their changes for certification of civil aircraft in icing conditions p 450 N92-21683
CAUDLE, MARK D.
An analysis of total quality management in Aeronautical Systems Division
[AD-A246661] p 772 N92-27760
CAUGHEY, DAVID A.
Parallel computing strategies for block multigrid implicit solution of the Euler equations p 812 A92-46894
Improved calculation of transonic potential flow past swept wings p 1031 A92-56179
CAVAILLER, C.
The DAM vertical shock-tube p 880 A92-45096
CAVALLI, J. R.
The SnoDog: Preliminary design of a close air support aircraft
[NASA-CR-189990] p 462 N92-21489
CAVALLO, ALBERTO
Robust flight control systems - A parameter space design p 976 A92-50503
CAVATORTA, ENRICO
A study on vortex flow control of inlet distortion in the re-engined 727-100 center inlet duct using computational fluid dynamics
[AIAA PAPER 92-0152] p 253 A92-23767
A study on vortex flow control on inlet distortion in the re-engined 727-100 center inlet duct using computational fluid dynamics
[NASA-TM-105321] p 179 N92-13998
CAVAZOS, ODILON V.
Pitch rate/sideslip effects on leading-edge extension vortices of an F/A-18 aircraft model
p 874 A92-46810
CAVENAGH, RICHARD A.
Air cushion vehicle conductive/semiconductive flexible skirt, and method
[AD-D015160] p 400 N92-18187
CAVES, ROBERT
A comparison between the consequences of the liberal and non-liberal UK-Europe bilaterals
[TT-9101] p 18 N92-10018
A review of UK aviation policy
[TT-9107] p 61 N92-12988
CAVOLOWSKY, JOHN A.
Reactivation and upgrade of the NASA Ames 16-Inch Shock Tunnel - Status report
[AIAA PAPER 92-0327] p 383 A92-25774
Flow characterization in the NASA Ames 16-inch Shock Tunnel
[AIAA PAPER 92-3810] p 1090 A92-54180
CAVONE, ANGELO A.
Signal processing schemes for Doppler global velocimetry p 1115 A92-54338
CAYSE, ROBERT W.
Transient aerodynamics of a high dynamic pressure shroud separation for a ground-based interceptor missile
[AIAA PAPER 92-2820] p 705 A92-41348
CAZES, R. J.
Aircraft tracking optimization of parameters selection
p 361 N92-18585
CEBECI, T.
An approach to the design of wings - The role of mathematics, physics and economics
[AIAA PAPER 92-0286] p 319 A92-25739
Analysis of iced wings
[NASA-TM-105773] p 1042 N92-34144
CEBECI, TUNCER
Three-dimensional linear stability approach to transition on wings and bodies of revolution at incidence
p 172 A92-18361
A turbulence model for iced airfoils and its validation
[AIAA PAPER 92-0417] p 326 A92-26267
Analysis of iced wings
[AIAA PAPER 92-0416] p 423 A92-29972
An economic approach to accurate wing design
[SAE PAPER 912008] p 789 A92-45408
Numerical method for predicting transition in three-dimensional flows by spatial amplification theory
p 812 A92-46886
A turbulence model for iced airfoils and its validation
[NASA-TM-105373] p 186 N92-15052
CEBECI, TUNCER
An interactive boundary-layer approach to multielement airfoils at high lift
[AIAA PAPER 92-0404] p 324 A92-26257
CEDAR, R. D.
An inverse method for the aerodynamic design of three-dimensional aircraft engine nacelles
p 194 N92-13958
CELENLIGIL, M. C.
Flat-ended circular cylinder in hypersonic rarefied flow
p 174 A92-20304
Hypersonic rarefied flow about a delta wing - direct simulation and comparison with experiment
p 812 A92-46892
Application of the DSMC method to hypersonic flow about a delta wing p 940 A92-52775
CELESTINA, M. L.
The role of tip clearance in high-speed fan stall
[ASME PAPER 91-GT-83] p 69 A92-15550
CELI, ROBERTO
Forward flight trim calculation and frequency response validation of a high-order helicopter simulation model
p 132 A92-14337
Coupled rotor-fuselage dynamics and aeroelasticity in turning flight
[AIAA PAPER 92-2109] p 544 A92-35680
High-order state space simulation models of helicopter flight mechanics p 569 A92-35777
Helicopter rotor blade aeroelasticity in forward flight with an implicit structural formulation p 958 A92-50315
CELIK, ZEKI Z.
Aircraft control at high-alpha by tangential blowing
[AIAA PAPER 92-0021] p 281 A92-22143
Vortical flow control on a wing-body combination using tangential blowing
[AIAA PAPER 92-4430] p 1081 A92-55354
CENCULA, J. E.
Stress concentration effects of oblique holes in aspirated-cooled turbine engine liners
[AIAA PAPER 92-1130] p 581 A92-33282
CENKO, A.
Flight test validation of tow target trajectory predictions
[AIAA PAPER 92-0209] p 271 A92-23814
Evaluation of methods for estimating store carriage loads
[AIAA PAPER 92-0675] p 379 A92-27043
CERBE, T. M.
Short takeoff optimization for the XV-15 tiltrotor aircraft p 1056 A92-56302
CERIANI, S.
An application of distributed environment in flight simulation p 602 A92-35739
CERRO, JEFFREY A.
Combined load test apparatus for flat panels
[NASA-CASE-LAR-14698-1] p 911 N92-30028

CERUTI, MARION G.
Information Management Engineering (IME) laboratory: A database development facility
[AD-A243191] p 305 N92-17369
CHA, JAMES T.
Power beaming - Energy transmission at 35 GHz and higher frequencies
[AIAA PAPER 92-2027] p 471 A92-29944
CHADERJIAN, NEAL M.
Transonic Navier-Stokes computations for an oscillating wing using zonal grids p 701 A92-41217
Navier-Stokes predictions for the F-18 wing and fuselage at large incidence p 810 A92-46783
Navier-Stokes prediction of large-amplitude delta-wing roll oscillations characterizing wing rock
[AIAA PAPER 92-4428] p 1080 A92-55352
CHADSEY, HAROLD
LORAN-C data reduction at the US Naval Observatory p 1050 N92-33358
CHAFFEE, JAMES W.
Integrating GPS with ranging transponders p 95 A92-16627
CHAIMOVICH, M.
A generic harmonic rotor model for helicopter flight simulation p 1086 A92-56333
CHAIMOVICH, MENAHEM
Modeling methods for high-fidelity rotorcraft flight mechanics simulation
[NASA-TM-103842] p 482 N92-21440
CHAIT, YOSSI
Parametric robust control by quantitative feedback theory p 302 A92-21176
CHAKKAEV, T. A.
A test bench for evaluating powerplant electrization p 138 A92-16830
CHAKRABARTI, A. K.
Ti-6Al-4V forgings with enhanced fatigue characteristics for engine and airframe applications p 288 A92-22757
CHAKRABARTI, S.
Software package for preliminary design of helicopter p 775 A92-41195
CHAKRAVARTHY, S. R.
Application of a universe-series code for inviscid flow over complex 3-dimensional configurations
[AIAA PAPER 92-0150] p 253 A92-23765
CHAKRAVARTHY, SUKUMAR R.
A user guide for the EMTAC-MZ CFD code
[NASA-CR-4283] p 678 N92-24242
CHAMBERLAIN, GEORGE A., JR.
Aerodynamic coefficients of a symmetrical airfoil in an oscillating flow
[AD-A241073] p 89 N92-13035
CHAMBERLAIN, R.
Evaluation of the ATD-GASP for endo-leap applications
[AIAA PAPER 92-2771] p 704 A92-41318
CHAMBERLAIN, STEVEN M.
Global satellite navigation using both GPS and GLONASS p 99 A92-16938
CHAMBERLIN, E.
Integrated Russian VLF/Omega receiver design
[PB92-193390] p 1051 N92-33809
CHAMBERLIN, ROY W.
Rejected takeoffs - Causes, problems, and consequences p 835 A92-45052
CHAMBERS, A. C.
Creep-fatigue crack growth in Jethete M152 at 550 C under mixed mode conditions p 288 A92-21490
CHAMIS, CHRISTOS C.
Structural tailoring/analysis for hypersonic components - Executive system development
[AIAA PAPER 92-2471] p 583 A92-34360
Analysis of aircraft engine blade subject to ice impact
[NASA-TM-105336] p 229 N92-15402
Coupled multi-disciplinary simulation of composite engine structures in propulsion environment
[NASA-TM-105575] p 596 N92-23267
Computational Structures Technology for Airframes and Propulsion Systems
[NASA-CP-3142] p 683 N92-25911
Computer codes developed and under development at Lewis p 692 N92-25913
CHAMITOFF, GREGORY ERROL
Robust intelligent flight control for hypersonic vehicles
[NASA-CR-185680] p 746 N92-28209
CHAMPAGNE, FRANK H.
Expand turbulence laboratory facilities to meet new DOD research interest
[AD-A248581] p 883 N92-28388
CHAMPAGNE, G. A.
A low noise propulsion concept for the supersonic transport
[ASME PAPER 91-GT-397] p 127 A92-15727
CHAMPAGNE, VICTOR K., JR.
Failure analysis of the Apache mixer pivot support
[AD-A240858] p 116 N92-13061
CHAMPAIGNE, JACK
Shot peening - Theory and applications
[ISBN 2-907669-18-4] p 676 A92-40400
CHAMPION, J. H.
Finite element analysis of tire critical speeds p 762 A92-42949
CHAMPION, M.
Determination of tire-wheel interface loads for aircraft wheels
[AIAA PAPER 92-2482] p 543 A92-34599
CHAN, JOHN
The SnoDog: Preliminary design of a close air support aircraft
[NASA-CR-189990] p 462 N92-21489
CHAN, JOHN S.
Viscous supersonic flow computations over a delta-rectangular wing with slanting surfaces p 441 A92-32178
CHAN, JYH-JANG
Numerical investigation of supersonic mixed-compression inlet using an implicit upwind scheme p 243 A92-21073
CHAN, S. C.
Numerical study of the 3-D flowfield for a supersonic jet exiting into a hypersonic stream from a conical surface
[AIAA PAPER 92-3675] p 1022 A92-54118
CHAN, SAMUEL Y.
Aeroservoelastic stabilization techniques for hypersonic flight vehicles
[AIAA PAPER 91-5056] p 203 A92-17839
CHAN, STEPHEN C.
Numerical investigation of a transverse jet for supersonic aerodynamic control
[AIAA PAPER 92-0639] p 334 A92-27017
CHAN, WAI Y.
Aeromechanical stability of hingeless helicopter rotors in forward flight p 874 A92-46923
CHAN, WILLIAM M.
Numerical methods for the simulation of complex multi-body flows with applications for the integrated Space Shuttle vehicle
[NASA-CR-190045] p 945 N92-30740
Numerical methods for the simulation of complex multi-body flows with applications for the integrated Space Shuttle vehicle p 945 N92-30741
Application of the Chimera overlapped grid scheme to simulation of Space Shuttle ascent flows p 945 N92-30742
CHAN, Y. S.
Nonstationary gasdynamics p 220 N92-13985
CHAN, Y. Y.
An analysis of the sidewall boundary layer effect in two-dimensional wind tunnel testing p 626 N92-24856
CHANA, K. S.
Predictions and measurements of 3D viscous flow in a transonic turbine nozzle guide vane row p 741 N92-27466
CHANA, WILLIAM F.
High speed VSTOL on the horizon - The answer to congestion?
[SAE PAPER 911976] p 843 A92-45383
CHANANI, G. R.
Supportability evaluation of thermoplastic and thermoset composites p 1108 N92-32576
CHAND, SUJEET
Fuzzy controller design and stability analysis for an aircraft model p 478 A92-29124
CHANDRA, RAMESH
Experimental and theoretical analysis of composite I-beams with elastic couplings p 216 A92-18377
CHANDRAN, RAVI
Pulse jet one-way valve performance
[AIAA PAPER 92-3169] p 863 A92-48790
CHANDRASEKHAR, R.
Thermochemical nonequilibrium and radiative interactions in supersonic hydrogen-air combustion
[AIAA PAPER 92-0340] p 394 A92-25786
CHANDRASEKHARA, M. S.
Leading edge velocity field of an oscillating airfoil in compressible dynamic stall
[AIAA PAPER 92-0193] p 257 A92-23802
Oscillating airfoil velocity field during large amplitude dynamic stall p 622 A92-40171
Design and development of a compressible dynamic stall facility p 747 A92-41215
A quantitative study of unsteady compressible flow on an oscillating airfoil
[AD-A244572] p 445 N92-21012
Laser velocimetry measurements of oscillating airfoil dynamic stall flow field
[AD-A244546] p 502 N92-21297
CHANDRASEKHARAN, REUBEN M.
Aerodynamic design with CFD p 447 N92-21514
CHANETZ, B.
New hypersonic test methods developed at ONERA - The R5 and F4 wind tunnels
[ONERA, TP NO. 1992-39] p 882 A92-48600
CHANEY, VAN G.
Development of a multi-computer in-flight data acquisition and analysis system for general aviation aircraft
[AIAA PAPER 92-1037] p 553 A92-33218
CHANG, CHAU-LYAN
Validation of three-dimensional incompressible spatial direct numerical simulation code: A comparison with linear stability and parabolic stability equation theories for boundary-layer transition on a flat plate
[NASA-TP-3205] p 943 N92-30295
CHANG, CHU-YIN
Quantitative Feedback Theory approach to AIAA Controls Design Challenge
[AIAA PAPER 92-4626] p 1077 A92-55303
CHANG, HO-PEN
Particle trajectory computer program for icing analysis of axisymmetric bodies
[NASA-CR-189134] p 352 N92-19276
CHANG, HONGZHE
An improved computation for gas-turbine combustion chamber flow p 375 A92-28479
CHANG, I. C.
Prediction of drag at subsonic and transonic speeds using Euler methods
[AIAA PAPER 92-0169] p 255 A92-23780
CHANG, I-CHUNG
Transonic aeroelasticity analysis for rotor blades p 758 A92-41238
CHANG, IKE
The rise of active-element phased-array radar
[RAND-P-7747-RGS] p 999 N92-30755
CHANG, IKE Y.
Thermal properties of high performance thermoplastic composites based on poly(ether ketone ketone) (PEKK) p 34 A92-10238
LDF thermoplastic composites technology p 34 A92-13243
CHANG, JEN-FU
Minimizing supersonic wave drag with physical constraints at design and off-design Mach numbers p 811 A92-46808
CHANG, JING-TANG
Transverse shear effect on flutter of composite panels p 1122 A92-56607
CHANG, JINHWA
Hypersonic waveriders - Effects of chemically reacting flow and viscous interaction
[AIAA PAPER 92-0302] p 320 A92-25754
A study of viscous interaction effects on hypersonic waveriders
[NASA-CR-189587] p 625 N92-24680
CHANG, K. C.
An algorithm for predicting the flow past fuselage-mounted engine arrangements
[AIAA PAPER 92-0151] p 253 A92-23766
CHANG, K.-M.
Cold-crucible directional solidification of refractory metal-silicide eutectics p 755 A92-43684
CHANG, LIMIN
The dimensional reconstruction of vortex cross-section images p 339 A92-27833
CHANG, MIN-I J.
Robust pole assignment using closed loop controllability conditions p 49 A92-11417
CHANG, MIN-I. J.
Flight test data analysis of a low cost GPS/IMU integrated navigation system p 638 A92-39560
CHANG, P. S.
Active control of structurally-coupled sound fields generated by localized force inputs p 694 A92-39106
CHANG, R. C.
Control system design for the free drop test of external stores in a wind tunnel
[IAF PAPER ST-91-002] p 207 A92-20650
Nonuniform motion of leading-edge vortex breakdown on ramp pitching delta wings p 808 A92-45828
Forcing level effects of internal acoustic excitation on the improvement of airfoil performance p 1136 A92-56162
CHANG, S.
Study of the flow field and molecular radiation heating around a reentry vehicle p 711 A92-43227
CHANG, S. H.
Steady supersonic and hypersonic flow computations using Eulerian and new Lagrangian formulations
[AIAA PAPER 92-0055] p 249 A92-22170
CHANG, STEPHEN
New, unusual and nonclassical behavior of thin-walled composite structures p 580 A92-32746

Modeling and analysis methodology for aeroelastically tailored chordwise deformable wings
[NASA-CR-189620] p 961 N92-30304
CHANG, TSU-SHUAN
Quantitative Feedback Theory approach to AIAA Controls Design Challenge
[AIAA PAPER 92-4626] p 1077 A92-55303
CHANG, XIN-YU
Radiative heat transfer from nonequilibrium shock layer to a hypersonic reentry body p 1019 A92-53579
Three-dimensional calculation of radiative field in hypersonic air shock layers p 1023 A92-54498
CHANG, XINYU
Test on high enthalpy hypersonic flow using a ballistic range p 747 A92-43097
CHAO, JIN-RONG
An investigation of real-time diagnostic technique for DEEC system p 470 A92-29742
CHAO, TZE-YUEN
An investigation of real-time diagnostic technique for DEEC system p 470 A92-29742
CHAPDELAINE, E. R.
Statistics on aircraft gas turbine engine rotor failures that occurred in US commercial aviation during 1989
[DOT/FAA/CT-92/5] p 971 N92-30303
Statistics on aircraft gas turbine engine rotor failures that occurred in US commercial aviation during 1988
[DOT/FAA/CT-91/28] p 1071 N92-33105
CHAPIN, V.
Generalized expression of chorochronic periodicity in turbomachinery blade-row interaction
p 423 A92-30000
CHAPLESKI, ROBERT C.
An anthropometric evaluation of the TH-57 Jetranger helicopter p 46 A92-11164
CHAPMAN, C. E.
Inspection of aircraft engine components using automated eddy current and pattern recognition techniques
[NRC-LTR-ST-1834] p 504 N92-22029
CHAPMAN, DEAN R.
A perspective on aerospace CFD p 169 A92-20145
CHAPMAN, GARY T.
Multibody interference at transonic Mach numbers
[AIAA PAPER 92-0651] p 334 A92-27023
Streamlines, vorticity lines, and vortices around three-dimensional bodies p 808 A92-45845
CHAPPELL, SHERYL L.
Who or what saved the day? A comparison of traditional and glass cockpits p 833 A92-44931
CHAPUT, ARMAND J.
Preliminary sizing methodology for hypersonic vehicles
p 460 A92-32233
CHAR, J. M.
Study on supersonic combustion in a hypersonic flight
[IAF PAPER 92-0661] p 1106 A92-57101
CHARGIN, MLADEN K.
Static aeroelastic analysis for generic configuration wing p 174 A92-20201
CHARLES, B. D.
Blade-mounted trailing edge flap control for BVI noise reduction
[NASA-CR-4426] p 512 N92-21173
CHARLES, D.
Addressing the challenge of aircraft component design and manufacture from metal matrix composites
p 985 A92-50007
CHARLES, JEAN-PAUL
Impact damage tolerance of helicopter sandwich structures p 958 A92-51506
CHATEL, G.
Active control of airborne noise transmitted through a ribbed panel p 695 A92-39111
CHATRENET, D.
Flight simulation and digital flight controls
p 884 N92-28526
CHATTERJI, G. B.
Vision-based stereo ranging as an optimal control problem
[AIAA PAPER 92-4418] p 1045 A92-55211
CHATTOPADHYAY, ADITI
Optimum design of helicopter rotor blades with multidisciplinary couplings
[AIAA PAPER 92-0214] p 357 A92-25687
Dynamics of an optimized rotor blade at off-design flight conditions p 461 A92-32250
A design optimization procedure for high-speed prop-rotors
[AIAA PAPER 92-2375] p 542 A92-34545
CHATTOPADHYAY, H.
Heat transfer in a channel with built-in wing-type vortex generators p 757 A92-41082
CHAUMETTE, D.
Structures and materials technologies for hypersonic vehicles - Lessons from Hermes experience
[AIAA PAPER 91-5098] p 486 A92-31697
CHAUVE, M. P.
Hot jet dilutor
[ETN-92-90860] p 366 N92-19225
CHAVEZ, FRANK
Dynamics and control of hypersonic vehicles - The integration challenge for the 1990's
[AIAA PAPER 91-5057] p 203 A92-17840
CHAVEZ, FRANK R.
An integrated analytical aeropropulsive/aeroelastic model for the dynamic analysis of hypersonic vehicles
[AIAA PAPER 92-4567] p 1035 A92-57034
CHAVIAROPOULOS, P.
Unsteady Euler calculations in 2-D internal aerodynamics with introduced vorticity
[ASME PAPER 91-GT-168] p 73 A92-15603
Arbitrary blade section design based on viscous considerations - Blade optimization p 523 A92-36030
An inverse inviscid method for the design of quasi-three dimensional turbomachinery cascades
p 523 A92-36033
Unsteady Euler calculations in 3D internal aerodynamics p 768 N92-27470
CHEATHAM, PATRICK L.
Computation of vectoring nozzle performance
p 10 A92-13213
CHEATWOOD, F. M.
An approximate viscous shock layer technique for calculating nonequilibrium hypersonic flows about blunt-nosed bodies
[AIAA PAPER 92-0498] p 329 A92-26326
CHEATWOOD, FOY MCNEIL
An approximate viscous shock layer technique for calculating chemically reacting hypersonic flows about blunt-nosed bodies p 1041 N92-33837
CHEDRIK, V. V.
Reduction of computational models in strength problems p 496 A92-31858
CHEESEMAN, I. C.
A high speed edgewise rotor using circulation control only in the reversed flow area p 1059 A92-56347
CHEKALOVA, IU. S.
Nonstationary forces on a wing airfoil
p 4 A92-10825
CHELARU, V.
Some considerations on modeling flight vehicles movement p 281 A92-21311
CHELLMAN, D. J.
Development and characterization of Powder Metallurgy (PM) 2XXX series Al alloy products and Metal Matrix Composite (MMC) 2XXX Al/SiC materials for high temperature aircraft structural applications
[NASA-CR-187631] p 390 N92-19290
CHEN, B. M.
Design of localizer capture and track hold for a transport airplane - An H(infinity)/LTR approach
p 52 A92-11583
CHEN, BENGANG
Predictive control for optimal path terrain following system p 955 A92-50207
CHEN, BINGLU
An investigation on flame stability by fuel permeability in a flame holder made of porous ceramic material
p 375 A92-28435
CHEN, BINGYONG
The computation of transonic viscous flow
p 338 A92-27831
CHEN, C. L.
Multizonal Navier-Stokes solutions for the multibody Space Shuttle configuration p 310 A92-24667
Scale effects on the flow past the mated Space Shuttle configuration
[AIAA PAPER 92-2680] p 799 A92-45532
CHEN, C.-H.
Low earth orbit satellite concepts for air traffic control *applications*
[AIAA PAPER 92-1927] p 453 A92-29856
CHEN, CHENG W.
Quantitative Feedback Theory approach to AIAA Controls Design Challenge
[AIAA PAPER 92-4626] p 1077 A92-55303
CHEN, CHUAN-YAO
The maintenance economy and economic life of structures p 37 A92-10673
Economic life analysis for replacing components
p 785 A92-47670
CHEN, CHUNG-LUNG
Computation of saddle point of attachment
p 703 A92-41276
CHEN, D.
Bulging of fatigue cracks in a pressurized aircraft fuselage
[LR-655] p 196 N92-14045
CHEN, F.-J.
Supersonic and hypersonic quiet tunnel technology at NASA Langley
[AIAA PAPER 92-3908] p 1094 A92-56743
CHEN, FANG-JENG
Gortler instability and supersonic quiet nozzle design
p 813 A92-46902
CHEN, FU-QUN
A new method for predicting the end wall boundary layers and the blade force defects inside the passage of axial compressor cascades p 819 A92-47691
CHEN, FUQUN
On velocity profile models for predicting end wall boundary layers and their blade force defects in axial compressor cascades p 311 A92-24877
New model for predicting end wall boundary layer in an axial cascade p 611 A92-37389
CHEN, G.
Lower-end dynamic characteristics of a magnetically coupled free-piston Stirling engine/compressor system
p 992 A92-50795
CHEN, GONG
Proof of concept of a magnetically coupled Stirling engine-driven heat pump
[DE92-017129] p 1129 N92-33271
CHEN, GUIBIN
A study of active flutter suppression for a wing/store system p 379 A92-27826
CHEN, GUOPING
A superelement simplified analysis for the vibration systems of the complex structures p 398 A92-27903
CHEN, H. C.
An installed nacelle design code using a multiblock Euler solver. Volume 1: Theory document
[NASA-CR-189652-VOL-1] p 950 N92-32226
An installed nacelle design code using a multiblock Euler solver. Volume 2: User guide
[NASA-CR-189652-VOL-2] p 951 N92-32228
CHEN, H. H.
Three-dimensional linear stability approach to transition on wings and bodies of revolution at incidence
p 172 A92-18361
An approach to the design of wings - The role of mathematics, physics and economics
[AIAA PAPER 92-0286] p 319 A92-25739
Analysis of iced wings
[AIAA PAPER 92-0416] p 423 A92-29972
Analysis of iced wings
[NASA-TM-105773] p 1042 N92-34144
CHEN, H. Y.
Failure analysis and reliability improvement of small turbine engine blades p 993 A92-50860
CHEN, HONGQUAN
An AF3 algorithm for the calculation of transonic nonconservative full potential flow around axisymmetric inlet cowls p 251 A92-23380
CHEN, HSUN H.
A turbulence model for iced airfoils and its validation
[AIAA PAPER 92-0417] p 326 A92-26267
Numerical method for predicting transition in three-dimensional flows by spatial amplification theory
p 812 A92-46886
A turbulence model for iced airfoils and its validation
[NASA-TM-105373] p 186 N92-15052
CHEN, I.
Measurements and correlation of two-phase pressure drop under microgravity conditions p 37 A92-10435
CHEN, J.
Fly-by-light technology development plan
[NASA-CR-181954] p 1086 N92-32778
CHEN, J. L.
The initial development of an expert system for designing composite material wing structures p 599 A92-32542
CHEN, J.-Y.
A new unsteady mixing model to predict NO(x) production during rapid mixing in a dual-stage combustor
[AIAA PAPER 92-0233] p 372 A92-25696
Interaction between chemical reaction and turbulence in supersonic nonpremixed H2-air combustion
p 1117 A92-54931
CHEN, JERRY M.
Model oscillations at high angle of attack in a low speed wind tunnel test
[IAF PAPER ST-91-001] p 175 A92-20649
CHEN, JINGSONG
Pitching derivatives of wing in supersonic and hypersonic stream - Method for local flow piston theory
p 312 A92-25012
CHEN, JUNYUE
Strategies for optimal design of gas turbine disks
p 371 A92-24741
CHEN, KAI-PIN
Adaptive mesh for turbulent hypersonic flow
[AIAA PAPER 92-2776] p 704 A92-41322
CHEN, L. T.
An approach to the design of wings - The role of mathematics, physics and economics
[AIAA PAPER 92-0286] p 319 A92-25739

CHEN, M.
Electronics/avionics integrity - Definition, measurement and improvement p 1120 A92-56252
CHEN, M. Z.
Similarity transformations for compressor blading
[ASME PAPER 91-GT-123] p 70 A92-15568
CHEN, MAOZHANG
A circumferential non-uniform effect model for multistage axial-flow compressor throughflow p 588 A92-35572
Mixing for multi-stage axial-flow compressors
p 996 A92-53015
CHEN, MING-HUA
Numerical simulation of twin-jet impingement on a flat plate coupled with cross-flow p 315 A92-25374
CHEN, O.
State-of-the-art materials for future gas turbine engines p 1070 A92-56122
CHEN, P. C.
Comment on 'Canard-wing interaction in unsteady supersonic flow' p 812 A92-46820
CHEN, P. H.
Convective transport phenomena on the suction surface of a turbine blade including the influence of secondary flows near the endwall
[ASME PAPER 91-GT-35] p 147 A92-15518
CHEN, PING
Relationship between the instability waves and noise of high-speed jets p 924 A92-45835
CHEN, PUHUI
Damage tolerance and durability design of composite aircraft structures p 996 A92-53067
CHEN, QING
Identification of the transfer function between turbulence and aircraft p 743 A92-41226
Reconstruction of flight path in turbulence
p 874 A92-46777
The relation among the general unsteady aerodynamic coefficients of a wing in subsonic and supersonic speed
p 941 A92-53022
Some important factors in turbulence in flight measurement p 1063 A92-54324
CHEN, S.
Analysis and prediction of transonic turbine blade losses
[ASME PAPER 91-GT-183] p 73 A92-15615
CHEN, S. K.
Factors influencing the effective spray cone angle of pressure-swirl atomizers p 295 A92-23300
CHEN, SHAOSONG
Wind tunnel study of aerodynamic characteristics of base combustion p 666 A92-36967
CHEN, SHIH H.
Prediction of periodic loadings on single rotation propfan with off-axis inflow p 277 A92-21071
Turbomachinery unsteady load predictions with nonuniform inflow p 611 A92-36972
CHEN, SHILU
Dynamic stability of elastic vehicles with unsteady aerodynamic force modeling p 509 A92-29326
Stability and dynamic coupling of elastic vehicles with unsteady aerodynamic forces considered
p 1102 A92-53545
CHEN, SHIZHONG
Fracture analysis on compressor blades
p 37 A92-10672
CHEN, SHYI-YAUNG
Evaluation of an advanced finite element analysis for rotor blades p 109 A92-14426
CHEN, STEPHEN P.
Interlaminar fracture characteristics of bonding concepts for thermoplastic primary structures p 758 A92-41282
CHEN, T. H.
Laser diagnostics for velocity measurements in supersonic combusting environments
[AIAA PAPER 92-0008] p 288 A92-22133
CHEN, TINGNAN
The research on Pilot Induced Oscillation
p 977 A92-53088
CHEN, WEIPING
Stability, control and gust response characteristics of an ultralight freewing airplane
[AIAA PAPER 92-4342] p 1079 A92-55331
CHEN, X. J.
Dynamic analysis technique of rotating centrifugal impeller
[ASME PAPER 91-GT-50] p 148 A92-15528
CHEN, XIA
H2/air subsystem combustion kinetics in aerospaceplane powerplants
[IAF PAPER 91-276] p 25 A92-12600
CHEN, XIANGJUN
Dynamic analysis of annular cascade shrouded blades
p 397 A92-27856
CHEN, XIAO
Flow characteristic and flow control of high aspect ratio and highly curved S-bend diffuser p 245 A92-21743
Separation control by vortex generators in subsonic diffuser p 338 A92-27829
Design and calculation of performance of a subsonic inlet duct p 343 A92-28478
Application of submerged vortex generators for separation control of a subsonic diffuser
p 933 A92-49832
CHEN, XIN
The measurement of flutter derivatives using mechanical admittance p 393 A92-25014
CHEN, Y.-J. D.
Application of face-gear drives in helicopter transmissions
[NASA-TM-105655] p 908 N92-28434
CHEN, Y.-M.
Preconditioned upwind methods to solve incompressible Navier-Stokes equations p 395 A92-26436
CHEN, YAN-QIU
The influences of forced oscillations toward vortex-breakdown p 934 A92-50210
CHEN, YOU-PING
The maintenance economy and economic life of structures p 37 A92-10673
Economic life analysis for replacing components
p 785 A92-47670
CHEN, YUANZHONG
3D LDA measurement in an axial fan rotor
p 391 A92-24730
CHEN, YUNG-YAW
Using new aggregation operators in rule-based intelligent control p 51 A92-11456
CHEN, ZEMIN
Efficient lifting line method for computing performance of propeller p 24 A92-10956
CHEN, ZHEN
Investigations of the laws of surge and rotating stall forecast in aeronautical engine p 470 A92-29739
CHEN, ZHIWEI
From fatigue test life to structure safe life
p 997 A92-53099
CHEN, ZONGJI
Reliability aspects in computer integrated manufacturing systems p 397 A92-27838
CHEN, ZUOBIN
Numerical simulations of flow fields over aircrafts
p 313 A92-25042
The study of inverse boundary layer algorithm for transonic flows over aerofoils p 315 A92-25140
CHEN, ZUOYI
Design of transonic compressor cascades using hodograph method p 202 N92-13973
The research progress on Hodograph Method of aerodynamic design at Tsinghua University
p 177 N92-13974
CHENAULT, CLARENCE
CFD calculations of closely coupled scissor wings - Inviscid, viscous, and vortex lattice with rollup results
[SAE PAPER 912150] p 619 A92-39986
CHENG, BUSHI
The 'derivative' and 'synthetic' approaches in aircraft design p 358 A92-27901
CHENG, C. W.
Reduction of the side force on pointed forebodies through add-on tip devices p 1024 A92-54918
CHENG, DEJIN
Engine flight load reliability analysis
p 968 A92-49827
CHENG, EDWARD S.
Resonant cryogenic chopper p 294 A92-22796
CHENG, FUQUN
A random vortex method for prediction of maximum instantaneous inlet total pressure distortion
p 311 A92-24731
CHENG, GENGDONG
Strategies for optimal design of gas turbine disks
p 371 A92-24741
Structural optimization and vibration control of composite rotor blades p 960 A92-53056
CHENG, H. K.
Perspectives on hypersonic viscous and nonequilibrium flow research
[NASA-CR-190817] p 1039 N92-33413
CHENG, J.
Detection and identification of axial flow compressor instabilities p 969 A92-50504
CHENG, KEMING
An investigation on detached shock waves ahead of bodies of revolution at transonic speeds
p 251 A92-23381
Analysis of transonic flow past an axisymmetric convex corner p 312 A92-25015
On the sensitivity of transonic flow
p 315 A92-25132
The lateral shock wave family on the surface of a cone-cylinder in transonic flowfield p 315 A92-25136
Some problems on the sidewall interference in two-dimensional subsonic and transonic wind tunnel testing p 747 A92-41929
Discussion on sidewall suction in two-dimensional wind tunnel p 997 A92-53263
CHENG, L.
Vibroacoustic simulation of an airplane structure
p 629 N92-24871
CHENG, LIN
Numerical simulations of flow fields over aircrafts
p 313 A92-25042
CHENG, MAOZHANG
A large-scale axial flow compressor facility and dynamic measurement techniques for rotor flow study
p 382 A92-24729
CHENG, PETER
Quantitative Feedback Theory approach to AIAA Controls Design Challenge
[AIAA PAPER 92-4626] p 1077 A92-55303
CHENG, PETER Y.
Aeroservoelastic stabilization techniques for hypersonic flight vehicles
[AIAA PAPER 91-5056] p 203 A92-17839
Aircraft aeroservoelastic compensation using constrained optimization
[AIAA PAPER 92-2399] p 564 A92-34470
Automated procedures for aircraft aeroservoelastic compensation
[AIAA PAPER 92-4606] p 1077 A92-55284
CHENG, R. M. H.
Application of a double actuator electronic fuel control unit on a small gas turbine engine
[SAE PAPER 912160] p 655 A92-39993
CHENG, RENDY
Scorpion: Close Air Support (CAS) aircraft
[NASA-CR-189974] p 462 N92-20664
CHENG, V. H. L.
Concepts for pilot interaction with an automated NOE obstacle-avoidance system
[AIAA PAPER 92-4472] p 1076 A92-55232
CHENG, VICTOR H. L.
Simulation of automatic rotorcraft nap-of-the-earth flight in graphics workstation environment
[AIAA PAPER 92-4131] p 981 A92-52428
Status of automatic guidance systems for rotorcraft in low altitude flight p 727 N92-27894
CHENG, XINGANG
A new study on a class of discrete event dynamic systems p 48 A92-11377
CHENG, Y. M.
Limitations to the large strain theory
p 219 A92-20356
CHEREMENSKI, ALEKSANDR G.
Robust frequency design of linear stationary systems in aeroautoelastics p 690 A92-37791
CHERN, JENG-SHING
Ideal proportional navigation p 976 A92-50497
CHERNOVA, T. A.
An automated workstation for the half-scale testing of the flight vehicle stabilization circuit p 664 A92-40622
CHERNYI, M. S.
A method for estimating the efficiency of gas turbine blade cooling systems p 657 A92-40606
CHERNYI, S. G.
On marching algorithms for solving stationary problems p 311 A92-24976
CHERNYSHOVA, S. M.
Interference of high-mounted propfan nacelles with an unswept wing and ways to attenuate it
p 460 A92-31881
CHERRETT, M. A.
Unsteady viscous flow in a high speed core compressor
[ASME PAPER 91-GT-91] p 70 A92-15555
CHESSHIRE, GEOFFREY
On constructing three-dimensional overlapping grids with CMPGRD p 691 N92-24424
CHESTER, R. J.
Minimum surface treatments for adhesively bonded repairs p 754 A92-42501
CHETTY, SHYAM
Computer aided evaluation of aircraft handling qualities and flight control system robustness
[AIAA PAPER 92-4423] p 1080 A92-55347
CHEUNG, SAMSON H.
Application of computational fluid dynamics to sonic boom near- and mid-field prediction
p 1031 A92-56173
CHEVRIER, NOEL
Human factors and simulation p 951 A92-53236
CHEW, G.
Investigation of hypersonic ramjet propulsion cycles using a ram accelerator test facility
[IAF PAPER 91-275] p 278 A92-22482

CHEW, J. W.
Performance of radial clearance rim seals in upstream and downstream rotor-stator wheelspaces
[ASME PAPER 91-GT-32] p 147 A92-15516
Rim sealing of rotor-stator wheelspaces in the absence of external flow
[ASME PAPER 91-GT-33] p 147 A92-15517
CHHOTE, L. SARAF
Criteria for use of seal coats on airport pavements
[DOT/FAA/RD-92/18] p 1102 N92-34247
CHI, C. T.
Control system design for the free drop test of external stores in a wind tunnel
[IAF PAPER ST-91-002] p 207 A92-20650
CHI, RAY M.
An unsteady lifting surface theory for ducted fan blades
[ASME PAPER 91-GT-131] p 71 A92-15575
CHIANG, C. H.
Fundamental studies on droplet interactions in dense sprays
[AD-A246918] p 770 N92-27546
CHIANG, HSIAO-WEI D.
Recent advancements in turbomachinery forced response analyses
[AIAA PAPER 92-0012] p 278 A92-22136
CHIANG, R. Y.
A hierarchical data structure and new capabilities of the Robust-Control Toolbox p 507 A92-29155
H-infinity synthesis using a bilinear pole shifting transform p 1007 A92-50490
CHIANG, RICHARD Y.
H(infinity) robust control synthesis for a fighter performing a coordinated bank turn p 29 A92-11585
CHIANG, WUYING
Dynamic analysis of rotor flex-structure based on nonlinear anisotropic shell models p 899 A92-46946
CHIDESTER, THOMAS R.
The impact of cockpit automation on crew coordination and communication. Volume 1: Overview, LOFT evaluations, error severity, and questionnaire data
[NASA-CR-177587] p 93 N92-13044
CHIEN, FEN-REN
Cyclic hot corrosion of Haynes 230 alloy p 754 A92-41091
CHIEN, LAI-CHEN
Fuel injection in hypersonic airbreathing engine
[IAF PAPER 91-273] p 120 A92-14710
Fair weather convection and light aircraft accidents
[IAF PAPER ST-91-004] p 186 A92-20651
Adaptive mesh for turbulent hypersonic flow
[AIAA PAPER 92-2776] p 704 A92-41322
CHIENG, CHING-CHANG
Navier-Stokes computations for turbulent transonic projectile with a two layer model combining the ASM model of turbulence and the k-epsilon model near the wall
[AIAA PAPER 92-0518] p 331 A92-26943
CHIESI, BRIAN
Concurrent engineering at Boeing Helicopters p 162 A92-14393
CHIH, MICHAEL H.
Instrumented blade experiments using a light autogiro p 555 A92-35773
CHILDS, D. W.
Pressure oscillation in the leakage annulus between a shrouded impeller and its housing due to impeller-discharge-pressure disturbances p 580 A92-32942
CHILDS, DARA W.
Test results for rotordynamic coefficients of the SSME HPOTP turbine interstage seal with two swirl brakes p 223 N92-14357
CHILDS, P. N.
The construction, application and interpretation of three-dimensional hybrid meshes p 919 A92-47089
Generation of unstructured grids within a hybrid multi-block environment p 818 A92-47090
CHIMA, RODRICK V.
Viscous three-dimensional calculations of transonic fan performance
[NASA-TM-103800] p 242 N92-17346
TCGRID: A three dimensional C-grid generator for turbomachinery p 659 N92-25716
Viscous three-dimensional calculations of transonic fan performance p 768 N92-27467
NASA. Lewis Research Center supersonic throughflow fan program
[NASA-TM-103248] p 972 N92-31250
CHIMENE, BEAU C.
Atmospheric disturbance model for aircraft and space capable vehicles
[AIAA PAPER 92-0294] p 407 A92-25747
CHIN, GERALD Y.
RAIM - Will it meet the RTCA GPS minimum operational performance standards? p 96 A92-16635
CHIN, H.
The development and test of thermoplastic composite speed brake p 272 A92-24178
CHIN, J. S.
Experimental techniques for the assessment of fuel thermal stability
[AIAA PAPER 92-0685] p 389 A92-27052
CHIN, SUEI
Fourier functional analysis for unsteady aerodynamic modeling p 935 A92-50313
CHIN, VINCENT D.
Maximum lift prediction for multielement wings
[AIAA PAPER 92-0401] p 324 A92-26254
Transonic calculations for wings with deflected control surfaces
[AIAA PAPER 92-2617] p 805 A92-45572
CHIN, YU-CHI
The navigation data logger for a suitcase navigation system
[AD-A245997] p 727 N92-26756
CHINITZ, W.
Hypersonic mixing and combustion studies in the hypulse facility p 737 A92-44526
CHINITZ, WALLACE
High pressure hypervelocity electrothermal wind tunnel performance study and subscale tests
[AIAA PAPER 92-0329] p 383 A92-25776
CHINZEI, NOBUO
Conceptual design of scramjet engine p 1065 A92-53490
Scramjet engine and its flying test bed p 1066 A92-53492
Performance analysis of idealized scramjet p 1066 A92-53493
Flow measurements in scramjet inlets p 1102 A92-53565
CHIOZZINI, C.
Heterodyne techniques in the I.R. bandwidth for laser obstacle detection p 533 A92-35740
CHISHOLM, D. M.
Flight simulation p 207 N92-13982
CHISHOLM, JOHN D.
In-flight optimization of the total propulsion system
[AIAA PAPER 92-3744] p 1068 A92-54146
CHISNALL, G.
British Aerospace Hawk into the 1990s p 957 A92-50009
CHISTOLINOV, V. G.
Influence of atmospheric rarefaction on aerodynamic characteristics of flying vehicles p 938 A92-52750
CHIU, S. A.
Thermal response of rigid and flexible insulations and reflective coating in an aeroconvective heating environment
[NASA-TM-103925] p 852 N92-28721
CHIU, STEPHEN
Fuzzy controller design and stability analysis for an aircraft model p 478 A92-29124
CHIU, Y. D.
Aerodynamic parametric studies and sensitivity analysis for rotor blades in axial flight p 816 A92-46959
CHIZECK, HOWARD J.
A horizon-recursive form for predictors and their computation p 50 A92-11427
CHMIELNIAK, TADEUSZ
Estimation of the size of separation zone in a turbine stage under small load p 10 A92-13235
CHO, K. N.
Forced vibration of rectangular laminated plates with material damping p 294 A92-23167
CHO, PETER
Pocono Mountain SAR data analysis for testing slant range to ground range conversion p 587 A92-35142
CHOCHOD, A.
A radar signal processing ASIC and a VME interface circuit p 859 N92-28380
CHOCKIE, ALAN
Effective maintenance practices to manage system aging p 1119 A92-56215
CHOI, DOCHUL
3D Navier-Stokes analysis for a tip leakage flow in a low aspect ratio turbine
[AIAA PAPER 92-0395] p 278 A92-23816
CHOI, JANG-SOO
Aerodynamic characteristics of a wing near its tip using panel method p 251 A92-22524
CHOI, JANGSOO
Aerodynamic characteristics near the tip of a finite wing by a panel method
[SAE PAPER 912020] p 790 A92-45413
CHOI, K. Y.
Organized structure in a Mach 5/Mach 3 turbulent shear layer
[AIAA PAPER 92-0180] p 256 A92-23790
CHOKANI, N.
Navier-Stokes study of supersonic cavity flowfield with passive control p 442 A92-32239
Passive control of supersonic cavity flowfields
[SAE PAPER 912153] p 619 A92-39988
CHOKANI, NDAONA
Experimental design of a supersonic shock wave/vortex interaction at Mach 3 p 521 A92-35988
The effects of nozzle exit geometry on forebody vortex control using blowing
[AIAA PAPER 92-2603] p 792 A92-45480
Numerical modeling of transonic juncture flow
[AIAA PAPER 92-4036] p 1035 A92-56858
A study of juncture flow in the NASA Langley 0.3-meter transonic cryogenic tunnel
[NASA-CR-190430] p 773 N92-27880
CHOLLET, J. P.
Reactive mixing layer between pressure reflecting boundaries p 656 A92-40144
CHOO, Y. K.
NASA Workshop on future directions in surface modeling and grid generation
[NASA-CP-10092] p 831 N92-29625
CHOO, YUNG K.
Interactive solution-adaptive grid generation procedure
[NASA-TM-105432] p 528 N92-23563
CHOPRA, INDERJIT
Dynamics of helicopters with dissimilar blades p 133 A92-14427
Experimental and theoretical analysis of composite I-beams with elastic couplings p 216 A92-18377
Aeroelastic analysis of swept, anhedral, and tapered tip rotor blades p 316 A92-25577
Aeroelastic response and blade loads of a composite rotor in forward flight
[AIAA PAPER 92-2566] p 564 A92-34480
Aeroelastic response of helicopters with flexible fuselage modeling
[AIAA PAPER 92-2567] p 564 A92-34481
Aeroelastic optimization of an advanced geometry helicopter rotor
[AIAA PAPER 92-2360] p 543 A92-34592
Dynamics of helicopters in ground resonance with and without blade dissimilarities
[AIAA PAPER 92-2108] p 544 A92-35679
Bearingless rotor aeromechanical stability measurements and correlations using nonlinear aerodynamics p 547 A92-35772
Nonlinear damping estimation from rotor stability data using time and frequency domain techniques p 641 A92-36855
Effects of higher harmonic control on rotor performance and control loads p 729 A92-41218
Aeromechanical stability of hingeless helicopter rotors in forward flight p 874 A92-46923
Dynamics of helicopters with dissimilar blades in forward flight p 1056 A92-56288
CHOU, HSING-TUNG
A robust filter configuration for DGPS users p 101 A92-16967
An adaptive correction technique for Differential Global Positioning System p 726 N92-26623
CHOU, J.
A numerical study of isothermal flows of a slit V-gutter
[AIAA PAPER 92-0100] p 293 A92-22203
CHOU, J. H.
Nonuniform motion of leading-edge vortex breakdown on ramp pitching delta wings p 808 A92-45828
CHOU, M. S.
Laser-initiated conical detonation wave for supersonic combustion, part 3
[AD-A250522] p 989 N92-32076
CHOU, M.-S.
Laser-initiated conical detonation wave for supersonic combustion. III
[AIAA PAPER 92-3247] p 893 A92-48846
CHOUDHARI, MEELAN
Distributed acoustic receptivity in laminar flow control configurations
[NASA-CR-4438] p 765 N92-26680
CHOUDHURY, DIPANKAR
Numerical analysis of airflow in aircraft cabins
[SAE PAPER 911441] p 245 A92-21837
Computational fluid dynamics applications in airplane cabin ventilation system design
[SAE PAPER 911992] p 788 A92-45394
CHOW, CHUEN-YEN
Transonic aeroelasticity analysis for rotor blades p 758 A92-41238
CHOY, FRED K.
Modal simulation of gearbox vibration with experimental correlation
[AIAA PAPER 92-3494] p 1112 A92-54036
Modal simulation of gearbox vibration with experimental correlation
[NASA-TM-105702] p 1002 N92-31485

CHPOUN, A.
Numerical and experimental investigation of rarefied compression corner flow
[AIAA PAPER 92-2900] p 820 A92-47876
Flat plates placed in depleted hypersonic flow
[SESSIA-430/91.960] p 947 N92-31508
CHRISS, RANDALL MARSHALL
A laser velocimeter investigation of the normal shockwave boundary layer interaction
p 500 N92-20485
CHRISTHILF, DAVID M.
Parameter insensitive control utilizing eigenspace methods p 204 A92-18615
Multifunction tests of a frequency domain based flutter suppression system
[AIAA PAPER 92-2096] p 566 A92-35667
Multifunction tests of a frequency domain based flutter suppression system
[NASA-TM-107615] p 662 N92-25607
CHRISTIAN, T. F., JR.
Composite material repairs to metallic airframe components p 699 A92-41237
CHRISTIE, P. I.
Vibration analysis of gas turbines by an intelligent knowledge-based system p 656 A92-40548
CHRISTODOULOU, L.
Axial alignment of short-fiber titanium aluminide composites by directional solidification
p 892 A92-46838
CHRONOPOULOS, A. T.
Efficient iterative methods for the transonic small disturbance equation p 1025 A92-54933
CHRUSCIEL, G. T.
Approximate aerodynamic analysis of jet interaction
[AIAA PAPER 92-4640] p 1027 A92-55387
CHU, JULIO
Measurements of fluctuating pressure in a rectangular cavity in transonic flow at high Reynolds numbers
[NASA-TM-4363] p 633 N92-25752
High Reynolds number test of the Boeing TR77 airfoil in the Langley 0.3-meter transonic cryogenic tunnel
[NASA-TM-4189] p 947 N92-31246
CHU, M. C.
Adhesive shear strength of impact ice
p 30 A92-11068
CHUA, KIAT
Mechanisms resulting in accreted ice roughness
[AIAA PAPER 92-0297] p 351 A92-25750
A fast three-dimensional vortex method for unsteady wake calculations
[AIAA PAPER 92-2624] p 794 A92-45496
CHUANG, CHE-CHUN
Navier-Stokes computations for turbulent transonic projectile with a two layer model combining the ASM model of turbulence and the k-epsilon model near the wall
[AIAA PAPER 92-0518] p 331 A92-26943
CHUANG, CHING H.
Shape-sensitivity analysis and design optimization of linear, thermoelastic solids p 395 A92-26433
CHUANG, SHU-HAO
Numerical simulation of twin-jet impingement on a flat plate coupled with cross-flow p 315 A92-25374
CHUKHLANTSEV, S. G.
Acoustic emission during changes in the aerodynamic load on the surface of a fan blade p 511 A92-30318
CHUN, CH.-H.
Experiments on separation at a compression corner in rarefied hypersonic flows p 938 A92-52755
CHUN, CLAYTON K. S.
The Lockheed F-117A
[RAND-P-7746-RGS] p 731 N92-26673
CHUNG, JASON
The SnoDog: Preliminary design of a close air support aircraft
[NASA-CR-189990] p 462 N92-21489
CHUNG, T. J.
Numerical studies of supersonic/hypersonic combustion
[AIAA PAPER 92-0094] p 293 A92-22200
CHUPP, RAYMOND E.
Performance characteristics of brush seals for limited-life engines
[ASME PAPER 91-GT-281] p 152 A92-15676
Simple effective thickness model for circular brush seals
[AIAA PAPER 92-3192] p 903 A92-48803
CHUSHKIN, P. I.
Numerical simulation of three-dimensional supersonic flow around aerodynamic configurations
p 434 A92-31492
CHYU, W. J.
Navier-Stokes simulation of flow through a highly contoured subsonic diffuser p 433 A92-31491
Bleed-boundary conditions for numerically simulated mixed-compression supersonic inlet flow
p 713 A92-44520
CIANCI, M.
Manufacture of XD gamma titanium aluminide airfoils via investment casting and machining
p 494 A92-30603
CIARAMELLA, KATHRYN M.
Validation and verification flight test for TCAS-2 logic changes (MOPS Change 6)
[DOT/FAA/CT-TN91/46] p 268 N92-15981
CICCOLI, M. C.
Efficient methods for inviscid non-equilibrium hypersonic flow fields p 1024 A92-54571
CICHON, DIETER J.
Estimation of the P-3/SAR L-, C- and X-band antenna directivity in range direction based on corner reflector measurements within the absolute SAR calibration
p 587 A92-35055
CIMBALA, J. M.
Suppression of the wing-body junction vortex by body surface suction p 309 A92-24417
CINCOTTA, MANUAL
Improved articulated fin/wing control system statement of government interests
[AD-D015268] p 1088 N92-34131
CINNELLA, PASQUALE
Characteristic-based algorithms for flows in thermochemical nonequilibrium p 670 A92-36846
CLARK, ANNE W.
A DSP-based microwave landing system (MLS) post-IF processor p 955 A92-49306
CLARK, B. E.
A model of the ADA avionics real-time system: An example of the benefits of the hardware/software codesign approach in development of real-time systems
[AD-A248893] p 967 N92-30524
CLARK, COLIN C.
Trends in the selection of airliners
p 417 A92-28183
CLARK, D.
Characteristics of thunderstorm-generated low altitude wind shear - A survey based on nationwide terminal Doppler weather radar testbed measurements
p 45 A92-11378
CLARK, DAVID R.
A re-examination of the aerodynamics of hovering rotors including the presence of the fuselage
p 66 A92-14446
CLARK, E. L.
Pressure measurements in high speed water tunnels
[DE92-004891] p 386 N92-19978
CLARK, EDWARD L.
Calibration of hemispherical-head flow angularity probes
[AIAA PAPER 92-4005] p 1122 A92-56828
CLARK, J. P.
Turbulent spot generation and growth rates in a transonic boundary layer
[AD-A250221] p 909 N92-29118
CLARK, J. W., JR.
United States Navy ski jump experience and future applications p 465 N92-21968
CLARK, JOHN C., JR.
Rolling element bearing member
[PATENT-1-271-213] p 158 N92-13434
CLARK, R. L.
A time-integrated image model for aero-optic analysis
[AIAA PAPER 92-2793] p 779 A92-41332
CLARK, ROD
A validated code to predict the performance of onboard broadband optical seekers through a turbulent transonic flow
[AIAA PAPER 92-2792] p 778 A92-41331
CLARK, STEVEN W.
Numerical investigation of a transverse jet for supersonic aerodynamic control
[AIAA PAPER 92-0639] p 334 A92-27017
CLARK, VICTOR R.
Engineering Graphical Analysis Tool (EGAT) development program p 164 N92-12542
CLARKE, J. F.
Aero-propulsive effects on configuration shaping
[AIAA PAPER 91-5064] p 459 A92-31691
CLARKSON, JEFFREY D.
A computational investigation of airfoil stall flutter
[AD-A247302] p 947 N92-31300
CLAUS, RICHARD O.
Fabry-Perot fiber-optic sensors in full-scale fatigue testing on an F-15 aircraft p 391 A92-24553
CLAUS, RUSSELL W.
The NASA Computational Aerosciences Program - Toward teraFLOPS computing
[AIAA PAPER 92-0558] p 411 A92-26968
CLAWSON, K. L.
Vortex characteristics of C5A/B, C141B and C130E aircraft applicable to ATC terminal flight operations tower fly-by-data
[PB92-114586] p 449 N92-20318
CLEAK, J. G. E.
Turbulence modelling for secondary flow prediction in a turbine cascade
[ASME PAPER 91-GT-57] p 68 A92-15535
CLEARY, JOSEPH W.
Flow over an all-body hypersonic aircraft - Experiment and computation p 310 A92-24651
CLEM, B. C.
Recent CFD applications on jet transport configurations
[AIAA PAPER 92-2658] p 844 A92-45519
CLEMENS, N. T.
Effects of sidewall disturbances on the supersonic mixing layer p 290 A92-21085
Two- and three-dimensional effects in the supersonic mixing layer p 432 A92-31165
CLEMENT, WARREN F.
Development of a real-time simulation of a ship-correlated airwake model interfaced with a rotorcraft dynamic model
[AIAA PAPER 92-4149] p 1007 A92-52440
CLEMENTS, A.
Comparison of two-way satellite time transfer and GPS common-view time transfer between OCA and TUG
p 1050 N92-33356
CLEMENTS, NANCY L.
Avionics standardization in the USAF: 1980 to 1990
p 198 N92-14048
CLEVELAND, JEFF I., II
High performance flight simulation at NASA Langley
[AIAA PAPER 92-4179] p 982 A92-52460
Application of technology developed for flight simulation at NASA. Langley Research Center p 573 N92-22437
CLIFF, EUGENE M.
Energy-heading transients in atmospheric flight guidance for airbreathing hypersonic vehicles
[AIAA PAPER 91-5065] p 480 A92-31692
CLIFF, S. E.
Practical design optimization of wing/body configurations using the Euler equations
[AIAA PAPER 92-2633] p 795 A92-45505
CLIFFORD, B. R.
Harrier GR MK 5/7 mission simulators for the Royal Air Force p 885 N92-28540
CLIFFORD, G. A.
Traditional finite element analysis - Opportunities for parallelism? p 40 A92-12354
CLINE, J. L.
X-ray computed tomographic inspection of castings
p 492 A92-28725
X-ray computed tomography for the aircraft/aerospace industry p 492 A92-28750
CLOUGH, BRUCE T.
A review of digital flight control system upsets caused by electromagnetic interference
[AIAA PAPER 91-3765] p 215 A92-17627
On upsets of analog portions of digital flight control systems due to electromagnetic interference
[SAE PAPER 912144] p 651 A92-39982
CLOUGH, SID A.
Mesoscale dynamics of cold fronts - Structures described by dropsoundings in Fronts 87
p 230 A92-18902
CLOUSER, S.
Development of an innovative high-temperature gas turbine fuel nozzle
[ASME PAPER 91-GT-36] p 121 A92-15519
CLUKEY, PATRICIA G.
The NASA Langley laminar-flow-control experiment on a swept, supercritical airfoil: Evaluation of initial perforated configuration
[NASA-TM-4309] p 525 N92-22196
CLYMER, JOHN R.
Discrete event fuzzy airport control
p 1046 A92-55973
COAKLEY, T. J.
Turbulence modeling for high speed flows
[AIAA PAPER 92-0436] p 327 A92-26283
An assessment and application of turbulence models for hypersonic flows
[NASA-TM-105124] p 82 N92-11984
COBBETT, JOHN A.
Progress report of Scot's Laser Ordnance Initiator System for crew escape p 580 A92-32988
COBLE, DONNA
A flight test study to determine aircraft propulsive efficiency and aerodynamic drag using two parameter identification methods and Lock's propeller model
[AIAA PAPER 92-0170] p 271 A92-23781
COCHER, G.
Use of relative humidity sensors for planes measurement p 467 A92-32080
COCHRAN, J. B.
Composite material repairs to metallic airframe components p 699 A92-41237

COCHRAN, J. E., JR.
Dynamics and control of maneuverable towed flight vehicles p 976 A92-50508
COCHRAN, KEITH G.
Artificial intelligence techniques applied to vehicle management system diagnostics p 965 A92-49315
COCKRELL, DAVID J.
Small two-dimensional surface excrescences on aircraft wings approaching separation p 1031 A92-56170
CODER, DAVID W.
On the measurement of subsonic flow around an appended body of revolution at cryogenic conditions in the NTF p 880 A92-45265
CODY, WILLIAM J.
An exploration of function analysis and function allocation in the commercial flight domain
[NASA-CR-4374] p 368 N92-19871
COEL, V.
Lightning activity in microburst producing storm cells
[ONERA, TP NO. 1991-98] p 161 A92-16080
COEN, P. G.
Application of multidisciplinary optimization methods to the design of a supersonic transport
p 550 N92-23230
COEN, PETER G.
Preliminary results from the High Speed Airframe Integration Research project
[AIAA PAPER 92-1004] p 536 A92-33196
Integrating aerodynamics and structures in the minimum weight design of a supersonic transport wing
[NASA-TM-107586] p 850 N92-28435
COET, M.-C.
New hypersonic test methods developed at ONERA - The R5 and F4 wind tunnels
[ONERA, TP NO. 1992-39] p 882 A92-48600
COFFEE, JOHN R.
GPS-INS integration requirements for robust NOE helicopter navigation p 94 A92-14404
COFFEN, CHARLES D.
Flow visualization and flow field measurements of a 1/12 scale tilt rotor aircraft in hover
[NASA-CR-189456] p 82 N92-11983
A comparative analysis of XV-15 tiltrotor hover test data and WOPWOP predictions incorporating the fountain effect
[NASA-CR-189455] p 114 N92-11992
COHEN, DOROTHEA
Rapid development of the X-31 simulation to support flight-testing
[NASA-TM-104256] p 1060 N92-33149
COHEN, GERALD C.
Design of an integrated airframe/propulsion control system architecture
[NASA-CR-182004] p 602 N92-22643
Design of an integrated airframe/propulsion control system architecture
[NASA-CR-182007] p 602 N92-22644
COIFFIER, B.
Structural optimization of aircraft practice and trends
p 551 N92-23239
COIRIER, WILLIAM J.
Cartesian based grid generation/adaptive mesh refinement p 682 N92-25722
COIRO, D. P.
Numerical predictions of transonic viscous flows around aerofoils through an Euler/boundary layer interaction method p 624 A92-40600
Wake effects on the prediction of transonic viscous flows around airfoils p 702 A92-41232
COLANTUONI, S.
Numerical computations of transonic flows through cascades
[AIAA PAPER 92-3041] p 822 A92-48702
COLE, GARY L.
Supersonic propulsion simulation by incorporating component models in the large perturbation inlet (LAPIN) computer code
[NASA-TM-105193] p 279 N92-15993
COLE, HAL L.
A new aircraft universal lightweight digital dropsonde
p 467 A92-32089
COLE, J. D.
Optimum hypersonic wings and wave riders
p 706 A92-42531
Asymptotic theory of transonic wind tunnel wall interference
[AD-A244075] p 403 N92-19080
COLE, RICHARD J.
Experimental and numerical investigation of anti-icing phenomena on a NACA 0012 assembly
[AIAA PAPER 92-0531] p 459 A92-31669
COLE, STANLEY R.
A summary of the Active Flexible Wing program
[AIAA PAPER 92-2080] p 565 A92-35652
Aeroelastic effects of spoiler surfaces on a low-aspect-ratio rectangular wing p 1030 A92-56154
Technical activities of the configuration aeroelasticity branch
[NASA-TM-104146] p 159 N92-13458
A summary of the active flexible wing program
[NASA-TM-107655] p 962 N92-31264
COLE, T. C.
Degenerate four-wave mixing for measurement of NO2 and smoke concentration in jet engine exhaust
[AIAA PAPER 92-3658] p 1113 A92-54108
COLE, W. A.
Degenerate four-wave mixing for measurement of NO2 and smoke concentration in jet engine exhaust
[AIAA PAPER 92-3658] p 1113 A92-54108
COLEHOUR, J. L.
Subsonic propulsion system installation analysis and optimization
[ASME PAPER 91-GT-167] p 111 A92-15602
COLEMAN, G. N.
Simulation and modeling of homogeneous compressible turbulence under isotropic mean compression
p 622 A92-40134
COLEMAN, HUGH W.
Using uncertainty analysis in the debugging and qualification of a turbulent heat transfer test facility
p 138 A92-17224
COLEMAN, M. M.
Advanced thermally stable jet fuel development program. Volume 2: Compositional factors affecting thermal degradation of jet fuels
[AD-A252656] p 987 N92-31399
COLLARD, DUDLEY
Supersonic transport in the 21st century
p 308 A92-26793
COLLE, A. R.
A probabilistic procedure for aircraft fleet management
p 360 N92-18576
COLLERCANDY, RANJIT
An improved approach for the computation of transonic/supersonic flows with applications to aerospace configurations
[AIAA PAPER 92-2613] p 793 A92-45487
COLLETTE, J. G. R.
Results of the space shuttle vehicle ascent air data system probe calibration test using a 0.07-scale external tank forebody model (68T) in the AEDC 16-foot transonic wind tunnel (IA-310), volume 1
[NASA-CR-167696] p 286 N92-17167
Results of the space shuttle vehicle ascent air data system probe calibration test using a 0.07-scale external tank forebody model (68T) in the AEDC 16-foot transonic wind tunnel (IA-310), volume 2
[NASA-CR-167697] p 286 N92-17214
COLLIER, ARNOLD S.
Aero-optical testing in the NSWC Hypervelocity Tunnel No. 9
[AIAA PAPER 92-2797] p 747 A92-41336
COLLIER, DON
Single slotted array achieves multimode performance
p 726 A92-44428
COLLIER, F. S., JR.
Application of laminar flow control to high-bypass-ratio turbofan engine nacelles
[SAE PAPER 912114] p 618 A92-39965
COLLIER, FAYETTE S., JR.
Design of a hybrid laminar flow control nacelle
[AIAA PAPER 92-0400] p 373 A92-26253
Crossflow vortex and transition measurements by use of multielement hot films p 935 A92-50307
COLLIER, RICHARD S.
Analysis and modeling of lightning strikes to the F106B, CVF580, and C160 aircraft p 186 A92-20129
COLLIN, G.
CARS temperature measurements and validation of a computing code on a gas-turbine combustor
[ONERA, TP NO. 1991-224] p 373 A92-26376
COLLINS, CHRISTOPHER C.
Preliminary investigation of the shock-boundary layer interaction in a simulated fan passage
[AD-A242656] p 185 N92-15045
COLLINS, D. J.
X-29 H-infinity controller synthesis
p 873 A92-46749
COLLINS, E. G., JR.
Real parameter uncertainty and phase information in the robust control of flexible structures
p 32 A92-11345
COLLINS, EMMANUEL G., JR.
Experimental demonstration of active vibration control for flexible structures p 50 A92-11442
COLLINS, ROBERT J.
Examination of ultraviolet radiation theory for bow shock rocket experiments
[AIAA PAPER 92-2871] p 901 A92-47853
COLLINS, W. T.
Ceramic component processing development for advanced gas-turbine engines
[ASME PAPER 91-GT-120] p 142 A92-15567
COLON, ANDY
High Capacity Voice Recorder (HCVR) Operational Test and Evaluation (OT and E)/integration test plan
[DOT/FAA/CT-TN91/55] p 402 N92-18959
COLOVIN, J. E., JR.
Aeroassist flight experiment heating-rate sensitivity study p 3 A92-10427
COLUCCI, FRANK
Hypersonic materials p 212 A92-18002
COLVIN, G.
Manufacture of XD gamma titanium aluminide airfoils via investment casting and machining
p 494 A92-30603
COLWELL, GENE T.
Heat pipe and surface mass transfer cooling of hypersonic vehicle structures p 763 A92-44380
Surface cooling of scramjet engine inlets using heat pipe, transpiration, and film cooling p 763 A92-44381
COMBS, S. R.
Flight management system integration on the F-117A
[AIAA PAPER 92-1077] p 563 A92-33246
Pilot activated automatic recovery system on the F-117A
[AIAA PAPER 92-1126] p 563 A92-33278
Flight management system of the F-117A
p 1082 A92-55910
COMSTOCK, J. RAYMOND, JR.
The multi-attribute task battery for human operator workload and strategic behavior research
[NASA-TM-104174] p 303 N92-17130
CONCILIO, A.
Active vibrations and noise control for turboprop application research program activities
p 1138 N92-32962
CONDIT, PHIL
777 - The airlines' higher-order technology airplane
p 1052 A92-55104
CONDRA, LLOYD
Using design of experiments to improve product and process integrity p 928 A92-48555
CONE, SCOTT M.
An evaluation of four F-16 vertical velocity indicator configurations
[AD-A243629] p 370 N92-18014
CONLEY, JOSEPH L.
User's manual for AeroFcn: A FORTRAN program to compute aerodynamic parameters
[NASA-TM-104237] p 1133 N92-32507
CONLEY, ROB
SATZAP - A novel approach to GPS integrity
p 99 A92-16947
CONLISK, A. T.
An experimental and analytical study of the interaction of a vortex with an airframe
[AIAA PAPER 92-0319] p 321 A92-25766
A simplified model for the interaction of a rotor tip vortex with an airframe
[AIAA PAPER 92-0320] p 321 A92-25767
The unsteady interaction of a 3-dimensional vortex filament with a cylinder p 813 A92-46934
CONNELL, J. R.
Calibration data for improved correction of UVW propeller anemometers
[DE92-002935] p 297 N92-16281
CONNELL, JOHN W.
Poly 1, 2, 4-triazoles via aromatic nucleophilic displacement
[NASA-CASE-LAR-14440-1] p 35 N92-10066
CONNELLY, JOHN DAVID
The dynamics of flexible multibody systems: A finite segment approach p 1128 N92-34036
CONNER, R. S.
PAN AIR: A computer program for predicting subsonic or supersonic linear potential flows about arbitrary configurations using a higher order panel method. Volume 2: User's manual (version 3.0)
[NASA-CR-3252] p 527 N92-22865
CONNERS, TIMOTHY R.
Thrust stand evaluation of engine performance improvement algorithms in an F-15 airplane
[AIAA PAPER 92-3747] p 866 A92-49111
Flight evaluation of an extended engine life mode on an F-15 airplane
[NASA-TM-104240] p 871 N92-29659
Thrust stand evaluation of engine performance improvement algorithms in an F-15 airplane
[NASA-TM-104252] p 971 N92-30518
CONNOLLY, C. F.
Use of CFD in the design of a modern multistage aero engine LP turbine design
[PNR-90862] p 472 N92-20179

CONOVER, ROBERT A.
JPL's Real-Time Weather Processor project (RWP) metrics and observations at system completion
p 413 N92-19428
CONRAD, GEORGE R.
Determination of balloon drag
[AIAA PAPER 91-3666] p 5 A92-11013
CONRAD, HANS
Electrorheological fluids; Proceedings of the 2nd International Conference, Raleigh, NC, Aug. 7-9, 1989
p 40 A92-12625
CONROY, CAROL
Fatal occupational injury related to helicopters in the United States 1980-1985 p 186 A92-20720
CONSOLI, ROBERT D.
Application of advanced multidisciplinary analysis and optimization methods to vehicle design synthesis
p 1054 A92-56160
CONSTANCIS, PIERRE
Wideband control of gyro/accelerometer multisensors in a strapdown guidance system p 856 A92-46736
CONSTANTIKES, KIM T.
Using fractal dimension for target detection in clutter
p 410 A92-24423
CONSTANTINESCU, V. N.
A lifting line theory for supersonic flow applications
[AIAA PAPER 91-5058] p 171 A92-17841
CONTI, RAUL J.
Navier-Stokes computation of hypersonic near wakes with foreign gas injection
[AIAA PAPER 92-0838] p 422 A92-29604
CONWAY, JOHN T.
Further development of the CANAERO computer code to include propulsor modelling
[DREA-CR-90-425] p 1038 N92-32811
CONWAY, SCOTT
Technology needs for high speed rotorcraft (3)
[NASA-CR-177592] p 195 N92-14039
COOK, HENRY L.
Stop, look and learn from accident investigation
p 834 A92-44996
COOK, JEFFREY
Tensile and interlaminar properties of GLARE (trade name) laminates
[AD-A250188] p 895 N92-28921
COOK, ROBERT L.
Laser velocimetry measurements in an MHD aerodynamic duct
[AIAA PAPER 92-2986] p 899 A92-46996
COOK, ROBERT M.
Airfoil Vibration Dampers program
[NASA-CR-184276] p 225 N92-14391
COOK, S.
Laser-initiated conical detonation wave for supersonic combustion p 375 A92-28531
COOK, T. S.
TMFSLAM - Design analysis tool for coated structures
[ASME PAPER 91-GT-141] p 690 A92-36895
COOKE, JOSEPH M.
NPSNET: Flight simulation dynamic modeling using quaternions
[AD-A247484] p 923 N92-28245
COOKSEY, DAVID L.
Evaluation of grounding and mooring points for Army aircraft
[AD-A250749] p 953 N92-31193
COOLEY, JOHN W.
Geometry acquisition and grid generation: Recent experiences with complex aircraft configurations
p 691 N92-24400
COONCE, KENNETH G.
Design and implementation of a total flight test system
p 189 A92-19278
COOPER, J. E.
Model parameter identification techniques for flight flutter testing
[AERO-REPT-9105] p 380 N92-18294
COOPER, M. I.
F-111C flight dynamic model aerodynamic data-base development and verification
[AD-A246356] p 715 N92-26947
COOPER, S. P.
Emergence of coherent patterns of vortex stretching during reconnection - A scattering paradigm
p 38 A92-11041
COOPER, THOMAS D.
ASNT and aerospace - What about the next 50 years?
p 215 A92-17293
Proceedings of the USAF Structural Integrity Program Conference
[AD-A242943] p 279 N92-17204
COOPRIDER, KAREN K.
X-ray computed tomography of composites
p 36 A92-10143
COPPENBARGER, R. A.
Concepts for pilot interaction with an automated NOE obstacle-avoidance system
[AIAA PAPER 92-4472] p 1076 A92-55232
COQUEL, F.
Numerical simulation of thermochemical non-equilibrium viscous flows around reentry bodies
p 227 N92-15029
CORBAN, J. E.
Rapid near-optimal aerospace plane trajectory generation and guidance
[NASA-CR-189469] p 205 N92-14066
CORBIN, MALCOLM
A NASA/RAE cooperation in the development of a real-time knowledge based autopilot
p 164 N92-12528
CORD, THOMAS J.
Agility and high angle of attack - An Air Force research perspective
[SAE PAPER 912145] p 608 A92-39983
CORDA, S.
The F/A-18 external burning flight test
[AIAA PAPER 91-5050] p 731 A92-44547
COREY, PHILIP D.
Discrete event fuzzy airport control
p 1046 A92-55973
CORKE, T. C.
Three-dimensional-mode resonance in far wakes
p 898 A92-46252
CORNELISON, CHARLES J.
Reactivation and upgrade of the NASA Ames 16-Inch Shock Tunnel - Status report
[AIAA PAPER 92-0327] p 383 A92-25774
CORNELIUS, KENNETH C.
An experimental study of pneumatic vortex flow control on high angle of attack forebody model
[AIAA PAPER 92-0018] p 247 A92-22140
CORNUAULT, C.
Structural optimization of aircraft practice and trends
p 551 N92-23239
Structural optimization of aircraft p 851 N92-28472
CORNWELL, PHILLIP J.
Trajectory control for a low-lift maneuverable reentry vehicle
[AIAA PAPER 92-1146] p 574 A92-33287
CORR, R. A.
Evaluation of NO(x) mechanisms for lean, premixed combustion
[ASME PAPER 91-GT-257] p 668 A92-36900
CORREA, S. M.
Local extinction mechanisms in non-premixed turbulent combustion
[AD-A242027] p 290 N92-17682
CORRIVEAU, PAUL
Development of the Basic Flight Instruction Tutoring System (BFITS)
[AD-A246458] p 751 N92-27836
CORSIGLIA, VICTOR
Large-scale wind tunnel studies of a jet-engined powered ejector-lift STOVL aircraft p 842 A92-45313
CORSIGLIA, VICTOR R.
NASA aerodynamics program
[NASA-TM-4368] p 609 N92-24678
On the anomalies in single-jet hover suckdown data
[NASA-TM-102261] p 1038 N92-33306
Dynamic response of induced pressures, suckdown, and temperatures for two tandem jet STOVL configurations
[NASA-TM-103934] p 1039 N92-33581
On the estimation of jet-induced fountain lift and additional suckdown in hover for two-jet configurations
[NASA-TM-102268] p 1040 N92-33618
CORWIN, WILLIAM H.
Data Link integration in commercial transport operations p 839 A92-44919
Knowledge-sensitive task manipulation - Acquiring knowledge from pilots flying a motion-based flight simulator p 916 A92-45064
COSGROVE, B. A.
Aging fleet: Maintaining airworthiness
p 953 N92-31862
COSTA, P.
Structures and materials technologies for hypersonic vehicles - Lessons from Hermes experience
[AIAA PAPER 91-5098] p 486 A92-31697
COSTELLO, MARK
Some issues on modeling atmospheric turbulence experienced by helicopter rotor blades
p 647 A92-40885
COSTES, J.-J.
Theoretical and experimental study of a model rotor
p 547 A92-35781
COSTES, M.
Aerodynamic and acoustic calculations of transonic nonlifting hovering rotors
[ONERA, TP NO. 1991-178] p 77 A92-16140
Weak coupling between an unsteady 3D full potential code and an unsteady turbulent boundary layer code - Application to a helicopter rotor in forward flight
[AIAA PAPER 92-0029] p 249 A92-22151
COSTES, P.
Integration of flight and carrier landing aid systems for shipboard operations
[ONERA, TP NO. 1991-113] p 134 A92-16092
Integration of flight and carrier landing aid systems for shipboard operations p 456 N92-21958
COSTIN, DANIEL P.
Approximate closed-form buckling solutions for the optimization of aircraft structures p 579 A92-32578
COTON, F. N.
Two-dimensional, incompressible aerofoil design and analysis p 247 A92-21987
COTTER, GLADYS A.
An international aerospace information system: A cooperative opportunity
[NASA-TM-108171] p 1142 N92-33237
COUAILLIER, V.
Validation of a 3D Navier-Stokes code on experimental compressor bladings
[ONERA, TP NO. 1991-229] p 330 A92-26381
COULTON, DAVID G.
Recent developments in data acquisition and control systems at the Aircraft Research Association Limited
p 1091 A92-54323
COURTRIGHT, JOHN F.
Requirements for an aircraft mishap analysis system
p 16 A92-11170
COUSINS, W. T.
Distortion tolerance of the T800-LHT-800 turboshaft engine p 120 A92-14409
COUSTEIX, J.
Calculation methods of three-dimensional boundary layers p 245 A92-21978
Asymptotic defect boundary-layer theory applied to hypersonic flows p 610 A92-36839
Influence of suction through a slot on a turbulent boundary layer p 622 A92-40127
Analysis of turbulence models for hypersonic boundary layers p 623 A92-40182
Characteristics of a boundary layer in a leading edge vortex p 86 N92-13012
COUSTEIX, JEAN
Basic concepts on boundary layers
p 717 N92-27707
COUSTOLS, E.
Turbulent friction drag reduction: Boundary layer manipulators
[CERT-RSF-DERAT-62/5004-31] p 43 N92-11309
Turbulent skin-friction drag reduction by active and passive means, part 1 p 718 N92-27714
COVELL, PETER F.
Euler code evaluation of a transatmospheric vehicle at supersonic speeds p 9 A92-13202
Longitudinal and lateral-directional aerodynamic characteristics of a wing-cone configuration at Mach numbers from 2.5 to 4.5
[NASA-TM-4337] p 630 N92-24977
COVINGTON, C. E.
V-22 propulsion system design p 1070 A92-56300
COWLES, LISA
Military utility of medium speed V/STOL designs
p 841 A92-45308
COX, J. C.
Use of CFD in the design of a modern multistage aero engine LP turbine design
[PNR-90862] p 472 N92-20179
COX, M. E.
GPS - Can it contribute to European ATC?
p 637 A92-38380
European studies to investigate the feasibility of using 1000 ft vertical separation minima above FL 290. Part 1: Overview of organisation, techniques employed, and conclusions
[NLR-TP-91062-U-PT-1] p 841 N92-29605
COX, P. C.
A method to determine propagation direction of compressive fracture in carbon-fibre composites
p 672 A92-38770
COX, TYLER G.
An investigation of two cooling technologies as applied to a distributed propulsion control architecture
[ASME PAPER 91-GT-341] p 111 A92-15705
COY, JOHN J.
Rotorcraft transmissions p 560 N92-22533
COYETTE, J. P.
Ritz vectors synthesis versus modal synthesis for fluid-structure interaction modeling p 898 A92-45885
COYNE, B. J.
Stress concentration effects of oblique holes in aspirated-cooled turbine engine liners
[AIAA PAPER 92-1130] p 581 A92-33282

COZART, AARON B.
Leading edge sweep effects in generic three-dimensional sidewall compression scramjet inlets
[AIAA PAPER 92-0674] p 343 A92-28218
CRABB, C. A.
A unique approach to aircraft conflict resolution using artificial intelligence techniques p 190 N92-14029
CRABILL, NORMAN L.
Pilot's Automated Weather Support System (PAWSS) concepts demonstration project. Phase 1: Pilot's weather information requirements and implications for weather data systems design
[NASA-CR-188228] p 46 N92-11593
CRAFT, D. WILLIAM
High accuracy fuel flowmeter. Phase 2C and 3: The mass flowrate calibration of high accuracy fuel flowmeters
[NASA-CR-187108] p 406 N92-19775
CRAIG, KEN
Computational study of the aerodynamics and control by blowing of asymmetric vortical flows over delta wings
[AIAA PAPER 92-0410] p 325 A92-26263
Computational study of the aerodynamics and control by blowing of asymmetric vortical flows over delta wings
[NASA-CR-187979] p 14 N92-10990
CRAIG, P. A.
Effect of sustained high temperature exposure on the mechanical properties of Nicalon/Al2O3 composites
p 668 A92-39672
CRAIG, T.
Helicopter handling: Experience and new developments p 465 N92-21969
CRAIGHEAD, I. A.
The application of a cylindrical-spherical floating ring bearing as a device to control stability of turbogenerators p 224 N92-14371
CRAMER, EVIN J.
The application of direct transcription to commercial aircraft trajectory optimization
[AIAA PAPER 92-4528] p 1077 A92-55246
CRAMER, M. S.
Prandtl-Meyer function for dense gases
p 415 A92-26441
Critical Mach number estimates for dense gases
p 933 A92-49498
Transonic flows of Bethe-Zel'dovich-Thompson fluids
p 935 A92-50293
CRAMER, S. G.
Supportability evaluation of thermoplastic and thermoset composites p 1108 N92-32576
CRANE, D. A.
Mechanics of curved fiber composites
p 140 A92-14346
Mechanics of curved fiber composites
p 757 A92-41034
CRASSIDIS, JOHN L.
Robust control design of an automatic carrier landing system
[AIAA PAPER 92-4619] p 1077 A92-55296
CRAVEN, B. K.
Microwave landing system autoland system analysis
[NASA-CR-189551] p 191 N92-15060
CRAVEY, ROBIN L.
Finite difference time domain grid generation from AMC helicopter models
[NASA-TM-107679] p 1128 N92-34017
CRAWFORD, CHARLES C., JR.
Damage tolerance analysis for rotorcraft - What the issues are p 1058 A92-56336
CRAWFORD, D.
Turbulent flow in the wake of an idealized wing-body junction
[AIAA PAPER 92-0282] p 435 A92-31652
CRAWFORD, TIMOTHY L.
A sensitive fast-response probe to measure turbulence and heat flux from any airplane p 775 A92-42097
CRAWLEY, EDWARD F.
Static aeroelastic control using strain actuated adaptive structures p 26 A92-11122
CREAMER, PAUL M.
Precision approach using GPS and GLONASS
p 97 A92-16649
CREASMAN, SON F.
Evaluation of Euler solvers for transonic wing-fuselage geometries p 174 A92-20214
CRESPI, G.
Aluminium-lithium alloys - Application on helicopters
p 1106 A92-56326
CRESS, DANIEL H.
Passive acoustic range estimation of helicopters
[AD-A248033] p 926 N92-28302
CREWS, CURTIS T.
Technology developments applied to the AH-1W SuperCobra
[AIAA PAPER 91-3071] p 21 A92-11607
Expanding U.S.M.C. roles for the AH-1W SuperCobra
p 59 A92-14347
CREWS, JOHN H., JR.
Effects of T-tabs and large deflections in double cantilever beam specimen tests p 673 A92-39009
CRICELLI, A. S.
A time-dependent tip loss formula for rotor blade dynamic analysis p 1057 A92-56310
CRICELLI, ANTONIO S.
Unsteady airfoil flow solutions on moving zonal grids
[AIAA PAPER 92-0543] p 342 A92-28200
CRICKENBERGER, A. B.
Prandtl-Meyer function for dense gases
p 415 A92-26441
CRIGHTON, D. G.
The jet edge-tone feedback cycle - Linear theory for the operating stages p 392 A92-24758
CRIGHTON, DAVID G.
Airframe noise p 55 N92-10605
CRISCOE, J. C.
Assessment of valve actuator motor rotor degradation by Fourier Analysis of current waveform
[DE92-013233] p 909 N92-28814
CRITES, R. C.
Aerodynamic applications of pressure-sensitive paint
[AIAA PAPER 92-0264] p 394 A92-25720
CRITES, ROGER C.
Simulation of wind tunnel flowfields
[AIAA PAPER 92-0034] p 249 A92-22155
Modeling the ventilated wind tunnel wall
[AIAA PAPER 92-0035] p 249 A92-22156
Wind tunnel boundary interference prediction and correction
[AIAA PAPER 92-0036] p 249 A92-22157
CRIVELLI VISCONTI, I.
Structural design and testing results of composite landing gear components p 1057 A92-56328
CROCKER, MALCOLM J.
International Congress on Recent Developments in Air- and Structure-Borne Sound and Vibration, Auburn University, AL, Mar. 6-8, 1990, Proceedings. Vols. 1 & 2
p 924 A92-45876
New methods to determine the transmission loss of partitions using sound intensity measurements
p 924 A92-45879
CROKE, DON
The use of high voltage direct current in aircraft electrical systems - A Navy perspective
[SAE PAPER 912173] p 655 A92-39998
CROLL, J. B.
Flight evaluation of curved MLS precision approaches in a twin otter aircraft, phase 2
[AD-A243025] p 268 N92-17568
CRONE, DAVID
Manx: Close air support aircraft preliminary design
[NASA-CR-189992] p 463 N92-21565
CRONIN, M.
Advanced balancing using laser machining
[SAE PAPER 912218] p 674 A92-40020
CRONIN, MICHAEL J.
Advanced power generation systems for more electric aircraft
[SAE PAPER 912186] p 656 A92-40006
CRONKHITE, JAMES D.
The NASA/Industry Design Analysis Methods for Vibrations (DAMVIBS) Program - Bell Helicopter Textron accomplishments
[AIAA PAPER 92-2201] p 539 A92-34391
Design of helicopter composite structures for crashworthiness p 848 A92-47408
CROOK, ANDREW
Precipitation development in Colorado Front Range snowstorms - 15 November 1987 case study
p 301 A92-23008
CROSO, H.
The DAM vertical shock-tube p 880 A92-45096
CROSS, JOHN
Single slotted array achieves multimode performance
p 726 A92-44428
CROSS, KENNETH D.
Assessment of army aviators' ability to perform individual and collective tasks in the aviation networked simulator
[AD-A250293] p 888 N92-29709
CROSS, S. A.
Parallel knowledge based systems architectures for in-flight mission management p 728 N92-27904
CROSSLEY, WILLIAM A.
A structural design and optimization tool for ducted rotor/wing blades
[AIAA PAPER 92-2361] p 543 A92-34593
CROSSWY, F. L.
Testing capabilities at AEDC for development of hypersonic vehicles
[AIAA PAPER 91-5027] p 483 A92-31686
CROUCH, MICHAEL
The V-22: Can the nation afford to forgo its production?
[AD-A243158] p 242 N92-17477
CROUCH, PETER E.
Dynamic interpolation for linear systems
p 52 A92-11465
CROUSE, G. L., JR.
Transonic aeroelasticity analysis using state-space unsteady aerodynamic modeling p 310 A92-24422
CROUSE, WILLIAM E.
Fatal occupational injury related to helicopters in the United States 1980-1985 p 186 A92-20720
CROWELL, CYNTHIA A.
Helicopter low-speed yaw control
[NASA-CASE-LAR-14219-1] p 879 N92-30025
Two-dimensional aerodynamic characteristics of several polygon-shaped cross-sectional models applicable to helicopter fuselages
[NASA-TP-3233] p 944 N92-30394
CROWNE, D. H.
Optically powered and interrogated rotary position sensor for aircraft engine control applications
p 370 A92-27777
CRUSE, T. A.
System reliability and risk assessment
[AIAA PAPER 92-2345] p 582 A92-34320
CRUSE, THOMAS A.
Thermal barrier coating life prediction model development
[ASME PAPER 91-GT-40] p 147 A92-15523
Failure model development for an integrally bladed turbine wheel
[AIAA PAPER 92-3420] p 865 A92-48979
CRUZ, CHRISTOPHER I.
Predicted aerodynamic characteristics for HL-20 lifting-body using the aerodynamic preliminary analysis system (APAS)
[AIAA PAPER 92-3941] p 1033 A92-56771
Preliminary subsonic aerodynamic model for simulation studies of the HL-20 lifting body
[NASA-TM-4302] p 978 N92-31175
CRUZ, JUAN R.
Optimization of composite sandwich cover panels subjected to compressive loadings
[NASA-TP-3173] p 489 N92-20679
CSAVINA, FRANK L.
A global approach in evaluating inlet/engine compatibility
[ASME PAPER 91-GT-402] p 127 A92-15732
CUCCIO, J.
Impact design methods for ceramic components in gas turbine engines
[ASME PAPER 91-GT-115] p 123 A92-15566
CUELLAR, JOHN P.
High-temperature miniaturized turbine engine lubrication system simulator
[AD-A249259] p 868 N92-28294
CUENCA, P. V.
Fuzzy guidance system evaluation
p 778 N92-27903
CUI, DEGANG
Development of data base system in CIEM project
p 1009 A92-53093
CUI, E. J.
Investigation of unsteady excitation effects on aerodynamic properties of airfoils p 66 A92-15335
CUI, ER-JIE
The numerical simulation of compressible flow around an airfoil at high angle of attack p 818 A92-47686
CUI, ERJIE
A flow visualization experiment on the unsteady flow around two-dimensional airfoil p 615 A92-38913
The numerical simulation of transonic inviscid flow over oscillating airfoils p 616 A92-38918
The numerical simulation of separation control using moving surface effect p 616 A92-38924
CUI, JI-YA
Numerical investigation of axial flow compressor casing treatment p 934 A92-50216
CUI, JIYA
A numerical investigation of axial flow compressor casing treatment p 942 A92-53381
CUI, NAIMING
Application of the wall pressure method to wall interference corrections for model tests at high angle of attack in high speed wind tunnel p 315 A92-25134
CUI, PINGYUAN
Maximum likelihood algorithm and its application to parameter identification of closed-loop flight vehicles
p 1008 A92-53023
CULLEN, J.
Characteristics of thunderstorm-generated low altitude wind shear - A survey based on nationwide terminal Doppler weather radar testbed measurements
p 45 A92-11378

CULLEN, J. A.
The 1990 Airport Surveillance Radar Wind Shear Processor (ASR-WSP) operational test at Orlando International Airport
[AD-A239852] p 18 N92-10019
CULLEN, JOSEPH A.
Predicting summer microburst hazard from thunderstorm day statistics p 407 A92-27960
CULP, J. D.
Free vibration analysis of branched blades by the integrating matrix method p 847 A92-47122
CULPEPPER, STEVEN D.
Structural considerations for aircraft payload Modification: P-3C zero fuel weight increase
[AD-A242690] p 196 N92-15068
CUMMINGS, RUSSELL M.
Computation of three-dimensional turbulent vortical flows on bodies at high incidence p 9 A92-13203
Computational investigation of slot blowing for fuselage forebody flow control
[AIAA PAPER 92-0020] p 248 A92-22142
Turbulence model effects on separated flow about a prolate spheroid p 340 A92-28036
Computational evaluation of an airfoil with a Gurney flap
[AIAA PAPER 92-2708] p 802 A92-45550
Navier-Stokes predictions for the F-18 wing and fuselage at large incidence p 810 A92-46783
Computation of three-dimensional effects on two dimensional wings
[NASA-CR-190576] p 832 N92-29691
CUMPSTY, N. A.
Surge dynamics in a free-spool centrifugal compressor system
[ASME PAPER 91-GT-31] p 68 A92-15515
Method for the prediction of supersonic compressor blade performance p 277 A92-21078
CUNNAN, WALTER S.
Supersonic Throughflow Fan Test Facility at NASA. Lewis Research Center
[NASA-TP-3038] p 983 N92-31640
CUNNINGHAM, A. M., JR.
Steady and unsteady aerodynamics of a pitching straked wing model at high angles of attack p 87 N92-13024
Analysis of unsteady force, pressure, and flow-visualization data for a pitching straked wing model at high angles of attack p 364 N92-18784
Development of a method to predict transonic limit cycle oscillation characteristics of fighter aircraft
p 746 N92-27958
CUNNINGHAM, ATLEE M., JR.
Transonic wind tunnel investigation of limit cycle oscillations on fighter type wings - Update
[AIAA PAPER 92-2125] p 572 A92-35692
Understanding and development of a prediction method of transonic limit cycle oscillation characteristics of fighter aircraft
[AIAA PAPER 92-4501] p 1026 A92-55369
Transonic wind tunnel investigation of limit cycle oscillations on fighter type wings p 721 N92-27959
CUNNINGHAM, ROBERT
Neutron radiography with SNRS p 492 A92-28747
CUPPERNULL, MICHAEL J.
The H-53E Super Stallion - A cost-effective solution to multi-service medium/heavy lift requirements
p 647 A92-40388
CURCHITSER, ENRIQUE N.
Solution of the Euler and Navier-Stokes equations on MIMD distributed memory multiprocessors using cyclic reduction
[AIAA PAPER 92-0561] p 411 A92-26970
CURLEE, T. R.
The cost of silicon nitride powder: What must it be to compete?
[DE92-008710] p 669 N92-25223
CURLETT, BRIAN P.
The aerodynamic effect of fillet radius in a low speed compressor cascade
[NASA-TM-105347] p 202 N92-14063
A graphical user-interface for propulsion system analysis
[NASA-TM-105696] p 1134 N92-33894
CURLEY, CHARLES H.
Global positioning system supported pilot's display
p 534 N92-22436
CURLEY, JOHN A.
Development of pitot static flightline testing
p 556 A92-35953
CURLISS, D. B.
Fluid effects: Thermoset and thermoplastic matrix composites p 1110 N92-33049
CURLISS, DAVID B.
The effect of jet fuel exposure on advanced aerospace composites. Part 1: Thermal and chemical analysis
[AD-A246559] p 756 N92-27531
CURRAN, E. T.
High-speed flight propulsion systems
[ISBN 1-56347-011-X] p 862 A92-46426
Introduction p 862 A92-46427
CURRAN, EDWARD T.
Further studies of kinetic energy methods in high speed ramjet cycle analysis
[AIAA PAPER 92-3805] p 1069 A92-54177
CURRAN, JIM
Multidimensional ELS user interface
[SAE PAPER 912108] p 691 A92-39961
CURREN, A. N.
A low-power, high-efficiency Ka-band TWTA
p 671 A92-38163
CURRERI, P. A.
Experimental results and numerical modeling of solidification during aircraft high-g arcs
[AIAA PAPER 92-0843] p 493 A92-29609
CURRERI, PETER A.
The effectiveness of Coriolis dampening of convection during aircraft high-g arcs p 581 A92-33847
CURRIER, JEFFREY M.
Analysis of the onset of dynamic stall
p 1024 A92-54919
CURRY, D. M.
Aeroassist flight experiment heating-rate sensitivity study p 3 A92-10427
Aerodynamic heating on AFE due to nonequilibrium flow with variable entropy at boundary layer edge
p 183 N92-15020
CURRY, RENWICK E.
The impact of cockpit automation on crew coordination and communication. Volume 1: Overview, LOFT evaluations, error severity, and questionnaire data
[NASA-CR-177587] p 93 N92-13044
CURTIS, DAYTON
The FAA aging airplane program plan for transport aircraft p 838 N92-30128
CURTISS, H. C.
A simulation study of tiltrotor vertical takeoff procedures using conventional and variable diameter rotor systems
p 1056 A92-56301
CURTISS, H. C., JR.
On the calculation of the response of helicopters to control inputs
[NASA-CR-190812] p 1088 N92-33536
CURTISS, HOWARD C., JR.
Approximations for inclusion of rotor lag dynamics in helicopter flight dynamics models p 1060 A92-56354
CUSHMAN, ARTHUR
Effect of guard band reduction on marker beacon receiver performance
[DOT/FAA/CT-TN92/18] p 1002 N92-31617
CUSWORTH, R. A.
An experimental and computational investigation of an annular reverse-flow combustor
[UTIAS-338] p 129 N92-11996
CUTCHINS, MALCOLM A.
Joined-wing model vibrations using PC-based modal testing and finite element analysis
[AIAA PAPER 92-2260] p 541 A92-34417
CUTLER, A. D.
CARS temperature measurements in a hypersonic propulsion test facility p 140 N92-12049
CYCON, JAMES P.
Sikorsky Aircraft UAV program p 646 A92-40385
CYNAMON, LOUISA J.
A processor-in-the-loop simulation using an XANALOG computer p 232 A92-19094
CZECH, J.
Evaluation of human response to structural vibrations induced by sonic booms
[NASA-CR-189584] p 697 N92-26130
CZYSZ, P.
Energy analysis of high-speed flight systems
p 925 A92-46430

D

D'ANGELO, JOHN
Finite element analysis of large wavelength antenna radome problems for leading edge and radar phased arrays p 267 A92-23984
D'AULERIO, LOU
Navy Aircrew Common Ejection Seat (NACES) program summary p 104 A92-13465
D'AZZO, J. J.
Automatic formation flight control
[AIAA PAPER 92-4473] p 1076 A92-55233
D'ESPINEY, P.
Three-dimensional thin-layer and space-marching Navier-Stokes computations using an implicit MUSCL approach - Comparison with experiments and Euler computations
[ONERA, TP NO. 1991-131] p 77 A92-16107
D'URSO, STEVEN J.
Integration of supportability elements into the conceptual design process
[AIAA PAPER 92-1194] p 600 A92-33306
DABUNDO, C.
Flying qualities evaluation of the V22 tiltrotor
p 131 A92-14334
DACOSTA, J. L.
Analysis tools of ONERA and DLR for the aerothermodynamics of reentry vehicles
p 211 N92-14977
Hypersonic inviscid flow field simulations around reentry vehicles with flap deflection p 184 N92-15025
DADKHAN, S.
Performance of radial clearance rim seals in upstream and downstream rotor-stator wheelspaces
[ASME PAPER 91-GT-32] p 147 A92-15516
Rim sealing of rotor-stator wheelspaces in the absence of external flow
[ASME PAPER 91-GT-33] p 147 A92-15517
DADONE, L.
The effects of inner wake modelling on blade airloads
p 521 A92-35784
DAEUBLER, M. A.
Applications of IMI 834 in aeroengines - A collaborative IMI/MTU programme p 288 A92-22754
Influence of long time exposure at elevated temperatures in air on mechanical properties of the high temperature titanium alloy IMI 834 p 289 A92-22767
DAGENHART, J. R.
Computational study of transition front on a swept wing leading-edge model
[AIAA PAPER 92-2630] p 795 A92-45502
DAGG, JAMES M.
An exploratory application of neural networks to the sortie generation forecasting problem
[AD-A246626] p 778 N92-27980
DAHLEH, MUNTHER A.
Optimal rejection of bounded persistent disturbances in periodic systems p 51 A92-11464
DAHM, WERNER K.
Hypersonic merged layer blunt body flows with wakes
p 939 A92-52757
DAI, XIAOWEN
Simulation research on the dynamic characteristics of steam-injected gas turbine p 971 A92-53389
DAIGUJI, HISAAKI
Unsteady Navier-Stokes simulation of turbulent flows through a supersonic compressor cascade
p 523 A92-36036
A higher-order accurate Navier-Stokes solver for transonic and supersonic flows in turbomachinery
[AIAA PAPER 92-3044] p 822 A92-48704
DAILEY, G. M.
The effect of blade tip geometry on the tip leakage flow in axial turbine cascades
[ASME PAPER 91-GT-135] p 72 A92-15577
Use of CFD in the design of a modern multistage aero engine LP turbine design
[PNR-90862] p 472 N92-20179
DAILY, JOHN W.
Low-frequency pressure oscillations in a model ramjet combustor p 154 A92-16026
Flame sheet algorithm for use in numerical modeling of ramjet combustion instability p 390 A92-28503
DAINEKO, V. I.
Plotting the universal characteristic of a compressor in low-rpm and autorotation regimes p 657 A92-40607
DALE, ROGER J.
Laser ordnance initiation system p 577 A92-35465
DALLEMAGNE, P. C.
Comparison between computational and experimental data for a hypersonic laser propelled vehicle
[AIAA PAPER 92-3808] p 1023 A92-54179
DALLEY, S.
Flow regimes of the cove regions between a slat and wing and between a wing and flap of a multielement airfoil p 614 A92-38858
DALLMANN, UWE
On the footprints of three-dimensional separated vortex flows around blunt bodies: Attempts of defining and analyzing complex flow structures p 84 N92-13005
DALPIAZ, G.
Monitoring fatigue cracks in gears
p 1116 A92-54496
DALTON, FRANK
Aviation meteorology p 685 A92-38383
DALTON, K. K.
Distortion tolerance of the T800-LHT-800 turboshaft engine p 120 A92-14409
DALY, JOHN H., III
Judgement training for Alaskan pilots
p 835 A92-45048
DALY, KIERAN
The real TCAS p 350 A92-25521

DALY, P.
Comparison of GLONASS and GPS time transfers between two west European time laboratories and VNIIFTRI p 1050 N92-33381
DALZELL, W. G.
The LISA 6000 - A highly integrated IRS/GPS navigation system p 267 A92-22088
DAMODARAN, K. A.
Estimation of overall drag coefficient of an aerospace plane p 700 A92-41188
DANAILA, S.
An improvement of the double-point method for unsteady subsonic flow p 243 A92-21315
DANBERG, JAMES E.
Analysis of the flight performance of the 155 mm M864 base burn projectile
[BRL-TR-3083] p 1041 N92-33699
DANCEY, C. L.
LDA measurements in a Mach 2 flow over a rearward facing step with staged transverse injection
[AIAA PAPER 92-2692] p 800 A92-45539
DANDO, ANDREW
The inviscid compressible Goertler problem in three-dimensional boundary layers p 809 A92-46441
DANE, CARL W.
Exploratory experimental investigation of a wave propeller
[AD-A252175] p 949 N92-32062
DANESH, MO R.
Mobile Microwave Landing System (MMLS): Operational requirements for setup accuracy
[AD-A241844] p 103 N92-13052
DANG, A.
Evaluation of the ATD-GASP for endo-leap applications
[AIAA PAPER 92-2771] p 704 A92-41318
DANG, T. Q.
Design of turbomachinery blading in transonic flows by the circulation method p 311 A92-24725
DANIELS, TAUMI
Present status of the MIT/NASA Langley 6-inch MSBS p 750 N92-27802
DANIELS, W. A.
Turbine disk cavity aerodynamics and heat transfer p 1124 N92-32265
DANILOV, ANATOLII N.
Fundamentals of applied aerogasdynamics. II - Viscous flow past bodies. Control devices p 64 A92-14281
DANKERT, C.
Preliminary laser induced fluorescence measurements in several facilities in preparation for application to studies in the high enthalpy shock tunnel Goettingen (HEG)
[AIAA PAPER 92-0143] p 284 A92-23761
DANSBERRY, BRYAN E.
NACA 0012 benchmark model experimental flutter results with unsteady pressure distributions
[AIAA PAPER 92-2396] p 517 A92-34469
Dynamic characteristics of a Benchmark models program supercritical wing
[AIAA PAPER 92-2368] p 571 A92-34596
The benchmark aeroelastic models program: Description and highlights of initial results
[NASA-TM-104180] p 185 N92-15049
NACA0012 benchmark model experimental flutter results with unsteady pressure distributions
[NASA-TM-107581] p 526 N92-22507
The benchmark aeroelastic models program: Description and highlights of initial results p 721 N92-27960
Pressure measurements on a rectangular wing with a NACA0012 airfoil during conventional flutter
[NASA-TM-104211] p 1042 N92-34147
DANZER, G.
Fatigue of repaired composite structures p 214 N92-14411
DARCY, SIMON C.
F/A-18 stabilator: Equivalent set of point forces required for pneumatic bag load case simulation
[AD-A242637] p 206 N92-15073
DARDEN, CHRISTINE M.
High-Speed Research: Sonic Boom, volume 1
[NASA-CP-3172] p 1061 N92-33874
DARDIS, WILLIAM J.
An acceptance process for the evaluation of inlet distortion
[AIAA PAPER 92-3918] p 1032 A92-56750
DARGAN, J. L.
Automatic formation flight control
[AIAA PAPER 92-4473] p 1076 A92-55233
DARGAN, JOHN L.
Proportional plus integral control of aircraft for automated maneuvering formation flight
[AD-A243792] p 382 N92-19505
DARGUE, JIM
Evaluation of advanced microwave landing system procedures in the New York terminal area
[DOT/FAA/ND-91/1] p 354 N92-18967
DARGUSH, G. F.
Development of an integrated BEM approach for hot fluid structure interaction: BEST-FSI: Boundary Element Solution Technique for Fluid Structure Interaction
[NASA-CR-189202] p 574 N92-22211
DARLING, DOUGLAS
A fast, uncoupled, compressible, two-dimensional, unsteady boundary layer algorithm with separation for engine inlets
[AIAA PAPER 92-3082] p 823 A92-48729
Interface of an uncoupled boundary layer algorithm with an inviscid core flow algorithm for unsteady supersonic engine inlets
[AIAA PAPER 92-3083] p 823 A92-48730
Interface of an uncoupled boundary layer algorithm with an inviscid core flow algorithm for unsteady supersonic engine inlets
[NASA-TM-105684] p 739 N92-27037
A fast, uncoupled, compressible, two-dimensional, unsteady boundary layer algorithm with separation for engine inlets
[NASA-TM-105686] p 770 N92-27653
DAS, A.
Analysis of spiraling vortical flows around slender delta wings moving in an inviscid medium p 173 A92-18900
DAS, S.
The cost of silicon nitride powder: What must it be to compete?
[DE92-008710] p 669 N92-25223
DASGUPTA, SAMHITA
Fiber optic controls for aircraft engines - Issues and implications p 856 A92-46244
Design issues in a fiber optic sensor system architecture for aircraft engine control
[AIAA PAPER 92-3483] p 866 A92-49023
DASH, ERNIE R.
Pilot's Automated Weather Support System (PAWSS) concepts demonstration project. Phase 1: Pilot's weather information requirements and implications for weather data systems design
[NASA-CR-188228] p 46 N92-11593
DASH, S. M.
Applications of an implicit, upwind Navier-Stokes code, CRAFT, to steady/unsteady reacting, multi-phase flowfields
[AIAA PAPER 92-0837] p 422 A92-29603
Progress towards the development of transient ram accelerator simulation as part of the U.S. Air Force Armament Directorate Research Program
[AIAA PAPER 92-3248] p 904 A92-48847
DASILVA, VICTOR
Nondestructive depth profiling of the protective coating on a turbine blade p 144 A92-13641
DASO, ENDWELL O.
Full Navier-Stokes analysis of a three-dimensional scramjet inlet p 934 A92-50272
DAU, K.
Computation of viscous phenomena in unsteady transonic flow p 720 N92-27949
DAUDPOTA, Q. I.
Numerical studies of transverse curvature effects on transonic flow stability p 524 A92-36186
DAVENPORT, W. J.
An experimental study of the relationship between velocity and pressure fluctuations in a wing-body junction
[AD-A249628] p 946 N92-31122
DAVID, TIM
Parallel algorithms for panel methods p 293 A92-22346
DAVIDSON, J. J.
AI for RPVs, Sensor Driven Airborne Replanner (SDAR), for a Robotic Aircraft Sensor Platform (RASP) p 114 N92-12534
DAVIDSON, KENNETH L.
Relating the microwave radar cross section to the sea surface stress - Physics and algorithms p 597 A92-35028
DAVIDSON, LARS
Navier-Stokes computation of airfoil in stall using algebraic Reynolds-stress model
[AIAA PAPER 92-0195] p 257 A92-23803
DAVIDSON, LAURIE
Controller memory enhancement: Field facility concepts and techniques
[DOT/FAA/CT-TN92/7] p 640 N92-24799
DAVIES, CAROL B.
Application of a solution adaptive grid scheme to complex three-dimensional flows p 935 A92-50309
DAVIES, M. R. D.
The torsional stability of a compressor cascade
[ASME PAPER 91-GT-180] p 123 A92-15612
DAVINSON, IAN
The use of optical sensors and signal processing gas turbine engines p 856 A92-46247
DAVIS, D. D., JR.
Coupled 2D-3D finite element method for analysis of a skin panel with a discontinuous stiffener
[AIAA PAPER 92-2474] p 583 A92-34363
Detailed analysis and test correlation of a stiffened composite wing panel p 1121 A92-56324
DAVIS, D. DALE, JR.
Detailed analysis and test correlation of a stiffened composite wing panel
[NASA-TM-104154] p 159 N92-13460
DAVIS, D. L.
Numerical analysis of techniques for efficient generation of vorticity in supersonic flows
[AIAA PAPER 92-0828] p 422 A92-29596
DAVIS, D. O.
Surface and flow field measurements in a symmetric crossing shock wave/turbulent boundary layer flow
[AIAA PAPER 92-2634] p 806 A92-45574
DAVIS, DARRELL W.
Omega - GPS integration platform p 98 A92-16660
DAVIS, DENNIS D.
Atmospheric pressure flow reactor: Gas phase chemical kinetics under tropospheric conditions without wall effects
[NASA-CASE-MSC-21384-1] p 297 N92-16243
DAVIS, E. S.
NASA's GPS tracking system for Aristoteles p 576 N92-23919
DAVIS, FRANCIS L.
Compact range test applications, phase 2
[AD-A248790] p 999 N92-3[illegible]83
DAVIS, GARY A.
Unsteady transonic Euler solutions using finite elements
[AIAA PAPER 92-2504] p 518 A[illegible]34499
DAVIS, GEOFFREY C. R.
Composite gearbox housing p 110 A92-14448
DAVIS, JAMES D.
An appraisal of cost-effectiveness models used in the Air Force and Navy aircraft engine component improvement programs
[AD-A245910] p 743 N92-28162
DAVIS, JOEL
Robotic non-destructive inspection of aircraft, phase 1
[AD-A240777] p 44 N92-11367
DAVIS, L. M.
Initial calibration of the HEAT-H2 arc-heated wind tunnel
[AD-A245072] p 484 N92-20898
DAVIS, LARRY P.
CFD helps the Air Force fly right p 169 A92-20146
DAVIS, M. W.
DYNamic Turbine Engine Compressor Code (DYNTECC) - Theory and capabilities
[AIAA PAPER 92-3190] p 923 A92-48802
DAVIS, M. W., JR.
Stage-by-stage poststall compression system modeling technique p 80 A92-17194
DAVIS, PAMELA A.
26 x 6.6 radial-belted aircraft tire performance
[SAE PAPER 912157] p 644 A92-39992
DAVIS, PAUL CHRISTOPHER
A study of transonic aerodynamic analysis methods for use with a hypersonic aircraft synthesis code
[NASA-CR-189854] p 625 N92-24803
DAVIS, R.
Advanced tactical fighter engine
[ETN-92-90840] p 376 N92-18728
DAVIS, ROGER L.
Unsteady analysis of hot streak migration in a turbine stage p 399 A92-28537
Numerical simulation of turbine 'hot spot' alleviation using film cooling
[AIAA PAPER 92-3309] p 904 A92-48896
Navier-Stokes analysis of turbine blade heat transfer and performance p 768 N92-27468
DAVIS, S.
Preliminary screening procedures and criteria for replacements for Halons 1211 and 1301
[AD-A252912] p 1126 N92-33501
DAVOUDZADEH, FARHAD
Three-dimensional blade vortex interactions p 815 A92-46953
DAWES, W. N.
The simulation of three-dimensional viscous flow in turbomachinery geometries using a solution-adaptive unstructured mesh methodology
[ASME PAPER 91-GT-124] p 71 A92-15569
Multi-blade row Navier-Stokes simulations of fan-bypass configurations
[ASME PAPER 91-GT-148] p 73 A92-15586

DAWICKE, D. S.
Proof test and fatigue crack growth modeling on 2024-T3 aluminum alloy p 213 A92-19828
DAWSON, DONNA K.
Organic Matrix Composite Helicopter Internal/External Cargo Pallet System (OMC INTEX)
[AD-A251127] p 961 N92-30878
DAWSON, DOUGLAS J.
Composite cylinder blast overpressure testing p 529 A92-32984
DAWSON, F.
The F/A-18 external burning flight test
[AIAA PAPER 91-5050] p 731 A92-44547
DAWSON, FRANK G.
National Aerospace Plane flight test - External burning on the F/A-18 p 645 A92-40032
DAWSON, RONALD A.
Supersonic Throughflow Fan Test Facility at NASA. Lewis Research Center
[NASA-TP-3038] p 983 N92-31640
DAWSON, W. D.
C-130 glass cockpit system development program
[AIAA PAPER 92-1050] p 553 A92-33230
DAY, DELBERT E.
Fabrication and mechanical properties of an optically transparent glass fiber/polymer matrix composite p 891 A92-45630
DAY, I. J.
Stall inception in axial flow compressors
[ASME PAPER 91-GT-86] p 69 A92-15551
Active suppression of rotating stall and surge in axial compressors
[ASME PAPER 91-GT-87] p 122 A92-15552
DAYAL, H. M.
Microbiological spoilage of aviation turbine fuel. II - Evaluation of a suitable biocide p 891 A92-45600
DAYS, COLIN
A NASA/RAE cooperation in the development of a real-time knowledge based autopilot p 164 N92-12528
DAYTON, A., JR.
A low-power, high-efficiency Ka-band TWTA p 671 A92-38163
DAYTON, RON
Programs at Wright-Patterson Air Force Base p 228 N92-15092
DAYWITT, JAMES E.
Navier-Stokes cavity solutions based on second-order turbulence modeling
[AIAA PAPER 92-2765] p 704 A92-41314
DE CARO, CHUCK
Aerobureau - Strategic television airmobile reports via satellite p 218 A92-19988
DE GROOT, W. A.
Turbulent diffusion flame properties behind a backward-facing step p 985 A92-50255
DE JONG, FREDERIK J.
Hybrid Navier-Stokes/Monte Carlo method for reacting flow calculations p 715 A92-41537
DE LA CHAPELLE, M.
A novel avionic sensor for fly-by-light controls p 650 A92-38128
DE LA VIUDA, JOSE M.
Patch-independent structured multiblock grids for CFD computations p 919 A92-47078
DE MARIA, GIUSEPPE
Robust flight control systems - A parameter space design p 971 A92-50503
DE MATTEIS, GUIDO
Dynamics of hang-gliders p 204 A92-18608
Hang-glider response to atmospheric inputs p 874 A92-46765
DE MATTEIS, P.
Numerical predictions of transonic viscous flows around aerofoils through an Euler/boundary layer interaction method p 624 A92-40630
Wake effects on the prediction of transonic viscous flows around airfoils p 702 A92-41232
DE MELO, DENISE A.
Analysis of aircraft performance during lateral maneuvering for microburst avoidance p 205 A92-20207
DE PRITER, KIRK
Flexible manufacturing in repair of gas turbine engine components
[AIAA PAPER 92-3524] p 786 A92-49049
DE REYES, EDWARD M.
C.A.T.C.H. - Computer aided test conductor handbook: A method for reducing cost, time and effort in an aircraft test and certification program p 602 A92-35943
DE ROSA, S.
Incompressible steady aerodynamics using a standard finite element code p 174 A92-20218
DE TURENNE, J. A.
Investigation of hypersonic ramjet propulsion cycles using a ram accelerator test facility
[IAF PAPER 91-275] p 278 A92-22482
DE WITT, KENNETH J.
Heat transfer measurements from a smooth NACA 0012 airfoil p 218 A92-20215
Roughness effects on heat transfer from a NACA 0012 airfoil p 219 A92-20217
Development of an improved model for runback water on aircraft surfaces
[AIAA PAPER 92-0042] p 270 A92-22160
Further developments in three-dimensional simulation of electrothermal deicing systems
[AIAA PAPER 92-0528] p 459 A92-31668
Experimental and numerical investigation of anti-icing phenomena on a NACA 0012 assembly
[AIAA PAPER 92-0531] p 459 A92-31669
An efficient finite element method for aircraft de-icing problems
[AIAA PAPER 92-0532] p 459 A92-31670
DE ZEEUW, DARREN
Euler calculations of axisymmetric under-expanded jets by an adaptive-refinement method
[AIAA PAPER 92-0321] p 321 A92-25768
A wave-model-based refinement criterion for adaptive-grid computation of compressible flows
[AIAA PAPER 92-0322] p 321 A92-25769
DEABREU-GARCIA, J. ALEX
Improved large perturbation propulsion models for control system design (1988-1989) and large perturbation models of high velocity propulsion systems (1989-1990) and reduced order propulsion models for control system design (1990-1991)
[NASA-CR-190148] p 593 N92-22491
Approximate truncated balanced realizations for infinite dimensional systems p 602 N92-22493
DEABREU, ALEX
A hierarchy for modeling high speed propulsion systems
[NASA-CR-186984] p 387 N92-19934
A hierarchy for modeling high speed propulsion systems p 559 N92-22492
DEAN, P.
Heat flux sensor research and development: The cool film calorimeter
[NASA-CR-189789] p 298 N92-17006
DEANGELIS, V. M.
A historical overview of high-temperature structural testing at the NASA Dryden Flight Research Facility p 981 A92-51407
DEANGELIS, V. MICHAEL
Thermal-structural test facilities at NASA Dryden
[NASA-TM-104249] p 1062 N92-34202
DEAR, ROGER G.
Z-Basic algorithm for collision avoidance system p 188 A92-18482
DEARNALEY, G.
Report on the workshop on Ion Implantation and Ion Beam Assisted Deposition
[AD-A250561] p 927 N92-28923
DEATON, JERRY W.
Residual strength of repaired graphite/epoxy laminates after 5 years of outdoor exposure p 1108 N92-32577
DEBOER, W. P.
Aircraft simulation and pilot proficiency: From surrogate flying towards effective training p 884 N92-28532
Some longitudinal handling qualities design guidelines for active control technology transport aircraft
[NLR-TP-90129-U] p 878 N92-28652
DEBONIS, J. R.
Three-dimensional compressible turbulent computations for a diffusing S-duct
[NASA-CR-4392] p 526 N92-22249
Three-dimensional compressible turbulent computations for a nondiffusing S-duct
[NASA-CR-4391] p 951 N92-32240
DEBONIS, JAMES R.
Full Navier-Stokes analysis of a two-dimensional mixer/ejector nozzle for noise suppression
[AIAA PAPER 92-3570] p 1067 A92-54059
Full Navier-Stokes analysis of a two-dimensional mixer/ejector nozzle for noise suppression
[NASA-TM-105715] p 868 N92-28419
DEBOUT, BRUNO
French research and technology program on advanced hypersonic propulsion
[AIAA PAPER 91-5003] p 471 A92-31683
DEBRY, B.
Definition of the unsteady vortex flow over a wing/body configuration
[NASA-CR-180083] p 178 N92-13995
DEBRY, BENOIT
Measurements of the unsteady vortex flow over a wing-body at angle of attack
[AIAA PAPER 92-2729] p 808 A92-45598
DEBURE, KELLY R.
Advanced Transport Operating System (ATOPS) control display unit software description
[NASA-CR-189606] p 652 N92-24689
DECHAUMPHAI, PRAMOTE
Evaluation of an adaptive unstructured remeshing technique for integrated fluid-thermal-structural analysis p 37 A92-10445
Three-dimensional thermal structural analysis of a swept cowl leading edge subjected to skewed shock-shock interference heating p 174 A92-20306
Progress in integrated analysis with adaptive unstructured meshing p 683 N92-25914
DECKER, HARRY J.
Full-scale transmission testing to evaluate advanced lubricants
[NASA-TM-105668] p 764 N92-26560
Analysis and modification of a single-mesh gear fatigue rig for use in diagnostic studies
[NASA-TM-105416] p 773 N92-27879
Development of a full-scale transmission testing procedure to evaluate advanced lubricants
[NASA-TP-3265] p 998 N92-30396
DECONINCK, H.
A frontal approach for node generation in Delaunay triangulations p 771 N92-27680
DECOOK, S. J.
Wake mixing and performance measurements in a linear compressor cascade with crenulated trailing edges
[AIAA PAPER 92-3188] p 824 A92-48800
DECOOK, STEVEN J.
Experimental investigation of trailing edge crenulation effects on losses in a compressor cascade
[AD-A243902] p 377 N92-19329
DEDIEU, J. P.
AS 332 MKII - Development and certification p 1059 A92-56343
DEDOES, DIRK
INS alignment using GPS Phase III user equipment computed corrections p 100 A92-16955
DEEDS, RICHARD A.
Noise abatement procedures vs. safety
[SAE PAPER 912137] p 635 A92-39977
DEESE, JERRY E.
Simulation of wind tunnel flowfields
[AIAA PAPER 92-0034] p 249 A92-22155
DEFIORE, THOMAS
Status of the FAA flight loads monitoring program p 914 N92-30113
DEFOSSE, P.
Aircraft tracking optimization of parameters selection p 361 N92-18585
DEFOUR, MARTIN
A cable detection lidar system for helicopters p 1001 N92-31068
DEGANI, ASAF
Who or what saved the day? A comparison of traditional and glass cockpits p 833 A92-44931
DEGANI, DAVID
Computation of three-dimensional turbulent vortical flows on bodies at high incidence p 9 A92-13203
Numerical prediction of subsonic turbulent flows over slender bodies at high incidence p 172 A92-18358
Instabilities of flows over bodies at large incidence p 176 A92-20738
Surface flow patterns on an ogive-cylinder at incidence p 176 A92-20762
Effect of upstream disturbance on flow asymmetry
[AIAA PAPER 92-0408] p 325 A92-26261
Numerical simulation of vortex unsteadiness on a slender body at high incidence p 340 A92-28062
Asymmetric turbulent vortical flows over slender bodies p 935 A92-50314
DEHAYE, V.
Fatigue safety factor: Assessment of associated safety level p 401 N92-18573
DEHOFF, RONALD L.
Turbine engine diagnostics system study
[DOT/FAA/CT-91/16] p 202 N92-14064
DEICH, M. E.
Pulsation characteristics of one-phase and two-phase steam flows in Laval nozzles under off-design conditions p 1019 A92-53882
DEINEKO, P. S.
Methyl-tert-butyl ether as a component of aviation gasolines p 34 A92-12146
DEITRICH, BRIAN
Systems simulation of an advanced avionics COMSEC unit p 921 A92-48485
DEJAGER, ALAN W.
Commercial airplane air distribution system development through the use of computational fluid dynamics
[AIAA PAPER 92-0987] p 535 A92-33182

DEJARNETTE, F. R.
An approximate viscous shock layer technique for calculating nonequilibrium hypersonic flows about blunt-nosed bodies
[AIAA PAPER 92-0498] p 329 A92-26326
DEJARNETTE, FRED R.
Effect of nose shape on three-dimensional stagnation region streamlines and heating rates
[AIAA PAPER 91-5032] p 171 A92-17822
Engineering method for calculating surface pressures and heating rates on vehicles with embedded shocks
[AIAA PAPER 91-5060] p 171 A92-17842
Engineering calculations of three-dimensional inviscid hypersonic flowfields p 175 A92-20378
Wall interference calculation in a transonic test section including simulation of discrete slots
[AIAA PAPER 92-0032] p 249 A92-22153
An engineering aerodynamic heating method for hypersonic flow
[AIAA PAPER 92-0499] p 329 A92-26327
Engineering aerodynamic heating method for hypersonic flow p 705 A92-41539
Boundary layer study on nozzle wall at hypersonic velocities
[AIAA PAPER 92-4013] p 1034 A92-56836
Second-order shock-expansion theory extended to include real gas effects
[AD-A247191] p 831 N92-29539
DEJONGE, J. B.
Monitoring load experience of individual aircraft
[NLR-TP-90084-U] p 196 N92-15065
Ageing aircraft research in the Netherlands p 838 N92-30129
DEL CASTILLO CABRERIZO, LORENZO
Iberia's Aeronautical Mapping Application (ACAI) p 637 A92-37073
DEL ROSARIO, RUBEN
Advanced nozzle and engine components test facility
[AIAA PAPER 92-3993] p 1099 A92-56816
DEL ROSO, RICHARD L.
Advanced nozzle and engine components test facility
[AIAA PAPER 92-3993] p 1099 A92-56816
DELAAT, JOHN C.
Real-time fault diagnosis for propulsion systems
[NASA-TM-105303] p 26 N92-11017
DELANEY, R. A.
Vane-blade interaction in a transonic turbine. I - Aerodynamics
[AIAA PAPER 92-3323] p 825 A92-48906
Vane-blade interaction in a transonic turbine. II - Heat transfer
[AIAA PAPER 92-3324] p 904 A92-48907
DELANEY, ROBERT A.
Time-dependent aerodynamic analysis of ducted and unducted propfans at angle of attack
[ASME PAPER 91-GT-190] p 74 A92-15616
DELAURIER, J. D.
Aerodynamics p 202 N92-13977
DELEEUW, J. H.
Flight research p 194 N92-13981
An evaluation of IFR approach techniques: Generic helicopter simulation compared with actual flight p 886 N92-28550
An evaluation of decelerating IFR approaches utilizing a helicopter flight simulator
[CTN-92-60348] p 1048 N92-32845
DELEEUW, JAAP H.
Identification techniques: Model structure and time domain methods p 273 N92-17157
DELERY, J.
Physics of vortical flow p 86 N92-13016
DELERY, JEAN
Basic experiment on a supersonic vortex flow around a missile body p 705 A92-41545
Experimental investigation of the reflection of a shock wave on a heated surface in presence of a turbulent boundary layer p 1023 A92-54569
DELERY, JEAN M.
Separation and vortex formation in turbulent flows
[ONERA, TP NO. 1992-7] p 822 A92-48579
Physics of vortical flows p 1031 A92-56166
DELESTRADE, P.
Preliminary evaluation of new control laws on the experimental fly-by-wire Dauphin helicopter p 568 A92-35756
DELETOMBE, E.
Airplane crashes on the runway. Fine modeling of the behavior after burning of a frame submitted to linear crushing
[IMFL-90-64] p 353 N92-19350
DELFRATE, JOHN H.
In-flight flow visualization and pressure measurements at low speeds on the NASA F-18 high alpha research vehicle p 85 N92-13009
DELIKARAOGLOU, D.
A consistency test of airborne GPS using multiple monitor stations p 454 A92-30651
DELLACORTE, CHRISTOPHER
High temperature dynamic engine seal technology development
[NASA-TM-105641] p 596 N92-23435
DELOGU, A.
Parametric bicubic spline and CAD tools for complex targets shape modelling in physical optics radar cross section prediction p 403 N92-19151
DELPECH, P.
Application of infrared thermography to thermal flux measurement in wind tunnels
[AAAF-NT-89-12] p 31 N92-11020
DELUCA, DANIEL P.
Fatigue in single crystal nickel superalloys
[AD-A248190] p 896 N92-29408
DELUCA, L.
Infrared measurements of aerodynamic heating in hypersonic wind tunnel p 208 N92-15002
DELUCIA, R. A.
Statistics on aircraft gas turbine engine rotor failures that occurred in US commercial aviation during 1989
[DOT/FAA/CT-92/5] p 971 N92-30303
Statistics on aircraft gas turbine engine rotor failures that occurred in US commercial aviation during 1988
[DOT/FAA/CT-91/28] p 1071 N92-33105
DELUISI, JOHN J.
Measured and calculated optical property profiles in the mixed layer and free troposphere p 1129 A92-54630
DELVIGS, PETER
Vinyl capped addition polyimides
[NASA-CASE-LEW-15027-2] p 579 N92-24053
DELVILLE, J.
Compressibility effects in turbulent far wakes p 622 A92-40140
DEMARTINO, JOSEPH
Naval aircraft/engine mission payoff analyses
[AIAA PAPER 92-3473] p 865 A92-49019
DEMEIS, RICHARD
Comanche - The armed scout p 103 A92-13291
An airlifter for the long haul p 358 A92-28493
Paint under pressure p 399 A92-28495
DEMENT, D. K.
System considerations, projected requirements and applications for aeronautical mobile satellite communications for air traffic services p 677 N92-24163
DEMERS, R. N.
Susceptibility of a parallelogram type skin friction balance to rotational motion
[AD-A241348] p 139 N92-13078
DEMETRIADES, ANTHONY
Supersonic and hypersonic boundary-layer transition induced by discrete trips p 522 A92-36023
DEMIN, A. E.
Analysis of transonic flow over plane compressor cascades using the large-particle method p 79 A92-16812
DEMMEL, JOHANN
The icing of the wing upper side and bottom side of the icing research aircraft of the DLR p 724 N92-26349
The icing of the elevator of the DLR icing research aircraft of Do 28 type
[DLR-MITT-91-12] p 953 N92-31813
Analysis of three icing test flights reaching the aircraft-referred icing degree of severe
[ESA-TT-1254] p 954 N92-31943
DEMO, WAYNE A.
Brazing method helps repair aircraft gas-turbine nozzles p 492 A92-29504
DEMOSS, SHANE
Preliminary design studies of an advanced general aviation aircraft
[NASA-CR-190024] p 461 N92-20064
DEN BOER, RUUD G.
Transonic wind tunnel investigation of limit cycle oscillations on fighter type wings - Update
[AIAA PAPER 92-2125] p 572 A92-35692
DEN BRAVEN, WIM
Profile negotiation - A concept for integrating airborne and ground-based automation for managing arrival traffic p 531 A92-33432
DENBOER, R. G.
Steady and unsteady aerodynamics of a pitching straked wing model at high angles of attack p 87 N92-13024
Analysis of unsteady force, pressure, and flow-visualization data for a pitching straked wing model at high angles of attack p 364 N92-18784
DENBOER, RUUD G.
Transonic wind tunnel investigation of limit cycle oscillations on fighter type wings p 721 N92-27959
DENBRAVEN, W.
NARSIM: A real-time simulator for air traffic control research
[NLR-TP-90147-U] p 888 N92-29204
DENBRAVEN, WIM
Design and evaluation of an advanced air-ground data-link system for air traffic control
[NASA-TM-103899] p 1050 N92-33407
DENDA, TAKESHI
Inclusion size effect on the fatigue crack propagation mechanism and fracture mechanics of a superalloy p 388 A92-24831
DENER, C.
An integrated CFD system for 3D turbomachinery applications p 741 N92-27464
DENERY, DALLAS G.
A review of recent programs and future plans for rotorcraft in-flight simulation at Ames Research Center
[SAE PAPER 912121] p 608 A92-39969
Rotorcraft In-Flight Simulation Research at NASA Ames Research Center: A Review of the 1980's and plans for the 1990's
[NASA-TM-103873] p 853 N92-28926
DENG, CIPING
A new method for orientation calculation of the electromagnetic helmet-mounted sighting unit p 370 A92-27837
DENG, CONG
Classification of radar clutter using neural networks p 145 A92-14252
A multi-layer neural network classifier for radar clutter p 291 A92-21691
DENG, G. B.
Navier-Stokes computations of horseshoe vortex flows p 990 A92-49516
DENG, XUEYING
A study of flow patterns and behaviours of 3D separated flow on a simplified Shuttle model p 615 A92-38906
Prediction for the incipient separation of fin-generated three-dimensional shock wave turbulent boundary layer interactions p 615 A92-38909
DENG, ZHENG-TAO
Numerical simulation of droplet deformation in convective flows p 670 A92-36844
DENIS, R.
Measurement of acoustic properties of the composite materials constituting the main rotor hub of the Agusta-Westland helicopter EH-101 (civil version) p 1010 A92-49475
DENNEY, RUSSELL K.
A global approach in evaluating inlet/engine compatibility
[ASME PAPER 91-GT-402] p 127 A92-15732
DENTON, J. D.
Inviscid-viscous coupled solution for unsteady flows through vibrating blades. II - Computational results
[ASME PAPER 91-GT-126] p 71 A92-15571
An experiment on unsteady flow over an oscillating airfoil
[ASME PAPER 91-GT-181] p 73 A92-15613
DEODHARE, GIRISH
Design of non-overshooting feedback control systems p 50 A92-11431
DEOM, A.
Application of infrared thermography to thermal flux measurement in wind tunnels
[AAAF-NT-89-12] p 31 N92-11020
DEOM, A. A.
Measurement of convective heat-transfer coefficients on a wind tunnel model by passive and stimulated infrared thermography p 291 A92-21450
Measurement of convective heat-transfer coefficients in wind tunnels using passive and stimulated infrared thermography p 390 A92-24430
Heat transfer measurements in ONERA supersonic and hypersonic wind tunnels using passive and active infrared thermography p 208 N92-15003
Ablation and temperature sensors for flight measurements in reentry body heat shields p 227 N92-15004
DEOTTE, ROBERT E., JR.
LDV measurements of the velocity field in an underexpanded supersonic jet (Ma = 1.5)
[AIAA PAPER 92-0504] p 341 A92-28196
DEPAULA, RAMON P.
Fiber optic and laser sensors VIII; Proceedings of the Meeting, San Jose, CA, Sept. 17-19, 1990
[SPIE-1367] p 901 A92-48026
DEPONTE, S.
Numerical simulation of vortex flows past impulsively started wings p 88 N92-13028
DEPRIEST, MICHAEL S.
Aviation Diagnostics And Maintenance (ADAM) system preliminary concept of operation and functional description
[AD-A242598] p 170 N92-14966

DERIABIN, A. D.
Calculation of the aerodynamic characteristics of bodies of revolution in incompressible flow by the vortex surface method p 428 A92-30375
DERSHOWITZ, ADAM
Experimental investigation of passive infrared ice detection for helicopter applications p 265 N92-17986
DESAI, C.
Three-dimensional buoyancy-induced flow and heat transfer around the wheel outboard of an aircraft p 397 A92-27773
Characterization of thermal performance of wheel outboard of an aircraft p 849 A92-48352
DESAINT-VICTOR, X.
Resolution of the Navier-Stokes equations applied to the computation of the laminar flow around a two dimensional wing profile
[CERT-RT-65/5604-35] p 43 N92-11307
DESAULTY, M.
Supersonic combustion studies p 211 N92-14984
DESAUTEL, D.
Development and integration of modern laboratories in aerospace education
[AIAA PAPER 92-4022] p 1141 A92-56844
DESIDERI, J. A.
Efficient methods for inviscid non-equilibrium hypersonic flow fields p 1024 A92-54571
DESJARDINS, R. L.
Airborne tests of flux measurement by the relaxed eddy accumulation technique p 504 A92-32052
DESJARDINS, RENE A.
Design and flight test evaluation of the Fantail antitorque system p 110 A92-14456
DESJARDINS, S. P.
Structural testing of commercial rotorcraft seats - An overview p 544 A92-35437
DESJONQUERES, P.
Theoretical study (Lagrangian modeling) of turbulent particulate dispersion
[ETN-91-99909] p 42 N92-11287
DESNOYER, D.
Large thin composite thermostructural parts p 576 N92-23821
DESNOYER, M.
Structures and materials technologies for hypersonic vehicles - Lessons from Hermes experience
[AIAA PAPER 91-5098] p 486 A92-31697
DESOPPER, A.
Weak coupling between an unsteady 3D full potential code and an unsteady turbulent boundary layer code - Application to a helicopter rotor in forward flight
[AIAA PAPER 92-0029] p 249 A92-22151
Experimental and theoretical studies on helicopter rotor fuselage interaction
[ONERA, TP NO. 1991-197] p 329 A92-26356
Theoretical and experimental studies of helicopter rotor/fuselage interaction
[ONERA, TP NO. 1991-198] p 329 A92-26357
DESSE, J. M.
Influence of flight parameters on air intake internal flow distortions due to gun blast-air interaction p 310 A92-24426
DESTUYNDER, PHILIPPE
A simplified model for aerodynamic flows around streamlined models p 63 A92-13816
DESWAANARONS, HINDRIK
Delfi: Design, development, and applicability of expert systems shells
[ISBN-90-6275-734-0] p 692 N92-25306
DETORE, JACK
Technology needs for high speed rotorcraft (3)
[NASA-CR-177592] p 195 N92-14039
DETROIT, MARK J.
Agility and high angle of attack - An Air Force research perspective
[SAE PAPER 912145] p 608 A92-39983
DEUERMEYER, D. W.
Traditional finite element analysis - Opportunities for parallelism? p 40 A92-12354
DEUR, J. M.
A simplified reaction mechanism for prediction of NO(x) emissions in the combustion of hydrocarbons
[AIAA PAPER 92-3340] p 894 A92-48919
Applied analytical combustion/emissions research at the NASA Lewis Research Center - A progress report
[AIAA PAPER 92-3338] p 1067 A92-54025
Applied analytical combustion/emissions research at the NASA Lewis Research Center
[NASA-TM-105731] p 890 N92-29343
DEUTERMANN, ALAN
Compression techniques for video telemetry p 188 A92-19214
DEUTSCH, S.
Particle image velocimetry
[AD-A246638] p 750 N92-27753
DEV, S. P.
Emerging technologies for gas turbine engines - U.A.V. synergies
[AIAA PAPER 92-3757] p 867 A92-49114
DEVENPORT, W. J.
An experimental study of a turbulent wing-body junction and wake flow
[AIAA PAPER 92-0434] p 327 A92-26281
An experimental study of a turbulent wing-body junction and wake flow
[AD-A243388] p 260 N92-17222
DEVENPORT, WILLIAM J.
Far-field turbulence structure of the tip vortex shed by a single rectangular wing p 620 A92-40084
Effects of a leading-edge fillet on the flow past an appendage-body junction p 935 A92-50301
The application of experimental data to blade wake interaction noise prediction
[NASA-CR-189461] p 237 N92-14789
DEVEZEAUX, D.
Analysis tools of ONERA and DLR for the aerothermodynamics of reentry vehicles p 211 N92-14977
DEVILBISS, DAVID W.
Preliminary results from the White Sands Missile Range sonic boom propagation experiment p 1140 N92-33884
DEVIN, ROBERT M.
A holistic approach to support p 60 A92-14413
DEWEESE, RICHARD
Evaluation of head impact kinematics for passengers seated behind interior walls
[AD-A252651] p 952 N92-30551
DEWEY, DONALD E.
Technical evaluation report on the 52nd Symposium on Software for Guidance and Control
[AGARD-AR-302] p 303 N92-17498
DEWHURST, T. B.
The impact load on containment rings during a multiple blade shed in aircraft gas turbine engines
[ASME PAPER 91-GT-163] p 123 A92-15598
DEWITT, K. J.
Numerical analysis of a thermal deicer
[AIAA PAPER 92-0527] p 357 A92-26950
DEWITT, RICHARD L.
Slush hydrogen (SLH2) technology development for application to the National Aerospace Plane (NASP) p 144 A92-13432
DEWITT, T. G.
An iodine hypersonic wind tunnel for the study of nonequilibrium reacting flows
[AIAA PAPER 92-0566] p 383 A92-26974
DEWITT, WARD S.
Proposal for a low cost close air support aircraft for the year 2000: The Raptor
[NASA-CR-190023] p 367 N92-19496
DEWITZ, MICHAEL B.
Effects of a leading-edge fillet on the flow past an appendage-body junction p 935 A92-50301
DEXTER, H. B.
New materials drive high-performance aircraft p 1105 A92-55134
DEXTER, H. BENSON
RTM: Cost-effective processing of composite structures p 578 N92-22678
Flight service environmental effects on composite materials and structures p 1110 N92-33054
DHAR, D.
Design of bearings for rotor systems based on stability p 773 N92-27799
DI GIROLAMO, S.
Aircraft navigation using Global Positioning System improved with geostationary satellites p 99 A92-16934
DI MARTINO, P.
Numerical computations of transonic flows through cascades
[AIAA PAPER 92-3041] p 822 A92-48702
DIBARTOLOMEO, W.
Preparation of the ice certification of the Dornier 328 regional airliner by numerical simulation and by ground test p 451 N92-21693
DIBBLE, R. W.
Experiments on the structure of an annular compressible reacting shear layer p 969 A92-50311
DIBIASE, DON
One joule output from a diode-array-pumped Nd:YAG laser with side-pumped rod geometry p 671 A92-37188
DICARLO, JAMES A.
Ceramics for engines p 578 N92-22517
DICICCO, L. D.
Description of a pressure measurement technique for obtaining surface static pressures of a radial turbine
[AIAA PAPER 92-4006] p 1123 A92-56829
DICICCO, L. DANIELLE
Description of a pressure measurement technique for obtaining surface static pressures of a radial turbine
[NASA-TM-105643] p 680 N92-24959
DICKERSON, TERRY
Fault Tree Interpreter
[AIAA PAPER 91-3789] p 232 A92-17645
DICKSON, RICHARD W.
Advanced Transport Operating System (ATOPS) color displays software description: MicroVAX system
[NASA-CR-189603] p 556 N92-22395
Advanced Transport Operating System (ATOPS) color displays software description microprocessor system
[NASA-CR-189605] p 556 N92-22645
DIDONE, M.
A module-level testing environment for safety-critical software systems p 1132 A92-56293
DIDRIKSON, S. R.
Transport Canada aging aircraft activities p 838 N92-30131
DIEHL, ALAN
The effectiveness of training programs for preventing aircrew 'error' p 834 A92-44997
DIEMUNSCH, JOSEPH R.
Engineering Graphical Analysis Tool (EGAT) development program p 164 N92-12542
DIEROFF, MANFRED
Integrated navigation for approach guidance using differential GPS p 101 A92-16970
DIESEL, JOHN W.
A synergistic solution to the GPS integrity problem p 96 A92-16641
DIET, JEAN
Patch-independent structured multiblock grids for CFD computations p 919 A92-47078
DIETERICH, WILLIAM
A 3-degree-of-freedom flight simulator evaluation of unsteady aerodynamics effects
[AD-A241540] p 139 N92-13079
DIETL, LOTHAR
Test and integration concept for complex helicopter avionic systems p 1064 A92-56292
DIETZ, ANTHONY JOHN
Blade surface pressure measurements on the rotor of a model turbine stage in a transient flow facility p 157 N92-12206
DIGIROLAMO, R.
Flight control law synthesis using neural network theory
[AIAA PAPER 92-4390] p 1074 A92-55191
DIGIROLAMO, ROBERT D.
Neural network and fuzzy logic technology for naval flight control
[AD-A242650] p 206 N92-15074
DIK, I. G.
Calculation of gas combustion regimes in a counterflow vortex chamber p 34 A92-12209
DIKOVSKAIA, N. D.
Pressure on a cylinder with a screen in transverse flow p 6 A92-12164
DILLIES, B.
The coherent flamelet model for propulsion applications p 756 N92-27486
DILLING, WENDELL L.
Development and tribological properties of new cyclotriphosphazene high temperature lubricants for aircraft gas turbine engines p 287 A92-21327
DIMARANAN, LIZA
The SnoDog: Preliminary design of a close air support aircraft
[NASA-CR-189990] p 462 N92-21489
DIMARZIO, CHARLES
Ship airwake measurement and modeling options for rotorcraft applications p 503 N92-21954
DIMICCO, R. G.
A new look at surface flow visualization to provide insight into complex fluid dynamic behavior p 1090 A92-54307
DIMIDUK, D. M.
Development of intermetallic materials for aerospace systems p 754 A92-41874
DIMITRIADIS, E. K.
Active control of sound transmission through elastic plates using piezoelectric actuators p 53 A92-11052
DIN, JIAXI
Numerical simulation of two incoming streams in a dual-combustion ramjet combustor p 375 A92-28419
DINDAR, MUSTAFA
Effect of turbulence modeling on dynamic stall of a NACA0012 airfoil
[AIAA PAPER 92-0027] p 248 A92-22149
Nonequilibrium turbulence modeling effects on transonic vortical flows about delta wings p 85 N92-13007
DING, ZESHENG
Wind tunnel study of aerodynamic characteristics of base combustion p 666 A92-36967

DINI, PAOLO
Simplified linear stability transition prediction method for separated boundary layers p 812 A92-46883
DION, M.
An improved model-creation program for EM interaction analysis
[NRC-31764] p 155 N92-12153
DION, MARC
Analysis of EMP response of structures using frequency domain electromagnetic interaction codes
[AD-A245758] p 765 N92-26592
DIRKZWAGER, AB
Preliminary design studies of an advanced general aviation aircraft
[NASA-CR-190024] p 461 N92-20064
DIRLIK, S. P.
Experimental evaluation of a 50-percent thick airfoil with blowing and suction boundary layer control
[AIAA PAPER 92-4500] p 1026 A92-55368
DIRUSSO, ELISEO
Performance tests of a cryogenic hybrid magnetic bearing for turbopumps
[NASA-TM-105627] p 473 N92-20523
Determining structural performance
p 560 N92-22519
DISARIO, R.
Controller response to conflict resolution advisory prototype
[PB92-190032] p 1050 N92-33596
DISARIO, ROBERT
Design considerations for IAP charts: Approach course track and communication frequencies
[AD-A241482] p 103 N92-13051
DISARIO, ROBERT M.
CDI sensitivity and crosstrack error on nonprecision approaches
[AD-A243981] p 356 N92-19391
DISIMILE, P. J.
Wedge-induced turbulent boundary-layer separation on a roughened surface at Mach 6.0 p 175 A92-20379
Turbulent boundary-layer characteristics over a flat-plate/wedge configuration at Mach 6
p 176 A92-20761
A new look at surface flow visualization to provide insight into complex fluid dynamic behavior
p 1090 A92-54307
DISTEFANO, J.
Characteristics of thunderstorm-generated low altitude wind shear - A survey based on nationwide terminal Doppler weather radar testbed measurements
p 45 A92-11378
DITTMAR, JAMES H.
Detailed noise measurements on the SR-7A propeller: Tone behavior with helical tip Mach number
[NASA-TM-105206] p 304 N92-16705
An evaluation of some alternative approaches for reducing fan tone noise
[NASA-TM-105356] p 416 N92-18282
DITTMER, W.
Applications of advanced composites in a 3/4 air transportable rack p 36 A92-10314
Application of resin and metal matrix composites to advanced avionics enclosure p 985 A92-51921
DIVITO, BEN L.
Formal design and verification of a reliable computing platform for real-time control. Phase 2: Results
[NASA-TM-104196] p 602 N92-22320
DIWAKAR, PHILIP M.
Prediction of wake in a curved duct p 3 A92-10487
DIXON, C. S.
Probability distributions that are important when assessing barometric aiding to GPS p 100 A92-16952
DIXON, CHARLES J.
Development of a high-angle-of-attack stability and control prediction code
[AIAA PAPER 92-4354] p 1079 A92-55340
DMITRIEV, S. I.
From the history of Soviet aviation - Aircraft of the Il'iushin design bureau (2nd revised and enlarged edition)
p 61 A92-15022
DO NASCIMENTO, MARCO A. R.
The selective bleed variable cycle engine
[ASME PAPER 91-GT-388] p 126 A92-15720
DOAN, D. B.
Rigid and flexible joint modelling in multibody dynamics using finite elements p 671 A92-37559
DOANE, P. M.
A methodology for the analysis and modeling of thrust vectoring usage
[AIAA PAPER 92-0389] p 357 A92-26245
DOBOSY, RONALD J.
A sensitive fast-response probe to measure turbulence and heat flux from any airplane p 775 A92-42097
DOBRZYNSKI, W.
Azimuthal noise characteristics of contra-rotating propellers - Results of a wind tunnel model test
p 693 A92-39066
DOBYNS, ALAN
Turning up the heat on aircraft structures
p 1052 A92-55131
DOD, L. R.
Retrieval of total precipitable water over high latitude regions using radiometric measurements near 90 and 183 GHz p 505 A92-32129
DODBELE, SIMHA S.
Design optimization of natural laminar flow bodies in compressible flow p 701 A92-41219
DODD, H. M.
The status of the US VAWT program
[DE92-002931] p 505 N92-21040
DODD, ROBERT S.
A review and discussion of flight management system incidents reported to the aviation safety reporting system
[AD-A252438] p 1043 N92-32941
DODDS, W.
A distributed vaporization time-lag model for gas turbine combustor dynamics
[AIAA PAPER 92-3465] p 865 A92-49014
DODDS, WILLARD J.
High-speed civil transport aircraft emissions
p 408 N92-19122
DODGE, L.
A distributed vaporization time-lag model for gas turbine combustor dynamics
[AIAA PAPER 92-3465] p 865 A92-49014
DOEHNEL, W.
Experience with piloted simulation in the development of helicopters p 884 N92-28528
Experience with piloted simulation in the development of helicopters
[MBB-UD-0610-91-PUB] p 889 N92-30076
DOELLNER, O. LEONARD
Radiant energy power source for jet aircraft
[DE92-008726] p 648 N92-24556
DOELLNER, OSCAR LEONARD
Aircraft photovoltaic power-generating system
p 775 N92-26581
DOERR, STEVE
Measurement of a three-dimensional hypersonic density field
[AIAA PAPER 92-0383] p 323 A92-26240
DOGAN, BILAL
Mechanical and fracture behaviour of Ti-6Al-2Sn-4Zr-2Mo-0.1Si alloys p 288 A92-22755
DOGGETT, ROBERT V., JR.
Low-speed flutter characteristics of some simple low-aspect-ratio delta-wing models p 460 A92-32247
On simple aerodynamic sensitivity derivatives for use in interdisciplinary optimization
[NASA-TM-104145] p 82 N92-11985
DOGRA, V. K.
Aerothermodynamics of a 1.6-meter-diameter sphere in hypersonic rarefied flow p 808 A92-45840
DOGRA, VIRENDRA K.
Hypersonic rarefied flow past spheres including wake structure
[AIAA PAPER 92-0495] p 329 A92-26325
DOHMEN, H.-J.
Computation of 3D flow phenomena in axial flow compressor blade rows
[ASME PAPER 91-GT-78] p 69 A92-15547
Boundary layer flow in axial compressors (theoretical part)
[ETN-92-91006] p 501 N92-21232
Boundary layer flow in axial compressors (theoretical part)
[ETN-92-91007] p 501 N92-21233
Boundary layer flow in axial compressors (theoretical part)
[ETN-92-91008] p 502 N92-21234
DOLLING, D. S.
Correlation of separation shock motion with pressure fluctuations in the incoming boundary layer
p 5 A92-11061
Organized structure in a Mach 5/Mach 3 turbulent shear layer
[AIAA PAPER 92-0180] p 256 A92-23790
Effects of sweepback on unsteady separation in Mach 5 compression ramp interactions
[AIAA PAPER 92-0430] p 435 A92-31663
A preliminary study of the turbulent structures associated with unsteady separation shock motion in a Mach 5 compression ramp interaction
[AIAA PAPER 92-0744] p 436 A92-31677
Unsteady separation in sharp fin-induced shock wave/turbulent boundary layer interaction at Mach 5
[AIAA PAPER 92-0748] p 436 A92-31678
Computation of turbulent, separated, unswept compression ramp interactions p 813 A92-46897
Effects of vortex generators on the growth of a compressible shear layer
[AIAA PAPER 90-1979] p 934 A92-50269
An experimental examination of the effects of incoming boundary layer modifications on the dynamics of a turbulent compression corner interaction
[AIAA PAPER 92-3667] p 1022 A92-54111
DOLLING, DAVID S.
An experimental/computational study of sharp fin induced shock wave/turbulent boundary layer interactions at Mach 5 - Experimental results
[AIAA PAPER 92-0749] p 335 A92-27093
Navier-Stokes computations for pointed, spherical, and flat tipped shell at Mach 3 p 705 A92-41536
Exploratory study of wall pressure fluctuations in a Mach 5, sharp fin-induced turbulent interaction
p 935 A92-50304
DOLLYHIGH, SAMUEL M.
Preliminary results from the High Speed Airframe Integration Research project
[AIAA PAPER 92-1004] p 536 A92-33196
DOLTSINIS, IOANNIS ST.
An exploration of chemically reacting viscous hypersonic flow p 612 A92-37550
DOMALEWSKI, STEVE
New insulation constructions for aerospace wiring applications. Volume 1: Testing and evaluation
[AD-A240638] p 22 N92-11006
New insulation constructions for aerospace wiring applications. Volume 2: The 270 VDC arc tracking testing with power controllers
[AD-A240639] p 23 N92-11007
DOMBRO, L.
A low-power, high-efficiency Ka-band TWTA
p 671 A92-38163
DOMINEK, A.
Analysis of lossy composite terminating structures
[NASA-CR-189901] p 404 N92-19217
DOMINIK, D. F.
Scale effects on the flow past the mated Space Shuttle configuration
[AIAA PAPER 92-2680] p 799 A92-45532
DOMINIQUE, H. P.
Filter debris analysis: A concrete approach to wear diagnosis
[DREP-TM-88-20] p 222 N92-14345
DOMINY, R. G.
Flat-ended circular cylinder in hypersonic rarefied flow
p 174 A92-20304
DOMPKA, ROBERT V.
Finite element correlation of the U.S. Army/BHTI ACAP composite airframe helicopter p 108 A92-14399
DONAHUE, D. J.
Development of the full-envelope Performance Seeking Control algorithm
[AIAA PAPER 92-3748] p 1068 A92-54148
DONE, G. T. S.
Relative energy concepts in helicopter dynamics
p 846 A92-46925
DONES, F.
A novel avionic sensor for fly-by-light controls
p 650 A92-38128
DONG, BENGHAN
Cyclic symmetric contact stress analysis of aeroengine rotor assembly p 470 A92-29733
DONG, BENHAN
Predication of fastening capacity of screwed joint structure with cone assembly p 391 A92-24737
DONG, BONIAN
Numerical simulations of wakes, blade-vortex interaction, flutter, and flutter suppression by feedback control p 597 N92-23997
DONG, CONG
Reliability analysis of fatigue life of a structural system
p 671 A92-37395
DONG, JINZHONG
Investigation on vortex control technique of flow separation in diffuser p 338 A92-27828
DONG, XINMIN
Steady state and quasi-transient analysis of aircraft hydraulic system with network theory
p 642 A92-37391
DONG, YANG
A horizon-recursive form for predictors and their computation p 50 A92-11427
DONG, YUAN
China's first variable stability aircraft: The BW-1-Gets its pre-acceptance flight tests
[AD-A240941] p 116 N92-13062
DONKER, J. C.
A knowledge-based assistant for diagnosis in aircraft maintenance p 61 N92-12538
Application of knowledge-based systems for diagnosis of aircraft systems
[NLR-TP-90192-U] p 837 N92-28655

DONNELLAN, MARY E.
Tensile and interlaminar properties of GLARE (trade name) laminates
[AD-A250188] p 895 N92-28921
DONNELLY, RUSSELL J.
High Reynolds number flows using liquid and gaseous helium
[ISBN 0-387-97475-X] p 897 A92-45261
DONOHUE, K.
Aerothermodynamic radiation studies
[NASA-CR-185666] p 284 N92-15998
DONOVAN, J. F.
Aerodynamic applications of pressure-sensitive paint
[AIAA PAPER 92-0264] p 394 A92-25720
An improved analysis method for cross-wire signals obtained in supersonic flow p 614 A92-38456
DONOVAN, JOHN F.
Experimental investigation of terminal shock sensors for mixed-compression inlets p 276 A92-21074
DONOVAN, M.
Characteristics of thunderstorm-generated low altitude wind shear - A survey based on nationwide terminal Doppler weather radar testbed measurements
p 45 A92-11378
DONOVAN, M. F.
A comparison of the performance of two gust front detection algorithms using a length-based scoring technique
[AD-A250862] p 1004 N92-32103
DONZELLI, G.
Aluminium-lithium alloys - Application on helicopters
p 1106 A92-56326
DOONAN, J. G.
Scale model test results of a multi-slotted vectoring 2DCD ejector nozzle
[AIAA PAPER 92-3264] p 864 A92-48859
DORATO, P.
Applications of robust control theory - Educational implications
[AIAA PAPER 92-4559] p 1131 A92-55271
DORATO, PETER
U-parameter design example - Robust flight control for wind-shear protection p 28 A92-11502
Trajectory shaping by the U-parameter design method
p 479 A92-29361
DOREY, GERARD
Productivity and quality in the Modane and Fauga wind tunnels - Prospects for the 90s
[ONERA, TP NO. 1991-203] p 383 A92-26360
DORIA, MICHAEL L.
Experiences with optimizing airfoil shapes for maximum lift over drag p 90 N92-13838
DORMAN, J. I.
Flight simulation modeling in support of engine/airframe integration p 1055 A92-56279
DORNEY, DANIEL J.
Unsteady analysis of hot streak migration in a turbine stage p 399 A92-28537
Numerical simulation of turbine 'hot spot' alleviation using film cooling
[AIAA PAPER 92-3309] p 904 A92-48896
Navier-Stokes analysis of turbine blade heat transfer and performance p 768 N92-27468
DORNHEIM, MICHAEL A.
Japan pushes high speed research
p 1015 A92-53434
Instrumentation key to NASP combustor tests
p 1092 A92-55100
DORRANCE, DANIEL R.
Radar troubleshooting assistant expert system
[AIAA PAPER 91-3764] p 231 A92-17626
DOTY, JOHN HOWARD
Performance prediction and design of maximum thrust planar supersonic nozzles using a flux-difference-splitting technique p 738 N92-26480
DOTY, MARK C.
Dynamics of an aircraft-towed body during release
[AIAA PAPER 92-0130] p 295 A92-23750
DOU, HUASHU
Prediction for the incipient separation of fin-generated three-dimensional shock wave turbulent boundary layer interactions p 615 A92-38909
DOUGHERTY, F. C.
Aerodynamic interference between stores
[AD-A247207] p 715 N92-27172
DOUGHERTY, JULIE A.
A modeling strategy for large-scale optimization based on analysis and visualization principles
[AD-A246570] p 777 N92-26620
DOUGHTY, R. L.
The effect of blade solidity on the aerodynamic loss of a transonic turbine cascade
[AIAA PAPER 92-0393] p 323 A92-26248
DOUGLAS, LAURA M.
Development of a lubrication system for the T800-LHT-800 turboshaft engine
[ASME PAPER 91-GT-398] p 127 A92-15728
DOUGLASS, ANNE R.
The atmospheric effects of stratospheric aircraft: A first program report
[NASA-RP-1272] p 408 N92-19121
Natural cycles, gases p 408 N92-19123
Ozone response to aircraft emissions: Sensitivity studies with two-dimensional models p 409 N92-19126
DOVGAL', A. V.
Control of laminar boundary layer separation
p 393 A92-24980
DOVI, A. R.
Application of multidisciplinary optimization methods to the design of a supersonic transport
p 550 N92-23230
DOVI, AUGUSTINE R.
Integrating aerodynamics and structures in the minimum weight design of a supersonic transport wing
[NASA-TM-107586] p 850 N92-28435
DOW, JOHN M.
Current activities and future plans for GPS applications p 640 N92-24735
DOWDEN, R. L.
Stratospheric electrodynamics from superpressure balloons - A technical challenge for small payload environments
[AIAA PAPER 91-3674] p 14 A92-11019
DOWELL, E. H.
Comparison of theory and experiment for nonlinear flutter and stall response of a helicopter blade
p 65 A92-14428
Experimental and theoretical study for nonlinear aeroelastic behavior of a flexible rotor blade
[AIAA PAPER 92-2253] p 584 A92-34410
Chaotic stall response of helicopter rotor in forward flight p 730 A92-43046
Chaotic oscillation in helicopter blade stall response
p 846 A92-46922
Flutter and stall response of a helicopter blade with structural nonlinearity p 1055 A92-56178
DOWELL, EARL H.
Eigenvalue calculation procedure for an Euler/Navier-Stokes solver with application to flows over airfoils p 170 A92-17429
A modern view of Theodore Theodorsen
[ISBN 0-930403-85-1] p 307 A92-26250
DOWLER, CONSTANCE A.
Performance characteristics of brush seals for limited-life engines
[ASME PAPER 91-GT-281] p 152 A92-15676
Simple effective thickness model for circular brush seals
[AIAA PAPER 92-3192] p 903 A92-48803
DOWNEY, J. P.
Experimental results and numerical modeling of solidification during aircraft high-g arcs
[AIAA PAPER 92-0843] p 493 A92-29609
DOWNIE, BRUCE
Effectiveness of an onboard water spray system during an oxygen enriched cabin fire
[DOT/FAA/CT-TN91/51] p 264 N92-17149
DOWNIE, JOHN D.
Optical computing at NASA Ames Research Center
[AIAA PAPER 91-3779] p 231 A92-17637
Binary optical filters for scale invariant pattern recognition
[NASA-TM-103902] p 853 N92-28910
DOWNING, J. M.
Sonic booms produced by US Air Force and US Navy aircraft: Measured data
[AD-A244804] p 512 N92-21719
DOWNING, J. MICAH
Lateral spread of sonic boom measurements from US Air Force boomfile flight tests p 1140 N92-33883
DOWNING, R.
Measurements and correlation of two-phase pressure drop under microgravity conditions p 37 A92-10435
DOXSTADER, ROY
Surfprep flash-lamp depaint system evaluation
p 497 A92-32411
DOYLE, JOHN
New methods in robust control
[AD-A240221] p 29 N92-11018
DRABCZUK, R.
Progress towards the development of transient ram accelerator simulation as part of the U.S. Air Force Armament Directorate Research Program
[AIAA PAPER 92-3248] p 904 A92-48847
DRACOPOULOS, THEODORE N.
Integrated aeroelastic control optimization of laminated composite lifting surfaces p 481 A92-32248
DRAGO, R. J.
Analytical evaluation of resonant response of spiral bevel gears in the RAH-66 helicopter Fantail transmission
[AIAA PAPER 92-3495] p 906 A92-49031
DRAPER, ALFRED C.
Evolution and development of hypersonic configurations 1958-1990
[AD-A242768] p 197 N92-15069
DREHER, G.
Stability failure of sandwich structures
[MBB-UD-0613-92-PUB] p 1111 N92-33994
DREIER, MARK E.
Development of an advanced piloted helicopter simulation p 105 A92-14363
DRELA, MARK
Modeling of heavy-gas effects on airfoil flows
[NASA-CR-190357] p 716 N92-27558
DRESSER, H. S.
Multizonal Navier-Stokes solutions for the multibody *Space Shuttle configuration* p 310 A92-24667
DREXLER, JAN
Discs low cycle fatigue life predictions for gas turbine engines in CSFR by using fractographic information
p 995 A92-51950
DRIFTMYER, RICHARD T.
Window cooling for high speed flight
[AD-D015145] p 344 N92-18193
DRIKAKIS, D.
Upwind schemes for Navier-Stokes computations at subsonic through hypersonic speeds
p 708 A92-43071
DRISCOLL, JOSEPH T.
Handling qualities of the H-76 Fantail Demonstrator
p 131 A92-14335
DRIVER, D.
Materials and process directions for advanced aero-engine design
[PNR-90814] p 378 N92-19938
Powder processing of aero-engine components
[PNR-90813] p 756 N92-27044
DRONNIK, A. IU.
Effect of Eulerian inertia forces on the stressed state of the rotating components of aircraft turbomachines
p 128 A92-16828
DROZDOV, V. V.
A criterion for estimating the economic and operational efficiency of the power distribution systems of commercial aircraft p 657 A92-40611
DRUHAN, BARRY B.
An explanation-based-learning approach to knowledge compilation - A Pilot's Associate application
p 920 A92-48220
DRUMMOND, A. M.
Trajectories and stability of trailing vortices very near the ground
[NRC-32151] p 716 N92-27344
DRUMMOND, COLIN K.
Preliminary dynamic tests of a flight-type ejector
[AIAA PAPER 92-3261] p 1066 A92-54020
Preliminary dynamic tests of a flight-type ejector
[NASA-TM-105814] p 972 N92-30998
DRUMMOND, J. P.
Supersonic reacting internal flowfields
p 155 A92-16989
An assumed joint-Beta PDF approach for supersonic turbulent combustion
[AIAA PAPER 92-3844] p 1113 A92-54199
DRUMMOND, J. PHILIP
Direct simulation of high-speed mixing layers
[NASA-TP-3186] p 945 N92-30909
DRUMMOND, SHARON L.
Rotorcraft Maneuverability and Agility Survivability Sensitivity Analysis (RMASSA) p 161 A92-14351
DU VAL, RONALD W.
A piloted comparison of elastic and rigid blade-element rotor models using parallel processing technology
p 546 A92-35751
Comparison of elastic and rigid blade-element rotor models using parallel processing technology for piloted simulations
[SAE PAPER 912120] p 608 A92-39968
DU, BINLAO
Digital simulation and experimental modal analysis of dynamic characteristics of a propeller hub
p 38 A92-10965
DU, GUANG-WU
Engine panel seals for hypersonic engine applications: High temperature leakage assessments and flow modelling
[NASA-TM-105260] p 298 N92-16336
High temperature dynamic engine seal technology development
[NASA-TM-105641] p 596 N92-23435

DU, JIAN-YI
Pseudostream function formulation - A method of solving three-dimensional aerodynamic analysis and design problems in turbomachinery p 996 A92-52981
DU, SHENGTONG
An investigation on flame stability by fuel permeability in a flame holder made of porous ceramic material p 375 A92-28435
DUBERSHTEIN, V. H.
Gas-generator with high-temperature path ceramic components
[ASME PAPER 91-GT-152] p 148 A92-15594
DUBINSKII, A. V.
Calculation of rotational derivatives in the case of local interaction between flow and a body surface p 624 A92-40746
DUBINSKY, RICHARD
A study of atmospheric optical scattering parameters at 1.5 and 2 micron region for solid state Doppler lidar applications p 1001 N92-31067
DUBLINSKI, ALEX C.
Producibility Demonstrator Program - Technological preeminence through concurrent engineering p 146 A92-14449
DUCK, P. W.
Boundary-layer receptivity due to a wall suction and control of Tollmien-Schlichting waves p 616 A92-39333
DUCK, PETER W.
The inviscid stability of supersonic flow past heated or cooled axisymmetric bodies p 712 A92-44363
DUCKETT, DONALD P., JR.
The application of statistical estimation techniques to terrain modeling
[AD-A243799] p 409 N92-19231
DUDEK, H.-L.
Knowledge-based planning for controlled airspace flight operation as part of a cockpit assistant p 727 N92-27895
DUDERSTADT, E. C.
Thermal barrier coatings for gas turbine use p 142 A92-15245
DUDLEY, MICHAEL R.
Large-scale wind tunnel studies of a jet-engined powered ejector-lift STOVL aircraft p 842 A92-45313
Potential flow theory and operation guide for the panel code PMARC
[NASA-TM-102851] p 1036 N92-32422
DUFFY, KEITH S.
NASA TSRV essential flight control system requirements via object oriented analysis
[NASA-CR-189573] p 381 N92-19499
DUFFY, PAUL
Russian realities p 932 A92-53250
DUGAN, JOANNE B.
Modular techniques for dynamic fault-tree analysis p 1120 A92-56241
HiRel - Reliability/availability integrated workstation tool p 1120 A92-56257
DUGEAI, A.
Prediction of generalized aerodynamic forces following linearized supersonic theory
[ONERA, TP NO. 1991-114] p 76 A92-16093
DUGUNDJI, JOHN
Nonlinear stall flutter and divergence analysis of cantilevered graphite/epoxy wings p 219 A92-20746
Nonlinear large amplitude aeroelastic behavior of composite rotor blades at large static deflection
[AIAA PAPER 92-2257] p 540 A92-34412
DUKE, EUGENE L.
A NASA/RAE cooperation in the development of a real-time knowledge based autopilot p 164 N92-12528
DULIKRAVICH, GEORGE S.
Minimization of the number of cooling holes in internally cooled turbine blades
[ASME PAPER 91-GT-52] p 121 A92-15530
Aerodynamic shape optimization of hypersonic configurations including viscous effects
[AIAA PAPER 92-2635] p 795 A92-45506
Third International Conference on Inverse Design Concepts and Optimization in Engineering Sciences (ICIDES-3)
[NASA-CR-188125] p 170 N92-13928
Aerodynamic shape optimization of arbitrary hypersonic vehicles p 194 N92-13954
DULL, TOM
The ATF YF-23 Vehicle Management System
[AIAA PAPER 92-1076] p 563 A92-33245
DUMARS, WILLIAM
Low VOC primer for structural bonding p 892 A92-47338
DUMITRESCU, LUCIEN Z.
Flow near the trailing edge of an airfoil p 431 A92-31151
DUNAVANT, JAMES C.
Shuttle Infrared Leeside Temperature Sensing (SILTS) experiment - STS-35 and STS-40 preliminary results
[AIAA PAPER 92-0126] p 286 A92-23746
DUNCAN, BEVERLY
Computational analysis of ramjet engine inlet interaction
[AIAA PAPER 92-3102] p 824 A92-48744
DUNFORD, PHIL
1991-92 AHS Technical Committee highlights - Test and evaluation p 609 A92-40398
DUNFORD, PHILIP
The V-22 Osprey - A significant flight test challenge p 546 A92-35766
DUNHAM, DANA J.
A summary of NASA research on effects of heavy rain on airfoils p 452 N92-21694
DUNHAM, DANA MORRIS
Effect of solidity and inclination on propeller-nacelle force coefficients
[NASA-TM-4316] p 90 N92-13038
DUNHAM, J.
The changing role of experimentation in aeroengine R and D: The point of view of the research worker
[AD-A246372] p 740 N92-27062
DUNHAM, R. EARL, JR.
A summary of NASA research on effects of heavy rain on airfoils p 452 N92-21694
Wind tunnel aerodynamic characteristics of a transport-type airfoil in a simulated heavy rain environment
[NASA-TP-3184] p 948 N92-31532
DUNLAVY, S.
Statistical prediction of maximum buffet loads on the F/A-18 vertical fin p 811 A92-46816
DUNMIRE, B.
Investigation of hypersonic ramjet propulsion cycles using a ram accelerator test facility
[IAF PAPER 91-275] p 278 A92-22482
DUNN, M. G.
Vane-blade interaction in a transonic turbine. I - Aerodynamics
[AIAA PAPER 92-3323] p 825 A92-48906
Vane-blade interaction in a transonic turbine. II - Heat transfer
[AIAA PAPER 92-3324] p 904 A92-48907
DUNN, MARK H.
High-speed propeller noise prediction - A multidisciplinary approach p 924 A92-45831
The solution of a singular integral equation arising from a lifting surface theory for rotating blades p 260 N92-17303
DUNN, PETER
Nonlinear stall flutter and divergence analysis of cantilevered graphite/epoxy wings p 219 A92-20746
DUPOIRIEUX, FRANCIS
Three-dimensional calculations of reactive flows in aircraft combustion chambers performed using two combustion models
[ONERA, TP NO. 1991-110] p 154 A92-16089
Three dimensional calculations of reactive flows within aircraft combustion chambers including some combustion models p 770 N92-27490
DUPONCHEL, JEAN PIERRE
Steady and transient performance calculation method for prediction, analysis, and identification p 869 N92-28461
DUPONT, P.
Hot-wire measurements in turbulent transonic flows p 941 A92-53078
DUPRIEZ, F.
Design and manufacturing of torsional flexible blade models p 547 A92-35780
Flutter models: Their design, manufacture, and ground testing p 1089 N92-34164
DUPUY, PHILIPPE
A simplified model for aerodynamic flows around streamlined models p 63 A92-13816
DUQUE, E. P.
Flowfield analysis of modern helicopter rotors in hover by Navier-Stokes method
[AD-A245011] p 446 N92-21333
DURAND, J.-M.
GPS availability. I - Availability of service achievable for different categories of civil users. II - Evaluation of state probabilities for 21-satellite and 24-satellite constellations p 99 A92-16949
DURAO, D. F. G.
Turbulent energy budgets in impinging zones p 620 A92-40081
DURHAM, MICHAEL H.
NACA 0012 benchmark model experimental flutter results with unsteady pressure distributions
[AIAA PAPER 92-2396] p 517 A92-34469
The benchmark aeroelastic models program: Description and highlights of initial results
[NASA-TM-104180] p 185 N92-15049
NACA0012 benchmark model experimental flutter results with unsteady pressure distributions
[NASA-TM-107581] p 526 N92-22507
The benchmark aeroelastic models program: Description and highlights of initial results p 721 N92-27960
Pressure measurements on a rectangular wing with a NACA0012 airfoil during conventional flutter
[NASA-TM-104211] p 1042 N92-34147
DURHAM, WAYNE C.
Constrained control allocation
[AIAA PAPER 92-4550] p 1131 A92-55262
Nonlinear model-following control application to airplane control (1992 AIAA Controls Design Challenge)
[AIAA PAPER 92-4625] p 1077 A92-55302
DURKIN, EDWARD
Future military APU requirements
[SAE PAPER 912176] p 655 A92-40001
DURST, FRANZ
Semiconductor laser Doppler anemometer for applications in aerodynamic research p 495 A92-31173
DUSSAUGE, J. P.
Hot-wire measurements in turbulent transonic flows p 941 A92-53078
DUTOYA, D.
Presentation of a computational code for 3-D compressible flow in complex channels and cavities p 769 N92-27475
DUTTON, J. C.
Development and application of a particle image velocimeter for high-speed flows
[AIAA PAPER 92-0004] p 292 A92-22129
Multiple normal shock wave/turbulent boundary-layer interactions p 344 A92-28527
Two-stream, supersonic, wake flowfield behind a thick base. I - General features p 813 A92-46895
DUVAL, RONALD W.
Application areas for rotorcraft system identification: Simulation model validation p 274 N92-17164
DUYAR, AHMET
Real-time fault diagnosis for propulsion systems
[NASA-TM-105303] p 26 N92-11017
A simplified dynamic model of the T700 turboshaft engine
[NASA-TM-105805] p 1009 N92-30898
DVORSCAK, B. J.
The Hummingbird experience at Lockheed Georgia p 646 A92-40041
DWYER, JOHN P.
Assessment of cockpit interface concepts for data link retrofit
[NASA-CR-187615] p 268 N92-17512
An exploration of function analysis and function allocation in the commercial flight domain
[NASA-CR-4374] p 368 N92-19871
DYER, C. S.
Surface activation of Concorde by Be-7 p 605 N92-23295
DYKE, RAYMOND W.
Air cushion vehicle conductive/semiconductive flexible skirt, and method
[AD-D015160] p 400 N92-18187
DYKMAN, JOHN R.
Design and analysis issues of integrated control systems for high-speed civil transports
[NASA-CR-186022] p 979 N92-31656
DZAMBA, L. D.
Analysis of helicopter accident risk exposure near heliports, airports, and unimproved sites
[SCT-91RR-13] p 637 N92-26028
Composite profiles of helicopter mishaps at heliports and airports
[AD-A248887] p 724 N92-28052
DZAMBA, LEN D.
Rotorcraft low altitude IFR benefit/cost analysis: Operations analysis
[SCT-90RR-44] p 191 N92-15061
DZIEDZIC, WILLIAM M.
Analysis of cooling systems for hypersonic aircraft
[AIAA PAPER 91-5063] p 216 A92-17843
Integrated numerical methods for hypersonic aircraft cooling systems analysis
[AIAA PAPER 92-0254] p 357 A92-25712
DZIELSKI, JOHN E.
Equivalence of optimal control problems and the use of parameterization methods p 52 A92-11466

E

EAGLE, KENNETH H.
Redundancy design philosophy for catastrophic loss protection p 1119 A92-56202
EAGLESON, L. A.
A review of computational/experimental methodology developments in aeroacoustics p 695 A92-39241
EARLS, MICHAEL
Experience with Ada on the F-18 High Alpha Research Vehicle Flight Test Program
[NASA-TM-104259] p 1062 N92-34039
EARLY, KEVIN
Engineering model for analysis of scramjet combustor performance with finite-rate chemistry
p 129 A92-17202
EAST, R. A.
Aero-propulsive effects on configuration shaping
[AIAA PAPER 91-5064] p 459 A92-31691
Interference heating near fin/body junctions on hypersonic vehicles p 182 N92-14996
EASTIN, ROBERT G.
System for generating sequences of phased gust or taxi loadings p 845 A92-46800
EASTMAN, PAUL F.
Moldless composite aircraft wing structural design modifications p 958 A92-51527
EASTON, ROGER L., JR.
Digital analysis of wind tunnel imagery to measure fluid thickness
[NASA-CR-189234] p 983 N92-31252
EASTWOOD, RAYMOND A.
Global satellite navigation using both GPS and GLONASS p 99 A92-16938
EATON, R. A.
The impact of air transport on the environment
[PNR-90876] p 1129 N92-33751
EATWELL, G. P.
A survey of active control in aircraft cabins
p 643 A92-39084
EBADIAN, M. A.
Heat transfer in the entrance region of semicircular ducts with internal fins p 497 A92-32264
EBENHOCH, G.
Thermal management of propulsion systems in hypersonic vehicles
[AIAA PAPER 92-0516] p 373 A92-26942
EBERHARDT, SCOTT
Numerical simulation of total temperature separation in jets
[AIAA PAPER 92-0535] p 396 A92-26952
Diagonal implicit scheme for computing flows with finite rate chemistry p 488 A92-32253
BUWICE - An interactive icing program applied to engine inlets
[AIAA PAPER 92-3179] p 922 A92-48794
Optimization of a 2D scramjet-vehicle using CFD and simplified approximate flow analysis techniques
[AIAA PAPER 92-3673] p 1022 A92-54116
EBERLE, A.
Application of the Euler method EUFLEX to a fighter-type airplane configuration at transonic speed
[AIAA PAPER 92-2620] p 845 A92-45573
CFD contributions during hypersonic airplane intake design p 769 N92-27472
Evaluation of an unsteady implicit Euler code against two and three-dimensional standard configurations
p 719 N92-27945
CFD contributions during hypersonic airplane intake design
[MBB/FE213/S/PUB/459] p 944 N92-30676
EBERSOLE, TAMMY S.
Development of composite structures with enhanced damage tolerance p 985 A92-51555
EBRAHIMI, HOUSHANG B.
Two and three dimensional parabolized Navier-Stokes code for scramjet combustor, nozzle, and film cooling analysis
[AIAA PAPER 92-0391] p 372 A92-26247
EBRAHIMI, NADER
Estimating the reliability of a system on the basis of sample paths
[AD-A248585] p 774 N92-28171
EBRAHIMI, Y. S.
Design of localizer capture and track hold for a transport airplane - An H(infinity)/LTR approach
p 52 A92-11583
ECCLES, E. S.
Applications of silicon hybrid multi-chip modules to avionics p 859 N92-28379
ECCLES, LEE H.
New Boeing flight test data acquisition systems
p 920 A92-47537
ECHIN, A. I.
Viscosity characteristics of synthetic aviation oils at low temperatures p 1105 A92-53875
ECIJA, J. B.
Fuzzy guidance system evaluation
p 778 N92-27903
ECKBRETH, ALAN C.
CARS temperature/multi-species measurement strategies for high speed airbreathing and rocket propulsion testing p 154 A92-16615
Simultaneous coherent anti-Stokes Raman *spectroscopy measurements in hydrogen-fueled* supersonic combustion p 287 A92-21052
ECKERLE, W. A.
Aerating fuel nozzle design influences on airflow features p 129 A92-17176
Experimental measurement of the vortex development downstream of a lobed forced mixer
[ASME PAPER 90-GT-27] p 295 A92-23299
ECKERSEY, JOHN S.
Shot peening - Theory and applications
[ISBN 2-907669-18-4] p 676 A92-40400
ECKERT, E. R.
Studies of gas turbine heat transfer: Airfoil surfaces and end-wall cooling effects
[AD-A244055] p 376 N92-19097
ECKSTROM, CLINTON V.
The benchmark aeroelastic models program: Description and highlights of initial results
[NASA-TM-104180] p 185 N92-15049
Unsteady-pressure and dynamic-deflection measurements on an aeroelastic supercritical wing
[NASA-TM-4278] p 445 N92-20654
The benchmark aeroelastic models program: Description and highlights of initial results
p 721 N92-27960
EDIE, JOSEPH
IsoDoppler and mocomp corrections improve MTI radar p 898 A92-45774
EDINGTON, LARRY
PAYCOS, a multidisciplinary sizing code for hypersonic vehicles
[AIAA PAPER 92-4564] p 1132 A92-55376
EDMONDS, JAE
Designing a methodology for future air travel scenarios p 409 N92-19125
EDWARDS, DAVID E.
Unsteady analysis of hot streak migration in a turbine stage p 399 A92-28537
EDWARDS, GERALDINE F.
Dynamic wind tunnel tests on control of forebody vortices with suction p 380 N92-18793
EDWARDS, JACK R.
A nonlinear relaxation/quasi-Newton algorithm for the compressible Navier-Stokes equations
[AIAA PAPER 92-2643] p 796 A92-45510
Numerical simulations using a dynamic solution-adaptive grid algorithm, with applications to unsteady internal flows
[AIAA PAPER 92-2719] p 803 A92-45557
EDWARDS, JOAN
A full mission simulation data system
p 162 A92-14367
EDWARDS, JOHN A.
Experimental investigation of supersonic flow over two cavities in tandem p 610 A92-36830
EDWARDS, JOHN W.
Current status of computational methods for transonic unsteady aerodynamics and aeroelastic applications
[NASA-TM-104191] p 446 N92-21432
Current status of computational methods for transonic unsteady aerodynamics and aeroelastic applications
p 718 N92-27937
EDWARDS, R. W.
An approach for increasing aeroelastic divergence dynamic pressure of wind-tunnel models
[AIAA PAPER 92-4002] p 1099 A92-56825
EDWARDS, T.
High temperature, thermally stable JP fuels - An overview
[AIAA PAPER 92-0683] p 389 A92-27050
EDWARDS, THOMAS A.
Application of computational fluid dynamics to sonic boom near- and mid-field prediction
p 1031 A92-56173
EDWARDS, TIM
Deposition during vaporization of jet fuel in a heated tube
[AIAA PAPER 92-0687] p 390 A92-27054
EFIMOV, O. E.
A second-order control optimization method for *nonlinear dynamic systems* and its use for calculating optimal aircraft trajectories p 460 A92-31894
EFIMTSOV, B. M.
Transverse correlation of the spectral components of pressure fluctuations on a plate ahead of a step
p 426 A92-30187
EFREMOV, I. I.
Vibration of a wing of finite span in subsonic flow at small distances from a solid boundary p 9 A92-12808
An aerodynamic hypothesis for the wing aeroelasticity problem p 761 A92-42665
EGENBURG, LAZAR' I.
Evolution of ejection systems p 262 A92-21684
EGOLF, T. A.
Navier-Stokes and Euler solutions for an unmanned *aerial vehicle*
[AIAA PAPER 92-2609] p 792 A92-45483
Initial validation of an unsteady Euler/Navier-Stokes flow solver for helicopter rotor airloads in forward flight
p 815 A92-46956
EGOROV, IU. A.
From the history of Soviet aviation - Aircraft of the Il'iushin design bureau (2nd revised and enlarged edition)
p 61 A92-15022
EGUCHI, K.
Advanced SCRAM-LACE system concept for single-stage-to-orbit space plane
[IAF PAPER 91-272] p 32 A92-12599
EGUCHI, KUNIHISA
Key design considerations for scramjet powered space plane p 1066 A92-53491
An advanced scramjet propulsion concept for a 350 MG SSTO space plane - External nozzle performance
[AIAA PAPER 92-3719] p 1067 A92-54134
EHERNBERGER, L. J.
Atmospheric analysis for airdata calibration on research aircraft
[AIAA PAPER 92-0293] p 369 A92-25746
EHLER, T.
Gamma Group-The Pale Horse: A proposal in response to a commercial air transportation study ort study
[NASA-CR-190019] p 731 N92-26435
EHLERS, STEVEN M.
Effect of adaptive material properties on static aeroelastic control
[AIAA PAPER 92-2526] p 539 A92-34373
EHLERS, STEVEN MICHAEL
Aeroelastic behavior of an adaptive lifting surface
p 443 N92-20378
EHRENFRIED, K.
Sound produced by vortex-airfoil interaction
p 1136 A92-56345
EIBERT, MAX
Laser-radar based obstacle avoidance system for helicopters p 1064 A92-56295
EICH, T.
Particle image velocimetry measurements of the aerodynamics of a wind turbine p 1115 A92-54337
EICK, C. D.
Experimental modeling of film-cooled axial turbine tip seals
[AIAA PAPER 92-4058] p 1119 A92-56141
EICKHOFF, H.
Particle dispersion in highly swirling, turbulent flows
p 675 A92-40093
EIDELMAN, S.
Review of propulsion applications and numerical simulations of the pulsed detonation engine concept
p 129 A92-17177
A parametric study of airbreathing Pulsed Detonation Engine
[AIAA PAPER 92-0392] p 471 A92-31660
EIDINOFF, HARVEY
Computational structures technology at Grumman: Current practice/future needs p 684 N92-25930
EIGL, CHRISTIAN
International standardization p 533 A92-33441
EIKEL, HARVEY A.
Aviation Diagnostics And Maintenance (ADAM) system preliminary concept of operation and functional *description*
[AD-A242598] p 170 N92-14966
EISEMAN, P. R.
Numerical grid generation in computational fluid dynamics and related fields; Proceedings of the 3rd International Conference, Universidad Politecnica de Cataluna, Barcelona, Spain, June 3-7, 1991
[ISBN 0-444-88948-5] p 918 A92-47035
EISENBERG, B.
Design and testing of a controlled diffusion airfoil cascade for industrial axial flow compressor application
[ASME PAPER 90-GT-140] p 6 A92-11286
EISENHOWER, E. H.
Criteria for the operation of federally-owned secondary calibration laboratories (ionizing radiation)
[PB92-112481] p 485 N92-21777
EISLER, G. R.
A guidance law for hypersonic descent to a point
[AIAA PAPER 92-4303] p 1104 A92-55311
EISSFELLER, B.
Navsat - A civil complement to GPS and Glonass
[IAF PAPER 91-490] p 188 A92-18505

EITELBERG, G.
Preliminary laser induced fluorescence measurements in several facilities in preparation for application to studies in the high enthalpy shock tunnel Goettingen (HEG)
[AIAA PAPER 92-0143] p 284 A92-23761
The high enthalpy shock tunnel in Goettingen
[AIAA PAPER 92-3942] p 1104 A92-56772
EJIRI, M.
Polar patrol balloon
[AIAA PAPER 91-3688] p 15 A92-11031
EKATERINARIS, JOHN A.
Unsteady airfoil flow solutions on moving zonal grids
[AIAA PAPER 92-0543] p 342 A92-28200
EKLUND, DEAN R.
A numerical study of the effects of geometry on the performance of a supersonic combustor
[AIAA PAPER 92-0624] p 342 A92-28213
EL-BANNA, HESHAM M.
Determination of aerodynamic sensitivity coefficients for wings in transonic flow
[NASA-CR-190570] p 832 N92-29657
EL-HADY, NABIL M.
Secondary instability of high-speed flows and the influence of wall cooling and suction
p 435 A92-31640
Secondary instability of high-speed flows and the influence of wall cooling and suction
[NASA-CR-4427] p 406 N92-19844
EL-SHAFEI, A.
Stability of intershaft squeeze film dampers
p 222 N92-14351
EL-SHAFEL, A.
Experimental and analytical investigation of hybrid squeeze film dampers
[ASME PAPER 91-GT-250] p 150 A92-15655
EL-SHARAWY, EL-BUDAWY
Advanced electromagnetic methods for aerospace vehicles
[NASA-CR-188630] p 488 N92-20193
Advanced electromagnetic methods for aerospace vehicles
[NASA-CR-190650] p 1001 N92-31156
ELALDI, F.
Processing and environmental effects on mechanical properties of composite repairs
[NRC-LTR-ST-1826] p 1109 N92-32791
ELARIO, DAVID S.
NASA advanced aeronautics design solar powered remotely piloted vehicle
[NASA-CR-190007] p 462 N92-20665
ELAZAR, DAVID
NASA/DOD Aerospace Knowledge Diffusion Research Project. Paper 14: An analysis of the technical communications practices reported by Israeli and US aerospace engineers and scientists
[NASA-TM-107924] p 782 N92-28183
ELBANNA, HESHAM M.
Determination of aerodynamic sensitivity coefficients based on the three-dimensional full potential equation
[AIAA PAPER 92-2670] p 798 A92-45525
ELBER, WOLF
Probabilistic fatigue methodology for six nines reliability p 145 A92-14342
ELDER, J.
Recombination-dominated nonequilibrium heat transfer to arbitrarily catalytic hypersonic vehicles
p 2 A92-10426
ELDER, M. G.
Analytical and experimental studies of heat pipe radiation cooling of hypersonic propulsion systems
[AIAA PAPER 92-3809] p 867 A92-49128
Analytical and experimental studies of heat pipe radiation cooling of hypersonic propulsion systems
[DE92-013428] p 973 N92-31817
ELDER, R. L.
Fibre optic laser anemometry for turbomachinery applications p 397 A92-27783
Radial inflow turbine study
[AD-A240169] p 26 N92-11015
Radial inflow turbine study
[AD-A246938] p 743 N92-28073
Radial inflow turbine study
[AD-A252783] p 1127 N92-33538
ELDREDGE, DONALD
A review and discussion of flight management system incidents reported to the aviation safety reporting system
[AD-A252438] p 1043 N92-32941
ELENEVSKII, D. S.
Holographic-interferometry methods employed for vibration-strength testing of aviation-engine workpieces
p 219 A92-20771
ELESHAKY, MOHAMAD E.
Aerodynamic design optimization using sensitivity analysis and computational fluid dynamics
[NASA-CASE-LAR-14815-1-CU] p 910 N92-29830
ELESHAKY, MOHAMED E.
Aerodynamic sensitivity analysis methods for the compressible Euler equations p 233 A92-19619
Aerodynamic design optimization using sensitivity analysis and computational fluid dynamics
p 340 A92-28044
Computations of multispecies mixing between scramjet nozzle flow and hypersonic freestream
p 376 A92-28534
ELGERSMA, MIKE
New methods in robust control
[AD-A240221] p 29 N92-11018
ELGHOBASHI, S.
Three-dimensional flow computation for two interacting, moving droplets
[AIAA PAPER 92-0343] p 496 A92-31655
ELGHOBASHI, S. E.
Fundamental studies on droplet interactions in dense sprays
[AD-A246918] p 770 N92-27546
ELIASSON, P.
Hypersonic flow past delta wing flow simulated by Navier-Stokes solutions p 180 N92-14981
ELIASSON, PETER
Generation of efficient multiblock grids for Navier-Stokes computations p 919 A92-47081
Calculation of hypersonic leeside vortices over blunt delta wings p 84 N92-13004
Hypersonic laminar flow computations over a blunt leading edged delta wing at three different chord Reynolds numbers
[FFA-TN-1991-40] p 528 N92-23168
ELIZAROV, A. M.
Design and optimization of airfoils in non-stalling incompressible flow with a prescribed range of the angle of attack p 933 A92-49556
Aerodynamic airfoils design by quasi-solutions method of inverse boundary-value problems
p 1020 A92-53998
ELLIN, A. D. S.
Tail rotor aerodynamic features recorded in flight
p 546 A92-35752
ELLIOT, SIMON
Flying on thin ice p 634 A92-38375
ELLIOTT, ANDREW S.
Dynamic response of a variable-speed rotor during rapid shaft tilt p 132 A92-14400
ELLIOTT, J. K.
Recent CFD applications on jet transport configurations
[AIAA PAPER 92-2658] p 844 A92-45519
Computational and experimental studies of flow in multi-lobed forced mixers
[AIAA PAPER 92-3568] p 1112 A92-54057
ELLIOTT, JOE W.
Comparison of frequency domain and time domain laser velocimeter signal processors p 1114 A92-54314
ELLIOTT, S. J.
Active control of sound transmission through stiff lightweight composite fuselage constructions
p 1137 N92-32957
ELLIOTT, SIMON
Damping down the fires p 350 A92-25075
Mass-transporter p 543 A92-34650
ELLIS, JOHN
Test plan for the international aircraft operator information system
[DOT/FAA/CT-91/18] p 781 N92-26830
ELLIS, KEN
Airbus - The family expands p 419 A92-30092
ELLIS, S. C.
The effects of inner wake modelling on blade airloads
p 521 A92-35784
ELLROTT, ANTJE
Preliminary design and lay-out of an infant restraint system p 449 N92-21513
ELLSWORTH, R. H.
Airfoil boundary layer measurements at low Re in an accelerating flow from a nonzero velocity
p 62 A92-13673
ELROD, W. C.
Wake mixing and performance measurements in a linear compressor cascade with crenulated trailing edges
[AIAA PAPER 92-3188] p 824 A92-48800
ELSENAAR, A.
An experimental study of the flow over a sharp-edged delta wing at subsonic and transonic speeds
p 85 N92-13011
The windtunnel as a tool for laminar flow research
[NLR-TP-90145-U] p 887 N92-28661
Instrumentation requirements for laminar flow research in the NLR high speed wind tunnel HST
[NLR-TP-89158-U] p 887 N92-28669
An experimental study of the flow over a sharp-edged delta wing at subsonic and transonic speeds
[NLR-TP-91117-U] p 1037 N92-32732
ELSNER, JANUSZ W.
An analysis of the flow-pattern at the exit of a single-stage turbine p 10 A92-13234
ELWELL, D.
Avionic data bus integration technology
[DOT/FAA/CT-91/19] p 736 N92-27973
ELY, W. L.
A computational exploration of the importance of three-dimensionality, boundary layer development, and flow chemistry to the prediction of scramjet nozzle performance
[AIAA PAPER 91-5059] p 472 A92-31689
EMAMI-NAEINI, ABBAS
Robust control law development for a hypersonic cruise aircraft p 478 A92-29127
EMANUEL, G.
Oblique shock wave with sweep p 613 A92-38370
EMANUELY, J. L.
Study of simulated lightning discharge effects on wires of a rotorcraft
[ONERA, TP NO. 1991-173] p 92 A92-16137
EMBORG, URBAN
Coupled propeller contributions to aircraft noise and vibration p 694 A92-39085
Advanced Study for Active Noise Control in Aircraft (ASANCA)
[AIAA PAPER 92-2092] p 1137 N92-32956
EMEL'IANOV, V. E.
Methyl-tert-butyl ether as a component of aviation gasolines p 34 A92-12146
EMMERSON, A. J.
Aging commuter aeroplanes: Fatigue evaluation and control methods p 915 N92-30132
EMO, S. M.
Integrated optic components for advanced turbine engine control systems p 925 A92-46248
ENDE, H.
Millisecond aerodynamic force measurement with side-jet model in the ISL shock tunnel
[AIAA PAPER 92-3963] p 1097 A92-56790
ENDOH, M.
Conceptual study of separated core ultra high bypass engine
[AIAA PAPER 92-3775] p 867 A92-49119
ENDOH, MASANORI
Research on a low-noise engine for a high-speed VTOL aircraft p 737 A92-43239
Design and off-design point characteristics of Separated Core Ultra High Bypass Engine (SCUBE)
[AIAA PAPER 92-3776] p 867 A92-49120
ENGE, JAMES
Digital analysis of wind tunnel imagery to measure fluid thickness
[NASA-CR-189234] p 983 N92-31252
ENGEL, GEORGE BRYAN
The FM-007: An advanced jet commuter for HUB to spoke transportation
[NASA-CR-189988] p 461 N92-20267
ENGELUND, WALTER C.
Computations of multispecies mixing between scramjet nozzle flow and hypersonic freestream
p 376 A92-28534
Viscous computations of cold air/air flow around scramjet nozzle afterbody
[NASA-CR-4406] p 13 N92-10982
ENGHOLM, C.
Lightning activity in microburst producing storm cells
[ONERA, TP NO. 1991-98] p 161 A92-16080
ENGLER, P.
The use of CT for dimensional measurements of green and sintered ceramic components p 490 A92-28592
ENGLER, R. H.
Aerodynamic assessment of an optical pressure measurement system (OPMS) by comparison with conventional pressure measurements in a high speed wind tunnel p 1114 A92-54304
ENGLISH, C.
Inertia-friction welding of an advanced rapidly solidified titanium alloy p 212 A92-18898
ENGLISH, THOMAS
Tactical Rubidium Frequency Standard (TRFS)
[AD-A243934] p 401 N92-18897
ENGLUND, DAVID R.
Research sensors p 594 N92-22526
ENIUTIN, G. V.
Effect of the longitudinal and transverse riblets of a flat plate on laminar-to-turbulent transition
p 428 A92-30210
ENNS, DALE
Abstract model and controller design for an unstable aircraft p 380 A92-28153
ENNS, DALE F.
Nonlinear control law with application to high angle-of-attack flight p 661 A92-39904
Nonlinear inversion flight control for a supermaneuverable aircraft p 873 A92-46751

Application of nonlinear feedback control theory to supermaneuverable aircraft
[NASA-CR-190336] p 663 N92-25648
ENTSTRASSER, NORBERT
Measurements in the inhomogeneous convective boundary layer using three powered gliders
p 775 N92-26350
ENVIA, EDMANE
Prediction of noise field of a propfan at angle of attack
[NASA-CR-189047] p 166 N92-13759
ENYA, SHINTARO
Fundamental studies on Marangoni convection related to Bridgman crystal growth p 1111 A92-53758
EPSTEIN, A. H.
Active control of rotating stall in a low speed axial compressor
[ASME PAPER 91-GT-88] p 122 A92-15553
Comparison of time-resolved turbine rotor blade heat transfer measurements and numerical calculations
[ASME PAPER 91-GT-268] p 151 A92-15666
Parameter identification of compressor dynamics during closed-loop operation p 508 A92-29313
Self-adaptive aeropropulsion components-enhancing axial compressor performance
[AD-A246123] p 743 N92-27817
Dynamic control of aerodynamic instabilities in gas turbine engines p 870 N92-28466
Active control of compressor surge and stall
[AD-A252771] p 1126 N92-33498
EPSTEIN, B.
Euler solver for arbitrary configurations: Further applications p 949 N92-31888
EPSTEIN, BORIS
Cartesian Euler method for arbitrary aircraft configurations p 340 A92-28039
EPTON, MICHAEL A.
PAN AIR: A computer program for predicting subsonic or supersonic linear potential flows about arbitrary configurations using a higher order panel method. Volume 1: Theory document (version 3.0)
[NASA-CR-3251] p 526 N92-22648
ERB, DONA M.
Case for real-time systems development - Quo vadis?
[AIAA PAPER 91-3726] p 231 A92-17594
ERBLAND, PETER J.
Fiber optics for the National Aero-Space Plane
p 386 A92-24780
ERCOLINE, WILLIAM R.
Effects of variations in head-up display airspeed and altitude representations on basic flight performance
p 46 A92-11204
The standardization of military head-up display symbology p 855 A92-44929
An aircraft landing accident caused by visually induced spatial disorientation p 834 A92-44993
The utility of analog vertical velocity information during instrument flight with a Head-Up Display (HUD)
[AD-A252863] p 1065 N92-33277
ERDMAN, PETER W.
Examination of ultraviolet radiation theory for bow shock rocket experiments
[AIAA PAPER 92-2871] p 901 A92-47853
ERDOGAN, TEMEL
Global positioning system supported pilot's display
p 534 N92-22436
ERDOS, J. I.
Hypersonic mixing and combustion studies in the hypulse facility p 737 A92-44526
ERDOS, JOHN
Engineering model for analysis of scramjet combustor performance with finite-rate chemistry
p 129 A92-17202
Experiments on shear layer mixing at hypervelocity conditions
[AIAA PAPER 92-0628] p 396 A92-27009
ERDOS, JOHN I.
Pioneering scramjet developments by Antonio Ferri
p 474 N92-21519
ERENGIL, M. E.
Correlation of separation shock motion with pressure fluctuations in the incoming boundary layer
p 5 A92-11061
Effects of sweepback on unsteady separation in Mach 5 compression ramp interactions
[AIAA PAPER 92-0430] p 435 A92-31663
EREZA, A. G.
Reducing the background noise level in the test section *of a wind tunnel for transonic flow velocities*
p 511 A92-30143
ERHART, J. J.
Application of computational fluid dynamics to pitch/yaw thrust vectoring spherical convergent flap nozzles
p 737 A92-44511
ERICKSON, GARY E.
Wind tunnel investigation of the interaction and breakdown characteristics of slender wing vortices at subsonic, transonic, and supersonic speeds
[NASA-TP-3114] p 82 N92-12994
Wind tunnel investigation of vortex flows on F/A-18 configuration at subsonic through transonic speed
[NASA-TP-3111] p 179 N92-14968
ERICKSON, J. C.
A wall interference assessment/correction system
[NASA-CR-189785] p 259 N92-15974
ERICKSON, J. J.
Detailed investigation of causes of avionics field failures p 995 A92-51925
ERICKSON, JEFFERY B.
Assessment of cockpit interface concepts for data link retrofit
[NASA-CR-187615] p 268 N92-17512
An exploration of function analysis and function *allocation in the commercial flight domain*
[NASA-CR-4374] p 368 N92-19871
ERICKSON, RICHARD A.
Development of an annoyance model based upon elementary auditory sensations for steady-state aircraft interior noise containing tonal components
[NASA-TM-104147] p 166 N92-13758
ERICKSON, WAYNE D.
Analysis of hypersonic nozzles including vibrational nonequilibrium and intermolecular force effects
[AIAA PAPER 92-0330] p 322 A92-25777
ERICSSON, K. ANDERS
Introduction to cognitive processes of expert pilots
[DOT/FAA/RD-92/12] p 952 N92-30980
ERICSSON, L. E.
Future experimental needs in high-alpha vehicle dynamics
[AIAA PAPER 92-0159] p 254 A92-23774
Effect of leading-edge cross-sectional geometry on slender wing unsteady aerodynamics
[AIAA PAPER 92-0173] p 255 A92-23784
Rapid prediction of high-alpha unsteady aerodynamics of slender-wing aircraft p 309 A92-24412
Unique high-alpha roll dynamics of a sharp-edged 65 deg delta wing
[AIAA PAPER 92-0276] p 318 A92-25730
Some thoughts on conical flow asymmetry
[AIAA PAPER 92-0427] p 326 A92-26275
Separation-induced self-excited structural oscillations
[AIAA PAPER 92-0486] p 328 A92-26317
Ground facility interference on aircraft configurations with separated flow
[AIAA PAPER 92-0673] p 384 A92-27042
Dynamic LEX/forebody vortex interaction effects
[AIAA PAPER 92-2732] p 804 A92-45566
Multiple roll attractors of a delta wing at high incidence p 88 N92-13026
ERICSSON, LARS E.
Fickle effect of nose microasymmetry on the high-alpha aerodynamics p 10 A92-13217
ERIKSON, CAROL A.
Getting expert systems off the ground: Lessons learned from integrating model-based diagnostics with prototype flight hardware p 220 N92-14217
ERIKSSON, K. G.
Analysis of Euler's and stress tensor methods for calculating power consumption of high speed centrifugal fans and turbocompressors
[DE92-728396] p 298 N92-16325
Calculation of local power consumptions and efficiencies of centrifugal fans and turbocompressors
[DE92-728402] p 298 N92-16326
ERKELENS, L. J. J.
Development of new flight procedures for the Microwave Landing System (MLS)
[NLR-TP-91156-U] p 1047 N92-32830
ERLEBACHER, GORDON
On the nonlinear stability of a high-speed, axisymmetric boundary layer p 78 A92-16457
Secondary instabilities in compressible boundary layers p 435 A92-31639
A weakly nonlinear theory for wave-vortex interactions in curved channel flow
[NASA-TP-3158] p 347 N92-19175
ERM, L. P.
A review of Australian activity on modelling the helicopter/ship dynamic interface p 465 N92-21967
ERMAK, IU. N.
Flow of a viscous twisted fluid film on the surface of a blunt body in supersonic flow of a gas
p 424 A92-30146
A study of flow of a fluid film on the surface of a plate in the case of slot injection p 496 A92-31892
ERMAKOVA, E. V.
Determination of physicochemical constant in the wake of a body from ballistic experiments p 609 A92-36549
ERMOLAEV, V. P.
Control of the development of boundary layer disturbances p 423 A92-30126
Flight studies of the riblet effect on drag variation
p 438 A92-31871
ERNST, MICHAEL A.
Determining structural performance
p 560 N92-22519
EROGLU, HASAN
LDV measurements and investigation of flow field through radial turbine guide vanes p 217 A92-19618
ERRERA, M.
Presentation of a computational code for 3-D compressible flow in complex channels and cavities
p 769 N92-27475
ERSHOV, B. A.
A mathematical model for the hydroelasticity problem concerning the motion of two flexible profiles in an ideal incompressible fluid. I p 712 A92-44127
ERSHOV, V. N.
Analysis of transonic flow over plane compressor cascades using the large-particle method
p 79 A92-16812
ERUSALIMSKII, M. A.
Determination of the mean duration of normal acceleration loads at the center of mass of aircraft during a flight in a turbulent atmosphere p 480 A92-30192
ERVIN, CAY A.
Improving reliability and maintainability through process management p 1141 A92-56212
ERWIN, D. A.
An iodine hypersonic wind tunnel for the study of nonequilibrium reacting flows
[AIAA PAPER 92-0566] p 383 A92-26974
A code validation strategy and facility for nonequilibrium, reacting flows
[AIAA PAPER 92-3970] p 1098 A92-56796
ERWIN, DANIEL
Experimental unsteady pressures on an oscillating cascade with supersonic leading edge locus
[AIAA PAPER 92-4035] p 1035 A92-56857
ERWIN, DANIEL A.
A new technique for temperature and specie concentration measurements in unseeded supersonic and hypersonic gas flows
[AD-A241536] p 158 N92-13409
ERZBERGER, HEINZ
CTAS: Computer intelligence for air traffic control in the terminal area
[NASA-TM-103959] p 1044 N92-33080
Analysis of delay reducing and fuel saving sequencing and spacing algorithms for arrival traffic
[NASA-TM-103880] p 1044 N92-33194
ESCANDE, B.
Comparison between two 3D-NS-codes and experiment on a turbine stator
[AIAA PAPER 92-3042] p 822 A92-48703
ESCANDE, BEATRICE
Validation of a CANARI code by the computation of three dimensional turbulent flow in turbine valve
p 741 N92-27462
ESCHBAUMER, HERMANN
Repair procedures for advanced composites for helicopters p 1016 A92-56277
Repair procedures for advanced composites for helicopters
[MBB-UD-0606-91-PUB] p 787 N92-29874
ESCHENAUER, H. A.
Multidisciplinary optimization of fiber composite aircraft structures
[MBB/FW321/S/PUB/476] p 961 N92-30424
ESCHER, WILLIAM J. D.
Cryogenic hydrogen-induced air-liquefaction technologies for combined-cycle propulsion applications
p 487 N92-21526
ESCOBAR, D. E.
A high resolution multispectral video system
p 587 A92-35479
ESER, S.
Advanced thermally stable jet fuel development program. Volume 2: Compositional factors affecting thermal degradation of jet fuels
[AD-A252656] p 987 N92-31399
ESFAHANIAN, V.
Computation of laminar flow over a long slender axisymmetric blunted cone in hypersonic flow
[AIAA PAPER 92-0756] p 336 A92-27098
ESFAHANIAN, VAHID
Computation and stability analysis of laminar flow over a blunt cone in hypersonic flow p 1041 N92-33839
ESHOW, MICHELLE M.
Flight investigation of variations in rotorcraft control and display dynamics for hover p 379 A92-28151
A review of recent programs and future plans for rotorcraft in-flight simulation at Ames Research Center
[SAE PAPER 912121] p 608 A92-39969

Rotorcraft In-Flight Simulation Research at NASA Ames Research Center: A Review of the 1980's and plans for the 1990's
[NASA-TM-103873] p 853 N92-28926
ESKELINEN, PEKKA
A computerized flight inspection system
p 726 A92-43881
ESKER, BARBARA S.
Experimental performance of three design factors for ventral nozzles for SSTOVL aircraft
[AIAA PAPER 92-3789] p 1069 A92-54168
Internal reversing flow in a tailpipe offtake configuration for SSTOVL aircraft
[AIAA PAPER 92-3790] p 1069 A92-54169
Experimental performance of three design factors for ventral nozzles for SSTOVL aircraft
[NASA-TM-105697] p 742 N92-27669
Internal reversing flow in a tailpipe offtake configuration for SSTOVL aircraft
[NASA-TM-105698] p 868 N92-28418
ESPINOSA, PAUL S.
Tiltrotor research aircraft composite blade repairs: Lessons learned
[NASA-TM-103875] p 367 N92-19563
ESTABROOK, POLLY
ACTS aeronautical experiments
[AIAA PAPER 92-2042] p 485 A92-29956
ESTEN, GUY M.
National airspace data interchange network analysis
[AD-A247345] p 727 N92-27217
ESTRADA ALVES, CARLOS F.
Some thermodynamical aspects in the optimization of supersonic combustors p 1065 A92-53486
The behaviour of the pressure temperature and density in an inviscid unsteady transonic axisymmetric flow with shock waves p 1018 A92-53553
ESWARA, VENKATASAM
The relationship between mode localization and energy transmission parameters in the vibration of coupled structures p 925 A92-45921
ETTER, S.
Design of a small axial compressor for high efficiency over a wide operating range
[ASME PAPER 91-GT-195] p 124 A92-15620
EUFRI, D.
An application of distributed environment in flight simulation p 602 A92-35739
EULER, HANS-JUERGEN
A system for precise real-time differential GPS positioning in the decimeter range p 638 A92-39569
EUSTACE, JOHN G.
Wavelength-multiplexed fiber-optic position encoder for aircraft control systems p 734 A92-42602
EUSTACE, R. W.
F-111C flight dynamic model aerodynamic data-base development and verification
[AD-A246356] p 715 N92-26947
EVANOFF, GEORGE A., JR.
Mid-range UV communications
[AD-D015213] p 770 N92-27615
EVANS-MORGIS, JEANNETTE
Pocono Mountain SAR data analysis for testing slant range to ground range conversion p 587 A92-35142
EVANS, A.
Mesh adaptivity with the quadtree method
p 816 A92-47041
EVANS, AUSTIN L.
Activities for numerical propulsion systems simulation program p 692 N92-25726
EVANS, DARRYL
Preliminary design studies of an advanced general aviation aircraft
[NASA-CR-190024] p 461 N92-20064
EVANS, JAMES M.
Testing of the high accuracy inertial navigation system in the Shuttle Avionics Integration Lab
p 210 N92-14087
EVANS, R. H.
Lightning protection requirements for aircraft: A proposed specification
[RAE-TM-FS(F)-632-REV-ISSUE] p 187 N92-14007
EVANS, R. W.
Prediction of long-term creep rupture properties for an aluminium alloy for airframe applications
p 141 A92-15206
EVANS, RICHARD H.
The utility of analog vertical velocity information during instrument flight with a Head-Up Display (HUD)
[AD-A252863] p 1065 N92-33277
EVDOKIMOV, A. I.
A method for estimating the technological and economic efficiency of measures enhancing the reliability of aviation gas turbine engines p 657 A92-40621
EVEKER, K. M.
Model development for active surge control/rotating stall avoidance in aircraft gas turbine engines
p 468 A92-29375
EVEREST, A. W.
Prototype instrumentation and design studies
[AD-A248378] p 736 N92-28004
EVERETT, R. A.
Fatigue crack initiation and small crack growth in several airframe alloys p 212 A92-19754
EVERETT, RICHARD A., JR.
Probabilistic fatigue methodology for six nines reliability p 145 A92-14342
A comparison of fatigue life prediction methodologies for rotorcraft p 647 A92-40884
EVERHART, JOEL L.
Engineering method for aero-propulsive characteristics at hypersonic Mach numbers
[AIAA PAPER 91-5061] p 437 A92-31690
Test description and preliminary pitot-pressure surveys for Langley Test Technique Demonstrator at Mach 6
[AIAA PAPER 92-3940] p 1096 A92-56770
Mass flux similarity for slotted transonic-wind-tunnel walls
[NASA-TM-4281] p 11 N92-10006
EVERITT, J. H.
A high resolution multispectral video system
p 587 A92-35479
EVERSMAN, WALTER
Chaotic and nonlinear dynamic response of aerosurfaces with structural nonlinearities
[AIAA PAPER 92-2547] p 518 A92-34517
Theoretical models for duct acoustic propagation and radiation p 236 N92-14782
EVERSON, H.
Steels for aerospace applications p 986 A92-52983
EVERSON, R. M.
Eigenfunction analysis of turbulent mixing phenomena
p 898 A92-45826
EVERTON, E. L.
Gridding strategies and associated results for winged entry vehicles p 918 A92-47051
Grid generation and compressible flow computations about a high-speed civil transport configuration
p 919 A92-47055
EVSEEV, D. D.
Reduction of computational models in strength problems p 496 A92-31858
EWALD, B.
The cryogenic balance design and balance calibration methods
[AIAA PAPER 92-4001] p 1122 A92-56824
EWALD, J.
FALKE and COBRA technology development in aerodynamics and aerothermodynamics
p 183 N92-15017
EXLEY, J. T.
Mixed flow compressor surge margin gain using a manifolded diffuser system
[AIAA PAPER 92-3753] p 1068 A92-54151
EYTH, JACOB, JR.
Design and performance of the centrifuge-based Dynamic Flight Simulator
[AIAA PAPER 92-4156] p 981 A92-52446
EZZO, MAUREEN B.
Flight service evaluation of composite helicopter components p 106 A92-14372

F

FADLALLA, A. A.
Prediction of long-term creep rupture properties for an aluminium alloy for airframe applications
p 141 A92-15206
FAGAN, J. R.
Impeller flow field measurement and analysis
[ASME PAPER 90-GT-146] p 38 A92-11288
FAGAN, JOHN R.
LDV measurements of a mixed-flow impeller at design and near stall
[ASME PAPER 91-GT-310] p 153 A92-15688
FAHEY, DAVID W.
Natural cycles, gases p 408 N92-19123
FAHNENBRUCK, GERHARD
Flying an aircraft as a problem-solving process: About the Instrument-Failure-Simulator (IFS) as a test for pilot-candidates
[DLR-FB-91-23] p 455 N92-20902
FAHR, A.
Inspection of compressor discs by ultrasonic leaky waves using an automated C-scan system
p 144 A92-13584
Inspection of aircraft engine components using automated eddy current and pattern recognition techniques
[NRC-LTR-ST-1834] p 504 N92-22029
FAHY, F. J.
Evaluation of sound transmission into aircraft fuselages by a reciprocity technique p 694 A92-39086
FAIRCHILD, JERRY F.
Boiling and condensing pumped loop microgravity experiment - Challenges of testing in both aircraft and rocket environments p 992 A92-50611
FAIRFIELD, M. S.
Aerodynamic effects on fuel spray structure - Experiment and theory
[AIAA PAPER 92-0227] p 317 A92-25691
FAL'KOV, ALEKSANDR I.
Flight test control p 136 A92-15021
FALASCO, THOMAS
H-76B Fantail demonstrator composite fan blade fabrication p 145 A92-14356
FALCHETTI, FREDERIC
Advanced CFD simulation and testing of compressor blading in the multistage environment
[AIAA PAPER 92-3040] p 822 A92-48701
FALCINELLI, D.
Limitations on helicopter operations in the aeronaval environment p 466 N92-21973
FALCOVITZ, JOSEPH
Semi-inverse marching characteristics scheme for supersonic flows p 432 A92-31187
FAN, GUANGHUA
Structural optimization and vibration control of composite rotor blades p 960 A92-53056
FAN, S.
Numerical simulation of turbomachinery flows with advanced turbulence models p 1124 N92-32270
FAN, YEPING
Experimental investigation on the structure of flow field and the total pressure loss in an atomizing channel injector p 375 A92-28436
Experimental technique of measuring fuel concentration in non-uniform flowfield p 734 A92-41928
FAN, YINHE
Prediction of low cycle fatigue life of engine cases
p 295 A92-23385
FAN, ZHAOLIN
Application of the wall pressure method to wall interference corrections for model tests at high angle of attack in high speed wind tunnel p 315 A92-25134
FAN, ZUOMIN
Integral minimization of engine fault equations based on least fault principle p 374 A92-27857
FANELLI, MADDALENA
Experimental and numerical investigation of anti-icing phenomena on a NACA 0012 assembly
[AIAA PAPER 92-0531] p 459 A92-31669
FANG, GANG
Second order perturbation method of gas turbine performance calculation p 759 A92-41834
FANG, J.
Aerodynamics of loaded cascades in subsonic flows subject to unsteady three-dimensional vortical disturbances
[AIAA PAPER 92-0146] p 253 A92-23762
FANG, K. C.
Tow-tank study of nonlinear aerodynamics of a 2-D airfoil
[AIAA PAPER 92-4499] p 1026 A92-55367
Nonlinear normal and axial force indicial responses for a two dimensional airfoil
[AD-A247196] p 830 N92-28888
FANG, LIANGWEI
Separation control by vortex generators in subsonic diffuser p 338 A92-27829
FANG, R.
Determination of limitations for helicopter ship-borne operations p 465 N92-21965
FANG, W.
Approximation methods for control of acoustic/structure models with piezoceramic actuators
[NASA-CR-189578] p 234 N92-15658
Active noise control: Piezoceramic actuators in fluid/structure interaction models
[NASA-CR-190328] p 685 N92-26125
FANG, XIAOQING
A new study on a class of discrete event dynamic systems p 48 A92-11377
FANG, ZONGDE
Vibration of gear system with web structure
p 588 A92-35573
Optimization of longitudinal corrections of helical gears p 990 A92-49578
On travelling wave vibration of high-speed duplex helical gears p 990 A92-49580

FANKHAUSER, JAMES C.
Use of distance-measuring equipment (DME) for correcting errors in position, velocity, and wind measurements from aircraft inertial navigation systems
p 188 A92-18172
FANNIN, HOMER W., JR.
Integration of supportability elements into the conceptual design process
[AIAA PAPER 92-1194] p 600 A92-33306
FANUCCI, JEROME P.
Measurement of basic material and processing properties affecting injection-pultrusion technology
p 580 A92-32636
FARASSAT, F.
Development of a shock noise prediction code for high-speed helicopters - The subsonically moving shock
p 165 A92-14384
High-speed propeller noise prediction - A multidisciplinary approach p 924 A92-45831
FARD, NASSER S.
Maintenance scheduling for critical parts of aircraft
p 699 A92-42054
FAREED, A. S.
Effect of sustained high temperature exposure on the mechanical properties of Nicalon/Al2O3 composites
p 668 A92-39672
FAREED, ALI S.
Fabrication and properties of fiber-reinforced ceramic composites made by directed metal oxidation
p 669 A92-39861
FARGE, TALIB Z.
Effect of flow rate on loss mechanisms in a backswept centrifugal impeller p 897 A92-45606
FARLEY, HAROLD C., JR.
F-117A flight test program p 112 A92-16061
FARMER, MOSES G.
The benchmark aeroelastic models program: Description and highlights of initial results
[NASA-TM-104180] p 185 N92-15049
The benchmark aeroelastic models program: Description and highlights of initial results
p 721 N92-27960
FARMER, ROY
The Mission Computer/Electronic Display Subsystem for the United States Air Force C-17A transport aircraft
[AIAA PAPER 92-1244] p 553 A92-33337
FARN, C. L. S.
Analysis and prediction of transonic turbine blade losses
[ASME PAPER 91-GT-183] p 73 A92-15615
FAROKHI, S.
Modern developments in shear flow control with swirl
p 703 A92-41265
A computational study of advanced exhaust system transition ducts with experimental validation
[AIAA PAPER 92-3794] p 907 A92-49126
FAROKHI, SAEED
A study of three dimensional turbulent boundary layer separation and vortex flow control using the reduced Navier Stokes equations p 621 A92-40105
Active flow control for twenty-first century high-performance aircraft with applications to land and sea vehicles p 447 N92-21504
FAROUK, B.
Numerical simulations of the structure of supersonic shear layers p 3 A92-10574
FARQUHAR, B. W.
Subsonic propulsion system installation analysis and optimization
[ASME PAPER 91-GT-167] p 111 A92-15602
FARR, N.
Grid generation and compressible flow computations about a high-speed civil transport configuration
p 919 A92-47055
FARRELL, JAMES L.
That all-important interface p 100 A92-16953
Receiver autonomous integrity monitoring (RAIM) - Techniques, performance and potential
p 638 A92-39567
FARRELL, MICHAEL K.
V-22 flight test aerodynamics p 104 A92-14333
FARSHCHI, MOHAMMAD
Automatic grid generation for iced airfoil flowfield predictions
[AIAA PAPER 92-0415] p 326 A92-26266
FASANELLA, EDWIN L.
Experimental and analytical study of the effects of floor location on response of composite fuselage frames
[AIAA PAPER 92-2473] p 539 A92-34362
FASEL, H.
Evolution of coherent structures during transition in a flat-plate boundary layer p 621 A92-40126
FASSI, F.
AM-X flight simulator from engineering tool to training device p 884 N92-28536
FASTL, HUGO
Trading number of operations versus loudness of aircraft p 688 A92-39102
FAUBERT, D.
Multiple phase centre DPCA for airborne radar
p 95 A92-16257
FAULKNER, A.
Experience with piloted simulation in the development of helicopters p 884 N92-28528
Experience with piloted simulation in the development of helicopters
[MBB-UD-0610-91-PUB] p 889 N92-30076
FAULKNER, H. B.
Currently available fuel gas booster compressor equipment for small gas turbine engines
[PB92-127026] p 499 N92-20265
FAULSTICH, RAYMOND J.
Common airborne instrumentation system (CAIS)
p 856 A92-47538
FAURE, J. C.
Mechanical qualification tests for materials used in the fabrication of aircraft parts
[CEAT-M5-5443/01] p 195 N92-14042
FAVINI, B.
Nonequilibrium hypersonic inviscid steady flows
p 176 A92-20737
Influence of chemical modeling on the solution of hypersonic shock layers p 183 N92-15016
FAVORSKII, V. S.
Effect of rarefaction on the nonstationary interaction of a supersonic underexpanded jet with a perpendicular obstacle p 337 A92-27594
FAVOT, JEAN-JACQUES
Concept for future cockpits p 118 A92-16148
FAWCETT, P. A.
Quantification of canard and wing interactions using spatial correlation velocimetry
[AIAA PAPER 92-2687] p 807 A92-45588
A multi-diagnostic approach to testing V/STOL craft
[AIAA PAPER 92-4008] p 1099 A92-56831
FAY, JOHN F.
Aerobrake aerothermodynamic environment predictions in support of the Aeroassist Flight Experiment
[TABES PAPER 91-278] p 519 A92-34683
Laminar hypersonic flow over a compression using the HANA code
[AIAA PAPER 92-2896] p 820 A92-47872
FEARN, RICHARD L.
Evaluation of a Navier-Stokes prediction of a jet in a crossflow p 441 A92-32235
FEATHER, J. B.
Microwave landing system autoland system analysis
[NASA-CR-189551] p 191 N92-15060
Evaluation of microwave landing system approaches in a wide-body transport simulator
[NASA-CR-4450] p 957 N92-30978
FEATHER, JOHN B.
Design and analysis issues of integrated control systems for high-speed civil transports
[NASA-CR-186022] p 979 N92-31656
FEATHER, TIMOTHY D.
Reducing environmental noise impacts: A USAREUR noise management program handbook
[AD-A240797] p 237 N92-14791
FECKE, THEODORE
Aero mechanics in the twenty-first century
[AIAA PAPER 92-3194] p 863 A92-48805
FEDORCHENKO, D. G.
A method for determining equivalent stresses in aviation gas turbine engine blades p 559 A92-36421
FEDORENKO, G. A.
Approximate determination of the effect of deviations of wing and tail geometry from design parameters on the drag coefficient of subsonic aircraft p 460 A92-31878
FEDOROV, A. V.
Problems of laminar-turbulent transition control in a boundary layer p 312 A92-24979
Investigation of the effect of an ultrasonic acoustic field on boundary layer separation on an airfoil
p 511 A92-30205
Susceptibility of a supersonic boundary layer to acoustic perturbations p 707 A92-42730
FEDOROV, L. P.
Investigation of extremal field behavior for two-dimensional linear problems in flight mechanics
p 509 A92-30130
Horizontal flight of an aircraft with periodic thrust reversal p 480 A92-31876
FEE, JOSEPH J.
The technological revolution in oceanic air traffic control p 531 A92-33431
FEERRAR, WALLACE R.
The technological revolution in oceanic air traffic control p 531 A92-33431
FEESS, W. A.
Evaluation of GPS/UTC steering performance
p 1049 N92-33353
FEFERMAN, BEN
Inspection of fabricated fuselage panels using electronic shearography
[DOT/FAA/CT-TN92/26] p 1127 N92-33627
FEGGETTER, AMANDA J. W.
The development of an intelligent human factors data base as an aid for the investigation of aircraft accidents
p 928 A92-44994
FEIG, P. D.
A propulsion perspective of the next generation supersonic transport
[ASME PAPER 91-GT-385] p 126 A92-15719
FEIJOO, C.
New practical method for measurement error determination in radar systems under real traffic conditions p 155 A92-17238
FEJTEK, IAN
Navier-Stokes computation of wing leading edge tangential blowing for a tilt rotor in hover
[AIAA PAPER 92-2608] p 805 A92-45568
FELDMANN, ROBERT J.
Intra-flight laser data links - Technology focus
p 725 A92-41472
FELIZIANI, C.
Prediction of gas turbine combustor flow by a finite element code
[AIAA PAPER 92-3469] p 906 A92-49016
FELKER, FORT F.
Results from a test of a 2/3-scale V-22 rotor and wing in the 40- by 80-Foot Wind Tunnel p 104 A92-14332
A new method for transonic static aeroelasticity problems
[AIAA PAPER 92-2123] p 589 A92-35691
Wing force and surface pressure data from a hover test of a 0.658-scale V-22 rotor and wing
[NASA-TM-102244] p 550 N92-22864
FELSMAN, JOHN
An airborne multimode radar display processor
p 965 A92-49308
FELTROP, E.
An experimental system to investigate subsonic aeroelastic behavior of lifting surfaces
[AIAA PAPER 92-0061] p 250 A92-22176
FENDELL, F.
Laser-initiated conical detonation wave for supersonic combustion. II
[AIAA PAPER 92-0088] p 292 A92-22195
Laser-initiated conical detonation wave for supersonic combustion p 375 A92-28531
FENDELL, F. E.
Laser-initiated conical detonation wave for supersonic combustion. III
[AIAA PAPER 92-3247] p 893 A92-48846
Laser-initiated conical detonation wave for supersonic combustion, part 3
[AD-A250522] p 989 N92-32076
FENG, GUOTAI
Application of compound leaned blades to controlling secondary flow p 5 A92-10975
A new calculating method for the flowfield in turbomachinery - The study on the application of the vorticity-velocity equations for the numerical solution of the flowfield in turbomachinery p 338 A92-27803
A direct-problem calculation method for gas turbines with bowed and twisted blades p 519 A92-35571
FENG, JIN Z.
Unsteady flows in rotor-stator cascades
[AD-A241593] p 158 N92-13410
FENG, Y.
Application of smart structures to aircraft health monitoring p 20 A92-11123
FENG, YANAN
Delay of wing vortex bursting by using favorable interaction of vortices p 615 A92-38910
FENG, YUANSHENG
The system reliability analysis and optimization design for wing-box structures p 997 A92-53292
FENG, YUCHENG
An aeroacoustic model about the rotating stall of a compressor p 416 A92-27855
FENG, ZHENXING
Calculation of fuel sloshing and its coupling vibration with a tank p 991 A92-50204
FENNELL, P. J.
Passenger knowledge of airline safety information
[CRANFIELD-AERO-9111] p 187 N92-15054
FENNELL, ROBERT E.
Parameter insensitive control utilizing eigenspace methods p 204 A92-18615
FENNO, CHARLES C., JR.
Use of finite volume schemes for transition simulation
p 432 A92-31185

FENTON, B. C.
Statistics on aircraft gas turbine engine rotor failures that occurred in US commercial aviation during 1989
[DOT/FAA/CT-92/5] p 971 N92-30303
Statistics on aircraft gas turbine engine rotor failures that occurred in US commercial aviation during 1988
[DOT/FAA/CT-91/28] p 1071 N92-33105
FENTON, J.
An evaluation of a simple PID controller designed using optimal control theory when applied to helicopter stabilisation p 569 A92-35785
FEO, A.
The measurement of water film thickness on airfoils in heavy rain conditions using conductance sensors
p 452 N92-21695
FEOKTISTOV, A. A.
Automated thematic processing of aircraft scanner data gathered over pasture territory in Turkmenia
p 406 A92-25330
FERBER, JACQUES
From concept to model: Conception and evaluation of an architecture for a distributed system with SAHARA - Some reflections on results of the utilization of SAHARA in the framework of the Electronic Copilot
[ONERA, TP NO. 1991-216] p 411 A92-26368
FERBER, M. K.
Evaluation of the elevated-temperature mechanical reliability of a HIPed silicon nitride
[DE92-007838] p 579 N92-23223
FERGUSON, DAVID L.
YF-22A prototype advanced tactical fighter demonstration/validation flight test program overview
p 646 A92-40037
FERGUSON, F. T.
Microgravity nucleation and particle coagulation experiments support
[NASA-CR-190159] p 502 N92-21385
Microgravity nucleation and particle coagulation experiments support
[NASA-CR-189899] p 502 N92-21433
FERGUSON, SAMUEL W.
Rotorwash computer model: User's guide
[DOT/FAA/RD-90/25] p 346 N92-18345
FERLITA, FRANK
Rotor support for the STME oxygen turbopump
[AIAA PAPER 92-3282] p 904 A92-48872
FERNANDEZ DE LA MORA, J.
Brownian-motion limited aerodynamic focusing of heavy molecules p 995 A92-52722
FERNANDEZ-FERIA, R.
Brownian-motion limited aerodynamic focusing of heavy molecules p 995 A92-52722
FERNANDEZ, BENITO
A novel associative memory for high level control functions p 52 A92-11472
FERNANDEZDELAMORA, G.
A methodology for software specification and development based on simulation p 135 N92-12458
FERO, RALPH D.
Investigation of the influence of rotary aerodynamics on the study of high angle of attack dynamics of the F-15B using bifurcation analysis
[AD-A243969] p 348 N92-19367
FERRANTI, MICHAEL J.
Engineering development simulation - Test vehicle of the future p 483 A92-29674
Full mission simulation: A view into the future
p 884 N92-28537
FERREIRA, MICHAEL J.
NASA advanced aeronautics design solar powered remotely piloted vehicle
[NASA-CR-190007] p 462 N92-20665
FERRET, B.
Establishment and characterization of a reproducible vortex for use in studying nonsteady two-dimensional phenomena p 310 A92-24428
FERRETTI, A.
Prediction of aerodynamic phenomena limiting aircraft manoeuvrability p 364 N92-18781
FERRIER, BERNARD
Helicopter/ship analytic dynamic interface
p 464 N92-21962
FERRIGNO, STEPHEN J.
Brazing method helps repair aircraft gas-turbine nozzles p 492 A92-29504
FERTALA, REMI
A cable detection lidar system for helicopters
p 1001 N92-31068
FERTIG, K. W.
Design sheet - An environment for facilitating flexible trade studies during conceptual design
[AIAA PAPER 92-1191] p 600 A92-33303
FERTIS, D. G.
Engine dynamic analysis with general nonlinear finite element codes
[NASA-CR-187222] p 44 N92-11379
FERZIGER, J. H.
Effect of walls on the supersonic reacting mixing layer
p 912 N92-30065
FEY, J.
Expert system for the Tornado ground-based check-out system p 118 N92-12536
FEZOUI, L.
Efficient methods for inviscid non-equilibrium hypersonic flow fields p 1024 A92-54571
FICKIE, K.
Visualization and analysis of hypersonic flows and comparison to experimental data
[AIAA PAPER 92-2774] p 704 A92-41320
FIDDES, S. P.
An efficient Euler solver for predominantly supersonic flows with embedded subsonic pockets
[AIAA PAPER 92-0323] p 322 A92-25770
FIDELL, S. A.
NSBIT program - Development of assessment system for aircraft noise and research on human impacts due to aircraft noise p 688 A92-39100
FIDELL, SANFORD
Relating the annoyance of aircraft overflights to their audibility by outdoor recreationists p 689 A92-39240
FIDRANSKY, JIRI
The FALSTAFF program - A standard spectrum for simulating the service loading of aircraft with prevailing maneuver loads p 284 A92-21922
FIEBIG, M.
Embedded longitudinal vortex arrays, velocity and temperature fields, loss and heat transfer augmentation
p 621 A92-40121
FIEDBERG, ROBERT
Suppression of radiating harmonics Electro-Impulse Deicing (EIDI) systems
[DOT/FAA/CT-TN90/33] p 405 N92-19764
FIELDS, JAMES M.
Human response to aircraft noise p 236 N92-14780
FIELKE, G.
Buffered serial data card
[AD-A246435] p 727 N92-26948
FILIMONOV, M. IU.
Application of special series for studying nonstationary transonic gas flows p 311 A92-24904
FILIPPENKO, V. A.
Two-phase flows at supersonic velocities
p 4 A92-10907
FILIPPOVA, R. D.
Reducing the background noise level in the test section of a wind tunnel for transonic flow velocities
p 511 A92-30143
FILKINS, PETER C.
Algorithms for blending surface generation
[AD-A245686] p 777 N92-26524
FILLER, RAYMOND L.
Low-noise oscillators for airborne radar applications
[AD-A242264] p 300 N92-17258
FIMPEL, H. P.
Airflow effects about PMS probes on the DLR Falcon
p 467 A92-32060
FINAISH, F.
An experimental system to investigate subsonic aeroelastic behavior of lifting surfaces
[AIAA PAPER 92-0061] p 250 A92-22176
FINDLAY, JOHN T.
STS-40 descent BET products: Development and results
[NASA-CR-189570] p 286 N92-16012
FINDLER, N. V.
Distributed artificial intelligence approach to air traffic control p 161 A92-13436
FINEGOLD, L. S.
NSBIT program - Development of assessment system for aircraft noise and research on human impacts due to aircraft noise p 688 A92-39100
FINELLI, GEORGE B.
Analysis of data from a DO-178A software development process p 1134 N92-32880
FINFROCK, GREGORY P.
Geometry acquisition and grid generation: Recent experiences with complex aircraft configurations
p 691 N92-24400
FINK, D. A.
Surge dynamics in a free-spool centrifugal compressor system
[ASME PAPER 91-GT-31] p 68 A92-15515
FINK, MARTIN R.
Propulsive lift noise p 55 N92-10606
FINK, PAMELA K.
Research into the development of a knowledge acquisition taxonomy
[NASA-CR-189939] p 778 N92-28150
FINKENZELLER, H.
Preconsiderations on aircraft integration
p 599 N92-23402
FINLAY, B. A.
United Kingdom approach to deriving military ship helicopter operating limits p 465 N92-21966
FINLEY, TOM D.
Model attitude measurements at NASA Langley Research Center
[AIAA PAPER 92-0763] p 398 A92-28226
FINSTAD, RANDY
Evolutionary upgrade and application of the C-130H simple-cycle refrigeration system
[SAE PAPER 911439] p 270 A92-21836
FINTEL, BRADLEY W.
An experimental analysis of lateral jet injection into confined swirling crossflows p 156 N92-12199
FISCHER, MICHAEL C.
Application of laminar flow control to the High Speed Civil Transport - The NASA Supersonic Laminar Flow Control Program
[SAE PAPER 912115] p 643 A92-39966
FISCHER, NORMAN H.
Verification of flight software by embedding software simulation in simulation of external environment
p 232 A92-19084
FISCHER, R.
Two-phase flow correlations in air/oil systems of aero engines
[ASME PAPER 91-GT-54] p 121 A92-15532
FISCHER, T.
Evaluation of triple simultaneous parallel ILS approaches spaced 5000 feet apart, phase 4.b
[DOT/FAA/CT-91/31] p 456 N92-21404
FISCHER, TERENCE
Simulation of triple simultaneous parallel ILS approaches p 880 A92-45025
Evaluation of triple simultaneous parallel ILS approaches spaced 4300 feet apart, phase 4a
[ACD-340] p 191 N92-14034
FISCHER, W.-G.
Design and development of test rigs for main rotor and main rotor transmission of a helicopter in the 6-ton-class
p 1093 A92-56280
FISCHERSWORRING-BUNK, A.
Multiaxial load spectra in a cooled gas turbine blade under in-service conditions p 201 A92-19696
FISCHL, ROBERT
Formulation of a strategy for monitoring control integrity in critical digital control systems
[NASA-TM-104158] p 206 N92-15075
FISCHMEISTER, H.
Probabilistic lifing approach for aero engine disks made of powder nickel base alloys containing ceramic defects
p 226 N92-14424
FISH, JOHN C.
Torsion and twisting of symmetric composite laminates
[AIAA PAPER 92-2425] p 582 A92-34354
Interlaminar fracture characteristics of bonding concepts for thermoplastic primary structures p 758 A92-41282
FISHER, C. J.
Flow contamination and flow quality in arc heaters used for hypersonic testing
[AIAA PAPER 92-4028] p 1100 A92-56850
FISHER, DAVID F.
In-flight flow visualization and pressure measurements at low speeds on the NASA F-18 high alpha research vehicle p 85 N92-13009
In-flight leading-edge extension vortex flow-field survey measurements on a F-18 aircraft at high angle of attack
[NASA-TM-4398] p 947 N92-31276
FISHER, EDWARD A.
Experimental pyrometer system for a gas turbine engine
[AIAA PAPER 92-3482] p 859 A92-49022
FISHER, M.
Numerical calculation of modulation transfer functions for low frequency mechanical vibrations
p 235 A92-19982
FISHER, M. S.
Computational icing analysis for aircraft inlets
[AIAA PAPER 92-3178] p 836 A92-48793
FITSCHEN, KEITH
Autonomous landing - Functional requirements
p 840 A92-48470
FITZGERALD, JAMES P.
ES-3A flight test program
[AIAA PAPER 92-1230] p 538 A92-33327
FITZGERALD, TIMOTHY R.
Use of high-fidelity simulation in the development of an F/A-18 active ground collision avoidance system
[AIAA PAPER 92-4140] p 959 A92-52434
Use of high-fidelity simulation in the development of an F/A-18 active ground collision avoidance system
p 837 N92-28530

FLAHERTY, JOSEPH E.
Compressible laminar boundary layers for perfect and real gases in equilibrium at Mach numbers to 30
[AIAA PAPER 92-0757] p 336 A92-27099
FLAMENT, C.
Numerical simulation of thermochemical non-equilibrium viscous flows around reentry bodies
p 227 N92-15029
FLANAGAN, M. J., JR.
Operation and design considerations for unsteady data acquisition with PC-based systems in high Reynolds number hypersonic flowfields
[AIAA PAPER 92-0204] p 284 A92-23810
FLANDERS, JOEY B.
Expert system for real-time aircraft monitoring
p 410 A92-24411
FLANDRO, G. A.
Dynamic interactions between hypersonic vehicle aerodynamics and propulsion system performance
[NASA-CR-190638] p 1038 N92-33304
FLATICO, JOSEPH M.
Wavelength-multiplexed fiber-optic position encoder for aircraft control systems p 734 A92-42602
FLATMAN, J. C.
Surface activation of Concorde by Be-7
p 605 N92-23295
FLECHNER, S. G.
On the measurement of subsonic flow around an appended body of revolution at cryogenic conditions in the NTF p 880 A92-45265
FLECHNER, STUART G.
High Reynolds number test of the Boeing TR77 airfoil in the Langley 0.3-meter transonic cryogenic tunnel
[NASA-TM-4189] p 947 N92-31246
FLECK, V. J.
Mechanical design of a rotary balance system for NASA. Langley Research Center's vertical spin tunnel
p 664 N92-25090
FLECKENSTEIN, H.
A systematic formulation, as an approach to air traffic
[MBB-Z-0371-91-PUB] p 19 N92-10996
FLEETER, S.
Impeller flow field measurement and analysis
[ASME PAPER 90-GT-146] p 38 A92-11288
Wind tunnel wall effects in a linear oscillating cascade
[ASME PAPER 91-GT-133] p 72 A92-15576
FLEETER, SANFORD
LDV measurements of a mixed-flow impeller at design and near stall
[ASME PAPER 91-GT-310] p 153 A92-15688
Compressor blade row unsteady aerodynamic response to attached and separated flow forcing functions
[AIAA PAPER 92-0147] p 253 A92-23763
The unresolved unsteady flow in multistage compressor blade rows p 421 A92-29472
Airfoil wake and linear theory gust response including sub and superresonant flow conditions
[AIAA PAPER 92-3074] p 823 A92-48724
Research on aero-thermodynamic distortion induced structural dynamic response of multistage compressor blading
[AD-A250865] p 974 N92-32059
FLEISCHMANN, A.
AS 332 MKII - Development and certification
p 1059 A92-56343
FLEMING, A. J.
Acoustic interactions between an altitude test facility and jet engine plumes: Theory and experiments
[NASA-CR-190423] p 738 N92-26405
FLEMING, DAVID
Determining structural performance
p 560 N92-22519
FLEMING, DAVID C.
Determination of the energy absorption of composite structures under combined loadings p 145 A92-14441
Crashworthiness of truncated composite cones under side loads p 590 A92-35746
FLEMING, J. L.
An experimental study of a turbulent wing-body junction and wake flow
[AIAA PAPER 92-0434] p 327 A92-26281
An experimental study of a turbulent wing-body junction and wake flow
[AD-A243388] p 260 N92-17222
FLEMMING, KEVIN J.
A case study of the Claycomo, Missouri microburst on July 30, 1989 p 407 A92-27961
FLEMMING, ROBERT J.
Model rotor icing tests in the NASA. Lewis Icing Research Tunnel p 450 N92-21688
FLESNER, RICHARD W.
GPS integration improves mission capabilities of CH-47D aircraft p 966 A92-49340
FLETCHER, DOUGLAS G.
Laser-spectroscopic measurement techniques for hypersonic, turbulent wind tunnel flows
[NASA-TM-103928] p 405 N92-19596
FLEURY, ANDRE
Navigation and flight management systems - Thoughts of a user p 354 A92-26848
FLEYGNAC, D.
Dynamic performance of an aircraft on its landing gear: Test and evaluation on a dihedral p 466 N92-21970
FLITCROFT, J. E.
Prediction and measurement of jet flowfield features for ASTOVL aircraft p 787 A92-45318
FLITMAN, L. M.
Subsonic axisymmetric viscoelastic flow past thin tapered bodies of revolution p 6 A92-12134
FLOM, YURY
Superconducting bearings with levitation control configurations
[NASA-CASE-GSC-13346-1] p 909 N92-29099
FLOOD, JOSEPH D.
Hot gas ingestion characteristics and flow visualization of a vectored thrust STOVL concept
p 860 A92-45316
FLORJANCIC, S.
Annular seals of high energy centrifugal pumps: Presentation of full scale measurement
p 224 N92-14362
FLORYAN, J. M.
Stability of plane nonorthogonal stagnation flow
p 704 A92-41291
Laminar-turbulent transition process in the presence of simulated wall roughness p 626 N92-24858
Flow visualization using computer animation
p 629 N92-24870
FLOUTI, REALY
Mathematical modeling of the flight of passenger aircraft in the case of engine failure p 875 A92-47777
FLOWERS, GEORGE T.
Chaotic dynamic behavior in a simplified rotor blade lag model p 846 A92-46926
FLOYD, ROBERT L., JR.
Anodize and prime your aluminum without environmental headaches p 892 A92-47340
FOCH, RICHARD J.
Low Reynolds number, long endurance aircraft design
[AIAA PAPER 92-1263] p 538 A92-33343
FOERSCHING, H.
A parametric study of the aeroelastic stability of a binary wing-with-engine nacelle flutter system in incompressible flow p 270 A92-22472
Wind tunnel wall corrections for unsteady flow applying steady wall adaptation and CFD-techniques
p 706 A92-42533
FOGARTY, P. J.
Scoping studies for small steady-state tokamaks for divertor testing
[DE92-000740] p 238 N92-15761
FOKIN, D. A.
Design and optimization of airfoils in non-stalling incompressible flow with a prescribed range of the angle of attack p 933 A92-49556
FOLEY, S. M.
A multi-diagnostic approach to testing V/STOL craft
[AIAA PAPER 92-4008] p 1099 A92-56831
FOLEY, STEPHEN F.
Utility management system for hypersonic vehicles
p 964 A92-49252
FOMICHEV, V. P.
Experimental and theoretical study of the improvement of the aerodynamic characteristics of supersonic flow past bodies with surface injection of a gas jet with particles
p 8 A92-12204
FOMIN, G. M.
Problems of strength and aeroelasticity of present-day propfans p 471 A92-30133
FOMIN, V. M.
Experimental and theoretical study of the improvement of the aerodynamic characteristics of supersonic flow past bodies with surface injection of a gas jet with particles
p 8 A92-12204
Control of the development of boundary layer disturbances p 423 A92-30126
Flight studies of the riblet effect on drag variation
p 438 A92-31871
Boundary-layer-separation control p 440 A92-31886
FONAREV, A. S.
A shock and an expansion wave in transonic flow
p 440 A92-31961
FONG, C. VANESSA
Automated problem resolution prototype in automated en route air traffic control p 190 N92-14028
FONT, G. I.
High alpha aerodynamic control by tangential fuselage blowing p 611 A92-36848
Force production mechanisms of a tangential jet on bodies at high alpha
[AIAA PAPER 92-4648] p 1082 A92-55393
FOO, W. P.
Fracture mechanics approach to creep growth in welded IN738LC gas turbine blades
[ASME PAPER 91-GT-119] p 670 A92-36893
FORBRICH, D.
Application of direct inverse analogy method (DIVA) and viscous design optimization techniques
p 176 N92-13951
FORCE, D. A.
A low-power, high-efficiency Ka-band TWTA
p 671 A92-38163
FORD, BRIAN
The application of multimedia expert systems to the depot level maintenance environment
p 922 A92-48557
FORD, D. A.
Present and future trends in turbine blade material and manufacturing technology
[PNR-90825] p 488 N92-20164
FORDHAM, KARI SUZANNE
The FM-007: An advanced jet commuter for HUB to spoke transportation
[NASA-CR-189988] p 461 N92-20267
FORKEY, J.
Rayleigh imaging and flow tagging in ground test facilities p 1115 A92-54330
FORMAGGIA, L.
Simulation of hypersonic flows on unstructured grids
p 434 A92-31496
Vortical flow simulation by using structured and unstructured grids p 83 N92-12999
FORMAGGIA, LUCA
An unstructured mesh generation algorithm for three-dimensional aeronautical configurations
p 918 A92-47053
FORMALEV, V. F.
Numerical study of coupled heat transfer under conditions of filtering and film cooling of blunt anisotropic bodies p 610 A92-36552
FORMANEK, B.
Corrosion damage and regeneration of aluminide coatings on aircraft turbine blades p 142 A92-15244
FORNASIER, L.
Application of the Euler method EUFLEX to a fighter-type airplane configuration at transonic speed
[AIAA PAPER 92-2620] p 845 A92-45573
FORNASIER, LUCIANO
Numerical optimization in Germany: A non-exhaustive survey on current activities with emphasis on aeronautics
[MBB/FE211/S/PUB/474] p 932 N92-30675
FORNEY, DON M., JR.
Evolving partnership for NDE in materials engineering and extended life cycle performance
p 490 A92-28556
FORRESTER, D. A.
Probability distributions that are important when assessing barometric aiding to GPS p 100 A92-16952
European studies to investigate the feasibility of using 1000 ft vertical separation minima above FL 290. Part 1: Overview of organisation, techniques employed, and conclusions
[NLR-TP-91062-U-PT-1] p 841 N92-29605
FORSSELL, BORJE
On the calculation of repeatable accuracy, with special reference to GPS p 955 A92-49383
FORSTER, C. P.
Fibre optic laser anemometry for turbomachinery applications p 397 A92-27783
FORSTER, JOHN V.
Controls for agility research in the NASA High-Alpha Technology Program
[SAE PAPER 912148] p 661 A92-39984
FOSS, G. C.
Enhancement of modal swept sine data by control of exciting forces p 215 A92-17562
FOSTER, JOHN V.
Application of piloted simulation to high-angle-of-attack flight-dynamics research for fighter aircraft
p 886 N92-28551
FOSTER, ROBERT G.
The effect of droplet sizing uncertainty on ice accretions p 679 N92-24874
FOSTER, STEPHEN P.
Ideal efficiency of propellers based on Theodorsen's theory: A review and computer study, with extended plus simplified charts
[UTIAS-TN-271] p 1071 N92-33102
FOTTNER, LEONARD
Performance improvements of compressor cascades by controlling the profile and sidewall boundary layers
[ASME PAPER 91-GT-260] p 75 A92-15662

FOULADI, K.
Interference flows past cylinder-fin-sting-cavity assemblies p 442 A92-32236
FOULADI, KAMRAN
Viscous simulation method for unsteady flows past multicomponent configurations p 714 A92-44671
Viscous flow past a nacelle isolated and in proximity of a flat plate
[AIAA PAPER 92-2723] p 803 A92-45560
FOULKE, KENNETH W.
Controlling radar signature p 967 A92-52018
FOURGUETTE, D. C.
Experiments on the structure of an annular compressible reacting shear layer p 969 A92-50311
FOURNIER, E.
Effects of vortex generators on the growth of a compressible shear layer
[AIAA PAPER 90-1979] p 934 A92-50269
FOURNIER, G.
Combat aircraft jet engine noise studies
[ONERA, TP NO. 1991-192] p 415 A92-26353
FOURNIER, J.
Measurement of convective heat-transfer coefficients in wind tunnels using passive and stimulated infrared thermography p 390 A92-24430
Application of infrared thermography to thermal flux measurement in wind tunnels
[AAAF-NT-89-12] p 31 N92-11020
FOURNIER, JEAN
GPS tests during approach at Singapore and Roissy p 956 A92-53240
FOUTTER, R. R.
Supersonic combustor testing using optical diagnostics and a high enthalpy shock tunnel
[AIAA PAPER 92-0761] p 384 A92-27102
FOWLER, J. O.
Superplastic applications in aero engines
[PNR-90788] p 473 N92-20436
FOWLER, THOMAS D.
A CLIPS-based tool for aircraft pilot-vehicle interface design p 303 N92-16605
FOX, BRUCE A.
Investigation of advanced aircraft performance measures of merit including new agility metrics
[AD-A242016] p 272 N92-15990
FOX, ROBERT D.
Committees, their importance to the structures of the Helicopter Association International p 59 A92-14411
FOX, T. A.
End plate interference effects on the aerodynamics of a circular cylinder in uniform flow p 313 A92-25097
Flow around two circular cylinders arranged perpendicular to each other
[PB91-238279] p 297 N92-16225
FOYE, R. L.
The effect of composite material allowable changes on VTOL airframe weights p 848 A92-47629
FRAAS, PAUL
Tornado structural fatigue life assessment of the German Air Force p 363 N92-18592
FRADENBURGH, EVAN A.
The high speed challenge for rotary wing aircraft
[SAE PAPER 911974] p 842 A92-45381
FRAEDRICH, WERNER M.
Tool supported software development experiences from the EFA project p 163 N92-12451
FRANC, O.
Materials and structures for Hermes p 666 A92-38213
FRANCES, A.
Active control of airborne noise transmitted through a ribbed panel p 695 A92-39111
FRANCOIS, G.
New hypersonic test methods developed at ONERA - The R5 and F4 wind tunnels
[ONERA, TP NO. 1992-39] p 882 A92-48600
FRANGOS, C.
The application of parameter optimisation techniques to linear optimal control system design p 302 A92-23038
FRANK, J. M.
Operational and economic benefits of area navigation from the perspective of a major air carrier p 96 A92-16632
FRANK, P. D.
A comparison of two closely-related approaches to aerodynamic design optimization p 193 N92-13933
FRANK, PAUL D.
A comparison of optimization-based approaches for a model computational aerodynamics design problem p 316 A92-25636
FRANK, ROBERT S.
High-speed cinematography of supersonic mixing layers
[AIAA PAPER 92-3545] p 1112 A92-54044
FRANKE, M. E.
Navier-Stokes methods to predict circulation control airfoil performance p 442 A92-32243
FRANKEL, S. H.
Modeling of the reactant conversion rate in a turbulent shear flow p 829 N92-28820
FRANKLIN, J. A.
Collaborative research on V/STOL control system/cockpit display tradeoffs under the NASA/MOD joint aeronautical program
[NASA-TM-103910] p 1087 N92-32788
FRANKLIN, JAMES A.
Integrated flight/propulsion control for supersonic STOVL aircraft p 872 A92-45320
FRANKLIN, JERROLD E.
Ceramic regenerator program
[NASA-CR-189053] p 225 N92-14374
FRANKLIN, WALTER M.
Composite material stub-blade wing joint p 763 A92-44618
FRANKLIN, WESLEY D.
Rotor-to-stator partial rubbing and its effects on rotor dynamic response p 224 N92-14367
FRASER, CLIVE S.
Dimensional characterization of a large aircraft structure by photogrammetry p 607 A92-37061
FRASER, K. F.
General requirements and techniques for component fatigue life substantiation in Australian service helicopters
[AD-A242881] p 275 N92-17565
FRATELLO, DAVID J.
Wind-tunnel and flight tests of a delta-wing remotely piloted vehicle p 21 A92-13208
FRAZIER, W. E.
The microstructural stability of TiC reinforced rapidly solidified Al-Fe-V-Si composite structures p 141 A92-15169
FREDETTE, R. E.
A USAF assessment of STOVL fighter options p 842 A92-45310
FREDRIKSSON, BILLY
A manufacturer's approach to ensure long term structural integrity p 838 N92-30133
FREED, A. D.
A viscoplastic theory for anisotropic materials
[ONERA, TP NO. 1992-90] p 391 A92-24721
FREEDMAN, A. P.
A demonstration of centimeter-level monitoring of polar motion with the Global Positioning System p 639 N92-24302
FREEDMAN, MARC R.
Reliability analysis of a structural ceramic combustion chamber
[ASME PAPER 91-GT-155] p 123 A92-15591
FREELS, J. D.
Recent advances on a finite element algorithm for computational aerodynamics: Transonics-hypersonics
[DE91-018176] p 11 N92-10010
FREEMAN, B. D.
Evaluation of metal hydride compressors for applications in Joule-Thomson cryocoolers p 296 A92-23835
FREEMAN, C.
Method for the prediction of supersonic compressor blade performance p 277 A92-21078
FREEMAN, JEANNINE
The Center/TRACON Automation System (CTAS): A video presentation
[NASA-TM-103887] p 356 N92-20029
FREEMAN, LEONARD S.
An overview of US Navy and Marine Corps V/STOL p 783 A92-45303
FREESE, MIKE
The SnoDog: Preliminary design of a close air support aircraft
[NASA-CR-189990] p 462 N92-21489
FRENCH, J. R.
Crew transportation for the 1990s. I - Commercializing manned flight with today's propulsion p 889 A92-46726
FRENCH, JAMES E.
Future air traffic control and navigation systems; Proceedings of the AIAA International Civil Aviation Seminar, Paris, France, June 12, 1991
[AIAA SP-050-1991] p 532 A92-33433
FRENCH, MARK
Demonstration of structural optimization applied to wind-tunnel model design p 1119 A92-56181
FREY, M. O.
Experimental investigation of coannular jet flow with swirl along a centerbody p 172 A92-18367
FREY, THOMAS J.
Flight test of a GPS-aided low-cost inertial navigation system programmed in Ada p 101 A92-16973
FREYMUTH, PETER
The anchored and loose vortex systems of finite wings
[AIAA PAPER 92-0318] p 321 A92-25765
Visualization of stopping flow over airfoils
[AIAA PAPER 92-2730] p 804 A92-45564
FRICKER, D. M.
Calculations of hot gas ingestion for a STOVL aircraft model
[AIAA PAPER 92-0385] p 374 A92-28191
FRICKER, DAVID M.
Calculations of hot gas ingestion for a STOVL aircraft model
[NASA-TM-105437] p 350 N92-19993
FRIDLENDER, O. G.
On thermal-stress gas flows p 37 A92-10657
Approximate aerodynamic analysis for complicated bodies in rarefied gas flows p 938 A92-52754
FRIDMAN, A. G.
High-temperature metal matrix composite p 1105 A92-53878
FRIEBEL, C.
FALKE and COBRA technology development in aerodynamics and aerothermodynamics p 183 N92-15017
FRIED, ZOLTAN
Functionally integrated aircraft instrumentation for the next generation commercial helicopter p 117 A92-14402
FRIEDMAN, GERALD
The role of PM in the design of lightweight aircraft engine components p 991 A92-50137
FRIEDMAN, INGER P.
Weight, center of gravity and modal test report for NTF fan blade set no. 3
[NASA-CR-189583] p 498 N92-20072
FRIEDMAN, PAUL J.
An integrated real-time turbine engine flight test system p 201 A92-19275
FRIEDMAN, W. D.
The use of CT for dimensional measurements of green and sintered ceramic components p 490 A92-28592
FRIEDMANN, P. P.
Helicopter air resonance modeling and suppression using active control p 204 A92-18625
Vibration reduction in helicopter rotors using an active control surface located on the blade
[AIAA PAPER 92-2451] p 564 A92-34478
A study of coupled rotor-fuselage vibration with higher harmonic control using a symbolic computing facility p 569 A92-35770
Exploratory design studies of actively controlled wings using integrated multidisciplinary synthesis p 641 A92-36828
Integrated aeroservoelastic wing synthesis by nonlinear programming/approximation concepts p 873 A92-46752
Coupled rotor-fuselage vibration reduction with multiple frequency blade pitch control p 1085 A92-56315
FRIEDMANN, PERETZ P.
Impact of structural optimization with aeroelastic/multidisciplinary constraints on helicopter rotor design
[AIAA PAPER 92-1001] p 535 A92-33193
A new aeroelastic model for composite rotor blades with straight and swept tips
[AIAA PAPER 92-2259] p 541 A92-34414
New time-domain technique for flutter boundary identification
[AIAA PAPER 92-2102] p 588 A92-35673
Rotary-wing aeroservoelastic problems
[AIAA PAPER 92-2107] p 567 A92-35678
Helicopter aeroelastic stability and response - Current topics and future trends p 730 A92-43100
Control augmented structural optimization of aeroelasticity tailored fiber composite wings
[AD-A241464] p 135 N92-13075
FRIEDRICH, H.-E.
Examples of advanced near-net shape manufacturing techniques for aerospace
[MBB-Z-0399-91-PUB] p 1125 N92-32742
FRIEDRICHS, R.
Automatic control of test parameters for intake measurements in a low-speed wind tunnel p 1091 A92-54341
FRIES, SYLVIA DOUGHTY
NASA engineers and the age of Apollo
[NASA-SP-4104] p 929 N92-28344
FRINK, NEAL T.
Upwind scheme for solving the Euler equations on unstructured tetrahedral meshes p 175 A92-20735
Estimation of propulsion-induced effects on transonic flows over a hypersonic configuration
[AIAA PAPER 92-0523] p 341 A92-28197

FRINK, NEAL TILSON
Three-dimensional upwind scheme for solving the Euler equations on unstructured tetrahedral grids
p 714 N92-26585
FRINK, WILLIAM D., JR.
Hot-wire surveys in the vortex wake downstream of a three-percent fighter aircraft model at high angles of attack
[AD-A241869] p 259 N92-15975
FRITSCH, EDWARD V.
Balloon altitude control by valving - A review and comparison of actual flight data and vertical performance analysis results
[AIAA PAPER 91-3669] p 14 A92-11016
FRITSCH, KLAUS
Wavelength-multiplexed fiber-optic position encoder for aircraft control systems p 734 A92-42602
FRIZ, HEINZ
An exploration of chemically reacting viscous hypersonic flow p 612 A92-37550
FROEBEL, ARNOLD T.
V-22 pilot-in-the-loop aeroelastic stability analysis
p 133 A92-14422
FROLOFF, WALT
Ames life science telescience testbed evaluation
[NASA-CR-188856] p 140 N92-12033
FROLOVA, A. A.
Calculation of flow of a radiating gas in axisymmetric nozzles of specified shape p 7 A92-12179
FRONEK, DENNIS L.
Supersonic Throughflow Fan Test Facility at NASA. Lewis Research Center
[NASA-TP-3038] p 983 N92-31640
FROOM, DOUGLAS A.
Nondestructive inspection perspectives
p 915 N92-30121
FROST, WALTER
Particle trajectory computer program for icing analysis of axisymmetric bodies
[NASA-CR-189134] p 352 N92-19276
FROUDE, F. A.
Digital ozonesondes - Examples of results from the EMEFS experiments of 1988 and 1990
p 468 A92-32140
FRYE, G. C.
Method and apparatus for acoustic plate mode liquid-solid phase transition detection
[DE92-003778] p 401 N92-18705
Monitoring jet fuel degradation using quartz crystal microbalances
[DE92-004730] p 489 N92-20858
FRYE, JOHN W.
Collision probability estimate method for impact generated low earth orbit space debris clouds
[AAS PAPER 91-369] p 752 A92-43269
FU, AN-KUO
An experimental investigation of the effect of leading-edge extensions on directional stability and the effectiveness of forebody nose strakes
[AIAA PAPER 92-2715] p 802 A92-45554
FU, DEXUN
Numerical simulation of the flow around rectangular cylinder p 339 A92-27851
FU, G. M.
Investigation of unsteady excitation effects on aerodynamic properties of airfoils p 66 A92-15335
FU, GUANGMING
A flow visualization experiment on the unsteady flow around two-dimensional airfoil p 615 A92-38913
FU, GUOZHENG
Safety factor and reliability for composite laminates
p 996 A92-53070
FU, HUIMIN
A method of reliability analysis for propeller blades
p 25 A92-10968
FU, K.-H.
Frequency-domain identification of BO 105 derivative models with rotor degrees of freedom
p 104 A92-14327
FU, Y.
Nonlinear development and secondary instability of large-amplitude Goertler vortices in hypersonic boundary layers p 942 A92-53080
FUCHS, J.
Shock wave reflection close to the leading edge of a wedge p 37 A92-10660
FUCHS, R.
Inlet flow angle determination of transonic compressor cascades
[ASME PAPER 91-GT-274] p 75 A92-15671
FUGLSANG, D. F.
Design load predictions on a fighter-like aircraft wing
p 811 A92-46797
FUGLSANG, DENNIS F.
Evaluation of shear layer cavity resonance mechanisms by numerical simulation
[AIAA PAPER 92-0555] p 333 A92-26965
A numerical study of control surface buzz using computational fluid dynamic methods
[AIAA PAPER 92-2654] p 806 A92-45578
Aeroelastic calculations for fighter aircraft using the transonic small disturbance equation
p 720 N92-27951
FUH, YIIN-KUEN
Fuel injection in hypersonic airbreathing engine
[IAF PAPER 91-273] p 120 A92-14710
FUHS, ALLEN E.
Semi-inverse marching characteristics scheme for supersonic flows p 432 A92-31187
FUJIEDA, HIROTOSHI
Low-speed wind tunnel testing of the lateral control force for the upper rudder surface of a joined-wing airfoil
p 711 A92-43228
Low-speed wind tunnel testing of a joined-wing airfoil
p 711 A92-43229
Effectiveness of aircraft aerodynamic performance on each part of a joined wing p 712 A92-43230
Experimental studies on aerodynamic characteristics of SSTO vehicle at low subsonic speeds
[SAE PAPER 911981] p 788 A92-45386
Wind tunnel investigation of an improved upper surface blown flap transport semi-span model
[SAE PAPER 911993] p 789 A92-45395
Aerodynamic development of boundary layer control system for NAL QSTOL research aircraft 'ASKA'
[SAE PAPER 912010] p 843 A92-45410
A low speed wind tunnel investigation of a joined-wing aircraft with an overhanging fin p 1030 A92-56078
A low speed wind tunnel investigation of the direct side force control of a joined-wing aircraft with overhanging fin p 1084 A92-56079
Improvement of data processing system for gust wind tunnel data acquisition part: System conversion from off-line to on-line processing
[NAL-TM-611] p 285 N92-17756
An approach to flow field measurement by Laser 2-Focus velocimeter (L2F) in gust wind tunnel
[NAL-TM-617] p 346 N92-18484
A pressure measurement method using Electronically Scanner Pressure sensors (ESP) installed in a gust wind tunnel
[NAL-TM-638] p 749 N92-27428
Upgrading the data processing section of the NAL Gust Wind Tunnel data processing system
[NAL-TM-635] p 888 N92-28833
FUJII, K.
Navier-Stokes code development for transonic flow simulations p 246 A92-21985
Gust load alleviation control design for the accuracy of an aeroelastic active control model
p 745 A92-43134
ACT wind tunnel experiment on gust load alleviation. II - Wind tunnel test with active support facility
p 745 A92-43135
Transonic wind tunnel tests of flutter suppression equipment (Wing response data processing)
p 748 A92-43136
FUJII, KENJI
Synthesis of gust load alleviation with flutter margin augmentation p 1082 A92-56021
Generalized aerodynamics analysis by the boundary element method p 1030 A92-56050
Flight evaluation of navigation systems including MLS using NAL Do228 - Outline p 1047 A92-56116
Static aeroelastic analysis of ACT wind tunnel model aircraft
[NAL-TM-624] p 632 N92-25366
Vibration tests and structural modeling of an aircraft model for active control technology experiments
[NAL-TM-626] p 662 N92-25401
FUJII, KOZO
Numerical computation of supersonic intakes
p 430 A92-30539
Aerodynamic design tool development for the calculation code of hypersonic flow p 711 A92-43198
Recent applications of the FNS zonal Method to complex flow problems
[SAE PAPER 912003] p 789 A92-45404
Numerical simulations of hypersonic real-gas flows over space vehicles
[SAE PAPER 912045] p 791 A92-45429
Aerodynamic aircraft design methods and their notable applications: Survey of the activity in Japan
p 193 N92-13930
FUJII, R.
Polar patrol balloon
[AIAA PAPER 91-3688] p 15 A92-11031
FUJIMORI, SHUNRO
Study on two-dimensional jet mixing with a vertical supersonic flow p 429 A92-30530
FUJIMORI, TOSHIRO
CFD application to 2D/3D flow fields in Scramjet engine p 170 A92-17501
FUJIMOTO, AKIRA
Numerical investigation of supersonic inlet with realistic bleed and bypass systems p 713 A92-44519
Wind tunnel test of M = 2.5 mixed compression inlet
p 1028 A92-56008
FUJIMOTO, ATSUSHI
Experimental and numerical investigations on separated flows around pitching airfoils p 710 A92-43166
FUJIMOTO, T.
High enthalpy wind tunnel for erosion testing of advanced materials
[AIAA PAPER 92-3888] p 1094 A92-56729
FUJITA, H.
Study on transonic cascade performance by use of newly built facility p 136 A92-15328
FUJITA, MITSUHIRO
An experimental program concerning a satellite data link for oceanic ATC p 1046 A92-56093
FUJITA, TOSHIMI
Low-speed wind tunnel testing of the lateral control force for the upper rudder surface of a joined-wing airfoil
p 711 A92-43228
Low-speed wind tunnel testing of a joined-wing airfoil
p 711 A92-43229
Effectiveness of aircraft aerodynamic performance on each part of a joined wing p 712 A92-43230
Experimental studies on aerodynamic characteristics of SSTO vehicle at low subsonic speeds
[SAE PAPER 911981] p 788 A92-45386
Wind tunnel investigation of an improved upper surface blown flap transport semi-span model
[SAE PAPER 911993] p 789 A92-45395
A low speed wind tunnel investigation of a joined-wing aircraft with an overhanging fin p 1030 A92-56078
A low speed wind tunnel investigation of the direct side force control of a joined-wing aircraft with overhanging fin p 1084 A92-56079
Improvement of data processing system for gust wind tunnel data acquisition part: System conversion from off-line to on-line processing
[NAL-TM-611] p 285 N92-17756
An approach to flow field measurement by Laser 2-Focus velocimeter (L2F) in gust wind tunnel
[NAL-TM-617] p 346 N92-18484
A pressure measurement method using Electronically Scanner Pressure sensors (ESP) installed in a gust wind tunnel
[NAL-TM-638] p 749 N92-27428
Upgrading the data processing section of the NAL Gust Wind Tunnel data processing system
[NAL-TM-635] p 888 N92-28833
FUJITSUNA, Y.
A conceptual study for future engine test facility
[AIAA PAPER 92-3992] p 1099 A92-56815
FUJIWARA, GENKICHI
Cabin structural vibration and noise for transport aircraft p 192 A92-17876
Fatigue cracking threshold prediction of transport airplanes p 1118 A92-56094
FUJIWARA, KAZUHITO
Flow around two square cylinders in staggered arrangements p 761 A92-42797
FUJIWARA, KENJI
Scramjet engine and its flying test bed
p 1066 A92-53492
FUJIWARA, MICHIO
Reduction of torque pulsation of Stirling engine-compressor system p 992 A92-50785
FUJIWARA, T.
Test on high enthalpy hypersonic flow using a ballistic range p 747 A92-43097
Study of the flow field and molecular radiation heating around a reentry vehicle p 711 A92-43227
FUJIWARA, TOSHI
Numerical simulation of a supersonic jet impingement on a ground
[SAE PAPER 912014] p 789 A92-45412
Numerical analysis of RCS jet in hypersonic flights
[SAE PAPER 912063] p 791 A92-45445
Detailed numerical analysis of standing oblique detonation p 1111 A92-53550
Radiative heat transfer from nonequilibrium shock layer to a hypersonic reentry body p 1019 A92-53579
Thermally and chemically nonequilibrium hypersonic flow in three-dimensional geometry
p 1019 A92-53580
Three-dimensional calculation of radiative field in hypersonic air shock layers p 1023 A92-54498

FUJIWARA, TSUTOMU
Key design considerations for scramjet powered space plane p 1066 A92-53491
An advanced scramjet propulsion concept for a 350 MG SSTO space plane - External nozzle performance
[AIAA PAPER 92-3719] p 1067 A92-54134
FUKUDA, MASAHIRO
Finite elements analysis of flexural edge wave for composite fan blades
[SAE PAPER 912048] p 861 A92-45432
FUKUDA, TOYO
Introduction to the traffic alert and collision avoidance system (TCAS) III p 734 A92-43150
FUKUI, K.
Outflow boundary conditions for Euler analysis of flow in turbine scroll p 591 A92-36037
FUKUI, YOSHIOKI
Weathering test of AFRP composites for the application of helicopter fuselage p 142 A92-15309
FUKUSHIMA, CHIHARU
Effect of controlled longitudinal vortex arrays on the development of a turbulent boundary layer p 614 A92-38856
FUKUSHIMA, SOUNOSUKE
Flight evaluation of navigation systems including MLS using NAL Do228 - Results of GPS p 1047 A92-56118
FUKUSHIMA, YASUO
A study on the rotating stall of centrifugal compressors. II - Effect of vaneless diffuser inlet shape on rotating stall p 497 A92-32508
FULACHIER, L.
Influence of suction through a slot on a turbulent boundary layer p 622 A92-40127
Experimental and numerical investigation of a turbulent boundary layer over riblets p 622 A92-40128
FULCHER, KAREN
On the aerodynamics/dynamics of store separation from hypersonic aircraft
[AIAA PAPER 92-2722] p 807 A92-45595
FULLER, ANDREW
Rapid systems integration of navigation avionics p 858 A92-48473
FULLER, C. R.
Active control of sound transmission through elastic plates using piezoelectric actuators p 53 A92-11052
A neural network for the identification of measured helicopter noise p 162 A92-14387
FULLER, CHRIS R.
Identification of helicopter noise using a neural network p 416 A92-28032
FULLER, E. J.
Mixing studies of helium in air at high supersonic speeds p 935 A92-50310
FULLER, GERRY
Are we doing HIRF testing sensibly? p 931 A92-49305
FULLER, JAMES WILLARD
Helicopter active rotor control p 570 N92-22157
FULLER, RAY
Fatigue and accidents - A comparison across modes of transport p 17 A92-13025
FULTON, KEN
CIS engines. I - The range revealed p 786 A92-47821
CIS engines - The range revealed. II p 1069 A92-54546
FULTON, MARK V.
Application of composite rotor blade stability analysis to extension-twist coupled blades
[AIAA PAPER 92-2254] p 564 A92-34479
FUNABIKI, KATSUSHI
Effect of streamwise pressure gradient on the supersonic mixing layer p 1025 A92-54936
FUNABIKI, KOHEI
Flight test of a flight reference display for powered-lift STOL aircraft p 1064 A92-56059
FUNG, K.-Y.
Analysis of the onset of dynamic stall p 1024 A92-54919
FUNK, R. B.
Quantification of canard and wing interactions using spatial correlation velocimetry
[AIAA PAPER 92-2687] p 807 A92-45588
A multi-diagnostic approach to testing V/STOL craft
[AIAA PAPER 92-4008] p 1099 A92-56831
FUQUN, CHEN
Influence of air liquefaction cycle on performance of combined cycle engine p 372 A92-24878
FURINI, F.
Parametric bicubic spline and CAD tools for complex targets shape modelling in physical optics radar cross section prediction p 403 N92-19151
FURNISS, TIM
The Delta Clipper dream p 574 A92-36127
FURUKAWA, M.
Unsteady Navier-Stokes simulation of transonic cascade flow using an unfactored implicit upwind relaxation scheme with inner iterations
[ASME PAPER 91-GT-223] p 74 A92-15637
Outflow boundary conditions for Euler analysis of flow in turbine scroll p 591 A92-36037
FURUKAWA, MASATO
Three-dimensional relaxation effect on quasi-3D flow in a blade row with spanwise loading distribution p 936 A92-51593
FUSARO, ROBERT L.
Tribology needs for future space and aeronautical systems
[NASA-TM-104525] p 214 N92-15191
Liquid lubricants for advanced aircraft engines
[NASA-TM-104531] p 1109 N92-32863
FUYKSCHOT, P. H.
Model incidence measurement using SAAB ELOPTOPOS system
[NLR-TP-89182-U] p 385 N92-18416

G

GABEL, R.
The NASA/Industry Design Analysis Methods for Vibrations (DAMVIBS) Program - Boeing helicopters airframe finite element modeling
[AIAA PAPER 92-2202] p 539 A92-34392
GABRIELE, G. A.
Improved coordination in non-hierarchic system optimization
[AIAA PAPER 92-2497] p 601 A92-34554
GAGLIARDI, ROBERT M.
Code Division Multiple Access (CDMA) system candidate for integrated modular avionics p 725 A92-42604
GAI, S. L.
Stagnation point heat flux in hypersonic high enthalpy flow p 613 A92-38373
Laminar heat transfer to blunt cones in high-enthalpy hypervelocity flows p 713 A92-44372
Separated high enthalpy dissociated laminar hypersonic flow behind a step - Pressure measurements p 809 A92-45858
GAIFULLIN, A. M.
A method for calculating the separated flow past a circular cone, taking viscous-inviscid interaction into account p 427 A92-30203
GAILLARD, R.
Aerodynamic measuring techniques for transonic and supersonic flow in cascades and turbomachines
[ONERA, TP NO. 1991-170] p 137 A92-16135
GAILLARDON, J. M.
Ageing airplane repair assessment program for Airbus A300 p 838 N92-30123
GAINER, CHARLES
The use of a dedicated testbed to evaluate simulator training effectiveness p 884 N92-28533
GAITONDE, DATTA
Numerical investigation of bleed on three-dimensional turbulent interactions due to sharp fins p 5 A92-11062
An examination of several high resolution schemes applied to complex problems in high speed flows
[AD-A250814] p 1124 N92-32632
GAJENDRAN, F.
Stability of an adaptive controller for aircraft. I - Analysis via Liapunov theory p 976 A92-51940
GAJIC, ZORAN
Study of the discrete singularly perturbed linear-quadratic control problem by a bilinear transformation p 163 A92-16072
GAL-OR, BENJAMIN Z.
Maximizing thrust-vectoring control power and agility metrics p 874 A92-46794
GALAMBOS, J. D.
Scoping studies for small steady-state tokamaks for divertor testing
[DE92-000740] p 238 N92-15761
GALANT, DAVID
Optical computing at NASA Ames Research Center
[AIAA PAPER 91-3779] p 231 A92-17637
GALATOLO, R.
Prediction of fatigue crack growth in a Ti-6Al-4V fan disk forging under spectrum loading p 213 A92-19817
GALBRAITH, R. A.
Two-dimensional, incompressible aerofoil design and analysis p 247 A92-21987
GALBRAITH, R. A. MCD.
An experimental investigation of the oblique blade-vortex interaction p 712 A92-43447
Measurements of the dynamic stall vortex convection speed p 1032 A92-56351
GALEMIN, E. K.
An approximate method for calculating flow past solid wings of small aspect ratio based on a nonlinear theory of a continuous vortex surface p 428 A92-30373
GALIAVIEVA, M. S.
Synthesis of wing profiles from chord velocity diagrams using quasi-solutions for inverse boundary value problems p 80 A92-16815
GALICA, M. A.
High-temperature combustor and seal for a water piston propulsor
[AD-A242493] p 229 N92-15385
GALINSKII, V. P.
Quick calculation of three-dimensional supersonic flow past nearly axisymmetric bodies p 624 A92-40605
GALKIN, M. N.
A method for estimating the efficiency of gas turbine blade cooling systems p 657 A92-40606
GALKOWSKI, PEGGY J.
An alternative derivation of the modified gain function of Song and Speyer p 232 A92-18464
GALLAGHER, JOHN E., JR.
Bell's OH-58D proves its reliability p 458 A92-29670
GALLAGHER, MICHAEL J.
Development of telemetry for the agility flight test of a radio controlled fighter model
[AD-A248653] p 753 N92-27994
GALLIANO, J.
High altitude airborne remote sensing mission using the advanced microwave precipitation radiometer (AMPR) p 574 A92-34893
GALLINGTON, ROGER W.
Propulsion requirements for high altitude long endurance flight
[ASME PAPER 91-GT-393] p 127 A92-15723
GALLOPS, G. W.
Real-time estimation of gas turbine engine damage using a control based Kalman filter algorithm
[ASME PAPER 91-GT-216] p 124 A92-15633
In-flight performance diagnostic capability of an adaptive engine model
[AIAA PAPER 92-3746] p 1068 A92-54147
Performance benefits of adaptive in-flight propulsion system optimization
[AIAA PAPER 92-3749] p 1068 A92-54149
GALLOTTI, ALBERTO
Time Resolved Lidar Fluorosensor operating from helicopter p 1121 A92-56296
GALLOWAY, E. M.
Heat transfer to a delta wing and two waverider wings in rarefied hypersonic flow p 937 A92-52748
GALLOWAY, GORDON L.
Modular simulation of HEI fragments and blast pressure
[AD-A248205] p 910 N92-29191
GALLUS, H. E.
Effects of stator wakes and spanwise nonuniform inlet conditions on the rotor flow of an axial turbine stage
[ASME PAPER 91-GT-93] p 70 A92-15557
GALLUS, HEINZ E.
Inviscid and viscous transonic flows in cascades using an implicit upwind algorithm p 344 A92-28522
GAMBILL, J. M.
Computational icing analysis for aircraft inlets
[AIAA PAPER 92-3178] p 836 A92-48793
GAN, SU
An impact dynamics investigation on some problems in bird strike on windshields of high-speed aircrafts p 986 A92-53330
GAN, XIAOHUA
An investigation of fuel nozzles for combustion performance p 278 A92-21745
GANGULI, RANJAN
Aeroelastic optimization of an advanced geometry helicopter rotor
[AIAA PAPER 92-2360] p 543 A92-34592
GANN, R. G.
Preliminary screening procedures and criteria for replacements for Halons 1211 and 1301
[AD-A252912] p 1126 N92-33501
GANY, ALON
Similarity and scale effects in solid-fuel ramjet combustors p 666 A92-36965
Fuel regression mechanism in a solid fuel ramjet p 860 A92-44898
GAO, BENQING
A new method for orientation calculation of the electromagnetic helmet-mounted sighting unit p 370 A92-27837
GAO, CHUNFENG
Surface flow visualization of rotating propeller p 4 A92-10959
GAO, DEPING
The selection of bird impact load types p 448 A92-29732

Analysis of tenon and mortise contact problems by boundary element methods p 587 A92-35554
GAO, JINYUAN
Optimal implicit model-following approach with frequency-shaped weighting and its application to design of flight control system p 977 A92-53094
GAO, KELING
Simulation research on the dynamic characteristics of steam-injected gas turbine p 971 A92-53389
GAO, M.
Emergence of coherent patterns of vortex stretching during reconnection - A scattering paradigm p 38 A92-11041
GAO, PENGFEI
Predication of fastening capacity of screwed joint structure with cone assembly p 391 A92-24737
GAO, PING
Design variables and constraint derivatives in aeroelastic tailoring p 997 A92-53074
GAO, SHUCHUN
Numerical simulation of supersonic separated flow over blunt cones at high angles of attack p 313 A92-25039
Numerical simulation and analysis for hypersonic flow with separation over blunt cone at angle of attack p 314 A92-25126
GAO, XIANGQUN
On travelling wave vibration of high-speed duplex helical gears p 990 A92-49580
GAO, ZEJUN
Dynamic behavior analysis for landing-gear with different types of dual-chamber shock-struts p 111 A92-15342
GAO, ZHEJUN
Mechanical model of landing impact of three dimensional fuselage landing gear p 960 A92-53090
GAO, ZHENG
A new method for calculation of helicopter maneuvering flight p 282 A92-23382
A study on rotor induced sand and dust environment and its harmfulness to helicopter p 960 A92-53012
GAO, ZHENTONG
A method of reliability analysis for propeller blades p 25 A92-10968
GAONKAR, G. H.
A new method for simulating atmospheric turbulence for rotorcraft applications p 162 A92-14368
Some issues on modeling atmospheric turbulence experienced by helicopter rotor blades p 647 A92-40885
Adequacy of modeling turbulence and related effects on helicopter response p 730 A92-41263
Computational aspects of helicopter trim analysis and damping levels from Floquet theory p 875 A92-46933
On the adequacy of modeling turbulence and related effects on helicopter response p 847 A92-46945
A new method for simulating atmospheric turbulence for rotorcraft applications p 464 N92-21956
GAONKAR, GOPAL H.
Computational aspects of helicopter trim analysis and damping levels from Floquet theory
[NASA-CR-190736] p 1087 N92-33107
GAPONOV, S. A.
Evolution of perturbations in a supersonic boundary layer p 337 A92-27596
Effect of a fan of rarefaction waves on the development of disturbances in a supersonic boundary layer p 809 A92-46519
GARBER, DONALD P.
Advanced subsonic transport approach noise: The relative contribution of airframe noise
[NASA-TM-104112] p 1140 N92-34148
GARBO, SAMUEL P.
Composites usage on the RAH-66 Comanche p 457 A92-29669
GARBUTT, K.
Propulsion simulator for magnetically suspended wind tunnel models p 750 N92-27801
GARCIAFOGEDA, P.
Unsteady transonic aerodynamics of pointed bodies of revolution in supersonic freestream p 719 N92-27946
GARDAREIN, P.
Aerodynamic computations of high-speed transonic propellers
[ONERA, TP NO. 1991-218] p 330 A92-26370
GARDETTE, G.
Measurement of convective heat-transfer coefficients in wind tunnels using passive and stimulated infrared thermography p 390 A92-24430
Application of infrared thermography to thermal flux measurement in wind tunnels
[AAAF-NT-89-12] p 31 N92-11020
Heat transfer measurements in ONERA supersonic and hypersonic wind tunnels using passive and active infrared thermography p 208 N92-15003
GARDINER, PETER T.
Fibre optic rotary position sensors for vehicle and propulsion controls p 855 A92-46243
GARDNER, BRYCE K.
Interior noise prediction methodology: ATDAC theory and validation
[NASA-CR-187626] p 697 N92-25368
GARDNER, J. H.
Numerical simulations of unsteady reactive flows in a combustion chamber p 39 A92-11761
GARDNER, JUDITH A.
Discrete event fuzzy airport control p 1046 A92-55973
GAREM, H.
Control aspects of the transition from transversal to transonic flow, step effects
[ETN-91-90106] p 82 N92-11981
GARG, S.
Design and evaluation of a robust dynamic neurocontroller for a multivariable aircraft control problem
[NASA-TM-105579] p 481 N92-20586
GARG, SANJAY
Integrated flight/propulsion control design for a STOVL aircraft using H-infinity control design techniques p 476 A92-29093
IMPAC - An integrated methodology for propulsion and airframe control p 477 A92-29118
Decentralized hierarchical partitioning of centralized integrated controllers p 477 A92-29119
Propulsion system performance resulting from an Integrated Flight/Propulsion Control design
[AIAA PAPER 92-4602] p 1069 A92-55281
A parameter optimization approach to controller partitioning for integrated flight/propulsion control application
[NASA-TM-105826] p 979 N92-32241
GARLAND, DOUG
Aerodynamic performance of a full-scale lifting ejector system in a STOVL fighter aircraft
[AIAA PAPER 92-3094] p 824 A92-48738
GARNIER, J. E.
Effect of sustained high temperature exposure on the mechanical properties of Nicalon/Al2O3 composites p 668 A92-39672
GARODZ, L. J.
Vortex characteristics of C5A/B, C141B and C130E aircraft applicable to ATC terminal flight operations tower fly-by-data
[PB92-114586] p 449 N92-20318
GARRARD, G. D.
Hydrogen exhaust gas disposition by afterburning
[AIAA PAPER 91-5075] p 200 A92-17848
GARRARD, WILLIAM L.
Achievement of rotorcraft handling qualities specifications via feedback control p 568 A92-35747
Robust dynamic inversion control laws for aircraft control
[AIAA PAPER 92-4329] p 1073 A92-55173
Robustness of a helicopter flight control system designed using eigenstructure assignment
[AIAA PAPER 92-4469] p 1076 A92-55229
Application of nonlinear feedback control theory to supermaneuverable aircraft
[NASA-CR-190336] p 663 N92-25648
Feedback control laws for highly maneuverable aircraft
[NASA-CR-190535] p 879 N92-29654
GARRARD, WILLIAM L., JR.
Nonlinear inversion flight control for a supermaneuverable aircraft p 873 A92-46751
GARRETT, STEVEN L.
Thermoacoustic refrigeration p 595 N92-22720
GARRETTE, DOUG
Advancing airlift avionics - C-17 avionics suite
[AIAA PAPER 92-1243] p 553 A92-33336
GARRIS, C. A.
Flow induction by pressure forces
[AIAA PAPER 92-3571] p 1067 A92-54060
GARRISON, T. J.
Flowfield visualization of crossing shock-wave/boundary-layer interactions
[AIAA PAPER 92-0750] p 335 A92-27094
Structure of crossing-shock wave/turbulent boundary-layer interactions
[AIAA PAPER 92-3670] p 1022 A92-54113
GARRIZ, JAVIER A.
User guide for WIACX: A transonic wind-tunnel wall interference assessment and correction procedure for the NTF
[NASA-TM-104168] p 261 N92-17547
GARRONE, ANGELO
An overview of the planned aerospace test facilities at Capua, Italy
[AIAA PAPER 92-3944] p 1097 A92-56773
GARTENBERG, EHUD
Twenty-five years of aerodynamic research with infrared imaging p 497 A92-32232
Problems and solutions for transition detection in cryogenic wind tunnels by infrared imaging p 1090 A92-54319
GARVEY, DENNIS M.
Measured and calculated optical property profiles in the mixed layer and free troposphere p 1129 A92-54630
GARY, BRUCE L.
Microwave temperature profiler for clear air turbulence prediction
[NASA-CASE-NPO-18115-1-CU] p 916 N92-29148
GARY, CHARLES K.
Optical computing at NASA Ames Research Center
[AIAA PAPER 91-3779] p 231 A92-17637
GARZON, SHERRY B.
Eighth DOD/NASA/FAA Conference on Fibrous Composites in Structural Design, part 1
[NASA-CP-3087-PT-1] p 1106 N92-32513
GASBARRI, P.
Gust effects on a flexible aircraft p 270 A92-22474
GASKIN, G. B.
Characterization of stainless steel pretreatments for adhesive bonding p 994 A92-51546
GASPERAS, GEDIMINIS
High speed transition prediction
[NASA-CR-190836] p 1039 N92-33424
GASTER, M.
Separation of relaminarised boundary layers
[CUED/A-AERO/TR-16] p 592 N92-22209
GASTINEAU, ZANE
Intelligent Engine Control (IEC)
[AIAA PAPER 92-3484] p 866 A92-49024
GATES, DAVID, III
MLS/RNAV control display unit development p 965 A92-49303
GATES, THOMAS S.
Effects of elevated temperature on the viscoplastic modeling of graphite/polymeric composites
[NASA-TM-104160] p 35 N92-11149
Apparatus for elevated temperature compression or tension testing of specimens
[NASA-CASE-LAR-14775-1] p 912 N92-30099
Isothermal aging of IM7/8320 and IM7/5260
[NASA-TM-107666] p 1110 N92-33423
GATHMANN, R. J.
Reactive mixing layer between pressure reflecting boundaries p 656 A92-40144
GATINEAU, R. J.
Development and testing of cabin sidewall acoustic resonators for the reduction of cabin tone levels in propfan-powered aircraft
[NASA-CR-4388] p 166 N92-13757
GATINEAU, ROBERT J.
Laboratory testing of a high transmission loss aircraft cabin structure p 663 A92-39229
GATLIN, DONALD
The F-18 high alpha research vehicle: A high-angle-of-attack testbed aircraft
[NASA-TM-104253] p 1060 N92-33404
GATLIN, DONALD H.
Flight-determined benefits of integrated flight-propulsion control systems
[NASA-TM-4393] p 742 N92-27587
GATLIN, JAMES A.
The application of high spectral and spatial resolution imaging spectrometers for locating downed aircraft p 598 A92-35132
GATZKE, TIMOTHY D.
Geometry acquisition and grid generation: Recent experiences with complex aircraft configurations p 691 N92-24400
GAUME, BRUNO
A cognitive temporal model for the planning in aircraft maintenance p 307 A92-25178
GAUSTAD, ALICE
A noise survey around Oslo Airport Fornebu p 687 A92-39061
GAUTHIER, BENOIT
Improved articulated fin/wing control system statement of government interests
[AD-D015268] p 1088 N92-34131
GAVAN, J.
RFI effects analysis of an airport-installed HF transmitter on aircraft COMM/NAV receivers p 725 A92-42313
GAVAN, JACQUES
An investigation of the desensitizing effects by high power HF broadcast transmitters on HF airborne receivers p 726 A92-43937
GAYDA, JOHN
Creep and fatigue research efforts on advanced materials p 593 N92-22514
GAYET, J.-F.
Industrial measurement of microphysical parameters - Application to natural and simulated icing clouds p 262 A92-23302

GAZZANIGA, JOHN A.
Wind tunnel performance results of swirl recovery vanes as tested with an advanced high speed propeller
[AIAA PAPER 92-3770] p 1068 A92-54159
GAZZOLA, WILLIAM L.
Gas turbine engine control
[PATENT-1-274-606] p 130 N92-13069
GE, GUO H.
Studying method of measuring flow-field between stages in axial-flow compressor p 423 A92-29720
GE, SEN
Research on sonic fatigue calculation and test for aircraft panel p 958 A92-50203
GEA, LIE-MINE
Transonic aeroelasticity analysis for rotor blades p 758 A92-41238
GEARHART, LARRY
Design and implementation of a generic Kalman filter in Ada p 858 A92-48475
GEDDES, NORMAN D.
Knowledge maintenance in an evolving system using a deep structure representation
[AIAA PAPER 91-3941] p 231 A92-17605
Verification and validation testing of the pilot's associate p 966 A92-49318
GEE, KEN
Turbulence model effects on separated flow about a prolate spheroid p 340 A92-28036
Numerical investigation of tail buffet on F-18 aircraft
[AIAA PAPER 92-2673] p 798 A92-45528
Analysis of a pneumatic forebody flow control concept about a full aircraft geometry
[AIAA PAPER 92-2678] p 799 A92-45530
GEENEN, ROBERT
Piloted simulation study of a balloon-assisted deployment of an aircraft at high altitude
[NASA-TM-104245] p 272 N92-15986
GEESEY, ROGER A.
Automated planning with special relevance to associate systems technology and mission planning
[AD-A241924] p 303 N92-17438
GEHLAR, B.
Azimuthal noise characteristics of contra-rotating propellers - Results of a wind tunnel model test p 693 A92-39066
GEIGER, DAVID L.
Static tests for the evaluation of fuel additives
[AIAA PAPER 92-0686] p 389 A92-27053
GEIST, DOUG
Functionally integrated aircraft instrumentation for the next generation commercial helicopter p 117 A92-14402
GELDER, THOMAS F.
Design and performance of controlled-diffusion stator compared with original double-circular-arc stator
[NASA-TP-2852] p 562 N92-22863
GELHAUSEN, P.
ACSYNT - A standards-based system for parametric, computer aided conceptual design of aircraft
[AIAA PAPER 92-1268] p 601 A92-33345
GELLER, M. J.
Operating principles for integrated sensor processing p 966 A92-49336
GELLER, MYER
Mid-range UV communications
[AD-D015213] p 770 N92-27615
GENERALOV, A. V.
Effect of the wake flow on the soundproofing of aircraft structures p 166 A92-16824
GENG, YIPING
Numerical comparison of experimentally measured ultrasound through a multilayered specimen p 510 A92-28682
GENGLER, J. E.
Subsonic propulsion system installation analysis and optimization
[ASME PAPER 91-GT-167] p 111 A92-15602
GENNARETTI, M.
A boundary element method for the potential, compressible aerodynamics of bodies in arbitrary motion p 314 A92-25098
A new integral equation for potential compressible aerodynamics of rotors in forward flight p 815 A92-46958
GENT, R. W.
A review of icing research at the Royal Aerospace Establishment p 451 N92-21689
GENTRY, G. L., JR.
Aerodynamic characteristics of a propeller powered high lift semispan wing
[AIAA PAPER 92-0388] p 323 A92-26244
GENTRY, GARL L., JR.
Effect of solidity and inclination on propeller-nacelle force coefficients
[NASA-TM-4316] p 90 N92-13038
Wind tunnel aerodynamic characteristics of a transport-type airfoil in a simulated heavy rain environment
[NASA-TP-3184] p 948 N92-31532
GEOFFROY, P.
Design and manufacturing of torsional flexible blade models p 547 A92-35780
Airplane crashes on the runway. Fine modeling of the behavior after burning of a frame submitted to linear crushing
[IMFL-90-64] p 353 N92-19350
GEORGALA, J. M.
The construction, application and interpretation of three-dimensional hybrid meshes p 919 A92-47089
GEORGANTAS, A. I.
Application of a double actuator electronic fuel control unit on a small gas turbine engine
[SAE PAPER 912160] p 655 A92-39993
GEORGE, A.
Laser velocimetry measurements in an MHD aerodynamic duct
[AIAA PAPER 92-2986] p 899 A92-46996
Millisecond aerodynamic force measurement with side-jet model in the ISL shock tunnel
[AIAA PAPER 92-3963] p 1097 A92-56790
GEORGE, ALBERT R.
Flow visualization and flow field measurements of a 1/12 scale tilt rotor aircraft in hover
[NASA-CR-189456] p 82 N92-11983
A comparative analysis of XV-15 tiltrotor hover test data and WOPWOP predictions incorporating the fountain effect
[NASA-CR-189455] p 114 N92-11992
GEORGE, V. V.
Adequacy of modeling turbulence and related effects on helicopter response p 730 A92-41263
On the adequacy of modeling turbulence and related effects on helicopter response p 847 A92-46945
GEORGESON, G. E.
X-ray computed tomographic inspection of castings p 492 A92-28725
X-ray computed tomography for the aircraft/aerospace industry p 492 A92-28750
GEORGESON, GARY E.
X-ray computed tomography of composites p 36 A92-10143
GERADIN, M.
Rigid and flexible joint modelling in multibody dynamics using finite elements p 671 A92-37559
GERARDI, J. J.
Application of smart structures to aircraft health monitoring p 20 A92-11123
GERBSCH, R. A.
Solution of the parabolized Navier-Stokes equations using Osher's upwind scheme p 713 A92-44371
GERHARZ, J. J.
Fatigue of repaired composite structures p 214 N92-14411
GERMANY, D. M.
STS-41 Space Shuttle mission report
[NASA-TM-105479] p 286 N92-16973
GERNERT, NELSON
Flexible heat pipe cold plates for aircraft thermal control
[SAE PAPER 912105] p 674 A92-39959
GEROLYMOS, G. A.
Generalized expression of chorochronic periodicity in turbomachinery blade-row interaction p 423 A92-30000
GEROLYMOS, GEORG A.
On the computation of unsteady turbomachinery flows. Part 1: Euler equations in vibrating cascades p 768 N92-27460
GERSTENFELD, ARTHUR
Expert system management system
[AD-A247102] p 781 N92-26863
GERSTLE, JOHN H.
High-speed civil transport aircraft emissions p 408 N92-19122
Designing a methodology for future air travel scenarios p 409 N92-19125
GERTEISEN, EDGAR A.
Computations of unsteady flows around airfoil sections by explicit and implicit methods solving the Euler and Navier-Stokes equations p 720 N92-27948
GESSNER, F. B.
Experimental investigation of coannular jet flow with swirl along a centerbody p 172 A92-18367
GETSOV, L. B.
Technique for estimating the strength of gas turbine guide vanes with stress raisers p 761 A92-42653
GEYER, CAROLYN R.
Active noise reduction p 603 A92-32980
GEYER, E. M.
Precision approach using GPS and GLONASS p 97 A92-16649
GHAOUI, LAURENT E.
Linear quadratic minimax controllers p 917 A92-46748
GHASSEMI, M.
Three-dimensional-mode resonance in far wakes p 898 A92-46252
GHAYEM, SHAHROKH
F-16 failure detection isolation and estimation study p 876 A92-48490
GHAZI, M. A.
Aircraft spoiler effects under wind shear
[AIAA PAPER 92-2642] p 796 A92-45509
GHAZI, MOHAMMAD
Effect of wing tip vortices on a trailing aircraft p 935 A92-50303
GHAZI, MUHAMMAD A.
Effect of atmospheric disturbances on airplane response
[AIAA PAPER 92-4340] p 1078 A92-55329
GHEE, TERENCE A.
Unsteady circulation control aerodynamics of a circular cylinder with periodic jet blowing p 330 A92-26401
GHIA, K. N.
A semi-elliptic analysis for 2-D viscous flows through cascade configurations p 3 A92-10688
Study of role of unsteady separation in formation of dynamic stall vortex
[AIAA PAPER 92-0196] p 257 A92-23804
GHIA, U.
A semi-elliptic analysis for 2-D viscous flows through cascade configurations p 3 A92-10688
Study of role of unsteady separation in formation of dynamic stall vortex
[AIAA PAPER 92-0196] p 257 A92-23804
GHIRINGHELLI, GIAN L.
Linear analysis of naturally curved and twisted anisotropic beam p 899 A92-46936
Composite beam analysis linear analysis of naturally curved and twisted anisotropic beams
[AD-A252652] p 999 N92-30766
GHOSH, AJOY K.
Parameter estimation of an augmented airplane with unsteady aerodynamics modelling p 1073 A92-53546
GIACOBBE, T.
Proposal for the new fatigue management system for the AMX p 361 N92-18580
GIANNAKIDIS, GEORGE
Calculation of potential flow around airfoils using a discrete vortex method p 808 A92-45827
GIANNAKOGLOU, K.
Turbine cascade calculations through a fractional step Navier-Stokes algorithm
[ASME PAPER 91-GT-55] p 68 A92-15533
Arbitrary blade section design based on viscous considerations - Background information p 523 A92-36029
GIBB, GERALD D.
Full model simulation of the National Airspace System - Research and training platform p 880 A92-45042
GIBB, JAMES
Application of computational fluid dynamics to the study of vortex flow control for the management of inlet distortion
[AIAA PAPER 92-3177] p 1020 A92-54013
Application of computational fluid dynamics to the study of vortex flow control for the management of inlet distortion
[NASA-TM-105672] p 1128 N92-34112
GIBBONS, MICHAEL D.
Extending a transonic small disturbance code to treat swept vertical surfaces
[AIAA PAPER 92-2503] p 518 A92-34498
GIBBS, MARTIN
Nortec 30 Eddyscan - Portable flaw imaging for aging aircraft p 492 A92-28745
GIBELING, H. J.
Computation of flow past a turbine blade with and without tip clearance
[ASME PAPER 91-GT-56] p 68 A92-15534
GIBSON, BERRY T.
Exploratory study of wall pressure fluctuations in a Mach 5, sharp fin-induced turbulent interaction p 935 A92-50304
GIBSON, C.
The application of lattice-structure adaptive filters to clutter-suppression for scanning radar p 403 N92-19154
GIBSON, RONALD F.
Nonlinear flutter of orthotropic composite panel under aerodynamic heating
[AIAA PAPER 92-2132] p 589 A92-35699
GIBSON, TERRY L.
Radar Detection Analysis of Rotor Systems (RADARS) p 117 A92-14350

GIBSON, WARREN C.
Preservation and utilization of finite element models of USAF aircraft structures
[AD-A241657] p 160 N92-13470
GIEL, P. W.
Three-dimensional Navier-Stokes heat transfer predictions for turbine blade rows
[AIAA PAPER 92-3068] p 1020 A92-54003
GIEMULLA, ELMAR
Legal problems in aircraft towing using the PTS procedure p 56 A92-11214
GILBANK, PASCALE
Three-dimensional calculations of reactive flows in aircraft combustion chambers performed using two combustion models
[ONERA, TP NO. 1991-110] p 154 A92-16089
Three dimensional calculations of reactive flows within aircraft combustion chambers including some combustion models p 770 N92-27490
Contribution to the modelling of turbulent combustion in the case of stabilisation by flame-lock
[ESA-TT-1229] p 988 N92-31942
GILBERT, ELMER G.
Linear systems with output constraints - The theory and application of maximal output admissible sets
p 506 A92-29066
GILBERT, N. E.
A review of Australian activity on modelling the helicopter/ship dynamic interface p 465 N92-21967
GILBERT, NEIL
Lifting line predictions for a swept tip rotor blade
p 65 A92-14424
GILBERTSON, MIKE
Two and three dimensional parabolized Navier-Stokes code for scramjet combustor, nozzle, and film cooling analysis
[AIAA PAPER 92-0391] p 372 A92-26247
GILE, BRENDA E.
The effects of blowing on delta wing vortices during dynamic pitching at high angles of attack
[AIAA PAPER 92-0407] p 325 A92-26260
GILES, M. B.
Comparison of time-resolved turbine rotor blade heat transfer measurements and numerical calculations
[ASME PAPER 91-GT-268] p 151 A92-15666
GILES, MICHAEL
Validation of a numerical method for unsteady flow calculations
[ASME PAPER 91-GT-271] p 151 A92-15668
GILHAM, S.
Self-induced flow in a stepped rotating tube
[ASME PAPER 91-GT-276] p 152 A92-15673
GILKEY, S. C.
A propulsion perspective of the next generation supersonic transport
[ASME PAPER 91-GT-385] p 126 A92-15719
GILL, JANET A.
Software safety analysis in heterogeneous multiprocessor control systems p 776 A92-42073
GILLARD, WILLIAM J.
High angle-of-attack control enhancement on a forward swept wing aircraft
[AIAA PAPER 92-4427] p 1080 A92-55351
GILLCRIST, M.
Obtaining the velocity field required for the calculation of propeller unsteady forces using 'traditional' approximate methods and CFD
[AIAA PAPER 92-0520] p 331 A92-26945
GILLES, A.
A parallel architecture adapted to onboard multiexpert systems p 276 A92-23040
GILLETTE, D.
Continuous flying quality improvement - The measure and the payoff
[AIAA PAPER 92-4327] p 1073 A92-55171
GILLETTE, RICHARD
Automatic production test equipment (APTE) for the B-2 p 997 A92-53107
GILLIAM, D.
Decentralized-feedback pole placement of linear systems p 411 A92-27347
GILLINGHAM, KENT K.
Effects of variations in head-up display airspeed and altitude representations on basic flight performance
p 46 A92-11204
An aircraft landing accident caused by visually induced spatial disorientation p 834 A92-44993
Reference mode effect on the auditory display of aircraft bank angle
[AD-A247825] p 728 N92-27916
GILMER, JOHN B.
Automated planning with special relevance to associate systems technology and mission planning
[AD-A241924] p 303 N92-17438
GILMORE, M. R.
Flat-ended circular cylinder in hypersonic rarefied flow
p 174 A92-20304
Heat transfer to a delta wing and two waverider wings in rarefied hypersonic flow p 937 A92-52748
GILREATH, H. E.
Stratified flow around an axisymmetric body at small angle of attack p 172 A92-18385
GILYARD, GLENN B.
Subsonic flight test evaluation of a performance seeking control algorithm on an F-15 airplane
[AIAA PAPER 92-3743] p 878 A92-49109
Subsonic flight test evaluation of a propulsion system parameter estimation process for the F100 engine
[AIAA PAPER 92-3745] p 866 A92-49110
Subsonic flight test evaluation of a performance seeking control algorithm on an F-15 airplane
[NASA-TM-4400] p 973 N92-31275
GIMLETT, JAMES I.
Modulation transfer function degradation in segmented windows p 733 A92-41431
GINDER, R. B.
Design and performance of advanced blading for a high-speed HP compressor
[ASME PAPER 91-GT-374] p 76 A92-15718
GINGRICH, C.
Structural design for durability - Lessons learned from service and test data
[AIAA PAPER 92-1129] p 537 A92-33281
GINZBURG, A. E.
Gas-generator with high-temperature path ceramic components
[ASME PAPER 91-GT-152] p 148 A92-15594
GIONFRIDDO, THOMAS A.
Analysis of sonic boom data to quantify distortions of shock profiles p 1139 N92-33879
GIORDANO, D.
SIMOUN and Scirocco wind tunnel nozzle viscous flow study p 208 N92-14999
GIRAGOSIAN, PAKRAD A.
Rapid synthesis for evaluating missile maneuverability parameters
[AIAA PAPER 92-2615] p 873 A92-45488
GIRARD, ANDRE
Environmental impact of a future supersonic transport aircraft
[ONERA, TP NO. 1991-132] p 161 A92-16108
GIRARD, M.
Thermographic gust wind tunnel measurements
[ONERA-RF-31/3409-PY] p 81 N92-11972
GIRIJA, G.
Estimation of lift and drag characteristics of an aircraft from flight data p 959 A92-51942
GIRODROUX-LAVIGNE, P.
Calculation of fully three-dimensional separated flows with an unsteady viscous-inviscid interaction method
[ONERA, TP NO. 1992-1] p 821 A92-48577
Development of an unsteady three-dimensional viscous-inviscid interaction numerical method for the calculation of airfoils vibration
[ONERA-RSF-7/3617-AY-022A] p 830 N92-29206
GISQUET, D.
Detailed analysis of wing-nacelle interaction for commercial transport aircraft
[ONERA, TP NO. 1991-152] p 77 A92-16122
GITTNER, NATHAN M.
The effects of nozzle exit geometry on forebody vortex control using blowing
[AIAA PAPER 92-2603] p 792 A92-45480
GIVI, P.
Modeling of the reactant conversion rate in a turbulent shear flow p 829 N92-28820
GIZA, DAVID A.
U.S. Coast Guard aviation life support and rescue equipment p 529 A92-32999
GIZDOVA, N. D.
Investigation of the structural inhomogeneity of a titanium alloy p 893 A92-47958
GJESTLAND, TRULS
A noise survey around Oslo Airport Fornebu
p 687 A92-39061
GLASS, CHRISTOPHER E.
Three-dimensional thermal structural analysis of a swept cowl leading edge subjected to skewed shock-shock interference heating p 174 A92-20306
GLASS, ROBERT
An artificial intelligence approach for the verification of requirements for aircraft electrical power systems
p 863 A92-48481
GLASSMAN, ARTHUR J.
Computer code for preliminary sizing analysis of axial-flow turbines
[NASA-CR-4430] p 473 N92-20196
Users manual and modeling improvements for axial turbine design and performance computer code TD2-2
[NASA-CR-189118] p 716 N92-27376
Users manual for updated computer code for axial-flow compressor conceptual design
[NASA-CR-189171] p 924 N92-30207
Trends in aeropropulsion research and their impact on engineering education
[NASA-TM-105682] p 972 N92-31172
GLASSON, DOUGLAS P.
Adaptive tactical navigation program
p 102 N92-12529
GLATT, L.
Hypersonic plasma predictions at nonzero angle of attack
[AIAA PAPER 92-3027] p 925 A92-47028
GLATZ, J. D.
Energy attenuation for crashworthy seating systems - Past, present, and possible future development
p 544 A92-35452
GLATZ, JOHN
Applications of advanced composites in a 3/4 air transportable rack p 36 A92-10314
Application of resin and metal matrix composites to advanced avionics enclosure p 985 A92-51921
Application of advanced composites in SEM-E heatsinks for the thermal management of avionics
p 986 A92-51922
GLAUSER, M.
Multifractal analysis of a lobed mixer flowfield utilizing the proper orthogonal decomposition
p 611 A92-36840
GLAZKOV, S. A.
Subsonic flow past a thin airfoil in a channel with porous walls p 438 A92-31867
Determination of the mass-flow-rate characteristics of porous panels p 439 A92-31875
GLAZNEV, V. N.
Feedback mechanism of self-oscillations in the case of an underexpanded supersonic jet impinging on a plane obstacle p 79 A92-16682
GLEASON, DANIEL
Estimation of flying qualities using a leastsquares lower-order equivalent systems technique
p 570 A92-35947
Flight test results using a low order equivalent systems technique to estimate flying qualities
[AIAA PAPER 92-4425] p 1080 A92-55349
Use of simulation in the USAF Test Pilot School curriculum p 884 N92-28535
GLEGG, STEWART A. L.
The application of experimental data to blade wake interaction noise prediction
[NASA-CR-189461] p 237 N92-14789
GLENDENING, J. W.
Boundary-layer transition across a stratocumulus cloud edge in a coastal zone p 45 A92-10489
GLESK, I.
Rayleigh imaging and flow tagging in ground test facilities p 1115 A92-54330
GLEZER, A.
The dynamics and control of fluctuating pressure loads in the reattachment region of a supersonic free shear layer
[AIAA PAPER 92-0178] p 255 A92-23788
GLEZER, B.
Turbine blade tip clearance improvement
[ASME PAPER 91-GT-164] p 123 A92-15599
GLICKSTEIN, IRA
Route planning p 1006 A92-49317
GLIEBE, P. R.
Jet noise suppression p 236 N92-14784
High speed turboprop aeroacoustic study (counterrotation). Volume 2: Computer programs
[NASA-CR-185242] p 1011 N92-31248
GLIEBE, PHILLIP R.
Turbomachinery noise p 54 N92-10601
GLODOWSKI, KAREN A.
Real-time microfocus radiography for electronic failure analysis p 214 A92-17289
GLOMB, WALTER L., JR.
Fiber-optic position transducers for aircraft controls
p 857 A92-48041
GLOSS, BLAIR B.
Future experimental needs to support applied aerodynamics - A transonic perspective
[AIAA PAPER 92-0156] p 254 A92-23771
GLOVER, K.
VSTOL aircraft flight control system design using H(infinity) controllers and a switching strategy
p 28 A92-11561
Meeting VSTOL aircraft performance requirements using scheduled H(infinity) controllers p 477 A92-29094
GLOVER, V. M.
An airborne Doppler lidar for meteorological research
p 467 A92-32082
GLOVER, VINCE
Modifications to and data correction methods for some radiometers used on aircraft p 467 A92-32062

GLOWER, JAKE
Model-reference adaptive control for systems with D matrices p 506 A92-29052
GLUSHCHENKO, G. N.
A computational study of flow past bodies and heat transfer for isentropic compression flows p 425 A92-30158
GLUSMAN, STEVEN I.
1991-92 AHS Technical Committee highlights - Handling qualities p 662 A92-40395
GLYNN, MICHAEL S.
High Intensity Radiated Fields (HIRF) project plan [DOT/FAA/CT-TN91/1] p 297 N92-16181
GNEMMI, P.
Computation of the BVI noise for the BO105 Model Rotor in forward flight and comparison with wind tunnel tests p 165 A92-14386
GNOFFO, P. A.
Application of program LAURA to perfect gas shock tube flows: A parametric study [NASA-TM-104190] p 298 N92-17002
GNOFFO, PEPTER A.
Computation of near-wake, aerobrake flowfields p 441 A92-32181
GNOFFO, PETER A.
Application of the LAURA code for slender-vehicle aerothermodynamics p 310 A92-24652
GOATHAM, JULIE
An evaluation of the Royal Air Force Shorts Tucano Navigation Instruments Trainer: The NAVIT [ETN-92-90841] p 354 N92-18729
GODARD, J. L.
Detailed analysis of wing-nacelle interaction for commercial transport aircraft [ONERA, TP NO. 1991-152] p 77 A92-16122
Drag prediction using computation methods [ONERA-RSF-82/1685-AY-154-4] p 349 N92-19682
GODARD, J.-L.
Investigations of propulsion integration interference effects on a transport aircraft configuration [AIAA PAPER 92-3097] p 849 A92-48739
GODDARD, K.
Environmentally sound [PNR-90776] p 506 N92-21743
Re-engining for real stage 3 compliance [PNR-90872] p 1072 N92-33748
GOEL, SANJAY
Integration of artificial intelligence and numerical optimization techniques for the design of complex aerospace systems [AIAA PAPER 92-1189] p 600 A92-33301
GOEL, SURESH
Dead reckoning for aircraft in distributed interactive simulation [AIAA PAPER 92-4171] p 1008 A92-52456
GOELLNER, AMBROS
Tornado structural fatigue life assessment of the German Air Force p 363 N92-18592
GOELZENLEUCHTER, HORST
Test and integration concept for complex helicopter avionic systems p 1064 A92-56292
GOERANSSON, PETER
Advanced Study for Active Noise Control in Aircraft (ASANCA) [AIAA PAPER 92-2092] p 1137 N92-32956
GOETZENDORF-GRABOWSKI, TOMASZ
Calculation of the aerodynamic derivatives of aircraft in the supersonic region using the Mach box method p 875 A92-47779
GOGGIN, PATRICK J.
A general gust and maneuver load analysis method to account for the effects of active control saturation and nonlinear aerodynamics [AIAA PAPER 92-2126] p 567 A92-35693
GOGINENI, SIVARAM
Experimental observations of instability modes in a rectangular jet p 1135 A92-54908
GOGISH, LEV V.
Separated and cavitation flows - Principal properties and computational models [ISBN 5-02-014005-8] p 610 A92-36600
GOGOLIN, V. P.
Maximum mass allowance to justify passenger-carrying aircraft modification p 113 A92-16802
GOINS, RICHARD T.
Identification of high-level functional/system requirements for future civil transports [NASA-CR-189561] p 276 N92-15991
An exploration of function analysis and function allocation in the commercial flight domain [NASA-CR-4374] p 368 N92-19871
High speed research system study. Advanced flight deck configuration effects [NASA-CR-189650] p 967 N92-30965
GOITIA, C. B.
World Administrative Radio Conference ends favourably for air transport sector p 956 A92-52650
GOKA, TSUYOSHI
MLS/RNAV control display unit development p 965 A92-49303
Evaluation of advanced microwave landing system procedures in the New York terminal area [DOT/FAA/ND-91/1] p 354 N92-18967
GOKER, MEHMET H.
The TSE 310 troubleshooting expert prototype for the Airbus A-310 commercial aircraft p 307 A92-25180
GOLDBERG, DAVID E.
Control system optimization using genetic algorithms p 661 A92-39900
GOLDBERG, JOSHUA
Improvements to expulsive separation ice protection blankets [AIAA PAPER 92-0533] p 358 A92-26951
GOLDBERG, NORMAN
Generators inside small engines [AIAA PAPER 92-3755] p 867 A92-49113
GOLDEN, K.
Hypersonic plasma predictions at nonzero angle of attack [AIAA PAPER 92-3027] p 925 A92-47028
GOLDEY, C. L.
Propulsion simulator for magnetically suspended wind tunnel models p 750 N92-27801
GOLDLSTEIN, R. J.
Studies of gas turbine heat transfer: Airfoil surfaces and end-wall cooling effects [AD-A244055] p 376 N92-19097
GOLDMAN, A.
A preliminary study on damage detection using piezoelectric film [AD-A246350] p 733 N92-28118
GOLDMAN, LOUIS J.
Laser anemometer measurements and computations in an annular cascade of high turning core turbine vanes [NASA-TP-3252] p 830 N92-28980
GOLDSTEIN, HOWARD E.
Performance of uncoated AFRSI blankets during multiple Space Shuttle flights [NASA-TM-103892] p 890 N92-29104
GOLDSTEIN, M. E.
Noise from turbulent shear flows p 55 N92-10603
GOLDSTEIN, R. J.
Convective transport phenomena on the suction surface of a turbine blade including the influence of secondary flows near the endwall [ASME PAPER 91-GT-35] p 147 A92-15518
GOLDSTONE, LEN
Single slotted array achieves multimode performance p 726 A92-44428
GOLDTHORPE, S.
Fly-by-light technology development plan [NASA-CR-181954] p 1086 N92-32778
GOLIA, C.
Stokes flows in superposed immiscible liquids with horizontal heating [IAF PAPER 92-0909] p 1123 A92-57288
GOLOVIZNIN, V. P.
Interaction between a body flying at a supersonic velocity and a point explosion p 1019 A92-53867
GOLOVKINA, T. E.
High-temperature metal matrix composite p 1105 A92-53878
GOLUBKIN, V. N.
Optimization of the three-dimensional shape of lifting bodies of small aspect ratio at hypersonic velocities p 244 A92-21602
GOMAN, M.
Stochastic self-induced roll oscillations of slender delta wing at high angles of attack [AIAA PAPER 92-4498] p 1081 A92-55366
State-space representation of aerodynamic characteristics of an aircraft at high angels of attack [AIAA PAPER 92-4651] p 1028 A92-55395
GOMER, CHARLES
Preliminary design studies of an advanced general aviation aircraft [NASA-CR-190024] p 461 N92-20064
GONDA, MASAHIRO
Experiments on turbulent flow due to an enclosed rotating disk p 615 A92-38863
GONG, BENQUAN
An experimental investigation of the swirling combustor for integral liquid fuel ramjet p 557 A92-35541
GONG, LEI
Polygon interval arithmetic and design of robust control systems p 49 A92-11418
GONG, MENGXIAN
Experimental research on blade containment p 557 A92-35561
GONG, WEI-BO
A new class of gradient estimators for queueing systems with real-time constraints p 49 A92-11395
GONG, YAO-NAN
Bird impact analysis of aircraft windshield transparency p 958 A92-50236
GONSALVES, PAUL G.
An alternative concept for aeroassisted orbit transfers [AD-A243409] p 287 N92-17325
GONZALEZ, W. D.
Stratospheric electrodynamics from superpressure balloons - A technical challenge for small payload environments [AIAA PAPER 91-3674] p 14 A92-11019
GOODALL, COLIN
Bird ingestion into large turbofan engines [DOT/FAA/CT-91/17] p 1043 N92-33005
GOODEN, J. H. M.
Comparison of LDA and LTA applications for propeller tests in wind tunnels [NLR-MP-88031-U] p 827 N92-28658
Flow gradient corrections on hot-wire measurements using an X-wire probe [NLR-TP-90255-U] p 829 N92-28713
GOODISMAN, M. I.
An Axial Turbobrake [ASME PAPER 91-GT-1] p 147 A92-15501
GOODMAN, CHARLES E.
FAMUSS - A new aeroservoelastic modeling tool [AIAA PAPER 92-2395] p 541 A92-34468
GOODMAN, ROBERT K.
Analysis of rotor blade dynamics using experimental UH-60A airloads obtained at the DNW p 107 A92-14394
GOODRICH, R. K.
Enclosing shapes for single-Doppler radar features p 494 A92-30476
GOODSELL, AGA M.
Euler/experiment correlation of a generic fighter p 1031 A92-56164
Transonic and supersonic Euler computations of vortex-dominated flow fields about a generic fighter [NASA-TP-3156] p 11 N92-10011
GOODSON, JOHN H.
Gulf Range Drone Control Upgrade System Mobile Control System p 882 A92-47567
GOODYER, M.
Propulsion simulator for magnetically suspended wind tunnel models p 750 N92-27801
GOODYER, MICHAEL J.
Wind tunnel magnetic Suspension Systems at the University of Southampton, England p 751 N92-27804
GOOLD, IAN
Dornier Do.328 special - Examining the high-speed commuter p 21 A92-11882
Ageing airliner census - Still flying safely p 634 A92-38374
GOPALRATNAM, GIRIJA
Graphics for interactive PC based parameter estimation package [NAL-PD-FC-9117] p 412 N92-18252
PC based flight path reconstruction using UD factorization filtering algorithm [NAL-PD-FC-9201] p 534 N92-22389
GOPALSWAMY, SWAMINATHAN
Robust adaptive nonlinear control of high performance aircraft p 478 A92-29188
GOPINATH, K. V.
Structural airworthiness of aging Boeing jet transports - 747 fuselage fatigue test program [AIAA PAPER 92-1128] p 537 A92-33280
GORADIA, SURESH
Engineering method for aero-propulsive characteristics at hypersonic Mach numbers [AIAA PAPER 91-5061] p 437 A92-31690
GORADIA, SURESH H.
Mass flux similarity for slotted transonic-wind-tunnel walls [NASA-TM-4281] p 11 N92-10006
GORANSON, ULF G.
Structural airworthiness of aging Boeing jet transports p 362 N92-18590
Structural integrity of future aging airplanes p 913 N92-30107
GORANSSON, PETER
Propeller aircraft interior noise - Physical background and possible treatments p 642 A92-39082
GORBUSHIN, A. R.
Determination of the mass-flow-rate characteristics of porous panels p 439 A92-31875
GORDER, P. J.
Quantitative Feedback Theory (QFT) applied to the design of a rotorcraft flight control system [AIAA PAPER 92-0044] p 281 A92-22161

GORDER, PETER J.
Development of a real-time simulation of a ship-correlated airwake model interfaced with a rotorcraft dynamic model
[AIAA PAPER 92-4149] p 1007 A92-52440
GORDIS, JOSHUA H.
A frequency domain theory for structural identification
p 590 A92-35745
GORDNIER, RAYMOND E.
Computation of a Kelvin-Helmholtz instability for delta wing vortex flows
[AD-A244320] p 346 N92-18825
GORDON, ALASTAIR C.
The 1991 Cierva Lecture - Aberdeen and its influence on the evolution of the commercial IFR twin engined helicopter p 723 A92-43446
GORDON, G.
Direct computation of turbulence and noise
[NASA-CR-187616] p 236 N92-14788
GORDON, IRA
The application of multimedia expert systems to the depot level maintenance environment
p 922 A92-48557
GORDON, J. M.
General performance characteristics of real heat engine p 1011 A92-50401
GORE, ALBERT, JR.
National Aeronautics and Space Administration Authorization Act, 1993
[S-2558-IS] p 698 N92-25606
GORELOV, S. L.
Approximate aerodynamic analysis for complicated bodies in rarefied gas flows p 938 A92-52754
GORELOV, V. A.
The flow pattern and external heat transfer investigation for gas turbine vanes end surfaces
[AIAA PAPER 92-3071] p 903 A92-48722
GORENBUKH, P. I.
Effect of viscosity on the drag of slender axisymmetric bodies in hypersonic flow p 425 A92-30154
The lift-drag ratio of a slender cone in viscous hypersonic gas flow p 425 A92-30172
Analytical and experimental studies of the aerodynamic characteristics of a delta wing at a slip angle at high supersonic velocities p 437 A92-31854
GORETSKII, LEONID I.
Airfield construction (3rd revised and enlarged edition)
[ISBN 5-277-01070-X] p 670 A92-36606
GORIN, VADIM V.
Flight test control p 136 A92-15021
GORSHENIN, D. S.
Lift characteristics of an infinite-span cylindrical wing of a thick symmetric profile at low subsonic velocities
p 440 A92-31897
GORSHKOV, ANATOLII G.
Nonstationary aerohydroelasticity of spherical bodies
[ISBN 5-02-014006-6] p 670 A92-36611
GORSHKOV, G. F.
Self-oscillatory interaction of an underexpanded jet with an obstacle in the presence of a supersonic wake
p 79 A92-16681
GORSKI, J.
Navier-Stokes analysis of turbulent boundary layer and wake for two-dimensional lifting bodies
p 221 N92-14309
GOSHEN-MESKIN, D.
Observability analysis of piece-wise constant systems with application to inertial navigation p 49 A92-11391
GOSLING, GEOFFREY
Tilt rotors and the Port Authority of New York and New Jersey Airport System
[RAND-R-3971/1-PA-SUMM] p 636 N92-25262
GOSS, L. P.
Laser diagnostics for velocity measurements in supersonic combusting environments
[AIAA PAPER 92-0008] p 288 A92-22133
GOSWAMI, TARUN
Fatigue testing of a gas turbine fan disc
p 217 A92-19818
GOTO, AKIRA
Three-dimensional flow and mixing in a axial flow compressor with different rotor tip clearances
[ASME PAPER 91-GT-89] p 70 A92-15554
GOTO, N.
Nonstationary manual control. III p 776 A92-43187
GOTO, NORIHIRO
Manual control of vehicles with time-varying dynamics
[SAE PAPER 912078] p 917 A92-45454
An identification procedure for a system with a choice of feedback structures p 1132 A92-55426
GOTTESDIENER, L.
Flat plates placed in depleted hypersonic flow
[SESSIA-430/91.960] p 947 N92-31508
GOTTLIEB, J. J.
Computational fluid dynamics p 177 N92-13979
Nonstationary gasdynamics p 220 N92-13985
TVD finite-difference solutions of nonequilibrium vibrationally relaxing and chemically reacting gaseous flows p 626 N92-24854
GOTTLIEB, JAMES
Rarefaction wave eliminator design study
[AD-A244401] p 484 N92-20455
GOUDENOVE, FRANCOIS
ELS for the A340
[SAE PAPER 912111] p 651 A92-39963
GOUEDARD, G.
Reaction speed constant for the reactions between N + O2 and between O + N2
[ETN-92-90861] p 347 N92-19252
GOULAIN, M.
Study model for the reduction of noise through double wall cylindrical shells - Comparison with experimentation
p 694 A92-39088
Noise inside aircraft fuselages subjected to airborne excitation p 643 A92-39089
GOULD, RONALD W.
Enhanced visual technique for rapid inspection of aircraft structures p 214 A92-17290
GOUNET, H.
Modification of the radiated sound directivity due to ground reflections - Application to static tests of helicopter turboshaft engines
[ONERA, TP NO. 1991-210] p 415 A92-26362
GOUSMAN, K. G.
Pilot activated automatic recovery system on the F-117A
[AIAA PAPER 92-1126] p 563 A92-33278
GOVINDARAJ, K. S.
The VISTA/F-16 programmable feel system
[AIAA PAPER 92-4172] p 977 A92-52457
GOWDY, VAN
Evaluation of head impact kinematics for passengers seated behind interior walls
[AD-A252651] p 952 N92-30551
GRABE, W.
Humidity effects on gas turbine performance
[NRC-30241] p 130 N92-11998
Fuel flow measurement in gas turbine testing
[NRC-29808] p 130 N92-12000
GRABER, EDWIN J.
Overview of NASA PTA propfan flight test program
p 561 N92-22536
GRACHEVA, L. I.
Thermal deformation of a polymer heat shield material on the descent trajectory p 754 A92-42655
GRAEBEL, B.
Solid-vapor adsorption refrigeration system development
[PB92-164383] p 771 N92-27715
GRAEWE, E.
The cryogenic balance design and balance calibration methods
[AIAA PAPER 92-4001] p 1122 A92-56824
GRAF, W. O.
Flight simulation p 207 N92-13982
GRAFFSTEIN, JERZY
Selected models of aircraft navigation space
p 839 A92-45373
GRAFTON, M.
Compensating for manufacturing and life-cycle variations in aircraft engine control systems
[AIAA PAPER 92-3869] p 868 A92-49139
GRAHAM, DARIN P. W.
Constraint propagation through electromagnetic interaction topologies
[NRC-31761] p 155 N92-12154
GRAHAM, DUNSTAN
Retrospective essay on nonlinearities in aircraft flight control p 204 A92-18601
GRAHAM, G. M.
Time-average loading on a two-dimensional airfoil in a large amplitude motion p 811 A92-46805
Tow-tank study of nonlinear aerodynamics of a 2-D airfoil
[AIAA PAPER 92-4499] p 1026 A92-55367
Nonlinear normal and axial force indicial responses for a two dimensional airfoil
[AD-A247196] p 830 N92-28888
GRAHAM, J. M. R.
Numerical simulation of vortex street-edge interaction
p 88 N92-13027
GRAHAM, L. J.
Realistic real-time ground testing
[AIAA PAPER 92-0197] p 284 A92-23805
GRAHAM, ROBERT G.
Implementation of a personal computer based parameter estimation program
[AD-A252914] p 1061 N92-33502
GRAHAM, ROBERT H.
Al-Li alloys find their niche p 755 A92-43685
GRAHAM, TERENCE ARTHUR
Pitch-heave dynamics models for an air cushion vehicle
[ISBN-0-315-51095-1] p 716 N92-27624
GRAHAM, W. R.
Boundary layer induced noise in aircraft
[CUED/A-AERO/TR-18] p 927 N92-29201
GRAHL, K. G.
Computation of 3D flow phenomena in axial flow compressor blade rows
[ASME PAPER 91-GT-78] p 69 A92-15547
GRALLERT, H.
Acquisition of an aerothermodynamic data base by means of a winged experimental reentry vehicle
p 486 A92-30685
Acquisition of an aerothermodynamic data base by means of a winged experimental reentry vehicle
[MBB/FE202/S/PUB/461] p 787 N92-30232
GRAMANN, R. A.
A preliminary study of the turbulent structures associated with unsteady separation shock motion in a Mach 5 compression ramp interaction
[AIAA PAPER 92-0744] p 436 A92-31677
GRAMBOW, K.
Process/object-oriented Ada software design for an experimental helicopter p 164 N92-12461
GRANBERG, HARDY B.
Interactive graphics method for removal of helicopter motions from laser profile data p 598 A92-35109
GRANCHER, M. S.
Theoretical study (Lagrangian modeling) of turbulent particulate dispersion
[ETN-91-99909] p 42 N92-11287
GRANDHI, R. V.
Automated trajectory synthesis for hypersonic vehicles using energy management and variational calculus techniques p 210 A92-19061
Control strategy for maximizing reconnaissance range of hypersonic cruise vehicles p 729 A92-41222
GRANOIEN, I. L. N.
Advanced method for single event aircraft noise analysis p 693 A92-39060
GRANOIEN, IDAR
A noise survey around Oslo Airport Fornebu
p 687 A92-39061
GRANOIEN, IDAR L. N.
Computation of aircraft noise exposure using digitized topography data p 687 A92-39058
GRANOVSKAIA, E. A.
Development and bench test of high-temperature combustion chamber with structural ceramic components
[ASME PAPER 91-GT-315] p 126 A92-15691
GRANT, GAYLE
An ultrareliable integrated digital computer for helicopters p 964 A92-49273
GRANT, H. P.
High temperature static strain gage development
[NASA-CR-189044] p 195 N92-14037
High temperature strain gage technology for hypersonic aircraft development applications
[NASA-CR-189101] p 592 N92-22239
GRANT, I.
Particle image velocimetry measurements of the aerodynamics of a wind turbine p 1115 A92-54337
GRANT, P. R.
Flight simulation p 207 N92-13982
GRANT, TED
Current nondestructive inspection methods for aging aircraft
[DOT/FAA/CT-91/5] p 1126 N92-33480
GRANTHAM, WALTER J.
A DFW microburst model based on DL-191 data
p 17 A92-11380
GRANVILLE, PAUL S.
Comment on 'Modification of the van Driest damping function to include the effects on surface roughness'
p 758 A92-41297
GRAS'KIN, S. S.
A discrete vortex study of stationary flow past three-dimensional lifting systems at subsonic and supersonic velocities p 79 A92-16813
GRASSIN, CHRISTOPHE
Computation of aerodynamic coefficients on Hermes-Ariane5 configuration p 184 N92-15040
GRASSO, F.
Viscous high-speed flow computations by adaptive mesh embedding techniques p 808 A92-45839
Lower upper implicit total variation diminishing solution of viscous hypersonic flows p 935 A92-50302
GRAU, RICHARD H.
Evaluation of grounding and mooring points for Army aircraft
[AD-A250749] p 953 N92-31193
GRAUER, WILLIAM K.
V-22 flight test aerodynamics p 104 A92-14333

GRAVELLE, A.
Aircraft ground vibration test by means of flight control surfaces
[ONERA, TP NO. 1991-96] p 133 A92-16079
GRAVELLE, ALAIN
Advances in aircraft modal identification
[ONERA, TP NO. 1992-47] p 877 A92-48608
GRAVES, MICHAEL J.
Composite fuselage technology (summary of year 2)
[NASA-CR-190434] p 731 N92-26655
GRAWE, J.
Grid impact on 3D hypersonic flows
p 184 N92-15041
GRAY, CARL E., JR.
Large-amplitude finite element flutter analysis of composite panels in hypersonic flow
[AIAA PAPER 92-2130] p 589 A92-35697
Thermal/structural analysis of a transpiration cooled nozzle
[NASA-TM-104184] p 401 N92-18877
GRAY, DAVID L.
Active thermal isolation for temperature responsive sensors
[NASA-CASE-LAR-14612-1] p 911 N92-29954
GRAY, F. G.
A model of the ADA avionics real-time system: An example of the benefits of the hardware/software codesign approach in development of real-time systems
[AD-A248893] p 967 N92-30524
GRAY, J.
New developments in the computer simulation of X-ray nondestructive evaluation process p 490 A92-28588
GRAY, L. J.
Simulation of 3D non-planar fatigue crack growth in a turbine blade root
[DE92-006859] p 739 N92-26697
GRAY, ROBIN B.
Vortex modeling for rotor aerodynamics - The 1991 Alexander A. Nikolsky Lecture p 315 A92-25576
GRAY, ROGER L.
Method of guiding an in-flight vehicle to a designed flight path
[AD-D015061] p 268 N92-17707
GRAY, T. A.
A new method to estimate the effective geometric focal length and radius of ultrasonic focused probes
p 490 A92-28633
A technique for quantitatively measuring microstructurally induced ultrasonic noise
p 510 A92-28720
GRAYSTON, ALAN M.
Data reduction formulas for the 16-foot transonic tunnel: NASA Langley Research Center, revision 2
[NASA-TM-107646] p 984 N92-31900
GRAZIANI, F.
Aircraft navigation using Global Positioning System improved with geostationary satellites
p 99 A92-16934
GRAZIANI, R. A.
Heat transfer in rotating serpentine passages with trips normal to the flow
[ASME PAPER 91-GT-265] p 151 A92-15663
GREBENSHCHIKOV, V. P.
Methyl-tert-butyl ether as a component of aviation gasolines p 34 A92-12146
GREBER, ISAAC
The structure and development of streamwise vortex arrays embedded in a turbulent boundary layer
[AIAA PAPER 92-0551] p 342 A92-28204
GRECHIKHA, G. E.
A method for determining the optimal composition of the measured parameters in diagnosing gas turbine engines p 128 A92-16819
GREELEY, RONALD
Aerodynamic roughness measured in the field and simulated in a wind tunnel
[NASA-CR-4422] p 347 N92-19354
GREEN-THOMAS, T.
Institute for experimental fluid mechanics: Results for 1990
[IB-222-90-A-46] p 400 N92-18244
GREEN, EDWIN W.
Aviation products liability and navigation - Recent developments and future directions p 697 A92-39563
GREEN, INGE S.
Vibro-acoustic FE analyses of the Saab 2000 aircraft
p 1137 N92-32952
GREEN, J. E.
The Second Goldstein Lecture: Modern developments in fluid dynamics - An addendum p 442 A92-32323
GREEN, JOHN A.
A piloted comparison of elastic and rigid blade-element rotor models using parallel processing technology
p 546 A92-35751
Comparison of elastic and rigid blade-element rotor models using parallel processing technology for piloted simulations
[SAE PAPER 912120] p 608 A92-39968
GREEN, LAWRENCE L.
Wall interference assessment/correction for transonic airfoil data p 30 A92-13214
GREEN, MICHAEL D.
Effect of blade planform variation on the forward-flight performance of small-scale rotors
[NASA-TM-4345] p 630 N92-24885
GREEN, R. B.
Measurements of the dynamic stall vortex convection speed p 1032 A92-56351
GREEN, STEVEN M.
Profile negotiation - A concept for integrating airborne and ground-based automation for managing arrival traffic
p 531 A92-33432
The Center/TRACON Automation System (CTAS): A video presentation
[NASA-TM-103887] p 356 N92-20029
GREEN, STUART
Aspects of compression in aerospace composites: Future requirements p 1109 N92-33036
GREENBERG, I.
Evaluation of parallel injector configurations for Mach 2 combustion p 376 A92-28533
GREENDYKE, ROBERT B.
A parametric analysis of radiative structure in aerobrake shock layers
[AIAA PAPER 92-2970] p 816 A92-46985
GREENE, FRANCIS A.
Comparison of heating calculations with experimental data on a modified Shuttle Orbiter p 441 A92-32184
GREENE, G. C.
High-Reynolds-number test requirements in low-speed aerodynamics p 787 A92-45263
GREENE, J. B.
Nonflammable hydraulic power system for tactical aircraft. Volume 2: Equipment and systems test and evaluation
[AD-A239805] p 35 N92-10100
GREENHALGH, E. S.
A method to determine propagation direction of compressive fracture in carbon-fibre composites
p 672 A92-38770
GREENING, DENIS A.
An electronically scanned precision runway monitor
p 98 A92-16654
GREENWOOD, DAN
The application of neural networks to drone control
p 205 A92-19273
GREENWOOD, STUART W.
The application of imaging sensors to aircraft landings in adverse weather p 1045 A92-54902
GREFF, E.
Application of direct inverse analogy method (DIVA) and viscous design optimization techniques
p 176 N92-13951
GREGOREK, G. M.
Experimental unsteady pressures on an oscillating cascade with supersonic leading edge locus
[AIAA PAPER 92-4035] p 1035 A92-56857
GREGORICH, STEVEN E.
The impact of cockpit automation on crew coordination and communication. Volume 1: Overview, LOFT evaluations, error severity, and questionnaire data
[NASA-CR-177587] p 93 N92-13044
GREGORY-SMITH, D. G.
Turbulence modelling for secondary flow prediction in a turbine cascade
[ASME PAPER 91-GT-57] p 68 A92-15535
GREGORY, B. A.
The effect of blade solidity on the aerodynamic loss of a transonic turbine cascade
[AIAA PAPER 92-0393] p 323 A92-26248
GREGORY, IRENE M.
Trim drag reduction concepts for horizontal takeoff single-stage-to-Orbit vehicles
[NASA-TM-102687] p 206 N92-15076
GREGORY, PEYTON B.
Thermal/structural analysis of a transpiration cooled nozzle
[NASA-TM-104184] p 401 N92-18877
GREIF, R.
Current DOT research on the effect of multiple site damage on structural integrity p 913 N92-30112
GREIN, H.-D.
Supercritical blade design on stream surfaces of revolution with an inverse method p 220 N92-13950
GREINER, HAROLD F.
Seal related development activities at EG/G
p 228 N92-15095
GREITZER, E. M.
Surge dynamics in a free-spool centrifugal compressor system
[ASME PAPER 91-GT-31] p 68 A92-15515
The role of tip clearance in high-speed fan stall
[ASME PAPER 91-GT-83] p 69 A92-15550
Active control of rotating stall in a low speed axial compressor
[ASME PAPER 91-GT-88] p 122 A92-15553
Computational and experimental studies of flow in multi-lobed forced mixers
[AIAA PAPER 92-3568] p 1112 A92-54057
Inlet distortion effects in aircraft propulsion system integration p 869 N92-28464
Dynamic control of aerodynamic instabilities in gas turbine engines p 870 N92-28466
Active control of compressor surge and stall
[AD-A252771] p 1126 N92-33498
GRELLA, RAY
PDES application protocol suite for composites (PAS-C). Functional needs report for the PAS-C program
[AD-A247886] p 1108 N92-32629
GRENIER, T.
Mechanical testing of glass-ceramic matrix composites
[ONERA, TP NO. 1991-182] p 388 A92-26351
GRETLER, W.
Calculation of three-dimensional turbulent flow in wind tunnel entry section p 708 A92-43055
GRETSCH, W. R.
Developments in airborne surveillance and control systems p 98 A92-16655
GRIBBLE, J. J.
Multivariable methods for helicopter flight control law design - A review p 568 A92-35748
Command following control law design by linear quadratic optimisation p 568 A92-35749
GRIDLEY, MARVIN C.
Computation of vectoring nozzle performance
p 10 A92-13213
GRIDNEV, N. P.
Experimental and theoretical study of the improvement of the aerodynamic characteristics of supersonic flow past bodies with surface injection of a gas jet with particles
p 8 A92-12204
Changing the structure and improving the aerodynamic characteristics of supersonic flow past bodies through ejection of a gas jet with particles p 78 A92-16680
GRIEB, H.
High speed airbreathing propulsion in Europe
p 575 N92-22277
GRIFFIN, J. H.
Optimizing instrumentation when measuring jet engine blade vibration
[ASME PAPER 91-GT-71] p 148 A92-15540
GRIFFIN, M. A.
Performance of aluminum honeycomb panels with structural defects and core anomalies. II - Specimen description and test results p 591 A92-36156
GRIFFIN, O. HAYDEN, JR.
Global/local methods research using the CSM testbed
p 1107 N92-32528
GRIFFITH, WAYLAND C.
A ballistic investigation of the aerodynamic characteristics of a blunt vehicle at hypersonic speeds in carbon dioxide and air
[AIAA PAPER 92-0328] p 322 A92-25775
A fine-wire thermocouple probe for measurement of stagnation temperatures in real gas hypersonic flows of nitrogen p 1114 A92-54317
Boundary layer study on nozzle wall at hypersonic velocities
[AIAA PAPER 92-4013] p 1034 A92-56836
GRIFFITHS, ROBERT C.
Study of theoretical and wind tunnel results on flight performance degradation due to leading edge rime ice accretion
[AIAA PAPER 92-0038] p 262 A92-22158
A theoretical analysis utilizing the LEWICE and EPPLER numerical analyses to predict flight performance degradation under icing conditions
[AIAA PAPER 92-0134] p 263 A92-23754
GRIGOR'EV, V. A.
Characteristics of the phugoid motion of nonmaneuverable aircraft p 480 A92-30190
GRIGUERE, HENRI
Flight management system back-up navigation for the A330/A340 aircraft p 975 A92-49326
GRIMM, ALBRECHT
Computer-Controlled Navigation System/General Positioning System (CCNS/GPS) - A guidance, positioning, and management system for remote sensing flights
p 840 A92-47630
GRISHIN, A. M.
Mathematical modeling of supersonic flow over a convex-concave formed body based on the Euler and Navier-Stokes equations p 252 A92-23416

GRISHIN, V. I.
Determination of the objective-function gradient in the problem of minimizing stress concentration using the finite element method p 494 A92-30170
GRISSOM, MARK P.
The role of stealth in naval aviation and joint/combined operations
[AD-A240595] p 22 N92-11005
GRISVAL, J. P.
Direct coupling of fluid structure in transonic aeroelasticity p 721 N92-27954
GRITTER, RICHARD J.
Flight testing a high performance kit built aircraft
[AIAA PAPER 92-1240] p 538 A92-33333
GROENEWEG, J. F.
Unsteady blade-surface pressures on a large-scale advanced propeller - Prediction and data
p 80 A92-17178
Unsteady Euler analysis of the flowfield of a propfan at an angle of attack p 242 A92-21070
GROENEWEG, JOHN F.
Turbomachinery noise p 54 N92-10601
GROENIG, H.
Vortex interaction in the wake behind an oscillating airfoil p 623 A92-40175
High enthalpy testing in the Aachen (Fed. Republic of Germany) shock tunnel TH 2 p 208 N92-15021
GROEPLER, DAVID R.
Tiltrotor research aircraft composite blade repairs: Lessons learned
[NASA-TM-103875] p 367 N92-19563
GROHMAN, KENNETH M.
Radar troubleshooting assistant expert system
[AIAA PAPER 91-3764] p 231 A92-17626
GROHSMEYER, STEVEN P.
Numerical investigation of the effect of leading edge geometry on dynamic stall of airfoils
[AD-A239949] p 12 N92-10015
GROMELSKI, STAN
Controller memory enhancement: Field facility concepts and techniques
[DOT/FAA/CT-TN92/7] p 640 N92-24799
GRONSKI, ROBERT S.
Small engine components test facility compressor testing cell at NASA Lewis Research Center
[AIAA PAPER 92-3980] p 1098 A92-56806
Small engine components test facility compressor testing cell at NASA Lewis Research Center
[NASA-TM-105685] p 982 N92-30508
GROOM, NELSON J.
International Symposium on Magnetic Suspension Technology, part 2
[NASA-CP-3152-PT-2] p 753 N92-27788
GROPENGIESSER, F.
Hypersonic flow calculations around a 3D delta wing at low Knudsen numbers p 937 A92-52734
Rarefied gas flow around a disc with different angles of attack p 938 A92-52753
GROSCH, C. E.
Inviscid spatial stability of a three-dimensional compressible mixing layer p 39 A92-11816
Solutions of acoustic field problems using parallel computers p 925 A92-45929
GROSECLOSE, L. E.
Design and analysis of ceramic and CMC components for advanced gas turbines
[ASME PAPER 91-GT-156] p 142 A92-15592
GROSS, BENJAMIN J.
Inviscid analysis of a dual mode scramjet inlet
p 80 A92-17198
GROSS, K.
Integrated Russian VLF/Omega receiver design
[PB92-193390] p 1051 N92-33809
GROSS, MARILYN
Bibliography of technical reports, 1980 - 1990
[PB92-110691] p 417 N92-18814
GROSSIN, J.
The cockpit of a modern aircraft - The Airbus A340 considered as an example p 357 A92-26849
GROSSMAN, B.
Variable-complexity aerodynamic optimization of an HSCT wing using structural wing-weight equations
[AIAA PAPER 92-0212] p 317 A92-25685
Least-squares/parabolized Navier-Stokes procedure for optimizing hypersonic wind-tunnel nozzles
p 980 A92-50270
Design optimization of transonic airfoils
p 177 N92-13961
GROSSMANN, BENOIST
A cable detection lidar system for helicopters
p 1001 N92-31068
GROSSMANN, W.
Review of propulsion applications and numerical simulations of the pulsed detonation engine concept
p 129 A92-17177
A parametric study of airbreathing Pulsed Detonation Engine
[AIAA PAPER 92-0392] p 471 A92-31660
GROSVELD, F. W.
Transition control of instability waves over an acoustically excited flexible surface p 416 A92-28037
GROSVELD, FERDINAND
The 'White Pelican' project - Design and construction of the world's largest paper airplane
p 931 A92-51400
GROTH, C. P. T.
Computational fluid dynamics p 177 N92-13979
Nonstationary gasdynamics p 220 N92-13985
TVD finite-difference solutions of nonequilibrium vibrationally relaxing and chemically reacting gaseous flows p 626 N92-24854
GROTOWSKY, I.
Supersonic flow in compression stages and inlets
p 625 N92-24395
GROUND, JOHN R.
Small balloon ballistic tracing and behavior anomalies
[AIAA PAPER 91-3682] p 15 A92-11026
GROVE, RANDALL D.
High performance flight simulation at NASA Langley
[AIAA PAPER 92-4179] p 982 A92-52460
GRUBB, J. P.
Applications of hot-film anemometers in hypersonic shear layers
[AIAA PAPER 91-5028] p 436 A92-31687
GRUDLER, P.
Comparison of two-way satellite time transfer and GPS common-view time transfer between OCA and TUG
p 1050 N92-33356
GRUEN, ARMIN
Close-range photogrammetry meets machine vision; Proceedings of the Meeting, Zurich, Switzerland, Sept. 3-7, 1990
[SPIE-1395] p 994 A92-51626
GRUENEWALD, ALFRED
Resonance and control response tests using a control stimulation drive
[MBB-UD-0586-90-PUB] p 134 N92-12003
GRUENEWALD, M.
Summary of Dornier 328 interior noise control study
p 643 A92-39083
GRUNDMANN, R.
Introduction to three dimensional boundary layers
p 245 A92-21977
GRUNDY, I. H.
An outline of a numerical scheme for calculating two-dimensional time linearised transonic flow using the Green's function method
[AD-A246349] p 764 N92-26258
GRUNNET, J. L.
A model study on diffuser pressure recovery in NAL scramjet test facility with simulated hydrogen combustion
[AIAA PAPER 92-3979] p 1071 A92-56805
GRUZDEV, V. N.
The aviation kerosene burning in the non-uniform air flow p 487 A92-29728
GU, C. W.
A numerical procedure of three-dimensional design problem in turbomachinery
[ASME PAPER 91-GT-144] p 72 A92-15583
GU, CHUANGANG
Study of a new airfoil used in reversible axial fans
p 177 N92-13970
GU, CHUN-WEI
Pseudostream function formulation - A method of solving three-dimensional aerodynamic analysis and design problems in turbomachinery p 996 A92-52981
GU, CHUNWEI
Three-dimensional compressible flows in turbo-machinery solved by the pseudostream function formulation p 338 A92-27801
GU, GAOCHI
Aerodynamic modification of a propeller
p 4 A92-10958
GU, JIAJIN
Experimental study of the equivalent sound source center of the propeller rotating noise
p 1011 A92-53257
GU, JIALIU
Vibration control of rotor-bearing system by controlled squeeze-film damper bearings p 990 A92-49579
Transient response of the rotor-support system of aeroengines p 997 A92-53293
GU, SONGNIAN
Open-loop model reduction and parameter perturbation for active flutter suppression system
p 379 A92-24879
GU, WEN-YING
Aerodynamic sensitivities for subsonic lifting-surface
p 819 A92-47695
GU, YIDONG
China-Soviet long duration balloon flight project
[AIAA PAPER 91-3678] p 1 A92-11036
GU, YUANXIAN
Structural optimization and vibration control of composite rotor blades p 960 A92-53056
GU, Z. Q.
Robustness characteristics of fast-sampling digital controllers for active flutter suppression
[AIAA PAPER 92-2104] p 567 A92-35675
Design of adaptive fast-sampling digital controllers for active flutter suppression
[AIAA PAPER 92-2105] p 567 A92-35676
GU, ZHEN
A simplified dynamic model of the T700 turboshaft engine
[NASA-TM-105805] p 1009 N92-30898
GU, ZHONG-QUAN
A study on mechanical model of the helicopter 'ground resonance' p 955 A92-50214
GUAN, JIANCHENG
A study on the marginal analysis method for the airline yield management p 951 A92-53018
GUAN, YAN-SHEN
On modelling of aero-gas turbine engine for real-time digital simulator p 471 A92-29743
GUBAREV, B. A.
Design method of a helicopter cockpit
p 1058 A92-56337
GUEDRA-DEGEORGES, DIDIER
Impact damage tolerance of helicopter sandwich structures p 958 A92-51506
GUEGAN, M. C.
Hypersonic wakes
[ETN-92-91082] p 349 N92-19925
GUENETTE, G. R.
Active control of rotating stall in a low speed axial compressor
[ASME PAPER 91-GT-88] p 122 A92-15553
Comparison of time-resolved turbine rotor blade heat transfer measurements and numerical calculations
[ASME PAPER 91-GT-268] p 151 A92-15666
Dynamic control of aerodynamic instabilities in gas turbine engines p 870 N92-28466
GUENTHER, G.
Rapid repair of integrally stiffened carbon fibre composite structures by bolted aluminium elements
[MBB-FE202-S-PUB-0453-A] p 290 N92-17310
GUERNIGOU, J.
Indirect measurements of convective flow by IR thermography
[ONERA, TP NO. 1992-46] p 902 A92-48607
GUERNSEY, D.
On the choice of appropriate bases for nonlinear dynamic modal analysis p 847 A92-46927
GUERRA, ROSEMARIE
An experimental investigation of the combustion of a hydrogen jet injected parallel in a supersonic air stream
[AIAA PAPER 91-5102] p 212 A92-17861
GUEVREMONT, G.
Finite element vorticity based methods for the solution of the compressible Navier-Stokes equations
p 246 A92-21983
GUEZ, ALLON
On-line identification and control of linearized aircraft dynamics p 1082 A92-55911
GUFFOND, D.
Development of a three-dimensional icing code - Comparison with experimental shapes
[AIAA PAPER 92-0041] p 262 A92-22159
GUFFOND, DIDIER
Aircraft icing
[ONERA, TP NO. 1991-202] p 351 A92-26359
GUGLIELMO, JAMES J.
High-speed cinematography of supersonic mixing layers
[AIAA PAPER 92-3545] p 1112 A92-54044
GUGLIERI, G.
Experimental investigation of vortex dynamics on delta wings
[AIAA PAPER 92-2731] p 804 A92-45565
GUIBERT, L.
Avionics standardization in Europe
p 199 N92-14050
GUICE, ROBERT L.
Rarefaction wave eliminator design study
[AD-A244401] p 484 N92-20455
GUICHETEAU, PH.
Utilization of a research simulator for the development of new flight control concepts
[ONERA, TP NO. 1991-161] p 137 A92-16128
Use of a research simulator for the development of new concepts of flight control p 885 N92-28543
GUIDOS, BERNARD J.
Navier-Stokes computations for pointed, spherical, and flat tipped shell at Mach 3 p 705 A92-41536

GUILE, R. N.
Hydrocarbon-fueled scramjet combustor investigation
p 376 A92-28535
GUILLMETTE, NEAL H.
NASA advanced aeronautics design solar powered remotely piloted vehicle
[NASA-CR-190007] p 462 N92-20665
GUILLOT, J.
International standardisation of regulations for gust loading calculations p 270 A92-22473
GUILLOT, JEAN
New ramjet configurations p 736 A92-41822
GUIVER, E. J.
Approach and landing guidance p 457 N92-21960
GULATI, A.
Local extinction mechanisms in non-premixed turbulent combustion
[AD-A242027] p 290 N92-17682
GULATI, ANIL
Measurement of scalar flowfield at exit of combustor sector using Raman diagnostics
[AIAA PAPER 92-3350] p 894 A92-48927
GULCAT, U.
3-D numerical grid generation for the transonic flow analysis about multi-bodies p 817 A92-47061
GUMMLICH, HEINZ J.
Comparison of aircraft noise indices for noise zoning at military airfields p 687 A92-39056
GUNDLACH, G.
Preliminary laser induced fluorescence measurements in several facilities in preparation for application to studies in the high enthalpy shock tunnel Goettingen (HEG)
[AIAA PAPER 92-0143] p 284 A92-23761
GUNDY-BURLET, KAREN L.
Computations of unsteady multistage compressor flows in a workstation environment
[ASME PAPER 91-GT-336] p 163 A92-15701
Computations of unsteady multistage compressor flows in a workstation environment
[NASA-TM-103839] p 1071 N92-32452
GUNDY-BURLET, KAREN LEANN
Computations of unsteady multistage turbomachinery flows p 562 N92-23671
GUNN, JAMES A.
Performance evaluation of a transonic wind tunnel compressor
[AIAA PAPER 92-3927] p 1096 A92-56758
GUNN, W. H.
Airline deregulation - Impact on human factors
p 834 A92-44999
GUNNINK, JAN W.
Aerospace Arall - A challenge for the aircraft designer
p 33 A92-10232
GUNSALLUS, C.
Continuation of the AHS round robin on fatigue reliability and damage tolerance p 59 A92-14341
GUNTER, EDGAR J.
Dynamic characteristics and stability analysis of space shuttle main engine oxygen pump p 224 N92-14366
GUNTHER, MICHAEL F.
Fabry-Perot fiber-optic sensors in full-scale fatigue testing on an F-15 aircraft p 391 A92-24553
GUNZBURGER, M.
Experiences with finite element methods for the velocity-vorticity formulation of three-dimensional, viscous, incompressible flows p 246 A92-21984
GUNZBURGER, M. D.
Optimal boundary control of nonsteady incompressible flow with an application to viscous drag reduction
p 39 A92-11344
GUO, JINGRONG
Design of transonic compressor cascades using hodograph method p 202 N92-13973
The research progress on Hodograph Method of aerodynamic design at Tsinghua University
p 177 N92-13974
GUO, R. W.
A new approach to swirl control in an S-duct
p 422 A92-29710
New method of swirl control in a diffusing S-duct
p 809 A92-45859
GUO, RONGWEI
The unsteady flow characteristics of an S-shaped inlet at high incidence p 339 A92-27905
GUO, TEN-HUEI
Real-time fault diagnosis for propulsion systems
[NASA-TM-105303] p 26 N92-11017
GUO, WEN-HAI
An improved multiple line-vortex method for simulation of separated vortices of slender wings
p 819 A92-47694
GUO, XIAOLIANG
An approach to the low-speed longitudinal aerodynamic characteristics of the joined wing configuration
p 339 A92-27909
GUO, ZHIQUAN
Space-marching calculations of hypersonic inviscid flowfield p 313 A92-25040
Study of numerical computation of inviscid flow field about complex configuration of re-entry vehicle
p 313 A92-25041
GUPTA, A. K.
Aerodynamic effects on fuel spray structure - Experiment and theory
[AIAA PAPER 92-0227] p 317 A92-25691
GUPTA, K. K.
Multidisciplinary modeling and simulation of a generic hypersonic vehicle
[AIAA PAPER 91-5015] p 232 A92-17813
GUPTA, ROOP N.
Enhancements to viscous-shock-layer technique
[AIAA PAPER 92-2897] p 820 A92-47873
Stagnation-point heat-transfer rate predictions at aeroassist flight conditions
[NASA-TP-3208] p 1001 N92-31281
GUPTA, S. C.
Current growth in the aeronautics p 701 A92-41196
Multi-constraint wing optimization p 701 A92-41197
GUPTA, S. K.
Surfprep flash-lamp depaint system evaluation
p 497 A92-32411
GUR'IANOV, I. A.
Mathematical modeling of nonstationary viscous flow over a solid angle of finite span p 440 A92-31890
GURGANUS, T. B.
Development and characterization of Powder Metallurgy (PM) 2XXX series Al alloy products and Metal Matrix Composite (MMC) 2XXX Al/SiC materials for high temperature aircraft structural applications
[NASA-CR-187631] p 390 N92-19290
GURGUIS, RAAFAT H.
Underwater turbojet engine
[AD-D015017] p 279 N92-15992
GURLEY, SYDNEY E.
Civil development and certification of a helicopter automatic approach and hover system on the Sikorsky S-76
[SAE PAPER 911975] p 872 A92-45382
GURSUL, ISMET
High aerodynamic loads on an airfoil submerged in an unsteady stream p 432 A92-31183
GURUSWAMY, GURU P.
Transonic Navier-Stokes computations for an oscillating wing using zonal grids p 701 A92-41217
Numerical investigation of tail buffet on F-18 aircraft
[AIAA PAPER 92-2673] p 798 A92-45528
Navier-Stokes computations on swept-tapered wings, including flexibility p 810 A92-46786
Vortical flow computations on a flexible blended wing-body configuration p 1024 A92-54922
Navier-Stokes computations for oscillating control surfaces
[AIAA PAPER 92-4431] p 1026 A92-55355
Unsteady shock-vortex interaction on a flexible delta wing p 1030 A92-56157
Transonic aeroelastic computations on wings using Navier-Stokes equations p 721 N92-27957
GURYLEV, V. G.
Aerodynamic characteristics of slender sharp-leading-edge delta wings with air scooping through the air intake at hypersonic velocities. I
p 427 A92-30206
Aerodynamic characteristics of a blunt delta wing with air bleed through an intake at supersonic and hypersonic velocities. II p 437 A92-31855
GUSAK, IU. V.
Generation of loads for finite-element models of large aircraft p 459 A92-30209
GUSTAFSON, STEVEN C.
Locally linear neural networks for aerospace navigation systems p 103 N92-12530
GUSTAVSSON, LARS
Propeller sound excitation on an aircraft fuselage using a loudspeaker ring p 643 A92-39087
GUTIERREZ, PIERRE J.
High-temperature miniaturized turbine engine lubrication system simulator
[AD-A249259] p 868 N92-28294
GUTMARK, E.
Thermal imaging of afterburning plumes
p 129 A92-17179
Effect of carbon particles and mixing on afterburning of exhaust plumes
[AIAA PAPER 92-0767] p 387 A92-27107
Combustion instability related to vortex shedding in dump combustors and their passive control
p 374 A92-27354
Flow and acoustic features of a supersonic tapered nozzle p 712 A92-44328
Supersonic flow mixing and combustion using RAMP nozzle
[AIAA PAPER 92-3840] p 1113 A92-54198
GUTSCHOW, TODD
Processing complexity of two approaches to object detection and recognition p 234 N92-14677
GUYTON, BOB W.
An experimental study of pneumatic vortex flow control on high angle of attack forebody model
[AIAA PAPER 92-0018] p 247 A92-22140
GUYTON, ROBERT W.
X-29 forebody jet blowing
[AIAA PAPER 92-0017] p 247 A92-22139
High angle-of-attack control enhancement on a forward swept wing aircraft
[AIAA PAPER 92-4427] p 1080 A92-55351
Forebody vortex control aeromechanics
p 380 N92-18792
GUZAS, DANIELJUS
Acoustic isolation of layers p 54 A92-12345
GWILLIAM, DAVID J., JR.
Poststall airfoil response to a periodic freestream
p 10 A92-13218
GYEKENYESI, JOHN P.
Reliability analysis of a structural ceramic combustion chamber
[ASME PAPER 91-GT-155] p 123 A92-15591
GYSLING, D. L.
A theoretical study of sensor-actuator schemes for rotating stall control
[AIAA PAPER 92-3486] p 878 A92-49025
Dynamic control of aerodynamic instabilities in gas turbine engines p 870 N92-28466

H

HA, CHEOLKEUN
Optimal discrete-time static output-feedback design - A W-domain approach p 1007 A92-50499
HAAG, JONATHAN
The Guardian: Preliminary design of a close air support aircraft
[NASA-CR-189991] p 463 N92-21566
HAARMEYER, J.
Computation and visualization of specific flow phenomena in turbomachinery application
p 741 N92-27463
HAAS, DAVID J.
Identification of helicopter component loads using multiple regression
[AIAA PAPER 92-2110] p 544 A92-35681
HAAS, J. F.
The DAM vertical shock-tube p 880 A92-45096
HAAS, R. J.
Flow visualization of a prop-fan leading-edge vortex
[AIAA PAPER 92-0386] p 323 A92-26242
HAAS, W.
The influence of density difference between hot and coolant gas on film cooling by a row of holes - Predictions and experiments
[ASME PAPER 91-GT-255] p 151 A92-15660
HABASHI, W. G.
Finite element solutions of the Euler equations for transonic external flows p 5 A92-11063
Finite element vorticity based methods for the solution of the compressible Navier-Stokes equations
p 246 A92-21983
Efficient direct solvers for large-scale computational fluid dynamics problems p 690 A92-37534
HABIGER, H.
The IRS plasma wind tunnels for the investigation of thermal protection materials for reentry vehicles
p 208 N92-15009
HACKESCHMIDT, M.
A new method for visualization and measurement of turbulent flow patterns p 619 A92-40063
HACKETT, CHARLES M.
Computational and numerical analysis of hypersonic nozzle flows with comparisons to wind tunnel calibration data
[AIAA PAPER 92-4011] p 1033 A92-56834
HACKSTEIN, H. J.
Interior noise reduction program for the Dornier 328
p 114 A92-17254
Summary of Dornier 328 interior noise control study
p 643 A92-39083
HACKSTEIN, H. JOSEF
The Dornier 328 Acoustic Test Cell (ATC) for interior noise tests and selected test results
[AIAA PAPER 92-2164] p 1137 N92-32951
HADAR, ILAN
Fuel regression mechanism in a solid fuel ramjet
p 860 A92-44898

HADAR, O.
Numerical calculation of modulation transfer functions for low frequency mechanical vibrations
p 235 A92-19982
HADDAD, RAYMOND C.
Flow field over the wing of a delta-wing fighter model with vortex control devices at Mach 0.6 to 1.2
[NASA-TM-4296] p 526 N92-22506
HADDAD, WASSIM M.
Robust stabilization with positive real uncertainty - Beyond the small gain theorem p 50 A92-11444
HADDEN, G.
Distributed health management systems technology for future propulsion control systems
[SAE PAPER 912167] p 655 A92-39995
HADFIELD, CHRIS A.
National Aerospace Plane flight test - External burning on the F/A-18 p 645 A92-40032
HADZIDAKIS, M.
Unsteady Euler calculations in 2-D internal aerodynamics with introduced vorticity
[ASME PAPER 91-GT-168] p 73 A92-15603
Unsteady Euler calculations in 3D internal aerodynamics p 768 N92-27470
HAEHNLEIN, GEORG
Pallet for helicopter testing instrumentation
p 652 N92-25598
HAERING, EDWARD A., JR.
Atmospheric analysis for airdata calibration on research aircraft
[AIAA PAPER 92-0293] p 369 A92-25746
Airdata calibration techniques for measuring atmospheric wind profiles p 856 A92-46792
HAERTIG, J.
Computation of the BVI noise for the BO105 Model Rotor in forward flight and comparison with wind tunnel tests
p 165 A92-14386
HAESELER, D.
Landing spacecraft gently on earth - The Soviet parachute systems p 33 A92-13227
HAEUSER, J.
Numerical grid generation in computational fluid dynamics and related fields; Proceedings of the 3rd International Conference, Universidad Politecnica de Cataluna, Barcelona, Spain, June 3-7, 1991
[ISBN 0-444-88948-5] p 918 A92-47035
Aerothermodynamic calculations for the Space Shuttle Orbiter
[AIAA PAPER 92-2953] p 821 A92-47917
Equilibrium solution of the Euler and Navier-Stokes equations around a double ellipsoidal shape with mono- and multi-blocks including real gas effects, part 1
p 227 N92-15030
Grid impact on 3D hypersonic flows
p 184 N92-15041
HAFERMAN, J. L.
Thermal radiation effects on a shocked particle-laden gas p 780 A92-44377
HAFEZ, M. M.
Finite element solutions of the Euler equations for transonic external flows p 5 A92-11063
Finite element vorticity based methods for the solution of the compressible Navier-Stokes equations
p 246 A92-21983
HAFTKA, R. T.
Variable-complexity aerodynamic optimization of an HSCT wing using structural wing-weight equations
[AIAA PAPER 92-0212] p 317 A92-25685
Design optimization of transonic airfoils
p 177 N92-13961
HAFTKA, RAPHAEL T.
Initial postbuckling response of an unsymmetrically laminated rectangular plate p 1108 N92-32586
HAGA, KAZUO
Study of potassium turbine electric generator system
p 1129 N92-33794
HAGEMAIER, DONALD J.
Nondestructive testing developments in the aircraft industry p 214 A92-17288
Inspection of aging aircraft: A manufacturer's perspective p 914 N92-30117
HAGMANN, DEAN B.
Stationary neutron radiography system
p 144 A92-13589
HAGUE, C. W.
EH101 helicopter development p 112 A92-16060
HAH, C.
Navier-Stokes analysis of three-dimensional unsteady flows inside turbine stages
[AIAA PAPER 92-3211] p 1021 A92-54016
A critical evaluation of a three-dimensional Navier-Stokes CFD as a tool to design supersonic turbine stages p 1124 N92-32268
HAH, CHUNILL
A viscous flow study of shock-boundary layer interaction, radial transport, and wake development in a transonic compressor
[ASME PAPER 91-GT-69] p 68 A92-15539
A critical evaluation of a three-dimensional Navier-Stokes method as a tool to calculate transonic flows inside a low-aspect-ratio compressor
p 768 N92-27459
HAHN, K.-U.
ATTAS flight test and simulation results of the advanced gust management system LARS
[AIAA PAPER 92-4343] p 1079 A92-55332
HAHNE, DAVID E.
Wind-tunnel static and free-flight investigation of high-angle-of-attack stability and control characteristics of a model of the EA-6B airplane
[NASA-TP-3194] p 631 N92-25276
HAIGLER, KARA J.
User guide for WIACX: A transonic wind-tunnel wall interference assessment and correction procedure for the NTF
[NASA-TM-104168] p 261 N92-17547
HAILYE, MICHAEL
The flip flop nozzle extended to supersonic flows
[AIAA PAPER 92-2724] p 803 A92-45561
HAIMES, ROBERT
Validation of a numerical method for unsteady flow calculations
[ASME PAPER 91-GT-271] p 151 A92-15668
HAINES, A. B.
Survey of experimental techniques for performance prediction p 552 N92-23954
HAINES, RICHARD F.
Ames life science telescience testbed evaluation
[NASA-CR-188856] p 140 N92-12033
HAJ-HARIRI, HOSSEIN
A numerical investigation of hydrogen combustion in Mach 2 flow
[AIAA PAPER 92-0341] p 388 A92-25787
HAJ, ANWAR MOHAMMED
Dynamics and control of a five degree-of-freedom magnetic suspension system
[NASA-CR-191259] p 1102 N92-34222
HAJJ, G.
NASA's GPS tracking system for Aristoteles
p 576 N92-23919
HAKUI, MASATAKA
Flight tests on the structures of the STOL research aircraft Asuka p 730 A92-43143
Study on the maintainability and inspection of the STOL research aircraft Asuka p 700 A92-43148
HALDEMAN, C. W.
Force measurement on rotating, ablating models using an air bearing balance p 483 A92-31174
HALE, A. A.
DYNamic Turbine Engine Compressor Code (DYNTECC) - Theory and capabilities
[AIAA PAPER 92-3190] p 923 A92-48802
HALEVI, YORAM
Observability under recurrent loss of data
p 302 A92-21191
HALL, CHARLES E., JR.
Formulation of the linear model from the nonlinear simulation for the F18 HARV p 117 N92-13842
HALL, DAVID G.
Detailed noise measurements on the SR-7A propeller: Tone behavior with helical tip Mach number
[NASA-TM-105206] p 304 N92-16705
A sophisticated, multi-channel data acquisition and processing system for high frequency noise research
[NASA-CR-189137] p 696 N92-24688
HALL, EDWARD J.
Time-dependent aerodynamic analysis of ducted and unducted propfans at angle of attack
[ASME PAPER 91-GT-190] p 74 A92-15616
HALL, I. M.
Marching with the parabolized Navier-Stokes equations. Problem 1: Numerical study of hypersonic viscous cone flow
[AERO-REPT-9007] p 344 N92-18231
Marching with the parabolized Navier-Stokes equations. Problem 2: Hypersonic viscous flow over a flat plate
[AERO-REPT-9008] p 345 N92-18232
Zonal solutions for a double-ellipse in a hypersonic flowfield
[AERO-REPT-9009] p 345 N92-18233
HALL, J. R.
Initial validation of a R/D simulator with large amplitude motion p 886 N92-28546
HALL, KENNETH
A flight test study to determine aircraft propulsive efficiency and aerodynamic drag using two parameter identification methods and Lock's propeller model
[AIAA PAPER 92-0170] p 271 A92-23781
HALL, KENNETH C.
A deforming grid variational principle and finite element method for computing unsteady small disturbance flows in cascades
[AIAA PAPER 92-0665] p 335 A92-27036
Development of unsteady aerodynamic analyses for turbomachinery aeroelastic and aeroacoustic applications
[NASA-CR-4405] p 12 N92-10979
HALL, KENNETH R.
Development of a multi-computer in-flight data acquisition and analysis system for general aviation aircraft
[AIAA PAPER 92-1037] p 553 A92-33218
HALL, L. E.
Application of multidisciplinary optimization methods to the design of a supersonic transport
p 550 N92-23230
HALL, LAURA E.
Integrating aerodynamics and structures in the minimum weight design of a supersonic transport wing
[NASA-TM-107586] p 850 N92-28435
HALL, MARSHALL C., III
Managing simulator wiring information and deriving system continuity p 964 A92-49287
HALL, NEIL S.
Velocity dependence of high angle of attack longitudinal flying qualities criteria
[SAE PAPER 912149] p 662 A92-39985
HALL, OLIVER K.
Distributed flight control system using fiber distributed data interface (FDDI) p 976 A92-51004
HALL, P.
Nonlinear development and secondary instability of large-amplitude Goertler vortices in hypersonic boundary layers p 942 A92-53080
HALL, PATRICK G.
Tiltrotor UAV - The next generation unmanned system
p 646 A92-40384
HALL, PHILIP
On the instability of boundary layers on heated flat plates
[NASA-CR-187581] p 347 N92-19250
HALL, S. R.
A proposed composite repair methodology for primary structure
[NRC-LTR-ST-1658] p 115 N92-13056
HALLER, R. L.
On-line adaptive control of unstable aircraft wing flutter p 27 A92-11374
HALLETT, J.
Influence of air velocity on the habit of ice crystal growth from the vapor p 668 A92-38111
HALLETT, JOHN
Size and critical supersaturation for condensation of jet engine exhaust particles p 161 A92-15884
HALLIKAINEN, M.
Development of a helicopter-borne 8-channel ranging scatterometer
[PB92-141977] p 599 N92-23441
HALLIKAINEN, MARTTI
Development of a 3-D remote sensing radar
p 597 A92-34908
X-band side-looking airborne radar for remote sensing
p 554 A92-34976
Mechanical design of an airborne imaging microwave radiometer p 554 A92-35276
HALLIWELL, I.
Investigation of three-dimensional flow field in a turbine including rotor/stator interaction. I - Design development and performance of the research facility
[AIAA PAPER 92-3325] p 883 A92-48908
HALLOWELL, R.
Characteristics of thunderstorm-generated low altitude wind shear - A survey based on nationwide terminal Doppler weather radar testbed measurements
p 45 A92-11378
HALLOWELL, ROBERT G.
Aspect angle dependence of outflow strength in Denver microbursts - Spatial and temporal variations
p 408 A92-27963
HALSKI, D. J.
ICAAS piloted simulation evaluation
p 735 N92-27906
HALSMER, ROBERT A.
Smoothing CFM56 engine removal rate at USAir
[AIAA PAPER 92-3928] p 1070 A92-56759
HALT, D. W.
A compact higher order Euler solver for unstructured grids with curved boundaries
[AIAA PAPER 92-2696] p 807 A92-45590
Compact higher order characteristic-based Euler solver for unstructured grids p 812 A92-46889
HALT, DAVID
Characteristic-based algorithms for flows in thermochemical nonequilibrium p 670 A92-36846

HALUCK, DAVID
Rotor support for the STME oxygen turbopump
[AIAA PAPER 92-3282] p 904 A92-48872
HALVORSEN, WILLIAM G.
Coupled propeller contributions to aircraft noise and vibration p 694 A92-39085
HAM, JOHNNIE A.
Flight testing the handling qualities requirements of ADS-33C - Lessons learned at ATTC
p 104 A92-14339
Frequency domain flight testing and analysis of an OH-58D helicopter p 847 A92-46943
HAM, NANCY M.
Tooling for C-17 composite parts p 900 A92-47412
HAM, NORMAN D.
Research on measurement and control of helicopter rotor response using blade-mounted accelerometers 1990-91 p 1057 A92-56316
HAMADA, Y.
Thermal measurement test in a shock wind tunnel
p 748 A92-43104
HAMAI, SHOHEI
Titanium alloy casting for aerospace
p 1106 A92-56103
HAMAN, KRZYSZTOF E.
A new thermometric instrument for airborne measurements in clouds p 368 A92-24918
HAMED, A.
High temperature erosion resistance of coatings for gas turbine
[ASME PAPER 91-GT-213] p 143 A92-15632
Investigation of oblique shock/boundary-layer bleed interaction p 344 A92-28524
Inviscid and viscous quasi-three-dimensional flow solutions in a transonic turbine cascade
p 523 A92-36035
An investigation in the variance in particle surface interactions and their effects in gas turbines
[ASME PAPER 91-GT-380] p 653 A92-36891
A study on the impact of shroud geometry on ejector pumping performance
[AIAA PAPER 92-3260] p 864 A92-48856
HAMED, AWATEF A.
Numerical simulations in turbomachinery; Proceedings of the Symposium, ASME and JSME Joint Fluids Engineering Conference, 1st, Portland, OR, June 23-27, 1991
[ISBN 0-7918-0714-2] p 522 A92-36028
HAMI, S.
Radial inflow turbine study
[AD-A246938] p 743 N92-28073
HAMID, S.
Fibre optic laser anemometry for turbomachinery applications p 397 A92-27783
Radial inflow turbine study
[AD-A240169] p 26 N92-11015
Radial inflow turbine study
[AD-A252783] p 1127 N92-33538
HAMILTON-JONES, LYNNE T.
Analysis of the VISTA longitudinal simulation capability for a cruise flight condition p 876 A92-48488
HAMILTON, B. K.
A general purpose nonlinear rigid body mass finite element for application to rotary wing dynamics
p 846 A92-46924
HAMILTON, H. H., II
Comparison of heating calculations with experimental data on a modified Shuttle Orbiter p 441 A92-32184
HAMILTON, SCOTT A.
Finite element analysis of a riveted repair on a curved composite panel
[AD-A243916] p 404 N92-19384
HAMMER, JACOB
State feedback for nonlinear continuous-time systems - Stabilization and the creation of invariant subspaces
p 52 A92-11587
HAMMERTON, P. W.
Leading-edge receptivity for blunt-nose bodies
[NASA-CR-190563] p 1036 N92-32648
HAMMETT, ROBERT
Application of syndrome pattern-matching approach to fault isolation in avionic systems p 1005 A92-49261
HAMMOND, D. C., JR.
Optimization of bluff body for minimum drag in ground proximity p 431 A92-31154
HAMMOND, D. L.
A USAF assessment of STOVL fighter options
p 842 A92-45310
HAMMOND, D. O.
Composite material repairs to metallic airframe components p 699 A92-41237
HAMOUDA, M.-N. H.
Recent rotorcraft aeroelastic testing in the Langley Transonic Dynamics Tunnel p 136 A92-14377
HAN, JIAKUN
New method for boundary layer thickness control on ground plate in wind tunnel p 383 A92-25110
HAN, T.
Optimization of bluff body for minimum drag in ground proximity p 431 A92-31154
HANAGUD, S.
Smart structures for helicopters p 516 A92-35727
Smart structures in the active control of blade vortex interaction p 1085 A92-56314
HANAMI, S.
Experimental study of the aerodynamic characteristics at Mach 3 of an air-intake model p 711 A92-43204
HANATANI, K.
Shafranov shift in low-aspect-ratio heliotron/torsatron CHS
[NIFS-110] p 1138 N92-33743
HANAWA, KIRK
High enthalpy wind tunnel for erosion testing of advanced materials
[AIAA PAPER 92-3888] p 1094 A92-56729
HANDSCHUH, R.
Experimental testing of prototype face gears for helicopter transmissions
[NASA-TM-105434] p 1002 N92-31349
HANDSCHUH, ROBERT F.
Recent manufacturing advances for spiral bevel gears
[SAE PAPER 912229] p 674 A92-40024
HANE, F.
Study of the flight control of remotely piloted helicopters p 745 A92-43183
HANEDA, HIROMASA
Polygon interval arithmetic and design of robust control systems p 49 A92-11418
HANFF, E. S.
Unique high-alpha roll dynamics of a sharp-edged 65 deg delta wing
[AIAA PAPER 92-0276] p 318 A92-25730
Prediction of leading-edge vortex breakdown on a delta wing oscillating in roll
[AIAA PAPER 92-2677] p 807 A92-45585
Multiple roll attractors of a delta wing at high incidence p 88 N92-13026
Non-linear airloads hypersurface representation: A time domain perspective p 346 N92-18783
HANGEN, J. A.
Application of a local panel buckling constraint within automated multidisciplinary structural analysis and design
[AIAA PAPER 92-1116] p 537 A92-33271
Finite element analysis of ASTOVL fighter structure
[AD-A243724] p 275 N92-17513
HANINE, F.
Performance of turbulence models to predict supersonic boundary layer flows p 613 A92-37553
HANKE, D.
The role of systems simulation for the development and qualification of ATTAS p 886 N92-28548
HANKEY, W. L.
Automated trajectory synthesis for hypersonic vehicles using energy management and variational calculus techniques p 210 A92-19061
Control strategy for maximizing reconnaissance range of hypersonic cruise vehicles p 729 A92-41222
HANLEY, ARTHUR
Automated mission planning - A striking capability
p 412 A92-28494
HANNEMANN, K.
Review of the European hypersonic wind tunnel performance and simulation requirements
p 209 N92-15043
HANOTEL, R.
Experimental and theoretical studies on helicopter rotor fuselage interaction
[ONERA, TP NO. 1991-197] p 329 A92-26356
Theoretical and experimental studies of helicopter rotor/fuselage interaction
[ONERA, TP NO. 1991-198] p 329 A92-26357
HANRAHAN, T.
Hypersonic plasma predictions at nonzero angle of attack
[AIAA PAPER 92-3027] p 925 A92-47028
HANSEN, A. C.
Dynamic stall on wind turbine blades
[DE92-001157] p 262 N92-17874
Yaw dynamics of horizontal axis wind turbines
[DE92-001245] p 1004 N92-30837
HANSEN, IRVING G.
Electromechanical systems with transient high power response operating from a resonant AC link
[NASA-TM-105716] p 870 N92-28985
HANSEN, J. G. R.
Report on aerospace structures and structural materials R and D in Europe
[PB92-123553] p 550 N92-22785
HANSEN, JAMES C.
A high performance general purpose processing element for avionic applications p 920 A92-48440
HANSMAN, JOHN
A data fusion algorithm for multi-sensor microburst hazard assessment
[AIAA PAPER 92-4339] p 1063 A92-55328
HANSMAN, R. J., JR.
Analysis of aircraft performance during lateral maneuvering for microburst avoidance
p 205 A92-20207
Experimental evaluation of candidate graphical microburst alert displays
[AIAA PAPER 92-0292] p 369 A92-25745
Electronic presentation of instrument approach information p 855 A92-44923
HANSMAN, R. JOHN
Experimental evaluation of candidate graphical microburst alert displays
[NASA-CR-189633] p 735 N92-27424
HANSMAN, R. JOHN, JR.
Experimental investigation of passive infrared ice detection for helicopter applications p 265 N92-17986
Deterministic multi-zone ice accretion modeling
p 265 N92-17987
Alert generation and cockpit presentation for an integrated microburst alerting system
p 265 N92-17988
Cockpit display of hazardous weather information
p 277 N92-17989
HANSON, A. W.
Lightning protection requirements for aircraft: A proposed specification
[RAE-TM-FS(F)-632-REV-ISSUE] p 187 N92-14007
HANSON, D. B.
Unsteady airloading panel method for propfans
p 780 A92-44512
Propeller and propfan noise p 54 N92-10599
HANSON, R. K.
Planar fluorescence imaging of a transverse jet in a supersonic crossflow p 755 A92-44501
Turbulent reacting flows and supersonic combustion
[AD-A251065] p 986 N92-30256
HANSON, W.
Comparison of two-way satellite time transfer and GPS common-view time transfer between OCA and TUG
p 1050 N92-33356
HAQ, Z. U.
Interference heating near fin/body junctions on hypersonic vehicles p 182 N92-14996
HARA, K.
Outflow boundary conditions for Euler analysis of flow in turbine scroll p 591 A92-36037
HARADA, K.
Integrated system to support computer analysis in conceptual aerospace design p 1130 A92-53596
HARADA, WASASHI
Optimal design of wing shape by use of neural-network p 1054 A92-56112
HARAKI, NOBUO
Sand erosion behavior of GFRP p 576 A92-32662
HARASGAMA, S. P.
Film cooling research on the endwall of a turbine nozzle guide vane in a short duration annular cascade. I - Experimental technique and results
[ASME PAPER 91-GT-252] p 150 A92-15657
Film cooling research on the endwall of a turbine nozzle guide vane in a short duration annular cascade. II - Analysis and correlation of results
[ASME PAPER 91-GT-253] p 150 A92-15658
The application of particle image velocimetry (PIV) in a short-duration transonic annular turbine cascade
[ASME PAPER 91-GT-221] p 899 A92-46825
Predictions and measurements of 3D viscous flow in a transonic turbine nozzle guide vane row
p 741 N92-27466
HARDIN, J. C.
Sound generation by a stenosis in a pipe
p 415 A92-26405
HARDIN, JAY C.
Removal of spurious reflections from computational fluid dynamic solutions with the complex cepstrum
p 235 A92-20729
HARDING, J. W.
Flight simulation modeling in support of engine/airframe integration p 1055 A92-56279
HARDING, JEFF W.
Assessment of rotorcraft system identification as applied to the AH-64 p 274 N92-17160
Industry view on rotorcraft system identification
p 274 N92-17163
HARDINGE, HAL
Flow visualization and flow field measurements of a 1/12 scale tilt rotor aircraft in hover
[NASA-CR-189456] p 82 N92-11983

HARDY, TERRY L.
Slush hydrogen (SLH2) technology development for application to the National Aerospace Plane (NASP)
p 144 A92-13432

HARGIS, ROWENA L.
Robust controller design for an advanced fighter aircraft p 28 A92-11500

HARGROVE, WILLIAM T.
Methodology for the determination of criticality codes and recertification intervals for Tank Mounted Air Compressors (TMAC) and Base Mounted Air Compressors (BMAC)
[NASA-CR-189268] p 770 N92-27649

HARIGAE, MASATOSHI
Flight evaluation of navigation systems including MLS using NAL Do228 - Results of GPS
p 1047 A92-56118

HARIGAE, SHOWA
Navigation experiment on an aircraft using the GPS-INS navigation system. I - Introduction to the system
p 726 A92-43122
Navigation experiment on aircraft flight using the GPS-INS navigation system. II - Test results
p 726 A92-43123

HARIHARAN, S. I.
Time domain numerical calculations of unsteady vortical flows about a flat plate airfoil p 936 A92-50473

HARLOFF, G. J.
Three-dimensional compressible turbulent computations for a diffusing S-duct
[NASA-CR-4392] p 526 N92-22249
Navier-Stokes analysis and experimental data comparison of compressible flow within ducts
[NASA-TM-105796] p 972 N92-30972
Three-dimensional compressible turbulent computations for a nondiffusing S-duct
[NASA-CR-4391] p 951 N92-32240

HARLOFF, GARY J.
Navier-Stokes analysis and experimental data comparison of compressible flow in a diffusing S-duct
[AIAA PAPER 92-2699] p 800 A92-45541
Navier-Stokes analysis and experimental data comparison of compressible flow in a diffusing S-duct
[NASA-TM-105683] p 1072 N92-33746

HARLOWE, W. W.
Ignition delays, heats of combustion, and reaction rates of aluminum alkyl derivatives used as ignition and combustion enhancers for supersonic combustors
[AIAA PAPER 92-3841] p 894 A92-49134

HARM, C.
Analysis of general aviation accidents during operations under instrument flight rules p 16 A92-11172

HARMON, A. O.
Nonflammable hydraulic power system for tactical aircraft. Volume 2: Equipment and systems test and evaluation
[AD-A239805] p 35 N92-10100

HARMON, C. B.
A 3-degree-of-freedom flight simulator evaluation of unsteady aerodynamics effects
[AD-A241540] p 139 N92-13079

HARNEY, R. J.
Single engine testing of the F-14A(PLUS) airplane in the power approach configuration p 645 A92-40036

HARPER, JOHN A.
DC-3 handling qualities flight tests: NACA - 1950
p 646 A92-40042

HARPER, RICHARD E.
An ultrareliable integrated digital computer for helicopters p 964 A92-49273

HARRADINE, P. J.
Assurance of safety in the aging aircraft fleet
p 635 A92-39305

HARRAND, V. J.
Visualization and analysis of hypersonic flows and comparison to experimental data
[AIAA PAPER 92-2774] p 704 A92-41320

HARRIS, C. S.
Effects of military training route noise on human annoyance p 689 A92-39237

HARRIS, CHARLES D.
The NASA Langley laminar-flow-control experiment on a swept, supercritical airfoil: Evaluation of initial perforated configuration
[NASA-TM-4309] p 525 N92-22196

HARRIS, CHARLES E.
Recent fracture mechanics results from NASA research related to the aging commercial transport fleet
p 362 N92-18589
The 1991 International Conference on Aging Aircraft and Structural Airworthiness
[NASA-CP-3160] p 912 N92-30106
Fracture mechanics research at NASA related to the aging commercial transport fleet p 913 N92-30110

HARRIS, J. R.
Passenger knowledge of airline safety information
[CRANFIELD-AERO-9111] p 187 N92-15054

HARRIS, J. S.
Preliminary screening procedures and criteria for replacements for Halons 1211 and 1301
[AD-A252912] p 1126 N92-33501

HARRIS, JULIUS E.
Numerical solution of the boundary-layer equations for a general aviation fuselage p 174 A92-20211
A new approach for the calculation of transitional flows
[AIAA PAPER 92-2669] p 798 A92-45524

HARRIS, KEVIN
Acoustic testing at elevated temperatures
p 981 A92-51405

HARRIS, L. P.
Compressor modeling and active control of stall/surge
p 508 A92-29315

HARRIS, MIKE J.
Core avionics and standardization
[AD-A248326] p 735 N92-27925

HARRIS, R. H.
Preliminary screening procedures and criteria for replacements for Halons 1211 and 1301
[AD-A252912] p 1126 N92-33501

HARRIS, ROY V., JR.
On the threshold - The outlook for supersonic and hypersonic aircraft p 356 A92-24402

HARRIS, T. M.
Unsteady aerodynamics for aeroelasticity at the Flight Dynamics Directorate p 718 N92-27939

HARRISON, D.
European studies to investigate the feasibility of using 1000 ft vertical separation minima above FL 290. II - Precision radar data analysis and collision risk assessment p 353 A92-24946

HARRISON, J. M.
Flight simulation modeling in support of engine/airframe integration p 1055 A92-56279

HARRISON, KENNETH R.
Simulation of radar clutter and jet engine modulation using digital quadrature modulator p 216 A92-19091

HARRISON, L.
Avionic data bus integration technology
[DOT/FAA/CT-91/19] p 736 N92-27973

HARRISON, MICHAEL J.
Runway incursions and airport surface traffic automation
[SAE PAPER 912123] p 635 A92-39970

HARRISON, ROBIN T.
Annoyance from aircraft overflights in wilderness
p 689 A92-39239

HARRISON, W. E., III
High temperature, thermally stable JP fuels - An overview
[AIAA PAPER 92-0683] p 389 A92-27050

HART, DANIEL C.
Helicopter control response types for hover and low-speed near-earth tasks in degraded visual conditions
p 132 A92-14338

HARTLEY, TOM T.
A hierarchy for modeling high speed propulsion systems
[NASA-CR-186984] p 387 N92-19934
Improved large perturbation propulsion models for control system design (1988-1989) and large perturbation models of high velocity propulsion systems (1989-1990) and reduced order propulsion models for control system design (1990-1991)
[NASA-CR-190148] p 593 N92-22491
A hierarchy for modeling high speed propulsion systems p 559 N92-22492
Approximate truncated balanced realizations for infinite dimensional systems p 602 N92-22493
Modeling of linear isentropic flow systems
p 593 N92-22495

HARTMAN, G.
Implicit solutions of three-dimensional viscous hypersonic flows p 434 A92-31549

HARTMAN, P.
Viscous flow analysis of advanced particle separators
p 737 A92-44517

HARTMANN, G.
Aerothermodynamics of nozzle flows for advanced hypersonic propulsion systems p 769 N92-27478

HARTMANN, GARY L.
Thermal control for hypersonic vehicle propulsion
p 468 A92-29356

HARTMANN, K.
Aerodynamic assessment of an optical pressure measurement system (OPMS) by comparison with conventional pressure measurements in a high speed wind tunnel p 1114 A92-54304

HARTMANN, LAWRENCE, A.
Annoyance from aircraft overflights in wilderness
p 689 A92-39239

HARTUNG, THOMAS A.
Ground collision avoidance using a variable incidence altitude measurement system for the A-7 aircraft
[AD-A243880] p 352 N92-19259

HARTWICH, P.
A Navier-Stokes solution of Hull-ring wing-thruster interaction p 221 N92-14310

HARTWICH, PETER M.
Estimation of propulsion-induced effects on transonic flows over a hypersonic configuration
[AIAA PAPER 92-0523] p 341 A92-28197

HARTZHEIM, W.
Multidisciplinary optimization of fiber composite aircraft structures
[MBB/FW321/S/PUB/476] p 961 N92-30424

HARVEY, ALBERT D., III
Solution-adaptive grid procedure for the parabolized Navier-Stokes equations p 432 A92-31163

HARVEY, GILES
The Rolls-Royce Trent
[PNR-90875] p 1061 N92-33750

HARVEY, J. K.
Flat-ended circular cylinder in hypersonic rarefied flow
p 174 A92-20304
Heat transfer to a delta wing and two waverider wings in rarefied hypersonic flow p 937 A92-52748

HARVEY, R. J.
Development of an innovative high-temperature gas turbine fuel nozzle
[ASME PAPER 91-GT-36] p 121 A92-15519

HARVEY, W. L.
A low-power, high-efficiency Ka-band TWTA
p 671 A92-38163

HASAN, M. A. Z.
The flow over a backward-facing step under controlled perturbation - Laminar separation p 705 A92-41653

HASE, YOSHIHIRO
Experiments on aeronautical satellite communications using ETS-V p 395 A92-26779
Experiments on aeronautical satellite communications using ETS-V satellite p 639 A92-40187

HASEGAWA, GIZO
Analysis of the aerodynamic performance of rotors with the boundary element method p 709 A92-43119
Multiharmonic control response of a rotor blade during forward flight (Test) p 744 A92-43120
Multiharmonic control response of a rotor blade during forward flight (Analysis) p 744 A92-43121
Free wake analyses of a hovering rotor using panel method
[SAE PAPER 912004] p 789 A92-45405
Prediction of dynamic hub load of a rotor executing multiple sinusoidal blade pitch variations
p 846 A92-46921

HASEGAWA, HIROSHI
Performance of a high-pressure-ratio centrifugal compressor influenced by distribution of tip clearance of the mixed-flow impeller p 498 A92-32509

HASEGAWA, S.
Turbine drive system of the high pressure LOX turbopump test facility
[DE92-783191] p 680 N92-25342

HASEGAWA, SEIICHI
Research on hypersonic wind tunnel methods in the 90's p 748 A92-43105

HASEGAWA, TAKAHISA
Application of automation for structural-composites production p 1119 A92-56109

HASEGAWA, YASUMICHI
A calculation method to predict helicopter noise and its verification p 1135 A92-56074

HASEL, K. L.
High-speed civil transport aircraft emissions
p 408 N92-19122

HASH, DAVID B.
Monte Carlo simulation of entry in the Martian atmosphere
[AIAA PAPER 92-0494] p 329 A92-26324

HASHEMI-KIA, MOSTAFA
The NASA/Industry Design Analysis Methods for Vibrations (DAMVIBS) program - McDonnell Douglas Helicopter Company achievements
[AIAA PAPER 92-2203] p 540 A92-34393

HASHEMI-YEGANEH, SHAHROKH
Advanced electromagnetic methods for aerospace vehicles
[NASA-CR-188630] p 488 N92-20193

HASHIDA, YOSHIKAZU
Space plane navigation simulation
p 1103 A92-53603

HASHIDATE, MASATAKA
Design - Analysis and experimental verification of a propeller working in the low Reynolds number range p 710 A92-43174
Low-speed wind tunnel testing for the high-speed propeller at high shaft angle of attack p 1030 A92-56054
HASHIDATE, N.
Noise test of high-speed counterrotation propeller in low-speed wind tunnel p 1135 A92-56055
HASHIMOTO, R.
Turbine drive system of the high pressure LOX turbopump test facility
[DE92-783191] p 680 N92-25342
HASHIMOTO, RYOSAKU
Nonlinear transient analysis of composite ATP blade model p 294 A92-23111
HASHISH, M.
Precision drilling of ceramic-coated components with abrasive-waterjets
[ASME PAPER 91-GT-232] p 149 A92-15641
HASHITADE, M.
Wind tunnel test for a high speed propeller with coaxial contrarotation p 737 A92-43195
HASKELL, MARGARET F.
Precision of the long baseline acoustic navigation system used by Pegasus
[AD-A246598] p 727 N92-26795
HASKO, GREG
RTM: Cost-effective processing of composite structures p 578 N92-22678
HASSA, C.
Particle dispersion in highly swirling, turbulent flows p 675 A92-40093
HASSAN, A. A.
Separation control using moving surface effects - A numerical simulation p 309 A92-24419
Blade-mounted trailing edge flap control for BVI noise reduction
[NASA-CR-4426] p 512 N92-21173
HASSAN, AHMED A.
Effects of leading and trailing edge flaps on the aerodynamics of airfoil/vortex interactions p 815 A92-46957
HASSAN, BASIL
Effect of nose shape on three-dimensional stagnation region streamlines and heating rates
[AIAA PAPER 91-5032] p 171 A92-17822
HASSAN, H. A.
Monte Carlo simulation of reentry flows with ionization
[AIAA PAPER 92-0493] p 328 A92-26323
Monte Carlo simulation of entry in the Martian atmosphere
[AIAA PAPER 92-0494] p 329 A92-26324
Use of finite volume schemes for transition simulation p 432 A92-31185
Direct simulation of re-entry flows with ionization p 713 A92-44367
A new approach for the calculation of transitional flows
[AIAA PAPER 92-2669] p 798 A92-45524
An assumed joint-Beta PDF approach for supersonic turbulent combustion
[AIAA PAPER 92-3844] p 1113 A92-54199
HASSAN, O.
The computation of three-dimensional flows using unstructured grids p 612 A92-37539
The numerical simulation of flow about installed aero engine nacelle using a finite element Euler solver on unstructured meshes p 941 A92-52848
HASSENPFLUG, WOLFGANG
Inertial reference units with integrated air speed determination for helicopters p 554 A92-35764
HASSOUN, JOHN A.
An evaluation of four F-16 vertical velocity indicator configurations
[AD-A243629] p 370 N92-18014
HASTIE, ROBERT L., JR.
The effect of physical aging on the creep response of a thermoplastic composite
[AD-A243600] p 290 N92-17932
HASTINGS, D. E.
Ionospheric plasma flow over large high-voltage space platforms. I - Ion-plasma-time scale interactions of a plate at zero angle of attack. II - The formation and structure of plasma wake p 779 A92-41359
HASTINGS, DANIEL E.
The formation and structure of plasma wakes behind large high-voltage space platforms in ionosphere
[AIAA PAPER 92-0577] p 407 A92-26984
HASTINGS, P. R.
High density fuel qualification for a gas turbine engine
[AIAA PAPER 92-0684] p 389 A92-27051
HASTINGS, W. J.
Condor - An all electric airplane
[SAE PAPER 912184] p 644 A92-40004
HATCHER, P. G.
Advanced thermally stable jet fuel development program. Volume 2: Compositional factors affecting thermal degradation of jet fuels
[AD-A252656] p 987 N92-31399
HATHAWAY, M. D.
NASA low-speed centrifugal compressor for 3-D viscous code assessment and fundamental flow physics research
[ASME PAPER 91-GT-140] p 72 A92-15580
HATHAWAY, MICHAEL D.
Design and performance of controlled-diffusion stator compared with original double-circular-arc stator
[NASA-TP-2852] p 562 N92-22863
HATTA, KEIZO
Technical history of aircraft engines p 558 A92-35911
HATTESTAD, BJARNE
Mandatory psychological testing of pilots as a requirement for licensing in Norway? p 835 A92-45081
HAUCK, HELMUTH
The German Hypersonics Technology Programme - Status report 1992
[IAF PAPER 92-0867] p 1105 A92-57258
HAUENSTEIN, ANTHONY J.
Chaotic and nonlinear dynamic response of aerosurfaces with structural nonlinearities
[AIAA PAPER 92-2547] p 518 A92-34517
HAUGER, MICHAEL
German-GUS cooperation in civil aviation p 785 A92-47592
HAUGH, JAMES M.
Never make the same mistake twice - Using configuration control and error analysis to improve software quality p 601 A92-33603
HAUNSCHILD, M.
Navsat - A civil complement to GPS and Glonass
[IAF PAPER 91-490] p 188 A92-18505
HAUSER, JOHN
Nonlinear control design for slightly nonminimum phase systems - Application to V/STOL aircraft p 876 A92-48160
HAVENER, GEORGE
Holographic and PLIF measurements of free-flight hypervelocity flows in the AEDC Range G facility
[AIAA PAPER 92-3935] p 1122 A92-56765
HAVILAND, JOHN K.
Pulse response method for vibration reduction in periodic dynamic systems p 661 A92-39909
HAWBOLDT, R. J.
Nonstationary gasdynamics p 220 N92-13985
HAWKEN, D. F.
Computational fluid dynamics p 177 N92-13979
Nonstationary gasdynamics p 220 N92-13985
HAWKINS, J.
Gamma Group-The Pale Horse: A proposal in response to a commercial air transportation study ort study
[NASA-CR-190019] p 731 N92-26435
HAWKINS, J. M.
High speed rotorcraft propulsion concepts to control power/speed characteristics
[AIAA PAPER 92-3367] p 865 A92-48940
HAWKINSON, TODD D.
Multiple input sliding mode control for autonomous diving and steering of underwater vehicles
[AD-A241935] p 283 N92-17442
HAWKSHAW, JOHN K.
Fire bombing and fire bombers
[CA-PATENT-1-268-164] p 1061 N92-33582
HAWLEY, ROBERT J.
Heliport VFR airspace design based on helicopter performance
[SCT-90RR-34] p 103 N92-13049
Helicopter rejected takeoff airspace requirements
[SCT-91RR-28] p 116 N92-13058
HAWSEY, R. A.
Counterrotating brushless DC permanent magnet motor
[DE92-003825] p 401 N92-18550
HAY, D. R.
Inspection of aircraft engine components using automated eddy current and pattern recognition techniques
[NRC-LTR-ST-1834] p 504 N92-22029
HAY, J.
Fly-by-light technology development plan
[NASA-CR-181954] p 1086 N92-32778
HAY, N.
Discharge coefficients of cooling holes with radiused and chamfered inlets
[ASME PAPER 91-GT-269] p 151 A92-15667
HAYAKAWA, K.
A model study on diffuser pressure recovery in NAL scramjet test facility with simulated hydrogen combustion
[AIAA PAPER 92-3979] p 1071 A92-56805
HAYAMA, KENJI
Experimental and numerical study of aerodynamic characteristics for second generation SST
[SAE PAPER 912056] p 844 A92-45439
HAYAMA, S.
The effectiveness of the warp shape airfoil of a supersonic transport p 711 A92-43203
HAYAMI, HIROSHI
Performance of a high-pressure-ratio centrifugal compressor influenced by distribution of tip clearance of the mixed-flow impeller p 498 A92-32509
HAYASHI, A. K.
Numerical simulation of a supersonic jet impingement on a ground
[SAE PAPER 912014] p 789 A92-45412
Numerical analysis of RCS jet in hypersonic flights
[SAE PAPER 912063] p 791 A92-45445
HAYASHI, H.
Working together in the development of the B777 p 1015 A92-56080
HAYASHI, M.
Aerodynamic heating measurement in hypersonic flow p 709 A92-43102
HAYASHI, MASANORI
Experimental and numerical investigations on separated flows around pitching airfoils p 710 A92-43166
Numerical simulations of separated flows around oscillating airfoil for dynamic stall phenomena
[SAE PAPER 911991] p 788 A92-45393
Aerodynamic heating in three-dimensional shock wave turbulent boundary layer interaction induced by sweptback sharp fins in hypersonic flows
[SAE PAPER 912044] p 791 A92-45428
Numerical experiments on unsteady shock reflection processes using the thin-layer Navier-Stokes equations p 818 A92-47155
Experimental investigation on turbulent phenomena in three-dimensional shock wave/turbulent boundary layer interaction induced by blunt fin p 1018 A92-53557
HAYASHI, TSUTOMO
An analytical evaluation of the aerodynamic forces acting on a circular cylinder in a uniform shear flow p 522 A92-35995
HAYASHI, TSUTOMU
The effect of a velocity gradient on the aerodynamic forces of a circular cylinder with tangential blowing p 614 A92-38859
HAYASHI, Y.
Scrutinizing k-epsilon EVM and ASM by means of LES and wind tunnel for flowfield around cube p 621 A92-40119
Aerodynamic model identification of a spaceplane model from a cable-mount dynamic wind-tunnel test p 1093 A92-56114
HAYASHI, YOICHI
Structural concept of main wings of high altitude unmanned aerial vehicle and basic properties of thermoplastic composites as candidate material
[SAE PAPER 912053] p 843 A92-45437
HAYASHI, YOSHIO
The quiet STOL research aircraft ASUKA p 642 A92-38206
The progress of a STOL project p 699 A92-43137
The main wing boundary layer separation pattern of STOL research aircraft Asuka p 709 A92-43144
HAYASHI,KOICHI
Numerical study on the secondary jet into a supersonic flow p 1018 A92-53556
HAYASHIDA, ROBERT D.
Rotor-to-stator partial rubbing and its effects on rotor dynamic response p 224 N92-14367
HAYBALL, C.
Aerodynamics p 202 N92-13977
HAYES, MICHAEL S.
Who or what saved the day? A comparison of traditional and glass cockpits p 833 A92-44931
HAYHURST, KELLY J.
Analysis of data from a DO-178A software development process p 1134 N92-32880
HAYKIN, SIMON
Classification of radar clutter using neural networks p 145 A92-14252
A multi-layer neural network classifier for radar clutter p 291 A92-21691
HAYMAN, T. E.
Noise generated by wind turbines p 686 A92-39045
HAYNES, ALFRED C.
United 232 - Coping with the 'one-in-a-billion' loss of all flight controls p 530 A92-36349

HAYNES, J.
Dynamic control of aerodynamic instabilities in gas turbine engines p 870 N92-28466
HAYRE, AVTAR
The ATF YF-23 Vehicle Management System
[AIAA PAPER 92-1076] p 563 A92-33245
HAZLETT, ROBERT N.
Thermal oxidation stability of aviation turbine fuels
[ISBN 0-8031-1248-3] p 669 A92-40409
HAZLEWOOD, K. H.
An air-launched balloon system for a 230 lb gross inflation
[AIAA PAPER 91-3689] p 16 A92-11032
HE, CHENG J.
An aeroelastic analysis with a generalized dynamic wake p 847 A92-46932
HE, DAWEI
Vibration of gear system with web structure
p 588 A92-35573
Optimization of longitudinal corrections of helical gears p 990 A92-49578
On travelling wave vibration of high-speed duplex helical gears p 990 A92-49580
HE, DEXIN
The measurement of flutter derivatives using mechanical *admittance* p 393 A92-25014
HE, ERMING
Vibration control of rotor-bearing system by controlled squeeze-film damper bearings p 990 A92-49579
HE, HONGQING
Ablative control mechanism in nozzle thermo-protection
[AIAA PAPER 92-3054] p 889 A92-48712
HE, J.
An algebraic model for dissipation in supersonic boundary layers
[AIAA PAPER 92-0311] p 320 A92-25759
HE, JIA J.
The research of reducing 3-D low supersonic shock wave reflection in a 2-D transonic flexible walls adaptive wind *tunnel*
[AIAA PAPER 92-3924] p 1095 A92-56755
HE, JINGYANG
Engine flight load reliability analysis
p 968 A92-49827
HE, L.
Inviscid-viscous coupled solution for unsteady flows through vibrating blades. II - Computational results
[ASME PAPER 91-GT-126] p 71 A92-15571
An experiment on unsteady flow over an oscillating airfoil
[ASME PAPER 91-GT-181] p 73 A92-15613
HE, LI X.
Location and tracking technique in a multistatic system established by multiple bistatic systems
p 840 A92-48480
HE, LIANZHU
Study of dynamic strength on composite wing
p 996 A92-53071
HE, LINSHU
Application researches on expert system used for structural layout optimization of wings
p 398 A92-27865
HE, QINGZHI
Applied fracture mechanics research in the aerospace field p 37 A92-10375
HE, WENYUE
Flow characteristic and flow control of high aspect ratio and highly curved S-bend diffuser p 245 A92-21743
HE, Z. W.
Control of strong shock-turbulent boundary layer interaction in rectangular channels p 422 A92-29714
HE, ZENG
Open-loop model reduction and parameter perturbation for active flutter suppression system
p 379 A92-24879
HE, ZHIDAI
A study on the stability of aircraft at high angles-of-attack and state vector propagation sensitivity
p 978 A92-53394
HEALEY, J. V.
Control of turbulent flow on a backward-facing step
[AIAA PAPER 92-0066] p 250 A92-22179
A data base for flight in the wake of a ship
[AIAA PAPER 92-0295] p 319 A92-25748
Establishing a database for flight in the wakes of structures p 810 A92-46782
Flight deck aerodynamics of a nonaviation ship
p 810 A92-46790
The aerodynamics of ship superstructures
p 503 N92-21953
HEALY, EDWARD A., JR.
Studies in chaos using stochastic methods
[AD-A246919] p 780 N92-27171
HEAPHY, WILLIAM J.
Advanced Transport Operating System (ATOPS) control display unit software description
[NASA-CR-189606] p 652 N92-24689
HEARD, P. J.
Aircraft gas turbine emissions: Their nature, technology for reduction, and a pollution comparison with channel tunnel transport
[ETN-92-91056] p 559 N92-22406
HEARNE, PETER A.
Anglo-American avionics p 307 A92-25575
HEATH, G.
Application of face-gear drives in helicopter transmissions
[NASA-TM-105655] p 908 N92-28434
HEATH, GREGORY F.
Advanced Rotorcraft Transmission program summary
[AIAA PAPER 92-3363] p 905 A92-48936
HEBBAR, S. K.
Flow visualization and wake analysis for complex three-dimensional bluff bodies at subcritical through critical Reynolds numbers
[AIAA PAPER 92-0155] p 253 A92-23770
HEBBAR, SHESHAGIRI K.
Pitch rate/sideslip effects on leading-edge extension *vortices of an F/A-18 aircraft model*
p 874 A92-46810
HECHT-NIELSEN, ROBERT
Processing complexity of two approaches to object detection and recognition p 234 N92-14677
HECHT, F.
Anisotropic control of mesh generation based upon a Voronoi type method p 918 A92-47043
HECHT, Y.
Response of helicopter blades to a sharp collective increase p 1084 A92-56282
HECK, BONNIE S.
Reaching conditions in variable structure systems for output feedback control p 506 A92-29037
HEDDE, T.
Development of a three-dimensional icing code - Comparison with experimental shapes
[AIAA PAPER 92-0041] p 262 A92-22159
HEDDERGOTT, A.
Application of a wall pressure method in a wind tunnel test section with adjustable longitudinal slots
p 1091 A92-54336
HEDGE, B.
Electronically steerable antenna for aircraft
p 229 N92-15272
HEDGES, LINDA S.
Numerical simulation of total temperature separation in jets
[AIAA PAPER 92-0535] p 396 A92-26952
HEDLUND, ERIC R.
Aero-optical testing in the NSWC Hypervelocity Tunnel No. 9
[AIAA PAPER 92-2797] p 747 A92-41336
HEDMAN, SVEN G.
MATGRID: A program for generation of C-H and C-O topology grids around wing/body configurations. Mathematical definition document
[FFA-TN-1990-19] p 444 N92-20468
MATGRID, a program for generation of C-H and C-O topology grids around wing/body configurations: Software description document
[FFA-TN-1990-20] p 945 N92-30713
HEDRICK, J. K.
Robust adaptive nonlinear control of high performance aircraft p 478 A92-29188
HEEG, JENNIFER
Simulation and model reduction for the AFW program
[AIAA PAPER 92-2081] p 572 A92-35653
An analytical and experimental investigation of flutter suppression via piezoelectric actuation
[AIAA PAPER 92-2106] p 567 A92-35677
An analytical and experimental study to investigate flutter *suppression via piezoelectric actuation*
[NASA-TM-893240] p 156 N92-12173
Flutter suppression via piezoelectric actuation
[NASA-TM-104120] p 197 N92-15070
An analytical and experimental investigation of flutter suppression via piezoelectric actuation
[NASA-TM-107653] p 962 N92-31174
HEFFERNAN, RUTH M.
Wing force and surface pressure data from a hover test of a 0.658-scale V-22 rotor and wing
[NASA-TM-102244] p 550 N92-22864
HEFFNER, K. S.
Numerical and experimental investigation of rarefied compression corner flow
[AIAA PAPER 92-2900] p 820 A92-47876
HEFFNER, MICHAEL
Further wind tunnel investigation of the SM701 airfoil with aileron and turbulators
[NASA-CR-190702] p 1038 N92-33063
HEFFNER, PEGGY L.
Design and performance of the centrifuge-based Dynamic Flight Simulator
[AIAA PAPER 92-4156] p 981 A92-52446
HEGEN, G. H.
Application of electronically scanned pressure measurement system for engine simulation tests in the German-Dutch Wind Tunnel
[AIAA PAPER 92-4003] p 1122 A92-56826
HEIDENREICH, R.
Probabilistic lifing approach for aero engine disks made of powder nickel base alloys containing ceramic defects
p 226 N92-14424
HEIDLEBAUGH, D. L.
Current stabilizing of fastened composite joints to improve non-sparking lightning current performance
p 213 A92-20130
HEIGES, M. W.
Synthesis of a helicopter full-authority controller
p 280 A92-21178
HEIMBERG, F.
Construction of a real-time DGPS experimental system
p 840 A92-47631
HEIMERDINGER, M. W.
Supportability evaluation of thermoplastic and thermoset *composites* p 1108 N92-32576
HEINDEL, TROY A.
Real Time Data System (RTDS) p 140 N92-12025
HEINZE, P.
Simultaneous stress and flutter optimization for the wing of a transport aircraft equipped with four engines
p 571 N92-23238
HEISER, W.
Investigation of a plate-ramp-configuration by means of laser Doppler anemometry at Mach 2.95
[AIAA PAPER 92-3956] p 1097 A92-56784
The trisonic wind tunnel Muenchen and its involvement in the German SAeNGER-programme
[AIAA PAPER 92-4019] p 1100 A92-56841
HEISER, WILLIAM H.
Improvements in teaching aircraft engine design
[AIAA PAPER 92-3758] p 1141 A92-54152
HEISS, S.
Application of the Euler method EUFLEX to a fighter-type airplane configuration at transonic speed
[AIAA PAPER 92-2620] p 845 A92-45573
HEITOR, M. V.
Turbulent energy budgets in impinging zones
p 620 A92-40081
HELD, T. W.
Explicit finite element method for transparency impact analysis
[AD-A243527] p 264 N92-17478
HELLER, GERARD H.
Impact of a process improvement program in a production software environment: Are we any better?
p 413 N92-19422
HELM, D.
Applications of IMI 834 in aeroengines - A collaborative IMI/MTU programme p 288 A92-22754
Influence of long time exposure at elevated temperatures in air on mechanical properties of the high temperature titanium alloy IMI 834 p 289 A92-22767
HEMDAN, HAMDI T.
Similarity solutions for supersonic axisymmetric flows
p 173 A92-18387
Hypersonic flows over slender circular cones at small angles of attack p 173 A92-19068
Oscillating two-dimensional hypersonic airfoils at small angles of attack p 340 A92-28042
On hypersonic flow over two-dimensional aerofoils
p 433 A92-31425
Three-dimensional wings and waveriders with attached shock waves p 936 A92-50322
Supersonic flow past pointed-nose thin airfoils
p 940 A92-52844
HEMINWAY, ROBERT
LH wind tunnel testing - Key to advanced aerodynamic design p 104 A92-14331
HEMSCH, MICHAEL J.
Alleviation of side force on tangent-ogive forebodies using passive porosity
[AIAA PAPER 92-2711] p 802 A92-45552
HENCKELS, A.
Experimental study of hypersonic shock wave boundary layer interactions by means of infrared technique
p 182 N92-14994
HENDERSON, GREGORY H.
Airfoil wake and linear theory gust response including sub and superresonant flow conditions
[AIAA PAPER 92-3074] p 823 A92-48724
HENDERSON, J. K.
Core avionics and standardization
[AD-A248326] p 735 N92-27925

HENDERSON, JOHN F.
Forebody vortex flow control on the F-16C using tangential slot and jet nozzle blowing
[AIAA PAPER 92-0019] p 247 A92-22141
HENDERSON, MICHAEL E.
On constructing three-dimensional overlapping grids with CMPGRD p 691 N92-24424
HENDERSON, TODD L.
Interactive solution-adaptive grid generation procedure
[NASA-TM-105432] p 528 N92-23563
HENDRICKS, G.
Active control of compressor surge and stall
[AD-A252771] p 1126 N92-33498
HENDRICKS, G. J.
A theoretical study of sensor-actuator schemes for rotating stall control
[AIAA PAPER 92-3486] p 878 A92-49025
Dynamic control of aerodynamic instabilities in gas turbine engines p 870 N92-28466
HENDRICKS, R. C.
A finite-volume numerical method to calculate fluid forces and rotordynamic coefficients in seals
[AIAA PAPER 92-3712] p 1113 A92-54132
HENDRICKS, ROBERT C.
Brush seal leakage performance with gaseous working fluids at static and low rotor speed conditions
[NASA-TM-105400] p 297 N92-16265
HENDRICKSON, HEIDI
Manx: Close air support aircraft preliminary design
[NASA-CR-189992] p 463 N92-21565
HENDRIX, R. E.
Developments in airborne surveillance and control systems p 98 A92-16655
HENEGHAN, S. P.
Isothermal flow fields in a research combustor for lean blowout studies
[ASME PAPER 91-GT-37] p 121 A92-15520
Lean blowout in a research combustor at simulated low pressures
[ASME PAPER 91-GT-359] p 137 A92-15713
HENEGHAN, SHAWN P.
Static tests for the evaluation of fuel additives
[AIAA PAPER 92-0686] p 389 A92-27053
HENFLING, JOHN F.
Calibration of hemispherical-head flow angularity probes
[AIAA PAPER 92-4005] p 1122 A92-56828
HENGST, R. R.
Ceramic component processing development for advanced gas-turbine engines
[ASME PAPER 91-GT-120] p 142 A92-15567
HENKE, ANDREA
Case-based reasoning - Taming the similarity heuristic p 47 A92-11153
HENKE, H.
Computation of viscous phenomena in unsteady transonic flow p 720 N92-27949
Computation of flutter boundaries in the time and frequency domain p 720 N92-27952
HENLEY, A. J.
An integrated navigation system manager using federated Kalman filtering p 858 A92-48477
HENLINE, WILLIAM D.
Thermal protection analysis of Mars-earth return vehicles p 497 A92-32183
HENNINGER, SANDRA
Guidelines for integrating helicopter assets into emergency planning
[SCT-91RR-18] p 18 N92-10993
HENRY, R.
Development of an electrothermal de-icing/anti-icing model
[AIAA PAPER 92-0526] p 351 A92-26949
HENRY, Z. S.
Advanced Rotorcraft Transmission (ART) - Component test results
[AIAA PAPER 92-3366] p 905 A92-48939
HENSHAW, WILLIAM D.
On constructing three-dimensional overlapping grids with CMPGRD p 691 N92-24424
HENSYL, J.
Avionic data bus integration technology
[DOT/FAA/CT-91/19] p 736 N92-27973
HERAGU, SRINATH S.
Prediction of turbulent flow behavior over a slotted flap p 309 A92-24407
HERBELL, THOMAS P.
Monolithic ceramics p 668 A92-39854
HERBERT, K.
The measurement of plate vibration and sound radiation from a turbulent boundary layer manipulator
[AD-A240127] p 42 N92-10206
HERBERT, TH.
Computation of laminar flow over a long slender axisymmetric blunted cone in hypersonic flow
[AIAA PAPER 92-0756] p 336 A92-27098
HERDEG, WOLFGANG F.
Bistatic scattering on a monostatic radar range p 849 A92-48408
HERGENROTHER, PAUL M.
Poly 1, 2, 4-triazoles via aromatic nucleophilic displacement
[NASA-CASE-LAR-14440-1] p 35 N92-10066
HERGERT, DENNIS W.
Buffet test in the National Transonic Facility
[AIAA PAPER 92-4032] p 1100 A92-56854
Buffet test in the National Transonic Facility
[NASA-CR-189595] p 888 N92-29352
HERMANO, CHRISTINE
SHARP: Subsonic High Altitude Research Platform
[NASA-CR-190004] p 648 N92-25263
HERMANS, C.
LAH main rotor model test at the DNW p 547 A92-35771
LAH-main rotor model test at the DNW
[NLR-TP-90305-U] p 852 N92-28687
HERMANSON, J. C.
Structure and penetration of a transverse fluid jet injected at supercritical pressure in supersonic flow
[AIAA PAPER 92-3652] p 1113 A92-54105
HERMSEN, P. A.
Wind loads on a mirage III O aircraft mounted above a ground plane
[AD-A243004] p 275 N92-17266
HERNANZ, M.
Electronically steerable antenna for aircraft p 229 N92-15272
HERNANZ, M. L.
Electronically steerable antenna for aircraft p 229 N92-15272
HERON, K. H.
Path identification in structural acoustics p 1059 A92-56346
HERRING, FRED M.
Buffet test in the National Transonic Facility
[AIAA PAPER 92-4032] p 1100 A92-56854
Buffet test in the National Transonic Facility
[NASA-CR-189595] p 888 N92-29352
HERRMANN, H.
Propulsion aspects of hypersonic turbo-ramjet-engines with special emphasis on nozzle/aftbody integration
[ASME PAPER 91-GT-395] p 127 A92-15725
HERSBACH, H. J. C.
NLR experience with high velocity burner rig testing, 1979-1989
[NLR-TP-89152-U] p 385 N92-18415
HERTEL, J.
Complete Euler-solution for a rotor in hover and a propeller in forward flight p 520 A92-35755
HERTEMAN, JEAN-PAUL
Manufacturing process control as a damage tolerance concept p 403 N92-19006
HERZOG, M.
BMI/bis (allylphenoxyphthalimide)-copolymers - A new family of resins for advanced composites with improved thermal oxidative stability p 33 A92-10213
HERZOG, P.
Experimental study of hypersonic shock wave boundary layer interactions by means of infrared technique p 182 N92-14994
HESHMAT, H.
Rotordynamic evaluation of an advanced multi-squeeze film damper - Imbalance response and bladeless simulation
[ASME PAPER 91-GT-242] p 149 A92-15647
High-temperature powder-lubricated dampers for gas turbine engines p 399 A92-28528
HESHMAT, HOOSHANG
Advanced multi-squeeze film dampers for rotor vibration control p 36 A92-10102
The basics of powder lubrication in high-temperature powder-lubricated dampers
[ASME PAPER 91-GT-248] p 150 A92-15653
HESS, ANDREW
The development and integration of an engine monitoring system for the F-14A+/D Super Tomcat
[SAE PAPER 912094] p 654 A92-39951
HESS, CECIL F.
An optical microphone for the detection of hidden helicopters
[AIAA PAPER 92-0377] p 395 A92-26235
HESS, PAUL J.
Engine aircraft systems integration course
[AIAA PAPER 92-3762] p 928 A92-49117
HESS, R. A.
Quantitative Feedback Theory (QFT) applied to the design of a rotorcraft flight control system
[AIAA PAPER 92-0044] p 281 A92-22161
An framework for robust flight control design using constrained optimization
[AIAA PAPER 92-4603] p 1131 A92-55282
Flight simulator fidelity assessment in a rotorcraft lateral translation maneuver
[AIAA PAPER 92-4424] p 1092 A92-55348
HESS, RICHARD F.
Fly-by-light technology development plan
[NASA-CR-181954] p 1086 N92-32778
HESS, RONALD A.
Analyzing the flared landing task with pitch-rate flight control systems p 661 A92-39905
HESS, RONALD W.
Advanced airframe structural materials: A primer and cost estimating methodology
[AD-A253371] p 1062 N92-34182
HESSENIUS, KRISTIN A.
Computational aerodynamics - The next generation
[SAE PAPER 911988] p 788 A92-45390
NASA aerodynamics program
[NASA-TM-4368] p 609 N92-24678
HETSKO, JEAN
Accomplishments under the Airport Improvement Program, FY 1991
[AD-A253046] p 1101 N92-33434
HETTENA, E.
Vortical flow simulation by using structured and unstructured grids p 83 N92-12999
HETTINGER, LAWRENCE J.
Toward an integrated multimodal approach to flight simulation p 880 A92-45026
HEUDIN, J.-C.
A parallel architecture adapted to onboard multiexpert systems p 276 A92-23040
HEWETT, MARLE D.
High-speed civil transport issues and technology program
[NASA-CR-186020] p 962 N92-31208
HEWITT, F. A.
Propulsion system performance and integration for high Mach air breathing flight p 862 A92-46429
HEWITT, K. L.
On the accuracy of an aircraft-borne ambient electric-field measuring system p 186 A92-20127
HEYDEN, J.
Opportunities for flight simulation to improve operational effectiveness p 883 N92-28523
HEYES, F. J. G.
The effect of blade tip geometry on the tip leakage flow in axial turbine cascades
[ASME PAPER 91-GT-135] p 72 A92-15577
HEYMAN, JOSEPH S.
Large area QNDE inspection for airframe integrity p 362 N92-18588
HIBNER, DAVID
Feasibility of magnetic bearings for advanced gas turbine engines p 772 N92-27738
HICKEY, ALBERT E.
Design specifications for the Advanced Instructional Design Advisor (AIDA), volume 2
[AD-A248202] p 923 N92-29188
HICKMAN, G. A.
Application of smart structures to aircraft health monitoring p 20 A92-11123
HICKMAN, R. A.
Operational design factors for NASP derived vehicles
[AIAA PAPER 91-5081] p 210 A92-17851
HICKS, GARY
NASA aerodynamics program
[NASA-TM-4368] p 609 N92-24678
HICKS, P.
Quick-look system p 599 N92-23393
HICKS, R.
Subsonic and transonic low-Reynolds-number airfoils with reduced pitching moments p 701 A92-41211
HICKS, R. M.
Practical design optimization of wing/body configurations using the Euler equations
[AIAA PAPER 92-2633] p 795 A92-45505
HIGASHINO, FUMIO
Oscillation of oblique shock waves generated in a two dimensional asymmetric nozzle
[SAE PAPER 912061] p 791 A92-45443
HIGASHINO, KAZUYUKI
Test results of the expander cycle air turbo ramjet for a future space plane
[IAF PAPER 91-271] p 120 A92-14709
HIGGINBOTHAM, G. J. S.
Present and future trends in turbine blade material and manufacturing technology
[PNR-90825] p 488 N92-20164
HIGGINS, CHRISTOPHER
A comparison between the consequences of the liberal and non-liberal UK-Europe bilaterals
[TT-9101] p 18 N92-10018
HILGENSTOCK, ACHIM
On the simulation of compressible turbulent flows past delta wing, delta wing-body and delta wing-canard p 84 N92-13003

On the footprints of three-dimensional separated vortex flows around blunt bodies: Attempts of defining and analyzing complex flow structures p 84 N92-13005
HILL, ACQUILLA S.
High Reynolds number test of the Boeing TR77 airfoil in the Langley 0.3-meter transonic cryogenic tunnel
[NASA-TM-4189] p 947 N92-31246
HILL, BERNARD
Suit study - The impact of VMS in subsystem integration
[AIAA PAPER 92-1078] p 563 A92-33247
HILL, C. J.
Ground surface erosion - British Aerospace test facility and experimental studies p 881 A92-45323
HILL, EUGENE G.
Wind tunnel investigation of the aerodynamic effects of aircraft ground deicing/anti-icing fluids and criteria for aerodynamic acceptance p 452 N92-21698
Lewis icing research tunnel test of the aerodynamic effects of aircraft ground deicing/anti-icing fluids
[NASA-TP-3238] p 952 N92-30395
HILL, GARY
A piloted comparison of elastic and rigid blade-element rotor models using parallel processing technology p 546 A92-35751
Comparison of elastic and rigid blade-element rotor models using parallel processing technology for piloted simulations
[SAE PAPER 912120] p 608 A92-39968
HILL, GARY C.
Improving designer productivity
[AIAA PAPER 92-1187] p 1130 A92-54285
Improving designer productivity
[NASA-TM-103929] p 854 N92-29417
HILL, PHILIP G.
Mechanics and thermodynamics of propulsion (2nd revised and enlarged edition)
[ISBN 0-201-14659-2] p 672 A92-38275
HILL, R. J.
Compressing the compressor
[PNR-90824] p 476 N92-21848
HILL, RALPH H.
Laser induced fluorescence detection of gums in jet fuels
[AD-A252685] p 987 N92-30767
HILL, RICHARD G.
Development and evaluation of an onboard aircraft cabin water spray system for postcrash fire protection
[SAE PAPER 912224] p 636 A92-40022
HILL, S. H.
The design and testing of a radial flow turbine for aerodynamic research
[ASME PAPER 91-GT-220] p 124 A92-15636
HILLENBRAND, CHRISTOPHER F.
Thrust test fixture
[AD-D015259] p 983 N92-31192
HILLESHEIMER, M.
Optimization of two stage reusable space transportation systems with rocket and airbreathing propulsion concepts
[IAF PAPER 92-0863] p 1104 A92-57254
HINDEL, JAMES T.
Low energy ice protection for helicopters p 1059 A92-56348
HINDS, BRUCE J.
The flight test pilot's display - A CRT system for test maneuvers p 118 A92-16057
HINDSON, WILLIAM S.
A review of recent programs and future plans for rotorcraft in-flight simulation at Ames Research Center
[SAE PAPER 912121] p 608 A92-39969
Rotorcraft In-Flight Simulation Research at NASA Ames Research Center: A Review of the 1980's and plans for the 1990's
[NASA-TM-103873] p 853 N92-28926
HINE, BUTLER P.
Optical computing at NASA Ames Research Center
[AIAA PAPER 91-3779] p 231 A92-17637
Binary optical filters for scale invariant pattern recognition
[NASA-TM-103902] p 853 N92-28910
HINGST, W. R.
Surface and flow field measurements in a symmetric crossing shock wave/turbulent boundary layer flow
[AIAA PAPER 92-2634] p 806 A92-45574
HINGST, WARREN R.
The structure and development of streamwise vortex arrays embedded in a turbulent boundary layer
[AIAA PAPER 92-0551] p 342 A92-28204
HINKEY, J. B.
High spatial resolution measurements of ram accelerator gas dynamic phenomena
[AIAA PAPER 92-3244] p 903 A92-48844
HINKLE, A. J.
Methodology for the assessment of material quality effects on airframe fatigue durability p 213 A92-19820
HINTON, DAVID A.
Forward-look wind-shear detection for microburst recovery p 378 A92-24408
HINTZE, M. MARX
High Intensity Radiated Fields (HIRF) project plan
[DOT/FAA/CT-TN91/1] p 297 N92-16181
HIRABAYASHI, N.
New 1.27-m leg of the National Aerospace Laboratory hypersonic wind tunnel p 1092 A92-56003
HIRAMOTO, M.
Study on transonic cascade performance by use of newly built facility p 136 A92-15328
HIRAOKA, KATSUMI
Effect of streamwise pressure gradient on the supersonic mixing layer p 1025 A92-54936
HIRAOKA, KOICHI
Roles of wind tunnel tests and CFD analyses in the design of energy-efficient SST
[AIAA PAPER 92-3923] p 1133 A92-56754
HIRASAWA, T.
Polar patrol balloon
[AIAA PAPER 91-3688] p 15 A92-11031
HIRATA, T.
Numerical simulation of supersonic nozzle flow p 430 A92-30540
HIRD, GEOFFREY R.
Formal specification and verification of Ada software
[AIAA PAPER 91-3713] p 230 A92-17585
HIRNER, TIMOTHY J.
Aircraft aeroservoelastic compensation using constrained optimization
[AIAA PAPER 92-2399] p 564 A92-34470
Automated procedures for aircraft aeroservoelastic compensation
[AIAA PAPER 92-4606] p 1077 A92-55284
HIROE, TETSUYUKI
Flow around two square cylinders in staggered arrangements p 761 A92-42797
HIROSE, HIDEHIRO
Design and wind tunnel test of low-Reynolds-number airfoil p 1029 A92-56047
HIROSE, MASANORI
Robotics application in aerospace manufacturing p 671 A92-38216
HIROSE, NAOKI
Euler flow analysis of turbine powered simulator and fanjet engine p 80 A92-17196
Proceedings of the Seminar on Investigation and Control of Boundary-Layer Transition
[NAL-SP-11] p 400 N92-18483
HIRSCH, C.
Computer-based areal surface temperature and local heat transfer measurements with thermochromic liquid crystals (TLC) p 763 A92-44326
An integrated CFD system for 3D turbomachinery applications p 741 N92-27464
HIRSCH, CH.
Three dimensional flow in a linear compressor cascade at design conditions
[ASME PAPER 91-GT-114] p 70 A92-15565
Genuinely upwind algorithms for the multidimensional Euler equations p 175 A92-20733
HIRSCHBERG, MARVIN H.
Aircraft engine hot section technology: An overview of the HOST Project p 561 N92-22535
HIRSCHEL, E. H.
Acquisition of an aerothermodynamic data base by means of a winged experimental reentry vehicle p 486 A92-30685
Aerothermodynamic challenges of the Saenger space-transportation system p 184 N92-15042
Modelling of chemical and physical effects with respect to flows around reentry bodies
[MBB-FE-211/S/PUB/0465/A] p 347 N92-19296
Saenger: The reference concept and its technological requirements - aerothermodynamics
[MBB-FE-202-S-PUB-0463-A] p 890 N92-29629
Technology programme: Aerothermodynamics and propulsion integration. Numerical and experimental aerothermodynamics
[MBB-FE-202-S-PUB-0464-A] p 831 N92-29648
Aerothermodynamics and propulsion integration in the Saenger technology programme
[MBB-FE-202-S-PUB-0469-A] p 831 N92-29649
Aerothermodynamic challenges of the Saenger space-transportation system
[MBB-FE-202-S-PUB-0462-A] p 890 N92-29680
Hypersonic flow past radiation-cooled surfaces
[MBB-FE-202-S-PUB-0468-A] p 832 N92-29713
Acquisition of an aerothermodynamic data base by means of a winged experimental reentry vehicle
[MBB/FE202/S/PUB/461] p 787 N92-30232
HIRSHMAN, S. P.
Scoping studies for small steady-state tokamaks for divertor testing
[DE92-000740] p 238 N92-15761
Shafranov shift in low-aspect-ratio heliotron/torsatron CHS
[NIFS-110] p 1138 N92-33743
HISCOCKS, R. J.
A parametric approach to spectrum development p 360 N92-18578
HITCH, BRADLEY D.
Thermal management systems for high Mach airbreathing propulsion
[AIAA PAPER 92-0515] p 373 A92-26941
HITCHCOCK, L.
Evaluation of triple simultaneous parallel ILS approaches spaced 5000 feet apart, phase 4.b
[DOT/FAA/CT-91/31] p 456 N92-21404
HITCHCOCK, LLOYD
Evaluation of triple simultaneous parallel ILS approaches spaced 4300 feet apart, phase 4a
[ACD-340] p 191 N92-14034
HITT, ELLIS F.
Fault tolerant avionics display system p 965 A92-49312
HIX, C. E.
Auxiliary power system requirements for commercial air transports - Past, present and future
[SAE PAPER 912188] p 656 A92-40007
HO, CHIEN-KO
Numerical investigation of unsteady transonic nozzle flows p 331 A92-26443
HO, CHIH-MING
High aerodynamic loads on an airfoil submerged in an unsteady stream p 432 A92-31183
HO, M. J.
A surface definition code for turbine blade surfaces
[DE92-010574] p 1004 N92-31498
HO, YAOLONG
Investigation on effects on enhancing lift by acoustic excitation p 693 A92-38923
HOA, SUONG V.
Development and design with advanced materials
[ISBN 0-444-88706-7] p 296 A92-24176
HOAD, DANNY R.
Helicopter local blade circulation calculations for a model rotor in forward flight using laser velocimeter measurements p 65 A92-14362
HOADLEY, SHERWOOD T.
Application of aeroservoelastic modeling using minimum-state unsteady aerodynamic approximations p 204 A92-18622
The multiple-function multi-input/multi-output digital controller system for the AFW wind tunnel model
[AIAA PAPER 92-2083] p 565 A92-35655
On-line analysis capabilities developed to support the AFW wind-tunnel tests
[AIAA PAPER 92-2084] p 572 A92-35656
On-line performance evaluation of multiloop digital control systems p 873 A92-46739
On-line analysis capabilities developed to support the AFW wind-tunnel tests
[NASA-TM-107651] p 961 N92-30752
The multiple-function multi-input/multi-output digital controller system for the AFW wind-tunnel model
[NASA-TM-107600] p 1060 N92-32536
HOANG, KIET D.
Expert system management system
[AD-A247102] p 781 N92-26863
HOANG, N. T.
The dynamic character of the wake of an axisymmetric body at an angle of attack
[AIAA PAPER 91-3268] p 8 A92-12741
Pitch-up motions of delta wings
[AIAA PAPER 92-0278] p 318 A92-25732
HOANG, STEPHEN
Piloted simulation study of a balloon-assisted deployment of an aircraft at high altitude
[NASA-TM-104245] p 272 N92-15986
HOBBS, PETER V.
Twenty years of airborne research at the University of Washington p 161 A92-14925
HOBEIKA, A. G.
Runway exit designs for capacity improvement demonstrations. Phase 2: Computer model development
[NASA-CR-190166] p 484 N92-21162
HOBSON, G. V.
A turbulence model based on RNG for quasi-three-dimensional cascade flows
[AIAA PAPER 92-3312] p 825 A92-48898
HOBSON, GARTH V.
A Navier-Stokes analysis of a controlled-diffusion compressor cascade at increasing inlet-flow angles
[AIAA PAPER 92-3313] p 825 A92-48899
HOCEVAR, SUSAN P.
Profile of an effective engineering manager
[AD-A246525] p 781 N92-27528
HOCH, OSWALD
Evaluating the use of satellite communications in the government of Canada p 594 N92-22577

HOCK, S. M.
An overview: Challenges in wind technology development
[DE92-001190] p 302 N92-17875
HOCK, TERRENCE F.
A new aircraft universal lightweight digital dropsonde
p 467 A92-32089
HOCKADAY, STEPHEN
Human factors issues in the use of artificial intelligence in air traffic control. October 1990 Workshop
[NASA-CR-190925] p 1051 N92-34203
HOCKBRUCKNER, MARTY
Stellar inertial navigation growing with the times upgrading of the LN-20 integrated inertial navigation system p 97 A92-16646
HODAPP, J. F.
Using satellite communication for aircraft Automatic Dependent Surveillance p 725 A92-42486
HODGE, CHARLES G.
Quiet aircraft design and operational characteristics
p 236 N92-14787
HODGE, JEFFREY S.
The Langley 15-inch Mach 6 High Temperature Tunnel
[AIAA PAPER 92-3938] p 1096 A92-56768
HODGES, DEWEY H.
Application of composite rotor blade stability analysis to extension-twist coupled blades
[AIAA PAPER 92-2254] p 564 A92-34479
HODGKINSON, J.
Continuous flying quality improvement - The measure and the payoff
[AIAA PAPER 92-4327] p 1073 A92-55171
The use and effectiveness of piloted simulation in transport aircraft research and development
p 886 N92-28549
HODGKINSON, JOHN
Design and analysis issues of integrated control systems for high-speed civil transports
[NASA-CR-186022] p 979 N92-31656
HODSON, H. P.
The effect of blade tip geometry on the tip leakage flow in axial turbine cascades
[ASME PAPER 91-GT-135] p 72 A92-15577
The design and testing of a radial flow turbine for aerodynamic research
[ASME PAPER 91-GT-220] p 124 A92-15636
Modelling of unsteady transitional boundary layers
[ASME PAPER 91-GT-282] p 152 A92-15677
Aspects of unsteady blade-surface boundary layers and transition in axial turbomachines p 658 N92-24340
HOEFT, L. O.
Using the single point excitation technique to measure aperture impedance over a broad frequency range
p 761 A92-42320
HOEFT, LOTHAR O.
Comparison of R2SPG waveforms with simulated EMP
p 760 A92-42317
HOEG, J. G.
Aircraft ship operations
[AGARD-AR-312] p 850 N92-28468
HOEIJMAKERS, H. W. M.
Numerical investigation into high-angle-of-attack leading-edge vortex flow
[AIAA PAPER 92-2600] p 791 A92-45477
Modeling and numerical simulation of vortex flow in aerodynamics
[AD-B163670L] p 83 N92-12997
Comparison of solution of various Euler solvers and one Navier-Stokes solver for the flow about a sharp-edged cropped delta wing
[AD-B163639L] p 83 N92-12998
Analysis of results of an Euler-equation method applied to leading-edge vortex flow p 84 N92-13000
An experimental study of the flow over a sharp-edged delta wing at subsonic and transonic speeds
p 85 N92-13011
Numerical simulation of vortical flow over a delta wing at subsonic and transonic speeds
[NLR-TP-90029-U] p 444 N92-20498
Panel methods for aerodynamic analysis and design
p 552 N92-23955
Analysis of results of an Euler-equation method applied to leading-edge vortex flow
[NLR-TP-90368-U] p 827 N92-28657
A method for computing the 3-dimensional flow about wings with leading-edge vortex separation. Part 2: Description of computer program VORSEP
[NLR-TR-86006-U] p 833 N92-29916
Modeling and numerical simulation of vortex flow in aerodynamics
[NLR-TP-91154-U] p 1037 N92-32673
An experimental study of the flow over a sharp-edged delta wing at subsonic and transonic speeds
[NLR-TP-91117-U] p 1037 N92-32732
HOELD, R.
Cases 6.1 and 6.8 double ellipsoid: Navier-Stokes calculation p 525 N92-22181
Case 7.4 delta wing: Navier-Stokes calculation
p 525 N92-22182
HOELD, ROLAND K.
Viscous shock-layer equations for the calculation of reentry aerothermodynamics p 183 N92-15008
HOERNLEIN, H. R. E. M.
First approach to an integrated fin design
p 551 N92-23236
HOFF, FREDERICK G.
Wavelength encoded fiber optic angular displacement sensor p 857 A92-48046
HOFF, R. M.
Digital ozonesondes - Examples of results from the EMEFS experiments of 1988 and 1990
p 468 A92-32140
HOFFLER, KEITH D.
Application of piloted simulation to high-angle-of-attack flight-dynamics research for fighter aircraft
p 886 N92-28551
Simulation model of a twin-tail, high performance airplane
[NASA-TM-107601] p 1088 N92-33537
HOFFMAN, J. J.
Low density real gas flows about hypersonic vehicles
[AD-A250048] p 949 N92-31777
HOFFMAN, KNUT
Pilots noise exposure during a Boeing 747-400 round trip: Ambient noise and acoustic-head recording and analysis of data p 1137 N92-32960
HOFFMAN, M. J.
Trajectory optimization for hypersonic aircraft guidance p 728 N92-27898
HOFFMAN, MARK
The importance of implicit and explicit knowledge in a pilot's associate system p 858 A92-48567
HOFFMAN, MARK A.
An explanation-based-learning approach to knowledge compilation - A Pilot's Associate application
p 920 A92-48220
HOFFMAN, WENDY B.
Simulation of 3-D shear flows around a nozzle-afterbody at high speeds p 519 A92-34826
HOFFMANN, HANS-EBERHARD
The icing of the wing upper side and bottom side of the icing research aircraft of the DLR
p 724 N92-26349
The icing of the elevator of the DLR icing research aircraft of Do 28 type
[DLR-MITT-91-12] p 953 N92-31813
Analysis of three icing test flights reaching the aircraft-referred icing degree of severe
[ESA-TT-1254] p 954 N92-31943
HOFFMANN, KLAUS A.
Grid sensitivity in low Reynolds number hypersonic continuum flows p 817 A92-47057
Effect of the grid system on heat transfer computations for high speed flows p 900 A92-47071
HOFFMANN, W.
Analysis of helicopter rotor-fuselage interference with time averaged pressure distribution
p 1032 A92-56331
HOFLER, THOMAS J.
Thermoacoustic refrigeration p 595 N92-22720
HOFSTRA, J. S.
Using the single point excitation technique to measure aperture impedance over a broad frequency range
p 761 A92-42320
HOFSTRA, JOSEPH S.
Comparison of R2SPG waveforms with simulated EMP
p 760 A92-42317
HOGABOOM, R.
GLONASS data analysis - Interim results
p 955 A92-49382
HOGAN, AUSTIN W.
Effects of the abrasiveness of test and training site soils on parachute life
[AD-A252389] p 1038 N92-32900
HOGAN, DAVID B.
PDFIII - A flight control system for EW UAV's
[TABES PAPER 91-315] p 565 A92-34688
HOGGARD, AMOS W.
Maintaining the safety of an aging fleet of aircraft
p 837 N92-30108
HOGUE, JEFFREY R.
Parachute canopy control simulation - A solution for aircrew emergency training p 572 A92-35428
HOH, R.
Tracking performance requirements for rotorcraft instrument approaches to reduced minima. Phase 1: Preliminary study
[NRC-32137-PHASE-1] p 102 N92-11988
HOH, ROGER
An exploratory investigation into the definition of tracking standards for IFR helicopter approaches to reduced minima p 533 A92-35726
HOH, ROGER H.
Helicopter control response types for hover and low-speed near-earth tasks in degraded visual conditions
p 132 A92-14338
Assessment of flying-quality criteria for air-breathing aerospacecraft
[NASA-CR-4442] p 663 N92-25982
The use of ground based simulation for handling qualities research: A new assessment p 885 N92-28545
HOHEISEL, H.
Investigations of propulsion integration interference effects on a transport aircraft configuration
[AIAA PAPER 92-3097] p 849 A92-48739
HOJO, HIDEMITSU
Sand erosion behavior of GFRP p 576 A92-32662
HOKE, MICHAEL J.
A field repair of advanced helicopter vertical fin structure p 785 A92-47417
HOLDEMAN, J. D.
CFD analysis of jet mixing in low NO(x) flametube combustors
[ASME PAPER 91-GT-217] p 124 A92-15634
Calculations of hot gas ingestion for a STOVL aircraft model
[AIAA PAPER 92-0385] p 374 A92-28191
Experimental study of cross-stream mixing in a rectangular duct
[AIAA PAPER 92-3090] p 903 A92-48735
A parametric numerical study of mixing in a cylindrical duct
[NASA-TM-105695] p 738 N92-26553
CFD mixing analysis of jets injected from straight and slanted slots into confined crossflow in rectangular ducts
[NASA-TM-105699] p 738 N92-26561
Experimental study of cross-stream mixing in a rectangular duct
[NASA-TM-105694] p 742 N92-27652
HOLDEMAN, JAMES D.
Studies of the effects of curvature on dilution jet mixing p 290 A92-21079
Calculations of hot gas ingestion for a STOVL aircraft model
[NASA-TM-105437] p 350 N92-19993
HOLDEN, M. S.
Ground test facilities for aerothermal and aero-optical evaluation of hypersonic interceptors
[AIAA PAPER 92-1074] p 573 A92-33244
A database of aerothermal measurements in hypersonic flow for CFD validation
[AIAA PAPER 92-4023] p 1034 A92-56845
HOLDEN, MICHAEL S.
Studies of aerothermal loads generated in regions of shock/shock interaction in hypersonic flow
[NASA-CR-181893] p 43 N92-11319
HOLDEN, S. J.
Whole aircraft lightning indirect effects evaluation using low level injection techniques p 192 A92-20134
HOLDER, DARRYL
Design and construction of a Helmholtz coil magnetic test cell
[AD-A249944] p 983 N92-30849
HOLEMAN, ERNEST G.
Prototype instrumentation and design studies
[AD-A248378] p 736 N92-28004
HOLL, DAVID
Parameter identification of AV-8B wingborne aerodynamics for flight simulator model updates
[AIAA PAPER 92-4506] p 1027 A92-55373
HOLL, JUDITH A.
Fatal occupational injury related to helicopters in the United States 1980-1985 p 186 A92-20720
HOLLAND, SCOTT D.
Leading edge sweep effects in generic three-dimensional sidewall compression scramjet inlets
[AIAA PAPER 92-0674] p 343 A92-28218
Internal shock interactions in propulsion/airframe integrated three-dimensional sidewall compression scramjet inlets
[AIAA PAPER 92-3099] p 824 A92-48741
HOLLAND, SCOTT DOUGLAS
A computational and experimental investigation of a three-dimensional hypersonic scramjet inlet flow field
p 11 N92-10007
HOLLE, GLENN F.
Simple effective thickness model for circular brush seals
[AIAA PAPER 92-3192] p 903 A92-48803
HOLLIS, BRIAN R.
A fine-wire thermocouple probe for measurement of stagnation temperatures in real gas hypersonic flows of nitrogen p 1114 A92-54317

HOLLMANN, MARTIN
Modern aircraft design. Vol. 1 (2nd Edition)
p 647 A92-40897
Modern aerodynamic flutter analysis
p 676 A92-40898
HOLLO, S. D.
KrF laser-induced OH fluorescence imaging in a supersonic combustion tunnel
[AIAA PAPER 92-3346] p 905 A92-48923
HOLLOT, C. V.
On the Nyquist envelope of an interval plant family
p 507 A92-29132
HOLLOWELL, S.
Application of multidisciplinary optimization to conceptual aircraft design at Rockwell International - A status report
[AIAA PAPER 92-1196] p 537 A92-33307
HOLLY, L.
'A new proposal for an old problem' - The right engine for the right helicopter p 1070 A92-56281
HOLM, INGVAR
A manufacturer's approach to ensure long term structural integrity p 838 N92-30133
HOLMES, B. J.
Experimental investigation on the effect of crescent planform on lift and drag p 9 A92-13206
HOLMES, BRUCE J.
Aeronautical research in the United States: Challenges for the 1990's p 420 N92-21502
Serrated trailing edges for improving lift and drag characteristics of lifting surfaces
[NASA-CASE-LAR-13870-1-CU] p 463 N92-21587
HOLMES, R.
The effects of manufacturing tolerances on the vibration of aero-engine rotor-damper assemblies
p 222 N92-14349
HOLMES, S. C.
Numerical studies of supersonic flow over a compression corner p 442 A92-32324
HOLOWECKY, BRIAN
A parameter optimization approach to controller partitioning for integrated flight/propulsion control application
[NASA-TM-105826] p 979 N92-32241
HOLST, H.
Application of a wall pressure method in a wind tunnel test section with adjustable longitudinal slots
p 1091 A92-54336
HOLST, TERRY L.
The NASA Computational Aerosciences Program - Toward teraFLOPS computing
[AIAA PAPER 92-0558] p 411 A92-26968
HOLT, GEORGE
Preliminary design of axial compressors using artificial intelligence and numerical optimization techniques
[ASME PAPER 91-GT-334] p 126 A92-15699
HOLT, R. T.
The hardness and toughness of HIPed silicon nitride
p 668 A92-39682
HOLTHOFF, H.
Finite-element algorithm for chemically reacting hypersonic flow
[AIAA PAPER 92-0754] p 336 A92-27097
Numerical approximation of hypersonic shocks in a finite-element method using flux-corrected transport (FCT) p 708 A92-43060
HOLTZ, H.
Evaluation of GPS/UTC steering performance
p 1049 N92-33353
HOLZ, R.
Development of a shock noise prediction code for high-speed helicopters - The subsonically moving shock
p 165 A92-14384
HOLZWORTH, R. H.
Stratospheric electrodynamics from superpressure balloons - A technical challenge for small payload environments
[AIAA PAPER 91-3674] p 14 A92-11019
HOMAMI, S.
Effects of attack angle on leg portion of the horseshoe vortex around the idealized wing p 623 A92-40177
HOMICZ, G. F.
Numerical simulation of VAWT stochastic aerodynamic loads produced by atmospheric turbulence: VAWT-SAL code
[DE92-000597] p 229 N92-15392
HOMILLER, MICHAEL D.
Value of survivability enhancement techniques
p 59 A92-14349
HONAMI, SHINJI
Mach 3 wind tunnel test of mixed compression supersonic inlet
[AIAA PAPER 92-3625] p 1021 A92-54092
HONDA, TAKEKAZU
Development study on air turbo-ramjet engine for space plane p 1065 A92-53487
HONERMANN, ANDREAS
Three-dimensional visualizations of the aerodynamic characteristics of delta wings for the transition from subsonic to supersonic leading edges in supersonic-hypersonic flow p 709 A92-43073
HONG, C. S.
Three-dimensional finite-element analysis of interlaminar stresses in thick composite laminates
p 39 A92-11791
Fiber-coupled position sensors for aerospace applications p 370 A92-27776
HONG, JINSEN
The dimensional reconstruction of vortex cross-section images p 339 A92-27833
HONG, LIU
Flow analysis of rectangular wind tunnel contraction
p 312 A92-25001
HONG, QILIN
A new method for calculating burst speed of aeroengine disks
[ASME PAPER 91-GT-121] p 670 A92-36899
HONG, STEVE W.
Helicopter modeling requirements for full mission simulation and handling qualities assessment
p 105 A92-14364
HONG, YOUNG S.
Computation of the hydrodynamic forces and moments on a body of revolution with and without appendages
[AD-A243033] p 298 N92-16978
HONKA, PAUL
Processing parameters for carbon/PMR-15 composite flat panels p 34 A92-11812
HONMA, HIROKI
A two-stage-diaphragm free-piston shock tube for a strong shock wave p 748 A92-43098
Experimental and numerical studies of radiation emission from high-temperature air behind 10 km/s shock waves
[SAE PAPER 912025] p 790 A92-45417
HOOD, ROBBIE
High altitude airborne remote sensing mission using the advanced microwave precipitation radiometer (AMPR)
p 574 A92-34893
HOOD, ROBERT C.
Day/Night Adverse weather Pilotage System (D/NAPS) p 94 A92-14429
HOOK, M.
Application of advanced composites in SEM-E heatsinks for the thermal management of avionics
p 986 A92-51922
HOOKER, JOHN R.
Spatial and temporal adaptive procedures for the unsteady aerodynamic analysis of airfoils using unstructured meshes
[AIAA PAPER 92-2694] p 800 A92-45540
Spatial and temporal adaptive procedures for the unsteady aerodynamic analysis of airfoils using unstructured meshes
[NASA-TM-107635] p 831 N92-29445
HOOLE, S. R. H.
Reflections off aircraft and the shape optimization of a ridged waveguide p 267 A92-23967
HOOMAN, HANS JUERGEN
Pilot noise exposure during a Boeing 747-400 round trip: Judgement of noise and analysis in respect to hearing impairment of pilots p 1138 N92-32961
HOOPER, EUAN
The Civil Rotorcraft Initiative - An action agenda
p 241 A92-22707
HOOPER, W. E.
Rotor revolutions in the Far East - Helicopters in China, Mongolia, and Siberia p 241 A92-22711
HOOS, JON A.
Boundary-layer receptivity of sound with roughness
p 604 A92-36006
HOOVER, BRIAN D.
Human response to helicopter noise: A test of A-weighting
[AD-A243719] p 304 N92-17506
HOPKINS, DALE A.
Structural tailoring/analysis for hypersonic components - Executive system development
[AIAA PAPER 92-2471] p 583 A92-34360
Computational Structures Technology for Airframes and Propulsion Systems
[NASA-CP-3142] p 683 N92-25911
A brief overview of computational structures technology related activities at NASA Lewis Research Center
p 683 N92-25915
HOPKINS, HARRY
Flying the A340 iron bird p 20 A92-10666
Delivered with feeling p 134 A92-16621
Feeling normal p 134 A92-16623
Through the looking glass p 856 A92-46449
Regional challenge p 961 A92-53121
HOPKINS, ROY C.
V-22 flight test p 112 A92-16056
HOPPE, A.
Flight simulation p 207 N92-13982
HOPPE, G.
The Berlin oil channel for drag reduction research
p 571 A92-34219
HOPWOOD, S. T.
The application of particle image velocimetry (PIV) in a short-duration transonic annular turbine cascade
[ASME PAPER 91-GT-221] p 899 A92-46825
HORISAWA, HIDEYUKI
Studies on the mechanism of ignition and flameholding by plasma jets p 755 A92-42798
HORIUCHI, SHOUJI
Hydrogen fueled subsonic-ram-combustor model tests for an air-turbo-ram engine
[NAL-TR-1064T] p 280 N92-17855
HORN, D. D.
Flow contamination and flow quality in arc heaters used for hypersonic testing
[AIAA PAPER 92-4028] p 1100 A92-56850
HORN, RANDY D.
The DLR Lyman-alpha hygrometer
p 467 A92-32091
HORN, ROGER D.
Prediction of helicopter simulator sickness
p 46 A92-11473
HORNER, M. B.
An experimental investigation of the oblique blade-vortex interaction p 712 A92-43447
HORNG, H. H.
Numerical and experimental analysis of vortex sheets behind lifting surfaces
[AIAA PAPER 92-0409] p 325 A92-26262
HORNSBY, MARY E.
Engine monitoring display study
[NASA-CR-4463] p 979 N92-32175
HORNUNG, H. G.
The G-range impulse facility - A high-performance free-piston shock tunnel
[AIAA PAPER 92-3946] p 1097 A92-56774
HORNUNG, HANS G.
Effects of tip Reynolds number and tip asymmetry on vortex wakes of axisymmetric bodies at various angles of attack
[AIAA PAPER 92-0406] p 324 A92-26259
Analysis of thermo-chemical nonequilibrium models for carbon dioxide flows
[AIAA PAPER 92-2852] p 892 A92-47835
Performance data of the new free-piston shock tunnel at GALCIT
[AIAA PAPER 92-3943] p 1033 A92-56776
HOROWITZ, I. M.
Robust discrete controller design for an unmanned research vehicle (URV) using discrete quantitative feedback theory p 877 A92-48495
HOROWITZ, ISAAC
Application of quantitative feedback theory (QFT) to flight control problems p 27 A92-11499
HORSTMAN, C. C.
Structure of supersonic turbulent flow past a swept compression corner p 431 A92-31155
Hypersonic shock-wave turbulent-boundary-layer interaction flows p 703 A92-41264
Interaction between crossing oblique shocks and a turbulent boundary layer p 812 A92-46882
Heat transfer measurements and CFD comparison of swept shock wave/boundary-layer interactions
[AIAA PAPER 92-3665] p 1021 A92-54110
HORSTMAN, HOWARD Z.
Unsteady flowfield simulation of ducted prop-fan configurations
[AIAA PAPER 92-0521] p 332 A92-26946
HORTON, G. C.
Predictions and measurements of 3D viscous flow in a transonic turbine nozzle guide vane row
p 741 N92-27466
HORTON, J.
Space Shuttle Orbiter auxiliary power unit status
[SAE PAPER 912060] p 889 A92-45442
HORTON, KEITH
The Langley turbo-prop commuter design: A complete project description
[NASA-CR-189987] p 463 N92-21540
HOSANGADI, A.
Applications of an implicit, upwind Navier-Stokes code, CRAFT, to steady/unsteady reacting, multi-phase flowfields
[AIAA PAPER 92-0837] p 422 A92-29603
HOSINO, HIDEO
On the effect of canards on NAL spaceplane model (0 order) in low speed area p 1030 A92-56052
HOSNI, M. H.
Using uncertainty analysis in the debugging and qualification of a turbulent heat transfer test facility
p 138 A92-17224

HOSNY, W. M.
Active stabilization of multistage axial-compressor aerodynamic system instabilities
[ASME PAPER 91-GT-403] p 76 A92-15733
HOSOE, NOBUYUKI
Development of wall pressure measuring apparatus for an existing transonic wind tunnel test section
[NAL-TM-565] p 573 N92-23778
HOSOKAWA, SHIGEO
Influence of inlet conditions on the flowfield in a model gas turbine combustor p 672 A92-38866
HOSOKAWA, SHIGERU
Pre-flight physical simulation test of HIMES reentry test vehicle p 1103 A92-53640
HOSOKAWA, SHUNSUKE
Experimental study of convection effects around the phase charge interface p 1111 A92-53755
HOTATE, KAZUO
Bias of an optical passive ring-resonator gyro caused by the misalignment of the polarization axis in the polarization-maintaining fiber resonator
p 652 A92-40262
HOU, G. J.-W.
Observations on computational methodologies for use in large-scale, gradient-based, multidisciplinary design incorporating advanced CFD codes
[NASA-TM-104206] p 630 N92-24956
HOU, GENE J. W.
Shape-sensitivity analysis and design optimization of linear, thermoelastic solids p 395 A92-26433
HOU, GENE W.
Taylor series approximation of geometric shape variation for the Euler equations p 899 A92-46916
Methodology for calculating aerodynamic sensitivity derivatives p 1024 A92-54911
Methodology for sensitivity analysis, approximate analysis, and design optimization in CFD for multidisciplinary applications
[NASA-CR-190201] p 595 N92-22662
An incremental strategy for calculating consistent discrete CFD sensitivity derivatives
[NASA-TM-104207] p 625 N92-24681
HOU, GUICANG
A new method for calculating burst speed of aeroengine disks
[ASME PAPER 91-GT-121] p 670 A92-36899
HOU, GUICHANG
Research on damage tolerance of compressor blade
p 588 A92-35556
HOU, L. S.
Optimal boundary control of nonsteady incompressible flow with an application to viscous drag reduction
p 39 A92-11344
HOU, LIN-JUN
Periodic trim solutions with hp-version finite elements in time p 874 A92-46931
HOU, RULIANG
Structural optimization and vibration control of composite rotor blades p 960 A92-53056
HOUCK, JACOB
Simulation and model reduction for the AFW program
[AIAA PAPER 92-2081] p 572 A92-35653
HOUCK, S.
The F/A-18 external burning flight test
[AIAA PAPER 91-5050] p 731 A92-44547
HOUCK, SHARON W.
National Aerospace Plane flight test - External burning on the F/A-18 p 645 A92-40032
HOUNJET, M. H. L.
Panel method control in 3-D hyperbolic grid generation
p 617 A92-39940
CAR 88: A method to calculate subsonic and supersonic, steady and unsteady, potential flow about complex configurations
[NLR-TR-88154-U] p 400 N92-18221
NLR inviscid transonic unsteady loads prediction methods in aeroelasticity p 720 N92-27947
Hyperbolic grid generation with BEM source terms
[NLR-TP-90334-U] p 923 N92-28635
Calculation of unsteady subsonic and supersonic flow about oscillating wings and bodies by new panel methods
[NLR-TP-89119-U] p 827 N92-28659
Hyperbolic grid generation control by panel methods
[NLR-TP-91061-U] p 924 N92-29604
HOUPIS, C. H.
Robust discrete controller design for an unmanned research vehicle (URV) using discrete quantitative feedback theory p 877 A92-48495
HOUPT, TRACY
The Air Force Manufacturing Technology (MANTECH): Technology transfer methodology as exemplified by the radar transmit/receive module program
p 593 N92-22451
HOURIGAN, K.
Acoustic sources in a tripped flow past a resonator tube p 778 A92-41266
HOURMOUZIADIS, J.
High-speed civil transport aircraft emissions
p 408 N92-19122
HOUSNER, JERROLD M.
Computational Structures Technology for Airframes and Propulsion Systems
[NASA-CP-3142] p 683 N92-25911
CSM activities at the NASA Langley Research Center
p 683 N92-25916
HOUTMAN, E. M.
Comparison of interferometric measurements with 3-D Euler computations for circular cones in supersonic flow
[AIAA PAPER 92-2691] p 800 A92-45538
Experimental and numerical investigation of the vortex flow over a delta wing at transonic speed
p 84 N92-13001
HOVEY, PETER W.
Study of the engine bird ingestion experience of the Boeing 737 aircraft
[DOT/FAA/CT-89/16] p 187 N92-15053
Engine bird ingestion experience of the Boeing 737 aircraft: Expanded data base
[DOT/FAA/CT-91/32] p 1045 N92-34151
HOWARD, FLOYD G.
Serrated trailing edges for improving lift and drag characteristics of lifting surfaces
[NASA-CASE-LAR-13870-1-CU] p 463 N92-21587
HOWARD, J. H. G.
Wind-tunnel investigation of aerodynamic and stability characteristics of a forward swept wing X-29 model
p 627 N92-24862
HOWARD, R. M.
Flight test of a half-scale unmanned air vehicle
p 193 A92-20208
HOWARD, RICHARD M.
Poststall airfoil response to a periodic freestream
p 10 A92-13218
Research flight test of a scaled unmanned air vehicle
p 549 A92-35944
Data analysis for unsteady turbulence measurements over airfoils p 701 A92-41214
Aerodynamic analysis of the Pioneer unmanned air vehicle
[AIAA PAPER 92-4635] p 1027 A92-55382
Escape strategies for turboprop aircraft in microburst windshear p 1084 A92-56151
HOWARD, S.
Hypersonic plasma predictions at nonzero angle of attack
[AIAA PAPER 92-3027] p 925 A92-47028
HOWE, G. W.
Bleed-boundary conditions for numerically simulated mixed-compression supersonic inlet flow
p 713 A92-44520
HOWE, H. C.
Shafranov shift in low-aspect-ratio heliotron/torsatron CHS
[NIFS-110] p 1138 N92-33743
HOWE, M. S.
Sound produced by an aerodynamic source adjacent to a partly coated, finite elastic plate
p 414 A92-25365
HOWE, R. M.
A new approach to the real-time simulation of control systems with discontinuities p 508 A92-29291
HOWELL, DOROTHY T.
Longitudinal and lateral-directional aerodynamic characteristics of a wing-cone configuration at Mach numbers from 2.5 to 4.5
[NASA-TM-4337] p 630 N92-24977
HOWLAND, CHRIS
The role of crack growth in defect assessment
[PNR-90798] p 501 N92-20909
HOWLETT, CARL L.
Examination of ultraviolet radiation theory for bow shock rocket experiments
[AIAA PAPER 92-2871] p 901 A92-47853
HOWLETT, JAMES T.
Calculation of unsteady transonic flows with mild separation by viscous-inviscid interaction
[NASA-TP-3197] p 827 N92-28477
HOWSON, TIMOTHY E.
Modeling the heat treatment of superalloys
p 755 A92-43679
HOYNIAK, DANIEL
Development of a steady potential solver for use with linearized, unsteady aerodynamic analyses
[NASA-TM-105288] p 473 N92-20525
HOYT, W. ANDES
Automated screening of propulsion system test data by neural networks, phase 1
[NASA-CR-184329] p 753 N92-27403
HOZA, BRADLEY J.
NASA TSRV essential flight control system requirements via object oriented analysis
[NASA-CR-189573] p 381 N92-19499
HOZUMI, HIROICHI
A thin metal model for aerodynamic heating tests of shock wave interaction p 709 A92-43103
HOZUMI, K.
New 1.27-m leg of the National Aerospace Laboratory hypersonic wind tunnel p 1092 A92-56003
HOZUMI, KOICHI
Aerodynamic studies on space plane configuration at hypersonic speed p 1019 A92-53641
Aerothermodynamic test of spaceplane by thin-skin method p 1093 A92-56043
HOZUMI, KOKI
Flight evaluation of navigation systems including MLS using NAL Do228 - Results of GPS
p 1047 A92-56118
HOZUMI, KOKUICHI
Aerodynamic study of H-II Orbiting Plane, HOPE
p 1103 A92-53639
HOZUMI, KOUICHI
Aerodynamic heating characteristics of space planes tested by NAL hypersonic wind tunnel
p 1017 A92-53547
HRACH, FRANK
Method of reducing drag in aerodynamic systems
[NASA-CASE-LEW-14791-1] p 1043 N92-34243
HRUSCH, LOUIS C.
Landing gear mechanism including runway-roughness restrictor assembly
[CA-PATENT-1-257-618] p 1061 N92-33585
HSIA, Y.-C.
FNS analysis of an axisymmetric scramjet inlet
[AIAA PAPER 92-3100] p 824 A92-48742
HSIA, YEU-CHUAN
Inviscid analysis of a dual mode scramjet inlet
p 80 A92-17198
Full Navier-Stokes analysis of a three-dimensional scramjet inlet p 934 A92-50272
HSIAO, BENJAMIN S.
Thermal properties of high performance thermoplastic composites based on poly(ether ketone ketone) (PEKK)
p 34 A92-10238
HSIAO, C. Y.
Control system design for the free drop test of external stores in a wind tunnel
[IAF PAPER ST-91-002] p 207 A92-20650
HSIAO, CHINGTENG
Finite element Euler calculations of unsteady transonic cascade flows
[AIAA PAPER 92-2120] p 520 A92-35689
HSIAO, F.-B.
Forcing level effects of internal acoustic excitation on the improvement of airfoil performance
p 1136 A92-56162
HSIEH, T.
Comparison of two flux splitting schemes for calculation of ogive-cylinder at M = 3.5 and alpha = 18 deg
[AIAA PAPER 92-2667] p 806 A92-45582
Separation patterns and flow structures about a hemisphere-cylinder at high incidences
[AIAA PAPER 92-2712] p 807 A92-45593
HSING, F. C.
Gas turbine main shaft internal flow and heat transfer
[ASME PAPER 91-GT-165] p 123 A92-15600
HSU, C. F.
Control system design for the free drop test of external stores in a wind tunnel
[IAF PAPER ST-91-002] p 207 A92-20650
HSU, C.-H.
Preconditioned upwind methods to solve incompressible Navier-Stokes equations p 395 A92-26436
Numerical study of vortex-dominated flows for wings at high incidence and sideslip p 702 A92-41227
HSU, J. C.
Holographic flowfield density measurements in swept shock wave/boundary-layer interactions
[AIAA PAPER 92-0746] p 335 A92-27092
HSU, MING-HWANG
Development of the DDV actuation system on the IDF aircraft
[SAE PAPER 912080] p 844 A92-45455
HSU, YEN-NIEN
Development of the DDV actuation system on the IDF aircraft
[SAE PAPER 912080] p 844 A92-45455
HU, BAIAN
Cyclic symmetric contact stress analysis of aeroengine rotor assembly p 470 A92-29733
HU, C. C.
Identification of aerodynamic models for maneuvering aircraft
[NASA-CR-190039] p 348 N92-19359

Identification of aerodynamic models for maneuvering aircraft
[NASA-CR-190444] p 852 N92-28720
HU, GUOQING
Steady state and quasi-transient analysis of aircraft hydraulic system with network theory
p 642 A92-37391
HU, H.
Stratospheric electrodynamics from superpressure balloons - A technical challenge for small payload environments
[AIAA PAPER 91-3674] p 14 A92-11019
HU, HESONG
An improved computation for gas-turbine combustion chamber flow p 375 A92-28479
HU, J.
Heat induced transient behaviours of axial compressors p 469 A92-29721
HU, SI-MING
A study of surge control using fuel pulse cutoff for dual spool turbo-jet engine p 470 A92-29737
HU, T. C. J.
An experimental and computational investigation of an annular reverse-flow combustor
[UTIAS-338] p 129 N92-11996
HU, ZHON-HAN
The design and simulation of an intelligence flight control system p 976 A92-50237
HU, ZHONGHAN
A reversed-frame normalization design of robust flight control system p 1009 A92-53382
HU, ZONGAN
Aeroacoustical modification of a propeller
p 24 A92-10961
An aeroacoustic model about the rotating stall of a compressor p 416 A92-27855
HUA, JUN
Aerodynamic analysis and modification design of NPU airfoils p 613 A92-38270
HUA, KAI
Study on two variable control plan for twin spool turbojet engine p 862 A92-47697
HUAN, FUMING
Dynamic stability of elastic vehicles with unsteady aerodynamic force modeling p 509 A92-29326
HUANG, CHIEN Y.
Application of nonlinear control strategies to aircraft at high angle of attack p 26 A92-11329
HUANG, CHUANQI
Aeroelastic tailoring of aeronautical composite wing structures p 146 A92-15343
HUANG, G. M.
Control design via TAM and H-infinity approaches - A flexible beam case study p 51 A92-11445
HUANG, H.-S.
Transition to turbulence in confined, compressible mixing layers. I - 3D numerical simulations with excitation of random, broadband white noise
[AIAA PAPER 92-0553] p 332 A92-26964
HUANG, J. R.
An efficient finite element method for aircraft de-icing problems
[AIAA PAPER 92-0532] p 459 A92-31670
HUANG, JOHN
A parallel-series-fed microstrip array with high efficiency and low cross-polarization p 496 A92-31630
HUANG, L.
Noise-driven flow p 173 A92-18680
HUANG, L. J.
Assessment of calculation methods for efficiency of straight fins of rectangular profile p 1121 A92-56374
HUANG, MINGKE
An AF3 algorithm for the calculation of transonic nonconservative full potential flow around axisymmetric inlet cowls p 251 A92-23380
Computations of the flow past bodies and wings using Euler equations p 312 A92-25038
Numerical simulation of separation flow on bodies of revolution at high angle of attack using Euler equations
p 616 A92-38919
Calculation of the transonic full-potential flowfield about 3D fuselage p 941 A92-53021
HUANG, P. G.
Turbulence modeling for high speed flows
[AIAA PAPER 92-0436] p 327 A92-26283
An assessment and application of turbulence models for hypersonic flows
[NASA-TM-105124] p 82 N92-11984
HUANG, PAO S.
A study on vortex flow control of inlet distortion in the re-engined 727-100 center inlet duct using computational fluid dynamics
[AIAA PAPER 92-0152] p 253 A92-23767
Design and analysis of reengine Boeing 727-100 center inlet S duct by a reduced Navier-Stokes code
[AIAA PAPER 92-1221] p 517 A92-33320
Design and analysis of vortex generators on reengined Boeing 727-100QF center inlet S-duct by a reduced Navier-Stokes code
[AIAA PAPER 92-2700] p 800 A92-45542
A study on vortex flow control on inlet distortion in the re-engined 727-100 center inlet duct using computational fluid dynamics
[NASA-TM-105321] p 179 N92-13998
HUANG, Q.
System reliability and risk assessment
[AIAA PAPER 92-2345] p 582 A92-34320
HUANG, T. T.
Three-dimensional linear stability approach to transition on wings and bodies of revolution at incidence
p 172 A92-18361
HUANG, TAIPING
Some rotordynamic problems in small turbo-engines
p 470 A92-29736
HUANG, TAO
Precision analysis on static measurement of radar cross section p 370 A92-27906
HUANG, TSAIR G.
Model oscillations at high angle of attack in a low speed wind tunnel test
[IAF PAPER ST-91-001] p 175 A92-20649
HUANG, X. Z.
Prediction of leading-edge vortex breakdown on a delta wing oscillating in roll
[AIAA PAPER 92-2677] p 807 A92-45585
HUANG, XI-JUN
A time marching method in finite volume for transonic diffuser turbulent flows p 819 A92-47690
HUANG, XIAN
Study on two variable control plan for twin spool turbojet engine p 862 A92-47697
HUANG, XIJIN
Preliminary investigation of inlet dynamic distortion and it's passive control p 245 A92-21742
HUANG, XIJUN
Investigation on vortex control technique of flow separation in diffuser p 338 A92-27828
HUANG, YINGHONG
A direct-problem calculation method for gas turbines with bowed and twisted blades p 519 A92-35571
HUANG, YIYI
High speed wind tunnel wall interference research progress at Nanjing Aeronautical Institute
p 136 A92-15338
An investigation on detached shock waves ahead of bodies of revolution at transonic speeds
p 251 A92-23381
Some problems on the sidewall interference in two-dimensional subsonic and transonic wind tunnel testing p 747 A92-41929
HUANG, Z.
Structural features of a heated round turbulent jet in a cross-flow p 676 A92-40148
HUANG, ZHI-TAO
A new method for predicting the end wall boundary layers and the blade force defects inside the passage of axial compressor cascades p 819 A92-47691
HUANG, ZHICHENG
Application of the multiplier penalty function method to the optimum design of wing configurations of aerospace vehicle p 356 A92-25013
HUBBARD, HARVEY H.
Aeroacoustics of flight vehicles: Theory and practice. Volume 1: Noise sources
[NASA-RP-1258-VOL-1] p 54 N92-10598
Aeroacoustics of flight vehicles: Theory and practice. Volume 2: Noise control
[NASA-RP-1258-VOL-2] p 235 N92-14779
Building vibrations induced by noise from rotorcraft and propeller aircraft flyovers
[NASA-TM-104170] p 1138 N92-33160
HUBER, ALAN C.
Prototype instrumentation and design studies
[AD-A248378] p 736 N92-28004
HUBER, DAVID
The Guardian: Preliminary design of a close air support aircraft
[NASA-CR-189991] p 463 N92-21566
HUBER, F. W.
Computation of flow past a turbine blade with and without tip clearance
[ASME PAPER 91-GT-56] p 68 A92-15534
HUBER, H.
The Eurofar program - An European overview on advanced VTOL civil transportation system
p 1016 A92-56299
The Eurofar program: An European overview on advanced VTOL civil transportation system
[MBB-UD-0611-91-PUB] p 952 N92-30418
HUCKABONE, THOMAS C.
An algorithm for robust eigenstructure assignment using the linear quadratic regulator
[AD-A244267] p 412 N92-19335
HUDDLESTON, R. L.
Ultra-high temperature (greater than 2000 C) testing capability at Oak Ridge National Laboratory for carbon materials in air, inert gas and vacuum
[DE92-004445] p 385 N92-18069
HUDGENS, JULIE A.
Three-dimensional simulation of a translating strut inlet
[AIAA PAPER 92-0270] p 317 A92-25726
Operating characteristics at Mach 4 of an inlet having forward-swept, sidewall-compression surfaces
[AIAA PAPER 92-3101] p 863 A92-48743
HUDSON, JAMES G.
Size and critical supersaturation for condensation of jet engine exhaust particles p 161 A92-15884
HUDSON, MAURICE G.
Airport technology international 1992
p 664 A92-39514
HUEBERT, BARRY
Meeting Review: Airborne Aerosol Inlet Workshop
[NASA-CR-189814] p 301 N92-17393
HUETTIG, GERHARD
Centre for Flight Simulation Berlin Airbus 340 simulator for research and training p 880 A92-45028
HUFF, DENNIS L.
Euler flow predictions for an oscillating cascade using a high resolution wave-split scheme
[ASME PAPER 91-GT-198] p 74 A92-15623
Pressure wave propagation studies for oscillating cascades
[AIAA PAPER 92-0145] p 316 A92-25682
Analysis of cascades using a two dimensional Euler aeroelastic solver
[AIAA PAPER 92-2370] p 556 A92-34598
Numerical analysis of flow through oscillating cascade sections p 713 A92-44513
Unsteady-flow-field predictions for oscillating cascades
[NASA-TM-105283] p 348 N92-19437
HUFF, R. W.
Enhanced displays, flight controls, and guidance systems for approach and landing p 456 N92-21957
HUGGINS, R. W.
Fiber-coupled position sensors for aerospace applications p 370 A92-27776
HUGGINS, RAYMOND W.
Multi-analog track fiber coupled position sensor
p 857 A92-48043
HUGHES, DAVID
Canada making many changes in wake of Dryden crash report p 529 A92-33799
HUGHES, G.
Eigenstructure assignment for handling qualities in helicopter flight control law design p 570 A92-35786
HUGHES, JOHN R.
Composite strengthening of Nb-Ti base alloys
p 577 A92-36380
HUGHES, R. C.
Method and apparatus for acoustic plate mode liquid-solid phase transition detection
[DE92-003778] p 401 N92-18705
HUGHES, THOMAS J. R.
A new finite element formulation for computational fluid dynamics. X - The compressible Euler and Navier-Stokes equations p 612 A92-37552
HUGHES, WILL
One joule output from a diode-array-pumped Nd:YAG laser with side-pumped rod geometry
p 671 A92-37188
HUGO, RONALD J.
Controlling unsteady lift using unsteady trailing-edge flap motions
[AIAA PAPER 92-0275] p 318 A92-25729
HUI, W. H.
Steady supersonic and hypersonic flow computations using Eulerian and new Lagrangian formulations
[AIAA PAPER 92-0055] p 249 A92-22170
HULEIHIL, MAHMOUD
General performance characteristics of real heat engine p 1011 A92-50401
HULEK, TOMAS
Numerical solution of steady incompressible viscous flows over airfoils p 8 A92-12649
HULL, DAVID G.
A guidance law for hypersonic descent to a point
[AIAA PAPER 92-4303] p 1104 A92-55311
HULLIGAN, DAVID D.
Safety considerations in testing a fuel-rich aeropropulsion gas generator
[NASA-TM-105258] p 279 N92-17061
HULSE, C. O.
High temperature static strain gage development
[NASA-CR-189044] p 195 N92-14037

HULSHOFF, S.
Aerodynamics p 202 N92-13977
HUMI, MAYER
Drag computation by vortex methods p 1031 A92-56161
HUMMEL, D.
Vortex formation over a close-coupled canard-wing-body configuration in unsymmetrical flow p 85 N92-13010
HUMPHRIS, R. R.
Professor Jesse W. Beams and the first practical magnetic suspension p 771 N92-27723
Low power magnetic bearing design for high speed rotating machinery p 772 N92-27739
HUNG, CHING-MAO
Computation of saddle point of attachment p 703 A92-41276
HUNGENBERG, H. G.
Thrust nozzle test facility at DLR Cologne
[AIAA PAPER 91-5024] p 206 A92-17818
HUNT, BARRY
Knowledge-based nonlinear boundary integral models of compressible viscous flows over arbitrary bodies - Taking CFD back to basics p 617 A92-39941
HUNT, GRAHAM J. F.
Getting test items to measure knowledge at the level of complexity which licensing authorities desire - Another dimension to test validity p 835 A92-45080
HUNT, L. R.
Axial compression corner flow with shock impingement p 441 A92-32196
HUNT, L. ROANE
Computational method to predict thermodynamic, transport, and flow properties for the modified Langley 8-foot high-temperature tunnel
[NASA-TM-4374] p 767 N92-27193
HUNTEN, KEITH
PDES application protocol suite for composites (PAS-C). Functional needs report for the PAS-C program
[AD-A247886] p 1108 N92-32629
HUNTER, N.
Development and integration of modern laboratories in aerospace education
[AIAA PAPER 92-4022] p 1141 A92-56844
HUNTLEY, M. S., JR.
Design considerations for IAP charts: Approach course track and communication frequencies
[AD-A241482] p 103 N92-13051
CDI sensitivity and crosstrack error on nonprecision approaches
[AD-A243981] p 356 N92-19391
HUNTSMAN, I.
The design and testing of a radial flow turbine for aerodynamic research
[ASME PAPER 91-GT-220] p 124 A92-15636
HUNTSMAN, STEVEN D.
Filament winding of composite isogrid fuselage structures p 784 A92-47405
HUO, WINIFRED M.
Rate parameters for coupled vibration-dissociation in a generalized SSH approximation p 235 A92-20301
HUO, XIUFANG
Dynamic stability of elastic vehicles with unsteady aerodynamic force modeling p 509 A92-29326
Stability and dynamic coupling of elastic vehicles with unsteady aerodynamic forces considered p 1102 A92-53545
HURLBUT, F. C.
Rarefied gas research at Berkeley - Current studies and future potentials
[AIAA PAPER 92-3971] p 1098 A92-56797
HURRASS, KARLHEINZ
Ground and satellite supported flight trajectory measurement by example of the avionics flight test system AFES p 641 N92-25600
Board-autonomous flight trajectory measurement by example of an ILS measuring system p 641 N92-25601
HUSSAIN, FAZLE
Direct evaluation of aeroacoustic theory in a jet p 1010 A92-50296
HUSSEY, I. W.
Short fatigue crack growth from blunt notches in an aero-engine alloy p 212 A92-19760
Fatigue crack growth of small corner defects from blunt notches in an aeroengine alloy
[PNR-90860] p 1111 N92-34019
HUSSIEN, B.
Passive range estimation for rotorcraft low-altitude flight
[NASA-TM-103897] p 2 N92-10003
HUSSIEN, BASSAM
Vision-based obstacle detection for rotorcraft flight p 967 A92-52465
Vision-based range estimation using helicopter flight data
[NASA-TM-103930] p 1047 N92-32424
HUTCHINSON, JOHN J.
Wichita State University 1986 aviation safety research projects
[DOT/FAA/CT-91/4] p 263 N92-16986
Program plans: Aviation safety research
[NIAR-91-30] p 264 N92-17587
Test plan for the international aircraft operator information system
[DOT/FAA/CT-91/18] p 781 N92-26830
HUTCHINSON, JOHN W.
Preliminary results on the fracture analysis of multi-site cracking of lap joints in aircraft skins p 913 N92-30111
HUTCHISON, M. G.
Variable-complexity aerodynamic optimization of an HSCT wing using structural wing-weight equations
[AIAA PAPER 92-0212] p 317 A92-25685
HUTH, H.
Environmental fatigue tests with composite materials p 214 N92-14413
HUTIN, P. M.
Unsteady wind tunnel tests p 1089 N92-34166
HUTTSELL, L. J.
Unsteady aerodynamics for aeroelasticity at the Flight Dynamics Directorate p 718 N92-27939
HUYER, S.
Recent results from data analysis of dynamic stall on wind turbine blades
[DE92-001200] p 505 N92-20245
HUYER, S. A.
Unsteady aerodynamic loading produced by a sinusoidally oscillating delta wing p 701 A92-41223
HUYNH, H. T.
Some longitudinal handling qualities design guidelines for active control technology transport aircraft
[NLR-TP-90129-U] p 878 N92-28652
HUYNH, HUNG T.
Numerical experiments on a new class of nonoscillatory schemes
[AIAA PAPER 92-0421] p 341 A92-28193
HUYNH, LOC C.
A piloted comparison of elastic and rigid blade-element rotor models using parallel processing technology p 546 A92-35751
Comparison of elastic and rigid blade-element rotor models using parallel processing technology for piloted simulations
[SAE PAPER 912120] p 608 A92-39968
Analysis of a hydrocarbon scramjet with augmented preburning
[AIAA PAPER 92-3425] p 865 A92-48984
HWANG, C. J.
Locally implicit hybrid algorithm for steady and unsteady viscous flows p 610 A92-36836
HWANG, DANNY
Grid management p 632 N92-25713
HWANG, PATRICK Y. C.
Kinematic GPS for differential positioning - Resolving integer ambiguities on the fly p 19 A92-10472
HWANG, W.-C.
The initial development of an expert system for designing composite material wing structures p 599 A92-32542
HYDE, R. A.
VSTOL aircraft flight control system design using H(infinity) controllers and a switching strategy p 28 A92-11561
Meeting VSTOL aircraft performance requirements using scheduled H(infinity) controllers p 477 A92-29094
HYDE, T. H.
Creep-fatigue crack growth in Jethete M152 at 550 C under mixed mode conditions p 288 A92-21490
HYLAND, D. C.
Real parameter uncertainty and phase information in the robust control of flexible structures p 32 A92-11345
HYLAND, DAVID C.
Experimental demonstration of active vibration control for flexible structures p 50 A92-11442
HYLL, LESLIE
Design and implementation of a generic Kalman filter in Ada p 858 A92-48475
HYNES, JEFFREY T.
High temperature thermoplastic and polyimide processing using CARE-MOLD wash-out tooling p 36 A92-10259
HYYPPAE, J.
Development of a helicopter-borne 8-channel ranging scatterometer
[PB92-141977] p 599 N92-23441

I

IACOVIDES, H.
Computational modelling of turbulent flow in S-bends p 769 N92-27480
IAKOVENKO, V. A.
A numerical study of flow of a viscous gas in a Laval nozzle in the narrow channel approximation p 706 A92-42680
IAKOVLEV, I. I.
Comparative analysis of the lift-drag ratio and heat flows toward the surface of wave riders of different configurations p 7 A92-12173
Aerodynamics of two-shock bodies derived by the gasdynamic design method p 707 A92-42683
IAKOVLEV, L. V.
Heat transfer in supersonic flow past a single crater p 63 A92-13741
IAKOVLEV, VIKTOR N.
Flight test control p 136 A92-15021
IAKUNINA, G. E.
Minimum-drag bodies moving in locality-law media p 779 A92-42732
IANCULESCU, GEORGE D.
Thermal control for hypersonic vehicle propulsion p 468 A92-29356
System controls challenges of hypersonic combined-cycle engine powered vehicles p 475 N92-21533
IANELLI, G. S.
Recent advances on a finite element algorithm for computational aerodynamics: Transonics-hypersonics
[DE91-018176] p 11 N92-10010
IANISHEVSKII, D. V.
Flow of a viscous twisted fluid film on the surface of a blunt body in supersonic flow of a gas p 424 A92-30146
IANNELLI, G. S.
A non-linearly stable implicit finite element algorithm for hypersonic aerodynamics p 433 A92-31487
IANNIELLO, JOSEPH W.
An airborne multimode radar display processor p 965 A92-49308
IATSENKO, V. K.
Calculation of the hardening factor for gas turbine engine components shot blasted in an ultrasonic field p 38 A92-10850
IBOSHI, NAOHIRO
Measurements of blade flapping motion on a wind tunnel model p 1093 A92-56023
Structural optimization of a cantilevered beam subject to combined static loadings p 1118 A92-56024
IBRAHIM, MOUNIR
Analysis of an advanced ducted propeller subsonic inlet
[AIAA PAPER 92-0274] p 318 A92-25728
Use of an approximate similarity principle for the thermal scaling of a full-scale thrust augmenting ejector
[AIAA PAPER 92-3792] p 1069 A92-54171
Analysis of an advanced ducted propeller subsonic inlet
[NASA-TM-105393] p 179 N92-14002
IBRAHIM, MOUNIR B.
Use of an approximate similarity principle for the thermal scaling of a full-scale thrust augmenting ejector
[NASA-TM-105724] p 739 N92-26613
IBRAHIM, R. A.
Nonlinear flutter of orthotropic composite panel under aerodynamic heating
[AIAA PAPER 92-2132] p 589 A92-35699
ICHIHASHI, TAKAHIRO
Design and testing of a composite hingeless hub for rotary-wing aircraft p 1053 A92-56075
ICHIKAWA, AKIO
Error characteristics of a vortex panel method in two-dimensional flow p 421 A92-29521
ICHIKAWA, M.
A development of computer support system for wing design p 162 A92-15332
IDA, K.
Shafranov shift in low-aspect-ratio heliotron/torsatron CHS
[NIFS-110] p 1138 N92-33743
IDAN, M.
Parameter identification of linear systems based on smoothing p 873 A92-46742
IDE, TOSHIYUKI
Experiments on aeronautical satellite communications using ETS-V p 395 A92-26779
IDELSOHN, S. R.
Improving the convergence rate of the Petrov-Galerkin techniques for the solution of transonic and supersonic flows p 434 A92-31495
IDEO, L.
Heterodyne techniques in the I.R. bandwidth for laser obstacle detection p 533 A92-35740
IDZOREK, JULIAN J.
Experience in the operation of a hypersonic nozzle static thrust stand
[AIAA PAPER 92-3292] p 882 A92-48881

IEK, CHANTHY
Analysis of an advanced ducted propeller subsonic inlet
[AIAA PAPER 92-0274] p 318 A92-25728
Analysis of an advanced ducted propeller subsonic inlet
[NASA-TM-105393] p 179 N92-14002
IEMMA, U.
A boundary integral formulation for unsteady transonic potential flows p 719 N92-27942
IGARASHI, S.
Force and heat transfer on a disc in rarefied flow p 939 A92-52764
IGNAT'EV, S. G.
Experimental investigation of the optimal deflection of a single-slotted flap with different degrees of extension on a modern supercritical profile p 439 A92-31879
IGUCHI, H.
Shafranov shift in low-aspect-ratio heliotron/torsatron CHS
[NIFS-110] p 1138 N92-33743
IGUCHI, STEVE K.
Potential flow theory and operation guide for the panel code PMARC
[NASA-TM-102851] p 1036 N92-32422
II, JACK M.
Convergence of subsonic unsteady aerodynamics evaluated by a finite element concept based on Huygeuns' wave propagation
[AIAA PAPER 92-2502] p 518 A92-34497
IIDA, A.
Combustion of solid fueled ramjet. II
[AIAA PAPER 92-3728] p 894 A92-49106
IIDA, HIROSHI
Flight evaluation of navigation systems including MLS using NAL Do228 - Results of MLS p 1047 A92-56117
IIZUKA, HIROYUKI
A two-stage-diaphragm free-piston shock tube for a strong shock wave p 748 A92-43098
Experimental and numerical studies of radiation emission from high-temperature air behind 10 km/s shock waves
[SAE PAPER 912025] p 790 A92-45417
IIZUKA, TOSHIO
Evaluation of a IMU with optical fiber gyros in dynamic windtunnel tests p 1104 A92-56121
IKAWA, KATUYA
Euler flow analysis of turbine powered simulator and fanjet engine p 80 A92-17196
IKEDA, K.
Demonstration performance of an aircraft liquid crystal display p 735 A92-43224
IKEDA, YUJI
Influence of inlet conditions on the flowfield in a model gas turbine combustor p 672 A92-38866
IKEDA, YUTAKA
Robust controller design for an advanced fighter aircraft p 28 A92-11500
Quantitative Feedback Theory approach to AIAA Controls Design Challenge
[AIAA PAPER 92-4626] p 1077 A92-55303
IKEGAWA, MASAHIRO
Numerical analysis of three-dimensional unsteady turbulent flows in a turbine stage p 443 A92-32501
Large eddy simulation of unsteady turbulent wake of a circular cylinder using the finite element method p 587 A92-34825
IKELER, TIMOTHY J.
Integrated flight/propulsion control for flight critical applications - A propulsion system perspective
[ASME PAPER 91-GT-284] p 125 A92-15679
IKEUCHI, MASAYUKI
Navigation experiment on an aircraft using the GPS-INS navigation system. I - Introduction to the system p 726 A92-43122
Flight evaluation of navigation systems including MLS using NAL Do228 - Results of GPS p 1047 A92-56118
IKEYAMA, M.
Analytical condition inspection and extension of time between overhaul of F3-30 engine
[ASME PAPER 91-GT-277] p 653 A92-36888
IKUSHIMA, YASUO
Prospects of turbulence research by means of testing bodies in motion p 30 A92-12194
IL'IN, V. A.
A method for estimating the minimum distance between two flight vehicles during their separation p 486 A92-30139
IL'INSKII, N. B.
Construction of a wing profile with a flap modeled by a point vortex p 707 A92-42726
Aerodynamic airfoils design by quasi-solutions method of inverse boundary-value problems p 1020 A92-53998
ILACQUA, PAUL N.
Data analysis for unsteady turbulence measurements over airfoils p 701 A92-41214
ILBAS, D.
Experimental and theoretical studies on helicopter rotor fuselage interaction
[ONERA, TP NO. 1991-197] p 329 A92-26356
Theoretical and experimental studies of helicopter rotor/fuselage interaction
[ONERA, TP NO. 1991-198] p 329 A92-26357
ILINCA, A.
Prediction of laminar boundary layer using cubic splines
[AIAA PAPER 92-2702] p 801 A92-45544
IMACHI, UICHI
Outline and discussion of the cooling loop of the heating control system in the exposed facility of the Japanese Experiment Module (JEM) p 574 A92-35610
IMADO, F.
The acceleration control system design of a flight vehicle using a two-wing control method p 745 A92-43185
IMADO, FUMIAKI
Aircraft evasive maneuvers against flying objects p 744 A92-43128
Three-dimensional game for two aircraft p 744 A92-43129
IMAMURA, TSUGIO
Light metal materials for aircraft structure p 140 A92-13444
IMANARI, KUNIYUKI
Application of non-reflecting boundary conditions to three-dimensional Euler equation calculations for thick strut cascades
[AIAA PAPER 92-3045] p 822 A92-48705
IMAO, SHIGEKI
Experiments on turbulent flow due to an enclosed rotating disk p 615 A92-38863
IMBER, ROBIN
Identification of helicopter component loads using multiple regression
[AIAA PAPER 92-2110] p 544 A92-35681
IMBERT, BEATRICE
Theoretical simulation of a 2 micron airborne solid state laser anemometer p 1000 N92-31059
IMBERT, CLEMENT
Magnetic particle testing of turbine blades mounted on the turbine rotor shaft p 898 A92-46498
IMLAY, SCOTT
Diagonal implicit scheme for computing flows with finite rate chemistry p 488 A92-32253
IMLAY, SCOTT T.
Solution of the Burnett equations for hypersonic flows near the continuum limit
[AIAA PAPER 92-2922] p 821 A92-47894
Numerical simulations of the transdetonative ram accelerator combusting flow field on a parallel computer
[AIAA PAPER 92-3249] p 894 A92-48848
Comparison of turbulence models for powered-lift flow fields
[AIAA PAPER 92-3674] p 1022 A92-54117
IMMARIGEON, J.-P.
Evaluation and qualification of diffusion braze repair techniques for superalloy gas turbine components
[NRC-LTR-ST-1839] p 504 N92-22028
IMUTA, MAMORU
Mechanical properties of laminate aluminum matrix composites p 1106 A92-56102
INABA, MOTOYUKI
Concepts of flight experiments for HOPE development p 1103 A92-53635
Design of orbital re-entry experiment vehicle and outline of the experiment p 667 N92-25374
INAGAKI, S.
Flight evaluations on in-flight simulation of unstable aircraft p 744 A92-43115
INAGAKI, TOSHIHARU
In-flight simulation of backside operating models using direct lift controller
[SAE PAPER 912069] p 872 A92-45450
Flight test of a flight reference display for powered-lift STOL aircraft p 1064 A92-56059
Synthesis of a MLS automatic landing control law for the NAL experimental research aircraft Do-228 p 1084 A92-56062
Flight evaluation of navigation systems including MLS using NAL Do228 - Results of MLS p 1047 A92-56117
Flight evaluation of navigation systems including MLS using NAL Do228 - Results of GPS p 1047 A92-56118
INANC, F.
New developments in the computer simulation of X-ray nondestructive evaluation process p 490 A92-28588
INATANI, YOSHIFUMI
Pre-flight physical simulation test of HIMES reentry test vehicle p 1103 A92-53640
INFIELD, D.
Particle image velocimetry measurements of the aerodynamics of a wind turbine p 1115 A92-54337
ING, D. N.
The experimental and computational study of jet impingement flowfields with reference to VSTOL aircraft performance p 787 A92-45324
INGER, G. R.
Recombination-dominated nonequilibrium heat transfer to arbitrarily catalytic hypersonic vehicles p 2 A92-10426
INGLES, FRANK M.
Development of a multi-computer in-flight data acquisition and analysis system for general aviation aircraft
[AIAA PAPER 92-1037] p 553 A92-33218
INGRAFFEA, A. R.
Simulation of 3D non-planar fatigue crack growth in a turbine blade root
[DE92-006859] p 739 N92-26697
INGRAFFEA, ANTHONY R.
Simulation of arbitrary crack propagation in three-dimensions p 393 A92-25535
INGRALDI, ANTHONY M.
Interference effects of very high bypass ratio nacelle installations on a low-wing transport
[ASME PAPER 91-GT-241] p 75 A92-15646
Experimental study of pylon geometries for transport aircraft
[AIAA PAPER 92-0153] p 271 A92-23768
Installation effects of wing-mounted turbofan nacelle-pylons on a 1/17-scale, twin-engine, low-wing transport model
[NASA-TP-3168] p 346 N92-19002
INKPEN, STUART
Development of a sensor for the detection of aircraft wing contaminants
[AIAA PAPER 92-0300] p 369 A92-25752
INNOCENTI, M.
Dynamics and control of maneuverable towed flight vehicles p 976 A92-50508
INNOCENTI, MARIO
Roll-performance criteria for high augmented aircraft p 204 A92-18623
Roll metrics for handling qualities - The landing approach p 976 A92-50520
INOKA, H.
A study of a ground support equipment (GSE) network p 748 A92-43158
INOKUCHI, H.
Analysis of the main wing lift distribution of the STOL research aircraft Asuka p 1053 A92-56051
INOUE, H.
New-type of ultralight flexible a-Si solar cell and its application on an airplane p 970 A92-53181
INOUE, KATSUTO
Outline and discussion of the cooling loop of the heating control system in the exposed facility of the Japanese Experiment Module (JEM) p 574 A92-35610
INOUE, KOICHI
Optimal design of wing shape by use of neural-network p 1054 A92-56112
INOUE, M.
Unsteady Navier-Stokes simulation of transonic cascade flow using an unfactored implicit upwind relaxation scheme with inner iterations
[ASME PAPER 91-GT-223] p 74 A92-15637
Outflow boundary conditions for Euler analysis of flow in turbine scroll p 591 A92-36037
INOUE, MASAHIRO
Three-dimensional relaxation effect on quasi-3D flow in a blade row with spanwise loading distribution p 936 A92-51593
INOUE, TAKASHI
The main wing boundary layer separation pattern of STOL research aircraft Asuka p 709 A92-43144
INOUE, YASUTOSHI
A thin metal model for aerodynamic heating tests of shock wave interaction p 709 A92-43103
Aerodynamic heating characteristics of space planes tested by NAL hypersonic wind tunnel p 1017 A92-53547
Aerothermodynamic test of spaceplane by thin-skin method p 1093 A92-56043
INOUE, YUMIKO
Numerical analysis of RCS jet in hypersonic flights
[SAE PAPER 912063] p 791 A92-45445
IOANNOU, P. A.
Identification and control of aircraft dynamics using radial basis function neural networks
[AIAA PAPER 92-4393] p 1074 A92-55194
IONOV, A. A.
Stability of stiffened panels with allowance for plasticity under nonstationary heating and loading p 493 A92-30152

IONTA, P.
Prediction of gas turbine combustor flow by a finite element code
[AIAA PAPER 92-3469] p 906 A92-49016
IORDANOV, D. V.
Investigation of the structural inhomogeneity of a titanium alloy p 893 A92-47958
IRANI, E.
Simple method of supersonic flow visualization using smoke p 219 A92-20764
IRONS, JAMES R.
The application of high spectral and spatial resolution imaging spectrometers for locating downed aircraft p 598 A92-35132
ISAAC, KAKKATTUKUZHY M.
Navier-Stokes simulation for cone-derived waverider p 703 A92-41271
ISAJI, HAJIME
Wind tunnel test of M = 2.5 mixed compression inlet p 1028 A92-56008
ISAMINGER, M.
Characteristics of thunderstorm-generated low altitude wind shear - A survey based on nationwide terminal Doppler weather radar testbed measurements p 45 A92-11378
ISAMINGER, MARK A.
A case study of the Claycomo, Missouri microburst on July 30, 1989 p 407 A92-27961
A prototype microburst prediction product for the Terminal Doppler Weather Radar p 408 A92-27962
ISERMANN, U.
Calculation of aircraft noise contours taking into account the lateral flight track dispersion p 687 A92-39059
ISHERWOOD, DAVID A.
Rates and risk factors for accidents and incidents versus violations for U.S. airmen p 91 A92-14048
ISHIDA, Y.
Numerical analysis on laminar flow control of transonic airfoils p 430 A92-30557
ISHIDA, YOJI
High subsonic wind tunnel test of a two-dimensional hybrid-laminar-flow-control airfoil with slotted surface p 1029 A92-56045
Proceedings of the Seminar on Investigation and Control of Boundary-Layer Transition
[NAL-SP-11] p 400 N92-18483
ISHIDE, AKIRE
An experimental program concerning a satellite data link for oceanic ATC p 1046 A92-56093
ISHIGAWA, W.
Navigation experiment on aircraft flight using the GPS-INS navigation system. II - Test results p 726 A92-43123
ISHIGURO, NORIYOSHIKO
Numerical computation of compressible flow around an object of complex shape p 429 A92-30517
ISHIGURO, NORIYOSHUIKO
Computation of scramjet inlet flow p 430 A92-30541
ISHIHARA, T.
Three-dimensional game for two aircraft p 744 A92-43129
ISHII, H.
Numerical investigation of surge and rotating stall in multistage axial compressors
[AIAA PAPER 92-3193] p 825 A92-48804
ISHII, M.
High enthalpy wind tunnel for erosion testing of advanced materials
[AIAA PAPER 92-3888] p 1094 A92-56729
ISHIKAWA, KAZUTOSHI
Synthesis of a MLS automatic landing control law for the NAL experimental research aircraft Do-228 p 1084 A92-56062
Flight evaluation of navigation systems including MLS using NAL Do228 - Results of GPS p 1047 A92-56118
Identification of the stability and control derivatives of a DLC-flap system for VSRA
[NAL-TR-1116] p 283 N92-17917
ISHIKAWA, MUNENORI
An autorotation-entry control for a helicopter with a fuzzy controller p 1083 A92-56032
ISHIKAWA, TADASHI
A shock tunnel experiment on aerodynamic interference induced by RCS jet p 1029 A92-56042
ISHIKAWA, TAKASHI
Structural concept of main wings of high altitude unmanned aerial vehicle and basic properties of thermoplastic composites as candidate material
[SAE PAPER 912053] p 843 A92-45437
ISHIMOTO, KATSUYA
Application of fuzzy control to aircraft guidance p 1083 A92-56033
ISHIMURA, JUN
Hunting phenomena of the balloon motions observed over Antarctica
[AIAA PAPER 91-3667] p 14 A92-11014
ISHIZAWA, H.
Jet engine test system including expert system for diagnosis
[ASME PAPER 91-GT-408] p 137 A92-15737
ISHMAEL, STEPHEN D.
X-29 high angle of attack p 111 A92-16052
ISII, KUNIYOSHI
Field telemetry of blade-rotor coupled torsional vibration at Matuura Power Station Number 1 unit p 222 N92-14348
ISKAKOV, K. M.
Local heat transfer in the perforation channels of turbine nozzle vanes p 657 A92-40615
ISKRA, ANTON L.
Cryogenic test rig with an aerodynamic magnetically levitated carriage p 750 N92-27792
ISLAM, M.
Time-average loading on a two-dimensional airfoil in a large amplitude motion p 811 A92-46805
Tow-tank study of nonlinear aerodynamics of a 2-D airfoil
[AIAA PAPER 92-4499] p 1026 A92-55367
Nonlinear normal and axial force indicial responses for a two dimensional airfoil
[AD-A247196] p 830 N92-28888
ISLAM, M. Q.
Secondary flow investigation inside the passage of a compressor cascade p 706 A92-42124
ISLAM, MOHAMMED A.
An alternative derivation of the modified gain function of Song and Speyer p 232 A92-18464
ISMAIL, I. H.
A simple model to simulate subsonic intakes and propelling nozzles of aircraft gas turbine engines
[ASME PAPER 91-GT-392] p 153 A92-15722
ISO, HIDEO
Aerodynamic characteristics of a high-speed composite airfoil p 712 A92-43231
ISOGAI, K.
Numerical simulation of shock-stall flutter of an airfoil using the Navier-Stokes equations p 746 N92-27956
ISOGAI, KOJI
Research on aeroelastic tailoring at NAL p 1053 A92-56019
ISOM, JEFFREY L.
A guide for the consideration of composite material impacts on airframe costs
[AD-A243928] p 417 N92-19466
ISSAC, KAKKATTUKUZHY M.
Computation of turbulent flow about cone-derived waverider
[AIAA PAPER 92-2726] p 804 A92-45562
ISSEN, HAROLD S.
Space Shuttle airframe inspection trend-analysis report p 759 A92-42052
ITAGAKI, HIROSHI
Bayesian reliability analysis in connection with the evaluation of multiple-site damage p 762 A92-43126
ITO, AKIHIRO
Flight simulator test of cockpit advisory system p 1054 A92-56115
ITO, AKIRA
Proceedings of the Seminar on Investigation and Control of Boundary-Layer Transition
[NAL-SP-11] p 400 N92-18483
ITO, FUMIKO
Investigation on freezing and sticking phenomena of slush on airplane surfaces when taxiing on the ground and the succeeding take-off run phase
[NAL-TR-1026] p 352 N92-18182
ITO, H.
Study on transonic cascade performance by use of newly built facility p 136 A92-15328
The low-turbulence wind tunnel at Tohoku University p 623 A92-40598
Tohoku University low-turbulence wind tunnel
[AIAA PAPER 92-3913] p 1095 A92-56746
ITO, JUNICHI
Development of an automatic drilling system. II p 1118 A92-56107
ITO, K.
Ranging and positioning experiments for aircraft using Engineering Test Satellite V p 102 A92-17242
ITO, NOBUTAKE
Proceedings of the Seminar on Investigation and Control of Boundary-Layer Transition
[NAL-SP-11] p 400 N92-18483
Cross-flow instabilities and pressure gradients in boundary layers p 767 N92-26922
ITO, S.
Bayesian reliability analysis in connection with the evaluation of multiple-site damage p 762 A92-43126
ITO, T.
Supersonic wind tunnel test of airintake/airframe integrated models p 1028 A92-56006
ITO, TETSUICHI
Hypersonic testing technology of HOPE (H-II orbiting plane) p 747 A92-43096
Concepts of flight experiments for HOPE development p 1103 A92-53635
Aerodynamic study of H-II Orbiting Plane, HOPE p 1103 A92-53639
ITODA, NORIHIKO
Spaceplane aerodynamic heating and thermal protection design method p 1102 A92-53578
ITOH, KOJI
Weathering test of AFRP composites for the application of helicopter fuselage p 142 A92-15309
ITOH, MOTOYUKI
Experiments on turbulent flow due to an enclosed rotating disk p 615 A92-38863
ITOU, FUMIKO
A pressure measurement method using Electronically Scanner Pressure sensors (ESP) installed in a gust wind tunnel
[NAL-TM-638] p 749 N92-27428
ITTY, I. P.
The vortical structure in the wake during dynamic stall
[AIAA PAPER 92-4496] p 1026 A92-55364
IUDIN, IU. I.
From the history of Soviet aviation - Aircraft of the Il'iushin design bureau (2nd revised and enlarged edition) p 61 A92-15022
IUDIN, V. G.
Aerodynamic characteristics of the combination of a wing with a cambered middle surface with a fuselage p 439 A92-31880
IUSHIN, A. IA.
The effect of the angle-of-attack on laminar-turbulent boundary transition near the lower surface of triangular plates in a supersonic gas flow p 426 A92-30180
A heat flow peak on the upwind surface of a blunt-leading-edge delta wing p 438 A92-31862
IUSO, G.
Skin friction measurements in 3-D boundary layers p 1092 A92-54351
IVANOV, A.
Simulation of vibrational status of gas-turbine engine p 470 A92-29731
IVANOV, A. I.
Consideration of the effect of viscosity in the problem of porous-wall induction p 440 A92-31887
IVANOV, M. IA.
Soviet CFD - An international perspective p 233 A92-20150
IVANOV, M. S.
Influence of atmospheric rarefaction on aerodynamic characteristics of flying vehicles p 938 A92-52750
Aerodynamics of complex shape bodies within a wide range of supersonic flows of rarefied gases p 939 A92-52767
IVERSEN, ARTHUR
Next generation power electronics for space and aircraft. II - Packaging p 992 A92-50553
IVERSEN, ARTHUR H.
Thermal management of high heat flux electronic components in space and aircraft systems, phase 1
[AD-A239982] p 41 N92-10157
IVERSON, D. J.
Thermal response of rigid and flexible insulations and reflective coating in an aeroconvective heating environment
[NASA-TM-103925] p 852 N92-28721
IVEY, P. C.
Self-induced flow in a stepped rotating tube
[ASME PAPER 91-GT-276] p 152 A92-15673
IWAGAMI, S.
A model study on diffuser pressure recovery in NAL scramjet test facility with simulated hydrogen combustion
[AIAA PAPER 92-3979] p 1071 A92-56805
IWAHORI, YUTAKA
Propeller-nacelle whirl flutter analysis and wind tunnel test p 1052 A92-56016
IWAI, MINORU
Configuration of flexible-skirts for an ACV and its CAD p 1118 A92-56036
IWAKI, TAKEO
Study on international cooperative test facilities for future SST/HST
[AIAA PAPER 92-3945] p 1097 A92-56775
IWAMURA, N.
Using helicopters for coastal alert p 723 A92-43164
IWASAKI, AKIHITO
Low-speed wind tunnel testing of the lateral control force for the upper rudder surface of a joined-wing airfoil p 711 A92-43228

Low-speed wind tunnel testing of a joined-wing airfoil
p 711 A92-43229
Effectiveness of aircraft aerodynamic performance on each part of a joined wing p 712 A92-43230
Experimental studies on aerodynamic characteristics of SSTO vehicle at low subsonic speeds
[SAE PAPER 911981] p 788 A92-45386
Wind tunnel investigation of an improved upper surface blown flap transport semi-span model
[SAE PAPER 911993] p 789 A92-45395
A low speed wind tunnel investigation of a joined-wing aircraft with an overhanging fin p 1030 A92-56078
A low speed wind tunnel investigation of the direct side force control of a joined-wing aircraft with overhanging fin p 1084 A92-56079
Improvement of data processing system for gust wind tunnel data acquisition part: System conversion from off-line to on-line processing
[NAL-TM-611] p 285 N92-17756
An approach to flow field measurement by Laser 2-Focus velocimeter (L2F) in gust wind tunnel
[NAL-TM-617] p 346 N92-18484
A pressure measurement method using Electronically Scanner Pressure sensors (ESP) installed in a gust wind tunnel
[NAL-TM-638] p 749 N92-27428
Upgrading the data processing section of the NAL Gust Wind Tunnel data processing system
[NAL-TM-635] p 888 N92-28833

IWASAKI, AKIRA
Experimental study of convection effects around the phase charge interface p 1111 A92-53755

IWATSUBO, T.
Experiment of static and dynamic characteristics of spiral grooved seals p 223 N92-14361

IYER, VENKIT
Application of linear stability theory in laminar flow design
[SAE PAPER 912116] p 618 A92-39967
Computational study of transition front on a swept wing leading-edge model
[AIAA PAPER 92-2630] p 795 A92-45502

IZUMI, TATSUSHI
Design of orbital re-entry experiment vehicle and outline of the experiment p 667 N92-25374

IZUMIDA, S.
Using helicopters for the erection of power transmission lines p 723 A92-43162

IZUMIKAWA, MUNEO
A preliminary study of a supersonic wind tunnel for a ram jet test facility p 1089 A92-53564

IZYGON, MICHEL
Advanced software development workstation: Effectiveness of constraint-checking
[NASA-CR-190712] p 1134 N92-32865

J

JACHIMOWSKI, CASIMIR J.
An analysis of combustion studies in shock expansion tunnels and reflected shock tunnels
[NASA-TP-3224] p 895 N92-28374

JACK, C. D.
The proposed revision to RTCA DO178A and its influence on system design
[PNR-90821] p 510 N92-21847

JACKLIN, STEPHEN A.
Comprehensive helicopter rotor instrumentation - A retrofit approach using miniature transducers
[AIAA PAPER 92-0268] p 369 A92-25724

JACKMAN, CHARLES H.
Natural cycles, gases p 408 N92-19123
Ozone response to aircraft emissions: Sensitivity studies with two-dimensional models p 409 N92-19126

JACKSON, A. G.
Turbine engine hot-part temperature measurement techniques
[AIAA PAPER 92-3960] p 1122 A92-56788

JACKSON, E.
Direct computation of turbulence and noise
[NASA-CR-187616] p 236 N92-14788

JACKSON, E. B.
Piloted simulator studies of the HL-20 Lifting Body
p 666 A92-40033

JACKSON, E. BRUCE
Preliminary subsonic aerodynamic model for simulation studies of the HL-20 lifting body
[NASA-TM-4302] p 978 N92-31175

JACKSON, JOSEPH W.
Dynamic interpolation for linear systems
p 52 A92-11465

JACKSON, M. R.
Cold-crucible directional solidification of refractory metal-silicide eutectics p 755 A92-43684

JACKSON, MELVIN R.
Composite strengthening of Nb-Ti base alloys
p 577 A92-36380

JACKSON, P.
Harrier GR MK 5/7 mission simulators for the Royal Air Force p 885 N92-28540

JACKSON, P. S.
Thin-airfoil correction for panel methods
p 811 A92-46811

JACKSON, PAUL
Applying mu-synthesis to missile autopilot design
p 28 A92-11564

JACKSON, RAYMOND H.
Combined compressive and shear buckling analysis of hypersonic aircraft sandwich panels
[AIAA PAPER 92-2487] p 586 A92-34603

JACKSON, T. L.
Inviscid spatial stability of a three-dimensional compressible mixing layer p 39 A92-11816
Stability of a nonorthogonal stagnation flow to three-dimensional disturbances p 495 A92-31194
Solutions of acoustic field problems using parallel computers p 925 A92-45929

JACOB, THOMAS
Integrated navigation for approach guidance using differential GPS p 101 A92-16970

JACOBS, ERIC W.
Stage 2 noise certification of the Sikorsky S-76A and S-76C helicopters p 91 A92-14388

JACOBS, HERBERT
Corrosion prevention field test utilizing water displacement compounds p 110 A92-14436

JACOBS, J. M. J. W.
Analysis of results of an Euler-equation method applied to leading-edge vortex flow p 84 N92-13000
Numerical simulation of vortical flow over a delta wing at subsonic and transonic speeds
[NLR-TP-90029-U] p 444 N92-20498
Analysis of results of an Euler-equation method applied to leading-edge vortex flow
[NLR-TP-90368-U] p 827 N92-28657

JACOBS, P. A.
Mach 4 and Mach 8 axisymmetric nozzles for a high-enthalpy shock tunnel p 78 A92-16668
Flow establishment in a generic scramjet combustor
p 737 A92-44525
Approximate Riemann solver for hypervelocity flows
p 1117 A92-54934
Numerical simulation of transient hypervelocity flow in an expansion tube
[NASA-CR-189601] p 402 N92-18965
Numerical simulation of transient hypervelocity flow in an expansion tube
[NASA-CR-189615] p 592 N92-22228

JACOBS, S. W.
Development of the full-envelope Performance Seeking Control algorithm
[AIAA PAPER 92-3748] p 1068 A92-54148

JACOBSON, NATHAN S.
High-temperature durability considerations for HSCT combustor
[NASA-TP-3162] p 289 N92-17070

JACOBUS, CHARLES H.
Tiltrotor UAV - The next generation unmanned system
p 646 A92-40384

JACOCKS, J. L.
Calculation of the carriage loads of tandem stores on a fighter aircraft
[AIAA PAPER 92-0283] p 319 A92-25736

JACQUES, R.
Low temperature environment operations of turboengines (design and user's problems)
p 450 N92-21682

JACQUOTTE, O.-P.
Detailed analysis of wing-nacelle interaction for commercial transport aircraft
[ONERA, TP NO. 1991-152] p 77 A92-16122

JACQUOTTE, OLIVIER-PIERRE
Recent progress in inverse methods in France
p 201 N92-13938

JADIC, I.
A lifting line theory for supersonic flow applications
[AIAA PAPER 91-5058] p 171 A92-17841

JAECKELS, H.
Probabilistic lifing approach for aero engine disks made of powder nickel base alloys containing ceramic defects
p 226 N92-14424

JAENSCH, PETER
Pallet for helicopter testing instrumentation
p 652 N92-25598

JAFFE, MICHAEL
Polymer blends, volume 1
[AD-A252112] p 987 N92-31419

JAFROUDI, H.
Asymptotic theory of transonic wind tunnel wall interference
[AD-A244075] p 403 N92-19080

JAGER, D.
SERI advanced wind turbine blades
[DE92-001216] p 598 N92-22971
Measured and predicted rotor performance for the SERI advanced wind turbine blades
[DE92-001215] p 598 N92-23119

JAGODA, J. I.
Turbulent diffusion flame properties behind a backward-facing step p 985 A92-50255

JAGODA, JECHIAL I.
Fractal image compression of Rayleigh, Raman, LIF and LDV data in turbulent reacting flows
[AD-A246960] p 767 N92-27352

JAHNS, T. M.
A new resonant link aircraft power generating system
p 970 A92-50528

JAIN, AMOLAK C.
Hypersonic merged layer blunt body flows with wakes
p 939 A92-52757

JAKOBSEN, JORGEN
Noise from turbine generators - Noise control, propagation, and assessment p 686 A92-39044

JAMES, KEVIN D.
Full-scale high angle-of-attack tests of an F/A-18
[AIAA PAPER 92-2676] p 806 A92-45584

JAMES, RICHARD M.
Slenderness approximations in RCS estimation - The simplest 2-D case p 533 A92-33622

JAMESON, ANTONY
Control theory for optimum design of aerodynamic shapes p 6 A92-11328
Multigrid Navier-Stokes calculations for three dimensional cascades
[AIAA PAPER 92-0190] p 256 A92-23799
Automatic design of transonic airfoils to reduce the shock induced pressure drag p 949 N92-31863

JAMET, J. F.
Structures and materials technologies for hypersonic vehicles - Lessons from Hermes experience
[AIAA PAPER 91-5098] p 486 A92-31697

JANABI-SHARIFI, F.
A torque-free flexible model gyro p 495 A92-31552

JANAK, ANTONIN
Discs low cycle fatigue life predictions for gas turbine engines in CSFR by using fractographic information
p 995 A92-51950

JANETZKE, D. C.
Parallel computation of aerodynamic influence coefficients for aeroelastic analysis on a transputer network p 53 A92-12367

JANETZKE, DAVID
Determining structural performance
p 560 N92-22519

JANG, CORY S.
Computational evaluation of an airfoil with a Gurney flap
[AIAA PAPER 92-2708] p 802 A92-45550

JANIK, TAD
Comparison between imposed-periodicity and marching-in-time solutions of helicopter rotor blade steady-state response problem
[AIAA PAPER 92-2256] p 540 A92-34411

JANKOWSKI, M. A.
Structural assessment of ultralightweight composites
p 1107 N92-32525

JANSSEN, M.
Computation of 3D flow phenomena in axial flow compressor blade rows
[ASME PAPER 91-GT-78] p 69 A92-15547
Boundary layer flow in axial compressors (theoretical part)
[ETN-92-91007] p 501 N92-21233
Boundary layer flow in axial compressors (theoretical part)
[ETN-92-91008] p 502 N92-21234

JANTZEN, HANS-ARNO
Compressible turbulent boundary layers with heat addition by homogeneous condensation
p 611 A92-36843

JANUS, J. M.
Unsteady flowfield simulation of ducted prop-fan configurations
[AIAA PAPER 92-0521] p 332 A92-26946

JANUS, J. MARK
TIGER: Turbomachinery interactive grid generation
p 659 N92-25718

JANZEN, D. B.
Utility of ground simulation in flight control problem identification, solution development, and verification
p 883 N92-28525

JARBOE, T. R.
Formation and sustainment of a very low aspect ratio tokamak using coaxial helicity injection: Helicity Injected Torus (HIT) experiment
[DE92-014311] p 1136 N92-32595
JAROUX, B.
Turbine blade tip and seal clearance excitation forces
[NASA-CR-184341] p 973 N92-31910
JARRETT, OLIN, JR.
CARS temperature measurements in a hypersonic propulsion test facility p 140 N92-12049
JATEGAONKAR, R. V.
Identification of aerodynamic effectiveness and interference effects of direct-lift-control flaps from flight data
[AIAA PAPER 92-0171] p 271 A92-23782
JAU, JULAN
An interactive boundary-layer approach to multielement airfoils at high lift
[AIAA PAPER 92-0404] p 324 A92-26257
JAW, LINK C.
Modeling rotor dynamics with rotor speed degree of freedom for drive train torsional stability analysis
p 547 A92-35779
JAW, LINK CHING
Control of a helicopter engine in low altitude flight
p 562 N92-23122
JAYARAM, S.
ACSYNT - A standards-based system for parametric, computer aided conceptual design of aircraft
[AIAA PAPER 92-1268] p 601 A92-33345
JAYASURIYA, SUHADA
Parametric robust control by quantitative feedback theory p 302 A92-21176
JECK, D.
Volume spectra in supercooled clouds for several research flights
[AIAA PAPER 92-0167] p 350 A92-25683
JECK, RICHARD K.
Examination of a numerical icing-severity scale
[AIAA PAPER 92-0164] p 263 A92-23777
JECKO, B.
Mechanisms of high-current pulses in lightning and long-spark stepped leaders p 1116 A92-54678
JEFFERIES, E. B.
Control of forebody vortices by suction at the nose of the RAE high incidence research model
p 87 N92-13022
Dynamic wind tunnel tests on control of forebody vortices with suction p 380 N92-18793
JEFFERY, R. W.
Heat transfer to a delta wing and two waverider wings in rarefied hypersonic flow p 937 A92-52748
JENG, SAN-MOU
Numerical simulation of droplet deformation in convective flows p 670 A92-36844
JENG, YIH N.
Numerical study on a supersonic open cavity flow with geometric modification of aft bulkhead
[AIAA PAPER 92-2627] p 794 A92-45499
JENG, YUAN-LIANG
Principles and computer simulations of intercooled-turbocharged gas generator/expander engine p 592 N92-22132
JENKINS, J. E.
Non-linear airloads hypersurface representation: A time domain perspective p 346 N92-18783
JENKINS, JAMES P.
Empirical foundations and sensitivity testing - Is it enough for the 90's? p 835 A92-45054
JENKINS, M. G.
Evaluation of the elevated-temperature mechanical reliability of a HIPed silicon nitride
[DE92-007838] p 579 N92-23223
JENKINS, RHONALD M.
A direct optimization procedure for spanwise work distribution in non-free vortex turbine stages
[ASME PAPER 91-GT-204] p 124 A92-15626
JENNEY, GAVIN D.
Simple fly-by-wire actuator p 876 A92-48491
JENNINGS, NICHOLAS
Aerospace software engineering in the United Kingdom p 233 A92-19405
JENSCHKE, ERWIN B., JR.
F-15 STOL/Maneuvering Technology Demonstrator. Phase III - Thrust vectoring, reversing and STOL operation p 112 A92-16054
JENSEN, FRANK L., JR.
Maintenance, Malfunction Information Report system
p 60 A92-14414
JENSEN, JORGEN B.
The 1988 Australian Winter Storms Experiment - Case study: 6 August 1988 p 301 A92-23009
JENSEN, RONALD N.
Multi-colored layers for visualizing aerodynamic flow effects
[NASA-CASE-LAR-13742-1] p 447 N92-21588
JENSEN, STEPHEN C.
A fiber optic temperature sensor for aerospace applications p 761 A92-42607
JENTINK, H. W.
Potential applications of laser Doppler anemometry for in-flight measurements
[NLR-TP-90163-U] p 859 N92-28654
JEONG, DAVID Y.
Current DOT research on the effect of multiple site damage on structural integrity p 913 N92-30112
JESIONEK, KRZYSZTOF J.
Total losses in turbulent flows inside conical diffusers
p 819 A92-47782
JESSEE, E.
An aircraft manufacturer's perspective
p 515 A92-33430
JETT, B. W.
Single engine testing of the F-14A(PLUS) airplane in the power approach configuration p 645 A92-40036
JEWELL, DONNA M.
AGSSS: The Airborne Graphics Software Support System; an Ada/PHIGS-based display editor for the rapid development of cockpit display software systems
[AD-A243224] p 277 N92-17221
JEWELL, WAYNE F.
Development of a real-time simulation of a ship-correlated airwake model interfaced with a rotorcraft dynamic model
[AIAA PAPER 92-4149] p 1007 A92-52440
JI, JUN
The performance evaluation of aeroderivative gas turbines p 119 A92-13296
JIA, GUO-RONG
Durability analysis for a main bulkhead subjected to load on the body of an aircraft p 848 A92-47664
JIA, GUORONG
A full-scale fatigue test and failure analyses research of F-X fighters p 960 A92-53092
JIANG, CAI-HONG
A study of surge control using fuel pulse cutoff for dual spool turbo-jet engine p 470 A92-29737
JIANG, CHANG-SHENG
The design and simulation of an intelligence flight control system p 976 A92-50237
JIANG, CHANGSHENG
A reversed-frame normalization design of robust flight control system p 1009 A92-53382
JIANG, DAZHONG
Aeroengine sensor failure detection by Bayesian multiple hypothesis testing p 391 A92-24747
JIANG, GUIQING
The wall interference correction and test data processing methods for airfoil wind tunnel test with endplates
p 942 A92-53087
An improved wall correction method for the longitudinal stability p 978 A92-53388
JIANG, HAOKANG
A large-scale axial flow compressor facility and dynamic measurement techniques for rotor flow study
p 382 A92-24729
A method for measuring high-subsonic two-dimensional periodic flow field using a single-hole high-response cylindrical pressure probe p 588 A92-35567
JIANG, JUN
Durability analysis for a main bulkhead subjected to load on the body of an aircraft p 848 A92-47664
JIANG, LUHUA
China-Soviet long duration balloon flight project
[AIAA PAPER 91-3678] p 1 A92-11036
JIANG, PING
Application of submerged vortex generators for separation control of a subsonic diffuser
p 933 A92-49832
JIANG, YEON F.
Error estimation of INS ground alignment through observability analysis p 639 A92-40226
JIE, OUYANG
On multiple grid method p 1006 A92-49585
JIN, SHENG
A bi-directional marching finite element algorithm for three-dimensional boundary layer separation flow computations p 942 A92-53288
JIN, XIN
The rolling-up and interaction of the leading-edge and trailing-edge vortex sheets of a delta wing
p 314 A92-25101
JOCHUM, ANNE M.
Simple models for the description of turbulence in the atmospheric boundary layer
[DLR-FB-90-17] p 410 N92-19292
Measurements in the inhomogeneous convective boundary layer using three powered gliders
p 775 N92-26350
JOE, W. S.
Laminar heat transfer to blunt cones in high-enthalpy hypervelocity flows p 713 A92-44372
JOFFE, ELYA B.
RFI effects analysis of an airport-installed HF transmitter on aircraft COMM/NAV receivers p 725 A92-42313
An investigation of the desensitizing effects by high power HF broadcast transmitters on HF airborne receivers p 726 A92-43937
JOGLEKAR, M.
Flying qualities evaluation of the V22 tiltrotor
p 131 A92-14334
JOGLEKAR, MUKUND
V-22 thrust power management control law development p 132 A92-14405
Tiltrotor control law design for rotor loads alleviation using modern control techniques p 478 A92-29331
JOH, C.-Y.
Design optimization of transonic airfoils
p 177 N92-13961
JOH, CHANGYEOL
Efficient and robust design optimization of transonic airfoils p 528 N92-23717
JOHAN, ZDENEK
A new finite element formulation for computational fluid dynamics. X - The compressible Euler and Navier-Stokes equations p 612 A92-37552
JOHANNESSEN, J. A.
Comparison of aircraft synthetic aperture radar and buoy spectra during NORCSEX '88 p 597 A92-34878
JOHANNESSEN, R.
Probability distributions that are important when assessing barometric aiding to GPS p 100 A92-16952
JOHANNSMEIER, DIETER
Behaviour and modelling of the aerothermodynamics of ballistic entry vehicles in the high altitude flow regimes
p 184 N92-15031
JOHANSSON, MELKER
Mechanical noise from large wind turbines - Experiences from Swedish prototypes p 686 A92-39046
JOHN, L. K.
Wing leading edge design with composites to meet bird strike requirements p 848 A92-47404
JOHNS, ALBERT L.
Acoustic characteristics and dynamic structural loading of an ASTOVL aircraft in hover
[AIAA PAPER 92-0370] p 416 A92-28190
Hot gas ingestion characteristics and flow visualization of a vectored thrust STOVL concept
p 860 A92-45316
JOHNS, ROBERT
Turning up the heat on aircraft structures
p 1052 A92-55131
JOHNSON, B. V.
Heat transfer in rotating serpentine passages with trips normal to the flow
[ASME PAPER 91-GT-265] p 151 A92-15663
Heat transfer in rotating serpentine passages with trips skewed to the flow
[NASA-TM-105581] p 499 N92-20235
Turbine disk cavity aerodynamics and heat transfer
p 1124 N92-32265
JOHNSON, D. A.
Nonequilibrium algebraic turbulence modeling considerations for transonic airfoils and wings
[AIAA PAPER 92-0026] p 248 A92-22148
JOHNSON, D. R.
Ceramic technology for Advanced Heat Engines Project
[DE92-002397] p 289 N92-16128
JOHNSON, DANIEL P.
Integrated GPS/INS for the National Aerospace Plane
p 102 A92-16975
JOHNSON, DONALD K.
Data analysis for unsteady turbulence measurements over airfoils p 701 A92-41214
JOHNSON, ERIC G.
Binary optic-corrected conformal windows for optical seekers
[AIAA PAPER 92-2802] p 779 A92-41340
JOHNSON, ERIC P.
Composite strength statistics from fiber strength statistics
[AD-A245616] p 755 N92-26383
JOHNSON, ERIC R.
Initial postbuckling response of an unsymmetrically laminated rectangular plate p 1108 N92-32586
JOHNSON, ERWIN H.
Comment on 'Canard-wing interaction in unsteady supersonic flow' p 812 A92-46820

JOHNSON, F. T.
Analysis of unsteady aerodynamic and flutter characteristics of an aeroelastic model in transonic flow
p 720 N92-27953
JOHNSON, G.
Steady flow of a fluid-solid mixture in a circular cylinder
[DE91-018698] p 41 N92-10174
JOHNSON, GREGORY B.
Closed-loop operation of GPS aided INS
p 100 A92-16954
JOHNSON, JAMES R.
Stage 2 noise certification of the Sikorsky S-76A and S-76C helicopters p 91 A92-14388
JOHNSON, JERRY
Design, analysis, testing, and certification of composite primary structure for the Piaggio P-180 Avanti
p 535 A92-32553
JOHNSON, JERRY G.
Simulation of wind tunnel flowfields
[AIAA PAPER 92-0034] p 249 A92-22155
JOHNSON, K. L.
F15E terrain following system development
[AIAA PAPER 92-1079] p 563 A92-33248
JOHNSON, LESLIE D.
Flexible manufacturing in repair of gas turbine engine components
[AIAA PAPER 92-3524] p 786 A92-49049
JOHNSON, M. C.
Propulsion system performance and integration for high Mach air breathing flight p 862 A92-46429
JOHNSON, M. R.
New processes in commercial airplane design
p 607 A92-38218
An independent review of the Multi-Path Redundant Avionics Suite (MPRAS) architecture assessment and characterization report
[NASA-CR-188126] p 163 N92-12440
JOHNSON, MARK S.
One-dimensional, stage-by-stage, axial compressor performance model
[ASME PAPER 91-GT-192] p 124 A92-15618
JOHNSON, MARK W.
Effect of flow rate on loss mechanisms in a backswept centrifugal impeller p 897 A92-45606
JOHNSON, P. D.
Computation of flow past a turbine blade with and without tip clearance
[ASME PAPER 91-GT-56] p 68 A92-15534
JOHNSON, PAUL D.
Application of an unsteady Navier-Stokes solver to transonic turbine design p 935 A92-50273
JOHNSON, R. N.
Condor - An all electric airplane
[SAE PAPER 912184] p 644 A92-40004
JOHNSON, RICHARD
Aging aircraft and structural airworthiness
[SAE PAPER 912212] p 635 A92-40016
JOHNSON, SALLY C.
Design for validation p 601 A92-33607
JOHNSON, STEVEN A.
Aircraft ground test and subscale model results of axial thrust loss caused by thrust vectoring using turning vanes
[NASA-TM-4341] p 273 N92-17071
JOHNSON, VICKI
Ames life science telescience testbed evaluation
[NASA-CR-188856] p 140 N92-12033
JOHNSON, VICKI S.
Tying it all together - The NASA/USRA University Advanced Design Program
[AIAA PAPER 92-1040] p 605 A92-33221
JOHNSON, W. P.
Aging aircraft structural damage analysis
p 360 N92-18575
JOHNSON, W. STEVEN
Stress-strain analysis of a (0/90)sub 2 symmetric titanium matrix laminate subjected to a generic hypersonic flight profile
[NASA-TM-107584] p 685 N92-26128
JOHNSON, WALTER A.
Identification of higher-order helicopter dynamics using linear modeling methods p 131 A92-14336
Parachute canopy control simulation - A solution for aircrew emergency training p 572 A92-35428
JOHNSON, WILLIAM B.
Advanced technology for aviation maintenance training - An industry status report and development plan
p 47 A92-11180
JOHNSTON, DONALD E.
Identification of higher-order helicopter dynamics using linear modeling methods p 131 A92-14336
Assessment of flying-quality criteria for air-breathing aerospacecraft
[NASA-CR-4442] p 663 N92-25982
JOHNSTON, G. W.
Aerodynamics p 202 N92-13977
Computational fluid dynamics p 177 N92-13979
Nonliner aspects of transonic aeroelasticity
p 628 N92-24864
Automated grid generation for high-lift configurations
p 628 N92-24869
JOHNSTON, JAMES P.
Evolution of three-dimensionality in stable and unstable curved mixing layers p 619 A92-40059
JOHNSTON, L. J.
Solution of the Reynolds-averaged Navier-Stokes equations for transonic aerofoil flows p 9 A92-13198
JOHNSTON, LESLIE J.
Application of an unstructured Navier-Stokes solver to multi-element airfoils operating at transonic maneuver conditions
[AIAA PAPER 92-2638] p 796 A92-45507
Prediction of the viscous transonic aerodynamic performance of supercritical aerofoil sections
[AIAA PAPER 92-2653] p 805 A92-45569
JOHNSTON, NEIL
Organizational factors in human factors accident investigation p 834 A92-45000
JOHNSTON, R. T.
Unsteady wing surface pressures in the wake of a propeller
[AIAA PAPER 92-0277] p 318 A92-25731
JOHNSTON, RICHARD P.
A preliminary design and analysis of an advanced heat-rejection system for an extreme altitude advanced variable cycle diesel engine installed in a high-altitude advanced research platform
[NASA-CR-186021] p 871 N92-29427
JOLLY, BRUCE A.
An unstructured approach to the design of multiple-element airfoils
[AIAA PAPER 92-2709] p 807 A92-45592
JOLY, V.
Numerical simulation of thermochemical non-equilibrium viscous flows around reentry bodies
p 227 N92-15029
JONASSON, HANS G.
Inter-noise 90; Proceedings of the International Conference on Noise Control Engineering, Goteborg, Sweden, Aug. 13-15, 1990. Vols. 1 & 2
[ISBN 91-7848-224-0] p 693 A92-39042
JONCKHEERE, EDMOND A.
Practical method's for robust multivariable control
[AD-A248473] p 1009 N92-30322
JONES, A. H.
Rule based identifier for unknown systems
p 509 A92-31430
JONES, ANNA
Ozone response to aircraft emissions: Sensitivity studies with two-dimensional models p 409 N92-19126
JONES, CHARLES H.
Expert system for real-time aircraft monitoring
p 410 A92-24411
JONES, D. J.
An analysis of the sidewall boundary layer effect in two-dimensional wind tunnel testing p 626 N92-24856
JONES, G.
Multiple aperture window and seeker concepts for endo KEW applications
[AIAA PAPER 92-2806] p 752 A92-41344
JONES, H. E.
Observations on computational methodologies for use in large-scale, gradient-based, multidisciplinary design incorporating advanced CFD codes
[NASA-TM-104206] p 630 N92-24956
JONES, H. W.
Noise generated by wind turbines p 686 A92-39045
JONES, HENRY
Dynamics of an optimized rotor blade at off-design flight conditions p 461 A92-32250
JONES, HENRY E.
An incremental strategy for calculating consistent discrete CFD sensitivity derivatives
[NASA-TM-104207] p 625 N92-24681
JONES, J. C.
Experimental results and numerical modeling of solidification during aircraft high-g arcs
[AIAA PAPER 92-0843] p 493 A92-29609
JONES, J. D.
Active control of structurally-coupled sound fields generated by localized force inputs p 694 A92-39106
JONES, J. D. C.
Fibre optic laser anemometry for turbomachinery applications p 397 A92-27783
JONES, JACK A.
Multicomponent gas sorption Joule-Thomson refrigeration
[NASA-CASE-NPO-17569-1-CU] p 228 N92-15203
Three-stage sorption type cryogenic refrigeration system and method employing heat regeneration
[NASA-CASE-NPO-18366-1-CU] p 300 N92-17674
JONES, JIM J.
Stagnation-point heat-transfer rate predictions at aeroassist flight conditions
[NASA-TP-3208] p 1001 N92-31281
JONES, KATHLEEN M.
The data flow simulator, a tool for system simulation
p 1006 A92-49329
JONES, KENNETH M.
Boundary layer study on nozzle wall at hypersonic velocities
[AIAA PAPER 92-4013] p 1034 A92-56836
JONES, KENNETH R.
Nickel hydrogen common pressure vessel battery development p 598 N92-22770
JONES, LISA E.
Experimental and analytical study of the effects of floor location on response of composite fuselage frames
[AIAA PAPER 92-2473] p 539 A92-34362
JONES, R.
Environmental evaluation of repairs to fuselage lap joints p 699 A92-41534
Evaluation of triple simultaneous parallel ILS approaches spaced 5000 feet apart, phase 4.b
[DOT/FAA/CT-91/31] p 456 N92-21404
A preliminary study on damage detection using piezoelectric film
[AD-A246350] p 733 N92-28118
JONES, R. R., III
Acoustic interactions between an altitude test facility and jet engine plumes: Theory and experiments
[NASA-CR-190423] p 738 N92-26405
JONES, RICKIE
Evaluation of triple simultaneous parallel ILS approaches spaced 4300 feet apart, phase 4a
[ACD-340] p 191 N92-14034
JONES, STUART C.
A comparison of cooling methods for the airframe nozzle of a single-stage-to-orbit aircraft
[AIAA PAPER 91-5036] p 210 A92-17825
Analysis of cooling systems for hypersonic aircraft
[AIAA PAPER 91-5063] p 216 A92-17843
Integrated numerical methods for hypersonic aircraft cooling systems analysis
[AIAA PAPER 92-0254] p 357 A92-25712
Thermal management for a Mach 5 cruise aircraft using endothermic fuel p 736 A92-41225
JONES, T. V.
An Axial Turbobrake
[ASME PAPER 91-GT-1] p 147 A92-15501
Turbulent spot generation and growth rates in a transonic boundary layer
[AD-A250221] p 909 N92-29118
JONES, TOM
SHARP: Subsonic High Altitude Research Platform
[NASA-CR-190004] p 648 N92-25263
JONES, W. H.
Probability of cycle jumps in Omega receivers and other phase locked loop applications
[PB92-128891] p 455 N92-21279
JONES, WILLIAM T.
Computational analysis of drag reduction techniques for afterbody/nozzle/empennage configurations
[SAE PAPER 912127] p 618 A92-39974
JOO, GENE
Dynamic response and aeroelastic analysis of a propeller blade of a prop-fan engine p 762 A92-43109
JORDAN, D. T.
Whole aircraft lightning indirect effects evaluation using low level injection techniques p 192 A92-20134
JORDAN, DAVID
Acoustic results of the Boeing model 360 whirl tower test p 603 A92-35741
JORDAN, E. H.
A viscoplastic model for single crystals
p 391 A92-24717
JORDAN, FRANK L., JR.
Wind-tunnel static and free-flight investigation of high-angle-of-attack stability and control characteristics of a model of the EA-6B airplane
[NASA-TP-3194] p 631 N92-25276
JORDAN, THOMAS
Present status of the MIT/NASA Langley 6-inch MSBS p 750 N92-27802
JORGENSEN, OLE
Optimization of the flutter load by material orientation
p 146 A92-15222
JORNA, P. G. A. M.
Aircraft simulation and pilot proficiency: From surrogate flying towards effective training p 884 N92-28532
JOSHI, P. B.
Propulsion simulator for magnetically suspended wind tunnel models p 750 N92-27801

JOSHI, PRAKASH B.
Laser-driven hypersonic air-breathing propulsion simulator
[AIAA PAPER 92-3922] p 1095 A92-56753
JOSLIN, RONALD D.
Validation of three-dimensional incompressible spatial direct numerical simulation code: A comparison with linear stability and parabolic stability equation theories for boundary-layer transition on a flat plate
[NASA-TP-3205] p 943 N92-30295
JOSSO, P.
Aluminides modified by palladium - Protection of new parts by local finishing
[ONERA, TP NO. 1992-49] p 893 A92-48610
JOSYULA, ESWAR
Computation of hypersonic flowfields in thermal and chemical nonequilibrium
[AIAA PAPER 92-2874] p 819 A92-47856
JOUET, C.
Three-dimensional thin-layer and space-marching Navier-Stokes computations using an implicit MUSCL approach - Comparison with experiments and Euler computations
[ONERA, TP NO. 1991-131] p 77 A92-16107
JOUIN, PIERRE
Manufacture of a primary flight structure using thermoplastics p 1 A92-10197
JOURDEN, C.
Comparison between two 3D-NS-codes and experiment on a turbine stator
[AIAA PAPER 92-3042] p 822 A92-48703
JOVIC, SRBOLJUB
An experimental investigation of the separating/reattaching flow over a backstep
[NASA-CR-190426] p 716 N92-27399
JOY, V. A.
Technological excellence in honeycomb sandwich and composite structures for aerospace applications
p 757 A92-41180
JOYNES, DONALD
Design of advanced composite components for maintainability based on inservice experience
[AIAA PAPER 92-1085] p 537 A92-33251
JUBE, MICHEL
The European ATC challenge p 19 A92-11877
JUDD, JON
PDES application protocol suite for composites (PAS-C). Functional needs report for the PAS-C program
[AD-A247886] p 1108 N92-32629
JUDGE, CAROL L.
Lessons learned about information management within the Pilot's Associate program p 916 A92-44909
JUDGE, T. R.
The application of particle image velocimetry (PIV) in a short-duration transonic annular turbine cascade
[ASME PAPER 91-GT-221] p 899 A92-46825
JUILLEN, J. C.
The effects of wall suction on laminar-turbulent transition in three-dimensional flow p 522 A92-36021
JULLIARD, J.
Experimental study of noise generation and propagation in a turbofan model p 1136 A92-56169
JUMPER, ERIC J.
Controlling unsteady lift using unsteady trailing-edge flap motions
[AIAA PAPER 92-0275] p 318 A92-25729
JUNE, REID B.
New materials drive high-performance aircraft
p 1105 A92-55134

K

KACIK, RICHARD J.
Optimization of tangential mass injection for minimizing flow separation in a scramjet inlet
[AD-A243868] p 376 N92-18867
KACPRZYNSKI, J. J.
Numerical verification of NISA 2 finite element analysis of the cracked 5th stage compressor disc of J-85 jet engine
[NRC-LTR-ST-1792] p 129 N92-11997
Verification of NISA 2 and ENDURE fracture mechanics capability
[NRC-ST-621] p 159 N92-13453
KADAMBI, JAIKRISHNAN R.
The effect of steady aerodynamic loading on the flutter stability of turbomachinery blading
[ASME PAPER 91-GT-130] p 71 A92-15574
KADOKURA, A.
Polar patrol balloon
[AIAA PAPER 91-3688] p 15 A92-11031
KADOTA, KOSYU
Step response of unsteady aerodynamics acting on a plane swept wing in incompressible flow for finite state modeling p 63 A92-14031
KAGEYAMA, ISAO
The progress of a STOL project p 699 A92-43137
KAGEYAMA, TAROU
Outlines of parabolic flight p 764 N92-26441
KAHLON, G.
Developments in airborne surveillance and control systems p 98 A92-16655
KAIDEN, T.
Non-planar wing design by Navier-Stokes inverse computation
[AIAA PAPER 92-0285] p 319 A92-25738
KAILASANATH, K.
Numerical simulations of the structure of supersonic shear layers p 3 A92-10574
Numerical simulations of unsteady reactive flows in a combustion chamber p 39 A92-11761
Supersonic flow over an axisymmetric backward-facing step p 705 A92-41542
KAINUMA, FUMIKAZU
A physical approach to the estimation of aerodynamic characteristics from flight data p 1030 A92-56058
KAISER, E. O.
V-22 propulsion system design p 1070 A92-56300
KAISER, STEFAN A.
A new aspect of future air navigation systems - How Secondary Surveillance Radar Mode S could protect civil aviation p 1012 A92-51424
KAITALA, VEIJO
Aircraft control for take-off in windshear
p 660 A92-36990
KAJI, S.
Study on transonic cascade performance by use of newly built facility p 136 A92-15328
KAJI, SHOJIRO
Theoretical study on the unsteady aerodynamic characteristics of an oscillating cascade with tip clearance (In the case of loaded cascade) p 331 A92-26797
Analytical study on plate edge noise. I - Trailing edge noise caused by vorticity waves p 511 A92-32502
Perspective on future aircraft engines
p 558 A92-35921
KAJITA, HIROSHI
Evaluation method of longitudinal static stability of tailless airplane p 282 A92-22520
KAJOKA, HIROSHI
Evaluation of a IMU with optical fiber gyros in dynamic windtunnel tests p 1104 A92-56121
KAKINUMA, ASAO
Design and testing of a composite hingeless hub for rotary-wing aircraft p 1053 A92-56075
KALDELLIS, J. K.
3-D loss prediction based on secondary flow and blade shear layer interaction
[ASME PAPER 91-GT-59] p 68 A92-15536
The influence of shock waves on the viscous flow field of axial compressors
[ASME PAPER 91-GT-173] p 73 A92-15608
Simulation of turbulent velocity profiles appearing on rotating and stationary parts of subsonic compressors and turbines p 676 A92-40172
KALENICHENKO, V. V.
Stability and inherent precision of two methods for solving motion and ablation equations for fireball-forming bodies in the earth atmosphere p 929 A92-46595
KALETKA, J.
Frequency-domain identification of BO 105 derivative models with rotor degrees of freedom
p 104 A92-14327
KALETKA, JUERGEN
Instrumentation and data processing
p 273 N92-17155
BO 105 identification results p 274 N92-17161
KALIAMIN, D. V.
Analysis of transonic flow over plane compressor cascades using the large-particle method
p 79 A92-16812
KALIN, D. A.
Crossed beam correlation modeling and experimental techniques for measuring density fluctuations in hypersonic flows
[AIAA PAPER 92-2779] p 758 A92-41323
Experimentally supported investigations into the optical performance of multi-aperture window concepts
[AIAA PAPER 92-2781] p 778 A92-41324
A time-integrated image model for aero-optic analysis
[AIAA PAPER 92-2793] p 779 A92-41332
Simultaneous imaging and interferometric turbule visualization in a high-velocity mixing/shear layer
p 896 A92-45130
KALKHORAN, I.
Hypersonic shock tunnel testing for undergraduate laboratory instruction
[AIAA PAPER 92-4021] p 1100 A92-56843
KALKHORAN, IRAJ M.
Experimental investigation of the perpendicular rotor blade-vortex interaction at transonic speeds
p 340 A92-28047
Airfoil pressure measurements during oblique shock wave-vortex interaction in a Mach 3 stream
[AIAA PAPER 92-2631] p 795 A92-45503
Experimental investigation of the parallel vortex-airfoil interaction at transonic speeds p 813 A92-46901
KALLINDERIS, J. G.
The finite volume approach for the Navier-Stokes equations p 246 A92-21980
Adaptation methods for viscous flows
p 246 A92-21982
KALLINDERIS, Y.
Prismatic grid generation with an efficient algebraic method for aircraft configurations
[AIAA PAPER 92-2721] p 803 A92-45559
KALLINDERIS, YANNIS
Algebraic turbulence modeling for adaptive unstructured grids p 398 A92-28033
A new adaptive algorithm for turbulent flows
p 434 A92-31547
KALLIS, J. M.
Detailed investigation of causes of avionics field failures p 995 A92-51925
KALLMES, MICHELLE H.
A new class of gradient estimators for queueing systems with real-time constraints p 49 A92-11395
KALMAN, H.
The effect of tip convection on the performance and optimum dimensions of cooling fins p 902 A92-48354
KALVISTE, JURI
Measures of merit for aircraft dynamic maneuvering
p 642 A92-37825
KAM, MOSHE
Neural networks for feedback linearization in aircraft control
[AIAA PAPER 92-4391] p 1074 A92-55192
Formulation of a strategy for monitoring control integrity in critical digital control systems
[NASA-TM-104158] p 206 N92-15075
KAMADA, R. F.
Boundary-layer transition across a stratocumulus cloud edge in a coastal zone p 45 A92-10489
KAMATA, YUKIO
Flight evaluation of navigation systems including MLS using NAL Do228 - Outline p 1047 A92-56116
KAMATSU, NOBUO
Distance and angle measuring method using laser light and rereflection plates p 762 A92-43206
KAMESAKI, KAZUHIKO
Outline and discussion of the cooling loop of the heating control system in the exposed facility of the Japanese Experiment Module (JEM) p 574 A92-35610
KAMIJO, K.
Turbine drive system of the high pressure LOX turbopump test facility
[DE92-783191] p 680 N92-25342
KAMINER, ARKADII A.
Aerodynamic damping of blade vibrations in turbomachines p 200 A92-18198
KAMINER, ISAAC
Design of the flare control law for longitudinal autopilot using H(infinity) synthesis p 28 A92-11562
KAMIYA, NOBUHIKO
Aero-structural integrated design of forward swept wing
[SAE PAPER 912021] p 790 A92-45414
KAMMERER, A.
Two-phase flow correlations in air/oil systems of aero engines
[ASME PAPER 91-GT-54] p 121 A92-15532
KAMPA, K.
Mission oriented investigation of handling qualities through simulation p 1059 A92-56353
Experience with piloted simulation in the development of helicopters p 884 N92-28528
Experience with piloted simulation in the development of helicopters
[MBB-UD-0610-91-PUB] p 889 N92-30076
KAMPE, S. L.
Axial alignment of short-fiber titanium aluminide composites by directional solidification
p 892 A92-46838
KAN, HAN PIN
Out of plane analysis for composite structures
p 1107 N92-32527
Damage tolerance certification methodology for composite structures p 1108 N92-32579
KANAI, KIMIO
Application of the delta-operator in MIMO discrete-time adaptive flight control systems p 479 A92-29516
A restructurable flight control system design using nonlinear compensation p 745 A92-43184

The acceleration control system design of a flight vehicle using a two-wing control method p 745 A92-43185
Design of a flight control system using a feedback-error-learning-type neural network p 1132 A92-56067

KANCHIRA, TOKUNO
Experiment on pitching moments of separated flow around airfoil profiles p 429 A92-30527

KANDA, H.
Recent airfoil tests in NAL 2D high Reynolds number wind tunnel p 748 A92-43171
Transonic visualization test for the airframe shape improvement of a spaceplane p 752 A92-43200
BGK airfoil oil flow test in a two-dimensional transonic wind tunnel p 711 A92-43201
Buffeting characteristics of a transonic airfoil p 711 A92-43202

KANDA, HIROSHI
The Bauer-Garabedian-Korn airfoil test in a two-dimensional wind tunnel p 429 A92-30532
On the structure of unsteady shock induced separation of the transonic airfoil in the NAL two-dimensional wind tunnel p 1029 A92-56010
Evaluation of sidewall interference in the NAL two-dimensional transonic wind tunnel p 1092 A92-56011
BGK1 airfoil oilflow tests in the NAL two-dimensional wind tunnel. II p 1029 A92-56044
High subsonic wind tunnel test of a two-dimensional hybrid-laminar-flow-control airfoil with slotted surface p 1029 A92-56045
Evaluation of NACA0012 airfoil test results in the NAL two-dimensional transonic wind tunnel [NAL-TR-1109T] p 445 N92-21287
Study of the NAL's 0.1 x 0.1 m magnetic suspension and balance system [NAL-TM-623] p 665 N92-25365
NACA0012 airfoil data corrected for sidewall boundary-layer effects in the NAL two-dimensional transonic wind tunnel [NAL-TM-640T] p 722 N92-28151
Force measurements on AGARD calibration model-B at transonic speeds in the NAL two-dimensional wind tunnel [NAL-TM-639] p 722 N92-28190

KANDA, TAKESHI
Effectiveness of plasma torches for ignition and flameholding in scramjet p 737 A92-44524
Performance analysis of idealized scramjet p 1066 A92-53493
Flow measurements in scramjet inlets p 1102 A92-53565

KANDARPA, S.
Determination of tire-wheel interface loads for aircraft wheels [AIAA PAPER 92-2482] p 543 A92-34599

KANDEBO, STANLEY W.
P&W F119 - Vectored thrust for the F-22 p 25 A92-13219
Sikorsky S-92 - Bold bid for future p 457 A92-29557
Russians want U.S. to join scramjet tests p 472 A92-32296
Russians say D-30F6 engine used in MiG-31 is highly reliable p 472 A92-32298
Russia bids to salvage development of Soyuz-powered VTOL fighter p 472 A92-32300
Airlines could reap big saving with new Pratt common core p 736 A92-42400

KANDIL, HAMDY A.
Critical effects of downstream boundary conditions on vortex breakdown [AIAA PAPER 92-2601] p 792 A92-45478

KANDIL, OSAMA
Critical effects of downstream boundary conditions on vortex breakdown [AIAA PAPER 92-2601] p 792 A92-45478

KANDIL, OSAMA A.
Prediction of steady and unsteady asymmetric vortical flows around circular cones p 172 A92-18372
Three-dimensional simulation of slender delta wing rock and divergence [AIAA PAPER 92-0280] p 318 A92-25734
Active control of asymmetric vortical flows around cones using injection and heating [AIAA PAPER 92-4426] p 1025 A92-55350
Computation of vortex wake flows and control of their effects on trailing wings [AIAA PAPER 92-4429] p 1025 A92-55353

KANDO, T.
Flight simulation of a spaceplane p 752 A92-43190

KANE, DAVID M.
Structural assessment of ultralightweight composites p 1107 N92-32525

KANEHIRA, NORIYUKI
Experimental and numerical investigations on separated flows around pitching airfoils p 710 A92-43166

KANEKO, A.
Noise test of high-speed counterrotation propeller in low-speed wind tunnel p 1135 A92-56055

KANEKO, O.
Shafranov shift in low-aspect-ratio heliotron/torsatron CHS [NIFS-110] p 1138 N92-33743

KANEMATSU, EMI
Rarefied gas numerical wind tunnel p 995 A92-52763
Rarefied gas numerical wind tunnel p 1017 A92-53552

KANG, H.
Detection and identification of axial flow compressor instabilities p 969 A92-50504

KANG, H. S.
Optimization of a thermally non-symmetric fin - Preliminary evaluation p 992 A92-50448

KANG, JONGMIN
The effect of molecular relaxation processes in air on the rise time of sonic booms p 898 A92-45883
Nonlinear acoustic propagation of shock waves through the atmosphere with molecular relaxation p 511 N92-20360

KANG, SHUN
Three dimensional flow in a linear compressor cascade at design conditions [ASME PAPER 91-GT-114] p 70 A92-15565

KANIA, LEE
Three-dimensional adaptive grid generation with applications in nonlinear fluid dynamics [AIAA PAPER 92-0661] p 397 A92-27032

KANKAINEN, P.
Wind-tunnel investigation of aerodynamic and stability characteristics of a forward swept wing X-29 model p 627 N92-24862

KANKI, BARBARA G.
Cockpit crew research p 951 A92-51440
The impact of cockpit automation on crew coordination and communication. Volume 1: Overview, LOFT evaluations, error severity, and questionnaire data [NASA-CR-177587] p 93 N92-13044

KANMURI, AKIO
Performance analysis of idealized scramjet p 1066 A92-53493

KANNMACHER, K. D.
Design and analysis of ceramic and CMC components for advanced gas turbines [ASME PAPER 91-GT-156] p 142 A92-15592

KAO, PI-JEN
Coupled Rayleigh-Ritz/finite element structural analysis using penalty function method [AIAA PAPER 92-2238] p 581 A92-34292

KAO, T. J.
Three-dimensional orthogonal-to-surface structured grid generation with transonic Navier-Stokes flow solutions for a commercial transport configuration [AIAA PAPER 92-2616] p 793 A92-45490
An interactive multi-block grid generation system p 691 N92-24419

KAPANIA, RAKESH K.
Analytical shape sensitivities and approximations of modal response of generally laminated tapered skew plates [AIAA PAPER 92-2391] p 585 A92-34465
Sensitivity analysis of dynamic aeroelastic responses p 571 N92-23229

KAPOOR, K.
Subcritical flow studies on two-dimensional external compression supersonic inlets p 713 A92-44518

KAPOOR, KAMLESH
Comparative study of turbulence models in predicting hypersonic inlet flows [AIAA PAPER 92-3098] p 824 A92-48740
Comparative study of turbulence models in predicting hypersonic inlet flows [NASA-TM-105720] p 722 N92-28102

KAPTEIN, DICK
Active synchrophasing of propeller unbalance p 1138 N92-32963

KAPUSTIN, N. IU.
Uniqueness of solutions of the generalized Tricomi problem arising in the theory of the Laval nozzle p 428 A92-30319

KAR, KISHORE K.
Development and tribological properties of new cyclotriphosphazene high temperature lubricants for aircraft gas turbine engines p 287 A92-21327

KARADIMAS, GEORGES
The position of the unsteady flow computation in the compressor and turbine design and analysis process [AIAA PAPER 92-0015] p 278 A92-22137

KARAGIANNIS, F.
Unsteady Euler calculations in 2-D internal aerodynamics with introduced vorticity [ASME PAPER 91-GT-168] p 73 A92-15603
Arbitrary blade section design based on viscous considerations - Background information p 523 A92-36029
Arbitrary blade section design based on viscous considerations - Blade optimization p 523 A92-36030
Unsteady Euler calculations in 3D internal aerodynamics p 768 N92-27470

KARAMYSHEV, V. B.
Computation of transonic flow over an airfoil at large Reynolds numbers p 252 A92-23414

KARAS', O. V.
Characteristics of transonic flow past a configuration comprising a wing and a fuselage with a large midsection ratio p 439 A92-31882

KARASAWA, KENJI
An experiment on the weight vs control relations of subsonic airplanes p 357 A92-25502
The relationship between the weight and flight characteristics of a transonic aircraft p 731 A92-43189

KARASHIMA, KEIICHI
Approximate analysis of aerodynamic heating at hypersonic speed p 430 A92-30551
Nonlinear dynamic stability characteristics of recovery bodies p 977 A92-52041

KARASKIEWICZ, RONALD J.
Comparison of R2SPG waveforms with simulated EMP p 760 A92-42317

KARCHMER, ALLEN
Combustion and core noise p 55 N92-10607

KARIYA, TIMMY T.
Interference effects of very high bypass ratio nacelle installations on a low-wing transport [ASME PAPER 91-GT-241] p 75 A92-15646
A user's guide to the Langley 16- by 24-inch water tunnel [NASA-TM-104200] p 385 N92-18956
Installation effects of wing-mounted turbofan nacelle-pylons on a 1/17-scale, twin-engine, low-wing transport model [NASA-TP-3168] p 346 N92-19002

KARNI, SMADAR
Accelerated convergence to steady state by gradual far-field damping p 610 A92-36835

KARNIADAKIS, G.
Direct computation of turbulence and noise [NASA-CR-187616] p 236 N92-14788

KARPEL, M.
Time simulation of flutter with large stiffness changes [AIAA PAPER 92-2394] p 585 A92-34467

KARPEL, MORDECHAY
Extensions to the minimum-state aeroelastic modeling method p 20 A92-11081
Application of aeroservoelastic modeling using minimum-state unsteady aerodynamic approximations p 204 A92-18622
Multidisciplinary optimization of aeroservoelastic systems using reduced-size models p 1054 A92-56176
Multi-disciplinary optimization of aeroservoelastic systems [NASA-CR-188983] p 44 N92-11377
Time simulation of flutter with large stiffness changes [NASA-TM-107650] p 963 N92-32111

KARPOUZIAN, G.
The equations governing the motion of wing-aileron structural systems constructed from advanced anisotropic composite materials [AIAA PAPER 92-2469] p 564 A92-34359

KASAI, TOKIO
Path angular control of the STOL research aircraft Asuka p 745 A92-43146

KASCAK, ALBERT
Determining structural performance p 560 N92-22519

KASHIWABARA, Y.
Numerical investigation of surge and rotating stall in multistage axial compressors [AIAA PAPER 92-3193] p 825 A92-48804

KASHIWAGI, TAKAO
Three-dimensional flow visualization of shock wave using double-pulsed holographic interferometry. II - Flow visualization for three-dimensional shock structures in rotating aeroengine fan blade rows p 497 A92-32507

KASHKOVSKII, A. V.
Influence of atmospheric rarefaction on aerodynamic characteristics of flying vehicles p 938 A92-52750

KASHYAP, S.
An improved model-creation program for EM interaction analysis [NRC-31764] p 155 N92-12153

KASHYAP, SATISH
Analysis of EMP response of structures using frequency domain electromagnetic interaction codes
[AD-A245758] p 765 N92-26592
KASINSKI, JEFFREY J.
One joule output from a diode-array-pumped Nd:YAG laser with side-pumped rod geometry
p 671 A92-37188
KASISCHKE, ERIC S.
Estimation of the P-3/SAR L-, C- and X-band antenna directivity in range direction based on corner reflector measurements within the absolute SAR calibration
p 587 A92-35055
KASSAPOGLOU, CHRISTOS
KGR-1 thick adherend specimen evaluation for the determination of adhesive mechanical properties
p 994 A92-51513
KASSIES, A.
Boundary conditions for Euler equations at internal block faces of multi-block domains using local grid refinement
[NLR-TP-90134-U] p 908 N92-28712
KASTELLA, KEITH
Aircraft route optimization using adaptive simulated annealing p 922 A92-48565
KATAOKA, HAJIME
Study of potassium turbine electric generator system
p 1129 N92-33794
KATAOKA, HIROYUKI
An experimental study on variable pressure hydraulic flight control system p 1084 A92-56119
KATAYANAGI, RYOJI
Inspection of stability deterioration with an adaptive regulator p 776 A92-43178
MIMO state-feedback control system considering phase stability by -90 deg phase-locus method
p 1084 A92-56066
KATHEDER, K.
The 3-D Navier-Stokes flow and temperature field computation for a forced mixer nozzle
p 770 N92-27482
KATHMAN, A. D.
Crossed beam correlation modeling and experimental techniques for measuring density fluctuations in hypersonic flows
[AIAA PAPER 92-2779] p 758 A92-41323
A time-integrated image model for aero-optic analysis
[AIAA PAPER 92-2793] p 779 A92-41332
KATHMAN, ALAN
A validated code to predict the performance of onboard broadband optical seekers through a turbulent transonic flow
[AIAA PAPER 92-2792] p 778 A92-41331
KATO, CHISACHI
Large eddy simulation of unsteady turbulent wake of a circular cylinder using the finite element method
p 587 A92-34825
KATO, H.
Model reference adaptive flight control system (MRAFCS) design with consideration of the balance point p 745 A92-43182
KATO, KANICHIRO
An experiment on the weight vs control relations of subsonic airplanes p 357 A92-25502
On the skip flight of a spaceplane
p 387 A92-25503
A note on thrust control for jetliner during approach
p 457 A92-29518
The relationship between the weight and flight characteristics of a transonic aircraft
p 731 A92-43189
A note on thrust control for jetliner during approach
p 1053 A92-56061
KATO, MICHIYO
PAR-WIG performance prediction during acceleration from water-borne to air-borne p 291 A92-21721
A quick automatic method for computing performance of nonducted propeller with constant-revolutional-speed
p 393 A92-25505
A quick automatic method for computing performance of ducted-propeller p 736 A92-42800
KATO, T.
Outline and discussion of the cooling loop of the heating control system in the exposed facility of the Japanese Experiment Module (JEM) p 574 A92-35610
KATOOZI, MEHDI
Built-in testable error detection and correction
p 394 A92-25846
KATOU, KAZUNOBU
Design of a flight control system using a feedback-error-learning-type neural network
p 1132 A92-56067
KATRAMATOS, D. T.
3-D loss prediction based on secondary flow and blade shear layer interaction
[ASME PAPER 91-GT-59] p 68 A92-15536
The influence of shock waves on the viscous flow field of axial compressors
[ASME PAPER 91-GT-173] p 73 A92-15608
KATSNEL'SON, S. S.
Experimental and theoretical study of the improvement of the aerodynamic characteristics of supersonic flow past bodies with surface injection of a gas jet with particles
p 8 A92-12204
KATSURAHARA, TADASHI
Numerical analysis of RCS jet in hypersonic flights
[SAE PAPER 912063] p 791 A92-45445
A hypersonic wind tunnel test of a mixed-compression air inlet model p 1028 A92-56007
Aerothermodynamic test of spaceplane by thin-skin method p 1093 A92-56043
KATTA, V. R.
A numerical method for simulating the fluid-dynamic and heat-transfer changes in a jet engine injector feed-arm due to fouling
[AIAA PAPER 92-0768] p 374 A92-27108
KATZ, AMNON
Flight model for unmanned simulated helicopters
p 874 A92-46776
Special Rotation Vectors quaternions in three components
[AIAA PAPER 92-4168] p 1008 A92-52454
KATZ, ERIC S.
Prototype runway hold-short lighting system
[DOT/FAA/CT-TN91/43] p 31 N92-11028
Comparative evaluation of internally and externally lighted taxiway guidance signs
[DOT/FAA/CT-TN92/2] p 573 N92-22237
Evaluation of a tritium runway lighting system
[DOT/FAA/CT-TN92/15] p 665 N92-25733
KATZ, JOSEPH
Reduction of wing rock amplitudes using leading-edge vortex manipulations
[AIAA PAPER 92-0279] p 379 A92-25733
Effect of airfoil (trailing-edge) thickness on the numerical solution of panel methods based on the Dirichlet boundary condition p 340 A92-28041
Self-induced roll oscillations of low-aspect-ratio rectangular wings p 874 A92-46802
Potential flow theory and operation guide for the panel code PMARC
[NASA-TM-102851] p 1036 N92-32422
KATZ, KENNETH P.
Flight testing the avionics system of the V-22 Osprey
p 117 A92-14378
KAUFFMAN, H. G.
Control strategy for maximizing reconnaissance range of hypersonic cruise vehicles p 729 A92-41222
KAUFFMAN, R. E.
Lubricant evaluation and performance 2
[AD-A247464] p 895 N92-28398
KAUKLER, WILLIAM F.
Convective flow analysis on the KC-135 aircraft
[AIAA PAPER 92-0844] p 493 A92-29610
KAUPS, K.
Analysis of iced wings
[AIAA PAPER 92-0416] p 423 A92-29972
Analysis of iced wings
[NASA-TM-105773] p 1042 N92-34144
KAUTZ, EDWARD F.
Out of plane analysis for composite structures
p 1107 N92-32527
Damage tolerance certification methodology for composite structures p 1108 N92-32579
KAWABATA, HITOSHI
Hypersonic flows with air chemistry over a reentry vehicle at high altitudes p 1017 A92-53549
KAWABATA, N.
The maneuver performance and control of a hovercraft p 763 A92-43240
KAWACHI, KEIJI
Navier-Stokes analysis of blade tip shape in hover
p 521 A92-35758
An adaptive flight control for use in connection with helicopter engine failure p 745 A92-43159
Optimal control of helicopters following power failure
[AIAA PAPER 92-4471] p 1076 A92-55231
A calculation method to predict helicopter noise and its verification p 1135 A92-56074
Optimal control of tiltrotor aircraft following power failure p 1085 A92-56303
KAWAGOE, SHIGETOSHI
Flow unsteadiness by weak normal shock wave/turbulent boundary layer interaction in internal flow
p 67 A92-15359
KAWAGOE, YASUHITO
A preliminary flight test on a basic performance of the flight research airplane Do 228: Velocity vs glide path angle
[NAL-TM-613] p 359 N92-18482
KAWAGUCHI, JUN'ICHIRO
Pre-flight physical simulation test of HIMES reentry test vehicle p 1103 A92-53640
KAWAHARA, HIROYASU
Evaluation test on the simulator of the liquid crystal flat display. II p 734 A92-43209
A simulator study of a flight reference display for powered-lift STOL aircraft
[SAE PAPER 912067] p 855 A92-45449
Flight test of a flight reference display for powered-lift STOL aircraft p 1064 A92-56059
Flight simulator test of cockpit advisory system
p 1054 A92-56115
KAWAHATA, NAGAKATU
In-flight simulation of backside operating models using direct lift controller
[SAE PAPER 912069] p 872 A92-45450
Gust response and cross wind performance of a hovercraft with vertical wings p 1118 A92-56034
KAWAI, M.
Integrated system to support computer analysis in conceptual aerospace design p 1130 A92-53596
KAWAI, MASAFUMI
CFD application to 2D/3D flow fields in Scramjet engine p 170 A92-17501
Study on two-dimensional jet mixing with a vertical supersonic flow p 429 A92-30530
KAWAI, N.
Numerical analysis on laminar flow control of transonic airfoils p 430 A92-30557
KAWAJI, M.
Forced-injection quenching of a hot-tube under microgravity p 590 A92-35977
KAWAKAMI, YOSHIFUMI
Impact response of composite UHB propeller blades
[SAE PAPER 912046] p 861 A92-45430
Predicted pressure distribution on a prop-fan blade through Euler analysis p 810 A92-46791
KAWALL, J. G.
Structural features of a heated round turbulent jet in a cross-flow p 676 A92-40148
KAWAMOTO, I.
Recent airfoil tests in NAL 2D high Reynolds number wind tunnel p 748 A92-43171
KAWAMOTO, IWAO
BGK airfoil oil flow test in a two-dimensional transonic wind tunnel p 711 A92-43201
Buffeting characteristics of a transonic airfoil
p 711 A92-43202
Aerodynamic study of H-II Orbiting Plane, HOPE
p 1103 A92-53639
Force measurements on AGARD calibration model-B at transonic speeds in the NAL two-dimensional wind tunnel
[NAL-TM-639] p 722 N92-28190
KAWAMURA, HIDEO
Study of grinding process and strength for ceramic heat insulated engine
[SME PAPER MR91-177] p 897 A92-45260
KAWAMURA, NAOKO
Propeller-nacelle whirl flutter analysis and wind tunnel test p 1052 A92-56016
KAWAMURA, RYUMA
Euler flow analysis of turbine powered simulator and fanjet engine p 80 A92-17196
KAWANO, ISAO
Design of orbital re-entry experiment vehicle and outline of the experiment p 667 N92-25374
KAWASHIMA, TOSHIHIRO
Nonlinear transient analysis of composite ATP blade model p 294 A92-23111
Numerical simulation of impact resistance on composite blade p 738 A92-44734
KAWASHIMA, Y.
Aircraft reliability and maintainability
p 700 A92-43141
KAWAUCHI, H.
The fluid-dynamic measurement of the fling motion of a three-dimensional flat plate p 710 A92-43194
KAWAUCHI, K.
Numerical analysis of helicopter rotor blades
p 430 A92-30558
KAWIECKI, GRZEGORZ
Comparison between imposed-periodicity and marching-in-time solutions of helicopter rotor blade steady-state response problem
[AIAA PAPER 92-2256] p 540 A92-34411
Bilinear formulation applied to the stability and response of helicopter rotor blade p 847 A92-46930
Helicopter rotor blade dynamics with bilinear formulation p 463 N92-21856
KAY, I. W.
Hydrocarbon-fueled scramjet combustor investigation
p 376 A92-28535

Structure and penetration of a transverse fluid jet injected at supercritical pressure in supersonic flow
[AIAA PAPER 92-3652] p 1113 A92-54105
KAYA, KEMAL
Computer simulation of an unsteady flow around an airfoil with a spoiler p 710 A92-43167
KAYA, M. O.
Numerical simulation of vortex street-edge interaction
p 88 N92-13027
KAYABA, S.
Aerodynamic model identification of a spaceplane model from a cable-mount dynamic wind-tunnel test
p 1093 A92-56114
KAYABA, SHIGEO
Estimation of spaceplane lateral-directional stability and control derivatives from dynamic wind tunnel test
[SAE PAPER 911979] p 872 A92-45384
Measurements of longitudinal static aerodynamic coefficients with cable mount system
p 1093 A92-56013
The fibre optic three dimensional laser two focus velocimeter for the low-speed windtunnel. Part 1: Two-dimensional measurement evaluations
[NAL-TM-627] p 665 N92-25402
KAYABA, SIGEO
A gust generation method for full configuration aircraft tests in a low speed wind tunnel. Part 1: Design and preliminary experiments
[NAL-TR-1115-PT-1] p 722 N92-28192
KAYKAYOGLU, C. R.
Computer simulation of an unsteady flow around an airfoil with a spoiler p 710 A92-43167
Numerical simulation of vortex street-edge interaction
p 88 N92-13027
KAYNAK, UNVER
Effect of turbulence modeling on dynamic stall of a NACA0012 airfoil
[AIAA PAPER 92-0027] p 248 A92-22149
Nonequilibrium turbulence modeling effects on transonic vortical flows about delta wings p 85 N92-13007
KAYTON, MYRON
Navigation - Land, sea, air, and space
[ISBN 0-87942-257-2] p 496 A92-31778
KAZA, KRISHNA
Determining structural performance
p 560 N92-22519
KAZA, KRISHNA RAO V.
Semi-empirical model for prediction of unsteady forces on an airfoil with application to flutter
[NASA-TM-105414] p 346 N92-18760
KAZAHARA, M.
A thin metal model for aerodynamic heating tests of shock wave interaction p 709 A92-43103
KAZAKIA, J. Y.
An algebraic model for dissipation in supersonic boundary layers
[AIAA PAPER 92-0311] p 320 A92-25759
KAZEMPOUR, AMIR
Aircraft landing-induced tire spinup
p 193 A92-20209
KAZMIERCZAK, MICHAEL
Deterministic multi-zone ice accretion modeling
p 265 N92-17987
KAZMIN, VYACHESLAV
History of EPOS air-launched spaceplane project
p 211 N92-14103
KEARY, PAUL E.
A full scale airframe high cycle fatigue test methodology and its application to the SH-2G helicopter
p 105 A92-14345
KEDDY, E. S.
Analytical and experimental studies of heat pipe radiation cooling of hypersonic propulsion systems
[AIAA PAPER 92-3809] p 867 A92-49128
Analytical and experimental studies of heat pipe radiation cooling of hypersonic propulsion systems
[DE92-013428] p 973 N92-31817
KEEFE, LAURENCE R.
Turbulence amplification through a shock wave
[AIAA PAPER 92-0313] p 320 A92-25761
KEEFER, THOMAS N., JR.
A summary of XB-70 sonic boom signature data
[NASA-CR-189630] p 696 N92-24800
KEEN, DANNY W.
Graceful degradation of GPS/INS performance with fewer than four satellites p 97 A92-16644
KEENAN, JAMES A.
The effects of winglets on low aspect ratio wings at supersonic Mach numbers
[NASA-CR-4407] p 178 N92-13996
KEENER, EARL R.
Boundary-layer and wake measurements on a swept, circulation-control wing p 9 A92-13205
Single expansion ramp nozzle simulations
[AIAA PAPER 92-0387] p 323 A92-26243
Experimental results for a hypersonic nozzle/afterbody flow field
[AIAA PAPER 92-3915] p 1032 A92-56747
Experimental research of the aerodynamics of nozzles and plumes at hypersonic speeds
[NASA-CR-187316] p 185 N92-15048
KEESEE, JOHN M.
Magnetic bearing design and control optimization for a four-stage centrifugal compressor p 900 A92-47188
KEETER, TIM
The Langley turbo-prop commuter design: A complete project description
[NASA-CR-189987] p 463 N92-21540
KEFFER, J. F.
Structural features of a heated round turbulent jet in a cross-flow p 676 A92-40148
KEGELMAN, J. T.
Aerodynamic applications of pressure-sensitive paint
[AIAA PAPER 92-0264] p 394 A92-25720
KEHAYAS, N.
ASTOVL combat aircraft design synthesis and optimization
[CRANFIELD-AERO-9201] p 963 N92-31515
KEHOE, M. W.
Digital time series analysis for flutter test data
[AIAA PAPER 92-2103] p 589 A92-35674
KEHOE, MICHAEL W.
High temperature ground vibration test techniques
p 980 A92-51404
Getting up to speed in hypersonic structures
p 1117 A92-55127
KEITER, JERRY
Preliminary design studies of an advanced general aviation aircraft
[NASA-CR-190024] p 461 N92-20064
KEITH, B. D.
Commercial turbofan engine exhaust nozzle flow analyses using PAB3D
[AIAA PAPER 92-2701] p 801 A92-45543
KEITH, T. G.
Results from computational analysis of a mixed compression supersonic inlet
[NASA-TM-104475] p 12 N92-10976
KEITH, T. G., JR.
Cascade flutter analysis with transient response aerodynamics p 154 A92-15972
Numerical analysis of a thermal deicer
[AIAA PAPER 92-0527] p 357 A92-26950
KEITH, THEO G., JR.
Time domain flutter analysis of cascades using a full-potential solver p 176 A92-20747
Development of an improved model for runback water on aircraft surfaces
[AIAA PAPER 92-0042] p 270 A92-22160
Investigation of the diffuser flow quality in an icing research wind tunnel p 382 A92-24406
Further developments in three-dimensional simulation of electrothermal deicing systems
[AIAA PAPER 92-0528] p 459 A92-31668
Experimental and numerical investigation of anti-icing phenomena on a NACA 0012 assembly
[AIAA PAPER 92-0531] p 459 A92-31669
An efficient finite element method for aircraft de-icing problems
[AIAA PAPER 92-0532] p 459 A92-31670
An investigation of cascade flutter using a two-dimensional full-potential solver
[AIAA PAPER 92-2119] p 558 A92-35688
KELDYSH, V. V.
Computational studies of the aerodynamic characteristics of delta wings with a subsonic leading edge p 439 A92-31874
KELLER, A.
Development of hardness cycles for fiber bound materials, using DSC: From laboratory specimens to complex high duty structural members
[MBB-Z-0409-91-PUB] p 987 N92-30969
KELLER, DONALD F.
Planform curvature effects on flutter characteristics of a wing with 56 deg leading-edge sweep and panel aspect ratio of 1.14
[NASA-TP-3116] p 115 N92-13054
KELLER, JOHN
US Navy revisits escape modules p 849 A92-47975
KELLER, K. L.
Utility of ground simulation in flight control problem identification, solution development, and verification
p 883 N92-28525
KELLER, M. A.
Lubricant evaluation and performance 2
[AD-A247464] p 895 N92-28398
KELLER, V. W.
Influence of air velocity on the habit of ice crystal growth from the vapor p 668 A92-38111
KELLEY, HENRY L.
Helicopter low-speed yaw control
[NASA-CASE-LAR-14219-1] p 879 N92-30025
Two-dimensional aerodynamic characteristics of several polygon-shaped cross-sectional models applicable to helicopter fuselages
[NASA-TP-3233] p 944 N92-30394
KELLEY, N.
Measured and predicted rotor performance for the SERI advanced wind turbine blades
[DE92-001215] p 598 N92-23119
KELLEY, RONALD T.
Flight test results of an Ada coded INS/GPS open loop Kalman filter design p 100 A92-16958
KELLOG, DAVID L.
Core avionics and standardization
[AD-A248326] p 735 N92-27925
KELLOGG, GARY
Rapid development of the X-31 simulation to support flight-testing
[NASA-TM-104256] p 1060 N92-33149
KELLY, G. M.
Skin-friction gauge for use in hypervelocity impulse facilities p 398 A92-28063
KELLY, P. G.
Results of a perturbation analysis correlating flows entering and exiting an aircraft inlet system
[AIAA PAPER 92-3624] p 1021 A92-54091
KELLY, R. J.
MLS system error model identification and synthesis
p 639 A92-40232
MLS system error model identification and synthesis
p 189 N92-14015
KELLY, SHAWN L.
Limitations of a holographic 3-D pixel projector for cockpit displays
[AD-A241295] p 119 N92-13067
KELLY, T. J.
A preliminary study of the microstructure-property relationships in cast gamma titanium aluminide alloys
p 487 A92-30596
KEMPEL, ROBERT
The F-18 high alpha research vehicle: A high-angle-of-attack testbed aircraft
[NASA-TM-104253] p 1060 N92-33404
KEMPPINEN, MARTTI
Mechanical design of an airborne imaging microwave radiometer p 554 A92-35276
KENDALL, CHRIS
Low cost HIRF troubleshooting and verification method for digital avionics systems p 990 A92-49304
KENDALL, E. R.
The use and effectiveness of piloted simulation in transport aircraft research and development
p 886 N92-28549
KENDALL, JAMES M.
Studies on laminar boundary-layer receptivity to freestream turbulence near a leading edge
p 591 A92-36007
KENNEDY, BETTY R.
A revolution in air transport - Acquiring the C-141 Starlifter p 607 A92-38101
KENNEDY, DAVID
Manipulation and management of data collected at the Crew Station Research and Development Facility - A case study
[AIAA PAPER 92-4162] p 1008 A92-52451
KENNEDY, JOHN M.
NASA/DOD Aerospace Knowledge Diffusion Research Project. Paper 14: An analysis of the technical communications practices reported by Israeli and US aerospace engineers and scientists
[NASA-TM-107924] p 782 N92-28183
KENNELLY, ROBERT A., JR.
Transonic wind tunnel test of a 14 percent thick oblique wing
[NASA-TM-102230] p 950 N92-32213
KERELIUK, S.
Tracking performance requirements for rotorcraft instrument approaches to reduced minima. Phase 1: Preliminary study
[NRC-32137-PHASE-1] p 102 N92-11988
KERELIUK, STAN
An exploratory investigation into the definition of tracking standards for IFR helicopter approaches to reduced minima p 533 A92-35726
KERHERVE, YVES
Rafale: Program update - Development of a naval version p 645 A92-40035
KERHO, M.
Finite wing aerodynamics with simulated glaze ice
[AIAA PAPER 92-0414] p 325 A92-26265
Helium bubble flow visualization of the spanwise separation on a NACA 0012 with simulated glaze ice
[AIAA PAPER 92-0413] p 341 A92-28192

LDV measurements on a rectangular wing with a simulated glaze ice accretion
[AIAA PAPER 92-2690] p 800 A92-45537
Helium bubble flow visualization of the spanwise separation on a NACA 0012 with simulated glaze ice
[NASA-TM-105742] p 714 N92-26612
KERN, STEVEN B.
A numerical investigation of vortex flow control through small geometry modifications at the strake/wing junction of a cropped double-delta wing
[AIAA PAPER 92-0411] p 435 A92-31661
KERNS, KAROL
Data-link communication between controllers and pilots - A review and synthesis of the simulation literature
p 94 A92-14045
KERR, L. J.
Real-time estimation of gas turbine engine damage using a control based Kalman filter algorithm
[ASME PAPER 91-GT-216] p 124 A92-15633
KERR, P. W.
Grid generation and compressible flow computations about a high-speed civil transport configuration
p 919 A92-47055
KERREBROCK, JACK L.
Some readily quantifiable aspects of scramjet engine performance p 969 A92-50278
Aircraft engines and gas turbines (2nd revised and enlarged edition)
[ISBN 0-262-11162-4] p 970 A92-53336
KERSCHEN, E. J.
Leading-edge receptivity for blunt-nose bodies
[NASA-CR-190563] p 1036 N92-32648
KERSTEIN, ALAN R.
A new unsteady mixing model to predict NO(x) production during rapid mixing in a dual-stage combustor
[AIAA PAPER 92-0233] p 372 A92-25696
KESHOCK, E. G.
Measurements and correlation of two-phase pressure drop under microgravity conditions p 37 A92-10435
KESSINGER, CATHY
Precipitation development in Colorado Front Range snowstorms - 15 November 1987 case study
p 301 A92-23008
KESSLER, G. K.
Enhanced displays, flight controls, and guidance systems for approach and landing p 456 N92-21957
KESTLER, MAUREEN A.
Performance of insulated pavements at Newton Fields, Jackman, Maine
[CRREL-92-9] p 1101 N92-32903
KEY, DAVID L.
The use of ground based simulation for handling qualities research: A new assessment p 885 N92-28545
KEY, M. K.
Downwash for joined-wing airframe with control surface deflections p 702 A92-41235
KEYS, CHARLES
LH wind tunnel testing - Key to advanced aerodynamic design p 104 A92-14331
KEYSON, RON
International SAMPE Electronics Conference, 5th, Los Angeles, CA, June 18-20, 1991, Proceedings
[ISBN 0-938994-58-1] p 985 A92-51901
KHALATOV, A. A.
A method for determining the parameters of mathematical generalizations of experimental data on convective heat transfer p 41 A92-12803
The flow pattern and external heat transfer investigation for gas turbine vanes end surfaces
[AIAA PAPER 92-3071] p 903 A92-48722
KHALID, M.
A scheme for two dimensional Euler and boundary layer interactive solutions p 627 N92-24860
KHALID, S. J.
Role of dynamic simulation in fighter engine design and development p 277 A92-21080
KHALIDOV, I. A.
Determination of duty factors from experimental data in local interaction theory p 338 A92-27645
KHALIDOV, ISKANDER A.
Local interaction theory
[ISBN 5-288-00516-8] p 779 A92-42778
KHAN, M. J.
Experimental investigation of a three-dimensional bluff-body wake
[AIAA PAPER 92-0429] p 326 A92-26277
KHAN, S.
A methodology for software specification and development based on simulation p 135 N92-12458
KHAN, T.
Advanced superalloys for turbine blade and vane applications
[ONERA, TP NO. 1992-2] p 893 A92-48578
KHARCHENKO, A. V.
An approach to the organization of an adaptive man-machine system for flight vehicle control
p 1133 A92-57445
KHARGONEKAR, PRAMOD P.
H(infinity) control of linear systems with nonzero initial conditions p 50 A92-11430
Design of the flare control law for longitudinal autopilot using H(infinity) synthesis p 28 A92-11562
KHATTAB, A. A.
An approach to the design of wings - The role of mathematics, physics and economics
[AIAA PAPER 92-0286] p 319 A92-25739
KHAVARAN, A.
Computation of supersonic jet mixing noise for an axisymmetric CD nozzle using k-epsilon turbulence model
[AIAA PAPER 92-0500] p 414 A92-26328
KHAVARAN, ABBAS
A survey of the broadband shock associated noise prediction methods
[AIAA PAPER 92-0501] p 415 A92-26930
Computation of supersonic jet mixing noise for an axisymmetric CD nozzle using k-epsilon turbulence model
[NASA-TM-105338] p 237 N92-14795
A survey of the broadband shock associated noise prediction methods
[NASA-TM-105365] p 237 N92-14797
KHLUPNOV, ALEKSANDR I.
Fundamentals of applied aerogasdynamics. I - Aerodynamics of wings (profiles), airframes, and their combinations p 64 A92-14280
KHMEL'NITSKII, A. A.
Approximate aerodynamic analysis for complicated bodies in rarefied gas flows p 938 A92-52754
KHODADOUST, A.
Finite wing aerodynamics with simulated glaze ice
[AIAA PAPER 92-0414] p 325 A92-26265
Measurements in a leading-edge separation bubble due to a simulated airfoil ice accretion p 723 A92-41262
LDV measurements on a rectangular wing with a simulated glaze ice accretion
[AIAA PAPER 92-2690] p 800 A92-45537
KHODADOUST, ABDI
Effect of a simulated glaze ice shape on the aerodynamic performance of a rectangular wing
[AIAA PAPER 92-4042] p 1035 A92-56861
KHOKHLOV, A. P.
Susceptibility of a supersonic boundary layer to acoustic perturbations p 707 A92-42730
KHOKHLOV, D. L.
Base pressure on an axisymmetric finned body during forced rotation in the autorotation regime
p 7 A92-12165
KHORRAMABADI, DELNAZ
A walk through the planned CS building
[NASA-CR-189963] p 386 N92-19675
KHORRAMI, MEHDI R.
Behavior of asymmetric unstable modes of a trailing line vortex near the upper neutral curve p 617 A92-39340
KHOSLA, P. K.
Transient behavior of supersonic flow through inlets
p 340 A92-28043
KHOZIAENKO, N. N.
Determination of the mass-flow-rate characteristics of porous panels p 439 A92-31875
KHRABROV, A.
Stochastic self-induced roll oscillations of slender delta wing at high angles of attack
[AIAA PAPER 92-4498] p 1081 A92-55366
State-space representation of aerodynamic characteristics of an aircraft at high angels of attack
[AIAA PAPER 92-4651] p 1028 A92-55395
KHRAMOV, A. G.
Holographic-interferometry methods employed for vibration-strength testing of aviation-engine workpieces
p 219 A92-20771
KIANG, R. L.
Power performance of a nonisentropic Brayton cycle
p 54 A92-11281
KIDA, TAKASHI
Quaternion and Euler angles in kinematics
[NAL-TM-636] p 909 N92-28836
KIDA, TERUHIKO
Three-dimensional numerical analysis of impinging circular jet - Discrete vortex method
p 1029 A92-56040
KIEFER, DENNIS A.
Developmental evaluation of a centrifuge flight simulator as an enhanced maneuverability flying qualities tool
[AIAA PAPER 92-4157] p 982 A92-52447
KIELB, ROBERT
Determining structural performance
p 560 N92-22519
KIELB, ROBERT E.
Recent advancements in turbomachinery forced response analyses
[AIAA PAPER 92-0012] p 278 A92-22136
KIENEL, GERHARD
PVD coatings for aircraft turbine blades
p 216 A92-17950
KIENITZ, K. H.
Robust stabilization of a helicopter model
p 28 A92-11501
KIKKAWA, S.
An experimental and numerical study of confined axisymmetric jet with a bluff body p 621 A92-40106
KIKUCHI, HIDEKATSU
An aircraft controller and its development
p 558 A92-35917
KIKUCHI, KAZUO
Numerical simulations of the flow through cascades with tip clearance p 523 A92-36038
KIKUCHI, TAKEO
The landing equipment of a high-tech aircraft
p 730 A92-43149
KIKUHARA, S.
Aircraft design experience p 110 A92-15326
KILGORE, D. R.
Transfer function between airborne VLF transmit and receive loop antenna p 1045 A92-54754
KILGORE, ROBERT A.
Magnetic suspension and balance systems: A comprehensive, annotated bibliography
[NASA-TM-4318] p 32 N92-11030
KILGORE, W. A.
Control of large cryogenic tunnels
[AIAA PAPER 92-3930] p 1096 A92-56761
KILGORE, W. ALLEN
The NASA Langley Research Center 0.3-meter transonic cryogenic tunnel microcomputer controller source code
[NASA-CR-189556] p 209 N92-15077
KIM, B. J.
Runway exit designs for capacity improvement demonstrations. Phase 2: Computer model development
[NASA-CR-190166] p 484 N92-21162
KIM, BYOUNG S.
Neural networks for feedback linearization in aircraft control
[AIAA PAPER 92-4391] p 1074 A92-55192
KIM, BYOUNGSOO
BUWICE - An interactive icing program applied to engine inlets
[AIAA PAPER 92-3179] p 922 A92-48794
KIM, C. M.
Computation of supersonic jet mixing noise for an axisymmetric CD nozzle using k-epsilon turbulence model
[AIAA PAPER 92-0500] p 414 A92-26328
KIM, CHAN M.
A survey of the broadband shock associated noise prediction methods
[AIAA PAPER 92-0501] p 415 A92-26930
Computation of supersonic jet mixing noise for an axisymmetric CD nozzle using k-epsilon turbulence model
[NASA-TM-105338] p 237 N92-14795
A survey of the broadband shock associated noise prediction methods
[NASA-TM-105365] p 237 N92-14797
KIM, CHANG H.
Flow visualization studies of a sideslipping, canard-configured X-31A-Like fighter aircraft model
[AD-A245940] p 829 N92-28883
KIM, CHANGJU
Time accurate computation of unsteady transonic flows around an airfoil with oscillating flap on dynamic grid
[AIAA PAPER 92-2733] p 805 A92-45567
KIM, FREDERICK D.
Forward flight trim calculation and frequency response validation of a high-order helicopter simulation model
p 132 A92-14337
High-order state space simulation models of helicopter flight mechanics p 569 A92-35777
Analysis of propulsion system dynamics in the validation of a high-order state space model of the UH-60
[AIAA PAPER 92-4150] p 959 A92-52441
KIM, HEUY-DONG
Flow unsteadiness by weak normal shock wave/turbulent boundary layer interaction in internal flow
p 67 A92-15359
KIM, I.
Three-dimensional flow computation for two interacting, moving droplets
[AIAA PAPER 92-0343] p 496 A92-31655
Navier-Stokes study of supersonic cavity flowfield with passive control p 442 A92-32239
Passive control of supersonic cavity flowfields
[SAE PAPER 912153] p 619 A92-39988

Detection and identification of axial flow compressor instabilities p 969 A92-50504
Fundamental studies on droplet interactions in dense sprays
[AD-A246918] p 770 N92-27546

KIM, INSUN
Numerical investigation of unsteady supersonic cavity flowfield with passive control p 88 N92-13029

KIM, J. J.
Study of turbulence structure through numerical simulations: The perspective of drag and reduction p 717 N92-27713

KIM, J. M.
An experimental and analytical study of the interaction of a vortex with an airframe
[AIAA PAPER 92-0319] p 321 A92-25766
Flow over a twin-tailed aircraft at angle of attack. I - Spatial characteristics p 702 A92-41229
Flow over a twin-tailed aircraft at angle of attack. II - Temporal characteristics p 810 A92-46781

KIM, J. Y.
Three-dimensional finite-element analysis of interlaminar stresses in thick composite laminates p 39 A92-11791

KIM, JAI-MOO
Interaction between a rotor tip vortex and a separated flowfield p 814 A92-46947

KIM, JAY C.
Computational and experimental investigation of annulus heat transfer with swirl
[AIAA PAPER 92-4060] p 1119 A92-56143

KIM, KI-CHUNG
Aeroelastic analysis of swept, anhedral, and tapered tip rotor blades p 316 A92-25577

KIM, KUK H.
Compressor blade row unsteady aerodynamic response to attached and separated flow forcing functions
[AIAA PAPER 92-0147] p 253 A92-23763

KIM, SANGHO
Observation and measurements of flow structures in the stagnation region of a wing-body junction p 714 N92-26616

KIM, TAE W.
Three-dimensional relaxation effect on quasi-3D flow in a blade row with spanwise loading distribution p 936 A92-51593

KIM, TAEHYOUN
Nonlinear large amplitude aeroelastic behavior of composite rotor blades at large static deflection
[AIAA PAPER 92-2257] p 540 A92-34412

KIM, WON-JONG
Application of recursive partially unknown system identification to aerodynamic coefficients estimation
[AIAA PAPER 92-4504] p 1081 A92-55371

KIM, Y.
Electronics/avionics integrity - Definition, measurement and improvement p 1120 A92-56252

KIM, YONG H.
Aircraft landing-induced tire spinup p 193 A92-20209

KIM, YOUNG
Measured and calculated optical property profiles in the mixed layer and free troposphere p 1129 A92-54630

KIM, YOUNG KIL
A numerical solution of implicit nonlinear equations of motion for rotor blades p 115 N92-13053

KIM, YOUNG R.
Measurement of basic material and processing properties affecting injection-pultrusion technology p 580 A92-32636

KIMBLE, KENNETH R.
Particle trajectory computer program for icing analysis of axisymmetric bodies
[NASA-CR-189134] p 352 N92-19276

KIMMEL, K. R.
Experimental evaluation of a 50-percent thick airfoil with blowing and suction boundary layer control
[AIAA PAPER 92-4500] p 1026 A92-55368

KIMMEL, ROGER L.
On hypersonic boundary-layer stability
[AIAA PAPER 92-0737] p 335 A92-27088

KIMURA, C. Y.
World commercial aircraft accidents: 1st edition, 1946-1991
[DE92-009801] p 636 N92-24713

KIMURA, ITSURO
Studies on the mechanism of ignition and flameholding by plasma jets p 755 A92-42798

KIMURA, MOTOAKIRA
Study on nozzle flow diffusion p 429 A92-30531

KIMURA, TAKASI
Flight control system design using H(infinity) optimal control p 1083 A92-56030

KIMURA, YUKIKO
Rarefied gas numerical wind tunnel p 995 A92-52763
Rarefied gas numerical wind tunnel p 1017 A92-53552

KINARD, THOMAS A.
Supersonic boundary-layer stability analysis on an aircraft wing p 9 A92-13207

KIND, R. J.
Effects of simulated rotation on tip leakage in a planar cascade of turbine blades. II - Downstream flow field and blade loading
[ASME PAPER 91-GT-128] p 71 A92-15573
Aerodynamic characteristics of hoar frost roughness p 808 A92-45829
Effects of frost on wing aerodynamics and take-off performance p 450 N92-21687
Performance degradation due to hoar frost on lifting surfaces p 628 N92-24866

KINDLER, A.
Thermally regenerative fuel cells
[AD-A242900] p 300 N92-17629

KING, C. H.
Analysis technique for lightning attachment zoning of aircraft p 186 A92-20126

KING, E. W.
Application of computational fluid dynamics to pitch/yaw thrust vectoring spherical convergent flap nozzles p 737 A92-44511

KING, H. H. C.
Effect of leading-edge cross-sectional geometry on slender wing unsteady aerodynamics
[AIAA PAPER 92-0173] p 255 A92-23784
Rapid prediction of high-alpha unsteady aerodynamics of slender-wing aircraft p 309 A92-24412

KING, J. E.
Crack initiation and the short-to-long crack growth transition in a Ni-base superalloy p 213 A92-19767

KING, JAMES A.
Case-based reasoning - Taming the similarity heuristic p 47 A92-11153

KING, JEFF
Advanced thermoplastic nose landing gear door development p 20 A92-10275

KING, JOHN E.
An economic approach to accurate wing design
[SAE PAPER 912008] p 789 A92-45408

KING, MING-DAH
Experimental investigation of the stability of a clearance-excited rotor system with optimal parameters p 1114 A92-54223

KING, P. I.
Wake mixing and performance measurements in a linear compressor cascade with crenulated trailing edges
[AIAA PAPER 92-3188] p 824 A92-48800

KINGCOMBE, R. C.
An Axial Turbobrake
[ASME PAPER 91-GT-1] p 147 A92-15501

KINGSLEY, J. P.
Prediction of a high bypass ratio engine exhaust nozzle flowfield
[AIAA PAPER 92-3259] p 864 A92-48855

KINGTON, H.
Impact design methods for ceramic components in gas turbine engines
[ASME PAPER 91-GT-115] p 123 A92-15566

KINNEY, T. R.
Integrated optic components for advanced turbine engine control systems p 925 A92-46248

KINNISON, DOUGLAS E.
Designing a methodology for future air travel scenarios p 409 N92-19125
Ozone response to aircraft emissions: Sensitivity studies with two-dimensional models p 409 N92-19126

KINOSITA, TETSUHIKO
Flow unsteadiness by weak normal shock wave/turbulent boundary layer interaction in internal flow p 67 A92-15359

KINSEY, DON W.
An unstructured approach to the design of multiple-element airfoils
[AIAA PAPER 92-2709] p 807 A92-45592

KINZIE, KEVIN W.
An experimental investigation of large scale instabilities in a low Reynolds number two-stream supersonic shear layer
[AIAA PAPER 92-0177] p 255 A92-23787

KIRALY, LOUIS J.
Determining structural performance p 560 N92-22519

KIRBY, M. W.
Eddy current imaging of aircraft using real time image signal processing p 144 A92-13594

KIRCHER, ROBERT C., JR.
Managing simulator wiring information and deriving system continuity p 964 A92-49287

KIRCHNER, DIETER
Comparison of two-way satellite time transfer and GPS common-view time transfer between OCA and TUG p 1050 N92-33356

KIRDEIKIS, J.
Adaptive simulator motion software with supervisory control p 412 A92-28136
Flight simulation p 207 N92-13982

KIRINOV, IU. V.
Control of the development of boundary layer disturbances p 423 A92-30126

KIRKHAM, ANTHONY J.
Optical design of dual combiner head-up displays p 414 A92-24628

KIRKKOPRU, K.
Secondary separation from a slender wing p 62 A92-13448
Laminar-flow secondary separation on a slender wing p 85 N92-13006

KIRKNER, D. J.
Determination of tire-wheel interface loads for aircraft wheels
[AIAA PAPER 92-2482] p 543 A92-34599

KIRKPATRICK, CAROL M.
Development of an advanced piloted helicopter simulation p 105 A92-14363

KIROL, L.
Solid-vapor adsorption refrigeration system development
[PB92-164383] p 771 N92-27715

KIRTLEY, K. R.
Deterministic blade row interactions in a centrifugal compressor stage
[ASME PAPER 91-GT-273] p 75 A92-15670
Renormalization group based algebraic turbulence model for three-dimensional turbomachinery flows p 703 A92-41268

KIRTS, RICHARD E.
Paint removal using cryogenic processes
[AD-A247668] p 895 N92-28912

KISER, JAMES D.
Ceramics for engines p 578 N92-22517

KISH, J. G.
Advanced Rotorcraft Transmission (ART) Program summary
[AIAA PAPER 92-3365] p 905 A92-48938
Advanced Rotorcraft Transmission (ART) program summary
[NASA-TM-105665] p 680 N92-24984

KISHI, Y.
New-type of ultralight flexible a-Si solar cell and its application on an airplane p 970 A92-53181

KISHIMOTO, TAKUJI
Multidimensional Euler/Navier-Stokes analysis for hypersonic equilibrium gas
[SAE PAPER 912026] p 790 A92-45418

KISHIMOTO, YASUO
Application of the delta-operator in MIMO discrete-time adaptive flight control systems p 479 A92-29516

KISSLINGER, R. L.
Verification and validation of F-15 and S/MTD unique software p 921 A92-48515

KITAJIMA, M.
Numerical simulation of supersonic nozzle flow p 430 A92-30540

KITAPLIOGLU, CAHIT
Three-dimensional blade vortex interactions p 815 A92-46953

KITCHEN, E. H.
The application of a Navier-Stokes CFD method to civil engine intake flows p 769 N92-27471

KITOWSKI, J. V.
Fighter airframe/propulsion integration - A General Dynamics perspective
[AIAA PAPER 92-3332] p 850 A92-48915

KITTL, PABLO A.
Mechanics Pan-America 1991; Pan-American Congress of Applied Mechanics, 2nd (PACAM II), Universidad Tecnica, Valparaiso, Chile, Jan. 2-5, 1991, Selected and Revised Proceedings p 673 A92-39930

KIURKCHAN, A. G.
Decoupling of antennas using periodic structures p 725 A92-42634

KJOME, N. T.
A valve-down technique for small balloons
[AIAA PAPER 91-3681] p 15 A92-11025

KLANN, GARY A.
Contingency power for a small turboshaft engine by using water injection into turbine cooling air
[NASA-TM-105680] p 871 N92-29661

KLARER, P. R.
Techniques for autonomous navigation
[DE92-013458] p 957 N92-31746

KLAVETTER, E. A.
In situ measurement of particle formation in heated jet fuels: A new application of photon correlation spectroscopy
[DE92-003641] p 488 N92-20132
Monitoring jet fuel degradation using quartz crystal microbalances
[DE92-004730] p 489 N92-20858
KLAVETTER, ELMER
Advanced thermally stable, jet fuels development program annual report. Volume 1: Model and experiment system development
[AD-A249625] p 988 N92-31462
KLEB, W. L.
Temporal adaptive Euler/Navier-Stokes algorithm involving unstructured dynamic meshes
p 812 A92-46887
KLEB, WILLIAM L.
Characteristics of the Shuttle Orbiter leeside flow during a reentry condition
[AIAA PAPER 92-2951] p 821 A92-47915
A high angle of attack inviscid shuttle orbiter computation
[NASA-TM-107606] p 685 N92-25964
Unstructured-grid methods development for unsteady aerodynamic and aeroelastic analyses
p 718 N92-27938
KLEBELSBERG, ANJA
Measurements in the inhomogeneous convective boundary layer using three powered gliders
p 775 N92-26350
KLEIN, K.
Construction of a real-time DGPS experimental system
p 840 A92-47631
KLEIN, VLADISLAV
Aerodynamic parameters of the X-31 drop model estimated from flight-data at high angles of attack
[AIAA PAPER 92-4357] p 1080 A92-55343
KLEINLE, MARK
A lightweight loudspeaker for aircraft communications and active noise control p 1125 N92-32964
KLEMBOWSKI, WIESLAW
Polish radar technology. II - Adaptive radar AVIA CM
p 39 A92-12290
Polish radar technology. III - Weather channel for primary surveillance radar p 40 A92-12291
KLEMM, R.
Adaptive airborne MTI with two-dimensional motion compensation p 102 A92-17240
KLEPL, M. J.
A flutter suppression system using strain gages applied to Active Flexible Wing Technology - Design and test
[AIAA PAPER 92-2098] p 566 A92-35669
KLEUSBERG, ALFRED
Dredging research program: Global positioning system bibliography
[AD-A248954] p 729 N92-28079
KLEVENOW, F. T.
Automated composite ellipsoid modelling for high frequency GTD analysis
[NASA-CR-189853] p 275 N92-17316
KLEYN, B.
Manufacture of XD gamma titanium aluminide airfoils via investment casting and machining
p 494 A92-30603
KLIMA, STANLEY J.
NDE of advanced turbine engine components and materials by computed tomography
[ASME PAPER 91-GT-287] p 152 A92-15681
KLINE, PAUL A.
Availability of positioning and receiver autonomous integrity monitoring for the global positioning system
p 100 A92-16963
KLINGE, MARK D.
Some practical aspects of viscous drag reduction concepts
[SAE PAPER 912129] p 618 A92-39976
KLINGLE-WILSON, D.
Characteristics of thunderstorm-generated low altitude wind shear - A survey based on nationwide terminal Doppler weather radar testbed measurements
p 45 A92-11378
KLINGLE-WILSON, D. L.
A comparison of the performance of two gust front detection algorithms using a length-based scoring technique
[AD-A250862] p 1004 N92-32103
KLUTE, S. M.
Pitch-up motions of delta wings
[AIAA PAPER 92-0278] p 318 A92-25732
KLYDE, DAVID H.
Aeroservoelastic stabilization techniques for hypersonic flight vehicles
[AIAA PAPER 91-5056] p 203 A92-17839
Effects of cockpit lateral stick characteristics on handling qualities and pilot dynamics
[NASA-CR-4443] p 878 N92-28584
KNABE, F.
Image-supported navigation for testing instrument landing systems p 189 N92-14012
KNEELING, W. D.
Modeling supersonic inlet boundary layer bleed roughness
[AIAA PAPER 92-0269] p 317 A92-25725
Evaluation of two flow analyses for subsonic diffuser design
[AIAA PAPER 92-0273] p 317 A92-25727
KNIEF, RONALD A.
Risk management - Expanding horizons in nuclear power and other industries
[ISBN 1-56032-231-4] p 993 A92-51438
KNIGHT, D.
A three-dimensional supersonic turbulent boundary layer generated by an isentropic compression
[AIAA PAPER 92-0310] p 320 A92-25758
Interaction between crossing oblique shocks and a turbulent boundary layer p 812 A92-46882
KNIGHT, D. D.
Structure of crossing-shock wave/turbulent boundary-layer interactions
[AIAA PAPER 92-3670] p 1022 A92-54113
KNIGHT, DOYLE
Numerical investigation of bleed on three-dimensional turbulent interactions due to sharp fins
p 5 A92-11062
KNIGHT, DOYLE D.
Structure of supersonic turbulent flow past a swept compression corner p 431 A92-31155
KNIGHT, NORMAN F., JR.
Global/local methods research using the CSM testbed
p 1107 N92-32528
Computational methods for global/local analysis
[NASA-TM-107591] p 1125 N92-33104
KNIGHT, PAUL D.
Design considerations for a modern telemetry processing and display system p 882 A92-47584
KNIPP, DARREN
Preliminary design studies of an advanced general aviation aircraft
[NASA-CR-190024] p 461 N92-20064
KNOSPE, C. R.
Stability and performance of notch filter control for unbalance response p 771 N92-27731
Design of bearings for rotor systems based on stability
p 773 N92-27799
KNOSPE, CARL R.
Pulse response method for vibration reduction in periodic dynamic systems p 661 A92-39909
KNOTT, M. J.
Transonic aeroelastic calculations in both the time and frequency domains p 720 N92-27950
KNOTT, P. G.
Configuration effects on the ingestion of hot gas into the engine intake p 842 A92-45315
Some implications for advanced STOVL operation from invincible class ships p 466 N92-21971
KNOWLEN, CARL
Theoretical and experimental investigation of the thermodynamics of the thermally choked ram accelerator p 604 N92-22137
KNOWLES, GARETH J.
Application of nonlinear control strategies to aircraft at high angle of attack p 26 A92-11329
KNOWLES, K.
Computation of normal impinging jets in cross-flow and comparison with experiment p 250 A92-22446
A review of impinging jets in cross-flows - Experimentation and computation
[AIAA PAPER 92-0633] p 333 A92-27011
Recent research into the aerodynamics of ASTOVL aircraft in ground environment p 623 A92-40549
KNOX, FRED D.
X-31 flight test update p 645 A92-40034
KNUTSON, B. W.
X-ray computed tomography for the aircraft/aerospace industry p 492 A92-28750
KNYSH, IU.
Carcinogenic hydrocarbons emission with gas-turbine engines exhaust gases p 504 A92-29726
KO, B. N.
Solid-fuel ramjet fuel regression rate/thrust modulation
p 666 A92-36966
KO, FRANK
Engine panel seals for hypersonic engine applications: High temperature leakage assessments and flow modelling
[NASA-TM-105260] p 298 N92-16336
High temperature dynamic engine seal technology development
[NASA-TM-105641] p 596 N92-23435
KO, MALCOLM K. W.
Impact of heterogeneous chemistry on model-calculated ozone change due to high speed civil transport aircraft
p 45 A92-12941
The atmospheric effects of stratospheric aircraft: A first program report
[NASA-RP-1272] p 408 N92-19121
Ozone response to aircraft emissions: Sensitivity studies with two-dimensional models p 409 N92-19126
KO, S. H.
Thermal details in a rotor-stator cavity at engine conditions with a mainstream
[ASME PAPER 91-GT-275] p 151 A92-15672
Turbine disk temperatures resulting from the hot mainstream at engine conditions
[AIAA PAPER 92-0398] p 373 A92-26252
KO, WILLIAM L.
Combined compressive and shear buckling analysis of hypersonic aircraft sandwich panels
[AIAA PAPER 92-2487] p 586 A92-34603
KOBAYAKAWA, MAKOTO
Predicted pressure distribution on a prop-fan blade through Euler analysis p 810 A92-46791
KOBAYASHI, A. S.
Tear straps in airplane fuselage
[AD-A248543] p 854 N92-29511
KOBAYASHI, H.
A conceptual study for future engine test facility
[AIAA PAPER 92-3992] p 1099 A92-56815
KOBAYASHI, HIROMI
A study on the rotating stall of centrifugal compressors. II - Effect of vaneless diffuser inlet shape on rotating stall p 497 A92-32508
KOBAYASHI, ICHIZO
Digital mapping display technology
p 735 A92-43225
KOBAYASHI, M. H.
Predictions of compressible viscous flows at all Mach number using pressure correction, collocated primitive variables and non-orthogonal meshes
[AIAA PAPER 92-0426] p 326 A92-26274
KOBAYASHI, MAKOTO
Aerodynamic design of an advanced turboprop using Euler codes p 737 A92-43196
KOBAYASHI, OSAMU
Static and dynamic flight-path stability of airplanes
p 977 A92-52043
Estimation of aerodynamic characteristics from flight-test data. I - Multicollinearity in the equation error method p 960 A92-53007
A physical approach to the estimation of aerodynamic characteristics from flight data p 1030 A92-56058
KOBAYASHI, R.
The low-turbulence wind tunnel at Tohoku University
p 623 A92-40598
Tohoku University low-turbulence wind tunnel
[AIAA PAPER 92-3913] p 1095 A92-56746
KOBAYASHI, REIMON
Impact response of composite UHB propeller blades
[SAE PAPER 912046] p 861 A92-45430
KOBAYASHI, TOMOYUKI
Fabrication test and evaluation of graphite/PMR-15 polyimide for HOPE primary structure
p 1105 A92-53516
Design of orbital re-entry experiment vehicle and outline of the experiment p 667 N92-25374
KOBE, A.
Using helicopters for coastal alert p 723 A92-43164
KOBYZHSKII, S.
Experimental investigation of liquid carbonhydrogen fuel combustion in channel at supersonic velocities
[AIAA PAPER 92-3429] p 894 A92-48986
KOBYZHSKII, S. A.
An experimental study of supersonic H2 combustion and heat transfer in a circular duct p 388 A92-25997
KOC, A.
Hypersonic flow past radiation-cooled surfaces
[MBB-FE-202-S-PUB-0468-A] p 832 N92-29713
KOCAAYDIN, C. S.
Some aerodynamic mechanisms of impulsive noise during blade-vortex-interaction p 604 A92-35782
KOCH-PETERS, DOROTHEA
Materials and Structures Research Department: Scientific report (1990)
[ETN-92-90727] p 466 N92-22000
KOCH, J.-U.
Report of the working group Future CNS Systems - Applications and impact on the German air transport system p 266 A92-21325
KOCH, PAUL A.
Flight testing of a half-scale remotely piloted vehicle
[AD-A248568] p 733 N92-28123
KOCUREK, J. DAVID
Rotorwash computer model: User's guide
[DOT/FAA/RD-90/25] p 346 N92-18345

KOCZAK, M. J.
The microstructural stability of TiC reinforced rapidly solidified Al-Fe-V-Si composite structures p 141 A92-15169
KOCZO, STEVE
A DSP-based microwave landing system (MLS) post-IF processor p 955 A92-49306
KODA, TOSHIHIDE
Reduction of torque pulsation of Stirling engine-compressor system p 992 A92-50785
KODAMA, HIDEKAZU
Unsteady lifting surface theory for a rotating transonic cascade of swept blades
[ASME PAPER 91-GT-178] p 73 A92-15610
Application of non-reflecting boundary conditions to three-dimensional Euler equation calculations for thick strut cascades
[AIAA PAPER 92-3045] p 822 A92-48705
KODAMA, MASARU
Numerical simulation of a supersonic jet impingement on a ground
[SAE PAPER 912014] p 789 A92-45412
KODAMA, YOSHIAKI
Research activities on CFD at the Ship Research Institute p 766 N92-26908
KODIYALAM, SRINIVAS
Shape optimization of three-dimensional structures with adaptive meshing
[AIAA PAPER 92-2434] p 586 A92-34548
KOECHLER, CLAUDIO
Time Resolved Lidar Fluorosensor operating from helicopter p 1121 A92-56296
KOEHLER, GRANT
Scorpion: Close Air Support (CAS) aircraft
[NASA-CR-189974] p 462 N92-20664
KOENIG, G.
Probabilistic lifing approach for aero engine disks made of powder nickel base alloys containing ceramic defects p 226 N92-14424
KOENIG, K.
Comparative study of fatigue in various materials and designs under sonic loading p 287 A92-21003
KOENIG, KLAUS
Short time force measurement system p 208 N92-15001
KOENIG, P.
BMI/bis (allylphenoxyphthalimide)-copolymers - A new family of resins for advanced composites with improved thermal oxidative stability p 33 A92-10213
KOENIG, R.
ATTAS flight test and simulation results of the advanced gust management system LARS
[AIAA PAPER 92-4343] p 1079 A92-55332
KOERT, PETER
Power beaming - Energy transmission at 35 GHz and higher frequencies
[AIAA PAPER 92-2027] p 471 A92-29944
KOESTER, KENNETH L.
Talons 95 GHz radar sensor for autonomous landing guidance p 1063 A92-55908
KOGA, KAZUYA
An experimental study on variable pressure hydraulic flight control system p 1084 A92-56119
KOGAN, A.
The calculation of incompressible separated turbulent boundary layers p 1003 N92-31886
KOGANE, SHIN
Engine maintenance technology and its development p 516 A92-35918
KOHALMI, DIANE
A new development in embedded computer performance measurement p 921 A92-48506
A new approach to embedded computer performance measurement p 1005 A92-49288
KOHAMA, Y.
The low-turbulence wind tunnel at Tohoku University p 623 A92-40598
Tohoku University low-turbulence wind tunnel
[AIAA PAPER 92-3913] p 1095 A92-56746
KOHAMA, YASUAKI
Proceedings of the Seminar on Investigation and Control of Boundary-Layer Transition
[NAL-SP-11] p 400 N92-18483
Three dimensional boundary layer transition on a yawed cylinder p 766 N92-26909
KOHDA, TAKEHISA
Optimal design of wing shape by use of neural-network p 1054 A92-56112
KOHL, RONALD H.
Development of local nonintrusive measurements of inlet and exhaust flows for the ground testing of air-breathing engines
[AIAA PAPER 92-3899] p 1122 A92-56735
KOHRS, R.
On board planning of 4D-trajectories p 728 N92-27897
KOIFMAN, M.
Autonomously aided strapdown attitude reference system p 204 A92-18610
Estimation of aircraft attitude by angular rate measurements p 963 N92-31881
KOIKE, AKIRA
Results of measured temperature distribution on an adiabatic wing model with radiation thermometer
[NAL-TM-610] p 261 N92-17755
KOIVULA, JUHA
Development of a 3-D remote sensing radar p 597 A92-34908
KOJIMA, KUNIHIKO
Development of pre- and post-processor system for structural analysis
[NAL-TM-628] p 681 N92-25403
KOJIMA, TOSHIRO
Aeronautical satellite communications system p 1046 A92-56089
KOKOTOVIC, PETER V.
Nonlinear system design: Adaptive feedback linearization with unmodeled dynamics
[AD-A248484] p 1009 N92-30335
KOKUBUN, S.
Polar patrol balloon
[AIAA PAPER 91-3688] p 15 A92-11031
KOLAR, R.
A time-dependent tip loss formula for rotor blade dynamic analysis p 1057 A92-56310
KOLAR, RAMESH
Approach for analysis and design of composite rotor blades p 899 A92-46801
KOLARIK, W.
Electronics/avionics integrity - Definition, measurement and improvement p 1120 A92-56252
KOLB, MARK A.
Constraint-based component-modeling for knowledge-based design
[AIAA PAPER 92-1192] p 600 A92-33304
KOLDEN, JENNIFER
Propulsion system evaluation for an unmanned high altitude long endurance RPV
[ASME PAPER 91-GT-409] p 128 A92-15738
KOLINA, N. P.
A computational study of flow past bodies and heat transfer for isentropic compression flows p 425 A92-30158
The effect of the angle-of-attack on laminar-turbulent boundary transition near the lower surface of triangular plates in a supersonic gas flow p 426 A92-30180
KOLKMAN, H. J.
Examination of aircraft warning and caution lights after shock testing
[NLR-TP-89284-U] p 952 N92-30474
KOLOBKOV, A. N.
Optimization of a lifting surface for minimum induced drag p 437 A92-31853
KOLONAY, RAYMOND M.
Demonstration of structural optimization applied to wind-tunnel model design p 1119 A92-56181
KOLOSKOVA, V. N.
Thermal deformation of a polymer heat shield material on the descent trajectory p 754 A92-42655
KOMAI, I.
Combustion of solid fueled ramjet. II
[AIAA PAPER 92-3728] p 894 A92-49106
KOMATSU, MASATOMO
Active control of the hydraulic forces of a body by a splitter plate p 591 A92-36351
KOMATSU, N.
Measurement of position and attitude using laser and retro-reflectors p 1047 A92-56120
KOMATSU, YUKIO
Results of measured temperature distribution on an adiabatic wing model with radiation thermometer
[NAL-TM-610] p 261 N92-17755
KOMERATH, N. M.
An experimental and analytical study of the interaction of a vortex with an airframe
[AIAA PAPER 92-0319] p 321 A92-25766
Measurements of the inflow to a vibrating rotor blade
[AIAA PAPER 92-0634] p 333 A92-27012
Flow over a twin-tailed aircraft at angle of attack. I - Spatial characteristics p 702 A92-41229
Quantification of canard and wing interactions using spatial correlation velocimetry
[AIAA PAPER 92-2687] p 807 A92-45588
Flow over a twin-tailed aircraft at angle of attack. II - Temporal characteristics p 810 A92-46781
A multi-diagnostic approach to testing V/STOL craft
[AIAA PAPER 92-4008] p 1099 A92-56831
Definition of the unsteady vortex flow over a wing/body configuration
[NASA-CR-180083] p 178 N92-13995
KOMERATH, NARAYANAN M.
Measurements of the unsteady vortex flow over a wing-body at angle of attack
[AIAA PAPER 92-2729] p 808 A92-45598
Interaction between a rotor tip vortex and a separated flowfield p 814 A92-46947
Image processing in the undergraduate fluid dynamics laboratory
[AIAA PAPER 92-4020] p 1141 A92-56842
KOMODA, MASAKI
In-flight simulation of backside operating models using direct lift controller
[SAE PAPER 912069] p 872 A92-45450
An investigation of the automation of emergency landings for helicopters p 1083 A92-56026
Multiaxis control in longitudinal mode of aircraft p 1083 A92-56027
KOMOROWSKI, J. P.
Photoelastic coating study of CT-114 coupon joint test specimen for horizontal stabilizer rear attachment fitting to vertical stabilizer rear spar
[NRC-LTR-ST-1689] p 489 N92-21018
KOMOROWSKI, JERZY P.
Enhanced visual technique for rapid inspection of aircraft structures p 214 A92-17290
KOMPANETS, V. K.
Technical tools of test automation for gas-turbine engines based on cluster CAMAC modules with an increased number of channels p 980 A92-51348
KOMPELLA, MURTY S.
The development of multiple-input models for airborne noise prediction p 695 A92-39243
KOMURO, TOMOYUKI
Effectiveness of plasma torches for ignition and flameholding in scramjet p 737 A92-44524
Flow measurements in scramjet inlets p 1102 A92-53565
KONDO, HIROHUMI
On the effect of canards on NAL spaceplane model (0 order) in low speed area p 1030 A92-56052
KONDO, KIMIO
ETS-V/EMSS mobile satellite communication experiments p 395 A92-26776
KONDO, T.
Research on state equations of unsteady aerodynamics p 709 A92-43132
KONDRAT'EV, I. A.
A heat flow peak on the upwind surface of a blunt-leading-edge delta wing p 438 A92-31862
KONDRAT'EVA, N. E.
Methods for determining atmospheric correction for radio-rangefinder measurements of inclined trajectories p 775 A92-44070
KONDRATENKOV, V. A.
Using the simulation modeling method to estimate the reliability of the crew-flight vehicle system p 1133 A92-57444
KONG, RUILIAN
Vibration characteristic analysis of a propeller blade p 38 A92-10967
KONONOV, K. M.
Technique for estimating the strength of gas turbine guide vanes with stress raisers p 761 A92-42653
KONOVALOV, S. F.
Characteristics of transonic flow past a configuration comprising a wing and a fuselage with a large midsection ratio p 439 A92-31882
Effect of the fuselage midsection ratio on the character of wing-fuselage aerodynamic interference p 439 A92-31883
KONRAD, W.
A three-dimensional supersonic turbulent boundary layer generated by an isentropic compression
[AIAA PAPER 92-0310] p 320 A92-25758
KONSTANTAKIS, GEORGE C.
NASA advanced aeronautics design solar powered remotely piloted vehicle
[NASA-CR-190007] p 462 N92-20665
KOOB, GARY M.
The Office of Naval Research initiative on ultradependable multicomputers and electronic systems p 1005 A92-49278
KOOI, J. W.
Application of electronically scanned pressure measurement system for engine simulation tests in the German-Dutch Wind Tunnel
[AIAA PAPER 92-4003] p 1122 A92-56826
Comparison of LDA and LTA applications for propeller tests in wind tunnels
[NLR-MP-88031-U] p 827 N92-28658
KOOL, G. A.
NLR experience with high velocity burner rig testing, 1979-1989
[NLR-TP-89152-U] p 385 N92-18415
Diffuser casing upgrade for an advanced turbofan
[NLR-TP-90097-U] p 870 N92-28711

KOONCE, JEFFERSON M.
Development of the Basic Flight Instruction Tutoring System (BFITS)
[AD-A246458] p 751 N92-27836
KOONTZ, STEVEN L.
Atmospheric pressure flow reactor: Gas phase chemical kinetics under tropospheric conditions without wall effects
[NASA-CASE-MSC-21384-1] p 297 N92-16243
KOPCHENOV, V. I.
The enhancement of the mixing and combustion processes in supersonic flow applied to scramjet engine
[AIAA PAPER 92-3428] p 1112 A92-54029
KOPEIKA, N. S.
Numerical calculation of modulation transfer functions for low frequency mechanical vibrations
p 235 A92-19982
KOPPENWALLNER, GEORG
FALKE and COBRA technology development in aerodynamics and aerothermodynamics
p 183 N92-15017
Behaviour and modelling of the aerothermodynamics of ballistic entry vehicles in the high altitude flow regimes
p 184 N92-15031
Review of the European hypersonic wind tunnel performance and simulation requirements
p 209 N92-15043
KOPPERNAES, CHRISTIAN
Measurement of basic material and processing properties affecting injection-pultrusion technology
p 580 A92-32636
KOPRIVA, DAVID A.
Multidomain spectral solutions of high-speed flows over blunt cones
[AIAA PAPER 92-0324] p 322 A92-25771
Spectral solution of inviscid supersonic flows over wedges and axisymmetric cones p 524 A92-36359
KORAKIANITIS, T.
On the prediction of unsteady forces on gas turbine blades. I - Description of the approach. II - Analysis of the results p 311 A92-24724
KORDULLA, W.
Comparison of solution of various Euler solvers and one Navier-Stokes solver for the flow about a sharp-edged cropped delta wing
[AD-B163639L] p 83 N92-12998
KOREJWO, H. A.
Ground test facilities for aerothermal and aero-optical evaluation of hypersonic interceptors
[AIAA PAPER 92-1074] p 573 A92-33244
KOREN, S.
Measurements of lateral aerodynamics characteristics of forebodies at high angle of attack in subsonic and transonic flows
[AIAA PAPER 92-0174] p 255 A92-23785
KORIVI, V. M.
Observations on computational methodologies for use in large-scale, gradient-based, multidisciplinary design incorporating advanced CFD codes
[NASA-TM-104206] p 630 N92-24956
KORIVI, VAMSHI M.
Taylor series approximation of geometric shape variation for the Euler equations p 899 A92-46916
Methodology for calculating aerodynamic sensitivity derivatives p 1024 A92-54911
KORIVI, VAMSHI MOHAN
An incremental strategy for calculating consistent discrete CFD sensitivity derivatives
[NASA-TM-104207] p 625 N92-24681
KORKACH, V. G.
Transverse correlation of the spectral components of pressure fluctuations on a plate ahead of a step
p 426 A92-30187
KORKAN, KENNETH
Experimental study of performance degradation of a rotating system in the NASA Lewis RC icing tunnel
[NASA-CR-190684] p 1102 N92-34141
KORKAN, KENNETH D.
Study of theoretical and wind tunnel results on flight performance degradation due to leading edge rime ice accretion
[AIAA PAPER 92-0038] p 262 A92-22158
KORNILOV, V. I.
A method for the optical measurement of surface friction in supersonic flow p 337 A92-27537
KOROITAMANA, JONE
A view from the Pacific Basin p 532 A92-33440
KOROLEV, A. S.
The lift-drag ratio of a slender cone in viscous hypersonic gas flow p 425 A92-30172
KORTE, JOHN J.
Numerical simulation of the actuation system for the ALDF's propulsion control valve p 41 A92-13204
Implementation of Vigneron's streamwise pressure gradient approximation in the PNS equations
[AIAA PAPER 92-0189] p 256 A92-23798
Aerodynamic design of axisymmetric hypersonic wind-tunnel nozzles using least-squares/parabolized Navier-Stokes procedure
[AIAA PAPER 92-0332] p 322 A92-25779
Least-squares/parabolized Navier-Stokes procedure for optimizing hypersonic wind-tunnel nozzles
p 980 A92-50270
CAN-DO, CFD-based Aerodynamic Nozzle Design and Optimization program for supersonic/hypersonic wind tunnels
[AIAA PAPER 92-4009] p 1033 A92-56832
KORTING, P. A. O. G.
Symposium on High Speed Airbreathing Propulsion: The Solid Fuel Combustion Chamber and Beyond
[ETN-92-90685] p 575 N92-22268
KOSAI, M.
Tear straps in airplane fuselage
[AD-A248543] p 854 N92-29511
KOSCHEL, W.
Design considerations for nozzles of hypersonic airbreathing propulsion
[AIAA PAPER 91-5019] p 471 A92-31685
Application of finite element method to hypersonic nozzle flow computations p 769 N92-27479
KOSHELYAEVSKY, N. B.
Comparison of GLONASS and GPS time transfers between two west European time laboratories and VNIIFTRI p 1050 N92-33381
KOSHEVOI, VSEVOLOD N.
Fundamentals of applied aerogasdynamics. II - Viscous flow past bodies. Control devices p 64 A92-14281
KOSHIOKA, Y.
Aerodynamic characteristics of a high-speed composite airfoil p 712 A92-43231
KOSHORST, J.
Advanced composite components in airline service status and repair p 785 A92-47416
KOSINOV, A. D.
Effect of a fan of rarefaction waves on the development of disturbances in a supersonic boundary layer
p 809 A92-46519
KOSITSKY, J.
On the accuracy of an aircraft-borne ambient electric-field measuring system p 186 A92-20127
KOSMATKA, J. B.
On the behavior of pretwisted beams with irregular cross-sections p 495 A92-31564
Flexure-torsion behavior of sheat-deformable beams with applications to aircraft wing sections
[AIAA PAPER 92-2467] p 582 A92-34357
KOSOVIC, BRANKO
Minimization of the number of cooling holes in internally cooled turbine blades
[ASME PAPER 91-GT-52] p 121 A92-15530
KOSOWSKI, JANALEE M.
EICAS in an integrated cockpit p 855 A92-44922
KOSTEN, SUE E.
Modifications to the rapid melt/rapid quench and transparent polymer video furnaces for the KC-135
[NASA-CR-184215] p 157 N92-12231
KOSTENKO, P. P.
A model of the operation of the pulsejet engine and a study of its characteristics p 657 A92-40608
KOSTOPOULOS, V.
Jet fuel absorption and dynamic mechanical analysis of carbon fibre composites p 1110 N92-33050
KOSYKH, A. P.
Aerodynamic characteristics of slender sharp-leading-edge delta wings with air scooping through the air intake at hypersonic velocities. I
p 427 A92-30206
Aerodynamic characteristics of a blunt delta wing with air bleed through an intake at supersonic and hypersonic velocities. II p 437 A92-31855
KOTAKE, MUTSUO
Experimental investigation of the boundary layer in a corner formed by two circular arc airfoils
p 1029 A92-56046
KOTELKIN, V. D.
Construction of aerodynamic profiles
p 315 A92-25299
KOTLAR, ANTHONY J.
Application of digital measurement techniques to analysis of range shadowgraphs
[AD-A241554] p 139 N92-13080
KOTOV, V. M.
Aerodynamics of complex shape bodies within a wide range of supersonic flows of rarefied gases
p 939 A92-52767
KOTOVSKII, V. N.
Mathematical modeling of nonstationary viscous flow over a solid angle of finite span p 440 A92-31890
KOTTAPALLI, SESI
Analytical aeroelastic stability considerations and conversion loads for an XV-15 tilt-rotor in a wind tunnel simulation
[AIAA PAPER 92-2258] p 540 A92-34413
Blade root torsional dampers to reduce hub loads
[AIAA PAPER 92-2449] p 541 A92-34476
Analysis of open loop higher harmonic control at high airspeeds on a modern four-bladed articulated rotor
[AIAA PAPER 92-2450] p 542 A92-34477
Analysis of open loop higher harmonic control at high airspeeds on a modern four-bladed articulated rotor
[NASA-TM-103876] p 21 N92-11000
KOUL, A. K.
Inspection of compressor discs by ultrasonic leaky waves using an automated C-scan system
p 144 A92-13584
KOURA, KATSUHIKA
Rarefied gas numerical wind tunnel
p 1017 A92-53552
KOURA, KATSUHISA
Rarefied gas numerical wind tunnel
p 995 A92-52763
Direct simulation of vortex shedding in dilute gas flows past bluff bodies p 939 A92-52766
KOURTA, A.
Performance of turbulence models to predict supersonic boundary layer flows p 613 A92-37553
KOURTIDES, D. A.
Thermal response of rigid and flexible insulations and reflective coating in an aeroconvective heating environment
[NASA-TM-103925] p 852 N92-28721
KOUTMOS, P.
Isothermal modeling of gas turbine combustors - Computational study p 129 A92-17203
KOUZUMA, S.
New-type of ultralight flexible a-Si solar cell and its application on an airplane p 970 A92-53181
KOVACH, KARL
SATZAP - A novel approach to GPS integrity
p 99 A92-16947
KOVAL'NOGOV, S. A.
Experimental investigation of the air bypass effect in the shock-wave region on the aerodynamic characteristics of a wing profile p 439 A92-31877
Investigation of the aerodynamic features of flows past models using thin-film capacitance-type sensors of pressure oscillations p 440 A92-31884
KOVALENKO, V. M.
Base pressure on an axisymmetric finned body during forced rotation in the autorotation regime
p 7 A92-12165
KOVALENKO, V. V.
Computational studies of the aerodynamic characteristics of delta wings with a subsonic leading edge p 439 A92-31874
KOVALEV, V. A.
Several results of lidar measurements of the characteristics of oblique visibility at an airfield
p 45 A92-12844
KOVALEVA, N. A.
The effect of the angle-of-attack on laminar-turbulent boundary transition near the lower surface of triangular plates in a supersonic gas flow p 426 A92-30180
KOVALEVSKII, A. K.
Selection of efficient primary-structure/force configurations for aircraft lifting surfaces subjected to displacement constraints p 458 A92-30140
KOVALEVSKII, V. P.
Gas-generator with high-temperature path ceramic components
[ASME PAPER 91-GT-152] p 148 A92-15594
KOVBASKO, O. N.
Dynamic synthesis of mechanical systems with a finite number of degrees of freedom p 603 A92-33790
KOVENIA, V. M.
On marching algorithms for solving stationary problems p 311 A92-24976
KOWAL, BRIAN F.
C-17 flight control system overview
p 1082 A92-55906
KOWALSKI, EDWARD J.
Propulsion system evaluation for an unmanned high altitude long endurance RPV
[ASME PAPER 91-GT-409] p 128 A92-15738
KOYAMA, H.
Transient aerodynamic behaviours associated with stepwise incidence variation of airfoils
p 66 A92-15327
KOYAMA, T.
New 1.27-m leg of the National Aerospace Laboratory hypersonic wind tunnel p 1092 A92-56003

KOYAMA, TADAO
Aerodynamic heating characteristics of space planes tested by NAL hypersonic wind tunnel
p 1017 A92-53547
KOZAROV, M.
Linear panel flutter of an elliptic cylindrical shell
p 291 A92-21216
KOZEL, KAREL
Numerical solution of steady incompressible viscous flows over airfoils p 8 A92-12649
KOZLOV, V. V.
Control of laminar boundary layer separation
p 393 A92-24980
KOZLOVA, Z. M.
Oscillations of balloon-flight altitude
p 836 A92-46660
KOZOL, J.
In-service evaluation of 2090 aluminum-lithium alloy on F/A-18 aircraft
[AD-A248472] p 986 N92-30321
KRAEMER, E.
Complete Euler-solution for a rotor in hover and a propeller in forward flight p 520 A92-35755
KRAEMER, JOHN H.
RAIM - Will it meet the RTCA GPS minimum operational performance standards? p 96 A92-16635
KRAEUTLE, K.
Supersonic flow mixing and combustion using RAMP nozzle
[AIAA PAPER 92-3840] p 1113 A92-54198
KRAEUTLE, K. J.
Effect of carbon particles and mixing on afterburning of exhaust plumes
[AIAA PAPER 92-0767] p 387 A92-27107
KRAFT, R. E.
Design and performance of duct acoustic treatment
p 236 N92-14783
KRAINIUKOV, N. I.
Holographic-interferometry methods employed for vibration-strength testing of aviation-engine workpieces
p 219 A92-20771
KRAL, L. D.
Development and application of a zonal k-epsilon turbulence model for complex 3-D flowfields
[AIAA PAPER 92-3176] p 903 A92-48792
KRAMER, BRIAN R.
Forebody vortex control for suppressing wing rock on a highly-swept wing configuration
[AIAA PAPER 92-2716] p 803 A92-45555
KRAMER, JANE R.
Structural tailoring/analysis for hypersonic components - Executive system development
[AIAA PAPER 92-2471] p 583 A92-34360
KRAMER, MARK T.
Aviation Diagnostics And Maintenance (ADAM) system preliminary concept of operation and functional description
[AD-A242598] p 170 N92-14966
KRAMMER, J.
First approach to an integrated fin design
p 551 N92-23236
Practical architecture of design optimisation software for aircraft structures taking the MBB-Lagrange code as an example p 851 N92-28471
Concurrent engineering in design of aircraft structures
[MBB-FE-2-S-PUB-472] p 854 N92-29650
KRAMMER, PAUL
Saenger and the German Hypersonics Technology Programme - Status report 1991
[IAF PAPER 91-198] p 32 A92-12570
KRANTZ, T. L.
Advanced Rotorcraft Transmission (ART) Program summary
[AIAA PAPER 92-3365] p 905 A92-48938
Advanced Rotorcraft Transmission (ART) program summary
[NASA-TM-105665] p 680 N92-24984
KRANTZ, TIMOTHY
Dynamics of a split torque helicopter transmission
[NASA-TM-105681] p 910 N92-29136
KRANTZ, TIMOTHY L.
Gear tooth stress measurements of two helicopter planetary stages
[NASA-TM-105651] p 764 N92-26555
KRASIL'NIKOV, A. V.
Experimental studies of the interaction of converging axisymmetric shock waves with sharp and blunt cones in supersonic flow p 63 A92-13749
KRASNOV, NIKOLAI F.
Fundamentals of applied aerogasdynamics. I - Aerodynamics of wings (profiles), airframes, and their combinations p 64 A92-14280
Fundamentals of applied aerogasdynamics. II - Viscous flow past bodies. Control devices p 64 A92-14281
KRASNOWSKI, BOGDAN R.
Reliability of helicopter composite dynamic components p 145 A92-14344
KRASOVSKAIA, I. V.
Interaction between a body flying at a supersonic velocity and a point explosion p 1019 A92-53867
KRASOWSKI, MICHAEL J.
Wavelength-multiplexed fiber-optic position encoder for aircraft control systems p 734 A92-42602
KRASZNAY, STEPHEN
Pocono Mountain SAR data analysis for testing slant range to ground range conversion p 587 A92-35142
KRAULAND, KONRAD L.
Universal weaving for turbine engine composite preforms
[AD-A237667] p 202 N92-14059
KRAUS, W.
X-31: Discussion of steady state and rotary derivatives
p 365 N92-18789
KRAUS, WERNER
Aerodynamic development of the X-31 aircraft for the high angle of attack region
[MBB-FE211-S-PUB-452] p 275 N92-17313
KRAUSE, E.
The calculation of a compressible boundary layer past a pointed body and a delta wing p 622 A92-40173
KRAUSE, F. H.
High-speed civil transport aircraft emissions
p 408 N92-19122
KRAUSE, JAMES M.
Thermal control for hypersonic vehicle propulsion
p 468 A92-29356
KRAUSS, J. K.
Low density real gas flows about hypersonic vehicles
[AD-A250048] p 949 N92-31777
KRAUSS, R. H.
Evaluation of OH laser-induced fluorescence techniques for supersonic combustion diagnostics
[AIAA PAPER 92-0508] p 396 A92-26935
KrF laser-induced OH fluorescence imaging in a supersonic combustion tunnel
[AIAA PAPER 92-3346] p 905 A92-48923
A clean air continuous flow propulsion facility
[AIAA PAPER 92-3912] p 1094 A92-56745
KRAUSS, ROLAND H.
Experimental investigation of a supersonic combustion flowfield employing staged transverse injection behind a rearward-facing step
[AIAA PAPER 92-0090] p 292 A92-22196
KRAVCHENKO, I. V.
On the experimental investigation of air-breathing engine of new schemes p 469 A92-29711
KRAVCHENKO, S. A.
Calculation of three-dimensional separated flows in the framework of the unsteady Euler equations
p 438 A92-31870
KRAVETZ, J.
Fly-by-light technology development plan
[NASA-CR-181954] p 1086 N92-32778
KRECH, R. H.
Aerothermodynamic radiation studies
[NASA-CR-185666] p 284 N92-15998
KREIMENDAHL, BRYAN W.
Composite material stub-blade wing joint
p 763 A92-44618
KREJSA, E. A.
Computation of supersonic jet mixing noise for an axisymmetric CD nozzle using k-epsilon turbulence model
[AIAA PAPER 92-0500] p 414 A92-26328
KREJSA, EUGENE A.
A survey of the broadband shock associated noise prediction methods
[AIAA PAPER 92-0501] p 415 A92-26930
Computation of supersonic jet mixing noise for an axisymmetric CD nozzle using k-epsilon turbulence model
[NASA-TM-105338] p 237 N92-14795
A survey of the broadband shock associated noise prediction methods
[NASA-TM-105365] p 237 N92-14797
KREPEC, T.
Application of a double actuator electronic fuel control unit on a small gas turbine engine
[SAE PAPER 912160] p 655 A92-39993
KRICKE, DIETER
Use of a virtual cockpit for the development of a future transport aircraft p 886 N92-28547
KRIEBEL, J.
Hypersonic plasma predictions at nonzero angle of attack
[AIAA PAPER 92-3027] p 925 A92-47028
KRIEBEL, JAMIE
Computations of hypersonic flows around a three-dimensional concave/convex body
[AIAA PAPER 92-2606] p 805 A92-45570
KRIJN, ROBERT
Results of a test program for the use of differential GPS for approach guidance p 101 A92-16969
Approach flight trials in the Netherlands for the Navstar GPS Joint Program Office International Test Program
p 533 A92-35928
KRISHEN, KUMAR
Issues in developing control zones for international space operations p 1141 A92-56602
KRISHNA, H. R.
Self reliance in aerospace structures
p 758 A92-41190
KRISHNAKUMAR, K.
Robust wind shear stochastic controller-estimator
p 661 A92-39893
Control system optimization using genetic algorithms
p 661 A92-39900
Robust flight reconstruction for helicopter simulation and training p 747 A92-41230
KRISHNAMURTHY, M.
A correlation study of the wing-body interference factor for high angles of attack p 700 A92-41179
KRISHNAMURTHY, T.
An independent refinement and integration procedure in multiregion finite element analysis
[AIAA PAPER 92-2290] p 582 A92-34307
Coupled 2D-3D finite element method for analysis of a skin panel with a discontinuous stiffener
[AIAA PAPER 92-2474] p 583 A92-34363
KRISHNAN, R.
On the interaction between first- and second-mode waves in a supersonic boundary layer
p 78 A92-16462
KRISHNAPPA, G.
Preliminary analysis of baseline vibration data from Allison T56-A-14LFE engine and reduction gearbox
[NRC-31578] p 130 N92-11999
A preliminary study in the use of phase demodulation techniques for the analysis of gear vibration data
[NRC-32083] p 1002 N92-31469
KRISHNAPRASAD, P. S.
A multibody analog of the dual-spin problem
p 49 A92-11426
KRISTENSEN, L.
Surface-layer gusts for aircraft operation
p 774 A92-42095
KRIUCHENKO, V. V.
Aerospace plane hydrogen scramjet boosting
[SAE PAPER 912071] p 891 A92-45451
KRIVENTSEV, V. I.
A criterion for estimating the economic and operational efficiency of the power distribution systems of commercial aircraft p 657 A92-40611
KROGMANN, UWE K.
Introduction to neural computing and categories of neural network applications to guidance, navigation and control p 234 N92-14674
KROLL, N.
Steps towards an efficient and accurate method solving the Euler equations around a re-entry configuration at super- and hypersonic speed p 181 N92-14987
KROLL, NORBERT
An examination of several high resolution schemes applied to complex problems in high speed flows
[AD-A250814] p 1124 N92-32632
KRONE, NORRIS J., JR.
EVS could expand all-weather landing capability of airliners p 556 A92-36125
KROO, ILAN
Navier-Stokes analysis of blunt trailing edge airfoils
[AIAA PAPER 92-0024] p 248 A92-22146
Vortex-in-cell analysis of wing wake roll-up
[AIAA PAPER 92-2703] p 801 A92-45545
Nonlinear aerodynamics and the design of wing tips
[NASA-CR-190649] p 946 N92-31157
KROO, ILAN M.
An interactive system for aircraft design and optimization
[AIAA PAPER 92-1190] p 600 A92-33302
Transonic wind tunnel test of a 14 percent thick oblique wing
[NASA-TM-102230] p 950 N92-32213
KROPFLI, R. A.
Progress report on analysis of differential attenuation radar data obtained during WISP-91
[PB92-133800] p 503 N92-21828
KROTHAPALLI, A.
Unsteady flow past an airfoil pitching at a constant rate p 610 A92-36826
The enhancement of mixing in high-speed heated jets using a counterflowing nozzle
[AIAA PAPER 92-3262] p 825 A92-48857
KROTHAPALLI, ANJANEYULU
Experimental observations of instability modes in a rectangular jet p 1135 A92-54908

KROUTIL, J. C.
Confined normal-shock/turbulent-boundary-layer interaction followed by an adverse pressure gradient p 172 A92-18365
Experimental investigation of normal-shock/turbulent-boundary-layer interactions with and without mass removal p 330 A92-26411
KRUCH, S.
Numerical analysis of an engine turbine disk loaded with a large number of thermomechanical cycles
[ONERA, TP NO. 1992-31] p 902 A92-48592
KRUCZYNSKI, D. L.
Experimental and computational investigation of scaling phenomena in a large caliber ram accelerator
[AIAA PAPER 92-3245] p 1103 A92-54019
KRUGLOV, V. I.
An automated workstation for the half-scale testing of the flight vehicle stabilization circuit p 664 A92-40622
KRUKOVSKII, P. G.
A method for determining the parameters of mathematical generalizations of experimental data on convective heat transfer p 41 A92-12803
KRULL, J. D.
Three-dimensional-mode resonance in far wakes p 898 A92-46252
KRULL, NICK
Designing a methodology for future air travel scenarios p 409 N92-19125
KRUMENACKER, JOSEPH
X-29 high angle of attack flight test procedures, results, and lessons learned p 548 A92-35934
KRUSE, R. J.
X-ray computed tomography for the aircraft/aerospace industry p 492 A92-28750
KRUTOVA, I. N.
Robustness of control systems with nonlinear parametric correction for certain types of perturbations p 509 A92-30311
KRYLOV, A. N.
Aerodynamics of complex shape bodies within a wide range of supersonic flows of rarefied gases p 939 A92-52767
KTENIDIS, P. D.
The influence of shock waves on the viscous flow field of axial compressors
[ASME PAPER 91-GT-173] p 73 A92-15608
KUBE, R.
Evaluation of a constant feedback gain for closed loop higher harmonic control p 568 A92-35768
KUBE, ROLAND
BVI impulsive noise reduction by higher harmonic pitch control - Results of a scaled model rotor experiment in the DNW p 1136 A92-56344
KUBINA, S. J.
RCS of four fuselage-like scatterers at HF frequencies p 533 A92-33632
KUBO, YOSHIHARU
An autorotation-entry control for a helicopter with a fuzzy controller p 1083 A92-56032
KUBOTA, H.
Low speed aerodynamic performance of a capsule-shaped flying object p 430 A92-30559
KUBOTA, HIROTO
Air flow under a flight-vehicle engine p 429 A92-30528
KUBOTA, HIROTOSHI
Effects of gas-surface interaction models on aerodynamic characteristics p 244 A92-21718
Spaceplane aerodynamic heating and thermal protection design method p 1102 A92-53578
Study on international cooperative test facilities for future SST/HST
[AIAA PAPER 92-3945] p 1097 A92-56775
KUBOTA, TOSHI
An analytical and computational investigation of shock-induced vortical flows
[AIAA PAPER 92-0316] p 321 A92-25763
KUBRYNSKI, K.
Two-point optimization of complete three-dimensional airplane configuration
[AIAA PAPER 92-2618] p 844 A92-45491
KUBRYNSKI, KRZYSZTOF
Design of 3-dimensional complex airplane configurations with specified pressure distribution via optimization p 194 N92-13948
KUCHAR, A. P.
Scale model test results of a multi-slotted vectoring 2DCD ejector nozzle
[AIAA PAPER 92-3264] p 864 A92-48859
KUCHAR, JAMES K.
Electronic presentation of instrument approach information p 855 A92-44923
KUCHER, A. G.
A probabilistic method for monitoring the remaining life of aircraft gas turbine engine components using the temperature limit criterion p 201 A92-18292
KUCZERA, HERIBERT
Saenger and the German Hypersonics Technology Programme - Status report 1991
[IAF PAPER 91-198] p 32 A92-12570
The German Hypersonics Technology Programme - Status report 1992
[IAF PAPER 92-0867] p 1105 A92-57258
KUDLICK, D. A.
Approximate aerodynamic analysis of jet interaction
[AIAA PAPER 92-4640] p 1027 A92-55387
KUDO, ISAO
Experimental study of convection effects around the phase charge interface p 1111 A92-53755
KUDO, MASATO
On the skip flight of a spaceplane p 387 A92-25503
KUDO, NATSUKO
Analysis of the aerodynamic characteristics of a simple remotely piloted research vehicle (RPRV) p 710 A92-43191
KUDOU, KENJI
Effectiveness of plasma torches for ignition and flameholding in scramjet p 737 A92-44524
Flow measurements in scramjet inlets p 1102 A92-53565
KUDRIAVTSEV, A. N.
Stability of a viscous compressible shear layer with a temperature drop p 79 A92-16684
On an adaptive numerical method for solution of high gradient problems p 410 A92-24905
KUDVA, J. N.
An expert system to aid real world finite element analysis
[AIAA PAPER 92-2488] p 601 A92-34604
Overview of computational structural methods for modern military aircraft p 684 N92-25928
KUECK, J. D.
Assessment of valve actuator motor rotor degradation by Fourier Analysis of current waveform
[DE92-013233] p 909 N92-28814
KUERTEN, J. G. M.
Improved shock-capturing of Jameson's scheme for the Euler equations
[PB92-148758] p 596 N92-23251
KUGLER, B. A.
NSBIT program - Development of assessment system for aircraft noise and research on human impacts due to aircraft noise p 688 A92-39100
KUHLENSCHMIDT, SHARON
Human factors issues in the use of artificial intelligence in air traffic control. October 1990 Workshop
[NASA-CR-190925] p 1051 N92-34203
KUHLMAN, G. W.
Ti-6Al-4V forgings with enhanced fatigue characteristics for engine and airframe applications p 288 A92-22757
A critical appraisal of thermomechanical processing of structural titanium alloys p 488 A92-30611
KUHLMAN, JOHN M.
The effects of winglets on low aspect ratio wings at supersonic Mach numbers
[NASA-CR-4407] p 178 N92-13996
KUHN, GARY D.
Postflight aerothermodynamic analysis of Pegasus(tm) using computational fluid dynamic techniques
[NASA-CR-186017] p 445 N92-21188
KUHN, RICHARD E.
On the anomalies in single-jet hover suckdown data
[NASA-TM-102261] p 1038 N92-33306
Dynamic response of induced pressures, suckdown, and temperatures for two tandem jet STOVL configurations
[NASA-TM-103934] p 1039 N92-33581
On the estimation of jet-induced fountain lift and additional suckdown in hover for two-jet configurations
[NASA-TM-102268] p 1040 N92-33618
KUKREJA, R. T.
Segmental heat transfer in a pin fin channel with ejection holes p 900 A92-47267
KUL, H. R.
3-D numerical grid generation for the transonic flow analysis about multi-bodies p 817 A92-47061
KULHMAN, JOHN M.
Experimental investigation of the effects of blowing on bursting of strake vortices
[AD-A240256] p 13 N92-10985
KULL, ROBERT
A model for the effects of aircraft overflight noise on the reproductive success of raptorial birds p 688 A92-39101
KUMAGAI, TATSUO
A preliminary study of a supersonic wind tunnel for a ram jet test facility p 1089 A92-53564
KUMAKURA, IKUO
Research on aeroelastic tailoring at NAL p 1053 A92-56019
KUMAKURA, KUNIO
Vibration tests of long plate structural model
[NAL-TM-625] p 400 N92-18485
KUMAR, AJAY
Numerical study of the effects of reverse sweep on scramjet inlet performance p 611 A92-36979
Least-squares/parabolized Navier-Stokes procedure for optimizing hypersonic wind-tunnel nozzles p 980 A92-50270
CAN-DO, CFD-based Aerodynamic Nozzle Design and Optimization program for supersonic/hypersonic wind tunnels
[AIAA PAPER 92-4009] p 1033 A92-56832
Direct simulation of high-speed mixing layers
[NASA-TP-3186] p 945 N92-30909
KUMAR, GANESH N.
Aerobrake aerothermodynamic environment predictions in support of the Aeroassist Flight Experiment
[TABES PAPER 91-278] p 519 A92-34683
KUMAR, RAMOHALLI
Free-radicals aided combustion with scramjet applications
[IAF PAPER 92-0659] p 1106 A92-57100
KUMAR, S. N.
The hardness and toughness of HIPed silicon nitride p 668 A92-39682
KUMAR, V. R.
Criteria for use of seal coats on airport pavements
[DOT/FAA/RD-92/18] p 1102 N92-34247
KUMM, EMERSON L.
Flat belt continuously variable high speed drive
[DE92-008952] p 680 N92-25054
KUNC, J. A.
An iodine hypersonic wind tunnel for the study of nonequilibrium reacting flows
[AIAA PAPER 92-0566] p 383 A92-26974
A code validation strategy and facility for nonequilibrium, reacting flows
[AIAA PAPER 92-3970] p 1098 A92-56796
KUNC, JOSEPH A.
A new technique for temperature and specie concentration measurements in unseeded supersonic and hypersonic gas flows
[AD-A241536] p 158 N92-13409
KUNDU, K. P.
A simplified reaction mechanism for prediction of NO(x) emissions in the combustion of hydrocarbons
[AIAA PAPER 92-3340] p 894 A92-48919
Applied analytical combustion/emissions research at the NASA Lewis Research Center - A progress report
[AIAA PAPER 92-3338] p 1067 A92-54025
Applied analytical combustion/emissions research at the NASA Lewis Research Center
[NASA-TM-105731] p 890 N92-29343
KUNKEL, B.
The imaging spectrometer p 599 N92-23387
KUNKEL, MATTHEW W.
Spectrum modal analysis for the detection of low-altitude windshear with airborne Doppler radar
[NASA-CR-4457] p 953 N92-31549
KUNTZ, D. W.
Two-stream, supersonic, wake flowfield behind a thick base. I - General features p 813 A92-46895
KUNTZ, H. L.
Development and testing of cabin sidewall acoustic resonators for the reduction of cabin tone levels in propfan-powered aircraft
[NASA-CR-4388] p 166 N92-13757
KUNTZ, HERBERT L.
Laboratory testing of a high transmission loss aircraft cabin structure p 663 A92-39229
KUNZ, DONALD L.
A multibody approach to modeling tilt-wing rotorcraft dynamics
[AIAA PAPER 92-0487] p 328 A92-26318
KUNZ, KARL S.
Finite difference time domain modeling of steady state scattering from jet engines with moving turbine blades
[NASA-CR-190290] p 971 N92-30753
KUNZ, R.
Numerical simulation of turbomachinery flows with advanced turbulence models p 1124 N92-32270
KUNZ, R. F.
Three-dimensional Navier-Stokes computation of turbomachinery flows using an explicit numerical procedure and a coupled k-epsilon turbulence model
[ASME PAPER 91-GT-146] p 72 A92-15584
Navier-Stokes investigation of a transonic centrifugal compressor stage using an algebraic Reynolds stress model
[AIAA PAPER 92-3311] p 825 A92-48897
KUNZ, ROBERT
Explicit Navier-Stokes computation of turbomachinery flows
[AD-A249284] p 909 N92-28879

KUNZ, ROBERT F.
Explicit Navier-Stokes computation of cascade flows using the k-epsilon turbulence model
p 175 A92-20727
Explicit Navier-Stokes computation of turbomachinery flows
[AD-A248458] p 911 N92-29933
KUNZ, STEVEN
Trajectory analysis of the G-11 family of clustered parachutes to determine minimum altitude
[AD-A243375] p 261 N92-17404
KUO, TZE
On modelling of aero-gas turbine engine for real-time digital simulator p 471 A92-29743
KUPCIS, EDGARS A.
Manually flown windshear recovery technique
p 27 A92-11386
KURANAGA, SEISHI
Experimental investigation on turbulent phenomena in three-dimensional shock wave/turbulent boundary layer interaction induced by blunt fin p 1018 A92-53557
KURATA, KAZUO
Computation of the potential flow through cascades using the conformal mapping and the singularity method
p 66 A92-15356
KURIAN, THOMAS
Basic design concepts for smart actuators for aerospace plane control p 752 A92-41193
KURILENKO, IU. V.
Iterative algorithms for solving problems of the shaping of three-dimensional ducts p 428 A92-30212
KURIYAMA, MASAMICHI
Flight test results and upper surface blowing (USB) technology of the STOL research aircraft Asuka
p 730 A92-43142
KURKOV, A. A.
Lift characteristics of an infinite-span cylindrical wing of a thick symmetric profile at low subsonic velocities
p 440 A92-31897
KURKOV, ANATOLE P.
Optical measurements of unducted fan flutter
[ASME PAPER 91-GT-19] p 147 A92-15510
KURNIAWAN, ANTONIUS S.
Thermal mechanical analysis of sprag clutches
[NASA-CR-190686] p 1128 N92-34207
KURODA, KEN
The acceleration control system design of a flight vehicle using a two-wing control method p 745 A92-43185
KURODA, SHIN-ICHI
Supersonic inlet flow computation
p 171 A92-17502
KURODA, SHINICHI
Numerical computation of supersonic intakes
p 430 A92-30539
KURODA, TAKESHI
Aircraft evasive maneuvers against flying objects
p 744 A92-43128
KUROSAKA, M.
Vortex-induced energy separation in shear flows
[AIAA PAPER 92-0192] p 257 A92-23801
KUROSAKA, T.
A model study on diffuser pressure recovery in NAL scramjet test facility with simulated hydrogen combustion
[AIAA PAPER 92-3979] p 1071 A92-56805
Numerical prediction of the flow characteristics in an arc wind tunnel
[AIAA PAPER 92-4016] p 1100 A92-56838
KUROSAWA, MINORU
Ultrasonic motor utilizing elastic fin rotor
p 215 A92-17414
KURSINSKI, E. R.
NASA's GPS tracking system for Aristoteles
p 576 N92-23919
KURTS, DAVID
The use of a dedicated testbed to evaluate simulator training effectiveness p 884 N92-28533
KURU, SELAHATTIN
The TSE 310 troubleshooting expert prototype for the Airbus A-310 commercial aircraft p 307 A92-25180
KURUVILA, G.
Aerodynamic design and optimization in one shot
[AIAA PAPER 92-0025] p 248 A92-22147
KURZKE, J.
Calculation of installation effects within performance computer programs p 869 N92-28465
KUSAKABE, MASAYUKI
Analyses of heat isolation property for metallic multiwall thermal protection system p 40 A92-12422
KUSHIKI, KENICHI
Analyses of heat isolation property for metallic multiwall thermal protection system p 40 A92-12422
KUSHMAN, KEITH L.
Integrated test and evaluation for hypervelocity systems
[AIAA PAPER 92-3901] p 1017 A92-56736
KUT'ENKOV, V. A.
High-temperature metal matrix composite
p 1105 A92-53878
KUTSCHENREUTER, PAUL
Inlet technology p 447 N92-21528
KUWAHARA, KEIICHI
Fundamental studies on Marangoni convection related to Bridgman crystal growth p 1111 A92-53758
KUWAHARA, T.
Combustion of solid fueled ramjet. I
[AIAA PAPER 92-3727] p 894 A92-49105
KUWANO, N.
Noise test of high-speed counterrotation propeller in low-speed wind tunnel p 1135 A92-56055
KUWANO, NAOAKI
The fibre optic three dimensional laser two focus velocimeter for the low-speed windtunnel. Part 1: Two-dimensional measurement evaluations
[NAL-TM-627] p 665 N92-25402
KUWANO, SONOKO
Temporal change of noisiness of helicopter noise
p 689 A92-39103
Temporal change of timbre of helicopter noise
p 694 A92-39104
KUYVENHOVEN, J. L.
Domain modeling and grid generation for multi-block structured grids with application to aerodynamic and hydrodynamic configurations p 691 N92-24411
KUZ'MIN, V. P.
Estimating the probability of a safe flight for an aircraft flying under the effect of disturbances
p 479 A92-30132
KUZIN, A. V.
An electromagnetic suspension system for aerodynamic studies p 483 A92-30409
Progress of magnetic suspension systems and magnetic bearings in the USSR p 772 N92-27740
Progress of magnetic suspension and balance systems for wind tunnels in the USSR p 751 N92-27803
KUZNETSOV, A. E.
Influence of three-dimensional effects on hydrodynamics and heat transfer in subsonic flow of a viscous compressible gas in the initial section of a rectangular duct p 66 A92-15031
KUZNETSOV, ANATOLIY A.
Levitation of YBa2Cu3O(7-x) superconductor in a variable magnetic field p 771 N92-27735
KUZNETSOV, E. N.
A study of flow past bodies of revolution with a Riabushinskii generatrix p 252 A92-23502
Bodies of revolution with minimal wave drag at transonic gas flow velocities p 424 A92-30135
KUZNETSOV, V. V.
A study of the nonlinear stress-strain state of spring-type landing gear p 154 A92-16825
KUZOVKIN, K. N.
Aerodynamic characteristics of a standard corrugated body in a free-molecular flow p 940 A92-52818
KUZUHARA, M.
Wind tunnel test of a supersonic air intake
p 711 A92-43205
KUZUU, KAZUTO
Effects of gas-surface interaction models on aerodynamic characteristics p 244 A92-21718
KVATERNIK, RAYMOND G.
The NASA/Industry Design Analysis Methods for Vibrations (DAMVIBS) Program - A government overview
[AIAA PAPER 92-2200] p 539 A92-34390
DAMVIBS looks at rotorcraft vibration
p 1052 A92-55128
Experiences at Langley Research Center in the application of optimization techniques to helicopter airframes for vibration reduction
[NASA-TM-104193] p 299 N92-17033
The NASA/industry design analysis methods for vibrations (DAMVIBS) program: Accomplishments and contributions
[NASA-TM-104192] p 299 N92-17034
A historical overview of tiltrotor aeroelastic research at Langley Research Center
[NASA-TM-107578] p 502 N92-21460
The NASA/industry Design Analysis Methods for Vibrations (DAMVIBS) Program: A government overview
[NASA-TM-107579] p 680 N92-25267
KWAK, DOCHAN
Efficient simulation of incompressible viscous flow over single and multi-element airfoils
[AIAA PAPER 92-0405] p 324 A92-26258
KWAK, MOON K.
Inclusion principle for the Rayleigh-Ritz based substructure synthesis p 670 A92-36851
KWAK, YEONG-LAE
Development of a flight information system using the structured method
[AD-A248207] p 859 N92-29222
KWATNY, HARRY G.
Regulation of relaxed static stability aircraft
p 203 A92-18463
KWON, HUI M.
Water tunnel flow visualization studies of a canard-configured X-31A-like fighter aircraft model
[AD-A241362] p 90 N92-13037
KWON, O.
A critical evaluation of a three-dimensional Navier-Stokes CFD as a tool to design supersonic turbine stages p 1124 N92-32268
KWON, O. J.
Simulation of iced wing aerodynamics
p 450 N92-21686
KWON, OH J.
Numerical investigation of performance degradation of wings and rotors due to icing
[AIAA PAPER 92-0412] p 325 A92-26264
KYRIACOU, C.
NASA's GPS tracking system for Aristoteles
p 576 N92-23919

L

LA BARBERA, A.
Fracture analysis and crack propagation in pressurized fuselage structures - Experimental and numerical investigations p 217 A92-19812
LAANANEN, DAVID H.
A structural design and optimization tool for ducted rotor/wing blades
[AIAA PAPER 92-2361] p 543 A92-34593
LABELLE, LINDA J.
Rotorcraft low altitude IFR benefit/cost analysis: Operations analysis
[SCT-90RR-44] p 191 N92-15061
LABOURDETTE, ROGER
Survey of French activities concerning structural airworthiness and aging aircraft p 838 N92-30130
LABOZZETTA, WALTER F.
Geometry acquisition and grid generation: Recent experiences with complex aircraft configurations
p 691 N92-24400
LABRUJERE, T. E.
Evaluation of measured-boundary-condition methods for 3D subsonic wall interference
[NLR-TR-88072-U] p 832 N92-29884
LABRUJERE, TH. E.
Review of aerodynamic design in the Netherlands
p 193 N92-13929
LACAS, F.
Turbulent combustion modelling in a side dump ramjet combustor
[AIAA PAPER 92-3599] p 1112 A92-54075
The coherent flamelet model for propulsion applications p 756 N92-27486
LACEY, DONALD J., JR.
A robust digital flight control system for an unfanned research vehicle using discrete quantitative feedback theory
[AD-A243638] p 283 N92-17748
LACEY, J.
The high enthalpy shock tunnel in Goettingen
[AIAA PAPER 92-3942] p 1104 A92-56772
LACHENMEIER, T. T.
Design of a trans-global manned balloon system with relevance to scientific ballooning
[AIAA PAPER 91-3687] p 15 A92-11030
LACHER, STEVEN J.
An experimental study of a sting-mounted circulation control wing
[AD-A243912] p 346 N92-18895
LACOMBE, A.
Large thin composite thermostructural parts
p 576 N92-23821
LACOR, C.
Genuinely upwind algorithms for the multidimensional Euler equations p 175 A92-20733
An integrated CFD system for 3D turbomachinery applications p 741 N92-27464
LACROIX, J. P.
Mixed approach towards modular avionics conflicting requirements p 199 N92-14051
LACROIX, JEAN P.
Digital technology applied to airborne receivers
p 98 A92-16927
LACY, JAMES A.
An overview of systems engineering management methods and processes
[AIAA PAPER 92-1539] p 690 A92-38636
LADD, J. A.
Development and application of a zonal k-epsilon turbulence model for complex 3-D flowfields
[AIAA PAPER 92-3176] p 903 A92-48792

LADDA, V.
The Operational Loads Monitoring System, OLMS
p 361 N92-18586
LADEN, T.
Study of detached turbulent flow in an air intake by means of high speed tomography and laser velocimetry
[REPT-90/55] p 157 N92-12216
LADERACH, G. E.
Repetitive High Energy Pulsed Power (RHEPP) temperature monitoring system utilizing Luxtron fluoroptic sensors and thermocouples technical reference manual
[DE92-013461] p 999 N92-30893
LADYGIN, V. S.
Dynamics of aerospace shuttles p 667 N92-24760
LAEMMERMANN, HELMUT
PVD coatings for aircraft turbine blades
p 216 A92-17950
LAFLAMME, J. C. G.
Compressor coating effects on gas turbine engine performance p 25 A92-11282
Implanted component faults and their effects on gas turbine engine performance
[ASME PAPER 91-GT-41] p 121 A92-15524
LAFLEUR, R. S.
A basis for ice formation design p 146 A92-14556
LAFON, J.
Acquisition of an aerothermodynamic data base by means of a winged experimental reentry vehicle
p 486 A92-30685
Acquisition of an aerothermodynamic data base by means of a winged experimental reentry vehicle
[MBB/FE202/S/PUB/461] p 787 N92-30232
LAFON, P.
High-speed impulsive noise and aerodynamic results for rectangular and swept rotor blade tip tests in S1-Modane wind tunnel
[ONERA, TP NO. 1991-124] p 76 A92-16102
LAFORCE, SOREN
Algorithmic improvements for simulator motion drive
[AIAA PAPER 92-4158] p 1007 A92-52448
LAFREY, R.
Integrated use of GPS and GLONASS in civil aviation navigation. I - Coverage and data models
p 99 A92-16950
GLONASS data analysis - Interim results
p 955 A92-49382
LAGACE, PAUL A.
Composite fuselage technology (summary of year 2)
[NASA-CR-190434] p 731 N92-26655
LAGANELLI, ANTHONY L.
Hypersonic wind tunnel nozzle study
[AIAA PAPER 92-4012] p 1033 A92-56835
LAGREE, PIERRE-YVES
Influence of the entropy layer on the separation length in hypersonic aerodynamics in the triple-deck framework. II p 63 A92-13815
LAI, CHEN-YAN
Development of the DDV actuation system on the IDF aircraft
[SAE PAPER 912080] p 844 A92-45455
LAI, M. C.
CFD analysis of jet mixing in low NO(x) flametube combustors
[ASME PAPER 91-GT-217] p 124 A92-15634
LAIBLE, CHRISTOPH
An experimental investigation of the combustion of a hydrogen jet injected parallel in a supersonic air stream
[AIAA PAPER 91-5102] p 212 A92-17861
LAKE, R. C.
A demonstration of passive blade twist control using extension-twist coupling
[AIAA PAPER 92-2468] p 539 A92-34358
LAKE, RENEE C.
A demonstration of passive blade twist control using extension-twist coupling
[NASA-TM-107642] p 1001 N92-31155
LAKESTANI, F.
Measurement of acoustic properties of the composite materials constituting the main rotor hub of the Agusta-Westland helicopter EH-101 (civil version)
p 1010 A92-49475
LAKEY, MARY J.
Statistical analysis of field data for aircraft warranties
p 760 A92-42077
LAKIN, WILLIAM D.
CSM solutions of rotating blade dynamics using integrating matrices
[NASA-CR-190577] p 1003 N92-31619
LAKSHMINARAYANA, B.
Three-dimensional Navier-Stokes computation of turbomachinery flows using an explicit numerical procedure and a coupled k-epsilon turbulence model
[ASME PAPER 91-GT-146] p 72 A92-15584
Numerical prediction of wakes in cascades and compressor rotors including the effects of mixing. I - Cascade wakes including the effects of incidence and freestream turbulence
[ASME PAPER 91-GT-225] p 74 A92-15638
Numerical prediction of wakes in cascades and compressor rotors including the effects of mixing. II - Rotor passage flow and wakes including the effects of spanwise mixing
[ASME PAPER 91-GT-222] p 74 A92-15639
Navier-Stokes investigation of a transonic centrifugal compressor stage using an algebraic Reynolds stress model
[AIAA PAPER 92-3311] p 825 A92-48897
Investigation of three-dimensional flow field in a turbine including rotor/stator interaction. I - Design development and performance of the research facility
[AIAA PAPER 92-3325] p 883 A92-48908
Investigation of three-dimensional flow field in a turbine including rotor/stator interaction. II - Three-dimensional flow field at the exit of the nozzle
[AIAA PAPER 92-3326] p 826 A92-48909
Explicit Navier-Stokes computation of turbomachinery flows
[AD-A249284] p 909 N92-28879
Numerical simulation of turbomachinery flows with advanced turbulence models p 1124 N92-32270
LAKSHMINARAYANA, BUDUGUR
Explicit Navier-Stokes computation of cascade flows using the k-epsilon turbulence model
p 175 A92-20727
Explicit Navier-Stokes computation of turbomachinery flows
[AD-A248458] p 911 N92-29933
LALLMAN, FREDERICK J.
Control concept for maneuvering in hypersonic flight
[AIAA PAPER 91-5055] p 203 A92-17838
Control integration concept for hypersonic cruise-turn maneuvers
[NASA-TP-3136] p 481 N92-20195
LALLO, ART
H-76B Fantail demonstrator composite fan blade fabrication p 145 A92-14356
LALLY, VINCENT E.
Manned orbital balloon flight - Available techniques
[AIAA PAPER 91-3675] p 15 A92-11020
LAM, C. G.
Efficient high-resolution rotor wake calculations using flow field reconstruction p 814 A92-46951
LAM, F.
A theoretical investigation of the induced drag of wing of finite aspect ratio
[CUED/A-AERO/TR-17(1991)] p 525 N92-22193
LAM, T.
Simulation of automatic rotorcraft nap-of-the-earth flight in graphics workstation environment
[AIAA PAPER 92-4131] p 981 A92-52428
LAMAR, JOHN E.
High angle of attack: Aerodynamics
p 528 N92-23956
LAMARRE, FRANCOIS
Efficient panel method for vortex sheet roll-up
p 309 A92-24404
LAMARSH, WILLIAM J., II
Fully integrated aerodynamic/dynamic optimization of helicopter rotor blades
[AIAA PAPER 92-2374] p 542 A92-34544
Fully integrated aerodynamic/dynamic optimization of helicopter rotor blades
[NASA-TM-104226] p 461 N92-20417
LAMBERTI, R.
A survey of composite structure technology at the Aerospatiale Helicopter Division p 546 A92-35754
LAMBREGTS, A. A.
High-speed civil transport flight- and propulsion-control technological issues
[NASA-CR-186015] p 482 N92-21253
LAMERIS, J.
The use of load enhancement factors in the certification of composite aircraft structures
[NLR-TP-90068-U] p 852 N92-28649
LAMONICA, GARY L.
Reconfigurable Mobile System - Ground, sea and air applications p 218 A92-19986
LAMPINEN, M. J.
Analysis of Euler's and stress tensor methods for calculating power consumption of high speed centrifugal fans and turbocompressors
[DE92-728396] p 298 N92-16325
Calculation of local power consumptions and efficiencies of centrifugal fans and turbocompressors
[DE92-728402] p 298 N92-16326
LAN, C. E.
Effect of thrust vectoring on level-turn performance
p 729 A92-41243
An experimental investigation of the effect of leading-edge extensions on directional stability and the effectiveness of forebody nose strakes
[AIAA PAPER 92-2715] p 802 A92-45554
Fourier functional analysis for unsteady aerodynamic modeling p 935 A92-50313
LAN, C. EDWARD
Identification of aerodynamic models for maneuvering aircraft
[NASA-CR-190039] p 348 N92-19359
Identification of aerodynamic models for maneuvering aircraft
[NASA-CR-190444] p 852 N92-28720
LANCIA, M. R.
A boundary integral formulation for the kinetic field in aerodynamics. I - Mathematical analysis
p 243 A92-21504
A boundary integral formulation for the kinetic field in aerodynamics. II - Applications to unsteady 2D flows
p 339 A92-28005
LANCIOTTI, A.
Effects of spectrum variations on fatigue crack growth
p 1123 A92-57399
The G-222 aircraft individual tracking programme
p 361 N92-18582
LANDAU, HERBERT
A system for precise real-time differential GPS positioning in the decimeter range p 638 A92-39569
LANDGRAF, R. W.
Advances in fatigue lifetime predictive techniques; Proceedings of the Symposium, San Francisco, CA, Apr. 24, 1990
[ASTM STP-1122] p 896 A92-45226
LANDMANN, A. E.
Application of analysis techniques for low frequency interior noise and vibration of commercial aircraft
[NASA-CR-189555] p 481 N92-20376
LANDRUM, D. B.
Engineering method for calculating surface pressures and heating rates on vehicles with embedded shocks
[AIAA PAPER 91-5060] p 171 A92-17842
LANDRY, L. M., JR.
Simulation software flowdown in the aircraft design process - Problems and solutions
[AIAA PAPER 92-4160] p 1008 A92-52450
LANDRY, MURPHY J.
Progress report of Scot's Laser Ordnance Initiator System for crew escape p 580 A92-32988
LANDY, R. J.
ICAAS piloted simulation evaluation
p 735 N92-27906
LANEN, T. A. W. M.
Comparison of interferometric measurements with 3-D Euler computations for circular cones in supersonic flow
[AIAA PAPER 92-2691] p 800 A92-45538
LANG, M. A.
MD-80 aft cabin noise control: A case history
p 1137 N92-32950
LANG, P.
The NASA/Industry Design Analysis Methods for Vibrations (DAMVIBS) Program - Boeing helicopters airframe finite element modeling
[AIAA PAPER 92-2202] p 539 A92-34392
LANGARI, G.
Design of compensators for linear parameter-varying feedback systems by the gain scheduling technique
p 507 A92-29101
LANGDON, H. SCOTT
Finite difference time domain modeling of steady state scattering from jet engines with moving turbine blades
[NASA-CR-190290] p 971 N92-30753
LANGE, H.-H.
The role of systems simulation for the development and qualification of ATTAS p 886 N92-28548
LANGER, H. J.
Correlation of flight, tunnel and prediction data on a helicopter main rotor p 1059 A92-56350
LANGER, H.-J.
LAH main rotor model test at the DNW
p 547 A92-35771
LAH-main rotor model test at the DNW
[NLR-TP-90305-U] p 852 N92-28687
LANGHALS, TAMMY J.
Experimental ice shape and performance characteristics for a multi-element airfoil in the NASA Lewis Icing Research Tunnel
[NASA-TM-105380] p 261 N92-17347
LANGLEY, R. S.
A dynamic stiffness technique for the vibration analysis of stiffened shell structures p 1123 A92-56866
LANGLOIS, ELENA B.
Some experiences with community response to low levels of aircraft noise p 689 A92-39235

LANGSTON, CHESTER W.
An experimental study of the sensitivity of helicopter rotor blade tracking to root pitch adjustment in hover
[NASA-TM-4313] p 61 N92-12989
LANGSTON, PAUL R.
Design and use of aramid fiber in aircraft structures
p 784 A92-47407
LANOUE, J. C.
Combined VISAR and flash x ray testing techniques
[DE92-004732] p 385 N92-18290
LANSER, WENDY R.
Analysis of a pneumatic forebody flow control concept about a full aircraft geometry
[AIAA PAPER 92-2678] p 799 A92-45530
Forebody flow control on a full-scale F/A-18 aircraft
[AIAA PAPER 92-2674] p 806 A92-45583
Full-scale high angle-of-attack tests of an F/A-18
[AIAA PAPER 92-2676] p 806 A92-45584
LANSHIN, A. I.
Aerospace plane hydrogen scramjet boosting
[SAE PAPER 912071] p 891 A92-45451
LANTZ, EDWARD
Accelerators and decelerators for large hypersonic aircraft p 665 A92-36952
LANTZ, RICHARD L.
Supersonic Throughflow Fan Test Facility at NASA. Lewis Research Center
[NASA-TP-3038] p 983 N92-31640
LAOR, K.
The effect of tip convection on the performance and optimum dimensions of cooling fins p 902 A92-48354
LAPATI, ANDREW J.
Helicopter in-flight frequency response test techniques
p 548 A92-35938
LAPLANTE, JOHN R.
An integrated analysis and simulation tool for avionics system development p 1005 A92-49289
LAPPOS, NICHOLAS D.
Results of flight tests of the Boeing Sikorsky Fantail demonstrator p 106 A92-14376
LAR'KIN, NIKOLAI A.
Smooth solutions for transonic gasdynamic equations
[ISBN 5-02-029345-8] p 809 A92-46626
LARDIERE, BENJAMIN, JR.
Improvements to expulsive separation ice protection blankets
[AIAA PAPER 92-0533] p 358 A92-26951
LARE, G. A.
Combined VISAR and flash x ray testing techniques
[DE92-004732] p 385 N92-18290
LAREAU, J. P.
Eddy current imaging of aircraft using real time image signal processing p 144 A92-13594
LARICHKIN, V. V.
Pressure on a cylinder with a screen in transverse flow p 6 A92-12164
LARIGALDIE, S.
Mechanisms of high-current pulses in lightning and long-spark stepped leaders p 1116 A92-54678
LARIMER, J.
Sensor fusion for synthetic vision
[AIAA PAPER 91-3730] p 197 A92-17597
LARINA, I. N.
Influence of internal molecular degrees of freedom on the hypersonic rarefied gas flow about a conical body
p 938 A92-52752
LARKIN, MICHAEL J.
Ultra high bypass Nacelle aerodynamics inlet flow-through high angle of attack distortion test
[NASA-CR-189149] p 943 N92-30298
LAROCCA, FRANCESCO
Research on inverse methods and optimization in Italy
p 202 N92-13956
LAROCHE, P.
Lightning activity in microburst producing storm cells
[ONERA, TP NO. 1991-98] p 161 A92-16080
LAROSE, C.
RCS of four fuselage-like scatterers at HF frequencies
p 533 A92-33632
LARROQUE, PIERRE
The role of simulation for the study of APIS (piloting support by synthetic imagery) p 885 N92-28544
LARSEN, PETER N.
Advanced Study for Active Noise Control in Aircraft (ASANCA)
[AIAA PAPER 92-2092] p 1137 N92-32956
LARSON, D. S.
Computer simulation of weapon blast pressures on flexible surfaces p 39 A92-12115
LARSON, KEVIN P.
Visual photometric experiment data processing system
[AD-A248657] p 729 N92-27964
LARSON, TERRY J.
High angle-of-attack flush airdata sensing system
p 1064 A92-56172
LARUELLE, GERARD
Potential hypersonic vehicles applications
[AIAA PAPER 91-5086] p 169 A92-17854
LASHKOV, V. A.
Aerodynamic drag of a cylinder in two-phase flow
p 707 A92-42735
LASSEIGNE, D. G.
Stability of a nonorthogonal stagnation flow to three-dimensional disturbances p 495 A92-31194
LAST, DAVID
The accuracy and coverage of Loran-C and of the Decca Navigator System - and the fallacy of fixed errors
p 353 A92-24944
LAST, STEVE
British Airways Airbus A320 pilots' autothrust survey
[SAE PAPER 912225] p 636 A92-40023
LASTER, M. L.
The G-range impulse facility - A high-performance free-piston shock tunnel
[AIAA PAPER 92-3946] p 1097 A92-56774
LATAPY, M. O.
Scale model test of an isolated turbofan nacelle with riblets
[SAE PAPER 912128] p 618 A92-39975
LAU, S. C.
Segmental heat transfer in a pin fin channel with ejection holes p 900 A92-47267
LAUB, JAMES
The FML compressor as a drive system for the LFSWT: A narrative p 751 N92-27978
LAUCHLE, G. C.
Basic hydrodynamics
[AD-A243513] p 300 N92-17387
LAUDIEN, E.
Noise level reduction inside helicopter cabins
p 545 A92-35733
LAUER, R. F., JR.
On-line distortion analysis system for inlet-engine testing
[ASME PAPER 91-GT-166] p 136 A92-15601
LAUFER, G.
Evaluation of OH laser-induced fluorescence techniques for supersonic combustion diagnostics
[AIAA PAPER 92-0508] p 396 A92-26935
KrF laser-induced OH fluorescence imaging in a supersonic combustion tunnel
[AIAA PAPER 92-3346] p 905 A92-48923
LAUGHREY, JAMES A.
Results and lessons learned from the STOL and Maneuver Demonstration Program
[SAE PAPER 912005] p 843 A92-45406
LAUMONIER, J.
Active control of pulsed flow for low frequency noises attenuation p 694 A92-39109
LAUNDER, B. E.
Towards the computation of turbulent hypersonic flows
[AERO-REPT-9106] p 345 N92-18318
Computational modelling of turbulent flow in S-bends
p 769 N92-27480
LAUNIUS, ROGER D.
A revolution in air transport - Acquiring the C-141 Starlifter p 607 A92-38101
LAURE, S.
The IRS plasma wind tunnels for the investigation of thermal protection materials for reentry vehicles
p 208 N92-15009
LAURIEN, E.
Finite-element algorithm for chemically reacting hypersonic flow
[AIAA PAPER 92-0754] p 336 A92-27097
Numerical approximation of hypersonic shocks in a finite-element method using flux-corrected transport (FCT) p 708 A92-43060
LAUZE, Y.
Interactive generation of structured/unstructured surface meshes using adaptivity p 919 A92-47066
LAVERNIA, E. J.
Mechanical behavior and processing of aluminum metal matrix composites
[AD-A249918] p 987 N92-30874
LAVIRON, M.
Optimization of the calculation margins of landing gears under extreme loads. Rupture static tests. Part 1: Program and test implantation
[CEAT-S8-6551-PARTIEL-1-PT-] p 195 N92-14043
LAW, HOWARD G.
Shuttle autoland status summary
[AIAA PAPER 92-1273] p 666 A92-38478
LAWING, P.
Propulsion simulator for magnetically suspended wind tunnel models p 750 N92-27801
LAWRENCE, CHARLES
Determining structural performance
p 560 N92-22519
LAWRENCE, DAVID
The Civil Rotorcraft Initiative - An action agenda
p 241 A92-22707
LAWRENCE, DAVID L.
Development of a multi-computer in-flight data acquisition and analysis system for general aviation aircraft
[AIAA PAPER 92-1037] p 553 A92-33218
LAWRENCE, SCOTT L.
Flow over an all-body hypersonic aircraft - Experiment and computation p 310 A92-24651
Solution-adaptive grid procedure for the parabolized Navier-Stokes equations p 432 A92-31163
Application of computational fluid dynamics to sonic boom near- and mid-field prediction
p 1031 A92-56173
LAWRENCE, STELLA
Development of a calibrated software reliability model for flight and supporting ground software for avionic systems p 234 N92-15870
LAWRYSYN, M. A.
Aerodynamic characteristics of hoar frost roughness
p 808 A92-45829
Effects of frost on wing aerodynamics and take-off performance p 450 N92-21687
Performance degradation due to hoar frost on lifting surfaces p 628 N92-24866
LAWSON, C. L.
Multidisciplinary modeling and simulation of a generic hypersonic vehicle
[AIAA PAPER 91-5015] p 232 A92-17813
LAWSON, R. P.
Design and preliminary tests of a new airborne thermometer p 468 A92-32097
LAWTON, B. W.
Risk to hearing from overflight noise of military aircraft
[ISVR-TR-194] p 604 N92-22241
LAYNE, STEVEN JAMES
The FM-007: An advanced jet commuter for HUB to spoke transportation
[NASA-CR-189988] p 461 N92-20267
LAZALIER, GLEN R.
On-line distortion analysis system for inlet-engine testing
[ASME PAPER 91-GT-166] p 136 A92-15601
LAZARUS, KENNETH B.
Static aeroelastic control using strain actuated adaptive structures p 26 A92-11122
LAZZERI, L.
Effects of spectrum variations on fatigue crack growth
p 1123 A92-57399
The G-222 aircraft individual tracking programme
p 361 N92-18582
LE BALLEUR, J. C.
Calculation of fully three-dimensional separated flows with an unsteady viscous-inviscid interaction method
[ONERA, TP NO. 1992-1] p 821 A92-48577
LE LETTY, L.
A two-feedback-loop robust helicopter controller based on eigenspace techniques and H(infinity) synthesis
p 29 A92-11582
LE MEUR, A.
Comparison between two 3D-NS-codes and experiment on a turbine stator
[AIAA PAPER 92-3042] p 822 A92-48703
LE MOING, T.
Integration of flight and carrier landing aid systems for shipboard operations
[ONERA, TP NO. 1991-113] p 134 A92-16092
LE, DY D.
Engine fan blade low cycle fatigue testing
[AIAA PAPER 92-3478] p 866 A92-49021
LE, JEANETTE
Experience with Ada on the F-18 High Alpha Research Vehicle Flight Test Program
[NASA-TM-104259] p 1062 N92-34039
LE, T. H.
Numerical simulation of vortex breakdown by solving the Euler equations for an incompressible fluid
p 41 N92-10163
Numerical simulation of vortex breakdown via 3-D Euler equations p 41 N92-10164
Determination of vortex-breakdown criteria by solving the Euler and Navier-Stokes equations
p 87 N92-13018
LEA, T. C., III
United States Navy ski jump experience and future applications p 465 N92-21968
LEACH, B. W.
A Kalman filter integrated navigation design for the IAR Twin Otter Atmospheric Research Aircraft
[NRC-32148] p 1048 N92-32849
The use of Kalman filtering techniques to improve the accuracy of flight test data
[NRC-32139] p 1064 N92-32850

LEAK, CHRIS E.
Durability analysis using fracture mechanics for avionics integrity p 396 A92-26799
LEATHERWOOD, J. D.
Application of magnitude estimation scaling to the assessment of subjective loudness response to simulated sonic booms
[NASA-TM-107657] p 1138 N92-33719
LEATHERWOOD, JACK D.
A new simulator for assessing subjective effects of sonic booms
[NASA-TM-104150] p 56 N92-11759
Subjective loudness response to simulated sonic booms p 1140 N92-33885
LEBACQZ, J. V.
A review of recent programs and future plans for rotorcraft in-flight simulation at Ames Research Center
[SAE PAPER 912121] p 608 A92-39969
LEBACQZ, J. VICTOR
Rotorcraft In-Flight Simulation Research at NASA Ames Research Center: A Review of the 1980's and plans for the 1990's
[NASA-TM-103873] p 853 N92-28926
LEBALLEUR, J. C.
Development of an unsteady three-dimensional viscous-inviscid interaction numerical method for the calculation of airfoils vibration
[ONERA-RSF-7/3617-AY-022A] p 830 N92-29206
LEBEAU, RAYMOND P.
Aviation Diagnostics And Maintenance (ADAM) system preliminary concept of operation and functional description
[AD-A242598] p 170 N92-14966
LEBED'KO, E. G.
Selection of the time parameters of the probing pulse during the nonstationary irradiation of flight vehicles p 454 A92-31951
Characteristics of the energy analysis of optical radar in the case of nonstationary irradiation of flying objects p 454 A92-31955
LEBIGA, V. A.
A hot-wire anemometer in compressible subsonic flow p 244 A92-21623
LEBLANC, L.
Tutor aft fuselage and empennage full-scale fatigue test: Resolution of horizontal stabilizer installation difficulties
[NRC-LTR-ST-1804] p 114 N92-11990
LEBLANC, R.
Control aspects of the transition from transversal to transonic flow, step effects
[ETN-91-90106] p 82 N92-11981
LECCE, LEONARDO V.
Active vibrations and noise control for turboprop application research program activities p 1138 N92-32962
LECKMAN, PAUL R.
Enhanced vision system option on future aircraft
[SAE PAPER 912204] p 651 A92-40014
LECLERCQ, M. C.
Industrial practice in aeronautical maintenance p 786 A92-47774
LECOINTE, Y.
Computation of unsteady, laminar, incompressible, viscous flows using the vorticity streamfunction formulation p 245 A92-21979
LECOMTE, CLAUDE
The sonic boom and problems related to supersonic flights of military aircraft
[ONERA, TP NO. 1991-162] p 77 A92-16129
LECOSTAOUEC, JEAN F.
Ceramic matrix composites and its application in gas turbine engines
[ASME PAPER 91-GT-338] p 143 A92-15702
LECREN, R. T.
High-temperature combustor and seal for a water piston propulsor
[AD-A242493] p 229 N92-15385
LEDERER, R.
Hypersonic airbreathing propulsion activities for Saenger
[AIAA PAPER 91-5040] p 200 A92-17828
LEE, B. H. K.
Effects of trailing-edge flap on buffet characteristics of a supercritical airfoil p 378 A92-24413
Wind-tunnel studies of F/A-18 tail buffet p 310 A92-24421
Development and analysis of flight flutter prediction methods
[AIAA PAPER 92-2101] p 588 A92-35672
Buffet load measurements on an F/A-18 vertical fin at high-angle-of-attack
[AIAA PAPER 92-2127] p 520 A92-35694
Unsteady pressure and load measurements on an F/A-18 vertical fin at high-angle-of-attack
[AIAA PAPER 92-2675] p 798 A92-45529
Statistical prediction of maximum buffet loads on the F/A-18 vertical fin p 811 A92-46816
Some characteristics and effects of the F/A-18 LEX vortices p 88 N92-13025
Flowfield in the vicinity of the F/A-18 vertical fin at high-angle-of-attack p 628 N92-24865
A time-linearization approach for unsteady transonic flows p 719 N92-27941
LEE, C. T.
Fabrication and properties of fiber-reinforced ceramic composites made by directed metal oxidation p 669 A92-39861
LEE, C. WILLIAM
Design of an integrated airframe/propulsion control system architecture
[NASA-CR-182004] p 602 N92-22643
Design of an integrated airframe/propulsion control system architecture
[NASA-CR-182007] p 602 N92-22644
LEE, CHANGDON
Wide area differential GPS p 101 A92-16966
LEE, CHAU-LIN
On a multi-block method for transonic turbulent flows past a wing-fuselage configuration p 632 N92-25569
LEE, CHUN-HIAN
The influences of forced oscillations toward vortex-breakdown p 934 A92-50210
A bi-directional marching finite element algorithm for three-dimensional boundary layer separation flow computations p 942 A92-53288
LEE, CLAUDIA J.
Standardization of NATOPS emergency egress procedures p 529 A92-32998
LEE, D.
A numerical study of isothermal flows of a slit V-gutter
[AIAA PAPER 92-0100] p 293 A92-22203
LEE, D. K.
Shafranov shift in low-aspect-ratio heliotron/torsatron CHS
[NIFS-110] p 1138 N92-33743
LEE, DAL H.
Application of recursive partially unknown system identification to aerodynamic coefficients estimation
[AIAA PAPER 92-4504] p 1081 A92-55371
LEE, DANIEL M.
Development of a 1/7th scale fighter UAV for flight research
[AD-A240703] p 23 N92-11008
LEE, DONGHO
Time accurate computation of unsteady transonic flows around an airfoil with oscillating flap on dynamic grid
[AIAA PAPER 92-2733] p 805 A92-45567
LEE, ELIZABETH M.
Unstructured-grid methods development for unsteady aerodynamic and aeroelastic analyses p 718 N92-27938
LEE, GEORGE
Two-dimensional adaptive-wall tests in the NASA Ames two- by two-foot transonic wind tunnel p 30 A92-13201
Study of optical techniques for the Ames unitary wind tunnels. Part 1: Schlieren
[NASA-CR-189951] p 385 N92-19218
Study of optical techniques for the Ames unitary wind tunnels. Part 2: Light sheet and vapor screen
[NASA-CR-190217] p 573 N92-22195
Study of optical techniques for the Ames unitary wind tunnels. Part 3: Angle of attack
[NASA-CR-190541] p 888 N92-29655
LEE, HAE-KYUNG
Dynamic response and aeroelastic analysis of a propeller blade of a prop-fan engine p 762 A92-43109
LEE, HSIEN-CHIARN
Washout filters in the bifurcation control of high alpha flight dynamics p 476 A92-29061
LEE, IN
Resonance prediction for slotted circular wind tunnel using finite element p 235 A92-18388
Static aeroelastic analysis for generic configuration wing p 174 A92-20201
LEE, JAEWOO
Inverse solution uniqueness and domain of existence for supersonic space marching applications
[AIAA PAPER 92-0028] p 248 A92-22150
Aerodynamically blunt and sharp bodies
[AIAA PAPER 92-2727] p 808 A92-45597
LEE, JANG G.
Application of recursive partially unknown system identification to aerodynamic coefficients estimation
[AIAA PAPER 92-4504] p 1081 A92-55371
LEE, JINHO
Studies of aerothermal loads generated in regions of shock/shock interaction in hypersonic flow
[NASA-CR-181893] p 43 N92-11319
LEE, JOSEPH W.
Signal processing schemes for Doppler global velocimetry p 1115 A92-54338
LEE, K. D.
An inviscid/viscous coupling approach for vortex flow field calculations p 933 A92-49510
LEE, KAM-PUI
Enhancements to viscous-shock-layer technique
[AIAA PAPER 92-2897] p 820 A92-47873
LEE, KI D.
Interactive solution-adaptive grid generation procedure
[NASA-TM-105432] p 528 N92-23563
LEE, KUOK-MING
Calculation of hypersonic leeside vortices over blunt delta wings p 84 N92-13004
LEE, M. J.
Effect of carbon particles and mixing on afterburning of exhaust plumes
[AIAA PAPER 92-0767] p 387 A92-27107
LEE, M. P.
Planar fluorescence imaging of a transverse jet in a supersonic crossflow p 755 A92-44501
LEE, MARK
Application of Active Flexible Wing technology to the Agile Falcon p 729 A92-41233
LEE, PAI-HUNG
Effect of thrust vectoring on level-turn performance p 729 A92-41243
LEE, Q. M.
A new vane swirler as applied to dual-inlet side-dump combustor
[AIAA PAPER 92-3654] p 906 A92-49085
LEE, R.
Jet noise suppression p 236 N92-14784
LEE, R. A.
Sonic booms produced by US Air Force and US Navy aircraft: Measured data
[AD-A244804] p 512 N92-21719
LEE, R. E.
Tangential mass addition for shock/boundary-layer interaction control in scramjet inlets p 80 A92-17197
LEE, R. N.
Development of active control technology for the next generation of combat aircraft p 975 A92-50008
LEE, ROBERT A.
Noisemap 6.0 - The USAF microcomputer program for airport noise analysis p 686 A92-39051
LEE, ROBERT B.
Risk management - Expanding horizons in nuclear power and other industries
[ISBN 1-56032-231-4] p 993 A92-51438
LEE, S.
Processing and environmental effects on mechanical properties of composite repairs
[NRC-LTR-ST-1826] p 1109 N92-32791
LEE, S. C.
A fast viscous correction method for transonic aerodynamics p 247 A92-21986
LEE, SEUNG-HO
Single expansion ramp nozzle simulations
[AIAA PAPER 92-0387] p 323 A92-26243
LEE, SUNHEE
The 1988 Australian Winter Storms Experiment - Case study: 6 August 1988 p 301 A92-23009
LEE, SUSAN
SHARP: Subsonic High Altitude Research Platform
[NASA-CR-190004] p 648 N92-25263
LEE, T-H.
Bistatic image processing for a 32 x 19 inch model aircraft using scattered fields obtained in the OSU-ESL compact range
[NASA-CR-189932] p 499 N92-20197
LEE, TAE-HO
A study of the flammability limit of the backward facing step flow combustion
[AIAA PAPER 92-3846] p 895 A92-49136
LEE, THOMAS
Manufacture of a primary flight structure using thermoplastics p 1 A92-10197
LEE, THOMAS R.
The design and manufacture of an advanced thermoplastic horizontal stabilator for the AH-64A p 59 A92-14354
LEE, TING-WHAI
Dynamic response of landing gears on rough repaired runway
[SAE PAPER 912154] p 644 A92-39989
LEE, Y.
Heat transfer measurements and CFD comparison of swept shock wave/boundary-layer interactions
[AIAA PAPER 92-3665] p 1021 A92-54110
Swept shock/boundary layer interaction experiments in support of CFD code validation
[NASA-CR-190583] p 1036 N92-32494
LEE, YOUNG C.
GPS for precision approaches p 139 A92-16648

Receiver Autonomous Integrity Monitoring (RAIM) capability for sole-means GPS navigation in the oceanic phase of flight p 956 A92-51012
LEE, YU-TAI
Unsteady flows in rotor-stator cascades
[AD-A241593] p 158 N92-13410
LEE, YUN-KUN
Development of the DDV actuation system on the IDF aircraft
[SAE PAPER 912080] p 844 A92-45455
LEE, YUNG-JANG
Development of a shock noise prediction code for high-speed helicopters - The subsonically moving shock
p 165 A92-14384
LEEDOM, DENNIS K.
A model for evaluation and training in aircrew coordination and cockpit resource management
p 46 A92-11191
LEEHEY, P.
The measurement of plate vibration and sound radiation from a turbulent boundary layer manipulator
[AD-A240127] p 42 N92-10206
LEEPER, KENNETH R.
Global memory in the Pave Pace architecture
p 920 A92-48447
LEESER, DANIEL
New thermoplastic composites for aircraft structures and interiors p 34 A92-10271
LEFAS, C.
GPS - Can it contribute to European ATC?
p 637 A92-38380
LEFAS, C. C.
Computation of aircraft geometric height under radar surveillance p 639 A92-40239
LEFEBVRE, A. H.
Weak extinction limits of large scale flameholders
[ASME PAPER 91-GT-234] p 125 A92-15643
Factors influencing the effective spray cone angle of pressure-swirl atomizers p 295 A92-23300
Experimental techniques for the assessment of fuel thermal stability
[AIAA PAPER 92-0685] p 389 A92-27052
LEFFERTS, A. N.
NATO CCMS aircraft noise study on receiver technology p 686 A92-39050
Aircraft noise - The calculation of the noise exposure by aircraft in the Netherlands p 687 A92-39054
LEGENDRE, PHILIPPE
Experimenting a new composite rotor on an Aerospatiale Dauphin helicopter p 546 A92-35744
LEGENDRE, R.
Topology of steady flows of low viscosity fluids
p 38 A92-11219
LEGER, KENNETH B.
Simulation of high heat flux levels with graphite heating and arc lamps p 980 A92-51402
LEGER, P.
Efficient evaluation of the flexibility of tapered I-beams accounting for shear deformations p 295 A92-23269
LEGGE, H.
Force and heat transfer on a disc in rarefied flow
p 939 A92-52764
LEGGETT, DAVID B.
Analysis of the VISTA longitudinal simulation capability for a cruise flight condition p 876 A92-48488
LEGNER, H. H.
Supersonic combustor testing using optical diagnostics and a high enthalpy shock tunnel
[AIAA PAPER 92-0761] p 384 A92-27102
LEGOSTAEV, A. A.
Hypersonic flow of a viscous gas past sharp elliptical cones at angles of attack and slip p 336 A92-27531
LEGRAFF, J. E.
Turbulent spot generation and growth rates in a transonic boundary layer
[AD-A250221] p 909 N92-29118
LEGUILLOUX, Y.
Approach and landing assisted by onboard image processing p 457 N92-21959
LEHNER, PAUL E.
Automated planning with special relevance to associate systems technology and mission planning
[AD-A241924] p 303 N92-17438
LEHNIG, T.
Investigation of oblique shock/boundary-layer bleed interaction p 344 A92-28524
LEHNIG, T. R.
Computational fluid dynamics based three-dimensional turbofan inlet/fan cowl analysis system
p 243 A92-21075
LEINENWEVER, ROGER W.
Transport delay measurements: Methodology and analysis for the F-16C combat engagement trainer, the display for advanced research and training, and the F-16A limited field of view
[AD-A248519] p 888 N92-29505
LEINGANG, J. L.
Advanced ramjet concepts program
p 474 N92-21520
Scramjet analysis, testing p 475 N92-21532
LEINGANG, JOHN L.
Further studies of kinetic energy methods in high speed ramjet cycle analysis
[AIAA PAPER 92-3805] p 1069 A92-54177
LEISHMAN, J. G.
Analysis of unsteady pressures induced on a body by a rotor p 10 A92-13212
An analysis of pitch and plunge effects on unsteady airfoil behavior p 65 A92-14359
Transonic aeroelasticity analysis using state-space unsteady aerodynamic modeling p 310 A92-24422
Unsteady circulation control aerodynamics of a circular cylinder with periodic jet blowing p 330 A92-26401
Measurements of a rotor flowfield and the effects on a fuselage in forward flight p 521 A92-35787
A study of rotor wake development and wake/body interactions in hover p 813 A92-46935
LEITER, M.
Technical feasibility of digital three-dimensional cellular communications for air traffic control applications. Volume 1: Introduction and summary
[AD-A244573] p 534 N92-22104
Technical feasibility of digital three-dimensional cellular communications for air traffic control applications. Volume 2: Example system design details
[AD-A244574] p 534 N92-22105
Technical feasibility of digital three-dimensional cellular communications for air traffic control applications. Volume 3: Ground network architecture
[AD-A244575] p 534 N92-22106
LEITH, D. J.
The identification of coupled flapping/inflow models for hovering flight p 1058 A92-56335
LEITH, J. R.
The vortical structure in the wake during dynamic stall
[AIAA PAPER 92-4496] p 1026 A92-55364
LEITMANN, GEORGE
Aircraft control under conditions of windshear
p 27 A92-11384
Aircraft control for take-off in windshear
p 660 A92-36990
LELE, SANJIVA K.
Direct computation of the sound from a compressible co-rotating vortex pair
[AIAA PAPER 92-0374] p 414 A92-26232
LEMAN, JEAN-LUC
Experimenting a new composite rotor on an Aerospatiale Dauphin helicopter p 546 A92-35744
LEMASURIER, PHILIP
Helicopter far-field acoustic levels as a function of reduced rotor speeds p 695 A92-39228
LEMAY, SCOTT P.
Forebody vortex flow control on the F-16C using tangential slot and jet nozzle blowing
[AIAA PAPER 92-0019] p 247 A92-22141
Forebody vortex control aeromechanics
p 380 N92-18792
Vortex flow visualization using colored and fluorescent dyes on flat plate delta wing with leading edge extension
[AD-A251139] p 1036 N92-32651
LEMEUR, ALAIN
Steady and unsteady 3D flow computation through a transonic turbine stage p 742 N92-27469
LEMISTRE, M.
Study of simulated lightning discharge effects on wires of a rotorcraft
[ONERA, TP NO. 1991-173] p 92 A92-16137
LEMMER, L.
Design, analysis, and testing of integrally stiffened composite centre fuselage skin for future fighter aircraft
p 535 A92-32554
Design, analysis, and testing of integrally stiffened composite centre fuselage skin for future fighter aircraft
[MBB-FE2-PUB-S-450] p 359 N92-18333
LEMOING, T.
Integration of flight and carrier landing aid systems for shipboard operations p 456 N92-21958
LEMPEREUR, C.
Application of infrared thermography to thermal flux measurement in wind tunnels
[AAAF-NT-89-12] p 31 N92-11020
LEMPERT, W. R.
Rayleigh imaging and flow tagging in ground test facilities p 1115 A92-54330
LENAKOS, J.
Definition of the unsteady vortex flow over a wing/body configuration
[NASA-CR-180083] p 178 N92-13995
LENAKOS, JASON
Measurements of the unsteady vortex flow over a wing-body at angle of attack
[AIAA PAPER 92-2729] p 808 A92-45598
LENGRAND, J. C.
Numerical and experimental investigation of rarefied compression corner flow
[AIAA PAPER 92-2900] p 820 A92-47876
Flat plates placed in depleted hypersonic flow
[SESSIA-430/91.960] p 947 N92-31508
LENOROVITZ, JEFFREY M.
First flight for Airbus A340 p 21 A92-12750
LENSKI, JOSEPH W., JR.
Boeing Helicopters Advanced Rotorcraft Transmission (ART) Program summary of component tests
[AIAA PAPER 92-3364] p 905 A92-48937
LENTINI, D.
Prediction of gas turbine combustor flow by a finite element code
[AIAA PAPER 92-3469] p 906 A92-49016
LENTS, C. E.
Optimal thermal management system for HALE UAV
[ASME PAPER 91-GT-396] p 111 A92-15726
LENTZ, CHRISTOPHER A.
Structural design considerations for a Personnel Launch System p 386 A92-24668
LENZO, G.
Description and simulation results of the Italsat AOCS advanced flight simulator p 667 N92-24472
LENZO, J. J., JR.
Transition of GPS user equipment testing from Yuma Proving Ground to Holloman AFB p 138 A92-16972
LEODOLTER, WALTER
Process control challenges during the manufacture of large superplastically formed/diffusion bonded structure
[SAE PAPER 912195] p 674 A92-40012
LEON-SALAMANCA, TEODORO
Surface residual stress analysis of metals and alloys
[AD-A248372] p 895 N92-28426
LEON, J.
Applications of advanced composites in a 3/4 air transportable rack p 36 A92-10314
LEON, R. M.
Computational fluid dynamics based three-dimensional turbofan inlet/fan cowl analysis system
p 243 A92-21075
LEONARD, DESIREE M.
Analysis of objects in binary images
[NASA-CR-4420] p 234 N92-14598
LEONARD, O.
Design method for subsonic and transonic cascade with prescribed Mach number distribution
[ASME PAPER 91-GT-18] p 67 A92-15509
LEONDES, CORNELIUS T.
Pneumatic distortion compensation for aircraft surface pressure sensing devices p 218 A92-20206
Failure detection and fault management techniques for flush airdata sensing systems
[AIAA PAPER 92-0263] p 369 A92-25719
Failure detection and fault management techniques for flush airdata sensing systems
[NASA-TM-4335] p 276 N92-17128
LEONE, G.
High enthalpy nozzle flows p 182 N92-15000
LEOUTSAKOS, G.
Arbitrary blade section design based on viscous considerations - Background information
p 523 A92-36029
LEPAPE, MARIE-CLAIRE
Recent progress in inverse methods in France
p 201 N92-13938
LEPART, M.
Aircraft ground vibration test by means of flight control surfaces
[ONERA, TP NO. 1991-96] p 133 A92-16079
LEPART, MARC
Dynamic characterization and identification of nonlinear systems application to aeronautical structures
p 39 A92-11830
LEPICOVSKY, JAN
Engine component instrumentation development facility at NASA Lewis Research Center
[AIAA PAPER 92-3995] p 1099 A92-56818
Engine component instrumentation development facility at NASA Lewis Research Center
[NASA-TM-105644] p 665 N92-25449
LERBS, S.
The trisonic wind tunnel Muenchen and its involvement in the German SAeNGER-programme
[AIAA PAPER 92-4019] p 1100 A92-56841
LERCH, MANFRED
A semi empirical method for the analytical representation of stationary measured profile coefficients for applications of rotary wing aerodynamics
[ETN-92-91491] p 832 N92-29741
LERWICK, TRYGVE R.
System for generating sequences of phased gust or taxi loadings p 845 A92-46800

LESCHING, A.
Theoretical model to calculate aerodynamic interference effects between rotor and wing of tiltrotors
p 521 A92-35788
LESCHIUTTA, S.
Navsat - A civil complement to GPS and Glonass
[IAF PAPER 91-490] p 188 A92-18505
LESCO, DANIEL J.
Optical measurement systems p 594 N92-22527
LESHCHINER, DMITRII V.
From the history of Soviet aviation - Aircraft of the Il'iushin design bureau (2nd revised and enlarged edition)
p 61 A92-15022
LESHCHITSKAIA, T. P.
Airfield construction (3rd revised and enlarged edition)
[ISBN 5-277-01070-X] p 670 A92-36606
LESIEUR, M.
Numerical simulation of turbulence at the back of the *airplane*
[ETN-92-91664] p 1037 N92-32769
LESIEUTRE, DANIEL J.
Prediction of vortex shedding from forebodies with chines p 702 A92-41228
LESMERISES, A. L.
Isothermal flow fields in a research combustor for lean blowout studies
[ASME PAPER 91-GT-37] p 121 A92-15520
Lean blowout in a research combustor at simulated low *pressures*
[ASME PAPER 91-GT-359] p 137 A92-15713
LESTEL, J. C.
Ablation and temperature sensors for flight measurements in reentry body heat shields
p 227 N92-15004
LESTER, H. C.
Active control of interior noise in a large scale cylinder using piezoelectric actuators p 1137 N92-32958
LESUEUR, C.
Noise inside aircraft fuselages subjected to airborne excitation p 643 A92-39089
Acoustic transmission through a 2-D orthotropic multi-layered infinite cylindrical shell p 780 A92-44197
LETNIKOV, VIKTOR B.
An analytical study of the helicopter flight safety under an engine failure in proximity of ground
p 91 A92-14454
LEUGERS, J. E.
Susceptibility of a parallelogram type skin friction balance to rotational motion
[AD-A241348] p 139 N92-13078
LEUNG, P. S.
The application of a cylindrical-spherical floating ring bearing as a device to control stability of turbogenerators p 224 N92-14371
LEUNG, R. W.
Interference flows past cylinder-fin-sting-cavity assemblies p 442 A92-32236
LEUTHAEUSSER, U.
An efficient method for three-dimensional route planning with different strategies and constraints
p 728 N92-27901
LEUTIN, A. P.
A method for estimating the minimum distance between two flight vehicles during their separation
p 486 A92-30139
LEVALLOIS, J. M.
Modelling the vaporiser and primary zone flows for a modern gas turbine combustion chamber
p 742 N92-27484
LEVASSEUR, ROBERT
Liquid cooled approaches for high density avionics
p 989 A92-49274
LEVASSEUR, ROBERT D.
High performance heat sink for surface mount applications p 989 A92-49275
LEVCHENKO, V. IA.
Problems of laminar-turbulent transition control in a boundary layer p 312 A92-24979
LEVENTHAL, L.
Active stabilization of multistage axial-compressor aerodynamic system instabilities
[ASME PAPER 91-GT-403] p 76 A92-15733
LEVERTON, JOHN W.
The Civil Rotorcraft Initiative - An action agenda
p 241 A92-22707
Helicopter/heliport operations - Environmental implications p 241 A92-22708
LEVI, KEITH R.
An explanation-based-learning approach to knowledge compilation - A Pilot's Associate application
p 920 A92-48220
The importance of implicit and explicit knowledge in a pilot's associate system p 858 A92-48567
LEVIN, D.
Improved measurement of the dynamic loads acting on rotating parachutes p 702 A92-41236
LEVIN, DANIEL
Self-induced roll oscillations of low-aspect-ratio rectangular wings p 874 A92-46802
LEVIN, DEBORAH A.
Examination of ultraviolet radiation theory for bow shock rocket experiments
[AIAA PAPER 92-2871] p 901 A92-47853
LEVIN, EUGENE
H-N2 interaction energies, transport cross sections, and collision integrals p 1135 A92-54660
LEVIN, I. A.
EIPOS for ice-formation control on aircraft in flight - An alternative technique p 647 A92-40545
LEVIN, M. P.
Iterative algorithms for solving problems of the shaping of three-dimensional ducts p 428 A92-30212
LEVIN, V. M.
Wide-range combustion chamber of ramjet
[AIAA PAPER 91-5094] p 472 A92-31696
LEVINE, S. R.
Ceramic composites: Enabling aerospace materials
[NASA-TM-105599] p 756 N92-27378
LEVINE, STANLEY R.
Ceramics and ceramic matrix composites - Aerospace potential and status
[AIAA PAPER 92-2445] p 577 A92-34474
Flight-vehicle materials, structures, and dynamics - Assessment and future directions. Vol. 3 - Ceramics and *ceramic-matrix composites*
[ISBN 0-7918-0661-8] p 668 A92-39852
Ceramics for engines p 578 N92-22517
LEVITT, RICK
The SnoDog: Preliminary design of a close air support aircraft
[NASA-CR-189990] p 462 N92-21489
LEVKOVSKII, IU. L.
Nonstationary forces on a wing airfoil
p 4 A92-10825
LEVOCI, PETER A.
V-22 full scale development testing
p 646 A92-40038
LEVRAEA, VINCENT
Add-on damping treatment for life extension of the F-15 upper-outer wing skin
[AD-A246149] p 746 N92-27577
LEVY, DAVID W.
Prediction of average downwash gradient for canard configurations
[AIAA PAPER 92-0284] p 319 A92-25737
LEVY, R. L.
Aerodynamic applications of pressure-sensitive paint
[AIAA PAPER 92-0264] p 394 A92-25720
LEVY, RALPH
Vortex generator design for aircraft inlet distortion as a numerical optimization problem p 194 N92-13959
LEVY, YUVAL
Numerical prediction of subsonic turbulent flows over slender bodies at high incidence p 172 A92-18358
Asymmetric turbulent vortical flows over slender bodies p 935 A92-50314
LEWANDOWSKI, JANUSZ
Concept of a one-dimensional model of the dynamic behavior of a gas turbine p 862 A92-47791
LEWANDOWSKI, WLODZIMIERZ
Comparison of GLONASS and GPS time transfers between two west European time laboratories and VNIIFTRI p 1050 N92-33381
LEWANDOWSKI, WLODZIMIERZ W.
The need for GPS standardization
p 1049 N92-33351
Precise GPS ephemerides from DMA and NGS tested by time transfer p 1049 N92-33355
Comparison of two-way satellite time transfer and GPS common-view time transfer between OCA and TUG
p 1050 N92-33356
LEWANTOWICZ, ZDZISLAW H.
Graceful degradation of GPS/INS performance with fewer than four satellites p 97 A92-16644
Closed-loop operation of GPS aided INS
p 100 A92-16954
Architectures and GPS/INS integration - Impact on mission accomplishment p 967 A92-51003
LEWICKI, D.
Experimental testing of prototype face gears for helicopter transmissions
[NASA-TM-105434] p 1002 N92-31349
LEWICKI, D. G.
Transmission overhaul and component replacement predictions using Weibull and renewal theory
p 155 A92-17201
Application of face-gear drives in helicopter transmissions
[NASA-TM-105655] p 908 N92-28434
LEWICKI, DAVID G.
Full-scale transmission testing to evaluate advanced lubricants
[NASA-TM-105668] p 764 N92-26560
Development of a full-scale transmission testing procedure to evaluate advanced lubricants
[NASA-TP-3265] p 998 N92-30396
LEWIS, CLARK H.
Improved nonequilibrium viscous shock-layer scheme for hypersonic blunt-body flowfields p 310 A92-24653
Low-to-high altitude predictions of three-dimensional ablative reentry flowfields
[AIAA PAPER 92-0366] p 394 A92-26227
An improved PNS scheme for predicting complex three-dimensional hypersonic flows
[AIAA PAPER 92-0753] p 436 A92-31679
LEWIS, D. W.
Professor Jesse W. Beams and the first practical magnetic suspension p 771 N92-27723
LEWIS, F. L.
Aircraft flight controls design using output feedback
p 280 A92-21180
Negative state weighting in the linear quadratic regulator for aircraft control p 1007 A92-50513
LEWIS, FRANK L.
Aircraft control and simulation
[ISBN 0-471-61397-5] p 480 A92-31021
LEWIS, G. M.
The 60 years of Bristol engines
[PNR-90845] p 473 N92-20460
The evolution of the bypass engine
[PNR-90832] p 476 N92-21850
LEWIS, JESS
The FAA aging airplane program plan for transport aircraft p 838 N92-30128
LEWIS, LIANE C.
Experimental study of vortex flows over delta wings in wing-rock motion p 810 A92-46787
LEWIS, MARK J.
Application of waverider-based configurations to hypersonic vehicle design
[AIAA PAPER 91-3304] p 32 A92-12742
Navier-Stokes computations of a viscous optimized waverider
[AIAA PAPER 92-0305] p 435 A92-31653
Design tradeoffs on engine-integrated hypersonic vehicles
[AIAA PAPER 92-1205] p 537 A92-33313
LEWIS, NORRIS E.
Fiber optic systems for mobile platforms IV; Proceedings of the Meeting, San Jose, CA, Sept. 18, 1990
[SPIE-1369] p 779 A92-42601
Fiber optic data busses for aircraft
p 736 N92-28093
LEWIS, RICHARD
Visibility measurements for the Automated Surface Observing System (ASOS) p 468 A92-32095
LEWIS, SCOTT W.
Stellar inertial navigation growing with the times upgrading of the LN-20 integrated inertial navigation system p 97 A92-16646
LEWIS, TIMOTHY J.
Experimental pyrometer system for a gas turbine engine
[AIAA PAPER 92-3482] p 859 A92-49022
LEWIS, W. D.
Performance and handling qualities criteria for low cost real time rotorcraft simulators - A methodology development p 136 A92-14365
LEWIS, W., III
Fiber-sensor design for turbine engines
[DE92-003539] p 376 N92-18230
LEWIS, WARREN H.
Singlemode fiber optic rotary joint for aircraft applications p 779 A92-42606
LEWY, S.
Combat aircraft jet engine noise studies
[ONERA, TP NO. 1991-192] p 415 A92-26353
Modification of the radiated sound directivity due to ground reflections - Application to static tests of helicopter turboshaft engines
[ONERA, TP NO. 1991-210] p 415 A92-26362
Experimental study of the effects of atmospheric turbulence on sound propagation over the ground
[ONERA, TP NO. 1991-211] p 415 A92-26363
Experimental study of noise generation and propagation in a turbofan model p 1136 A92-56169
LEWY, SERGE
Research and studies on quiet helicopters
[ONERA, TP NO. 1992-59] p 926 A92-48618
LEWYCKYJ, JULES Z.
Helmet-mounted image intensification analysis
p 554 A92-35454

LEYLAND, JANE
Analysis of open loop higher harmonic control at high airspeeds on a modern four-bladed articulated rotor
[AIAA PAPER 92-2450] p 542 A92-34477
Analysis of open loop higher harmonic control at high airspeeds on a modern four-bladed articulated rotor
[NASA-TM-103876] p 21 N92-11000
LEYLAND, JANE A.
Comparison of three controllers applied to helicopter vibration
[NASA-TM-102192] p 878 N92-28457
LEYLAND, P.
Mesh adaption for 2D transsonic Euler flows on unstructured meshes p 816 A92-47038
LEYNAERT, J.
Recent development of wind-tunnel test techniques at ONERA
[ONERA, TP NO. 1991-135] p 137 A92-16110
Tests of models equipped with a turbofan powered simulator in the ONERA F1 low-speed pressurized wind tunnel
[ONERA, TP NO. 1991-219] p 383 A92-26371
LI, CHANGLIN
Numerical modelling for gas duct in tuboannular combustor p 371 A92-24738
On performance calculation of centrifugal dish atomizer combustor p 654 A92-37390
LI, CHAOJUN
Study of a new airfoil used in reversible axial fans p 177 N92-13970
LI, CHIEN-PENG
Computational methods for shock waves in three-dimensional supersonic flow p 611 A92-37537
LI, CHUN
A new calculating method for the flowfield in turbomachinery - The study on the application of the vorticity-velocity equations for the numerical solution of the flowfield in turbomachinery p 338 A92-27803
LI, F. B.
Control of strong shock-turbulent boundary layer interaction in rectangular channels p 422 A92-29714
LI, FENG
The numerical simulation of transonic inviscid flow over oscillating airfoils p 616 A92-38918
The numerical simulation of separation control using moving surface effect p 616 A92-38924
Numerical simulation of interaction between vortexes and shocks in jet flow field p 616 A92-38925
The numerical simulation of compressible flow around an airfoil at high angle of attack p 818 A92-47686
LI, FENG-HSI
Static and dynamic flow visualization studies of two double-delta wing models at high angles of attack
[AD-A252878] p 1040 N92-33678
LI, GAIQI
Experimental investigation on the mechanism of flame stabilization in afterburner with V-gutter flameholder p 487 A92-29725
LI, GUI-WEN
Durability analysis for a main bulkhead subjected to load on the body of an aircraft p 848 A92-47664
LI, HONGMIN
Experimental characteristics comparison between two scale-model propellers p 24 A92-10962
LI, HUA X.
The research of reducing 3-D low supersonic shock wave reflection in a 2-D transonic flexible walls adaptive wind tunnel
[AIAA PAPER 92-3924] p 1095 A92-56755
LI, JIA
Statistical analysis and prediction of aeroengine deterioration p 557 A92-35570
LI, JILU
A study on the stability of aircraft at high angles-of-attack and state vector propagation sensitivity p 978 A92-53394
LI, JINGYUAN
Wind tunnel study of aerodynamic characteristics of base combustion p 666 A92-36967
LI, JINXIAN
Numerical simulation of three-dimensional turbulent flows in combustion chambers p 970 A92-53276
LI, KEDONG
Digital simulation and experimental modal analysis of dynamic characteristics of a propeller hub p 38 A92-10965
LI, LIGUO
A numerical study of the radiation characteristic of an elliptical exhaust jet p 970 A92-53258
LI, MINGSHUI
The measurement of flutter derivatives using mechanical admittance p 393 A92-25014
LI, PING
Flow analysis for axial compressor including secondary flow effects p 759 A92-41835
LI, QIHAN
Experiments on the blade loss transient response of rotor with flexible damped support
[ASME PAPER 91-GT-149] p 148 A92-15587
Experimental investigation on blade loss transient response of rotor with flexible damped support p 557 A92-35551
LI, QINGHONG
Effect of different force-functions and initial shock pressure on blade response p 374 A92-27913
LI, QINGQUAN
Hypersonic turbulent separated flow past an unswept circular cylinder on a flat plate p 615 A92-38908
LI, RUHUI
Energy analysis of aeroengine and its significance p 557 A92-35569
LI, SHIMING
A circumferential non-uniform effect model for multistage axial-flow compressor throughflow p 588 A92-35572
Mixing for multi-stage axial-flow compressors p 996 A92-53015
LI, SUXUN
Separated flow over the protuberances in hypersonic flow p 615 A92-38907
LI, TING-JIE
A calculating method of the kill probability attack area for AAM p 975 A92-50212
LI, WEI-LIN
BUWICE - An interactive icing program applied to engine inlets
[AIAA PAPER 92-3179] p 922 A92-48794
LI, WENLAN
The engineering prediction for aircraft noise p 1010 A92-50206
LI, X. J.
Heat induced transient behaviours of axial compressors p 469 A92-29721
LI, XIAODONG
Aeroacoustical modification of a propeller p 24 A92-10961
LI, YAN-SHENG
A 3D FEM variational aerodynamic calculation and performance analysis of a leaned turbine stator cascade
[ASME PAPER 91-GT-79] p 69 A92-15548
LI, YIDONG
Measurement and analysis of the flow field above a wing/body configuration p 616 A92-38917
The flow field characteristics about a fighter configuration at high angles of attack
[AIAA PAPER 92-4358] p 1025 A92-55344
LI, YING
Three-dimensional optimal reentry trajectory and aerodynamic heating history of the Space Shuttle p 984 A92-49582
LI, YONGXIN
A real-time rain-flow method of cycle counting and its program design for aeroengine service loads p 557 A92-35560
LI, YOURONG
The study of inverse boundary layer algorithm for transonic flows over aerofoils p 315 A92-25140
LI, YUCHUN
A large-scale axial flow compressor facility and dynamic measurement techniques for rotor flow study p 382 A92-24729
A method for measuring high-subsonic two-dimensional periodic flow field using a single-hole high-response cylindrical pressure probe p 588 A92-35567
LIAGUSHIN, B. E.
Structure of the separated flow region in a dihedral corner in front of an obstacle in supersonic flow p 524 A92-36420
LIAN, XIAOCHUN
Influence of air liquefaction cycle on performance of combined cycle engine p 372 A92-24878
LIANDRAT, J.
Experimental and numerical investigation of a turbulent boundary layer over riblets p 622 A92-40128
LIANG, D. W.
Estimation of the maximum instantaneous distortion p 242 A92-21051
Improved method for estimation of the maximum instantaneous distortion values
[AIAA PAPER 92-3623] p 826 A92-49076
LIANG, DEWANG
Design and calculation of performance of a subsonic inlet duct p 343 A92-28478
LIANG, FANG-PEI
An inviscid stability analysis of unbounded supersonic mixing layer flows p 443 N92-20332
LIANG, SHEN-MIN
Numerical investigation of supersonic mixed-compression inlet using an implicit upwind scheme p 243 A92-21073
Numerical investigation of unsteady transonic nozzle flows p 331 A92-26443
LIANG, SI
An experimental investigation of the inlet exit flow field improved by aerodynamic grid p 343 A92-28477
LIANG, YE P.
Effects of bleed and power extraction on the operating line of engines p 469 A92-29717
Investigation and application of compressor loading technique p 469 A92-29718
LIANN, W. C.
Fair weather convection and light aircraft accidents
[IAF PAPER ST-91-004] p 186 A92-20651
LIAO, JIUN-RONG
Navier-Stokes simulation for cone-derived waverider p 703 A92-41271
LIASJO, K. H.
Advanced method for single event aircraft noise analysis p 693 A92-39060
LIASJO, KARE
A noise survey around Oslo Airport Fornebu p 687 A92-39061
LIASJO, KARE H.
Computation of aircraft noise exposure using digitized topography data p 687 A92-39058
A mobile system for measuring airport noise p 688 A92-39099
LIAW, DER-CHERNG
Two-parameter bifurcation analysis of axial flow compressor dynamics p 421 A92-29355
LIAW, S. P.
Boiling heat transfer from an excavated fin p 498 A92-32523
LIBBY, P. A.
Theories of turbulent combustion in high speed flows
[AD-A253032] p 1111 N92-33624
LIBERATI, F.
Innovation in the laser warning sensor field p 554 A92-35742
LIBERATORE, E. K.
Cold-cycle pressure-jet helicopters: Ventures, designs, and developments. III - Costs and developments p 458 A92-29675
Cold-cycle pressure-jet helicopters: Ventures, designs, and developments. I - Ventures p 459 A92-31325
LIBERATORE, EUGENE K.
Cold-cycle pressure-jet helicopters - Ventures, designs, and developments. II - Design p 271 A92-22712
LIBERATORE, FEDERICO D.
An investigation of the energy loss and near wake flow field of trailing edge injection p 456 N92-21839
LIBESKIND, MARK
Design, evaluation and experimental effort toward development of a high strain composite wing for Navy aircraft p 1107 N92-32514
LIBRESCU, L.
The equations governing the motion of wing-aileron structural systems constructed from advanced anisotropic composite materials
[AIAA PAPER 92-2469] p 564 A92-34359
Dynamic response to time-dependent excitations of cantilevered aircraft wing structures modelled as thin-walled beams
[AIAA PAPER 92-2213] p 584 A92-34403
LIBRESCU, LIVIU
Static aeroelastic tailoring of composite aircraft swept wings modelled as thin-walled beam structures p 294 A92-23114
Adaptive response control of wing structures carrying heavy tip weights
[AIAA PAPER 92-2527] p 583 A92-34374
Behavior of thin-walled beams made of advanced composite materials and incorporating non-classical effects p 673 A92-39944
LICINA, JOSEPH R.
Concept evaluation of the UH-60 externally mounted rescue hoist
[AD-A240545] p 22 N92-11004
LIEBE, DETLEF
Application of MSC/DYNA to shock and impact problems in aircraft industry
[MBB-UD-0593-91-PUB] p 225 N92-14382
LIEBECK, R. H.
Laminar separation bubbles and airfoil design at low Reynolds numbers
[AIAA PAPER 92-2735] p 797 A92-45515
LIEBST, BRAD S.
An algorithm for robust eigenstructure assignment using the Linear Quadratic Regulator
[AIAA PAPER 92-4478] p 1131 A92-55237
LIEPINS, M.
Characteristics of thunderstorm-generated low altitude wind shear - A survey based on nationwide terminal Doppler weather radar testbed measurements p 45 A92-11378

LIESEBERG, A.
Finite-element algorithm for chemically reacting hypersonic flow
[AIAA PAPER 92-0754] p 336 A92-27097
LIFSHITZ, S.
Adaptive suppression of biodynamic interference in helmet-mounted displays and head teleoperation
p 197 A92-18611
LIGHTSTONE, L.
Multiple phase centre DPCA for airborne radar
p 95 A92-16257
LIGRANI, P. M.
Surface heat transfer and flow properties of vortex arrays induced artificially and from centrifugal instabilities
p 1121 A92-56371
LIGTHART, L. P.
Quantitative estimation of secondary surveillance radar information p 353 A92-24943
LII, SHEN-WU
Numerical simulation of twin-jet impingement on a flat plate coupled with cross-flow p 315 A92-25374
LILEK, Z.
Measurements and simulation of the flow around a poppet valve p 675 A92-40103
LILLELEHT, L. U.
Microgravity nucleation and particle coagulation experiments support
[NASA-CR-190159] p 502 N92-21385
Microgravity nucleation and particle coagulation experiments support
[NASA-CR-189899] p 502 N92-21433
LILLEY, G. M.
Jet noise classical theory and experiments
p 54 N92-10602
LILLEY, ROBERT W.
Investigation of air transportation technology at Ohio University, 1990-1991 p 265 N92-17990
Loran-C performance assurance assessment program
[NASA-CR-190469] p 840 N92-28718
LIM, DON
A-2000: Close air support aircraft design team
[NASA-CR-190022] p 463 N92-21567
LIM, HOCK-BIN
Analysis of a dusty wall jet
[NASA-CR-189759] p 257 N92-15965
LIMANSKII, A. V.
A parametric study of the lift-drag ratio of blunt cones
p 437 A92-31860
LIN, C. A.
Predictions of a turbulent backward-facing-step flow with a cubic pressure-strain model
[AIAA PAPER 92-2647] p 796 A92-45514
LIN, C. K.
A numerical study of isothermal flows of a slit V-gutter
[AIAA PAPER 92-0100] p 293 A92-22203
Nonuniform motion of leading-edge vortex breakdown on ramp pitching delta wings p 808 A92-45828
LIN, C.-M.
Robust stabilisation of multivariable feedback systems with desired performance requirement
p 776 A92-42172
LIN, CHAOQIANG
Flow analysis of rectangular wind tunnel contraction
p 312 A92-25001
Singular perturbation theory of hypersonic flow over blunt bodies p 313 A92-25048
LIN, CHING-FANG
Modern navigation, guidance, and control processing
[ISBN 0-13-596230-7] p 639 A92-40199
LIN, CHONGPING
A microprocessor-based automation test system for the experiment of the multi-stage compressor
p 997 A92-53100
LIN, FU-JIA
Probability analysis of structure failure for the wings with main and subordinate components p 848 A92-47657
LIN, GUOCHANG
Quasi-static analysis of roller bearing
p 391 A92-24732
LIN, JISHU
Quasi-static analysis of roller bearing
p 391 A92-24732
LIN, JOHN C.
Separation control on high Reynolds number multi-element airfoils
[AIAA PAPER 92-2636] p 806 A92-45575
LIN, JUANG-LU
Numerical modeling technique for field-to-cable coupling through advanced composite material
p 146 A92-14684
LIN, K. C.
A new approach to the real-time simulation of control systems with discontinuities p 508 A92-29291
LIN, KUO-JIUN
Flutter analysis of anisotropic panels with patched cracks p 219 A92-20216
LIN, KUO-WEI
Fuel injection in hypersonic airbreathing engine
[IAF PAPER 91-273] p 120 A92-14710
LIN, QI
The unsteady flow characteristics of an S-shaped inlet at high incidence p 339 A92-27905
LIN, RUMOU
Second order perturbation method of gas turbine performance calculation p 759 A92-41834
LIN, SONG
Steady state and quasi-transient analysis of aircraft hydraulic system with network theory
p 642 A92-37391
LIN, TONGJI
An experimental study of the flow past spheres at transonic speeds and high Reynolds numbers
p 312 A92-25002
Analysis of transonic flow past an axisymmetric convex corner p 312 A92-25015
On the sensitivity of transonic flow
p 315 A92-25132
LIN, Y.-C.
New systolic array for all-nearest-neighbours problem
p 776 A92-41419
LIN, YU P.
Error estimation of INS ground alignment through observability analysis p 639 A92-40226
LIN, YUAN
Reconstruction of flight path in turbulence
p 874 A92-46777
LIN, ZHAOFU
Integral minimization of engine fault equations based on least fault principle p 374 A92-27857
LINAN, A.
Compressibility effects in thin channels with injection
p 216 A92-18369
LINCOLN, JOHN W.
Proceedings of the USAF Structural Integrity Program Conference
[AD-A242943] p 279 N92-17204
Life management approach for USAF aircraft
p 362 N92-18587
Damage tolerance for commuter aircraft
p 914 N92-30114
LIND, EDWARD
High Capacity Voice Recorder (HCVR) Operational Test and Evaluation (OT and E)/integration test plan
[DOT/FAA/CT-TN91/55] p 402 N92-18959
LIND, GREGORY S.
NASA advanced aeronautics design solar powered remotely piloted vehicle
[NASA-CR-190007] p 462 N92-20665
LINDE, MAGNUS
Temperature effects in FFA HYP 500 at M = 7 in a flow with strong expansion
[FFA-TN-1991-27] p 443 N92-20229
LINDEMANN, ULRICH
Project of an adaptive multiaxial autopilot with learning pilot control
[ETN-92-90592] p 205 N92-15072
LINDGREN, RANDAHL N.
Rotorcraft low altitude IFR benefit/cost analysis: Operations analysis
[SCT-90RR-44] p 191 N92-15061
LINDHOLM, ARNE
JAS 39 Gripen progress report p 112 A92-16058
JAS 39 Gripen flight test report p 645 A92-40030
LINDLEY, CHARLES A.
Combined exo/endoatmospheric transport alternatives
[IAF PAPER 92-0663] p 1104 A92-57102
LINDQWISTER, U. J.
A demonstration of centimeter-level monitoring of polar motion with the Global Positioning System
p 639 N92-24302
LINDSLEY, MICHELLE
Using design of experiments to improve product and process integrity p 928 A92-48555
LINEBARGER, R. S.
Laser-based ultrasonics on GR/epoxy composite - Interferometric detection p 144 A92-13554
LINSE, DENNIS J.
Identification of aerodynamic coefficients using computational neural networks
[AIAA PAPER 92-0172] p 255 A92-23783
A system identification model for adaptive nonlinear control p 508 A92-29248
Neural networks for aircraft system identification
p 303 N92-17998
Identification of aerodynamic coefficients using computational neural networks
[AD-A244711] p 447 N92-21753
LIOU, LUEN-WOEI
A stochastic regulator for integrated communication and control systems. I - Formulation of control law. II - Numerical analysis and simulation p 233 A92-19605
LIOU, MENG-SING
Navier-Stokes solution of transonic cascade flows using nonperiodic C-type grids p 344 A92-28523
Development of a new flux splitting scheme
p 596 N92-23352
Development of new flux splitting schemes
p 682 N92-25809
A new Lagrangian method for real gases at supersonic speed p 633 N92-25814
LIOU, S. G.
Flow over a twin-tailed aircraft at angle of attack. I - Spatial characteristics p 702 A92-41229
Definition of the unsteady vortex flow over a wing/body configuration
[NASA-CR-180083] p 178 N92-13995
LIOU, S.-G.
Measurements of the inflow to a vibrating rotor blade
[AIAA PAPER 92-0634] p 333 A92-27012
LIOU, SHIUH-GUANG
Measurements of the unsteady vortex flow over a wing-body at angle of attack
[AIAA PAPER 92-2729] p 808 A92-45598
Interaction between a rotor tip vortex and a separated flowfield p 814 A92-46947
LIOU, T.-M.
LDV measurements of the flowfield in a simulated combustor with axial and side inlets p 672 A92-38867
LIOU, W. W.
Workshop on Engineering Turbulence Modeling
[NASA-CP-10088] p 678 N92-24514
LIPCHENKO, V. I.
System of cryogenic security of the superconducting accelerator of relativistic nuclei-nuclotron
[DE91-643289] p 304 N92-16789
LIPIN, E. K.
Reduction of computational models in strength problems p 496 A92-31858
Lifting surface design using the principle of passive control of elastic characteristics p 480 A92-31865
LIPKENS, BART
Model experiment to study the effect of turbulence on risetime and waveform of N waves
p 1139 N92-33881
LISCINSKY, D. S.
Experimental study of cross-stream mixing in a rectangular duct
[AIAA PAPER 92-3090] p 903 A92-48735
Experimental study of cross-stream mixing in a rectangular duct
[NASA-TM-105694] p 742 N92-27652
LISOV, A. A.
An automated workstation for the half-scale testing of the flight vehicle stabilization circuit p 664 A92-40622
LITT, JONATHAN S.
A simplified dynamic model of the T700 turboshaft engine
[NASA-TM-105805] p 1009 N92-30898
LITTLE, DAVID D.
Personal air transport: State of the art
[PB91-204768] p 18 N92-10991
LITTLE, ERIC J.
Flexible manufacturing in repair of gas turbine engine components
[AIAA PAPER 92-3524] p 786 A92-49049
LITTLE, GORDON R.
Locally linear neural networks for aerospace navigation systems p 103 N92-12530
LITTLE, T. E.
Structures technology applications for the National AeroSpace Plane p 649 N92-25920
LITVIN, F. L.
Application of face-gear drives in helicopter transmissions
[NASA-TM-105655] p 908 N92-28434
LITVINENKO, A. A.
Generation of loads for finite-element models of large aircraft p 459 A92-30209
LITVINOV, V. M.
Investigating the feasibility of controlling the laminar-turbulent transition by means of laminarizing plates p 493 A92-30161
Effect of the longitudinal and transverse riblets of a flat plate on laminar-to-turbulent transition
p 428 A92-30210
LIU, A.
Particle image velocimetry measurements of the aerodynamics of a wind turbine p 1115 A92-54337
LIU, BIN
China-Soviet long duration balloon flight project
[AIAA PAPER 91-3678] p 1 A92-11036
LIU, C. H.
Prediction of steady and unsteady asymmetric vortical flows around circular cones p 172 A92-18372
Preconditioned upwind methods to solve incompressible Navier-Stokes equations p 395 A92-26436

Numerical study of vortex-dominated flows for wings at high incidence and sideslip p 702 A92-41227
Critical effects of downstream boundary conditions on vortex breakdown
[AIAA PAPER 92-2601] p 792 A92-45478
Active control of asymmetric vortical flows around cones using injection and heating
[AIAA PAPER 92-4426] p 1025 A92-55350
Computation of vortex wake flows and control of their effects on trailing wings
[AIAA PAPER 92-4429] p 1025 A92-55353

LIU, D. D.
Comment on 'Canard-wing interaction in unsteady supersonic flow' p 812 A92-46820

LIU, DAO-ZHI
Analytical investigation of the rules of component matching in turbojet engines
[ASME PAPER 91-GT-170] p 123 A92-15605
Transonic flow calculation of Euler equations by implicit iterating scheme with flux splitting p 934 A92-50215

LIU, DEZHANG
Flow pattern characterization and heat transfer behavior in a boiling two-phase flow in an inclined pipe p 493 A92-29722
The numerical method for calculating the flow field, temperature field and radiation fluxfield in the pipe p 587 A92-35546
The mechanism of liquid-cooling of vane in high-temperature turbine p 969 A92-49841

LIU, FENG
Multigrid Navier-Stokes calculations for three dimensional cascades
[AIAA PAPER 92-0190] p 256 A92-23799

LIU, FENGJUN
A direct-problem calculation method for gas turbines with bowed and twisted blades p 519 A92-35571

LIU, GAO-LIAN
Simple formulae for optimal solidity of two-dimensional compressor cascades based on diffusion concept
[ASME PAPER 91-GT-308] p 126 A92-15687
Research on inverse, hybrid and optimization problems in engineering sciences with emphasis on turbomachine aerodynamics: Review of Chinese advances p 201 N92-13939
Variational formulation of hybrid problems for fully 3-D transonic flow with shocks in rotor p 176 N92-13953

LIU, GENG
On travelling wave vibration of high-speed duplex helical gears p 990 A92-49580

LIU, H. Z.
Fault diagnostics on jet engine starting p 1116 A92-54345

LIU, H.-T.
Effects of ambient turbulence on the decay of a trailing vortex wake p 442 A92-32245
Unsteady aerodynamics of a Wortmann wing at low Reynolds numbers p 810 A92-46778

LIU, J. L.
Locally implicit hybrid algorithm for steady and unsteady viscous flows p 610 A92-36836

LIU, J.-K.
Bifurcation analysis of airfoils in incompressible flow p 623 A92-40580

LIU, JIANYE
GPS integrated system application in aircraft approach landing p 266 A92-21466

LIU, KETAO
Closed-loop identification and iterative controller design p 48 A92-11362

LIU, MINHOU
The mechanism of liquid-cooling of vane in high-temperature turbine p 969 A92-49841

LIU, QIANGANG
The calculation of the static elastic aerodynamic distribution for the rolling maneuver aircraft p 379 A92-25010
Comparison of two flutter analysis methods for elastic aircraft p 660 A92-37394

LIU, REX
1991-92 AHS Technical Committee highlights - Structures and materials p 609 A92-40397

LIU, RIZHI
Delay of wing vortex bursting by using favorable interaction of vortices p 615 A92-38910

LIU, RUN-QUAN
A calculating method of the kill probability attack area for AAM p 975 A92-50212

LIU, SANDY R.
Acoustic predictions using measured pressures from a model rotor in the DNW p 165 A92-14385

LIU, SHAOBO
An experimental investigation of the swirling combustor for integral liquid fuel ramjet p 557 A92-35541

LIU, SHOUSHEN
A study on rotor induced sand and dust environment and its harmfulness to helicopter p 960 A92-53012

LIU, SONG-LING
A new method for predicting the end wall boundary layers and the blade force defects inside the passage of axial compressor cascades p 819 A92-47691

LIU, SONGLING
On velocity profile models for predicting end wall boundary layers and their blade force defects in axial compressor cascades p 311 A92-24877
New model for predicting end wall boundary layer in an axial cascade p 611 A92-37389

LIU, T.
Thermal paints for shock/boundary layer interaction in inlet flows
[AIAA PAPER 92-3626] p 1113 A92-54093

LIU, WEI
Numerical modelling for gas duct in tuboannular combustor p 371 A92-24738

LIU, WEN-TING
A study on crack initiation method for durability analysis p 901 A92-47663
Durability analysis for a main bulkhead subjected to load on the body of an aircraft p 848 A92-47664

LIU, XANGSHENG
Life prediction of local stress-strain method p 588 A92-35564

LIU, XIANGSHENG
Strategies for optimal design of gas turbine disks p 371 A92-24741

LIU, XIAOFENG
Delay of wing vortex bursting by using favorable interaction of vortices p 615 A92-38910

LIU, XINGZHI
Fracture analysis on compressor blades p 37 A92-10672

LIU, YAFEI
Wind tunnel study of aerodynamic characteristics of base combustion p 666 A92-36967

LIU, YIYU
Study on the reliability evaluation of engine fuel accessories p 392 A92-24749

LIU, YUQI
Calculation of fuel sloshing and its coupling vibration with a tank p 991 A92-50204

LIU, ZHENXIA
The engineering prediction for aircraft noise p 1010 A92-50206

LIU, ZHIGANG
Experimental investigation on the mechanism of flame stabilization in afterburner with V-gutter flameholder p 487 A92-29725

LIUBCHIK, G. N.
Development and bench test of high-temperature combustion chamber with structural ceramic components
[ASME PAPER 91-GT-315] p 126 A92-15691

LIUBIMOV, D. A.
An efficient method for calculating three-dimensional transonic flow past air intakes p 7 A92-12178

LIVINE, E.
Exploratory design studies of actively controlled wings using integrated multidisciplinary synthesis p 641 A92-36828

LIVNE, E.
Integrated aeroservoelastic wing synthesis by nonlinear programming/approximation concepts p 873 A92-46752

LIVNE, ELI
New complex pole and gust response approximations for integrated aeroservoelastic synthesis
[AIAA PAPER 92-2377] p 565 A92-34547
Optimization of a 2D scramjet-vehicle using CFD and simplified approximate flow analysis techniques
[AIAA PAPER 92-3673] p 1022 A92-54116

LIVNEH, RAFAEL
New literal approximations for the longitudinal dynamic characteristics of flexible flight vehicles
[AIAA PAPER 92-4411] p 1075 A92-55205

LIZZA, CARL S.
Pilot's associate: Evolution of a functional prototype p 118 N92-12531

LJUNGGREN, STEN
Mechanical noise from large wind turbines - Experiences from Swedish prototypes p 686 A92-39046

LLEWELYN-DAVIES, D. I. T. P.
An investigation into the interface between three closely spaced axi-symmetric bodies at subsonic speed
[CRANFIELD-AERO-9114] p 948 N92-31514

LO, C. F.
Experimental results on a wall interference correction method with interface measurements
[AIAA PAPER 92-0570] p 333 A92-26978
Blockage correction in three-dimensional wind tunnel testing based on the wall signature method
[AIAA PAPER 92-3925] p 1095 A92-56756
A wall interference assessment/correction system
[NASA-CR-189785] p 259 N92-15974

LO, CHING F.
Wind-tunnel compressor stall monitoring using neural networks p 918 A92-46817

LO, EDMOND Y.
Laser-driven hypersonic air-breathing propulsion simulator
[AIAA PAPER 92-3922] p 1095 A92-56753

LO, R.
Distributed artificial intelligence approach to air traffic control p 161 A92-13436

LOBANOVSKII, IU. I.
The effect of wing twist optimized in the framework of the plane cross section hypothesis on the aerodynamic characteristics of a wing-body combination at hypersonic speeds p 424 A92-30129

LOBOSCO, ROY
New York Downtown Manhattan (Wall Street) Heliport: Operations analysis
[DOT/FAA/RD-91/12] p 139 N92-13077

LOCATELLI, J.
Structural optimization at Aerospatiale Aircraft
[AIAA PAPER 92-2371] p 601 A92-34542

LOCK, G. D.
Nonstationary gasdynamics p 220 N92-13985

LOCK, WILTON P.
Variable-camber systems integration and operational performance of the AFTI/F-111 mission adaptive wing
[NASA-TM-4370] p 570 N92-22194

LOCKE, W.
Fatigue crack growth of small corner defects from blunt notches in an aeroengine alloy
[PNR-90860] p 1111 N92-34019

LOCKHART, MARY G.
Atmospheric analysis for airdata calibration on research aircraft
[AIAA PAPER 92-0293] p 369 A92-25746

LOCKHART, THOMAS J.
Relative accuracy of wind tunnel calibration speeds p 484 A92-32056

LOCKLEAR, STACY L.
Static tests for the evaluation of fuel additives
[AIAA PAPER 92-0686] p 389 A92-27053

LOCKMAN, WILLIAM K.
Flow over an all-body hypersonic aircraft - Experiment and computation p 310 A92-24651

LODGE, JOHN H.
A TMS320-based modem for the aeronautical-satellite core data service p 594 N92-22562

LODGE, M. A.
Noise generated by wind turbines p 686 A92-39045

LOEBERT, G.
Turbulent drag reduction by laminar sublayer thickening
[AIAA PAPER 92-2707] p 801 A92-45549

LOEHNER, R.
Supersonic flow over an axisymmetric backward-facing step p 705 A92-41542

LOESH, ROBERT E.
JPL's Real-Time Weather Processor project (RWP) metrics and observations at system completion p 413 N92-19428

LOEWY, R. G.
Dynamic analysis of rotor blades with root retention design variations p 1054 A92-56156

LOEWY, ROBERT G.
Aeroelasticity and the Tiltrotor VTOL aircraft p 647 A92-40389

LOFARO, RONALD JOHN
Workshop on integrated Crew Resource Management (CRM)
[DOT/FAA/RD-92/5] p 781 N92-27518
Workshop on Aeronautical Decision Making (ADM). Volume 1: Executive summary
[DOT/FAA/RD-92/14-VOL-1] p 1142 N92-33305

LOFTIN, R. B.
Advanced training systems for the next decade and beyond
[AIAA PAPER 92-1626] p 690 A92-38699

LOH, C. Y.
A new Lagrangian method for real gases at supersonic speed p 633 N92-25814

LOH, ROBERT
GPS for precision approaches p 139 A92-16648
Analysis of stand-alone differential GPS for precision approach p 638 A92-38381

LOHMANN, R. P.
High-speed civil transport aircraft emissions p 408 N92-19122

LOHNER, R.
Three-dimensional space-marching algorithm on unstructured grids p 5 A92-11058
Formation of shocks within axisymmetric nozzles p 176 A92-20760

LOIKKANEN, M. J.
Multidisciplinary design optimization of a large transport aircraft wing
[AIAA PAPER 92-1002] p 536 A92-33194
LOISY, JEAN
Steady and transient performance calculation method for prediction, analysis, and identification
p 869 N92-28461
LOKEN, G.
Space Shuttle Orbiter auxiliary power unit status
[SAE PAPER 912060] p 889 A92-45442
LOKHOV, G. M.
Development of a combined fast method for studying the plane motions of rigid bodies in the atmosphere around the center of mass in the presence of perturbations
p 304 A92-23563
Singularity bypass algorithms in the numerical solution of equations of body motion relative to a center of mass in the atmosphere in the presence of disturbances
p 437 A92-31857
LOKOS, WILLIAM A.
Predicted and measured in-flight wing deformations of a forward-swept-wing aircraft p 548 A92-35936
LOKOTKO, A. V.
A method for determining the internal force characteristics of a model in external supersonic flow
p 706 A92-42682
LOKUTA, ROBERT S.
JTIDS electromagnetic compatibility in the 960-1215 MHz band
[AD-A247834] p 773 N92-27864
LOMBARD, CHARLES
Accurate, productive aerodynamic simulation on patched mesh systems
[AD-A243977] p 405 N92-19386
LOMKOV, K. E.
The enhancement of the mixing and combustion processes in supersonic flow applied to scramjet engine
[AIAA PAPER 92-3428] p 1112 A92-54029
LONDON, B.
A preliminary study of the microstructure-property relationships in cast gamma titanium aluminide alloys
p 487 A92-30596
LONG, ALEXIS B.
The 1988 Australian Winter Storms Experiment - Case study: 6 August 1988 p 301 A92-23009
LONG, ARLEN N.
The Software Factory, version 5.0
[AIAA PAPER 92-0590] p 411 A92-26992
LONG, CHRISTOPHER A.
Rotational coherent anti-Stokes Raman spectroscopy measurements in a rotating cavity with axial throughflow of cooling air - Oxygen concentration measurements
p 990 A92-49574
LONG, LYLE N.
Prediction of forces and moments for hypersonic flight vehicle control effectors
[NASA-CR-188954] p 33 N92-11070
LONG, MARY J.
Experimental investigation of an ejector-powered free-jet facility
[AIAA PAPER 92-3569] p 1090 A92-54058
LONG, ROBERT L.
Risk management - Expanding horizons in nuclear power and other industries
[ISBN 1-56032-231-4] p 993 A92-51438
LONG, RONALD R.
How to support the 'little guy' p 60 A92-14437
LONG, YU-QIU
Combined application of the energy method and the weighted residual method - A new way to construct the finite elements p 991 A92-50239
LONGLEY, J. P.
Active control of rotating stall in a low speed axial compressor
[ASME PAPER 91-GT-88] p 122 A92-15553
Inlet distortion effects in aircraft propulsion system integration p 869 N92-28464
LONGMAN, CHICK
Strategic vs tactical air traffic control utilizing ADS and earth reference area NAV p 96 A92-16631
LONGO, J. M. A.
Vortical flow simulation by the solution of the Navier-Stokes equations p 620 A92-40104
LONGOBARDI, R.
EH 101 ship interface trials: Flight test programme and preliminary results p 465 N92-21964
LONSINGER, H.
Design, analysis, and testing of integrally stiffened composite centre fuselage skin for future fighter aircraft
p 535 A92-32554
Design, analysis, and testing of integrally stiffened composite centre fuselage skin for future fighter aircraft
[MBB-FE2-PUB-S-450] p 359 N92-18333
LOOIJE, C. E. W.
Diffuser casing upgrade for an advanced turbofan
[NLR-TP-90097-U] p 870 N92-28711
LOOK, D. C., JR.
Optimization of a thermally non-symmetric fin - Preliminary evaluation p 992 A92-50448
LOOMIS, MARK P.
Flow characterization in the NASA Ames 16-inch Shock Tunnel
[AIAA PAPER 92-3810] p 1090 A92-54180
LOOMIS, WILLIAM R.
Liquid lubricants for advanced aircraft engines
[NASA-TM-104531] p 1109 N92-32863
LOONEY, ALAN
Welding technology transfer task/laser based weld joint tracking system for compressor girth welds
p 593 N92-22426
LOPEZ, A. R.
Numerical calculations of two-dimensional single and multi-material flow fields with CCICE
[DE92-015778] p 1000 N92-30903
LOPEZ, HENRY J.
The NASA hypersonic research engine program
p 474 N92-21521
LOPEZ, ISAAC
Transonic turbine blade cascade testing facility
[AIAA PAPER 92-4034] p 1101 A92-56856
Transonic turbine blade cascade testing facility
[NASA-TM-105646] p 667 N92-26129
LOPEZ, S. B.
Detailed investigation of causes of avionics field failures p 995 A92-51925
LORBER, PETER F.
Compressibility effects on the dynamic stall of a three-dimensional wing
[AIAA PAPER 92-0191] p 256 A92-23800
LORCH, D. R.
MD-80 aft cabin noise control: A case history
p 1137 N92-32950
LORD, JEFFREY R.
Wavelength encoded fiber optic angular displacement sensor p 857 A92-48046
LORDON, J.
A new automatic grid generation environment for CFD applications
[AIAA PAPER 92-2720] p 803 A92-45558
LORENZ, DAVID A.
Recent advances in restraint technology
p 535 A92-32979
LORENZO, CARL F.
IMPAC - An integrated methodology for propulsion and airframe control p 477 A92-29118
Directions in propulsion control p 560 N92-22530
LORIER, PHILIPPE
Space software is first of all software
p 509 N92-20590
LOSCHKE, R. C.
Flight management system of the F-117A
p 1082 A92-55910
LOTH, E.
Formation of shocks within axisymmetric nozzles
p 176 A92-20760
Supersonic flow over an axisymmetric backward-facing step p 705 A92-41542
LOTH, ERIC
High-speed cinematography of supersonic mixing layers
[AIAA PAPER 92-3545] p 1112 A92-54044
LOTH, JOHN L.
Pulse jet one-way valve performance
[AIAA PAPER 92-3169] p 863 A92-48790
LOTTATI, I.
Review of propulsion applications and numerical simulations of the pulsed detonation engine concept
p 129 A92-17177
A parametric study of airbreathing Pulsed Detonation Engine
[AIAA PAPER 92-0392] p 471 A92-31660
LOTTS, C. G.
Coupled 2D-3D finite element method for analysis of a skin panel with a discontinuous stiffener
[AIAA PAPER 92-2474] p 583 A92-34363
LOU, KEN A.
Development of a reclined crashworthy crewseat for rotorcraft p 105 A92-14370
LOU, Y. W.
A simulator and performance criteria for evaluation of ground and space-based ATC surveillance
p 96 A92-16639
LOUIE, A.
An improved model-creation program for EM interaction analysis
[NRC-31764] p 155 N92-12153
LOUIE, C. M.
Numerical simulation of leading-edge vortex breakdown using an Euler code p 701 A92-41213
LOUKIS, E.
Combination of different unsteady quantity measurements for gas turbine blade fault diagnosis
[ASME PAPER 91-GT-201] p 149 A92-15624
A procedure for automated gas turbine blade fault identification based on spectral pattern analysis
[ASME PAPER 91-GT-259] p 151 A92-15661
LOURENCO, L.
Unsteady flow past an airfoil pitching at a constant rate p 610 A92-36826
LOURME, D.
Review of the European hypersonic wind tunnel performance and simulation requirements
p 209 N92-15043
LOUTON, STEVEN E.
Use of simulation in the USAF Test Pilot School curriculum p 884 N92-28535
LOVATO, J. A.
Active control of vortex structures in a separating flow over an airfoil
[AIAA PAPER 92-2728] p 804 A92-45563
LOVATO, JULIE A.
Active control of the separation region on a two-dimensional airfoil
[AD-A249739] p 948 N92-31622
LOVE, MICHAEL H.
Application of analytical and design tools for fighter wing aeroelastic tailoring
[AIAA PAPER 92-2373] p 542 A92-34543
Application of analytical and design tools for fighter wing aeroelastic tailoring p 550 N92-23231
LOVELL, D. A.
An experimental investigation of vortex flaps on a canard combat-aircraft configuration p 87 N92-13023
LOVETRI, JOE
Constraint propagation through electromagnetic interaction topologies
[NRC-31761] p 155 N92-12154
LOW, EICHER
Achievement of rotorcraft handling qualities specifications via feedback control p 568 A92-35747
Robustness of a helicopter flight control system designed using eigenstructure assignment
[AIAA PAPER 92-4469] p 1076 A92-55229
Design of helicopter flight control systems for hover and low speed using eigenstructure assignment
p 1061 N92-33952
LOW, M. S.
Structural features of a heated round turbulent jet in a cross-flow p 676 A92-40148
LOWE, D. M.
Thermal response of rigid and flexible insulations and reflective coating in an aeroconvective heating environment
[NASA-TM-103925] p 852 N92-28721
LOWE, J. D.
Aerodynamics p 202 N92-13977
LOWE, S. R.
Solid-fuel ramjet fuel regression rate/thrust modulation
p 666 A92-36966
LOWELL, T. A.
Analysis of airframe/engine interactions for a STOVL aircraft with integrated flight/propulsion control
[AIAA PAPER 92-4623] p 1052 A92-55300
LOWRIE, ROBERT B.
Evaluation of Euler solvers for transonic wing-fuselage geometries p 174 A92-20214
LOWSON, M. V.
The evaluation of canard couplings at high angles of attack
[AIAA PAPER 92-0281] p 318 A92-25735
Symmetry breaking in vortex flows on conical bodies
p 703 A92-41278
Progress towards quieter civil helicopters
p 1011 A92-52847
LOYALKA, S. K.
Motion of a sphere in a gas - Numerical solution of the linearized Boltzmann equation p 591 A92-36194
LU, BO
Experimental investigation on reducing fluctuating pressures of launch vehicles by passive shock-wave/boundary-layer control p 616 A92-38916
LU, FRANK K.
Initial operation of the UTA shock tunnel
[AIAA PAPER 92-0331] p 383 A92-25778
Experimental studies of hypersonic shock-wave boundary-layer interactions
[NASA-CR-190731] p 950 N92-32162
LU, HONGYU
Measurement and analysis of the flow field above a wing/body configuration p 616 A92-38917
The flow field characteristics about a fighter configuration at high angles of attack
[AIAA PAPER 92-4358] p 1025 A92-55344

LU, JIHUAI
A study on rotor induced sand and dust environment and its harmfulness to helicopter p 960 A92-53012
LU, JUN
Three-dimensional compressible flows in turbo-machinery solved by the pseudostream function formulation p 338 A92-27801
LU, PANMING
Loss prediction of annular cascade flow based upon *S1/S2 stream surface Navier-Stokes analysis* p 338 A92-27802
LU, PING
Optimal control problems with maximum functional p 232 A92-18616
Trajectory optimization for the National Aerospace Plane
[NASA-CR-190355] p 650 N92-26017
LU, PONG-JEU
Flutter analysis of anisotropic panels with patched cracks p 219 A92-20216
LU, QINGFENG
An approach to the low-speed longitudinal aerodynamic characteristics of the joined wing configuration p 339 A92-27909
LU, QIZHENG
Experimental investigation on reducing fluctuating pressures of launch vehicles by passive shock-wave/boundary-layer control p 616 A92-38916
Investigation on effects on enhancing lift by acoustic excitation p 693 A92-38923
LU, YA-JUN
Numerical investigation of axial flow compressor casing treatment p 934 A92-50216
LU, YAJUN
A numerical investigation of axial flow compressor casing treatment p 942 A92-53381
LU, YI
Sensitivity analysis of discrete periodic systems with applications to helicopter rotor dynamics p 846 A92-46884
LU, ZHI-YONG
The influences of forced oscillations toward vortex-breakdown p 934 A92-50210
LU, ZHIYONG
Measurement and analysis of the flow field above a wing/body configuration p 616 A92-38917
The flow field characteristics about a fighter configuration at high angles of attack
[AIAA PAPER 92-4358] p 1025 A92-55344
LUBNER, MAXINE E.
Rates and risk factors for accidents and incidents versus violations for U.S. airmen p 91 A92-14048
LUBRINA, P.
Aircraft ground vibration test by means of flight control surfaces
[ONERA, TP NO. 1991-96] p 133 A92-16079
LUCAS, EVANGELINE
A-2000: Close air support aircraft design team
[NASA-CR-190022] p 463 N92-21567
LUCAS, JEFFERY C.
Enhanced autopilot design through hardware-in-the-loop simulation p 204 A92-19103
LUCHINI, P.
A fast conformal mapping algorithm with no FFT p 1007 A92-50471
LUCHT, BRAD
Advanced experimental design applied to damage tolerance of composite materials p 993 A92-51505
LUCJANEK, WIESLAW
General model of isolated helicopter blade for stability investigation p 547 A92-35774
Modeling of the control systems of rotary wing aircraft (Review) p 875 A92-47783
A new method of helicopter rotor blade motion control p 875 A92-47786
Simulation of helicopter see-saw rotor motion p 1055 A92-56287
LUCK, ROGELIO
Observability under recurrent loss of data p 302 A92-21191
LUCKRING, JAMES M.
Recent progress in computational vortex-flow aerodynamics p 84 N92-13002
LUDTKE, WILLIAM P.
Notes on the cause of parachute critical velocity
[AD-A244417] p 347 N92-19085
LUDWIG, F. A.
Thermally regenerative fuel cells
[AD-A242900] p 300 N92-17629
LUDWIG, GARY L.
Evolution of avionic systems architecture, from the 1950's to the present p 198 N92-14047
LUDWIG, REINHOLD
Numerical comparison of experimentally measured ultrasound through a multilayered specimen p 510 A92-28682
LUEBBERS, RAYMOND J.
Finite difference time domain modeling of steady state scattering from jet engines with moving turbine blades
[NASA-CR-190290] p 971 N92-30753
LUEHRSEN, RUSSELL P.
Solid fuel ramjet infrared signature
[AD-A246299] p 753 N92-26362
LUFFY, RONALD J.
A study on the impact of shroud geometry on ejector pumping performance
[AIAA PAPER 92-3260] p 864 A92-48856
LUKASHCHIK, E. P.
Vibration of a wing of finite span in subsonic flow at small distances from a solid boundary p 9 A92-12808
LUKENS, W.
Space Shuttle Orbiter auxiliary power unit status
[SAE PAPER 912060] p 889 A92-45442
LUKOWICZ, HENRYK
Estimation of the size of separation zone in a turbine stage under small load p 10 A92-13235
LUKSAK, D. A.
Methodology for the assessment of material quality effects on airframe fatigue durability p 213 A92-19820
LUM, K. K.
The design and development of a portable, DSP micro-processor based, high-accuracy data acquisition system
[NRC-32146] p 1134 N92-32851
LUMB, S. B.
Transient aerodynamics of a high dynamic pressure shroud separation for a ground-based interceptor missile
[AIAA PAPER 92-2820] p 705 A92-41348
LUNDBERG, JOHN B.
Simulation of GRM drag compensation system p 285 A92-21023
LUNDBERG, WAYNE R.
Analysis of measured environmental noise levels: An assessment of the effects of airbase operational model variables on predicted noise exposure levels
[AD-A244805] p 485 N92-21720
LUNDGREN, T. S.
Microburst modelling and scaling p 915 A92-46262
LUNN, KEN
The V-22 Osprey - A significant flight test challenge p 546 A92-35766
LUNTZ, A. L.
Euler solver for arbitrary configurations: Further applications p 949 N92-31888
LUNTZ, ALEXANDER L.
Cartesian Euler method for arbitrary aircraft configurations p 340 A92-28039
LUO, J.
Numerical simulation of turbomachinery flows with advanced turbulence models p 1124 N92-32270
LUO, JIAN
Robustness analysis of a model reference adaptive control system p 412 A92-27859
LUO, RONG
Wind tunnel study of aerodynamic characteristics of base combustion p 666 A92-36967
LUO, SHIJUN
Multiple line-vortex model of vortex flows around body of revolution at high angles of attack up to 60 degrees p 314 A92-25104
LUONGO, R.
Evaluation of triple simultaneous parallel ILS approaches spaced 5000 feet apart, phase 4.b
[DOT/FAA/CT-91/31] p 456 N92-21404
LUONGO, RENEE
Evaluation of triple simultaneous parallel ILS approaches spaced 4300 feet apart, phase 4a
[ACD-340] p 191 N92-14034
LUPINC, V.
Creep fracture mechanisms in single crystal superalloys p 388 A92-25031
LUPPOLD, ROBERT
Application of syndrome pattern-matching approach to fault isolation in avionic systems p 1005 A92-49261
LURIA, FRANK
High angle-of-attack control enhancement on a forward swept wing aircraft
[AIAA PAPER 92-4427] p 1080 A92-55351
LUSCH, THOMAS G.
Real targets, unreal displays - The inadvertent suppression of critical radar data p 839 A92-44969
LUSHIN, V. N.
Comparative studies of flow around a wing profile in two wind tunnels p 7 A92-12170
LUSTIG, S.
A history of high-temperature testing at WPAFB p 981 A92-51406
LUSTIGER, A.
Processing effects and damage tolerance in poly(etheretherketone) composites p 388 A92-26152
LUTON, J. A.
Numerical simulations of flutter and its suppression by active control
[AIAA PAPER 92-4652] p 1082 A92-55396
LUTTGES, M. W.
Unsteady aerodynamic loading produced by a sinusoidally oscillating delta wing p 701 A92-41223
LUTTGES, MARVIN W.
Flow visualization image analysis of high-rate roll *experiments on a delta wing*
[AIAA PAPER 92-0317] p 321 A92-25764
Static and dynamic flow field development about a porous suction surface wing
[AIAA PAPER 92-2628] p 795 A92-45500
LUTZ, A. E.
Simulation of chemical kinetics in turbulent natural gas combustion
[PB92-123660] p 488 N92-20329
LUTZE, FREDERICK H.
Nonlinear model-following control application to airplane control (1992 AIAA Controls Design Challenge)
[AIAA PAPER 92-4625] p 1077 A92-55302
LUTZE, FREDERICK H., JR.
Enhanced energy maneuverability for attack helicopters using continuous, variable (C-V) rotor speed control p 132 A92-14421
LY, UY-LOI
Design of localizer capture and track hold for a transport airplane - An H(infinity)/LTR approach p 52 A92-11583
Optimal discrete-time static output-feedback design - A W-domain approach p 1007 A92-50499
Control design of a UH-60 rotorcraft via CLTR and direct optimization
[AIAA PAPER 92-4470] p 1076 A92-55230
Advanced rotorcraft control using parameter optimization
[NASA-CR-189502] p 135 N92-13073
LYCANS, RANDAL W.
Heat transfer to a cylinder submerged in a rectangular cavity in supersonic flow
[AIAA PAPER 92-2949] p 901 A92-47913
LYDON, T.
Remote telemetry concepts p 882 A92-47562
LYKOV, O. P.
Enhancing the performance characteristics of engine fuels by means of surfactant additives p 892 A92-46631
LYKOV, V. A.
Methods for determining atmospheric correction for radio-rangefinder measurements of inclined trajectories p 775 A92-44070
LYNCH, F. T.
Experimental necessities for subsonic transport configuration development
[AIAA PAPER 92-0158] p 254 A92-23773
LYNCH, FRANK T.
Some practical aspects of viscous drag reduction concepts
[SAE PAPER 912129] p 618 A92-39976
The adverse aerodynamic impact of very small leading-edge ice (roughness) buildups on wings and tails p 451 N92-21691
LYNCH, PRISCA L.
Multibody interference at transonic Mach numbers
[AIAA PAPER 92-0651] p 334 A92-27023
LYNE, GEORGE W.
A testability-dependent maintainability-prediction technique p 1120 A92-56222
LYNE, J. E.
Earth aerobraking strategies for manned return from Mars p 752 A92-41535
LYNN, STEVEN G.
New processes in commercial airplane design p 607 A92-38218
LYON, ERVIN F.
Airport Surface Traffic Automation p 95 A92-16228
LYON, SEAN
Scorpion: Close Air Support (CAS) aircraft
[NASA-CR-189974] p 462 N92-20664
LYONS, ARTHUR
Fault tolerant EHA architectures p 763 A92-43885
LYONS, D. F.
Flight test of a half-scale unmanned air vehicle p 193 A92-20208
LYONS, DANIEL F.
Research flight test of a scaled unmanned air vehicle p 549 A92-35944
Aerodynamic analysis of the Pioneer unmanned air vehicle
[AIAA PAPER 92-4635] p 1027 A92-55382
LYONS, R.
An aircraft Earth station for general aviation p 678 N92-24194

LYRINTZIS, A. S.
Efficient iterative methods for the transonic small disturbance equation p 1025 A92-54933
LYSENKO, K. V.
Processing of axisymmetric flow interferograms with density profile bends or discontinuities p 993 A92-51316
LYTLE, DREW B.
Commercial airplane air distribution system development through the use of computational fluid dynamics
[AIAA PAPER 92-0987] p 535 A92-33182

M

M'SAAD, M.
On the adaptive control of missile autopilots p 477 A92-29102
MA, CAIFEN
Experimental investigation on gas-particle flow in cascades p 62 A92-13300
MA, DONG-LI
The effect of atmospheric turbulence on the external store separation from an aircraft p 934 A92-50233
MA, EDWARD C.
A transonic/supersonic/hypersonic CFD analysis of the entry Space Shuttle Orbiter
[AIAA PAPER 92-2614] p 805 A92-45571
MA, HANDONG
Numerical simulation of interaction between vortexes and shocks in jet flow field p 616 A92-38925
MA, HUIYANG
The rolling-up and interaction of the leading-edge and trailing-edge vortex sheets of a delta wing p 314 A92-25101
MA, JIAJU
Experimental study of a two-dimensional random frequency generator p 483 A92-29712
MA, JIHUA
Numerical simulation of two incoming streams in a dual-combustion ramjet combustor p 375 A92-28419
MA, PAUL W.
Optical computing at NASA Ames Research Center
[AIAA PAPER 91-3779] p 231 A92-17637
MA, SHULIN
The effect of afterbody devices on drag reduction p 942 A92-53097
MA, XIA
The computation of transonic viscous flow p 338 A92-27831
MA, YANWEN
Numerical simulation of 2-D separated flows caused by suddenly change of the body section p 312 A92-25004
Numerical simulation of the flow around rectangular cylinder p 339 A92-27851
MA, YUWEN
A full-scale fatigue test and failure analyses research of F-X fighters p 960 A92-53092
MA, ZUKANG
Safety factor and reliability for composite laminates p 996 A92-53070
MAARSINGH, T. A.
Evaluation of measured-boundary-condition methods for 3D subsonic wall interference
[NLR-TR-88072-U] p 832 N92-29884
MABEY, D. G.
A review of rigid body response on sting supported models at high angles of incidence p 66 A92-15345
Heat transfer effects on aerodynamics and implications for wind-tunnel tests p 497 A92-32240
Comment on 'Transition effects on airfoil dynamics and implications for subscale tests' p 703 A92-41247
Effect of model cooling on periodic transonic flow p 813 A92-46900
A review of scale effects in unsteady aerodynamics p 934 A92-50121
Review of aircraft dynamic loads due to flow separation p 85 N92-13008
Further investigation of the effect of model cooling on periodic transonic flow p 721 N92-27961
A review of scale effects on surfaces in unsteady motion p 722 N92-27962
MACARAEG, M. G.
Numerical studies of transverse curvature effects on transonic flow stability p 524 A92-36186
MACCAGNO, T. M.
The hardness and toughness of HIPed silicon nitride p 668 A92-39682
MACCONOCHIE, IAN O.
Structural design considerations for a Personnel Launch System p 386 A92-24668
MACCORMACK, ROBERT W.
Navier-Stokes computation of hypersonic near wakes with foreign gas injection
[AIAA PAPER 92-0838] p 422 A92-29604
MACDERMOTT, W. N.
Flow contamination and flow quality in arc heaters used for hypersonic testing
[AIAA PAPER 92-4028] p 1100 A92-56850
MACDONALD, DAVID
Concorde, fifteen years on the front line
[SAE PAPER 912193] p 644 A92-40010
MACE, JAMES
Integration of supportability elements into the conceptual design process
[AIAA PAPER 92-1194] p 600 A92-33306
Fighter airframe/propulsion integration - A McDonnell Aircraft perspective
[AIAA PAPER 92-3333] p 850 A92-48916
MACE, W. D., JR.
Comparison of frequency domain and time domain laser velocimeter signal processors p 1114 A92-54314
MACEDO MAURA, GERALDO A.
Approach for analysis and design of composite rotor blades p 899 A92-46801
MACGREGOR, G. R.
Application of analysis techniques for low frequency interior noise and vibration of commercial aircraft
[NASA-CR-189555] p 481 N92-20376
MACGUGAN, DOUGLAS C.
Testability of the PAALS auto-align sensor system p 965 A92-49310
MACH, R.
Managing airborne assets through loads monitoring p 363 N92-18594
MACHIDA, Y.
Study on transonic cascade performance by use of newly built facility p 136 A92-15328
MACHINA, MARK H.
Power beaming - Energy transmission at 35 GHz and higher frequencies
[AIAA PAPER 92-2027] p 471 A92-29944
MACHINCHICK, MICHAEL
High temperature dynamic engine seal technology development
[NASA-TM-105641] p 596 N92-23435
MACIEJNY, A.
Corrosion damage and regeneration of aluminide coatings on aircraft turbine blades p 142 A92-15244
MACINA, O.
A new integral equation for potential compressible aerodynamics of rotors in forward flight p 815 A92-46958
MACISAAC, B. D.
Engine performance and health monitoring models using steady state and transient prediction methods p 870 N92-28467
MACK, J. R.
Development of natural gas rotary engines
[PB92-149665] p 765 N92-26816
MACK, M. D.
High Reynolds number testing in support of transport airplane development
[AIAA PAPER 92-3982] p 1099 A92-56807
MACKALL, DALE
System overview of the NASA Dryden Integrated Test Facility
[NASA-TM-104250] p 984 N92-32201
Rapid development of the X-31 simulation to support flight-testing
[NASA-TM-104256] p 1060 N92-33149
MACKENZIE, ANNE I.
Radar multipath study for rain-on-radome experiments at the Aircraft Landing Dynamics Facility
[NASA-TM-101657] p 680 N92-25137
MACKENZIE, FRANKLIN D.
Loran time difference correction factors - Valid information or blue smoke and mirrors? p 96 A92-16633
MACKIN, CLIFFORD
Joint Federal Aviation Administration (FAA)/Civil Aviation Authority (CAA) Microwave Landing System (MLS) Area Navigation (RNAV) flight evaluations
[DOT/FAA/CT-TN91/17] p 268 N92-15983
Comparison of the performance of a microwave landing system elevation station with the instrument landing system end-fire glide slope at Yeager Airport, Charleston, West Virginia
[DOT/FAA/CT-TN91/22] p 534 N92-22210
MACKNIGHT, NIGEL
NASA's quiet side. I p 607 A92-37875
MACKOWSKI, MICHAEL J.
Requirements for high flux cooling of future avionics systems
[SAE PAPER 912104] p 673 A92-39958
MACLEAN, R.
Hot gas environment around STOVL aircraft in ground proximity. I - Experimental study p 371 A92-24409
MACLEOD, J. D.
Compressor coating effects on gas turbine engine performance p 25 A92-11282
Implanted component faults and their effects on gas turbine engine performance
[ASME PAPER 91-GT-41] p 121 A92-15524
Investigation of engine thrust correlation methods for enclosed test cells
[ASME PAPER 91-GT-68] p 121 A92-15538
High density fuel qualification for a gas turbine engine
[AIAA PAPER 92-0684] p 389 A92-27051
MACLEOD, JAMES D.
A derivation of gross thrust for a sea-level jet engine test cell
[NRC-30165] p 130 N92-12001
MACLIN, JAMES R.
Performance of fuselage pressure structure p 913 N92-30109
MACPHERSON, J. I.
Airborne tests of flux measurement by the relaxed eddy accumulation technique p 504 A92-32052
Airflow effects about PMS probes on the DLR Falcon p 467 A92-32060
The use of Kalman filtering techniques to improve the accuracy of flight test data
[NRC-32139] p 1064 N92-32850
MACRET, J. L.
Materials and structures for Hermes p 666 A92-38213
MACRORIE, MICHAEL
Experimental development of spanwise vortex models with streamwise decay due to wall interaction
[AIAA PAPER 92-2688] p 799 A92-45535
MACUMBER, HOWARD L.
Evaluating the use of satellite communications in the government of Canada p 594 N92-22577
MACY, WILLIAM W.
Testing of a titanium matrix composite landing gear
[SAE PAPER 912175] p 644 A92-40000
MADAVAN, NATERI K.
Unsteady analysis of hot streak migration in a turbine stage p 399 A92-28537
Application of an unsteady Navier-Stokes solver to transonic turbine design p 935 A92-50273
MADDALON, DAL V.
Crossflow vortex and transition measurements by use of multielement hot films p 935 A92-50307
Method of measuring cross-flow vortices by use of an array of hot-film sensors
[NASA-CASE-LAR-14824-1-SB] p 998 N92-30390
MADDOCK, BLAIR C.
Anodize and prime your aluminum without environmental headaches p 892 A92-47340
MADHAVAN, N. S.
On the application of parabolized Navier-Stokes equations to flow field simulations p 936 A92-51943
MADISON, ROBIN M.
Expert system for real-time aircraft monitoring p 410 A92-24411
MADLEY, W. B.
Durability and damage tolerance testing and fatigue life management: A CF-18 experience p 361 N92-18581
MADNIA, C. K.
Modeling of the reactant conversion rate in a turbulent shear flow p 829 N92-28820
MAEDA, TATSUO
Aerodynamic drag on the bullet trains p 766 N92-26911
MAEDA, Y.
Navigation experiment on aircraft flight using the GPS-INS navigation system. II - Test results p 726 A92-43123
MAEKAWA, SHOUZO
Aerodynamic heating in three-dimensional shock wave turbulent boundary layer interaction induced by sweptback sharp fins in hypersonic flows
[SAE PAPER 912044] p 791 A92-45428
Three-dimensional shock wave-turbulent boundary layer interaction induced by blunt body and protuberance p 1029 A92-56009
MAEKAWA, SYOUZOU
A study on the interaction between a bow shock wave generated by a blunt body and a turbulent boundary layer p 8 A92-12424
MAEKAWA, SYOZO
Experimental study on three-dimensional shock wave-turbulent boundary layer interaction induced by protuberance p 1019 A92-53997
MAERKI, GLENN
X-29 forebody jet blowing
[AIAA PAPER 92-0017] p 247 A92-22139
MAESTRELLO, L.
On the interaction between first- and second-mode waves in a supersonic boundary layer p 78 A92-16462
Transition control of instability waves over an acoustically excited flexible surface p 416 A92-28037

MAFFEO, R. J.
The 3D inelastic analysis methods for hot section components
[NASA-CR-189089] p 402 N92-18971
Component-specific modeling
[NASA-CR-189088] p 377 N92-19726
MAFFIONE, R. A.
On the accuracy of an aircraft-borne ambient electric-field measuring system p 186 A92-20127
MAGDALENO, RAYMOND E.
Identification of higher-order helicopter dynamics using linear modeling methods p 131 A92-14336
MAGIAWALA, K.
Laser-initiated conical detonation wave for supersonic combustion. II
[AIAA PAPER 92-0088] p 292 A92-22195
MAGLIERI, DOMENIC J.
Sonic boom p 55 N92-10608
A summary of XB-70 sonic boom signature data
[NASA-CR-189630] p 696 N92-24800
MAGLIOZZI, B.
Propeller and propfan noise p 54 N92-10599
MAGNESS, C.
Unsteady crossflow on a delta wing using particle image velocimetry p 811 A92-46804
MAGNESS, CHARLES LEE
Unsteady response of the leading-edge vortices on a pitching delta wing p 1041 N92-33851
MAGNI, GABRIO
Transmission vibration monitoring - A single board computer architecture p 554 A92-35765
MAGNI, JEAN-FRANCOIS
Double loop control law strategy and applications to helicopter
[CERT-2/7724-DERA] p 381 N92-19295
MAGNUS, ALFRED E.
PAN AIR: A computer program for predicting subsonic or supersonic linear potential flows about arbitrary configurations using a higher order panel method. Volume 1: Theory document (version 3.0)
[NASA-CR-3251] p 526 N92-22648
MAGNUSEN, P. E.
Methodology for the assessment of material quality effects on airframe fatigue durability p 213 A92-19820
MAGNUSON, RON
The V-22 Osprey - A significant flight test challenge p 546 A92-35766
MAGRE, P.
CARS temperature measurements and validation of a computing code on a gas-turbine combustor
[ONERA, TP NO. 1991-224] p 373 A92-26376
MAGROGAN, MICHAEL
Joint Federal Aviation Administration (FAA)/Civil Aviation Authority (CAA) Microwave Landing System (MLS) Area Navigation (RNAV) flight evaluations
[DOT/FAA/CT-TN91/17] p 268 N92-15983
MAHADEVAN, R.
High-speed cinematography of supersonic mixing layers
[AIAA PAPER 92-3545] p 1112 A92-54044
MAHADEVAN, S.
System reliability and risk assessment
[AIAA PAPER 92-2345] p 582 A92-34320
MAHAFFEY, JAY D.
The V-22 tilt rotor: A comparison with existing Coast Guard aircraft
[AD-A245843] p 650 N92-26039
MAHAJAN, A. J.
Cascade flutter analysis with transient response aerodynamics p 154 A92-15972
MAHAJAN, APARAJIT J.
Eigenvalue calculation procedure for an Euler/Navier-Stokes solver with application to flows over airfoils p 170 A92-17429
Semi-empirical model for prediction of unsteady forces on an airfoil with application to flutter
[NASA-TM-105414] p 346 N92-18760
MAHAN, J. ROBERT
Combustion and core noise p 55 N92-10607
MAHAPATRA, PRAVAS R.
Sensors and systems to enhance aviation safety against weather hazards p 160 A92-14265
MAHLER, M. A.
Out of plane analysis for composite structures p 1107 N92-32527
MAHMOOD, M.
Experimental investigations of the vortex flow on delta wings at high incidence p 432 A92-31172
MAHN, JEFFREY A.
Risk management - Expanding horizons in nuclear power and other industries
[ISBN 1-56032-231-4] p 993 A92-51438
MAHON, J.
Induction bonding procedures for graphite reinforced thermoplastic assemblies p 994 A92-51545
MAIDA, JOHN L.
Fiber optic speed sensor for advanced gas turbine engine control p 857 A92-48044
MAIDEN, JANICE R.
Development of composite structures with enhanced damage tolerance p 985 A92-51555
MAIER, A.
Fatigue of repaired composite structures p 214 N92-14411
MAIER, THOMAS H.
Lifting line predictions for a swept tip rotor blade p 65 A92-14424
MAIKAPAR, G. I.
Possibility of reducing the wave drag of a hypersonic flight vehicle (wave rider) p 438 A92-31863
MAILLETTE, J.
Nonstationary gasdynamics p 220 N92-13985
MAINE, TRINDEL
Flight testing and simulation of an F-15 airplane using throttles for flight control
[NASA-TM-104255] p 1087 N92-32864
MAININI, M.
Test Engineering Language for Avionic Systems p 554 A92-35763
MAINVILLE, D.
A universal turboprop engine dynamometer test cell
[ASME PAPER 91-GT-343] p 137 A92-15706
MAIR, W. A.
Aircraft performance
[ISBN 0-521-36264-4] p 538 A92-33919
MAITA, M.
Airbreathing engine selection criteria for SSTO propulsion system
[IAF PAPER 92-0658] p 1071 A92-57099
MAITA, MASATAKA
Spaceplane system studies p 285 A92-22632
MAJID, A. A.
Legal capacity of Eurocontrol to ensure smooth aviation in Europe p 167 A92-16134
MAJIDZADEH, KAMRAN
Criteria for use of seal coats on airport pavements
[DOT/FAA/RD-92/18] p 1102 N92-34247
MAJJIGI, R. K.
Jet noise suppression p 236 N92-14784
MAJKA, KRZYSZTOF
Blade defect force investigation in a compressor cascade p 10 A92-13233
MAJOR, STEPHANE R.
Indicial method calculating dynamic stall on a vertical axis wind turbine p 714 A92-44528
MAK, A.
Reduction of the side force on pointed forebodies through add-on tip devices p 1024 A92-54918
MAKAROV, A. A.
Nonparametric methods of regression analysis in problems related to the processing of aerodynamic balance calibration tests p 602 A92-36417
MAKAROV, L. G.
System of cryogenic security of the superconducting accelerator of relativistic nuclei-nuclotron
[DE91-643289] p 304 N92-16789
MAKASHEVA, O. V.
Effect of turbulent mixing on the characteristics of a turbofan-engine nozzle p 493 A92-30162
MAKEL, WILLIAM J.
Annoyance from aircraft overflights in wilderness p 689 A92-39239
MAKHORTYKH, G. V.
Experimental investigation of the coefficients of the normal-force derivatives for rectangular wings with translational oscillations p 423 A92-30127
MAKI, STAN C.
A proposal for a dynamic test platform for inertial units and/or GPS p 138 A92-16653
MAKINO, MITSUO
Boundary layer flows around an airship p 430 A92-30560
MAKITA, H.
Three-dimensional vortical structure of a large-scale coherent vortex in a turbulent boundary layer p 619 A92-40056
MAKITA, HIDEHARU
Realization of a large-scale turbulence field in a small wind tunnel p 67 A92-15487
MAKOWIEC, GEORGE M.
Wind-tunnel and flight tests of a delta-wing remotely piloted vehicle p 21 A92-13208
MAKRIS, R.
The Berlin oil channel for drag reduction research p 571 A92-34219
MAKSIMOV, A. I.
Evolution of three-dimensional flows during the interaction between conical shock waves and a turbulent boundary layer p 7 A92-12169
MAL'TSEV, IU. I.
Optimization of the aerodynamic balance and parameters of the horizontal tail surfaces of the three-surface aircraft configuration with allowance for the capabilities of the stability and control augmentation system p 134 A92-16803
MALARIK, DIANE C.
Vinyl capped addition polyimides
[NASA-CASE-LEW-15027-2] p 579 N92-24053
MALCHODI, LAWRENCE A.
New Boeing flight test data acquisition systems p 920 A92-47537
MALCOLM, GERALD N.
Forebody vortex control with miniature, rotatable nose-boom strakes
[AIAA PAPER 92-0022] p 281 A92-22144
Forebody vortex control p 251 A92-22517
Forebody vortex control for suppressing wing rock on a highly-swept wing configuration
[AIAA PAPER 92-2716] p 803 A92-45555
Experimental study of vortex flows over delta wings in wing-rock motion p 810 A92-46787
Forebody vortex control using small, rotatable strakes p 811 A92-46798
Aerodynamic control of fighter aircraft by manipulation of forebody vortices p 380 N92-18791
MALDINI, M.
Creep fracture mechanisms in single crystal superalloys p 388 A92-25031
MALDONADO, M. A.
A new resonant link aircraft power generating system p 970 A92-50528
MALE, HERB
An advanced flight path management system for low-altitude helicopter flight p 975 A92-49330
MALEK, ALBERT
H2 fueled flightweight ramjet construction and test p 475 N92-21531
MALHERBE, C.
Lightning activity in microburst producing storm cells
[ONERA, TP NO. 1991-98] p 161 A92-16080
MALHOTRA, SHAN
JPL's Real-Time Weather Processor project (RWP) metrics and observations at system completion p 413 N92-19428
MALHOTRA, SUBHASH
Optics in aircraft engines p 926 A92-48500
MALIK, M. R.
Linear stability of three-dimensional boundary layers over axisymmetric bodies at incidence p 431 A92-31157
Discrete modes and continuous spectra in supersonic boundary layers p 809 A92-46264
MALIK, MUJEEB R.
Gortler instability and supersonic quiet nozzle design p 813 A92-46902
MALINOVSKII, K. A.
A method for estimating the efficiency of gas turbine blade cooling systems p 657 A92-40606
MALKOV, V. A.
The flow pattern and external heat transfer investigation for gas turbine vanes end surfaces
[AIAA PAPER 92-3071] p 903 A92-48722
MALL, S.
Thermo-mechanical fatigue crack growth in aircraft engine materials p 213 A92-19799
MALL, SHANKAR
Elevated temperature crack growth in aircraft engine materials p 891 A92-45234
MALLISON, JAMES A.
Dimensional characterization of a large aircraft structure by photogrammetry p 607 A92-37061
MALLOS, SAMUEL T.
Managing simulator wiring information and deriving system continuity p 964 A92-49287
MALLOY, DONALD J.
Test data models to characterize turbine engine operation in altitude test facilities
[AIAA PAPER 92-3917] p 1095 A92-56749
MALLOY, P. J.
Design load predictions on a fighter-like aircraft wing p 811 A92-46797
MALMUTH, N. D.
Asymptotic theory of transonic wind tunnel wall interference
[AD-A244075] p 403 N92-19080
MALONE, ERLE W.
MIL-STD-1553 data bus/PCM multiplexer system p 188 A92-19211
MALONE, J. B.
Inverse airfoil design procedure using a multigrid Navier-Stokes method p 193 N92-13932
MALONE, JOHN B.
Current status of computational methods for transonic unsteady aerodynamics and aeroelastic applications
[NASA-TM-104191] p 446 N92-21432

Current status of computational methods for transonic unsteady aerodynamics and aeroelastic applications
p 718 N92-27937

MALONSON, M. R.
Propulsion simulator for magnetically suspended wind tunnel models p 750 N92-27801

MALSBURY, T.
Flight simulator fidelity assessment in a rotorcraft lateral translation maneuver
[AIAA PAPER 92-4424] p 1092 A92-55348

MALTE, P. C.
Evaluation of NO(x) mechanisms for lean, premixed combustion
[ASME PAPER 91-GT-257] p 668 A92-36900

MALYGIN, V. V.
A method for determining equivalent stresses in aviation gas turbine engine blades p 559 A92-36421

MAMICH, HARVEY
Dynamics and control of hypersonic vehicles - The integration challenge for the 1990's
[AIAA PAPER 91-5057] p 203 A92-17840

MAN, YOSHIHIRO
Wing test at the cryogenic wind tunnel of the National Defense Academy p 749 A92-43199

MANDAI, KATSUMI
Super plastic forming technology applied to aeroengine and space equipment p 764 A92-44732

MANDERS, P. J. H. M.
Application of VME-technology on an airborne data link processor unit
[NLR-MP-88040-U] p 841 N92-29615

MANDERSCHEID, JANE M.
Reliability analysis of a structural ceramic combustion chamber
[ASME PAPER 91-GT-155] p 123 A92-15591

MANENTE, D.
Evaluation and qualification of diffusion braze repair techniques for superalloy gas turbine components
[NRC-LTR-ST-1839] p 504 N92-22028

MANGALAM, SIVA M.
Crossflow vortex and transition measurements by use of multielement hot films p 935 A92-50307
Method of measuring cross-flow vortices by use of an array of hot-film sensors
[NASA-CASE-LAR-14824-1-SB] p 998 N92-30390

MANGOLD, PETER
Transformation of flightmechanical design requirements for modern fighters into aerodynamic characteristics
p 365 N92-18794

MANGOLD, SUSAN J.
A review and discussion of flight management system incidents reported to the aviation safety reporting system
[AD-A252438] p 1043 N92-32941

MANI, R.
High speed turboprop aeroacoustic study (counterrotation). Volume 2: Computer programs
[NASA-CR-185242] p 1011 N92-31248

MANIE, F.
Wing tip turbine: Analysis of the results of S2MA sounding of marginal vortex of the A320, technical summary
[ONERA-RTS-21/4365-AY-056A] p 23 N92-11009

MANN, D. L.
Application of a water droplet trajectory prediction code to the design of inlet particle separator anti-icing systems
[PNR-90839] p 474 N92-20573

MANN, MICHAEL J.
Survey and analysis of research on supersonic drag-due-to-lift minimization with recommendations for wing design
[NASA-TP-3202] p 1040 N92-33656

MANNESS, M. A.
Multivariable methods for helicopter flight control law design - A review p 568 A92-35748
Eigenstructure assignment for handling qualities in helicopter flight control law design p 570 A92-35786

MANNING, CLARKE O.
Estimation of flying qualities using a leastsquares lower-order equivalent systems technique
p 570 A92-35947
Flight test results using a low order equivalent systems technique to estimate flying qualities
[AIAA PAPER 92-4425] p 1080 A92-55349

MANNING, JAMES C.
Study of external dynamic flap loads on a 6 percent B-1B model
[ASME PAPER 91-GT-236] p 125 A92-15645

MANNING, JEROME E.
Use of SEA to predict structure-borne noise in aircraft
p 1137 N92-32955

MANNING, S. D.
Reliability centered maintenance for metallic airframes based on a stochastic crack growth approach
p 897 A92-45242

MANNING, T. A.
Computational and experimental studies of flow in multi-lobed forced mixers
[AIAA PAPER 92-3568] p 1112 A92-54057

MANOHA, ERIC
Wall pressure wavenumber-frequency spectrum beneath a turbulent boundary layer measured with transducer arrays calibrated with an acoustical method
[ONERA, TP NO. 1991-212] p 329 A92-26364

MANOLAKIS, D. E.
Computation of aircraft geometric height under radar surveillance p 639 A92-40239

MANSEL, W.
Expert system for the Tornado ground-based check-out system p 118 N92-12536

MANSFELD, G.
Development of flight testing of a fault tolerant fly-by-light yaw control system p 662 N92-25599

MANSFIELD, F. A.
Numerical investigation of laminar separated trailing-edge flows p 339 A92-28026

MANSFIELD, FRANK A.
Investigation of solution operators for the three-dimensional Euler equations
[AIAA PAPER 92-2666] p 797 A92-45522

MANSOUR, M.
Robust stabilization of a helicopter model
p 28 A92-11501

MANSOUR, N. N.
Compressibility effects on the growth and structure of homogeneous turbulent shear flow p 675 A92-40052
Simulation and modeling of homogeneous compressible turbulence under isotropic mean compression
p 622 A92-40134
Microburst modelling and scaling p 915 A92-46262

MANSUR, M. HOSSEIN
Modeling methods for high-fidelity rotorcraft flight mechanics simulation
[NASA-TM-103842] p 482 N92-21440

MANTAY, WAYNE R.
Integrated multidisciplinary rotorcraft optimization research at the NASA Langley Research Center
p 419 A92-29673

MANTEL, B.
Anisotropic control of mesh generation based upon a Voronoi type method p 918 A92-47043

MANTIN, MICHEL J.
The helicopter commuter - A perspective on regular passenger transportation by rotary wing
p 634 A92-38208

MANUEL, G. S.
Effect of collector configuration on test section turbulence levels in an open-jet wind tunnel
[NASA-TM-4333] p 750 N92-27670

MANUILOVICH, S. V.
A method of boundary layer laminarization on an oscillating wing p 441 A92-31969

MANWARING, STEVEN R.
The unresolved unsteady flow in multistage compressor blade rows p 421 A92-29472

MANZO, F.
A fast conformal mapping algorithm with no FFT
p 1007 A92-50471

MANZOLILLO, DOMINIC
A digital Doppler Rate of Descent Indicator (DRODI)
p 555 A92-35927

MAO, GENWANG
Numerical simulation of three-dimensional turbulent flows in combustion chambers p 970 A92-53276

MAO, JIAN-GUO
An investigation of real-time diagnostic technique for DEEC system p 470 A92-29742

MAO, KEJIU
Simulation research on the dynamic characteristics of steam-injected gas turbine p 971 A92-53389

MAO, XICHANG
Surface flow visualization of rotating propeller
p 4 A92-10959
Experimental characteristics comparison between two scale-model propellers p 24 A92-10962

MARANGOS, J.
Expert system for the Tornado ground-based check-out system p 118 N92-12536

MARBLE, FRANK E.
A systematic experimental and computational investigation of a class of contoured wall fuel injectors
[AIAA PAPER 92-0625] p 374 A92-27007
Shock enhancement and control of hypersonic combustion
[AD-A248558] p 896 N92-29580

MARCEAU, J. A.
Design for Corrosion Prevention
[AIAA PAPER 92-1127] p 577 A92-33279

MARCHANT, M. J.
Mesh adaptivity with the quadtree method
p 816 A92-47041

MARCHELLO, JOSEPH M.
Polymer infiltration studies
[NASA-CR-189773] p 289 N92-17004
Polymer infiltration studies
[NASA-CR-190204] p 578 N92-22486

MARCHESE, MICHAEL
Real-time microfocus radiography for electronic failure analysis p 214 A92-17289

MARCHETTI, M.
Fracture analysis and crack propagation in pressurized fuselage structures - Experimental and numerical investigations p 217 A92-19812

MARCHETTI, R.
Heterodyne techniques in the I.R. bandwidth for laser obstacle detection p 533 A92-35740

MARCHIONNI, M.
High temperature low cycle fatigue of single crystal nickel base superalloys p 213 A92-19796

MARCI, G.
A fatigue crack growth threshold p 389 A92-26667

MARCILLAT, J.
Experimental and numerical study of flow around helicopter rotor blade tips p 814 A92-46948

MARCOCCI, L.
A module-level testing environment for safety-critical software systems p 1132 A92-56293

MARCOLINI, MICHAEL A.
Acoustic predictions using measured pressures from a model rotor in the DNW p 165 A92-14385

MARCONI, F.
Orthogonal grids for multiple airfoils
p 818 A92-47096

MARCONI, FRANK
Solution of the Euler and Navier-Stokes equations on MIMD distributed memory multiprocessors using cyclic reduction
[AIAA PAPER 92-0561] p 411 A92-26970

MARCUM, D. L.
Finite element Navier-Stokes solver for unstructured grids p 398 A92-28035

MARDOIAN, GEORGE H.
Flight service evaluation of composite helicopter components p 106 A92-14372

MAREC, J.-P.
Eighty years of aerospace technique through ATMA bulletins
[ETN-91-90097] p 57 N92-11963

MAREC, JEAN-PIERRE
Trends in commercial aircraft design - What evolution factors and what approach?
[ONERA, TP NO. 1992-25] p 786 A92-48587

MARESH, JEFF
The development of a real time visual flight simulator for tactical operations research and measurement
p 880 A92-45027

MARGALIT, ELI
A study of atmospheric optical scattering parameters at 1.5 and 2 micron region for solid state Doppler lidar applications p 1001 N92-31067

MARGETAN, F. J.
A new method to estimate the effective geometric focal length and radius of ultrasonic focused probes
p 490 A92-28633
A technique for quantitatively measuring microstructurally induced ultrasonic noise
p 510 A92-28720

MARGUET, ROGER
Generalities on the ramjet p 736 A92-41819

MARHEFKA, R. J.
SATCOM antenna siting study on P-3C aircraft, volume 1
[NASA-CR-189514] p 221 N92-14262
SATCOM antenna siting study on P-3C aircraft, volume 2
[NASA-CR-189515] p 221 N92-14263

MARHEFKA, RONALD J.
Antennas on complex platforms p 494 A92-31084

MARIANI, G. P.
Test Engineering Language for Avionic Systems
p 554 A92-35763

MARINELLI, RICK
Evaluation of two high-speed runway exits
[DOT/FAA/CT-TN91/36] p 31 N92-11021

MARINELLI, W. J.
Aerothermodynamic radiation studies
[NASA-CR-185666] p 284 N92-15998

MARINI, M.
Viscous high-speed flow computations by adaptive mesh embedding techniques p 808 A92-45839
Lower upper implicit total variation diminishing solution of viscous hypersonic flows p 935 A92-50302

MARINOV, N. M.
Evaluation of NO(x) mechanisms for lean, premixed combustion
[ASME PAPER 91-GT-257] p 668 A92-36900

MARITAN, M.
A high gain antenna system for airborne satellite communication applications p 677 N92-24096
MARK, H.
Thermal management of propulsion systems in hypersonic vehicles
[AIAA PAPER 92-0516] p 373 A92-26942
MARKER, JESSE L.
Flight operations safety management
[SAE PAPER 912124] p 635 A92-39971
MARKER, TIMOTHTY R.
Development and evaluation of an onboard aircraft cabin water spray system for postcrash fire protection
[SAE PAPER 912224] p 636 A92-40022
MARKER, TIMOTHY
Onboard cabin water spray system under various discharge configurations
[DOT/FAA/CT-TN91/42] p 93 N92-13043
Effectiveness of an onboard water spray system during an oxygen enriched cabin fire
[DOT/FAA/CT-TN91/51] p 264 N92-17149
MARKES, J.
Digital ozonesondes - Examples of results from the EMEFS experiments of 1988 and 1990
p 468 A92-32140
MARKHAM, BRIAN L.
Radiometric properties of the NS001 Thematic Mapper Simulator aircraft multispectral scanner
p 155 A92-17110
MARKHAM, K. C.
Time-to-go estimation from infrared images
p 840 A92-48308
MARKHARDT, TIM W.
Recent developments in the use of thin-film polyethylene balloons for meteorological applications
p 16 A92-11033
MARKIEWICZ, JANUSZ
Modeling of the control systems of rotary wing aircraft (Review) p 875 A92-47783
MARKIEWICZ, R. H.
A study of the aeroelastic behaviour of helicopter rotor blades featuring swept tips p 367 N92-19701
MARKIN, ROBERT E.
Specifying exhaust nozzle contours in real-time using genetic algorithm trained neural networks
[AIAA PAPER 92-3328] p 865 A92-48911
MARKOPOULOS, N.
Rapid near-optimal aerospace plane trajectory generation and guidance
[NASA-CR-189469] p 205 N92-14066
MARKOV, A. A.
Nonstationary viscous shock layer in supersonic motion over an inhomogeneity p 708 A92-42737
MARKOV, V. P.
A ionospheric-sounding experiment from an aircraft
p 160 A92-13809
MARKOWITZ, JEFFREY S.
Rates and risk factors for accidents and incidents versus violations for U.S. airmen p 91 A92-14048
MARKSTALLER, MATTHEW G.
Moldless composite aircraft wing structural design modifications p 958 A92-51527
MARLER, J. E.
Reliability centered maintenance for metallic airframes based on a stochastic crack growth approach
p 897 A92-45242
MARMIGNON, C.
Numerical simulation of thermochemical non-equilibrium viscous flows around reentry bodies
p 227 N92-15029
MAROHN, HEINZ-DIETER
Comparison of aircraft noise indices for noise zoning at military airfields p 687 A92-39056
MARQUETTE, THOMAS J.
Computational fluid dynamics as a tool for aerodynamic analysis of ejection seats p 519 A92-35444
MARR, ROGER
The V-22 Osprey - A significant flight test challenge
p 546 A92-35766
MARRAFFA, L.
SIMOUN and Scirocco wind tunnel nozzle viscous flow study p 208 N92-14999
MARRISON, CLAIRE
The effect on aircraft evacuations of passenger behaviour and smoke in the cabin p 834 A92-44998
MARSDEN, D. J.
Variable geometry sailplanes Minisigma
p 629 N92-24877
MARSH, S.
An explosively driven, fast shock tube
[DE92-008437] p 749 N92-26720
MARSHALL, DAVID L.
NASA advanced aeronautics design solar powered remotely piloted vehicle
[NASA-CR-190007] p 462 N92-20665
MARSHALL, FRANK P.
Pneumatically actuated multiple store launcher
[AD-D015237] p 732 N92-27188
MARSHALL, T. A.
Computation of turbulent, separated, unswept compression ramp interactions p 813 A92-46897
MARSTERS, G. F.
Corrosion and your aircraft
[NRC-30465] p 114 N92-11991
MARTENS, STEVEN
An experimental investigation of large scale instabilities in a low Reynolds number two-stream supersonic shear layer
[AIAA PAPER 92-0177] p 255 A92-23787
MARTHA, LUIZ F.
Simulation of arbitrary crack propagation in three-dimensions p 393 A92-25535
MARTIN-DUPONT, FRANCOIS
Data processing aspects of the Hermes Flight Control Center p 513 N92-20629
MARTIN, C.
Electronically steerable antenna for aircraft
p 229 N92-15272
MARTIN, C. A.
Surface pressure measurements on the wing of a wind tunnel model during steady rotation
[AD-A243047] p 260 N92-17281
Scale model measurements of fin buffet due to vortex bursting on F/A-18 p 365 N92-18788
F-111C flight dynamic model aerodynamic data-base development and verification
[AD-A246356] p 715 N92-26947
MARTIN, C. F.
Decentralized-feedback pole placement of linear systems p 411 A92-27347
MARTIN, CARL J., JR.
Combined load test apparatus for flat panels
[NASA-CASE-LAR-14698-1] p 911 N92-30028
MARTIN, CHARLES A.
Experimental and numerical investigation of anti-icing phenomena on a NACA 0012 assembly
[AIAA PAPER 92-0531] p 459 A92-31669
Advanced pneumatic impulse ice protection system (PIIP) for aircraft p 845 A92-46807
MARTIN, D. L.
A novel avionic sensor for fly-by-light controls
p 650 A92-38128
MARTIN, D. M.
Hub and pylon fairing integration for helicopter drag reduction p 107 A92-14391
Experimental study of an independently deflected wingtip mounted on a semispan wing
[NASA-TM-102842] p 13 N92-10983
MARTIN, GLENN L.
A study of altitude-constrained supersonic cruise transport concepts
[AIAA PAPER 92-1027] p 536 A92-33208
MARTIN, J. R.
Fuzzy guidance system evaluation
p 778 N92-27903
MARTIN, J. S.-T.
Use of the thrust-weight diagram versus transport cargo in the initial dimensioning of passenger-transport aircraft
p 642 A92-37074
MARTIN, JOSE M. H.
Possible utilization of GPS in precision approach maneuvers p 637 A92-37075
MARTIN, M.
A chambered porous damper for rotor vibration control. II - Imbalance response and bladeless simulation
[ASME PAPER 91-GT-243] p 149 A92-15648
MARTIN, OLGA
The static and fatigue computation of the propeller blades retention system p 995 A92-51895
MARTIN, R. A.
Analytical and experimental studies of heat pipe radiation cooling of hypersonic propulsion systems
[AIAA PAPER 92-3809] p 867 A92-49128
Analytical and experimental studies of heat pipe radiation cooling of hypersonic propulsion systems
[DE92-013428] p 973 N92-31817
MARTIN, RODERICK H.
Isothermal aging of IM7/8320 and IM7/5260
[NASA-TM-107666] p 1110 N92-33423
MARTIN, S. J.
Method and apparatus for acoustic plate mode liquid-solid phase transition detection
[DE92-003778] p 401 N92-18705
Monitoring jet fuel degradation using quartz crystal microbalances
[DE92-004730] p 489 N92-20858
MARTIN, STEVE
Advanced thermally stable, jet fuels development program annual report. Volume 1: Model and experiment system development
[AD-A249625] p 988 N92-31462
MARTIN, VINCENT
Advanced Study for Active Noise Control in Aircraft (ASANCA)
[AIAA PAPER 92-2092] p 1137 N92-32956
MARTINDALE, W. R.
Performance evaluation of a transonic wind tunnel compressor
[AIAA PAPER 92-3927] p 1096 A92-56758
MARTINEZ-SANCHEZ, M.
Turbine blade tip and seal clearance excitation forces
[NASA-CR-184341] p 973 N92-31910
MARTINEZ-VAL, RODRIGO
Optimum cruise lift coefficient in initial design of jet aircraft p 845 A92-46806
MARTINEZ, F. E.
Low volatile organic compound paints
[DE91-017984] p 35 N92-11203
MARTINSON, SCOTT D.
Active thermal isolation for temperature responsive sensors
[NASA-CASE-LAR-14612-1] p 911 N92-29954
MARTINSON, VELORIA J.
26 x 6.6 radial-belted aircraft tire performance
[SAE PAPER 912157] p 644 A92-39992
MARTNER, B. E.
Progress report on analysis of differential attenuation radar data obtained during WISP-91
[PB92-133800] p 503 N92-21828
MARTYNOV, B. B.
Problems of strength and aeroelasticity of present-day propfans p 471 A92-30133
MARVILLET, C.
Experimental methods to determine heat exchanger performances p 682 N92-25667
MARVIN, JOSEPH G.
CFD validation experiments for hypersonic flows
[AIAA PAPER 92-4024] p 1034 A92-56846
MARYNIAK, JERZY
Mathematical modeling of the flight of passenger aircraft in the case of engine failure p 875 A92-47777
Mathematical modeling of the effect of windshear on the dynamics of a landing aircraft p 875 A92-47784
MARZANO, A.
Aerothermodynamic development of the CARINA re-entry vehicle: CFD analyses and experimental tests
p 211 N92-14980
MARZE, HENRI-JAMES
Research and studies on quiet helicopters
[ONERA, TP NO. 1992-59] p 926 A92-48618
MASAD, J. A.
Effect of suction on the stability of supersonic boundary layers. I - Second-mode waves. II - First-mode waves
p 174 A92-19611
Laminar flow control of subsonic boundary layers by suction and heat transfer strips p 617 A92-39338
Effect of a bulge on the subharmonic instability of subsonic boundary layers p 898 A92-45833
MASAKI, SHOJU
Current repair technologies for jet engine components
p 1016 A92-56085
MASALOV, V. K.
Calculation of the base pressure and enthalpy behind a step in the path of two supersonic streams with allowance for the effect of boundary layers and heat fluxes
p 63 A92-13748
Calculation of the parameters of separated flow behind a plane rounded body in the path of two supersonic flows p 244 A92-21624
MASIULANIEC, K. C.
Experimental and numerical investigation of anti-icing phenomena on a NACA 0012 assembly
[AIAA PAPER 92-0531] p 459 A92-31669
MASKEW, BRIAN
A re-examination of the aerodynamics of hovering rotors including the presence of the fuselage
p 66 A92-14446
MASLEN, E. H.
Low power magnetic bearing design for high speed rotating machinery p 772 N92-27739
MASLOV, A. A.
Effect of a fan of rarefaction waves on the development of disturbances in a supersonic boundary layer
p 809 A92-46519
MASON, J. M.
Evaluation of sound transmission into aircraft fuselages by a reciprocity technique p 694 A92-39086
MASON, JOHN L.
The impact of advanced materials on small turbine engines
[SAE PAPER 911207] p 862 A92-48021
MASON, MARY L.
A static investigation of the thrust vectoring system of the F/A-18 high-alpha research vehicle
[NASA-TM-4359] p 633 N92-25967

MASON, W. H.
Inverse solution uniqueness and domain of existence for supersonic space marching applications
[AIAA PAPER 92-0028] p 248 A92-22150
What we need in experimental aerodynamics - One engineering educator's view
[AIAA PAPER 92-0161] p 241 A92-23776
Variable-complexity aerodynamic optimization of an HSCT wing using structural wing-weight equations
[AIAA PAPER 92-0212] p 317 A92-25685
Applied Computational Aerodynamics - Case studies
[AIAA PAPER 92-2661] p 845 A92-45580
Aerodynamically blunt and sharp bodies
[AIAA PAPER 92-2727] p 808 A92-45597
MASON, WILLIAM H.
A computational study on directional stability of chine-shaped forebodies at high-alpha
[AIAA PAPER 92-0030] p 249 A92-22152
Hi-alpha forebody design. Part 1: Methodology base and initial parametrics
[NASA-CR-189849] p 358 N92-18024
Hi-alpha forebody design. Part 2: Determination of body shapes for positive directional stability
[NASA-CR-189850] p 359 N92-18038
A computational examination of directional stability for smooth and chined forebodies at high-alpha
[NASA-CR-4465] p 950 N92-32114
MASOTTO, THOMAS K.
Applications of an automated programming system
[AIAA PAPER 91-3767] p 231 A92-17629
MASOTTO, TOM
Advanced information processing system: Inter-computer communication services
[NASA-CR-187556] p 53 N92-11706
MASSAR, ANDREW
Ceramic matrix composites and its application in gas turbine engines
[ASME PAPER 91-GT-338] p 143 A92-15702
MASSEY, C. P.
Carefree handling systems for helicopters
p 975 A92-50010
MASSEY, K. C.
Acoustic interactions between an altitude test facility and jet engine plumes: Theory and experiments
[NASA-CR-190423] p 738 N92-26405
MASSIMI, J. M.
Preliminary evaluation of new control laws on the experimental fly-by-wire Dauphin helicopter
p 568 A92-35756
MASSOGLIA, PETER
Automatic Dependent Surveillance (ADS) Pacific Engineering Trials (PET)
[AIAA PAPER 92-1812] p 453 A92-29760
MASSON, A.
New hypersonic test methods developed at ONERA - The R5 and F4 wind tunnels
[ONERA, TP NO. 1992-39] p 882 A92-48600
MASSOUDI, M.
Steady flow of a fluid-solid mixture in a circular cylinder
[DE91-018698] p 41 N92-10174
MASSY-GREENE, DAVID
Halfway around the world is far enough
p 516 A92-33462
MASTER, CHARLES O.
Aircraft ground deicing
[SAE PAPER 912222] p 635 A92-40021
MASTERS, CHARLES O.
Evaluation of the aerodynamic effects of commuter class (type 1-1/2) anti-icing fluids on small general aviation airplanes
[AIAA PAPER 92-0643] p 459 A92-31675
MASTRODDI, F.
A boundary integral formulation for unsteady transonic potential flows p 719 N92-27942
MASUE, TATSUYA
Review on the abatement of helicopter noise
p 406 A92-25501
Efficiency and accuracy in helicopter hovering performance calculation p 1053 A92-56072
MASUGO, T.
A perspective on helicopter noise p 780 A92-43160
MASUYA, GORO
Effectiveness of plasma torches for ignition and flameholding in scramjet p 737 A92-44524
Conceptual design of scramjet engine
p 1065 A92-53490
Scramjet engine and its flying test bed
p 1066 A92-53492
Performance analysis of idealized scramjet
p 1066 A92-53493
Flow measurements in scramjet inlets
p 1102 A92-53565
MASUZAWA, HIDEO
Flight simulator test of cockpit advisory system
p 1054 A92-56115
MATARRESE, M. D.
Control of hypersonic aerodynamic forces with surface blowing p 172 A92-18363
MATEESCO MATE, NICOLAS
Annals of air and space law. Vol. 16
p 1012 A92-51450
MATEESCU, D.
Analysis of flexible-membrane and jet-flapped airfoils using velocity singularities p 10 A92-13216
MATHE, J. M.
Application of infrared thermography to thermal flux measurement in wind tunnels
[AAAF-NT-89-12] p 31 N92-11020
MATHENY, NEIL
The F-18 high alpha research vehicle: A high-angle-of-attack testbed aircraft
[NASA-TM-104253] p 1060 N92-33404
MATHEW, M. B.
Dynamic analysis of rotor blades with root retention design variations p 1054 A92-56156
MATHEWS, BRUCE D.
Saberliner flight test and results for forward looking detection and avoidance of airborne windshear
p 98 A92-16656
MATHIEU, G.
Millisecond aerodynamic force measurement with side-jet model in the ISL shock tunnel
[AIAA PAPER 92-3963] p 1097 A92-56790
MATHIOUDAKIS, K.
Combination of different unsteady quantity measurements for gas turbine blade fault diagnosis
[ASME PAPER 91-GT-201] p 149 A92-15624
A procedure for automated gas turbine blade fault identification based on spectral pattern analysis
[ASME PAPER 91-GT-259] p 151 A92-15661
Jet engine fault detection with discrete operating points gas path analysis p 129 A92-17200
Optimal measurement and health index selection for gas turbine performance status and fault diagnosis
[ASME PAPER 91-GT-294] p 653 A92-36889
MATHIS, JULIE A.
Examination of energy spectra moments in a developing turbulent flow
[NIAR-91-28] p 399 N92-18116
MATHUR, A. B.
Flowpath optimization for hypersonic vehicles
[AIAA PAPER 91-5043] p 437 A92-31688
MATHUR, GOPAL P.
Interior noise prediction methodology: ATDAC theory and validation
[NASA-CR-187626] p 697 N92-25368
MATHUR, J. S.
The simulation of inviscid, compressible flows using an upwind kinetic method on unstructured grids
p 933 A92-49515
MATHUR, M. P.
Steady flow of a fluid-solid mixture in a circular cylinder
[DE91-018698] p 41 N92-10174
MATHUR, SANJAY R.
Three dimensional analysis of a rotor in forward flight
p 64 A92-14329
MATSON, ROBERT E.
Smoothing CFM56 engine removal rate at USAir
[AIAA PAPER 92-3928] p 1070 A92-56759
MATSSON, O. J. E.
Transition to turbulence in curved channel flow
p 621 A92-40125
MATSUBARA, MANABU
Analysis of the aerodynamic characteristics of a simple remotely piloted research vehicle (RPRV)
p 710 A92-43191
MATSUDA, K.
The concept of an unmanned flying vehicle at high altitude p 731 A92-43242
MATSUDA, MASAMI
Application of fuzzy control to aircraft guidance
p 1083 A92-56033
MATSUDA, SEIJI
Structure/control design synthesis of active flutter suppression system by goal programming
p 204 A92-18621
MATSUDA, T.
Thermal measurement test in a shock wind tunnel
p 748 A92-43104
MATSUDA, YUKIO
Research on a low-noise engine for a high-speed VTOL aircraft p 737 A92-43239
Design and off-design point characteristics of Separated Core Ultra High Bypass Engine (SCUBE)
[AIAA PAPER 92-3776] p 867 A92-49120
MATSUHAMA, M.
A conceptual study for future engine test facility
[AIAA PAPER 92-3992] p 1099 A92-56815
MATSUHAMA, MASAAKI
Key design considerations for scramjet powered space plane p 1066 A92-53491
MATSUI, TOSHIO
Study on effectiveness of the front wedge shape in hypersonic flow p 430 A92-30552
MATSUMOTO, H.
Nonstationary manual control. III p 776 A92-43187
MATSUMOTO, HIROYUKI
Manual control of vehicles with time-varying dynamics
[SAE PAPER 912078] p 917 A92-45454
MATSUMOTO, K.
A study of the pilot's associate system
p 745 A92-43218
Integrated system to support computer analysis in conceptual aerospace design p 1130 A92-53596
MATSUMOTO, KOHTARO
Flight simulator test of cockpit advisory system
p 1054 A92-56115
MATSUMOTO, M.
High enthalpy wind tunnel for erosion testing of advanced materials
[AIAA PAPER 92-3888] p 1094 A92-56729
MATSUMOTO, MASASHI
Experimental validation of scramjet nozzle performance
[AIAA PAPER 92-3290] p 864 A92-48879
MATSUMURA, KENJI
Development of the D-size liquid crystal flat panel display for aircraft p 734 A92-43208
Evaluation test on the simulator of the liquid crystal flat display. II p 734 A92-43209
MATSUNAGA, KOJI
Numerical simulation for various flowfields of aero-engine components p 200 A92-17503
MATSUNO, KENICHI
Multi-block airfoil profile of grid formation
p 429 A92-30523
BGK1 airfoil oilflow tests in the NAL two-dimensional wind tunnel. II p 1029 A92-56044
Evaluation of NACA0012 airfoil test results in the NAL two-dimensional transonic wind tunnel
[NAL-TR-1109T] p 445 N92-21287
NACA0012 airfoil data corrected for sidewall boundary-layer effects in the NAL two-dimensional transonic wind tunnel
[NAL-TM-640T] p 722 N92-28151
MATSUO, AKIKO
Detailed numerical analysis of standing oblique detonation p 1111 A92-53550
MATSUO, HIDEO
Flow around two square cylinders in staggered arrangements p 761 A92-42797
Planning method of skirt systems for small ACVs
p 1118 A92-56038
MATSUO, KAZUYASU
Flow unsteadiness by weak normal shock wave/turbulent boundary layer interaction in internal flow
p 67 A92-15359
MATSUO, KENSUKE
Planning method of skirt systems for small ACVs
p 1118 A92-56038
MATSUO, SHIGERU
Oscillation of oblique shock waves generated in a two dimensional asymmetric nozzle
[SAE PAPER 912061] p 791 A92-45443
MATSUOKA, H.
Operational progress of the STOL research aircraft Asuka p 730 A92-43138
MATSUSHIMA, HIROICHI
Navigation experiment on an aircraft using the GPS-INS navigation system. I - Introduction to the system
p 726 A92-43122
MATSUSHIMA, K.
Integrated system to support computer analysis in conceptual aerospace design p 1130 A92-53596
MATSUSHIMA, KOICHI
Flight simulation and its application
p 284 A92-22634
Space plane navigation simulation
p 1103 A92-53603
MATSUSHIMA, MASAMICHI
Structural concept of main wings of high altitude unmanned aerial vehicle and basic properties of thermoplastic composites as candidate material
[SAE PAPER 912053] p 843 A92-45437
MATSUSHITA, H.
Gust load alleviation control design for the accuracy of an aeroelastic active control model
p 745 A92-43134
ACT wind tunnel experiment on gust load alleviation. II - Wind tunnel test with active support facility
p 745 A92-43135
Transonic wind tunnel tests of flutter suppression equipment (Wing response data processing)
p 748 A92-43136

MATSUSHITA, HIROSHI
Synthesis of gust load alleviation with flutter margin augmentation p 1082 A92-56021
Static aeroelastic analysis of ACT wind tunnel model aircraft
[NAL-TM-624] p 632 N92-25366
MATSUSHITA, MITSUNORI
Generalized aerodynamics analysis by the boundary element method p 1030 A92-56050
MATSUURA, TSUKASA
A consideration on air traffic control processing capability in terminal area p 1047 A92-56110
MATSUZAKI, KATSUYA
Preliminary study of algorithm for real-time flutter monitoring
[SAE PAPER 912001] p 897 A92-45403
MATSUZAKI, YUJI
Subcritical flutter characteristics of a swept-back wing in a turbulent supersonic flow - Comparison between analysis and experiment
[AIAA PAPER 92-2393] p 517 A92-34466
Response characteristics of a wing in supersonic flow near flutter boundary
[SAE PAPER 911999] p 789 A92-45401
Vibration tests of long plate structural model
[NAL-TM-625] p 400 N92-18485
MATTERN, DUANE
Propulsion system performance resulting from an Integrated Flight/Propulsion Control design
[AIAA PAPER 92-4602] p 1069 A92-55281
MATTERN, DUANE L.
IMPAC - An integrated methodology for propulsion and airframe control p 477 A92-29118
MATTHEWS, A.
Comparison of Hemispherical Resonator Gyro and optical Gyros p 993 A92-51014
MATTHEWS, R. K.
Testing capabilities at AEDC for development of hypersonic vehicles
[AIAA PAPER 91-5027] p 483 A92-31686
MATTHEWS, RAYMOND H.
Rotorcraft terminal ATC route standards
[SCT-90RR-33] p 641 N92-26101
MATTHEWS, WILLIAM T.
A sensitivity analysis on component reliability from *fatigue life computations*
[AD-A247430] p 908 N92-28425
MATTINGLY, JACK D.
Developing undergraduate gas turbine and turbomachinery courses
[AIAA PAPER 91-2509] p 56 A92-12700
Improvements in teaching aircraft engine design
[AIAA PAPER 92-3758] p 1141 A92-54152
MATTISSEK, A.
Development and verification of software for flight safety critical systems p 164 N92-12469
MATULAITIS, J. A.
High-speed civil transport aircraft emissions
p 408 N92-19122
MATULICH, DAN
Evolutionary upgrade and application of the C-130H simple-cycle refrigeration system
[SAE PAPER 911439] p 270 A92-21836
MATVIENKO, O. V.
Calculation of gas combustion regimes in a counterflow vortex chamber p 34 A92-12209
MATYAS, R.
An aircraft Earth station for general aviation
p 678 N92-24194
MAUGHMER, MARK D.
Multipoint inverse airfoil design method based on conformal mapping p 610 A92-36827
Simplified linear stability transition prediction method for separated boundary layers p 812 A92-46883
Prediction of forces and moments for hypersonic flight vehicle control effectors
[NASA-CR-188954] p 33 N92-11070
Analysis and design of planar and non-planar wings for induced drag minimization
[NASA-CR-189509] p 179 N92-13999
MAURER, F.
Experimental study of hypersonic shock wave boundary layer interactions by means of infrared technique
p 182 N92-14994
MAURICE, MARK S.
Laser velocimetry seed particles within compressible, vortical flows p 395 A92-26413
MAURINO, DANIEL
Management decisions have an impact on flight safety
p 92 A92-15175
MAURINO, DANIEL E.
ICAO Flight Safety and Human Factors Programme
p 835 A92-45055
MAUS, J. R.
Calculation of high speed base flows
[AIAA PAPER 92-2679] p 799 A92-45531
The G-range impulse facility - A high-performance free-piston shock tunnel
[AIAA PAPER 92-3946] p 1097 A92-56774
MAUTNER, T.
Obtaining the velocity field required for the calculation of propeller unsteady forces using 'traditional' approximate methods and CFD
[AIAA PAPER 92-0520] p 331 A92-26945
MAVRIPLIS, D. J.
Unstructured and adaptive mesh generation for high Reynolds number viscous flows p 816 A92-47042
MAVRIPLIS, DIMITRI J.
Turbulent flow calculations using unstructured and adaptive meshes p 153 A92-15823
Algebraic turbulence modeling for unstructured and adaptive meshes p 216 A92-18362
MAX, HEINZ
Air transport research in Germany p 61 A92-17095
Air transport research in Germany
p 241 A92-21014
MAY, D. N.
MD-80 aft cabin noise control: A case history
p 1137 N92-32950
MAY, KIMBERLY A.
Nationwide system delay study of the microwave landing system in the New York terminal area, volume 1
[DOT/FAA/CT-TN91/59-VOL-1] p 640 N92-25098
MAY, MARVIN
INS alignment using GPS Phase III user equipment computed corrections p 100 A92-16955
MAY, MATTHEW J.
Flapping inertia for selected rotor blades
[NASA-TM-104125] p 115 N92-13057
MAY, NOAL D.
Exposures from headset interference tones
[AD-A247175] p 1136 N92-32697
MAYANAGI, MITSUYOSHI
Development and future view of the technology for fly-by-light control system elements p 131 A92-14027
Development of digital/optical rotary position transducer
[NAL-TR-1106] p 29 N92-10028
MAYDEW, R. C.
Design and testing of high-performance parachutes
[AGARD-AG-319] p 345 N92-18269
MAYER, DAVID W.
Evaluation of two flow analyses for subsonic diffuser design
[AIAA PAPER 92-0273] p 317 A92-25727
MAYER, ERNST W.
Similarity solutions for viscous vortex cores
p 759 A92-41658
MAYER, JUERGEN F.
Three-dimensional calculation of low-frequency unsteady transonic flow in axial turbine stages
p 174 A92-19110
MAYHEW, ELLEN R.
An acceptance process for the evaluation of inlet distortion
[AIAA PAPER 92-3918] p 1032 A92-56750
MAYLE, R. E.
Boundary-layer measurements during a parallel blade-vortex interaction
[AIAA PAPER 92-2623] p 794 A92-45495
MAYLE, ROBERT E.
The role of laminar-turbulent transition in gas turbine engines p 120 A92-14868
Fundamental aspects of boundary layers and transition in turbomachines p 658 N92-24337
MAYMON, GIORA
Response of plate-like structures to correlated random pressure fluctuations
[AIAA PAPER 92-2378] p 584 A92-34452
MAYNE, D. Q.
A method of centers based on barrier functions for solving optimal control problems with continuum state and control constraints p 52 A92-11467
MAYO, JOHN R.
Helicopter modeling requirements for full mission simulation and handling qualities assessment
p 105 A92-14364
MAYS, R. B.
Mixing studies of helium in air at high supersonic speeds p 935 A92-50310
MAYWALD, P. V.
Development of a freejet capability for evaluating inlet-engine compatibility
[ASME PAPER 91-GT-401] p 137 A92-15731
MAZARSKIJ, V. L.
System of cryogenic security of the superconducting accelerator of relativistic nuclei-nuclotron
[DE91-643289] p 304 N92-16789
MAZHUL', I. I.
Comparative analysis of the lift-drag ratio and heat flows toward the surface of wave riders of different *configurations* p 7 A92-12173
Aerodynamics of two-shock bodies derived by the gasdynamic design method p 707 A92-42683
MAZUR, VLADISLAV
Aircraft-triggered lightning - Processes following strike initiation that affect aircraft p 836 A92-46784
MAZZELLA, ANDREW J., JR.
Visual photometric experiment data processing system
[AD-A248657] p 729 N92-27964
MAZZUCCHELLI, C.
The achievement of aerodynamic goals on the EH101 project through the 'single site' concept
p 1058 A92-56342
MBA, M. N.
The computation and validation of hovering rotor performance p 1055 A92-56285
MCALISTER, K. W.
NACA 0015 wing pressure and trailing vortex measurements
[NASA-TP-3151] p 13 N92-10981
MCARDLE, JACK G.
Flow in a ventral nozzle for short takeoff and vertical landing aircraft p 376 A92-28538
Experimental and analytical study of close-coupled ventral nozzles for ASTOVL aircraft p 861 A92-45325
Internal reversing flow in a tailpipe offtake configuration for SSTOVL aircraft
[AIAA PAPER 92-3790] p 1069 A92-54169
Flow studies in close-coupled ventral nozzles for STOVL aircraft
[NASA-TM-102554] p 445 N92-20934
Internal reversing flow in a tailpipe offtake configuration for SSTOVL aircraft
[NASA-TM-105698] p 868 N92-28418
MCBRIDE, STUART
Acoustic emission monitoring of a ground durability and damage tolerance test p 492 A92-28737
MCCALLUM, A. T.
A study of helicopter rotor/fuselage response in *low-speed manoeuvres - Comparison of theory with* flight p 1086 A92-56334
MCCARTHY, THOMAS R.
Optimum design of helicopter rotor blades with multidisciplinary couplings
[AIAA PAPER 92-0214] p 357 A92-25687
MCCARTY, CRAIG A.
Design and analysis issues of integrated control systems for high-speed civil transports
[NASA-CR-186022] p 979 N92-31656
MCCAULEY, HUGH W.
Assessment of cockpit interface concepts for data link retrofit
[NASA-CR-187615] p 268 N92-17512
MCCAULEY, STEPHEN G.
The Flight Simulation Facility at the Wichita State University p 484 N92-21511
MCCLARY, CHARLES R.
A fault-tolerant Air Data/Inertial Reference System
p 967 A92-51011
MCCLEARY, S. L.
Coupled analysis of independently modeled finite element subdomains
[AIAA PAPER 92-2235] p 581 A92-34289
MCCLEARY, SUSAN L.
Computational methods for global/local analysis
[NASA-TM-107591] p 1125 N92-33104
MCCLELLAND, I. W.
Tomorrow's cockpit displays p 117 A92-13699
MCCLINTICK, BRUCE C.
Computational structures technology engine/airframe coupling p 649 N92-25935
MCCLINTON, C. R.
A computational investigation of mixing and reacting flows in supersonic combustors
[AIAA PAPER 92-0626] p 278 A92-23817
A comparative study of scramjet injection strategies for high Mach numbers flows
[AIAA PAPER 92-3287] p 904 A92-48876
MCCLOSKEY, T.
Annular seals of high energy centrifugal pumps: Presentation of full scale measurement
p 224 N92-14362
MCCLURE, MARK A.
Development of high angle of attack control laws for an unstable, non-minimum phase aircraft using variations of the quantitative feedback technique
[AD-A243698] p 282 N92-17096
MCCLURE, W. B.
An experimental examination of the effects of incoming boundary layer modifications on the dynamics of a turbulent compression corner interaction
[AIAA PAPER 92-3667] p 1022 A92-54111
MCCONKEY, E. D.
Analysis of helicopter accident risk exposure near heliports, airports, and unimproved sites
[SCT-91RR-13] p 637 N92-26028

MCCONKEY, EDWIN D.
Heliport VFR airspace design based on helicopter performance
[SCT-90RR-34] p 103 N92-13049
Helicopter rejected takeoff airspace requirements
[SCT-91RR-28] p 116 N92-13058
Rotorcraft acceleration and climb performance model
[SCT-90RR-30] p 116 N92-13059
Helicopter physical and performance data
[SCT-91RR-27] p 116 N92-13060
MCCONNELL, VICKI P.
Flight vehicles of the future p 419 A92-31525
MCCORMICK, D. C.
Shock-boundary layer interaction control with low-profile vortex generators and passive cavity
[AIAA PAPER 92-0064] p 250 A92-22178
Flow visualization of a prop-fan leading-edge vortex
[AIAA PAPER 92-0386] p 323 A92-26242
MCCORMICK, M. P.
Natural cycles, gases p 408 N92-19123
MCCORRY, DAN
The NASP Program - An update p 61 A92-16059
MCCOY, C. ELAINE
Cooperative planning in aviation contexts
p 456 N92-21509
MCCROSKEY, W. J.
Navier-Stokes analysis of blunt trailing edge airfoils
[AIAA PAPER 92-0024] p 248 A92-22146
Flowfield of a lifting rotor in hover - A Navier-Stokes simulation p 1024 A92-54906
MCCULLERS, L. A.
Analysis for the application of hybrid laminar flow control to a long-range subsonic transport aircraft
[SAE PAPER 912113] p 617 A92-39964
MCCURDY, DAVID A.
Annoyance caused by advanced turboprop aircraft flyover noise: Comparison of different propeller configurations
[NASA-TP-3104] p 56 N92-11758
Development of an annoyance model based upon elementary auditory sensations for steady-state aircraft interior noise containing tonal components
[NASA-TM-104147] p 166 N92-13758
Annoyance caused by aircraft en route noise
[NASA-TP-3165] p 512 N92-20479
MCDANIEL, J. C., JR.
Evaluation of OH laser-induced fluorescence techniques for supersonic combustion diagnostics
[AIAA PAPER 92-0508] p 396 A92-26935
KrF laser-induced OH fluorescence imaging in a supersonic combustion tunnel
[AIAA PAPER 92-3346] p 905 A92-48923
A clean air continuous flow propulsion facility
[AIAA PAPER 92-3912] p 1094 A92-56745
MCDANIEL, JAMES C.
Experimental investigation of a supersonic combustion flowfield employing staged transverse injection behind a rearward-facing step
[AIAA PAPER 92-0090] p 292 A92-22196
A numerical investigation of hydrogen combustion in Mach 2 flow
[AIAA PAPER 92-0341] p 388 A92-25787
MCDANIEL, S.
Application of magnitude estimation scaling to the assessment of subjective loudness response to simulated sonic booms
[NASA-TM-107657] p 1138 N92-33719
MCDEVITT, T. K.
Two-dimensional adaptive-wall tests in the NASA Ames two- by two-foot transonic wind tunnel
p 30 A92-13201
MCDEVITT, T. KEVIN
Measurement of vortex flow fields
[NASA-CR-189543] p 443 N92-20283
MCDONALD, GARY H.
Redesign of flight space shuttle main engine nozzle G-15 seal area based on the thermal analysis and flow models p 212 N92-15877
MCDONALD, HENRY
Hybrid Navier-Stokes/Monte Carlo method for reacting flow calculations p 705 A92-41537
MCDONALD, K. D.
System considerations, projected requirements and applications for aeronautical mobile satellite communications for air traffic services
p 677 N92-24163
MCDONALD, MARK
Proposal for a low cost close air support aircraft for the year 2000: The Raptor
[NASA-CR-190023] p 367 N92-19496
MCDONALD, NICK
Fatigue and accidents - A comparison across modes of transport p 17 A92-13025
MCDONELL, V. G.
Characterization of a two-phase flow field downstream of a 3x-scale gas turbine co-axial, counter-swirling, combustor dome swirl cup
[AIAA PAPER 92-0229] p 393 A92-25693
The influence of spray angle on the continuous- and discrete-phase flowfield downstream of an engine combustor swirl cup
[AIAA PAPER 92-3231] p 863 A92-48832
MCDOUGALL, J. M.
Preliminary analysis of baseline vibration data from Allison T56-A-14LFE engine and reduction gearbox
[NRC-31578] p 130 N92-11999
MCDOWELL, PAUL H.
Robust controller design for an advanced fighter aircraft p 28 A92-11500
MCENTEE, J.
Lower-end dynamic characteristics of a magnetically coupled free-piston Stirling engine/compressor system
p 992 A92-50795
Proof of concept of a magnetically coupled Stirling engine-driven heat pump
[DE92-017129] p 1129 N92-33271
MCENTIRE, B. J.
Ceramic component processing development for advanced gas-turbine engines
[ASME PAPER 91-GT-120] p 142 A92-15567
MCFADDEN, JOHN J.
NASA's rotary engine technology enablement program: 1983-1991
[NASA-TM-105562] p 378 N92-20033
MCFARLAND, DAVID M.
Modifications to and data correction methods for some radiometers used on aircraft p 467 A92-32062
MCFARLAND, ERIC
Aerodynamics and heat transfer investigations on a high Reynolds number turbine cascade
[ASME PAPER 91-GT-157] p 148 A92-15593
MCFARLAND, R. H.
New siting techniques for the ILS glide slope
p 188 A92-17422
MCFARLAND, RICHARD H.
Curved landing approaches using ILS and Loran C
p 94 A92-13854
The appropriate concern for possible aberrations in landing guidance signals p 839 A92-44932
MCFAWN, LESTER
Avionics technology beyond 2000
p 200 N92-14058
MCFEETERS, LARRY
The INFO-ROC technique - A method for comparing and optimizing inspection systems p 144 A92-13563
MCGANN, EDWARD L.
A prelude to interoperability - Comments on the lack of Federal Radionavigation Plan procedures for assessing the potential of a candidate system to fit into the mix of domestic radionavigation systems p 97 A92-16651
MCGARITY, JOHN O.
Prototype instrumentation and design studies
[AD-A248378] p 736 N92-28004
MCGARRY, FRANK
Towards understanding software: 15 years in the SEL
p 413 N92-19423
MCGAW, MICHAEL A.
Life prediction technologies for aeronautical propulsion systems p 560 N92-22520
MCGEE, O. G.
On the three-dimensional vibration analysis of simultaneously skewed and twisted cantilevered parallelepipeds p 759 A92-41801
MCGHEE, ROBERT J.
Separation control on high Reynolds number multi-element airfoils
[AIAA PAPER 92-2636] p 806 A92-45575
The adverse aerodynamic impact of very small leading-edge ice (roughness) buildups on wings and tails
p 451 N92-21691
MCGLAUN, M.
Eulerian computational methods
[DE92-008017] p 765 N92-26853
MCGOVERN, JAMES J.
Flight operations for higher harmonic control research
[AD-A242478] p 196 N92-15067
MCGOWAN, DAVID M.
A simplified method for thermal analysis of a cowl leading edge subject to intense local shock-wave-interference heating
[NASA-TP-3167] p 679 N92-24797
MCGRANE, KEVIN
Analysis and design optimization of monopulse receivers for secondary surveillance radar p 40 A92-12299
MCGRATH, BRIAN E.
Euler code evaluation of a transatmospheric vehicle at supersonic speeds p 9 A92-13202
MCGRATTAN, KEVIN
Comparison of transonic flow models
p 936 A92-50325
MCGRAW, RICHARD J., JR.
Software safety analysis in heterogeneous multiprocessor control systems p 776 A92-42073
MCGRAW, SANDRA M.
The multiple-function multi-input/multi-output digital controller system for the AFW wind tunnel model
[AIAA PAPER 92-2083] p 565 A92-35655
On-line analysis capabilities developed to support the AFW wind-tunnel tests
[AIAA PAPER 92-2084] p 572 A92-35656
On-line analysis capabilities developed to support the AFW wind-tunnel tests
[NASA-TM-107651] p 961 N92-30752
The multiple-function multi-input/multi-output digital controller system for the AFW wind-tunnel model
[NASA-TM-107600] p 1060 N92-32536
MCGREGOR, R.
Laser-initiated conical detonation wave for supersonic combustion. II
[AIAA PAPER 92-0088] p 292 A92-22195
Laser-initiated conical detonation wave for supersonic combustion p 375 A92-28531
MCGRORY, W. D.
Three-dimensional space-marching algorithm on unstructured grids p 5 A92-11058
MCGUIRE, FRANK G.
Airport X-ray screening technology becomes a viable explosives detector p 836 A92-47925
MCGUIRE, JACK F.
Structural airworthiness of aging Boeing jet transports
p 362 N92-18590
Structural integrity of future aging airplanes
p 913 N92-30107
MCGUIRE, JAMES C.
An exploration of function analysis and function allocation in the commercial flight domain
[NASA-CR-4374] p 368 N92-19871
MCGUIRE, ROBERT
Drop test: Cessna Golden Eagle 421B
[DOT/FAA/CT-TN91/32] p 837 N92-28900
MCGUIRK, J.
Prediction and measurement of jet flowfield features for ASTOVL aircraft p 787 A92-45318
MCGUIRK, J. J.
Isothermal modeling of gas turbine combustors - Computational study p 129 A92-17203
Calculations of the dilution system in an annular gas turbine combustor p 494 A92-31164
Second moment closure predictions of jet-on-jet impingement flows p 675 A92-40102
MCHARDY, J.
Thermally regenerative fuel cells
[AD-A242900] p 300 N92-17629
MCINERNEY, KELLY
The Guardian: Preliminary design of a close air support aircraft
[NASA-CR-189991] p 463 N92-21566
MCINTIRE, ALLEN J.
Bearingless main rotor system composite component fabrication techniques p 110 A92-14453
MCINTYRE, T. J.
The high enthalpy shock tunnel in Goettingen
[AIAA PAPER 92-3942] p 1104 A92-56772
MCIVER, DUNCAN E.
Validation of flight critical control systems
[AGARD-AR-274] p 382 N92-20026
Proceedings of the 53rd Symposium on Air Vehicle Mission Control and Management
[AGARD-AR-310] p 1010 N92-32229
MCKAVITT, THOMAS P., JR.
Parameter identification studies on the NASA/Ames Research Center Advanced Concepts Flight Simulator
[NASA-TM-105126] p 31 N92-11024
MCKELVEY, MICHAEL H.
Engineering reliability and maintainability review - A regimen for discovering production deficiencies
p 1120 A92-56254
MCKENNA, P. M.
The use of finite difference electromagnetic analysis in the design and verification of modern aircraft
p 192 A92-20136
MCKENZIE, A. J.
Filter debris analysis: A concrete approach to wear diagnosis
[DREP-TM-88-20] p 222 N92-14345
MCKENZIE, ROBERT L.
Laser-spectroscopic measurement techniques for hypersonic, turbulent wind tunnel flows
[NASA-TM-103928] p 405 N92-19596
MCKENZIE, SAMUEL D.
Investigation of the effects of aeroelastic deformations on the radar cross section of aircraft
[AD-A243889] p 402 N92-18940

MCKEON, MARK F.
Tasking and communication flows in the F/A-18D cockpit: Issues, problems, and possible solutions
[AD-A245977] p 853 N92-28802
MCKEOWN, STEPHEN A.
High performance heat sink for surface mount applications p 989 A92-49275
MCKILLIP, ROBERT M., JR.
Instrumented blade experiments using a light autogiro p 555 A92-35773
Research on measurement and control of helicopter rotor response using blade-mounted accelerometers 1990-91 p 1057 A92-56316
MCKILLIP, ROBERT, JR.
Approximations for inclusion of rotor lag dynamics in helicopter flight dynamics models p 1060 A92-56354
MCKINNEY, BARRY T.
Designing through test
[AIAA PAPER 91-3822] p 232 A92-17664
MCKINNEY, W. D.
Aerodynamics p 202 N92-13977
MCKNIGHT, R. L.
TMFSLAM - Design analysis tool for coated structures
[ASME PAPER 91-GT-141] p 690 A92-36895
The 3D inelastic analysis methods for hot section components
[NASA-CR-189089] p 402 N92-18971
Component-specific modeling
[NASA-CR-189088] p 377 N92-19726
High speed civil transport p 649 N92-25919
MCLACHLAN, R.
Asymptotic theory of transonic wind tunnel wall interference
[AD-A244075] p 403 N92-19080
MCLAUGHLIN, DENNIS K.
An experimental investigation of large scale instabilities in a low Reynolds number two-stream supersonic shear layer
[AIAA PAPER 92-0177] p 255 A92-23787
MCLAUGHLIN, J. C.
Fabrication and testing of corrosion resistant coatings
[DE92-003553] p 490 N92-21063
MCLAUGHLIN, MICHAEL P.
Safety study of TCAS 2 for logic version 6.04
[DOT/FAA/RD-92/22] p 1047 N92-32537
MCLAUGHLIN, THOMAS A.
Hypersonic waveriders - Effects of chemically reacting flow and viscous interaction
[AIAA PAPER 92-0302] p 320 A92-25754
MCLAUGHLIN, THOMAS E.
Flow visualization image analysis of high-rate roll experiments on a delta wing
[AIAA PAPER 92-0317] p 321 A92-25764
MCLVER, DOUGLAS W.
Developing robust support structures for high-technology subsystems: The AH-64 Apache helicopter
[AD-A252773] p 1017 N92-33499
MCMASTERS, J. H.
High Reynolds number testing in support of transport airplane development
[AIAA PAPER 92-3982] p 1099 A92-56807
MCMILLIN, B. K.
Planar fluorescence imaging of a transverse jet in a supersonic crossflow p 755 A92-44501
MCMILLIN, R. D.
Segmental heat transfer in a pin fin channel with ejection holes p 900 A92-47267
MCMILLIN, S. N.
Computational study of incipient leading-edge separation on a supersonic delta wing p 442 A92-32237
MCMINN, JOHN D.
Atmospheric disturbance model for aircraft and space capable vehicles
[AIAA PAPER 92-0294] p 407 A92-25747
MCMURTRY, PATRICK A.
A new unsteady mixing model to predict NO(x) production during rapid mixing in a dual-stage combustor
[AIAA PAPER 92-0233] p 372 A92-25696
MCNAB, ROBERT B.
Rotor blade preservation - Getting the most service life with lowest operational costs p 108 A92-14412
MCNEESE, MICHAEL D.
Identifying design requirements using integrated analysis structures p 922 A92-48527
MCQUADE, PETER D.
Optimization of a 2D scramjet-vehicle using CFD and simplified approximate flow analysis techniques
[AIAA PAPER 92-3673] p 1022 A92-54116
MCQUISTON, BARBARA K.
Turbine engine diagnostics system study
[DOT/FAA/CT-91/16] p 202 N92-14064
MCRAE, D. S.
Newton's method solver for high-speed viscous separated flowfields p 176 A92-20736
Newton's method solver for the axisymmetric Navier-Stokes equations p 703 A92-41269
A nonlinear relaxation/quasi-Newton algorithm for the compressible Navier-Stokes equations
[AIAA PAPER 92-2643] p 796 A92-45510
Numerical simulations using a dynamic solution-adaptive grid algorithm, with applications to unsteady internal flows
[AIAA PAPER 92-2719] p 803 A92-45557
MCRAE, M. M.
Manufacturing technology methodology for propulsion system parts
[AIAA PAPER 92-3525] p 906 A92-49048
MCRUE, DUANE T.
Aeroservoelastic stabilization techniques for hypersonic flight vehicles
[AIAA PAPER 91-5056] p 203 A92-17839
MCRUER, DUANE
Retrospective essay on nonlinearities in aircraft flight control p 204 A92-18601
Design and modeling issues for integrated airframe/propulsion control of hypersonic flight vehicles p 477 A92-29115
MCRUER, DUANE T.
Assessment of flying-quality criteria for air-breathing aerospacecraft
[NASA-CR-4442] p 663 N92-25982
MCWHORTER, JOHN C., III
Analysis and testing of a composite sandwich shell horizontal tail p 755 A92-44617
MCWHORTER, LARRY B.
Shuttle autoland status summary
[AIAA PAPER 92-1273] p 666 A92-38478
MCWITHEY, ROBERT R.
Combined load test apparatus for flat panels
[NASA-CASE-LAR-14698-1] p 911 N92-30028
MEADE, ANDREW J., JR.
Calculation of compressible boundary layer flow about airfoils by a finite element/finite difference method
[AIAA PAPER 92-0524] p 332 A92-26948
The use of artificial neural networks in experimental data acquisition and aerodynamic design p 90 N92-13848
MEADE, L. E.
Manufacturing development of pultruded composite panels
[NASA-CR-181780] p 578 N92-22637
MEADE, PERRY
Manipulation and management of data collected at the Crew Station Research and Development Facility - A case study
[AIAA PAPER 92-4162] p 1008 A92-52451
MEADOR, MARY A. B.
Addition curing thermosets endcapped with 4-amino (2,2) paracyclophane p 577 A92-33918
MEADOR, MICHAEL A.
Addition curing thermosets endcapped with 4-amino (2,2) paracyclophane p 577 A92-33918
High-temperature polymer matrix composites p 578 N92-22513
MEADOWS, KRISTINE R.
Removal of spurious reflections from computational fluid dynamic solutions with the complex cepstrum p 235 A92-20729
MEAKIN, ROBERT L.
Computations of the unsteady flow about a generic wing/pylon/finned-store configuration
[AIAA PAPER 92-4568] p 1027 A92-55377
MEASE, KENNETH D.
A geometric approach to regulator and tracker design for an aerospace plane
[AIAA PAPER 91-5054] p 203 A92-17837
Aerospace plane guidance using time-scale decomposition and feedback linearization p 984 A92-50498
MEASURES, R. M.
Damage assessment for composite smart structures p 140 A92-13601
MEASURES, RAYMOND M.
Progress towards fiber optic smart structures at UTIAS p 368 A92-24781
The detection of damage and the measurement of strain within composites by means of embedded optical fiber sensors p 491 A92-28669
MECHAM, MICHAEL
Dornier 328 first flight p 192 A92-19924
Evaluations of X-29 high-AOA regime show promise for future fighters p 192 A92-19925
MEDAN, RICHARD T.
PAN AIR: A computer program for predicting subsonic or supersonic linear potential flows about arbitrary configurations using a higher order panel method. Volume 2: User's manual (version 3.0)
[NASA-CR-3252] p 527 N92-22865
MEDANIC, J. V.
Design of reliable control systems p 49 A92-11420
MEDEPALLI, SUDHAKAR
A Lie Bracket solution of the optimal thrust magnitude on a singular arc in atmospheric flight
[AIAA PAPER 92-4345] p 1079 A92-55334
MEDOVIKOV, A. S.
Methods for determining atmospheric correction for radio-rangefinder measurements of inclined trajectories p 775 A92-44070
MEDZORIAN, J. P.
Finite element analysis of tire critical speeds p 762 A92-42949
MEE, D. J.
Large chord turbine cascade testing at engine Mach and Reynolds number p 173 A92-18771
MEEHAN, T. K.
NASA's GPS tracking system for Aristoteles p 576 N92-23919
MEERKOETTER, R.
A comparison of measured and modeled broadband fluxes from aircraft data during the ICE '89 field experiment p 1003 A92-49771
MEERWIJK, L.
Real-time helicopter simulation using the blade element method p 1132 A92-56278
Development of nonlinear real-time helicopter simulation using a blade element method
[NLR-TP-90115-U] p 381 N92-18893
MEGE, P.
Numerical simulation of vortex breakdown by solving the Euler equations for an incompressible fluid p 41 N92-10163
Numerical simulation of vortex breakdown via 3-D Euler equations p 41 N92-10164
MEGE, PH.
Determination of vortex-breakdown criteria by solving the Euler and Navier-Stokes equations p 87 N92-13018
MEHDI, I. S.
Condor - An all electric airplane
[SAE PAPER 912184] p 644 A92-40004
MEHLMAN, B. P.
Experimental investigation of film cooling effectiveness for slots of various exit geometries p 497 A92-32265
MEHMED, O.
Aeroelastic analysis of advanced propellers using an efficient Euler solver
[AIAA PAPER 92-0488] p 341 A92-28194
A numerical classical flutter analysis of advanced propellers
[AIAA PAPER 92-2118] p 557 A92-35687
MEHMED, ORAL
Optical measurements of unducted fan flutter
[ASME PAPER 91-GT-19] p 147 A92-15510
MEHTA, JAYESH M.
A distributed vaporization time-lag model for gas turbine combustor dynamics
[AIAA PAPER 92-3465] p 865 A92-49014
MEHTA, R. D.
Three-dimensional structure of a curved wake
[AIAA PAPER 92-0541] p 341 A92-28199
MEHTA, RABINDRA D.
Evolution of three-dimensionality in stable and unstable curved mixing layers p 619 A92-40059
MEHTA, RAMESH
Advanced balancing using laser machining
[SAE PAPER 912218] p 674 A92-40020
MEHTA, S.
System reliability and risk assessment
[AIAA PAPER 92-2345] p 582 A92-34320
MEHTA, U. B.
Some Aspects of uncertainty in computational fluid dynamics results p 233 A92-19609
MEHU, BRUNO
Space software is first of all software p 509 N92-20590
MEI, CHUH
Finite element nonlinear panel flutter with arbitrary temperatures in supersonic flow
[AIAA PAPER 92-2129] p 589 A92-35696
Large-amplitude finite element flutter analysis of composite panels in hypersonic flow
[AIAA PAPER 92-2130] p 589 A92-35697
Prediction of response of aircraft panels subjected to acoustic and thermal loads
[NASA-CR-190305] p 678 N92-24345
Nonlinear analyses of composite aerospace structures in sonic fatigue
[NASA-CR-190565] p 854 N92-30209
MEI, ZUYAN
Inverse solution of 3D incompressible turbulent boundary layer with separated bubbles p 522 A92-35992
MEIER, C.
Construction of a real-time DGPS experimental system p 840 A92-47631

MEIER, G. E. A.
Sound produced by vortex-airfoil interaction
p 1136 A92-56345
MEIER, SUSAN M.
Thermal barrier coating life prediction model development
[ASME PAPER 91-GT-40] p 147 A92-15523
MEIJER, J. J.
Investigation of a semi-empirical method to predict limit cycle oscillations of modern fighter aircraft
[NLR-TP-90087-U] p 481 N92-20475
Development of a method to predict transonic limit cycle oscillation characteristics of fighter aircraft
p 746 N92-27958
MEIJER, JOS J.
Understanding and development of a prediction method of transonic limit cycle oscillation characteristics of fighter aircraft
[AIAA PAPER 92-4501] p 1026 A92-55369
MEILE, W.
Calculation of three-dimensional turbulent flow in wind tunnel entry section p 708 A92-43055
MEIROVITCH, LEONARD
Inclusion principle for the Rayleigh-Ritz based substructure synthesis p 670 A92-36851
MEISNER, JOHN W.
Field test of an advanced maintenance-system
p 1016 A92-56221
MEIZOSO, J. C.
ARINC and commercial aircraft avionics. I
p 353 A92-25655
ARINC and the avionics of commercial aircraft. II
p 637 A92-37072
MEJZAK, RICHARD S.
JIAWG module fault coverage metrics methodology
p 989 A92-49279
MEL'NIK, VALERII I.
Flight test control p 136 A92-15021
MELACHRINOUDIS, EMANUEL
Maintenance scheduling for critical parts of aircraft
p 699 A92-42054
MELAKE, A.
Numerical flow simulation and analysis of a shrouded propfan rotor
[AIAA PAPER 92-3773] p 826 A92-49118
MELBOURNE, WILLIAM G.
NASA's GPS tracking system for Aristoteles
p 576 N92-23919
MELBOURNE, WILLIAM H.
Operating ranges of meteorological wind tunnels for the simulation of convective boundary layer phenomena
[AD-A244153] p 409 N92-19195
MELCONIAN, JERRY O.
The VRT gas turbine combustor - Phase II
[AIAA PAPER 92-3471] p 1067 A92-54035
MELFI, D.
A universal turboprop engine dynamometer test cell
[ASME PAPER 91-GT-343] p 137 A92-15706
MELNIK, ROBERT E.
Industry warms to CFD p 392 A92-24908
MELSON, N. DUANE
Comparison of jet plume shape predictions and plume influence on sonic boom signature
[NASA-TP-3172] p 631 N92-25133
MELSON, W. E., JR.
Observation and comparison of rainfall measured at a high sample rate p 505 A92-32073
MELSON, W. EDWARD, JR.
Wind tunnel aerodynamic characteristics of a transport-type airfoil in a simulated heavy rain environment
[NASA-TP-3184] p 948 N92-31532
MELTON, JOHN E.
Transonic and supersonic Euler computations of vortex-dominated flow fields about a generic fighter
[NASA-TP-3156] p 11 N92-10011
MELVIN, R. G.
Analysis of unsteady aerodynamic and flutter characteristics of an aeroelastic model in transonic flow
p 720 N92-27953
MEN'SHIKOV, V. A.
Solution of the problem of three-dimensional flow past the blade rows of turbomachines with allowance for viscosity effects p 244 A92-21618
MEN'SHOV, I. S.
Increasing the accuracy of the Godunov scheme for calculating steady-state supersonic gas flows by solving the generalized Riemann problem p 1035 A92-57499
MENDENHALL, MICHAEL R.
Computational analysis of high-speed ejection seats
[AIAA PAPER 92-0403] p 324 A92-26256
Prediction of vortex shedding from forebodies with chines p 702 A92-41228
MENDEZ, ANTONIO J.
Efficiency of a 5V/5mW power by light power supply for avionics applications p 734 A92-42603
Code Division Multiple Access (CDMA) system candidate for integrated modular avionics
p 725 A92-42604
MENEGHETTI, U.
Monitoring fatigue cracks in gears
p 1116 A92-54496
MENEGOZZI, LIONEL
A neural network based postattack damage assessment system p 922 A92-48520
MENG, GUANG
The stability of the steady state and bistable response of a flexible rotor supported on squeeze film dampers
p 222 N92-14350
MENGERT, P.
Controller response to conflict resolution advisory prototype
[PB92-190032] p 1050 N92-33596
MENITSKII, VALERII E.
MiG-29 prototype and development flight tests - General overview and high angle of attack investigation
p 113 A92-16064
MENNE, S.
Computation of 3-D hypersonic flows in chemical non-equilibrium including transport phenomena
[AIAA PAPER 92-2876] p 820 A92-47858
Three-dimensional simulations of hypersonic flows
[MBB-UK-0155-89-PUB] p 447 N92-21703
Aerothermodynamics of nozzle flows for advanced hypersonic propulsion systems p 769 N92-27478
MENON, P. K. A.
Nonlinear control of a twin-lift helicopter configuration
p 204 A92-18624
Synthesis of a helicopter full-authority controller
p 280 A92-21178
Aerobrake guidance law synthesis using feedback linearization p 485 A92-29304
Synthesis of robust nonlinear autopilots using differential game theory p 478 A92-29330
Vision-based stereo ranging as an optimal control problem
[AIAA PAPER 92-4418] p 1045 A92-55211
Image-based ranging and guidance for rotorcraft
[NASA-CR-184829] p 191 N92-14036
MENON, SURESH
A new unsteady mixing model to predict NO(x) production during rapid mixing in a dual-stage combustor
[AIAA PAPER 92-0233] p 372 A92-25696
A numerical study of secondary fuel injection techniques for active control of combustion instability in a ramjet
[AIAA PAPER 92-0777] p 374 A92-27114
Computations of hypersonic flows around a three-dimensional concave/convex body
[AIAA PAPER 92-2606] p 805 A92-45570
A new unsteady mixing model to predict NO(x) production during rapid mixing in a dual-stage combustor
[NASA-CR-189155] p 971 N92-30569
MENSEN, H.
Report of the working group Future CNS Systems - Applications and impact on the German air transport system p 266 A92-21325
MENTASTI, A.
Parametric effects of some aircraft components on high-alpha aerodynamic characteristics
p 364 N92-18782
MENZIES, K. R.
Modelling the vaporiser and primary zone flows for a modern gas turbine combustion chamber
p 742 N92-27484
MERATI, PARVIZ
The interaction between a plane shear layer and a slender body p 991 A92-49790
MERBOTH, LAWRENCE J.
A high performance general purpose processing element for avionic applications p 920 A92-48440
MERCER, B. P.
Technology exploitation for in-service support of future rotorcraft p 1016 A92-56327
MERCER, CHARLES E.
Data reduction formulas for the 16-foot transonic tunnel: NASA Langley Research Center, revision 2
[NASA-TM-107646] p 984 N92-31900
MERCURIO, U.
CFRP stiffened panels under compression
p 1109 N92-33044
MERDGEN, DAVID B.
Zonal analysis - The final step in system safety assessment p 760 A92-42071
MERET, G.
Industrial practice in aeronautical maintenance
p 786 A92-47774
MERHAV, S. J.
Autonomously aided strapdown attitude reference system p 204 A92-18610
Adaptive suppression of biodynamic interference in helmet-mounted displays and head teleoperation
p 197 A92-18611
Estimation of aircraft attitude by angular rate measurements p 963 N92-31881
MERIENNE, M. C.
Feasibility study of hypersonic clinometric measurements at R3Ch
[ONERA-RSF-136/1865-AY-728-] p 829 N92-28789
MERKEL, J.
Navsat - A civil complement to GPS and Glonass
[IAF PAPER 91-490] p 188 A92-18505
MERKEL, PHILIP A.
Automated planning with special relevance to associate systems technology and mission planning
[AD-A241924] p 303 N92-17438
MERKLE, CHARLES L.
Unsteady flows in rotor-stator cascades
[AD-A241593] p 158 N92-13410
MERLINI, TEODORO
Linear analysis of naturally curved and twisted anisotropic beam p 899 A92-46936
Composite beam analysis linear analysis of naturally curved and twisted anisotropic beams
[AD-A252652] p 999 N92-30766
MERLO, A.
Numerical simulations around models in hypersonic wind tunnels p 182 N92-14998
MERONEY, ROBERT N.
Operating ranges of meteorological wind tunnels for the simulation of convective boundary layer phenomena
[AD-A244153] p 409 N92-19195
MERRICK, V. K.
Control and display combinations for blind vertical landings p 661 A92-39903
MERRIGAN, M. A.
Analytical and experimental studies of heat pipe radiation cooling of hypersonic propulsion systems
[AIAA PAPER 92-3809] p 867 A92-49128
Analytical and experimental studies of heat pipe radiation cooling of hypersonic propulsion systems
[DE92-013428] p 973 N92-31817
MERRILL, W.
Design and evaluation of a robust dynamic neurocontroller for a multivariable aircraft control problem
[NASA-TM-105579] p 481 N92-20586
MERRILL, WALTER C.
Real-time fault diagnosis for propulsion systems
[NASA-TM-105303] p 26 N92-11017
MERSCH, T.
Flow field measurement and visualization using projected smoke trails
[AIAA PAPER 92-0384] p 323 A92-26241
MERSCH, THOMAS
Computational vorticity capturing - Application to helicopter rotor flows
[AIAA PAPER 92-0056] p 250 A92-22171
MERTENS, JOSEF
Short time force measurement system
p 208 N92-15001
MERX, M.
Expert system for the Tornado ground-based check-out system p 118 N92-12536
MERZ, A. W.
Maximum-miss aircraft collision avoidance
p 660 A92-37077
MERZOUGUI, T.
Robustness characteristics of fast-sampling digital controllers for active flutter suppression
[AIAA PAPER 92-2104] p 567 A92-35675
Design of adaptive fast-sampling digital controllers for active flutter suppression
[AIAA PAPER 92-2105] p 567 A92-35676
MESANDER, GEERT A.
Advanced ice protection systems test in the NASA Lewis Icing Research Tunnel p 108 A92-14406
Results of a low power ice protection system test and a new method of imaging data analysis
[NASA-TM-105745] p 828 N92-28696
MESCHWITZ, STEVEN
The effect of angle of incidence and Reynolds number on heat transfer in a linear turbine cascade
[AD-A243900] p 377 N92-19328
MESSERSCHMID, E.
Optimization of two stage reusable space transportation systems with rocket and airbreathing propulsion concepts
[IAF PAPER 92-0863] p 1104 A92-57254
MESSERSCHMID, E. W.
The IRS plasma wind tunnels for the investigation of thermal protection materials for reentry vehicles
p 208 N92-15009
MESSERSCHMID, ERNST
IRS organigram p 33 N92-10053
MESSITER, A. F.
Control of hypersonic aerodynamic forces with surface blowing p 172 A92-18363

MESSITT, D. G.
Comparison between computational and experimental data for a hypersonic laser propelled vehicle
[AIAA PAPER 92-3808] p 1023 A92-54179
METCALF, FREDERIC T.
On the overdetermined celestial fix p 19 A92-10475
METCALF, THOMAS R.
On the overdetermined celestial fix p 19 A92-10475
METCALFE, M. T.
Emissions from aircraft: Standards and potential for improvement
[PNR-90768] p 476 N92-21740
The impact of air transport on the environment
[PNR-90876] p 1129 N92-33751
METWALLY, M.
High temperature erosion resistance of coatings for gas turbine
[ASME PAPER 91-GT-213] p 143 A92-15632
Coating effect on particle trajectories and turbine blade erosion p 653 A92-36892
METWALLY, METWALLY H.
Unsteady pressure field and vorticity production over a pitching airfoil p 330 A92-26416
METWALLY, MUNIR
Designing a methodology for future air travel scenarios p 409 N92-19125
METZ, PAUL
YF-23A preliminary flight test results p 112 A92-16063
METZGER, D. E.
Computer-based areal surface temperature and local heat transfer measurements with thermochromic liquid crystals (TLC) p 763 A92-44326
Experimental modeling of film-cooled axial turbine tip seals
[AIAA PAPER 92-4058] p 1119 A92-56141
METZGER, FREDERICK B.
Predicted pressure distribution on a prop-fan blade through Euler analysis p 810 A92-46791
METZGER, MICHAEL A.
Notes on the use of fusible temperature indicators to bound the temperature of hot graphite in the NAVSWC hypervelocity wind tunnel facility p 1090 A92-54315
MEURZEC, J. L.
Direct coupling of fluid structure in transonic aeroelasticity p 721 N92-27954
MEYER, FRIEDRICH-WILHELM
A Mach-scaled powered model for rotor-fuselage interactional aerodynamics and flight mechanics investigations p 847 A92-46960
MEYER, GEORGE
Nonlinear control design for slightly nonminimum phase systems - Application to V/STOL aircraft p 876 A92-48160
MEYER, H.-J.
A concept for the revisions of structural inspection schedules p 226 N92-14431
The Operational Loads Monitoring System, OLMS p 361 N92-18586
MEYER, HANS-L.
The DLR test aircraft in FZ-BS VFW614/ATTAS, Dornier DO228-101, MBB BO 105-S-3 p 648 N92-25591
MEYER, J.
Effects of the roll angle on cruciform wing-body configurations at high incidences
[AIAA PAPER 92-4356] p 1079 A92-55342
Pulsating spanwise blowing on a fighter aircraft
[AIAA PAPER 92-4359] p 1025 A92-55345
MEYER, R. P.
ICAAS piloted simulation evaluation p 735 N92-27906
MEYER, ROBERT R., JR.
Overview of the NASA Dryden Flight Research Facility aeronautical flight projects
[NASA-TM-104254] p 962 N92-31261
MEYER, STEPHAN S.
Resonant cryogenic chopper p 294 A92-22796
MEYER, T. G.
Life prediction and constitutive models for engine hot section anisotropic materials program
[NASA-CR-189222] p 973 N92-31534
Life prediction and constitutive models for engine hot section anisotropic materials program
[NASA-CR-189223] p 1072 N92-33479
MEYER, THOMAS J.
Distribution of maximum levels of aircraft noise around their mean value p 693 A92-39062
Robust identification of nonlinear aerodynamic model structure
[AIAA PAPER 92-4503] p 1081 A92-55370
MEYERS, JAMES F.
Doppler global velocimeter measurements of the vortical flow above a thin delta wing
[AIAA PAPER 92-0005] p 292 A92-22130
Signal processing schemes for Doppler global velocimetry p 1115 A92-54338
MEYN, FRED
The ATF YF-23 Vehicle Management System
[AIAA PAPER 92-1076] p 563 A92-33245
MEYN, LARRY A.
Analysis of a pneumatic forebody flow control concept about a full aircraft geometry
[AIAA PAPER 92-2678] p 799 A92-45530
Forebody flow control on a full-scale F/A-18 aircraft
[AIAA PAPER 92-2674] p 806 A92-45583
Full-scale high angle-of-attack tests of an F/A-18
[AIAA PAPER 92-2676] p 806 A92-45584
MEZA, VICTOR
Analytical aeroelastic stability considerations and conversion loads for an XV-15 tilt-rotor in a wind tunnel simulation
[AIAA PAPER 92-2258] p 540 A92-34413
MIAGKOV, IU. A.
Oscillations of an anisotropic rotor on an elastic anisotropic support p 1057 A92-56311
MIAILLIER, BERNARD
The Automatic Dependent Surveillance (ADS) system p 724 A92-41208
MIAKE-LYE, RICHARD C.
The atmospheric effects of stratospheric aircraft: A first program report
[NASA-RP-1272] p 408 N92-19121
High-speed civil transport aircraft emissions p 408 N92-19122
MIAO, YONGMIAO
An analysis method and applications for 3-D viscous internal flows with complex geometry p 143 A92-13299
A calculation procedure for three-dimensional turbulent flow in a centrifugal impeller with any blade geometry
[ASME PAPER 91-GT-171] p 73 A92-15606
MIAU, J. J.
Nonuniform motion of leading-edge vortex breakdown on ramp pitching delta wings p 808 A92-45828
MICHAEL, M.
Developments in airborne surveillance and control systems p 98 A92-16655
MICHAL, T.
GPS availability. I - Availability of service achievable for different categories of civil users. II - Evaluation of state probabilities for 21-satellite and 24-satellite constellations p 99 A92-16949
MICHALEK, DONNA J.
A nearly-monotone genuinely multidimensional scheme for the Euler equations
[AIAA PAPER 92-0325] p 322 A92-25772
MICHALKE, A.
On the effect of external flow and shear-layer thickness on the expansion cells of under-expanded supersonic circular jets p 969 A92-50478
MICHALSKI, WIESLAW J. J.
Aircraft stabilization at large angles of attack p 875 A92-47785
MICHARD, MARC
Inhomogeneous turbulence beyond spectral equilibria: Aeronautical applications
[ETN-92-90867] p 404 N92-19349
MICHARD, P. J.
Presentation of a computational code for 3-D compressible flow in complex channels and cavities p 769 N92-27475
MICHEL, ULF
Jet aircraft noise at high subsonic flight Mach numbers
[DLR-FB-91-28] p 928 N92-29997
MICHELI, F.
Nonstationary flight aerodynamics in a turbulent environment
[ETN-91-90102] p 82 N92-11980
MICKLE, R. E.
Digital ozonesondes - Examples of results from the EMEFS experiments of 1988 and 1990 p 468 A92-32140
MICOL, JOHN R.
Simulation of real-gas effects on pressure distributions for aeroassist flight experiment vehicle and comparison with prediction
[NASA-TP-3157] p 501 N92-20677
MIDDLETON, D. H.
The first fifty years of composite materials in aircraft construction p 461 A92-32325
MIDDLETON, DAVID B.
Takeoff Performance Monitoring System display options
[AIAA PAPER 92-4138] p 967 A92-52433
MIDDLETON, ELIZABETH M.
The application of high spectral and spatial resolution imaging spectrometers for locating downed aircraft p 598 A92-35132
MIDKIFF, M.
Liquid flow-through cooling for avionics applications p 902 A92-48448
MIELE, A.
Optimal trajectories and guidance trajectories for aircraft flight through windshears p 27 A92-11383
MIGEMI, S.
The calculation of incompressible separated turbulent boundary layers p 1003 N92-31886
MIGINIAC, ROLAND
The role of simulation for the study of APIS (piloting support by synthetic imagery) p 885 N92-28544
MIGUET, B.
Successful transfer of technology from a research and development laboratory to an Aerospatiale production unit p 931 A92-51808
MIHALOEW, JAMES R.
Integrated flight/propulsion control for supersonic STOVL aircraft p 872 A92-45320
MIKAMI, SHINICHI
Low speed aerodynamic performance of a capsule-shaped flying object p 430 A92-30559
MIKAMI, TADASHI
Experimental investigation of the boundary layer in a corner formed by two circular arc airfoils p 1029 A92-56046
MIKAMI, TATSUO
Space plane navigation simulation p 1103 A92-53603
MIKELADZE, V. G.
Reducing the background noise level in the test section of a wind tunnel for transonic flow velocities p 511 A92-30143
MIKHAILOVA, L. K.
Evaluation of the fungicide properties of antifreeze additives for jet fuels p 141 A92-15070
MIKI, Y.
Advanced SCRAM-LACE system concept for single-stage-to-orbit space plane
[IAF PAPER 91-272] p 32 A92-12599
MIKI, YOICHIRO
An advanced scramjet propulsion concept for a 350 MG SSTO space plane - External nozzle performance
[AIAA PAPER 92-3719] p 1067 A92-54134
MIKI, YOUICHIRO
Key design considerations for scramjet powered space plane p 1066 A92-53491
MIKKELSEN, KEVIN L.
Experience in the operation of a hypersonic nozzle static thrust stand
[AIAA PAPER 92-3292] p 882 A92-48881
MILES, JOHN B.
Navier-Stokes simulation for cone-derived waverider p 703 A92-41271
Computation of turbulent flow about cone-derived waverider
[AIAA PAPER 92-2726] p 804 A92-45562
MILES, R.
Rayleigh imaging and flow tagging in ground test facilities p 1115 A92-54330
MILES, R. N.
Acoustic fatigue life prediction for nonlinear structures with multiple resonant modes
[NASA-CR-190471] p 1000 N92-30988
MILES, WILLIAM L.
Assessment of cockpit interface concepts for data link retrofit
[NASA-CR-187615] p 268 N92-17512
MILFORD, C. M.
Configuration effects on the ingestion of hot gas into the engine intake p 842 A92-45315
MILHOLEN, WILLIAM E., II
Numerical modeling of transonic juncture flow
[AIAA PAPER 92-4036] p 1035 A92-56858
MILLAR, R. I.
Technical feasibility of digital three-dimensional cellular communications for air traffic control applications. Volume 1: Introduction and summary
[AD-A244573] p 534 N92-22104
Technical feasibility of digital three-dimensional cellular communications for air traffic control applications. Volume 2: Example system design details
[AD-A244574] p 534 N92-22105
Technical feasibility of digital three-dimensional cellular communications for air traffic control applications. Volume 3: Ground network architecture
[AD-A244575] p 534 N92-22106
MILLER, ALLEN R.
Traveling on the curved earth p 19 A92-10474
MILLER, ANDRZEJ
Concept of a one-dimensional model of the dynamic behavior of a gas turbine p 862 A92-47791
MILLER, B. M.
Conditions of optimality in problems of generalized control. II - Sufficient conditions of optimality p 1007 A92-51328
MILLER, BARRY
High costs force avionics links p 276 A92-22000

MILLER, C.
Shipboard mission training effectiveness of the Naval Air Warfare Center's V-22 Government Test Pilot Trainer
[AIAA PAPER 92-4130] p 959 A92-52427
MILLER, C. G., III
Hypersonic aerodynamic/aerothermodynamic testing capabilities at Langley Research Center
[AIAA PAPER 92-3937] p 1096 A92-56767
MILLER, C. M.
System considerations, projected requirements and applications for aeronautical mobile satellite communications for air traffic services
p 677 N92-24163
MILLER, CHRISTOPHER A.
An explanation-based-learning approach to knowledge compilation - A Pilot's Associate application
p 920 A92-48220
MILLER, D. C.
An improved compressor performance prediction model
[PNR-90873] p 1072 N92-33749
MILLER, DAVID G.
V-22 pilot-in-the-loop aeroelastic stability analysis
p 133 A92-14422
Tiltrotor control law design for rotor loads alleviation using modern control techniques p 478 A92-29331
MILLER, DAVID P.
TIGGERC: Turbomachinery interactive grid generator energy distributor and restart code p 659 N92-25719
MILLER, G. E.
Fiber-coupled position sensors for aerospace applications p 370 A92-27776
MILLER, GERALD D.
A summary of the Active Flexible Wing program
[AIAA PAPER 92-2080] p 565 A92-35652
A summary of the active flexible wing program
[NASA-TM-107655] p 962 N92-31264
MILLER, GLEN E.
Application of analog fiber optic position sensors to flight control systems p 857 A92-48042
MILLER, JAMES G.
Failure environment analysis tool (FEAT) development status
[AIAA PAPER 91-3803] p 232 A92-17654
MILLER, JEFFREY H.
Engine panel seals for hypersonic engine applications: High temperature leakage assessments and flow modelling
[NASA-TM-105260] p 298 N92-16336
High temperature dynamic engine seal technology development
[NASA-TM-105641] p 596 N92-23435
MILLER, JOHN I.
MD-11 status report p 646 A92-40040
MILLER, L. S.
Simple method of supersonic flow visualization using smoke p 219 A92-20764
Doppler global velocimeter measurements of the vortical flow above a thin delta wing
[AIAA PAPER 92-0005] p 292 A92-22130
The effects of blowing on delta wing vortices during dynamic pitching at high angles of attack
[AIAA PAPER 92-0407] p 325 A92-26260
Experimental and computational investigation of wind tunnel effects on airfoil flow fields
[AIAA PAPER 92-0672] p 431 A92-30624
A simple three component velocity measurement method using a rotated split-film sensor
p 1115 A92-54333
MILLER, L. SCOTT
An evaluation of preliminary Doppler global velocimetry measurements p 90 N92-13849
MILLER, M. M.
Transition of GPS user equipment testing from Yuma Proving Ground to Holloman AFB p 138 A92-16972
MILLER, M. P.
Auxiliary power system requirements for commercial air transports - Past, present and future
[SAE PAPER 912188] p 656 A92-40007
MILLER, MICHAEL B.
Singlemode fiber optic rotary joint for aircraft applications p 779 A92-42606
MILLER, MILES C.
Experimental aerodynamic facilities of the Aerodynamics Research and Concepts Assistance Branch
[AD-A247489] p 883 N92-28248
MILLER, NICHOLAS P.
Some experiences with community response to low levels of aircraft noise p 689 A92-39235
MILLER, P.
The application of high pressure ejectors to reaction control systems p 128 A92-16666
MILLER, R. E.
Distortion tolerance of the T800-LHT-800 turboshaft engine p 120 A92-14409
MILLER, R. H.
The effects of inner wake modelling on blade airloads
p 521 A92-35784
MILLER, ROBERT J.
Reactivation and upgrade of the NASA Ames 16-Inch Shock Tunnel - Status report
[AIAA PAPER 92-0327] p 383 A92-25774
MILLER, S. C.
The search for new materials
[PNR-90777] p 490 N92-21744
MILLER, WAYNE OWEN
Analytical/numerical matching and periodic inversion: Two advances in free wake analysis
p 178 N92-13994
MILLHOUSE, PAUL
The Langley turbo-prop commuter design: A complete project description
[NASA-CR-189987] p 463 N92-21540
MILLOTT, T. A.
Vibration reduction in helicopter rotors using an active control surface located on the blade
[AIAA PAPER 92-2451] p 564 A92-34478
MILLS, H. L.
24-bit flight test data recording format
p 900 A92-47528
MILLS, HARLAN D.
Cleanroom - An alternative software development process p 233 A92-19386
MILTHORPE, J. F.
Simulation of supersonic and hypersonic flows
p 251 A92-22790
MIN, J. B.
Study of weld offset in longitudinally welded SSME HPFTP inlet
[AIAA PAPER 92-2305] p 586 A92-34525
MINAS, CONSTANTINOS
Experimental active control of a two-dimensional truss
p 47 A92-11346
MINCIOTTI, R. L.
Description and simulation results of the Italsat AOCS advanced flight simulator p 667 N92-24472
MINECK, RAYMOND E.
Wall interference assessment/correction for transonic airfoil data p 30 A92-13214
Comparison of a two-dimensional adaptive-wall technique with analytical wall interference correction techniques
[NASA-TP-3132] p 444 N92-20494
MINECK, RAYMOND EDWARD
Assessment of potential aerodynamic benefits from spanwise blowing at the wing tip
[NASA-TM-107847] p 631 N92-25261
MINEGISHI, MASAKATSU
Vibration tests of long plate structural model
[NAL-TM-625] p 400 N92-18485
MINEO, SHINICHI
Development of pre- and post-processor system for structural analysis
[NAL-TM-628] p 681 N92-25403
MINGES, MARK E.
Integrated Communications, Navigation, Identification, Avionics (ICNIA) expert system for fault tolerant avionics
p 118 N92-12539
MINGUEZ, R.
A methodology for software specification and development based on simulation p 135 N92-12458
MINK, K.-H.
Steps toward acceptance p 355 N92-19046
MINNICH, STEVE
F-14 dual hydraulic failure flying qualities evaluation
p 645 A92-40029
MINTO, K. D.
Compensating for manufacturing and life-cycle variations in aircraft engine control systems
[AIAA PAPER 92-3869] p 868 A92-49139
MINUCCI, M. A. S.
Experimental study of a two-dimensional scramjet inset, M(freestream) = 10.1-25.1 p 611 A92-36974
MINUTO, A.
The G-222 aircraft individual tracking programme
p 361 N92-18582
MIRACLE, D. B.
Development of intermetallic materials for aerospace systems p 754 A92-41874
MIRDAMADI, MASSOUD
Stress-strain analysis of a (0/90)sub 2 symmetric titanium matrix laminate subjected to a generic hypersonic flight profile
[NASA-TM-107584] p 685 N92-26128
MIRESSI, MICHAEL J.
Loran time difference correction factors - Valid information or blue smoke and mirrors?
p 96 A92-16633
MIRICA, D.
An aerodynamical analysis of 'seesaw' type rotor for autogyro p 937 A92-52034
MIRICK, P. H.
A demonstration of passive blade twist control using extension-twist coupling
[AIAA PAPER 92-2468] p 539 A92-34358
MIRICK, PAUL H.
Recent rotorcraft aeroelastic testing in the Langley Transonic Dynamics Tunnel p 136 A92-14377
An experimental study of the sensitivity of helicopter rotor blade tracking to root pitch adjustment in hover
[NASA-TM-4313] p 61 N92-12989
A demonstration of passive blade twist control using extension-twist coupling
[NASA-TM-107642] p 1001 N92-31155
MIRONOV, S. G.
Characteristics of the mechanism of separated flow pulsation ahead of a spike-tipped cylinder in supersonic flow p 337 A92-27597
MIROSHIN, ROMAN N.
Local interaction theory
[ISBN 5-288-00516-8] p 779 A92-42778
MIRZA-BAIG, F. S.
Off-design performance prediction of turbofans using gasdynamics
[ASME PAPER 91-GT-389] p 126 A92-15721
MISHIWAKI, OSAMU
Present status of Al-Li alloys p 1106 A92-56105
MISHLER, R.
Emerging airframe/propulsion integration technologies at General Electric
[AIAA PAPER 92-3335] p 850 A92-48917
MISHRA, S. R.
RCS of four fuselage-like scatterers at HF frequencies
p 533 A92-33632
MISRA, P.
Integrated use of GPS and GLONASS in civil aviation navigation. I - Coverage and data models
p 99 A92-16950
GLONASS data analysis - Interim results
p 955 A92-49382
MITANI, TOHRU
Experimental validation of scramjet nozzle performance
[AIAA PAPER 92-3290] p 864 A92-48879
A preliminary study of a supersonic wind tunnel for a ram jet test facility p 1089 A92-53564
MITCHELL, BRIAN E.
Direct computation of the sound from a compressible co-rotating vortex pair
[AIAA PAPER 92-0374] p 414 A92-26232
MITCHELL, DAVID G.
The use of ground based simulation for handling qualities research: A new assessment p 885 N92-28545
Effects of cockpit lateral stick characteristics on handling qualities and pilot dynamics
[NASA-CR-4443] p 878 N92-28584
MITCHELL, GEORGE D., JR.
Manufacturing techniques - Split torque path helicopter transmission p 110 A92-14452
MITCHELL, J.
Laser-initiated conical detonation wave for supersonic combustion. II
[AIAA PAPER 92-0088] p 292 A92-22195
MITCHELL, L. K.
Acoustic characteristics and dynamic structural loading of an ASTOVL aircraft in hover
[AIAA PAPER 92-0370] p 416 A92-28190
MITCHELL, M. R.
Advances in fatigue lifetime predictive techniques; Proceedings of the Symposium, San Francisco, CA, Apr. 24, 1990
[ASTM STP-1122] p 896 A92-45226
MITCHELL, MARK D.
Feasibility of systematic recycling of aircraft Halon extinguishing agents
[DOT/FAA/CT-91/21] p 352 N92-18259
MITCHELL, N. A.
ASTOVL propulsion systems configuration and concept choice p 842 A92-45312
ASTOVL propulsion systems: Configuration and concept choice
[PNR-90809] p 740 N92-27041
MITCHELL, RICK
Implementation and usage of the RJ program Data Acquisition System Ground Station p 210 A92-19257
MITCHELTREE, R. A.
Plasmadynamic effects in thermochemical nonequilibrium aerobrake flows
[AIAA PAPER 92-0573] p 333 A92-26980
Plasmadynamic effects in thermochemical nonequilibrium aerobrake flows p 705 A92-41538
Application of program LAURA to perfect gas shock tube flows: A parametric study
[NASA-TM-104190] p 298 N92-17002

MITRA, N. K.
Embedded longitudinal vortex arrays, velocity and temperature fields, loss and heat transfer augmentation p 621 A92-40121
MITRAMAJUMDAR, D.
Fracture behaviour of high-temperature polymer composites p 34 A92-11993
MITROKHIN, N. M.
Interaction of jets ejected from two-dimensional nozzles with a curved surface p 438 A92-31869
MITRY, SAMEH A.
Transfer function between airborne VLF transmit and receive loop antenna p 1045 A92-54754
MITSUDA, M.
Numerical prediction of the flow characteristics in an arc wind tunnel
[AIAA PAPER 92-4016] p 1100 A92-56838
MITSUMA, HIDEHIKO
Fabrication test and evaluation of graphite/PMR-15 polyimide for HOPE primary structure p 1105 A92-53516
MITTAL, S.
Unsteady incompressible flow computations with quadrilateral elements p 394 A92-26219
MITTERER, K. F.
Application of program LAURA to perfect gas shock tube flows: A parametric study
[NASA-TM-104190] p 298 N92-17002
MIURA, HIROKAZU
Static aeroelastic analysis for generic configuration wing p 174 A92-20201
MIURA, Y.
The maneuver performance and control of a hovercraft p 763 A92-43240
MIURA, YOSIHIRO
Gust response and cross wind performance of a hovercraft with vertical wings p 1118 A92-56034
MIWA, H.
Recent airfoil tests in NAL 2D high Reynolds number wind tunnel p 748 A92-43171
MIWA, HITOSHI
On the structure of unsteady shock induced separation of the transonic airfoil in the NAL two-dimensional wind tunnel p 1029 A92-56010
BGK1 airfoil oilflow tests in the NAL two-dimensional wind tunnel. II p 1029 A92-56044
Evaluation of NACA0012 airfoil test results in the NAL two-dimensional transonic wind tunnel
[NAL-TR-1109T] p 445 N92-21287
NACA0012 airfoil data corrected for sidewall boundary-layer effects in the NAL two-dimensional transonic wind tunnel
[NAL-TM-640T] p 722 N92-28151
Force measurements on AGARD calibration model-B at transonic speeds in the NAL two-dimensional wind tunnel
[NAL-TM-639] p 722 N92-28190
MIXSON, JOHN S.
Interior noise p 236 N92-14785
MIYABA, HIROSHI
Concepts of flight experiments for HOPE development p 1103 A92-53635
MIYACHI, T.
An analysis of impact resistance of composite blades for turbo-fan engines p 294 A92-23109
MIYACHI, TOSHIO
An analysis of impact resistance of composite fan blade p 293 A92-22523
An analysis of impact resistance of composite blades for aircraft engines (Analysis with two dimensional and three dimensional finite elements) p 579 A92-32562
An analysis of the effect of centrifugal force on the impact resistance of composite fan blades for turbo-fan engines
[SAE PAPER 912047] p 861 A92-45431
Finite elements analysis of flexural edge wave for composite fan blades
[SAE PAPER 912048] p 861 A92-45432
MIYAJIMA, H.
A model study on diffuser pressure recovery in NAL scramjet test facility with simulated hydrogen combustion
[AIAA PAPER 92-3979] p 1071 A92-56805
MIYAJIMA, HIROSHI
Scramjet research at the National Aerospace Laboratory
[AIAA PAPER 91-5076] p 200 A92-17849
Experimental validation of scramjet nozzle performance
[AIAA PAPER 92-3290] p 864 A92-48879
MIYAKAWA, JUNICHI
Aero-structural integrated design of forward swept wing
[SAE PAPER 912021] p 790 A92-45414
MIYAKE, S.
Strength evaluation and safety of machine/structure. III - Case examples on strength and safety evaluation of machine/structure 3.2 aircraft (airframe) p 882 A92-47303
MIYAKE, SHO
Numerical analysis of RCS jet in hypersonic flights
[SAE PAPER 912063] p 791 A92-45445
HOPE re-entry experimental vehicle p 1103 A92-55098
MIYAMOTO, YOSHIT
Aerodynamic development of boundary layer control system for NAL QSTOL research aircraft 'ASKA'
[SAE PAPER 912010] p 843 A92-45410
MIYAMOTO, YOSHITO
Experimental studies on aerodynamic characteristics of SSTO vehicle at low subsonic speeds
[SAE PAPER 911981] p 788 A92-45386
MIYASHITA, JUNICHI
Prospects for a commercial STOL transportation system p 634 A92-38207
Aerodynamic development of boundary layer control system for NAL QSTOL research aircraft 'ASKA'
[SAE PAPER 912010] p 843 A92-45410
MIYATAKE, HIROKAZU
Operational progress of the STOL research aircraft Asuka p 730 A92-43138
MIYAUCHI, T.
Numerical simulation of supersonic nozzle flow p 430 A92-30540
MIYAZAWA, Y.
Robust flight control system design using a multimodel approach. II p 745 A92-43180
MIYAZAWA, YOSHIKAZU
Robust flight control system design with multiple model approach p 661 A92-39910
Gust load alleviation control design for the accuracy of an aeroelastic active control model p 745 A92-43134
Multiple delay model approach applied to the AIAA 1922 Controls Design Challenge
[AIAA PAPER 92-4630] p 1078 A92-55305
Synthesis of gust load alleviation with flutter margin augmentation p 1082 A92-56021
Robust control system design with multiple model approach p 1083 A92-56029
Flight evaluation of navigation systems including MLS using NAL Do228 - Outline p 1047 A92-56116
A preliminary flight test on a basic performance of the flight research airplane Do 228: Velocity vs glide path angle
[NAL-TM-613] p 359 N92-18482
MIYOSHI, HAJIME
Ultra High Speed Numerical Wind Tunnel (UHSNWT) initiative at National Aerospace Laboratory numerical simulator - second generation
[NAL-TR-1108] p 384 N92-18037
MIZUKI, S.
Unsteady flow within centrifugal compressor channels under rotating stall and surge
[ASME PAPER 91-GT-85] p 670 A92-36901
MIZUTANI, TOMOAKI
Test results of the expander cycle air turbo ramjet for a future space plane
[IAF PAPER 91-271] p 120 A92-14709
MNICH, JASON
Non-chromated anodize process for corrosion resistance and adhesive bonding p 892 A92-47341
MO, G.
Visualization and analysis of hypersonic flows and comparison to experimental data
[AIAA PAPER 92-2774] p 704 A92-41320
MOBLEY, MICHAEL D.
Flight test of a GPS-aided low-cost inertial navigation system programmed in Ada p 101 A92-16973
MOCARSKI, S. J.
Durability and damage tolerance of aluminum castings
[AD-A245237] p 490 N92-21159
MOCHIDA, A.
Scrutinizing k-epsilon EVM and ASM by means of LES and wind tunnel for flowfield around cube p 621 A92-40119
MOCHIZUKI, OSAMU
Development of pre- and post-processor system for structural analysis
[NAL-TM-628] p 681 N92-25403
MODI, V. J.
Approach to side force alleviation through modification of the pointed forebody geometry p 309 A92-24418
Drag reduction of bluff bodies through momentum injection p 702 A92-41231
Reduction of the side force on pointed forebodies through add-on tip devices p 1024 A92-54918
MODLIN, JAMES M.
Heat pipe and surface mass transfer cooling of hypersonic vehicle structures p 763 A92-44380
Surface cooling of scramjet engine inlets using heat pipe, transpiration, and film cooling p 763 A92-44381
MODLIN, JAMES MICHAEL
Hypersonic aerospace vehicle leading edge cooling using heat pipe, transpiration and film cooling techniques p 780 N92-26733
MODZELEWSKI, STEPHEN A.
Computer program for calculating in-flight aircraft-store interface reaction loads
[AD-A245782] p 731 N92-26896
MOEK, G.
European studies to investigate the feasibility of using 1000 ft vertical separation minima above FL 290. II - Precision radar data analysis and collision risk assessment p 353 A92-24946
Estimating the probability of vertical overlap from the paired aircraft data obtained in the European vertical data collection using the program DGLDiF
[NLR-TR-88108-U] p 356 N92-19491
MOENS, F.
Construction of a numerical optimization method for the definition of hypersupported profiles
[ONERA-RSF-43/1736-AY-146A] p 908 N92-28788
MOES, TIMOTHY
Piloted simulation study of a balloon-assisted deployment of an aircraft at high altitude
[NASA-TM-104245] p 272 N92-15986
MOES, TIMOTHY R.
Failure detection and fault management techniques for flush airdata sensing systems
[AIAA PAPER 92-0263] p 369 A92-25719
High angle-of-attack flush airdata sensing system p 1064 A92-56172
Failure detection and fault management techniques for flush airdata sensing systems
[NASA-TM-4335] p 276 N92-17128
MOFFATT, ALAN W.
The V-22 Osprey - Preparing for fleet operations p 458 A92-29671
MOFFITT, ROBERT
1991-92 AHS Technical Committee highlights - Aerodynamics p 623 A92-40391
MOHAGHEGH, M.
Design for Corrosion Prevention
[AIAA PAPER 92-1127] p 577 A92-33279
MOHAMED, F. A.
Mechanical behavior and processing of aluminum metal matrix composites
[AD-A249918] p 987 N92-30874
MOHER, MICHAEL L.
A TMS320-based modem for the aeronautical-satellite core data service p 594 N92-22562
MOHLER, R. R.
Nonlinear stability and control study of highly maneuverable high performance aircraft, phase 2
[NASA-CR-189911] p 382 N92-19841
Nonlinear stability and control study of highly maneuverable high performance aircraft, phase 2
[NASA-CR-190667] p 978 N92-30922
MOHLER, STANLEY H., JR.
Predicting droplet impingement on yawed wings p 1043 A92-56180
MOHLER, STANLEY R., JR.
Comparison of two-dimensional and three-dimensional droplet trajectory calculations in the vicinity of finite wings
[AIAA PAPER 92-0645] p 342 A92-28215
Comparison of two-dimensional and three-dimensional droplet trajectory calculations in the vicinity of finite wings
[NASA-TM-105617] p 596 N92-23154
MOIN, PARVIZ
Direct computation of the sound from a compressible co-rotating vortex pair
[AIAA PAPER 92-0374] p 414 A92-26232
On the mechanics of 3-D turbulent boundary layers p 620 A92-40068
MOIR, I. R. M.
An experimental investigation of the effect of fineness ratio on lateral force on a pointed slender body of revolution p 86 N92-13015
MOITRA, ANUTOSH
Enthalpy damping for high Mach number Euler solutions p 330 A92-26402
Two- and three-dimensional grid generation by an algebraic homotopy procedure p 611 A92-36861
MOIZIS, S. E.
The lift-drag ratio of a slender cone in viscous hypersonic gas flow p 425 A92-30172
Numerical determination of the regions of existence of two types of shock-wave interaction p 428 A92-30211
MOKHTARIAN, FARZAD
On the coupling of Euler/boundary-layer equations p 627 N92-24859

MOKRY, M.
Complex variable boundary element method for external potential flows p 172 A92-18353
A scheme for two dimensional Euler and boundary layer interactive solutions p 627 N92-24860
MOLDER, S.
Applications of Busemann inlet designs for flight at hypersonic speeds
[AIAA PAPER 92-1210] p 517 A92-33314
MOLENT, L.
Environmental evaluation of repairs to fuselage lap joints p 699 A92-41534
MOLEZZI, M. J.
Development and application of a particle image velocimeter for high-speed flows
[AIAA PAPER 92-0004] p 292 A92-22129
MOLLOY, JOHN K.
Effect of collector configuration on test section turbulence levels in an open-jet wind tunnel
[NASA-TM-4333] p 750 N92-27670
MOLTON, PASCAL
Basic experiment on a supersonic vortex flow around a missile body p 705 A92-41545
MOLVIK, G. A.
Calculation of high speed base flows
[AIAA PAPER 92-2679] p 799 A92-45531
MOLVIK, GREGORY A.
Analysis of a hydrocarbon scramjet with augmented preburning
[AIAA PAPER 92-3425] p 865 A92-48984
MOM, A. J. A.
NLR experience with high velocity burner rig testing, 1979-1989
[NLR-TP-89152-U] p 385 N92-18415
MOMIGLIANO, ALBERTO
A constraint satisfaction approach to operative management of aircraft routing p 350 A92-25181
MONAGHAN, TIMOTHY P.
The concept exploration stage of a dependable avionic system p 1006 A92-49339
MONAN, WILLIAM P.
Cockpit distractions - Precursors to emergencies p 16 A92-11178
MONGEAU, LUC
Experimental study of the mechanism of sound generation by rotating stall in centrifugal turbomachines p 605 N92-23726
MONGIA, H. C.
Lean low NO(x) combustion concept evaluation p 143 A92-16583
A parametric numerical study of mixing in a cylindrical duct
[NASA-TM-105695] p 738 N92-26553
MONGIA, HUKAM C.
Analytical design and demonstration of a low-cost expendable turbine engine combustor
[AIAA PAPER 92-3754] p 867 A92-49112
The VRT gas turbine combustor - Phase II
[AIAA PAPER 92-3471] p 1067 A92-54035
MONNIER, J. C.
Study of detached turbulent flow in an air intake by means of high speed tomography and laser velocimetry
[REPT-90/55] p 157 N92-12216
MONNOYER, F.
Calculation of hypersonic non-equilibrium viscous flow using second order boundary layer theory
[MBB-FE122-S-PUB-434] p 345 N92-18316
MONNOYER, FRANCOIS
Contributions of MBB-FE211 to the 2nd Antibes Workshop on Hypersonic Flows
[MBB-FE211-S-PUB-449] p 524 N92-22179
Case 7.4: Blunt nose delta wing Euler-boundary layer calculation p 525 N92-22184
MONTA, WILLIAM J.
Test description and preliminary pitot-pressure surveys for Langley Test Technique Demonstrator at Mach 6
[AIAA PAPER 92-3940] p 1096 A92-56770
MONTAGUE, T.
Integrated Russian VLF/Omega receiver design
[PB92-193390] p 1051 N92-33809
MONTANO, WILLIAM G.
High rate PCM data receiving, recording and relying p 189 A92-19279
MONTAZEL, X.
Turbulent combustion modelling in a side dump ramjet combustor
[AIAA PAPER 92-3599] p 1112 A92-54075
MONTERO, EUGENIO O.
Iberia's Aeronautical Mapping Application (ACAI) p 637 A92-37073
MONTESARCHIO, B.
Structural design and testing results of composite landing gear components p 1057 A92-56328
MONTGOMERY, LEON
Pulse jet one-way valve performance
[AIAA PAPER 92-3169] p 863 A92-48790
MONTI, RODOLFO
Detecting 3-D, turbulent separation regions using unsteady computerized thermographic technique p 1023 A92-54308
MONTIGNY-RANNOU, F.
Resolution of Navier-Stokes equations around profiles: Drag evolution
[ONERA-RTS-86/1685-AY-156A] p 43 N92-11310
Drag prediction using computation methods
[ONERA-RSF-82/1685-AY-154-4] p 349 N92-19682
MONTOYA, R. J.
AGSSS: The Airborne Graphics Software Support System; an Ada/PHIGS-based display editor for the rapid development of cockpit display software systems
[AD-A243224] p 277 N92-17221
MOODY, CHRIS
Operational evaluation of a tower workstation for clearance delivery p 879 A92-44981
MOODY, LARRY A.
Generic helicopter for multiship simulations
[AIAA PAPER 92-4151] p 959 A92-52442
MOOK, D. J.
Nonlinear aircraft tracking filter utilizing control variable estimation p 302 A92-21179
Improved noise rejection in automatic carrier landing systems p 380 A92-28154
Robust control design of an automatic carrier landing system
[AIAA PAPER 92-4619] p 1077 A92-55296
Robust identification of nonlinear aerodynamic model structure
[AIAA PAPER 92-4503] p 1081 A92-55370
MOOK, DEAN T.
Mechanics Pan-America 1991; Pan-American Congress of Applied Mechanics, 2nd (PACAM II), Universidad Tecnica, Valparaiso, Chile, Jan. 2-5, 1991, Selected and Revised Proceedings p 673 A92-39930
Numerical simulations of flutter and its suppression by active control
[AIAA PAPER 92-4652] p 1082 A92-55396
MOON, BONG C.
Fault tolerant control based on a new accommodation filter p 51 A92-11453
MOONEY, JOHN
Perspectives on the cooperative air traffic management concept - Far East/Pacific point of view p 606 A92-33428
MOORE, ALAN
The development of a requirement specification for an experimental active flight control system for a variable stability helicopter: An Ada simulation in JSD p 135 N92-12466
MOORE, DEBORAH L.
Magnetic suspension and balance systems: A comprehensive, annotated bibliography
[NASA-TM-4318] p 32 N92-11030
MOORE, DOUG
Maneuver load control using optimized feedforward commands
[AIAA PAPER 92-2100] p 567 A92-35671
MOORE, EMERY L.
Fiber optic systems for mobile platforms IV; Proceedings of the Meeting, San Jose, CA, Sept. 18, 1990
[SPIE-1369] p 779 A92-42601
MOORE, FRANK G.
Second-order shock-expansion theory extended to include real gas effects
[AD-A247191] p 831 N92-29539
MOORE, GARY
United States Air Force summer research program 1991. Volume 1: Program management report
[AD-A248763] p 1142 N92-32338
MOORE, JAMES A.
The relationship between mode localization and energy transmission parameters in the vibration of coupled structures p 925 A92-45921
MOORE, JOAN G.
Effects of curvature and rotation on turbulence in the NASA low-speed centrifugal compressor impeller p 1124 N92-32292
MOORE, JOEL DAVID
The FM-007: An advanced jet commuter for HUB to spoke transportation
[NASA-CR-189988] p 461 N92-20267
MOORE, JOHN
Effects of curvature and rotation on turbulence in the NASA low-speed centrifugal compressor impeller p 1124 N92-32292
MOORE, MICHAEL J.
Flight vibration testing of the V-22 tiltrotor aircraft p 107 A92-14397
MOORE, ROYCE D.
Supersonic throughflow fans for high-speed aircraft p 561 N92-22541
NASA. Lewis Research Center supersonic throughflow fan program
[NASA-TM-103248] p 972 N92-31250
MOORE, THOMAS E.
Space shuttle entry terminal area energy management
[NASA-TM-104744] p 308 N92-19930
MOORHOUSE, DAVID J.
Results and lessons learned from the STOL and Maneuver Demonstration Program
[SAE PAPER 912005] p 843 A92-45406
MOOZ, WILLIAM E.
Developing robust support structures for high-technology subsystems: The AH-64 Apache helicopter
[AD-A252773] p 1017 N92-33499
MORAES, AUGUSTO C. M.
Compressible laminar boundary layers for perfect and real gases in equilibrium at Mach numbers to 30
[AIAA PAPER 92-0757] p 336 A92-27099
MORAN, FRANCIS J.
A workstation-based evaluation of a far-field route planner for helicopters
[NASA-TM-102882] p 1051 N92-33609
MORAN, ROBERT D., JR.
Simulation of a rotorcraft in turbulent flows
[AD-A245742] p 650 N92-26155
MORAN, SUSANNE I.
Transport delay measurements: Methodology and analysis for the F-16C combat engagement trainer, the display for advanced research and training, and the F-16A limited field of view
[AD-A248519] p 888 N92-29505
MORAWSKI, JANUSZ M.
Safety vs. economy, system-theoretic approach to the problem analysis p 916 A92-45002
MORCHOISNE, Y.
Numerical simulation of vortex breakdown by solving the Euler equations for an incompressible fluid p 41 N92-10163
Numerical simulation of vortex breakdown via 3-D Euler equations p 41 N92-10164
Determination of vortex-breakdown criteria by solving the Euler and Navier-Stokes equations p 87 N92-13018
MOREAU, JEAN-PATRICK
Aircraft-triggered lightning - Processes following strike initiation that affect aircraft p 836 A92-46784
MORELLI, EUGENE ARCANGELO
Practical input optimization for aircraft parameter estimation experiments p 114 N92-11989
MORETTI, G.
Orthogonal grids for multiple airfoils p 818 A92-47096
MORETTI, GINO
Orthogonal grids around difficult bodies p 432 A92-31160
MOREUX, V.
A new automatic grid generation environment for CFD applications
[AIAA PAPER 92-2720] p 803 A92-45558
MORGAN, BEN B., JR.
An analysis of aircrew communication patterns and content
[AD-A246618] p 907 N92-28253
MORGAN, D. R.
Avionics technology beyond 2000 p 200 N92-14058
MORGAN, K.
The computation of three-dimensional flows using unstructured grids p 612 A92-37539
The numerical simulation of flow about installed aero engine nacelle using a finite element Euler solver on unstructured meshes p 941 A92-52848
Finite element methods for integrated aerodynamic heating analysis
[NASA-CR-190353] p 633 N92-25959
MORGAN, R.
Applications of advanced composites in a 3/4 air transportable rack p 36 A92-10314
Application of resin and metal matrix composites to advanced avionics enclosure p 985 A92-51921
MORGAN, R. G.
Effects of oxygen dissociation on hypervelocity combustion experiments
[AIAA PAPER 92-3964] p 1098 A92-56791
MORGAN, ROBERT E.
Applications of composite material systems to avionic systems packaging p 576 A92-32564
MORGAN, TED A.
Development and tribological properties of new cyclotriphosphazene high temperature lubricants for aircraft gas turbine engines p 287 A92-21327
MORGENFELD, THOMAS A.
YF-22A prototype Advanced Tactical Fighter demonstration/validation flight test program overview
[AIAA PAPER 92-1087] p 537 A92-33253

MORI, MIKIHIKO
The progress of a STOL project p 699 A92-43137
MORI, YASUHIKO H.
Observational study of pool boiling under microgravity p 757 A92-41060
MORIKAWA, K.
Vortex interaction in the wake behind an oscillating airfoil p 623 A92-40175
MORIKAWA, YASUSHI
The concept of an unmanned flying vehicle at high altitude p 731 A92-43242
An acrobatic airship 'Acrostat'
[SAE PAPER 911994] p 843 A92-45396
High-altitude lighter-than-air powered platform
[SAE PAPER 912054] p 844 A92-45438
MORIMOTO, MITSUO
A320 flight control from the pilot's point of view p 1083 A92-56028
MORIMOTO, S.
High enthalpy wind tunnel for erosion testing of advanced materials
[AIAA PAPER 92-3888] p 1094 A92-56729
MORIMOTO, TOSIYUKI
Three-dimensional numerical analysis of impinging circular jet - Discrete vortex method p 1029 A92-56040
MORIN, P.
Effects of ionizing and nonionizing radiation on aircraft p 295 A92-23301
MORINISHI, KOJI
A numerical solution of inviscid transonic flow using the Boltzmann equation p 443 A92-32504
A finite difference solution of the Euler equations on *non-body-fitted Cartesian grids* p 818 A92-47153
Numerical solutions of unsteady oscillating flows past an airfoil
[AIAA PAPER 92-3212] p 825 A92-48817
MORINO, L.
A boundary element method for the potential, compressible aerodynamics of bodies in arbitrary motion p 314 A92-25098
A new integral equation for potential compressible aerodynamics of rotors in forward flight p 815 A92-46958
A boundary integral formulation for unsteady transonic potential flows p 719 N92-27942
MORISHITA, ETSUO
Study on effectiveness of the front wedge shape in *hypersonic flow* p 430 A92-30552
MORITA, S.
Shafranov shift in low-aspect-ratio heliotron/torsatron CHS
[NIFS-110] p 1138 N92-33743
MORITA, YOSHIO
Aerodynamic development of boundary layer control system for NAL QSTOL research aircraft 'ASKA'
[SAE PAPER 912010] p 843 A92-45410
MORIYAMA, KAZUO
An identification procedure for a system with a choice of feedback structures p 1132 A92-55426
MORO, MIKE
An integrated real-time turbine engine flight test system p 201 A92-19275
MOROOKIAN, JOHN-MICHAEL
Efficiency of a 5V/5mW power by light power supply for avionics applications p 734 A92-42603
MORRELL, FREDERICK R.
Joint University Program for Air Transportation Research, 1990-1991
[NASA-CP-3131] p 242 N92-17984
MORRIS, A. J.
Fundamentals of structural optimisation p 851 N92-28470
MORRIS, ANDREW
The evaluation of simulator effectiveness for the training of high speed, low level, tactical flight operations p 885 N92-28539
MORRIS, CHARLES E. K., JR.
Technologies for the National Aero-Space Plane
[IAF PAPER 92-0868] p 1105 A92-57259
MORRIS, DAVID L.
Testing of a titanium matrix composite landing gear
[SAE PAPER 912175] p 644 A92-40000
MORRIS, HELEN
On the instability of boundary layers on heated flat plates
[NASA-CR-187581] p 347 N92-19250
MORRIS, KENNETH D.
Dead reckoning for aircraft in distributed interactive simulation
[AIAA PAPER 92-4171] p 1008 A92-52456
MORRIS, LESTER
Non-curing fuel and water resistant sealant compositions p 985 A92-51906
MORRIS, M. J.
Confined normal-shock/turbulent-boundary-layer interaction followed by an adverse pressure gradient p 172 A92-18365
Aerodynamic applications of pressure-sensitive paint
[AIAA PAPER 92-0264] p 394 A92-25720
Experimental investigation of normal-shock/turbulent-boundary-layer interactions with and without mass removal p 330 A92-26411
MORRIS, MARTIN J.
Experimental investigation of terminal shock sensors for mixed-compression inlets p 276 A92-21074
Numerical simulation of a confined transonic normal shock wave/turbulent boundary layer interaction
[AIAA PAPER 92-3668] p 826 A92-49088
MORRIS, V. R.
Calibration data for improved correction of UVW propeller anemometers
[DE92-002935] p 297 N92-16281
MORRISON, DWAYNE
Comprehensive helicopter rotor instrumentation - A retrofit approach using miniature transducers
[AIAA PAPER 92-0268] p 369 A92-25724
MORRISON, GERALD L.
LDV measurements of the velocity field in an underexpanded supersonic jet (Ma = 1.5)
[AIAA PAPER 92-0504] p 341 A92-28196
MORRISON, J. F.
Bursts and sources of pressure fluctuation in turbulent boundary layers p 619 A92-40055
MORRISON, J. T.
A model of the ADA avionics real-time system: An example of the benefits of the hardware/software codesign approach in development of real-time systems
[AD-A248893] p 967 N92-30524
MORRISON, JOSEPH H.
Implementation of Vigneron's streamwise pressure gradient approximation in the PNS equations
[AIAA PAPER 92-0189] p 256 A92-23798
A compressible Navier-Stokes solver with two-equation and Reynolds stress turbulence closure models
[NASA-CR-4440] p 681 N92-25376
MORRISON, RUSSELL H.
System controls challenges of hypersonic combined-cycle engine powered vehicles p 475 N92-21533
MORROCCO, JOHN D.
Soviet aerospace in turmoil p 2 A92-13220
MORT, R. W.
Hub and pylon fairing integration for helicopter drag reduction p 107 A92-14391
MORT, RAY
Comprehensive helicopter rotor instrumentation - A retrofit approach using miniature transducers
[AIAA PAPER 92-0268] p 369 A92-25724
MORTARA, K.
Analysis and design of planar and non-planar wings for induced drag minimization
[NASA-CR-189509] p 179 N92-13999
MORTCHELEWICZ, G. D.
Solution of Euler equations with unstructured mesh - 3-D case p 941 A92-52973
MORTLOCK, ALAN
Designing a methodology for future air travel scenarios p 409 N92-19125
MORTON, BLAISE
New methods in robust control
[AD-A240221] p 29 N92-11018
MORTON, WAYNE K.
On-line distortion analysis system for inlet-engine *testing*
[ASME PAPER 91-GT-166] p 136 A92-15601
MOSELLE, J. R.
A database of aerothermal measurements in hypersonic flow for CFD validation
[AIAA PAPER 92-4023] p 1034 A92-56845
MOSELLE, JOHN R.
Studies of aerothermal loads generated in regions of *shock/shock interaction in hypersonic flow*
[NASA-CR-181893] p 43 N92-11319
MOSES, CLIFFORD A.
High-temperature miniaturized turbine engine lubrication system simulator
[AD-A249259] p 868 N92-28294
MOSES, H. L.
The effect of blade solidity on the aerodynamic loss of a transonic turbine cascade
[AIAA PAPER 92-0393] p 323 A92-26248
MOSKOW, HARRY J.
A lightweight loudspeaker for aircraft communications and active noise control p 1125 N92-32964
MOSKOWITZ, IRA S.
Traveling on the curved earth p 19 A92-10474
MOSS, J. E.
Qualification test report. Fuel pump test stand 3C3965G05
[AD-A242929] p 280 N92-17552
MOSS, J. N.
Aerothermodynamics of a 1.6-meter-diameter sphere in hypersonic rarefied flow p 808 A92-45840
MOSS, JAMES N.
Hypersonic flow simulations using DSMC (direct simulation Monte Carlo) p 323 A92-26216
Hypersonic rarefied flow past spheres including wake structure
[AIAA PAPER 92-0495] p 329 A92-26325
Hypersonic rarefied flow about a delta wing - direct simulation and comparison with experiment p 812 A92-46892
Enhancements and applications of DSMC for hypersonic rarefied flows p 939 A92-52761
Application of the DSMC method to hypersonic flow *about a delta wing* p 940 A92-52775
MOSS, JIM
NASA aerodynamics program
[NASA-TM-4368] p 609 N92-24678
MOSSER, P. E.
The beta-CEZ - A high performance titanium alloy for aerospace engines p 289 A92-22760
MOSSMAN, DOUGLAS
The INFO-ROC technique - A method for comparing and optimizing inspection systems p 144 A92-13563
MOSTAFA, A.
Viscous flow analysis of advanced particle separators p 737 A92-44517
MOTAMED, FARZIN
Evaluation and comparison of triple and quadruple flight control architectures p 745 A92-43884
MOTODA, TOSHIKAZU
An identification procedure for a system with a choice of feedback structures p 1132 A92-55426
MOTOHASHI, TATSUO
Flow around an isolated surface roughness in the laminar boundary layer p 766 N92-26913
MOTSINGER, R. E.
Design and performance of duct acoustic treatment p 236 N92-14783
MOULDEN, TREVOR H.
A double chaotic attractor in transonic flow p 1019 A92-53561
MOULTON, BRYAN
Piloted simulation study of a balloon-assisted deployment of an aircraft at high altitude
[NASA-TM-104245] p 272 N92-15986
MOUNT, DAVID M.
Delaunay triangulation and computational fluid dynamics meshes
[NASA-TM-107663] p 1010 N92-30907
MOUNTS, JON S.
Numerical analysis of shock-induced separation alleviation using vortex generators
[AIAA PAPER 92-0751] p 335 A92-27095
MOURING, CHRIS A.
Thermal/structural analysis of a transpiration cooled nozzle
[NASA-TM-104184] p 401 N92-18877
MOURTOS, N.
Development and integration of modern laboratories in aerospace education
[AIAA PAPER 92-4022] p 1141 A92-56844
MOUSTAPHA, S. H.
Establishing two-dimensional flow in a large-scale planar turbine cascade
[AIAA PAPER 92-3066] p 823 A92-48720
MOUYON, PHILIPPE
Double loop control law strategy and applications to helicopter
[CERT-2/7724-DERA] p 381 N92-19295
MOXON, JULIAN
Dornier Do.328 special - Examining the high-speed commuter p 21 A92-11882
Behind the screens p 353 A92-25520
MOYLE, I. N.
Stator averaged, rotor blade-to-blade near wall flow in a multistage axial compressor with tip clearance variation
[ASME PAPER 91-GT-30] p 67 A92-15514
MOZHAROV, E. E.
Several results of lidar measurements of the characteristics of oblique visibility at an airfield p 45 A92-12844
MU, J. S.
Study on supersonic combustion in a hypersonic flight
[IAF PAPER 92-0661] p 1106 A92-57101
MU, XINHUA
The computer analysis of the prediction of aircraft electrical power supply system reliability p 690 A92-37950

MUDFORD, N. R.
Stagnation point heat flux in hypersonic high enthalpy flow p 613 A92-38373
Unsteady shock propagation in a steady flow nozzle expansion p 1023 A92-54489
MUEFFELMANN, W. H.
Multiple aperture window and seeker concepts for endo KEW applications
[AIAA PAPER 92-2806] p 752 A92-41344
MUELLER, ALAN
Computations of hypersonic flows around a three-dimensional concave/convex body
[AIAA PAPER 92-2606] p 805 A92-45570
MUELLER, ARNOLD W.
Helicopter far-field acoustic levels as a function of reduced rotor speeds p 695 A92-39228
Helicopter main-rotor speed effects: A comparison of predicted ranges of detection from the aural detection program ICHIN and the electronic detection program ARCAS
[NASA-TM-104134] p 166 N92-12598
MUELLER, C.-A.
Hypersonic configurations in slow speed flight p 624 N92-24394
MUELLER, HUBERT
Resonance and control response tests using a control stimulation drive
[MBB-UD-0586-90-PUB] p 134 N92-12003
Resonance and control response tests using a control simulation device
[MBB-UD-0608-91-PUB] p 978 N92-30439
MUELLER, J.-D.
A frontal approach for node generation in Delaunay triangulations p 771 N92-27680
MUELLER, R. H. G.
A new method for visualization and measurement of turbulent flow patterns p 619 A92-40063
A small light-weight rotor platform for ground observation and pollution control p 1057 A92-56329
MUELLER, REINER
Semiconductor laser Doppler anemometer for applications in aerodynamic research p 495 A92-31173
MUELLER, REINERT H. G.
Visualization and measurement of helicopter rotor flow using projected smoke filaments and digital image processing p 520 A92-35728
MUELLER, S.
Simulation of the flow on a space glider. Stagnation point calculation using the 2D Navier-Stokes equations including chemical effects p 624 N92-24393
MUELLER, S. R.
Aeroassist flight experiment heating-rate sensitivity study p 3 A92-10427
MUELLER, T.
Construction of a real-time DGPS experimental system p 840 A92-47631
MUELLER, T. J.
Airfoil boundary layer measurements at low Re in an accelerating flow from a nonzero velocity p 62 A92-13673
The design of a subsonic low-noise, low-turbulence wind tunnel for acoustic measurements
[AIAA PAPER 92-3883] p 1094 A92-56726
MUELLER, THOMAS J.
Experimental study of a low Reynolds number tandem airfoil configuration p 442 A92-32241
MUELLER, U. R.
Computation of viscous phenomena in unsteady transonic flow p 720 N92-27949
MUENKEL, C.
Trial of a slant visual range measuring device p 1000 N92-31043
MUGGLI, W.
'A new proposal for an old problem' - The right engine for the right helicopter p 1070 A92-56281
MUIR, H. C.
Passenger knowledge of airline safety information
[CRANFIELD-AERO-9111] p 187 N92-15054
MUIR, HELEN
The effect on aircraft evacuations of passenger behaviour and smoke in the cabin p 834 A92-44998
MUKHOPADHYAY, VIVEK
Flutter suppression digital control law design and testing for the AFW wind tunnel model
[AIAA PAPER 92-2095] p 566 A92-35668
On-line performance evaluation of multiloop digital control systems p 873 A92-46739
Flutter suppression digital control law design and testing for the AFW wind-tunnel model
[NASA-TM-107652] p 962 N92-31350
MUKUNDA, H. S.
Direct simulation of high-speed mixing layers
[NASA-TP-3186] p 945 N92-30909
MULAC, RICHARD A.
The numerical simulation of a high-speed axial flow compressor
[ASME PAPER 91-GT-272] p 75 A92-15669
MULDER, WIM A.
A high-resolution Euler solver based on multigrid, semi-coarsening, and defect correction p 671 A92-37868
MULE, A.
Design and testing leading to certification of the Airbus A340 nose landing gear doors p 272 A92-24192
MULERO, M.
Measurement of the flow distribution over the flight deck of an aircraft carrier p 504 N92-21955
MULGUND, SANDEEP S.
Target pitch angle for the microburst escape maneuver
[AIAA PAPER 92-0730] p 379 A92-27082
Optimal recovery from microburst wind shear
[AIAA PAPER 92-4338] p 1078 A92-55327
Target pitch angle for the microburst escape maneuver p 266 N92-17996
MULHOLLAND, S. L.
The Catalyst software engineering environment p 1005 A92-49300
MULLEN, ORLIN L.
RAH-66 Comanche - A cut above the rest p 61 A92-16675
MULLEN, ROBERT L.
Thermal mechanical analysis of sprag clutches
[NASA-CR-190686] p 1128 N92-34207
MULLER, M.
Statistics on aircraft gas turbine engine rotor failures that occurred in US commercial aviation during 1989
[DOT/FAA/CT-92/5] p 971 N92-30303
MULLIGAN, GREG
The Guardian: Preliminary design of a close air support aircraft
[NASA-CR-189991] p 463 N92-21566
MULLIGAN, M. F.
Investigation of engine thrust correlation methods for enclosed test cells
[ASME PAPER 91-GT-68] p 121 A92-15538
MULTER, JORDAN
Design considerations for IAP charts: Approach course track and communication frequencies
[AD-A241482] p 103 N92-13051
MULVEHILL, ALICE M.
Expert knowledge techniques applied to the analysis of electric field mill data p 408 A92-27991
MUNAFO, C. F.
Evaluation of the aerodynamic effects of commuter class (type 1-1/2) anti-icing fluids on small general aviation airplanes
[AIAA PAPER 92-0643] p 459 A92-31675
MUNDINGER, GERD
Similarity and resistance in near-sonic flows for given heat conduction p 708 A92-43065
MUNDT, C.
Calculation of hypersonic non-equilibrium viscous flow using second order boundary layer theory
[MBB-FE122-S-PUB-434] p 345 N92-18316
Modelling of chemical and physical effects with respect to flows around reentry bodies
[MBB-FE-211/S/PUB/0465/A] p 347 N92-19296
MUNDT, CH.
Calculation of hypersonic, viscous, non-equilibrium flows around reentry bodies using a coupled boundary layer/Euler method
[AIAA PAPER 92-2856] p 819 A92-47839
MUNDT, M.
Experiences with finite element methods for the velocity-vorticity formulation of three-dimensional, viscous, incompressible flows p 246 A92-21984
MUNDUS, BERNHARD
Influence of the swirl producing construction in the flow and reaction field of turbulent diffusion flames
[ETN-92-92103] p 1127 N92-33916
MUNGAL, M. G.
Effects of sidewall disturbances on the supersonic mixing layer p 290 A92-21085
Two- and three-dimensional effects in the supersonic mixing layer p 432 A92-31165
Experiments on the structure of an annular compressible reacting shear layer p 969 A92-50311
Turbulent reacting flows and supersonic combustion
[AD-A251065] p 986 N92-30256
MUNGUR, P.
A distributed vaporization time-lag model for gas turbine combustor dynamics
[AIAA PAPER 92-3465] p 865 A92-49014
MUNIN, A. G.
Reducing the background noise level in the test section of a wind tunnel for transonic flow velocities p 511 A92-30143
An experimental study of tone-like noise in the flow past a wing at low flow velocities p 425 A92-30160
An experimental study of the noise of flow past a wing at low velocities p 603 A92-33771
MUNIR, N. I.
An expert system to aid real world finite element analysis
[AIAA PAPER 92-2488] p 601 A92-34604
MUNJAL, M. L.
Theoretical and experimental methods in acoustics of ducts and mufflers - A critical review p 693 A92-39068
MUNK, J.
Analysis of lossy composite terminating structures
[NASA-CR-189901] p 404 N92-19217
MUNRO, BRUCE C.
Nonlinear model-following control application to airplane control (1992 AIAA Controls Design Challenge)
[AIAA PAPER 92-4625] p 1077 A92-55302
MUNSELL, PETER M.
Gas turbine main shaft internal flow and heat transfer
[ASME PAPER 91-GT-165] p 123 A92-15600
MUNSHTUKOV, D. A.
A model of the operation of the pulsejet engine and a study of its characteristics p 657 A92-40608
MUNSON, JOHN
Development of film riding face seals for a gas turbine engine p 291 A92-21330
Seal development activities at Allison Turbine Division p 228 N92-15093
MUNSON, JOHN H.
Development of high performance compressor discharge seal
[AIAA PAPER 92-3714] p 907 A92-49096
MUNTZ, E. P.
An iodine hypersonic wind tunnel for the study of nonequilibrium reacting flows
[AIAA PAPER 92-0566] p 383 A92-26974
A code validation strategy and facility for nonequilibrium, reacting flows
[AIAA PAPER 92-3970] p 1098 A92-56796
A new technique for temperature and specie concentration measurements in unseeded supersonic and hypersonic gas flows
[AD-A241536] p 158 N92-13409
MURAGISHI, OSAMU
Demonstration of gas liquid separation under the microgravity by aircraft KC-135
[SAE PAPER 912024] p 897 A92-45416
MURAIDA, DANIEL J.
Design specifications for the Advanced Instructional Design Advisor (AIDA), volume 2
[AD-A248202] p 923 N92-29188
MURAKAMI, A.
Experimental study of the aerodynamic characteristics at Mach 3 of an air-intake model p 711 A92-43204
Supersonic wind tunnel test of airintake/airframe integrated models p 1028 A92-56006
MURAKAMI, AKIRA
Mach 3 wind tunnel test of mixed compression supersonic inlet
[AIAA PAPER 92-3625] p 1021 A92-54092
MURAKAMI, ATSUO
Effectiveness of plasma torches for ignition and flameholding in scramjet p 737 A92-44524
Flow measurements in scramjet inlets p 1102 A92-53565
MURAKAMI, HIDEAKI
Field telemetry of blade-rotor coupled torsional vibration at Matuura Power Station Number 1 unit p 222 N92-14348
MURAKAMI, S.
Scrutinizing k-epsilon EVM and ASM by means of LES and wind tunnel for flowfield around cube p 621 A92-40119
Aircraft accidents and human factors p 723 A92-43219
MURAKAMI, TETSU
Study of cavity pumping in supersonic internal flow p 429 A92-30538
MURAKAMI, YOSHITAKA
Flight evaluation of navigation systems including MLS using NAL Do228 - Results of MLS p 1047 A92-56117
MURAO, RINICHI
On the maneuvering tests of an ACV model p 1118 A92-56035
Configuration of flexible-skirts for an ACV and its CAD p 1118 A92-56036
MURASE, T.
Laminar-turbulent transition process in the presence of simulated wall roughness p 626 N92-24858
MURATA, K.
New-type of ultralight flexible a-Si solar cell and its application on an airplane p 970 A92-53181

MURATA, MASAAKI
Space plane navigation simulation
p 1103 A92-53603
MURATA, MASAKI
Flight evaluation of navigation systems including MLS using NAL Do228 - Outline p 1047 A92-56116
MURATA, SHIGERU
Numerical solutions of unsteady oscillating flows past an airfoil
[AIAA PAPER 92-3212] p 825 A92-48817
MURATA, SUSUMU
Computation of the potential flow through cascades using the conformal mapping and the singularity method
p 66 A92-15356
MURAV'EV, G. B.
A test bench for evaluating powerplant electrization
p 138 A92-16830
MURAYAMA, T.
Study of the flow field and molecular radiation heating around a reentry vehicle p 711 A92-43227
MURAYAMA, TOSHI
Thermally and chemically nonequilibrium hypersonic flow in three-dimensional geometry
p 1019 A92-53580
MURAYAMA, TOSHIYUKI
Three-dimensional calculation of radiative field in hypersonic air shock layers p 1023 A92-54498
MURCHIE, GATES S.
The army special operations aircraft integrated avionics subsystem - An operational perspective
p 966 A92-49332
MURDAUGH, WILLIAM O.
Aero-optical testing in the NSWC Hypervelocity Tunnel No. 9
[AIAA PAPER 92-2797] p 747 A92-41336
MURMAN, EARLL M.
Calculation of hypersonic leeside vortices over blunt delta wings p 84 N92-13004
MURMAN, SCOTT M.
Computational investigation of slot blowing for fuselage forebody flow control
[AIAA PAPER 92-0020] p 248 A92-22142
Coupled numerical simulation of the external and engine inlet flows for the F-18 at large incidence
[AIAA PAPER 92-2621] p 793 A92-45493
Analysis of a pneumatic forebody flow control concept about a full aircraft geometry
[AIAA PAPER 92-2678] p 799 A92-45530
MUROTA, K.
Aerodynamic model identification of a spaceplane model from a cable-mount dynamic wind-tunnel test
p 1093 A92-56114
MUROTA, KATSUICHI
Estimation of spaceplane lateral-directional stability and control derivatives from dynamic wind tunnel test
[SAE PAPER 911979] p 872 A92-45384
Measurements of longitudinal static aerodynamic coefficients with cable mount system
p 1093 A92-56013
The fibre optic three dimensional laser two focus velocimeter for the low-speed windtunnel. Part 1: Two-dimensional measurement evaluations
[NAL-TM-627] p 665 N92-25402
MUROTSU, Y.
A development of computer support system for wing design p 162 A92-15332
MUROTSU, YOSHISADA
A development of hypermedia type database system for instruction of aircraft conceptual design
p 1132 A92-56113
MUROZONO, MASAHIKO
Analyses of heat isolation property for metallic multiwall thermal protection system p 40 A92-12422
MURPHY, CHARLES H.
Symptom of payload-induced flight instability
p 873 A92-46761
MURPHY, DEBORAH W.
Aircraft noise and the elderly p 689 A92-39236
MURPHY, JAY
Comparison of frequency domain and time domain laser velocimeter signal processors p 1114 A92-54314
MURPHY, KENT A.
Fabry-Perot fiber-optic sensors in full-scale fatigue testing on an F-15 aircraft p 391 A92-24553
MURPHY, KEVIN J.
Operational noise data for OH-58D Army helicopters
[AD-A246822] p 926 N92-28292
MURPHY, PEG
Reference mode effect on the auditory display of aircraft bank angle
[AD-A247825] p 728 N92-27916
MURPHY, TIMOTHY A.
Flight test of ARINC 741 configuration low gain SATCOM system on Boeing 747-400 aircraft p 677 N92-24097
MURRAY-SMITH, D. J.
Multivariable methods for helicopter flight control law design - A review p 568 A92-35748
Command following control law design by linear quadratic optimisation p 568 A92-35749
Eigenstructure assignment for handling qualities in helicopter flight control law design p 570 A92-35786
The identification of coupled flapping/inflow models for hovering flight p 1058 A92-56335
MURRAY-SMITH, DAVID J.
Design of experiments p 273 N92-17154
Modelling aspects and robustness issues in rotorcraft system identification p 274 N92-17159
MURRAY, B. D.
Aerodynamic design and analysis of a light aircraft propeller p 629 N92-24876
MURRAY, JAMES
Piloted simulation study of a balloon-assisted deployment of an aircraft at high altitude
[NASA-TM-104245] p 272 N92-15986
MURTHY, D. V.
Parallel computation of aerodynamic influence coefficients for aeroelastic analysis on a transputer network p 53 A92-12367
MURTHY, DURBHA V.
FREPS - A forced response prediction system for turbomachinery blade rows
[AIAA PAPER 92-3072] p 1130 A92-54006
Aeroelastic modal characteristics of mistuned blade assemblies - Mode localization and loss of eigenstructure p 1117 A92-54921
MURTHY, K. N.
Technological excellence in honeycomb sandwich and composite structures for aerospace applications
p 757 A92-41180
MURTHY, P. L. N.
Analysis of aircraft engine blade subject to ice impact
[NASA-TM-105336] p 229 N92-15402
MURTHY, S. N. B.
Thermodynamic structural analysis of high speed propulsion systems
[IAF PAPER 91-278] p 120 A92-14711
Hot gas environment around STOVL aircraft in ground proximity. I - Experimental study p 371 A92-24409
High-speed flight propulsion systems
[ISBN 1-56347-011-X] p 862 A92-46426
Energy analysis of high-speed flight systems
p 925 A92-46430
Flowpath and sensitivity analyses of high speed propulsion systems
[AIAA PAPER 92-3806] p 1069 A92-54178
MURTHY, T. K. S.
Computational methods in viscous aerodynamics
p 245 A92-21976
MURTHY, T. S.
Rotorcraft airframe structural optimization for combined vibration and fatigue constraints p 106 A92-14390
MURTHY, T. SREEKANTA
Experiences at Langley Research Center in the application of optimization techniques to helicopter airframes for vibration reduction
[NASA-TM-104193] p 299 N92-17033
MURTHY, V. R.
Sensitivity analysis of discrete periodic systems with applications to helicopter rotor dynamics
p 846 A92-46884
Free vibration analysis of branched blades by the integrating matrix method p 847 A92-47122
MURTY, H.
Aerodynamics p 202 N92-13977
Computational fluid dynamics p 177 N92-13979
MURTY, H. S.
Nonliner aspects of transonic aeroelasticity
p 628 N92-24864
Nonunique solutions in unsteady transonic flow
p 629 N92-24872
A time-linearization approach for unsteady transonic flows p 719 N92-27941
MURYN, ROMAN
Development testing of the EH101 Flight Control System p 132 A92-14380
MUSAT, V.
A direct viscous-inviscid interaction method for the flow calculation around airfoils p 936 A92-52028
MUSSELMAN, STEPHEN
Simulator data integrity program: Process standard development
[AD-A242207] p 386 N92-19642
MUSTAFA, DENIS
Reduced-order robust controllers - H(infinity)-balanced truncation and optimal projection p 48 A92-11363
MUSZYNSKA, AGNES
Rotor-to-stator partial rubbing and its effects on rotor dynamic response p 224 N92-14367
Comments on frequency swept rotating input perturbation techniques and identification of the fluid force models in rotor/bearing/seal systems and fluid handling machines p 224 N92-14370
MUTHARASAN, RAJAKKANNU
Engine panel seals for hypersonic engine applications: High temperature leakage assessments and flow modelling
[NASA-TM-105260] p 298 N92-16336
High temperature dynamic engine seal technology development
[NASA-TM-105641] p 596 N92-23435
MUTHUNAYAGAM, A. E.
Trends in propulsion technology p 757 A92-41186
MUYLAERT, J.
Aerothermodynamic calculations for the Space Shuttle Orbiter
[AIAA PAPER 92-2953] p 821 A92-47917
Review of the European hypersonic wind tunnel performance and simulation requirements
p 209 N92-15043
MYATT, J. H.
Preliminary design of an intermittent smoke flow visualization system
[AIAA PAPER 92-1028] p 580 A92-33209
MYERS, G. D.
Development of an innovative high-temperature gas turbine fuel nozzle
[ASME PAPER 91-GT-36] p 121 A92-15519
MYERS, JERRY A.
VHDL design and simulation for airborne graphics generation requirements p 902 A92-48465
MYERS, LAWRENCE P.
Performance improvements of an F-15 airplane with an integrated engine-flight control system
p 205 A92-20204
Flight evaluation of an extended engine life mode on an F-15 airplane
[NASA-TM-104240] p 871 N92-29659
MYERS, THOMAS T.
Aeroservoelastic stabilization techniques for hypersonic flight vehicles
[AIAA PAPER 91-5056] p 203 A92-17839
Assessment of flying-quality criteria for air-breathing aerospacecraft
[NASA-CR-4442] p 663 N92-25982
MYERS, WILLIAM
Analytical modeling of SH-2F helicopter shipboard operation p 464 N92-21961
MYHRE, GRETE
Mandatory psychological testing of pilots as a requirement for licensing in Norway?
p 835 A92-45081
MYKITYSHYN, MARK G.
Electronic presentation of instrument approach information p 855 A92-44923
MYKLEBUST, A.
ACSYNT - A standards-based system for parametric, computer aided conceptual design of aircraft
[AIAA PAPER 92-1268] p 601 A92-33345
MYRABO, L. N.
Comparison between computational and experimental data for a hypersonic laser propelled vehicle
[AIAA PAPER 92-3808] p 1023 A92-54179
MYRICK, DAVID L.
Shuttle Infrared Leeside Temperature Sensing (SILTS) experiment - STS-35 and STS-40 preliminary results
[AIAA PAPER 92-0126] p 286 A92-23746

N

NACHSHON, A.
Euler solver for arbitrary configurations: Further applications p 949 N92-31888
NACHSHON, AHARON
Cartesian Euler method for arbitrary aircraft configurations p 340 A92-28039
NADARAJAH, S.
Measurements and simulation of the flow around a poppet valve p 675 A92-40103
NADER, BASSAM S.
Development and tribological properties of new cyclotriphosphazene high temperature lubricants for aircraft gas turbine engines p 287 A92-21327
NADER, BLAIR A.
Issues in developing control zones for international space operations p 1141 A92-56602
NAEGELI, DAVID W.
Laser induced fluorescence detection of gums in jet fuels
[AD-A252685] p 987 N92-30767
NAGABHUSHAN, B. L.
Analysis of airship lateral maneuverability
[AIAA PAPER 91-1274] p 743 A92-41212

NAGABHUSHANAM, J.
Software package for preliminary design of helicopter p 775 A92-41195
NAGAHATA, M.
Flutter analysis and wind tunnel test with respect to a low-aspect-ratio wing with free-rotational control surface p 1052 A92-56014
Whirl flutter analysis and application to aircraft design p 1053 A92-56017
NAGAHATA, MASASHI
Propeller-nacelle whirl flutter analysis and wind tunnel test p 1052 A92-56016
NAGAHITA, MASASHI
Analysis and wind tunnel test of low aspect wing gust load alleviation p 1053 A92-56020
NAGAI, K.
Optimization of blade structure to reduce rotor vibration p 730 A92-43118
NAGAMATSU, H. T.
Experimental study of a two-dimensional scramjet inset, M(freestream) = 10.1-25.1 p 611 A92-36974
Comparison between computational and experimental data for a hypersonic laser propelled vehicle [AIAA PAPER 92-3808] p 1023 A92-54179
NAGAMATSU, HENRY T.
Compressible laminar boundary layers for perfect and real gases in equilibrium at Mach numbers to 30 [AIAA PAPER 92-0757] p 336 A92-27099
NAGAMO, T.
Thermal fiber-reinforced-plastic composite technology for aircraft structures p 755 A92-43237
NAGANO, KOUTAROU
Analysis of spacecraft entry into Mars atmosphere p 1105 N92-33763
NAGANO, SUSUMU
Three-dimensional flow visualization of shock wave using double-pulsed holographic interferometry. II - Flow visualization for three-dimensional shock structures in rotating aeroengine fan blade rows p 497 A92-32507
NAGAO, T.
Helicopter rotor testing using scaled model p 1093 A92-56076
NAGAO, TORU
An experimental study on variable pressure hydraulic flight control system p 1084 A92-56119
NAGAOKA, SAKAE
Height keeping performance requirements for reducing vertical separation minima used for air traffic control p 1046 A92-56081
NAGARAJ, B. A.
Thermal barrier coatings for gas turbine use p 142 A92-15245
NAGARAJA, K. S.
Low density heat transfer phenomena [AIAA PAPER 92-2899] p 820 A92-47875
The wind tunnel, its evolution for aerospace test purposes, perspective for curriculum development [AIAA PAPER 92-4017] p 1100 A92-56839
NAGASHIMA, AKIRA
Observational study of pool boiling under microgravity p 757 A92-41060
NAGASHIMA, TETSUYA
Shock interaction induced by two hemisphere-cylinders [SAE PAPER 912043] p 790 A92-45427
NAGASHIMA, TOMOARI
Analysis of the aerodynamic performance of rotors with the boundary element method p 709 A92-43119
Multiharmonic control response of a rotor blade during forward flight (Test) p 744 A92-43120
Multiharmonic control response of a rotor blade during forward flight (Analysis) p 744 A92-43121
Free wake analyses of a hovering rotor using panel method [SAE PAPER 912004] p 789 A92-45405
Prediction of dynamic hub load of a rotor executing multiple sinusoidal blade pitch variations p 846 A92-46921
Measurements of blade flapping motion on a wind tunnel model p 1093 A92-56023
Structural optimization of a cantilevered beam subject to combined static loadings p 1118 A92-56024
Optimization approach for helicopter maneuverability with a point mass model p 1083 A92-56025
NAGASU, H.
Navier-Stokes code development for transonic flow simulations p 246 A92-21985
NAGATI, M. G.
An efficient algorithm for optimal aircraft trajectories [AIAA PAPER 92-4412] p 1076 A92-55206
NAGAYASU, M.
Aerodynamic model identification of a spaceplane model from a cable-mount dynamic wind-tunnel test p 1093 A92-56114
NAGAYASU, MASAHIKO
Wind tunnel tests on the motion of a spaceplane simulation for cable mount p 752 A92-43192
Motion estimation for cable-mount dynamic wind-tunnel test p 749 A92-43210
Estimation of spaceplane longitudinal stability and control derivatives from dynamic wind tunnel test p 752 A92-43211
Estimation of spaceplane model inertia characteristics p 752 A92-43212
On the characteristics of servo actuators attached to a model spaceplane for dynamic wind-tunnel test p 762 A92-43213
Flight simulator test of cockpit advisory system p 1054 A92-56115
Evaluation of a IMU with optical fiber gyros in dynamic windtunnel tests p 1104 A92-56121
Estimation of cable-mounted model inertia characteristics for dynamic wind-tunnel test [NAL-TM-641] p 722 N92-28152
NAGESH BABU, G. L.
Smart structures in the active control of blade vortex interaction p 1085 A92-56314
NAGLE, AMBER L.
Cost effectiveness of environmental stress screening (ESS) - A case history p 760 A92-42084
NAGPAL, KRISHAN M.
H(infinity) control of linear systems with nonzero initial conditions p 50 A92-11430
NAGUMO, T.
New thermoplastic polyimide composite for supersonic aircraft structures p 985 A92-51512
NAHM, ALEXANDER H.
Rolling element bearing member [PATENT-1-271-213] p 158 N92-13434
NAHON, M. A.
Adaptive simulator motion software with supervisory control p 412 A92-28136
NAIDA, M. A.
A study of flow of a fluid film on the surface of a plate in the case of slot injection p 496 A92-31892
NAIK, DINESH A.
Experimental study of pylon geometries for transport aircraft [AIAA PAPER 92-0153] p 271 A92-23768
NAIK, RAJIV A.
Effects of T-tabs and large deflections in double cantilever beam specimen tests p 673 A92-39009
NAIK, SUBHASH K.
Ceramic matrix composites and its application in gas turbine engines [ASME PAPER 91-GT-338] p 143 A92-15702
NAIR, C. G. K.
Technological excellence in honeycomb sandwich and composite structures for aerospace applications p 757 A92-41180
NAIR, VINOD K.
Numerical comparison of experimentally measured ultrasound through a multilayered specimen p 510 A92-28682
NAKA, M.
Integrated system to support computer analysis in conceptual aerospace design p 1130 A92-53596
NAKADATE, M.
Helicopter rotor testing using scaled model p 1093 A92-56076
NAKAGAWA, H.
Analysis of the aerodynamic performance of rotors with the boundary element method p 709 A92-43119
NAKAGAWA, HIROYUKI
Free wake analyses of a hovering rotor using panel method [SAE PAPER 912004] p 789 A92-45405
NAKAGAWA, I.
Combustion of solid fueled ramjet. I [AIAA PAPER 92-3727] p 894 A92-49105
NAKAHASHI, K.
Optimized control of structured grids p 429 A92-30520
NAKAJIMA, KEN
Analysis of spacecraft entry into Mars atmosphere p 1105 N92-33763
NAKAJIMA, TENRYUKI
Numerical computation and experimental study of shock wave reflection p 430 A92-30542
NAKAJIMA, TOMOYA
Three-dimensional numerical analysis of impinging circular jet - Discrete vortex method p 1029 A92-56040
NAKAJIMA, TSUYOSHI
Influence of inlet conditions on the flowfield in a model gas turbine combustor p 672 A92-38866
NAKAJIMA, YOSHIJI
Flow field around thick delta wing with rounded leading edge [SAE PAPER 912009] p 789 A92-45409
NAKAKURA, T.
New thermoplastic polyimide composite for supersonic aircraft structures p 985 A92-51512
NAKAKURA, TOSHIYUKI
Thermal fiber-reinforced-plastic composite technology for aircraft structures p 755 A92-43237
NAKAMICHI, JIRO
Research on aeroelastic tailoring at NAL p 1053 A92-56019
NAKAMURA, H.
New thermoplastic polyimide composite for supersonic aircraft structures p 985 A92-51512
NAKAMURA, HIROKA
Thermal fiber-reinforced-plastic composite technology for aircraft structures p 755 A92-43237
NAKAMURA, KATSUYA
A numerical solution of inviscid transonic flow using the Boltzmann equation p 443 A92-32504
NAKAMURA, KENTARO
Ultrasonic motor utilizing elastic fin rotor p 215 A92-17414
NAKAMURA, M.
Wind tunnel test for a high speed propeller with coaxial contrarotation p 737 A92-43195
NAKAMURA, MASARU
A simulator study of a flight reference display for powered-lift STOL aircraft [SAE PAPER 912067] p 855 A92-45449
Flight test of a flight reference display for powered-lift STOL aircraft p 1064 A92-56059
Flight evaluation of navigation systems including MLS using NAL Do228 - Outline p 1047 A92-56116
NAKAMURA, S.
Noise test of high-speed counterrotation propeller in low-speed wind tunnel p 1135 A92-56055
Grid generation research at OSU p 633 N92-25723
NAKAMURA, SEIGO
Results of measured temperature distribution on an adiabatic wing model with radiation thermometer [NAL-TM-610] p 261 N92-17755
Development of wall pressure measuring apparatus for an existing transonic wind tunnel test section [NAL-TM-565] p 573 N92-23778
NAKAMURA, SYUNRO
A potential flow theory of two-dimensional bifurcated curtain jets. II p 1118 A92-56039
NAKAMURA, TAKASHI
Finite elements analysis of flexural edge wave for composite fan blades [SAE PAPER 912048] p 861 A92-45432
NAKAMURA, YOSHIAKI
Flow field around thick delta wing with rounded leading edge [SAE PAPER 912009] p 789 A92-45409
Shock interaction induced by two hemisphere-cylinders [SAE PAPER 912043] p 790 A92-45427
DSMC simulation of hypersonic flows past 2-dimensional bodies p 939 A92-52772
NAKAMURA, YUKINOBU
Improvement of atmospheric flight performance of a space vehicle through H infinity-control theory p 1130 A92-53785
NAKANISHI, HIDEKI
Roles of wind tunnel tests and CFD analyses in the design of energy-efficient SST [AIAA PAPER 92-3923] p 1133 A92-56754
NAKANO, EIICHIRO
Air flow under a flight-vehicle engine p 429 A92-30528
NAKANO, T.
Unsteady Navier-Stokes simulation of transonic cascade flow using an unfactored implicit upwind relaxation scheme with inner iterations [ASME PAPER 91-GT-223] p 74 A92-15637
NAKAO, M.
Analytical condition inspection and extension of time between overhaul of F3-30 engine [ASME PAPER 91-GT-277] p 653 A92-36888
Aerodynamic design tool development for the calculation code of hypersonic flow p 711 A92-43198
NAKAO, MASAHIRO
Numerical simulations of hypersonic real-gas flows over space vehicles [SAE PAPER 912045] p 791 A92-45429
NAKAO, SHIGEHIDE
A study on the interaction between a bow shock wave generated by a blunt body and a turbulent boundary layer p 8 A92-12424
Experimental investigation on turbulent phenomena in three-dimensional shock wave/turbulent boundary layer interaction induced by blunt fin p 1018 A92-53557
Experimental study on three-dimensional shock wave-turbulent boundary layer interaction induced by protuberance p 1019 A92-53997

Three-dimensional shock wave-turbulent boundary layer interaction induced by blunt body and protuberance
p 1029 A92-56009

NAKAO, SHINICHI
Application of riblet surface to pipe flow
p 766 N92-26915

NAKAO, YOSHIYUKI
Flow field around thick delta wing with rounded leading edge
[SAE PAPER 912009] p 789 A92-45409

NAKATANI, HIROSHI
Mechanical properties of laminate aluminum matrix composites p 1106 A92-56102

NAKAUCHI, Y.
Wing test at the cryogenic wind tunnel of the National Defense Academy p 749 A92-43199

NAKAUCHI, YASUO
Preliminary airfoil testing experience in the NDA cryogenic wind tunnel p 1091 A92-54326

NAKAYAMA, A.
Turbulent flow in the wake of an idealized wing-body junction
[AIAA PAPER 92-0282] p 435 A92-31652
Phase-averaged turbulence statistics in a near wake with an asymmetric vortex shedding p 620 A92-40086

NAKAYAMA, CHUICHI
Analysis of the aerodynamic characteristics of a simple remotely piloted research vehicle (RPRV)
p 710 A92-43191

NAKAYAMA, HIROTOSHI
Mechanical properties of laminate aluminum matrix composites p 1106 A92-56102

NAKAZAWA, TORU
Ultrasonic motor utilizing elastic fin rotor
p 215 A92-17414

NALLASAMY, M.
Unsteady blade-surface pressures on a large-scale advanced propeller - Prediction and data
p 80 A92-17178
Unsteady Euler analysis of the flowfield of a propfan at an angle of attack p 242 A92-21070
Unsteady blade pressures on a propfan at takeoff - Euler analysis and flight data
[AIAA PAPER 92-0376] p 372 A92-26234
Unsteady blade pressures on a propfan - Predicted and measured compressibility effects
[AIAA PAPER 92-3774] p 1023 A92-54161
Unsteady blade pressures on a propfan at takeoff: Euler analysis and flight data
[NASA-CR-189076] p 130 N92-13071

NAMBA, MASANOBU
Unsteady lifting surface theory for a rotating transonic cascade of swept blades
[ASME PAPER 91-GT-178] p 73 A92-15610

NAMBA, SEIICHIRO
Temporal change of noisiness of helicopter noise
p 689 A92-39103
Temporal change of timbre of helicopter noise
p 694 A92-39104

NAMDAR, BAHMAN
BUWICE - An interactive icing program applied to engine inlets
[AIAA PAPER 92-3179] p 922 A92-48794

NAMDAR, BAHMAN S.
Experimental ice shape and performance characteristics for a multi-element airfoil in the NASA Lewis Icing Research Tunnel
[NASA-TM-105380] p 261 N92-17347

NANBU, K.
Force and heat transfer on a disc in rarefied flow
p 939 A92-52764

NANNONI, F.
Correlation of flight, tunnel and prediction data on a helicopter main rotor p 1059 A92-56350

NAPIER, JAMES C.
Development of T-100 multipurpose small power unit
[ASME PAPER 91-GT-327] p 153 A92-15697

NAPOLITANO, LUIGI G.
Linear acoustics in gas mixtures with rate processes
p 238 N92-15013

NAQWI, AMIR A.
Semiconductor laser Doppler anemometer for applications in aerodynamic research
p 495 A92-31173

NARASIMHAN, J. L.
Prediction of wake in a curved duct p 3 A92-10487

NARAYAN, JOHNNY R.
A design optimization procedure for high-speed prop-rotors
[AIAA PAPER 92-2375] p 542 A92-34545

NARAYANAN, G. V.
Structural tailoring/analysis for hypersonic components - Executive system development
[AIAA PAPER 92-2471] p 583 A92-34360

NARAYANSWAMI, N.
Interaction between crossing oblique shocks and a turbulent boundary layer p 812 A92-46882
Structure of crossing-shock wave/turbulent boundary-layer interactions
[AIAA PAPER 92-3670] p 1022 A92-54113

NARKIEWICZ, JANUSZ
General model of isolated helicopter blade for stability investigation p 547 A92-35774
A new method of helicopter rotor blade motion control
p 875 A92-47786
Simulation of helicopter see-saw rotor motion
p 1055 A92-56287

NARRAMORE, J. C.
Navier-Stokes calculations of inboard stall delay due to rotation p 309 A92-24410
Numerical simulation of multizone two-dimensional transonic flows using the full Navier-Stokes equations
p 815 A92-46955

NARUO, YOSHIHIRO
Test results of the expander cycle air turbo ramjet for a future space plane
[IAF PAPER 91-271] p 120 A92-14709
Development study on air turbo-ramjet engine for space plane p 1065 A92-53487
Tests results on Air Turbo Ramjet for a future space plane
[IAF PAPER 92-0657] p 1071 A92-57098

NARVESON, MARSHALL L.
Flow modification over a backward facing step
[AD-A241351] p 158 N92-13406

NASR, HATEM
Study objectives: Will commercial avionics do the job? Improvements needed? p 1065 N92-33340

NAST, T. C.
Computer simulation model for Lucas Stirling refrigerators p 296 A92-23837

NASTASE, ADRIANA
The design of fully-optimized configurations by using the iterative optimum-optimorum theory p 709 A92-43072
Three-dimensional visualizations of the aerodynamic characteristics of delta wings for the transition from subsonic to supersonic leading edges in supersonic-hypersonic flow p 709 A92-43073

NATH, G.
Unsteady hypersonic boundary layers for slender axisymmetric bodies with large injection rates
p 524 A92-36100

NATHAN, ARNOLD
A review of aging aircraft technology: An IAI perspective
[IAITIC-91-1018] p 461 N92-20500

NATSUMURA, TADASHI
Numerical simulation of impact resistance on composite blade p 738 A92-44734

NATUMURA, TADASHI
Nonlinear transient analysis of composite ATP blade model p 294 A92-23111

NAUGHTON, J. W.
Experiments on the enhancement of compressible mixing via streamwise vorticity. I - Optical measurements
[AIAA PAPER 92-3549] p 906 A92-49064

NAUMANN, K. W.
Millisecond aerodynamic force measurement with side-jet model in the ISL shock tunnel
[AIAA PAPER 92-3963] p 1097 A92-56790

NAYFEH, A. H.
Effect of suction on the stability of supersonic boundary layers. I - Second-mode waves. II - First-mode waves
p 174 A92-19611
Laminar flow control of subsonic boundary layers by suction and heat transfer strips p 617 A92-39338
Effect of a bulge on the subharmonic instability of subsonic boundary layers p 898 A92-45833

NAYFEH, ALI H.
Triple-deck structure p 3 A92-10690

NEAL, D. F.
Applications of IMI 834 in aeroengines - A collaborative IMI/MTU programme p 288 A92-22754

NEAL, DONALD M.
A sensitivity analysis on component reliability from fatigue life computations
[AD-A247430] p 908 N92-28425

NEBRES, J. V.
Flow about cylinders with helical surface protrusions
[AIAA PAPER 92-0540] p 332 A92-26957

NEESE, RICHARD E.
Partitioned software support concept for modular embedded computer software p 922 A92-48518

NEESE, WILLIAM A.
Aircraft hydraulic systems (3rd revised and enlarged edition)
[ISBN 0-89464-562-5] p 642 A92-38316

NEGAARD, GORDON N.
Preservation and utilization of finite element models of USAF aircraft structures
[AD-A241657] p 160 N92-13470

NEGODA, V. V.
Optimization of the three-dimensional shape of lifting bodies of small aspect ratio at hypersonic velocities
p 244 A92-21602

NEILAN, R. E.
NASA's GPS tracking system for Aristoteles
p 576 N92-23919

NEILAND, V. M.
Computations of a transonic flow about an airfoil in a wind tunnel with porous walls p 423 A92-30128
An asymptotic transonic theory and optimal porosity of wind tunnel walls at M greater than about 1
p 425 A92-30159

NEILAND, V. YA.
Aerothermodynamic configuration of first generation aerospace planes (of Buran-type) and first flight results
p 211 N92-14975

NEILLEY, D.
Characteristics of thunderstorm-generated low altitude wind shear - A survey based on nationwide terminal Doppler weather radar testbed measurements
p 45 A92-11378

NEINER, GEORGE H.
Hot gas ingestion characteristics and flow visualization of a vectored thrust STOVL concept
p 860 A92-45316

NEJAD, A. S.
Laser diagnostics for velocity measurements in supersonic combusting environments
[AIAA PAPER 92-0008] p 288 A92-22133
Premixed, turbulent combustion of axisymmetric sudden expansion flows p 397 A92-27770
Swirl effects on confined flows in axisymmetric geometries p 399 A92-28513
Swirl number effects on confined flows in a model of a dump combustor p 896 A92-45202

NEKOHASHI, TOSHIFUMI
Multiharmonic control response of a rotor blade during forward flight (Analysis) p 744 A92-43121
Prediction of dynamic hub load of a rotor executing multiple sinusoidal blade pitch variations
p 846 A92-46921
Structural optimization of a cantilevered beam subject to combined static loadings p 1118 A92-56024
Optimization approach for helicopter maneuverability with a point mass model p 1083 A92-56025

NELSON, B. A.
Formation and sustainment of a very low aspect ratio tokamak using coaxial helicity injection: Helicity Injected Torus (HIT) experiment
[DE92-014311] p 1136 N92-32595

NELSON, B. E.
Scoping studies for small steady-state tokamaks for divertor testing
[DE92-000740] p 238 N92-15761

NELSON, C. P.
Effects of wing planform on HSCT off-design aerodynamics
[AIAA PAPER 92-2629] p 844 A92-45501

NELSON, CHRIS
A fast, uncoupled, compressible, two-dimensional, unsteady boundary layer algorithm with separation for engine inlets
[AIAA PAPER 92-3082] p 823 A92-48729
A fast, uncoupled, compressible, two-dimensional, unsteady boundary layer algorithm with separation for engine inlets
[NASA-TM-105686] p 770 N92-27653

NELSON, HAROLD, JR.
Monitoring operational concept
[DOT/FAA/SE-91/3] p 268 N92-15980
National Airspace System maintenance and support operational concept
[DOT/FAA/SE-92/1] p 308 N92-18969
National airspace system: System effectiveness operational concept NAS-SR-138
[DOT/FAA/SE-92/2] p 535 N92-23096
National airspace system. Air defense and law enforcement surveillance operational concept NAS-SR-135
[DOT/FAA/SE-92/3] p 953 N92-31211

NELSON, JOHN E.
State-of-the-art airborne video recording
p 555 A92-35932

NELSON, MICHAEL D.
An experimental investigation of leading edge vortical flow about a delta wing during wing rock
[AD-A243363] p 260 N92-17114

NELSON, O. E.
The compatibility and tradeoffs of titanium and composites p 288 A92-22758

NELSON, P. A.
Active control of sound transmission through stiff lightweight composite fuselage constructions
p 1137 N92-32957
NELSON, R. C.
Breaking down the delta wing vortex: The role of vorticity in the breakdown process p 86 N92-13017
NELSON, ROBERT C.
A discrete vortex model for predicting wing rock of slender wings
[AIAA PAPER 92-4497] p 1026 A92-55365
Wind tunnel blockage effects on slender wings undergoing large amplitude motions
[AIAA PAPER 92-3926] p 1096 A92-56757
Aerodynamic and flowfield hysteresis of slender wing aircraft undergoing large-amplitude motions
p 364 N92-18780
NELSON, T.
Computational fluid dynamics p 177 N92-13979
NELSON, T. E.
Automated grid generation for high-lift configurations
p 628 N92-24869
NEMEC, T. S.
Real-time estimation of gas turbine engine damage using a control based Kalman filter algorithm
[ASME PAPER 91-GT-216] p 124 A92-15633
NERSESOV, G. G.
A computational study of flow past bodies and heat transfer for isentropic compression flows
p 425 A92-30158
NESTEROV, M. E.
The effect of wing twist optimized in the framework of the plane cross section hypothesis on the aerodynamic characteristics of a wing-body combination at hypersonic speeds p 424 A92-30129
NESTOR, DUANE E.
Calibration of the Naval Postgraduate School 3.5' x 5.0' academic wind tunnel
[AD-A240614] p 31 N92-11025
NETSVETAILOV, E. M.
A study of the base pressure behind circular steps
p 426 A92-30196
NETT, C. N.
A general nonlinear dynamical analysis of a second-order, one-dimensional, theoretical compression system model p 509 A92-29374
Model development for active surge control/rotating stall avoidance in aircraft gas turbine engines
p 468 A92-29375
An integrated, full-range surge control/rotating stall avoidance compressor control system
p 469 A92-29376
NETTER, GASTON
FALKE: Winged re-entry vehicle flight control
p 667 N92-24454
NETTERFIELD, M. P.
Hypersonic aerothermodynamic computations using a point-implicit TVD method p 183 N92-15006
NETZER, ALLAN
Airborne Data Acquisition and Relay System
p 839 A92-47574
NETZER, D. W.
Solid-fuel ramjet fuel regression rate/thrust modulation
p 666 A92-36966
NETZER, DAVID W.
A study of the flammability limit of the backward facing step flow combustion
[AIAA PAPER 92-3846] p 895 A92-49136
NEU, C. E.
In-service evaluation of 2090 aluminum-lithium alloy on F/A-18 aircraft
[AD-A248472] p 986 N92-30321
NEUBAUER, JAY C.
Reference mode effect on the auditory display of aircraft bank angle
[AD-A247825] p 728 N92-27916
NEUHART, DAN H.
A laser fluorescence anemometer system for the Langley 16- by 24-inch water tunnel
p 1092 A92-54347
A user's guide to the Langley 16- by 24-inch water tunnel
[NASA-TM-104200] p 385 N92-18956
NEUMAN, FRANK
Analysis of delay reducing and fuel saving sequencing and spacing algorithms for arrival traffic
[NASA-TM-103880] p 1044 N92-33194
NEUMANN, BENJAMIN
NASA aerodynamics program
[NASA-TM-4368] p 609 N92-24678
NEUMANN, RICHARD D.
The value of sub-scale flight tests in the development of NASP vehicles
[AIAA PAPER 91-5048] p 210 A92-17834
The wind tunnel test 'system' of 1995 - Cost effective experimentation through a fusion of related technologies
p 1091 A92-54342
Hypersonic wind tunnel nozzle study
[AIAA PAPER 92-4012] p 1033 A92-56835
NEUMEIER, MARK E.
Mode S data link pilot-system interface - A blessing in de skies or a beast of burden? p 839 A92-44920
NEUNABER, R.
Aircraft tracking for structural fatigue
p 361 N92-18584
NEUNZERT, H.
Hypersonic flow calculations around a 3D delta wing at low Knudsen numbers p 937 A92-52734
Rarefied gas flow around a disc with different angles of attack p 938 A92-52753
NEURAUTER, DAVE
Realistic real-time ground testing
[AIAA PAPER 92-0197] p 284 A92-23805
NEWAZ, G. M.
Processing effects and damage tolerance in poly(etheretherketone) composites p 388 A92-26152
NEWBERRY, CONRAD F.
Applied aerodynamics education - Design and science
[AIAA PAPER 92-2662] p 928 A92-45581
NEWBERRY, KELLI
The Langley turbo-prop commuter design: A complete project description
[NASA-CR-189987] p 463 N92-21540
NEWELL, DOUGLAS F.
Hypervelocity Wind Tunnel 9 control system
p 1092 A92-54343
NEWELL, J.
Gamma Group-The Pale Horse: A proposal in response to a commercial air transportation study ort study
[NASA-CR-190019] p 731 N92-26435
NEWELL, O. J.
The 1990 Airport Surveillance Radar Wind Shear Processor (ASR-WSP) operational test at Orlando International Airport
[AD-A239852] p 18 N92-10019
NEWFIELD, MARK E.
Reactivation and upgrade of the NASA Ames 16-Inch Shock Tunnel - Status report
[AIAA PAPER 92-0327] p 383 A92-25774
Flow characterization in the NASA Ames 16-inch Shock Tunnel
[AIAA PAPER 92-3810] p 1090 A92-54180
NEWMAN, B. G.
Analysis of flexible-membrane and jet-flapped airfoils using velocity singularities p 10 A92-13216
Incompressible flow past a flat plate aerofoil with leading edge separation bubble p 421 A92-28943
NEWMAN, GARY
On the aerodynamics/dynamics of store separation from hypersonic aircraft
[AIAA PAPER 92-2722] p 807 A92-45595
NEWMAN, J. C., JR.
Fatigue crack initiation and small crack growth in several airframe alloys p 212 A92-19754
Proof test and fatigue crack growth modeling on 2024-T3 aluminum alloy p 213 A92-19828
Effects of constraint on crack growth under aircraft spectrum loading
[NASA-TM-107677] p 1128 N92-34178
NEWMAN, JAMES C., JR.
Fracture mechanics research at NASA related to the aging commercial transport fleet p 913 N92-30110
NEWMAN, M. J.
Kestrel balloon launch system
[AIAA PAPER 91-3684] p 15 A92-11027
NEWMAN, P. A.
Observations on computational methodologies for use in large-scale, gradient-based, multidisciplinary design incorporating advanced CFD codes
[NASA-TM-104206] p 630 N92-24956
NEWMAN, PERRY A.
An incremental strategy for calculating consistent discrete CFD sensitivity derivatives
[NASA-TM-104207] p 625 N92-24681
NEWMAN, ROBERT B.
Rotorcraft low altitude IFR benefit/cost analysis: Operations analysis
[SCT-90RR-44] p 191 N92-15061
NEWMAN, S. J.
The application of a theoretical blade sailing model to predict the behaviour of articulated helicopter rotors
p 960 A92-52849
NEWPORT, JOHN
A new development in embedded computer performance measurement p 921 A92-48506
A new approach to embedded computer performance measurement p 1005 A92-49288
NEWTON, JAMES E.
Heat transfer measurements from a smooth NACA 0012 airfoil p 218 A92-20215
NG, JAMES
Suppression of radiating harmonics Electro-Impulse Deicing (EIDI) systems
[DOT/FAA/CT-TN90/33] p 405 N92-19764
NG, LIAN L.
On the nonlinear stability of a high-speed, axisymmetric boundary layer p 78 A92-16457
Secondary instability mechanisms in compressible, axisymmetric boundary layers
[AIAA PAPER 92-0743] p 343 A92-28224
Secondary instabilities in compressible boundary layers p 435 A92-31639
NG, POH H.
Nonlinear triggered lightning models for use in finite difference calculations p 230 A92-20128
NG, T. T.
Forebody vortex control with miniature, rotatable nose-boom strakes
[AIAA PAPER 92-0022] p 281 A92-22144
Experimental study of vortex flows over delta wings in wing-rock motion p 810 A92-46787
Forebody vortex control using small, rotatable strakes
p 811 A92-46798
Effect of a nose-boom on forebody vortex flow
p 812 A92-46818
NG, T. TERRY
Aerodynamic control of fighter aircraft by manipulation of forebody vortices p 380 N92-18791
NG, W. F.
The Baldwin-Lomax model for separated and wake flows using the entropy envelope concept
[AIAA PAPER 92-0148] p 253 A92-23764
A concentration probe for the study of mixing in supersonic shear flows p 991 A92-50039
NGUYEN, BA T.
Analysis of the VISTA longitudinal simulation capability for a cruise flight condition p 876 A92-48488
NGUYEN, DUC T.
A parallel-vector algorithm for rapid structural analysis on high-performance computers
[NASA-TM-102614] p 595 N92-22649
NGUYEN, H.
Two-dimensional effects in a triangular convecting fin
p 219 A92-20324
NGUYEN, H. L.
Applied analytical combustion/emissions research at the NASA Lewis Research Center - A progress report
[AIAA PAPER 92-3338] p 1067 A92-54025
Applied analytical combustion/emissions research at the NASA Lewis Research Center
[NASA-TM-105731] p 890 N92-29343
NGUYEN, HUNG L.
The VRT gas turbine combustor - Phase II
[AIAA PAPER 92-3471] p 1067 A92-54035
NGUYEN, KHANH
Effects of higher harmonic control on rotor performance and control loads p 729 A92-41218
NGUYEN, PHUC
Navier-Stokes analysis of turbulent boundary layer and wake for two-dimensional lifting bodies
p 221 N92-14309
NGUYEN, PHUC N.
Use of Navier-Stokes analysis in section design
[AD-A242074] p 299 N92-17168
NGUYEN, TIEN M.
ACTS aeronautical experiments
[AIAA PAPER 92-2042] p 485 A92-29956
NGUYEN, V. D.
Wind tunnel investigation of a wing-propeller model performance degradation due to distributed upper-surface roughness and leading edge shape modification
p 451 N92-21690
NGUYEN, V.-N.
Efficient direct solvers for large-scale computational fluid dynamics problems p 690 A92-37534
NI, GANG
The dimensional reconstruction of vortex cross-section images p 339 A92-27833
NI, X. Q.
Fault diagnostics on jet engine starting
p 1116 A92-54345
NI, YONGXI
GPS integrated system application in aircraft approach landing p 266 A92-21466
NICHOLAS, D. J.
Compressing the compressor
[PNR-90824] p 476 N92-21848
NICHOLAS, O. P.
A progress report on ASTOVL control concept studies under the VAAC programme p 871 A92-45319
Some longitudinal handling qualities design guidelines for active control technology transport aircraft
[NLR-TP-90129-U] p 878 N92-28652

Collaborative research on V/STOL control system/cockpit display tradeoffs under the NASA/MOD joint aeronautical program
[NASA-TM-103910] p 1087 N92-32788
NICHOLAS, T.
Thermo-mechanical fatigue crack growth in aircraft engine materials p 213 A92-19799
NICHOLAS, THEODORE
Elevated temperature crack growth in aircraft engine materials p 891 A92-45234
NICHOLS, LESTER D.
Aeropropulsion structures p 559 N92-22518
NICHOLS, LYNNE
Putting the control back in air traffic control - An enhanced Universal Development Simulation System p 916 A92-44982
NICHOLS, R. H.
Calculation of the carriage loads of tandem stores on a fighter aircraft
[AIAA PAPER 92-0283] p 319 A92-25736
Calculation of high speed base flows
[AIAA PAPER 92-2679] p 799 A92-45531
NICHOLS, TIMOTHY C.
Testing and analysis of a 'smart' interface to connect two complex avionics bus systems without significant modification to the software of either system p 964 A92-49254
NICHOLSON, JAMES R.
Expert knowledge techniques applied to the analysis of electric field mill data p 408 A92-27991
NICHOLSON, LEONARD S.
STS-41 Space Shuttle mission report
[NASA-TM-105479] p 286 N92-16973
NICHOLSON, ROGER K.
Flight testing of the Boeing 747-400 Central Maintenance Computer system p 555 A92-35950
NICKERSON, JOSEPH D., JR.
Handling qualities of the H-76 Fantail Demonstrator p 131 A92-14335
NICKS, J.
Preliminary analysis of baseline vibration data from Allison T56-A-14LFE engine and reduction gearbox
[NRC-31578] p 130 N92-11999
A preliminary study in the use of phase demodulation techniques for the analysis of gear vibration data
[NRC-32083] p 1002 N92-31469
NICKS, ORAN
Further wind tunnel investigation of the SM701 airfoil with aileron and turbulators
[NASA-CR-190702] p 1038 N92-33063
NICOL, D. J.
An evaluation of in-cabin safety features in passenger aircraft
[ETN-92-90656] p 449 N92-20794
NICOL, DAVID M.
Advanced techniques in reliability model representation and solution
[NASA-TP-3242] p 1134 N92-33483
NICOLAES, J. M. J. A.
Fokker 50 flameouts in icing conditions p 548 A92-35940
NICOLAI, LELAND M.
Designing a better engineer p 606 A92-34771
NICOLAS, J.
Vibroacoustic simulation of an airplane structure p 629 N92-24871
NICOUT, D.
New hypersonic test methods developed at ONERA - The R5 and F4 wind tunnels
[ONERA, TP NO. 1992-39] p 882 A92-48600
NIE, HONG
Dynamic behavior analysis for landing-gear with different types of dual-chamber shock-struts p 111 A92-15342
NIE, JINGXU
Cyclic symmetric contact stress analysis of aeroengine rotor assembly p 470 A92-29733
A compound fatigue investigation of plate specimen under low-cycle load superposed on high cycle load p 587 A92-35555
NIE, TIEJUN
On multiple grid method p 1006 A92-49585
NIEDERDRENK, P.
Analysis tools of ONERA and DLR for the aerothermodynamics of reentry vehicles p 211 N92-14977
NIEDERSTRASSER, HELMUT
Investigation of the dynamic behaviour and the frequency response of the GG 1342 laser gyro
[ESA-TT-1236] p 595 N92-22641
NIEDZWIECKI, RICHARD W.
Small engine technology programs p 560 N92-22532
NIELSEN, T.
Airbus Industrie A330/A340: Full scale fatigue test of center fuselage and wing p 226 N92-14425
NIEMI, EUGENE E., JR.
Selection of opening model for parachute scaling studies
[AD-A250882] p 943 N92-30239
NIERENBERG, MICHELE R.
The development and integration of an engine monitoring system for the F-14A+/D Super Tomcat
[SAE PAPER 912094] p 654 A92-39951
NIESL, G.
Noise level reduction inside helicopter cabins p 545 A92-35733
NIESL, GEORG
BVI impulsive noise reduction by higher harmonic pitch control - Results of a scaled model rotor experiment in the DNW p 1136 A92-56344
NIEUWKERK, L. R.
Quantitative estimation of secondary surveillance radar information p 353 A92-24943
NIEUWPOORT, A. M. H.
A simulator evaluation of various manual control concepts for fly-by-wire transport aircraft
[AIAA PAPER 92-4328] p 1073 A92-55172
NIGGEMANN, R. E.
270-Vdc/hydrid 115-Vac electric power generating system technology demonstrator evolution to a dual-channel, more electric aircraft technology development testbed
[SAE PAPER 912183] p 655 A92-40003
270-Vdc/hybrid 115 Vac electric power generating system technology demonstrator
[SAE PAPER 912051] p 861 A92-45435
NIIMI, KENJI
An experimental program concerning a satellite data link for oceanic ATC p 1046 A92-56093
NIINO, MASAYUKI
Conceptual design of scramjet engine p 1065 A92-53490
NIKAI, M.
Quality management of landing gear with pulling support system p 762 A92-43156
NIKFETRAT, K.
Prediction of drag at subsonic and transonic speeds using Euler methods
[AIAA PAPER 92-0169] p 255 A92-23780
Accurate prediction of drag using Euler methods p 703 A92-41246
NIKIFOROVA, L. N.
The solution of the helicopter flight dynamics tasks by the methods of optimal control theory p 1085 A92-56284
NIKITINA, E. A.
Methyl-tert-butyl ether as a component of aviation gasolines p 34 A92-12146
NIKLASCH, N.
Navsat - A civil complement to GPS and Glonass
[IAF PAPER 91-490] p 188 A92-18505
NIKOLAEV, K. V.
Flow of a rarefied gas over a cylinder at angle of sideslip p 708 A92-42738
NIKOLAEV, M. I.
Optimization of a lifting surface for minimum induced drag p 437 A92-31853
NIKOLAEV, V. S.
Analytical and experimental studies of the aerodynamic characteristics of a delta wing at a slip angle at high supersonic velocities p 437 A92-31854
NIKRAVESH, PARVIZ E.
A multibody approach to modeling tilt-wing rotorcraft dynamics
[AIAA PAPER 92-0487] p 328 A92-26318
NIKSCH, RICHARD A.
ASTOVL flexibility in the 21st century p 783 A92-45309
NILSEN, JOHN
Visibility measurements for the Automated Surface Observing System (ASOS) p 468 A92-32095
NILSSON, JOHNNY
GPS/GLONASS user systems in Sweden p 638 A92-38384
NINNEMANN, T. A.
A concentration probe for the study of mixing in supersonic shear flows p 991 A92-50039
NINO, MASAYUKI
Scramjet engine and its flying test bed p 1066 A92-53492
NIPPRESS, K. R.
Sentinel 1000 flight test programme overview and preliminary results
[AIAA PAPER 92-1229] p 538 A92-33326
NIRANJANA, T.
Dynamic flying investigations on 1/13.5 NALLA model (Longitudinal Results)
[NAL-PD-FC-9113] p 359 N92-18073
NIRENBERG, ALLAN
IsoDoppler and mocomp corrections improve MTI radar p 898 A92-45774
NISHIDA, HIDEO
A study on the rotating stall of centrifugal compressors. II - Effect of vaneless diffuser inlet shape on rotating stall p 497 A92-32508
NISHIDA, M.
Numerical computation and experimental study of shock wave reflection p 430 A92-30542
Numerical simulation of opposing sonic jets p 524 A92-36357
NISHIDA, MICHIO
Thermal and chemical nonequilibrium viscous shock layer flows over a blunt body at high altitudes p 938 A92-52749
Hypersonic flows with air chemistry over a reentry vehicle at high altitudes p 1017 A92-53549
NISHIKUNI, M.
New-type of ultralight flexible a-Si solar cell and its application on an airplane p 970 A92-53181
NISHIMURA, HIROFUMI
Estimation of aircraft inertial characteristics using maximum likelihood estimation p 1084 A92-56057
NISHIMURA, J.
Polar patrol balloon
[AIAA PAPER 91-3688] p 15 A92-11031
NISHIMURA, Y.
Wind tunnel tests on A4, A4.1, and A4.2 2-D airfoil models in the IAR 5-ft. wind tunnel: Boeing Commercial Airplane Company and Institute for Aerospace Research collaborative work program
[NRC-IAR-C3] p 81 N92-11975
The BCAC/IAR collaborative research program to investigate the sidewall boundary layer effects in the IAR/NRC 2-D High Reynolds Number Test Facility
[NRC-HSA-434] p 81 N92-11976
NISHIO, SEIJI
Demonstration of gas liquid separation under the microgravity by aircraft KC-135
[SAE PAPER 912024] p 897 A92-45416
NISHIOKA, MICHIO
Observation and testing on supersonic multiphase flow p 429 A92-30502
Proceedings of the Seminar on Investigation and Control of Boundary-Layer Transition
[NAL-SP-11] p 400 N92-18483
NISHIWAKI, H.
New-type of ultralight flexible a-Si solar cell and its application on an airplane p 970 A92-53181
NISHT, M. I.
Mathematical modeling of nonstationary viscous flow over a solid angle of finite span p 440 A92-31890
NISIOKA, JUN
An experimental study on variable pressure hydraulic flight control system p 1084 A92-56119
NISSLEY, D. M.
Life prediction and constitutive models for engine hot section anisotropic materials program
[NASA-CR-189222] p 973 N92-31534
Life prediction and constitutive models for engine hot section anisotropic materials program
[NASA-CR-189223] p 1072 N92-33479
NISSLEY, DAVID M.
Thermal barrier coating life prediction model development
[ASME PAPER 91-GT-40] p 147 A92-15523
NISSLEY, WILLIAM
Drop test: Cessna Golden Eagle 421B
[DOT/FAA/CT-TN91/32] p 837 N92-28900
NISTLER, NOEL F.
A learning enhanced flight control system for high performance aircraft
[AD-A252520] p 1086 N92-32435
NITA, M. M.
Control surfaces correlation in DLC maneuvers p 280 A92-21301
Control surfaces correlation in DSFC maneuvers p 281 A92-21307
Some considerations on modeling flight vehicles movement p 281 A92-21311
NITSCHE, W.
Shock detection on airfoils by means of piezo foil- and hot film arrays p 1115 A92-54334
NITSOPOULOS, IOANNIS
Application of MSC/DYNA to shock and impact problems in aircraft industry
[MBB-UD-0593-91-PUB] p 225 N92-14382
NITTA, KYOKO
Finite difference numerical prediction of aerodynamics of an airfoil flying over wavy wall p 64 A92-14033
Analysis of a 2-D airfoil motion flying in-proximity-to a wavy-wall surface-lifting surface-scheme p 315 A92-25506
Analysis of a 2-D airfoil motion flying in-proximity-to a wavy-wall surface - Finite difference method p 421 A92-29517
Analysis of motion of airfoil flying over wavy-wall surface (lifting surface method) p 818 A92-47100

Motion analysis of 2-dimensional flat plate in ground effect p 1030 A92-56053
NITTA, UYAKO
Reevaluation of the motion of an airship p 731 A92-43243
NITZSCHE, F.
A study on the feasibility of using adaptive structures in the attenuation of vibration characteristics of rotary wings
[AIAA PAPER 92-2452] p 541 A92-34415
Whirl-flutter stability of a pusher configuration in nonuniform flow p 845 A92-46813
NIVEN, A. J.
Measurements of the dynamic stall vortex convection speed p 1032 A92-56351
NIWA, M.
Measurement of position and attitude using laser and retro-reflectors p 1047 A92-56120
NIWA, NOBUO
Numerical investigation of supersonic inlet with realistic bleed and bypass systems p 713 A92-44519
Wind tunnel test of M = 2.5 mixed compression intet p 1028 A92-56008
NIWA, SHOHEI
Ducted fan VTOL for working platform
[SAE PAPER 911995] p 843 A92-45397
A design of strongly stabilizing controller
[SAE PAPER 912081] p 917 A92-45456
NIXON, DAVID
Turbulence amplification through a shock wave
[AIAA PAPER 92-0313] p 320 A92-25761
Outflow boundary conditions using Duhamel's equation p 813 A92-46913
NIXON, M. W.
A demonstration of passive blade twist control using extension-twist coupling
[AIAA PAPER 92-2468] p 539 A92-34358
NIXON, MARK W.
Parametric studies for tiltrotor aeroelastic stability in high-speed flight
[AIAA PAPER 92-2568] p 565 A92-34482
A demonstration of passive blade twist control using extension-twist coupling
[NASA-TM-107642] p 1001 N92-31155
NO, T. S.
Dynamics and control of maneuverable towed flight vehicles p 976 A92-50508
NOAH, SHERIF T.
Nonlinear rotordynamics analysis
[NASA-CR-184263] p 221 N92-14344
NOBACK, R.
Response of helicopters to gusts
[NLR-TP-90159-U] p 879 N92-28653
Atmospheric turbulence spectra and correlation functions
[NLR-TP-89217-U] p 915 N92-28689
NOBBS, S. G.
Development of the full-envelope Performance Seeking Control algorithm
[AIAA PAPER 92-3748] p 1068 A92-54148
NODA, J.
Supersonic wind tunnel test of airintake/airframe integrated models p 1028 A92-56006
NODERER, KEITH D.
Aerodynamic parameters of the X-31 drop model estimated from flight-data at high angles of attack
[AIAA PAPER 92-4357] p 1080 A92-55343
NOEHREN, WILLIAM L.
Design and flight test evaluation of the Fantail antitorque system p 110 A92-14456
NOEL, B. W.
Fiber-sensor design for turbine engines
[DE92-003539] p 376 N92-18230
NOGUCHI, MASAYOSHI
High subsonic wind tunnel test of a two-dimensional hybrid-laminar-flow-control airfoil with slotted surface p 1029 A92-56045
NOGUCHI, TOSHIHIKO
Engine condition monitoring system for B747-400 p 1064 A92-56082
NOLAN, CHRIS
Development of a sensor for the detection of aircraft wing contaminants
[AIAA PAPER 92-0300] p 369 A92-25752
NOLET, STEPHEN C.
Measurement of basic material and processing properties affecting injection-pultrusion technology p 580 A92-32636
NOLL, BERTHOLD
Evaluation of a bounded high-resolution scheme for combustor flow computations p 201 A92-20734
NOMIZO, KUNIO
An improved method for simulating supersonic flow past a wedge shaped body
[NAL-TR-1097] p 345 N92-18239
NOMOTO, HIDEKI
Wind tunnel test of a supersonic air intake p 711 A92-43205
A hypersonic wind tunnel test of a mixed-compression air inlet model p 1028 A92-56007
NOMURA, H.
Numerical simulation of opposing sonic jets p 524 A92-36357
NOMURA, S.
New 1.27-m leg of the National Aerospace Laboratory hypersonic wind tunnel p 1092 A92-56003
NOMURA, SHIGEAKI
Experimental studies on aerodynamic heating and thermal protection in hypersonic flight p 709 A92-43101
Aerodynamic studies on space plane configuration at hypersonic speed p 1019 A92-53641
NOMURA, SIGEAKI
Computational aerodynamic simulation on HOPE p 251 A92-22635
NONAKA, O.
Aerodynamic model identification of a spaceplane model from a cable-mount dynamic wind-tunnel test p 1093 A92-56114
NONAKA, OSAMU
Spaceplane longitudinal aerodynamic parameter estimation by cable-mount dynamic wind-tunnel test
[SAE PAPER 911980] p 788 A92-45385
On improvements of three-dimensional position measuring system for dynamic wind tunnel testing p 1093 A92-56012
NONWEILER, T. R. F.
Aero-propulsive effects on configuration shaping
[AIAA PAPER 91-5064] p 459 A92-31691
NOONAN, KEVIN W.
Effect of blade planform variation on the forward-flight performance of small-scale rotors
[NASA-TM-4345] p 630 N92-24885
NOOR, AHMED K.
Reduced basis technique for evaluating the sensitivity coefficients of the nonlinear tire response
[AIAA PAPER 92-2530] p 583 A92-34376
Overview and major characteristics of future aeronautical and space systems
[AIAA PAPER 92-2441] p 585 A92-34472
Computational structures technology
[AIAA PAPER 92-2442] p 585 A92-34473
Sensitivity of tire response to variations in material and geometric parameters p 900 A92-47128
Computational Structures Technology for Airframes and Propulsion Systems
[NASA-CP-3142] p 683 N92-25911
Computational structures technology and UVA Center for CST p 683 N92-25912
NORDMANN, R.
Evaluation of rotordynamic coefficients of look-through labyrinths by means of a three volume bulk flow model p 223 N92-14356
Determination of rotordynamic coefficients for labyrinth seals and application to rotordynamic design calculations p 223 N92-14360
NORDSIECK, ARNOLD W.
Built-in testable error detection and correction p 394 A92-25846
NORDSTROM, JAN
Extrapolation procedures for the time-dependent Navier-Stokes equations p 704 A92-41289
NORDWALL, BRUCE D.
European ATC integration faces dual challenges p 534 A92-36076
Modified Doppler detects wind shear more reliably p 1015 A92-55099
NOREN, GEORGE
Retrofit provides navigation enhancement for older aircraft p 198 A92-20025
NORIEGA, J.
A high resolution multispectral video system p 587 A92-35479
NORLIN, KEN
Piloted simulation study of a balloon-assisted deployment of an aircraft at high altitude
[NASA-TM-104245] p 272 N92-15986
NORLIN, KENNETH
Rapid development of the X-31 simulation to support flight-testing
[NASA-TM-104256] p 1060 N92-33149
NORMAN, THOMAS R.
Full-scale investigation of aerodynamic interactions between a rotor and fuselage p 105 A92-14361
NORRIS, GUY
The engine inside p 558 A92-36126
Shear progress p 609 A92-40880
777 shaping up p 959 A92-52300
NORTH, DAVID M.
A340 handling, cockpit design improve on predecessor A320 p 849 A92-47969
NORTH, JIM
Test plan for the international aircraft operator information system
[DOT/FAA/CT-91/18] p 781 N92-26830
NORTH, RON
FANS implementation planning under way in Canada p 267 A92-23298
NORTHAM, G. B.
A numerical study of the effects of geometry on the performance of a supersonic combustor
[AIAA PAPER 92-0624] p 342 A92-28213
Evaluation of parallel injector configurations for Mach 2 combustion p 376 A92-28533
Strain-induced extinction of hydrogen-air counterflow diffusion flames - Effects of steam, CO2, N2, and O2 additives to air
[AIAA PAPER 92-0877] p 487 A92-29639
NORTHAM, G. BURT
CARS temperature measurements in a hypersonic propulsion test facility p 140 N92-12049
NORTHAM, G. BURTON
Hypersonic propulsion research p 561 N92-22543
NORTON, R. J. G.
Prediction of a high bypass ratio engine exhaust nozzle flowfield
[AIAA PAPER 92-3259] p 864 A92-48855
The application of a Navier-Stokes CFD method to civil engine intake flows p 769 N92-27471
NORTON, WILLIAM J.
Limit cycle oscillation and flight flutter testing p 570 A92-35939
NORUM, THOMAS D.
Acoustic characteristics and dynamic structural loading of an ASTOVL aircraft in hover
[AIAA PAPER 92-0370] p 416 A92-28190
NORVILLE, K. W.
Stratospheric electrodynamics from superpressure balloons - A technical challenge for small payload environments
[AIAA PAPER 91-3674] p 14 A92-11019
NORY, PASCAL
From concept to model: Conception and evaluation of an architecture for a distributed system with SAHARA - Some reflections on results of the utilization of SAHARA in the framework of the Electronic Copilot
[ONERA, TP NO. 1991-216] p 411 A92-26368
NOUAILHAS, D.
A viscoplastic theory for anisotropic materials
[ONERA, TP NO. 1992-90] p 391 A92-24721
NOURSE, R. W.
Ablation performance characterization of thermal protection materials using a Mach 4.4 Sled Test
[AIAA PAPER 92-3055] p 893 A92-48713
Aerothermal ablation behavior of selected candidate external insulation materials
[AIAA PAPER 92-3056] p 893 A92-48714
NOURY, ROGER
Improved noise rejection in automatic carrier landing systems p 380 A92-28154
NOVIKOV, VLADIMIR S.
Processing and displaying radio navigation data p 266 A92-21683
NOVOZHILOV, GENRIKH V.
From the history of Soviet aviation - Aircraft of the Il'iushin design bureau (2nd revised and enlarged edition) p 61 A92-15022
NOWLIN, BRENT C.
Description of a pressure measurement technique for obtaining surface static pressures of a radial turbine
[AIAA PAPER 92-4006] p 1123 A92-56829
Description of a pressure measurement technique for obtaining surface static pressures of a radial turbine
[NASA-TM-105643] p 680 N92-24959
NOYES, T. A.
The 1990 Airport Surveillance Radar Wind Shear Processor (ASR-WSP) operational test at Orlando International Airport
[AD-A239852] p 18 N92-10019
NOZAKI, OSAMU
Numerical simulations of the flow through cascades with tip clearance p 523 A92-36038
NOZUMI, KOKI
Synthesis of a MLS automatic landing control law for the NAL experimental research aircraft Do-228 p 1084 A92-56062
NSI MBA, M.
Experimental and computational studies of hovering rotor flows p 815 A92-46954
NTUEN, CELESTINE A.
Model analysis and expert system development for planning and scheduling teleoperations for aircraft turnaround functions, volume 1
[AD-A251037] p 932 N92-30253

Model analysis and expert system development for planning and scheduling teleoperations for aircraft turnaround functions. Volume 2: Top user's guide
[AD-A251083] p 932 N92-30258
NUCCI, LOUIS M.
Pioneering scramjet developments by Antonio Ferri
p 474 N92-21519
NUNNA, V.
Runway exit designs for capacity improvement demonstrations. Phase 2: Computer model development
[NASA-CR-190166] p 484 N92-21162
NUSCA, M. J.
Experimental and computational investigation of scaling phenomena in a large caliber ram accelerator
[AIAA PAPER 92-3245] p 1103 A92-54019
NUSSBAUM, DAVID M.
Advanced ASDE provides new eyes and ears for controllers p 453 A92-29506
NUZZI, STEPHEN F.
From Russia and beyond p 96 A92-16638
NWOKAH, O. D. I.
Full envelope multivariable control of a gas turbine engine p 468 A92-29116
NWOKAH, OSITA
Parametric robust control by quantitative feedback theory p 302 A92-21176
NWOKAH, OSITA D. I.
Frequency response specifications and sensitivity functions in quantitative feedback theory
p 508 A92-29280
NYBERG, GREGORY
Fighter airframe/propulsion integration - A McDonnell Aircraft perspective
[AIAA PAPER 92-3333] p 850 A92-48916
NYGARD, M. K.
Probabilistic design and fatigue management based on probabilistic fatigue models with reliability updating
p 360 N92-18574

O

O'BRIEN, J.
Brownian-motion limited aerodynamic focusing of heavy molecules p 995 A92-52722
O'BRIEN, MICHAEL
Nondestructive depth profiling of the protective coating on a turbine blade p 144 A92-13641
O'BRIEN, RUSSELL
The 1988 Australian Winter Storms Experiment - Case study: 6 August 1988 p 301 A92-23009
O'BRIEN, W. F.
A neural network for the identification of measured helicopter noise p 162 A92-14387
Stage-by-stage poststall compression system modeling technique p 80 A92-17194
O'BRIEN, WALTER F.
Identification of helicopter noise using a neural network p 416 A92-28032
O'BRIMSKI, FRANCIS J.
An overview of US Navy and Marine Corps V/STOL
p 783 A92-45303
O'CALLAGHAN, J. J.
Vortex-induced energy separation in shear flows
[AIAA PAPER 92-0192] p 257 A92-23801
O'CONNOR, J.
Design of a small axial compressor for high efficiency over a wide operating range
[ASME PAPER 91-GT-195] p 124 A92-15620
O'CONNOR, LEO
Active magnetic bearings give systems a lift
p 901 A92-48201
O'HERON, PATRICK J.
A multibody approach to modeling tilt-wing rotorcraft dynamics
[AIAA PAPER 92-0487] p 328 A92-26318
O'KEEFFE, H. B.
The ICAO Future Air Navigation System
p 532 A92-33435
O'NEIL, P. J.
Numerical simulation of leading-edge vortex breakdown using an Euler code p 701 A92-41213
O'NEILL, MARY KAE L.
Design tradeoffs on engine-integrated hypersonic vehicles
[AIAA PAPER 92-1205] p 537 A92-33313
O'RENDY, JOSEPH E.
Retrofit provides navigation enhancement for older aircraft p 198 A92-20025
O'ROURKE, MATTHEW J.
A simulation model for tail rotor failure
[AIAA PAPER 92-4633] p 1081 A92-55380
OAKES, KEVIN F.
STS-40 descent BET products: Development and results
[NASA-CR-189570] p 286 N92-16012
OBAL, M. B.
Smart structures for helicopters p 516 A92-35727
OBATA, SYOICHI
Test results of the expander cycle air turbo ramjet for a future space plane
[IAF PAPER 91-271] p 120 A92-14709
OBAYASHI, S.
Flowfield of a lifting rotor in hover - A Navier-Stokes simulation p 1024 A92-54906
OBAYASHI, SHIGERU
Freestream capturing for moving coordinates in three dimensions p 432 A92-31186
Navier-Stokes computations for oscillating control surfaces
[AIAA PAPER 92-4431] p 1026 A92-55355
Unsteady shock-vortex interaction on a flexible delta wing p 1030 A92-56157
Algorithm and code development for unsteady three-dimensional Navier-Stokes equations
[NASA-CR-190077] p 692 N92-25264
Transonic aeroelastic computations on wings using Navier-Stokes equations p 721 N92-27957
OBERKAMPF, W. L.
Joint computational and experimental aerodynamics research on a hypersonic vehicle
[DE92-013439] p 943 N92-30367
OBERKAMPF, WILLIAM L.
Joint computational/experimental aerodynamics research on a hypersonic vehicle. I - Experimental results p 812 A92-46890
Joint computational/experimental aerodynamics research on hypersonic vehicle. II - Computational results p 812 A92-46891
OBERMAYER, M.
Experience with piloted simulation in the development of helicopters p 884 N92-28528
Experience with piloted simulation in the development of helicopters
[MBB-UD-0610-91-PUB] p 889 N92-30076
OBERMEIER, F.
Sound produced by vortex-airfoil interaction
p 1136 A92-56345
OBRIEN, WALTER F.
Dynamic simulation of compressor and gas turbine performance p 869 N92-28463
OBRUBOV, A. G.
Improving the efficiency of passenger aircraft during the landing approach p 460 A92-31893
OBUKATA, M.
Helicopter rotor testing using scaled model
p 1093 A92-56076
OBYRNE, BRIAN
The Langley turbo-prop commuter design: A complete project description
[NASA-CR-189987] p 463 N92-21540
OCCHIATO, JOHN J.
Helicopter modeling requirements for full mission simulation and handling qualities assessment
p 105 A92-14364
OCHADLICK, ANDREW R., JR.
Pocono Mountain SAR data analysis for testing slant range to ground range conversion p 587 A92-35142
OCHI, K.
Study on a flight simulator of time delays
p 744 A92-43112
OCHI, YOSHIMASA
Application of the delta-operator in MIMO discrete-time adaptive flight control systems p 479 A92-29516
A restructurable flight control system design using nonlinear compensation p 745 A92-43184
The acceleration control system design of a flight vehicle using a two-wing control method p 745 A92-43185
Design of a flight control system using a feedback-error-learning-type neural network
p 1132 A92-56067
Application of restructurable flight control system using nonlinear control to an airliner p 1084 A92-56068
OCHIAI, JUN-ICHI
Fundamental studies on Marangoni convection related to Bridgman crystal growth p 1111 A92-53758
OCONNOR, D. G.
Ultra-high temperature (greater than 2000 C) testing capability at Oak Ridge National Laboratory for carbon materials in air, inert gas and vacuum
[DE92-004445] p 385 N92-18069
ODAM, G. A. M.
Lightning protection requirements for aircraft: A proposed specification
[RAE-TM-FS(F)-632-REV-ISSUE] p 187 N92-14007
ODGERS, J.
Acoustic control of combustor primary zone air-jet mixing
[AIAA PAPER 92-3651] p 1067 A92-54104
OECHSLE, V. L.
A parametric numerical study of mixing in a cylindrical duct
[NASA-TM-105695] p 738 N92-26553
OELCHER, W.
Induction bonding procedures for graphite reinforced thermoplastic assemblies p 994 A92-51545
OELKER, H.-CHR.
Vortex formation over a close-coupled canard-wing-body configuration in unsymmetrical flow p 85 N92-13010
OGATA, TAKASHI
Change and reliability of the DC-9-81 digital flight guidance system p 1084 A92-56086
OGAWA, AKINORI
Nonlinear transient analysis of composite ATP blade model p 294 A92-23111
OGAWA, S.
Computation of scramjet inlet flow
p 430 A92-30541
OGAWA, SATORU
Computational aerodynamic simulation on HOPE
p 251 A92-22635
HOPE looks to CFD for help p 386 A92-24910
OGAWA, TETSU
Numerical computation of compressible flow around an object of complex shape p 429 A92-30517
OGAWA, TOSHIO
Functional mock-up tests for flight control system of the NAL QSTOL research aircraft 'ASKA'
[SAE PAPER 912036] p 881 A92-45422
OGBURN, MARILYN E.
Application of piloted simulation to high-angle-of-attack flight-dynamics research for fighter aircraft
p 886 N92-28551
OGDEN, T. P.
Analysis technique for lightning attachment zoning of aircraft p 186 A92-20126
OGINO, J.
Non-planar wing design by Navier-Stokes inverse computation
[AIAA PAPER 92-0285] p 319 A92-25738
OGINO, JUN
Aerodynamic design of a nonplanar airfoil by an inverse method with Navier-Stokes equations
p 711 A92-43197
OGUMA, MASATO
Test results of the expander cycle air turbo ramjet for a future space plane
[IAF PAPER 91-271] p 120 A92-14709
OHAMA, Y.
Aerodynamic characteristics of a hypersonic aircraft
p 711 A92-43226
OHARA, M.
Gamma Group-The Pale Horse: A proposal in response to a commercial air transportation study ort study
[NASA-CR-190019] p 731 N92-26435
OHASHI, TOSHIJI
Advanced display system for an aircraft payload
p 735 A92-43221
OHERN, T. J.
In situ measurement of particle formation in heated jet fuels: A new application of photon correlation spectroscopy
[DE92-003641] p 488 N92-20132
Reynolds number dependence of the drag coefficient for laminar flow through fine-scale screens
[DE92-002930] p 765 N92-26698
OHERN, TIM
Advanced thermally stable, jet fuels development program annual report. Volume 1: Model and experiment system development
[AD-A249625] p 988 N92-31462
OHJI, MICHIO
Prospects of turbulence research by means of testing bodies in motion p 30 A92-12194
OHKAMI, Y.
Airbreathing engine selection criteria for SSTO propulsion system
[IAF PAPER 92-0658] p 1071 A92-57099
OHMOMO, MITSUHARA
Development of ITS90 small gas turbine engine
p 1070 A92-55500
OHMORI, H.
New robust adaptive control system using multiple regularization parameters p 51 A92-11455
OHMORI, SHINGO
ETS-V/EMSS mobile satellite communication experiments p 395 A92-26776
Experiments on aeronautical satellite communications using ETS-V p 395 A92-26779
High gain airborne antenna for satellite communications p 354 A92-26780
Experiments on aeronautical satellite communications using ETS-V satellite p 639 A92-40187
High gain airborne antenna for satellite communications p 639 A92-40188

Beam scanning error of phased array antenna
p 676 A92-40189
History of aeronautical satellite communications
p 1046 A92-56088

OHMORI, YASUNORI
CFD application to 2D/3D flow fields in Scramjet engine p 170 A92-17501
Conceptual design of scramjet engine
p 1065 A92-53490

OHNO, MASAHIRO
Flight control system design using H(infinity) optimal control p 1083 A92-56030

OHNSORG, R. W.
Development and characterization of high strength SiC rotors
[ASME PAPER 91-GT-191] p 149 A92-15617
The use of CT for dimensional measurements of green and sintered ceramic components p 490 A92-28592

OHNUKI, TAKESHI
Aero-structural integrated design of forward swept wing
[SAE PAPER 912021] p 790 A92-45414

OHOTA, S.
Polar patrol balloon
[AIAA PAPER 91-3688] p 15 A92-11031

OHTA, HIROBUMI
Measurement of angle of attack using a five-hole arrow head pitot tube p 941 A92-53009
Motion analysis of 2-dimensional flat plate in ground effect p 1030 A92-56053
Estimation of aircraft inertial characteristics using maximum likelihood estimation p 1084 A92-56057

OHTA, YUZO
Polygon interval arithmetic and design of robust control systems p 49 A92-11418

OHTAKE, K.
An analysis of impact resistance of composite blades for turbo-fan engines p 294 A92-23109

OHTAKE, KUNIHIKO
An analysis of impact resistance of composite fan blade p 293 A92-22523
Nonlinear transient analysis of composite ATP blade model p 294 A92-23111
An analysis of impact resistance of composite blades for aircraft engines (Analysis with two dimensional and three dimensional finite elements) p 579 A92-32562
An analysis of the effect of centrifugal force on the impact resistance of composite fan blades for turbo-fan engines
[SAE PAPER 912047] p 861 A92-45431
Finite elements analysis of flexural edge wave for composite fan blades
[SAE PAPER 912048] p 861 A92-45432

OHWAKI, KATSURA
Effectiveness of plasma torches for ignition and flameholding in scramjet p 737 A92-44524

OI, M.
Study on the lower aspect view of a helicopter simulator p 748 A92-43110

OJHA, SHIVA K.
Optimization of constant altitude-constant airspeed flight of turbojet aircraft p 845 A92-46815

OJI, MICHIO
Proceedings of the Seminar on Investigation and Control of Boundary-Layer Transition
[NAL-SP-11] p 400 N92-18483

OK, HONAM
BUWICE - An interactive icing program applied to engine inlets
[AIAA PAPER 92-3179] p 922 A92-48794

OKA, MASARU
Navigation experiment on an aircraft using the GPS-INS navigation system. I - Introduction to the system
p 726 A92-43122

OKA, T.
Operation of the on-board measuring system of the STOL research aircraft Asuka p 734 A92-43139

OKA, TOSHIHARU
Observational study of pool boiling under microgravity
p 757 A92-41060

OKABE, AKIRA
Field telemetry of blade-rotor coupled torsional vibration at Matuura Power Station Number 1 unit
p 222 N92-14348

OKADA, H.
Operation of the on-board measuring system of the STOL research aircraft Asuka p 734 A92-43139

OKADA, NORIAKI
Flight test results and upper surface blowing (USB) technology of the STOL research aircraft Asuka
p 730 A92-43142
Path angular control of the STOL research aircraft Asuka p 745 A92-43146
Functional mock-up tests for flight control system of the NAL QSTOL research aircraft 'ASKA'
[SAE PAPER 912036] p 881 A92-45422

OKAJIMA, ATSUSHI
Change of flow about an elongated rectangular cylinder in a range of Reynolds numbers of 200 to 0.7 x 10 exp 4 p 522 A92-35997

OKAMOTO, OSAMU
Quaternion and Euler angles in kinematics
[NAL-TM-636] p 909 N92-28836

OKAMOTO, S.
An experimental and numerical study of confined axisymmetric jet with a bluff body p 621 A92-40106

OKAYAMA, YUICHI
Numerical simulation of supersonic unsteady flow using a panel method p 1030 A92-56048

OKAZAKI, TAKURO
Research on aircraft engines p 558 A92-35912

OKAZAWA, SHIN
A design of strongly stabilizing controller
[SAE PAPER 912081] p 917 A92-45456

OKEEFE, A.
Laser based, non-intrusive measurement system for analysis of jet engine flows
[AD-A242398] p 279 N92-17011

OKIISHI, T. H.
An experimental investigation of the flow in a diffusing S-duct
[AIAA PAPER 92-3622] p 1021 A92-54090

OKIISHI, THEODORE H.
Visualization of boundary-layer development on turbomachine blades with liquid crystals
[NASA-CR-190433] p 742 N92-27519

OKLADNIKOV, D. E.
Interference of high-mounted propfan nacelles with an unswept wing and ways to attenuate it
p 460 A92-31881

OKU, H.
Study on the effective utilization of the current flight simulator p 748 A92-43113

OKUBA, T.
Measurement of position and attitude using laser and retro-reflectors p 1047 A92-56120

OKUMURA, H.
An analysis of impact resistance of composite blades for turbo-fan engines p 294 A92-23109

OKUMURA, HIDEHITO
An analysis of impact resistance of composite fan blade p 293 A92-22523
Nonlinear transient analysis of composite ATP blade model p 294 A92-23111
An analysis of impact resistance of composite blades for aircraft engines (Analysis with two dimensional and three dimensional finite elements) p 579 A92-32562
An analysis of the effect of centrifugal force on the impact resistance of composite fan blades for turbo-fan engines
[SAE PAPER 912047] p 861 A92-45431
Finite elements analysis of flexural edge wave for composite fan blades
[SAE PAPER 912048] p 861 A92-45432
Development of pre- and post-processor system for structural analysis
[NAL-TM-628] p 681 N92-25403

OKUNO, YOSHINORI
An adaptive flight control for use in connection with helicopter engine failure p 745 A92-43159
Optimal control of helicopters following power failure
[AIAA PAPER 92-4471] p 1076 A92-55231
Optimal launch trajectory of a hypersonic research vehicle
[AIAA PAPER 92-4302] p 1103 A92-55310
Flight evaluation of navigation systems including MLS using NAL Do228 - Results of MLS
p 1047 A92-56117
Optimal control of tiltrotor aircraft following power failure p 1085 A92-56303

OKUNUKI, T.
Measurements of turbulence in hypersonic flow
p 1092 A92-56005

OKURA, K.
Noise test of high-speed counterrotation propeller in low-speed wind tunnel p 1135 A92-56055

OKUYAMA, MASAHIRO
Wind tunnel investigation of an improved upper surface blown flap transport semi-span model
[SAE PAPER 911993] p 789 A92-45395

OKUYAMA, TETSU
Study on two-dimensional jet mixing with a vertical supersonic flow p 429 A92-30530

OLCMEN, SEMIH M.
Influence of wing shapes on the surface pressure fluctuations of a wing-body junction
[AIAA PAPER 92-0433] p 327 A92-26280
An experimental evaluation of some turbulence models from a three-dimensional turbulent boundary layer around a wing-body junction p 620 A92-40087

OLDFIELD, M. L. G.
An Axial Turbobrake
[ASME PAPER 91-GT-1] p 147 A92-15501

OLEARY, C. O.
Measurement of derivatives due to acceleration in heave and sideslip p 364 N92-18785

OLEJAK, D.
Investigation of a plate-ramp-configuration by means of laser Doppler anemometry at Mach 2.95
[AIAA PAPER 92-3956] p 1097 A92-56784

OLEJNIK, A.
A model of a deformable aeroplane with a wing of low aspect ratio and movable control surfaces for studying natural vibrations p 744 A92-41528

OLESKIW, M. M.
Laboratory evaluation of a sensor for detection of aircraft wing contaminants
[AIAA PAPER 92-0301] p 369 A92-25753
Freezing precipitation on lifting surfaces
[NRC-32124] p 448 N92-20156

OLIANIUK, PETR V.
Processing and displaying radio navigation data
p 266 A92-21683

OLIVA, PAUL V.
Integral wing/fuel box p 958 A92-51569

OLIVA, S. M.
A general nonlinear dynamical analysis of a second-order, one-dimensional, theoretical compression system model p 509 A92-29374

OLIVERO, PHILIPPE
Experimental study of the wall pressure fluctuations under a turbulent boundary layer downstream of tandem aerofoil external manipulators
[REPT-207-90-78] p 500 N92-20497

OLIVIER, H.
High enthalpy testing in the Aachen (Fed. Republic of Germany) shock tunnel TH 2 p 208 N92-15021

OLLERHEAD, J. B.
Airport noise contours - Converting from NNI to Leq
p 686 A92-39053

OLLEVIER, THOMAS E.
DRES unmanned aerial vehicle data link research
[AD-A244272] p 365 N92-19030

OLMOS, M.
Hypersonic plasma predictions at nonzero angle of attack
[AIAA PAPER 92-3027] p 925 A92-47028

OLSEN, GEROLD
Computation of aircraft noise exposure using digitized topography data p 687 A92-39058

OLSEN, H.
Advanced method for single event aircraft noise analysis p 693 A92-39060

OLSEN, MICHAEL E.
Low aspect ratio wing code validation experiment
[AIAA PAPER 92-0402] p 324 A92-26255

OLSON, JAMES R.
Fabrication and mechanical properties of an optically transparent glass fiber/polymer matrix composite
p 891 A92-45630

OLSON, JOHN
The H-53E Super Stallion - A cost-effective solution to multi-service medium/heavy lift requirements
p 647 A92-40388

OLSON, LARRY E.
The design of test-section inserts for higher speed aeroacoustic testing in the Ames 80- by 120-foot wind tunnel
[NASA-TM-103915] p 927 N92-28909

OLSON, LAWRENCE E.
Future experimental needs in low-speed aerodynamics
[AIAA PAPER 92-0157] p 254 A92-23772

OLSON, REO
Passive acoustic range estimation of helicopters
[AD-A248033] p 926 N92-28302

OLSON, RICHARD F.
Simulation of radar clutter and jet engine modulation using digital quadrature modulator p 216 A92-19091

OLSON, ROHN
V-22 Osprey tiltrotor blade fold/wing stow system design and testing p 109 A92-14420

OLSON, S. H.
A comparison of the performance of two gust front detection algorithms using a length-based scoring technique
[AD-A250862] p 1004 N92-32103

OLSSON, MATS-OLOF
Damage tolerance of the fighter aircraft 37 Viggen. I - Analytical assessment. II - Experimental verification
p 192 A92-19819

OLWI, I. A.
Aircraft spoiler effects under wind shear
[AIAA PAPER 92-2642] p 796 A92-45509

OLWI, IBRAHIM
Effect of wing tip vortices on a trailing aircraft
p 935 A92-50303

OMIYAYAMA, FUMIO
Study of cavity pumping in supersonic internal flow
p 429 A92-30538

OMKAR, S. N.
Software package for preliminary design of helicopter p 775 A92-41195
ONATE, E.
Flow and temperature computations for space vehicles using adaptive finite element techniques p 181 N92-14990
ONDA, M.
Stratospheric lighter-than-air powered platform p 110 A92-15334
The concept of an unmanned flying vehicle at high altitude p 731 A92-43242
ONDA, MASAHIKO
An acrobatic airship 'Acrostat'
[SAE PAPER 911994] p 843 A92-45396
High-altitude lighter-than-air powered platform
[SAE PAPER 912054] p 844 A92-45438
ONG, C. L.
Some results on metal and composite patch reinforcement of aluminum honeycomb panel p 216 A92-18830
ONG, C.-L.
The development and test of thermoplastic composite speed brake p 272 A92-24178
The reinforcing effect of composite patch repairs on metallic aircraft structures p 419 A92-30498
The evaluation of non-tank surface treatments for aluminium bonding repairs p 761 A92-42502
ONG, CHING-LONG
The study on the composite-patching repairs for metallic aircraft structures p 36 A92-10285
ONG, SHAW Y.
2-D and 3-D minimum-time-to-turn flights via parameter optimization
[AIAA PAPER 92-0731] p 379 A92-27083
ONISHCHENKO, T. S.
Evaluation of the fungicide properties of antifreeze additives for jet fuels p 141 A92-15070
ONISHI, T.
Optimization of composite material wing of fighter type aircrafts p 1053 A92-56018
ONKEN, R.
Knowledge-based planning for controlled airspace flight operation as part of a cockpit assistant p 727 N92-27895
ONNO, R.
Trajectories and stability of trailing vortices very near the ground
[NRC-32151] p 716 N92-27344
ONO, KENJI
Flow around two square cylinders in staggered arrangements p 761 A92-42797
ONO, KIYOAKI
Study on nozzle flow diffusion p 429 A92-30531
ONO, KOJI
Navigation experiment on aircraft flight using the GPS-INS navigation system. II - Test results p 726 A92-43123
ONO, M.
Experiment of static and dynamic characteristics of spiral grooved seals p 223 N92-14361
ONO, TAKATSUGU
Flight test of a flight reference display for powered-lift STOL aircraft p 1064 A92-56059
Flight evaluation of navigation systems including MLS using NAL Do228 - Outline p 1047 A92-56116
Flight evaluation of navigation systems including MLS using NAL Do228 - Results of MLS p 1047 A92-56117
Identification of the stability and control derivatives of a DLC-flap system for VSRA
[NAL-TR-1116] p 283 N92-17917
A preliminary flight test on a basic performance of the flight research airplane Do 228: Velocity vs glide path angle
[NAL-TM-613] p 359 N92-18482
NAL Dornier 228-200 flight research airplane: Present status and outline of the installed equipment
[NAL-TM-637] p 732 N92-27429
ONODERA, H.
Double piston shock-wave valve p 1117 A92-54938
ONOFRI, M.
Nonequilibrium hypersonic inviscid steady flows p 176 A92-20737
Influence of chemical modeling on the solution of hypersonic shock layers p 183 N92-15016
ONOPRIENKO, E. I.
Synthesis of the algorithm of a spatial-temporal discriminator and the potential accuracy of the velocity meter p 41 A92-12828
ONORATO, M.
Skin friction measurements in 3-D boundary layers p 1092 A92-54351
ONOZUKA, SACHIKO
A consideration on air traffic control processing capability in terminal area p 1047 A92-56110
ONUSTACK, STEVEN A.
The large scale test control systems designed and built by the Boeing Company to support the 757 and 767 major fatigue tests
[SAE PAPER 911985] p 881 A92-45388
OOKAMI, YOSHIAKI
Quaternion and Euler angles in kinematics
[NAL-TM-636] p 909 N92-28836
OONUMA, MASAHIKO
An experimental program concerning a satellite data link for oceanic ATC p 1046 A92-56093
OOSAWA, Y.
Unsteady flow within centrifugal compressor channels under rotating stall and surge
[ASME PAPER 91-GT-85] p 670 A92-36901
OOTAKE, KUNIHIKO
Development of pre- and post-processor system for structural analysis
[NAL-TM-628] p 681 N92-25403
OOTSUBO, AKIRA
Study of potassium turbine electric generator system p 1129 N92-33794
ORAN, E. S.
Numerical simulations of the structure of supersonic shear layers p 3 A92-10574
Numerical simulations of unsteady reactive flows in a combustion chamber p 39 A92-11761
The effects of viscosity and diffusion on a supersonic mixing layer p 622 A92-40143
ORBANSKI, B.
High density fuel qualification for a gas turbine engine
[AIAA PAPER 92-0684] p 389 A92-27051
OREN, N.
The influence of a retarding rocket on parameter limits for reentry trajectories p 211 N92-15037
ORF, M. A.
Nonflammable hydraulic power system for tactical aircraft. Volume 2: Equipment and systems test and evaluation
[AD-A239805] p 35 N92-10100
ORKISZ, M.
An estimate of the influence of the compressor stability margin on the pick-up time of a turbojet engine p 654 A92-37423
An estimate of the influence of the compressor stability margin on the thrust of a turbojet engine p 654 A92-37424
Simulation analysis of the influence of variation in some selected design and control parameters on the acceleration time of a turbojet engine p 970 A92-52890
ORKISZ, MAREK
The effect of air-compressor adjustment by means of air-bleed on the reserve of its stable operation p 471 A92-29973
ORKWIS, PAUL D.
Newton's method solver for high-speed viscous separated flowfields p 176 A92-20736
Newton's method solver for the axisymmetric Navier-Stokes equations p 703 A92-41269
ORLIK-RUECKEMANN, K. J.
Design and testing of high-performance parachutes
[AGARD-AG-319] p 345 N92-18269
ORLINO, DREW G.
1991-92 AHS Technical Committee highlights - Manufacturing and product assurance p 609 A92-40396
ORLINSKA, MALGORZATA
Automation of the measurement process in the N2 wind tunnel with the SPITA N-3 system p 30 A92-12347
ORME, JOHN S.
Subsonic flight test evaluation of a performance seeking control algorithm on an F-15 airplane
[AIAA PAPER 92-3743] p 878 A92-49109
Subsonic flight test evaluation of a propulsion system parameter estimation process for the F100 engine
[AIAA PAPER 92-3745] p 866 A92-49110
Subsonic flight test evaluation of a performance seeking control algorithm on an F-15 airplane
[NASA-TM-4400] p 973 N92-31275
ORMISTON, ROBERT A.
Finite-element analysis and multibody dynamics issues in rotorcraft dynamic analysis p 1055 A92-56286
First level release of 2GCHAS for comprehensive helicopter analysis p 1133 A92-56339
ORNGARD, GARY M.
A laser fluorescence anemometer system for the Langley 16- by 24-inch water tunnel p 1092 A92-54347
Measurement of vortex flow fields
[NASA-CR-189543] p 443 N92-20283
ORR, G. D.
Balloon altitude control by valving - A review and comparison of actual flight data and vertical performance analysis results
[AIAA PAPER 91-3669] p 14 A92-11016
ORSZAG, S.
Direct computation of turbulence and noise
[NASA-CR-187616] p 236 N92-14788
ORTWERTH, J. P.
Inviscid analysis of a dual mode scramjet inlet p 80 A92-17198
ORTWERTH, P. J.
Flowpath optimization for hypersonic vehicles
[AIAA PAPER 91-5043] p 437 A92-31688
ORTWERTH, PAUL J.
Three dimensional hypersonic inlets - Low speed performance
[AIAA PAPER 91-5021] p 171 A92-17817
ORYANG, D.
A surface definition code for turbine blade surfaces
[DE92-010574] p 1004 N92-31498
OSAKA, HIDEO
Effect of controlled longitudinal vortex arrays on the development of a turbulent boundary layer p 614 A92-38856
OSBORN, RUSS F.
An experimental study of pneumatic vortex flow control on high angle of attack forebody model
[AIAA PAPER 92-0018] p 247 A92-22140
OSBORN, RUSSELL F.
Forebody vortex control aeromechanics p 380 N92-18792
OSDER, STEPHEN
Practical robustness testing for helicopter flight control systems p 132 A92-14340
OSE, K.
Introduction to the traffic alert and collision avoidance system (TCAS) III p 734 A92-43150
OSEGUERA, ROSA M.
Airborne in situ computation of the wind shear hazard index
[AIAA PAPER 92-0291] p 351 A92-25744
OSER, RANDALL L.
An analysis of aircrew communication patterns and content
[AD-A246618] p 907 N92-28253
OSHCHEPKOV, M. IU.
Pulsation characteristics of one-phase and two-phase steam flows in Laval nozzles under off-design conditions p 1019 A92-53882
OSHIMA, H.
Measurements of the velocity and vorticity fields around a pitching airfoil
[AIAA PAPER 92-2626] p 794 A92-45498
OSHIMA, SHUZO
Oscillation of nearly circular shock waves p 146 A92-15358
Resonance of circular shock waves p 395 A92-26795
OSLAC, MICHAEL J.
A lightweight loudspeaker for aircraft communications and active noise control p 1125 N92-32964
OSMUNDSEN, EYJOLF
A mobile system for measuring airport noise p 688 A92-39099
OSSWALD, G. A.
Study of role of unsteady separation in formation of dynamic stall vortex
[AIAA PAPER 92-0196] p 257 A92-23804
OSTAPENKO, N. A.
Minimum-drag bodies moving in locality-law media p 779 A92-42732
OSTER, REINHOLD
Computed tomography (CT) as a nondestructive test method used for composite helicopter components p 1121 A92-56276
Computed Tomography (CT) as a nondestructive test method used for composite helicopter components
[MBB-UD-0603-91-PUB] p 910 N92-29873
OSTIGUY, N. J. G.
Potential impact of FANS - Far-reaching and positive p 267 A92-23296
OSTROFF, AARON J.
High-alpha application of variable-gain output feedback control p 380 A92-28152
OSWALD, FRED B.
Modal simulation of gearbox vibration with experimental correlation
[AIAA PAPER 92-3494] p 1112 A92-54036
Analysis and modification of a single-mesh gear fatigue rig for use in diagnostic studies
[NASA-TM-105416] p 773 N92-27879
Modal simulation of gearbox vibration with experimental correlation
[NASA-TM-105702] p 1002 N92-31485
OTA, H.
Flight control system design p 776 A92-43181
OTA, T.
Study on small stalker tube performance and numerical calculation p 748 A92-43099

OTAWARA, YASUHIKO
Field telemetry of blade-rotor coupled torsional vibration at Matuura Power Station Number 1 unit
p 222 N92-14348
OTHMER, P.
Detonation duct gas generator demonstration program
[AIAA PAPER 92-3174] p 1066 A92-54011
OTT, JEAN E.
Smart structures - A damage detection concept
p 491 A92-28672
OUYANG, NING
Flow pattern characterization and heat transfer behavior in a boiling two-phase flow in an inclined pipe
p 493 A92-29722
OUZTS, PETER J.
Integrated flight/propulsion control design for a STOVL aircraft using H-infinity control design techniques
p 476 A92-29093
IMPAC - An integrated methodology for propulsion and airframe control p 477 A92-29118
OVERSTREET, MARK A.
Fiber optic speed sensor for advanced gas turbine engine control p 857 A92-48044
OWA, H.
Flight test results and upper surface blowing (USB) technology of the STOL research aircraft Asuka
p 730 A92-43142
OWEN, ALBERT K.
A comparison of predicted and measured inlet distortion flows in a subsonic axial inlet flow compressor rotor
[NASA-TM-105427] p 633 N92-26104
OWEN, ALBERT KARL
Effects of inlet distortion on the development of secondary flows in a subsonic axial inlet compressor rotor p 89 N92-13030
OWEN, F. K.
An assessment of particle velocimetry potential in hypersonic flow
[AIAA PAPER 92-0010] p 247 A92-22135
A laser fluorescence anemometer system for the Langley 16- by 24-inch water tunnel
p 1092 A92-54347
OWEN, F. KEVIN
Measurement of vortex flow fields
[NASA-CR-189543] p 443 N92-20283
OWEN, J. M.
Self-induced flow in a stepped rotating tube
[ASME PAPER 91-GT-276] p 152 A92-15673
OWEN, STEPHEN J.
Navier-Stokes and Euler solutions for an unmanned aerial vehicle
[AIAA PAPER 92-2609] p 792 A92-45483
OWEN, T. E.
Evaluating the velocity accuracy of an integrated GPS/INS system: Flight test results
[DE92-007519] p 640 N92-25470
OWENS, JOHN K.
Development of a multi-computer in-flight data acquisition and analysis system for general aviation aircraft
[AIAA PAPER 92-1037] p 553 A92-33218
OWSLEY, LISA
Artificial intelligence in the helicopter cockpit of the future p 964 A92-49271
OYAMA, O.
Development of the D-size liquid crystal flat panel display for aircraft p 734 A92-43208
Evaluation test on the simulator of the liquid crystal flat display. II p 734 A92-43209
OYAMA, TOSHIO
Magnetohydrodynamic boundary layer flow over a rotating disk p 304 A92-21338
OYANAGI, YUKIO
The traffic alert and collision avoidance system (TCAS) for air navigation p 734 A92-43151
OZ, HAYRANI
Integrated aeroelastic control optimization of laminated composite lifting surfaces p 481 A92-32248
OZBAY, HITAY
Abstract model and controller design for an unstable aircraft p 380 A92-28153
OZCAN, OKTAY
Cylinder-induced shock-wave boundary-layer interaction p 433 A92-31188
OZELTON, M. W.
Durability and damage tolerance of aluminum castings
[AD-A245237] p 490 N92-21159
OZEROV, V. N.
Control of the development of boundary layer disturbances p 423 A92-30126
Flight studies of the riblet effect on drag variation
p 438 A92-31871
OZGUR, DINCER
Gas turbine exhaust system silencing design
p 882 A92-47365

P

PACHTER, M.
Automatic formation flight control
[AIAA PAPER 92-4473] p 1076 A92-55233
PACIA, ARNEL
Acoustic testing at elevated temperatures
p 981 A92-51405
Add-on damping treatment for life extension of the F-15 upper-outer wing skin
[AD-A246149] p 746 N92-27577
PACKARD, JAMES D.
A ballistic investigation of the aerodynamic characteristics of a blunt vehicle at hypersonic speeds in carbon dioxide and air
[AIAA PAPER 92-0328] p 322 A92-25775
PADFIELD, G. D.
Creation of a living specification for an experimental helicopter active flight control system through incremental simulation p 1057 A92-56312
PADFIELD, GARETH D.
The development of a requirement specification for an experimental active flight control system for a variable stability helicopter: An Ada simulation in JSD
p 135 N92-12466
Design of experiments p 273 N92-17154
SA 330 Puma identification results
p 274 N92-17162
Application areas for rotorcraft system identification: Simulation model validation p 274 N92-17164
PADHYE, VIDYA A.
Full Navier-Stokes analysis of a three-dimensional scramjet inlet p 934 A92-50272
PADOVAN, J.
Engine dynamic analysis with general nonlinear finite element codes
[NASA-CR-187222] p 44 N92-11379
PADOVAN, JOE
Aircraft landing-induced tire spinup
p 193 A92-20209
PADUANO, J.
Active control of rotating stall in a low speed axial compressor
[ASME PAPER 91-GT-88] p 122 A92-15553
Parameter identification of compressor dynamics during closed-loop operation p 508 A92-29313
Dynamic control of aerodynamic instabilities in gas turbine engines p 870 N92-28466
Active control of compressor surge and stall
[AD-A252771] p 1126 N92-33498
PAGAN, DIDIER
Basic experiment on a supersonic vortex flow around a missile body p 705 A92-41545
PAGAN, G.
Aero-propulsive effects on configuration shaping
[AIAA PAPER 91-5064] p 459 A92-31691
PAGANO, PETER J.
Prediction of forces and moments for hypersonic flight vehicle control effectors
[NASA-CR-188954] p 33 N92-11070
PAGE, G. J.
Prediction and measurement of jet flowfield features for ASTOVL aircraft p 787 A92-45318
PAGE, GERALD T.
Impact of a process improvement program in a production software environment: Are we any better?
p 413 N92-19422
PAGE, LYMAN A.
Resonant cryogenic chopper p 294 A92-22796
PAGE, M.
Continuous flying quality improvement - The measure and the payoff
[AIAA PAPER 92-4327] p 1073 A92-55171
PAGE, MARK A.
Design and analysis issues of integrated control systems for high-speed civil transports
[NASA-CR-186022] p 979 N92-31656
PAGGI, B.
EH 101 ship interface trials: Flight test programme and preliminary results p 465 N92-21964
PAGNANO, G.
Current European research activities in helicopter interactional aerodynamics p 1058 A92-56330
Correlation of flight, tunnel and prediction data on a helicopter main rotor p 1059 A92-56350
PAGNANO, GIUSEPPE
EUROFAR airframe aerodynamic design
p 546 A92-35750
PAGNIEZ, PIERRE
The role of simulation for the study of APIS (piloting support by synthetic imagery) p 885 N92-28544
PAGUIO, CECILIA
Scorpion: Close Air Support (CAS) aircraft
[NASA-CR-189974] p 462 N92-20664
PAHLE, JOSEPH W.
Controls for agility research in the NASA High-Alpha Technology Program
[SAE PAPER 912148] p 661 A92-39984
PAI, D. M.
Behavior of aircraft tire coupons under various loading conditions
[AD-A241416] p 116 N92-13063
PAI, T. G.
Subcritical flow studies on two-dimensional external compression supersonic inlets p 713 A92-44518
PAILHAS, G.
Influence of suction through a slot on a turbulent boundary layer p 622 A92-40127
Characteristics of a boundary layer in a leading edge vortex p 86 N92-13012
PAILLARD, JACQUES
Advanced Study for Active Noise Control in Aircraft (ASANCA)
[AIAA PAPER 92-2092] p 1137 N92-32956
PAILLERE, HENRI
A wave-model-based refinement criterion for adaptive-grid computation of compressible flows
[AIAA PAPER 92-0322] p 321 A92-25769
PAIPETIS, S. A.
Jet fuel absorption and dynamic mechanical analysis of carbon fibre composites p 1110 N92-33050
PAISLEY, D. J.
The aerodynamic assistant - A tool for V/STOL aircraft conceptual design p 545 A92-35737
PAJERSKI, ROSE
Towards understanding software: 15 years in the SEL
p 413 N92-19423
PAK, A. S.
Several results of lidar measurements of the characteristics of oblique visibility at an airfield
p 45 A92-12844
PAK, CHAN-GI
New time-domain technique for flutter boundary identification
[AIAA PAPER 92-2102] p 588 A92-35673
Adaptive active flutter suppression of wings in subsonic and transonic flight regimes p 553 N92-24010
PALASIS, D.
Development of a conceptual design method for rotary-wing aircraft using digital computers
p 1058 A92-56340
PALAZOGLU, A.
An framework for robust flight control design using constrained optimization
[AIAA PAPER 92-4603] p 1131 A92-55282
PALKIN, V. A.
The study of experimental turboramjets
[AIAA PAPER 92-3720] p 1067 A92-54135
PALLEGOIX, JEAN-FRANCOIS
Transitional flows around re-entry bodies
p 184 N92-15035
PALLISTER, KEITH
Comparison of recent results from different wind tunnel facilities along with comparisons of measured flight results and wind tunnel based predictions
[AIAA PAPER 92-3985] p 1060 A92-56809
PALLONEN, JORMA
X-band side-looking airborne radar for remote sensing
p 554 A92-34976
PALMA, J. M. L. M.
Calculations of the dilution system in an annular gas turbine combustor p 494 A92-31164
PALMBERG, BJORN
Damage tolerance of the fighter aircraft 37 Viggen. I - Analytical assessment. II - Experimental verification
p 192 A92-19819
PALMER, CARL ALEXANDER
Dynamic simulation of a solid fuelled gas turbine system p 592 N92-22315
PALMER, EVERETT A.
The impact of cockpit automation on crew coordination and communication. Volume 1: Overview, LOFT evaluations, error severity, and questionnaire data
[NASA-CR-177587] p 93 N92-13044
PALMER, G. E.
Earth atmospheric entry studies for manned Mars missions p 442 A92-32251
PALMER, GRANT
Effective treatments of the singular line boundary problem for three dimensional grids
[AIAA PAPER 92-0545] p 342 A92-28202
Thermochemical nonequilibrium flow computations of flow around the aeroassist flight experiment
p 713 A92-44368
PALMER, J. L.
Planar fluorescence imaging of a transverse jet in a supersonic crossflow p 755 A92-44501
PALMER, R. W.
A low-power, high-efficiency Ka-band TWTA
p 671 A92-38163

PALMIERI, M.
A low noise propulsion concept for the supersonic transport
[ASME PAPER 91-GT-397] p 127 A92-15727
PALOTAS, P. A.
Analysis of unsteady aerodynamic and flutter characteristics of an aeroelastic model in transonic flow
p 720 N92-27953
PALTRINIERI, MASSIMO
A constraint satisfaction approach to operative management of aircraft routing p 350 A92-25181
PALUCH, B.
Design and manufacturing of torsional flexible blade models p 547 A92-35780
A finite element method for shear stresses calculation in composite blade models p 1121 A92-56322
PALUMBO, DAN
A low maintenance and highly reliable fly-by-light architecture p 975 A92-49325
PALUMBO, DANIEL L.
Advanced techniques in reliability model representation and solution
[NASA-TP-3242] p 1134 N92-33483
PAMADI, B. N.
Subcritical flow studies on two-dimensional external compression supersonic inlets p 713 A92-44518
PAN, JIAZHENG
The experimental approach to the LEBU on turbulent drag reduction p 243 A92-21469
An approach to the low-speed longitudinal aerodynamic characteristics of the joined wing configuration
p 339 A92-27909
PAN, JIEYUAN
Efficient lifting line method for computing performance of propeller p 24 A92-10956
Aerodynamic design of propeller by numerical optimization p 24 A92-10957
The effects of unsteady perturbation on vortex breakdown p 672 A92-38922
PAN, XIAOLI
The effects of unsteady perturbation on vortex breakdown *p 672 A92-38922*
PANARAS, ARGYRIS G.
Numerical investigation of the high-speed conical flow past a sharp fin p 433 A92-31468
Numerical study of secondary separation in glancing shock/turbulent boundary layer interactions
[AIAA PAPER 92-3666] p 907 A92-49087
PANATTIL, TOM X.
Stability of an adaptive controller for aircraft. I - Analysis via Liapunov theory p 976 A92-51940
PANDA, J.
Experimental investigation of the flowfield of an oscillating airfoil
[AIAA PAPER 92-2622] p 793 A92-45494
Experimental investigation of the flowfield of an oscillating airfoil
[NASA-TM-105675] p 833 N92-30182
PANDEY, AJAY K.
Three-dimensional thermal structural analysis of a swept cowl leading edge subjected to skewed shock-shock interference heating p 174 A92-20306
Thermoviscoplastic analysis of engine cowl leading edge subjected to oscillating shock-shock interaction
[AIAA PAPER 92-2537] p 583 A92-34381
PANDEY, SANDEEP
Aircraft control under conditions of windshear
p 27 A92-11384
Aircraft control for take-off in windshear
p 660 A92-36990
PANDIT, NOORULHAQ
An experimental study of pneumatic vortex flow control on high angle of attack forebody model
[AIAA PAPER 92-0018] p 247 A92-22140
PANKOW, RICHARD J.
Integrating a radar/ESM antenna suite with the S-70 helicopter p 957 A92-49333
PANNETON, B.
Trajectories and stability of trailing vortices very near the ground
[NRC-32151] p 716 N92-27344
PANOV, IU. A.
Structure of the separated flow region in a dihedral corner in front of an obstacle in supersonic flow
p 524 A92-36420
PANTON, RONALD L.
Experimental study of a vortex subjected to imposed strain
[NASA-CR-189757] p 258 N92-15969
PAO, S. P.
Computational investigation of circular-to-rectangular transition ducts
[AIAA PAPER 91-3342] p 6 A92-11605
Grid adaptation to multiple functions for applied aerodynamic analysis p 817 A92-47045
PAOLETTI, STEFANO
An unfactored implicit scheme for 3D inviscid transonic flows
[AIAA PAPER 92-2668] p 798 A92-45523
PAONESSA, A.
Active vibrations and noise control for turboprop application research program activities
p 1138 N92-32962
PAPADAKIS, MICHAEL
Experimental and computational investigation of wind tunnel effects on airfoil flow fields
[AIAA PAPER 92-0672] p 431 A92-30624
PAPAILIOU, K.
Combination of different unsteady quantity measurements for gas turbine blade fault diagnosis
[ASME PAPER 91-GT-201] p 149 A92-15624
A procedure for automated gas turbine blade fault identification based on spectral pattern analysis
[ASME PAPER 91-GT-259] p 151 A92-15661
Jet engine fault detection with discrete operating points gas path analysis p 129 A92-17200
Optimal measurement and health index selection for gas turbine performance status and fault diagnosis
[ASME PAPER 91-GT-294] p 653 A92-36889
PAPAILIOU, K. D.
Turbine cascade calculations through a fractional step Navier-Stokes algorithm
[ASME PAPER 91-GT-55] p 68 A92-15533
Unsteady Euler calculations in 2-D internal aerodynamics with introduced vorticity
[ASME PAPER 91-GT-168] p 73 A92-15603
Arbitrary blade section design based on viscous considerations - Background information
p 523 A92-36029
Arbitrary blade section design based on viscous considerations - Blade optimization p 523 A92-36030
An inverse inviscid method for the design of quasi-three dimensional turbomachinery cascades
p 523 A92-36033
Unsteady Euler calculations in 3D internal aerodynamics p 768 N92-27470
PAPAS, P.
Structure and penetration of a transverse fluid jet injected at supercritical pressure in supersonic flow
[AIAA PAPER 92-3652] p 1113 A92-54105
PAPATHANASIOU, A.
Combination of different unsteady quantity measurements for gas turbine blade fault diagnosis
[ASME PAPER 91-GT-201] p 149 A92-15624
PAPAVASSILIOU, I.
A study of coupled rotor-fuselage vibration with higher harmonic control using a symbolic computing facility
p 569 A92-35770
Coupled rotor-fuselage vibration reduction with multiple frequency blade pitch control p 1085 A92-56315
PAPAVERGOS, PANAYIOTIS G.
Spray nozzle for fire control
[CA-PATENT-APPL-SN-2-011-94] p 1125 N92-32856
PAPIRNYK, O.
Review of the European hypersonic wind tunnel performance and simulation requirements
p 209 N92-15043
PAPPAS, PAUL
An analysis of fixed wing tactical airlifter characteristics using an intra-theater airlift computer model
[AD-A246908] p 732 N92-27719
PAPROCKI, THOMAS H.
Prototype runway hold-short lighting system
[DOT/FAA/CT-TN91/43] p 31 N92-11028
Surface painted taxiway markings at Seattle-Tacoma International Airport
[DOT/FAA/CT-TN91/49] p 32 N92-11029
PARAMESWARAN, V.
Estimation of lift and drag characteristics of an aircraft from flight data p 959 A92-51942
PARASCHIVOIU, ION
Efficient panel method for vortex sheet roll-up
p 309 A92-24404
Indicial method calculating dynamic stall on a vertical *axis wind turbine* p 714 A92-44528
Navier-Stokes simulation of dynamic stall on a rotating airfoil p 626 N92-24853
PARASCHIVOIU, M.
Periodic Euler and Navier-Stokes solutions about oscillating airfoils p 626 N92-24850
PARASCHIVOIU, MARIUS
Unsteady Euler solution for oscillatory airfoil and oscillating flap
[AIAA PAPER 92-0131] p 252 A92-23751
PARASIDA, TONY
Concurrent engineering at Boeing Helicopters
p 162 A92-14393
PARDINI, S.
Use of target spectrum for detection enhancement and identification p 404 N92-19155
PAREKH, D. E.
The combined wake of an array of oscillating ribbons
p 623 A92-40180
PARET, A.
Structural optimization of aircraft practice and trends
p 551 N92-23239
PARFENENKO, N. I.
A variational method for solving the problem of motion of a profile of complex geometry in a fluid
p 397 A92-27482
PARHAM, TOM, JR.
V-22 pilot-in-the-loop aeroelastic stability analysis
p 133 A92-14422
PARIN, MICHAEL
Add-on damping treatment for life extension of the F-15 upper-outer wing skin
[AD-A246149] p 746 N92-27577
PARK, C. S.
A development of computer support system for wing design p 162 A92-15332
PARK, CHOONG S.
A development of hypermedia type database system for instruction of aircraft conceptual design
p 1132 A92-56113
PARK, CHUL
Rate parameters for coupled vibration-dissociation in a generalized SSH approximation p 235 A92-20301
Calculation of real-gas effects on blunt-body trim angles p 432 A92-31169
Laboratory simulation of aerothermodynamic phenomena - A review
[AIAA PAPER 92-4025] p 1104 A92-56847
PARK, EUI H.
Model analysis and expert system development for planning and scheduling teleoperations for aircraft turnaround functions, volume 1
[AD-A251037] p 932 N92-30253
Model analysis and expert system development for planning and scheduling teleoperations for aircraft turnaround functions. Volume 2: Top user's guide
[AD-A251083] p 932 N92-30258
PARK, K. H.
Parallel solver for trajectory optimization search directions *p 777 A92-43399*
PARK, KIHONG
Thrust laws for microburst wind shear penetration
p 873 A92-46750
PARK, MYEONG-KWAN
Oscillation of nearly circular shock waves
p 146 A92-15358
Resonance of circular shock waves
p 395 A92-26795
PARK, S. O.
Reynolds stress budget in the outwash jet arising from colliding curved wall jets p 614 A92-38860
PARK, YOUNG W.
Atmospheric disturbance model for aircraft and space capable vehicles
[AIAA PAPER 92-0294] p 407 A92-25747
PARKER, E. A.
Aero-propulsive effects on configuration shaping
[AIAA PAPER 91-5064] p 459 A92-31691
PARKER, JOHN T.
Naval Postgraduate School aircraft synthesis program (user's manual)
[AD-A246198] p 777 N92-26458
PARKER, JON
Comparison of recent results from different wind tunnel facilities along with comparisons of measured flight results and wind tunnel based predictions
[AIAA PAPER 92-3985] p 1060 A92-56809
PARKER, NIGEL
Design and flight test of a differential GPS/inertial navigation system for approach/landing guidance
p 97 A92-16650
Differential GPS/inertial navigation approach/landing flight test results p 956 A92-51009
PARKER, R. J.
Holographic flow visualization in rotating turbomachinery
[PNR-90837] p 500 N92-20491
PARKER, T. E.
Supersonic combustor testing using optical diagnostics and a high enthalpy shock tunnel
[AIAA PAPER 92-0761] p 384 A92-27102
PARKINSON, BRADFORD W.
Wide area differential GPS p 101 A92-16966
PARKS, EDWIN K.
A DFW microburst model based on DL-191 data
p 17 A92-11380
Correction of sideslip-induced static pressure errors in flight-test measurements p 309 A92-24416
PARKS, MARK A.
Advanced Transport Operating System (ATOPS) control display unit software description
[NASA-CR-189606] p 652 N92-24689

PARKS, STEVEN J.
Application of the Chimera overlapped grid scheme to simulation of Space Shuttle ascent flows
p 945 N92-30742
PARLIER, M.
Mechanical testing of glass-ceramic matrix composites
[ONERA, TP NO. 1991-182] p 388 A92-26351
PARLOS, ALEXANDER
A novel associative memory for high level control functions p 52 A92-11472
PARNAS, LEVEND
Buckling, postbuckling and crippling of thin walled composite airframe structures under compression
p 899 A92-46940
PARPIA, IJAZ H.
A nearly-monotone genuinely multidimensional scheme for the Euler equations
[AIAA PAPER 92-0325] p 322 A92-25772
PARR, C. H.
Performance of aluminum honeycomb panels with structural defects and core anomalies. II - Specimen description and test results p 591 A92-36156
PARR, T.
Supersonic flow mixing and combustion using RAMP nozzle
[AIAA PAPER 92-3840] p 1113 A92-54198
PARR, T. P.
Thermal imaging of afterburning plumes
p 129 A92-17179
PARRISH, RUSSELL V.
Effect of short-term exposure to stereoscopic three-dimensional flight displays on real-world depth perception
[NASA-TP-3117] p 119 N92-13065
Computational algorithms for increased control of depth-viewing volume for stereo three-dimensional graphic displays
[NASA-TM-4379] p 1065 N92-34109
PARROTT, TONY L.
Sound transmission through a high-temperature acoustic probe tube p 415 A92-26406
PARTHASARATHY, V. N.
Shape optimization of three-dimensional structures with adaptive meshing
[AIAA PAPER 92-2434] p 586 A92-34548
PARTHIER, W.
Extension of the Frankfurt COMPAS for general application p 355 N92-19048
PARTRIDGE, HARRY
H-N2 interaction energies, transport cross sections, and collision integrals p 1135 A92-54660
PARVU, P.
Some considerations on modeling flight vehicles movement p 281 A92-21311
PASCHAL, WILLIAM
Design and analysis of reengine Boeing 727-100 center inlet S duct by a reduced Navier-Stokes code
[AIAA PAPER 92-1221] p 517 A92-33320
PASCHAL, WILLIAM A.
A study on vortex flow control of inlet distortion in the re-engined 727-100 center inlet duct using computational fluid dynamics
[AIAA PAPER 92-0152] p 253 A92-23767
A study on vortex flow control on inlet distortion in the re-engined 727-100 center inlet duct using computational fluid dynamics
[NASA-TM-105321] p 179 N92-13998
PASHA, RAMIN P. K.
Analysis of airship lateral maneuverability
[AIAA PAPER 91-1274] p 743 A92-41212
PASHCHENKO, O. B.
Computer-aided equipment layout for the fuselage of maneuverable aircraft p 113 A92-16833
PASHINTSEV, V. T.
The analysis and approximate representation of the optimal control law for a maneuverable aircraft
p 479 A92-30131
PASIN, M.
High temperature erosion resistance of coatings for gas turbine
[ASME PAPER 91-GT-213] p 143 A92-15632
Laser measurements of unsteady flow field in a radial turbine guide vanes
[AIAA PAPER 92-0394] p 395 A92-26249
PASQUALE, LINDA
MLS mathematical modeling study of Philadelphia International Airport runway 27L
[DOT/FAA/CT-TN91/54] p 573 N92-22503
PASSALACQUA, M.
Viscous high-speed flow computations by adaptive mesh embedding techniques p 808 A92-45839
PASSINO, KEVIN M.
Optimal stabilization of discrete event systems
p 48 A92-11376
PASTUKHOV, A. I.
An approximate method for calculating flow past solid wings of small aspect ratio based on a nonlinear theory of a continuous vortex surface p 428 A92-30373
Calculation of the aerodynamic characteristics of bodies of revolution in incompressible flow by the vortex surface method p 428 A92-30375
PATANKAR, S. V.
Studies of gas turbine heat transfer: Airfoil surfaces and end-wall cooling effects
[AD-A244055] p 376 N92-19097
PATEL, R. S.
Optimal thermal management system for HALE UAV
[ASME PAPER 91-GT-396] p 111 A92-15726
PATERSON, R. W.
Enhanced mixing of supersonic jets
p 80 A92-17195
Supersonic nozzle mixer ejector p 376 A92-28536
PATHAK, PRABHAKAR H.
High-frequency techniques for antenna analysis
p 494 A92-31071
PATRICK, W. P.
Enhanced mixing of supersonic jets
p 80 A92-17195
PATRIQUIN, DOUGLAS R.
Wavelength encoded fiber optic angular displacement sensor p 857 A92-48046
PATTERSON-HINE, F. A.
Modular techniques for dynamic fault-tree analysis
p 1120 A92-56241
PATTISON, J. H.
Deck motion criteria for carrier aircraft operations
p 464 N92-21952
PATTON, R.
A two-feedback-loop robust helicopter controller based on eigenspace techniques and H(infinity) synthesis
p 29 A92-11582
PATTON, R. J.
An assessment of robustness of variable structure control systems for advanced aircraft manoeuvres
p 29 A92-11595
Frequency domain testing of helicopter dynamics using automated input signals p 545 A92-35731
Improvement of helicopter robustness and performance control law using eigenstructure techniques and H-infinity synthesis p 569 A92-35776
Design of low-sensitivity modalized observers using left eigenstructure assignment p 661 A92-39908
PATUREAU, PHILLIPPE
Real time presentation for RAFALE in-flight tests
p 882 A92-47522
PAUL, BERNARD P., JR.
Analysis of junction flowfields using the incompressible Navier-Stokes equations
[AIAA PAPER 92-0519] p 331 A92-26944
PAUL, BETH E.
Application of analytical and design tools for fighter wing aeroelastic tailoring
[AIAA PAPER 92-2373] p 542 A92-34543
Application of analytical and design tools for fighter wing aeroelastic tailoring p 550 N92-23231
PAUL, DIANE
A new development in embedded computer performance measurement p 921 A92-48506
A new approach to embedded computer performance measurement p 1005 A92-49288
PAUL, GREG
PDES application protocol suite for composites (PAS-C). Functional needs report for the PAS-C program
[AD-A247886] p 1108 N92-32629
PAUL, J.
A preliminary study on damage detection using piezoelectric film
[AD-A246350] p 733 N92-28118
PAUL, LORI
Proceedings of the Workshop on Advanced Network and Technology Concepts for Mobile, Micro, and Personal Communications
[NASA-CR-190459] p 1000 N92-30923
PAUL, P. C.
Out of plane analysis for composite structures
p 1107 N92-32527
PAUL, W.
Application of the Euler method EUFLEX to a fighter-type airplane configuration at transonic speed
[AIAA PAPER 92-2620] p 845 A92-45573
PAULEY, WAYNE R.
Experimental development of spanwise vortex models with streamwise decay due to wall interaction
[AIAA PAPER 92-2688] p 799 A92-45535
PAULL, A.
Skin-friction gauge for use in hypervelocity impulse facilities p 398 A92-28063
PAULO, EUGENE P.
Comparison of Janus and field test aircraft detection ranges for the line-of-sight forward heavy system
[AD-A246047] p 770 N92-27600
PAULSON, G. A.
Transition to cooperative ATM system requires commitment p 267 A92-23297
PAULSON, GEORGE A.
A European perspective on the co-operative air traffic management concept p 531 A92-33427
PAUS, M.
A general approach to optimal real-time guidance of dynamic systems based on nonlinear programming
[AIAA PAPER 92-4378] p 1131 A92-55182
PAUSDER, H. J.
Experiences with high authority helicopter flight control
p 568 A92-35757
PAVEL, M.
Sensor fusion for synthetic vision
[AIAA PAPER 91-3730] p 197 A92-17597
PAVLIUCHENKO, A. M.
A study of aerophysical and dynamic characteristics using an axisymmetric flight test vehicle with a reusable nose section p 707 A92-42684
PAVLOV, A. A.
A method for the optical measurement of surface friction in supersonic flow p 337 A92-27537
PAWLIK, EUGENE A., SR.
A model for evaluation and training in aircrew coordination and cockpit resource management
p 46 A92-11191
PAWLIK, SIMON R., SR.
Development of rating instruments and procedures for aviation mishap investigation
[AD-A253072] p 1044 N92-33288
PAWLOSKI, CHESTER E.
Development and tribological properties of new cyclotriphosphazene high temperature lubricants for aircraft gas turbine engines p 287 A92-21327
PAXSON, DANIEL W.
A general numerical model for wave rotor analysis
[NASA-TM-105740] p 1002 N92-31484
PAYNE, GORDON A.
Variable-camber systems integration and operational performance of the AFTI/F-111 mission adaptive wing
[NASA-TM-4370] p 570 N92-22194
PAYNE, LEE
Lighter than air - An illustrated history of the airship (Revised edition) p 418 A92-25680
PAYNTER, GERALD C.
Modeling supersonic inlet boundary layer bleed roughness
[AIAA PAPER 92-0269] p 317 A92-25725
PEACE, A. J.
The construction, application and interpretation of three-dimensional hybrid meshes p 919 A92-47089
PEACOCK, N. J.
Advanced propulsion systems for large subsonic transports p 653 A92-36977
PEAKE, N.
The interaction between a high-frequency gust and a blade row p 1135 A92-54484
PEAL, RICHARD A.
Avionics flight systems for the 21st century
[SAE PAPER 912033] p 784 A92-45421
PEARCE, J. A.
High temperature, thermally stable JP fuels - An overview
[AIAA PAPER 92-0683] p 389 A92-27050
PEARSON, ALLAN E.
Parameter identification for nonlinear aerodynamic systems
[NASA-CR-188985] p 53 N92-10347
Parameter identification for nonlinear aerodynamic systems
[NASA-CR-190264] p 830 N92-29329
PEARSON, M. S.
Computational fluid dynamics based three-dimensional turbofan inlet/fan cowl analysis system
p 243 A92-21075
PEART, NOEL A.
Flyover-noise measurement and prediction
p 236 N92-14786
PECHT, GLENN
Development of film riding face seals for a gas turbine engine p 291 A92-21330
PECORA, M.
A boundary integral formulation for unsteady transonic potential flows p 719 N92-27942
PEDRO, JIMOH
Mathematical modeling of the effect of windshear on the dynamics of a landing aircraft p 875 A92-47784

PEECHER, S.
270-Vdc/hydrid 115-Vac electric power generating system technology demonstrator evolution to a dual-channel, more electric aircraft technology development testbed
[SAE PAPER 912183] p 655 A92-40003
270-Vdc/hybrid 115 Vac electric power generating system technology demonstrator
[SAE PAPER 912051] p 861 A92-45435
PEETERS, M. F.
Finite element vorticity based methods for the solution of the compressible Navier-Stokes equations
p 246 A92-21983
PEGAH, M.
Model based reasoning in the aerospace domain
[AIAA PAPER 91-3709] p 230 A92-17582
PEIGIN, S. V.
Hypersonic flow of a viscous gas past sharp elliptical cones at angles of attack and slip p 336 A92-27531
PEIN, R.
Swirl and fuel composition effects on boron combustion in solid-fuel ramjets p 668 A92-36964
PEIRO, J.
The computation of three-dimensional flows using unstructured grids p 612 A92-37539
The numerical simulation of flow about installed aero engine nacelle using a finite element Euler solver on unstructured meshes p 941 A92-52848
PEISEN, DEBORAH
The Civil Rotorcraft Initiative - An action agenda
p 241 A92-22707
PEISEN, DEBORAH J.
New York Downtown Manhattan (Wall Street) Heliport: Operations analysis
[DOT/FAA/RD-91/12] p 139 N92-13077
Rotorcraft low altitude IFR benefit/cost analysis: Operations analysis
[SCT-90RR-44] p 191 N92-15061
PELLAZAR, MILES B.
Advanced avionics system development environment
[AIAA PAPER 91-3944] p 231 A92-17608
PELLEBERGS, PER
JAS 39 Gripen flight test report p 645 A92-40030
PELLEGRINI, P. F.
Use of target spectrum for detection enhancement and identification p 404 N92-19155
PELLETIER, A.
Inspection of aircraft engine components using automated eddy current and pattern recognition techniques
[NRC-LTR-ST-1834] p 504 N92-22029
PELLETT, G. L.
Strain-induced extinction of hydrogen-air counterflow diffusion flames - Effects of steam, CO2, N2, and O2 additives to air
[AIAA PAPER 92-0877] p 487 A92-29639
PELLICANO, PAUL
X-29 high angle of attack flight test procedures, results, and lessons learned p 548 A92-35934
PELOUBET, R. P., JR.
On-line adaptive control of unstable aircraft wing flutter p 27 A92-11374
PELUSO, JAMES D.
Turboshaft/turboprop cycle sensitivity analysis
[AIAA PAPER 92-3476] p 865 A92-49020
PELZ, R. B.
Emergence of coherent patterns of vortex stretching during reconnection - A scattering paradigm
p 38 A92-11041
PELZ, RICHARD B.
Solution of the Euler and Navier-Stokes equations on MIMD distributed memory multiprocessors using cyclic reduction
[AIAA PAPER 92-0561] p 411 A92-26970
PELZL, J.
Cutting treatment by drilling of fiber bound synthetic materials
[MBB-UD-0609-91-PUB] p 988 N92-31716
PEN, JIBING
The computer analysis of the prediction of aircraft electrical power supply system reliability
p 690 A92-37950
PENDERGRAFT, ODIS C., JR.
Study of external dynamic flap loads on a 6 percent B-1B model
[ASME PAPER 91-GT-236] p 125 A92-15645
Interference effects of very high bypass ratio nacelle installations on a low-wing transport
[ASME PAPER 91-GT-241] p 75 A92-15646
Experimental study of pylon geometries for transport aircraft
[AIAA PAPER 92-0153] p 271 A92-23768
A user's guide to the Langley 16- by 24-inch water tunnel
[NASA-TM-104200] p 385 N92-18956
Installation effects of wing-mounted turbofan nacelle-pylons on a 1/17-scale, twin-engine, low-wing transport model
[NASA-TP-3168] p 346 N92-19002
PENDLETON, EDMUND
Application of Active Flexible Wing technology to the Agile Falcon p 729 A92-41233
PENG, CHENGYI
Experimental study of a two-dimensional random frequency generator p 483 A92-29712
PENG, HAIXIN
A theoretical study on helicopter alert time without maintenance p 358 A92-27836
PENG, JIAN
Advanced electromagnetic methods for aerospace vehicles
[NASA-CR-190650] p 1001 N92-31156
PENG, XU
Preliminary investigation of inlet dynamic distortion and it's passive control p 245 A92-21742
PENG, Y. K. M.
Scoping studies for small steady-state tokamaks for divertor testing
[DE92-000740] p 238 N92-15761
PENN, JAY
Combined exo/endoatmospheric transport alternatives
[IAF PAPER 92-0663] p 1104 A92-57102
PENNA, SERGIO D.
On-board data acquisition system for Embraer's CBA123 p 198 A92-19251
PEPI, MARC S.
Failure analysis of the Apache mixer pivot support
[AD-A240858] p 116 N92-13061
PEPPI, K. M.
Application of a universe-series code for inviscid flow over complex 3-dimensional configurations
[AIAA PAPER 92-0150] p 253 A92-23765
PERAIRE, J.
The computation of three-dimensional flows using unstructured grids p 612 A92-37539
The numerical simulation of flow about installed aero engine nacelle using a finite element Euler solver on unstructured meshes p 941 A92-52848
Finite element methods for integrated aerodynamic heating analysis
[NASA-CR-190353] p 633 N92-25959
PERALA, R. A.
The use of finite difference electromagnetic analysis in the design and verification of modern aircraft
p 192 A92-20136
PERALA, RODNEY A.
Nonlinear triggered lightning models for use in finite difference calculations p 230 A92-20128
Analysis and modeling of lightning strikes to the F106B, CVF580, and C160 aircraft p 186 A92-20129
PERBET, JEAN-NOEL
Concept for future cockpits p 118 A92-16148
PERCIVAL, L. D.
Metal-metal bondline NDE methods
[AD-A244429] p 503 N92-21730
PERDICHIZZI, ANTONIO
Reynolds stress distribution downstream of a turbine cascade p 614 A92-38861
PEREIRA, J. C. F.
Predictions of compressible viscous flows at all Mach number using pressure correction, collocated primitive variables and non-orthogonal meshes
[AIAA PAPER 92-0426] p 326 A92-26274
PEREZ, EMILIO
Optimum cruise lift coefficient in initial design of jet aircraft p 845 A92-46806
PEREZ, F.
New practical method for measurement error determination in radar systems under real traffic conditions p 155 A92-17238
PEREZ, GREGORY, JR.
An eight month gearbox development program
[AIAA PAPER 92-3368] p 850 A92-48941
PEREZ, R. A.
Full envelope multivariable control of a gas turbine engine p 468 A92-29116
PERIC, M.
Measurements and simulation of the flow around a poppet valve p 675 A92-40103
PERKINS, A. R.
Use of stepwise regression techniques and kinematic compatibility for the analysis of EAP flight data
p 365 N92-18790
PERKINS, JOHN N.
Analysis of hypersonic nozzles including vibrational nonequilibrium and intermolecular force effects
[AIAA PAPER 92-0330] p 322 A92-25777
Leading edge sweep effects in generic three-dimensional sidewall compression scramjet inlets
[AIAA PAPER 92-0674] p 343 A92-28218
Internal shock interactions in propulsion/airframe integrated three-dimensional sidewall compression scramjet inlets
[AIAA PAPER 92-3099] p 824 A92-48741
PERKINS, W. R.
Design of reliable control systems p 49 A92-11420
PERLEY, JEFF
Realistic real-time ground testing
[AIAA PAPER 92-0197] p 284 A92-23805
PERMINOV, V. D.
Approximate aerodynamic analysis for complicated bodies in rarefied gas flows p 938 A92-52754
PERNICKA, H.
Development and integration of modern laboratories in aerospace education
[AIAA PAPER 92-4022] p 1141 A92-56844
PERON, LEE R.
Thrust vectoring for lateral-directional stability
[NASA-CR-186016] p 482 N92-21357
PERREY, G.
HEPO mission simulator - Development and usage for NH90 helicopter p 1094 A92-56313
PERRIER, P.
Computational procedures for preliminary design
p 552 N92-23952
PERRIN, M. Y.
A unified nonequilibrium model for hypersonic flows
p 3 A92-10575
Hypersonic viscous shock layer in thermochemical nonequilibrium p 183 N92-15014
PERRY, BOYD, III
Determining design gust loads for nonlinear aircraft similarity between methods based on matched filter theory and on stochastic simulation
[AIAA PAPER 92-2369] p 518 A92-34597
A summary of the Active Flexible Wing program
[AIAA PAPER 92-2080] p 565 A92-35652
Maximized gust loads for a nonlinear airplane using matched filter theory and constrained optimization
[NASA-TM-104138] p 23 N92-11010
A summary of the active flexible wing program
[NASA-TM-107655] p 962 N92-31264
PERRY, DOUGLAS
Verification of flight software by embedding software simulation in simulation of external environment
p 232 A92-19084
PERSCHBACHER, DAVID L.
An explanation-based-learning approach to knowledge compilation - A Pilot's Associate application
p 920 A92-48220
The importance of implicit and explicit knowledge in a pilot's associate system p 858 A92-48567
PERSON, LEE H., JR.
Takeoff Performance Monitoring System display options
[AIAA PAPER 92-4138] p 967 A92-52433
PERTILE, R.
Parametric effects of some aircraft components on high-alpha aerodynamic characteristics
p 364 N92-18782
PERUCCHINI, J.
Indirect measurements of convective flow by IR thermography
[ONERA, TP NO. 1992-46] p 902 A92-48607
PERUSEK, GAIL P.
Experimental performance of three design factors for ventral nozzles for SSTOVL aircraft
[AIAA PAPER 92-3789] p 1069 A92-54168
Use of an approximate similarity principle for the thermal scaling of a full-scale thrust augmenting ejector
[AIAA PAPER 92-3792] p 1069 A92-54171
Use of an approximate similarity principle for the thermal scaling of a full-scale thrust augmenting ejector
[NASA-TM-105724] p 739 N92-26613
Experimental performance of three design factors for ventral nozzles for SSTOVL aircraft
[NASA-TM-105697] p 742 N92-27669
PESCHKE, W. T.
Hydrocarbon-fueled scramjet combustor investigation
p 376 A92-28535
PESSIN, DAVID
The Guardian: Preliminary design of a close air support aircraft
[NASA-CR-189991] p 463 N92-21566
PETERS, B. R.
Crossed beam correlation modeling and experimental techniques for measuring density fluctuations in hypersonic flows
[AIAA PAPER 92-2779] p 758 A92-41323
PETERS, C.
Comparison between hot/wet test and RT/dry test on the Seastar horizontal stabilizer and fin
p 226 N92-14414
PETERS, DAVID A.
An integrated airloads-inflow model for use in rotor aeroelasticity and control analysis p 64 A92-14328

Extension and validation of an unsteady wake model for rotors p 702 A92-41224
Periodic trim solutions with hp-version finite elements in time p 874 A92-46931
An aeroelastic analysis with a generalized dynamic wake p 847 A92-46932
Aerodynamic parametric studies and sensitivity analysis for rotor blades in axial flight p 816 A92-46959
Integration of dynamic, aerodynamic, and structural optimization of helicopter rotor blades
[NASA-CR-189018] p 195 N92-14038

PETERS, JEANNE M.
Reduced basis technique for evaluating the sensitivity coefficients of the nonlinear tire response
[AIAA PAPER 92-2530] p 583 A92-34376
Sensitivity of tire response to variations in material and geometric parameters p 900 A92-47128

PETERS, RICKY L.
The challenge of commercial aircraft survivability p 931 A92-52022

PETERSEN, K. L.
Multidisciplinary modeling and simulation of a generic hypersonic vehicle
[AIAA PAPER 91-5015] p 232 A92-17813

PETERSEN, T. J.
Systems engineering as applied to the Boeing 777
[AIAA PAPER 92-1010] p 515 A92-33198

PETERSON, B.
Integrated Russian VLF/Omega receiver design
[PB92-193390] p 1051 N92-33809

PETERSON, B. B.
Measurement of LORAN-C envelope to cycle difference in the far field
[PB92-128909] p 455 N92-21263
Probability of cycle jumps in Omega receivers and other phase locked loop applications
[PB92-128891] p 455 N92-21279

PETERSON, C. W.
Design and testing of high-performance parachutes
[AGARD-AG-319] p 345 N92-18269

PETERSON, CARL R.
Mechanics and thermodynamics of propulsion (2nd revised and enlarged edition)
[ISBN 0-201-14659-2] p 672 A92-38275

PETERSON, J.
Experiences with finite element methods for the velocity-vorticity formulation of three-dimensional, viscous, incompressible flows p 246 A92-21984

PETERSON, J. B., JR.
On the measurement of subsonic flow around an appended body of revolution at cryogenic conditions in the NTF p 880 A92-45265

PETERSON, JAMES M.
Flammability, smoke and toxic gas combustion products of composites used in aircraft cabins p 14 A92-10257

PETERSON, JOHN B., JR.
Computer programs for the calculation of dual sting pitch and roll angles required for an articulated sting to obtain angles of attack and sideslip on wind-tunnel models
[NASA-TM-104161] p 138 N92-12007

PETERSON, STEVEN W.
Local bridging to predict aerodynamic coefficients in hypersonic, rarefied flow p 705 A92-41541

PETESCH, D. J.
Traditional finite element analysis - Opportunities for parallelism? p 40 A92-12354

PETIAU, C.
Structural optimization of aircraft practice and trends p 551 N92-23239
Structural optimization of aircraft p 851 N92-28472

PETIT, GERARD
The need for GPS standardization p 1049 N92-33351
Precise GPS ephemerides from DMA and NGS tested by time transfer p 1049 N92-33355
Comparison of GLONASS and GPS time transfers between two west European time laboratories and VNIIFTRI p 1050 N92-33381

PETLEY, DENNIS H.
A comparison of cooling methods for the airframe nozzle of a single-stage-to-orbit aircraft
[AIAA PAPER 91-5036] p 210 A92-17825
Analysis of cooling systems for hypersonic aircraft
[AIAA PAPER 91-5063] p 216 A92-17843
Integrated numerical methods for hypersonic aircraft cooling systems analysis
[AIAA PAPER 92-0254] p 357 A92-25712
Thermal management for a Mach 5 cruise aircraft using endothermic fuel p 736 A92-41225

PETRI, MICHAEL C.
Validation and verification flight test for TCAS-2 logic changes (MOPS Change 6)
[DOT/FAA/CT-TN91/46] p 268 N92-15981

PETRICK, S. WALTER
Multicomponent gas sorption Joule-Thomson refrigeration
[NASA-CASE-NPO-17569-1-CU] p 228 N92-15203

PETRIE, HOWARD L.
A study of the diffusion of slot-injected drag-reducing polymer solution in a turbulent boundary layer modified by large-eddy breakup devices
[AD-A243411] p 344 N92-18007

PETRINI, G. L.
Nonstationary gasdynamics p 220 N92-13985

PETROV, A. S.
The total drag of a body in the flow of a viscous heat-conducting gas p 439 A92-31873

PETROV, A. V.
Flow past a highly curved wing with tangential jet ejection p 438 A92-31868
Interaction of jets ejected from two-dimensional nozzles with a curved surface p 438 A92-31869

PETROV, K. P.
The aerodynamic characteristics of grid fin wings p 427 A92-30201

PETROV, M.
Experimental investigation of liquid carbonhydrogen fuel combustion in channel at supersonic velocities
[AIAA PAPER 92-3429] p 894 A92-48986

PETTERS, DEAN P.
Further studies of kinetic energy methods in high speed ramjet cycle analysis
[AIAA PAPER 92-3805] p 1069 A92-54177

PEUBE, J.
Establishment and characterization of a reproducible vortex for use in studying nonsteady two-dimensional phenomena p 310 A92-24428

PEUBE, J. L.
Active control of pulsed flow for low frequency noises attenuation p 694 A92-39109

PEYRAN, R. J.
The effect of composite material allowable changes on VTOL airframe weights p 848 A92-47629

PEZZULLO, G.
Incompressible steady aerodynamics using a standard finite element code p 174 A92-20218

PFAFFENBERGER, EUGENE E.
Performance of hybrid ball bearings in oil and jet fuel p 900 A92-47176

PFAIFLE, E. E.
Effect of the blade height of the nozzle ring of axial-flow microturbines on the flow velocity factor and exit angle p 128 A92-16831

PFANNESCHLAG, LISA J.
An overview of US Navy and Marine Corps V/STOL p 783 A92-45303

PFEIFFER, NEAL J.
One view of experimental aerodynamics
[AIAA PAPER 92-0160] p 254 A92-23775

PFENNINGER, WERNER
Design of a hybrid laminar flow control nacelle
[AIAA PAPER 92-0400] p 373 A92-26253

PFITZNER, M.
Computation of 3-D hypersonic flows in chemical non-equilibrium including transport phenomena
[AIAA PAPER 92-2876] p 820 A92-47858

PFITZNER, MICHAEL
Three-dimensional simulations of hypersonic flows
[MBB-UK-0155-89-PUB] p 447 N92-21703

PHAM-VAN-DIEP, G.
A code validation strategy and facility for nonequilibrium, reacting flows
[AIAA PAPER 92-3970] p 1098 A92-56796

PHAM-VAN-DIEP, G. C.
An iodine hypersonic wind tunnel for the study of nonequilibrium reacting flows
[AIAA PAPER 92-0566] p 383 A92-26974

PHAM, TUAN M.
Kalman filter mechanization for INS airstart p 574 A92-33602

PHATAK, ANIL V.
Analysis of image-based navigation system for rotorcraft low-altitude flight p 1046 A92-55968

PHELPS, KEVIN D.
Results of flight tests of the Boeing Sikorsky Fantail demonstrator p 106 A92-14376

PHILATOV, ANATOLY P.
Cryogenic test rig with an aerodynamic magnetically levitated carriage p 750 N92-27792

PHILBECK, THOMAS E., JR.
Testing and evaluation of the Vanner electrical inverters, models 24-1500 and SP 00112
[AD-A241914] p 299 N92-17216

PHILIPPE, JEAN-JACQUES
Research on helicopter rotors - Progress in aerodynamics, aeroelasticity and acoustics
[ONERA, TP NO. 1992-27] p 849 A92-48589

PHILIPS, D. B.
Suppression of the wing-body junction vortex by body surface suction p 309 A92-24417

PHILLIPS, D.
Inertia-friction welding of an advanced rapidly solidified titanium alloy p 212 A92-18898

PHILLIPS, DOUGLAS J.
Experimental demonstration of active vibration control for flexible structures p 50 A92-11442

PHILLIPS, E. P.
Fatigue crack initiation and small crack growth in several airframe alloys p 212 A92-19754

PHILLIPS, EDWARD H.
NASA research program directed at reducing supersonic transport noise p 61 A92-16150

PHILLIPS, EDWARD P.
Measurements of fuselage skin strains and displacements near a longitudinal lap joint in a pressurized aircraft
[NASA-TM-104163] p 159 N92-13455

PHILLIPS, H. I.
Harrier international programme p 841 A92-45305

PHILLIPS, J. R.
Evaluation of metal hydride compressors for applications in Joule-Thomson cryocoolers p 296 A92-23835

PHILLIPS, M.
The measurement of plate vibration and sound radiation from a turbulent boundary layer manipulator
[AD-A240127] p 42 N92-10206

PHILLIPS, RICHARD W.
A fiber optic temperature sensor for aerospace applications p 761 A92-42607

PHILPOT, M. G.
Practical considerations in designing the engine cycle p 869 N92-28460

PIAN, THEODORE H. H.
Advanced stress analysis methods applicable to turbine engine structures
[NASA-CR-187235] p 44 N92-11378

PIANKO, M.
Combat aircraft jet engine noise studies
[ONERA, TP NO. 1991-192] p 415 A92-26353

PICCINI, P.
Use of target spectrum for detection enhancement and identification p 404 N92-19155

PICCO, E.
High temperature low cycle fatigue of single crystal nickel base superalloys p 213 A92-19796

PICCOLO, ANTONIO
Design and analysis of reengine Boeing 727-100 center inlet S duct by a reduced Navier-Stokes code
[AIAA PAPER 92-1221] p 517 A92-33320
Design and analysis of vortex generators on reengined Boeing 727-100QF center inlet S-duct by a reduced Navier-Stokes code
[AIAA PAPER 92-2700] p 800 A92-45542

PICKARD, A. C.
Introduction: Needs and approaches to reliability and quality assurance in design and manufacture p 402 N92-19005
Application of finite element methods to fracture mechanics
[PNR-90770] p 503 N92-21741

PICKERELL, THOMAS
Monitoring operational concept
[DOT/FAA/SE-91/3] p 268 N92-15980
National Airspace System maintenance and support operational concept
[DOT/FAA/SE-92/1] p 308 N92-18969
National airspace system: System effectiveness operational concept NAS-SR-138
[DOT/FAA/SE-92/2] p 535 N92-23096
National airspace system. Air defense and law enforcement surveillance operational concept NAS-SR-135
[DOT/FAA/SE-92/3] p 953 N92-31211

PICKET, J. S.
Nonstationary gasdynamics p 220 N92-13985

PICKETT, MARK T.
Flow quality studies of the NASA Lewis Research Center 8- by 6-foot supersonic/9- by 15-foot Low Speed Wind Tunnel
[AIAA PAPER 92-3916] p 1095 A92-56748
Flow quality studies of the NASA Lewis Research Center 8- by 6-foot supersonic/9- by 15-foot low speed wind tunnel
[NASA-TM-105417] p 887 N92-28673

PIDAPARTI, R. M. V.
Structural and aerodynamic data transformation using inverse isoparametric mapping p 758 A92-41242

PIDD, M.
Asymmetric vortex flow over circular cones p 86 N92-13014

PIELLISCH, RICHARD
Weaving an aircraft p 392 A92-24911

PIERCE, ALLAN D.
The effect of molecular relaxation processes in air on the rise time of sonic booms p 898 A92-45883
Wave equations and computational models for sonic boom propagation through a turbulent atmosphere p 1139 N92-33877
Simulations of sonic boom ray tube area fluctuations for propagation through atmospheric turbulence including caustics via a Monte Carlo method p 1139 N92-33878

PIERCE, CARL H.
Two crew stations for dynamic flight simulation p 572 A92-35443

PIERCE, M. A.
A computational exploration of the importance of three-dimensionality, boundary layer development, and flow chemistry to the prediction of scramjet nozzle performance
[AIAA PAPER 91-5059] p 472 A92-31689

PIERENS, DAVID A.
Stagnation and dynamic pressure limits for the S1 wind tunnel
[AD-A242989] p 285 N92-17297

PIERRE, CHRISTOPHE
Aeroelastic modal characteristics of mistuned blade assemblies - Mode localization and loss of eigenstructure p 1117 A92-54921

PIERS, M. A.
A knowledge-based assistant for diagnosis in aircraft maintenance p 61 N92-12538
Application of knowledge-based systems for diagnosis of aircraft systems
[NLR-TP-90192-U] p 837 N92-28655

PIERSON, BION L.
2-D and 3-D minimum-time-to-turn flights via parameter optimization
[AIAA PAPER 92-0731] p 379 A92-27083

PIFKO, ALLAN B.
Computational structures technology at Grumman: Current practice/future needs p 684 N92-25930

PIKE, J.
Aero-propulsive effects on configuration shaping
[AIAA PAPER 91-5064] p 459 A92-31691

PIKIELNY, JERZY
Polish radar technology. II - Adaptive radar AVIA CM p 39 A92-12290

PILAND, WILLIAM M.
Aerothermodynamics for United States advanced programs p 184 N92-15039

PILIDIS, PERICLES
The selective bleed variable cycle engine
[ASME PAPER 91-GT-388] p 126 A92-15720

PILIUGIN, N. N.
Calculation of heat transfer and friction for a blunt body in the path of supersonic flow of a chemically equilibrium air-xenon mixture p 336 A92-27532
Determination of physicochemical constant in the wake of a body from ballistic experiments p 609 A92-36549

PILKINGTON, G.
The environmental impact of commercial aviation: The evolution of exhaust emissions legislation and control technology
[PNR-90847] p 505 N92-20574

PIMM, JOHN H.
Design and test of aircraft aft fuselage structure using postbuckled shear panels p 848 A92-47406

PINCHUKOV, V. I.
Computation of transonic flow over an airfoil at large Reynolds numbers p 252 A92-23414
On one method of constructing adaptive difference grids in aerodynamics problems p 311 A92-24902

PINCKNEY, FRANK D.
Magnetic bearing design and control optimization for a four-stage centrifugal compressor p 900 A92-47188

PINCKNEY, S. Z.
A configuration development strategy for the NASP
[AIAA PAPER 91-5044] p 210 A92-17830

PINDERA, JERZY T.
Development and design with advanced materials
[ISBN 0-444-88706-7] p 296 A92-24176

PINDERA, M. Z.
Visualization and analysis of hypersonic flows and comparison to experimental data
[AIAA PAPER 92-2774] p 704 A92-41320

PINE, NICHOLSON L.
Fiber-optic pressure sensor system for gas turbine engine control p 857 A92-48047

PINELLI, THOMAS E.
NASA/DOD Aerospace Knowledge Diffusion Research Project. Paper 13: The information-seeking habits and practices of engineers
[NASA-TM-107931] p 782 N92-28114
NASA/DOD Aerospace Knowledge Diffusion Research Project. Paper 14: An analysis of the technical communications practices reported by Israeli and US aerospace engineers and scientists
[NASA-TM-107924] p 782 N92-28183

PINEO, FREDERICK J.
Gas turbine engine control
[PATENT-1-274-606] p 130 N92-13069

PINES, V. N.
Technical tools of test automation for gas-turbine engines based on cluster CAMAC modules with an increased number of channels p 980 A92-51348

PING, YU
Time domain numerical calculations of unsteady vortical flows about a flat plate airfoil p 936 A92-50473

PINKERTON, THERESA L.
Planform curvature effects on flutter characteristics of a wing with 56 deg leading-edge sweep and panel aspect ratio of 1.14
[NASA-TP-3116] p 115 N92-13054

PINNEY, MARK
On the aerodynamics/dynamics of store separation from hypersonic aircraft
[AIAA PAPER 92-2722] p 807 A92-45595

PINNINGTON, R. J.
Active control of sound transmission through stiff lightweight composite fuselage constructions p 1137 N92-32957

PINSKY, MARK A.
The generalized normal forms and method of resonance control of nonlinear dynamical systems p 507 A92-29189

PINTO, O., JR.
Stratospheric electrodynamics from superpressure balloons - A technical challenge for small payload environments
[AIAA PAPER 91-3674] p 14 A92-11019

PIOU, J. E.
A time approach to robustness of LTI systems with structured uncertainty and unmodelled dynamics p 48 A92-11356

PIOU, JEAN E.
Robust sampled data eigenstructure assignment using the delta operator
[AIAA PAPER 92-4400] p 1075 A92-55200

PIPERIAS, P.
Reduction and analysis of F-111C flight data
[AD-A250341] p 853 N92-28771

PIPES, R. BYRON
Continuation of tailored composite structures of ordered staple thermoplastic material
[NASA-CR-189671] p 1110 N92-33613

PIQUET, J.
Computation of unsteady, laminar, incompressible, viscous flows using the vorticity streamfunction formulation p 245 A92-21979
Navier-Stokes computations of horseshoe vortex flows p 990 A92-49516

PISANOV, E. V.
Experimental investigation of the optimal deflection of a single-slotted flap with different degrees of extension on a modern supercritical profile p 439 A92-31879

PISARENKO, GEORGII S.
Aerodynamic damping of blade vibrations in turbomachines p 200 A92-18198

PISCITELLE, LOUIS J.
Dynamical systems analysis of an aerodynamic decelerator's behavior during the initial opening process
[AD-A244194] p 348 N92-19394

PIT, FABIENNE
Three-dimensional calculations of reactive flows in aircraft combustion chambers performed using two combustion models
[ONERA, TP NO. 1991-110] p 154 A92-16089
Three dimensional calculations of reactive flows within aircraft combustion chambers including some combustion models p 770 N92-27490

PITARYS, MARC J.
Avionics software reusability observations and recommendations p 921 A92-48502
Partitioned software support concept for modular embedded computer software p 922 A92-48518
A development-memory approach for enhancing avionics software logistics p 119 N92-12540

PITCHFORD, MARC
Size and critical supersaturation for condensation of jet engine exhaust particles p 161 A92-15884

PITT, DALE M.
FAMUSS - A new aeroservoelastic modeling tool
[AIAA PAPER 92-2395] p 541 A92-34468
Design of a fighter aircraft vertical tail enhanced buffet environment survivability p 551 N92-23235
Aeroelastic calculations for fighter aircraft using the transonic small disturbance equation p 720 N92-27951

PITTMAN, JAMES L.
Computational study of incipient leading-edge separation on a supersonic delta wing p 442 A92-32237

PITTS, JULIE
Navier-Stokes analysis of helicopter plume flowfield for infrared calculations
[AIAA PAPER 92-0983] p 580 A92-33185

PITZ, R. W.
Degenerate four-wave mixing for measurement of NO2 and smoke concentration in jet engine exhaust
[AIAA PAPER 92-3658] p 1113 A92-54108
Interaction between chemical reaction and turbulence in supersonic nonpremixed H2-air combustion p 1117 A92-54931

PIVA, R.
A boundary integral formulation for the kinetic field in aerodynamics. I - Mathematical analysis p 243 A92-21504
A boundary integral formulation for the kinetic field in aerodynamics. II - Applications to unsteady 2D flows p 339 A92-28005

PLANCHE, O. H.
Direct simulation of a supersonic reacting mixing-layer p 676 A92-40132

PLANT, WILLIAM J.
Relating the microwave radar cross section to the sea surface stress - Physics and algorithms p 597 A92-35028

PLATT, J. T.
Evolution of ASTOVL aircraft design p 842 A92-45311

PLATT, R. H.
High altitude airborne remote sensing mission using the advanced microwave precipitation radiometer (AMPR) p 574 A92-34893

PLATZ, K.
The impact of COMPAS on the future Cooperative Air Traffic Management Concept (CATMAC) p 355 N92-19049

PLATZER, K.-H.
Computer-based areal surface temperature and local heat transfer measurements with thermochromic liquid crystals (TLC) p 763 A92-44326

PLATZER, M. F.
Flow visualization and wake analysis for complex three-dimensional bluff bodies at subcritical through critical Reynolds numbers
[AIAA PAPER 92-0155] p 253 A92-23770

PLATZER, MAX F.
Unsteady airfoil flow solutions on moving zonal grids
[AIAA PAPER 92-0543] p 342 A92-28200
Pitch rate/sideslip effects on leading-edge extension vortices of an F/A-18 aircraft model p 874 A92-46810

PLENTOVICH, E. B.
Measurements of fluctuating pressure in a rectangular cavity in transonic flow at high Reynolds numbers
[NASA-TM-4363] p 633 N92-25752

PLESNIAK, MICHAEL W.
Evolution of three-dimensionality in stable and unstable curved mixing layers p 619 A92-40059

PLETCHER, R. H.
Wall functions for the kappa-epsilon turbulence model in generalized nonorthogonal curvilinear coordinates
[NASA-CR-190368] p 685 N92-25962

PLETTA, J. B.
Techniques for autonomous navigation
[DE92-013458] p 957 N92-31746

PLISSONNEAU, B.
The development of a new light, single engine helicopter family p 545 A92-35734

PLOSENSKI, M.
Flowfield in the vicinity of the F/A-18 vertical fin at high-angle-of-attack p 628 N92-24865

PLOT-LOCATELLI, SYLVIE
Research on some centered implicit methods for calculating transonic flows by solving Navier-Stokes equations
[ONERA-RSF-24/1408-AY-150A] p 1037 N92-32773

PLOTKIN, ALLEN
Effect of airfoil (trailing-edge) thickness on the numerical solution of panel methods based on the Dirichlet boundary condition p 340 A92-28041

PLOTKIN, KENNETH J.
Sonic boom p 55 N92-10608
The effect of turbulence on the loudness of minimized sonic boom signatures p 1139 N92-33880

PLOVSING, BIRGER
DANSIM - Danish Airport Noise Simulation Model - Basic principles, experience, and improvements p 687 A92-39055
DANSIM applications - Development of airport noise reduction strategies and environmental policy p 687 A92-39057

PLYLER, VALERIE E.
Advanced Transport Operating System (ATOPS) color displays software description: MicroVAX system
[NASA-CR-189603] p 556 N92-22395
Advanced Transport Operating System (ATOPS) color displays software description microprocessor system
[NASA-CR-189605] p 556 N92-22645
PODGORSKI, ANDREW S.
Lightning standards for aircraft protection
p 91 A92-14688
Composite electromagnetic pulse threat
p 146 A92-14689
PODNEY, WALTER N.
Development of an electromagnetic microscope for eddy current evaluation of materials
[AD-A242007] p 406 N92-19873
PODOBEDOV, V. A.
A discrete vortex study of stationary flow past three-dimensional lifting systems at subsonic and supersonic velocities p 79 A92-16813
PODZOROV, S. I.
Development of a combined fast method for studying the plane motions of rigid bodies in the atmosphere around the center of mass in the presence of perturbations
p 304 A92-23563
Singularity bypass algorithms in the numerical solution of equations of body motion relative to a center of mass in the atmosphere in the presence of disturbances
p 437 A92-31857
POE, C. C., JR.
Proof test and fatigue crack growth modeling on 2024-T3 aluminum alloy p 213 A92-19828
Overview of mechanics of materials branch activities in the computational structures area
p 684 N92-25917
POENSGEN, C.
Experimental investigation of the unsteady pressure field around an oscillating blade
[MITT-90-01] p 768 N92-27407
POERTNER, T.
Simulation requirements for RCS plume: Flowfield interaction modelling on a winged reentry vehicle
p 181 N92-14985
POESTKOKE, R.
Instrumentation requirements for laminar flow research in the NLR high speed wind tunnel HST
[NLR-TP-89158-U] p 887 N92-28669
POFF, RONALD
Low profile microsensor for aerodynamic pressure measurement p 555 A92-35949
POGGIE, J.
The dynamics and control of fluctuating pressure loads in the reattachment region of a supersonic free shear layer
[AIAA PAPER 92-0178] p 255 A92-23788
POGODAEV, A. A.
Improving the efficiency of passenger aircraft during the landing approach p 460 A92-31893
POGORELOV, O. I.
Mathematical modeling of supersonic flow over a convex-concave formed body based on the Euler and Navier-Stokes equations p 252 A92-23416
POGU, M.
Concerning the functional solution of transonic flows
p 243 A92-21318
POHLCHUCK, BOBBY
Preliminary evaluation of adhesion strength measurement devices for ceramic/titanium matrix composite bonds
[NASA-TM-105803] p 932 N92-31267
POINSATTE, PHILIP E.
Heat transfer measurements from a smooth NACA 0012 airfoil p 218 A92-20215
Roughness effects on heat transfer from a NACA 0012 airfoil p 219 A92-20217
POINSOT, T.
Turbulent combustion modelling in a side dump ramjet combustor
[AIAA PAPER 92-3599] p 1112 A92-54075
The coherent flamelet model for propulsion applications p 756 N92-27486
POLACSEK, C.
High-speed impulsive noise and aerodynamic results for rectangular and swept rotor blade tip tests in S1-Modane wind tunnel
[ONERA, TP NO. 1991-124] p 76 A92-16102
Basic experiments on the directivity of the sound radiation emitted by a turboshaft engine
[ONERA, TP NO. 1992-36] p 926 A92-48597
Influence of geometrical parameters on helicopter rotor high speed impulsive noise
[ONERA, TP NO. 1992-40] p 926 A92-48601
POLAK, E.
A method of centers based on barrier functions for solving optimal control problems with continuum state and control constraints p 52 A92-11467
POLANSKI, L.
The cryogenic balance design and balance calibration methods
[AIAA PAPER 92-4001] p 1122 A92-56824
POLANSKY, G. F.
Center of pressure calculations for a bent-axis vehicle
[AIAA PAPER 92-0168] p 254 A92-23779
Center of pressure calculations for a bent-axis vehicle
[DE92-005186] p 498 N92-20143
POLESKY, SANDRA P.
Three-dimensional thermal structural analysis of a swept cowl leading edge subjected to skewed shock-shock interference heating p 174 A92-20306
POLHEMUS, WILLIAM L.
Greater RNAV utilization could expand system capacity p 448 A92-29507
POLICHAR, RAULF
Neutron radiography with SNRS p 492 A92-28747
POLING, DAVID R.
Fundamental research in helicopter rotor blade-vortex interaction modeling p 65 A92-14358
POLL, D. I. A.
Boundary-layer transition and heat transfer on slender delta wings
[AERO-REPT-8904] p 262 N92-17849
Marching with the parabolized Navier-Stokes equations. Problem 1: Numerical study of hypersonic viscous cone flow
[AERO-REPT-9007] p 344 N92-18231
Marching with the parabolized Navier-Stokes equations. Problem 2: Hypersonic viscous flow over a flat plate
[AERO-REPT-9008] p 345 N92-18232
Zonal solutions for a double-ellipse in a hypersonic flowfield
[AERO-REPT-9009] p 345 N92-18233
Towards the computation of turbulent hypersonic flows
[AERO-REPT-9106] p 345 N92-18318
The installation of the AVRO 9 by 7 foot low-speed wind tunnel at the University of Manchester (England)
[AERO-REPT-9005] p 385 N92-18341
POLLACK, M.
A simulation study of tiltrotor vertical takeoff procedures using conventional and variable diameter rotor systems
p 1056 A92-56301
POLLANO, G.
A fin optimisation study p 551 N92-23237
POLLARD, MICHAEL
Acoustic emission monitoring of a ground durability and damage tolerance test p 492 A92-28737
POLLINGER, J. P.
Development of silicon nitride rotors for the ATTAP program at Garrett Ceramic Components
[ASME PAPER 91-GT-154] p 142 A92-15590
The use of NDE as a process development tool for ceramic engine components
[ASME PAPER 91-GT-290] p 152 A92-15682
POLOSIN-NIKITIN, S. M.
Airfield construction (3rd revised and enlarged edition)
[ISBN 5-277-01070-X] p 670 A92-36606
POLVI, HENRY
Helicopter/ship analytic dynamic interface
p 464 N92-21962
POLYCARPOU, M. M.
Identification and control of aircraft dynamics using radial basis function neural networks
[AIAA PAPER 92-4393] p 1074 A92-55194
POLYCHRONIADIS, MICHEL
Generalized higher harmonic control - Ten years of Aerospatiale experience p 569 A92-35769
POLZ, G.
Current European rotorcraft research activities on development of advanced CFD methods for the design of rotor blades (BRITE/EURAM 'DACRO' project)
p 1032 A92-56332
POMERANTZ, ARTHUR P.
Nationwide system delay study of the microwave landing system in the New York terminal area, volume 1
[DOT/FAA/CT-TN91/59-VOL-1] p 640 N92-25098
POMPONI, R. A.
Low earth orbit satellite concepts for air traffic control applications
[AIAA PAPER 92-1927] p 453 A92-29856
PONTON, A. J.
The evaluation of canard couplings at high angles of attack
[AIAA PAPER 92-0281] p 318 A92-25735
PONTON, A. J. C.
Symmetry breaking in vortex flows on conical bodies
p 703 A92-41278
PONZI, C.
Metal matrix composite fabrication processes for high performance aerospace structures p 760 A92-42145
POOLLA, KAMESHWAR R.
H(infinity) control of linear systems with nonzero initial conditions p 50 A92-11430
POON, C.
Preliminary finite element analysis of unloaded and loaded notched composite laminated plates
[NRC-LTR-ST-1806] p 159 N92-13454
POOR, W. A.
The statistical estimation of navigation errors
p 97 A92-16652
POPE, A. NELSON
Areas of seal R/D at GE p 228 N92-15094
POPE, D. S.
Sound generation by a stenosis in a pipe
p 415 A92-26405
POPE, JOHN A.
Midair collision - The links in a chain
p 951 A92-52645
POPELKA, DAVID
V-22 pilot-in-the-loop aeroelastic stability analysis
p 133 A92-14422
POPLAVSKAIA, T. V.
On the calculation of the compressible boundary layer on a nonplanar delta wing with supersonic leading edges
p 252 A92-23409
The calculation of a compressible boundary layer past a pointed body and a delta wing p 622 A92-40173
POPPE, M.
Construction of a real-time DGPS experimental system
p 840 A92-47631
POPPEL, GARY L.
Fiber optic controls for aircraft engines - Issues and implications p 856 A92-46244
POPPEN, WILLIAM A.
Aerodynamic performance of a full-scale lifting ejector system in a STOVL fighter aircraft
[AIAA PAPER 92-3094] p 824 A92-48738
PORCHER, BRYAN
Advanced flight software reconfiguraton
p 287 N92-17350
PORDAL, H. S.
Transient behavior of supersonic flow through inlets
p 340 A92-28043
PORTABELLA, F. GOMEZ
Measurement of the flow distribution over the flight deck of an aircraft carrier p 504 N92-21955
PORTER, B.
Robustness characteristics of fast-sampling digital controllers for active flutter suppression
[AIAA PAPER 92-2104] p 567 A92-35675
Design of adaptive fast-sampling digital controllers for active flutter suppression
[AIAA PAPER 92-2105] p 567 A92-35676
Robustness characteristics of fast-sampling digital PI controllers for high-performance aircraft with impaired control surfaces p 877 A92-48496
PORTER, C. R.
Fiber-coupled position sensors for aerospace applications p 370 A92-27776
A novel avionic sensor for fly-by-light controls
p 650 A92-38128
PORTER, G.
Research, services, and facilities (National Institute of Standards and Technology)
[PB92-109172] p 485 N92-21870
PORTER, P. G.
Durability and damage tolerance of aluminum castings
[AD-A245237] p 490 N92-21159
POSENAU, MARY-ANNE K.
Delaunay triangulation and computational fluid dynamics meshes
[NASA-TM-107663] p 1010 N92-30907
POST, M. J.
Measured and calculated optical property profiles in the mixed layer and free troposphere p 1129 A92-54630
POSTLETHWAITE, I.
Full authority active control system design for a high performance helicopter p 567 A92-35732
POT, T.
New hypersonic test methods developed at ONERA - The R5 and F4 wind tunnels
[ONERA, TP NO. 1992-39] p 882 A92-48600
POTAPCZUK, M. G.
Icing simulation: A survey of computer models and experimental facilities p 450 N92-21684
Simulation of iced wing aerodynamics
p 450 N92-21686
POTAPCZUK, MARK G.
LEWICE/E - An Euler based ice accretion code
[AIAA PAPER 92-0037] p 316 A92-25676
LEWICE/E: An Euler based ice accretion code
[NASA-TM-105389] p 179 N92-14001
Experimental ice shape and performance characteristics for a multi-element airfoil in the NASA Lewis Icing Research Tunnel
[NASA-TM-105380] p 261 N92-17347
POTAPOV, G. P.
A test bench for evaluating powerplant electrization
p 138 A92-16830

POTASHEV, A. V.
Design of wing profiles with tangential suction or injection p 624 A92-40602
Construction of a wing profile with a flap modeled by a point vortex p 707 A92-42726
Aerodynamic airfoils design by quasi-solutions method of inverse boundary-value problems p 1020 A92-53998
POTOCKI DE MONTALK, J. P. P.
Computer software in civil aircraft p 1006 A92-49302
POTOTZKY, ANTHONY
On-line performance evaluation of multiloop digital control systems p 873 A92-46739
POTOTZKY, ANTHONY S.
Determining design gust loads for nonlinear aircraft similarity between methods based on matched filter theory and on stochastic simulation
[AIAA PAPER 92-2369] p 518 A92-34597
Rolling Maneuver Load Alleviation using active controls
[AIAA PAPER 92-2099] p 566 A92-35670
Maximized gust loads for a nonlinear airplane using matched filter theory and constrained optimization
[NASA-TM-104138] p 23 N92-11010
Rolling maneuver load alleviation using active controls
[NASA-TM-107654] p 962 N92-31351
POTTER, J. L.
Local bridging to predict aerodynamic coefficients in hypersonic, rarefied flow p 705 A92-41541
POTTER, J. LEITH
Rarefied-flow aerodynamics
[NASA-CR-190452] p 715 N92-27191
POTTER, K. J.
An evaluation of a simple PID controller designed using optimal control theory when applied to helicopter stabilisation p 569 A92-35785
POTYONDY, D. O.
Simulation of 3D non-planar fatigue crack growth in a turbine blade root
[DE92-006859] p 739 N92-26697
POULIN, RICHARD G.
Flight testing the avionics system of the V-22 Osprey p 117 A92-14378
POULOSE, M. M.
Microwave landing system modeling with application to air traffic control automation p 725 A92-41220
POVAROV, O. A.
Two-phase flows at supersonic velocities p 4 A92-10907
POVAROVA, K. B.
High-temperature metal matrix composite p 1105 A92-53878
POVINELLI, LOUIS A.
Navier-Stokes solution of transonic cascade flows using nonperiodic C-type grids p 344 A92-28523
Workshop on Engineering Turbulence Modeling
[NASA-CP-10088] p 678 N92-24514
Trends in aeropropulsion research and their impact on engineering education
[NASA-TM-105682] p 972 N92-31172
POVINELLI, MARK J.
Finite element analysis of large wavelength antenna radome problems for leading edge and radar phased arrays p 267 A92-23984
POWELL, ARTHUR G.
Supersonic boundary-layer stability analysis on an aircraft wing p 9 A92-13207
POWELL, CLEMANS A.
Human response to aircraft noise p 236 N92-14780
POWELL, DAVID
Integration of artificial intelligence and numerical optimization techniques for the design of complex aerospace systems
[AIAA PAPER 92-1189] p 600 A92-33301
POWELL, FREDERIC D.
Mobile Microwave Landing System (MMLS): Operational requirements for setup accuracy
[AD-A241844] p 103 N92-13052
POWELL, FREDERICK D.
The problem of multiple solutions in area navigation and computed centerline operations with the microwave landing system
[AD-A242757] p 191 N92-15058
POWELL, KENNETH G.
Euler calculations of axisymmetric under-expanded jets by an adaptive-refinement method
[AIAA PAPER 92-0321] p 321 A92-25768
A wave-model-based refinement criterion for adaptive-grid computation of compressible flows
[AIAA PAPER 92-0322] p 321 A92-25769
Similarity solutions for viscous vortex cores p 759 A92-41658
POWELL, RICHARD KARL
Computered tomography: Experimental data acquisition and parallelization of reconstruction algorithm
[DE92-005151] p 499 N92-20301
POWELL, RICHARD W.
A six-degree-of-freedom guidance and control analysis of Mars aerocapture
[AIAA PAPER 92-0736] p 486 A92-31676
Earth aerobraking strategies for manned return from Mars p 752 A92-41535
POWELL, WILLIAM E.
NASP - A status report
[AIAA PAPER 92-1417] p 666 A92-38569
NASP X-30 Propulsion technology status p 475 N92-21534
PRABHU, DINESH K.
Numerical simulation of unsteady flow in a hypersonic shock tunnel facility
[AIAA PAPER 92-4029] p 1034 A92-56851
PRABHU, RAMADAS K.
Computational method to predict thermodynamic, transport, and flow properties for the modified Langley 8-foot high-temperature tunnel
[NASA-TM-4374] p 767 N92-27193
PRANDI, B.
The beta-CEZ - A high performance titanium alloy for aerospace engines p 289 A92-22760
PRANG, LOTHAR
Interdependencies of aircraft-/airport-noise and urban- and regional-planning standards p 688 A92-39063
PRASAD, ANIL
Numerical and experimental investigations of rarefied gas flows through nozzles and composite systems p 940 A92-52797
PRASAD, C. B.
A Protection And Detection Surface (PADS) for damage tolerance p 1107 N92-32523
PRASAD, DILIP
Numerical and experimental investigations of rarefied gas flows through nozzles and composite systems p 940 A92-52797
PRASAD, J. V. R.
Performance and handling qualities criteria for low cost real time rotorcraft simulators - A methodology development p 136 A92-14365
A new method for simulating atmospheric turbulence for rotorcraft applications p 162 A92-14368
Nonlinear control of a twin-lift helicopter configuration p 204 A92-18624
Active vibration control using fixed order dynamic compensation with frequency shaped cost functionals p 508 A92-29324
Some issues on modeling atmospheric turbulence experienced by helicopter rotor blades p 647 A92-40885
Adequacy of modeling turbulence and related effects on helicopter response p 730 A92-41263
Active control of blade vortex interaction p 814 A92-46944
On the adequacy of modeling turbulence and related effects on helicopter response p 847 A92-46945
Smart structures in the active control of blade vortex interaction p 1085 A92-56314
Helicopter nonlinear flight control system development p 1085 A92-56317
A new method for simulating atmospheric turbulence for rotorcraft applications p 464 N92-21956
PRASANTH, R. K.
Robust wind shear stochastic controller-estimator p 661 A92-39893
Robust flight reconstruction for helicopter simulation and training p 747 A92-41230
PRASANTH, RAVI K.
Specifying exhaust nozzle contours in real-time using genetic algorithm trained neural networks
[AIAA PAPER 92-3328] p 865 A92-48911
PRATHER, MICHAEL J.
The atmospheric effects of stratospheric aircraft: A first program report
[NASA-RP-1272] p 408 N92-19121
Designing a methodology for future air travel scenarios p 409 N92-19125
PRATHER, WILLIAM D.
Comparison of R2SPG waveforms with simulated EMP p 760 A92-42317
Using the single point excitation technique to measure aperture impedance over a broad frequency range p 761 A92-42320
PRATT, M.
Integrated use of GPS and GLONASS in civil aviation navigation. I - Coverage and data models p 99 A92-16950
GLONASS data analysis - Interim results p 955 A92-49382
PRATTE, JAMES F.
LDF thermoplastic composites technology p 34 A92-13243
PREEN, PHILIP J.
Testing and evaluation of the Vanner electrical inverters, models 24-1500 and SP 00112
[AD-A241914] p 299 N92-17216
PREISIGKE, HANS-JOERG
Calculation of transonic flow in turbomachine cascades p 708 A92-43067
PREL, P.
Method for calculating the three-dimensional water concentration coefficients and its industrial applications p 502 N92-21685
PREOBRAZHENSKII, A. S.
Technique for estimating the strength of gas turbine guide vanes with stress raisers p 761 A92-42653
PRESSER, C.
Aerodynamic effects on fuel spray structure - Experiment and theory
[AIAA PAPER 92-0227] p 317 A92-25691
PRESTON, J.
Continuous flying quality improvement - The measure and the payoff
[AIAA PAPER 92-4327] p 1073 A92-55171
PRESZ, W. M., JR.
Supersonic nozzle mixer ejector p 376 A92-28536
PRETZER, F. L.
Reliability centered maintenance for metallic airframes based on a stochastic crack growth approach p 897 A92-45242
PREVALLET, L. C.
Single lever power management of turboprop engines
[SAE PAPER 912200] p 656 A92-40013
PREVOT, T.
Knowledge-based planning for controlled airspace flight operation as part of a cockpit assistant p 727 N92-27895
PRICE, JOSEPH M.
Hypersonic rarefied flow past spheres including wake structure
[AIAA PAPER 92-0495] p 329 A92-26325
Computation of near-wake, aerobrake flowfields p 441 A92-32181
PRICE, ROBERT C.
V-22 full scale development testing p 646 A92-40038
PRICE, S. J.
Development and analysis of flight flutter prediction methods
[AIAA PAPER 92-2101] p 588 A92-35672
PRIDGEON, SCOTT P.
Cost/benefit analysis of the AH-64 (Apache) helicopter Automated Test Equipment (ATE)
[AD-A252909] p 1101 N92-33398
PRIEL, BENI I.
The effect of gyro nonorthogonality error on gyrocompassing p 1045 A92-55955
PRIEUR, J.
Aerodynamic and acoustic calculations of transonic nonlifting hovering rotors
[ONERA, TP NO. 1991-178] p 77 A92-16140
Influence of geometrical parameters on helicopter rotor high speed impulsive noise
[ONERA, TP NO. 1992-40] p 926 A92-48601
PRIEUR, JEAN
Importance of an accurate prediction of shock curvature for high-speed rotor noise p 414 A92-25578
PRILL, ROBERT S.
Programmable channelized digital radio/modem p 955 A92-49291
PRILLWITZ, RONALD D.
Stage 2 noise certification of the Sikorsky S-76A and S-76C helicopters p 91 A92-14388
PRINCE, CAROLYN
An analysis of aircrew communication patterns and content
[AD-A246618] p 907 N92-28253
PRINZ, U.
Numerical simulation of chemical and thermal nonequilibrium flows behind compression shocks
[AIAA PAPER 92-2879] p 820 A92-47860
PRISCO, GIULIO
Parallelization of a Direct Simulation Monte Carlo (DSMC) code for fluid dynamics p 227 N92-15033
PRITCHARD, JOCELYN I.
Integrated multidisciplinary rotorcraft optimization research at the NASA Langley Research Center p 419 A92-29673
Optimizing tuning masses for helicopter rotor blade vibration reduction including computed airloads and comparison with test data
[AIAA PAPER 92-2376] p 542 A92-34546

Optimizing tuning masses for helicopter rotor blade vibration reduction including computed airloads and comparison with test data
[NASA-TM-104194] p 367 N92-19846
PRITTS, DOUGLAS P.
Concept evaluation of the UH-60 externally mounted rescue hoist
[AD-A240545] p 22 N92-11004
PRITULO, T. M.
Calculation of the rolling moment for a wing with a supersonic leading edge in the presence of sideslip
p 426 A92-30186
PROBERT, BRIAN
Comparison of recent results from different wind tunnel facilities along with comparisons of measured flight results and wind tunnel based predictions
[AIAA PAPER 92-3985] p 1060 A92-56809
PROCTOR, F. H.
Evaluation of a technique to quantify microburst windshear hazard potential to aircraft p 17 A92-11379
PROCTOR, FRED H.
Three-dimensional simulation of the Denver 11 July Storm of 1988 - An intense microburst event
p 407 A92-27958
PROSKAWETZ, K.-O.
System-identification of airplanes using the 'estimation before modelling' technique p 269 A92-21007
PROVENCIO, ANTONIO C.
Iberia's Aeronautical Mapping Application (ACAI)
p 637 A92-37073
PROVOTOROV, V. P.
Effect of viscosity on the drag of slender axisymmetric bodies in hypersonic flow p 425 A92-30154
PROZOROV, A. G.
An experimental study of tone-like noise in the flow past a wing at low flow velocities p 425 A92-30160
An experimental study of the noise of flow past a wing at low velocities p 603 A92-33771
PRUETT, C. D.
On the nonlinear stability of a high-speed, axisymmetric boundary layer p 78 A92-16457
Direct numerical simulation of laminar breakdown in high-speed, axisymmetric boundary layers
[AIAA PAPER 92-0742] p 343 A92-28223
PRUFERT, M. B.
Turbine engine hot-part temperature measurement techniques
[AIAA PAPER 92-3960] p 1122 A92-56788
Turbine engine performance test and evaluation techniques
[AIAA PAPER 92-3977] p 1071 A92-56803
PRUITT, GERALD R.
Reliability growth of coolers for advanced optical systems and instruments p 294 A92-22879
PRUVOST, M.
Study of interactions on anemoclinometric sensors
[REPT-90/30] p 138 N92-12006
PRUYN, RICHARD R.
Testing and analysis of a 'smart' interface to connect two complex avionics bus systems without significant modification to the software of either system
p 964 A92-49254
PRYDZ, R. A.
Development and testing of cabin sidewall acoustic resonators for the reduction of cabin tone levels in propfan-powered aircraft
[NASA-CR-4388] p 166 N92-13757
PRYOR, ANNA H.
Optical computing at NASA Ames Research Center
[AIAA PAPER 91-3779] p 231 A92-17637
PRZEKWAS, A. J.
Prediction of shock pattern dynamics at hypersonic angle of attack maneuvers of endo-KEW missile forebodies
[AIAA PAPER 92-2768] p 704 A92-41317
A finite-volume numerical method to calculate fluid forces and rotordynamic coefficients in seals
[AIAA PAPER 92-3712] p 1113 A92-54132
Pressure-based high-order TVD methodology for dynamic stall control
[AD-A247056] p 774 N92-27918
PRZEKWAS, ANDRZEJ J.
Development of a CFD code for analysis of fluid dynamic forces in seals p 228 N92-15084
PRZYBYSZEWSKI, J. S.
High temperature static strain gage development
[NASA-CR-189044] p 195 N92-14037
PRZYBYTKOWSKI, S. M.
Finite element vorticity based methods for the solution of the compressible Navier-Stokes equations
p 246 A92-21983
PSIAKI, M. L.
Parallel solver for trajectory optimization search directions p 777 A92-43399
PSIAKI, MARK L.
Thrust laws for microburst wind shear penetration
p 873 A92-46750
Optimal aircraft performance during microburst encounter p 266 N92-17999
PUCHE, T. M.
Investigation of the tail buffeting of the C-101
p 942 A92-53253
PUECH, J. F.
Stretched skin concept for the entry aerodynamic decelerator system of planetary probes
p 576 N92-23836
PUGH, EVAN R.
Laser-driven hypersonic air-breathing propulsion simulator
[AIAA PAPER 92-3922] p 1095 A92-56753
PUGH, THOMAS S.
The U-2A flight test program
[AIAA PAPER 92-1086] p 537 A92-33252
PULSONETTI, M. V.
Hypersonic mixing and combustion studies in the hypulse facility p 737 A92-44526
PULSONETTI, MARIA V.
Engineering model for analysis of scramjet combustor performance with finite-rate chemistry
p 129 A92-17202
PULVIN, P.
The combined wake of an array of oscillating ribbons
p 623 A92-40180
PURDON, DAVID J.
PAN AIR: A computer program for predicting subsonic or supersonic linear potential flows about arbitrary configurations using a higher order panel method. Volume 2: User's manual (version 3.0)
[NASA-CR-3252] p 527 N92-22865
PURIFOY, DANA D.
X-29 high angle of attack p 111 A92-16052
PURSEL, ROBERT
Joint Federal Aviation Administration (FAA)/Civil Aviation Authority (CAA) Microwave Landing System (MLS) Area Navigation (RNAV) flight evaluations
[DOT/FAA/CT-TN91/17] p 268 N92-15983
PUSTER, RICHARD L.
Research capabilities of the NASA Langley 8-foot high temperature tunnel p 980 A92-51403
PUTERBAUGH, STEVEN L.
A critical evaluation of a three-dimensional Navier-Stokes method as a tool to calculate transonic flows inside a low-aspect-ratio compressor
p 768 N92-27459
PUTT, JAMES C.
Advanced pneumatic impulse ice protection system (PIIP) for aircraft p 845 A92-46807
PUZACH, S. V.
Effect of supersonic diffuser geometry on operation conditions p 310 A92-24599
PYLE, J.
Ozone response to aircraft emissions: Sensitivity studies with two-dimensional models p 409 N92-19126
PYNE, C. R.
A review of rigid body response on sting supported models at high angles of incidence p 66 A92-15345
PYNE, TONY
The law in Australia relating to negligence of aircrew and engineers p 606 A92-33463

Q

QI, FENG
Effects of bleed and power extraction on the operating line of engines p 469 A92-29717
QIAN, HUEDE
Aerodynamic design of propeller by numerical optimization p 24 A92-10957
QIAN, Y. J.
Extended mapping and characteristics techniques for inverse aerodynamic design p 194 N92-13949
QIAN, Z.
Fracture behaviour of high-temperature polymer composites p 34 A92-11993
QIAO, WEIYANG
The engineering prediction for aircraft noise
p 1010 A92-50206
QIAO, XIN
Dynamic behavior analysis for landing-gear with different types of dual-chamber shock-struts p 111 A92-15342
Aeroelastic tailoring of aeronautical composite wing structures p 146 A92-15343
The stability analysis of the nonlinear shimmy
p 358 A92-27902
QIU, TAO
Experimental investigation on flutter characteristics of composite torsion-box p 996 A92-53055
QIU, X. Y.
A new vane swirler as applied to dual-inlet side-dump combustor
[AIAA PAPER 92-3654] p 906 A92-49085
QIU, XIAOMEI
Energy analysis of aeroengine and its significance
p 557 A92-35569
QIU, XINYU
An experimental investigation of the swirling combustor for integral liquid fuel ramjet p 557 A92-35541
QIU, Y. J.
Computational and experimental studies of flow in multi-lobed forced mixers
[AIAA PAPER 92-3568] p 1112 A92-54057
QU, BENHE
Joined-wing model vibrations using PC-based modal testing and finite element analysis
[AIAA PAPER 92-2260] p 541 A92-34417
QUACH, TAI
Flight research p 194 N92-13981
QUACKENBUSH, TODD R.
Prediction of high-resolution flowfields for rotorcraft aeroacoustics p 53 A92-11053
A fast three-dimensional vortex method for unsteady wake calculations
[AIAA PAPER 92-2624] p 794 A92-45496
Efficient high-resolution rotor wake calculations using flow field reconstruction p 814 A92-46951
Analysis of rotor vibratory loads using higher harmonic pitch control
[NASA-CR-189591] p 696 N92-24251
QUADFASEL, U.
Probabilistic lifing approach for aero engine disks made of powder nickel base alloys containing ceramic defects
p 226 N92-14424
QUAGLIAROLI, T. M.
Evaluation of OH laser-induced fluorescence techniques for supersonic combustion diagnostics
[AIAA PAPER 92-0508] p 396 A92-26935
KrF laser-induced OH fluorescence imaging in a supersonic combustion tunnel
[AIAA PAPER 92-3346] p 905 A92-48923
QUAGLIOTTI, F. B.
Experimental investigation of vortex dynamics on delta wings
[AIAA PAPER 92-2731] p 804 A92-45565
QUAN, ZHONG
An investigation of fuel nozzles for combustion performance p 278 A92-21745
QUART, BARRY
Implementation and usage of the RJ program Data Acquisition System Ground Station p 210 A92-19257
QUAST, A.
The A320 laminar fin programme
[ONERA, TP NO. 1992-23] p 849 A92-48586
QUEENEY, P. J.
Developments in airborne surveillance and control systems p 98 A92-16655
QUELLMANN, WILFRIED
Use of a virtual cockpit for the development of a future transport aircraft p 886 N92-28547
QUENTMEYER, RICHARD J.
An experimental investigation of high-aspect-ratio cooling passages
[AIAA PAPER 92-3154] p 890 A92-48780
QUERIN, OSVALDO M.
Flow visualisation of a small diameter rotor operating at high rotational speeds with blades at small pitch angles p 814 A92-46949
QUEROL, HENRI
The obstacle avoidance radar - A safety mean for low altitude flights in adverse weather conditions
p 554 A92-35743
QUINLIVAN, RICHARD
C-17 flight control system overview
p 1082 A92-55906
QUINN, B. J.
ASTOVL engine control p 860 A92-45321
ASTOVL engine control
[PNR-90808] p 740 N92-27040
QUINTAL, JOSEPH
MLS/RNAV control display unit development
p 965 A92-49303
QUINTANA, F.
Flow and temperature computations for space vehicles using adaptive finite element techniques
p 181 N92-14990
QUIRK, JAMES J.
An alternative to unstructured grids for computing gas dynamic flows around arbitrarily complex two-dimensional bodies
[NASA-CR-189612] p 447 N92-21465
QUMEI, IYAD K.
Chaotic and nonlinear dynamic response of aerosurfaces with structural nonlinearities
[AIAA PAPER 92-2547] p 518 A92-34517

R

RACHELE, HENRY
Assessment of one-dimensional icing forecast model applied to stratiform clouds p 915 A92-46803
RADDATZ, J.
Analysis of helicopter rotor-fuselage interference with time averaged pressure distribution p 1032 A92-56331
RADEMAKER, E. R.
Experimental validation of a line-duct acoustics model including flow
[NLR-TP-90223-U] p 927 N92-28695
RADER, JOCK A.
Automatic document generation with case on a DOD avionics project p 1005 A92-49299
RADESPIEL, R.
Vortical flow simulation by the solution of the Navier-Stokes equations p 620 A92-40104
Analysis tools of ONERA and DLR for the aerothermodynamics of reentry vehicles p 211 N92-14977
Progress with multigrid schemes for hypersonic flow problems
[NASA-CR-189579] p 185 N92-15047
RADEZTSKY, RONALD H.
Boundary-layer receptivity of sound with roughness p 604 A92-36006
RADLOFF, BRIAN
SHARP: Subsonic High Altitude Research Platform
[NASA-CR-190004] p 648 N92-25263
RADMAND, MANSOUR
A state-of-the-art data acquisition system p 217 A92-19231
RADYSH, IU. V.
Dynamic synthesis of mechanical systems with a finite number of degrees of freedom p 603 A92-33790
RAFFA, ANTHONY
Improved articulated fin/wing control system statement of government interests
[AD-D015268] p 1088 N92-34131
RAFFIN, G.
Flight crew integration in the maintenance chain of a commercial aircraft (A 320) p 1012 N92-30957
RAFFIN, M.
Experimental investigation of transverse jet effects related to hypersonic space vehicles p 182 N92-14995
Flat plates placed in depleted hypersonic flow
[SESSIA-430/91.960] p 947 N92-31508
RAFIN, C.
Flight crew integration in the maintenance chain of a commercial aircraft (A 320) p 1012 N92-30957
RAGHAVAN, V.
Flowfield analysis of modern helicopter rotors in hover by Navier-Stokes method
[AD-A245011] p 446 N92-21333
RAGHUNATHAN, S.
Effect of model cooling on periodic transonic flow p 813 A92-46900
Further investigation of the effect of model cooling on periodic transonic flow p 721 N92-27961
RAGSDALE, W. A.
Piloted simulator studies of the HL-20 Lifting Body p 666 A92-40033
RAHAI, H. R.
Turbulent flow in the wake of an idealized wing-body junction
[AIAA PAPER 92-0282] p 435 A92-31652
Phase-averaged turbulence statistics in a near wake with an asymmetric vortex shedding p 620 A92-40086
RAHAINGOMANANA, M.
Weak coupling between an unsteady 3D full potential code and an unsteady turbulent boundary layer code - Application to a helicopter rotor in forward flight
[AIAA PAPER 92-0029] p 249 A92-22151
RAHIER, G.
Blade-vortex noise on a helicopter main rotor. Study of the strong two dimensional incompressible interaction
[ONERA-RT-96/5094-PY] p 511 N92-20388
RAHIER, GILLES
Theoretical study and prediction of BVI noise including close interactions
[ONERA, TP NO. 1991-174] p 165 A92-16138
RAHN, ROBERT O.
Design is the name of the game - Comparison of the F5D Skylancer to the F4D Skyray p 167 A92-16062
RAI, H. G.
Mechanics of curved fiber composites p 140 A92-14346
Mechanics of curved fiber composites p 757 A92-41034
RAIS-ROHANI, MASOUD
Integrated aerodynamic-structural-control wing design p 349 N92-19698
RAISINGHANI, S. C.
Parameter estimation of an augmented airplane with unsteady aerodynamics modelling p 1073 A92-53546
RAITI, PETER
Fiber optic sensors for smart skins applications p 392 A92-24778
RAIZENNE, M. D.
Review of methods for crack growth testing in gas turbine engine disc materials p 296 A92-24193
A proposed composite repair methodology for primary structure
[NRC-LTR-ST-1658] p 115 N92-13056
RAJ, P.
Computational aerodynamics in aircraft design - Challenges and opportunities for Euler/Navier-Stokes methods
[SAE PAPER 911990] p 788 A92-45392
RAJAGOPAL, K.
Multizonal Navier-Stokes solutions for the multibody Space Shuttle configuration p 310 A92-24667
RAJAGOPAL, K. R.
Steady flow of a fluid-solid mixture in a circular cylinder
[DE91-018698] p 41 N92-10174
RAJAGOPALAN, R. G.
Three dimensional analysis of a rotor in forward flight p 64 A92-14329
A comparative study of turbulence models for overset grids
[AIAA PAPER 92-0437] p 327 A92-26284
A unified procedure for solving rotor flowfield, performance and interference p 814 A92-46950
RAJAMURTHY, M. S.
Dynamic flying investigations on 1/13.5 NALLA model (Longitudinal Results)
[NAL-PD-FC-9113] p 359 N92-18073
RAJAN, S. R.
Dynamic flying investigations on 1/13.5 NALLA model (Longitudinal Results)
[NAL-PD-FC-9113] p 359 N92-18073
RAJAOFETRA, MAURICE
Future air navigation systems for Africa p 532 A92-33439
RAJCZEWSKI, DAVID M.
X-29 high angle-of-attack flight test air data comparisons of an inertial navigation system and noseboom probe p 549 A92-35945
RAJU, I. S.
An independent refinement and integration procedure in multiregion finite element analysis
[AIAA PAPER 92-2290] p 582 A92-34307
RAJU, SAVITHRI
Multisensor data fusion and decision support for airborne target identification p 454 A92-31063
RALLO, R.
An investigation of passive control methods for shock-induced separation at hypersonic speeds
[AIAA PAPER 92-2725] p 808 A92-45596
RAM, G. R.
A unique approach to aircraft conflict resolution using artificial intelligence techniques p 190 N92-14029
RAMACHANDRAN, K.
Experimental and computational studies of hovering rotor flows p 815 A92-46954
The computation and validation of hovering rotor performance p 1055 A92-56285
RAMACHANDRAN, N.
Experimental results and numerical modeling of solidification during aircraft high-g arcs
[AIAA PAPER 92-0843] p 493 A92-29609
RAMAKRISHNAN, R.
Numerical simulation of aerothermal loads in hypersonic engine inlets due to shock impingement
[AIAA PAPER 92-2605] p 792 A92-45482
Mixing and combustion effects in a sliding-wedge ram accelerator with hydrogen injection
[AIAA PAPER 92-3251] p 890 A92-48849
RAMAKRISHNAN, RAMANATH I.
Modeling the heat treatment of superalloys p 755 A92-43679
RAMAKRISHNAN, S.
Multizonal Navier-Stokes solutions for the multibody Space Shuttle configuration p 310 A92-24667
RAMAKRISHNAN, S. V.
Scale effects on the flow past the mated Space Shuttle configuration
[AIAA PAPER 92-2680] p 799 A92-45532
RAMALINGAM, T.
Estimating the reliability of a system on the basis of sample paths
[AD-A248585] p 774 N92-28171
RAMAMOORTHY, R. P.
Nonlinear landing gear behavior at touchdown p 192 A92-19606
RAMAMURTI, R.
A semi-elliptic analysis for 2-D viscous flows through cascade configurations p 3 A92-10688
RAMAN, GANESH
The flip flop nozzle extended to supersonic flows
[AIAA PAPER 92-2724] p 803 A92-45561
RAMAPRAIN, B. R.
Study of the leading-edge vortex dynamics in the unsteady flow over an airfoil
[AD-A247532] p 829 N92-28865
RAMAPRIAN, B. R.
LDV measurements in the unsteady tip-vortex behind an oscillating rectangular wing p 620 A92-40085
Measurements of the velocity and vorticity fields around a pitching airfoil
[AIAA PAPER 92-2626] p 794 A92-45498
LDV measurements in the three-dimensional near wake of a stationary and oscillating rectangular wind
[AIAA PAPER 92-2689] p 799 A92-45536
RAMASWAMY, M. A.
Prediction of separation point in compressible turbulent boundary layers by Green's lag-entrainment method p 700 A92-41178
RAMBONE, JAMES D.
ILS mathematical modeling study of an ILS localizer and glide slope proposed for runway 32R, Moffett Field Airport, California
[DOT/FAA/CT-TN92/28] p 1048 N92-33308
RAMESH, V.
Prediction of separation point in compressible turbulent boundary layers by Green's lag-entrainment method p 700 A92-41178
Acoustic control of combustor primary zone air-jet mixing
[AIAA PAPER 92-3651] p 1067 A92-54104
RAMETTE, PHILIPPE
Potential hypersonic vehicles applications
[AIAA PAPER 91-5086] p 169 A92-17854
RAMIZ, ANWAR
Dynamical scaling of a model unsteady separating flow p 1117 A92-54932
RAMIZ, M. A.
Detection of flow state in an unsteady separating flow p 219 A92-20741
RAMJEE, V.
Prediction of wake in a curved duct p 3 A92-10487
RAMKUMAR, R. L.
Manufacturing cost model for composites p 1012 A92-51565
RAMOND, J. P.
The advantages of digital engine control as compared with traditional systems (hydraulic or pneumatic) p 1070 A92-56338
RAMPERSAD, KRISHNA
Magnetic particle testing of turbine blades mounted on the turbine rotor shaft p 898 A92-46498
RAMSDEN, J. M.
Review of aviation record p 634 A92-39302
BA's 777 p 958 A92-51580
RAMSEY, CHRISTOPHER
Test results for rotordynamic coefficients of the SSME HPOTP turbine interstage seal with two swirl brakes p 223 N92-14357
RAMSEY, J. L.
Technical feasibility of digital three-dimensional cellular communications for air traffic control applications. Volume 1: Introduction and summary
[AD-A244573] p 534 N92-22104
Technical feasibility of digital three-dimensional cellular communications for air traffic control applications. Volume 2: Example system design details
[AD-A244574] p 534 N92-22105
Technical feasibility of digital three-dimensional cellular communications for air traffic control applications. Volume 3: Ground network architecture
[AD-A244575] p 534 N92-22106
RAMSEY, JOHN
Experimental unsteady pressures on an oscillating cascade with supersonic leading edge locus
[AIAA PAPER 92-4035] p 1035 A92-56857
RAMSTEDT, CLARENCE F.
Pulsed field system for detecting the presence of a target in a subsurface environment
[AD-D015074] p 296 N92-16174
RAMULU, M.
Tear straps in airplane fuselage
[AD-A248543] p 854 N92-29511
RAN, ZHENG
A calculating method of shock wave oscillating frequency due to turbulent shear layer fluctuations in supersonic flow p 251 A92-22720
RAND, O.
Experimental investigation of periodically excited rotating composite rotor blades p 218 A92-20213
Response of helicopter blades to a sharp collective increase p 1084 A92-56282

A generic harmonic rotor model for helicopter flight simulation p 1086 A92-56333
RAND, OMRI
Modeling methods for high-fidelity rotorcraft flight mechanics simulation
[NASA-TM-103842] p 482 N92-21440
RANEY, DAVID L.
Control concept for maneuvering in hypersonic flight
[AIAA PAPER 91-5055] p 203 A92-17838
Control integration concept for hypersonic cruise-turn maneuvers
[NASA-TP-3136] p 481 N92-20195
RANGACHARYULU, M. A.
Flight vibration testing of the V-22 tiltrotor aircraft
p 107 A92-14397
RANGWALLA, AKIL A.
Application of an unsteady Navier-Stokes solver to transonic turbine design p 935 A92-50273
RANKIN, JAMES
Avionics systems engineering education
p 1012 A92-49269
RANKINE, ROBERT R., JR.
Total quality treatment for science and technology
p 697 A92-36950
RANOUX, GILBERT
Patch-independent structured multiblock grids for CFD computations p 919 A92-47078
RANSFORD, KEVIN M.
Baseline vibration measurements of remotely piloted helicopters for higher harmonic control research
[AD-A244669] p 482 N92-21360
RANSHAW, M. J.
Coherence multiplexed polarimetric fibre sensor arrays for aerospace applications p 370 A92-27785
RANSOM, J. B.
Coupled analysis of independently modeled finite element subdomains
[AIAA PAPER 92-2235] p 581 A92-34289
RANSOM, JONATHAN B.
Global/local methods research using the CSM testbed
p 1107 N92-32528
Computational methods for global/local analysis
[NASA-TM-107591] p 1125 N92-33104
RANUCCI, D.
High temperature low cycle fatigue of single crystal nickel base superalloys p 213 A92-19796
RAO, DHANVADA M.
A LEX blowing technique for post-stall lateral control of trapezoidal wings
[AIAA PAPER 92-2714] p 802 A92-45553
Exploratory investigation of a spanwise blowing concept for tip-stall control on cranked-arrow wings
[AIAA PAPER 92-2637] p 806 A92-45576
Vortex control: Further encounters p 87 N92-13020
A low-speed wind tunnel study of vortex interaction control techniques on a chine-forebody/delta-wing configuration
[NASA-CR-189616] p 632 N92-25510
High-alpha vortex decoupling investigations on a chine forebody/Delta wing configuration at transonic Mach numbers
[NASA-CR-189642] p 715 N92-26651
Subsonic investigations of vortex interaction control for enhanced high-alpha aerodynamics of a chine forebody/Delta wing configuration
[NASA-CR-189641] p 715 N92-26652
RAO, G. N. V.
Measurement of magnus derivatives with an elastically forced oscillation rig p 749 A92-43172
RAO, K. V.
Vane-blade interaction in a transonic turbine. I - Aerodynamics
[AIAA PAPER 92-3323] p 825 A92-48906
Vane-blade interaction in a transonic turbine. II - Heat transfer
[AIAA PAPER 92-3324] p 904 A92-48907
RAOL, J. R.
Estimation of lift and drag characteristics of an aircraft from flight data p 959 A92-51942
Computer aided evaluation of aircraft handling qualities and flight control system robustness
[AIAA PAPER 92-4423] p 1080 A92-55347
PC based flight path reconstruction using UD factorization filtering algorithm
[NAL-PD-FC-9201] p 534 N92-22389
RAPP, HELMUT
Non-homogeneous bars under tension, pure bending and thermal loads p 495 A92-31198
Influence of cross section variations on the structural behaviour of composite rotor blades
p 1121 A92-56320
Avionics systems development: Technological trends, conflicts, and cost issues in a changing European environment p 199 N92-14054
RAPUC, M.
Acquisition of an aerothermodynamic data base by means of a winged experimental reentry vehicle
p 486 A92-30685
Acquisition of an aerothermodynamic data base by means of a winged experimental reentry vehicle
[MBB/FE202/S/PUB/461] p 787 N92-30232
RAQUET, CHARLES A.
ACTS aeronautical experiments
[AIAA PAPER 92-2042] p 485 A92-29956
RASHIDI, MAJID
Dynamics of a split torque helicopter transmission
[NASA-TM-105681] p 910 N92-29136
RASHIDIAN, B.
An efficient algorithm for optimal aircraft trajectories
[AIAA PAPER 92-4412] p 1076 A92-55206
RASMUSSEN, ROY M.
Precipitation development in Colorado Front Range snowstorms - 15 November 1987 case study
p 301 A92-23008
RASMUSSEN, STEVEN J.
Application of nonlinear QFT to flight control design for high angle of attack maneuvers with thrust vectoring
[AD-A243821] p 381 N92-19241
RASPET, RICHARD
Steady state risetimes of shock waves in the atmosphere p 1140 N92-33882
RASTY, J.
Electronics/avionics integrity - Definition, measurement and improvement p 1120 A92-56252
RATCLIFF, ROBERT R.
Direct-inverse transonic wing-design method in curvilinear coordinates including viscous interaction
p 193 A92-20202
RATHINAM, R.
Estimation of overall drag coefficient of an aerospace plane p 700 A92-41188
RAULT, DIDIER F. G.
Aerodynamic characteristics of a hypersonic viscous optimized waverider at high altitudes
[AIAA PAPER 92-0306] p 320 A92-25755
RAUPP, F.
An efficient method for three-dimensional route planning with different strategies and constraints
p 728 N92-27901
RAUSCH, RUSS D.
Three-dimensional time-marching aeroelastic analyses using an unstructured-grid Euler method
[AIAA PAPER 92-2506] p 542 A92-34500
Spatial adaptation of unstructured meshes for unsteady aerodynamic flow computations p 610 A92-36838
Three-dimensional time-marching aeroelastic analyses using an unstructured-grid Euler method
[NASA-TM-107567] p 527 N92-23116
Unstructured-grid methods development for unsteady aerodynamic and aeroelastic analyses
p 718 N92-27938
RAUSCH, VINCENT L.
Technologies for the National Aero-Space Plane
[IAF PAPER 92-0868] p 1105 A92-57259
RAUSCHER, MARK E.
Space Shuttle shell structure waffle panel optimization
[AIAA PAPER 92-2359] p 586 A92-34591
RAVI, R.
A computational study on directional stability of chine-shaped forebodies at high-alpha
[AIAA PAPER 92-0030] p 249 A92-22152
Compensating for manufacturing and life-cycle variations in aircraft engine control systems
[AIAA PAPER 92-3869] p 868 A92-49139
Hi-alpha forebody design. Part 1: Methodology base and initial parametrics
[NASA-CR-189849] p 358 N92-18024
Hi-alpha forebody design. Part 2: Determination of body shapes for positive directional stability
[NASA-CR-189850] p 359 N92-18038
RAVI, RAMAKRISHNAN
A computational examination of directional stability for smooth and chined forebodies at high-alpha
[NASA-CR-4465] p 950 N92-32114
RAWLINGS, R. C.
GPS - Can it contribute to European ATC?
p 637 A92-38380
RAWLINS, W. T.
Supersonic combustor testing using optical diagnostics and a high enthalpy shock tunnel
[AIAA PAPER 92-0761] p 384 A92-27102
RAWNSLEY, B. W.
An evaluation of a simple PID controller designed using optimal control theory when applied to helicopter stabilisation p 569 A92-35785
RAY, ASOK
A stochastic regulator for integrated communication and control systems. I - Formulation of control law. II - Numerical analysis and simulation p 233 A92-19605
Observability under recurrent loss of data
p 302 A92-21191
RAY, J. K.
High-speed civil transport flight- and propulsion-control technological issues
[NASA-CR-186015] p 482 N92-21253
RAY, LAURA R.
Application of stochastic robustness to aircraft control systems p 204 A92-18620
Technical notes and correspondence: Stochastic robustness of linear time-invariant control systems
p 303 N92-18002
RAY, ROBERT
On the aerodynamics/dynamics of store separation from hypersonic aircraft
[AIAA PAPER 92-2722] p 807 A92-45595
RAY, RONALD J.
Effects of bleed air extraction of thrust levels on the F404-GE-400 turbofan engine
[AIAA PAPER 92-3092] p 1066 A92-54009
Effects of bleed air extraction on thrust levels on the F404-GE-400 turbofan engine
[NASA-TM-104247] p 871 N92-29425
RAYMER, DANIEL P.
Configuration development p 552 N92-23953
RAZANI, A.
Optimum dimensions of convective-radiative spines using a temperature correlated profile
p 676 A92-40869
The optimization of variable cross-section spines with temperature dependent thermal parameters
p 901 A92-48353
RAZETO, W.
Structural design for durability - Lessons learned from service and test data
[AIAA PAPER 92-1129] p 537 A92-33281
RE, RICHARD J.
Interference effects of very high bypass ratio nacelle installations on a low-wing transport
[ASME PAPER 91-GT-241] p 75 A92-15646
Static internal performance of ventral and rear nozzle concepts for short-takeoff and vertical-landing aircraft
[NASA-TP-3103] p 12 N92-10975
Installation effects of wing-mounted turbofan nacelle-pylons on a 1/17-scale, twin-engine, low-wing transport model
[NASA-TP-3168] p 346 N92-19002
Parametric investigation of single-expansion-ramp nozzles at Mach numbers from 0.60 to 1.20
[NASA-TP-3240] p 1042 N92-34193
READ, WILLIAM J.
An evaluation of superresolution methods for tactical radio direction finding
[AD-A246316] p 726 N92-26291
REARDON, J.
The optimization of variable cross-section spines with temperature dependent thermal parameters
p 901 A92-48353
REARDON, K.
Evaluation of triple simultaneous parallel ILS approaches spaced 5000 feet apart, phase 4.b
[DOT/FAA/CT-91/31] p 456 N92-21404
REARDON, KIMBERLY
Evaluation of triple simultaneous parallel ILS approaches spaced 4300 feet apart, phase 4a
[ACD-340] p 191 N92-14034
REASON, JAMES
How to promote error tolerance in complex systems in the context of ships and aircraft p 673 A92-39308
REBARBER, RICHARD
Robustness of distributed systems with respect to small time delays p 47 A92-11351
REBAY, S.
Transonic and supersonic inviscid computations in cascades using adaptive unstructured meshes
[ASME PAPER 91-GT-312] p 75 A92-15689
REBER, RON
The Civil Rotorcraft Initiative - An action agenda
p 241 A92-22707
REBHAN, D.
Two-phase flow correlations in air/oil systems of aero engines
[ASME PAPER 91-GT-54] p 121 A92-15532
RECK, M.
Space Shuttle Orbiter auxiliary power unit status
[SAE PAPER 912060] p 889 A92-45442
REDA, D. C.
Liquid crystal coatings for surface shear-stress visualization in hypersonic flows p 496 A92-32177
REDA, DANIEL C.
Active thermal isolation for temperature responsive sensors
[NASA-CASE-LAR-14612-1] p 911 N92-29954
REDD, JUSTIN D.
Design of a fiber optic image transmission link
[AD-A243686] p 304 N92-17088

REDDAN, MICHEL
The new airport aeronautic meteorological codes
p 160 A92-13855
REDDINGIUS, N. H.
NSBIT program - Development of assessment system for aircraft noise and research on human impacts due to aircraft noise p 688 A92-39100
REDDY, BILL
Ship airwake measurement and modeling options for rotorcraft applications p 503 N92-21954
REDDY, D. R.
Three-dimensional viscous analysis of a Mach 5 inlet and comparison with experimental data
p 344 A92-28526
REDDY, E. S.
Analysis of aircraft engine blade subject to ice impact
[NASA-TM-105336] p 229 N92-15402
REDDY, N. N.
Acoustic loads prediction on jet aircraft
p 1136 N92-32949
REDDY, T. S. R.
Euler flow predictions for an oscillating cascade using a high resolution wave-split scheme
[ASME PAPER 91-GT-198] p 74 A92-15623
Time domain flutter analysis of cascades using a full-potential solver p 176 A92-20747
Aeroelastic analysis of advanced propellers using an efficient Euler solver
[AIAA PAPER 92-0488] p 341 A92-28194
Analysis of cascades using a two dimensional Euler aeroelastic solver
[AIAA PAPER 92-2370] p 556 A92-34598
A numerical classical flutter analysis of advanced propellers
[AIAA PAPER 92-2118] p 557 A92-35687
An investigation of cascade flutter using a two-dimensional full-potential solver
[AIAA PAPER 92-2119] p 558 A92-35688
REDEKER, G.
Aerodynamic analysis and modification design of NPU airfoils p 613 A92-38270
Concepts for the stability analysis of NLF-experiments on swept wings
[AIAA PAPER 92-2706] p 801 A92-45548
REDIN, L. V.
Experimental study of an adjustable plane supersonic diffusor p 426 A92-30173
REDINIOTIS, O. K.
Pitch-up motions of delta wings
[AIAA PAPER 92-0278] p 318 A92-25732
REDOLFI, J.
What is an ASIC? p 859 N92-28377
REED, D.
The NASA/Industry Design Analysis Methods for Vibrations (DAMVIBS) Program - Boeing helicopters airframe finite element modeling
[AIAA PAPER 92-2202] p 539 A92-34392
REED, HELEN
Linear stability of supersonic cone boundary layers
p 1024 A92-54910
REED, HELEN L.
Numerical simulation of swept-wing flows
[NASA-CR-189457] p 180 N92-14969
Stability and transition of hypersonic boundary-layer flows
[AD-A250279] p 948 N92-31555
REED, L. H. K.
Recent developments at the Shoeburyness STOVL test facility p 881 A92-45314
Recent developments at the Shoeburyness (England) STOVL Test Facility
[PNR-90806] p 572 N92-22096
REED, S. E.
Absolute fiber optic pressure transducer for aircraft air data measurement p 858 A92-48501
REEDER, M. F.
Effect of tabs on the evolution of an axisymmetric jet
p 656 A92-40151
Supersonic jet mixing enhancement by 'delta-tabs'
[AIAA PAPER 92-3548] p 826 A92-49063
Supersonic jet mixing enhancement by delta-tabs
[NASA-TM-105664] p 630 N92-24958
REEHORST, ANDREW L.
Prediction of ice accretion on a swept NACA 0012 airfoil and comparisons to flight test results
[AIAA PAPER 92-0043] p 316 A92-25677
Prediction of ice accretion on a swept NACA 0012 airfoil and comparisons to flight test results
[NASA-TM-105368] p 258 N92-15968
REES, D.
Environmental evaluation of repairs to fuselage lap joints p 699 A92-41534
REEVE, JOHN
Stellar inertial navigation growing with the times upgrading of the LN-20 integrated inertial navigation system p 97 A92-16646
REEVES, B. L.
Multiple aperture window and seeker concepts for endo KEW applications
[AIAA PAPER 92-2806] p 752 A92-41344
REEVES, M.
Holographic flow visualization in rotating turbomachinery
[PNR-90837] p 500 N92-20491
REGENIE, VICTORIA
The F-18 high alpha research vehicle: A high-angle-of-attack testbed aircraft
[NASA-TM-104253] p 1060 N92-33404
REGENIE, VICTORIA A.
Experience with Ada on the F-18 High Alpha Research Vehicle Flight Test Program
[NASA-TM-104259] p 1062 N92-34039
REGGIO, M.
A Navier-Stokes solver for stretched triangular grids
[AIAA PAPER 92-0183] p 256 A92-23793
Periodic Euler and Navier-Stokes solutions about oscillating airfoils p 626 N92-24850
REGISTER, JEFF
Current and future developments in civil aircraft non-destructive evaluation from an operator's point of view p 787 N92-30122
REHFIELD, LAWRENCE W.
New, unusual and nonclassical behavior of thin-walled composite structures p 580 A92-32746
Modeling and analysis methodology for aeroelastically tailored chordwise deformable wings
[NASA-CR-189620] p 961 N92-30304
REICH, A. D.
Ice property/structure variations across the glaze/rime transition
[AIAA PAPER 92-0296] p 351 A92-25749
REICHERT, B. A.
An experimental investigation of the flow in a diffusing S-duct
[AIAA PAPER 92-3622] p 1021 A92-54090
Navier-Stokes analysis and experimental data comparison of compressible flow within ducts
[NASA-TM-105796] p 972 N92-30972
REICHERT, BRUCE A.
Navier-Stokes analysis and experimental data comparison of compressible flow in a diffusing S-duct
[AIAA PAPER 92-2699] p 800 A92-45541
Trends in aeropropulsion research and their impact on engineering education
[NASA-TM-105682] p 972 N92-31172
Navier-Stokes analysis and experimental data comparison of compressible flow in a diffusing S-duct
[NASA-TM-105683] p 1072 N92-33746
REICHERT, G.
Active control of helicopter ground and air resonance
p 568 A92-35762
Short takeoff optimization for the XV-15 tiltrotor aircraft p 1056 A92-56302
REICHERT, ROBERT T.
Robust autopilot design for aircraft with multiple lateral-axes controls using H(infinity) synthesis
p 28 A92-11563
REID, L. D.
Adaptive simulator motion software with supervisory control p 412 A92-28136
Flight simulation p 207 N92-13982
An evaluation of IFR approach techniques: Generic helicopter simulation compared with actual flight
p 886 N92-28550
An evaluation of decelerating IFR approaches utilizing a helicopter flight simulator
[CTN-92-60348] p 1048 N92-32845
REID, LONNIE
A viscous flow study of shock-boundary layer interaction, radial transport, and wake development in a transonic compressor
[ASME PAPER 91-GT-69] p 68 A92-15539
REID, MAX B.
Optical computing at NASA Ames Research Center
[AIAA PAPER 91-3779] p 231 A92-17637
Binary optical filters for scale invariant pattern recognition
[NASA-TM-103902] p 853 N92-28910
REIFER, DONALD J.
Reuse metrics and measurement: A framework
p 413 N92-19432
REIGHARD, M. K.
Rapid ultrasonic scanning of aircraft structures
p 215 A92-17292
REIMERING, W. R. M.
Helicopter handling: Experience and new developments p 465 N92-21969
REINECKE, W. G.
Supersonic combustor testing using optical diagnostics and a high enthalpy shock tunnel
[AIAA PAPER 92-0761] p 384 A92-27102
Aerothermodynamic radiation studies
[NASA-CR-185666] p 284 N92-15998
REINER, JAKOB
Robust dynamic inversion control laws for aircraft *control*
[AIAA PAPER 92-4329] p 1073 A92-55173
REINHARDT, M. E.
Studies on the effect of high-flying air-traffic on the atmosphere
[IAF PAPER 91-737] p 301 A92-22495
REINHART, EUGENE R.
Surface residual stress analysis of metals and alloys
[AD-A248372] p 895 N92-28426
REINKENHOF, JOSEF
Thermodynamic behaviour of hydrogen-powered hypersonic ramjets flying along ideal trajectories
[IAF PAPER 91-277] p 25 A92-12601
REINL, WERNER
Modern helicopter technologies at MBB and the application in future programmes p 1016 A92-56304
REINMANN, J. J.
Technical evaluation report, AGARD Fluid Dynamics Panel Symposium on Effects of Adverse Weather on Aerodynamics
[NASA-TM-105192] p 2 N92-10002
Icing simulation: A survey of computer models and experimental facilities p 450 N92-21684
REINMANN, JOHN J.
Technical evaluation report on the Fluid Dynamics Panel Specialists' Meeting on Effects of Adverse Weather on Aerodynamics
[AGARD-AR-306] p 352 N92-18242
The NASA aircraft icing research program
p 549 N92-22534
NASA's aircraft icing technology program
[NASA-TM-104518] p 527 N92-23105
REISINGER, D.
Investigation of a plate-ramp-configuration by means of laser Doppler anemometry at Mach 2.95
[AIAA PAPER 92-3956] p 1097 A92-56784
The trisonic wind tunnel Muenchen and its involvement in the German SAeNGER-programme
[AIAA PAPER 92-4019] p 1100 A92-56841
REITZ, R. D.
Three-dimensional modeling of diesel engine intake flow, combustion and emissions
[NASA-CR-189126] p 658 N92-24539
REKKAS, C. M.
Computation of aircraft geometric height under radar surveillance p 639 A92-40239
RELOTIUS, KLAUS-DIETER
FALKE: Winged re-entry vehicle flight control
p 667 N92-24454
REMPEL, G.
Multiple phase centre DPCA for airborne radar
p 95 A92-16257
REMPFER, D.
Evolution of coherent structures during transition in a flat-plate boundary layer p 621 A92-40126
REN, XINGMIN
Transient response of the rotor-support system of aeroengines p 997 A92-53293
RENAUD, J.
The Eurofar program - An European overview on advanced VTOL civil transportation system
p 1016 A92-56299
The Eurofar program: An European overview on advanced VTOL civil transportation system
[MBB-UD-0611-91-PUB] p 952 N92-30418
RENAUD, J. E.
Improved coordination in non-hierarchic system optimization
[AIAA PAPER 92-2497] p 601 A92-34554
RENAUDIE, J. F.
Flight in adverse environmental conditions
p 449 N92-21680
RENDER, M. E. J.
Aircraft fatigue management in the Royal Air Force
p 363 N92-18591
RENEAUX, J.
The design and testing of an airfoil with hybrid laminar flow control
[ONERA, TP NO. 1992-22] p 822 A92-48585
RENGER, KLAUS
The Dornier 328 Acoustic Test Cell (ATC) for interior noise tests and selected test results
[AIAA PAPER 92-2164] p 1137 N92-32951
RENIER, O.
Characterization of unsteady aerodynamic phenomena at high angles p 364 N92-18787
RENKSIZBULUT, M.
A piezoelectric droplet generator for use in wind tunnels p 291 A92-21374

RENNARD, ROBERT
A digital P-code GPS receiver embedded in the AN/APN-217(V)5 Doppler Navigator p 102 A92-16976
RENTON, MARGARET B.
Heliport VFR airspace design based on helicopter performance
[SCT-90RR-34] p 103 N92-13049
Helicopter physical and performance data
[SCT-91RR-27] p 116 N92-13060
RENZE, KEVIN J.
A comparative study of turbulence models for overset grids
[AIAA PAPER 92-0437] p 327 A92-26284
Application of the Chimera overlapped grid scheme to simulation of Space Shuttle ascent flows p 945 N92-30742
REPIK, E. U.
Effect of compressibility on the value of the acceptable roughness Reynolds number p 427 A92-30197
RESENDE, HUGO B.
Temperature and initial curvature effects in low-density panel flutter
[AIAA PAPER 92-2128] p 589 A92-35695
RESETAR, SUSAN A.
Advanced airframe structural materials: A primer and cost estimating methodology
[AD-A253371] p 1062 N92-34182
RESHETIN, A. G.
Aerodynamics of complex shape bodies within a wide range of supersonic flows of rarefied gases p 939 A92-52767
RESHOTKO, E.
Turbulent heat flux measurements in a transitional boundary layer
[NASA-TM-105623] p 716 N92-27377
RESSLER, H.
Comparison of two-way satellite time transfer and GPS common-view time transfer between OCA and TUG p 1050 N92-33356
RESTER, AUSTIN
Restart of theory of air-breathing engines
[AIAA PAPER 92-3472] p 906 A92-49018
RETIF, F.
Industrial measurement of microphysical parameters - Application to natural and simulated icing clouds p 262 A92-23302
REUBUSH, DAVID E.
Flow field over the wing of a delta-wing fighter model with vortex control devices at Mach 0.6 to 1.2
[NASA-TM-4296] p 526 N92-22506
REULAND, R. S.
Pusher turboprop installation technology for the Embraer CBA-123 vector
[SAE PAPER 911030] p 658 A92-40943
REUTHER, J.
Subsonic and transonic low-Reynolds-number airfoils with reduced pitching moments p 701 A92-41211
Practical design optimization of wing/body configurations using the Euler equations
[AIAA PAPER 92-2633] p 795 A92-45505
REW, H. S.
Reynolds stress budget in the outwash jet arising from colliding curved wall jets p 614 A92-38860
REYHNER, T. A.
Subsonic propulsion system installation analysis and optimization
[ASME PAPER 91-GT-167] p 111 A92-15602
REYNOLDS, B.
Design of a small axial compressor for high efficiency over a wide operating range
[ASME PAPER 91-GT-195] p 124 A92-15620
REYNOLDS, MICHAEL C.
Mode S data link pilot-system interface - A blessing in de skies or a beast of burden? p 839 A92-44920
REYNOLDS, R. A.
Ablation performance characterization of thermal protection materials using a Mach 4.4 Sled Test
[AIAA PAPER 92-3055] p 893 A92-48713
Aerothermal ablation behavior of selected candidate external insulation materials
[AIAA PAPER 92-3056] p 893 A92-48714
REYNOLDS, ROBERT S.
Studies of the effects of curvature on dilution jet mixing p 290 A92-21079
REYNOLDS, THOMAS L.
Aircraft Command in Emergency Situations (ACES)
[SAE PAPER 912039] p 835 A92-45424
REYNOLDS, W. C.
Compressibility effects on the growth and structure of homogeneous turbulent shear flow p 675 A92-40052
Direct simulation of a supersonic reacting mixing-layer p 676 A92-40132
Turbulent reacting flows and supersonic combustion
[AD-A251065] p 986 N92-30256
RHIE, CHAE M.
Full Navier-Stokes analysis of a three-dimensional hypersonic mixed compression inlet p 343 A92-28501
RHOADES, M. M.
Flight deck aerodynamics of a nonaviation ship p 810 A92-46790
RHOADES, MARK M.
A study of the airwake aerodynamics over the flight deck of an AOR model ship
[AD-A241008] p 89 N92-13034
RHODE, D. L.
Thermal details in a rotor-stator cavity at engine conditions with a mainstream
[ASME PAPER 91-GT-275] p 151 A92-15672
Turbine disk temperatures resulting from the hot mainstream at engine conditions
[AIAA PAPER 92-0398] p 373 A92-26252
RHODES, JAMES A.
Internal reversing flow in a tailpipe offtake configuration for SSTOVL aircraft
[AIAA PAPER 92-3790] p 1069 A92-54169
Internal reversing flow in a tailpipe offtake configuration for SSTOVL aircraft
[NASA-TM-105698] p 868 N92-28418
RHYS-JONES, T. N.
Thermally sprayed coating systems for surface protection and clearance control applications in aero engines p 488 A92-32394
Thermally sprayed coating systems for surface protection and clearance control applications in aero engines
[PNR-90802] p 741 N92-27422
RIAZ, J.
A new method for simulating atmospheric turbulence for rotorcraft applications p 162 A92-14368
A new method for simulating atmospheric turbulence for rotorcraft applications p 464 N92-21956
RIBEIRO, RENATO S.
Vortex-in-cell analysis of wing wake roll-up
[AIAA PAPER 92-2703] p 801 A92-45545
RIBNER, H. S.
Ideal efficiency of propellers based on Theodorsen's theory: A review and computer study, with extended plus simplified charts
[UTIAS-TN-271] p 1071 N92-33102
RICCIO, GARY E.
Toward an integrated multimodal approach to flight simulation p 880 A92-45026
RICCO, A. J.
Method and apparatus for acoustic plate mode liquid-solid phase transition detection
[DE92-003778] p 401 N92-18705
Monitoring jet fuel degradation using quartz crystal microbalances
[DE92-004730] p 489 N92-20858
RICE, C. K.
Benchmark performance analysis of an ECM-modulated air-to-air heat pump with a reciprocating compressor
[DE92-004478] p 500 N92-20341
RICE, E. J.
Screech noise source structure of a supersonic rectangular jet
[AIAA PAPER 92-0503] p 331 A92-26932
Modern developments in shear flow control with swirl p 703 A92-41265
RICE, EDWARD J.
The flip flop nozzle extended to supersonic flows
[AIAA PAPER 92-2724] p 803 A92-45561
Turbomachinery noise p 54 N92-10601
Inlets, ducts, and nozzles p 593 N92-22523
RICE, RICHARD C.
Generation of spectra and stress histories for fatigue and damage tolerance analysis of fuselage repairs
[AD-A250390] p 854 N92-29180
RICE, WILLIAM A.
High rate PCM data receiving, recording and relying p 189 A92-19279
RICH, MICHAEL D.
When should we start high-rate production of the B-2? An analysis based on flight test results
[RAND/P-7757] p 697 N92-25204
RICHARD, JACQUES C.
Supersonic propulsion simulation by incorporating component models in the large perturbation inlet (LAPIN) computer code
[NASA-TM-105193] p 279 N92-15993
RICHARDS, C. D.
The role of primary jet injection on mixing in gas turbine combustion p 128 A92-16584
RICHARDS, KATHY M.
Visual approach data collection at San Francisco International Airport (SFO)
[DOT/FAA/CT-90/23] p 354 N92-18112
RICHARDS, W. J.
An advanced neutron radiography system p 492 A92-28748
RICHARDS, W. L.
Thermal-structural panel buckling tests p 993 A92-51409
RICHARDSON, CECIL
Formation flight system design concept p 954 A92-49255
RICHARDSON, JOHN G.
Managing Europe's air traffic system p 19 A92-11876
RICHARDSON, P.
Flight test validation of tow target trajectory predictions
[AIAA PAPER 92-0209] p 271 A92-23814
RICHARDSON, PAMELA F.
Computational aerodynamics - The next generation
[SAE PAPER 911988] p 788 A92-45390
NASA aerodynamics program
[NASA-TM-4368] p 609 N92-24678
RICHARDSON, Z. C.
Detailed investigation of causes of avionics field failures p 995 A92-51925
RICHIE, JOSEPH M.
Nationwide system delay study of the microwave landing system in the New York terminal area, volume 1
[DOT/FAA/CT-TN91/59-VOL-1] p 640 N92-25098
RICHTER, A. BRUCE
Turbine aircraft engine operational trending and JT8D static component reliability study
[DOT/FAA/CT-91/10] p 870 N92-28686
RICHTER, G. P.
Slush hydrogen (SLH2) technology development for application to the National Aerospace Plane (NASP) p 144 A92-13432
RICHTER, P.
Design and development of test rigs for main rotor and main rotor transmission of a helicopter in the 6-ton-class p 1093 A92-56280
RICHTER, R.
Mesh adaption for 2D transsonic Euler flows on unstructured meshes p 816 A92-47038
RICHWINE, DAVID M.
In-flight leading-edge extension vortex flow-field survey measurements on a F-18 aircraft at high angle of attack
[NASA-TM-4398] p 947 N92-31276
RICK, H.
Propulsion aspects of hypersonic turbo-ramjet-engines with special emphasis on nozzle/aftbody integration
[ASME PAPER 91-GT-395] p 127 A92-15725
RICK, W.
Design considerations for nozzles of hypersonic airbreathing propulsion
[AIAA PAPER 91-5019] p 471 A92-31685
Application of finite element method to hypersonic nozzle flow computations p 769 N92-27479
RICKER, WILLIAM G.
A new 1553 all-bus instrumentation monitor p 198 A92-19252
RICKETTS, RODNEY H.
Getting up to speed in hypersonic structures p 1117 A92-55127
RICKS, WENDELL R.
Feasibility of using a knowledge-based system concept for in-flight primary flight display research
[NASA-TM-4279] p 17 N92-10017
RIDDER, SVEN-OLOF
Performance improvements and fuel cost savings due to leading edge modification of a vintage delta wing jet fighter
[FFA-TN-1991-22] p 114 N92-11993
RIDENOUR-BENDER, MARGARET
Turbine aircraft engine operational trending and JT8D static component reliability study
[DOT/FAA/CT-91/10] p 870 N92-28686
RIDGELY, D. B.
Loop shaping in mixed H2 and H-infinity optimal control p 507 A92-29177
RIDGELY, MARGARET
The Air Force Manufacturing Technology (MANTECH): Technology transfer methodology as exemplified by the radar transmit/receive module program p 593 N92-22451
RIECHERS, JOHN T.
A methodology for the evaluation of runway roughness for repair
[AD-A250407] p 887 N92-28772
An assessment of the B-747's capability to operate on rough surfaces
[AD-A250134] p 963 N92-31793
RIEDELBAUCH, S.
Hypersonic flow past radiation-cooled surfaces
[MBB-FE-202-S-PUB-0468-A] p 832 N92-29713
RIEDELBAUCH, STEFAN
On the footprints of three-dimensional separated vortex flows around blunt bodies: Attempts of defining and analyzing complex flow structures p 84 N92-13005

RIEDER, R. J.
Aircraft lidar sensitivity study for measuring water vapor
[AD-A240549] p 42 N92-11237
RIEGER, H.
Computational aerothermodynamic methods for industrial applications to re-entry and hypersonic cruise problems p 227 N92-15027
RIEGER, JAMES L.
Telemetry antenna patterns for single and multi-element arrays p 188 A92-19216
RIENSTRA, S. W.
A note on the Kutta condition in Glauert's solution of the thin aerofoil problem p 613 A92-37933
RIESCO-CHUECA, P.
Brownian-motion limited aerodynamic focusing of heavy molecules p 995 A92-52722
RIESTER, JOHN E.
Helical-perturbation device for cylinder-wing vortex generators p 432 A92-31167
RIESTER, L.
Fabrication and testing of corrosion resistant coatings
[DE92-003553] p 490 N92-21063
RIEUTORD, E.
Analysis of criteria predicting the tendency of pilot induced oscillation for linear non-linear system
p 133 A92-15340
RIFE, M. C.
An experimental study of the relationship between velocity and pressure fluctuations in a wing-body junction
[AD-A249628] p 946 N92-31122
RIFFE, J.
Measurement of LORAN-C envelope to cycle difference in the far field
[PB92-128909] p 455 N92-21263
RIGAULT, M.
Stretched skin concept for the entry aerodynamic decelerator system of planetary probes
p 576 N92-23836
RIGBY, D. L.
Increased heat transfer to elliptical leading edges due to spanwise variations in the freestream momentum - Numerical and experimental results
[AIAA PAPER 92-3070] p 1020 A92-54005
RIGBY, M. J.
Effects of wake and shock passing on the heat transfer to a film cooled transonic turbine blade
p 156 N92-12201
RIGGINS, D. W.
A computational investigation of mixing and reacting flows in supersonic combustors
[AIAA PAPER 92-0626] p 278 A92-23817
A comparative study of scramjet injection strategies for high Mach numbers flows
[AIAA PAPER 92-3287] p 904 A92-48876
RIGLEY, J.
An aircraft Earth station for general aviation
p 678 N92-24194
RIGLEY, JACK
Aeronautical mobile satellite service: An overview
p 594 N92-22573
RILEY, B. R.
Kinetic theory model for the flow of a simple gas from a three-dimensional axisymmetric nozzle
p 937 A92-52730
RILEY, CHRISTOPHER J.
Engineering calculations of three-dimensional inviscid hypersonic flowfields p 175 A92-20378
An engineering aerodynamic heating method for hypersonic flow
[AIAA PAPER 92-0499] p 329 A92-26327
Engineering aerodynamic heating method for hypersonic flow p 705 A92-41539
An engineering method for interactive inviscid-boundary layers in three-dimensional hypersonic flows
[NASA-TM-107838] p 632 N92-25279
RILEY, DAVID R.
Velocity dependence of high angle of attack longitudinal flying qualities criteria
[SAE PAPER 912149] p 662 A92-39985
RILEY, J.
Volume spectra in supercooled clouds for several research flights
[AIAA PAPER 92-0167] p 350 A92-25683
RILEY, J. J.
Transition to turbulence in confined, compressible mixing layers. I - 3D numerical simulations with excitation of random, broadband white noise
[AIAA PAPER 92-0553] p 332 A92-26964
RILEY, JOHN W.
Proposal for a low cost close air support aircraft for the year 2000: The Raptor
[NASA-CR-190023] p 367 N92-19496
RILEY, M. F.
Application of multidisciplinary optimization methods to the design of a supersonic transport
p 550 N92-23230
RILEY, N.
Secondary separation from a slender wing
p 62 A92-13448
Laminar-flow secondary separation on a slender wing
p 85 N92-13006
RILL, S.
Simulation of transonic flow over twin-jet transport aircraft p 811 A92-46793
RIMBOS, PETER G.
Study of materials and structures for the High-Speed Civil Transport
[AIAA PAPER 92-1080] p 536 A92-33249
RIMROTT, F. P. J.
A torque-free flexible model gyro p 495 A92-31552
RINALDI, STEPHEN F.
Hypervelocity Wind Tunnel 9 control system
p 1092 A92-54343
RINGENBACH, DANIEL P.
Use of simulation in the USAF Test Pilot School curriculum p 884 N92-28535
RINGERTZ, ULF TORBJOERN
Optimal design of nonlinear shell structures
[FFA-TN-1991-18] p 157 N92-12312
RINOIE, K.
Experimental studies of vortex flaps and vortex plates. Part 1: 0.53 m span 60 deg delta wing
[CRANFIELD-AERO-9113-PT-1] p 349 N92-19679
RINOIE, KENICHI
An approach to flow field measurement by Laser 2-Focus velocimeter (L2F) in gust wind tunnel
[NAL-TM-617] p 346 N92-18484
RIOJA, ROBERTO J.
Al-Li alloys find their niche p 755 A92-43685
RIPLE, J. C.
H2-fueled high-bypass turbofan p 475 N92-21529
RIQNEY, DONALD
Thin bondline measurement of adhesively bonded metallic aircraft structures using an ultrasonic analyzer
p 491 A92-28684
RISPOLI, F.
Prediction of gas turbine combustor flow by a finite element code
[AIAA PAPER 92-3469] p 906 A92-49016
RISSE, ALAN
A-2000: Close air support aircraft design team
[NASA-CR-190022] p 463 N92-21567
RISSER, DANIEL T.
A model for evaluation and training in aircrew coordination and cockpit resource management
p 46 A92-11191
RIST, M. J.
Calculation of the carriage loads of tandem stores on a fighter aircraft
[AIAA PAPER 92-0283] p 319 A92-25736
RISTIC, S.
Disturbance of transonic wind tunnel flow by a slot in the tunnel wall p 135 A92-13675
RISTORI, A.
Indirect measurements of convective flow by IR thermography
[ONERA, TP NO. 1992-46] p 902 A92-48607
Presentation of a computational code for 3-D compressible flow in complex channels and cavities
p 769 N92-27475
RITTY, M. H.
Mechanical testing of glass-ceramic matrix composites
[ONERA, TP NO. 1991-182] p 388 A92-26351
RIVERA, JOSE A., JR.
NACA 0012 benchmark model experimental flutter results with unsteady pressure distributions
[AIAA PAPER 92-2396] p 517 A92-34469
RIVERA, JOSE A., JR.
The benchmark aeroelastic models program: Description and highlights of initial results
[NASA-TM-104180] p 185 N92-15049
NACA0012 benchmark model experimental flutter results with unsteady pressure distributions
[NASA-TM-107581] p 526 N92-22507
The benchmark aeroelastic models program: Description and highlights of initial results
p 721 N92-27960
Pressure measurements on a rectangular wing with a NACA0012 airfoil during conventional flutter
[NASA-TM-104211] p 1042 N92-34147
RIVERS, ROBERT A.
Piloted simulator studies of the HL-20 Lifting Body
p 666 A92-40033
RIZETTA, DONALD P.
Numerical simulation of slot injection into a turbulent supersonic stream p 1024 A92-54914
RIZK, N. K.
Lean low NO(x) combustion concept evaluation
p 143 A92-16583
RIZK, YEHIA M.
Computational investigation of slot blowing for fuselage forebody flow control
[AIAA PAPER 92-0020] p 248 A92-22142
Coupled numerical simulation of the external and engine inlet flows for the F-18 at large incidence
[AIAA PAPER 92-2621] p 793 A92-45493
Numerical investigation of tail buffet on F-18 aircraft
[AIAA PAPER 92-2673] p 798 A92-45528
Analysis of a pneumatic forebody flow control concept about a full aircraft geometry
[AIAA PAPER 92-2678] p 799 A92-45530
Navier-Stokes predictions for the F-18 wing and fuselage at large incidence p 810 A92-46783
RIZKALLA, O.
Hypersonic mixing and combustion studies in the hypulse facility p 737 A92-44526
RIZKALLA, OUSSAMA F.
High pressure hypervelocity electrothermal wind tunnel performance study and subscale tests
[AIAA PAPER 92-0329] p 383 A92-25776
RIZZETTA, DONALD P.
Numerical simulation of slot injection into a turbulent supersonic stream
[AIAA PAPER 92-0827] p 421 A92-29595
Comparative numerical study of two turbulence models for airfoil static and dynamic stall
[AIAA PAPER 92-4649] p 1028 A92-55394
RIZZI, A.
Hypersonic flow past delta wing flow simulated by Navier-Stokes solutions p 180 N92-14981
RIZZI, ARTHUR
Navier-Stokes computation of airfoil in stall using algebraic Reynolds-stress model
[AIAA PAPER 92-0195] p 257 A92-23803
Calculation of hypersonic leeside vortices over blunt delta wings p 84 N92-13004
Hypersonic laminar flow computations over a blunt leading edged delta wing at three different chord Reynolds numbers
[FFA-TN-1991-40] p 528 N92-23168
RIZZO, ROBERT
Thin bondline measurement of adhesively bonded metallic aircraft structures using an ultrasonic analyzer
p 491 A92-28684
RO, KAPSCONG
Integrated flight control law synthesis for an aeroelastic forward-swept wing aircraft
[AIAA PAPER 92-0046] p 281 A92-22163
ROACH, G. F.
Inverse problems and imaging (Pitman research notes in mathematics series Number 245)
[AD-A240333] p 53 N92-11737
ROACH, R. L.
Dynamic interactions between hypersonic vehicle aerodynamics and propulsion system performance
[NASA-CR-190638] p 1038 N92-33304
ROACH, ROBERT ALLEN
Experimental investigation of the effects of blowing on bursting of strake vortices
[AD-A240256] p 13 N92-10985
ROACH, ROBERT L.
A fast, uncoupled, compressible, two-dimensional, unsteady boundary layer algorithm with separation for engine inlets
[AIAA PAPER 92-3082] p 823 A92-48729
A fast, uncoupled, compressible, two-dimensional, unsteady boundary layer algorithm with separation for engine inlets
[NASA-TM-105686] p 770 N92-27653
ROARK, CHUCK
A new development in embedded computer performance measurement p 921 A92-48506
A new approach to embedded computer performance measurement p 1005 A92-49288
ROBBINS, EDWARD J.
Determination of balloon drag
[AIAA PAPER 91-3666] p 5 A92-11013
ROBBINS, MARC L.
Developing robust support structures for high-technology subsystems: The AH-64 Apache helicopter
[AD-A252773] p 1017 N92-33499
ROBELEN, DAVID B.
Wind-tunnel and flight tests of a delta-wing remotely piloted vehicle p 21 A92-13208
Model flight tests of a spin-resistant trainer configuration p 1054 A92-56158
ROBERT, J. P.
The A320 laminar fin programme
[ONERA, TP NO. 1992-23] p 849 A92-48586
Drag reduction: An industrial challenge
p 717 N92-27708

ROBERTS, A. S., JR.
Twenty-five years of aerodynamic research with infrared imaging p 497 A92-32232
ROBERTS, ANTHONY E.
Proposal for a low cost close air support aircraft for the year 2000: The Raptor
[NASA-CR-190023] p 367 N92-19496
ROBERTS, BARRY
Inertial navigation sensor integrated motion analysis for obstacle detection p 954 A92-49272
Inertial navigation sensor integrated motion analysis for autonomous vehicle navigation p 995 A92-52470
ROBERTS, DONALD W.
Numerical simulations of the transdetonative ram accelerator combusting flow field on a parallel computer
[AIAA PAPER 92-3249] p 894 A92-48848
Comparison of turbulence models for powered-lift flow fields
[AIAA PAPER 92-3674] p 1022 A92-54117
ROBERTS, G. T.
Interference heating near fin/body junctions on hypersonic vehicles p 182 N92-14996
ROBERTS, JAMES W.
Further calculations of the performance of turbofan engines incorporating a wave rotor
[AD-A240867] p 131 N92-13072
ROBERTS, LEONARD
Aircraft control at high-alpha by tangential blowing
[AIAA PAPER 92-0021] p 281 A92-22143
Navier-Stokes computation of wing leading edge tangential blowing for a tilt rotor in hover
[AIAA PAPER 92-2608] p 805 A92-45568
Vortical flow control on a wing-body combination using tangential blowing
[AIAA PAPER 92-4430] p 1081 A92-55354
Analysis of a dusty wall jet
[NASA-CR-189759] p 257 N92-15965
High speed transport cruise drag
[NASA-CR-190248] p 527 N92-23103
ROBERTS, PAUL W.
Dual strain gage balance system for measuring light loads
[NASA-CASE-LAR-14419-1] p 42 N92-10185
ROBERTSON, R. S.
A Ka-band instrumentation radar with one foot range resolution p 95 A92-16252
ROBIKOV, D. G.
Power spectrum of ring modes of pressure fluctuations at the surface of a cylinder in axial flow
p 603 A92-33770
ROBINSON, B. A.
A simple numerical criterion for vortex breakdown
[AIAA PAPER 92-0057] p 250 A92-22172
Investigation of vortex breakdown on a delta wing using Euler and Navier-Stokes equations p 87 N92-13019
ROBINSON, BRIAN A.
Aeroelastic analysis of wings using the Euler equations with a deforming mesh p 10 A92-13215
Numerical investigation of vortex breakdown on a delta wing p 340 A92-28027
ROBINSON, CHARLES T.
Limitations of a holographic 3-D pixel projector for cockpit displays
[AD-A241295] p 119 N92-13067
ROBINSON, D. W.
Risk to hearing from overflight noise of military aircraft
[ISVR-TR-194] p 604 N92-22241
ROBINSON, JAMES C.
Structural design considerations for a Personnel Launch System p 386 A92-24668
ROBINSON, JON W.
The application of high spectral and spatial resolution imaging spectrometers for locating downed aircraft
p 598 A92-35132
ROBINSON, LEICK D.
A numerical model for sonic boom propagation through an inhomogeneous, windy atmosphere
p 1138 N92-33876
ROBINSON, M. C.
Unsteady aerodynamic loading produced by a sinusoidally oscillating delta wing p 701 A92-41223
ROBINSON, MARK S.
A knowledge acquisition approach for an on-board mission planner
[AIAA PAPER 92-1021] p 531 A92-33204
ROBINSON, MARTHA
Experimental and analytical study of the effects of floor location on response of composite fuselage frames
[AIAA PAPER 92-2473] p 539 A92-34362
ROBINSON, O.
Unsteady crossflow on a delta wing using particle image velocimetry p 811 A92-46804
ROBINSON, P. A.
Flight simulation p 207 N92-13982
ROBINSON, PAUL
Automatic production test equipment (APTE) for the B-2 p 997 A92-53107
ROBINSON, PAUL A.
Airborne in situ computation of the wind shear hazard index
[AIAA PAPER 92-0291] p 351 A92-25744
ROBINSON, PAUL AARON
The modelling of turbulence and downbursts for flight simulators
[UTIAS-339] p 161 N92-12373
The modelling of turbulence and downbursts for flight simulators
[ISBN-0-315-59945-6] p 749 N92-27645
ROBINSON, STEPHEN K.
Separation control on high Reynolds number multi-element airfoils
[AIAA PAPER 92-2636] p 806 A92-45575
ROBNIK, R.
Comparison of two-way satellite time transfer and GPS common-view time transfer between OCA and TUG
p 1050 N92-33356
ROCHAT, PHILIPPE
The view from the airport p 532 A92-33438
ROCHE, JOHN
The role of crack growth in defect assessment
[PNR-90798] p 501 N92-20909
ROCHELLE, W. C.
Aeroassist flight experiment heating-rate sensitivity study p 3 A92-10427
Aerodynamic heating on AFE due to nonequilibrium flow with variable entropy at boundary layer edge
p 183 N92-15020
ROCHELLE, WILLIAM C.
Stagnation-point heat-transfer rate predictions at aeroassist flight conditions
[NASA-TP-3208] p 1001 N92-31281
ROCK, STACEY G.
Analysis of thermo-chemical nonequilibrium models for carbon dioxide flows
[AIAA PAPER 92-2852] p 892 A92-47835
ROCK, STEPHEN M.
Integrated flight/propulsion control specifications for systems with two-way coupling p 477 A92-29117
ROCKENFELLER, U.
Solid-vapor adsorption refrigeration system development
[PB92-164383] p 771 N92-27715
ROCKWELL, D.
Unsteady crossflow on a delta wing using particle image velocimetry p 811 A92-46804
RODCHENKO, V. V.
Estimation of the optimal load characteristics of aircraft control levers p 479 A92-30150
RODDEN, WILLIAM P.
Comment on 'Canard-wing interaction in unsteady supersonic flow' p 812 A92-46820
RODGER, P.
Establishing two-dimensional flow in a large-scale planar turbine cascade
[AIAA PAPER 92-3066] p 823 A92-48720
RODGERS, C.
The efficiencies of single-stage centrifugal compressors for aircraft applications
[ASME PAPER 91-GT-77] p 122 A92-15546
RODGERS, COLIN
Challenging power-density requirements for future fighter APUs
[SAE PAPER 912177] p 655 A92-40002
Auxiliary power units for current and future aircraft
[SAE PAPER 912059] p 862 A92-45441
RODGERS, JOHN P.
Aerothermoelastic analysis of a NASP-like vertical fin
[AIAA PAPER 92-2400] p 541 A92-34471
RODI, ALFRED R.
Use of distance-measuring equipment (DME) for correcting errors in position, velocity, and wind measurements from aircraft inertial navigation systems
p 188 A92-18172
RODI, PATRICK E.
An experimental/computational study of sharp fin induced shock wave/turbulent boundary layer interactions at Mach 5 - Experimental results
[AIAA PAPER 92-0749] p 335 A92-27093
RODI, W.
The influence of density difference between hot and coolant gas on film cooling by a row of holes - Predictions and experiments
[ASME PAPER 91-GT-255] p 151 A92-15660
International Symposium on Engineering Turbulence Modelling and Measurements, Dubrovnik, Yugoslavia, Sept. 24-24, 1990, Selected Papers p 672 A92-38851
RODMAN, LAURA C.
Turbulence amplification through a shock wave
[AIAA PAPER 92-0313] p 320 A92-25761
RODRIGUES, E. A.
Whirl-flutter stability of a pusher configuration in nonuniform flow p 845 A92-46813
RODRIGUEZ, G.
The DAM vertical shock-tube p 880 A92-45096
RODRIGUEZ, JOSE M.
Impact of heterogeneous chemistry on model-calculated ozone change due to high speed civil transport aircraft
p 45 A92-12941
RODRIGUEZ, L. M.
Fuzzy guidance system evaluation
p 778 N92-27903
RODRIGUEZ, O.
Phenomenological modeling of the wake produced by a straight two dimensional base in subsonic flow
[REPT-90/59] p 82 N92-11982
ROE, P. L.
A frontal approach for node generation in Delaunay triangulations p 771 N92-27680
ROEBROEKS, GERARDUS HUBERTUS JOANNES J.
Towards GLARE: The development of a fatigue insensitive and damage tolerant aircraft material
[ETN-92-91301] p 648 N92-24966
ROECK, W.
The IRS plasma wind tunnels for the investigation of thermal protection materials for reentry vehicles
p 208 N92-15009
ROEMER, MICHAEL J.
Improved noise rejection in automatic carrier landing systems p 380 A92-28154
ROEMER, W.
BMI/bis (allylphenoxyphthalimide)-copolymers - A new family of resins for advanced composites with improved thermal oxidative stability p 33 A92-10213
ROENNEKE, AXEL J.
Trajectory control for a low-lift maneuverable reentry vehicle
[AIAA PAPER 92-1146] p 574 A92-33287
ROESLER, TIMOTHY C.
Analytical design and demonstration of a low-cost expendable turbine engine combustor
[AIAA PAPER 92-3754] p 867 A92-49112
ROGACKI, J.
Thermoviscoplastic response of Ti-15-3 under various loading conditions
[NASA-CR-187621] p 45 N92-11391
ROGER, R. P.
Numerical study of the 3-D flowfield for a supersonic jet exiting into a hypersonic stream from a conical surface
[AIAA PAPER 92-3675] p 1022 A92-54118
ROGERS, BRIAN K.
Microcomputer-based instrument flight simulation: Undergraduate pilot training student attitude assessment
[AD-A245449] p 749 N92-26527
ROGERS, C. W.
Mechanics of curved fiber composites
p 140 A92-14346
Mechanics of curved fiber composites
p 757 A92-41034
ROGERS, CRAIG A.
Adaptive response control of wing structures carrying heavy tip weights
[AIAA PAPER 92-2527] p 583 A92-34374
ROGERS, D. H., JR.
Scale model test of an isolated turbofan nacelle with riblets
[SAE PAPER 912128] p 618 A92-39975
ROGERS, ERNEST O.
Hover evaluation of an integrated pneumatic lift/reaction-drive rotor system
[AIAA PAPER 92-0630] p 333 A92-27010
ROGERS, HARVEY N.
Cyclic fatigue behavior of silica fiber
p 754 A92-42040
ROGERS, J. C.
Advanced airframe structural materials: A primer and cost estimating methodology
[AD-A253371] p 1062 N92-34182
ROGERS, JOEL C. W.
Critical problems of computational aeroacoustics
p 167 N92-13857
ROGERS, LAWRENCE C.
Computational analysis of inertial effects on the stability of an ACES-II ejection seat p 543 A92-35436
ROGERS, LYNN
Add-on damping treatment for life extension of the F-15 upper-outer wing skin
[AD-A246149] p 746 N92-27577
ROGERS, R. C.
Flow establishment in a generic scramjet combustor
p 737 A92-44525
A comparative study of scramjet injection strategies for high Mach numbers flows
[AIAA PAPER 92-3287] p 904 A92-48876

ROGERS, STEVEN B.
Manipulation and management of data collected at the Crew Station Research and Development Facility - A case study
[AIAA PAPER 92-4162] p 1008 A92-52451
ROGERS, STEVEN P.
A CLIPS-based tool for aircraft pilot-vehicle interface design p 303 N92-16605
ROGERS, STUART E.
Efficient simulation of incompressible viscous flow over single and multi-element airfoils
[AIAA PAPER 92-0405] p 324 A92-26258
ROGERS, W. L.
X-29 H-infinity controller synthesis
p 873 A92-46749
ROGERS, WILLIAM A.
Application of analytical and design tools for fighter wing aeroelastic tailoring
[AIAA PAPER 92-2373] p 542 A92-34543
Application of analytical and design tools for fighter wing aeroelastic tailoring p 550 N92-23231
ROGLES, F.
The measurement of water film thickness on airfoils in heavy rain conditions using conductance sensors
p 452 N92-21695
ROHDE, JOHN
Airbreathing combined cycle engine systems
p 475 N92-21523
ROHLING, H.
Construction of a real-time DGPS experimental system
p 840 A92-47631
ROHNE, K.-H.
Investigation of the flow at the exit of an unshrouded centrifugal impeller and comparison with the 'classical' jet-wake theory
[ASME PAPER 90-GT-124] p 6 A92-11287
ROHNE, P. B.
Instrumentation requirements for laminar flow research in the NLR high speed wind tunnel HST
[NLR-TP-89158-U] p 887 N92-28669
ROISMAN, W. P.
Identification of dynamic characteristics of flexible rotors as dynamic inverse problem p 220 N92-13962
ROJAS, R. G.
Automated composite ellipsoid modelling for high frequency GTD analysis
[NASA-CR-189853] p 275 N92-17316
ROKHSAZ, K.
Use of neural networks in control of high alpha maneuvers
[AIAA PAPER 92-0048] p 282 A92-22164
ROKHSAZ, KAMRAN
Effect of viscous drag on optimum spanwise lift distribution
[AIAA PAPER 92-0287] p 319 A92-25740
A study in dynamic control of a super maneuver with neural networks p 463 N92-21510
ROKUTANDA, ITARU
Test results of the expander cycle air turbo ramjet for a future space plane
[IAF PAPER 91-271] p 120 A92-14709
Tests results on Air Turbo Ramjet for a future space plane
[IAF PAPER 92-0657] p 1071 A92-57098
ROLADER, G. E.
Progress towards the development of transient ram accelerator simulation as part of the U.S. Air Force Armament Directorate Research Program
[AIAA PAPER 92-3248] p 904 A92-48847
ROLF, R. L.
Methodology for the assessment of material quality effects on airframe fatigue durability p 213 A92-19820
ROLFGEN, J. W.
G-Field Control of nonlinear systems
[AIAA PAPER 92-4555] p 1131 A92-55267
ROLLBUHLER, J.
Factors influencing the effective spray cone angle of pressure-swirl atomizers p 295 A92-23300
ROLLBUHLER, R. JAMES
Safety considerations in testing a fuel-rich aeropropulsion gas generator
[NASA-TM-105258] p 279 N92-17061
ROLLET, PHILIPPE
EUROFAR airframe aerodynamic design
p 546 A92-35750
ROLTGEN, J.
Hover control of a PVTOL using nonlinear regulator theory p 478 A92-29171
ROM, J.
Measurements of lateral aerodynamics characteristics of forebodies at high angle of attack in subsonic and transonic flows
[AIAA PAPER 92-0174] p 255 A92-23785
ROM, JOSEF
High angle of attack aerodynamics - Subsonic, transonic, and supersonic flows
[ISBN 0-387-97672-8] p 431 A92-30850
The External Propulsion Accelerator - Scramjet thrust without interaction with accelerator barrel
[AIAA PAPER 92-3717] p 866 A92-49098
ROMAN, ALAN
Parameter identification of AV-8B wingborne aerodynamics for flight simulator model updates
[AIAA PAPER 92-4506] p 1027 A92-55373
ROMANO, R. A.
Flight simulation p 207 N92-13982
ROMANOWSKY, H. E.
The Catalyst software engineering environment
p 1005 A92-49300
ROME, H. J.
Potential impact of GPS and automatic dependent surveillance on air lane separation in the North Atlantic Organized Track System p 99 A92-16935
RONALD, TERENCE M. F.
Structural materials for NASP
[AIAA PAPER 91-5101] p 486 A92-31698
RONZHEIMER, A.
Multi-block grid generation around wing-body-engine-pylon configurations
p 817 A92-47060
ROOD, R. B.
Natural cycles, gases p 408 N92-19123
ROQUEMORE, W. M.
A numerical method for simulating the fluid-dynamic and heat-transfer changes in a jet engine injector feed-arm due to fouling
[AIAA PAPER 92-0768] p 374 A92-27108
ROSA, PEDRO
Harmonisation and integration of air traffic control in Europe p 532 A92-33437
ROSADO, LEWIS
Feasibility of magnetic bearings for advanced gas turbine engines p 772 N92-27738
ROSCOE, D. V.
Computation of flow past a turbine blade with and without tip clearance
[ASME PAPER 91-GT-56] p 68 A92-15534
ROSCOE, DAVID V.
Gas turbine main shaft internal flow and heat transfer
[ASME PAPER 91-GT-165] p 123 A92-15600
ROSE, C. D.
On-line distortion analysis system for inlet-engine testing
[ASME PAPER 91-GT-166] p 136 A92-15601
ROSE, DAVE
Scenario analysis of thigh gap related ejection injuries
p 834 A92-44995
ROSE, GAYLE E.
Wind tunnel performance results of swirl recovery vanes as tested with an advanced high speed propeller
[AIAA PAPER 92-3770] p 1068 A92-54159
ROSE, WILLIAM C.
Numerical investigations in three-dimensional internal flows
[NASA-CR-189467] p 221 N92-14313
Numerical investigations in three-dimensional internal flows
[NASA-CR-190498] p 998 N92-30380
ROSELL-LLOMPART, J.
Brownian-motion limited aerodynamic focusing of heavy molecules p 995 A92-52722
ROSEN, A.
Dynamic analysis of rotor blades with root retention design variations p 1054 A92-56156
A generic harmonic rotor model for helicopter flight simulation p 1086 A92-56333
A simulation model of a single rotor helicopter
p 979 N92-31865
ROSEN, AVIV
Modeling methods for high-fidelity rotorcraft flight mechanics simulation
[NASA-TM-103842] p 482 N92-21440
ROSEN, JAMES M.
Measured and calculated optical property profiles in the mixed layer and free troposphere p 1129 A92-54630
ROSEN, KENNETH M.
Composites usage on the RAH-66 Comanche
p 457 A92-29669
ROSEN, ROBERT
The future challenge for aeropropulsion
[NASA-TM-105613] p 658 N92-25164
ROSENBLATT, MARTIN
Navier-Stokes cavity solutions based on second-order turbulence modeling
[AIAA PAPER 92-2765] p 704 A92-41314
ROSEVEAR, JERRY
Supercharged ejector ramjet p 475 N92-21527
ROSFJORD, T. J.
Aerating fuel nozzle design influences on airflow features p 129 A92-17176
ROSHKO, ANATOL
Transmission of thin light beams through turbulent mixing layers
[AIAA PAPER 92-0658] p 396 A92-27029
ROSKAM, JAN
Facing the crisis in aircraft design education
p 606 A92-34770
ROSNER, DANIEL E.
Transport phenomena and interfacial kinetics in multiphase combustion systems
[AD-A244849] p 489 N92-20695
ROSS, A. JEAN
Control of forebody vortices by suction at the nose of the RAE high incidence research model
p 87 N92-13022
Dynamic wind tunnel tests on control of forebody vortices with suction p 380 N92-18793
ROSS, HANNES
X-31 enhancement of aerodynamics for maneuvering beyond stall p 363 N92-18779
ROSS, HOLLY M.
Model flight tests of a spin-resistant trainer configuration p 1054 A92-56158
ROSS, I. M.
Aerobang - A new synergetic plane-change maneuver
[AAS PAPER 91-418] p 753 A92-43356
ROSS, JAMES C.
Computational evaluation of an airfoil with a Gurney flap
[AIAA PAPER 92-2708] p 802 A92-45550
ROSSI, D.
Aerothermodynamic radiation studies
[NASA-CR-185666] p 284 N92-15998
ROSSITTO, K. F.
The use and effectiveness of piloted simulation in transport aircraft research and development
p 886 N92-28549
ROSSOW, C.-C.
Multi-block grid generation around wing-body-engine-pylon configurations
p 817 A92-47060
Investigations of propulsion integration interference effects on a transport aircraft configuration
[AIAA PAPER 92-3097] p 849 A92-48739
ROSSOW, VERNON J.
Two-fence concept for efficient trapping of vortices on airfoils p 1031 A92-56165
ROSSOW, VERNON, J.
Probe shapes for streamwise momentum and cross-stream turbulence intensity p 9 A92-13210
Probe systems for static pressure and cross-stream turbulence intensity p 10 A92-13211
ROSTAFINSKI, W.
Detonation duct gas generator demonstration program
[AIAA PAPER 92-3174] p 1066 A92-54011
ROTH, KARLIN R.
Evaluation of a Navier-Stokes prediction of a jet in a crossflow p 441 A92-32235
ROTH, PAUL
Double Density recording acquisition and playback
p 920 A92-47534
ROTHENFLUE, JAMES A.
Experimental investigation into the effects of riblets on compressor cascade performance
[AD-A243881] p 377 N92-19235
ROTKIN, A. N.
A study of a version of the boundary conditions of a two-dimensional spline in surface and line modeling
p 163 A92-16826
ROTT, D.
Environmental fatigue tests with composite materials
p 214 N92-14413
ROTTMAN, MICHAEL S.
Implementation of non-dedicated redundancy in a fault tolerant multiprocessor testbed p 974 A92-49294
ROTZ, CHRISTOPHER A.
Filament winding of composite isogrid fuselage structures p 784 A92-47405
ROUCHON, JEAN
Evaluation of the effects of the environment on the behavior of the primary structures of composite material aircraft in service: Historic and current situation
p 1110 N92-33048
ROUGES, J. M.
Large thin composite thermostructural parts
p 576 N92-23821
ROURE, A.
Active control of airborne noise transmitted through a ribbed panel p 695 A92-39111
ROURKE, CHRISTOPHER J.
CDI sensitivity and crosstrack error on nonprecision approaches
[AD-A243981] p 356 N92-19391

ROUSE, WILLIAM B.
Specification of adaptive aiding systems - Information requirements for designers p 916 A92-44915
An exploration of function analysis and function allocation in the commercial flight domain
[NASA-CR-4374] p 368 N92-19871
ROUSSAUD, A.
Mechanisms of high-current pulses in lightning and long-spark stepped leaders p 1116 A92-54678
ROWELL, C. M.
Application of a universe-series code for inviscid flow over complex 3-dimensional configurations
[AIAA PAPER 92-0150] p 253 A92-23765
ROWLES, STEVE H.
Second-order shock-expansion theory extended to include real gas effects
[AD-A247191] p 831 N92-29539
ROY, S.
Unsteady hypersonic boundary layers for slender axisymmetric bodies with large injection rates
p 524 A92-36100
ROYSTON, JAMES D.
Superconducting bearings with levitation control configurations
[NASA-CASE-GSC-13346-1] p 909 N92-29099
ROZENDAAL, ROGER A.
High Reynolds number test of the Boeing TR77 airfoil in the Langley 0.3-meter transonic cryogenic tunnel
[NASA-TM-4189] p 947 N92-31246
ROZENDAL, D.
Instrumentation requirements for laminar flow research in the NLR high speed wind tunnel HST
[NLR-TP-89158-U] p 887 N92-28669
ROZHDESTVENSKII, MIKHAIL
Helicopter tail rotor stall flutter p 1056 A92-56290
ROZHKOVA, L. G.
Base pressure on an axisymmetric finned body during forced rotation in the autorotation regime
p 7 A92-12165
ROZMAN, G.
270-Vdc/hybrid 115 Vac electric power generating system technology demonstrator
[SAE PAPER 912051] p 861 A92-45435
ROZMAN, G. I.
270-Vdc/hydrid 115-Vac electric power generating system technology demonstrator evolution to a dual-channel, more electric aircraft technology development testbed
[SAE PAPER 912183] p 655 A92-40003
RUAN, YEEFENG F.
Modal simulation of gearbox vibration with experimental correlation
[AIAA PAPER 92-3494] p 1112 A92-54036
Modal simulation of gearbox vibration with experimental correlation
[NASA-TM-105702] p 1002 N92-31485
RUAN, YINGZHENG
Scattering mechanism and RCS reduction of antennas
p 726 A92-44850
RUBAN, A. I.
An algebraic model for dissipation in supersonic boundary layers
[AIAA PAPER 92-0311] p 320 A92-25759
Numerical methods in the theory of boundary layer interaction with nonviscous flow p 426 A92-30185
RUBBERT, PAUL E.
The impact of CFD on the airplane design process - Today and tomorrow
[SAE PAPER 911989] p 788 A92-45391
RUBENSON, DAVID
Tilt rotors and the Port Authority of New York and New Jersey Airport System
[RAND-R-3971/1-PA-SUMM] p 636 N92-25262
RUBERT, KENNEDY F.
The NASA hypersonic research engine program
p 474 N92-21521
RUBESIN, M. W.
An assessment and application of turbulence models for hypersonic flows
[NASA-TM-105124] p 82 N92-11984
RUBESIN, MORRIS W.
Assessment of compressibility corrections to the k-epsilon model in high-speed shear layers
p 1024 A92-54905
RUBIN, S. G.
Transient behavior of supersonic flow through inlets
p 340 A92-28043
RUDAKOV, A. S.
Aerospace plane hydrogen scramjet boosting
[SAE PAPER 912071] p 891 A92-45451
RUDALEVIGE, TREVOR
A sensitivity analysis on component reliability from fatigue life computations
[AD-A247430] p 908 N92-28425
RUDD, ROBERT E., III
Wavelength encoded fiber optic angular displacement sensor p 857 A92-48046
RUDNIK, R.
Extension of a three-dimensional Euler method for calculating the flowfield around bypass engines with fan and core jet p 62 A92-13690
RUDNIK, RALF
Extension of a three dimensional Euler-code for the investigation of the flow field around bypass engines with fan and core jet
[DLR-FB-91-13] p 503 N92-21699
RUDOLPH, TERENCE
Nonlinear triggered lightning models for use in finite difference calculations p 230 A92-20128
Analysis and modeling of lightning strikes to the F106B, CVF580, and C160 aircraft p 186 A92-20129
RUDRAIAH, N.
Axisymmetric potential flow calculations. II - Design mode p 8 A92-12399
RUED, K.
Thermal management of propulsion systems in hypersonic vehicles
[AIAA PAPER 92-0516] p 373 A92-26942
RUEGER, MATHEW L.
Simulation of wind tunnel flowfields
[AIAA PAPER 92-0034] p 249 A92-22155
Modeling the ventilated wind tunnel wall
[AIAA PAPER 92-0035] p 249 A92-22156
Wind tunnel boundary interference prediction and correction
[AIAA PAPER 92-0036] p 249 A92-22157
RUFENACH, C. L.
Comparison of aircraft synthetic aperture radar and buoy spectra during NORCSEX '88 p 597 A92-34878
RUFFIN, STEPHEN M.
Single expansion ramp nozzle simulations
[AIAA PAPER 92-0387] p 323 A92-26243
RUHMANN, DOUGLAS C.
New materials drive high-performance aircraft
p 1105 A92-55134
RUIJGROK, G. J. J.
Elements of airplane performance
[ISBN 90-6275-608-5] p 357 A92-26550
Propeller-driven-small airplane noise certification
[LR-650] p 237 N92-14798
RUMBERGER, WILLIAM
V-22 Osprey tiltrotor blade fold/wing stow system design and testing p 109 A92-14420
RUNYAN, L. JAMES
Lewis icing research tunnel test of the aerodynamic effects of aircraft ground deicing/anti-icing fluids
[NASA-TP-3238] p 952 N92-30395
RUNYAN, R. B.
Thrust stand design principles
[AIAA PAPER 92-3976] p 1098 A92-56802
RUSAK, Z.
The subsonic and transonic flow around the leading edge of a thin airfoil with a parabolic nose
[AIAA PAPER 92-2649] p 797 A92-45516
The three-dimensional stability of the Foeppl vortices
p 949 N92-31889
RUSAKOV, V. V.
Axisymmetric analogy for three-dimensional viscous flow problems p 244 A92-21617
Similarity relations for calculating three-dimensional chemically nonequilibrium viscous flows
p 827 A92-49188
RUSCELLO, ANTHONY
Conceptual design and analysis of a special operations transport
[AIAA PAPER 92-1066] p 536 A92-33239
Conceptual design and analysis of a special operations transport p 646 A92-40387
RUSNAK, ILAN
On-line identification and control of linearized aircraft dynamics p 1082 A92-55911
RUSSELL, ALAN J.
A damage tolerance assessment of bonded repairs to CF-18 composite components. Part 1: Adhesive properties
[DREP-TM-88-25-PT-1] p 143 N92-12060
RUSSELL, C. RAY
Background issues for on-line aircraft documentation
p 119 N92-13858
RUSSELL, G. W.
Ablation performance characterization of thermal protection materials using a Mach 4.4 Sled Test
[AIAA PAPER 92-3055] p 893 A92-48713
Aerothermal ablation behavior of selected candidate external insulation materials
[AIAA PAPER 92-3056] p 893 A92-48714
RUSSELL, JULIE C.
Fatal occupational injury related to helicopters in the United States 1980-1985 p 186 A92-20720
RUSSELL, L. M.
Full field flow visualization and computer-aided velocity measurements in a bank of cylinders in a wind tunnel
p 991 A92-50040
RUSSELL, MARK S.
A high performance general purpose processing element for avionic applications p 920 A92-48440
RUSSELL, ROBERT J.
A continuing study of altitude determination deficiencies of the Service Aircraft Instrumentation Package (SAIP)
[AD-A245952] p 968 N92-32051
RUSSELL, STEVEN G.
A Rayleigh-Ritz design methodology for cutouts in composite structures
[AIAA PAPER 92-2278] p 582 A92-34297
RUSSIER, M.
P120 programme - First results of the pre-development phase p 60 A92-14447
The development of a new light, single engine helicopter family p 545 A92-35734
RUSSO, G.
SIMOUN and Scirocco wind tunnel nozzle viscous flow study p 208 N92-14999
High enthalpy nozzle flows p 182 N92-15000
RUSSOW, J.
Flight in a steady wind field p 131 A92-13696
RUTAN, DICK
The Pond Racer preliminary flight test report
p 645 A92-40031
RUTH, JOHN C.
Historical perspective on the evolution of avionics standards p 198 N92-14049
RUTHERFORD, JOHN W.
A structural design and optimization tool for ducted rotor/wing blades
[AIAA PAPER 92-2361] p 543 A92-34593
RUTKOVSKII, V. IU.
Robustness of control systems with nonlinear parametric correction for certain types of perturbations
p 509 A92-30311
RUTKOWSKI, C.
Induction bonding procedures for graphite reinforced thermoplastic assemblies p 994 A92-51545
RUTKOWSKI, MICHAEL J.
First level release of 2GCHAS for comprehensive helicopter analysis p 1133 A92-56339
RUTLAND, C. J.
Three-dimensional modeling of diesel engine intake flow, combustion and emissions
[NASA-CR-189126] p 658 N92-24539
RUTLEDGE, CHARLES K.
A comparative analysis of XV-15 tiltrotor hover test data and WOPWOP predictions incorporating the fountain effect
[NASA-CR-189455] p 114 N92-11992
RUTLEDGE, W. H.
Center of pressure calculations for a bent-axis vehicle
[AIAA PAPER 92-0168] p 254 A92-23779
Center of pressure calculations for a bent-axis vehicle
[DE92-005186] p 498 N92-20143
RUTLEDGE, WALTER H.
Grid sensitivity in low Reynolds number hypersonic continuum flows p 817 A92-47057
Effect of the grid system on heat transfer computations for high speed flows p 900 A92-47071
RUZICKA, G. C.
A general purpose nonlinear rigid body mass finite element for application to rotary wing dynamics
p 846 A92-46924
RUZICKA, GENE C.
Finite-element analysis and multibody dynamics issues in rotorcraft dynamic analysis p 1055 A92-56286
First level release of 2GCHAS for comprehensive helicopter analysis p 1133 A92-56339
RYALL, KATHLEEN
A graphical user-interface for propulsion system analysis
[NASA-TM-105696] p 1134 N92-33894
RYAN, DEIRDRE A.
Finite difference time domain modeling of steady state scattering from jet engines with moving turbine blades
[NASA-CR-190290] p 971 N92-30753
RYAN, S. G.
Limit cycle vibrations in turbomachinery
[NASA-TP-3181] p 211 N92-14108
RYAN, T. W., III
Ignition delays, heats of combustion, and reaction rates of aluminum alkyl derivatives used as ignition and combustion enhancers for supersonic combustors
[AIAA PAPER 92-3841] p 894 A92-49134
RYBAK, F. J.
Comparison of Hemispherical Resonator Gyro and optical Gyros p 993 A92-51014

RYBAKOV, E. E.
Several results of lidar measurements of the characteristics of oblique visibility at an airfield
p 45 A92-12844
RYBAKOV, F. V.
Determination of the objective-function gradient in the problem of minimizing stress concentration using the finite element method p 494 A92-30170
RYDAEV, A. I.
A method for estimating the technological and economic efficiency of measures enhancing the reliability of aviation gas turbine engines p 657 A92-40621
RYKOV, V. A.
Influence of internal molecular degrees of freedom on the hypersonic rarefied gas flow about a conical body
p 938 A92-52752
RYND, J. P., JR.
Thrust stand design principles
[AIAA PAPER 92-3976] p 1098 A92-56802
RYZHKOV, M. I.
Synthesis of optimal digital systems for the stabilization of stochastically perturbed unstable dynamic systems
p 601 A92-33754
RYZHKOV, O. S.
Wave motions in a three-dimensional boundary layer
p 244 A92-21629
RYZHOV, IU. A.
Aerodynamic characteristics of a standard corrugated body in a free-molecular flow p 940 A92-52818

S

SAAGER, P.
The role of systems simulation for the development and qualification of ATTAS p 886 N92-28548
SAARENVIRTA, G.
Aerodynamics p 202 N92-13977
SABA, COSTANDY S.
Improving sample introduction for total wear metal determination by atomic emission spectroscopy
p 389 A92-26850
Lubricant evaluation and performance 2
[AD-A247464] p 895 N92-28398
SABER, AARON J.
H2/air subsystem combustion kinetics in aerospaceplane powerplants
[IAF PAPER 91-276] p 25 A92-12600
SABERI, A.
Design of localizer capture and track hold for a transport airplane - An H(infinity)/LTR approach
p 52 A92-11583
SABETTA, F.
Nonequilibrium hypersonic inviscid steady flows
p 176 A92-20737
Influence of chemical modeling on the solution of hypersonic shock layers p 183 N92-15016
SABIROV, R. KH.
A test bench for evaluating powerplant electrization
p 138 A92-16830
SABITOV, K. B.
Uniqueness of solutions of the generalized Tricomi problem arising in the theory of the Laval nozzle
p 428 A92-30319
SABNIS, J. S.
Computation of flow past a turbine blade with and without tip clearance
[ASME PAPER 91-GT-56] p 68 A92-15534
SABNIS, JAYANT S.
Hybrid Navier-Stokes/Monte Carlo method for reacting flow calculations p 705 A92-41537
SABUNCU, M.
Vibration characteristics of pretwisted aerofoil cross-section blade packets under rotating conditions
p 219 A92-20756
SACCO, G. P.
Propulsion simulator for magnetically suspended wind tunnel models p 750 N92-27801
SACHER, P. W.
Introduction to Special Course on Engineering Methods in Aerodynamic Analysis and Design of Aircraft
p 552 N92-23951
SACHER, PETER
Saenger and the German Hypersonics Technology Programme - Status report 1991
[IAF PAPER 91-198] p 32 A92-12570
SACHS, GOTTFRIED
A new method for increasing maximum flight endurance p 280 A92-21006
Thrust/speed effects on long-term dynamics of aerospace planes p 889 A92-46766
SACKLEH, F. J.
Testing capabilities at AEDC for development of hypersonic vehicles
[AIAA PAPER 91-5027] p 483 A92-31686
SACZALSKI, TODD
Advanced experimental design applied to damage tolerance of composite materials p 993 A92-51505
SADDOUGHI, SEYED G.
A preliminary experimental investigation of local isotropy in high-Reynolds-number turbulence
p 912 N92-30042
SADEGHI, TOM
Evaluation and comparison of triple and quadruple flight control architectures p 745 A92-43884
Fault tolerant EHA architectures p 763 A92-43885
SADLER, J. H. R.
Advanced propulsion systems for large subsonic transports p 653 A92-36977
SADLER, R. L.
Behavior of aircraft tire coupons under various loading conditions
[AD-A241416] p 116 N92-13063
SADREHAGHIGHI, I.
An analytical approach to grid sensitivity analysis for NACA four-digit wing sections
[NASA-CR-190251] p 631 N92-25175
SADREHAGHIGHI, IDEEN
An analytical approach to grid sensitivity analysis
[AIAA PAPER 92-0660] p 334 A92-27031
SAFF, C. R.
Application of integrated structural analysis to the high speed civil transport p 684 N92-25927
Out of plane analysis for composite structures
p 1107 N92-32527
SAFF, CHARLES
Turning up the heat on aircraft structures
p 1052 A92-55131
SAFFOLD, J. A.
A multidimensional terrain model for low altitude tracking scenarios p 205 A92-19107
SAFONOV, M. G.
A hierarchical data structure and new capabilities of the Robust-Control Toolbox p 507 A92-29155
H-infinity synthesis using a bilinear pole shifting transform p 1007 A92-50490
SAFONOV, MICHAEL G.
Practical method's for robust multivariable control
[AD-A248473] p 1009 N92-30322
SAFRONOV, A. V.
Effect of shock waves on the critical rate of bending-torsional flutter of an airfoil p 494 A92-30208
Aerodynamic effect of compression shocks on an oscillating aileron in transonic flow p 440 A92-31898
SAGENDORPH, FRANK
Algorithmic development in structures technology
p 684 N92-25924
SAGI, C. J.
Optimization of bluff body for minimum drag in ground proximity p 431 A92-31154
SAGNIER, P.
Analysis tools of ONERA and DLR for the aerothermodynamics of reentry vehicles
p 211 N92-14977
Review of the European hypersonic wind tunnel performance and simulation requirements
p 209 N92-15043
SAHA, S. K.
Manufacturing cost model for composites
p 1012 A92-51565
SAHELI, FARI
Navier-Stokes analysis of helicopter plume flowfield for infrared calculations
[AIAA PAPER 92-0983] p 580 A92-33185
SAHOO, P.
The microstructural stability of TiC reinforced rapidly solidified Al-Fe-V-Si composite structures
p 141 A92-15169
SAHU, JUBARAJ
Transonic Navier-Stokes computations for a spinning body of revolution
[AD-A241015] p 180 N92-14972
SAID, WALEED
An artificial intelligence approach for the verification of requirements for aircraft electrical power systems
p 863 A92-48481
SAITO, HIROSHI
An investigation of the automation of emergency landings for helicopters p 1083 A92-56026
SAITO, K.
Research on a low-noise engine for a high-speed VTOL aircraft p 737 A92-43239
Noise test of high-speed counterrotation propeller in low-speed wind tunnel p 1135 A92-56055
SAITO, M.
Wind tunnel test for a high speed propeller with coaxial contrarotation p 737 A92-43195
SAITO, MASAKI
The main wing boundary layer separation pattern of STOL research aircraft Asuka p 709 A92-43144
SAITO, SHIGERU
Numerical analysis of helicopter rotor blades
p 430 A92-30558
Navier-Stokes analysis of blade tip shape in hover
p 521 A92-35758
Wind tunnel test for a high speed propeller with coaxial contrarotation p 737 A92-43195
Low-speed wind tunnel testing for the high-speed propeller at high shaft angle of attack
p 1030 A92-56054
SAITO, TERUO
Preliminary airfoil testing experience in the NDA cryogenic wind tunnel p 1091 A92-54326
SAITO, Y.
Conceptual study of separated core ultra high bypass engine
[AIAA PAPER 92-3775] p 867 A92-49119
SAITO, YOSHIO
Design and off-design point characteristics of Separated Core Ultra High Bypass Engine (SCUBE)
[AIAA PAPER 92-3776] p 867 A92-49120
SAITOH, TAKASHI
Hydrogen fueled subsonic-ram-combustor model tests for an air-turbo-ram engine
[NAL-TR-1064T] p 280 N92-17855
SAITOH, TAMOTSU
Conceptual design of scramjet engine
p 1065 A92-53490
SAJBEN, M.
Confined normal-shock/turbulent-boundary-layer interaction followed by an adverse pressure gradient
p 172 A92-18365
Experimental investigation of normal-shock/turbulent-boundary-layer interactions with and without mass removal p 330 A92-26411
SAJBEN, MIKLOS
Experimental investigation of terminal shock sensors for mixed-compression inlets p 276 A92-21074
SAKA, MITSUO
On the possibility of freezing and sticking phenomena in a transport during the ground taxiing and takeoff run and on the preventions of the hazard
[SAE PAPER 912042] p 836 A92-45426
SAKA, T.
The acceleration control system design of a flight vehicle using a two-wing control method p 745 A92-43185
SAKAGUCHI, HAJIME
Air ejector experiments using the two-dimensional supersonic cascade tunnel: Zero secondary flow performance
[NAL-TM-632] p 887 N92-28829
SAKAI, H.
New thermoplastic polyimide composite for supersonic aircraft structures p 985 A92-51512
SAKAI, HIDEO
Thermal fiber-reinforced-plastic composite technology for aircraft structures p 755 A92-43237
SAKAI, KENJI
Aerodynamic development of boundary layer control system for NAL QSTOL research aircraft 'ASKA'
[SAE PAPER 912010] p 843 A92-45410
SAKAI, S.
New-type of ultralight flexible a-Si solar cell and its application on an airplane p 970 A92-53181
SAKAI, T.
Model reference adaptive flight control system (MRAFCS) design with consideration of the balance point p 745 A92-43182
SAKAI, TETSU
Analysis of a 2-D airfoil motion flying in-proximity-to a wavy-wall surface-lifting surface-scheme
p 315 A92-25506
Analysis of motion of airfoil flying over wavy-wall surface (lifting surface method) p 818 A92-47100
SAKAI, TOSHIHO
Synthesis of a MLS automatic landing control law for the NAL experimental research aircraft Do-228
p 1084 A92-56062
Flight evaluation of navigation systems including MLS using NAL Do228 - Outline p 1047 A92-56116
SAKAKIBARA, S.
New 1.27-m leg of the National Aerospace Laboratory hypersonic wind tunnel p 1092 A92-56003
SAKAKIBARA, SEIZO
Development of wall pressure measuring apparatus for an existing transonic wind tunnel test section
[NAL-TM-565] p 573 N92-23778
SAKAKIBARA, SEIZOU
Aerodynamic study of H-II Orbiting Plane, HOPE
p 1103 A92-53639
SAKAKIBARA, TOSIO
Present status of Al-Li alloys p 1106 A92-56105
SAKAMOTO, AKIRA
Current status of R&D on materials for super/hypersonic transports p 1106 A92-56002

SAKAMOTO, ATSUHIRO
A numerical simulation of separated flows around bodies p 8 A92-12423
Numerical simulations of separated flows around oscillating airfoil for dynamic stall phenomena
[SAE PAPER 911991] p 788 A92-45393
SAKAMOTO, R. D.
Technical feasibility of digital three-dimensional cellular communications for air traffic control applications. Volume 1: Introduction and summary
[AD-A244573] p 534 N92-22104
SAKAMOTO, Y.
Numerical prediction of the flow characteristics in an arc wind tunnel
[AIAA PAPER 92-4016] p 1100 A92-56838
Turbine drive system of the high pressure LOX turbopump test facility
[DE92-783191] p 680 N92-25342
SAKAMOTOR, R. D.
Technical feasibility of digital three-dimensional cellular communications for air traffic control applications. Volume 3: Ground network architecture
[AD-A244575] p 534 N92-22106
SAKAMURA, YOSHITAKA
Thermal and chemical nonequilibrium viscous shock layer flows over a blunt body at high altitudes
p 938 A92-52749
Hypersonic flows with air chemistry over a reentry vehicle at high altitudes p 1017 A92-53549
SAKATA, K.
Study of cavity pumping in supersonic internal flow
p 429 A92-30538
Supersonic wind tunnel test of airintake/airframe integrated models p 1028 A92-56006
SAKATA, KIMIO
Mach 3 wind tunnel test of mixed compression supersonic inlet
[AIAA PAPER 92-3625] p 1021 A92-54092
SAKELLARIOU, N.
Prediction and measurement of jet flowfield features for ASTOVL aircraft p 787 A92-45318
SAKHAROV, V. I.
Radiant heat transfer in supersonic three-dimensional and axisymmetric flow of air past evaporating bodies
p 337 A92-27533
SAKHNENKO, T. M.
An experimental study of transonic flow of a gas past wedges p 424 A92-30153
SAKOWSKI, BARBARA
A fast, uncoupled, compressible, two-dimensional, unsteady boundary layer algorithm with separation for engine inlets
[AIAA PAPER 92-3082] p 823 A92-48729
Interface of an uncoupled boundary layer algorithm with an inviscid core flow algorithm for unsteady supersonic engine inlets
[AIAA PAPER 92-3083] p 823 A92-48730
Interface of an uncoupled boundary layer algorithm with an inviscid core flow algorithm for unsteady supersonic engine inlets
[NASA-TM-105684] p 739 N92-27037
A fast, uncoupled, compressible, two-dimensional, unsteady boundary layer algorithm with separation for engine inlets
[NASA-TM-105686] p 770 N92-27653
SAKUMA, HIDETAKE
Aircraft accidents and human factors
p 723 A92-43219
SAKURAI, AKIRA
Analysis of the aerodynamic characteristics of a simple remotely piloted research vehicle (RPRV)
p 710 A92-43191
SAKURAI, YOSHIO
Operation of the on-board measuring system of the STOL research aircraft Asuka p 734 A92-43139
SAKURANAKA, NOBORU
A preliminary study of a supersonic wind tunnel for a ram jet test facility p 1089 A92-53564
SALAM, A.
Secondary flow investigation inside the passage of a compressor cascade p 706 A92-42124
SALAMINUCCI, MARCO ANTONIO
An experimental investigation of a 2-D scramjet inlet at flow Mach numbers of 8 to 25 and stagnation temperatures of 800 to 4,100 K p 739 N92-26586
SALAS, M. D.
Aerodynamic design and optimization in one shot
[AIAA PAPER 92-0025] p 248 A92-22147
SALAS, MANUEL D.
The NASA Computational Aerosciences Program - Toward teraFLOPS computing
[AIAA PAPER 92-0558] p 411 A92-26968
SALEIN, MARIANNE
Materials and Structures Research Department: Scientific report (1990)
[ETN-92-90727] p 466 N92-22000
SALEM, JONATHAN A.
Reliability analysis of a structural ceramic combustion chamber
[ASME PAPER 91-GT-155] p 123 A92-15591
SALITSKY, GEORGE J.
A prototype semantic integrity front end expert system for a relational database
[AD-A246084] p 781 N92-26765
SALIVEROS, E.
An experimental investigation of the oblique blade-vortex interaction p 712 A92-43447
SALLEY, THOMAS
An alternative method for acquiring avionic bus data in a class I PCM telemetry system p 217 A92-19202
SALMAN, AHMED A.
Three-dimensional simulation of slender delta wing rock and divergence
[AIAA PAPER 92-0280] p 318 A92-25734
SALMINEN, E.
Modernized MBB panel code: User's guide including background theory
[PB92-136431] p 526 N92-22233
SALMIRS, SEYMOUR
Prediction of the pressure loss coefficient of wind tunnel turbulence reducing screens
[AIAA PAPER 92-0568] p 384 A92-26976
SALMONS, JAMES D.
Developmental flight testing of a half scale unmanned air vehicle
[AD-A240347] p 22 N92-11002
SALOV, N. N.
Heat transfer on a cylindrical surface in the cavities of gas turbine engine rotors p 657 A92-40609
SALVANERA, ROLANDO C.
Implementing total quality management at the intermediate level of aircraft maintenance
[AD-A241768] p 62 N92-12992
SALVATORE, A.
Prediction of aerodynamic phenomena limiting aircraft manoeuvrability p 364 N92-18781
SAMAK, D. K.
A study of rotor wake development and wake/body interactions in hover p 813 A92-46935
SAMAK, DHANANJAY K.
Effect of blade planform variation on the forward-flight performance of small-scale rotors
[NASA-TM-4345] p 630 N92-24885
SAMANIEGO, J. M.
Turbulent combustion modelling in a side dump ramjet combustor
[AIAA PAPER 92-3599] p 1112 A92-54075
The coherent flamelet model for propulsion applications p 756 N92-27486
SAMAREH-ABOLHASSANI, JAMSHID
Surface grid generation in a parameter space
[AIAA PAPER 92-2717] p 803 A92-45556
SAMBAMURTHI, JAY
Laminar hypersonic flow over a compression using the HANA code
[AIAA PAPER 92-2896] p 820 A92-47872
SAMBLANCAT, C.
A two-feedback-loop robust helicopter controller based on eigenspace techniques and H(infinity) synthesis
p 29 A92-11582
Improvement of helicopter robustness and performance control law using eigenstructure techniques and H-infinity synthesis p 569 A92-35776
SAMBLANCAT, CHRISTIANE
Double loop control law strategy and applications to helicopter
[CERT-2/7724-DERA] p 381 N92-19295
SAMIMY, M.
Effect of tabs on the evolution of an axisymmetric jet
p 656 A92-40151
Supersonic jet mixing enhancement by 'delta-tabs'
[AIAA PAPER 92-3548] p 826 A92-49063
Supersonic jet mixing enhancement by delta-tabs
[NASA-TM-105664] p 630 N92-24958
SAMOKHIN, V.
Simulation of vibrational status of gas-turbine engine
p 470 A92-29731
SAMPATH, SAM N.
Current DOT research on the effect of multiple site damage on structural integrity p 913 N92-30112
SAMPSON, W. T., III
Composite profiles of helicopter mishaps at heliports and airports
[AD-A248887] p 724 N92-28052
SAMUELSEN, G. S.
The role of primary jet injection on mixing in gas turbine combustion p 128 A92-16584
Active control for gas turbine combustors
p 128 A92-16585
Characterization of a two-phase flow field downstream of a 3x-scale gas turbine co-axial, counter-swirling, combustor dome swirl cup
[AIAA PAPER 92-0229] p 393 A92-25693
Mixing in the dome region of a staged gas turbine combustor
[AIAA PAPER 92-3089] p 903 A92-48734
The influence of spray angle on the continuous- and discrete-phase flowfield downstream of an engine combustor swirl cup
[AIAA PAPER 92-3231] p 863 A92-48832
SAN ANDRES, LUIS A.
A gas operated bearing damper for turbomachinery
[ASME PAPER 91-GT-249] p 150 A92-15654
SANANDRES, LUIS A.
Effect of eccentricity on the static and dynamic performance of a turbulent hybrid bearing
p 225 N92-14373
SANCHEZ-CHEW, A. P.
Flight management system integration on the F-117A
[AIAA PAPER 92-1077] p 563 A92-33246
SANCHEZ, D. H.
Combined VISAR and flash x ray testing techniques
[DE92-004732] p 385 N92-18290
SANCHEZ, F.
Fuzzy guidance system evaluation
p 778 N92-27903
SANCHEZ, LUIS M.
Madrid's double airport p 138 A92-16231
SANDA, TOMIO
An example of whirl flutter analysis
p 1052 A92-56015
SANDERS, B.
Acoustic control of combustor primary zone air-jet mixing
[AIAA PAPER 92-3651] p 1067 A92-54104
SANDERS, WILLIAM A.
Monolithic ceramics p 668 A92-39854
SANDERSON, S. R.
Drag balance for hypervelocity impulse facilities
p 207 A92-18375
SANDFORD, MAYNARD C.
Planform curvature effects on flutter characteristics of a wing with 56 deg leading-edge sweep and panel aspect ratio of 1.14
[NASA-TP-3116] p 115 N92-13054
Unsteady-pressure and dynamic-deflection measurements on an aeroelastic supercritical wing
[NASA-TM-4278] p 445 N92-20654
SANDLIN, DORAL R.
A study of transonic aerodynamic analysis methods for use with a hypersonic aircraft synthesis code
[NASA-CR-189854] p 625 N92-24803
SANGER, KENNETH B.
Out of plane analysis for composite structures
p 1107 N92-32527
SANI, A. P.
Prototyping the IRDS: An airport application
[PB92-112580] p 484 N92-20448
SANKAR, L. N.
Separation control using moving surface effects - A numerical simulation p 309 A92-24419
An inverse method for the design of transonic wings
[AIAA PAPER 92-1025] p 517 A92-33206
Numerical simulation of multizone two-dimensional transonic flows using the full Navier-Stokes equations
p 815 A92-46955
Effects of leading and trailing edge flaps on the aerodynamics of airfoil/vortex interactions
p 815 A92-46957
Blade-mounted trailing edge flap control for BVI noise reduction
[NASA-CR-4426] p 512 N92-21173
Simulation of iced wing aerodynamics
p 450 N92-21686
Numerical investigation of the effects of icing on fixed and rotary wing aircraft
[NASA-CR-190542] p 1044 N92-34105
SANKAR, LAKSHMI N.
Numerical investigation of performance degradation of wings and rotors due to icing
[AIAA PAPER 92-0412] p 325 A92-26264
Numerical simulation of flow separation for rotors and fixed wings
[AIAA PAPER 92-0635] p 334 A92-27013
Numerical simulation of three-dimensional supersonic free shear layers p 431 A92-31152
Unsteady aerodynamic characteristics of a dual-element airfoil
[AIAA PAPER 92-2508] p 518 A92-34501
Numerical solution of three-dimensional unsteady viscous flows
[AD-A244274] p 403 N92-19052
SANO, A.
New robust adaptive control system using multiple regularization parameters p 51 A92-11455

SANO, H.
Automation of composite material structure installation
p 700 A92-43248
SANO, MASAAKI
Flight tests on the structures of the STOL research aircraft Asuka p 730 A92-43143
SANRYO, TAKUJI
Flow of a rarefied gas past a two-dimensional body of an arbitrary shape at small Mach numbers
p 937 A92-52726
SANSONE, A.
Aerothermodynamic development of the CARINA re-entry vehicle: CFD analyses and experimental tests
p 211 N92-14980
SANTANA, M. W.
The use of CT for dimensional measurements of green and sintered ceramic components p 490 A92-28592
SANTARE, MICHAEL H.
Continuation of tailored composite structures of ordered staple thermoplastic material
[NASA-CR-189671] p 1110 N92-33613
SANTI, FRANCOISE
A simplified model for aerodynamic flows around streamlined models p 63 A92-13816
SANTILLAN, S.
Vortical flow simulation by using structured and unstructured grids p 83 N92-12999
SANTINI, P.
Gust effects on a flexible aircraft p 270 A92-22474
SANTOS, DANIEL
Fatigue management for the A-7P
p 363 N92-18593
SANZ, A.
Unsteady transonic aerodynamics of pointed bodies of revolution in supersonic freestream p 719 N92-27946
SAPIN, S.
Compressibility effects in turbulent far wakes
p 622 A92-40140
SAPORITI, A.
Current European research activities in helicopter interactional aerodynamics p 1058 A92-56330
SARANTOPOULOS, ATHAN D.
Modeling of linear isentropic flow systems
p 593 N92-22495
SARANTSEV, A. I.
A supplement to the second-order shock-expansion method p 437 A92-31861
SARAVANAMUTTOO, H. I. H.
Off-design performance prediction of turbofans using gasdynamics
[ASME PAPER 91-GT-389] p 126 A92-15721
Overview on basis and use of performance prediction methods p 869 N92-28459
Component performance requirements
p 869 N92-28462
SARAVIA, H. E.
Aerodynamic calculation of an elliptic ring wing
[AIAA PAPER 91-0068] p 1035 A92-57035
SAREEN, ASHISH K.
Rotorcraft airframe structural optimization for combined vibration and fatigue constraints p 106 A92-14390
SAREN, V. E.
Flow and shape correction problems for thin profiles in incompressible stream p 707 A92-42736
SARIC, WILLIAM S.
Boundary-layer receptivity of sound with roughness
p 604 A92-36006
The ASU Transition Research Facility
[AIAA PAPER 92-3910] p 1094 A92-56744
Laminar-turbulent transition: Fundamentals
p 717 N92-27710
Stability and transition of hypersonic boundary-layer flows
[AD-A250279] p 948 N92-31555
SARIGUL, NESRIN
A novel approach in formulation of special transition elements: Mesh interface elements
[NASA-CR-189050] p 501 N92-20954
SARKISIAN, A. K.
Selection of the time parameters of the probing pulse during the nonstationary irradiation of flight vehicles
p 454 A92-31951
Characteristics of the energy analysis of optical radar in the case of nonstationary irradiation of flying objects
p 454 A92-31955
SARKOS, CONSTANTINE P.
Development and evaluation of an onboard aircraft cabin water spray system for postcrash fire protection
[SAE PAPER 912224] p 636 A92-40022
SARLIN, P.
Certifying composite helicopter structures
p 110 A92-14443
SARMA, V. V. S.
Multisensor data fusion and decision support for airborne target identification p 454 A92-31063
SARRAF, DAVID
Flexible heat pipe cold plates for aircraft thermal control
[SAE PAPER 912105] p 674 A92-39959
SASA, S.
Aerodynamic model identification of a spaceplane model from a cable-mount dynamic wind-tunnel test
p 1093 A92-56114
SASA, SHUICHI
Aerodynamic drag as determined from flight test data of the STOL research aircraft Asuka
p 709 A92-43145
Motion estimation for cable-mount dynamic wind-tunnel test p 749 A92-43210
Estimation of spaceplane longitudinal stability and control derivatives from dynamic wind tunnel test
p 752 A92-43211
Estimation of spaceplane model inertia characteristics
p 752 A92-43212
On the characteristics of servo actuators attached to a model spaceplane for dynamic wind-tunnel test
p 762 A92-43213
Spaceplane longitudinal aerodynamic parameter estimation by cable-mount dynamic wind-tunnel test
[SAE PAPER 911980] p 788 A92-45385
On improvements of three-dimensional position measuring system for dynamic wind tunnel testing
p 1093 A92-56012
Evaluation of a IMU with optical fiber gyros in dynamic windtunnel tests p 1104 A92-56121
SASA, SHUUICHI
Estimation of cable-mounted model inertia characteristics for dynamic wind-tunnel test
[NAL-TM-641] p 722 N92-28152
SASAKI, GLEN E.
The 12-foot pressure wind tunnel restoration project model support systems p 664 N92-25091
SASAKI, HIROSHI
Concepts of flight experiments for HOPE development
p 1103 A92-53635
SASAKI, KUZUTO
Three-dimensional relaxation effect on quasi-3D flow in a blade row with spanwise loading distribution
p 936 A92-51593
SASAKI, MAKOTO
Operational progress of the STOL research aircraft Asuka p 730 A92-43138
SASAKI, SHIGERU
Optimization approach for helicopter maneuverability with a point mass model p 1083 A92-56025
SASHIKUMA, HIROFUMI
An example of whirl flutter analysis
p 1052 A92-56015
SASO, AKIHIRO
Test on high enthalpy hypersonic flow using a ballistic range p 747 A92-43097
SASOH, AKIHIRO
Radiative heat transfer from nonequilibrium shock layer to a hypersonic reentry body p 1019 A92-53579
Three-dimensional calculation of radiative field in hypersonic air shock layers p 1023 A92-54498
SASSA, K.
Three-dimensional vortical structure of a large-scale coherent vortex in a turbulent boundary layer
p 619 A92-40056
SASSA, SHUICHI
Wind tunnel tests on the motion of a spaceplane simulation for cable mount p 752 A92-43192
SASSO, M.
Description and simulation results of the Italsat AOCS advanced flight simulator p 667 N92-24472
SASTRY, S. S.
Adaptive control of nonlinear systems with applications to the control of flexible robot arms
[AD-A244409] p 413 N92-19397
SASTRY, SHANKAR
Nonlinear control design for slightly nonminimum phase systems - Application to V/STOL aircraft
p 876 A92-48160
SATERLIE, S. F.
Hypersonic plasma predictions at nonzero angle of attack
[AIAA PAPER 92-3027] p 925 A92-47028
SATIN, A. L.
Evaluation of GPS/UTC steering performance
p 1049 N92-33353
SATO, AKIO
Repair operation on a composite material structure
p 700 A92-43153
SATO, HIROKI
A data processing system for oceanic air traffic control p 1046 A92-56090
SATO, HISASI
A low speed wind tunnel investigation of a joined-wing aircraft with an overhanging fin p 1030 A92-56078
A low speed wind tunnel investigation of the direct side force control of a joined-wing aircraft with overhanging fin p 1084 A92-56079
SATO, JUNICHI
Low speed aerodynamic performance of a capsule-shaped flying object p 430 A92-30559
SATO, KIYOSHI
Approximate analysis of aerodynamic heating at hypersonic speed p 430 A92-30551
Nonlinear dynamic stability characteristics of recovery bodies p 977 A92-52041
SATO, M.
Recent airfoil tests in NAL 2D high Reynolds number wind tunnel p 748 A92-43171
SATO, MAMORU
Transonic visualization test for the airframe shape improvement of a spaceplane p 752 A92-43200
BGK airfoil oil flow test in a two-dimensional transonic wind tunnel p 711 A92-43201
Buffeting characteristics of a transonic airfoil
p 711 A92-43202
On the structure of unsteady shock induced separation of the transonic airfoil in the NAL two-dimensional wind tunnel p 1029 A92-56010
Evaluation of sidewall interference in the NAL two-dimensional transonic wind tunnel
p 1092 A92-56011
BGK1 airfoil oilflow tests in the NAL two-dimensional wind tunnel. II p 1029 A92-56044
High subsonic wind tunnel test of a two-dimensional hybrid-laminar-flow-control airfoil with slotted surface
p 1029 A92-56045
Evaluation of NACA0012 airfoil test results in the NAL two-dimensional transonic wind tunnel
[NAL-TR-1109T] p 445 N92-21287
NACA0012 airfoil data corrected for sidewall boundary-layer effects in the NAL two-dimensional transonic wind tunnel
[NAL-TM-640T] p 722 N92-28151
SATO, SHIGERU
Experimental validation of scramjet nozzle performance
[AIAA PAPER 92-3290] p 864 A92-48879
A preliminary study of a supersonic wind tunnel for a ram jet test facility p 1089 A92-53564
Propeller-nacelle whirl flutter analysis and wind tunnel test p 1052 A92-56016
SATO, TAKASHI
Free wake analyses of a hovering rotor using panel method
[SAE PAPER 912004] p 789 A92-45405
SATO, TATSUO
Structural concept of main wings of high altitude unmanned aerial vehicle and basic properties of thermoplastic composites as candidate material
[SAE PAPER 912053] p 843 A92-45437
SATO, TOMOHIKO
Film cooling on a gas turbine rotor blade
[ASME PAPER 91-GT-279] p 152 A92-15675
SATO, Y.
Integrated system to support computer analysis in conceptual aerospace design p 1130 A92-53596
SATO, YUKINORI
Effectiveness of plasma torches for ignition and flameholding in scramjet p 737 A92-44524
SATOFUKA, NOBUYUKI
A numerical solution of inviscid transonic flow using the Boltzmann equation p 443 A92-32504
SATONAKA, K.
Selection of sampling rate for nonlinear flight trajectory controller of aircraft p 1084 A92-56070
SATOSHI, YONEZAWA
Optimum structural design of a cantilevered rectangular elastic wing with a gust load alleviation system
p 762 A92-43133
SATOU, MAMORU
Force measurements on AGARD calibration model-B at transonic speeds in the NAL two-dimensional wind tunnel
[NAL-TM-639] p 722 N92-28190
SAUCEDO, V. E.
Integrated wiring system
[SAE PAPER 912058] p 897 A92-45440
SAUCEREAU, D.
Supersonic combustion studies p 211 N92-14984
SAUCRAY, J. M.
International standardisation of regulations for gust loading calculations p 270 A92-22473
SAUER, GREGORY
Self-compensating carrier aircraft recovery system
p 448 A92-32238
SAUL, G. W.
The aerodynamic assistant - A tool for V/STOL aircraft conceptual design p 545 A92-35737

SAUNDERS, J. D.
Results from computational analysis of a mixed compression supersonic inlet
[NASA-TM-104475] p 12 N92-10976
SAUNDERS, NEAL T.
Impact and promise of NASA aeropropulsion technology p 559 N92-22511
SAUNDERS, R. W.
A comparison of measured and modeled broadband fluxes from aircraft data during the ICE '89 field experiment p 1003 A92-49771
SAVAGE, M.
Transmission overhaul and component replacement predictions using Weibull and renewal theory p 155 A92-17201
SAVELLE, S. A.
Turbine engine performance test and evaluation techniques
[AIAA PAPER 92-3977] p 1071 A92-56803
SAVELY, ROBERT T.
Advanced training systems for the next decade and beyond
[AIAA PAPER 92-1626] p 690 A92-38699
SAVILL, A. M.
Turbulent skin-friction drag reduction by active and passive means, part 1 p 718 N92-27714
SAVIN, A. V.
Effect of rarefaction on the nonstationary interaction of a supersonic underexpanded jet with a perpendicular obstacle p 337 A92-27594
SAVINI, M.
Transonic and supersonic inviscid computations in cascades using adaptive unstructured meshes
[ASME PAPER 91-GT-312] p 75 A92-15689
SAVORY, E.
Flow regimes of the cove regions between a slat and wing and between a wing and flap of a multielement airfoil p 614 A92-38858
SAVU, G.
On a global aerodynamic optimization of a civil transport aircraft p 193 N92-13931
SAWADA, HIDEO
Results of measured temperature distribution on an adiabatic wing model with radiation thermometer
[NAL-TM-610] p 261 N92-17755
Development of wall pressure measuring apparatus for an existing transonic wind tunnel test section
[NAL-TM-565] p 573 N92-23778
Study of the NAL's 0.1 x 0.1 m magnetic suspension and balance system
[NAL-TM-623] p 665 N92-25365
SAWADA, KEISUKE
Numerical investigation of supersonic inlet with realistic bleed and bypass systems p 713 A92-44519
SAWADA, TERUO
Numerical simulation of supersonic unsteady flow using a panel method p 1030 A92-56048
SAWAI, TADAO
A gust generation method for full configuration aircraft tests in a low speed wind tunnel. Part 1: Design and preliminary experiments
[NAL-TR-1115-PT-1] p 722 N92-28192
SAWKO, PAUL M.
Performance of uncoated AFRSI blankets during multiple Space Shuttle flights
[NASA-TM-103892] p 890 N92-29104
SAWLEY, M. L.
Non-equilibrium hypersonic flow simulations using the second-order boundary layer equations p 612 A92-37551
SAWYER, BRIAN M.
Rotorcraft terminal ATC route standards
[SCT-90RR-33] p 641 N92-26101
SAWYER, R. S.
Lift development of delta wings undergoing constant acceleration from rest p 9 A92-13209
SAYA, S.
Transonic visualization test for the airframe shape improvement of a spaceplane p 752 A92-43200
BGK airfoil oil flow test in a two-dimensional transonic wind tunnel p 711 A92-43201
Buffeting characteristics of a transonic airfoil p 711 A92-43202
SAYAMA, MASAMI
Studies on the mechanism of ignition and flameholding by plasma jets p 755 A92-42798
Effectiveness of plasma torches for ignition and flameholding in scramjet p 737 A92-44524
SAYLOR, BRETT D.
Flexible manufacturing in repair of gas turbine engine components
[AIAA PAPER 92-3524] p 786 A92-49049
SAYLOR, D. A.
Simultaneous imaging and interferometric turbule visualization in a high-velocity mixing/shear layer p 896 A92-45130
SCAGGS, N. E.
Wedge-induced turbulent boundary-layer separation on a roughened surface at Mach 6.0 p 175 A92-20379
Turbulent boundary-layer characteristics over a flat-plate/wedge configuration at Mach 6 p 176 A92-20761
SCAGGS, NORMAN E.
Future requirements for hypersonic aerodynamic and aerothermodynamic facilities
[AIAA PAPER 92-3903] p 1094 A92-56738
Hypersonic wind tunnel nozzle study
[AIAA PAPER 92-4012] p 1033 A92-56835
SCALES, W. C.
System considerations, projected requirements and applications for aeronautical mobile satellite communications for air traffic services p 677 N92-24163
SCANLAN, ROBERT H.
Aeroelasticity of bluff bodies p 1089 N92-34165
SCANLON, CHARLES H.
Cockpit weather information needs p 449 N92-21503
A graphical weather system design for the NASA transport systems research vehicle B-737
[NASA-TM-104205] p 556 N92-22504
SCANLON, ROBERT W.
Design of a fighter aircraft vertical tail enhanced buffet environment survivability p 551 N92-23235
SCAVUZZO, R. J.
Adhesive shear strength of impact ice p 30 A92-11068
SCHABER, VEIT
Three-dimensional calculation of low-frequency unsteady transonic flow in axial turbine stages p 174 A92-19110
SCHADOW, K.
Supersonic flow mixing and combustion using RAMP nozzle
[AIAA PAPER 92-3840] p 1113 A92-54198
SCHADOW, K. C.
Thermal imaging of afterburning plumes p 129 A92-17179
Effect of carbon particles and mixing on afterburning of exhaust plumes
[AIAA PAPER 92-0767] p 387 A92-27107
Combustion instability related to vortex shedding in dump combustors and their passive control p 374 A92-27354
Flow and acoustic features of a supersonic tapered nozzle p 712 A92-44328
SCHAEFER, CARL G., JR.
Enhanced energy maneuverability for attack helicopters using continuous, variable (C-V) rotor speed control p 132 A92-14421
SCHAEFER, CHRISTOPH H.
Laser-radar based obstacle avoidance system for helicopters p 1064 A92-56295
SCHAEFER, W.
Navsat - A civil complement to GPS and Glonass
[IAF PAPER 91-490] p 188 A92-18505
SCHAEFFER, JOSEPH
V-22 thrust power management control law development p 132 A92-14405
SCHAENZER, GUNTHER
Identification of the transfer function between turbulence and aircraft p 743 A92-41226
SCHAFFAR, M.
Computation of the BVI noise for the BO105 Model Rotor in forward flight and comparison with wind tunnel tests p 165 A92-14386
SCHAFRANEK, D.
Some longitudinal handling qualities design guidelines for active control technology transport aircraft
[NLR-TP-90129-U] p 878 N92-28652
SCHAIRER, EDWARD T.
Two-dimensional adaptive-wall tests in the NASA Ames two- by two-foot transonic wind tunnel p 30 A92-13201
SCHANK, JOHN F.
Developing robust support structures for high-technology subsystems: The AH-64 Apache helicopter
[AD-A252773] p 1017 N92-33499
SCHAPHORST, RICHARD
Compression techniques for video telemetry p 188 A92-19214
SCHARPF, D. F.
The design of a subsonic low-noise, low-turbulence wind tunnel for acoustic measurements
[AIAA PAPER 92-3883] p 1094 A92-56726
SCHARPF, DANIEL F.
Experimental study of a low Reynolds number tandem airfoil configuration p 442 A92-32241
SCHARTON, TERRY D.
Force limited vibration testing p 595 N92-22688
SCHAUB, WILLIAM R., JR.
C-29A aircraft altimeter errors
[AD-A240486] p 23 N92-11011
SCHECHTER, JACOB
Modern techniques for monitoring airborne telemetry p 857 A92-47560
SCHEICK, J. T.
Automated composite ellipsoid modelling for high frequency GTD analysis
[NASA-CR-189853] p 275 N92-17316
SCHEITLE, H.
Influences of wind tunnel parameters on airfoil characteristics at high subsonic speeds p 173 A92-18769
SCHELL, ALLAN C.
CFD helps the Air Force fly right p 169 A92-20146
SCHELLENBERG, CARL B.
Future considerations for vertical flight p 608 A92-40383
SCHENEWERK, MARK S.
GPS orbit determination at the National Geodetic Survey p 1049 N92-33354
SCHENK, A.
Modal identification in the presence of steady excitation p 131 A92-13693
SCHENK, H.-D.
Experiences developed in transfering the experimental COMPAS system to an operational prototype version p 355 N92-19045
SCHERZ, CARL J.
C-17 flight control system overview p 1082 A92-55906
SCHETTINO, ANTONIO
High enthalpy nozzle flows p 182 N92-15000
SCHETZ, J. A.
Effects of unsteady shock impingement on high-speed gaseous mixing
[AIAA PAPER 91-5091] p 172 A92-17857
Mixing studies of helium in air at high supersonic speeds p 935 A92-50310
SCHEUGENPFLUG, HERMANN
Performance improvements of compressor cascades by controlling the profile and sidewall boundary layers
[ASME PAPER 91-GT-260] p 75 A92-15662
SCHIAVONE, ANTHONY J.
Core avionics and standardization
[AD-A248326] p 735 N92-27925
SCHICK, FRED V.
The COMPAS system in the ATC environment
[DLR-MITT-91-08] p 354 N92-19041
Evaluation of the COMPAS experimental system p 355 N92-19044
Evaluation of the COMPAS operational system p 355 N92-19047
SCHIERENBECK, D.
Simultaneous stress and flutter optimization for the wing of a transport aircraft equipped with four engines p 571 N92-23238
SCHIERMAN, JOHN D.
A framework for the analysis of airframe/engine interactions and integrated flight/propulsion control p 478 A92-29120
Analysis of airframe/engine interactions for a STOVL aircraft with integrated flight/propulsion control
[AIAA PAPER 92-4623] p 1052 A92-55300
SCHIFF, LEWIS B.
Computation of three-dimensional turbulent vortical flows on bodies at high incidence p 9 A92-13203
Numerical prediction of subsonic turbulent flows over slender bodies at high incidence p 172 A92-18358
Computational investigation of slot blowing for fuselage forebody flow control
[AIAA PAPER 92-0020] p 248 A92-22142
Turbulence model effects on separated flow about a prolate spheroid p 340 A92-28036
Coupled numerical simulation of the external and engine inlet flows for the F-18 at large incidence
[AIAA PAPER 92-2621] p 793 A92-45493
Analysis of a pneumatic forebody flow control concept about a full aircraft geometry
[AIAA PAPER 92-2678] p 799 A92-45530
Navier-Stokes predictions for the F-18 wing and fuselage at large incidence p 810 A92-46783
SCHIJVE, J.
Bulging of fatigue cracks in a pressurized aircraft fuselage
[LR-655] p 196 N92-14045
SCHILLING, LAWRENCE
Rapid development of the X-31 simulation to support flight-testing
[NASA-TM-104256] p 1060 N92-33149
SCHIMKE, D.
Mission oriented investigation of handling qualities through simulation p 1059 A92-56353

SCHIMKE, S.
Analysis of iced wings
[AIAA PAPER 92-0416] p 423 A92-29972
Analysis of iced wings
[NASA-TM-105773] p 1042 N92-34144
SCHIPPER, BRIAN
Design and flight test of a differential GPS/inertial navigation system for approach/landing guidance
p 97 A92-16650
Differential GPS/inertial navigation approach/landing flight test results p 956 A92-51009
SCHIROKY, GERHARD H.
Fabrication and properties of fiber-reinforced ceramic composites made by directed metal oxidation
p 669 A92-39861
SCHLAGER, LYNN M.
Boiling and condensation in microfin tubes
p 682 N92-25660
SCHLEICHER, MARCEL
Theoretical principles of a Euler method for the calculation of three dimensional flows
[F+W-TF-2012] p 767 N92-27045
SCHLINGELHOF, MARIUS
The electronic aeronautical chart for general aeronautics: A system specification
[ILR-MITT-263(1991)] p 20 N92-10997
SCHLUTER, L. L.
The status of the US VAWT program
[DE92-002931] p 505 N92-21040
SCHMAELZLE, U.
Methodology for assessment of skin repairs on Airbus aircraft p 226 N92-14428
SCHMATZ, M.
Cases 6.1 and 6.8 double ellipsoid: Navier-Stokes calculation p 525 N92-22181
Case 7.4 delta wing: Navier-Stokes calculation
p 525 N92-22182
SCHMATZ, M. A.
Verification and application of the NSFLEX method for hypersonic flow conditions p 182 N92-15005
SCHMELTEKOPF, ARTHUR L.
The atmospheric effects of stratospheric aircraft: A first program report
[NASA-RP-1272] p 408 N92-19121
Lower stratospheric measurement issues workshop report p 409 N92-19127
SCHMID, RONALD
Legal problems in aircraft towing using the PTS procedure p 56 A92-11214
SCHMIDT, ARLEN
Airborne/shipborne PSK telemetry data link
p 839 A92-47511
SCHMIDT, B.
Shock wave reflection close to the leading edge of a wedge p 37 A92-10660
SCHMIDT, DAVID K.
Dynamics and control of hypersonic vehicles - The integration challenge for the 1990's
[AIAA PAPER 91-5057] p 203 A92-17840
A framework for the analysis of airframe/engine interactions and integrated flight/propulsion control
p 478 A92-29120
Dynamics and control of hypersonic aeropropulsive/aeroelastic vehicles
[AIAA PAPER 92-4326] p 1073 A92-55170
New literal approximations for the longitudinal dynamic characteristics of flexible flight vehicles
[AIAA PAPER 92-4411] p 1075 A92-55205
An integrated development of the equations of motion for elastic hypersonic flight vehicles
[AIAA PAPER 92-4605] p 1077 A92-55283
An integrated analytical aeropropulsive/aeroelastic model for the dynamic analysis of hypersonic vehicles
[AIAA PAPER 92-4567] p 1035 A92-57034
SCHMIDT, E.
Supercritical blade design on stream surfaces of revolution with an inverse method p 220 N92-13950
SCHMIDT, FRED
Characteristics of a future aeronautical satellite communications system
[AIAA PAPER 92-2058] p 453 A92-29889
SCHMIDT, HANS-J.
Ageing airplane repair assessment program for Airbus A300 p 838 N92-30123
SCHMIDT, JAMES F.
Design and performance of controlled-diffusion stator compared with original double-circular-arc stator
[NASA-TP-2852] p 562 N92-22863
SCHMIDT, JOHN
Scenario analysis of thigh gap related ejection injuries
p 834 A92-44995
SCHMIDT, PHILLIP
Decentralized hierarchical partitioning of centralized integrated controllers p 477 A92-29119
A parameter optimization approach to controller partitioning for integrated flight/propulsion control application
[NASA-TM-105826] p 979 N92-32241
SCHMIDT, WOLFGANG
Europe presents a united CFD front
p 392 A92-24909
SCHMIDTKE, KLAUS
Development of hardness cycles for fiber bound materials, using DSC: From laboratory specimens to complex high duty structural members
[MBB-Z-0409-91-PUB] p 987 N92-30969
SCHMIERER, KIRK T.
JIAWG module fault coverage metrics methodology
p 989 A92-49279
SCHMISSEUR, J. D.
Unsteady separation in sharp fin-induced shock wave/turbulent boundary layer interaction at Mach 5
[AIAA PAPER 92-0748] p 436 A92-31678
SCHMIT, L. A.
Exploratory design studies of actively controlled wings using integrated multidisciplinary synthesis
p 641 A92-36828
Integrated aeroservoelastic wing synthesis by nonlinear programming/approximation concepts
p 873 A92-46752
SCHMIT, LUCIEN A., JR.
Control augmented structural optimization of aeroelasticity tailored fiber composite wings
[AD-A241464] p 135 N92-13075
SCHMITT, R. G.
Thermal radiation effects on a shocked particle-laden gas p 780 A92-44377
SCHMITT, V.
Investigations of propulsion integration interference effects on a transport aircraft configuration
[AIAA PAPER 92-3097] p 849 A92-48739
SCHMITZ, F. H.
Rotor noise p 54 N92-10600
SCHNEIDER, G.
Continuation of the AHS round robin on fatigue reliability and damage tolerance p 59 A92-14341
First approach to an integrated fin design
p 551 N92-23236
SCHNEIDER, STEVEN P.
A quiet-flow Ludwieg tube for experimental study of high speed boundary layer transition
[AIAA PAPER 91-5026] p 207 A92-17819
A quiet-flow Ludwieg tube for experimental study of high speed boundary layer transition
[AIAA PAPER 92-3885] p 1094 A92-56727
Aerodynamics laboratory education at Purdue University - Ground testing facilities
[AIAA PAPER 92-4018] p 1100 A92-56840
SCHNELL, RUSSELL C.
Measured and calculated optical property profiles in the mixed layer and free troposphere p 1129 A92-54630
SCHNERR, G. H.
The just attached shock-wave at the leading edge of a profile p 3 A92-10663
SCHNERR, GUENTER H.
Compressible turbulent boundary layers with heat addition by homogeneous condensation
p 611 A92-36843
Similarity and resistance in near-sonic flows for given heat conduction p 708 A92-43065
SCHOBEIRI, TAHER
Aerodynamics and heat transfer investigations on a high Reynolds number turbine cascade
[ASME PAPER 91-GT-157] p 148 A92-15593
SCHOBERT, H. H.
Advanced thermally stable jet fuel development program. Volume 2: Compositional factors affecting thermal degradation of jet fuels
[AD-A252656] p 987 N92-31399
SCHOBIERI, T.
Row-by-row off-design performance calculation method for turbines p 737 A92-44514
SCHOENE, J.
Analysis tools of ONERA and DLR for the aerothermodynamics of reentry vehicles
p 211 N92-14977
Steps towards an efficient and accurate method solving the Euler equations around a re-entry configuration at super- and hypersonic speed p 181 N92-14987
SCHOENUNG, B.
The influence of density difference between hot and coolant gas on film cooling by a row of holes - Predictions and experiments
[ASME PAPER 91-GT-255] p 151 A92-15660
SCHOEPFEL, A.
Review of investigations on aeronautical fatigue in the Federal Republic of Germany
[ETN-92-90317] p 225 N92-14397
SCHOESS, J.
Distributed health management systems technology for future propulsion control systems
[SAE PAPER 912167] p 655 A92-39995
SCHOETTLE, U. M.
Optimization of two stage reusable space transportation systems with rocket and airbreathing propulsion concepts
[IAF PAPER 92-0863] p 1104 A92-57254
SCHOFIELD, B. L.
The flight test pilot's display - A CRT system for test maneuvers p 118 A92-16057
SCHOMER, PAUL D.
Human response to helicopter noise: A test of A-weighting
[AD-A243719] p 304 N92-17506
SCHOMMER, D. G.
Laser diagnostics for velocity measurements in supersonic combusting environments
[AIAA PAPER 92-0008] p 288 A92-22133
SCHOONMAKER, PETER M.
Preliminary experience with an expert system providing initial centrifugal compressor sizing for performance prediction and analysis
[ASME PAPER 91-GT-28] p 162 A92-15513
SCHORK, F. J.
An integrated, full-range surge control/rotating stall avoidance compressor control system
p 469 A92-29376
SCHOTT, TIMOTHY
Present status of the MIT/NASA Langley 6-inch MSBS p 750 N92-27802
SCHOULTZ, MICHAEL
Formation flight system design concept
p 954 A92-49255
SCHRA, L.
Short cracks and durability analysis of the Fokker 100 wing/fuselage structure
[NLR-TP-90336-U] p 910 N92-29603
SCHRADER, STEPHEN M.
Performance of hybrid ball bearings in oil and jet fuel
p 900 A92-47176
Performance of a hybrid cylindrical roller bearing
p 995 A92-51845
SCHRAGE, D. P.
Performance and handling qualities criteria for low cost real time rotorcraft simulators - A methodology development p 136 A92-14365
A new method for simulating atmospheric turbulence for rotorcraft applications p 162 A92-14368
Nonlinear control of a twin-lift helicopter configuration
p 204 A92-18624
Some issues on modeling atmospheric turbulence experienced by helicopter rotor blades
p 647 A92-40885
Adequacy of modeling turbulence and related effects on helicopter response p 730 A92-41263
On the adequacy of modeling turbulence and related effects on helicopter response p 847 A92-46945
Short takeoff optimization for the XV-15 tiltrotor aircraft p 1056 A92-56302
Helicopter nonlinear flight control system development
p 1085 A92-56317
A new method for simulating atmospheric turbulence for rotorcraft applications p 464 N92-21956
SCHRAGE, DANIEL P.
Rotorcraft airframe structural optimization for combined vibration and fatigue constraints p 106 A92-14390
Relating economics to design parameters through a criterion function p 271 A92-22709
Optimal output feedback for linear time-periodic systems p 412 A92-28142
SCHRAGER, D. P.
Synthesis of a helicopter full-authority controller
p 280 A92-21178
SCHRAMM, F. M.
Development of an advanced piloted helicopter simulation p 105 A92-14363
SCHRAUF, G.
Curvature effects for three-dimensional compressible boundary-layer stability p 701 A92-41207
SCHRECK, SCOTT J.
Static and dynamic flow field development about a porous suction surface wing
[AIAA PAPER 92-2628] p 795 A92-45500
SCHREIBER, FABIO A.
State and time granularity in system description: An example
[REPT-91-040] p 603 N92-22673
SCHREIBER, H. A.
An investigation of a strong shock-wave turbulent boundary layer interaction in a supersonic compressor cascade
[ASME PAPER 91-GT-92] p 70 A92-15556

SCHROEDER, J. A.
Control and display combinations for blind vertical landings p 661 A92-39903
SCHROEDER, JOHN B.
Field test of an advanced maintenance-system p 1016 A92-56221
SCHROEDER, TH.
Investigations of blade row interaction and boundary layer transition phenomena in a multistage aero engine low-pressure turbine by measurements with hot-film probes and surface-mounted hot-film gauges p 658 N92-24338
SCHROEDER, W.
Implicit solutions of three-dimensional viscous hypersonic flows p 434 A92-31549
Three-dimensional simulations of hypersonic flows [MBB-UK-0155-89-PUB] p 447 N92-21703
SCHUBERT, M.
COMPAS system concept p 354 N92-19043
Implementation and operational experience with a new arrival traffic management system at the Frankfurt ATC-Center p 728 N92-27905
SCHUDT, KARL
Gamma Group-The Pale Horse: A proposal in response to a commercial air transportation study ort study [NASA-CR-190019] p 731 N92-26435
SCHUETTE, R.
A small light-weight rotor platform for ground observation and pollution control p 1057 A92-56329
SCHUHMACHER, G.
Multidisciplinary optimization of fiber composite aircraft structures [MBB/FW321/S/PUB/476] p 961 N92-30424
SCHULTE-WERNING, BURKHARD
On the footprints of three-dimensional separated vortex flows around blunt bodies: Attempts of defining and analyzing complex flow structures p 84 N92-13005
SCHULTZ, KLAUS-J.
BVI impulsive noise reduction by higher harmonic pitch control - Results of a scaled model rotor experiment in the DNW p 1136 A92-56344
SCHULTZ, MICHAEL
Inertia reels for aircrew restraint systems p 529 A92-32982
SCHULTZ, R. E.
Application of a universe-series code for inviscid flow over complex 3-dimensional configurations [AIAA PAPER 92-0150] p 253 A92-23765
SCHULTZ, R. L.
Trajectory optimization for hypersonic aircraft guidance p 728 N92-27898
SCHULTZ, ROBERT B.
Navigation charts on trial - How safe is safe? p 1012 A92-49380
SCHULTZ, WILLIAM D.
Static tests for the evaluation of fuel additives [AIAA PAPER 92-0686] p 389 A92-27053
SCHULZ, A.
Life time prediction for ceramic gas turbine components [ASME PAPER 91-GT-96] p 122 A92-15560
SCHULZE, B.
Aerodynamic assessment of an optical pressure measurement system (OPMS) by comparison with conventional pressure measurements in a high speed wind tunnel p 1114 A92-54304
Computation of flutter boundaries in the time and frequency domain p 720 N92-27952
SCHUMACHER, GARY A.
Design and implementation of a total flight test system p 189 A92-19278
SCHUMANN, U.
Studies on the effect of high-flying air-traffic on the atmosphere [IAF PAPER 91-737] p 301 A92-22495
SCHUR, WILLI W.
Structural behavior of scientific balloons - Finite element simulation and verification [AIAA PAPER 91-3668] p 20 A92-11015
SCHUSTER, E. P.
Computational icing analysis for aircraft inlets [AIAA PAPER 92-3178] p 836 A92-48793
SCHUSTER, JOACHIM
The icing of the elevator of the DLR icing research aircraft of Do 28 type [DLR-MITT-91-12] p 953 N92-31813
SCHUTZ, BOB E.
Simulation of GRM drag compensation system p 285 A92-21023
SCHWAB, R. R.
Hypersonic airbreathing propulsion activities for Saenger [AIAA PAPER 91-5040] p 200 A92-17828
SCHWAB, RUDOLPH T.
Day/Night Adverse weather Pilotage System (D/NAPS) p 94 A92-14429
SCHWAB, S.
Ignition delays, heats of combustion, and reaction rates of aluminum alkyl derivatives used as ignition and combustion enhancers for supersonic combustors [AIAA PAPER 92-3841] p 894 A92-49134
SCHWAB, S. D.
Aerodynamic applications of pressure-sensitive paint [AIAA PAPER 92-0264] p 394 A92-25720
SCHWALB, ANDREW P.
Global positioning system supported pilot's display p 534 N92-22436
SCHWALBE, KARL-HEINZ
Mechanical and fracture behaviour of Ti-6Al-2Sn-4Zr-2Mo-0.1Si alloys p 288 A92-22755
SCHWARMANN, L.
A concept for the revisions of structural inspection schedules p 226 N92-14431
SCHWARTEN, H.
Application of direct inverse analogy method (DIVA) and viscous design optimization techniques p 176 N92-13951
SCHWARTZ, ADAM L.
Comments on 'Fuzzy logic for control of roll and moment for a flexible wing aircraft' p 480 A92-30995
SCHWARTZ, ALAN W.
Hover evaluation of an integrated pneumatic lift/reaction-drive rotor system [AIAA PAPER 92-0630] p 333 A92-27010
SCHWARTZ, F.
The beta-CEZ - A high performance titanium alloy for aerospace engines p 289 A92-22760
SCHWARTZ, KENNETH P.
Foreign object damage to tires operating in a wartime environment [AD-A247195] p 724 N92-27682
SCHWARTZ, R. J.
Flow over a twin-tailed aircraft at angle of attack. I - Spatial characteristics p 702 A92-41229
Flow over a twin-tailed aircraft at angle of attack. II - Temporal characteristics p 810 A92-46781
SCHWARTZ, SUSAN K.
Surface generation and editing operations applied to structural support of aerospace vehicle fuselages p 777 N92-27831
SCHWARZ, K. P.
A consistency test of airborne GPS using multiple monitor stations p 454 A92-30651
SCHWEIGER, PAUL S.
Ultra high bypass Nacelle aerodynamics inlet flow-through high angle of attack distortion test [NASA-CR-189149] p 943 N92-30298
SCHWEIKHARD, WILLIAM G.
An alternative source of flight test services [AIAA PAPER 92-1088] p 515 A92-33254
SCHWENK, R.
Report of the working group Future CNS Systems - Applications and impact on the German air transport system p 266 A92-21325
SCHWERTASSEK, RICHARD
Representation of geometric stiffening in multibody system simulation p 217 A92-19463
SCHWIESOW, R. L.
An airborne Doppler lidar for meteorological research p 467 A92-32082
Simplified signal processing for an airborne CO2 Doppler lidar p 1000 N92-31023
SCHWIRZKE, M.
Analysis of accidents during instrument approaches p 529 A92-34253
SCHWIRZKE, MARTIN
Analysis of general aviation accidents during operations under instrument flight rules p 16 A92-11172
SCHWIRZKE, MARTIN F. J.
A re-analysis of the causes of Boeing 727 'black hole landing' crashes p 833 A92-44985
SCHYMANIETZ, KLAUS
Tiger development status p 458 A92-29672
SCIAMMARELLA, CESAR A.
Electro optical system to measure strains at high temperature [NASA-CR-190450] p 1127 N92-33696
SCOTT, BARRY C.
MLS/RNAV control display unit development p 965 A92-49303
Evaluation of advanced microwave landing system procedures in the New York terminal area [DOT/FAA/ND-91/1] p 354 N92-18967
SCOTT, C. D.
Aeroassist flight experiment heating-rate sensitivity study p 3 A92-10427
Aerodynamic heating on AFE due to nonequilibrium flow with variable entropy at boundary layer edge p 183 N92-15020
SCOTT, G.
Dynamic stall on wind turbine blades [DE92-001157] p 262 N92-17874
SCOTT, J. R.
Time domain numerical calculations of unsteady vortical flows about a flat plate airfoil p 936 A92-50473
SCOTT, JOHN E., JR.
Test facilities and instrumentation for research in rarefied gas dynamics - An historical perspective [AIAA PAPER 92-3969] p 1098 A92-56795
SCOTT, MARSHALL M., JR.
Global positioning system supported pilot's display p 534 N92-22436
SCOTT, R. F.
Processing and environmental effects on mechanical properties of composite repairs [NRC-LTR-ST-1826] p 1109 N92-32791
SCOTT, ROBERT C.
Determining design gust loads for nonlinear aircraft similarity between methods based on matched filter theory and on stochastic simulation [AIAA PAPER 92-2369] p 518 A92-34597
Maximized gust loads for a nonlinear airplane using matched filter theory and constrained optimization [NASA-TM-104138] p 23 N92-11010
SCOTT, W.
Space Shuttle Orbiter auxiliary power unit status [SAE PAPER 912060] p 889 A92-45442
SCOTT, WILLIAM B.
Renewed interest in pulsed engines may be linked to 'black' aircraft p 24 A92-10600
Evaluations of X-29 high-AOA regime show promise for future fighters p 192 A92-19925
B-2 handling, automation tailored to two-pilot crew p 643 A92-39725
B-1B excels in conventional role p 786 A92-47971
SCOTTI, STEPHEN J.
A simplified method for thermal analysis of a cowl leading edge subject to intense local shock-wave-interference heating [NASA-TP-3167] p 679 N92-24797
SCRIVENER, C. T. J.
Use of CFD in the design of a modern multistage aero engine LP turbine design [PNR-90862] p 472 N92-20179
SCURLOCK, R. G.
Magnetic suspension using high temperature superconducting cores p 772 N92-27789
SEAFORD, C. M.
Aerobrake aerothermodynamic environment predictions in support of the Aeroassist Flight Experiment [TABES PAPER 91-278] p 519 A92-34683
SEAGLE, S. R.
Ti-6Al-4V forgings with enhanced fatigue characteristics for engine and airframe applications p 288 A92-22757
SEALS, D.
Liquid flow-through cooling for avionics applications p 902 A92-48448
SEALS, J. D.
Putting ten pounds of avionics in a one pound package (Can we do it again?) [AIAA PAPER 91-3766] p 197 A92-17628
Next-generation avionics packaging and cooling 'test results from a prototype system' p 989 A92-49277
SEASHOLTZ, RICHARD G.
Laser anemometer measurements and computations in an annular cascade of high turning core turbine vanes [NASA-TP-3252] p 830 N92-28980
SEATH, DONALD D.
Experimental investigation of the perpendicular rotor blade-vortex interaction at transonic speeds p 340 A92-28047
SEAVER, D. W.
Nickel base alloy GTD-222 - A new gas turbine nozzle alloy [ASME PAPER 91-GT-73] p 142 A92-15542
SEDBON, GILBERT
Mirage 2000-5 - Dassault's delta described p 113 A92-16622
SEDDOUGUI, SHARON O.
The effects of suction on the nonlinear stability of the three-dimensional boundary layer above a rotating disc p 393 A92-25366
SEEGMILLER, H. L.
Low aspect ratio wing code validation experiment [AIAA PAPER 92-0402] p 324 A92-26255
SEEL, M. W. R.
The application of high pressure ejectors to reaction control systems p 128 A92-16666
SEELOS, MICHAEL
The Guardian: Preliminary design of a close air support aircraft [NASA-CR-189991] p 463 N92-21566
SEELY, J. F.
Thrust stand design principles [AIAA PAPER 92-3976] p 1098 A92-56802

SEGAL, CORIN
Experimental investigation of a supersonic combustion flowfield employing staged transverse injection behind a rearward-facing step
[AIAA PAPER 92-0090] p 292 A92-22196
A numerical investigation of hydrogen combustion in Mach 2 flow
[AIAA PAPER 92-0341] p 388 A92-25787
SEGAL, H. M.
EDMS: Microcomputer pollution model for civilian airports and Air Force bases, (user's guide)
[AD-A240528] p 45 N92-11578
SEGINER, A.
Pulsating spanwise blowing on a fighter aircraft
[AIAA PAPER 92-4359] p 1025 A92-55345
The three-dimensional stability of the Foeppl vortices
p 949 N92-31889
SEHER, CHRIS
National research program for nondestructive inspection of aging aircraft p 169 A92-17294
SEHER, CHRIS C.
Federal Aviation Administration aging aircraft nondestructive inspection research plan
p 914 N92-30116
SEHGAL, A. K.
Effects of nose bluntness and angle of attack on slender bodies in hypersonic flows
[AIAA PAPER 92-0638] p 334 A92-27016
Combined effect of nose bluntness and angle of attack on slender bodies in viscous hypersonic flows
[AIAA PAPER 92-0755] p 436 A92-31680
SEHRA, A.
Viscous flow analysis of advanced particle separators
p 737 A92-44517
SEHRA, ARUN K.
Application of CFD in the design of gas turbine engine components p 741 N92-27461
SEIBERT, G. L.
Nonintrusive measurements in fluid dynamic flows from Mach .0005 to 14 p 1090 A92-54311
SEIBERT, ROBERT
The Mission Computer/Electronic Display Subsystem for the United States Air Force C-17A transport aircraft
[AIAA PAPER 92-1244] p 553 A92-33337
SEIDEL, DAVID A.
Unsteady-pressure and dynamic-deflection measurements on an aeroelastic supercritical wing
[NASA-TM-4278] p 445 N92-20654
SEIER, GLEN
Preliminary design studies of an advanced general aviation aircraft
[NASA-CR-190024] p 461 N92-20064
SEILER, F.
Expansion tube experiments for the investigation of ram-accelerator-related combustion and gasdynamic problems
[AIAA PAPER 92-3246] p 904 A92-48845
SEINER, J. M.
Relationship between the instability waves and noise of high-speed jets p 924 A92-45835
SEINER, JOHN M.
Study of external dynamic flap loads on a 6 percent B-1B model
[ASME PAPER 91-GT-236] p 125 A92-15645
SEINO, HIROSHI
Study of potassium turbine electric generator system
p 1129 N92-33794
SEINO, YOSHINORI
Aircraft satellite communication systems
p 1046 A92-56091
SEKAR, B.
Direct simulation of high-speed mixing layers
[NASA-TP-3186] p 945 N92-30909
SEKELSKY, A.
Experimental evaluation of a 50-percent thick airfoil with blowing and suction boundary layer control
[AIAA PAPER 92-4500] p 1026 A92-55368
SEKIGUCHI, T.
Helicopter rotor testing using scaled model
p 1093 A92-56076
SEKINE, SHIZUO
Operational progress of the STOL research aircraft Asuka p 730 A92-43138
SELBERG, BRUCE P.
Non linear induced drag study of generically cambered closely coupled dual wings
[SAE PAPER 912126] p 618 A92-39973
CFD calculations of closely coupled scissor wings - Inviscid, viscous, and vortex lattice with rollup results
[SAE PAPER 912150] p 619 A92-39986
SELIG, MICHAEL S.
Multipoint inverse airfoil design method based on conformal mapping p 610 A92-36827
Multi-point inverse design of an infinite cascade of airfoils
[AIAA PAPER 92-2650] p 797 A92-45517
Simplified linear stability transition prediction method for separated boundary layers p 812 A92-46883
SELIKHOV, A. F.
Main concepts of providing the static/fatigue strength of helicopters in the USSR p 110 A92-14455
SELIM, ABDULFATAH A.
Supersonic flow past pointed-nose thin airfoils
p 940 A92-52844
SELLAR, M. R.
Re-engining for real stage 3 compliance
[PNR-90872] p 1072 N92-33748
SELMIN, V.
Simulation of hypersonic flows on unstructured grids
p 434 A92-31496
Vortical flow simulation by using structured and unstructured grids p 83 N92-12999
SEMENOV, A. V.
Consideration of the effect of viscosity in the problem of porous-wall induction p 440 A92-31887
SEMENOV, P. K.
Consideration of the time lag of engine processes in the problem of VTOL aircraft control synthesis
p 134 A92-16807
SEMENOVA, O. K.
Consideration of the effect of viscosity in the problem of porous-wall induction p 440 A92-31887
SEMERJIAN, H. G.
Aerodynamic effects on fuel spray structure - Experiment and theory
[AIAA PAPER 92-0227] p 317 A92-25691
SENA, J. T.
Analytical and experimental studies of heat pipe radiation cooling of hypersonic propulsion systems
[AIAA PAPER 92-3809] p 867 A92-49128
Analytical and experimental studies of heat pipe radiation cooling of hypersonic propulsion systems
[DE92-013428] p 973 N92-31817
SEND, WOLFGANG
The mean power of forces and moments in unsteady aerodynamics p 421 A92-28949
SENDA, M.
An experimental and numerical study of confined axisymmetric jet with a bluff body p 621 A92-40106
SENDECKYJ, G. P.
Airframe life prediction p 649 N92-25931
SENDSTAD, O.
Structure of three-dimensional turbulent boundary layers p 999 N92-30654
SENDSTAD, OLAV
On the mechanics of 3-D turbulent boundary layers
p 620 A92-40068
SENFT, A.
A parametric study of the aeroelastic stability of a binary wing-with-engine nacelle flutter system in incompressible flow p 270 A92-22472
SENFT, J. R.
Pressurization effects in kinematic heat engines
p 696 A92-40866
SENG, GARY T.
Fiber optics for controls p 570 N92-22529
SENGE, HEINRICH
Computational vorticity capturing - Application to helicopter rotor flows
[AIAA PAPER 92-0056] p 250 A92-22171
An Eulerian/Lagrangian method for computing blade/vortex impingement p 814 A92-46952
SENGUPTA, G.
Analysis of unsteady aerodynamic and flutter characteristics of an aeroelastic model in transonic flow
p 720 N92-27953
SENGUPTA, JAY R.
Inmarsat aeronautical mobile satellite system: Internetworking issues p 677 N92-24098
SENICK, PAUL F.
Effects of turbine cooling assumptions on performance and sizing of high-speed civil transport
[NASA-TM-105610] p 562 N92-23537
SENIK, V. IA.
Analysis of the efficiency of some structural-inspection strategies in aircraft maintenance p 419 A92-30141
SENN, C. P.
Evaluating fixed wing aircraft in the aircraft carrier environment p 464 N92-21963
United States Navy ski jump experience and future applications p 465 N92-21968
SENNOTT, J. W.
A simulator and performance criteria for evaluation of ground and space-based ATC surveillance
p 96 A92-16639
SENOO, YASUTOSHI
Performance of a high-pressure-ratio centrifugal compressor influenced by distribution of tip clearance of the mixed-flow impeller p 498 A92-32509
SENS, ANNE-SOPHIE
Computation of unsteady transonic flows using an implicit centered Euler solver without artificial viscosity
[ESA-TT-1235] p 944 N92-30514
SENSBURG, O.
Concurrent engineering in design of aircraft structures
[MBB-FE-2-S-PUB-472] p 854 N92-29650
SENSBURG, OTTO
Mathematical optimization: A powerful tool for aircraft design p 851 N92-28474
SENTOH, ETSUROH
Inverse and optimal control for desired outputs
p 661 A92-39894
SEREBRENIKOV, VADIM A.
Airfield construction (3rd revised and enlarged edition)
[ISBN 5-277-01070-X] p 670 A92-36606
SERGEEV, A. A.
A procedure for calculating the static aeroelasticity characteristics of flight vehicles by the influence coefficient method using three-dimensional finite element schemes
p 460 A92-31896
SERGIENKO, A. A.
A model of gasdynamic loads on an oscillating nozzle shell p 80 A92-16817
SERR, CHRISTOPHE
Studying dynamic behavior of X380 helicopter equipped with a new 5-blade composite rotor p 108 A92-14398
SETTLES, G. S.
Experiments on shock/vortex interactions
[AIAA PAPER 92-0315] p 320 A92-25762
Holographic flowfield density measurements in swept shock wave/boundary-layer interactions
[AIAA PAPER 92-0746] p 335 A92-27092
Flowfield visualization of crossing shock-wave/boundary-layer interactions
[AIAA PAPER 92-0750] p 335 A92-27094
Experiments on the enhancement of compressible mixing via streamwise vorticity. I - Optical measurements
[AIAA PAPER 92-3549] p 906 A92-49064
Physical model of the swept shock wave/boundary-layer interaction flowfield p 935 A92-50312
Heat transfer measurements and CFD comparison of swept shock wave/boundary-layer interactions
[AIAA PAPER 92-3665] p 1021 A92-54110
Structure of crossing-shock wave/turbulent boundary-layer interactions
[AIAA PAPER 92-3670] p 1022 A92-54113
Swept shock/boundary layer interaction experiments in support of CFD code validation
[NASA-CR-190583] p 1036 N92-32494
SEUBERT, R.
Preparation of the ice certification of the Dornier 328 regional airliner by numerical simulation and by ground test p 451 N92-21693
SEVEROV, A. A.
Thermal deformation of a polymer heat shield material on the descent trajectory p 754 A92-42655
SEWALL, WILLIAM G.
Forebody vortex flow control on the F-16C using tangential slot and jet nozzle blowing
[AIAA PAPER 92-0019] p 247 A92-22141
SEWELL, ROBERT D.
LDV measurements of the velocity field in an underexpanded supersonic jet (Ma = 1.5)
[AIAA PAPER 92-0504] p 341 A92-28196
SEYBERT, A. F.
Fatigue due to noise-induced pressure
[ASME PAPER 91-GT-150] p 148 A92-15588
SEYMOUR, THEODORE D.
Life cycle costs of the C-130 electrical power system upgrade
[AD-A246759] p 786 N92-28348
SFORZA, P. M.
Hypersonic shock tunnel testing for undergraduate laboratory instruction
[AIAA PAPER 92-4021] p 1100 A92-56843
SFORZA, PASQUALE M.
Airfoil pressure measurements during oblique shock wave-vortex interaction in a Mach 3 stream
[AIAA PAPER 92-2631] p 795 A92-45503
SHABBIR, A.
Workshop on Engineering Turbulence Modeling
[NASA-CP-10088] p 678 N92-24514
SHAFER, MARY F.
In-flight simulation studies at the NASA Dryden Flight Research Facility
[NASA-TM-4396] p 853 N92-29110
SHAFFER, ROBERT D.
Historical development of eddy current testing in aircraft maintenance p 292 A92-21900
SHAFFER, S. A.
Research, services, and facilities (National Institute of Standards and Technology)
[PB92-109172] p 485 N92-21870

SHAH, GOURANG
Added mass of high-altitude balloons
[AIAA PAPER 91-3693] p 16 A92-11034
SHAH, R. K.
Assessment of calculation methods for efficiency of straight fins of rectangular profile p 1121 A92-56374
SHAHPAR, S.
Marching with the parabolized Navier-Stokes equations. Problem 1: Numerical study of hypersonic viscous cone flow
[AERO-REPT-9007] p 344 N92-18231
Marching with the parabolized Navier-Stokes equations. Problem 2: Hypersonic viscous flow over a flat plate
[AERO-REPT-9008] p 345 N92-18232
Zonal solutions for a double-ellipse in a hypersonic flowfield
[AERO-REPT-9009] p 345 N92-18233
SHAHRUZ, S. M.
Design of compensators for linear parameter-varying feedback systems by the gain scheduling technique
p 507 A92-29101
SHAKHOV, EVGENII
One-dimensional kinetic model for flows near a stagnation point of a highly cooled body in hypersonic rarefied streams p 938 A92-52751
SHAKIB, FARZIN
A new finite element formulation for computational fluid dynamics. X - The compressible Euler and Navier-Stokes equations p 612 A92-37552
SHALAEV, V. I.
Boundary layer on slender wings of small aspect ratio
p 441 A92-31963
SHALIN, VALERIE L.
Knowledge-sensitive task manipulation - Acquiring knowledge from pilots flying a motion-based flight simulator p 916 A92-45064
An explanation-based-learning approach to knowledge compilation - A Pilot's Associate application
p 920 A92-48220
SHAMOLIN, M. V.
The problem of body motion in a medium with resistance p 604 A92-36416
SHAMROTH, STEPHEN J.
Three-dimensional blade vortex interactions
p 815 A92-46953
SHANE, DOUGLAS B.
Agile responsive effective support - Design and testing of the ARES concept demonstrator aircraft
[AIAA PAPER 92-1038] p 536 A92-33219
SHANE, S. J.
Structural testing of commercial rotorcraft seats - An overview p 544 A92-35437
SHANG, JOSEPH S.
Computation of hypersonic flowfields in thermal and chemical nonequilibrium
[AIAA PAPER 92-2874] p 819 A92-47856
SHANKAR, DOC
AI technology and application development on the Shuttle project p 302 A92-23693
SHANNON, JENIFER M.
An investigation of switched reluctance rotor position estimation using neural networks
[AD-A252846] p 1061 N92-33414
SHANTHAKUMARAN, P.
The application of flight simulation models in support of rotorcraft design and development
p 884 N92-28527
SHAPIRO, E. Y.
A time approach to robustness of LTI systems with structured uncertainty and unmodelled dynamics
p 48 A92-11356
SHAPIRO, WILBUR
Industrial code development p 227 N92-15083
SHAPOSHNIKOV, IU. N.
Holographic-interferometry methods employed for vibration-strength testing of aviation-engine workpieces
p 219 A92-20771
SHAPOVALOV, G. K.
Experimental investigation of the air bypass effect in the shock-wave region on the aerodynamic characteristics of a wing profile p 439 A92-31877
Investigation of the aerodynamic features of flows past models using thin-film capacitance-type sensors of pressure oscillations p 440 A92-31884
Progress of magnetic suspension and balance systems for wind tunnels in the USSR p 751 N92-27803
SHAPPELL, SCOTT A.
Use of a commercially available flight simulator during aircrew performance testing
[AD-A245922] p 883 N92-28407
SHARAF, HAZEM H.
Active control of asymmetric vortical flows around cones using injection and heating
[AIAA PAPER 92-4426] p 1025 A92-55350
SHARLAND, M. S.
Harrier international programme p 841 A92-45305
SHARMA, A. K.
Retrieval of total precipitable water over high latitude regions using radiometric measurements near 90 and 183 GHz p 505 A92-32129
SHARMA, GAUTAM
Far-field turbulence structure of the tip vortex shed by a single rectangular wing p 620 A92-40084
SHARMA, SURENDRA P.
Rate parameters for coupled vibration-dissociation in a generalized SSH approximation p 235 A92-20301
SHARMA, TILAK C.
New aircraft technologies - Challenges for dependability p 1120 A92-56225
SHARP, TIMOTHY J.
Improving reliability and maintainability through process management p 1141 A92-56212
SHASHKINA, G. N.
Modeling of the vortex structure at delta wings of low aspect ratio by the discrete vortex method
p 7 A92-12203
SHATAEV, V. G.
A study of a version of the boundary conditions of a two-dimensional spline in surface and line modeling
p 163 A92-16826
SHATALOV, I. V.
Effect of rarefaction on the nonstationary interaction of a supersonic underexpanded jet with a perpendicular obstacle p 337 A92-27594
SHAU, Y. R.
Organized structure in a Mach 5/Mach 3 turbulent shear layer
[AIAA PAPER 92-0180] p 256 A92-23790
Effects of vortex generators on the growth of a compressible shear layer
[AIAA PAPER 90-1979] p 934 A92-50269
SHAUGHNESSY, JOHN D.
Atmospheric disturbance model for aircraft and space capable vehicles
[AIAA PAPER 92-0294] p 407 A92-25747
Trim drag reduction concepts for horizontal takeoff single-stage-to-Orbit vehicles
[NASA-TM-102687] p 206 N92-15076
SHAVER, B. E.
Tutor aft fuselage and empennage full-scale fatigue test: Resolution of horizontal stabilizer installation difficulties
[NRC-LTR-ST-1804] p 114 N92-11990
SHAVER, FREDERICK MARTIN
The FM-007: An advanced jet commuter for HUB to spoke transportation
[NASA-CR-189988] p 461 N92-20267
SHAW, J. A.
The construction, application and interpretation of three-dimensional hybrid meshes p 919 A92-47089
SHAW, JILL L.
Thermal nonequilibrium effects on turbine cascade aerodynamics
[AD-A244049] p 404 N92-19183
SHAW, JOB J.
Simulator data integrity program: Process standard development
[AD-A242207] p 386 N92-19642
SHAW, ROBERT J.
Comparative study of turbulence models in predicting hypersonic inlet flows
[AIAA PAPER 92-3098] p 824 A92-48740
The NASA aircraft icing research program
p 549 N92-22534
Comparative study of turbulence models in predicting hypersonic inlet flows
[NASA-TM-105720] p 722 N92-28102
SHAW, STEPHEN J.
The inviscid stability of supersonic flow past heated or cooled axisymmetric bodies p 712 A92-44363
SHAW, THOMAS E.
An overview of systems engineering management methods and processes
[AIAA PAPER 92-1539] p 690 A92-38636
SHAW, WILLIAM J.
Relating the microwave radar cross section to the sea surface stress - Physics and algorithms
p 597 A92-35028
SHCHEGLOVA, M. G.
Experimental investigation of the coefficients of the normal-force derivatives for rectangular wings with translational oscillations p 423 A92-30127
SHCHEPANOVSKII, VLADIMIR A.
Gasdynamic design
[ISBN 5-02-029715-1] p 708 A92-42777
SHCHERBAK, V. G.
Axisymmetric analogy for three-dimensional viscous flow problems p 244 A92-21617
Vibrational relaxation effects in hypersonic flows of a viscous gas p 609 A92-36550
Similarity relations for calculating three-dimensional chemically nonequilibrium viscous flows
p 827 A92-49188
SHCHUROV, A. A.
Boundary-layer-separation control p 440 A92-31886
SHEA, MARK A.
Testing of a titanium matrix composite landing gear
[SAE PAPER 912175] p 644 A92-40000
SHEAHAN, J. J.
Nonflammable hydraulic power system for tactical aircraft. Volume 2: Equipment and systems test and evaluation
[AD-A239805] p 35 N92-10100
SHEBALIN, J. V.
Plasmadynamic effects in thermochemical nonequilibrium aerobrake flows
[AIAA PAPER 92-0573] p 333 A92-26980
Plasmadynamic effects in thermochemical nonequilibrium aerobrake flows p 705 A92-41538
SHEE, H. K.
Failure analysis and reliability improvement of small turbine engine blades p 993 A92-50860
SHEEHY, HUGH F.
Wing force and surface pressure data from a hover test of a 0.658-scale V-22 rotor and wing
[NASA-TM-102244] p 550 N92-22864
SHEEN, DAN R.
Estimation of the P-3/SAR L-, C- and X-band antenna directivity in range direction based on corner reflector measurements within the absolute SAR calibration
p 587 A92-35055
SHEEN, JEEN S.
Shape-sensitivity analysis and design optimization of linear, thermoelastic solids p 395 A92-26433
SHEEN, JOHN
Rapid development of the X-31 simulation to support flight-testing
[NASA-TM-104256] p 1060 N92-33149
SHEEN, QUEN Y.
Model oscillations at high angle of attack in a low speed wind tunnel test
[IAF PAPER ST-91-001] p 175 A92-20649
SHEFFER, SCOTT G.
Aerodynamic shape optimization of hypersonic configurations including viscous effects
[AIAA PAPER 92-2635] p 795 A92-45506
Aerodynamic shape optimization of arbitrary hypersonic vehicles p 194 N92-13954
SHEFFIELD, M.
Laser-initiated conical detonation wave for supersonic combustion. II
[AIAA PAPER 92-0088] p 292 A92-22195
SHEFFIELD, RICHARD E.
An analysis tool for UAV effectiveness evaluation
p 608 A92-40386
SHEFFLER, KEITH D.
Thermal barrier coating life prediction model development
[ASME PAPER 91-GT-40] p 147 A92-15523
SHEFFLER, MARC
LH wind tunnel testing - Key to advanced aerodynamic design p 104 A92-14331
SHEFTIC, J. S.
Interference flows past cylinder-fin-sting-cavity assemblies p 442 A92-32236
SHEIBANI, H.
Experimental measurement of the vortex development downstream of a lobed forced mixer
[ASME PAPER 90-GT-27] p 295 A92-23299
SHEIKH, S. I.
Trajectory optimization for hypersonic aircraft guidance p 728 N92-27898
SHEININ, VIKTOR M.
From the history of Soviet aviation - Aircraft of the Il'iushin design bureau (2nd revised and enlarged edition)
p 61 A92-15022
SHEKELL, TED K.
Reducing environmental noise impacts: A USAREUR noise management program handbook
[AD-A240797] p 237 N92-14791
SHEKLETON, JACK
Challenging power-density requirements for future fighter APUs
[SAE PAPER 912177] p 655 A92-40002
SHELBURNE, BRIAN J.
Avionics software reusability observations and recommendations p 921 A92-48502
SHELDAHL, R. E.
Measurement of the freestream density for re-entry vehicles - A design study p 940 A92-52821
SHELKONOGOV, A. M.
Aerodynamics of complex shape bodies within a wide range of supersonic flows of rarefied gases
p 939 A92-52767
SHELLMAN, C. H.
Feasibility of measuring transverse electric noise at VLF and LF on an ice cap
[AD-A252280] p 1129 N92-33220

SHEN, CHENGWU
Calculation of fuel sloshing and its coupling vibration with a tank p 991 A92-50204
SHEN, CHUN-LIN
U-parameter design example - Robust flight control for wind-shear protection p 28 A92-11502
Trajectory shaping by the U-parameter design method p 479 A92-29361
The design and simulation of an intelligence flight control system p 976 A92-50237
SHEN, CHUNLIN
A reversed-frame normalization design of robust flight control system p 1009 A92-53382
SHEN, HUILI
Solution of Euler equations for fighter forebody-inlet combinations at high angles of attack p 613 A92-38269
SHEN, JOHN P.
Behavior-based fault monitoring [AD-A241254] p 164 N92-13746
SHEN, LI-ZHONG
Durability analysis for a main bulkhead subjected to load on the body of an aircraft p 848 A92-47664
SHEN, QING
Numerical simulation of supersonic separated flow over blunt cones at high angles of attack p 313 A92-25039
Numerical simulation and analysis for hypersonic flow with separation over blunt cone at angle of attack p 314 A92-25126
SHEN, S. B.
Some results on metal and composite patch reinforcement of aluminum honeycomb panel p 216 A92-18830
The reinforcing effect of composite patch repairs on metallic aircraft structures p 419 A92-30498
The evaluation of non-tank surface treatments for aluminium bonding repairs p 761 A92-42502
SHEN, SHYAN B.
The study on the composite-patching repairs for metallic aircraft structures p 36 A92-10285
SHEN, XUE-MIN
Study of the discrete singularly perturbed linear-quadratic control problem by a bilinear transformation p 163 A92-16072
SHEN, YUNWEN
Vibration of gear system with web structure p 588 A92-35573
On travelling wave vibration of high-speed duplex helical gears p 990 A92-49580
SHEN, ZHEN
Damage tolerance and durability design of composite aircraft structures p 996 A92-53067
SHENG, B. C.
Experiment of static and dynamic characteristics of spiral grooved seals p 223 N92-14361
SHENG, YIXING
Simulation of commercial-aircraft reliability p 759 A92-42057
SHENOY, AJIT R.
Aircraft longitudinal dynamics equations including wind shear effects p 977 A92-51946
SHEPHERD, KEVIN P.
Loudness of shaped sonic booms p 695 A92-39238
A new simulator for assessing subjective effects of sonic booms [NASA-TM-104150] p 56 N92-11759
A loudness calculation procedure applied to shaped sonic booms [NASA-TP-3134] p 56 N92-11765
Building vibrations induced by noise from rotorcraft and propeller aircraft flyovers [NASA-TM-104170] p 1138 N92-33160
SHEPHERD, O.
Aircraft lidar sensitivity study for measuring water vapor [AD-A240549] p 42 N92-11237
SHEPPARD, JOHN W.
Developing intelligent automatic test equipment p 922 A92-48569
SHERIDAN, PATRICK J.
Measured and calculated optical property profiles in the mixed layer and free troposphere p 1129 A92-54630
SHERIF, YOSEF S.
Z-Basic algorithm for collision avoidance system p 188 A92-18482
SHERMAN, B.
Fly-by-light technology development plan [NASA-CR-181954] p 1086 N92-32778
SHERMAN, BRADLEY D.
Efficiency of a 5V/5mW power by light power supply for avionics applications p 734 A92-42603
SHERROUSE, MARK A.
Analysis and testing of a composite sandwich shell horizontal tail p 755 A92-44617
SHEVCHENKO, I. V.
A method for estimating the efficiency of gas turbine blade cooling systems p 657 A92-40606
SHEVCHENKO, V. E.
An automated workstation for the half-scale testing of the flight vehicle stabilization circuit p 664 A92-40622
SHEVEL'KOV, S. G.
Effect of a fan of rarefaction waves on the development of disturbances in a supersonic boundary layer p 809 A92-46519
SHEVOROSHKIN, A. V.
Radiant heat transfer in supersonic three-dimensional and axisymmetric flow of air past evaporating bodies p 337 A92-27533
SHI, G. Z.
Wind-tunnel compressor stall monitoring using neural networks p 918 A92-46817
SHI, JIAN-CHENG
Pseudostream function formulation - A method of solving three-dimensional aerodynamic analysis and design problems in turbomachinery p 996 A92-52981
SHI, JINYUAN
Study on reliability design of turbine blade p 371 A92-24739
SHI, LIMING
Improvement in transmission loss of aircraft double wall with resonators p 1011 A92-53091
SHI, RONG-MING
Durability analysis for a main bulkhead subjected to load on the body of an aircraft p 848 A92-47664
SHI, SHAOQIU
An impact dynamics investigation on some problems in bird strike on windshields of high-speed aircrafts p 986 A92-53330
SHI, WANGXING
The experimental investigation on the diffuser flow distortion p 519 A92-35543
SHI, WEIMIN
Precision analysis on static measurement of radar cross section p 370 A92-27906
SHI, WENJIE
Experimental technique of measuring fuel concentration in non-uniform flowfield p 734 A92-41928
SHI, Y.
Development of an integrated BEM approach for hot fluid structure interaction: BEST-FSI: Boundary Element Solution Technique for Fluid Structure Interaction [NASA-CR-189202] p 574 N92-22211
SHI, YUEDING
Separated flow over the protuberances in hypersonic flow p 615 A92-38907
SHI, ZHONG-KE
On-line state estimation and parameter identification for flight p 50 A92-11429
SHI, ZHONGKE
A separated algorithm and application to flight test p 690 A92-38273
SHIAU, LE-CHUNG
Transverse shear effect on flutter of composite panels p 1122 A92-56607
SHIBATA, KATSUHIKO
Preliminary study of algorithm for real-time flutter monitoring [SAE PAPER 912001] p 897 A92-45403
SHIBATA, M.
Display trends in aircraft cockpits p 734 A92-43217
SHIBUYA, H.
New-type of ultralight flexible a-Si solar cell and its application on an airplane p 970 A92-53181
SHIDLOVSKII, V. P.
Method of large particles in arbitrary curvilinear orthogonal coordinates for the solution of problems of hydro and aerodynamics p 937 A92-52035
SHIEH, CHIH F.
Navier-Stokes solutions of transonic nozzle flow with shock-induced flow separations p 713 A92-44515
SHIEH, TENG-HUA
Prediction and analysis of wing flutter at transonic speeds p 662 N92-25555
SHIFRIN, CAROLE A.
Saab 2000 begins 1,200-hr. test program at Skavsta site p 538 A92-33800
SHIH, C.
Unsteady flow past an airfoil pitching at a constant rate p 610 A92-36826
SHIH, CHIANG
Experimental observations of instability modes in a rectangular jet p 1135 A92-54908
SHIH, E.
Drag reduction of bluff bodies through momentum injection p 702 A92-41231
SHIH, MING-HSIN
TIGER: Turbomachinery interactive grid generation p 659 N92-25718
SHIH, PETER K.
The value of sub-scale flight tests in the development of NASP vehicles [AIAA PAPER 91-5048] p 210 A92-17834
SHIH, R.
Unsteady incompressible flow computations with quadrilateral elements p 394 A92-26219
SHIH, T. I-P.
Bleed-boundary conditions for numerically simulated mixed-compression supersonic inlet flow p 713 A92-44520
SHIH, T.-H.
Workshop on Engineering Turbulence Modeling [NASA-CP-10088] p 678 N92-24514
SHIKANO, YOSHIO
Numerical analysis of three-dimensional unsteady turbulent flows in a turbine stage p 443 A92-32501
SHILU, CHEN
Parameter identification of unsteady aerodynamic forces for elastic vehicles [AIAA PAPER 92-4505] p 1027 A92-55372
SHIMA, EIJI
The unstructured upwind method p 429 A92-30522
SHIMA, NOBUYUKI
Prediction of three-dimensional turbulent boundary layers using a second-moment closure p 675 A92-40080
SHIMADA, TORU
Direct simulation of hypersonic rarefied flows about atmospheric re-entry vehicles p 710 A92-43169
SHIMADA, YUZO
Model reference adaptive flight control system (MRAFCS) design with consideration of the balance point p 745 A92-43182
SHIMEALL, TIMOTHY J.
Software safety analysis in heterogeneous multiprocessor control systems p 776 A92-42073
SHIMIZU, TATSUO
Development of the D-size liquid crystal flat panel display for aircraft p 734 A92-43208
Evaluation test on the simulator of the liquid crystal flat display. II p 734 A92-43209
SHIMIZU, TETSUO
Space plane navigation simulation p 1103 A92-53603
SHIMODAIRA, KAZUO
Hydrogen fueled subsonic-ram-combustor model tests for an air-turbo-ram engine [NAL-TR-1064T] p 280 N92-17855
SHIMOMURA, T.
STOL research aircraft Asuka flight analysis in connection with the operation of the monitoring system p 730 A92-43140
Aerodynamic model identification of a spaceplane model from a cable-mount dynamic wind-tunnel test p 1093 A92-56114
SHIMOMURA, TAKASHI
Motion estimation for cable-mount dynamic wind-tunnel test p 749 A92-43210
Estimation of spaceplane longitudinal stability and control derivatives from dynamic wind tunnel test p 752 A92-43211
Estimation of spaceplane model inertia characteristics p 752 A92-43212
On the characteristics of servo actuators attached to a model spaceplane for dynamic wind-tunnel test p 762 A92-43213
Spaceplane longitudinal aerodynamic parameter estimation by cable-mount dynamic wind-tunnel test [SAE PAPER 911980] p 788 A92-45385
Estimation of cable-mounted model inertia characteristics for dynamic wind-tunnel test [NAL-TM-641] p 722 N92-28152
SHIMOMURA, TOYO
Flight tests on the structures of the STOL research aircraft Asuka p 730 A92-43143
SHIMSKI, JOHN T.
Full-scale transmission testing to evaluate advanced lubricants [NASA-TM-105668] p 764 N92-26560
Development of a full-scale transmission testing procedure to evaluate advanced lubricants [NASA-TP-3265] p 998 N92-30396
SHIN, D. S.
Effect of walls on the supersonic reacting mixing layer p 912 N92-30065
SHIN, J.
Helium bubble flow visualization of the spanwise separation on a NACA 0012 with simulated glaze ice [AIAA PAPER 92-0413] p 341 A92-28192
Helium bubble flow visualization of the spanwise separation on a NACA 0012 with simulated glaze ice [NASA-TM-105742] p 714 N92-26612
Analysis of iced wings [NASA-TM-105773] p 1042 N92-34144

SHIN, JAIWAN
Advanced ice protection systems test in the NASA Lewis Icing Research Tunnel p 108 A92-14406
SHIN, JAIWON
A turbulence model for iced airfoils and its validation
[AIAA PAPER 92-0417] p 326 A92-26267
Results of an icing test on a NACA 0012 airfoil in the NASA Lewis Icing Research Tunnel
[AIAA PAPER 92-0647] p 334 A92-27021
Analysis of iced wings
[AIAA PAPER 92-0416] p 423 A92-29972
Results of an Icing test on a NACA 0012 airfoil in the NASA Lewis Icing Research Tunnel
[NASA-TM-105374] p 185 N92-15051
A turbulence model for iced airfoils and its validation
[NASA-TM-105373] p 186 N92-15052
Experimental and computational ice shapes and resulting drag increase for a NACA 0012 airfoil
[NASA-TM-105743] p 828 N92-28674
Results of a low power ice protection system test and a new method of imaging data analysis
[NASA-TM-105745] p 828 N92-28696
SHIN, KWANG S.
Interlaminar fracture characteristics of bonding concepts for thermoplastic primary structures p 758 A92-41282
SHIN, SEIICHI
A design of continuous-time model reference adaptive control based on a function estimation of periodically time varying linear system p 51 A92-11454
SHINAGAWA, TAKASHI
Application of fuzzy control to aircraft guidance p 1083 A92-56033
SHINAGAWA, YUJI
Development of an automatic drilling system. II p 1118 A92-56107
SHINDO, S.
Experimental study of the aerodynamic characteristics at Mach 3 of an air-intake model p 711 A92-43204
Supersonic wind tunnel test of airintake/airframe integrated models p 1028 A92-56006
SHINDO, SHIGEMI
Mach 3 wind tunnel test of mixed compression supersonic inlet
[AIAA PAPER 92-3625] p 1021 A92-54092
SHINER, ROBERT J.
Man-Vehicle Systems Research Facility - Design and operating characteristics
[AIAA PAPER 92-4177] p 982 A92-52458
SHINGU, HIROKIMI
Navigation experiment on an aircraft using the GPS-INS navigation system. I - Introduction to the system p 726 A92-43122
Space plane navigation simulation p 1103 A92-53603
Flight evaluation of navigation systems including MLS using NAL Do228 - Results of GPS p 1047 A92-56118
SHINKU, HIROKIMI
Navigation experiment on aircraft flight using the GPS-INS navigation system. II - Test results p 726 A92-43123
SHINODA, PATRICK R.
Wing force and surface pressure data from a hover test of a 0.658-scale V-22 rotor and wing
[NASA-TM-102244] p 550 N92-22864
SHINOHARA, KENJI
Development of pre- and post-processor system for structural analysis
[NAL-TM-628] p 681 N92-25403
SHIOIRI, JUMPEI
Research and development of aircraft engine materials p 577 A92-35916
SHIRAHATTI, U. S.
Solutions of acoustic field problems using parallel computers p 925 A92-45929
SHIRAI, YUJIRO
Analysis and wind tunnel test of low aspect wing gust load alleviation p 1053 A92-56020
SHIRAISHI, KAZUO
Experimental study of the aerodynamic characteristics at Mach 3 of an air-intake model p 711 A92-43204
Mach 3 wind tunnel test of mixed compression supersonic inlet
[AIAA PAPER 92-3625] p 1021 A92-54092
SHIRAKAWA, KENICHI
Flight evaluation of navigation systems including MLS using NAL Do228 - Results of MLS p 1047 A92-56117
SHIRAKAWA, M.
Introduction to the traffic alert and collision avoidance system (TCAS) III p 734 A92-43150
SHIRAYAMA, SUSUMU
Flow past a sphere - Topological transitions of the vorticity field p 330 A92-26410
Simple diagnosis for the quality of generated grid systems p 919 A92-47069
SHIRAZI, SIAMACK A.
Simple turbulence models for supersonic flows - Bodies at incidence and compression corners p 5 A92-11059
SHIRER, HEYWOOD O.
The 1990 Federal Radionavigation Plan and its impact on the Omega Navigation System p 98 A92-16658
SHIRLEY, JOHN A.
UV laser spectroscopic measurements in jet engine combustion exit flows
[AIAA PAPER 92-0513] p 396 A92-26939
SHIROKOV, P. E.
Methods for determining atmospheric correction for radio-rangefinder measurements of inclined trajectories p 775 A92-44070
SHIROUZU, MASAO
Weight evaluation and sensitivity analysis for space plane. Part 2: TSTO
[NAL-TM-602-PT-2] p 287 N92-17754
SHIVAKUMAR, KUNIGAL N.
Effects of T-tabs and large deflections in double cantilever beam specimen tests p 673 A92-39009
SHIVELY, CURTIS A.
Capacity as a consideration for providing aeronautical mobile satellite air traffic services in the U.S. domestic airspace p 956 A92-51007
SHIVELY, ROBERT J.
Pre-flight risk assessment in emergency medical service (EMS) helicopters p 16 A92-11171
SHIZAWA, T.
Effects of attack angle on leg portion of the horseshoe vortex around the idealized wing p 623 A92-40177
SHKIRIN, N. N.
A computational study of flow past bodies and heat transfer for isentropic compression flows p 425 A92-30158
SHLIAGUN, A. N.
Reducing the background noise level in the test section of a wind tunnel for transonic flow velocities p 511 A92-30143
SHMILOVICH, ARVIN
An algorithm for predicting the flow past fuselage-mounted engine arrangements
[AIAA PAPER 92-0151] p 253 A92-23766
SHOEMAKER, M.
A critical evaluation of a three-dimensional Navier-Stokes CFD as a tool to design supersonic turbine stages p 1124 N92-32268
SHOHAM, BARACK
Timing analysis of parallel algorithms on a MIMD multiprocessor
[ITN-92-85153] p 510 N92-20905
SHONDER, J. A.
Proof of concept of a magnetically coupled Stirling engine-driven heat pump
[DE92-017129] p 1129 N92-33271
SHONG, LIMIN
Strategies for optimal design of gas turbine disks p 371 A92-24741
SHOPE, FREDERICK L.
Conjugate conduction/convection/nucleate-boiling heat transfer with a high-speed boundary layer
[AIAA PAPER 91-5033] p 215 A92-17823
SHOPOV, A. V.
Investigation of the structural inhomogeneity of a titanium alloy p 893 A92-47958
SHOWS, FRED
Standardizing operational flight data handling p 1009 A92-53109
SHPAK, S. I.
A method for the optical measurement of surface friction in supersonic flow p 337 A92-27537
SHPUND, Z.
Improved measurement of the dynamic loads acting on rotating parachutes p 702 A92-41236
SHREEVE, R. P.
Stator averaged, rotor blade-to-blade near wall flow in a multistage axial compressor with tip clearance variation
[ASME PAPER 91-GT-30] p 67 A92-15514
SHROFF, DINIAR M.
A proposal for a dynamic test platform for inertial units and/or GPS p 138 A92-16653
SHU, W.-Y.
The evaluation of non-tank surface treatments for aluminium bonding repairs p 761 A92-42502
SHUART, M. J.
A Protection And Detection Surface (PADS) for damage tolerance p 1107 N92-32523
SHUBIN, G. R.
A comparison of two closely-related approaches to aerodynamic design optimization p 193 N92-13933
SHUBIN, GREGORY R.
A comparison of optimization-based approaches for a model computational aerodynamics design problem p 316 A92-25636
SHUCHMAN, R. A.
Comparison of aircraft synthetic aperture radar and buoy spectra during NORCSEX '88 p 597 A92-34878
SHUI, V. H.
Multiple aperture window and seeker concepts for endo KEW applications
[AIAA PAPER 92-2806] p 752 A92-41344
SHULTZ, JEFF
Quantitative Feedback Theory approach to AIAA Controls Design Challenge
[AIAA PAPER 92-4626] p 1077 A92-55303
SHUMSKII, G. M.
Numerical modeling of self-oscillations for a small-aspect-ratio delta wing using measurements of roll motion at large angles of attack p 424 A92-30138
SHUR, M. L.
Influence of three-dimensional effects on hydrodynamics and heat transfer in subsonic flow of a viscous compressible gas in the initial section of a rectangular duct p 66 A92-15031
SHUROV, A. A.
Control of the development of boundary layer disturbances p 423 A92-30126
SHURYGIN, V. M.
Combined method for the solution of plane direct problems of flow past bodies with jets p 427 A92-30200
SHUSHIN, N. A.
Experimental study of an adjustable plane supersonic diffusor p 426 A92-30173
SHUSTOV, V. I.
The lift-drag ratio of a slender cone in viscous hypersonic gas flow p 425 A92-30172
SHVETS, A. I.
An experimental study of subsonic separated flow over parawings p 4 A92-10901
Aerodynamic characteristics of curved delta wings in the case of subsonic separated flow p 712 A92-44121
SHVETS, ALEKSANDR I.
Aerodynamics of lifting configurations p 712 A92-44125
SHVETS, IVAN T.
Aerodynamics of lifting configurations p 712 A92-44125
SHYU, IN-MING
Nonlinear aircraft tracking filter utilizing control variable estimation p 302 A92-21179
SHYU, LIH-SHYUNG
An experimental investigation of the effect of leading-edge extensions on directional stability and the effectiveness of forebody nose strakes
[AIAA PAPER 92-2715] p 802 A92-45554
SHYU, R.-N.
Forcing level effects of internal acoustic excitation on the improvement of airfoil performance p 1136 A92-56162
SI, ZHONGKE
A new U-D factorization-based fixed-point smoother and application to flight test p 411 A92-27858
SIBIO, SCOTT A.
Shock fitting with a finite volume approximation to the Euler equations
[AIAA PAPER 92-2646] p 796 A92-45513
SICLARI, M. J.
Asymmetric separated flows at supersonic speeds p 176 A92-20742
SIDDIQUI, M. S.
Effect of the grid system on heat transfer computations for high speed flows p 900 A92-47071
SIDES, J.
Solution of the compressible Euler equations for steady flows around helicopter rotor blades by an implicit space-centered method
[ONERA, TP NO. 1991-177] p 77 A92-16139
Resolution of the Euler equations applied to a helicopter rotor in forward flight
[ONERA-RSF-2/3731-AY-004A] p 406 N92-19976
SIDWELL, KENNETH W.
PAN AIR: A computer program for predicting subsonic or supersonic linear potential flows about arbitrary configurations using a higher order panel method. Volume 2: User's manual (version 3.0)
[NASA-CR-3252] p 527 N92-22865
SIEBERT, R.
Automatic control of test parameters for intake measurements in a low-speed wind tunnel p 1091 A92-54341
SIENER, MICHAEL P.
Stress field sensitivity of a composite patch repair as a result of varying patch thickness p 763 A92-44630
SIERON, THOMAS R.
Evolution and development of hypersonic configurations 1958-1990
[AD-A242768] p 197 N92-15069

SIEVERS, G. KEITH
Overview of the subsonic propulsion technology session p 560 N92-22531
SIGURDSSON, G.
Probabilistic design and fatigue management based on probabilistic fatigue models with reliability updating p 360 N92-18574
SIH, GEORGE C.
Development and design with advanced materials
[ISBN 0-444-88706-7] p 296 A92-24176
SIIKONEN, T.
Two-dimensional transonic flow calculation by interaction of Euler and boundary layer equations
[PB92-136449] p 448 N92-21784
Three-dimensional multigrid algorithm for the Euler and the thin-layer Navier-Stokes equations
[PB92-134329] p 602 N92-22216
SIKES, G. D.
Multidisciplinary design optimization of a large transport aircraft wing
[AIAA PAPER 92-1002] p 536 A92-33194
SIKHARULIDZE, Y. G.
Dynamics of aerospace shuttles p 667 N92-24760
SIKORA, TIMOTHY P.
Simulation of high heat flux levels with graphite heating and arc lamps p 980 A92-51402
SILCOX, R. J.
Approximation methods for control of acoustic/structure models with piezoceramic actuators
[NASA-CR-189578] p 234 N92-15658
Active control of interior noise in a large scale cylinder using piezoelectric actuators p 1137 N92-32958
SILDER, STEPHEN H., JR.
Full mission simulation: A view into the future p 884 N92-28537
SILVA, A.
A module-level testing environment for safety-critical software systems p 1132 A92-56293
SILVA, D. H.
An inverse method for the design of transonic wings
[AIAA PAPER 92-1025] p 517 A92-33206
SILVA, VINCE
Manx: Close air support aircraft preliminary design
[NASA-CR-189992] p 463 N92-21565
SILVA, WALTER A.
NACA 0012 benchmark model experimental flutter results with unsteady pressure distributions
[AIAA PAPER 92-2396] p 517 A92-34469
Further investigations of the aeroelastic behavior of the AFW wind-tunnel model using transonic small disturbance theory
[AIAA PAPER 92-2082] p 565 A92-35654
Investigation of the aeroelastic stability of the AFW wind-tunnel model using CAP-TSD
[NASA-TM-104142] p 81 N92-11977
Further investigations of the aeroelastic behavior of the AFW wind-tunnel model using transonic small disturbance theory
[NASA-TM-107576] p 526 N92-22240
NACA0012 benchmark model experimental flutter results with unsteady pressure distributions
[NASA-TM-107581] p 526 N92-22507
Investigation of the aeroelastic stability of the AFW wind-tunnel model using CAP-TSD p 721 N92-27955
Pressure measurements on a rectangular wing with a NACA0012 airfoil during conventional flutter
[NASA-TM-104211] p 1042 N92-34147
SILVATI, LAURA
Relating the annoyance of aircraft overflights to their audibility by outdoor recreationists p 689 A92-39240
SILVER, D.
Emergence of coherent patterns of vortex stretching during reconnection - A scattering paradigm p 38 A92-11041
SILVERSTEIN, C. C.
Analytical and experimental studies of heat pipe radiation cooling of hypersonic propulsion systems
[AIAA PAPER 92-3809] p 867 A92-49128
Analytical and experimental studies of heat pipe radiation cooling of hypersonic propulsion systems
[DE92-013428] p 973 N92-31817
SILVIA, PETER A.
Revolution at sea: Aircraft options for the year 2030 p 466 N92-21974
SIM, DAVE
Aeronautical mobile satellite service: Air traffic control applications p 677 N92-24164
SIMANDIRAKIS, G.
Turbine cascade calculations through a fractional step Navier-Stokes algorithm
[ASME PAPER 91-GT-55] p 68 A92-15533
SIMBIRSKII, V. L.
A model of the operation of the pulsejet engine and a study of its characteristics p 657 A92-40608
SIMEONIDES, G.
Quantitative heat transfer measurements in hypersonic wind tunnels by means of infrared thermography p 1115 A92-54321
SIMEONOVA, IU. M.
Investigation of the structural inhomogeneity of a titanium alloy p 893 A92-47958
SIMMEN, JEFF
Traveling on the curved earth p 19 A92-10474
SIMMON, DAVID A.
Airline industry safety management systems and feedback p 951 A92-51439
SIMMONS, J. M.
Drag balance for hypervelocity impulse facilities p 207 A92-18375
Skin-friction gauge for use in hypervelocity impulse facilities p 398 A92-28063
Measurement of shock-wave/boundary-layer interaction in a free-piston shock tunnel p 813 A92-46903
SIMMS, D.
Dynamic stall on wind turbine blades
[DE92-001157] p 262 N92-17874
Recent results from data analysis of dynamic stall on wind turbine blades
[DE92-001200] p 505 N92-20245
SIMMS, D. A.
A comparison of spanwise aerodynamic loads estimated from measured bending moments versus direct pressure measurements on horizontal axis wind turbine blades
[DE92-001158] p 301 N92-16458
SIMO, CONSTANCE
Development of fuel neutralizing agents to prevent flashback on aircraft fires
[AD-A242828] p 264 N92-17259
SIMO, J. C.
Mathematical modeling and numerical simulation of the dynamics of flexible structures undergoing large overall motions
[AD-A250202] p 979 N92-31967
SIMOMURA, TAKASHI
On improvements of three-dimensional position measuring system for dynamic wind tunnel testing p 1093 A92-56012
SIMON, DONALD L.
Piloted evaluation of an integrated propulsion and flight control simulator
[AIAA PAPER 92-4178] p 960 A92-52459
Piloted evaluation of an integrated propulsion and flight control simulator
[NASA-TM-105797] p 1088 N92-34107
SIMON, F. J.
Investigation of the tail buffeting of the C-101 p 942 A92-53253
SIMON, HORST D.
Future directions in computing and CFD
[AIAA PAPER 92-2734] p 917 A92-45489
SIMON, J. S.
A Lyapunov based nonlinear control scheme for stabilizing a basic compression system using a close-coupled control valve p 508 A92-29316
Dynamic control of aerodynamic instabilities in gas turbine engines p 870 N92-28466
SIMON, JAMES M.
Dynamic derivative data for high angle of attack simulation
[AIAA PAPER 92-4355] p 1079 A92-55341
SIMON, ROBERT
A model for evaluation and training in aircrew coordination and cockpit resource management p 46 A92-11191
SIMON, T. W.
Studies of gas turbine heat transfer: Airfoil surfaces and end-wall cooling effects
[AD-A244055] p 376 N92-19097
SIMONI, M.
Correlation of flight, tunnel and prediction data on a helicopter main rotor p 1059 A92-56350
SIMONIAN, S. O.
The method of determinant equations in the applied theory of optimal systems - Systems with 'rigid' constraints and with fixed boundary conditions p 917 A92-46629
SIMONICH, J. C.
Flow visualization of a prop-fan leading-edge vortex
[AIAA PAPER 92-0386] p 323 A92-26242
SIMONICH, JOHN C.
Loading and vibration reduction through active aerodynamic control
[AD-A242321] p 283 N92-17243
SIMONSSON, BENGT
Propeller sound excitation on an aircraft fuselage using a loudspeaker ring p 643 A92-39087
SIMPSON, A.
The use of Stodola modes in rotor-blade aeroelastic studies p 590 A92-35729
SIMPSON, D. L.
A proposed composite repair methodology for primary structure
[NRC-LTR-ST-1658] p 115 N92-13056
A parametric approach to spectrum development p 360 N92-18578
SIMPSON, DAVID L.
Enhanced visual technique for rapid inspection of aircraft structures p 214 A92-17290
SIMPSON, DENNIS J.
An application of the object-oriented paradigm to a flight simulator
[AD-A243624] p 384 N92-18012
SIMPSON, JOEL M.
Overpressurized zero pressure balloon system
[AIAA PAPER 91-3671] p 14 A92-11018
SIMPSON, L. B.
Flux-difference split algorithm for unsteady thin-layer Navier-Stokes solutions p 431 A92-31158
SIMPSON, M. A.
MD-80 aft cabin noise control: A case history p 1137 N92-32950
SIMPSON, R. L.
An experimental study of a turbulent wing-body junction and wake flow
[AIAA PAPER 92-0434] p 327 A92-26281
An experimental study of a turbulent wing-body junction and wake flow
[AD-A243388] p 260 N92-17222
An experimental study of the relationship between velocity and pressure fluctuations in a wing-body junction
[AD-A249628] p 946 N92-31122
SIMPSON, ROBERT W.
An investigation of air transportation technology at the Massachusetts Institute of Technology, 1990-1991 p 265 N92-17985
Impacts of technology on the capacity needs of the US national airspace system
[NASA-CR-4470] p 1045 N92-34192
SIMPSON, ROGER L.
Cross-flow separation on a prolate spheroid at angles of attack
[AIAA PAPER 92-0428] p 326 A92-26276
Influence of wing shapes on the surface pressure fluctuations of a wing-body junction
[AIAA PAPER 92-0433] p 327 A92-26280
An experimental evaluation of some turbulence models from a three-dimensional turbulent boundary layer around a wing-body junction p 620 A92-40087
Effects of a leading-edge fillet on the flow past an appendage-body junction p 935 A92-50301
SIMPSON, STEVEN S.
An analysis of aircrew communication patterns and content
[AD-A246618] p 907 N92-28253
SIMPSON, WILLIAM R.
Developing intelligent automatic test equipment p 922 A92-48569
SIMS, J. TERRY
Advanced information processing system: Inter-computer communication services
[NASA-CR-187556] p 53 N92-11706
SIMSIC, CRAIG J.
Electric actuation system duty cycles p 877 A92-48494
SINAY, LEON R.
Some thermodynamical aspects in the optimization of supersonic combustors p 1065 A92-53486
SINCLAIR, ANTHONY
Nondestructive depth profiling of the protective coating on a turbine blade p 144 A92-13641
SINCLAIR, D. W.
A comparison of transition Reynolds number measured in a wind tunnel and in flight p 522 A92-36026
SINDIR, MUNIR M.
Some comments on turbulence modeling from an industrial perspective p 678 N92-24531
SINGER, A. C. B.
Tomorrow's cockpit displays p 117 A92-13699
SINGER, B.
RAE Bedford VAAC research project p 662 A92-40039
SINGER, BART A.
A weakly nonlinear theory for wave-vortex interactions in curved channel flow
[NASA-TP-3158] p 347 N92-19175
SINGER, S. W.
Computational aerodynamics in aircraft design - Challenges and opportunities for Euler/Navier-Stokes methods
[SAE PAPER 911990] p 788 A92-45392
SINGH, D. J.
Three-dimensional simulation of a translating strut inlet
[AIAA PAPER 92-0270] p 317 A92-25726

Effects of nose bluntness and angle of attack on slender bodies in hypersonic flows
[AIAA PAPER 92-0638] p 334 A92-27016
Combined effect of nose bluntness and angle of attack on slender bodies in viscous hypersonic flows
[AIAA PAPER 92-0755] p 436 A92-31680
Numerical study of the effects of reverse sweep on scramjet inlet performance p 611 A92-36979
Mixing and combustion effects in a sliding-wedge ram accelerator with hydrogen injection
[AIAA PAPER 92-3251] p 890 A92-48849
Least-squares/parabolized Navier-Stokes procedure for optimizing hypersonic wind-tunnel nozzles
p 980 A92-50270
CAN-DO, CFD-based Aerodynamic Nozzle Design and Optimization program for supersonic/hypersonic wind tunnels
[AIAA PAPER 92-4009] p 1033 A92-56832

SINGH, K. ROMI
A strategy for exploiting the full potential of MLS based terminal procedures in Canada p 190 N92-14025

SINGH, M.
Non-slender shapes of minimum drag
p 937 A92-52029

SINGH, SAHJENDRA N.
Invertibility and trajectory control for nonlinear maneuvers of aircraft
[AIAA PAPER 92-4410] p 1075 A92-55204

SINGH, V. P.
Coupled vibrations of turbomachine blades
p 738 A92-44545

SINGHAL, A. C.
Computer simulation of weapon blast pressures on flexible surfaces p 39 A92-12115

SINGHAL, ASHOK K.
Development of a CFD code for analysis of fluid dynamic forces in seals p 228 N92-15084

SINGHAL, SURENDRA N.
Coupled multi-disciplinary simulation of composite engine structures in propulsion environment
[NASA-TM-105575] p 596 N92-23267

SINGHVI, SARVESH
Analytical shape sensitivities and approximations of modal response of generally laminated tapered skew plates
[AIAA PAPER 92-2391] p 585 A92-34465

SINGLETON, J. D.
A demonstration of passive blade twist control using extension-twist coupling
[AIAA PAPER 92-2468] p 539 A92-34358

SINGLETON, JEFFREY D.
Recent rotorcraft aeroelastic testing in the Langley Transonic Dynamics Tunnel p 136 A92-14377
An experimental study of the sensitivity of helicopter rotor blade tracking to root pitch adjustment in hover
[NASA-TM-4313] p 61 N92-12989
A demonstration of passive blade twist control using extension-twist coupling
[NASA-TM-107642] p 1001 N92-31155

SINHA, N.
Applications of an implicit, upwind Navier-Stokes code, CRAFT, to steady/unsteady reacting, multi-phase flowfields
[AIAA PAPER 92-0837] p 422 A92-29603
Progress towards the development of transient ram accelerator simulation as part of the U.S. Air Force Armament Directorate Research Program
[AIAA PAPER 92-3248] p 904 A92-48847

SINHA, PRASUN K.
INS alignment using GPS Phase III user equipment computed corrections p 100 A92-16955

SINSKY, ALLEN I.
An electronically scanned precision runway monitor
p 98 A92-16654

SIOCHI, EMILIE J.
Isothermal aging of IM7/8320 and IM7/5260
[NASA-TM-107666] p 1110 N92-33423

SIOSHANSI, PIRAN
Improving the properties of titanium alloys by ion implantation p 289 A92-22771

SIRA-RAMIREZ, HEBERTT
The differential algebraic approach in nonlinear dynamical feedback controlled landing maneuvers
p 574 A92-33639

SIRACUSE, R. J.
The VISTA/F-16 programmable feel system
[AIAA PAPER 92-4172] p 977 A92-52457

SIRBAUGH, J. R.
Navier-Stokes analysis and experimental data comparison of compressible flow within ducts
[NASA-TM-105796] p 972 N92-30972

SIRCAR, SUBRATA
Computer-aided design of flight control systems
[AD-A244657] p 483 N92-21752

SIRGNANO, W. A.
Fundamental studies on droplet interactions in dense sprays
[AD-A246918] p 770 N92-27546

SIRIGNANO, W. A.
One-dimensional analysis of liquid-fueled combustion instability p 143 A92-17188
Three-dimensional flow computation for two interacting, moving droplets
[AIAA PAPER 92-0343] p 496 A92-31655

SIRIKUMARAN, SAKUNTHALA
Reflections off aircraft and the shape optimization of a ridged waveguide p 267 A92-23967

SIROCKY, PAUL J.
High temperature dynamic engine seal technology development
[NASA-TM-105641] p 596 N92-23435

SIROTINSKII, B. S.
Composite blades for helicopter main and tail rotors developed by Mil Design Bureau p 1057 A92-56325

SIROVICH, L.
Eigenfunction analysis of turbulent mixing phenomena
p 898 A92-45826

SISLIAN, J. P.
An experimental and computational investigation of an annular reverse-flow combustor
[UTIAS-338] p 129 N92-11996

SISTO, F.
Computational study of stall flutter in linear cascades
[ASME PAPER 91-GT-5] p 67 A92-15503

SITNIKOV, V. G.
Dynamics of the three-dimensional angular motions of rotating flight vehicles in the presence of the aerodynamic hysteresis of the moment characteristic
p 428 A92-30371

SITU, M.
A new vane swirler as applied to dual-inlet side-dump combustor
[AIAA PAPER 92-3654] p 906 A92-49085

SIVAKUMARAN, K. S.
Response of symmetrically laminated rectangular plates subjected to heating p 296 A92-24186

SIVANERI, NITHIAM T.
Comparison between imposed-periodicity and marching-in-time solutions of helicopter rotor blade steady-state response problem
[AIAA PAPER 92-2256] p 540 A92-34411
Bilinear formulation applied to the stability and response of helicopter rotor blade p 847 A92-46930

SIZUN, M.
Reaction speed constant for the reactions between N + O2 and between O + N2
[ETN-92-90861] p 347 N92-19252

SJOLANDER, S. A.
Effects of simulated rotation on tip leakage in a planar cascade of turbine blades. I - Tip gap flow
[ASME PAPER 91-GT-127] p 71 A92-15572
Effects of simulated rotation on tip leakage in a planar cascade of turbine blades. II - Downstream flow field and blade loading
[ASME PAPER 91-GT-128] p 71 A92-15573
Establishing two-dimensional flow in a large-scale planar turbine cascade
[AIAA PAPER 92-3066] p 823 A92-48720

SJOSTEDT, ROB J.
Organic Matrix Composite Helicopter Internal/External Cargo Pallet System (OMC INTEX)
[AD-A251127] p 961 N92-30878

SKELTON, E. A.
Acoustic scattering by a disk or annulus linking two concentric cylindrical shells. I - Theory and results for heavy exterior fluid loading. II - Results for heavy exterior fluid loading on both shells p 696 A92-40588

SKELTON, ROBERT
Closed-loop identification and iterative controller design p 48 A92-11362

SKINN, DONALD A.
Study of the engine bird ingestion experience of the Boeing 737 aircraft
[DOT/FAA/CT-89/16] p 187 N92-15053
Engine bird ingestion experience of the Boeing 737 aircraft: Expanded data base
[DOT/FAA/CT-91/32] p 1045 N92-34151

SKINNER, D. J.
The microstructural stability of TiC reinforced rapidly solidified Al-Fe-V-Si composite structures
p 141 A92-15169

SKINNER, M. J.
Blade repair with adaptive vision tracking
[ASME PAPER 91-GT-208] p 607 A92-36897

SKIRA, CHARLES A.
Control systems for the next century's fighter engines
[ASME PAPER 91-GT-278] p 125 A92-15674

SKJONG, R.
Probabilistic design and fatigue management based on probabilistic fatigue models with reliability updating
p 360 N92-18574

SKOB, IU. A.
Solution of the problem of three-dimensional flow past the blade rows of turbomachines with allowance for viscosity effects p 244 A92-21618

SKOBELEV, O. P.
Technical tools of test automation for gas-turbine engines based on cluster CAMAC modules with an increased number of channels p 980 A92-51348

SKOCH, GARY J.
A 4-spot time-of-flight anemometer for small centrifugal compressor velocity measurements
[NASA-TM-105717] p 909 N92-29105

SKODA, ZDENEK
Application of holomorphic vectors theory in three-dimensional potential flow problem
p 292 A92-21923
Effect of a deicing device on the induced drag of a lifting airfoil p 959 A92-51947

SKOMOROKHOV, S. I.
Aerodynamic wing-nacelle integration
p 458 A92-30134

SKOVORODKO, P. A.
A numerical study of flow of a viscous gas in a Laval nozzle in the narrow channel approximation
p 706 A92-42680

SKOW, ANDREW M.
Agility as a contributor to design balance
p 356 A92-24405

SKRIBACHILIN, V. B.
Evaluation of the fungicide properties of antifreeze additives for jet fuels p 141 A92-15070

SKUPNIEWICZ, C. E.
Boundary-layer transition across a stratocumulus cloud edge in a coastal zone p 45 A92-10489

SLACK, DAVID C.
Characteristic-based algorithms for flows in thermochemical nonequilibrium p 670 A92-36846

SLATER, ANDY
Design and analysis of vortex generators on reengined Boeing 727-100QF center inlet S-duct by a reduced Navier-Stokes code
[AIAA PAPER 92-2700] p 800 A92-45542

SLATTERY, K. P.
Low cost HIRF troubleshooting and verification method for digital avionics systems p 990 A92-49304

SLAUERHOFF, J. F.
Application of electronically scanned pressure measurement system for engine simulation tests in the German-Dutch Wind Tunnel
[AIAA PAPER 92-4003] p 1122 A92-56826

SLINGERLAND, FRANK W.
Spectrogram diagnosis of aircraft disasters
[SAE PAPER 912041] p 836 A92-45425

SLOMINSKI, CHRISTOPHER J.
Advanced Transport Operating System (ATOPS) color displays software description: MicroVAX system
[NASA-CR-189603] p 556 N92-22395
Advanced Transport Operating System (ATOPS) color displays software description microprocessor system
[NASA-CR-189605] p 556 N92-22645
Advanced Transport Operating System (ATOPS) control display unit software description
[NASA-CR-189606] p 652 N92-24689

SLOMSKI, J. F.
Compressible Navier-Stokes solutions for a suction boundary control airfoil
[AIAA PAPER 92-2710] p 802 A92-45551
Experimental evaluation of a 50-percent thick airfoil with blowing and suction boundary layer control
[AIAA PAPER 92-4500] p 1026 A92-55368

SLOOFF, J. W.
Technical evaluation report on the Fluid Dynamics Panel Specialists' Meeting on Effects of Adverse Weather on Aerodynamics
[AGARD-AR-306] p 352 N92-18242

SLUSARCZUK, MARKO
DARPA high resolution display technologies
p 218 A92-19977

SMALL, J. F.
Flow visualization and wake analysis for complex three-dimensional bluff bodies at subcritical through critical Reynolds numbers
[AIAA PAPER 92-0155] p 253 A92-23770

SMALL, JAMES F.
Flow visualization and wake analysis for standard and modified configurations of the AN/ALQ-78 antenna pod
[AD-A243552] p 260 N92-17339

SMART, ANTHONY E.
Optical velocity sensor for air data applications
p 368 A92-24575

SMART, K. P. R.
Learning from aircraft accidents and incidents
p 635 A92-39310
SMEETS, G.
Expansion tube experiments for the investigation of ram-accelerator-related combustion and gasdynamic problems
[AIAA PAPER 92-3246] p 904 A92-48845
SMELT, RONALD
Power economy in high-speed wind tunnels by choice of working fluid and temperature p 881 A92-45275
SMERECZNIAK, P.
Comparative investigation of multiplane thrust vectoring nozzles
[AIAA PAPER 92-3263] p 864 A92-48858
SMIRNOV, A. P.
Method of large particles in arbitrary curvilinear orthogonal coordinates for the solution of problems of hydro and aerodynamics p 937 A92-52035
SMIRNOV, A. V.
Development of a method for calculating the effect of the propeller slipstream on transonic flow over the wing
p 424 A92-30144
SMIT, KEVIN L.
A geometry-integrated approach to multiblock grid generation p 919 A92-47083
SMITH-BAILEY, SHERYL
Design considerations for a generic E.V.M.
[SAE PAPER 912095] p 651 A92-39952
SMITH, A. F.
Aluminium-lithium alloys - Application on helicopters
p 1106 A92-56326
SMITH, A. G.
The experimental and computational study of jet impingement flowfields with reference to VSTOL aircraft performance p 787 A92-45324
SMITH, A. J.
Approach and landing guidance p 457 N92-21960
SMITH, B.
SERI advanced wind turbine blades
[DE92-001216] p 598 N92-22971
Measured and predicted rotor performance for the SERI advanced wind turbine blades
[DE92-001215] p 598 N92-23119
SMITH, BARBARA K.
Test plan for the international aircraft operator information system
[DOT/FAA/CT-91/18] p 781 N92-26830
SMITH, BETH W.
Assessment of army aviators' ability to perform individual and collective tasks in the aviation networked simulator
[AD-A250293] p 888 N92-29709
SMITH, BRAD
Flight testing a digital terrain following system
p 548 A92-35929
SMITH, BRIAN E.
Large-scale wind tunnel studies of a jet-engined powered ejector-lift STOVL aircraft p 842 A92-45313
Aerodynamic performance of a full-scale lifting ejector system in a STOVL fighter aircraft
[AIAA PAPER 92-3094] p 824 A92-48738
SMITH, BROOKE C.
Dynamically enhanced sustained lift using oscillating leading-edge flaps
[AIAA PAPER 92-2625] p 794 A92-45497
SMITH, C. E.
CFD analysis of jet mixing in low NO(x) flametube combustors
[ASME PAPER 91-GT-217] p 124 A92-15634
CFD mixing analysis of jets injected from straight and slanted slots into confined crossflow in rectangular ducts
[NASA-TM-105699] p 738 N92-26561
SMITH, C. F.
Experimental and analytical study of close-coupled ventral nozzles for ASTOVL aircraft p 861 A92-45325
Full Navier-Stokes calculations on the installed F/A-18 inlet at a high angle of attack
[AIAA PAPER 92-3175] p 1020 A92-54012
Three-dimensional compressible turbulent computations for a diffusing S-duct
[NASA-CR-4392] p 526 N92-22249
Three-dimensional compressible turbulent computations for a nondiffusing S-duct
[NASA-CR-4391] p 951 N92-32240
SMITH, C. FREDERIC
Flow studies in close-coupled ventral nozzles for STOVL aircraft
[NASA-TM-102554] p 445 N92-20934
SMITH, CAREY
Systems commonality - Integrated avionics for the MH-47E and the MH-60K p 966 A92-49331
SMITH, CHARLES D.
Helicopter far-field acoustic levels as a function of reduced rotor speeds p 695 A92-39228
Helicopter main-rotor speed effects: A comparison of predicted ranges of detection from the aural detection program ICHIN and the electronic detection program ARCAS
[NASA-TM-104134] p 166 N92-12598
SMITH, COLIN A.
The B-2 radar p 956 A92-53102
SMITH, CRAWFORD F.
Flow in a ventral nozzle for short takeoff and vertical landing aircraft p 376 A92-28538
SMITH, D. E.
Design sheet - An environment for facilitating flexible trade studies during conceptual design
[AIAA PAPER 92-1191] p 600 A92-33303
SMITH, D. P.
Lightning strike tests of composite connectors
[AD-A252281] p 1044 N92-33249
SMITH, DOUGLAS
Neutron radiography with SNRS p 492 A92-28747
SMITH, DOUGLAS R.
The effect of successive distortions of the boundary layer in a supersonic flow
[AIAA PAPER 92-0309] p 320 A92-25757
SMITH, EDWARD C.
Aeroelastic response and blade loads of a composite rotor in forward flight
[AIAA PAPER 92-2566] p 564 A92-34480
SMITH, G. H.
Particle image velocimetry measurements of the aerodynamics of a wind turbine p 1115 A92-54337
SMITH, GARY M.
Field test of an advanced maintenance-system
p 1016 A92-56221
SMITH, GILES K.
When should we start high-rate production of the B-2? An analysis based on flight test results
[RAND/P-7757] p 697 N92-25204
SMITH, GUY A.
Modifications to the rapid melt/rapid quench and transparent polymer video furnaces for the KC-135
[NASA-CR-184215] p 157 N92-12231
SMITH, H. A.
Lubricant evaluation and performance 2
[AD-A247464] p 895 N92-28398
SMITH, HOWARD R.
An intelligent pilot vehicle interface for a day/night adverse weather pilotage system (D/NAPS)
[AIAA PAPER 91-3729] p 197 A92-17596
SMITH, I. G.
A unique approach to aircraft conflict resolution using artificial intelligence techniques p 190 N92-14029
SMITH, I. S., JR.
NASA test flights with increased flight stress indices
[AIAA PAPER 91-3665] p 20 A92-11012
SMITH, J.
Evaluation of measured-boundary-condition methods for 3D subsonic wall interference
[NLR-TR-88072-U] p 832 N92-29884
Integration of wall interference assessment and wall adaptation
[NLR-TP-91119-U] p 1101 N92-32734
SMITH, J. H. B.
Asymmetric vortex flow over circular cones
p 86 N92-13014
Vortex flow aerodynamics
[AGARD-AR-299] p 946 N92-30947
SMITH, JAMES E., JR.
High temperature aircraft research furnace facilities
[NASA-CR-184384] p 1101 N92-33826
SMITH, JOHN W.
Variable-camber systems integration and operational performance of the AFTI/F-111 mission adaptive wing
[NASA-TM-4370] p 570 N92-22194
SMITH, KEITH
Aeronautical satellite system test and implementation
p 676 N92-24095
SMITH, KENT F.
Development of a reclined crashworthy crewseat for rotorcraft p 105 A92-14370
SMITH, LEIGH ANN
Applications of a direct/iterative design method to complex transonic configurations
[NASA-TP-3234] p 1039 N92-33484
SMITH, M. J. T.
Do we really need 57 ways of rating aircraft noise?
p 688 A92-39065
Re-engining appears to offer best payback for young: Chapter 2 compliant aircraft
[PNR-90848] p 378 N92-19939
The impact of aircraft noise control technology
[PNR-90846] p 512 N92-20461
The environmental challenges for the next supersonic aircraft
[PNR-90782] p 505 N92-20928
Environmentally sound
[PNR-90776] p 506 N92-21743
SMITH, M. W.
CARS temperature measurements in a hypersonic propulsion test facility p 140 N92-12049
SMITH, MICHAEL S.
Operational evaluation of recently developed balloon fabrication methods
[AIAA PAPER 91-3670] p 1 A92-11017
Holographic and PLIF measurements of free-flight hypervelocity flows in the AEDC Range G facility
[AIAA PAPER 92-3935] p 1122 A92-56765
SMITH, P. R.
Application of Eigenstructure Assignment to the control of powered lift combat aircraft
[RAE-TM-FS-1009] p 135 N92-12004
SMITH, PHILIP N.
Vision-based range estimation using helicopter flight data
[NASA-TM-103930] p 1047 N92-32424
SMITH, PHILLIP
Vision-based obstacle detection for rotorcraft flight
p 967 A92-52465
SMITH, PHILLIP N.
A rotorcraft flight database for validation of vision-based ranging algorithms
[NASA-TM-103906] p 841 N92-29103
SMITH, R.
Supersonic flow mixing and combustion using RAMP nozzle
[AIAA PAPER 92-3840] p 1113 A92-54198
SMITH, R. C.
Approximation methods for control of acoustic/structure models with piezoceramic actuators
[NASA-CR-189578] p 234 N92-15658
Active noise control: Piezoceramic actuators in fluid/structure interaction models
[NASA-CR-190328] p 685 N92-26125
SMITH, R. D.
Analysis of helicopter accident risk exposure near heliports, airports, and unimproved sites
[SCT-91RR-13] p 637 N92-26028
SMITH, R. E.
Gridding strategies and associated results for winged entry vehicles p 918 A92-47051
Grid generation and compressible flow computations about a high-speed civil transport configuration
p 919 A92-47055
NASA Workshop on future directions in surface modeling and grid generation
[NASA-CP-10092] p 831 N92-29625
SMITH, RICHARD B.
Integrated flight control systems - Architectural considerations for future aircraft concepts
p 872 A92-45322
SMITH, RICHARD H.
Why not a safety rating? p 530 A92-36200
SMITH, ROBERT D.
FAA vertical flight research, engineering, and development bibliography, 1962 - 1991
[FAA/ARD-30] p 462 N92-21210
SMITH, ROBERT E.
An analytical approach to grid sensitivity analysis
[AIAA PAPER 92-0660] p 334 A92-27031
An adaptive grid method for computing the high speed 3D viscous flow about a re-entry vehicle
[AIAA PAPER 92-2685] p 799 A92-45534
Software Surface Modeling and Grid Generation Steering Committee
[NASA-CP-3143] p 691 N92-24397
SMITH, ROGERS E.
X-29 high angle of attack p 111 A92-16052
SMITH, ROY S.
The army special operations aircraft integrated avionics subsystem - An operational perspective
p 966 A92-49332
SMITH, S. F.
Advanced techniques in current signature analysis
[DE92-007680] p 679 N92-24892
SMITH, SAMUEL H.
Generation of spectra and stress histories for fatigue and damage tolerance analysis of fuselage repairs
[AD-A250390] p 854 N92-29180
SMITH, STEVE
Preliminary design studies of an advanced general aviation aircraft
[NASA-CR-190024] p 461 N92-20064
SMITH, T. F.
Thermal radiation effects on a shocked particle-laden gas p 780 A92-44377
SMITH, TODD E.
The effect of steady aerodynamic loading on the flutter stability of turbomachinery blading
[ASME PAPER 91-GT-130] p 71 A92-15574

SMITS, A. J.
The dynamics and control of fluctuating pressure loads in the reattachment region of a supersonic free shear layer
[AIAA PAPER 92-0178] p 255 A92-23788
A three-dimensional supersonic turbulent boundary layer generated by an isentropic compression
[AIAA PAPER 92-0310] p 320 A92-25758
SMITS, ALEXANDER J.
The effect of successive distortions of the boundary layer in a supersonic flow
[AIAA PAPER 92-0309] p 320 A92-25757
The structure and control of three-dimensional shock wave turbulent boundary layer interactions
[AD-A250209] p 1003 N92-31824
SMOUT, P. D.
The problem of static pressure measurement in turbomachinery annuli using traversable instrumentation
[PNR-90791] p 591 N92-22099
SMYTH, J. R.
Garrett GTP50-1 multipurpose small power unit technology demonstrator program
[ASME PAPER 91-GT-328] p 153 A92-15698
Advanced ceramic engine technology for gas turbines
[ASME PAPER 91-GT-368] p 153 A92-15716
SNAPE, D. M.
Emissions from aircraft: Standards and potential for improvement
[PNR-90768] p 476 N92-21740
The impact of air transport on the environment
[PNR-90876] p 1129 N92-33751
SNEE, J. M. D.
Simultaneous stress and flutter optimization for the wing of a transport aircraft equipped with four engines
p 571 N92-23238
SNEGIREV, N. A.
A probabilistic method for monitoring the remaining life of aircraft gas turbine engine components using the temperature limit criterion p 201 A92-18292
SNELL, S. A.
Nonlinear inversion flight control for a supermaneuverable aircraft p 873 A92-46751
Preliminary assessment of the robustness of dynamic inversion based flight control laws
[AIAA PAPER 92-4330] p 1074 A92-55174
SNELL, SIDNEY ANTONY
Nonlinear dynamic-inversion flight control of supermaneuverable aircraft p 1062 N92-33953
SNELLING, SANDRA L.
Effect of nonuniform entrance flow profile on hypersonic nozzle pitching moment
[AD-A244050] p 377 N92-19184
SNIDER, J. B.
Remote measurements of supercooled integrated liquid water during WISP/FAA aircraft icing program
p 915 A92-46788
Progress report on analysis of differential attenuation radar data obtained during WISP-91
[PB92-133800] p 503 N92-21828
SNIGIREV, V. F.
A study of a version of the boundary conditions of a two-dimensional spline in surface and line modeling
p 163 A92-16826
SNYDER, CHRISTOPHER A.
Effects of chemical equilibrium on turbine engine performance for various fuels and combustor temperatures
[NASA-TM-105399] p 562 N92-23254
SNYDER, CURTIS D.
A configuration development strategy for the NASP
[AIAA PAPER 91-5044] p 210 A92-17830
SNYDER, DANIEL E.
Identifying design requirements using integrated analysis structures p 922 A92-48527
SNYDER, H. T.
High temperature ground vibration test techniques
p 980 A92-51404
SNYDER, PHILIP H.
Cooled high-temperature radial turbine program 2
[NASA-CR-189122] p 1073 N92-34236
SNYDER, SCOTT
Design and flight test of a differential GPS/inertial navigation system for approach/landing guidance
p 97 A92-16650
Differential GPS/inertial navigation approach/landing flight test results p 956 A92-51009
SNYDER, STEVEN P.
Analysis of an advanced fighter aircraft using jet flap techniques and the vortex lattice method
[AD-A244051] p 366 N92-19185
SNYMAN, J. A.
The application of parameter optimisation techniques to linear optimal control system design
p 302 A92-23038
SOBAN, DANI
The SnoDog: Preliminary design of a close air support aircraft
[NASA-CR-189990] p 462 N92-21489
SOBEL, K. M.
A time approach to robustness of LTI systems with structured uncertainty and unmodelled dynamics
p 48 A92-11356
SOBEL, KENNETH M.
Robust sampled data eigenstructure assignment using the delta operator
[AIAA PAPER 92-4400] p 1075 A92-55200
SOBH, NAHIL ATEF
Iterative methods for large scale static analysis of structures on a scalable multiprocessor supercomputer
[NASA-CR-190369] p 692 N92-26018
SOBIECZKY, H.
Extended mapping and characteristics techniques for inverse aerodynamic design p 194 N92-13949
SOBIESZCZANSKI-SOBIESKI, JAROSLAW
Preliminary results from the High Speed Airframe Integration Research project
[AIAA PAPER 92-1004] p 536 A92-33196
Application of advanced multidisciplinary analysis and optimization methods to vehicle design synthesis
p 1054 A92-56160
A system approach to aircraft optimization
p 550 N92-23228
Aircraft optimization by a system approach: Achievements and trends
[NASA-TM-107622] p 650 N92-25995
Multidisciplinary design and optimization
[AGARD-PAPER-2] p 851 N92-28473
SOBOL', S. B.
Safety provision against 'ground resonance' free vibration of a coaxial helicopter p 1056 A92-56289
SODERMAN, PAUL T.
The design of test-section inserts for higher speed aeroacoustic testing in the Ames 80- by 120-foot wind tunnel
[NASA-TM-103915] p 927 N92-28909
SOEDEL, SVEN M.
System for generating sequences of phased gust or taxi loadings p 845 A92-46800
SOELTER, HARALD
A multivariable control concept for a gas turbine engine
[ETN-92-92104] p 1072 N92-33645
SOESMAN, J. L.
On the optimization of windshear warning and guidance systems
[NLR-TP-90196-U] p 837 N92-29703
SOETRISNO, MOELJO
Numerical simulations of the transdetonative ram accelerator combusting flow field on a parallel computer
[AIAA PAPER 92-3249] p 894 A92-48848
SOFRIN, THOMAS G.
Turbomachinery noise p 54 N92-10601
SOFUE, Y.
An analysis of impact resistance of composite blades for turbo-fan engines p 294 A92-23109
SOFUE, YASUSHI
An analysis of impact resistance of composite fan blade p 293 A92-22523
SOGA, K.
Thermal measurement test in a shock wind tunnel
p 748 A92-43104
New 1.27-m leg of the National Aerospace Laboratory hypersonic wind tunnel p 1092 A92-56003
SOGA, KUNIO
A shock tunnel experiment on aerodynamic interference induced by RCS jet p 1029 A92-56042
SOGA, TOMOKATSU
The operational status of automated aircraft washing system p 1016 A92-56087
SOHA, G.
Gamma Group-The Pale Horse: A proposal in response to a commercial air transportation study ort study
[NASA-CR-190019] p 731 N92-26435
SOHN, K. H.
Turbulent heat flux measurements in a transitional boundary layer
[NASA-TM-105623] p 716 N92-27377
SOHN, PHILIP Y.
Characteristics of a future aeronautical satellite communications system
[AIAA PAPER 92-2058] p 453 A92-29889
SOINIKOV, IU. V.
A study of the nonlinear stress-strain state of spring-type landing gear p 154 A92-16825
SOISTMANN, DAVID L.
Low-speed flutter characteristics of some simple low-aspect-ratio delta-wing models p 460 A92-32247
An experimental and analytical investigation of wing flutter on a trail rotor V/STOL aircraft
[AIAA PAPER 92-2112] p 544 A92-35682
SOIZE, C.
Numerical methods in elastoacoustics in the nonmodal domain
[ONERA, TP NO. 1991-232] p 415 A92-26383
Perfect compressible two dimensional boundary layer strong fluid coupling in the case of sharp leading edge profiles. Unsteady case of isolated profiles and steady case of blade grids
[ONERA-RT-43/1621-RY-006-R] p 43 N92-11311
Strong coupling between inviscid fluid and boundary layer of sharp leading edges: Two-dimensional stationary and turbulent cases for isolated profiles and guard vanes
[ONERA-RT-44/1621-RY-016-R] p 1125 N92-32776
SOKOLOV, E. I.
Effect of rarefaction on the nonstationary interaction of a supersonic underexpanded jet with a perpendicular obstacle p 337 A92-27594
SOKOLOVA, O. N.
Calculating the steady-state nonlinear aerodynamic characteristics of thin wings near the interface between two fluids p 426 A92-30181
SOKOLOWSKI, DANIEL E.
Aircraft engine hot section technology: An overview of the HOST Project p 561 N92-22535
SOLAZZO, M.
Aerothermodynamic development of the CARINA re-entry vehicle: CFD analyses and experimental tests
p 211 N92-14980
SOLIES, U. P.
Flight measurements of downwash on the Ball-Bartoe Jetwing powered lift aircraft p 1054 A92-56174
SOLIMAN, M. M. E.
A high speed edgewise rotor using circulation control only in the reversed flow area p 1059 A92-56347
SOLLO, ANTONIO
Advanced Study for Active Noise Control in Aircraft (ASANCA)
[AIAA PAPER 92-2092] p 1137 N92-32956
SOLNTSEV, I. A.
Theoretical analysis of the effect of the porous walls of a wind tunnel on transonic flow past bodies of cone-cylinder type p 427 A92-30202
SOLODOVNIKOV, O. E.
Local heat transfer in the perforation channels of turbine nozzle vanes p 657 A92-40615
SOLOMAN, RON
New insulation constructions for aerospace wiring applications. Volume 1: Testing and evaluation
[AD-A240638] p 22 N92-11006
New insulation constructions for aerospace wiring applications. Volume 2: The 270 VDC arc tracking testing with power controllers
[AD-A240639] p 23 N92-11007
SOLONIN, V. I.
The study of experimental turboramjets
[AIAA PAPER 92-3720] p 1067 A92-54135
SOLOTCHIN, A. V.
Three-dimensional singularity of flow structure in an underexpanded supersonic jet p 78 A92-16679
SOLOV'EV, A. S.
Stability of a viscous compressible shear layer with a temperature drop p 79 A92-16684
On an adaptive numerical method for solution of high gradient problems p 410 A92-24905
SOLTANI, M. R.
Finite wing aerodynamics with simulated glaze ice
[AIAA PAPER 92-0414] p 325 A92-26265
SOM, AMIT K.
Characterization of diffusion bonds using an acoustic microscope p 491 A92-28686
SOMAKUMAR, R.
Flight control system design using eigenstructure assignment for rolling the aircraft around the velocity vector p 977 A92-51945
SOMMER, STEVEN T.
A study of the diffusion of slot-injected drag-reducing polymer solution in a turbulent boundary layer modified by large-eddy breakup devices
[AD-A243411] p 344 N92-18007
SOMOZA, EUGENE
The INFO-ROC technique - A method for comparing and optimizing inspection systems p 144 A92-13563
SONDAK, D. L.
Wall functions for the kappa-epsilon turbulence model in generalized nonorthogonal curvilinear coordinates
[NASA-CR-190368] p 685 N92-25962
SONG, BIFENG
The system reliability analysis and optimization design for wing-box structures p 997 A92-53292
SONG, C.
Advanced thermally stable jet fuel development program. Volume 2: Compositional factors affecting thermal degradation of jet fuels
[AD-A252656] p 987 N92-31399

SONG, J.
Impact design methods for ceramic components in gas turbine engines
[ASME PAPER 91-GT-115] p 123 A92-15566
SONG, O.
Dynamic response to time-dependent excitations of cantilevered aircraft wing structures modelled as thin-walled beams
[AIAA PAPER 92-2213] p 584 A92-34403
SONG, OHSEOP
Static aeroelastic tailoring of composite aircraft swept wings modelled as thin-walled beam structures
p 294 A92-23114
Adaptive response control of wing structures carrying heavy tip weights
[AIAA PAPER 92-2527] p 583 A92-34374
Behavior of thin-walled beams made of advanced composite materials and incorporating non-classical effects p 673 A92-39944
SONG, SHOUFENG
The relation among the general unsteady aerodynamic coefficients of a wing in subsonic and supersonic speed
p 941 A92-53022
SONG, SHUXIAN
A new method for orientation calculation of the electromagnetic helmet-mounted sighting unit
p 370 A92-27837
SONG, WEIPING
A calculation of influence of vortex breakdown on aerodynamic characteristics for slender wings
p 616 A92-38920
SONI, BHARAT K.
Simulation of wind tunnel flowfields
[AIAA PAPER 92-0034] p 249 A92-22155
TIGER: Turbomachinery interactive grid generation
p 659 N92-25718
SONNEBORN, W. G.
V-22 propulsion system design p 1070 A92-56300
SONSINO, C. M.
Low cycle fatigue of cast nickel base turbine rotors
p 226 N92-14405
SONTI, V. R.
Active control of structurally-coupled sound fields generated by localized force inputs p 694 A92-39106
SONUPARLAK, B.
Effect of sustained high temperature exposure on the mechanical properties of Nicalon/Al2O3 composites
p 668 A92-39672
SONUPARLAK, BIROL
Fabrication and properties of fiber-reinforced ceramic composites made by directed metal oxidation
p 669 A92-39861
SOOSAAR, R. J.
Flight simulation p 207 N92-13982
SOPHER, ROBERT
Evaluation of an advanced finite element analysis for rotor blades p 109 A92-14426
SORAKU, TAKIHIKO
A study of aircraft surface coating technology
p 700 A92-43147
SORENSEN, THOMAS
Airfoil optimization with efficient gradient calculations
p 177 N92-13960
SORENSON, BOYD W.
Fabrication and properties of fiber-reinforced ceramic composites made by directed metal oxidation
p 669 A92-39861
SORINE, MICHEL
Wideband control of gyro/accelerometer multisensors in a strapdown guidance system p 856 A92-46736
SORTORE, C. K.
Low power magnetic bearing design for high speed rotating machinery p 772 N92-27739
SOSOUNOV, V. A.
The study of experimental turboramjets
[AIAA PAPER 92-3720] p 1067 A92-54135
SOSUNOV, V. A.
Soviet CFD - An international perspective
p 233 A92-20150
SOTHCOTT, VICTOR E.
A summary of XB-70 sonic boom signature data
[NASA-CR-189630] p 696 N92-24800
SOTOMAYER, W. A.
Unsteady aerodynamics for aeroelasticity at the Flight Dynamics Directorate p 718 N92-27939
SOTOMAYOR, JORGE L.
Wavelength-multiplexed fiber-optic position encoder for aircraft control systems p 734 A92-42602
SOTOZAKI, TOKUO
Development of an instrument for measuring runway roughness p 748 A92-43124
A proposed method for evaluating runway roughness
p 748 A92-43125
Grooved runway surface texture before and after rubber removal p 1093 A92-56111
SOVIERO, P. A. O.
Jet inflow simulation and its downwash effect on lifting surfaces p 9 A92-13200
SOWA, W. A.
Characterization of a two-phase flow field downstream of a 3x-scale gas turbine co-axial, counter-swirling, combustor dome swirl cup
[AIAA PAPER 92-0229] p 393 A92-25693
Mixing in the dome region of a staged gas turbine combustor
[AIAA PAPER 92-3089] p 903 A92-48734
SPAID, FRANK W.
Boundary-layer and wake measurements on a swept, circulation-control wing p 9 A92-13205
Single expansion ramp nozzle simulations
[AIAA PAPER 92-0387] p 323 A92-26243
Experimental results for a hypersonic nozzle/afterbody flow field
[AIAA PAPER 92-3915] p 1032 A92-56747
SPALART, P. R.
A one-equation turbulence model for aerodynamic flows
[AIAA PAPER 92-0439] p 327 A92-26285
SPALDING, KEVIN J.
Flight test of a GPS-aided low-cost inertial navigation system programmed in Ada p 101 A92-16973
SPALL, R. E.
Linear stability of three-dimensional boundary layers over axisymmetric bodies at incidence
p 431 A92-31157
SPALL, ROBERT
Application of linear stability theory in laminar flow design
[SAE PAPER 912116] p 618 A92-39967
SPALL, ROBERT E.
Computational study of transition front on a swept wing leading-edge model
[AIAA PAPER 92-2630] p 795 A92-45502
SPANG, H. A., III
Compressor modeling and active control of stall/surge
p 508 A92-29315
SPANYER, K. S.
Study of weld offset in longitudinally welded SSME HPFTP inlet
[AIAA PAPER 92-2305] p 586 A92-34525
SPARAGGIS, PANAYOTIS D.
Stochastic ordering properties and optimal routing control for a class of finite capacity queueing systems
p 48 A92-11375
SPARKS, ANDREW G.
Combined H(2)/H(infinity) optimal control design applied to an advanced fighter aircraft
[AIAA PAPER 92-0045] p 281 A92-22162
Loop shaping in mixed H2 and H-infinity optimal control p 507 A92-29177
SPARROW, DAVID A.
Modeling radar clutter
[AD-A240965] p 158 N92-13351
SPARROW, VICTOR W.
Simulations of sonic boom ray tube area fluctuations for propagation through atmospheric turbulence including caustics via a Monte Carlo method
p 1139 N92-33878
SPAZZINI, P. G.
Skin friction measurements in 3-D boundary layers
p 1092 A92-54351
SPEARMAN, M. L.
An aerodynamic design study of a series of lifting bodies at angles of attack from 10 to 53 degrees at Mach numbers from 2.30 to 4.62 p 442 A92-32500
SPECK, ERIC
The use of high voltage direct current in aircraft electrical systems - A Navy perspective
[SAE PAPER 912173] p 655 A92-39998
SPECTOR, J. MICHAEL
Design specifications for the Advanced Instructional Design Advisor (AIDA), volume 2
[AD-A248202] p 923 N92-29188
SPEED, F. M., JR.
Designing through test
[AIAA PAPER 91-3822] p 232 A92-17664
SPEKREIJSE, S. P.
The design of a system of codes for industrial calculations of flows around aircraft and other complex aerodynamic configurations
[AIAA PAPER 92-2619] p 917 A92-45492
Domain modeling and grid generation for multi-block structured grids with application to aerodynamic and hydrodynamic configurations p 691 N92-24411
New concepts for multi-block grid generation for flow domains around complex aerodynamic configurations
[NLR-TP-91046-U] p 1037 N92-32730
SPEKREYSE, S. P.
An information system for the numerical simulation of 3D Euler flows around aircraft p 613 A92-37554
New concepts for multi-block grid generation for flow domains around complex aerodynamic configurations
p 817 A92-47079
SPEL, M.
Aerothermodynamic calculations for the Space Shuttle Orbiter
[AIAA PAPER 92-2953] p 821 A92-47917
SPELTEN, ROBERT
Production of periodical Mach number variations in high subsonic flow in a blow down wind tunnel, and its influence on profile measurements
[ETN-92-91492] p 833 N92-29889
SPENCE, ANNE M.
Coupled rotor-fuselage dynamics and aeroelasticity in turning flight
[AIAA PAPER 92-2109] p 544 A92-35680
SPENCER, A.
Discharge coefficients of cooling holes with radiused and chamfered inlets
[ASME PAPER 91-GT-269] p 151 A92-15667
SPENCER, B. F., JR.
Determination of tire-wheel interface loads for aircraft wheels
[AIAA PAPER 92-2482] p 543 A92-34599
SPENCER, ROY
High altitude airborne remote sensing mission using the advanced microwave precipitation radiometer (AMPR)
p 574 A92-34893
SPENLER, S.
An aircraft Earth station for general aviation
p 678 N92-24194
SPERRY, DAVID J.
Prototype instrumentation and design studies
[AD-A248378] p 736 N92-28004
SPETNAGEL, D.
Comparative investigation of multiplane thrust vectoring nozzles
[AIAA PAPER 92-3263] p 864 A92-48858
SPEZIALE, C. G.
Application of a new K-tau model to near wall turbulent flows p 395 A92-26437
SPIEGEL, P.
Prediction of helicopter noise: Adaptation of noise load calculations to the blade-vortex interaction
[ONERA-RS-97/5094-PY] p 513 N92-21736
SPIEGEL, PIERRE
Theoretical study and prediction of BVI noise including close interactions
[ONERA, TP NO. 1991-174] p 165 A92-16138
SPILLMAN, J. J.
The use of variable camber to reduce drag, weight and costs of transport aircraft p 313 A92-25096
SPILLMAN, W. B., JR.
Optically powered and interrogated rotary position sensor for aircraft engine control applications
p 370 A92-27777
SPILLMAN, WILLIAM B., JR.
Wavelength encoded fiber optic angular displacement sensor p 857 A92-48046
SPINA, E. F.
An improved analysis method for cross-wire signals obtained in supersonic flow p 614 A92-38456
SPINA, ERIC F.
Constant-temperature anemometry measurements in hypersonic boundary layers p 90 N92-13861
SPINETTI, R. L.
Calculation of high speed base flows
[AIAA PAPER 92-2679] p 799 A92-45531
SPIRKL, A.
'A new proposal for an old problem' - The right engine for the right helicopter p 1070 A92-56281
SPIRKOVSKA, LILLY
Optical computing at NASA Ames Research Center
[AIAA PAPER 91-3779] p 231 A92-17637
SPITZER, CARY
Design and flight test of a differential GPS/inertial navigation system for approach/landing guidance
p 97 A92-16650
Differential GPS/inertial navigation approach/landing flight test results p 956 A92-51009
SPLETTSTOESSER, WOLF R.
BVI impulsive noise reduction by higher harmonic pitch control - Results of a scaled model rotor experiment in the DNW p 1136 A92-56344
SPOWART, M. P.
An airborne Doppler lidar for meteorological research
p 467 A92-32082
Simplified signal processing for an airborne CO2 Doppler lidar p 1000 N92-31023
SPRADLEY, I. E.
Computer simulation model for Lucas Stirling refrigerators p 296 A92-23837
SPRAGUE, JOHN R.
Current technology propulsion systems meet the STOVL window of opportunity p 860 A92-45307

SPRECHER, A. F.
Electrorheological fluids; Proceedings of the 2nd International Conference, Raleigh, NC, Aug. 7-9, 1989 p 40 A92-12625
SPRING, DONALD J.
Downwash for joined-wing airframe with control surface deflections p 702 A92-41235
SPRING, S. A.
Measurements in a leading-edge separation bubble due to a simulated airfoil ice accretion p 723 A92-41262
SPRING, S. D.
Experimental investigation of film cooling effectiveness for slots of various exit geometries p 497 A92-32265
SPURGEON, S. K.
An assessment of robustness of variable structure control systems for advanced aircraft manoeuvres p 29 A92-11595
SPYERS-DURAN, PAUL A.
An airborne cryogenic frost-point hygrometer p 467 A92-32090
SQUEGLIA, G.
International standardisation of regulations for gust loading calculations p 270 A92-22473
SQUIRE, C.
A study of the interaction of a normal shock wave with a turbulent boundary layer at Mach numbers between 1.30 and 1.55 p 339 A92-28006
SQUIRE, L. C.
Numerical studies of supersonic flow over a compression corner p 442 A92-32324
SQUIRES, P. K.
Hub and pylon fairing integration for helicopter drag reduction p 107 A92-14391
SREEKANTH, A. K.
Numerical and experimental investigations of rarefied gas flows through nozzles and composite systems p 940 A92-52797
SREENIVASAN, K. R.
Remarks on high-Reynolds-number turbulence experiments and facilities p 881 A92-45267
SRIDHAR, B.
Vision-based stereo ranging as an optimal control problem
[AIAA PAPER 92-4418] p 1045 A92-55211
Passive range estimation for rotorcraft low-altitude flight
[NASA-TM-103897] p 2 N92-10003
SRIDHAR, BANAVAR
Inertial navigation sensor integrated motion analysis for obstacle detection p 954 A92-49272
Vision-based obstacle detection for rotorcraft flight p 967 A92-52465
Analysis of image-based navigation system for rotorcraft low-altitude flight p 1046 A92-55968
Status of automatic guidance systems for rotorcraft in low altitude flight p 727 N92-27894
Vision-based range estimation using helicopter flight data
[NASA-TM-103930] p 1047 N92-32424
SRINATHKUMAR, S.
Flutter suppression for the Active Flexible Wing - Control system design and experimental validation
[AIAA PAPER 92-2097] p 566 A92-35666
Estimation of lift and drag characteristics of an aircraft from flight data p 959 A92-51942
Design and experimental validation of a flutter suppression controller for the active flexible wing
[NASA-TM-4381] p 979 N92-31240
SRINIVASA RAO, B. R.
Measurement of magnus derivatives with an elastically forced oscillation rig p 749 A92-43172
SRINIVASAN, G. R.
Flowfield of a lifting rotor in hover - A Navier-Stokes simulation p 1024 A92-54906
Flowfield analysis of modern helicopter rotors in hover by Navier-Stokes method
[AD-A245011] p 446 N92-21333
SRINIVASAN, G. V.
Development and characterization of high strength SiC rotors
[ASME PAPER 91-GT-191] p 149 A92-15617
SRINIVASAN, RAM
Studies of the effects of curvature on dilution jet mixing p 290 A92-21079
SRINIVASAN, S.
Hypersonic flow past delta wing flow simulated by Navier-Stokes solutions p 180 N92-14981
SRINIVASAN, SHIVAKUMAR
Hypersonic laminar flow computations over a blunt leading edged delta wing at three different chord Reynolds numbers
[FFA-TN-1991-40] p 528 N92-23168
SRINIVASSAN, R.
Tracking performance requirements for rotorcraft instrument approaches to reduced minima. Phase 1: Preliminary study
[NRC-32137-PHASE-1] p 102 N92-11988
SRIRAM, P.
Buckling, postbuckling and crippling of thin walled composite airframe structures under compression p 899 A92-46940
SRIVASTAVA, R.
An unsteady Euler scheme for the analysis of ducted propellers
[AIAA PAPER 92-0522] p 332 A92-26947
Aeroelastic analysis of advanced propellers using an efficient Euler solver
[AIAA PAPER 92-0488] p 341 A92-28194
A numerical classical flutter analysis of advanced propellers
[AIAA PAPER 92-2118] p 557 A92-35687
SRIVATSAN, RAGHAVACHARI
Takeoff Performance Monitoring System display options
[AIAA PAPER 92-4138] p 967 A92-52433
SRULIJES, J.
Expansion tube experiments for the investigation of ram-accelerator-related combustion and gasdynamic problems
[AIAA PAPER 92-3246] p 904 A92-48845
STACEY, C. H. B.
Measurement of shock-wave/boundary-layer interaction in a free-piston shock tunnel p 813 A92-46903
STACHTCHENKO, LEONID
Yaw dynamics of a coaxial rotor helicopter p 378 A92-24427
STACK, JOHN P.
The NASA Langley laminar-flow-control experiment on a swept, supercritical airfoil: Evaluation of initial perforated configuration
[NASA-TM-4309] p 525 N92-22196
STACK, SHARON H.
Engineering method for aero-propulsive characteristics at hypersonic Mach numbers
[AIAA PAPER 91-5061] p 437 A92-31690
STAEHLE, ROBERT
Crew transportation for the 1990s. I - Commercializing manned flight with today's propulsion p 889 A92-46726
STAHL, W. H.
Experimental investigations of the vortex flow on delta wings at high incidence p 432 A92-31172
STAHR, R. S.
Implementing data link across the Pacific
[SAE PAPER 912235] p 638 A92-40027
STALKER, R. J.
Mach 4 and Mach 8 axisymmetric nozzles for a high-enthalpy shock tunnel p 78 A92-16668
Waves and thermodynamics in high Mach number propulsive ducts p 809 A92-46431
Unsteady shock propagation in a steady flow nozzle expansion p 1023 A92-54489
STALLARD, PAUL
The development of an engine air particle separator system for the CH-47 helicopter p 545 A92-35736
STALLCOP, JAMES R.
H-N2 interaction energies, transport cross sections, and collision integrals p 1135 A92-54660
STAMATIS, A.
Jet engine fault detection with discrete operating points gas path analysis p 129 A92-17200
Optimal measurement and health index selection for gas turbine performance status and fault diagnosis
[ASME PAPER 91-GT-294] p 653 A92-36889
STAMP, JEFF
Engine air particle separator panels for helicopter engine protection p 545 A92-35735
STANAWAY, SHARON
Navier-Stokes analysis of blunt trailing edge airfoils
[AIAA PAPER 92-0024] p 248 A92-22146
STANDER, C.
High-speed civil transport aircraft emissions p 408 N92-19122
STANDLEY, VAUGHN H.
Boiling and condensing pumped loop microgravity experiment - Challenges of testing in both aircraft and rocket environments p 992 A92-50611
STANEWSKY, EGON
Numerical study of secondary separation in glancing shock/turbulent boundary layer interactions
[AIAA PAPER 92-3666] p 907 A92-49087
STANISLAS, M.
Study of detached turbulent flow in an air intake by means of high speed tomography and laser velocimetry
[REPT-90/55] p 157 N92-12216
STANKOV, B. B.
Remote measurements of supercooled integrated liquid water during WISP/FAA aircraft icing program p 915 A92-46788
STANLEY, SCOTT A.
Effects of shock wave precursors ahead of hypersonic entry vehicles p 441 A92-32182
STANZIONE, KAYDON A.
Technology developments applied to the AH-1W SuperCobra
[AIAA PAPER 91-3071] p 21 A92-11607
Expanding U.S.M.C. roles for the AH-1W SuperCobra p 59 A92-14347
STAPLE, ALAN E.
The development and testing of an active control of structural response system for the EH101 helicopter p 569 A92-35775
STAPLETON, BRIAN P.
Flight test of ARINC 741 configuration low gain SATCOM system on Boeing 747-400 aircraft p 677 N92-24097
STARK, GEORGE E.
Software reliability for flight crew training simulators p 747 A92-41221
STARK, MICHAEL E.
Software Engineering Laboratory (SEL) Ada performance study report
[NASA-TM-105510] p 412 N92-18125
STARKEN, H.
Design and testing of a controlled diffusion airfoil cascade for industrial axial flow compressor application
[ASME PAPER 90-GT-140] p 6 A92-11286
An investigation of a strong shock-wave turbulent boundary layer interaction in a supersonic compressor cascade
[ASME PAPER 91-GT-92] p 70 A92-15556
Inlet flow angle determination of transonic compressor cascades
[ASME PAPER 91-GT-274] p 75 A92-15671
Design and analysis of a high pitch to chord ratio cascade representative of ducted propfans
[ASME PAPER 91-GT-335] p 126 A92-15700
STARLEY, BRUCE B.
Damage tolerant design of critical aircraft structural components
[AIAA PAPER 92-4041] p 1123 A92-56860
STARNES, JAMES H., JR.
Computational Structures Technology for Airframes and Propulsion Systems
[NASA-CP-3142] p 683 N92-25911
Analysis and design technology for high-speed aircraft structures p 684 N92-25918
Damaged stiffened shell research at NASA. Langley Research Center p 914 N92-30115
Eighth DOD/NASA/FAA Conference on Fibrous Composites in Structural Design, part 1
[NASA-CP-3087-PT-1] p 1106 N92-32513
STAROVATOV, A. A.
A ionospheric-sounding experiment from an aircraft p 160 A92-13809
STARTZEL-DEHEL, B.
Evaluation of triple simultaneous parallel ILS approaches spaced 5000 feet apart, phase 4.b
[DOT/FAA/CT-91/31] p 456 N92-21404
STARZEL-DEHEL, BARBARA
Evaluation of triple simultaneous parallel ILS approaches spaced 4300 feet apart, phase 4a
[ACD-340] p 191 N92-14034
STATECNY, JIRI
Discs low cycle fatigue life predictions for gas turbine engines in CSFR by using fractographic information p 995 A92-51950
STATON, LEO D.
Radar multipath study for rain-on-radome experiments at the Aircraft Landing Dynamics Facility
[NASA-TM-101657] p 680 N92-25137
STAUFENBIEL, R.
On aircraft wake properties and some methods for stimulating decay and breakdown of tip vortices p 87 N92-13021
STAVRAKAKIS, G. S.
Computation of aircraft geometric height under radar surveillance p 639 A92-40239
STECCO, S. S.
Transonic cascade flow prediction using the Navier-Stokes equations
[ASME PAPER 91-GT-313] p 76 A92-15690
STECK, J. E.
Use of neural networks in control of high alpha maneuvers
[AIAA PAPER 92-0048] p 282 A92-22164
STECK, JAMES E.
A study in dynamic control of a super maneuver with neural networks p 463 N92-21510

STECKEMETZ, B.
FALKE and COBRA technology development in aerodynamics and aerothermodynamics
p 183 N92-15017
STECKLEIN, GREGORY O.
A comparative study of numerical versus analytical waverider solutions
[AD-A244183] p 347 N92-19304
STEEB, DOUG
Advanced experimental design applied to damage tolerance of composite materials p 993 A92-51505
STEEN, GREGORY
Further wind tunnel investigation of the SM701 airfoil with aileron and turbulators
[NASA-CR-190702] p 1038 N92-33063
STEENKEN, W. G.
Active stabilization of multistage axial-compressor aerodynamic system instabilities
[ASME PAPER 91-GT-403] p 76 A92-15733
STEFFEN, CHRISTOPHER J., JR.
Development of a new flux splitting scheme
p 596 N92-23352
Development of new flux splitting schemes
p 682 N92-25809
STEFKO, G. L.
Cascade flutter analysis with transient response aerodynamics p 154 A92-15972
STEFKO, GEORGE L.
FREPS - A forced response prediction system for turbomachinery blade rows
[AIAA PAPER 92-3072] p 1130 A92-54006
STEHWIEN, WOLFGANG
Radar clutter classification
[ISBN-0-315-57981-1] p 1126 N92-33440
STEICH, DAVID J.
Finite difference time domain modeling of steady state scattering from jet engines with moving turbine blades
[NASA-CR-190290] p 971 N92-30753
STEIN, A.
Towards coherent hypermedia navigation by pragmatic dialogue modeling
[PB92-114735] p 455 N92-20818
STEIN, EARL S.
Controller memory enhancement: Field facility concepts and techniques
[DOT/FAA/CT-TN92/7] p 640 N92-24799
STEIN, PAMELA B.
The price of success - Mitigation and litigation in airport growth p 417 A92-27450
STEINBACH, DIETER
Calculation of support interferences on the aerodynamic coefficients for a wind tunnel calibration model
[ESA-TT-1247] p 830 N92-29159
STEINBERG, MARC
Robust optimal control with a worst case time domain performance criterion p 509 A92-29368
Potential role of neural networks and fuzzy logic in flight control design and development
[AIAA PAPER 92-0999] p 600 A92-33191
Flexible heat pipe cold plates for aircraft thermal control
[SAE PAPER 912105] p 674 A92-39959
A fuzzy logic based F/A-18 automatic carrier landing system
[AIAA PAPER 92-4392] p 1074 A92-55193
On-line identification and control of linearized aircraft dynamics p 1082 A92-55911
STEINBERG, MARC L.
Neural network and fuzzy logic technology for naval flight control
[AD-A242650] p 206 N92-15074
STEINDL, A.
Chaotic motion in mechanical and engineering systems p 695 A92-39480
STEINERT, W.
Design and testing of a controlled diffusion airfoil cascade for industrial axial flow compressor application
[ASME PAPER 90-GT-140] p 6 A92-11286
Inlet flow angle determination of transonic compressor cascades
[ASME PAPER 91-GT-274] p 75 A92-15671
Design and analysis of a high pitch to chord ratio cascade representative of ducted propfans
[ASME PAPER 91-GT-335] p 126 A92-15700
STEINETZ, BRUCE M.
Engine panel seals for hypersonic engine applications: High temperature leakage assessments and flow modelling
[NASA-TM-105260] p 298 N92-16336
High temperature dynamic engine seal technology development
[NASA-TM-105641] p 596 N92-23435
STEINETZ, BRUCE MICHAEL
Evaluation of an innovative high-temperature ceramic wafer seal for hypersonic engine applications
p 578 N92-22205
STEINHOFF, J. S.
Flow field measurement and visualization using projected smoke trails
[AIAA PAPER 92-0384] p 323 A92-26241
STEINHOFF, JOHN
Computational vorticity capturing - Application to helicopter rotor flows
[AIAA PAPER 92-0056] p 250 A92-22171
An Eulerian/Lagrangian method for computing blade/vortex impingement p 814 A92-46952
Development of a multigrid transonic potential flow code for cascades
[NASA-CR-190480] p 830 N92-29361
STEINLE, F. W., JR.
Blockage correction in three-dimensional wind tunnel testing based on the wall signature method
[AIAA PAPER 92-3925] p 1095 A92-56756
STEINMETZ, P.
Aluminides modified by palladium - Protection of new parts by local finishing
[ONERA, TP NO. 1992-49] p 893 A92-48610
STEMPLE, ALAN D.
The design and manufacture of an advanced thermoplastic horizontal stabilator for the AH-64A
p 59 A92-14354
STENGEL, ROBERT F.
Stochastic prediction techniques for wind shear hazard assessment p 48 A92-11381
Application of stochastic robustness to aircraft control systems p 204 A92-18620
Probabilistic reasoning for intelligent wind shear avoidance p 302 A92-21181
Identification of aerodynamic coefficients using computational neural networks
[AIAA PAPER 92-0172] p 255 A92-23783
Real-time decision aiding - Aircraft guidance for wind shear avoidance
[AIAA PAPER 92-0290] p 350 A92-25743
Target pitch angle for the microburst escape maneuver
[AIAA PAPER 92-0730] p 379 A92-27082
A system identification model for adaptive nonlinear control p 508 A92-29248
Comment on 'Effect of thrust/speed dependence on long-period dynamics in supersonic flight'
p 643 A92-39913
Stochastic prediction techniques for wind shear hazard assessment p 1007 A92-50505
Optimal recovery from microburst wind shear
[AIAA PAPER 92-4338] p 1078 A92-55327
Investigation of air transportation technology at Princeton University, 1990-1991 p 266 N92-17995
Optimal aircraft performance during microburst encounter p 266 N92-17999
Technical notes and correspondence: Stochastic robustness of linear time-invariant control systems
p 303 N92-18002
Computer-aided design of flight control systems
[AD-A244657] p 483 N92-21752
Identification of aerodynamic coefficients using computational neural networks
[AD-A244711] p 447 N92-21753
STENZENBERGER, H. D.
BMI/bis (allylphenoxyphthalimide)-copolymers - A new family of resins for advanced composites with improved thermal oxidative stability p 33 A92-10213
STEPANOV, GEORGII IU.
Separated and cavitation flows - Principal properties and computational models
[ISBN 5-02-014005-8] p 610 A92-36600
STEPANOV, V. A.
Numerical and experimental investigation of airframe-integrated inlet for high velocities
p 243 A92-21072
STEPHAN, AMY
Getting expert systems off the ground: Lessons learned from integrating model-based diagnostics with prototype flight hardware p 220 N92-14217
STEPHEN, ERIC J.
Flow visualization image analysis of high-rate roll experiments on a delta wing
[AIAA PAPER 92-0317] p 321 A92-25764
STEPHENS, DAVID G.
Fourth Aircraft Interior Noise Workshop
[NASA-CP-10103] p 1136 N92-32948
STEPHENS, J. R.
Microgravity nucleation and particle coagulation experiments support
[NASA-CR-190159] p 502 N92-21385
Microgravity nucleation and particle coagulation experiments support
[NASA-CR-189899] p 502 N92-21433
STEPHENS, JOSEPH R.
Intermetallic and ceramic matrix composites for 815 to 1370 C (1500 to 2500 F) gas turbine engine applications
p 141 A92-15128
STERN, ALAN
Characteristics of a future aeronautical satellite communications system
[AIAA PAPER 92-2058] p 453 A92-29889
STERNER, SUSANA C.
A unified numerical approach for the analysis of rotating disks including turbine rotors
[AIAA PAPER 92-2303] p 585 A92-34524
STETSON, KENNETH F.
On hypersonic boundary-layer stability
[AIAA PAPER 92-0737] p 335 A92-27088
STETTER, H.
Experimental investigations of exciting forces caused by flow in labyrinth seals p 223 N92-14354
STETTER, HEINZ
Three-dimensional calculation of low-frequency unsteady transonic flow in axial turbine stages
p 174 A92-19110
STEUBER, G. D.
New applications of liquid-crystal thermography in rotating turbomachinery heat transfer research
[ASME PAPER 91-GT-354] p 153 A92-15710
Heat transfer in rotating serpentine passages with trips skewed to the flow
[NASA-TM-105581] p 499 N92-20235
STEVENS, B. L.
Derivation of aircraft linear state equations from implicit nonlinear equations p 27 A92-11361
Aircraft flight controls design using output feedback
p 280 A92-21180
Negative state weighting in the linear quadratic regulator for aircraft control p 1007 A92-50513
STEVENS, BRIAN L.
Aircraft control and simulation
[ISBN 0-471-61397-5] p 480 A92-31021
STEVENS, E. G.
Whole aircraft lightning indirect effects evaluation using low level injection techniques p 192 A92-20134
STEVENS, J. E.
Aircraft fatigue management in the Royal Air Force
p 363 N92-18591
STEVENS, J. M. G. F.
A computer programme for the certification of helicopter vertical take-off and landing operations and an application to the S-76B helicopter p 106 A92-14379
S-76B certification for vertical take-off and landing operations from confined areas p 530 A92-35760
S-76B certification for vertical take-off and landing operations from confined areas
[NLR-TP-90286-U] p 852 N92-28714
STEVENS, LISA
Scenario analysis of thigh gap related ejection injuries
p 834 A92-44995
STEVENS, S. J.
The influence of blade leaning on the performance of an integrated OGV-diffuser system
[ASME PAPER 91-GT-104] p 122 A92-15561
STEVENSON, ROBERT W.
Failure environment analysis tool (FEAT) development status
[AIAA PAPER 91-3803] p 232 A92-17654
STEVENSON, RYAN
Flow visualization and flow field measurements of a 1/12 scale tilt rotor aircraft in hover
[NASA-CR-189456] p 82 N92-11983
STEVENSON, SCOTT W.
Parameter identification of AV-8B wingborne aerodynamics for flight simulator model updates
[AIAA PAPER 92-4506] p 1027 A92-55373
STEWART, A. C.
Approach to side force alleviation through modification of the pointed forebody geometry p 309 A92-24418
STEWART, ERIC C.
A comparison of airborne wake vortex detection measurements with values predicted from potential theory
[NASA-TP-3125] p 18 N92-10994
STEWART, J. E.
Grid generation and compressible flow computations about a high-speed civil transport configuration
p 919 A92-47055
STEWART, JAMES F.
Integrated flight propulsion control research results using the NASA F-15 HIDEC Flight Research Facility
[NASA-TM-4394] p 740 N92-27379
Flight-determined benefits of integrated flight-propulsion control systems
[NASA-TM-4393] p 742 N92-27587
STEWART, JOHN E.
Surface grid generation in a parameter space
[AIAA PAPER 92-2717] p 803 A92-45556
STEWART, MARK E. M.
Euler solutions for an unbladed jet engine configuration
[AIAA PAPER 92-0544] p 398 A92-28201

Domain-decomposition algorithm applied to multielement airfoil grids p 703 A92-41261
Euler solutions for an unbladed jet engine configuration
[NASA-TM-105332] p 44 N92-11328
A two-dimensional Euler solution for an unbladed jet engine configuration
[NASA-TM-105329] p 597 N92-23560
A multiblock grid generation technique applied to a jet engine configuration p 692 N92-24428
A two-dimensional Euler solution for an unbladed jet engine configuration p 627 N92-24861
Multiblock grid generation for jet engine configurations p 659 N92-25720

STICH, HUBERT
Laser-radar based obstacle avoidance system for helicopters p 1064 A92-56295

STICKLEN, JON
Model based reasoning in the aerospace domain
[AIAA PAPER 91-3709] p 230 A92-17582

STIELER, BERNHARD
Ground and satellite supported flight trajectory measurement by example of the avionics flight test system AFES p 641 N92-25600
Board-autonomous flight trajectory measurement by example of an ILS measuring system p 641 N92-25601

STIERS, R.
Remote telemetry concepts p 882 A92-47562

STIFLE, KIRK E.
Experimental study of a vortex subjected to imposed strain
[NASA-CR-189757] p 258 N92-15969

STIGALL, PAUL D.
Distributed flight control system using fiber distributed data interface (FDDI) p 976 A92-51004

STIHARU-ALEXE, I.
On automatic control of aeroelastic vehicles p 509 A92-29327

STILES, PETER
Route planning p 1006 A92-49317

STINTON, D. P.
Fabrication and testing of corrosion resistant coatings
[DE92-003553] p 490 N92-21063

STOCK, H.
Computational aerothermodynamic methods for industrial applications to re-entry and hypersonic cruise problems p 227 N92-15027

STOCKER, HAROLD L.
Analytical design and demonstration of a low-cost expendable turbine engine combustor
[AIAA PAPER 92-3754] p 867 A92-49112

STOCKFISH, BRUCE
Opening closed skies - The prospects for further liberalization of trade in international air transport services p 697 A92-39244

STOCKMAN, N. O.
Scale model test of an isolated turbofan nacelle with riblets
[SAE PAPER 912128] p 618 A92-39975

STOFFER, JAMES O.
Fabrication and mechanical properties of an optically transparent glass fiber/polymer matrix composite p 891 A92-45630

STOKES, ALAN F.
MIDIS - A microcomputer flight decision simulator p 136 A92-13845

STOKES, W. L.
Crossing shock wave turbulent boundary layer interactions - Variable angle and shock generator length geometry effects at Mach 3
[AIAA PAPER 92-0636] p 334 A92-27014

STOLARSKI, R. S.
Natural cycles, gases p 408 N92-19123

STOLCIS, LUCA
Application of an unstructured Navier-Stokes solver to multi-element airfoils operating at transonic maneuver conditions
[AIAA PAPER 92-2638] p 796 A92-45507

STOLIAROV, E. P.
Reducing the background noise level in the test section of a wind tunnel for transonic flow velocities p 511 A92-30143

STOLLERY, J. L.
Flow over a delta wing at hypersonic speeds p 181 N92-14993
Experimental studies of vortex flaps and vortex plates. Part 1: 0.53 m span 60 deg delta wing
[CRANFIELD-AERO-9113-PT-1] p 349 N92-19679

STOLZE, DETLEF
The electronic aeronautical chart for general aeronautics: A system specification
[ILR-MITT-263(1991)] p 20 N92-10997

STONE, BONNIE K.
Space Shuttle airframe inspection trend-analysis report p 759 A92-42052

STONE, MARK H., JR.
Development of a knowledge base for use in an Expert System Advisor for Aircraft Maintenance Scheduling (ESAAMS)
[AD-A243435] p 305 N92-17687

STONE, PHILIP L.
Paint removal using cryogenic processes
[AD-A247668] p 895 N92-28912

STOOKESBERRY, D.
Prediction of inviscid supersonic/hypersonic aircraft flowfields p 810 A92-46785

STORAASLI, OLAF O.
A parallel-vector algorithm for rapid structural analysis on high-performance computers
[NASA-TM-102614] p 595 N92-22649

STORACE, A. F.
Interactive engine system dynamics analysis
[ASME PAPER 91-GT-193] p 124 A92-15619

STORACE, ALBERT F.
A gas operated bearing damper for turbomachinery
[ASME PAPER 91-GT-249] p 150 A92-15654
A simplified method for predicting the stability of aerodynamically excited turbomachinery p 224 N92-14364

STORMER, WILLIAM H.
Frequency domain flight testing and analysis of an OH-58D helicopter p 847 A92-46943

STORMVANLEEUWEN, S.
A simple and low cost system to measure delay times in pneumatic systems
[NLR-TP-90174-U] p 859 N92-28644

STORTI, M. A.
Improving the convergence rate of the Petrov-Galerkin techniques for the solution of transonic and supersonic flows p 434 A92-31495

STORTZ, MICHAEL W.
Integrated flight/propulsion control for supersonic STOVL aircraft p 872 A92-45320

STOTT, G.
Evolution of ASTOVL aircraft design p 842 A92-45311

STOTTLER, RICHARD H.
Case-based reasoning - Taming the similarity heuristic p 47 A92-11153

STOUTE, P.
Inspection of compressor discs by ultrasonic leaky waves using an automated C-scan system p 144 A92-13584
Evaluation and qualification of diffusion braze repair techniques for superalloy gas turbine components
[NRC-LTR-ST-1839] p 504 N92-22028

STOW, PETER
An unfactored implicit scheme for 3D inviscid transonic flows
[AIAA PAPER 92-2668] p 798 A92-45523

STOWE, MIKE
PDES application protocol suite for composites (PAS-C). Functional needs report for the PAS-C program
[AD-A247886] p 1108 N92-32629

STOWELL, STEVEN C.
Properties of a TZP/Al2O3 composite after long-term exposure at 1000 C
[AD-A246407] p 757 N92-27752

STRACENER, JERRELL T.
Designing to cost effectiveness - Enhancing quality p 1119 A92-56209

STRACHAN, RUSSELL L.
Testing of the high accuracy inertial navigation system in the Shuttle Avionics Integration Lab p 210 N92-14087

STRACK, WILLIAM C.
Propulsion challenges and opportunities for high-speed transport aircraft p 561 N92-22540

STRAHLE, W. C.
Turbulent diffusion flame properties behind a backward-facing step p 985 A92-50255

STRAHLE, WARREN C.
Fractal image compression of Rayleigh, Raman, LIF and LDV data in turbulent reacting flows
[AD-A246960] p 767 N92-27352

STRASH, DANIEL J.
Zonal flow analysis method for two-dimensional airfoils p 330 A92-26435

STRATTON, ANDREW
Omega/VLF now and into the 21st century p 98 A92-16659

STRATTON, D. A.
Stochastic prediction techniques for wind shear hazard assessment p 48 A92-11381
Probabilistic reasoning for intelligent wind shear avoidance p 302 A92-21181
Real-time decision aiding - Aircraft guidance for wind shear avoidance
[AIAA PAPER 92-0290] p 350 A92-25743
Stochastic prediction techniques for wind shear hazard assessment p 1007 A92-50505

STRAUB, F. K.
A general purpose nonlinear rigid body mass finite element for application to rotary wing dynamics p 846 A92-46924
Flight simulation modeling in support of engine/airframe integration p 1055 A92-56279

STRAUB, FRIEDRICH K.
Design optimization of rotor blades for improved performance and vibration p 106 A92-14389

STRAUS, J.
Boundary-layer measurements during a parallel blade-vortex interaction
[AIAA PAPER 92-2623] p 794 A92-45495

STRAUS, JOHN
Pressure and velocity measurements about an airfoil during a parallel blade-vortex interaction p 446 N92-21429

STRAUSSFOGEL, DENNIS M.
Analysis and design of planar and non-planar wings for induced drag minimization
[NASA-CR-189509] p 179 N92-13999

STRAWA, ANTHONY W.
A ballistic investigation of the aerodynamic characteristics of a blunt vehicle at hypersonic speeds in carbon dioxide and air
[AIAA PAPER 92-0328] p 322 A92-25775

STRAWN, ROGER C.
Wing tip vortex calculations with an unstructured adaptive-grid Euler solver p 64 A92-14330

STRAZZULLO, FRANCO
Transmission vibration monitoring - A single board computer architecture p 554 A92-35765

STREBINGER, R. B.
The design of a subsonic low-noise, low-turbulence wind tunnel for acoustic measurements
[AIAA PAPER 92-3883] p 1094 A92-56726

STREBY, OLIVIER
BVI impulsive noise reduction by higher harmonic pitch control - Results of a scaled model rotor experiment in the DNW p 1136 A92-56344

STREET, A. B.
VSTOL engine design evolution - Growth of the Pegasus engine for Harrier p 860 A92-45306
VSTOL engine design evolution: Growth of the Pegasus engine for Harrier
[PNR-90805] p 739 N92-27039

STREET, T.
Simultaneous imaging and interferometric turbule visualization in a high-velocity mixing/shear layer p 896 A92-45130

STREETER, C. A. C.
Boundary singularities in steady potential compressible flow through plane two-dimensional channels p 336 A92-27384

STREETT, CRAIG L.
Use of finite volume schemes for transition simulation p 432 A92-31185
Validation of three-dimensional incompressible spatial direct numerical simulation code: A comparison with linear stability and parabolic stability equation theories for boundary-layer transition on a flat plate
[NASA-TP-3205] p 943 N92-30295

STREICHER, J.
Trial of a slant visual range measuring device p 1000 N92-31043

STREIT, T.
Steps towards an efficient and accurate method solving the Euler equations around a re-entry configuration at super- and hypersonic speed p 181 N92-14987

STRELETS, M. KH.
Influence of three-dimensional effects on hydrodynamics and heat transfer in subsonic flow of a viscous compressible gas in the initial section of a rectangular duct p 66 A92-15031

STRELKOVSKAIA, I. I.
A mathematical model for the hydroelasticity problem concerning the motion of two flexible profiles in an ideal incompressible fluid. I p 712 A92-44127

STRICKLAND, J. H.
Axisymmetric bluff-body flow: A vortex solver for thin shells
[DE92-016748] p 1003 N92-31933

STRICKLAND, MICHAEL J.
Design of an integrated airframe/propulsion control system architecture
[NASA-CR-182004] p 602 N92-22643
Design of an integrated airframe/propulsion control system architecture
[NASA-CR-182007] p 602 N92-22644

STRICKLAND, PETER C.
Low cost, electronically steered phased array for general aviation p 677 N92-24099

STRIKE, W. T.
Applications of hot-film anemometers in hypersonic shear layers
[AIAA PAPER 91-5028] p 436 A92-31687

STRINGFIELD, MIKE
Determination of liquid water content in the AEDC engine test cells
[AIAA PAPER 92-0165] p 263 A92-23778
STRIZ, A. G.
Forced vibration of rectangular laminated plates with material damping p 294 A92-23167
STRIZ, ALFRED G.
Multidisciplinary optimization studies using ASTROS
p 571 N92-23234
Influence of structural and aerodynamic modeling on flutter analysis and structural optimization
[AD-A248487] p 978 N92-30323
STROCK, THOMAS W.
Hot gas ingestion characteristics and flow visualization of a vectored thrust STOVL concept
p 860 A92-45316
STROME, ROBERT W.
E-6 flutter investigation and experience
[AIAA PAPER 92-4601] p 1077 A92-55280
STRONG, A. B.
A piezoelectric droplet generator for use in wind tunnels p 291 A92-21374
Composites in manufacturing - Case studies
[ISBN 0-87263-406-X] p 784 A92-47403
Filament winding of composite isogrid fuselage structures p 784 A92-47405
STRONG, JAMES M.
Transonic wind tunnel test of a 14 percent thick oblique wing
[NASA-TM-102230] p 950 N92-32213
STRONG, STUART L.
Calculation of compressible boundary layer flow about airfoils by a finite element/finite difference method
[AIAA PAPER 92-0524] p 332 A92-26948
STROUB, ROBERT H.
Low-speed cruise aerodynamics of the stopped rotor/disk rotorcraft concept
[AIAA PAPER 92-1067] p 517 A92-33240
STROWEIS, JEAN-PIERRE
From IGES to STEP
[REPT-3.1.6] p 603 N92-23881
STRUBLE, DAVID G.
A new development in embedded computer performance measurement p 921 A92-48506
A new approach to embedded computer performance measurement p 1005 A92-49288
STRUCKMEIER, J.
Hypersonic flow calculations around a 3D delta wing at low Knudsen numbers p 937 A92-52734
Rarefied gas flow around a disc with different angles of attack p 938 A92-52753
STRYKOWSKI, P. J.
The enhancement of mixing in high-speed heated jets using a counterflowing nozzle
[AIAA PAPER 92-3262] p 825 A92-48857
STUBBS, SANDY M.
26 x 6.6 radial-belted aircraft tire performance
[SAE PAPER 912157] p 644 A92-39992
STUBERT, B.
Computation and visualization of specific flow phenomena in turbomachinery application
p 741 N92-27463
STUCHLIK, DAVID
The NASA long duration balloon project
[AIAA PAPER 91-3680] p 15 A92-11024
STUCKERT, GREG
Linear stability of supersonic cone boundary layers
p 1024 A92-54910
STUCKEY, C. I.
Heat transfer to a cylinder submerged in a rectangular cavity in supersonic flow
[AIAA PAPER 92-2949] p 901 A92-47913
STUDER, P. A.
Low power magnetic bearing design for high speed rotating machinery p 772 N92-27739
STUDNEV, A.
Stochastic self-induced roll oscillations of slender delta wing at high angles of attack
[AIAA PAPER 92-4498] p 1081 A92-55366
STUERCHLER, R.
Annular seals of high energy centrifugal pumps: Presentation of full scale measurement
p 224 N92-14362
STUERMER, G.
Life time prediction for ceramic gas turbine components
[ASME PAPER 91-GT-96] p 122 A92-15560
STULL, F. D.
Scramjet analysis, testing p 475 N92-21532
STURGEON, WAYNE R.
Development of an emergency underwater escape breathing system for CH124 seaking aircrew
[DCIEM-87-TR-11] p 92 N92-13041
STURGES, JAMES W.
Reconfigurable Mobile System - Ground, sea and air applications p 218 A92-19986
STURGESS, G. J.
Isothermal flow fields in a research combustor for lean blowout studies
[ASME PAPER 91-GT-37] p 121 A92-15520
Lean blowout in a research combustor at simulated low pressures
[ASME PAPER 91-GT-359] p 137 A92-15713
STURM, WOLFGANG
Performance improvements of compressor cascades by controlling the profile and sidewall boundary layers
[ASME PAPER 91-GT-260] p 75 A92-15662
STURSBERG, K. H.
Thrust nozzle test facility at DLR Cologne
[AIAA PAPER 91-5024] p 206 A92-17818
STURZA, MARK A.
Comparison of fixed and variable threshold RAIM algorithms p 100 A92-16951
SU, AY
An integrated airloads-inflow model for use in rotor aeroelasticity and control analysis p 64 A92-14328
Extension and validation of an unsteady wake model for rotors p 702 A92-41224
SU, JICHAO
A new method for solving the kernel equations of transonic flows - An auxiliary kernel method
p 410 A92-25108
Time marching integral equation method for the solutions of unsteady transonic flows p 314 A92-25129
Time marching integral equation method for unsteady transonic flows around airfoils p 433 A92-31489
SU, JIEXIAN
Application of compound leaned blades to controlling secondary flow p 5 A92-10975
SU, T. Y.
A geometry-integrated approach to multiblock grid generation p 919 A92-47083
An interactive multi-block grid generation system
p 691 N92-24419
SU, YAO-XI
Flow analysis and design of three-dimensional wind tunnel contractions p 5 A92-11067
SU, YAOXI
Flow analysis of rectangular wind tunnel contraction
p 312 A92-25001
SUAREZ, CARLOS J.
Forebody vortex control with miniature, rotatable nose-boom strakes
[AIAA PAPER 92-0022] p 281 A92-22144
Forebody vortex control for suppressing wing rock on a highly-swept wing configuration
[AIAA PAPER 92-2716] p 803 A92-45555
SUBRAHMANYAM, M. B.
Robust optimal control with a worst case time domain performance criterion p 509 A92-29368
SUBRAMANIAN, C. S.
Surface heat transfer and flow properties of vortex arrays induced artificially and from centrifugal instabilities
p 1121 A92-56371
SUBRAMANIAN, S.
The design of a subsonic low-noise, low-turbulence wind tunnel for acoustic measurements
[AIAA PAPER 92-3883] p 1094 A92-56726
SUDAKOV, G. G.
Asymptotic solution of the problem of ideal-fluid flow past the vertices of bodies and wings
p 427 A92-30199
SUDANI, N.
Recent airfoil tests in NAL 2D high Reynolds number wind tunnel p 748 A92-43171
SUDANI, NORIKAZU
Evaluation of sidewall interference in the NAL two-dimensional transonic wind tunnel
p 1092 A92-56011
BGK1 airfoil oilflow tests in the NAL two-dimensional wind tunnel. II p 1029 A92-56044
Evaluation of NACA0012 airfoil test results in the NAL two-dimensional transonic wind tunnel
[NAL-TR-1109T] p 445 N92-21287
NACA0012 airfoil data corrected for sidewall boundary-layer effects in the NAL two-dimensional transonic wind tunnel
[NAL-TM-640T] p 722 N92-28151
Force measurements on AGARD calibration model-B at transonic speeds in the NAL two-dimensional wind tunnel
[NAL-TM-639] p 722 N92-28190
SUDAREV, A. V.
Gas-generator with high-temperature path ceramic components
[ASME PAPER 91-GT-152] p 148 A92-15594
Development and bench test of high-temperature combustion chamber with structural ceramic components
[ASME PAPER 91-GT-315] p 126 A92-15691
SUDER, KENNETH L.
Design and performance of controlled-diffusion stator compared with original double-circular-arc stator
[NASA-TP-2852] p 562 N92-22863
SUDHAKAR, K.
Aircraft longitudinal dynamics equations including wind shear effects p 977 A92-51946
SUDIK, STEVEN J.
High performance flight simulation at NASA Langley
[AIAA PAPER 92-4179] p 982 A92-52460
SUDO, NAOKI
An autorotation-entry control for a helicopter with a fuzzy controller p 1083 A92-56032
SUE, MILES K.
ACTS aeronautical experiments
[AIAA PAPER 92-2042] p 485 A92-29956
SUENAGA, HISASHI
Study of the NAL's 0.1 x 0.1 m magnetic suspension and balance system
[NAL-TM-623] p 665 N92-25365
Replacement of the NAL high pressure air storage system
[NAL-TM-634] p 888 N92-28835
SUGAHARA, N.
Conceptual study of separated core ultra high bypass engine
[AIAA PAPER 92-3775] p 867 A92-49119
SUGANAMI, TAKUYA
Reduction of torque pulsation of Stirling engine-compressor system p 992 A92-50785
SUGANO, M.
Navigation preparations for passenger helicopters
p 723 A92-43155
SUGIMOTO, HIROSHI
Optimization of blade structure to reduce rotor vibration p 730 A92-43118
SUGIMOTO, HIROYUKI
Sensitivity analysis for structural optimization of helicopter rotor blades p 1053 A92-56073
SUGIMOTO, TAKESHI
Analysis of circular elastic membrane wings
p 245 A92-21722
Wing design for hanggliders having minimum induced drag p 811 A92-46814
SUGIYAMA, NANAHISA
Derivation of ABCD system matrices from nonlinear dynamic simulation of jet engines
[AIAA PAPER 92-3319] p 923 A92-48903
Design and off-design point characteristics of Separated Core Ultra High Bypass Engine (SCUBE)
[AIAA PAPER 92-3776] p 867 A92-49120
SUGIYAMA, YOSHIYUKI
Aerodynamic characteristics of a wing near its tip using panel method p 251 A92-22524
Aerodynamic characteristics near the tip of a finite wing by a panel method
[SAE PAPER 912020] p 790 A92-45413
A calculation of penetration of the jet issuing normally into a cross flow across a wall boundary layer
[SAE PAPER 912029] p 790 A92-45419
SUH, JUNG-CHUN
Some exact and numerical results for plane steady sheared flow of an incompressible inviscid fluid
p 821 A92-48019
SUI, HAI
A real-time rain-flow method of cycle counting and its program design for aeroengine service loads
p 557 A92-35560
SUI, YONGKONG
Strategies for optimal design of gas turbine disks
p 371 A92-24741
SUK, GO H.
The design of broadband radar absorbing surfaces
[AD-A240521] p 42 N92-11235
SUKHANOVA, A. K.
System of cryogenic security of the superconducting accelerator of relativistic nuclei-nuclotron
[DE91-643289] p 304 N92-16789
SUKOV, A. I.
Decoupling of antennas using periodic structures
p 725 A92-42634
SULLIVAN, B. M.
Application of magnitude estimation scaling to the assessment of subjective loudness response to simulated sonic booms
[NASA-TM-107657] p 1138 N92-33719
SULLIVAN, BARRY T.
Man-Vehicle Systems Research Facility - Design and operating characteristics
[AIAA PAPER 92-4177] p 982 A92-52458

SULLIVAN, BRENDA M.
Loudness of shaped sonic booms
p 695 A92-39238
A new simulator for assessing subjective effects of sonic booms
[NASA-TM-104150] p 56 N92-11759
A loudness calculation procedure applied to shaped sonic booms
[NASA-TP-3134] p 56 N92-11765
Subjective loudness response to simulated sonic booms p 1140 N92-33885
SULLIVAN, C. J.
The design of a subsonic low-noise, low-turbulence wind tunnel for acoustic measurements
[AIAA PAPER 92-3683] p 1094 A92-56726
SULLIVAN, J.
Hot gas environment around STOVL aircraft in ground proximity. I - Experimental study p 371 A92-24409
SULLIVAN, J. P.
Unsteady wing surface pressures in the wake of a propeller
[AIAA PAPER 92-0277] p 318 A92-25731
Thermal paints for shock/boundary layer interaction in inlet flows
[AIAA PAPER 92-3626] p 1113 A92-54093
SULLIVAN, JOHN M., JR.
Numerical comparison of experimentally measured ultrasound through a multilayered specimen
p 510 A92-28682
SULLIVAN, JOHN P.
Lift development of delta wings undergoing constant acceleration from rest p 9 A92-13209
Aerodynamics laboratory education at Purdue University - Ground testing facilities
[AIAA PAPER 92-4018] p 1100 A92-56840
SULLIVAN, P.
Compressibility effects in turbulent far wakes
p 622 A92-40140
SULLIVAN, P. A.
Computational fluid dynamics p 177 N92-13979
SULLIVAN, ROBERT
Aerodynamic roughness measured in the field and simulated in a wind tunnel
[NASA-CR-4422] p 347 N92-19354
SULLIVAN, WILLIAM
Conducting the NASP ground test program
[AIAA PAPER 91-5029] p 209 A92-17820
SUMI, SEINOSUKE
Analyses of heat isolation property for metallic multiwall thermal protection system p 40 A92-12422
SUMMA, J. M.
Zonal flow analysis method for two-dimensional airfoils p 330 A92-26435
SUMMERFIELD, P. H.
36th Roy Chadwick Lecture - Manufacturing breakout 1941-1991: Development in aerospace industry manufacturing techniques p 419 A92-28941
SUMMERS, L. G.
Evaluation of microwave landing system approaches in a wide-body transport simulator
[NASA-CR-4450] p 957 N92-30978
SUMWALT, ROBERT L., III
Eliminating pilot-caused altitude deviations - A human factors approach p 834 A92-45041
SUN, CHUNLIN
Integral minimization of engine fault equations based on least fault principle p 374 A92-27857
SUN, HUIXIAN
An investigation on flame stability by fuel permeability in a flame holder made of porous ceramic material
p 375 A92-28435
SUN, JIAN-GUO
A study of surge control using fuel pulse cutoff for dual spool turbo-jet engine p 470 A92-29737
SUN, JINCAI
Improvement in transmission loss of aircraft double wall with resonators p 1011 A92-53091
SUN, S.-H.
The initial development of an expert system for designing composite material wing structures p 599 A92-32542
SUN, SHULING
Calculation of fuel sloshing and its coupling vibration with a tank p 991 A92-50204
SUN, WEIMIN
Advanced electromagnetic methods for aerospace vehicles
[NASA-CR-190650] p 1001 N92-31156
SUN, XIAOFENG
An aeroacoustic model about the rotating stall of a compressor p 416 A92-27855
SUN, ZHONGKANG
Location and tracking technique in a multistatic system established by multiple bistatic systems
p 840 A92-48480
SUNADA, S.
The fluid-dynamic measurement of the fling motion of a three-dimensional flat plate p 710 A92-43194
SUNAKAWA, MEGUMI
Current status of R&D on materials for super/hypersonic transports p 1106 A92-56002
SUNDARAM, P.
A Navier-Stokes solution of Hull-ring wing-thruster interaction p 221 N92-14310
SUNDER, R.
Contribution of individual load cycles to crack growth under aircraft spectrum loading p 891 A92-45236
SUNG, CHAO-HO
Computation of saddle point of attachment
p 703 A92-41276
SUNILKUMAR, C.
Graphics for interactive PC based parameter estimation package
[NAL-PD-FC-9117] p 412 N92-18252
SUORSA, R.
Passive range estimation for rotorcraft low-altitude flight
[NASA-TM-103897] p 2 N92-10003
SUORSA, RAY
Vision-based obstacle detection for rotorcraft flight
p 967 A92-52465
SURESH, AMBADY
Numerical experiments on a new class of nonoscillatory schemes
[AIAA PAPER 92-0421] p 341 A92-28193
SURESH, B. N.
Basic design concepts for smart actuators for aerospace plane control p 752 A92-41193
SURESH, RAMASUBRAMANIAN
AGSSS: The Airborne Graphics Software Support System; an Ada/PHIGS-based display editor for the rapid development of cockpit display software systems
[AD-A243224] p 277 N92-17221
SURIN, V. P.
Optimization of the aerodynamic balance and parameters of the horizontal tail surfaces of the three-surface aircraft configuration with allowance for the capabilities of the stability and control augmentation system p 134 A92-16803
SUROVTSEVA, N. I.
Evaluation of the fungicide properties of antifreeze additives for jet fuels p 141 A92-15070
SURYAVAMSHI, N.
Numerical prediction of wakes in cascades and compressor rotors including the effects of mixing. I - Cascade wakes including the effects of incidence and freestream turbulence
[ASME PAPER 91-GT-225] p 74 A92-15638
Numerical prediction of wakes in cascades and compressor rotors including the effects of mixing. II - Rotor passage flow and wakes including the effects of spanwise mixing
[ASME PAPER 91-GT-222] p 74 A92-15639
SUSKI, HARALD
Application of MSC/DYNA to shock and impact problems in aircraft industry
[MBB-UD-0593-91-PUB] p 225 N92-14382
SUTCLIFFE, P. L.
Systems engineering as applied to the Boeing 777
[AIAA PAPER 92-1010] p 515 A92-33198
SUTHERLAND, H. J.
The status of the US VAWT program
[DE92-002931] p 505 N92-21040
Fatigue life variability and reliability analysis of a wind turbine blade
[DE92-008673] p 689 N92-25049
SUTHERLAND, LOUIS C.
Evaluation of human response to structural vibrations induced by sonic booms
[NASA-CR-189584] p 697 N92-26130
Evaluation of outdoor-to-indoor response to minimized sonic booms
[NASA-CR-189643] p 927 N92-28556
SUTLIFF, J. A.
Cold-crucible directional solidification of refractory metal-silicide eutectics p 755 A92-43684
SUTTAN, J.
Shock detection on airfoils by means of piezo foil- and hot film arrays p 1115 A92-54334
SUTTER, JAMES K.
Addition curing thermosets endcapped with 4-amino (2.2) paracyclophane p 577 A92-33918
SUYA, S.
The Bauer-Garabedian-Korn airfoil test in a two-dimensional wind tunnel p 429 A92-30532
SUZUKI, H.
Low speed aerodynamic performance of a capsule-shaped flying object p 430 A92-30559
SUZUKI, K.
Jet engine test system including expert system for diagnosis
[ASME PAPER 91-GT-408] p 137 A92-15737
SUZUKI, KOICHI
Results of measured temperature distribution on an adiabatic wing model with radiation thermometer
[NAL-TM-610] p 261 N92-17755
Development of wall pressure measuring apparatus for an existing transonic wind tunnel test section
[NAL-TM-565] p 573 N92-23778
SUZUKI, MASAAKI
A320 flight control from the pilot's point of view
p 1083 A92-56028
SUZUKI, MASAMITU
Replacement of the NAL high pressure air storage system
[NAL-TM-634] p 888 N92-28835
SUZUKI, MASAYUKI
Ducted fan VTOL for working platform
[SAE PAPER 911995] p 843 A92-45397
A design of strongly stabilizing controller
[SAE PAPER 912081] p 917 A92-45456
SUZUKI, NORIO
Hypersonic testing technology of HOPE (H-II orbiting plane) p 747 A92-43096
Aerodynamic study of H-II Orbiting Plane, HOPE
p 1103 A92-53639
SUZUKI, S.
ACT wind tunnel experiment on gust load alleviation. II - Wind tunnel test with active support facility
p 745 A92-43135
Transonic wind tunnel tests of flutter suppression equipment (Wing response data processing)
p 748 A92-43136
Flight simulation of a spaceplane p 752 A92-43190
Aerodynamic model identification of a spaceplane model from a cable-mount dynamic wind-tunnel test
p 1093 A92-56114
SUZUKI, SEIZO
Wind tunnel tests on the motion of a spaceplane simulation for cable mount p 752 A92-43192
Motion estimation for cable-mount dynamic wind-tunnel test p 749 A92-43210
Estimation of spaceplane longitudinal stability and control derivatives from dynamic wind tunnel test
p 752 A92-43211
Estimation of spaceplane lateral-directional stability and control derivatives from dynamic wind tunnel test
[SAE PAPER 911979] p 872 A92-45384
On improvements of three-dimensional position measuring system for dynamic wind tunnel testing
p 1093 A92-56012
On the effect of canards on NAL spaceplane model (0 order) in low speed area p 1030 A92-56052
SUZUKI, SEIZOU
A gust generation method for full configuration aircraft tests in a low speed wind tunnel. Part 1: Design and preliminary experiments
[NAL-TR-1115-PT-1] p 722 N92-28192
SUZUKI, SHINJI
Step response of unsteady aerodynamics acting on a plane swept wing in incompressible flow for finite state modeling p 63 A92-14031
Structure/control design synthesis of active flutter suppression system by goal programming
p 204 A92-18621
Step response of incompressible unsteady aerodynamic modeling p 744 A92-43131
Research on state equations of unsteady aerodynamics p 709 A92-43132
Optimum structural design of a cantilevered rectangular elastic wing with a gust load alleviation system
p 762 A92-43133
Optimization of aeroelastic system with active control
p 1083 A92-56022
Lateral control of spaceplane at hypersonic flight
p 1104 A92-56069
SUZUKI, TAKAKO
CFD application to 2D/3D flow fields in Scramjet engine p 170 A92-17501
SVANE, CHRISTIAN
DANSIM - Danish Airport Noise Simulation Model - Basic principles, experience, and improvements
p 687 A92-39055
DANSIM applications - Development of airport noise reduction strategies and environmental policy
p 687 A92-39057
SVIATODUKH, V. K.
Characteristics of the phugoid motion of nonmaneuverable aircraft p 480 A92-30190
SVIRCHEVSKII, S. B.
Aerodynamic characteristics of a standard corrugated body in a free-molecular flow p 940 A92-52818

SVISHCHEV, G. P.
Control of the development of boundary layer disturbances p 423 A92-30126
SVOBODNY, T. P.
Optimal boundary control of nonsteady incompressible flow with an application to viscous drag reduction p 39 A92-11344
SWAB, JEFFREY J.
Properties of a TZP/Al2O3 composite after long-term exposure at 1000 C
[AD-A246407] p 757 N92-27752
SWADZBA, L.
Corrosion damage and regeneration of aluminide coatings on aircraft turbine blades p 142 A92-15244
SWAFFORD, TIMOTHY W.
Euler flow predictions for an oscillating cascade using a high resolution wave-split scheme
[ASME PAPER 91-GT-198] p 74 A92-15623
Analysis of cascades using a two dimensional Euler aeroelastic solver
[AIAA PAPER 92-2370] p 556 A92-34598
SWAIN, M. H.
Fatigue crack initiation and small crack growth in several airframe alloys p 212 A92-19754
SWALE, R.
Cost effective solutions for titanium sheet metal forming p 293 A92-22785
SWALE, W.
Cost effective solutions for titanium sheet metal forming p 293 A92-22785
SWALES, MICHAEL R.
Helicopter NVG testing in the United Kingdom p 112 A92-16053
SWAMINATHAN, V.
On the application of parabolized Navier-Stokes equations to flow field simulations p 936 A92-51943
SWANBOROUGH, GORDON
Dornier 328 - A Daimler for commuters p 458 A92-30091
SWANSON, DOUGLAS A.
Improved noise rejection in automatic carrier landing systems p 380 A92-28154
SWANSON, R. C.
On central-difference and upwind schemes p 1007 A92-50466
Inverse airfoil design procedure using a multigrid Navier-Stokes method p 193 N92-13932
Progress with multigrid schemes for hypersonic flow problems
[NASA-CR-189579] p 185 N92-15047
SWANSON, STEPHEN M.
Low-speed cruise aerodynamics of the stopped rotor/disk rotorcraft concept
[AIAA PAPER 92-1067] p 517 A92-33240
SWANSSON, N. S.
Research into improving the durability of the hot section in the aircraft turbine engine
[AD-A250342] p 973 N92-31439
SWART, PAUL W.
RTOK elimination with TSMM p 902 A92-48446
SWEETING, T. J.
A method for the construction of safe S-N curves p 586 A92-34759
SWEETMAN, BILL
Infra-red offers new landing aid competition p 198 A92-18937
The stealth master p 307 A92-25175
Why composites wait in the wings p 577 A92-35475
SWENSEN, KEITH A.
Further studies in filmwise condensation of steam on horizontal finned tubes
[AD-A252705] p 1011 N92-31767
SWENSON, HARRY N.
Computer aiding for low-altitude helicopter flight p 94 A92-14444
Status of automatic guidance systems for rotorcraft in low altitude flight p 727 N92-27894
SWIDER, ANDRZEJ
Experimental determination of the center of mass, the principal central axes of inertia and moments of inertia p 40 A92-12346
SWIFT, GERALD A.
Model identification and control system design for the lambda unmanned research vehicle
[AD-A241859] p 299 N92-17024
SWIFT, JOE B.
Malfunction/discrepancy reporting p 60 A92-14438
SWIFT, R. A.
Damage tolerant structural design using neural networks
[AIAA PAPER 92-1097] p 581 A92-33261
SWINFORD, SCOTT
A new system for recording unstable aerodynamic phenomena in NAVSWC Hypervelocity Wind Tunnel No. 9 p 1091 A92-54325
SWINK, JAY R.
Identification of high-level functional/system requirements for future civil transports
[NASA-CR-189561] p 276 N92-15991
High speed research system study. Advanced flight deck configuration effects
[NASA-CR-189650] p 967 N92-30965
SWINSICK, SCOTT R.
Rotorcraft Maneuverability and Agility Survivability Sensitivity Analysis (RMASSA) p 161 A92-14351
SWIRSKI, KONRAD
Concept of a one-dimensional model of the dynamic behavior of a gas turbine p 862 A92-47791
SWOBODA, M.
Shock detection on airfoils by means of piezo foil- and hot film arrays p 1115 A92-54334
SWOPE, G. H.
Axial alignment of short-fiber titanium aluminide composites by directional solidification p 892 A92-46838
SYCHEV, VIK. V.
Breakdown of an axisymmetric laminar wake p 424 A92-30145
SYDOR, JOHN T.
Design considerations for general aviation mobile satellite terminals p 594 N92-22572
SYED, S. A.
Application of computational fluid dynamics to pitch/yaw thrust vectoring spherical convergent flap nozzles p 737 A92-44511
SYKES, J. E. H.
The effects of manufacturing tolerances on the vibration of aero-engine rotor-damper assemblies p 222 N92-14349
SYMS, RAYMOND A.
Operational survey: VFR heliport approaches and departures
[SCT-91RR-26] p 190 N92-14033
SYRYCZYNSKI, JACEK
A new method of helicopter rotor blade motion control p 875 A92-47786
SYSKOV, L. V.
A method for determining the parameters of mathematical generalizations of experimental data on convective heat transfer p 41 A92-12803
SYTSMA, H. A.
Numerical investigation into high-angle-of-attack leading-edge vortex flow
[AIAA PAPER 92-2600] p 791 A92-45477
SZALAI, KENNETH J.
Validation of flight critical control systems
[AGARD-AR-274] p 382 N92-20026
SZE, K. Y.
Automated composite ellipsoid modelling for high frequency GTD analysis
[NASA-CR-189853] p 275 N92-17316
SZE, NIEN-DAK
Impact of heterogeneous chemistry on model-calculated ozone change due to high speed civil transport aircraft p 45 A92-12941
SZEMA, K. Y.
Multizonal Navier-Stokes solutions for the multibody Space Shuttle configuration p 310 A92-24667
SZEMA, K.-Y.
Application of a universe-series code for inviscid flow over complex 3-dimensional configurations
[AIAA PAPER 92-0150] p 253 A92-23765
SZEMA, KUO-YEN
A user guide for the EMTAC-MZ CFD code
[NASA-CR-4283] p 678 N92-24242
SZMELTER, J.
Mesh adaptivity with the quadtree method p 816 A92-47041
SZUMANSKI, KAZIMIERZ
Transgressions in a pilot-helicopter system p 358 A92-27394

T

TA'ASAN, SHLOMO
Aerodynamic design and optimization in one shot
[AIAA PAPER 92-0025] p 248 A92-22147
TABAKOFF, W.
High temperature erosion resistance of coatings for gas turbine
[ASME PAPER 91-GT-213] p 143 A92-15632
Laser measurements of unsteady flow field in a radial turbine guide vanes
[AIAA PAPER 92-0394] p 395 A92-26249
Inviscid and viscous quasi-three-dimensional flow solutions in a transonic turbine cascade p 523 A92-36035
Coating effect on particle trajectories and turbine blade erosion p 653 A92-36892
TABAKOFF, WIDEN
LDV measurements and investigation of flow field through radial turbine guide vanes p 217 A92-19618
TABUYO, IGNACIO G.
Iberia's Aeronautical Mapping Application (ACAI) p 637 A92-37073
TACHIBANA, MASAKAZU
Navier-Stokes simulation for the winged space vehicle 'HOPE' at subsonic, transonic, and supersonic regimes p 1018 A92-53559
TADA, AKIRA
Functional mock-up tests for flight control system of the NAL QSTOL research aircraft 'ASKA'
[SAE PAPER 912036] p 881 A92-45422
Flight evaluation of navigation systems including MLS using NAL Do228 - Outline p 1047 A92-56116
TADGHIGHI, H.
Development of a shock noise prediction code for high-speed helicopters - The subsonically moving shock p 165 A92-14384
Effects of leading and trailing edge flaps on the aerodynamics of airfoil/vortex interactions p 815 A92-46957
Blade-mounted trailing edge flap control for BVI noise reduction
[NASA-CR-4426] p 512 N92-21173
TAFLIN, DAVE
BUWICE - An interactive icing program applied to engine inlets
[AIAA PAPER 92-3179] p 922 A92-48794
TAFTI, D. K.
Hot gas environment around STOVL aircraft in ground proximity. II - Numerical study p 371 A92-24403
TAGAO, KICHIRO
Study on an induction method for a flying object, taking accelerating targets into account p 744 A92-43127
TAGG, BRUCE A.
Design-for-reliability through durability analysis p 760 A92-42086
TAGHAVI, R.
Screech noise source structure of a supersonic rectangular jet
[AIAA PAPER 92-0503] p 331 A92-26932
Modern developments in shear flow control with swirl p 703 A92-41265
A computational study of advanced exhaust system transition ducts with experimental validation
[AIAA PAPER 92-3794] p 907 A92-49126
TAGIROV, R. K.
Calculation of the base pressure and enthalpy behind a step in the path of two supersonic streams with allowance for the effect of boundary layers and heat fluxes p 63 A92-13748
Calculation of the parameters of separated flow behind a plane rounded body in the path of two supersonic flows p 244 A92-21624
TAGLIALAVORE, A. P.
Ceramic component processing development for advanced gas-turbine engines
[ASME PAPER 91-GT-120] p 142 A92-15567
TAHOURI, B.
Flow regimes of the cove regions between a slat and wing and between a wing and flap of a multielement airfoil p 614 A92-38858
TAI, FANG-MEI
Numerical simulation of twin-jet impingement on a flat plate coupled with cross-flow p 315 A92-25374
TAI, TSZE C.
Flow separation patterns over an F-14A aircraft wing p 174 A92-20205
Direct simulation of low-density flow over airfoils p 1030 A92-56159
TAIRA, SHINICHI
Experiments on aeronautical satellite communications using ETS-V p 395 A92-26779
High gain airborne antenna for satellite communications p 354 A92-26780
Experiments on aeronautical satellite communications using ETS-V satellite p 639 A92-40187
High gain airborne antenna for satellite communications p 639 A92-40188
Beam scanning error of phased array antenna p 676 A92-40189
TAJIMA, HIROHISA
Flight evaluation of navigation systems including MLS using NAL Do228 - Results of MLS p 1047 A92-56117
TAKAGAWA, KINGO
Investigation on freezing and sticking phenomena of slush on airplane surfaces when taxiing on the ground and the succeeding take-off run phase
[NAL-TR-1026] p 352 N92-18182
TAKAGI, AKITO
Analysis and wind tunnel test of low aspect wing gust load alleviation p 1053 A92-56020

TAKAGI, SHOHEI
Proceedings of the Seminar on Investigation and Control of Boundary-Layer Transition
[NAL-SP-11] p 400 N92-18483
The fibre optic three dimensional laser two focus velocimeter for the low-speed windtunnel. Part 1: Two-dimensional measurement evaluations
[NAL-TM-627] p 665 N92-25402
TAKAGI, TAKEO
A study on the rotating stall of centrifugal compressors. II - Effect of vaneless diffuser inlet shape on rotating stall p 497 A92-32508
TAKAHAMA, MORLO
Flight control system design using H(infinity) optimal control p 1083 A92-56030
TAKAHASHI, HIDEAKI
Aerodynamic performances of spoiler motion p 429 A92-30526
TAKAHASHI, HITOSHI
Wind tunnel investigation of an improved upper surface blown flap transport semi-span model
[SAE PAPER 911993] p 789 A92-45395
Aerodynamic development of boundary layer control system for NAL QSTOL research aircraft 'ASKA'
[SAE PAPER 912010] p 843 A92-45410
TAKAHASHI, KOJI
Analytical study on plate edge noise. I - Trailing edge noise caused by vorticity waves p 511 A92-32502
TAKAHASHI, M. D.
Helicopter air resonance modeling and suppression using active control p 204 A92-18625
TAKAHASHI, MASAHIRO
Numerical study on the secondary jet into a supersonic flow p 1018 A92-53556
TAKAHASHI, R. K.
NACA 0015 wing pressure and trailing vortex measurements
[NASA-TP-3151] p 13 N92-10981
TAKAHATA, RYOICHI
Characterization of superconducting magnetic bearings (dynamic stiffness and damping coefficient in axial direction) p 772 N92-27737
TAKAHIRA, KEN-ICHI
Wind tunnel test of M = 2.5 mixed compression inlet p 1028 A92-56008
TAKAI, M.
Outline and discussion of the cooling loop of the heating control system in the exposed facility of the Japanese Experiment Module (JEM) p 574 A92-35610
TAKAKI, R.
Aerodynamic design of an advanced turboprop using Euler codes p 737 A92-43196
TAKAKI, RYOJI
Predicted pressure distribution on a prop-fan blade through Euler analysis p 810 A92-46791
TAKAKURA, HAKO
Numerical computation of compressible flow around an object of complex shape p 429 A92-30517
TAKALLU, M. A.
Aerodynamic characteristics of a propeller powered high lift semispan wing
[AIAA PAPER 92-0388] p 323 A92-26244
Effect of solidity and inclination on propeller-nacelle force coefficients
[NASA-TM-4316] p 90 N92-13038
TAKAMORI, SUSUMU
Air ejector experiments using the two-dimensional supersonic cascade tunnel: Zero secondary flow performance
[NAL-TM-632] p 887 N92-28829
TAKANASHI, S.
Non-planar wing design by Navier-Stokes inverse computation
[AIAA PAPER 92-0285] p 319 A92-25738
TAKANASHI, SUSUMU
Computational aerodynamic simulation on HOPE p 251 A92-22635
HOPE looks to CFD for help p 386 A92-24910
Aerodynamic design of a nonplanar airfoil by an inverse method with Navier-Stokes equations p 711 A92-43197
Navier-Stokes simulation for the winged space vehicle 'HOPE' at subsonic, transonic, and supersonic regimes p 1018 A92-53559
Aerodynamic aircraft design methods and their notable applications: Survey of the activity in Japan p 193 N92-13930
Evaluation of NACA0012 airfoil test results in the NAL two-dimensional transonic wind tunnel
[NAL-TR-1109T] p 445 N92-21287
TAKANO, MASANORI
Numerical simulations of shock reflections by a TVD scheme p 1018 A92-53558
TAKAO, K.
Selection of sampling rate for nonlinear flight trajectory controller of aircraft p 1084 A92-56070
TAKASAKI, NOBUYUKI
The progress of a STOL project p 699 A92-43137
TAKASAWA, KINGO
Design - Analysis and experimental verification of a propeller working in the low Reynolds number range p 710 A92-43174
Feasibility study on a microwave-powered unmanned aerial vehicle for the communication relay utilization
[SAE PAPER 912052] p 843 A92-45436
Structural concept of main wings of high altitude unmanned aerial vehicle and basic properties of thermoplastic composites as candidate material
[SAE PAPER 912053] p 843 A92-45437
TAKASHIMA, NARUHISA
Navier-Stokes computations of a viscous optimized waverider
[AIAA PAPER 92-0305] p 435 A92-31653
Navier-Stokes computations of a viscous optimized waverider
[NASA-CR-189658] p 944 N92-30392
TAKATA, H.
Study on transonic cascade performance by use of newly built facility p 136 A92-15328
TAKATA, HIROYUKI
Current topics connected with rotating stall p 521 A92-35913
TAKAYAMA, S.
Study on small stalker tube performance and numerical calculation p 748 A92-43099
TAKEDA, HIROMICHI
Automatic function testing in the aircraft production p 1015 A92-56083
TAKEDA, NOBUO
Impact response of composite UHB propeller blades
[SAE PAPER 912046] p 861 A92-45430
TAKEI, YOICHI
Aerodynamic drag as determined from flight test data of the STOL research aircraft Asuka p 709 A92-43145
TAKEISHI, KENICHIRO
Film cooling on a gas turbine rotor blade
[ASME PAPER 91-GT-279] p 152 A92-15675
TAKEUCHI, YASURO
Functional mock-up tests for flight control system of the NAL QSTOL research aircraft 'ASKA'
[SAE PAPER 912036] p 881 A92-45422
TAKI, MASATO
Sensitivity analysis for structural optimization of helicopter rotor blades p 1053 A92-56073
TAKIGUCHI, KOICHI
Bias of an optical passive ring-resonator gyro caused by the misalignment of the polarization axis in the polarization-maintaining fiber resonator p 652 A92-40262
TAKIZAWA, M.
Aerodynamic model identification of a spaceplane model from a cable-mount dynamic wind-tunnel test p 1093 A92-56114
TAKIZAWA, MINORU
Motion estimation for cable-mount dynamic wind-tunnel test p 749 A92-43210
Estimation of spaceplane longitudinal stability and control derivatives from dynamic wind tunnel test p 752 A92-43211
Spaceplane longitudinal aerodynamic parameter estimation by cable-mount dynamic wind-tunnel test
[SAE PAPER 911980] p 788 A92-45385
On improvements of three-dimensional position measuring system for dynamic wind tunnel testing p 1093 A92-56012
Evaluation of a IMU with optical fiber gyros in dynamic windtunnel tests p 1104 A92-56121
Development of digital/optical rotary position transducer
[NAL-TR-1106] p 29 N92-10028
TAKIZAWA, NAOTO
Low-speed wind tunnel testing of the lateral control force for the upper rudder surface of a joined-wing airfoil p 711 A92-43228
Low-speed wind tunnel testing of a joined-wing airfoil p 711 A92-43229
Effectiveness of aircraft aerodynamic performance on each part of a joined wing p 712 A92-43230
A low speed wind tunnel investigation of a joined-wing aircraft with an overhanging fin p 1030 A92-56078
A low speed wind tunnel investigation of the direct side force control of a joined-wing aircraft with overhanging fin p 1084 A92-56079
TAKSAWA, KINGO
On the possibility of freezing and sticking phenomena in a transport during the ground taxiing and takeoff run and on the preventions of the hazard
[SAE PAPER 912042] p 836 A92-45426
TALAT, KAUSAR
Smart skins and fiber-optic sensors application and issues p 368 A92-24785
TALBOT, N.
Helicopter fog flying trials p 530 A92-35759
TALBOT, PETER D.
High speed rotorcraft - Comparison of leading concepts and technology needs p 108 A92-14415
TALMADGE, RICHARD D.
A state-of-the-art data acquisition system p 217 A92-19231
TALPALLIKAR, M. V.
CFD analysis of jet mixing in low NO(x) flametube combustors
[ASME PAPER 91-GT-217] p 124 A92-15634
TALUY, ATILLA M.
The background and the development of the TAL-WAR (Rose) shape blimp with the articulated thruster
[AIAA PAPER 91-3692] p 17 A92-12749
TALYZIN, V. A.
Problem of the optimal correction of a flight test program for an aircraft system p 113 A92-16809
TAM, C. K.
Acoustic interactions between an altitude test facility and jet engine plumes: Theory and experiments
[NASA-CR-190423] p 738 N92-26405
TAM, C. K. W.
Broadband shock-associated noise from supersonic jets in flight p 235 A92-18683
TAM, CHRISTOPHER K. W.
Broadband shock associated noise from supersonic jets measured by a ground observer
[AIAA PAPER 92-0502] p 416 A92-26931
Relationship between the instability waves and noise of high-speed jets p 924 A92-45835
Broadband shock associated noise from supersonic jets measured by a ground observer p 1135 A92-54909
Jet noise generated by large-scale coherent motion p 55 N92-10604
TAM, L. T.
LU-SGS implicit scheme for entry vehicle flow computation and comparison with aerodynamic data
[AIAA PAPER 92-2671] p 798 A92-45526
Aerodynamic heating on AFE due to nonequilibrium flow with variable entropy at boundary layer edge p 183 N92-15020
TAM, TIM C.
Flow characterization in the NASA Ames 16-inch Shock Tunnel
[AIAA PAPER 92-3810] p 1090 A92-54180
TAMAGNO, J.
Hypersonic mixing and combustion studies in the hypulse facility p 737 A92-44526
Effects of oxygen dissociation on hypervelocity combustion experiments
[AIAA PAPER 92-3964] p 1098 A92-56791
TAMAKI, TEIICHI
Three-dimensional flow visualization of shock wave using double-pulsed holographic interferometry. II - Flow visualization for three-dimensional shock structures in rotating aeroengine fan blade rows p 497 A92-32507
Conceptual design of scramjet engine p 1065 A92-53490
TAMANGO, JOSE
Experiments on shear layer mixing at hypervelocity conditions
[AIAA PAPER 92-0628] p 396 A92-27009
TAMARU, TAKASHI
Combustion research and design technology of aircraft engines p 558 A92-35915
Hydrogen fueled subsonic-ram-combustor model tests for an air-turbo-ram engine
[NAL-TR-1064T] p 280 N92-17855
TAMASHIRO, R. N.
A low-power, high-efficiency Ka-band TWTA p 671 A92-38163
TAMIGNIAUX, T. L. B.
Recent CFD applications on jet transport configurations
[AIAA PAPER 92-2658] p 844 A92-45519
TAMPLIN, G. C.
A USAF assessment of STOVL fighter options p 842 A92-45310
TAMURA, ATSUHIRO
Numerical simulations of the flow through cascades with tip clearance p 523 A92-36038
TAMURA, HIROBUMI
Fabrication test and evaluation of graphite/PMR-15 polyimide for HOPE primary structure p 1105 A92-53516
TAMURA, T.
Measurements of turbulence in hypersonic flow p 1092 A92-56005
TAMURA, YOSHIAKI
Recent applications of the FNS zonal Method to complex flow problems
[SAE PAPER 912003] p 789 A92-45404

TAN, C. S.
Computational and experimental studies of flow in multi-lobed forced mixers
[AIAA PAPER 92-3568] p 1112 A92-54057
TAN, CARINA M.
First level release of 2GCHAS for comprehensive helicopter analysis p 1133 A92-56339
TAN, KOK T.
Linear systems with output constraints - The theory and application of maximal output admissible sets
p 506 A92-29066
TAN, S. C.
Application of a water droplet trajectory prediction code to the design of inlet particle separator anti-icing systems
[PNR-90839] p 474 N92-20573
TAN, T. H.
An explosively driven, fast shock tube
[DE92-008437] p 749 N92-26720
TANABE, W.
Stringer subsystem automation p 700 A92-43246
TANABE, YOSHIKAZU
Discussion for possibility of some aerodynamic ground effect craft
[NAL-TM-619] p 300 N92-17757
TANAHASHI, YOSHIHARU
A thin metal model for aerodynamic heating tests of shock wave interaction p 709 A92-43103
Aerothermodynamic test of spaceplane by thin-skin method p 1093 A92-56043
TANAKA, A.
Supersonic wind tunnel test of airintake/airframe integrated models p 1028 A92-56006
A conceptual study for future engine test facility
[AIAA PAPER 92-3992] p 1099 A92-56815
TANAKA, ATSUSHIGE
Numerical simulation for various flowfields of aero-engine components p 200 A92-17503
Experimental study of the aerodynamic characteristics at Mach 3 of an air-intake model p 711 A92-43204
Mach 3 wind tunnel test of mixed compression supersonic inlet
[AIAA PAPER 92-3625] p 1021 A92-54092
TANAKA, H.
New-type of ultralight flexible a-Si solar cell and its application on an airplane p 970 A92-53181
TANAKA, HIDEO
Trends of research on cascade flutter
p 558 A92-35914
TANAKA, HIROYUKI
Analysis and wind tunnel test of low aspect wing gust load alleviation p 1053 A92-56020
TANAKA, JUNICHI
DSMC simulation of hypersonic flows past 2-dimensional bodies p 939 A92-52772
TANAKA, K.
A study of the pilot's associate system
p 745 A92-43218
TANAKA, KEIJI
A simulator study of a flight reference display for powered-lift STOL aircraft
[SAE PAPER 912067] p 855 A92-45449
Flight test of a flight reference display for powered-lift STOL aircraft p 1064 A92-56059
Flight simulator test of cockpit advisory system
p 1054 A92-56115
TANAKA, KOTARO
Observational study of pool boiling under microgravity
p 757 A92-41060
TANAKA, KOUHEI
A shock tunnel experiment on aerodynamic interference induced by RCS jet p 1029 A92-56042
TANAKA, MASATO
High gain airborne antenna for satellite communications p 354 A92-26780
High gain airborne antenna for satellite communications p 639 A92-40188
TANAKA, NAOYUKI
Weathering test of AFRP composites for the application of helicopter fuselage p 142 A92-15309
TANAKA, SHUJI
Computation of the potential flow through cascades using the conformal mapping and the singularity method
p 66 A92-15356
TANAKA, TOSHIYUKI
A robust gain scheduler interpolated into multiple models by membership functions
[AIAA PAPER 92-4553] p 1131 A92-55265
TANAKA, YASUHIKO
Experimental investigation of the boundary layer in a corner formed by two circular arc airfoils
p 1029 A92-56046
TANAKA, YASUO
Helicopters for public services, including rescue, fire fighting, and medical emergency p 723 A92-43163
TANAKA, YASUYUKI
Nonlinear transient analysis of composite ATP blade model p 294 A92-23111
Numerical simulation of impact resistance on composite blade p 738 A92-44734
TANASE, SHOJI
Piloted simulation for the BK117 FBW demonstrator
p 1053 A92-56077
TANATSUGU, NOBUHIRO
Test results of the expander cycle air turbo ramjet for a future space plane
[IAF PAPER 91-271] p 120 A92-14709
Development study on air turbo-ramjet engine for space plane p 1065 A92-53487
Tests results on Air Turbo Ramjet for a future space plane
[IAF PAPER 92-0657] p 1071 A92-57098
TAND, DIYI
A dynamic digital model for the turbojet with pulse-monitored fueller p 654 A92-38267
TANDON, G. P.
Microbiological spoilage of aviation turbine fuel. II - Evaluation of a suitable biocide p 891 A92-45600
TANEDA, H.
Flutter analysis and wind tunnel test with respect to a low-aspect-ratio wing with free-rotational control surface
p 1052 A92-56014
TANG, D. M.
Comparison of theory and experiment for nonlinear flutter and stall response of a helicopter blade
p 65 A92-14428
Experimental and theoretical study for nonlinear aeroelastic behavior of a flexible rotor blade
[AIAA PAPER 92-2253] p 584 A92-34410
Chaotic stall response of helicopter rotor in forward flight p 730 A92-43046
Chaotic oscillation in helicopter blade stall response
p 846 A92-46922
Flutter and stall response of a helicopter blade with structural nonlinearity p 1055 A92-56178
TANG, DENG-BIN
The calculation of three-dimensional compressible boundary layer stability on swept wings
p 818 A92-47684
TANG, DIYI
The engineering prediction for aircraft noise
p 1010 A92-50206
TANG, F. C.
Buffet load measurements on an F/A-18 vertical fin at high-angle-of-attack
[AIAA PAPER 92-2127] p 520 A92-35694
Unsteady pressure and load measurements on an F/A-18 vertical fin at high-angle-of-attack
[AIAA PAPER 92-2675] p 798 A92-45529
Some characteristics and effects of the F/A-18 LEX vortices p 88 N92-13025
Experimental investigation of heavy rainfall effect on a 2-D high lift airfoil p 452 N92-21696
Flowfield in the vicinity of the F/A-18 vertical fin at high-angle-of-attack p 628 N92-24865
TANG, G. C.
Heat induced transient behaviours of axial compressors p 469 A92-29721
TANG, MING
An investigation on flame stability by fuel permeability in a flame holder made of porous ceramic material
p 375 A92-28435
On performance calculation of centrifugal dish atomizer combustor p 654 A92-37390
TANG, MINZHONG
The LDV measurement of three-component velocity of complex vortex flow in the wind tunnel
p 393 A92-25109
TANG, SHOU
Stability and dynamic coupling of elastic vehicles with unsteady aerodynamic forces considered
p 1102 A92-53545
TANG, T. S.
Control design via TAM and H-infinity approaches - A flexible beam case study p 51 A92-11445
TANG, XIAODONG
Damage tolerance and durability design of composite aircraft structures p 996 A92-53067
TANGLER, J.
SERI advanced wind turbine blades
[DE92-001216] p 598 N92-22971
Measured and predicted rotor performance for the SERI advanced wind turbine blades
[DE92-001215] p 598 N92-23119
TANI, ICHIRO
Proceedings of the Seminar on Investigation and Control of Boundary-Layer Transition
[NAL-SP-11] p 400 N92-18483
TANI, KOICHIRO
Experimental validation of scramjet nozzle performance
[AIAA PAPER 92-3290] p 864 A92-48879
TANI, KOUICHIRO
Effectiveness of plasma torches for ignition and flameholding in scramjet p 737 A92-44524
Flow measurements in scramjet inlets
p 1102 A92-53565
TANIKAWA, EIJI
Present status of Al-Li alloys p 1106 A92-56105
TANIKAWA, K.
Utilizing the fault monitoring system for the A320 aircraft p 700 A92-43157
TANIMOTO, MITSUMORI
Experimental study of convection effects around the phase charge interface p 1111 A92-53755
TANIOKA, TADAYUKI
Engineering and technology Japanese aircraft/spacecraft p 699 A92-41781
TANIS, FRED J.
Concept design phase expendable holographic sensor to measure ocean small angle optical scattering
[AD-A245067] p 501 N92-20997
TANKINS, E. S.
In-service evaluation of 2090 aluminum-lithium alloy on F/A-18 aircraft
[AD-A248472] p 986 N92-30321
TANNEHILL, J. C.
New nonequilibrium turbulence model for calculating flows over airfoils p 330 A92-26403
Development of a 3-D upwind PNS code for chemically reacting hypersonic flowfields
[NASA-CR-190182] p 946 N92-30977
TANNENBAUM, ALLEN
Abstract model and controller design for an unstable aircraft p 380 A92-28153
TANNER, J. C.
Flight test of a half-scale unmanned air vehicle
p 193 A92-20208
TANNER, JAMES C.
Research flight test of a scaled unmanned air vehicle
p 549 A92-35944
TANNER, JOHN A.
Reduced basis technique for evaluating the sensitivity coefficients of the nonlinear tire response
[AIAA PAPER 92-2530] p 583 A92-34376
Sensitivity of tire response to variations in material and geometric parameters p 900 A92-47128
TANNER, M.
Base pressure measurements on a cone at Mach numbers from M sub infinity = 5 to 7
p 173 A92-18770
Base pressure measurements on a cone at hypersonic Mach numbers: A contribution to aerothermodynamics for space vehicles p 181 N92-14992
TANNER, MAURI
Base pressure in supersonic flow - Further thoughts about a theory p 331 A92-26442
TAO, DE-PING
Concerning a basic assumption for aeroelasticity in turbomachinery p 373 A92-26920
TAO, ZENGYUAN
Statistical analysis and prediction of aeroengine deterioration p 557 A92-35570
TAO, ZHENQU
A new approach to determining control surface's moments of inertia with test-twice vibrations approach
p 379 A92-27914
TAPOSU, I.
A theory for mechanical flight control linkages
p 269 A92-21312
TARANNIKOVA, T. N.
Viscosity characteristics of synthetic aviation oils at low temperatures p 1105 A92-53875
TARDITI, S.
Vortical flow simulation by using structured and unstructured grids p 83 N92-12999
TARKENTON, G. M.
Critical Mach number estimates for dense gases
p 933 A92-49498
Transonic flows of Bethe-Zel'dovich-Thompson fluids
p 935 A92-50293
TARKENTON, L. M.
Critical Mach number estimates for dense gases
p 933 A92-49498
TARLAKOVSKII, DMITRII V.
Nonstationary aerohydroelasticity of spherical bodies
[ISBN 5-02-014006-6] p 670 A92-36611
TARN, JIANN-QUO
Flutter analysis of anisotropic panels with patched cracks p 219 A92-20216
TARTARIN, J.
Active control of pulsed flow for low frequency noises attenuation p 694 A92-39109

TARTER, JAMES F.
Quantification of aircraft carbon brake wear using regression analysis and periodic wave forms
[SAE PAPER 912174] p 644 A92-39999
TARTTELIN, P. C.
Rotor aeromechanics research with the RAE research Lynx - The experimental facility and test programme
p 547 A92-35767
TARZANIN, FRANK J., JR.
Structural optimization and Mach scale test validation of a low vibration rotor p 107 A92-14395
TASKER, FREDERICK
Nonlinear damping estimation from rotor stability data using time and frequency domain techniques
p 641 A92-36855
TASLIM, M. E.
Experimental investigation of film cooling effectiveness for slots of various exit geometries p 497 A92-32265
TATAM, R. P.
Fibre optic laser anemometry for turbomachinery applications p 397 A92-27783
TATE, TOKUSHI
Safety test on the rolling angles of a winged vehicle in hypersonic speed p 480 A92-30549
TATGE, R. B.
Gas turbine exhaust system silencing design
p 882 A92-47365
TATTERSALL, P.
Prediction and measurement of jet flowfield features for ASTOVL aircraft p 787 A92-45318
TAUBER, M. E.
Earth atmospheric entry studies for manned Mars missions p 442 A92-32251
TAUKE, G. J.
Flight management system integration on the F-117A
[AIAA PAPER 92-1077] p 563 A92-33246
Pilot activated automatic recovery system on the F-117A
[AIAA PAPER 92-1126] p 563 A92-33278
Flight management system of the F-117A
p 1082 A92-55910
TAURA, S.
Optimization of composite material wing of fighter type aircrafts p 1053 A92-56018
TAVELLA, D. A.
High alpha aerodynamic control by tangential fuselage blowing p 611 A92-36848
TAVERNETTI, LEONARD R.
The C-17 - Modern airlift technology
[AIAA PAPER 92-1262] p 538 A92-33342
TAYLOR, A. C., III
Observations on computational methodologies for use in large-scale, gradient-based, multidisciplinary design incorporating advanced CFD codes
[NASA-TM-104206] p 630 N92-24956
TAYLOR, ARTHUR C., III
Taylor series approximation of geometric shape variation for the Euler equations p 899 A92-46916
Methodology for calculating aerodynamic sensitivity derivatives p 1024 A92-54911
Methodology for sensitivity analysis, approximate analysis, and design optimization in CFD for multidisciplinary applications
[NASA-CR-190201] p 595 N92-22662
An incremental strategy for calculating consistent discrete CFD sensitivity derivatives
[NASA-TM-104207] p 625 N92-24681
TAYLOR, D. J.
CARS temperature measurements in a hypersonic propulsion test facility p 140 N92-12049
TAYLOR, DANIEL E.
Allocation and recovery of federal airport and airway costs, 1991
[AD-A249436] p 983 N92-30777
TAYLOR, ED
The use of high voltage direct current in aircraft electrical systems - A Navy perspective
[SAE PAPER 912173] p 655 A92-39998
TAYLOR, JAMES C.
Organizational context for aircraft maintenance and inspection p 2 A92-11181
TAYLOR, JEFF C.
Monte Carlo simulation of reentry flows with ionization
[AIAA PAPER 92-0493] p 328 A92-26323
TAYLOR, JOHN A.
Flying qualities testing on the modern technology airship p 570 A92-35933
TAYLOR, KEVIN J.
Characterization of diffusion bonds using an acoustic microscope p 491 A92-28686
TAYLOR, P.
Frequency domain testing of helicopter dynamics using automated input signals p 545 A92-35731
TAYLOR, R. M.
Coherence multiplexed polarimetric fibre sensor arrays for aerospace applications p 370 A92-27785
TAYLOR, ROBERT P.
Using uncertainty analysis in the debugging and qualification of a turbulent heat transfer test facility
p 138 A92-17224
TAYLOR, ROGER
The mechanical properties of metal-void composites
[AD-A246087] p 757 N92-27749
TAYLOR, TERRY
A flight test study to determine aircraft propulsive efficiency and aerodynamic drag using two parameter identification methods and Lock's propeller model
[AIAA PAPER 92-0170] p 271 A92-23781
TAYLOR, TERRY L.
Development of a multi-computer in-flight data acquisition and analysis system for general aviation aircraft
[AIAA PAPER 92-1037] p 553 A92-33218
TAYLOR, V.
Implanted component faults and their effects on gas turbine engine performance
[ASME PAPER 91-GT-41] p 121 A92-15524
TCHENG, PING
Model attitude measurements at NASA Langley Research Center
[AIAA PAPER 92-0763] p 398 A92-28226
TCHON, KO-FOA
Navier-Stokes simulation of dynamic stall on a rotating airfoil p 626 N92-24853
TEAGER, STEPHEN A.
Flight test investigation of the wake vortices generated by helicopters p 270 A92-21925
TEAL, R. S.
A novel avionic sensor for fly-by-light controls
p 650 A92-38128
TEAS, DON C.
Reference mode effect on the auditory display of aircraft bank angle
[AD-A247825] p 728 N92-27916
TEASLEY, STEWART P.
The evolution of military GPS technology into the Navcore V receiver engine p 651 A92-39570
TECZA, J.
A chambered porous damper for rotor vibration control. I - Concept development
[ASME PAPER 91-GT-244] p 150 A92-15649
TEETS, EDWARD H.
Atmospheric analysis for airdata calibration on research aircraft
[AIAA PAPER 92-0293] p 369 A92-25746
TEGTMEIER, A.
FALKE and COBRA technology development in aerodynamics and aerothermodynamics
p 183 N92-15017
TELFER, ROSS
A training program for airline line instructors
p 835 A92-45044
TELIONIS, D. P.
The dynamic character of the wake of an axisymmetric body at an angle of attack
[AIAA PAPER 91-3268] p 8 A92-12741
Pitch-up motions of delta wings
[AIAA PAPER 92-0278] p 318 A92-25732
TELIONIS, DEMETRI P.
Fundamental research in helicopter rotor blade-vortex interaction modeling p 65 A92-14358
TEMPELMAN, W. G.
Performance benefits of adaptive in-flight propulsion system optimization
[AIAA PAPER 92-3749] p 1068 A92-54149
TEMPO, R.
On the Nyquist envelope of an interval plant family
p 507 A92-29132
TENAUD, C.
Hypersonic wakes
[ETN-92-91082] p 349 N92-19925
TENHAVE, J. M.
NARSIM: A real-time simulator for air traffic control research
[NLR-TP-90147-U] p 888 N92-29204
European studies to investigate the feasibility of using 1000 ft vertical separation minima above FL 290. Part 1: Overview of organisation, techniques employed, and conclusions
[NLR-TP-91062-U-PT-1] p 841 N92-29605
TENIAEVA, V. E.
Lifting surface design using the principle of passive control of elastic characteristics p 480 A92-31865
TENNING, CARL
Electric power generating system for the Boeing 777 airplane
[SAE PAPER 912050] p 861 A92-45434
Design of the Boeing 777 electric system
p 1070 A92-55902
TENSI, J.
Instantaneous visualization of surface flows
p 763 A92-44327
TENTI, L.
Measurement of acoustic properties of the composite materials constituting the main rotor hub of the Agusta-Westland helicopter EH-101 (civil version)
p 1010 A92-49475
TENTO, SCOTT W.
The implicit function theorem and robust root locus
p 507 A92-29134
TEODORESCU, B.
Control surfaces correlation in DLC maneuvers
p 280 A92-21301
Control surfaces correlation in DSFC maneuvers
p 281 A92-21307
TEPERIN, L. L.
Aerodynamic wing-nacelle integration
p 458 A92-30134
A pressure-drag-determination method for aerodynamic-interference problems p 425 A92-30157
TER-GRIGORIAN, V. IU.
Investigation of the aerodynamic features of flows past models using thin-film capacitance-type sensors of pressure oscillations p 440 A92-31884
TERADA, HIROYUKI
Some consideration for evaluation of structural integrity of aging aircraft p 762 A92-43107
TEREKHOV, N. S.
From the history of Soviet aviation - Aircraft of the Il'iushin design bureau (2nd revised and enlarged edition)
p 61 A92-15022
TERENT'EV, E. D.
Wave motions in a three-dimensional boundary layer
p 244 A92-21629
TERENTIEV, ALEXANDER N.
Levitation of YBa2Cu3O(7-x) superconductor in a variable magnetic field p 771 N92-27735
TERESHKIN, A. A.
An experimental study of organismic principles of the functioning of the crew-transport aircraft system
p 1133 A92-57446
TERESHKIN, G. A.
Using the simulation modeling method to estimate the reliability of the crew-flight vehicle system
p 1133 A92-57444
TERLIZZI, A.
Numerical computations of transonic flows through cascades
[AIAA PAPER 92-3041] p 822 A92-48702
TERSTEEGEN, J.
Development of flight testing of a fault tolerant fly-by-light yaw control system p 662 N92-25599
TERUI, SUKEYUKI
Flight test results and upper surface blowing (USB) technology of the STOL research aircraft Asuka
p 730 A92-43142
TERUI, YUSHI
A simulator study of a flight reference display for powered-lift STOL aircraft
[SAE PAPER 912067] p 855 A92-45449
Flight test of a flight reference display for powered-lift STOL aircraft p 1064 A92-56059
Flight evaluation of navigation systems including MLS using NAL Do228 - Outline p 1047 A92-56116
TESARIK, D. R.
Two-dimensional heat transfer from a rectangular fin with asymmetrical thermal boundary conditions
p 498 A92-32524
TESHIMA, KOJI
Experimental and numerical investigation of a supersonic free jet impinging on a perpendicular surface
p 1018 A92-53555
TETZLAFF, JUERGEN
Arrangements and methods for the survey of aircraft radio components and systems p 652 N92-25603
TEWARI, K. C.
Microbiological spoilage of aviation turbine fuel. II - Evaluation of a suitable biocide p 891 A92-45600
TEZDUYAR, T. E.
Unsteady incompressible flow computations with quadrilateral elements p 394 A92-26219
THACKER, CHRISTOPHER
State-of-the-art airborne video recording
p 555 A92-35932
THACKRAY, RICHARD I.
Human factors evaluation of the work environment of operators engaged in the inspection and repair of aging aircraft
[AD-A246445] p 724 N92-27914
THAKKER, A. B.
Surfprep flash-lamp depaint system evaluation
p 497 A92-32411
THAKUR, SIDDHARTH S.
Evaluation of a Navier-Stokes prediction of a jet in a crossflow p 441 A92-32235
THANGAM, S.
Computational study of stall flutter in linear cascades
[ASME PAPER 91-GT-5] p 67 A92-15503

Application of a new K-tau model to near wall turbulent flows p 395 A92-26437
THAYER, E.
Comparative investigation of multiplane thrust vectoring nozzles
[AIAA PAPER 92-3263] p 864 A92-48858
THAYER, J. S.
On the accuracy of an aircraft-borne ambient electric-field measuring system p 186 A92-20127
THEOFILIS, VASSILIOS
A numerical study of the stability of the swept attachment line boundary layer
[AERO-REPT-9103] p 345 N92-18293
THERIAULT, Y.
A probabilistic procedure for aircraft fleet management p 360 N92-18576
THERY, CHRISTIAN
The sonic boom and problems related to supersonic flights of military aircraft
[ONERA, TP NO. 1991-162] p 77 A92-16129
THIBERT, J. J.
The A320 laminar fin programme
[ONERA, TP NO. 1992-23] p 849 A92-48586
Drag prediction using computation methods
[ONERA-RSF-82/1685-AY-154-4] p 349 N92-19682
THIBODEAU, FRANCOIS A.
Helicopter/ship analytic dynamic interface p 464 N92-21962
THIBODEAUX, J. J.
Control of large cryogenic tunnels
[AIAA PAPER 92-3930] p 1096 A92-56761
THIEL, U.
Towards coherent hypermedia navigation by pragmatic dialogue modeling
[PB92-114735] p 455 N92-20818
THIELE, THOMAS
Lightning protection for the Dornier 328 p 113 A92-17253
THIELEKE, G.
Experimental investigations of exciting forces caused by flow in labyrinth seals p 223 N92-14354
THIVET, F.
A unified nonequilibrium model for hypersonic flows p 3 A92-10575
Hypersonic viscous shock layer in thermochemical nonequilibrium p 183 N92-15014
THOM, JAMES
An artificial intelligence approach for the verification of requirements for aircraft electrical power systems p 863 A92-48481
THOMADAKIS, M. P.
Transonic unsteady inviscid and viscous flow's simulation around 2-D moving bodies
[AIAA PAPER 92-2704] p 801 A92-45546
Improved artificial dissipation schemes for the Euler equations p 933 A92-49508
THOMAS, A. M.
Investigation of advancing front method for generating unstructured grid
[NASA-CR-190902] p 1128 N92-34043
THOMAS, CLAUDINE
The need for GPS standardization p 1049 N92-33351
Precise GPS ephemerides from DMA and NGS tested by time transfer p 1049 N92-33355
Comparison of GLONASS and GPS time transfers between two west European time laboratories and VNIIFTRI p 1050 N92-33381
THOMAS, D. R.
Active control of sound transmission through stiff lightweight composite fuselage constructions p 1137 N92-32957
THOMAS, DAVID C.
A fiber optic temperature sensor for aerospace applications p 761 A92-42607
THOMAS, GAIL F.
Profile of an effective engineering manager
[AD-A246525] p 781 N92-27528
THOMAS, GEOFF
New Airbus Industrie airliners on course for long-haul era p 308 A92-26792
THOMAS, HALL
Map projections and airborne moving map displays p 966 A92-49327
THOMAS, J.
Vibration characteristics of pretwisted aerofoil cross-section blade packets under rotating conditions p 219 A92-20756
THOMAS, J. L.
Navier-Stokes computations for aerodynamic configurations at high angles of attack p 246 A92-21981
THOMAS, JAMES L.
Computational study of incipient leading-edge separation on a supersonic delta wing p 442 A92-32237
THOMAS, JOHN P., JR.
NASP - A status report
[AIAA PAPER 92-1417] p 666 A92-38569
THOMAS, KENNETH W.
Profile of an effective engineering manager
[AD-A246525] p 781 N92-27528
THOMAS, M.
Design and testing leading to certification of the Airbus A340 nose landing gear doors p 272 A92-24192
THOMAS, R. H.
Mixing studies of helium in air at high supersonic speeds p 935 A92-50310
THOMAS, SCOTT
Computational analysis of ramjet engine inlet interaction
[AIAA PAPER 92-3102] p 824 A92-48744
THOMPSON, D.
Application of an automated multidisciplinary analysis and optimisation system to the design of aircraft structures p 551 N92-23233
THOMPSON, D. H.
Scale model measurements of fin buffet due to vortex bursting on F/A-18 p 365 N92-18788
Visualisation in water of vortex flow over sharp-edged canard configurations
[ARL-FLIGHT-MECH-R-189] p 632 N92-25410
THOMPSON, DANIEL B.
Implementation of non-dedicated redundancy in a fault tolerant multiprocessor testbed p 974 A92-49294
THOMPSON, DANNIELLA M.
Global/local methods research using the CSM testbed p 1107 N92-32528
THOMPSON, DAVID F.
Frequency response specifications and sensitivity functions in quantitative feedback theory p 508 A92-29280
THOMPSON, DONALD O.
NDE research efforts at the FAA Center for Aviation Systems Reliability p 914 N92-30119
THOMPSON, HAYDN ASHLEY
Parallel processing applications for gas turbine engine control p 25 N92-11012
THOMPSON, J. F.
Numerical grid generation in computational fluid dynamics and related fields; Proceedings of the 3rd International Conference, Universidad Politecnica de Cataluna, Barcelona, Spain, June 3-7, 1991
[ISBN 0-444-88948-5] p 918 A92-47035
THOMPSON, J. J.
In-service evaluation of 2090 aluminum-lithium alloy on F/A-18 aircraft
[AD-A248472] p 986 N92-30321
THOMPSON, JACK
Guidelines for integrating helicopter assets into emergency planning
[SCT-91RR-18] p 18 N92-10993
THOMPSON, JOE F.
Three-dimensional solution-adaptive grid generation on composite configurations p 172 A92-18352
THOMPSON, JON E.
Thermal/structural analysis of a transpiration cooled nozzle
[NASA-TM-104184] p 401 N92-18877
THOMPSON, M. C.
Acoustic sources in a tripped flow past a resonator tube p 778 A92-41266
THOMPSON, M. W.
Tangential mass addition for shock/boundary-layer interaction control in scramjet inlets p 80 A92-17197
THOMPSON, PETER M.
H(infinity) robust control synthesis for a fighter performing a coordinated bank turn p 29 A92-11585
THOMPSON, R. B.
A technique for quantitatively measuring microstructurally induced ultrasonic noise p 510 A92-28720
THOMPSON, RANDOLPH C.
Thermal-structural panel buckling tests p 993 A92-51409
THOMPSON, RICHARD A.
Application of the LAURA code for slender-vehicle aerothermodynamics p 310 A92-24652
THOMPSON, SCOTT A.
Wind tunnel blockage effects on slender wings undergoing large amplitude motions
[AIAA PAPER 92-3926] p 1096 A92-56757
Aerodynamic and flowfield hysteresis of slender wing aircraft undergoing large-amplitude motions p 364 N92-18780
THOMSON, BRUCE
Ceramic matrix composites and its application in gas turbine engines
[ASME PAPER 91-GT-338] p 143 A92-15702
THOMSON, D. G.
The use of inverse simulation for conceptual design p 546 A92-35738
THOMSON, DANIEL E.
Military engine computational structures technology p 660 N92-25934
THOMSON, MICHAEL
Experience with Ada on the F-18 High Alpha Research Vehicle Flight Test Program
[NASA-TM-104259] p 1062 N92-34039
THOMSON, T. N.
Measurement of LORAN-C envelope to cycle difference in the far field
[PB92-128909] p 455 N92-21263
THORESON, SHARILYN A.
The Software Factory, version 5.0
[AIAA PAPER 92-0590] p 411 A92-26992
THORNTON, DOUGLAS HERSHAL, JR.
The FM-007: An advanced jet commuter for HUB to spoke transportation
[NASA-CR-189988] p 461 N92-20267
THORNTON, EARL A.
Thermoviscoplastic response of thin plates subjected to intense local heating
[AIAA PAPER 92-2538] p 584 A92-34382
Thermal structures and materials for high-speed flight; Collection of Papers of the 1st Thermal Structures Conference, University of Virginia, Charlottesville, Nov. 13-15, 1990
[ISBN 1-56347-017-9] p 590 A92-35847
Thermal structures - Four decades of progress p 729 A92-41239
Light thermal structures and materials for high speed flight p 649 N92-25922
THORP, SCOTT A.
Integrating aerodynamic surface modeling for computational fluid dynamics with computer aided structural analysis, design, and manufacturing p 682 N92-25727
THORPE, ALAN J.
Mesoscale dynamics of cold fronts - Structures described by dropsoundings in Fronts 87 p 230 A92-18902
THORSSELL, STEVEN E.
An alternative method for acquiring avionic bus data in a class I PCM telemetry system p 217 A92-19202
THOUVENOT, JEAN-LUC
Optimization of a light helicopter with Arrius power plants p 120 A92-14408
THRESHER, R. W.
An overview: Challenges in wind technology development
[DE92-001190] p 302 N92-17875
THROCKMORTON, DAVID A.
Shuttle Infrared Leeside Temperature Sensing (SILTS) experiment - STS-35 and STS-40 preliminary results
[AIAA PAPER 92-0126] p 286 A92-23746
THUKRAL, A.
Dynamics and control of maneuverable towed flight vehicles p 976 A92-50508
THUKRAL, AJAY
Roll-performance criteria for high augmented aircraft p 204 A92-18623
Roll metrics for handling qualities - The landing approach p 976 A92-50520
THYR, U.
Comparison of two-way satellite time transfer and GPS common-view time transfer between OCA and TUG p 1050 N92-33356
THYSON, N. A.
Multiple aperture window and seeker concepts for endo KEW applications
[AIAA PAPER 92-2806] p 752 A92-41344
TIAN, JIFENG
Fracture analysis on compressor blades p 37 A92-10672
TIBBALS, TOM
Determination of liquid water content in the AEDC engine test cells
[AIAA PAPER 92-0165] p 263 A92-23778
TICE, DAVID C.
A study of altitude-constrained supersonic cruise transport concepts
[AIAA PAPER 92-1027] p 536 A92-33208
TICHTINSKY, HELENE
Three-dimensional calculations of reactive flows in aircraft combustion chambers performed using two combustion models
[ONERA, TP NO. 1991-110] p 154 A92-16089
Three dimensional calculations of reactive flows within aircraft combustion chambers including some combustion models p 770 N92-27490
TIEN, JOHN K.
Inclusion size effect on the fatigue crack propagation mechanism and fracture mechanics of a superalloy p 388 A92-24831

TIKHONOV, N. T.
Effect of the blade height of the nozzle ring of axial-flow microturbines on the flow velocity factor and exit angle
p 128 A92-16831
TILL, ROBERT
Automatic Dependent Surveillance (ADS) Pacific Engineering Trials (PET)
[AIAA PAPER 92-1812] p 453 A92-29760
TILLEMA, H. F.
Application of analysis techniques for low frequency interior noise and vibration of commercial aircraft
[NASA-CR-189555] p 481 N92-20376
TILLERY, KEVIN
The NASA long duration balloon project
[AIAA PAPER 91-3680] p 15 A92-11024
TILLMAN, KENNETH D.
Integrated flight/propulsion control for flight critical applications - A propulsion system perspective
[ASME PAPER 91-GT-284] p 125 A92-15679
TILLMAN, T. G.
Enhanced mixing of supersonic jets
p 80 A92-17195
Supersonic nozzle mixer ejector p 376 A92-28536
Computational and experimental studies of flow in multi-lobed forced mixers
[AIAA PAPER 92-3568] p 1112 A92-54057
TILSTRA, SHELLE D.
A fiber optic temperature sensor for aerospace applications p 761 A92-42607
TIMERBULATOV, A. M.
Effect of the fuselage midsection ratio on the character of wing-fuselage aerodynamic interference
p 439 A92-31883
TIMONIN, V. A.
Experimental study of an adjustable plane supersonic diffusor p 426 A92-30173
TIMOSHENKO, V. I.
A parametric study of the lift-drag ratio of blunt cones
p 437 A92-31860
Quick calculation of three-dimensional supersonic flow past nearly axisymmetric bodies p 624 A92-40605
TIMOSHIN, S. N.
Asymptotic form of the lower branch of the neutral curve in a transonic boundary layer p 427 A92-30204
TIMOTEO, DOMINIC
Visual approach data collection at San Francisco International Airport (SFO)
[DOT/FAA/CT-90/23] p 354 N92-18112
TINCHER, D. J.
A hypersonic waverider test vehicle - The logical next step
[AIAA PAPER 92-0308] p 387 A92-25756
TINDAL, M. J.
Measurements and simulation of the flow around a poppet valve p 675 A92-40103
TING, P. C.
Aeroassist flight experiment heating-rate sensitivity study p 3 A92-10427
Aerodynamic heating on AFE due to nonequilibrium flow with variable entropy at boundary layer edge
p 183 N92-15020
TING, Z.
A simulator and performance criteria for evaluation of ground and space-based ATC surveillance
p 96 A92-16639
TINOCO, E. N.
Recent CFD applications on jet transport configurations
[AIAA PAPER 92-2658] p 844 A92-45519
TIPPEY, D. K.
AV-8B V/STOL performance analysis
p 549 A92-35948
TIPTON, M. T.
The 3D inelastic analysis methods for hot section components
[NASA-CR-189089] p 402 N92-18971
Component-specific modeling
[NASA-CR-189088] p 377 N92-19726
TIRKAS, PANAYIOTIS A.
Advanced electromagnetic methods for aerospace vehicles
[NASA-CR-190650] p 1001 N92-31156
TIRRE, WILLIAM C.
Development of the Basic Flight Instruction Tutoring System (BFITS)
[AD-A246458] p 751 N92-27836
TIRRES, LIZET
A comparison of the calculated and experimental off-design performance of a radial flow turbine
[AIAA PAPER 92-3069] p 1020 A92-54004
Description of a pressure measurement technique for obtaining surface static pressures of a radial turbine
[AIAA PAPER 92-4006] p 1123 A92-56829
Description of a pressure measurement technique for obtaining surface static pressures of a radial turbine
[NASA-TM-105643] p 680 N92-24959
A comparison of the calculated and experimental off-design performance of a radial flow turbine
[NASA-CR-189207] p 831 N92-29402
TISCHLER, MARK B.
Forward flight trim calculation and frequency response validation of a high-order helicopter simulation model
p 132 A92-14337
System identification requirements for high-bandwidth rotorcraft flight control system design
p 479 A92-29332
High-order state space simulation models of helicopter flight mechanics p 569 A92-35777
Identification techniques: Frequency domain methods
p 273 N92-17158
System identification methods for handling-qualities evaluation p 274 N92-17165
System identification requirements for high-bandwidth rotorcraft flight control system design
p 282 N92-17166
Modeling methods for high-fidelity rotorcraft flight mechanics simulation
[NASA-TM-103842] p 482 N92-21440
TISHCHENKO, A. A.
Pulsation characteristics of one-phase and two-phase steam flows in Laval nozzles under off-design conditions
p 1019 A92-53882
TISHKOFF, J. M.
Contractors Meeting in Propulsion
[AD-A240057] p 33 N92-10062
TISSEN, A.
Towards coherent hypermedia navigation by pragmatic dialogue modeling
[PB92-114735] p 455 N92-20818
TITTMANN, B. R.
Laser-based ultrasonics on GR/epoxy composite - Interferometric detection p 144 A92-13554
TIVENDALE, CHARLES
The 1988 Australian Winter Storms Experiment - Case study: 6 August 1988 p 301 A92-23009
TIWARI, S. N.
Thermochemical nonequilibrium and radiative interactions in supersonic hydrogen-air combustion
[AIAA PAPER 92-0340] p 394 A92-25786
Effects of nose bluntness and angle of attack on slender bodies in hypersonic flows
[AIAA PAPER 92-0638] p 334 A92-27016
Combined effect of nose bluntness and angle of attack on slender bodies in viscous hypersonic flows
[AIAA PAPER 92-0755] p 436 A92-31680
An analytical approach to grid sensitivity analysis for NACA four-digit wing sections
[NASA-CR-190251] p 631 N92-25175
Investigation of advancing front method for generating unstructured grid
[NASA-CR-190902] p 1128 N92-34043
TIWARI, SURENDRA N.
An analytical approach to grid sensitivity analysis
[AIAA PAPER 92-0660] p 334 A92-27031
TKACHENKO, V. M.
Power spectrum of ring modes of pressure fluctuations at the surface of a cylinder in axial flow
p 603 A92-33770
TOBAK, MURRAY
Surface flow patterns on an ogive-cylinder at incidence p 176 A92-20762
Effect of upstream disturbance on flow asymmetry
[AIAA PAPER 92-0408] p 325 A92-26261
TOBIN, K. W., JR.
Fiber-sensor design for turbine engines
[DE92-003539] p 376 N92-18230
TOBINAGA, YOSHINARI
Flight test results and upper surface blowing (USB) technology of the STOL research aircraft Asuka
p 730 A92-43142
TODA, N.
Flutter analysis and wind tunnel test with respect to a low-aspect-ratio wing with free-rotational control surface
p 1052 A92-56014
TODA, NOBUHIRO
Replacement of the NAL high pressure air storage system
[NAL-TM-634] p 888 N92-28835
TODA, NOBUO
Propeller-nacelle whirl flutter analysis and wind tunnel test p 1052 A92-56016
TODD, J. R.
Critical digital systems - A fly-by-light consideration
p 974 A92-49324
Fly-by-light technology development plan
[NASA-CR-181954] p 1086 N92-32778
TODD, JOHN R.
Development of fly-by-light systems for commercial aircraft p 744 A92-42605
Modular avionics - A commercial perspective
p 858 A92-48427
Making fly-by-light a reality p 877 A92-48499
Digital flight control systems - Some new commercial twists p 974 A92-49264
TOFUKUJI, NORIYASU
A consideration on air traffic control processing capability in terminal area p 1047 A92-56110
TOGAWA, M.
Advanced SCRAM-LACE system concept for single-stage-to-orbit space plane
[IAF PAPER 91-272] p 32 A92-12599
TOGAWA, MORITO
Key design considerations for scramjet powered space plane p 1066 A92-53491
An advanced scramjet propulsion concept for a 350 MG SSTO space plane - External nozzle performance
[AIAA PAPER 92-3719] p 1067 A92-54134
TOGNACCINI, R.
Boundary conditions for Euler equations at internal block faces of multi-block domains using local grid refinement
[NLR-TP-90134-U] p 908 N92-28712
TOH, HIDEMI
Numerical simulation for various flowfields of aero-engine components p 200 A92-17503
TOH, K. H.
Flow induction by pressure forces
[AIAA PAPER 92-3571] p 1067 A92-54060
TOKAR', V. L.
A procedure for calculating the static aeroelasticity characteristics of flight vehicles by the influence coefficient method using three-dimensional finite element schemes
p 460 A92-31896
TOKARCIK, SUSAN
Numerical simulation of unsteady flow in a hypersonic shock tunnel facility
[AIAA PAPER 92-4029] p 1034 A92-56851
TOKI, MASATO
Optimization of blade structure to reduce rotor vibration p 730 A92-43118
TOKUDA, EI
Flight control system design using H(infinity) optimal control p 1083 A92-56030
TOKUMARU, PHILLIP TAKEO
Active control of the flow past a cylinder executing rotary motions p 349 N92-19623
TOKUNAGA, T.
Advanced SCRAM-LACE system concept for single-stage-to-orbit space plane
[IAF PAPER 91-272] p 32 A92-12599
TOKUNAGA, TATSURU
Key design considerations for scramjet powered space plane p 1066 A92-53491
An advanced scramjet propulsion concept for a 350 MG SSTO space plane - External nozzle performance
[AIAA PAPER 92-3719] p 1067 A92-54134
TOLMACHEV, A. N.
Theoretical analysis of a suction diffuser in the porous test section of a wind tunnel p 428 A92-30207
TOLPADI, A. K.
A numerical study of two-phase flow in gas turbine combustors
[AIAA PAPER 92-3468] p 905 A92-49015
TOLPADI, ANIL K.
Numerical study of branched turboprop inlet ducts using a multiple block grid procedure
[ASME PAPER 91-GT-339] p 76 A92-15703
TOMASHOFSKI, CHRIS A.
A full scale airframe high cycle fatigue test methodology and its application to the SH-2G helicopter
p 105 A92-14345
TOMBS, MICHAEL STANLEY
Robust control system design with application to high performance helicopters p 382 N92-19621
TOMESCU, N. S.
A study of supersonic flow over the ogival bodies with attached shock waves at zero incidence
p 936 A92-51896
TOMESCU, N.-S.
A method of calculation for the radius of curvature of the attached shock waves in front of a sharp-nosed axi-symmetrical body placed in a uniform stream
p 243 A92-21319
TOMIOKA, KENJI
A study on the interaction between a bow shock wave generated by a blunt body and a turbulent boundary layer p 8 A92-12424
Experimental study on three-dimensional shock wave-turbulent boundary layer interaction induced by protuberance p 1019 A92-53997
Three-dimensional shock wave-turbulent boundary layer interaction induced by blunt body and protuberance
p 1029 A92-56009
TOMIOKA, Y.
High enthalpy wind tunnel for erosion testing of advanced materials
[AIAA PAPER 92-3888] p 1094 A92-56729

TOMITA, CHOJI
A helicopter transportation system
p 723 A92-43161
TOMITA, HIROSHI
Flight evaluation of navigation systems including MLS using NAL Do228 - Results of GPS
p 1047 A92-56118
TOMLINSON, B. N.
Initial validation of a R/D simulator with large amplitude motion p 886 N92-28546
TONE, S.
Turbine drive system of the high pressure LOX turbopump test facility
[DE92-783191] p 680 N92-25342
TONG, P.
Current DOT research on the effect of multiple site damage on structural integrity p 913 N92-30112
TONG, SIU S.
Integration of artificial intelligence and numerical optimization techniques for the design of complex aerospace systems
[AIAA PAPER 92-1189] p 600 A92-33301
TONGUE, BENSON H.
Chaotic dynamic behavior in a simplified rotor blade lag model p 846 A92-46926
TOOGOOD, R. D.
Preparation of the ice certification of the Dornier 328 regional airliner by numerical simulation and by ground test p 451 N92-21693
TOON, JOHN J.
Metal fibers and fabrics as shielding materials for composites, missiles and airframes p 141 A92-14680
TOOSSI, MOSTAFA
The NASA/Industry Design Analysis Methods for Vibrations (DAMVIBS) program - McDonnell Douglas Helicopter Company achievements
[AIAA PAPER 92-2203] p 540 A92-34393
TOPOROV, A. V.
An experimental study of tone-like noise in the flow past a wing at low flow velocities p 425 A92-30160
An experimental study of the noise of flow past a wing at low velocities p 603 A92-33771
TORCZYNSKI, J. R.
Reynolds number dependence of the drag coefficient for laminar flow through fine-scale screens
[DE92-002930] p 765 N92-26698
TORELLA, GIOVANNI
Expert systems for the trouble-shooting and the diagnostics of engines
[AIAA PAPER 92-3327] p 923 A92-48910
The numerical simulation of the main fuel control unit of gas turbine engines
[AIAA PAPER 92-3760] p 867 A92-49115
TORII, HIROSHI
Subcritical flutter characteristics of a swept-back wing in a turbulent supersonic flow - Comparison between analysis and experiment
[AIAA PAPER 92-2393] p 517 A92-34466
Response characteristics of a wing in supersonic flow near flutter boundary
[SAE PAPER 911999] p 789 A92-45401
TORII, KAHORU
Enhancement of laminar boundary layer heat transfer by a vortex generator p 1118 A92-55453
TORIKAI, TSURUO
Production technologies and aircraft design
p 608 A92-38220
TORINOUMI, S.
Flight simulation of a spaceplane p 752 A92-43190
TORIUMI, MASAKI
Lateral control of spaceplane at hypersonic flight
p 1104 A92-56069
TORIZ, F. C.
Surfprep flash-lamp depaint system evaluation
p 497 A92-32411
TORKELSON, THOMAS C.
Design of an integrated airframe/propulsion control system architecture
[NASA-CR-182007] p 602 N92-22644
TORLUND, PER-AKE
Wind tunnel force measurements and visualization on a 60-deg delta wing in oscillation, stepwise motion, and gusts p 364 N92-18786
TOROK, MICHAEL S.
Analysis of rotor blade dynamics using experimental UH-60A airloads obtained at the DNW
p 107 A92-14394
TORONY, J.
Design of a small axial compressor for high efficiency over a wide operating range
[ASME PAPER 91-GT-195] p 124 A92-15620
TORQUATI, FRANCO
A constraint satisfaction approach to operative management of aircraft routing p 350 A92-25181
TORRES, ABEL O.
Engineering method for aero-propulsive characteristics at hypersonic Mach numbers
[AIAA PAPER 91-5061] p 437 A92-31690
An aerodynamic design study of a series of lifting bodies at angles of attack from 10 to 53 degrees at Mach numbers from 2.30 to 4.62 p 442 A92-32500
TOTAH, JOSEPH J.
Description of a tilt wing mathematical model for piloted simulation p 133 A92-14445
A mathematical model of a tilt-wing aircraft for piloted simulation
[NASA-TM-103864] p 368 N92-19847
TOTH, D. K.
Lubricant evaluation and performance 2
[AD-A247464] p 895 N92-28398
TOULMAY, FRANCOIS
Lifting line predictions for a swept tip rotor blade
p 65 A92-14424
TOURJANSKY, N.
Theoretical and experimental study of a model rotor
p 547 A92-35781
TOURNEMINE, G.
Concerning the functional solution of transonic flows
p 243 A92-21318
TOUSSAINT, GREGORY J.
Intra-flight laser data links - Technology focus
p 725 A92-41472
TOWERS, C. E.
The application of particle image velocimetry (PIV) in a short-duration transonic annular turbine cascade
[ASME PAPER 91-GT-221] p 899 A92-46825
TOWERS, D. P.
The application of particle image velocimetry (PIV) in a short-duration transonic annular turbine cascade
[ASME PAPER 91-GT-221] p 899 A92-46825
TOWNEND, L. H.
Aero-propulsive effects on configuration shaping
[AIAA PAPER 91-5064] p 459 A92-31691
TOWNES, RICHARD
Acceptance of two identical radars in the absence of a precision reference p 533 A92-35931
TOWNSEND, DENNIS P.
Analysis and modification of a single-mesh gear fatigue rig for use in diagnostic studies
[NASA-TM-105416] p 773 N92-27879
TOWSLEY, DON
Stochastic ordering properties and optimal routing control for a class of finite capacity queueing systems
p 48 A92-11375
TOY, N.
Flow regimes of the cove regions between a slat and wing and between a wing and flap of a multielement airfoil p 614 A92-38858
TRACY, M. B.
Measurements of fluctuating pressure in a rectangular cavity in transonic flow at high Reynolds numbers
[NASA-TM-4363] p 633 N92-25752
TRAN, DONALD H.
Effects of chemical equilibrium on turbine engine performance for various fuels and combustor temperatures
[NASA-TM-105399] p 562 N92-23254
TRAN, DUC
Correction of sideslip-induced static pressure errors in flight-test measurements p 309 A92-24416
TRAN, TUAN A.
Television Microwave Link (TML) Operational Test and Evaluation (OT/E)/integration test report
[DOT/FAA/CT-TN91/57] p 500 N92-20653
TRANI, A. A.
Runway exit designs for capacity improvement demonstrations. Phase 2: Computer model development
[NASA-CR-190166] p 484 N92-21162
TRANSUE, AMY E.
Visual approach data collection at San Francisco International Airport (SFO)
[DOT/FAA/CT-90/23] p 354 N92-18112
TRAVOR, BRUCE W.
Pneumatically actuated multiple store launcher
[AD-D015237] p 732 N92-27188
TRAXLER, BOB
Departments of Veterans Affairs and Housing and Urban Development, and independent agencies appropriations for 1993, part 6
[GAO-55-636-PT-6] p 1141 N92-32505
TREASTER, A. L.
Suppression of the wing-body junction vortex by body surface suction p 309 A92-24417
TREFNY, C.
The F/A-18 external burning flight test
[AIAA PAPER 91-5050] p 731 A92-44547
TREFNY, CHARLES J.
Experiments and analysis concerning the use of external burning to reduce aerospace vehicle transonic drag
[NASA-TM-105397] p 279 N92-17546
TREIBER, DAVID A.
Modeling supersonic inlet boundary layer bleed roughness
[AIAA PAPER 92-0269] p 317 A92-25725
TRENT, WILLIAM
Monitoring operational concept
[DOT/FAA/SE-91/3] p 268 N92-15980
National Airspace System maintenance and support operational concept
[DOT/FAA/SE-92/1] p 308 N92-18969
National airspace system: System effectiveness operational concept NAS-SR-138
[DOT/FAA/SE-92/2] p 535 N92-23096
National airspace system. Air defense and law enforcement surveillance operational concept NAS-SR-135
[DOT/FAA/SE-92/3] p 953 N92-31211
TREPANIER, J. Y.
A Navier-Stokes solver for stretched triangular grids
[AIAA PAPER 92-0183] p 256 A92-23793
Periodic Euler and Navier-Stokes solutions about oscillating airfoils p 626 N92-24850
TREXLER, CARL A.
Three-dimensional simulation of a translating strut inlet
[AIAA PAPER 92-0270] p 317 A92-25726
Leading edge sweep effects in generic three-dimensional sidewall compression scramjet inlets
[AIAA PAPER 92-0674] p 343 A92-28218
Numerical study of the effects of reverse sweep on scramjet inlet performance p 611 A92-36979
Operating characteristics at Mach 4 of an inlet having forward-swept, sidewall-compression surfaces
[AIAA PAPER 92-3101] p 863 A92-48743
TRIFU, O.
On a global aerodynamic optimization of a civil transport aircraft p 193 N92-13931
TRIMARCHI, PAUL A.
Inflatable traversing probe seal p 595 N92-22692
TRIPATHI, SATISH
Distributed systems: Interconnection and fault tolerance studies
[AD-A252869] p 1135 N92-33920
TRIPP, JAMES S.
Communication: An important element of maintenance and repair p 838 N92-30124
TRIPPENSEE, GARY
Update of the X-29 high-angle-of-attack program
[SAE PAPER 912006] p 783 A92-45407
TROCHALIDIS, V.
The aerodynamic interference between a flapped tanker aircraft and a receiver aircraft during air-to-air refuelling
p 29 A92-13199
TROCHALIDIS, VASSILIOS
Aircraft aerodynamics and stability and control during air-to-air refueling
[AERO-REPT-9017] p 380 N92-18321
TROGER, H.
Chaotic motion in mechanical and engineering systems p 695 A92-39480
TROTT, W. M.
In situ measurement of particle formation in heated jet fuels: A new application of photon correlation spectroscopy
[DE92-003641] p 488 N92-20132
TROTT, WAYNE
Advanced thermally stable, jet fuels development program annual report. Volume 1: Model and experiment system development
[AD-A249625] p 988 N92-31462
TROUDET, T.
Design and evaluation of a robust dynamic neurocontroller for a multivariable aircraft control problem
[NASA-TM-105579] p 481 N92-20586
TROUTT, T. R.
Active control of vortex structures in a separating flow over an airfoil
[AIAA PAPER 92-2728] p 804 A92-45563
TROUVE, ARNAUD
Low-frequency pressure oscillations in a model ramjet combustor p 154 A92-16026
TROUVE, MICHEL
Studying dynamic behavior of X380 helicopter equipped with a new 5-blade composite rotor p 108 A92-14398
TROXEL, S. W.
The 1990 Airport Surveillance Radar Wind Shear Processor (ASR-WSP) operational test at Orlando International Airport
[AD-A239852] p 18 N92-10019
TRUBSHAW, E. B.
Concorde flight testing - Powerplant and performance flying
[SAE PAPER 912192] p 644 A92-40009

TRUCCO, RICHARD
Experiments on shear layer mixing at hypervelocity conditions
[AIAA PAPER 92-0628] p 396 A92-27009
TRUDEAU, ALLEN E.
Automated composite lay-up p 146 A92-14450
TRUE, B.
Experimental study of cross-stream mixing in a rectangular duct
[AIAA PAPER 92-3090] p 903 A92-48735
Experimental study of cross-stream mixing in a rectangular duct
[NASA-TM-105694] p 742 N92-27652
TRUEMAN, C. W.
RCS of four fuselage-like scatterers at HF frequencies
p 533 A92-33632
TRUMAN, C. R.
Simple turbulence models for supersonic flows - Bodies at incidence and compression corners p 5 A92-11059
TRUONG, Y. VIET
Effect of guard band reduction on marker beacon receiver performance
[DOT/FAA/CT-TN92/18] p 1002 N92-31617
TRUSCOTT, P. R.
Surface activation of Concorde by Be-7
p 605 N92-23295
TRYON, ROBERT G.
Failure model development for an integrally bladed turbine wheel
[AIAA PAPER 92-3420] p 865 A92-48979
TRZCINSKI, MAREK
An analysis of the flow-pattern at the exit of a single-stage turbine p 10 A92-13234
TSAI, BOR-JANG
Navier-Stokes simulation for cone-derived waverider
p 703 A92-41271
Computation of turbulent flow about cone-derived waverider
[AIAA PAPER 92-2726] p 804 A92-45562
TSAI, CHOU-JIU
Numerical investigation of unsteady transonic nozzle flows p 331 A92-26443
TSAI, F. P.
Evaluation of the ATD-GASP for endo-leap applications
[AIAA PAPER 92-2771] p 704 A92-41318
TSAI, WEI K.
A novel associative memory for high level control functions p 52 A92-11472
TSAMOURTZIS, V.
Quasi-three-dimensional characteristics method for a supersonic compressor rotor
[ASME PAPER 91-GT-81] p 69 A92-15549
TSANGARIS, PARRY
A lightweight loudspeaker for aircraft communications and active noise control p 1125 N92-32964
TSANGARIS, S.
Upwind schemes for Navier-Stokes computations at subsonic through hypersonic speeds
p 708 A92-43071
Transonic unsteady inviscid and viscous flow's simulation around 2-D moving bodies
[AIAA PAPER 92-2704] p 801 A92-45546
Improved artificial dissipation schemes for the Euler equations p 933 A92-49508
TSAO, MIKE
Turbine aircraft engine operational trending and JT8D static component reliability study
[DOT/FAA/CT-91/10] p 870 N92-28686
TSE, M.-C.
Incompressible flow past a flat plate aerofoil with leading edge separation bubble p 421 A92-28943
TSENG, LI-KENG
Near-injector structure of non-evaporating pressure-atomized sprays at various ambient densities
p 681 N92-25571
TSKHOVREBOV, M. M.
The study of experimental turboramjets
[AIAA PAPER 92-3720] p 1067 A92-54135
TSO, JIN
Vortex trapping on a 60 degree delta wing
[AIAA PAPER 92-2639] p 796 A92-45508
TSUBAKI, KENJI
Application of X-ray image radiography system for aircraft p 1118 A92-56084
TSUBOI, KIYOSHI
Shock interaction induced by two hemisphere-cylinders
[SAE PAPER 912043] p 790 A92-45427
TSUBOI, NOBUYUKI
Numerical simulation of a supersonic jet impingement on a ground
[SAE PAPER 912014] p 789 A92-45412
TSUBOKAWA, N.
Boundary layer flows around an airship
p 430 A92-30560
TSUCHIYA, KEIICHI
Evaluation report of an experimental Satcom operation by a Japan Airline's B747 passenger plane
p 1046 A92-56092
TSUDA, KEN
Sand erosion behavior of GFRP p 576 A92-32662
TSUEI, Y. M.
A numerical study of isothermal flows of a slit V-gutter
[AIAA PAPER 92-0100] p 293 A92-22203
TSUI, Y.
Limitations to the large strain theory
p 219 A92-20356
TSUJIMOTO, H.
Path angular control of the STOL research aircraft Asuka p 745 A92-43146
TSUJIMOTO, TAKASHI
Roles of wind tunnel tests and CFD analyses in the design of energy-efficient SST
[AIAA PAPER 92-3923] p 1133 A92-56754
Study on international cooperative test facilities for future SST/HST
[AIAA PAPER 92-3945] p 1097 A92-56775
TSUJIO, SHOWZOW
A development of hypermedia type database system for instruction of aircraft conceptual design
p 1132 A92-56113
TSUKAGOSHI, KEIZO
Film cooling on a gas turbine rotor blade
[ASME PAPER 91-GT-279] p 152 A92-15675
TSUKAMOTO, MASATO
Aircraft maintenance support system
p 607 A92-38217
TSUKANO, YUKICHI
In-flight simulation of backside operating models using direct lift controller
[SAE PAPER 912069] p 872 A92-45450
Flight test of a flight reference display for powered-lift STOL aircraft p 1064 A92-56059
Identification of the stability and control derivatives of a DLC-flap system for VSRA
[NAL-TR-1116] p 283 N92-17917
TSUKANO, YUKIICHI
Flight evaluations on in-flight simulation of unstable aircraft p 744 A92-43115
TSUMURA, S.
Distance and angle measuring method using laser light and rereflection plates p 762 A92-43206
TSUMURA, T.
Measurement of position and attitude using laser and retro-reflectors p 1047 A92-56120
TSUNG, FU-LIN
Numerical simulation of flow separation for rotors and fixed wings
[AIAA PAPER 92-0635] p 334 A92-27013
TSUYUKI, TARO
Oscillation of oblique shock waves generated in a two dimensional asymmetric nozzle
[SAE PAPER 912061] p 791 A92-45443
TSYBIZOV, IU. I.
Low-frequency vibrations of the shutters of the variable Laval nozzle of gas turbine engines p 657 A92-40610
TU, EUGENE
Nonequilibrium turbulence modeling effects on transonic vortical flows about delta wings p 85 N92-13007
TU, EUGENE L.
Effect of canard deflection on close-coupled canard-wing-body aerodynamics
[AIAA PAPER 92-2602] p 792 A92-45479
Navier-Stokes simulation of a close-coupled canard-wing-body configuration p 1031 A92-56163
TU, M.-H.
Robust stabilisation of multivariable feedback systems with desired performance requirement
p 776 A92-42172
TU, QINGCI
Simulation of commercial-aircraft reliability
p 759 A92-42057
TU, YEN
Three-dimensional solution-adaptive grid generation on composite configurations p 172 A92-18352
Unsteady Navier-Stokes simulations of supersonic flow over a three-dimensional cavity
[AIAA PAPER 92-2632] p 795 A92-45504
TUBANOS, N.
The IRS plasma wind tunnels for the investigation of thermal protection materials for reentry vehicles
p 208 N92-15009
TUBBS, H.
Compressing the compressor
[PNR-90824] p 476 N92-21848
TUCK, PAUL D.
Enhancement of ground handling through optimum selection/use of Ground Support Equipment (GSE)
[SAE PAPER 911973] p 881 A92-45380
TUCKER, RONALD
Automatic production test equipment (APTE) for the B-2 p 997 A92-53107
TUDA, S.
New 1.27-m leg of the National Aerospace Laboratory hypersonic wind tunnel p 1092 A92-56003
TUDES, BULENT
Rub induced rotor/stator vibration analysis on CF700 engine
[NRC-TR-ENG-007] p 202 N92-14060
TULAPURKARA, E. G.
Prediction of wake in a curved duct p 3 A92-10487
TULEY, M. T.
A multidimensional terrain model for low altitude tracking scenarios p 205 A92-19107
TULPULE, BHAL R.
Achieving fault tolerance in multichannel control systems p 974 A92-49296
TUMIN, A. M.
Problems of laminar-turbulent transition control in a boundary layer p 312 A92-24979
TUNCER, ISMAIL H.
Numerical simulation of three-dimensional supersonic free shear layers p 431 A92-31152
Unsteady aerodynamic characteristics of a dual-element airfoil
[AIAA PAPER 92-2508] p 518 A92-34501
TUNG, CHEE
Aerodynamic design of a Coanda induced force and thruster anti-torque system p 109 A92-14419
TUNICK, ARNOLD
Assessment of one-dimensional icing forecast model applied to stratiform clouds p 915 A92-46803
TUNIK, A. A.
Synthesis of optimal digital systems for the stabilization of stochastically perturbed unstable dynamic systems
p 601 A92-33754
TURCAT, A.
The turbo-ramjet Griffon p 782 A92-41820
TURCO, RICHARD P.
The atmospheric effects of stratospheric aircraft: A first program report
[NASA-RP-1272] p 408 N92-19121
TURKEL, ELI
On central-difference and upwind schemes
p 1007 A92-50466
TURKOVICH, JOHN J.
Applications of an automated programming system
[AIAA PAPER 91-3767] p 231 A92-17629
TURLEY, W. D.
Fiber-sensor design for turbine engines
[DE92-003539] p 376 N92-18230
TURNER, A. B.
Performance of radial clearance rim seals in upstream and downstream rotor-stator wheelspaces
[ASME PAPER 91-GT-32] p 147 A92-15516
Rim sealing of rotor-stator wheelspaces in the absence of external flow
[ASME PAPER 91-GT-33] p 147 A92-15517
TURNER, ELIJAH W.
An assessment of the B-747's capability to operate on rough surfaces
[AD-A250134] p 963 N92-31793
TURNER, JOSEPH G.
Calibration of an aircraft control surface using a tri-axial accelerometer package p 555 A92-35942
TURNER, TIMOTHY L.
AGSSS: The Airborne Graphics Software Support System; an Ada/PHIGS-based display editor for the rapid development of cockpit display software systems
[AD-A243224] p 277 N92-17221
TURTON, JOHN A.
Avionics software evolution p 199 N92-14052
TURVER, K. D.
24-bit flight test data recording format
p 900 A92-47528
TUSZYNSKI, MICHAL
Polish radar technology. V - Adaptive MTI filters for uniform and staggered sampling p 40 A92-12293
TUTTLE, F. L.
Verification and validation of F-15 and S/MTD unique software p 921 A92-48515
TUTTLE, M. E.
Thermoviscoplastic response of Ti-15-3 under various loading conditions
[NASA-CR-187621] p 45 N92-11391
TUTTLE, MARIE H.
Magnetic suspension and balance systems: A comprehensive, annotated bibliography
[NASA-TM-4318] p 32 N92-11030
TUTYNIN, V. K.
Technique for estimating the strength of gas turbine guide vanes with stress raisers p 761 A92-42653

TUZZOLO, M. F.
Surface heat transfer and flow properties of vortex arrays induced artificially and from centrifugal instabilities
p 1121 A92-56371
TWEEDT, DANIEL L.
NASA. Lewis Research Center supersonic throughflow fan program
[NASA-TM-103248] p 972 N92-31250
TWOMEY, WILLIAM J.
The NASA/Industry Design Analysis Methods for Vibrations (DAMVIBS) Program - Sikorsky Aircraft - Advances toward interacting with the airframe design process
[AIAA PAPER 92-2204] p 540 A92-34394
TYLER, JOSEPH C.
An analysis of pitch and plunge effects on unsteady airfoil behavior p 65 A92-14359
TYMCZYSZYN, JOSEPH J.
Flight test investigation of the wake vortices generated by helicopters p 270 A92-21925
TYSELL, LARS G.
MATGRID: A program for generation of C-H and C-O topology grids around wing/body configurations. Mathematical definition document
[FFA-TN-1990-19] p 444 N92-20468
MATGRID, a program for generation of C-H and C-O topology grids around wing/body configurations: Software description document
[FFA-TN-1990-20] p 945 N92-30713
TYSON, JOHN, II
Inspection of fabricated fuselage panels using electronic shearography
[DOT/FAA/CT-TN92/26] p 1127 N92-33627
TZENG, M. J.
Active vibration control of smart structural materials
p 673 A92-39281
TZONG, T. J.
Multidisciplinary design optimization of a large transport aircraft wing
[AIAA PAPER 92-1002] p 536 A92-33194

U

UBALDI, MARINA
Reynolds stress distribution downstream of a turbine cascade p 614 A92-38861
UCHIDA, HIROYUKI
Fundamental studies on Marangoni convection related to Bridgman crystal growth p 1111 A92-53758
UCHIDA, TADAO
Navigation experiment on an aircraft using the GPS-INS navigation system. I - Introduction to the system
p 726 A92-43122
Functional mock-up tests for flight control system of the NAL QSTOL research aircraft 'ASKA'
[SAE PAPER 912036] p 881 A92-45422
Synthesis of a MLS automatic landing control law for the NAL experimental research aircraft Do-228
p 1084 A92-56062
Flight evaluation of navigation systems including MLS using NAL Do228 - Outline p 1047 A92-56116
Development of digital/optical rotary position transducer
[NAL-TR-1106] p 29 N92-10028
UCHIDA, TAKASHI
Wind tunnel test of M ≈ 2.5 mixed compression inlet
p 1028 A92-56008
UCHIKI, TATSUYA
Ultrasonic motor utilizing elastic fin rotor
p 215 A92-17414
UCIKAWA, ISOROKU
Functional mock-up tests for flight control system of the NAL QSTOL research aircraft 'ASKA'
[SAE PAPER 912036] p 881 A92-45422
UDD, ERIC
Fiber optic and laser sensors VIII; Proceedings of the Meeting, San Jose, CA, Sept. 17-19, 1990
[SPIE-1367] p 901 A92-48026
UDIN, SERGEI V.
Wing mass formula for subsonic aircraft
p 845 A92-46812
Wing mass formula for twin fuselage aircraft
p 1054 A92-56171
UDZHUKHU, A. IU.
A pressure-drag-determination method for aerodynamic-interference problems p 425 A92-30157
UEDA, FUMIO
On the relation between cumulus cloud lines and surface shear lines p 410 N92-19667
UEDA, TETSUHIKO
Unsteady aerodynamic calculations for general configurations by the double-point method
[NAL-TR-1101T] p 12 N92-10980
Static aeroelastic analysis of ACT wind tunnel model aircraft
[NAL-TM-624] p 632 N92-25366
Vibration tests and structural modeling of an aircraft model for active control technology experiments
[NAL-TM-626] p 662 N92-25401
UEHA, SADAYUKI
Ultrasonic motor utilizing elastic fin rotor
p 215 A92-17414
UEMURA, M.
Study on the lower aspect view of a helicopter simulator p 748 A92-43110
UEMURA, NAKOTO
An autorotation-entry control for a helicopter with a fuzzy controller p 1083 A92-56032
UEMURA, TSUNEHARU
A note on thrust control for jetliner during approach
p 457 A92-29518
A note on thrust control for jetliner during approach
p 1053 A92-56061
UENISHI, K.
Computational fluid dynamics based three-dimensional turbofan inlet/fan cowl analysis system
p 243 A92-21075
Commercial turbofan engine exhaust nozzle flow analyses using PAB3D
[AIAA PAPER 92-2701] p 801 A92-45543
UENO, TORU
A consideration on air traffic control processing capability in terminal area p 1047 A92-56110
UEYAMA, HIROCHIKA
Characterization of superconducting magnetic bearings (dynamic stiffness and damping coefficient in axial direction) p 772 N92-27737
UGRIUMOV, M. L.
Solution of the problem of three-dimensional flow past the blade rows of turbomachines with allowance for viscosity effects p 244 A92-21618
UKEILEY, L.
Multifractal analysis of a lobed mixer flowfield utilizing the proper orthogonal decomposition
p 611 A92-36840
UL'IANOV, G. C.
Aerodynamic characteristics of curved delta wings in the case of subsonic separated flow
p 712 A92-44121
ULBRICH, HEINZ
Hydraulic actuator system for rotor control
p 224 N92-14363
ULBRICH, N.
Experimental results on a wall interference correction method with interface measurements
[AIAA PAPER 92-0570] p 333 A92-26978
Blockage correction in three-dimensional wind tunnel testing based on the wall signature method
[AIAA PAPER 92-3925] p 1095 A92-56756
A wall interference assessment/correction system
[NASA-CR-189785] p 259 N92-15974
ULLAH, DOUGLAS
Real time presentation for RAFALE in-flight tests
p 882 A92-47522
ULLYOTT, RICHARD
Secondary power system preliminary design
[SAE PAPER 912189] p 656 A92-40008
ULMER, LON
94 GHz MMW imaging radar system
[SAE PAPER 912208] p 651 A92-40015
UMENE, K.
Jet engine test system including expert system for diagnosis
[ASME PAPER 91-GT-408] p 137 A92-15737
UMIDA, T.
Aerodynamic design of a nonplanar airfoil by an inverse method with Navier-Stokes equations
p 711 A92-43197
UNDERWOOD, DAVID
Growing need to replace ILS can best be met by MLS
p 534 A92-36124
UNDERWOOD, HAROLD W.
Avionics reliability, durability, and integrity: Can they be independent of application? p 200 N92-14056
UNGER, E. R.
Variable-complexity aerodynamic optimization of an HSCT wing using structural wing-weight equations
[AIAA PAPER 92-0212] p 317 A92-25685
UNGER, GEORGE
Research needs for a commercial passenger tiltrotor
p 1056 A92-56298
NASA aerodynamics program
[NASA-TM-4368] p 609 N92-24678
UNRUH, JAMES F.
Structure-borne noise transmission in the Propfan Test Assessment aircraft p 778 A92-41240
UNT, H.
Phase-averaged turbulence statistics in a near wake with an asymmetric vortex shedding p 620 A92-40086
UPADHYA, K.
Composite materials for aerospace applications
p 577 A92-36377
URALIL, F. S.
Processing effects and damage tolerance in poly(etheretherketone) composites p 388 A92-26152
URASEK, DONALD C.
Supersonic Throughflow Fan Test Facility at NASA. Lewis Research Center
[NASA-TP-3038] p 983 N92-31640
URBAN, JUERGEN
An exploration of chemically reacting viscous hypersonic flow p 612 A92-37550
URDIALES, M.
The measurement of water film thickness on airfoils in heavy rain conditions using conductance sensors
p 452 N92-21695
USHAKOV, A. P.
Self-oscillatory interaction of an underexpanded jet with an obstacle in the presence of a supersonic wake
p 79 A92-16681
USKOV, V. N.
Self-oscillatory interaction of an underexpanded jet with an obstacle in the presence of a supersonic wake
p 79 A92-16681
USRY, JIMMY W.
Doppler global velocimeter measurements of the vortical flow above a thin delta wing
[AIAA PAPER 92-0005] p 292 A92-22130

V

VACHON, JAMES
Optics in aircraft engines p 926 A92-48500
VACHTSEVANOS, G.
Detection and identification of axial flow compressor instabilities p 969 A92-50504
VAFAI, K.
Three-dimensional buoyancy-induced flow and heat transfer around the wheel outboard of an aircraft
p 397 A92-27773
Characterization of thermal performance of wheel outboard of an aircraft p 849 A92-48352
VAGHELA, NARESH P.
Design analysis of the T-800 inlet particle separator/air oil cooler blower p 579 A92-32556
VAILLANCOURT, WALTER
Talons 95 GHz radar sensor for autonomous landing guidance p 1063 A92-55908
VAJINGORTIN, L. D.
Identification of dynamic characteristics of flexible rotors as dynamic inverse problem p 220 N92-13962
VAKILI, A. D.
Review of the physics of enhancing vortex lift by unsteady excitation p 66 A92-15344
VALAREZO, WALTER O.
Maximum lift prediction for multielement wings
[AIAA PAPER 92-0401] p 324 A92-26254
Separation control on high Reynolds number multi-element airfoils
[AIAA PAPER 92-2636] p 806 A92-45575
High-lift testing at high Reynolds numbers
[AIAA PAPER 92-3986] p 1033 A92-56810
The adverse aerodynamic impact of very small leading-edge ice (roughness) buildups on wings and tails
p 451 N92-21691
VALAVANI, L.
Active control of rotating stall in a low speed axial compressor
[ASME PAPER 91-GT-88] p 122 A92-15553
Parameter identification of compressor dynamics during closed-loop operation p 508 A92-29313
A Lyapunov based nonlinear control scheme for stabilizing a basic compression system using a close-coupled control valve p 508 A92-29316
Dynamic control of aerodynamic instabilities in gas turbine engines p 870 N92-28466
VALAVANI, LENA S.
Optimal rejection of bounded persistent disturbances in periodic systems p 51 A92-11464
VALC, ZDENEK
New methods to determine the transmission loss of partitions using sound intensity measurements
p 924 A92-45879
VALCO, MARK J.
Boeing Helicopters Advanced Rotorcraft Transmission (ART) Program summary of component tests
[AIAA PAPER 92-3364] p 905 A92-48937
VALENTINE, D.
Multifractal analysis of a lobed mixer flowfield utilizing the proper orthogonal decomposition
p 611 A92-36840
VALKOV, THEODORE
Yaw dynamics of a coaxial rotor helicopter
p 378 A92-24427

VALLET, M. G.
Anisotropic control of mesh generation based upon a Voronoi type method p 918 A92-47043
VALLOT, LARRY
Differential GPS/inertial navigation approach/landing flight test results p 956 A92-51009
VALLOT, LAWRENCE
Design and flight test of a differential GPS/inertial navigation system for approach/landing guidance p 97 A92-16650
VALORANI, M.
Nonequilibrium hypersonic inviscid steady flows p 176 A92-20737
VALUISKII, A. M.
A discrete vortex study of stationary flow past three-dimensional lifting systems at subsonic and supersonic velocities p 79 A92-16813
VAN AKEN, JOHANNES M.
Alleviation of whirl-flutter on tilt-rotor aircraft using active controls p 133 A92-14423
VAN BUREN, MARK A.
A geometric approach to regulator and tracker design for an aerospace plane
[AIAA PAPER 91-5054] p 203 A92-17837
Aerospace plane guidance using time-scale decomposition and feedback linearization p 984 A92-50498
VAN DALSEM, WILLIAM R.
Flowfield simulation about the SOFIA Airborne Observatory
[AIAA PAPER 92-0656] p 342 A92-28217
VAN DAM, C. P.
Experimental investigation on the effect of crescent planform on lift and drag p 9 A92-13206
Prediction of drag at subsonic and transonic speeds using Euler methods
[AIAA PAPER 92-0169] p 255 A92-23780
Subsonic and transonic low-Reynolds-number airfoils with reduced pitching moments p 701 A92-41211
Accurate prediction of drag using Euler methods p 703 A92-41246
Practical design optimization of wing/body configurations using the Euler equations
[AIAA PAPER 92-2633] p 795 A92-45505
VAN DE WALL, ALLAN G.
A fast, uncoupled, compressible, two-dimensional, unsteady boundary layer algorithm with separation for engine inlets
[AIAA PAPER 92-3082] p 823 A92-48729
VAN DEN BERG, J. I.
Numerical investigation into high-angle-of-attack leading-edge vortex flow
[AIAA PAPER 92-2600] p 791 A92-45477
VAN DEN BRAEMBUSSCHE, R.
Experimental study of the swirling flow in the internal volute of a centrifugal compressor
[ASME PAPER 91-GT-7] p 67 A92-15505
VAN DEN BRAEMBUSSCHE, R. A.
Design method for subsonic and transonic cascade with prescribed Mach number distribution
[ASME PAPER 91-GT-18] p 67 A92-15509
VAN DER GEEST, P. J.
A simulator evaluation of various manual control concepts for fly-by-wire transport aircraft
[AIAA PAPER 92-4328] p 1073 A92-55172
VAN DER HOEVEN, J. G. TH.
The Berlin oil channel for drag reduction research p 571 A92-34219
VAN DER KLEIN, D. C. M.
Quantitative estimation of secondary surveillance radar information p 353 A92-24943
VAN DER KRAAN, P.
GPS - Can it contribute to European ATC? p 637 A92-38380
VAN DER VOOREN, J.
Inviscid drag prediction for transonic transport wings using a full-potential method p 174 A92-20212
VAN DER WEES, A. J.
Inviscid drag prediction for transonic transport wings using a full-potential method p 174 A92-20212
VAN DEVENTER, B.
Fiber-coupled position sensors for aerospace applications p 370 A92-27776
VAN DIERENDONCK, A. J.
Concepts for replacing shipboard TACAN with differential GPS p 101 A92-16971
VAN DOMMELEN, L.
Unsteady flow past an airfoil pitching at a constant rate p 610 A92-36826
VAN DRIEL, NICO
Results of a test program for the use of differential GPS for approach guidance p 101 A92-16969
Approach flight trials in the Netherlands for the Navstar GPS Joint Program Office International Test Program p 533 A92-35928
VAN DYKEN, R. D.
Oscillating airfoil velocity field during large amplitude dynamic stall p 622 A92-40171
VAN FOSSEN, G. J.
Heat transfer measurements from a smooth NACA 0012 airfoil p 218 A92-20215
Roughness effects on heat transfer from a NACA 0012 airfoil p 219 A92-20217
Increased heat transfer to elliptical leading edges due to spanwise variations in the freestream momentum - Numerical and experimental results
[AIAA PAPER 92-3070] p 1020 A92-54005
VAN GRAAS, FRANK
In-flight demonstration of hybrid GPS/Loran RAIM p 96 A92-16643
That all-important interface p 100 A92-16953
GPS interferometric attitude and heading determination - Initial flight test results p 454 A92-30023
GPS interferometric attitude and heading determination - Flight test results p 650 A92-39561
Receiver autonomous integrity monitoring (RAIM) - Techniques, performance and potential p 638 A92-39567
VAN LEER, BRAM
An investigation of passive control methods for shock-induced separation at hypersonic speeds
[AIAA PAPER 92-2725] p 808 A92-45596
VAN NUNEN, J. W. G.
LAH main rotor model test at the DNW p 547 A92-35771
VAN OORDT, T. W.
Rapid ultrasonic scanning of aircraft structures p 215 A92-17292
VAN REENEN, M.
A piezoelectric droplet generator for use in wind tunnels p 291 A92-21374
VAN SUETENDAEL, RICHARD
GNAS Maintenance Control Center (GMCC) Design Qualification Test and Evaluation (DQT/E) test procedures
[DOT/FAA/CT-TN91/40] p 983 N92-30976
VAN VEGGEL, L. H.
The evolution from bonded F27 aircraft to Arall structures p 699 A92-41177
VAN WESTERHUYZEN, D. H.
Detailed investigation of causes of avionics field failures p 995 A92-51925
VAN WIE, D. M.
Applications of Busemann inlet designs for flight at hypersonic speeds
[AIAA PAPER 92-1210] p 517 A92-33314
VANCE, JOHN M.
A gas operated bearing damper for turbomachinery
[ASME PAPER 91-GT-249] p 150 A92-15654
AFRAPT Program at Texas A and M University research for advanced aircraft engine structures
[AD-A247040] p 743 N92-28076
VANDALSEM, W. R.
Wall functions for the kappa-epsilon turbulence model in generalized nonorthogonal curvilinear coordinates
[NASA-CR-190368] p 685 N92-25962
NASA Workshop on future directions in surface modeling and grid generation
[NASA-CP-10092] p 831 N92-29625
VANDEKERCKHOVE, D.
Active control of blade vortex interaction p 814 A92-46944
VANDENBERG, J. I.
Analysis of results of an Euler-equation method applied to leading-edge vortex flow p 84 N92-13000
Numerical simulation of vortical flow over a delta wing at subsonic and transonic speeds
[NLR-TP-90029-U] p 444 N92-20498
Analysis of results of an Euler-equation method applied to leading-edge vortex flow
[NLR-TP-90368-U] p 827 N92-28657
Development and validation of a characteristic boundary condition for a cell-centered Euler method
[NLR-TP-90144-U] p 828 N92-28692
VANDENBERG, S.
Gamma Group-The Pale Horse: A proposal in response to a commercial air transportation study ort study
[NASA-CR-190019] p 731 N92-26435
VANDENDAM, R. F.
Constrained spanload optimization for minimum drag of multi-lifting-surface configurations
[NLR-TP-89126-U] p 828 N92-28660
VANDENKERCKHOVE, J.
The thermodynamic approach in the study of large systems - Application to high-velocity airbreathing propulsion p 654 A92-37824
VANDERBERG, B.
Turbulence modeling: Survey of activities in Belgium and the Netherlands, and appraisal of the status and a view on the prospects
[NLR-TP-90184-U] p 908 N92-28694
VANDERBURG, J. W.
Improved shock-capturing of Jameson's scheme for the Euler equations
[PB92-148758] p 596 N92-23251
VANDERHOEK, M. W.
Calibration of GPS antennas
[ETN-92-92034] p 1051 N92-33693
VANDERLEEST, L.
Manufacture of XD gamma titanium aluminide airfoils via investment casting and machining p 494 A92-30603
VANDERVEGT, J. J. W.
Methods for direct simulation of transition in hypersonic boundary layers 2 p 912 N92-30064
VANDERVLIET, G.
Shipboard mission training effectiveness of the Naval Air Warfare Center's V-22 Government Test Pilot Trainer
[AIAA PAPER 92-4130] p 959 A92-52427
VANDERVOOREN, J.
Inviscid drag prediction for transonic transport wings using a full-potential method
[NLR-TP-89365-U] p 444 N92-20473
Wave drag determination in the transonic full-potential flow code MATRICS
[NLR-TP-90062-U] p 828 N92-28709
VANDERWAL, J. M. M.
Evaluation of the applicability of Helmholtz resonators for low frequency acoustic liners
[PB92-138544] p 605 N92-23588
VANDERWEES, A. J.
Inviscid drag prediction for transonic transport wings using a full-potential method
[NLR-TP-89365-U] p 444 N92-20473
Wave drag determination in the transonic full-potential flow code MATRICS
[NLR-TP-90062-U] p 828 N92-28709
VANDEWALL, ALLAN G.
A fast, uncoupled, compressible, two-dimensional, unsteady boundary layer algorithm with separation for engine inlets
[NASA-TM-105686] p 770 N92-27653
VANDYKEN, R. D.
Leading edge velocity field of an oscillating airfoil in compressible dynamic stall
[AIAA PAPER 92-0193] p 257 A92-23802
VANENGELEN, J. A. J.
Some longitudinal handling qualities design guidelines for active control technology transport aircraft
[NLR-TP-90129-U] p 878 N92-28652
Results of a flight simulator experiment to establish handling quality guidelines for the design of future transport aircraft
[NLR-MP-88044-U] p 854 N92-29616
VANGEL, MARK G.
A sensitivity analysis on component reliability from fatigue life computations
[AD-A247430] p 908 N92-28425
VANGERPEN, JON H.
A two-stroke diesel engine simulation program
[NASA-CR-185155] p 562 N92-22647
VANGRAAS, FRANK
GPS interferometric attitude and heading determination: Initial flight test results p 269 N92-17994
VANGSNESS, M. D.
Isothermal flow fields in a research combustor for lean blowout studies
[ASME PAPER 91-GT-37] p 121 A92-15520
Lean blowout in a research combustor at simulated low pressures
[ASME PAPER 91-GT-359] p 137 A92-15713
VANHEMEL, PAUL E.
The evaluation of simulator effectiveness for the training of high speed, low level, tactical flight operations p 885 N92-28539
VANHENGST, J.
The effect of hoar-frosted wings on the Fokker 50 take-off characteristics p 451 N92-21692
VANHOY, DAVID
X-29 high angle of attack flight test procedures, results, and lessons learned p 548 A92-35934
VANHOY, LARRY N.
Airport smart power lighting system
[DOT/FAA/CT-TN91/12] p 573 N92-22966
VANKA, S. P.
Hot gas environment around STOVL aircraft in ground proximity. II - Numerical study p 371 A92-24403
Calculations of hot gas ingestion for a STOVL aircraft model
[AIAA PAPER 92-0385] p 374 A92-28191
VANKA, SURYA P.
Calculations of hot gas ingestion for a STOVL aircraft model
[NASA-TM-105437] p 350 N92-19993
VANKLEEF, E. R. A.
Aircraft simulation and pilot proficiency: From surrogate flying towards effective training p 884 N92-28532

VANKUIK, GIJSBERTUS ARNOLDUS MARIA
On the limitations of Froude's actuator disc concept
[ETN-91-90136] p 81 N92-11973
VANLENT, M.
Flow gradient corrections on hot-wire measurements using an X-wire probe
[NLR-TP-90255-U] p 829 N92-28713
VANMOL, DENIS O.
Heat transfer characteristics of hypersonic waveriders with an emphasis on leading edge effects
[AIAA PAPER 92-2920] p 821 A92-47892
Heat transfer characteristics of hypersonic waveriders with an emphasis on the leading edge effects
[NASA-CR-189586] p 525 N92-22215
VANN, F. W.
Aircraft structural design p 643 A92-39304
VANNIER, JEAN-CLAUDE
Is the avionics system of the Hermes Spaceplane centralized or decentralized? p 984 A92-49258
VANNUCCI, RAYMOND D.
Vinyl capped addition polyimides
[NASA-CASE-LEW-15027-2] p 579 N92-24053
VANNUNEN, J. W. G.
LAH-main rotor model test at the DNW
[NLR-TP-90305-U] p 852 N92-28687
VANPAASSEN, D. M.
Propeller-driven-small airplane noise certification
[LR-650] p 237 N92-14798
VANSTEENWYK, BRETT
Control design of a UH-60 rotorcraft via CLTR and direct optimization
[AIAA PAPER 92-4470] p 1076 A92-55230
Advanced rotorcraft control using parameter optimization
[NASA-CR-189502] p 135 N92-13073
VANSUETENDAEL, N.
Avionic data bus integration technology
[DOT/FAA/CT-91/19] p 736 N92-27973
VANSUETENDAEL, RICHARD
GNAS Maintenance Control Center (GMCC) Design Qualification Test and Evaluation (DQT/E) test report
[DOT/FAA/CT-TN91/39] p 932 N92-31615
VANZANTE, DALE E.
Visualization of boundary-layer development on turbomachine blades with liquid crystals
[NASA-CR-190433] p 742 N92-27519
VARESHNYA, DEEPAK
Fiber optic speed sensor for advanced gas turbine engine control p 857 A92-48044
VARGHESE, M.
Multifractal analysis of a lobed mixer flowfield utilizing the proper orthogonal decomposition
p 611 A92-36840
VASANTH, T. R.
Software package for preliminary design of helicopter
p 775 A92-41195
VASENIN, V. A.
Nonparametric methods of regression analysis in problems related to the processing of aerodynamic balance calibration tests p 602 A92-36417
VASIL'EVA, K. I.
Modeling the effect of helicopter downwash on warm fog p 775 A92-44081
VASSALLO, J.
Electronically steerable antenna for aircraft
p 229 N92-15272
VASSBERG, JOHN C.
A fast, implicit unstructured-mesh Euler method
[AIAA PAPER 92-2693] p 917 A92-45589
VASSEL, A.
The beta-CEZ - A high performance titanium alloy for aerospace engines p 289 A92-22760
VASTAVA, R. B.
Manufacturing cost model for composites
p 1012 A92-51565
VATSA, VEER N.
Viscous flow solutions for slender bodies of revolution at incidence p 4 A92-10692
Evaluation of a multigrid-based Navier-Stokes solver for aerothermodynamic computations
[AIAA PAPER 92-4563] p 1027 A92-55375
VAUGHAN, ROBIN L.
Use of distance-measuring equipment (DME) for correcting errors in position, velocity, and wind measurements from aircraft inertial navigation systems
p 188 A92-18172
VAUGHN, MICHELLE
FAA vertical flight research, engineering, and development bibliography, 1962 - 1991
[FAA/ARD-30] p 462 N92-21210
VAVRECK, ANDREW N.
Flexible manufacturing in repair of gas turbine engine components
[AIAA PAPER 92-3524] p 786 A92-49049
VAZIRANI, M.
Laser-initiated conical detonation wave for supersonic combustion p 375 A92-28531
VEERAVALLI, SRINIVAS V.
A preliminary experimental investigation of local isotropy in high-Reynolds-number turbulence
p 912 N92-30042
VEERS, P. S.
Fatigue life variability and reliability analysis of a wind turbine blade
[DE92-008673] p 689 N92-25049
VEILLET, CHRISTIAN
Comparison of two-way satellite time transfer and GPS common-view time transfer between OCA and TUG
p 1050 N92-33356
VEILLETTE, R. J.
Design of reliable control systems p 49 A92-11420
VELICHKO, S. A.
Bodies of revolution with minimal wave drag at transonic gas flow velocities p 424 A92-30135
Theoretical analysis of the effect of the porous walls of a wind tunnel on transonic flow past bodies of cone-cylinder type p 427 A92-30202
VELICKI, A.
Design for the relief of thermal stresses in a large high-speed wing
[AIAA PAPER 92-1082] p 536 A92-33250
VELKOFF, HENRY R.
Aerodynamic design of a Coanda induced force and thruster anti-torque system p 109 A92-14419
VELLAICHAMY, SENTHILVEL
Aeroelastic response of helicopters with flexible fuselage modeling
[AIAA PAPER 92-2567] p 564 A92-34481
VELOVICH, ALEXANDER
Mikoyan's market-buster p 1052 A92-54981
VEMURU, CHANDRA S.
Application of laminar flow control to the High Speed Civil Transport - The NASA Supersonic Laminar Flow Control Program
[SAE PAPER 912115] p 643 A92-39966
VENET, GERARD
Advanced Study for Active Noise Control in Aircraft (ASANCA)
[AIAA PAPER 92-2092] p 1137 N92-32956
VENGSARKAR, ASHISH M.
Fabry-Perot fiber-optic sensors in full-scale fatigue testing on an F-15 aircraft p 391 A92-24553
VENGZHEN, VAD. V.
Thermal deformation of a polymer heat shield material on the descent trajectory p 754 A92-42655
VENKATAPATHY, ETHIRAJ
Single expansion ramp nozzle simulations
[AIAA PAPER 92-0387] p 323 A92-26243
Effective treatments of the singular line boundary problem for three dimensional grids
[AIAA PAPER 92-0545] p 342 A92-28202
Free-flight trim-angle predictions for the aeroassist flight experiment p 705 A92-41540
Application of a solution adaptive grid scheme to complex three-dimensional flows p 935 A92-50309
Development and application of computational aerothermodynamics flowfield computer codes
[NASA-CR-190294] p 624 N92-24229
VENKATESAN, C.
A study of coupled rotor-fuselage vibration with higher harmonic control using a symbolic computing facility
p 569 A92-35770
Coupled rotor-fuselage vibration reduction with multiple frequency blade pitch control p 1085 A92-56315
VENKATESAN, COMANDUR
A new aeroelastic model for composite rotor blades with straight and swept tips
[AIAA PAPER 92-2259] p 541 A92-34414
VENKATESWARAN, S.
Axial compression corner flow with shock impingement p 441 A92-32196
Computational method to predict thermodynamic, transport, and flow properties for the modified Langley 8-foot high-temperature tunnel
[NASA-TM-4374] p 767 N92-27193
VENKAYYA, VIPPERIA B.
Large scale optimization using ASTROS: An overview
p 649 N92-25921
VENKAYYA, VIPPERLA B.
Multidisciplinary optimization studies using ASTROS
p 571 N92-23234
VENN, G.
The Eurofar program - An European overview on advanced VTOL civil transportation system
p 1016 A92-56299
The Eurofar program: An European overview on advanced VTOL civil transportation system
[MBB-UD-0611-91-PUB] p 952 N92-30418
VENNEMANN, D.
New hypersonic test methods developed at ONERA - The R5 and F4 wind tunnels
[ONERA, TP NO. 1992-39] p 882 A92-48600
VENNERI, SAMUEL L.
Overview and major characteristics of future aeronautical and space systems
[AIAA PAPER 92-2441] p 585 A92-34472
VENUGOPAL, N.
Automated trajectory synthesis for hypersonic vehicles using energy management and variational calculus techniques p 210 A92-19061
VENUGOPAL, S.
A correlation study of the wing-body interference factor for high angles of attack p 700 A92-41179
VERDE, LEOPOLDO
Robust flight control systems - A parameter space design p 976 A92-50503
VERDEBOUT, JEAN
Time Resolved Lidar Fluorosensor operating from helicopter p 1121 A92-56296
VERDON, J. M.
Development of an efficient analysis for high Reynolds number inviscid/viscid interactions in cascades
[AIAA PAPER 92-3073] p 823 A92-48723
VERDON, JOSEPH M.
Unsteady aerodynamic methods for turbomachinery aeroelastic and aeroacoustic applications
[AIAA PAPER 92-0011] p 252 A92-23730
Development of unsteady aerodynamic analyses for turbomachinery aeroelastic and aeroacoustic applications
[NASA-CR-4405] p 12 N92-10979
Development of a steady potential solver for use with linearized, unsteady aerodynamic analyses
[NASA-TM-105288] p 473 N92-20525
VERES, JOSEPH P.
A survey of instabilities within centrifugal pumps and concepts for improving the flow range of pumps in rocket engines
[NASA-TM-105439] p 387 N92-18280
VERETENNIKOV, V. F.
Calculation of the aerodynamic characteristics of bodies of revolution in incompressible flow by the vortex surface method p 428 A92-30375
VERHOFF, A.
Prediction of inviscid supersonic/hypersonic aircraft flowfields p 810 A92-46785
VERHOFF, AUGUST
Industry warms to CFD p 392 A92-24908
VERHOFF, VINCENT G.
Transonic turbine blade cascade testing facility
[AIAA PAPER 92-4034] p 1101 A92-56856
Transonic turbine blade cascade testing facility
[NASA-TM-105646] p 667 N92-26129
Three-dimensional laser window formation
[NASA-RP-1280] p 984 N92-30307
VERMELAND, R.
Navier-Stokes calculations of inboard stall delay due to rotation p 309 A92-24410
VERMEULEN, J. P.
Quantitative heat transfer measurements in hypersonic wind tunnels by means of infrared thermography
p 1115 A92-54321
VERMEULEN, P. J.
Acoustic control of combustor primary zone air-jet mixing
[AIAA PAPER 92-3651] p 1067 A92-54104
VERTATSCHITSCH, E. J.
A novel avionic sensor for fly-by-light controls
p 650 A92-38128
VETLUTSKII, V. N.
On the calculation of the compressible boundary layer on a nonplanar delta wing with supersonic leading edges
p 252 A92-23409
The calculation of a compressible boundary layer past a pointed body and a delta wing p 622 A92-40173
VETROV, A. N.
A probabilistic method for monitoring the remaining life of aircraft gas turbine engine components using the temperature limit criterion p 201 A92-18292
VETTER, M.
High enthalpy testing in the Aachen (Fed. Republic of Germany) shock tunnel TH 2 p 208 N92-15021
VEUILLOT, J. P.
Resolution of Navier-Stokes equations around profiles: Drag evolution
[ONERA-RTS-86/1685-AY-156A] p 43 N92-11310
VEYNANTE, D.
The coherent flamelet model for propulsion applications p 756 N92-27486
VEYSSEYRE, PH.
Validation of a 3D Navier-Stokes code on experimental compressor bladings
[ONERA, TP NO. 1991-229] p 330 A92-26381

VIALLE, MICHEL
Tiger MGB - High reliability low weight
p 109 A92-14418
VICHI, FRANK
Current nondestructive inspection methods for aging aircraft
[DOT/FAA/CT-91/5] p 1126 N92-33480
VID, VIL'GEL'M V.
Flight test control p 136 A92-15021
VIDERMAN, ZVI
On the stability of a dual spin satellite with asymmetric rotor and flexible platform
[ISBN-0-315-54650-6] p 753 N92-27613
VIDIL, R.
Experimental methods to determine heat exchanger performances p 682 N92-25667
VIDYASAGAR, M.
Design of non-overshooting feedback control systems
p 50 A92-11431
VIEGAS, J. R.
An assessment and application of turbulence models for hypersonic flows
[NASA-TM-105124] p 82 N92-11984
VIEGAS, JOHN R.
Assessment of compressibility corrections to the k-epsilon model in high-speed shear layers
p 1024 A92-54905
VIETEN, K. W.
High-performance fighter fly-by-wire flight control actuation system
[AIAA PAPER 92-1123] p 563 A92-33277
VIG, JOHN R.
Low-noise oscillators for airborne radar applications
[AD-A242264] p 300 N92-17258
VIGNERON, YVON
EUROFAR airframe aerodynamic design
p 546 A92-35750
VIGUE, J.
Reaction speed constant for the reactions between N + O2 and between O + N2
[ETN-92-90861] p 347 N92-19252
VIJGEN, P. M. H. W.
Experimental investigation on the effect of crescent planform on lift and drag p 9 A92-13206
Prediction of drag at subsonic and transonic speeds using Euler methods
[AIAA PAPER 92-0169] p 255 A92-23780
VIJGEN, PAUL M. H. W.
Serrated trailing edges for improving lift and drag characteristics of lifting surfaces
[NASA-CASE-LAR-13870-1-CU] p 463 N92-21587
VIKEN, JEFFERY K.
Design of a hybrid laminar flow control nacelle
[AIAA PAPER 92-0400] p 373 A92-26253
VILLA, J. R.
A methodology for software specification and development based on simulation p 135 N92-12458
VILLASENOR, R.
Interaction between chemical reaction and turbulence in supersonic nonpremixed H2-air combustion
p 1117 A92-54931
VILSMEIER, J.
Rapid repair of integrally stiffened carbon fibre composite structures by bolted aluminium elements
[MBB-FE202-S-PUB-0453-A] p 290 N92-17310
Concurrent engineering in design of aircraft structures
[MBB-FE-2-S-PUB-472] p 854 N92-29650
VINALL, PETER D.
Engine reliability p 654 A92-39309
VINCENT, JAMES H.
Robust control law development for a hypersonic cruise aircraft p 478 A92-29127
VINER, MELVYN
Acoustic emission monitoring of a ground durability and damage tolerance test p 492 A92-28737
VINH, N. X.
A Lie Bracket solution of the optimal thrust magnitude on a singular arc in atmospheric flight
[AIAA PAPER 92-4345] p 1079 A92-55334
VINH, NGUYEN X.
Optimal control problems with maximum functional
p 232 A92-18616
VINNEMEIER, F.
Swirl and fuel composition effects on boron combustion in solid-fuel ramjets p 668 A92-36964
VINOGRADOV, B. S.
Diffuser efficiency estimation parameters
p 79 A92-16814
VINOGRADOV, V.
Experimental investigation of liquid carbonhydrogen fuel combustion in channel at supersonic velocities
[AIAA PAPER 92-3429] p 894 A92-48986
VINOGRADOV, V. A.
Numerical and experimental investigation of airframe-integrated inlet for high velocities
p 243 A92-21072
An experimental study of supersonic H2 combustion and heat transfer in a circular duct p 388 A92-25997
VISBAL, MIGUEL R.
Comparative numerical study of two turbulence models for airfoil static and dynamic stall
[AIAA PAPER 92-4649] p 1028 A92-55394
VISINTAINER, JOSEPH A.
Acoustic predictions using measured pressures from a model rotor in the DNW p 165 A92-14385
VISINTINI, L.
Parametric effects of some aircraft components on high-alpha aerodynamic characteristics
p 364 N92-18782
VISKOV, A. N.
Experimental investigation of the optimal deflection of a single-slotted flap with different degrees of extension on a modern supercritical profile p 439 A92-31879
Interference of high-mounted propfan nacelles with an unswept wing and ways to attenuate it
p 460 A92-31881
VISMARA, G.
EH 101 ship interface trials: Flight test programme and preliminary results p 465 N92-21964
VISSER, H. G.
Terminal area traffic management
p 955 A92-50122
VISSER, KENNETH DALE
Breaking down the delta wing vortex: The role of vorticity in the breakdown process p 86 N92-13017
An experimental analysis of critical factors involved in the breakdown process of leading edge vortex flows
p 89 N92-13031
VISWANATHAN, KRISHNAMURTHY
Turbulent mixing in supersonic jets
p 715 N92-27054
VISWANATHAN, SATHY P.
Reliability of helicopter composite dynamic components p 145 A92-14344
VITAGILANO, P. L.
New concepts for multi-block grid generation for flow domains around complex aerodynamic configurations
[NLR-TP-91046-U] p 1037 N92-32730
VITAGLIANO, P. L.
The design of a system of codes for industrial calculations of flows around aircraft and other complex aerodynamic configurations
[AIAA PAPER 92-2619] p 917 A92-45492
New concepts for multi-block grid generation for flow domains around complex aerodynamic configurations
p 817 A92-47079
Domain modeling and grid generation for multi-block structured grids with application to aerodynamic and hydrodynamic configurations p 691 N92-24411
VITALETTI, MARCELLO
An unfactored implicit scheme for 3D inviscid transonic flows
[AIAA PAPER 92-2668] p 798 A92-45523
VITIELLO, DOMINICO
An interactive boundary-layer approach to multielement airfoils at high lift
[AIAA PAPER 92-0404] p 324 A92-26257
VITLIP, MARCIA L.
The design and manufacture of an advanced thermoplastic horizontal stabilator for the AH-64A
p 59 A92-14354
Interlaminar fracture characteristics of bonding concepts for thermoplastic primary structures p 758 A92-41282
VITLIP, ROBERT
Manufacture of a primary flight structure using thermoplastics p 1 A92-10197
VITTING, T.
On aircraft wake properties and some methods for stimulating decay and breakdown of tip vortices
p 87 N92-13021
VIVIANI, A.
Stokes flows in superposed immiscible liquids with horizontal heating
[IAF PAPER 92-0909] p 1123 A92-57288
VIZZINI, ANTHONY J.
Determination of the energy absorption of composite structures under combined loadings p 145 A92-14441
Crashworthiness of truncated composite cones under side loads p 590 A92-35746
VLADIMIROV, A. V.
Analysis of the stability of the lateral motion of aircraft
p 480 A92-30191
VLADIMIROVA, N. A.
Computational studies of transonic flow past a swept wing and the boundary layer characteristics
p 438 A92-31872
VLOT, ARIE
Low-velocity impact loading on fibre reinforced aluminum laminates (ARALL) and other aircraft sheet materials
[ETN-92-91613] p 987 N92-30414
VODEGEL, H. J. G. C.
A computer programme for the certification of helicopter vertical take-off and landing operations and an application to the S-76B helicopter p 106 A92-14379
S-76B certification for vertical take-off and landing operations from confined areas p 530 A92-35760
S-76B certification for vertical take-off and landing operations from confined areas
[NLR-TP-90286-U] p 852 N92-28714
VODENICHAROVA, T.
Linear panel flutter of an elliptic cylindrical shell
p 291 A92-21216
VOELCKERS, U.
A Taxi And Ramp Management And Control system (TARMAC) p 207 N92-14027
Implementation and operational experience with a new arrival traffic management system at the Frankfurt ATC-Center p 728 N92-27905
VOELCKERS, UWE
The COMPAS system in the ATC environment
[DLR-MITT-91-08] p 354 N92-19041
Design principles of automation aids for ATC approach control p 354 N92-19042
VOGEL, A. A.
NASA Workshop on future directions in surface modeling and grid generation
[NASA-CP-10092] p 831 N92-29625
VOGEL, S.
Computation of flutter boundaries in the time and frequency domain p 720 N92-27952
VOGELBACHER, THOMAS
Engine air inlet and de-icing system - At -30 C in the icing tunnel of NRC Ottawa p 92 A92-17252
VOGELESANG, BOUD
Aerospace Arall - A challenge for the aircraft designer
p 33 A92-10232
VOGELS, M. E. S.
WP 4b compressible flow simulation: Information System for flow simulation based on the Navier-Stokes equation (ISNaS). Requirements grid generation for the ISNaS compressible flow solver
[NLR-TR-88103-U] p 405 N92-19490
VOGELSONG, KRISTOFER H.
Ames life science telescience testbed evaluation
[NASA-CR-188856] p 140 N92-12033
VOGT, ANN T.
Cost/benefit analysis of the AH-64 (Apache) helicopter Automated Test Equipment (ATE)
[AD-A252909] p 1101 N92-33398
VOGT, KONRAD
The Dornier 328 Acoustic Test Cell (ATC) for interior noise tests and selected test results
[AIAA PAPER 92-2164] p 1137 N92-32951
VOGT, ROBERT L.
Future trends in turboshaft engines up to 5000 horsepower class
[ASME PAPER 91-GT-74] p 122 A92-15543
VOIRON, T.
Aerothermodynamic calculations for the Space Shuttle Orbiter
[AIAA PAPER 92-2953] p 821 A92-47917
Review of the European hypersonic wind tunnel performance and simulation requirements
p 209 N92-15043
VOKITS, RONALD S.
Avionics modernization/upgrades in the late 1990s
p 199 N92-14055
VOLAKIS, JOHN L.
Development of 3D electromagnetic modeling tools for airborne vehicles
[NASA-CR-190810] p 1126 N92-33307
VOLCHENKO, E. IA.
Automated thematic processing of aircraft scanner data gathered over pasture territory in Turkmenia
p 406 A92-25330
VOLK, J. A.
Multidisciplinary design environment development for air vehicle engineering
[AIAA PAPER 92-1113] p 605 A92-33269
VOLLMERS, HEINRICH
On the simulation of compressible turbulent flows past delta wing, delta wing-body and delta wing-canard
p 84 N92-13003
On the footprints of three-dimensional separated vortex flows around blunt bodies: Attempts of defining and analyzing complex flow structures p 84 N92-13005
VOLODIN, VIACHESLAV V.
Automation of flight vehicle design
[ISBN 5-217-01447-4] p 776 A92-42780
VOLODKO, A. M.
Dynamics of helicopter tip-over during taxiing
p 479 A92-30149
VON GRUENHAGEN, W.
Experiences with high authority helicopter flight control
p 568 A92-35757

VON RETH, R. D.
Status of the NH90 European Helicopter Program
p 113 A92-16676
Organization and technical status of the NH90 European helicopter programme p 1016 A92-56306
VOROB'EV, N. F.
Modeling of the vortex structure at delta wings of low aspect ratio by the discrete vortex method
p 7 A92-12203
An exact solution to edge effect problem for a finite-span wing in supersonic flow p 441 A92-31962
VOROB'EV, V. M.
Restoration of aircraft engine nozzle block blades by vacuum arc brazing with controlled current
p 471 A92-30381
VORONIN, V. I.
An experimental study of subsonic separated flow over parawings p 4 A92-10901
Aerodynamic characteristics of curved delta wings in the case of subsonic separated flow
p 712 A92-44121
VORONKOV, A. Z.
Safety provision against 'ground resonance' free vibration of a coaxial helicopter p 1056 A92-56289
VORONOVA, G. G.
A parametric study of the lift-drag ratio of blunt cones
p 437 A92-31860
VORUM, PETER C.
Cut progression during dynamometer testing of foreign object damaged type VII extra high pressure aircraft tires
[SAE PAPER 912155] p 644 A92-39990
VOS, JAN B.
A multiblock flow solver for inviscid hypersonic flows
p 181 N92-14986
VOSKRESENSKII, G. P.
Numerical simulation of three-dimensional supersonic flow around aerodynamic configurations
p 434 A92-31492
VOSS, N.
Hypersonic airbreathing propulsion activities for Saenger
[AIAA PAPER 91-5040] p 200 A92-17828
VOSS, R.
Comparison of Euler and full potential methods for unsteady transonic flow calculations
p 719 N92-27943
VOTHANH, TAM
A full scale airframe high cycle fatigue test methodology and its application to the SH-2G helicopter
p 105 A92-14345
VOULGARIS, PETROS G.
Optimal rejection of bounded persistent disturbances in periodic systems p 51 A92-11464
VRABLIK, G. R.
Networked simulation of multiple aircraft using Semi-Automated Forces
[AIAA PAPER 92-4170] p 1008 A92-52455
VRANOS, A.
Experimental study of cross-stream mixing in a rectangular duct
[AIAA PAPER 92-3090] p 903 A92-48735
Experimental study of cross-stream mixing in a rectangular duct
[NASA-TM-105694] p 742 N92-27652
VRIES-BAAYENS, ANNE ELISABETH
CAD product data exchange: Conversions for curves and surfaces
[ISBN-90-6275-723-9] p 648 N92-24964
VU-QUOC, L.
Efficient evaluation of the flexibility of tapered I-beams accounting for shear deformations p 295 A92-23269
VU, B. D.
Integration of flight and carrier landing aid systems for shipboard operations
[ONERA, TP NO. 1991-113] p 134 A92-16092
VU, B. DANG
Integration of flight and carrier landing aid systems for shipboard operations p 456 N92-21958
VUCINIC, D.
An integrated CFD system for 3D turbomachinery applications p 741 N92-27464
VUILLERMOZ, P.
The effects of viscosity and diffusion on a supersonic mixing layer p 622 A92-40143
VUILLOT, A. M.
Validation of a 3D Navier-Stokes code on experimental compressor bladings
[ONERA, TP NO. 1991-229] p 330 A92-26381
VUONG, T. M.
Remote sensing of trapping layer base height using ATIS transmissions
[AD-A250074] p 1004 N92-31362
VYSHINSKII, V. V.
A study of flow past bodies of revolution with a Riabushinskii generatrix p 252 A92-23502
Bodies of revolution with minimal wave drag at transonic gas flow velocities p 424 A92-30135
Calculation of three-dimensional separated flows in the framework of the unsteady Euler equations
p 438 A92-31870
VYSHKOV, Y. D.
Progress of magnetic suspension and balance systems for wind tunnels in the USSR p 751 N92-27803

W

WAALAND, I. T.
Technology in the lives of an aircraft designer
[AIAA PAPER 91-3069] p 192 A92-20000
WACHINGER, G.
Development of hardness cycles for fiber bound materials, using DSC: From laboratory specimens to complex high duty structural members
[MBB-Z-0409-91-PUB] p 987 N92-30969
WACHSPRESS, DANIEL A.
Analysis of rotor vibratory loads using higher harmonic pitch control
[NASA-CR-189591] p 696 N92-24251
WADA, Y.
Computation of scramjet inlet flow
p 430 A92-30541
WADA, YASUHIRO
Numerical computation of compressible flow around an object of complex shape p 429 A92-30517
WADAWADIGI, G.
Development of a 3-D upwind PNS code for chemically reacting hypersonic flowfields
[NASA-CR-190182] p 946 N92-30977
WADIER, J. F.
The beta-CEZ - A high performance titanium alloy for aerospace engines p 289 A92-22760
WADSWORTH, MARK
Resin transfer molding of a complex composite aircraft structure p 784 A92-47410
WAGGONER, LARRY P.
Cost/benefit analysis of the AH-64 (Apache) helicopter Automated Test Equipment (ATE)
[AD-A252909] p 1101 N92-33398
WAGNER, B.
Computational aerothermodynamic methods for industrial applications to re-entry and hypersonic cruise problems p 227 N92-15027
WAGNER, D. W.
Performance evaluation of a transonic wind tunnel compressor
[AIAA PAPER 92-3927] p 1096 A92-56758
WAGNER, J. H.
Heat transfer in rotating serpentine passages with trips normal to the flow
[ASME PAPER 91-GT-265] p 151 A92-15663
New applications of liquid-crystal thermography in rotating turbomachinery heat transfer research
[ASME PAPER 91-GT-354] p 153 A92-15710
Heat transfer in rotating serpentine passages with trips skewed to the flow
[NASA-TM-105581] p 499 N92-20235
WAGNER, LEE R.
Human response to helicopter noise: A test of A-weighting
[AD-A243719] p 304 N92-17506
WAGNER, R. D.
Application of laminar flow control to high-bypass-ratio turbofan engine nacelles
[SAE PAPER 912114] p 618 A92-39965
WAGNER, RICHARD D.
Design of a hybrid laminar flow control nacelle
[AIAA PAPER 92-0400] p 373 A92-26253
WAGNER, S.
Influences of wind tunnel parameters on airfoil characteristics at high subsonic speeds
p 173 A92-18769
Complete Euler-solution for a rotor in hover and a propeller in forward flight p 520 A92-35755
Theoretical model to calculate aerodynamic interference effects between rotor and wing of tiltrotors
p 521 A92-35788
Development of a conceptual design method for rotary-wing aircraft using digital computers
p 1058 A92-56340
Investigation of a plate-ramp-configuration by means of laser Doppler anemometry at Mach 2.95
[AIAA PAPER 92-3956] p 1097 A92-56784
The trisonic wind tunnel Muenchen and its involvement in the German SAeNGER-programme
[AIAA PAPER 92-4019] p 1100 A92-56841
WAGNER, STEVEN M.
Gulf Range Drone Control Upgrade System Mobile Control System p 882 A92-47567
WAHLGREN, B. I.
The use of finite difference electromagnetic analysis in the design and verification of modern aircraft
p 192 A92-20136
WAIDMANN, WINFRIED
An experimental investigation of the combustion of a hydrogen jet injected parallel in a supersonic air stream
[AIAA PAPER 91-5102] p 212 A92-17861
WAITZ, IAN A.
A systematic experimental and computational investigation of a class of contoured wall fuel injectors
[AIAA PAPER 92-0625] p 374 A92-27007
WAKA, RYOJI
An analytical evaluation of the aerodynamic forces acting on a circular cylinder in a uniform shear flow
p 522 A92-35995
WAKAHAR, H.
Analysis of the main wing lift distribution of the STOL research aircraft Asuka p 1053 A92-56051
WAKAI, HIROSHI
A shock tunnel experiment on aerodynamic interference induced by RCS jet p 1029 A92-56042
WAKAIRO, KAORU
Evaluation test on the simulator of the liquid crystal flat display. II p 734 A92-43209
WAKAMATSU, NAOYA
Measurement of angle of attack using a five-hole arrow head pitot tube p 941 A92-53009
WAKAMATSU, YOSHIO
Effectiveness of plasma torches for ignition and flameholding in scramjet p 737 A92-44524
Conceptual design of scramjet engine
p 1065 A92-53490
Scramjet engine and its flying test bed
p 1066 A92-53492
Performance analysis of idealized scramjet
p 1066 A92-53493
Flow measurements in scramjet inlets
p 1102 A92-53565
WAKANA, HIROMITSU
Experiments on aeronautical satellite communications using ETS-V p 395 A92-26779
Experiments on aeronautical satellite communications using ETS-V satellite p 639 A92-40187
WAKANA, K.
Aerodynamic characteristics of a hypersonic aircraft
p 711 A92-43226
WAKAYAMA, SEAN
Nonlinear aerodynamics and the design of wing tips
[NASA-CR-190649] p 946 N92-31157
WAKE, ALISON J.
Ground surface erosion - British Aerospace test facility and experimental studies p 881 A92-45323
WAKE, BRIAN E.
Navier-Stokes and Euler solutions for an unmanned aerial vehicle
[AIAA PAPER 92-2609] p 792 A92-45483
Initial validation of an unsteady Euler/Navier-Stokes flow solver for helicopter rotor airloads in forward flight
p 815 A92-46956
WAKISAKA, K.
New-type of ultralight flexible a-Si solar cell and its application on an airplane p 970 A92-53181
WAKU, HIROYUKI
Finite difference numerical prediction of aerodynamics of an airfoil flying over wavy wall p 64 A92-14033
WALCH, STEPHEN P.
H-N2 interaction energies, transport cross sections, and collision integrals p 1135 A92-54660
WALCHLI, LAWRENCE A.
High angle-of-attack control enhancement on a forward swept wing aircraft
[AIAA PAPER 92-4427] p 1080 A92-55351
WALD, J.
Distributed health management systems technology for future propulsion control systems
[SAE PAPER 912167] p 655 A92-39995
WALDER, RAY
Aging aircraft programme entails major effort and expense p 169 A92-20023
WALDO, RICHARD K.
Utility management system for hypersonic vehicles
p 964 A92-49252
WALEFFE, FABIAN
Non-linear interactions in homogeneous turbulence with and without background rotation p 912 N92-30044
WALITT, LEONARD
Navier-Stokes cavity solutions based on second-order turbulence modeling
[AIAA PAPER 92-2765] p 704 A92-41314
WALKER, CARRIE K.
Applications of an automated programming system
[AIAA PAPER 91-3767] p 231 A92-17629
WALKER, D.
Full authority active control system design for a high performance helicopter p 567 A92-35732

WALKER, G. J.
Stator averaged, rotor blade-to-blade near wall flow in a multistage axial compressor with tip clearance variation
[ASME PAPER 91-GT-30] p 67 A92-15514
WALKER, IRA J.
Euler code evaluation of a transatmospheric vehicle at supersonic speeds p 9 A92-13202
Longitudinal and lateral-directional aerodynamic characteristics of a wing-cone configuration at Mach numbers from 2.5 to 4.5
[NASA-TM-4337] p 630 N92-24977
WALKER, J. A.
Development and characterization of Powder Metallurgy (PM) 2XXX series Al alloy products and Metal Matrix Composite (MMC) 2XXX Al/SiC materials for high temperature aircraft structural applications
[NASA-CR-187631] p 390 N92-19290
WALKER, J. D. A.
An algebraic model for dissipation in supersonic boundary layers
[AIAA PAPER 92-0311] p 320 A92-25759
WALKER, J. M.
Measurement of derivatives due to acceleration in heave and sideslip p 364 N92-18785
WALKER, JAMES L., II
Ultimate strength prediction of ASTM D - 3039 tensile specimens from acoustic emission amplitude data
[AIAA PAPER 92-0258] p 394 A92-25716
WALKER, K. P.
A viscoplastic model for single crystals
p 391 A92-24717
Life prediction and constitutive models for engine hot section anisotropic materials program
[NASA-CR-189223] p 1072 N92-33479
WALKER, LAURENCE A.
F-15 STOL/Maneuvering Technology Demonstrator. Phase III - Thrust vectoring, reversing and STOL operation p 112 A92-16054
WALKER, M. M.
Joint computational and experimental aerodynamics research on a hypersonic vehicle
[DE92-013439] p 943 N92-30367
WALKER, MARY M.
Joint computational/experimental aerodynamics research on hypersonic vehicle. II - Computational results p 812 A92-46891
WALKER, ROBERT R.
Spares support of your Rotary-Wing Jenny
p 60 A92-14435
WALKER, STEVEN H.
Computation of vectoring nozzle performance
p 10 A92-13213
WALLACE, F. B.
Regional airline and equipment review - Evolution, trends, and future prospects p 1015 A92-55102
WALLER, G. C.
VORVISC: A vortex lattice method with viscous and compressibility corrections for full aircraft configurations including propulsion p 626 N92-24857
WALLER, MARVIN C.
Flight deck benefits of integrated data link communication
[NASA-TP-3219] p 456 N92-21459
WALLISER, ERIC
Concurrent engineering at Boeing Helicopters
p 162 A92-14393
WALLRAPP, OSKAR
Representation of geometric stiffening in multibody system simulation p 217 A92-19463
WALSH, C.
Computational fluid dynamics p 177 N92-13979
WALSH, JOANNE L.
Integrated multidisciplinary rotorcraft optimization research at the NASA Langley Research Center
p 419 A92-29673
Fully integrated aerodynamic/dynamic optimization of helicopter rotor blades
[AIAA PAPER 92-2374] p 542 A92-34544
Optimizing tuning masses for helicopter rotor blade vibration reduction including computed airloads and comparison with test data
[AIAA PAPER 92-2376] p 542 A92-34546
Optimizing tuning masses for helicopter rotor blade vibration reduction including computed airloads and comparison with test data
[NASA-TM-104194] p 367 N92-19846
Fully integrated aerodynamic/dynamic optimization of helicopter rotor blades
[NASA-TM-104226] p 461 N92-20417
WALSH, JOSEPH
TCAS in the 1990s p 98 A92-16657
WALSH, KEVIN R.
Performance improvements of an F-15 airplane with an integrated engine-flight control system
p 205 A92-20204
Summary of the effects of engine throttle response on airplane formation-flying qualities
[AIAA PAPER 92-3318] p 877 A92-48902
WALSH, M.
An investigation of passive control methods for shock-induced separation at hypersonic speeds
[AIAA PAPER 92-2725] p 808 A92-45596
WALSH, M. J.
Application of finite element methods to fracture mechanics
[PNR-90770] p 503 N92-21741
WALTER, P. L.
Aging Aircraft NDI Development and Demonstration Center (AANC): An overview
[DE92-002358] p 241 N92-15962
WALTER, PATRICK L.
Aging aircraft NDI Development and Demonstration Center (AANC): An overview p 915 N92-30120
WALTERICK, R. E.
Turbulent diffusion flame properties behind a backward-facing step p 985 A92-50255
WALTERS, KEVIN D.
Solutions to supportability concerns related to reduced-signature aircraft p 1055 A92-56220
WALTERS, R. W.
Three-dimensional space-marching algorithm on unstructured grids p 5 A92-11058
Navier-Stokes computations for aerodynamic configurations at high angles of attack
p 246 A92-21981
WALTERS, ROBERT W.
Characteristic-based algorithms for flows in thermochemical nonequilibrium p 670 A92-36846
WALTON, J.
A chambered porous damper for rotor vibration control. II - Imbalance response and bladeless simulation
[ASME PAPER 91-GT-243] p 149 A92-15648
A chambered porous damper for rotor vibration control. I - Concept development
[ASME PAPER 91-GT-244] p 150 A92-15649
WALTON, J. F.
High-temperature powder-lubricated dampers for gas turbine engines p 399 A92-28528
Advanced balancing using laser machining
[SAE PAPER 912218] p 674 A92-40020
WALTON, J. F., II
Rotordynamic evaluation of an advanced multi-squeeze film damper - Imbalance response and bladeless simulation
[ASME PAPER 91-GT-242] p 149 A92-15647
WALTON, JAMES
Reduction of wing rock amplitudes using leading-edge vortex manipulations
[AIAA PAPER 92-0279] p 379 A92-25733
WALTON, JAMES F.
Advanced multi-squeeze film dampers for rotor vibration control p 36 A92-10102
The basics of powder lubrication in high-temperature powder-lubricated dampers
[ASME PAPER 91-GT-248] p 150 A92-15653
WAN, T.
Aerodynamic calculation of an elliptic ring wing
[AIAA PAPER 91-0068] p 1035 A92-57035
WANDER, STEVE
NASA's hypersonic propulsion program: History and direction p 476 N92-21535
WANDERLEY, J. B. V.
Jet inflow simulation and its downwash effect on lifting surfaces p 9 A92-13200
WANG, BO P.
Approximate closed-form buckling solutions for the optimization of aircraft structures p 579 A92-32578
WANG, C. Y.
Numerical and experimental study of jet impingement or interaction effects at hypersonic and supersonic speeds
[AIAA PAPER 91-5038] p 171 A92-17826
WANG, C.-W.
A turbulence model based on RNG for quasi-three-dimensional cascade flows
[AIAA PAPER 92-3312] p 825 A92-48898
WANG, CHAO-ZHI
A calculating method of the kill probability attack area for AAM p 975 A92-50212
WANG, DAOBO
Electronic control of a turbine power unit
p 470 A92-29741
WANG, H.
Rule based identifier for unknown systems
p 509 A92-31430
WANG, H. M.
Fault diagnostics on jet engine starting
p 1116 A92-54345
WANG, H. Y.
Characterization of a two-phase flow field downstream of a 3x-scale gas turbine co-axial, counter-swirling, combustor dome swirl cup
[AIAA PAPER 92-0229] p 393 A92-25693
The influence of spray angle on the continuous- and discrete-phase flowfield downstream of an engine combustor swirl cup
[AIAA PAPER 92-3231] p 863 A92-48832
WANG, HONGMING
An investigation of fuel nozzles for combustion performance p 278 A92-21745
WANG, J.
The formation and structure of plasma wakes behind large high-voltage space platforms in ionosphere
[AIAA PAPER 92-0577] p 407 A92-26984
Ionospheric plasma flow over large high-voltage space platforms. I - Ion-plasma-time scale interactions of a plate at zero angle of attack. II - The formation and structure of plasma wake p 779 A92-41359
WANG, J. J.
Fatigue due to noise-induced pressure
[ASME PAPER 91-GT-150] p 148 A92-15588
WANG, J. R.
Retrieval of total precipitable water over high latitude regions using radiometric measurements near 90 and 183 GHz p 505 A92-32129
WANG, J. T.
Coupled 2D-3D finite element method for analysis of a skin panel with a discontinuous stiffener
[AIAA PAPER 92-2474] p 583 A92-34363
WANG, J.-A.
LDA measurements in a Mach 2 flow over a rearward facing step with staged transverse injection
[AIAA PAPER 92-2692] p 800 A92-45539
WANG, J.-C.
Application of face-gear drives in helicopter transmissions
[NASA-TM-105655] p 908 N92-28434
WANG, JAMES M.
Dynamics of helicopters with dissimilar blades
p 133 A92-14427
Dynamics of helicopters in ground resonance with and without blade dissimilarities
[AIAA PAPER 92-2108] p 544 A92-35679
Bearingless rotor aeromechanical stability measurements and correlations using nonlinear aerodynamics p 547 A92-35772
Dynamics of helicopters with dissimilar blades in forward flight p 1056 A92-56288
WANG, JHY-HORNG
Experimental investigation of the stability of a clearance-excited rotor system with optimal parameters
p 1114 A92-54223
WANG, JIAHUA
Experimental investigation on the structure of flow field and the total pressure loss in an atomizing channel injector p 375 A92-28436
Experimental investigation on the mechanism of flame stabilization in afterburner with V-gutter flameholder
p 487 A92-29725
WANG, JIEBING
Experimental characteristics comparison between two scale-model propellers p 24 A92-10962
WANG, JUNYUAN
Experimental technique of measuring fuel concentration in non-uniform flowfield p 734 A92-41928
WANG, K. C.
Separation patterns and flow structures about a hemisphere-cylinder at high incidences
[AIAA PAPER 92-2712] p 807 A92-45593
WANG, L. C.
Calculation of 3D flow field in a single transonic compressor stage p 422 A92-29719
WANG, LI
Numerical simulation of the flow around rectangular cylinder p 339 A92-27851
WANG, LI-SHENG
A multibody analog of the dual-spin problem
p 49 A92-11426
WANG, LI-ZHEN
A calculating method of the kill probability attack area for AAM p 975 A92-50212
WANG, LIANGYI
Study on calculating the subsonic and supersonic aerodynamic characteristics of slender wing-body combinations at large angles of attack
p 706 A92-41926
WANG, LIANQYI
An efficient calculation method of subsonic aerodynamic characteristics for a Space Shuttle orbiter in the reentry attitude p 252 A92-23383
WANG, LILI
An impact dynamics investigation on some problems in bird strike on windshields of high-speed aircrafts
p 986 A92-53330

WANG, LIXIA
Improved calculation of transonic potential flow past swept wings p 1031 A92-56179
WANG, LU S.
Experimental research on blade containment p 557 A92-35561
WANG, N.
Analysis of lossy composite terminating structures [NASA-CR-189901] p 404 N92-19217
WANG, PAUL
A neural network based postattack damage assessment system p 922 A92-48520
WANG, PEIDE
A separated algorithm and application to flight test p 690 A92-38273
WANG, PING
A new method for calculating burst speed of aeroengine disks [ASME PAPER 91-GT-121] p 670 A92-36899
WANG, QIAN-XI
Analysis of slender bodies of revolution with curved-ground effect and waving-water effect p 524 A92-36151
WANG, RUGEN
Effect of thermodynamic parameters on performance and cost of turbine engines p 969 A92-49834
Research on aircraft life cycle cost reduction p 1012 A92-49835
WANG, SHANGJIN
An analysis method and applications for 3-D viscous internal flows with complex geometry p 143 A92-13299
A calculation procedure for three-dimensional turbulent flow in a centrifugal impeller with any blade geometry [ASME PAPER 91-GT-171] p 73 A92-15606
WANG, SHAOJIAN
Development of an advanced composite material on vertical stabilizer of F-X aircraft p 579 A92-32555
WANG, SHAOQING
Calculation of combustion efficiency of dump combustor in ramjet engine p 375 A92-28480
Calculation methods on equivalence ratio of multi-propellant for propulsion system p 893 A92-48269
WANG, SHENGYUAN
Failure detection of engine sensors with a bank of Kalman filters p 392 A92-24748
WANG, SHIFEN
Hypersonic turbulent separated flow past an unswept circular cylinder on a flat plate p 615 A92-38908
WANG, SHIH H.
Quantitative Feedback Theory approach to AIAA Controls Design Challenge [AIAA PAPER 92-4626] p 1077 A92-55303
WANG, SHUYUAN
A flow visualization experiment on the unsteady flow around two-dimensional airfoil p 615 A92-38913
WANG, T. P.
5,000-hour stability tests of metal sheathed thermocouples at respective temperatures of 538 C and 875 C [ASME PAPER 91-GT-182] p 148 A92-15614
WANG, W. L.
Dynamic analysis technique of rotating centrifugal impeller [ASME PAPER 91-GT-50] p 148 A92-15528
WANG, WEI
Robustness analysis of a model reference adaptive control system p 412 A92-27859
WANG, WEI-GUO
Prospects of turbulence research by means of testing bodies in motion p 30 A92-12194
WANG, WENLIANG
Dynamic analysis of annular cascade shrouded blades p 397 A92-27856
WANG, X.
Decentralized-feedback pole placement of linear systems p 411 A92-27347
WANG, XIANFU
A numerical method for solving the circulation control airfoil with wall jet p 314 A92-25103
WANG, XIAOKUI
Aeroengine sensor failure detection by Bayesian multiple hypothesis testing p 391 A92-24747
WANG, XIAOYU
3D LDA measurement in an axial fan rotor p 391 A92-24730
WANG, XUEJUN
The stability analysis of the nonlinear shimmy p 358 A92-27902
WANG, XUEXIAO
Maximum likelihood algorithm and its application to parameter identification of closed-loop flight vehicles p 1008 A92-53023
WANG, YANRONG
Vibration characteristic analysis of a propeller blade p 38 A92-10967
WANG, YI-YUN
The numerical simulation of compressible flow around an airfoil at high angle of attack p 818 A92-47686
WANG, YIYUN
The numerical simulation of transonic inviscid flow over oscillating airfoils p 616 A92-38918
The numerical simulation of separation control using moving surface effect p 616 A92-38924
WANG, YONGMING
Optimization of multistage axial-flow compressor vane setting p 371 A92-24746
WANG, YUNLIANG
Performance predictions for centrifugal compressor impellers p 759 A92-41836
WANG, Z. H.
Numerical and experimental study of jet impingement or interaction effects at hypersonic and supersonic speeds [AIAA PAPER 91-5038] p 171 A92-17826
WANG, ZHENGMING
An improved method for aerodynamic design of centrifugal impeller blades [ASME PAPER 91-GT-76] p 69 A92-15545
WANG, ZHONGQI
Application of compound leaned blades to controlling secondary flow p 5 A92-10975
A new calculating method for the flowfield in turbomachinery - The study on the application of the vorticity-velocity equations for the numerical solution of the flowfield in turbomachinery p 338 A92-27803
A direct-problem calculation method for gas turbines with bowed and twisted blades p 519 A92-35571
WANG, ZIMING
Investigation of a method for determining machining stress in polymethylmethacrylate (PMMA) of airplane canopies p 986 A92-53096
WANHILL, R. J. H.
NLR experience with high velocity burner rig testing, 1979-1989 [NLR-TP-89152-U] p 385 N92-18415
Diffuser casing upgrade for an advanced turbofan [NLR-TP-90097-U] p 870 N92-28711
Short cracks and durability analysis of the Fokker 100 wing/fuselage structure [NLR-TP-90336-U] p 910 N92-29603
WANIE, K. M.
Verification and application of the NSFLEX method for hypersonic flow conditions p 182 N92-15005
WANKE, CRAIG
Experimental evaluation of candidate graphical microburst alert displays [AIAA PAPER 92-0292] p 369 A92-25745
Alert generation and cockpit presentation for an integrated microburst alerting system p 265 N92-17988
Cockpit display of hazardous weather information p 277 N92-17989
WANKE, CRAIG R.
A data fusion algorithm for multi-sensor microburst hazard assessment [AIAA PAPER 92-4339] p 1063 A92-55328
Experimental evaluation of candidate graphical microburst alert displays [NASA-CR-189633] p 735 N92-27424
WARBURTON, F.
A simulation study of tiltrotor vertical takeoff procedures using conventional and variable diameter rotor systems p 1056 A92-56301
WARD, A. P.
The development of fatigue management requirements and techniques p 360 N92-18572
WARD, C. H.
Development of intermetallic materials for aerospace systems p 754 A92-41874
WARD, D. T.
Preliminary design of an intermittent smoke flow visualization system [AIAA PAPER 92-1028] p 580 A92-33209
WARD, JOHN F.
The practical application of new technology to the civil rotorcraft need p 108 A92-14410
WARD, S.
Prismatic grid generation with an efficient algebraic method for aircraft configurations [AIAA PAPER 92-2721] p 803 A92-45559
WARDI, YORAI
A new class of gradient estimators for queueing systems with real-time constraints p 49 A92-11395
WARDLAW, A. B., JR.
Comparison of two flux splitting schemes for calculation of ogive-cylinder at M = 3.5 and alpha = 18 deg [AIAA PAPER 92-2667] p 806 A92-45582
WARDLAW, R.
Evaluating the velocity accuracy of an integrated GPS/INS system: Flight test results [DE92-007519] p 640 N92-25470
WARDWELL, DOUGLAS A.
On the anomalies in single-jet hover suckdown data [NASA-TM-102261] p 1038 N92-33306
Dynamic response of induced pressures, suckdown, and temperatures for two tandem jet STOVL configurations [NASA-TM-103934] p 1039 N92-33581
On the estimation of jet-induced fountain lift and additional suckdown in hover for two-jet configurations [NASA-TM-102268] p 1040 N92-33618
WARE, GEORGE M.
Predicted aerodynamic characteristics for HL-20 lifting-body using the aerodynamic preliminary analysis system (APAS) [AIAA PAPER 92-3941] p 1033 A92-56771
WARFIELD, MATTHEW J.
Numerical analysis of airflow in aircraft cabins [SAE PAPER 911441] p 245 A92-21837
Computational fluid dynamics applications in airplane cabin ventilation system design [SAE PAPER 911992] p 788 A92-45394
WARNAKA, GLENN E.
A lightweight loudspeaker for aircraft communications and active noise control p 1125 N92-32964
WARNER, DAVID N., JR.
A workstation-based evaluation of a far-field route planner for helicopters [NASA-TM-102882] p 1051 N92-33609
WARNER, J. D.
Assurance of safety in the aging aircraft fleet p 635 A92-39305
WARNER, M.
Controller response to conflict resolution advisory prototype [PB92-190032] p 1050 N92-33596
WARNER, MARGARET
Design considerations for IAP charts: Approach course track and communication frequencies [AD-A241482] p 103 N92-13051
WARNICA, W. D.
A piezoelectric droplet generator for use in wind tunnels p 291 A92-21374
WARREN, DALE S.
Air transports in the 21st century p 1015 A92-55103
WARREN, ERIC S.
A new approach for the calculation of transitional flows [AIAA PAPER 92-2669] p 798 A92-45524
WARREN, STEVEN M.
Dual mode shock absorber and method [PATENT-1-265-541] p 115 N92-13055
WARSHAWSKY, ARNOLD S.
Effectiveness of V-22 tiltrotors in support of land combat operations p 60 A92-14442
WARWICK, GRAHAM
Clever cockpits p 241 A92-21700
Tilting at targets p 357 A92-25074
Flying on thin ice p 634 A92-38375
Shear progress p 609 A92-40880
777 shaping up p 959 A92-52300
Silent solutions p 970 A92-53120
WARZECHA, M. P.
Numerical and experimental analysis of vortex sheets behind lifting surfaces [AIAA PAPER 92-0409] p 325 A92-26262
WASHBURN, ANTHONY E.
Effects of external influences in subsonic delta wing vortices [AIAA PAPER 92-4033] p 1034 A92-56855
WASHBURN, ANTHONY EUGENE
The effect of freestream turbulence on the vortical flow over a delta wing p 261 N92-17681
WASHIDA, T.
Numerical prediction of the flow characteristics in an arc wind tunnel [AIAA PAPER 92-4016] p 1100 A92-56838
WASHIZU, TADAHIRO
Basic study of adhesive bonding for fiber-composites - Adhesive bonding technologies on jet engine parts p 764 A92-44733
WASIKOWSKI, MARK E.
Optimal output feedback for linear time-periodic systems p 412 A92-28142
WASSELL, A. B.
The environmental impact of commercial aviation: The evolution of exhaust emissions legislation and control technology [PNR-90847] p 505 N92-20574

WASSERBAUER, C. A.
NASA low-speed centrifugal compressor for 3-D viscous code assessment and fundamental flow physics research
[ASME PAPER 91-GT-140] p 72 A92-15580
WASSERMAN, LEE
Application of Active Flexible Wing technology to the Agile Falcon p 729 A92-41233
WASZAK, M. R.
Flutter suppression for the Active Flexible Wing - Control system design and experimental validation
[AIAA PAPER 92-2097] p 566 A92-35666
WASZAK, MARTIN R.
A methodology for computing uncertainty bounds of multivariable systems based on sector stability theory concepts
[NASA-TP-3166] p 482 N92-21410
Design and experimental validation of a flutter suppression controller for the active flexible wing
[NASA-TM-4381] p 979 N92-31240
WATABE, T.
The fluid-dynamic measurement of the fling motion of a three-dimensional flat plate p 710 A92-43194
WATANABE, AKIRA
Evaluation test on the simulator of the liquid crystal flat display. II p 734 A92-43209
WATANABE, ATSUSHI
Flight simulator test of cockpit advisory system p 1054 A92-56115
WATANABE, K.
Safety test on the rolling angles of a winged vehicle in hypersonic speed p 480 A92-30549
WATANABE, M.
Development of an automatic metal sheet working machine for interior structure p 700 A92-43247
WATANABE, SEIWA
Experimental operation of aircraft-engine turbine blade materials p 737 A92-43233
WATANABE, SHIGEYA
Safety test on the rolling angles of a winged vehicle in hypersonic speed p 480 A92-30549
Measurement on hypersonic dynamic stable coefficients of a winged vehicle p 430 A92-30550
A scramjet nozzle experiment with hypersonic external flow
[AIAA PAPER 92-3289] p 864 A92-48878
Aerodynamic studies on space plane configuration at hypersonic speed p 1019 A92-53641
Optimal launch trajectory of a hypersonic research vehicle
[AIAA PAPER 92-4302] p 1103 A92-55310
WATANABE, TAKASHI
Magnetohydrodynamic boundary layer flow over a rotating disk p 304 A92-21338
WATANABE, TOSHINORI
Theoretical study on the unsteady aerodynamic characteristics of an oscillating cascade with tip clearance (In the case of loaded cascade) p 331 A92-26797
Numerical simulations of the flow through cascades with tip clearance p 523 A92-36038
WATANABE, Y.
Noise test of high-speed counterrotation propeller in low-speed wind tunnel p 1135 A92-56055
Turbine drive system of the high pressure LOX turbopump test facility
[DE92-783191] p 680 N92-25342
WATANUKI, TADAHARU
Low speed aerodynamic performance of a capsule-shaped flying object p 430 A92-30559
WATERHOUSE, R. B.
Fretting fatigue p 672 A92-38225
WATERMAN, ELLY H.
Advanced Study for Active Noise Control in Aircraft (ASANCA)
[AIAA PAPER 92-2092] p 1137 N92-32956
WATERS, JOHN F.
Addition curing thermosets endcapped with 4-amino (2,2) paracyclophane p 577 A92-33918
WATKINS, MIKE
Advancing airlift avionics - C-17 avionics suite
[AIAA PAPER 92-1243] p 553 A92-33336
WATKINS, R. D.
Development of a wind chamber for model testing of tornado forces on structures
[PB92-104165] p 386 N92-19940
WATSON, SEAN
Proposal for a low cost close air support aircraft for the year 2000: The Raptor
[NASA-CR-190023] p 367 N92-19496
WATTS, MICHAEL E.
Acoustic results of the Boeing model 360 whirl tower test p 603 A92-35741
WATTS, ROLAND
Suit study - The impact of VMS in subsystem integration
[AIAA PAPER 92-1078] p 563 A92-33247
WATZLAWICK, ROBERT
Examination of the main error factors with regards to secondary losses in compression and turbine cascades by variations of the blade picture ratio
[ETN-92-91493] p 871 N92-29927
WAWRZYNEK, PAUL A.
Simulation of arbitrary crack propagation in three-dimensions p 393 A92-25535
WAZYNIAK, JOSEPH A.
Current technology propulsion systems meet the STOVL window of opportunity p 860 A92-45307
WEATHERILL, N. P.
Mesh adaptivity with the quadtree method p 816 A92-47041
Generation of unstructured grids within a hybrid multi-block environment p 818 A92-47090
The simulation of inviscid, compressible flows using an upwind kinetic method on unstructured grids p 933 A92-49515
WEATHERILL, WARREN H.
Flutter in the transonic flight regime p 1089 N92-34167
Flutter analyses using high speed computers. Part 1: Flutter analyses for large aircraft p 1089 N92-34168
Flutter analyses using high speed computers. Part 2: Aerodynamic procedures p 1089 N92-34169
WEAVER, D. P.
An iodine hypersonic wind tunnel for the study of nonequilibrium reacting flows
[AIAA PAPER 92-0566] p 383 A92-26974
WEAVER, DAVE
A-2000: Close air support aircraft design team
[NASA-CR-190022] p 463 N92-21567
WEAVER, K. A.
An airborne Doppler lidar for meteorological research p 467 A92-32082
WEBB, CHARLES D.
Initial design study of existing flight control system of RPH and feasibility study of implementing HHC on the SH-60B
[AD-A240522] p 30 N92-11019
WEBB, DAVID B.
Canadian CF-18 aircraft ejection seat parachute update p 529 A92-32983
WEBB, STEVEN G.
Time-periodic control of a multi-blade helicopter p 204 A92-18626
WEBBER, M. L.
Helicopter fog flying trials p 530 A92-35759
WEBER, A.
Design and analysis of a high pitch to chord ratio cascade representative of ducted propfans
[ASME PAPER 91-GT-335] p 126 A92-15700
WEBER, G.
The 3D inelastic analysis methods for hot section components
[NASA-CR-189089] p 402 N92-18971
Component-specific modeling
[NASA-CR-189088] p 377 N92-19726
WEBER, HELMUT E.
Wave engine aerothermodynamic design
[ASME PAPER 91-GT-4] p 120 A92-15502
WEBER, M.
Lightning activity in microburst producing storm cells
[ONERA, TP NO. 1991-98] p 161 A92-16080
WEBER, M. E.
The 1990 Airport Surveillance Radar Wind Shear Processor (ASR-WSP) operational test at Orlando International Airport
[AD-A239852] p 18 N92-10019
Airport Surveillance Radar (ASR-9) wind shear processor: 1991 test at Orlando, Florida
[AD-A252246] p 1124 N92-32686
WEBER, R. L.
Remote measurements of supercooled integrated liquid water during WISP/FAA aircraft icing program p 915 A92-46788
WEBER, TIMOTHY LAVERN
Turbulence-induced loads on a teetered rotor p 1042 N92-34029
WEBSTER, B. E.
The subsonic and transonic flow around the leading edge of a thin airfoil with a parabolic nose
[AIAA PAPER 92-2649] p 797 A92-45516
WEBSTER, JOHN A.
Extreme wide field-of-view displays and the enclosed cockpit p 965 A92-49313
WEBSTER, JONATHAN D.
NASA advanced aeronautics design solar powered remotely piloted vehicle
[NASA-CR-190007] p 462 N92-20665
WEBSTER, LEE
The wind tunnel test 'system' of 1995 - Cost effective experimentation through a fusion of related technologies p 1091 A92-54342
WECHSLER, GARY
Failure analysis of the Apache mixer pivot support
[AD-A240858] p 116 N92-13061
WEEDA, D. J. A.
Quantitative estimation of secondary surveillance radar information p 353 A92-24943
WEGENER, D.
Comparison between two 3D-NS-codes and experiment on a turbine stator
[AIAA PAPER 92-3042] p 822 A92-48703
WEGER, JAMES
Experimental design of a supersonic shock wave/vortex interaction at Mach 3 p 521 A92-35988
WEGER, PETER
European Fighter Aircraft (EFA) programme status report p 646 A92-40043
WEGNER, W.
Comparison of Euler and full potential methods for unsteady transonic flow calculations p 719 N92-27943
WEI, BAOSUO
Study of a new airfoil used in reversible axial fans p 177 N92-13970
WEI, FU-SHANG
Analytical modeling of SH-2F helicopter shipboard operation p 464 N92-21961
WEI, JIAN-QIU
A method of failure analysis of complicated structures p 901 A92-47656
WEI, JINZHONG
Optimal implicit model-following approach with frequency-shaped weighting and its application to design of flight control system p 977 A92-53094
WEI, M.
A consistency test of airborne GPS using multiple monitor stations p 454 A92-30651
WEI, W.
High temperature MMCs for aero-engines - Challenge and potential p 986 A92-52982
WEI, XINGLU
Triple contra-rotating turbine and its basic analysis p 371 A92-24745
WEI, YANG
U-parameter design example - Robust flight control for wind-shear protection p 28 A92-11502
Trajectory shaping by the U-parameter design method p 479 A92-29361
WEI, YING-JYI P.
F-16 failure detection isolation and estimation study p 876 A92-48490
Intelligent control law tuning for AIAA Controls Design Challenge
[AIAA PAPER 92-4631] p 1132 A92-55306
WEIDEMANN, WERNER
Tactical Rubidium Frequency Standard (TRFS)
[AD-A243934] p 401 N92-18897
WEIDNER, E. H.
Flow establishment in a generic scramjet combustor p 737 A92-44525
WEIDNER, JOHN P.
Hypersonic airbreathing propulsion/airframe integration p 474 N92-21522
WEILAND, C.
Computation of 3-D hypersonic flows in chemical non-equilibrium including transport phenomena
[AIAA PAPER 92-2876] p 820 A92-47858
Aerothermodynamics of nozzle flows for advanced hypersonic propulsion systems p 769 N92-27478
WEILAND, CLAUS
Three-dimensional simulations of hypersonic flows
[MBB-UK-0155-89-PUB] p 447 N92-21703
WEILAND, PETER LAWRENCE
A connectionist approach to autonomous robotic navigation p 454 N92-20356
WEILMUENSTER, K. J.
Comparison of heating calculations with experimental data on a modified Shuttle Orbiter p 441 A92-32184
Gridding strategies and associated results for winged entry vehicles p 918 A92-47051
Characteristics of the Shuttle Orbiter leeside flow during a reentry condition
[AIAA PAPER 92-2951] p 821 A92-47915
WEILMUENSTER, K. JAMES
A high angle of attack inviscid shuttle orbiter computation
[NASA-TM-107606] p 685 N92-25964
WEIMER, M. M.
Design and test of an Active Tip Clearance System for centrifugal compressors
[AIAA PAPER 92-3189] p 863 A92-48801
WEINACHT, PAUL
Navier-Stokes computations for pointed, spherical, and flat tipped shell at Mach 3 p 705 A92-41536
WEINBERG, A. D.
Force measurement on rotating, ablating models using an air bearing balance p 483 A92-31174

WEINBERG, ZVI
Effect of tunnel walls on vortex breakdown location over delta wings p 703 A92-41279
WEINDORF, PAUL
The C-17 Multifunction Display - A building block for avionic systems p 1063 A92-55907
WEINER, STEVEN
LH wind tunnel testing - Key to advanced aerodynamic design p 104 A92-14331
WEINSTEIN, CLIFFORD J.
Opportunities for advanced speech processing in military computer-based systems p 293 A92-22299
WEINSTEIN, LEONARD M.
Reflection type skin friction meter
[NASA-CASE-LAR-14520-1-SB] p 11 N92-10008
Vaporizing particle velocimeter
[NASA-CASE-LAR-14685-1] p 1042 N92-34172
WEINSTEIN, LISA F.
The standardization of military head-up display symbology p 855 A92-44929
An aircraft landing accident caused by visually induced spatial disorientation p 834 A92-44993
The utility of analog vertical velocity information during instrument flight with a Head-Up Display (HUD)
[AD-A252863] p 1065 N92-33277
WEINSTOCK, S.
Formulation of a simplified model of rotor-horizontal stabilizer interactions and comparison with experimental measurements
[ONERA, TP NO. 1991-157] p 77 A92-16125
WEIR, B.
Measurement of derivatives due to acceleration in heave and sideslip p 364 N92-18785
WEIR, L. J.
Three-dimensional viscous analysis of a Mach 5 inlet and comparison with experimental data
p 344 A92-28526
WEISENBURGER, RICHARD
The NASA/Industry Design Analysis Methods for Vibrations (DAMVIBS) program - McDonnell Douglas Helicopter Company achievements
[AIAA PAPER 92-2203] p 540 A92-34393
WEISEND, NORBERT A.
Low energy ice protection for helicopters
p 1059 A92-56348
WEISENSTEIN, DEBRA
Ozone response to aircraft emissions: Sensitivity studies with two-dimensional models p 409 N92-19126
WEISENSTEIN, DEBRA K.
Impact of heterogeneous chemistry on model-calculated ozone change due to high speed civil transport aircraft
p 45 A92-12941
WEISER, P.
Evaluation of rotordynamic coefficients of look-through labyrinths by means of a three volume bulk flow model
p 223 N92-14356
Determination of rotordynamic coefficients for labyrinth seals and application to rotordynamic design calculations p 223 N92-14360
WEISS, CARL F.
An investigation of two cooling technologies as applied to a distributed propulsion control architecture
[ASME PAPER 91-GT-341] p 111 A92-15705
WEISS, GEORGE
Robustness of distributed systems with respect to small time delays p 47 A92-11351
WEISS, HARVEY
A digital Doppler Rate of Descent Indicator (DRODI)
p 555 A92-35927
WEISS, ROSANNE M.
Helicopter nighttime parking test results - UH-1
[DOT/FAA/CT-TN92/1] p 961 N92-31165
WEISSHAAR, TERRENCE A.
Effect of adaptive material properties on static aeroelastic control
[AIAA PAPER 92-2526] p 539 A92-34373
Aeroelasticity - Advances and future directions
[AIAA PAPER 92-2446] p 585 A92-34475
WEISSMAN, DAVID E.
Relating the microwave radar cross section to the sea surface stress - Physics and algorithms
p 597 A92-35028
WELCH, STEVEN R.
MassInfo - An intelligent mass properties information system p 928 A92-47628
WELL, KLAUS-H.
Energy-heading transients in atmospheric flight guidance for airbreathing hypersonic vehicles
[AIAA PAPER 91-5065] p 480 A92-31692
WELLBORN, S. R.
An experimental investigation of the flow in a diffusing S-duct
[AIAA PAPER 92-3622] p 1021 A92-54090
Navier-Stokes analysis and experimental data comparison of compressible flow within ducts
[NASA-TM-105796] p 972 N92-30972
WELLBORN, STEVEN R.
Navier-Stokes analysis and experimental data comparison of compressible flow in a diffusing S-duct
[AIAA PAPER 92-2699] p 800 A92-45541
Navier-Stokes analysis and experimental data comparison of compressible flow in a diffusing S-duct
[NASA-TM-105683] p 1072 N92-33746
WELLER, WILLIAM H.
Variation in hover aeromechanical stability trends with bearingless main rotor design p 109 A92-14425
1991-92 AHS Technical Committee highlights - Dynamics p 647 A92-40393
WELLS, A.
5,000-hour stability tests of metal sheathed thermocouples at respective temperatures of 538 C and 875 C
[ASME PAPER 91-GT-182] p 148 A92-15614
WELLS, DANIEL M.
The development and testing of an active control of structural response system for the EH101 helicopter
p 569 A92-35775
WELLS, DAVID E.
Dredging research program: Global positioning system bibliography
[AD-A248954] p 729 N92-28079
WELLS, S.
Finite wing aerodynamics with simulated glaze ice
[AIAA PAPER 92-0414] p 325 A92-26265
WELLS, WENDLYNN
Dredging research program: Global positioning system bibliography
[AD-A248954] p 729 N92-28079
WELSH, B. L.
A review of rigid body response on sting supported models at high angles of incidence p 66 A92-15345
WELSH, M. C.
Acoustic sources in a tripped flow past a resonator tube p 778 A92-41266
WELTE, D.
Preparation of the ice certification of the Dornier 328 regional airliner by numerical simulation and by ground test p 451 N92-21693
WELTON, W. C.
Compressible Navier-Stokes solutions for a suction boundary control airfoil
[AIAA PAPER 92-2710] p 802 A92-45551
WEN, CHUANYUAN
Reliability aspects in computer integrated manufacturing systems p 397 A92-27838
WEN, WEIDONG
Analysis of tenon and mortise contact problems by boundary element methods p 587 A92-35554
WENDEL, HORST
Bistatic scattering on a monostatic radar range
p 849 A92-48408
WENDL, M.
F15E terrain following system development
[AIAA PAPER 92-1079] p 563 A92-33248
WENDLING, P.
A comparison of measured and modeled broadband fluxes from aircraft data during the ICE '89 field experiment p 1003 A92-49771
WENDT, BRUCE J.
The structure and development of streamwise vortex arrays embedded in a turbulent boundary layer
[AIAA PAPER 92-0551] p 342 A92-28204
WENDT, J. F.
Quantitative heat transfer measurements in hypersonic wind tunnels by means of infrared thermography
p 1115 A92-54321
WENG, P. F.
A new approach to swirl control in an S-duct
p 422 A92-29710
New method of swirl control in a diffusing S-duct
p 809 A92-45859
WENGLARZ, R. A.
An approach for evaluation of gas turbine deposition
[ASME PAPER 91-GT-214] p 653 A92-36890
WENIGWIESER, C.
Summary of Dornier 328 interior noise control study
p 643 A92-39083
WENIGWIESER, CHRISTIAN
Interior noise reduction program for the Dornier 328
p 114 A92-17254
WENNINGER, ED
Preliminary design studies of an advanced general aviation aircraft
[NASA-CR-190024] p 461 N92-20064
WENTZ, KENNETH R.
Acoustic testing at elevated temperatures
p 981 A92-51405
WENTZ, WILLIAM H.
Program plans: Aviation safety research
[NIAR-91-30] p 264 N92-17587
WENZLER, THOMAS
Registration of aircraft in the aircraft registrar using the 'Leasing Decree' of the Federal Minister of Transport of February 12, 1991 p 56 A92-11215
WERLE, H.
Hydrodynamic flow visualization around an oscillating vane. Extension of study to the case of higher incidences and amplitudes and the starting off phase from permanent regime
[ONERA-RT-56/1369-AN] p 43 N92-11312
WERNER, J. S.
Multiple aperture window and seeker concepts for endo KEW applications
[AIAA PAPER 92-2806] p 752 A92-41344
WERNET, MARK P.
A 4-spot time-of-flight anemometer for small centrifugal compressor velocity measurements
[NASA-TM-105717] p 909 N92-29105
WESOKY, HOWARD L.
The atmospheric effects of stratospheric aircraft: A first program report
[NASA-RP-1272] p 408 N92-19121
WESSELMANN, GARY F.
Influence of airfoil geometry on delta wing leading-edge vortices and vortex-induced aerodynamics at supersonic speeds
[NASA-TP-3105] p 350 N92-20038
WESSON, LAURENCE N.
Fiber-optic pressure sensor system for gas turbine engine control p 857 A92-48047
WEST, M. G.
The aerodynamic interference between a flapped tanker aircraft and a receiver aircraft during air-to-air refuelling
p 29 A92-13199
WESTBYE, C. J.
Forced-injection quenching of a hot-tube under microgravity p 590 A92-35977
WESTON, B. A.
Metal-metal bondline NDE methods
[AD-A244429] p 503 N92-21730
WESTON, JOSEPH C.
Helmet-mounted image intensification analysis
p 554 A92-35454
WESTON, RALPH J.
Noise from military airfields in the United Kingdom
p 686 A92-39052
WESTPHAL, R. V.
Measurements of the flow around a lifting-wing/body junction p 175 A92-20726
WESTWATER, E. R.
Remote measurements of supercooled integrated liquid water during WISP/FAA aircraft icing program
p 915 A92-46788
WETTA, P.
Combination of different unsteady quantity measurements for gas turbine blade fault diagnosis
[ASME PAPER 91-GT-201] p 149 A92-15624
WEUBBLES, DONALD J.
Ozone response to aircraft emissions: Sensitivity studies with two-dimensional models p 409 N92-19126
WEYER, H. B.
Thrust nozzle test facility at DLR Cologne
[AIAA PAPER 91-5024] p 206 A92-17818
WEYER, THOMAS H.
DLR-news: Announcements of the German Research Institute for Aeronautics and Astronautics
p 698 N92-25413
DLR-News: Announcements of the German Research Institute for Aeronautics and Astronautics
p 698 N92-26086
WEYGANDT, J. H.
Three-dimensional structure of a curved wake
[AIAA PAPER 92-0541] p 341 A92-28199
WHALEN, J.
Precision drilling of ceramic-coated components with abrasive-waterjets
[ASME PAPER 91-GT-232] p 149 A92-15641
WHALEN, MARGARET V.
Slush hydrogen (SLH2) technology development for application to the National Aerospace Plane (NASP)
p 144 A92-13432
WHEATON, D. G.
Robust discrete controller design for an unmanned research vehicle (URV) using discrete quantitative feedback theory p 877 A92-48495
WHELAN, MARGARET M.
Proposal for a low cost close air support aircraft for the year 2000: The Raptor
[NASA-CR-190023] p 367 N92-19496
WHELAN, MICHAEL A.
Pilot's associate: Evolution of a functional prototype
p 118 N92-12531
WHIRLOW, D. K.
Analysis and prediction of transonic turbine blade losses
[ASME PAPER 91-GT-183] p 73 A92-15615

WHITAKER, KEVIN W.
Turbine blade heat transfer prediction using coupled turbulent Prandtl number and transition models
[SAE PAPER 912152] p 674 A92-39987
Specifying exhaust nozzle contours in real-time using genetic algorithm trained neural networks
[AIAA PAPER 92-3328] p 865 A92-48911
WHITAKER, LESLIE A.
Case-based reasoning - Taming the similarity heuristic
p 47 A92-11153
WHITE, A. D.
Initial validation of a R/D simulator with large amplitude motion p 886 N92-28546
WHITE, B. E.
Low earth orbit satellite concepts for air traffic control applications
[AIAA PAPER 92-1927] p 453 A92-29856
Technical feasibility of digital three-dimensional cellular communications for air traffic control applications. Volume 1: Introduction and summary
[AD-A244573] p 534 N92-22104
Technical feasibility of digital three-dimensional cellular communications for air traffic control applications. Volume 2: Example system design details
[AD-A244574] p 534 N92-22105
Technical feasibility of digital three-dimensional cellular communications for air traffic control applications. Volume 3: Ground network architecture
[AD-A244575] p 534 N92-22106
WHITE, C. D.
Development of an innovative high-temperature gas turbine fuel nozzle
[ASME PAPER 91-GT-36] p 121 A92-15519
WHITE, CRAIG D.
Studies of the effects of curvature on dilution jet mixing p 290 A92-21079
WHITE, D. A.
The use of CT for dimensional measurements of green and sintered ceramic components p 490 A92-28592
WHITE, D. R.
Prediction and measurement of jet flowfield features for ASTOVL aircraft p 787 A92-45318
WHITE, GEORGE
Fatigue and accidents - A comparison across modes of transport p 17 A92-13025
WHITE, J.
Flying qualities evaluation of the V22 tiltrotor
p 131 A92-14334
WHITE, J. A.
CAN-DO, CFD-based Aerodynamic Nozzle Design and Optimization program for supersonic/hypersonic wind tunnels
[AIAA PAPER 92-4009] p 1033 A92-56832
WHITE, JEFFERY A.
Full Navier-Stokes analysis of a three-dimensional hypersonic mixed compression inlet p 343 A92-28501
WHITE, M. E.
Tangential mass addition for shock/boundary-layer interaction control in scramjet inlets p 80 A92-17197
WHITE, MICHAEL E.
The National Aerospace Plane program and the APL role p 666 A92-37375
WHITE, MICHEAL J.
Operational noise data for OH-58D Army helicopters
[AD-A246822] p 926 N92-28292
WHITE, PAUL
Use of Markov methods in analysis of fault-tolerant systems with flexible repair policies
[PNR-90801] p 767 N92-27038
WHITE, ROLAND J.
Effect of wind shear on airspeed during airplane landing approach p 481 A92-32242
WHITE, T. S.
A model of the ADA avionics real-time system: An example of the benefits of the hardware/software codesign approach in development of real-time systems
[AD-A248893] p 967 N92-30524
WHITEHEAD, BRUCE A.
Automated screening of propulsion system test data by neural networks, phase 1
[NASA-CR-184329] p 753 N92-27403
WHITEHEAD, ROBIN S.
Structural assessment of ultralightweight composites
p 1107 N92-32525
Damage tolerance certification methodology for composite structures p 1108 N92-32579
WHITEHURST, R. B., III
KrF laser-induced OH fluorescence imaging in a supersonic combustion tunnel
[AIAA PAPER 92-3346] p 905 A92-48923
WHITEHURST, ROBERT B.
Experimental investigation of a supersonic combustion flowfield employing staged transverse injection behind a rearward-facing step
[AIAA PAPER 92-0090] p 292 A92-22196
WHITFIELD, C. E.
High speed turboprop aeroacoustic study (counterrotation). Volume 2: Computer programs
[NASA-CR-185242] p 1011 N92-31248
WHITFIELD, DAVID
Investigation of solution operators for the three-dimensional Euler equations
[AIAA PAPER 92-2666] p 797 A92-45522
WHITFIELD, DAVID L.
Unsteady flowfield simulation of ducted prop-fan configurations
[AIAA PAPER 92-0521] p 332 A92-26946
Flux-difference split algorithm for unsteady thin-layer Navier-Stokes solutions p 431 A92-31158
WHITFIELD, KENNETH W.
Flight testing of the Boeing 747-400 Central Maintenance Computer system p 555 A92-35950
WHITFORD, RAY
Four decades of transonic fighter design
p 193 A92-20203
The use of large teams in conceptual aircraft design
[AIAA PAPER 92-1092] p 605 A92-33257
WHITING, ELLIS E.
Decoupled predictions of radiative heating in air using a particle simulation method
[AIAA PAPER 92-2971] p 816 A92-46986
WHITING, M.
A universal turboprop engine dynamometer test cell
[ASME PAPER 91-GT-343] p 137 A92-15706
WHITMAN, GARY
Scenario analysis of thigh gap related ejection injuries
p 834 A92-44995
WHITMORE, STEPHEN A.
Pneumatic distortion compensation for aircraft surface pressure sensing devices p 218 A92-20206
Failure detection and fault management techniques for flush airdata sensing systems
[AIAA PAPER 92-0263] p 369 A92-25719
Development of a pneumatic high-angle-of-attack flush airdata sensing system
[SAE PAPER 912142] p 651 A92-39980
High angle-of-attack flush airdata sensing system
p 1064 A92-56172
Development of a pneumatic high-angle-of-attack flush airdata sensing (HI-FADS) system
[NASA-TM-104241] p 118 N92-11994
Failure detection and fault management techniques for flush airdata sensing systems
[NASA-TM-4335] p 276 N92-17128
WHITTREDGE, ROY
Advanced information processing system: Inter-computer communication services
[NASA-CR-187556] p 53 N92-11706
WICHMANN, G.
Aerodynamic analysis and modification design of NPU airfoils p 613 A92-38270
WICHMANN, G. R.
The aerodynamic assistant - A tool for V/STOL aircraft conceptual design p 545 A92-35737
WICKENS, R. H.
Wind tunnel investigation of a wing-propeller model performance degradation due to distributed upper-surface roughness and leading edge shape modification
p 451 N92-21690
WIE, Y. S.
Application of laminar flow control to high-bypass-ratio turbofan engine nacelles
[SAE PAPER 912114] p 618 A92-39965
WIE, YONG-SUN
Numerical solution of the boundary-layer equations for a general aviation fuselage p 174 A92-20211
Design of a hybrid laminar flow control nacelle
[AIAA PAPER 92-0400] p 373 A92-26253
A three-dimensional, compressible, laminar boundary-layer method for general fuselages. Volume 2: User's manual
[NASA-CR-4292-VOL-2] p 678 N92-24344
A three-dimensional, compressible, laminar boundary-layer method for general fuselages. Volume 1: Numerical method
[NASA-CR-4292-VOL-1] p 679 N92-24547
WIEDEMANN, RANDAL A.
Operational survey: VFR heliport approaches and departures
[SCT-91RR-26] p 190 N92-14033
WIELDT, J. A.
Nonflammable hydraulic power system for tactical aircraft. Volume 2: Equipment and systems test and evaluation
[AD-A239805] p 35 N92-10100
WIENER, EARL L.
The impact of cockpit automation on crew coordination and communication. Volume 1: Overview, LOFT evaluations, error severity, and questionnaire data
[NASA-CR-177587] p 93 N92-13044
WIENSS, W.
FALKE and COBRA technology development in aerodynamics and aerothermodynamics
p 183 N92-15017
WIERZBANOWSKI, TED
The NASP Program - An update p 61 A92-16059
WIESBAUM, J.
Finite-element algorithm for chemically reacting hypersonic flow
[AIAA PAPER 92-0754] p 336 A92-27097
WIESE, DOUGLAS E.
Thermal management of hypersonic aircraft using noncryogenic fuels
[SAE PAPER 911443] p 270 A92-21839
WIESEL, WILLIAM E.
Time-periodic control of a multi-blade helicopter
p 204 A92-18626
WIESEMAN, C. D.
Time simulation of flutter with large stiffness changes
[AIAA PAPER 92-2394] p 585 A92-34467
WIESEMAN, CAROL
On-line performance evaluation of multiloop digital control systems p 873 A92-46739
WIESEMAN, CAROL D.
On-line analysis capabilities developed to support the AFW wind-tunnel tests
[AIAA PAPER 92-2084] p 572 A92-35656
On-line analysis capabilities developed to support the AFW wind-tunnel tests
[NASA-TM-107651] p 961 N92-30752
Time simulation of flutter with large stiffness changes
[NASA-TM-107650] p 963 N92-32111
WIESEN, B.
Hypersonic flow calculations around a 3D delta wing at low Knudsen numbers p 937 A92-52734
Rarefied gas flow around a disc with different angles of attack p 938 A92-52753
WIETING, ALLAN R.
Multiple shock-shock interference on a cylindrical leading edge p 813 A92-46899
WIGDOROWITZ, B.
Application of linearization analysis to aircraft dynamics p 661 A92-39902
WIGGENRAAD, J. F. M.
Global/local interlaminar stress analysis of a grid-stiffened composite panel
[NASA-CR-190822] p 1125 N92-33139
WIKSE, STEVE
A-2000: Close air support aircraft design team
[NASA-CR-190022] p 463 N92-21567
WILBUR, M. L.
A demonstration of passive blade twist control using extension-twist coupling
[AIAA PAPER 92-2468] p 539 A92-34358
WILBUR, MATTHEW L.
Recent rotorcraft aeroelastic testing in the Langley Transonic Dynamics Tunnel p 136 A92-14377
Experimental investigation of helicopter vibration reduction using rotor blade aeroelastic tailoring
p 107 A92-14396
Optimizing tuning masses for helicopter rotor blade vibration reduction including computed airloads and comparison with test data
[AIAA PAPER 92-2376] p 542 A92-34546
An experimental study of the sensitivity of helicopter rotor blade tracking to root pitch adjustment in hover
[NASA-TM-4313] p 61 N92-12989
Optimizing tuning masses for helicopter rotor blade vibration reduction including computed airloads and comparison with test data
[NASA-TM-104194] p 367 N92-19846
A demonstration of passive blade twist control using extension-twist coupling
[NASA-TM-107642] p 1001 N92-31155
WILBY, JOHN F.
Interior noise p 236 N92-14785
WILCZYNSKI, VINCENT
Organized turbulent structures and their induced wall pressure fluctuations p 949 N92-31853
WILDER, MICHAEL C.
Fundamental research in helicopter rotor blade-vortex interaction modeling p 65 A92-14358
Control of unsteady separated flow associated with the dynamic stall of airfoils
[NASA-CR-190688] p 950 N92-32177
WILKE, ULRICH
Beriev Be-42 - A unique jet-propelled seaplane
p 269 A92-21010
WILKERSON, JOSEPH
1991-92 AHS Technical Committee highlights - Aircraft design p 608 A92-40392
WILKIE, W. K.
Recent rotorcraft aeroelastic testing in the Langley Transonic Dynamics Tunnel p 136 A92-14377

WILKIE, W. KEATS
An experimental study of the sensitivity of helicopter rotor blade tracking to root pitch adjustment in hover
[NASA-TM-4313] p 61 N92-12989
WILKINSON, R. E.
Liquid cooled turbocharged propulsion system for HALE application
[ASME PAPER 91-GT-399] p 127 A92-15729
WILKINSON, S. P.
Supersonic and hypersonic quiet tunnel technology at NASA Langley
[AIAA PAPER 92-3908] p 1094 A92-56743
WILKINSON, T.
Emerging airframe/propulsion integration technologies at General Electric
[AIAA PAPER 92-3335] p 850 A92-48917
WILKINSON, T. S.
The application of a cylindrical-spherical floating ring bearing as a device to control stability of turbogenerators p 224 N92-14371
WILLEKE, HERMANN
Measurements in the inhomogeneous convective boundary layer using three powered gliders
p 775 N92-26350
WILLIAMS, B. R.
Comparison of solution of various Euler solvers and one Navier-Stokes solver for the flow about a sharp-edged cropped delta wing
[AD-B163639L] p 83 N92-12998
WILLIAMS, BEN R.
Hot gas ingestion characteristics and flow visualization of a vectored thrust STOVL concept
p 860 A92-45316
WILLIAMS, D. D.
Hot-gas reingestion - Engine response considerations
p 860 A92-45317
Hot-gas reingestion engine response considerations
[PNR-90810] p 740 N92-27042
WILLIAMS, DAVID H.
Profile negotiation - A concept for integrating airborne and ground-based automation for managing arrival traffic
p 531 A92-33432
WILLIAMS, F. A.
Compressibility effects in thin channels with injection
p 216 A92-18369
Theories of turbulent combustion in high speed flows
[AD-A253032] p 1111 N92-33624
WILLIAMS, GEORGE M., JR.
A high-performance LLLTV CCD camera for nighttime pilotage p 855 A92-46227
WILLIAMS, JAMES C.
Advanced materials for aircraft engine applications
p 390 A92-28251
WILLIAMS, JOHN R.
Dealing with pilot response in failure case testing
p 549 A92-35952
WILLIAMS, LOUIS J.
NASA aerodynamics program
[NASA-TM-4368] p 609 N92-24678
WILLIAMS, M. H.
Temporal adaptive Euler/Navier-Stokes algorithm involving unstructured dynamic meshes
p 812 A92-46887
WILLIAMS, MARC H.
Spatial and temporal adaptive procedures for the unsteady aerodynamic analysis of airfoils using unstructured meshes
[AIAA PAPER 92-2694] p 800 A92-45540
Spatial and temporal adaptive procedures for the unsteady aerodynamic analysis of airfoils using unstructured meshes
[NASA-TM-107635] p 831 N92-29445
Extension of the integral equation formulation of linearized time dependent subsonic flow
[AD-A250654] p 947 N92-31171
WILLIAMS, MARK J.
Military utility of medium speed V/STOL designs
p 841 A92-45308
WILLIAMS, R. M.
PAYCOS, a multidisciplinary sizing code for hypersonic vehicles
[AIAA PAPER 92-4564] p 1132 A92-55376
AI for RPVs, Sensor Driven Airborne Replanner (SDAR), for a Robotic Aircraft Sensor Platform (RASP)
p 114 N92-12534
WILLIAMS, ROGER L.
A common engineering-to-manufacturing-to-field test strategy to achieve systems readiness beyond the '90s
p 931 A92-53111
WILLIAMS, ROY
Adaptive parallel meshes with complex geometry
p 918 A92-47050
WILLIAMS, S. L.
Navier-Stokes methods to predict circulation control airfoil performance p 442 A92-32243
WILLIAMS, STEVEN P.
Effect of short-term exposure to stereoscopic three-dimensional flight displays on real-world depth perception
[NASA-TP-3117] p 119 N92-13065
Computational algorithms for increased control of depth-viewing volume for stereo three-dimensional graphic displays
[NASA-TM-4379] p 1065 N92-34109
WILLIAMS, T.
Fly-by-light technology development plan
[NASA-CR-181954] p 1086 N92-32778
WILLIAMSON, C. H. K.
The natural and forced formation of spot-like Lambda-structures caused by vortex dislocations in a wake p 621 A92-40111
WILLIAMSON, JAMES S.
Expert Avionics Code Modification
p 921 A92-48513
WILLIS, EDWARD A.
NASA's rotary engine technology enablement program: 1983-1991
[NASA-TM-105562] p 378 N92-20033
Rotary engine performance limits predicted by a zero-dimensional model
[NASA-CR-189129] p 474 N92-20650
WILLIS, RANDY
Manx: Close air support aircraft preliminary design
[NASA-CR-189992] p 463 N92-21565
WILLSHIRE, WILLIAM L., JR.
Preliminary results from the White Sands Missile Range sonic boom propagation experiment
p 1140 N92-33884
Advanced subsonic transport approach noise: The relative contribution of airframe noise
[NASA-TM-104112] p 1140 N92-34148
WILMOTH, R. G.
Aerothermodynamics of a 1.6-meter-diameter sphere in hypersonic rarefied flow p 808 A92-45840
WILMOTH, RICHARD G.
Shock interference prediction using direct simulation Monte Carlo
[AIAA PAPER 92-0492] p 328 A92-26322
Hypersonic rarefied flow past spheres including wake structure
[AIAA PAPER 92-0495] p 329 A92-26325
Application of a parallel direct simulation Monte Carlo method to hypersonic rarefied flows
p 1024 A92-54916
WILSHIRE, B.
Prediction of long-term creep rupture properties for an aluminium alloy for airframe applications
p 141 A92-15206
WILSON, ANTHONY
Drop test: Cessna Golden Eagle 421B
[DOT/FAA/CT-TN91/32] p 837 N92-28900
WILSON, B.
Sentinel 1000 flight test programme overview and preliminary results
[AIAA PAPER 92-1229] p 538 A92-33326
WILSON, CHUCK
Meeting Review: Airborne Aerosol Inlet Workshop
[NASA-CR-189814] p 301 N92-17393
WILSON, DAVID J.
Velocity dependence of high angle of attack longitudinal flying qualities criteria
[SAE PAPER 912149] p 662 A92-39985
WILSON, DENNIS
The effect of a type 3 and type 4 shock/shock interaction on heat transfer in the stagnation region
p 160 N92-13867
WILSON, DONALD R.
Experimental investigation of the perpendicular rotor blade-vortex interaction at transonic speeds
p 340 A92-28047
Experimental investigation of the parallel vortex-airfoil interaction at transonic speeds p 813 A92-46901
WILSON, F. T.
The achievement of aerodynamic goals on the EH101 project through the 'single site' concept
p 1058 A92-56342
WILSON, F. W.
A comparison of the performance of two gust front detection algorithms using a length-based scoring technique
[AD-A250862] p 1004 N92-32103
WILSON, F. W., JR.
Enclosing shapes for single-Doppler radar features
p 494 A92-30476
WILSON, J. F.
A low-power, high-efficiency Ka-band TWTA
p 671 A92-38163
WILSON, JOHN C.
Experimental evaluation of a flat wake theory for predicting rotor inflow-wake velocities
[NASA-TM-4334] p 630 N92-24882
Helicopter low-speed yaw control
[NASA-CASE-LAR-14219-1] p 879 N92-30025
Two-dimensional aerodynamic characteristics of several polygon-shaped cross-sectional models applicable to helicopter fuselages
[NASA-TP-3233] p 944 N92-30394
WILSON, JOSEPH J.
Study of the engine bird ingestion experience of the Boeing 737 aircraft
[DOT/FAA/CT-89/16] p 187 N92-15053
Engine bird ingestion experience of the Boeing 737 aircraft: Expanded data base
[DOT/FAA/CT-91/32] p 1045 N92-34151
WILSON, K.
Supersonic flow mixing and combustion using RAMP nozzle
[AIAA PAPER 92-3840] p 1113 A92-54198
V-22 propulsion system design p 1070 A92-56300
WILSON, K. J.
Thermal imaging of afterburning plumes
p 129 A92-17179
Effect of carbon particles and mixing on afterburning of exhaust plumes
[AIAA PAPER 92-0767] p 387 A92-27107
WILSON, L. G.
Strain-induced extinction of hydrogen-air counterflow diffusion flames - Effects of steam, CO2, N2, and O2 additives to air
[AIAA PAPER 92-0877] p 487 A92-29639
WILSON, MARK R.
An introduction to high speed aircraft noise prediction
[NASA-CR-189582] p 416 N92-19672
WILSON, R.
A time approach to robustness of LTI systems with structured uncertainty and unmodelled dynamics
p 48 A92-11356
WILSON, R. B.
Computational structural analysis and advanced commercial engines p 660 N92-25933
WILSON, R. N.
Prediction of long-term creep rupture properties for an aluminium alloy for airframe applications
p 141 A92-15206
WILSON, ROBERT J.
Decision-making guide for the proposed Coast Guard differential global positioning system
[AD-A246046] p 957 N92-32054
WILSON, TOM M.
Experimental and numerical investigation of anti-icing phenomena on a NACA 0012 assembly
[AIAA PAPER 92-0531] p 459 A92-31669
WILSON, W. J.
Technical feasibility of digital three-dimensional cellular communications for air traffic control applications. Volume 2: Example system design details
[AD-A244574] p 534 N92-22105
WILSON, W. W.
Laser velocimetry measurements in an MHD aerodynamic duct
[AIAA PAPER 92-2986] p 899 A92-46996
WILTBERGER, N. L.
Efficient simulation of incompressible viscous flow over single and multi-element airfoils
[AIAA PAPER 92-0405] p 324 A92-26258
WIMPENNY, J. C.
Civil aircraft design in relation to airworthiness
p 635 A92-39303
WINDT, CARI L.
NASA advanced aeronautics design solar powered remotely piloted vehicle
[NASA-CR-190007] p 462 N92-20665
WINFREE, WILLIAM P.
Thermal imaging of graphite/epoxy composite samples with fabricated defects p 491 A92-28655
Large area QNDE inspection for airframe integrity
p 362 N92-18588
Thermal QNDE detection of airframe disbonds
p 914 N92-30118
WING, DAVID J.
Static performance of a cruciform nozzle with multiaxis thrust-vectoring and reverse-thrust capabilities
[NASA-TP-3188] p 527 N92-23095
WINGROVE, R. C.
Severe turbulence and maneuvering from airline flight records
[AIAA PAPER 92-4341] p 1078 A92-55330
WINKELMANN, ALLEN E.
Studies in general aviation aerodynamics
[NASA-CR-190431] p 827 N92-28511
WINKER, J. A.
Whither scientific ballooning?
[AIAA PAPER 91-3676] p 1 A92-11021
WINKLER, P.-J.
Examples of advanced near-net shape manufacturing techniques for aerospace
[MBB-Z-0399-91-PUB] p 1125 N92-32742

WINOWICH, NICHOLAS S.
Numerical simulation of the reactive flow in advanced (HSR) combustors using KIVA-2
[NASA-CR-188996] p 26 N92-11014
WINTER, H.
The role of planning systems in future air traffic management p 355 N92-19050
WINTER, M.
Eigenfunction analysis of turbulent mixing phenomena p 898 A92-45826
WINYARD, DAVID C.
Single screw mechanism with gaterotor housing at intermediate pressure
[AD-D015140] p 400 N92-18120
WINZELL, BENGT
Recent applications of linear and nonlinear unsteady aerodynamics for aeroelastic analysis p 718 N92-27940
WIRYOHADIATMOJO, E. S. L. H.
Inverse control problems: Mathematical preliminaries, system theoretical approaches, and their applications to aircraft dynamics
[LR-665] p 923 N92-28581
WISE, KEVIN A.
Comparison of six robustness tests evaluating missile autopilot robustness to uncertain aerodynamics p 873 A92-46737
WISHART, D.
The enhancement of mixing in high-speed heated jets using a counterflowing nozzle
[AIAA PAPER 92-3262] p 825 A92-48857
WISNOM, MICHAEL R.
The relationship between tensile and flexural strength of unidirectional composites p 891 A92-45629
WISSINK, A. M.
Efficient iterative methods for the transonic small disturbance equation p 1025 A92-54933
WISSLER, JOHN B.
Transmission of thin light beams through turbulent mixing layers
[AIAA PAPER 92-0658] p 396 A92-27029
WISTON, EDWARD J., II
Nationwide system delay study of the microwave landing system in the New York terminal area, volume 1
[DOT/FAA/CT-TN91/59-VOL-1] p 640 N92-25098
WITHERSPOON, F. D.
High pressure hypervelocity electrothermal wind tunnel performance study and subscale tests
[AIAA PAPER 92-0329] p 383 A92-25776
WITTE, DAVID W.
Axial compression corner flow with shock impingement p 441 A92-32196
WITTENBERG, H.
Symposium on High Speed Airbreathing Propulsion: The Solid Fuel Combustion Chamber and Beyond
[ETN-92-90685] p 575 N92-22268
WITTIG, S.
Life time prediction for ceramic gas turbine components
[ASME PAPER 91-GT-96] p 122 A92-15560
Computer-based areal surface temperature and local heat transfer measurements with thermochromic liquid crystals (TLC) p 763 A92-44326
WOERNDLE, RUDOLF
Influence of cross section variations on the structural behaviour of composite rotor blades p 1121 A92-56320
WOESTE, TIMOTHY J.
Shuttle Entry Air Data System - An experimental investigation of calibration for ascent flight
[AIAA PAPER 92-0133] p 286 A92-23753
WOHLRATH, W.
Preparation of the ice certification of the Dornier 328 regional airliner by numerical simulation and by ground test p 451 N92-21693
WOITHE, K.
Fatigue life behaviour of composite structures p 390 N92-18577
WOJCIECH, JOHN
TCAS in the 1990s p 98 A92-16657
WOJTKIEWICZ, ANDRZEJ
Polish radar technology. V - Adaptive MTI filters for uniform and staggered sampling p 40 A92-12293
WOLF, JOHN D.
Air transports in the 21st century p 1015 A92-55103
WOLF, KLAUS
Application of MSC/DYNA to shock and impact problems in aircraft industry
[MBB-UD-0593-91-PUB] p 225 N92-14382
WOLF, PETER
Poly 1, 2, 4-triazoles via aromatic nucleophilic displacement
[NASA-CASE-LAR-14440-1] p 35 N92-10066
WOLF, STEPHEN
The FML compressor as a drive system for the LFSWT: A narrative p 751 N92-27978
WOLF, STEPHEN W. D.
Development of a quiet supersonic wind tunnel with a cryogenic adaptive nozzle
[NASA-CR-188055] p 751 N92-27976
Development of a quiet supersonic wind tunnel with a cryogenic adaptive nozzle p 751 N92-27977
WOLF, T.
Design of a variable contraction for a full-scale automotive wind tunnel
[AIAA PAPER 92-3929] p 1096 A92-56760
WOLF, THOMAS
Flight testing and simulation of an F-15 airplane using throttles for flight control
[NASA-TM-104255] p 1087 N92-32864
WOLFE, D.
Performance and handling qualities criteria for low cost real time rotorcraft simulators - A methodology development p 136 A92-14365
WOLFE, HOWARD F.
Nonlinear aspects of aerospace structures at high excitation levels flat aluminum beams and plates studied
[AD-A240600] p 44 N92-11383
WOLFRAMM, A. P.
The imaging radar system p 599 N92-23391
WOLFSON, M.
Characteristics of thunderstorm-generated low altitude wind shear - A survey based on nationwide terminal Doppler weather radar testbed measurements p 45 A92-11378
WOLFSON, MARILYN M.
Understanding and predicting microbursts p 407 A92-27953
Predicting summer microburst hazard from thunderstorm day statistics p 407 A92-27960
WOLKE, W.
DLR research reports and communications
[ETN-92-91391] p 929 N92-29218
WOMER, RODNEY K.
X-29 high angle of attack p 111 A92-16052
WON, C. C.
Smart structures for helicopters p 516 A92-35727
WONG, BOON
International SAMPE Electronics Conference, 5th, Los Angeles, CA, June 18-20, 1991, Proceedings
[ISBN 0-938994-58-1] p 985 A92-51901
WONG, C. H.
Nonstationary gasdynamics p 220 N92-13985
WONG, DOUGLAS T.
Evaluation of electrolytic tilt sensors for wind tunnel model angle-of-attack (AOA) measurements p 1116 A92-54344
Evaluation of electrolytic tilt sensors for measuring model angle of attack in wind tunnel tests
[NASA-TM-4315] p 297 N92-16283
WONG, H.
Aerothermodynamic calculations for the Space Shuttle Orbiter
[AIAA PAPER 92-2953] p 821 A92-47917
Equilibrium solution of the Euler and Navier-Stokes equations around a double ellipsoidal shape with mono- and multi-blocks including real gas effects, part 1 p 227 N92-15030
Grid impact on 3D hypersonic flows p 184 N92-15041
WONG, JIM L.
Computations of hypersonic flows around a three-dimensional concave/convex body
[AIAA PAPER 92-2606] p 805 A92-45570
WONG, KA-KHA
Integrated optic components for advanced turbine engine control systems p 925 A92-46248
WONG, R. S.
Low density real gas flows about hypersonic vehicles
[AD-A250048] p 949 N92-31777
WONG, TIN-CHEE
Prediction of steady and unsteady asymmetric vortical flows around circular cones p 172 A92-18372
Computation of vortex wake flows and control of their effects on trailing wings
[AIAA PAPER 92-4429] p 1025 A92-55353
Prediction and control of asymmetric vortical flows around slender bodies using Navier-Stokes equations p 1127 N92-33968
WONG, Y. S.
A time-linearization approach for unsteady transonic flows p 719 N92-27941
WONGWIWAT, WOODY
Thin bondline measurement of adhesively bonded metallic aircraft structures using an ultrasonic analyzer p 491 A92-28684
WOOD, C. W.
Effects of unsteady shock impingement on high-speed gaseous mixing
[AIAA PAPER 91-5091] p 172 A92-17857
WOOD, CHARLES WADE
Oscillating shock impingement on low-angle gas injection into a supersonic flow p 89 N92-13032
WOOD, D. H.
Measurements of the flow around a lifting-wing/body junction p 175 A92-20726
WOOD, DAVID
Simulation and model reduction for the AFW program
[AIAA PAPER 92-2081] p 572 A92-35653
WOOD, E. R.
A time-dependent tip loss formula for rotor blade dynamic analysis p 1057 A92-56310
WOOD, J. R.
NASA low-speed centrifugal compressor for 3-D viscous code assessment and fundamental flow physics research
[ASME PAPER 91-GT-140] p 72 A92-15580
WOOD, JAMES S.
STS-40 descent BET products: Development and results
[NASA-CR-189570] p 286 N92-16012
WOOD, N. B.
Experience with the Johnson-King turbulence model in a transonic turbine cascade flow solver p 821 A92-48207
WOOD, N. L.
Rapid ultrasonic scanning of aircraft structures p 215 A92-17292
WOOD, PETER
Future developments in aeronautical satellite communications p 678 N92-24167
WOOD, RICHARD J.
Architecture for Survivable System Processing (ASSP) p 220 N92-14210
WOOD, RICHARD M.
Assessment of passive porosity with free and fixed separation on a tangent ogive forebody
[AIAA PAPER 92-4494] p 1081 A92-55363
Influence of airfoil geometry on delta wing leading-edge vortices and vortex-induced aerodynamics at supersonic speeds
[NASA-TP-3105] p 350 N92-20038
The natural flow wing-design concept
[NASA-TP-3193] p 631 N92-25202
Natural flow wing
[NASA-CASE-LAR-14281-1] p 829 N92-28729
WOODARD, PAUL R.
Quality assessment of two- and three-dimensional unstructured meshes and validation of an upwind Euler flow solver
[AIAA PAPER 92-0444] p 328 A92-26288
Quality assessment of two- and three-dimensional unstructured meshes and validation of an upwind Euler flow solver
[NASA-TM-104215] p 444 N92-20480
WOODBERRY, R. F. H.
Design and testing leading to certification of the Airbus A340 nose landing gear doors p 272 A92-24192
WOODCOCK, B.
Aerodynamics p 202 N92-13977
WOODFIELD, A. A.
Validation of simulation systems for aircraft acceptance testing p 852 N92-28531
WOODFIELD, A. P.
Inertia-friction welding of an advanced rapidly solidified titanium alloy p 212 A92-18898
WOODFORD, LYNN
New insulation constructions for aerospace wiring applications. Volume 1: Testing and evaluation
[AD-A240638] p 22 N92-11006
New insulation constructions for aerospace wiring applications. Volume 2: The 270 VDC arc tracking testing with power controllers
[AD-A240639] p 23 N92-11007
WOODRUM, LARRY C.
Concept evaluation of the UH-60 externally mounted rescue hoist
[AD-A240545] p 22 N92-11004
WOODS-VEDELER, JESSICA A.
Rolling Maneuver Load Alleviation using active controls
[AIAA PAPER 92-2099] p 566 A92-35670
Rolling maneuver load alleviation using active controls
[NASA-TM-107654] p 962 N92-31351
WOODS, EDWARD, J.
High speed civil transport electrical power system technology requirements
[SAE PAPER 912185] p 655 A92-40005
WOODWARD, D. W.
Optically powered and interrogated rotary position sensor for aircraft engine control applications p 370 A92-27777

WOODWARD, RICHARD P.
Noise of two high-speed model counter-rotation propellers at takeoff/approach conditions p 925 A92-46799
An evaluation of some alternative approaches for reducing fan tone noise
[NASA-TM-105356] p 416 N92-18282
WORKMAN, GARY L.
Convective flow analysis on the KC-135 aircraft
[AIAA PAPER 92-0844] p 493 A92-29610
Modifications to the rapid melt/rapid quench and transparent polymer video furnaces for the KC-135
[NASA-CR-184215] p 157 N92-12231
Process modeling KC-135 aircraft
[NASA-CR-184278] p 359 N92-18347
Materials processing in low gravity
[NASA-CR-184280] p 499 N92-20198
WORKMAN, THOMAS P.
The future of Loran-C navigation, instrument approaches and flight following for air traffic management p 95 A92-16630
WORNOM, STEPHEN F.
Comparison of two Navier-Stokes codes for attached transonic wing flows p 309 A92-24414
WORTMAN, A.
Detonation duct gas generator demonstration program
[AIAA PAPER 92-3174] p 1066 A92-54011
WORTMAN, D. J.
Thermal barrier coatings for gas turbine use p 142 A92-15245
WRAY, A. P.
The influence of blade leaning on the performance of an integrated OGV-diffuser system
[ASME PAPER 91-GT-104] p 122 A92-15561
WRENN, G. A.
Application of multidisciplinary optimization methods to the design of a supersonic transport p 550 N92-23230
WRENN, GREGORY A.
Integrating aerodynamics and structures in the minimum weight design of a supersonic transport wing
[NASA-TM-107586] p 850 N92-28435
WRIGHT, A. D.
The NREL teetering hub rotor code: Final results and conclusions
[DE92-001187] p 410 N92-19633
WRIGHT, GREGORY P.
Handling qualities of the H-76 Fantail Demonstrator p 131 A92-14335
WRIGHT, JAN R.
Elementary flutter analysis p 1088 N92-34162
Flight flutter testing p 1089 N92-34163
WRIGHT, K. W.
Military and civil software standards and guidelines for guidance and control p 163 N92-12452
WRIGHT, P. I.
An improved compressor performance prediction model
[PNR-90873] p 1072 N92-33749
WRIGHT, ROBERT E., JR.
Problems and solutions for transition detection in cryogenic wind tunnels by infrared imaging p 1090 A92-54319
WRIGHT, STEPHANIE
Radio Technical Commission for Aeronautics, Technical Symposium, Washington, DC, Nov. 18-20, 1991, Proceedings p 531 A92-33426
WRIGHT, STEVEN R.
A wing rock model for the F-14A aircraft
[AD-A243109] p 275 N92-17300
WRIGHT, W. B.
Numerical analysis of a thermal deicer
[AIAA PAPER 92-0527] p 357 A92-26950
WRIGHT, WILLIAM B.
Experimental and numerical investigation of anti-icing phenomena on a NACA 0012 assembly
[AIAA PAPER 92-0531] p 459 A92-31669
WU, BANGXIAN
An improved method for aerodynamic design of centrifugal impeller blades
[ASME PAPER 91-GT-76] p 69 A92-15545
WU, C.
Power performance of a nonisentropic Brayton cycle p 54 A92-11281
A computational study of advanced exhaust system transition ducts with experimental validation
[AIAA PAPER 92-3794] p 907 A92-49126
WU, C. C.
Asymptotic theory of transonic wind tunnel wall interference
[AD-A244075] p 403 N92-19080
WU, CHANGMING
A small five-hole spherical pressure probe for compressor experiments p 38 A92-10970
WU, CHIVEY C.
Navier-Stokes calculation of transonic flow past the NTF 65 deg delta wing p 91 N92-13868
WU, FEN
The study of constant value thresholds of FDI in strapdown inertial navigation p 267 A92-22087
WU, GUOCHUAN
Analysis of effects of freestream turbulence on cascade performance p 422 A92-29716
Finite analytic numerical solution of Navier-Stokes equations p 996 A92-53011
WU, HU
A random vortex method for prediction of maximum instantaneous inlet total pressure distortion p 311 A92-24731
On velocity profile models for predicting end wall boundary layers and their blade force defects in axial compressor cascades p 311 A92-24877
New model for predicting end wall boundary layer in an axial cascade p 611 A92-37389
A new method for predicting the end wall boundary layers and the blade force defects inside the passage of axial compressor cascades p 819 A92-47691
WU, J.
A general explicit or semi-explicit algorithm for compressible and incompressible flows p 937 A92-52682
WU, J. M.
Review of the physics of enhancing vortex lift by unsteady excitation p 66 A92-15344
WU, J. T.
Compensating user position for GPS ephemeris error p 101 A92-16968
WU, J. Z.
Review of the physics of enhancing vortex lift by unsteady excitation p 66 A92-15344
WU, LIYI
Time marching integral equation method for the solutions of unsteady transonic flows p 314 A92-25129
An inverse method with regularity condition for transonic airfoil design p 177 N92-13969
WU, M. Z.
Turbulent diffusion flame properties behind a backward-facing step p 985 A92-50255
WU, Q.-H.
Robust stabilization of a helicopter model p 28 A92-11501
WU, SHEN
Fatigue life estimation of fastener holes without load transfer p 291 A92-21472
WU, T. W.
Fatigue due to noise-induced pressure
[ASME PAPER 91-GT-150] p 148 A92-15588
WU, TIN-JUEI
Numerical study on a supersonic open cavity flow with geometric modification of aft bulkhead
[AIAA PAPER 92-2627] p 794 A92-45499
WU, W. B.
Active vibration control of smart structural materials p 673 A92-39281
WU, WEIDONG
The mechanism of liquid-cooling of vane in high-temperature turbine p 969 A92-49841
WU, WENLIANG
Steady state risetimes of shock waves in the atmosphere p 1140 N92-33882
WU, XINPIN
Numerical simulation of three-dimensional turbulent flows in combustion chambers p 970 A92-53276
WU, XUEREN
Solution of stress intensity factor by weight function for small surface cracks in plates p 998 A92-53332
WU, Y.-Y.
LDV measurements of the flowfield in a simulated combustor with axial and side inlets p 672 A92-38867
WU, YAOHUA
Maximum likelihood algorithm and its application to parameter identification of closed-loop flight vehicles p 1008 A92-53023
WU, YINGXIANG
An experimental study of the flow past spheres at transonic speeds and high Reynolds numbers p 312 A92-25002
WU, YUE G.
Studying method of measuring flow-field between stages in axial-flow compressor p 423 A92-29720
WU, YULIN
Inverse solution of 3D incompressible turbulent boundary layer with separated bubbles p 522 A92-35992
WU, ZHE
Optimal maintenance program of damage tolerance structure p 785 A92-47660
WUEBBLES, D. J.
NASA High Speed Research Program, Emissions Scenarios Committee report of meetings on 26 September 1991 and 9 January 1992
[NASA-CR-190379] p 1004 N92-32147
WUEBBLES, DONALD J.
The atmospheric effects of stratospheric aircraft: A first program report
[NASA-RP-1272] p 408 N92-19121
Designing a methodology for future air travel scenarios p 409 N92-19125
WUETHRICH, S.
Non-equilibrium hypersonic flow simulations using the second-order boundary layer equations p 612 A92-37551
WULFF, D.
Measurements of the pressure and velocity distribution in low-speed turbomachinery by means of high-frequency pressure transducers p 391 A92-24723
WYNNE, ELEANOR C.
Structural dynamics division research and technology accomplishments for F.Y. 1991 and plans for F.Y. 1992
[NASA-TM-104188] p 261 N92-17509

X

XI, GUANG
An analysis method and applications for 3-D viscous internal flows with complex geometry p 143 A92-13299
A calculation procedure for three-dimensional turbulent flow in a centrifugal impeller with any blade geometry
[ASME PAPER 91-GT-171] p 73 A92-15606
XI, PING
An investigation on the characteristics of combustor with oblique air jet p 375 A92-28434
XIA, XUEJIAN
Delay of wing vortex bursting by using favorable interaction of vortices p 615 A92-38910
The effect of afterbody devices on drag reduction p 942 A92-53097
XIA, ZHIXUN
An inverse method with regularity condition for transonic airfoil design p 177 N92-13969
XIAO, CHENGSHU
Investigation on vortex control technique of flow separation in diffuser p 338 A92-27828
XIAO, SHUNDA
A low-altitude breakthrough system using optimal path terrain following p 205 A92-20483
Robustness analysis of a model reference adaptive control system p 412 A92-27859
Predictive control for optimal path terrain following system p 955 A92-50207
A fuel-optimal 4D guidance algorithm p 978 A92-53095
XIAO, YE-LUN
Some problems on atmospheric turbulence spectrum and aircraft response p 975 A92-50235
XIE, XIAOBIN
The canard-wing interference and stall safety of light canard aircraft p 111 A92-15341
XIE, YUNWU
Investigation on opening and ejection of an aircraft canopy by using a solid rocket engine p 358 A92-28489
XIN, ZHIMING
Experimental investigation of in-flight oscillation on helicopters and its prevention p 977 A92-53089
XING, BIN
Anti-fatigue optimization design by artificial intelligence strategy p 996 A92-53013
XING, DING-DING
An improved multiple line-vortex method for simulation of separated vortices of slender wings p 819 A92-47694
XING, JUNBO
Experimental investigation on performances of two-dimensional inlet at supersonic speed p 519 A92-35544
XIONG, CHANGBING
Stress analysis of a propeller blade p 38 A92-10963
Stress analysis of a propeller hub p 38 A92-10964
XIONG, HAIQUAN
Analysis of criteria predicting the tendency of pilot induced oscillation for linear non-linear system p 133 A92-15340
XIONG, JUN-JIANG
A study on crack initiation method for durability analysis p 901 A92-47663
XIONG, SHANWEN
A calculation of influence of vortex breakdown on aerodynamic characteristics for slender wings p 616 A92-38920

XIONG, XIAOFEI
Parameter identification of unsteady aerodynamic forces for elastic vehicles
[AIAA PAPER 92-4505] p 1027 A92-55372
XIONG, XINMIN
A numerical method for solving the circulation control airfoil with wall jet p 314 A92-25103
XIONG, ZHANG
A large-scale axial flow compressor facility and dynamic measurement techniques for rotor flow study p 382 A92-24729
XU, CONGRU
Quasi-static analysis of roller bearing p 391 A92-24732
XU, DIAO
Finite analytic numerical solution of Navier-Stokes equations p 996 A92-53011
XU, FENGJING
A compound fatigue investigation of plate specimen under low-cycle load superposed on high cycle load p 587 A92-35555
XU, FUREN
Calculation of the exerting force necessary to form the aircraft hull plate in the symmetry plate bender with three rolls and the feeding value of the centre roll p 998 A92-53297
XU, HAOJUN
The research on Pilot Induced Oscillation p 977 A92-53088
XU, J. Z.
A numerical procedure of three-dimensional design problem in turbomachinery
[ASME PAPER 91-GT-144] p 72 A92-15583
XU, JIAN-ZHONG
Pseudostream function formulation - A method of solving three-dimensional aerodynamic analysis and design problems in turbomachinery p 996 A92-52981
XU, JIANZHONG
Three-dimensional compressible flows in turbo-machinery solved by the pseudostream function formulation p 338 A92-27801
XU, JIBIN
Application of the multiplier penalty function method to the optimum design of wing configurations of aerospace vehicle p 356 A92-25013
XU, KE
Some problems on atmospheric turbulence spectrum and aircraft response p 975 A92-50235
XU, L.
Similarity transformations for compressor blading
[ASME PAPER 91-GT-123] p 70 A92-15568
XU, LI-GONG
A calculating method of shock wave oscillating frequency due to turbulent shear layer fluctuations in supersonic flow p 251 A92-22720
XU, LIPIN
A large-scale axial flow compressor facility and dynamic measurement techniques for rotor flow study p 382 A92-24729
XU, LIPING
3D LDA measurement in an axial fan rotor p 391 A92-24730
XU, MIN
The research of reducing 3-D low supersonic shock wave reflection in a 2-D transonic flexible walls adaptive wind tunnel
[AIAA PAPER 92-3924] p 1095 A92-56755
XU, MING
A study on rotor induced sand and dust environment and its harmfulness to helicopter p 960 A92-53012
XU, MING-CHU
Aerodynamic sensitivities for subsonic lifting-surface p 819 A92-47695
XU, QIHUA
A fuel-optimal 4D guidance algorithm p 978 A92-53095
XU, SU-QIANG
Bird impact analysis of aircraft windshield transparency p 958 A92-50236
XU, TANG
Prediction of low cycle fatigue life of engine cases p 295 A92-23385
XU, XINYU
The response of a helicopter to windshear p 269 A92-21470
XU, YONGDING
New method for boundary layer thickness control on ground plate in wind tunnel p 383 A92-25110
XU, ZHONG
Performance predictions for centrifugal compressor impellers p 759 A92-41836
A failure analysis for landing gear structural system p 849 A92-47667
XU, ZONGQING
A study of dynamic response to bird impact on arc windshields of aircrafts p 952 A92-53340
XUE, DAVID Y.
Finite element nonlinear panel flutter with arbitrary temperatures in supersonic flow
[AIAA PAPER 92-2129] p 589 A92-35696
XUE, DAVID YONGXIANG
Finite element frequency domain solution of nonlinear panel flutter with temperature effects and fatigue life analysis p 682 N92-25589
XUE, JIANHUA
Study on the reliability evaluation of engine fuel accessories p 392 A92-24749

Y

YACAVONE, D. W.
Loss of cabin pressurization in U.S. naval aircraft - 1969-90 p 634 A92-37168
YADAV, D.
Nonlinear landing gear behavior at touchdown p 192 A92-19606
YADLIN, YORAM
Parallel computing strategies for block multigrid implicit solution of the Euler equations p 812 A92-46894
YAGER, RONALD R.
Using new aggregation operators in rule-based intelligent control p 51 A92-11456
YAGER, THOMAS J.
Runway drainage characteristics related to tire friction performance
[SAE PAPER 912156] p 664 A92-39991
26 x 6.6 radial-belted aircraft tire performance
[SAE PAPER 912157] p 644 A92-39992
YAHIA, H.
FCS skewed sensors array: Practical considerations p 968 N92-31868
YAJIMA, N.
Polar patrol balloon
[AIAA PAPER 91-3688] p 15 A92-11031
YALLAPRAGADA, SUBBARAO V.
Reaching conditions in variable structure systems for output feedback control p 506 A92-29037
YAMADA, H.
Shafranov shift in low-aspect-ratio heliotron/torsatron CHS
[NIFS-110] p 1138 N92-33743
YAMADA, HIDESHI
Hydrogen fueled subsonic-ram-combustor model tests for an air-turbo-ram engine
[NAL-TR-1064T] p 280 N92-17855
YAMADA, RYOJI
Current status and future tasks of a cockpit liquid crystal display p 735 A92-43222
YAMADA, YUTAKA
Experiments on turbulent flow due to an enclosed rotating disk p 615 A92-38863
YAMAGAMI, T.
Polar patrol balloon
[AIAA PAPER 91-3688] p 15 A92-11031
YAMAGUCHI, ISAO
Quaternion and Euler angles in kinematics
[NAL-TM-636] p 909 N92-28836
YAMAGUCHI, K.
Deterministic multi-zone ice accretion modeling p 265 N92-17987
YAMAGUCHI, MAKOTO
Study on an induction method for a flying object, taking accelerating targets into account p 744 A92-43127
YAMAGUCHI, SUMIO
Three-dimensional relaxation effect on quasi-3D flow in a blade row with spanwise loading distribution p 936 A92-51593
YAMAGUCHI, YUTAKA
Wing test at the cryogenic wind tunnel of the National Defense Academy p 749 A92-43199
Preliminary airfoil testing experience in the NDA cryogenic wind tunnel p 1091 A92-54326
YAMAME, KOSABURO
Grooved runway surface texture before and after rubber removal p 1093 A92-56111
YAMAMOTO, H.
Integrated system to support computer analysis in conceptual aerospace design p 1130 A92-53596
YAMAMOTO, K.
Conceptual study of separated core ultra high bypass engine
[AIAA PAPER 92-3775] p 867 A92-49119
Laminar-turbulent transition process in the presence of simulated wall roughness p 626 N92-24858
YAMAMOTO, KEIZOU
Design and testing of a composite hingeless hub for rotary-wing aircraft p 1053 A92-56075
YAMAMOTO, KISHI
Study of the flight control of remotely piloted helicopters p 745 A92-43183
YAMAMOTO, KIYOSHI
Spaceplane aerodynamic heating and thermal protection design method p 1102 A92-53578
Proceedings of the Seminar on Investigation and Control of Boundary-Layer Transition
[NAL-SP-11] p 400 N92-18483
YAMAMOTO, KYOJI
Flow of a rarefied gas past a two-dimensional body of an arbitrary shape at small Mach numbers p 937 A92-52726
YAMAMOTO, M.
Effects of attack angle on leg portion of the horseshoe vortex around the idealized wing p 623 A92-40177
YAMAMOTO, MASATAKA
Conceptional design to heat-resistant airframe of HOPE p 575 N92-23820
YAMAMOTO, O.
Structural and aerodynamic analysis of a large-scale advanced propeller blade p 375 A92-28517
Numerical calculations of propfan/swirl recovery vane flow field
[AIAA PAPER 92-3771] p 1022 A92-54160
YAMAMOTO, S.
Demonstration performance of an aircraft liquid crystal display p 735 A92-43224
YAMAMOTO, SATORU
Unsteady Navier-Stokes simulation of turbulent flows through a supersonic compressor cascade p 523 A92-36036
A higher-order accurate Navier-Stokes solver for transonic and supersonic flows in turbomachinery
[AIAA PAPER 92-3044] p 822 A92-48704
YAMAMOTO, SHIRO
Effect of porosity in transpiration cooling system p 1112 A92-53786
YAMAMOTO, YUKIMITSU
HOPE looks to CFD for help p 386 A92-24910
Numerical simulation of hypersonic viscous flow for the design of H-II orbiting plane (HOPE) p 612 A92-37549
Spaceplane aerodynamic heating and thermal protection design method p 1102 A92-53578
Numerical simulation of hypersonic viscous flow for the design of H-2 orbiting plane (HOPE-2)
[NAL-TR-1093] p 11 N92-10009
YAMAMOTO, YUKIMITU
Computational aerodynamic simulation on HOPE p 251 A92-22635
Aerothermodynamic test of spaceplane by thin-skin method p 1093 A92-56043
YAMAMOTO, YUZO
Minimum induced drag of a wing in a circular open wind tunnel p 251 A92-22521
Induced drag of a wing in a circular wind tunnel p 936 A92-50327
YAMAMURA, T.
A model study on diffuser pressure recovery in NAL scramjet test facility with simulated hydrogen combustion
[AIAA PAPER 92-3979] p 1071 A92-56805
YAMANAKA, T.
Advanced SCRAM-LACE system concept for single-stage-to-orbit space plane
[IAF PAPER 91-272] p 32 A92-12599
Airbreathing engine selection criteria for SSTO propulsion system
[IAF PAPER 92-0658] p 1071 A92-57099
YAMANAKA, TATSUO
'Spaceplanes' R&D status of Japan
[AIAA PAPER 91-5002] p 209 A92-17802
Key design considerations for scramjet powered space plane p 1066 A92-53491
An advanced scramjet propulsion concept for a 350 MG SSTO space plane - External nozzle performance
[AIAA PAPER 92-3719] p 1067 A92-54134
YAMANASHI, AKIRA
Development of aircraft bonded structure and the NDI method p 1016 A92-56100
YAMANE, KOSABURO
Development of an instrument for measuring runway roughness p 748 A92-43124
A proposed method for evaluating runway roughness p 748 A92-43125
YAMANE, RYUICHIRO
Oscillation of nearly circular shock waves p 146 A92-15358
Resonance of circular shock waves p 395 A92-26795
YAMANE, TAKASHI
Aeroelastic tailoring analysis for advanced turbo propellers with composite blades p 558 A92-36358
YAMAO, HIROYUKI
A study on the interaction between a bow shock wave generated by a blunt body and a turbulent boundary layer p 8 A92-12424

Experimental study on three-dimensional shock wave-turbulent boundary layer interaction induced by protuberance p 1019 A92-53997
Three-dimensional shock wave-turbulent boundary layer interaction induced by blunt body and protuberance p 1029 A92-56009

YAMATO, HIDEYUKI
Functional mock-up tests for flight control system of the NAL QSTOL research aircraft 'ASKA'
[SAE PAPER 912036] p 881 A92-45422

YAMAUCHI, GLORIA K.
Full-scale investigation of aerodynamic interactions between a rotor and fuselage p 105 A92-14361

YAMAZAKI, TAKASHI
Thermal measurement test in a shock wind tunnel p 748 A92-43104

YAMAZAKI, TETSUO
Design and wind tunnel test of low-Reynolds-number airfoil p 1029 A92-56047

YAN, CHAO
Inverse solution of 3D incompressible turbulent boundary layer with separated bubbles p 522 A92-35992

YAN, CHUANJUN
Numerical simulation of interaction of diffusion flame with vortex pair in a recirculation zone p 390 A92-28433

YAN, HENGYUAN
Numerical calculation of subsonic and supersonic aerodynamic loads around complex configuration vehicle p 175 A92-20488
Dynamic stability of elastic vehicles with unsteady aerodynamic force modeling p 509 A92-29326
Three-dimensional optimal reentry trajectory and aerodynamic heating history of the Space Shuttle p 984 A92-49582
Stability and dynamic coupling of elastic vehicles with unsteady aerodynamic forces considered p 1102 A92-53545

YAN, JIAXIANG
A numerical calculation of three dimensional incompressible laminar, transition and turbulent boundary layers p 393 A92-25138

YAN, JIUKUN
A small five-hole spherical pressure probe for compressor experiments p 38 A92-10970

YAN, LITANG
Experiments on the blade loss transient response of rotor with flexible damped support
[ASME PAPER 91-GT-149] p 148 A92-15587

YAN, MINGGAO
Solution of stress intensity factor by weight function for small surface cracks in plates p 998 A92-53332

YAN, YANGGUANG
The computer analysis of the prediction of aircraft electrical power supply system reliability p 690 A92-37950

YANAGI, R.
Experimental study of the aerodynamic characteristics at Mach 3 of an air-intake model p 711 A92-43204

YANAGI, RYOJI
Mach 3 wind tunnel test of mixed compression supersonic inlet
[AIAA PAPER 92-3625] p 1021 A92-54092

YANAGIHARA, JURANDIR I.
Enhancement of laminar boundary layer heat transfer by a vortex generator p 1118 A92-55453

YANAGIHARA, M.
Aerodynamic model identification of a spaceplane model from a cable-mount dynamic wind-tunnel test p 1093 A92-56114

YANAGIHARA, MASAAKI
Aerodynamic drag as determined from flight test data of the STOL research aircraft Asuka p 709 A92-43145
Motion estimation for cable-mount dynamic wind-tunnel test p 749 A92-43210
Estimation of spaceplane longitudinal stability and control derivatives from dynamic wind tunnel test p 752 A92-43211
Estimation of spaceplane model inertia characteristics p 752 A92-43212
On the characteristics of servo actuators attached to a model spaceplane for dynamic wind-tunnel test p 762 A92-43213
Estimation of spaceplane lateral-directional stability and control derivatives from dynamic wind tunnel test
[SAE PAPER 911979] p 872 A92-45384
Measurements of longitudinal static aerodynamic coefficients with cable mount system p 1093 A92-56013
On the effect of canards on NAL spaceplane model (0 order) in low speed area p 1030 A92-56052
Estimation of cable-mounted model inertia characteristics for dynamic wind-tunnel test
[NAL-TM-641] p 722 N92-28152

YANAGISAWA, MITSUNORI
Static aeroelastic analysis of ACT wind tunnel model aircraft
[NAL-TM-624] p 632 N92-25366

YANAGISAWA, YUJI
Influence of inlet conditions on the flowfield in a model gas turbine combustor p 672 A92-38866

YANAGIZAWA, MITSUNORI
Calculations for aerodynamic characteristics of HOPE type vehicle in subsonic and hypersonic flow p 1018 A92-53560
Calculations of aerodynamic forces on a wing with thrust using B.E.M p 1030 A92-56049
Generalized aerodynamics analysis by the boundary element method p 1030 A92-56050

YANAGIZAWA, MITUNORI
Computational aerodynamic simulation on HOPE p 251 A92-22635

YANAZAKI, TAKASHI
A shock tunnel experiment on aerodynamic interference induced by RCS jet p 1029 A92-56042

YANCEY, R. N.
NDE of advanced turbine engine components and materials by computed tomography
[ASME PAPER 91-GT-287] p 152 A92-15681

YANG, C.-I.
A Navier-Stokes solution of Hull-ring wing-thruster interaction p 221 N92-14310

YANG, CHUN
LOS rate estimation in inertial navigation using landmarks p 453 A92-29360

YANG, DI
Maximum likelihood algorithm and its application to parameter identification of closed-loop flight vehicles p 1008 A92-53023

YANG, GUOCAI
An investigation of the swirl in an S-shaped inlet p 343 A92-28476

YANG, H.
Interactive generation of structured/unstructured surface meshes using adaptivity p 919 A92-47066

YANG, H. Q.
Interfacial instability between a liquid film and the surrounding compressible gas
[AIAA PAPER 92-0461] p 395 A92-26302
Prediction of shock pattern dynamics at hypersonic angle of attack maneuvers of endo-KEW missile forebodies
[AIAA PAPER 92-2768] p 704 A92-41317
Pressure-based high-order TVD methodology for dynamic stall control
[AD-A247056] p 774 N92-27918

YANG, HENRY T. Y.
Aeroelastic analysis of wings using the Euler equations with a deforming mesh p 10 A92-13215
Quality assessment of two- and three-dimensional unstructured meshes and validation of an upwind Euler flow solver
[AIAA PAPER 92-0444] p 328 A92-26288
Three-dimensional time-marching aeroelastic analyses using an unstructured-grid Euler method
[AIAA PAPER 92-2506] p 542 A92-34500
Spatial adaptation of unstructured meshes for unsteady aerodynamic flow computations p 610 A92-36838
Quality assessment of two- and three-dimensional unstructured meshes and validation of an upwind Euler flow solver
[NASA-TM-104215] p 444 N92-20480
Three-dimensional time-marching aeroelastic analyses using an unstructured-grid Euler method
[NASA-TM-107567] p 527 N92-23116

YANG, HONG
A direct-problem calculation method for gas turbines with bowed and twisted blades p 519 A92-35571

YANG, HONGLI
Investigations of the laws of surge and rotating stall forecast in aeronautical engine p 470 A92-29739

YANG, J.
Study of role of unsteady separation in formation of dynamic stall vortex
[AIAA PAPER 92-0196] p 257 A92-23804

YANG, J. N.
Reliability centered maintenance for metallic airframes based on a stochastic crack growth approach p 897 A92-45242

YANG, J. Y.
Steady supersonic and hypersonic flow computations using Eulerian and new Lagrangian formulations
[AIAA PAPER 92-0055] p 249 A92-22170

YANG, JIANN-SHIOU
Controller design for the F-14 pitch axis control problem using the quantitative feedback theory approach p 478 A92-29128

YANG, JOSEPH
An analytical and computational investigation of shock-induced vortical flows
[AIAA PAPER 92-0316] p 321 A92-25763
An analytical and computational investigation of shock-induced vortical flows with applications to supersonic combustion p 405 N92-19538

YANG, KAITIAN
Turbofan with a small bypass ratio for first stage of a two-stage to-orbit vehicle p 968 A92-49833

YANG, LIFA
Comparison of two flutter analysis methods for elastic aircraft p 660 A92-37394

YANG, LILY
Earth atmospheric entry studies for manned Mars missions p 442 A92-32251

YANG, LING
Safety factor and reliability for composite laminates p 996 A92-53070

YANG, P. M.
Computer simulation model for Lucas Stirling refrigerators p 296 A92-23837

YANG, QINGXIONG
Reliability analysis of fatigue life of a structural system p 671 A92-37395
Anti-fatigue optimization design by artificial intelligence strategy p 996 A92-53013

YANG, S. L.
A surface definition code for turbine blade surfaces
[DE92-010574] p 1004 N92-31498

YANG, T. H.
A method of centers based on barrier functions for solving optimal control problems with continuum state and control constraints p 52 A92-11467

YANG, T. W.
Failure analysis and reliability improvement of small turbine engine blades p 993 A92-50860

YANG, WEIMIN
Simulation of commercial-aircraft reliability p 759 A92-42057

YANG, XIAO-DONG
Concerning a basic assumption for aeroelasticity in turbomachinery p 373 A92-26920

YANG, XIAODONG
Aeroacoustical modification of a propeller p 24 A92-10961

YANG, YONGJIAN
Numerical simulation of inviscid flow over a complicated body using an overlapping grid technique p 313 A92-25043

YANG, YONGNIAN
On vortex interference for canard configuration p 64 A92-14071

YANG, YONGSHENG
Free-radicals aided combustion with scramjet applications
[IAF PAPER 92-0659] p 1106 A92-57100

YANG, ZHI-CHUN
Transition of the flutter mode of a two-dimensional section with an external store p 758 A92-41244

YANG, ZHILI
Measurement and analysis of the flow field above a wing/body configuration p 616 A92-38917
The flow field characteristics about a fighter configuration at high angles of attack
[AIAA PAPER 92-4358] p 1025 A92-55344

YANG, ZUO-SHENG
A complete boundary integral formulation for steady compressible inviscid flows governed by nonlinear equations p 934 A92-50211

YANG, ZUOSHENG
Recent progress in finite element method and boundary integral equation method for nonviscous transonic flows p 314 A92-25127

YANIV, GERSHON
Development of a reclined crashworthy crewseat for rotorcraft p 105 A92-14370

YANO, K.
A simple three component velocity measurement method using a rotated split-film sensor p 1115 A92-54333

YANTA, W. J.
Tangential mass addition for shock/boundary-layer interaction control in scramjet inlets p 80 A92-17197

YANTA, WILLIAM J.
A fine-wire thermocouple probe for measurement of stagnation temperatures in real gas hypersonic flows of nitrogen p 1114 A92-54317
Boundary layer study on nozzle wall at hypersonic velocities
[AIAA PAPER 92-4013] p 1034 A92-56836

YAO, HUA
An investigation of real-time diagnostic technique for DEEC system p 470 A92-29742

YAO, HUIZHONG
Transient aerodynamic behaviours associated with stepwise incidence variation of airfoils p 66 A92-15327

YAO, J.
Microburst modelling and scaling p 915 A92-46262

YAO, JIXIAN
Numerical modelling for gas duct in tuboannular combustor p 371 A92-24738
YAO, LIXIN
Steady state risetimes of shock waves in the atmosphere p 1140 N92-33882
YAO, YONGMEI
The performance evaluation of aeroderivative gas turbines p 119 A92-13296
YARAS, M. I.
Effects of simulated rotation on tip leakage in a planar cascade of turbine blades. I - Tip gap flow
[ASME PAPER 91-GT-127] p 71 A92-15572
Effects of simulated rotation on tip leakage in a planar cascade of turbine blades. II - Downstream flow field and blade loading
[ASME PAPER 91-GT-128] p 71 A92-15573
YASHIMA, SATOSHI
Research and development of turbofan engine for supersonic aircraft p 654 A92-38025
YASHIMA, SOTOSHI
Development trends of recent aircraft engines p 558 A92-35919
YASLIK, ALAN D.
Further developments in three-dimensional simulation of electrothermal deicing systems
[AIAA PAPER 92-0528] p 459 A92-31668
YASTROP, G.
Evaluation of triple simultaneous parallel ILS approaches spaced 5000 feet apart, phase 4.b
[DOT/FAA/CT-91/31] p 456 N92-21404
YASTROP, GLORIA
Evaluation of triple simultaneous parallel ILS approaches spaced 4300 feet apart, phase 4a
[ACD-340] p 191 N92-14034
YASU, SHOHACHI
Three-dimensional flow visualization of shock wave using double-pulsed holographic interferometry. II - Flow visualization for three-dimensional shock structures in rotating aeroengine fan blade rows p 497 A92-32507
YASU, SHOUHACHI
Experimental validation of scramjet nozzle performance
[AIAA PAPER 92-3290] p 864 A92-48879
YASUHARA, MICHIRU
The problem of transition from continuum to rarefied gas flows p 251 A92-22519
Flow field around thick delta wing with rounded leading edge
[SAE PAPER 912009] p 789 A92-45409
Shock interaction induced by two hemisphere-cylinders
[SAE PAPER 912043] p 790 A92-45427
DSMC simulation of hypersonic flows past 2-dimensional bodies p 939 A92-52772
YASUTOMI, ZENSABURO
Three-dimensional numerical analysis of impinging circular jet - Discrete vortex method p 1029 A92-56040
YATES, E. C., JR.
Integral equation methods for linear and nonlinear aerodynamics p 617 A92-39949
YATES, JOHN E.
A unified viscous theory of lift and drag of 2-D thin airfoils and 3-D thin wings
[NASA-CR-4414] p 178 N92-13997
YATES, KEN R.
JPATS escape system development p 543 A92-35434
YATES, LESLIE A.
A ballistic investigation of the aerodynamic characteristics of a blunt vehicle at hypersonic speeds in carbon dioxide and air
[AIAA PAPER 92-0328] p 322 A92-25775
Free-flight trim-angle predictions for the aeroassist flight experiment p 705 A92-41540
Streamlines, vorticity lines, and vortices around three-dimensional bodies p 808 A92-45845
Interferograms, schlieren, and shadowgraphs constructed from real- and ideal-gas, two- and three-dimensional computed flowfields
[NASA-CR-190054] p 446 N92-21356
YAZAWA, K.
STOL research aircraft Asuka flight analysis in connection with the operation of the monitoring system p 730 A92-43140
Analysis of the main wing lift distribution of the STOL research aircraft Asuka p 1053 A92-56051
YE, BIQUAN
Calculation of fuel sloshing and its coupling vibration with a tank p 991 A92-50204
YE, XINING
Improvement in transmission loss of aircraft double wall with resonators p 1011 A92-53091
YE, YOUDA
Space-marching calculations of hypersonic inviscid flowfield p 313 A92-25040
YE, ZHENGYIN
A simplified method for simulating steady, unsteady flow around canard wing configuration p 311 A92-24876
A numerical method for analyzing the nonlinear flutter of wings at high angles of attack p 338 A92-27827
YEAGER, WILLIAM T., JR.
Recent rotorcraft aeroelastic testing in the Langley Transonic Dynamics Tunnel p 136 A92-14377
An experimental study of the sensitivity of helicopter rotor blade tracking to root pitch adjustment in hover
[NASA-TM-4313] p 61 N92-12989
YECKLEY, R. L.
Ceramic component processing development for advanced gas-turbine engines
[ASME PAPER 91-GT-120] p 142 A92-15567
YEDAVALLI, R. K.
Aircraft ride quality controller design using new robust root clustering theory for linear uncertain systems
[AIAA PAPER 92-4399] p 1075 A92-55199
YEDAVLLI, R. K.
Applications of robust control theory - Educational implications
[AIAA PAPER 92-4559] p 1131 A92-55271
YEH, F. C.
Heat transfer in rotating serpentine passages with trips normal to the flow
[ASME PAPER 91-GT-265] p 151 A92-15663
Heat transfer in rotating serpentine passages with trips skewed to the flow
[NASA-TM-105581] p 499 N92-20235
YEH, FREDERICK
Aerodynamics and heat transfer investigations on a high Reynolds number turbine cascade
[ASME PAPER 91-GT-157] p 148 A92-15593
YEH, HSI-HAN
Combined H(2)/H(infinity) optimal control design applied to an advanced fighter aircraft
[AIAA PAPER 92-0045] p 281 A92-22162
Loop shaping in mixed H2 and H-infinity optimal control p 507 A92-29177
YEH, J. H.
Study on supersonic combustion in a hypersonic flight
[IAF PAPER 92-0661] p 1106 A92-57101
YEH, R. H.
Boiling heat transfer from an excavated fin p 498 A92-32523
YEH, T. K.
Fair weather convection and light aircraft accidents
[IAF PAPER ST-91-004] p 186 A92-20651
YEN, GUAN-WEI
Computing high-speed flows past an oscillating cylinder near a vertical wall
[AIAA PAPER 92-4653] p 1028 A92-55397
YEN, JING G.
Calculation of pitch-link loads in deep stall using state-of-the-art methodology p 520 A92-35753
YERU, R.
Compressibility effects in turbulent far wakes p 622 A92-40140
YEUAN, J. J.
Inviscid and viscous quasi-three-dimensional flow solutions in a transonic turbine cascade p 523 A92-36035
YI, GUANG-QU
The study of constant value thresholds of FDI in strapdown inertial navigation p 267 A92-22087
YI, JINGHAI
Experimental investigation on gas-particle flow in cascades p 62 A92-13300
YIANNESKIS, M.
Measurements and simulation of the flow around a poppet valve p 675 A92-40103
YILLIKCI, Y. K.
Trimming rotor blades with periodically deflecting trailing edge flaps p 1085 A92-56283
YILMAZ, S.
Determination of aircraft noise levels while the engine is running on the ground - An approach from the point of urbanization and architecture p 688 A92-39064
YIN, DAH N.
Space Shuttle shell structure waffle panel optimization
[AIAA PAPER 92-2359] p 586 A92-34591
YIN, JING
Effect of some load factors of bird impact on blade response p 371 A92-24740
Effect of different force-functions and initial shock pressure on blade response p 374 A92-27913
The selection of bird impact load types p 448 A92-29732
YIN, QUN
The jet screen ignition scheme and its experimental verification p 388 A92-24744
YIN, XIEZHEN
Aerodynamic performances of spoiler motion p 429 A92-30526
YIN, ZEYONG
Cyclic symmetric contact stress analysis of aeroengine rotor assembly p 470 A92-29733
YING, B.
Drag reduction of bluff bodies through momentum injection p 702 A92-41231
YINGER, COLLEEN H.
Evaluation of GPS/UTC steering performance p 1049 N92-33353
YIP, LONG P.
Wind-tunnel and flight tests of a delta-wing remotely piloted vehicle p 21 A92-13208
Model flight tests of a spin-resistant trainer configuration p 1054 A92-56158
YOAHIZAWA, AKIRA
A thin metal model for aerodynamic heating tests of shock wave interaction p 709 A92-43103
YODER, DENNIS A.
Brush seal leakage performance with gaseous working fluids at static and low rotor speed conditions
[NASA-TM-105400] p 297 N92-16265
YOERKIE, CHARLES A., JR.
Stage 2 noise certification of the Sikorsky S-76A and S-76C helicopters p 91 A92-14388
YOKOKURA, SHUICHI
Research on a helicopter information control system p 735 A92-43220
YOKOMIZO, T.
Drag reduction of bluff bodies through momentum injection p 702 A92-41231
Reduction of the side force on pointed forebodies through add-on tip devices p 1024 A92-54918
YON, STEVEN
Effect of airfoil (trailing-edge) thickness on the numerical solution of panel methods based on the Dirichlet boundary condition p 340 A92-28041
YONEMOTO, K.
Wind tunnel tests on the motion of a spaceplane simulation for cable mount p 752 A92-43192
YONEMOTO, KOICHI
Scramjet engine and its flying test bed p 1066 A92-53492
Pre-flight physical simulation test of HIMES reentry test vehicle p 1103 A92-53640
YONEZAWA, SATOSHI
Optimization of aeroelastic system with active control p 1083 A92-56022
YONGHU, WENREN
Computational vorticity capturing - Application to helicopter rotor flows
[AIAA PAPER 92-0056] p 250 A92-22171
An Eulerian/Lagrangian method for computing blade/vortex impingement p 814 A92-46952
YOO, KYUNG M.
Extension and validation of an unsteady wake model for rotors p 702 A92-41224
Prediction of rotor unsteady airloads using vortex filament theory
[AIAA PAPER 92-2610] p 792 A92-45484
YOO, SUNGYUL
Zonal flow analysis method for two-dimensional airfoils p 330 A92-26435
YOON, SEOKKWAN
Calculation of real-gas effects on blunt-body trim angles p 432 A92-31169
YOON, W. S.
Numerical studies of supersonic/hypersonic combustion
[AIAA PAPER 92-0094] p 293 A92-22200
YORK, B. J.
Progress towards the development of transient ram accelerator simulation as part of the U.S. Air Force Armament Directorate Research Program
[AIAA PAPER 92-3248] p 904 A92-48847
YOROZU, MASAHIRO
Preliminary airfoil testing experience in the NDA cryogenic wind tunnel p 1091 A92-54326
YOSHIDA, K.
A conceptual study for future engine test facility
[AIAA PAPER 92-3992] p 1099 A92-56815
YOSHIDA, KENJI
Experimental and numerical study of aerodynamic characteristics for second generation SST
[SAE PAPER 912056] p 844 A92-45439
YOSHIDA, NORIMASA
A gust generation method for full configuration aircraft tests in a low speed wind tunnel. Part 1: Design and preliminary experiments
[NAL-TR-1115-PT-1] p 722 N92-28192
YOSHIDA, T.
The effectiveness of the warp shape airfoil of a supersonic transport p 711 A92-43203

YOSHINAGA, A.
Safety test on the rolling angles of a winged vehicle in hypersonic speed p 480 A92-30549
Measurement on hypersonic dynamic stable coefficients of a winged vehicle p 430 A92-30550
YOSHINO, FUMIO
An analytical evaluation of the aerodynamic forces acting on a circular cylinder in a uniform shear flow p 522 A92-35995
The effect of a velocity gradient on the aerodynamic forces of a circular cylinder with tangential blowing p 614 A92-38859
YOSHIOKA, E.
Research on hypersonic wind tunnel methods in the 90's p 748 A92-43105
YOSHIZAWA, AKIRA
Measurement on hypersonic dynamic stable coefficients of a winged vehicle p 430 A92-30550
Aerodynamic heating characteristics of space planes tested by NAL hypersonic wind tunnel p 1017 A92-53547
Aerothermodynamic test of spaceplane by thin-skin method p 1093 A92-56043
YOSIBASH, ZOHAR
Structural risk assessment in the Israel Air Force for fleet management p 836 A92-46779
YOST, PETER
Navy Aircrew Common Ejection Seat (NACES) program summary p 104 A92-13465
Methods for predicting successful ejection seat canopy penetration p 544 A92-35441
YOTSUYA, TSUTOM
Characterization of superconducting magnetic bearings (dynamic stiffness and damping coefficient in axial direction) p 772 N92-27737
YOU, LIXIN
Advances of cryogenics in aeronautics and astronautics p 398 A92-27908
YOUNG, A. D.
Vortex flow aerodynamics
[AGARD-AR-299] p 946 N92-30947
YOUNG, CLARENCE P., JR.
Buffet test in the National Transonic Facility
[AIAA PAPER 92-4032] p 1100 A92-56854
Buffet test in the National Transonic Facility
[NASA-CR-189595] p 888 N92-29352
YOUNG, COLIN
Lifting line predictions for a swept tip rotor blade p 65 A92-14424
YOUNG, D. P.
Analysis of unsteady aerodynamic and flutter characteristics of an aeroelastic model in transonic flow p 720 N92-27953
YOUNG, DARRELL K.
Structural optimization and Mach scale test validation of a low vibration rotor p 107 A92-14395
YOUNG, G. S.
Surface-layer gusts for aircraft operation p 774 A92-42095
YOUNG, JAMES
Helicopter physical and performance data
[SCT-91RR-27] p 116 N92-13060
YOUNG, L. A.
Hub and pylon fairing integration for helicopter drag reduction p 107 A92-14391
Experimental study of an independently deflected wingtip mounted on a semispan wing
[NASA-TM-102842] p 13 N92-10983
YOUNG, L. E.
NASA's GPS tracking system for Aristoteles p 576 N92-23919
YOUNG, MAURICE I.
Structural dynamics and vibrations of damped, aircraft-type structures
[NASA-CR-4424] p 499 N92-20194
YOUNG, P.
Frequency domain testing of helicopter dynamics using automated input signals p 545 A92-35731
YOUNG, T. W.
A new approach for the calculation of transitional flows
[AIAA PAPER 92-2669] p 798 A92-45524
YOUNT, LARRY J.
Development of fly-by-light systems for commercial aircraft p 744 A92-42605
Digital flight control systems - Some new commercial twists p 974 A92-49264
Fly-by-light technology development plan
[NASA-CR-181954] p 1086 N92-32778
YOUSEFPOR, M.
An framework for robust flight control design using constrained optimization
[AIAA PAPER 92-4603] p 1131 A92-55282
YOUSEFPOR, MARDUKE
Analyzing the flared landing task with pitch-rate flight control systems p 661 A92-39905
YOUSSEF, H. M.
Identification and control of aircraft dynamics using radial basis function neural networks
[AIAA PAPER 92-4393] p 1074 A92-55194
YU, BIN
A numerical calculation of three dimensional incompressible laminar, transition and turbulent boundary layers p 393 A92-25138
YU, JIAN
China's first variable stability aircraft: The BW-1-Gets its pre-acceptance flight tests
[AD-A240941] p 116 N92-13062
YU, JUANHONG
Research on damage tolerance of compressor blade p 588 A92-35556
YU, K.
Supersonic flow mixing and combustion using RAMP nozzle
[AIAA PAPER 92-3840] p 1113 A92-54198
YU, K. H.
Effect of carbon particles and mixing on afterburning of exhaust plumes
[AIAA PAPER 92-0767] p 387 A92-27107
YU, KEN H.
Low-frequency pressure oscillations in a model ramjet combustor p 154 A92-16026
YU, LI J.
Investigation and application of compressor loading technique p 469 A92-29718
YU, N. J.
Transonic airfoil and wing design using Navier-Stokes codes
[AIAA PAPER 92-2651] p 797 A92-45518
YU, Q.
A new vane swirler as applied to dual-inlet side-dump combustor
[AIAA PAPER 92-3654] p 906 A92-49085
YU, SHOUQIN
Finite element method for computing nonisentropic potential transonic flow with shock waves p 312 A92-25009
A penalty-Galerkin finite element method for calculating transonic flow over wings p 943 A92-53386
YU, SHU-KUI
Research of environmental spectrum for aircraft structure p 785 A92-47655
YU, TAO
A numerical method for unsteady transonic flow about wings with control surface p 314 A92-25107
YU, W.
A time approach to robustness of LTI systems with structured uncertainty and unmodelled dynamics p 48 A92-11356
YU, WEIFENG
A simplified method of transient mathematical model for non-augmentation engine p 372 A92-24750
YU, X. T.
Investigation of unsteady excitation effects on aerodynamic properties of airfoils p 66 A92-15335
YU, XINTIAN
A flow visualization experiment on the unsteady flow around two-dimensional airfoil p 615 A92-38913
YUAN, F. G.
Composite laminated shells under internal pressure p 758 A92-41296
YUAN, KUO-AN
A new aeroelastic model for composite rotor blades with straight and swept tips
[AIAA PAPER 92-2259] p 541 A92-34414
YUAN, PIN-JAR
Ideal proportional navigation p 976 A92-50497
YUAN, S. W. K.
Computer simulation model for Lucas Stirling refrigerators p 296 A92-23837
YUAN, XIN
GPS integrated system application in aircraft approach landing p 266 A92-21466
YUCE, MITHAT
Calculation of pitch-link loads in deep stall using state-of-the-art methodology p 520 A92-35753
YUCEIL, BULENT K.
Cylinder-induced shock-wave boundary-layer interaction p 433 A92-31188
YUHAS, ANDREW J.
Effects of bleed air extraction of thrust levels on the F404-GE-400 turbofan engine
[AIAA PAPER 92-3092] p 1066 A92-54009
Effects of bleed air extraction on thrust levels on the F404-GE-400 turbofan engine
[NASA-TM-104247] p 871 N92-29425
YUKAWA, KIYOSHI
An experimental program concerning a satellite data link for oceanic ATC p 1046 A92-56093
YUMITE, YOSHIYUKI
Development of ITS90 small gas turbine engine p 1070 A92-55500
YUN, QILIN
Application of the wall pressure method to wall interference corrections for model tests at high angle of attack in high speed wind tunnel p 315 A92-25134
Measurement of turbulent boundary layer in transonic flow p 941 A92-53010
YUNCK, THOMAS P.
NASA's GPS tracking system for Aristoteles p 576 N92-23919
YUNGKURTH, C.
The F/A-18 external burning flight test
[AIAA PAPER 91-5050] p 731 A92-44547
YUNGSTER, S.
Computational studies of a superdetonative ram accelerator mode p 399 A92-28529
YUNGSTER, SHAYNE
Study of shock-induced combustion using an implicit TVD scheme p 669 N92-25816
YURKANIN, D. J.
Proposal for a 3-D, vectorized, adaptable, algorithm for modeling the randomness, unsteadiness, and microphysical properties of ice accretion
[AIAA PAPER 92-0299] p 351 A92-25751
YUTO, T.
Operation of the on-board measuring system of the STOL research aircraft Asuka p 734 A92-43139

Z

ZAAL, K. J. J. M.
The two-bay crack problem in fuselages built in GLARE and ARALL
[LR-653] p 196 N92-14044
ZAB, RONALD JOSEPH
Thermal mechanical analysis of sprag clutches
[NASA-CR-190686] p 1128 N92-34207
ZABUSKY, N. J.
Emergence of coherent patterns of vortex stretching during reconnection - A scattering paradigm p 38 A92-11041
ZACCARIA, M.
Investigation of three-dimensional flow field in a turbine including rotor/stator interaction. I - Design development and performance of the research facility
[AIAA PAPER 92-3325] p 883 A92-48908
Investigation of three-dimensional flow field in a turbine including rotor/stator interaction. II - Three-dimensional flow field at the exit of the nozzle
[AIAA PAPER 92-3326] p 826 A92-48909
ZACHAR, EDWARD
H-76B Fantail demonstrator composite fan blade fabrication p 145 A92-14356
ZACHO, LEON H.
An overview of the planned aerospace test facilities at Capua, Italy
[AIAA PAPER 92-3944] p 1097 A92-56773
ZADNEV, A. A.
A test bench for evaluating powerplant electrization p 138 A92-16830
ZAFF, BRIAN S.
Identifying design requirements using integrated analysis structures p 922 A92-48527
ZAGRODNIK, JEFFREY P.
Nickel hydrogen common pressure vessel battery development p 598 N92-22770
ZAICHIK, L. E.
Estimation of the optimal load characteristics of aircraft control levers p 479 A92-30150
ZAKHARCHENKO, VADIM F.
Fundamentals of applied aerogasdynamics. II - Viscous flow past bodies. Control devices p 64 A92-14281
ZAKHARENKOV, M. N.
Unsteady incompressible viscous flow past an airfoil p 3 A92-10662
ZAKHAROV, IU. I.
Development and bench test of high-temperature combustion chamber with structural ceramic components
[ASME PAPER 91-GT-315] p 126 A92-15691
ZAKHAROV, S. B.
A method for calculating the separated flow past a circular cone, taking viscous-inviscid interaction into account p 427 A92-30203
The effect of rounding the leading edges on the characteristics of separated flow past delta wings of low aspect ratio
[RAE-LIB-TRANS-2164] p 257 N92-15964
ZAKHAROVA, I. M.
Use of the TMS-65 heating equipment at airports to create fog-dispersal zones above the runway to facilitate takeoff p 775 A92-44084
ZAKRAJSEK, JAMES J.
Modal simulation of gearbox vibration with experimental correlation
[AIAA PAPER 92-3494] p 1112 A92-54036

Analysis and modification of a single-mesh gear fatigue rig for use in diagnostic studies
[NASA-TM-105416] p 773 N92-27879
Modal simulation of gearbox vibration with experimental correlation
[NASA-TM-105702] p 1002 N92-31485
ZAKRENT, ANDRZEJ
Radioaltimeter RWL-750 p 855 A92-45374
ZALAMEDA, JOSEPH N.
Thermal imaging of graphite/epoxy composite samples with fabricated defects p 491 A92-28655
ZALAUTDINOV, S. R.
A method for determining equivalent stresses in aviation gas turbine engine blades p 559 A92-36421
ZALEWSKI, P.
A model of a deformable aeroplane with a wing of low aspect ratio and movable control surfaces for studying natural vibrations p 744 A92-41528
ZAMAN, K. B. M. Q.
Effect of tabs on the evolution of an axisymmetric jet p 656 A92-40151
Effect of acoustic excitation on stalled flows over an airfoil p 703 A92-41267
Experimental investigation of the flowfield of an oscillating airfoil
[AIAA PAPER 92-2622] p 793 A92-45494
Supersonic jet mixing enhancement by 'delta-tabs'
[AIAA PAPER 92-3548] p 826 A92-49063
Supersonic jet mixing enhancement by delta-tabs
[NASA-TM-105664] p 630 N92-24958
Turbulent heat flux measurements in a transitional boundary layer
[NASA-TM-105623] p 716 N92-27377
Experimental investigation of the flowfield of an oscillating airfoil
[NASA-TM-105675] p 833 N92-30182
ZAMBRANA, HORACIO A.
Reactivation and upgrade of the NASA Ames 16-Inch Shock Tunnel - Status report
[AIAA PAPER 92-0327] p 383 A92-25774
Flow characterization in the NASA Ames 16-inch Shock Tunnel
[AIAA PAPER 92-3810] p 1090 A92-54180
ZAMMIT, ROSE M.
CH-53E/AV-8B aircraft sling load recovery system analysis
[AD-A239950] p 21 N92-10022
ZANDBERGEN, P. J.
Improved shock-capturing of Jameson's scheme for the Euler equations
[PB92-148758] p 596 N92-23251
ZANG, JUN
Dynamic analysis of annular cascade shrouded blades p 397 A92-27856
ZANG, T. A.
Direct numerical simulation of laminar breakdown in high-speed, axisymmetric boundary layers
[AIAA PAPER 92-0742] p 343 A92-28223
ZANG, THOMAS A.
Secondary instability mechanisms in compressible, axisymmetric boundary layers
[AIAA PAPER 92-0743] p 343 A92-28224
A weakly nonlinear theory for wave-vortex interactions in curved channel flow
[NASA-TP-3158] p 347 N92-19175
ZANIN, B. IU.
Comparative studies of flow around a wing profile in two wind tunnels p 7 A92-12170
Generation of several wave packets in the boundary layer of a wing profile p 424 A92-30136
Structure of a boundary layer on the lower surface of a wing in flight and in a wind tunnel p 440 A92-31899
ZANOTTI, C.
Aluminium-lithium alloys - Application on helicopters p 1106 A92-56326
ZAPRIAGAEV, V. I.
Three-dimensional singularity of flow structure in an underexpanded supersonic jet p 78 A92-16679
Characteristics of the mechanism of separated flow pulsation ahead of a spike-tipped cylinder in supersonic flow p 337 A92-27597
ZARA, JAMES A.
Chaotic and nonlinear dynamic response of aerosurfaces with structural nonlinearities
[AIAA PAPER 92-2547] p 518 A92-34517
ZARIANKIN, ARKADII E.
Total losses in turbulent flows inside conical diffusers p 819 A92-47782
ZARIFI-RAD, F.
Effect of model cooling on periodic transonic flow p 813 A92-46900
Further investigation of the effect of model cooling on periodic transonic flow p 721 N92-27961
ZARKHIN, V. I.
Power spectrum of ring modes of pressure fluctuations at the surface of a cylinder in axial flow p 603 A92-33770
ZARUBIN, V. A.
The designer-FEM model interface based on the data base management concept p 163 A92-16832
ZAVALA, MARK A.
Performance and stability analysis of the non-linear dynamics of a simple powered lifting hypersonic vehicle flying on a minor circle
[AD-A243933] p 366 N92-19192
ZAVARZINA, E. K.
High-temperature metal matrix composite p 1105 A92-53878
ZAVITZ, D.
A parametric approach to spectrum development p 360 N92-18578
ZEDALIS, M. S.
The microstructural stability of TiC reinforced rapidly solidified Al-Fe-V-Si composite structures p 141 A92-15169
ZEDAN, M.
Viscous flow analysis of advanced particle separators p 737 A92-44517
ZEDAN, MOHAMED G.
Application of CFD in the design of gas turbine engine components p 741 N92-27461
ZEITLIN, ANDREW D.
Safety study of TCAS 2 for logic version 6.04
[DOT/FAA/RD-92/22] p 1047 N92-32537
ZELENAK, M.
Development and validation of a freejet technique for inlet-engine compatibility testing
[AIAA PAPER 92-3921] p 1033 A92-56752
ZELENIN, V. A.
Automated thematic processing of aircraft scanner data gathered over pasture territory in Turkmenia p 406 A92-25330
ZELENKA, RICHARD E.
Integration of radar altimeter, precision navigation, and digital terrain data for low-altitude flight
[AIAA PAPER 92-4420] p 1063 A92-55212
ZELLER, H.
Supersonic combustion studies p 211 N92-14984
ZELLER, MARY V.
Preliminary evaluation of adhesion strength measurement devices for ceramic/titanium matrix composite bonds
[NASA-TM-105803] p 932 N92-31267
ZEMAN, OTTO
Similarity in supersonic mixing layers p 611 A92-36842
ZEMBOWER, ANDY
Autonomous landing - Functional requirements p 840 A92-48470
ZENG, MING
Aerodynamic modification of a propeller p 4 A92-10958
Surface flow visualization of rotating propeller p 4 A92-10959
ZENG, XIAOPING
Application researches on expert system used for structural layout optimization of wings p 398 A92-27865
ZESCHKY, J.
Effects of stator wakes and spanwise nonuniform inlet conditions on the rotor flow of an axial turbine stage
[ASME PAPER 91-GT-93] p 70 A92-15557
ZETZL, LARRY
Rapid systems integration of navigation avionics p 858 A92-48473
ZGELA, M. B.
Durability and damage tolerance testing and fatigue life management: A CF-18 experience p 361 N92-18581
ZHA, GE-CHENG
An efficient upwind relaxation-sweeping algorithm for three-dimensional Navier-Stokes equations
[AIAA PAPER 92-0023] p 248 A92-22145
Effect of throat contouring on two-dimensional converging-diverging nozzles using URS method
[AIAA PAPER 92-2659] p 797 A92-45520
Transonic flow calculation of Euler equations by implicit iterating scheme with flux splitting p 934 A92-50215
ZHADAN, G. G.
An experimental study of supersonic H2 combustion and heat transfer in a circular duct p 388 A92-25997
ZHANG, AIKUN
Effect of antiicer on propeller performance p 25 A92-10969
ZHANG, B.
Rayleigh imaging and flow tagging in ground test facilities p 1115 A92-54330
ZHANG, BINQIAN
On vortex interference for canard configuration p 64 A92-14071
ZHANG, CHANMIN
An experimental investigation of the inlet exit flow field improved by aerodynamic grid p 343 A92-28477
ZHANG, CHUANMIN
Experimental investigation on performances of two-dimensional inlet at supersonic speed p 519 A92-35544
ZHANG, DONGXU
Strategies for optimal design of gas turbine disks p 371 A92-24741
ZHANG, FU-ZE
The fatigue scatter factors and reduction factors in the design of aircraft and helicopter's structural lives
[SAE PAPER 911984] p 843 A92-45387
ZHANG, GUI-LIAN
Some problems on atmospheric turbulence spectrum and aircraft response p 975 A92-50235
ZHANG, GUOZHENG
Limit point flow mode analysis of exhaust diffuser and operation characteristics of injector p 968 A92-49830
ZHANG, H.
A Navier-Stokes solver for stretched triangular grids
[AIAA PAPER 92-0183] p 256 A92-23793
Periodic Euler and Navier-Stokes solutions about oscillating airfoils p 626 N92-24850
ZHANG, H. Y.
Heat transfer in the entrance region of semicircular ducts with internal fins p 497 A92-32264
ZHANG, HANXIN
Numerical simulation of supersonic separated flow over blunt cones at high angles of attack p 313 A92-25039
Space-marching calculations of hypersonic inviscid flowfield p 313 A92-25040
Numerical simulation and analysis for hypersonic flow with separation over blunt cone at angle of attack p 314 A92-25126
ZHANG, HONG
A large-scale axial flow compressor facility and dynamic measurement techniques for rotor flow study p 382 A92-24729
ZHANG, HONGWEI
A study of flow patterns and behaviours of 3D separated flow on a simplified Shuttle model p 615 A92-38906
ZHANG, HONGYUE
Failure detection and identification for aircraft sensors p 370 A92-27832
ZHANG, HUISHENG
A microprocessor-based automation test system for the experiment of the multi-stage compressor p 997 A92-53100
ZHANG, JIA-ZHEN
Study on two variable control plan for twin spool turbojet engine p 862 A92-47697
ZHANG, JIANBAI
A numerical method for unsteady transonic flow about wings with control surface p 314 A92-25107
ZHANG, JIN
Dynamic analysis technique of rotating centrifugal impeller
[ASME PAPER 91-GT-50] p 148 A92-15528
Dynamic analysis of annular cascade shrouded blades p 397 A92-27856
ZHANG, LI
Calculation of the transonic full-potential flowfield about 3D fuselage p 941 A92-53021
ZHANG, LINRUI
A review of some computer programs of composites p 1009 A92-53069
ZHANG, LONG
An experimental investigation of the inlet exit flow field improved by aerodynamic grid p 343 A92-28477
ZHANG, LUMIN
Numerical simulation of inviscid flow over a complicated body using an overlapping grid technique p 313 A92-25043
ZHANG, QIANG
Experimental study of the equivalent sound source center of the propeller rotating noise p 1011 A92-53257
ZHANG, QING-FAN
Experimental investigation on combustor with double co-axial swirlers p 469 A92-29729
ZHANG, QINGBING
Finite element method for computing nonisentropic potential transonic flow with shock waves p 312 A92-25009
A penalty-Galerkin finite element method for calculating transonic flow over wings p 943 A92-53386
ZHANG, QINGFAN
An investigation on the characteristics of combustor with oblique air jet p 375 A92-28434
ZHANG, QIQIAO
A study of dynamic response to bird impact on arc windshields of aircrafts p 952 A92-53340

ZHANG, QIWEI
High speed wind tunnel wall interference research progress at Nanjing Aeronautical Institute p 136 A92-15338
ZHANG, RIXIN
Mechanical model of landing impact of three dimensional fuselage landing gear p 960 A92-53090
ZHANG, S.
Axisymmetric potential flow calculations. II - Design mode p 8 A92-12399
ZHANG, S. Y.
Estimation of the maximum instantaneous distortion p 242 A92-21051
Improved method for estimation of the maximum instantaneous distortion values
[AIAA PAPER 92-3623] p 826 A92-49076
ZHANG, SHAOJI
A simplified method of transient mathematical model for non-augmentation engine p 372 A92-24750
Real-time simulation and adaptive PID control of QSK-06A control for gas turbine p 470 A92-29740
A simplified real-time engine model for developing aeroengine control system
[AIAA PAPER 92-3321] p 864 A92-48904
ZHANG, SHIPING
Experiments on the blade loss transient response of rotor with flexible damped support
[ASME PAPER 91-GT-149] p 148 A92-15587
Experimental investigation on blade loss transient response of rotor with flexible damped support p 557 A92-35551
ZHANG, SHIZHENG
The performance evaluation of aeroderivative gas turbines p 119 A92-13296
ZHANG, SHU-CHENG
A time marching method in finite volume for transonic diffuser turbulent flows p 819 A92-47690
ZHANG, SONG L.
Studying method of measuring flow-field between stages in axial-flow compressor p 423 A92-29720
ZHANG, WEI
Probability analysis of structure failure for the wings with main and subordinate components p 848 A92-47657
ZHANG, WU
An improved method for aerodynamic design of centrifugal impeller blades
[ASME PAPER 91-GT-76] p 69 A92-15545
Multiple line-vortex model of vortex flows around body of revolution at high angles of attack up to 60 degrees p 314 A92-25104
ZHANG, XIANGLIN
Cyclic symmetric contact stress analysis of aeroengine rotor assembly p 470 A92-29733
ZHANG, XIAOMEI
An investigation on the characteristics of combustor with oblique air jet p 375 A92-28434
ZHANG, XIN
Experimental investigation of supersonic flow over two cavities in tandem p 610 A92-36830
ZHANG, XIU-YI
Sonic fatigue analysis and anti-sonic fatigue design of aircraft structure p 848 A92-47666
ZHANG, XIZHEN
A full-scale fatigue test and failure analyses research of F-X fighters p 960 A92-53092
ZHANG, YI
The response of a helicopter to windshear p 269 A92-21470
ZHANG, YULUN
Numerical simulations of flow fields over aircrafts p 313 A92-25042
The study of inverse boundary layer algorithm for transonic flows over aerofoils p 315 A92-25140
ZHANG, ZHAOWEN
The dimensional reconstruction of vortex cross-section images p 339 A92-27833
ZHANG, ZHI-FANG
Calculation of 3D flow field in a single transonic compressor stage p 422 A92-29719
ZHANG, ZHI-GANG
A 3D FEM variational aerodynamic calculation and performance analysis of a leaned turbine stator cascade
[ASME PAPER 91-GT-79] p 69 A92-15548
ZHANG, ZHILONG
Design variables and constraint derivatives in aeroelastic tailoring p 997 A92-53074
ZHANG, ZHONGYIN
Aerodynamic analysis and modification design of NPU airfoils p 613 A92-38270
ZHAO, CHANGAN
Measurement of turbulent boundary layer in transonic flow p 941 A92-53010
ZHAO, CHANGZHAN
A compound fatigue investigation of plate specimen under low-cycle load superposed on high cycle load p 587 A92-35555
ZHAO, DONGMEI
The numerical method for calculating the flow field, temperature field and radiation fluxfield in the pipe p 587 A92-35546
ZHAO, FUAN
Experiments on the blade loss transient response of rotor with flexible damped support
[ASME PAPER 91-GT-149] p 148 A92-15587
Experimental investigation on blade loss transient response of rotor with flexible damped support p 557 A92-35551
ZHAO, JIAXING
A numerical study of the radiation characteristic of an elliptical exhaust jet p 970 A92-53258
ZHAO, JUJUN
Noise control used for turbojet engine test bench p 284 A92-21749
ZHAO, JUN-QING
Combined application of the energy method and the weighted residual method - A new way to construct the finite elements p 991 A92-50239
ZHAO, KEYUN
An experimental investigation on aft bypass supersonic inlet performance at high angle of attack and yaw p 862 A92-48268
ZHAO, L.-C.
Bifurcation analysis of airfoils in incompressible flow p 623 A92-40580
ZHAO, LING-CHENG
Transition of the flutter mode of a two-dimensional section with an external store p 758 A92-41244
ZHAO, LINGCHENG
A numerical method for analyzing the nonlinear flutter of wings at high angles of attack p 338 A92-27827
ZHAO, MINGGUI
Precision analysis on static measurement of radar cross section p 370 A92-27906
ZHAO, NING
A flow visualization experiment on the unsteady flow around two-dimensional airfoil p 615 A92-38913
ZHAO, WEI
Solution of stress intensity factor by weight function for small surface cracks in plates p 998 A92-53332
ZHAO, YIYUAN
Aircraft control in a downburst on takeoff and landing p 27 A92-11385
Approach guidance in a downburst p 873 A92-46741
ZHAO, ZHEN-YAN
The effect of atmospheric turbulence on the external store separation from an aircraft p 934 A92-50233
ZHELEZNIAK, N. I.
The feasibility of reducing induced wing drag by using crescent planform wings p 425 A92-30167
ZHELTOVODOV, A. A.
Evolution of three-dimensional flows during the interaction between conical shock waves and a turbulent boundary layer p 7 A92-12169
ZHENG, GUANGHUA
Research on damage tolerance of compressor blade p 588 A92-35556
ZHENG, QING-PING
Experimental investigation on combustor with double co-axial swirlers p 469 A92-29729
ZHENG, QINGXIONG
Influence of air liquefaction cycle on performance of combined cycle engine p 372 A92-24878
ZHENG, QIXUAN
A new method for calculating burst speed of aeroengine disks
[ASME PAPER 91-GT-121] p 670 A92-36899
ZHENG, QUAN
Numerical calculation of subsonic and supersonic aerodynamic loads around complex configuration vehicle p 175 A92-20488
ZHENG, SUI
An investigation of the swirl in an S-shaped inlet p 343 A92-28476
ZHENG, XIAOQING
Solution of Euler equations for fighter forebody-inlet combinations at high angles of attack p 613 A92-38269
ZHENG, Y.
LDV measurements in the three-dimensional near wake of a stationary and oscillating rectangular wind
[AIAA PAPER 92-2689] p 799 A92-45536
ZHENG, YINGPING
A new study on a class of discrete event dynamic systems p 48 A92-11377
ZHENG, YOUXIN
LDV measurements in the unsteady tip-vortex behind an oscillating rectangular wing p 620 A92-40085
ZHENG, Z.
Viscous effects on a vortex wake in ground effect
[NASA-CR-190400] p 907 N92-28361
ZHENG, ZHICHU
An experimental study of the flow past spheres at transonic speeds and high Reynolds numbers p 312 A92-25002
ZHIGULEV, S. V.
Experimental study of the characteristics of boundary-layer development on an airfoil p 425 A92-30171
Investigation of the effect of an ultrasonic acoustic field on boundary layer separation on an airfoil p 511 A92-30205
ZHIQIN, LING
Soviet electronic display systems under research and manufactured for the civil aviation aircraft of the 1990's
[AD-A240933] p 119 N92-13066
ZHITKO, A. V.
Lift characteristics of an infinite-span cylindrical wing of a thick symmetric profile at low subsonic velocities p 440 A92-31897
ZHOKHOV, V. A.
Gasdynamic calculation of an impulse wind tunnel with a two-section plenum p 493 A92-30147
ZHONG, C.
Runway exit designs for capacity improvement demonstrations. Phase 2: Computer model development
[NASA-CR-190166] p 484 N92-21162
ZHONG, QIANG
An investigation on the characteristics of combustor with oblique air jet p 375 A92-28434
ZHOU, ANNING
Calculation of fuel sloshing and its coupling vibration with a tank p 991 A92-50204
ZHOU, BIAO
Experimental investigation on combustor with double co-axial swirlers p 469 A92-29729
ZHOU, DONG-MEI
A 3D FEM variational aerodynamic calculation and performance analysis of a leaned turbine stator cascade
[ASME PAPER 91-GT-79] p 69 A92-15548
ZHOU, JIAN-SHENG
Approximate analysis for failure probability of structural systems p 901 A92-47671
ZHOU, JUYUAN
A theoretical study on helicopter alert time without maintenance p 358 A92-27836
ZHOU, LANQIN
Dynamic behavior analysis for landing-gear with different types of dual-chamber shock-struts p 111 A92-15342
ZHOU, MENG
An analysis of boundary layer for droplet aerodynamic stripped in high speed gas flow p 1116 A92-54563
ZHOU, SHENG
Aeroelastic stability analysis of aerial propellers p 24 A92-10955
Concerning a basic assumption for aeroelasticity in turbomachinery p 373 A92-26920
An aeroacoustic model about the rotating stall of a compressor p 416 A92-27855
ZHOU, WEIJIANG
Numerical simulation of 2-D separated flows caused by suddenly change of the body section p 312 A92-25004
Numerical simulation of interaction between vortexes and shocks in jet flow field p 616 A92-38925
ZHOU, XI-YUAN
Research of environmental spectrum for aircraft structure p 785 A92-47655
ZHOU, XIN XIN
Propagation of shock waves through clouds
[AERO-REPT-9104] p 400 N92-18317
ZHOU, XINHAI
Flow analysis for axial compressor including secondary flow effects p 759 A92-41835
ZHOU, XU
Ablative control mechanism in nozzle thermo-protection
[AIAA PAPER 92-3054] p 889 A92-48712
ZHOU, XUEHUA
Integrated electric density and scaling law for hypersonic blunt-body wakes p 714 A92-44865
ZHOU, ZHILUN
Research on sonic fatigue calculation and test for aircraft panel p 958 A92-50203
ZHOU, ZHIQIANG
The calculation of the static elastic aerodynamic distribution for the rolling maneuver aircraft p 379 A92-25010
ZHU, DEMAO
A superelement simplified analysis for the vibration systems of the complex structures p 398 A92-27903
ZHU, FENGHUI
Experimental investigation on flutter characteristics of composite torsion-box p 996 A92-53055
ZHU, GU-XIANG
A calculating method of the kill probability attack area for AAM p 975 A92-50212

ZHU, J. X.
Embedded longitudinal vortex arrays, velocity and temperature fields, loss and heat transfer augmentation
p 621 A92-40121
ZHU, KE-QIN
A study on the superconvergence of Multhopp's discretization in vortex-lattice methods
p 336 A92-27381
ZHU, N. G.
Similarity transformations for compressor blading
[ASME PAPER 91-GT-123] p 70 A92-15568
ZHU, PEIYE
Multiple line-vortex model of vortex flows around body of revolution at high angles of attack up to 60 degrees
p 314 A92-25104
ZHU, QING
Surge-troubleshooting of a twin-spool turbojet engine tested at a high altitude test facility p 375 A92-28459
Research on altitude simulation of starting for a single-spool small turbojet p 969 A92-49836
ZHU, XIXIONG
An impact dynamics investigation on some problems in bird strike on windshields of high-speed aircrafts
p 986 A92-53330
ZHU, YAN
3D LDA measurement in an axial fan rotor
p 391 A92-24730
ZHU, YUAN
Simulation of commercial-aircraft reliability
p 759 A92-42057
ZHU, ZI-QIANG
Numerical computation of improved transonic potential method p 441 A92-32234
ZHU, ZIQIANG
The computation of transonic viscous flow
p 338 A92-27831
Discussion of improved transonic potential method
p 942 A92-53290
An inverse method with regularity condition for transonic airfoil design p 177 N92-13969
ZHUANG, F. C.
An analysis of boundary layer for droplet aerodynamic stripped in high speed gas flow p 1116 A92-54563
ZHUANG, FENG-GAN
An improved multiple line-vortex method for simulation of separated vortices of slender wings
p 819 A92-47694
ZHUANG, PING
Numerical investigation of axial flow compressor casing treatment p 934 A92-50216
A numerical investigation of axial flow compressor casing treatment p 942 A92-53381
ZHUK, V. I.
Asymptotics of the upper branch of the neutral curve at subsonic and transonic external flow velocities
p 79 A92-16705
ZICH, JOHN A.
An exploration of function analysis and function allocation in the commercial flight domain
[NASA-CR-4374] p 368 N92-19871
ZIEGLER, BERNARD
New way of flying (1990 Sir Charles Kingsford Smith Lecture) p 515 A92-33461
ZIEMIANSKI, JOSEPH A.
NASA thrusts in high-speed aeropropulsion research and development: An overview p 561 N92-22538
ZIENKIEWICZ, O. C.
Computational mechanics today p 399 A92-28464
A general explicit or semi-explicit algorithm for compressible and incompressible flows
p 937 A92-52682
ZIEREP, J.
The just attached shock-wave at the leading edge of a profile p 3 A92-10663
ZIERTEN, THOMAS A.
Wind tunnel investigation of the aerodynamic effects of aircraft ground deicing/anti-icing fluids and criteria for aerodynamic acceptance p 452 N92-21698
Lewis icing research tunnel test of the aerodynamic effects of aircraft ground deicing/anti-icing fluids
[NASA-TP-3238] p 952 N92-30395
ZIEVE, PETER
Suppression of radiating harmonics Electro-Impulse Deicing (EIDI) systems
[DOT/FAA/CT-TN90/33] p 405 N92-19764
ZILLIAC, G. G.
Surface flow patterns on an ogive-cylinder at incidence p 176 A92-20762
ZIMMERMAN, JOHN
Trends in the selection of airliners
p 417 A92-28183
ZIMMERMANN, H.
Two-phase flow correlations in air/oil systems of aero engines
[ASME PAPER 91-GT-54] p 121 A92-15532
Calculation of three-dimensional transonic turbine cascade flow p 344 A92-28519
Simultaneous stress and flutter optimization for the wing of a transport aircraft equipped with four engines
p 571 N92-23238
Computation of flutter boundaries in the time and frequency domain p 720 N92-27952
ZIMMERMANN, HELGA
DLR-news: Announcements of the German Research Institute for Aeronautics and Astronautics
p 698 N92-25413
DLR-News: Announcements of the German Research Institute for Aeronautics and Astronautics
p 698 N92-26086
ZIMMERMANN, HELMUT
Aeroservoelasticity p 642 A92-37577
ZIMONT, E. L.
Analysis of the efficiency of some structural-inspection strategies in aircraft maintenance p 419 A92-30141
ZIMONT, V. L.
Effect of turbulent mixing on the characteristics of a turbofan-engine nozzle p 493 A92-30162
ZINCHENKO, V. I.
Calculation of three-dimensional flow past blunt cones near the plane of symmetry for different flow regimes in the shock layer and in the presence of gas injection from the surface p 337 A92-27593
ZINGG, D. W.
Grid studies for thin-layer Navier-Stokes computations of airfoil flowfields
[AIAA PAPER 92-0184] p 256 A92-23794
Grid studies for thin-layer Navier-Stokes computations of airfoil flowfields p 1025 A92-54935
Aerodynamics p 202 N92-13977
Computational fluid dynamics p 177 N92-13979
Automated grid generation for high-lift configurations
p 628 N92-24869
Boundary layer computations using a generalized formulation p 679 N92-24873
ZION, H. L.
Safe life reliability - Evaluation of new statistical methods p 104 A92-14343
ZIPF, EDWARD C.
Examination of ultraviolet radiation theory for bow shock rocket experiments
[AIAA PAPER 92-2871] p 901 A92-47853
ZIQIANG, Z.
Two-dimensional transonic flow calculation by interaction of Euler and boundary layer equations
[PB92-136449] p 448 N92-21784
ZISCHKA, PETER J.
Modeling and analysis methodology for aeroelastically tailored chordwise deformable wings
[NASA-CR-189620] p 961 N92-30304
ZLOCKA, MARIA
Aircraft stabilization at large angles of attack
p 875 A92-47785
ZOBY, E. V.
Effect of nose shape on three-dimensional stagnation region streamlines and heating rates
[AIAA PAPER 91-5032] p 171 A92-17822
Shuttle Infrared Leeside Temperature Sensing (SILTS) experiment - STS-35 and STS-40 preliminary results
[AIAA PAPER 92-0126] p 286 A92-23746
ZOBY, ERNEST V.
Enhancements to viscous-shock-layer technique
[AIAA PAPER 92-2897] p 820 A92-47873
ZOHOOR, H.
Optimum dimensions of convective-radiative spines using a temperature correlated profile
p 676 A92-40869
ZOLOTOVSKY, S.
Successful transfer of technology from a research and development laboratory to an Aerospatiale production unit p 931 A92-51808
ZORINA, O. P.
Optimization of the aerodynamic balance and parameters of the horizontal tail surfaces of the three-surface aircraft configuration with allowance for the capabilities of the stability and control augmentation system p 134 A92-16803
ZORUMSKI, WILLIAM E.
Sound transmission through a high-temperature acoustic probe tube p 415 A92-26406
ZOTEEV, A. I.
Control of the landing of a flight vehicle in the grazing-incidence mode p 134 A92-16808
ZOTEMANTEL, RAINER
MBB-LAGRANGE: A general structural reliability and optimization structural system
[MBB/FW321/S/PUB/467] p 998 N92-30423
ZOTTO, M.
Dynamic analysis of rotor blades with root retention design variations p 1054 A92-56156
ZRNIC, DUSAN S.
Sensors and systems to enhance aviation safety against weather hazards p 160 A92-14265
ZUBAIR, M.
Solutions of acoustic field problems using parallel computers p 925 A92-45929
ZUBKOV, A. I.
Structure of the separated flow region in a dihedral corner in front of an obstacle in supersonic flow
p 524 A92-36420
ZUKOSKI, EDWARD E.
An analytical and computational investigation of shock-induced vortical flows
[AIAA PAPER 92-0316] p 321 A92-25763
A systematic experimental and computational investigation of a class of contoured wall fuel injectors
[AIAA PAPER 92-0625] p 374 A92-27007
ZUMWALT, GLEN W.
Experimental studies of a two-element airfoil with large separation
[AIAA PAPER 92-0267] p 317 A92-25723
ZUNIGA, FANNY A.
In-flight flow visualization and pressure measurements at low speeds on the NASA F-18 high alpha research vehicle p 85 N92-13009
ZUNINO, PIETRO
Reynolds stress distribution downstream of a turbine cascade p 614 A92-38861
ZUO, PEI C.
The research of reducing 3-D low supersonic shock wave reflection in a 2-D transonic flexible walls adaptive wind tunnel
[AIAA PAPER 92-3924] p 1095 A92-56755
ZUPPARDI, GENNARO
Detecting 3-D, turbulent separation regions using unsteady computerized thermographic technique
p 1023 A92-54308
ZVEREV, O. V.
Calculation of heat transfer and friction for a blunt body in the path of supersonic flow of a chemically equilibrium air-xenon mixture p 336 A92-27532
ZWAAN, R. J.
Investigation of a semi-empirical method to predict limit cycle oscillations of modern fighter aircraft
[NLR-TP-90087-U] p 481 N92-20475
ZWEBEN, MONTE
Constraint-based scheduling
[NASA-TM-107873] p 692 N92-25190
ZYZYS, EDMUND
Comparison of the performance of a microwave landing system elevation station with the instrument landing system end-fire glide slope at Yeager Airport, Charleston, West Virginia
[DOT/FAA/CT-TN91/22] p 534 N92-22210

Typical Corporate Source Index Listing

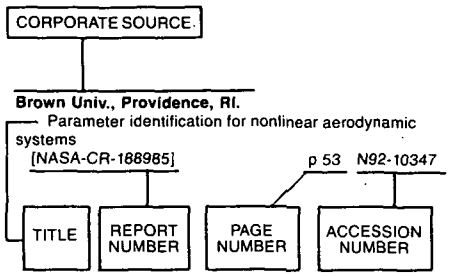

Listings in this index are arranged alphabetically by corporate source. The title of the document is used to provide a brief description of the subject matter. The page number and the accession number are included in each entry to assist the user in locating the abstract in the abstract section. If applicable, a report number is also included as an aid in identifying the document.

A

Academy of Sciences (USSR), Moscow.
Dynamics of aerospace shuttles p 667 N92-24760
Levitation of YBa2Cu3O(7-x) superconductor in a variable magnetic field p 771 N92-27735
Cryogenic test rig with an aerodynamic magnetically levitated carriage p 750 N92-27792

Adsystech, Inc., Silver Spring, MD.
General aviation activity and avionics survey, calendar year 1989
[PB91-179234] p 169 N92-13926

Advanced Aviation Concepts, Jupiter, FL.
Introduction to cognitive processes of expert pilots
[DOT/FAA/RD-92/12] p 952 N92-30980
Workshop on Aeronautical Decision Making (ADM). Volume 1: Executive summary
[DOT/FAA/RD-92/14-VOL-1] p 1142 N92-33305

Advisory Group for Aerospace Research and Development, Neuilly-Sur-Seine (France).
Rotorcraft system identification
[AGARD-AR-280] p 22 N92-11001
Machine Intelligence for Aerospace Electronic Systems
[AGARD-CP-499] p 164 N92-12517
Vortex Flow Aerodynamics
[AGARD-CP-494] p 83 N92-12996
Knowledge based system applications for guidance and control
[AGARD-AR-284] p 205 N92-14065
Artificial Neural Network Approaches in Guidance and Control
[AGARD-LS-179] p 234 N92-14673
Rotorcraft System Identification
[AGARD-LS-178] p 273 N92-17153
Technical evaluation report on the 52nd Symposium on Software for Guidance and Control
[AGARD-AR-302] p 303 N92-17498
Technical evaluation report on the Fluid Dynamics Panel Specialists' Meeting on Effects of Adverse Weather on Aerodynamics
[AGARD-AR-306] p 352 N92-18242
Design and testing of high-performance parachutes
[AGARD-AG-319] p 345 N92-18269
Fatigue Management
[AGARD-CP-506] p 360 N92-18571
Manoeuvring Aerodynamics
[AGARD-CP-497] p 363 N92-18778
AGARD/SMP Review: Damage Tolerance for Engine Structures. 4: Reliability and Quality Assurance
[AGARD-R-773] p 402 N92-19004
Validation of flight critical control systems
[AGARD-AR-274] p 382 N92-20026
Air intakes for high speed vehicles
[AGARD-AR-270] p 445 N92-20797
Effects of Adverse Weather on Aerodynamics
[AGARD-CP-496] p 449 N92-21679
Aircraft Ship Operations
[AGARD-CP-509] p 464 N92-21951
Integrated Design Analysis and Optimisation of Aircraft Structures
[AGARD-R-784] p 550 N92-23227
Special Course on Engineering Methods in Aerodynamic Analysis and Design of Aircraft
[AGARD-R-783] p 552 N92-23950
Special Course on Unstructured Grid Methods for Advection Dominated Flows
[AGARD-R-787] p 771 N92-27671
Special Course on Skin Friction Drag Reduction
[AGARD-R-786] p 717 N92-27706
Technical evaluation report on the Flight Mechanics Panel Symposium on Flying Qualities
[AGARD-AR-311] p 733 N92-27870
Transonic Unsteady Aerodynamics and Aeroelasticity
[AGARD-CP-507] p 718 N92-27936
Advances in Fibre-Optic Technology in Communications and for Guidance and Control
[AGARD-LS-184] p 774 N92-28084
Applications of ASICs to avionics
[AGARD-AG-329] p 859 N92-28376
Steady and Transient Performance Prediction of Gas Turbine Engines
[AGARD-LS-183] p 868 N92-28458
Aircraft ship operations
[AGARD-AR-312] p 850 N92-28468
Integrated Design Analysis and Optimisation of Aircraft Structures
[AGARD-LS-186] p 851 N92-28469
Piloted Simulation Effectiveness
[AGARD-CP-513] p 786 N92-28522
Technical evaluation report on the Flight Mechanics Panel Symposium on Piloted Simulation Effectiveness
[AGARD-AR-315] p 983 N92-30769
Vortex flow aerodynamics
[AGARD-AR-299] p 946 N92-30947
Proceedings of the 53rd Symposium on Air Vehicle Mission Control and Management
[AGARD-AR-310] p 1010 N92-32229
The Utilization of Advanced Composites in Military Aircraft
[AGARD-R-785] p 1109 N92-33033

AEG-Electrocom G.m.b.H., Konstanz (Germany).
Extension of the Frankfurt COMPAS for general application p 355 N92-19048

Aeritalia S.p.A., Naples (Italy).
The G-222 aircraft individual tracking programme p 361 N92-18582
Boundary conditions for Euler equations at internal block faces of multi-block domains using local grid refinement
[NLR-TP-90134-U] p 908 N92-28712

Aeritalia S.p.A., Rome (Italy).
Use of target spectrum for detection enhancement and identification p 404 N92-19155

Aeritalia S.p.A., Turin (Italy).
Vortical flow simulation by using structured and unstructured grids p 83 N92-12999

AeroChem Research Labs., Inc., Princeton, NJ.
Direct computation of turbulence and noise
[NASA-CR-187616] p 236 N92-14788

Aerodyne Research, Inc., Billerica, MA.
High-speed civil transport aircraft emissions p 408 N92-19122

Aerojet-General Corp., Sacramento, CA.
Ceramic regenerator program
[NASA-CR-189053] p 225 N92-14374

Aeronautica Macchi S.p.A., Varese (Italy).
Parametric effects of some aircraft components on high-alpha aerodynamic characteristics p 364 N92-18782

Aeronautical Research Inst. of Sweden, Bromma.
Calculation of hypersonic leeside vortices over blunt delta wings p 84 N92-13004
Hypersonic flow past delta wing flow simulated by Navier-Stokes solutions p 180 N92-14981
Wind tunnel force measurements and visualization on a 60-deg delta wing in oscillation, stepwise motion, and gusts p 364 N92-18786

Aeronautical Research Inst. of Sweden, Stockholm.
Performance improvements and fuel cost savings due to leading edge modification of a vintage delta wing jet fighter
[FFA-TN-1991-22] p 114 N92-11993
Optimal design of nonlinear shell structures
[FFA-TN-1991-18] p 157 N92-12312
A review of aeronautical fatigue investigations in Sweden during the period May 1989 to April 1991
[FFA-TN-1991-24] p 158 N92-12313
Temperature effects in FFA HYP 500 at M = 7 in a flow with strong expansion
[FFA-TN-1991-27] p 443 N92-20229
MATGRID: A program for generation of C-H and C-O topology grids around wing/body configurations. Mathematical definition document
[FFA-TN-1990-19] p 444 N92-20468
Hypersonic laminar flow computations over a blunt leading edged delta wing at three different chord Reynolds numbers
[FFA-TN-1991-40] p 528 N92-23168
MATGRID, a program for generation of C-H and C-O topology grids around wing/body configurations: Software description document
[FFA-TN-1990-20] p 945 N92-30713

Aeronautical Research Labs., Melbourne (Australia).
Critical appraisal of the McDonnell Douglas closure model for predicting fatigue crack growth
[ARL-STRUC-R-444] p 44 N92-11376
F/A-18 stabilator: Equivalent set of point forces required for pneumatic bag load case simulation
[AD-A242637] p 206 N92-15073
Modification of Jindivik air intake duct with an auxiliary intake static aerodynamic tests
[AD-A243002] p 275 N92-17234
Wind loads on a mirage III O aircraft mounted above a ground plane
[AD-A243004] p 275 N92-17266
Surface pressure measurements on the wing of a wind tunnel model during steady rotation
[AD-A243047] p 260 N92-17281
Stagnation and dynamic pressure limits for the S1 wind tunnel
[AD-A242989] p 285 N92-17297
General requirements and techniques for component fatigue life substantiation in Australian service helicopters
[AD-A242881] p 275 N92-17565
Scale model measurements of fin buffet due to vortex bursting on F/A-18 p 365 N92-18788
A review of Australian activity on modelling the helicopter/ship dynamic interface p 465 N92-21967
Visualisation in water of vortex flow over sharp-edged canard configurations
[ARL-FLIGHT-MECH-R-189] p 632 N92-25410
An outline of a numerical scheme for calculating two-dimensional time linearised transonic flow using the Green's function method
[AD-A246349] p 764 N92-26258
F-111C flight dynamic model aerodynamic data-base development and verification
[AD-A246356] p 715 N92-26947

SOURCE

A preliminary study on damage detection using piezoelectric film
[AD-A246350] p 733 N92-28118
Reduction and analysis of F-111C flight data
[AD-A250341] p 853 N92-28771
Activities of the Aeronautical Research Laboratory
p 1013 N92-30768
Research into improving the durability of the hot section in the aircraft turbine engine
[AD-A250342] p 973 N92-31439

Aeronautical Systems Div., Wright-Patterson AFB, OH.
Evolution of avionic systems architecture, from the 1950's to the present p 198 N92-14047
Avionics standardization in the USAF: 1980 to 1990
p 198 N92-14048
Common avionics baseline: The product of the joint integrated avionics working group p 199 N92-14053
Avionics modernization/upgrades in the late 1990s
p 199 N92-14055
Avionics reliability, durability, and integrity: Can they be independent of application? p 200 N92-14056
An evaluation of four F-16 vertical velocity indicator configurations
[AD-A243629] p 370 N92-18014
Life management approach for USAF aircraft
p 362 N92-18587
Managing airborne assets through loads monitoring
p 363 N92-18594
Approach to crew training in support of the USAF Aircraft Structural Integrity Program (ASIP) p 363 N92-18595
Damage tolerance for commuter aircraft
p 914 N92-30114

Aeroplane and Armament Experimental Establishment, Boscombe Down (England).
United Kingdom approach to deriving military ship helicopter operating limits p 465 N92-21966

Aerospace Corp., El Segundo, CA.
Operational design factors for NASP derived vehicles
[AIAA PAPER 91-5081] p 210 A92-17851
Evaluation of GPS/UTC steering performance
p 1049 N92-33353

Aerospace Medical Research Labs., Brooks AFB, TX.
Sonic booms produced by US Air Force and US Navy aircraft: Measured data
[AD-A244804] p 512 N92-21719
Analysis of measured environmental noise levels: An assessment of the effects of airbase operational model variables on predicted noise exposure levels
[AD-A244805] p 485 N92-21720
Microcomputer-based instrument flight simulation: Undergraduate pilot training student attitude assessment
[AD-A245449] p 749 N92-26527

Aerospatiale, Les Mureaux (France).
Transitional flows around re-entry bodies
p 184 N92-15035
Computation of aerodynamic coefficients on Hermes-Ariane5 configuration p 184 N92-15040

Aerospatiale, Toulouse (France).
Fatigue testing and tear down operations on Airbus A320 forward fuselage p 360 N92-18579
Method for calculating the three-dimensional water concentration coefficients and its industrial applications
p 502 N92-21685
Flight simulation and digital flight controls
p 884 N92-28526

Agusta Sistemi S.p.A., Tradate (Italy).
RAMREQ: A computerized tool for the definition of RAM (Reliability, Availability, Maintainability) requirements of complex systems p 412 N92-18647

Agusta Sistemi S.p.A., Varese (Italy).
EH 101 ship interface trials: Flight test programme and preliminary results p 465 N92-21964

Air Force Academy, CO.
Effects of unsteady shock impingement on high-speed gaseous mixing
[AIAA PAPER 91-5091] p 172 A92-17857
Downwash measurements on a pitching canard-wing configuration
[AD-A239956] p 12 N92-10016
A 3-degree-of-freedom flight simulator evaluation of unsteady aerodynamics effects
[AD-A241540] p 139 N92-13079
Active control of the separation region on a two-dimensional airfoil
[AD-A249739] p 948 N92-31622

Air Force Environmental Technical Applications Center, Scott AFB, IL.
C-29A aircraft altimeter errors
[AD-A240486] p 23 N92-11011

Air Force Flight Test Center, Edwards AFB, CA.
X-29 high angle of attack p 111 A92-16052
Utility of ground simulation in flight control problem identification, solution development, and verification
p 883 N92-28525
Use of simulation in the USAF Test Pilot School curriculum p 884 N92-28535

Air Force Inst. of Tech., Wright-Patterson AFB, OH.
Investigation of advanced aircraft performance measures of merit including new agility metrics
[AD-A242016] p 272 N92-15990
Model identification and control system design for the lambda unmanned research vehicle
[AD-A241859] p 299 N92-17024
Design of a fiber optic image transmission link
[AD-A243686] p 304 N92-17088
Development of high angle of attack control laws for an unstable, non-minimum phase aircraft using variations of the quantitative feedback technique
[AD-A243698] p 282 N92-17096
Implementation of an object-oriented flight simulator D.C. electrical system on a hypercube architecture
[AD-A243700] p 284 N92-17097
An experimental investigation of leading edge vortical flow about a delta wing during wing rock
[AD-A243363] p 260 N92-17114
A robust digital flight control system for an unfanned research vehicle using discrete quantitative feedback theory
[AD-A243638] p 283 N92-17748
The effect of physical aging on the creep response of a thermoplastic composite
[AD-A243600] p 290 N92-17932
An application of the object-oriented paradigm to a flight simulator
[AD-A243624] p 384 N92-18012
Optimization of tangential mass injection for minimizing flow separation in a scramjet inlet
[AD-A243868] p 376 N92-18867
An experimental study of a sting-mounted circulation control wing
[AD-A243912] p 346 N92-18895
Investigation of the effects of aeroelastic deformations on the radar cross section of aircraft
[AD-A243889] p 402 N92-18940
Thrust vector control of an overexpanded supersonic nozzle using pin insertion and rotating airfoils
[AD-A243891] p 387 N92-18942
Analysis of the effects of removing nose ballast from the F-15 eagle
[AD-A244044] p 366 N92-19178
Thermal nonequilibrium effects on turbine cascade aerodynamics
[AD-A244049] p 404 N92-19183
Effect of nonuniform entrance flow profile on hypersonic nozzle pitching moment
[AD-A244050] p 377 N92-19184
Analysis of an advanced fighter aircraft using jet flap techniques and the vortex lattice method
[AD-A244051] p 366 N92-19185
Performance and stability analysis of the non-linear dynamics of a simple powered lifting hypersonic vehicle flying on a minor circle
[AD-A243933] p 366 N92-19192
The application of statistical estimation techniques to terrain modeling
[AD-A243799] p 409 N92-19231
Experimental investigation into the effects of riblets on compressor cascade performance
[AD-A243881] p 377 N92-19235
Application of nonlinear QFT to flight control design for high angle of attack maneuvers with thrust vectoring
[AD-A243821] p 381 N92-19241
Ground collision avoidance using a variable incidence altitude measurement system for the A-7 aircraft
[AD-A243880] p 352 N92-19259
A comparative study of numerical versus analytical waverider solutions
[AD-A244183] p 347 N92-19304
The effect of angle of incidence and Reynolds number on heat transfer in a linear turbine cascade
[AD-A243900] p 377 N92-19328
Experimental investigation of trailing edge crenulation effects on losses in a compressor cascade
[AD-A243902] p 377 N92-19329
An algorithm for robust eigenstructure assignment using the linear quadratic regulator
[AD-A244267] p 412 N92-19335
Structured Hypermedia Application Development Model (SHADM): A structured model for technical documentation application design
[AD-A244268] p 417 N92-19336
Investigation of the influence of rotary aerodynamics on the study of high angle of attack dynamics of the F-15B using bifurcation analysis
[AD-A243969] p 348 N92-19367
Finite element analysis of a riveted repair on a curved composite panel
[AD-A243916] p 404 N92-19384
A guide for the consideration of composite material impacts on airframe costs
[AD-A243928] p 417 N92-19466
Proportional plus integral control of aircraft for automated maneuvering formation flight
[AD-A243792] p 382 N92-19505
GPS/INS integration for improved aircraft attitude estimates
[AD-A243947] p 356 N92-19604
An analysis of fixed wing tactical airlifter characteristics using an intra-theater airlift computer model
[AD-A246908] p 732 N92-27719
An analysis of total quality management in Aeronautical Systems Division
[AD-A246661] p 772 N92-27760
An exploratory application of neural networks to the sortie generation forecasting problem
[AD-A246626] p 778 N92-27980
A formal definition of the object-oriented paradigm for requirements analysis
[AD-A246814] p 729 N92-28132
Life cycle costs of the C-130 electrical power system upgrade
[AD-A246759] p 786 N92-28348
Modular simulation of HEI fragments and blast pressure
[AD-A248205] p 910 N92-29191
Development of a flight information system using the structured method
[AD-A248207] p 859 N92-29222
Thermomechanical fatigue behavior of a silicone carbide fiber-reinforced calcium aluminosilicate glass-ceramic matrix composite
[AD-A249870] p 988 N92-31823
A learning enhanced flight control system for high performance aircraft
[AD-A252520] p 1086 N92-32435

Air Force Logistics Command, Tinker AFB, OK.
Advanced ice protection systems test in the NASA Lewis Icing Research Tunnel p 108 A92-14406

Air Force Systems Command, Brooks AFB, TX.
Testing and evaluation of the Vanner electrical inverters, models 24-1500 and SP 00112
[AD-A241914] p 299 N92-17216

Air Force Systems Command, Wright-Patterson AFB, OH.
China's first variable stability aircraft: The BW-1-Gets its pre-acceptance flight tests
[AD-A240941] p 116 N92-13062
Soviet electronic display systems under research and manufactured for the civil aviation aircraft of the 1990's
[AD-A240933] p 119 N92-13066
International aviation (selected article)
[AD-A240986] p 170 N92-13991
International aviation (selected article)
[AD-A240987] p 170 N92-13992
International aviation (selected articles)
[AD-A241119] p 170 N92-13993
Programs at Wright-Patterson Air Force Base
p 228 N92-15092
Ferrundi Company supplies 4500 model head up display devices to India's MIG-21 aircraft
[AD-A241044] p 229 N92-15367
Design challenges for the National Aero-Space Plane
p 551 N92-23822
Lateral spread of sonic boom measurements from US Air Force boomfile flight tests p 1140 N92-33883

Air Force Wright Aeronautical Labs., Wright-Patterson AFB, OH.
Forebody vortex flow control on the F-16C using tangential slot and jet nozzle blowing
[AIAA PAPER 92-0019] p 247 A92-22141
Avionics technology beyond 2000
p 200 N92-14058

Air Inter, Lignes Aeriennes Interieures, Paris (France).
Preparation for a new plane (A 320): Experience reviewed p 1010 N92-30954
Flight crew integration in the maintenance chain of a commercial aircraft (A 320) p 1012 N92-30957

Airbus Industrie, Blagnac (France).
Drag reduction: An industrial challenge
p 717 N92-27708
Ageing airplane repair assessment program for Airbus A300 p 838 N92-30123

Aircraft Research Association Ltd., Bedford (England).
Survey of experimental techniques for performance prediction p 552 N92-23954

Aix-Marseilles Univ. (France).
Hot jet dilutor
[ETN-92-90860] p 366 N92-19225
Experimental study of the wall pressure fluctuations under a turbulent boundary layer downstream of tandem aerofoil external manipulators
[REPT-207-90-78] p 500 N92-20497

Akron Univ., OH.
Transmission overhaul and component replacement predictions using Weibull and renewal theory
p 155 A92-17201

Engine dynamic analysis with general nonlinear finite element codes
[NASA-CR-187222] p 44 N92-11379
A hierarchy for modeling high speed propulsion systems
[NASA-CR-186984] p 387 N92-19934
Improved large perturbation propulsion models for control system design (1988-1989) and large perturbation models of high velocity propulsion systems (1989-1990) and reduced order propulsion models for control system design (1990-1991)
[NASA-CR-190148] p 593 N92-22491
A hierarchy for modeling high speed propulsion systems p 559 N92-22492
Approximate truncated balanced realizations for infinite dimensional systems p 602 N92-22493
Modeling of linear isentropic flow systems
p 593 N92-22495

Alabama Univ., Huntsville.
Modifications to the rapid melt/rapid quench and transparent polymer video furnaces for the KC-135
[NASA-CR-184215] p 157 N92-12231
Process modeling KC-135 aircraft
[NASA-CR-184278] p 359 N92-18347
Materials processing in low gravity
[NASA-CR-184280] p 499 N92-20198
High temperature aircraft research furnace facilities
[NASA-CR-184384] p 1101 N92-33826

Alberta Research Council, Edmonton (Canada).
The application of lattice-structure adaptive filters to clutter-suppression for scanning radar
p 403 N92-19154

Alberta Univ., Edmonton.
Aerodynamic design and analysis of a light aircraft propeller p 629 N92-24876
Variable geometry sailplanes Minisigma
p 629 N92-24877
A time-linearization approach for unsteady transonic flows p 719 N92-27941

Alenia, Foggia (Italy).
CFRP stiffened panels under compression
p 1109 N92-33044

Alenia, Torino (Italy).
Proposal for the new fatigue management system for the AMX p 361 N92-18580
Prediction of aerodynamic phenomena limiting aircraft manoeuvrability p 364 N92-18781
Parametric bicubic spline and CAD tools for complex targets shape modelling in physical optics radar cross section prediction p 403 N92-19151
A fin optimisation study p 551 N92-23237
AM-X flight simulator from engineering tool to training device p 884 N92-28536

Alenia Aeronautica, Naples (Italy).
Active vibrations and noise control for turboprop application research program activities
p 1138 N92-32962

Alenia Spazio S.p.A., Naples (Italy).
Aerothermodynamic development of the CARINA re-entry vehicle: CFD analyses and experimental tests
p 211 N92-14980

Allied-Signal Aerospace Co., Baltimore, MD.
MLS system error model identification and synthesis
p 189 N92-14015

Allied-Signal Aerospace Co., Phoenix, AZ.
Impact design methods for ceramic components in gas turbine engines
[ASME PAPER 91-GT-115] p 123 A92-15566
Studies of the effects of curvature on dilution jet mixing p 290 A92-21079

Allied-Signal Aerospace Co., Torrance, CA.
Development of silicon nitride rotors for the ATTAP program at Garrett Ceramic Components
[ASME PAPER 91-GT-154] p 142 A92-15590
H2-fueled high-bypass turbofan p 475 N92-21529

Ames Lab., IA.
Computered tomography: Experimental data acquisition and parallelization of reconstruction algorithm
[DE92-005151] p 499 N92-20301

Ametek, Inc., Wilmington, MA.
High accuracy fuel flowmeter. Phase 2C and 3: The mass flowrate calibration of high accuracy fuel flowmeters
[NASA-CR-187108] p 406 N92-19775

Amptek, Inc., Bedford, MA.
Prototype instrumentation and design studies
[AD-A248378] p 736 N92-28004

Anacapa Sciences, Inc., Fort Rucker, AL.
Assessment of army aviators' ability to perform individual and collective tasks in the aviation networked simulator
[AD-A250293] p 888 N92-29709

Analytical Services and Materials, Inc., Hampton, VA.
Computational investigation of circular-to-rectangular transition ducts
[AIAA PAPER 91-3342] p 6 A92-11605
On the nonlinear stability of a high-speed, axisymmetric boundary layer p 78 A92-16457
Proof test and fatigue crack growth modeling on 2024-T3 aluminum alloy p 213 A92-19828
Secondary instability of high-speed flows and the influence of wall cooling and suction
[NASA-CR-4427] p 406 N92-19844
A compressible Navier-Stokes solver with two-equation and Reynolds stress turbulence closure models
[NASA-CR-4440] p 681 N92-25376
Preliminary structural sizing of a Mach 3.0 high-speed civil transport model
[NASA-CR-189631] p 685 N92-25960

Anderson Associates, Glenville, NY.
Spectrum sharing between AMSS(R) and MSS
p 677 N92-24165

Appalachian State Univ., Boone, NC.
Background issues for on-line aircraft documentation
p 119 N92-13858

Applied Acoustic Research, State College, PA.
A lightweight loudspeaker for aircraft communications and active noise control p 1125 N92-32964

Applied Research Associates, Inc., Lakewood, CO.
Rarefaction wave eliminator design study
[AD-A244401] p 484 N92-20455

Applied Research Lab., State College, PA.
Basic hydrodynamics
[AD-A243513] p 300 N92-17387
A study of the diffusion of slot-injected drag-reducing polymer solution in a turbulent boundary layer modified by large-eddy breakup devices
[AD-A243411] p 344 N92-18007

Arizona State Univ., Tempe.
Dynamics and control of hypersonic vehicles - The integration challenge for the 1990's
[AIAA PAPER 91-5057] p 203 A92-17840
Numerical simulation of swept-wing flows
[NASA-CR-189457] p 180 N92-14969
Aerodynamic roughness measured in the field and simulated in a wind tunnel
[NASA-CR-4422] p 347 N92-19354
Advanced electromagnetic methods for aerospace vehicles
[NASA-CR-188630] p 488 N92-20193
Laminar-turbulent transition: Fundamentals
p 717 N92-27710
Advanced electromagnetic methods for aerospace vehicles
[NASA-CR-190650] p 1001 N92-31156
Stability and transition of hypersonic boundary-layer flows
[AD-A250279] p 948 N92-31555

Arizona Univ., Tucson.
A DFW microburst model based on DL-191 data
p 17 A92-11380
Prediction and analysis of wing flutter at transonic speeds p 662 N92-25555
Aircraft photovoltaic power-generating system
p 775 N92-26581
Expand turbulence laboratory facilities to meet new DOD research interest
[AD-A248581] p 883 N92-28388
Leading-edge receptivity for blunt-nose bodies
[NASA-CR-190563] p 1036 N92-32648

Army Aeromedical Research Lab., Fort Rucker, AL.
Concept evaluation of the UH-60 externally mounted rescue hoist
[AD-A240545] p 22 N92-11004

Army Aerostructures Directorate, Hampton, VA.
Recent rotorcraft aeroelastic testing in the Langley Transonic Dynamics Tunnel p 136 A92-14377
Experimental investigation of helicopter vibration reduction using rotor blade aeroelastic tailoring
p 107 A92-14396
Fatigue crack initiation and small crack growth in several airframe alloys p 212 A92-19754

Army Aviation Research and Development Command, Moffett Field, CA.
Pre-flight risk assessment in emergency medical service (EMS) helicopters p 16 A92-11171
Analysis of general aviation accidents during operations under instrument flight rules p 16 A92-11172

Army Aviation Systems Command, Cleveland, OH.
NASA low-speed centrifugal compressor for 3-D viscous code assessment and fundamental flow physics research
[ASME PAPER 91-GT-140] p 72 A92-15580
A comparison of predicted and measured inlet distortion flows in a subsonic axial inlet flow compressor rotor
[NASA-TM-105427] p 633 N92-26104
Experimental testing of prototype face gears for helicopter transmissions
[NASA-TM-105434] p 1002 N92-31349

Army Aviation Systems Command, Hampton, VA.
Detailed analysis and test correlation of a stiffened composite wing panel
[NASA-TM-104154] p 159 N92-13460
Experimental evaluation of a flat wake theory for predicting rotor inflow-wake velocities
[NASA-TM-4334] p 630 N92-24882
Evaluation of composite components on the Bell 206L and Sikorsky S-76 helicopters p 1107 N92-32575

Army Aviation Systems Command, Moffett Field, CA.
Wing tip vortex calculations with an unstructured adaptive-grid Euler solver p 64 A92-14330
Forward flight trim calculation and frequency response validation of a high-order helicopter simulation model
p 132 A92-14337
Helicopter control response types for hover and low-speed near-earth tasks in degraded visual conditions
p 132 A92-14338
Acoustic predictions using measured pressures from a model rotor in the DNW p 165 A92-14385
Aerodynamic design of a Coanda induced force and thruster anti-torque system p 109 A92-14419
Helicopter air resonance modeling and suppression using active control p 204 A92-18625
Navier-Stokes analysis of blunt trailing edge airfoils
[AIAA PAPER 92-0024] p 248 A92-22146
Identification techniques: Frequency domain methods
p 273 N92-17158
System identification methods for handling-qualities evaluation p 274 N92-17165
System identification requirements for high-bandwidth rotorcraft flight control system design
p 282 N92-17166

Army Aviation Technical Test Center, Fort Rucker, AL.
Steady-state acoustical noise measurements in aviation systems
[AD-A247831] p 780 N92-27924

Army Aviation Test Board, Fort Rucker, AL.
Ingress, emergency egress, and emergency evacuation testing of army aircraft
[AD-A246398] p 724 N92-27750

Army Cold Regions Research and Engineering Lab., Hanover, NH.
Effects of the abrasiveness of test and training site soils on parachute life
[AD-A252389] p 1038 N92-32900
Performance of insulated pavements at Newton Fields, Jackman, Maine
[CRREL-92-9] p 1101 N92-32903

Army Construction Engineering Research Lab., Champaign, IL.
Human response to helicopter noise: A test of A-weighting
[AD-A243719] p 304 N92-17506
Operational noise data for OH-58D Army helicopters
[AD-A246822] p 926 N92-28292

Army Electronic Proving Ground, Fort Huachuca, AZ.
Antenna pattern measurement facilities
[AD-A248964] p 982 N92-30329
Compact range test applications, phase 2
[AD-A248790] p 999 N92-30583

Army Engineer Waterways Experiment Station, Vicksburg, MS.
Alternate/modified binders for asphalt airfield pavements
[AD-A242829] p 285 N92-17260
Passive acoustic range estimation of helicopters
[AD-A248033] p 926 N92-28302
Evaluation of grounding and mooring points for Army aircraft
[AD-A250749] p 953 N92-31193

Army Lab. Command, Fort Monmouth, NJ.
Low-noise oscillators for airborne radar applications
[AD-A242264] p 300 N92-17258

Army Lab. Command, Watertown, MA.
Failure analysis of the Apache mixer pivot support
[AD-A240858] p 116 N92-13061
A sensitivity analysis on component reliability from fatigue life computations
[AD-A247430] p 908 N92-28425

Army Materials Technology Lab., Watertown, MA.
Properties of a TZP/Al2O3 composite after long-term exposure at 1000 C
[AD-A246407] p 757 N92-27752

Army Materiel Systems Analysis Activity, Aberdeen Proving Ground, MD.
Cost/benefit analysis of the AH-64 (Apache) helicopter Automated Test Equipment (ATE)
[AD-A252909] p 1101 N92-33398

Army Missile Command, Redstone Arsenal, AL.
Design and construction of a Helmholtz coil magnetic test cell
[AD-A249944] p 983 N92-30849

Army Natick Labs., MA.
Dynamical systems analysis of an aerodynamic decelerator's behavior during the initial opening process
[AD-A244194] p 348 N92-19394

Army Natick Research and Development Command, MA.
Trajectory analysis of the G-11 family of clustered parachutes to determine minimum altitude
[AD-A243375] p 261 N92-17404
Army Propulsion Lab., Cleveland, OH.
Army research concerns in engine sealing
p 228 N92-15089
Arnold Engineering Development Center, Arnold AFS, TN.
Asymptotic theory of transonic wind tunnel wall interference
[AD-A244075] p 403 N92-19080
Initial calibration of the HEAT-H2 arc-heated wind tunnel
[AD-A245072] p 484 N92-20898
Association Aeronautique et Astronautique de France, Paris.
Application of infrared thermography to thermal flux measurement in wind tunnels
[AAAF-NT-89-12] p 31 N92-11020
ATConsult, Frankfurt (Germany).
Steps toward acceptance p 355 N92-19046
Atlantic Research Corp., Landover, MD.
Revolution at sea: Aircraft options for the year 2030
p 466 N92-21974
Atmospheric and Environmental Research, Inc., Cambridge, MA.
Impact of heterogeneous chemistry on model-calculated ozone change due to high speed civil transport aircraft
p 45 A92-12941
Auburn Univ., AL.
The FM-007: An advanced jet commuter for HUB to spoke transportation
[NASA-CR-189988] p 461 N92-20267
The Langley turbo-prop commuter design: A complete project description
[NASA-CR-189987] p 463 N92-21540
Aviation Inst., Bucharest (Romania).
On a global aerodynamic optimization of a civil transport aircraft p 193 N92-13931
Aviation Planning Services Ltd., Montreal (Quebec).
A strategy for exploiting the full potential of MLS based terminal procedures in Canada p 190 N92-14025
Avions Marcel Dassault-Breguet Aviation, Saint-Cloud (France).
Stretched skin concept for the entry aerodynamic decelerator system of planetary probes
p 576 N92-23836

B

Ballistic Research Labs., Aberdeen Proving Ground, MD.
Application of digital measurement techniques to analysis of range shadowgraphs
[AD-A241554] p 139 N92-13080
Transonic Navier-Stokes computations for a spinning body of revolution
[AD-A241015] p 180 N92-14972
Analysis of the flight performance of the 155 mm M864 base burn projectile
[BRL-TR-3083] p 1041 N92-33699
Bath Univ. (England).
An evaluation of some strategies for vibration control of flexible rotors p 773 N92-27800
Battelle Columbus Labs., OH.
A review and discussion of flight management system incidents reported to the aviation safety reporting system
[AD-A252438] p 1043 N92-32941
Battelle Memorial Inst., Columbus, OH.
Generation of spectra and stress histories for fatigue and damage tolerance analysis of fuselage repairs
[AD-A250390] p 854 N92-29180
BBN Systems and Technologies Corp., Cambridge, MA.
MULTIRAD
[AD-A244211] p 412 N92-19247
SIMNET plan view display user manual
[AD-A244617] p 510 N92-21392
BDM International, Inc., Arlington, VA.
Automated planning with special relevance to associate systems technology and mission planning
[AD-A241924] p 303 N92-17438
Beijing Univ. (China).
An inverse method with regularity condition for transonic airfoil design p 177 N92-13969
Bell Helicopter Co., Fort Worth, TX.
Hub and pylon fairing integration for helicopter drag reduction p 107 A92-14391
Beltran, Inc., Brooklyn, NY.
Development of fuel neutralizing agents to prevent flashback on aircraft fires
[AD-A242828] p 264 N92-17259
Bently Rotor Dynamics Research Corp., Minden, NV.
Rotor-to-stator partial rubbing and its effects on rotor dynamic response p 224 N92-14367
Comments on frequency swept rotating input perturbation techniques and identification of the fluid force models in rotor/bearing/seal systems and fluid handling machines p 224 N92-14370
Bodenseewerk Geraetetechnik G.m.b.H., Ueberlingen (Germany).
Introduction to neural computing and categories of neural network applications to guidance, navigation and control p 234 N92-14674
Boeing Advanced Systems Co., Seattle, WA.
Design of an integrated airframe/propulsion control system architecture
[NASA-CR-182004] p 602 N92-22643
Design of an integrated airframe/propulsion control system architecture
[NASA-CR-182007] p 602 N92-22644
Boeing Aerospace and Electronics Co., Seattle, WA.
Low density real gas flows about hypersonic vehicles
[AD-A250048] p 949 N92-31777
Boeing Co., Seattle, WA.
Dual mode shock absorber and method
[PATENT-1-265-541] p 115 N92-13055
Flyover-noise measurement and prediction
p 236 N92-14786
Quiet aircraft design and operational characteristics
p 236 N92-14787
Application of analysis techniques for low frequency interior noise and vibration of commercial aircraft
[NASA-CR-189555] p 481 N92-20376
Analysis of unsteady aerodynamic and flutter characteristics of an aeroelastic model in transonic flow
p 720 N92-27953
Buffet test in the National Transonic Facility
[NASA-CR-189595] p 888 N92-29352
Boeing Commercial Airplane Co., Seattle, WA.
Design of localizer capture and track hold for a transport airplane - An H(infinity)/LTR approach
p 52 A92-11583
Structural airworthiness of aging Boeing jet transports
p 362 N92-18590
NASA TSRV essential flight control system requirements via object oriented analysis
[NASA-CR-189573] p 381 N92-19499
High-speed civil transport flight- and propulsion-control technological issues
[NASA-CR-186015] p 482 N92-21253
Wind tunnel investigation of the aerodynamic effects of aircraft ground deicing/anti-icing fluids and criteria for aerodynamic acceptance p 452 N92-21698
Flight test of ARINC 741 configuration low gain SATCOM system on Boeing 747-400 aircraft p 677 N92-24097
An interactive multi-block grid generation system
p 691 N92-24419
Structural analysis for preliminary design of High Speed Civil Transport (HSCT) p 684 N92-25926
Structural integrity of future aging airplanes
p 913 N92-30107
Performance of fuselage pressure structure
p 913 N92-30109
Aging fleet: Maintaining airworthiness
p 953 N92-31862
Integrated computer systems in aircraft design and manufacture: Difficulties and implications
p 1010 N92-31864
Engine monitoring display study
[NASA-CR-4463] p 979 N92-32175
An installed nacelle design code using a multiblock Euler solver. Volume 1: Theory document
[NASA-CR-189652-VOL-1] p 950 N92-32226
An installed nacelle design code using a multiblock Euler solver. Volume 2: User guide
[NASA-CR-189652-VOL-2] p 951 N92-32228
Flutter in the transonic flight regime
p 1089 N92-34167
Flutter analyses using high speed computers. Part 1: Flutter analyses for large aircraft p 1089 N92-34168
Flutter analyses using high speed computers. Part 2: Aerodynamic procedures p 1089 N92-34169
Boeing Computer Services Co., Seattle, WA.
A comparison of two closely-related approaches to aerodynamic design optimization p 193 N92-13933
PAN AIR: A computer program for predicting subsonic or supersonic linear potential flows about arbitrary configurations using a higher order panel method. Volume 1: Theory document (version 3.0)
[NASA-CR-3251] p 526 N92-22648
Boeing Military Airplane Development, Seattle, WA.
Historical perspective on the evolution of avionics standards p 198 N92-14049
PAN AIR: A computer program for predicting subsonic or supersonic linear potential flows about arbitrary configurations using a higher order panel method. Volume 2: User's manual (version 3.0)
[NASA-CR-3252] p 527 N92-22865
Boeing Military Airplane Development, Wichita, KS.
Development of thermoplastic components for structural validation p 1107 N92-32522
Bombardier, Inc., Montreal (Quebec).
On the coupling of Euler/boundary-layer equations
p 627 N92-24859
Further development of the CANAERO computer code to include propulsor modelling
[DREA-CR-90-425] p 1038 N92-32811
Booz-Allen and Hamilton, Inc., Bethesda, MD.
Heavy duty transport research needs assessment
[DE92-010622] p 767 N92-27394
Booz-Allen and Hamilton, Inc., Houston, TX.
Attributes of winged manned space vehicles and their relationship to ground site characteristics and facilities
p 487 N92-20776
British Aerospace Aircraft Group, Kingston-upon-Thames (England).
Transonic aeroelastic calculations in both the time and frequency domains p 720 N92-27950
British Aerospace Aircraft Group, Warton (England).
Aspects of compression in aerospace composites: Future requirements p 1109 N92-33036
British Aerospace Public Ltd. Co., Bristol (England).
Simultaneous stress and flutter optimization for the wing of a transport aircraft equipped with four engines
p 571 N92-23238
British Aerospace Public Ltd. Co., Lancashire (England).
Some implications for advanced STOVL operation from invincible class ships p 466 N92-21971
Application of an automated multidisciplinary analysis and optimisation system to the design of aircraft structures p 551 N92-23233
Effective cueing during approach and touchdown: Comparison with flight p 886 N92-28552
British Aerospace Public Ltd. Co., Preston (England).
The development of fatigue management requirements and techniques p 360 N92-18572
Use of stepwise regression techniques and kinematic compatibility for the analysis of EAP flight data
p 365 N92-18790
British Petroleum Co. Ltd., London (England).
Spray nozzle for fire control
[CA-PATENT-APPL-SN-2-011-94] p 1125 N92-32856
Brown Univ., Providence, RI.
Parameter identification for nonlinear aerodynamic systems
[NASA-CR-188985] p 53 N92-10347
Parameter identification for nonlinear aerodynamic systems
[NASA-CR-190264] p 830 N92-29329
Bundesamt fuer Wehrtechnik und Beschaffung, Munich (Germany).
Tornado structural fatigue life assessment of the German Air Force p 363 N92-18592
Bundesanstalt fuer Flugsicherung, Frankfurt am Main (Germany).
The impact of COMPAS on the future Cooperative Air Traffic Management Concept (CATMAC)
p 355 N92-19049
Bureau International des Poids et Mesures, Sevres (France).
The need for GPS standardization
p 1049 N92-33351
Precise GPS ephemerides from DMA and NGS tested by time transfer p 1049 N92-33355

C

CAE Electronics Ltd., Montreal (Quebec).
The use of a dedicated testbed to evaluate simulator training effectiveness p 884 N92-28533
CAE Electronics Ltd., Saint Laurent (Quebec).
The evaluation of simulator effectiveness for the training of high speed, low level, tactical flight operations
p 885 N92-28539
California Inst. of Tech., Pasadena.
Experimental simulation and diagnostics of high-enthalpy real-gas flows
[AD-A241286] p 166 N92-13822
An analytical and computational investigation of shock-induced vortical flows with applications to supersonic combustion p 405 N92-19538
Active control of the flow past a cylinder executing rotary motions p 349 N92-19623
Shock enhancement and control of hypersonic combustion
[AD-A248558] p 896 N92-29580

California Polytechnic State Univ., San Luis Obispo.
Computational investigation of slot blowing for fuselage forebody flow control
[AIAA PAPER 92-0020] p 248 A92-22142
A CLIPS-based tool for aircraft pilot-vehicle interface design p 303 N92-16605
Proposal for a low cost close air support aircraft for the year 2000: The Raptor
[NASA-CR-190023] p 367 N92-19496
Scorpion: Close Air Support (CAS) aircraft
[NASA-CR-189974] p 462 N92-20664
The SnoDog: Preliminary design of a close air support aircraft
[NASA-CR-189990] p 462 N92-21489
Manx: Close air support aircraft preliminary design
[NASA-CR-189992] p 463 N92-21565
The Guardian: Preliminary design of a close air support aircraft
[NASA-CR-189991] p 463 N92-21566
A-2000: Close air support aircraft design team
[NASA-CR-190022] p 463 N92-21567
A study of transonic aerodynamic analysis methods for use with a hypersonic aircraft synthesis code
[NASA-CR-189854] p 625 N92-24803
Computation of three-dimensional effects on two dimensional wings
[NASA-CR-190576] p 832 N92-29691
Human factors issues in the use of artificial intelligence in air traffic control. October 1990 Workshop
[NASA-CR-190925] p 1051 N92-34203
California State Polytechnic Univ., Pomona.
SHARP: Subsonic High Altitude Research Platform
[NASA-CR-190004] p 648 N92-25263
California State Univ., Fullerton.
Z-Basic algorithm for collision avoidance system p 188 A92-18482
California State Univ., Los Angeles.
Navier-Stokes calculation of transonic flow past the NTF 65 deg delta wing p 91 N92-13868
California Univ., Berkeley.
Personal air transport: State of the art
[PB91-204768] p 18 N92-10991
Adaptive control of nonlinear systems with applications to the control of flexible robot arms
[AD-A244409] p 413 N92-19397
A walk through the planned CS building
[NASA-CR-189963] p 386 N92-19675
Experimental studies of compact toroids
[DE92-003469] p 512 N92-21046
California Univ., Davis.
Experimental investigation on the effect of crescent planform on lift and drag p 9 A92-13206
Quantitative Feedback Theory (QFT) applied to the design of a rotorcraft flight control system
[AIAA PAPER 92-0044] p 281 A92-22161
Modeling and analysis methodology for aeroelastically tailored chordwise deformable wings
[NASA-CR-189620] p 961 N92-30304
California Univ., Irvine.
Fundamental studies on droplet interactions in dense sprays
[AD-A246918] p 770 N92-27546
Mechanical behavior and processing of aluminum metal matrix composites
[AD-A249918] p 987 N92-30874
California Univ., Los Angeles.
Helicopter air resonance modeling and suppression using active control p 204 A92-18625
Control augmented structural optimization of aeroelasticity tailored fiber composite wings
[AD-A241464] p 135 N92-13075
Adaptive active flutter suppression of wings in subsonic and transonic flight regimes p 553 N92-24010
California Univ., San Diego, La Jolla.
Processing complexity of two approaches to object detection and recognition p 234 N92-14677
Theories of turbulent combustion in high speed flows
[AD-A253032] p 1111 N92-33624
Calspan-Buffalo Univ. Research Center, NY.
Studies of aerothermal loads generated in regions of shock/shock interaction in hypersonic flow
[NASA-CR-181893] p 43 N92-11319
Development of an integrated BEM approach for hot fluid structure interaction: BEST-FSI: Boundary Element Solution Technique for Fluid Structure Interaction
[NASA-CR-189202] p 574 N92-22211
Calspan Corp., Arnold AFS, TN.
Initial calibration of the HEAT-H2 arc-heated wind tunnel
[AD-A245072] p 484 N92-20898
Cambridge Collaborative, Inc., MA.
Use of SEA to predict structure-borne noise in aircraft p 1137 N92-32955
Cambridge Univ. (England).
Airframe noise p 55 N92-10605
A theoretical investigation of the induced drag of wing of finite aspect ratio
[CUED/A-AERO/TR-17(1991)] p 525 N92-22193
Separation of relaminarised boundary layers
[CUED/A-AERO/TR-16] p 592 N92-22209
Aspects of unsteady blade-surface boundary layers and transition in axial turbomachines p 658 N92-24340
Inlet distortion effects in aircraft propulsion system integration p 869 N92-28464
Boundary layer induced noise in aircraft
[CUED/A-AERO/TR-18] p 927 N92-29201
Canadair Ltd., Montreal (Quebec).
A probabilistic procedure for aircraft fleet management p 360 N92-18576
Helicopter/ship analytic dynamic interface p 464 N92-21962
Canadian Aeronautics and Space Inst., Montreal (Quebec).
Proceedings of the 3rd Canadian Symposium on Aerodynamics
[CTN-92-60420] p 625 N92-24849
Canadian Astronautics Ltd., Ottawa (Ontario).
Low cost, electronically steered phased array for general aviation p 677 N92-24099
An aircraft Earth station for general aviation p 678 N92-24194
Canadian Forces Headquarters, Ottawa (Ontario).
The effect of droplet sizing uncertainty on ice accretions p 679 N92-24874
Canadian Marconi Co. Ltd., Kanata (Ontario).
A high gain antenna system for airborne satellite communication applications p 677 N92-24096
Canadian Petroleum Association, Calgary (Alberta).
A report on enhancements for existing and future helicopters supporting operations of the Canadian oil and gas industry
[CTN-91-60126] p 636 N92-25350
Carleton Univ., Ottawa (Ontario).
Effects of frost on wing aerodynamics and take-off performance p 450 N92-21687
Performance degradation due to hoar frost on lifting surfaces p 628 N92-24866
Overview on basis and use of performance prediction methods p 869 N92-28459
Component performance requirements p 869 N92-28462
Carnegie-Mellon Univ., Pittsburgh, PA.
Behavior-based fault monitoring
[AD-A241254] p 164 N92-13746
Case Western Reserve Univ., Cleveland, OH.
The effect of steady aerodynamic loading on the flutter stability of turbomachinery blading
[ASME PAPER 91-GT-130] p 71 A92-15574
An inviscid stability analysis of unbounded supersonic mixing layer flows p 443 N92-20332
Conceptual design of two-stage-to-orbit hybrid launch vehicle
[NASA-CR-190006] p 486 N92-20666
Evaluation of an innovative high-temperature ceramic wafer seal for hypersonic engine applications p 578 N92-22205
Thermal mechanical analysis of sprag clutches
[NASA-CR-190686] p 1128 N92-34207
Catholic Univ. of America, Washington, DC.
Organized turbulent structures and their induced wall pressure fluctuations p 949 N92-31853
Centre d'Essais Aeronautique Toulouse (France).
Mechanical qualification tests for materials used in the fabrication of aircraft parts
[CEAT-M5-5443/01] p 195 N92-14042
Optimization of the calculation margins of landing gears under extreme loads. Rupture static tests. Part 1: Program and test implantation
[CEAT-S8-6551-PARTIEL-1-PT-] p 195 N92-14043
Fatigue safety factor: Assessment of associated safety level p 401 N92-18573
Evaluation of the effects of the environment on the behavior of the primary structures of composite material aircraft in service: Historic and current situation p 1110 N92-33048
Centre d'Essais en Vol, Istres (France).
Regulations and their changes for certification of civil aircraft in icing conditions p 450 N92-21683
Centre d'Etudes Aerodynamiques et Thermiques, Poitiers (France).
Control aspects of the transition from transversal to transonic flow, step effects
[ETN-91-90106] p 82 N92-11981
Hypersonic wakes
[ETN-92-91082] p 349 N92-19925
Centre d'Etudes et de Recherches, Toulouse (France).
Resolution of the Navier-Stokes equations applied to the computation of the laminar flow around a two dimensional wing profile
[CERT-RT-65/5604-35] p 43 N92-11307
Turbulent friction drag reduction: Boundary layer manipulators
[CERT-RSF-DERAT-62/5004-31] p 43 N92-11309
Double loop control law strategy and applications to helicopter
[CERT-2/7724-DERA] p 381 N92-19295
Basic concepts on boundary layers p 717 N92-27707
Boundary layer transition: Prediction, application to drag reduction p 717 N92-27711
Turbulent skin-friction drag reduction by active and passive means, part 1 p 718 N92-27714
Centre National de la Recherche Scientifique, Chatenay-Malabry (France).
Hypersonic viscous shock layer in thermochemical nonequilibrium p 183 N92-15014
The coherent flamelet model for propulsion applications p 756 N92-27486
Centre National de la Recherche Scientifique, Marseilles (France).
Numerical simulations around models in hypersonic wind tunnels p 182 N92-14998
Centro Italiano Ricerche Aerospaziali, Naples.
High enthalpy nozzle flows p 182 N92-15000
CFD Research Corp., Huntsville, AL.
CFD analysis of jet mixing in low NO(x) flametube combustors
[ASME PAPER 91-GT-217] p 124 A92-15634
Development of a CFD code for analysis of fluid dynamic forces in seals p 228 N92-15084
Pressure-based high-order TVD methodology for dynamic stall control
[AD-A247056] p 774 N92-27918
Charles River Analytics, Inc., Cambridge, MA.
An alternative concept for aeroassisted orbit transfers
[AD-A243409] p 287 N92-17325
Chemical Research and Development Center, Aberdeen Proving Ground, MD.
Experimental aerodynamic facilities of the Aerodynamics Research and Concepts Assistance Branch
[AD-A247489] p 883 N92-28248
Chrysler Corp., New Orleans, LA.
Results of the space shuttle vehicle ascent air data system probe calibration test using a 0.07-scale external tank forebody model (68T) in the AEDC 16-foot transonic wind tunnel (IA-310), volume 1
[NASA-CR-167696] p 286 N92-17167
Results of the space shuttle vehicle ascent air data system probe calibration test using a 0.07-scale external tank forebody model (68T) in the AEDC 16-foot transonic wind tunnel (IA-310), volume 2
[NASA-CR-167697] p 286 N92-17214
Cincinnati Univ., OH.
A semi-elliptic analysis for 2-D viscous flows through cascade configurations p 3 A92-10688
The dynamics of flexible multibody systems: A finite segment approach p 1128 N92-34036
City Univ. of New York, Bronx.
Development of a calibrated software reliability model for flight and supporting ground software for avionic systems p 234 N92-15870
Civil Aviation Authority, Canberra (Australia).
Aging commuter aeroplanes: Fatigue evaluation and control methods p 915 N92-30132
Civil Aviation Authority, London (England).
UK airmisses involving commercial air transport: September - December 1990
[ETN-92-91050] p 452 N92-21746
Clemson Univ., SC.
Parameter insensitive control utilizing eigenspace methods p 204 A92-18615
Spectrum modal analysis for the detection of low-altitude windshear with airborne Doppler radar
[NASA-CR-4457] p 953 N92-31549
Real-time processing of radar return on a parallel computer
[NASA-CR-4456] p 1043 N92-32606
Coast Guard Academy, New London, CT.
Measurement of LORAN-C envelope to cycle difference in the far field
[PB92-128909] p 455 N92-21263
Probability of cycle jumps in Omega receivers and other phase locked loop applications
[PB92-128891] p 455 N92-21279
Integrated Russian VLF/Omega receiver design
[PB92-193390] p 1051 N92-33809
Colorado State Univ., Fort Collins.
Operating ranges of meteorological wind tunnels for the simulation of convective boundary layer phenomena
[AD-A244153] p 409 N92-19195
Colorado Univ., Boulder.
Simulation of GRM drag compensation system p 285 A92-21023
Contractors Meeting in Propulsion
[AD-A240057] p 33 N92-10062

Aerodynamic interference between stores
[AD-A247207] p 715 N92-27172
Commissariat a l'Energie Atomique, Grenoble (France).
Experimental methods to determine heat exchanger performances p 682 N92-25667
Committee of Conference (U.S. Congress).
National Aeronautics and Space Administration research and development p 238 N92-15937
Committee on Appropriations (U.S. House).
National Aeronautics and Space Administration
p 417 N92-18309
Departments of Veterans Affairs and Housing and Urban Development, and independent agencies appropriations for 1993, part 6
[GAO-55-636-PT-6] p 1141 N92-32505
Committee on Appropriations (U.S. Senate).
National Aeronautics and Space Administration
p 238 N92-14925
National Aeronautics and Space Administration
p 238 N92-14927
Committee on Commerce, Science, and Transportation (U.S. Senate).
National Aeronautics and Space Administration Authorization Act, 1993
[S-2558-IS] p 698 N92-25606
Committee on Science, Space and Technology (U.S. House).
NASA authorization, 1993, volume 1
[GPO-55-260-VOL-1] p 1142 N92-33147
Communications Gillies, Inc., Sainte Lambert (Quebec).
Electronic systems in transportation
[TP-9983] p 189 N92-14009
Communications Research Centre, Ottawa (Ontario).
A TMS320-based modem for the aeronautical-satellite core data service p 594 N92-22562
CompEngServ Ltd., Ottawa (Ontario).
A unique approach to aircraft conflict resolution using artificial intelligence techniques p 190 N92-14029
Complere, Inc., Palo Alto, CA.
Two-dimensional adaptive-wall tests in the NASA Ames two- by two-foot transonic wind tunnel
p 30 A92-13201
An assessment of particle velocimetry potential in hypersonic flow
[AIAA PAPER 92-0010] p 247 A92-22135
Measurement of vortex flow fields
[NASA-CR-189543] p 443 N92-20283
Computational Methodology Associates, Hurst, TX.
Rotorwash computer model: User's guide
[DOT/FAA/RD-90/25] p 346 N92-18345
Computer Resource Management, Inc., Herndon, VA.
Monitoring operational concept
[DOT/FAA/SE-91/3] p 268 N92-15980
National airspace system: System effectiveness operational concept NAS-SR-138
[DOT/FAA/SE-92/2] p 535 N92-23096
National airspace system. Air defense and law enforcement surveillance operational concept NAS-SR-135
[DOT/FAA/SE-92/3] p 953 N92-31211
Computer Resource Management, Inc., Pleasantville, NJ.
Avionic data bus integration technology
[DOT/FAA/CT-91/19] p 736 N92-27973
Computer Sciences Corp., Hampton, VA.
Analysis of objects in binary images
[NASA-CR-4420] p 234 N92-14598
Advanced Transport Operating System (ATOPS) color displays software description: MicroVAX system
[NASA-CR-189603] p 556 N92-22395
Advanced Transport Operating System (ATOPS) color displays software description microprocessor system
[NASA-CR-189605] p 556 N92-22645
Advanced Transport Operating System (ATOPS) control display unit software description
[NASA-CR-189606] p 652 N92-24689
Computer Sciences Corp., Lanham, MD.
Impact of a process improvement program in a production software environment: Are we any better?
p 413 N92-19422
Computer Technology Associates, Inc., McKee City, NJ.
Evaluation of triple simultaneous parallel ILS approaches spaced 4300 feet apart, phase 4a
[ACD-340] p 191 N92-14034
Evaluation of triple simultaneous parallel ILS approaches spaced 5000 feet apart, phase 4.b
[DOT/FAA/CT-91/31] p 456 N92-21404
Conceptual Research Corp., Sylmar, CA.
Configuration development p 552 N92-23953
Congress of the United States, Washington, DC.
National Aeronautics and Space Administration
p 238 N92-14923
The 1991 Federal Aviation Administration plan for research, engineering and development
p 1142 N92-32453
Continuum Dynamics, Inc., Princeton, NJ.
Prediction of high-resolution flowfields for rotorcraft aeroacoustics p 53 A92-11053
Analysis of rotor vibratory loads using higher harmonic pitch control
[NASA-CR-189591] p 696 N92-24251
Coriolis Corp., Saratoga, CA.
Thermal management of high heat flux electronic components in space and aircraft systems, phase 1
[AD-A239982] p 41 N92-10157
Cornell Univ., Ithaca, NY.
Flow visualization and flow field measurements of a 1/12 scale tilt rotor aircraft in hover
[NASA-CR-189456] p 82 N92-11983
Optimal aircraft performance during microburst encounter p 266 N92-17999
Council for National Academic Awards (England).
Variable impedance journal bearings for rotor-bearing systems p 157 N92-12270
Cranfield Inst. of Tech., Bedford (England).
Radial inflow turbine study
[AD-A240169] p 26 N92-11015
Flow over a delta wing at hypersonic speeds
p 181 N92-14993
Passenger knowledge of airline safety information
[CRANFIELD-AERO-9111] p 187 N92-15054
Advanced tactical fighter engine
[ETN-92-90840] p 376 N92-18728
Experimental studies of vortex flaps and vortex plates. Part 1: 0.53 m span 60 deg delta wing
[CRANFIELD-AERO-9113-PT-1] p 349 N92-19679
A study of the aeroelastic behaviour of helicopter rotor blades featuring swept tips p 367 N92-19701
An evaluation of in-cabin safety features in passenger aircraft
[ETN-92-90656] p 449 N92-20794
Radial inflow turbine study
[AD-A246938] p 743 N92-28073
Fundamentals of structural optimisation
p 851 N92-28470
An investigation into the interface between three closely spaced axi-symmetric bodies at subsonic speed
[CRANFIELD-AERO-9114] p 948 N92-31514
ASTOVL combat aircraft design synthesis and optimization
[CRANFIELD-AERO-9201] p 963 N92-31515
Radial inflow turbine study
[AD-A252783] p 1127 N92-33538
CSA Engineering, Inc., Palo Alto, CA.
Preservation and utilization of finite element models of USAF aircraft structures
[AD-A241657] p 160 N92-13470

D

Dassault (E. M.) Co., Saint Cloud (France).
Structural optimization of aircraft p 851 N92-28472
Dassault-Breguet Aviation, Saint Cloud (France).
Aircraft tracking optimization of parameters selection
p 361 N92-18585
Dynamic performance of an aircraft on its landing gear: Test and evaluation on a dihedral p 466 N92-21970
The role of simulation for the study of APIS (piloting support by synthetic imagery) p 885 N92-28544
Dassault Espace, Saint-Cloud (France).
Structural optimization of aircraft practice and trends
p 551 N92-23239
Computational procedures for preliminary design
p 552 N92-23952
David Taylor Research Center, Bethesda, MD.
Unsteady flows in rotor-stator cascades
[AD-A241593] p 158 N92-13410
Navier-Stokes analysis of turbulent boundary layer and wake for two-dimensional lifting bodies
p 221 N92-14309
Aviation Diagnostics And Maintenance (ADAM) system preliminary concept of operation and functional description
[AD-A242598] p 170 N92-14966
Computation of the hydrodynamic forces and moments on a body of revolution with and without appendages
[AD-A243033] p 298 N92-16978
Use of Navier-Stokes analysis in section design
[AD-A242074] p 299 N92-17168
Dayton Univ., OH.
Locally linear neural networks for aerospace navigation systems p 103 N92-12530
Explicit finite element method for transparency impact analysis
[AD-A243527] p 264 N92-17478
Lubricant evaluation and performance 2
[AD-A247464] p 895 N92-28398
Dayton Univ. Research Inst., OH.
Study of the engine bird ingestion experience of the Boeing 737 aircraft
[DOT/FAA/CT-89/16] p 187 N92-15053
Engine bird ingestion experience of the Boeing 737 aircraft: Expanded data base
[DOT/FAA/CT-91/32] p 1045 N92-34151
De Havilland Aircraft Co. of Canada Ltd., Ottawa (Ontario).
VORVISC: A vortex lattice method with viscous and compressibility corrections for full aircraft configurations including propulsion p 626 N92-24857
Deacon Research, Palo Alto, CA.
Laser based, non-intrusive measurement system for analysis of jet engine flows
[AD-A242398] p 279 N92-17011
Defence and Civil Inst. of Environmental Medicine, Downsview (Ontario).
Development of an emergency underwater escape breathing system for CH124 seaking aircrew
[DCIEM-87-TR-11] p 92 N92-13041
Canadian aircrew sea water survival, 1952-1987
[DCIEM-88-RR-39] p 954 N92-32219
Defence Research Agency, Bedford (England).
Initial validation of a R/D simulator with large amplitude motion p 886 N92-28546
Defence Research Establishment, Ottawa (Ontario).
An improved model-creation program for EM interaction analysis
[NRC-31764] p 155 N92-12153
An evaluation of superresolution methods for tactical radio direction finding
[AD-A246316] p 726 N92-26291
Analysis of EMP response of structures using frequency domain electromagnetic interaction codes
[AD-A245758] p 765 N92-26592
Defence Research Establishment Pacific, Victoria (British Columbia).
A damage tolerance assessment of bonded repairs to CF-18 composite components. Part 1: Adhesive properties
[DREP-TM-88-25-PT-1] p 143 N92-12060
Filter debris analysis: A concrete approach to wear diagnosis
[DREP-TM-88-20] p 222 N92-14345
Detection of honeycomb damage using hexagonal grid discontinuities
[DREP-89-9] p 1109 N92-32846
Defence Research Establishment Suffield, Ralston (Alberta).
DRES unmanned aerial vehicle data link research
[AD-A244272] p 365 N92-19030
Boundary layer computations using a generalized formulation p 679 N92-24873
Delaware Univ., Newark.
Continuation of tailored composite structures of ordered staple thermoplastic material
[NASA-CR-189671] p 1110 N92-33613
Department of Communications, Ottawa (Ontario).
Design considerations for general aviation mobile satellite terminals p 594 N92-22572
Evaluating the use of satellite communications in the government of Canada p 594 N92-22577
Department of Defense, Washington, DC.
DoD key technologies plan
[AD-A253692] p 1142 N92-33238
Department of Energy, Washington, DC.
Report of the aviation safety review of Department of Energy helicopter operations
[DE92-016346] p 954 N92-31928
Department of the Navy, Washington, DC.
Stabilized square parachute
[AD-D015014] p 90 N92-13036
Underwater turbojet engine
[AD-D015017] p 279 N92-15992
Pulsed field system for detecting the presence of a target in a subsurface environment
[AD-D015074] p 296 N92-16174
Method of guiding an in-flight vehicle to a designed flight path
[AD-D015061] p 268 N92-17707
Single screw mechanism with gaterotor housing at intermediate pressure
[AD-D015140] p 400 N92-18120
Air cushion vehicle conductive/semiconductive flexible skirt, and method
[AD-D015160] p 400 N92-18187
Window cooling for high speed flight
[AD-D015145] p 344 N92-18193
A method of passive range determination using only two bearing measurements
[AD-D015182] p 455 N92-20834
High lift aircraft
[AD-D015215] p 732 N92-27185
Pneumatically actuated multiple store launcher
[AD-D015237] p 732 N92-27188

Mid-range UV communications
[AD-D015213] p 770 N92-27615
Multi-channel fiber optic rotary joint for single-mode fiber
[AD-D015273] p 927 N92-29095
Thrust test fixture
[AD-D015259] p 983 N92-31192
Improved articulated fin/wing control system statement of government interests
[AD-D015268] p 1088 N92-34131

Department of Transport, Ottawa (Ontario).
Transport Canada aging aircraft activities
p 838 N92-30131

Detroit Diesel Allison, MI.
Seal development activities at Allison Turbine Division
p 228 N92-15093

Detroit Diesel Allison, Indianapolis, IN.
Advanced Turbine Technology Applications Project (ATTAP)
[NASA-CR-189142] p 682 N92-25649

Deutsche Airbus G.m.b.H., Bremen (Germany).
Application of direct inverse analogy method (DIVA) and viscous design optimization techniques
p 176 N92-13951
A concept for the revisions of structural inspection schedules p 226 N92-14431
Short time force measurement system
p 208 N92-15001
The Operational Loads Monitoring System, OLMS
p 361 N92-18586
Computation of viscous phenomena in unsteady transonic flow p 720 N92-27949
Computation of flutter boundaries in the time and frequency domain p 720 N92-27952

Deutsche Airbus G.m.b.H., Hamburg (Germany).
Airbus Industrie A330/A340: Full scale fatigue test of center fuselage and wing p 226 N92-14425
Methodology for assessment of skin repairs on Airbus aircraft p 226 N92-14428
Use of a virtual cockpit for the development of a future transport aircraft p 886 N92-28547

Deutsche Forschungs- und Versuchsanstalt fuer Luft- und Raumfahrt, Brunswick (Germany).
Image-supported navigation for testing instrument landing systems p 189 N92-14012
DME growth elements and their use with MLS
p 189 N92-14018
A Taxi And Ramp Management And Control system (TARMAC) p 207 N92-14027

Deutsche Forschungs- und Versuchsanstalt fuer Luft- und Raumfahrt, Goettingen (Germany).
Comparison of Euler and full potential methods for unsteady transonic flow calculations
p 719 N92-27943
Computation of the unsteady transonic 2D cascade flow by an Euler algorithm with interactive grid generation
p 719 N92-27944

Deutsche Forschungsanstalt fuer Luft- und Raumfahrt, Brunswick (Germany).
Steps towards an efficient and accurate method solving the Euler equations around a re-entry configuration at super- and hypersonic speed p 181 N92-14987
Instrumentation and data processing
p 273 N92-17155
BO 105 identification results p 274 N92-17161
The COMPAS system in the ATC environment
[DLR-MITT-91-08] p 354 N92-19041
Design principles of automation aids for ATC approach control p 354 N92-19042
COMPAS system concept p 354 N92-19043
Evaluation of the COMPAS experimental system
p 355 N92-19044
Experiences developed in transfering the experimental COMPAS system to an operational prototype version
p 355 N92-19045
Evaluation of the COMPAS operational system
p 355 N92-19047
The role of planning systems in future air traffic management p 355 N92-19050
Extension of a three dimensional Euler-code for the investigation of the flow field around bypass engines with fan and core jet
[DLR-FB-91-13] p 503 N92-21699
Flight test of avionic and air-traffic control systems
[ETN-92-91063] p 640 N92-25590
The DLR test aircraft in FZ-BS VFW614/ATTAS, Dornier DO228-101, MBB BO 105-S-3 p 648 N92-25591
The basic measuring technical equipment of the DLR test aircraft p 652 N92-25592
Ground installations for the preparation and evaluation of flight tests p 665 N92-25593
Introduction and execution of flight tests at the DLR
p 648 N92-25594
ATTAS experimental cockpit and ATMOS for flight control components and systems investigations
p 641 N92-25595
Testing of an experimental FMS p 648 N92-25596
Testing concept of a movement area guidance
p 641 N92-25597
Pallet for helicopter testing instrumentation
p 652 N92-25598
Development of flight testing of a fault tolerant fly-by-light yaw control system p 662 N92-25599
Ground and satellite supported flight trajectory measurement by example of the avionics flight test system AFES p 641 N92-25600
Board-autonomous flight trajectory measurement by example of an ILS measuring system
p 641 N92-25601
Arrangements and methods for the survey of aircraft radio components and systems p 652 N92-25603
On board planning of 4D-trajectories
p 728 N92-27897
Implementation and operational experience with a new arrival traffic management system at the Frankfurt ATC-Center p 728 N92-27905
The role of systems simulation for the development and qualification of ATTAS p 886 N92-28548
Sensor fault detection on board an aircraft with observer and polynomial classifier
[DLR-FB-91-34] p 859 N92-29870
Jet aircraft noise at high subsonic flight Mach numbers
[DLR-FB-91-28] p 928 N92-29997

Deutsche Forschungsanstalt fuer Luft- und Raumfahrt, Cologne (Germany).
Experimental study of hypersonic shock wave boundary layer interactions by means of infrared technique
p 182 N92-14994
Preconsiderations on aircraft integration
p 599 N92-23402
DLR-news: Announcements of the German Research Institute for Aeronautics and Astronautics
p 698 N92-25413
DLR-News: Announcements of the German Research Institute for Aeronautics and Astronautics
p 698 N92-26086
DLR research reports and communications
[ETN-92-91391] p 929 N92-29218

Deutsche Forschungsanstalt fuer Luft- und Raumfahrt, Goettingen (Germany).
On the simulation of compressible turbulent flows past delta wing, delta wing-body and delta wing-canard
p 84 N92-13003
On the footprints of three-dimensional separated vortex flows around blunt bodies: Attempts of defining and analyzing complex flow structures p 84 N92-13005
Extended mapping and characteristics techniques for inverse aerodynamic design p 194 N92-13949
Simulation requirements for RCS plume: Flowfield interaction modelling on a winged reentry vehicle
p 181 N92-14985
Base pressure measurements on a cone at hypersonic Mach numbers: A contribution to aerothermodynamics for space vehicles p 181 N92-14992
Applicability of bridging methods to hypersonic rarefied flow aerodynamics of reentry vehicles
p 184 N92-15032
Institute for experimental fluid mechanics: Results for 1990
[IB-222-90-A-46] p 400 N92-18244

Deutsche Forschungsanstalt fuer Luft- und Raumfahrt, Hamburg (Germany).
Flying an aircraft as a problem-solving process: About the Instrument-Failure-Simulator (IFS) as a test for pilot-candidates
[DLR-FB-91-23] p 455 N92-20902

Deutsche Forschungsanstalt fuer Luft- und Raumfahrt, Munich (Germany).
Materials and Structures Research Department: Scientific report (1990)
[ETN-92-90727] p 466 N92-22000

Deutsche Forschungsanstalt fuer Luft- und Raumfahrt, Oberpfaffenhofen (Germany).
Simple models for the description of turbulence in the atmospheric boundary layer
[DLR-FB-90-17] p 410 N92-19292
The icing of the wing upper side and bottom side of the icing research aircraft of the DLR
p 724 N92-26349
Measurements in the inhomogeneous convective boundary layer using three powered gliders
p 775 N92-26350
Global and high resolution radar cross section measurements and two-dimensional microwave images of a scaled aircraft model from the type Airbus A 310
[DLR-MITT-91-10] p 911 N92-29877
Trial of a slant visual range measuring device
p 1000 N92-31043
The icing of the elevator of the DLR icing research aircraft of Do 28 type
[DLR-MITT-91-12] p 953 N92-31813

Deutsche Insurance Germany (F.R.).
Pilot noise exposure during a Boeing 747-400 round trip: Judgement of noise and analysis in respect to hearing impairment of pilots p 1138 N92-32961

Deutsche Lufthansa A.G., Frankfurt am Main (Germany).
Pilots noise exposure during a Boeing 747-400 round trip: Ambient noise and acoustic-head recording and analysis of data p 1137 N92-32960

Diagnostic Equipment Development, Inc., Boca Raton, FL.
CH-46 and OH-58 transmission stress wave analysis
[AD-A244321] p 365 N92-18826

Diamond Air Service, Inc. (Japan).
Outlines of parabolic flight p 764 N92-26441

DieselDyne Corp., Morrow, OH.
A preliminary design and analysis of an advanced heat-rejection system for an extreme altitude advanced variable cycle diesel engine installed in a high-altitude advanced research platform
[NASA-CR-186021] p 871 N92-29427

Doellner (O. Leonard), Tucson, AZ.
Radiant energy power source for jet aircraft
[DE92-008726] p 648 N92-24556

Dornier Luftfahrt G.m.b.H., Friedrichshafen (Germany).
Transformation of flightmechanical design requirements for modern fighters into aerodynamic characteristics
p 365 N92-18794
Preparation of the ice certification of the Dornier 328 regional airliner by numerical simulation and by ground test p 451 N92-21693
Computations of unsteady flows around airfoil sections by explicit and implicit methods solving the Euler and Navier-Stokes equations p 720 N92-27948
The Dornier 328 Acoustic Test Cell (ATC) for interior noise tests and selected test results
[AIAA PAPER 92-2164] p 1137 N92-32951
Advanced Study for Active Noise Control in Aircraft (ASANCA)
[AIAA PAPER 92-2092] p 1137 N92-32956

Dornier System G.m.b.H., Friedrichshafen (Germany).
Computational aerothermodynamic methods for industrial applications to re-entry and hypersonic cruise problems p 227 N92-15027

Douglas Aircraft Co., Inc., Long Beach, CA.
Supersonic boundary-layer stability analysis on an aircraft wing p 9 A92-13207
Microwave landing system autoland system analysis
[NASA-CR-189551] p 191 N92-15060
Identification of high-level functional/system requirements for future civil transports
[NASA-CR-189561] p 276 N92-15991
Assessment of cockpit interface concepts for data link retrofit
[NASA-CR-187615] p 268 N92-17512
High-speed civil transport aircraft emissions
p 408 N92-19122
An exploration of function analysis and function allocation in the commercial flight domain
[NASA-CR-4374] p 368 N92-19871
The effect of wing ice contamination on essential flight characteristics p 449 N92-21681
Interior noise prediction methodology: ATDAC theory and validation
[NASA-CR-187626] p 697 N92-25368
Evaluation of human response to structural vibrations induced by sonic booms
[NASA-CR-189584] p 697 N92-26130
The use and effectiveness of piloted simulation in transport aircraft research and development
p 886 N92-28549
Maintaining the safety of an aging fleet of aircraft
p 837 N92-30108
Inspection of aging aircraft: A manufacturer's perspective p 914 N92-30117
High speed research system study. Advanced flight deck configuration effects
[NASA-CR-189650] p 967 N92-30965
Evaluation of microwave landing system approaches in a wide-body transport simulator
[NASA-CR-4450] p 957 N92-30978
Design and analysis issues of integrated control systems for high-speed civil transports
[NASA-CR-186022] p 979 N92-31656
Fly-by-light technology development plan
[NASA-CR-181954] p 1086 N92-32778
MD-80 aft cabin noise control: A case history
p 1137 N92-32950

Draper (Charles Stark) Lab., Inc., Cambridge, MA.
Applications of an automated programming system
[AIAA PAPER 91-3767] p 231 A92-17629
Advanced information processing system: Inter-computer communication services
[NASA-CR-187556] p 53 N92-11706

Design of an integrated airframe/propulsion control system architecture
[NASA-CR-182007] p 602 N92-22644
Robust intelligent flight control for hypersonic vehicles
[NASA-CR-185680] p 746 N92-28209

Duisburg Univ. (Germany).
Boundary layer flow in axial compressors (theoretical part)
[ETN-92-91006] p 501 N92-21232
Boundary layer flow in axial compressors (theoretical part)
[ETN-92-91007] p 501 N92-21233
Boundary layer flow in axial compressors (theoretical part)
[ETN-92-91008] p 502 N92-21234

Duke Univ., Durham, NC.
Prediction of high-resolution flowfields for rotorcraft aeroacoustics p 53 A92-11053
Eigenvalue calculation procedure for an Euler/Navier-Stokes solver with application to flows over airfoils p 170 A92-17429
Analytical/numerical matching and periodic inversion: Two advances in free wake analysis
p 178 N92-13994

Dynamic Engineering, Inc., Newport News, VA.
Weight, center of gravity and modal test report for NTF fan blade set no. 3
[NASA-CR-189583] p 498 N92-20072

Dynamics Research Corp., Wilmington, MA.
Development of rating instruments and procedures for aviation mishap investigation
[AD-A253072] p 1044 N92-33288

E

Eagle Engineering, Inc., Hampton, VA.
Sonic boom p 55 N92-10608
A summary of XB-70 sonic boom signature data
[NASA-CR-189630] p 696 N92-24800

East Anglia Univ., Norwich (England).
Laminar-flow secondary separation on a slender wing
p 85 N92-13006

Ecole Nationale Superieure de Mecanique et d'Aerotechnique, Poitiers (France).
Nonstationary flight aerodynamics in a turbulent environment
[ETN-91-90102] p 82 N92-11980

Ecole Normale Superieure, Paris (France).
Reaction speed constant for the reactions between N + O2 and between O + N2
[ETN-92-90861] p 347 N92-19252

Ecole Polytechnique, Montreal (Quebec).
Periodic Euler and Navier-Stokes solutions about oscillating airfoils p 626 N92-24850
Navier-Stokes simulation of dynamic stall on a rotating airfoil p 626 N92-24853

Ecole Polytechnique Federale de Lausanne (Switzerland).
A multiblock flow solver for inviscid hypersonic flows
p 181 N92-14986

Ecole Royale Militaire, Brussels (Belgium).
Low temperature environment operations of turboengines (design and user's problems)
p 450 N92-21682

Edgerton, Germeshausen and Grier, Inc., Idaho Falls, ID.
An independent review of the Multi-Path Redundant Avionics Suite (MPRAS) architecture assessment and characterization report
[NASA-CR-188126] p 163 N92-12440

Edgerton, Germeshausen and Grier, Inc., Wellesley, MA.
Seal related development activities at EG/G
p 228 N92-15095

Edinburgh Univ. (Scotland).
Ozone response to aircraft emissions: Sensitivity studies with two-dimensional models p 409 N92-19126

Efratom Systems Corp., Irvine, CA.
Tactical Rubidium Frequency Standard (TRFS)
[AD-A243934] p 401 N92-18897

EG and G Energy Measurements, Inc., Woburn, MA.
Controller response to conflict resolution advisory prototype
[PB92-190032] p 1050 N92-33596

Eidetics International, Inc., Torrance, CA.
Forebody vortex control with miniature, rotatable nose-boom strakes
[AIAA PAPER 92-0022] p 281 A92-22144
Aerodynamic control of fighter aircraft by manipulation of forebody vortices p 380 N92-18791

Eidgenoessisches Flugzeugwerk, Emmen (Switzerland).
Separation of external stores: Comparison of results
[F+W-TF-2058] p 732 N92-26944
Theoretical principles of a Euler method for the calculation of three dimensional flows
[F+W-TF-2012] p 767 N92-27045

Electro Magnetic Applications, Inc., Lakewood, CO.
Nonlinear triggered lightning models for use in finite difference calculations p 230 A92-20128

Electroimpact, Inc., Seattle, WA.
Suppression of radiating harmonics Electro-Impulse Deicing (EIDI) systems
[DOT/FAA/CT-TN90/33] p 405 N92-19764

Electronic System G.m.b.H., Munich (Germany).
Process/object-oriented Ada software design for an experimental helicopter p 164 N92-12461
An efficient method for three-dimensional route planning with different strategies and constraints
p 728 N92-27901

Electronique Serge Dassault, Saint Cloud (France).
Space software is first of all software
p 509 N92-20590

Eloret Corp., Palo Alto, CA.
Interferograms, schlieren, and shadowgraphs constructed from real- and ideal-gas, two- and three-dimensional computed flowfields
[NASA-CR-190054] p 446 N92-21356

Eloret Corp., Sunnyvale, CA.
Experimental research of the aerodynamics of nozzles and plumes at hypersonic speeds
[NASA-CR-187316] p 185 N92-15048
Development and application of computational aerothermodynamics flowfield computer codes
[NASA-CR-190294] p 624 N92-24229
Experimental investigation of nozzle/plume aerodynamics at hypersonic speeds
[NASA-CR-190074] p 664 N92-25162
An experimental investigation of the separating/reattaching flow over a backstep
[NASA-CR-190426] p 716 N92-27399

EMA, Mansfield, TX.
Rotorwash computer model: User's guide
[DOT/FAA/RD-90/25] p 346 N92-18345

Embraer S.A., Sao Jose dos Campos (Brazil).
Analysis of aircraft performance during lateral maneuvering for microburst avoidance
p 205 A92-20207

Engineering Research and Consulting, Inc., Tullahoma, TN.
Automated screening of propulsion system test data by neural networks, phase 1
[NASA-CR-184329] p 753 N92-27403

Environmental Protection Agency, Research Triangle Park, NC.
A model of the ADA avionics real-time system: An example of the benefits of the hardware/software codesign approach in development of real-time systems
[AD-A248893] p 967 N92-30524

Environmental Research Inst. of Michigan, Ann Arbor.
Concept design phase expendable holographic sensor to measure ocean small angle optical scattering
[AD-A245067] p 501 N92-20997

Erno Raumfahrttechnik G.m.b.H., Bremen (Germany).
FALKE: Winged re-entry vehicle flight control
p 667 N92-24454

Escuela Tecnica Superior de Ingenieros Aeronauticos, Madrid (Spain).
Unsteady transonic aerodynamics of pointed bodies of revolution in supersonic freestream p 719 N92-27946

ESDU International Ltd., London (England).
Effect of twin fins on isolated tailplane lift-curve slope
[ESDU-91009] p 80 N92-11969
Maximum lift of wings with trailing-edge flaps at low speeds
[ESDU-91014] p 81 N92-11970
A method of estimating a flow breakdown boundary for aerofoils and swept wings in transonic flows
[ESDU-91021] p 258 N92-15970
Contribution of fin and tailplane to sideforce and yawing moment derivatives due to sideslip at supersonic speeds at low angles of attack
[ESDU-91031] p 259 N92-15971
Simplified method for the prediction of aerofoil excrescence drag magnification factor for turbulent boundary layers at subcritical Mach numbers
[ESDU-91028] p 259 N92-15972
Excrescence drag magnification factors at the drag-rise condition for aerofoils with a specified form of upper-surface pressure distribution
[ESDU-91029] p 259 N92-15973
Energy height method for flight path optimisation. Addendum A: Numerical method suitable for rapid use on IBM PC compatible computers
[ESDU-91016-ADD] p 272 N92-15987
Estimation of airborne performance in landing
[ESDU-91032] p 272 N92-15988
Example of statistical techniques applied to cruise performance guarantees (Student's t distribution)
[ESDU-91018] p 276 N92-17843
Example of statistical techniques applied to autoland touchdown dispersion (confidence intervals for normal and skew distributions)
[ESDU-91019] p 268 N92-17844
Variability of standard aircraft performance parameters
[ESDU-91020] p 276 N92-17847
Prediction of far-field harmonic noise from propellers
[ESDU-91033] p 416 N92-18074
Response of structures to galloping excitation: Background and approximate estimation
[ESDU-91010] p 399 N92-18091
Statistical methods applicable to analysis of aircraft performance data
[ESDU-91017] p 359 N92-18096
Normal force of low aspect ratio wing-body combinations up to high angles of attack at supersonic speeds
[ESDU-91042] p 553 N92-24009
Aerodynamic centre of wing-body combinations
[ESDU-92024] p 1036 N92-32479
Contribution of tailplane-mounted twin fins to sideforce, yawing moment, and rolling moment derivatives due to sideslip
[ESDU-92007] p 1086 N92-32487
A background to the handling qualities of aircraft
[ESDU-92006] p 1087 N92-32780
Lift and rolling moment due to spoilers on wings with trailing-edge flaps deflected at subsonic speeds
[ESDU-92002-SUPPL] p 1037 N92-32782

European Office of Aerospace Research and Development, FPO New York, NY.
Report on aerospace structures and structural materials R and D in Europe
[PB92-123553] p 550 N92-22785

European Space Agency, Paris (France).
Aerothermodynamics for Space Vehicles
[ESA-SP-318] p 180 N92-14973
Investigation of the dynamic behaviour and the frequency response of the GG 1342 laser gyro
[ESA-TT-1236] p 595 N92-22641
Calculation of support interferences on the aerodynamic coefficients for a wind tunnel calibration model
[ESA-TT-1247] p 830 N92-29159
Computation of unsteady transonic flows using an implicit centered Euler solver without artificial viscosity
[ESA-TT-1235] p 944 N92-30514
Contribution to the modelling of turbulent combustion in the case of stabilisation by flame-lock
[ESA-TT-1229] p 988 N92-31942
Analysis of three icing test flights reaching the aircraft-referred icing degree of severe
[ESA-TT-1254] p 954 N92-31943

European Space Agency. European Space Operations Center, Darmstadt (Germany).
Current activities and future plans for GPS applications p 640 N92-24735

European Space Agency. European Space Research and Technology Center, ESTEC, Noordwijk (Netherlands).
Aerothermodynamic challenges for ESA programmes
p 180 N92-14974
SIMOUN and Scirocco wind tunnel nozzle viscous flow study p 208 N92-14999
Equilibrium solution of the Euler and Navier-Stokes equations around a double ellipsoidal shape with mono- and multi-blocks including real gas effects, part 1
p 227 N92-15030
Parallelization of a Direct Simulation Monte Carlo (DSMC) code for fluid dynamics p 227 N92-15033
Grid impact on 3D hypersonic flows
p 184 N92-15041
Review of the European hypersonic wind tunnel performance and simulation requirements
p 209 N92-15043

Executive Resource Associates, Inc., Arlington, VA.
General aviation activity and avionics survey, calendar year 1989
[PB91-179234] p 169 N92-13926

F

Fairfax Materials Research, Inc., Alexandria, VA.
The mechanical properties of metal-void composites
[AD-A246087] p 757 N92-27749

Federal Aviation Administration, Atlantic City, NJ.
Solid-State Radar Beacon Decoder (SSRBD) Operational Test and Evaluation (OT/E) integration test plan
[DOT/FAA/CT-TN91/30] p 19 N92-10020
Program plan: National aging aircraft research program
[DOT/FAA/CT-88/32-1] p 18 N92-10992
Evaluation of two high-speed runway exits
[DOT/FAA/CT-TN91/36] p 31 N92-11021
Prototype runway hold-short lighting system
[DOT/FAA/CT-TN91/43] p 31 N92-11028

Surface painted taxiway markings at Seattle-Tacoma International Airport
[DOT/FAA/CT-TN91/49] p 32 N92-11029
Onboard cabin water spray system under various discharge configurations
[DOT/FAA/CT-TN91/42] p 93 N92-13043
Data Multiplexing Network (DMN) phase 3 equipment Operational Test and Evaluation (OT and E)/integration test report
[DOT/FAA/CT-TN91/50] p 221 N92-14270
Validation and verification flight test for TCAS-2 logic changes (MOPS Change 6)
[DOT/FAA/CT-TN91/46] p 268 N92-15981
Joint Federal Aviation Administration (FAA)/Civil Aviation Authority (CAA) Microwave Landing System (MLS) Area Navigation (RNAV) flight evaluations
[DOT/FAA/CT-TN91/17] p 268 N92-15983
Effectiveness of an onboard water spray system during an oxygen enriched cabin fire
[DOT/FAA/CT-TN91/51] p 264 N92-17149
Visual approach data collection at San Francisco International Airport (SFO)
[DOT/FAA/CT-90/23] p 354 N92-18112
High Capacity Voice Recorder (HCVR) Operational Test and Evaluation (OT and E)/integration test plan
[DOT/FAA/CT-TN91/55] p 402 N92-18959
Television Microwave Link (TML) Operational Test and Evaluation (OT/E)/integration test report
[DOT/FAA/CT-TN91/57] p 500 N92-20653
Comparison of the performance of a microwave landing system elevation station with the instrument landing system end-fire glide slope at Yeager Airport, Charleston, West Virginia
[DOT/FAA/CT-TN91/22] p 534 N92-22210
Comparative evaluation of internally and externally lighted taxiway guidance signs
[DOT/FAA/CT-TN92/2] p 573 N92-22237
MLS mathematical modeling study of Philadelphia International Airport runway 27L
[DOT/FAA/CT-TN91/54] p 573 N92-22503
Airport smart power lighting system
[DOT/FAA/CT-TN91/12] p 573 N92-22966
MLS and DME/P multipath simulation model user's manual. Volume 1: Operating instructions
[DOT/FAA/CT-TN91/47] p 640 N92-24888
Nationwide system delay study of the microwave landing system in the New York terminal area, volume 1
[DOT/FAA/CT-TN91/59-VOL-1] p 640 N92-25098
Evaluation of a tritium runway lighting system
[DOT/FAA/CT-TN92/15] p 665 N92-25733
Drop test: Cessna Golden Eagle 421B
[DOT/FAA/CT-TN91/32] p 837 N92-28900
Federal Aviation Administration aging aircraft nondestructive inspection research plan
p 914 N92-30116
GNAS Maintenance Control Center (GMCC) Design Qualification Test and Evaluation (DQT/E) test procedures
[DOT/FAA/CT-TN91/40] p 983 N92-30976
Helicopter nighttime parking test results - UH-1
[DOT/FAA/CT-TN92/1] p 961 N92-31165
GNAS Maintenance Control Center (GMCC) Design Qualification Test and Evaluation (DQT/E) test report
[DOT/FAA/CT-TN91/39] p 932 N92-31615
Effect of guard band reduction on marker beacon receiver performance
[DOT/FAA/CT-TN92/18] p 1002 N92-31617
Global positioning system runway incursion program static ground tests
[DOT/FAA/CT-TN91/44] p 957 N92-31838
Bird ingestion into large turbofan engines
[DOT/FAA/CT-91/17] p 1043 N92-33005
ILS mathematical modeling study of an ILS localizer and glide slope proposed for runway 32R, Moffett Field Airport, California
[DOT/FAA/CT-TN92/28] p 1048 N92-33308

Federal Aviation Administration, Cambridge, MA.
Design considerations for IAP charts: Approach course track and communication frequencies
[AD-A241482] p 103 N92-13051
Bibliography of technical reports, 1980 - 1990
[PB92-110691] p 417 N92-18814
CDI sensitivity and crosstrack error on nonprecision approaches
[AD-A243981] p 356 N92-19391
Current DOT research on the effect of multiple site damage on structural integrity p 913 N92-30112
Controller response to conflict resolution advisory prototype
[PB92-190032] p 1050 N92-33596

Federal Aviation Administration, Seattle, WA.
Status of the FAA flight loads monitoring program
p 914 N92-30113
The FAA aging airplane program plan for transport aircraft p 838 N92-30128

Federal Aviation Administration, Washington, DC.
EDMS: Microcomputer pollution model for civilian airports and Air Force bases, (user's guide)
[AD-A240528] p 45 N92-11578
Pilot's Automated Weather Support System (PAWSS) concepts demonstration project. Phase 1: Pilot's weather information requirements and implications for weather data systems design
[NASA-CR-188228] p 46 N92-11593
Airport activity statistics of certificated route air carriers: Calendar year 1990
[AD-A241483] p 93 N92-13045
FAA air traffic activity: FY 1990. Addendum
[AD-A241484] p 93 N92-13046
FAA statistical handbook of aviation: Calendar year 1989
[PB91-202051] p 170 N92-13927
Evaluation of advanced microwave landing system procedures in the New York terminal area
[DOT/FAA/ND-91/1] p 354 N92-18967
National Airspace System maintenance and support operational concept
[DOT/FAA/SE-92/1] p 308 N92-18969
FAA vertical flight research, engineering, and development bibliography, 1962 - 1991
[FAA/ARD-30] p 462 N92-21210
Advisory Circular: Corrosion control for aircraft
[FAA-AC-43-4A] p 420 N92-21834
System considerations, projected requirements and applications for aeronautical mobile satellite communications for air traffic services
p 677 N92-24163
Aviation system: Capital investment plan
p 636 N92-25297
General maintenance handbook for airway facilities
[PB92-147586] p 640 N92-25518
Human factors evaluation of the work environment of operators engaged in the inspection and repair of aging aircraft
[AD-A246445] p 724 N92-27914
FAA aviation forecasts
[AD-A250412] p 837 N92-29182
Evaluation of head impact kinematics for passengers seated behind interior walls
[AD-A252651] p 952 N92-30551
Allocation and recovery of federal airport and airway costs, 1991
[AD-A249436] p 983 N92-30777
The 1991 Federal Aviation Administration plan for research, engineering and development
p 1142 N92-32453
Exposures from headset interference tones
[AD-A247175] p 1136 N92-32697
Federal aviation regulations. Part 91: General operating *and flight rules*
[PB92-197334] p 1017 N92-33176
Accomplishments under the Airport Improvement Program, FY 1991
[AD-A253046] p 1101 N92-33434

Federal Express Corp., Memphis, TN.
Communication: An important element of maintenance and repair p 838 N92-30124

Federal Ministry for Defence, Bonn (Germany).
Tool supported software development experiences from the EFA project p 163 N92-12451
Opportunities for flight simulation to improve operational effectiveness p 883 N92-28523

Fiat Aviazione S.p.A., Turin (Italy).
Research on inverse methods and optimization in Italy
p 202 N92-13956

Field Aviation Co., Inc., Mississauga (Ontario).
Fire bombing and fire bombers
[CA-PATENT-1-268-164] p 1061 N92-33582

Flight Mechanics and Control, Inc., Hampton, VA.
STS-40 descent BET products: Development and results
[NASA-CR-189570] p 286 N92-16012

Florence Univ. (Italy).
Transonic cascade flow prediction using the Navier-Stokes equations
[ASME PAPER 91-GT-313] p 76 A92-15690

Florida Atlantic Univ., Boca Raton.
A new method for simulating atmospheric turbulence for rotorcraft applications p 162 A92-14368
The application of experimental data to blade wake interaction noise prediction
[NASA-CR-189461] p 237 N92-14789
A numerical study of fuselage scattering effects on rotor noise p 511 N92-20428
Computational aspects of helicopter trim analysis and damping levels from Floquet theory
[NASA-CR-190736] p 1087 N92-33107

Florida State Univ., Tallahassee.
Broadband shock-associated noise from supersonic jets in flight p 235 A92-18683
Jet noise generated by large-scale coherent motion
p 55 N92-10604

Florida Univ., Gainesville.
Experimental investigation of a supersonic combustion flowfield employing staged transverse injection behind a rearward-facing step
[AIAA PAPER 92-0090] p 292 A92-22196
On a multi-block method for transonic turbulent flows past a wing-fuselage configuration p 632 N92-25569

Fluid Gravity Engineering Ltd., Witley (England).
Hypersonic aerothermodynamic computations using a point-implicit TVD method p 183 N92-15006

Fokker B.V., Schipol-Oost (Netherlands).
The effect of hoar-frosted wings on the Fokker 50 take-off characteristics p 451 N92-21692
Active synchrophasing of propeller unbalance
p 1138 N92-32963

Forschungszentrum Juelich G.m.b.H. (Germany).
Wide gap, permanent magnet biased magnetic bearing system p 773 N92-27794

Fraunhofer-Inst. fuer Betriebsfestigkeit, Darmstadt (Germany).
Review of investigations on aeronautical fatigue in the Federal Republic of Germany
[ETN-92-90317] p 225 N92-14397
Fatigue of repaired composite structures
p 214 N92-14411
Environmental fatigue tests with composite materials
p 214 N92-14413

FWG Associates, Inc., Tullahoma, TN.
Particle trajectory computer program for icing analysis of axisymmetric bodies
[NASA-CR-189134] p 352 N92-19276

G

G and C Systems, Inc., San Juan Capistrano, CA.
High-speed civil transport issues and technology program
[NASA-CR-186020] p 962 N92-31208

Galaxy Scientific Corp., Mays Landing, NJ.
Statistics on aircraft gas turbine engine rotor failures that occurred in US commercial aviation during 1989
[DOT/FAA/CT-92/5] p 971 N92-30303
Current nondestructive inspection methods for aging aircraft
[DOT/FAA/CT-91/5] p 1126 N92-33480

GasTOPS Ltd., Gloucester (Ontario).
Engine performance and health monitoring models using steady state and transient prediction methods
p 870 N92-28467

General Accounting Office, Washington, DC.
Aerospace plane technology: Research and *development efforts in Japan and Australia*
[AD-A241641] p 62 N92-12991
Aerospace technology: Technical data and information on foreign test facilities
[GAO/NSIAD-90-71FS] p 139 N92-13076
B-2 program: Trends in manufacturing
[AD-A242141] p 242 N92-15963
Aviation safety: Changes needed in FAA's service difficulty reporting program
[GAO/RCED-91-24] p 953 N92-31453
Aviation noise: Costs of phasing out noisy aircraft
[GAO/RCED-91-128] p 1011 N92-31454
Air traffic control: FAA's advanced automation system contract
[GAO/IMTEC-91-25] p 1048 N92-32861

General Applied Science Labs., Inc., Ronkonkoma, NY.
Pioneering scramjet developments by Antonio Ferri
p 474 N92-21519

General Dynamics Corp., Fort Worth, TX.
Forebody vortex flow control on the F-16C using tangential slot and jet nozzle blowing
[AIAA PAPER 92-0019] p 247 A92-22141
Steady and unsteady aerodynamics of a pitching straked wing model at high angles of attack p 87 N92-13024
Analysis of unsteady force, pressure, and flow-visualization data for a pitching straked wing model at high angles of attack p 364 N92-18784
Application of analytical and design tools for fighter wing aeroelastic tailoring p 550 N92-23231
Core avionics and standardization
[AD-A248326] p 735 N92-27925
Transonic wind tunnel investigation of limit cycle oscillations on fighter type wings p 721 N92-27959

General Electric Co., Cincinnati, OH.
An inverse method for the aerodynamic design of three-dimensional aircraft engine nacelles
p 194 N92-13958
A simplified method for predicting the stability of aerodynamically excited turbomachinery
p 224 N92-14364
Design and performance of duct acoustic treatment
p 236 N92-14783

Jet noise suppression p 236 N92-14784
Areas of seal R/D at GE p 228 N92-15094
Qualification test report. Fuel pump test stand 3C3965G05
[AD-A242929] p 280 N92-17552
The 3D inelastic analysis methods for hot section components
[NASA-CR-189089] p 402 N92-18971
Engine Structures Modeling Software System (ESMOSS)
[NASA-CR-187227] p 404 N92-19277
Component-specific modeling
[NASA-CR-189088] p 377 N92-19726
Inlet technology p 447 N92-21528
High speed civil transport p 649 N92-25919
Algorithmic development in structures technology p 684 N92-25924
Computational structures technology engine/airframe coupling p 649 N92-25935
High speed turboprop aeroacoustic study (counterrotation). Volume 2: Computer programs
[NASA-CR-185242] p 1011 N92-31248

General Electric Co., Fairfield, CT.
Gas turbine engine control
[PATENT-1-274-606] p 130 N92-13069
Rolling element bearing member
[PATENT-1-271-213] p 158 N92-13434

General Electric Co., Gilbert, AZ.
Transport delay measurements: Methodology and analysis for the F-16C combat engagement trainer, the display for advanced research and training, and the F-16A limited field of view
[AD-A248519] p 888 N92-29505

General Electric Co., Schenectady, NY.
Local extinction mechanisms in non-premixed turbulent combustion
[AD-A242027] p 290 N92-17682

General Motors Corp., Indianapolis, IN.
Time-dependent aerodynamic analysis of ducted and unducted propfans at angle of attack
[ASME PAPER 91-GT-190] p 74 A92-15616
Cooled high-temperature radial turbine program 2
[NASA-CR-189122] p 1073 N92-34236

George Washington Univ., Washington, DC.
Three-dimensional space-marching algorithm on unstructured grids p 5 A92-11058
Practical input optimization for aircraft parameter estimation experiments p 114 N92-11989
The effect of freestream turbulence on the vortical flow over a delta wing p 261 N92-17681

Georgia Inst. of Tech., Atlanta.
A new class of gradient estimators for queueing systems with real-time constraints p 49 A92-11395
An integrated airloads-inflow model for use in rotor aeroelasticity and control analysis p 64 A92-14328
A new method for simulating atmospheric turbulence for rotorcraft applications p 162 A92-14368
Rotorcraft airframe structural optimization for combined vibration and fatigue constraints p 106 A92-14390
Synthesis of a helicopter full-authority controller p 280 A92-21178
A numerical solution of implicit nonlinear equations of motion for rotor blades p 115 N92-13053
Definition of the unsteady vortex flow over a wing/body configuration
[NASA-CR-180083] p 178 N92-13995
Image-based ranging and guidance for rotorcraft
[NASA-CR-184829] p 191 N92-14036
Integration of dynamic, aerodynamic, and structural optimization of helicopter rotor blades
[NASA-CR-189018] p 195 N92-14038
Rapid near-optimal aerospace plane trajectory generation and guidance
[NASA-CR-189469] p 205 N92-14066
Periodic trim solutions with HP-version finite elements in time
[NASA-CR-189778] p 282 N92-17019
Numerical solution of three-dimensional unsteady viscous flows
[AD-A244274] p 403 N92-19052
A new method for simulating atmospheric turbulence for rotorcraft applications p 464 N92-21956
Hypersonic aerospace vehicle leading edge cooling using heat pipe, transpiration and film cooling techniques p 780 N92-26733
Fractal image compression of Rayleigh, Raman, LIF and LDV data in turbulent reacting flows
[AD-A246960] p 767 N92-27352
Numerical investigation of the effects of icing on fixed and rotary wing aircraft
[NASA-CR-190542] p 1044 N92-34105

Georgia Tech Research Inst., Atlanta.
Acoustic interactions between an altitude test facility and jet engine plumes: Theory and experiments
[NASA-CR-190423] p 738 N92-26405

Gesellschaft fuer Mathematik und Datenverarbeitung, Saint Augustin (Germany).
Towards coherent hypermedia navigation by pragmatic dialogue modeling
[PB92-114735] p 455 N92-20818

Glasgow Univ. (Scotland).
Design of experiments p 273 N92-17154
Modelling aspects and robustness issues in rotorcraft system identification p 274 N92-17159

Goldsworthy Engineering, Inc., Springville, UT.
Organic Matrix Composite Helicopter Internal/External Cargo Pallet System (OMC INTEX)
[AD-A251127] p 961 N92-30878

Grumman Aerospace Corp., Bethpage, NY.
Aircraft drag analysis methods p 552 N92-23957
Computational structures technology at Grumman: Current practice/future needs p 684 N92-25930
Design, evaluation and experimental effort toward development of a high strain composite wing for Navy aircraft p 1107 N92-32514

H

Hamilton Standard, Windsor Locks, CT.
Propeller and propfan noise p 54 N92-10599

Harris Government Aerospace Systems Div., Melbourne, FL.
Experimental demonstration of active vibration control for flexible structures p 50 A92-11442

Harvard Univ., Cambridge, MA.
Preliminary results on the fracture analysis of multi-site cracking of lap joints in aircraft skins p 913 N92-30111

HCC Science and Technology Co., Summit, NJ.
Polymer blends, volume 1
[AD-A252112] p 987 N92-31419

Hecht-Nielsen Neurocomputer Corp., Inc., San Diego, CA.
Processing complexity of two approaches to object detection and recognition p 234 N92-14677

Helsinki Univ. of Technology, Espoo (Finland).
Two-dimensional transonic flow calculation by interaction of Euler and boundary layer equations
[PB92-136449] p 448 N92-21784
Three-dimensional multigrid algorithm for the Euler and the thin-layer Navier-Stokes equations
[PB92-134329] p 602 N92-22216
Modernized MBB panel code: User's guide including background theory
[PB92-136431] p 526 N92-22233
Development of a helicopter-borne 8-channel ranging scatterometer
[PB92-141977] p 599 N92-23441
Analysis of a 37 kW cage-induction motor
[PB92-142116] p 597 N92-23496

Helsinki Univ. of Technology, Otaniemi (Finland).
Analysis of Euler's and stress tensor methods for calculating power consumption of high speed centrifugal fans and turbocompressors
[DE92-728396] p 298 N92-16325
Calculation of local power consumptions and efficiencies of centrifugal fans and turbocompressors
[DE92-728402] p 298 N92-16326

High Technology Corp., Hampton, VA.
Experimental investigation on the effect of crescent planform on lift and drag p 9 A92-13206
Numerical solution of the boundary-layer equations for a general aviation fuselage p 174 A92-20211
A three-dimensional, compressible, laminar boundary-layer method for general fuselages. Volume 2: User's manual
[NASA-CR-4292-VOL-2] p 678 N92-24344
A three-dimensional, compressible, laminar boundary-layer method for general fuselages. Volume 1: Numerical method
[NASA-CR-4292-VOL-1] p 679 N92-24547
Distributed acoustic receptivity in laminar flow control configurations
[NASA-CR-4438] p 765 N92-26680

Hoh Aeronautics, Inc., Lomita, CA.
Helicopter control response types for hover and low-speed near-earth tasks in degraded visual conditions p 132 A92-14338

Honeywell, Inc., Clearwater, FL.
Design and flight test of a differential GPS/inertial navigation system for approach/landing guidance p 97 A92-16650

Honeywell, Inc., Minneapolis, MN.
Design and flight test of a differential GPS/inertial navigation system for approach/landing guidance p 97 A92-16650
New methods in robust control
[AD-A240221] p 29 N92-11018
Trajectory optimization for hypersonic aircraft guidance p 728 N92-27898
Study objectives: Will commercial avionics do the job? Improvements needed? p 1065 N92-33340

Hughes Aircraft Co., El Segundo, CA.
Thermally regenerative fuel cells
[AD-A242900] p 300 N92-17629

Hyperschall-Technologie-Goettingen (Germany).
Behaviour and modelling of the aerothermodynamics of ballistic entry vehicles in the high altitude flow regimes p 184 N92-15031

I

IIT Research Inst., Lanham, MD.
Development statistics for the UH-1 Ada feasibility study
[AD-A252404] p 982 N92-30547

Illinois Inst. of Tech., Chicago.
Electro optical system to measure strains at high temperature
[NASA-CR-190450] p 1127 N92-33696

Illinois Univ., Urbana.
Nonlinear system design: Adaptive feedback linearization with unmodeled dynamics
[AD-A248484] p 1009 N92-30335

Imperial Coll. of Science and Technology, London (England).
The 8th Symposium on Turbulent Shear Flows. Volume 1: Sessions 1-18
[AD-A243809] p 402 N92-18933
Finite element methods for integrated aerodynamic heating analysis
[NASA-CR-190353] p 633 N92-25959

Indiana Univ.-Purdue Univ., Fort Wayne.
Boiling and condensation in microfin tubes p 682 N92-25660

Industrieanlagen-Betriebsgesellschaft m.b.H., Ottobrunn (Germany).
Low cycle fatigue of cast nickel base turbine rotors p 226 N92-14405
Comparison between hot/wet test and RT/dry test on the Seastar horizontal stabilizer and fin p 226 N92-14414
Probabilistic lifing approach for aero engine disks made of powder nickel base alloys containing ceramic defects p 226 N92-14424
Fatigue life behaviour of composite structures p 390 N92-18577
Aircraft tracking for structural fatigue p 361 N92-18584

Innovative Textile Applications Co., Grand Junction, CO.
Universal weaving for turbine engine composite preforms
[AD-A237667] p 202 N92-14059

Institut de Mecanique de Grenoble (France).
Numerical simulation of turbulence at the back of the airplane
[ETN-92-91664] p 1037 N92-32769

Institut de Mecanique des Fluides de Lille (France).
Phenomenological modeling of the wake produced by a straight two dimensional base in subsonic flow
[REPT-90/59] p 82 N92-11982
Study of interactions on anemoclinometric sensors
[REPT-90/30] p 138 N92-12006
Study of detached turbulent flow in an air intake by means of high speed tomography and laser velocimetry
[REPT-90/55] p 157 N92-12216
Characterization of unsteady aerodynamic phenomena at high angles p 364 N92-18787
Airplane crashes on the runway. Fine modeling of the behavior after burning of a frame submitted to linear crushing
[IMFL-90-64] p 353 N92-19350

Institut National de Recherche d'Informatique et d'Automatique, Valbonne (France).
Numerical simulations around models in hypersonic wind tunnels p 182 N92-14998

Institut National des Sciences Appliquees de Rouen, Mont Saint Aignan (France).
Theoretical study (Lagrangian modeling) of turbulent particulate dispersion
[ETN-91-99909] p 42 N92-11287

Institute for Aerospace Research, Ottawa (Ontario).
Trajectories and stability of trailing vortices very near the ground
[NRC-32151] p 716 N92-27344
Processing and environmental effects on mechanical properties of composite repairs
[NRC-LTR-ST-1826] p 1109 N92-32791
A Kalman filter integrated navigation design for the IAR Twin Otter Atmospheric Research Aircraft
[NRC-32148] p 1048 N92-32849

Institute for Computer Applications in Science and Engineering, Hampton, VA.
Turbulent flow calculations using unstructured and adaptive meshes p 153 A92-15823
On the nonlinear stability of a high-speed, axisymmetric boundary layer p 78 A92-16457
Mach 4 and Mach 8 axisymmetric nozzles for a high-enthalpy shock tunnel p 78 A92-16668
Aerodynamic design and optimization in one shot [AIAA PAPER 92-0025] p 248 A92-22147
Progress with multigrid schemes for hypersonic flow problems [NASA-CR-189579] p 185 N92-15047
Approximation methods for control of acoustic/structure models with piezoceramic actuators [NASA-CR-189578] p 234 N92-15658
Numerical simulation of transient hypervelocity flow in an expansion tube [NASA-CR-189601] p 402 N92-18965
On the instability of boundary layers on heated flat plates [NASA-CR-187581] p 347 N92-19250
An alternative to unstructured grids for computing gas dynamic flows around arbitrarily complex two-dimensional bodies [NASA-CR-189612] p 447 N92-21465
Numerical simulation of transient hypervelocity flow in an expansion tube [NASA-CR-189615] p 592 N92-22228
Institute for Defense Analyses, Alexandria, VA.
Modeling radar clutter [AD-A240965] p 158 N92-13351
Institute for Water Resources, Fort Belvoir, VA.
Reducing environmental noise impacts: A USAREUR noise management program handbook [AD-A240797] p 237 N92-14791
Instituto de Pesquisas Espaciais, Sao Jose dos Campos (Brazil).
Stratospheric electrodynamics from superpressure balloons - A technical challenge for small payload environments [AIAA PAPER 91-3674] p 14 A92-11019
The influence of a retarding rocket on parameter limits for reentry trajectories p 211 N92-15037
Instituto Nacional de Tecnica Aeroespacial, Madrid (Spain).
The measurement of water film thickness on airfoils in heavy rain conditions using conductance sensors p 452 N92-21695
Measurement of the flow distribution over the flight deck of an aircraft carrier p 504 N92-21955
Fuzzy guidance system evaluation p 778 N92-27903
International Business Machines Corp., Yorktown Heights, NY.
On constructing three-dimensional overlapping grids with CMPGRD p 691 N92-24424
International Centre for Numerical Methods in Engineering, Barcelona (Spain).
Flow and temperature computations for space vehicles using adaptive finite element techniques p 181 N92-14990
International Maritime Satellite Organization, London (England).
Aeronautical satellite system test and implementation p 676 N92-24095
Inmarsat aeronautical mobile satellite system: Internetworking issues p 677 N92-24098
Future developments in aeronautical satellite communications p 678 N92-24167
Iona Coll., New Rochelle, NY.
Using new aggregation operators in rule-based intelligent control p 51 A92-11456
Iowa State Univ. of Science and Technology, Ames.
A two-stroke diesel engine simulation program [NASA-CR-185155] p 562 N92-22647
Wall functions for the kappa-epsilon turbulence model in generalized nonorthogonal curvilinear coordinates [NASA-CR-190368] p 685 N92-25962
Trajectory optimization for the National Aerospace Plane [NASA-CR-190355] p 650 N92-26017
Visualization of boundary-layer development on turbomachine blades with liquid crystals [NASA-CR-190433] p 742 N92-27519
NDE research efforts at the FAA Center for Aviation Systems Reliability p 914 N92-30119
Development of a 3-D upwind PNS code for chemically reacting hypersonic flowfields [NASA-CR-190182] p 946 N92-30977
Israel Aircraft Industries Ltd., Ben-Gurion Airport.
A review of aging aircraft technology: An IAI perspective [IAITIC-91-1018] p 461 N92-20500
Some interesting phenomena from Lavi test flights relating to aircraft stability and control [IAITIC-91-1017] p 482 N92-20849
From IGES to STEP [REPT-3.1.6] p 603 N92-23881
The calculation of incompressible separated turbulent boundary layers p 1003 N92-31886
Euler solver for arbitrary configurations: Further applications p 949 N92-31888
Israel Aircraft Industries Ltd., Lod.
FCS skewed sensors array: Practical considerations p 968 N92-31868
Israel Military Industries, Ramat-Hasharon (Israel).
Optimal trajectories for an unmanned air vehicle p 963 N92-31880
Israel Society of Aeronautics and Astronautics, Tel Aviv.
Collection of papers of the 31st Israel Annual Conference on Aviation and Astronautics [ITN-92-85124] p 932 N92-31861

J

JAI Associates, Inc., Mountain View, CA.
Flowfield analysis of modern helicopter rotors in hover by Navier-Stokes method [AD-A245011] p 446 N92-21333
Jet Propulsion Lab., California Inst. of Tech., Pasadena.
Compensating user position for GPS ephemeris error p 101 A92-16968
Z-Basic algorithm for collision avoidance system p 188 A92-18482
The formation and structure of plasma wakes behind large high-voltage space platforms in ionosphere [AIAA PAPER 92-0577] p 407 A92-26984
ACTS aeronautical experiments [AIAA PAPER 92-2042] p 485 A92-29956
A parallel-series-fed microstrip array with high efficiency and low cross-polarization p 496 A92-31630
Studies on laminar boundary-layer receptivity to freestream turbulence near a leading edge p 591 A92-36007
A low-power, high-efficiency Ka-band TWTA p 671 A92-38163
Ionospheric plasma flow over large high-voltage space platforms. I - Ion-plasma-time scale interactions of a plate at zero angle of attack. II - The formation and structure of plasma wake p 779 A92-41359
H-infinity synthesis using a bilinear pole shifting transform p 1007 A92-50490
Multicomponent gas sorption Joule-Thomson refrigeration [NASA-CASE-NPO-17569-1-CU] p 228 N92-15203
Three-stage sorption type cryogenic refrigeration system and method employing heat regeneration [NASA-CASE-NPO-18366-1-CU] p 300 N92-17674
JPL's Real-Time Weather Processor project (RWP) metrics and observations at system completion p 413 N92-19428
Force limited vibration testing p 595 N92-22688
NASA's GPS tracking system for Aristoteles p 576 N92-23919
A demonstration of centimeter-level monitoring of polar motion with the Global Positioning System p 639 N92-24302
Microwave temperature profiler for clear air turbulence prediction [NASA-CASE-NPO-18115-1-CU] p 916 N92-29148
Proceedings of the Workshop on Advanced Network and Technology Concepts for Mobile, Micro, and Personal Communications [NASA-CR-190459] p 1000 N92-30923
John Deere Technologies International, Inc., Wood-Ridge, NJ.
Development of natural gas rotary engines [PB92-149665] p 765 N92-26816
Johns Hopkins Univ., Baltimore, MD.
Aeroelasticity of bluff bodies p 1089 N92-34165
Johnson Controls, Inc., Milwaukee, WI.
Nickel hydrogen common pressure vessel battery development p 598 N92-22770
Joint Inst. for Nuclear Research, Dubna (USSR).
System of cryogenic security of the superconducting accelerator of relativistic nuclei-nuclotron [DE91-643289] p 304 N92-16789
Joint Publications Research Service, Arlington, VA.
JPRS report: Science and technology. USSR: Space [JPRS-USP-91-007] p 211 N92-14101
History of EPOS air-launched spaceplane project p 211 N92-14103
JPRS report: Science and technology. USSR: Engineering and equipment [JPRS-UEQ-92-001] p 592 N92-22296
JPRS report: Science and technology. Central Eurasia: Engineering and equipment [JPRS-UEQ-92-002] p 592 N92-22298
JPRS report: Science and technology. USSR: Engineering and equipment [JPRS-UEQ-91-010] p 593 N92-22397
JPRS report: Science and technology. Central Eurasia: Space [JPRS-USP-92-002] p 575 N92-23705

K

Kaiserslautern Univ. (Germany).
Evaluation of rotordynamic coefficients of look-through labyrinths by means of a three volume bulk flow model p 223 N92-14356
Determination of rotordynamic coefficients for labyrinth seals and application to rotordynamic design calculations p 223 N92-14360
Kaman Aerospace Corp., Bloomfield, CT.
Analytical modeling of SH-2F helicopter shipboard operation p 464 N92-21961
Kansas Univ., Lawrence.
Preliminary design studies of an advanced general aviation aircraft [NASA-CR-190024] p 461 N92-20064
Active flow control for twenty-first century high-performance aircraft with applications to land and sea vehicles p 447 N92-21504
Preliminary design and lay-out of an infant restraint system p 449 N92-21513
Kansas Univ. Center for Research, Inc., Lawrence.
Identification of aerodynamic models for maneuvering aircraft [NASA-CR-190039] p 348 N92-19359
Identification of aerodynamic models for maneuvering aircraft [NASA-CR-190444] p 852 N92-28720
Khmelnitsky Technological Inst. (USSR).
Identification of dynamic characteristics of flexible rotors as dynamic inverse problem p 220 N92-13962
Kobe Univ. (Japan).
Experiment of static and dynamic characteristics of spiral grooved seals p 223 N92-14361
Koyo Seiko Co. Ltd., Kokubuhiganjo (Japan).
Characterization of superconducting magnetic bearings (dynamic stiffness and damping coefficient in axial direction) p 772 N92-27737
Krug Life Sciences, Inc., San Antonio, TX.
Reference mode effect on the auditory display of aircraft bank angle [AD-A247825] p 728 N92-27916
The utility of analog vertical velocity information during instrument flight with a Head-Up Display (HUD) [AD-A252863] p 1065 N92-33277
Kumm (Emerson L.), Tempe, AZ.
Flat belt continuously variable high speed drive [DE92-008952] p 680 N92-25054
Kyushu Electric Power Co., Inc., Fukuoka (Japan).
Field telemetry of blade-rotor coupled torsional vibration at Matuura Power Station Number 1 unit p 222 N92-14348

L

Laboratoire d'Aerothermique du CNRS, Meudon (France).
Flat plates placed in depleted hypersonic flow [SESSIA-430/91.960] p 947 N92-31508
Lancaster Univ. (England).
An evaluation of the Royal Air Force Shorts Tucano Navigation Instruments Trainer: The NAVIT [ETN-92-90841] p 354 N92-18729
Laser Technology, Inc., Norristown, PA
Inspection of fabricated fuselage panels using electronic shearography [DOT/FAA/CT-TN92/26] p 1127 N92-33627
Lawrence Livermore National Lab., CA.
World commercial aircraft accidents: 1st edition, 1946-1991 [DE92-009801] p 636 N92-24713
Composition monitoring of electron beam melting processes using diode lasers [DE92-009527] p 669 N92-25259
NASA High Speed Research Program, Emissions Scenarios Committee report of meetings on 26 September 1991 and 9 January 1992 [NASA-CR-190379] p 1004 N92-32147
Lear Jet Industries, Inc., Wichita, KS.
Aerodynamic design with CFD p 447 N92-21514
Leeds Univ. (England).
Comparison of GLONASS and GPS time transfers between two west European time laboratories and VNIIFTRI p 1050 N92-33381

Lehigh Univ., Bethlehem, PA.
Unsteady response of the leading-edge vortices on a pitching delta wing p 1041 N92-33851
LITEF, Freiburg (Germany).
Development and verification of software for flight safety critical systems p 164 N92-12469
Litton Industries, Blacksburg, VA.
Fiber optic data busses for aircraft p 736 N92-26093
Litton Industries, Moorpark, CA.
A study of atmospheric optical scattering parameters at 1.5 and 2 micron region for solid state Doppler lidar applications p 1001 N92-31067
Lockheed Aeronautical Systems Co., Burbank, CA.
Development and testing of cabin sidewall acoustic resonators for the reduction of cabin tone levels in propfan-powered aircraft
[NASA-CR-4388] p 166 N92-13757
Heat flux sensor research and development: The cool film calorimeter
[NASA-CR-189789] p 298 N92-17006
Manufacturing development of pultruded composite panels
[NASA-CR-181780] p 578 N92-22637
Lockheed Aeronautical Systems Co., Marietta, GA.
Development and characterization of Powder Metallurgy (PM) 2XXX series Al alloy products and Metal Matrix Composite (MMC) 2XXX Al/SiC materials for high temperature aircraft structural applications
[NASA-CR-187631] p 390 N92-19290
Acoustic loads prediction on jet aircraft p 1136 N92-32949
Lockheed Engineering and Sciences Co., Hampton, VA.
Euler code evaluation of a transatmospheric vehicle at supersonic speeds p 9 A92-13202
Recent rotorcraft aeroelastic testing in the Langley Transonic Dynamics Tunnel p 136 A92-14377
Rotorcraft airframe structural optimization for combined vibration and fatigue constraints p 106 A92-14390
A comparison of cooling methods for the airframe nozzle of a single-stage-to-orbit aircraft
[AIAA PAPER 91-5036] p 210 A92-17825
Analysis of cooling systems for hypersonic aircraft
[AIAA PAPER 91-5063] p 216 A92-17843
Parameter insensitive control utilizing eigenspace methods p 204 A92-18615
Fatigue crack initiation and small crack growth in several airframe alloys p 212 A92-19754
Three-dimensional thermal structural analysis of a swept cowl leading edge subjected to skewed shock-shock interference heating p 174 A92-20306
A comparative analysis of XV-15 tiltrotor hover test data and WOPWOP predictions incorporating the fountain effect
[NASA-CR-189455] p 114 N92-11992
An introduction to high speed aircraft noise prediction
[NASA-CR-189582] p 416 N92-19672
Lockheed Engineering and Sciences Co., Houston, TX.
Aeroassist flight experiment heating-rate sensitivity study p 3 A92-10427
Los Alamos National Lab., NM.
An explosively driven, fast shock tube
[DE92-008437] p 749 N92-26720
Analytical and experimental studies of heat pipe radiation cooling of hypersonic propulsion systems
[DE92-013428] p 973 N92-31817
Loughborough Univ. of Technology (England).
A comparison between the consequences of the liberal and non-liberal UK-Europe bilaterals
[TT-9101] p 18 N92-10018
A review of UK aviation policy
[TT-9107] p 61 N92-12988
Aircraft gas turbine emissions: Their nature, technology for reduction, and a pollution comparison with channel tunnel transport
[ETN-92-91056] p 559 N92-22406
An investigation into the feasibility of providing a proximity warning device for search and rescue helicopters
[ETN-92-91057] p 530 N92-22408
Lowell Univ., MA.
Selection of opening model for parachute scaling studies
[AD-A250882] p 943 N92-30239

M

Maine Univ., Orono.
Numerical simulation of the reactive flow in advanced (HSR) combustors using KIVA-2
[NASA-CR-188996] p 26 N92-11014
Manchester Coll. of Science and Technology (England).
Computational modelling of turbulent flow in S-bends p 769 N92-27480
Manchester Univ. (England).
Boundary-layer transition and heat transfer on slender delta wings
[AERO-REPT-8904] p 262 N92-17849
Marching with the parabolized Navier-Stokes equations. Problem 1: Numerical study of hypersonic viscous cone flow
[AERO-REPT-9007] p 344 N92-18231
Marching with the parabolized Navier-Stokes equations. Problem 2: Hypersonic viscous flow over a flat plate
[AERO-REPT-9008] p 345 N92-18232
Zonal solutions for a double-ellipse in a hypersonic flowfield
[AERO-REPT-9009] p 345 N92-18233
A numerical study of the stability of the swept attachment line boundary layer
[AERO-REPT-9103] p 345 N92-18293
Model parameter identification techniques for flight flutter testing
[AERO-REPT-9105] p 380 N92-18294
Propagation of shock waves through clouds
[AERO-REPT-9104] p 400 N92-18317
Towards the computation of turbulent hypersonic flows
[AERO-REPT-9106] p 345 N92-18318
Aircraft aerodynamics and stability and control during air-to-air refueling
[AERO-REPT-9017] p 380 N92-18321
The Goldstein Engineering Research Laboratory
[AERO-REPT-8906] p 308 N92-18322
The installation of the AVRO 9 by 7 foot low-speed wind tunnel at the University of Manchester (England)
[AERO-REPT-9005] p 385 N92-18341
Aeronautical Engineering Group publications, 1950 - present
[AERO-REPT-8907] p 910 N92-29683
Elementary flutter analysis p 1088 N92-34162
Flight flutter testing p 1089 N92-34163
Marquardt Corp., Van Nuys, CA.
Supercharged ejector ramjet p 475 N92-21527
H2 fueled flightweight ramjet construction and test p 475 N92-21531
Maryland Univ., College Park.
Application of waverider-based configurations to hypersonic vehicle design
[AIAA PAPER 91-3304] p 32 A92-12742
Analysis of unsteady pressures induced on a body by a rotor p 10 A92-13212
Forward flight trim calculation and frequency response validation of a high-order helicopter simulation model p 132 A92-14337
Dynamics of helicopters with dissimilar blades p 133 A92-14427
Heat transfer characteristics of hypersonic waveriders with an emphasis on the leading edge effects
[NASA-CR-189586] p 525 N92-22215
A study of viscous interaction effects on hypersonic waveriders
[NASA-CR-189587] p 625 N92-24680
Studies in general aviation aerodynamics
[NASA-CR-190431] p 827 N92-28511
Navier-Stokes computations of a viscous optimized waverider
[NASA-CR-189658] p 944 N92-30392
Distributed systems: Interconnection and fault tolerance studies
[AD-A252869] p 1135 N92-33920
Massachusetts Inst. of Tech., Cambridge.
Optimal rejection of bounded persistent disturbances in periodic systems p 51 A92-11464
The role of tip clearance in high-speed fan stall
[ASME PAPER 91-GT-83] p 69 A92-15550
Analysis of aircraft performance during lateral maneuvering for microburst avoidance p 205 A92-20207
The measurement of plate vibration and sound radiation from a turbulent boundary layer manipulator
[AD-A240127] p 42 N92-10206
Advanced stress analysis methods applicable to turbine engine structures
[NASA-CR-187235] p 44 N92-11378
Airfoil optimization with efficient gradient calculations p 177 N92-13960
An investigation of air transportation technology at the Massachusetts Institute of Technology, 1990-1991 p 265 N92-17985
Experimental investigation of passive infrared ice detection for helicopter applications p 265 N92-17986
Deterministic multi-zone ice accretion modeling p 265 N92-17987
Alert generation and cockpit presentation for an integrated microburst alerting system p 265 N92-17988
Cockpit display of hazardous weather information p 277 N92-17989
Algorithms for blending surface generation
[AD-A245686] p 777 N92-26524
Composite fuselage technology (summary of year 2)
[NASA-CR-190434] p 731 N92-26655
Experimental evaluation of candidate graphical microburst alert displays
[NASA-CR-189633] p 735 N92-27424
Modeling of heavy-gas effects on airfoil flows
[NASA-CR-190357] p 716 N92-27558
Self-adaptive aeropropulsion components-enhancing axial compressor performance
[AD-A246123] p 743 N92-27817
Dynamic control of aerodynamic instabilities in gas turbine engines p 870 N92-28466
Turbine blade tip and seal clearance excitation forces
[NASA-CR-184341] p 973 N92-31910
A comparison of the performance of two gust front detection algorithms using a length-based scoring technique
[AD-A250862] p 1004 N92-32103
Active control of compressor surge and stall
[AD-A252771] p 1126 N92-33498
Impacts of technology on the capacity needs of the US national airspace system
[NASA-CR-4470] p 1045 N92-34192
Massachusetts Inst. of Tech., Lexington.
The 1990 Airport Surveillance Radar Wind Shear Processor (ASR-WSP) operational test at Orlando International Airport
[AD-A239852] p 18 N92-10019
Air-to-air visual acquisition handbook
[ATC-151] p 93 N92-13042
Terminal Doppler weather radar test bed operation, Orlando: January-June 1990
[AD-A242890] p 301 N92-17028
Airport Surveillance Radar (ASR-9) wind shear processor: 1991 test at Orlando, Florida
[AD-A252246] p 1124 N92-32686
Massachusetts Univ., Amherst.
Stochastic ordering properties and optimal routing control for a class of finite capacity queueing systems p 48 A92-11375
A new class of gradient estimators for queueing systems with real-time constraints p 49 A92-11395
Matrix Corp., Santa Fe, NM.
Microgravity nucleation and particle coagulation experiments support
[NASA-CR-189899] p 502 N92-21433
Max-Planck-Inst. fuer Stroemungsforschung, Goettingen (Germany).
Development of an electronic high speed camera system for the quantitative analysis of unsteady flows
[MPIS-100/1991] p 300 N92-17344
MCAT Inst., Moffett Field, CA.
Computational investigation of slot blowing for fuselage forebody flow control
[AIAA PAPER 92-0020] p 248 A92-22142
MCAT Inst., San Jose, CA.
Control of unsteady separated flow associated with the dynamic pitching of airfoils
[NASA-CR-189758] p 258 N92-15966
Study of optical techniques for the Ames unitary wind tunnels. Part 1: Schlieren
[NASA-CR-189951] p 385 N92-19218
Study of optical techniques for the Ames unitary wind tunnels. Part 2: Light sheet and vapor screen
[NASA-CR-190217] p 573 N92-22195
Turbulence modeling for hypersonic flight
[NASA-CR-190313] p 630 N92-24898
Algorithm and code development for unsteady three-dimensional Navier-Stokes equations
[NASA-CR-190077] p 692 N92-25264
Development of a quiet supersonic wind tunnel with a cryogenic adaptive nozzle
[NASA-CR-188055] p 751 N92-27976
Development of a quiet supersonic wind tunnel with a cryogenic adaptive nozzle p 751 N92-27977
The FML compressor as a drive system for the LFSWT: A narrative p 751 N92-27978
Study of optical techniques for the Ames unitary wind tunnels. Part 3: Angle of attack
[NASA-CR-190541] p 888 N92-29655
Numerical methods for the simulation of complex multi-body flows with applications for the integrated Space Shuttle vehicle
[NASA-CR-190045] p 945 N92-30740
Numerical methods for the simulation of complex multi-body flows with applications for the integrated Space Shuttle vehicle p 945 N92-30741

Application of the Chimera overlapped grid scheme to simulation of Space Shuttle ascent flows
p 945 N92-30742
Hypersonic code efficiency and validation studies
[NASA-CR-190680] p 948 N92-31533
Control of unsteady separated flow associated with the dynamic stall of airfoils
[NASA-CR-190688] p 950 N92-32177
High speed transition prediction
[NASA-CR-190836] p 1039 N92-33424

McDonnell Aircraft Co., Saint Louis, MO.
Supersonic boundary-layer stability analysis on an aircraft wing p 9 A92-13207
Aeroservoelastic stabilization techniques for hypersonic flight vehicles
[AIAA PAPER 91-5056] p 203 A92-17839
Nonflammable hydraulic power system for tactical aircraft. Volume 2: Equipment and systems test and evaluation
[AD-A239805] p 35 N92-10100
Investigation of vortex breakdown on a delta wing using Euler and Navier-Stokes equations p 87 N92-13019
Design of a fighter aircraft vertical tail enhanced buffet environment survivability p 551 N92-23235
Geometry acquisition and grid generation: Recent experiences with complex aircraft configurations
p 691 N92-24400
ICAAS piloted simulation evaluation
p 735 N92-27906
Aeroelastic calculations for fighter aircraft using the transonic small disturbance equation
p 720 N92-27951
Out of plane analysis for composite structures
p 1107 N92-32527

McDonnell-Douglas Corp., Long Beach, CA.
Evaluation of outdoor-to-indoor response to minimized sonic booms
[NASA-CR-189643] p 927 N92-28556

McDonnell-Douglas Corp., Saint Louis, MO.
Boundary-layer and wake measurements on a swept, circulation-control wing p 9 A92-13205
New insulation constructions for aerospace wiring applications. Volume 1: Testing and evaluation
[AD-A240638] p 22 N92-11006
New insulation constructions for aerospace wiring applications. Volume 2: The 270 VDC arc tracking testing with power controllers
[AD-A240639] p 23 N92-11007
Application of integrated structural analysis to the high speed civil transport p 684 N92-25927

McDonnell-Douglas Helicopter Co., Mesa, AZ.
Development of a shock noise prediction code for high-speed helicopters - The subsonically moving shock
p 165 A92-14384
Assessment of rotorcraft system identification as applied to the AH-64 p 274 N92-17160
Industry view on rotorcraft system identification
p 274 N92-17163
Blade-mounted trailing edge flap control for BVI noise reduction
[NASA-CR-4426] p 512 N92-21173
The application of flight simulation models in support of rotorcraft design and development
p 884 N92-28527

McDonnell-Douglas Research Labs., Saint Louis, MO.
Experimental investigation of terminal shock sensors for mixed-compression inlets p 276 A92-21074

McMaster Univ., Hamilton (Ontario).
Radar clutter classification
[ISBN-0-315-57981-1] p 1126 N92-33440

Mechanical Technology, Inc., Latham, NY.
Industrial code development p 227 N92-15083

Mei Associates, Inc., Lexington, MA.
Design specifications for the Advanced Instructional Design Advisor (AIDA), volume 2
[AD-A248202] p 923 N92-29188

Messerschmitt-Boelkow-Blohm G.m.b.H., Bremen (Germany).
FALKE: Winged re-entry vehicle flight control
p 667 N92-24454

Messerschmitt-Boelkow-Blohm G.m.b.H., Munich (Germany).
A systematic formulation, as an approach to air traffic
[MBB-Z-0371-91-PUB] p 19 N92-10996
Resonance and control response tests using a control stimulation drive
[MBB-UD-0586-90-PUB] p 134 N92-12003
Expert system for the Tornado ground-based check-out system p 118 N92-12536
Avionics systems development: Technological trends, conflicts, and cost issues in a changing European environment p 199 N92-14054
Application of MSC/DYNA to shock and impact problems in aircraft industry
[MBB-UD-0593-91-PUB] p 225 N92-14382
Verification and application of the NSFLEX method for hypersonic flow conditions p 182 N92-15005
Viscous shock-layer equations for the calculation of reentry aerothermodynamics p 183 N92-15008
Aerothermodynamic challenges of the Saenger space-transportation system p 184 N92-15042
Development and evaluation of a finite element model for a fiber composite helicopter fuselage
[MBB-UD-0584-90-PUB] p 196 N92-15066
The acoustic flashlight
[MBB-Z-0359-90-PUB] p 239 N92-15938
Aerodynamic development of the X-31 aircraft for the high angle of attack region
[MBB-FE211-S-PUB-452] p 275 N92-17313
Calculation of hypersonic non-equilibrium viscous flow using second order boundary layer theory
[MBB-FE122-S-PUB-434] p 345 N92-18316
Design, analysis, and testing of integrally stiffened composite centre fuselage skin for future fighter aircraft
[MBB-FE2-PUB-S-450] p 359 N92-18333
X-31 enhancement of aerodynamics for maneuvering beyond stall p 363 N92-18779
X-31: Discussion of steady state and rotary derivatives
p 365 N92-18789
Aeroservoelastic stability of aircraft at high incidence
p 381 N92-18795
Modelling of chemical and physical effects with respect to flows around reentry bodies
[MBB-FE-211/S/PUB/0465/A] p 347 N92-19296
Three-dimensional simulations of hypersonic flows
[MBB-UK-0155-89-PUB] p 447 N92-21703
Contributions of MBB-FE211 to the 2nd Antibes Workshop on Hypersonic Flows
[MBB-FE211-S-PUB-449] p 524 N92-22179
Cases 6.1 and 6.8 double ellipsoid: Navier-Stokes calculation p 525 N92-22181
Case 7.4 delta wing: Navier-Stokes calculation
p 525 N92-22182
Case 7.4: Blunt nose delta wing Euler-boundary layer calculation p 525 N92-22184
First approach to an integrated fin design
p 551 N92-23236
Recommended system concept p 599 N92-23383
The imaging spectrometer p 599 N92-23387
The imaging radar system p 599 N92-23391
Quick-look system p 599 N92-23393
Sensor compatibility/optimal sensor combinations
p 599 N92-23403
Symposium on Marketing for Technological Products
[MBB-UE-0014-90-PUB] p 606 N92-23928
Introduction to Special Course on Engineering Methods in Aerodynamic Analysis and Design of Aircraft
p 552 N92-23951
CFD contributions during hypersonic airplane intake design p 769 N92-27472
Aerothermodynamics of nozzle flows for advanced hypersonic propulsion systems p 769 N92-27478
Evaluation of an unsteady implicit Euler code against two and three-dimensional standard configurations
p 719 N92-27945
Practical architecture of design optimisation software for aircraft structures taking the MBB-Lagrange code as an example p 851 N92-28471
Mathematical optimization: A powerful tool for aircraft design p 851 N92-28474
Experience with piloted simulation in the development of helicopters p 884 N92-28528
Saenger: The reference concept and its technological requirements - aerothermodynamics
[MBB-FE-202-S-PUB-0463-A] p 890 N92-29629
Technology programme: Aerothermodynamics and propulsion integration. Numerical and experimental aerothermodynamics
[MBB-FE-202-S-PUB-0464-A] p 831 N92-29648
Aerothermodynamics and propulsion integration in the Saenger technology programme
[MBB-FE-202-S-PUB-0469-A] p 831 N92-29649
Concurrent engineering in design of aircraft structures
[MBB-FE-2-S-PUB-472] p 854 N92-29650
Aerothermodynamic challenges of the Saenger space-transportation system
[MBB-FE-202-S-PUB-0462-A] p 890 N92-29680
Hypersonic flow past radiation-cooled surfaces
[MBB-FE-202-S-PUB-0468-A] p 832 N92-29713
Computed Tomography (CT) as a nondestructive test method used for composite helicopter components
[MBB-UD-0603-91-PUB] p 910 N92-29873
Repair procedures for advanced composites for helicopters
[MBB-UD-0606-91-PUB] p 787 N92-29874
Experience with piloted simulation in the development of helicopters
[MBB-UD-0610-91-PUB] p 889 N92-30076
Acquisition of an aerothermodynamic data base by means of a winged experimental reentry vehicle
[MBB/FE202/S/PUB/461] p 787 N92-30232
The Eurofar program: An European overview on advanced VTOL civil transportation system
[MBB-UD-0611-91-PUB] p 952 N92-30418
MBB-LAGRANGE: A general structural reliability and optimization structural system
[MBB/FW321/S/PUB/467] p 998 N92-30423
Multidisciplinary optimization of fiber composite aircraft structures
[MBB/FW321/S/PUB/476] p 961 N92-30424
Resonance and control response tests using a control simulation device
[MBB-UD-0608-91-PUB] p 978 N92-30439
Numerical optimization in Germany: A non-exhaustive survey on current activities with emphasis on aeronautics
[MBB/FE211/S/PUB/474] p 932 N92-30675
CFD contributions during hypersonic airplane intake design
[MBB/FE213/S/PUB/459] p 944 N92-30676
Development of hardness cycles for fiber bound materials, using DSC: From laboratory specimens to complex high duty structural members
[MBB-Z-0409-91-PUB] p 987 N92-30969
Cutting treatment by drilling of fiber bound synthetic materials
[MBB-UD-0609-91-PUB] p 988 N92-31716
Stability failure of sandwich structures
[MBB-UD-0613-92-PUB] p 1111 N92-33994

Messerschmitt-Boelkow-Blohm G.m.b.H., Ottobrunn (Germany).
Rapid repair of integrally stiffened carbon fibre composite structures by bolted aluminium elements
[MBB-FE202-S-PUB-0453-A] p 290 N92-17310
Examples of advanced near-net shape manufacturing techniques for aerospace
[MBB-Z-0399-91-PUB] p 1125 N92-32742

Meteorological Satellite Center, Tokyo (Japan).
On the relation between cumulus cloud lines and surface shear lines p 410 N92-19667

Metraflu, Ecully (France).
Inhomogeneous turbulence beyond spectral equilibria: Aeronautical applications
[ETN-92-90867] p 404 N92-19349

Miami Univ., Coral Gables, FL.
The impact of cockpit automation on crew coordination and communication. Volume 1: Overview, LOFT evaluations, error severity, and questionnaire data
[NASA-CR-177587] p 93 N92-13044

Michigan Univ., Ann Arbor.
Near-injector structure of non-evaporating pressure-atomized sprays at various ambient densities
p 681 N92-25571
Development of 3D electromagnetic modeling tools for airborne vehicles
[NASA-CR-190810] p 1126 N92-33307

Micro Circuit Engineering Ltd., Tewkesbury (England).
Applications of silicon hybrid multi-chip modules to avionics p 859 N92-28379

Micro Craft, Inc., Tullahoma, TN.
Computation of a Kelvin-Helmholtz instability for delta wing vortex flows
[AD-A244320] p 346 N92-18825

Midwest Research Inst., Golden, CO.
A comparison of spanwise aerodynamic loads estimated from measured bending moments versus direct pressure measurements on horizontal axis wind turbine blades
[DE92-001158] p 301 N92-16458
Dynamic stall on wind turbine blades
[DE92-001157] p 262 N92-17874
An overview: Challenges in wind technology development
[DE92-001190] p 302 N92-17875
The NREL teetering hub rotor code: Final results and conclusions
[DE92-001187] p 410 N92-19633
Recent results from data analysis of dynamic stall on wind turbine blades
[DE92-001200] p 505 N92-20245
SERI advanced wind turbine blades
[DE92-001216] p 598 N92-22971
Measured and predicted rotor performance for the SERI advanced wind turbine blades
[DE92-001215] p 598 N92-23119
Wind energy program overview
[DE91-002178] p 689 N92-25498
Yaw dynamics of horizontal axis wind turbines
[DE92-001245] p 1004 N92-30837
A surface definition code for turbine blade surfaces
[DE92-010574] p 1004 N92-31498

Ministry of Defence, London (England).
Avionics software evolution p 199 N92-14052
Aircraft fatigue management in the Royal Air Force
p 363 N92-18591
Harrier GR MK 5/7 mission simulators for the Royal Air Force p 885 N92-28540

Ministry of Defence, Paris (France).
Avionics standardization in Europe
p 199 N92-14050
Minnesota Univ., Minneapolis.
Aircraft control in a downburst on takeoff and landing
p 27 A92-11385
Studies of gas turbine heat transfer: Airfoil surfaces and end-wall cooling effects
[AD-A244055] p 376 N92-19097
Application of nonlinear feedback control theory to supermaneuverable aircraft
[NASA-CR-190336] p 663 N92-25648
Feedback control laws for highly maneuverable aircraft
[NASA-CR-190535] p 879 N92-29654
Design of helicopter flight control systems for hover and low speed using eigenstructure assignment
p 1061 N92-33952
Nonlinear dynamic-inversion flight control of supermaneuverable aircraft p 1062 N92-33953
Mississippi State Univ., Mississippi State.
Euler flow predictions for an oscillating cascade using a high resolution wave-split scheme
[ASME PAPER 91-GT-198] p 74 A92-15623
Observability under recurrent loss of data
p 302 A92-21191
Mississippi State Univ., State College.
TIGER: Turbomachinery interactive grid generation
p 659 N92-25718
Mississippi Univ., University.
Steady state risetimes of shock waves in the atmosphere p 1140 N92-33882
Missouri Univ., Rolla.
Theoretical models for duct acoustic propagation and radiation p 236 N92-14782
MITech, Inc., Washington, DC.
Workshop on integrated Crew Resource Management (CRM)
[DOT/FAA/RD-92/5] p 781 N92-27518
Mitre Corp., Bedford, MA.
Mobile Microwave Landing System (MMLS): Operational requirements for setup accuracy
[AD-A241844] p 103 N92-13052
The problem of multiple solutions in area navigation and computed centerline operations with the microwave landing system
[AD-A242757] p 191 N92-15058
Technical feasibility of digital three-dimensional cellular communications for air traffic control applications. Volume 1: Introduction and summary
[AD-A244573] p 534 N92-22104
Technical feasibility of digital three-dimensional cellular communications for air traffic control applications. Volume 2: Example system design details
[AD-A244574] p 534 N92-22105
Technical feasibility of digital three-dimensional cellular *communications for air traffic control applications. Volume* 3: Ground network architecture
[AD-A244575] p 534 N92-22106
JTIDS electromagnetic compatibility in the 960-1215 MHz band
[AD-A247834] p 773 N92-27864
Mitre Corp., Houston, TX.
Case for real-time systems development - Quo vadis?
[AIAA PAPER 91-3726] p 231 A92-17594
Mitre Corp., McLean, VA.
Automated problem resolution prototype in automated en route air traffic control p 190 N92-14028
Safety study of TCAS 2 for logic version 6.04
[DOT/FAA/RD-92/22] p 1047 N92-32537
Simulation test and evaluation of TCAS 2 logic version 6.04
[DOT/FAA/RD-92/23] p 1048 N92-33098
Mitsubishi Space Software Corp. (Japan).
Analysis of spacecraft entry into Mars atmosphere
p 1105 N92-33763
Moscow Inst. of Aviation Technology (USSR).
Progress of magnetic suspension systems and magnetic bearings in the USSR p 772 N92-27740
Progress of magnetic suspension and balance systems for wind tunnels in the USSR p 751 N92-27803
Motoren- und Turbinen-Union Muenchen G.m.b.H. (Germany).
High speed airbreathing propulsion in Europe
p 575 N92-22277
Investigations of blade row interaction and boundary layer transition phenomena in a multistage aero engine low-pressure turbine by measurements with hot-film probes and surface-mounted hot-film gauges
p 658 N92-24338
Computation and visualization of specific flow phenomena in turbomachinery application
p 741 N92-27463
The 3-D Navier-Stokes flow and temperature field computation for a forced mixer nozzle
p 770 N92-27482

N

Naples Univ. (Italy).
Infrared measurements of aerodynamic heating in hypersonic wind tunnel p 208 N92-15002
Linear acoustics in gas mixtures with rate processes
p 238 N92-15013
National Academy of Sciences - National Research Council, Washington, DC.
Development of an improved model for runback water on aircraft surfaces
[AIAA PAPER 92-0042] p 270 A92-22160
Winds of change: Domestic air transport since deregulation
[NRC-SR-230] p 92 N92-13040
National Aero-Space Plane Joint Program Office, Wright-Patterson AFB, OH.
The NASP Program - An update p 61 A92-16059
Conducting the NASP ground test program
[AIAA PAPER 91-5029] p 209 A92-17820
A configuration development strategy for the NASP
[AIAA PAPER 91-5044] p 210 A92-17830
NASP X-30 Propulsion technology status
p 475 N92-21534
National Aeronautical Establishment, Ottawa (Ontario).
Multiple roll attractors of a delta wing at high incidence p 88 N92-13026
A parametric approach to spectrum development
p 360 N92-18578
The use of Kalman filtering techniques to improve the accuracy of flight test data
[NRC-32139] p 1064 N92-32850
National Aeronautical Lab., Bangalore (India).
Dynamic flying investigations on 1/13.5 NALLA model *(Longitudinal Results)*
[NAL-PD-FC-9113] p 359 N92-18073
Graphics for interactive PC based parameter estimation package
[NAL-PD-FC-9117] p 412 N92-18252
PC based flight path reconstruction using UD factorization filtering algorithm
[NAL-PD-FC-9201] p 534 N92-22389
National Aeronautics and Space Administration, Washington, DC.
Resonant cryogenic chopper p 294 A92-22796
Identification of aerodynamic coefficients using computational neural networks
[AIAA PAPER 92-0172] p 255 A92-23783
Operation and design considerations for unsteady data acquisition with PC-based systems in high Reynolds number hypersonic flowfields
[AIAA PAPER 92-0204] p 284 A92-23810
Space Cryogenics Workshop, 10th, Cleveland, OH, June 18-20, 1991, Proceedings p 295 A92-23826
Fiber optics for the National Aero-Space Plane
p 386 A92-24780
Vortex modeling for rotor aerodynamics - The 1991 Alexander A. Nikolsky Lecture p 315 A92-25576
Experimental evaluation of candidate graphical microburst alert displays
[AIAA PAPER 92-0292] p 369 A92-25745
A ballistic investigation of the aerodynamic characteristics of a blunt vehicle at hypersonic speeds in carbon dioxide and air
[AIAA PAPER 92-0328] p 322 A92-25775
Analysis of hypersonic nozzles including vibrational nonequilibrium and intermolecular force effects
[AIAA PAPER 92-0330] p 322 A92-25777
A numerical investigation of hydrogen combustion in Mach 2 flow
[AIAA PAPER 92-0341] p 388 A92-25787
A comparative study of turbulence models for overset grids
[AIAA PAPER 92-0437] p 327 A92-26284
Monte Carlo simulation of reentry flows with ionization
[AIAA PAPER 92-0493] p 328 A92-26323
Monte Carlo simulation of entry in the Martian atmosphere
[AIAA PAPER 92-0494] p 329 A92-26324
Evaluation of OH laser-induced fluorescence techniques for supersonic combustion diagnostics
[AIAA PAPER 92-0508] p 396 A92-26935
An iodine hypersonic wind tunnel for the study of nonequilibrium reacting flows
[AIAA PAPER 92-0566] p 383 A92-26974
Target pitch angle for the microburst escape maneuver
[AIAA PAPER 92-0730] p 379 A92-27082
An experimental/computational study of sharp fin induced shock wave/turbulent boundary layer interactions at Mach 5 - Experimental results
[AIAA PAPER 92-0749] p 335 A92-27093
Skin-friction gauge for use in hypervelocity impulse facilities p 398 A92-28063
Leading edge sweep effects in generic three-dimensional sidewall compression scramjet inlets
[AIAA PAPER 92-0674] p 343 A92-28218
A system identification model for adaptive nonlinear control p 508 A92-29248
Experimental results and numerical modeling of solidification during aircraft high-g arcs
[AIAA PAPER 92-0843] p 493 A92-29609
GPS interferometric attitude and heading determination - Initial flight test results p 454 A92-30023
Use of finite volume schemes for transition simulation
p 432 A92-31185
System design from mission definition to flight validation
[AIAA PAPER 92-1091] p 605 A92-33256
The effectiveness of Coriolis dampening of convection during aircraft high-g arcs p 581 A92-33847
Reduced basis technique for evaluating the sensitivity coefficients of the nonlinear tire response
[AIAA PAPER 92-2530] p 583 A92-34376
Time simulation of flutter with large stiffness changes
[AIAA PAPER 92-2394] p 585 A92-34467
Overview and major characteristics of future aeronautical and space systems
[AIAA PAPER 92-2441] p 585 A92-34472
Vibration reduction in helicopter rotors using an active *control surface located on the blade*
[AIAA PAPER 92-2451] p 564 A92-34478
Three-dimensional time-marching aeroelastic analyses *using an unstructured-grid Euler method*
[AIAA PAPER 92-2506] p 542 A92-34500
Relating the microwave radar cross section to the sea surface stress - Physics and algorithms
p 597 A92-35028
Temperature and initial curvature effects in low-density panel flutter
[AIAA PAPER 92-2128] p 589 A92-35695
Multipoint inverse airfoil design method based on conformal mapping p 610 A92-36827
Spatial adaptation of unstructured meshes for unsteady aerodynamic flow computations p 610 A92-36838
Multifractal analysis of a lobed mixer flowfield utilizing the proper orthogonal decomposition
p 611 A92-36840
The computation of three-dimensional flows using unstructured grids p 612 A92-37539
NASP - A status report
[AIAA PAPER 92-1417] p 666 A92-38569
GPS interferometric attitude and heading determination - Flight test results p 650 A92-39561
Receiver autonomous integrity monitoring (RAIM) - Techniques, performance and potential
p 638 A92-39567
Passive control of supersonic cavity flowfields
[SAE PAPER 912153] p 619 A92-39988
Oscillating airfoil velocity field during large amplitude *dynamic stall* p 622 A92-40171
Composite laminated shells under internal pressure
p 758 A92-41296
Direct simulation of re-entry flows with ionization
p 713 A92-44367
Heat pipe and surface mass transfer cooling of hypersonic vehicle structures p 763 A92-44380
Hypersonic mixing and combustion studies in the hypulse facility p 737 A92-44526
Who or what saved the day? A comparison of traditional and glass cockpits p 833 A92-44931
Empirical foundations and sensitivity testing - Is it enough for the 90's? p 835 A92-45054
Computational aerodynamics - The next generation
[SAE PAPER 911988] p 788 A92-45390
A nonlinear relaxation/quasi-Newton algorithm for the *compressible Navier-Stokes equations*
[AIAA PAPER 92-2643] p 796 A92-45510
Multi-point inverse design of an infinite cascade of airfoils
[AIAA PAPER 92-2650] p 797 A92-45517
A new approach for the calculation of transitional flows
[AIAA PAPER 92-2669] p 798 A92-45524
Numerical simulations using a dynamic solution-adaptive grid algorithm, with applications to unsteady internal flows
[AIAA PAPER 92-2719] p 803 A92-45557
Waves and thermodynamics in high Mach number *propulsive ducts* p 809 A92-46431
Airdata calibration techniques for measuring atmospheric wind profiles p 856 A92-46792
Wind-tunnel compressor stall monitoring using neural networks p 918 A92-46817
Computation of turbulent, separated, unswept compression ramp interactions p 813 A92-46897
Unstructured and adaptive mesh generation for high Reynolds number viscous flows p 816 A92-47042

Analysis of thermo-chemical nonequilibrium models for carbon dioxide flows
[AIAA PAPER 92-2852] p 892 A92-47835
Fiber optic and laser sensors VIII; Proceedings of the Meeting, San Jose, CA, Sept. 17-19, 1990
[SPIE-1367] p 901 A92-48026
Comparative study of turbulence models in predicting hypersonic inlet flows
[AIAA PAPER 92-3098] p 824 A92-48740
Advanced Rotorcraft Transmission (ART) Program summary
[AIAA PAPER 92-3365] p 905 A92-48938
Experiments on the enhancement of compressible mixing via streamwise vorticity. I - Optical measurements
[AIAA PAPER 92-3549] p 906 A92-49064
Exploratory study of wall pressure fluctuations in a Mach 5, sharp fin-induced turbulent interaction
p 935 A92-50304
Time domain numerical calculations of unsteady vortical flows about a flat plate airfoil p 936 A92-50473
A general explicit or semi-explicit algorithm for compressible and incompressible flows
p 937 A92-52682
An experimental examination of the effects of incoming boundary layer modifications on the dynamics of a turbulent compression corner interaction
[AIAA PAPER 92-3667] p 1022 A92-54111
Comparison between computational and experimental data for a hypersonic laser propelled vehicle
[AIAA PAPER 92-3808] p 1023 A92-54179
An assumed joint-Beta PDF approach for supersonic turbulent combustion
[AIAA PAPER 92-3844] p 1113 A92-54199
A fine-wire thermocouple probe for measurement of stagnation temperatures in real gas hypersonic flows of nitrogen p 1114 A92-54317
Measured and calculated optical property profiles in the mixed layer and free troposphere p 1129 A92-54630
Optimal recovery from microburst wind shear
[AIAA PAPER 92-4338] p 1078 A92-55327
A data fusion algorithm for multi-sensor microburst hazard assessment
[AIAA PAPER 92-4339] p 1063 A92-55328
Multidisciplinary optimization of aeroservoelastic systems using reduced-size models
p 1054 A92-56176
Research needs for a commercial passenger tiltrotor
p 1056 A92-56298
Effects of oxygen dissociation on hypervelocity combustion experiments
[AIAA PAPER 92-3964] p 1098 A92-56791
A code validation strategy and facility for nonequilibrium, reacting flows
[AIAA PAPER 92-3970] p 1098 A92-56796
Small engine components test facility compressor testing cell at NASA Lewis Research Center
[AIAA PAPER 92-3980] p 1098 A92-56806
Advanced nozzle and engine components test facility
[AIAA PAPER 92-3993] p 1099 A92-56816
Engine component instrumentation development facility at NASA Lewis Research Center
[AIAA PAPER 92-3995] p 1099 A92-56818
Description of a pressure measurement technique for obtaining surface static pressures of a radial turbine
[AIAA PAPER 92-4006] p 1123 A92-56829
Boundary layer study on nozzle wall at hypersonic velocities
[AIAA PAPER 92-4013] p 1034 A92-56836
A database of aerothermal measurements in hypersonic flow for CFD validation
[AIAA PAPER 92-4023] p 1034 A92-56845
Free-radicals aided combustion with scramjet applications
[IAF PAPER 92-0659] p 1106 A92-57100
Technologies for the National Aero-Space Plane
[IAF PAPER 92-0868] p 1105 A92-57259
NASA reliability preferred practices for design and test
[NASA-TM-4322] p 157 N92-12286
The atmospheric effects of stratospheric aircraft: A first program report
[NASA-RP-1272] p 408 N92-19121
Cryogenic hydrogen-induced air-liquefaction technologies for combined-cycle propulsion applications
p 487 N92-21526
NASA's hypersonic propulsion program: History and direction p 476 N92-21535
NASA aerodynamics program
[NASA-TM-4368] p 609 N92-24678
NASA engineers and the age of Apollo
[NASA-SP-4104] p 929 N92-28344
An international aerospace information system: A cooperative opportunity
[NASA-TM-108171] p 1142 N92-33237

National Aeronautics and Space Administration. Ames Research Center, Moffett Field, CA.

Pre-flight risk assessment in emergency medical service (EMS) helicopters p 16 A92-11171
Analysis of general aviation accidents during operations under instrument flight rules p 16 A92-11172
Using new aggregation operators in rule-based intelligent control p 51 A92-11456
Two-dimensional adaptive-wall tests in the NASA Ames two- by two-foot transonic wind tunnel
p 30 A92-13201
Computation of three-dimensional turbulent vortical flows on bodies at high incidence p 9 A92-13203
Boundary-layer and wake measurements on a swept, circulation-control wing p 9 A92-13205
Probe shapes for streamwise momentum and cross-stream turbulence intensity p 9 A92-13210
Probe systems for static pressure and cross-stream turbulence intensity p 10 A92-13211
Wing tip vortex calculations with an unstructured adaptive-grid Euler solver p 64 A92-14330
Results from a test of a 2/3-scale V-22 rotor and wing in the 40- by 80-Foot Wind Tunnel p 104 A92-14332
Forward flight trim calculation and frequency response validation of a high-order helicopter simulation model
p 132 A92-14337
Helicopter control response types for hover and low-speed near-earth tasks in degraded visual conditions
p 132 A92-14338
Full-scale investigation of aerodynamic interactions between a rotor and fuselage p 105 A92-14361
Hub and pylon fairing integration for helicopter drag reduction p 107 A92-14391
High speed rotorcraft - Comparison of leading concepts and technology needs p 108 A92-14415
Aerodynamic design of a Coanda induced force and thruster anti-torque system p 109 A92-14419
Computer aiding for low-altitude helicopter flight
p 94 A92-14444
Description of a tilt wing mathematical model for piloted simulation p 133 A92-14445
Computations of unsteady multistage compressor flows in a workstation environment
[ASME PAPER 91-GT-336] p 163 A92-15701
Sensor fusion for synthetic vision
[AIAA PAPER 91-3730] p 197 A92-17597
Optical computing at NASA Ames Research Center
[AIAA PAPER 91-3779] p 231 A92-17637
Numerical prediction of subsonic turbulent flows over slender bodies at high incidence p 172 A92-18358
Some Aspects of uncertainty in computational fluid dynamics results p 233 A92-19609
Static aeroelastic analysis for generic configuration wing p 174 A92-20201
Rate parameters for coupled vibration-dissociation in a generalized SSH approximation p 235 A92-20301
Measurements of the flow around a lifting-wing/body junction p 175 A92-20726
Instabilities of flows over bodies at large incidence
p 176 A92-20738
Surface flow patterns on an ogive-cylinder at incidence p 176 A92-20762
Synthesis of a helicopter full-authority controller
p 280 A92-21178
Computational investigation of slot blowing for fuselage forebody flow control
[AIAA PAPER 92-0020] p 248 A92-22142
Navier-Stokes analysis of blunt trailing edge airfoils
[AIAA PAPER 92-0024] p 248 A92-22146
Nonequilibrium algebraic turbulence modeling considerations for transonic airfoils and wings
[AIAA PAPER 92-0026] p 248 A92-22148
Future experimental needs in low-speed aerodynamics
[AIAA PAPER 92-0157] p 254 A92-23772
Prediction of drag at subsonic and transonic speeds using Euler methods
[AIAA PAPER 92-0169] p 255 A92-23780
Leading edge velocity field of an oscillating airfoil in compressible dynamic stall
[AIAA PAPER 92-0193] p 257 A92-23802
Correction of sideslip-induced static pressure errors in flight-test measurements p 309 A92-24416
Flow over an all-body hypersonic aircraft - Experiment and computation p 310 A92-24651
Comprehensive helicopter rotor instrumentation - A retrofit approach using miniature transducers
[AIAA PAPER 92-0268] p 369 A92-25724
Reduction of wing rock amplitudes using leading-edge vortex manipulations
[AIAA PAPER 92-0279] p 379 A92-25733
Experiments on shock/vortex interactions
[AIAA PAPER 92-0315] p 320 A92-25762
Reactivation and upgrade of the NASA Ames 16-Inch Shock Tunnel - Status report
[AIAA PAPER 92-0327] p 383 A92-25774
A ballistic investigation of the aerodynamic characteristics of a blunt vehicle at hypersonic speeds in carbon dioxide and air
[AIAA PAPER 92-0328] p 322 A92-25775
Direct computation of the sound from a compressible co-rotating vortex pair
[AIAA PAPER 92-0374] p 414 A92-26232
Single expansion ramp nozzle simulations
[AIAA PAPER 92-0387] p 323 A92-26243
Low aspect ratio wing code validation experiment
[AIAA PAPER 92-0402] p 324 A92-26255
Efficient simulation of incompressible viscous flow over single and multi-element airfoils
[AIAA PAPER 92-0405] p 324 A92-26258
Effect of upstream disturbance on flow asymmetry
[AIAA PAPER 92-0408] p 325 A92-26261
Computational study of the aerodynamics and control by blowing of asymmetric vortical flows over delta wings
[AIAA PAPER 92-0410] p 325 A92-26263
Turbulence modeling for high speed flows
[AIAA PAPER 92-0436] p 327 A92-26283
A comparative study of turbulence models for overset grids
[AIAA PAPER 92-0437] p 327 A92-26284
Zonal flow analysis method for two-dimensional airfoils p 330 A92-26435
The NASA Computational Aerosciences Program - Toward teraFLOPS computing
[AIAA PAPER 92-0558] p 411 A92-26968
Experimental results on a wall interference correction method with interface measurements
[AIAA PAPER 92-0570] p 333 A92-26978
Crossing shock wave turbulent boundary layer interactions - Variable angle and shock generator length geometry effects at Mach 3
[AIAA PAPER 92-0636] p 334 A92-27014
Multibody interference at transonic Mach numbers
[AIAA PAPER 92-0651] p 334 A92-27023
An experimental/computational study of sharp fin induced shock wave/turbulent boundary layer interactions at Mach 5 - Experimental results
[AIAA PAPER 92-0749] p 335 A92-27093
Decentralized-feedback pole placement of linear systems p 411 A92-27347
Turbulence model effects on separated flow about a prolate spheroid p 340 A92-28036
Effect of airfoil (trailing-edge) thickness on the numerical solution of panel methods based on the Dirichlet boundary condition p 340 A92-28041
Numerical simulation of vortex unsteadiness on a slender body at high incidence p 340 A92-28062
Flight investigation of variations in rotorcraft control and display dynamics for hover p 379 A92-28151
Three-dimensional structure of a curved wake
[AIAA PAPER 92-0541] p 341 A92-28199
Unsteady airfoil flow solutions on moving zonal grids
[AIAA PAPER 92-0543] p 342 A92-28200
Effective treatments of the singular line boundary problem for three dimensional grids
[AIAA PAPER 92-0545] p 342 A92-28202
Flowfield simulation about the SOFIA Airborne Observatory
[AIAA PAPER 92-0656] p 342 A92-28217
Unsteady analysis of hot streak migration in a turbine stage p 399 A92-28537
Aerobrake guidance law synthesis using feedback linearization p 485 A92-29304
Synthesis of robust nonlinear autopilots using differential game theory p 478 A92-29330
System identification requirements for high-bandwidth rotorcraft flight control system design
p 479 A92-29332
Structure of supersonic turbulent flow past a swept compression corner p 431 A92-31155
Solution-adaptive grid procedure for the parabolized Navier-Stokes equations p 432 A92-31163
Two- and three-dimensional effects in the supersonic mixing layer p 432 A92-31165
Calculation of real-gas effects on blunt-body trim angles p 432 A92-31169
Freestream capturing for moving coordinates in three dimensions p 432 A92-31186
A non-linearly stable implicit finite element algorithm for hypersonic aerodynamics p 433 A92-31487
Navier-Stokes simulation of flow through a highly contoured subsonic diffuser p 433 A92-31491
Unsteady separation in sharp fin-induced shock wave/turbulent boundary layer interaction at Mach 5
[AIAA PAPER 92-0748] p 436 A92-31678
Liquid crystal coatings for surface shear-stress visualization in hypersonic flows p 496 A92-32177
Thermal protection analysis of Mars-earth return vehicles p 497 A92-32183
Evaluation of a Navier-Stokes prediction of a jet in a crossflow p 441 A92-32235

Earth atmospheric entry studies for manned Mars missions p 442 A92-32251
Preliminary design of an intermittent smoke flow visualization system
[AIAA PAPER 92-1028] p 580 A92-33209
Low-speed cruise aerodynamics of the stopped rotor/disk rotorcraft concept
[AIAA PAPER 92-1067] p 517 A92-33240
An interactive system for aircraft design and optimization
[AIAA PAPER 92-1190] p 600 A92-33302
Constraint-based component-modeling for knowledge-based design
[AIAA PAPER 92-1192] p 600 A92-33304
Design tradeoffs on engine-integrated hypersonic vehicles
[AIAA PAPER 92-1205] p 537 A92-33313
ACSYNT - A standards-based system for parametric, computer aided conceptual design of aircraft
[AIAA PAPER 92-1268] p 601 A92-33345
Profile negotiation - A concept for integrating airborne and ground-based automation for managing arrival traffic p 531 A92-33432
Analysis of accidents during instrument approaches p 529 A92-34253
Analytical aeroelastic stability considerations and conversion loads for an XV-15 tilt-rotor in a wind tunnel simulation
[AIAA PAPER 92-2258] p 540 A92-34413
Blade root torsional dampers to reduce hub loads
[AIAA PAPER 92-2449] p 541 A92-34476
Analysis of open loop higher harmonic control at high airspeeds on a modern four-bladed articulated rotor
[AIAA PAPER 92-2450] p 542 A92-34477
Vibration reduction in helicopter rotors using an active control surface located on the blade
[AIAA PAPER 92-2451] p 564 A92-34478
Unsteady transonic Euler solutions using finite elements
[AIAA PAPER 92-2504] p 518 A92-34499
New time-domain technique for flutter boundary identification
[AIAA PAPER 92-2102] p 588 A92-35673
Digital time series analysis for flutter test data
[AIAA PAPER 92-2103] p 589 A92-35674
Rotary-wing aeroservoelastic problems
[AIAA PAPER 92-2107] p 567 A92-35678
Role of shock dynamics in transonic flutter
[AIAA PAPER 92-2121] p 520 A92-35690
A new method for transonic static aeroelasticity problems
[AIAA PAPER 92-2123] p 589 A92-35691
Acoustic results of the Boeing model 360 whirl tower test p 603 A92-35741
A piloted comparison of elastic and rigid blade-element rotor models using parallel processing technology p 546 A92-35751
A study of coupled rotor-fuselage vibration with higher harmonic control using a symbolic computing facility p 569 A92-35770
Bearingless rotor aeromechanical stability measurements and correlations using nonlinear aerodynamics p 547 A92-35772
High-order state space simulation models of helicopter flight mechanics p 569 A92-35777
Boundary-layer receptivity of sound with roughness p 604 A92-36006
High alpha aerodynamic control by tangential fuselage blowing p 611 A92-36848
Control and display combinations for blind vertical landings p 661 A92-39903
Analyzing the flared landing task with pitch-rate flight *control systems* p 661 A92-39905
Comparison of elastic and rigid blade-element rotor models using parallel processing technology for piloted simulations
[SAE PAPER 912120] p 608 A92-39968
A review of recent programs and future plans for rotorcraft in-flight simulation at Ames Research Center
[SAE PAPER 912121] p 608 A92-39969
Compressibility effects on the growth and structure of homogeneous turbulent shear flow p 675 A92-40052
Evolution of three-dimensionality in stable and unstable curved mixing layers p 619 A92-40059
Simulation and modeling of homogeneous compressible *turbulence under isotropic mean compression* p 622 A92-40134
Oscillating airfoil velocity field during large amplitude dynamic stall p 622 A92-40171
1991-92 AHS Technical Committee highlights - Flight simulation p 609 A92-40394
Some issues on modeling atmospheric turbulence experienced by helicopter rotor blades p 647 A92-40885
Subsonic and transonic low-Reynolds-number airfoils with reduced pitching moments p 701 A92-41211
Design and development of a compressible dynamic stall facility p 747 A92-41215
Transonic Navier-Stokes computations for an oscillating wing using zonal grids p 701 A92-41217
Effects of higher harmonic control on rotor performance and control loads p 729 A92-41218
Microwave landing system modeling with application to air traffic control automation p 725 A92-41220
Extension and validation of an unsteady wake model for rotors p 702 A92-41224
Transonic aeroelasticity analysis for rotor blades p 758 A92-41238
Accurate prediction of drag using Euler methods p 703 A92-41246
Adequacy of modeling turbulence and related effects on helicopter response p 730 A92-41263
Hypersonic shock-wave turbulent-boundary-layer interaction flows p 703 A92-41264
Computation of saddle point of attachment p 703 A92-41276
Free-flight trim-angle predictions for the aeroassist flight experiment p 705 A92-41540
Helicopter aeroelastic stability and response - Current topics and future trends p 730 A92-43100
Thermochemical nonequilibrium flow computations of *flow around the aeroassist flight experiment* p 713 A92-44368
Bleed-boundary conditions for numerically simulated mixed-compression supersonic inlet flow p 713 A92-44520
Who or what saved the day? A comparison of traditional and glass cockpits p 833 A92-44931
A re-analysis of the causes of Boeing 727 'black hole landing' crashes p 833 A92-44985
Jet-powered V/STOL aircraft - Lessons learned p 841 A92-45304
Large-scale wind tunnel studies of a jet-engined powered ejector-lift STOVL aircraft p 842 A92-45313
Integrated flight/propulsion control for supersonic STOVL aircraft p 872 A92-45320
Effect of canard deflection on close-coupled canard-wing-body aerodynamics
[AIAA PAPER 92-2602] p 792 A92-45479
High speed aerodynamics of upper surface blowing aircraft configurations
[AIAA PAPER 92-2611] p 793 A92-45485
Future directions in computing and CFD
[AIAA PAPER 92-2734] p 917 A92-45489
Coupled numerical simulation of the external and engine inlet flows for the F-18 at large incidence
[AIAA PAPER 92-2621] p 793 A92-45493
Practical design optimization of wing/body configurations using the Euler equations
[AIAA PAPER 92-2633] p 795 A92-45505
Vortex trapping on a 60 degree delta wing
[AIAA PAPER 92-2639] p 796 A92-45508
Numerical investigation of tail buffet on F-18 aircraft
[AIAA PAPER 92-2673] p 798 A92-45528
Analysis of a pneumatic forebody flow control concept about a full aircraft geometry
[AIAA PAPER 92-2678] p 799 A92-45530
Computational evaluation of an airfoil with a Gurney flap
[AIAA PAPER 92-2708] p 802 A92-45550
Forebody vortex control for suppressing wing rock on a highly-swept wing configuration
[AIAA PAPER 92-2716] p 803 A92-45555
Navier-Stokes computation of wing leading edge tangential blowing for a tilt rotor in hover
[AIAA PAPER 92-2608] p 805 A92-45568
Forebody flow control on a full-scale F/A-18 aircraft
[AIAA PAPER 92-2674] p 806 A92-45583
Full-scale high angle-of-attack tests of an F/A-18
[AIAA PAPER 92-2676] p 806 A92-45584
Streamlines, vorticity lines, and vortices around three-dimensional bodies p 808 A92-45845
Microburst modelling and scaling p 915 A92-46262
Parameter identification of linear systems based on smoothing p 873 A92-46742
Navier-Stokes predictions for the F-18 wing and fuselage at large incidence p 810 A92-46783
Navier-Stokes computations on swept-tapered wings, including flexibility p 810 A92-46786
Experimental study of vortex flows over delta wings in *wing-rock motion* p 810 A92-46787
Forebody vortex control using small, rotatable strakes p 811 A92-46798
Self-induced roll oscillations of low-aspect-ratio rectangular wings p 874 A92-46802
Wind-tunnel compressor stall monitoring using neural networks p 918 A92-46817
Interaction between crossing oblique shocks and a turbulent boundary layer p 812 A92-46882
Parallel computing strategies for block multigrid implicit solution of the Euler equations p 812 A92-46894
A general purpose nonlinear rigid body mass finite element for application to rotary wing dynamics p 846 A92-46924
A study of rotor wake development and wake/body interactions in hover p 813 A92-46935
On the adequacy of modeling turbulence and related effects on helicopter response p 847 A92-46945
An Eulerian/Lagrangian method for computing blade/vortex impingement p 814 A92-46952
Three-dimensional blade vortex interactions p 815 A92-46953
Experimental and computational studies of hovering rotor flows p 815 A92-46954
Decoupled predictions of radiative heating in air using a particle simulation method
[AIAA PAPER 92-2971] p 816 A92-46986
Nonlinear control design for slightly nonminimum phase systems - Application to V/STOL aircraft p 876 A92-48160
Aerodynamic performance of a full-scale lifting ejector system in a STOVL fighter aircraft
[AIAA PAPER 92-3094] p 824 A92-48738
High speed rotorcraft propulsion concepts to control *power/speed characteristics*
[AIAA PAPER 92-3367] p 865 A92-48940
Analysis of a hydrocarbon scramjet with augmented *preburning*
[AIAA PAPER 92-3425] p 865 A92-48984
Inertial navigation sensor integrated motion analysis for obstacle detection p 954 A92-49272
Application of a solution adaptive grid scheme to complex three-dimensional flows p 935 A92-50309
Asymmetric turbulent vortical flows over slender bodies p 935 A92-50314
Cockpit crew research p 951 A92-51440
Simulation of automatic rotorcraft nap-of-the-earth flight in graphics workstation environment
[AIAA PAPER 92-4131] p 981 A92-52428
Analysis of propulsion system dynamics in the validation of a high-order state space model of the UH-60
[AIAA PAPER 92-4150] p 959 A92-52441
Algorithmic improvements for simulator motion drive
[AIAA PAPER 92-4158] p 1007 A92-52448
Man-Vehicle Systems Research Facility - Design and operating characteristics
[AIAA PAPER 92-4177] p 982 A92-52458
Vision-based obstacle detection for rotorcraft flight p 967 A92-52465
Inertial navigation sensor integrated motion analysis for *autonomous vehicle navigation* p 995 A92-52470
A general explicit or semi-explicit algorithm for compressible and incompressible flows p 937 A92-52682
Monte Carlo study of vibrational relaxation processes p 940 A92-52777
Heat transfer measurements and CFD comparison of swept shock wave/boundary-layer interactions
[AIAA PAPER 92-3665] p 1021 A92-54110
Comparison of turbulence models for powered-lift flow fields
[AIAA PAPER 92-3674] p 1022 A92-54117
Flow characterization in the NASA Ames 16-inch Shock Tunnel
[AIAA PAPER 92-3810] p 1090 A92-54180
Improving designer productivity
[AIAA PAPER 92-1187] p 1130 A92-54285
H-N2 interaction energies, transport cross sections, and collision integrals p 1135 A92-54660
Assessment of compressibility corrections to the k-epsilon model in high-speed shear layers p 1024 A92-54905
Flowfield of a lifting rotor in hover - A Navier-Stokes *simulation* p 1024 A92-54906
Analysis of the onset of dynamic stall p 1024 A92-54919
Vortical flow computations on a flexible blended wing-body configuration p 1024 A92-54922
Vision-based stereo ranging as an optimal control problem
[AIAA PAPER 92-4418] p 1045 A92-55211
Integration of radar altimeter, precision navigation, and digital terrain data for low-altitude flight
[AIAA PAPER 92-4420] p 1063 A92-55212
Control design of a UH-60 rotorcraft via CLTR and direct optimization
[AIAA PAPER 92-4470] p 1076 A92-55230
Concepts for pilot interaction with an automated NOE obstacle-avoidance system
[AIAA PAPER 92-4472] p 1076 A92-55232
An framework for robust flight control design using constrained optimization
[AIAA PAPER 92-4603] p 1131 A92-55282
Severe turbulence and maneuvering from airline flight records
[AIAA PAPER 92-4341] p 1078 A92-55330

Flight simulator fidelity assessment in a rotorcraft lateral translation maneuver
[AIAA PAPER 92-4424] p 1092 A92-55348
Navier-Stokes prediction of large-amplitude delta-wing roll oscillations characterizing wing rock
[AIAA PAPER 92-4428] p 1080 A92-55352
Vortical flow control on a wing-body combination using tangential blowing
[AIAA PAPER 92-4430] p 1081 A92-55354
Navier-Stokes computations for oscillating control surfaces
[AIAA PAPER 92-4431] p 1026 A92-55355
A discrete vortex model for predicting wing rock of slender wings
[AIAA PAPER 92-4497] p 1026 A92-55365
Computations of the unsteady flow about a generic wing/pylon/finned-store configuration
[AIAA PAPER 92-4568] p 1027 A92-55377
Force production mechanisms of a tangential jet on bodies at high alpha
[AIAA PAPER 92-4648] p 1082 A92-55393
Analysis of image-based navigation system for rotorcraft low-altitude flight p 1046 A92-55968
Unsteady shock-vortex interaction on a flexible delta wing p 1030 A92-56157
Navier-Stokes simulation of a close-coupled canard-wing-body configuration p 1031 A92-56163
Euler/experiment correlation of a generic fighter p 1031 A92-56164
Two-fence concept for efficient trapping of vortices on airfoils p 1031 A92-56165
Application of computational fluid dynamics to sonic boom near- and mid-field prediction p 1031 A92-56173
Modular techniques for dynamic fault-tree analysis p 1120 A92-56241
The computation and validation of hovering rotor performance p 1055 A92-56285
Finite-element analysis and multibody dynamics issues in rotorcraft dynamic analysis p 1055 A92-56286
Coupled rotor-fuselage vibration reduction with multiple frequency blade pitch control p 1085 A92-56315
Research on measurement and control of helicopter rotor response using blade-mounted accelerometers 1990-91 p 1057 A92-56316
First level release of 2GCHAS for comprehensive helicopter analysis p 1133 A92-56339
Approximations for inclusion of rotor lag dynamics in helicopter flight dynamics models p 1060 A92-56354
Experimental results for a hypersonic nozzle/afterbody flow field
[AIAA PAPER 92-3915] p 1032 A92-56747
Blockage correction in three-dimensional wind tunnel testing based on the wall signature method
[AIAA PAPER 92-3925] p 1095 A92-56756
Development and integration of modern laboratories in aerospace education
[AIAA PAPER 92-4022] p 1141 A92-56844
CFD validation experiments for hypersonic flows
[AIAA PAPER 92-4024] p 1034 A92-56846
Laboratory simulation of aerothermodynamic phenomena - A review
[AIAA PAPER 92-4025] p 1104 A92-56847
Numerical simulation of unsteady flow in a hypersonic shock tunnel facility
[AIAA PAPER 92-4029] p 1034 A92-56851
Passive range estimation for rotorcraft low-altitude flight
[NASA-TM-103897] p 2 N92-10003
Transonic and supersonic Euler computations of vortex-dominated flow fields about a generic fighter
[NASA-TP-3156] p 11 N92-10011
Rotor noise p 54 N92-10600
NACA 0015 wing pressure and trailing vortex measurements
[NASA-TP-3151] p 13 N92-10981
Experimental study of an independently deflected wingtip mounted on a semispan wing
[NASA-TM-102842] p 13 N92-10983
Analysis of open loop higher harmonic control at high airspeeds on a modern four-bladed articulated rotor
[NASA-TM-103876] p 21 N92-11000
An assessment and application of turbulence models for hypersonic flows
[NASA-TM-105124] p 82 N92-11984
A NASA/RAE cooperation in the development of a real-time knowledge based autopilot p 164 N92-12528
Nonequilibrium turbulence modeling effects on transonic vortical flows about delta wings p 85 N92-13007
Tiltrotor research aircraft composite blade repairs: Lessons learned
[NASA-TM-103875] p 367 N92-19563
Laser-spectroscopic measurement techniques for hypersonic, turbulent wind tunnel flows
[NASA-TM-103928] p 405 N92-19596
A mathematical model of a tilt-wing aircraft for piloted simulation
[NASA-TM-103864] p 368 N92-19847
The Center/TRACON Automation System (CTAS): A video presentation
[NASA-TM-103887] p 356 N92-20029
Modeling methods for high-fidelity rotorcraft flight mechanics simulation
[NASA-TM-103842] p 482 N92-21440
Wing force and surface pressure data from a hover test of a 0.658-scale V-22 rotor and wing
[NASA-TM-102244] p 550 N92-22864
The 12-foot pressure wind tunnel restoration project model support systems p 664 N92-25091
Constraint-based scheduling
[NASA-TM-107873] p 692 N92-25190
Study of turbulence structure through numerical simulations: The perspective of drag and reduction p 717 N92-27713
Status of automatic guidance systems for rotorcraft in low altitude flight p 727 N92-27894
Transonic aeroelastic computations on wings using Navier-Stokes equations p 721 N92-27957
Comparison of three controllers applied to helicopter vibration
[NASA-TM-102192] p 878 N92-28457
Thermal response of rigid and flexible insulations and reflective coating in an aeroconvective heating environment
[NASA-TM-103925] p 852 N92-28721
The design of test-section inserts for higher speed aeroacoustic testing in the Ames 80- by 120-foot wind tunnel
[NASA-TM-103915] p 927 N92-28909
Binary optical filters for scale invariant pattern recognition
[NASA-TM-103902] p 853 N92-28910
Rotorcraft In-Flight Simulation Research at NASA Ames Research Center: A Review of the 1980's and plans for the 1990's
[NASA-TM-103873] p 853 N92-28926
A rotorcraft flight database for validation of vision-based ranging algorithms
[NASA-TM-103906] p 841 N92-29103
Performance of uncoated AFRSI blankets during multiple Space Shuttle flights
[NASA-TM-103892] p 890 N92-29104
Improving designer productivity
[NASA-TM-103929] p 854 N92-29417
NASA Workshop on future directions in surface modeling and grid generation
[NASA-CP-10092] p 831 N92-29625
NAS (Numerical Aerodynamic Simulation Program) technical summaries, March 1989 - February 1990
[NASA-TM-107960] p 1013 N92-31852
Transonic wind tunnel test of a 14 percent thick oblique wing
[NASA-TM-102230] p 950 N92-32213
Potential flow theory and operation guide for the panel code PMARC
[NASA-TM-102851] p 1036 N92-32422
Vision-based range estimation using helicopter flight data
[NASA-TM-103930] p 1047 N92-32424
Computations of unsteady multistage compressor flows in a workstation environment
[NASA-TM-103839] p 1071 N92-32452
Collaborative research on V/STOL control system/cockpit display tradeoffs under the NASA/MOD joint aeronautical program
[NASA-TM-103910] p 1087 N92-32788
Ski jump takeoff performance predictions for a mixed-flow, remote-lift STOVL aircraft
[NASA-TM-103866] p 1060 N92-32887
CTAS: Computer intelligence for air traffic control in the terminal area
[NASA-TM-103959] p 1044 N92-33080
Analysis of delay reducing and fuel saving sequencing and spacing algorithms for arrival traffic
[NASA-TM-103880] p 1044 N92-33194
On the anomalies in single-jet hover suckdown data
[NASA-TM-102261] p 1038 N92-33306
Design and evaluation of an advanced air-ground data-link system for air traffic control
[NASA-TM-103899] p 1050 N92-33407
Dynamic response of induced pressures, suckdown, and temperatures for two tandem jet STOVL configurations
[NASA-TM-103934] p 1039 N92-33581
A workstation-based evaluation of a far-field route planner for helicopters
[NASA-TM-102882] p 1051 N92-33609
On the estimation of jet-induced fountain lift and additional suckdown in hover for two-jet configurations
[NASA-TM-102268] p 1040 N92-33618
Research and technology, 1990
[NASA-TM-107967] p 1143 N92-33948

National Aeronautics and Space Administration. Goddard Inst. for Space Studies, New York, NY.
Designing a methodology for future air travel scenarios p 409 N92-19125

National Aeronautics and Space Administration. Goddard Space Flight Center, Greenbelt, MD.
Radiometric properties of the NS001 Thematic Mapper Simulator aircraft multispectral scanner p 155 A92-17110
Resonant cryogenic chopper p 294 A92-22796
Retrieval of total precipitable water over high latitude regions using radiometric measurements near 90 and 183 GHz p 505 A92-32129
The application of high spectral and spatial resolution imaging spectrometers for locating downed aircraft p 598 A92-35132
Software Engineering Laboratory (SEL) Ada performance study report
[NASA-TM-105510] p 412 N92-18125
Natural cycles, gases p 408 N92-19123
Ozone response to aircraft emissions: Sensitivity studies with two-dimensional models p 409 N92-19126
Towards understanding software: 15 years in the SEL p 413 N92-19423
Superconducting bearings with levitation control configurations
[NASA-CASE-GSC-13346-1] p 909 N92-29099

National Aeronautics and Space Administration. Hugh L. Dryden Flight Research Center, Edwards, CA.
Piloted simulation study of a balloon-assisted deployment of an aircraft at high altitude
[NASA-TM-104245] p 272 N92-15986
In-flight simulation studies at the NASA Dryden Flight Research Facility
[NASA-TM-4396] p 853 N92-29110
Experience with Ada on the F-18 High Alpha Research Vehicle Flight Test Program
[NASA-TM-104259] p 1062 N92-34039

National Aeronautics and Space Administration. Hugh L. Dryden Flight Research Facility, Edwards, CA.
X-29 high angle of attack p 111 A92-16052
Multidisciplinary modeling and simulation of a generic hypersonic vehicle
[AIAA PAPER 91-5015] p 232 A92-17813
Performance improvements of an F-15 airplane with an integrated engine-flight control system p 205 A92-20204
Pneumatic distortion compensation for aircraft surface pressure sensing devices p 218 A92-20206
Failure detection and fault management techniques for flush airdata sensing systems
[AIAA PAPER 92-0263] p 369 A92-25719
Atmospheric analysis for airdata calibration on research aircraft
[AIAA PAPER 92-0293] p 369 A92-25746
ACSYNT - A standards-based system for parametric, computer aided conceptual design of aircraft
[AIAA PAPER 92-1268] p 601 A92-33345
Combined compressive and shear buckling analysis of hypersonic aircraft sandwich panels
[AIAA PAPER 92-2487] p 586 A92-34603
Digital time series analysis for flutter test data
[AIAA PAPER 92-2103] p 589 A92-35674
Predicted and measured in-flight wing deformations of a forward-swept-wing aircraft p 548 A92-35936
Development of a pneumatic high-angle-of-attack flush airdata sensing system
[SAE PAPER 912142] p 651 A92-39980
Controls for agility research in the NASA High-Alpha Technology Program
[SAE PAPER 912148] p 661 A92-39984
The F/A-18 external burning flight test
[AIAA PAPER 91-5050] p 731 A92-44547
Water tunnels p 880 A92-45266
Update of the X-29 high-angle-of-attack program
[SAE PAPER 912006] p 783 A92-45407
Airdata calibration techniques for measuring atmospheric wind profiles p 856 A92-46792
Summary of the effects of engine throttle response on airplane formation-flying qualities
[AIAA PAPER 92-3318] p 877 A92-48902
Subsonic flight test evaluation of a performance seeking control algorithm on an F-15 airplane
[AIAA PAPER 92-3743] p 878 A92-49109
Subsonic flight test evaluation of a propulsion system parameter estimation process for the F100 engine
[AIAA PAPER 92-3745] p 866 A92-49110
Thrust stand evaluation of engine performance improvement algorithms in an F-15 airplane
[AIAA PAPER 92-3747] p 866 A92-49111
High temperature ground vibration test techniques p 980 A92-51404
A historical overview of high-temperature structural testing at the NASA Dryden Flight Research Facility p 981 A92-51407

Thermal-structural panel buckling tests
p 993 A92-51409
Effects of bleed air extraction of thrust levels on the F404-GE-400 turbofan engine
[AIAA PAPER 92-3092] p 1066 A92-54009
Getting up to speed in hypersonic structures
p 1117 A92-55127
Flight-determined stability analysis of multiple-input-multiple-output control systems
[AIAA PAPER 92-4396] p 1074 A92-55196
High angle-of-attack flush airdata sensing system
p 1064 A92-56172
Development of a pneumatic high-angle-of-attack flush airdata sensing (HI-FADS) system
[NASA-TM-104241] p 118 N92-11994
In-flight flow visualization and pressure measurements at low speeds on the NASA F-18 high alpha research vehicle p 85 N92-13009
Aircraft ground test and subscale model results of axial thrust loss caused by thrust vectoring using turning vanes
[NASA-TM-4341] p 273 N92-17071
Failure detection and fault management techniques for flush airdata sensing systems
[NASA-TM-4335] p 276 N92-17128
Linearized aerodynamic and control law models of the X-29A airplane and comparison with flight data
[NASA-TM-4356] p 381 N92-19174
High-speed civil transport flight- and propulsion-control technological issues
[NASA-CR-186015] p 482 N92-21253
Thrust vectoring for lateral-directional stability
[NASA-CR-186016] p 482 N92-21357
Variable-camber systems integration and operational performance of the AFTI/F-111 mission adaptive wing
[NASA-TM-4370] p 570 N92-22194
A preliminary look at an optimal multivariable design for propulsion-only flight control of jet-transport aircraft
[NASA-CR-186014] p 663 N92-25734
Integrated flight propulsion control research results using the NASA F-15 HIDEC Flight Research Facility
[NASA-TM-4394] p 740 N92-27379
Flight-determined benefits of integrated flight-propulsion control systems
[NASA-TM-4393] p 742 N92-27587
Effects of bleed air extraction on thrust levels on the F404-GE-400 turbofan engine
[NASA-TM-104247] p 871 N92-29425
Flight evaluation of an extended engine life mode on an F-15 airplane
[NASA-TM-104240] p 871 N92-29659
Thrust stand evaluation of engine performance improvement algorithms in an F-15 airplane
[NASA-TM-104252] p 971 N92-30518
Overview of the NASA Dryden Flight Research Facility aeronautical flight projects
[NASA-TM-104254] p 962 N92-31261
Subsonic flight test evaluation of a performance seeking control algorithm on an F-15 airplane
[NASA-TM-4400] p 973 N92-31275
In-flight leading-edge extension vortex flow-field survey measurements on a F-18 aircraft at high angle of attack
[NASA-TM-4398] p 947 N92-31276
System overview of the NASA Dryden Integrated Test Facility
[NASA-TM-104250] p 984 N92-32201
User's manual for AeroFcn: A FORTRAN program to compute aerodynamic parameters
[NASA-TM-104237] p 1133 N92-32507
Flight testing and simulation of an F-15 airplane using throttles for flight control
[NASA-TM-104255] p 1087 N92-32864
The development of an airborne information management system for flight test
[NASA-TM-104251] p 1065 N92-32866
Rapid development of the X-31 simulation to support flight-testing
[NASA-TM-104256] p 1060 N92-33149
The F-18 high alpha research vehicle: A high-angle-of-attack testbed aircraft
[NASA-TM-104253] p 1060 N92-33404
Thermal-structural test facilities at NASA Dryden
[NASA-TM-104249] p 1062 N92-34202

National Aeronautics and Space Administration. John F. Kennedy Space Center, Cocoa Beach, FL.

Expert knowledge techniques applied to the analysis of electric field mill data p 408 A92-27991
Global positioning system supported pilot's display
p 534 N92-22436

National Aeronautics and Space Administration. Lyndon B. Johnson Space Center, Houston, TX.

Aeroassist flight experiment heating-rate sensitivity study p 3 A92-10427
Unsteady incompressible flow computations with quadrilateral elements p 394 A92-26219
Computational methods for shock waves in three-dimensional supersonic flow p 611 A92-37537
Shuttle autoland status summary
[AIAA PAPER 92-1273] p 666 A92-38478
Advanced training systems for the next decade and beyond
[AIAA PAPER 92-1626] p 690 A92-38699
Space Shuttle Orbiter auxiliary power unit status
[SAE PAPER 912060] p 889 A92-45442
Issues in developing control zones for international space operations p 1141 A92-56602
Real Time Data System (RTDS) p 140 N92-12025
Aerodynamic heating on AFE due to nonequilibrium flow with variable entropy at boundary layer edge
p 183 N92-15020
Atmospheric pressure flow reactor: Gas phase chemical kinetics under tropospheric conditions without wall effects
[NASA-CASE-MSC-21384-1] p 297 N92-16243
STS-41 Space Shuttle mission report
[NASA-TM-105479] p 286 N92-16973
Advanced flight software reconfiguraton
p 287 N92-17350
Space shuttle entry terminal area energy management
[NASA-TM-104744] p 308 N92-19930
Bearing servicing tool
[NASA-CASE-MSC-21881-1] p 912 N92-30082
SATWG networked quality function deployment
p 1134 N92-33339

National Aeronautics and Space Administration. Langley Research Center, Hampton, VA.

Evaluation of an adaptive unstructured remeshing technique for integrated fluid-thermal-structural analysis
p 37 A92-10445
Viscous flow solutions for slender bodies of revolution at incidence p 4 A92-10692
Implicit flux-split Euler schemes for unsteady aerodynamic analysis involving unstructured dynamic meshes p 5 A92-11057
Evaluation of a technique to quantify microburst windshear hazard potential to aircraft p 17 A92-11379
Windshear detection and avoidance - Airborne systems survey p 17 A92-11382
Computational investigation of circular-to-rectangular transition ducts
[AIAA PAPER 91-3342] p 6 A92-11605
Euler code evaluation of a transatmospheric vehicle at supersonic speeds p 9 A92-13202
Numerical simulation of the actuation system for the ALDF's propulsion control valve p 41 A92-13204
Experimental investigation on the effect of crescent planform on lift and drag p 9 A92-13206
Wind-tunnel and flight tests of a delta-wing remotely piloted vehicle p 21 A92-13208
Wall interference assessment/correction for transonic airfoil data p 30 A92-13214
Aeroelastic analysis of wings using the Euler equations with a deforming mesh p 10 A92-13215
Helicopter local blade circulation calculations for a model rotor in forward flight using laser velocimeter measurements p 65 A92-14362
Recent rotorcraft aeroelastic testing in the Langley Transonic Dynamics Tunnel p 136 A92-14377
Development of a shock noise prediction code for high-speed helicopters - The subsonically moving shock
p 165 A92-14384
Acoustic predictions using measured pressures from a model rotor in the DNW p 165 A92-14385
Experimental investigation of helicopter vibration reduction using rotor blade aeroelastic tailoring
p 107 A92-14396
Study of external dynamic flap loads on a 6 percent B-1B model
[ASME PAPER 91-GT-236] p 125 A92-15645
Interference effects of very high bypass ratio nacelle installations on a low-wing transport
[ASME PAPER 91-GT-241] p 75 A92-15646
Turbulent flow calculations using unstructured and adaptive meshes p 153 A92-15823
On the nonlinear stability of a high-speed, axisymmetric boundary layer p 78 A92-16457
On the interaction between first- and second-mode waves in a supersonic boundary layer
p 78 A92-16462
Design and flight test of a differential GPS/inertial navigation system for approach/landing guidance
p 97 A92-16650
Mach 4 and Mach 8 axisymmetric nozzles for a high-enthalpy shock tunnel p 78 A92-16668
Supersonic reacting internal flowfields
p 155 A92-16989
Applications of an automated programming system
[AIAA PAPER 91-3767] p 231 A92-17629
Effect of nose shape on three-dimensional stagnation region streamlines and heating rates
[AIAA PAPER 91-5032] p 171 A92-17822
A comparison of cooling methods for the airframe nozzle of a single-stage-to-orbit aircraft
[AIAA PAPER 91-5036] p 210 A92-17825
Control concept for maneuvering in hypersonic flight
[AIAA PAPER 91-5055] p 203 A92-17838
Analysis of cooling systems for hypersonic aircraft
[AIAA PAPER 91-5063] p 216 A92-17843
Algebraic turbulence modeling for unstructured and adaptive meshes p 216 A92-18362
Prediction of steady and unsteady asymmetric vortical flows around circular cones p 172 A92-18372
Numerical study on using sulfur hexafluoride as a wind tunnel test gas p 216 A92-18373
Parameter insensitive control utilizing eigenspace methods p 204 A92-18615
Application of aeroservoelastic modeling using minimum-state unsteady aerodynamic approximations
p 204 A92-18622
Fatigue crack initiation and small crack growth in several airframe alloys p 212 A92-19754
Proof test and fatigue crack growth modeling on 2024-T3 aluminum alloy p 213 A92-19828
Numerical solution of the boundary-layer equations for a general aviation fuselage p 174 A92-20211
Three-dimensional thermal structural analysis of a swept cowl leading edge subjected to skewed shock-shock interference heating p 174 A92-20306
Engineering calculations of three-dimensional inviscid hypersonic flowfields p 175 A92-20378
Removal of spurious reflections from computational fluid dynamic solutions with the complex cepstrum
p 235 A92-20729
Upwind scheme for solving the Euler equations on unstructured tetrahedral meshes p 175 A92-20735
Navier-Stokes computations for aerodynamic configurations at high angles of attack
p 246 A92-21981
Doppler global velocimeter measurements of the vortical flow above a thin delta wing
[AIAA PAPER 92-0005] p 292 A92-22130
Forebody vortex flow control on the F-16C using tangential slot and jet nozzle blowing
[AIAA PAPER 92-0019] p 247 A92-22141
Aerodynamic design and optimization in one shot
[AIAA PAPER 92-0025] p 248 A92-22147
Wall interference calculation in a transonic test section including simulation of discrete slots
[AIAA PAPER 92-0032] p 249 A92-22153
Shuttle Infrared Leeside Temperature Sensing (SILTS) experiment - STS-35 and STS-40 preliminary results
[AIAA PAPER 92-0126] p 286 A92-23746
Experimental study of pylon geometries for transport aircraft
[AIAA PAPER 92-0153] p 271 A92-23768
Future experimental needs to support applied aerodynamics - A transonic perspective
[AIAA PAPER 92-0156] p 254 A92-23771
Prediction of drag at subsonic and transonic speeds using Euler methods
[AIAA PAPER 92-0169] p 255 A92-23780
Identification of aerodynamic coefficients using computational neural networks
[AIAA PAPER 92-0172] p 255 A92-23783
The dynamics and control of fluctuating pressure loads in the reattachment region of a supersonic free shear layer
[AIAA PAPER 92-0178] p 255 A92-23788
Implementation of Vigneron's streamwise pressure gradient approximation in the PNS equations
[AIAA PAPER 92-0189] p 256 A92-23798
A computational investigation of mixing and reacting flows in supersonic combustors
[AIAA PAPER 92-0626] p 278 A92-23817
On the threshold - The outlook for supersonic and hypersonic aircraft p 356 A92-24402
Forward-look wind-shear detection for microburst recovery p 378 A92-24408
Comparison of two Navier-Stokes codes for attached transonic wing flows p 309 A92-24414
Application of the LAURA code for slender-vehicle aerothermodynamics p 310 A92-24652
Structural design considerations for a Personnel Launch System p 386 A92-24668
Variable-complexity aerodynamic optimization of an HSCT wing using structural wing-weight equations
[AIAA PAPER 92-0212] p 317 A92-25685
Integrated numerical methods for hypersonic aircraft cooling systems analysis
[AIAA PAPER 92-0254] p 357 A92-25712
Three-dimensional simulation of a translating strut inlet
[AIAA PAPER 92-0270] p 317 A92-25726
Three-dimensional simulation of slender delta wing rock and divergence
[AIAA PAPER 92-0280] p 318 A92-25734

Real-time decision aiding - Aircraft guidance for wind shear avoidance
[AIAA PAPER 92-0290] p 350 A92-25743
Airborne in situ computation of the wind shear hazard index
[AIAA PAPER 92-0291] p 351 A92-25744
Atmospheric disturbance model for aircraft and space capable vehicles
[AIAA PAPER 92-0294] p 407 A92-25747
Aerodynamic characteristics of a hypersonic viscous optimized waverider at high altitudes
[AIAA PAPER 92-0306] p 320 A92-25755
An algebraic model for dissipation in supersonic boundary layers
[AIAA PAPER 92-0311] p 320 A92-25759
Multidomain spectral solutions of high-speed flows over blunt cones
[AIAA PAPER 92-0324] p 322 A92-25771
A nearly-monotone genuinely multidimensional scheme for the Euler equations
[AIAA PAPER 92-0325] p 322 A92-25772
High pressure hypervelocity electrothermal wind tunnel performance study and subscale tests
[AIAA PAPER 92-0329] p 383 A92-25776
Initial operation of the UTA shock tunnel
[AIAA PAPER 92-0331] p 383 A92-25778
Aerodynamic design of axisymmetric hypersonic wind-tunnel nozzles using least-squares/parabolized Navier-Stokes procedure
[AIAA PAPER 92-0332] p 322 A92-25779
Thermochemical nonequilibrium and radiative interactions in supersonic hydrogen-air combustion
[AIAA PAPER 92-0340] p 394 A92-25786
A numerical investigation of hydrogen combustion in Mach 2 flow
[AIAA PAPER 92-0341] p 388 A92-25787
Hypersonic flow simulations using DSMC (direct simulation Monte Carlo) p 323 A92-26216
Flow field measurement and visualization using projected smoke trails
[AIAA PAPER 92-0384] p 323 A92-26241
Aerodynamic characteristics of a propeller powered high lift semispan wing
[AIAA PAPER 92-0388] p 323 A92-26244
Design of a hybrid laminar flow control nacelle
[AIAA PAPER 92-0400] p 373 A92-26253
The effects of blowing on delta wing vortices during dynamic pitching at high angles of attack
[AIAA PAPER 92-0407] p 325 A92-26260
Quality assessment of two- and three-dimensional unstructured meshes and validation of an upwind Euler flow solver
[AIAA PAPER 92-0444] p 328 A92-26288
A fast implicit upwind solution algorithm for three-dimensional unstructured dynamic meshes
[AIAA PAPER 92-0447] p 328 A92-26291
Shock interference prediction using direct simulation Monte Carlo
[AIAA PAPER 92-0492] p 328 A92-26322
Monte Carlo simulation of reentry flows with ionization
[AIAA PAPER 92-0493] p 328 A92-26323
Monte Carlo simulation of entry in the Martian atmosphere
[AIAA PAPER 92-0494] p 329 A92-26324
Hypersonic rarefied flow past spheres including wake structure
[AIAA PAPER 92-0495] p 329 A92-26325
An approximate viscous shock layer technique for calculating nonequilibrium hypersonic flows about blunt-nosed bodies
[AIAA PAPER 92-0498] p 329 A92-26326
An engineering aerodynamic heating method for hypersonic flow
[AIAA PAPER 92-0499] p 329 A92-26327
Enthalpy damping for high Mach number Euler solutions p 330 A92-26402
New nonequilibrium turbulence model for calculating flows over airfoils p 330 A92-26403
Sound generation by a stenosis in a pipe
p 415 A92-26405
Sound transmission through a high-temperature acoustic probe tube p 415 A92-26406
Preconditioned upwind methods to solve incompressible Navier-Stokes equations p 395 A92-26436
Application of a new K-tau model to near wall turbulent flows p 395 A92-26437
Broadband shock associated noise from supersonic jets measured by a ground observer
[AIAA PAPER 92-0502] p 416 A92-26931
Calculation of compressible boundary layer flow about airfoils by a finite element/finite difference method
[AIAA PAPER 92-0524] p 332 A92-26948
The NASA Computational Aerosciences Program - Toward teraFLOPS computing
[AIAA PAPER 92-0558] p 411 A92-26968
Plasmadynamic effects in thermochemical nonequilibrium aerobrake flows
[AIAA PAPER 92-0573] p 333 A92-26980
A systematic experimental and computational investigation of a class of contoured wall fuel injectors
[AIAA PAPER 92-0625] p 374 A92-27007
Experiments on shear layer mixing at hypervelocity conditions
[AIAA PAPER 92-0628] p 396 A92-27009
Effects of nose bluntness and angle of attack on slender bodies in hypersonic flows
[AIAA PAPER 92-0638] p 334 A92-27016
An analytical approach to grid sensitivity analysis
[AIAA PAPER 92-0660] p 334 A92-27031
Target pitch angle for the microburst escape maneuver
[AIAA PAPER 92-0730] p 379 A92-27082
Three-dimensional simulation of the Denver 11 July Storm of 1988 - An intense microburst event
p 407 A92-27958
Models of space-averaged energetics of plates
p 398 A92-28031
Identification of helicopter noise using a neural network p 416 A92-28032
Transition control of instability waves over an acoustically excited flexible surface p 416 A92-28037
Aerodynamic design optimization using sensitivity analysis and computational fluid dynamics
p 340 A92-28044
High-alpha application of variable-gain output feedback control p 380 A92-28152
Acoustic characteristics and dynamic structural loading of an ASTOVL aircraft in hover
[AIAA PAPER 92-0370] p 416 A92-28190
Estimation of propulsion-induced effects on transonic flows over a hypersonic configuration
[AIAA PAPER 92-0523] p 341 A92-28197
A numerical study of the effects of geometry on the performance of a supersonic combustor
[AIAA PAPER 92-0624] p 342 A92-28213
Leading edge sweep effects in generic three-dimensional sidewall compression scramjet inlets
[AIAA PAPER 92-0674] p 343 A92-28218
Direct numerical simulation of laminar breakdown in high-speed, axisymmetric boundary layers
[AIAA PAPER 92-0742] p 343 A92-28223
Secondary instability mechanisms in compressible, axisymmetric boundary layers
[AIAA PAPER 92-0743] p 343 A92-28224
Model attitude measurements at NASA Langley Research Center
[AIAA PAPER 92-0763] p 398 A92-28226
Evaluation of parallel injector configurations for Mach 2 combustion p 376 A92-28533
Computations of multispecies mixing between scramjet nozzle flow and hypersonic freestream
p 376 A92-28534
Hydrocarbon-fueled scramjet combustor investigation
p 376 A92-28535
Thermal imaging of graphite/epoxy composite samples with fabricated defects p 491 A92-28655
A system identification model for adaptive nonlinear control p 508 A92-29248
Strain-induced extinction of hydrogen-air counterflow diffusion flames - Effects of steam, CO2, N2, and O2 additives to air
[AIAA PAPER 92-0877] p 487 A92-29639
Integrated multidisciplinary rotorcraft optimization research at the NASA Langley Research Center
p 419 A92-29673
Nonadiabatic and three-dimensional effects in compressible turbulent boundary layers
p 431 A92-31156
Linear stability of three-dimensional boundary layers over axisymmetric bodies at incidence
p 431 A92-31157
Helical-perturbation device for cylinder-wing vortex generators p 432 A92-31167
Use of finite volume schemes for transition simulation
p 432 A92-31185
Stability of a nonorthogonal stagnation flow to three-dimensional disturbances p 495 A92-31194
Secondary instabilities in compressible boundary layers p 435 A92-31639
Secondary instability of high-speed flows and the influence of wall cooling and suction
p 435 A92-31640
A six-degree-of-freedom guidance and control analysis of Mars aerocapture
[AIAA PAPER 92-0736] p 486 A92-31676
Combined effect of nose bluntness and angle of attack on slender bodies in viscous hypersonic flows
[AIAA PAPER 92-0755] p 436 A92-31680
Applications of hot-film anemometers in hypersonic shear layers
[AIAA PAPER 91-5028] p 436 A92-31687
Engineering method for aero-propulsive characteristics at hypersonic Mach numbers
[AIAA PAPER 91-5061] p 437 A92-31690
Energy-heading transients in atmospheric flight guidance for airbreathing hypersonic vehicles
[AIAA PAPER 91-5065] p 480 A92-31692
Computation of near-wake, aerobrake flowfields
p 441 A92-32181
Effects of shock wave precursors ahead of hypersonic entry vehicles p 441 A92-32182
Comparison of heating calculations with experimental data on a modified Shuttle Orbiter p 441 A92-32184
Axial compression corner flow with shock impingement p 441 A92-32196
Twenty-five years of aerodynamic research with infrared imaging p 497 A92-32232
Interference flows past cylinder-fin-sting-cavity assemblies p 442 A92-32236
Computational study of incipient leading-edge separation on a supersonic delta wing
p 442 A92-32237
Navier-Stokes study of supersonic cavity flowfield with passive control p 442 A92-32239
Low-speed flutter characteristics of some simple low-aspect-ratio delta-wing models p 460 A92-32247
Dynamics of an optimized rotor blade at off-design flight conditions p 461 A92-32250
An aerodynamic design study of a series of lifting bodies at angles of attack from 10 to 53 degrees at Mach numbers from 2.30 to 4.62 p 442 A92-32500
New, unusual and nonclassical behavior of thin-walled composite structures p 580 A92-32746
Impact of structural optimization with aeroelastic/multidisciplinary constraints on helicopter rotor design
[AIAA PAPER 92-1001] p 535 A92-33193
Preliminary results from the High Speed Airframe Integration Research project
[AIAA PAPER 92-1004] p 536 A92-33196
A study of altitude-constrained supersonic cruise transport concepts
[AIAA PAPER 92-1027] p 536 A92-33208
An interactive system for aircraft design and optimization
[AIAA PAPER 92-1190] p 600 A92-33302
Profile negotiation - A concept for integrating airborne and ground-based automation for managing arrival traffic
p 531 A92-33432
Design for validation p 601 A92-33607
Coupled analysis of independently modeled finite element subdomains
[AIAA PAPER 92-2235] p 581 A92-34289
A Rayleigh-Ritz design methodology for cutouts in composite structures
[AIAA PAPER 92-2278] p 582 A92-34297
An independent refinement and integration procedure in multiregion finite element analysis
[AIAA PAPER 92-2290] p 582 A92-34307
Flexure-torsion behavior of sheat-deformable beams with applications to aircraft wing sections
[AIAA PAPER 92-2467] p 582 A92-34357
A demonstration of passive blade twist control using extension-twist coupling
[AIAA PAPER 92-2468] p 539 A92-34358
Experimental and analytical study of the effects of floor location on response of composite fuselage frames
[AIAA PAPER 92-2473] p 539 A92-34362
Coupled 2D-3D finite element method for analysis of a skin panel with a discontinuous stiffener
[AIAA PAPER 92-2474] p 583 A92-34363
Reduced basis technique for evaluating the sensitivity coefficients of the nonlinear tire response
[AIAA PAPER 92-2530] p 583 A92-34376
Thermoviscoplastic analysis of engine cowl leading edge subjected to oscillating shock-shock interaction
[AIAA PAPER 92-2537] p 583 A92-34381
Thermoviscoplastic response of thin plates subjected to intense local heating
[AIAA PAPER 92-2538] p 584 A92-34382
The NASA/Industry Design Analysis Methods for Vibrations (DAMVIBS) Program - A government overview
[AIAA PAPER 92-2200] p 539 A92-34390
The NASA/Industry Design Analysis Methods for Vibrations (DAMVIBS) Program - Boeing helicopters airframe finite element modeling
[AIAA PAPER 92-2202] p 539 A92-34392
A new aeroelastic model for composite rotor blades with straight and swept tips
[AIAA PAPER 92-2259] p 541 A92-34414
Analytical shape sensitivities and approximations of modal response of generally laminated tapered skew plates
[AIAA PAPER 92-2391] p 585 A92-34465
Time simulation of flutter with large stiffness changes
[AIAA PAPER 92-2394] p 585 A92-34467

NACA 0012 benchmark model experimental flutter results with unsteady pressure distributions
[AIAA PAPER 92-2396] p 517 A92-34469
Computational structures technology
[AIAA PAPER 92-2442] p 585 A92-34473
Aeroelastic response and blade loads of a composite rotor in forward flight
[AIAA PAPER 92-2566] p 564 A92-34480
Parametric studies for tiltrotor aeroelastic stability in high-speed flight
[AIAA PAPER 92-2568] p 565 A92-34482
Extending a transonic small disturbance code to treat swept vertical surfaces
[AIAA PAPER 92-2503] p 518 A92-34498
Three-dimensional time-marching aeroelastic analyses using an unstructured-grid Euler method
[AIAA PAPER 92-2506] p 542 A92-34500
Fully integrated aerodynamic/dynamic optimization of helicopter rotor blades
[AIAA PAPER 92-2374] p 542 A92-34544
Optimizing tuning masses for helicopter rotor blade vibration reduction including computed airloads and comparison with test data
[AIAA PAPER 92-2376] p 542 A92-34546
Aeroelastic optimization of an advanced geometry helicopter rotor
[AIAA PAPER 92-2360] p 543 A92-34592
Dynamic characteristics of a Benchmark models program supercritical wing
[AIAA PAPER 92-2368] p 571 A92-34596
Determining design gust loads for nonlinear aircraft similarity between methods based on matched filter theory and on stochastic simulation
[AIAA PAPER 92-2369] p 518 A92-34597
Simulation of 3-D shear flows around a nozzle-afterbody at high speeds p 519 A92-34826
A summary of the Active Flexible Wing program
[AIAA PAPER 92-2080] p 565 A92-35652
Simulation and model reduction for the AFW program
[AIAA PAPER 92-2081] p 572 A92-35653
Further investigations of the aeroelastic behavior of the AFW wind-tunnel model using transonic small disturbance theory
[AIAA PAPER 92-2082] p 565 A92-35654
The multiple-function multi-input/multi-output digital controller system for the AFW wind tunnel model
[AIAA PAPER 92-2083] p 565 A92-35655
On-line analysis capabilities developed to support the AFW wind-tunnel tests
[AIAA PAPER 92-2084] p 572 A92-35656
Flutter suppression for the Active Flexible Wing - Control system design and experimental validation
[AIAA PAPER 92-2097] p 566 A92-35666
Multifunction tests of a frequency domain based flutter suppression system
[AIAA PAPER 92-2096] p 566 A92-35667
Flutter suppression digital control law design and testing for the AFW wind tunnel model
[AIAA PAPER 92-2095] p 566 A92-35668
Rolling Maneuver Load Alleviation using active controls
[AIAA PAPER 92-2099] p 566 A92-35670
An analytical and experimental investigation of flutter suppression via piezoelectric actuation
[AIAA PAPER 92-2106] p 567 A92-35677
Finite element nonlinear panel flutter with arbitrary temperatures in supersonic flow
[AIAA PAPER 92-2129] p 589 A92-35696
Large-amplitude finite element flutter analysis of composite panels in hypersonic flow
[AIAA PAPER 92-2130] p 589 A92-35697
Rotor blade-vortex interaction noise reduction and vibration using higher harmonic control
p 604 A92-35778
Numerical studies of transverse curvature effects on transonic flow stability p 524 A92-36186
Spectral solution of inviscid supersonic flows over wedges and axisymmetric cones p 524 A92-36359
Multipoint inverse airfoil design method based on conformal mapping p 610 A92-36827
Evaluation of a finite volume method for compressible shear layers p 610 A92-36834
Spatial adaptation of unstructured meshes for unsteady aerodynamic flow computations p 610 A92-36838
Characteristic-based algorithms for flows in thermochemical nonequilibrium p 670 A92-36846
Two- and three-dimensional grid generation by an algebraic homotopy procedure p 611 A92-36861
Numerical study of the effects of reverse sweep on scramjet inlet performance p 611 A92-36979
One joule output from a diode-array-pumped Nd:YAG laser with side-pumped rod geometry
p 671 A92-37188
A new finite element formulation for computational fluid dynamics. X - The compressible Euler and Navier-Stokes equations p 612 A92-37552
Oblique shock wave with sweep p 613 A92-38370
Effects of T-tabs and large deflections in double cantilever beam specimen tests p 673 A92-39009
Helicopter far-field acoustic levels as a function of reduced rotor speeds p 695 A92-39228
Laboratory testing of a high transmission loss aircraft cabin structure p 663 A92-39229
Loudness of shaped sonic booms
p 695 A92-39238
Boundary-layer receptivity due to a wall suction and control of Tollmien-Schlichting waves
p 616 A92-39333
Behavior of asymmetric unstable modes of a trailing line vortex near the upper neutral curve p 617 A92-39340
Receiver autonomous integrity monitoring (RAIM) - Techniques, performance and potential
p 638 A92-39567
Analysis for the application of hybrid laminar flow control to a long-range subsonic transport aircraft
[SAE PAPER 912113] p 617 A92-39964
Application of laminar flow control to high-bypass-ratio turbofan engine nacelles
[SAE PAPER 912114] p 618 A92-39965
Application of laminar flow control to the High Speed Civil Transport - The NASA Supersonic Laminar Flow Control Program
[SAE PAPER 912115] p 643 A92-39966
Application of linear stability theory in laminar flow design
[SAE PAPER 912116] p 618 A92-39967
Controls for agility research in the NASA High-Alpha Technology Program
[SAE PAPER 912148] p 661 A92-39984
Passive control of supersonic cavity flowfields
[SAE PAPER 912153] p 619 A92-39988
Runway drainage characteristics related to tire friction performance
[SAE PAPER 912156] p 664 A92-39991
26 x 6.6 radial-belted aircraft tire performance
[SAE PAPER 912157] p 644 A92-39992
Piloted simulator studies of the HL-20 Lifting Body
p 666 A92-40033
1991-92 AHS Technical Committee highlights - Acoustics p 696 A92-40390
Design optimization of natural laminar flow bodies in compressible flow p 701 A92-41219
Thermal management for a Mach 5 cruise aircraft using endothermic fuel p 736 A92-41225
Numerical study of vortex-dominated flows for wings at high incidence and sideslip p 702 A92-41227
Prediction of vortex shedding from forebodies with chines p 702 A92-41228
Thermal structures - Four decades of progress
p 729 A92-41239
Accurate prediction of drag using Euler methods
p 703 A92-41246
Earth aerobraking strategies for manned return from Mars p 752 A92-41535
Plasmadynamic effects in thermochemical nonequilibrium aerobrake flows p 705 A92-41538
Engineering aerodynamic heating method for hypersonic flow p 705 A92-41539
Local bridging to predict aerodynamic coefficients in hypersonic, rarefied flow p 705 A92-41541
Parallel solver for trajectory optimization search directions p 777 A92-43399
The inviscid stability of supersonic flow past heated or cooled axisymmetric bodies p 712 A92-44363
Direct simulation of re-entry flows with ionization
p 713 A92-44367
Flow establishment in a generic scramjet combustor
p 737 A92-44525
Viscous simulation method for unsteady flows past multicomponent configurations p 714 A92-44671
High-Reynolds-number test requirements in low-speed aerodynamics p 787 A92-45263
On the measurement of subsonic flow around an appended body of revolution at cryogenic conditions in the NTF p 880 A92-45265
Critical effects of downstream boundary conditions on vortex breakdown
[AIAA PAPER 92-2601] p 792 A92-45478
The effects of nozzle exit geometry on forebody vortex control using blowing
[AIAA PAPER 92-2603] p 792 A92-45480
Numerical simulation of aerothermal loads in hypersonic engine inlets due to shock impingement
[AIAA PAPER 92-2605] p 792 A92-45482
Computational study of transition front on a swept wing leading-edge model
[AIAA PAPER 92-2630] p 795 A92-45502
Transonic airfoil and wing design using Navier-Stokes codes
[AIAA PAPER 92-2651] p 797 A92-45518
A new approach for the calculation of transitional flows
[AIAA PAPER 92-2669] p 798 A92-45524
Determination of aerodynamic sensitivity coefficients based on the three-dimensional full potential equation
[AIAA PAPER 92-2670] p 798 A92-45525
An adaptive grid method for computing the high speed 3D viscous flow about a re-entry vehicle
[AIAA PAPER 92-2685] p 799 A92-45534
LDA measurements in a Mach 2 flow over a rearward facing step with staged transverse injection
[AIAA PAPER 92-2692] p 800 A92-45539
Spatial and temporal adaptive procedures for the unsteady aerodynamic analysis of airfoils using unstructured meshes
[AIAA PAPER 92-2694] p 800 A92-45540
Commercial turbofan engine exhaust nozzle flow analyses using PAB3D
[AIAA PAPER 92-2701] p 801 A92-45543
Alleviation of side force on tangent-ogive forebodies using passive porosity
[AIAA PAPER 92-2711] p 802 A92-45552
A LEX blowing technique for post-stall lateral control of trapezoidal wings
[AIAA PAPER 92-2714] p 802 A92-45553
Viscous flow past a nacelle isolated and in proximity of a flat plate
[AIAA PAPER 92-2723] p 803 A92-45560
Separation control on high Reynolds number multi-element airfoils
[AIAA PAPER 92-2636] p 806 A92-45575
Exploratory investigation of a spanwise blowing concept for tip-stall control on cranked-arrow wings
[AIAA PAPER 92-2637] p 806 A92-45576
An investigation of passive control methods for shock-induced separation at hypersonic speeds
[AIAA PAPER 92-2725] p 808 A92-45596
Measurements of the unsteady vortex flow over a wing-body at angle of attack
[AIAA PAPER 92-2729] p 808 A92-45598
High-speed propeller noise prediction - A multidisciplinary approach p 924 A92-45831
Relationship between the instability waves and noise of high-speed jets p 924 A92-45835
Aerothermodynamics of a 1.6-meter-diameter sphere in hypersonic rarefied flow p 808 A92-45840
The effect of molecular relaxation processes in air on the rise time of sonic booms p 898 A92-45883
Discrete modes and continuous spectra in supersonic boundary layers p 809 A92-46264
On-line performance evaluation of multiloop digital control systems p 873 A92-46739
Nonlinear inversion flight control for a supermaneuverable aircraft p 873 A92-46751
Temporal adaptive Euler/Navier-Stokes algorithm involving unstructured dynamic meshes
p 812 A92-46887
Hypersonic rarefied flow about a delta wing - direct simulation and comparison with experiment
p 812 A92-46892
Multiple shock-shock interference on a cylindrical leading edge p 813 A92-46899
Gortler instability and supersonic quiet nozzle design
p 813 A92-46902
Periodic trim solutions with hp-version finite elements in time p 874 A92-46931
An aeroelastic analysis with a generalized dynamic wake p 847 A92-46932
Efficient high-resolution rotor wake calculations using flow field reconstruction p 814 A92-46951
Effects of leading and trailing edge flaps on the aerodynamics of airfoil/vortex interactions
p 815 A92-46957
Aerodynamic parametric studies and sensitivity analysis for rotor blades in axial flight p 816 A92-46959
A parametric analysis of radiative structure in aerobrake shock layers
[AIAA PAPER 92-2970] p 816 A92-46985
Unstructured and adaptive mesh generation for high Reynolds number viscous flows p 816 A92-47042
Grid adaptation to multiple functions for applied aerodynamic analysis p 817 A92-47045
Gridding strategies and associated results for winged entry vehicles p 918 A92-47051
Grid generation and compressible flow computations about a high-speed civil transport configuration
p 919 A92-47055
Sensitivity of tire response to variations in material and geometric parameters p 900 A92-47128
Analysis of thermo-chemical nonequilibrium models for carbon dioxide flows
[AIAA PAPER 92-2852] p 892 A92-47835
Enhancements to viscous-shock-layer technique
[AIAA PAPER 92-2897] p 820 A92-47873

Heat transfer characteristics of hypersonic waveriders with an emphasis on leading edge effects
[AIAA PAPER 92-2920] p 821 A92-47892
Characteristics of the Shuttle Orbiter leeside flow during a reentry condition
[AIAA PAPER 92-2951] p 821 A92-47915
Thrust vectoring characteristics of the F-18 high alpha research vehicle at angles of attack from 0 to 70 deg
[AIAA PAPER 92-3095] p 877 A92-48737
Internal shock interactions in propulsion/airframe integrated three-dimensional sidewall compression scramjet inlets
[AIAA PAPER 92-3099] p 824 A92-48741
Operating characteristics at Mach 4 of an inlet having forward-swept, sidewall-compression surfaces
[AIAA PAPER 92-3101] p 863 A92-48743
High spatial resolution measurements of ram accelerator gas dynamic phenomena
[AIAA PAPER 92-3244] p 903 A92-48844
Mixing and combustion effects in a sliding-wedge ram accelerator with hydrogen injection
[AIAA PAPER 92-3251] p 890 A92-48849
Comparative investigation of multiplane thrust vectoring nozzles
[AIAA PAPER 92-3263] p 864 A92-48858
A comparative study of scramjet injection strategies for high Mach numbers flows
[AIAA PAPER 92-3287] p 904 A92-48876
KrF laser-induced OH fluorescence imaging in a supersonic combustion tunnel
[AIAA PAPER 92-3346] p 905 A92-48923
Experiments on the enhancement of compressible mixing via streamwise vorticity. I - Optical measurements
[AIAA PAPER 92-3549] p 906 A92-49064
Ignition delays, heats of combustion, and reaction rates of aluminum alkyl derivatives used as ignition and combustion enhancers for supersonic combustors
[AIAA PAPER 92-3841] p 894 A92-49134
An ultrareliable integrated digital computer for helicopters p 964 A92-49273
A fault-tolerant network architecture for integrated avionics p 965 A92-49297
A low maintenance and highly reliable fly-by-light architecture p 975 A92-49325
Least-squares/parabolized Navier-Stokes procedure for optimizing hypersonic wind-tunnel nozzles
p 980 A92-50270
Exploratory study of wall pressure fluctuations in a Mach 5, sharp fin-induced turbulent interaction
p 935 A92-50304
Crossflow vortex and transition measurements by use of multielement hot films p 935 A92-50307
Mixing studies of helium in air at high supersonic speeds p 935 A92-50310
Fourier functional analysis for unsteady aerodynamic modeling p 935 A92-50313
On central-difference and upwind schemes
p 1007 A92-50466
Aerospace plane guidance using time-scale decomposition and feedback linearization
p 984 A92-50498
Stochastic prediction techniques for wind shear hazard assessment p 1007 A92-50505
Differential GPS/inertial navigation approach/landing flight test results p 956 A92-51009
Research capabilities of the NASA Langley 8-foot high temperature tunnel p 980 A92-51403
Takeoff Performance Monitoring System display options
[AIAA PAPER 92-4138] p 967 A92-52433
High performance flight simulation at NASA Langley
[AIAA PAPER 92-4179] p 982 A92-52460
Enhancements and applications of DSMC for hypersonic rarefied flows p 939 A92-52761
Application of the DSMC method to hypersonic flow about a delta wing p 940 A92-52775
Nonlinear development and secondary instability of large-amplitude Goertler vortices in hypersonic boundary layers p 942 A92-53080
An assumed joint-Beta PDF approach for supersonic turbulent combustion
[AIAA PAPER 92-3844] p 1113 A92-54199
Comparison of frequency domain and time domain laser velocimeter signal processors p 1114 A92-54314
Problems and solutions for transition detection in cryogenic wind tunnels by infrared imaging
p 1090 A92-54319
Signal processing schemes for Doppler global velocimetry p 1115 A92-54338
Evaluation of electrolytic tilt sensors for wind tunnel model angle-of-attack (AOA) measurements
p 1116 A92-54344
A laser fluorescence anemometer system for the Langley 16- by 24-inch water tunnel
p 1092 A92-54347

The use of silicon microsensors in smart skins for aerodynamic research p 1116 A92-54348
Broadband shock associated noise from supersonic jets measured by a ground observer p 1135 A92-54909
Methodology for calculating aerodynamic sensitivity derivatives p 1024 A92-54911
Application of a parallel direct simulation Monte Carlo method to hypersonic rarefied flows
p 1024 A92-54916
Approximate Riemann solver for hypervelocity flows
p 1117 A92-54934
Getting up to speed in hypersonic structures
p 1117 A92-55127
DAMVIBS looks at rotorcraft vibration
p 1052 A92-55128
New materials drive high-performance aircraft
p 1105 A92-55134
Dynamics and control of hypersonic aeropropulsive/aeroelastic vehicles
[AIAA PAPER 92-4326] p 1073 A92-55170
Robust dynamic inversion control laws for aircraft control
[AIAA PAPER 92-4329] p 1073 A92-55173
Preliminary assessment of the robustness of dynamic inversion based flight control laws
[AIAA PAPER 92-4330] p 1074 A92-55174
Aircraft ride quality controller design using new robust root clustering theory for linear uncertain systems
[AIAA PAPER 92-4399] p 1075 A92-55199
New literal approximations for the longitudinal dynamic characteristics of flexible flight vehicles
[AIAA PAPER 92-4411] p 1075 A92-55205
Constrained control allocation
[AIAA PAPER 92-4550] p 1131 A92-55262
Applications of robust control theory - Educational implications
[AIAA PAPER 92-4559] p 1131 A92-55271
An integrated development of the equations of motion for elastic hypersonic flight vehicles
[AIAA PAPER 92-4605] p 1077 A92-55283
Aerodynamic parameters of the X-31 drop model estimated from flight-data at high angles of attack
[AIAA PAPER 92-4357] p 1080 A92-55343
Active control of asymmetric vortical flows around cones using injection and heating
[AIAA PAPER 92-4426] p 1025 A92-55350
Computation of vortex wake flows and control of their effects on trailing wings
[AIAA PAPER 92-4429] p 1025 A92-55353
Assessment of passive porosity with free and fixed separation on a tangent ogive forebody
[AIAA PAPER 92-4494] p 1081 A92-55363
Evaluation of a multigrid-based Navier-Stokes solver for aerothermodynamic computations
[AIAA PAPER 92-4563] p 1027 A92-55375
PAYCOS, a multidisciplinary sizing code for hypersonic vehicles
[AIAA PAPER 92-4564] p 1132 A92-55376
Computing high-speed flows past an oscillating cylinder near a vertical wall
[AIAA PAPER 92-4653] p 1028 A92-55397
Aeroelastic effects of spoiler surfaces on a low-aspect-ratio rectangular wing p 1030 A92-56154
Model flight tests of a spin-resistant trainer configuration p 1054 A92-56158
Application of advanced multidisciplinary analysis and optimization methods to vehicle design synthesis
p 1054 A92-56160
HiRel - Reliability/availability integrated workstation tool p 1120 A92-56257
Detailed analysis and test correlation of a stiffened composite wing panel p 1121 A92-56324
BVI impulsive noise reduction by higher harmonic pitch control - Results of a scaled model rotor experiment in the DNW p 1136 A92-56344
A quiet-flow Ludwieg tube for experimental study of high speed boundary layer transition
[AIAA PAPER 92-3885] p 1094 A92-56727
Supersonic and hypersonic quiet tunnel technology at NASA Langley
[AIAA PAPER 92-3908] p 1094 A92-56743
The ASU Transition Research Facility
[AIAA PAPER 92-3910] p 1094 A92-56744
A clean air continuous flow propulsion facility
[AIAA PAPER 92-3912] p 1094 A92-56745
Control of large cryogenic tunnels
[AIAA PAPER 92-3930] p 1096 A92-56761
Hypersonic aerodynamic/aerothermodynamic testing capabilities at Langley Research Center
[AIAA PAPER 92-3937] p 1096 A92-56767
The Langley 15-inch Mach 6 High Temperature Tunnel
[AIAA PAPER 92-3938] p 1096 A92-56768
Test description and preliminary pitot-pressure surveys for Langley Test Technique Demonstrator at Mach 6
[AIAA PAPER 92-3940] p 1096 A92-56770

Predicted aerodynamic characteristics for HL-20 lifting-body using the aerodynamic preliminary analysis system (APAS)
[AIAA PAPER 92-3941] p 1033 A92-56771
Performance data of the new free-piston shock tunnel at GALCIT
[AIAA PAPER 92-3943] p 1033 A92-56776
Effects of oxygen dissociation on hypervelocity combustion experiments
[AIAA PAPER 92-3964] p 1098 A92-56791
An approach for increasing aeroelastic divergence dynamic pressure of wind-tunnel models
[AIAA PAPER 92-4002] p 1099 A92-56825
CAN-DO, CFD-based Aerodynamic Nozzle Design and Optimization program for supersonic/hypersonic wind tunnels
[AIAA PAPER 92-4009] p 1033 A92-56832
Computational and numerical analysis of hypersonic nozzle flows with comparisons to wind tunnel calibration data
[AIAA PAPER 92-4011] p 1033 A92-56834
Buffet test in the National Transonic Facility
[AIAA PAPER 92-4032] p 1100 A92-56854
Effects of external influences in subsonic delta wing vortices
[AIAA PAPER 92-4033] p 1034 A92-56855
Numerical modeling of transonic juncture flow
[AIAA PAPER 92-4036] p 1035 A92-56858
An integrated analytical aeropropulsive/aeroelastic model for the dynamic analysis of hypersonic vehicles
[AIAA PAPER 92-4567] p 1035 A92-57034
Mass flux similarity for slotted transonic-wind-tunnel walls
[NASA-TM-4281] p 11 N92-10006
Reflection type skin friction meter
[NASA-CASE-LAR-14520-1-SB] p 11 N92-10008
Feasibility of using a knowledge-based system concept for in-flight primary flight display research
[NASA-TM-4279] p 17 N92-10017
A compensatory algorithm for the slow-down effect on constant-time-separation approaches
[NASA-TM-4285] p 23 N92-10024
Poly 1, 2, 4-triazoles via aromatic nucleophilic displacement
[NASA-CASE-LAR-14440-1] p 35 N92-10066
Dual strain gage balance system for measuring light loads
[NASA-CASE-LAR-14419-1] p 42 N92-10185
Aeroacoustics of flight vehicles: Theory and practice. Volume 1: Noise sources
[NASA-RP-1258-VOL-1] p 54 N92-10598
Static internal performance of ventral and rear nozzle concepts for short-takeoff and vertical-landing aircraft
[NASA-TP-3103] p 12 N92-10975
A comparison of airborne wake vortex detection measurements with values predicted from potential theory
[NASA-TP-3125] p 18 N92-10994
Maximized gust loads for a nonlinear airplane using matched filter theory and constrained optimization
[NASA-TM-104138] p 23 N92-11010
Model representation in the PANCOR wall interference assessment code
[NASA-TM-104152] p 31 N92-11022
Magnetic suspension and balance systems: A comprehensive, annotated bibliography
[NASA-TM-4318] p 32 N92-11030
Effects of elevated temperature on the viscoplastic modeling of graphite/polymeric composites
[NASA-TM-104160] p 35 N92-11149
Annoyance caused by advanced turboprop aircraft flyover noise: Comparison of different propeller configurations
[NASA-TP-3104] p 56 N92-11758
A new simulator for assessing subjective effects of sonic booms
[NASA-TM-104150] p 56 N92-11759
A loudness calculation procedure applied to shaped sonic booms
[NASA-TP-3134] p 56 N92-11765
Investigation of the aeroelastic stability of the AFW wind-tunnel model using CAP-TSD
[NASA-TM-104142] p 81 N92-11977
On simple aerodynamic sensitivity derivatives for use in interdisciplinary optimization
[NASA-TM-104145] p 82 N92-11985
Computer programs for the calculation of dual sting pitch and roll angles required for an articulated sting to obtain angles of attack and sideslip on wind-tunnel models
[NASA-TM-104161] p 138 N92-12007
CARS temperature measurements in a hypersonic propulsion test facility p 140 N92-12049
An analytical and experimental study to investigate flutter suppression via piezoelectric actuation
[NASA-TM-893240] p 156 N92-12173

Helicopter main-rotor speed effects: A comparison of predicted ranges of detection from the aural detection program ICHIN and the electronic detection program ARCAS
[NASA-TM-104134] p 166 N92-12598
An experimental study of the sensitivity of helicopter rotor blade tracking to root pitch adjustment in hover
[NASA-TM-4313] p 61 N92-12989
Wind tunnel investigation of the interaction and breakdown characteristics of slender wing vortices at subsonic, transonic, and supersonic speeds
[NASA-TP-3114] p 82 N92-12994
Recent progress in computational vortex-flow aerodynamics p 84 N92-13002
Effect of solidity and inclination on propeller-nacelle force coefficients
[NASA-TM-4316] p 90 N92-13038
Planform curvature effects on flutter characteristics of a wing with 56 deg leading-edge sweep and panel aspect ratio of 1.14
[NASA-TP-3116] p 115 N92-13054
Flapping inertia for selected rotor blades
[NASA-TM-104125] p 115 N92-13057
Effect of short-term exposure to stereoscopic three-dimensional flight displays on real-world depth perception
[NASA-TP-3117] p 119 N92-13065
Measurements of fuselage skin strains and displacements near a longitudinal lap joint in a pressurized aircraft
[NASA-TM-104163] p 159 N92-13455
Technical activities of the configuration aeroelasticity branch
[NASA-TM-104146] p 159 N92-13458
Detailed analysis and test correlation of a stiffened composite wing panel
[NASA-TM-104154] p 159 N92-13460
Development of an annoyance model based upon elementary auditory sensations for steady-state aircraft interior noise containing tonal components
[NASA-TM-104147] p 166 N92-13758
Inverse airfoil design procedure using a multigrid Navier-Stokes method p 193 N92-13932
A Navier-Stokes solution of Hull-ring wing-thruster interaction p 221 N92-14310
Aeroacoustics of flight vehicles: Theory and practice. Volume 2: Noise control
[NASA-RP-1258-VOL-2] p 235 N92-14779
Human response to aircraft noise p 236 N92-14780
Interior noise p 236 N92-14785
Aerothermodynamics for United States advanced programs p 184 N92-15039
The benchmark aeroelastic models program: Description and highlights of initial results
[NASA-TM-104180] p 185 N92-15049
A fast implicit upwind solution algorithm for three-dimensional unstructured dynamic meshes
[NASA-TM-104186] p 185 N92-15050
Flutter suppression via piezoelectric actuation
[NASA-TM-104120] p 197 N92-15070
Formulation of a strategy for monitoring control integrity in critical digital control systems
[NASA-TM-104158] p 206 N92-15075
Trim drag reduction concepts for horizontal takeoff single-stage-to-Orbit vehicles
[NASA-TM-102687] p 206 N92-15076
Evaluation of electrolytic tilt sensors for measuring model angle of attack in wind tunnel tests
[NASA-TM-4315] p 297 N92-16283
Application of program LAURA to perfect gas shock tube flows: A parametric study
[NASA-TM-104190] p 298 N92-17002
Experiences at Langley Research Center in the application of optimization techniques to helicopter airframes for vibration reduction
[NASA-TM-104193] p 299 N92-17033
The NASA/industry design analysis methods for vibrations (DAMVIBS) program: Accomplishments and contributions
[NASA-TM-104192] p 299 N92-17034
The multi-attribute task battery for human operator workload and strategic behavior research
[NASA-TM-104174] p 303 N92-17130
Structural dynamics division research and technology accomplishments for F.Y. 1991 and plans for F.Y. 1992
[NASA-TM-104188] p 261 N92-17509
User guide for WIACX: A transonic wind-tunnel wall interference assessment and correction procedure for the NTF
[NASA-TM-104168] p 261 N92-17547
Joint University Program for Air Transportation Research, 1990-1991
[NASA-CP-3131] p 242 N92-17984
Effect of crash pulse shape on seat stroke requirements for limiting loads on occupants of aircraft
[NASA-TP-3126] p 399 N92-18053
Large area QNDE inspection for airframe integrity
p 362 N92-18588
Recent fracture mechanics results from NASA research related to the aging commercial transport fleet
p 362 N92-18589
Thermal/structural analysis of a transpiration cooled nozzle
[NASA-TM-104184] p 401 N92-18877
A user's guide to the Langley 16- by 24-inch water tunnel
[NASA-TM-104200] p 385 N92-18956
Installation effects of wing-mounted turbofan nacelle-pylons on a 1/17-scale, twin-engine, low-wing transport model
[NASA-TP-3168] p 346 N92-19002
Ozone response to aircraft emissions: Sensitivity studies with two-dimensional models p 409 N92-19126
A weakly nonlinear theory for wave-vortex interactions in curved channel flow
[NASA-TP-3158] p 347 N92-19175
Experimental validation of structural optimization methods
[NASA-TM-104203] p 404 N92-19258
Optimizing tuning masses for helicopter rotor blade vibration reduction including computed airloads and comparison with test data
[NASA-TM-104194] p 367 N92-19846
Influence of airfoil geometry on delta wing leading-edge vortices and vortex-induced aerodynamics at supersonic speeds
[NASA-TP-3105] p 350 N92-20038
Control integration concept for hypersonic cruise-turn maneuvers
[NASA-TP-3136] p 481 N92-20195
Fully integrated aerodynamic/dynamic optimization of helicopter rotor blades
[NASA-TM-104226] p 461 N92-20417
Annoyance caused by aircraft en route noise
[NASA-TP-3165] p 512 N92-20479
Quality assessment of two- and three-dimensional unstructured meshes and validation of an upwind Euler flow solver
[NASA-TM-104215] p 444 N92-20480
Comparison of a two-dimensional adaptive-wall technique with analytical wall interference correction techniques
[NASA-TP-3132] p 444 N92-20494
Diffracted and head waves associated with waves on nonseparable surfaces
[NASA-TP-3169] p 444 N92-20545
Unsteady-pressure and dynamic-deflection measurements on an aeroelastic supercritical wing
[NASA-TM-4278] p 445 N92-20654
Simulation of real-gas effects on pressure distributions for aeroassist flight experiment vehicle and comparison with prediction
[NASA-TP-3157] p 501 N92-20677
Optimization of composite sandwich cover panels subjected to compressive loadings
[NASA-TP-3173] p 489 N92-20679
A methodology for computing uncertainty bounds of multivariable systems based on sector stability theory concepts
[NASA-TP-3166] p 482 N92-21410
Current status of computational methods for transonic unsteady aerodynamics and aeroelastic applications
[NASA-TM-104191] p 446 N92-21432
Flight deck benefits of integrated data link communication
[NASA-TP-3219] p 456 N92-21459
A historical overview of tiltrotor aeroelastic research at Langley Research Center
[NASA-TM-107578] p 502 N92-21460
Aeronautical research in the United States: Challenges for the 1990's p 420 N92-21502
Cockpit weather information needs
p 449 N92-21503
The NASA hypersonic research engine program
p 474 N92-21521
Hypersonic airbreathing propulsion/airframe integration p 474 N92-21522
Serrated trailing edges for improving lift and drag characteristics of lifting surfaces
[NASA-CASE-LAR-13870-1-CU] p 463 N92-21587
Multi-colored layers for visualizing aerodynamic flow effects
[NASA-CASE-LAR-13742-1] p 447 N92-21588
The adverse aerodynamic impact of very small leading-edge ice (roughness) buildups on wings and tails
p 451 N92-21691
A summary of NASA research on effects of heavy rain on airfoils p 452 N92-21694
The NASA Langley laminar-flow-control experiment on a swept, supercritical airfoil: Evaluation of initial perforated configuration
[NASA-TM-4309] p 525 N92-22196
Experimental study of a generic high-speed civil transport: Tabulated data
[NASA-TM-104216] p 525 N92-22232
Further investigations of the aeroelastic behavior of the AFW wind-tunnel model using transonic small disturbance theory
[NASA-TM-107576] p 526 N92-22240
Formal design and verification of a reliable computing platform for real-time control. Phase 2: Results
[NASA-TM-104196] p 602 N92-22320
Application of technology developed for flight simulation at NASA. Langley Research Center p 573 N92-22437
A graphical weather system design for the NASA transport systems research vehicle B-737
[NASA-TM-104205] p 556 N92-22504
Flow field over the wing of a delta-wing fighter model with vortex control devices at Mach 0.6 to 1.2
[NASA-TM-4296] p 526 N92-22506
NACA0012 benchmark model experimental flutter results with unsteady pressure distributions
[NASA-TM-107581] p 526 N92-22507
Hypersonic propulsion research p 561 N92-22543
A parallel-vector algorithm for rapid structural analysis on high-performance computers
[NASA-TM-102614] p 595 N92-22649
RTM: Cost-effective processing of composite structures p 578 N92-22678
Static performance of a cruciform nozzle with multiaxis thrust-vectoring and reverse-thrust capabilities
[NASA-TP-3188] p 527 N92-23095
Three-dimensional time-marching aeroelastic analyses using an unstructured-grid Euler method
[NASA-TM-107567] p 527 N92-23116
A system approach to aircraft optimization
p 550 N92-23228
Application of multidisciplinary optimization methods to the design of a supersonic transport
p 550 N92-23230
Grid generation and flow solution method for Euler equations on unstructured grids
[NASA-TM-4295] p 528 N92-23533
High angle of attack: Aerodynamics
p 528 N92-23956
Software Surface Modeling and Grid Generation Steering Committee
[NASA-CP-3143] p 691 N92-24397
An incremental strategy for calculating consistent discrete CFD sensitivity derivatives
[NASA-TM-104207] p 625 N92-24681
A simplified method for thermal analysis of a cowl leading edge subject to intense local shock-wave-interference heating
[NASA-TP-3167] p 679 N92-24797
Experimental evaluation of a flat wake theory for predicting rotor inflow-wake velocities
[NASA-TM-4334] p 630 N92-24882
Effect of blade planform variation on the forward-flight performance of small-scale rotors
[NASA-TM-4345] p 630 N92-24885
Observations on computational methodologies for use in large-scale, gradient-based, multidisciplinary design incorporating advanced CFD codes
[NASA-TM-104206] p 630 N92-24956
Longitudinal and lateral-directional aerodynamic characteristics of a wing-cone configuration at Mach numbers from 2.5 to 4.5
[NASA-TM-4337] p 630 N92-24977
Mechanical design of a rotary balance system for NASA. Langley Research Center's vertical spin tunnel
p 664 N92-25090
Comparison of jet plume shape predictions and plume influence on sonic boom signature
[NASA-TP-3172] p 631 N92-25133
Radar multipath study for rain-on-radome experiments at the Aircraft Landing Dynamics Facility
[NASA-TM-101657] p 680 N92-25137
The natural flow wing-design concept
[NASA-TP-3193] p 631 N92-25202
Assessment of potential aerodynamic benefits from spanwise blowing at the wing tip
[NASA-TM-107847] p 631 N92-25261
The NASA/industry Design Analysis Methods for Vibrations (DAMVIBS) Program: A government overview
[NASA-TM-107579] p 680 N92-25267
Wind-tunnel static and free-flight investigation of high-angle-of-attack stability and control characteristics of a model of the EA-6B airplane
[NASA-TP-3194] p 631 N92-25276
An engineering method for interactive inviscid-boundary layers in three-dimensional hypersonic flows
[NASA-TM-107838] p 632 N92-25279
Multifunction tests of a frequency domain based flutter suppression system
[NASA-TM-107615] p 662 N92-25607

Measurements of fluctuating pressure in a rectangular cavity in transonic flow at high Reynolds numbers
[NASA-TM-4363] p 633 N92-25752
Computational Structures Technology for Airframes and Propulsion Systems
[NASA-CP-3142] p 683 N92-25911
Progress in integrated analysis with adaptive unstructured meshing p 683 N92-25914
CSM activities at the NASA Langley Research Center p 683 N92-25916
Overview of mechanics of materials branch activities in the computational structures area p 684 N92-25917
Analysis and design technology for high-speed aircraft structures p 684 N92-25918
A high angle of attack inviscid shuttle orbiter computation
[NASA-TM-107606] p 685 N92-25964
A static investigation of the thrust vectoring system of the F/A-18 high-alpha research vehicle
[NASA-TM-4359] p 633 N92-25967
Aircraft optimization by a system approach: Achievements and trends
[NASA-TM-107622] p 650 N92-25995
Stress-strain analysis of a (0/90)sub 2 symmetric titanium matrix laminate subjected to a generic hypersonic flight profile
[NASA-TM-107584] p 685 N92-26128
Computational method to predict thermodynamic, transport, and flow properties for the modified Langley 8-foot high-temperature tunnel
[NASA-TM-4374] p 767 N92-27193
Effect of collector configuration on test section turbulence levels in an open-jet wind tunnel
[NASA-TM-4333] p 750 N92-27670
Aircraft drag reduction p 717 N92-27709
International Symposium on Magnetic Suspension Technology, part 2
[NASA-CP-3152-PT-2] p 753 N92-27788
Propulsion simulator for magnetically suspended wind tunnel models p 750 N92-27801
Present status of the MIT/NASA Langley 6-inch MSBS p 750 N92-27802
Current status of computational methods for transonic unsteady aerodynamics and aeroelastic applications p 718 N92-27937
Unstructured-grid methods development for unsteady aerodynamic and aeroelastic analyses p 718 N92-27938
Investigation of the aeroelastic stability of the AFW wind-tunnel model using CAP-TSD p 721 N92-27955
The benchmark aeroelastic models program: Description and highlights of initial results p 721 N92-27960
NASA/DOD Aerospace Knowledge Diffusion Research Project. Paper 13: The information-seeking habits and practices of engineers
[NASA-TM-107931] p 782 N92-28114
NASA/DOD Aerospace Knowledge Diffusion Research Project. Paper 14: An analysis of the technical communications practices reported by Israeli and US aerospace engineers and scientists
[NASA-TM-107924] p 782 N92-28183
An analysis of combustion studies in shock expansion tunnels and reflected shock tunnels
[NASA-TP-3224] p 895 N92-28374
Integrating aerodynamics and structures in the minimum weight design of a supersonic transport wing
[NASA-TM-107586] p 850 N92-28435
Multidisciplinary design and optimization
[AGARD-PAPER-2] p 851 N92-28473
Calculation of unsteady transonic flows with mild separation by viscous-inviscid interaction
[NASA-TP-3197] p 827 N92-28477
Application of piloted simulation to high-angle-of-attack flight-dynamics research for fighter aircraft p 886 N92-28551
Natural flow wing
[NASA-CASE-LAR-14281-1] p 829 N92-28729
Spatial and temporal adaptive procedures for the unsteady aerodynamic analysis of airfoils using unstructured meshes
[NASA-TM-107635] p 831 N92-29445
Aerodynamic design optimization using sensitivity analysis and computational fluid dynamics
[NASA-CASE-LAR-14815-1-CU] p 910 N92-29830
Active thermal isolation for temperature responsive sensors
[NASA-CASE-LAR-14612-1] p 911 N92-29954
Helicopter low-speed yaw control
[NASA-CASE-LAR-14219-1] p 879 N92-30025
Combined load test apparatus for flat panels
[NASA-CASE-LAR-14698-1] p 911 N92-30028
Apparatus for elevated temperature compression or tension testing of specimens
[NASA-CASE-LAR-14775-1] p 912 N92-30099
The 1991 International Conference on Aging Aircraft and Structural Airworthiness
[NASA-CP-3160] p 912 N92-30106
Fracture mechanics research at NASA related to the aging commercial transport fleet p 913 N92-30110
Damaged stiffened shell research at NASA, Langley Research Center p 914 N92-30115
Thermal QNDE detection of airframe disbonds p 914 N92-30118
Validation of three-dimensional incompressible spatial direct numerical simulation code: A comparison with linear stability and parabolic stability equation theories for boundary-layer transition on a flat plate
[NASA-TP-3205] p 943 N92-30295
Method of measuring cross-flow vortices by use of an array of hot-film sensors
[NASA-CASE-LAR-14824-1-SB] p 998 N92-30390
Progress in unstructured-grid methods development for unsteady aerodynamic applications
[NASA-TM-107643] p 944 N92-30393
Two-dimensional aerodynamic characteristics of several polygon-shaped cross-sectional models applicable to helicopter fuselages
[NASA-TP-3233] p 944 N92-30394
A gridless Euler/Navier-Stokes solution algorithm for complex two-dimensional applications
[NASA-TM-107631] p 944 N92-30570
Implicit upwind-Euler solution algorithms for unstructured-grid applications
[NASA-TM-107645] p 945 N92-30691
Research and technology, 1991. Langley Research Center
[NASA-TM-4331] p 1013 N92-30733
Trajectory fitting in function space with application to analytic modeling of surfaces
[NASA-TP-3232] p 945 N92-30747
On-line analysis capabilities developed to support the AFW wind-tunnel tests
[NASA-TM-107651] p 961 N92-30752
Delaunay triangulation and computational fluid dynamics meshes
[NASA-TM-107663] p 1010 N92-30907
Direct simulation of high-speed mixing layers
[NASA-TP-3186] p 945 N92-30909
A demonstration of passive blade twist control using extension-twist coupling
[NASA-TM-107642] p 1001 N92-31155
An analytical and experimental investigation of flutter suppression via piezoelectric actuation
[NASA-TM-107653] p 962 N92-31174
Preliminary subsonic aerodynamic model for simulation studies of the HL-20 lifting body
[NASA-TM-4302] p 978 N92-31175
CFD methods development considerations for unsteady aerodynamic analysis
[NASA-TM-107644] p 947 N92-31239
Design and experimental validation of a flutter suppression controller for the active flexible wing
[NASA-TM-4381] p 979 N92-31240
High Reynolds number test of the Boeing TR77 airfoil in the Langley 0.3-meter transonic cryogenic tunnel
[NASA-TM-4189] p 947 N92-31246
A summary of the active flexible wing program
[NASA-TM-107655] p 962 N92-31264
Stagnation-point heat-transfer rate predictions at aeroassist flight conditions
[NASA-TP-3208] p 1001 N92-31281
Flutter suppression digital control law design and testing for the AFW wind-tunnel model
[NASA-TM-107652] p 962 N92-31350
Rolling maneuver load alleviation using active controls
[NASA-TM-107654] p 962 N92-31351
Wind tunnel aerodynamic characteristics of a transport-type airfoil in a simulated heavy rain environment
[NASA-TP-3184] p 948 N92-31532
Data reduction formulas for the 16-foot transonic tunnel: NASA Langley Research Center, revision 2
[NASA-TM-107646] p 984 N92-31900
Time simulation of flutter with large stiffness changes
[NASA-TM-107650] p 963 N92-32111
A method for designing blended wing-body configurations for low wave drag
[NASA-TP-3261] p 1036 N92-32480
Eighth DOD/NASA/FAA Conference on Fibrous Composites in Structural Design, part 1
[NASA-CP-3087-PT-1] p 1106 N92-32513
A Protection And Detection Surface (PADS) for damage tolerance p 1107 N92-32523
Global/local methods research using the CSM testbed p 1107 N92-32528
The multiple-function multi-input/multi-output digital controller system for the AFW wind-tunnel model
[NASA-TM-107600] p 1060 N92-32536
Residual strength of repaired graphite/epoxy laminates after 5 years of outdoor exposure p 1108 N92-32577
Analysis of data from a DO-178A software development process p 1134 N92-32880
Fourth Aircraft Interior Noise Workshop
[NASA-CP-10103] p 1136 N92-32948
Active control of interior noise in a large scale cylinder using piezoelectric actuators p 1137 N92-32958
Flight service environmental effects on composite materials and structures p 1110 N92-33054
Computational methods for global/local analysis
[NASA-TM-107591] p 1125 N92-33104
Building vibrations induced by noise from rotorcraft and propeller aircraft flyovers
[NASA-TM-104170] p 1138 N92-33160
Isothermal aging of IM7/8320 and IM7/5260
[NASA-TM-107666] p 1110 N92-33423
Advanced techniques in reliability model representation and solution
[NASA-TP-3242] p 1134 N92-33483
Applications of a direct/iterative design method to complex transonic configurations
[NASA-TP-3234] p 1039 N92-33484
Simulation model of a twin-tail, high performance airplane
[NASA-TM-107601] p 1088 N92-33537
A nozzle internal performance prediction method
[NASA-TP-3221] p 1040 N92-33625
Experimental study of a generic high-speed civil transport
[NASA-TM-4382] p 1040 N92-33631
Survey and analysis of research on supersonic drag-due-to-lift minimization with recommendations for wing design
[NASA-TP-3202] p 1040 N92-33656
Effect of afterbody geometry on aerodynamic characteristics of isolated nonaxisymmetric afterbodies at transonic Mach numbers
[NASA-TP-3236] p 1041 N92-33706
Application of magnitude estimation scaling to the assessment of subjective loudness response to simulated sonic booms
[NASA-TM-107657] p 1138 N92-33719
High-Speed Research: Sonic Boom, volume 1
[NASA-CP-3172] p 1061 N92-33874
Preliminary results from the White Sands Missile Range sonic boom propagation experiment p 1140 N92-33884
Subjective loudness response to simulated sonic booms p 1140 N92-33885
Finite difference time domain grid generation from AMC helicopter models
[NASA-TM-107679] p 1128 N92-34017
Computational algorithms for increased control of depth-viewing volume for stereo three-dimensional graphic displays
[NASA-TM-4379] p 1065 N92-34109
Pressure measurements on a rectangular wing with a NACA0012 airfoil during conventional flutter
[NASA-TM-104211] p 1042 N92-34147
Advanced subsonic transport approach noise: The relative contribution of airframe noise
[NASA-TM-104112] p 1140 N92-34148
Vaporizing particle velocimeter
[NASA-CASE-LAR-14685-1] p 1042 N92-34172
Effects of constraint on crack growth under aircraft spectrum loading
[NASA-TM-107677] p 1128 N92-34178
Parametric investigation of single-expansion-ramp nozzles at Mach numbers from 0.60 to 1.20
[NASA-TP-3240] p 1042 N92-34193
Pilot-pressure probe for measuring pressure in a hypersonic wind tunnel
[NASA-CASE-LAR-14232-1] p 1102 N92-34213

National Aeronautics and Space Administration. Lewis Research Center, Cleveland, OH.

Parallel computation of aerodynamic influence coefficients for aeroelastic analysis on a transputer network p 53 A92-12367
Slush hydrogen (SLH2) technology development for application to the National Aerospace Plane (NASP) p 144 A92-13432
Advanced ice protection systems test in the NASA Lewis Icing Research Tunnel p 108 A92-14406
Ongoing development of a computer jobstream to predict helicopter main rotor performance in icing conditions p 65 A92-14407
Intermetallic and ceramic matrix composites for 815 to 1370 C (1500 to 2500 F) gas turbine engine applications p 141 A92-15128
Optical measurements of unducted fan flutter
[ASME PAPER 91-GT-19] p 147 A92-15510
A viscous flow study of shock-boundary layer interaction, radial transport, and wake development in a transonic compressor
[ASME PAPER 91-GT-69] p 68 A92-15539
The role of tip clearance in high-speed fan stall
[ASME PAPER 91-GT-83] p 69 A92-15550

The effect of steady aerodynamic loading on the flutter stability of turbomachinery blading
[ASME PAPER 91-GT-130] p 71 A92-15574
Wind tunnel wall effects in a linear oscillating cascade
[ASME PAPER 91-GT-133] p 72 A92-15576
NASA low-speed centrifugal compressor for 3-D viscous code assessment and fundamental flow physics research
[ASME PAPER 91-GT-140] p 72 A92-15580
Reliability analysis of a structural ceramic combustion chamber
[ASME PAPER 91-GT-155] p 123 A92-15591
Aerodynamics and heat transfer investigations on a high Reynolds number turbine cascade
[ASME PAPER 91-GT-157] p 148 A92-15593
Euler flow predictions for an oscillating cascade using a high resolution wave-split scheme
[ASME PAPER 91-GT-198] p 74 A92-15623
CFD analysis of jet mixing in low NO(x) flametube combustors
[ASME PAPER 91-GT-217] p 124 A92-15634
Heat transfer in rotating serpentine passages with trips normal to the flow
[ASME PAPER 91-GT-265] p 151 A92-15663
The numerical simulation of a high-speed axial flow compressor
[ASME PAPER 91-GT-272] p 75 A92-15669
Deterministic blade row interactions in a centrifugal compressor stage
[ASME PAPER 91-GT-273] p 75 A92-15670
NDE of advanced turbine engine components and materials by computed tomography
[ASME PAPER 91-GT-287] p 152 A92-15681
Cascade flutter analysis with transient response aerodynamics p 154 A92-15972
Unsteady blade-surface pressures on a large-scale advanced propeller - Prediction and data
p 80 A92-17178
Transmission overhaul and component replacement predictions using Weibull and renewal theory
p 155 A92-17201
Eigenvalue calculation procedure for an Euler/Navier-Stokes solver with application to flows over airfoils p 170 A92-17429
Heat transfer measurements from a smooth NACA 0012 airfoil p 218 A92-20215
Roughness effects on heat transfer from a NACA 0012 airfoil p 219 A92-20217
Unsteady Euler analysis of the flowfield of a propfan at an angle of attack p 242 A92-21070
Studies of the effects of curvature on dilution jet mixing p 290 A92-21079
Factors influencing the effective spray cone angle of pressure-swirl atomizers p 295 A92-23300
Aerodynamics of loaded cascades in subsonic flows subject to unsteady three-dimensional vortical disturbances
[AIAA PAPER 92-0146] p 253 A92-23762
The Baldwin-Lomax model for separated and wake flows using the entropy envelope concept
[AIAA PAPER 92-0148] p 253 A92-23764
A study on vortex flow control of inlet distortion in the re-engined 727-100 center inlet duct using computational fluid dynamics
[AIAA PAPER 92-0152] p 253 A92-23767
Hot gas environment around STOVL aircraft in ground proximity. II - Numerical study p 371 A92-24403
Investigation of the diffuser flow quality in an icing research wind tunnel p 382 A92-24406
Improved nonequilibrium viscous shock-layer scheme for hypersonic blunt-body flowfields p 310 A92-24653
A viscoplastic model for single crystals
p 391 A92-24717
A viscoplastic theory for anisotropic materials
[ONERA, TP NO. 1992-90] p 391 A92-24721
LEWICE/E - An Euler based ice accretion code
[AIAA PAPER 92-0037] p 316 A92-25676
Prediction of ice accretion on a swept NACA 0012 airfoil and comparisons to flight test results
[AIAA PAPER 92-0043] p 316 A92-25677
Pressure wave propagation studies for oscillating cascades
[AIAA PAPER 92-0145] p 316 A92-25682
A new unsteady mixing model to predict NO(x) production during rapid mixing in a dual-stage combustor
[AIAA PAPER 92-0233] p 372 A92-25696
Analysis of an advanced ducted propeller subsonic inlet
[AIAA PAPER 92-0274] p 318 A92-25728
Unsteady wing surface pressures in the wake of a propeller
[AIAA PAPER 92-0277] p 318 A92-25731
Mechanisms resulting in accreted ice roughness
[AIAA PAPER 92-0297] p 351 A92-25750
Low-to-high altitude predictions of three-dimensional ablative reentry flowfields
[AIAA PAPER 92-0366] p 394 A92-26227
Unsteady blade pressures on a propfan at takeoff - Euler analysis and flight data
[AIAA PAPER 92-0376] p 372 A92-26234
Numerical investigation of performance degradation of wings and rotors due to icing
[AIAA PAPER 92-0412] p 325 A92-26264
Finite wing aerodynamics with simulated glaze ice
[AIAA PAPER 92-0414] p 325 A92-26265
Automatic grid generation for iced airfoil flowfield predictions
[AIAA PAPER 92-0415] p 326 A92-26266
A turbulence model for iced airfoils and its validation
[AIAA PAPER 92-0417] p 326 A92-26267
Computation of supersonic jet mixing noise for an axisymmetric CD nozzle using k-epsilon turbulence model
[AIAA PAPER 92-0500] p 414 A92-26328
A survey of the broadband shock associated noise prediction methods
[AIAA PAPER 92-0501] p 415 A92-26930
Screech noise source structure of a supersonic rectangular jet
[AIAA PAPER 92-0503] p 331 A92-26932
Unsteady flowfield simulation of ducted prop-fan configurations
[AIAA PAPER 92-0521] p 332 A92-26946
An unsteady Euler scheme for the analysis of ducted propellers
[AIAA PAPER 92-0522] p 332 A92-26947
Numerical analysis of a thermal deicer
[AIAA PAPER 92-0527] p 357 A92-26950
The NASA Computational Aerosciences Program - Toward teraFLOPS computing
[AIAA PAPER 92-0558] p 411 A92-26968
The formation and structure of plasma wakes behind large high-voltage space platforms in ionosphere
[AIAA PAPER 92-0577] p 407 A92-26984
Crossing shock wave turbulent boundary layer interactions - Variable angle and shock generator length geometry effects at Mach 3
[AIAA PAPER 92-0636] p 334 A92-27014
Results of an icing test on a NACA 0012 airfoil in the NASA Lewis Icing Research Tunnel
[AIAA PAPER 92-0647] p 334 A92-27021
Transient behavior of supersonic flow through inlets
p 340 A92-28043
Unsteady aerodynamic interaction effects on turbomachinery blade life and performance
[AIAA PAPER 92-0149] p 341 A92-28186
Acoustic characteristics and dynamic structural loading of an ASTOVL aircraft in hover
[AIAA PAPER 92-0370] p 416 A92-28190
Calculations of hot gas ingestion for a STOVL aircraft model
[AIAA PAPER 92-0385] p 374 A92-28191
Helium bubble flow visualization of the spanwise separation on a NACA 0012 with simulated glaze ice
[AIAA PAPER 92-0413] p 341 A92-28192
Numerical experiments on a new class of nonoscillatory schemes
[AIAA PAPER 92-0421] p 341 A92-28193
Aeroelastic analysis of advanced propellers using an efficient Euler solver
[AIAA PAPER 92-0488] p 341 A92-28194
Euler solutions for an unbladed jet engine configuration
[AIAA PAPER 92-0544] p 398 A92-28201
The structure and development of streamwise vortex arrays embedded in a turbulent boundary layer
[AIAA PAPER 92-0551] p 342 A92-28204
Comparison of two-dimensional and three-dimensional droplet trajectory calculations in the vicinity of finite wings
[AIAA PAPER 92-0645] p 342 A92-28215
Navier-Stokes solution of transonic cascade flows using nonperiodic C-type grids p 344 A92-28523
Three-dimensional viscous analysis of a Mach 5 inlet and comparison with experimental data
p 344 A92-28526
Flow in a ventral nozzle for short takeoff and vertical landing aircraft p 376 A92-28538
Integrated flight/propulsion control design for a STOVL aircraft using H-infinity control design techniques
p 476 A92-29093
Integrated flight/propulsion control specifications for systems with two-way coupling p 477 A92-29117
IMPAC - An integrated methodology for propulsion and airframe control p 477 A92-29118
Decentralized hierarchical partitioning of centralized integrated controllers p 477 A92-29119
A framework for the analysis of airframe/engine interactions and integrated flight/propulsion control
p 478 A92-29120
A Lyapunov based nonlinear control scheme for stabilizing a basic compression system using a close-coupled control valve p 508 A92-29316
Characteristics of a future aeronautical satellite communications system
[AIAA PAPER 92-2058] p 453 A92-29889
ACTS aeronautical experiments
[AIAA PAPER 92-2042] p 485 A92-29956
Analysis of iced wings
[AIAA PAPER 92-0416] p 423 A92-29972
An efficient finite element method for aircraft de-icing problems
[AIAA PAPER 92-0532] p 459 A92-31670
An improved PNS scheme for predicting complex three-dimensional hypersonic flows
[AIAA PAPER 92-0753] p 436 A92-31679
Design and analysis of reengine Boeing 727-100 center inlet S duct by a reduced Navier-Stokes code
[AIAA PAPER 92-1221] p 517 A92-33320
Addition curing thermosets endcapped with 4-amino (2.2) paracyclophane p 577 A92-33918
Structural tailoring/analysis for hypersonic components - Executive system development
[AIAA PAPER 92-2471] p 583 A92-34360
Ceramics and ceramic matrix composites - Aerospace potential and status
[AIAA PAPER 92-2445] p 577 A92-34474
Unsteady transonic Euler solutions using finite elements
[AIAA PAPER 92-2504] p 518 A92-34499
Analysis of cascades using a two dimensional Euler aeroelastic solver
[AIAA PAPER 92-2370] p 556 A92-34598
A numerical classical flutter analysis of advanced propellers
[AIAA PAPER 92-2118] p 557 A92-35687
Finite element Euler calculations of unsteady transonic cascade flows
[AIAA PAPER 92-2120] p 520 A92-35689
A low-power, high-efficiency Ka-band TWTA
p 671 A92-38163
A review of computational/experimental methodology developments in aeroacoustics p 695 A92-39241
Flight-vehicle materials, structures, and dynamics - Assessment and future directions. Vol. 3 - Ceramics and ceramic-matrix composites
[ISBN 0-7918-0661-8] p 668 A92-39852
Monolithic ceramics p 668 A92-39854
Recent manufacturing advances for spiral bevel gears
[SAE PAPER 912229] p 674 A92-40024
A study of three dimensional turbulent boundary layer separation and vortex flow control using the reduced Navier Stokes equations p 621 A92-40105
Effect of tabs on the evolution of an axisymmetric jet
p 656 A92-40151
Domain-decomposition algorithm applied to multielement airfoil grids p 703 A92-41261
Measurements in a leading-edge separation bubble due to a simulated airfoil ice accretion p 723 A92-41262
Modern developments in shear flow control with swirl
p 703 A92-41265
Effect of acoustic excitation on stalled flows over an airfoil p 703 A92-41267
Renormalization group based algebraic turbulence model for three-dimensional turbomachinery flows
p 703 A92-41268
Ionospheric plasma flow over large high-voltage space platforms. I - Ion-plasma-time scale interactions of a plate at zero angle of attack. II - The formation and structure of plasma wake p 779 A92-41359
Wavelength-multiplexed fiber-optic position encoder for aircraft control systems p 734 A92-42602
Unsteady airloading panel method for propfans
p 780 A92-44512
Numerical analysis of flow through oscillating cascade sections p 713 A92-44513
Row-by-row off-design performance calculation method for turbines p 737 A92-44514
The F/A-18 external burning flight test
[AIAA PAPER 91-5050] p 731 A92-44547
Hot gas ingestion characteristics and flow visualization of a vectored thrust STOVL concept
p 860 A92-45316
Integrated flight/propulsion control for supersonic STOVL aircraft p 872 A92-45320
Experimental and analytical study of close-coupled ventral nozzles for ASTOVL aircraft p 861 A92-45325
Experimental investigation of the flowfield of an oscillating airfoil
[AIAA PAPER 92-2622] p 793 A92-45494
LDV measurements on a rectangular wing with a simulated glaze ice accretion
[AIAA PAPER 92-2690] p 800 A92-45537
Navier-Stokes analysis and experimental data comparison of compressible flow in a diffusing S-duct
[AIAA PAPER 92-2699] p 800 A92-45541

Design and analysis of vortex generators on reengined Boeing 727-100QF center inlet S-duct by a reduced Navier-Stokes code
[AIAA PAPER 92-2700] p 800 A92-45542
The flip flop nozzle extended to supersonic flows
[AIAA PAPER 92-2724] p 803 A92-45561
Surface and flow field measurements in a symmetric crossing shock wave/turbulent boundary layer flow
[AIAA PAPER 92-2634] p 806 A92-45574
Fiber optic controls for aircraft engines - Issues and implications p 856 A92-46244
Potential for integrated optical circuits in advanced aircraft with fiber optic control and monitoring systems
p 856 A92-46246
Predicted pressure distribution on a prop-fan blade through Euler analysis p 810 A92-46791
Noise of two high-speed model counter-rotation propellers at takeoff/approach conditions
p 925 A92-46799
Development of an efficient analysis for high Reynolds number inviscid/viscid interactions in cascades
[AIAA PAPER 92-3073] p 823 A92-48723
Airfoil wake and linear theory gust response including sub and superresonant flow conditions
[AIAA PAPER 92-3074] p 823 A92-48724
A fast, uncoupled, compressible, two-dimensional, unsteady boundary layer algorithm with separation for engine inlets
[AIAA PAPER 92-3082] p 823 A92-48729
Interface of an uncoupled boundary layer algorithm with an inviscid core flow algorithm for unsteady supersonic engine inlets
[AIAA PAPER 92-3083] p 823 A92-48730
Mixing in the dome region of a staged gas turbine combustor
[AIAA PAPER 92-3089] p 903 A92-48734
Experimental study of cross-stream mixing in a rectangular duct
[AIAA PAPER 92-3090] p 903 A92-48735
Comparative study of turbulence models in predicting hypersonic inlet flows
[AIAA PAPER 92-3098] p 824 A92-48740
Computational analysis of ramjet engine inlet interaction
[AIAA PAPER 92-3102] p 824 A92-48744
An experimental investigation of high-aspect-ratio cooling passages
[AIAA PAPER 92-3154] p 890 A92-48780
Investigation of three-dimensional flow field in a turbine including rotor/stator interaction. I - Design development and performance of the research facility
[AIAA PAPER 92-3325] p 883 A92-48908
Investigation of three-dimensional flow field in a turbine including rotor/stator interaction. II - Three-dimensional flow field at the exit of the nozzle
[AIAA PAPER 92-3326] p 826 A92-48909
A simplified reaction mechanism for prediction of NO(x) emissions in the combustion of hydrocarbons
[AIAA PAPER 92-3340] p 894 A92-48919
Advanced Rotorcraft Transmission program summary
[AIAA PAPER 92-3363] p 905 A92-48936
Boeing Helicopters Advanced Rotorcraft Transmission (ART) Program summary of component tests
[AIAA PAPER 92-3364] p 905 A92-48937
Advanced Rotorcraft Transmission (ART) Program summary
[AIAA PAPER 92-3365] p 905 A92-48938
Advanced Rotorcraft Transmission (ART) - Component test results
[AIAA PAPER 92-3366] p 905 A92-48939
Supersonic jet mixing enhancement by 'delta-tabs'
[AIAA PAPER 92-3548] p 826 A92-49063
A computational study of advanced exhaust system transition ducts with experimental validation
[AIAA PAPER 92-3794] p 907 A92-49126
Analytical and experimental studies of heat pipe radiation cooling of hypersonic propulsion systems
[AIAA PAPER 92-3809] p 867 A92-49128
Full field flow visualization and computer-aided velocity measurements in a bank of cylinders in a wind tunnel
p 991 A92-50040
Direct evaluation of aeroacoustic theory in a jet
p 1010 A92-50296
Time domain numerical calculations of unsteady vortical flows about a flat plate airfoil p 936 A92-50473
Piloted evaluation of an integrated propulsion and flight control simulator
[AIAA PAPER 92-4178] p 960 A92-52459
Kinetic theory model for the flow of a simple gas from a three-dimensional axisymmetric nozzle
p 937 A92-52730
Three-dimensional Navier-Stokes heat transfer predictions for turbine blade rows
[AIAA PAPER 92-3068] p 1020 A92-54003
A comparison of the calculated and experimental off-design performance of a radial flow turbine
[AIAA PAPER 92-3069] p 1020 A92-54004
Increased heat transfer to elliptical leading edges due to spanwise variations in the freestream momentum - Numerical and experimental results
[AIAA PAPER 92-3070] p 1020 A92-54005
FREPS - A forced response prediction system for turbomachinery blade rows
[AIAA PAPER 92-3072] p 1130 A92-54006
Detonation duct gas generator demonstration program
[AIAA PAPER 92-3174] p 1066 A92-54011
Full Navier-Stokes calculations on the installed F/A-18 inlet at a high angle of attack
[AIAA PAPER 92-3175] p 1020 A92-54012
Application of computational fluid dynamics to the study of vortex flow control for the management of inlet distortion
[AIAA PAPER 92-3177] p 1020 A92-54013
Navier-Stokes analysis of three-dimensional unsteady flows inside turbine stages
[AIAA PAPER 92-3211] p 1021 A92-54016
Preliminary dynamic tests of a flight-type ejector
[AIAA PAPER 92-3261] p 1066 A92-54020
Applied analytical combustion/emissions research at the NASA Lewis Research Center - A progress report
[AIAA PAPER 92-3338] p 1067 A92-54025
Summary highlights of the Advanced Rotorcraft Transmission (ART) program
[AIAA PAPER 92-3362] p 1051 A92-54026
The VRT gas turbine combustor - Phase II
[AIAA PAPER 92-3471] p 1067 A92-54035
Modal simulation of gearbox vibration with experimental correlation
[AIAA PAPER 92-3494] p 1112 A92-54036
Experimental investigation of an ejector-powered free-jet facility
[AIAA PAPER 92-3569] p 1090 A92-54058
Full Navier-Stokes analysis of a two-dimensional mixer/ejector nozzle for noise suppression
[AIAA PAPER 92-3570] p 1067 A92-54059
Flow induction by pressure forces
[AIAA PAPER 92-3571] p 1067 A92-54060
An experimental investigation of the flow in a diffusing S-duct
[AIAA PAPER 92-3622] p 1021 A92-54090
A finite-volume numerical method to calculate fluid forces and rotordynamic coefficients in seals
[AIAA PAPER 92-3712] p 1113 A92-54132
Wind tunnel performance results of swirl recovery vanes as tested with an advanced high speed propeller
[AIAA PAPER 92-3770] p 1068 A92-54159
Unsteady blade pressures on a propfan - Predicted and measured compressibility effects
[AIAA PAPER 92-3774] p 1023 A92-54161
Experimental performance of three design factors for ventral nozzles for SSTOVL aircraft
[AIAA PAPER 92-3789] p 1069 A92-54168
Internal reversing flow in a tailpipe offtake configuration for SSTOVL aircraft
[AIAA PAPER 92-3790] p 1069 A92-54169
Use of an approximate similarity principle for the thermal scaling of a full-scale thrust augmenting ejector
[AIAA PAPER 92-3792] p 1069 A92-54171
Aeroelastic modal characteristics of mistuned blade assemblies - Mode localization and loss of eigenstructure p 1117 A92-54921
Turning up the heat on aircraft structures
p 1052 A92-55131
Propulsion system performance resulting from an Integrated Flight/Propulsion Control design
[AIAA PAPER 92-4602] p 1069 A92-55281
Analysis of airframe/engine interactions for a STOVL aircraft with integrated flight/propulsion control
[AIAA PAPER 92-4623] p 1052 A92-55300
Surface heat transfer and flow properties of vortex arrays induced artificially and from centrifugal instabilities
p 1121 A92-56371
Flow quality studies of the NASA Lewis Research Center 8- by 6-foot supersonic/9- by 15-foot Low Speed Wind Tunnel
[AIAA PAPER 92-3916] p 1095 A92-56748
Laser-driven hypersonic air-breathing propulsion simulator
[AIAA PAPER 92-3922] p 1095 A92-56753
Small engine components test facility compressor testing cell at NASA Lewis Research Center
[AIAA PAPER 92-3980] p 1098 A92-56806
Advanced nozzle and engine components test facility
[AIAA PAPER 92-3993] p 1099 A92-56816
Engine component instrumentation development facility at NASA Lewis Research Center
[AIAA PAPER 92-3995] p 1099 A92-56818
Calibration of hemispherical-head flow angularity probes
[AIAA PAPER 92-4005] p 1122 A92-56828
Description of a pressure measurement technique for obtaining surface static pressures of a radial turbine
[AIAA PAPER 92-4006] p 1123 A92-56829
Transonic turbine blade cascade testing facility
[AIAA PAPER 92-4034] p 1101 A92-56856
Experimental unsteady pressures on an oscillating cascade with supersonic leading edge locus
[AIAA PAPER 92-4035] p 1035 A92-56857
Effect of a simulated glaze ice shape on the aerodynamic performance of a rectangular wing
[AIAA PAPER 92-4042] p 1035 A92-56861
Technical evaluation report, AGARD Fluid Dynamics Panel Symposium on Effects of Adverse Weather on Aerodynamics
[NASA-TM-105192] p 2 N92-10002
Turbomachinery noise p 54 N92-10601
Noise from turbulent shear flows p 55 N92-10603
Combustion and core noise p 55 N92-10607
Results from computational analysis of a mixed compression supersonic inlet
[NASA-TM-104475] p 12 N92-10976
Real-time fault diagnosis for propulsion systems
[NASA-TM-105303] p 26 N92-11017
Euler solutions for an unbladed jet engine configuration
[NASA-TM-105332] p 44 N92-11328
Computers in aeronautics and space research at the Lewis Research Center
[NASA-TM-105096] p 53 N92-11642
Vortex generator design for aircraft inlet distortion as a numerical optimization problem p 194 N92-13959
A study on vortex flow control on inlet distortion in the re-engined 727-100 center inlet duct using computational fluid dynamics
[NASA-TM-105321] p 179 N92-13998
LEWICE/E: An Euler based ice accretion code
[NASA-TM-105389] p 179 N92-14001
Analysis of an advanced ducted propeller subsonic inlet
[NASA-TM-105393] p 179 N92-14002
The aerodynamic effect of fillet radius in a low speed compressor cascade
[NASA-TM-105347] p 202 N92-14063
Rotordynamic Instability Problems in High-Performance Turbomachinery, 1990
[NASA-CP-3122] p 222 N92-14346
Computation of supersonic jet mixing noise for an axisymmetric CD nozzle using k-epsilon turbulence model
[NASA-TM-105338] p 237 N92-14795
A survey of the broadband shock associated noise prediction methods
[NASA-TM-105365] p 237 N92-14797
Wind tunnel investigation of vortex flows on F/A-18 configuration at subsonic through transonic speed
[NASA-TP-3111] p 179 N92-14968
Results of an Icing test on a NACA 0012 airfoil in the NASA Lewis Icing Research Tunnel
[NASA-TM-105374] p 185 N92-15051
A turbulence model for iced airfoils and its validation
[NASA-TM-105373] p 186 N92-15052
Tribology needs for future space and aeronautical systems
[NASA-TM-104525] p 214 N92-15191
Analysis of aircraft engine blade subject to ice impact
[NASA-TM-105336] p 229 N92-15402
Structural Dynamics Branch research and accomplishments for FY 1990
[NASA-TM-103747] p 230 N92-15406
Prediction of ice accretion on a swept NACA 0012 airfoil and comparisons to flight test results
[NASA-TM-105368] p 258 N92-15968
Supersonic propulsion simulation by incorporating component models in the large perturbation inlet (LAPIN) computer code
[NASA-TM-105193] p 279 N92-15993
Brush seal leakage performance with gaseous working fluids at static and low rotor speed conditions
[NASA-TM-105400] p 297 N92-16265
Engine panel seals for hypersonic engine applications: High temperature leakage assessments and flow modelling
[NASA-TM-105260] p 298 N92-16336
Detailed noise measurements on the SR-7A propeller: Tone behavior with helical tip Mach number
[NASA-TM-105206] p 304 N92-16705
Safety considerations in testing a fuel-rich aeropropulsion gas generator
[NASA-TM-105258] p 279 N92-17061
High-temperature durability considerations for HSCT combustor
[NASA-TP-3162] p 289 N92-17070
Viscous three-dimensional calculations of transonic fan performance
[NASA-TM-103800] p 242 N92-17346

Experimental ice shape and performance characteristics for a multi-element airfoil in the NASA Lewis Icing Research Tunnel
[NASA-TM-105380] p 261 N92-17347
Experiments and analysis concerning the use of external burning to reduce aerospace vehicle transonic drag
[NASA-TM-105397] p 279 N92-17546
A survey of instabilities within centrifugal pumps and concepts for improving the flow range of pumps in rocket engines
[NASA-TM-105439] p 387 N92-18280
An evaluation of some alternative approaches for reducing fan tone noise
[NASA-TM-105356] p 416 N92-18282
Semi-empirical model for prediction of unsteady forces on an airfoil with application to flutter
[NASA-TM-105414] p 346 N92-18760
Unsteady-flow-field predictions for oscillating cascades
[NASA-TM-105283] p 348 N92-19437
Calculations of hot gas ingestion for a STOVL aircraft model
[NASA-TM-105437] p 350 N92-19993
NASA's rotary engine technology enablement program: 1983-1991
[NASA-TM-105562] p 378 N92-20033
Heat transfer in rotating serpentine passages with trips skewed to the flow
[NASA-TM-105581] p 499 N92-20235
Performance tests of a cryogenic hybrid magnetic bearing for turbopumps
[NASA-TM-105627] p 473 N92-20523
Development of a steady potential solver for use with linearized, unsteady aerodynamic analyses
[NASA-TM-105288] p 473 N92-20525
Design and evaluation of a robust dynamic neurocontroller for a multivariable aircraft control problem
[NASA-TM-105579] p 481 N92-20586
Flow studies in close-coupled ventral nozzles for STOVL aircraft
[NASA-TM-102554] p 445 N92-20934
Airbreathing combined cycle engine systems
p 475 N92-21523
Icing simulation: A survey of computer models and experimental facilities p 450 N92-21684
Simulation of iced wing aerodynamics
p 450 N92-21686
Model rotor icing tests in the NASA. Lewis Icing Research Tunnel p 450 N92-21688
Aeropropulsion 1987
[NASA-CP-3049] p 559 N92-22510
Impact and promise of NASA aeropropulsion technology p 559 N92-22511
High-temperature polymer matrix composites
p 578 N92-22513
Creep and fatigue research efforts on advanced materials p 593 N92-22514
Development of a new generation of high-temperature composite materials p 578 N92-22515
Ceramics for engines p 578 N92-22517
Aeropropulsion structures p 559 N92-22518
Determining structural performance
p 560 N92-22519
Life prediction technologies for aeronautical propulsion systems p 560 N92-22520
Inlets, ducts, and nozzles p 593 N92-22523
Research sensors p 594 N92-22526
Optical measurement systems p 594 N92-22527
Fiber optics for controls p 570 N92-22529
Directions in propulsion control p 560 N92-22530
Overview of the subsonic propulsion technology session p 560 N92-22531
Small engine technology programs
p 560 N92-22532
Rotorcraft transmissions p 560 N92-22533
The NASA aircraft icing research program
p 549 N92-22534
Aircraft engine hot section technology: An overview of the HOST Project p 561 N92-22535
Overview of NASA PTA propfan flight test program
p 561 N92-22536
NASA thrusts in high-speed aeropropulsion research and development: An overview p 561 N92-22538
Supersonic STOVL propulsion technology program: An overview p 561 N92-22539
Propulsion challenges and opportunities for high-speed transport aircraft p 561 N92-22540
Supersonic throughflow fans for high-speed aircraft
p 561 N92-22541
Research and technology, 1991
[NASA-TM-105320] p 516 N92-22659
Inflatable traversing probe seal p 595 N92-22692
Design and performance of controlled-diffusion stator compared with original double-circular-arc stator
[NASA-TP-2852] p 562 N92-22863
NASA's aircraft icing technology program
[NASA-TM-104518] p 527 N92-23105
Comparison of two-dimensional and three-dimensional droplet trajectory calculations in the vicinity of finite wings
[NASA-TM-105617] p 596 N92-23154
Effects of chemical equilibrium on turbine engine performance for various fuels and combustor temperatures
[NASA-TM-105399] p 562 N92-23254
Coupled multi-disciplinary simulation of composite engine structures in propulsion environment
[NASA-TM-105575] p 596 N92-23267
Development of a new flux splitting scheme
p 596 N92-23352
High temperature dynamic engine seal technology development
[NASA-TM-105641] p 596 N92-23435
Effects of turbine cooling assumptions on performance and sizing of high-speed civil transport
[NASA-TM-105610] p 562 N92-23537
A two-dimensional Euler solution for an unbladed jet engine configuration
[NASA-TM-105329] p 597 N92-23560
Interactive solution-adaptive grid generation procedure
[NASA-TM-105432] p 528 N92-23563
Vinyl capped addition polyimides
[NASA-CASE-LEW-15027-2] p 579 N92-24053
A multiblock grid generation technique applied to a jet engine configuration p 692 N92-24428
Workshop on Engineering Turbulence Modeling
[NASA-CP-10088] p 678 N92-24514
A two-dimensional Euler solution for an unbladed jet engine configuration p 627 N92-24861
Supersonic jet mixing enhancement by delta-tabs
[NASA-TM-105664] p 630 N92-24958
Description of a pressure measurement technique for obtaining surface static pressures of a radial turbine
[NASA-TM-105643] p 680 N92-24959
Advanced Rotorcraft Transmission (ART) program summary
[NASA-TM-105665] p 680 N92-24984
The future challenge for aeropropulsion
[NASA-TM-105613] p 658 N92-25164
Engine component instrumentation development facility at NASA Lewis Research Center
[NASA-TM-105644] p 665 N92-25449
Workshop on Grid Generation and Related Areas
[NASA-CP-10089] p 659 N92-25712
Grid management p 632 N92-25713
TCGRID: A three dimensional C-grid generator for turbomachinery p 659 N92-25716
TIGGERC: Turbomachinery interactive grid generator energy distributor and restart code p 659 N92-25719
Multiblock grid generation for jet engine configurations
p 659 N92-25720
Cartesian based grid generation/adaptive mesh refinement p 682 N92-25722
Activities for numerical propulsion systems simulation program p 692 N92-25726
Integrating aerodynamic surface modeling for computational fluid dynamics with computer aided structural analysis, design, and manufacturing
p 682 N92-25727
Computational Fluid Dynamics
[NASA-CP-10078] p 660 N92-25808
Development of new flux splitting schemes
p 682 N92-25809
A new Lagrangian method for real gases at supersonic speed p 633 N92-25814
Study of shock-induced combustion using an implicit TVD scheme p 669 N92-25816
Computer codes developed and under development at Lewis p 692 N92-25913
A brief overview of computational structures technology related activities at NASA Lewis Research Center
p 683 N92-25915
A comparison of predicted and measured inlet distortion flows in a subsonic axial inlet flow compressor rotor
[NASA-TM-105427] p 633 N92-26104
Transonic turbine blade cascade testing facility
[NASA-TM-105646] p 667 N92-26129
A parametric numerical study of mixing in a cylindrical duct
[NASA-TM-105695] p 738 N92-26553
Gear tooth stress measurements of two helicopter planetary stages
[NASA-TM-105651] p 764 N92-26555
Full-scale transmission testing to evaluate advanced lubricants
[NASA-TM-105668] p 764 N92-26560
CFD mixing analysis of jets injected from straight and slanted slots into confined crossflow in rectangular ducts
[NASA-TM-105699] p 738 N92-26561
Helium bubble flow visualization of the spanwise separation on a NACA 0012 with simulated glaze ice
[NASA-TM-105742] p 714 N92-26612
Use of an approximate similarity principle for the thermal scaling of a full-scale thrust augmenting ejector
[NASA-TM-105724] p 739 N92-26613
Interface of an uncoupled boundary layer algorithm with an inviscid core flow algorithm for unsteady supersonic engine inlets
[NASA-TM-105684] p 739 N92-27037
Turbulent heat flux measurements in a transitional boundary layer
[NASA-TM-105623] p 716 N92-27377
Ceramic composites: Enabling aerospace materials
[NASA-TM-105599] p 756 N92-27378
A critical evaluation of a three-dimensional Navier-Stokes method as a tool to calculate transonic flows inside a low-aspect-ratio compressor
p 768 N92-27459
Viscous three-dimensional calculations of transonic fan performance p 768 N92-27467
Experimental study of cross-stream mixing in a rectangular duct
[NASA-TM-105694] p 742 N92-27652
A fast, uncoupled, compressible, two-dimensional, unsteady boundary layer algorithm with separation for engine inlets
[NASA-TM-105686] p 770 N92-27653
Experimental performance of three design factors for ventral nozzles for SSTOVL aircraft
[NASA-TM-105697] p 742 N92-27669
Analysis and modification of a single-mesh gear fatigue rig for use in diagnostic studies
[NASA-TM-105416] p 773 N92-27879
Comparative study of turbulence models in predicting hypersonic inlet flows
[NASA-TM-105720] p 722 N92-28102
Internal reversing flow in a tailpipe offtake configuration for SSTOVL aircraft
[NASA-TM-105698] p 868 N92-28418
Full Navier-Stokes analysis of a two-dimensional mixer/ejector nozzle for noise suppression
[NASA-TM-105715] p 868 N92-28419
Application of face-gear drives in helicopter transmissions
[NASA-TM-105655] p 908 N92-28434
Flow quality studies of the NASA Lewis Research Center 8- by 6-foot supersonic/9- by 15-foot low speed wind tunnel
[NASA-TM-105417] p 887 N92-28673
Experimental and computational ice shapes and resulting drag increase for a NACA 0012 airfoil
[NASA-TM-105743] p 828 N92-28674
Results of a low power ice protection system test and a new method of imaging data analysis
[NASA-TM-105745] p 828 N92-28696
Laser anemometer measurements and computations in an annular cascade of high turning core turbine vanes
[NASA-TP-3252] p 830 N92-28980
Electromechanical systems with transient high power response operating from a resonant AC link
[NASA-TM-105716] p 870 N92-28985
A 4-spot time-of-flight anemometer for small centrifugal compressor velocity measurements
[NASA-TM-105717] p 909 N92-29105
Dynamics of a split torque helicopter transmission
[NASA-TM-105681] p 910 N92-29136
Applied analytical combustion/emissions research at the NASA Lewis Research Center
[NASA-TM-105731] p 890 N92-29343
Contingency power for a small turboshaft engine by using water injection into turbine cooling air
[NASA-TM-105680] p 871 N92-29661
Experimental investigation of the flowfield of an oscillating airfoil
[NASA-TM-105675] p 833 N92-30182
Three-dimensional laser window formation
[NASA-RP-1280] p 984 N92-30307
Lewis icing research tunnel test of the aerodynamic effects of aircraft ground deicing/anti-icing fluids
[NASA-TP-3238] p 952 N92-30395
Development of a full-scale transmission testing procedure to evaluate advanced lubricants
[NASA-TP-3265] p 998 N92-30396
Small engine components test facility compressor testing cell at NASA Lewis Research Center
[NASA-TM-105685] p 982 N92-30508
A simplified dynamic model of the T700 turboshaft engine
[NASA-TM-105805] p 1009 N92-30898
Navier-Stokes analysis and experimental data comparison of compressible flow within ducts
[NASA-TM-105796] p 972 N92-30972
Preliminary dynamic tests of a flight-type ejector
[NASA-TM-105814] p 972 N92-30998

Trends in aeropropulsion research and their impact on engineering education
[NASA-TM-105682] p 972 N92-31172
NASA. Lewis Research Center supersonic throughflow fan program
[NASA-TM-103248] p 972 N92-31250
Preliminary evaluation of adhesion strength measurement devices for ceramic/titanium matrix composite bonds
[NASA-TM-105803] p 932 N92-31267
Experimental testing of prototype face gears for helicopter transmissions
[NASA-TM-105434] p 1002 N92-31349
A general numerical model for wave rotor analysis
[NASA-TM-105740] p 1002 N92-31484
Modal simulation of gearbox vibration with experimental correlation
[NASA-TM-105702] p 1002 N92-31485
Supersonic Throughflow Fan Test Facility at NASA. Lewis Research Center
[NASA-TP-3038] p 983 N92-31640
A parameter optimization approach to controller partitioning for integrated flight/propulsion control application
[NASA-TM-105826] p 979 N92-32241
A critical evaluation of a three-dimensional Navier-Stokes CFD as a tool to design supersonic turbine stages p 1124 N92-32268
Liquid lubricants for advanced aircraft engines
[NASA-TM-104531] p 1109 N92-32863
Navier-Stokes analysis and experimental data comparison of compressible flow in a diffusing S-duct
[NASA-TM-105683] p 1072 N92-33746
A graphical user-interface for propulsion system analysis
[NASA-TM-105696] p 1134 N92-33894
Piloted evaluation of an integrated propulsion and flight control simulator
[NASA-TM-105797] p 1088 N92-34107
Application of computational fluid dynamics to the study of vortex flow control for the management of inlet distortion
[NASA-TM-105672] p 1128 N92-34112
Analysis of iced wings
[NASA-TM-105773] p 1042 N92-34144
Method of reducing drag in aerodynamic systems
[NASA-CASE-LEW-14791-1] p 1043 N92-34243

National Aeronautics and Space Administration. Marshall Space Flight Center, Huntsville, AL.
Experimental results and numerical modeling of solidification during aircraft high-g arcs
[AIAA PAPER 92-0843] p 493 A92-29609
Convective flow analysis on the KC-135 aircraft
[AIAA PAPER 92-0844] p 493 A92-29610
Diagonal implicit scheme for computing flows with finite rate chemistry p 488 A92-32253
Pressure oscillation in the leakage annulus between a shrouded impeller and its housing due to impeller-discharge-pressure disturbances p 580 A92-32942
The effectiveness of Coriolis dampening of convection during aircraft high-g arcs p 581 A92-33847
Study of weld offset in longitudinally welded SSME HPFTP inlet
[AIAA PAPER 92-2305] p 586 A92-34525
Aerobrake aerothermodynamic environment predictions in support of the Aeroassist Flight Experiment
[TABES PAPER 91-278] p 519 A92-34683
High altitude airborne remote sensing mission using the advanced microwave precipitation radiometer (AMPR) p 574 A92-34893
Influence of air velocity on the habit of ice crystal growth from the vapor p 668 A92-38111
Laminar hypersonic flow over a compression using the HANA code
[AIAA PAPER 92-2896] p 820 A92-47872
Solution of the Burnett equations for hypersonic flows near the continuum limit
[AIAA PAPER 92-2922] p 821 A92-47894
Application of an unsteady Navier-Stokes solver to transonic turbine design p 935 A92-50273
Hypersonic merged layer blunt body flows with wakes p 939 A92-52757
Limit cycle vibrations in turbomachinery
[NASA-TP-3181] p 211 N92-14108
High altitude solar power platform
[NASA-TM-103578] p 506 N92-21546
Welding technology transfer task/laser based weld joint tracking system for compressor girth welds p 593 N92-22426

National Aeronautics and Space Administration. Pasadena Office, CA.
Multicomponent gas sorption Joule-Thomson refrigeration
[NASA-CASE-NPO-17569-1-CU] p 228 N92-15203
Three-stage sorption type cryogenic refrigeration system and method employing heat regeneration
[NASA-CASE-NPO-18366-1-CU] p 300 N92-17674
Microwave temperature profiler for clear air turbulence prediction
[NASA-CASE-NPO-18115-1-CU] p 916 N92-29148

National Aeronautics and Space Administration. Wallops Flight Facility, Wallops Island, VA.
NASA test flights with increased flight stress indices
[AIAA PAPER 91-3665] p 20 A92-11012
Determination of balloon drag
[AIAA PAPER 91-3666] p 5 A92-11013
Structural behavior of scientific balloons - Finite element simulation and verification
[AIAA PAPER 91-3668] p 20 A92-11015
Overpressurized zero pressure balloon system
[AIAA PAPER 91-3671] p 14 A92-11018
The NASA long duration balloon project
[AIAA PAPER 91-3680] p 15 A92-11024
Observation and comparison of rainfall measured at a high sample rate p 505 A92-32073
Agreements/subagreements applicable to Wallops, 12 Nov. 1991 p 575 N92-22598

National Aerospace Lab., Amsterdam (Netherlands).
A knowledge-based assistant for diagnosis in aircraft maintenance p 61 N92-12538
Modeling and numerical simulation of vortex flow in aerodynamics
[AD-B163670L] p 83 N92-12997
Analysis of results of an Euler-equation method applied to leading-edge vortex flow p 84 N92-13000
An experimental study of the flow over a sharp-edged delta wing at subsonic and transonic speeds p 85 N92-13011
Review of aerodynamic design in the Netherlands p 193 N92-13929
Monitoring load experience of individual aircraft
[NLR-TP-90084-U] p 196 N92-15065
CAR 88: A method to calculate subsonic and supersonic, steady and unsteady, potential flow about complex configurations
[NLR-TR-88154-U] p 400 N92-18221
NLR experience with high velocity burner rig testing, 1979-1989
[NLR-TP-89152-U] p 385 N92-18415
Model incidence measurement using SAAB ELOPTOPOS system
[NLR-TP-89182-U] p 385 N92-18416
Analysis of unsteady force, pressure, and flow-visualization data for a pitching straked wing model at high angles of attack p 364 N92-18784
Development of nonlinear real-time helicopter simulation using a blade element method
[NLR-TP-90115-U] p 381 N92-18893
WP 4b compressible flow simulation: Information System for flow simulation based on the Navier-Stokes equation (ISNaS). Requirements grid generation for the ISNaS compressible flow solver
[NLR-TR-88103-U] p 405 N92-19490
Estimating the probability of vertical overlap from the paired aircraft data obtained in the European vertical data collection using the program DGLDiF
[NLR-TR-88108-U] p 356 N92-19491
Inviscid drag prediction for transonic transport wings using a full-potential method
[NLR-TP-89365-U] p 444 N92-20473
Investigation of a semi-empirical method to predict limit cycle oscillations of modern fighter aircraft
[NLR-TP-90087-U] p 481 N92-20475
Numerical simulation of vortical flow over a delta wing at subsonic and transonic speeds
[NLR-TP-90029-U] p 444 N92-20498
Determination of limitations for helicopter ship-borne operations p 465 N92-21965
Evaluation of the applicability of Helmholtz resonators for low frequency acoustic liners
[PB92-138544] p 605 N92-23588
Panel methods for aerodynamic analysis and design p 552 N92-23955
Domain modeling and grid generation for multi-block structured grids with application to aerodynamic and hydrodynamic configurations p 691 N92-24411
NLR inviscid transonic unsteady loads prediction methods in aeroelasticity p 720 N92-27947
Development of a method to predict transonic limit cycle oscillation characteristics of fighter aircraft p 746 N92-27958
Aircraft simulation and pilot proficiency: From surrogate flying towards effective training p 884 N92-28532
Hyperbolic grid generation with BEM source terms
[NLR-TP-90334-U] p 923 N92-28635
A simple and low cost system to measure delay times in pneumatic systems
[NLR-TP-90174-U] p 859 N92-28644
The use of load enhancement factors in the certification of composite aircraft structures
[NLR-TP-90068-U] p 852 N92-28649
Some longitudinal handling qualities design guidelines for active control technology transport aircraft
[NLR-TP-90129-U] p 878 N92-28652
Response of helicopters to gusts
[NLR-TP-90159-U] p 879 N92-28653
Potential applications of laser Doppler anemometry for in-flight measurements
[NLR-TP-90163-U] p 859 N92-28654
Application of knowledge-based systems for diagnosis of aircraft systems
[NLR-TP-90192-U] p 837 N92-28655
Analysis of results of an Euler-equation method applied to leading-edge vortex flow
[NLR-TP-90368-U] p 827 N92-28657
Comparison of LDA and LTA applications for propeller tests in wind tunnels
[NLR-MP-88031-U] p 827 N92-28658
Calculation of unsteady subsonic and supersonic flow about oscillating wings and bodies by new panel methods
[NLR-TP-89119-U] p 827 N92-28659
Constrained spanload optimization for minimum drag of multi-lifting-surface configurations
[NLR-TP-89126-U] p 828 N92-28660
The windtunnel as a tool for laminar flow research
[NLR-TP-90145-U] p 887 N92-28661
Instrumentation requirements for laminar flow research in the NLR high speed wind tunnel HST
[NLR-TP-89158-U] p 887 N92-28669
LAH-main rotor model test at the DNW
[NLR-TP-90305-U] p 852 N92-28687
Atmospheric turbulence spectra and correlation functions
[NLR-TP-89217-U] p 915 N92-28689
Development and validation of a characteristic boundary condition for a cell-centered Euler method
[NLR-TP-90144-U] p 828 N92-28692
Turbulence modeling: Survey of activities in Belgium and the Netherlands, and appraisal of the status and a view on the prospects
[NLR-TP-90184-U] p 908 N92-28694
Experimental validation of a line-duct acoustics model including flow
[NLR-TP-90223-U] p 927 N92-28695
Wave drag determination in the transonic full-potential flow code MATRICS
[NLR-TP-90062-U] p 828 N92-28709
Diffuser casing upgrade for an advanced turbofan
[NLR-TP-90097-U] p 870 N92-28711
Boundary conditions for Euler equations at internal block faces of multi-block domains using local grid refinement
[NLR-TP-90134-U] p 908 N92-28712
Flow gradient corrections on hot-wire measurements using an X-wire probe
[NLR-TP-90255-U] p 829 N92-28713
S-76B certification for vertical take-off and landing operations from confined areas
[NLR-TP-90286-U] p 852 N92-28714
NARSIM: A real-time simulator for air traffic control research
[NLR-TP-90147-U] p 888 N92-29204
Short cracks and durability analysis of the Fokker 100 wing/fuselage structure
[NLR-TP-90336-U] p 910 N92-29603
Hyperbolic grid generation control by panel methods
[NLR-TP-91061-U] p 924 N92-29604
European studies to investigate the feasibility of using 1000 ft vertical separation minima above FL 290. Part 1: Overview of organisation, techniques employed, and conclusions
[NLR-TP-91062-U-PT-1] p 841 N92-29605
Application of VME-technology on an airborne data link processor unit
[NLR-MP-88040-U] p 841 N92-29615
Results of a flight simulator experiment to establish handling quality guidelines for the design of future transport aircraft
[NLR-MP-88044-U] p 854 N92-29616
On the optimization of windshear warning and guidance systems
[NLR-TP-90196-U] p 837 N92-29703
Evaluation of measured-boundary-condition methods for 3D subsonic wall interference
[NLR-TR-88072-U] p 832 N92-29884
A method for computing the 3-dimensional flow about wings with leading-edge vortex separation. Part 2: Description of computer program VORSEP
[NLR-TR-86006-U] p 833 N92-29916
Examination of aircraft warning and caution lights after shock testing
[NLR-TP-89284-U] p 952 N92-30474

Modeling and numerical simulation of vortex flow in aerodynamics
[NLR-TP-91154-U] p 1037 N92-32673
New concepts for multi-block grid generation for flow domains around complex aerodynamic configurations
[NLR-TP-91046-U] p 1037 N92-32730
An experimental study of the flow over a sharp-edged delta wing at subsonic and transonic speeds
[NLR-TP-91117-U] p 1037 N92-32732
Integration of wall interference assessment and wall adaptation
[NLR-TP-91119-U] p 1101 N92-32734
Development of new flight procedures for the Microwave Landing System (MLS)
[NLR-TP-91156-U] p 1047 N92-32830
Global/local interlaminar stress analysis of a grid-stiffened composite panel
[NASA-CR-190822] p 1125 N92-33139
Activities report of the National Aerospace Laboratory
[ETN-92-92053] p 1143 N92-33694

National Aerospace Lab., Emmeloord (Netherlands).
Ageing aircraft research in the Netherlands
p 838 N92-30129

National Aerospace Lab., Tokyo (Japan).
Numerical simulation of hypersonic viscous flow for the design of H-2 orbiting plane (HOPE-2)
[NAL-TR-1093] p 11 N92-10009
Development of digital/optical rotary position transducer
[NAL-TR-1106] p 29 N92-10028
Unsteady aerodynamic calculations for general configurations by the double-point method
[NAL-TR-1101T] p 12 N92-10980
Weight evaluation and sensitivity analysis for space plane. Part 2: TSTO
[NAL-TM-602-PT-2] p 287 N92-17754
Results of measured temperature distribution on an adiabatic wing model with radiation thermometer
[NAL-TM-610] p 261 N92-17755
Improvement of data processing system for gust wind tunnel data acquisition part: System conversion from off-line to on-line processing
[NAL-TM-611] p 285 N92-17756
Discussion for possibility of some aerodynamic ground effect craft
[NAL-TM-619] p 300 N92-17757
Hydrogen fueled subsonic-ram-combustor model tests for an air-turbo-ram engine
[NAL-TR-1064T] p 280 N92-17855
Identification of the stability and control derivatives of a DLC-flap system for VSRA
[NAL-TR-1116] p 283 N92-17917
Ultra High Speed Numerical Wind Tunnel (UHSNWT) initiative at National Aerospace Laboratory numerical simulator - second generation
[NAL-TR-1108] p 384 N92-18037
Investigation on freezing and sticking phenomena of slush on airplane surfaces when taxiing on the ground and the succeeding take-off run phase
[NAL-TR-1026] p 352 N92-18182
An improved method for simulating supersonic flow past a wedge shaped body
[NAL-TR-1097] p 345 N92-18239
A preliminary flight test on a basic performance of the flight research airplane Do 228: Velocity vs glide path angle
[NAL-TM-613] p 359 N92-18482
Proceedings of the Seminar on Investigation and Control of Boundary-Layer Transition
[NAL-SP-11] p 400 N92-18483
An approach to flow field measurement by Laser 2-Focus velocimeter (L2F) in gust wind tunnel
[NAL-TM-617] p 346 N92-18484
Vibration tests of long plate structural model
[NAL-TM-625] p 400 N92-18485
Evaluation of NACA0012 airfoil test results in the NAL two-dimensional transonic wind tunnel
[NAL-TR-1109T] p 445 N92-21287
Development of wall pressure measuring apparatus for an existing transonic wind tunnel test section
[NAL-TM-565] p 573 N92-23778
Turbine drive system of the high pressure LOX turbopump test facility
[DE92-783191] p 680 N92-25342
Study of the NAL's 0.1 x 0.1 m magnetic suspension and balance system
[NAL-TM-623] p 665 N92-25365
Static aeroelastic analysis of ACT wind tunnel model aircraft
[NAL-TM-624] p 632 N92-25366
Vibration tests and structural modeling of an aircraft model for active control technology experiments
[NAL-TM-626] p 662 N92-25401
The fibre optic three dimensional laser two focus velocimeter for the low-speed windtunnel. Part 1: Two-dimensional measurement evaluations
[NAL-TM-627] p 665 N92-25402
Development of pre- and post-processor system for structural analysis
[NAL-TM-628] p 681 N92-25403
Cross-flow instabilities and pressure gradients in boundary layers p 767 N92-26922
A pressure measurement method using Electronically Scanner Pressure sensors (ESP) installed in a gust wind tunnel
[NAL-TM-638] p 749 N92-27428
NAL Dornier 228-200 flight research airplane: Present status and outline of the installed equipment
[NAL-TM-637] p 732 N92-27429
Numerical simulation of shock-stall flutter of an airfoil using the Navier-Stokes equations p 746 N92-27956
NACA0012 airfoil data corrected for sidewall boundary-layer effects in the NAL two-dimensional transonic wind tunnel
[NAL-TM-640T] p 722 N92-28151
Estimation of cable-mounted model inertia characteristics for dynamic wind-tunnel test
[NAL-TM-641] p 722 N92-28152
Evaluation of high lift devices of the quiet STOL experimental aircraft ASKA
[NAL-TR-1102] p 733 N92-28153
Note on flight measured control effectiveness of the quiet STOL experimental aircraft ASKA
[NAL-TR-1103] p 746 N92-28154
Force measurements on AGARD calibration model-B at transonic speeds in the NAL two-dimensional wind tunnel
[NAL-TM-639] p 722 N92-28190
Evaluation of landing configuration by flight test of the quiet STOL experimental aircraft ASKA
[NAL-TR-1113] p 733 N92-28191
A gust generation method for full configuration aircraft tests in a low speed wind tunnel. Part 1: Design and preliminary experiments
[NAL-TR-1115-PT-1] p 722 N92-28192
Air ejector experiments using the two-dimensional supersonic cascade tunnel: Zero secondary flow performance
[NAL-TM-632] p 887 N92-28829
Upgrading the data processing section of the NAL Gust Wind Tunnel data processing system
[NAL-TM-635] p 888 N92-28833
Replacement of the NAL high pressure air storage system
[NAL-TM-634] p 888 N92-28835
Quaternion and Euler angles in kinematics
[NAL-TM-636] p 909 N92-28836
Aerodynamic characteristics obtained from alpha sweep test of the quiet STOL experimental aircraft ASKA
[NAL-TR-1112] p 853 N92-28901

National Center for Atmospheric Research, Boulder, CO.
Meeting Review: Airborne Aerosol Inlet Workshop
[NASA-CR-189814] p 301 N92-17393
Simplified signal processing for an airborne CO2 Doppler lidar p 1000 N92-31023

National Defence Headquarters, Ottawa (Ontario).
Durability and damage tolerance testing and fatigue life management: A CF-18 experience p 361 N92-18581

National Inst. for Fusion Science, Nagoya (Japan).
Shafranov shift in low-aspect-ratio heliotron/torsatron CHS
[NIFS-110] p 1138 N92-33743

National Inst. of Standards and Technology, Gaithersburg, MD.
Prototyping the IRDS: An airport application
[PB92-112580] p 484 N92-20448
Criteria for the operation of federally-owned secondary calibration laboratories (ionizing radiation)
[PB92-112481] p 485 N92-21777
Research, services, and facilities (National Institute of Standards and Technology)
[PB92-109172] p 485 N92-21870
Preliminary screening procedures and criteria for replacements for Halons 1211 and 1301
[AD-A252912] p 1126 N92-33501

National Oceanic and Atmospheric Administration, Boulder, CO.
Lower stratospheric measurement issues workshop report p 409 N92-19127
Progress report on analysis of differential attenuation radar data obtained during WISP-91
[PB92-133800] p 503 N92-21828

National Oceanic and Atmospheric Administration, Rockville, MD.
GPS orbit determination at the National Geodetic Survey p 1049 N92-33354

National Oceanic and Atmospheric Administration, Silver Spring, MD.
Vortex characteristics of C5A/B, C141B and C130E aircraft applicable to ATC terminal flight operations tower fly-by-data
[PB92-114586] p 449 N92-20318

National Park Service, Washington, DC.
Study of alternatives: Dayton's Aviation heritage, Ohio
[PB91-202275] p 2 N92-10972

National Research Council of Canada, Ottawa (Ontario).
Wind tunnel tests on A4, A4.1, and A4.2 2-D airfoil models in the IAR 5-ft. wind tunnel: Boeing Commercial Airplane Company and Institute for Aerospace Research collaborative work program
[NRC-IAR-C3] p 81 N92-11975
The BCAC/IAR collaborative research program to investigate the sidewall boundary layer effects in the IAR/NRC 2-D High Reynolds Number Test Facility
[NRC-HSA-434] p 81 N92-11976
Tracking performance requirements for rotorcraft instrument approaches to reduced minima. Phase 1: Preliminary study
[NRC-32137-PHASE-1] p 102 N92-11988
Tutor aft fuselage and empennage full-scale fatigue test: Resolution of horizontal stabilizer installation difficulties
[NRC-LTR-ST-1804] p 114 N92-11990
Corrosion and your aircraft
[NRC-30465] p 114 N92-11991
Numerical verification of NISA 2 finite element analysis of the cracked 5th stage compressor disc of J-85 jet engine
[NRC-LTR-ST-1792] p 129 N92-11997
Humidity effects on gas turbine performance
[NRC-30241] p 130 N92-11998
Preliminary analysis of baseline vibration data from Allison T56-A-14LFE engine and reduction gearbox
[NRC-31578] p 130 N92-11999
Fuel flow measurement in gas turbine testing
[NRC-29808] p 130 N92-12000
A derivation of gross thrust for a sea-level jet engine test cell
[NRC-30165] p 130 N92-12001
Constraint propagation through electromagnetic interaction topologies
[NRC-31761] p 155 N92-12154
Some characteristics and effects of the F/A-18 LEX vortices p 88 N92-13025
A proposed composite repair methodology for primary structure
[NRC-LTR-ST-1658] p 115 N92-13056
Verification of NISA 2 and ENDURE fracture mechanics capability
[NRC-ST-621] p 159 N92-13453
Preliminary finite element analysis of unloaded and loaded notched composite laminated plates
[NRC-LTR-ST-1806] p 159 N92-13454
Rub induced rotor/stator vibration analysis on CF700 engine
[NRC-TR-ENG-007] p 202 N92-14060
Flight evaluation of curved MLS precision approaches in a twin otter aircraft, phase 2
[AD-A243025] p 268 N92-17568
Freezing precipitation on lifting surfaces
[NRC-32124] p 448 N92-20156
Activities of NRC-CNRC, Institute for Aerospace Research
[CTN-92-60431] p 420 N92-20204
Activities of NRC-CNRC, Institute for Aerospace Research, Flight Research Lab.
[CTN-92-60432] p 420 N92-20205
Photoelastic coating study of CT-114 coupon joint test specimen for horizontal stabilizer rear attachment fitting to vertical stabilizer rear spar
[NRC-LTR-ST-1689] p 489 N92-21018
Wind tunnel investigation of a wing-propeller model performance degradation due to distributed upper-surface roughness and leading edge shape modification
p 451 N92-21690
Experimental investigation of heavy rainfall effect on a 2-D high lift airfoil p 452 N92-21696
Evaluation and qualification of diffusion braze repair techniques for superalloy gas turbine components
[NRC-LTR-ST-1839] p 504 N92-22028
Inspection of aircraft engine components using automated eddy current and pattern recognition techniques
[NRC-LTR-ST-1834] p 504 N92-22029
Proceedings of the 3rd Canadian Symposium on Aerodynamics
[CTN-92-60420] p 625 N92-24849
An analysis of the sidewall boundary layer effect in two-dimensional wind tunnel testing p 626 N92-24856
A scheme for two dimensional Euler and boundary layer interactive solutions p 627 N92-24860
Propeller noise research at NRC p 628 N92-24863

Flowfield in the vicinity of the F/A-18 vertical fin at high-angle-of-attack p 628 N92-24865
A preliminary study in the use of phase demodulation techniques for the analysis of gear vibration data
[NRC-32083] p 1002 N92-31469
The design and development of a portable, DSP micro-processor based, high-accuracy data acquisition system
[NRC-32146] p 1134 N92-32851

National Research Lab. of Metrology, Tokyo (Japan).
Application of riblet surface to pipe flow
p 766 N92-26915

National Space Development Agency, Ibaraki (Japan).
Conceptional design to heat-resistant airframe of HOPE p 575 N92-23820
Design of orbital re-entry experiment vehicle and outline of the experiment p 667 N92-25374

National Technical Univ., Athens (Greece).
Unsteady Euler calculations in 3D internal aerodynamics p 768 N92-27470

National Transportation Safety Board, Washington, DC.
Aircraft accident report: MarkAir, Inc., Boeing 737-2X6C, N670MA, controlled flight into terrain, Unalakleet, Alaska, 2 June 1990
[PB91-910402] p 92 N92-13039
Aircraft accident report: Northwest Airlines, Inc., Flights 1482 and 299. Runway incursion and collision, Detroit Metropolitan/Wayne County Airport, Romulus, Michigan, December 3, 1990
[PB91-910405] p 187 N92-14006
Aircraft accident/incident summary report: Midair collision involving Lycoming Air Services Piper Aerostar PA-60 and Sun Company Aviation Department Bell 412, Merion, Pennsylvania, April 4, 1991
[PB91-910407] p 187 N92-15055
Aircraft accident reports: Brief format US civil and foreign aviation issue number 2 of 1989 accidents
[PB90-916902] p 263 N92-15978
Aircraft accident reports: Brief format US civil and foreign aviation issue number 3 of 1989 accidents
[PB90-916903] p 263 N92-15979
Aircraft accident reports: Brief format. US civil and foreign aviation issue number 4 of 1989 accidents
[PB90-916904] p 263 N92-17133
Aircraft accident report: Northwest Airlines, Inc., Flights 1482 and 299. Runway incursion and collision, Detroit Metropolitan/Wayne County Airport, Romulus, Michigan, December 3, 1990
[PB91-910405] p 264 N92-17213
Aircraft accident reports: Brief format U.S. Civil and Foreign Aviation Issue Number 5 of 1989 accidents
[PB90-916905] p 452 N92-21833
Aircraft accident report: Unstabilized approach and loss of control NPA, Inc. dba United Express Flight 2415, British Aerospace BA-3101, N41OUE, Tri-Cities Airport, Pasco, Washington, December 26, 1989
[PB91-910406] p 453 N92-21873
Aircraft accident report: Runway collision of USAir Flight 1493, Boeing 737 and Skywest Flight 5569 Fairchild Metroliner, Los Angeles International Airport, Los Angeles, CA, February 1, 1991
[PB91-910409] p 530 N92-23596
Aircraft accident report: Ryan International Airlines DC-9-15, N565PC, loss of control on takeoff, Cleveland-Hopkins International Airport, Cleveland, Ohio, February 17, 1991
[PB91-910410] p 530 N92-23597
Aircraft accident report: Explosive decompression - loss of cargo door in flight, United Airlines Flight 811, Boeing 747-122, N4713U, Honolulu, Hawaii, February 24, 1989
[PB92-910402] p 953 N92-31159
Aircraft accident report: L'Express Airlines, Inc., Flight 508, Beech C99, N7217L weather encounter and crash near Birmingham, Alabama, July 10, 1991
[PB92-910401] p 1043 N92-32455
Aircraft accident/incident summary report: Controlled flight into terrain Bruno's Inc., Beechjet, N25BR, Rome, Georgia, 11 December 1991
[PB92-910404] p 1044 N92-34081

Naval Aerospace Medical Research Lab., Pensacola, FL.
Use of a commercially available flight simulator during aircrew performance testing
[AD-A245922] p 883 N92-28407

Naval Air Development Center, Warminster, PA.
AI for RPVs, Sensor Driven Airborne Replanner (SDAR), for a Robotic Aircraft Sensor Platform (RASP)
p 114 N92-12534
Neural network and fuzzy logic technology for naval flight control
[AD-A242650] p 206 N92-15074
Tensile and interlaminar properties of GLARE (trade name) laminates
[AD-A250188] p 895 N92-28921
In-service evaluation of 2090 aluminum-lithium alloy on F/A-18 aircraft
[AD-A248472] p 986 N92-30321

Naval Air Propulsion Test Center, Trenton, NJ.
Statistics on aircraft gas turbine engine rotor faitures that occurred in US commercial aviation during 1988
[DOT/FAA/CT-91/28] p 1071 N92-33105

Naval Air Test Center, Patuxent River, MD.
Ship airwake measurement and modeling options for rotorcraft applications p 503 N92-21954
Enhanced displays, flight controls, and guidance systems for approach and landing p 456 N92-21957
Evaluating fixed wing aircraft in the aircraft carrier environment p 464 N92-21963
United States Navy ski jump experience and future applications p 465 N92-21968
Use of high-fidelity simulation in the development of an F/A-18 active ground collision avoidance system
p 837 N92-28530

Naval Air Warfare Center, Warminster, PA.
An investigation of switched reluctance rotor position estimation using neural networks
[AD-A252846] p 1061 N92-33414

Naval Civil Engineering Lab., Port Hueneme, CA.
Paint removal using cryogenic processes
[AD-A247668] p 895 N92-28912

Naval Observatory, Washington, DC.
LORAN-C data reduction at the US Naval Observatory
p 1050 N92-33358

Naval Ocean Systems Center, San Diego, CA.
Information Management Engineering (IME) laboratory: A database development facility
[AD-A243191] p 305 N92-17369
Remote sensing of trapping layer base height using ATIS transmissions
[AD-A250074] p 1004 N92-31362
Feasibility of measuring transverse electric noise at VLF and LF on an ice cap
[AD-A252280] p 1129 N92-33220

Naval Postgraduate School, Monterey, CA.
Numerical investigation of the effect of leading edge geometry on dynamic stall of airfoils
[AD-A239949] p 12 N92-10015
CH-53E/AV-8B aircraft sling load recovery system analysis
[AD-A239950] p 21 N92-10022
Developmental flight testing of a half scale unmanned air vehicle
[AD-A240347] p 22 N92-11002
Development of a 1/7th scale fighter UAV for flight research
[AD-A240703] p 23 N92-11008
Initial design study of existing flight control system of RPH and feasibility study of implementing HHC on the SH-60B
[AD-A240522] p 30 N92-11019
Parameter identification studies on the NASA/Ames Research Center Advanced Concepts Flight Simulator
[NASA-TM-105126] p 31 N92-11024
Calibration of the Naval Postgraduate School 3.5' x 5.0' academic wind tunnel
[AD-A240614] p 31 N92-11025
The design of broadband radar absorbing surfaces
[AD-A240521] p 42 N92-11235
Implementing total quality management at the intermediate level of aircraft maintenance
[AD-A241768] p 62 N92-12992
A study of the airwake aerodynamics over the flight deck of an AOR model ship
[AD-A241008] p 89 N92-13034
Aerodynamic coefficients of a symmetrical airfoil in an oscillating flow
[AD-A241073] p 89 N92-13035
Water tunnel flow visualization studies of a canard-configured X-31A-like fighter aircraft model
[AD-A241362] p 90 N92-13037
Further calculations of the performance of turbofan engines incorporating a wave rotor
[AD-A240867] p 131 N92-13072
Flow modification over a backward facing step
[AD-A241351] p 158 N92-13406
Preliminary investigation of the shock-boundary layer interaction in a simulated fan passage
[AD-A242656] p 185 N92-15045
Flight operations for higher harmonic control research
[AD-A242478] p 196 N92-15067
Structural considerations for aircraft payload Modification: P-3C zero fuel weight increase
[AD-A242690] p 196 N92-15068
Hot-wire surveys in the vortex wake downstream of a three-percent fighter aircraft model at high angles of attack
[AD-A241869] p 259 N92-15975
Escape strategies for turboprop aircraft in a microburst windshear
[AD-A243090] p 264 N92-17217
A wing rock model for the F-14A aircraft
[AD-A243109] p 275 N92-17300
Flow visualization and wake analysis for standard and modified configurations of the AN/ALQ-78 antenna pod
[AD-A243552] p 260 N92-17339
Multiple input sliding mode control for autonomous diving and steering of underwater vehicles
[AD-A241935] p 283 N92-17442
The V-22: Can the nation afford to forgo its production?
[AD-A243158] p 242 N92-17477
Development of a knowledge base for use in an Expert System Advisor for Aircraft Maintenance Scheduling (ESAAMS)
[AD-A243435] p 305 N92-17687
An analysis of the aircraft engine Component Improvement Program (CIP): A life cycle cost approach
[AD-A243346] p 280 N92-17729
A quantitative study of unsteady compressible flow on an oscillating airfoil
[AD-A244572] p 445 N92-21012
Laser velocimetry measurements of oscillating airfoil dynamic stall flow field
[AD-A244546] p 502 N92-21297
Baseline vibration measurements of remotely piloted helicopters for higher harmonic control research
[AD-A244669] p 482 N92-21360
The aerodynamics of ship superstructures
p 503 N92-21953
Thermoacoustic refrigeration p 595 N92-22720
The V-22 tilt rotor: A comparison with existing Coast Guard aircraft
[AD-A245843] p 650 N92-26039
Simulation of a rotorcraft in turbulent flows
[AD-A245742] p 650 N92-26155
Solid fuel ramjet infrared signature
[AD-A246299] p 753 N92-26362
Composite strength statistics from fiber strength statistics
[AD-A245616] p 755 N92-26383
Naval Postgraduate School aircraft synthesis program (user's manual)
[AD-A246198] p 777 N92-26458
A modeling strategy for large-scale optimization based on analysis and visualization principles
[AD-A246570] p 777 N92-26620
The navigation data logger for a suitcase navigation system
[AD-A245997] p 727 N92-26756
A prototype semantic integrity front end expert system for a relational database
[AD-A246084] p 781 N92-26765
Precision of the long baseline acoustic navigation system used by Pegasus
[AD-A246598] p 727 N92-26795
Computer program for calculating in-flight aircraft-store interface reaction loads
[AD-A245782] p 731 N92-26896
Studies in chaos using stochastic methods
[AD-A246919] p 780 N92-27171
National airspace data interchange network analysis
[AD-A247345] p 727 N92-27217
A wind tunnel study of the pioneer remotely piloted vehicle
[AD-A247028] p 732 N92-27335
Application of neural network to adaptive control theory for super-augmented aircraft
[AD-A246596] p 745 N92-27505
Profile of an effective engineering manager
[AD-A246525] p 781 N92-27528
Comparison of Janus and field test aircraft detection ranges for the line-of-sight forward heavy system
[AD-A246047] p 770 N92-27600
Development of telemetry for the agility flight test of a radio controlled fighter model
[AD-A248653] p 753 N92-27994
Flight testing of a half-scale remotely piloted vehicle
[AD-A248568] p 733 N92-28123
An appraisal of cost-effectiveness models used in the Air Force and Navy aircraft engine component improvement programs
[AD-A245910] p 743 N92-28162
NPSNET: Flight simulation dynamic modeling using quaternions
[AD-A247484] p 923 N92-28245
Stability and control flight testing of a half-scale Pioneer remotely piloted vehicle
[AD-A245973] p 879 N92-28801
Tasking and communication flows in the F/A-18D cockpit: Issues, problems, and possible solutions
[AD-A245977] p 853 N92-28802
Flow visualization studies of a sideslipping, canard-configured X-31A-Like fighter aircraft model
[AD-A245940] p 829 N92-28883

Improving the LAMP Mk 3 SH-60B HF communication system
[AD-A245970] p 910 N92-29344
A computational investigation of airfoil stall flutter
[AD-A247302] p 947 N92-31300
Further studies in filmwise condensation of steam on horizontal finned tubes
[AD-A252705] p 1011 N92-31767
A continuing study of altitude determination deficiencies of the Service Aircraft Instrumentation Package (SAIP)
[AD-A245952] p 968 N92-32051
Decision-making guide for the proposed Coast Guard differential global positioning system
[AD-A246046] p 957 N92-32054
Exploratory experimental investigation of a wave propeller
[AD-A252175] p 949 N92-32062
Investigation of the flight control requirements of a half-scale ducted fan unmanned aerial vehicle
[AD-A252730] p 1087 N92-32988
Implementation of a personal computer based parameter estimation program
[AD-A252914] p 1061 N92-33502
Static and dynamic flow visualization studies of two double-delta wing models at high angles of attack
[AD-A252878] p 1040 N92-33678

Naval Research Lab., Washington, DC.
Lightning strike tests of composite connectors
[AD-A252281] p 1044 N92-33249

Naval Sea Systems Command, Washington, DC.
Deck motion criteria for carrier aircraft operations
p 464 N92-21952

Naval Surface Warfare Center, Dahlgren, VA.
Second-order shock-expansion theory extended to include real gas effects
[AD-A247191] p 831 N92-29539

Naval Surface Warfare Center, Silver Spring, MD.
Notes on the cause of parachute critical velocity
[AD-A244417] p 347 N92-19085

Naval Training Systems Center, Orlando, FL.
An analysis of aircrew communication patterns and content
[AD-A246618] p 907 N92-28253

Naval War Coll., Newport, RI.
The role of stealth in naval aviation and joint/combined operations
[AD-A240595] p 22 N92-11005

Navy Clothing and Textile Research Facility, Natick, MA.
Thermal energy test apparatus
[AD-A243526] p 305 N92-17537

Nebraska Univ., Omaha.
Cooperative planning in aviation contexts
p 456 N92-21509

Netrologic, Inc., San Diego, CA.
Robotic non-destructive inspection of aircraft, phase 1
[AD-A240777] p 44 N92-11367

Nevada Univ., Reno.
Numerical investigations in three-dimensional internal flows
[NASA-CR-189467] p 221 N92-14313
Numerical investigations in three-dimensional internal flows
[NASA-CR-190498] p 998 N92-30380

New Brunswick Univ., Fredericton.
Dredging research program: Global positioning system bibliography
[AD-A248954] p 729 N92-28079

New Mexico State Univ., Las Cruces.
Determination of balloon drag
[AIAA PAPER 91-3666] p 5 A92-11013
Structural behavior of scientific balloons - Finite element simulation and verification
[AIAA PAPER 91-3668] p 20 A92-11015
The NASA long duration balloon project
[AIAA PAPER 91-3680] p 15 A92-11024

Newcastle Polytechnic, Newcastle-upon-Tyne (England).
The application of a cylindrical-spherical floating ring bearing as a device to control stability of turbogenerators p 224 N92-14371

Nielsen Engineering and Research, Inc., Mountain View, CA.
Postflight aerothermodynamic analysis of Pegasus(tm) using computational fluid dynamic techniques
[NASA-CR-186017] p 445 N92-21188

Nihon Univ., Tokyo (Japan).
Flow around an isolated surface roughness in the laminar boundary layer p 766 N92-26913

Norden, Norwalk, CT.
Propulsive lift noise p 55 N92-10606

North Carolina Agricultural and Technical State Univ., Greensboro.
Behavior of aircraft tire coupons under various loading conditions
[AD-A241416] p 116 N92-13063

Model analysis and expert system development for planning and scheduling teleoperations for aircraft turnaround functions, volume 1
[AD-A251037] p 932 N92-30253
Model analysis and expert system development for planning and scheduling teleoperations for aircraft turnaround functions. Volume 2: Top user's guide
[AD-A251083] p 932 N92-30258

North Carolina State Univ., Raleigh.
Effect of nose shape on three-dimensional stagnation region streamlines and heating rates
[AIAA PAPER 91-5032] p 171 A92-17822
Engineering calculations of three-dimensional inviscid hypersonic flowfields p 175 A92-20378
Wall interference calculation in a transonic test section including simulation of discrete slots
[AIAA PAPER 92-0032] p 249 A92-22153
A computational and experimental investigation of a three-dimensional hypersonic scramjet inlet flow field
p 11 N92-10007
Wall interference calculation in a transonic wind tunnel with discrete slots p 83 N92-12995
Numerical investigation of unsteady supersonic cavity flowfield with passive control p 88 N92-13029
Formulation of the linear model from the nonlinear simulation for the F18 HARV p 117 N92-13842
A study of juncture flow in the NASA Langley 0.3-meter transonic cryogenic tunnel
[NASA-CR-190430] p 773 N92-27880
Buffet test in the National Transonic Facility
[NASA-CR-189595] p 888 N92-29352
An approximate viscous shock layer technique for calculating chemically reacting hypersonic flows about blunt-nosed bodies p 1041 N92-33837

Northern Research and Engineering Corp., Woburn, MA.
Currently available fuel gas booster compressor equipment for small gas turbine engines
[PB92-127026] p 499 N92-20265
Turbocharged pressurized combustion system
[PB92-142579] p 756 N92-26521

Northrop Corp., Hawthorne, CA.
Finite element analysis of ASTOVL fighter structure
[AD-A243724] p 275 N92-17513
Durability and damage tolerance of aluminum castings
[AD-A245237] p 490 N92-21159
Overview of computational structural methods for modern military aircraft p 684 N92-25928
Structural assessment of ultralightweight composites
p 1107 N92-32525
Supportability evaluation of thermoplastic and thermoset composites p 1108 N92-32576
Damage tolerance certification methodology for composite structures p 1108 N92-32579

Northwest Airlines, Inc., Minneapolis, MN.
Current and future developments in civil aircraft non-destructive evaluation from an operator's point of view p 787 N92-30122

Northwestern Polytechnical Univ., Xian (China).
The stability of the steady state and bistable response of a flexible rotor supported on squeeze film dampers
p 222 N92-14350

Northwestern Univ., Evanston, IL.
On the interaction between first- and second-mode waves in a supersonic boundary layer
p 78 A92-16462

Norton Co., Northboro, MA.
Ceramic component processing development for advanced gas-turbine engines
[ASME PAPER 91-GT-120] p 142 A92-15567

Notre Dame Univ., IN.
Optimal stabilization of discrete event systems
p 48 A92-11376
Breaking down the delta wing vortex: The role of vorticity in the breakdown process p 86 N92-13017
An experimental analysis of critical factors involved in the breakdown process of leading edge vortex flows
p 89 N92-13031
Aerodynamic and flowfield hysteresis of slender wing aircraft undergoing large-amplitude motions
p 364 N92-18780
Kappa Group: The initial guess. A proposal in response to a commercial air transportation study
[NASA-CR-189981] p 366 N92-19374
Alpha Group: The Behemoth Apteryx. Final design proposal
[NASA-CR-190026] p 462 N92-20951
Gamma Group-The Pale Horse: A proposal in response to a commercial air transportation study ort study
[NASA-CR-190019] p 731 N92-26435
Experimental investigation of turbulence behavior in shock wave/turbulent boundary layer interactions
[AD-A247792] p 774 N92-27886

NSI Technology Services Corp., Research Triangle Park, NC.
Methodology for the determination of criticality codes and recertification intervals for Tank Mounted Air Compressors (TMAC) and Base Mounted Air Compressors (BMAC)
[NASA-CR-189268] p 770 N92-27649

O

Oak Ridge Associated Universities, Inc., TN.
Steady flow of a fluid-solid mixture in a circular cylinder
[DE91-018698] p 41 N92-10174

Oak Ridge National Lab., TN.
Recent advances on a finite element algorithm for computational aerodynamics: Transonics-hypersonics
[DE91-018176] p 11 N92-10010
Scoping studies for small steady-state tokamaks for divertor testing
[DE92-000740] p 238 N92-15761
Ceramic technology for Advanced Heat Engines Project
[DE92-002397] p 289 N92-16128
Ultra-high temperature (greater than 2000 C) testing capability at Oak Ridge National Laboratory for carbon materials in air, inert gas and vacuum
[DE92-004445] p 385 N92-18069
Fiber-sensor design for turbine engines
[DE92-003539] p 376 N92-18230
Counterrotating brushless DC permanent magnet motor
[DE92-003825] p 401 N92-18550
Benchmark performance analysis of an ECM-modulated air-to-air heat pump with a reciprocating compressor
[DE92-004478] p 500 N92-20341
Fabrication and testing of corrosion resistant coatings
[DE92-003553] p 490 N92-21063
Terrain following of arbitrary surfaces using a high intensity LED proximity sensor
[DE92-007161] p 455 N92-21201
Evaluation of the elevated-temperature mechanical reliability of a HIPed silicon nitride
[DE92-007838] p 579 N92-23223
Advanced techniques in current signature analysis
[DE92-007680] p 679 N92-24892
The cost of silicon nitride powder: What must it be to compete?
[DE92-008710] p 669 N92-25223
Simulation of 3D non-planar fatigue crack growth in a turbine blade root
[DE92-006859] p 739 N92-26697
Assessment of valve actuator motor rotor degradation by Fourier Analysis of current waveform
[DE92-013233] p 909 N92-28814
Proof of concept of a magnetically coupled Stirling engine-driven heat pump
[DE92-017129] p 1129 N92-33271

Office National d'Etudes et de Recherches Aeronautiques, Paris (France).
Physics of vortical flow p 86 N92-13016
Determination of vortex-breakdown criteria by solving the Euler and Navier-Stokes equations
p 87 N92-13018

Office National d'Etudes et de Recherches Aerospatiales, Meundon (France).
Theoretical simulation of a 2 micron airborne solid state laser anemometer p 1000 N92-31059

Office National d'Etudes et de Recherches Aerospatiales, Paris (France).
Numerical simulation of vortex breakdown by solving the Euler equations for an incompressible fluid
p 41 N92-10163
Numerical simulation of vortex breakdown via 3-D Euler equations p 41 N92-10164
Three dimensional numerical method for resolving small transonic perturbations in unstructured mesh
[ONERA-RT-56/3064-RY-006-R] p 13 N92-10989
Wing tip turbine: Analysis of the results of S2MA sounding of marginal vortex of the A320, technical summary
[ONERA-RTS-21/4365-AY-056A] p 23 N92-11009
Resolution of Navier-Stokes equations around profiles: Drag evolution
[ONERA-RTS-86/1685-AY-156A] p 43 N92-11310
Perfect compressible two dimensional boundary layer strong fluid coupling in the case of sharp leading edge profiles. Unsteady case of isolated profiles and steady case of blade grids
[ONERA-RT-43/1621-RY-006-R] p 43 N92-11311
Hydrodynamic flow visualization around an oscillating vane. Extension of study to the case of higher incidences and amplitudes and the starting off phase from permanent regime
[ONERA-RT-56/1369-AN] p 43 N92-11312

Eighty years of aerospace technique through ATMA bulletins
[ETN-91-90097] p 57 N92-11963
Thermographic gust wind tunnel measurements
[ONERA-RF-31/3409-PY] p 81 N92-11972
Analysis tools of ONERA and DLR for the aerothermodynamics of reentry vehicles
p 211 N92-14977
Heat transfer measurements in ONERA supersonic and hypersonic wind tunnels using passive and active infrared thermography p 208 N92-15003
Ablation and temperature sensors for flight measurements in reentry body heat shields
p 227 N92-15004
Hypersonic inviscid flow field simulations around reentry vehicles with flap deflection p 184 N92-15025
Numerical simulation of thermochemical non-equilibrium viscous flows around reentry bodies
p 227 N92-15029
Drag prediction using computation methods
[ONERA-RSF-82/1685-AY-154-4] p 349 N92-19682
Resolution of the Euler equations applied to a helicopter rotor in forward flight
[ONERA-RSF-2/3731-AY-004A] p 406 N92-19976
Blade-vortex noise on a helicopter main rotor. Study of the strong two dimensional incompressible interaction
[ONERA-RT-96/5094-PY] p 511 N92-20388
Prediction of helicopter noise: Adaptation of noise load calculations to the blade-vortex interaction
[ONERA-RS-97/5094-PY] p 513 N92-21736
Integration of flight and carrier landing aid systems for shipboard operations p 456 N92-21958
Validation of a CANARI code by the computation of three dimensional turbulent flow in turbine valve
p 741 N92-27462
Steady and unsteady 3D flow computation through a transonic turbine stage p 742 N92-27469
Presentation of a computational code for 3-D compressible flow in complex channels and cavities
p 769 N92-27475
Three dimensional calculations of reactive flows within aircraft combustion chambers including some combustion models p 770 N92-27490
Direct coupling of fluid structure in transonic aeroelasticity p 721 N92-27954
Use of a research simulator for the development of new concepts of flight control p 885 N92-28543
Construction of a numerical optimization method for the definition of hypersupported profiles
[ONERA-RSF-43/1736-AY-146A] p 908 N92-28788
Feasibility study of hypersonic clinometric measurements at R3Ch
[ONERA-RSF-136/1865-AY-728-] p 829 N92-28789
Development of an unsteady three-dimensional viscous-inviscid interaction numerical method for the calculation of airfoils vibration
[ONERA-RSF-7/3617-AY-022A] p 830 N92-29206
Survey of French activities concerning structural airworthiness and aging aircraft p 838 N92-30130
Research on some centered implicit methods for calculating transonic flows by solving Navier-Stokes equations
[ONERA-RSF-24/1408-AY-150A] p 1037 N92-32773
Strong coupling between inviscid fluid and boundary layer of sharp leading edges: Two-dimensional stationary and turbulent cases for isolated profiles and guard vanes
[ONERA-RT-44/1621-RY-016-R] p 1125 N92-32776
Flutter models: Their design, manufacture, and ground testing p 1089 N92-34164
Unsteady wind tunnel tests p 1089 N92-34166

Office National d'Etudes et de Recherches Aerospatiales, Toulouse (France).
Characteristics of a boundary layer in a leading edge vortex p 86 N92-13012

Office of Technology Assessment, Washington, DC.
New Ways: Tiltrotor aircraft and magnetically levitated vehicles
[OTA-SET-507] p 238 N92-14933

OHB-System G.m.b.H., Bremen (Germany).
FALKE and COBRA technology development in aerodynamics and aerothermodynamics
p 183 N92-15017

Ohio State Univ., Columbus.
Optimal stabilization of discrete event systems
p 48 A92-11376
SATCOM antenna siting study on P-3C aircraft, volume 1
[NASA-CR-189514] p 221 N92-14262
SATCOM antenna siting study on P-3C aircraft, volume 2
[NASA-CR-189515] p 221 N92-14263
Automated composite ellipsoid modelling for high frequency GTD analysis
[NASA-CR-189853] p 275 N92-17316
Analysis of lossy composite terminating structures
[NASA-CR-189901] p 404 N92-19217
Bistatic image processing for a 32 x 19 inch model aircraft using scattered fields obtained in the OSU-ESL compact range
[NASA-CR-189932] p 499 N92-20197
A novel approach in formulation of special transition elements: Mesh interface elements
[NASA-CR-189050] p 501 N92-20954
Two stage to orbit design
[NASA-CR-189994] p 575 N92-22625
Grid generation research at OSU p 633 N92-25723
Computation and stability analysis of laminar flow over a blunt cone in hypersonic flow p 1041 N92-33839

Ohio Univ., Athens.
In-flight demonstration of hybrid GPS/Loran RAIM
p 96 A92-16643
Availability of positioning and receiver autonomous integrity monitoring for the global positioning system
p 100 A92-16963
Investigation of air transportation technology at Ohio University, 1990-1991 p 265 N92-17990
GPS interferometric attitude and heading determination: Initial flight test results p 269 N92-17994
Loran-C performance assurance assessment program
[NASA-CR-190469] p 840 N92-28718
Nonlinear normal and axial force indicial responses for a two dimensional airfoil
[AD-A247196] p 830 N92-28888

Oklahoma Univ., Norman.
Multidisciplinary optimization studies using ASTROS
p 571 N92-23234
Influence of structural and aerodynamic modeling on flutter analysis and structural optimization
[AD-A248487] p 978 N92-30323

Old Dominion Univ., Norfolk, VA.
Prediction of steady and unsteady asymmetric vortical flows around circular cones p 172 A92-18372
Aerodynamic sensitivity analysis methods for the compressible Euler equations p 233 A92-19619
Viscous computations of cold air/air flow around scramjet nozzle afterbody
[NASA-CR-4406] p 13 N92-10982
Further developments relating to the NASA Langley Research Center 13-inch magnetic suspension and balance system
[NASA-CR-188995] p 31 N92-11023
Polymer infiltration studies
[NASA-CR-189773] p 289 N92-17004
The solution of a singular integral equation arising from a lifting surface theory for rotating blades
p 260 N92-17303
Flow analysis and design optimization methods for nozzle afterbody of a hypersonic vehicle
[NASA-CR-4431] p 446 N92-21456
Polymer infiltration studies
[NASA-CR-190204] p 578 N92-22486
Methodology for sensitivity analysis, approximate analysis, and design optimization in CFD for multidisciplinary applications
[NASA-CR-190201] p 595 N92-22662
Prediction of response of aircraft panels subjected to acoustic and thermal loads
[NASA-CR-190305] p 678 N92-24345
An analytical approach to grid sensitivity analysis for NACA four-digit wing sections
[NASA-CR-190251] p 631 N92-25175
Finite element frequency domain solution of nonlinear panel flutter with temperature effects and fatigue life analysis p 682 N92-25589
Iterative methods for large scale static analysis of structures on a scalable multiprocessor supercomputer
[NASA-CR-190369] p 692 N92-26018
System requirements specification for SMART structures mode p 777 N92-27830
Surface generation and editing operations applied to structural support of aerospace vehicle fuselages
p 777 N92-27831
Viscous effects on a vortex wake in ground effect
[NASA-CR-190400] p 907 N92-28361
Nonlinear analyses of composite aerospace structures in sonic fatigue
[NASA-CR-190565] p 854 N92-30209
Prediction and control of asymmetric vortical flows around slender bodies using Navier-Stokes equations
p 1127 N92-33968
Investigation of advancing front method for generating unstructured grid
[NASA-CR-190902] p 1128 N92-34043
Dynamics and control of a five degree-of-freedom magnetic suspension system
[NASA-CR-191259] p 1102 N92-34222

Omega Navigation System Center, Alexandria, VA.
US Coast Guard GPS Information Center (GPSIC) and its function within the Civil GPS Service (CGS)
p 1049 N92-33352

ORA Corp., Ithaca, NY.
Formal specification and verification of Ada software
[AIAA PAPER 91-3713] p 230 A92-17585

Oregon State Univ., Corvallis.
Nonlinear stability and control study of highly maneuverable high performance aircraft, phase 2
[NASA-CR-189911] p 382 N92-19841
Nonlinear stability and control study of highly maneuverable high performance aircraft, phase 2
[NASA-CR-190667] p 978 N92-30922
Turbulence-induced loads on a teetered rotor
p 1042 N92-34029

Oslo Univ. (Norway).
Ozone response to aircraft emissions: Sensitivity studies with two-dimensional models p 409 N92-19126

Otago Univ., Dunedin (New Zealand).
Stratospheric electrodynamics from superpressure balloons - A technical challenge for small payload environments
[AIAA PAPER 91-3674] p 14 A92-11019

Ottawa Univ. (Ontario).
Nonliner aspects of transonic aeroelasticity
p 628 N92-24864
Nonunique solutions in unsteady transonic flow
p 629 N92-24872

Oxford Univ. (England).
Effects of wake and shock passing on the heat transfer to a film cooled transonic turbine blade
p 156 N92-12201
Heat transfer and instrumentation studies on rotating turbine blades in a transient facility p 156 N92-12203
Blade surface pressure measurements on the rotor of a model turbine stage in a transient flow facility
p 157 N92-12206
Robust control system design with application to high performance helicopters p 382 N92-19621
Turbulent spot generation and growth rates in a transonic boundary layer
[AD-A250221] p 909 N92-29118

P

Pacific Northwest Lab., Richland, WA.
Calibration data for improved correction of UVW propeller anemometers
[DE92-002935] p 297 N92-16281

Paris VI Univ. (France).
On the computation of unsteady turbomachinery flows. Part 1: Euler equations in vibrating cascades
p 768 N92-27460

Patras Univ. (Greece).
Jet fuel absorption and dynamic mechanical analysis of carbon fibre composites p 1110 N92-33050

PEDA Corp., Palo Alto, CA.
Accurate, productive aerodynamic simulation on patched mesh systems
[AD-A243977] p 405 N92-19386

Pennsylvania State Univ., University Park.
Numerical prediction of wakes in cascades and compressor rotors including the effects of mixing. I - Cascade wakes including the effects of incidence and freestream turbulence
[ASME PAPER 91-GT-225] p 74 A92-15638
Numerical prediction of wakes in cascades and compressor rotors including the effects of mixing. II - Rotor passage flow and wakes including the effects of spanwise mixing
[ASME PAPER 91-GT-222] p 74 A92-15639
A stochastic regulator for integrated communication and control systems. I - Formulation of control law. II - Numerical analysis and simulation p 233 A92-19605
Observability under recurrent loss of data
p 302 A92-21191
Prediction of forces and moments for hypersonic flight vehicle control effectors
[NASA-CR-188954] p 33 N92-11070
Third International Conference on Inverse Design Concepts and Optimization in Engineering Sciences (ICIDES-3)
[NASA-CR-188125] p 170 N92-13928
Aerodynamic shape optimization of arbitrary hypersonic vehicles p 194 N92-13954
Analysis and design of planar and non-planar wings for induced drag minimization
[NASA-CR-189509] p 179 N92-13999
Nonlinear acoustic propagation of shock waves through the atmosphere with molecular relaxation
p 511 N92-20360
Experimental study of the mechanism of sound generation by rotating stall in centrifugal turbomachines
p 605 N92-23726
Turbulent mixing in supersonic jets
p 715 N92-27054
Particle image velocimetry
[AD-A246638] p 750 N92-27753

Explicit Navier-Stokes computation of turbomachinery flows
[AD-A249284] p 909 N92-28879
Explicit Navier-Stokes computation of turbomachinery flows
[AD-A248458] p 911 N92-29933
Finite difference time domain modeling of steady state scattering from jet engines with moving turbine blades
[NASA-CR-190290] p 971 N92-30753
Advanced thermally stable jet fuel development program. Volume 2: Compositional factors affecting thermal degradation of jet fuels
[AD-A252656] p 987 N92-31399
Numerical simulation of turbomachinery flows with advanced turbulence models p 1124 N92-32270
Swept shock/boundary layer interaction experiments in support of CFD code validation
[NASA-CR-190583] p 1036 N92-32494
Wave equations and computational models for sonic boom propagation through a turbulent atmosphere
p 1139 N92-33877
Simulations of sonic boom ray tube area fluctuations for propagation through atmospheric turbulence including caustics via a Monte Carlo method
p 1139 N92-33878
Analysis of sonic boom data to quantify distortions of shock profiles p 1139 N92-33879

PERI, Inc., Princeton, NJ.
Controller memory enhancement: Field facility concepts and techniques
[DOT/FAA/CT-TN92/7] p 640 N92-24799

Physical Sciences, Inc., Andover, MA.
Aerothermodynamic radiation studies
[NASA-CR-185666] p 284 N92-15998

Pittsburgh Energy Technology Center, PA.
Steady flow of a fluid-solid mixture in a circular cylinder
[DE91-018698] p 41 N92-10174

Planning and Management Consultants Ltd., Carbondale, IL.
Reducing environmental noise impacts: A USAREUR noise management program handbook
[AD-A240797] p 237 N92-14791

Pneumo Corp., Boston, MA.
Landing gear mechanism including runway-roughness restrictor assembly
[CA-PATENT-1-257-618] p 1061 N92-33585

Politecnico di Milano (Italy).
Numerical simulation of vortex flows past impulsively started wings p 88 N92-13028
State and time granularity in system description: An example
[REPT-91-040] p 603 N92-22673
Composite beam analysis linear analysis of naturally curved and twisted anisotropic beams
[AD-A252652] p 999 N92-30766

Polytechnic Univ., Brooklyn, NY.
Critical problems of computational aeroacoustics
p 167 N92-13857

Port Authority of New York and New Jersey, Jersey City.
Tilt rotors and the Port Authority of New York and New Jersey Airport System
[RAND-R-3971/1-PA-SUMM] p 636 N92-25262

Portuguese Air Force, Alfragide.
Fatigue management for the A-7P
p 363 N92-18593

Power Reactor and Nuclear Fuel Development Corp., Oarai (Japan).
Study of potassium turbine electric generator system
p 1129 N92-33794

Pratt and Whitney Aircraft, East Hartford, CT.
High temperature strain gage technology for hypersonic aircraft development applications
[NASA-CR-189101] p 592 N92-22239
Computational structural analysis and advanced commercial engines p 660 N92-25933
Feasibility of magnetic bearings for advanced gas turbine engines p 772 N92-27738
Ultra high bypass Nacelle aerodynamics inlet flow-through high angle of attack distortion test
[NASA-CR-189149] p 943 N92-30298

Pratt and Whitney Aircraft, West Palm Beach, FL.
Properties of aircraft fuels and related materials
[AD-A240650] p 35 N92-11213
Fatigue in single crystal nickel superalloys
[AD-A243453] p 290 N92-17653
Fatigue in single crystal nickel superalloys
[AD-A244815] p 489 N92-21015
Metal-metal bondline NDE methods
[AD-A244429] p 503 N92-21730
Structures technology applications for the National AeroSpace Plane p 649 N92-25920
Fatigue in single crystal nickel superalloys
[AD-A248190] p 896 N92-29408
Fatigue in single crystal nickel superalloys
[AD-A250068] p 987 N92-31360
Fatigue in single crystal nickel superalloys
[AD-A252492] p 988 N92-32066

Pratt and Whitney Aircraft Group, East Hartford, CT.
Thermal barrier coating life prediction model development
[ASME PAPER 91-GT-40] p 147 A92-15523
Heat transfer in rotating serpentine passages with trips normal to the flow
[ASME PAPER 91-GT-265] p 151 A92-15663
New applications of liquid-crystal thermography in rotating turbomachinery heat transfer research
[ASME PAPER 91-GT-354] p 153 A92-15710
Life prediction and constitutive models for engine hot section anisotropic materials program
[NASA-CR-189223] p 1072 N92-33479

PRC Kentron, Inc., Edwards, CA.
Postflight aerothermodynamic analysis of Pegasus(tm) using computational fluid dynamic techniques
[NASA-CR-186017] p 445 N92-21188
High-speed civil transport flight- and propulsion-control technological issues
[NASA-CR-186015] p 482 N92-21253
Assessment of flying-quality criteria for air-breathing *aerospacecraft*
[NASA-CR-4442] p 663 N92-25982
High-speed civil transport issues and technology program
[NASA-CR-186020] p 962 N92-31208
Design and analysis issues of integrated control systems for high-speed civil transports
[NASA-CR-186022] p 979 N92-31656

PRC Systems Services Co., Edwards, CA.
An aircraft model for the AIAA controls design challenge
[NASA-CR-186019] p 117 N92-13064

Princeton Univ., NJ.
Stochastic prediction techniques for wind shear hazard assessment p 48 A92-11381
A geometric approach to regulator and tracker design for an aerospace plane
[AIAA PAPER 91-5054] p 203 A92-17837
Application of stochastic robustness to aircraft control systems p 204 A92-18620
Probabilistic reasoning for intelligent wind shear avoidance p 302 A92-21181
Investigation of air transportation technology at *Princeton University, 1990-1991* p 266 N92-17995
Target pitch angle for the microburst escape maneuver p 266 N92-17996
Neural networks for aircraft system identification
p 303 N92-17998
Technical notes and correspondence: Stochastic robustness of linear time-invariant control systems
p 303 N92-18002
Computer-aided design of flight control systems
[AD-A244657] p 483 N92-21752
Identification of aerodynamic coefficients using computational neural networks
[AD-A244711] p 447 N92-21753
The structure and control of three-dimensional shock wave turbulent boundary layer interactions
[AD-A250209] p 1003 N92-31824
Automatic design of transonic airfoils to reduce the shock induced pressure drag p 949 N92-31863
On the calculation of the response of helicopters to control inputs
[NASA-CR-190812] p 1088 N92-33536

Purdue Univ., West Lafayette, IN.
Impeller flow field measurement and analysis
[ASME PAPER 90-GT-146] p 38 A92-11288
Aeroelastic analysis of wings using the Euler equations with a deforming mesh p 10 A92-13215
Wind tunnel wall effects in a linear oscillating cascade
[ASME PAPER 91-GT-133] p 72 A92-15576
A quiet-flow Ludwieg tube for experimental study of high speed boundary layer transition
[AIAA PAPER 91-5026] p 207 A92-17819
Invariant boundary conditions for cascade flows
p 498 N92-20147
Design of a turbofan powered regional transport aircraft
[NASA-CR-190130] p 461 N92-20280
Aeroelastic behavior of an adaptive lifting surface
p 443 N92-20378
Performance prediction and design of maximum thrust planar supersonic nozzles using a flux-difference-splitting technique p 738 N92-26480
Extension of the integral equation formulation of linearized time dependent subsonic flow
[AD-A250654] p 947 N92-31171
Research on aero-thermodynamic distortion induced structural dynamic response of multistage compressor blading
[AD-A250865] p 974 N92-32059

Q

Queens Univ., Belfast (Northern Ireland).
Further investigation of the effect of model cooling on periodic transonic flow p 721 N92-27961

Queensland Univ., Brisbane (Australia).
Flow around two circular cylinders arranged perpendicular to each other
[PB91-238279] p 297 N92-16225

Queensland Univ., Saint Lucia (Australia).
Mach 4 and Mach 8 axisymmetric nozzles for a high-enthalpy shock tunnel p 78 A92-16668

Quest Integrated, Inc., Kent, WA.
A new unsteady mixing model to predict NO(x) production during rapid mixing in a dual-stage combustor
[NASA-CR-189155] p 971 N92-30569

R

Railway Technical Research Inst., Tokyo (Japan).
Aerodynamic drag on the bullet trains
p 766 N92-26911

RAND Corp., Santa Monica, CA.
When should we start high-rate production of the B-2? An analysis based on flight test results
[RAND/P-7757] p 697 N92-25204
Tilt rotors and the Port Authority of New York and New Jersey Airport System
[RAND-R-3971/1-PA-SUMM] p 636 N92-25262
Developing robust support structures for high-technology subsystems: The AH-64 Apache helicopter
[AD-A252773] p 1017 N92-33499
Advanced airframe structural materials: A primer and cost estimating methodology
[AD-A253371] p 1062 N92-34182

Rand Graduate Inst. for Policies Study, Santa Monica, CA.
The Lockheed F-117A
[RAND-P-7746-RGS] p 731 N92-26673
The rise of active-element phased-array radar
[RAND-P-7747-RGS] p 999 N92-30755

RDM Technology, Rotterdam (Netherlands).
Helicopter handling: Experience and new developments p 465 N92-21969

RDP, Inc., Waltham, MA.
Visual photometric experiment data processing system
[AD-A248657] p 729 N92-27964

Reifer Consultants, Inc., Torrance, CA.
Reuse metrics and measurement: A framework
p 413 N92-19432

Reinhart and Associates, Inc., Austin, TX.
Surface residual stress analysis of metals and alloys
[AD-A248372] p 895 N92-28426

Renaudie (J. F.), Versailles (France).
Flight in adverse environmental conditions
p 449 N92-21680

Rensselaer Polytechnic Inst., Troy, NY.
Pressure and velocity measurements about an airfoil during a parallel blade-vortex interaction
p 446 N92-21429
An investigation of the energy loss and near wake flow field of trailing edge injection p 456 N92-21839
Fundamental aspects of boundary layers and transition in turbomachines p 658 N92-24337
An experimental investigation of a 2-D scramjet inlet at flow Mach numbers of 8 to 25 and stagnation temperatures of 800 to 4,100 K p 739 N92-26586

Research and Development Labs., Culver City, CA.
United States Air Force summer research program 1991. Volume 1: Program management report
[AD-A248763] p 1142 N92-32338

Research Inst. for Advanced Computer Science, Moffett Field, CA.
Ames life science telescience testbed evaluation
[NASA-CR-188856] p 140 N92-12033

Research Inst. for Computing and Information Systems, Houston, TX.
Research into the development of a knowledge acquisition taxonomy
[NASA-CR-189939] p 778 N92-28150
Advanced software development workstation: Effectiveness of constraint-checking
[NASA-CR-190712] p 1134 N92-32865

Research Triangle Inst., Research Triangle Park, NC.
AGSSS: The Airborne Graphics Software Support System; an Ada/PHIGS-based display editor for the rapid development of cockpit display software systems
[AD-A243224] p 277 N92-17221

Resource International, Inc., Westerville, OH.
Criteria for use of seal coats on airport pavements
[DOT/FAA/RD-92/18] p 1102 N92-34247

Rice Univ., Houston, TX.
Optimal trajectories and guidance trajectories for aircraft flight through windshears p 27 A92-11383

The use of artificial neural networks in experimental data acquisition and aerodynamic design p 90 N92-13848
A connectionist approach to autonomous robotic navigation p 454 N92-20356

Rochester Inst. of Tech., NY.
Digital analysis of wind tunnel imagery to measure fluid thickness
[NASA-CR-189234] p 983 N92-31252

Rockwell International Corp., Canoga Park, CA.
Airfoil Vibration Dampers program
[NASA-CR-184276] p 225 N92-14391
System controls challenges of hypersonic combined-cycle engine powered vehicles
p 475 N92-21533
Some comments on turbulence modeling from an industrial perspective p 678 N92-24531

Rockwell International Corp., Downey, CA.
Results of the space shuttle vehicle ascent air data system probe calibration test using a 0.07-scale external tank forebody model (68T) in the AEDC 16-foot transonic wind tunnel (IA-310), volume 1
[NASA-CR-167696] p 286 N92-17167
Results of the space shuttle vehicle ascent air data system probe calibration test using a 0.07-scale external tank forebody model (68T) in the AEDC 16-foot transonic wind tunnel (IA-310), volume 2
[NASA-CR-167697] p 286 N92-17214

Rockwell International Science Center, Thousand Oaks, CA.
A user guide for the EMTAC-MZ CFD code
[NASA-CR-4283] p 678 N92-24242

Rockwell Space Operations Co., Houston, TX.
Testing of the high accuracy inertial navigation system in the Shuttle Avionics Integration Lab
p 210 N92-14087

Rocky Research Corp., Boulder City, NV.
Solid-vapor adsorption refrigeration system development
[PB92-164383] p 771 N92-27715

Rolls-Royce Ltd., Bristol (England).
The 60 years of Bristol engines
[PNR-90845] p 473 N92-20460
Recent developments at the Shoeburyness (England) STOVL Test Facility
[PNR-90806] p 572 N92-22096
VSTOL engine design evolution: Growth of the Pegasus engine for Harrier
[PNR-90805] p 739 N92-27039
ASTOVL engine control
[PNR-90808] p 740 N92-27040
Hot-gas reingestion engine response considerations
[PNR-90810] p 740 N92-27042
Thermally sprayed coating systems for surface protection and clearance control applications in aero engines
[PNR-90802] p 741 N92-27422
Modelling the vaporiser and primary zone flows for a modern gas turbine combustion chamber
p 742 N92-27484
Joint study on the computerisation of in-field aero engines vibration diagnosis
[PNR-90799] p 1072 N92-33815

Rolls-Royce Ltd., Colne (England).
Superplastic applications in aero engines
[PNR-90788] p 473 N92-20436

Rolls-Royce Ltd., Derby (England).
Introduction: Needs and approaches to reliability and quality assurance in design and manufacture
p 402 N92-19005
Materials and process directions for advanced aero-engine design
[PNR-90814] p 378 N92-19938
Re-engining appears to offer best payback for young: Chapter 2 compliant aircraft
[PNR-90848] p 378 N92-19939
Present and future trends in turbine blade material and manufacturing technology
[PNR-90825] p 488 N92-20164
Use of CFD in the design of a modern multistage aero engine LP turbine design
[PNR-90862] p 472 N92-20179
ETOPS: A developing scene
[PNR-90844] p 473 N92-20459
The impact of aircraft noise control technology
[PNR-90846] p 512 N92-20461
Holographic flow visualization in rotating turbomachinery
[PNR-90837] p 500 N92-20491
The environmental impact of commercial aviation: The evolution of exhaust emissions legislation and control technology
[PNR-90847] p 505 N92-20574
The role of crack growth in defect assessment
[PNR-90798] p 501 N92-20909
The environmental challenges for the next supersonic aircraft
[PNR-90782] p 505 N92-20928
Emissions from aircraft: Standards and potential for improvement
[PNR-90768] p 476 N92-21740
Application of finite element methods to fracture mechanics
[PNR-90770] p 503 N92-21741
Environmentally sound
[PNR-90776] p 506 N92-21743
The search for new materials
[PNR-90777] p 490 N92-21744
The proposed revision to RTCA DO178A and its influence on system design
[PNR-90821] p 510 N92-21847
Compressing the compressor
[PNR-90824] p 476 N92-21848
The evolution of the bypass engine
[PNR-90832] p 476 N92-21850
Impact of regulation changes on engine design and certification
[PNR-90789] p 559 N92-22098
The problem of static pressure measurement in turbomachinery annuli using traversable instrumentation
[PNR-90791] p 591 N92-22099
Use of Markov methods in analysis of fault-tolerant systems with flexible repair policies
[PNR-90801] p 767 N92-27038
ASTOVL propulsion systems: Configuration and concept choice
[PNR-90809] p 740 N92-27041
Simultaneous engineering in aero-gas turbine design and manufacture
[PNR-90811] p 740 N92-27043
Powder processing of aero-engine components
[PNR-90813] p 756 N92-27044
The application of a Navier-Stokes CFD method to civil engine intake flows p 769 N92-27471
Re-engining for real stage 3 compliance
[PNR-90872] p 1072 N92-33748
An improved compressor performance prediction model
[PNR-90873] p 1072 N92-33749
The Rolls-Royce Trent
[PNR-90875] p 1061 N92-33750
The impact of air transport on the environment
[PNR-90876] p 1129 N92-33751
Fatigue crack growth of small corner defects from blunt notches in an aeroengine alloy
[PNR-90860] p 1111 N92-34019

Rolls-Royce Ltd., Leavesden (England).
Application of a water droplet trajectory prediction code to the design of inlet particle separator anti-icing systems
[PNR-90839] p 474 N92-20573

Rome Air Development Center, Griffiss AFB, NY.
Heuristic route optimization: A model for force level route planning p 164 N92-12520
Architecture for Survivable System Processing (ASSP)
p 220 N92-14210

Rome Univ. (Italy).
Influence of chemical modeling on the solution of hypersonic shock layers p 183 N92-15016
A boundary integral formulation for unsteady transonic potential flows p 719 N92-27942

Royal Aerospace Establishment, Bedford (England).
Application of Eigenstructure Assignment to the control of powered lift combat aircraft
[RAE-TM-FS-1009] p 135 N92-12004
The development of a requirement specification for an experimental active flight control system for a variable stability helicopter: An Ada simulation in JSD
p 135 N92-12466
SA 330 Puma identification results
p 274 N92-17162
Application areas for rotorcraft system identification: Simulation model validation p 274 N92-17164
Measurement of derivatives due to acceleration in heave and sideslip p 364 N92-18785
Approach and landing guidance p 457 N92-21960
A review of scale effects on surfaces in unsteady motion p 722 N92-27962
Validation of simulation systems for aircraft acceptance testing p 852 N92-28531

Royal Aerospace Establishment, Farnborough (England).
Lightning protection requirements for aircraft: A proposed specification
[RAE-TM-FS(F)-632-REV-ISSUE] p 187 N92-14007
Dynamic wind tunnel tests on control of forebody vortices with suction p 380 N92-18793
A review of icing research at the Royal Aerospace Establishment p 451 N92-21689
Application of S1BYL2 to the AGARD WG18 compressor test cases p 768 N92-27452
Predictions and measurements of 3D viscous flow in a transonic turbine nozzle guide vane row
p 741 N92-27466
Practical considerations in designing the engine cycle
p 869 N92-28460

Royal Air Force Coll., Cranwell (England).
Aircraft gas turbine emissions: Their nature, technology for reduction, and a pollution comparison with channel tunnel transport
[ETN-92-91056] p 559 N92-22406
An investigation into the feasibility of providing a proximity warning device for search and rescue helicopters
[ETN-92-91057] p 530 N92-22408

Royal Aircraft Establishment, Farnborough (England).
Comparison of solution of various Euler solvers and one Navier-Stokes solver for the flow about a sharp-edged cropped delta wing
[AD-B163639L] p 83 N92-12998
Review of aircraft dynamic loads due to flow separation p 85 N92-13008
Asymmetric vortex flow over circular cones
p 86 N92-13014
An experimental investigation of the effect of fineness ratio on lateral force on a pointed slender body of revolution p 86 N92-13015
Control of forebody vortices by suction at the nose of the RAE high incidence research model
p 87 N92-13022
An experimental investigation of vortex flaps on a canard combat-aircraft configuration p 87 N92-13023
The effect of rounding the leading edges on the characteristics of separated flow past delta wings of low aspect ratio
[RAE-LIB-TRANS-2164] p 257 N92-15964
Surface activation of Concorde by Be-7
p 605 N92-23295
The changing role of experimentation in aeroengine R and D: The point of view of the research worker
[AD-A246372] p 740 N92-27062
Parallel knowledge based systems architectures for in-flight mission management p 728 N92-27904

Royal Netherlands Air Force, The Hague.
Diffuser casing upgrade for an advanced turbofan
[NLR-TP-90097-U] p 870 N92-28711

Ruhr Univ., Bochum (Germany).
Influence of the swirl producing construction in the flow and reaction field of turbulent diffusion flames
[ETN-92-92103] p 1127 N92-33916

S

Saab Aircraft Co., Linkoping (Sweden).
Recent applications of linear and nonlinear unsteady aerodynamics for aeroelastic analysis
p 718 N92-27940
Vibro-acoustic FE analyses of the Saab 2000 aircraft
p 1137 N92-32952

Saab-Scania, Linkoping (Sweden).
The structural optimization system OPTSYS: Current status and applications p 550 N92-23232
A manufacturer's approach to ensure long term structural integrity p 838 N92-30133

Sacramento Air Logistics Center, McClellan AFB, CA.
Nondestructive inspection perspectives
p 915 N92-30121

San Jose State Univ., CA.
Analysis of general aviation accidents during operations under instrument flight rules p 16 A92-11172

Sandia National Labs., Albuquerque, NM.
Low volatile organic compound paints
[DE91-017984] p 35 N92-11203
Numerical simulation of VAWT stochastic aerodynamic loads produced by atmospheric turbulence: VAWT-SAL code
[DE92-000597] p 229 N92-15392
Aging Aircraft NDI Development and Demonstration Center (AANC): An overview
[DE92-002358] p 241 N92-15962
Combined VISAR and flash x ray testing techniques
[DE92-004732] p 385 N92-18290
Method and apparatus for acoustic plate mode liquid-solid phase transition detection
[DE92-003778] p 401 N92-18705
Pressure measurements in high speed water tunnels
[DE92-004891] p 386 N92-19978
In situ measurement of particle formation in heated jet fuels: A new application of photon correlation spectroscopy
[DE92-003641] p 488 N92-20132
Center of pressure calculations for a bent-axis vehicle
[DE92-005186] p 498 N92-20143
Monitoring jet fuel degradation using quartz crystal microbalances
[DE92-004730] p 489 N92-20858

The status of the US VAWT program
[DE92-002931] p 505 N92-21040
Fatigue life variability and reliability analysis of a wind turbine blade
[DE92-008673] p 689 N92-25049
Joint computational and experimental aerodynamics research on a reentry vehicle
[DE91-017315] p 667 N92-25315
Evaluating the velocity accuracy of an integrated GPS/INS system: Flight test results
[DE92-007519] p 640 N92-25470
Reynolds number dependence of the drag coefficient for laminar flow through fine-scale screens
[DE92-002930] p 765 N92-26698
Eulerian computational methods
[DE92-008017] p 765 N92-26853
Aging aircraft NDI Development and Demonstration Center (AANC): An overview p 915 N92-30120
Joint computational and experimental aerodynamics research on a hypersonic vehicle
[DE92-013439] p 943 N92-30367
Repetitive High Energy Pulsed Power (RHEPP) temperature monitoring system utilizing Luxtron fluoroptic sensors and thermocouples technical reference manual
[DE92-013461] p 999 N92-30893
Numerical calculations of two-dimensional single and multi-material flow fields with CCICE
[DE92-015778] p 1000 N92-30903
Advanced thermally stable, jet fuels development program annual report. Volume 1: Model and experiment system development
[AD-A249625] p 988 N92-31462
Techniques for autonomous navigation
[DE92-013458] p 957 N92-31746
Axisymmetric bluff-body flow: A vortex solver for thin shells
[DE92-016748] p 1003 N92-31933

Sandia National Labs., Livermore, CA.
Simulation of chemical kinetics in turbulent natural gas combustion
[PB92-123660] p 488 N92-20329

Science Applications International Corp., San Antonio, TX.
Turbine aircraft engine operational trending and JT8D static component reliability study
[DOT/FAA/CT-91/10] p 870 N92-28686

Scientech, Inc., Idaho Falls, ID.
High Intensity Radiated Fields (HIRF) project plan
[DOT/FAA/CT-TN91/1] p 297 N92-16181

Sener Ingenieria y Sistemas S.A., Madrid (Spain).
A methodology for software specification and development based on simulation p 135 N92-12458

Shanghai Inst. of Mechanical Engineering (China).
Research on inverse, hybrid and optimization problems in engineering sciences with emphasis on turbomachine aerodynamics: Review of Chinese advances
p 201 N92-13939
Variational formulation of hybrid problems for fully 3-D transonic flow with shocks in rotor p 176 N92-13953

Sherbrooke Univ. (Quebec).
Vibroacoustic simulation of an airplane structure
p 629 N92-24871

Ship Research Inst., Tokyo (Japan).
Research activities on CFD at the Ship Research Institute p 766 N92-26908

Sikorsky Aircraft, Stratford, CT.
Acoustic predictions using measured pressures from a model rotor in the DNW p 165 A92-14385
Manufacturing techniques - Split torque path helicopter transmission p 110 A92-14452
Full mission simulation: A view into the future
p 884 N92-28537

Simtec, Inc., Manassas, VA.
Simulator data integrity program: Process standard development
[AD-A242207] p 386 N92-19642

Smiths Industries Aerospace and Defence Systems Ltd., Cheltenham (England).
Military and civil software standards and guidelines for guidance and control p 163 N92-12452

Societe Anonyme de Telecommunications, Toulouse (France).
Data processing aspects of the Hermes Flight Control Center p 513 N92-20629

Societe d'Applications Generales d'Electricite et de Mecanique, Paris (France).
Approach and landing assisted by onboard image processing p 457 N92-21959

Societe d'Etudes et de Services pour Souffleries et Installations Aerothermodynamiques, Paris (France).
Experimental investigation of transverse jet effects related to hypersonic space vehicles
p 182 N92-14995

Societe Europeenne de Propulsion, Saint-Medard-en-Jalles (France).
Large thin composite thermostructural parts
p 576 N92-23821

Societe Europeenne de Propulsion, Vernon (France).
Supersonic combustion studies p 211 N92-14984

Societe Nationale d'Etude et de Construction de Moteurs d'Aviation, Cincinnati, OH.
Recent progress in inverse methods in France
p 201 N92-13938

Societe Nationale d'Etude et de Construction de Moteurs d'Aviation, Evry Cedex (France).
Manufacturing process control as a damage tolerance concept p 403 N92-19006

Societe Nationale d'Etude et de Construction de Moteurs d'Aviation, Moissy-Cramayel (France).
Steady and transient performance calculation method for prediction, analysis, and identification
p 869 N92-28461

Solar Turbines, Inc. San Diego, CA.
High-temperature combustor and seal for a water piston propulsor
[AD-A242493] p 229 N92-15385

South Carolina Research Authority. Charleston.
PDES application protocol suite for composites (PAS-C). Functional needs report for the PAS-C program
[AD-A247886] p 1108 N92-32629

Southampton Univ. (England).
Jet noise classical theory and experiments
p 54 N92-10602
The effects of manufacturing tolerances on the vibration of aero-engine rotor-damper assemblies
p 222 N92-14349
Interference heating near fin/body junctions on hypersonic vehicles p 182 N92-14996
Risk to hearing from overflight noise of military aircraft
[ISVR-TR-194] p 604 N92-22241
Magnetic suspension using high temperature superconducting cores p 772 N92-27789
Wind tunnel magnetic Suspension Systems at the University of Southampton, England
p 751 N92-27804
Active control of sound transmission through stiff lightweight composite fuselage constructions
p 1137 N92-32957

Southwest Research Inst., San Antonio, TX.
High-temperature miniaturized turbine engine lubrication system simulator
[AD-A249259] p 868 N92-28294
Laser induced fluorescence detection of gums in jet fuels
[AD-A252685] p 987 N92-30767

SQM Technology, Inc., La Jolla, CA.
Development of an electromagnetic microscope for eddy current evaluation of materials
[AD-A242007] p 406 N92-19873

ST Systems Corp., Lanham, MD.
Radiometric properties of the NS001 Thematic Mapper Simulator aircraft multispectral scanner
p 155 A92-17110

Stanford Univ., CA.
Aircraft control in a downburst on takeoff and landing
p 27 A92-11385
Aircraft control at high-alpha by tangential blowing
[AIAA PAPER 92-0021] p 281 A92-22143
Navier-Stokes analysis of blunt trailing edge airfoils
[AIAA PAPER 92-0024] p 248 A92-22146
Computational study of the aerodynamics and control by blowing of asymmetric vortical flows over delta wings
[NASA-CR-187979] p 14 N92-10990
Analysis of a dusty wall jet
[NASA-CR-189759] p 257 N92-15965
Helicopter active rotor control p 570 N92-22157
High speed transport cruise drag
[NASA-CR-190248] p 527 N92-23103
Control of a helicopter engine in low altitude flight
p 562 N92-23122
Computations of unsteady multistage turbomachinery flows p 562 N92-23671
An adaptive correction technique for Differential Global Positioning System p 726 N92-26623
A preliminary experimental investigation of local isotropy in high-Reynolds-number turbulence
p 912 N92-30042
Non-linear interactions in homogeneous turbulence with and without background rotation p 912 N92-30044
Methods for direct simulation of transition in hypersonic boundary layers 2 p 912 N92-30064
Effect of walls on the supersonic reacting mixing layer
p 912 N92-30065
Turbulent reacting flows and supersonic combustion
[AD-A251065] p 986 N92-30256
Structure of three-dimensional turbulent boundary layers p 999 N92-30654
Nonlinear aerodynamics and the design of wing tips
[NASA-CR-190649] p 946 N92-31157
Mathematical modeling and numerical simulation of the dynamics of flexible structures undergoing large overall motions
[AD-A250202] p 979 N92-31967

State Univ. of New York, Binghamton.
Acoustic fatigue life prediction for nonlinear structures with multiple resonant modes
[NASA-CR-190471] p 1000 N92-30988

State Univ. of New York, Brockport.
Evaluation of a technique to quantify microburst windshear hazard potential to aircraft p 17 A92-11379

State Univ. of New York, Buffalo.
Modeling of the reactant conversion rate in a turbulent shear flow p 829 N92-28820

State Univ. of New York, Stony Brook.
Principles and computer simulations of intercooled-turbocharged gas generator/expander engine p 592 N92-22132

Stato Maggiore Marina, Rome (Italy).
Limitations on helicopter operations in the aeronaval environment p 466 N92-21973

Sterling Federal Systems, Inc., Moffett Field, CA.
Using new aggregation operators in rule-based intelligent control p 51 A92-11456
Aerodynamic design of a Coanda induced force and thruster anti-torque system p 109 A92-14419

Sterling Software, Palo Alto, CA.
Hub and pylon fairing integration for helicopter drag reduction p 107 A92-14391

Strathclyde Univ., Glasgow (Scotland).
Inverse problems and imaging (Pitman research notes in mathematics series Number 245)
[AD-A240333] p 53 N92-11737

Stuttgart Univ. (Germany).
IRS organigram p 33 N92-10053
Supercritical blade design on stream surfaces of revolution with an inverse method p 220 N92-13950
Experimental investigations of exciting forces caused by flow in labyrinth seals p 223 N92-14354
The IRS plasma wind tunnels for the investigation of thermal protection materials for reentry vehicles
p 208 N92-15009

Sulzer Bros. Ltd., Winterthur (Switzerland).
Annular seals of high energy centrifugal pumps: Presentation of full scale measurement
p 224 N92-14362

Sundstrand Corp., Rockford, IL.
Measurements and correlation of two-phase pressure drop under microgravity conditions p 37 A92-10435

Surveillance Research Lab., Salisbury (Australia).
Buffered serial data card
[AD-A246435] p 727 N92-26948

Survival Systems Ltd. (Alberta).
A report on enhancements for existing and future helicopters supporting operations of the Canadian oil and gas industry
[CTN-91-60126] p 636 N92-25350

Sverdrup Technology, Inc., Brook Park, OH.
Ongoing development of a computer jobstream to predict helicopter main rotor performance in icing conditions p 65 A92-14407
The effect of steady aerodynamic loading on the flutter stability of turbomachinery blading
[ASME PAPER 91-GT-130] p 71 A92-15574
Deterministic blade row interactions in a centrifugal compressor stage
[ASME PAPER 91-GT-273] p 75 A92-15670
Unsteady blade-surface pressures on a large-scale advanced propeller - Prediction and data
p 80 A92-17178
Unsteady Euler analysis of the flowfield of a propfan at an angle of attack p 242 A92-21070
Unsteady blade pressures on a propfan at takeoff: Euler analysis and flight data
[NASA-CR-189076] p 130 N92-13071
Prediction of noise field of a propfan at angle of attack
[NASA-CR-189047] p 166 N92-13759
Development of an analytical method to predict helicopter main rotor performance in icing conditions
[NASA-CR-189110] p 258 N92-15967
Rotary engine performance limits predicted by a zero-dimensional model
[NASA-CR-189129] p 474 N92-20650
Three-dimensional compressible turbulent computations for a diffusing S-duct
[NASA-CR-4392] p 526 N92-22249
A sophisticated, multi-channel data acquisition and processing system for high frequency noise research
[NASA-CR-189137] p 696 N92-24688
A comparison of the calculated and experimental off-design performance of a radial flow turbine
[NASA-CR-189207] p 831 N92-29402
Three-dimensional compressible turbulent computations for a nondiffusing S-duct
[NASA-CR-4391] p 951 N92-32240

Sverdrup Technology, Inc., Cleveland, OH.
The role of tip clearance in high-speed fan stall
[ASME PAPER 91-GT-83] p 69 A92-15550
NASA low-speed centrifugal compressor for 3-D viscous code assessment and fundamental flow physics research
[ASME PAPER 91-GT-140] p 72 A92-15580
The numerical simulation of a high-speed axial flow compressor
[ASME PAPER 91-GT-272] p 75 A92-15669
Computers in aeronautics and space research at the Lewis Research Center
[NASA-TM-105096] p 53 N92-11642
Grid generation for a complex aircraft configuration
p 649 N92-25714
An interactive grid generation technique for turbomachinery p 659 N92-25717
Sydney Univ. (Australia).
Development of a wind chamber for model testing of tornado forces on structures
[PB92-104165] p 386 N92-19940
Syms (Raymond A.) and Associates, Bridge Water, NJ.
Operational survey: VFR heliport approaches and departures
[SCT-91RR-26] p 190 N92-14033
Syracuse Univ., NY.
Constant-temperature anemometry measurements in hypersonic boundary layers p 90 N92-13861
Systems Control Technology, Inc., Arlington, VA.
Guidelines for integrating helicopter assets into emergency planning
[SCT-91RR-18] p 18 N92-10993
Heliport VFR airspace design based on helicopter performance
[SCT-90RR-34] p 103 N92-13049
Helicopter rejected takeoff airspace requirements
[SCT-91RR-28] p 116 N92-13058
Rotorcraft acceleration and climb performance model
[SCT-90RR-30] p 116 N92-13059
Helicopter physical and performance data
[SCT-91RR-27] p 116 N92-13060
New York Downtown Manhattan (Wall Street) Heliport: Operations analysis
[DOT/FAA/RD-91/12] p 139 N92-13077
Operational survey: VFR heliport approaches and departures
[SCT-91RR-26] p 190 N92-14033
Rotorcraft low altitude IFR benefit/cost analysis: Operations analysis
[SCT-90RR-44] p 191 N92-15061
Analysis of helicopter accident risk exposure near heliports, airports, and unimproved sites
[SCT-91RR-13] p 637 N92-26028
Rotorcraft terminal ATC route standards
[SCT-90RR-33] p 641 N92-26101
Composite profiles of helicopter mishaps at heliports and airports
[AD-A248887] p 724 N92-28052
Systems Control Technology, Inc., Palo Alto, CA.
Turbine engine diagnostics system study
[DOT/FAA/CT-91/16] p 202 N92-14064
Systems Technology, Inc., Hawthorne, CA.
Aeroservoelastic stabilization techniques for hypersonic flight vehicles
[AIAA PAPER 91-5056] p 203 A92-17839
Assessment of flying-quality criteria for air-breathing aerospacecraft
[NASA-CR-4442] p 663 N92-25982
The use of ground based simulation for handling qualities research: A new assessment p 885 N92-28545
Effects of cockpit lateral stick characteristics on handling qualities and pilot dynamics
[NASA-CR-4443] p 878 N92-28584

T

Technical Univ. of Istanbul (Turkey).
Numerical simulation of vortex street-edge interaction
p 88 N92-13027
Technion - Israel Inst. of Tech., Haifa.
Numerical prediction of subsonic turbulent flows over slender bodies at high incidence p 172 A92-18358
Adaptive suppression of biodynamic interference in helmet-mounted displays and head teleoperation
p 197 A92-18611
Application of aeroservoelastic modeling using minimum-state unsteady aerodynamic approximations
p 204 A92-18622
Observability under recurrent loss of data
p 302 A92-21191
A simulation model of a single rotor helicopter
p 979 N92-31865
Estimation of aircraft attitude by angular rate measurements p 963 N92-31881
The three-dimensional stability of the Foeppl vortices
p 949 N92-31889
Technion Research and Development Foundation Ltd., Haifa (Israel).
Multi-disciplinary optimization of aeroservoelastic systems
[NASA-CR-188983] p 44 N92-11377
Technische Hochschule, Aachen (Germany).
High enthalpy testing in the Aachen (Fed. Republic of Germany) shock tunnel TH 2 p 208 N92-15021
Simulation of the flow on a space glider. Stagnation point calculation using the 2D Navier-Stokes equations including chemical effects p 624 N92-24393
Hypersonic configurations in slow speed flight
p 624 N92-24394
Supersonic flow in compression stages and inlets
p 625 N92-24395
Experimental investigation of the unsteady pressure field around an oscillating blade
[MITT-90-01] p 768 N92-27407
Technische Univ., Aachen (Germany).
On aircraft wake properties and some methods for stimulating decay and breakdown of tip vortices
p 87 N92-13021
Application of finite element method to hypersonic nozzle flow computations p 769 N92-27479
Technische Univ., Berlin (Germany).
The electronic aeronautical chart for general aeronautics: A system specification
[ILR-MITT-263(1991)] p 20 N92-10997
Technische Univ., Brunswick (Germany).
Vortex formation over a close-coupled canard-wing-body configuration in unsymmetrical flow p 85 N92-13010
Project of an adaptive multiaxial autopilot with learning pilot control
[ETN-92-90592] p 205 N92-15072
A multivariable control concept for a gas turbine engine
[ETN-92-92104] p 1072 N92-33645
Technische Univ., Delft (Netherlands).
Experimental and numerical investigation of the vortex flow over a delta wing at transonic speed
p 84 N92-13001
The two-bay crack problem in fuselages built in GLARE and ARALL
[LR-653] p 196 N92-14044
Bulging of fatigue cracks in a pressurized aircraft fuselage
[LR-655] p 196 N92-14045
Propeller-driven-small airplane noise certification
[LR-650] p 237 N92-14798
- Symposium on High Speed Airbreathing Propulsion: The Solid Fuel Combustion Chamber and Beyond
[ETN-92-90685] p 575 N92-22268
CAD product data exchange: Conversions for curves and surfaces
[ISBN-90-6275-723-9] p 648 N92-24964
Towards GLARE: The development of a fatigue insensitive and damage tolerant aircraft material
[ETN-92-91301] p 648 N92-24966
Delfi: Design, development, and applicability of expert systems shells
[ISBN-90-6275-734-0] p 692 N92-25306
The basic research simulator programme and the industrial and aerospace community: Opportunities for cooperative research
[LR-662] p 887 N92-28579
Inverse control problems: Mathematical preliminaries, system theoretical approaches, and their applications to aircraft dynamics
[LR-665] p 923 N92-28581
Low-velocity impact loading on fibre reinforced aluminum laminates (ARALL) and other aircraft sheet materials
[ETN-92-91613] p 987 N92-30414
Calibration of GPS antennas
[ETN-92-92034] p 1051 N92-33693
Technische Univ., Eindhoven (Netherlands).
On the limitations of Froude's actuator disc concept
[ETN-91-90136] p 81 N92-11973
Technische Univ., Graz (Austria).
Comparison of two-way satellite time transfer and GPS common-view time transfer between OCA and TUG
p 1050 N92-33356
Technische Univ., Munich (Germany).
Hydraulic actuator system for rotor control
p 224 N92-14363
Calculation of installation effects within performance computer programs p 869 N92-28465
Technische Univ., Twente (Netherlands).
Improved shock-capturing of Jameson's scheme for the Euler equations
[PB92-148758] p 596 N92-23251
Technology Development Corp., Madrid (Spain).
Electronically steerable antenna for aircraft
p 229 N92-15272
Technology Systems, Inc., North Edgecomb, ME.
Development of the Basic Flight Instruction Tutoring System (BFITS)
[AD-A246458] p 751 N92-27836
Tel-Aviv Univ. (Israel).
Timing analysis of parallel algorithms on a MIMD multiprocessor
[ITN-92-85153] p 510 N92-20905
Telespazio, S.p.A., Rome (Italy).
Description and simulation results of the Italsat AOCS advanced flight simulator p 667 N92-24472
Tennessee Univ., Chattanooga.
Redesign of flight space shuttle main engine nozzle G-15 seal area based on the thermal analysis and flow models p 212 N92-15877
Tennessee Univ., Knoxville.
Measurements and correlation of two-phase pressure drop under microgravity conditions p 37 A92-10435
Tennessee Univ., Tullahoma.
Development of a multigrid transonic potential flow code for cascades
[NASA-CR-190480] p 830 N92-29361
Tennessee Univ. Space Inst., Tullahoma.
Review of the physics of enhancing vortex lift by unsteady excitation p 66 A92-15344
A wall interference assessment/correction system
[NASA-CR-189785] p 259 N92-15974
Dynamic interactions between hypersonic vehicle aerodynamics and propulsion system performance
[NASA-CR-190638] p 1038 N92-33304
Test Group (6585th), Holloman AFB, NM.
The use and misuse of aircraft and missile RCS statistics
[AD-A239892] p 41 N92-10141
Texas A&M Univ., College Station.
Aerodynamics and heat transfer investigations on a high Reynolds number turbine cascade
[ASME PAPER 91-GT-157] p 148 A92-15593
Direct-inverse transonic wing-design method in curvilinear coordinates including viscous interaction
p 193 A92-20202
Nonlinear rotordynamics analysis
[NASA-CR-184263] p 221 N92-14344
Test results for rotordynamic coefficients of the SSME HPOTP turbine interstage seal with two swirl brakes
p 223 N92-14357
Effect of eccentricity on the static and dynamic performance of a turbulent hybrid bearing
p 225 N92-14373
An initial investigation into methods of computing transonic aerodynamic sensitivity coefficients
[NASA-CR-190040] p 348 N92-19545
An experimental investigation of the surface flow and wake dynamics associated with transverse flow over wavy cylinders p 681 N92-25547
AFRAPT Program at Texas A and M University research for advanced aircraft engine structures
[AD-A247040] p 743 N92-28076
Determination of aerodynamic sensitivity coefficients for wings in transonic flow
[NASA-CR-190570] p 832 N92-29657
Further wind tunnel investigation of the SM701 airfoil with aileron and turbulators
[NASA-CR-190702] p 1038 N92-33063
Experimental study of performance degradation of a rotating system in the NASA Lewis RC icing tunnel
[NASA-CR-190684] p 1102 N92-34141
Texas Univ., Arlington.
Experimental studies of hypersonic shock-wave boundary-layer interactions
[NASA-CR-190731] p 950 N92-32162
Texas Univ., Austin.
Simulation of GRM drag compensation system
p 285 A92-21023
The effect of a type 3 and type 4 shock/shock interaction on heat transfer in the stagnation region
p 160 N92-13867
Experimental study of a vortex subjected to imposed strain
[NASA-CR-189757] p 258 N92-15969
A numerical model for sonic boom propagation through an inhomogeneous, windy atmosphere
p 1138 N92-33876
Model experiment to study the effect of turbulence on risetime and waveform of N waves
p 1139 N92-33881
Textron Bell Helicopter, Fort Worth, TX.
Synthesis of a helicopter full-authority controller
p 280 A92-21178
Technology needs for high speed rotorcraft (3)
[NASA-CR-177592] p 195 N92-14039
Textron Lycoming, Stratford, CT.
Application of CFD in the design of gas turbine engine components p 741 N92-27461
Thomson Composants, Saint Egreve (France).
What is an ASIC? p 859 N92-28377

Thomson-CSF, Malakoff (France).
Mixed approach towards modular avionics conflicting requirements p 199 N92-14051
Thomson-CSF, Montrouge (France).
A radar signal processing ASIC and a VME interface circuit p 859 N92-28380
Thomson-TRT Defense, Guyancourt (France).
A cable detection lidar system for helicopters p 1001 N92-31068
Titan Systems, Inc., Princeton, NJ.
A unified viscous theory of lift and drag of 2-D thin airfoils and 3-D thin wings
[NASA-CR-4414] p 178 N92-13997
Tohoku Univ., Sendai (Japan).
Three dimensional boundary layer transition on a yawed cylinder p 766 N92-26909
Tokyo Univ., Sagamihara (Japan).
Aerodynamic aircraft design methods and their notable applications: Survey of the activity in Japan p 193 N92-13930
Toledo Univ., OH.
Parallel computation of aerodynamic influence coefficients for aeroelastic analysis on a transputer network p 53 A92-12367
Euler flow predictions for an oscillating cascade using a high resolution wave-split scheme
[ASME PAPER 91-GT-198] p 74 A92-15623
Cascade flutter analysis with transient response aerodynamics p 154 A92-15972
Eigenvalue calculation procedure for an Euler/Navier-Stokes solver with application to flows over airfoils p 170 A92-17429
Heat transfer measurements from a smooth NACA 0012 airfoil p 218 A92-20215
Roughness effects on heat transfer from a NACA 0012 airfoil p 219 A92-20217
Time domain flutter analysis of cascades using a full-potential solver p 176 A92-20747
Forebody vortex control with miniature, rotatable nose-boom strakes
[AIAA PAPER 92-0022] p 281 A92-22144
Development of an improved model for runback water on aircraft surfaces
[AIAA PAPER 92-0042] p 270 A92-22160
An experimental analysis of lateral jet injection into confined swirling crossflows p 156 N92-12199
Effects of inlet distortion on the development of secondary flows in a subsonic axial inlet compressor rotor p 89 N92-13030
Computer code for preliminary sizing analysis of axial-flow turbines
[NASA-CR-4430] p 473 N92-20196
Numerical simulation of an aircraft anti-icing system incorporating a rivulet model for the runback water p 448 N92-20303
A laser velocimeter investigation of the normal shockwave boundary layer interaction p 500 N92-20485
Users manual and modeling improvements for axial turbine design and performance computer code TD2-2
[NASA-CR-189118] p 716 N92-27376
Users manual for updated computer code for axial-flow compressor conceptual design
[NASA-CR-189171] p 924 N92-30207
Toronto Univ., Downsview (Ontario).
Aerodynamics p 202 N92-13977
Computational fluid dynamics p 177 N92-13979
Flight research p 194 N92-13981
Flight simulation p 207 N92-13982
Nonstationary gasdynamics p 220 N92-13985
An evaluation of IFR approach techniques: Generic helicopter simulation compared with actual flight p 886 N92-28550
Toronto Univ. (Ontario).
An experimental and computational investigation of an annular reverse-flow combustor
[UTIAS-338] p 129 N92-11996
The modelling of turbulence and downbursts for flight simulators
[UTIAS-339] p 161 N92-12373
Identification techniques: Model structure and time domain methods p 273 N92-17157
TVD finite-difference solutions of nonequilibrium vibrationally relaxing and chemically reacting gaseous flows p 626 N92-24854
Automated grid generation for high-lift configurations p 628 N92-24869
On the stability of a dual spin satellite with asymmetric rotor and flexible platform
[ISBN-0-315-54650-6] p 753 N92-27613
Pitch-heave dynamics models for an air cushion vehicle
[ISBN-0-315-51095-1] p 716 N92-27624
The modelling of turbulence and downbursts for flight simulators
[ISBN-0-315-59945-6] p 749 N92-27645
An evaluation of decelerating IFR approaches utilizing a helicopter flight simulator
[CTN-92-60348] p 1048 N92-32845
Ideal efficiency of propellers based on Theodorsen's theory: A review and computer study, with extended plus simplified charts
[UTIAS-TN-271] p 1071 N92-33102
Transport Canada Aviation, Ottawa (Ontario).
Aeronautical mobile satellite service: An overview p 594 N92-22573
Aeronautical mobile satellite service: Air traffic control applications p 677 N92-24164
Transportation Research Board, Washington, DC.
Public-sector aviation issues: Graduate research award papers, 1989 - 1990
[PB91-242271] p 308 N92-19662
TRW, Inc., Beavercreek, OH.
A model of the ADA avionics real-time system: An example of the benefits of the hardware/software codesign approach in development of real-time systems
[AD-A248893] p 967 N92-30524
TRW Space Technology Labs., Redondo Beach, CA.
Getting expert systems off the ground: Lessons learned from integrating model-based diagnostics with prototype flight hardware p 220 N92-14217
Laser-initiated conical detonation wave for supersonic combustion, part 3
[AD-A250522] p 989 N92-32076
Tsentralni Aerogidrodinamicheskii Inst., Moscow (USSR).
Aerothermodynamic configuration of first generation aerospace planes (of Buran-type) and first flight results p 211 N92-14975
Tsinghua Univ., Bejing (China).
Design of transonic compressor cascades using hodograph method p 202 N92-13973
The research progress on Hodograph Method of aerodynamic design at Tsinghua University p 177 N92-13974
Turbine Support Europa, Tilburg (Netherlands).
Diffuser casing upgrade for an advanced turbofan
[NLR-TP-90097-U] p 870 N92-28711

U

UFA, Inc., Newton, MA.
Expert system management system
[AD-A247102] p 781 N92-26863
United Kingdom Atomic Energy Authority, Harwell (England).
Report on the workshop on Ion Implantation and Ion Beam Assisted Deposition
[AD-A250561] p 927 N92-28923
United Technologies Corp., East Hartford, CT.
Structural tailoring of advanced turboprops (STAT): User's manual
[NASA-CR-187101] p 26 N92-11016
Life prediction and constitutive models for engine hot section anisotropic materials program
[NASA-CR-189222] p 973 N92-31534
United Technologies Optical Systems, Inc., West Palm Beach, FL.
Navier-Stokes analysis of turbine blade heat transfer and performance p 768 N92-27468
United Technologies Research Center, East Hartford, CT.
Heat transfer in rotating serpentine passages with trips normal to the flow
[ASME PAPER 91-GT-265] p 151 A92-15663
New applications of liquid-crystal thermography in rotating turbomachinery heat transfer research
[ASME PAPER 91-GT-354] p 153 A92-15710
Development of unsteady aerodynamic analyses for turbomachinery aeroelastic and aeroacoustic applications
[NASA-CR-4405] p 12 N92-10979
The effects of Reynolds number, rotor incidence angle and surface roughness on the heat transfer distribution in a large-scale turbine rotor passage
[NASA-CR-184260] p 42 N92-11297
High temperature static strain gage development
[NASA-CR-189044] p 195 N92-14037
Loading and vibration reduction through active aerodynamic control
[AD-A242321] p 283 N92-17243
Turbine disk cavity aerodynamics and heat transfer p 1124 N92-32265
Universitaet der Bundeswehr Muenchen, Neubiberg (Germany).
Knowledge-based planning for controlled airspace flight operation as part of a cockpit assistant p 727 N92-27895
A semi empirical method for the analytical representation of stationary measured profile coefficients for applications of rotary wing aerodynamics
[ETN-92-91491] p 832 N92-29741
Production of periodical Mach number variations in high subsonic flow in a blow down wind tunnel, and its influence on profile measurements
[ETN-92-91492] p 833 N92-29889
Examination of the main error factors with regards to secondary losses in compression and turbine cascades by variations of the blade picture ratio
[ETN-92-91493] p 871 N92-29927
Universiteit Twente, Enschede (Netherlands).
On the origin and acoustical behaviour of cloud cavitation
[ISBN-90-9004317-9] p 1125 N92-33066
University Coll. of North Wales, Bangor.
Parallel processing applications for gas turbine engine control p 25 N92-11012
University of Northern Illinois, De Kalb.
Estimating the reliability of a system on the basis of sample paths
[AD-A248585] p 774 N92-28171
University of South Florida, Tampa.
Comparison of polynomial approximations and artificial neural nets for response surfaces in engineering optimization p 165 N92-13835
Stability of intershaft squeeze film dampers p 222 N92-14351
University of Southern California, Los Angeles.
A new technique for temperature and specie concentration measurements in unseeded supersonic and hypersonic gas flows
[AD-A241536] p 158 N92-13409
Active noise control: Piezoceramic actuators in fluid/structure interaction models
[NASA-CR-190328] p 685 N92-26125
The eddy structures in bounded shear flows p 717 N92-27712
Practical method's for robust multivariable control
[AD-A248473] p 1009 N92-30322
Perspectives on hypersonic viscous and nonequilibrium flow research
[NASA-CR-190817] p 1039 N92-33413
University of Western Ontario, London.
Laminar-turbulent transition process in the presence of simulated wall roughness p 626 N92-24858
Flow visualization using computer animation p 629 N92-24870

V

Valparaiso Univ., IN.
Experiences with optimizing airfoil shapes for maximum lift over drag p 90 N92-13838
Vanderbilt Univ., Nashville, TN.
Thermal barrier coating life prediction model development
[ASME PAPER 91-GT-40] p 147 A92-15523
Rarefied-flow aerodynamics
[NASA-CR-190452] p 715 N92-27191
Vatell Corp., Blacksburg, VA.
Eddy current transducing system
[DE91-018924] p 401 N92-18515
Veritas Research A.S., Hovik (Norway).
Probabilistic design and fatigue management based on probabilistic fatigue models with reliability updating p 360 N92-18574
Vermont Univ., Burlington.
CSM solutions of rotating blade dynamics using integrating matrices
[NASA-CR-190577] p 1003 N92-31619
Vigyan Research Associates, Inc., Hampton, VA.
Wind-tunnel and flight tests of a delta-wing remotely piloted vehicle p 21 A92-13208
Interference effects of very high bypass ratio nacelle installations on a low-wing transport
[ASME PAPER 91-GT-241] p 75 A92-15646
On the interaction between first- and second-mode waves in a supersonic boundary layer p 78 A92-16462
Aerodynamic design and optimization in one shot
[AIAA PAPER 92-0025] p 248 A92-22147
Vortex control: Further encounters p 87 N92-13020
The NASA Langley Research Center 0.3-meter transonic cryogenic tunnel microcomputer controller source code
[NASA-CR-189556] p 209 N92-15077
Structural dynamics and vibrations of damped, aircraft-type structures
[NASA-CR-4424] p 499 N92-20194
A low-speed wind tunnel study of vortex interaction control techniques on a chine-forebody/delta-wing configuration
[NASA-CR-189616] p 632 N92-25510

High-alpha vortex decoupling investigations on a chine forebody/Delta wing configuration at transonic Mach numbers
[NASA-CR-189642] p 715 N92-26651
Subsonic investigations of vortex interaction control for enhanced high-alpha aerodynamics of a chine forebody/Delta wing configuration
[NASA-CR-189641] p 715 N92-26652

Virginia Polytechnic Inst. and State Univ., Blacksburg.
Three-dimensional space-marching algorithm on unstructured grids p 5 A92-11058
The dynamic character of the wake of an axisymmetric body at an angle of attack
[AIAA PAPER 91-3268] p 8 A92-12741
A neural network for the identification of measured helicopter noise p 162 A92-14387
Effects of unsteady shock impingement on high-speed gaseous mixing
[AIAA PAPER 91-5091] p 172 A92-17857
Navier-Stokes computations for aerodynamic configurations at high angles of attack
p 246 A92-21981
A computational study on directional stability of chine-shaped forebodies at high-alpha
[AIAA PAPER 92-0030] p 249 A92-22152
Oscillating shock impingement on low-angle gas injection into a supersonic flow p 89 N92-13032
Design optimization of transonic airfoils
p 177 N92-13961
An experimental study of a turbulent wing-body junction and wake flow
[AD-A243388] p 260 N92-17222
Hi-alpha forebody design. Part 1: Methodology base and initial parametrics
[NASA-CR-189849] p 358 N92-18024
Hi-alpha forebody design. Part 2: Determination of body shapes for positive directional stability
[NASA-CR-189850] p 359 N92-18038
Integrated aerodynamic-structural-control wing design
p 349 N92-19698
A multi-loop guidance scheme using singular perturbation and linear quadratic regulator techniques simultaneously p 481 N92-20148
Runway exit designs for capacity improvement demonstrations. Phase 2: Computer model development
[NASA-CR-190166] p 484 N92-21162
Time-optimal reorientation maneuvers of an aircraft
p 549 N92-22605
Sensitivity analysis of dynamic aeroelastic responses
p 571 N92-23229
Efficient and robust design optimization of transonic airfoils p 528 N92-23717
Numerical simulations of wakes, blade-vortex interaction, flutter, and flutter suppression by feedback control p 597 N92-23997
Three-dimensional upwind scheme for solving the Euler equations on unstructured tetrahedral grids
p 714 N92-26585
Observation and measurements of flow structures in the stagnation region of a wing-body junction
p 714 N92-26616
Dynamic simulation of compressor and gas turbine performance p 869 N92-28463
A model of the ADA avionics real-time system: An example of the benefits of the hardware/software codesign approach in development of real-time systems
[AD-A248893] p 967 N92-30524
An experimental study of the relationship between velocity and pressure fluctuations in a wing-body junction
[AD-A249628] p 946 N92-31122
A computational examination of directional stability for smooth and chined forebodies at high-alpha
[NASA-CR-4465] p 950 N92-32114
Effects of curvature and rotation on turbulence in the NASA low-speed centrifugal compressor impeller
p 1124 N92-32292
Initial postbuckling response of an unsymmetrically laminated rectangular plate p 1108 N92-32586

Virginia Univ., Charlottesville.
Experimental investigation of a supersonic combustion flowfield employing staged transverse injection behind a rearward-facing step
[AIAA PAPER 92-0090] p 292 A92-22196
Dynamic characteristics and stability analysis of space shuttle main engine oxygen pump p 224 N92-14366
Microgravity nucleation and particle coagulation experiments support
[NASA-CR-190159] p 502 N92-21385
Microgravity nucleation and particle coagulation experiments support
[NASA-CR-189899] p 502 N92-21433
Computational structures technology and UVA Center for CST p 683 N92-25912
Light thermal structures and materials for high speed flight p 649 N92-25922
Professor Jesse W. Beams and the first practical magnetic suspension p 771 N92-27723
Stability and performance of notch filter control for unbalance response p 771 N92-27731
Low power magnetic bearing design for high speed rotating machinery p 772 N92-27739
Design of bearings for rotor systems based on stability
p 773 N92-27799

Visidyne, Inc., Burlington, MA.
Aircraft lidar sensitivity study for measuring water vapor
[AD-A240549] p 42 N92-11237

Von Karman Inst. for Fluid Dynamics, Rhode-Saint-Genese (Belgium).
Aerodynamic effects of de/anti-icing fluids and description of a facility and test technique for their assessment p 452 N92-21697
Boundary Layers in Turbomachines
[VKI-LS-1991-06] p 658 N92-24336
A frontal approach for node generation in Delaunay triangulations p 771 N92-27680
Introduction to Flutter of Winged Aircraft, volume 2
[VKI-LS-1992-01-VOL-2] p 1088 N92-34161

Vrije Univ., Brussels (Belgium).
An integrated CFD system for 3D turbomachinery applications p 741 N92-27464

W

Walter Kidde Aerospace, Inc., Wilson, NC.
Feasibility of systematic recycling of aircraft Halon extinguishing agents
[DOT/FAA/CT-91/21] p 352 N92-18259

Warsaw Technical Univ. (Poland).
Design of 3-dimensional complex airplane configurations with specified pressure distribution via optimization
p 194 N92-13948

Washington State Univ., Pullman.
A DFW microburst model based on DL-191 data
p 17 A92-11380
Design of localizer capture and track hold for a transport airplane - An H(infinity)/LTR approach
p 52 A92-11583
Study of the leading-edge vortex dynamics in the unsteady flow over an airfoil
[AD-A247532] p 829 N92-28865

Washington Univ., Seattle.
Stratospheric electrodynamics from superpressure balloons - A technical challenge for small payload environments
[AIAA PAPER 91-3674] p 14 A92-11019
Design of localizer capture and track hold for a transport airplane - An H(infinity)/LTR approach
p 52 A92-11583
Pneumatic distortion compensation for aircraft surface pressure sensing devices p 218 A92-20206
Investigation of hypersonic ramjet propulsion cycles using a ram accelerator test facility
[IAF PAPER 91-275] p 278 A92-22482
Thermoviscoplastic response of Ti-15-3 under various loading conditions
[NASA-CR-187621] p 45 N92-11391
Advanced rotorcraft control using parameter optimization
[NASA-CR-189502] p 135 N92-13073
Theoretical and experimental investigation of the thermodynamics of the thermally choked ram accelerator p 604 N92-22137
Tear straps in airplane fuselage
[AD-A248543] p 854 N92-29511
Formation and sustainment of a very low aspect ratio tokamak using coaxial helicity injection: Helicity Injected Torus (HIT) experiment
[DE92-014311] p 1136 N92-32595

Waterloo Univ. (Ontario).
Wind-tunnel investigation of aerodynamic and stability characteristics of a forward swept wing X-29 model
p 627 N92-24862

Wayne State Univ., Detroit, MI.
CFD analysis of jet mixing in low NO(x) flametube combustors
[ASME PAPER 91-GT-217] p 124 A92-15634

Weizmann Inst. of Science, Rehovoth (Israel).
Aerodynamic design and optimization in one shot
[AIAA PAPER 92-0025] p 248 A92-22147

West Virginia Univ., Morgantown.
Experimental investigation of the effects of blowing on bursting of strake vortices
[AD-A240256] p 13 N92-10985
The effects of winglets on low aspect ratio wings at supersonic Mach numbers
[NASA-CR-4407] p 178 N92-13996
Helicopter rotor blade dynamics with bilinear formulation p 463 N92-21856

Wichita State Univ., KS.
Doppler global velocimeter measurements of the vortical flow above a thin delta wing
[AIAA PAPER 92-0005] p 292 A92-22130
An evaluation of preliminary Doppler global velocimetry measurements p 90 N92-13849
Wichita State University 1986 aviation safety research projects
[DOT/FAA/CT-91/4] p 263 N92-16986
Program plans: Aviation safety research
[NIAR-91-30] p 264 N92-17587
Examination of energy spectra moments in a developing turbulent flow
[NIAR-91-28] p 399 N92-18116
Techfest 18 Proceedings
[NIAR-92-1] p 420 N92-21501
A study in dynamic control of a super maneuver with neural networks p 463 N92-21510
The Flight Simulation Facility at the Wichita State University p 484 N92-21511
Test plan for the international aircraft operator information system
[DOT/FAA/CT-91/18] p 781 N92-26830

Windsor Univ. (Ontario).
Analysis and design of transonic airfoils using streamwise coordinates p 194 N92-13955

Wisconsin Univ., Madison.
Dynamic simulation of a solid fuelled gas turbine system p 592 N92-22315
Three-dimensional modeling of diesel engine intake flow, combustion and emissions
[NASA-CR-189126] p 658 N92-24539

Worcester Polytechnic Inst., MA.
NASA advanced aeronautics design solar powered remotely piloted vehicle
[NASA-CR-190007] p 462 N92-20665

Wright Lab., Wright-Patterson AFB, OH.
Subsonic wind tunnel testing handbook
[AD-A240263] p 13 N92-10986
Nonlinear aspects of aerospace structures at high excitation levels flat aluminum beams and plates studied
[AD-A240600] p 44 N92-11383
Adaptive tactical navigation program
p 102 N92-12529
Pilot's associate: Evolution of a functional prototype
p 118 N92-12531
Integrated Communications, Navigation, Identification, Avionics (ICNIA) expert system for fault tolerant avionics
p 118 N92-12539
A development-memory approach for enhancing avionics software logistics p 119 N92-12540
Engineering Graphical Analysis Tool (EGAT) development program p 164 N92-12542
Limitations of a holographic 3-D pixel projector for cockpit displays
[AD-A241295] p 119 N92-13067
Susceptibility of a parallelogram type skin friction balance to rotational motion
[AD-A241348] p 139 N92-13078
Proceedings of Damping 1991, volume 3
[AD-A241313] p 225 N92-14386
Evolution and development of hypersonic configurations 1958-1990
[AD-A242768] p 197 N92-15069
Proceedings of the USAF Structural Integrity Program Conference
[AD-A242943] p 279 N92-17204
Aging aircraft structural damage analysis
p 360 N92-18575
Non-linear airloads hypersurface representation: A time domain perspective p 346 N92-18783
Forebody vortex control aeromechanics
p 380 N92-18792
The Air Force Manufacturing Technology (MANTECH): Technology transfer methodology as exemplified by the radar transmit/receive module program
p 593 N92-22451
Large scale optimization using ASTROS: An overview
p 649 N92-25921
Airframe life prediction p 649 N92-25931
Military engine computational structures technology
p 660 N92-25934
The effect of jet fuel exposure on advanced aerospace composites. Part 1: Thermal and chemical analysis
[AD-A246559] p 756 N92-27531
Add-on damping treatment for life extension of the F-15 upper-outer wing skin
[AD-A246149] p 746 N92-27577
Foreign object damage to tires operating in a wartime environment
[AD-A247195] p 724 N92-27682
Unsteady aerodynamics for aeroelasticity at the Flight Dynamics Directorate p 718 N92-27939
Piloted simulation effectiveness development applications and limitations p 883 N92-28524

A methodology for the evaluation of runway roughness for repair
[AD-A250407] p 887 N92-28772
An assessment of the B-747's capability to operate on rough surfaces
[AD-A250134] p 963 N92-31793
An examination of several high resolution schemes applied to complex problems in high speed flows
[AD-A250814] p 1124 N92-32632
Vortex flow visualization using colored and fluorescent dyes on flat plate delta wing with leading edge extension
[AD-A251139] p 1036 N92-32651
Fluid effects: Thermoset and thermoplastic matrix composites p 1110 N92-33049

Wright Research Development Center, Wright-Patterson AFB, OH.
Advanced ramjet concepts program
p 474 N92-21520
Scramjet analysis, testing p 475 N92-21532

Wyle Labs., Inc., Arlington, VA.
The effect of turbulence on the loudness of minimized sonic boom signatures p 1139 N92-33880

Wyle Labs., Inc., El Segundo, CA.
Evaluation of human response to structural vibrations induced by sonic booms
[NASA-CR-189584] p 697 N92-26130
Evaluation of outdoor-to-indoor response to minimized sonic booms
[NASA-CR-189643] p 927 N92-28556

X

Xian Jiaotong Univ. (China).
Study of a new airfoil used in reversible axial fans
p 177 N92-13970

Y

Yale Univ., New Haven, CT.
Transport phenomena and interfacial kinetics in multiphase combustion systems
[AD-A244849] p 489 N92-20695

Z

Zeiss (Carl), Oberkochen (Germany).
Airborne experimental FLIR program
p 1064 N92-32447

Typical Foreign Technology Index Listing

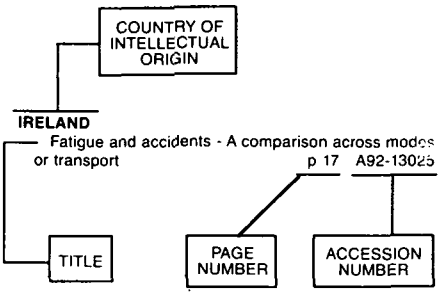

Listings in this index are arranged alphabetically by country of intellectual origin. The title of the document is used to provide a brief description of the subject matter. The page number and the accession number are included in each entry to assist the user in locating the citation in the abstract section. If applicable, a report number is also included as an aid in identifying the document.

A

ARGENTINA
Improving the convergence rate of the Petrov-Galerkin techniques for the solution of transonic and supersonic flows p 434 A92-31495
Rigid and flexible joint modelling in multibody dynamics using finite elements p 671 A92-37559
World Administrative Radio Conference ends favourably for air transport sector p 956 A92-52650

AUSTRALIA
Drag balance for hypervelocity impulse facilities p 207 A92-18375
Fatigue testing of a gas turbine fan disc p 217 A92-19818
Simulation of supersonic and hypersonic flows p 251 A92-22790
The 1988 Australian Winter Storms Experiment - Case study: 6 August 1988 p 301 A92-23009
End plate interference effects on the aerodynamics of a circular cylinder in uniform flow p 313 A92-25097
Skin-friction gauge for use in hypervelocity impulse facilities p 398 A92-28063
The ICAO Future Air Navigation System p 532 A92-33435
Australian aeronautics, 1989-90 p 515 A92-33460
Halfway around the world is far enough p 516 A92-33462
The law in Australia relating to negligence of aircrew and engineers p 606 A92-33463
Why not a safety rating? p 530 A92-36200
Stagnation point heat flux in hypersonic high enthalpy flow p 613 A92-38373
Beam scanning error of phased array antenna p 676 A92-40189
Acoustic sources in a tripped flow past a resonator tube p 778 A92-41266
Environmental evaluation of repairs to fuselage lap joints p 699 A92-41534
Minimum surface treatments for adhesively bonded repairs p 754 A92-42501
Laminar heat transfer to blunt cones in high-enthalpy hypervelocity flows p 713 A92-44372
A training program for airline line instructors p 835 A92-45044
Separated high enthalpy dissociated laminar hypersonic flow behind a step - Pressure measurements p 809 A92-45858
Waves and thermodynamics in high Mach number propulsive ducts p 809 A92-46431
Measurement of shock-wave/boundary-layer interaction in a free-piston shock tunnel p 813 A92-46903
Flow visualisation of a small diameter rotor operating at high rotational speeds with blades at small pitch angles p 814 A92-46949
Unsteady shock propagation in a steady flow nozzle expansion p 1023 A92-54489
Effects of oxygen dissociation on hypervelocity combustion experiments
[AIAA PAPER 92-3964] p 1098 A92-56791
Critical appraisal of the McDonnell Douglas closure model for predicting fatigue crack growth
[ARL-STRUC-R-444] p 44 N92-11376
F/A-18 stabilator: Equivalent set of point forces required for pneumatic bag load case simulation
[AD-A242637] p 206 N92-15073
Flow around two circular cylinders arranged perpendicular to each other
[PB91-238279] p 297 N92-16225
Modification of Jindivik air intake duct with an auxiliary intake static aerodynamic tests
[AD-A243002] p 275 N92-17234
Wind loads on a mirage III O aircraft mounted above a ground plane
[AD-A243004] p 275 N92-17266
Surface pressure measurements on the wing of a wind tunnel model during steady rotation
[AD-A243047] p 260 N92-17281
Stagnation and dynamic pressure limits for the S1 wind tunnel
[AD-A242989] p 285 N92-17297
General requirements and techniques for component fatigue life substantiation in Australian service helicopters
[AD-A242881] p 275 N92-17565
Scale model measurements of fin buffet due to vortex bursting on F/A-18 p 365 N92-18788
Development of a wind chamber for model testing of tornado forces on structures
[PB92-104165] p 386 N92-19940
A review of Australian activity on modelling the helicopter/ship dynamic interface p 465 N92-21967
Visualisation in water of vortex flow over sharp-edged canard configurations
[ARL-FLIGHT-MECH-R-189] p 632 N92-25410
An outline of a numerical scheme for calculating two-dimensional time linearised transonic flow using the Green's function method
[AD-A246349] p 764 N92-26258
F-111C flight dynamic model aerodynamic data-base development and verification
[AD-A246356] p 715 N92-26947
Buffered serial data card
[AD-A246435] p 727 N92-26948
A preliminary study on damage detection using piezoelectric film
[AD-A246350] p 733 N92-28118
Reduction and analysis of F-111C flight data
[AD-A250341] p 853 N92-28771
Aging commuter aeroplanes: Fatigue evaluation and control methods p 915 N92-30132
Activities of the Aeronautical Research Laboratory p 1013 N92-30768
Research into improving the durability of the hot section in the aircraft turbine engine
[AD-A250342] p 973 N92-31439

AUSTRIA
Chaotic motion in mechanical and engineering systems p 695 A92-39480
Calculation of three-dimensional turbulent flow in wind tunnel entry section p 708 A92-43055
Comparison of two-way satellite time transfer and GPS common-view time transfer between OCA and TUG p 1050 N92-33356

B

BELGIUM
Three dimensional flow in a linear compressor cascade at design conditions
[ASME PAPER 91-GT-114] p 70 A92-15565
Genuinely upwind algorithms for the multidimensional Euler equations p 175 A92-20733
Secondary flow investigation inside the passage of a compressor cascade p 706 A92-42124
Quantitative heat transfer measurements in hypersonic wind tunnels by means of infrared thermography p 1115 A92-54321
Low temperature environment operations of turboengines (design and user's problems) p 450 N92-21682
Aerodynamic effects of de/anti-icing fluids and description of a facility and test technique for their assessment p 452 N92-21697
Boundary Layers in Turbomachines
[VKI-LS-1991-06] p 658 N92-24336
An integrated CFD system for 3D turbomachinery applications p 741 N92-27464
A frontal approach for node generation in Delaunay triangulations p 771 N92-27680
Introduction to Flutter of Winged Aircraft, volume 2
[VKI-LS-1992-01-VOL-2] p 1088 N92-34161

BRAZIL
Kernel function occurring in supersonic unsteady potential flow p 6 A92-11080
Jet inflow simulation and its downwash effect on lifting surfaces p 9 A92-13200
On-board data acquisition system for Embraer's CBA123 p 198 A92-19251
Analysis of aircraft performance during lateral maneuvering for microburst avoidance p 205 A92-20207
An inverse method for the design of transonic wings
[AIAA PAPER 92-1025] p 517 A92-33206
Experimental study of a two-dimensional scramjet inset, M(freestream) = 10.1-25.1 p 611 A92-36974
Mixed volume boundary element approach for aerodynamics p 617 A92-39934
Coalescence of aeroelastic modes in flutter analysis p 758 A92-41241
Approach for analysis and design of composite rotor blades p 899 A92-46801
Whirl-flutter stability of a pusher configuration in nonuniform flow p 845 A92-46813
Some thermodynamical aspects in the optimization of supersonic combustors p 1065 A92-53486
The behaviour of the pressure temperature and density in an inviscid unsteady transonic axisymmetric flow with shock waves p 1018 A92-53553
Enhancement of laminar boundary layer heat transfer by a vortex generator p 1118 A92-55453
The influence of a retarding rocket on parameter limits for reentry trajectories p 211 N92-15037

BRUNEI DARUSSALAMY
Microwave landing system modeling with application to air traffic control automation p 725 A92-41220

BULGARIA
Linear panel flutter of an elliptic cylindrical shell p 291 A92-21216
Robust frequency design of linear stationary systems in aeroautoelastics p 690 A92-37791
Investigation of the structural inhomogeneity of a titanium alloy p 893 A92-47958

C

CANADA
Finite element solutions of the Euler equations for transonic external flows p 5 A92-11063
Compressor coating effects on gas turbine engine performance p 25 A92-11282

FOREIGN

Axisymmetric potential flow calculations. II - Design mode p 8 A92-12399
H2/air subsystem combustion kinetics in aerospaceplane powerplants
[IAF PAPER 91-276] p 25 A92-12600
Analysis of flexible-membrane and jet-flapped airfoils using velocity singularities p 10 A92-13216
Inspection of compressor discs by ultrasonic leaky waves using an automated C-scan system p 144 A92-13584
Damage assessment for composite smart structures p 140 A92-13601
Nondestructive depth profiling of the protective coating on a turbine blade p 144 A92-13641
Classification of radar clutter using neural networks p 145 A92-14252
Lightning standards for aircraft protection p 91 A92-14688
Composite electromagnetic pulse threat p 146 A92-14689
Implanted component faults and their effects on gas turbine engine performance
[ASME PAPER 91-GT-41] p 121 A92-15524
Investigation of engine thrust correlation methods for enclosed test cells
[ASME PAPER 91-GT-68] p 121 A92-15538
Effects of simulated rotation on tip leakage in a planar cascade of turbine blades. I - Tip gap flow
[ASME PAPER 91-GT-127] p 71 A92-15572
Effects of simulated rotation on tip leakage in a planar cascade of turbine blades. II - Downstream flow field and blade loading
[ASME PAPER 91-GT-128] p 71 A92-15573
A universal turboprop engine dynamometer test cell
[ASME PAPER 91-GT-343] p 137 A92-15706
Off-design performance prediction of turbofans using gasdynamics
[ASME PAPER 91-GT-389] p 126 A92-15721
Multiple phase centre DPCA for airborne radar p 95 A92-16257
Enhanced visual technique for rapid inspection of aircraft structures p 214 A92-17290
Complex variable boundary element method for external potential flows p 172 A92-18353
Implementation and usage of the RJ program Data Acquisition System Ground Station p 210 A92-19257
F27 aging aircraft programme emphasizes corrosion prevention p 186 A92-20024
A piezoelectric droplet generator for use in wind tunnels p 291 A92-21374
A multi-layer neural network classifier for radar clutter p 291 A92-21691
Finite element vorticity based methods for the solution of the compressible Navier-Stokes equations p 246 A92-21983
An efficient upwind relaxation-sweeping algorithm for three-dimensional Navier-Stokes equations
[AIAA PAPER 92-0023] p 248 A92-22145
FANS implementation planning under way in Canada p 267 A92-23298
Unsteady Euler solution for oscillatory airfoil and oscillating flap
[AIAA PAPER 92-0131] p 252 A92-23751
A Navier-Stokes solver for stretched triangular grids
[AIAA PAPER 92-0183] p 256 A92-23793
Grid studies for thin-layer Navier-Stokes computations of airfoil flowfields
[AIAA PAPER 92-0184] p 256 A92-23794
Response of symmetrically laminated rectangular plates subjected to heating p 296 A92-24186
Design and testing leading to certification of the Airbus A340 nose landing gear doors p 272 A92-24192
Review of methods for crack growth testing in gas turbine engine disc materials p 296 A92-24193
Efficient panel method for vortex sheet roll-up p 309 A92-24404
Effects of trailing-edge flap on buffet characteristics of a supercritical airfoil p 378 A92-24413
Approach to side force alleviation through modification of the pointed forebody geometry p 309 A92-24418
Wind-tunnel studies of F/A-18 tail buffet p 310 A92-24421
Yaw dynamics of a coaxial rotor helicopter p 378 A92-24427
Progress towards fiber optic smart structures at UTIAS p 368 A92-24781
Development of a sensor for the detection of aircraft wing contaminants
[AIAA PAPER 92-0300] p 369 A92-25752
Laboratory evaluation of a sensor for detection of aircraft wing contaminants
[AIAA PAPER 92-0301] p 369 A92-25753
High density fuel qualification for a gas turbine engine
[AIAA PAPER 92-0684] p 389 A92-27051
Adaptive simulator motion software with supervisory control p 412 A92-28136
The detection of damage and the measurement of strain within composites by means of embedded optical fiber sensors p 491 A92-28669
Acoustic emission monitoring of a ground durability and damage tolerance test p 492 A92-28737
Incompressible flow past a flat plate aerofoil with leading edge separation bubble p 421 A92-28943
New specifications proposed for taxiing guidance signs p 483 A92-29505
A consistency test of airborne GPS using multiple monitor stations p 454 A92-30651
A torque-free flexible model gyro p 495 A92-31552
Airborne tests of flux measurement by the relaxed eddy accumulation technique p 504 A92-32052
Airflow effects about PMS probes on the DLR Falcon p 467 A92-32060
Digital ozonesondes - Examples of results from the EMEFS experiments of 1988 and 1990 p 468 A92-32140
Canadian CF-18 aircraft ejection seat parachute update p 529 A92-32983
RCS of four fuselage-like scatterers at HF frequencies p 533 A92-33632
Interactive graphics method for removal of helicopter motions from laser profile data p 598 A92-35109
Development and analysis of flight flutter prediction methods
[AIAA PAPER 92-2101] p 588 A92-35672
Buffet load measurements on an F/A-18 vertical fin at high-angle-of-attack
[AIAA PAPER 92-2127] p 520 A92-35694
An exploratory investigation into the definition of tracking standards for IFR helicopter approaches to reduced minima p 533 A92-35726
Forced-injection quenching of a hot-tube under microgravity p 590 A92-35977
Growing need to replace ILS can best be met by MLS p 534 A92-36124
Fracture mechanics approach to creep growth in welded IN738LC gas turbine blades
[ASME PAPER 91-GT-119] p 670 A92-36893
Efficient direct solvers for large-scale computational fluid dynamics problems p 690 A92-37534
Mechanics and thermodynamics of propulsion (2nd revised and enlarged edition)
[ISBN 0-201-14659-2] p 672 A92-38275
Noise generated by wind turbines p 686 A92-39045
Opening closed skies - The prospects for further liberalization of trade in international air transport services p 697 A92-39244
The hardness and toughness of HIPed silicon nitride p 668 A92-39682
Application of a double actuator electronic fuel control unit on a small gas turbine engine
[SAE PAPER 912160] p 655 A92-39993
Secondary power system preliminary design
[SAE PAPER 912189] p 656 A92-40008
Structural features of a heated round turbulent jet in a cross-flow p 676 A92-40148
Drag reduction of bluff bodies through momentum injection p 702 A92-41231
Stability of plane nonorthogonal stagnation flow p 704 A92-41291
Indicial method calculating dynamic stall on a vertical axis wind turbine p 714 A92-44528
Spectrogram diagnosis of aircraft disasters
[SAE PAPER 912041] p 836 A92-45425
Effect of throat contouring on two-dimensional converging-diverging nozzles using URS method
[AIAA PAPER 92-2659] p 797 A92-45520
Unsteady pressure and load measurements on an F/A-18 vertical fin at high-angle-of-attack
[AIAA PAPER 92-2675] p 798 A92-45529
Prediction of laminar boundary layer using cubic splines
[AIAA PAPER 92-2702] p 801 A92-45544
Prediction of leading-edge vortex breakdown on a delta wing oscillating in roll
[AIAA PAPER 92-2677] p 807 A92-45585
Aerodynamic characteristics of hoar frost roughness p 808 A92-45829
Statistical prediction of maximum buffet loads on the F/A-18 vertical fin p 811 A92-46816
Interactive generation of structured/unstructured surface meshes using adaptivity p 919 A92-47066
Wing leading edge design with composites to meet bird strike requirements p 848 A92-47404
Establishing two-dimensional flow in a large-scale planar turbine cascade
[AIAA PAPER 92-3066] p 823 A92-48720
Annals of air and space law. Vol. 16 p 1012 A92-51450
Acoustic control of combustor primary zone air-jet mixing
[AIAA PAPER 92-3651] p 1067 A92-54104
Reduction of the side force on pointed forebodies through add-on tip devices p 1024 A92-54918
Grid studies for thin-layer Navier-Stokes computations of airfoil flowfields p 1025 A92-54935
Wind tunnel tests on A4, A4.1, and A4.2 2-D airfoil models in the IAR 5-ft. wind tunnel: Boeing Commercial Airplane Company and Institute for Aerospace Research collaborative work program
[NRC-IAR-C3] p 81 N92-11975
The BCAC/IAR collaborative research program to investigate the sidewall boundary layer effects in the IAR/NRC 2-D High Reynolds Number Test Facility
[NRC-HSA-434] p 81 N92-11976
Tracking performance requirements for rotorcraft instrument approaches to reduced minima. Phase 1: Preliminary study
[NRC-32137-PHASE-1] p 102 N92-11988
Tutor aft fuselage and empennage full-scale fatigue test: Resolution of horizontal stabilizer installation difficulties
[NRC-LTR-ST-1804] p 114 N92-11990
Corrosion and your aircraft
[NRC-30465] p 114 N92-11991
An experimental and computational investigation of an annular reverse-flow combustor
[UTIAS-338] p 129 N92-11996
Numerical verification of NISA 2 finite element analysis of the cracked 5th stage compressor disc of J-85 jet engine
[NRC-LTR-ST-1792] p 129 N92-11997
Humidity effects on gas turbine performance
[NRC-30241] p 130 N92-11998
Preliminary analysis of baseline vibration data from Allison T56-A-14LFE engine and reduction gearbox
[NRC-31578] p 130 N92-11999
Fuel flow measurement in gas turbine testing
[NRC-29808] p 130 N92-12000
A derivation of gross thrust for a sea-level jet engine test cell
[NRC-30165] p 130 N92-12001
A damage tolerance assessment of bonded repairs to CF-18 composite components. Part 1: Adhesive properties
[DREP-TM-88-25-PT-1] p 143 N92-12060
An improved model-creation program for EM interaction analysis
[NRC-31764] p 155 N92-12153
Constraint propagation through electromagnetic interaction topologies
[NRC-31761] p 155 N92-12154
The modelling of turbulence and downbursts for flight simulators
[UTIAS-339] p 161 N92-12373
Some characteristics and effects of the F/A-18 LEX vortices p 88 N92-13025
Multiple roll attractors of a delta wing at high incidence p 88 N92-13026
Development of an emergency underwater escape breathing system for CH124 seaking aircrew
[DCIEM-87-TR-11] p 92 N92-13041
A proposed composite repair methodology for primary structure
[NRC-LTR-ST-1658] p 115 N92-13056
Verification of NISA 2 and ENDURE fracture mechanics capability
[NRC-ST-621] p 159 N92-13453
Preliminary finite element analysis of unloaded and loaded notched composite laminated plates
[NRC-LTR-ST-1806] p 159 N92-13454
Analysis and design of transonic airfoils using streamwise coordinates p 194 N92-13955
Aerodynamics p 202 N92-13977
Computational fluid dynamics p 177 N92-13979
Flight research p 194 N92-13981
Flight simulation p 207 N92-13982
Nonstationary gasdynamics p 220 N92-13985
Electronic systems in transportation
[TP-9983] p 189 N92-14009
A strategy for exploiting the full potential of MLS based terminal procedures in Canada p 190 N92-14025
A unique approach to aircraft conflict resolution using artificial intelligence techniques p 190 N92-14029
Rub induced rotor/stator vibration analysis on CF700 engine
[NRC-TR-ENG-007] p 202 N92-14060
Filter debris analysis: A concrete approach to wear diagnosis
[DREP-TM-88-20] p 222 N92-14345
Identification techniques: Model structure and time domain methods p 273 N92-17157
Flight evaluation of curved MLS precision approaches in a twin otter aircraft, phase 2
[AD-A243025] p 268 N92-17568
A probabilistic procedure for aircraft fleet management p 360 N92-18576
A parametric approach to spectrum development p 360 N92-18578

Durability and damage tolerance testing and fatigue life management: A CF-18 experience p 361 N92-18581
DRES unmanned aerial vehicle data link research
[AD-A244272] p 365 N92-19030
The application of lattice-structure adaptive filters to clutter-suppression for scanning radar
p 403 N92-19154
Freezing precipitation on lifting surfaces
[NRC-32124] p 448 N92-20156
Activities of NRC-CNRC, Institute for Aerospace Research
[CTN-92-60431] p 420 N92-20204
Activities of NRC-CNRC, Institute for Aerospace Research, Flight Research Lab.
[CTN-92-60432] p 420 N92-20205
Prototyping the IRDS: An airport application
[PB92-112580] p 484 N92-20448
Photoelastic coating study of CT-114 coupon joint test specimen for horizontal stabilizer rear attachment fitting to vertical stabilizer rear spar
[NRC-LTR-ST-1689] p 489 N92-21018
Effects of frost on wing aerodynamics and take-off performance p 450 N92-21687
Wind tunnel investigation of a wing-propeller model performance degradation due to distributed upper-surface roughness and leading edge shape modification
p 451 N92-21690
Experimental investigation of heavy rainfall effect on a 2-D high lift airfoil p 452 N92-21696
Helicopter/ship analytic dynamic interface
p 464 N92-21962
Evaluation and qualification of diffusion braze repair techniques for superalloy gas turbine components
[NRC-LTR-ST-1839] p 504 N92-22028
Inspection of aircraft engine components using automated eddy current and pattern recognition techniques
[NRC-LTR-ST-1834] p 504 N92-22029
A TMS320-based modem for the aeronautical-satellite core data service p 594 N92-22562
Design considerations for general aviation mobile satellite terminals p 594 N92-22572
Aeronautical mobile satellite service: An overview
p 594 N92-22573
Evaluating the use of satellite communications in the government of Canada p 594 N92-22577
A high gain antenna system for airborne satellite communication applications p 677 N92-24096
Low cost, electronically steered phased array for general aviation p 677 N92-24099
Aeronautical mobile satellite service: Air traffic control applications p 677 N92-24164
An aircraft Earth station for general aviation
p 678 N92-24194
Proceedings of the 3rd Canadian Symposium on Aerodynamics
[CTN-92-60420] p 625 N92-24849
Periodic Euler and Navier-Stokes solutions about oscillating airfoils p 626 N92-24850
Navier-Stokes simulation of dynamic stall on a rotating airfoil p 626 N92-24853
TVD finite-difference solutions of nonequilibrium vibrationally relaxing and chemically reacting gaseous flows p 626 N92-24854
An analysis of the sidewall boundary layer effect in two-dimensional wind tunnel testing p 626 N92-24856
VORVISC: A vortex lattice method with viscous and compressibility corrections for full aircraft configurations including propulsion p 626 N92-24857
Laminar-turbulent transition process in the presence of simulated wall roughness p 626 N92-24858
On the coupling of Euler/boundary-layer equations
p 627 N92-24859
A scheme for two dimensional Euler and boundary layer interactive solutions p 627 N92-24860
Wind-tunnel investigation of aerodynamic and stability characteristics of a forward swept wing X-29 model
p 627 N92-24862
Propeller noise research at NRC p 628 N92-24863
Nonliner aspects of transonic aeroelasticity
p 628 N92-24864
Flowfield in the vicinity of the F/A-18 vertical fin at high-angle-of-attack p 628 N92-24865
Performance degradation due to hoar frost on lifting surfaces p 628 N92-24866
Automated grid generation for high-lift configurations
p 628 N92-24869
Flow visualization using computer animation
p 629 N92-24870
Vibroacoustic simulation of an airplane structure
p 629 N92-24871
Nonunique solutions in unsteady transonic flow
p 629 N92-24872
Boundary layer computations using a generalized formulation p 679 N92-24873
The effect of droplet sizing uncertainty on ice accretions p 679 N92-24874
Aerodynamic design and analysis of a light aircraft propeller p 629 N92-24876
Variable geometry sailplanes Minisigma
p 629 N92-24877
A report on enhancements for existing and future helicopters supporting operations of the Canadian oil and gas industry
[CTN-91-60126] p 636 N92-25350
An evaluation of superresolution methods for tactical radio direction finding
[AD-A246316] p 726 N92-26291
Analysis of EMP response of structures using frequency domain electromagnetic interaction codes
[AD-A245758] p 765 N92-26592
Trajectories and stability of trailing vortices very near the ground
[NRC-32151] p 716 N92-27344
On the stability of a dual spin satellite with asymmetric rotor and flexible platform
[ISBN-0-315-54650-6] p 753 N92-27613
Pitch-heave dynamics models for an air cushion vehicle
[ISBN-0-315-51095-1] p 716 N92-27624
The modelling of turbulence and downbursts for flight simulators
[ISBN-0-315-59945-6] p 749 N92-27645
Overview on basis and use of performance prediction methods p 869 N92-28459
Component performance requirements
p 869 N92-28462
Engine performance and health monitoring models using steady state and transient prediction methods
p 870 N92-28467
The use of a dedicated testbed to evaluate simulator training effectiveness p 884 N92-28533
The evaluation of simulator effectiveness for the training of high speed, low level, tactical flight operations
p 885 N92-28539
An evaluation of IFR approach techniques: Generic helicopter simulation compared with actual flight
p 886 N92-28550
Transport Canada aging aircraft activities
p 838 N92-30131
A preliminary study in the use of phase demodulation techniques for the analysis of gear vibration data
[NRC-32083] p 1002 N92-31469
Canadian aircrew sea water survival, 1952-1987
[DCIEM-88-RR-39] p 954 N92-32219
Processing and environmental effects on mechanical properties of composite repairs
[NRC-LTR-ST-1826] p 1109 N92-32791
Further development of the CANAERO computer code to include propulsor modelling
[DREA-CR-90-425] p 1038 N92-32811
An evaluation of decelerating IFR approaches utilizing a helicopter flight simulator
[CTN-92-60348] p 1048 N92-32845
Detection of honeycomb damage using hexagonal grid discontinuities
[DREP-89-9] p 1109 N92-32846
A Kalman filter integrated navigation design for the IAR Twin Otter Atmospheric Research Aircraft
[NRC-32148] p 1048 N92-32849
The use of Kalman filtering techniques to improve the accuracy of flight test data
[NRC-32139] p 1064 N92-32850
The design and development of a portable, DSP micro-processor based, high-accuracy data acquisition system
[NRC-32146] p 1134 N92-32851
Ideal efficiency of propellers based on Theodorsen's theory: A review and computer study, with extended plus simplified charts
[UTIAS-TN-271] p 1071 N92-33102
Radar clutter classification
[ISBN-0-315-57981-1] p 1126 N92-33440
Fire bombing and fire bombers
[CA-PATENT-1-268-164] p 1061 N92-33582

CHILE

Mechanics Pan-America 1991; Pan-American Congress of Applied Mechanics, 2nd (PACAM II), Universidad Tecnica, Valparaiso, Chile, Jan. 2-5, 1991, Selected and Revised Proceedings p 673 A92-39930

CHINA

Applied fracture mechanics research in the aerospace field p 37 A92-10375
Fracture analysis on compressor blades
p 37 A92-10672
The maintenance economy and economic life of structures p 37 A92-10673
Aeroelastic stability analysis of aerial propellers
p 24 A92-10955
Efficient lifting line method for computing performance of propeller p 24 A92-10956
Aerodynamic design of propeller by numerical optimization p 24 A92-10957
Aerodynamic modification of a propeller
p 4 A92-10958
Surface flow visualization of rotating propeller
p 4 A92-10959
Aeroacoustical modification of a propeller
p 24 A92-10961
Experimental characteristics comparison between two scale-model propellers p 24 A92-10962
Stress analysis of a propeller blade
p 38 A92-10963
Stress analysis of a propeller hub p 38 A92-10964
Digital simulation and experimental modal analysis of dynamic characteristics of a propeller hub
p 38 A92-10965
Vibration characteristic analysis of a propeller blade
p 38 A92-10967
A method of reliability analysis for propeller blades
p 25 A92-10968
Effect of antiicer on propeller performance
p 25 A92-10969
A small five-hole spherical pressure probe for compressor experiments p 38 A92-10970
Application of compound leaned blades to controlling secondary flow p 5 A92-10975
China-Soviet long duration balloon flight project
[AIAA PAPER 91-3678] p 1 A92-11036
Flow analysis and design of three-dimensional wind tunnel contractions p 5 A92-11067
A new study on a class of discrete event dynamic systems p 48 A92-11377
On-line state estimation and parameter identification for flight p 50 A92-11429
U-parameter design example - Robust flight control for wind-shear protection p 28 A92-11502
The performance evaluation of aeroderivative gas turbines p 119 A92-13296
An analysis method and applications for 3-D viscous internal flows with complex geometry
p 143 A92-13299
Experimental investigation on gas-particle flow in cascades p 62 A92-13300
On vortex interference for canard configuration
p 64 A92-14071
Investigation of unsteady excitation effects on aerodynamic properties of airfoils p 66 A92-15335
High speed wind tunnel wall interference research progress at Nanjing Aeronautical Institute
p 136 A92-15338
Analysis of criteria predicting the tendency of pilot induced oscillation for linear non-linear system
p 133 A92-15340
The canard-wing interference and stall safety of light canard aircraft p 111 A92-15341
Dynamic behavior analysis for landing-gear with different types of dual-chamber shock-struts p 111 A92-15342
Aeroelastic tailoring of aeronautical composite wing structures p 146 A92-15343
Dynamic analysis technique of rotating centrifugal impeller
[ASME PAPER 91-GT-50] p 148 A92-15528
An improved method for aerodynamic design of centrifugal impeller blades
[ASME PAPER 91-GT-76] p 69 A92-15545
A 3D FEM variational aerodynamic calculation and performance analysis of a leaned turbine stator cascade
[ASME PAPER 91-GT-79] p 69 A92-15548
Similarity transformations for compressor blading
[ASME PAPER 91-GT-123] p 70 A92-15568
A numerical procedure of three-dimensional design problem in turbomachinery
[ASME PAPER 91-GT-144] p 72 A92-15583
Experiments on the blade loss transient response of rotor with flexible damped support
[ASME PAPER 91-GT-149] p 148 A92-15587
Analytical investigation of the rules of component matching in turbojet engines
[ASME PAPER 91-GT-170] p 123 A92-15605
A calculation procedure for three-dimensional turbulent flow in a centrifugal impeller with any blade geometry
[ASME PAPER 91-GT-171] p 73 A92-15606
Simple formulae for optimal solidity of two-dimensional compressor cascades based on diffusion concept
[ASME PAPER 91-GT-308] p 126 A92-15687
Numerical and experimental study of jet impingement or interaction effects at hypersonic and supersonic speeds
[AIAA PAPER 91-5038] p 171 A92-17826
A low-altitude breakthrough system using optimal path terrain following p 205 A92-20483
Numerical calculation of subsonic and supersonic aerodynamic loads around complex configuration vehicle
p 175 A92-20488
Estimation of the maximum instantaneous distortion
p 242 A92-21051

GPS integrated system application in aircraft approach landing p 266 A92-21466
The experimental approach to the LEBU on turbulent drag reduction p 243 A92-21469
The response of a helicopter to windshear p 269 A92-21470
Fatigue life estimation of fastener holes without load transfer p 291 A92-21472
Preliminary investigation of inlet dynamic distortion and it's passive control p 245 A92-21742
Flow characteristic and flow control of high aspect ratio and highly curved S-bend diffuser p 245 A92-21743
An investigation of fuel nozzles for combustion performance p 278 A92-21745
Noise control used for turbojet engine test bench p 284 A92-21749
The study of constant value thresholds of FDI in strapdown inertial navigation p 267 A92-22087
A calculating method of shock wave oscillating frequency due to turbulent shear layer fluctuations in supersonic flow p 251 A92-22720
An AF3 algorithm for the calculation of transonic nonconservative full potential flow around axisymmetric inlet cowls p 251 A92-23380
An investigation on detached shock waves ahead of bodies of revolution at transonic speeds p 251 A92-23381
A new method for calculation of helicopter maneuvering flight p 282 A92-23382
An efficient calculation method of subsonic aerodynamic characteristics for a Space Shuttle orbiter in the reentry attitude p 252 A92-23383
Prediction of low cycle fatigue life of engine cases p 295 A92-23385
A large-scale axial flow compressor facility and dynamic measurement techniques for rotor flow study p 382 A92-24729
3D LDA measurement in an axial fan rotor p 391 A92-24730
A random vortex method for prediction of maximum instantaneous inlet total pressure distortion p 311 A92-24731
Quasi-static analysis of roller bearing p 391 A92-24732
Predication of fastening capacity of screwed joint structure with cone assembly p 391 A92-24737
Numerical modelling for gas duct in tuboannular combustor p 371 A92-24738
Study on reliability design of turbine blade p 371 A92-24739
Effect of some load factors of bird impact on blade response p 371 A92-24740
Strategies for optimal design of gas turbine disks p 371 A92-24741
The jet screen ignition scheme and its experimental verification p 388 A92-24744
Triple contra-rotating turbine and its basic analysis p 371 A92-24745
Optimization of multistage axial-flow compressor vane setting p 371 A92-24746
Aeroengine sensor failure detection by Bayesian multiple hypothesis testing p 391 A92-24747
Failure detection of engine sensors with a bank of Kalman filters p 392 A92-24748
Study on the reliability evaluation of engine fuel accessories p 392 A92-24749
A simplified method of transient mathematical model for non-augmentation engine p 372 A92-24750
A simplified method for simulating steady, unsteady flow around canard wing configuration p 311 A92-24876
On velocity profile models for predicting end wall boundary layers and their blade force defects in axial compressor cascades p 311 A92-24877
Influence of air liquefaction cycle on performance of combined cycle engine p 372 A92-24878
Open-loop model reduction and parameter perturbation for active flutter suppression system p 379 A92-24879
Flow analysis of rectangular wind tunnel contraction p 312 A92-25001
An experimental study of the flow past spheres at transonic speeds and high Reynolds numbers p 312 A92-25002
Numerical simulation of 2-D separated flows caused by *suddenly change of the body section* p 312 A92-25004
Finite element method for computing nonisentropic potential transonic flow with shock waves p 312 A92-25009
The calculation of the static elastic aerodynamic distribution for the rolling maneuver aircraft p 379 A92-25010
Pitching derivatives of wing in supersonic and hypersonic stream - Method for local flow piston theory p 312 A92-25012
Application of the multiplier penalty function method to the optimum design of wing configurations of aerospace vehicle p 356 A92-25013
The measurement of flutter derivatives using mechanical *admittance* p 393 A92-25014
Analysis of transonic flow past an axisymmetric convex corner p 312 A92-25015
Creep fracture mechanisms in single crystal superalloys p 388 A92-25031
Computations of the flow past bodies and wings using Euler equations p 312 A92-25038
Numerical simulation of supersonic separated flow over blunt cones at high angles of attack p 313 A92-25039
Space-marching calculations of hypersonic inviscid flowfield p 313 A92-25040
Study of numerical computation of inviscid flow field about complex configuration of re-entry vehicle p 313 A92-25041
Numerical simulations of flow fields over aircrafts p 313 A92-25042
Numerical simulation of inviscid flow over a complicated body using an overlapping grid technique p 313 A92-25043
Singular perturbation theory of hypersonic flow over blunt bodies p 313 A92-25048
The rolling-up and interaction of the leading-edge and trailing-edge vortex sheets of a delta wing p 314 A92-25101
A numerical method for solving the circulation control airfoil with wall jet p 314 A92-25103
Multiple line-vortex model of vortex flows around body of revolution at high angles of attack up to 60 degrees p 314 A92-25104
A numerical method for unsteady transonic flow about wings with control surface p 314 A92-25107
A new method for solving the kernel equations of transonic flows - An auxiliary kernel method p 410 A92-25108
The LDV measurement of three-component velocity of complex vortex flow in the wind tunnel p 393 A92-25109
New method for boundary layer thickness control on ground plate in wind tunnel p 383 A92-25110
Numerical simulation and analysis for hypersonic flow with separation over blunt cone at angle of attack p 314 A92-25126
Recent progress in finite element method and boundary integral equation method for nonviscous transonic flows p 314 A92-25127
Time marching integral equation method for the solutions of unsteady transonic flows p 314 A92-25129
On the sensitivity of transonic flow p 315 A92-25132
Application of the wall pressure method to wall interference corrections for model tests at high angle of attack in high speed wind tunnel p 315 A92-25134
The lateral shock wave family on the surface of a cone-cylinder in transonic flowfield p 315 A92-25136
A numerical calculation of three dimensional incompressible laminar, transition and turbulent boundary layers p 393 A92-25138
The study of inverse boundary layer algorithm for transonic flows over aerofoils p 315 A92-25140
Concerning a basic assumption for aeroelasticity in turbomachinery p 373 A92-26920
Three-dimensional compressible flows in turbo-machinery solved by the pseudostream function formulation p 338 A92-27801
Loss prediction of annular cascade flow based upon S1/S2 stream surface Navier-Stokes analysis p 338 A92-27802
A new calculating method for the flowfield in turbomachinery - The study on the application of the vorticity-velocity equations for the numerical solution of the flowfield in turbomachinery p 338 A92-27803
A study of active flutter suppression for a wing/store system p 379 A92-27826
A numerical method for analyzing the nonlinear flutter of wings at high angles of attack p 338 A92-27827
Investigation on vortex control technique of flow separation in diffuser p 338 A92-27828
Separation control by vortex generators in subsonic diffuser p 338 A92-27829
The computation of transonic viscous flow p 338 A92-27831
Failure detection and identification for aircraft sensors p 370 A92-27832
The dimensional reconstruction of vortex cross-section images p 339 A92-27833
A theoretical study on helicopter alert time without maintenance p 358 A92-27836
A new method for orientation calculation of the electromagnetic helmet-mounted sighting unit p 370 A92-27837
Reliability aspects in computer integrated manufacturing systems p 397 A92-27838
Numerical simulation of the flow around rectangular cylinder p 339 A92-27851
An aeroacoustic model about the rotating stall of a compressor p 416 A92-27855
Dynamic analysis of annular cascade shrouded blades p 397 A92-27856
Integral minimization of engine fault equations based on least fault principle p 374 A92-27857
A new U-D factorization-based fixed-point smoother and application to flight test p 411 A92-27858
Robustness analysis of a model reference adaptive control system p 412 A92-27859
Application researches on expert system used for structural layout optimization of wings p 398 A92-27865
The 'derivative' and 'synthetic' approaches in aircraft design p 358 A92-27901
The stability analysis of the nonlinear shimmy p 358 A92-27902
A superelement simplified analysis for the vibration systems of the complex structures p 398 A92-27903
The unsteady flow characteristics of an S-shaped inlet at high incidence p 339 A92-27905
Precision analysis on static measurement of radar cross section p 370 A92-27906
Advances of cryogenics in aeronautics and astronautics p 398 A92-27908
An approach to the low-speed longitudinal aerodynamic characteristics of the joined wing configuration p 339 A92-27909
Effect of different force-functions and initial shock pressure on blade response p 374 A92-27913
A new approach to determining control surface's moments of inertia with test-twice vibrations approach p 379 A92-27914
Numerical simulation of two incoming streams in a dual-combustion ramjet combustor p 375 A92-28419
Numerical simulation of interaction of diffusion flame with vortex pair in a recirculation zone p 390 A92-28433
An investigation on the characteristics of combustor with oblique air jet p 375 A92-28434
An investigation on flame stability by fuel permeability in a flame holder made of porous ceramic material p 375 A92-28435
Experimental investigation on the structure of flow field and the total pressure loss in an atomizing channel injector p 375 A92-28436
Surge-troubleshooting of a twin-spool turbojet engine tested at a high altitude test facility p 375 A92-28459
An investigation of the swirl in an S-shaped inlet p 343 A92-28476
An experimental investigation of the inlet exit flow field improved by aerodynamic grid p 343 A92-28477
Design and calculation of performance of a subsonic inlet duct p 343 A92-28478
An improved computation for gas-turbine combustion chamber flow p 375 A92-28479
Calculation of combustion efficiency of dump combustor in ramjet engine p 375 A92-28480
Investigation on opening and ejection of an aircraft canopy by using a solid rocket engine p 358 A92-28489
Dynamic stability of elastic vehicles with unsteady aerodynamic force modeling p 509 A92-29326
CUSAE '91; Proceedings of the 1st China-USSR Seminar on Aero Engines, Nanjing, People's Republic of China, Apr. 15-20, 1991 p 469 A92-29709
A new approach to swirl control in an S-duct p 422 A92-29710
Experimental study of a two-dimensional random frequency generator p 483 A92-29712
Control of strong shock-turbulent boundary layer interaction in rectangular channels p 422 A92-29714
Analysis of effects of freestream turbulence on cascade performance p 422 A92-29716
Effects of bleed and power extraction on the operating line of engines p 469 A92-29717
Investigation and application of compressor loading technique p 469 A92-29718
Calculation of 3D flow field in a single transonic compressor stage p 422 A92-29719
Studying method of measuring flow-field between stages in axial-flow compressor p 423 A92-29720
Heat induced transient behaviours of axial *compressors* p 469 A92-29721
Flow pattern characterization and heat transfer behavior in a boiling two-phase flow in an inclined pipe p 493 A92-29722
Experimental investigation on the mechanism of flame stabilization in afterburner with V-gutter flameholder p 487 A92-29725
Experimental investigation on combustor with double co-axial swirlers p 469 A92-29729
The selection of bird impact load types p 448 A92-29732

Cyclic symmetric contact stress analysis of aeroengine rotor assembly p 470 A92-29733
Some rotordynamic problems in small turbo-engines p 470 A92-29736
A study of surge control using fuel pulse cutoff for dual spool turbo-jet engine p 470 A92-29737
Investigations of the laws of surge and rotating stall forecast in aeronautical engine p 470 A92-29739
Real-time simulation and adaptive PID control of QSK-06A control for gas turbine p 470 A92-29740
Electronic control of a turbine power unit p 470 A92-29741
An investigation of real-time diagnostic technique for DEEC system p 470 A92-29742
On modelling of aero-gas turbine engine for real-time digital simulator p 471 A92-29743
Time marching integral equation method for unsteady transonic flows around airfoils p 433 A92-31489
Numerical computation of improved transonic potential method p 441 A92-32234
Development of an advanced composite material on vertical stabilizer of F-X aircraft p 579 A92-32555
An experimental investigation of the swirling combustor for integral liquid fuel ramjet p 557 A92-35541
The experimental investigation on the diffuser flow distortion p 519 A92-35543
Experimental investigation on performances of two-dimensional inlet at supersonic speed p 519 A92-35544
The numerical method for calculating the flow field, temperature field and radiation fluxfield in the pipe p 587 A92-35546
Experimental investigation on blade loss transient response of rotor with flexible damped support p 557 A92-35551
Analysis of tenon and mortise contact problems by boundary element methods p 587 A92-35554
A compound fatigue investigation of plate specimen under low-cycle load superposed on high cycle load p 587 A92-35555
Research on damage tolerance of compressor blade p 588 A92-35556
A real-time rain-flow method of cycle counting and its program design for aeroengine service loads p 557 A92-35560
Experimental research on blade containment p 557 A92-35561
Life prediction of local stress-strain method p 588 A92-35564
A method for measuring high-subsonic two-dimensional periodic flow field using a single-hole high-response cylindrical pressure probe p 588 A92-35567
Energy analysis of aeroengine and its significance p 557 A92-35569
Statistical analysis and prediction of aeroengine deterioration p 557 A92-35570
A direct-problem calculation method for gas turbines with bowed and twisted blades p 519 A92-35571
A circumferential non-uniform effect model for multistage axial-flow compressor throughflow p 588 A92-35572
Vibration of gear system with web structure p 588 A92-35573
Inverse solution of 3D incompressible turbulent boundary layer with separated bubbles p 522 A92-35992
Analysis of slender bodies of revolution with curved-ground effect and waving-water effect p 524 A92-36151
A new method for calculating burst speed of aeroengine disks
[ASME PAPER 91-GT-121] p 670 A92-36899
Wind tunnel study of aerodynamic characteristics of base combustion p 666 A92-36967
New model for predicting end wall boundary layer in an axial cascade p 611 A92-37389
On performance calculation of centrifugal dish atomizer combustor p 654 A92-37390
Steady state and quasi-transient analysis of aircraft hydraulic system with network theory p 642 A92-37391
Comparison of two flutter analysis methods for elastic aircraft p 660 A92-37394
Reliability analysis of fatigue life of a structural system p 671 A92-37395
The computer analysis of the prediction of aircraft electrical power supply system reliability p 690 A92-37950
Aerospace - Collected translations of selected papers p 608 A92-38266
A dynamic digital model for the turbojet with pulse-monitored fueller p 654 A92-38267
Solution of Euler equations for fighter forebody-inlet combinations at high angles of attack p 613 A92-38269
Aerodynamic analysis and modification design of NPU airfoils p 613 A92-38270
A separated algorithm and application to flight test p 690 A92-38273
A study of flow patterns and behaviours of 3D separated flow on a simplified Shuttle model p 615 A92-38906
Separated flow over the protuberances in hypersonic flow p 615 A92-38907
Hypersonic turbulent separated flow past an unswept circular cylinder on a flat plate p 615 A92-38908
Prediction for the incipient separation of fin-generated three-dimensional shock wave turbulent boundary layer interactions p 615 A92-38909
Delay of wing vortex bursting by using favorable interaction of vortices p 615 A92-38910
A flow visualization experiment on the unsteady flow around two-dimensional airfoil p 615 A92-38913
Experimental investigation on reducing fluctuating pressures of launch vehicles by passive shock-wave/boundary-layer control p 616 A92-38916
Measurement and analysis of the flow field above a wing/body configuration p 616 A92-38917
The numerical simulation of transonic inviscid flow over oscillating airfoils p 616 A92-38918
Numerical simulation of separation flow on bodies of revolution at high angle of attack using Euler equations p 616 A92-38919
A calculation of influence of vortex breakdown on aerodynamic characteristics for slender wings p 616 A92-38920
The effects of unsteady perturbation on vortex breakdown p 672 A92-38922
Investigation on effects on enhancing lift by acoustic excitation p 693 A92-38923
The numerical simulation of separation control using moving surface effect p 616 A92-38924
Numerical simulation of interaction between vortexes and shocks in jet flow field p 616 A92-38925
Bifurcation analysis of airfoils in incompressible flow p 623 A92-40580
Transition of the flutter mode of a two-dimensional section with an external store p 758 A92-41244
Second order perturbation method of gas turbine performance calculation p 759 A92-41834
Flow analysis for axial compressor including secondary flow effects p 759 A92-41835
Performance predictions for centrifugal compressor impellers p 759 A92-41836
Study on calculating the subsonic and supersonic aerodynamic characteristics of slender wing-body combinations at large angles of attack p 706 A92-41926
Experimental technique of measuring fuel concentration in non-uniform flowfield p 734 A92-41928
Some problems on the sidewall interference in two-dimensional subsonic and transonic wind tunnel testing p 747 A92-41929
Simulation of commercial-aircraft reliability p 759 A92-42057
Scattering mechanism and RCS reduction of antennas p 726 A92-44850
Integrated electric density and scaling law for hypersonic blunt-body wakes p 714 A92-44865
The fatigue scatter factors and reduction factors in the design of aircraft and helicopter's structural lives
[SAE PAPER 911984] p 843 A92-45387
New method of swirl control in a diffusing S-duct p 809 A92-45859
Research of environmental spectrum for aircraft structure p 785 A92-47655
A method of failure analysis of complicated structures p 901 A92-47656
Probability analysis of structure failure for the wings with main and subordinate components p 848 A92-47657
Optimal maintenance program of damage tolerance structure p 785 A92-47660
A study on crack initiation method for durability analysis p 901 A92-47663
Durability analysis for a main bulkhead subjected to load on the body of an aircraft p 848 A92-47664
Sonic fatigue analysis and anti-sonic fatigue design of aircraft structure p 848 A92-47666
A failure analysis for landing gear structural system p 849 A92-47667
Economic life analysis for replacing components p 785 A92-47670
Approximate analysis for failure probability of structural systems p 901 A92-47671
The calculation of three-dimensional compressible boundary layer stability on swept wings p 818 A92-47684
The numerical simulation of compressible flow around an airfoil at high angle of attack p 818 A92-47686
A time marching method in finite volume for transonic diffuser turbulent flows p 819 A92-47690
A new method for predicting the end wall boundary layers and the blade force defects inside the passage of axial compressor cascades p 819 A92-47691
Basic analysis of counter-rotating turbines p 862 A92-47692
An improved multiple line-vortex method for simulation of separated vortices of slender wings p 819 A92-47694
Aerodynamic sensitivities for subsonic lifting-surface p 819 A92-47695
Study on two variable control plan for twin spool turbojet engine p 862 A92-47697
An experimental investigation on aft bypass supersonic inlet performance at high angle of attack and yaw p 862 A92-48268
Calculation methods on equivalence ratio of multi-propellant for propulsion system p 893 A92-48269
Location and tracking technique in a multistatic system established by multiple bistatic systems p 840 A92-48480
Ablative control mechanism in nozzle thermo-protection
[AIAA PAPER 92-3054] p 889 A92-48712
A simplified real-time engine model for developing aeroengine control system
[AIAA PAPER 92-3321] p 864 A92-48904
Improved method for estimation of the maximum instantaneous distortion values
[AIAA PAPER 92-3623] p 826 A92-49076
A new vane swirler as applied to dual-inlet side-dump combustor
[AIAA PAPER 92-3654] p 906 A92-49085
Optimization of longitudinal corrections of helical gears p 990 A92-49578
Vibration control of rotor-bearing system by controlled squeeze-film damper bearings p 990 A92-49579
On travelling wave vibration of high-speed duplex helical gears p 990 A92-49580
Three-dimensional optimal reentry trajectory and aerodynamic heating history of the Space Shuttle p 984 A92-49582
On multiple grid method p 1006 A92-49585
Engine flight load reliability analysis p 968 A92-49827
Limit point flow mode analysis of exhaust diffuser and operation characteristics of injector p 968 A92-49830
Application of submerged vortex generators for separation control of a subsonic diffuser p 933 A92-49832
Turbofan with a small bypass ratio for first stage of a two-stage to-orbit vehicle p 968 A92-49833
Effect of thermodynamic parameters on performance and cost of turbine engines p 969 A92-49834
Research on aircraft life cycle cost reduction p 1012 A92-49835
Research on altitude simulation of starting for a single-spool small turbojet p 969 A92-49836
The mechanism of liquid-cooling of vane in high-temperature turbine p 969 A92-49841
Research on sonic fatigue calculation and test for aircraft panel p 958 A92-50203
Calculation of fuel sloshing and its coupling vibration with a tank p 991 A92-50204
The engineering prediction for aircraft noise p 1010 A92-50206
Predictive control for optimal path terrain following system p 955 A92-50207
The influences of forced oscillations toward vortex-breakdown p 934 A92-50210
A complete boundary integral formulation for steady compressible inviscid flows governed by nonlinear equations p 934 A92-50211
A calculating method of the kill probability attack area for AAM p 975 A92-50212
A study on mechanical model of the helicopter 'ground resonance' p 955 A92-50214
Transonic flow calculation of Euler equations by implicit iterating scheme with flux splitting p 934 A92-50215
Numerical investigation of axial flow compressor casing treatment p 934 A92-50216
The effect of atmospheric turbulence on the external store separation from an aircraft p 934 A92-50233
Some problems on atmospheric turbulence spectrum and aircraft response p 975 A92-50235
Bird impact analysis of aircraft windshield transparency p 958 A92-50236
The design and simulation of an intelligence flight control system p 976 A92-50237
Combined application of the energy method and the weighted residual method - A new way to construct the finite elements p 991 A92-50239
Pseudostream function formulation - A method of solving three-dimensional aerodynamic analysis and design problems in turbomachinery p 996 A92-52981
Measurement of turbulent boundary layer in transonic flow p 941 A92-53010
Finite analytic numerical solution of Navier-Stokes equations p 996 A92-53011

A study on rotor induced sand and dust environment and its harmfulness to helicopter p 960 A92-53012
Anti-fatigue optimization design by artificial intelligence strategy p 996 A92-53013
Mixing for multi-stage axial-flow compressors p 996 A92-53015
A study on the marginal analysis method for the airline yield management p 951 A92-53018
Calculation of the transonic full-potential flowfield about 3D fuselage p 941 A92-53021
The relation among the general unsteady aerodynamic coefficients of a wing in subsonic and supersonic speed p 941 A92-53022
Maximum likelihood algorithm and its application to parameter identification of closed-loop flight vehicles p 1008 A92-53023
Experimental investigation on flutter characteristics of composite torsion-box p 996 A92-53055
Structural optimization and vibration control of composite rotor blades p 960 A92-53056
Damage tolerance and durability design of composite aircraft structures p 996 A92-53067
A review of some computer programs of composites p 1009 A92-53069
Safety factor and reliability for composite laminates p 996 A92-53070
Study of dynamic strength on composite wing p 996 A92-53071
Design variables and constraint derivatives in aeroelastic tailoring p 997 A92-53074
The wall interference correction and test data processing methods for airfoil wind tunnel test with endplates p 942 A92-53087
The research on Pilot Induced Oscillation p 977 A92-53088
Experimental investigation of in-flight oscillation on helicopters and its prevention p 977 A92-53089
Mechanical model of landing impact of three dimensional fuselage landing gear p 960 A92-53090
Improvement in transmission loss of aircraft double wall with resonators p 1011 A92-53091
A full-scale fatigue test and failure analyses research of F-X fighters p 960 A92-53092
Development of data base system in CIEM project p 1009 A92-53093
Optimal implicit model-following approach with frequency-shaped weighting and its application to design of flight control system p 977 A92-53094
A fuel-optimal 4D guidance algorithm p 978 A92-53095
Investigation of a method for determining machining stress in polymethylmethacrylate (PMMA) of airplane canopies p 986 A92-53096
The effect of afterbody devices on drag reduction p 942 A92-53097
From fatigue test life to structure safe life p 997 A92-53099
A microprocessor-based automation test system for the experiment of the multi-stage compressor p 997 A92-53100
Experimental study of the equivalent sound source center of the propeller rotating noise p 1011 A92-53257
A numerical study of the radiation characteristic of an elliptical exhaust jet p 970 A92-53258
Discussion on sidewall suction in two-dimensional wind tunnel p 997 A92-53263
Numerical simulation of three-dimensional turbulent flows in combustion chambers p 970 A92-53276
A bi-directional marching finite element algorithm for three-dimensional boundary layer separation flow computations p 942 A92-53288
Discussion of improved transonic potential method p 942 A92-53290
The system reliability analysis and optimization design for wing-box structures p 997 A92-53292
Transient response of the rotor-support system of aeroengines p 997 A92-53293
Calculation of the exerting force necessary to form the aircraft hull plate in the symmetry plate bender with three rolls and the feeding value of the centre roll p 998 A92-53297
An impact dynamics investigation on some problems in bird strike on windshields of high-speed aircrafts p 986 A92-53330
Solution of stress intensity factor by weight function for small surface cracks in plates p 998 A92-53332
A study of dynamic response to bird impact on arc windshields of aircrafts p 952 A92-53340
A numerical investigation of axial flow compressor casing treatment p 942 A92-53381
A reversed-frame normalization design of robust flight control system p 1009 A92-53382
A penalty-Galerkin finite element method for calculating transonic flow over wings p 943 A92-53386
An improved wall correction method for the longitudinal stability p 978 A92-53388
Simulation research on the dynamic characteristics of steam-injected gas turbine p 971 A92-53389
A study on the stability of aircraft at high angles-of-attack and state vector propagation sensitivity p 978 A92-53394
Stability and dynamic coupling of elastic vehicles with unsteady aerodynamic forces considered p 1102 A92-53545
Fault diagnostics on jet engine starting p 1116 A92-54345
An analysis of boundary layer for droplet aerodynamic stripped in high speed gas flow p 1116 A92-54563
The flow field characteristics about a fighter configuration at high angles of attack
[AIAA PAPER 92-4358] p 1025 A92-55344
Parameter identification of unsteady aerodynamic forces for elastic vehicles
[AIAA PAPER 92-4505] p 1027 A92-55372
The research of reducing 3-D low supersonic shock wave reflection in a 2-D transonic flexible walls adaptive wind tunnel
[AIAA PAPER 92-3924] p 1095 A92-56755
Research on inverse, hybrid and optimization problems in engineering sciences with emphasis on turbomachine aerodynamics: Review of Chinese advances p 201 N92-13939
Variational formulation of hybrid problems for fully 3-D transonic flow with shocks in rotor p 176 N92-13953
An inverse method with regularity condition for transonic airfoil design p 177 N92-13969
Study of a new airfoil used in reversible axial fans p 177 N92-13970
Design of transonic compressor cascades using hodograph method p 202 N92-13973
The research progress on Hodograph Method of aerodynamic design at Tsinghua University p 177 N92-13974
The stability of the steady state and bistable response of a flexible rotor supported on squeeze film dampers p 222 N92-14350

CZECHOSLOVAKIA

Numerical solution of steady incompressible viscous flows over airfoils p 8 A92-12649
The FALSTAFF program - A standard spectrum for *simulating the service loading of aircraft with prevailing* maneuver loads p 284 A92-21922
Application of holomorphic vectors theory in three-dimensional potential flow problem p 292 A92-21923
Effect of a deicing device on the induced drag of a lifting airfoil p 959 A92-51947
Shimmy of nose undercarriage wheels p 959 A92-51948
Discs low cycle fatigue life predictions for gas turbine engines in CSFR by using fractographic information p 995 A92-51950

D

DENMARK

Optimization of the flutter load by material orientation p 146 A92-15222
The SAS Flight Analysis and Aircraft Monitoring System p 555 A92-35941
Noise from turbine generators - Noise control, propagation, and assessment p 686 A92-39044
DANSIM - Danish Airport Noise Simulation Model - Basic principles, experience, and improvements p 687 A92-39055
DANSIM applications - Development of airport noise reduction strategies and environmental policy p 687 A92-39057

E

EGYPT

Experimental and analytical investigation of hybrid squeeze film dampers
[ASME PAPER 91-GT-250] p 150 A92-15655

F

FINLAND

Development of a 3-D remote sensing radar p 597 A92-34908
X-band side-looking airborne radar for remote sensing p 554 A92-34976
Mechanical design of an airborne imaging microwave radiometer p 554 A92-35276
Aircraft control for take-off in windshear p 660 A92-36990
A computerized flight inspection system p 726 A92-43881
Analysis of Euler's and stress tensor methods for calculating power consumption of high speed centrifugal fans and turbocompressors
[DE92-728396] p 298 N92-16325
Calculation of local power consumptions and efficiencies of centrifugal fans and turbocompressors
[DE92-728402] p 298 N92-16326
Two-dimensional transonic flow calculation by interaction of Euler and boundary layer equations
[PB92-136449] p 448 N92-21784
Three-dimensional multigrid algorithm for the Euler and the thin-layer Navier-Stokes equations
[PB92-134329] p 602 N92-22216
Modernized MBB panel code: User's guide including background theory
[PB92-136431] p 526 N92-22233
Development of a helicopter-borne 8-channel ranging scatterometer
[PB92-141977] p 599 N92-23441
Analysis of a 37 kW cage-induction motor
[PB92-142116] p 597 N92-23496

FRANCE

A unified nonequilibrium model for hypersonic flows p 3 A92-10575
Topology of steady flows of low viscosity fluids p 38 A92-11219
A two-feedback-loop robust helicopter controller based on eigenspace techniques and H(infinity) synthesis p 29 A92-11582
Dynamic characterization and identification of nonlinear systems application to aeronautical structures p 39 A92-11830
The European ATC challenge p 19 A92-11877
Influence of the entropy layer on the separation length in hypersonic aerodynamics in the triple-deck framework. II p 63 A92-13815
A simplified model for aerodynamic flows around streamlined models p 63 A92-13816
The Aeronautical Mobile Satellite Service (AMSS). I - Architecture of the AMSS system p 93 A92-13851
The Aeronautical Mobile Satellite Service (AMSS). II - Frequency spectrum requirements for the Aeronautical *Mobile Satellite Service* p 94 A92-13852
The new airport aeronautic meteorological codes p 160 A92-13855
Studying dynamic behavior of X380 helicopter equipped with a new 5-blade composite rotor p 108 A92-14398
Optimization of a light helicopter with Arrius power plants p 120 A92-14408
Tiger MGB - High reliability low weight p 109 A92-14418
Certifying composite helicopter structures p 110 A92-14443
P120 programme - First results of the pre-development phase p 60 A92-14447
Aircraft ground vibration test by means of flight control surfaces
[ONERA, TP NO. 1991-96] p 133 A92-16079
Lightning activity in microburst producing storm cells
[ONERA, TP NO. 1991-98] p 161 A92-16080
Three-dimensional calculations of reactive flows in aircraft combustion chambers performed using two combustion models
[ONERA, TP NO. 1991-110] p 154 A92-16089
Integration of flight and carrier landing aid systems for shipboard operations
[ONERA, TP NO. 1991-113] p 134 A92-16092
Prediction of generalized aerodynamic forces following linearized supersonic theory
[ONERA, TP NO. 1991-114] p 76 A92-16093
High-speed impulsive noise and aerodynamic results for rectangular and swept rotor blade tip tests in S1-Modane wind tunnel
[ONERA, TP NO. 1991-124] p 76 A92-16102
Three-dimensional thin-layer and space-marching Navier-Stokes computations using an implicit MUSCL approach - Comparison with experiments and Euler computations
[ONERA, TP NO. 1991-131] p 77 A92-16107
Environmental impact of a future supersonic transport aircraft
[ONERA, TP NO. 1991-132] p 161 A92-16108
Recent development of wind-tunnel test techniques at ONERA
[ONERA, TP NO. 1991-135] p 137 A92-16110
Detailed analysis of wing-nacelle interaction for commercial transport aircraft
[ONERA, TP NO. 1991-152] p 77 A92-16122
Formulation of a simplified model of rotor-horizontal stabilizer interactions and comparison with experimental measurements
[ONERA, TP NO. 1991-157] p 77 A92-16125

Utilization of a research simulator for the development of new flight control concepts
[ONERA, TP NO. 1991-161] p 137 A92-16128
The sonic boom and problems related to supersonic flights of military aircraft
[ONERA, TP NO. 1991-162] p 77 A92-16129
Supersonic stator-rotor interaction in a turbine stage
[ONERA, TP NO. 1991-166] p 77 A92-16133
Aerodynamic measuring techniques for transonic and supersonic flow in cascades and turbomachines
[ONERA, TP NO. 1991-170] p 137 A92-16135
Study of simulated lightning discharge effects on wires of a rotorcraft
[ONERA, TP NO. 1991-173] p 92 A92-16137
Theoretical study and prediction of BVI noise including close interactions
[ONERA, TP NO. 1991-174] p 165 A92-16138
Solution of the compressible Euler equations for steady flows around helicopter rotor blades by an implicit space-centered method
[ONERA, TP NO. 1991-177] p 77 A92-16139
Aerodynamic and acoustic calculations of transonic nonlifting hovering rotors
[ONERA, TP NO. 1991-178] p 77 A92-16140
Numerical optimization of helicopter rotor blade airfoils using unsteady aerodynamic calculations
[ONERA, TP NO. 1991-187] p 78 A92-16141
Concept for future cockpits p 118 A92-16148
Status of the NH90 European Helicopter Program p 113 A92-16676
Digital technology applied to airborne receivers p 98 A92-16927
GPS availability. I - Availability of service achievable for different categories of civil users. II - Evaluation of state probabilities for 21-satellite and 24-satellite constellations p 99 A92-16949
Potential hypersonic vehicles applications
[AIAA PAPER 91-5086] p 169 A92-17854
Protective coatings of thermal barrier type p 214 A92-20349
Concerning the functional solution of transonic flows p 243 A92-21318
Measurement of convective heat-transfer coefficients on a wind tunnel model by passive and stimulated infrared thermography p 291 A92-21450
Calculation methods of three-dimensional boundary layers p 245 A92-21978
Computation of unsteady, laminar, incompressible, viscous flows using the vorticity streamfunction formulation p 245 A92-21979
The position of the unsteady flow computation in the compressor and turbine design and analysis process
[AIAA PAPER 92-0015] p 278 A92-22137
Weak coupling between an unsteady 3D full potential code and an unsteady turbulent boundary layer code - Application to a helicopter rotor in forward flight
[AIAA PAPER 92-0029] p 249 A92-22151
Development of a three-dimensional icing code - Comparison with experimental shapes
[AIAA PAPER 92-0041] p 262 A92-22159
International standardisation of regulations for gust loading calculations p 270 A92-22473
The beta-CEZ - A high performance titanium alloy for aerospace engines p 289 A92-22760
A parallel architecture adapted to onboard multiexpert systems p 276 A92-23040
Effects of ionizing and nonionizing radiation on aircraft p 295 A92-23301
Industrial measurement of microphysical parameters - Application to natural and simulated icing clouds p 262 A92-23302
Navier-Stokes computation of airfoil in stall using algebraic Reynolds-stress model
[AIAA PAPER 92-0195] p 257 A92-23803
Influence of flight parameters on air intake internal flow distortions due to gun blast-air interaction p 310 A92-24426
Establishment and characterization of a reproducible vortex for use in studying nonsteady two-dimensional phenomena p 310 A92-24428
Measurement of convective heat-transfer coefficients in wind tunnels using passive and stimulated infrared thermography p 390 A92-24430
A viscoplastic theory for anisotropic materials
[ONERA, TP NO. 1992-90] p 391 A92-24721
A cognitive temporal model for the planning in aircraft maintenance p 307 A92-25178
Importance of an accurate prediction of shock curvature for high-speed rotor noise p 414 A92-25578
Mechanical testing of glass-ceramic matrix composites
[ONERA, TP NO. 1991-182] p 388 A92-26351
Combat aircraft jet engine noise studies
[ONERA, TP NO. 1991-192] p 415 A92-26353
Experimental and theoretical studies on helicopter rotor fuselage interaction
[ONERA, TP NO. 1991-197] p 329 A92-26356
Theoretical and experimental studies of helicopter rotor/fuselage interaction
[ONERA, TP NO. 1991-198] p 329 A92-26357
Aircraft icing
[ONERA, TP NO. 1991-202] p 351 A92-26359
Productivity and quality in the Modane and Fauga wind tunnels - Prospects for the 90s
[ONERA, TP NO. 1991-203] p 383 A92-26360
Aircraft lightning strikes
[ONERA, TP NO. 1991-204] p 351 A92-26361
Modification of the radiated sound directivity due to ground reflections - Application to static tests of helicopter turboshaft engines
[ONERA, TP NO. 1991-210] p 415 A92-26362
Experimental study of the effects of atmospheric turbulence on sound propagation over the ground
[ONERA, TP NO. 1991-211] p 415 A92-26363
Wall pressure wavenumber-frequency spectrum beneath a turbulent boundary layer measured with transducer arrays calibrated with an acoustical method
[ONERA, TP NO. 1991-212] p 329 A92-26364
From concept to model: Conception and evaluation of an architecture for a distributed system with SAHARA - Some reflections on results of the utilization of SAHARA in the framework of the Electronic Copilot
[ONERA, TP NO. 1991-216] p 411 A92-26368
Aerodynamic computations of high-speed transonic propellers
[ONERA, TP NO. 1991-218] p 330 A92-26370
Tests of models equipped with a turbofan powered simulator in the ONERA F1 low-speed pressurized wind tunnel
[ONERA, TP NO. 1991-219] p 383 A92-26371
CARS temperature measurements and validation of a computing code on a gas-turbine combustor
[ONERA, TP NO. 1991-224] p 373 A92-26376
Validation of a 3D Navier-Stokes code on experimental compressor bladings
[ONERA, TP NO. 1991-229] p 330 A92-26381
Numerical methods in elastoacoustics in the nonmodal domain
[ONERA, TP NO. 1991-232] p 415 A92-26383
Supersonic transport in the 21st century p 308 A92-26793
Navigation and flight management systems - Thoughts of a user p 354 A92-26848
The cockpit of a modern aircraft - The Airbus A340 considered as an example p 357 A92-26849
Development of an electrothermal de-icing/anti-icing model
[AIAA PAPER 92-0526] p 351 A92-26949
On the adaptive control of missile autopilots p 477 A92-29102
Assessment of three models of turbulence in a shock-boundary layer interaction of a heated wall p 423 A92-29999
Generalized expression of chorochronic periodicity in turbomachinery blade-row interaction p 423 A92-30000
French research and technology program on advanced hypersonic propulsion
[AIAA PAPER 91-5003] p 471 A92-31683
Structures and materials technologies for hypersonic vehicles - Lessons from Hermes experience
[AIAA PAPER 91-5098] p 486 A92-31697
Use of relative humidity sensors for planes measurement p 467 A92-32080
Structural optimization at Aerospatiale Aircraft
[AIAA PAPER 92-2371] p 601 A92-34542
The development of a new light, single engine helicopter family p 545 A92-35734
The obstacle avoidance radar - A safety mean for low altitude flights in adverse weather conditions p 554 A92-35743
Experimenting a new composite rotor on an Aerospatiale Dauphin helicopter p 546 A92-35744
EUROFAR airframe aerodynamic design p 546 A92-35750
A survey of composite structure technology at the Aerospatiale Helicopter Division p 546 A92-35754
Preliminary evaluation of new control laws on the experimental fly-by-wire Dauphin helicopter p 568 A92-35756
Generalized higher harmonic control - Ten years of Aerospatiale experience p 569 A92-35769
Improvement of helicopter robustness and performance control law using eigenstructure techniques and H-infinity synthesis p 569 A92-35776
Design and manufacturing of torsional flexible blade models p 547 A92-35780
Theoretical and experimental study of a model rotor p 547 A92-35781
The effects of wall suction on laminar-turbulent transition in three-dimensional flow p 522 A92-36021
Asymptotic defect boundary-layer theory applied to hypersonic flows p 610 A92-36839
Performance of turbulence models to predict supersonic boundary layer flows p 613 A92-37553
The thermodynamic approach in the study of large systems - Application to high-velocity airbreathing propulsion p 654 A92-37824
Materials and structures for Hermes p 666 A92-38213
Study model for the reduction of noise through double wall cylindrical shells - Comparison with experimentation p 694 A92-39088
Noise inside aircraft fuselages subjected to airborne excitation p 643 A92-39089
Active control of pulsed flow for low frequency noises attenuation p 694 A92-39109
Active control of airborne noise transmitted through a ribbed panel p 695 A92-39111
ELS for the A340
[SAE PAPER 912111] p 651 A92-39963
Rafale: Program update - Development of a naval version p 645 A92-40035
Influence of suction through a slot on a turbulent boundary layer p 622 A92-40127
Experimental and numerical investigation of a turbulent boundary layer over riblets p 622 A92-40128
Compressibility effects in turbulent far wakes p 622 A92-40140
The effects of viscosity and diffusion on a supersonic mixing layer p 622 A92-40143
Reactive mixing layer between pressure reflecting boundaries p 656 A92-40144
Analysis of turbulence models for hypersonic boundary layers p 623 A92-40182
Simulation in the Air Force p 747 A92-41209
Simulation as applied to mission planning p 747 A92-41210
Basic experiment on a supersonic vortex flow around a missile body p 705 A92-41545
Models of turbulence in a hypersonic boundary layer p 705 A92-41817
Generalities on the ramjet p 736 A92-41819
The turbo-ramjet Griffon p 782 A92-41820
New ramjet configurations p 736 A92-41822
The beginnings of the hypersonic and the renewal of the supersonic ramjet p 782 A92-41824
Acoustic transmission through a 2-D orthotropic multi-layered infinite cylindrical shell p 780 A92-44197
Instantaneous visualization of surface flows p 763 A92-44327
The DAM vertical shock-tube p 880 A92-45096
An improved approach for the computation of transonic/supersonic flows with applications to aerospace configurations
[AIAA PAPER 92-2613] p 793 A92-45487
A new automatic grid generation environment for CFD applications
[AIAA PAPER 92-2720] p 803 A92-45558
Wideband control of gyro/accelerometer multisensors in a strapdown guidance system p 856 A92-46736
Experimental and numerical study of flow around helicopter rotor blade tips p 814 A92-46948
Experimental and computational studies of hovering rotor flows p 815 A92-46954
Anisotropic control of mesh generation based upon a Voronoi type method p 918 A92-47043
Real time presentation for RAFALE in-flight tests p 882 A92-47522
Industrial practice in aeronautical maintenance p 786 A92-47774
Numerical and experimental investigation of rarefied compression corner flow
[AIAA PAPER 92-2900] p 820 A92-47876
A340 handling, cockpit design improve on predecessor A320 p 849 A92-47969
Calculation of fully three-dimensional separated flows with an unsteady viscous-inviscid interaction method
[ONERA, TP NO. 1992-1] p 821 A92-48577
Advanced superalloys for turbine blade and vane applications
[ONERA, TP NO. 1992-2] p 893 A92-48578
Separation and vortex formation in turbulent flows
[ONERA, TP NO. 1992-7] p 822 A92-48579
The design and testing of an airfoil with hybrid laminar flow control
[ONERA, TP NO. 1992-22] p 822 A92-48585
The A320 laminar fin programme
[ONERA, TP NO. 1992-23] p 849 A92-48586
Trends in commercial aircraft design - What evolution factors and what approach?
[ONERA, TP NO. 1992-25] p 786 A92-48587
Research on helicopter rotors - Progress in aerodynamics, aeroelasticity and acoustics
[ONERA, TP NO. 1992-27] p 849 A92-48589
Numerical analysis of an engine turbine disk loaded with a large number of thermomechanical cycles
[ONERA, TP NO. 1992-31] p 902 A92-48592

Basic experiments on the directivity of the sound radiation emitted by a turboshaft engine
[ONERA, TP NO. 1992-36] p 926 A92-48597
New hypersonic test methods developed at ONERA - The R5 and F4 wind tunnels
[ONERA, TP NO. 1992-39] p 882 A92-48600
Influence of geometrical parameters on helicopter rotor high speed impulsive noise
[ONERA, TP NO. 1992-40] p 926 A92-48601
Acoustic spinning-mode analysis by iterative threshold method applied to a helicopter turboshaft engine
[ONERA, TP NO. 1992-41] p 926 A92-48602
Indirect measurements of convective flow by IR thermography
[ONERA, TP NO. 1992-46] p 902 A92-48607
Advances in aircraft modal identification
[ONERA, TP NO. 1992-47] p 877 A92-48608
Aluminides modified by palladium - Protection of new parts by local finishing
[ONERA, TP NO. 1992-49] p 893 A92-48610
Research and studies on quiet helicopters
[ONERA, TP NO. 1992-59] p 926 A92-48618
Advanced CFD simulation and testing of compressor blading in the multistage environment
[AIAA PAPER 92-3040] p 822 A92-48701
Is the avionics system of the Hermes Spaceplane centralized or decentralized? p 984 A92-49258
Computer software in civil aircraft
p 1006 A92-49302
Flight management system back-up navigation for the A330/A340 aircraft p 975 A92-49326
Navier-Stokes computations of horseshoe vortex flows
p 990 A92-49516
Impact damage tolerance of helicopter sandwich structures p 958 A92-51506
Successful transfer of technology from a research and development laboratory to an Aerospatiale production unit p 931 A92-51808
Solution of Euler equations with unstructured mesh - 3-D case p 941 A92-52973
Hot-wire measurements in turbulent transonic flows
p 941 A92-53078
Remarks on the relation between lift induced drag and vortex drag p 941 A92-53079
Human factors and simulation p 951 A92-53236
Monopulse secondary surveillance radar and the mode-S surveillance system p 956 A92-53239
GPS tests during approach at Singapore and Roissy
p 956 A92-53240
Turbulent combustion modelling in a side dump ramjet combustor
[AIAA PAPER 92-3599] p 1112 A92-54075
Experimental investigation of the reflection of a shock wave on a heated surface in presence of a turbulent boundary layer p 1023 A92-54569
Efficient methods for inviscid non-equilibrium hypersonic flow fields p 1024 A92-54571
Mechanisms of high-current pulses in lightning and long-spark stepped leaders p 1116 A92-54678
Physics of vortical flows p 1031 A92-56166
Experimental study of noise generation and propagation in a turbofan model p 1136 A92-56169
The computation and validation of hovering rotor performance p 1055 A92-56285
The Eurofar program - An European overview on advanced VTOL civil transportation system
p 1016 A92-56299
Organization and technical status of the NH90 European helicopter programme p 1016 A92-56306
A finite element method for shear stresses calculation in composite blade models p 1121 A92-56322
The advantages of digital engine control as compared with traditional systems (hydraulic or pneumatic)
p 1070 A92-56338
AS 332 MKII - Development and certification
p 1059 A92-56343
The SR3 low density wind tunnel - Facility capabilities and research development
[AIAA PAPER 92-3972] p 1098 A92-56798
Numerical simulation of vortex breakdown by solving the Euler equations for an incompressible fluid
p 41 N92-10163
Numerical simulation of vortex breakdown via 3-D Euler equations p 41 N92-10164
Three dimensional numerical method for resolving small transonic perturbations in unstructured mesh
[ONERA-RT-56/3064-RY-006-R] p 13 N92-10989
Rotorcraft system identification
[AGARD-AR-280] p 22 N92-11001
Wing tip turbine: Analysis of the results of S2MA sounding of marginal vortex of the A320, technical summary
[ONERA-RTS-21/4365-AY-056A] p 23 N92-11009
Application of infrared thermography to thermal flux measurement in wind tunnels
[AAAF-NT-89-12] p 31 N92-11020
Theoretical study (Lagrangian modeling) of turbulent particulate dispersion
[ETN-91-99909] p 42 N92-11287
Resolution of the Navier-Stokes equations applied to the computation of the laminar flow around a two dimensional wing profile
[CERT-RT-65/5604-35] p 43 N92-11307
Turbulent friction drag reduction: Boundary layer manipulators
[CERT-RSF-DERAT-62/5004-31] p 43 N92-11309
Resolution of Navier-Stokes equations around profiles: Drag evolution
[ONERA-RTS-86/1685-AY-156A] p 43 N92-11310
Perfect compressible two dimensional boundary layer strong fluid coupling in the case of sharp leading edge profiles. Unsteady case of isolated profiles and steady case of blade grids
[ONERA-RT-43/1621-RY-006-R] p 43 N92-11311
Hydrodynamic flow visualization around an oscillating vane. Extension of study to the case of higher incidences and amplitudes and the starting off phase from permanent regime
[ONERA-RT-56/1369-AN] p 43 N92-11312
Eighty years of aerospace technique through ATMA bulletins
[ETN-91-90097] p 57 N92-11963
Thermographic gust wind tunnel measurements
[ONERA-RF-31/3409-PY] p 81 N92-11972
Nonstationary flight aerodynamics in a turbulent environment
[ETN-91-90102] p 82 N92-11980
Control aspects of the transition from transversal to transonic flow, step effects
[ETN-91-90106] p 82 N92-11981
Phenomenological modeling of the wake produced by a straight two dimensional base in subsonic flow
[REPT-90/59] p 82 N92-11982
Study of interactions on anemoclinometric sensors
[REPT-90/30] p 138 N92-12006
Study of detached turbulent flow in an air intake by means of high speed tomography and laser velocimetry
[REPT-90/55] p 157 N92-12216
Machine Intelligence for Aerospace Electronic Systems
[AGARD-CP-499] p 164 N92-12517
Vortex Flow Aerodynamics
[AGARD-CP-494] p 83 N92-12996
Characteristics of a boundary layer in a leading edge vortex p 86 N92-13012
Physics of vortical flow p 86 N92-13016
Determination of vortex-breakdown criteria by solving the Euler and Navier-Stokes equations
p 87 N92-13018
Recent progress in inverse methods in France
p 201 N92-13938
Mechanical qualification tests for materials used in the fabrication of aircraft parts
[CEAT-M5-5443/01] p 195 N92-14042
Optimization of the calculation margins of landing gears under extreme loads. Rupture static tests. Part 1: Program and test implantation
[CEAT-S8-6551-PARTIEL-1-PT-] p 195 N92-14043
Avionics standardization in Europe
p 199 N92-14050
Mixed approach towards modular avionics conflicting requirements p 199 N92-14051
Artificial Neural Network Approaches in Guidance and Control
[AGARD-LS-179] p 234 N92-14673
Aerothermodynamics for Space Vehicles
[ESA-SP-318] p 180 N92-14973
Analysis tools of ONERA and DLR for the aerothermodynamics of reentry vehicles
p 211 N92-14977
Supersonic combustion studies p 211 N92-14984
Experimental investigation of transverse jet effects related to hypersonic space vehicles
p 182 N92-14995
Numerical simulations around models in hypersonic wind tunnels p 182 N92-14998
Heat transfer measurements in ONERA supersonic and hypersonic wind tunnels using passive and active infrared thermography p 208 N92-15003
Ablation and temperature sensors for flight measurements in reentry body heat shields
p 227 N92-15004
Hypersonic viscous shock layer in thermochemical nonequilibrium p 183 N92-15014
Hypersonic inviscid flow field simulations around reentry vehicles with flap deflection p 184 N92-15025
Numerical simulation of thermochemical non-equilibrium viscous flows around reentry bodies
p 227 N92-15029
Transitional flows around re-entry bodies
p 184 N92-15035
Computation of aerodynamic coefficients on Hermes-Ariane5 configuration p 184 N92-15040
Rotorcraft System Identification
[AGARD-LS-178] p 273 N92-17153
Technical evaluation report on the Fluid Dynamics Panel Specialists' Meeting on Effects of Adverse Weather on Aerodynamics
[AGARD-AR-306] p 352 N92-18242
Fatigue Management
[AGARD-CP-506] p 360 N92-18571
Fatigue safety factor: Assessment of associated safety level p 401 N92-18573
Fatigue testing and tear down operations on Airbus A320 forward fuselage p 360 N92-18579
Aircraft tracking optimization of parameters selection
p 361 N92-18585
Manoeuvring Aerodynamics
[AGARD-CP-497] p 363 N92-18778
Characterization of unsteady aerodynamic phenomena at high angles p 364 N92-18787
AGARD/SMP Review: Damage Tolerance for Engine Structures. 4: Reliability and Quality Assurance
[AGARD-R-773] p 402 N92-19004
Manufacturing process control as a damage tolerance concept p 403 N92-19006
Hot jet dilutor
[ETN-92-90860] p 366 N92-19225
Reaction speed constant for the reactions between N + O2 and between O + N2
[ETN-92-90861] p 347 N92-19252
Double loop control law strategy and applications to helicopter
[CERT-2/7724-DERA] p 381 N92-19295
Inhomogeneous turbulence beyond spectral equilibria: Aeronautical applications
[ETN-92-90867] p 404 N92-19349
Airplane crashes on the runway. Fine modeling of the behavior after burning of a frame submitted to linear crushing
[IMFL-90-64] p 353 N92-19350
Drag prediction using computation methods
[ONERA-RSF-82/1685-AY-154-4] p 349 N92-19682
Hypersonic wakes
[ETN-92-91082] p 349 N92-19925
Resolution of the Euler equations applied to a helicopter rotor in forward flight
[ONERA-RSF-2/3731-AY-004A] p 406 N92-19976
Validation of flight critical control systems
[AGARD-AR-274] p 382 N92-20026
Blade-vortex noise on a helicopter main rotor. Study of the strong two dimensional incompressible interaction
[ONERA-RT-96/5094-PY] p 511 N92-20388
Experimental study of the wall pressure fluctuations under a turbulent boundary layer downstream of tandem aerofoil external manipulators
[REPT-207-90-78] p 500 N92-20497
Space software is first of all software
p 509 N92-20590
Data processing aspects of the Hermes Flight Control Center p 513 N92-20629
Air intakes for high speed vehicles
[AGARD-AR-270] p 445 N92-20797
Effects of Adverse Weather on Aerodynamics
[AGARD-CP-496] p 449 N92-21679
Flight in adverse environmental conditions
p 449 N92-21680
Regulations and their changes for certification of civil aircraft in icing conditions p 450 N92-21683
Method for calculating the three-dimensional water concentration coefficients and its industrial applications
p 502 N92-21685
Prediction of helicopter noise: Adaptation of noise load calculations to the blade-vortex interaction
[ONERA-RS-97/5094-PY] p 513 N92-21736
Aircraft Ship Operations
[AGARD-CP-509] p 464 N92-21951
Integration of flight and carrier landing aid systems for shipboard operations p 456 N92-21958
Approach and landing assisted by onboard image processing p 457 N92-21959
Dynamic performance of an aircraft on its landing gear: Test and evaluation on a dihedral p 466 N92-21970
Integrated Design Analysis and Optimisation of Aircraft Structures
[AGARD-R-784] p 550 N92-23227
Structural optimization of aircraft practice and trends
p 551 N92-23239
Large thin composite thermostructural parts
p 576 N92-23821
Stretched skin concept for the entry aerodynamic decelerator system of planetary probes
p 576 N92-23836
Special Course on Engineering Methods in Aerodynamic Analysis and Design of Aircraft
[AGARD-R-783] p 552 N92-23950

Computational procedures for preliminary design
p 552 N92-23952
Experimental methods to determine heat exchanger performances p 682 N92-25667
On the computation of unsteady turbomachinery flows. Part 1: Euler equations in vibrating cascades
p 768 N92-27460
Validation of a CANARI code by the computation of three dimensional turbulent flow in turbine valve
p 741 N92-27462
Steady and unsteady 3D flow computation through a transonic turbine stage p 742 N92-27469
Presentation of a computational code for 3-D compressible flow in complex channels and cavities
p 769 N92-27475
The coherent flamelet model for propulsion applications p 756 N92-27486
Three dimensional calculations of reactive flows within aircraft combustion chambers including some combustion models p 770 N92-27490
Special Course on Unstructured Grid Methods for Advection Dominated Flows
[AGARD-R-787] p 771 N92-27671
Special Course on Skin Friction Drag Reduction
[AGARD-R-786] p 717 N92-27706
Basic concepts on boundary layers
p 717 N92-27707
Drag reduction: An industrial challenge
p 717 N92-27708
Boundary layer transition: Prediction, application to drag reduction p 717 N92-27711
Turbulent skin-friction drag reduction by active and passive means, part 1 p 718 N92-27714
Technical evaluation report on the Flight Mechanics Panel Symposium on Flying Qualities
[AGARD-AR-311] p 733 N92-27870
Transonic Unsteady Aerodynamics and Aeroelasticity
[AGARD-CP-507] p 718 N92-27936
Direct coupling of fluid structure in transonic aeroelasticity p 721 N92-27954
Advances in Fibre-Optic Technology in Communications and for Guidance and Control
[AGARD-LS-184] p 774 N92-28084
Applications of ASICs to avionics
[AGARD-AG-329] p 859 N92-28376
What is an ASIC? p 859 N92-28377
A radar signal processing ASIC and a VME interface circuit p 859 N92-28380
Steady and Transient Performance Prediction of Gas Turbine Engines
[AGARD-LS-183] p 868 N92-28458
Steady and transient performance calculation method for prediction, analysis, and identification
p 869 N92-28461
Aircraft ship operations
[AGARD-AR-312] p 850 N92-28468
Integrated Design Analysis and Optimisation of Aircraft Structures
[AGARD-LS-186] p 851 N92-28469
Structural optimization of aircraft p 851 N92-28472
Piloted Simulation Effectiveness
[AGARD-CP-513] p 786 N92-28522
Flight simulation and digital flight controls
p 884 N92-28526
Use of a research simulator for the development of new concepts of flight control p 885 N92-28543
The role of simulation for the study of APIS (piloting support by synthetic imagery) p 885 N92-28544
Construction of a numerical optimization method for the definition of hypersupported profiles
[ONERA-RSF-43/1736-AY-146A] p 908 N92-28788
Feasibility study of hypersonic clinometric measurements at R3Ch
[ONERA-RSF-136/1865-AY-728-] p 829 N92-28789
Development of an unsteady three-dimensional viscous-inviscid interaction numerical method for the calculation of airfoils vibration
[ONERA-RSF-7/3617-AY-022A] p 830 N92-29206
Ageing airplane repair assessment program for Airbus A300 p 838 N92-30123
Survey of French activities concerning structural airworthiness and aging aircraft p 838 N92-30130
Computation of unsteady transonic flows using an implicit centered Euler solver without artificial viscosity
[ESA-TT-1235] p 944 N92-30514
Vortex flow aerodynamics
[AGARD-AR-299] p 946 N92-30947
Preparation for a new plane (A 320): Experience reviewed p 1010 N92-30954
Flight crew integration in the maintenance chain of a commercial aircraft (A 320) p 1012 N92-30957
Theoretical simulation of a 2 micron airborne solid state laser anemometer p 1000 N92-31059
A cable detection lidar system for helicopters
p 1001 N92-31068
Flat plates placed in depleted hypersonic flow
[SESSIA-430/91.960] p 947 N92-31508
Contribution to the modelling of turbulent combustion in the case of stabilisation by flame-lock
[ESA-TT-1229] p 988 N92-31942
Proceedings of the 53rd Symposium on Air Vehicle Mission Control and Management
[AGARD-AR-310] p 1010 N92-32229
Numerical simulation of turbulence at the back of the airplane
[ETN-92-91664] p 1037 N92-32769
Research on some centered implicit methods for calculating transonic flows by solving Navier-Stokes equations
[ONERA-RSF-24/1408-AY-150A] p 1037 N92-32773
Strong coupling between inviscid fluid and boundary layer of sharp leading edges: Two-dimensional stationary and turbulent cases for isolated profiles and guard vanes
[ONERA-RT-44/1621-RY-016-R] p 1125 N92-32776
The Utilization of Advanced Composites in Military Aircraft
[AGARD-R-785] p 1109 N92-33033
Evaluation of the effects of the environment on the behavior of the primary structures of composite material aircraft in service: Historic and current situation
p 1110 N92-33048
The need for GPS standardization
p 1049 N92-33351
Precise GPS ephemerides from DMA and NGS tested by time transfer p 1049 N92-33355
Flutter models: Their design, manufacture, and ground testing p 1089 N92-34164
Unsteady wind tunnel tests p 1089 N92-34166

G

GERMANY

BMI/bis (allylphenoxyphthalimide)-copolymers - A new family of resins for advanced composites with improved thermal oxidative stability p 33 A92-10213
Shock wave reflection close to the leading edge of a wedge p 37 A92-10660
The just attached shock-wave at the leading edge of a profile p 3 A92-10663
Legal problems in aircraft towing using the PTS procedure p 56 A92-11214
Registration of aircraft in the aircraft registrar using the 'Leasing Decree' of the Federal Minister of Transport of February 12, 1991 p 56 A92-11215
Design and testing of a controlled diffusion airfoil cascade for industrial axial flow compressor application
[ASME PAPER 90-GT-140] p 6 A92-11286
Saenger and the German Hypersonics Technology Programme - Status report 1991
[IAF PAPER 91-198] p 32 A92-12570
Thermodynamic behaviour of hydrogen-powered hypersonic ramjets flying along ideal trajectories
[IAF PAPER 91-277] p 25 A92-12601
Landing spacecraft gently on earth - The Soviet parachute systems p 33 A92-13227
Extension of a three-dimensional Euler method for calculating the flowfield around bypass engines with fan and core jet p 62 A92-13690
Modal identification in the presence of steady excitation p 131 A92-13693
Flight in a steady wind field p 131 A92-13696
Frequency-domain identification of BO 105 derivative models with rotor degrees of freedom
p 104 A92-14327
Two-phase flow correlations in air/oil systems of aero engines
[ASME PAPER 91-GT-54] p 121 A92-15532
Computation of 3D flow phenomena in axial flow compressor blade rows
[ASME PAPER 91-GT-78] p 69 A92-15547
An investigation of a strong shock-wave turbulent boundary layer interaction in a supersonic compressor cascade
[ASME PAPER 91-GT-92] p 70 A92-15556
Effects of stator wakes and spanwise nonuniform inlet conditions on the rotor flow of an axial turbine stage
[ASME PAPER 91-GT-93] p 70 A92-15557
Life time prediction for ceramic gas turbine components
[ASME PAPER 91-GT-96] p 122 A92-15560
The influence of density difference between hot and coolant gas on film cooling by a row of holes - Predictions and experiments
[ASME PAPER 91-GT-255] p 151 A92-15660
Performance improvements of compressor cascades by controlling the profile and sidewall boundary layers
[ASME PAPER 91-GT-260] p 75 A92-15662
Inlet flow angle determination of transonic compressor cascades
[ASME PAPER 91-GT-274] p 75 A92-15671
Blade row interaction in a multistage low-pressure turbine
[ASME PAPER 91-GT-283] p 125 A92-15678
Design and analysis of a high pitch to chord ratio cascade representative of ducted propfans
[ASME PAPER 91-GT-335] p 126 A92-15700
Propulsion aspects of hypersonic turbo-ramjet-engines with special emphasis on nozzle/aftbody integration
[ASME PAPER 91-GT-395] p 127 A92-15725
Integrated navigation for approach guidance using differential GPS p 101 A92-16970
Dornier Do 328 - A start in the world market
p 113 A92-17093
The long-distance Airbus A340 - Europe's largest aircraft p 113 A92-17094
Air transport research in Germany p 61 A92-17095
German airports - Capacity crisis p 61 A92-17097
Adaptive airborne MTI with two-dimensional motion compensation p 102 A92-17240
Engine air inlet and de-icing system - At -30 C in the icing tunnel of NRC Ottawa p 92 A92-17252
Lightning protection for the Dornier 328
p 113 A92-17253
Interior noise reduction program for the Dornier 328
p 114 A92-17254
Thrust nozzle test facility at DLR Cologne
[AIAA PAPER 91-5024] p 206 A92-17818
Hypersonic airbreathing propulsion activities for Saenger
[AIAA PAPER 91-5040] p 200 A92-17828
An experimental investigation of the combustion of a hydrogen jet injected parallel in a supersonic air stream
[AIAA PAPER 91-5102] p 212 A92-17861
PVD coatings for aircraft turbine blades
p 216 A92-17950
Navsat - A civil complement to GPS and Glonass
[IAF PAPER 91-490] p 188 A92-18505
Influences of wind tunnel parameters on airfoil characteristics at high subsonic speeds
p 173 A92-18769
Base pressure measurements on a cone at Mach numbers from M sub infinity = 5 to 7
p 173 A92-18770
Analysis of spiraling vortical flows around slender delta wings moving in an inviscid medium p 173 A92-18900
Three-dimensional calculation of low-frequency unsteady transonic flow in axial turbine stages
p 174 A92-19110
Representation of geometric stiffening in multibody system simulation p 217 A92-19463
Multiaxial load spectra in a cooled gas turbine blade under in-service conditions p 201 A92-19696
Dornier 328 first flight p 192 A92-19924
Evaluation of a bounded high-resolution scheme for combustor flow computations p 201 A92-20734
Comparative study of fatigue in various materials and designs under sonic loading p 287 A92-21003
A new method for increasing maximum flight endurance p 280 A92-21006
System-identification of airplanes using the 'estimation before modelling' technique p 269 A92-21007
Beriev Be-42 - A unique jet-propelled seaplane
p 269 A92-21010
Airbus A340 - The first phase of flight testing
p 269 A92-21011
Pratt & Whitney PW300 for general aviation
p 277 A92-21012
Technology for tomorrow - Do 228 with laminar wings
p 269 A92-21013
Air transport research in Germany
p 241 A92-21014
Report of the working group Future CNS Systems - Applications and impact on the German air transport system p 266 A92-21325
A parametric study of the aeroelastic stability of a binary wing-with-engine nacelle flutter system in incompressible flow p 270 A92-22472
Studies on the effect of high-flying air-traffic on the atmosphere
[IAF PAPER 91-737] p 301 A92-22495
Applications of IMI 834 in aeroengines - A collaborative IMI/MTU programme p 288 A92-22754
Mechanical and fracture behaviour of Ti-6Al-2Sn-4Zr-2Mo-0.1Si alloys p 288 A92-22755
Influence of long time exposure at elevated temperatures in air on mechanical properties of the high temperature titanium alloy IMI 834 p 289 A92-22767
No end to incidents in airspace? III
p 262 A92-23172
Preliminary laser induced fluorescence measurements in several facilities in preparation for application to studies in the high enthalpy shock tunnel Goettingen (HEG)
[AIAA PAPER 92-0143] p 284 A92-23761

Identification of aerodynamic effectiveness and interference effects of direct-lift-control flaps from flight data
[AIAA PAPER 92-0171] p 271 A92-23782
Measurements of the pressure and velocity distribution in low-speed turbomachinery by means of high-frequency pressure transducers p 391 A92-24723
Europe presents a united CFD front p 392 A92-24909
Base pressure in supersonic flow - Further thoughts about a theory p 331 A92-26442
A fatigue crack growth threshold p 389 A92-26667
Thermal management of propulsion systems in hypersonic vehicles
[AIAA PAPER 92-0516] p 373 A92-26942
Finite-element algorithm for chemically reacting hypersonic flow
[AIAA PAPER 92-0754] p 336 A92-27097
A study on the superconvergence of Multhopp's discretization in vortex-lattice methods p 336 A92-27381
Calculation of three-dimensional transonic turbine cascade flow p 344 A92-28519
Inviscid and viscous transonic flows in cascades using an implicit upwind algorithm p 344 A92-28522
The mean power of forces and moments in unsteady aerodynamics p 421 A92-28949
Dornier 328 now in flight testing p 457 A92-29418
Tiger development status p 458 A92-29672
Acquisition of an aerothermodynamic data base by means of a winged experimental reentry vehicle p 486 A92-30685
Experimental investigations of the vortex flow on delta wings at high incidence p 432 A92-31172
Semiconductor laser Doppler anemometer for applications in aerodynamic research p 495 A92-31173
Non-homogeneous bars under tension, pure bending and thermal loads p 495 A92-31198
Numerical investigation of the high-speed conical flow past a sharp fin p 433 A92-31468
Implicit solutions of three-dimensional viscous hypersonic flows p 434 A92-31549
Design considerations for nozzles of hypersonic airbreathing propulsion
[AIAA PAPER 91-5019] p 471 A92-31685
The DLR Lyman-alpha hygrometer p 467 A92-32091
Design, analysis, and testing of integrally stiffened composite centre fuselage skin for future fighter aircraft p 535 A92-32554
CATMAC - A way to integrate ground ATC and airborne systems p 531 A92-33429
The Berlin oil channel for drag reduction research p 571 A92-34219
A study on the feasibility of using adaptive structures in the attenuation of vibration characteristics of rotary wings
[AIAA PAPER 92-2452] p 541 A92-34415
Estimation of the P-3/SAR L-, C- and X-band antenna directivity in range direction based on corner reflector measurements within the absolute SAR calibration p 587 A92-35055
Visualization and measurement of helicopter rotor flow using projected smoke filaments and digital image processing p 520 A92-35728
Noise level reduction inside helicopter cabins p 545 A92-35733
Complete Euler-solution for a rotor in hover and a propeller in forward flight p 520 A92-35755
Experiences with high authority helicopter flight control p 568 A92-35757
Active control of helicopter ground and air resonance p 568 A92-35762
Inertial reference units with integrated air speed determination for helicopters p 554 A92-35764
Evaluation of a constant feedback gain for closed loop higher harmonic control p 568 A92-35768
Some aerodynamic mechanisms of impulsive noise during blade-vortex-interaction p 604 A92-35782
On the influence of blade-vortex-interactions on vortex structure p 521 A92-35783
Theoretical model to calculate aerodynamic interference effects between rotor and wing of tiltrotors p 521 A92-35788
Compressible turbulent boundary layers with heat addition by homogeneous condensation p 611 A92-36843
Swirl and fuel composition effects on boron combustion in solid-fuel ramjets p 668 A92-36964
An exploration of chemically reacting viscous hypersonic flow p 612 A92-37550
Aeroservoelasticity p 642 A92-37577
International Symposium on Engineering Turbulence Modelling and Measurements, Dubrovnik, Yugoslavia, Sept. 24-24, 1990, Selected Papers p 672 A92-38851
Comparison of aircraft noise indices for noise zoning at military airfields p 687 A92-39056
Calculation of aircraft noise contours taking into account the lateral flight track dispersion p 687 A92-39059
Distribution of maximum levels of aircraft noise around their mean value p 693 A92-39062
Interdependencies of aircraft-/airport-noise and urban- and regional-planning standards p 688 A92-39063
Azimuthal noise characteristics of contra-rotating propellers - Results of a wind tunnel model test p 693 A92-39066
Summary of Dornier 328 interior noise control study p 643 A92-39083
Trading number of operations versus loudness of aircraft p 688 A92-39102
A system for precise real-time differential GPS positioning in the decimeter range p 638 A92-39569
European Fighter Aircraft (EFA) programme status report p 646 A92-40043
A new method for visualization and measurement of turbulent flow patterns p 619 A92-40063
Particle dispersion in highly swirling, turbulent flows p 675 A92-40093
Measurements and simulation of the flow around a poppet valve p 675 A92-40103
Vortical flow simulation by the solution of the Navier-Stokes equations p 620 A92-40104
Embedded longitudinal vortex arrays, velocity and temperature fields, loss and heat transfer augmentation p 621 A92-40121
Evolution of coherent structures during transition in a flat-plate boundary layer p 621 A92-40126
The calculation of a compressible boundary layer past a pointed body and a delta wing p 622 A92-40173
Vortex interaction in the wake behind an oscillating airfoil p 623 A92-40175
Curvature effects for three-dimensional compressible boundary-layer stability p 701 A92-41207
Identification of the transfer function between turbulence and aircraft p 743 A92-41226
Wind tunnel wall corrections for unsteady flow applying steady wall adaptation and CFD-techniques p 706 A92-42533
Numerical approximation of hypersonic shocks in a finite-element method using flux-corrected transport (FCT) p 708 A92-43060
Similarity and resistance in near-sonic flows for given heat conduction p 708 A92-43065
Calculation of transonic flow in turbomachine cascades p 708 A92-43067
The design of fully-optimized configurations by using the iterative optimum-optimorum theory p 709 A92-43072
Three-dimensional visualizations of the aerodynamic characteristics of delta wings for the transition from subsonic to supersonic leading edges in supersonic-hypersonic flow p 709 A92-43073
Computer-based areal surface temperature and local heat transfer measurements with thermochromic liquid crystals (TLC) p 763 A92-44326
Centre for Flight Simulation Berlin Airbus 340 simulator for research and training p 880 A92-45028
Concepts for the stability analysis of NLF-experiments on swept wings
[AIAA PAPER 92-2706] p 801 A92-45548
Turbulent drag reduction by laminar sublayer thickening
[AIAA PAPER 92-2707] p 801 A92-45549
Application of the Euler method EUFLEX to a fighter-type airplane configuration at transonic speed
[AIAA PAPER 92-2620] p 845 A92-45573
A new milestone in automatic aircraft control - Fly-by-light systems transmit commands optoelectronically p 784 A92-45699
Thrust/speed effects on long-term dynamics of aerospace planes p 889 A92-46766
Reconstruction of flight path in turbulence p 874 A92-46777
Calibration-related pseudo-Reynolds number trends in transonic wind tunnels p 882 A92-46780
Simulation of transonic flow over twin-jet transport aircraft p 811 A92-46793
A Mach-scaled powered model for rotor-fuselage interactional aerodynamics and flight mechanics investigations p 847 A92-46960
Multi-block grid generation around wing-body-engine-pylon configurations p 817 A92-47060
Interactive algebraic mesh generation for twin jet transport aircraft p 817 A92-47064
Airbus A319 - Completion of the standard fuselage family p 848 A92-47591
German-GUS cooperation in civil aviation p 785 A92-47592
Computer-Controlled Navigation System/General Positioning System (CCNS/GPS) - A guidance, positioning, and management system for remote sensing flights p 840 A92-47630
Construction of a real-time DGPS experimental system p 840 A92-47631
Calculation of hypersonic, viscous, non-equilibrium flows around reentry bodies using a coupled boundary layer/Euler method
[AIAA PAPER 92-2856] p 819 A92-47839
Computation of 3-D hypersonic flows in chemical non-equilibrium including transport phenomena
[AIAA PAPER 92-2876] p 820 A92-47858
Numerical simulation of chemical and thermal nonequilibrium flows behind compression shocks
[AIAA PAPER 92-2879] p 820 A92-47860
Bistatic scattering on a monostatic radar range p 849 A92-48408
Motion errors in an airborne synthetic aperture radar system p 840 A92-48416
Comparison between two 3D-NS-codes and experiment on a turbine stator
[AIAA PAPER 92-3042] p 822 A92-48703
Investigations of propulsion integration interference effects on a transport aircraft configuration
[AIAA PAPER 92-3097] p 849 A92-48739
Numerical study of secondary separation in glancing shock/turbulent boundary layer interactions
[AIAA PAPER 92-3666] p 907 A92-49087
Numerical flow simulation and analysis of a shrouded propfan rotor
[AIAA PAPER 92-3773] p 826 A92-49118
On the effect of external flow and shear-layer thickness on the expansion cells of under-expanded supersonic circular jets p 969 A92-50478
A new aspect of future air navigation systems - How Secondary Surveillance Radar Mode S could protect civil aviation p 1012 A92-51424
Hypersonic flow calculations around a 3D delta wing at low Knudsen numbers p 937 A92-52734
Rarefied gas flow around a disc with different angles of attack p 938 A92-52753
Experiments on separation at a compression corner in rarefied hypersonic flows p 938 A92-52755
Force and heat transfer on a disc in rarefied flow p 939 A92-52764
Monte Carlo simulation of the hypersonic mon- and diatomic gas flow past a disk at an angle of attack p 939 A92-52770
High temperature MMCs for aero-engines - Challenge and potential p 986 A92-52982
Aerodynamic assessment of an optical pressure measurement system (OPMS) by comparison with conventional pressure measurements in a high speed wind tunnel p 1114 A92-54304
Conception of a UHB engine simulator for the essential characteristics of a true-scale engine p 1090 A92-54322
Some important factors in turbulence in flight measurement p 1063 A92-54324
Shock detection on airfoils by means of piezo foil- and hot film arrays p 1115 A92-54334
Application of a wall pressure method in a wind tunnel test section with adjustable longitudinal slots p 1091 A92-54336
Automatic control of test parameters for intake measurements in a low-speed wind tunnel p 1091 A92-54341
A general approach to optimal real-time guidance of dynamic systems based on nonlinear programming
[AIAA PAPER 92-4378] p 1131 A92-55182
ATTAS flight test and simulation results of the advanced gust management system LARS
[AIAA PAPER 92-4343] p 1079 A92-55332
Computed tomography (CT) as a nondestructive test method used for composite helicopter components p 1121 A92-56276
Repair procedures for advanced composites for helicopters p 1016 A92-56277
Design and development of test rigs for main rotor and main rotor transmission of a helicopter in the 6-ton-class p 1093 A92-56280
'A new proposal for an old problem' - The right engine for the right helicopter p 1070 A92-56281
Test and integration concept for complex helicopter avionic systems p 1064 A92-56292
Laser-radar based obstacle avoidance system for helicopters p 1064 A92-56295
Short takeoff optimization for the XV-15 tiltrotor aircraft p 1056 A92-56302
Modern helicopter technologies at MBB and the application in future programmes p 1016 A92-56304
Blade instability of horizontally stoppable rotors p 1085 A92-56308
HEPO mission simulator - Development and usage for NH90 helicopter p 1094 A92-56313

Influence of cross section variations on the structural behaviour of composite rotor blades
p 1121 A92-56320
A small light-weight rotor platform for ground observation and pollution control p 1057 A92-56329
Analysis of helicopter rotor-fuselage interference with time averaged pressure distribution
p 1032 A92-56331
Current European rotorcraft research activities on development of advanced CFD methods for the design of rotor blades (BRITE/EURAM 'DACRO' project)
p 1032 A92-56332
Development of a conceptual design method for rotary-wing aircraft using digital computers
p 1058 A92-56340
BVI impulsive noise reduction by higher harmonic pitch control - Results of a scaled model rotor experiment in the DNW p 1136 A92-56344
Sound produced by vortex-airfoil interaction
p 1136 A92-56345
Mission oriented investigation of handling qualities through simulation p 1059 A92-56353
Design of a variable contraction for a full-scale automotive wind tunnel
[AIAA PAPER 92-3929] p 1096 A92-56760
The high enthalpy shock tunnel in Goettingen
[AIAA PAPER 92-3942] p 1104 A92-56772
Investigation of a plate-ramp-configuration by means of laser Doppler anemometry at Mach 2.95
[AIAA PAPER 92-3956] p 1097 A92-56784
The cryogenic balance design and balance calibration methods
[AIAA PAPER 92-4001] p 1122 A92-56824
The trisonic wind tunnel Muenchen and its involvement in the German SAeNGER-programme
[AIAA PAPER 92-4019] p 1100 A92-56841
Optimization of two stage reusable space transportation systems with rocket and airbreathing propulsion concepts
[IAF PAPER 92-0863] p 1104 A92-57254
The German Hypersonics Technology Programme - Status report 1992
[IAF PAPER 92-0867] p 1105 A92-57258
IRS organigram p 33 N92-10053
A systematic formulation, as an approach to air traffic
[MBB-Z-0371-91-PUB] p 19 N92-10996
The electronic aeronautical chart for general aeronautics: A system specification
[ILR-MITT-263(1991)] p 20 N92-10997
Resonance and control response tests using a control stimulation drive
[MBB-UD-0586-90-PUB] p 134 N92-12003
Tool supported software development experiences from the EFA project p 163 N92-12451
Process/object-oriented Ada software design for an experimental helicopter p 164 N92-12461
Development and verification of software for flight safety critical systems p 164 N92-12469
Expert system for the Tornado ground-based check-out system p 118 N92-12536
On the simulation of compressible turbulent flows past delta wing, delta wing-body and delta wing-canard
p 84 N92-13003
On the footprints of three-dimensional separated vortex flows around blunt bodies: Attempts of defining and analyzing complex flow structures p 84 N92-13005
Vortex formation over a close-coupled canard-wing-body configuration in unsymmetrical flow p 85 N92-13010
On aircraft wake properties and some methods for stimulating decay and breakdown of tip vortices
p 87 N92-13021
Extended mapping and characteristics techniques for inverse aerodynamic design p 194 N92-13949
Supercritical blade design on stream surfaces of revolution with an inverse method p 220 N92-13950
Application of direct inverse analogy method (DIVA) and viscous design optimization techniques
p 176 N92-13951
Image-supported navigation for testing instrument landing systems p 189 N92-14012
DME growth elements and their use with MLS
p 189 N92-14018
A Taxi And Ramp Management And Control system (TARMAC) p 207 N92-14027
Avionics systems development: Technological trends, conflicts, and cost issues in a changing European environment p 199 N92-14054
Experimental investigations of exciting forces caused by flow in labyrinth seals p 223 N92-14354
Evaluation of rotordynamic coefficients of look-through labyrinths by means of a three volume bulk flow model
p 223 N92-14356
Determination of rotordynamic coefficients for labyrinth seals and application to rotordynamic design calculations p 223 N92-14360
Hydraulic actuator system for rotor control
p 224 N92-14363
Application of MSC/DYNA to shock and impact problems in aircraft industry
[MBB-UD-0593-91-PUB] p 225 N92-14382
Review of investigations on aeronautical fatigue in the Federal Republic of Germany
[ETN-92-90317] p 225 N92-14397
Low cycle fatigue of cast nickel base turbine rotors
p 226 N92-14405
Fatigue of repaired composite structures
p 214 N92-14411
Environmental fatigue tests with composite materials
p 214 N92-14413
Comparison between hot/wet test and RT/dry test on the Seastar horizontal stabilizer and fin
p 226 N92-14414
Probabilistic lifing approach for aero engine disks made of powder nickel base alloys containing ceramic defects
p 226 N92-14424
Airbus Industrie A330/A340: Full scale fatigue test of center fuselage and wing p 226 N92-14425
Methodology for assessment of skin repairs on Airbus aircraft p 226 N92-14428
A concept for the revisions of structural inspection schedules p 226 N92-14431
Introduction to neural computing and categories of neural network applications to guidance, navigation and control p 234 N92-14674
Simulation requirements for RCS plume: Flowfield interaction modelling on a winged reentry vehicle
p 181 N92-14985
Steps towards an efficient and accurate method solving the Euler equations around a re-entry configuration at super- and hypersonic speed p 181 N92-14987
Base pressure measurements on a cone at hypersonic Mach numbers: A contribution to aerothermodynamics for space vehicles p 181 N92-14992
Experimental study of hypersonic shock wave boundary layer interactions by means of infrared technique
p 182 N92-14994
Short time force measurement system
p 208 N92-15001
Verification and application of the NSFLEX method for hypersonic flow conditions p 182 N92-15005
Viscous shock-layer equations for the calculation of reentry aerothermodynamics p 183 N92-15008
The IRS plasma wind tunnels for the investigation of thermal protection materials for reentry vehicles
p 208 N92-15009
FALKE and COBRA technology development in aerodynamics and aerothermodynamics
p 183 N92-15017
High enthalpy testing in the Aachen (Fed. Republic of Germany) shock tunnel TH 2 p 208 N92-15021
Computational aerothermodynamic methods for industrial applications to re-entry and hypersonic cruise problems p 227 N92-15027
Behaviour and modelling of the aerothermodynamics of ballistic entry vehicles in the high altitude flow regimes
p 184 N92-15031
Applicability of bridging methods to hypersonic rarefied flow aerodynamics of reentry vehicles
p 184 N92-15032
Aerothermodynamic challenges of the Saenger space-transportation system p 184 N92-15042
Development and evaluation of a finite element model for a fiber composite helicopter fuselage
[MBB-UD-0584-90-PUB] p 196 N92-15066
Project of an adaptive multiaxial autopilot with learning pilot control
[ETN-92-90592] p 205 N92-15072
The acoustic flashlight
[MBB-Z-0359-90-PUB] p 239 N92-15938
Instrumentation and data processing
p 273 N92-17155
BO 105 identification results p 274 N92-17161
Rapid repair of integrally stiffened carbon fibre composite structures by bolted aluminium elements
[MBB-FE202-S-PUB-0453-A] p 290 N92-17310
Aerodynamic development of the X-31 aircraft for the high angle of attack region
[MBB-FE211-S-PUB-452] p 275 N92-17313
Development of an electronic high speed camera system for the quantitative analysis of unsteady flows
[MPIS-100/1991] p 300 N92-17344
Institute for experimental fluid mechanics: Results for 1990
[IB-222-90-A-46] p 400 N92-18244
Calculation of hypersonic non-equilibrium viscous flow using second order boundary layer theory
[MBB-FE122-S-PUB-434] p 345 N92-18316
Design, analysis, and testing of integrally stiffened composite centre fuselage skin for future fighter aircraft
[MBB-FE2-PUB-S-450] p 359 N92-18333
Fatigue life behaviour of composite structures
p 390 N92-18577
Aircraft tracking for structural fatigue
p 361 N92-18584
The Operational Loads Monitoring System, OLMS
p 361 N92-18586
Tornado structural fatigue life assessment of the German Air Force p 363 N92-18592
X-31 enhancement of aerodynamics for maneuvering beyond stall p 363 N92-18779
X-31: Discussion of steady state and rotary derivatives
p 365 N92-18789
Transformation of flightmechanical design requirements for modern fighters into aerodynamic characteristics
p 365 N92-18794
Aeroservoelastic stability of aircraft at high incidence
p 381 N92-18795
The COMPAS system in the ATC environment
[DLR-MITT-91-08] p 354 N92-19041
Design principles of automation aids for ATC approach control p 354 N92-19042
COMPAS system concept p 354 N92-19043
Evaluation of the COMPAS experimental system
p 355 N92-19044
Experiences developed in transfering the experimental COMPAS system to an operational prototype version
p 355 N92-19045
Steps toward acceptance p 355 N92-19046
Evaluation of the COMPAS operational system
p 355 N92-19047
Extension of the Frankfurt COMPAS for general application p 355 N92-19048
The impact of COMPAS on the future Cooperative Air Traffic Management Concept (CATMAC)
p 355 N92-19049
The role of planning systems in future air traffic management p 355 N92-19050
Simple models for the description of turbulence in the atmospheric boundary layer
[DLR-FB-90-17] p 410 N92-19292
Modelling of chemical and physical effects with respect to flows around reentry bodies
[MBB-FE-211/S/PUB/0465/A] p 347 N92-19296
Towards coherent hypermedia navigation by pragmatic dialogue modeling
[PB92-114735] p 455 N92-20818
Flying an aircraft as a problem-solving process: About the Instrument-Failure-Simulator (IFS) as a test for pilot-candidates
[DLR-FB-91-23] p 455 N92-20902
Boundary layer flow in axial compressors (theoretical part)
[ETN-92-91006] p 501 N92-21232
Boundary layer flow in axial compressors (theoretical part)
[ETN-92-91007] p 501 N92-21233
Boundary layer flow in axial compressors (theoretical part)
[ETN-92-91008] p 502 N92-21234
Preparation of the ice certification of the Dornier 328 regional airliner by numerical simulation and by ground test p 451 N92-21693
Extension of a three dimensional Euler-code for the investigation of the flow field around bypass engines with fan and core jet
[DLR-FB-91-13] p 503 N92-21699
Three-dimensional simulations of hypersonic flows
[MBB-UK-0155-89-PUB] p 447 N92-21703
Materials and Structures Research Department: Scientific report (1990)
[ETN-92-90727] p 466 N92-22000
Contributions of MBB-FE211 to the 2nd Antibes Workshop on Hypersonic Flows
[MBB-FE211-S-PUB-449] p 524 N92-22179
Cases 6.1 and 6.8 double ellipsoid: Navier-Stokes calculation p 525 N92-22181
Case 7.4 delta wing: Navier-Stokes calculation
p 525 N92-22182
Case 7.4: Blunt nose delta wing Euler-boundary layer calculation p 525 N92-22184
High speed airbreathing propulsion in Europe
p 575 N92-22277
Investigation of the dynamic behaviour and the frequency response of the GG 1342 laser gyro
[ESA-TT-1236] p 595 N92-22641
First approach to an integrated fin design
p 551 N92-23236
Recommended system concept p 599 N92-23383
The imaging spectrometer p 599 N92-23387
The imaging radar system p 599 N92-23391
Quick-look system p 599 N92-23393
Preconsiderations on aircraft integration
p 599 N92-23402
Sensor compatibility/optimal sensor combinations
p 599 N92-23403

Symposium on Marketing for Technological Products
[MBB-UE-0014-90-PUB] p 606 N92-23928
Introduction to Special Course on Engineering Methods in Aerodynamic Analysis and Design of Aircraft
p 552 N92-23951
Investigations of blade row interaction and boundary layer transition phenomena in a multistage aero engine low-pressure turbine by measurements with hot-film probes and surface-mounted hot-film gauges
p 658 N92-24338
Simulation of the flow on a space glider. Stagnation point calculation using the 2D Navier-Stokes equations including chemical effects p 624 N92-24393
Hypersonic configurations in slow speed flight
p 624 N92-24394
Supersonic flow in compression stages and inlets
p 625 N92-24395
FALKE: Winged re-entry vehicle flight control
p 667 N92-24454
Current activities and future plans for GPS applications p 640 N92-24735
DLR-news: Announcements of the German Research Institute for Aeronautics and Astronautics
p 698 N92-25413
Flight test of avionic and air-traffic control systems
[ETN-92-91063] p 640 N92-25590
The DLR test aircraft in FZ-BS VFW614/ATTAS, Dornier DO228-101, MBB BO 105-S-3 p 648 N92-25591
The basic measuring technical equipment of the DLR test aircraft p 652 N92-25592
Ground installations for the preparation and evaluation of flight tests p 665 N92-25593
Introduction and execution of flight tests at the DLR
p 648 N92-25594
ATTAS experimental cockpit and ATMOS for flight control components and systems investigations
p 641 N92-25595
Testing of an experimental FMS p 648 N92-25596
Testing concept of a movement area guidance
p 641 N92-25597
Pallet for helicopter testing instrumentation
p 652 N92-25598
Development of flight testing of a fault tolerant fly-by-light yaw control system p 662 N92-25599
Ground and satellite supported flight trajectory measurement by example of the avionics flight test system AFES p 641 N92-25600
Board-autonomous flight trajectory measurement by example of an ILS measuring system
p 641 N92-25601
Arrangements and methods for the survey of aircraft radio components and systems p 652 N92-25603
DLR-News: Announcements of the German Research Institute for Aeronautics and Astronautics
p 698 N92-26086
The icing of the wing upper side and bottom side of the icing research aircraft of the DLR
p 724 N92-26349
Measurements in the inhomogeneous convective boundary layer using three powered gliders
p 775 N92-26350
Experimental investigation of the unsteady pressure field around an oscillating blade
[MITT-90-01] p 768 N92-27407
Computation and visualization of specific flow phenomena in turbomachinery application
p 741 N92-27463
CFD contributions during hypersonic airplane intake design p 769 N92-27472
Aerothermodynamics of nozzle flows for advanced hypersonic propulsion systems p 769 N92-27478
Application of finite element method to hypersonic nozzle flow computations p 769 N92-27479
The 3-D Navier-Stokes flow and temperature field computation for a forced mixer nozzle
p 770 N92-27482
Wide gap, permanent magnet biased magnetic bearing system p 773 N92-27794
Knowledge-based planning for controlled airspace flight operation as part of a cockpit assistant
p 727 N92-27895
On board planning of 4D-trajectories
p 728 N92-27897
An efficient method for three-dimensional route planning with different strategies and constraints
p 728 N92-27901
Implementation and operational experience with a new arrival traffic management system at the Frankfurt ATC-Center p 728 N92-27905
Comparison of Euler and full potential methods for unsteady transonic flow calculations
p 719 N92-27943
Computation of the unsteady transonic 2D cascade flow by an Euler algorithm with interactive grid generation
p 719 N92-27944
Evaluation of an unsteady implicit Euler code against two and three-dimensional standard configurations
p 719 N92-27945
Computations of unsteady flows around airfoil sections by explicit and implicit methods solving the Euler and Navier-Stokes equations p 720 N92-27948
Computation of viscous phenomena in unsteady transonic flow p 720 N92-27949
Computation of flutter boundaries in the time and frequency domain p 720 N92-27952
Calculation of installation effects within performance computer programs p 869 N92-28465
Practical architecture of design optimisation software for aircraft structures taking the MBB-Lagrange code as an example p 851 N92-28471
Mathematical optimization: A powerful tool for aircraft design p 851 N92-28474
Opportunities for flight simulation to improve operational effectiveness p 883 N92-28523
Experience with piloted simulation in the development of helicopters p 884 N92-28528
Use of a virtual cockpit for the development of a future transport aircraft p 886 N92-28547
The role of systems simulation for the development and qualification of ATTAS p 886 N92-28548
Calculation of support interferences on the aerodynamic coefficients for a wind tunnel calibration model
[ESA-TT-1247] p 830 N92-29159
DLR research reports and communications
[ETN-92-91391] p 929 N92-29218
Saenger: The reference concept and its technological requirements - aerothermodynamics
[MBB-FE-202-S-PUB-0463-A] p 890 N92-29629
Technology programme: Aerothermodynamics and propulsion integration. Numerical and experimental aerothermodynamics
[MBB-FE-202-S-PUB-0464-A] p 831 N92-29648
Aerothermodynamics and propulsion integration in the Saenger technology programme
[MBB-FE-202-S-PUB-0469-A] p 831 N92-29649
Concurrent engineering in design of aircraft structures
[MBB-FE-2-S-PUB-472] p 854 N92-29650
Aerothermodynamic challenges of the Saenger space-transportation system
[MBB-FE-202-S-PUB-0462-A] p 890 N92-29680
Hypersonic flow past radiation-cooled surfaces
[MBB-FE-202-S-PUB-0468-A] p 832 N92-29713
A semi empirical method for the analytical representation of stationary measured profile coefficients for applications of rotary wing aerodynamics
[ETN-92-91491] p 832 N92-29741
Sensor fault detection on board an aircraft with observer and polynomial classifier
[DLR-FB-91-34] p 859 N92-29870
Computed Tomography (CT) as a nondestructive test method used for composite helicopter components
[MBB-UD-0603-91-PUB] p 910 N92-29873
Repair procedures for advanced composites for helicopters
[MBB-UD-0606-91-PUB] p 787 N92-29874
Global and high resolution radar cross section measurements and two-dimensional microwave images of a scaled aircraft model from the type Airbus A 310
[DLR-MITT-91-10] p 911 N92-29877
Production of periodical Mach number variations in high subsonic flow in a blow down wind tunnel, and its influence on profile measurements
[ETN-92-91492] p 833 N92-29889
Examination of the main error factors with regards to secondary losses in compression and turbine cascades by variations of the blade picture ratio
[ETN-92-91493] p 871 N92-29927
Jet aircraft noise at high subsonic flight Mach numbers
[DLR-FB-91-28] p 928 N92-29997
Experience with piloted simulation in the development of helicopters
[MBB-UD-0610-91-PUB] p 889 N92-30076
Acquisition of an aerothermodynamic data base by means of a winged experimental reentry vehicle
[MBB/FE202/S/PUB/461] p 787 N92-30232
The Eurofar program: An European overview on advanced VTOL civil transportation system
[MBB-UD-0611-91-PUB] p 952 N92-30418
MBB-LAGRANGE: A general structural reliability and optimization structural system
[MBB/FW321/S/PUB/467] p 998 N92-30423
Multidisciplinary optimization of fiber composite aircraft structures
[MBB/FW321/S/PUB/476] p 961 N92-30424
Resonance and control response tests using a control simulation device
[MBB-UD-0608-91-PUB] p 978 N92-30439
Numerical optimization in Germany: A non-exhaustive survey on current activities with emphasis on aeronautics
[MBB/FE211/S/PUB/474] p 932 N92-30675
CFD contributions during hypersonic airplane intake design
[MBB/FE213/S/PUB/459] p 944 N92-30676
Development of hardness cycles for fiber bound materials, using DSC: From laboratory specimens to complex high duty structural members
[MBB-Z-0409-91-PUB] p 987 N92-30969
Trial of a slant visual range measuring device
p 1000 N92-31043
Cutting treatment by drilling of fiber bound synthetic materials
[MBB-UD-0609-91-PUB] p 988 N92-31716
The icing of the elevator of the DLR icing research aircraft of Do 28 type
[DLR-MITT-91-12] p 953 N92-31813
Analysis of three icing test flights reaching the aircraft-referred icing degree of severe
[ESA-TT-1254] p 954 N92-31943
Airborne experimental FLIR program
p 1064 N92-32447
Examples of advanced near-net shape manufacturing techniques for aerospace
[MBB-Z-0399-91-PUB] p 1125 N92-32742
The Dornier 328 Acoustic Test Cell (ATC) for interior noise tests and selected test results
[AIAA PAPER 92-2164] p 1137 N92-32951
Advanced Study for Active Noise Control in Aircraft (ASANCA)
[AIAA PAPER 92-2092] p 1137 N92-32956
Pilots noise exposure during a Boeing 747-400 round trip: Ambient noise and acoustic-head recording and analysis of data p 1137 N92-32960
Pilot noise exposure during a Boeing 747-400 round trip: Judgement of noise and analysis in respect to hearing impairment of pilots p 1138 N92-32961
A multivariable control concept for a gas turbine engine
[ETN-92-92104] p 1072 N92-33645
Influence of the swirl producing construction in the flow and reaction field of turbulent diffusion flames
[ETN-92-92103] p 1127 N92-33916
Stability failure of sandwich structures
[MBB-UD-0613-92-PUB] p 1111 N92-33994

GREECE

Turbine cascade calculations through a fractional step Navier-Stokes algorithm
[ASME PAPER 91-GT-55] p 68 A92-15533
3-D loss prediction based on secondary flow and blade shear layer interaction
[ASME PAPER 91-GT-59] p 68 A92-15536
Unsteady Euler calculations in 2-D internal aerodynamics with introduced vorticity
[ASME PAPER 91-GT-168] p 73 A92-15603
The influence of shock waves on the viscous flow field of axial compressors
[ASME PAPER 91-GT-173] p 73 A92-15608
Combination of different unsteady quantity measurements for gas turbine blade fault diagnosis
[ASME PAPER 91-GT-201] p 149 A92-15624
A procedure for automated gas turbine blade fault identification based on spectral pattern analysis
[ASME PAPER 91-GT-259] p 151 A92-15661
Jet engine fault detection with discrete operating points gas path analysis p 129 A92-17200
Arbitrary blade section design based on viscous considerations - Background information
p 523 A92-36029
Arbitrary blade section design based on viscous considerations - Blade optimization p 523 A92-36030
An inverse inviscid method for the design of quasi-three dimensional turbomachinery cascades
p 523 A92-36033
Optimal measurement and health index selection for gas turbine performance status and fault diagnosis
[ASME PAPER 91-GT-294] p 653 A92-36889
Simulation of turbulent velocity profiles appearing on rotating and stationary parts of subsonic compressors and turbines p 676 A92-40172
Computation of aircraft geometric height under radar surveillance p 639 A92-40239
Upwind schemes for Navier-Stokes computations at subsonic through hypersonic speeds
p 708 A92-43071
Transonic unsteady inviscid and viscous flow's simulation around 2-D moving bodies
[AIAA PAPER 92-2704] p 801 A92-45546
Improved artificial dissipation schemes for the Euler equations p 933 A92-49508
Unsteady Euler calculations in 3D internal aerodynamics p 768 N92-27470
Jet fuel absorption and dynamic mechanical analysis of carbon fibre composites p 1110 N92-33050

H

HONG KONG
Limitations to the large strain theory
p 219 A92-20356

I

INDIA
Prediction of wake in a curved duct p 3 A92-10487
Design of non-overshooting feedback control systems
p 50 A92-11431
Sensors and systems to enhance aviation safety against weather hazards p 160 A92-14265
Nonlinear landing gear behavior at touchdown
p 192 A92-19606
Prediction of turbulent flow behavior over a slotted flap p 309 A92-24407
Multisensor data fusion and decision support for airborne target identification p 454 A92-31063
Unsteady hypersonic boundary layers for slender axisymmetric bodies with large injection rates
p 524 A92-36100
Theoretical and experimental methods in acoustics of ducts and mufflers - A critical review
p 693 A92-39068
Heat transfer in a channel with built-in wing-type vortex generators p 757 A92-41082
A correlation study of the wing-body interference factor for high angles of attack p 700 A92-41179
Technological excellence in honeycomb sandwich and composite structures for aerospace applications
p 757 A92-41180
International Conference on Aerospace Trends...2001 - *From Aeroplane to Aerospace Plane*, Thiruvananthapuram, India, June 27, 28, 1991, Proceedings p 751 A92-41184
Trends in propulsion technology p 757 A92-41186
Estimation of overall drag coefficient of an aerospace plane p 700 A92-41188
Self reliance in aerospace structures
p 758 A92-41190
Basic design concepts for smart actuators for aerospace plane control p 752 A92-41193
Software package for preliminary design of helicopter
p 775 A92-41195
Current growth in the aeronautics p 701 A92-41196
Multi-constraint wing optimization p 701 A92-41197
Measurement of magnus derivatives with an elastically forced oscillation rig p 749 A92-43172
Subcritical flow studies on two-dimensional external compression supersonic inlets p 713 A92-44518
Coupled vibrations of turbomachine blades
p 738 A92-44545
Contribution of individual load cycles to crack growth under aircraft spectrum loading p 891 A92-45236
Microbiological spoilage of aviation turbine fuel. II - Evaluation of a suitable biocide p 891 A92-45600
Optimization of constant altitude-constant airspeed flight *of turbojet aircraft* p 845 A92-46815
Stability of an adaptive controller for aircraft. I - Analysis via Liapunov theory p 976 A92-51940
Estimation of lift and drag characteristics of an aircraft from flight data p 959 A92-51942
On the application of parabolized Navier-Stokes equations to flow field simulations p 936 A92-51943
Flight control system design using eigenstructure assignment for rolling the aircraft around the velocity vector p 977 A92-51945
Aircraft longitudinal dynamics equations including wind shear effects p 977 A92-51946
Non-slender shapes of minimum drag
p 937 A92-52029
Numerical and experimental investigations of rarefied gas flows through nozzles and composite systems
p 940 A92-52797
Parameter estimation of an augmented airplane with unsteady aerodynamics modelling p 1073 A92-53546
Computer aided evaluation of aircraft handling qualities and flight control system robustness
[AIAA PAPER 92-4423] p 1080 A92-55347
Dynamic flying investigations on 1/13.5 NALLA model (Longitudinal Results)
[NAL-PD-FC-9113] p 359 N92-18073
Graphics for interactive PC based parameter estimation package
[NAL-PD-FC-9117] p 412 N92-18252
PC based flight path reconstruction using UD factorization filtering algorithm
[NAL-PD-FC-9201] p 534 N92-22389

IRELAND
Fatigue and accidents - A comparison across modes of transport p 17 A92-13025
The torsional stability of a compressor cascade
[ASME PAPER 91-GT-180] p 123 A92-15612
Organizational factors in human factors accident investigation p 834 A92-45000
Further investigation of the effect of model cooling on periodic transonic flow p 721 N92-27961

ISRAEL
Extensions to the minimum-state aeroelastic modeling method p 20 A92-11081
Observability analysis of piece-wise constant systems with application to inertial navigation p 49 A92-11391
Numerical prediction of subsonic turbulent flows over slender bodies at high incidence p 172 A92-18358
Autonomously aided strapdown attitude reference system p 204 A92-18610
Adaptive suppression of biodynamic interference in helmet-mounted displays and head teleoperation
p 197 A92-18611
Numerical calculation of modulation transfer functions for low frequency mechanical vibrations
p 235 A92-19982
Experimental investigation of periodically excited rotating composite rotor blades p 218 A92-20213
Measurements of lateral aerodynamics characteristics of forebodies at high angle of attack in subsonic and transonic flows
[AIAA PAPER 92-0174] p 255 A92-23785
Effect of upstream disturbance on flow asymmetry
[AIAA PAPER 92-0408] p 325 A92-26261
Cartesian Euler method for arbitrary aircraft configurations p 340 A92-28039
High angle of attack aerodynamics - Subsonic, transonic, and supersonic flows
[ISBN 0-387-97672-8] p 431 A92-30850
Response of plate-like structures to correlated random pressure fluctuations
[AIAA PAPER 92-2378] p 584 A92-34452
Time simulation of flutter with large stiffness changes
[AIAA PAPER 92-2394] p 585 A92-34467
Similarity and scale effects in solid-fuel ramjet combustors p 666 A92-36965
Improved measurement of the dynamic loads acting on rotating parachutes p 702 A92-41236
RFI effects analysis of an airport-installed HF transmitter on aircraft COMM/NAV receivers p 725 A92-42313
An investigation of the desensitizing effects by high power HF broadcast transmitters on HF airborne receivers p 726 A92-43937
Fuel regression mechanism in a solid fuel ramjet
p 860 A92-44898
Structural risk assessment in the Israel Air Force for fleet management p 836 A92-46779
Maximizing thrust-vectoring control power and agility metrics p 874 A92-46794
Modern techniques for monitoring airborne telemetry
p 857 A92-47560
The effect of tip convection on the performance and optimum dimensions of cooling fins p 902 A92-48354
The External Propulsion Accelerator - Scramjet thrust without interaction with accelerator barrel
[AIAA PAPER 92-3717] p 866 A92-49098
Asymmetric turbulent vortical flows over slender bodies p 935 A92-50314
General performance characteristics of real heat engine p 1011 A92-50401
Optimal trajectories for an unmanned air-vehicle in the horizontal plane
[AIAA PAPER 92-4344] p 1079 A92-55333
Effects of the roll angle on cruciform wing-body configurations at high incidences
[AIAA PAPER 92-4356] p 1079 A92-55342
Pulsating spanwise blowing on a fighter aircraft
[AIAA PAPER 92-4359] p 1025 A92-55345
The effect of gyro nonorthogonality error on gyrocompassing p 1045 A92-55955
Multidisciplinary optimization of aeroservoelastic systems using reduced-size models
p 1054 A92-56176
Response of helicopter blades to a sharp collective increase p 1084 A92-56282
A generic harmonic rotor model for helicopter flight *simulation* p 1086 A92-56333
Multi-disciplinary optimization of aeroservoelastic systems
[NASA-CR-188983] p 44 N92-11377
A review of aging aircraft technology: An IAI perspective
[IAITIC-91-1018] p 461 N92-20500
Some interesting phenomena from Lavi test flights relating to aircraft stability and control
[IAITIC-91-1017] p 482 N92-20849
Timing analysis of parallel algorithms on a MIMD multiprocessor
[ITN-92-85153] p 510 N92-20905
From IGES to STEP
[REPT-3.1.6] p 603 N92-23881
Collection of papers of the 31st Israel Annual Conference on Aviation and Astronautics
[ITN-92-85124] p 932 N92-31861
A simulation model of a single rotor helicopter
p 979 N92-31865
FCS skewed sensors array: Practical considerations
p 968 N92-31868
Optimal trajectories for an unmanned air vehicle
p 963 N92-31880
Estimation of aircraft attitude by angular rate measurements p 963 N92-31881
The calculation of incompressible separated turbulent boundary layers p 1003 N92-31886
Euler solver for arbitrary configurations: Further applications p 949 N92-31888
The three-dimensional stability of the Foeppl vortices
p 949 N92-31889

ITALY
The Eurofar vehicle overview p 108 A92-14416
Transonic and supersonic inviscid computations in cascades using adaptive unstructured meshes
[ASME PAPER 91-GT-312] p 75 A92-15689
Transonic cascade flow prediction using the Navier-Stokes equations
[ASME PAPER 91-GT-313] p 76 A92-15690
Aircraft navigation using Global Positioning System improved with geostationary satellites
p 99 A92-16934
Dynamics of hang-gliders p 204 A92-18608
High temperature low cycle fatigue of single crystal nickel base superalloys p 213 A92-19796
Fracture analysis and crack propagation in pressurized fuselage structures - Experimental and numerical investigations p 217 A92-19812
Prediction of fatigue crack growth in a Ti-6Al-4V fan disk forging under spectrum loading p 213 A92-19817
Incompressible steady aerodynamics using a standard finite element code p 174 A92-20218
Nonequilibrium hypersonic inviscid steady flows
p 176 A92-20737
A boundary integral formulation for the kinetic field in aerodynamics. I - Mathematical analysis
p 243 A92-21504
The LISA 6000 - A highly integrated IRS/GPS navigation system p 267 A92-22088
Gust effects on a flexible aircraft p 270 A92-22474
A boundary element method for the potential, compressible aerodynamics of bodies in arbitrary motion
p 314 A92-25098
A constraint satisfaction approach to operative management of aircraft routing p 350 A92-25181
A boundary integral formulation for the kinetic field in aerodynamics. II - Applications to unsteady 2D flows
p 339 A92-28005
Navier-Stokes solution of transonic cascade flows using nonperiodic C-type grids p 344 A92-28523
Simulation of hypersonic flows on unstructured grids
p 434 A92-31496
An application of distributed environment in flight simulation p 602 A92-35739
Heterodyne techniques in the I.R. bandwidth for laser obstacle detection p 533 A92-35740
Innovation in the laser warning sensor field
p 554 A92-35742
Test Engineering Language for Avionic Systems
p 554 A92-35763
Transmission vibration monitoring - A single board computer architecture p 554 A92-35765
Reynolds stress distribution downstream of a turbine cascade p 614 A92-38861
Numerical predictions of transonic viscous flows around aerofoils through an Euler/boundary layer interaction method p 624 A92-40600
Wake effects on the prediction of transonic viscous flows around airfoils p 702 A92-41232
Metal matrix composite fabrication processes for high performance aerospace structures p 760 A92-42145
Radiation and coupling between antennas mounted on a complex metallic structure p 760 A92-42315
An unfactored implicit scheme for 3D inviscid transonic flows
[AIAA PAPER 92-2668] p 798 A92-45523
Experimental investigation of vortex dynamics on delta wings
[AIAA PAPER 92-2731] p 804 A92-45565
Viscous high-speed flow computations by adaptive mesh embedding techniques p 808 A92-45839
Hang-glider response to atmospheric inputs
p 874 A92-46765
Linear analysis of naturally curved and twisted anisotropic beam p 899 A92-46936
A new integral equation for potential compressible aerodynamics of rotors in forward flight
p 815 A92-46958

An unstructured mesh generation algorithm for three-dimensional aeronautical configurations p 918 A92-47053
Numerical computations of transonic flows through cascades
[AIAA PAPER 92-3041] p 822 A92-48702
Expert systems for the trouble-shooting and the diagnostics of engines
[AIAA PAPER 92-3327] p 923 A92-48910
Prediction of gas turbine combustor flow by a finite element code
[AIAA PAPER 92-3469] p 906 A92-49016
The numerical simulation of the main fuel control unit of gas turbine engines
[AIAA PAPER 92-3760] p 867 A92-49115
Measurement of acoustic properties of the composite materials constituting the main rotor hub of the Agusta-Westland helicopter EH-101 (civil version) p 1010 A92-49475
Detection and imaging of moving objects with synthetic aperture radar. I - Optimal detection and parameter estimation theory p 955 A92-50033
Lower upper implicit total variation diminishing solution of viscous hypersonic flows p 935 A92-50302
A fast conformal mapping algorithm with no FFT p 1007 A92-50471
Robust flight control systems - A parameter space design p 976 A92-50503
Detecting 3-D, turbulent separation regions using unsteady computerized thermographic technique p 1023 A92-54308
Skin friction measurements in 3-D boundary layers p 1092 A92-54351
Monitoring fatigue cracks in gears p 1116 A92-54496
A module-level testing environment for safety-critical software systems p 1132 A92-56293
Time Resolved Lidar Fluorosensor operating from helicopter p 1121 A92-56296
Aluminium-lithium alloys - Application on helicopters p 1106 A92-56326
Structural design and testing results of composite landing gear components p 1057 A92-56328
Current European research activities in helicopter interactional aerodynamics p 1058 A92-56330
The achievement of aerodynamic goals on the EH101 project through the 'single site' concept p 1058 A92-56342
Correlation of flight, tunnel and prediction data on a helicopter main rotor p 1059 A92-56350
Numerical simulation of unsteady rotor wakes p 1032 A92-56352
An overview of the planned aerospace test facilities at Capua, Italy
[AIAA PAPER 92-3944] p 1097 A92-56773
Stokes flows in superposed immiscible liquids with horizontal heating
[IAF PAPER 92-0909] p 1123 A92-57288
Effects of spectrum variations on fatigue crack growth p 1123 A92-57399
Vortical flow simulation by using structured and unstructured grids p 83 N92-12999
Numerical simulation of vortex flows past impulsively started wings p 88 N92-13028
Research on inverse methods and optimization in Italy p 202 N92-13956
Knowledge based system applications for guidance and control
[AGARD-AR-284] p 205 N92-14065
Aerothermodynamic development of the CARINA re-entry vehicle: CFD analyses and experimental tests p 211 N92-14980
High enthalpy nozzle flows p 182 N92-15000
Infrared measurements of aerodynamic heating in hypersonic wind tunnel p 208 N92-15002
Linear acoustics in gas mixtures with rate processes p 238 N92-15013
Influence of chemical modeling on the solution of hypersonic shock layers p 183 N92-15016
Proposal for the new fatigue management system for the AMX p 361 N92-18580
The G-222 aircraft individual tracking programme p 361 N92-18582
RAMREQ: A computerized tool for the definition of RAM (Reliability, Availability, Maintainability) requirements of complex systems p 412 N92-18647
Prediction of aerodynamic phenomena limiting aircraft manoeuvrability p 364 N92-18781
Parametric effects of some aircraft components on high-alpha aerodynamic characteristics p 364 N92-18782
Parametric bicubic spline and CAD tools for complex targets shape modelling in physical optics radar cross section prediction p 403 N92-19151
Use of target spectrum for detection enhancement and identification p 404 N92-19155
EH 101 ship interface trials: Flight test programme and preliminary results p 465 N92-21964
Limitations on helicopter operations in the aeronaval environment p 466 N92-21973
State and time granularity in system description: An example
[REPT-91-040] p 603 N92-22673
A fin optimisation study p 551 N92-23237
Description and simulation results of the Italsat AOCS advanced flight simulator p 667 N92-24472
A boundary integral formulation for unsteady transonic potential flows p 719 N92-27942
AM-X flight simulator from engineering tool to training device p 884 N92-28536
Composite beam analysis linear analysis of naturally curved and twisted anisotropic beams
[AD-A252652] p 999 N92-30766
Active vibrations and noise control for turboprop application research program activities p 1138 N92-32962
CFRP stiffened panels under compression p 1109 N92-33044

J

JAPAN

Hunting phenomena of the balloon motions observed over Antarctica
[AIAA PAPER 91-3667] p 14 A92-11014
Polar patrol balloon
[AIAA PAPER 91-3688] p 15 A92-11031
Polygon interval arithmetic and design of robust control systems p 49 A92-11418
A design of continuous-time model reference adaptive control based on a function estimation of periodically time varying linear system p 51 A92-11454
New robust adaptive control system using multiple regularization parameters p 51 A92-11455
Prospects of turbulence research by means of testing bodies in motion p 30 A92-12194
Analyses of heat isolation property for metallic multiwall thermal protection system p 40 A92-12422
A numerical simulation of separated flows around bodies p 8 A92-12423
A study on the interaction between a bow shock wave generated by a blunt body and a turbulent boundary layer p 8 A92-12424
Advanced SCRAM-LACE system concept for single-stage-to-orbit space plane
[IAF PAPER 91-272] p 32 A92-12599
Light metal materials for aircraft structure p 140 A92-13444
Development and future view of the technology for fly-by-light control system elements p 131 A92-14027
Step response of unsteady aerodynamics acting on a plane swept wing in incompressible flow for finite state modeling p 63 A92-14031
Finite difference numerical prediction of aerodynamics of an airfoil flying over wavy wall p 64 A92-14033
Test results of the expander cycle air turbo ramjet for a future space plane
[IAF PAPER 91-271] p 120 A92-14709
Weathering test of AFRP composites for the application of helicopter fuselage p 142 A92-15309
Aircraft design experience p 110 A92-15326
Transient aerodynamic behaviours associated with stepwise incidence variation of airfoils p 66 A92-15327
Study on transonic cascade performance by use of newly built facility p 136 A92-15328
A development of computer support system for wing design p 162 A92-15332
Stratospheric lighter-than-air powered platform p 110 A92-15334
Computation of the potential flow through cascades using the conformal mapping and the singularity method p 66 A92-15356
Oscillation of nearly circular shock waves p 146 A92-15358
Flow unsteadiness by weak normal shock wave/turbulent boundary layer interaction in internal flow p 67 A92-15359
Realization of a large-scale turbulence field in a small wind tunnel p 67 A92-15487
Three-dimensional flow and mixing in a axial flow compressor with different rotor tip clearances
[ASME PAPER 91-GT-89] p 70 A92-15554
Unsteady lifting surface theory for a rotating transonic cascade of swept blades
[ASME PAPER 91-GT-178] p 73 A92-15610
Unsteady Navier-Stokes simulation of transonic cascade flow using an unfactored implicit upwind relaxation scheme with inner iterations
[ASME PAPER 91-GT-223] p 74 A92-15637
Film cooling on a gas turbine rotor blade
[ASME PAPER 91-GT-279] p 152 A92-15675
Jet engine test system including expert system for diagnosis
[ASME PAPER 91-GT-408] p 137 A92-15737
Euler flow analysis of turbine powered simulator and fanjet engine p 80 A92-17196
Ranging and positioning experiments for aircraft using Engineering Test Satellite V p 102 A92-17242
Ultrasonic motor utilizing elastic fin rotor p 215 A92-17414
CFD application to 2D/3D flow fields in Scramjet engine p 170 A92-17501
Supersonic inlet flow computation p 171 A92-17502
Numerical simulation for various flowfields of aero-engine components p 200 A92-17503
'Spaceplanes' R&D status of Japan
[AIAA PAPER 91-5002] p 209 A92-17802
Scramjet research at the National Aerospace Laboratory
[AIAA PAPER 91-5076] p 200 A92-17849
Cabin structural vibration and noise for transport aircraft p 192 A92-17876
Structure/control design synthesis of active flutter suppression system by goal programming p 204 A92-18621
Magnetohydrodynamic boundary layer flow over a rotating disk p 304 A92-21338
Effects of gas-surface interaction models on aerodynamic characteristics p 244 A92-21718
PAR-WIG performance prediction during acceleration from water-borne to air-borne p 291 A92-21721
Analysis of circular elastic membrane wings p 245 A92-21722
Navier-Stokes code development for transonic flow simulations p 246 A92-21985
The problem of transition from continuum to rarefied gas flows p 251 A92-22519
Evaluation method of longitudinal static stability of tailless airplane p 282 A92-22520
Minimum induced drag of a wing in a circular open wind tunnel p 251 A92-22521
An analysis of impact resistance of composite fan blade p 293 A92-22523
Aerodynamic characteristics of a wing near its tip using panel method p 251 A92-22524
Spaceplane system studies p 285 A92-22632
Flight simulation and its application p 284 A92-22634
Computational aerodynamic simulation on HOPE p 251 A92-22635
An analysis of impact resistance of composite blades for turbo-fan engines p 294 A92-23109
Nonlinear transient analysis of composite ATP blade model p 294 A92-23111
Inclusion size effect on the fatigue crack propagation mechanism and fracture mechanics of a superalloy p 388 A92-24831
HOPE looks to CFD for help p 386 A92-24910
Review on the abatement of helicopter noise p 406 A92-25501
An experiment on the weight vs control relations of subsonic airplanes p 357 A92-25502
On the skip flight of a spaceplane p 387 A92-25503
A quick automatic method for computing performance of nonducted propeller with constant-revolutional-speed p 393 A92-25505
Analysis of a 2-D airfoil motion flying in-proximity-to a wavy-wall surface-lifting surface-scheme p 315 A92-25506
Non-planar wing design by Navier-Stokes inverse computation
[AIAA PAPER 92-0285] p 319 A92-25738
Flow past a sphere - Topological transitions of the vorticity field p 330 A92-26410
ETS-V/EMSS mobile satellite communication experiments p 395 A92-26776
Experiments on aeronautical satellite communications using ETS-V p 395 A92-26779
High gain airborne antenna for satellite communications p 354 A92-26780
Resonance of circular shock waves p 395 A92-26795
Theoretical study on the unsteady aerodynamic characteristics of an oscillating cascade with tip clearance (In the case of loaded cascade) p 331 A92-26797
Experiments to evaluate hot-jet simulation capabilities in Cryogenic Wind-Tunnel testing
[AIAA PAPER 92-0567] p 384 A92-26975
Application of the delta-operator in MIMO discrete-time adaptive flight control systems p 479 A92-29516
Analysis of a 2-D airfoil motion flying in-proximity-to a wavy-wall surface - Finite difference method p 421 A92-29517

A note on thrust control for jetliner during approach p 457 A92-29518
Error characteristics of a vortex panel method in two-dimensional flow p 421 A92-29521
Fluid Dynamics Conference, 22nd, Osaka, Japan, Nov. 15, 1990, Proceedings p 494 A92-30501
Observation and testing on supersonic multiphase flow p 429 A92-30502
Numerical computation of compressible flow around an object of complex shape p 429 A92-30517
Optimized control of structured grids p 429 A92-30520
The unstructured upwind method p 429 A92-30522
Multi-block airfoil profile of grid formation p 429 A92-30523
Aerodynamic performances of spoiler motion p 429 A92-30526
Experiment on pitching moments of separated flow around airfoil profiles p 429 A92-30527
Air flow under a flight-vehicle engine p 429 A92-30528
Study on two-dimensional jet mixing with a vertical supersonic flow p 429 A92-30530
Study on nozzle flow diffusion p 429 A92-30531
The Bauer-Garabedian-Korn airfoil test in a two-dimensional wind tunnel p 429 A92-30532
Study of cavity pumping in supersonic internal flow p 429 A92-30538
Numerical computation of supersonic intakes p 430 A92-30539
Numerical simulation of supersonic nozzle flow p 430 A92-30540
Computation of scramjet inlet flow p 430 A92-30541
Numerical computation and experimental study of shock wave reflection p 430 A92-30542
Safety test on the rolling angles of a winged vehicle in hypersonic speed p 480 A92-30549
Measurement on hypersonic dynamic stable coefficients of a winged vehicle p 430 A92-30550
Approximate analysis of aerodynamic heating at hypersonic speed p 430 A92-30551
Study on effectiveness of the front wedge shape in hypersonic flow p 430 A92-30552
Numerical analysis on laminar flow control of transonic airfoils p 430 A92-30557
Numerical analysis of helicopter rotor blades p 430 A92-30558
Low speed aerodynamic performance of a capsule-shaped flying object p 430 A92-30559
Boundary layer flows around an airship p 430 A92-30560
Numerical analysis of three-dimensional unsteady turbulent flows in a turbine stage p 443 A92-32501
Analytical study on plate edge noise. I - Trailing edge noise caused by vorticity waves p 511 A92-32502
A numerical solution of inviscid transonic flow using the Boltzmann equation p 443 A92-32504
Three-dimensional flow visualization of shock wave using double-pulsed holographic interferometry. II - Flow visualization for three-dimensional shock structures in rotating aeroengine fan blade rows p 497 A92-32507
A study on the rotating stall of centrifugal compressors. II - Effect of vaneless diffuser inlet shape on rotating stall p 497 A92-32508
Performance of a high-pressure-ratio centrifugal compressor influenced by distribution of tip clearance of the mixed-flow impeller p 498 A92-32509
An analysis of impact resistance of composite blades for aircraft engines (Analysis with two dimensional and three dimensional finite elements) p 579 A92-32562
Sand erosion behavior of GFRP p 576 A92-32662
Subcritical flutter characteristics of a swept-back wing in a turbulent supersonic flow - Comparison between analysis and experiment
[AIAA PAPER 92-2393] p 517 A92-34466
Large eddy simulation of unsteady turbulent wake of a circular cylinder using the finite element method p 587 A92-34825
Outline and discussion of the cooling loop of the heating control system in the exposed facility of the Japanese Experiment Module (JEM) p 574 A92-35610
Navier-Stokes analysis of blade tip shape in hover p 521 A92-35758
Technical history of aircraft engines p 558 A92-35911
Research on aircraft engines p 558 A92-35912
Current topics connected with rotating stall p 521 A92-35913
Trends of research on cascade flutter p 558 A92-35914
Combustion research and design technology of aircraft engines p 558 A92-35915
Research and development of aircraft engine materials p 577 A92-35916
An aircraft controller and its development p 558 A92-35917
Engine maintenance technology and its development p 516 A92-35918
Development trends of recent aircraft engines p 558 A92-35919
Perspective on future aircraft engines p 558 A92-35921
An analytical evaluation of the aerodynamic forces acting on a circular cylinder in a uniform shear flow p 522 A92-35995
Change of flow about an elongated rectangular cylinder in a range of Reynolds numbers of 200 to 0.7 x 10 exp 4 p 522 A92-35997
Unsteady Navier-Stokes simulation of turbulent flows through a supersonic compressor cascade p 523 A92-36036
Outflow boundary conditions for Euler analysis of flow in turbine scroll p 591 A92-36037
Numerical simulations of the flow through cascades with tip clearance p 523 A92-36038
Active control of the hydraulic forces of a body by a splitter plate p 591 A92-36351
Numerical simulation of opposing sonic jets p 524 A92-36357
Aeroelastic tailoring analysis for advanced turbo propellers with composite blades p 558 A92-36358
Analytical condition inspection and extension of time between overhaul of F3-30 engine
[ASME PAPER 91-GT-277] p 653 A92-36888
Unsteady flow within centrifugal compressor channels under rotating stall and surge
[ASME PAPER 91-GT-85] p 670 A92-36901
Numerical simulation of hypersonic viscous flow for the design of H-II orbiting plane (HOPE) p 612 A92-37549
Research and development of turbofan engine for supersonic aircraft p 654 A92-38025
International Aerospace Symposium 90, Nagoya, Japan, Nov. 26, 27, 1990, Proceedings p 607 A92-38201
The quiet STOL research aircraft ASUKA p 642 A92-38206
Prospects for a commercial STOL transportation system p 634 A92-38207
The helicopter commuter - A perspective on regular passenger transportation by rotary wing p 634 A92-38208
Robotics application in aerospace manufacturing p 671 A92-38216
Aircraft maintenance support system p 607 A92-38217
Production technologies and aircraft design p 608 A92-38220
Effect of controlled longitudinal vortex arrays on the development of a turbulent boundary layer p 614 A92-38856
The effect of a velocity gradient on the aerodynamic forces of a circular cylinder with tangential blowing p 614 A92-38859
Experiments on turbulent flow due to an enclosed rotating disk p 615 A92-38863
Influence of inlet conditions on the flowfield in a model gas turbine combustor p 672 A92-38866
Temporal change of noisiness of helicopter noise p 689 A92-39103
Temporal change of timbre of helicopter noise p 694 A92-39104
Robust flight control system design with multiple model approach p 661 A92-39910
Three-dimensional vortical structure of a large-scale coherent vortex in a turbulent boundary layer p 619 A92-40056
Prediction of three-dimensional turbulent boundary layers using a second-moment closure p 675 A92-40080
Phase-averaged turbulence statistics in a near wake with an asymmetric vortex shedding p 620 A92-40086
An experimental and numerical study of confined axisymmetric jet with a bluff body p 621 A92-40106
Scrutinizing k-epsilon EVM and ASM by means of LES and wind tunnel for flowfield around cube p 621 A92-40119
Effects of attack angle on leg portion of the horseshoe vortex around the idealized wing p 623 A92-40177
Experiments on aeronautical satellite communications using ETS-V satellite p 639 A92-40187
High gain airborne antenna for satellite communications p 639 A92-40188
Bias of an optical passive ring-resonator gyro caused by the misalignment of the polarization axis in the polarization-maintaining fiber resonator p 652 A92-40262
The low-turbulence wind tunnel at Tohoku University p 623 A92-40598
Observational study of pool boiling under microgravity p 757 A92-41060
Engineering and technology Japanese aircraft/spacecraft p 699 A92-41781
Flow around two square cylinders in staggered arrangements p 761 A92-42797
Studies on the mechanism of ignition and flameholding by plasma jets p 755 A92-42798
A quick automatic method for computing performance of ducted-propeller p 736 A92-42800
Aircraft Symposium, 28th, Tokyo, Japan, Nov. 7-9, 1990, Proceedings p 699 A92-43095
Hypersonic testing technology of HOPE (H-II orbiting plane) p 747 A92-43096
Test on high enthalpy hypersonic flow using a ballistic range p 747 A92-43097
A two-stage-diaphragm free-piston shock tube for a strong shock wave p 748 A92-43098
Study on small stalker tube performance and numerical calculation p 748 A92-43099
Experimental studies on aerodynamic heating and thermal protection in hypersonic flight p 709 A92-43101
Aerodynamic heating measurement in hypersonic flow p 709 A92-43102
A thin metal model for aerodynamic heating tests of shock wave interaction p 709 A92-43103
Thermal measurement test in a shock wind tunnel p 748 A92-43104
Research on hypersonic wind tunnel methods in the 90's p 748 A92-43105
Some consideration for evaluation of structural integrity of aging aircraft p 762 A92-43107
Study on the lower aspect view of a helicopter simulator p 748 A92-43110
Study on a flight simulator of time delays p 744 A92-43112
Study on the effective utilization of the current flight simulator p 748 A92-43113
Flight evaluations on in-flight simulation of unstable aircraft p 744 A92-43115
Optimization of blade structure to reduce rotor vibration p 730 A92-43118
Analysis of the aerodynamic performance of rotors with the boundary element method p 709 A92-43119
Multiharmonic control response of a rotor blade during forward flight (Test) p 744 A92-43120
Multiharmonic control response of a rotor blade during forward flight (Analysis) p 744 A92-43121
Navigation experiment on an aircraft using the GPS-INS navigation system. I - Introduction to the system p 726 A92-43122
Navigation experiment on aircraft flight using the GPS-INS navigation system. II - Test results p 726 A92-43123
Development of an instrument for measuring runway roughness p 748 A92-43124
A proposed method for evaluating runway roughness p 748 A92-43125
Bayesian reliability analysis in connection with the evaluation of multiple-site damage p 762 A92-43126
Study on an induction method for a flying object, taking accelerating targets into account p 744 A92-43127
Aircraft evasive maneuvers against flying objects p 744 A92-43128
Three-dimensional game for two aircraft p 744 A92-43129
Step response of incompressible unsteady aerodynamic modeling p 744 A92-43131
Research on state equations of unsteady aerodynamics p 709 A92-43132
Optimum structural design of a cantilevered rectangular elastic wing with a gust load alleviation system p 762 A92-43133
Gust load alleviation control design for the accuracy of an aeroelastic active control model p 745 A92-43134
ACT wind tunnel experiment on gust load alleviation. II - Wind tunnel test with active support facility p 745 A92-43135
Transonic wind tunnel tests of flutter suppression equipment (Wing response data processing) p 748 A92-43136
The progress of a STOL project p 699 A92-43137
Operational progress of the STOL research aircraft Asuka p 730 A92-43138
Operation of the on-board measuring system of the STOL research aircraft Asuka p 734 A92-43139
STOL research aircraft Asuka flight analysis in connection with the operation of the monitoring system p 730 A92-43140
Aircraft reliability and maintainability p 700 A92-43141
Flight test results and upper surface blowing (USB) technology of the STOL research aircraft Asuka p 730 A92-43142
Flight tests on the structures of the STOL research aircraft Asuka p 730 A92-43143

The main wing boundary layer separation pattern of STOL research aircraft Asuka p 709 A92-43144
Aerodynamic drag as determined from flight test data of the STOL research aircraft Asuka p 709 A92-43145
Path angular control of the STOL research aircraft Asuka p 745 A92-43146
A study of aircraft surface coating technology p 700 A92-43147
Study on the maintainability and inspection of the STOL research aircraft Asuka p 700 A92-43148
The landing equipment of a high-tech aircraft p 730 A92-43149
Introduction to the traffic alert and collision avoidance system (TCAS) III p 734 A92-43150
The traffic alert and collision avoidance system (TCAS) for air navigation p 734 A92-43151
Repair operation on a composite material structure p 700 A92-43153
Navigation preparations for passenger helicopters p 723 A92-43155
Quality management of landing gear with pulling support system p 762 A92-43156
Utilizing the fault monitoring system for the A320 aircraft p 700 A92-43157
A study of a ground support equipment (GSE) network p 748 A92-43158
An adaptive flight control for use in connection with helicopter engine failure p 745 A92-43159
A perspective on helicopter noise p 780 A92-43160
A helicopter transportation system p 723 A92-43161
Using helicopters for the erection of power transmission lines p 723 A92-43162
Helicopters for public services, including rescue, fire fighting, and medical emergency p 723 A92-43163
Using helicopters for coastal alert p 723 A92-43164
Experimental and numerical investigations on separated flows around pitching airfoils p 710 A92-43166
Direct simulation of hypersonic rarefied flows about atmospheric re-entry vehicles p 710 A92-43169
Recent airfoil tests in NAL 2D high Reynolds number wind tunnel p 748 A92-43171
Design - Analysis and experimental verification of a propeller working in the low Reynolds number range p 710 A92-43174
Inspection of stability deterioration with an adaptive regulator p 776 A92-43178
Robust flight control system design using a multimodel approach. II p 745 A92-43180
Flight control system design p 776 A92-43181
Model reference adaptive flight control system (MRAFCS) design with consideration of the balance point p 745 A92-43182
Study of the flight control of remotely piloted helicopters p 745 A92-43183
A restructurable flight control system design using nonlinear compensation p 745 A92-43184
The acceleration control system design of a flight vehicle using a two-wing control method p 745 A92-43185
Nonstationary manual control. III p 776 A92-43187
The relationship between the weight and flight characteristics of a transonic aircraft p 731 A92-43189
Flight simulation of a spaceplane p 752 A92-43190
Analysis of the aerodynamic characteristics of a simple remotely piloted research vehicle (RPRV) p 710 A92-43191
Wind tunnel tests on the motion of a spaceplane simulation for cable mount p 752 A92-43192
The fluid-dynamic measurement of the fling motion of a three-dimensional flat plate p 710 A92-43194
Wind tunnel test for a high speed propeller with coaxial contrarotation p 737 A92-43195
Aerodynamic design of an advanced turboprop using Euler codes p 737 A92-43196
Aerodynamic design of a nonplanar airfoil by an inverse method with Navier-Stokes equations p 711 A92-43197
Aerodynamic design tool development for the calculation code of hypersonic flow p 711 A92-43198
Wing test at the cryogenic wind tunnel of the National Defense Academy p 749 A92-43199
Transonic visualization test for the airframe shape improvement of a spaceplane p 752 A92-43200
BGK airfoil oil flow test in a two-dimensional transonic wind tunnel p 711 A92-43201
Buffeting characteristics of a transonic airfoil p 711 A92-43202
The effectiveness of the warp shape airfoil of a supersonic transport p 711 A92-43203
Experimental study of the aerodynamic characteristics at Mach 3 of an air-intake model p 711 A92-43204
Wind tunnel test of a supersonic air intake p 711 A92-43205
Distance and angle measuring method using laser light and rereflection plates p 762 A92-43206
Development of the D-size liquid crystal flat panel display for aircraft p 734 A92-43208
Evaluation test on the simulator of the liquid crystal flat display. II p 734 A92-43209
Motion estimation for cable-mount dynamic wind-tunnel test p 749 A92-43210
Estimation of spaceplane longitudinal stability and control derivatives from dynamic wind tunnel test p 752 A92-43211
Estimation of spaceplane model inertia characteristics p 752 A92-43212
On the characteristics of servo actuators attached to a model spaceplane for dynamic wind-tunnel test p 762 A92-43213
Display trends in aircraft cockpits p 734 A92-43217
A study of the pilot's associate system p 745 A92-43218
Aircraft accidents and human factors p 723 A92-43219
Research on a helicopter information control system p 735 A92-43220
Advanced display system for an aircraft payload p 735 A92-43221
Current status and future tasks of a cockpit liquid crystal display p 735 A92-43222
Demonstration performance of an aircraft liquid crystal display p 735 A92-43224
Digital mapping display technology p 735 A92-43225
Aerodynamic characteristics of a hypersonic aircraft p 711 A92-43226
Study of the flow field and molecular radiation heating around a reentry vehicle p 711 A92-43227
Low-speed wind tunnel testing of the lateral control force for the upper rudder surface of a joined-wing airfoil p 711 A92-43228
Low-speed wind tunnel testing of a joined-wing airfoil p 711 A92-43229
Effectiveness of aircraft aerodynamic performance on each part of a joined wing p 712 A92-43230
Aerodynamic characteristics of a high-speed composite airfoil p 712 A92-43231
Experimental operation of aircraft-engine turbine blade materials p 737 A92-43233
Thermal fiber-reinforced-plastic composite technology for aircraft structures p 755 A92-43237
Research on a low-noise engine for a high-speed VTOL aircraft p 737 A92-43239
The maneuver performance and control of a hovercraft p 763 A92-43240
WIG transportation efficiency considering the influence of no-load situation p 781 A92-43241
The concept of an unmanned flying vehicle at high altitude p 731 A92-43242
Reevaluation of the motion of an airship p 731 A92-43243
Small and cost-effective airship for transportation p 731 A92-43244
Stringer subsystem automation p 700 A92-43246
Development of an automatic metal sheet working machine for interior structure p 700 A92-43247
Automation of composite material structure installation p 700 A92-43248
Numerical investigation of supersonic inlet with realistic bleed and bypass systems p 713 A92-44519
Effectiveness of plasma torches for ignition and flameholding in scramjet p 737 A92-44524
Super plastic forming technology applied to aeroengine and space equipment p 764 A92-44732
Basic study of adhesive bonding for fiber-composites - Adhesive bonding technologies on jet engine parts p 764 A92-44733
Numerical simulation of impact resistance on composite blade p 738 A92-44734
Study of grinding process and strength for ceramic heat insulated engine [SME PAPER MR91-177] p 897 A92-45260
Estimation of spaceplane lateral-directional stability and control derivatives from dynamic wind tunnel test [SAE PAPER 911979] p 872 A92-45384
Spaceplane longitudinal aerodynamic parameter estimation by cable-mount dynamic wind-tunnel test [SAE PAPER 911980] p 788 A92-45385
Experimental studies on aerodynamic characteristics of SSTO vehicle at low subsonic speeds [SAE PAPER 911981] p 788 A92-45386
Numerical simulations of separated flows around oscillating airfoil for dynamic stall phenomena [SAE PAPER 911991] p 788 A92-45393
Wind tunnel investigation of an improved upper surface blown flap transport semi-span model [SAE PAPER 911993] p 789 A92-45395
An acrobatic airship 'Acrostat' [SAE PAPER 911994] p 843 A92-45396
Ducted fan VTOL for working platform [SAE PAPER 911995] p 843 A92-45397
Response characteristics of a wing in supersonic flow near flutter boundary [SAE PAPER 911999] p 789 A92-45401
Preliminary study of algorithm for real-time flutter monitoring [SAE PAPER 912001] p 897 A92-45403
Recent applications of the FNS zonal Method to complex flow problems [SAE PAPER 912003] p 789 A92-45404
Free wake analyses of a hovering rotor using panel method [SAE PAPER 912004] p 789 A92-45405
Flow field around thick delta wing with rounded leading edge [SAE PAPER 912009] p 789 A92-45409
Aerodynamic development of boundary layer control system for NAL QSTOL research aircraft 'ASKA' [SAE PAPER 912010] p 843 A92-45410
Numerical simulation of a supersonic jet impingement on a ground [SAE PAPER 912014] p 789 A92-45412
Aerodynamic characteristics near the tip of a finite wing by a panel method [SAE PAPER 912020] p 790 A92-45413
Aero-structural integrated design of forward swept wing [SAE PAPER 912021] p 790 A92-45414
Demonstration of gas liquid separation under the microgravity by aircraft KC-135 [SAE PAPER 912024] p 897 A92-45416
Experimental and numerical studies of radiation emission from high-temperature air behind 10 km/s shock waves [SAE PAPER 912025] p 790 A92-45417
Multidimensional Euler/Navier-Stokes analysis for hypersonic equilibrium gas [SAE PAPER 912026] p 790 A92-45418
A calculation of penetration of the jet issuing normally into a cross flow across a wall boundary layer [SAE PAPER 912029] p 790 A92-45419
Functional mock-up tests for flight control system of the NAL QSTOL research aircraft 'ASKA' [SAE PAPER 912036] p 881 A92-45422
On the possibility of freezing and sticking phenomena in a transport during the ground taxiing and takeoff run and on the preventions of the hazard [SAE PAPER 912042] p 836 A92-45426
Shock interaction induced by two hemisphere-cylinders [SAE PAPER 912043] p 790 A92-45427
Aerodynamic heating in three-dimensional shock wave turbulent boundary layer interaction induced by sweptback sharp fins in hypersonic flows [SAE PAPER 912044] p 791 A92-45428
Numerical simulations of hypersonic real-gas flows over space vehicles [SAE PAPER 912045] p 791 A92-45429
Impact response of composite UHB propeller blades [SAE PAPER 912046] p 861 A92-45430
An analysis of the effect of centrifugal force on the impact resistance of composite fan blades for turbo-fan engines [SAE PAPER 912047] p 861 A92-45431
Finite elements analysis of flexural edge wave for composite fan blades [SAE PAPER 912048] p 861 A92-45432
Feasibility study on a microwave-powered unmanned aerial vehicle for the communication relay utilization [SAE PAPER 912052] p 843 A92-45436
Structural concept of main wings of high altitude unmanned aerial vehicle and basic properties of thermoplastic composites as candidate material [SAE PAPER 912053] p 843 A92-45437
High-altitude lighter-than-air powered platform [SAE PAPER 912054] p 844 A92-45438
Experimental and numerical study of aerodynamic characteristics for second generation SST [SAE PAPER 912056] p 844 A92-45439
Oscillation of oblique shock waves generated in a two dimensional asymmetric nozzle [SAE PAPER 912061] p 791 A92-45443
Numerical analysis of RCS jet in hypersonic flights [SAE PAPER 912063] p 791 A92-45445
A simulator study of a flight reference display for powered-lift STOL aircraft [SAE PAPER 912067] p 855 A92-45449
In-flight simulation of backside operating models using direct lift controller [SAE PAPER 912069] p 872 A92-45450
Manual control of vehicles with time-varying dynamics [SAE PAPER 912078] p 917 A92-45454
A design of strongly stabilizing controller [SAE PAPER 912081] p 917 A92-45456
Predicted pressure distribution on a prop-fan blade through Euler analysis p 810 A92-46791

Wing design for hanggliders having minimum induced drag p 811 A92-46814
Prediction of dynamic hub load of a rotor executing multiple sinusoidal blade pitch variations p 846 A92-46921
Simple diagnosis for the quality of generated grid systems p 919 A92-47069
Analysis of motion of airfoil flying over wavy-wall surface (lifting surface method) p 818 A92-47100
A finite difference solution of the Euler equations on non-body-fitted Cartesian grids p 818 A92-47153
Numerical experiments on unsteady shock reflection processes using the thin-layer Navier-Stokes equations p 818 A92-47155
Strength evaluation and safety of machine/structure. III - Case examples on strength and safety evaluation of machine/structure 3.2 aircraft (airframe) p 882 A92-47303
A higher-order accurate Navier-Stokes solver for transonic and supersonic flows in turbomachinery [AIAA PAPER 92-3044] p 822 A92-48704
Application of non-reflecting boundary conditions to three-dimensional Euler equation calculations for thick strut cascades [AIAA PAPER 92-3045] p 822 A92-48705
Numerical investigation of surge and rotating stall in multistage axial compressors [AIAA PAPER 92-3193] p 825 A92-48804
Numerical solutions of unsteady oscillating flows past an airfoil [AIAA PAPER 92-3212] p 825 A92-48817
A scramjet nozzle experiment with hypersonic external flow [AIAA PAPER 92-3289] p 864 A92-48878
Experimental validation of scramjet nozzle performance [AIAA PAPER 92-3290] p 864 A92-48879
Derivation of ABCD system matrices from nonlinear dynamic simulation of jet engines [AIAA PAPER 92-3319] p 923 A92-48903
Combustion of solid fueled ramjet. I [AIAA PAPER 92-3727] p 894 A92-49105
Combustion of solid fueled ramjet. II [AIAA PAPER 92-3728] p 894 A92-49106
Conceptual study of separated core ultra high bypass engine [AIAA PAPER 92-3775] p 867 A92-49119
Design and off-design point characteristics of Separated Core Ultra High Bypass Engine (SCUBE) [AIAA PAPER 92-3776] p 867 A92-49120
Induced drag of a wing in a circular wind tunnel p 936 A92-50327
Reduction of torque pulsation of Stirling engine-compressor system p 992 A92-50785
New thermoplastic polyimide composite for supersonic aircraft structures p 985 A92-51512
Three-dimensional relaxation effect on quasi-3D flow in a blade row with spanwise loading distribution p 936 A92-51593
Nonlinear dynamic stability characteristics of recovery bodies p 977 A92-52041
Static and dynamic flight-path stability of airplanes p 977 A92-52043
Flow of a rarefied gas past a two-dimensional body of an arbitrary shape at small Mach numbers p 937 A92-52726
Thermal and chemical nonequilibrium viscous shock layer flows over a blunt body at high altitudes p 938 A92-52749
Rarefied gas numerical wind tunnel p 995 A92-52763
Direct simulation of vortex shedding in dilute gas flows past bluff bodies p 939 A92-52766
DSMC simulation of hypersonic flows past 2-dimensional bodies p 939 A92-52772
Estimation of aerodynamic characteristics from flight-test data. I - Multicollinearity in the equation error method p 960 A92-53007
Measurement of angle of attack using a five-hole arrow head pitot tube p 941 A92-53009
New-type of ultralight flexible a-Si solar cell and its application on an airplane p 970 A92-53181
Japan pushes high speed research p 1015 A92-53434
Development study on air turbo-ramjet engine for space plane p 1065 A92-53487
Conceptual design of scramjet engine p 1065 A92-53490
Key design considerations for scramjet powered space plane p 1066 A92-53491
Scramjet engine and its flying test bed p 1066 A92-53492
Performance analysis of idealized scramjet p 1066 A92-53493
Fabrication test and evaluation of graphite/PMR-15 polyimide for HOPE primary structure p 1105 A92-53516
Aerodynamic heating characteristics of space planes tested by NAL hypersonic wind tunnel p 1017 A92-53547
Hypersonic flows with air chemistry over a reentry vehicle at high altitudes p 1017 A92-53549
Detailed numerical analysis of standing oblique detonation p 1111 A92-53550
Rarefied gas numerical wind tunnel p 1017 A92-53552
Experimental and numerical investigation of a supersonic free jet impinging on a perpendicular surface p 1018 A92-53555
Numerical study on the secondary jet into a supersonic flow p 1018 A92-53556
Experimental investigation on turbulent phenomena in three-dimensional shock wave/turbulent boundary layer interaction induced by blunt fin p 1018 A92-53557
Numerical simulations of shock reflections by a TVD scheme p 1018 A92-53558
Navier-Stokes simulation for the winged space vehicle 'HOPE' at subsonic, transonic, and supersonic regimes p 1018 A92-53559
Calculations for aerodynamic characteristics of HOPE type vehicle in subsonic and hypersonic flow p 1018 A92-53560
A preliminary study of a supersonic wind tunnel for a ram jet test facility p 1089 A92-53564
Flow measurements in scramjet inlets p 1102 A92-53565
Spaceplane aerodynamic heating and thermal protection design method p 1102 A92-53578
Radiative heat transfer from nonequilibrium shock layer to a hypersonic reentry body p 1019 A92-53579
Thermally and chemically nonequilibrium hypersonic flow in three-dimensional geometry p 1019 A92-53580
Integrated system to support computer analysis in conceptual aerospace design p 1130 A92-53596
Space plane navigation simulation p 1103 A92-53603
Concepts of flight experiments for HOPE development p 1103 A92-53635
Aerodynamic study of H-II Orbiting Plane, HOPE p 1103 A92-53639
Pre-flight physical simulation test of HIMES reentry test vehicle p 1103 A92-53640
Aerodynamic studies on space plane configuration at hypersonic speed p 1019 A92-53641
Experimental study of convection effects around the phase charge interface p 1111 A92-53755
Fundamental studies on Marangoni convection related to Bridgman crystal growth p 1111 A92-53758
Improvement of atmospheric flight performance of a space vehicle through H infinity-control theory p 1130 A92-53785
Effect of porosity in transpiration cooling system p 1112 A92-53786
Experimental study on three-dimensional shock wave-turbulent boundary layer interaction induced by protuberance p 1019 A92-53997
Mach 3 wind tunnel test of mixed compression supersonic inlet [AIAA PAPER 92-3625] p 1021 A92-54092
An advanced scramjet propulsion concept for a 350 MG SSTO space plane - External nozzle performance [AIAA PAPER 92-3719] p 1067 A92-54134
Preliminary airfoil testing experience in the NDA cryogenic wind tunnel p 1091 A92-54326
Three-dimensional calculation of radiative field in hypersonic air shock layers p 1023 A92-54498
Effect of streamwise pressure gradient on the supersonic mixing layer p 1025 A92-54936
Double piston shock-wave valve p 1117 A92-54938
HOPE re-entry experimental vehicle p 1103 A92-55098
Optimal control of helicopters following power failure [AIAA PAPER 92-4471] p 1076 A92-55231
A robust gain scheduler interpolated into multiple models by membership functions [AIAA PAPER 92-4553] p 1131 A92-55265
Multiple delay model approach applied to the AIAA 1922 Controls Design Challenge [AIAA PAPER 92-4630] p 1078 A92-55305
Optimal launch trajectory of a hypersonic research vehicle [AIAA PAPER 92-4302] p 1103 A92-55310
An identification procedure for a system with a choice of feedback structures p 1132 A92-55426
Development of ITS90 small gas turbine engine p 1070 A92-55500
Aircraft Symposium, 29th, Gifu, Japan, Oct. 7-9, 1991, Proceedings p 1015 A92-56001
Current status of R&D on materials for super/hypersonic transports p 1106 A92-56002
New 1.27-m leg of the National Aerospace Laboratory hypersonic wind tunnel p 1092 A92-56003
Measurements of turbulence in hypersonic flow p 1092 A92-56005
Supersonic wind tunnel test of airintake/airframe integrated models p 1028 A92-56006
A hypersonic wind tunnel test of a mixed-compression air inlet model p 1028 A92-56007
Wind tunnel test of M = 2.5 mixed compression inlet p 1028 A92-56008
Three-dimensional shock wave-turbulent boundary layer interaction induced by blunt body and protuberance p 1029 A92-56009
On the structure of unsteady shock induced separation of the transonic airfoil in the NAL two-dimensional wind tunnel p 1029 A92-56010
Evaluation of sidewall interference in the NAL two-dimensional transonic wind tunnel p 1092 A92-56011
On improvements of three-dimensional position measuring system for dynamic wind tunnel testing p 1093 A92-56012
Measurements of longitudinal static aerodynamic coefficients with cable mount system p 1093 A92-56013
Flutter analysis and wind tunnel test with respect to a low-aspect-ratio wing with free-rotational control surface p 1052 A92-56014
An example of whirl flutter analysis p 1052 A92-56015
Propeller-nacelle whirl flutter analysis and wind tunnel test p 1052 A92-56016
Whirl flutter analysis and application to aircraft design p 1053 A92-56017
Optimization of composite material wing of fighter type aircrafts p 1053 A92-56018
Research on aeroelastic tailoring at NAL p 1053 A92-56019
Analysis and wind tunnel test of low aspect wing gust load alleviation p 1053 A92-56020
Synthesis of gust load alleviation with flutter margin augmentation p 1082 A92-56021
Optimization of aeroelastic system with active control p 1083 A92-56022
Measurements of blade flapping motion on a wind tunnel model p 1093 A92-56023
Structural optimization of a cantilevered beam subject to combined static loadings p 1118 A92-56024
Optimization approach for helicopter maneuverability with a point mass model p 1083 A92-56025
An investigation of the automation of emergency landings for helicopters p 1083 A92-56026
Multiaxis control in longitudinal mode of aircraft p 1083 A92-56027
A320 flight control from the pilot's point of view p 1083 A92-56028
Robust control system design with multiple model approach p 1083 A92-56029
Flight control system design using H(infinity) optimal control p 1083 A92-56030
An autorotation-entry control for a helicopter with a fuzzy controller p 1083 A92-56032
Application of fuzzy control to aircraft guidance p 1083 A92-56033
Gust response and cross wind performance of a hovercraft with vertical wings p 1118 A92-56034
On the maneuvering tests of an ACV model p 1118 A92-56035
Configuration of flexible-skirts for an ACV and its CAD p 1118 A92-56036
Planning method of skirt systems for small ACVs p 1118 A92-56038
A potential flow theory of two-dimensional bifurcated curtain jets. II p 1118 A92-56039
Three-dimensional numerical analysis of impinging circular jet - Discrete vortex method p 1029 A92-56040
A shock tunnel experiment on aerodynamic interference induced by RCS jet p 1029 A92-56042
Aerothermodynamic test of spaceplane by thin-skin method p 1093 A92-56043
BGK1 airfoil oilflow tests in the NAL two-dimensional wind tunnel. II p 1029 A92-56044
High subsonic wind tunnel test of a two-dimensional hybrid-laminar-flow-control airfoil with slotted surface p 1029 A92-56045
Experimental investigation of the boundary layer in a corner formed by two circular arc airfoils p 1029 A92-56046
Design and wind tunnel test of low-Reynolds-number airfoil p 1029 A92-56047
Numerical simulation of supersonic unsteady flow using a panel method p 1030 A92-56048

Calculations of aerodynamic forces on a wing with thrust using B.E.M p 1030 A92-56049
Generalized aerodynamics analysis by the boundary element method p 1030 A92-56050
Analysis of the main wing lift distribution of the STOL research aircraft Asuka p 1053 A92-56051
On the effect of canards on NAL spaceplane model (0 order) in low speed area p 1030 A92-56052
Motion analysis of 2-dimensional flat plate in ground effect p 1030 A92-56053
Low-speed wind tunnel testing for the high-speed propeller at high shaft angle of attack p 1030 A92-56054
Noise test of high-speed counterrotation propeller in low-speed wind tunnel p 1135 A92-56055
Estimation of aircraft inertial characteristics using maximum likelihood estimation p 1084 A92-56057
A physical approach to the estimation of aerodynamic characteristics from flight data p 1030 A92-56058
Flight test of a flight reference display for powered-lift STOL aircraft p 1064 A92-56059
A note on thrust control for jetliner during approach p 1053 A92-56061
Synthesis of a MLS automatic landing control law for the NAL experimental research aircraft Do-228 p 1084 A92-56062
MIMO state-feedback control system considering phase stability by -90 deg phase-locus method p 1084 A92-56066
Design of a flight control system using a feedback-error-learning-type neural network p 1132 A92-56067
Application of restructurable flight control system using nonlinear control to an airliner p 1084 A92-56068
Lateral control of spaceplane at hypersonic flight p 1104 A92-56069
Selection of sampling rate for nonlinear flight trajectory controller of aircraft p 1084 A92-56070
Efficiency and accuracy in helicopter hovering performance calculation p 1053 A92-56072
Sensitivity analysis for structural optimization of helicopter rotor blades p 1053 A92-56073
A calculation method to predict helicopter noise and its verification p 1135 A92-56074
Design and testing of a composite hingeless hub for rotary-wing aircraft p 1053 A92-56075
Helicopter rotor testing using scaled model p 1093 A92-56076
Piloted simulation for the BK117 FBW demonstrator p 1053 A92-56077
A low speed wind tunnel investigation of a joined-wing aircraft with an overhanging fin p 1030 A92-56078
A low speed wind tunnel investigation of the direct side force control of a joined-wing aircraft with overhanging fin p 1084 A92-56079
Working together in the development of the B777 p 1015 A92-56080
Height keeping performance requirements for reducing vertical separation minima used for air traffic control p 1046 A92-56081
Engine condition monitoring system for B747-400 p 1064 A92-56082
Automatic function testing in the aircraft production p 1015 A92-56083
Application of X-ray image radiography system for aircraft p 1118 A92-56084
Current repair technologies for jet engine components p 1016 A92-56085
Change and reliability of the DC-9-81 digital flight guidance system p 1084 A92-56086
The operational status of automated aircraft washing system p 1016 A92-56087
History of aeronautical satellite communications p 1046 A92-56088
Aeronautical satellite communications system p 1046 A92-56089
A data processing system for oceanic air traffic control p 1046 A92-56090
Aircraft satellite communication systems p 1046 A92-56091
Evaluation report of an experimental Satcom operation by a Japan Airline's B747 passenger plane p 1046 A92-56092
An experimental program concerning a satellite data link for oceanic ATC p 1046 A92-56093
Fatigue cracking threshold prediction of transport airplanes p 1118 A92-56094
Development of aircraft bonded structure and the NDI method p 1016 A92-56100
Mechanical properties of laminate aluminum matrix composites p 1106 A92-56102
Titanium alloy casting for aerospace p 1106 A92-56103
Present status of Al-Li alloys p 1106 A92-56105
Development of an automatic drilling system. II p 1118 A92-56107
Application of automation for structural-composites production p 1119 A92-56109
A consideration on air traffic control processing capability in terminal area p 1047 A92-56110
Grooved runway surface texture before and after rubber removal p 1093 A92-56111
Optimal design of wing shape by use of neural-network p 1054 A92-56112
A development of hypermedia type database system for instruction of aircraft conceptual design p 1132 A92-56113
Aerodynamic model identification of a spaceplane model from a cable-mount dynamic wind-tunnel test p 1093 A92-56114
Flight simulator test of cockpit advisory system p 1054 A92-56115
Flight evaluation of navigation systems including MLS using NAL Do228 - Outline p 1047 A92-56116
Flight evaluation of navigation systems including MLS using NAL Do228 - Results of MLS p 1047 A92-56117
Flight evaluation of navigation systems including MLS using NAL Do228 - Results of GPS p 1047 A92-56118
An experimental study on variable pressure hydraulic flight control system p 1084 A92-56119
Measurement of position and attitude using laser and retro-reflectors p 1047 A92-56120
Evaluation of a IMU with optical fiber gyros in dynamic windtunnel tests p 1104 A92-56121
Optimal control of tiltrotor aircraft following power failure p 1085 A92-56303
High enthalpy wind tunnel for erosion testing of advanced materials
[AIAA PAPER 92-3888] p 1094 A92-56729
Tohoku University low-turbulence wind tunnel
[AIAA PAPER 92-3913] p 1095 A92-56746
Roles of wind tunnel tests and CFD analyses in the design of energy-efficient SST
[AIAA PAPER 92-3923] p 1133 A92-56754
Study on international cooperative test facilities for future SST/HST
[AIAA PAPER 92-3945] p 1097 A92-56775
A model study on diffuser pressure recovery in NAL scramjet test facility with simulated hydrogen combustion
[AIAA PAPER 92-3979] p 1071 A92-56805
A conceptual study for future engine test facility
[AIAA PAPER 92-3992] p 1099 A92-56815
Numerical prediction of the flow characteristics in an arc wind tunnel
[AIAA PAPER 92-4016] p 1100 A92-56838
Tests results on Air Turbo Ramjet for a future space plane
[IAF PAPER 92-0657] p 1071 A92-57098
Airbreathing engine selection criteria for SSTO propulsion system
[IAF PAPER 92-0658] p 1071 A92-57099
Numerical simulation of hypersonic viscous flow for the design of H-2 orbiting plane (HOPE-2)
[NAL-TR-1093] p 11 N92-10009
Development of digital/optical rotary position transducer
[NAL-TR-1106] p 29 N92-10028
Unsteady aerodynamic calculations for general configurations by the double-point method
[NAL-TR-1101T] p 12 N92-10980
Aerodynamic aircraft design methods and their notable applications: Survey of the activity in Japan p 193 N92-13930
Field telemetry of blade-rotor coupled torsional vibration at Matuura Power Station Number 1 unit p 222 N92-14348
Experiment of static and dynamic characteristics of spiral grooved seals p 223 N92-14361
Weight evaluation and sensitivity analysis for space plane. Part 2: TSTO
[NAL-TM-602-PT-2] p 287 N92-17754
Results of measured temperature distribution on an adiabatic wing model with radiation thermometer
[NAL-TM-610] p 261 N92-17755
Improvement of data processing system for gust wind tunnel data acquisition part: System conversion from off-line to on-line processing
[NAL-TM-611] p 285 N92-17756
Discussion for possibility of some aerodynamic ground effect craft
[NAL-TM-619] p 300 N92-17757
Hydrogen fueled subsonic-ram-combustor model tests for an air-turbo-ram engine
[NAL-TR-1064T] p 280 N92-17855
Identification of the stability and control derivatives of a DLC-flap system for VSRA
[NAL-TR-1116] p 283 N92-17917
Ultra High Speed Numerical Wind Tunnel (UHSNWT) initiative at National Aerospace Laboratory numerical simulator - second generation
[NAL-TR-1108] p 384 N92-18037
Investigation on freezing and sticking phenomena of slush on airplane surfaces when taxiing on the ground and the succeeding take-off run phase
[NAL-TR-1026] p 352 N92-18182
An improved method for simulating supersonic flow past a wedge shaped body
[NAL-TR-1097] p 345 N92-18239
A preliminary flight test on a basic performance of the flight research airplane Do 228: Velocity vs glide path angle
[NAL-TM-613] p 359 N92-18482
Proceedings of the Seminar on Investigation and Control of Boundary-Layer Transition
[NAL-SP-11] p 400 N92-18483
An approach to flow field measurement by Laser 2-Focus velocimeter (L2F) in gust wind tunnel
[NAL-TM-617] p 346 N92-18484
Vibration tests of long plate structural model
[NAL-TM-625] p 400 N92-18485
On the relation between cumulus cloud lines and surface shear lines p 410 N92-19667
Evaluation of NACA0012 airfoil test results in the NAL two-dimensional transonic wind tunnel
[NAL-TR-1109T] p 445 N92-21287
Development of wall pressure measuring apparatus for an existing transonic wind tunnel test section
[NAL-TM-565] p 573 N92-23778
Conceptional design to heat-resistant airframe of HOPE p 575 N92-23820
Turbine drive system of the high pressure LOX turbopump test facility
[DE92-783191] p 680 N92-25342
Study of the NAL's 0.1 x 0.1 m magnetic suspension and balance system
[NAL-TM-623] p 665 N92-25365
Static aeroelastic analysis of ACT wind tunnel model aircraft
[NAL-TM-624] p 632 N92-25366
Design of orbital re-entry experiment vehicle and outline of the experiment p 667 N92-25374
Vibration tests and structural modeling of an aircraft model for active control technology experiments
[NAL-TM-626] p 662 N92-25401
The fibre optic three dimensional laser two focus velocimeter for the low-speed windtunnel. Part 1: Two-dimensional measurement evaluations
[NAL-TM-627] p 665 N92-25402
Development of pre- and post-processor system for structural analysis
[NAL-TM-628] p 681 N92-25403
Outlines of parabolic flight p 764 N92-26441
Research activities on CFD at the Ship Research Institute p 766 N92-26908
Three dimensional boundary layer transition on a yawed cylinder p 766 N92-26909
Aerodynamic drag on the bullet trains p 766 N92-26911
Flow around an isolated surface roughness in the laminar boundary layer p 766 N92-26913
Application of riblet surface to pipe flow p 766 N92-26915
Cross-flow instabilities and pressure gradients in boundary layers p 767 N92-26922
A pressure measurement method using Electronically Scanner Pressure sensors (ESP) installed in a gust wind tunnel
[NAL-TM-638] p 749 N92-27428
NAL Dornier 228-200 flight research airplane: Present status and outline of the installed equipment
[NAL-TM-637] p 732 N92-27429
Characterization of superconducting magnetic bearings (dynamic stiffness and damping coefficient in axial direction) p 772 N92-27737
Numerical simulation of shock-stall flutter of an airfoil using the Navier-Stokes equations p 746 N92-27956
NACA0012 airfoil data corrected for sidewall boundary-layer effects in the NAL two-dimensional transonic wind tunnel
[NAL-TM-640T] p 722 N92-28151
Estimation of cable-mounted model inertia characteristics for dynamic wind-tunnel test
[NAL-TM-641] p 722 N92-28152
Evaluation of high lift devices of the quiet STOL experimental aircraft ASKA
[NAL-TR-1102] p 733 N92-28153
Note on flight measured control effectiveness of the quiet STOL experimental aircraft ASKA
[NAL-TR-1103] p 746 N92-28154
Force measurements on AGARD calibration model-B at transonic speeds in the NAL two-dimensional wind tunnel
[NAL-TM-639] p 722 N92-28190

Evaluation of landing configuration by flight test of the quiet STOL experimental aircraft ASKA
[NAL-TR-1113] p 733 N92-28191
A gust generation method for full configuration aircraft tests in a low speed wind tunnel. Part 1: Design and preliminary experiments
[NAL-TR-1115-PT-1] p 722 N92-28192
Air ejector experiments using the two-dimensional supersonic cascade tunnel: Zero secondary flow performance
[NAL-TM-632] p 887 N92-28829
Upgrading the data processing section of the NAL Gust Wind Tunnel data processing system
[NAL-TM-635] p 888 N92-28833
Replacement of the NAL high pressure air storage system
[NAL-TM-634] p 888 N92-28835
Quaternion and Euler angles in kinematics
[NAL-TM-636] p 909 N92-28836
Aerodynamic characteristics obtained from alpha sweep test of the quiet STOL experimental aircraft ASKA
[NAL-TR-1112] p 853 N92-28901
Shafranov shift in low-aspect-ratio heliotron/torsatron CHS
[NIFS-110] p 1138 N92-33743
Analysis of spacecraft entry into Mars atmosphere
p 1105 N92-33763
Study of potassium turbine electric generator system
p 1129 N92-33794

JORDAN
Effect of suction on the stability of supersonic boundary layers. I - Second-mode waves. II - First-mode waves
p 174 A92-19611
Small two-dimensional surface excrescences on aircraft wings approaching separation p 1031 A92-56170

K

KOREA, REPUBLIC OF
Fault tolerant control based on a new accommodation filter p 51 A92-11453
Three-dimensional finite-element analysis of interlaminar stresses in thick composite laminates
p 39 A92-11791
Resonance prediction for slotted circular wind tunnel using finite element p 235 A92-18388
Static aeroelastic analysis for generic configuration wing p 174 A92-20201
Reynolds stress budget in the outwash jet arising from colliding curved wall jets p 614 A92-38860
Dynamic response and aeroelastic analysis of a propeller blade of a prop-fan engine p 762 A92-43109
Numerical simulation of unsteady hypersonic viscous flows in shock tunnel p 710 A92-43170
Prediction of rotor unsteady airloads using vortex filament theory
[AIAA PAPER 92-2610] p 792 A92-45484
Time accurate computation of unsteady transonic flows around an airfoil with oscillating flap on dynamic grid
[AIAA PAPER 92-2733] p 805 A92-45567
A study of the flammability limit of the backward facing step flow combustion
[AIAA PAPER 92-3846] p 895 A92-49136
Application of recursive partially unknown system identification to aerodynamic coefficients estimation
[AIAA PAPER 92-4504] p 1081 A92-55371

N

NETHERLANDS
Aerospace Arall - A challenge for the aircraft designer
p 33 A92-10232
A computer programme for the certification of helicopter vertical take-off and landing operations and an application to the S-76B helicopter p 106 A92-14379
Results of a test program for the use of differential GPS for approach guidance p 101 A92-16969
Inviscid drag prediction for transonic transport wings using a full-potential method p 174 A92-20212
Quantitative estimation of secondary surveillance radar information p 353 A92-24943
Elements of airplane performance
[ISBN 90-6275-608-5] p 357 A92-26550
An aircraft manufacturer's perspective
p 515 A92-33430
S-76B certification for vertical take-off and landing operations from confined areas p 530 A92-35760
LAH main rotor model test at the DNW
p 547 A92-35771
Approach flight trials in the Netherlands for the Navstar GPS Joint Program Office International Test Program
p 533 A92-35928
Fokker 50 flameouts in icing conditions
p 548 A92-35940
An information system for the numerical simulation of 3D Euler flows around aircraft p 613 A92-37554
A note on the Kutta condition in Glauert's solution of the thin aerofoil problem p 613 A92-37933
NATO CCMS aircraft noise study on receiver technology p 686 A92-39050
Aircraft noise - The calculation of the noise exposure by aircraft in the Netherlands p 687 A92-39054
Panel method control in 3-D hyperbolic grid generation
p 617 A92-39940
The evolution from bonded F27 aircraft to Arall structures p 699 A92-41177
Joint Aviation Authorities: Development of an international standard for safety regulation - The first steps are being taken by the JAA p 781 A92-43548
Numerical investigation into high-angle-of-attack leading-edge vortex flow
[AIAA PAPER 92-2600] p 791 A92-45477
The design of a system of codes for industrial calculations of flows around aircraft and other complex aerodynamic configurations
[AIAA PAPER 92-2619] p 917 A92-45492
Comparison of interferometric measurements with 3-D Euler computations for circular cones in supersonic flow
[AIAA PAPER 92-2691] p 800 A92-45538
New concepts for multi-block grid generation for flow domains around complex aerodynamic configurations
p 817 A92-47079
Terminal area traffic management
p 955 A92-50122
A simulator evaluation of various manual control concepts for fly-by-wire transport aircraft
[AIAA PAPER 92-4328] p 1073 A92-55172
Understanding and development of a prediction method of transonic limit cycle oscillation characteristics of fighter aircraft
[AIAA PAPER 92-4501] p 1026 A92-55369
Real-time helicopter simulation using the blade element method p 1132 A92-56278
Application of electronically scanned pressure measurement system for engine simulation tests in the German-Dutch Wind Tunnel
[AIAA PAPER 92-4003] p 1122 A92-56826
On the limitations of Froude's actuator disc concept
[ETN-91-90136] p 81 N92-11973
A knowledge-based assistant for diagnosis in aircraft maintenance p 61 N92-12538
Modeling and numerical simulation of vortex flow in aerodynamics
[AD-B163670L] p 83 N92-12997
Analysis of results of an Euler-equation method applied to leading-edge vortex flow p 84 N92-13000
Experimental and numerical investigation of the vortex flow over a delta wing at transonic speed
p 84 N92-13001
An experimental study of the flow over a sharp-edged delta wing at subsonic and transonic speeds
p 85 N92-13011
Review of aerodynamic design in the Netherlands
p 193 N92-13929
The two-bay crack problem in fuselages built in GLARE and ARALL
[LR-653] p 196 N92-14044
Bulging of fatigue cracks in a pressurized aircraft fuselage
[LR-655] p 196 N92-14045
Propeller-driven-small airplane noise certification
[LR-650] p 237 N92-14798
Aerothermodynamic challenges for ESA programmes
p 180 N92-14974
SIMOUN and Scirocco wind tunnel nozzle viscous flow study p 208 N92-14999
Equilibrium solution of the Euler and Navier-Stokes equations around a double ellipsoidal shape with mono- and multi-blocks including real gas effects, part 1
p 227 N92-15030
Parallelization of a Direct Simulation Monte Carlo (DSMC) code for fluid dynamics p 227 N92-15033
Grid impact on 3D hypersonic flows
p 184 N92-15041
Review of the European hypersonic wind tunnel performance and simulation requirements
p 209 N92-15043
Monitoring load experience of individual aircraft
[NLR-TP-90084-U] p 196 N92-15065
CAR 88: A method to calculate subsonic and supersonic, steady and unsteady, potential flow about complex configurations
[NLR-TR-88154-U] p 400 N92-18221
NLR experience with high velocity burner rig testing, 1979-1989
[NLR-TP-89152-U] p 385 N92-18415
Model incidence measurement using SAAB ELOPTOPOS system
[NLR-TP-89182-U] p 385 N92-18416
Development of nonlinear real-time helicopter simulation using a blade element method
[NLR-TP-90115-U] p 381 N92-18893
WP 4b compressible flow simulation: Information System for flow simulation based on the Navier-Stokes equation (ISNaS). Requirements grid generation for the ISNaS compressible flow solver
[NLR-TR-88103-U] p 405 N92-19490
Estimating the probability of vertical overlap from the paired aircraft data obtained in the European vertical data collection using the program DGLDiF
[NLR-TR-88108-U] p 356 N92-19491
Inviscid drag prediction for transonic transport wings using a full-potential method
[NLR-TP-89365-U] p 444 N92-20473
Investigation of a semi-empirical method to predict limit cycle oscillations of modern fighter aircraft
[NLR-TP-90087-U] p 481 N92-20475
Numerical simulation of vortical flow over a delta wing at subsonic and transonic speeds
[NLR-TP-90029-U] p 444 N92-20498
The effect of hoar-frosted wings on the Fokker 50 take-off characteristics p 451 N92-21692
Determination of limitations for helicopter ship-borne operations p 465 N92-21965
Helicopter handling: Experience and new developments p 465 N92-21969
Symposium on High Speed Airbreathing Propulsion: The Solid Fuel Combustion Chamber and Beyond
[ETN-92-90685] p 575 N92-22268
Improved shock-capturing of Jameson's scheme for the Euler equations
[PB92-148758] p 596 N92-23251
Evaluation of the applicability of Helmholtz resonators for low frequency acoustic liners
[PB92-138544] p 605 N92-23588
Panel methods for aerodynamic analysis and design
p 552 N92-23955
Domain modeling and grid generation for multi-block structured grids with application to aerodynamic and hydrodynamic configurations p 691 N92-24411
CAD product data exchange: Conversions for curves and surfaces
[ISBN-90-6275-723-9] p 648 N92-24964
Towards GLARE: The development of a fatigue insensitive and damage tolerant aircraft material
[ETN-92-91301] p 648 N92-24966
Delfi: Design, development, and applicability of expert systems shells
[ISBN-90-6275-734-0] p 692 N92-25306
NLR inviscid transonic unsteady loads prediction methods in aeroelasticity p 720 N92-27947
Development of a method to predict transonic limit cycle oscillation characteristics of fighter aircraft
p 746 N92-27958
Aircraft simulation and pilot proficiency: From surrogate flying towards effective training p 884 N92-28532
The basic research simulator programme and the industrial and aerospace community: Opportunities for cooperative research
[LR-662] p 887 N92-28579
Inverse control problems: Mathematical preliminaries, system theoretical approaches, and their applications to aircraft dynamics
[LR-665] p 923 N92-28581
Hyperbolic grid generation with BEM source terms
[NLR-TP-90334-U] p 923 N92-28635
A simple and low cost system to measure delay times in pneumatic systems
[NLR-TP-90174-U] p 859 N92-28644
The use of load enhancement factors in the certification of composite aircraft structures
[NLR-TP-90068-U] p 852 N92-28649
Some longitudinal handling qualities design guidelines for active control technology transport aircraft
[NLR-TP-90129-U] p 878 N92-28652
Response of helicopters to gusts
[NLR-TP-90159-U] p 879 N92-28653
Potential applications of laser Doppler anemometry for in-flight measurements
[NLR-TP-90163-U] p 859 N92-28654
Application of knowledge-based systems for diagnosis of aircraft systems
[NLR-TP-90192-U] p 837 N92-28655
Analysis of results of an Euler-equation method applied to leading-edge vortex flow
[NLR-TP-90368-U] p 827 N92-28657
Comparison of LDA and LTA applications for propeller tests in wind tunnels
[NLR-MP-88031-U] p 827 N92-28658
Calculation of unsteady subsonic and supersonic flow about oscillating wings and bodies by new panel methods
[NLR-TP-89119-U] p 827 N92-28659

Constrained spanload optimization for minimum drag of multi-lifting-surface configurations
[NLR-TP-89126-U] p 828 N92-28660
The windtunnel as a tool for laminar flow research
[NLR-TP-90145-U] p 887 N92-28661
Instrumentation requirements for laminar flow research in the NLR high speed wind tunnel HST
[NLR-TP-89158-U] p 887 N92-28669
LAH-main rotor model test at the DNW
[NLR-TP-90305-U] p 852 N92-28687
Atmospheric turbulence spectra and correlation functions
[NLR-TP-89217-U] p 915 N92-28689
Development and validation of a characteristic boundary condition for a cell-centered Euler method
[NLR-TP-90144-U] p 828 N92-28692
Turbulence modeling: Survey of activities in Belgium and the Netherlands, and appraisal of the status and a view on the prospects
[NLR-TP-90184-U] p 908 N92-28694
Experimental validation of a line-duct acoustics model including flow
[NLR-TP-90223-U] p 927 N92-28695
Wave drag determination in the transonic full-potential flow code MATRICS
[NLR-TP-90062-U] p 828 N92-28709
Diffuser casing upgrade for an advanced turbofan
[NLR-TP-90097-U] p 870 N92-28711
Boundary conditions for Euler equations at internal block faces of multi-block domains using local grid refinement
[NLR-TP-90134-U] p 908 N92-28712
Flow gradient corrections on hot-wire measurements using an X-wire probe
[NLR-TP-90255-U] p 829 N92-28713
S-76B certification for vertical take-off and landing operations from confined areas
[NLR-TP-90286-U] p 852 N92-28714
NARSIM: A real-time simulator for air traffic control research
[NLR-TP-90147-U] p 888 N92-29204
Short cracks and durability analysis of the Fokker 100 wing/fuselage structure
[NLR-TP-90336-U] p 910 N92-29603
Hyperbolic grid generation control by panel methods
[NLR-TP-91061-U] p 924 N92-29604
European studies to investigate the feasibility of using 1000 ft vertical separation minima above FL 290. Part 1: Overview of organisation, techniques employed, and conclusions
[NLR-TP-91062-U-PT-1] p 841 N92-29605
Application of VME-technology on an airborne data link processor unit
[NLR-MP-88040-U] p 841 N92-29615
Results of a flight simulator experiment to establish handling quality guidelines for the design of future transport aircraft
[NLR-MP-88044-U] p 854 N92-29616
On the optimization of windshear warning and guidance systems
[NLR-TP-90196-U] p 837 N92-29703
Evaluation of measured-boundary-condition methods for 3D subsonic wall interference
[NLR-TR-88072-U] p 832 N92-29884
A method for computing the 3-dimensional flow about wings with leading-edge vortex separation. Part 2: Description of computer program VORSEP
[NLR-TR-86006-U] p 833 N92-29916
Ageing aircraft research in the Netherlands
p 838 N92-30129
Low-velocity impact loading on fibre reinforced aluminum laminates (ARALL) and other aircraft sheet materials
[ETN-92-91613] p 987 N92-30414
Examination of aircraft warning and caution lights after shock testing
[NLR-TP-89284-U] p 952 N92-30474
Modeling and numerical simulation of vortex flow in aerodynamics
[NLR-TP-91154-U] p 1037 N92-32673
New concepts for multi-block grid generation for flow domains around complex aerodynamic configurations
[NLR-TP-91046-U] p 1037 N92-32730
An experimental study of the flow over a sharp-edged delta wing at subsonic and transonic speeds
[NLR-TP-91117-U] p 1037 N92-32732
Integration of wall interference assessment and wall adaptation
[NLR-TP-91119-U] p 1101 N92-32734
Development of new flight procedures for the Microwave Landing System (MLS)
[NLR-TP-91156-U] p 1047 N92-32830
Active synchrophasing of propeller unbalance
p 1138 N92-32963
On the origin and acoustical behaviour of cloud cavitation
[ISBN-90-9004317-9] p 1125 N92-33066
Global/local interlaminar stress analysis of a grid-stiffened composite panel
[NASA-CR-190822] p 1125 N92-33139
Calibration of GPS antennas
[ETN-92-92034] p 1051 N92-33693
Activities report of the National Aerospace Laboratory
[ETN-92-92053] p 1143 N92-33694

NEW ZEALAND

Perspectives on the cooperative air traffic management concept - Far East/Pacific point of view
p 606 A92-33428
Getting test items to measure knowledge at the level of complexity which licensing authorities desire - Another dimension to test validity p 835 A92-45080
Thin-airfoil correction for panel methods
p 811 A92-46811

NORWAY

Computation of aircraft noise exposure using digitized topography data p 687 A92-39058
Advanced method for single event aircraft noise analysis p 693 A92-39060
A noise survey around Oslo Airport Fornebu
p 687 A92-39061
A mobile system for measuring airport noise
p 688 A92-39099
Mandatory psychological testing of pilots as a requirement for licensing in Norway?
p 835 A92-45081
On the calculation of repeatable accuracy, with special reference to GPS p 955 A92-49383
Probabilistic design and fatigue management based on probabilistic fatigue models with reliability updating
p 360 N92-18574

P

POLAND

Biennial Fluid Dynamics Symposium on Advanced Problems and Methods in Fluid Mechanics, 19th, Kozubnik, Poland, Sept. 3-8, 1989, Selected Papers
p 37 A92-10654
Polish radar technology. II - Adaptive radar AVIA CM
p 39 A92-12290
Polish radar technology. III - Weather channel for primary surveillance radar p 40 A92-12291
Polish radar technology. V - Adaptive MTI filters for uniform and staggered sampling p 40 A92-12293
Acoustic isolation of layers p 54 A92-12345
Experimental determination of the center of mass, the principal central axes of inertia and moments of inertia
p 40 A92-12346
Automation of the measurement process in the N2 wind tunnel with the SPITA N-3 system p 30 A92-12347
Blade defect force investigation in a compressor cascade p 10 A92-13233
An analysis of the flow-pattern at the exit of a single-stage turbine p 10 A92-13234
Estimation of the size of separation zone in a turbine stage under small load p 10 A92-13235
Corrosion damage and regeneration of aluminide coatings on aircraft turbine blades p 142 A92-15244
A new thermometric instrument for airborne measurements in clouds p 368 A92-24918
Transgressions in a pilot-helicopter system
p 358 A92-27394
The effect of air-compressor adjustment by means of air-bleed on the reserve of its stable operation
p 471 A92-29973
General model of isolated helicopter blade for stability investigation p 547 A92-35774
An estimate of the influence of the compressor stability margin on the pick-up time of a turbojet engine
p 654 A92-37423
An estimate of the influence of the compressor stability margin on the thrust of a turbojet engine
p 654 A92-37424
A model of a deformable aeroplane with a wing of low aspect ratio and movable control surfaces for studying natural vibrations p 744 A92-41528
Biennial Fluid Dynamics Symposium on Advanced Problems and Methods in Fluid Mechanics, 19th, Kozubnik, Poland, Sept. 3-8, 1989, Selected Papers
p 761 A92-42529
Safety vs. economy, system-theoretic approach to the problem analysis p 916 A92-45002
Selected models of aircraft navigation space
p 839 A92-45373
Radioaltimeter RWL-750 p 855 A92-45374
Two-point optimization of complete three-dimensional airplane configuration
[AIAA PAPER 92-2618] p 844 A92-45491
Mathematical modeling of the flight of passenger aircraft in the case of engine failure p 875 A92-47777
Calculation of the aerodynamic derivatives of aircraft in the supersonic region using the Mach box method
p 875 A92-47779
Total losses in turbulent flows inside conical diffusers
p 819 A92-47782
Modeling of the control systems of rotary wing aircraft (Review) p 875 A92-47783
Mathematical modeling of the effect of windshear on the dynamics of a landing aircraft p 875 A92-47784
Aircraft stabilization at large angles of attack
p 875 A92-47785
A new method of helicopter rotor blade motion control
p 875 A92-47786
Concept of a one-dimensional model of the dynamic behavior of a gas turbine p 862 A92-47791
Simulation analysis of the influence of variation in some selected design and control parameters on the acceleration time of a turbojet engine
p 970 A92-52890
Simulation of helicopter see-saw rotor motion
p 1055 A92-56287
Design of 3-dimensional complex airplane configurations with specified pressure distribution via optimization
p 194 N92-13948

PORTUGAL

Predictions of compressible viscous flows at all Mach number using pressure correction, collocated primitive variables and non-orthogonal meshes
[AIAA PAPER 92-0426] p 326 A92-26274
Turbulent energy budgets in impinging zones
p 620 A92-40081
Fatigue management for the A-7P
p 363 N92-18593

R

ROMANIA

A lifting line theory for supersonic flow applications
[AIAA PAPER 91-5058] p 171 A92-17841
Control surfaces correlation in DLC maneuvers
p 280 A92-21301
Control surfaces correlation in DSFC maneuvers
p 281 A92-21307
Some considerations on modeling flight vehicles movement p 281 A92-21311
A theory for mechanical flight control linkages
p 269 A92-21312
An improvement of the double-point method for unsteady subsonic flow p 243 A92-21315
A method of calculation for the radius of curvature of the attached shock waves in front of a sharp-nosed axi-symmetrical body placed in a uniform stream
p 243 A92-21319
On automatic control of aeroelastic vehicles
p 509 A92-29327
Flow near the trailing edge of an airfoil
p 431 A92-31151
The static and fatigue computation of the propeller blades retention system p 995 A92-51895
A study of supersonic flow over the ogival bodies with attached shock waves at zero incidence
p 936 A92-51896
A direct viscous-inviscid interaction method for the flow calculation around airfoils p 936 A92-52028
An aerodynamical analysis of 'seesaw' type rotor for autogyro p 937 A92-52034
On a global aerodynamic optimization of a civil transport aircraft p 193 N92-13931

RUSSIA

The use of photogrammetry in aviation equipment flight testing p 994 A92-51649
Method of large particles in arbitrary curvilinear orthogonal coordinates for the solution of problems of hydro and aerodynamics p 937 A92-52035
Influence of atmospheric rarefaction on aerodynamic characteristics of flying vehicles p 938 A92-52750
One-dimensional kinetic model for flows near a stagnation point of a highly cooled body in hypersonic rarefied streams p 938 A92-52751
Influence of internal molecular degrees of freedom on the hypersonic rarefied gas flow about a conical body
p 938 A92-52752
Approximate aerodynamic analysis for complicated bodies in rarefied gas flows p 938 A92-52754
Aerodynamics of complex shape bodies within a wide range of supersonic flows of rarefied gases
p 939 A92-52767
Aerodynamic characteristics of a standard corrugated body in a free-molecular flow p 940 A92-52818
Interaction between a body flying at a supersonic velocity and a point explosion p 1019 A92-53867
Viscosity characteristics of synthetic aviation oils at low temperatures p 1105 A92-53875
High-temperature metal matrix composite
p 1105 A92-53878

Pulsation characteristics of one-phase and two-phase steam flows in Laval nozzles under off-design conditions p 1019 A92-53882
Aerodynamic airfoils design by quasi-solutions method of inverse boundary-value problems p 1020 A92-53998
The enhancement of the mixing and combustion processes in supersonic flow applied to scramjet engine [AIAA PAPER 92-3428] p 1112 A92-54029
The study of experimental turboramjets [AIAA PAPER 92-3720] p 1067 A92-54135
Stochastic self-induced roll oscillations of slender delta wing at high angles of attack [AIAA PAPER 92-4498] p 1081 A92-55366
State-space representation of aerodynamic characteristics of an aircraft at high angels of attack [AIAA PAPER 92-4651] p 1028 A92-55395
The solution of the helicopter flight dynamics tasks by the methods of optimal control theory p 1085 A92-56284
Safety provision against 'ground resonance' free vibration of a coaxial helicopter p 1056 A92-56289
Helicopter tail rotor stall flutter p 1056 A92-56290
Aeroelasticity of a coaxial helicopter rotor p 1057 A92-56309
Oscillations of an anisotropic rotor on an elastic anisotropic support p 1057 A92-56311
Composite blades for helicopter main and tail rotors developed by Mil Design Bureau p 1057 A92-56325
Design method of a helicopter cockpit p 1058 A92-56337
Aerodynamic features of a coaxial rotor helicopter p 1032 A92-56349
TSNIIMASH capabilities for aerogasdynamical and thermal testing of hypersonic vehicles [AIAA PAPER 92-3962] p 1097 A92-56789
Increasing the accuracy of the Godunov scheme for calculating steady-state supersonic gas flows by solving the generalized Riemann problem p 1035 A92-57499

S

SAUDI ARABIA

Similarity solutions for supersonic axisymmetric flows p 173 A92-18387
Hypersonic flows over slender circular cones at small angles of attack p 173 A92-19068
Oscillating two-dimensional hypersonic airfoils at small angles of attack p 340 A92-28042
On hypersonic flow over two-dimensional aerofoils p 433 A92-31425
The flow over a backward-facing step under controlled perturbation - Laminar separation p 705 A92-41653
Aircraft spoiler effects under wind shear [AIAA PAPER 92-2642] p 796 A92-45509
Effect of wing tip vortices on a trailing aircraft p 935 A92-50303
Three-dimensional wings and waveriders with attached shock waves p 936 A92-50322
Supersonic flow past pointed-nose thin airfoils p 940 A92-52844
Effect of atmospheric disturbances on airplane response [AIAA PAPER 92-4340] p 1078 A92-55329

SENEGAL

Future air navigation systems for Africa p 532 A92-33439

SINGAPORE

Robustness of a helicopter flight control system designed using eigenstructure assignment [AIAA PAPER 92-4469] p 1076 A92-55229

SPAIN

Madrid's double airport p 138 A92-16231
New practical method for measurement error determination in radar systems under real traffic conditions p 155 A92-17238
ARINC and commercial aircraft avionics. I p 353 A92-25655
ARINC and the avionics of commercial aircraft. II p 637 A92-37072
Iberia's Aeronautical Mapping Application (ACAI) p 637 A92-37073
Use of the thrust-weight diagram versus transport cargo in the initial dimensioning of passenger-transport aircraft p 642 A92-37074
Possible utilization of GPS in precision approach maneuvers p 637 A92-37075
Optimum cruise lift coefficient in initial design of jet aircraft p 845 A92-46806
Patch-independent structured multiblock grids for CFD computations p 919 A92-47078
Brownian-motion limited aerodynamic focusing of heavy molecules p 995 A92-52722
Investigation of the tail buffeting of the C-101 p 942 A92-53253
A methodology for software specification and development based on simulation p 135 N92-12458
Flow and temperature computations for space vehicles using adaptive finite element techniques p 181 N92-14990
Electronically steerable antenna for aircraft p 229 N92-15272
The measurement of water film thickness on airfoils in heavy rain conditions using conductance sensors p 452 N92-21695
Measurement of the flow distribution over the flight deck of an aircraft carrier p 504 N92-21955
Fuzzy guidance system evaluation p 778 N92-27903
Unsteady transonic aerodynamics of pointed bodies of revolution in supersonic freestream p 719 N92-27946

SWEDEN

JAS 39 Gripen progress report p 112 A92-16058
Aerospace software in Sweden p 233 A92-19406
Fatigue and damage tolerance verification of aircraft structures p 217 A92-19677
Damage tolerance of the fighter aircraft 37 Viggen. I - Analytical assessment. II - Experimental verification p 192 A92-19819
The use of finite difference electromagnetic analysis in the design and verification of modern aircraft p 192 A92-20136
GPS/GLONASS user systems in Sweden p 638 A92-38384
Inter-noise 90; Proceedings of the International Conference on Noise Control Engineering, Goteborg, Sweden, Aug. 13-15, 1990. Vols. 1 & 2 [ISBN 91-7848-224-0] p 693 A92-39042
Mechanical noise from large wind turbines - Experiences from Swedish prototypes p 686 A92-39046
Propeller aircraft interior noise - Physical background and possible treatments p 642 A92-39082
Coupled propeller contributions to aircraft noise and vibration p 694 A92-39085
Propeller sound excitation on an aircraft fuselage using a loudspeaker ring p 643 A92-39087
JAS 39 Gripen flight test report p 645 A92-40030
Transition to turbulence in curved channel flow p 621 A92-40125
Extrapolation procedures for the time-dependent Navier-Stokes equations p 704 A92-41289
Generation of efficient multiblock grids for Navier-Stokes computations p 919 A92-47081
Performance improvements and fuel cost savings due to leading edge modification of a vintage delta wing jet fighter [FFA-TN-1991-22] p 114 N92-11993
Optimal design of nonlinear shell structures [FFA-TN-1991-18] p 157 N92-12312
A review of aeronautical fatigue investigations in Sweden during the period May 1989 to April 1991 [FFA-TN-1991-24] p 158 N92-12313
Hypersonic flow past delta wing flow simulated by Navier-Stokes solutions p 180 N92-14981
Wind tunnel force measurements and visualization on a 60-deg delta wing in oscillation, stepwise motion, and gusts p 364 N92-18786
Temperature effects in FFA HYP 500 at M = 7 in a flow with strong expansion [FFA-TN-1991-27] p 443 N92-20229
MATGRID: A program for generation of C-H and C-O topology grids around wing/body configurations. Mathematical definition document [FFA-TN-1990-19] p 444 N92-20468
Hypersonic laminar flow computations over a blunt leading edged delta wing at three different chord Reynolds numbers [FFA-TN-1991-40] p 528 N92-23168
The structural optimization system OPTSYS: Current status and applications p 550 N92-23232
Recent applications of linear and nonlinear unsteady aerodynamics for aeroelastic analysis p 718 N92-27940
A manufacturer's approach to ensure long term structural integrity p 838 N92-30133
MATGRID, a program for generation of C-H and C-O topology grids around wing/body configurations: Software description document [FFA-TN-1990-20] p 945 N92-30713
Vibro-acoustic FE analyses of the Saab 2000 aircraft p 1137 N92-32952

SWITZERLAND

Investigation of the flow at the exit of an unshrouded centrifugal impeller and comparison with the 'classical' jet-wake theory [ASME PAPER 90-GT-124] p 6 A92-11287
Robust stabilization of a helicopter model p 28 A92-11501
Quasi-three-dimensional characteristics method for a supersonic compressor rotor [ASME PAPER 91-GT-81] p 69 A92-15549
The view from the airport p 532 A92-33438
Non-equilibrium hypersonic flow simulations using the second-order boundary layer equations p 612 A92-37551
Mesh adaption for 2D transsonic Euler flows on unstructured meshes p 816 A92-47038
Close-range photogrammetry meets machine vision; Proceedings of the Meeting, Zurich, Switzerland, Sept. 3-7, 1990 [SPIE-1395] p 994 A92-51626
Annular seals of high energy centrifugal pumps: Presentation of full scale measurement p 224 N92-14362
A multiblock flow solver for inviscid hypersonic flows p 181 N92-14986
Separation of external stores: Comparison of results [F+W-TF-2058] p 732 N92-26944
Theoretical principles of a Euler method for the calculation of three dimensional flows [F+W-TF-2012] p 767 N92-27045

U

UNITED KINGDOM

Flying the A340 iron bird p 20 A92-10666
VSTOL aircraft flight control system design using H(infinity) controllers and a switching strategy p 28 A92-11561
An assessment of robustness of variable structure control systems for advanced aircraft manoeuvres p 29 A92-11595
Dornier Do.328 special - Examining the high-speed commuter p 21 A92-11882
Analysis and design optimization of monopulse receivers for secondary surveillance radar p 40 A92-12299
Solution of the Reynolds-averaged Navier-Stokes equations for transonic aerofoil flows p 9 A92-13198
The aerodynamic interference between a flapped tanker aircraft and a receiver aircraft during air-to-air refuelling p 29 A92-13199
Secondary separation from a slender wing p 62 A92-13448
Tomorrow's cockpit displays p 117 A92-13699
Mind that restyle p 91 A92-13700
A 3-D separation model for arbitrary planforms p 65 A92-14360
Development testing of the EH101 Flight Control System p 132 A92-14380
Lifting line predictions for a swept tip rotor blade p 65 A92-14424
High temperature multiaxial creep testing of Nimonic 115 p 141 A92-15202
Prediction of long-term creep rupture properties for an aluminium alloy for airframe applications p 141 A92-15206
A review of rigid body response on sting supported models at high angles of incidence p 66 A92-15345
An Axial Turbobrake [ASME PAPER 91-GT-1] p 147 A92-15501
Performance of radial clearance rim seals in upstream and downstream rotor-stator wheelspaces [ASME PAPER 91-GT-32] p 147 A92-15516
Rim sealing of rotor-stator wheelspaces in the absence of external flow [ASME PAPER 91-GT-33] p 147 A92-15517
Turbulence modelling for secondary flow prediction in a turbine cascade [ASME PAPER 91-GT-57] p 68 A92-15535
Stall inception in axial flow compressors [ASME PAPER 91-GT-86] p 69 A92-15551
Active suppression of rotating stall and surge in axial compressors [ASME PAPER 91-GT-87] p 122 A92-15552
Unsteady viscous flow in a high speed core compressor [ASME PAPER 91-GT-91] p 70 A92-15555
The influence of blade leaning on the performance of an integrated OGV-diffuser system [ASME PAPER 91-GT-104] p 122 A92-15561
The simulation of three-dimensional viscous flow in turbomachinery geometries using a solution-adaptive unstructured mesh methodology [ASME PAPER 91-GT-124] p 71 A92-15569
Inviscid-viscous coupled solution for unsteady flows through vibrating blades. II - Computational results [ASME PAPER 91-GT-126] p 71 A92-15571
The effect of blade tip geometry on the tip leakage flow in axial turbine cascades [ASME PAPER 91-GT-135] p 72 A92-15577
Multi-blade row Navier-Stokes simulations of fan-bypass configurations [ASME PAPER 91-GT-148] p 73 A92-15586
An experiment on unsteady flow over an oscillating airfoil [ASME PAPER 91-GT-181] p 73 A92-15613

The design and testing of a radial flow turbine for aerodynamic research
[ASME PAPER 91-GT-220] p 124 A92-15636
Film cooling research on the endwall of a turbine nozzle guide vane in a short duration annular cascade. I - Experimental technique and results
[ASME PAPER 91-GT-252] p 150 A92-15657
Film cooling research on the endwall of a turbine nozzle guide vane in a short duration annular cascade. II - Analysis and correlation of results
[ASME PAPER 91-GT-253] p 150 A92-15658
Discharge coefficients of cooling holes with radiused and chamfered inlets
[ASME PAPER 91-GT-269] p 151 A92-15667
Self-induced flow in a stepped rotating tube
[ASME PAPER 91-GT-276] p 152 A92-15673
Modelling of unsteady transitional boundary layers
[ASME PAPER 91-GT-282] p 152 A92-15677
Design and performance of advanced blading for a high-speed HP compressor
[ASME PAPER 91-GT-374] p 76 A92-15718
The selective bleed variable cycle engine
[ASME PAPER 91-GT-388] p 126 A92-15720
A simple model to simulate subsonic intakes and propelling nozzles of aircraft gas turbine engines
[ASME PAPER 91-GT-392] p 153 A92-15722
Flight safety; Proceedings of the Conference, London, England, Nov. 21, 1991 p 92 A92-16050
EH101 helicopter development p 112 A92-16060
Legal capacity of Eurocontrol to ensure smooth aviation in Europe p 167 A92-16134
Delivered with feeling p 134 A92-16621
Mirage 2000-5 - Dassault's delta described p 113 A92-16622
Feeling normal p 134 A92-16623
The application of high pressure ejectors to reaction control systems p 128 A92-16666
Probability distributions that are important when assessing barometric aiding to GPS p 100 A92-16952
Isothermal modeling of gas turbine combustors - Computational study p 129 A92-17203
Hypersonic materials p 212 A92-18002
Rolling in the tolerance p 216 A92-18005
Heavy metal p 207 A92-18100
Noise-driven flow p 173 A92-18680
Large chord turbine cascade testing at engine Mach and Reynolds number p 173 A92-18771
Mesoscale dynamics of cold fronts - Structures described by dropsoundings in Fronts 87 p 230 A92-18902
Infra-red offers new landing aid competition p 198 A92-18937
Aerospace software engineering in the United Kingdom p 233 A92-19405
Short fatigue crack growth from blunt notches in an aero-engine alloy p 212 A92-19760
Crack initiation and the short-to-long crack growth transition in a Ni-base superalloy p 213 A92-19767
Whole aircraft lightning indirect effects evaluation using low level injection techniques p 192 A92-20134
Four decades of transonic fighter design p 193 A92-20203
Flat-ended circular cylinder in hypersonic rarefied flow p 174 A92-20304
Method for the prediction of supersonic compressor blade performance p 277 A92-21078
Airport terminals p 283 A92-21125
Creep-fatigue crack growth in Jethete M152 at 550 C under mixed mode conditions p 288 A92-21490
Clever cockpits p 241 A92-21700
Computational methods in viscous aerodynamics p 245 A92-21976
Two-dimensional, incompressible aerofoil design and analysis p 247 A92-21987
High costs force avionics links p 276 A92-22000
Parallel algorithms for panel methods p 293 A92-22346
Computation of normal impinging jets in cross-flow and comparison with experiment p 250 A92-22446
Cost effective solutions for titanium sheet metal forming p 293 A92-22785
Transition to cooperative ATM system requires commitment p 267 A92-23297
Optical design of dual combiner head-up displays p 414 A92-24628
The jet edge-tone feedback cycle - Linear theory for the operating stages p 392 A92-24758
The accuracy and coverage of Loran-C and of the Decca Navigator System - and the fallacy of fixed errors p 353 A92-24944
The avoidance of collisions for Newtonian bodies with hidden variables p 353 A92-24945
European studies to investigate the feasibility of using 1000 ft vertical separation minima above FL 290. II - Precision radar data analysis and collision risk assessment p 353 A92-24946
Tilting at targets p 357 A92-25074
Damping down the fires p 350 A92-25075
The use of variable camber to reduce drag, weight and costs of transport aircraft p 313 A92-25096
The effects of suction on the nonlinear stability of the three-dimensional boundary layer above a rotating disc p 393 A92-25366
Behind the screens p 353 A92-25520
The real TCAS p 350 A92-25521
Anglo-American avionics p 307 A92-25575
The evaluation of canard couplings at high angles of attack
[AIAA PAPER 92-0281] p 318 A92-25735
An efficient Euler solver for predominantly supersonic flows with embedded subsonic pockets
[AIAA PAPER 92-0323] p 322 A92-25770
A review of impinging jets in cross-flows - Experimentation and computation
[AIAA PAPER 92-0633] p 333 A92-27011
Embedded meshes of controllable quality synthesised from elementary geometric features
[AIAA PAPER 92-0663] p 411 A92-27034
Boundary singularities in steady potential compressible flow through plane two-dimensional channels p 336 A92-27384
Fibre optic laser anemometry for turbomachinery applications p 397 A92-27783
Coherence multiplexed polarimetric fibre sensor arrays for aerospace applications p 370 A92-27785
A study of the interaction of a normal shock wave with a turbulent boundary layer at Mach numbers between 1.30 and 1.55 p 339 A92-28006
Computational mechanics today p 399 A92-28464
Characterization of diffusion bonds using an acoustic microscope p 491 A92-28686
36th Roy Chadwick Lecture - Manufacturing breakout 1941-1991: Development in aerospace industry manufacturing techniques p 419 A92-28941
Meeting VSTOL aircraft performance requirements using scheduled H(infinity) controllers p 477 A92-29094
Fire-fighting foams must meet newly-developed ICAO standard p 448 A92-29508
Dornier 328 - A Daimler for commuters p 458 A92-30091
Airbus - The family expands p 419 A92-30092
Calculations of the dilution system in an annular gas turbine combustor p 494 A92-31164
Rule based identifier for unknown systems p 509 A92-31430
Aero-propulsive effects on configuration shaping
[AIAA PAPER 91-5064] p 459 A92-31691
Heat transfer effects on aerodynamics and implications for wind-tunnel tests p 497 A92-32240
The Second Goldstein Lecture: Modern developments in fluid dynamics - An addendum p 442 A92-32323
Numerical studies of supersonic flow over a compression corner p 442 A92-32324
The first fifty years of composite materials in aircraft construction p 461 A92-32325
Thermally sprayed coating systems for surface protection and clearance control applications in aero engines p 488 A92-32394
The use of large teams in conceptual aircraft design
[AIAA PAPER 92-1092] p 605 A92-33257
Sentinel 1000 flight test programme overview and preliminary results
[AIAA PAPER 92-1229] p 538 A92-33326
A European perspective on the co-operative air traffic management concept p 531 A92-33427
Aircraft performance
[ISBN 0-521-36264-4] p 538 A92-33919
Mass-transporter p 543 A92-34650
A method for the construction of safe S-N curves p 586 A92-34759
JPATS escape system development p 543 A92-35434
Why composites wait in the wings p 577 A92-35475
Robustness characteristics of fast-sampling digital controllers for active flutter suppression
[AIAA PAPER 92-2104] p 567 A92-35675
Design of adaptive fast-sampling digital controllers for active flutter suppression
[AIAA PAPER 92-2105] p 567 A92-35676
The use of Stodola modes in rotor-blade aeroelastic studies p 590 A92-35729
Frequency domain testing of helicopter dynamics using automated input signals p 545 A92-35731
Full authority active control system design for a high performance helicopter p 567 A92-35732
Engine air particle separator panels for helicopter engine protection p 545 A92-35735
The development of an engine air particle separator system for the CH-47 helicopter p 545 A92-35736
The use of inverse simulation for conceptual design p 546 A92-35738
Multivariable methods for helicopter flight control law design - A review p 568 A92-35748
Command following control law design by linear quadratic optimisation p 568 A92-35749
Tail rotor aerodynamic features recorded in flight p 546 A92-35752
Helicopter fog flying trials p 530 A92-35759
Rotor aeromechanics research with the RAE research Lynx - The experimental facility and test programme p 547 A92-35767
The development and testing of an active control of structural response system for the EH101 helicopter p 569 A92-35775
An evaluation of a simple PID controller designed using optimal control theory when applied to helicopter stabilisation p 569 A92-35785
Eigenstructure assignment for handling qualities in helicopter flight control law design p 570 A92-35786
Handling and performance considerations when conducting air-to-air refuelling of large aircraft by the probe and drogue system p 548 A92-35937
Dealing with pilot response in failure case testing p 549 A92-35952
The engine inside p 558 A92-36126
The Delta Clipper dream p 574 A92-36127
Experimental investigation of supersonic flow over two cavities in tandem p 610 A92-36830
Advanced propulsion systems for large subsonic transports p 653 A92-36977
The computation of three-dimensional flows using unstructured grids p 612 A92-37539
NASA's quiet side. I p 607 A92-37875
Fretting fatigue p 672 A92-38225
Ageing airliner census - Still flying safely p 634 A92-38374
Flying on thin ice p 634 A92-38375
Aviation meteorology p 685 A92-38383
A method to determine propagation direction of compressive fracture in carbon-fibre composites p 672 A92-38770
Flow regimes of the cove regions between a slat and wing and between a wing and flap of a multielement airfoil p 614 A92-38858
Noise from military airfields in the United Kingdom p 686 A92-39052
Airport noise contours - Converting from NNI to Leq p 686 A92-39053
Do we really need 57 ways of rating aircraft noise? p 688 A92-39065
A survey of active control in aircraft cabins p 643 A92-39084
Evaluation of sound transmission into aircraft fuselages by a reciprocity technique p 694 A92-39086
Safety at sea and in the air - Taking stock together; Proceedings of the Conference, London, England, Nov. 13-15, 1990
[ISBN 0-903409-78-X] p 634 A92-39301
Review of aviation record p 634 A92-39302
Civil aircraft design in relation to airworthiness p 635 A92-39303
Aircraft structural design p 643 A92-39304
How to promote error tolerance in complex systems in the context of ships and aircraft p 673 A92-39308
Engine reliability p 654 A92-39309
Learning from aircraft accidents and incidents p 635 A92-39310
Airport technology international 1992 p 664 A92-39514
Design of low-sensitivity modalized observers using left eigenstructure assignment p 661 A92-39908
Concorde flight testing - Powerplant and performance flying
[SAE PAPER 912192] p 644 A92-40009
Concorde, fifteen years on the front line
[SAE PAPER 912193] p 644 A92-40010
British Airways Airbus A320 pilots' autothrust survey
[SAE PAPER 912225] p 636 A92-40023
RAE Bedford VAAC research project p 662 A92-40039
Bursts and sources of pressure fluctuation in turbulent boundary layers p 619 A92-40055
Second moment closure predictions of jet-on-jet impingement flows p 675 A92-40102
Vibration analysis of gas turbines by an intelligent knowledge-based system p 656 A92-40548
Recent research into the aerodynamics of ASTOVL aircraft in ground environment p 623 A92-40549
Acoustic scattering by a disk or annulus linking two concentric cylindrical shells. I - Theory and results for heavy exterior fluid loading. II - Results for heavy exterior fluid loading on both shells p 696 A92-40588
In-flight evaluation of Mach number at hypersonic speeds p 624 A92-40599
Shear progress p 609 A92-40880
Comment on 'Transition effects on airfoil dynamics and implications for subscale tests' p 703 A92-41247

Symmetry breaking in vortex flows on conical bodies
p 703 A92-41278
Windscreen departure p 723 A92-42500
The 1991 Cierva Lecture - Aberdeen and its influence on the evolution of the commercial IFR twin engined helicopter p 723 A92-43446
An experimental investigation of the oblique blade-vortex interaction p 712 A92-43447
The inviscid stability of supersonic flow past heated or cooled axisymmetric bodies p 712 A92-44363
Assembling the future p 783 A92-44895
The development of an intelligent human factors data base as an aid for the investigation of aircraft accidents
p 928 A92-44994
The effect on aircraft evacuations of passenger behaviour and smoke in the cabin p 834 A92-44998
International Powered Lift Conference, London, England, Aug. 29-31, 1990, Proceedings
[ISBN 0-903409-68-2] p 783 A92-45302
VSTOL engine design evolution - Growth of the Pegasus engine for Harrier p 860 A92-45306
Evolution of ASTOVL aircraft design
p 842 A92-45311
ASTOVL propulsion systems configuration and concept choice p 842 A92-45312
Recent developments at the Shoeburyness STOVL test facility p 881 A92-45314
Configuration effects on the ingestion of hot gas into the engine intake p 842 A92-45315
Hot-gas reingestion - Engine response considerations
p 860 A92-45317
Prediction and measurement of jet flowfield features for ASTOVL aircraft p 787 A92-45318
A progress report on ASTOVL control concept studies under the VAAC programme p 871 A92-45319
ASTOVL engine control p 860 A92-45321
Integrated flight control systems - Architectural considerations for future aircraft concepts
p 872 A92-45322
Ground surface erosion - British Aerospace test facility and experimental studies p 881 A92-45323
The experimental and computational study of jet impingement flowfields with reference to VSTOL aircraft performance p 787 A92-45324
Application of an unstructured Navier-Stokes solver to multi-element airfoils operating at transonic maneuver conditions
[AIAA PAPER 92-2638] p 796 A92-45507
Prediction of the viscous transonic aerodynamic performance of supercritical aerofoil sections
[AIAA PAPER 92-2653] p 805 A92-45569
Effect of flow rate on loss mechanisms in a backswept centrifugal impeller p 897 A92-45606
The relationship between tensile and flexural strength of unidirectional composites p 891 A92-45629
Calculation of potential flow around airfoils using a discrete vortex method p 808 A92-45827
Fibre optic rotary position sensors for vehicle and propulsion controls p 855 A92-46243
The use of optical sensors and signal processing gas turbine engines p 856 A92-46247
Propulsion system performance and integration for high Mach air breathing flight p 862 A92-46429
The inviscid compressible Goertler problem in three-dimensional boundary layers p 809 A92-46441
Through the looking glass p 856 A92-46449
The application of particle image velocimetry (PIV) in a short-duration transonic annular turbine cascade
[ASME PAPER 91-GT-221] p 899 A92-46825
Effect of model cooling on periodic transonic flow
p 813 A92-46900
Relative energy concepts in helicopter dynamics
p 846 A92-46925
Mesh adaptivity with the quadtree method
p 816 A92-47041
The construction, application and interpretation of three-dimensional hybrid meshes p 919 A92-47089
Generation of unstructured grids within a hybrid multi-block environment p 818 A92-47090
CIS engines. I - The range revealed
p 786 A92-47821
US Navy revisits escape modules p 849 A92-47975
Experience with the Johnson-King turbulence model in a transonic turbine cascade flow solver
p 821 A92-48207
Time-to-go estimation from infrared images
p 840 A92-48308
An integrated navigation system manager using federated Kalman filtering p 858 A92-48477
Robustness characteristics of fast-sampling digital PI controllers for high-performance aircraft with impaired control surfaces p 877 A92-48496
The simulation of inviscid, compressible flows using an upwind kinetic method on unstructured grids
p 933 A92-49515
Rotational coherent anti-Stokes Raman spectroscopy measurements in a rotating cavity with axial throughflow of cooling air - Oxygen concentration measurements
p 990 A92-49574
A comparison of measured and modeled broadband fluxes from aircraft data during the ICE '89 field experiment p 1003 A92-49771
Addressing the challenge of aircraft component design and manufacture from metal matrix composites
p 985 A92-50007
Development of active control technology for the next generation of combat aircraft p 975 A92-50008
British Aerospace Hawk into the 1990s
p 957 A92-50009
Carefree handling systems for helicopters
p 975 A92-50010
The use of math-dynamic models to aid the development of integrated health and usage monitoring systems
p 1006 A92-50013
A review of scale effects in unsteady aerodynamics
p 934 A92-50121
BA's 777 p 958 A92-51580
777 shaping up p 959 A92-52300
A general explicit or semi-explicit algorithm for compressible and incompressible flows
p 937 A92-52682
Heat transfer to a delta wing and two waverider wings in rarefied hypersonic flow p 937 A92-52748
Progress towards quieter civil helicopters
p 1011 A92-52847
The numerical simulation of flow about installed aero engine nacelle using a finite element Euler solver on unstructured meshes p 941 A92-52848
The application of a theoretical blade sailing model to predict the behaviour of articulated helicopter rotors
p 960 A92-52849
Steels for aerospace applications p 986 A92-52983
Nonlinear development and secondary instability of large-amplitude Goertler vortices in hypersonic boundary layers p 942 A92-53080
Silent solutions p 970 A92-53120
Regional challenge p 961 A92-53121
Russian realities p 932 A92-53250
Recent developments in data acquisition and control systems at the Aircraft Research Association Limited
p 1091 A92-54323
Particle image velocimetry measurements of the aerodynamics of a wind turbine p 1115 A92-54337
The interaction between a high-frequency gust and a blade row p 1135 A92-54484
CIS engines - The range revealed. II
p 1069 A92-54546
Joining a Ni-based creep-resistant (ODS) alloy by brazing p 1116 A92-54867
Diffusion bonding a creep-resistant Fe-ODS alloy
p 1117 A92-54868
Mikoyan's market-buster p 1052 A92-54981
The application of math-dynamic models to characterise a range of helicopter rotor system faults
p 1056 A92-56297
Lynx - A 50 year product? p 1056 A92-56307
Creation of a living specification for an experimental helicopter active flight control system through incremental simulation p 1057 A92-56312
Experimental investigation of helicopter coupled rotor/body control p 1086 A92-56318
Technology exploitation for in-service support of future rotorcraft p 1016 A92-56327
A study of helicopter rotor/fuselage response in low-speed manoeuvres - Comparison of theory with flight p 1086 A92-56334
The identification of coupled flapping/inflow models for hovering flight p 1058 A92-56335
The compound helicopter - A concept revisited
p 1058 A92-56341
Path identification in structural acoustics
p 1059 A92-56346
A high speed edgewise rotor using circulation control only in the reversed flow area p 1059 A92-56347
Measurements of the dynamic stall vortex convection speed p 1032 A92-56351
Comparison of recent results from different wind tunnel facilities along with comparisons of measured flight results and wind tunnel based predictions
[AIAA PAPER 92-3985] p 1060 A92-56809
A dynamic stiffness technique for the vibration analysis of stiffened shell structures p 1123 A92-56866
A comparison between the consequences of the liberal and non-liberal UK-Europe bilaterals
[TT-9101] p 18 N92-10018
Jet noise classical theory and experiments
p 54 N92-10602
Airframe noise p 55 N92-10605
Parallel processing applications for gas turbine engine control p 25 N92-11012
Radial inflow turbine study
[AD-A240169] p 26 N92-11015
Inverse problems and imaging (Pitman research notes in mathematics series Number 245)
[AD-A240333] p 53 N92-11737
Effect of twin fins on isolated tailplane lift-curve slope
[ESDU-91009] p 80 N92-11969
Maximum lift of wings with trailing-edge flaps at low speeds
[ESDU-91014] p 81 N92-11970
Application of Eigenstructure Assignment to the control of powered lift combat aircraft
[RAE-TM-FS-1009] p 135 N92-12004
Effects of wake and shock passing on the heat transfer to a film cooled transonic turbine blade
p 156 N92-12201
Heat transfer and instrumentation studies on rotating turbine blades in a transient facility p 156 N92-12203
Blade surface pressure measurements on the rotor of a model turbine stage in a transient flow facility
p 157 N92-12206
Variable impedance journal bearings for rotor-bearing systems p 157 N92-12270
Military and civil software standards and guidelines for guidance and control p 163 N92-12452
The development of a requirement specification for an experimental active flight control system for a variable stability helicopter: An Ada simulation in JSD
p 135 N92-12466
A review of UK aviation policy
[TT-9107] p 61 N92-12988
Comparison of solution of various Euler solvers and one Navier-Stokes solver for the flow about a sharp-edged cropped delta wing
[AD-B163639L] p 83 N92-12998
Laminar-flow secondary separation on a slender wing
p 85 N92-13006
Review of aircraft dynamic loads due to flow separation p 85 N92-13008
Asymmetric vortex flow over circular cones
p 86 N92-13014
An experimental investigation of the effect of fineness ratio on lateral force on a pointed slender body of revolution p 86 N92-13015
Control of forebody vortices by suction at the nose of the RAE high incidence research model
p 87 N92-13022
An experimental investigation of vortex flaps on a canard combat-aircraft configuration p 87 N92-13023
Lightning protection requirements for aircraft: A proposed specification
[RAE-TM-FS(F)-632-REV-ISSUE] p 187 N92-14007
Avionics software evolution p 199 N92-14052
The effects of manufacturing tolerances on the vibration of aero-engine rotor-damper assemblies
p 222 N92-14349
The application of a cylindrical-spherical floating ring bearing as a device to control stability of turbogenerators p 224 N92-14371
Flow over a delta wing at hypersonic speeds
p 181 N92-14993
Interference heating near fin/body junctions on hypersonic vehicles p 182 N92-14996
Hypersonic aerothermodynamic computations using a point-implicit TVD method p 183 N92-15006
Passenger knowledge of airline safety information
[CRANFIELD-AERO-9111] p 187 N92-15054
A method of estimating a flow breakdown boundary for aerofoils and swept wings in transonic flows
[ESDU-91021] p 258 N92-15970
Contribution of fin and tailplane to sideforce and yawing moment derivatives due to sideslip at supersonic speeds at low angles of attack
[ESDU-91031] p 259 N92-15971
Simplified method for the prediction of aerofoil excrescence drag magnification factor for turbulent boundary layers at subcritical Mach numbers
[ESDU-91028] p 259 N92-15972
Excrescence drag magnification factors at the drag-rise condition for aerofoils with a specified form of upper-surface pressure distribution
[ESDU-91029] p 259 N92-15973
Energy height method for flight path optimisation. Addendum A: Numerical method suitable for rapid use on IBM PC compatible computers
[ESDU-91016-ADD] p 272 N92-15987
Estimation of airborne performance in landing
[ESDU-91032] p 272 N92-15988
Design of experiments p 273 N92-17154
Modelling aspects and robustness issues in rotorcraft system identification p 274 N92-17159
SA 330 Puma identification results
p 274 N92-17162
Application areas for rotorcraft system identification: Simulation model validation p 274 N92-17164

Example of statistical techniques applied to cruise performance guarantees (Student's t distribution)
[ESDU-91018] p 276 N92-17843
Example of statistical techniques applied to autoland touchdown dispersion (confidence intervals for normal and skew distributions)
[ESDU-91019] p 268 N92-17844
Variability of standard aircraft performance parameters
[ESDU-91020] p 276 N92-17847
Boundary-layer transition and heat transfer on slender delta wings
[AERO-REPT-8904] p 262 N92-17849
Prediction of far-field harmonic noise from propellers
[ESDU-91033] p 416 N92-18074
Response of structures to galloping excitation: Background and approximate estimation
[ESDU-91010] p 399 N92-18091
Statistical methods applicable to analysis of aircraft performance data
[ESDU-91017] p 359 N92-18096
Marching with the parabolized Navier-Stokes equations. Problem 1: Numerical study of hypersonic viscous cone flow
[AERO-REPT-9007] p 344 N92-18231
Marching with the parabolized Navier-Stokes equations. Problem 2: Hypersonic viscous flow over a flat plate
[AERO-REPT-9008] p 345 N92-18232
Zonal solutions for a double-ellipse in a hypersonic flowfield
[AERO-REPT-9009] p 345 N92-18233
A numerical study of the stability of the swept attachment line boundary layer
[AERO-REPT-9103] p 345 N92-18293
Model parameter identification techniques for flight flutter testing
[AERO-REPT-9105] p 380 N92-18294
Propagation of shock waves through clouds
[AERO-REPT-9104] p 400 N92-18317
Towards the computation of turbulent hypersonic flows
[AERO-REPT-9106] p 345 N92-18318
Aircraft aerodynamics and stability and control during air-to-air refueling
[AERO-REPT-9017] p 380 N92-18321
The Goldstein Engineering Research Laboratory
[AERO-REPT-8906] p 308 N92-18322
The installation of the AVRO 9 by 7 foot low-speed wind tunnel at the University of Manchester (England)
[AERO-REPT-9005] p 385 N92-18341
The development of fatigue management requirements and techniques p 360 N92-18572
Aircraft fatigue management in the Royal Air Force p 363 N92-18591
Advanced tactical fighter engine
[ETN-92-90840] p 376 N92-18728
An evaluation of the Royal Air Force Shorts Tucano Navigation Instruments Trainer: The NAVIT
[ETN-92-90841] p 354 N92-18729
Measurement of derivatives due to acceleration in heave and sideslip p 364 N92-18785
Use of stepwise regression techniques and kinematic compatibility for the analysis of EAP flight data p 365 N92-18790
Dynamic wind tunnel tests on control of forebody vortices with suction p 380 N92-18793
The 8th Symposium on Turbulent Shear Flows. Volume 1: Sessions 1-18
[AD-A243809] p 402 N92-18933
Introduction: Needs and approaches to reliability and quality assurance in design and manufacture p 402 N92-19005
Robust control system design with application to high performance helicopters p 382 N92-19621
Experimental studies of vortex flaps and vortex plates. Part 1: 0.53 m span 60 deg delta wing
[CRANFIELD-AERO-9113-PT-1] p 349 N92-19679
A study of the aeroelastic behaviour of helicopter rotor blades featuring swept tips p 367 N92-19701
Materials and process directions for advanced aero-engine design
[PNR-90814] p 378 N92-19938
Re-engining appears to offer best payback for young: Chapter 2 compliant aircraft
[PNR-90848] p 378 N92-19939
Present and future trends in turbine blade material and manufacturing technology
[PNR-90825] p 488 N92-20164
Use of CFD in the design of a modern multistage aero engine LP turbine design
[PNR-90862] p 472 N92-20179
Superplastic applications in aero engines
[PNR-90788] p 473 N92-20436
ETOPS: A developing scene
[PNR-90844] p 473 N92-20459
The 60 years of Bristol engines
[PNR-90845] p 473 N92-20460
The impact of aircraft noise control technology
[PNR-90846] p 512 N92-20461
Holographic flow visualization in rotating turbomachinery
[PNR-90837] p 500 N92-20491
Application of a water droplet trajectory prediction code to the design of inlet particle separator anti-icing systems
[PNR-90839] p 474 N92-20573
The environmental impact of commercial aviation: The evolution of exhaust emissions legislation and control technology
[PNR-90847] p 505 N92-20574
An evaluation of in-cabin safety features in passenger aircraft
[ETN-92-90656] p 449 N92-20794
The role of crack growth in defect assessment
[PNR-90798] p 501 N92-20909
The environmental challenges for the next supersonic aircraft
[PNR-90782] p 505 N92-20928
A review of icing research at the Royal Aerospace Establishment p 451 N92-21689
Emissions from aircraft: Standards and potential for improvement
[PNR-90768] p 476 N92-21740
Application of finite element methods to fracture mechanics
[PNR-90770] p 503 N92-21741
Environmentally sound
[PNR-90776] p 506 N92-21743
The search for new materials
[PNR-90777] p 490 N92-21744
UK airmisses involving commercial air transport: September - December 1990
[ETN-92-91050] p 452 N92-21746
The proposed revision to RTCA DO178A and its influence on system design
[PNR-90821] p 510 N92-21847
Compressing the compressor
[PNR-90824] p 476 N92-21848
The evolution of the bypass engine
[PNR-90832] p 476 N92-21850
Approach and landing guidance p 457 N92-21960
United Kingdom approach to deriving military ship helicopter operating limits p 465 N92-21966
Some implications for advanced STOVL operation from invincible class ships p 466 N92-21971
Recent developments at the Shoeburyness (England) STOVL Test Facility
[PNR-90806] p 572 N92-22096
Impact of regulation changes on engine design and certification
[PNR-90789] p 559 N92-22098
The problem of static pressure measurement in turbomachinery annuli using traversable instrumentation
[PNR-90791] p 591 N92-22099
A theoretical investigation of the induced drag of wing of finite aspect ratio
[CUED/A-AERO/TR-17(1991)] p 525 N92-22193
Separation of relaminarised boundary layers
[CUED/A-AERO/TR-16] p 592 N92-22209
Risk to hearing from overflight noise of military aircraft
[ISVR-TR-194] p 604 N92-22241
Aircraft gas turbine emissions: Their nature, technology for reduction, and a pollution comparison with channel tunnel transport
[ETN-92-91056] p 559 N92-22406
An investigation into the feasibility of providing a proximity warning device for search and rescue helicopters
[ETN-92-91057] p 530 N92-22408
Application of an automated multidisciplinary analysis and optimisation system to the design of aircraft structures p 551 N92-23233
Simultaneous stress and flutter optimization for the wing of a transport aircraft equipped with four engines p 571 N92-23238
Surface activation of Concorde by Be-7 p 605 N92-23295
Survey of experimental techniques for performance prediction p 552 N92-23954
Normal force of low aspect ratio wing-body combinations up to high angles of attack at supersonic speeds
[ESDU-91042] p 553 N92-24009
Aeronautical satellite system test and implementation p 676 N92-24095
Inmarsat aeronautical mobile satellite system: Internetworking issues p 677 N92-24098
Future developments in aeronautical satellite communications p 678 N92-24167
Aspects of unsteady blade-surface boundary layers and transition in axial turbomachines p 658 N92-24340
Finite element methods for integrated aerodynamic heating analysis
[NASA-CR-190353] p 633 N92-25959
Use of Markov methods in analysis of fault-tolerant systems with flexible repair policies
[PNR-90801] p 767 N92-27038
VSTOL engine design evolution: Growth of the Pegasus engine for Harrier
[PNR-90805] p 739 N92-27039
ASTOVL engine control
[PNR-90808] p 740 N92-27040
ASTOVL propulsion systems: Configuration and concept choice
[PNR-90809] p 740 N92-27041
Hot-gas reingestion engine response considerations
[PNR-90810] p 740 N92-27042
Simultaneous engineering in aero-gas turbine design and manufacture
[PNR-90811] p 740 N92-27043
Powder processing of aero-engine components
[PNR-90813] p 756 N92-27044
The changing role of experimentation in aeroengine R and D: The point of view of the research worker
[AD-A246372] p 740 N92-27062
Thermally sprayed coating systems for surface protection and clearance control applications in aero engines
[PNR-90802] p 741 N92-27422
Application of S1BYL2 to the AGARD WG18 compressor test cases p 768 N92-27452
Predictions and measurements of 3D viscous flow in a transonic turbine nozzle guide vane row p 741 N92-27466
The application of a Navier-Stokes CFD method to civil engine intake flows p 769 N92-27471
Computational modelling of turbulent flow in S-bends p 769 N92-27480
Modelling the vaporiser and primary zone flows for a modern gas turbine combustion chamber p 742 N92-27484
Magnetic suspension using high temperature superconducting cores p 772 N92-27789
An evaluation of some strategies for vibration control of flexible rotors p 773 N92-27800
Wind tunnel magnetic Suspension Systems at the University of Southampton, England p 751 N92-27804
Parallel knowledge based systems architectures for in-flight mission management p 728 N92-27904
Transonic aeroelastic calculations in both the time and frequency domains p 720 N92-27950
A review of scale effects on surfaces in unsteady motion p 722 N92-27962
Radial inflow turbine study
[AD-A246938] p 743 N92-28073
Applications of silicon hybrid multi-chip modules to avionics p 859 N92-28379
Practical considerations in designing the engine cycle p 869 N92-28460
Inlet distortion effects in aircraft propulsion system integration p 869 N92-28464
Fundamentals of structural optimisation p 851 N92-28470
Validation of simulation systems for aircraft acceptance testing p 852 N92-28531
Harrier GR MK 5/7 mission simulators for the Royal Air Force p 885 N92-28540
Initial validation of a R/D simulator with large amplitude motion p 886 N92-28546
Effective cueing during approach and touchdown: Comparison with flight p 886 N92-28552
Report on the workshop on Ion Implantation and Ion Beam Assisted Deposition
[AD-A250561] p 927 N92-28923
Turbulent spot generation and growth rates in a transonic boundary layer
[AD-A250221] p 909 N92-29118
Boundary layer induced noise in aircraft
[CUED/A-AERO/TR-18] p 927 N92-29201
Aeronautical Engineering Group publications, 1950 - present
[AERO-REPT-8907] p 910 N92-29683
Technical evaluation report on the Flight Mechanics Panel Symposium on Piloted Simulation Effectiveness
[AGARD-AR-315] p 983 N92-30769
An investigation into the interface between three closely spaced axi-symmetric bodies at subsonic speed
[CRANFIELD-AERO-9114] p 948 N92-31514
ASTOVL combat aircraft design synthesis and optimization
[CRANFIELD-AERO-9201] p 963 N92-31515
Aerodynamic centre of wing-body combinations
[ESDU-92024] p 1036 N92-32479
Contribution of tailplane-mounted twin fins to sideforce, yawing moment, and rolling moment derivatives due to sideslip
[ESDU-92007] p 1086 N92-32487
A background to the handling qualities of aircraft
[ESDU-92006] p 1087 N92-32780

Lift and rolling moment due to spoilers on wings with trailing-edge flaps deflected at subsonic speeds
[ESDU-92002;SUPPL] p 1037 N92-32782
Spray nozzle for fire control
[CA-PATENT-APPL-SN-2-011-94] p 1125 N92-32856
Active control of sound transmission through stiff lightweight composite fuselage constructions
p 1137 N92-32957
Aspects of compression in aerospace composites: Future requirements p 1109 N92-33036
Comparison of GLONASS and GPS time transfers between two west European time laboratories and VNIIFTRI p 1050 N92-33381
Radial inflow turbine study
[AD-A252783] p 1127 N92-33538
Re-engining for real stage 3 compliance
[PNR-90872] p 1072 N92-33748
An improved compressor performance prediction model
[PNR-90873] p 1072 N92-33749
The Rolls-Royce Trent
[PNR-90875] p 1061 N92-33750
The impact of air transport on the environment
[PNR-90876] p 1129 N92-33751
Joint study on the computerisation of in-field aero engines vibration diagnosis
[PNR-90799] p 1072 N92-33815
Fatigue crack growth of small corner defects from blunt notches in an aeroengine alloy
[PNR-90860] p 1111 N92-34019
Elementary flutter analysis p 1088 N92-34162
Flight flutter testing p 1089 N92-34163

USSR

On thermal-stress gas flows p 37 A92-10657
Unsteady incompressible viscous flow past an airfoil
p 3 A92-10662
Nonstationary forces on a wing airfoil
p 4 A92-10825
Calculation of the hardening factor for gas turbine engine components shot blasted in an ultrasonic field
p 38 A92-10850
An experimental study of subsonic separated flow over parawings p 4 A92-10901
Two-phase flows at supersonic velocities
p 4 A92-10907
Subsonic axisymmetric viscoelastic flow past thin tapered bodies of revolution p 6 A92-12134
Methyl-tert-butyl ether as a component of aviation gasolines p 34 A92-12146
Pressure on a cylinder with a screen in transverse flow p 6 A92-12164
Base pressure on an axisymmetric finned body during forced rotation in the autorotation regime
p 7 A92-12165
Evolution of three-dimensional flows during the interaction between conical shock waves and a turbulent boundary layer p 7 A92-12169
Comparative studies of flow around a wing profile in two wind tunnels p 7 A92-12170
Comparative analysis of the lift-drag ratio and heat flows toward the surface of wave riders of different configurations p 7 A92-12173
An efficient method for calculating three-dimensional transonic flow past air intakes p 7 A92-12178
Calculation of flow of a radiating gas in axisymmetric nozzles of specified shape p 7 A92-12179
Modeling of the vortex structure at delta wings of low aspect ratio by the discrete vortex method
p 7 A92-12203
Experimental and theoretical study of the improvement of the aerodynamic characteristics of supersonic flow past bodies with surface injection of a gas jet with particles
p 8 A92-12204
Calculation of gas combustion regimes in a counterflow vortex chamber p 34 A92-12209
A method for determining the parameters of mathematical generalizations of experimental data on convective heat transfer p 41 A92-12803
Vibration of a wing of finite span in subsonic flow at small distances from a solid boundary p 9 A92-12808
Synthesis of the algorithm of a spatial-temporal discriminator and the potential accuracy of the velocity meter p 41 A92-12828
Several results of lidar measurements of the characteristics of oblique visibility at an airfield
p 45 A92-12844
Heat transfer in supersonic flow past a single crater
p 63 A92-13741
Calculation of the base pressure and enthalpy behind a step in the path of two supersonic streams with allowance for the effect of boundary layers and heat fluxes
p 63 A92-13748
Experimental studies of the interaction of converging axisymmetric shock waves with sharp and blunt cones in supersonic flow p 63 A92-13749
A ionospheric-sounding experiment from an aircraft
p 160 A92-13809
Fundamentals of applied aerogasdynamics. I - Aerodynamics of wings (profiles), airframes, and their combinations p 64 A92-14280
Fundamentals of applied aerogasdynamics. II - Viscous flow past bodies. Control devices p 64 A92-14281
Main concepts of providing the static/fatigue strength of helicopters in the USSR p 110 A92-14455
Flight test control p 136 A92-15021
From the history of Soviet aviation - Aircraft of the Il'iushin design bureau (2nd revised and enlarged edition)
p 61 A92-15022
Influence of three-dimensional effects on hydrodynamics and heat transfer in subsonic flow of a viscous compressible gas in the initial section of a rectangular duct p 66 A92-15031
Evaluation of the fungicide properties of antifreeze additives for jet fuels p 141 A92-15070
Gas-generator with high-temperature path ceramic components
[ASME PAPER 91-GT-152] p 148 A92-15594
Development and bench test of high-temperature combustion chamber with structural ceramic components
[ASME PAPER 91-GT-315] p 126 A92-15691
MiG-29 prototype and development flight tests - General overview and high angle of attack investigation
p 113 A92-16064
Three-dimensional singularity of flow structure in an underexpanded supersonic jet p 78 A92-16679
Changing the structure and improving the aerodynamic characteristics of supersonic flow past bodies through ejection of a gas jet with particles p 78 A92-16680
Self-oscillatory interaction of an underexpanded jet with an obstacle in the presence of a supersonic wake
p 79 A92-16681
Feedback mechanism of self-oscillations in the case of an underexpanded supersonic jet impinging on a plane obstacle p 79 A92-16682
Stability of a viscous compressible shear layer with a temperature drop p 79 A92-16684
Asymptotics of the upper branch of the neutral curve at subsonic and transonic external flow velocities
p 79 A92-16705
Aerodynamic balance range of aircraft of different configurations p 134 A92-16801
Maximum mass allowance to justify passenger-carrying aircraft modification p 113 A92-16802
Optimization of the aerodynamic balance and parameters of the horizontal tail surfaces of the three-surface aircraft configuration with allowance for the capabilities of the stability and control augmentation system p 134 A92-16803
Consideration of the time lag of engine processes in the problem of VTOL aircraft control synthesis
p 134 A92-16807
Control of the landing of a flight vehicle in the grazing-incidence mode p 134 A92-16808
Problem of the optimal correction of a flight test program for an aircraft system p 113 A92-16809
Effect of inertia forces on the characteristics of a long hydrodynamic vibration damper in the mixed flow regime
p 154 A92-16811
Analysis of transonic flow over plane compressor cascades using the large-particle method
p 79 A92-16812
A discrete vortex study of stationary flow past three-dimensional lifting systems at subsonic and supersonic velocities p 79 A92-16813
Diffuser efficiency estimation parameters
p 79 A92-16814
Synthesis of wing profiles from chord velocity diagrams using quasi-solutions for inverse boundary value problems p 80 A92-16815
A model of gasdynamic loads on an oscillating nozzle shell p 80 A92-16817
Detuning from the natural resonances of the blade in the computer-aided design of blade rows for axial-flow compressors p 80 A92-16818
A method for determining the optimal composition of the measured parameters in diagnosing gas turbine engines p 128 A92-16819
Effect of the wake flow on the soundproofing of aircraft structures p 166 A92-16824
A study of the nonlinear stress-strain state of spring-type landing gear p 154 A92-16825
A study of a version of the boundary conditions of a two-dimensional spline in surface and line modeling
p 163 A92-16826
Effect of Eulerian inertia forces on the stressed state of the rotating components of aircraft turbomachines
p 128 A92-16828
A test bench for evaluating powerplant electrization
p 138 A92-16830
Effect of the blade height of the nozzle ring of axial-flow microturbines on the flow velocity factor and exit angle
p 128 A92-16831
The designer-FEM model interface based on the data base management concept p 163 A92-16832
Computer-aided equipment layout for the fuselage of maneuverable aircraft p 113 A92-16833
Aerodynamic damping of blade vibrations in turbomachines p 200 A92-18198
A probabilistic method for monitoring the remaining life of aircraft gas turbine engine components using the temperature limit criterion p 201 A92-18292
Soviet CFD - An international perspective
p 233 A92-20150
Holographic-interferometry methods employed for vibration-strength testing of aviation-engine workpieces
p 219 A92-20771
Numerical and experimental investigation of airframe-integrated inlet for high velocities
p 243 A92-21072
Optimization of the three-dimensional shape of lifting bodies of small aspect ratio at hypersonic velocities
p 244 A92-21602
Axisymmetric analogy for three-dimensional viscous flow problems p 244 A92-21617
Solution of the problem of three-dimensional flow past the blade rows of turbomachines with allowance for viscosity effects p 244 A92-21618
A hot-wire anemometer in compressible subsonic flow
p 244 A92-21623
Calculation of the parameters of separated flow behind a plane rounded body in the path of two supersonic flows p 244 A92-21624
Wave motions in a three-dimensional boundary layer
p 244 A92-21629
Processing and displaying radio navigation data
p 266 A92-21683
Evolution of ejection systems p 262 A92-21684
On the calculation of the compressible boundary layer on a nonplanar delta wing with supersonic leading edges
p 252 A92-23409
Computation of transonic flow over an airfoil at large Reynolds numbers p 252 A92-23414
Mathematical modeling of supersonic flow over a convex-concave formed body based on the Euler and Navier-Stokes equations p 252 A92-23416
A study of flow past bodies of revolution with a Riabushinskii generatrix p 252 A92-23502
Development of a combined fast method for studying the plane motions of rigid bodies in the atmosphere around the center of mass in the presence of perturbations
p 304 A92-23563
Effect of supersonic diffuser geometry on operation conditions p 310 A92-24599
On one method of constructing adaptive difference grids in aerodynamics problems p 311 A92-24902
Application of special series for studying nonstationary transonic gas flows p 311 A92-24904
On an adaptive numerical method for solution of high gradient problems p 410 A92-24905
On marching algorithms for solving stationary problems p 311 A92-24976
Problems of laminar-turbulent transition control in a boundary layer p 312 A92-24979
Control of laminar boundary layer separation
p 393 A92-24980
Construction of aerodynamic profiles
p 315 A92-25299
Automated thematic processing of aircraft scanner data gathered over pasture territory in Turkmenia
p 406 A92-25330
An experimental study of supersonic H2 combustion and heat transfer in a circular duct p 388 A92-25997
A variational method for solving the problem of motion of a profile of complex geometry in a fluid
p 397 A92-27482
Hypersonic flow of a viscous gas past sharp elliptical cones at angles of attack and slip p 336 A92-27531
Calculation of heat transfer and friction for a blunt body in the path of supersonic flow of a chemically equilibrium air-xenon mixture p 336 A92-27532
Radiant heat transfer in supersonic three-dimensional and axisymmetric flow of air past evaporating bodies
p 337 A92-27533
A method for the optical measurement of surface friction in supersonic flow p 337 A92-27537
Calculation of three-dimensional flow past blunt cones near the plane of symmetry for different flow regimes in the shock layer and in the presence of gas injection from the surface p 337 A92-27593
Effect of rarefaction on the nonstationary interaction of a supersonic underexpanded jet with a perpendicular obstacle p 337 A92-27594
Evolution of perturbations in a supersonic boundary layer p 337 A92-27596

Characteristics of the mechanism of separated flow pulsation ahead of a spike-tipped cylinder in supersonic flow p 337 A92-27597
Determination of duty factors from experimental data in local interaction theory p 338 A92-27645
On the experimental investigation of air-breathing engine of new schemes p 469 A92-29711
Carcinogenic hydrocarbons emission with gas-turbine engines exhaust gases p 504 A92-29726
The aviation kerosene burning in the non-uniform air flow p 487 A92-29728
Simulation of vibrational status of gas-turbine engine p 470 A92-29731
Control of the development of boundary layer disturbances p 423 A92-30126
Experimental investigation of the coefficients of the normal-force derivatives for rectangular wings with translational oscillations p 423 A92-30127
Computations of a transonic flow about an airfoil in a wind tunnel with porous walls p 423 A92-30128
The effect of wing twist optimized in the framework of the plane cross section hypothesis on the aerodynamic characteristics of a wing-body combination at hypersonic speeds p 424 A92-30129
Investigation of extremal field behavior for two-dimensional linear problems in flight mechanics p 509 A92-30130
The analysis and approximate representation of the optimal control law for a maneuverable aircraft p 479 A92-30131
Estimating the probability of a safe flight for an aircraft flying under the effect of disturbances p 479 A92-30132
Problems of strength and aeroelasticity of present-day propfans p 471 A92-30133
Aerodynamic wing-nacelle integration p 458 A92-30134
Bodies of revolution with minimal wave drag at transonic gas flow velocities p 424 A92-30135
Generation of several wave packets in the boundary layer of a wing profile p 424 A92-30136
Numerical modeling of self-oscillations for a small-aspect-ratio delta wing using measurements of roll motion at large angles of attack p 424 A92-30138
A method for estimating the minimum distance between two flight vehicles during their separation p 486 A92-30139
Selection of efficient primary-structure/force configurations for aircraft lifting surfaces subjected to displacement constraints p 458 A92-30140
Analysis of the efficiency of some structural-inspection strategies in aircraft maintenance p 419 A92-30141
Reducing the background noise level in the test section of a wind tunnel for transonic flow velocities p 511 A92-30143
Development of a method for calculating the effect of the propeller slipstream on transonic flow over the wing p 424 A92-30144
Breakdown of an axisymmetric laminar wake p 424 A92-30145
Flow of a viscous twisted fluid film on the surface of a blunt body in supersonic flow of a gas p 424 A92-30146
Gasdynamic calculation of an impulse wind tunnel with a two-section plenum p 493 A92-30147
Dynamics of helicopter tip-over during taxiing p 479 A92-30149
Estimation of the optimal load characteristics of aircraft control levers p 479 A92-30150
Stability of stiffened panels with allowance for plasticity under nonstationary heating and loading p 493 A92-30152
An experimental study of transonic flow of a gas past wedges p 424 A92-30153
Effect of viscosity on the drag of slender axisymmetric bodies in hypersonic flow p 425 A92-30154
A pressure-drag-determination method for aerodynamic-interference problems p 425 A92-30157
A computational study of flow past bodies and heat transfer for isentropic compression flows p 425 A92-30158
An asymptotic transonic theory and optimal porosity of wind tunnel walls at M greater than about 1 p 425 A92-30159
An experimental study of tone-like noise in the flow past a wing at low flow velocities p 425 A92-30160
Investigating the feasibility of controlling the laminar-turbulent transition by means of laminarizing plates p 493 A92-30161
Effect of turbulent mixing on the characteristics of a turbofan-engine nozzle p 493 A92-30162
The feasibility of reducing induced wing drag by using crescent planform wings p 425 A92-30167
Determination of the objective-function gradient in the problem of minimizing stress concentration using the finite element method p 494 A92-30170
Experimental study of the characteristics of boundary-layer development on an airfoil p 425 A92-30171
The lift-drag ratio of a slender cone in viscous hypersonic gas flow p 425 A92-30172
Experimental study of an adjustable plane supersonic diffusor p 426 A92-30173
The effect of the angle-of-attack on laminar-turbulent boundary transition near the lower surface of triangular plates in a supersonic gas flow p 426 A92-30180
Calculating the steady-state nonlinear aerodynamic characteristics of thin wings near the interface between two fluids p 426 A92-30181
Numerical methods in the theory of boundary layer interaction with nonviscous flow p 426 A92-30185
Calculation of the rolling moment for a wing with a supersonic leading edge in the presence of sideslip p 426 A92-30186
Transverse correlation of the spectral components of pressure fluctuations on a plate ahead of a step p 426 A92-30187
Cooling of a sharp nose by extraneous gas injection into the viscous shock layer p 426 A92-30188
Characteristics of the phugoid motion of nonmaneuverable aircraft p 480 A92-30190
Analysis of the stability of the lateral motion of aircraft p 480 A92-30191
Determination of the mean duration of normal acceleration loads at the center of mass of aircraft during a flight in a turbulent atmosphere p 480 A92-30192
A study of the base pressure behind circular steps p 426 A92-30196
Effect of compressibility on the value of the acceptable roughness Reynolds number p 427 A92-30197
Asymptotic solution of the problem of ideal-fluid flow past the vertices of bodies and wings p 427 A92-30199
Combined method for the solution of plane direct problems of flow past bodies with jets p 427 A92-30200
The aerodynamic characteristics of grid fin wings p 427 A92-30201
Theoretical analysis of the effect of the porous walls of a wind tunnel on transonic flow past bodies of cone-cylinder type p 427 A92-30202
A method for calculating the separated flow past a circular cone, taking viscous-inviscid interaction into account p 427 A92-30203
Asymptotic form of the lower branch of the neutral curve in a transonic boundary layer p 427 A92-30204
Investigation of the effect of an ultrasonic acoustic field on boundary layer separation on an airfoil p 511 A92-30205
Aerodynamic characteristics of slender sharp-leading-edge delta wings with air scooping through the air intake at hypersonic velocities. I p 427 A92-30206
Theoretical analysis of a suction diffuser in the porous test section of a wind tunnel p 428 A92-30207
Effect of shock waves on the critical rate of bending-torsional flutter of an airfoil p 494 A92-30208
Generation of loads for finite-element models of large aircraft p 459 A92-30209
Effect of the longitudinal and transverse riblets of a flat plate on laminar-to-turbulent transition p 428 A92-30210
Numerical determination of the regions of existence of two types of shock-wave interaction p 428 A92-30211
Iterative algorithms for solving problems of the shaping of three-dimensional ducts p 428 A92-30212
Robustness of control systems with nonlinear parametric correction for certain types of perturbations p 509 A92-30311
Acoustic emission during changes in the aerodynamic load on the surface of a fan blade p 511 A92-30318
Uniqueness of solutions of the generalized Tricomi problem arising in the theory of the Laval nozzle p 428 A92-30319
Dynamics of the three-dimensional angular motions of rotating flight vehicles in the presence of the aerodynamic hysteresis of the moment characteristic p 428 A92-30371
An approximate method for calculating flow past solid wings of small aspect ratio based on a nonlinear theory of a continuous vortex surface p 428 A92-30373
Calculation of the aerodynamic characteristics of bodies of revolution in incompressible flow by the vortex surface method p 428 A92-30375
Restoration of aircraft engine nozzle block blades by vacuum arc brazing with controlled current p 471 A92-30381
An electromagnetic suspension system for aerodynamic studies p 483 A92-30409
CFD state-of-the-art in the U.S.S.R p 495 A92-31486
Numerical simulation of three-dimensional supersonic flow around aerodynamic configurations p 434 A92-31492
Wide-range combustion chamber of ramjet [AIAA PAPER 91-5094] p 472 A92-31696
Optimization of a lifting surface for minimum induced drag p 437 A92-31853
Analytical and experimental studies of the aerodynamic characteristics of a delta wing at a slip angle at high supersonic velocities p 437 A92-31854
Aerodynamic characteristics of a blunt delta wing with air bleed through an intake at supersonic and hypersonic velocities. II p 437 A92-31855
Singularity bypass algorithms in the numerical solution of equations of body motion relative to a center of mass in the atmosphere in the presence of disturbances p 437 A92-31857
Reduction of computational models in strength problems p 496 A92-31858
A parametric study of the lift-drag ratio of blunt cones p 437 A92-31860
A supplement to the second-order shock-expansion method p 437 A92-31861
A heat flow peak on the upwind surface of a blunt-leading-edge delta wing p 438 A92-31862
Possibility of reducing the wave drag of a hypersonic flight vehicle (wave rider) p 438 A92-31863
Lifting surface design using the principle of passive control of elastic characteristics p 480 A92-31865
Subsonic flow past a thin airfoil in a channel with porous walls p 438 A92-31867
Flow past a highly curved wing with tangential jet ejection p 438 A92-31868
Interaction of jets ejected from two-dimensional nozzles with a curved surface p 438 A92-31869
Calculation of three-dimensional separated flows in the framework of the unsteady Euler equations p 438 A92-31870
Flight studies of the riblet effect on drag variation p 438 A92-31871
Computational studies of transonic flow past a swept wing and the boundary layer characteristics p 438 A92-31872
The total drag of a body in the flow of a viscous heat-conducting gas p 439 A92-31873
Computational studies of the aerodynamic characteristics of delta wings with a subsonic leading edge p 439 A92-31874
Determination of the mass-flow-rate characteristics of porous panels p 439 A92-31875
Horizontal flight of an aircraft with periodic thrust reversal p 480 A92-31876
Experimental investigation of the air bypass effect in the shock-wave region on the aerodynamic characteristics of a wing profile p 439 A92-31877
Approximate determination of the effect of deviations of wing and tail geometry from design parameters on the drag coefficient of subsonic aircraft p 460 A92-31878
Experimental investigation of the optimal deflection of a single-slotted flap with different degrees of extension on a modern supercritical profile p 439 A92-31879
Aerodynamic characteristics of the combination of a wing with a cambered middle surface with a fuselage p 439 A92-31880
Interference of high-mounted propfan nacelles with an unswept wing and ways to attenuate it p 460 A92-31881
Characteristics of transonic flow past a configuration comprising a wing and a fuselage with a large midsection ratio p 439 A92-31882
Effect of the fuselage midsection ratio on the character of wing-fuselage aerodynamic interference p 439 A92-31883
Investigation of the aerodynamic features of flows past models using thin-film capacitance-type sensors of pressure oscillations p 440 A92-31884
Some characteristics of transonic flow past an airfoil in the case of developed separation p 440 A92-31885
Boundary-layer-separation control p 440 A92-31886
Consideration of the effect of viscosity in the problem of porous-wall induction p 440 A92-31887
Mathematical modeling of nonstationary viscous flow over a solid angle of finite span p 440 A92-31890
A study of flow of a fluid film on the surface of a plate in the case of slot injection p 496 A92-31892
Improving the efficiency of passenger aircraft during the landing approach p 460 A92-31893
A second-order control optimization method for nonlinear dynamic systems and its use for calculating optimal aircraft trajectories p 460 A92-31894
A procedure for calculating the static aeroelasticity characteristics of flight vehicles by the influence coefficient method using three-dimensional finite element schemes p 460 A92-31896

Lift characteristics of an infinite-span cylindrical wing of a thick symmetric profile at low subsonic velocities p 440 A92-31897
Aerodynamic effect of compression shocks on an oscillating aileron in transonic flow p 440 A92-31898
Structure of a boundary layer on the lower surface of a wing in flight and in a wind tunnel p 440 A92-31899
Selection of the time parameters of the probing pulse during the nonstationary irradiation of flight vehicles p 454 A92-31951
Characteristics of the energy analysis of optical radar in the case of nonstationary irradiation of flying objects p 454 A92-31955
A shock and an expansion wave in transonic flow p 440 A92-31961
An exact solution to edge effect problem for a finite-span wing in supersonic flow p 441 A92-31962
Boundary layer on slender wings of small aspect ratio p 441 A92-31963
A method of boundary layer laminarization on an oscillating wing p 441 A92-31969
Relationship between the rotating stall and vibrations of a blade row p 496 A92-31988
Synthesis of optimal digital systems for the stabilization of stochastically perturbed unstable dynamic systems p 601 A92-33754
Power spectrum of ring modes of pressure fluctuations at the surface of a cylinder in axial flow p 603 A92-33770
An experimental study of the noise of flow past a wing at low velocities p 603 A92-33771
A study of the precision characteristics of a gyroscopic gravimeter p 581 A92-33778
Dynamic synthesis of mechanical systems with a finite number of degrees of freedom p 603 A92-33790
The problem of body motion in a medium with resistance p 604 A92-36416
Nonparametric methods of regression analysis in problems related to the processing of aerodynamic balance calibration tests p 602 A92-36417
Structure of the separated flow region in a dihedral corner in front of an obstacle in supersonic flow p 524 A92-36420
A method for determining equivalent stresses in aviation gas turbine engine blades p 559 A92-36421
Determination of physicochemical constant in the wake of a body from ballistic experiments p 609 A92-36549
Vibrational relaxation effects in hypersonic flows of a viscous gas p 609 A92-36550
Numerical study of coupled heat transfer under conditions of filtering and film cooling of blunt anisotropic bodies p 610 A92-36552
Separated and cavitation flows - Principal properties and computational models
[ISBN 5-02-014005-8] p 610 A92-36600
Airfield construction (3rd revised and enlarged edition)
[ISBN 5-277-01070-X] p 670 A92-36606
Nonstationary aerohydroelasticity of spherical bodies
[ISBN 5-02-014006-6] p 670 A92-36611
EIPOS for ice-formation control on aircraft in flight - An alternative technique p 647 A92-40545
Design of wing profiles with tangential suction or injection p 624 A92-40602
Quick calculation of three-dimensional supersonic flow past nearly axisymmetric bodies p 624 A92-40605
A method for estimating the efficiency of gas turbine blade cooling systems p 657 A92-40606
Plotting the universal characteristic of a compressor in low-rpm and autorotation regimes p 657 A92-40607
A model of the operation of the pulsejet engine and a study of its characteristics p 657 A92-40608
Heat transfer on a cylindrical surface in the cavities of gas turbine engine rotors p 657 A92-40609
Low-frequency vibrations of the shutters of the variable Laval nozzle of gas turbine engines p 657 A92-40610
A criterion for estimating the economic and operational efficiency of the power distribution systems of commercial aircraft p 657 A92-40611
Local heat transfer in the perforation channels of turbine nozzle vanes p 657 A92-40615
A method for estimating the technological and economic efficiency of measures enhancing the reliability of aviation gas turbine engines p 657 A92-40621
An automated workstation for the half-scale testing of the flight vehicle stabilization circuit p 664 A92-40622
Calculation of rotational derivatives in the case of local interaction between flow and a body surface p 624 A92-40746
Some aspects of advanced aircraft development p 729 A92-41176
Decoupling of antennas using periodic structures p 725 A92-42634
Technique for estimating the strength of gas turbine guide vanes with stress raisers p 761 A92-42653
Possibility of increasing durability of blades with damages p 761 A92-42654
Thermal deformation of a polymer heat shield material on the descent trajectory p 754 A92-42655
An aerodynamic hypothesis for the wing aeroelasticity problem p 761 A92-42665
A numerical study of flow of a viscous gas in a Laval nozzle in the narrow channel approximation p 706 A92-42680
A method for determining the internal force characteristics of a model in external supersonic flow p 706 A92-42682
Aerodynamics of two-shock bodies derived by the gasdynamic design method p 707 A92-42683
A study of aerophysical and dynamic characteristics using an axisymmetric flight test vehicle with a reusable nose section p 707 A92-42684
Construction of a wing profile with a flap modeled by a point vortex p 707 A92-42726
Susceptibility of a supersonic boundary layer to acoustic perturbations p 707 A92-42730
Minimum-drag bodies moving in locality-law media p 779 A92-42732
Aerodynamic drag of a cylinder in two-phase flow p 707 A92-42735
Flow and shape correction problems for thin profiles in incompressible stream p 707 A92-42736
Nonstationary viscous shock layer in supersonic motion over an inhomogeneity p 708 A92-42737
Flow of a rarefied gas over a cylinder at angle of sideslip p 708 A92-42738
Gasdynamic design
[ISBN 5-02-029715-1] p 708 A92-42777
Local interaction theory
[ISBN 5-288-00516-8] p 779 A92-42778
Automation of flight vehicle design
[ISBN 5-217-01447-4] p 776 A92-42780
Visibility in the atmosphere and flight safety
[ISBN 5-286-00416-4] p 775 A92-42785
Data processing in navigation complexes
[ISBN 5-217-01060-6] p 725 A92-42789
Methods for determining atmospheric correction for radio-rangefinder measurements of inclined trajectories p 775 A92-44070
Modeling the effect of helicopter downwash on warm fog p 775 A92-44081
Use of the TMS-65 heating equipment at airports to create fog-dispersal zones above the runway to facilitate takeoff p 775 A92-44084
Aerodynamic characteristics of curved delta wings in the case of subsonic separated flow p 712 A92-44121
Aerodynamics of lifting configurations p 712 A92-44125
A mathematical model for the hydroelasticity problem concerning the motion of two flexible profiles in an ideal incompressible fluid. I p 712 A92-44127
Aerospace plane hydrogen scramjet boosting
[SAE PAPER 912071] p 891 A92-45451
Effect of a fan of rarefaction waves on the development of disturbances in a supersonic boundary layer p 809 A92-46519
Stability and inherent precision of two methods for solving motion and ablation equations for fireball-forming bodies in the earth atmosphere p 929 A92-46595
Smooth solutions for transonic gasdynamic equations
[ISBN 5-02-029345-8] p 809 A92-46626
The method of determinant equations in the applied theory of optimal systems - Systems with 'rigid' constraints and with fixed boundary conditions p 917 A92-46629
Enhancing the performance characteristics of engine fuels by means of surfactant additives p 892 A92-46631
Oscillations of balloon-flight altitude p 836 A92-46660
The flow pattern and external heat transfer investigation for gas turbine vanes end surfaces
[AIAA PAPER 92-3071] p 903 A92-48722
Experimental investigation of liquid carbonhydrogen fuel combustion in channel at supersonic velocities
[AIAA PAPER 92-3429] p 894 A92-48986
Similarity relations for calculating three-dimensional chemically nonequilibrium viscous flows p 827 A92-49188
Design and optimization of airfoils in non-stalling incompressible flow with a prescribed range of the angle of attack p 933 A92-49556
All-Union Conference on Optical Methods of Flow Research, 1st, Novosibirsk, Russia, Apr. 1991, Proceedings p 993 A92-51311
Processing of axisymmetric flow interferograms with density profile bends or discontinuities p 993 A92-51316
Conditions of optimality in problems of generalized control. II - Sufficient conditions of optimality p 1007 A92-51328
Technical tools of test automation for gas-turbine engines based on cluster CAMAC modules with an increased number of channels p 980 A92-51348
Identification of dynamic characteristics of flexible rotors as dynamic inverse problem p 220 N92-13962
JPRS report: Science and technology. USSR: Space
[JPRS-USP-91-007] p 211 N92-14101
History of EPOS air-launched spaceplane project p 211 N92-14103
Aerothermodynamic configuration of first generation aerospace planes (of Buran-type) and first flight results p 211 N92-14975
The effect of rounding the leading edges on the characteristics of separated flow past delta wings of low aspect ratio
[RAE-LIB-TRANS-2164] p 257 N92-15964
System of cryogenic security of the superconducting accelerator of relativistic nuclei-nucloitron
[DE91-643289] p 304 N92-16789
JPRS report: Science and technology. USSR: Engineering and equipment
[JPRS-UEQ-92-001] p 592 N92-22296
JPRS report: Science and technology. Central Eurasia: Engineering and equipment
[JPRS-UEQ-92-002] p 592 N92-22298
JPRS report: Science and technology. USSR: Engineering and equipment
[JPRS-UEQ-91-010] p 593 N92-22397
JPRS report: Science and technology. Central Eurasia: Space
[JPRS-USP-92-002] p 575 N92-23705
Dynamics of aerospace shuttles p 667 N92-24760
Progress of magnetic suspension systems and magnetic bearings in the USSR p 772 N92-27740
Cryogenic test rig with an aerodynamic magnetically levitated carriage p 750 N92-27792
Progress of magnetic suspension and balance systems for wind tunnels in the USSR p 751 N92-27803

CONTRACT NUMBER INDEX

Typical Contract Number Index Listing

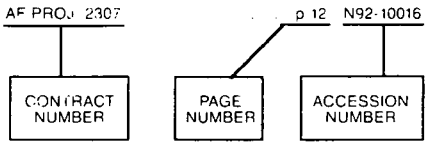

Listings in this index are arranged alphanumerically by contract number. Under each contract number, the accession numbers denoting documents that have been produced as a result of research done under the contract are shown. The accession number denotes the number by which the citation is identified in the abstract section. Preceding the accession number is the page number on which the citation may be found.

AF PROJ. 1123 ..... p 749 N92-26527
AF PROJ. 2300 ..... p 948 N92-31622
AF PROJ. 2307 ..... p 12 N92-10016
p 139 N92-13079
p 158 N92-13409
p 1124 N92-32632
AF PROJ. 2308 ..... p 33 N92-10062
p 896 N92-29580
AF PROJ. 2401 ..... p 225 N92-14386
AF PROJ. 2404 ..... p 13 N92-10986
p 139 N92-13078
p 197 N92-15069
AF PROJ. 2418 ..... p 279 N92-17204
AF PROJ. 2673 ..... p 285 N92-17260
AF PROJ. 3048 ..... p 988 N92-31462
AF PROJ. 3405 ..... p 888 N92-29709
AF PROJ. 7231 ..... p 512 N92-21719
p 485 N92-21720
AF-AFOSR-0004-87 ..... p 883 N92-28388
AF-AFOSR-0011-90 ..... p 1009 N92-30335
AF-AFOSR-0033-89 ..... p 1003 N92-31824
AF-AFOSR-0064-90 ..... p 770 N92-27546
AF-AFOSR-0091-90 ..... p 234 N92-15658
p 685 N92-26125
AF-AFOSR-0104-91 ..... p 1039 N92-33413
AF-AFOSR-0119-88 ..... p 158 N92-13409
AF-AFOSR-0131-90 ..... p 829 N92-28865
AF-AFOSR-0151-90 ..... p 986 N92-30256
AF-AFOSR-0188-90 ..... p 896 N92-29580
AF-AFOSR-0223-89 ..... p 489 N92-20695
AF-AFOSR-0235-89 ..... p 715 N92-27172
AF-AFOSR-0247-90 ..... p 767 N92-27352
AF-AFOSR-0294-89 ..... p 979 N92-31967
AF-AFOSR-0297-86 ..... p 743 N92-28076
AF-AFOSR-0310-89 ..... p 1111 N92-33624
AF-AFOSR-0321-90 ..... p 364 N92-18780
AF-AFOSR-0398-89 ..... p 1009 N92-30322
AF-AFOSR-0402-90 ..... p 774 N92-28171
AF-AFOSR-0427-89 ..... p 909 N92-29118
AF-AFOSR-0502-89 ..... p 830 N92-28888
AF-AFOSR-0541-89 ..... p 33 N92-10062
AF-AFOSR-82-0136 ..... p 246 A92-21980
p 246 A92-21982
p 434 A92-31547
AF-AFOSR-85-0075 ..... p 138 A92-17224
AF-AFOSR-85-0231 ..... p 3 A92-10688
AF-AFOSR-85-0273 ..... p 172 A92-18367
AF-AFOSR-85-0288 ..... p 1112 A92-54057
AF-AFOSR-86-0082 ..... p 335 A92-27092
AF-AFOSR-86-0112 ..... p 5 A92-11061
p 435 A92-31663
p 813 A92-46897
AF-AFOSR-86-0116 ..... p 52 A92-11467
AF-AFOSR-86-0178 ..... p 138 A92-17224
AF-AFOSR-86-0266 ..... p 5 A92-11062
p 320 A92-25758
p 431 A92-31155
p 812 A92-46882
p 1022 A92-54113
AF-AFOSR-87-0073 ..... p 49 A92-11426
AF-AFOSR-87-0074 ..... p 3 A92-10688
AF-AFOSR-87-0218 ..... p 434 A92-31547
AF-AFOSR-87-0312 ..... p 811 A92-46805
AF-AFOSR-87-0366 ..... p 176 A92-20739
AF-AFOSR-88-0001 ..... p 985 A92-50255
AF-AFOSR-88-0037 ..... p 706 A92-42531
AF-AFOSR-88-0076 ..... p 47 A92-11351
AF-AFOSR-88-0120 ..... p 614 A92-38456
AF-AFOSR-88-0163 ..... p 1024 A92-54919
AF-AFOSR-88-0197 ..... p 246 A92-21984
AF-AFOSR-88-0298 ..... p 197 A92-18611
AF-AFOSR-88-0309 ..... p 411 A92-27347
AF-AFOSR-89-0010 ..... p 1082 A92-55911
AF-AFOSR-89-0031 ..... p 47 A92-11351
AF-AFOSR-89-0033 ..... p 320 A92-25758
p 812 A92-46882
AF-AFOSR-89-0042 ..... p 942 A92-53080
AF-AFOSR-89-0276 ..... p 48 A92-11363
AF-AFOSR-89-0310 ..... p 216 A92-18369
AF-AFOSR-89-0315 ..... p 335 A92-27092
p 335 A92-27094
p 935 A92-50312
p 1022 A92-54113
AF-AFOSR-89-0397 ..... p 1032 A92-56351
AF-AFOSR-89-0487 ..... p 320 A92-25759
AF-AFOSR-89-0495 ..... p 47 A92-11347
AF-AFOSR-89-0502 ..... p 1026 A92-55367
AF-AFOSR-89-0552 ..... p 396 A92-27029
AF-AFOSR-90-0015 ..... p 476 A92-29061
p 421 A92-29355
AF-AFOSR-90-0024 ..... p 380 A92-28153
AF-AFOSR-90-0032 ..... p 1082 A92-55396
AF-AFOSR-90-0053 ..... p 50 A92-11430
AF-AFOSR-90-0064 ..... p 496 A92-31655
AF-AFOSR-90-0096 ..... p 340 A92-28043
AF-AFOSR-90-0105 ..... p 49 A92-11426
AF-AFOSR-90-0131 ..... p 620 A92-40085
p 794 A92-45498
p 804 A92-45563
AF-AFOSR-90-0173 ..... p 330 A92-26416
AF-AFOSR-90-0188 ..... p 321 A92-25763
AF-AFOSR-90-0217 ..... p 255 A92-23788
AF-AFOSR-90-0234 ..... p 604 A92-36006
p 1094 A92-56744
AF-AFOSR-90-0249 ..... p 257 A92-23804
AF-AFOSR-90-0261 ..... p 320 A92-25757
AF-AFOSR-90-0321 ..... p 1096 A92-56757
AF-AFOSR-91-0022 ..... p 803 A92-45559
AF-AFOSR-91-0042 ..... p 936 A92-50325
AF-AFOSR-91-0248 ..... p 38 A92-11041
AF-AFOSR-91-0310 ..... p 318 A92-25732
ARPA ORDER 6707 ..... p 303 N92-17438
ATD-88-STI-0221 ..... p 663 N92-25982
ATD-90-STI-6401 ..... p 878 N92-28584
ATD-91-BCA-7201 ..... p 482 N92-21253
ATD-91-DAC-7103 ..... p 979 N92-31656
ATD-91-GNC-7102 ..... p 962 N92-31208
BARR-10-119 ..... p 265 N92-17988
p 277 N92-17989
BMVG-T/RF41/I0008/I1407 ..... p 1058 A92-56340
CNR-88,00370,11 ..... p 217 A92-19812
CNR-89,01214,01 ..... p 243 A92-21504
CNR-90,01532,01 ..... p 243 A92-21504
p 339 A92-28005
CNR-91,01319,01 ..... p 339 A92-28005
CNT PROJ. 6902 ..... p 189 N92-14009
p 189 N92-14018
DA PROJ. 1E4-64804-D-279 ..... p 261 N92-17404
DA PROJ. 1L1-61102-AH-43 ..... p 180 N92-14972
DA PROJ. 1L1-61102-AH-45 ..... p 119 N92-13065
p 562 N92-22647
p 562 N92-22863
p 633 N92-26104
p 667 N92-26129
p 1009 N92-30898
DA PROJ. 1L1-61102-AH-52 ..... p 348 N92-19394
DA PROJ. 1L1-62101-AH-84 ..... p 757 N92-27752
DA PROJ. 1L1-62120-AH-25 ..... p 484 N92-20455
DA PROJ. 1L1-62211-A-47-AB ..... p 61 N92-12989
p 1001 N92-31155
DA PROJ. 1L1-62211-A-47-A ..... p 630 N92-24882
p 630 N92-24885
p 680 N92-24984
p 764 N92-26555
p 764 N92-26560
p 908 N92-28434
p 909 N92-29105
p 910 N92-29136
p 998 N92-30396
p 1002 N92-31349
p 1002 N92-31485
DA PROJ. 1L1-62211-A-47A ..... p 773 N92-27879
DA PROJ. 1L1-62618-AH-80 ..... p 1041 N92-33699
DA PROJ. 1L1-62705-AH-94 ..... p 300 N92-17258
DA PROJ. 1L2-36003-D-313 ..... p 944 N92-30394
DA PROJ. 1L6-2211-A-47-AA ..... p 367 N92-19846
DA PROJ. 3M4-63807-D-836 ..... p 22 N92-11004
DAAA15-87-C-0086 ..... p 484 N92-20455
DAAA15-91-C-0096 ..... p 704 A92-41320
DAAE07-89-C-R112 ..... p 674 A92-40020
DAAG29-82-K-0094 ..... p 516 A92-35727
DAAG29-84-K-0131 ..... p 813 A92-46901
DAAG29-84-K-131 ..... p 340 A92-28047
DAAG29-88-C-0003 ..... p 334 A92-27013
DAAH01-85-DA-015 ..... p 186 A92-20129
DAAH01-88-C-0341 ..... p 47 A92-11153
DAAH01-88-D-0002 ..... p 204 A92-19103
DAAH01-90-C-0373 ..... p 894 A92-48848
DAAH01-90-C-0813 ..... p 395 A92-26235
DAAH01-91-C-R061 ..... p 287 N92-17325
DAAJ02-86-C-0006 ..... p 153 A92-15698
DAAJ02-86-C-0009 ..... p 961 N92-30878
DAAJ02-89-C-0035 ..... p 122 A92-15543
DAAJ09-90-G-0022 ..... p 1055 A92-56279
DAAK51-79-C-0037 ..... p 848 A92-47408
DAAL03-86-D-0001 ..... p 562 N92-22647
p 729 N92-28079
DAAL03-86-G-0013 ..... p 883 A92-48908
DAAL03-86-G-0039 ..... p 176 A92-20736
p 703 A92-41269
DAAL03-86-G-0044 ..... p 72 A92-15584
p 175 A92-20727
p 825 A92-48897
p 909 N92-28879
p 911 N92-29933
DAAL03-86-G-0109 ..... p 569 A92-35770
DAAL03-86-K-0056 ..... p 568 A92-35747
p 1076 A92-55229
DAAL03-86-K-0171 ..... p 51 A92-11464
DAAL03-87-G-0011 ..... p 620 A92-40085
p 799 A92-45536
DAAL03-87-G-0017 ..... p 217 A92-19618
DAAL03-87-K-0010 ..... p 813 A92-46895
DAAL03-87-K-0023 ..... p 65 A92-14428
p 584 A92-34410
p 730 A92-43046
p 846 A92-46922
p 1055 A92-56178
DAAL03-87-K-0037 ..... p 875 A92-46933
DAAL03-87-K-0127 ..... p 995 A92-52722
DAAL03-88-C-0002 ..... p 10 A92-13212
p 65 A92-14359
p 564 A92-34480
p 564 A92-34481
p 547 A92-35772
p 521 A92-35787
p 874 A92-46923
p 813 A92-46935
p 958 A92-50315
DAAL03-88-C-0003 ..... p 321 A92-25766
p 412 A92-28142
p 807 A92-45588
p 814 A92-46947
p 1085 A92-56314
DAAL03-88-C-0004 ..... p 847 A92-46927
DAAL03-88-C-0006 ..... p 1024 A92-54906
DAAL03-88-C-0028 ..... p 705 A92-41537

DAAL03-88-C-002 ..... p 316 A92-25577
p 544 A92-35680
DAAL03-88-C-004 ..... p 1054 A92-56156
DAAL03-88-C-022 ..... p 216 A92-18377
DAAL03-88-K-0106 ..... p 413 N92-19397
DAAL03-89-C-0003 ..... p 66 A92-14446
DAAL03-89-C-0004 ..... p 794 A92-45496
DAAL03-89-C-0013 ..... p 256 A92-23800
DAAL03-89-C-0027 ..... p 250 A92-22171
DAAL03-89-K-0007 ..... p 580 A92-32746
p 564 A92-34479
DAAL03-89-K-0027 ..... p 987 N92-30874
DAAL03-89-K-0092 ..... p 255 A92-23783
p 508 A92-29248
p 483 N92-21752
p 447 N92-21753
DAAL03-90-C-0013 ..... p 1024 A92-54906
DAAL03-90-G-0008 ..... p 50 A92-11430
DAAL03-90-G-0021 ..... p 813 A92-46895
DAAL03-90-G-0096 ..... p 336 A92-27099
DAAL03-90-G-0129 ..... p 217 A92-19618
p 395 A92-26249
DAAL03-91-G-0019 ..... p 380 A92-28153
DAAL03-91-G-0023 ..... p 435 A92-31663
p 436 A92-31677
p 1022 A92-54111
DAAL03-91-G-0026 ..... p 620 A92-40085
DACA76-91-C-0005 ..... p 1008 A92-52455
DACA76-91-C-0006 ..... p 1008 A92-52455
DAHC35-89-D-0030 ..... p 46 A92-11191
p 1044 N92-33288
DAJA45-89-C-0006 ..... p 26 N92-11015
p 743 N92-28073
p 1127 N92-33538
DAJA45-89-M-0086 ..... p 53 N92-11737
DAJA45-90-C-0037 ..... p 999 N92-30766
DAJA45-91-M-0079 ..... p 402 N92-18933
DASG60-86-C-0013 ..... p 705 A92-41348
DASG60-87-C-0042 ..... p 758 A92-41323
p 778 A92-41324
p 779 A92-41332
p 896 A92-45130
DASG60-87-C-0066 ..... p 1135 N92-33920
DASG60-90-C-0134 ..... p 704 A92-41318
DE-AC01-89ER-30148 ..... p 767 N92-27394
DE-AC02-83CH-10093 ..... p 301 N92-16458
p 262 N92-17874
p 302 N92-17875
p 410 N92-19633
p 505 N92-20245
p 598 N92-22971
p 598 N92-23119
p 689 N92-25498
p 1004 N92-30837
p 1004 N92-31498
DE-AC02-88ER-13895 ..... p 391 A92-24717
DE-AC04-76DP-00789 ..... p 4 A92-10691
p 254 A92-23779
p 496 A92-32177
p 812 A92-46890
p 812 A92-46891
p 817 A92-47057
p 900 A92-47071
p 940 A92-52821
p 1104 A92-55311
p 1122 A92-56828
p 35 N92-11203
p 229 N92-15392
p 241 N92-15962
p 385 N92-18290
p 401 N92-18705
p 386 N92-19978
p 488 N92-20132
p 498 N92-20143
p 489 N92-20858
p 505 N92-21040
p 689 N92-25049
p 667 N92-25315
p 640 N92-25470
p 765 N92-26698
p 765 N92-26853
p 943 N92-30367
p 999 N92-30893
p 1000 N92-30903
p 957 N92-31746
p 1003 N92-31933
DE-AC05-76OR-00033 ..... p 41 N92-10174
DE-AC05-84OR-21400 ..... p 46 A92-11473
p 11 N92-10010
p 238 N92-15761
p 289 N92-16128
p 385 N92-18069
p 376 N92-18230
p 401 N92-18550
p 500 N92-20341
p 490 N92-21063
p 455 N92-21201
p 579 N92-23223
p 679 N92-24892
p 669 N92-25223
p 739 N92-26697
p 909 N92-28814
p 1129 N92-33271
DE-AC06-76RL-01830 ..... p 297 N92-16281
DE-AC07-76ID-01570 ..... p 163 N92-12440
DE-AI01-91CE-50306 ..... p 658 N92-24539
DE-FC05-85ER-25000 ..... p 322 A92-25771
p 524 A92-36359
DE-FG01-82CE-15144 ..... p 648 N92-24556
DE-FG01-86CE-15301 ..... p 648 N92-24556
DE-FG01-89CE-15426 ..... p 401 N92-18515
DE-FG01-90CE-15470 ..... p 680 N92-25054
DE-FG02-87ER-13750 ..... p 995 A92-52722
DE-FG02-88ER-25053 ..... p 936 A92-50325
DE-FG03-87ER-53262 ..... p 512 N92-21046
DE-FG05-91ER-81207 ..... p 794 A92-45496
DE-FG06-90ER-54095 ..... p 1136 N92-32595
DE-FG07-89ER-12893 ..... p 52 A92-11472
DEN3-335 ..... p 123 A92-15566
p 142 A92-15590
DEN3-336 ..... p 142 A92-15590
p 682 N92-25649
DFG-HU-254/8 ..... p 85 N92-13010
DFG-PE-350-2/2 ..... p 675 A92-40103
DFG-SFB-167 ..... p 763 A92-44326
DFG-SFB-204 ..... p 688 A92-39102
DFG-SFB-212 ..... p 269 A92-21007
p 271 A92-23782
DFG-SFB-253 ..... p 471 A92-31685
DFG-SFB-255 ..... p 1097 A92-56784
DFG-SFB-259 ..... p 1104 A92-57254
DFG-SFB-25 ..... p 521 A92-35783
DFG-ZI-18/32 ..... p 611 A92-36843
DND-FE-C0220788NRC21 ..... p 159 N92-13454
DND-FE-847787FACBF ..... p 489 N92-21018
DOD/FA7INA-AP ..... p 1071 N92-33105
DREA-W7707-8-1140-01-SC ..... p 1038 N92-32811
DRET-BC-87-001-54 ..... p 81 N92-11972
DRET-85-072 ..... p 82 N92-11980
DRET-85-092 ..... p 310 A92-24428
DRET-86-003-04 ..... p 353 N92-19350
DRET-86-003 ..... p 157 N92-12216
DRET-86-104 ..... p 990 A92-49516
DRET-88-218 ..... p 42 N92-11287
DRET-88-34-001 ..... p 349 N92-19682
DRET-88-351 ..... p 404 N92-19349
DRET-88-521 ..... p 947 N92-31508
DRET-89-001-118 ..... p 511 N92-20388
p 513 N92-21736
DRET-89-001-31 ..... p 411 A92-26368
DRET-89-002-36-1-3-4 ..... p 381 N92-19295
DRET-89-003-03 ..... p 138 N92-12006
DRET-89-003-07 ..... p 82 N92-11982
DRET-89-080 ..... p 820 A92-47876
DRET-89-1170 ..... p 82 N92-11981
DRET-89-117 ..... p 990 A92-49516
DRET-89-1433-DS-SR ..... p 1055 A92-56285
DRET-89-1433 ..... p 815 A92-46954
DRET-89-169 ..... p 366 N92-19225
DRET-89-174 ..... p 347 N92-19252
DRET-89-204 ..... p 1037 N92-32769
DRET-89-34-001 ..... p 13 N92-10989
p 43 N92-11310
p 406 N92-19976
p 908 N92-28788
p 829 N92-28789
p 1037 N92-32773
p 1125 N92-32776
DRET-89-34-01 ..... p 43 N92-11311
DRET-89-34-080-00-470-75-01 ..... p 349 N92-19925
DRET-89-34347 ..... p 411 A92-26368
DTFA 01-L-83-4-10579 ..... p 18 N92-10019
DTFA-01-84-Z-02030 ..... p 955 A92-49382
DTFA-02-90-C-90583 ..... p 916 A92-44982
DTFA01-L-83-4-10579 ..... p 301 N92-17028
DTFA01-82-Y-10513 ..... p 494 A92-30476
DTFA01-85-Z-02015 ..... p 93 N92-13042
DTFA01-87-C-00014 ..... p 18 N92-10993
p 103 N92-13049
p 116 N92-13058
p 116 N92-13059
p 116 N92-13060
p 139 N92-13077
p 190 N92-14033
p 202 N92-14064
p 191 N92-15061
p 462 N92-21210
p 637 N92-26028
p 641 N92-26101
DTFA01-87-C-0014 ..... p 724 N92-28052
DTFA01-89-C-00001 ..... p 1047 N92-32537
p 1048 N92-33098
DTFA01-89-Z-02030 ..... p 1124 N92-32686
DTFA01-89-Z-02033 ..... p 1004 N92-32103
DTFA01-89-Z-02050 ..... p 1101 N92-32903
DTFA01-90-C-00029 ..... p 1102 N92-34247
DTFA01-90-C-00042 ..... p 952 N92-30980
p 1142 N92-33305
DTFA01-90-P-01095 ..... p 96 A92-16639
DTFA01-90-Y-01009 ..... p 781 N92-27518
DTFA01-90-Z-02005 ..... p 915 A92-46788
DTFA01-90-4-01019 ..... p 46 N92-11593
DTFA01-91-Y-01004 ..... p 268 N92-15980
p 308 N92-18969
p 535 N92-23096
p 953 N92-31211
DTFA03-86-C-00041 ..... p 263 N92-16986
DTFA03-86-C-00042 ..... p 736 N92-27973
DTFA03-87-A-00021 ..... p 836 A92-46784
DTFA03-88-C-00024 ..... p 187 N92-15053
p 1045 N92-34151
DTFA03-89-A-00111 ..... p 297 N92-16181
DTFA03-89-C-00023 ..... p 191 N92-14034
p 456 N92-21404
DTFA03-89-C-00043 ..... p 971 N92-30303
p 1126 N92-33480
DTFA03-89-C-00050 ..... p 640 N92-24799
DTFA03-89-C-00057 ..... p 781 N92-26830
DTFA03-89-P-00692 ..... p 405 N92-19764
DTFA03-90-C-00039 ..... p 352 N92-18259
DTFA03-90-C-00050 ..... p 264 N92-17587
DTRS-57-87-C-00006 ..... p 638 A92-39567
DTRS-57-88-C-0078 ..... p 855 A92-44923
DTRS57-87-C-00006 ..... p 96 A92-16643
DTRS57-87-C-00109 ..... p 442 A92-32245
DTRS57-87-P-81048 ..... p 346 N92-18345
DTRS57-89-C-00006 ..... p 854 N92-29180
DTRS57-90-P-80922 ..... p 1127 N92-33627
EEC-AERO-0028-C ..... p 1137 N92-32956
EEC-EN3W-0035-GR ..... p 523 A92-36029
p 523 A92-36030
ERI PROJ. 3051 ..... p 946 N92-30977
ERI PROJ. 3067 ..... p 742 N92-27519
ESA-H-ST-13-01-AS ..... p 486 A92-30685
FAA-ADS-210 ..... p 855 A92-44923
FAA-T0603-B ..... p 573 N92-22503
FAA-T0603-S ..... p 1048 N92-33308
FAA-T0604-S ..... p 534 N92-22210
FAA-T0704-E ..... p 957 N92-31838
FAA-T0707-A ..... p 268 N92-15983
FA220787NRC06 ..... p 129 N92-11997
FE220787NRC01 ..... p 114 N92-11990
FFWF PROJECT P-7003 ..... p 695 A92-39480
FMV-FFL-82260-89-262-73-001 ..... p 114 N92-11993
FY1455-89-N-0635 ..... p 987 N92-31399
F04606-89-D-0036 ..... p 870 N92-28686
F04704-92-C-0006 ..... p 925 A92-47028
F08635-86-C-0309 ..... p 128 A92-16584
F08635-87-C-0003 ..... p 705 A92-41537
F08635-87-C-0302 ..... p 264 N92-17259
F08635-87-K-0031 ..... p 51 A92-11464
F08635-89-C-0196 ..... p 278 A92-22482
p 903 A92-48844
F09063-85-G-3104 ..... p 810 A92-46781
F19628-83-C-0173 ..... p 401 N92-18897
F19628-87-C-0065 ..... p 729 N92-27964
F19628-87-C-0094 ..... p 736 N92-28004
F19628-88-C-0013 ..... p 42 N92-11237
F19628-89-C-0001 ..... p 103 N92-13052
p 191 N92-15058
p 773 N92-27864
F19628-90-C-0001 ..... p 301 N92-17028
F19628-90-C-0002 ..... p 1063 A92-55328
p 18 N92-10019
p 93 N92-13042
p 735 N92-27424
F29601-85-C-0038 ..... p 1026 A92-55364
F30602-86-C-0124 ..... p 779 A92-42606
F33600-88-D-0414 ..... p 264 N92-17478
F33601-89-D-0045 ..... p 346 N92-18825
F33615-C-86-3401 ..... p 762 A92-42949
F33615-83-C-3253 ..... p 994 A92-51545
F33615-84-C-2454 ..... p 148 A92-15540
F33615-84-C-3200 ..... p 27 A92-11374
F33615-84-C-3202 ..... p 54 N92-10598
p 235 N92-14779
F33615-85-C-2508 ..... p 35 N92-11213
F33615-85-C-2515 ..... p 129 A92-17176
F33615-85-C-2518 ..... p 36 A92-10102
p 149 A92-15647
p 149 A92-15648
p 150 A92-15649
F33615-85-C-3804 ..... p 966 A92-49318
F33615-85-C-5015 ..... p 490 N92-21159
F33615-86-C-2600 ..... p 35 N92-10100
F33615-86-C-2695 ..... p 154 A92-16615
p 287 A92-21052
F33615-86-C-3006 ..... p 949 N92-31777

F33615-86-C-3602 ..... p 472 A92-31689
F33615-86-C-3606 ..... p 876 A92-48491
p 876 A92-48492
F33615-86-C-3623 ..... p 380 N92-18791
F33615-86-C-5008 ..... p 994 A92-51545
F33615-86-D-0554 ..... p 16 A92-11170
F33615-87-C-1531 ..... p 277 N92-17221
F33615-87-C-1550 ..... p 210 A92-19061
p 729 A92-41222
F33615-87-C-2702 ..... p 154 A92-16615
F33615-87-C-2767 ..... p 121 A92-15520
p 137 A92-15713
p 389 A92-27053
F33615-87-C-2806 ..... p 970 A92-50528
F33615-87-C-2808 ..... p 655 A92-40002
F33615-87-C-2822 ..... p 121 A92-15520
p 137 A92-15713
F33615-87-C-3228 ..... p 978 N92-30323
F33615-87-C-3402 ..... p 171 A92-17842
F33615-87-C-3403 ..... p 396 A92-26799
p 995 A92-51925
F33615-87-C-3413 ..... p 116 N92-13063
F33615-87-C-3607 ..... p 326 A92-26275
F33615-87-C-5232 ..... p 490 A92-28633
F33615-87-D-1451 ..... p 858 A92-48475
F33615-87-D-1452 ..... p 967 N92-30524
F33615-88-C-0003 ..... p 923 N92-29188
F33615-88-C-0014 ..... p 888 N92-29505
F33615-88-C-1713 ..... p 922 A92-48518
F33615-88-C-1720 ..... p 781 N92-26863
F33615-88-C-1739 ..... p 920 A92-48220
p 858 A92-48567
F33615-88-C-2816 ..... p 868 N92-28294
F33615-88-C-2817 ..... p 389 A92-26850
p 895 N92-28398
F33615-88-C-2823 ..... p 152 A92-15681
F33615-88-C-2832 ..... p 288 A92-22133
F33615-88-C-2907 ..... p 384 A92-27102
F33615-88-C-3014 ..... p 247 A92-22135
F33615-88-C-3205 ..... p 275 N92-17513
F33615-88-C-3400 ..... p 932 N92-30253
p 932 N92-30258
F33615-88-C-3606 ..... p 203 A92-18463
F33615-88-C-3612 ..... p 916 A92-44915
F33615-88-C-5433 ..... p 491 A92-28690
F33615-88-C-5447 ..... p 1107 N92-32525
F33615-89-C-0009 ..... p 751 N92-27836
F33615-89-C-0603 ..... p 728 N92-27916
p 1065 N92-33277
F33615-89-C-2970 ..... p 41 N92-10157
F33615-89-C-3001 ..... p 13 N92-10985
F33615-89-C-3205 ..... p 160 N92-13470
F33615-89-C-5605 ..... p 22 N92-11006
p 23 N92-11007
F33615-89-C-5616 ..... p 503 N92-21730
F33615-89-C-5618 ..... p 152 A92-15681
F33615-90-C-2028 ..... p 825 A92-48906
p 904 A92-48907
F33615-90-C-2033 ..... p 374 A92-27108
F33615-90-C-2050 ..... p 987 N92-30767
F33615-90-C-2066 ..... p 202 N92-14059
F33615-90-C-2077 ..... p 279 N92-17011
F33615-90-C-3206 ..... p 947 N92-31171
F33615-91-C-5713 ..... p 1108 N92-32629
F33657-79-C-0541 ..... p 277 A92-21080
F33657-81-C-2108 ..... p 845 A92-46800
F33657-83-C-0281 ..... p 149 A92-15641
F33657-84-C-2011 ..... p 280 N92-17552
F33657-84-C-2014 ..... p 277 A92-21080
F33657-87-C-2214 ..... p 468 A92-29356
p 934 A92-50272
F33657-88-C-2168 ..... p 386 N92-19642
F33657-89-C-2017 ..... p 122 A92-15543
F33657-91-C-2012 ..... p 824 A92-48742
F40600-84-C-0010 ..... p 403 N92-19080
F41608-87-D-A237 ..... p 591 A92-36156
F49620-84-C-0065 ..... p 701 A92-41223
F49620-85-C-0080 ..... p 717 N92-27712
F49620-85-C-0081 ..... p 405 N92-19386
F49620-86-C-0066 ..... p 219 A92-20746
F49620-86-C-0094 ..... p 431 A92-31155
F49620-86-C-0113 ..... p 321 A92-25763
p 374 A92-27007
F49620-86-C-0127 ..... p 281 A92-22162
F49620-86-C-0133 ..... p 219 A92-20741
p 1117 A92-54932
F49620-86-K-0022 ..... p 675 A92-40052
F49620-87-C-0081 ..... p 375 A92-28531
F49620-87-C-0108 ..... p 50 A92-11442
F49620-87-K-0003 ..... p 641 A92-36828
p 873 A92-46752
p 135 N92-13075
F49620-88-C-0006 ..... p 813 A92-46913
F49620-88-C-0014 ..... p 987 N92-31419
F49620-88-C-0022 ..... p 253 A92-23763
p 421 A92-29472
p 974 N92-32059
F49620-88-C-0041 ..... p 257 A92-23801
F49620-88-C-0047 ..... p 518 A92-34517
F49620-88-C-0053 ..... p 247 A92-22140
p 344 A92-28524
p 508 A92-29280
p 921 A92-48502
p 1075 A92-55200
F49620-88-C-0061 ..... p 432 A92-31183
F49620-88-C-0066 ..... p 290 N92-17682
F49620-88-C-0076 ..... p 1024 A92-54910
p 948 N92-31555
F49620-88-C-0077 ..... p 29 N92-11018
F49620-88-C-0082 ..... p 336 A92-27098
F49620-89-C-0011 ..... p 32 A92-11345
p 50 A92-11444
F49620-89-C-0014 ..... p 610 A92-36826
F49620-89-C-0029 ..... p 32 A92-11345
p 50 A92-11444
F49620-89-C-0045 ..... p 670 A92-36851
F49620-89-C-0060 ..... p 376 N92-19097
F49620-90-C-0058 ..... p 406 N92-19873
F49620-90-C-0070 ..... p 292 A92-22195
p 893 A92-48846
p 989 N92-32076
F49620-90-C-0076 ..... p 795 A92-45500
p 804 A92-45563
p 1142 N92-32338
F49620-91-C-0003 ..... p 1062 N92-34182
F49620-91-C-0042 ..... p 774 N92-27918
F49620-91-C-0085 ..... p 573 A92-33244
F49620-92-J-0014 ..... p 1007 A92-50490
F49620-92-J-0189 ..... p 803 A92-45557
F49629-88-C-0053 ..... p 302 A92-21176
GR/F/70495 ..... p 769 N92-27480
GRF/58646 ..... p 385 N92-18341
GRI-5086-233-1262 ..... p 765 N92-26816
GRI-5086-233-1436 ..... p 499 N92-20265
GRI-5087-234-1608 ..... p 756 N92-26521
GRI-5089-260-1893 ..... p 488 N92-20329
GRI-5089-296-1941 ..... p 771 N92-27715
IAR PROJ. 07332 ..... p 114 N92-11990
IAR PROJ. 07335 ..... p 129 N92-11997
MDA072-90-C-0039 ..... p 303 N92-17438
MDA903-87-C-0523 ..... p 888 N92-29709
MDA903-89-C-0003 ..... p 158 N92-13351
MDA903-91-C-0006 ..... p 1017 N92-33499
MDA904-90-H-4009 ..... p 411 A92-27347
MDA972-88-C-0047 ..... p 494 A92-30603
p 892 A92-46838
MDA972-89-C-0060 ..... p 412 N92-19247
p 510 N92-21392
MDA972-89-C-0061 ..... p 412 N92-19247
p 510 N92-21392
MDA972-90-C-0061 ..... p 1008 A92-52455
MIPR-ARO-114-91 ..... p 445 N92-21012
p 502 N92-21297
MIPR-N-86-28 ..... p 285 N92-17260
MIPR-N-87-5 ..... p 285 N92-17260
MIPR-N-88-15 ..... p 285 N92-17260
MOD-AT/2037/331 ..... p 937 A92-52748
MOD-2048/53/RAE(B) ..... p 568 A92-35748
p 568 A92-35749
p 570 A92-35786
MOESC-02252105 ..... p 790 A92-45417
MOESC-02452114 ..... p 822 A92-48704
MOESC-03238105 ..... p 790 A92-45417
MOESC-03238202 ..... p 822 A92-48704
MOESC-03750110 ..... p 822 A92-48704
MOESC-61420021 ..... p 790 A92-45417
MOESC-62850016 ..... p 843 A92-45397
MOESC-63302022 ..... p 790 A92-45417
MOESC-6355031 ..... p 49 A92-11418
NAC2-478 ..... p 1120 A92-56241
NAE PROJ. 03336 ..... p 489 N92-21018
NAE PROJ. 07335 ..... p 159 N92-13453
NAE PROJ. 07336 ..... p 159 N92-13454
NAGW-1022 ..... p 328 A92-26323
p 329 A92-26324
p 432 A92-31185
p 713 A92-44367
p 798 A92-45524
NAGW-1061 ..... p 1039 N92-33413
NAGW-1072 ..... p 171 A92-17822
p 619 A92-39988
p 796 A92-45510
p 803 A92-45557
p 1114 A92-54317
p 1034 A92-56836
NAGW-1128 ..... p 197 A92-18611
NAGW-1195 ..... p 918 A92-46817
NAGW-1331 ..... p 322 A92-25775
p 322 A92-25777
p 328 A92-26323
p 329 A92-26324
p 432 A92-31185
p 758 A92-41296
p 713 A92-44367
p 798 A92-45524
p 892 A92-47835
p 1113 A92-54199
NAGW-1708 ..... p 585 A92-34467
p 1054 A92-56176
p 44 N92-11377
p 963 N92-32111
NAGW-1809 ..... p 612 A92-37539
p 633 N92-25959
NAGW-1841 ..... p 294 A92-22796
NAGW-2127 ..... p 937 A92-52682
NAGW-674 ..... p 78 A92-16668
p 398 A92-28063
p 809 A92-46431
p 1098 A92-56791
NAGW-964 ..... p 935 A92-50304
p 1022 A92-54111
NAG1-1003 ..... p 441 A92-32182
NAG1-1005 ..... p 935 A92-50304
NAG1-1009 ..... p 777 A92-43399
NAG1-1013 ..... p 584 A92-34382
p 649 N92-25922
NAG1-1027 ..... p 874 A92-46931
p 282 N92-17019
NAG1-1032 ..... p 1094 A92-56744
NAG1-1037 ..... p 249 A92-22152
p 358 N92-18024
p 359 N92-18038
p 950 N92-32114
NAG1-1056 ..... p 1102 N92-34222
NAG1-1058 ..... p 275 N92-17316
NAG1-1061 ..... p 278 A92-22482
NAG1-1065 ..... p 53 N92-10347
p 830 N92-29329
NAG1-1067 ..... p 289 N92-17004
p 578 N92-22486
NAG1-1072 ..... p 255 A92-23788
NAG1-1081 ..... p 382 N92-19841
p 978 N92-30922
NAG1-1082 ..... p 488 N92-20193
p 1001 N92-31156
NAG1-1087 ..... p 935 A92-50313
p 348 N92-19359
p 852 N92-28720
NAG1-1097 ..... p 1003 N92-31619
NAG1-1111 ..... p 1094 A92-56744
NAG1-1116 ..... p 234 N92-15658
p 685 N92-26125
NAG1-1119 ..... p 237 N92-14789
NAG1-1133 ..... p 207 A92-17819
p 1094 A92-56727
NAG1-1135 ..... p 1036 N92-32648
NAG1-1142 ..... p 31 N92-11023
NAG1-1149 ..... p 1045 N92-34192
NAG1-1150 ..... p 1028 A92-55397
NAG1-1151 ..... p 582 A92-34357
NAG1-1156 ..... p 86 N92-13017
NAG1-1158 ..... p 180 N92-14969
NAG1-1160 ..... p 317 A92-25685
NAG1-1164 ..... p 1075 A92-55199
p 1131 A92-55271
NAG1-1180 ..... p 900 A92-47128
NAG1-1188 ..... p 233 A92-19619
p 340 A92-28044
p 446 N92-21456
p 910 N92-29830
NAG1-1192 ..... p 821 A92-47892
p 525 N92-22215
p 625 N92-24680
p 944 N92-30392
NAG1-1196 ..... p 332 A92-26948
NAG1-1197 ..... p 583 A92-34376
NAG1-1198 ..... p 179 N92-13999
NAG1-1201 ..... p 207 A92-17819
p 1094 A92-56727
NAG1-1205 ..... p 1038 N92-33304
NAG1-1207 ..... p 322 A92-25772
NAG1-1209 ..... p 1033 A92-56776
NAG1-1244 ..... p 480 A92-31692
NAG1-1253 ..... p 564 A92-34480
NAG1-1255 ..... p 650 N92-26017
NAG1-1260 ..... p 1038 N92-33063
NAG1-1265 ..... p 1024 A92-54911
p 595 N92-22662
NAG1-1278 ..... p 808 A92-45598
p 178 N92-13995
NAG1-1288 ..... p 903 A92-48844
NAG1-1291 ..... p 692 N92-26018
NAG1-1341 ..... p 203 A92-17840
p 1073 A92-55170
p 1075 A92-55205
p 1077 A92-55283
p 1132 A92-55376
p 1035 A92-57034

NAG1-1350 ..... p 971 N92-30753
NAG1-1358 ..... p 854 N92-30209
NAG1-1380 ..... p 1073 A92-55173
p 879 N92-29654
NAG1-168 ..... p 1108 N92-32586
NAG1-244 ..... p 1113 A92-54199
NAG1-321 ..... p 873 A92-46751
NAG1-327 ..... p 278 A92-22482
NAG1-361 ..... p 612 A92-37552
NAG1-363 ..... p 334 A92-27016
p 436 A92-31680
NAG1-372 ..... p 10 A92-13215
p 328 A92-26288
p 800 A92-45540
p 812 A92-46887
p 831 N92-29445
NAG1-421 ..... p 235 A92-18683
p 416 A92-26931
p 924 A92-45835
p 1135 A92-54909
NAG1-423 ..... p 394 A92-25786
p 334 A92-27016
p 436 A92-31680
NAG1-516 ..... p 27 A92-11383
NAG1-530 ..... p 432 A92-31167
NAG1-537 ..... p 1108 N92-32586
NAG1-560 ..... p 323 A92-26241
NAG1-58 ..... p 398 A92-28031
NAG1-619 ..... p 193 A92-20202
NAG1-645 ..... p 330 A92-26403
NAG1-648 ..... p 318 A92-25734
NAG1-664 ..... p 442 A92-32236
p 714 A92-44671
NAG1-681 ..... p 827 N92-28511
NAG1-690 ..... p 205 A92-20207
p 277 N92-17989
NAG1-710 ..... p 195 N92-14038
NAG1-727 ..... p 364 N92-18780
NAG1-732 ..... p 9 A92-13206
NAG1-739 ..... p 543 A92-34592
NAG1-745 ..... p 649 N92-25922
NAG1-776 ..... p 5 A92-11058
p 670 A92-36846
NAG1-793 ..... p 798 A92-45525
p 348 N92-19545
p 832 N92-29657
NAG1-795 ..... p 292 A92-22196
p 388 A92-25787
p 905 A92-48923
p 1094 A92-56745
NAG1-811 ..... p 376 A92-28534
p 519 A92-34826
p 13 N92-10982
p 446 N92-21456
NAG1-816 ..... p 840 N92-28718
NAG1-821 ..... p 1073 A92-55173
p 1074 A92-55174
p 663 N92-25648
NAG1-832 ..... p 320 A92-25759
NAG1-833 ..... p 535 A92-33193
p 541 A92-34414
NAG1-834 ..... p 48 A92-11381
p 302 A92-21181
p 350 A92-25743
p 1007 A92-50505
NAG1-838 ..... p 678 N92-24345
NAG1-842 ..... p 374 A92-27007
NAG1-844 ..... p 66 A92-15344
NAG1-849 ..... p 33 N92-11070
NAG1-858 ..... p 595 N92-22649
NAG1-862 ..... p 322 A92-25771
p 524 A92-36359
NAG1-872 ..... p 906 A92-49064
NAG1-878 ..... p 705 A92-41541
NAG1-886 ..... p 613 A92-38370
NAG1-891 ..... p 383 A92-25778
p 950 N92-32162
NAG1-907 ..... p 203 A92-17837
p 984 A92-50498
NAG1-921 ..... p 705 A92-41541
p 715 N92-27191
NAG1-922 ..... p 205 N92-14066
NAG1-928 ..... p 953 N92-31549
NAG1-937 ..... p 1094 A92-56744
NAG1-947 ..... p 1139 N92-33877
p 1139 N92-33878
p 1139 N92-33879
NAG1-951 ..... p 178 N92-13996
NAG1-974 ..... p 45 N92-11391
NAG1-978 ..... p 1000 N92-30988
NAG1-987 ..... p 907 N92-28361
NAG1-991 ..... p 731 N92-26655
NAG1-994 ..... p 792 A92-45478
p 1025 A92-55350
p 1025 A92-55353
NAG2-1005 ..... p 436 A92-31678
NAG2-191 ..... p 27 A92-11385
NAG2-209 ..... p 204 A92-18625
p 730 A92-43100
NAG2-243 ..... p 876 A92-48160
NAG2-297 ..... p 51 A92-11464
NAG2-389 ..... p 258 N92-15969
NAG2-409 ..... p 133 A92-14427
p 547 A92-35772
NAG2-462 ..... p 702 A92-41224
NAG2-477 ..... p 204 A92-18625
p 564 A92-34478
p 567 A92-35678
p 569 A92-35770
p 730 A92-43100
p 1085 A92-56315
NAG2-478 ..... p 600 A92-33304
NAG2-482 ..... p 1092 A92-55348
NAG2-490 ..... p 661 A92-39905
NAG2-502 ..... p 946 N92-30977
NAG2-541 ..... p 1126 N92-33307
NAG2-542 ..... p 221 N92-14262
p 221 N92-14263
p 499 N92-20197
NAG2-547 ..... p 1127 N92-33696
NAG2-554 ..... p 82 N92-11983
p 114 N92-11992
NAG2-561 ..... p 1060 A92-56354
p 1088 N92-33536
NAG2-575 ..... p 320 A92-25762
NAG2-591 ..... p 386 N92-19675
NAG2-592 ..... p 1021 A92-54110
p 1036 N92-32494
NAG2-595 ..... p 48 A92-11375
p 49 A92-11395
NAG2-596 ..... p 918 A92-46817
NAG2-607 ..... p 10 A92-13212
p 813 A92-46935
NAG2-629 ..... p 52 A92-11583
NAG2-651 ..... p 580 A92-33209
NAG2-654 ..... p 1131 A92-55282
NAG2-665 ..... p 812 A92-46894
NAG2-669 ..... p 1051 N92-34203
NAG2-691 ..... p 1076 A92-55230
p 135 N92-13073
NAG2-708 ..... p 716 N92-27558
NAG2-718 ..... p 334 A92-27014
NAG2-727 ..... p 1087 N92-33107
NAG2-733 ..... p 333 A92-26978
p 1095 A92-56756
p 259 N92-15974
NAG2-89 ..... p 411 A92-27347
NAG3-1000 ..... p 404 N92-19217
NAG3-1026 ..... p 371 A92-24403
NAG3-1087 ..... p 658 N92-24539
NAG3-1115 ..... p 26 N92-11014
NAG3-1124 ..... p 903 A92-48734
NAG3-1134 ..... p 341 A92-28192
p 723 A92-41262
NAG3-1137 ..... p 556 A92-34598
NAG3-1163 ..... p 1117 A92-54921
NAG3-1165 ..... p 473 N92-20196
p 716 N92-27376
p 924 N92-30207
NAG3-1177 ..... p 477 A92-29117
NAG3-1178 ..... p 340 A92-28043
NAG3-1198 ..... p 1009 N92-30898
NAG3-1202 ..... p 983 N92-31252
NAG3-1230 ..... p 557 A92-35687
NAG3-1275 ..... p 1021 A92-54090
NAG3-181 ..... p 223 N92-14357
NAG3-194 ..... p 3 A92-10688
NAG3-28 ..... p 723 A92-41262
NAG3-3139 ..... p 556 A92-34598
p 557 A92-35687
NAG3-323 ..... p 233 A92-19605
NAG3-33 ..... p 44 N92-11378
NAG3-354 ..... p 695 A92-39241
NAG3-398 ..... p 830 N92-29361
NAG3-512 ..... p 391 A92-24717
NAG3-520 ..... p 342 A92-28204
NAG3-639 ..... p 1010 A92-50296
NAG3-653 ..... p 1128 N92-34207
NAG3-666 ..... p 265 N92-17987
NAG3-695 ..... p 407 A92-26984
p 779 A92-41359
NAG3-712 ..... p 574 N92-22211
NAG3-724 ..... p 170 A92-17429
NAG3-72 ..... p 218 A92-20215
p 219 A92-20217
NAG3-730 ..... p 332 A92-26947
p 341 A92-28194
NAG3-732 ..... p 253 A92-23762
NAG3-746 ..... p 937 A92-52730
NAG3-767 ..... p 332 A92-26946
NAG3-768 ..... p 325 A92-26264
p 1044 N92-34105
NAG3-770 ..... p 508 A92-29316
NAG3-790 ..... p 501 N92-20954
NAG3-823 ..... p 302 A92-21191
NAG3-841 ..... p 907 A92-49126
NAG3-860 ..... p 1067 A92-54060
NAG3-904 ..... p 387 N92-19934
p 593 N92-22491
p 559 N92-22492
p 602 N92-22493
p 593 N92-22495
NAG3-917 ..... p 742 N92-27519
NAG3-927 ..... p 265 N92-17986
NAG3-983 ..... p 556 A92-34598
NAG3-998 ..... p 478 A92-29120
p 1052 A92-55300
NAG4-261 ..... p 601 A92-33345
NAG5-528 ..... p 285 A92-21023
NAG5-668 ..... p 14 A92-11019
NAG5-865 ..... p 502 N92-21385
p 502 N92-21433
NAG9-405 ..... p 690 A92-38699
NAL PROJ. FC-8-101 ..... p 412 N92-18252
NAL PROJ. ID-7-117H ..... p 359 N92-18073
NASA ORDER C-22955-P ..... p 1122 A92-56828
NASA ORDER C-30002-M ..... p 867 A92-49128
NASA ORDER C-30030-P ..... p 1121 A92-56371
NASA ORDER C-99066-G ..... p 44 N92-11328
p 597 N92-23560
p 678 N92-24514
NASA ORDER L-53177-C ..... p 163 N92-12440
NASA ORDER L-74809-C ..... p 178 N92-13997
NASA ORDER L-91172-C ..... p 735 N92-27424
NASA ORDER T-06038 ..... p 640 N92-24888
NASW-4162 ..... p 45 A92-12941
NASW-4234 ..... p 140 N92-12033
NASW-4430 ..... p 609 N92-24678
NASW-4435 ..... p 366 N92-19374
p 367 N92-19496
p 461 N92-20064
p 461 N92-20267
p 461 N92-20280
p 462 N92-20664
p 462 N92-20665
p 486 N92-20666
p 462 N92-20951
p 462 N92-21489
p 463 N92-21540
p 463 N92-21565
p 463 N92-21566
p 463 N92-21567
p 575 N92-22625
p 648 N92-25263
p 731 N92-26435
NAS1-15069 ..... p 578 N92-22637
NAS1-16048 ..... p 390 N92-19290
NAS1-16460 ..... p 539 A92-34392
NAS1-16984 ..... p 230 A92-20128
NAS1-17077 ..... p 702 A92-41228
NAS1-17492 ..... p 678 N92-24242
NAS1-17497 ..... p 539 A92-34392
NAS1-17721 ..... p 43 N92-11319
NAS1-17748 ..... p 230 A92-20128
NAS1-17794 ..... p 376 A92-28535
NAS1-17919 ..... p 271 A92-23768
NAS1-17925 ..... p 1125 N92-33139
NAS1-18027 ..... p 381 N92-19499
p 481 N92-20376
p 979 N92-32175
NAS1-18028 ..... p 191 N92-15060
p 276 N92-15991
p 268 N92-17512
p 368 N92-19871
p 957 N92-30978
p 1086 N92-32778
NAS1-18036 ..... p 663 A92-39229
p 166 N92-13757
NAS1-18037 ..... p 9 A92-13207
p 697 N92-25368
NAS1-18099 ..... p 602 N92-22643
p 602 N92-22644
NAS1-18107 ..... p 78 A92-16462
p 204 A92-18615
p 942 A92-53080
p 234 N92-15658
p 685 N92-26125
NAS1-18240 ..... p 9 A92-13206
p 174 A92-20211
p 255 A92-23780
p 431 A92-31157
p 617 A92-39340
p 618 A92-39965
p 618 A92-39967
p 703 A92-41246
p 809 A92-46264
p 678 N92-24344
p 679 N92-24547

	p 765	N92-26680
NAS1-18352	p 498	N92-20072
NAS1-18450	p 383	A92-25776
	p 396	A92-27009
NAS1-18458	p 106	A92-14390
	p 1094	A92-56743
NAS1-18471	p 8	A92-12741
	p 162	A92-14387
	p 416	A92-28032
	p 585	A92-34465
	p 800	A92-45539
	p 484	N92-21162
	p 571	N92-23229
NAS1-18565	p 964	A92-49273
	p 965	A92-49297
	p 53	N92-11706
NAS1-18570	p 298	N92-17006
NAS1-18584	p 172	A92-18372
	p 497	A92-32232
	p 589	A92-35696
	p 1090	A92-54319
NAS1-18585	p 395	A92-26436
	p 341	A92-28197
	p 618	A92-39967
	p 701	A92-41219
	p 702	A92-41227
	p 795	A92-45502
	p 1034	A92-56855
	p 46	N92-11593
	p 209	N92-15077
	p 261	N92-17547
	p 499	N92-20194
	p 1088	N92-33537
NAS1-18599	p 256	A92-23798
	p 343	A92-28224
	p 432	A92-31167
	p 435	A92-31639
	p 406	N92-19844
NAS1-18605	p 78	A92-16457
	p 78	A92-16462
	p 78	A92-16668
	p 395	A92-26437
	p 495	A92-31194
	p 585	A92-34467
	p 616	A92-39333
	p 712	A92-44363
	p 737	A92-44525
	p 816	A92-47042
	p 942	A92-53080
	p 185	N92-15047
	p 234	N92-15658
	p 402	N92-18965
	p 347	N92-19250
	p 447	N92-21465
	p 592	N92-22228
	p 963	N92-32111
NAS1-18607	p 53	A92-11053
NAS1-18667	p 1092	A92-54347
	p 443	N92-20283
NAS1-18703	p 950	N92-32226
	p 951	N92-32228
NAS1-18754	p 580	A92-32746
	p 961	N92-30304
NAS1-18758	p 1110	N92-33613
NAS1-18763	p 203	A92-17839
NAS1-18842	p 582	A92-34297
NAS1-18845	p 750	N92-27801
NAS1-18849	p 236	N92-14788
NAS1-18856	p 632	N92-25510
	p 715	N92-26651
	p 715	N92-26652
NAS1-18858	p 407	A92-27958
NAS1-18872	p 50	A92-11442
NAS1-18937	p 286	N92-16012
NAS1-18972	p 230	A92-17585
NAS1-19000	p 581	A92-34289
	p 583	A92-34381
	p 802	A92-45552
	p 803	A92-45560
	p 816	A92-46959
	p 114	N92-11992
	p 416	N92-19672
NAS1-1900	p 536	A92-33208
NAS1-19023	p 814	A92-46951
NAS1-19038	p 234	N92-14598
	p 556	N92-22395
	p 556	N92-22645
	p 652	N92-24689
NAS1-19060	p 697	N92-26130
	p 927	N92-28556
NAS1-19061	p 738	N92-26405
NAS1-19125	p 1096	A92-56761
NAS1-19136	p 815	A92-46957
	p 512	N92-21173
NAS1-19160	p 696	N92-24251
NAS1-19192	p 45	A92-12941
NAS1-19237	p 816	A92-46985
NAS1-19289	p 281	A92-22144
NAS1-19317	p 581	A92-34289
	p 582	A92-34307
	p 685	N92-25960
NAS1-19320	p 435	A92-31640
	p 890	A92-48849
	p 681	N92-25376
NAS1-19345	p 967	N92-30965
NAS10-11572	p 408	A92-27991
NAS2-11090	p 105	A92-14361
NAS2-12036	p 526	N92-22648
	p 527	N92-22865
NAS2-12343	p 846	A92-46924
NAS2-12568	p 433	A92-31487
NAS2-12635	p 815	A92-46953
NAS2-12722	p 117	N92-13064
	p 445	N92-21188
	p 482	N92-21253
	p 663	N92-25982
	p 878	N92-28584
	p 962	N92-31208
	p 979	N92-31656
NAS2-12787	p 810	A92-46787
NAS2-12800	p 995	A92-52470
NAS2-12853	p 247	A92-22135
NAS2-12961	p 917	A92-45489
NAS2-12962	p 330	A92-26435
NAS2-12989	p 803	A92-45555
NAS2-13072	p 195	N92-14039
NAS2-13079	p 814	A92-46952
NAS2-13127	p 885	N92-28545
NAS2-131313	p 871	N92-29427
NAS2-13155	p 811	A92-46798
	p 380	N92-18791
NAS2-13357	p 1022	A92-54117
NAS2-13391	p 303	N92-16605
NAS3-22448	p 352	N92-19276
NAS3-22767	p 404	N92-19277
NAS3-23687	p 377	N92-19726
NAS3-23691	p 151	A92-15663
NAS3-23698	p 402	N92-18971
NAS3-23720	p 780	A92-44512
NAS3-23721	p 1011	N92-31248
NAS3-23722	p 195	N92-14037
NAS3-23939	p 973	N92-31534
	p 1072	N92-33479
NAS3-23941	p 26	N92-11016
NAS3-23944	p 147	A92-15523
NAS3-24230	p 1073	N92-34236
NAS3-24357	p 406	N92-19775
NAS3-25266	p 65	A92-14407
	p 71	A92-15574
	p 75	A92-15670
	p 372	A92-26234
	p 331	A92-26932
	p 341	A92-28193
	p 344	A92-28526
	p 376	A92-28538
	p 583	A92-34360
	p 703	A92-41268
	p 800	A92-45541
	p 1020	A92-54004
	p 1020	A92-54012
	p 1023	A92-54161
	p 130	N92-13071
	p 166	N92-13759
	p 237	N92-14797
	p 258	N92-15967
	p 298	N92-16336
	p 261	N92-17347
	p 526	N92-22249
	p 596	N92-23267
	p 696	N92-24688
	p 887	N92-28673
	p 831	N92-29402
	p 972	N92-30972
	p 951	N92-32240
	p 1072	N92-33746
NAS3-25270	p 74	A92-15616
NAS3-25344	p 856	A92-46244
NAS3-25410	p 592	N92-22239
NAS3-25416	p 225	N92-14374
NAS3-25421	p 905	A92-48937
NAS3-25423	p 110	A92-14452
NAS3-25425	p 823	A92-48723
	p 12	N92-10979
NAS3-25446	p 276	A92-21074
NAS3-25450	p 310	A92-24653
	p 394	A92-26227
	p 436	A92-31679
NAS3-25453	p 1066	A92-54011
NAS3-25454	p 905	A92-48936
NAS3-25455	p 905	A92-48939
NAS3-25574	p 518	A92-34499
	p 520	A92-35689
NAS3-25644	p 1113	A92-54132
NAS3-25834	p 124	A92-15634
NAS3-25945	p 474	N92-20650
NAS3-25952	p 903	A92-48735
	p 943	N92-30298
NAS3-26059	p 326	A92-26266
NAS3-26146	p 1095	A92-56753
NAS3-26242	p 372	A92-25696
	p 971	N92-30569
NAS5-30343	p 770	N92-27649
NAS7-918	p 300	N92-17674
	p 413	N92-19428
	p 1000	N92-30923
NAS8-35018	p 973	N92-31910
NAS8-36719	p 224	N92-14367
NAS8-36720	p 225	N92-14391
NAS8-36955	p 493	A92-29610
	p 157	N92-12231
	p 359	N92-18347
	p 499	N92-20198
	p 1101	N92-33826
NAS8-37142	p 574	A92-34893
NAS8-37351	p 153	A92-15710
NAS8-37406	p 488	A92-32253
NAS8-37462	p 1124	N92-32265
NAS8-37465	p 221	N92-14344
NAS8-37814	p 820	A92-47872
NAS8-37821	p 580	A92-32942
NAS8-38870	p 42	N92-11297
NAS8-38892	p 821	A92-47894
NAS8-39184	p 753	N92-27403
NAS9-17195	p 37	A92-10435
NAS9-17840	p 286	N92-17167
	p 286	N92-17214
NAS9-17892	p 394	A92-26219
NAS9-17900	p 696	N92-24800
NAS9-18057	p 231	A92-17594
NAS9-18172	p 284	N92-15998
NAS9-18426	p 746	N92-28209
NCA2-216	p 17	A92-11380
NCA2-310	p 569	A92-35777
NCA2-326	p 432	A92-31163
NCA2-329	p 915	A92-46262
NCA2-397	p 9	A92-13206
	p 255	A92-23780
	p 703	A92-41246
NCA2-406	p 1026	A92-55365
	p 364	N92-18780
NCA2-417	p 322	A92-25775
NCA2-486	p 327	A92-26284
NCA2-512	p 162	A92-14368
	p 647	A92-40885
	p 730	A92-41263
	p 464	N92-21956
NCA2-526	p 685	N92-25962
NCA2-529	p 334	A92-27023
NCA2-548	p 589	A92-35674
NCA2-578	p 935	A92-50314
NCA2-581	p 255	A92-23780
NCCW-0011	p 583	A92-34376
NCC1-1002	p 171	A92-17822
NCC1-100	p 329	A92-26326
	p 329	A92-26327
	p 705	A92-41539
NCC1-112	p 328	A92-26323
	p 329	A92-26324
	p 713	A92-44367
NCC1-140	p 892	A92-47835
NCC1-141	p 1100	A92-56854
	p 888	N92-29352
NCC1-153	p 824	A92-48741
NCC1-158	p 1131	A92-55262
NCC1-22	p 432	A92-31185
	p 798	A92-45524
NCC1-29	p 1080	A92-55343
NCC1-46	p 442	A92-32239
	p 619	A92-39988
	p 792	A92-45480
NCC1-68	p 334	A92-27016
	p 631	N92-25175
	p 1128	N92-34043
NCC1-98	p 1035	A92-56858
	p 773	N92-27880
NCC1-99	p 777	N92-27831
NCC2-106	p 873	A92-46742
NCC2-237	p 833	A92-44931
NCC2-329	p 17	A92-11380
NCC2-346	p 347	N92-19354
NCC2-366	p 1057	A92-56316
NCC2-374	p 518	A92-34499
	p 588	A92-35673
	p 520	A92-35690
NCC2-387	p 1135	A92-54660
NCC2-420	p 342	A92-28202
	p 705	A92-41540
	p 935	A92-50309

NCC2-458 ..... p 379 A92-25733
p 874 A92-46802
NCC2-465 ..... p 716 N92-27399
NCC2-476 ..... p 685 N92-25962
NCC2-478 ..... p 1135 A92-54660
NCC2-487 ..... p 383 A92-25774
p 664 N92-25162
NCC2-498 ..... p 865 A92-48984
NCC2-507 ..... p 221 N92-14313
p 998 N92-30380
NCC2-508 ..... p 758 A92-41238
NCC2-522 ..... p 948 N92-31533
NCC2-536 ..... p 802 A92-45550
p 832 N92-29691
NCC2-553 ..... p 1032 A92-56747
p 185 N92-15048
NCC2-55 ..... p 281 A92-22143
p 341 A92-28199
p 611 A92-36848
p 619 A92-40059
p 805 A92-45568
p 1081 A92-55354
p 1082 A92-55393
NCC2-564 ..... p 248 A92-22142
p 340 A92-28036
NCC2-575 ..... p 1045 A92-55211
p 191 N92-14036
NCC2-581 ..... p 93 N92-13044
NCC2-582 ..... p 816 A92-46986
p 940 A92-52777
NCC2-583 ..... p 705 A92-41540
p 808 A92-45845
p 446 N92-21356
NCC2-585 ..... p 630 N92-24898
NCC2-586 ..... p 482 N92-21357
NCC2-596 ..... p 340 A92-28041
NCC2-604 ..... p 751 N92-27976
p 751 N92-27977
NCC2-605 ..... p 432 A92-31186
p 1026 A92-55355
p 692 N92-25264
NCC2-624 ..... p 281 A92-22161
NCC2-632 ..... p 325 A92-26261
NCC2-637 ..... p 258 N92-15966
p 950 N92-32177
NCC2-654 ..... p 945 N92-30740
NCC2-659 ..... p 604 A92-36006
NCC2-660 ..... p 625 N92-24803
NCC2-683 ..... p 946 N92-31157
NCC2-692 ..... p 1027 A92-55377
NCC2-704 ..... p 1039 N92-33424
NCC2-716 ..... p 385 N92-19218
p 573 N92-22195
p 888 N92-29655
NCC2-729 ..... p 793 A92-45493
NCC2-730 ..... p 796 A92-45508
NCC2-746 ..... p 865 A92-48984
NCC3-124 ..... p 716 N92-27377
NCC3-132 ..... p 1102 N92-34141
NCC3-165 ..... p 991 A92-50040
NCC3-189 ..... p 932 N92-31267
NCC9-16 ..... p 778 N92-28150
p 1134 N92-32865
NGL-05-020-243 ..... p 589 A92-35695
NGL-22-009-640 ..... p 205 A92-20207
p 369 A92-25745
p 1063 A92-55328
p 265 N92-17987
p 265 N92-17988
p 277 N92-17989
NGL-31-001-252 ..... p 204 A92-18620
p 255 A92-23783
p 379 A92-27082
p 508 A92-29248
p 1078 A92-55327
p 266 N92-17999
p 303 N92-18002
NGR-36-009-017 ..... p 96 A92-16643
p 100 A92-16963
p 454 A92-30023
p 650 A92-39561
p 269 N92-17994
NGR-36-009-17 ..... p 638 A92-39567
NGT-01-008-021 ..... p 234 N92-15870
p 212 N92-15877
NGT-40018 ..... p 327 A92-26284
NGT-50142 ..... p 292 A92-22196
NGT-50172 ..... p 335 A92-27093
NGT-50341 ..... p 610 A92-36827
p 797 A92-45517
NGT-50400 ..... p 906 A92-49064
NGT-50406 ..... p 542 A92-34500
p 610 A92-36838
NGT-50414 ..... p 1043 N92-32606
NGT-50444 ..... p 564 A92-34478
NGT-50714 ..... p 396 A92-26935
NGT-70161 ..... p 343 A92-28218
NIVR-RB-311.1-01501-N ..... p 828 N92-28709
NIVR-01101-N ..... p 828 N92-28660
NIVR-01501-N ..... p 444 N92-20473
NIVR-01502-N ..... p 829 N92-28713
NIVR-01604-N ..... p 691 N92-24411
p 908 N92-28712
p 1037 N92-32730
NIVR-01708-N ..... p 837 N92-28655
NIVR-01803-N ..... p 927 N92-28695
NIVR-01904-N ..... p 720 N92-27947
p 923 N92-28635
p 924 N92-29604
NIVR-03601-N ..... p 827 N92-28658
NIVR-07801-N ..... p 746 N92-27958
NR PROJ. C31-50 ..... p 229 N92-15385
NR PROJ. RB2-3-C-22 ..... p 299 N92-17168
NR PROJ. RM3-3-T-21 ..... p 907 N92-28253
NR PROJ. RR0-3308 ..... p 1129 N92-33220
NR PROJECT 432-5201 ..... p 174 A92-19611
NR PROJECT 4324-201 ..... p 3 A92-10690
NSCRC-77-0210-D006-14 ..... p 219 A92-20216
NSCRC-77-0401-E007-17 ..... p 1114 A92-54223
NSCRC-79-0210-D006-03 ..... p 1136 A92-56162
NSCRC-79-0401-E006-38 ..... p 331 A92-26443
NSCRC-80-0210-D006-04 ..... p 1106 A92-57101
NSCRC-80-0401-E006-41 ..... p 794 A92-45499
NSCRC-80-0401-E007-02 ..... p 672 A92-38867
NSCRC-80-0413-E007-11 ..... p 331 A92-26943
NSCRC-81-0401-E002-03 ..... p 249 A92-22170
NSCRC-81-0401-E019-01 ..... p 498 A92-32523
NSERC-A-1240 ..... p 50 A92-11431
NSERC-A-1671 ..... p 71 A92-15572
p 71 A92-15573
NSERC-A-2181 ..... p 309 A92-24418
p 702 A92-41231
p 1024 A92-54918
NSERC-A-2746 ..... p 676 A92-40148
NSERC-A-7801 ..... p 1067 A92-54104
NSERC-OGPIN-006 ..... p 295 A92-23269
NSERC-OGPIN-013 ..... p 690 A92-37534
NSERC-STREQ-040 ..... p 690 A92-37534
NSF ASC-87-19573 ..... p 78 A92-16462
NSF ATM-79-20399 ..... p 668 A92-38111
NSF ATM-82-05776 ..... p 188 A92-18172
NSF ATM-85-02517 ..... p 188 A92-18172
NSF ATM-87-02993 ..... p 188 A92-18172
NSF ATM-88-19676 ..... p 468 A92-32097
NSF ATM-89-12555 ..... p 188 A92-18172
NSF ATM-89-20428 ..... p 14 A92-11019
NSF CBT-87-05576 ..... p 696 A92-40866
NSF CBT-87-13833 ..... p 900 A92-47267
NSF CBT-88-09548 ..... p 995 A92-52722
NSF CBT-88-12070 ..... p 995 A92-52722
NSF CDR-88-03012 ..... p 49 A92-11426
p 476 A92-29061
p 421 A92-29355
NSF CTS-84-51610 ..... p 661 A92-39900
NSF CTS-86-57130 ..... p 1113 A92-54108
p 1117 A92-54931
NSF CTS-88-15670 ..... p 619 A92-40059
NSF CTS-89-13198 ..... p 415 A92-26441
p 933 A92-49498
p 935 A92-50293
NSF CTS-90-10594 ..... p 1112 A92-54044
NSF CTS-90-12309 ..... p 653 A92-36891
NSF CTS-90-17732 ..... p 497 A92-32264
NSF DDM-90-08451 ..... p 317 A92-25685
NSF DMC-86-15336 ..... p 177 N92-13961
NSF DMC-86-57917 ..... p 899 A92-46916
p 1024 A92-54911
NSF DMC-87-07648 ..... p 233 A92-19605
NSF DMS-88-11084 ..... p 380 A92-28153
NSF DMS-88-11863 ..... p 671 A92-37868
NSF DMS-89-01900 ..... p 38 A92-11041
NSF DMS-89-05334 ..... p 411 A92-27347
NSF DMS-89-10679 ..... p 432 A92-31160
NSF DMS-89-22805 ..... p 936 A92-50325
NSF DMS-90-0024 ..... p 936 A92-50325
NSF DMS-90-08223 ..... p 411 A92-27347
NSF ECD-88-03012 ..... p 421 A92-29355
NSF ECS-86-02524 ..... p 660 A92-36990
NSF ECS-86-12948 ..... p 507 A92-29132
NSF ECS-86-57561 ..... p 476 A92-29061
p 421 A92-29355
NSF ECS-87-13334 ..... p 52 A92-11467
NSF ECS-87-15092 ..... p 46 A92-11473
NSF ECS-88-01912 ..... p 48 A92-11375
p 49 A92-11395
NSF ECS-88-10178 ..... p 51 A92-11464
NSF ECS-89-57461 ..... p 50 A92-11430
NSF ECS-90-96109 ..... p 50 A92-11430
NSF EET-88-08780 ..... p 38 A92-11041
NSF EET-88-57500 ..... p 759 A92-41658
NSF INT-88-21843 ..... p 28 A92-11502
p 479 A92-29361
NSF INT-90-16501 ..... p 1131 A92-55271
NSF ISI-88-61052 ..... p 5 A92-11058
NSF MSM-87-96352 ..... p 394 A92-26219
NSF MSM-88-09132 ..... p 495 A92-31564
NSF MSM-88-10384 ..... p 694 A92-39106
NSF MSM-88-12779 ..... p 913 N92-30111
NSF MSM-88-21143 ..... p 759 A92-41801
NSF MSM-90-57055 ..... p 585 A92-34524
NSF MSS-89-09153 ..... p 295 A92-23269
NSF MSS-90-57602 ..... p 295 A92-23269
NSG-3139 ..... p 176 A92-20747
NSG-3208 ..... p 69 A92-15550
NSG-3266 ..... p 74 A92-15638
p 74 A92-15639
NSG-3283 ..... p 44 N92-11379
NSG-3555 ..... p 883 A92-48908
p 826 A92-48909
N00012-90-C-0091 ..... p 501 N92-20997
N00014-81-C-0692 ..... p 597 A92-34878
N00014-81-G-0010 ..... p 392 A92-24758
N00014-82-K-0084 ..... p 717 N92-27712
N00014-83-K-0239 ..... p 62 A92-13673
p 442 A92-32241
N00014-84-K-0372 ..... p 154 A92-16026
p 390 A92-28503
N00014-85-C-0214 ..... p 810 A92-46778
N00014-85-C-0506 ..... p 80 A92-17195
N00014-85-K-0011 ..... p 3 A92-10690
p 174 A92-19611
p 898 A92-45833
N00014-85-K-0527 ..... p 1094 A92-56744
N00014-85-K-0658 ..... p 143 A92-17188
N00014-86-G-0066 ..... p 392 A92-24758
N00014-86-K-0507 ..... p 164 N92-13746
N00014-86-K-0679 ..... p 717 N92-27712
N00014-86-K-0691 ..... p 671 A92-37868
N00014-86-K-0693 ..... p 204 A92-18615
N00014-86-K-0754 ..... p 898 A92-45826
N00014-87-K-0057 ..... p 453 A92-29360
N00014-87-K-0174 ..... p 332 A92-26964
N00014-87-K-0196 ..... p 300 N92-17387
N00014-87-K-0304 ..... p 48 A92-11375
N00014-87-K-0352 ..... p 743 N92-27817
N00014-87-K-0816 ..... p 326 A92-26276
N00014-88-C-0291 ..... p 327 A92-26280
p 935 A92-50301
N00014-88-C-0677 ..... p 399 A92-28537
p 904 A92-48896
N00014-88-K-0004 ..... p 494 A92-31071
N00014-88-K-0029 ..... p 409 N92-19195
N00014-88-K-0242 ..... p 255 A92-23787
N00014-88-K-0565 ..... p 399 A92-28529
N00014-88-K-0670 ..... p 774 N92-27886
N00014-88-K-0721 ..... p 53 A92-11052
N00014-89-C-0071 ..... p 300 N92-17629
N00014-89-J-1176 ..... p 42 N92-10206
N00014-89-J-1221 ..... p 256 A92-23790
p 934 A92-50269
N00014-89-J-1275 ..... p 327 A92-26281
p 260 N92-17222
N00014-89-J-1276 ..... p 854 N92-29511
N00014-89-J-1319 ..... p 403 N92-19052
N00014-89-J-1320 ..... p 38 A92-11041
N00014-89-J-1361 ..... p 1010 A92-50296
N00014-89-J-1783 ..... p 1094 A92-56726
N00014-89-J-3102 ..... p 799 A92-45535
N00014-90-C-0089 ..... p 374 A92-27114
N00014-90-J-1095 ..... p 38 A92-11041
N00014-90-J-1270 ..... p 49 A92-11420
N00014-90-J-1305 ..... p 324 A92-26259
p 1033 A92-56776
p 166 N92-13822
N00014-90-J-1420 ..... p 898 A92-46252
N00014-90-J-1513 ..... p 233 A92-19605
p 302 A92-21191
N00014-90-J-1686 ..... p 621 A92-40111
N00014-90-J-1909 ..... p 327 A92-26280
p 327 A92-26281
p 260 N92-17222
p 946 N92-31122
N00014-90-J-4012 ..... p 774 A92-42095
N00014-91-C-0095 ..... p 44 N92-11367
N00014-91-C-0124 ..... p 290 N92-17653
p 489 N92-21015
p 896 N92-29408
p 987 N92-31360
N00014-91-C-0148 ..... p 283 N92-17243
N00014-91-C-0233 ..... p 735 N92-27925
N00014-91-C-0247 ..... p 757 N92-27749
N00014-91-J-1309 ..... p 617 A92-39338
N00014-91-J-1575 ..... p 743 N92-27817
N00014-91-J-1608 ..... p 750 N92-27753
N00014-91-J-1646 ..... p 300 N92-17387
N00014-91-J-1925 ..... p 949 N92-31853
N00014-92-J-1406 ..... p 825 A92-48857
N00019-84-C-0240 ..... p 806 A92-45578

N00019-87-C-0195 ..... p 131 A92-14336
N00019-88-C-0029 ..... p 1112 A92-54057
N00019-89-C-0352 ..... p 122 A92-15543
N00019-90-C-0195 ..... p 21 A92-11607
p 59 A92-14347
N00019-91-C-0062 ..... p 895 N92-28426
N00019-91-C-0083 ..... p 794 A92-45497
N00019-91-C-0176 ..... p 1007 A92-52440
N00039-88-C-0043 ..... p 1138 N92-33876
N00039-88-C-0051 ..... p 786 A92-49049
p 344 N92-18007
N00039-89-C-5301 ..... p 172 A92-18385
N00039-91-C-0082 ..... p 1138 N92-33876
N00123-89-G-0580 ..... p 777 N92-26524
N00140-87-C-0836 ..... p 121 A92-15519
N00140-88-C-0677 ..... p 768 N92-27468
N00167-85-C-0042 ..... p 229 N92-15385
N00167-87-C-0021 ..... p 414 A92-25365
N60530-86-WR-30021 ..... p 666 A92-36966
N60530-89-C-0383 ..... p 780 A92-44377
N62269-85-R-0278 ..... p 365 N92-18826
N62269-87-C-0226 ..... p 1107 N92-32527
N62269-87-C-0259 ..... p 1108 N92-32579
N62269-88-C-0208 ..... p 690 A92-36895
N62269-90-C-0246 ..... p 518 A92-34501
N62269-90-C-0264 ..... p 324 A92-26256
N66001-88-D-0088 ..... p 129 A92-17177
N66604-87-R-1195 ..... p 779 A92-42606
OV/RLD-937/1 ..... p 915 N92-28689
OV/RLD-987 ..... p 852 N92-28649
PROJ. 3335 ..... p 685 N92-25962
RICIS PROJ. ET-26 ..... p 778 N92-28150
RICIS PROJ. SR-02 ..... p 1134 N92-32865
RLD-LVB/L-24575 ..... p 356 N92-19491
RNLAF-RB-KLU-1990/A.5 ..... p 879 N92-28653
RP-1884-10 ..... p 224 N92-14362
RTOP 324-02-00 ..... p 236 N92-14788
p 971 N92-30569
RTOP 505-52-62 ..... p 630 N92-24958
RTOP 505-59-00 ..... p 831 N92-29625
RTOP 505-59-10-03 ..... p 444 N92-20494
p 525 N92-22232
p 1039 N92-33484
p 1040 N92-33631
RTOP 505-59-30-01 ..... p 13 N92-10982
p 178 N92-13996
p 446 N92-21456
RTOP 505-59-30 ..... p 1060 N92-32887
RTOP 505-59-36-01 ..... p 115 N92-13057
p 630 N92-24882
p 944 N92-30394
RTOP 505-59-36 ..... p 21 N92-11000
p 482 N92-21440
p 853 N92-28926
RTOP 505-59-40-10 ..... p 525 N92-22215
p 625 N92-24680
p 944 N92-30392
RTOP 505-59-40 ..... p 405 N92-19596
RTOP 505-59-50-01 ..... p 347 N92-19175
p 406 N92-19844
p 681 N92-25376
p 943 N92-30295
RTOP 505-59-52 ..... p 927 N92-28909
RTOP 505-59-53-01 ..... p 261 N92-17547
p 444 N92-20545
p 528 N92-23533
p 625 N92-24681
p 630 N92-24956
p 631 N92-25133
p 945 N92-30747
p 1036 N92-32480
RTOP 505-59-54-01 ..... p 31 N92-11022
p 138 N92-12007
p 178 N92-13997
RTOP 505-59-54-02 ..... p 297 N92-16283
RTOP 505-59-54-07 ..... p 209 N92-15077
RTOP 505-59-85-01 ..... p 32 N92-11030
p 498 N92-20072
p 888 N92-29352
RTOP 505-59-87-54 ..... p 630 N92-24885
RTOP 505-60-00 ..... p 1071 N92-32452
RTOP 505-60-01-02 ..... p 678 N92-24242
RTOP 505-60-11 ..... p 11 N92-10011
RTOP 505-60-31 ..... p 678 N92-24344
p 679 N92-24547
RTOP 505-61-01-01 ..... p 947 N92-31246
RTOP 505-61-21-03 ..... p 525 N92-22196
RTOP 505-61-31-08 ..... p 630 N92-24977
RTOP 505-61-41-02 ..... p 750 N92-27670
RTOP 505-61-51 ..... p 13 N92-10981
p 13 N92-10983
p 367 N92-19563
p 368 N92-19847
p 878 N92-28457
RTOP 505-61-71-01 ..... p 350 N92-20038
p 631 N92-25202
RTOP 505-61-71-07 ..... p 631 N92-25276
RTOP 505-61-71 ..... p 1036 N92-32422
p 1038 N92-33306
p 1040 N92-33618
RTOP 505-62-OK ..... p 562 N92-22647
p 633 N92-26104
p 1073 N92-34236
RTOP 505-62-00 ..... p 658 N92-25164
RTOP 505-62-10 ..... p 473 N92-20525
p 1002 N92-31484
RTOP 505-62-12 ..... p 378 N92-20033
p 474 N92-20650
RTOP 505-62-20 ..... p 242 N92-17346
p 739 N92-27037
p 770 N92-27653
RTOP 505-62-21 ..... p 936 A92-50473
p 44 N92-11328
p 597 N92-23560
p 678 N92-24514
RTOP 505-62-3B ..... p 559 N92-22510
RTOP 505-62-30-01 ..... p 12 N92-10975
p 385 N92-18956
p 443 N92-20283
p 527 N92-23095
p 984 N92-31900
p 1040 N92-33625
p 1041 N92-33706
p 1042 N92-34193
RTOP 505-62-30 ..... p 972 N92-30998
RTOP 505-62-40-04 ..... p 895 N92-28374
RTOP 505-62-40-06 ..... p 945 N92-30909
RTOP 505-62-40 ..... p 824 A92-48740
p 722 N92-28102
p 1062 N92-34202
RTOP 505-62-50 ..... p 195 N92-14037
p 481 N92-20586
p 909 N92-29105
p 979 N92-32241
p 1088 N92-34107
RTOP 505-62-51 ..... p 562 N92-22863
RTOP 505-62-52 ..... p 179 N92-13998
p 499 N92-20235
p 528 N92-23563
p 659 N92-25712
p 660 N92-25808
p 716 N92-27377
p 830 N92-28980
p 833 N92-30182
p 972 N92-30972
p 972 N92-31172
p 1072 N92-33746
p 1128 N92-34112
RTOP 505-62-61 ..... p 972 N92-31250
p 983 N92-31640
RTOP 505-62-71 ..... p 445 N92-20934
p 739 N92-26613
RTOP 505-62-84 ..... p 1098 A92-56806
p 1099 A92-56816
p 1099 A92-56818
p 665 N92-25449
p 667 N92-26129
p 887 N92-28673
p 984 N92-30307
p 982 N92-30508
RTOP 505-63-01-06 ..... p 578 N92-22637
RTOP 505-63-01-09 ..... p 1106 N92-32513
RTOP 505-63-01-10 ..... p 595 N92-22649
RTOP 505-63-10-03 ..... p 159 N92-13455
RTOP 505-63-20 ..... p 289 N92-17070
RTOP 505-63-36-01 ..... p 299 N92-17033
p 299 N92-17034
p 499 N92-20194
p 502 N92-21460
p 680 N92-25267
RTOP 505-63-36-06 ..... p 404 N92-19258
p 367 N92-19846
p 461 N92-20417
RTOP 505-63-36 ..... p 905 A92-48938
p 61 N92-12989
p 512 N92-21173
p 680 N92-24984
p 764 N92-26555
p 764 N92-26560
p 773 N92-27879
p 908 N92-28434
p 910 N92-29136
p 998 N92-30396
p 1001 N92-31155
p 1002 N92-31349
p 1002 N92-31485
RTOP 505-63-5A ..... p 756 N92-27378
p 1109 N92-32863
RTOP 505-63-5B ..... p 12 N92-10979
p 44 N92-11378
p 44 N92-11379
p 214 N92-15191
p 230 N92-15406
p 298 N92-16336
p 404 N92-19277
p 377 N92-19726
p 501 N92-20954
RTOP 505-63-50-04 ..... p 35 N92-11149
p 45 N92-11391
p 1110 N92-33423
RTOP 505-63-50-06 ..... p 82 N92-11985
p 650 N92-25995
p 850 N92-28435
RTOP 505-63-50-08 ..... p 489 N92-20679
RTOP 505-63-50-09 ..... p 399 N92-18053
RTOP 505-63-50-12 ..... p 185 N92-15049
p 185 N92-15050
p 444 N92-20480
p 445 N92-20654
p 446 N92-21432
p 526 N92-22240
p 527 N92-23116
p 831 N92-29445
p 944 N92-30393
p 944 N92-30570
p 945 N92-30691
p 947 N92-31239
RTOP 505-63-50-13 ..... p 115 N92-13054
p 261 N92-17509
RTOP 505-63-50-15 ..... p 23 N92-11010
p 197 N92-15070
p 961 N92-30752
p 962 N92-31174
p 962 N92-31264
p 962 N92-31350
p 962 N92-31351
p 963 N92-32111
p 1060 N92-32536
RTOP 505-63-50 ..... p 159 N92-13458
p 526 N92-22507
p 1042 N92-34147
RTOP 505-63-51-09 ..... p 56 N92-11758
RTOP 505-63-53-01 ..... p 683 N92-25911
p 1125 N92-33104
RTOP 505-63-53 ..... p 159 N92-13460
p 596 N92-23267
RTOP 505-64-10-05 ..... p 602 N92-22320
RTOP 505-64-10-07 ..... p 1134 N92-33483
RTOP 505-64-10-10 ..... p 206 N92-15075
RTOP 505-64-12-01 ..... p 735 N92-27424
RTOP 505-64-12-02 ..... p 953 N92-31549
p 1043 N92-32606
RTOP 505-64-13-01 ..... p 456 N92-21459
p 556 N92-22504
RTOP 505-64-13-11 ..... p 556 N92-22395
p 556 N92-22645
p 652 N92-24689
RTOP 505-64-13-22 ..... p 17 N92-10017
RTOP 505-64-13-23 ..... p 276 N92-15991
RTOP 505-64-13-32 ..... p 119 N92-13065
RTOP 505-64-13 ..... p 23 N92-10024
p 303 N92-17130
p 356 N92-20029
p 1044 N92-33080
p 1044 N92-33194
p 1050 N92-33407
RTOP 505-64-20-01 ..... p 662 N92-25607
p 979 N92-31240
RTOP 505-64-20 ..... p 962 N92-31208
RTOP 505-64-30-01 ..... p 1088 N92-33537
RTOP 505-64-30 ..... p 117 N92-13064
p 878 N92-28584
p 853 N92-29110
p 1060 N92-33149
RTOP 505-64-36 ..... p 841 N92-29103
p 1047 N92-32424
RTOP 505-64-40-01 ..... p 206 N92-15076
p 481 N92-20195
p 978 N92-31175
RTOP 505-64-40 ..... p 663 N92-25982
RTOP 505-64-52-01 ..... p 242 N92-17984
RTOP 505-64-70-01 ..... p 1128 N92-34017
RTOP 505-66-11-07 ..... p 680 N92-25137
RTOP 505-66-11 ..... p 2 N92-10003
p 1051 N92-33609
RTOP 505-66-41-02 ..... p 268 N92-17512
RTOP 505-66-41-04 ..... p 381 N92-19499
p 979 N92-32175
RTOP 505-66-41-50 ..... p 191 N92-15060
RTOP 505-66-41-66 ..... p 957 N92-30978
RTOP 505-66-71-01 ..... p 482 N92-21410
RTOP 505-66-71-02 ..... p 602 N92-22643
p 602 N92-22644
RTOP 505-66-71 ..... p 445 N92-21188
RTOP 505-67-01-04 ..... p 1065 N92-34109
RTOP 505-67-21-02 ..... p 368 N92-19871
RTOP 505-68-00 ..... p 273 N92-17071
p 352 N92-19276

RTOP 505-68-01-02 ..... p 948 N92-31532
RTOP 505-68-1C ..... p 229 N92-15402
RTOP 505-68-10-01 ..... p 18 N92-10994
RTOP 505-68-10 ..... p 2 N92-10002
p 179 N92-14001
p 185 N92-15051
p 186 N92-15052
p 258 N92-15967
p 258 N92-15968
p 261 N92-17347
p 596 N92-23154
p 714 N92-26612
p 828 N92-28674
p 828 N92-28696
p 1042 N92-34144
p 1073 N92-34236
RTOP 505-68-11 ..... p 527 N92-23105
p 952 N92-30395
RTOP 505-68-27 ..... p 984 N92-32201
RTOP 505-68-30-03 ..... p 179 N92-14968
p 632 N92-25510
p 715 N92-26651
p 715 N92-26652
p 950 N92-32114
RTOP 505-68-30-07 ..... p 633 N92-25967
RTOP 505-68-30 ..... p 871 N92-29425
RTOP 505-68-31 ..... p 856 A92-46792
RTOP 505-68-32 ..... p 742 N92-27669
p 868 N92-28418
p 871 N92-29661
p 1039 N92-33581
RTOP 505-68-40 ..... p 118 N92-11994
p 276 N92-17128
RTOP 505-68-50 ..... p 272 N92-15986
p 962 N92-31261
p 1065 N92-32866
RTOP 505-68-70-02 ..... p 1040 N92-33656
RTOP 505-68-70-08 ..... p 633 N92-25752
RTOP 505-68-71-03 ..... p 82 N92-12994
RTOP 505-68-71 ..... p 350 N92-19993
p 947 N92-31276
RTOP 505-68-91-06 ..... p 526 N92-22506
RTOP 505-69-10 ..... p 202 N92-14063
RTOP 505-69-14 ..... p 871 N92-29427
RTOP 505-69-20-01 ..... p 1045 N92-34192
RTOP 505-69-40 ..... p 562 N92-23254
RTOP 505-69-50 ..... p 473 N92-20196
p 716 N92-27376
p 854 N92-29417
p 924 N92-30207
p 1134 N92-33894
RTOP 505-80-31-01 ..... p 401 N92-18877
RTOP 505-90-52-01 ..... p 816 A92-47042
p 185 N92-15047
p 234 N92-15658
p 402 N92-18965
p 347 N92-19250
p 447 N92-21465
p 592 N92-22228
RTOP 505-90-53-02 ..... p 691 N92-24397
p 1010 N92-30907
RTOP 506-40-21-01 ..... p 43 N92-11319
RTOP 506-40-41-01 ..... p 501 N92-20677
RTOP 506-40-41-02 ..... p 11 N92-10006
RTOP 506-40-91-01 ..... p 685 N92-25964
RTOP 506-40-91-02 ..... p 298 N92-17002
p 1001 N92-31281
RTOP 506-42-72 ..... p 297 N92-16265
p 387 N92-18280
RTOP 506-43-31-04 ..... p 679 N92-24797
RTOP 506-43-31-05 ..... p 767 N92-27193
RTOP 506-43-31 ..... p 852 N92-28721
p 890 N92-29104
RTOP 506-46-21-05 ..... p 1086 N92-32778
RTOP 506-46-21-56 ..... p 53 N92-11706
RTOP 506-48-11-01 ..... p 286 N92-16012
RTOP 506-51-31 ..... p 853 N92-28910
RTOP 509-10-02-03 ..... p 81 N92-11977
p 827 N92-28477
RTOP 509-10-03 ..... p 279 N92-15993
RTOP 510-02-12-01 ..... p 1110 N92-33613
RTOP 510-02-12-05 ..... p 685 N92-25960
RTOP 510-02-12-08 ..... p 961 N92-30304
RTOP 532-06-01 ..... p 550 N92-22864
RTOP 532-06-36-02 ..... p 166 N92-12598
RTOP 532-06-37 ..... p 696 N92-24251
RTOP 533-02-00 ..... p 570 N92-22194
RTOP 533-02-21 ..... p 663 N92-25734
RTOP 533-02-30 ..... p 526 N92-22249
p 951 N92-32240
RTOP 533-02-35 ..... p 482 N92-21357
p 1060 N92-33404
p 1062 N92-34039
RTOP 533-02-36 ..... p 740 N92-27379
p 742 N92-27587
p 871 N92-29659
p 971 N92-30518
p 973 N92-31275
p 1133 N92-32507
p 1087 N92-32864
RTOP 533-02-37 ..... p 1087 N92-32788
RTOP 533-02-38 ..... p 381 N92-19174
RTOP 533-06-01 ..... p 950 N92-32213
RTOP 535-03-10-01 ..... p 346 N92-19002
RTOP 535-03-10-02 ..... p 90 N92-13038
RTOP 535-03-10 ..... p 130 N92-13071
p 166 N92-13759
p 179 N92-14002
p 304 N92-16705
p 416 N92-18282
p 346 N92-18760
p 348 N92-19437
p 943 N92-30298
RTOP 535-03-11-03 ..... p 54 N92-10598
p 166 N92-13758
p 235 N92-14779
p 512 N92-20479
p 697 N92-25368
p 1136 N92-32948
p 1138 N92-33160
RTOP 535-03-11-04 ..... p 166 N92-13757
p 481 N92-20376
RTOP 535-05-01 ..... p 1011 N92-31248
RTOP 535-05-10 ..... p 1123 A92-56829
p 680 N92-24959
p 831 N92-29402
RTOP 537-01-22 ..... p 562 N92-23537
RTOP 537-02-02 ..... p 738 N92-26553
RTOP 537-02-20 ..... p 279 N92-17061
p 738 N92-26561
p 742 N92-27652
p 890 N92-29343
RTOP 537-02-23 ..... p 12 N92-10976
p 237 N92-14795
p 237 N92-14797
p 696 N92-24688
p 868 N92-28419
RTOP 537-03-20 ..... p 416 N92-19672
RTOP 537-03-21-01 ..... p 1061 N92-33874
RTOP 537-03-21-03 ..... p 56 N92-11759
p 56 N92-11765
p 697 N92-26130
p 927 N92-28556
p 1138 N92-33719
RTOP 537-03-21-04 ..... p 696 N92-24800
p 1140 N92-34148
RTOP 537-03-23-03 ..... p 765 N92-26680
RTOP 538-02-10-01 ..... p 912 N92-30106
p 1128 N92-34178
RTOP 551-15-12-16 ..... p 308 N92-19930
RTOP 553-13-00 ..... p 222 N92-14346
RTOP 582-01-11 ..... p 26 N92-11017
RTOP 590-14-11-02 ..... p 753 N92-27788
RTOP 590-21-11 ..... p 1072 N92-33479
RTOP 590-21-31 ..... p 12 N92-10979
p 473 N92-20523
RTOP 650-60-15-01-00 ..... p 1000 N92-30923
RTOP 763-01-21 ..... p 279 N92-17546
RTOP 763-22-41 ..... p 596 N92-23435
RTOP 763-22-51 ..... p 932 N92-31267
RTOP 763-23-41-85 ..... p 685 N92-26128
RTOP 778-34-2A ..... p 658 N92-24539
RTOP 906-11-03 ..... p 870 N92-28985
RTOP 992-16-04-05 ..... p 234 N92-14598
SBA-4-91-2-0357 ..... p 753 N92-27403
SERC-GR/E/06824 ..... p 718 N92-27714
SERC-GR/E/25702 ..... p 712 A92-44363
SERC-GR/E/77039 ..... p 718 N92-27714
SERC-GR/F/27062 ..... p 491 A92-28686
SERC-GR/XG/107732 ..... p 545 A92-35731
SERC-XG/10909 ..... p 491 A92-28686
STPA-85-95-009-51 ..... p 43 N92-11309
STPA-85-95-009 ..... p 23 N92-11009
p 830 N92-29206
T/RF42/E0013/E1413 ..... p 501 N92-21232
p 501 N92-21233
p 502 N92-21234
TEES PROJ. 30540-AE ..... p 1038 N92-33063
TTN77-1038 ..... p 1125 N92-33066
VUB-8356/89/NL/FG(SG) ..... p 528 N92-23168
W-7405-ENG-36 ..... p 376 N92-18230
p 749 N92-26720
p 973 N92-31817
W-7405-ENG-48 ..... p 15 A92-11027
p 60 A92-14442
p 636 N92-24713
p 669 N92-25259
p 1004 N92-32147
W-7405-ENG-82 ..... p 144 A92-13554
p 510 A92-28720
p 499 N92-20301
p 914 N92-30119
W2207-7-AF69/01-SS ..... p 886 N92-28550
p 1048 N92-32845
505-62-21 ..... p 44 N92-11328
p 597 N92-23560
p 678 N92-24514

Typical Report Number Index Listing

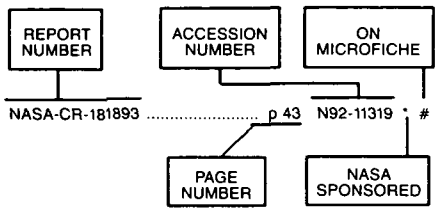

Listings in this index are arranged alphanumerically by report number. The page number indicates the page on which the citation is located. The accession number denotes the number by which the citation is identified. An asterisk (*) indicates that the item is a NASA report. A pound sign (#) indicates that the item is available on microfiche.

A-89130 ..... p 878 N92-28457 * #
A-89236 ..... p 950 N92-32213 * #
A-89267 ..... p 550 N92-22864 * #
A-90021 ..... p 1038 N92-33306 * #
A-90040 ..... p 1040 N92-33618 * #
A-90161 ..... p 11 N92-10011 * #
A-90210 ..... p 13 N92-10983 * #
A-90244 ..... p 1036 N92-32422 * #
A-90290 ..... p 1039 N92-33581 * #
A-91011 ..... p 1051 N92-33609 * #
A-91054 ..... p 1143 N92-33948 * #
A-91056 ..... p 13 N92-10981 * #
A-91074 ..... p 1071 N92-32452 * #
A-91080 ..... p 482 N92-21440 * #
A-91150 ..... p 368 N92-19847 * #
A-91156 ..... p 1060 N92-32887 * #
A-91178 ..... p 853 N92-28926 * #
A-91189 ..... p 367 N92-19563 * #
A-91190 ..... p 21 N92-11000 * #
A-91203 ..... p 1044 N92-33194 * #
A-91223 ..... p 356 N92-20029 * #
A-91237 ..... p 890 N92-29104 * #
A-91242 ..... p 2 N92-10003 * #
A-92003 ..... p 1050 N92-33407 * #
A-92013 ..... p 195 N92-14039 * #
A-92014 ..... p 853 N92-28910 * #
A-92021 ..... p 841 N92-29103 * #
A-92039 ..... p 1087 N92-32788 * #
A-92052 ..... p 927 N92-28909 * #
A-92064 ..... p 852 N92-28721 * #
A-92072 ..... p 831 N92-29625 * #
A-92076 ..... p 405 N92-19596 * #
A-92081 ..... p 854 N92-29417 * #
A-92085 ..... p 1047 N92-32424 * #
A-92156 ..... p 1044 N92-33080 * #

AAAF-NT-89-12 ..... p 31 N92-11020 #

AAS PAPER 91-369 ..... p 752 A92-43269
AAS PAPER 91-418 ..... p 753 A92-43356

AATTC-TOP-7-3-530 ..... p 780 N92-27924 #

ACD-330 ..... p 534 N92-22210 #
ACD-330 ..... p 573 N92-22503 #
ACD-340 ..... p 191 N92-14034 #

AD-A210523 ..... p 143 N92-12060 #
AD-A235634 ..... p 102 N92-11988 #
AD-A237667 ..... p 202 N92-14059 #
AD-A239805 ..... p 35 N92-10100 #
AD-A239852 ..... p 18 N92-10019 #
AD-A239892 ..... p 41 N92-10141 #
AD-A239949 ..... p 12 N92-10015 #
AD-A239950 ..... p 21 N92-10022 #
AD-A239956 ..... p 12 N92-10016 #
AD-A239982 ..... p 41 N92-10157 #
AD-A240057 ..... p 33 N92-10062 #
AD-A240127 ..... p 42 N92-10206 #
AD-A240169 ..... p 26 N92-11015 #
AD-A240221 ..... p 29 N92-11018 #
AD-A240256 ..... p 13 N92-10985 #
AD-A240263 ..... p 13 N92-10986 #
AD-A240333 ..... p 53 N92-11737 #
AD-A240347 ..... p 22 N92-11002 #
AD-A240486 ..... p 23 N92-11011 #
AD-A240521 ..... p 42 N92-11235 #
AD-A240522 ..... p 30 N92-11019 #
AD-A240528 ..... p 45 N92-11578 #
AD-A240545 ..... p 22 N92-11004 #
AD-A240549 ..... p 42 N92-11237 #
AD-A240587 ..... p 31 N92-11024 * #
AD-A240595 ..... p 22 N92-11005 #
AD-A240600 ..... p 44 N92-11383 #
AD-A240614 ..... p 31 N92-11025 #
AD-A240638 ..... p 22 N92-11006 #
AD-A240639 ..... p 23 N92-11007 #
AD-A240650 ..... p 35 N92-11213 #
AD-A240703 ..... p 23 N92-11008 #
AD-A240777 ..... p 44 N92-11367 #
AD-A240797 ..... p 237 N92-14791 #
AD-A240858 ..... p 116 N92-13061 #
AD-A240867 ..... p 131 N92-13072 #
AD-A240933 ..... p 119 N92-13066 #
AD-A240941 ..... p 116 N92-13062 #
AD-A240965 ..... p 158 N92-13351 #
AD-A240986 ..... p 170 N92-13991 #
AD-A240987 ..... p 170 N92-13992 #
AD-A241008 ..... p 89 N92-13034 #
AD-A241015 ..... p 180 N92-14972 #
AD-A241044 ..... p 229 N92-15367 #
AD-A241073 ..... p 89 N92-13035 #
AD-A241119 ..... p 170 N92-13993 #
AD-A241141 ..... p 54 N92-10598 * #
AD-A241254 ..... p 164 N92-13746 #
AD-A241286 ..... p 166 N92-13822 #
AD-A241295 ..... p 119 N92-13067 #
AD-A241313 ..... p 225 N92-14386 #
AD-A241348 ..... p 139 N92-13078 #
AD-A241351 ..... p 158 N92-13406 #
AD-A241357 ..... p 205 N92-14065 #
AD-A241362 ..... p 90 N92-13037 #
AD-A241416 ..... p 116 N92-13063 #
AD-A241464 ..... p 135 N92-13075 #
AD-A241482 ..... p 103 N92-13051 #
AD-A241483 ..... p 93 N92-13045 #
AD-A241484 ..... p 93 N92-13046 #
AD-A241536 ..... p 158 N92-13409 #
AD-A241540 ..... p 139 N92-13079 #
AD-A241554 ..... p 139 N92-13080 #
AD-A241593 ..... p 158 N92-13410 #
AD-A241641 ..... p 62 N92-12991 #
AD-A241657 ..... p 160 N92-13470 #
AD-A241768 ..... p 62 N92-12992 #
AD-A241844 ..... p 103 N92-13052 #
AD-A241859 ..... p 299 N92-17024 #
AD-A241869 ..... p 259 N92-15975 #
AD-A241914 ..... p 299 N92-17216 #
AD-A241924 ..... p 303 N92-17438 #
AD-A241935 ..... p 283 N92-17442 #
AD-A242007 ..... p 406 N92-19873 #
AD-A242016 ..... p 272 N92-15990 #
AD-A242025 ..... p 164 N92-12517 #
AD-A242027 ..... p 290 N92-17682 #
AD-A242074 ..... p 299 N92-17168 #
AD-A242141 ..... p 242 N92-15963 #
AD-A242207 ..... p 386 N92-19642 #
AD-A242212 ..... p 257 N92-15964 #
AD-A242264 ..... p 300 N92-17258 #
AD-A242321 ..... p 283 N92-17243 #
AD-A242333 ..... p 119 N92-13065 * #
AD-A242398 ..... p 279 N92-17011 #
AD-A242478 ..... p 196 N92-15067 #
AD-A242493 ..... p 229 N92-15385 #
AD-A242598 ..... p 170 N92-14966 #
AD-A242637 ..... p 206 N92-15073 #
AD-A242650 ..... p 206 N92-15074 #
AD-A242656 ..... p 185 N92-15045 #
AD-A242690 ..... p 196 N92-15068 #
AD-A242757 ..... p 191 N92-15058 #
AD-A242768 ..... p 197 N92-15069 #
AD-A242828 ..... p 264 N92-17259 #
AD-A242829 ..... p 285 N92-17260 #
AD-A242881 ..... p 275 N92-17565 #
AD-A242890 ..... p 301 N92-17028 #
AD-A242900 ..... p 300 N92-17629 #
AD-A242929 ..... p 280 N92-17552 #
AD-A242943 ..... p 279 N92-17204 #
AD-A242972 ..... p 44 N92-11376 #
AD-A242989 ..... p 285 N92-17297 #
AD-A243002 ..... p 275 N92-17234 #
AD-A243004 ..... p 275 N92-17266 #
AD-A243025 ..... p 268 N92-17568 #
AD-A243033 ..... p 298 N92-16978 #
AD-A243047 ..... p 260 N92-17281 #
AD-A243090 ..... p 264 N92-17217 #
AD-A243109 ..... p 275 N92-17300 #
AD-A243158 ..... p 242 N92-17477 #
AD-A243191 ..... p 305 N92-17369 #
AD-A243203 ..... p 46 N92-11593 * #
AD-A243207 ..... p 139 N92-13077 #
AD-A243224 ..... p 277 N92-17221 #
AD-A243346 ..... p 280 N92-17729 #
AD-A243363 ..... p 260 N92-17114 #
AD-A243375 ..... p 261 N92-17404 #
AD-A243383 ..... p 170 N92-13928 * #
AD-A243388 ..... p 260 N92-17222 #
AD-A243409 ..... p 287 N92-17325 #
AD-A243411 ..... p 344 N92-18007 #
AD-A243435 ..... p 305 N92-17687 #
AD-A243453 ..... p 290 N92-17653 #
AD-A243513 ..... p 300 N92-17387 #
AD-A243526 ..... p 305 N92-17537 #
AD-A243527 ..... p 264 N92-17478 #
AD-A243552 ..... p 260 N92-17339 #
AD-A243600 ..... p 290 N92-17932 #
AD-A243624 ..... p 384 N92-18012 #
AD-A243629 ..... p 370 N92-18014 #
AD-A243638 ..... p 283 N92-17748 #
AD-A243679 ..... p 61 N92-12989 * #
AD-A243686 ..... p 304 N92-17088 #
AD-A243698 ..... p 282 N92-17096 #
AD-A243700 ..... p 284 N92-17097 #
AD-A243719 ..... p 304 N92-17506 #
AD-A243724 ..... p 275 N92-17513 #
AD-A243737 ..... p 116 N92-13059 #
AD-A243738 ..... p 116 N92-13058 #
AD-A243739 ..... p 103 N92-13049 #
AD-A243792 ..... p 382 N92-19505 #
AD-A243799 ..... p 409 N92-19231 #
AD-A243804 ..... p 190 N92-14033 #
AD-A243805 ..... p 116 N92-13060 #
AD-A243807 ..... p 93 N92-13042 #
AD-A243809 ..... p 402 N92-18933 #
AD-A243812 ..... p 115 N92-13057 * #
AD-A243821 ..... p 381 N92-19241 #
AD-A243860 ..... p 191 N92-14034 #
AD-A243868 ..... p 376 N92-18867 #
AD-A243880 ..... p 352 N92-19259 #
AD-A243881 ..... p 377 N92-19235 #
AD-A243889 ..... p 402 N92-18940 #
AD-A243891 ..... p 387 N92-18942 #
AD-A243900 ..... p 377 N92-19328 #
AD-A243902 ..... p 377 N92-19329 #
AD-A243912 ..... p 346 N92-18895 #
AD-A243916 ..... p 404 N92-19384 #
AD-A243928 ..... p 417 N92-19466 #
AD-A243933 ..... p 366 N92-19192 #
AD-A243934 ..... p 401 N92-18897 #
AD-A243947 ..... p 356 N92-19604 #
AD-A243969 ..... p 348 N92-19367 #
AD-A243977 ..... p 405 N92-19386 #
AD-A243981 ..... p 356 N92-19391 #
AD-A244044 ..... p 366 N92-19178 #
AD-A244049 ..... p 404 N92-19183 #
AD-A244050 ..... p 377 N92-19184 #
AD-A244051 ..... p 366 N92-19185 #
AD-A244055 ..... p 376 N92-19097 #
AD-A244075 ..... p 403 N92-19080 #
AD-A244153 ..... p 409 N92-19195 #
AD-A244183 ..... p 347 N92-19304 #

AD-A244194 ..... p 348 N92-19394 #
AD-A244211 ..... p 412 N92-19247 #
AD-A244247 ..... p 234 N92-14673 #
AD-A244248 ..... p 273 N92-17153 #
AD-A244249 ..... p 83 N92-12996 #
AD-A244250 ..... p 22 N92-11001 #
AD-A244267 ..... p 412 N92-19335 #
AD-A244268 ..... p 417 N92-19336 #
AD-A244272 ..... p 365 N92-19030 #
AD-A244274 ..... p 403 N92-19052 #
AD-A244320 ..... p 346 N92-18825 #
AD-A244321 ..... p 365 N92-18826 #
AD-A244350 ..... p 234 N92-15658 * #
AD-A244353 ..... p 187 N92-15053 #
AD-A244401 ..... p 484 N92-20455 #
AD-A244409 ..... p 413 N92-19397 #
AD-A244417 ..... p 347 N92-19085 #
AD-A244429 ..... p 503 N92-21730 #
AD-A244546 ..... p 502 N92-21297 #
AD-A244572 ..... p 445 N92-21012 #
AD-A244573 ..... p 534 N92-22104 #
AD-A244574 ..... p 534 N92-22105 #
AD-A244575 ..... p 534 N92-22106 #
AD-A244595 ..... p 202 N92-14064 #
AD-A244617 ..... p 510 N92-21392 #
AD-A244657 ..... p 483 N92-21752 #
AD-A244669 ..... p 482 N92-21360 #
AD-A244711 ..... p 447 N92-21753 #
AD-A244804 ..... p 512 N92-21719 #
AD-A244805 ..... p 485 N92-21720 #
AD-A244815 ..... p 489 N92-21015 #
AD-A244822 ..... p 185 N92-15047 * #
AD-A244849 ..... p 489 N92-20695 #
AD-A244869 ..... p 464 N92-21951 #
AD-A245011 ..... p 446 N92-21333 #
AD-A245067 ..... p 501 N92-20997 #
AD-A245072 ..... p 484 N92-20898 #
AD-A245117 ..... p 352 N92-18242 #
AD-A245237 ..... p 490 N92-21159 #
AD-A245302 ..... p 363 N92-18778 #
AD-A245304 ..... p 402 N92-19004 #
AD-A245449 ..... p 749 N92-26527 #
AD-A245463 ..... p 738 N92-26405 * #
AD-A245616 ..... p 755 N92-26383 #
AD-A245686 ..... p 777 N92-26524 #
AD-A245742 ..... p 650 N92-26155 #
AD-A245758 ..... p 765 N92-26592 #
AD-A245782 ..... p 731 N92-26896 #
AD-A245843 ..... p 650 N92-26039 #
AD-A245910 ..... p 743 N92-28162 #
AD-A245922 ..... p 883 N92-28407 #
AD-A245940 ..... p 829 N92-28883 #
AD-A245952 ..... p 968 N92-32051 #
AD-A245970 ..... p 910 N92-29344 #
AD-A245973 ..... p 879 N92-28801 #
AD-A245977 ..... p 853 N92-28802 #
AD-A245997 ..... p 727 N92-26756 #
AD-A246046 ..... p 957 N92-32054 #
AD-A246047 ..... p 770 N92-27600 #
AD-A246084 ..... p 781 N92-26765 #
AD-A246087 ..... p 757 N92-27749 #
AD-A246123 ..... p 743 N92-27817 #
AD-A246149 ..... p 746 N92-27577 #
AD-A246198 ..... p 777 N92-26458 #
AD-A246297 ..... p 449 N92-21679 #
AD-A246299 ..... p 753 N92-26362 #
AD-A246316 ..... p 726 N92-26291 #
AD-A246343 ..... p 345 N92-18269 #
AD-A246349 ..... p 764 N92-26258 #
AD-A246350 ..... p 733 N92-28118 #
AD-A246356 ..... p 715 N92-26947 #
AD-A246372 ..... p 740 N92-27062 #
AD-A246398 ..... p 724 N92-27750 #
AD-A246407 ..... p 757 N92-27752 #
AD-A246435 ..... p 727 N92-26948 #
AD-A246445 ..... p 724 N92-27914 #
AD-A246458 ..... p 751 N92-27836 #
AD-A246525 ..... p 781 N92-27528 #
AD-A246559 ..... p 756 N92-27531 #
AD-A246570 ..... p 777 N92-26620 #
AD-A246596 ..... p 745 N92-27505 #
AD-A246598 ..... p 727 N92-26795 #
AD-A246618 ..... p 907 N92-28253 #
AD-A246626 ..... p 778 N92-27980 #
AD-A246638 ..... p 750 N92-27753 #
AD-A246661 ..... p 772 N92-27760 #
AD-A246692 ..... p 263 N92-16986 #
AD-A246759 ..... p 786 N92-28348 #
AD-A246814 ..... p 729 N92-28132 #
AD-A246822 ..... p 926 N92-28292 #
AD-A246823 ..... p 346 N92-18345 #
AD-A246865 ..... p 191 N92-15061 #
AD-A246908 ..... p 732 N92-27719 #
AD-A246918 ..... p 770 N92-27546 #
AD-A246919 ..... p 780 N92-27171 #
AD-A246938 ..... p 743 N92-28073 #
AD-A246959 ..... p 360 N92-18571 #
AD-A246960 ..... p 767 N92-27352 #
AD-A247028 ..... p 732 N92-27335 #
AD-A247040 ..... p 743 N92-28076 #
AD-A247056 ..... p 774 N92-27918 #
AD-A247102 ..... p 781 N92-26863 #
AD-A247175 ..... p 1136 N92-32697 #
AD-A247191 ..... p 831 N92-29539 #
AD-A247195 ..... p 724 N92-27682 #
AD-A247196 ..... p 830 N92-28888 #
AD-A247207 ..... p 715 N92-27172 #
AD-A247280 ..... p 352 N92-18259 #
AD-A247302 ..... p 947 N92-31300 #
AD-A247345 ..... p 727 N92-27217 #
AD-A247430 ..... p 908 N92-28425 #
AD-A247464 ..... p 895 N92-28398 #
AD-A247484 ..... p 923 N92-28245 #
AD-A247489 ..... p 883 N92-28248 #
AD-A247532 ..... p 829 N92-28865 #
AD-A247668 ..... p 895 N92-28912 #
AD-A247719 ..... p 552 N92-23950 #
AD-A247742 ..... p 382 N92-20026 #
AD-A247792 ..... p 774 N92-27886 #
AD-A247825 ..... p 728 N92-27916 #
AD-A247831 ..... p 780 N92-27924 #
AD-A247834 ..... p 773 N92-27864 #
AD-A247886 ..... p 1108 N92-32629 #
AD-A247937 ..... p 402 N92-18965 * #
AD-A248011 ..... p 354 N92-18967 #
AD-A248033 ..... p 926 N92-28302 #
AD-A248190 ..... p 896 N92-29408 #
AD-A248202 ..... p 923 N92-29188 #
AD-A248205 ..... p 910 N92-29191 #
AD-A248207 ..... p 859 N92-29222 #
AD-A248224 ..... p 462 N92-21210 #
AD-A248257 ..... p 550 N92-23227 #
AD-A248270 ..... p 445 N92-20797 #
AD-A248326 ..... p 735 N92-27925 #
AD-A248372 ..... p 895 N92-28426 #
AD-A248378 ..... p 736 N92-28004 #
AD-A248458 ..... p 911 N92-29933 #
AD-A248472 ..... p 986 N92-30321 #
AD-A248473 ..... p 1009 N92-30322 #
AD-A248484 ..... p 1009 N92-30335 #
AD-A248487 ..... p 978 N92-30323 #
AD-A248519 ..... p 888 N92-29505 #
AD-A248543 ..... p 854 N92-29511 #
AD-A248558 ..... p 896 N92-29580 #
AD-A248568 ..... p 733 N92-28123 #
AD-A248581 ..... p 883 N92-28388 #
AD-A248585 ..... p 774 N92-28171 #
AD-A248653 ..... p 753 N92-27994 #
AD-A248657 ..... p 729 N92-27964 #
AD-A248763 ..... p 1142 N92-32338 #
AD-A248783 ..... p 447 N92-21465 * #
AD-A248790 ..... p 999 N92-30583 #
AD-A248887 ..... p 724 N92-28052 #
AD-A248893 ..... p 967 N92-30524 #
AD-A248954 ..... p 729 N92-28079 #
AD-A248964 ..... p 982 N92-30329 #
AD-A249127 ..... p 637 N92-26028 #
AD-A249132 ..... p 641 N92-26101 #
AD-A249232 ..... p 592 N92-22228 * #
AD-A249259 ..... p 868 N92-28294 #
AD-A249284 ..... p 909 N92-28879 #
AD-A249436 ..... p 983 N92-30777 #
AD-A249625 ..... p 988 N92-31462 #
AD-A249628 ..... p 946 N92-31122 #
AD-A249739 ..... p 948 N92-31622 #
AD-A249807 ..... p 535 N92-23096 #
AD-A249870 ..... p 988 N92-31823 #
AD-A249918 ..... p 987 N92-30874 #
AD-A249944 ..... p 983 N92-30849 #
AD-A250048 ..... p 949 N92-31777 #
AD-A250068 ..... p 987 N92-31360 #
AD-A250074 ..... p 1004 N92-31362 #
AD-A250134 ..... p 963 N92-31793 #
AD-A250188 ..... p 895 N92-28921 #
AD-A250192 ..... p 630 N92-24882 * #
AD-A250202 ..... p 979 N92-31967 #
AD-A250209 ..... p 1003 N92-31824 #
AD-A250221 ..... p 909 N92-29118 #
AD-A250279 ..... p 948 N92-31555 #
AD-A250293 ..... p 888 N92-29709 #
AD-A250341 ..... p 853 N92-28771 #
AD-A250342 ..... p 973 N92-31439 #
AD-A250390 ..... p 854 N92-29180 #
AD-A250407 ..... p 887 N92-28772 #
AD-A250412 ..... p 837 N92-29182 #
AD-A250416 ..... p 308 N92-18969 #
AD-A250522 ..... p 989 N92-32076 #
AD-A250561 ..... p 927 N92-28923 #
AD-A250654 ..... p 947 N92-31171 #
AD-A250749 ..... p 953 N92-31193 #
AD-A250772 ..... p 630 N92-24885 * #
AD-A250782 ..... p 716 N92-27344 #
AD-A250814 ..... p 1124 N92-32632 #
AD-A250862 ..... p 1004 N92-32103 #
AD-A250865 ..... p 974 N92-32059 #
AD-A250882 ..... p 943 N92-30239 #
AD-A251037 ..... p 932 N92-30253 #
AD-A251065 ..... p 986 N92-30256 #
AD-A251083 ..... p 932 N92-30258 #
AD-A251127 ..... p 961 N92-30878 #
AD-A251139 ..... p 1036 N92-32651 #
AD-A251967 ..... p 782 N92-28114 * #
AD-A252112 ..... p 987 N92-31419 #
AD-A252175 ..... p 949 N92-32062 #
AD-A252246 ..... p 1124 N92-32686 #
AD-A252280 ..... p 1129 N92-33220 #
AD-A252281 ..... p 1044 N92-33249 #
AD-A252378 ..... p 764 N92-26555 * #
AD-A252379 ..... p 680 N92-24984 * #
AD-A252381 ..... p 773 N92-27879 * #
AD-A252382 ..... p 764 N92-26560 * #
AD-A252389 ..... p 1038 N92-32900 #
AD-A252404 ..... p 982 N92-30547 #
AD-A252406 ..... p 736 N92-27973 #
AD-A252438 ..... p 1043 N92-32941 #
AD-A252481 ..... p 609 N92-24678 * #
AD-A252492 ..... p 988 N92-32066 #
AD-A252497 ..... p 665 N92-25733 #
AD-A252520 ..... p 1086 N92-32435 #
AD-A252564 ..... p 782 N92-28183 * #
AD-A252651 ..... p 952 N92-30551 #
AD-A252652 ..... p 999 N92-30766 #
AD-A252656 ..... p 987 N92-31399 #
AD-A252685 ..... p 987 N92-30767 #
AD-A252705 ..... p 1011 N92-31767 #
AD-A252730 ..... p 1087 N92-32988 #
AD-A252734 ..... p 837 N92-28900 #
AD-A252771 ..... p 1126 N92-33498 #
AD-A252773 ..... p 1017 N92-33499 #
AD-A252778 ..... p 484 N92-21162 * #
AD-A252783 ..... p 1127 N92-33538 #
AD-A252846 ..... p 1061 N92-33414 #
AD-A252863 ..... p 1065 N92-33277 #
AD-A252869 ..... p 1135 N92-33920 #
AD-A252878 ..... p 1040 N92-33678 #
AD-A252909 ..... p 1101 N92-33398 #
AD-A252912 ..... p 1126 N92-33501 #
AD-A252914 ..... p 1061 N92-33502 #
AD-A252922 ..... p 1050 N92-33596 #
AD-A253004 ..... p 1109 N92-33033 #
AD-A253005 ..... p 717 N92-27706 #
AD-A253007 ..... p 786 N92-28522 #
AD-A253032 ..... p 1111 N92-33624 #
AD-A253040 ..... p 870 N92-28686 #
AD-A253046 ..... p 1101 N92-33434 #
AD-A253072 ..... p 1044 N92-33288 #
AD-A253127 ..... p 667 N92-26129 * #
AD-A253371 ..... p 1062 N92-34182 #
AD-A253603 ..... p 718 N92-27936 #
AD-A253692 ..... p 1142 N92-33238 #
AD-A253798 ..... p 961 N92-31165 #
AD-A253805 ..... p 850 N92-28468 #
AD-A253824 ..... p 868 N92-28458 #
AD-A253853 ..... p 983 N92-30976 #

AD-B123560L ..... p 92 N92-13041 #
AD-B156440L ..... p 196 N92-15065 #
AD-B157410L ..... p 161 N92-12373 #
AD-B158638L ..... p 381 N92-18893 #
AD-B158639L ..... p 444 N92-20473 #
AD-B158641L ..... p 385 N92-18416 #
AD-B158645L ..... p 444 N92-20498 #
AD-B158646L ..... p 481 N92-20475 #
AD-B158647L ..... p 385 N92-18415 #
AD-B159047L ..... p 356 N92-19491 #
AD-B159336L ..... p 400 N92-18221 #
AD-B163639L ..... p 83 N92-12998 #
AD-B163670L ..... p 83 N92-12997 #
AD-B165067L ..... p 697 N92-25204 #

AD-D015014 ..... p 90 N92-13036
AD-D015017 ..... p 279 N92-15992 #
AD-D015061 ..... p 268 N92-17707 #
AD-D015074 ..... p 296 N92-16174
AD-D015140 ..... p 400 N92-18120
AD-D015145 ..... p 344 N92-18193
AD-D015160 ..... p 400 N92-18187 #
AD-D015182 ..... p 455 N92-20834 #
AD-D015213 ..... p 770 N92-27615
AD-D015215 ..... p 732 N92-27185 #
AD-D015237 ..... p 732 N92-27188
AD-D015259 ..... p 983 N92-31192 #
AD-D015268 ..... p 1088 N92-34131 #
AD-D015273 ..... p 927 N92-29095 #

AD-E200941 ..... p 736 N92-28004 #
AD-E501424 ..... p 158 N92-13351 #
AD-E951786 ..... p 983 N92-30849 #

AEDC-TR-91-16 ..... p 484 N92-20898 #
AEDC-TR-91-20 ..... p 738 N92-26405 * #
AEDC-TR-91-24 ..... p 403 N92-19080 #

AERO-REPT-8904 ..... p 262 N92-17849 #
AERO-REPT-8906 ..... p 308 N92-18322 #
AERO-REPT-8907 ..... p 910 N92-29683 #
AERO-REPT-9005 ..... p 385 N92-18341 #
AERO-REPT-9007 ..... p 344 N92-18231 #
AERO-REPT-9008 ..... p 345 N92-18232 #
AERO-REPT-9009 ..... p 345 N92-18233 #
AERO-REPT-9017 ..... p 380 N92-18321 #
AERO-REPT-9103 ..... p 345 N92-18293 #
AERO-REPT-9104 ..... p 400 N92-18317 #
AERO-REPT-9105 ..... p 380 N92-18294 #
AERO-REPT-9106 ..... p 345 N92-18318 #

AFESC/ESL-TR-89-40 ..... p 285 N92-17260 #
AFESC/ESL-TR-90-60 ..... p 264 N92-17259 #

AFIT/CI/CIA-91-017D ..... p 290 N92-17932 #
AFIT/CI/CIA-91-066 ..... p 260 N92-17114 #
AFIT/CI/CIA-91-126 ..... p 988 N92-31823 #
AFIT/CI/CIA-92-039 ..... p 1086 N92-32435 #

AFIT/GA/ENY/91D-11 ..... p 366 N92-19192 #
AFIT/GA/ENY/91D-13 ..... p 377 N92-19184 #
AFIT/GA/ENY/91D-1 ..... p 366 N92-19178 #
AFIT/GA/ENY/91D-4 ..... p 348 N92-19367 #

AFIT/GAE/ENY/91D-15 ..... p 352 N92-19259 #
AFIT/GAE/ENY/91D-1 ..... p 377 N92-19329 #
AFIT/GAE/ENY/91D-25 ..... p 404 N92-19183 #
AFIT/GAE/ENY/91D-26 ..... p 347 N92-19304 #
AFIT/GAE/ENY/91D-27 ..... p 366 N92-19185 #
AFIT/GAE/ENY/91D-2 ..... p 376 N92-18867 #
AFIT/GAE/ENY/91D-3 ..... p 404 N92-19384 #
AFIT/GAE/ENY/91D-4 ..... p 346 N92-18895 #
AFIT/GAE/ENY/91D-5 ..... p 377 N92-19235 #
AFIT/GAE/ENY/91D-6 ..... p 377 N92-19328 #
AFIT/GAE/ENY/91D-7 ..... p 412 N92-19335 #
AFIT/GAE/ENY/91S-3 ..... p 272 N92-15990 #
AFIT/GAE/ENY/91S-4 ..... p 299 N92-17024 #

AFIT/GCA/LSQ/91S-3 ..... p 417 N92-19466 #

AFIT/GCE/ENG/91D-02 ..... p 409 N92-19231 #

AFIT/GCE/ENS/91D-01 ..... p 284 N92-17097 #

AFIT/GCS/ENG/91D-22 ..... p 384 N92-18012 #
AFIT/GCS/ENG/92M-03 ..... p 859 N92-29222 #

AFIT/GE/EN/91D-14 ..... p 382 N92-19505 #
AFIT/GE/EN/91D-44 ..... p 381 N92-19241 #

AFIT/GE/ENG/91D-04 ..... p 356 N92-19604 #
AFIT/GE/ENG/91D-33 ..... p 283 N92-17748 #
AFIT/GE/ENG/91D-39 ..... p 282 N92-17096 #
AFIT/GE/ENG/91D-40 ..... p 402 N92-18940 #
AFIT/GE/ENG/91D-45 ..... p 304 N92-17088 #

AFIT/GIR/LSY/91D-3 ..... p 417 N92-19336 #

AFIT/GLM/ENS/91S-50 ..... p 732 N92-27719 #

AFIT/GLM/LSM/91S-11 ..... p 778 N92-27980 #

AFIT/GLM/LSQ/91S-57 ..... p 786 N92-28348 #

AFIT/GOR/ENS/92M-11 ..... p 910 N92-29191 #

AFIT/GSM/LSG/91S-6 ..... p 772 N92-27760 #

AFIT/GSS/ENG/91D-3 ..... p 729 N92-28132 #

AFOSR-91-0713TR ..... p 33 N92-10062 #
AFOSR-91-0740TR ..... p 29 N92-11018 #
AFOSR-91-0785TR ..... p 406 N92-19873 #
AFOSR-91-0786TR ..... p 135 N92-13075 #
AFOSR-91-0808TR ..... p 158 N92-13409 #
AFOSR-91-0871TR ..... p 290 N92-17682 #
AFOSR-91-0954TR ..... p 376 N92-19097 #
AFOSR-91-0975TR ..... p 405 N92-19386 #
AFOSR-91-1035TR ..... p 489 N92-20695 #
AFOSR-92-0015TR ..... p 774 N92-27918 #
AFOSR-92-0077TR ..... p 830 N92-28888 #
AFOSR-92-0086TR ..... p 715 N92-27172 #
AFOSR-92-0088TR ..... p 767 N92-27352 #
AFOSR-92-0100TR ..... p 770 N92-27546 #
AFOSR-92-0163TR ..... p 743 N92-28076 #
AFOSR-92-0167TR-VOL-1 ..... p 1142 N92-32338 #
AFOSR-92-0215TR ..... p 1009 N92-30335 #
AFOSR-92-0222TR ..... p 829 N92-28865 #
AFOSR-92-0238TR ..... p 896 N92-29580 #
AFOSR-92-0257TR ..... p 774 N92-28171 #
AFOSR-92-0259TR ..... p 883 N92-28388 #
AFOSR-92-0287TR ..... p 979 N92-31967 #
AFOSR-92-0365TR ..... p 909 N92-29118 #
AFOSR-92-0388TR ..... p 1003 N92-31824 #
AFOSR-92-0399TR ..... p 948 N92-31555 #
AFOSR-92-0403TR ..... p 974 N92-32059 #
AFOSR-92-0415TR ..... p 987 N92-31419 #
AFOSR-92-0420TR ..... p 989 N92-32076 #
AFOSR-92-0456TR ..... p 986 N92-30256 #
AFOSR-92-0673TR ..... p 1111 N92-33624 #

AGARD-AG-319 ..... p 345 N92-18269 #
AGARD-AG-329 ..... p 859 N92-28376 #

AGARD-AR-270 ..... p 445 N92-20797 #
AGARD-AR-274 ..... p 382 N92-20026 #
AGARD-AR-280 ..... p 22 N92-11001 #
AGARD-AR-284 ..... p 205 N92-14065 #
AGARD-AR-299 ..... p 946 N92-30947 #
AGARD-AR-302 ..... p 303 N92-17498 #
AGARD-AR-306 ..... p 352 N92-18242 #
AGARD-AR-310 ..... p 1010 N92-32229 #
AGARD-AR-311 ..... p 733 N92-27870 #
AGARD-AR-312 ..... p 850 N92-28468 #
AGARD-AR-315 ..... p 983 N92-30769 #

AGARD-CP-494 ..... p 83 N92-12996 #
AGARD-CP-496 ..... p 449 N92-21679 #
AGARD-CP-497 ..... p 363 N92-18778 #
AGARD-CP-499 ..... p 164 N92-12517 #
AGARD-CP-506 ..... p 360 N92-18571 #
AGARD-CP-507 ..... p 718 N92-27936 #
AGARD-CP-509 ..... p 464 N92-21951 #
AGARD-CP-513 ..... p 786 N92-28522 #

AGARD-LS-178 ..... p 273 N92-17153 #
AGARD-LS-179 ..... p 234 N92-14673 #
AGARD-LS-183 ..... p 868 N92-28458 #
AGARD-LS-184 ..... p 774 N92-28084 #
AGARD-LS-186 ..... p 851 N92-28469 #

AGARD-PAPER-1 ..... p 446 N92-21432 * #
AGARD-PAPER-25 ..... p 185 N92-15049 * #
AGARD-PAPER-2 ..... p 851 N92-28473 * #

AGARD-R-773 ..... p 402 N92-19004 #
AGARD-R-783 ..... p 552 N92-23950 #
AGARD-R-784 ..... p 550 N92-23227 #
AGARD-R-785 ..... p 1109 N92-33033 #
AGARD-R-786 ..... p 717 N92-27706 #
AGARD-R-787 ..... p 771 N92-27671 #

AGARD-16 ..... p 962 N92-31261 * #

AIAA PAPER 90-1149 ..... p 595 N92-22649 * #
AIAA PAPER 90-1979 ..... p 934 A92-50269
AIAA PAPER 91-0068 ..... p 1035 A92-57035 #
AIAA PAPER 91-1274 ..... p 743 A92-41212
AIAA PAPER 91-2509 ..... p 56 A92-12700 #
AIAA PAPER 91-2581 ..... p 12 N92-10976 * #
AIAA PAPER 91-2631 ..... p 117 N92-13064 * #
AIAA PAPER 91-3069 ..... p 192 A92-20000 #
AIAA PAPER 91-3071 ..... p 21 A92-11607 #
AIAA PAPER 91-3268 ..... p 8 A92-12741 * #
AIAA PAPER 91-3304 ..... p 32 A92-12742 * #
AIAA PAPER 91-3342 ..... p 6 A92-11605 * #
AIAA PAPER 91-3665 ..... p 20 A92-11012 * #
AIAA PAPER 91-3666 ..... p 5 A92-11013 * #
AIAA PAPER 91-3667 ..... p 14 A92-11014 #
AIAA PAPER 91-3668 ..... p 20 A92-11015 * #
AIAA PAPER 91-3669 ..... p 14 A92-11016 #
AIAA PAPER 91-3670 ..... p 1 A92-11017 #
AIAA PAPER 91-3671 ..... p 14 A92-11018 * #
AIAA PAPER 91-3674 ..... p 14 A92-11019 * #
AIAA PAPER 91-3675 ..... p 15 A92-11020 #
AIAA PAPER 91-3676 ..... p 1 A92-11021 #
AIAA PAPER 91-3677 ..... p 1 A92-11022 #
AIAA PAPER 91-3678 ..... p 1 A92-11036 #
AIAA PAPER 91-3679 ..... p 15 A92-11023 #
AIAA PAPER 91-3680 ..... p 15 A92-11024 * #
AIAA PAPER 91-3681 ..... p 15 A92-11025 #
AIAA PAPER 91-3682 ..... p 15 A92-11026 #
AIAA PAPER 91-3684 ..... p 15 A92-11027 #
AIAA PAPER 91-3687 ..... p 15 A92-11030 #
AIAA PAPER 91-3688 ..... p 15 A92-11031 #
AIAA PAPER 91-3689 ..... p 16 A92-11032 #
AIAA PAPER 91-3692 ..... p 17 A92-12749 #
AIAA PAPER 91-3693 ..... p 16 A92-11034 #
AIAA PAPER 91-3709 ..... p 230 A92-17582 #
AIAA PAPER 91-3713 ..... p 230 A92-17585 * #
AIAA PAPER 91-3726 ..... p 231 A92-17594 * #
AIAA PAPER 91-3729 ..... p 197 A92-17596 #
AIAA PAPER 91-3730 ..... p 197 A92-17597 * #
AIAA PAPER 91-3764 ..... p 231 A92-17626 #
AIAA PAPER 91-3765 ..... p 215 A92-17627 #
AIAA PAPER 91-3766 ..... p 197 A92-17628 #
AIAA PAPER 91-3767 ..... p 231 A92-17629 * #
AIAA PAPER 91-3779 ..... p 231 A92-17637 * #
AIAA PAPER 91-3789 ..... p 232 A92-17645 #
AIAA PAPER 91-3803 ..... p 232 A92-17654 #
AIAA PAPER 91-3822 ..... p 232 A92-17664 #
AIAA PAPER 91-3941 ..... p 231 A92-17605 #
AIAA PAPER 91-3944 ..... p 231 A92-17608 #
AIAA PAPER 91-5002 ..... p 209 A92-17802 #
AIAA PAPER 91-5003 ..... p 471 A92-31683 #
AIAA PAPER 91-5015 ..... p 232 A92-17813 * #
AIAA PAPER 91-5019 ..... p 471 A92-31685 #
AIAA PAPER 91-5021 ..... p 171 A92-17817 #
AIAA PAPER 91-5024 ..... p 206 A92-17818 #
AIAA PAPER 91-5026 ..... p 207 A92-17819 * #
AIAA PAPER 91-5027 ..... p 483 A92-31686 #
AIAA PAPER 91-5028 ..... p 436 A92-31687 * #
AIAA PAPER 91-5029 ..... p 209 A92-17820 * #
AIAA PAPER 91-5031 ..... p 832 N92-29713 #
AIAA PAPER 91-5032 ..... p 171 A92-17822 #
AIAA PAPER 91-5033 ..... p 215 A92-17823 #
AIAA PAPER 91-5035 ..... p 209 A92-17824 #
AIAA PAPER 91-5036 ..... p 210 A92-17825 * #
AIAA PAPER 91-5038 ..... p 171 A92-17826 #
AIAA PAPER 91-5040 ..... p 200 A92-17828 #
AIAA PAPER 91-5041 ..... p 831 N92-29649 #
AIAA PAPER 91-5043 ..... p 437 A92-31688 #
AIAA PAPER 91-5044 ..... p 210 A92-17830 * #
AIAA PAPER 91-5048 ..... p 210 A92-17834 #
AIAA PAPER 91-5050 ..... p 731 A92-44547 #
AIAA PAPER 91-5054 ..... p 203 A92-17837 * #
AIAA PAPER 91-5055 ..... p 203 A92-17838 * #
AIAA PAPER 91-5056 ..... p 203 A92-17839 * #
AIAA PAPER 91-5057 ..... p 203 A92-17840 * #
AIAA PAPER 91-5058 ..... p 171 A92-17841 #
AIAA PAPER 91-5059 ..... p 472 A92-31689 #
AIAA PAPER 91-5060 ..... p 171 A92-17842 #
AIAA PAPER 91-5061 ..... p 437 A92-31690 * #
AIAA PAPER 91-5063 ..... p 216 A92-17843 * #
AIAA PAPER 91-5064 ..... p 459 A92-31691 #
AIAA PAPER 91-5065 ..... p 480 A92-31692 * #
AIAA PAPER 91-5075 ..... p 200 A92-17848 #
AIAA PAPER 91-5076 ..... p 200 A92-17849 #
AIAA PAPER 91-5081 ..... p 210 A92-17851 * #
AIAA PAPER 91-5086 ..... p 169 A92-17854 #
AIAA PAPER 91-5091 ..... p 172 A92-17857 * #
AIAA PAPER 91-5094 ..... p 472 A92-31696 #
AIAA PAPER 91-5098 ..... p 486 A92-31697 #
AIAA PAPER 91-5101 ..... p 486 A92-31698 #
AIAA PAPER 91-5102 ..... p 212 A92-17861 #
AIAA PAPER 92-0001 ..... p 278 A92-22126 #
AIAA PAPER 92-0004 ..... p 292 A92-22129 #
AIAA PAPER 92-0005 ..... p 292 A92-22130 * #
AIAA PAPER 92-0008 ..... p 288 A92-22133 #
AIAA PAPER 92-0010 ..... p 247 A92-22135 * #
AIAA PAPER 92-0011 ..... p 252 A92-23730 #
AIAA PAPER 92-0012 ..... p 278 A92-22136 #
AIAA PAPER 92-0015 ..... p 278 A92-22137 #
AIAA PAPER 92-0017 ..... p 247 A92-22139 #
AIAA PAPER 92-0018 ..... p 247 A92-22140 #
AIAA PAPER 92-0019 ..... p 247 A92-22141 * #
AIAA PAPER 92-0020 ..... p 248 A92-22142 * #
AIAA PAPER 92-0021 ..... p 281 A92-22143 * #
AIAA PAPER 92-0022 ..... p 281 A92-22144 * #
AIAA PAPER 92-0023 ..... p 248 A92-22145 #
AIAA PAPER 92-0024 ..... p 248 A92-22146 * #
AIAA PAPER 92-0025 ..... p 248 A92-22147 * #
AIAA PAPER 92-0026 ..... p 248 A92-22148 * #
AIAA PAPER 92-0027 ..... p 248 A92-22149 #
AIAA PAPER 92-0028 ..... p 248 A92-22150 #
AIAA PAPER 92-0029 ..... p 249 A92-22151 #
AIAA PAPER 92-0030 ..... p 249 A92-22152 * #
AIAA PAPER 92-0032 ..... p 249 A92-22153 * #
AIAA PAPER 92-0034 ..... p 249 A92-22155 #
AIAA PAPER 92-0035 ..... p 249 A92-22156 #
AIAA PAPER 92-0036 ..... p 249 A92-22157 #
AIAA PAPER 92-0037 ..... p 316 A92-25676 * #
AIAA PAPER 92-0037 ..... p 179 N92-14001 * #
AIAA PAPER 92-0038 ..... p 262 A92-22158 #
AIAA PAPER 92-0041 ..... p 262 A92-22159 #
AIAA PAPER 92-0042 ..... p 270 A92-22160 * #
AIAA PAPER 92-0043 ..... p 316 A92-25677 * #
AIAA PAPER 92-0043 ..... p 258 N92-15968 * #
AIAA PAPER 92-0044 ..... p 281 A92-22161 * #
AIAA PAPER 92-0045 ..... p 281 A92-22162 #
AIAA PAPER 92-0046 ..... p 281 A92-22163 #
AIAA PAPER 92-0048 ..... p 282 A92-22164 #
AIAA PAPER 92-0055 ..... p 249 A92-22170 #
AIAA PAPER 92-0056 ..... p 250 A92-22171 #
AIAA PAPER 92-0057 ..... p 250 A92-22172 #
AIAA PAPER 92-0061 ..... p 250 A92-22176 #
AIAA PAPER 92-0064 ..... p 250 A92-22178 #
AIAA PAPER 92-0066 ..... p 250 A92-22179 #
AIAA PAPER 92-0088 ..... p 292 A92-22195 #
AIAA PAPER 92-0090 ..... p 292 A92-22196 #
AIAA PAPER 92-0094 ..... p 293 A92-22200 #
AIAA PAPER 92-0100 ..... p 293 A92-22203 #

AIAA PAPER 92-0126 ..... p 286 A92-23746 * #
AIAA PAPER 92-0130 ..... p 295 A92-23750 #
AIAA PAPER 92-0131 ..... p 252 A92-23751 #
AIAA PAPER 92-0133 ..... p 286 A92-23753 #
AIAA PAPER 92-0134 ..... p 263 A92-23754 #
AIAA PAPER 92-0143 ..... p 284 A92-23761 #
AIAA PAPER 92-0145 ..... p 316 A92-25682 * #
AIAA PAPER 92-0146 ..... p 253 A92-23762 * #
AIAA PAPER 92-0147 ..... p 253 A92-23763 #
AIAA PAPER 92-0148 ..... p 253 A92-23764 * #
AIAA PAPER 92-0149 ..... p 341 A92-28186 * #
AIAA PAPER 92-0150 ..... p 253 A92-23765 #
AIAA PAPER 92-0151 ..... p 253 A92-23766 #
AIAA PAPER 92-0152 ..... p 253 A92-23767 * #
AIAA PAPER 92-0152 ..... p 179 N92-13998 * #
AIAA PAPER 92-0153 ..... p 271 A92-23768 * #
AIAA PAPER 92-0155 ..... p 253 A92-23770 #
AIAA PAPER 92-0156 ..... p 254 A92-23771 * #
AIAA PAPER 92-0157 ..... p 254 A92-23772 * #
AIAA PAPER 92-0158 ..... p 254 A92-23773 #
AIAA PAPER 92-0159 ..... p 254 A92-23774 #
AIAA PAPER 92-0160 ..... p 254 A92-23775 #
AIAA PAPER 92-0161 ..... p 241 A92-23776 #
AIAA PAPER 92-0164 ..... p 263 A92-23777 #
AIAA PAPER 92-0165 ..... p 263 A92-23778 #
AIAA PAPER 92-0167 ..... p 350 A92-25683 #
AIAA PAPER 92-0168 ..... p 254 A92-23779 #
AIAA PAPER 92-0168 ..... p 498 N92-20143 #
AIAA PAPER 92-0169 ..... p 255 A92-23780 #
AIAA PAPER 92-0170 ..... p 271 A92-23781 #
AIAA PAPER 92-0171 ..... p 271 A92-23782 #
AIAA PAPER 92-0172 ..... p 255 A92-23783 #
AIAA PAPER 92-0173 ..... p 255 A92-23784 #
AIAA PAPER 92-0174 ..... p 255 A92-23785 #
AIAA PAPER 92-0177 ..... p 255 A92-23787 #
AIAA PAPER 92-0178 ..... p 255 A92-23788 * #
AIAA PAPER 92-0180 ..... p 256 A92-23790 #
AIAA PAPER 92-0183 ..... p 256 A92-23793 #
AIAA PAPER 92-0184 ..... p 256 A92-23794 #
AIAA PAPER 92-0189 ..... p 256 A92-23798 * #
AIAA PAPER 92-0190 ..... p 256 A92-23799 #
AIAA PAPER 92-0191 ..... p 256 A92-23800 #
AIAA PAPER 92-0192 ..... p 257 A92-23801 #
AIAA PAPER 92-0193 ..... p 257 A92-23802 * #
AIAA PAPER 92-0195 ..... p 257 A92-23803 #
AIAA PAPER 92-0196 ..... p 257 A92-23804 #
AIAA PAPER 92-0197 ..... p 284 A92-23805 #
AIAA PAPER 92-0204 ..... p 284 A92-23810 * #
AIAA PAPER 92-0209 ..... p 271 A92-23814 #
AIAA PAPER 92-0212 ..... p 317 A92-25685 * #
AIAA PAPER 92-0214 ..... p 357 A92-25687 #
AIAA PAPER 92-0227 ..... p 317 A92-25691 #
AIAA PAPER 92-0229 ..... p 393 A92-25693 #
AIAA PAPER 92-0233 ..... p 372 A92-25696 * #
AIAA PAPER 92-0254 ..... p 357 A92-25712 * #
AIAA PAPER 92-0258 ..... p 394 A92-25716 #
AIAA PAPER 92-0263 ..... p 369 A92-25719 * #
AIAA PAPER 92-0264 ..... p 394 A92-25720 #
AIAA PAPER 92-0267 ..... p 317 A92-25723 #
AIAA PAPER 92-0268 ..... p 369 A92-25724 * #
AIAA PAPER 92-0269 ..... p 317 A92-25725 #
AIAA PAPER 92-0270 ..... p 317 A92-25726 * #
AIAA PAPER 92-0273 ..... p 317 A92-25727 #
AIAA PAPER 92-0274 ..... p 318 A92-25728 * #
AIAA PAPER 92-0274 ..... p 179 N92-14002 * #
AIAA PAPER 92-0275 ..... p 318 A92-25729 #
AIAA PAPER 92-0276 ..... p 318 A92-25730 #
AIAA PAPER 92-0277 ..... p 318 A92-25731 * #
AIAA PAPER 92-0278 ..... p 318 A92-25732 #
AIAA PAPER 92-0279 ..... p 379 A92-25733 * #
AIAA PAPER 92-0280 ..... p 318 A92-25734 * #
AIAA PAPER 92-0281 ..... p 318 A92-25735 #
AIAA PAPER 92-0282 ..... p 435 A92-31652 #
AIAA PAPER 92-0283 ..... p 319 A92-25736 #
AIAA PAPER 92-0284 ..... p 319 A92-25737 #
AIAA PAPER 92-0285 ..... p 319 A92-25738 #
AIAA PAPER 92-0286 ..... p 319 A92-25739 #
AIAA PAPER 92-0287 ..... p 319 A92-25740 #
AIAA PAPER 92-0290 ..... p 350 A92-25743 * #
AIAA PAPER 92-0291 ..... p 351 A92-25744 * #
AIAA PAPER 92-0292 ..... p 369 A92-25745 * #
AIAA PAPER 92-0293 ..... p 369 A92-25746 * #
AIAA PAPER 92-0294 ..... p 407 A92-25747 * #
AIAA PAPER 92-0295 ..... p 319 A92-25748 #
AIAA PAPER 92-0296 ..... p 351 A92-25749 #
AIAA PAPER 92-0297 ..... p 351 A92-25750 * #
AIAA PAPER 92-0299 ..... p 351 A92-25751 #
AIAA PAPER 92-0300 ..... p 369 A92-25752 #
AIAA PAPER 92-0301 ..... p 369 A92-25753 #
AIAA PAPER 92-0302 ..... p 320 A92-25754 #
AIAA PAPER 92-0305 ..... p 435 A92-31653 #
AIAA PAPER 92-0306 ..... p 320 A92-25755 * #
AIAA PAPER 92-0308 ..... p 387 A92-25756 #
AIAA PAPER 92-0309 ..... p 320 A92-25757 #
AIAA PAPER 92-0310 ..... p 320 A92-25758 #
AIAA PAPER 92-0311 ..... p 320 A92-25759 * #
AIAA PAPER 92-0313 ..... p 320 A92-25761 #
AIAA PAPER 92-0315 ..... p 320 A92-25762 * #
AIAA PAPER 92-0316 ..... p 321 A92-25763 #
AIAA PAPER 92-0317 ..... p 321 A92-25764 #
AIAA PAPER 92-0318 ..... p 321 A92-25765 #
AIAA PAPER 92-0319 ..... p 321 A92-25766 #
AIAA PAPER 92-0320 ..... p 321 A92-25767 #
AIAA PAPER 92-0321 ..... p 321 A92-25768 #
AIAA PAPER 92-0322 ..... p 321 A92-25769 #
AIAA PAPER 92-0323 ..... p 322 A92-25770 #
AIAA PAPER 92-0324 ..... p 322 A92-25771 * #
AIAA PAPER 92-0325 ..... p 322 A92-25772 * #
AIAA PAPER 92-0327 ..... p 383 A92-25774 * #
AIAA PAPER 92-0328 ..... p 322 A92-25775 #
AIAA PAPER 92-0329 ..... p 383 A92-25776 * #
AIAA PAPER 92-0330 ..... p 322 A92-25777 * #
AIAA PAPER 92-0331 ..... p 383 A92-25778 * #
AIAA PAPER 92-0332 ..... p 322 A92-25779 * #
AIAA PAPER 92-0340 ..... p 394 A92-25786 * #
AIAA PAPER 92-0341 ..... p 388 A92-25787 #
AIAA PAPER 92-0343 ..... p 496 A92-31655 #
AIAA PAPER 92-0366 ..... p 394 A92-26227 * #
AIAA PAPER 92-0370 ..... p 416 A92-28190 #
AIAA PAPER 92-0374 ..... p 414 A92-26232 * #
AIAA PAPER 92-0376 ..... p 372 A92-26234 * #
AIAA PAPER 92-0376 ..... p 130 N92-13071 * #
AIAA PAPER 92-0377 ..... p 395 A92-26235 #
AIAA PAPER 92-0383 ..... p 323 A92-26240 #
AIAA PAPER 92-0384 ..... p 323 A92-26241 * #
AIAA PAPER 92-0385 ..... p 374 A92-28191 * #
AIAA PAPER 92-0385 ..... p 350 N92-19993 * #
AIAA PAPER 92-0386 ..... p 323 A92-26242 #
AIAA PAPER 92-0387 ..... p 323 A92-26243 * #
AIAA PAPER 92-0388 ..... p 323 A92-26244 * #
AIAA PAPER 92-0389 ..... p 357 A92-26245 #
AIAA PAPER 92-0391 ..... p 372 A92-26247 #
AIAA PAPER 92-0392 ..... p 471 A92-31660 #
AIAA PAPER 92-0393 ..... p 323 A92-26248 #
AIAA PAPER 92-0394 ..... p 395 A92-26249 #
AIAA PAPER 92-0395 ..... p 278 A92-23816 #
AIAA PAPER 92-0398 ..... p 373 A92-26252 #
AIAA PAPER 92-0400 ..... p 373 A92-26253 * #
AIAA PAPER 92-0401 ..... p 324 A92-26254 #
AIAA PAPER 92-0402 ..... p 324 A92-26255 * #
AIAA PAPER 92-0403 ..... p 324 A92-26256 #
AIAA PAPER 92-0404 ..... p 324 A92-26257 #
AIAA PAPER 92-0405 ..... p 324 A92-26258 * #
AIAA PAPER 92-0406 ..... p 324 A92-26259 #
AIAA PAPER 92-0407 ..... p 325 A92-26260 * #
AIAA PAPER 92-0408 ..... p 325 A92-26261 * #
AIAA PAPER 92-0409 ..... p 325 A92-26262 #
AIAA PAPER 92-0410 ..... p 325 A92-26263 * #
AIAA PAPER 92-0411 ..... p 435 A92-31661 #
AIAA PAPER 92-0412 ..... p 325 A92-26264 * #
AIAA PAPER 92-0413 ..... p 341 A92-28192 * #
AIAA PAPER 92-0413 ..... p 714 N92-26612 * #
AIAA PAPER 92-0414 ..... p 325 A92-26265 * #
AIAA PAPER 92-0415 ..... p 326 A92-26266 * #
AIAA PAPER 92-0416 ..... p 423 A92-29972 * #
AIAA PAPER 92-0417 ..... p 326 A92-26267 * #
AIAA PAPER 92-0417 ..... p 186 N92-15052 * #
AIAA PAPER 92-0418 ..... p 326 A92-26268 #
AIAA PAPER 92-0418 ..... p 258 N92-15967 * #
AIAA PAPER 92-0421 ..... p 341 A92-28193 * #
AIAA PAPER 92-0426 ..... p 326 A92-26274 #
AIAA PAPER 92-0427 ..... p 326 A92-26275 #
AIAA PAPER 92-0428 ..... p 326 A92-26276 #
AIAA PAPER 92-0429 ..... p 326 A92-26277 #
AIAA PAPER 92-0430 ..... p 435 A92-31663 #
AIAA PAPER 92-0433 ..... p 327 A92-26280 #
AIAA PAPER 92-0434 ..... p 327 A92-26281 #
AIAA PAPER 92-0436 ..... p 327 A92-26283 * #
AIAA PAPER 92-0437 ..... p 327 A92-26284 #
AIAA PAPER 92-0439 ..... p 327 A92-26285 #
AIAA PAPER 92-0444 ..... p 328 A92-26288 * #
AIAA PAPER 92-0447 ..... p 328 A92-26291 * #
AIAA PAPER 92-0461 ..... p 395 A92-26302 #
AIAA PAPER 92-0486 ..... p 328 A92-26317 #
AIAA PAPER 92-0487 ..... p 328 A92-26318 #
AIAA PAPER 92-0488 ..... p 341 A92-28194 * #
AIAA PAPER 92-0492 ..... p 328 A92-26322 * #
AIAA PAPER 92-0493 ..... p 328 A92-26323 #
AIAA PAPER 92-0494 ..... p 329 A92-26324 #
AIAA PAPER 92-0495 ..... p 329 A92-26325 * #
AIAA PAPER 92-0498 ..... p 329 A92-26326 * #
AIAA PAPER 92-0499 ..... p 329 A92-26327 * #
AIAA PAPER 92-0500 ..... p 414 A92-26328 * #
AIAA PAPER 92-0500 ..... p 237 N92-14795 * #
AIAA PAPER 92-0501 ..... p 415 A92-26930 * #
AIAA PAPER 92-0501 ..... p 237 N92-14797 * #
AIAA PAPER 92-0502 ..... p 416 A92-26931 * #
AIAA PAPER 92-0503 ..... p 331 A92-26932 * #
AIAA PAPER 92-0504 ..... p 341 A92-28196 #
AIAA PAPER 92-0508 ..... p 396 A92-26935 * #
AIAA PAPER 92-0513 ..... p 396 A92-26939 #
AIAA PAPER 92-0514 ..... p 373 A92-26940 #
AIAA PAPER 92-0515 ..... p 373 A92-26941 #
AIAA PAPER 92-0516 ..... p 373 A92-26942 #
AIAA PAPER 92-0518 ..... p 331 A92-26943 #
AIAA PAPER 92-0519 ..... p 331 A92-26944 #
AIAA PAPER 92-0520 ..... p 331 A92-26945 #
AIAA PAPER 92-0521 ..... p 332 A92-26946 * #
AIAA PAPER 92-0522 ..... p 332 A92-26947 * #
AIAA PAPER 92-0523 ..... p 341 A92-28197 * #
AIAA PAPER 92-0524 ..... p 332 A92-26948 * #
AIAA PAPER 92-0526 ..... p 351 A92-26949 #
AIAA PAPER 92-0527 ..... p 357 A92-26950 * #
AIAA PAPER 92-0528 ..... p 459 A92-31668 #
AIAA PAPER 92-0531 ..... p 459 A92-31669 #
AIAA PAPER 92-0532 ..... p 459 A92-31670 * #
AIAA PAPER 92-0533 ..... p 358 A92-26951 #
AIAA PAPER 92-0535 ..... p 396 A92-26952 #
AIAA PAPER 92-0540 ..... p 332 A92-26957 #
AIAA PAPER 92-0541 ..... p 341 A92-28199 * #
AIAA PAPER 92-0543 ..... p 342 A92-28200 * #
AIAA PAPER 92-0544 ..... p 398 A92-28201 * #
AIAA PAPER 92-0545 ..... p 342 A92-28202 * #
AIAA PAPER 92-0551 ..... p 342 A92-28204 * #
AIAA PAPER 92-0553 ..... p 332 A92-26964 #
AIAA PAPER 92-0555 ..... p 333 A92-26965 #
AIAA PAPER 92-0558 ..... p 411 A92-26968 #
AIAA PAPER 92-0561 ..... p 411 A92-26970 #
AIAA PAPER 92-0566 ..... p 383 A92-26974 * #
AIAA PAPER 92-0567 ..... p 384 A92-26975 #
AIAA PAPER 92-0568 ..... p 384 A92-26976 #
AIAA PAPER 92-0570 ..... p 333 A92-26978 * #
AIAA PAPER 92-0573 ..... p 333 A92-26980 * #
AIAA PAPER 92-0577 ..... p 407 A92-26984 #
AIAA PAPER 92-0590 ..... p 411 A92-26992 #
AIAA PAPER 92-0624 ..... p 342 A92-28213 * #
AIAA PAPER 92-0625 ..... p 374 A92-27007 * #
AIAA PAPER 92-0626 ..... p 278 A92-23817 * #
AIAA PAPER 92-0628 ..... p 396 A92-27009 * #
AIAA PAPER 92-0630 ..... p 333 A92-27010 #
AIAA PAPER 92-0633 ..... p 333 A92-27011 #
AIAA PAPER 92-0634 ..... p 333 A92-27012 #
AIAA PAPER 92-0635 ..... p 334 A92-27013 #
AIAA PAPER 92-0636 ..... p 334 A92-27014 #
AIAA PAPER 92-0638 ..... p 334 A92-27016 * #
AIAA PAPER 92-0639 ..... p 334 A92-27017 #
AIAA PAPER 92-0643 ..... p 459 A92-31675 #
AIAA PAPER 92-0645 ..... p 342 A92-28215 * #
AIAA PAPER 92-0645 ..... p 596 N92-23154 * #
AIAA PAPER 92-0647 ..... p 334 A92-27021 * #
AIAA PAPER 92-0647 ..... p 185 N92-15051 * #
AIAA PAPER 92-0651 ..... p 334 A92-27023 * #
AIAA PAPER 92-0656 ..... p 342 A92-28217 * #
AIAA PAPER 92-0658 ..... p 396 A92-27029 #
AIAA PAPER 92-0660 ..... p 334 A92-27031 * #
AIAA PAPER 92-0661 ..... p 397 A92-27032 #
AIAA PAPER 92-0663 ..... p 411 A92-27034 #
AIAA PAPER 92-0665 ..... p 335 A92-27036 #
AIAA PAPER 92-0672 ..... p 431 A92-30624 #
AIAA PAPER 92-0673 ..... p 384 A92-27042 #
AIAA PAPER 92-0674 ..... p 343 A92-28218 #
AIAA PAPER 92-0675 ..... p 379 A92-27043 #
AIAA PAPER 92-0683 ..... p 389 A92-27050 #
AIAA PAPER 92-0684 ..... p 389 A92-27051 #
AIAA PAPER 92-0685 ..... p 389 A92-27052 #
AIAA PAPER 92-0686 ..... p 389 A92-27053 #
AIAA PAPER 92-0687 ..... p 390 A92-27054 #
AIAA PAPER 92-0730 ..... p 379 A92-27082 #
AIAA PAPER 92-0731 ..... p 379 A92-27083 #
AIAA PAPER 92-0736 ..... p 486 A92-31676 * #
AIAA PAPER 92-0737 ..... p 335 A92-27088 #
AIAA PAPER 92-0742 ..... p 343 A92-28223 * #
AIAA PAPER 92-0743 ..... p 343 A92-28224 * #
AIAA PAPER 92-0744 ..... p 436 A92-31677 #
AIAA PAPER 92-0746 ..... p 335 A92-27092 #
AIAA PAPER 92-0748 ..... p 436 A92-31678 * #
AIAA PAPER 92-0749 ..... p 335 A92-27093 #
AIAA PAPER 92-0750 ..... p 335 A92-27094 #
AIAA PAPER 92-0751 ..... p 335 A92-27095 #
AIAA PAPER 92-0753 ..... p 436 A92-31679 * #
AIAA PAPER 92-0754 ..... p 336 A92-27097 #
AIAA PAPER 92-0755 ..... p 436 A92-31680 * #
AIAA PAPER 92-0756 ..... p 336 A92-27098 #
AIAA PAPER 92-0757 ..... p 336 A92-27099 #
AIAA PAPER 92-0761 ..... p 384 A92-27102 #
AIAA PAPER 92-0763 ..... p 398 A92-28226 * #
AIAA PAPER 92-0767 ..... p 387 A92-27107 #
AIAA PAPER 92-0768 ..... p 374 A92-27108 #
AIAA PAPER 92-0777 ..... p 374 A92-27114 #
AIAA PAPER 92-0827 ..... p 421 A92-29595 #
AIAA PAPER 92-0828 ..... p 422 A92-29596 #
AIAA PAPER 92-0837 ..... p 422 A92-29603 #
AIAA PAPER 92-0838 ..... p 422 A92-29604 #
AIAA PAPER 92-0843 ..... p 493 A92-29609 #
AIAA PAPER 92-0844 ..... p 493 A92-29610 * #
AIAA PAPER 92-0877 ..... p 487 A92-29639 * #
AIAA PAPER 92-0983 ..... p 580 A92-33185 #
AIAA PAPER 92-0987 ..... p 535 A92-33182 #

AIAA PAPER 92-0999 ..... p 600 A92-33191 #
AIAA PAPER 92-1001 ..... p 535 A92-33193 * #
AIAA PAPER 92-1002 ..... p 536 A92-33194 #
AIAA PAPER 92-1004 ..... p 536 A92-33196 * #
AIAA PAPER 92-1010 ..... p 515 A92-33198 #
AIAA PAPER 92-1021 ..... p 531 A92-33204 #
AIAA PAPER 92-1025 ..... p 517 A92-33206 #
AIAA PAPER 92-1027 ..... p 536 A92-33208 * #
AIAA PAPER 92-1028 ..... p 580 A92-33209 * #
AIAA PAPER 92-1037 ..... p 553 A92-33218 #
AIAA PAPER 92-1038 ..... p 536 A92-33219 #
AIAA PAPER 92-1040 ..... p 605 A92-33221 #
AIAA PAPER 92-1050 ..... p 553 A92-33230 #
AIAA PAPER 92-1066 ..... p 536 A92-33239 #
AIAA PAPER 92-1067 ..... p 517 A92-33240 * #
AIAA PAPER 92-1074 ..... p 573 A92-33244 #
AIAA PAPER 92-1076 ..... p 563 A92-33245 #
AIAA PAPER 92-1077 ..... p 563 A92-33246 #
AIAA PAPER 92-1078 ..... p 563 A92-33247 #
AIAA PAPER 92-1079 ..... p 563 A92-33248 #
AIAA PAPER 92-1080 ..... p 536 A92-33249 #
AIAA PAPER 92-1082 ..... p 536 A92-33250 #
AIAA PAPER 92-1085 ..... p 537 A92-33251 #
AIAA PAPER 92-1086 ..... p 537 A92-33252 #
AIAA PAPER 92-1087 ..... p 537 A92-33253 #
AIAA PAPER 92-1088 ..... p 515 A92-33254 #
AIAA PAPER 92-1091 ..... p 605 A92-33256 * #
AIAA PAPER 92-1092 ..... p 605 A92-33257 #
AIAA PAPER 92-1097 ..... p 581 A92-33261 #
AIAA PAPER 92-1113 ..... p 605 A92-33269 #
AIAA PAPER 92-1116 ..... p 537 A92-33271 #
AIAA PAPER 92-1123 ..... p 563 A92-33277 #
AIAA PAPER 92-1126 ..... p 563 A92-33278 #
AIAA PAPER 92-1127 ..... p 577 A92-33279 #
AIAA PAPER 92-1128 ..... p 537 A92-33280 #
AIAA PAPER 92-1129 ..... p 537 A92-33281 #
AIAA PAPER 92-1130 ..... p 581 A92-33282 #
AIAA PAPER 92-1146 ..... p 574 A92-33287 #
AIAA PAPER 92-1187 ..... p 1130 A92-54285 * #
AIAA PAPER 92-1188 ..... p 600 A92-33300 #
AIAA PAPER 92-1189 ..... p 600 A92-33301 #
AIAA PAPER 92-1190 ..... p 600 A92-33302 #
AIAA PAPER 92-1191 ..... p 600 A92-33303 #
AIAA PAPER 92-1192 ..... p 600 A92-33304 * #
AIAA PAPER 92-1194 ..... p 600 A92-33306 #
AIAA PAPER 92-1196 ..... p 537 A92-33307 #
AIAA PAPER 92-1205 ..... p 537 A92-33313 * #
AIAA PAPER 92-1210 ..... p 517 A92-33314 #
AIAA PAPER 92-1221 ..... p 517 A92-33320 * #
AIAA PAPER 92-1229 ..... p 538 A92-33326 #
AIAA PAPER 92-1230 ..... p 538 A92-33327 #
AIAA PAPER 92-1240 ..... p 538 A92-33333 #
AIAA PAPER 92-1243 ..... p 553 A92-33336 #
AIAA PAPER 92-1244 ..... p 553 A92-33337 #
AIAA PAPER 92-1256 ..... p 515 A92-33339 #
AIAA PAPER 92-1262 ..... p 538 A92-33342 #
AIAA PAPER 92-1263 ..... p 538 A92-33343 #
AIAA PAPER 92-1268 ..... p 601 A92-33345 #
AIAA PAPER 92-1273 ..... p 666 A92-38478 * #
AIAA PAPER 92-1417 ..... p 666 A92-38569 * #
AIAA PAPER 92-1539 ..... p 690 A92-38636 #
AIAA PAPER 92-1626 ..... p 690 A92-38699 * #
AIAA PAPER 92-1812 ..... p 453 A92-29760 #
AIAA PAPER 92-1927 ..... p 453 A92-29856 #
AIAA PAPER 92-2027 ..... p 471 A92-29944 #
AIAA PAPER 92-2042 ..... p 485 A92-29956 #
AIAA PAPER 92-2058 ..... p 453 A92-29889 * #
AIAA PAPER 92-2080 ..... p 565 A92-35652 * #
AIAA PAPER 92-2081 ..... p 572 A92-35653 * #
AIAA PAPER 92-2082 ..... p 565 A92-35654 * #
AIAA PAPER 92-2083 ..... p 565 A92-35655 * #
AIAA PAPER 92-2084 ..... p 572 A92-35656 * #
AIAA PAPER 92-2092 ..... p 1137 N92-32956 * #
AIAA PAPER 92-2095-CP ..... p 962 N92-31350 * #
AIAA PAPER 92-2095 ..... p 566 A92-35668 * #
AIAA PAPER 92-2096 ..... p 566 A92-35667 * #
AIAA PAPER 92-2096 ..... p 662 N92-25607 * #
AIAA PAPER 92-2097 ..... p 566 A92-35666 * #
AIAA PAPER 92-2098 ..... p 566 A92-35669 #
AIAA PAPER 92-2099 ..... p 566 A92-35670 * #
AIAA PAPER 92-2100 ..... p 567 A92-35671 #
AIAA PAPER 92-2101 ..... p 588 A92-35672 #
AIAA PAPER 92-2102 ..... p 588 A92-35673 * #
AIAA PAPER 92-2103 ..... p 589 A92-35674 #
AIAA PAPER 92-2104 ..... p 567 A92-35675 #
AIAA PAPER 92-2105 ..... p 567 A92-35676 #
AIAA PAPER 92-2106 ..... p 567 A92-35677 * #
AIAA PAPER 92-2107 ..... p 567 A92-35678 * #
AIAA PAPER 92-2108 ..... p 544 A92-35679 #
AIAA PAPER 92-2109 ..... p 544 A92-35680 #
AIAA PAPER 92-2110 ..... p 544 A92-35681 #
AIAA PAPER 92-2112 ..... p 544 A92-35682 #
AIAA PAPER 92-2118 ..... p 557 A92-35687 * #
AIAA PAPER 92-2119 ..... p 558 A92-35688 #
AIAA PAPER 92-2120 ..... p 520 A92-35689 * #
AIAA PAPER 92-2121 ..... p 520 A92-35690 * #
AIAA PAPER 92-2123 ..... p 589 A92-35691 * #
AIAA PAPER 92-2125 ..... p 572 A92-35692 #
AIAA PAPER 92-2126 ..... p 567 A92-35693 #
AIAA PAPER 92-2127 ..... p 520 A92-35694 #
AIAA PAPER 92-2128 ..... p 589 A92-35695 * #
AIAA PAPER 92-2129 ..... p 589 A92-35696 * #
AIAA PAPER 92-2130 ..... p 589 A92-35697 * #
AIAA PAPER 92-2132 ..... p 589 A92-35699 #
AIAA PAPER 92-2164 ..... p 1137 N92-32951 * #
AIAA PAPER 92-2200 ..... p 539 A92-34390 * #
AIAA PAPER 92-2201 ..... p 539 A92-34391 #
AIAA PAPER 92-2202 ..... p 539 A92-34392 * #
AIAA PAPER 92-2203 ..... p 540 A92-34393 #
AIAA PAPER 92-2204 ..... p 540 A92-34394 #
AIAA PAPER 92-2213 ..... p 584 A92-34403 #
AIAA PAPER 92-2235 ..... p 581 A92-34289 * #
AIAA PAPER 92-2238 ..... p 581 A92-34292 #
AIAA PAPER 92-2253 ..... p 584 A92-34410 #
AIAA PAPER 92-2254 ..... p 564 A92-34479 #
AIAA PAPER 92-2256 ..... p 540 A92-34411 #
AIAA PAPER 92-2257 ..... p 540 A92-34412 #
AIAA PAPER 92-2258 ..... p 540 A92-34413 * #
AIAA PAPER 92-2259 ..... p 541 A92-34414 * #
AIAA PAPER 92-2260 ..... p 541 A92-34417 #
AIAA PAPER 92-2278 ..... p 582 A92-34297 * #
AIAA PAPER 92-2290 ..... p 582 A92-34307 * #
AIAA PAPER 92-2303 ..... p 585 A92-34524 #
AIAA PAPER 92-2305 ..... p 586 A92-34525 * #
AIAA PAPER 92-2345 ..... p 582 A92-34320 #
AIAA PAPER 92-2359 ..... p 586 A92-34591 #
AIAA PAPER 92-2360 ..... p 543 A92-34592 * #
AIAA PAPER 92-2361 ..... p 543 A92-34593 #
AIAA PAPER 92-2368 ..... p 571 A92-34596 * #
AIAA PAPER 92-2369 ..... p 518 A92-34597 * #
AIAA PAPER 92-2370 ..... p 556 A92-34598 * #
AIAA PAPER 92-2371 ..... p 601 A92-34542 #
AIAA PAPER 92-2373 ..... p 542 A92-34543 #
AIAA PAPER 92-2374 ..... p 542 A92-34544 * #
AIAA PAPER 92-2375 ..... p 542 A92-34545 #
AIAA PAPER 92-2376 ..... p 542 A92-34546 * #
AIAA PAPER 92-2377 ..... p 565 A92-34547 #
AIAA PAPER 92-2378 ..... p 584 A92-34452 #
AIAA PAPER 92-2391 ..... p 585 A92-34465 * #
AIAA PAPER 92-2393 ..... p 517 A92-34466 #
AIAA PAPER 92-2394 ..... p 585 A92-34467 #
AIAA PAPER 92-2395 ..... p 541 A92-34468 #
AIAA PAPER 92-2396 ..... p 517 A92-34469 * #
AIAA PAPER 92-2399 ..... p 564 A92-34470 #
AIAA PAPER 92-2400 ..... p 541 A92-34471 #
AIAA PAPER 92-2425 ..... p 582 A92-34354 #
AIAA PAPER 92-2434 ..... p 586 A92-34548 #
AIAA PAPER 92-2441 ..... p 585 A92-34472 * #
AIAA PAPER 92-2442 ..... p 585 A92-34473 * #
AIAA PAPER 92-2445 ..... p 577 A92-34474 * #
AIAA PAPER 92-2446 ..... p 585 A92-34475 #
AIAA PAPER 92-2449 ..... p 541 A92-34476 * #
AIAA PAPER 92-2450 ..... p 542 A92-34477 * #
AIAA PAPER 92-2451 ..... p 564 A92-34478 #
AIAA PAPER 92-2452 ..... p 541 A92-34415 #
AIAA PAPER 92-2467 ..... p 582 A92-34357 * #
AIAA PAPER 92-2468 ..... p 539 A92-34358 * #
AIAA PAPER 92-2469 ..... p 564 A92-34359 #
AIAA PAPER 92-2471 ..... p 583 A92-34360 * #
AIAA PAPER 92-2473 ..... p 539 A92-34362 * #
AIAA PAPER 92-2474 ..... p 583 A92-34363 * #
AIAA PAPER 92-2482 ..... p 543 A92-34599 #
AIAA PAPER 92-2487 ..... p 586 A92-34603 * #
AIAA PAPER 92-2488 ..... p 601 A92-34604 #
AIAA PAPER 92-2497 ..... p 601 A92-34554 #
AIAA PAPER 92-2502 ..... p 518 A92-34497 #
AIAA PAPER 92-2503 ..... p 518 A92-34498 * #
AIAA PAPER 92-2504 ..... p 518 A92-34499 #
AIAA PAPER 92-2506 ..... p 542 A92-34500 #
AIAA PAPER 92-2508 ..... p 518 A92-34501 #
AIAA PAPER 92-2526 ..... p 539 A92-34373 #
AIAA PAPER 92-2527 ..... p 583 A92-34374 #
AIAA PAPER 92-2530 ..... p 583 A92-34376 #
AIAA PAPER 92-2537 ..... p 583 A92-34381 * #
AIAA PAPER 92-2538 ..... p 584 A92-34382 * #
AIAA PAPER 92-2547 ..... p 518 A92-34517 #
AIAA PAPER 92-2566 ..... p 564 A92-34480 * #
AIAA PAPER 92-2567 ..... p 564 A92-34481 #
AIAA PAPER 92-2568 ..... p 565 A92-34482 * #
AIAA PAPER 92-2600 ..... p 791 A92-45477 #
AIAA PAPER 92-2601 ..... p 792 A92-45478 * #
AIAA PAPER 92-2602 ..... p 792 A92-45479 * #
AIAA PAPER 92-2603 ..... p 792 A92-45480 * #
AIAA PAPER 92-2605 ..... p 792 A92-45482 * #
AIAA PAPER 92-2606 ..... p 805 A92-45570 #
AIAA PAPER 92-2608 ..... p 805 A92-45568 * #
AIAA PAPER 92-2609 ..... p 792 A92-45483 #
AIAA PAPER 92-2610 ..... p 792 A92-45484 #
AIAA PAPER 92-2611 ..... p 793 A92-45485 * #
AIAA PAPER 92-2613 ..... p 793 A92-45487 #
AIAA PAPER 92-2614 ..... p 805 A92-45571 #
AIAA PAPER 92-2615 ..... p 873 A92-45488 #
AIAA PAPER 92-2616 ..... p 793 A92-45490 #
AIAA PAPER 92-2617 ..... p 805 A92-45572 #
AIAA PAPER 92-2618 ..... p 844 A92-45491 #
AIAA PAPER 92-2619 ..... p 917 A92-45492 #
AIAA PAPER 92-2620 ..... p 845 A92-45573 #
AIAA PAPER 92-2621 ..... p 793 A92-45493 * #
AIAA PAPER 92-2622-CP ..... p 833 N92-30182 * #
AIAA PAPER 92-2622 ..... p 793 A92-45494 * #
AIAA PAPER 92-2623 ..... p 794 A92-45495 #
AIAA PAPER 92-2624 ..... p 794 A92-45496 #
AIAA PAPER 92-2625 ..... p 794 A92-45497 #
AIAA PAPER 92-2626 ..... p 794 A92-45498 #
AIAA PAPER 92-2627 ..... p 794 A92-45499 #
AIAA PAPER 92-2628 ..... p 795 A92-45500 #
AIAA PAPER 92-2629 ..... p 844 A92-45501 #
AIAA PAPER 92-2630 ..... p 795 A92-45502 * #
AIAA PAPER 92-2631 ..... p 795 A92-45503 #
AIAA PAPER 92-2632 ..... p 795 A92-45504 #
AIAA PAPER 92-2633 ..... p 795 A92-45505 * #
AIAA PAPER 92-2634 ..... p 806 A92-45574 * #
AIAA PAPER 92-2635 ..... p 795 A92-45506 #
AIAA PAPER 92-2636 ..... p 806 A92-45575 * #
AIAA PAPER 92-2637 ..... p 806 A92-45576 * #
AIAA PAPER 92-2638 ..... p 796 A92-45507 #
AIAA PAPER 92-2639 ..... p 796 A92-45508 * #
AIAA PAPER 92-2642 ..... p 796 A92-45509 #
AIAA PAPER 92-2643 ..... p 796 A92-45510 * #
AIAA PAPER 92-2646 ..... p 796 A92-45513 #
AIAA PAPER 92-2647 ..... p 796 A92-45514 #
AIAA PAPER 92-2649 ..... p 797 A92-45516 #
AIAA PAPER 92-2650 ..... p 797 A92-45517 * #
AIAA PAPER 92-2651 ..... p 797 A92-45518 * #
AIAA PAPER 92-2653 ..... p 805 A92-45569 #
AIAA PAPER 92-2654 ..... p 806 A92-45578 #
AIAA PAPER 92-2658 ..... p 844 A92-45519 #
AIAA PAPER 92-2659 ..... p 797 A92-45520 #
AIAA PAPER 92-2661 ..... p 845 A92-45580 #
AIAA PAPER 92-2662 ..... p 928 A92-45581 #
AIAA PAPER 92-2666 ..... p 797 A92-45522 #
AIAA PAPER 92-2667 ..... p 806 A92-45582 #
AIAA PAPER 92-2668 ..... p 798 A92-45523 #
AIAA PAPER 92-2669 ..... p 798 A92-45524 #
AIAA PAPER 92-2670 ..... p 798 A92-45525 * #
AIAA PAPER 92-2671 ..... p 798 A92-45526 #
AIAA PAPER 92-2673 ..... p 798 A92-45528 * #
AIAA PAPER 92-2674 ..... p 806 A92-45583 * #
AIAA PAPER 92-2675 ..... p 798 A92-45529 #
AIAA PAPER 92-2676 ..... p 806 A92-45584 * #
AIAA PAPER 92-2677 ..... p 807 A92-45585 #
AIAA PAPER 92-2678 ..... p 799 A92-45530 * #
AIAA PAPER 92-2679 ..... p 799 A92-45531 #
AIAA PAPER 92-2680 ..... p 799 A92-45532 #
AIAA PAPER 92-2685 ..... p 799 A92-45534 * #
AIAA PAPER 92-2687 ..... p 807 A92-45588 #
AIAA PAPER 92-2688 ..... p 799 A92-45535 #
AIAA PAPER 92-2689 ..... p 799 A92-45536 #
AIAA PAPER 92-2690 ..... p 800 A92-45537 * #
AIAA PAPER 92-2691 ..... p 800 A92-45538 #
AIAA PAPER 92-2692 ..... p 800 A92-45539 * #
AIAA PAPER 92-2693 ..... p 917 A92-45589 #
AIAA PAPER 92-2694 ..... p 800 A92-45540 * #
AIAA PAPER 92-2696 ..... p 807 A92-45590 #
AIAA PAPER 92-2699 ..... p 800 A92-45541 * #
AIAA PAPER 92-2699 ..... p 1072 N92-33746 * #
AIAA PAPER 92-2700 ..... p 800 A92-45542 * #
AIAA PAPER 92-2701 ..... p 801 A92-45543 * #
AIAA PAPER 92-2702 ..... p 801 A92-45544 #
AIAA PAPER 92-2703 ..... p 801 A92-45545 #
AIAA PAPER 92-2704 ..... p 801 A92-45546 #
AIAA PAPER 92-2706 ..... p 801 A92-45548 #
AIAA PAPER 92-2707 ..... p 801 A92-45549 #
AIAA PAPER 92-2708 ..... p 802 A92-45550 * #
AIAA PAPER 92-2709 ..... p 807 A92-45592 #
AIAA PAPER 92-2710 ..... p 802 A92-45551 #
AIAA PAPER 92-2711 ..... p 802 A92-45552 * #
AIAA PAPER 92-2712 ..... p 807 A92-45593 #
AIAA PAPER 92-2714 ..... p 802 A92-45553 * #
AIAA PAPER 92-2715 ..... p 802 A92-45554 #
AIAA PAPER 92-2716 ..... p 803 A92-45555 * #
AIAA PAPER 92-2717 ..... p 803 A92-45556 #
AIAA PAPER 92-2719 ..... p 803 A92-45557 * #
AIAA PAPER 92-2720 ..... p 803 A92-45558 #
AIAA PAPER 92-2721 ..... p 803 A92-45559 #
AIAA PAPER 92-2722 ..... p 807 A92-45595 #
AIAA PAPER 92-2723 ..... p 803 A92-45560 * #
AIAA PAPER 92-2724 ..... p 803 A92-45561 * #
AIAA PAPER 92-2725 ..... p 808 A92-45596 * #
AIAA PAPER 92-2726 ..... p 804 A92-45562 #
AIAA PAPER 92-2727 ..... p 808 A92-45597 #
AIAA PAPER 92-2728 ..... p 804 A92-45563 #
AIAA PAPER 92-2729 ..... p 808 A92-45598 * #
AIAA PAPER 92-2730 ..... p 804 A92-45564 #
AIAA PAPER 92-2731 ..... p 804 A92-45565 #
AIAA PAPER 92-2732 ..... p 804 A92-45566 #
AIAA PAPER 92-2733 ..... p 805 A92-45567 #
AIAA PAPER 92-2734 ..... p 917 A92-45489 * #

AIAA PAPER 92-2735 ..... p 797 A92-45515 #
AIAA PAPER 92-2765 ..... p 704 A92-41314 #
AIAA PAPER 92-2768 ..... p 704 A92-41317 #
AIAA PAPER 92-2771 ..... p 704 A92-41318 #
AIAA PAPER 92-2774 ..... p 704 A92-41320 #
AIAA PAPER 92-2776 ..... p 704 A92-41322 #
AIAA PAPER 92-2779 ..... p 758 A92-41323 #
AIAA PAPER 92-2781 ..... p 778 A92-41324 #
AIAA PAPER 92-2792 ..... p 778 A92-41331 #
AIAA PAPER 92-2793 ..... p 779 A92-41332 #
AIAA PAPER 92-2797 ..... p 747 A92-41336 #
AIAA PAPER 92-2802 ..... p 779 A92-41340 #
AIAA PAPER 92-2806 ..... p 752 A92-41344 #
AIAA PAPER 92-2820 ..... p 705 A92-41348 #
AIAA PAPER 92-2852 ..... p 892 A92-47835 #
AIAA PAPER 92-2856 ..... p 819 A92-47839 #
AIAA PAPER 92-2871 ..... p 901 A92-47853 #
AIAA PAPER 92-2874 ..... p 819 A92-47856 #
AIAA PAPER 92-2876 ..... p 820 A92-47858 #
AIAA PAPER 92-2879 ..... p 820 A92-47860 #
AIAA PAPER 92-2896 ..... p 820 A92-47872 * #
AIAA PAPER 92-2897 ..... p 820 A92-47873 * #
AIAA PAPER 92-2899 ..... p 820 A92-47875 #
AIAA PAPER 92-2900 ..... p 820 A92-47876 #
AIAA PAPER 92-2920 ..... p 821 A92-47892 * #
AIAA PAPER 92-2922 ..... p 821 A92-47894 * #
AIAA PAPER 92-2949 ..... p 901 A92-47913 #
AIAA PAPER 92-2951 ..... p 821 A92-47915 * #
AIAA PAPER 92-2953 ..... p 821 A92-47917 #
AIAA PAPER 92-2970 ..... p 816 A92-46985 * #
AIAA PAPER 92-2971 ..... p 816 A92-46986 * #
AIAA PAPER 92-2986 ..... p 899 A92-46996 #
AIAA PAPER 92-3027 ..... p 925 A92-47028 #
AIAA PAPER 92-3040 ..... p 822 A92-48701 #
AIAA PAPER 92-3041 ..... p 822 A92-48702 #
AIAA PAPER 92-3042 ..... p 822 A92-48703 #
AIAA PAPER 92-3044 ..... p 822 A92-48704 #
AIAA PAPER 92-3045 ..... p 822 A92-48705 #
AIAA PAPER 92-3054 ..... p 889 A92-48712 #
AIAA PAPER 92-3055 ..... p 893 A92-48713 #
AIAA PAPER 92-3056 ..... p 893 A92-48714 #
AIAA PAPER 92-3066 ..... p 823 A92-48720 #
AIAA PAPER 92-3068 ..... p 1020 A92-54003 * #
AIAA PAPER 92-3069 ..... p 1020 A92-54004 * #
AIAA PAPER 92-3069 ..... p 831 N92-29402 * #
AIAA PAPER 92-3070 ..... p 1020 A92-54005 * #
AIAA PAPER 92-3071 ..... p 903 A92-48722 #
AIAA PAPER 92-3072 ..... p 1130 A92-54006 * #
AIAA PAPER 92-3073 ..... p 823 A92-48723 * #
AIAA PAPER 92-3074 ..... p 823 A92-48724 * #
AIAA PAPER 92-3082 ..... p 823 A92-48729 * #
AIAA PAPER 92-3082 ..... p 770 N92-27653 * #
AIAA PAPER 92-3083 ..... p 823 A92-48730 * #
AIAA PAPER 92-3083 ..... p 739 N92-27037 * #
AIAA PAPER 92-3087 ..... p 738 N92-26561 * #
AIAA PAPER 92-3089 ..... p 903 A92-48734 * #
AIAA PAPER 92-3090 ..... p 903 A92-48735 * #
AIAA PAPER 92-3090 ..... p 742 N92-27652 * #
AIAA PAPER 92-3092 ..... p 1066 A92-54009 * #
AIAA PAPER 92-3092 ..... p 871 N92-29425 * #
AIAA PAPER 92-3094 ..... p 824 A92-48738 * #
AIAA PAPER 92-3095 ..... p 877 A92-48737 * #
AIAA PAPER 92-3097 ..... p 849 A92-48739 #
AIAA PAPER 92-3098 ..... p 824 A92-48740 #
AIAA PAPER 92-3098 ..... p 722 N92-28102 * #
AIAA PAPER 92-3099 ..... p 824 A92-48741 * #
AIAA PAPER 92-3100 ..... p 824 A92-48742 #
AIAA PAPER 92-3101 ..... p 863 A92-48743 * #
AIAA PAPER 92-3102 ..... p 824 A92-48744 * #
AIAA PAPER 92-3154 ..... p 890 A92-48780 * #
AIAA PAPER 92-3169 ..... p 863 A92-48790 #
AIAA PAPER 92-3174 ..... p 1066 A92-54011 * #
AIAA PAPER 92-3175 ..... p 1020 A92-54012 * #
AIAA PAPER 92-3176 ..... p 903 A92-48792 #
AIAA PAPER 92-3177 ..... p 1020 A92-54013 * #
AIAA PAPER 92-3177 ..... p 1128 N92-34112 * #
AIAA PAPER 92-3178 ..... p 836 A92-48793 #
AIAA PAPER 92-3179 ..... p 922 A92-48794 #
AIAA PAPER 92-3188 ..... p 824 A92-48800 #
AIAA PAPER 92-3189 ..... p 863 A92-48801 #
AIAA PAPER 92-3190 ..... p 923 A92-48802 #
AIAA PAPER 92-3192 ..... p 903 A92-48803 #
AIAA PAPER 92-3193 ..... p 825 A92-48804 #
AIAA PAPER 92-3194 ..... p 863 A92-48805 #
AIAA PAPER 92-3211 ..... p 1021 A92-54016 * #
AIAA PAPER 92-3212 ..... p 825 A92-48817 #
AIAA PAPER 92-3231 ..... p 863 A92-48832 #
AIAA PAPER 92-3244 ..... p 903 A92-48844 * #
AIAA PAPER 92-3245 ..... p 1103 A92-54019 #
AIAA PAPER 92-3246 ..... p 904 A92-48845 #
AIAA PAPER 92-3247 ..... p 893 A92-48846 #
AIAA PAPER 92-3248 ..... p 904 A92-48847 #
AIAA PAPER 92-3249 ..... p 894 A92-48848 #
AIAA PAPER 92-3251 ..... p 890 A92-48849 * #
AIAA PAPER 92-3259 ..... p 864 A92-48855 #
AIAA PAPER 92-3260 ..... p 864 A92-48856 #
AIAA PAPER 92-3261 ..... p 1066 A92-54020 * #
AIAA PAPER 92-3262 ..... p 825 A92-48857 #
AIAA PAPER 92-3263 ..... p 864 A92-48858 * #
AIAA PAPER 92-3264 ..... p 864 A92-48859 #
AIAA PAPER 92-3282 ..... p 904 A92-48872 #
AIAA PAPER 92-3287 ..... p 904 A92-48876 * #
AIAA PAPER 92-3289 ..... p 864 A92-48878 #
AIAA PAPER 92-3290 ..... p 864 A92-48879 #
AIAA PAPER 92-3292 ..... p 882 A92-48881 #
AIAA PAPER 92-3309 ..... p 904 A92-48896 #
AIAA PAPER 92-3311 ..... p 825 A92-48897 #
AIAA PAPER 92-3312 ..... p 825 A92-48898 #
AIAA PAPER 92-3313 ..... p 825 A92-48899 #
AIAA PAPER 92-3318 ..... p 877 A92-48902 * #
AIAA PAPER 92-3319 ..... p 923 A92-48903 #
AIAA PAPER 92-3321 ..... p 864 A92-48904 #
AIAA PAPER 92-3323 ..... p 825 A92-48906 #
AIAA PAPER 92-3324 ..... p 904 A92-48907 #
AIAA PAPER 92-3325 ..... p 883 A92-48908 * #
AIAA PAPER 92-3326 ..... p 826 A92-48909 * #
AIAA PAPER 92-3327 ..... p 923 A92-48910 #
AIAA PAPER 92-3328 ..... p 865 A92-48911 #
AIAA PAPER 92-3332 ..... p 850 A92-48915 #
AIAA PAPER 92-3333 ..... p 850 A92-48916 #
AIAA PAPER 92-3335 ..... p 850 A92-48917 #
AIAA PAPER 92-3338 ..... p 1067 A92-54025 * #
AIAA PAPER 92-3338 ..... p 890 N92-29343 * #
AIAA PAPER 92-3340 ..... p 894 A92-48919 * #
AIAA PAPER 92-3346 ..... p 905 A92-48923 * #
AIAA PAPER 92-3350 ..... p 894 A92-48927 #
AIAA PAPER 92-3362 ..... p 1051 A92-54026 * #
AIAA PAPER 92-3363 ..... p 905 A92-48936 * #
AIAA PAPER 92-3364 ..... p 905 A92-48937 * #
AIAA PAPER 92-3365 ..... p 905 A92-48938 #
AIAA PAPER 92-3365 ..... p 680 N92-24984 * #
AIAA PAPER 92-3366 ..... p 905 A92-48939 * #
AIAA PAPER 92-3367 ..... p 865 A92-48940 * #
AIAA PAPER 92-3368 ..... p 850 A92-48941 #
AIAA PAPER 92-3420 ..... p 865 A92-48979 #
AIAA PAPER 92-3425 ..... p 865 A92-48984 * #
AIAA PAPER 92-3428 ..... p 1112 A92-54029 #
AIAA PAPER 92-3429 ..... p 894 A92-48986 #
AIAA PAPER 92-3465 ..... p 865 A92-49014 #
AIAA PAPER 92-3468 ..... p 905 A92-49015 #
AIAA PAPER 92-3469 ..... p 906 A92-49016 #
AIAA PAPER 92-3471 ..... p 1067 A92-54035 * #
AIAA PAPER 92-3472 ..... p 906 A92-49018 #
AIAA PAPER 92-3473 ..... p 865 A92-49019 #
AIAA PAPER 92-3476 ..... p 865 A92-49020 #
AIAA PAPER 92-3478 ..... p 866 A92-49021 #
AIAA PAPER 92-3482 ..... p 859 A92-49022 #
AIAA PAPER 92-3483 ..... p 866 A92-49023 #
AIAA PAPER 92-3484 ..... p 866 A92-49024 #
AIAA PAPER 92-3486 ..... p 878 A92-49025 #
AIAA PAPER 92-3491 ..... p 906 A92-49028 #
AIAA PAPER 92-3494 ..... p 1112 A92-54036 * #
AIAA PAPER 92-3494 ..... p 1002 N92-31485 * #
AIAA PAPER 92-3495 ..... p 906 A92-49031 #
AIAA PAPER 92-3524 ..... p 786 A92-49049 #
AIAA PAPER 92-3525 ..... p 906 A92-49048 #
AIAA PAPER 92-3545 ..... p 1112 A92-54044 #
AIAA PAPER 92-3548 ..... p 826 A92-49063 * #
AIAA PAPER 92-3548 ..... p 630 N92-24958 * #
AIAA PAPER 92-3549 ..... p 906 A92-49064 #
AIAA PAPER 92-3568 ..... p 1112 A92-54057 #
AIAA PAPER 92-3569 ..... p 1090 A92-54058 * #
AIAA PAPER 92-3570 ..... p 1067 A92-54059 * #
AIAA PAPER 92-3570 ..... p 868 N92-28419 * #
AIAA PAPER 92-3571 ..... p 1067 A92-54060 * #
AIAA PAPER 92-3599 ..... p 1112 A92-54075 #
AIAA PAPER 92-3622 ..... p 1021 A92-54090 * #
AIAA PAPER 92-3623 ..... p 826 A92-49076 #
AIAA PAPER 92-3624 ..... p 1021 A92-54091 #
AIAA PAPER 92-3625 ..... p 1021 A92-54092 #
AIAA PAPER 92-3626 ..... p 1113 A92-54093 #
AIAA PAPER 92-3651 ..... p 1067 A92-54104 #
AIAA PAPER 92-3652 ..... p 1113 A92-54105 #
AIAA PAPER 92-3654 ..... p 906 A92-49085 #
AIAA PAPER 92-3658 ..... p 1113 A92-54108 #
AIAA PAPER 92-3665 ..... p 1021 A92-54110 * #
AIAA PAPER 92-3666 ..... p 907 A92-49087 #
AIAA PAPER 92-3667 ..... p 1022 A92-54111 * #
AIAA PAPER 92-3668 ..... p 826 A92-49088 #
AIAA PAPER 92-3670 ..... p 1022 A92-54113 #
AIAA PAPER 92-3673 ..... p 1022 A92-54116 #
AIAA PAPER 92-3674 ..... p 1022 A92-54117 * #
AIAA PAPER 92-3675 ..... p 1022 A92-54118 #
AIAA PAPER 92-3712 ..... p 1113 A92-54132 * #
AIAA PAPER 92-3714 ..... p 907 A92-49096 #
AIAA PAPER 92-3717 ..... p 866 A92-49098 #
AIAA PAPER 92-3719 ..... p 1067 A92-54134 #
AIAA PAPER 92-3720 ..... p 1067 A92-54135 #
AIAA PAPER 92-3727 ..... p 894 A92-49105 #
AIAA PAPER 92-3728 ..... p 894 A92-49106 #
AIAA PAPER 92-3743 ..... p 878 A92-49109 * #
AIAA PAPER 92-3744 ..... p 1068 A92-54146 #
AIAA PAPER 92-3745 ..... p 866 A92-49110 * #
AIAA PAPER 92-3746 ..... p 1068 A92-54147 #
AIAA PAPER 92-3747 ..... p 866 A92-49111 * #
AIAA PAPER 92-3747 ..... p 971 N92-30518 * #
AIAA PAPER 92-3748 ..... p 1068 A92-54148 #
AIAA PAPER 92-3749 ..... p 1068 A92-54149 #
AIAA PAPER 92-3753 ..... p 1068 A92-54151 #
AIAA PAPER 92-3754 ..... p 867 A92-49112 #
AIAA PAPER 92-3755 ..... p 867 A92-49113 #
AIAA PAPER 92-3757 ..... p 867 A92-49114 #
AIAA PAPER 92-3758 ..... p 1141 A92-54152 #
AIAA PAPER 92-3760 ..... p 867 A92-49115 #
AIAA PAPER 92-3762 ..... p 928 A92-49117 #
AIAA PAPER 92-3770 ..... p 1068 A92-54159 * #
AIAA PAPER 92-3771 ..... p 1022 A92-54160 #
AIAA PAPER 92-3773 ..... p 826 A92-49118 #
AIAA PAPER 92-3774 ..... p 1023 A92-54161 * #
AIAA PAPER 92-3775 ..... p 867 A92-49119 #
AIAA PAPER 92-3776 ..... p 867 A92-49120 #
AIAA PAPER 92-3789 ..... p 1069 A92-54168 * #
AIAA PAPER 92-3789 ..... p 742 N92-27669 * #
AIAA PAPER 92-3790 ..... p 1069 A92-54169 * #
AIAA PAPER 92-3790 ..... p 868 N92-28418 * #
AIAA PAPER 92-3792 ..... p 1069 A92-54171 * #
AIAA PAPER 92-3792 ..... p 739 N92-26613 * #
AIAA PAPER 92-3794 ..... p 907 A92-49126 * #
AIAA PAPER 92-3805 ..... p 1069 A92-54177 #
AIAA PAPER 92-3806 ..... p 1069 A92-54178 #
AIAA PAPER 92-3808 ..... p 1023 A92-54179 * #
AIAA PAPER 92-3809 ..... p 867 A92-49128 * #
AIAA PAPER 92-3810 ..... p 1090 A92-54180 * #
AIAA PAPER 92-3840 ..... p 1113 A92-54198 #
AIAA PAPER 92-3841 ..... p 894 A92-49134 * #
AIAA PAPER 92-3844 ..... p 1113 A92-54199 #
AIAA PAPER 92-3846 ..... p 895 A92-49136 #
AIAA PAPER 92-3869 ..... p 868 A92-49139 #
AIAA PAPER 92-3883 ..... p 1094 A92-56726 #
AIAA PAPER 92-3885 ..... p 1094 A92-56727 * #
AIAA PAPER 92-3888 ..... p 1094 A92-56729 #
AIAA PAPER 92-3899 ..... p 1122 A92-56735 #
AIAA PAPER 92-3901 ..... p 1017 A92-56736 #
AIAA PAPER 92-3903 ..... p 1094 A92-56738 #
AIAA PAPER 92-3908 ..... p 1094 A92-56743 * #
AIAA PAPER 92-3910 ..... p 1094 A92-56744 * #
AIAA PAPER 92-3912 ..... p 1094 A92-56745 * #
AIAA PAPER 92-3913 ..... p 1095 A92-56746 #
AIAA PAPER 92-3915 ..... p 1032 A92-56747 * #
AIAA PAPER 92-3916 ..... p 1095 A92-56748 * #
AIAA PAPER 92-3916 ..... p 887 N92-28673 * #
AIAA PAPER 92-3917 ..... p 1095 A92-56749 #
AIAA PAPER 92-3918 ..... p 1032 A92-56750 #
AIAA PAPER 92-3921 ..... p 1033 A92-56752 #
AIAA PAPER 92-3922 ..... p 1095 A92-56753 * #
AIAA PAPER 92-3923 ..... p 1133 A92-56754 #
AIAA PAPER 92-3924 ..... p 1095 A92-56755 #
AIAA PAPER 92-3925 ..... p 1095 A92-56756 * #
AIAA PAPER 92-3926 ..... p 1096 A92-56757 #
AIAA PAPER 92-3927 ..... p 1096 A92-56758 #
AIAA PAPER 92-3928 ..... p 1070 A92-56759 #
AIAA PAPER 92-3929 ..... p 1096 A92-56760 #
AIAA PAPER 92-3930 ..... p 1096 A92-56761 * #
AIAA PAPER 92-3935 ..... p 1122 A92-56765 #
AIAA PAPER 92-3937 ..... p 1096 A92-56767 * #
AIAA PAPER 92-3938 ..... p 1096 A92-56768 * #
AIAA PAPER 92-3940 ..... p 1096 A92-56770 * #
AIAA PAPER 92-3941 ..... p 1033 A92-56771 * #
AIAA PAPER 92-3942 ..... p 1104 A92-56772 #
AIAA PAPER 92-3943 ..... p 1033 A92-56776 * #
AIAA PAPER 92-3944 ..... p 1097 A92-56773 #
AIAA PAPER 92-3945 ..... p 1097 A92-56775 #
AIAA PAPER 92-3946 ..... p 1097 A92-56774 #
AIAA PAPER 92-3953 ..... p 1133 A92-56781 #
AIAA PAPER 92-3956 ..... p 1097 A92-56784 #
AIAA PAPER 92-3960 ..... p 1122 A92-56788 #
AIAA PAPER 92-3962 ..... p 1097 A92-56789 #
AIAA PAPER 92-3963 ..... p 1097 A92-56790 #
AIAA PAPER 92-3964 ..... p 1098 A92-56791 #
AIAA PAPER 92-3969 ..... p 1098 A92-56795 #
AIAA PAPER 92-3970 ..... p 1098 A92-56796 * #
AIAA PAPER 92-3971 ..... p 1098 A92-56797 #
AIAA PAPER 92-3972 ..... p 1098 A92-56798 #
AIAA PAPER 92-3976 ..... p 1098 A92-56802 #
AIAA PAPER 92-3977 ..... p 1071 A92-56803 #
AIAA PAPER 92-3979 ..... p 1071 A92-56805 #
AIAA PAPER 92-3980 ..... p 1098 A92-56806 #
AIAA PAPER 92-3980 ..... p 982 N92-30508 * #
AIAA PAPER 92-3982 ..... p 1099 A92-56807 #
AIAA PAPER 92-3985 ..... p 1060 A92-56809 #
AIAA PAPER 92-3986 ..... p 1033 A92-56810 #
AIAA PAPER 92-3992 ..... p 1099 A92-56815 #
AIAA PAPER 92-3993 ..... p 1099 A92-56816 #
AIAA PAPER 92-3995 ..... p 1099 A92-56818 #
AIAA PAPER 92-3995 ..... p 665 N92-25449 * #
AIAA PAPER 92-4001 ..... p 1122 A92-56824 #
AIAA PAPER 92-4002 ..... p 1099 A92-56825 * #
AIAA PAPER 92-4003 ..... p 1122 A92-56826 #

AIAA PAPER 92-4005 ..... p 1122 A92-56828 * #
AIAA PAPER 92-4006 ..... p 1123 A92-56829 #
AIAA PAPER 92-4006 ..... p 680 N92-24959 * #
AIAA PAPER 92-4008 ..... p 1099 A92-56831 #
AIAA PAPER 92-4009 ..... p 1033 A92-56832 * #
AIAA PAPER 92-4011 ..... p 1033 A92-56834 * #
AIAA PAPER 92-4012 ..... p 1033 A92-56835 #
AIAA PAPER 92-4013 ..... p 1034 A92-56836 * #
AIAA PAPER 92-4016 ..... p 1100 A92-56838 #
AIAA PAPER 92-4017 ..... p 1100 A92-56839 #
AIAA PAPER 92-4018 ..... p 1100 A92-56840 #
AIAA PAPER 92-4019 ..... p 1100 A92-56841 #
AIAA PAPER 92-4020 ..... p 1141 A92-56842 #
AIAA PAPER 92-4021 ..... p 1100 A92-56843 #
AIAA PAPER 92-4022 ..... p 1141 A92-56844 * #
AIAA PAPER 92-4023 ..... p 1034 A92-56845 * #
AIAA PAPER 92-4024 ..... p 1034 A92-56846 * #
AIAA PAPER 92-4025 ..... p 1104 A92-56847 * #
AIAA PAPER 92-4028 ..... p 1100 A92-56850 #
AIAA PAPER 92-4029 ..... p 1034 A92-56851 * #
AIAA PAPER 92-4032 ..... p 1100 A92-56854 * #
AIAA PAPER 92-4033 ..... p 1034 A92-56855 * #
AIAA PAPER 92-4034 ..... p 1101 A92-56856 * #
AIAA PAPER 92-4034 ..... p 667 N92-26129 * #
AIAA PAPER 92-4035 ..... p 1035 A92-56857 * #
AIAA PAPER 92-4036 ..... p 1035 A92-56858 * #
AIAA PAPER 92-4041 ..... p 1123 A92-56860 #
AIAA PAPER 92-4042 ..... p 1035 A92-56861 * #
AIAA PAPER 92-4043 ..... p 1035 A92-56862 #
AIAA PAPER 92-4058 ..... p 1119 A92-56141 #
AIAA PAPER 92-4060 ..... p 1119 A92-56143 #
AIAA PAPER 92-4106 ..... p 740 N92-27379 * #
AIAA PAPER 92-4109 ..... p 1087 N92-32864 * #
AIAA PAPER 92-4113 ..... p 1065 N92-32866 * #
AIAA PAPER 92-4121 ..... p 1060 N92-33404 * #
AIAA PAPER 92-4130 ..... p 959 A92-52427 #
AIAA PAPER 92-4131 ..... p 981 A92-52428 * #
AIAA PAPER 92-4138 ..... p 967 A92-52433 * #
AIAA PAPER 92-4140 ..... p 959 A92-52434 #
AIAA PAPER 92-4149 ..... p 1007 A92-52440 #
AIAA PAPER 92-4150 ..... p 959 A92-52441 * #
AIAA PAPER 92-4151 ..... p 959 A92-52442 #
AIAA PAPER 92-4156 ..... p 981 A92-52446 #
AIAA PAPER 92-4157 ..... p 982 A92-52447 #
AIAA PAPER 92-4158 ..... p 1007 A92-52448 * #
AIAA PAPER 92-4160 ..... p 1008 A92-52450 #
AIAA PAPER 92-4162 ..... p 1008 A92-52451 #
AIAA PAPER 92-4168 ..... p 1008 A92-52454 #
AIAA PAPER 92-4170 ..... p 1008 A92-52455 #
AIAA PAPER 92-4171 ..... p 1008 A92-52456 #
AIAA PAPER 92-4172 ..... p 977 A92-52457 #
AIAA PAPER 92-4176 ..... p 1060 N92-33149 * #
AIAA PAPER 92-4177 ..... p 982 A92-52458 * #
AIAA PAPER 92-4178 ..... p 960 A92-52459 * #
AIAA PAPER 92-4179 ..... p 982 A92-52460 * #
AIAA PAPER 92-4302 ..... p 1103 A92-55310 #
AIAA PAPER 92-4303 ..... p 1104 A92-55311 #
AIAA PAPER 92-4326 ..... p 1073 A92-55170 * #
AIAA PAPER 92-4327 ..... p 1073 A92-55171 #
AIAA PAPER 92-4328 ..... p 1073 A92-55172 #
AIAA PAPER 92-4329 ..... p 1073 A92-55173 * #
AIAA PAPER 92-4330 ..... p 1074 A92-55174 * #
AIAA PAPER 92-4338 ..... p 1078 A92-55327 * #
AIAA PAPER 92-4339 ..... p 1063 A92-55328 * #
AIAA PAPER 92-4340 ..... p 1078 A92-55329 #
AIAA PAPER 92-4341 ..... p 1078 A92-55330 * #
AIAA PAPER 92-4342 ..... p 1079 A92-55331 #
AIAA PAPER 92-4343 ..... p 1079 A92-55332 #
AIAA PAPER 92-4344 ..... p 1079 A92-55333 #
AIAA PAPER 92-4345 ..... p 1079 A92-55334 #
AIAA PAPER 92-4354 ..... p 1079 A92-55340 #
AIAA PAPER 92-4355 ..... p 1079 A92-55341 #
AIAA PAPER 92-4356 ..... p 1079 A92-55342 #
AIAA PAPER 92-4357 ..... p 1080 A92-55343 * #
AIAA PAPER 92-4358 ..... p 1025 A92-55344 #
AIAA PAPER 92-4359 ..... p 1025 A92-55345 #
AIAA PAPER 92-4378 ..... p 1131 A92-55182 #
AIAA PAPER 92-4390 ..... p 1074 A92-55191 #
AIAA PAPER 92-4391 ..... p 1074 A92-55192 #
AIAA PAPER 92-4392 ..... p 1074 A92-55193 #
AIAA PAPER 92-4393 ..... p 1074 A92-55194 #
AIAA PAPER 92-4396 ..... p 1074 A92-55196 * #
AIAA PAPER 92-4399 ..... p 1075 A92-55199 * #
AIAA PAPER 92-4400 ..... p 1075 A92-55200 #
AIAA PAPER 92-4409 ..... p 1075 A92-55203 #
AIAA PAPER 92-4410 ..... p 1075 A92-55204 #
AIAA PAPER 92-4411 ..... p 1075 A92-55205 * #
AIAA PAPER 92-4412 ..... p 1076 A92-55206 #
AIAA PAPER 92-4418 ..... p 1045 A92-55211 * #
AIAA PAPER 92-4420 ..... p 1063 A92-55212 * #
AIAA PAPER 92-4422 ..... p 1080 A92-55346 #
AIAA PAPER 92-4423 ..... p 1080 A92-55347 #
AIAA PAPER 92-4424 ..... p 1092 A92-55348 * #
AIAA PAPER 92-4425 ..... p 1080 A92-55349 #
AIAA PAPER 92-4426 ..... p 1025 A92-55350 * #
AIAA PAPER 92-4427 ..... p 1080 A92-55351 #
AIAA PAPER 92-4428 ..... p 1080 A92-55352 * #
AIAA PAPER 92-4429 ..... p 1025 A92-55353 * #
AIAA PAPER 92-4430 ..... p 1081 A92-55354 * #
AIAA PAPER 92-4431 ..... p 1026 A92-55355 * #
AIAA PAPER 92-4469 ..... p 1076 A92-55229 #
AIAA PAPER 92-4470 ..... p 1076 A92-55230 * #
AIAA PAPER 92-4471 ..... p 1076 A92-55231 #
AIAA PAPER 92-4472 ..... p 1076 A92-55232 * #
AIAA PAPER 92-4473 ..... p 1076 A92-55233 #
AIAA PAPER 92-4478 ..... p 1131 A92-55237 #
AIAA PAPER 92-4494 ..... p 1081 A92-55363 * #
AIAA PAPER 92-4496 ..... p 1026 A92-55364 #
AIAA PAPER 92-4497 ..... p 1026 A92-55365 * #
AIAA PAPER 92-4498 ..... p 1081 A92-55366 #
AIAA PAPER 92-4499 ..... p 1026 A92-55367 #
AIAA PAPER 92-4500 ..... p 1026 A92-55368 #
AIAA PAPER 92-4501 ..... p 1026 A92-55369 #
AIAA PAPER 92-4503 ..... p 1081 A92-55370 #
AIAA PAPER 92-4504 ..... p 1081 A92-55371 #
AIAA PAPER 92-4505 ..... p 1027 A92-55372 #
AIAA PAPER 92-4506 ..... p 1027 A92-55373 #
AIAA PAPER 92-4528 ..... p 1077 A92-55246 #
AIAA PAPER 92-4550 ..... p 1131 A92-55262 * #
AIAA PAPER 92-4553 ..... p 1131 A92-55265 #
AIAA PAPER 92-4555 ..... p 1131 A92-55267 #
AIAA PAPER 92-4559 ..... p 1131 A92-55271 * #
AIAA PAPER 92-4560 ..... p 1141 A92-55272 #
AIAA PAPER 92-4563 ..... p 1027 A92-55375 * #
AIAA PAPER 92-4564 ..... p 1132 A92-55376 * #
AIAA PAPER 92-4567 ..... p 1035 A92-57034 * #
AIAA PAPER 92-4568 ..... p 1027 A92-55377 * #
AIAA PAPER 92-4601 ..... p 1077 A92-55280 #
AIAA PAPER 92-4602 ..... p 1069 A92-55281 * #
AIAA PAPER 92-4603 ..... p 1131 A92-55282 * #
AIAA PAPER 92-4605 ..... p 1077 A92-55283 * #
AIAA PAPER 92-4606 ..... p 1077 A92-55284 #
AIAA PAPER 92-4619 ..... p 1077 A92-55296 #
AIAA PAPER 92-4623 ..... p 1052 A92-55300 * #
AIAA PAPER 92-4625 ..... p 1077 A92-55302 #
AIAA PAPER 92-4626 ..... p 1077 A92-55303 #
AIAA PAPER 92-4629 ..... p 1078 A92-55304 #
AIAA PAPER 92-4630 ..... p 1078 A92-55305 #
AIAA PAPER 92-4631 ..... p 1132 A92-55306 #
AIAA PAPER 92-4633 ..... p 1081 A92-55380 #
AIAA PAPER 92-4635 ..... p 1027 A92-55382 #
AIAA PAPER 92-4640 ..... p 1027 A92-55387 #
AIAA PAPER 92-4648 ..... p 1082 A92-55393 * #
AIAA PAPER 92-4649 ..... p 1028 A92-55394 #
AIAA PAPER 92-4651 ..... p 1028 A92-55395 #
AIAA PAPER 92-4652 ..... p 1082 A92-55396 #
AIAA PAPER 92-4653 ..... p 1028 A92-55397 * #

AIAA SP-050-1991 ..... p 532 A92-33433

AL-TP-1992-0009 ..... p 888 N92-29505 #
AL-TP-1992-0021 ..... p 1065 N92-33277 #

AL-TR-1991-0039 ..... p 749 N92-26527 #
AL-TR-1991-0085-VOL-2 ..... p 923 N92-29188 #
AL-TR-1991-0094 ..... p 299 N92-17216 #
AL-TR-1991-0097 ..... p 485 N92-21720 #
AL-TR-1991-0099 ..... p 512 N92-21719 #
AL-TR-1991-0121 ..... p 728 N92-27916 #

AL-18 ..... p 751 N92-27836 #

AMSAA-TR-519 ..... p 1101 N92-33398 #

AMSMI/TR-RD-WS-92-1 ..... p 983 N92-30849 #

ANSI/AIAA S-017-1991 ..... p 634 A92-38000

AR-006-587 ..... p 632 N92-25410
AR-006-626 ..... p 44 N92-11376 #

ARA-5462 ..... p 484 N92-20455 #

ARI-RN-92-32 ..... p 888 N92-29709 #
ARI-RN-92-47 ..... p 1044 N92-33288 #

ARL-FLIGHT-MECH-R-189 ..... p 632 N92-25410

ARL-FLIGHT-MECH-TM-434 ..... p 275 N92-17266 #
ARL-FLIGHT-MECH-TM-435 ..... p 285 N92-17297 #
ARL-FLIGHT-MECH-TM-437 ..... p 715 N92-26947 #
ARL-FLIGHT-MECH-TM-443 ..... p 260 N92-17281 #

ARL-PROP-R-187 ..... p 275 N92-17565 #

ARL-PROP-TM-460 ..... p 275 N92-17234 #
ARL-PROP-TM-473 ..... p 973 N92-31439 #

ARL-STRUC-R-444 ..... p 44 N92-11376 #

ARL-STRUC-TM-527 ..... p 764 N92-26258 #
ARL-STRUC-TM-538 ..... p 733 N92-28118 #
ARL-STRUC-TM-544 ..... p 853 N92-28771 #
ARL-STRUC-TM-571 ..... p 206 N92-15073 #

ARL/PSU/TR-92-015 ..... p 344 N92-18007 #

ARO-25264.13-MA ..... p 447 N92-21753 #
ARO-25264.7-MA ..... p 483 N92-21752 #
ARO-25844.13-MA ..... p 413 N92-19397 #
ARO-26439.48-MS ..... p 987 N92-30874 #
ARO-27752.2-EG ..... p 446 N92-21333 #
ARO-27894.6-EG ..... p 502 N92-21297 #
ARO-27894.7-EG ..... p 445 N92-21012 #

ASD-TR-91-5007 ..... p 370 N92-18014 #
ASD-TR-91-5011 ..... p 386 N92-19642 #

ASIAC-1090.10 ..... p 978 N92-30323 #

ASL-91-2 ..... p 735 N92-27424 * #

ASME PAPER 90-GT-124 ..... p 6 A92-11287
ASME PAPER 90-GT-140 ..... p 6 A92-11286
ASME PAPER 90-GT-146 ..... p 38 A92-11288 *
ASME PAPER 90-GT-27 ..... p 295 A92-23299
ASME PAPER 91-GT-104 ..... p 122 A92-15561
ASME PAPER 91-GT-114 ..... p 70 A92-15565
ASME PAPER 91-GT-115 ..... p 123 A92-15566 *
ASME PAPER 91-GT-119 ..... p 670 A92-36893
ASME PAPER 91-GT-120 ..... p 142 A92-15567 *
ASME PAPER 91-GT-121 ..... p 670 A92-36899
ASME PAPER 91-GT-123 ..... p 70 A92-15568
ASME PAPER 91-GT-124 ..... p 71 A92-15569
ASME PAPER 91-GT-126 ..... p 71 A92-15571
ASME PAPER 91-GT-127 ..... p 71 A92-15572
ASME PAPER 91-GT-128 ..... p 71 A92-15573
ASME PAPER 91-GT-130 ..... p 71 A92-15574 *
ASME PAPER 91-GT-131 ..... p 71 A92-15575
ASME PAPER 91-GT-133 ..... p 72 A92-15576 *
ASME PAPER 91-GT-135 ..... p 72 A92-15577
ASME PAPER 91-GT-140 ..... p 72 A92-15580 *
ASME PAPER 91-GT-141 ..... p 690 A92-36895
ASME PAPER 91-GT-144 ..... p 72 A92-15583
ASME PAPER 91-GT-146 ..... p 72 A92-15584
ASME PAPER 91-GT-148 ..... p 73 A92-15586
ASME PAPER 91-GT-149 ..... p 148 A92-15587
ASME PAPER 91-GT-150 ..... p 148 A92-15588
ASME PAPER 91-GT-152 ..... p 148 A92-15594
ASME PAPER 91-GT-154 ..... p 142 A92-15590 *
ASME PAPER 91-GT-155 ..... p 123 A92-15591 *
ASME PAPER 91-GT-156 ..... p 142 A92-15592
ASME PAPER 91-GT-157 ..... p 148 A92-15593 *
ASME PAPER 91-GT-163 ..... p 123 A92-15598
ASME PAPER 91-GT-164 ..... p 123 A92-15599
ASME PAPER 91-GT-165 ..... p 123 A92-15600
ASME PAPER 91-GT-166 ..... p 136 A92-15601
ASME PAPER 91-GT-167 ..... p 111 A92-15602
ASME PAPER 91-GT-168 ..... p 73 A92-15603
ASME PAPER 91-GT-170 ..... p 123 A92-15605
ASME PAPER 91-GT-171 ..... p 73 A92-15606
ASME PAPER 91-GT-173 ..... p 73 A92-15608
ASME PAPER 91-GT-178 ..... p 73 A92-15610
ASME PAPER 91-GT-180 ..... p 123 A92-15612
ASME PAPER 91-GT-181 ..... p 73 A92-15613
ASME PAPER 91-GT-182 ..... p 148 A92-15614
ASME PAPER 91-GT-183 ..... p 73 A92-15615
ASME PAPER 91-GT-18 ..... p 67 A92-15509
ASME PAPER 91-GT-190 ..... p 74 A92-15616 *
ASME PAPER 91-GT-191 ..... p 149 A92-15617
ASME PAPER 91-GT-192 ..... p 124 A92-15618
ASME PAPER 91-GT-193 ..... p 124 A92-15619
ASME PAPER 91-GT-195 ..... p 124 A92-15620
ASME PAPER 91-GT-198 ..... p 74 A92-15623 *
ASME PAPER 91-GT-19 ..... p 147 A92-15510 *
ASME PAPER 91-GT-1 ..... p 147 A92-15501
ASME PAPER 91-GT-201 ..... p 149 A92-15624
ASME PAPER 91-GT-204 ..... p 124 A92-15626
ASME PAPER 91-GT-208 ..... p 607 A92-36897
ASME PAPER 91-GT-213 ..... p 143 A92-15632
ASME PAPER 91-GT-214 ..... p 653 A92-36890
ASME PAPER 91-GT-216 ..... p 124 A92-15633
ASME PAPER 91-GT-217 ..... p 124 A92-15634 *
ASME PAPER 91-GT-220 ..... p 124 A92-15636
ASME PAPER 91-GT-221 ..... p 899 A92-46825
ASME PAPER 91-GT-222 ..... p 74 A92-15639 *
ASME PAPER 91-GT-223 ..... p 74 A92-15637
ASME PAPER 91-GT-225 ..... p 74 A92-15638 *
ASME PAPER 91-GT-232 ..... p 149 A92-15641
ASME PAPER 91-GT-234 ..... p 125 A92-15643
ASME PAPER 91-GT-236 ..... p 125 A92-15645 *
ASME PAPER 91-GT-241 ..... p 75 A92-15646 *
ASME PAPER 91-GT-242 ..... p 149 A92-15647
ASME PAPER 91-GT-243 ..... p 149 A92-15648
ASME PAPER 91-GT-244 ..... p 150 A92-15649
ASME PAPER 91-GT-248 ..... p 150 A92-15653
ASME PAPER 91-GT-249 ..... p 150 A92-15654
ASME PAPER 91-GT-250 ..... p 150 A92-15655

ASME PAPER 91-GT-252 ..... p 150 A92-15657
ASME PAPER 91-GT-253 ..... p 150 A92-15658
ASME PAPER 91-GT-255 ..... p 151 A92-15660
ASME PAPER 91-GT-257 ..... p 668 A92-36900
ASME PAPER 91-GT-259 ..... p 151 A92-15661
ASME PAPER 91-GT-260 ..... p 75 A92-15662
ASME PAPER 91-GT-265 ..... p 151 A92-15663 *
ASME PAPER 91-GT-268 ..... p 151 A92-15666
ASME PAPER 91-GT-269 ..... p 151 A92-15667
ASME PAPER 91-GT-271 ..... p 151 A92-15668
ASME PAPER 91-GT-272 ..... p 75 A92-15669 *
ASME PAPER 91-GT-273 ..... p 75 A92-15670 *
ASME PAPER 91-GT-274 ..... p 75 A92-15671
ASME PAPER 91-GT-275 ..... p 151 A92-15672
ASME PAPER 91-GT-276 ..... p 152 A92-15673
ASME PAPER 91-GT-277 ..... p 653 A92-36888
ASME PAPER 91-GT-278 ..... p 125 A92-15674
ASME PAPER 91-GT-279 ..... p 152 A92-15675
ASME PAPER 91-GT-281 ..... p 152 A92-15676
ASME PAPER 91-GT-282 ..... p 152 A92-15677
ASME PAPER 91-GT-283 ..... p 125 A92-15678
ASME PAPER 91-GT-284 ..... p 125 A92-15679
ASME PAPER 91-GT-287 ..... p 152 A92-15681 *
ASME PAPER 91-GT-28 ..... p 162 A92-15513
ASME PAPER 91-GT-290 ..... p 152 A92-15682
ASME PAPER 91-GT-294 ..... p 653 A92-36889
ASME PAPER 91-GT-308 ..... p 126 A92-15687
ASME PAPER 91-GT-30 ..... p 67 A92-15514
ASME PAPER 91-GT-310 ..... p 153 A92-15688
ASME PAPER 91-GT-312 ..... p 75 A92-15689
ASME PAPER 91-GT-313 ..... p 76 A92-15690 *
ASME PAPER 91-GT-315 ..... p 126 A92-15691
ASME PAPER 91-GT-31 ..... p 68 A92-15515
ASME PAPER 91-GT-327 ..... p 153 A92-15697
ASME PAPER 91-GT-328 ..... p 153 A92-15698
ASME PAPER 91-GT-32 ..... p 147 A92-15516
ASME PAPER 91-GT-334 ..... p 126 A92-15699
ASME PAPER 91-GT-335 ..... p 126 A92-15700
ASME PAPER 91-GT-336 ..... p 163 A92-15701 *
ASME PAPER 91-GT-338 ..... p 143 A92-15702
ASME PAPER 91-GT-339 ..... p 76 A92-15703
ASME PAPER 91-GT-33 ..... p 147 A92-15517
ASME PAPER 91-GT-341 ..... p 111 A92-15705
ASME PAPER 91-GT-343 ..... p 137 A92-15706
ASME PAPER 91-GT-354 ..... p 153 A92-15710 *
ASME PAPER 91-GT-359 ..... p 137 A92-15713
ASME PAPER 91-GT-35 ..... p 147 A92-15518
ASME PAPER 91-GT-368 ..... p 153 A92-15716
ASME PAPER 91-GT-36 ..... p 121 A92-15519
ASME PAPER 91-GT-374 ..... p 76 A92-15718
ASME PAPER 91-GT-37 ..... p 121 A92-15520
ASME PAPER 91-GT-380 ..... p 653 A92-36891
ASME PAPER 91-GT-385 ..... p 126 A92-15719
ASME PAPER 91-GT-388 ..... p 126 A92-15720
ASME PAPER 91-GT-389 ..... p 126 A92-15721
ASME PAPER 91-GT-392 ..... p 153 A92-15722
ASME PAPER 91-GT-393 ..... p 127 A92-15723
ASME PAPER 91-GT-395 ..... p 127 A92-15725
ASME PAPER 91-GT-396 ..... p 111 A92-15726
ASME PAPER 91-GT-397 ..... p 127 A92-15727
ASME PAPER 91-GT-398 ..... p 127 A92-15728
ASME PAPER 91-GT-399 ..... p 127 A92-15729
ASME PAPER 91-GT-400 ..... p 76 A92-15730
ASME PAPER 91-GT-401 ..... p 137 A92-15731
ASME PAPER 91-GT-402 ..... p 127 A92-15732
ASME PAPER 91-GT-403 ..... p 76 A92-15733
ASME PAPER 91-GT-408 ..... p 137 A92-15737
ASME PAPER 91-GT-409 ..... p 128 A92-15738
ASME PAPER 91-GT-40 ..... p 147 A92-15523 *
ASME PAPER 91-GT-41 ..... p 121 A92-15524
ASME PAPER 91-GT-4 ..... p 120 A92-15502
ASME PAPER 91-GT-50 ..... p 148 A92-15528
ASME PAPER 91-GT-52 ..... p 121 A92-15530
ASME PAPER 91-GT-54 ..... p 121 A92-15532
ASME PAPER 91-GT-55 ..... p 68 A92-15533
ASME PAPER 91-GT-56 ..... p 68 A92-15534
ASME PAPER 91-GT-57 ..... p 68 A92-15535
ASME PAPER 91-GT-59 ..... p 68 A92-15536
ASME PAPER 91-GT-5 ..... p 67 A92-15503
ASME PAPER 91-GT-68 ..... p 121 A92-15538
ASME PAPER 91-GT-69 ..... p 68 A92-15539 *
ASME PAPER 91-GT-71 ..... p 148 A92-15540
ASME PAPER 91-GT-73 ..... p 142 A92-15542
ASME PAPER 91-GT-74 ..... p 122 A92-15543
ASME PAPER 91-GT-76 ..... p 69 A92-15545
ASME PAPER 91-GT-77 ..... p 122 A92-15546
ASME PAPER 91-GT-78 ..... p 69 A92-15547
ASME PAPER 91-GT-79 ..... p 69 A92-15548
ASME PAPER 91-GT-7 ..... p 67 A92-15505
ASME PAPER 91-GT-81 ..... p 69 A92-15549
ASME PAPER 91-GT-83 ..... p 69 A92-15550 *
ASME PAPER 91-GT-85 ..... p 670 A92-36901
ASME PAPER 91-GT-86 ..... p 69 A92-15551
ASME PAPER 91-GT-87 ..... p 122 A92-15552
ASME PAPER 91-GT-88 ..... p 122 A92-15553
ASME PAPER 91-GT-89 ..... p 70 A92-15554
ASME PAPER 91-GT-91 ..... p 70 A92-15555
ASME PAPER 91-GT-92 ..... p 70 A92-15556
ASME PAPER 91-GT-93 ..... p 70 A92-15557
ASME PAPER 91-GT-96 ..... p 122 A92-15560

ASTM STP-1122 ..... p 896 A92-45226

ATC-151 ..... p 93 N92-13042 #
ATC-178 ..... p 18 N92-10019 #
ATC-180 ..... p 301 N92-17028 #
ATC-185 ..... p 1004 N92-32103 #
ATC-189 ..... p 1124 N92-32686 #

AVSCOM-TR-C-016 ..... p 667 N92-26129 * #

AVSCOM-TR-88-C-013 ..... p 562 N92-22863 * #
AVSCOM-TR-88-C-024 ..... p 562 N92-22647 * #
AVSCOM-TR-91-A-003 ..... p 13 N92-10981 * #
AVSCOM-TR-91-B-014 ..... p 119 N92-13065 * #
AVSCOM-TR-91-B-015 ..... p 159 N92-13460 * #
AVSCOM-TR-91-B-017 ..... p 61 N92-12989 * #
AVSCOM-TR-91-B-019 ..... p 115 N92-13057 * #
AVSCOM-TR-91-B-020 ..... p 367 N92-19846 * #
AVSCOM-TR-91-C-026 ..... p 998 N92-30396 * #
AVSCOM-TR-91-C-035 ..... p 764 N92-26560 * #
AVSCOM-TR-91-C-036 ..... p 908 N92-28434 * #
AVSCOM-TR-91-C-038 ..... p 764 N92-26555 * #
AVSCOM-TR-91-C-043 ..... p 910 N92-29136 * #
AVSCOM-TR-91-C-049 ..... p 773 N92-27879 * #
AVSCOM-TR-91-C-053 ..... p 350 N92-19993 * #
AVSCOM-TR-92-B-002 ..... p 944 N92-30394 * #
AVSCOM-TR-92-B-004 ..... p 630 N92-24882 * #
AVSCOM-TR-92-B-005 ..... p 630 N92-24885 * #
AVSCOM-TR-92-B-006 ..... p 625 N92-24681 * #
AVSCOM-TR-92-B-007 ..... p 630 N92-24956 * #
AVSCOM-TR-92-C-001 ..... p 633 N92-26104 * #
AVSCOM-TR-92-C-008 ..... p 1002 N92-31349 * #
AVSCOM-TR-92-C-011 ..... p 680 N92-24984 * #
AVSCOM-TR-92-C-018 ..... p 1002 N92-31485 * #
AVSCOM-TR-92-C-019 ..... p 871 N92-29661 * #
AVSCOM-TR-92-C-024 ..... p 1009 N92-30898 * #
AVSCOM-TR-92-C-026 ..... p 909 N92-29105 * #
AVSCOM-TR-92-C-028 ..... p 1088 N92-34107 * #
AVSCOM-TR-92-E-002 ..... p 1065 N92-34109 * #

B-235387 ..... p 139 N92-13076 #
B-238393 ..... p 953 N92-31453 #
B-239410 ..... p 1011 N92-31454 #
B-242745 ..... p 1048 N92-32861 #

BBN-7618 ..... p 510 N92-21392 #
BBN-7621 ..... p 412 N92-19247 #

BDM/VSQ-91-0742-TR ..... p 303 N92-17438 #

BRL-CR-678 ..... p 484 N92-20455 #

BRL-TR-3083 ..... p 1041 N92-33699 #
BRL-TR-3265 ..... p 180 N92-14972 #
BRL-TR-3271 ..... p 139 N92-13080 #

BR302867 ..... p 135 N92-12004 #
BR303122 ..... p 187 N92-14007 #
BR305194 ..... p 257 N92-15964 #

CA-PATENT-APPL-SN-2-011-945 p 1125 N92-32856

CA-PATENT-1-257-618 ..... p 1061 N92-33585
CA-PATENT-1-268-164 ..... p 1061 N92-33582

CA/TL-91-03 ..... p 18 N92-10991 #

CDI-91-03 ..... p 696 N92-24251 * #

CEAT-M5-5443/01 ..... p 195 N92-14042 #

CEAT-S8-6551-PARTIEL-1-PT-1 .. p 195 N92-14043 #

CEP90-91-RNM-WNM-11 ..... p 409 N92-19195 #

CERL-N-92/07 ..... p 926 N92-28292 #

CERL-TR-N-91/13 ..... p 304 N92-17506 #

CERT-RSF-DERAT-62/5004-31 ... p 43 N92-11309 #

CERT-RT-65/5604-35 ..... p 43 N92-11307 #

CERT-2/7724-DERA ..... p 381 N92-19295 #

CESAR-92/01 ..... p 455 N92-21201 #

CFD-25 ..... p 685 N92-25962 * #
CFD-26 ..... p 946 N92-30977 * #

CIT-REF-06/769E(5) ..... p 26 N92-11015 #

CMOTT-92-02 ..... p 678 N92-24514 * #

CNRS-RC-91-1 ..... p 947 N92-31508 #

CONF-9101134-1 ..... p 689 N92-25049 #
CONF-910617-7 ..... p 490 N92-21063 #
CONF-910802-3 ..... p 598 N92-22971 #
CONF-9109112-3 ..... p 301 N92-16458 #
CONF-9109112-7 ..... p 262 N92-17874 #
CONF-9109112-8 ..... p 302 N92-17875 #
CONF-9109112-9 ..... p 598 N92-23119 #
CONF-9109230-7 ..... p 376 N92-18230 #
CONF-9109257-1 ..... p 11 N92-10010 #
CONF-9109274-1 ..... p 35 N92-11203 #
CONF-910968-10 ..... p 238 N92-15761 #
CONF-9110282-2-VUGRAPHS ..... p 385 N92-18290 #
CONF-911050-4 ..... p 579 N92-23223 #
CONF-9111112-1 ..... p 241 N92-15962 #
CONF-9111131-1 ..... p 505 N92-21040 #
CONF-911189-3 ..... p 669 N92-25259 #
CONF-911272-1 ..... p 385 N92-18069 #
CONF-911287-1 ..... p 505 N92-20245 #
CONF-920108-2 ..... p 500 N92-20341 #
CONF-920122-4 ..... p 410 N92-19633 #
CONF-920157-1 ..... p 498 N92-20143 #
CONF-920187-1 ..... p 640 N92-25470 #
CONF-920432-11 ..... p 909 N92-28814 #
CONF-920444-2 ..... p 488 N92-20132 #
CONF-920444-6 ..... p 489 N92-20858 #
CONF-920460-1 ..... p 386 N92-19978 #
CONF-920474-2 ..... p 679 N92-24892 #
CONF-920534-1-EXT-ABST ..... p 667 N92-25315 #
CONF-920534-2 ..... p 943 N92-30367 #
CONF-920605-2 ..... p 765 N92-26698 #
CONF-920631-7 ..... p 739 N92-26697 #
CONF-920688-5 ..... p 765 N92-26853 #
CONF-920688-7 ..... p 749 N92-26720 #
CONF-920747-2 ..... p 973 N92-31817 #
CONF-920801-15 ..... p 1129 N92-33271 #

CP-474 ..... p 205 N92-14065 #
CP-503 ..... p 303 N92-17498 #
CP-504S ..... p 1010 N92-32229 #
CP-504 ..... p 1010 N92-32229 #

CRANFIELD-AERO-9111 ..... p 187 N92-15054 #
CRANFIELD-AERO-9113-PT-1 ..... p 349 N92-19679 #
CRANFIELD-AERO-9114 ..... p 948 N92-31514 #
CRANFIELD-AERO-9201 ..... p 963 N92-31515 #

CRDEC-TR-309 ..... p 883 N92-28248 #

CRREL-SR-92-11 ..... p 1038 N92-32900 #

CRREL-92-9 ..... p 1101 N92-32903 #

CSA-91-01-02 ..... p 160 N92-13470 #

CSDL-T-1106 ..... p 746 N92-28209 * #

CTN-91-60126 ..... p 636 N92-25350 #
CTN-91-60132 ..... p 1061 N92-33582
CTN-91-60166 ..... p 1061 N92-33585
CTN-91-60227 ..... p 92 N92-13041 #
CTN-91-60231 ..... p 189 N92-14009
CTN-91-60232 ..... p 115 N92-13055 #
CTN-91-60234 ..... p 158 N92-13434 #
CTN-91-60235 ..... p 130 N92-13069 #
CTN-91-60242 ..... p 155 N92-12153 #
CTN-91-60243 ..... p 155 N92-12154 #
CTN-91-60253 ..... p 129 N92-11996 #
CTN-91-60255 ..... p 81 N92-11975 #
CTN-91-60256 ..... p 81 N92-11976 #
CTN-91-60258 ..... p 129 N92-11997 #
CTN-91-60261 ..... p 114 N92-11990 #
CTN-91-60269 ..... p 161 N92-12373 #
CTN-91-60270 ..... p 143 N92-12060 #
CTN-91-60271 ..... p 222 N92-14345 #
CTN-91-60273 ..... p 202 N92-14060 #
CTN-91-60275 ..... p 159 N92-13453 #
CTN-91-60276 ..... p 159 N92-13454 #
CTN-91-60278 ..... p 102 N92-11988 #
CTN-91-60285 ..... p 130 N92-11998 #
CTN-91-60290 ..... p 114 N92-11991 #
CTN-91-60291 ..... p 489 N92-21018 #
CTN-91-60292 ..... p 115 N92-13056 #
CTN-91-60298 ..... p 130 N92-11999 #
CTN-91-60303 ..... p 130 N92-12000 #
CTN-91-60304 ..... p 130 N92-12001 #
CTN-92-60310 ..... p 1002 N92-31469 #
CTN-92-60344 ..... p 954 N92-32219 #
CTN-92-60348 ..... p 1048 N92-32845 #
CTN-92-60350 ..... p 1109 N92-32846 #
CTN-92-60357 ..... p 1038 N92-32811 #
CTN-92-60369 ..... p 1048 N92-32849 #
CTN-92-60370 ..... p 1109 N92-32791 #

CTN-92-60371 ..... p 1064 N92-32850 #
CTN-92-60372 ..... p 1134 N92-32851 #
CTN-92-60378 ..... p 1071 N92-33102 #
CTN-92-60391 ..... p 1125 N92-32856
CTN-92-60410 ..... p 504 N92-22028 #
CTN-92-60411 ..... p 504 N92-22029 #
CTN-92-60420 ..... p 625 N92-24849 #
CTN-92-60430 ..... p 448 N92-20156 #
CTN-92-60431 ..... p 420 N92-20204 #
CTN-92-60432 ..... p 420 N92-20205 #
CTN-92-60468 ..... p 749 N92-27645 #
CTN-92-60471 ..... p 716 N92-27624 #
CTN-92-60472 ..... p 753 N92-27613 #
CTN-92-60537 ..... p 716 N92-27344 #
CTN-92-60565 ..... p 1126 N92-33440

CTR-R-1-92-PHASE-2 ..... p 484 N92-21162 * #

CU-TR-14 ..... p 1043 N92-32606 * #
CU-TR-15 ..... p 953 N92-31549 * #

CUED/A-AERO/TR-16 ..... p 592 N92-22209 #
CUED/A-AERO/TR-17(1991) ..... p 525 N92-22193 #
CUED/A-AERO/TR-18 ..... p 927 N92-29201 #

C1-1X2-TN-393 ..... p 191 N92-15060 * #

DCIEM-87-TR-11 ..... p 92 N92-13041 #
DCIEM-88-RR-39 ..... p 954 N92-32219 #

DEI-D-425 ..... p 498 N92-20072 * #

DE91-002178 ..... p 689 N92-25498 #
DE91-017315 ..... p 667 N92-25315 #
DE91-017984 ..... p 35 N92-11203 #
DE91-018176 ..... p 11 N92-10010 #
DE91-018692 ..... p 163 N92-12440 * #
DE91-018698 ..... p 41 N92-10174 #
DE91-018924 ..... p 401 N92-18515 #
DE91-643289 ..... p 304 N92-16789 #
DE92-000597 ..... p 229 N92-15392 #
DE92-000740 ..... p 238 N92-15761 #
DE92-001157 ..... p 262 N92-17874 #
DE92-001158 ..... p 301 N92-16458 #
DE92-001187 ..... p 410 N92-19633 #
DE92-001190 ..... p 302 N92-17875 #
DE92-001200 ..... p 505 N92-20245 #
DE92-001215 ..... p 598 N92-23119 #
DE92-001216 ..... p 598 N92-22971 #
DE92-001245 ..... p 1004 N92-30837 #
DE92-002358 ..... p 241 N92-15962 #
DE92-002397 ..... p 289 N92-16128 #
DE92-002930 ..... p 765 N92-26698 #
DE92-002931 ..... p 505 N92-21040 #
DE92-002935 ..... p 297 N92-16281 #
DE92-003469 ..... p 512 N92-21046 #
DE92-003539 ..... p 376 N92-18230 #
DE92-003553 ..... p 490 N92-21063 #
DE92-003641 ..... p 488 N92-20132 #
DE92-003778 ..... p 401 N92-18705 #
DE92-003825 ..... p 401 N92-18550 #
DE92-004445 ..... p 385 N92-18069 #
DE92-004478 ..... p 500 N92-20341 #
DE92-004730 ..... p 489 N92-20858 #
DE92-004732 ..... p 385 N92-18290 #
DE92-004891 ..... p 386 N92-19978 #
DE92-005151 ..... p 499 N92-20301 #
DE92-005186 ..... p 498 N92-20143 #
DE92-006859 ..... p 739 N92-26697 #
DE92-007161 ..... p 455 N92-21201 #
DE92-007519 ..... p 640 N92-25470 #
DE92-007680 ..... p 679 N92-24892 #
DE92-007838 ..... p 579 N92-23223 #
DE92-008017 ..... p 765 N92-26853 #
DE92-008437 ..... p 749 N92-26720 #
DE92-008673 ..... p 689 N92-25049 #
DE92-008710 ..... p 669 N92-25223 #
DE92-008726 ..... p 648 N92-24556 #
DE92-008952 ..... p 680 N92-25054 #
DE92-009527 ..... p 669 N92-25259 #
DE92-009801 ..... p 636 N92-24713 #
DE92-010574 ..... p 1004 N92-31498 #
DE92-010622 ..... p 767 N92-27394 #
DE92-012409 ..... p 1004 N92-32147 * #
DE92-013233 ..... p 909 N92-28814 #
DE92-013428 ..... p 973 N92-31817 #
DE92-013439 ..... p 943 N92-30367 #
DE92-013458 ..... p 957 N92-31746 #
DE92-013461 ..... p 999 N92-30893 #
DE92-014311 ..... p 1136 N92-32595 #
DE92-015778 ..... p 1000 N92-30903 #
DE92-016346 ..... p 954 N92-31928 #
DE92-016748 ..... p 1003 N92-31933 #
DE92-017129 ..... p 1129 N92-33271 #
DE92-526025 ..... p 283 N92-17917 #
DE92-728396 ..... p 298 N92-16325 #
DE92-728402 ..... p 298 N92-16326 #
DE92-783191 ..... p 680 N92-25342 #

DLR-FB-90-17 ..... p 410 N92-19292 #
DLR-FB-90-22 ..... p 595 N92-22641 #
DLR-FB-90-26 ..... p 830 N92-29159 #
DLR-FB-90-34 ..... p 954 N92-31943 #
DLR-FB-91-13 ..... p 503 N92-21699 #
DLR-FB-91-23 ..... p 455 N92-20902 #
DLR-FB-91-28 ..... p 928 N92-29997 #
DLR-FB-91-34 ..... p 859 N92-29870 #

DLR-MITT-91-08 ..... p 354 N92-19041 #
DLR-MITT-91-10 ..... p 911 N92-29877 #
DLR-MITT-91-12 ..... p 953 N92-31813 #

DMS-DR-2547-VOL-1 ..... p 286 N92-17167 * #
DMS-DR-2547-VOL-2 ..... p 286 N92-17214 * #

DODA-AR-006-091 ..... p 764 N92-26258 #
DODA-AR-006-123 ..... p 206 N92-15073 #
DODA-AR-006-440 ..... p 727 N92-26948 #
DODA-AR-006-590 ..... p 275 N92-17266 #
DODA-AR-006-591 ..... p 285 N92-17297 #
DODA-AR-006-595 ..... p 715 N92-26947 #
DODA-AR-006-600 ..... p 275 N92-17234 #
DODA-AR-006-614 ..... p 260 N92-17281 #
DODA-AR-006-619 ..... p 275 N92-17565 #
DODA-AR-006-620 ..... p 733 N92-28118 #
DODA-AR-006-633 ..... p 853 N92-28771 #
DODA-AR-006-651 ..... p 973 N92-31439 #

DOE/CE-15301/T15 ..... p 648 N92-24556 #
DOE/CE-15426/T9 ..... p 401 N92-18515 #
DOE/CE-15470/T7 ..... p 680 N92-25054 #

DOE/CH-10093/101 ..... p 689 N92-25498 #

DOE/EH-0242P ..... p 954 N92-31928 #

DOE/ER-30148/T1 ..... p 767 N92-27394 #
DOE/ER-53262/T2 ..... p 512 N92-21046 #
DOE/ER-54095/2 ..... p 1136 N92-32595 #

DOE/NASA/0336-3 ..... p 682 N92-25649 * #
DOE/NASA/1087-1 ..... p 658 N92-24539 * #

DOE/PETC-TR/91/10 ..... p 41 N92-10174 #

DOT-VNTSC-FAA-91-11 ..... p 103 N92-13051 #
DOT-VNTSC-FAA-92-1 ..... p 1050 N92-33596 #
DOT-VNTSC-FAA-92-2 ..... p 1043 N92-32941 #

DOT-VNTSC-RSPA-91-1 ..... p 417 N92-18814 #

DOT/FAA/AM-92-03 ..... p 1050 N92-33596 #
DOT/FAA/AM-92/20 ..... p 952 N92-30551 #
DOT/FAA/AM-92/3 ..... p 724 N92-27914 #
DOT/FAA/AM-92/4 ..... p 1136 N92-32697 #

DOT/FAA/CT-TN90/33 ..... p 405 N92-19764 #
DOT/FAA/CT-TN91/12 ..... p 573 N92-22966 #
DOT/FAA/CT-TN91/17 ..... p 268 N92-15983 #
DOT/FAA/CT-TN91/1 ..... p 297 N92-16181 #
DOT/FAA/CT-TN91/22 ..... p 534 N92-22210 #
DOT/FAA/CT-TN91/30 ..... p 19 N92-10020 #
DOT/FAA/CT-TN91/32 ..... p 837 N92-28900 #
DOT/FAA/CT-TN91/36 ..... p 31 N92-11021 #
DOT/FAA/CT-TN91/39 ..... p 932 N92-31615 #
DOT/FAA/CT-TN91/40 ..... p 983 N92-30976 #
DOT/FAA/CT-TN91/42 ..... p 93 N92-13043 #
DOT/FAA/CT-TN91/43 ..... p 31 N92-11028 #
DOT/FAA/CT-TN91/44 ..... p 957 N92-31838 #
DOT/FAA/CT-TN91/46 ..... p 268 N92-15981 #
DOT/FAA/CT-TN91/47 ..... p 640 N92-24888 #
DOT/FAA/CT-TN91/49 ..... p 32 N92-11029 #
DOT/FAA/CT-TN91/50 ..... p 221 N92-14270 #
DOT/FAA/CT-TN91/51 ..... p 264 N92-17149 #
DOT/FAA/CT-TN91/54 ..... p 573 N92-22503 #
DOT/FAA/CT-TN91/55 ..... p 402 N92-18959 #
DOT/FAA/CT-TN91/57 ..... p 500 N92-20653 #
DOT/FAA/CT-TN91/59-VOL-1 ..... p 640 N92-25098 #
DOT/FAA/CT-TN92/15 ..... p 665 N92-25733 #
DOT/FAA/CT-TN92/18 ..... p 1002 N92-31617 #
DOT/FAA/CT-TN92/1 ..... p 961 N92-31165 #
DOT/FAA/CT-TN92/26 ..... p 1127 N92-33627 #
DOT/FAA/CT-TN92/28 ..... p 1048 N92-33308 #
DOT/FAA/CT-TN92/2 ..... p 573 N92-22237 #
DOT/FAA/CT-TN92/7 ..... p 640 N92-24799 #

DOT/FAA/CT-88/32-1 ..... p 18 N92-10992 #
DOT/FAA/CT-89/16 ..... p 187 N92-15053 #
DOT/FAA/CT-89/29 ..... p 187 N92-15053 #
DOT/FAA/CT-90/23 ..... p 354 N92-18112 #
DOT/FAA/CT-90/28 ..... p 187 N92-15053 #
DOT/FAA/CT-91/10 ..... p 870 N92-28686 #
DOT/FAA/CT-91/16 ..... p 202 N92-14064 #
DOT/FAA/CT-91/17 ..... p 1043 N92-33005 #
DOT/FAA/CT-91/18 ..... p 781 N92-26830 #
DOT/FAA/CT-91/19 ..... p 736 N92-27973 #
DOT/FAA/CT-91/21 ..... p 352 N92-18259 #
DOT/FAA/CT-91/28 ..... p 1071 N92-33105 #
DOT/FAA/CT-91/31 ..... p 456 N92-21404 #
DOT/FAA/CT-91/32 ..... p 1045 N92-34151 #
DOT/FAA/CT-91/4 ..... p 263 N92-16986 #
DOT/FAA/CT-91/5 ..... p 1126 N92-33480 #
DOT/FAA/CT-91/6 ..... p 191 N92-14034 #
DOT/FAA/CT-92/5 ..... p 971 N92-30303 #

DOT/FAA/DS-89/10 ..... p 191 N92-15061 #

DOT/FAA/EE-88-6 ..... p 45 N92-11578 #
DOT/FAA/EE-91-3 ..... p 45 N92-11578 #

DOT/FAA/ND-91/1 ..... p 354 N92-18967 #

DOT/FAA/NR-91/1 ..... p 18 N92-10019 #
DOT/FAA/NR-92/1 ..... p 1004 N92-32103 #
DOT/FAA/NR-92/7 ..... p 1124 N92-32686 #

DOT/FAA/PM-87/30 ..... p 93 N92-13042 #

DOT/FAA/RD-90/11 ..... p 18 N92-10993 #
DOT/FAA/RD-90/18 ..... p 641 N92-26101 #
DOT/FAA/RD-90/25 ..... p 346 N92-18345 #
DOT/FAA/RD-90/3 ..... p 116 N92-13060 #
DOT/FAA/RD-90/4 ..... p 103 N92-13049 #
DOT/FAA/RD-90/5 ..... p 190 N92-14033 #
DOT/FAA/RD-90/6 ..... p 116 N92-13059 #
DOT/FAA/RD-90/7 ..... p 116 N92-13058 #
DOT/FAA/RD-90/9 ..... p 637 N92-26028 #
DOT/FAA/RD-91/12 ..... p 139 N92-13077 #
DOT/FAA/RD-91/18 ..... p 356 N92-19391 #
DOT/FAA/RD-91/19 ..... p 103 N92-13051 #
DOT/FAA/RD-91/1 ..... p 724 N92-28052 #
DOT/FAA/RD-91/9 ..... p 46 N92-11593 * #
DOT/FAA/RD-92/12 ..... p 952 N92-30980 #
DOT/FAA/RD-92/14-VOL-1 ..... p 1142 N92-33305 #
DOT/FAA/RD-92/18 ..... p 1102 N92-34247 #
DOT/FAA/RD-92/1 ..... p 462 N92-21210 #
DOT/FAA/RD-92/20 ..... p 1043 N92-32606 * #
DOT/FAA/RD-92/21 ..... p 953 N92-31549 * #
DOT/FAA/RD-92/22 ..... p 1047 N92-32537 #
DOT/FAA/RD-92/23 ..... p 1048 N92-33098 #
DOT/FAA/RD-92/2 ..... p 1043 N92-32941 #
DOT/FAA/RD-92/5 ..... p 781 N92-27518 #
DOT/FAA/RD-92/6-PHASE-2 ..... p 484 N92-21162 * #
DOT/FAA/RD-92/8 ..... p 1101 N92-32903 #

DOT/FAA/RP-92/3 ..... p 1101 N92-33434 #

DOT/FAA/SE-91/3 ..... p 268 N92-15980 #
DOT/FAA/SE-92/1 ..... p 308 N92-18969 #
DOT/FAA/SE-92/2 ..... p 535 N92-23096 #
DOT/FAA/SE-92/3 ..... p 953 N92-31211 #

DOT/VNTSC-FAA-91-16 ..... p 854 N92-29180 #

DOTVNTSC-FAA-91-2 ..... p 356 N92-19391 #

DREA-CR-90-425 ..... p 1038 N92-32811 #

DREO-1078 ..... p 765 N92-26592 #
DREO-1091 ..... p 726 N92-26291 #

DREP-TM-88-20 ..... p 222 N92-14345 #
DREP-TM-88-25-PT-1 ..... p 143 N92-12060 #

DREP-89-9 ..... p 1109 N92-32846 #

DRES-MEMO-1355 ..... p 365 N92-19030 #

DRIC-BR-307984 ..... p 740 N92-27062 #

DTRC-91/017 ..... p 170 N92-14966 #

DTRC/PAS-91/7 ..... p 158 N92-13410 #

DTRC/SD-CR-16/91 ..... p 229 N92-15385 #

DTRC/SHD-1003-06 ..... p 298 N92-16978 #
DTRC/SHD-1262-04 ..... p 299 N92-17168 #

D6-55817 ..... p 481 N92-20376 * #

E-3798 ..... p 559 N92-22510 * #
E-4195 ..... p 562 N92-22863 * #
E-5121 ..... p 562 N92-22647 * #
E-5369 ..... p 445 N92-20934 * #
E-5398 ..... p 983 N92-31640 * #
E-5628 ..... p 222 N92-14346 * #
E-5675 ..... p 972 N92-31250 * #

E-5808 ..... p 952 N92-30395 * #
E-5976 ..... p 279 N92-17061 * #
E-5993 ..... p 230 N92-15406 * #
E-6088 ..... p 242 N92-17346 * #
E-6096 ..... p 984 N92-30307 * #
E-6150 ..... p 473 N92-20196 * #
E-6172 ..... p 526 N92-22249 * #
E-6173 ..... p 951 N92-32240 * #
E-6322 ..... p 12 N92-10976 * #
E-6343 ..... p 289 N92-17070 * #
E-6354 ..... p 830 N92-28980 * #
E-6374 ..... p 660 N92-25808 * #
E-6388 ..... p 527 N92-23105 * #
E-6399 ..... p 214 N92-15191 * #
E-6407 ..... p 1109 N92-32863 * #
E-6460 ..... p 2 N92-10002 * #
E-6494 ..... p 279 N92-15993 * #
E-6519 ..... p 304 N92-16705 * #
E-6528 ..... p 12 N92-10979 * #
E-6531 ..... p 998 N92-30396 * #
E-6545 ..... p 298 N92-16336 * #
E-6613 ..... p 348 N92-19437 * #
E-6620 ..... p 473 N92-20525 * #
E-6645 ..... p 166 N92-13759 * #
E-6650 ..... p 26 N92-11017 * #
E-6677 ..... p 516 N92-22659 * #
E-6679 ..... p 179 N92-13998 * #
E-6691 ..... p 597 N92-23560 * #
E-6695 ..... p 44 N92-11328 * #
E-6703 ..... p 229 N92-15402 * #
E-6705 ..... p 237 N92-14795 * #
E-6706 ..... p 130 N92-13071 * #
E-6717 ..... p 202 N92-14063 * #
E-6730 ..... p 416 N92-18282 * #
E-6743 ..... p 237 N92-14797 * #
E-6746 ..... p 258 N92-15968 * #
E-6760 ..... p 186 N92-15052 * #
E-6761 ..... p 185 N92-15051 * #
E-6767 ..... p 261 N92-17347 * #
E-6775 ..... p 473 N92-20523 * #
E-6778 ..... p 179 N92-14001 * #
E-6779 ..... p 258 N92-15967 * #
E-6784 ..... p 179 N92-14002 * #
E-6789 ..... p 279 N92-17546 * #
E-6795 ..... p 562 N92-23254 * #
E-6796 ..... p 297 N92-16265 * #
E-6806 ..... p 596 N92-23154 * #
E-6808 ..... p 350 N92-19993 * #
E-6820 ..... p 346 N92-18760 * #
E-6823 ..... p 659 N92-25712 * #
E-6826 ..... p 773 N92-27879 * #
E-6827 ..... p 887 N92-28673 * #
E-6828 ..... p 716 N92-27376 * #
E-6830 ..... p 678 N92-24514 * #
E-6843 ..... p 633 N92-26104 * #
E-6853 ..... p 528 N92-23563 * #
E-6859 ..... p 387 N92-18280 * #
E-6868 ..... p 378 N92-20033 * #
E-6880 ..... p 474 N92-20650 * #
E-6901 ..... p 596 N92-23267 * #
E-6905 ..... p 481 N92-20586 * #
E-6908 ..... p 499 N92-20235 * #
E-6930 ..... p 828 N92-28696 * #
E-6935 ..... p 756 N92-27378 * #
E-6936 ..... p 696 N92-24688 * #
E-6943 ..... p 658 N92-25164 * #
E-6945 ..... p 596 N92-23435 * #
E-6948 ..... p 562 N92-23537 * #
E-6962 ..... p 716 N92-27377 * #
E-6989 ..... p 680 N92-24959 * #
E-6993 ..... p 630 N92-24958 * #
E-6999 ..... p 665 N92-25449 * #
E-7002 ..... p 667 N92-26129 * #
E-7003 ..... p 924 N92-30207 * #
E-7015 ..... p 764 N92-26555 * #
E-7019 ..... p 908 N92-28434 * #
E-7027 ..... p 680 N92-24984 * #
E-7032 ..... p 764 N92-26560 * #
E-7039 ..... p 1128 N92-34112 * #
E-7046 ..... p 833 N92-30182 * #
E-7058 ..... p 871 N92-29661 * #
E-7060 ..... p 910 N92-29136 * #
E-7061 ..... p 972 N92-31172 * #
E-7062 ..... p 1072 N92-33746 * #
E-7063 ..... p 739 N92-27037 * #
E-7064 ..... p 982 N92-30508 * #
E-7065 ..... p 770 N92-27653 * #
E-7082 ..... p 742 N92-27652 * #
E-7083 ..... p 738 N92-26553 * #
E-7084 ..... p 1002 N92-31349 * #
E-7085 ..... p 742 N92-27669 * #
E-7086 ..... p 868 N92-28418 * #
E-7087 ..... p 738 N92-26561 * #
E-7090 ..... p 1002 N92-31485 * #
E-7109 ..... p 868 N92-28419 * #
E-7112 ..... p 909 N92-29105 * #
E-7113 ..... p 870 N92-28985 * #
E-7116 ..... p 722 N92-28102 * #
E-7124 ..... p 739 N92-26613 * #
E-7135 ..... p 890 N92-29343 * #
E-7141 ..... p 1002 N92-31484 * #
E-7147 ..... p 714 N92-26612 * #
E-7148 ..... p 828 N92-28674 * #
E-7158 ..... p 1134 N92-33894 * #
E-7175 ..... p 831 N92-29402 * #
E-7201 ..... p 1042 N92-34144 * #
E-7226 ..... p 972 N92-30972 * #
E-7227 ..... p 1088 N92-34107 * #
E-7233 ..... p 932 N92-31267 * #
E-7235 ..... p 1009 N92-30898 * #
E-7245 ..... p 972 N92-30998 * #
E-7260 ..... p 979 N92-32241 * #

EDR-15593 ..... p 682 N92-25649 * #
EDR-15982 ..... p 1073 N92-34236 * #

EGG-EE-9479 ..... p 163 N92-12440 * #

EMA-TR-87-5-1 ..... p 346 N92-18345 #

EOARD-LR-91-008 ..... p 550 N92-22785 #

ERC-R-92-022 ..... p 753 N92-27403 * #

ERI-89179 ..... p 562 N92-22647 * #

ERIM-227000-1-F ..... p 501 N92-20997 #

ESA-SP-318 ..... p 180 N92-14973 #

ESA-TT-1229 ..... p 988 N92-31942 #
ESA-TT-1235 ..... p 944 N92-30514 #
ESA-TT-1236 ..... p 595 N92-22641 #
ESA-TT-1247 ..... p 830 N92-29159 #
ESA-TT-1254 ..... p 954 N92-31943 #

ESD-TR-91-211 ..... p 103 N92-13052 #
ESD-TR-91-213 ..... p 191 N92-15058 #
ESD-TR-91-224 ..... p 773 N92-27864 #

ESDU-AERO-C.01.01.02 ..... p 1086 N92-32487

ESDU-PERF-EG6/3 ..... p 272 N92-15988

ESDU-68022 ..... p 553 N92-24009
ESDU-90030 ..... p 1037 N92-32782
ESDU-91009 ..... p 80 N92-11969
ESDU-91010 ..... p 399 N92-18091
ESDU-91014 ..... p 81 N92-11970
ESDU-91016-ADD ..... p 272 N92-15987
ESDU-91017 ..... p 359 N92-18096
ESDU-91018 ..... p 276 N92-17843
ESDU-91019 ..... p 268 N92-17844
ESDU-91020 ..... p 276 N92-17847
ESDU-91021 ..... p 258 N92-15970
ESDU-91028 ..... p 259 N92-15972
ESDU-91029 ..... p 259 N92-15973
ESDU-91031 ..... p 259 N92-15971
ESDU-91032 ..... p 272 N92-15988
ESDU-91033 ..... p 416 N92-18074
ESDU-91042 ..... p 553 N92-24009
ESDU-92002-SUPPL ..... p 1037 N92-32782
ESDU-92006 ..... p 1087 N92-32780
ESDU-92007 ..... p 1086 N92-32487
ESDU-92024 ..... p 1036 N92-32479

ESL-TR-90-24 ..... p 1126 N92-33501 #
ESL-TR-91-31 ..... p 45 N92-11578 #

ETN-91-90080 ..... p 43 N92-11307 #
ETN-91-90082 ..... p 23 N92-11009 #
ETN-91-90085 ..... p 43 N92-11309 #
ETN-91-90086 ..... p 43 N92-11310 #
ETN-91-90087 ..... p 81 N92-11972 #
ETN-91-90094 ..... p 43 N92-11311 #
ETN-91-90095 ..... p 43 N92-11312 #
ETN-91-90096 ..... p 13 N92-10989 #
ETN-91-90097 ..... p 57 N92-11963 #
ETN-91-90102 ..... p 82 N92-11980 #
ETN-91-90106 ..... p 82 N92-11981 #
ETN-91-90108 ..... p 157 N92-12216 #
ETN-91-90109 ..... p 82 N92-11982 #
ETN-91-90110 ..... p 138 N92-12006 #
ETN-91-90136 ..... p 81 N92-11973 #
ETN-91-90194 ..... p 134 N92-12003 #
ETN-91-90195 ..... p 225 N92-14382 #
ETN-91-90199 ..... p 19 N92-10996 #
ETN-91-90209 ..... p 20 N92-10997 #
ETN-91-90286 ..... p 157 N92-12312 #
ETN-91-90287 ..... p 114 N92-11993 #
ETN-91-90288 ..... p 158 N92-12313 #
ETN-91-90293 ..... p 61 N92-12988 #
ETN-91-90294 ..... p 135 N92-12004 #
ETN-91-99891 ..... p 18 N92-10018 #
ETN-91-99909 ..... p 42 N92-11287 #
ETN-91-99953 ..... p 31 N92-11020 #
ETN-92-90317 ..... p 225 N92-14397 #
ETN-92-90319 ..... p 187 N92-14007 #
ETN-92-90417 ..... p 237 N92-14798 #
ETN-92-90418 ..... p 196 N92-14044 #
ETN-92-90420 ..... p 196 N92-14045 #
ETN-92-90432 ..... p 196 N92-15065 #
ETN-92-90592 ..... p 205 N92-15072 #
ETN-92-90610 ..... p 239 N92-15938 #
ETN-92-90612 ..... p 196 N92-15066 #
ETN-92-90614 ..... p 359 N92-18333 #
ETN-92-90615 ..... p 345 N92-18316 #
ETN-92-90616 ..... p 290 N92-17310 #
ETN-92-90619 ..... p 524 N92-22179 #
ETN-92-90620 ..... p 275 N92-17313 #
ETN-92-90624 ..... p 300 N92-17344 #
ETN-92-90656 ..... p 449 N92-20794 #
ETN-92-90680 ..... p 180 N92-14973 #
ETN-92-90685 ..... p 575 N92-22268 #
ETN-92-90704 ..... p 187 N92-15054 #
ETN-92-90727 ..... p 466 N92-22000 #
ETN-92-90729 ..... p 354 N92-19041 #
ETN-92-90731 ..... p 410 N92-19292 #
ETN-92-90732 ..... p 503 N92-21699 #
ETN-92-90738 ..... p 455 N92-20902 #
ETN-92-90760 ..... p 476 N92-21740 #
ETN-92-90761 ..... p 503 N92-21741 #
ETN-92-90764 ..... p 506 N92-21743 #
ETN-92-90765 ..... p 490 N92-21744 #
ETN-92-90768 ..... p 505 N92-20928 #
ETN-92-90772 ..... p 501 N92-20909 #
ETN-92-90774 ..... p 767 N92-27038 #
ETN-92-90775 ..... p 739 N92-27039 #
ETN-92-90776 ..... p 572 N92-22096 #
ETN-92-90777 ..... p 740 N92-27040 #
ETN-92-90778 ..... p 740 N92-27041 #
ETN-92-90779 ..... p 740 N92-27042 #
ETN-92-90780 ..... p 740 N92-27043 #
ETN-92-90781 ..... p 756 N92-27044 #
ETN-92-90782 ..... p 378 N92-19938 #
ETN-92-90785 ..... p 510 N92-21847 #
ETN-92-90786 ..... p 476 N92-21848 #
ETN-92-90788 ..... p 476 N92-21850 #
ETN-92-90791 ..... p 500 N92-20491 #
ETN-92-90792 ..... p 474 N92-20573 #
ETN-92-90794 ..... p 473 N92-20459 #
ETN-92-90795 ..... p 473 N92-20460 #
ETN-92-90796 ..... p 512 N92-20461 #
ETN-92-90797 ..... p 505 N92-20574 #
ETN-92-90798 ..... p 378 N92-19939 #
ETN-92-90819 ..... p 767 N92-27045 #
ETN-92-90820 ..... p 732 N92-26944 #
ETN-92-90829 ..... p 768 N92-27407 #
ETN-92-90840 ..... p 376 N92-18728 #
ETN-92-90841 ..... p 354 N92-18729 #
ETN-92-90842 ..... p 473 N92-20436 #
ETN-92-90843 ..... p 559 N92-22098 #
ETN-92-90844 ..... p 591 N92-22099 #
ETN-92-90845 ..... p 741 N92-27422 #
ETN-92-90847 ..... p 488 N92-20164 #
ETN-92-90851 ..... p 472 N92-20179 #
ETN-92-90860 ..... p 366 N92-19225 #
ETN-92-90861 ..... p 347 N92-19252 #
ETN-92-90867 ..... p 404 N92-19349 #
ETN-92-90868 ..... p 353 N92-19350 #
ETN-92-90871 ..... p 381 N92-19295 #
ETN-92-90872 ..... p 513 N92-21736 #
ETN-92-90876 ..... p 511 N92-20388 #
ETN-92-90913 ..... p 262 N92-17849 #
ETN-92-90922 ..... p 385 N92-18341 #
ETN-92-90924 ..... p 344 N92-18231 #
ETN-92-90925 ..... p 345 N92-18232 #
ETN-92-90926 ..... p 345 N92-18233 #
ETN-92-90934 ..... p 345 N92-18293 #
ETN-92-90935 ..... p 400 N92-18317 #
ETN-92-90936 ..... p 380 N92-18294 #
ETN-92-90937 ..... p 345 N92-18318 #
ETN-92-90940 ..... p 380 N92-18321 #
ETN-92-90941 ..... p 308 N92-18322 #
ETN-92-90951 ..... p 500 N92-20497 #
ETN-92-90953 ..... p 405 N92-19490 #
ETN-92-90954 ..... p 356 N92-19491 #
ETN-92-90956 ..... p 400 N92-18221 #
ETN-92-90958 ..... p 385 N92-18415 #
ETN-92-90959 ..... p 385 N92-18416 #
ETN-92-90961 ..... p 444 N92-20473 #
ETN-92-90962 ..... p 444 N92-20498 #
ETN-92-90965 ..... p 481 N92-20475 #
ETN-92-90969 ..... p 381 N92-18893 #
ETN-92-90998 ..... p 447 N92-21703 #
ETN-92-91000 ..... p 347 N92-19296 #
ETN-92-91006 ..... p 501 N92-21232 #
ETN-92-91007 ..... p 501 N92-21233 #

ETN-92-91008 ..... p 502 N92-21234 #
ETN-92-91050 ..... p 452 N92-21746
ETN-92-91052 ..... p 349 N92-19679 #
ETN-92-91056 ..... p 559 N92-22406 #
ETN-92-91057 ..... p 530 N92-22408 #
ETN-92-91058 ..... p 444 N92-20468 #
ETN-92-91059 ..... p 443 N92-20229 #
ETN-92-91063 ..... p 640 N92-25590 #
ETN-92-91074 ..... p 606 N92-23928 #
ETN-92-91080 ..... p 349 N92-19682 #
ETN-92-91081 ..... p 406 N92-19976 #
ETN-92-91082 ..... p 349 N92-19925 #
ETN-92-91177 ..... p 603 N92-22673
ETN-92-91194 ..... p 528 N92-23168 #
ETN-92-91197 ..... p 604 N92-22241 #
ETN-92-91206 ..... p 595 N92-22641 #
ETN-92-91207 ..... p 830 N92-29159 #
ETN-92-91262 ..... p 658 N92-24336 #
ETN-92-91295 ..... p 692 N92-25306 #
ETN-92-91300 ..... p 648 N92-24964 #
ETN-92-91301 ..... p 648 N92-24966 #
ETN-92-91319 ..... p 947 N92-31508 #
ETN-92-91325 ..... p 830 N92-29206 #
ETN-92-91326 ..... p 908 N92-28788 #
ETN-92-91327 ..... p 829 N92-28789 #
ETN-92-91342 ..... p 910 N92-29683 #
ETN-92-91387 ..... p 988 N92-31942 #
ETN-92-91390 ..... p 859 N92-29870 #
ETN-92-91391 ..... p 929 N92-29218 #
ETN-92-91401 ..... p 887 N92-28579 #
ETN-92-91403 ..... p 923 N92-28581 #
ETN-92-91432 ..... p 852 N92-28649 #
ETN-92-91435 ..... p 878 N92-28652 #
ETN-92-91436 ..... p 879 N92-28653 #
ETN-92-91437 ..... p 859 N92-28654 #
ETN-92-91438 ..... p 859 N92-28644 #
ETN-92-91439 ..... p 837 N92-28655 #
ETN-92-91440 ..... p 837 N92-29703 #
ETN-92-91446 ..... p 852 N92-28687 #
ETN-92-91448 ..... p 923 N92-28635 #
ETN-92-91449 ..... p 910 N92-29603 #
ETN-92-91450 ..... p 827 N92-28657 #
ETN-92-91453 ..... p 924 N92-29604 #
ETN-92-91454 ..... p 841 N92-29605 #
ETN-92-91491 ..... p 832 N92-29741 #
ETN-92-91492 ..... p 833 N92-29889 #
ETN-92-91493 ..... p 871 N92-29927 #
ETN-92-91495 ..... p 890 N92-29680 #
ETN-92-91496 ..... p 890 N92-29629 #
ETN-92-91497 ..... p 831 N92-29648 #
ETN-92-91498 ..... p 832 N92-29713 #
ETN-92-91499 ..... p 831 N92-29649 #
ETN-92-91500 ..... p 854 N92-29650 #
ETN-92-91512 ..... p 827 N92-28658 #
ETN-92-91513 ..... p 841 N92-29615 #
ETN-92-91514 ..... p 854 N92-29616 #
ETN-92-91518 ..... p 827 N92-28659 #
ETN-92-91519 ..... p 828 N92-28660 #
ETN-92-91520 ..... p 887 N92-28669 #
ETN-92-91523 ..... p 915 N92-28689 #
ETN-92-91525 ..... p 952 N92-30474 #
ETN-92-91530 ..... p 828 N92-28709 #
ETN-92-91531 ..... p 870 N92-28711 #
ETN-92-91533 ..... p 908 N92-28712 #
ETN-92-91535 ..... p 828 N92-28692 #
ETN-92-91536 ..... p 887 N92-28661 #
ETN-92-91537 ..... p 888 N92-29204 #
ETN-92-91540 ..... p 908 N92-28694 #
ETN-92-91541 ..... p 927 N92-28695 #
ETN-92-91543 ..... p 829 N92-28713 #
ETN-92-91544 ..... p 852 N92-28714 #
ETN-92-91546 ..... p 833 N92-29916 #
ETN-92-91547 ..... p 832 N92-29884 #
ETN-92-91613 ..... p 987 N92-30414 #
ETN-92-91664 ..... p 1037 N92-32769 #
ETN-92-91671 ..... p 1037 N92-32773 #
ETN-92-91675 ..... p 1125 N92-32776 #
ETN-92-91695 ..... p 910 N92-29873 #
ETN-92-91696 ..... p 787 N92-29874 #
ETN-92-91697 ..... p 889 N92-30076 #
ETN-92-91704 ..... p 945 N92-30713 #
ETN-92-91709 ..... p 944 N92-30514 #
ETN-92-91711 ..... p 954 N92-31943 #
ETN-92-91727 ..... p 948 N92-31514 #
ETN-92-91728 ..... p 963 N92-31515 #
ETN-92-91731 ..... p 911 N92-29877 #
ETN-92-91732 ..... p 953 N92-31813 #
ETN-92-91733 ..... p 928 N92-29997 #
ETN-92-91888 ..... p 978 N92-30439 #
ETN-92-91889 ..... p 988 N92-31716 #
ETN-92-91890 ..... p 952 N92-30418 #
ETN-92-91898 ..... p 987 N92-30969 #
ETN-92-91901 ..... p 998 N92-30423 #
ETN-92-91902 ..... p 961 N92-30424 #
ETN-92-91903 ..... p 787 N92-30232 #
ETN-92-91906 ..... p 932 N92-30675 #
ETN-92-91907 ..... p 944 N92-30676 #
ETN-92-91994 ..... p 1037 N92-32730 #
ETN-92-91996 ..... p 1125 N92-33139 * #
ETN-92-91997 ..... p 1037 N92-32732 #
ETN-92-91998 ..... p 1101 N92-32734 #
ETN-92-92000 ..... p 1037 N92-32673 #
ETN-92-92001 ..... p 1047 N92-32830 #
ETN-92-92034 ..... p 1051 N92-33693 #
ETN-92-92041 ..... p 1125 N92-33066 #
ETN-92-92053 ..... p 1143 N92-33694 #
ETN-92-92103 ..... p 1127 N92-33916 #
ETN-92-92104 ..... p 1072 N92-33645 #
ETN-92-92108 ..... p 1111 N92-33994 #
ETN-92-92118 ..... p 1125 N92-32742 #
ETN-92-92163 ..... p 1088 N92-34161 #
ETN-92-92177 ..... p 1072 N92-33815 #
ETN-92-92181 ..... p 1111 N92-34019 #
ETN-92-92183 ..... p 1072 N92-33748 #
ETN-92-92184 ..... p 1072 N92-33749 #
ETN-92-92185 ..... p 1061 N92-33750 #
ETN-92-92186 ..... p 1129 N92-33751 #
ETN-92-99978 ..... p 195 N92-14042 #
ETN-92-99979 ..... p 195 N92-14043 #

F+W-TF-2012 ..... p 767 N92-27045 #
F+W-TF-2058 ..... p 732 N92-26944 #

FAA-AC-43-4A ..... p 420 N92-21834 #

FAA-AMS-420 ..... p 169 N92-13926 #
FAA-AMS-420 ..... p 170 N92-13927 #

FAA-APO-92-1 ..... p 837 N92-29182 #

FAA/APO-210 ..... p 983 N92-30777 #
FAA/APO-91-4 ..... p 983 N92-30777 #

FAA/ARD-30 ..... p 462 N92-21210 #

FFA-TN-1990-19 ..... p 444 N92-20468 #
FFA-TN-1990-20 ..... p 945 N92-30713 #
FFA-TN-1991-18 ..... p 157 N92-12312 #
FFA-TN-1991-22 ..... p 114 N92-11993 #
FFA-TN-1991-24 ..... p 158 N92-12313 #
FFA-TN-1991-27 ..... p 443 N92-20229 #
FFA-TN-1991-40 ..... p 528 N92-23168 #

FIA-91-27 ..... p 692 N92-25190 * #

FJSRL-TR-91-0001 ..... p 12 N92-10016 #
FJSRL-TR-91-0002 ..... p 139 N92-13079 #
FJSRL-TR-92-0001 ..... p 948 N92-31622 #

FR-721711-4-VOL-1 ..... p 221 N92-14262 * #
FR-721711-4-VOL-2 ..... p 221 N92-14263 * #

FTD-ID(RS)T-0167-91 ..... p 170 N92-13991 #
FTD-ID(RS)T-0170-91 ..... p 170 N92-13992 #
FTD-ID(RS)T-0172-91 ..... p 229 N92-15367 #
FTD-ID(RS)T-0289-91 ..... p 119 N92-13066 #
FTD-ID(RS)T-0460-91 ..... p 116 N92-13062 #
FTD-ID(RS)T-0461-91 ..... p 170 N92-13993 #

FTL-R-91-7 ..... p 1045 N92-34192 * #

GAO-55-636-PT-6 ..... p 1141 N92-32505 #

GAO/IMTEC-91-25 ..... p 1048 N92-32861 #

GAO/NSIAD-90-71FS ..... p 139 N92-13076 #
GAO/NSIAD-91-211 ..... p 242 N92-15963 #
GAO/NSIAD-92-5 ..... p 62 N92-12991 #

GAO/RCED-91-128 ..... p 1011 N92-31454 #
GAO/RCED-91-24 ..... p 953 N92-31453 #

GARTEUR-TP-051 ..... p 854 N92-29616 #

GARTEUR/TP-056 ..... p 878 N92-28652 #

GITAER-91-6 ..... p 178 N92-13995 * #

GMD-580 ..... p 455 N92-20818 #

GPO-55-260-VOL-1 ..... p 1142 N92-33147 #

GRI-91/0180 ..... p 756 N92-26521 #
GRI-91/0282 ..... p 488 N92-20329 #
GRI-91/0290 ..... p 765 N92-26816 #
GRI-91/0328 ..... p 499 N92-20265 #
GRI-91/0382 ..... p 771 N92-27715 #

GTRI-A8612-001 ..... p 738 N92-26405 * #

H-1645 ..... p 482 N92-21357 * #
H-1675 ..... p 1133 N92-32507 * #
H-1676 ..... p 381 N92-19174 * #
H-1729 ..... p 663 N92-25734 * #
H-1743 ..... p 273 N92-17071 * #
H-1748 ..... p 570 N92-22194 * #
H-1758 ..... p 663 N92-25982 * #
H-1764 ..... p 871 N92-29659 * #
H-1765 ..... p 445 N92-21188 * #
H-1766 ..... p 118 N92-11994 * #
H-1769 ..... p 878 N92-28584 * #
H-1775 ..... p 871 N92-29427 * #
H-1777 ..... p 117 N92-13064 * #
H-1780 ..... p 276 N92-17128 * #
H-1783 ..... p 947 N92-31276 * #
H-1785 ..... p 272 N92-15986 * #
H-1787 ..... p 979 N92-31656 * #
H-1794 ..... p 482 N92-21253 * #
H-1795 ..... p 962 N92-31208 * #
H-1806 ..... p 871 N92-29425 * #
H-1808 ..... p 973 N92-31275 * #
H-1811 ..... p 742 N92-27587 * #
H-1817 ..... p 740 N92-27379 * #
H-1818 ..... p 1062 N92-34202 * #
H-1826 ..... p 1087 N92-32864 * #
H-1831 ..... p 984 N92-32201 * #
H-1833 ..... p 853 N92-29110 * #
H-1839 ..... p 1065 N92-32866 * #
H-1842 ..... p 971 N92-30518 * #
H-1846 ..... p 1060 N92-33404 * #
H-1847 ..... p 962 N92-31261 * #
H-1857 ..... p 1060 N92-33149 * #
H-1860 ..... p 1062 N92-34039 * #

HSRC-C910684 ..... p 29 N92-11018 #

HTL-55 ..... p 685 N92-25962 * #

IAF PAPER ST-91-001 ..... p 175 A92-20649
IAF PAPER ST-91-002 ..... p 207 A92-20650
IAF PAPER ST-91-004 ..... p 186 A92-20651

IAF PAPER 91-198 ..... p 32 A92-12570
IAF PAPER 91-271 ..... p 120 A92-14709
IAF PAPER 91-272 ..... p 32 A92-12599
IAF PAPER 91-273 ..... p 120 A92-14710
IAF PAPER 91-275 ..... p 278 A92-22482 *
IAF PAPER 91-276 ..... p 25 A92-12600
IAF PAPER 91-277 ..... p 25 A92-12601
IAF PAPER 91-278 ..... p 120 A92-14711
IAF PAPER 91-490 ..... p 188 A92-18505
IAF PAPER 91-737 ..... p 301 A92-22495
IAF PAPER 92-0657 ..... p 1071 A92-57098
IAF PAPER 92-0658 ..... p 1071 A92-57099
IAF PAPER 92-0659 ..... p 1106 A92-57100 *
IAF PAPER 92-0661 ..... p 1106 A92-57101
IAF PAPER 92-0663 ..... p 1104 A92-57102
IAF PAPER 92-0863 ..... p 1104 A92-57254
IAF PAPER 92-0867 ..... p 1105 A92-57258
IAF PAPER 92-0868 ..... p 1105 A92-57259 *
IAF PAPER 92-0909 ..... p 1123 A92-57288

IAITIC-91-1017 ..... p 482 N92-20849 #
IAITIC-91-1018 ..... p 461 N92-20500 #

IAR-AN-70-PHASE-1 ..... p 102 N92-11988 #
IAR-AN-72 ..... p 1048 N92-32849 #
IAR-AN-73 ..... p 268 N92-17568 #
IAR-AN-74 ..... p 716 N92-27344 #

IB-222-90-A-46 ..... p 400 N92-18244 #

ICASE-IR-20 ..... p 402 N92-18965 * #

ICASE-91-44 ..... p 347 N92-19250 * #
ICASE-91-88 ..... p 234 N92-15658 * #
ICASE-91-89 ..... p 185 N92-15047 * #
ICASE-92-10 ..... p 592 N92-22228 * #
ICASE-92-7 ..... p 447 N92-21465 * #

ICOMP-91-22 ..... p 597 N92-23560 * #
ICOMP-91-23 ..... p 44 N92-11328 * #
ICOMP-92-02 ..... p 678 N92-24514 * #

IDA-P-2464 ..... p 158 N92-13351 #

IDA/HQ-90-35838 ..... p 158 N92-13351 #

ILR-MITT-263(1991) ..... p 20 N92-10997 #

IME-CRE-TR-003 ..... p 448 N92-20156 #

IMFL-90-64 ..... p 353 N92-19350 #

INT-PATENT-CLASS-B05B-1/00 . p 1125 N92-32856
INT-PATENT-CLASS-B64C-21/10 p 463 N92-21587 *
INT-PATENT-CLASS-B64C-25/60 p 1061 N92-33585
INT-PATENT-CLASS-B64C-3/14 . p 829 N92-28729 *

INT-PATENT-CLASS-B64D-1/16 . p 1061 N92-33582

INT-PATENT-CLASS-F16C-32/04 p 909 N92-29099 *
INT-PATENT-CLASS-F16C-3330 . p 158 N92-13434 #
INT-PATENT-CLASS-F16F-948 .... p 115 N92-13055 #
INT-PATENT-CLASS-F17C-11/00 p 228 N92-15203 *

INT-PATENT-CLASS-G01C-21/00 p 916 N92-29148 *
INT-PATENT-CLASS-G01L-5/16 . p 42 N92-10185 *
INT-PATENT-CLASS-G01M-9/00 p 42 N92-10185 *
INT-PATENT-CLASS-G01M-9/00 p 447 N92-21588 *
INT-PATENT-CLASS-G01P-3/36 . p 1042 N92-34172 *
INT-PATENT-CLASS-G10L-908 ... p 130 N92-13069 #
INT-PATENT-CLASS-G10L-914 ... p 130 N92-13069 #

INT-PATENT-CLASS-H01N-1/26 . p 297 N92-16243 *
INT-PATENT-CLASS-H01N-17/00 p 297 N92-16243 *
INT-PATENT-CLASS-H02K-1/14 . p 909 N92-29099 *

IS-T-1551 ..... p 499 N92-20301 #

ISBN 0-0783-0123-4 ..... p 1114 A92-54301
ISBN 0-13-596230-7 ..... p 639 A92-40199
ISBN 0-201-14659-2 ..... p 672 A92-38275
ISBN 0-262-11162-4 ..... p 970 A92-53336
ISBN 0-387-97475-X ..... p 897 A92-45261
ISBN 0-387-97672-8 ..... p 431 A92-30850
ISBN 0-444-88706-7 ..... p 296 A92-24176
ISBN 0-444-88948-5 ..... p 918 A92-47035
ISBN 0-471-61397-5 ..... p 480 A92-31021
ISBN 0-521-36264-4 ..... p 538 A92-33919
ISBN 0-7803-0084-X ..... p 786 A92-48426
ISBN 0-7803-0115-3 ..... p 964 A92-49251
ISBN 0-7803-0521-3 ..... p 1119 A92-56201
ISBN 0-7918-0661-8 ..... p 668 A92-39852 *
ISBN 0-7918-0714-2 ..... p 522 A92-36028
ISBN 0-8031-1248-3 ..... p 669 A92-40409
ISBN 0-8031-1423-0 ..... p 896 A92-45226
ISBN 0-8194-0428-4 ..... p 901 A92-48026 *
ISBN 0-8194-0430-6 ..... p 779 A92-42601
ISBN 0-8194-0441-1 ..... p 994 A92-51626
ISBN 0-87263-406-X ..... p 784 A92-47403
ISBN 0-87942-257-2 ..... p 496 A92-31778
ISBN 0-87942-661-6 ..... p 759 A92-42051
ISBN 0-89448-163-0 ..... p 992 A92-50771
ISBN 0-89464-562-5 ..... p 642 A92-38316
ISBN 0-903409-68-2 ..... p 783 A92-45302
ISBN 0-903409-78-X ..... p 634 A92-39301
ISBN 0-912053-34-8 ..... p 980 A92-51401
ISBN 0-930403-85-1 ..... p 307 A92-26250
ISBN 0-930403-94-0 ..... p 634 A92-38000
ISBN 0-931784-21-2 ..... p 695 A92-39226
ISBN 0-938994-58-1 ..... p 985 A92-51901
ISBN 1-55831-117-1 ..... p 929 A92-46201
ISBN 1-56032-231-4 ..... p 993 A92-51438
ISBN 1-56091-146-8 ..... p 783 A92-45376
ISBN 1-56347-010-1 ..... p 459 A92-31606
ISBN 1-56347-011-X ..... p 862 A92-46426
ISBN 1-56347-017-9 ..... p 590 A92-35847
ISBN 1-56347-031-4 ..... p 1052 A92-54550
ISBN 1-56347 ..... p 532 A92-33433
ISBN 2-907669-18-4 ..... p 676 A92-40400
ISBN 5-02-014005-8 ..... p 610 A92-36600
ISBN 5-02-014006-6 ..... p 670 A92-36611
ISBN 5-02-029345-8 ..... p 809 A92-46626
ISBN 5-02-029715-1 ..... p 708 A92-42777
ISBN 5-217-01060-6 ..... p 725 A92-42789
ISBN 5-217-01447-4 ..... p 776 A92-42780
ISBN 5-277-01070-X ..... p 670 A92-36606
ISBN 5-286-00416-4 ..... p 775 A92-42785
ISBN 5-288-00516-8 ..... p 779 A92-42778
ISBN 90-6275-608-5 ..... p 357 A92-26550
ISBN 91-7848-224-0 ..... p 693 A92-39042

ISBN-0-16-035630-X ..... p 238 N92-14933 #
ISBN-0-16-036174-5 ..... p 929 N92-28344 * #
ISBN-0-16-038597-0 ..... p 1141 N92-32505 #
ISBN-0-16-038832-5 ..... p 1142 N92-33147 #
ISBN-0-309-05104-5 ..... p 92 N92-13040 #
ISBN-0-309-05107-X ..... p 308 N92-19662 #
ISBN-0-315-51095-1 ..... p 716 N92-27624 #
ISBN-0-315-54650-6 ..... p 753 N92-27613 #
ISBN-0-315-57981-1 ..... p 1126 N92-33440
ISBN-0-315-59945-6 ..... p 749 N92-27645 #
ISBN-0-8330-1193-6 ..... p 636 N92-25262
ISBN-0-85679-771-5 ..... p 80 N92-11969
ISBN-0-85679-772-3 ..... p 399 N92-18091
ISBN-0-85679-776-6 ..... p 81 N92-11970
ISBN-0-85679-778-2 ..... p 272 N92-15987
ISBN-0-85679-779-0 ..... p 359 N92-18096
ISBN-0-85679-780-4 ..... p 276 N92-17843
ISBN-0-85679-781-2 ..... p 268 N92-17844
ISBN-0-85679-782-0 ..... p 276 N92-17847
ISBN-0-85679-783-9 ..... p 258 N92-15970
ISBN-0-85679-790-1 ..... p 259 N92-15972
ISBN-0-85679-791-X ..... p 259 N92-15973
ISBN-0-85679-793-6 ..... p 272 N92-15988
ISBN-0-85679-794-4 ..... p 259 N92-15971
ISBN-0-85679-795-2 ..... p 416 N92-18074
ISBN-0-85679-804-5 ..... p 553 N92-24009
ISBN-0-85679-807-X ..... p 1037 N92-32782
ISBN-0-85679-811-8 ..... p 1087 N92-32780
ISBN-0-85679-812-6 ..... p 1086 N92-32487
ISBN-0-85679-829-0 ..... p 1036 N92-32479
ISBN-0-86776-418-X ..... p 297 N92-16225 #
ISBN-0-904947-30-0 ..... p 18 N92-10018 #
ISBN-0-904947-34-3 ..... p 61 N92-12988 #
ISBN-0309-7293 ..... p 592 N92-22209 #
ISBN-1-871564-31-X ..... p 187 N92-15054 #
ISBN-1-871564-33-6 ..... p 349 N92-19679 #
ISBN-1-871564-360 ..... p 963 N92-31515 #
ISBN-1-871564-387 ..... p 948 N92-31514 #
ISBN-2-7170-0945-0 ..... p 31 N92-11020 #
ISBN-90-6275-723-9 ..... p 648 N92-24964 #
ISBN-90-6275-734-0 ..... p 692 N92-25306 #
ISBN-90-9004317-9 ..... p 1125 N92-33066 #
ISBN-92-835-0623-5 ..... p 83 N92-12996 #
ISBN-92-835-0624-3 ..... p 205 N92-14065 #
ISBN-92-835-0628-6 ..... p 164 N92-12517 #
ISBN-92-835-0632-4 ..... p 22 N92-11001 #
ISBN-92-835-0635-9 ..... p 234 N92-14673 #
ISBN-92-835-0637-5 ..... p 445 N92-20797 #
ISBN-92-835-0640-5 ..... p 273 N92-17153 #
ISBN-92-835-0641-3 ..... p 464 N92-21951 #
ISBN-92-835-0642-1 ..... p 360 N92-18571 #
ISBN-92-835-0643-X ..... p 363 N92-18778 #
ISBN-92-835-0644-8 ..... p 449 N92-21679 #
ISBN-92-835-0646-4 ..... p 352 N92-18242 #
ISBN-92-835-0647-2 ..... p 303 N92-17498 #
ISBN-92-835-0648-0 ..... p 402 N92-19004 #
ISBN-92-835-0649-9 ..... p 345 N92-18269 #
ISBN-92-835-0650-2 ..... p 382 N92-20026 #
ISBN-92-835-0652-9 ..... p 552 N92-23950 #
ISBN-92-835-0653-7 ..... p 550 N92-23227 #
ISBN-92-835-0656-1 ..... p 786 N92-28522 #
ISBN-92-835-0657-X ..... p 859 N92-28376 #
ISBN-92-835-0660-X ..... p 718 N92-27936 #
ISBN-92-835-0661-8 ..... p 717 N92-27706 #
ISBN-92-835-0665-0 ..... p 733 N92-27870 #
ISBN-92-835-0666-9 ..... p 1109 N92-33033 #
ISBN-92-835-0668-5 ..... p 850 N92-28468 #
ISBN-92-835-0669-3 ..... p 983 N92-30769 #
ISBN-92-835-0670-7 ..... p 946 N92-30947 #
ISBN-92-835-0671-5 ..... p 771 N92-27671 #
ISBN-92-835-0673-1 ..... p 774 N92-28084 #
ISBN-92-835-0674-X ..... p 868 N92-28458 #
ISBN-92-835-0675-8 ..... p 851 N92-28469 #
ISBN-92-835-0678-2 ..... p 1010 N92-32229 #
ISBN-92-9092-114-5 ..... p 180 N92-14973 #
ISBN-951-22-0389-8 ..... p 448 N92-21784 #
ISBN-951-22-0602-3 ..... p 602 N92-22216 #
ISBN-951-22-0733-8 ..... p 599 N92-23441 #
ISBN-951-22-0757-5 ..... p 597 N92-23496 #
ISBN-951-22-0763-X ..... p 526 N92-22233 #

ISNAS-88-05-028 ..... p 405 N92-19490 #

ISSN-0939-298X ..... p 953 N92-31813 #

ISU-ERI-AMES-92114 ..... p 742 N92-27519 * #
ISU-ERI-AMES-92259 ..... p 685 N92-25962 * #

ISVR-TR-194 ..... p 604 N92-22241 #

ITN-92-85124 ..... p 932 N92-31861 #
ITN-92-85137 ..... p 482 N92-20849 #
ITN-92-85138 ..... p 461 N92-20500 #
ITN-92-85153 ..... p 510 N92-20905

IWR-91-R-5 ..... p 237 N92-14791 #

JIAA-TR-104 ..... p 14 N92-10990 * #
JIAA-TR-105 ..... p 257 N92-15965 * #
JIAA-TR-106 ..... p 527 N92-23103 * #

JINR-R-8-90-481 ..... p 304 N92-16789 #

JPL-PUBL-91-35 ..... p 1000 N92-30923 * #

JPRS-UEQ-91-010 ..... p 593 N92-22397 #
JPRS-UEQ-92-001 ..... p 592 N92-22296 #
JPRS-UEQ-92-002 ..... p 592 N92-22298 #

JPRS-USP-91-007 ..... p 211 N92-14101 #
JPRS-USP-92-002 ..... p 575 N92-23705 #

JTN-92-80241 ..... p 287 N92-17754 #
JTN-92-80246 ..... p 261 N92-17755 #
JTN-92-80247 ..... p 285 N92-17756 #
JTN-92-80249 ..... p 359 N92-18482 #
JTN-92-80287 ..... p 400 N92-18483 #
JTN-92-80289 ..... p 346 N92-18484 #
JTN-92-80290 ..... p 300 N92-17757 #
JTN-92-80293 ..... p 400 N92-18485 #
JTN-92-80298 ..... p 280 N92-17855 #
JTN-92-80309 ..... p 573 N92-23778 #
JTN-92-80311 ..... p 665 N92-25365 #
JTN-92-80312 ..... p 632 N92-25366 #
JTN-92-80313 ..... p 662 N92-25401 #
JTN-92-80314 ..... p 665 N92-25402 #
JTN-92-80315 ..... p 681 N92-25403 #
JTN-92-80350 ..... p 887 N92-28829 #
JTN-92-80352 ..... p 888 N92-28833 #
JTN-92-80362 ..... p 888 N92-28835 #
JTN-92-80363 ..... p 909 N92-28836 #
JTN-92-80364 ..... p 749 N92-27428 #
JTN-92-80375 ..... p 732 N92-27429 #
JTN-92-80376 ..... p 722 N92-28190 #
JTN-92-80377 ..... p 722 N92-28151 #
JTN-92-80378 ..... p 722 N92-28152 #
JTN-92-80379 ..... p 733 N92-28153 #
JTN-92-80380 ..... p 746 N92-28154 #
JTN-92-80381 ..... p 853 N92-28901 #
JTN-92-80382 ..... p 733 N92-28191 #
JTN-92-80383 ..... p 722 N92-28192 #

KFF-FR ..... p 225 N92-14374 * #

KU-FRL-872-4 ..... p 348 N92-19359 * #
KU-FRL-872-5 ..... p 852 N92-28720 * #

L-16505 ..... p 679 N92-24797 * #
L-16724 ..... p 947 N92-31246 * #
L-16799 ..... p 179 N92-14968 * #
L-16803 ..... p 82 N92-12994 * #
L-16813 ..... p 631 N92-25276 * #
L-16829 ..... p 1065 N92-34109 * #
L-16832-PT-1 ..... p 1106 N92-32513 * #
L-16834 ..... p 526 N92-22506 * #
L-16837 ..... p 631 N92-25202 * #
L-16838 ..... p 750 N92-27670 * #
L-16839 ..... p 630 N92-24977 * #
L-16845 ..... p 456 N92-21459 * #
L-16846 ..... p 482 N92-21410 * #
L-16850 ..... p 56 N92-11758 * #
L-16851 ..... p 350 N92-20038 * #
L-16856 ..... p 525 N92-22196 * #
L-16858 ..... p 115 N92-13054 * #
L-16859 ..... p 633 N92-25752 * #
L-16864 ..... p 11 N92-10006 * #
L-16897 ..... p 119 N92-13065 * #
L-16899 ..... p 18 N92-10994 * #
L-16902 ..... p 12 N92-10975 * #
L-16906 ..... p 445 N92-20654 * #
L-16911 ..... p 444 N92-20494 * #
L-16913 ..... p 56 N92-11765 * #
L-16917 ..... p 17 N92-10017 * #
L-16922 ..... p 23 N92-10024 * #
L-16923 ..... p 501 N92-20677 * #
L-16926-VOL-1 ..... p 54 N92-10598 * #
L-16926-VOL-2 ..... p 235 N92-14779 * #
L-16928 ..... p 481 N92-20195 * #
L-16929 ..... p 945 N92-30909 * #
L-16933 ..... p 90 N92-13038 * #
L-16938 ..... p 297 N92-16283 * #
L-16939 ..... p 61 N92-12989 * #
L-16941 ..... p 399 N92-18053 * #
L-16942 ..... p 489 N92-20679 * #
L-16951 ..... p 944 N92-30394 * #
L-16953 ..... p 630 N92-24882 * #
L-16956 ..... p 978 N92-31175 * #
L-16958 ..... p 527 N92-23095 * #
L-16959 ..... p 948 N92-31532 * #
L-16960 ..... p 346 N92-19002 * #
L-16962 ..... p 1039 N92-33484 * #
L-16963 ..... p 1040 N92-33656 * #
L-16965 ..... p 1040 N92-33625 * #
L-16968 ..... p 444 N92-20545 * #
L-16970 ..... p 631 N92-25133 * #
L-16974 ..... p 32 N92-11030 * #
L-16975 ..... p 512 N92-20479 * #
L-16977 ..... p 979 N92-31240 * #
L-16989 ..... p 347 N92-19175 * #
L-16994 ..... p 630 N92-24885 * #
L-16996 ..... p 827 N92-28477 * #
L-17002 ..... p 633 N92-25967 * #
L-17013 ..... p 767 N92-27193 * #
L-17017 ..... p 242 N92-17984 * #
L-17018 ..... p 1013 N92-30733 * #
L-17025 ..... p 895 N92-28374 * #
L-17026 ..... p 943 N92-30295 * #
L-17034 ..... p 1041 N92-33706 * #
L-17039 ..... p 1001 N92-31281 * #
L-17046 ..... p 1040 N92-33631 * #
L-17048 ..... p 1134 N92-33483 * #
L-17049 ..... p 683 N92-25911 * #
L-17054 ..... p 945 N92-30747 * #
L-17067 ..... p 1042 N92-34193 * #

L-17092-PT-2 p 753 N92-27788 * #
L-17093 p 691 N92-24397 * #
L-17094 p 912 N92-30106 * #
L-17095 p 1036 N92-32480 * #
L-17145-VOL-1 p 1061 N92-33874 * #

LA-UR-92-1390 p 973 N92-31817 #
LA-UR-92-356 p 749 N92-26720 #

LC-90-39761 p 929 N92-28344 * #
LC-91-22773 p 92 N92-13040 #
LC-91-24111 p 308 N92-19662 #

LG90ER0119 p 166 N92-13757 * #
LG92ER0022 p 390 N92-19290 * #

LR-31824 p 298 N92-17006 * #
LR-650 p 237 N92-14798 #
LR-653 p 196 N92-14044 #
LR-655 p 196 N92-14045 #
LR-662 p 887 N92-28579 #
LR-665 p 923 N92-28581 #

L16986 p 528 N92-23533 * #

M-676 p 211 N92-14108 * #

MBB-FE-2-S-PUB-472 p 854 N92-29650 #
MBB-FE-202-S-PUB-0462-A p 890 N92-29680 #
MBB-FE-202-S-PUB-0463-A p 890 N92-29629 #
MBB-FE-202-S-PUB-0464-A p 831 N92-29648 #
MBB-FE-202-S-PUB-0468-A p 832 N92-29713 #
MBB-FE-202-S-PUB-0469-A p 831 N92-29649 #
MBB-FE-211/S/PUB/0465/A p 347 N92-19296 #

MBB-FE122-S-PUB-434 p 345 N92-18316 #
MBB-FE2-PUB-S-450 p 359 N92-18333 #
MBB-FE202-S-PUB-0453-A p 290 N92-17310 #
MBB-FE211-S-PUB-449 p 524 N92-22179 #
MBB-FE211-S-PUB-452 p 275 N92-17313 #

MBB-UD-0584-90-PUB p 196 N92-15066 #
MBB-UD-0586-90-PUB p 134 N92-12003 #
MBB-UD-0593-91-PUB p 225 N92-14382 #
MBB-UD-0603-91-PUB p 910 N92-29873 #
MBB-UD-0606-91-PUB p 787 N92-29874 #
MBB-UD-0608-91-PUB p 978 N92-30439 #
MBB-UD-0609-91-PUB p 988 N92-31716 #
MBB-UD-0610-91-PUB p 889 N92-30076 #
MBB-UD-0611-91-PUB p 952 N92-30418 #
MBB-UD-0613-92-PUB p 1111 N92-33994 #

MBB-UE-0014-90-PUB p 606 N92-23928 #

MBB-UK-0155-89-PUB p 447 N92-21703 #

MBB-Z-0359-90-PUB p 239 N92-15938 #
MBB-Z-0371-91-PUB p 19 N92-10996 #
MBB-Z-0399-91-PUB p 1125 N92-32742 #
MBB-Z-0409-91-PUB p 987 N92-30969 #

MBB/FE202/S/PUB/461 p 787 N92-30232 #
MBB/FE211/S/PUB/474 p 932 N92-30675 #
MBB/FE213/S/PUB/459 p 944 N92-30676 #

MBB/FW321/S/PUB/467 p 998 N92-30423 #
MBB/FW321/S/PUB/476 p 961 N92-30424 #

MCAT-92-004 p 573 N92-22195 * #
MCAT-92-005 p 692 N92-25264 * #
MCAT-92-009 p 945 N92-30740 * #
MCAT-92-010 p 630 N92-24898 * #
MCAT-92-011-PT-3 p 888 N92-29655 * #
MCAT-92-012 p 751 N92-27976 * #
MCAT-92-014 p 948 N92-31533 * #
MCAT-92-015 p 950 N92-32177 * #
MCAT-92-017 p 1039 N92-33424 * #

MDC-91K0792 p 957 N92-30978 * #

MEMO-997 p 596 N92-23251 #

MITT-90-01 p 768 N92-27407 #

MPIS-100/1991 p 300 N92-17344 #

MTL-TR-91-25 p 116 N92-13061 #
MTL-TR-91-54 p 757 N92-27752 #
MTL-TR-92-5 p 908 N92-28425 #

MTR-11023 p 191 N92-15058 #
MTR-11120 p 103 N92-13052 #
MTR-11135 p 773 N92-27864 #

M91-122-VOL-1 p 534 N92-22104 #
M91-122-VOL-2 p 534 N92-22105 #
M91-122-VOL-3 p 534 N92-22106 #

NADC-91069-60 p 365 N92-18826 #
NADC-91078-60 p 986 N92-30321 #
NADC-91080-60 p 206 N92-15074 #
NADC-91087-60 p 895 N92-28921 #

NAE-MISC-63 p 114 N92-11991 #

NAL-PD-FC-9113 p 359 N92-18073 #
NAL-PD-FC-9117 p 412 N92-18252 #
NAL-PD-FC-9201 p 534 N92-22389 #

NAL-SP-11 p 400 N92-18483 #

NAL-TM-565 p 573 N92-23778 #
NAL-TM-602-PT-2 p 287 N92-17754 #
NAL-TM-610 p 261 N92-17755 #
NAL-TM-611 p 285 N92-17756 #
NAL-TM-613 p 359 N92-18482 #
NAL-TM-617 p 346 N92-18484 #
NAL-TM-619 p 300 N92-17757 #
NAL-TM-623 p 665 N92-25365 #
NAL-TM-624 p 632 N92-25366 #
NAL-TM-625 p 400 N92-18485 #
NAL-TM-626 p 662 N92-25401 #
NAL-TM-627 p 665 N92-25402 #
NAL-TM-628 p 681 N92-25403 #
NAL-TM-631 p 680 N92-25342 #
NAL-TM-632 p 887 N92-28829 #
NAL-TM-634 p 888 N92-28835 #
NAL-TM-635 p 888 N92-28833 #
NAL-TM-636 p 909 N92-28836 #
NAL-TM-637 p 732 N92-27429 #
NAL-TM-638 p 749 N92-27428 #
NAL-TM-639 p 722 N92-28190 #
NAL-TM-640T p 722 N92-28151 #
NAL-TM-641 p 722 N92-28152 #

NAL-TR-1026 p 352 N92-18182 #
NAL-TR-1064T p 280 N92-17855 #
NAL-TR-1093 p 11 N92-10009 #
NAL-TR-1097 p 345 N92-18239 #
NAL-TR-1101T p 12 N92-10980 #
NAL-TR-1102 p 733 N92-28153 #
NAL-TR-1103 p 746 N92-28154 #
NAL-TR-1106 p 29 N92-10028 #
NAL-TR-1108 p 384 N92-18037 #
NAL-TR-1109T p 445 N92-21287 #
NAL-TR-1112 p 853 N92-28901 #
NAL-TR-1113 p 733 N92-28191 #
NAL-TR-1115-PT-1 p 722 N92-28192 #
NAL-TR-1116 p 283 N92-17917 #

NAMRL-TM-91-2 p 883 N92-28407 #

NAS 1.15:101657 p 680 N92-25137 * #
NAS 1.15:102192 p 878 N92-28457 * #
NAS 1.15:102230 p 950 N92-32213 * #
NAS 1.15:102244 p 550 N92-22864 * #
NAS 1.15:102261 p 1038 N92-33306 * #
NAS 1.15:102268 p 1040 N92-33618 * #
NAS 1.15:102554 p 445 N92-20934 * #
NAS 1.15:102614 p 595 N92-22649 * #
NAS 1.15:102687 p 206 N92-15076 * #
NAS 1.15:102842 p 13 N92-10983 * #
NAS 1.15:102851 p 1036 N92-32422 * #
NAS 1.15:102882 p 1051 N92-33609 * #
NAS 1.15:103248 p 972 N92-31250 * #
NAS 1.15:103578 p 506 N92-21546 * #
NAS 1.15:103747 p 230 N92-15406 * #
NAS 1.15:103800 p 242 N92-17346 * #
NAS 1.15:103839 p 1071 N92-32452 * #
NAS 1.15:103842 p 482 N92-21440 * #
NAS 1.15:103864 p 368 N92-19847 * #
NAS 1.15:103866 p 1060 N92-32887 * #
NAS 1.15:103873 p 853 N92-28926 * #
NAS 1.15:103875 p 367 N92-19563 * #
NAS 1.15:103876 p 21 N92-11000 * #
NAS 1.15:103880 p 1044 N92-33194 * #
NAS 1.15:103887 p 356 N92-20029 * #
NAS 1.15:103892 p 890 N92-29104 * #
NAS 1.15:103897 p 2 N92-10003 * #
NAS 1.15:103899 p 1050 N92-33407 * #
NAS 1.15:103902 p 853 N92-28910 * #
NAS 1.15:103906 p 841 N92-29103 * #
NAS 1.15:103910 p 1087 N92-32788 * #
NAS 1.15:103915 p 927 N92-28909 * #
NAS 1.15:103925 p 852 N92-28721 * #
NAS 1.15:103928 p 405 N92-19596 * #
NAS 1.15:103929 p 854 N92-29417 * #
NAS 1.15:103930 p 1047 N92-32424 * #
NAS 1.15:103934 p 1039 N92-33581 * #
NAS 1.15:103959 p 1044 N92-33080 * #
NAS 1.15:104112 p 1140 N92-34148 * #
NAS 1.15:104120 p 197 N92-15070 * #
NAS 1.15:104125 p 115 N92-13057 * #
NAS 1.15:104134 p 166 N92-12598 * #
NAS 1.15:104138 p 23 N92-11010 * #
NAS 1.15:104142 p 81 N92-11977 * #
NAS 1.15:104145 p 82 N92-11985 * #
NAS 1.15:104146 p 159 N92-13458 * #
NAS 1.15:104147 p 166 N92-13758 * #
NAS 1.15:104150 p 56 N92-11759 * #
NAS 1.15:104152 p 31 N92-11022 * #
NAS 1.15:104154 p 159 N92-13460 * #
NAS 1.15:104158 p 206 N92-15075 * #
NAS 1.15:104160 p 35 N92-11149 * #
NAS 1.15:104161 p 138 N92-12007 * #
NAS 1.15:104163 p 159 N92-13455 * #
NAS 1.15:104168 p 261 N92-17547 * #
NAS 1.15:104170 p 1138 N92-33160 * #
NAS 1.15:104174 p 303 N92-17130 * #
NAS 1.15:104180 p 185 N92-15049 * #
NAS 1.15:104184 p 401 N92-18877 * #
NAS 1.15:104186 p 185 N92-15050 * #
NAS 1.15:104188 p 261 N92-17509 * #
NAS 1.15:104190 p 298 N92-17002 * #
NAS 1.15:104191 p 446 N92-21432 * #
NAS 1.15:104192 p 299 N92-17034 * #
NAS 1.15:104193 p 299 N92-17033 * #
NAS 1.15:104194 p 367 N92-19846 * #
NAS 1.15:104196 p 602 N92-22320 * #
NAS 1.15:104200 p 385 N92-18956 * #
NAS 1.15:104203 p 404 N92-19258 * #
NAS 1.15:104205 p 556 N92-22504 * #
NAS 1.15:104206 p 630 N92-24956 * #
NAS 1.15:104207 p 625 N92-24681 * #
NAS 1.15:104211 p 1042 N92-34147 * #
NAS 1.15:104215 p 444 N92-20480 * #
NAS 1.15:104216 p 525 N92-22232 * #
NAS 1.15:104226 p 461 N92-20417 * #
NAS 1.15:104237 p 1133 N92-32507 * #
NAS 1.15:104240 p 871 N92-29659 * #
NAS 1.15:104241 p 118 N92-11994 * #
NAS 1.15:104245 p 272 N92-15986 * #
NAS 1.15:104247 p 871 N92-29425 * #
NAS 1.15:104249 p 1062 N92-34202 * #
NAS 1.15:104250 p 984 N92-32201 * #
NAS 1.15:104251 p 1065 N92-32866 * #
NAS 1.15:104252 p 971 N92-30518 * #
NAS 1.15:104253 p 1060 N92-33404 * #
NAS 1.15:104254 p 962 N92-31261 * #
NAS 1.15:104255 p 1087 N92-32864 * #
NAS 1.15:104256 p 1060 N92-33149 * #
NAS 1.15:104259 p 1062 N92-34039 * #
NAS 1.15:104475 p 12 N92-10976 * #
NAS 1.15:104518 p 527 N92-23105 * #
NAS 1.15:104525 p 214 N92-15191 * #
NAS 1.15:104531 p 1109 N92-32863 * #
NAS 1.15:104744 p 308 N92-19930 * #
NAS 1.15:105096 p 53 N92-11642 * #
NAS 1.15:105124 p 82 N92-11984 * #
NAS 1.15:105126 p 31 N92-11024 * #
NAS 1.15:105192 p 2 N92-10002 * #
NAS 1.15:105193 p 279 N92-15993 * #
NAS 1.15:105206 p 304 N92-16705 * #
NAS 1.15:105258 p 279 N92-17061 * #
NAS 1.15:105260 p 298 N92-16336 * #
NAS 1.15:105283 p 348 N92-19437 * #
NAS 1.15:105288 p 473 N92-20525 * #
NAS 1.15:105303 p 26 N92-11017 * #
NAS 1.15:105320 p 516 N92-22659 * #
NAS 1.15:105321 p 179 N92-13998 * #
NAS 1.15:105329 p 597 N92-23560 * #
NAS 1.15:105332 p 44 N92-11328 * #
NAS 1.15:105336 p 229 N92-15402 * #
NAS 1.15:105338 p 237 N92-14795 * #
NAS 1.15:105347 p 202 N92-14063 * #
NAS 1.15:105356 p 416 N92-18282 * #
NAS 1.15:105365 p 237 N92-14797 * #
NAS 1.15:105368 p 258 N92-15968 * #
NAS 1.15:105373 p 186 N92-15052 * #
NAS 1.15:105374 p 185 N92-15051 * #
NAS 1.15:105380 p 261 N92-17347 * #
NAS 1.15:105389 p 179 N92-14001 * #
NAS 1.15:105393 p 179 N92-14002 * #
NAS 1.15:105397 p 279 N92-17546 * #
NAS 1.15:105399 p 562 N92-23254 * #
NAS 1.15:105400 p 297 N92-16265 * #
NAS 1.15:105414 p 346 N92-18760 * #
NAS 1.15:105416 p 773 N92-27879 * #
NAS 1.15:105417 p 887 N92-28673 * #
NAS 1.15:105427 p 633 N92-26104 * #
NAS 1.15:105432 p 528 N92-23563 * #
NAS 1.15:105434 p 1002 N92-31349 * #
NAS 1.15:105437 p 350 N92-19993 * #
NAS 1.15:105439 p 387 N92-18280 * #
NAS 1.15:105479 p 286 N92-16973 * #
NAS 1.15:105510 p 412 N92-18125 * #
NAS 1.15:105562 p 378 N92-20033 * #
NAS 1.15:105575 p 596 N92-23267 * #

NAS 1.15:105579 ..... p 481 N92-20586 * #
NAS 1.15:105581 ..... p 499 N92-20235 * #
NAS 1.15:105599 ..... p 756 N92-27378 * #
NAS 1.15:105610 ..... p 562 N92-23537 * #
NAS 1.15:105613 ..... p 658 N92-25164 * #
NAS 1.15:105617 ..... p 596 N92-23154 * #
NAS 1.15:105623 ..... p 716 N92-27377 * #
NAS 1.15:105627 ..... p 473 N92-20523 * #
NAS 1.15:105641 ..... p 596 N92-23435 * #
NAS 1.15:105643 ..... p 680 N92-24959 * #
NAS 1.15:105644 ..... p 665 N92-25449 * #
NAS 1.15:105646 ..... p 667 N92-26129 * #
NAS 1.15:105651 ..... p 764 N92-26555 * #
NAS 1.15:105655 ..... p 908 N92-28434 * #
NAS 1.15:105664 ..... p 630 N92-24958 * #
NAS 1.15:105665 ..... p 680 N92-24984 * #
NAS 1.15:105668 ..... p 764 N92-26560 * #
NAS 1.15:105672 ..... p 1128 N92-34112 * #
NAS 1.15:105675 ..... p 833 N92-30182 * #
NAS 1.15:105680 ..... p 871 N92-29661 * #
NAS 1.15:105681 ..... p 910 N92-29136 * #
NAS 1.15:105682 ..... p 972 N92-31172 * #
NAS 1.15:105683 ..... p 1072 N92-33746 * #
NAS 1.15:105684 ..... p 739 N92-27037 * #
NAS 1.15:105685 ..... p 982 N92-30508 * #
NAS 1.15:105686 ..... p 770 N92-27653 * #
NAS 1.15:105694 ..... p 742 N92-27652 * #
NAS 1.15:105695 ..... p 738 N92-26553 * #
NAS 1.15:105696 ..... p 1134 N92-33894 * #
NAS 1.15:105697 ..... p 742 N92-27669 * #
NAS 1.15:105698 ..... p 868 N92-28418 * #
NAS 1.15:105699 ..... p 738 N92-26561 * #
NAS 1.15:105702 ..... p 1002 N92-31485 * #
NAS 1.15:105715 ..... p 868 N92-28419 * #
NAS 1.15:105716 ..... p 870 N92-28985 * #
NAS 1.15:105717 ..... p 909 N92-29105 * #
NAS 1.15:105720 ..... p 722 N92-28102 * #
NAS 1.15:105724 ..... p 739 N92-26613 * #
NAS 1.15:105731 ..... p 890 N92-29343 * #
NAS 1.15:105740 ..... p 1002 N92-31484 * #
NAS 1.15:105742 ..... p 714 N92-26612 * #
NAS 1.15:105743 ..... p 828 N92-28674 * #
NAS 1.15:105745 ..... p 828 N92-28696 * #
NAS 1.15:105773 ..... p 1042 N92-34144 * #
NAS 1.15:105796 ..... p 972 N92-30972 * #
NAS 1.15:105797 ..... p 1088 N92-34107 * #
NAS 1.15:105803 ..... p 932 N92-31267 * #
NAS 1.15:105805 ..... p 1009 N92-30898 * #
NAS 1.15:105814 ..... p 972 N92-30998 * #
NAS 1.15:105826 ..... p 979 N92-32241 * #
NAS 1.15:107567 ..... p 527 N92-23116 * #
NAS 1.15:107576 ..... p 526 N92-22240 * #
NAS 1.15:107578 ..... p 502 N92-21460 * #
NAS 1.15:107579 ..... p 680 N92-25267 * #
NAS 1.15:107581 ..... p 526 N92-22507 * #
NAS 1.15:107584 ..... p 685 N92-26128 * #
NAS 1.15:107586 ..... p 850 N92-28435 * #
NAS 1.15:107591 ..... p 1125 N92-33104 * #
NAS 1.15:107600 ..... p 1060 N92-32536 * #
NAS 1.15:107601 ..... p 1088 N92-33537 * #
NAS 1.15:107606 ..... p 685 N92-25964 * #
NAS 1.15:107615 ..... p 662 N92-25607 * #
NAS 1.15:107622 ..... p 650 N92-25995 * #
NAS 1.15:107631 ..... p 944 N92-30570 * #
NAS 1.15:107635 ..... p 831 N92-29445 * #
NAS 1.15:107642 ..... p 1001 N92-31155 * #
NAS 1.15:107643 ..... p 944 N92-30393 * #
NAS 1.15:107644 ..... p 947 N92-31239 * #
NAS 1.15:107645 ..... p 945 N92-30691 * #
NAS 1.15:107646 ..... p 984 N92-31900 * #
NAS 1.15:107650 ..... p 963 N92-32111 * #
NAS 1.15:107651 ..... p 961 N92-30752 * #
NAS 1.15:107652 ..... p 962 N92-31350 * #
NAS 1.15:107653 ..... p 962 N92-31174 * #
NAS 1.15:107654 ..... p 962 N92-31351 * #
NAS 1.15:107655 ..... p 962 N92-31264 * #
NAS 1.15:107657 ..... p 1138 N92-33719 * #
NAS 1.15:107663 ..... p 1010 N92-30907 * #
NAS 1.15:107666 ..... p 1110 N92-33423 * #
NAS 1.15:107677 ..... p 1128 N92-34178 * #
NAS 1.15:107679 ..... p 1128 N92-34017 * #
NAS 1.15:107838 ..... p 632 N92-25279 * #
NAS 1.15:107847 ..... p 631 N92-25261 * #
NAS 1.15:107873 ..... p 692 N92-25190 * #
NAS 1.15:107924 ..... p 782 N92-28183 * #
NAS 1.15:107931 ..... p 782 N92-28114 * #
NAS 1.15:107960 ..... p 1013 N92-31852 * #
NAS 1.15:107967 ..... p 1143 N92-33948 * #
NAS 1.15:108171 ..... p 1142 N92-33237 * #
NAS 1.15:3238 ..... p 952 N92-30395 * #
NAS 1.15:4189 ..... p 947 N92-31246 * #
NAS 1.15:4278 ..... p 445 N92-20654 * #
NAS 1.15:4279 ..... p 17 N92-10017 * #
NAS 1.15:4281 ..... p 11 N92-10006 * #
NAS 1.15:4285 ..... p 23 N92-10024 * #
NAS 1.15:4295 ..... p 528 N92-23533 * #
NAS 1.15:4296 ..... p 526 N92-22506 * #
NAS 1.15:4302 ..... p 978 N92-31175 * #
NAS 1.15:4309 ..... p 525 N92-22196 * #
NAS 1.15:4313 ..... p 61 N92-12989 * #
NAS 1.15:4315 ..... p 297 N92-16283 * #
NAS 1.15:4316 ..... p 90 N92-13038 * #
NAS 1.15:4318 ..... p 32 N92-11030 * #
NAS 1.15:4322 ..... p 157 N92-12286 * #
NAS 1.15:4331 ..... p 1013 N92-30733 * #
NAS 1.15:4333 ..... p 750 N92-27670 * #
NAS 1.15:4334 ..... p 630 N92-24882 * #
NAS 1.15:4335 ..... p 276 N92-17128 * #
NAS 1.15:4337 ..... p 630 N92-24977 * #
NAS 1.15:4341 ..... p 273 N92-17071 * #
NAS 1.15:4345 ..... p 630 N92-24885 * #
NAS 1.15:4356 ..... p 381 N92-19174 * #
NAS 1.15:4359 ..... p 633 N92-25967 * #
NAS 1.15:4363 ..... p 633 N92-25752 * #
NAS 1.15:4368 ..... p 609 N92-24678 * #
NAS 1.15:4370 ..... p 570 N92-22194 * #
NAS 1.15:4374 ..... p 767 N92-27193 * #
NAS 1.15:4379 ..... p 1065 N92-34109 * #
NAS 1.15:4381 ..... p 979 N92-31240 * #
NAS 1.15:4382 ..... p 1040 N92-33631 * #
NAS 1.15:4393 ..... p 742 N92-27587 * #
NAS 1.15:4394 ..... p 740 N92-27379 * #
NAS 1.15:4396 ..... p 853 N92-29110 * #
NAS 1.15:4398 ..... p 947 N92-31276 * #
NAS 1.15:4400 ..... p 973 N92-31275 * #
NAS 1.15:893240 ..... p 156 N92-12173 * #
NAS 1.21:4104 ..... p 929 N92-28344 * #
NAS 1.26:167696 ..... p 286 N92-17167 * #
NAS 1.26:167697 ..... p 286 N92-17214 * #
NAS 1.26:177587 ..... p 93 N92-13044 * #
NAS 1.26:177592 ..... p 195 N92-14039 * #
NAS 1.26:180083 ..... p 178 N92-13995 * #
NAS 1.26:181780 ..... p 578 N92-22637 * #
NAS 1.26:181893 ..... p 43 N92-11319 * #
NAS 1.26:181954 ..... p 1086 N92-32778 * #
NAS 1.26:182004 ..... p 602 N92-22643 * #
NAS 1.26:182007 ..... p 602 N92-22644 * #
NAS 1.26:184215 ..... p 157 N92-12231 * #
NAS 1.26:184260 ..... p 42 N92-11297 * #
NAS 1.26:184263 ..... p 221 N92-14344 * #
NAS 1.26:184276 ..... p 225 N92-14391 * #
NAS 1.26:184278 ..... p 359 N92-18347 * #
NAS 1.26:184280 ..... p 499 N92-20198 * #
NAS 1.26:184329 ..... p 753 N92-27403 * #
NAS 1.26:184341 ..... p 973 N92-31910 * #
NAS 1.26:184384 ..... p 1101 N92-33826 * #
NAS 1.26:184829 ..... p 191 N92-14036 * #
NAS 1.26:185155 ..... p 562 N92-22647 * #
NAS 1.26:185242 ..... p 1011 N92-31248 * #
NAS 1.26:185666 ..... p 284 N92-15998 * #
NAS 1.26:185680 ..... p 746 N92-28209 * #
NAS 1.26:186014 ..... p 663 N92-25734 * #
NAS 1.26:186015 ..... p 482 N92-21253 * #
NAS 1.26:186016 ..... p 482 N92-21357 * #
NAS 1.26:186017 ..... p 445 N92-21188 * #
NAS 1.26:186019 ..... p 117 N92-13064 * #
NAS 1.26:186020 ..... p 962 N92-31208 * #
NAS 1.26:186021 ..... p 871 N92-29427 * #
NAS 1.26:186022 ..... p 979 N92-31656 * #
NAS 1.26:186984 ..... p 387 N92-19934 * #
NAS 1.26:187101 ..... p 26 N92-11016 * #
NAS 1.26:187108 ..... p 406 N92-19775 * #
NAS 1.26:187222 ..... p 44 N92-11379 * #
NAS 1.26:187227 ..... p 404 N92-19277 * #
NAS 1.26:187235 ..... p 44 N92-11378 * #
NAS 1.26:187316 ..... p 185 N92-15048 * #
NAS 1.26:187556 ..... p 53 N92-11706 * #
NAS 1.26:187581 ..... p 347 N92-19250 * #
NAS 1.26:187615 ..... p 268 N92-17512 * #
NAS 1.26:187616 ..... p 236 N92-14788 * #
NAS 1.26:187621 ..... p 45 N92-11391 * #
NAS 1.26:187626 ..... p 697 N92-25368 * #
NAS 1.26:187631 ..... p 390 N92-19290 * #
NAS 1.26:187979 ..... p 14 N92-10990 * #
NAS 1.26:188055 ..... p 751 N92-27976 * #
NAS 1.26:188125 ..... p 170 N92-13928 * #
NAS 1.26:188126 ..... p 163 N92-12440 * #
NAS 1.26:188228 ..... p 46 N92-11593 * #
NAS 1.26:188630 ..... p 488 N92-20193 * #
NAS 1.26:188856 ..... p 140 N92-12033 * #
NAS 1.26:188954 ..... p 33 N92-11070 * #
NAS 1.26:188983 ..... p 44 N92-11377 * #
NAS 1.26:188985 ..... p 53 N92-10347 * #
NAS 1.26:188995 ..... p 31 N92-11023 * #
NAS 1.26:188996 ..... p 26 N92-11014 * #
NAS 1.26:189018 ..... p 195 N92-14038 * #
NAS 1.26:189044 ..... p 195 N92-14037 * #
NAS 1.26:189047 ..... p 166 N92-13759 * #
NAS 1.26:189050 ..... p 501 N92-20954 * #
NAS 1.26:189053 ..... p 225 N92-14374 * #
NAS 1.26:189076 ..... p 130 N92-13071 * #
NAS 1.26:189088 ..... p 377 N92-19726 * #
NAS 1.26:189089 ..... p 402 N92-18971 * #
NAS 1.26:189101 ..... p 592 N92-22239 * #
NAS 1.26:189110 ..... p 258 N92-15967 * #
NAS 1.26:189118 ..... p 716 N92-27376 * #
NAS 1.26:189122 ..... p 1073 N92-34236 * #
NAS 1.26:189126 ..... p 658 N92-24539 * #
NAS 1.26:189129 ..... p 474 N92-20650 * #
NAS 1.26:189134 ..... p 352 N92-19276 * #
NAS 1.26:189137 ..... p 696 N92-24688 * #
NAS 1.26:189142 ..... p 682 N92-25649 * #
NAS 1.26:189149 ..... p 943 N92-30298 * #
NAS 1.26:189155 ..... p 971 N92-30569 * #
NAS 1.26:189171 ..... p 924 N92-30207 * #
NAS 1.26:189202 ..... p 574 N92-22211 * #
NAS 1.26:189207 ..... p 831 N92-29402 * #
NAS 1.26:189222 ..... p 973 N92-31534 * #
NAS 1.26:189223 ..... p 1072 N92-33479 * #
NAS 1.26:189234 ..... p 983 N92-31252 * #
NAS 1.26:189268 ..... p 770 N92-27649 * #
NAS 1.26:189455 ..... p 114 N92-11992 * #
NAS 1.26:189456 ..... p 82 N92-11983 * #
NAS 1.26:189457 ..... p 180 N92-14969 * #
NAS 1.26:189461 ..... p 237 N92-14789 * #
NAS 1.26:189467 ..... p 221 N92-14313 * #
NAS 1.26:189469 ..... p 205 N92-14066 * #
NAS 1.26:189502 ..... p 135 N92-13073 * #
NAS 1.26:189509 ..... p 179 N92-13999 * #
NAS 1.26:189514 ..... p 221 N92-14262 * #
NAS 1.26:189515 ..... p 221 N92-14263 * #
NAS 1.26:189543 ..... p 443 N92-20283 * #
NAS 1.26:189551 ..... p 191 N92-15060 * #
NAS 1.26:189555 ..... p 481 N92-20376 * #
NAS 1.26:189556 ..... p 209 N92-15077 * #
NAS 1.26:189561 ..... p 276 N92-15991 * #
NAS 1.26:189570 ..... p 286 N92-16012 * #
NAS 1.26:189573 ..... p 381 N92-19499 * #
NAS 1.26:189578 ..... p 234 N92-15658 * #
NAS 1.26:189579 ..... p 185 N92-15047 * #
NAS 1.26:189582 ..... p 416 N92-19672 * #
NAS 1.26:189583 ..... p 498 N92-20072 * #
NAS 1.26:189584 ..... p 697 N92-26130 * #
NAS 1.26:189586 ..... p 525 N92-22215 * #
NAS 1.26:189587 ..... p 625 N92-24680 * #
NAS 1.26:189591 ..... p 696 N92-24251 * #
NAS 1.26:189595 ..... p 888 N92-29352 * #
NAS 1.26:189601 ..... p 402 N92-18965 * #
NAS 1.26:189603 ..... p 556 N92-22395 * #
NAS 1.26:189605 ..... p 556 N92-22645 * #
NAS 1.26:189606 ..... p 652 N92-24689 * #
NAS 1.26:189612 ..... p 447 N92-21465 * #
NAS 1.26:189615 ..... p 592 N92-22228 * #
NAS 1.26:189616 ..... p 632 N92-25510 * #
NAS 1.26:189620 ..... p 961 N92-30304 * #
NAS 1.26:189630 ..... p 696 N92-24800 * #
NAS 1.26:189631 ..... p 685 N92-25960 * #
NAS 1.26:189633 ..... p 735 N92-27424 * #
NAS 1.26:189641 ..... p 715 N92-26652 * #
NAS 1.26:189642 ..... p 715 N92-26651 * #
NAS 1.26:189643 ..... p 927 N92-28556 * #
NAS 1.26:189650 ..... p 967 N92-30965 * #
NAS 1.26:189652-VOL-1 ..... p 950 N92-32226 * #
NAS 1.26:189652-VOL-2 ..... p 951 N92-32228 * #
NAS 1.26:189658 ..... p 944 N92-30392 * #
NAS 1.26:189671 ..... p 1110 N92-33613 * #
NAS 1.26:189757 ..... p 258 N92-15969 * #
NAS 1.26:189758 ..... p 258 N92-15966 * #
NAS 1.26:189759 ..... p 257 N92-15965 * #
NAS 1.26:189773 ..... p 289 N92-17004 * #
NAS 1.26:189778 ..... p 282 N92-17019 * #
NAS 1.26:189785 ..... p 259 N92-15974 * #
NAS 1.26:189789 ..... p 298 N92-17006 * #
NAS 1.26:189814 ..... p 301 N92-17393 * #
NAS 1.26:189849 ..... p 358 N92-18024 * #
NAS 1.26:189850 ..... p 359 N92-18038 * #
NAS 1.26:189853 ..... p 275 N92-17316 * #
NAS 1.26:189854 ..... p 625 N92-24803 * #
NAS 1.26:189899 ..... p 502 N92-21433 * #
NAS 1.26:189901 ..... p 404 N92-19217 * #
NAS 1.26:189911 ..... p 382 N92-19841 * #
NAS 1.26:189932 ..... p 499 N92-20197 * #
NAS 1.26:189939 ..... p 778 N92-28150 * #
NAS 1.26:189951 ..... p 385 N92-19218 * #
NAS 1.26:189963 ..... p 386 N92-19675 * #
NAS 1.26:189974 ..... p 462 N92-20664 * #
NAS 1.26:189981 ..... p 366 N92-19374 * #
NAS 1.26:189987 ..... p 463 N92-21540 * #
NAS 1.26:189988 ..... p 461 N92-20267 * #
NAS 1.26:189990 ..... p 462 N92-21489 * #
NAS 1.26:189991 ..... p 463 N92-21566 * #
NAS 1.26:189992 ..... p 463 N92-21565 * #
NAS 1.26:189994 ..... p 575 N92-22625 * #
NAS 1.26:190004 ..... p 648 N92-25263 * #
NAS 1.26:190006 ..... p 486 N92-20666 * #
NAS 1.26:190007 ..... p 462 N92-20665 * #
NAS 1.26:190019 ..... p 731 N92-26435 * #
NAS 1.26:190022 ..... p 463 N92-21567 * #

NAS 1.26:190023 ..... p 367 N92-19496 * #
NAS 1.26:190024 ..... p 461 N92-20064 * #
NAS 1.26:190026 ..... p 462 N92-20951 * #
NAS 1.26:190039 ..... p 348 N92-19359 * #
NAS 1.26:190040 ..... p 348 N92-19545 * #
NAS 1.26:190045 ..... p 945 N92-30740 * #
NAS 1.26:190054 ..... p 446 N92-21356 * #
NAS 1.26:190074 ..... p 664 N92-25162 * #
NAS 1.26:190077 ..... p 692 N92-25264 * #
NAS 1.26:190130 ..... p 461 N92-20280 * #
NAS 1.26:190148 ..... p 593 N92-22491 * #
NAS 1.26:190159 ..... p 502 N92-21385 * #
NAS 1.26:190166 ..... p 484 N92-21162 * #
NAS 1.26:190182 ..... p 946 N92-30977 * #
NAS 1.26:190201 ..... p 595 N92-22662 * #
NAS 1.26:190204 ..... p 578 N92-22486 * #
NAS 1.26:190217 ..... p 573 N92-22195 * #
NAS 1.26:190248 ..... p 527 N92-23103 * #
NAS 1.26:190251 ..... p 631 N92-25175 * #
NAS 1.26:190264 ..... p 830 N92-29329 * #
NAS 1.26:190290 ..... p 971 N92-30753 * #
NAS 1.26:190294 ..... p 624 N92-24229 * #
NAS 1.26:190305 ..... p 678 N92-24345 * #
NAS 1.26:190313 ..... p 630 N92-24898 * #
NAS 1.26:190328 ..... p 685 N92-26125 *
NAS 1.26:190336 ..... p 663 N92-25648 * #
NAS 1.26:190353 ..... p 633 N92-25959 * #
NAS 1.26:190355 ..... p 650 N92-26017 * #
NAS 1.26:190357 ..... p 716 N92-27558 * #
NAS 1.26:190368 ..... p 685 N92-25962 * #
NAS 1.26:190369 ..... p 692 N92-26018 * #
NAS 1.26:190379 ..... p 1004 N92-32147 * #
NAS 1.26:190400 ..... p 907 N92-28361 * #
NAS 1.26:190423 ..... p 738 N92-26405 * #
NAS 1.26:190426 ..... p 716 N92-27399 * #
NAS 1.26:190430 ..... p 773 N92-27880 * #
NAS 1.26:190431 ..... p 827 N92-28511 * #
NAS 1.26:190433 ..... p 742 N92-27519 * #
NAS 1.26:190434 ..... p 731 N92-26655 * #
NAS 1.26:190444 ..... p 852 N92-28720 * #
NAS 1.26:190450 ..... p 1127 N92-33696 * #
NAS 1.26:190452 ..... p 715 N92-27191 * #
NAS 1.26:190459 ..... p 1000 N92-30923 * #
NAS 1.26:190469 ..... p 840 N92-28718 * #
NAS 1.26:190471 ..... p 1000 N92-30988 * #
NAS 1.26:190480 ..... p 830 N92-29361 * #
NAS 1.26:190498 ..... p 998 N92-30380 * #
NAS 1.26:190535 ..... p 879 N92-29654 * #
NAS 1.26:190541 ..... p 888 N92-29655 * #
NAS 1.26:190542 ..... p 1044 N92-34105 * #
NAS 1.26:190563 ..... p 1036 N92-32648 * #
NAS 1.26:190565 ..... p 854 N92-30209 * #
NAS 1.26:190570 ..... p 832 N92-29657 * #
NAS 1.26:190576 ..... p 832 N92-29691 * #
NAS 1.26:190577 ..... p 1003 N92-31619 * #
NAS 1.26:190583 ..... p 1036 N92-32494 * #
NAS 1.26:190638 ..... p 1038 N92-33304 * #
NAS 1.26:190649 ..... p 946 N92-31157 * #
NAS 1.26:190650 ..... p 1001 N92-31156 * #
NAS 1.26:190667 ..... p 978 N92-30922 * #
NAS 1.26:190680 ..... p 948 N92-31533 * #
NAS 1.26:190684 ..... p 1102 N92-34141 * #
NAS 1.26:190686 ..... p 1128 N92-34207 * #
NAS 1.26:190688 ..... p 950 N92-32177 * #
NAS 1.26:190702 ..... p 1038 N92-33063 * #
NAS 1.26:190712 ..... p 1134 N92-32865 * #
NAS 1.26:190731 ..... p 950 N92-32162 * #
NAS 1.26:190736 ..... p 1087 N92-33107 * #
NAS 1.26:190810 ..... p 1126 N92-33307 * #
NAS 1.26:190812 ..... p 1088 N92-33536 * #
NAS 1.26:190817 ..... p 1039 N92-33413 * #
NAS 1.26:190822 ..... p 1125 N92-33139 * #
NAS 1.26:190836 ..... p 1039 N92-33424 * #
NAS 1.26:190902 ..... p 1128 N92-34043 * #
NAS 1.26:190925 ..... p 1051 N92-34203 * #
NAS 1.26:191259 ..... p 1102 N92-34222 * #
NAS 1.26:3251 ..... p 526 N92-22648 * #
NAS 1.26:3252 ..... p 527 N92-22865 * #
NAS 1.26:4283 ..... p 678 N92-24242 * #
NAS 1.26:4292-VOL-1 ..... p 679 N92-24547 *
NAS 1.26:4292-VOL-2 ..... p 678 N92-24344 * #
NAS 1.26:4374 ..... p 368 N92-19871 * #
NAS 1.26:4388 ..... p 166 N92-13757 * #
NAS 1.26:4391 ..... p 951 N92-32240 * #
NAS 1.26:4392 ..... p 526 N92-22249 * #
NAS 1.26:4405 ..... p 12 N92-10979 * #
NAS 1.26:4406 ..... p 13 N92-10982 * #
NAS 1.26:4407 ..... p 178 N92-13996 * #
NAS 1.26:4414 ..... p 178 N92-13997 * #
NAS 1.26:4420 ..... p 234 N92-14598 * #
NAS 1.26:4422 ..... p 347 N92-19354 * #
NAS 1.26:4424 ..... p 499 N92-20194 * #
NAS 1.26:4426 ..... p 512 N92-21173 * #
NAS 1.26:4427 ..... p 406 N92-19844 * #
NAS 1.26:4430 ..... p 473 N92-20196 * #
NAS 1.26:4431 ..... p 446 N92-21456 * #
NAS 1.26:4438 ..... p 765 N92-26680 * #
NAS 1.26:4440 ..... p 681 N92-25376 * #
NAS 1.26:4442 ..... p 663 N92-25982 * #
NAS 1.26:4443 ..... p 878 N92-28584 * #
NAS 1.26:4450 ..... p 957 N92-30978 * #
NAS 1.26:4456 ..... p 1043 N92-32606 * #
NAS 1.26:4457 ..... p 953 N92-31549 * #
NAS 1.26:4463 ..... p 979 N92-32175 * #
NAS 1.26:4465 ..... p 950 N92-32114 * #
NAS 1.26:4470 ..... p 1045 N92-34192 * #
NAS 1.55:10078 ..... p 660 N92-25808 * #
NAS 1.55:10088 ..... p 678 N92-24514 * #
NAS 1.55:10089 ..... p 659 N92-25712 * #
NAS 1.55:10092 ..... p 831 N92-29625 * #
NAS 1.55:10103 ..... p 1136 N92-32948 * #
NAS 1.55:3049 ..... p 559 N92-22510 * #
NAS 1.55:3087-PT-1 ..... p 1106 N92-32513 * #
NAS 1.55:3122 ..... p 222 N92-14346 * #
NAS 1.55:3131 ..... p 242 N92-17984 * #
NAS 1.55:3142 ..... p 683 N92-25911 * #
NAS 1.55:3143 ..... p 691 N92-24397 * #
NAS 1.55:3152-PT-2 ..... p 753 N92-27788 * #
NAS 1.55:3160 ..... p 912 N92-30106 * #
NAS 1.55:3172 ..... p 1061 N92-33874 * #
NAS 1.60:2852 ..... p 562 N92-22863 * #
NAS 1.60:3038 ..... p 983 N92-31640 * #
NAS 1.60:3103 ..... p 12 N92-10975 * #
NAS 1.60:3104 ..... p 56 N92-11758 * #
NAS 1.60:3105 ..... p 350 N92-20038 * #
NAS 1.60:3111 ..... p 179 N92-14968 * #
NAS 1.60:3114 ..... p 82 N92-12994 * #
NAS 1.60:3116 ..... p 115 N92-13054 * #
NAS 1.60:3117 ..... p 119 N92-13065 * #
NAS 1.60:3125 ..... p 18 N92-10994 * #
NAS 1.60:3126 ..... p 399 N92-18053 * #
NAS 1.60:3132 ..... p 444 N92-20494 * #
NAS 1.60:3134 ..... p 56 N92-11765 * #
NAS 1.60:3136 ..... p 481 N92-20195 * #
NAS 1.60:3151 ..... p 13 N92-10981 * #
NAS 1.60:3156 ..... p 11 N92-10011 * #
NAS 1.60:3157 ..... p 501 N92-20677 * #
NAS 1.60:3158 ..... p 347 N92-19175 * #
NAS 1.60:3162 ..... p 289 N92-17070 * #
NAS 1.60:3165 ..... p 512 N92-20479 * #
NAS 1.60:3166 ..... p 482 N92-21410 * #
NAS 1.60:3167 ..... p 679 N92-24797 * #
NAS 1.60:3168 ..... p 346 N92-19002 * #
NAS 1.60:3169 ..... p 444 N92-20545 * #
NAS 1.60:3172 ..... p 631 N92-25133 * #
NAS 1.60:3173 ..... p 489 N92-20679 * #
NAS 1.60:3181 ..... p 211 N92-14108 * #
NAS 1.60:3184 ..... p 948 N92-31532 * #
NAS 1.60:3186 ..... p 945 N92-30909 * #
NAS 1.60:3188 ..... p 527 N92-23095 * #
NAS 1.60:3193 ..... p 631 N92-25202 * #
NAS 1.60:3194 ..... p 631 N92-25276 * #
NAS 1.60:3197 ..... p 827 N92-28477 * #
NAS 1.60:3202 ..... p 1040 N92-33656 * #
NAS 1.60:3205 ..... p 943 N92-30295 * #
NAS 1.60:3208 ..... p 1001 N92-31281 * #
NAS 1.60:3219 ..... p 456 N92-21459 * #
NAS 1.60:3221 ..... p 1040 N92-33625 * #
NAS 1.60:3224 ..... p 895 N92-28374 * #
NAS 1.60:3232 ..... p 945 N92-30747 * #
NAS 1.60:3233 ..... p 944 N92-30394 * #
NAS 1.60:3234 ..... p 1039 N92-33484 * #
NAS 1.60:3236 ..... p 1041 N92-33706 * #
NAS 1.60:3240 ..... p 1042 N92-34193 * #
NAS 1.60:3242 ..... p 1134 N92-33483 * #
NAS 1.60:3252 ..... p 830 N92-28980 * #
NAS 1.60:3261 ..... p 1036 N92-32480 * #
NAS 1.60:3265 ..... p 998 N92-30396 * #
NAS 1.61:1258-VOL-1 ..... p 54 N92-10598 * #
NAS 1.61:1258-VOL-2 ..... p 235 N92-14779 * #
NAS 1.61:1272 ..... p 408 N92-19121 * #
NAS 1.61:1280 ..... p 984 N92-30307 * #
NAS 1.71:LAR-14219-1 ..... p 879 N92-30025 * #
NAS 1.71:LAR-14232-1 ..... p 1102 N92-34213 * #
NAS 1.71:LAR-14440-1 ..... p 35 N92-10066 * #
NAS 1.71:LAR-14520-1-SB ..... p 11 N92-10008 * #
NAS 1.71:LAR-14612-1 ..... p 911 N92-29954 * #
NAS 1.71:LAR-14698-1 ..... p 911 N92-30028 * #
NAS 1.71:LAR-14775-1 ..... p 912 N92-30099 * #
NAS 1.71:LAR-14815-1-CU ..... p 910 N92-29830 * #
NAS 1.71:LAR-14824-1-SB ..... p 998 N92-30390 * #
NAS 1.71:LEW-14791-1 ..... p 1043 N92-34243 * #
NAS 1.71:LEW-15027-2 ..... p 579 N92-24053 * #
NAS 1.71:MSC-21881-1 ..... p 912 N92-30082 * #
NAS 1.71:NPO-18366-1-CU ..... p 300 N92-17674 * #

NAS-SR-133 ..... p 268 N92-15980 #
NAS-SR-137 ..... p 308 N92-18969 #

NASA-CASE-GSC-13346-1 ..... p 909 N92-29099 *

NASA-CASE-LAR-13742-1 ..... p 447 N92-21588 *
NASA-CASE-LAR-13870-1-CU ..... p 463 N92-21587 *
NASA-CASE-LAR-14219-1 ..... p 879 N92-30025 * #
NASA-CASE-LAR-14232-1 ..... p 1102 N92-34213 * #
NASA-CASE-LAR-14281-1 ..... p 829 N92-28729 *
NASA-CASE-LAR-14419-1 ..... p 42 N92-10185 *
NASA-CASE-LAR-14440-1 ..... p 35 N92-10066 * #
NASA-CASE-LAR-14520-1-SB ..... p 11 N92-10008 * #
NASA-CASE-LAR-14612-1 ..... p 911 N92-29954 * #
NASA-CASE-LAR-14685-1 ..... p 1042 N92-34172 *
NASA-CASE-LAR-14698-1 ..... p 911 N92-30028 * #
NASA-CASE-LAR-14775-1 ..... p 912 N92-30099 * #
NASA-CASE-LAR-14815-1-CU ..... p 910 N92-29830 * #
NASA-CASE-LAR-14824-1-SB ..... p 998 N92-30390 * #

NASA-CASE-LEW-14791-1 ..... p 1043 N92-34243 * #
NASA-CASE-LEW-15027-2 ..... p 579 N92-24053 * #

NASA-CASE-MSC-21384-1 ..... p 297 N92-16243 *
NASA-CASE-MSC-21881-1 ..... p 912 N92-30082 * #

NASA-CASE-NPO-17569-1-CU ..... p 228 N92-15203 *
NASA-CASE-NPO-18115-1-CU ..... p 916 N92-29148 *
NASA-CASE-NPO-18366-1-CU ..... p 300 N92-17674 * #

NASA-CP-10078 ..... p 660 N92-25808 * #
NASA-CP-10088 ..... p 678 N92-24514 * #
NASA-CP-10089 ..... p 659 N92-25712 * #
NASA-CP-10092 ..... p 831 N92-29625 * #
NASA-CP-10103 ..... p 1136 N92-32948 * #
NASA-CP-3049 ..... p 559 N92-22510 * #
NASA-CP-3087-PT-1 ..... p 1106 N92-32513 * #
NASA-CP-3122 ..... p 222 N92-14346 * #
NASA-CP-3131 ..... p 242 N92-17984 * #
NASA-CP-3142 ..... p 683 N92-25911 * #
NASA-CP-3143 ..... p 691 N92-24397 * #
NASA-CP-3152-PT-2 ..... p 753 N92-27788 * #
NASA-CP-3160 ..... p 912 N92-30106 * #
NASA-CP-3172 ..... p 1061 N92-33874 * #

NASA-CR-167696 ..... p 286 N92-17167 * #
NASA-CR-167697 ..... p 286 N92-17214 * #
NASA-CR-177587 ..... p 93 N92-13044 * #
NASA-CR-177592 ..... p 195 N92-14039 * #
NASA-CR-180083 ..... p 178 N92-13995 * #
NASA-CR-181780 ..... p 578 N92-22637 * #
NASA-CR-181893 ..... p 43 N92-11319 * #
NASA-CR-181954 ..... p 1086 N92-32778 * #
NASA-CR-182004 ..... p 602 N92-22643 * #
NASA-CR-182007 ..... p 602 N92-22644 * #
NASA-CR-184215 ..... p 157 N92-12231 * #
NASA-CR-184260 ..... p 42 N92-11297 * #
NASA-CR-184263 ..... p 221 N92-14344 * #
NASA-CR-184276 ..... p 225 N92-14391 * #
NASA-CR-184278 ..... p 359 N92-18347 * #
NASA-CR-184280 ..... p 499 N92-20198 * #
NASA-CR-184329 ..... p 753 N92-27403 * #
NASA-CR-184341 ..... p 973 N92-31910 * #
NASA-CR-184384 ..... p 1101 N92-33826 * #
NASA-CR-184829 ..... p 191 N92-14036 * #
NASA-CR-185155 ..... p 562 N92-22647 * #
NASA-CR-185242 ..... p 1011 N92-31248 * #
NASA-CR-185666 ..... p 284 N92-15998 * #
NASA-CR-185680 ..... p 746 N92-28209 * #
NASA-CR-186014 ..... p 663 N92-25734 * #
NASA-CR-186015 ..... p 482 N92-21253 * #
NASA-CR-186016 ..... p 482 N92-21357 * #
NASA-CR-186017 ..... p 445 N92-21188 * #
NASA-CR-186019 ..... p 117 N92-13064 * #
NASA-CR-186020 ..... p 962 N92-31208 * #
NASA-CR-186021 ..... p 871 N92-29427 * #
NASA-CR-186022 ..... p 979 N92-31656 * #
NASA-CR-186984 ..... p 387 N92-19934 * #
NASA-CR-187101 ..... p 26 N92-11016 * #
NASA-CR-187108 ..... p 406 N92-19775 * #
NASA-CR-187222 ..... p 44 N92-11379 * #
NASA-CR-187227 ..... p 404 N92-19277 * #
NASA-CR-187235 ..... p 44 N92-11378 * #
NASA-CR-187316 ..... p 185 N92-15048 * #
NASA-CR-187556 ..... p 53 N92-11706 * #
NASA-CR-187581 ..... p 347 N92-19250 * #
NASA-CR-187615 ..... p 268 N92-17512 * #
NASA-CR-187616 ..... p 236 N92-14788 * #
NASA-CR-187621 ..... p 45 N92-11391 * #
NASA-CR-187626 ..... p 697 N92-25368 * #
NASA-CR-187631 ..... p 390 N92-19290 * #
NASA-CR-187979 ..... p 14 N92-10990 * #
NASA-CR-188055 ..... p 751 N92-27976 * #
NASA-CR-188125 ..... p 170 N92-13928 * #
NASA-CR-188126 ..... p 163 N92-12440 * #
NASA-CR-188228 ..... p 46 N92-11593 * #
NASA-CR-188630 ..... p 488 N92-20193 * #
NASA-CR-188856 ..... p 140 N92-12033 * #
NASA-CR-188954 ..... p 33 N92-11070 * #
NASA-CR-188983 ..... p 44 N92-11377 * #
NASA-CR-188985 ..... p 53 N92-10347 * #
NASA-CR-188995 ..... p 31 N92-11023 * #

NASA-CR-188996 ..... p 26 N92-11014 * #
NASA-CR-189018 ..... p 195 N92-14038 * #
NASA-CR-189044 ..... p 195 N92-14037 * #
NASA-CR-189047 ..... p 166 N92-13759 * #
NASA-CR-189050 ..... p 501 N92-20954 * #
NASA-CR-189053 ..... p 225 N92-14374 * #
NASA-CR-189076 ..... p 130 N92-13071 * #
NASA-CR-189088 ..... p 377 N92-19726 * #
NASA-CR-189089 ..... p 402 N92-18971 * #
NASA-CR-189101 ..... p 592 N92-22239 * #
NASA-CR-189110 ..... p 258 N92-15967 * #
NASA-CR-189118 ..... p 716 N92-27376 * #
NASA-CR-189122 ..... p 1073 N92-34236 * #
NASA-CR-189126 ..... p 658 N92-24539 * #
NASA-CR-189129 ..... p 474 N92-20650 * #
NASA-CR-189134 ..... p 352 N92-19276 * #
NASA-CR-189137 ..... p 696 N92-24688 * #
NASA-CR-189142 ..... p 682 N92-25649 * #
NASA-CR-189149 ..... p 943 N92-30298 * #
NASA-CR-189155 ..... p 971 N92-30569 * #
NASA-CR-189171 ..... p 924 N92-30207 * #
NASA-CR-189202 ..... p 574 N92-22211 * #
NASA-CR-189207 ..... p 831 N92-29402 * #
NASA-CR-189222 ..... p 973 N92-31534 * #
NASA-CR-189223 ..... p 1072 N92-33479 * #
NASA-CR-189234 ..... p 983 N92-31252 * #
NASA-CR-189268 ..... p 770 N92-27649 * #
NASA-CR-189455 ..... p 114 N92-11992 * #
NASA-CR-189456 ..... p 82 N92-11983 * #
NASA-CR-189457 ..... p 180 N92-14969 * #
NASA-CR-189461 ..... p 237 N92-14789 * #
NASA-CR-189467 ..... p 221 N92-14313 * #
NASA-CR-189469 ..... p 205 N92-14066 * #
NASA-CR-189502 ..... p 135 N92-13073 * #
NASA-CR-189509 ..... p 179 N92-13999 * #
NASA-CR-189514 ..... p 221 N92-14262 * #
NASA-CR-189515 ..... p 221 N92-14263 * #
NASA-CR-189543 ..... p 443 N92-20283 * #
NASA-CR-189551 ..... p 191 N92-15060 * #
NASA-CR-189555 ..... p 481 N92-20376 * #
NASA-CR-189556 ..... p 209 N92-15077 * #
NASA-CR-189561 ..... p 276 N92-15991 * #
NASA-CR-189570 ..... p 286 N92-16012 * #
NASA-CR-189573 ..... p 381 N92-19499 * #
NASA-CR-189578 ..... p 234 N92-15658 * #
NASA-CR-189579 ..... p 185 N92-15047 * #
NASA-CR-189582 ..... p 416 N92-19672 * #
NASA-CR-189583 ..... p 498 N92-20072 * #
NASA-CR-189584 ..... p 697 N92-26130 * #
NASA-CR-189586 ..... p 525 N92-22215 * #
NASA-CR-189587 ..... p 625 N92-24680 * #
NASA-CR-189591 ..... p 696 N92-24251 * #
NASA-CR-189595 ..... p 888 N92-29352 * #
NASA-CR-189601 ..... p 402 N92-18965 * #
NASA-CR-189603 ..... p 556 N92-22395 * #
NASA-CR-189605 ..... p 556 N92-22645 * #
NASA-CR-189606 ..... p 652 N92-24689 * #
NASA-CR-189612 ..... p 447 N92-21465 * #
NASA-CR-189615 ..... p 592 N92-22228 * #
NASA-CR-189616 ..... p 632 N92-25510 * #
NASA-CR-189620 ..... p 961 N92-30304 * #
NASA-CR-189630 ..... p 696 N92-24800 * #
NASA-CR-189631 ..... p 685 N92-25960 * #
NASA-CR-189633 ..... p 735 N92-27424 * #
NASA-CR-189641 ..... p 715 N92-26652 * #
NASA-CR-189642 ..... p 715 N92-26651 * #
NASA-CR-189643 ..... p 927 N92-28556 * #
NASA-CR-189650 ..... p 967 N92-30965 * #
NASA-CR-189652-VOL-1 ..... p 950 N92-32226 * #
NASA-CR-189652-VOL-2 ..... p 951 N92-32228 * #
NASA-CR-189658 ..... p 944 N92-30392 * #
NASA-CR-189671 ..... p 1110 N92-33613 * #
NASA-CR-189757 ..... p 258 N92-15969 * #
NASA-CR-189758 ..... p 258 N92-15966 * #
NASA-CR-189759 ..... p 257 N92-15965 * #
NASA-CR-189773 ..... p 289 N92-17004 * #
NASA-CR-189778 ..... p 282 N92-17019 * #
NASA-CR-189785 ..... p 259 N92-15974 * #
NASA-CR-189789 ..... p 298 N92-17006 * #
NASA-CR-189814 ..... p 301 N92-17393 * #
NASA-CR-189849 ..... p 358 N92-18024 * #
NASA-CR-189850 ..... p 359 N92-18038 * #
NASA-CR-189853 ..... p 275 N92-17316 * #
NASA-CR-189854 ..... p 625 N92-24803 * #
NASA-CR-189899 ..... p 502 N92-21433 * #
NASA-CR-189901 ..... p 404 N92-19217 * #
NASA-CR-189911 ..... p 382 N92-19841 * #
NASA-CR-189932 ..... p 499 N92-20197 * #
NASA-CR-189939 ..... p 778 N92-28150 * #
NASA-CR-189951 ..... p 385 N92-19218 * #
NASA-CR-189963 ..... p 386 N92-19675 * #
NASA-CR-189974 ..... p 462 N92-20664 * #
NASA-CR-189981 ..... p 366 N92-19374 * #
NASA-CR-189987 ..... p 463 N92-21540 * #
NASA-CR-189988 ..... p 461 N92-20267 * #
NASA-CR-189990 ..... p 462 N92-21489 * #
NASA-CR-189991 ..... p 463 N92-21566 * #
NASA-CR-189992 ..... p 463 N92-21565 * #
NASA-CR-189994 ..... p 575 N92-22625 * #
NASA-CR-190004 ..... p 648 N92-25263 * #
NASA-CR-190006 ..... p 486 N92-20666 * #
NASA-CR-190007 ..... p 462 N92-20665 * #
NASA-CR-190019 ..... p 731 N92-26435 * #
NASA-CR-190022 ..... p 463 N92-21567 * #
NASA-CR-190023 ..... p 367 N92-19496 * #
NASA-CR-190024 ..... p 461 N92-20064 * #
NASA-CR-190026 ..... p 462 N92-20951 * #
NASA-CR-190039 ..... p 348 N92-19359 * #
NASA-CR-190040 ..... p 348 N92-19545 * #
NASA-CR-190045 ..... p 945 N92-30740 * #
NASA-CR-190054 ..... p 446 N92-21356 * #
NASA-CR-190074 ..... p 664 N92-25162 * #
NASA-CR-190077 ..... p 692 N92-25264 * #
NASA-CR-190130 ..... p 461 N92-20280 * #
NASA-CR-190148 ..... p 593 N92-22491 * #
NASA-CR-190159 ..... p 502 N92-21385 * #
NASA-CR-190166 ..... p 484 N92-21162 * #
NASA-CR-190182 ..... p 946 N92-30977 * #
NASA-CR-190201 ..... p 595 N92-22662 * #
NASA-CR-190204 ..... p 578 N92-22486 * #
NASA-CR-190217 ..... p 573 N92-22195 * #
NASA-CR-190248 ..... p 527 N92-23103 * #
NASA-CR-190251 ..... p 631 N92-25175 * #
NASA-CR-190264 ..... p 830 N92-29329 * #
NASA-CR-190290 ..... p 971 N92-30753 * #
NASA-CR-190294 ..... p 624 N92-24229 * #
NASA-CR-190305 ..... p 678 N92-24345 * #
NASA-CR-190313 ..... p 630 N92-24898 * #
NASA-CR-190328 ..... p 685 N92-26125 *
NASA-CR-190336 ..... p 663 N92-25648 * #
NASA-CR-190353 ..... p 633 N92-25959 * #
NASA-CR-190355 ..... p 650 N92-26017 * #
NASA-CR-190357 ..... p 716 N92-27558 * #
NASA-CR-190368 ..... p 685 N92-25962 * #
NASA-CR-190369 ..... p 692 N92-26018 * #
NASA-CR-190379 ..... p 1004 N92-32147 * #
NASA-CR-190400 ..... p 907 N92-28361 * #
NASA-CR-190423 ..... p 738 N92-26405 * #
NASA-CR-190426 ..... p 716 N92-27399 * #
NASA-CR-190430 ..... p 773 N92-27880 * #
NASA-CR-190431 ..... p 827 N92-28511 * #
NASA-CR-190433 ..... p 742 N92-27519 * #
NASA-CR-190434 ..... p 731 N92-26655 * #
NASA-CR-190444 ..... p 852 N92-28720 * #
NASA-CR-190450 ..... p 1127 N92-33696 * #
NASA-CR-190452 ..... p 715 N92-27191 * #
NASA-CR-190459 ..... p 1000 N92-30923 * #
NASA-CR-190469 ..... p 840 N92-28718 * #
NASA-CR-190471 ..... p 1000 N92-30988 * #
NASA-CR-190480 ..... p 830 N92-29361 * #
NASA-CR-190498 ..... p 998 N92-30380 * #
NASA-CR-190535 ..... p 879 N92-29654 * #
NASA-CR-190541 ..... p 888 N92-29655 * #
NASA-CR-190542 ..... p 1044 N92-34105 * #
NASA-CR-190563 ..... p 1036 N92-32648 * #
NASA-CR-190565 ..... p 854 N92-30209 * #
NASA-CR-190570 ..... p 832 N92-29657 * #
NASA-CR-190576 ..... p 832 N92-29691 * #
NASA-CR-190577 ..... p 1003 N92-31619 * #
NASA-CR-190583 ..... p 1036 N92-32494 * #
NASA-CR-190638 ..... p 1038 N92-33304 * #
NASA-CR-190649 ..... p 946 N92-31157 * #
NASA-CR-190650 ..... p 1001 N92-31156 * #
NASA-CR-190667 ..... p 978 N92-30922 * #
NASA-CR-190680 ..... p 948 N92-31533 * #
NASA-CR-190684 ..... p 1102 N92-34141 * #
NASA-CR-190686 ..... p 1128 N92-34207 * #
NASA-CR-190688 ..... p 950 N92-32177 * #
NASA-CR-190702 ..... p 1038 N92-33063 * #
NASA-CR-190712 ..... p 1134 N92-32865 * #
NASA-CR-190731 ..... p 950 N92-32162 * #
NASA-CR-190736 ..... p 1087 N92-33107 * #
NASA-CR-190810 ..... p 1126 N92-33307 * #
NASA-CR-190812 ..... p 1088 N92-33536 * #
NASA-CR-190817 ..... p 1039 N92-33413 * #
NASA-CR-190822 ..... p 1125 N92-33139 * #
NASA-CR-190836 ..... p 1039 N92-33424 * #
NASA-CR-190902 ..... p 1128 N92-34043 * #
NASA-CR-190925 ..... p 1051 N92-34203 * #
NASA-CR-191259 ..... p 1102 N92-34222 * #
NASA-CR-3251 ..... p 526 N92-22648 * #
NASA-CR-3252 ..... p 527 N92-22865 * #
NASA-CR-4283 ..... p 678 N92-24242 * #
NASA-CR-4292-VOL-1 ..... p 679 N92-24547 *
NASA-CR-4292-VOL-2 ..... p 678 N92-24344 * #
NASA-CR-4374 ..... p 368 N92-19871 * #
NASA-CR-4388 ..... p 166 N92-13757 * #
NASA-CR-4391 ..... p 951 N92-32240 * #
NASA-CR-4392 ..... p 526 N92-22249 * #
NASA-CR-4405 ..... p 12 N92-10979 * #
NASA-CR-4406 ..... p 13 N92-10982 * #
NASA-CR-4407 ..... p 178 N92-13996 * #
NASA-CR-4414 ..... p 178 N92-13997 * #
NASA-CR-4420 ..... p 234 N92-14598 * #
NASA-CR-4422 ..... p 347 N92-19354 * #
NASA-CR-4424 ..... p 499 N92-20194 * #
NASA-CR-4426 ..... p 512 N92-21173 * #
NASA-CR-4427 ..... p 406 N92-19844 * #
NASA-CR-4430 ..... p 473 N92-20196 * #
NASA-CR-4431 ..... p 446 N92-21456 * #
NASA-CR-4438 ..... p 765 N92-26680 * #
NASA-CR-4440 ..... p 681 N92-25376 * #
NASA-CR-4442 ..... p 663 N92-25982 * #
NASA-CR-4443 ..... p 878 N92-28584 * #
NASA-CR-4450 ..... p 957 N92-30978 * #
NASA-CR-4456 ..... p 1043 N92-32606 * #
NASA-CR-4457 ..... p 953 N92-31549 * #
NASA-CR-4463 ..... p 979 N92-32175 * #
NASA-CR-4465 ..... p 950 N92-32114 * #
NASA-CR-4470 ..... p 1045 N92-34192 * #

NASA-RP-1258-VOL-1 ..... p 54 N92-10598 * #
NASA-RP-1258-VOL-2 ..... p 235 N92-14779 * #
NASA-RP-1272 ..... p 408 N92-19121 * #
NASA-RP-1280 ..... p 984 N92-30307 * #

NASA-SP-4104 ..... p 929 N92-28344 * #

NASA-TM-101657 ..... p 680 N92-25137 * #
NASA-TM-102192 ..... p 878 N92-28457 * #
NASA-TM-102230 ..... p 950 N92-32213 * #
NASA-TM-102244 ..... p 550 N92-22864 * #
NASA-TM-102261 ..... p 1038 N92-33306 * #
NASA-TM-102268 ..... p 1040 N92-33618 * #
NASA-TM-102554 ..... p 445 N92-20934 * #
NASA-TM-102614 ..... p 595 N92-22649 * #
NASA-TM-102687 ..... p 206 N92-15076 * #
NASA-TM-102842 ..... p 13 N92-10983 * #
NASA-TM-102851 ..... p 1036 N92-32422 * #
NASA-TM-102882 ..... p 1051 N92-33609 * #
NASA-TM-103248 ..... p 972 N92-31250 * #
NASA-TM-103578 ..... p 506 N92-21546 * #
NASA-TM-103747 ..... p 230 N92-15406 * #
NASA-TM-103800 ..... p 242 N92-17346 * #
NASA-TM-103839 ..... p 1071 N92-32452 * #
NASA-TM-103842 ..... p 482 N92-21440 * #
NASA-TM-103864 ..... p 368 N92-19847 * #
NASA-TM-103866 ..... p 1060 N92-32887 * #
NASA-TM-103873 ..... p 853 N92-28926 * #
NASA-TM-103875 ..... p 367 N92-19563 * #
NASA-TM-103876 ..... p 21 N92-11000 * #
NASA-TM-103880 ..... p 1044 N92-33194 * #
NASA-TM-103887 ..... p 356 N92-20029 * #
NASA-TM-103892 ..... p 890 N92-29104 * #
NASA-TM-103897 ..... p 2 N92-10003 * #
NASA-TM-103899 ..... p 1050 N92-33407 * #
NASA-TM-103902 ..... p 853 N92-28910 * #
NASA-TM-103906 ..... p 841 N92-29103 * #
NASA-TM-103910 ..... p 1087 N92-32788 * #
NASA-TM-103915 ..... p 927 N92-28909 * #
NASA-TM-103925 ..... p 852 N92-28721 * #
NASA-TM-103928 ..... p 405 N92-19596 * #
NASA-TM-103929 ..... p 854 N92-29417 * #
NASA-TM-103930 ..... p 1047 N92-32424 * #
NASA-TM-103934 ..... p 1039 N92-33581 * #
NASA-TM-103959 ..... p 1044 N92-33080 * #
NASA-TM-104112 ..... p 1140 N92-34148 * #
NASA-TM-104120 ..... p 197 N92-15070 * #
NASA-TM-104125 ..... p 115 N92-13057 * #
NASA-TM-104134 ..... p 166 N92-12598 * #
NASA-TM-104138 ..... p 23 N92-11010 * #
NASA-TM-104142 ..... p 81 N92-11977 * #
NASA-TM-104145 ..... p 82 N92-11985 * #
NASA-TM-104146 ..... p 159 N92-13458 * #
NASA-TM-104147 ..... p 166 N92-13758 * #
NASA-TM-104150 ..... p 56 N92-11759 * #
NASA-TM-104152 ..... p 31 N92-11022 * #
NASA-TM-104154 ..... p 159 N92-13460 * #
NASA-TM-104158 ..... p 206 N92-15075 * #
NASA-TM-104160 ..... p 35 N92-11149 * #
NASA-TM-104161 ..... p 138 N92-12007 * #
NASA-TM-104163 ..... p 159 N92-13455 * #
NASA-TM-104168 ..... p 261 N92-17547 * #
NASA-TM-104170 ..... p 1138 N92-33160 * #
NASA-TM-104174 ..... p 303 N92-17130 * #
NASA-TM-104180 ..... p 185 N92-15049 * #
NASA-TM-104184 ..... p 401 N92-18877 * #
NASA-TM-104186 ..... p 185 N92-15050 * #
NASA-TM-104188 ..... p 261 N92-17509 * #
NASA-TM-104190 ..... p 298 N92-17002 * #
NASA-TM-104191 ..... p 446 N92-21432 * #
NASA-TM-104192 ..... p 299 N92-17034 * #
NASA-TM-104193 ..... p 299 N92-17033 * #
NASA-TM-104194 ..... p 367 N92-19846 * #
NASA-TM-104196 ..... p 602 N92-22320 * #
NASA-TM-104200 ..... p 385 N92-18956 * #
NASA-TM-104203 ..... p 404 N92-19258 * #
NASA-TM-104205 ..... p 556 N92-22504 * #

NASA-TM-104206 ..... p 630 N92-24956 * #
NASA-TM-104207 ..... p 625 N92-24681 * #
NASA-TM-104211 ..... p 1042 N92-34147 * #
NASA-TM-104215 ..... p 444 N92-20480 * #
NASA-TM-104216 ..... p 525 N92-22232 * #
NASA-TM-104226 ..... p 461 N92-20417 * #
NASA-TM-104237 ..... p 1133 N92-32507 * #
NASA-TM-104240 ..... p 871 N92-29659 * #
NASA-TM-104241 ..... p 118 N92-11994 * #
NASA-TM-104245 ..... p 272 N92-15986 * #
NASA-TM-104247 ..... p 871 N92-29425 * #
NASA-TM-104249 ..... p 1062 N92-34202 * #
NASA-TM-104250 ..... p 984 N92-32201 * #
NASA-TM-104251 ..... p 1065 N92-32866 * #
NASA-TM-104252 ..... p 971 N92-30518 * #
NASA-TM-104253 ..... p 1060 N92-33404 * #
NASA-TM-104254 ..... p 962 N92-31261 * #
NASA-TM-104255 ..... p 1087 N92-32864 * #
NASA-TM-104256 ..... p 1060 N92-33149 * #
NASA-TM-104259 ..... p 1062 N92-34039 * #
NASA-TM-104475 ..... p 12 N92-10976 * #
NASA-TM-104518 ..... p 527 N92-23105 * #
NASA-TM-104525 ..... p 214 N92-15191 * #
NASA-TM-104531 ..... p 1109 N92-32863 * #
NASA-TM-104744 ..... p 308 N92-19930 * #
NASA-TM-105096 ..... p 53 N92-11642 * #
NASA-TM-105124 ..... p 82 N92-11984 * #
NASA-TM-105126 ..... p 31 N92-11024 * #
NASA-TM-105192 ..... p 2 N92-10002 * #
NASA-TM-105193 ..... p 279 N92-15993 * #
NASA-TM-105206 ..... p 304 N92-16705 * #
NASA-TM-105258 ..... p 279 N92-17061 * #
NASA-TM-105260 ..... p 298 N92-16336 * #
NASA-TM-105283 ..... p 348 N92-19437 * #
NASA-TM-105288 ..... p 473 N92-20525 * #
NASA-TM-105303 ..... p 26 N92-11017 * #
NASA-TM-105320 ..... p 516 N92-22659 * #
NASA-TM-105321 ..... p 179 N92-13998 * #
NASA-TM-105329 ..... p 597 N92-23560 * #
NASA-TM-105332 ..... p 44 N92-11328 * #
NASA-TM-105336 ..... p 229 N92-15402 * #
NASA-TM-105338 ..... p 237 N92-14795 * #
NASA-TM-105347 ..... p 202 N92-14063 * #
NASA-TM-105356 ..... p 416 N92-18282 * #
NASA-TM-105365 ..... p 237 N92-14797 * #
NASA-TM-105368 ..... p 258 N92-15968 * #
NASA-TM-105373 ..... p 186 N92-15052 * #
NASA-TM-105374 ..... p 185 N92-15051 * #
NASA-TM-105380 ..... p 261 N92-17347 * #
NASA-TM-105389 ..... p 179 N92-14001 * #
NASA-TM-105393 ..... p 179 N92-14002 * #
NASA-TM-105397 ..... p 279 N92-17546 * #
NASA-TM-105399 ..... p 562 N92-23254 * #
NASA-TM-105400 ..... p 297 N92-16265 * #
NASA-TM-105414 ..... p 346 N92-18760 * #
NASA-TM-105416 ..... p 773 N92-27879 * #
NASA-TM-105417 ..... p 887 N92-28673 * #
NASA-TM-105427 ..... p 633 N92-26104 * #
NASA-TM-105432 ..... p 528 N92-23563 * #
NASA-TM-105434 ..... p 1002 N92-31349 * #
NASA-TM-105437 ..... p 350 N92-19993 * #
NASA-TM-105439 ..... p 387 N92-18280 * #
NASA-TM-105479 ..... p 286 N92-16973 * #
NASA-TM-105510 ..... p 412 N92-18125 * #
NASA-TM-105562 ..... p 378 N92-20033 * #
NASA-TM-105575 ..... p 596 N92-23267 * #
NASA-TM-105579 ..... p 481 N92-20586 * #
NASA-TM-105581 ..... p 499 N92-20235 * #
NASA-TM-105599 ..... p 756 N92-27378 * #
NASA-TM-105610 ..... p 562 N92-23537 * #
NASA-TM-105613 ..... p 658 N92-25164 * #
NASA-TM-105617 ..... p 596 N92-23154 * #
NASA-TM-105623 ..... p 716 N92-27377 * #
NASA-TM-105627 ..... p 473 N92-20523 * #
NASA-TM-105641 ..... p 596 N92-23435 * #
NASA-TM-105643 ..... p 680 N92-24959 * #
NASA-TM-105644 ..... p 665 N92-25449 * #
NASA-TM-105646 ..... p 667 N92-26129 * #
NASA-TM-105651 ..... p 764 N92-26555 * #
NASA-TM-105655 ..... p 908 N92-28434 * #
NASA-TM-105664 ..... p 630 N92-24958 * #
NASA-TM-105665 ..... p 680 N92-24984 * #
NASA-TM-105668 ..... p 764 N92-26560 * #
NASA-TM-105672 ..... p 1128 N92-34112 * #
NASA-TM-105675 ..... p 833 N92-30182 * #
NASA-TM-105680 ..... p 871 N92-29661 * #
NASA-TM-105681 ..... p 910 N92-29136 * #
NASA-TM-105682 ..... p 972 N92-31172 * #
NASA-TM-105683 ..... p 1072 N92-33746 * #
NASA-TM-105684 ..... p 739 N92-27037 * #
NASA-TM-105685 ..... p 982 N92-30508 * #
NASA-TM-105686 ..... p 770 N92-27653 * #
NASA-TM-105694 ..... p 742 N92-27652 * #
NASA-TM-105695 ..... p 738 N92-26553 * #
NASA-TM-105696 ..... p 1134 N92-33894 * #
NASA-TM-105697 ..... p 742 N92-27669 * #
NASA-TM-105698 ..... p 868 N92-28418 * #
NASA-TM-105699 ..... p 738 N92-26561 * #
NASA-TM-105702 ..... p 1002 N92-31485 * #
NASA-TM-105715 ..... p 868 N92-28419 * #
NASA-TM-105716 ..... p 870 N92-28985 * #
NASA-TM-105717 ..... p 909 N92-29105 * #
NASA-TM-105720 ..... p 722 N92-28102 * #
NASA-TM-105724 ..... p 739 N92-26613 * #
NASA-TM-105731 ..... p 890 N92-29343 * #
NASA-TM-105740 ..... p 1002 N92-31484 * #
NASA-TM-105742 ..... p 714 N92-26612 * #
NASA-TM-105743 ..... p 828 N92-28674 * #
NASA-TM-105745 ..... p 828 N92-28696 * #
NASA-TM-105773 ..... p 1042 N92-34144 * #
NASA-TM-105796 ..... p 972 N92-30972 * #
NASA-TM-105797 ..... p 1088 N92-34107 * #
NASA-TM-105803 ..... p 932 N92-31267 * #
NASA-TM-105805 ..... p 1009 N92-30898 * #
NASA-TM-105814 ..... p 972 N92-30998 * #
NASA-TM-105826 ..... p 979 N92-32241 * #
NASA-TM-107567 ..... p 527 N92-23116 * #
NASA-TM-107576 ..... p 526 N92-22240 * #
NASA-TM-107578 ..... p 502 N92-21460 * #
NASA-TM-107579 ..... p 680 N92-25267 * #
NASA-TM-107581 ..... p 526 N92-22507 * #
NASA-TM-107584 ..... p 685 N92-26128 * #
NASA-TM-107586 ..... p 850 N92-28435 * #
NASA-TM-107591 ..... p 1125 N92-33104 * #
NASA-TM-107600 ..... p 1060 N92-32536 * #
NASA-TM-107601 ..... p 1088 N92-33537 * #
NASA-TM-107606 ..... p 685 N92-25964 * #
NASA-TM-107615 ..... p 662 N92-25607 * #
NASA-TM-107622 ..... p 650 N92-25995 * #
NASA-TM-107631 ..... p 944 N92-30570 * #
NASA-TM-107635 ..... p 831 N92-29445 * #
NASA-TM-107642 ..... p 1001 N92-31155 * #
NASA-TM-107643 ..... p 944 N92-30393 * #
NASA-TM-107644 ..... p 947 N92-31239 * #
NASA-TM-107645 ..... p 945 N92-30691 * #
NASA-TM-107646 ..... p 984 N92-31900 * #
NASA-TM-107650 ..... p 963 N92-32111 * #
NASA-TM-107651 ..... p 961 N92-30752 * #
NASA-TM-107652 ..... p 962 N92-31350 * #
NASA-TM-107653 ..... p 962 N92-31174 * #
NASA-TM-107654 ..... p 962 N92-31351 * #
NASA-TM-107655 ..... p 962 N92-31264 * #
NASA-TM-107657 ..... p 1138 N92-33719 * #
NASA-TM-107663 ..... p 1010 N92-30907 * #
NASA-TM-107666 ..... p 1110 N92-33423 * #
NASA-TM-107677 ..... p 1128 N92-34178 * #
NASA-TM-107679 ..... p 1128 N92-34017 * #
NASA-TM-107838 ..... p 632 N92-25279 * #
NASA-TM-107847 ..... p 631 N92-25261 * #
NASA-TM-107873 ..... p 692 N92-25190 * #
NASA-TM-107924 ..... p 782 N92-28183 * #
NASA-TM-107931 ..... p 782 N92-28114 * #
NASA-TM-107960 ..... p 1013 N92-31852 * #
NASA-TM-107967 ..... p 1143 N92-33948 * #
NASA-TM-108171 ..... p 1142 N92-33237 * #
NASA-TM-4189 ..... p 947 N92-31246 * #
NASA-TM-4278 ..... p 445 N92-20654 * #
NASA-TM-4279 ..... p 17 N92-10017 * #
NASA-TM-4281 ..... p 11 N92-10006 * #
NASA-TM-4285 ..... p 23 N92-10024 * #
NASA-TM-4295 ..... p 528 N92-23533 * #
NASA-TM-4296 ..... p 526 N92-22506 * #
NASA-TM-4302 ..... p 978 N92-31175 * #
NASA-TM-4309 ..... p 525 N92-22196 * #
NASA-TM-4313 ..... p 61 N92-12989 * #
NASA-TM-4315 ..... p 297 N92-16283 * #
NASA-TM-4316 ..... p 90 N92-13038 * #
NASA-TM-4318 ..... p 32 N92-11030 * #
NASA-TM-4322 ..... p 157 N92-12286 * #
NASA-TM-4331 ..... p 1013 N92-30733 * #
NASA-TM-4333 ..... p 750 N92-27670 * #
NASA-TM-4334 ..... p 630 N92-24882 * #
NASA-TM-4335 ..... p 276 N92-17128 * #
NASA-TM-4337 ..... p 630 N92-24977 * #
NASA-TM-4341 ..... p 273 N92-17071 * #
NASA-TM-4345 ..... p 630 N92-24885 * #
NASA-TM-4356 ..... p 381 N92-19174 * #
NASA-TM-4359 ..... p 633 N92-25967 * #
NASA-TM-4363 ..... p 633 N92-25752 * #
NASA-TM-4368 ..... p 609 N92-24678 * #
NASA-TM-4370 ..... p 570 N92-22194 * #
NASA-TM-4374 ..... p 767 N92-27193 * #
NASA-TM-4379 ..... p 1065 N92-34109 * #
NASA-TM-4381 ..... p 979 N92-31240 * #
NASA-TM-4382 ..... p 1040 N92-33631 * #
NASA-TM-4393 ..... p 742 N92-27587 * #
NASA-TM-4394 ..... p 740 N92-27379 * #
NASA-TM-4396 ..... p 853 N92-29110 * #
NASA-TM-4398 ..... p 947 N92-31276 * #
NASA-TM-4400 ..... p 973 N92-31275 * #
NASA-TM-80225 ..... p 32 N92-11030 * #
NASA-TM-84661 ..... p 32 N92-11030 * #
NASA-TM-893240 ..... p 156 N92-12173 * #

NASA-TP-2852 ..... p 562 N92-22863 * #
NASA-TP-3038 ..... p 983 N92-31640 * #
NASA-TP-3103 ..... p 12 N92-10975 * #
NASA-TP-3104 ..... p 56 N92-11758 * #
NASA-TP-3105 ..... p 350 N92-20038 * #
NASA-TP-3111 ..... p 179 N92-14968 * #
NASA-TP-3114 ..... p 82 N92-12994 * #
NASA-TP-3116 ..... p 115 N92-13054 * #
NASA-TP-3117 ..... p 119 N92-13065 * #
NASA-TP-3125 ..... p 18 N92-10994 * #
NASA-TP-3126 ..... p 399 N92-18053 * #
NASA-TP-3132 ..... p 444 N92-20494 * #
NASA-TP-3134 ..... p 56 N92-11765 * #
NASA-TP-3136 ..... p 481 N92-20195 * #
NASA-TP-3151 ..... p 13 N92-10981 * #
NASA-TP-3156 ..... p 11 N92-10011 * #
NASA-TP-3157 ..... p 501 N92-20677 * #
NASA-TP-3158 ..... p 347 N92-19175 * #
NASA-TP-3162 ..... p 289 N92-17070 * #
NASA-TP-3165 ..... p 512 N92-20479 * #
NASA-TP-3166 ..... p 482 N92-21410 * #
NASA-TP-3167 ..... p 679 N92-24797 * #
NASA-TP-3168 ..... p 346 N92-19002 * #
NASA-TP-3169 ..... p 444 N92-20545 * #
NASA-TP-3172 ..... p 631 N92-25133 * #
NASA-TP-3173 ..... p 489 N92-20679 * #
NASA-TP-3181 ..... p 211 N92-14108 * #
NASA-TP-3184 ..... p 948 N92-31532 * #
NASA-TP-3186 ..... p 945 N92-30909 * #
NASA-TP-3188 ..... p 527 N92-23095 * #
NASA-TP-3193 ..... p 631 N92-25202 * #
NASA-TP-3194 ..... p 631 N92-25276 * #
NASA-TP-3197 ..... p 827 N92-28477 * #
NASA-TP-3202 ..... p 1040 N92-33656 * #
NASA-TP-3205 ..... p 943 N92-30295 * #
NASA-TP-3208 ..... p 1001 N92-31281 * #
NASA-TP-3219 ..... p 456 N92-21459 * #
NASA-TP-3221 ..... p 1040 N92-33625 * #
NASA-TP-3224 ..... p 895 N92-28374 * #
NASA-TP-3232 ..... p 945 N92-30747 * #
NASA-TP-3233 ..... p 944 N92-30394 * #
NASA-TP-3234 ..... p 1039 N92-33484 * #
NASA-TP-3236 ..... p 1041 N92-33706 * #
NASA-TP-3238 ..... p 952 N92-30395 * #
NASA-TP-3240 ..... p 1042 N92-34193 * #
NASA-TP-3242 ..... p 1134 N92-33483 * #
NASA-TP-3252 ..... p 830 N92-28980 * #
NASA-TP-3261 ..... p 1036 N92-32480 * #
NASA-TP-3265 ..... p 998 N92-30396 * #

NATICK-TR-92/009 ..... p 943 N92-30239 #

NATICK/TR-92/005 ..... p 261 N92-17404 #
NATICK/TR-92/017 ..... p 348 N92-19394 #

NAVSWC-TR-90-683 ..... p 831 N92-29539 #
NAVSWC-TR-91-178 ..... p 347 N92-19085 #

NAVY-CASE-73152 ..... p 1088 N92-34131 #
NAVY-CASE-73256 ..... p 268 N92-17707 #

NAWCADWAR-92022-60 ..... p 1061 N92-33414 #

NCAR/TN-362+1A ..... p 301 N92-17393 * #

NCEL-TN-1839 ..... p 895 N92-28912 #

NCTRF-187 ..... p 305 N92-17537 #

NIAR-91-28 ..... p 399 N92-18116 #
NIAR-91-30 ..... p 264 N92-17587 #
NIAR-92-1 ..... p 420 N92-21501 #

NIFS-110 ..... p 1138 N92-33743 #

NIST-TN-1278 ..... p 1126 N92-33501 #

NIST/SP-812 ..... p 485 N92-21777 #
NIST/SP-817 ..... p 485 N92-21870 #

NISTIR-4688 ..... p 484 N92-20448 #

NLR-MP-88031-U ..... p 827 N92-28658 #
NLR-MP-88040-U ..... p 841 N92-29615 #
NLR-MP-88044-U ..... p 854 N92-29616 #

NLR-TP-89119-U ..... p 827 N92-28659 #
NLR-TP-89126-U ..... p 828 N92-28660 #
NLR-TP-89152-U ..... p 385 N92-18415 #
NLR-TP-89158-U ..... p 887 N92-28669 #
NLR-TP-89182-U ..... p 385 N92-18416 #
NLR-TP-89217-U ..... p 915 N92-28689 #
NLR-TP-89284-U ..... p 952 N92-30474 #
NLR-TP-89365-U ..... p 444 N92-20473 #

NLR-TP-90029-U ..... p 444 N92-20498 #
NLR-TP-90062-U ..... p 828 N92-28709 #
NLR-TP-90068-U ..... p 852 N92-28649 #
NLR-TP-90084-U ..... p 196 N92-15065 #
NLR-TP-90087-U ..... p 481 N92-20475 #
NLR-TP-90097-U ..... p 870 N92-28711 #
NLR-TP-90115-U ..... p 381 N92-18893 #
NLR-TP-90129-U ..... p 878 N92-28652 #
NLR-TP-90134-U ..... p 908 N92-28712 #
NLR-TP-90144-U ..... p 828 N92-28692 #
NLR-TP-90145-U ..... p 887 N92-28661 #
NLR-TP-90147-U ..... p 888 N92-29204 #
NLR-TP-90159-U ..... p 879 N92-28653 #
NLR-TP-90163-U ..... p 859 N92-28654 #
NLR-TP-90174-U ..... p 859 N92-28644 #
NLR-TP-90184-U ..... p 908 N92-28694 #
NLR-TP-90192-U ..... p 837 N92-28655 #
NLR-TP-90196-U ..... p 837 N92-29703 #
NLR-TP-90223-U ..... p 927 N92-28695 #
NLR-TP-90255-U ..... p 829 N92-28713 #
NLR-TP-90286-U ..... p 852 N92-28714 #
NLR-TP-90305-U ..... p 852 N92-28687 #
NLR-TP-90334-U ..... p 923 N92-28635 #
NLR-TP-90336-U ..... p 910 N92-29603 #
NLR-TP-90368-U ..... p 827 N92-28657 #
NLR-TP-91046-U ..... p 1037 N92-32730 #
NLR-TP-91052-U ..... p 1125 N92-33139 * #
NLR-TP-91061-U ..... p 924 N92-29604 #
NLR-TP-91062-U-PT-1 ..... p 841 N92-29605 #
NLR-TP-91117-U ..... p 1037 N92-32732 #
NLR-TP-91119-U ..... p 1101 N92-32734 #
NLR-TP-91154-U ..... p 1037 N92-32673 #
NLR-TP-91156-U ..... p 1047 N92-32830 #

NLR-TR-86006-U ..... p 833 N92-29916 #
NLR-TR-88072-U ..... p 832 N92-29884 #
NLR-TR-88103-U ..... p 405 N92-19490 #
NLR-TR-88108-U ..... p 356 N92-19491 #
NLR-TR-88148-U ..... p 605 N92-23588 #
NLR-TR-88154-U ..... p 400 N92-18221 #

NOAA-TM-ERL-ARL-190 ..... p 449 N92-20318 #

NOAA-TM-ERL-WPL-215 ..... p 503 N92-21828 #

NOR-89-101 ..... p 275 N92-17513 #
NOR-91-25 ..... p 490 N92-21159 #

NOSC-TD-2174 ..... p 305 N92-17369 #

NOSC/TR-1487 ..... p 1004 N92-31362 #
NOSC/TR-1492 ..... p 1129 N92-33220 #

NPS-AS-92-006 ..... p 781 N92-27528 #

NRC-DM-009 ..... p 130 N92-12001 #

NRC-HSA-434 ..... p 81 N92-11976 #

NRC-IAR-C3 ..... p 81 N92-11975 #

NRC-LTR-HA-5X5/0196 ..... p 81 N92-11975 #

NRC-LTR-ST-1658 ..... p 115 N92-13056 #
NRC-LTR-ST-1689 ..... p 489 N92-21018 #
NRC-LTR-ST-1792 ..... p 129 N92-11997 #
NRC-LTR-ST-1804 ..... p 114 N92-11990 #
NRC-LTR-ST-1806 ..... p 159 N92-13454 #
NRC-LTR-ST-1826 ..... p 1109 N92-32791 #
NRC-LTR-ST-1834 ..... p 504 N92-22029 #
NRC-LTR-ST-1839 ..... p 504 N92-22028 #

NRC-SR-230 ..... p 92 N92-13040 #

NRC-ST-621 ..... p 159 N92-13453 #

NRC-TR-ENG-001 ..... p 130 N92-12000 #
NRC-TR-ENG-003 ..... p 130 N92-11998 #
NRC-TR-ENG-005 ..... p 1002 N92-31469 #
NRC-TR-ENG-007 ..... p 202 N92-14060 #
NRC-TR-ENG-013 ..... p 130 N92-11999 #

NRC-29808 ..... p 130 N92-12000 #
NRC-30165 ..... p 130 N92-12001 #
NRC-30241 ..... p 130 N92-11998 #
NRC-30465 ..... p 114 N92-11991 #
NRC-31578 ..... p 130 N92-11999 #
NRC-31761 ..... p 155 N92-12154 #
NRC-31764 ..... p 155 N92-12153 #
NRC-32083 ..... p 1002 N92-31469 #
NRC-32124 ..... p 448 N92-20156 #
NRC-32137-PHASE-1 ..... p 102 N92-11988 #
NRC-32139 ..... p 1064 N92-32850 #
NRC-32146 ..... p 1134 N92-32851 #
NRC-32148 ..... p 1048 N92-32849 #
NRC-32149 ..... p 268 N92-17568 #

NRC-32151 ..... p 716 N92-27344 #

NREC-1656-1 ..... p 756 N92-26521 #

NREL/TP-257-4099 ..... p 1004 N92-31498 #
NREL/TP-257-4492 ..... p 598 N92-22971 #
NREL/TP-257-4507 ..... p 301 N92-16458 #
NREL/TP-257-4510 ..... p 262 N92-17874 #
NREL/TP-257-4517 ..... p 410 N92-19633 #
NREL/TP-257-4518 ..... p 302 N92-17875 #
NREL/TP-257-4594 ..... p 598 N92-23119 #
NREL/TP-257-4654 ..... p 505 N92-20245 #
NREL/TP-442-4822 ..... p 1004 N92-30837 #

NRL/MR/4654-92-6986 ..... p 1044 N92-33249 #

NSTS-08194 ..... p 286 N92-16973 * #

NTSB/AAB-90/02 ..... p 263 N92-15978 #
NTSB/AAB-90/03 ..... p 263 N92-15979 #
NTSB/AAB-90/04 ..... p 263 N92-17133 #
NTSB/AAB-90/05 ..... p 452 N92-21833 #

NTSB/AAR-90/01 ..... p 953 N92-31159 #
NTSB/AAR-91/01/SUM ..... p 187 N92-15055 #
NTSB/AAR-91/02 ..... p 92 N92-13039 #
NTSB/AAR-91/05 ..... p 187 N92-14006 #
NTSB/AAR-91/05 ..... p 264 N92-17213 #
NTSB/AAR-91/06 ..... p 453 N92-21873 #
NTSB/AAR-91/08 ..... p 530 N92-23596 #
NTSB/AAR-91/09 ..... p 530 N92-23597 #
NTSB/AAR-92/01/SUM ..... p 1044 N92-34081 #
NTSB/AAR-92/01 ..... p 1043 N92-32455 #
NTSB/AAR-92/02 ..... p 953 N92-31159 #

NTSC-TR-90-09 ..... p 907 N92-28253 #

ONERA-NT-1989-8 ..... p 988 N92-31942 #
ONERA-NT-1990-8 ..... p 944 N92-30514 #

ONERA-RF-31/3409-PY ..... p 81 N92-11972 #

ONERA-RS-97/5094-PY ..... p 513 N92-21736 #

ONERA-RSF-136/1865-AY-728-A p 829 N92-28789 #
ONERA-RSF-2/3731-AY-004A .... p 406 N92-19976 #
ONERA-RSF-24/1408-AY-150A .. p 1037 N92-32773 #
ONERA-RSF-43/1736-AY-146A .. p 908 N92-28788 #
ONERA-RSF-7/3617-AY-022A .... p 830 N92-29206 #
ONERA-RSF-82/1685-AY-154-4 .. p 349 N92-19682 #

ONERA-RT-43/1621-RY-006-R ... p 43 N92-11311 #
ONERA-RT-44/1621-RY-016-R ... p 1125 N92-32776 #
ONERA-RT-56/1369-AN ..... p 43 N92-11312 #
ONERA-RT-56/3064-RY-006-R ... p 13 N92-10989 #
ONERA-RT-96/5094-PY ..... p 511 N92-20388 #

ONERA-RTS-21/4365-AY-056A .. p 23 N92-11009 #
ONERA-RTS-86/1685-AY-156A .. p 43 N92-11310 #

ONERA, TP NO. 1991-110 ..... p 154 A92-16089
ONERA, TP NO. 1991-113 ..... p 134 A92-16092
ONERA, TP NO. 1991-114 ..... p 76 A92-16093
ONERA, TP NO. 1991-124 ..... p 76 A92-16102
ONERA, TP NO. 1991-131 ..... p 77 A92-16107
ONERA, TP NO. 1991-132 ..... p 161 A92-16108
ONERA, TP NO. 1991-135 ..... p 137 A92-16110
ONERA, TP NO. 1991-152 ..... p 77 A92-16122
ONERA, TP NO. 1991-157 ..... p 77 A92-16125
ONERA, TP NO. 1991-161 ..... p 137 A92-16128
ONERA, TP NO. 1991-162 ..... p 77 A92-16129
ONERA, TP NO. 1991-166 ..... p 77 A92-16133
ONERA, TP NO. 1991-170 ..... p 137 A92-16135
ONERA, TP NO. 1991-173 ..... p 92 A92-16137
ONERA, TP NO. 1991-174 ..... p 165 A92-16138
ONERA, TP NO. 1991-177 ..... p 77 A92-16139
ONERA, TP NO. 1991-178 ..... p 77 A92-16140
ONERA, TP NO. 1991-182 ..... p 388 A92-26351
ONERA, TP NO. 1991-187 ..... p 78 A92-16141
ONERA, TP NO. 1991-192 ..... p 415 A92-26353
ONERA, TP NO. 1991-197 ..... p 329 A92-26356
ONERA, TP NO. 1991-198 ..... p 329 A92-26357
ONERA, TP NO. 1991-202 ..... p 351 A92-26359
ONERA, TP NO. 1991-203 ..... p 383 A92-26360
ONERA, TP NO. 1991-204 ..... p 351 A92-26361
ONERA, TP NO. 1991-210 ..... p 415 A92-26362
ONERA, TP NO. 1991-211 ..... p 415 A92-26363
ONERA, TP NO. 1991-212 ..... p 329 A92-26364
ONERA, TP NO. 1991-216 ..... p 411 A92-26368
ONERA, TP NO. 1991-218 ..... p 330 A92-26370
ONERA, TP NO. 1991-219 ..... p 383 A92-26371
ONERA, TP NO. 1991-224 ..... p 373 A92-26376
ONERA, TP NO. 1991-229 ..... p 330 A92-26381
ONERA, TP NO. 1991-232 ..... p 415 A92-26383
ONERA, TP NO. 1991-96 ..... p 133 A92-16079
ONERA, TP NO. 1991-98 ..... p 161 A92-16080

ONERA, TP NO. 1992-1 ..... p 821 A92-48577
ONERA, TP NO. 1992-22 ..... p 822 A92-48585
ONERA, TP NO. 1992-23 ..... p 849 A92-48586
ONERA, TP NO. 1992-25 ..... p 786 A92-48587
ONERA, TP NO. 1992-27 ..... p 849 A92-48589
ONERA, TP NO. 1992-2 ..... p 893 A92-48578
ONERA, TP NO. 1992-31 ..... p 902 A92-48592
ONERA, TP NO. 1992-36 ..... p 926 A92-48597
ONERA, TP NO. 1992-39 ..... p 882 A92-48600
ONERA, TP NO. 1992-3 ..... p 249 A92-22151 #
ONERA, TP NO. 1992-40 ..... p 926 A92-48601
ONERA, TP NO. 1992-41 ..... p 926 A92-48602
ONERA, TP NO. 1992-46 ..... p 902 A92-48607
ONERA, TP NO. 1992-47 ..... p 877 A92-48608
ONERA, TP NO. 1992-49 ..... p 893 A92-48610
ONERA, TP NO. 1992-59 ..... p 926 A92-48618
ONERA, TP NO. 1992-5 ..... p 351 A92-26949 #
ONERA, TP NO. 1992-6 ..... p 262 A92-22159 #
ONERA, TP NO. 1992-7 ..... p 822 A92-48579
ONERA, TP NO. 1992-90 ..... p 391 A92-24721 *

ORNL-6694 ..... p 669 N92-25223 #

ORNL/TM-11859 ..... p 289 N92-16128 #
ORNL/TM-11991 ..... p 455 N92-21201 #

OSU-ECE-NASA-92-02 ..... p 978 N92-30922 * #

OSU-ECE-92-01 ..... p 382 N92-19841 * #

OTA-SET-507 ..... p 238 N92-14933 #

OTN-021385 ..... p 225 N92-14382 #
OTN-033124 ..... p 19 N92-10996 #

OU/AEC-EER-92-2 ..... p 840 N92-28718 * #

P/W-FR21998-2 ..... p 489 N92-21015 #

PAPER-F07 ..... p 1088 N92-33536 * #

PAPER-106 ..... p 82 N92-11984 * #
PAPER-92-2.9.1 ..... p 742 N92-27587 * #

PASC002-01-00 ..... p 1108 N92-32629 #

PATENT-1-265-541 ..... p 115 N92-13055 #
PATENT-1-271-213 ..... p 158 N92-13434 #
PATENT-1-274-606 ..... p 130 N92-13069 #

PATENTS-US-A7531492 ..... p 401 N92-18705 #
PATENTS-US-A7559030 ..... p 401 N92-18550 #

PB90-916902 ..... p 263 N92-15978 #
PB90-916903 ..... p 263 N92-15979 #
PB90-916904 ..... p 263 N92-17133 #
PB90-916905 ..... p 452 N92-21833 #
PB91-179234 ..... p 169 N92-13926 #
PB91-202051 ..... p 170 N92-13927 #
PB91-202275 ..... p 2 N92-10972 #
PB91-204768 ..... p 18 N92-10991 #
PB91-233783 ..... p 301 N92-17393 * #
PB91-238279 ..... p 297 N92-16225 #
PB91-242263 ..... p 92 N92-13040 #
PB91-242271 ..... p 308 N92-19662 #
PB91-910402 ..... p 92 N92-13039 #
PB91-910405 ..... p 187 N92-14006 #
PB91-910405 ..... p 264 N92-17213 #
PB91-910406 ..... p 453 N92-21873 #
PB91-910407 ..... p 187 N92-15055 #
PB91-910409 ..... p 530 N92-23596 #
PB91-910410 ..... p 530 N92-23597 #
PB92-104165 ..... p 386 N92-19940 #
PB92-109172 ..... p 485 N92-21870 #
PB92-110691 ..... p 417 N92-18814 #
PB92-112481 ..... p 485 N92-21777 #
PB92-112580 ..... p 484 N92-20448 #
PB92-114586 ..... p 449 N92-20318 #
PB92-114735 ..... p 455 N92-20818 #
PB92-120401 ..... p 170 N92-14966 #
PB92-121110 ..... p 356 N92-19391 #
PB92-123553 ..... p 550 N92-22785 #
PB92-123660 ..... p 488 N92-20329 #
PB92-127026 ..... p 499 N92-20265 #
PB92-127760 ..... p 237 N92-14798 #
PB92-128891 ..... p 455 N92-21279 #
PB92-128909 ..... p 455 N92-21263 #
PB92-133412 ..... p 196 N92-14044 #
PB92-133438 ..... p 196 N92-14045 #
PB92-133800 ..... p 503 N92-21828 #
PB92-134329 ..... p 602 N92-22216 #
PB92-136431 ..... p 526 N92-22233 #
PB92-136449 ..... p 448 N92-21784 #
PB92-136605 ..... p 298 N92-16325 #
PB92-136670 ..... p 298 N92-16326 #
PB92-138544 ..... p 605 N92-23588 #

PB92-138643 ..... p 196 N92-15065 #
PB92-141977 ..... p 599 N92-23441 #
PB92-142116 ..... p 597 N92-23496 #
PB92-142579 ..... p 756 N92-26521 #
PB92-147586 ..... p 640 N92-25518 #
PB92-148758 ..... p 596 N92-23251 #
PB92-149665 ..... p 765 N92-26816 #
PB92-164383 ..... p 771 N92-27715 #
PB92-178862 ..... p 445 N92-21287 #
PB92-190032 ..... p 1050 N92-33596 #
PB92-193390 ..... p 1051 N92-33809 #
PB92-197334 ..... p 1017 N92-33176 #
PB92-200963 ..... p 1043 N92-32941 #
PB92-910401 ..... p 1043 N92-32455 #
PB92-910402 ..... p 953 N92-31159 #
PB92-910404 ..... p 1044 N92-34081 #

PC-86-08 ..... p 961 N92-30878 #

PL-TR-91-2074 ..... p 42 N92-11237 #
PL-TR-91-2236 ..... p 736 N92-28004 #
PL-TR-91-2248 ..... p 729 N92-27964 #

PNL-7824 ..... p 297 N92-16281 #

PNR-90768 ..... p 476 N92-21740 #
PNR-90770 ..... p 503 N92-21741 #
PNR-90776 ..... p 506 N92-21743 #
PNR-90777 ..... p 490 N92-21744 #
PNR-90782 ..... p 505 N92-20928 #
PNR-90788 ..... p 473 N92-20436 #
PNR-90789 ..... p 559 N92-22098 #
PNR-90791 ..... p 591 N92-22099 #
PNR-90798 ..... p 501 N92-20909 #
PNR-90799 ..... p 1072 N92-33815 #
PNR-90801 ..... p 767 N92-27038 #
PNR-90802 ..... p 741 N92-27422 #
PNR-90805 ..... p 739 N92-27039 #
PNR-90806 ..... p 572 N92-22096 #
PNR-90808 ..... p 740 N92-27040 #
PNR-90809 ..... p 740 N92-27041 #
PNR-90810 ..... p 740 N92-27042 #
PNR-90811 ..... p 740 N92-27043 #
PNR-90813 ..... p 756 N92-27044 #
PNR-90814 ..... p 378 N92-19938 #
PNR-90821 ..... p 510 N92-21847 #
PNR-90824 ..... p 476 N92-21848 #
PNR-90825 ..... p 488 N92-20164 #
PNR-90832 ..... p 476 N92-21850 #
PNR-90837 ..... p 500 N92-20491 #
PNR-90839 ..... p 474 N92-20573 #
PNR-90844 ..... p 473 N92-20459 #
PNR-90845 ..... p 473 N92-20460 #
PNR-90846 ..... p 512 N92-20461 #
PNR-90847 ..... p 505 N92-20574 #
PNR-90848 ..... p 378 N92-19939 #
PNR-90860 ..... p 1111 N92-34019 #
PNR-90862 ..... p 472 N92-20179 #
PNR-90872 ..... p 1072 N92-33748 #
PNR-90873 ..... p 1072 N92-33749 #
PNR-90875 ..... p 1061 N92-33750 #
PNR-90876 ..... p 1129 N92-33751 #

PSI-2093/TR-1143 ..... p 284 N92-15998 * #

PSU-TURBO-R-9201 ..... p 909 N92-28879 #

PSU-TURBO-9201 ..... p 911 N92-29933 #

PSU/ARL-TM-91-299 ..... p 300 N92-17387 #

PW/GESP-FR2198-05 ..... p 896 N92-29408 #

PWA-FR-21509 ..... p 35 N92-11213 #

PWA-FR2198-06 ..... p 987 N92-31360 #
PWA-FR21998-08 ..... p 988 N92-32066 #
PWA-FR21998-1 ..... p 290 N92-17653 #

PWA-5967-43 ..... p 26 N92-11016 * #
PWA-5968-102 ..... p 1072 N92-33479 * #
PWA-5968-80 ..... p 973 N92-31534 * #
PWA-6141 ..... p 592 N92-22239 * #
PWA-6354 ..... p 943 N92-30298 * #

QTR-CDRL-29087 ..... p 280 N92-17552 #

QUEST-TR-534 ..... p 971 N92-30569 * #

R-638 ..... p 386 N92-19940 #

R/D-5824-AN-01 ..... p 26 N92-11015 #
R/D-5824-AN-01 ..... p 743 N92-28073 #
R/D-5824-AN-01 ..... p 1127 N92-33538 #
R/D-6105-MA-02 ..... p 53 N92-11737 #
R/D-6571-AN-01 ..... p 999 N92-30766 #
R/D-6662-AN-02 ..... p 402 N92-18933 #
R/D-6907-EE-06 ..... p 927 N92-28923 #

RAE-LIB-TRANS-2164 ..... p 257 N92-15964 #

RAE-TM-FS(F)-632-REV-ISSUE-1 p 187 N92-14007 #

RAE-TM-FS-1009 ..... p 135 N92-12004 #

RAE-TM-P-1216 ..... p 740 N92-27062 #

RAE-2029/236 ..... p 592 N92-22209 #

RAND-P-7746-RGS ..... p 731 N92-26673 #
RAND-P-7747-RGS ..... p 999 N92-30755 #

RAND-R-3971/1-PA-SUMM ..... p 636 N92-25262

RAND/P-7757 ..... p 697 N92-25204 #

RAND/R-3768-A ..... p 1017 N92-33499 #
RAND/R-4016-AF ..... p 1062 N92-34182 #

RATSCAT-TM-91-001 ..... p 41 N92-10141 #

REPT-160-573 ..... p 44 N92-11377 * #
REPT-207-90-78 ..... p 500 N92-20497 #
REPT-3.1.6 ..... p 603 N92-23881 #
REPT-3/1990 ..... p 239 N92-15938 #
REPT-4 ..... p 599 N92-23441 #
REPT-5416-B ..... p 187 N92-14006 #
REPT-61423 ..... p 352 N92-18259 #
REPT-71435-2 ..... p 42 N92-10206 #
REPT-722780-3 ..... p 499 N92-20197 * #
REPT-722792-2 ..... p 275 N92-17316 * #
REPT-90/30 ..... p 138 N92-12006 #
REPT-90/55 ..... p 157 N92-12216 #
REPT-90/59 ..... p 82 N92-11982 #
REPT-91-040 ..... p 603 N92-22673
REPT-91RC13695 ..... p 225 N92-14391 * #
REPT-91RR-12 ..... p 139 N92-13077 #
REPT-92-002 ..... p 385 N92-19218 * #

RI/RD-91-230 ..... p 225 N92-14391 * #

RIACS-TR-89-31 ..... p 140 N92-12033 * #

RL-TR-91-245 ..... p 401 N92-18897 #

RPT/F0094.93A ..... p 225 N92-14374 * #

RR-CE126 ..... p 297 N92-16225 #

RTI/3966/00-01F ..... p 277 N92-17221 #

RTOP 505-62-0K ..... p 1009 N92-30898 * #

R90-916528-80 ..... p 195 N92-14037 * #
R91-957907-3 ..... p 12 N92-10979 * #

S-2558-IS ..... p 698 N92-25606 #
S-661 ..... p 308 N92-19930 * #

SAE AIR 1168/3 ..... p 36 A92-10039
SAE AIR 1168/7 ..... p 849 A92-48022

SAE P-246 ..... p 783 A92-45376

SAE PAPER 911030 ..... p 658 A92-40943
SAE PAPER 911207 ..... p 862 A92-48021
SAE PAPER 911439 ..... p 270 A92-21836
SAE PAPER 911441 ..... p 245 A92-21837
SAE PAPER 911443 ..... p 270 A92-21839
SAE PAPER 911973 ..... p 881 A92-45380
SAE PAPER 911974 ..... p 842 A92-45381
SAE PAPER 911975 ..... p 872 A92-45382
SAE PAPER 911976 ..... p 843 A92-45383
SAE PAPER 911979 ..... p 872 A92-45384
SAE PAPER 911980 ..... p 788 A92-45385
SAE PAPER 911981 ..... p 788 A92-45386
SAE PAPER 911984 ..... p 843 A92-45387
SAE PAPER 911985 ..... p 881 A92-45388
SAE PAPER 911988 ..... p 788 A92-45390 *
SAE PAPER 911989 ..... p 788 A92-45391
SAE PAPER 911990 ..... p 788 A92-45392
SAE PAPER 911991 ..... p 788 A92-45393
SAE PAPER 911992 ..... p 788 A92-45394
SAE PAPER 911993 ..... p 789 A92-45395
SAE PAPER 911994 ..... p 843 A92-45396
SAE PAPER 911995 ..... p 843 A92-45397
SAE PAPER 911999 ..... p 789 A92-45401
SAE PAPER 912001 ..... p 897 A92-45403
SAE PAPER 912003 ..... p 789 A92-45404
SAE PAPER 912004 ..... p 789 A92-45405
SAE PAPER 912005 ..... p 843 A92-45406
SAE PAPER 912006 ..... p 783 A92-45407 *
SAE PAPER 912008 ..... p 789 A92-45408
SAE PAPER 912009 ..... p 789 A92-45409
SAE PAPER 912010 ..... p 843 A92-45410
SAE PAPER 912014 ..... p 789 A92-45412
SAE PAPER 912020 ..... p 790 A92-45413
SAE PAPER 912021 ..... p 790 A92-45414
SAE PAPER 912024 ..... p 897 A92-45416
SAE PAPER 912025 ..... p 790 A92-45417
SAE PAPER 912026 ..... p 790 A92-45418
SAE PAPER 912029 ..... p 790 A92-45419
SAE PAPER 912033 ..... p 784 A92-45421
SAE PAPER 912036 ..... p 881 A92-45422
SAE PAPER 912039 ..... p 835 A92-45424
SAE PAPER 912041 ..... p 836 A92-45425
SAE PAPER 912042 ..... p 836 A92-45426
SAE PAPER 912043 ..... p 790 A92-45427
SAE PAPER 912044 ..... p 791 A92-45428
SAE PAPER 912045 ..... p 791 A92-45429
SAE PAPER 912046 ..... p 861 A92-45430
SAE PAPER 912047 ..... p 861 A92-45431
SAE PAPER 912048 ..... p 861 A92-45432
SAE PAPER 912050 ..... p 861 A92-45434
SAE PAPER 912051 ..... p 861 A92-45435
SAE PAPER 912052 ..... p 843 A92-45436
SAE PAPER 912053 ..... p 843 A92-45437
SAE PAPER 912054 ..... p 844 A92-45438
SAE PAPER 912056 ..... p 844 A92-45439
SAE PAPER 912058 ..... p 897 A92-45440
SAE PAPER 912059 ..... p 862 A92-45441
SAE PAPER 912060 ..... p 889 A92-45442 *
SAE PAPER 912061 ..... p 791 A92-45443
SAE PAPER 912063 ..... p 791 A92-45445
SAE PAPER 912067 ..... p 855 A92-45449
SAE PAPER 912069 ..... p 872 A92-45450
SAE PAPER 912071 ..... p 891 A92-45451
SAE PAPER 912078 ..... p 917 A92-45454
SAE PAPER 912080 ..... p 844 A92-45455
SAE PAPER 912081 ..... p 917 A92-45456
SAE PAPER 912094 ..... p 654 A92-39951
SAE PAPER 912095 ..... p 651 A92-39952
SAE PAPER 912104 ..... p 673 A92-39958
SAE PAPER 912105 ..... p 674 A92-39959
SAE PAPER 912107 ..... p 691 A92-39960
SAE PAPER 912108 ..... p 691 A92-39961
SAE PAPER 912111 ..... p 651 A92-39963
SAE PAPER 912113 ..... p 617 A92-39964 *
SAE PAPER 912114 ..... p 618 A92-39965 *
SAE PAPER 912115 ..... p 643 A92-39966 *
SAE PAPER 912116 ..... p 618 A92-39967 *
SAE PAPER 912120 ..... p 608 A92-39968 *
SAE PAPER 912121 ..... p 608 A92-39969 *
SAE PAPER 912123 ..... p 635 A92-39970
SAE PAPER 912124 ..... p 635 A92-39971
SAE PAPER 912126 ..... p 618 A92-39973
SAE PAPER 912127 ..... p 618 A92-39974
SAE PAPER 912128 ..... p 618 A92-39975
SAE PAPER 912129 ..... p 618 A92-39976
SAE PAPER 912137 ..... p 635 A92-39977
SAE PAPER 912142 ..... p 651 A92-39980 *
SAE PAPER 912143 ..... p 651 A92-39981
SAE PAPER 912144 ..... p 651 A92-39982
SAE PAPER 912145 ..... p 608 A92-39983
SAE PAPER 912148 ..... p 661 A92-39984
SAE PAPER 912149 ..... p 662 A92-39985
SAE PAPER 912150 ..... p 619 A92-39986
SAE PAPER 912152 ..... p 674 A92-39987
SAE PAPER 912153 ..... p 619 A92-39988
SAE PAPER 912154 ..... p 644 A92-39989
SAE PAPER 912155 ..... p 644 A92-39990
SAE PAPER 912156 ..... p 664 A92-39991 *
SAE PAPER 912157 ..... p 644 A92-39992 *
SAE PAPER 912160 ..... p 655 A92-39993
SAE PAPER 912167 ..... p 655 A92-39995
SAE PAPER 912173 ..... p 655 A92-39998
SAE PAPER 912174 ..... p 644 A92-39999
SAE PAPER 912175 ..... p 644 A92-40000
SAE PAPER 912176 ..... p 655 A92-40001
SAE PAPER 912177 ..... p 655 A92-40002
SAE PAPER 912183 ..... p 655 A92-40003
SAE PAPER 912184 ..... p 644 A92-40004
SAE PAPER 912185 ..... p 655 A92-40005
SAE PAPER 912186 ..... p 656 A92-40006
SAE PAPER 912188 ..... p 656 A92-40007
SAE PAPER 912189 ..... p 656 A92-40008
SAE PAPER 912192 ..... p 644 A92-40009
SAE PAPER 912193 ..... p 644 A92-40010
SAE PAPER 912195 ..... p 674 A92-40012
SAE PAPER 912200 ..... p 656 A92-40013
SAE PAPER 912204 ..... p 651 A92-40014
SAE PAPER 912208 ..... p 651 A92-40015
SAE PAPER 912212 ..... p 635 A92-40016
SAE PAPER 912214 ..... p 652 A92-40017
SAE PAPER 912216 ..... p 674 A92-40018
SAE PAPER 912218 ..... p 674 A92-40020
SAE PAPER 912222 ..... p 635 A92-40021
SAE PAPER 912224 ..... p 636 A92-40022

SAE PAPER 912225 ..... p 636 A92-40023
SAE PAPER 912229 ..... p 674 A92-40024 *
SAE PAPER 912235 ..... p 638 A92-40027

SAE SP-871 ..... p 862 A92-48021

SAE-871783 ..... p 562 N92-22863 * #
SAE-901033 ..... p 445 N92-20934 * #

SAND-91-0028C ..... p 689 N92-25049 #
SAND-91-1124 ..... p 229 N92-15392 #
SAND-91-1429C ..... p 765 N92-26698 #
SAND-91-1624 ..... p 999 N92-30893 #
SAND-91-1839C ..... p 667 N92-25315 #
SAND-91-1894C ..... p 35 N92-11203 #
SAND-91-2309C ..... p 241 N92-15962 #
SAND-91-2376C ..... p 385 N92-18290 #
SAND-91-2386C ..... p 505 N92-21040 #
SAND-91-2422C ..... p 489 N92-20858 #
SAND-91-2444C ..... p 488 N92-20132 #
SAND-91-2584C ..... p 640 N92-25470 #
SAND-91-2650 ..... p 1000 N92-30903 #
SAND-91-2760 ..... p 1003 N92-31933 #
SAND-91-2851C ..... p 386 N92-19978 #
SAND-91-2865C ..... p 765 N92-26853 #
SAND-91-2936C ..... p 498 N92-20143 #
SAND-92-0457 ..... p 957 N92-31746 #
SAND-92-0919C ..... p 943 N92-30367 #

SBI-AD-E200944 ..... p 729 N92-27964 #

SCT-90RR-30 ..... p 116 N92-13059 #
SCT-90RR-33 ..... p 641 N92-26101 #
SCT-90RR-34 ..... p 103 N92-13049 #
SCT-90RR-44 ..... p 191 N92-15061 #
SCT-91RR-13 ..... p 637 N92-26028 #
SCT-91RR-18 ..... p 18 N92-10993 #
SCT-91RR-26 ..... p 190 N92-14033 #
SCT-91RR-27 ..... p 116 N92-13060 #
SCT-91RR-28 ..... p 116 N92-13058 #
SCT-91RR-31 ..... p 724 N92-28052 #

SEL-91-003 ..... p 412 N92-18125 * #

SER-A-91-A12 ..... p 602 N92-22216 #

SER-B-90-B27 ..... p 448 N92-21784 #
SER-B-91-B33 ..... p 526 N92-22233 #

SESSIA-430/91.960 ..... p 947 N92-31508 #

SIMTEC/TR-91-01 ..... p 386 N92-19642 #

SLCET-TR-91-26 ..... p 300 N92-17258 #

SME PAPER MR91-177 ..... p 897 A92-45260

SPIE-1367 ..... p 901 A92-48026 *
SPIE-1369 ..... p 779 A92-42601
SPIE-1395 ..... p 994 A92-51626

SQMT-91-101R ..... p 406 N92-19873 #

SR-1 ..... p 42 N92-11237 #
SR-3 ..... p 736 N92-28004 #

SRL-0058-TM ..... p 727 N92-26948 #

SR90-R-5253-76 ..... p 229 N92-15385 #

STI-TR-2361-2 ..... p 663 N92-25982 * #

SWRI-03-3685 ..... p 987 N92-30767 #

TABES PAPER 91-278 ..... p 519 A92-34683 *
TABES PAPER 91-315 ..... p 565 A92-34688
TABES PAPER 91-503 ..... p 606 A92-34692

TAMRF-5802-92-01 ..... p 348 N92-19545 * #
TAMRF-5802-92-02 ..... p 832 N92-29657 * #

TCRL-36 ..... p 742 N92-27519 * #

TELAC-91-17 ..... p 731 N92-26655 * #

TKK-KO/LTK-49 ..... p 298 N92-16325 #
TKK-KO/LTK-62 ..... p 298 N92-16326 #

TP-499 ..... p 236 N92-14788 * #
TP-9983 ..... p 189 N92-14009

TR-R90222 ..... p 287 N92-17325 #

TR-723224-3 ..... p 404 N92-19217 * #
TR-91-7 ..... p 1051 N92-34203 * #

TRB/TRR-1298 ..... p 308 N92-19662 #

TRC-EM-CAB-9203 ..... p 1001 N92-31156 * #

TSPC-TR-92-10 ..... p 974 N92-32059 #

TT-9101 ..... p 18 N92-10018 #
TT-9107 ..... p 61 N92-12988 #

UCB/CSD-91/652 ..... p 386 N92-19675 * #

UCRL-ID-109860 ..... p 1004 N92-32147 * #
UCRL-ID-110003 ..... p 636 N92-24713 #

UCRL-JC-107999 ..... p 669 N92-25259 #

UDR-TR-90-108 ..... p 187 N92-15053 #
UDR-TR-90-114 ..... p 264 N92-17478 #
UDR-TR-91-125 ..... p 1045 N92-34151 #
UDR-TR-91-53 ..... p 895 N92-28398 #

UM-AERO-91-42 ..... p 525 N92-22215 * #
UM-AERO-91-44 ..... p 625 N92-24680 * #
UM-AERO-92-08 ..... p 944 N92-30392 * #

UMICH-025921-32-T ..... p 1126 N92-33307 * #

US-PATENT-APPL-SN-032815 ..... p 296 N92-16174
US-PATENT-APPL-SN-279170 ..... p 297 N92-16243 *
US-PATENT-APPL-SN-318988 ..... p 770 N92-27615
US-PATENT-APPL-SN-359462 ..... p 400 N92-18120
US-PATENT-APPL-SN-429516 ..... p 463 N92-21587 *
US-PATENT-APPL-SN-453658 ..... p 732 N92-27185 #
US-PATENT-APPL-SN-487489 ..... p 400 N92-18187 #
US-PATENT-APPL-SN-517011 ..... p 344 N92-18193
US-PATENT-APPL-SN-518619 ..... p 90 N92-13036
US-PATENT-APPL-SN-531492 ..... p 401 N92-18705 #
US-PATENT-APPL-SN-545236 ..... p 228 N92-15203 *
US-PATENT-APPL-SN-559030 ..... p 401 N92-18550 #
US-PATENT-APPL-SN-560923 ..... p 829 N92-28729 *
US-PATENT-APPL-SN-584018 ..... p 42 N92-10185 *
US-PATENT-APPL-SN-605902 ..... p 732 N92-27188
US-PATENT-APPL-SN-618790 ..... p 916 N92-29148 *
US-PATENT-APPL-SN-621144 ..... p 447 N92-21588 *
US-PATENT-APPL-SN-650336 ..... p 35 N92-10066 * #
US-PATENT-APPL-SN-691609 ..... p 909 N92-29099 *
US-PATENT-APPL-SN-708991 ..... p 268 N92-17707 #
US-PATENT-APPL-SN-718313 ..... p 1042 N92-34172 *
US-PATENT-APPL-SN-724079 ..... p 279 N92-15992 #
US-PATENT-APPL-SN-743238 ..... p 11 N92-10008 * #
US-PATENT-APPL-SN-760635 ..... p 927 N92-29095 #
US-PATENT-APPL-SN-769685 ..... p 455 N92-20834 #
US-PATENT-APPL-SN-781520 ..... p 300 N92-17674 * #
US-PATENT-APPL-SN-785637 ..... p 912 N92-30082 * #
US-PATENT-APPL-SN-788908 ..... p 879 N92-30025 * #
US-PATENT-APPL-SN-790607 ..... p 1088 N92-34131 #
US-PATENT-APPL-SN-800785 ..... p 983 N92-31192 #
US-PATENT-APPL-SN-820431 ..... p 911 N92-29954 * #
US-PATENT-APPL-SN-820432 ..... p 910 N92-29830 * #
US-PATENT-APPL-SN-823805 ..... p 998 N92-30390 * #
US-PATENT-APPL-SN-824858 ..... p 579 N92-24053 * #
US-PATENT-APPL-SN-866769 ..... p 911 N92-30028 * #
US-PATENT-APPL-SN-881912 ..... p 912 N92-30099 * #
US-PATENT-APPL-SN-914905 ..... p 1102 N92-34213 * #
US-PATENT-APPL-SN-943659 ..... p 1043 N92-34243 * #

US-PATENT-CLASS-116-201 ..... p 447 N92-21588 *
US-PATENT-CLASS-116-207 ..... p 447 N92-21588 *
US-PATENT-CLASS-244-117 ..... p 344 N92-18193
US-PATENT-CLASS-244-12.1 ..... p 732 N92-27185 #
US-PATENT-CLASS-244-145 ..... p 90 N92-13036
US-PATENT-CLASS-244-198 ..... p 463 N92-21587 *
US-PATENT-CLASS-244-200 ..... p 463 N92-21587 *
US-PATENT-CLASS-244-212 ..... p 463 N92-21587 *
US-PATENT-CLASS-244-215 ..... p 463 N92-21587 *
US-PATENT-CLASS-244-35R ..... p 829 N92-28729 *
US-PATENT-CLASS-244-36 ..... p 829 N92-28729 *
US-PATENT-CLASS-310-90.5 ..... p 909 N92-29099 *
US-PATENT-CLASS-324-334 ..... p 296 N92-16174
US-PATENT-CLASS-356-28 ..... p 1042 N92-34172 *
US-PATENT-CLASS-356-318 ..... p 1042 N92-34172 *
US-PATENT-CLASS-359-154 ..... p 770 N92-27615
US-PATENT-CLASS-364-443 ..... p 916 N92-29148 *
US-PATENT-CLASS-374-112 ..... p 916 N92-29148 *
US-PATENT-CLASS-422-176 ..... p 297 N92-16243 *
US-PATENT-CLASS-422-83 ..... p 297 N92-16243 *
US-PATENT-CLASS-422-93 ..... p 297 N92-16243 *
US-PATENT-CLASS-505-876 ..... p 909 N92-29099 *
US-PATENT-CLASS-62-461 ..... p 228 N92-15203 *
US-PATENT-CLASS-624-3.2 ..... p 228 N92-15203 *
US-PATENT-CLASS-624-467 ..... p 228 N92-15203 *
US-PATENT-CLASS-624-500 ..... p 228 N92-15203 *
US-PATENT-CLASS-624-51.2 ..... p 228 N92-15203 *
US-PATENT-CLASS-73-147 ..... p 42 N92-10185 *
US-PATENT-CLASS-73-147 ..... p 447 N92-21588 *
US-PATENT-CLASS-73-178R ..... p 916 N92-29148 *
US-PATENT-CLASS-73-861.05 ..... p 1042 N92-34172 *
US-PATENT-CLASS-73-862.04 ..... p 42 N92-10185 *
US-PATENT-CLASS-73-862.65 ..... p 42 N92-10185 *
US-PATENT-CLASS-89-1.51 ..... p 732 N92-27188

US-PATENT-5,014,932 ..... p 344 N92-18193
US-PATENT-5,018,952 ..... p 400 N92-18120
US-PATENT-5,025,218 ..... p 296 N92-16174
US-PATENT-5,037,042 ..... p 90 N92-13036
US-PATENT-5,056,361 ..... p 42 N92-10185 *
US-PATENT-5,062,154 ..... p 770 N92-27615
US-PATENT-5,063,747 ..... p 228 N92-15203 *
US-PATENT-5,070,729 ..... p 447 N92-21588 *
US-PATENT-5,070,760 ..... p 732 N92-27188
US-PATENT-5,071,088 ..... p 732 N92-27185 #
US-PATENT-5,077,015 ..... p 297 N92-16243 *
US-PATENT-5,088,665 ..... p 463 N92-21587 *
US-PATENT-5,112,120 ..... p 829 N92-28729 *
US-PATENT-5,117,139 ..... p 909 N92-29099 *
US-PATENT-5,117,689 ..... p 916 N92-29148 *
US-PATENT-5,153,665 ..... p 1042 N92-34172 *

USAAVSCOM-TR-91-A-005 ..... p 482 N92-21440 * #
USAAVSCOM-TR-92-B-010 ..... p 1001 N92-31155 * #
USAAVSCOM-TR-92-C-010 ..... p 1073 N92-34236 * #
USAAVSCOM-TR-92-D-2 ..... p 961 N92-30878 #

USAEPG-FR-1420-PHASE-2 ..... p 999 N92-30583 #

USAFETAC/PR-91/011 ..... p 23 N92-11011 #

USCAE-151 ..... p 1039 N92-33413 * #

USCGA-TR-1-92 ..... p 1051 N92-33809 #
USCGA-TR-2-91 ..... p 455 N92-21263 #
USCGA-TR-6-91 ..... p 455 N92-21279 #

UTIAS-TN-271 ..... p 1071 N92-33102 #

UTIAS-338 ..... p 129 N92-11996 #
UTIAS-339 ..... p 161 N92-12373 #

UTRC-R91-970089-01 ..... p 283 N92-17243 #

UTRC/R91-970057-3 ..... p 42 N92-11297 * #

UVA/528260/CHE92/106 ..... p 502 N92-21433 * #
UVA/528260/CHE92/107 ..... p 502 N92-21385 * #

UWA/DME/TR-92/68 ..... p 854 N92-29511 #

UWAERP-35 ..... p 1136 N92-32595 #

VKI-LS-1991-06 ..... p 658 N92-24336 #
VKI-LS-1992-01-VOL-2 ..... p 1088 N92-34161 #

VPI-AERO-176-REV ..... p 358 N92-18024 * #
VPI-AERO-182-REV ..... p 359 N92-18038 * #
VPI-AERO-182 ..... p 950 N92-32114 * #

VPI-AOE-179 ..... p 260 N92-17222 #
VPI-AOE-188 ..... p 946 N92-31122 #

WES/MP/GL-92-10 ..... p 953 N92-31193 #

WES/TR/D-92-2 ..... p 729 N92-28079 #

WES/TR/EL-92-13 ..... p 926 N92-28302 #

WL-TM-02-307-FIBE ..... p 887 N92-28772 #
WL-TM-91-307-FIBG ..... p 746 N92-27577 #
WL-TM-91-311-FIBG ..... p 44 N92-11383 #
WL-TM-91-326 ..... p 139 N92-13078 #
WL-TM-91-601 ..... p 119 N92-13067 #
WL-TM-92-313-FIBE ..... p 963 N92-31793 #
WL-TM-92-323 ..... p 1036 N92-32651 #

WL-TR-91-1042 ..... p 277 N92-17221 #
WL-TR-91-1063 ..... p 781 N92-26863 #
WL-TR-91-2036 ..... p 35 N92-11213 #
WL-TR-91-2051 ..... p 202 N92-14059 #
WL-TR-91-2071 ..... p 279 N92-17204 #
WL-TR-91-2099 ..... p 988 N92-31462 #
WL-TR-91-2103 ..... p 868 N92-28294 #
WL-TR-91-2108 ..... p 279 N92-17011 #
WL-TR-91-2111 ..... p 895 N92-28398 #
WL-TR-91-2117-VOL-2 ..... p 987 N92-31399 #
WL-TR-91-3006 ..... p 264 N92-17478 #
WL-TR-91-3014 ..... p 724 N92-27682 #
WL-TR-91-3055 ..... p 160 N92-13470 #
WL-TR-91-3064 ..... p 978 N92-30323 #
WL-TR-91-3065 ..... p 13 N92-10985 #
WL-TR-91-3067 ..... p 197 N92-15069 #
WL-TR-91-3072 ..... p 949 N92-31777 #
WL-TR-91-3073 ..... p 13 N92-10986 #
WL-TR-91-3078-VOL-3 ..... p 225 N92-14386 #

WL-TR-91-3086 ..... p 116 N92-13063 #
WL-TR-91-3089 ..... p 1124 N92-32632 #
WL-TR-91-3098 ..... p 346 N92-18825 #
WL-TR-91-3104 ..... p 275 N92-17513 #
WL-TR-91-3107-VOL-1 ..... p 932 N92-30253 #
WL-TR-91-3107-VOL-2 ..... p 932 N92-30258 #
WL-TR-91-3120 ..... p 947 N92-31171 #
WL-TR-91-4017 ..... p 756 N92-27531 #
WL-TR-91-4066-VOL-1 ..... p 22 N92-11006 #
WL-TR-91-4066-VOL-2 ..... p 23 N92-11007 #
WL-TR-91-4111 ..... p 490 N92-21159 #
WL-TR-91-4135 ..... p 503 N92-21730 #
WL-TR-92-1022 ..... p 967 N92-30524 #
WL-TR-92-2015 ..... p 987 N92-30767 #
WL-TR-92-8017 ..... p 1108 N92-32629 #

WRDC-TR-89-2026-VOL-2 ..... p 35 N92-10100 #
WRDC-TR-90-2122-PHASE-1 ..... p 41 N92-10157 #
WRDC-TR-90-3052-VOL-1 ..... p 54 N92-10598 * #
WRDC-TR-90-3052-VOL-2 ..... p 235 N92-14779 * #

WYLE-TN-91-8 ..... p 927 N92-28556 * #

WYLE-WR-91-20 ..... p 697 N92-26130 * #

Typical Accession Number Index Listing

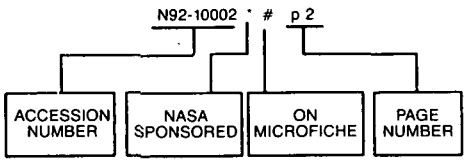

Listings in this index are arranged alphanumerically by accession number. The page number listed to the right indicates the page on which the citation is located. An asterisk (*) indicates that the item is a NASA report. A pound sign (#) indicates that the item is available on microfiche.

A92-10039 p 36
A92-10102 p 36
A92-10143 p 36
A92-10197 p 1
A92-10213 p 33
A92-10232 p 33
A92-10238 p 34
A92-10257 p 14
A92-10259 p 36
A92-10271 p 34
A92-10275 p 20
A92-10285 p 36
A92-10314 p 36
A92-10375 p 37
A92-10426 p 2
A92-10427 * p 3
A92-10435 * p 37
A92-10445 * p 37
A92-10472 p 19
A92-10474 p 19
A92-10475 p 19
A92-10487 p 3
A92-10489 p 45
A92-10574 p 3
A92-10575 p 3
A92-10600 p 24
A92-10654 p 37
A92-10657 p 37
A92-10660 p 37
A92-10662 p 3
A92-10663 p 3
A92-10666 p 20
A92-10672 p 37
A92-10673 p 37
A92-10688 * p 3
A92-10690 p 3
A92-10691 p 4
A92-10692 * p 4
A92-10825 p 4
A92-10850 p 38
A92-10901 p 4
A92-10907 p 4
A92-10955 p 24
A92-10956 p 24
A92-10957 p 24
A92-10958 p 4
A92-10959 p 4
A92-10961 p 24
A92-10962 p 24
A92-10963 p 38
A92-10964 p 38
A92-10965 p 38
A92-10967 p 38
A92-10968 p 25
A92-10969 p 25
A92-10970 p 38
A92-10975 p 5
A92-11001 p 1
A92-11012 * # p 20
A92-11013 * # p 5
A92-11014 # p 14
A92-11015 * # p 20
A92-11016 # p 14
A92-11017 # p 1
A92-11018 * # p 14
A92-11019 * # p 14
A92-11020 # p 15
A92-11021 # p 1
A92-11022 # p 1
A92-11023 # p 15
A92-11024 * # p 15
A92-11025 # p 15
A92-11026 # p 15
A92-11027 # p 15
A92-11030 # p 15
A92-11031 # p 15
A92-11032 # p 16
A92-11033 # p 16
A92-11034 # p 16
A92-11036 # p 1
A92-11041 p 38
A92-11051 p 5
A92-11052 p 53
A92-11053 * p 53
A92-11057 * p 5
A92-11058 * p 5
A92-11059 p 5
A92-11061 p 5
A92-11062 p 5
A92-11063 p 5
A92-11066 p 5
A92-11067 p 5
A92-11068 p 30
A92-11080 p 6
A92-11081 p 20
A92-11122 p 26
A92-11123 p 20
A92-11153 p 47
A92-11164 p 46
A92-11170 p 16
A92-11171 * p 16
A92-11172 * p 16
A92-11178 p 16
A92-11180 p 47
A92-11181 p 2
A92-11191 p 46
A92-11204 p 46
A92-11214 p 56
A92-11215 p 56
A92-11219 p 38
A92-11281 p 54
A92-11282 p 25
A92-11286 p 6
A92-11287 p 6
A92-11288 * p 38
A92-11312 p 47
A92-11328 p 6
A92-11329 p 26
A92-11344 p 39
A92-11345 p 32
A92-11346 p 47
A92-11347 p 47
A92-11351 p 47
A92-11356 p 48
A92-11361 p 27
A92-11362 p 48
A92-11363 p 48
A92-11374 p 27
A92-11375 * p 48
A92-11376 * p 48
A92-11377 p 48
A92-11378 p 45
A92-11379 * p 17
A92-11380 * p 17
A92-11381 * p 48
A92-11382 * p 17
A92-11383 * p 27
A92-11384 p 27
A92-11385 * p 27
A92-11386 p 27
A92-11391 p 49
A92-11395 * p 49
A92-11417 p 49
A92-11418 p 49
A92-11420 p 49
A92-11426 p 49
A92-11427 p 50
A92-11429 p 50
A92-11430 p 50
A92-11431 p 50
A92-11442 * p 50
A92-11444 p 50
A92-11445 p 51
A92-11453 p 51
A92-11454 p 51
A92-11455 p 51
A92-11456 * p 51
A92-11464 * p 51
A92-11465 p 52
A92-11466 p 52
A92-11467 p 52
A92-11472 p 52
A92-11473 p 46
A92-11499 p 27
A92-11500 p 28
A92-11501 p 28
A92-11502 p 28
A92-11553 p 52
A92-11561 p 28
A92-11562 p 28
A92-11563 p 28
A92-11564 p 28
A92-11582 p 29
A92-11583 * p 52
A92-11585 p 29
A92-11587 p 52
A92-11595 p 29
A92-11605 * # p 6
A92-11607 # p 21
A92-11761 p 39
A92-11791 p 39
A92-11812 p 34
A92-11816 p 39
A92-11830 p 39
A92-11876 p 19
A92-11877 p 19
A92-11882 p 21
A92-11993 p 34
A92-12115 p 39
A92-12134 p 6
A92-12146 p 34
A92-12164 p 6
A92-12165 p 7
A92-12169 p 7
A92-12170 p 7
A92-12173 p 7
A92-12178 p 7
A92-12179 p 7
A92-12194 p 30
A92-12203 p 7
A92-12204 p 8
A92-12209 p 34
A92-12290 p 39
A92-12291 p 40
A92-12293 p 40
A92-12299 p 40
A92-12345 p 54
A92-12346 p 40
A92-12347 p 30
A92-12354 p 40
A92-12367 * p 53
A92-12399 p 8
A92-12422 p 40
A92-12423 p 8
A92-12424 p 8
A92-12570 p 32
A92-12599 p 32
A92-12600 p 25
A92-12601 p 25
A92-12625 p 40
A92-12649 p 8
A92-12700 # p 56
A92-12741 * # p 8
A92-12742 * # p 32
A92-12749 # p 17
A92-12750 p 21
A92-12803 p 41
A92-12808 p 9
A92-12828 p 41
A92-12844 p 45
A92-12941 p 45
A92-13025 p 17
A92-13198 p 9
A92-13199 p 29
A92-13200 p 9
A92-13201 * p 30
A92-13202 * p 9
A92-13203 * p 9
A92-13204 * p 41
A92-13205 * p 9
A92-13206 p 9
A92-13207 * p 9
A92-13208 * p 21
A92-13209 p 9
A92-13210 * p 9
A92-13211 * p 10
A92-13212 * p 10
A92-13213 p 10
A92-13214 * p 30
A92-13215 * p 10
A92-13216 p 10
A92-13217 p 10
A92-13218 p 10
A92-13219 p 25
A92-13220 p 2
A92-13227 p 33
A92-13233 p 10
A92-13234 p 10
A92-13235 p 10
A92-13243 p 34
A92-13246 p 21
A92-13247 p 33
A92-13291 p 103
A92-13296 p 119
A92-13299 p 143
A92-13300 p 62
A92-13432 * p 144
A92-13436 p 161
A92-13444 p 140
A92-13448 p 62
A92-13463 p 103
A92-13465 p 104
A92-13554 p 144
A92-13563 p 144
A92-13584 p 144
A92-13589 p 144
A92-13594 p 144
A92-13601 p 140
A92-13641 p 144
A92-13657 p 145
A92-13673 p 62
A92-13675 p 135
A92-13690 p 62
A92-13693 p 131
A92-13696 p 131
A92-13699 p 117
A92-13700 p 91
A92-13741 p 63
A92-13748 p 63
A92-13749 p 63
A92-13809 p 160
A92-13815 p 63
A92-13816 p 63
A92-13845 p 136
A92-13851 p 93
A92-13852 p 94
A92-13854 p 94
A92-13855 p 160
A92-14027 p 131
A92-14031 p 63
A92-14033 p 64
A92-14045 p 94
A92-14048 p 91
A92-14071 p 64
A92-14252 p 145
A92-14265 p 160
A92-14280 p 64
A92-14281 p 64
A92-14326 p 59
A92-14327 p 104
A92-14328 * p 64
A92-14329 p 64
A92-14330 * p 64
A92-14331 p 104
A92-14332 * p 104
A92-14333 p 104
A92-14334 p 131
A92-14335 p 131
A92-14336 p 131
A92-14337 * p 132
A92-14338 * p 132
A92-14339 p 104
A92-14340 p 132
A92-14341 p 59
A92-14342 p 145
A92-14343 p 104
A92-14344 p 145
A92-14345 p 105
A92-14346 p 140
A92-14347 p 59
A92-14349 p 59
A92-14350 p 117
A92-14351 p 161
A92-14353 p 105
A92-14354 p 59
A92-14356 p 145
A92-14358 p 65
A92-14359 p 65
A92-14360 p 65
A92-14361 * p 105
A92-14362 * p 65
A92-14363 p 105
A92-14364 p 105
A92-14365 p 136
A92-14367 p 162
A92-14368 * p 162
A92-14369 p 105
A92-14370 p 105
A92-14372 p 106
A92-14374 p 141
A92-14376 p 106
A92-14377 * p 136
A92-14378 p 117
A92-14379 p 106
A92-14380 p 132
A92-14381 p 145
A92-14384 * p 165
A92-14385 * p 165
A92-14386 p 165

A92-14387 * p 162
A92-14388 p 91
A92-14389 p 106
A92-14390 * p 106
A92-14391 * p 107
A92-14392 p 107
A92-14393 p 162
A92-14394 p 107
A92-14395 p 107
A92-14396 * p 107
A92-14397 p 107
A92-14398 p 108
A92-14399 p 108
A92-14400 p 132
A92-14402 p 117
A92-14403 p 94
A92-14404 p 94
A92-14405 p 132
A92-14406 * p 108
A92-14407 * p 65
A92-14408 p 120
A92-14409 p 120
A92-14410 p 108
A92-14411 p 59
A92-14412 p 108
A92-14413 p 60
A92-14414 p 60
A92-14415 * p 108
A92-14416 p 108
A92-14417 p 109
A92-14418 p 109
A92-14419 * p 109
A92-14420 p 109
A92-14421 p 132
A92-14422 p 133
A92-14423 p 133
A92-14424 p 65
A92-14425 p 109
A92-14426 p 109
A92-14427 * p 133
A92-14428 p 65
A92-14429 p 94
A92-14435 p 60
A92-14436 p 110
A92-14437 p 60
A92-14438 p 60
A92-14441 p 145
A92-14442 p 60
A92-14443 p 110
A92-14444 * p 94
A92-14445 * p 133
A92-14446 p 66
A92-14447 p 60
A92-14448 p 110
A92-14449 p 146
A92-14450 p 146
A92-14452 * p 110
A92-14453 p 110
A92-14454 p 91
A92-14455 p 110
A92-14456 p 110
A92-14556 p 146
A92-14680 p 141
A92-14684 p 146
A92-14688 p 91
A92-14689 p 146
A92-14709 p 120
A92-14710 p 120
A92-14711 p 120
A92-14868 p 120
A92-14925 p 161
A92-15021 p 136
A92-15022 p 61
A92-15031 p 66
A92-15070 p 141
A92-15128 * p 141
A92-15169 p 141
A92-15175 p 92
A92-15202 p 141
A92-15206 p 141
A92-15222 p 146
A92-15244 p 142
A92-15245 p 142
A92-15309 p 142
A92-15326 p 110
A92-15327 p 66
A92-15328 p 136
A92-15332 p 162
A92-15334 p 110
A92-15335 p 66
A92-15338 p 136
A92-15340 p 133
A92-15341 p 111
A92-15342 p 111
A92-15343 p 146
A92-15344 * p 66
A92-15345 p 66
A92-15356 p 66
A92-15358 p 146
A92-15359 p 67
A92-15487 p 67
A92-15501 p 147
A92-15502 p 120
A92-15503 p 67
A92-15505 p 67
A92-15509 p 67
A92-15510 * p 147
A92-15513 p 162
A92-15514 p 67
A92-15515 p 68
A92-15516 p 147
A92-15517 p 147
A92-15518 p 147
A92-15519 p 121
A92-15520 p 121
A92-15523 * p 147
A92-15524 p 121
A92-15528 p 148
A92-15530 p 121
A92-15532 p 121
A92-15533 p 68
A92-15534 p 68
A92-15535 p 68
A92-15536 p 68
A92-15538 p 121
A92-15539 * p 68
A92-15540 p 148
A92-15542 p 142
A92-15543 p 122
A92-15545 p 69
A92-15546 p 122
A92-15547 p 69
A92-15548 p 69
A92-15549 p 69
A92-15550 * p 69
A92-15551 p 69
A92-15552 p 122
A92-15553 p 122
A92-15554 p 70
A92-15555 p 70
A92-15556 p 70
A92-15557 p 70
A92-15560 p 122
A92-15561 p 122
A92-15565 p 70
A92-15566 * p 123
A92-15567 * p 142
A92-15568 p 70
A92-15569 p 71
A92-15571 p 71
A92-15572 p 71
A92-15573 p 71
A92-15574 * p 71
A92-15575 p 71
A92-15576 * p 72
A92-15577 p 72
A92-15580 * p 72
A92-15583 p 72
A92-15584 p 72
A92-15586 p 73
A92-15587 p 148
A92-15588 p 148
A92-15590 * p 142
A92-15591 * p 123
A92-15592 p 142
A92-15593 * p 148
A92-15594 p 148
A92-15598 p 123
A92-15599 p 123
A92-15600 p 123
A92-15601 p 136
A92-15602 p 111
A92-15603 p 73
A92-15605 p 123
A92-15606 p 73
A92-15608 p 73
A92-15610 p 73
A92-15612 p 123
A92-15613 p 73
A92-15614 p 148
A92-15615 p 73
A92-15616 * p 74
A92-15617 p 149
A92-15618 p 124
A92-15619 p 124
A92-15620 p 124
A92-15623 * p 74
A92-15624 p 149
A92-15626 p 124
A92-15632 p 143
A92-15633 p 124
A92-15634 * p 124
A92-15636 p 124
A92-15637 p 74
A92-15638 * p 74
A92-15639 * p 74
A92-15641 p 149
A92-15643 p 125
A92-15645 * p 125
A92-15646 * p 75
A92-15647 p 149
A92-15648 p 149
A92-15649 p 150
A92-15653 p 150
A92-15654 p 150
A92-15655 p 150
A92-15657 p 150
A92-15658 p 150
A92-15660 p 151
A92-15661 p 151
A92-15662 p 75
A92-15663 * p 151
A92-15666 p 151
A92-15667 p 151
A92-15668 p 151
A92-15669 * p 75
A92-15670 * p 75
A92-15671 p 75
A92-15672 p 151
A92-15673 p 152
A92-15674 p 125
A92-15675 p 152
A92-15676 p 152
A92-15677 p 152
A92-15678 p 125
A92-15679 p 125
A92-15681 * p 152
A92-15682 p 152
A92-15687 p 126
A92-15688 p 153
A92-15689 p 75
A92-15690 * p 76
A92-15691 p 126
A92-15697 p 153
A92-15698 p 153
A92-15699 p 126
A92-15700 p 126
A92-15701 * p 163
A92-15702 p 143
A92-15703 p 76
A92-15705 p 111
A92-15706 p 137
A92-15710 * p 153
A92-15713 p 137
A92-15716 p 153
A92-15718 p 76
A92-15719 p 126
A92-15720 p 126
A92-15721 p 126
A92-15722 p 153
A92-15723 p 127
A92-15725 p 127
A92-15726 p 111
A92-15727 p 127
A92-15728 p 127
A92-15729 p 127
A92-15730 p 76
A92-15731 p 137
A92-15732 p 127
A92-15733 p 76
A92-15737 p 137
A92-15738 p 128
A92-15823 * p 153
A92-15884 p 161
A92-15972 * p 154
A92-16026 p 154
A92-16050 p 92
A92-16051 p 111
A92-16052 * p 111
A92-16053 p 112
A92-16054 p 112
A92-16055 p 112
A92-16056 p 112
A92-16057 p 118
A92-16058 p 112
A92-16059 * p 61
A92-16060 p 112
A92-16061 p 112
A92-16062 p 167
A92-16063 p 112
A92-16064 p 113
A92-16072 p 163
A92-16079 p 133
A92-16080 p 161
A92-16089 p 154
A92-16092 p 134
A92-16093 p 76
A92-16102 p 76
A92-16107 p 77
A92-16108 p 161
A92-16110 p 137
A92-16122 p 77
A92-16125 p 77
A92-16128 p 137
A92-16129 p 77
A92-16133 p 77
A92-16134 p 167
A92-16135 p 137
A92-16137 p 92
A92-16138 p 165
A92-16139 p 77
A92-16140 p 77
A92-16141 p 78
A92-16148 p 118
A92-16150 p 61
A92-16228 p 95
A92-16231 p 138
A92-16252 p 95
A92-16257 p 95
A92-16457 * p 78
A92-16462 * p 78
A92-16583 p 143
A92-16584 p 128
A92-16585 p 128
A92-16615 p 154
A92-16621 p 134
A92-16622 p 113
A92-16623 p 134
A92-16626 p 95
A92-16627 p 95
A92-16629 p 95
A92-16630 p 95
A92-16631 p 96
A92-16632 p 96
A92-16633 p 96
A92-16635 p 96
A92-16637 p 96
A92-16638 p 96
A92-16639 p 96
A92-16641 p 96
A92-16643 * p 96
A92-16644 p 97
A92-16646 p 97
A92-16647 p 97
A92-16648 p 139
A92-16649 p 97
A92-16650 * p 97
A92-16651 p 97
A92-16652 p 97
A92-16653 p 138
A92-16654 p 98
A92-16655 p 98
A92-16656 p 98
A92-16657 p 98
A92-16658 p 98
A92-16659 p 98
A92-16660 p 98
A92-16666 p 128
A92-16668 p 78
A92-16675 p 61
A92-16676 p 113
A92-16679 p 78
A92-16680 p 78
A92-16681 p 79
A92-16682 p 79
A92-16684 p 79
A92-16705 p 79
A92-16801 p 134
A92-16802 p 113
A92-16803 p 134
A92-16807 p 134
A92-16808 p 134
A92-16809 p 113
A92-16811 p 154
A92-16812 p 79
A92-16813 p 79
A92-16814 p 79
A92-16815 p 80
A92-16817 p 80
A92-16818 p 80
A92-16819 p 128
A92-16824 p 166
A92-16825 p 154
A92-16826 p 163
A92-16828 p 128
A92-16830 p 138
A92-16831 p 128
A92-16832 p 163
A92-16833 p 113
A92-16927 p 98
A92-16934 p 99
A92-16935 p 99
A92-16938 p 99
A92-16947 p 99
A92-16948 p 99
A92-16949 p 99
A92-16950 p 99
A92-16951 p 100
A92-16952 p 100
A92-16953 p 100
A92-16954 p 100
A92-16955 p 100
A92-16958 p 100
A92-16963 * p 100
A92-16966 p 101
A92-16967 p 101
A92-16968 * p 101
A92-16969 p 101
A92-16970 p 101
A92-16971 p 101
A92-16972 p 138
A92-16973 p 101
A92-16975 p 102
A92-16976 p 102
A92-16989 * p 155
A92-17093 p 113
A92-17094 p 113
A92-17095 p 61
A92-17097 p 61
A92-17110 p 155
A92-17176 p 129
A92-17177 p 129
A92-17178 * p 80
A92-17179 p 129
A92-17188 p 143
A92-17194 p 80
A92-17195 p 80
A92-17196 p 80
A92-17197 p 80
A92-17198 p 80
A92-17200 p 129
A92-17201 * p 155
A92-17202 p 129
A92-17203 p 129
A92-17224 p 138
A92-17238 p 155
A92-17240 p 102
A92-17242 p 102
A92-17252 p 92
A92-17253 p 113
A92-17254 p 114
A92-17288 p 214
A92-17289 p 214
A92-17290 p 214
A92-17292 p 215
A92-17293 p 215
A92-17294 p 169
A92-17348 p 215
A92-17349 p 209
A92-17414 p 215
A92-17422 p 188
A92-17429 * p 170
A92-17501 p 170
A92-17502 p 171
A92-17503 p 200
A92-17562 p 215
A92-17582 # p 230
A92-17585 * # p 230
A92-17594 * # p 231
A92-17596 # p 197
A92-17597 * # p 197
A92-17605 # p 231
A92-17608 # p 231
A92-17626 # p 231
A92-17627 # p 215
A92-17628 # p 197
A92-17629 * # p 231
A92-17637 * # p 231
A92-17645 # p 232
A92-17654 # p 232
A92-17664 # p 232
A92-17802 # p 209
A92-17813 * # p 232
A92-17817 # p 171
A92-17818 # p 206
A92-17819 * # p 207
A92-17820 * # p 209
A92-17822 # p 171
A92-17823 # p 215
A92-17824 # p 209
A92-17825 * # p 210
A92-17826 # p 171
A92-17828 # p 200
A92-17830 * # p 210
A92-17834 # p 210
A92-17837 * # p 203
A92-17838 * # p 203
A92-17839 * # p 203
A92-17840 * # p 203
A92-17841 # p 171

A92-17842 # p 171
A92-17843 *# p 216
A92-17848 # p 200
A92-17849 # p 200
A92-17851 *# p 210
A92-17854 # p 169
A92-17857 *# p 172
A92-17861 # p 212
A92-17876 p 192
A92-17950 p 216
A92-18002 p 212
A92-18005 p 216
A92-18100 p 207
A92-18172 p 188
A92-18198 p 200
A92-18292 p 201
A92-18352 p 172
A92-18353 p 172
A92-18358 * p 172
A92-18361 p 172
A92-18362 * p 216
A92-18363 p 172
A92-18365 p 172
A92-18367 p 172
A92-18369 p 216
A92-18372 * p 172
A92-18373 * p 216
A92-18375 p 207
A92-18377 p 216
A92-18385 p 172
A92-18387 p 173
A92-18388 p 235
A92-18463 p 203
A92-18464 p 232
A92-18482 * p 188
A92-18505 p 188
A92-18601 p 204
A92-18608 p 204
A92-18610 p 204
A92-18611 p 197
A92-18615 * p 204
A92-18616 p 232
A92-18620 p 204
A92-18621 p 204
A92-18622 * p 204
A92-18623 p 204
A92-18624 p 204
A92-18625 * p 204
A92-18626 p 204
A92-18680 p 173
A92-18683 * p 235
A92-18769 p 173
A92-18770 p 173
A92-18771 p 173
A92-18830 p 216
A92-18898 p 212
A92-18900 p 173
A92-18902 p 230
A92-18937 p 198
A92-19061 p 210
A92-19068 p 173
A92-19084 p 232
A92-19091 p 216
A92-19094 p 232
A92-19103 p 204
A92-19107 p 205
A92-19110 p 174
A92-19202 p 217
A92-19211 p 188
A92-19214 p 188
A92-19216 p 188
A92-19231 p 217
A92-19251 p 198
A92-19252 p 198
A92-19257 p 210
A92-19273 p 205
A92-19275 p 201
A92-19278 p 189
A92-19279 p 189
A92-19386 p 233
A92-19405 p 233
A92-19406 p 233
A92-19463 p 217
A92-19605 * p 233
A92-19606 p 192
A92-19609 * p 233
A92-19611 p 174
A92-19618 p 217
A92-19619 * p 233
A92-19677 p 217
A92-19696 p 201
A92-19754 * p 212
A92-19760 p 212
A92-19767 p 213
A92-19796 p 213
A92-19799 p 213
A92-19812 p 217
A92-19817 p 213
A92-19818 p 217
A92-19819 p 192
A92-19820 p 213
A92-19828 * p 213
A92-19924 p 192
A92-19925 p 192
A92-19977 p 218
A92-19982 p 235
A92-19986 p 218
A92-19988 p 218
A92-20000 # p 192
A92-20023 p 169
A92-20024 p 186
A92-20025 p 198
A92-20126 p 186
A92-20127 p 186
A92-20128 * p 230
A92-20129 p 186
A92-20130 p 213
A92-20134 p 192
A92-20136 p 192
A92-20145 p 169
A92-20146 p 169
A92-20150 p 233
A92-20201 * p 174
A92-20202 * p 193
A92-20203 p 193
A92-20204 * p 205
A92-20205 p 174
A92-20206 * p 218
A92-20207 p 205
A92-20208 p 193
A92-20209 p 193
A92-20211 * p 174
A92-20212 p 174
A92-20213 p 218
A92-20214 p 174
A92-20215 * p 218
A92-20216 p 219
A92-20217 * p 219
A92-20218 p 174
A92-20301 * p 235
A92-20304 p 174
A92-20306 * p 174
A92-20324 p 219
A92-20349 p 214
A92-20356 p 219
A92-20378 * p 175
A92-20379 p 175
A92-20483 p 205
A92-20488 p 175
A92-20649 p 175
A92-20650 p 207
A92-20651 p 186
A92-20720 p 186
A92-20722 p 187
A92-20726 * p 175
A92-20727 p 175
A92-20729 * p 235
A92-20733 p 175
A92-20734 p 201
A92-20735 * p 175
A92-20736 p 176
A92-20737 p 176
A92-20738 * p 176
A92-20739 p 176
A92-20741 p 219
A92-20742 p 176
A92-20746 p 219
A92-20747 * p 176
A92-20756 p 219
A92-20760 p 176
A92-20761 p 176
A92-20762 * p 176
A92-20764 p 219
A92-20771 p 219
A92-21003 p 287
A92-21006 p 280
A92-21007 p 269
A92-21010 p 269
A92-21011 p 269
A92-21012 p 277
A92-21013 p 269
A92-21014 p 241
A92-21023 * p 285
A92-21051 p 242
A92-21052 p 287
A92-21070 * p 242
A92-21071 p 277
A92-21072 p 243
A92-21073 p 243
A92-21074 * p 276
A92-21075 p 243
A92-21078 p 277
A92-21079 * p 290
A92-21080 p 277
A92-21085 p 290
A92-21125 p 283
A92-21176 p 302
A92-21178 * p 280
A92-21179 p 302
A92-21180 p 280
A92-21181 * p 302
A92-21191 * p 302
A92-21216 p 291
A92-21301 p 280
A92-21307 p 281
A92-21311 p 281
A92-21312 p 269
A92-21315 p 243
A92-21318 p 243
A92-21319 p 243
A92-21325 p 266
A92-21327 p 287
A92-21330 p 291
A92-21338 p 304
A92-21374 p 291
A92-21450 p 291
A92-21466 p 266
A92-21469 p 243
A92-21470 p 269
A92-21472 p 291
A92-21490 p 288
A92-21504 p 243
A92-21602 p 244
A92-21617 p 244
A92-21618 p 244
A92-21623 p 244
A92-21624 p 244
A92-21629 p 244
A92-21683 p 266
A92-21684 p 262
A92-21691 p 291
A92-21700 p 241
A92-21718 p 244
A92-21721 p 291
A92-21722 p 245
A92-21733 p 292
A92-21734 p 269
A92-21742 p 245
A92-21743 p 245
A92-21745 p 278
A92-21749 p 284
A92-21836 p 270
A92-21837 p 245
A92-21839 p 270
A92-21900 p 292
A92-21922 p 284
A92-21923 p 292
A92-21925 p 270
A92-21976 p 245
A92-21977 p 245
A92-21978 p 245
A92-21979 p 245
A92-21980 p 246
A92-21981 * p 246
A92-21982 p 246
A92-21983 p 246
A92-21984 p 246
A92-21985 p 246
A92-21986 p 247
A92-21987 p 247
A92-22000 p 276
A92-22087 p 267
A92-22088 p 267
A92-22126 # p 278
A92-22129 # p 292
A92-22130 *# p 292
A92-22133 # p 288
A92-22135 *# p 247
A92-22136 # p 278
A92-22137 # p 278
A92-22139 # p 247
A92-22140 # p 247
A92-22141 *# p 247
A92-22142 *# p 248
A92-22143 *# p 281
A92-22144 *# p 281
A92-22145 # p 248
A92-22146 *# p 248
A92-22147 *# p 248
A92-22148 *# p 248
A92-22149 # p 248
A92-22150 # p 248
A92-22151 # p 249
A92-22152 *# p 249
A92-22153 *# p 249
A92-22155 # p 249
A92-22156 # p 249
A92-22157 # p 249
A92-22158 # p 262
A92-22159 # p 262
A92-22160 *# p 270
A92-22161 *# p 281
A92-22162 # p 281
A92-22163 # p 281
A92-22164 # p 282
A92-22170 # p 249
A92-22171 # p 250
A92-22172 # p 250
A92-22176 # p 250
A92-22178 # p 250
A92-22179 # p 250
A92-22195 # p 292
A92-22196 # p 292
A92-22200 # p 293
A92-22203 # p 293
A92-22299 p 293
A92-22346 p 293
A92-22446 p 250
A92-22472 p 270
A92-22473 p 270
A92-22474 p 270
A92-22482 * p 278
A92-22495 p 301
A92-22517 p 251
A92-22519 p 251
A92-22520 p 282
A92-22521 p 251
A92-22523 p 293
A92-22524 p 251
A92-22632 p 285
A92-22634 p 284
A92-22635 p 251
A92-22707 p 241
A92-22708 p 241
A92-22709 p 271
A92-22710 p 271
A92-22711 p 241
A92-22712 p 271
A92-22720 p 251
A92-22754 p 288
A92-22755 p 288
A92-22757 p 288
A92-22758 p 288
A92-22760 p 289
A92-22767 p 289
A92-22771 p 289
A92-22785 p 293
A92-22790 p 251
A92-22796 p 294
A92-22879 p 294
A92-23008 p 301
A92-23009 p 301
A92-23038 p 302
A92-23040 p 276
A92-23109 p 294
A92-23111 p 294
A92-23114 p 294
A92-23167 p 294
A92-23172 p 262
A92-23269 p 295
A92-23296 p 267
A92-23297 p 267
A92-23298 p 267
A92-23299 p 295
A92-23300 * p 295
A92-23301 p 295
A92-23302 p 262
A92-23380 p 251
A92-23381 p 251
A92-23382 p 282
A92-23383 p 252
A92-23385 p 295
A92-23409 p 252
A92-23414 p 252
A92-23416 p 252
A92-23418 p 289
A92-23502 p 252
A92-23563 p 304
A92-23693 p 302
A92-23730 # p 252
A92-23746 *# p 286
A92-23750 # p 295
A92-23751 # p 252
A92-23753 # p 286
A92-23754 # p 263
A92-23761 # p 284
A92-23762 *# p 253
A92-23763 # p 253
A92-23764 *# p 253
A92-23765 # p 253
A92-23766 # p 253
A92-23767 *# p 253
A92-23768 *# p 271
A92-23770 # p 253
A92-23771 *# p 254
A92-23772 *# p 254
A92-23773 # p 254
A92-23774 # p 254
A92-23775 # p 254
A92-23776 # p 241
A92-23777 # p 263
A92-23778 # p 263
A92-23779 # p 254
A92-23780 # p 255
A92-23781 # p 271
A92-23782 # p 271
A92-23783 # p 255
A92-23784 # p 255
A92-23785 # p 255
A92-23787 # p 255
A92-23788 *# p 255
A92-23790 # p 256
A92-23793 # p 256
A92-23794 # p 256
A92-23798 *# p 256
A92-23799 # p 256
A92-23800 # p 256
A92-23801 # p 257
A92-23802 *# p 257
A92-23803 # p 257
A92-23804 # p 257
A92-23805 # p 284
A92-23810 *# p 284
A92-23814 # p 271
A92-23816 # p 278
A92-23817 *# p 278
A92-23826 * p 295
A92-23835 p 296
A92-23837 p 296
A92-23967 p 267
A92-23984 p 267
A92-24176 p 296
A92-24178 p 272
A92-24186 p 296
A92-24192 p 272
A92-24193 p 296
A92-24402 * p 356
A92-24403 * p 371
A92-24404 p 309
A92-24405 p 356
A92-24406 * p 382
A92-24407 p 309
A92-24408 * p 378
A92-24409 p 371
A92-24410 p 309
A92-24411 p 410
A92-24412 p 309
A92-24413 p 378
A92-24414 * p 309
A92-24416 * p 309
A92-24417 p 309
A92-24418 p 309
A92-24419 p 309
A92-24421 p 310
A92-24422 p 310
A92-24423 p 410
A92-24426 p 310
A92-24427 p 378
A92-24428 p 310
A92-24430 p 390
A92-24553 p 391
A92-24575 p 368
A92-24599 p 310
A92-24628 p 414
A92-24651 * p 310
A92-24652 * p 310
A92-24653 * p 310
A92-24667 p 310
A92-24668 * p 386
A92-24717 * p 391
A92-24721 * p 391
A92-24723 p 391
A92-24724 p 311
A92-24725 p 311
A92-24729 p 382
A92-24730 p 391
A92-24731 p 311
A92-24732 p 391
A92-24737 p 391
A92-24738 p 371
A92-24739 p 371
A92-24740 p 371
A92-24741 p 371
A92-24744 p 388
A92-24745 p 371
A92-24746 p 371
A92-24747 p 391
A92-24748 p 392
A92-24749 p 392
A92-24750 p 372

A92-24758 p 392
A92-24778 p 392
A92-24780 p 386
A92-24781 p 368
A92-24785 p 368
A92-24831 p 388
A92-24876 p 311
A92-24877 p 311
A92-24878 p 372
A92-24879 p 379
A92-24902 p 311
A92-24904 p 311
A92-24905 p 410
A92-24908 p 392
A92-24909 p 392
A92-24910 p 386
A92-24911 p 392
A92-24918 p 368
A92-24943 p 353
A92-24944 p 353
A92-24945 p 353
A92-24946 p 353
A92-24976 p 311
A92-24979 p 312
A92-24980 p 393
A92-25001 p 312
A92-25002 p 312
A92-25004 p 312
A92-25009 p 312
A92-25010 p 379
A92-25012 p 312
A92-25013 p 356
A92-25014 p 393
A92-25015 p 312
A92-25031 p 388
A92-25038 p 312
A92-25039 p 313
A92-25040 p 313
A92-25041 p 313
A92-25042 p 313
A92-25043 p 313
A92-25048 p 313
A92-25074 p 357
A92-25075 p 350
A92-25096 p 313
A92-25097 p 313
A92-25098 p 314
A92-25101 p 314
A92-25103 p 314
A92-25104 p 314
A92-25107 p 314
A92-25108 p 410
A92-25109 p 393
A92-25110 p 383
A92-25126 p 314
A92-25127 p 314
A92-25129 p 314
A92-25132 p 315
A92-25134 p 315
A92-25136 p 315
A92-25138 p 393
A92-25140 p 315
A92-25175 p 307
A92-25178 p 307
A92-25180 p 307
A92-25181 p 350
A92-25299 p 315
A92-25330 p 406
A92-25365 p 414
A92-25366 p 393
A92-25371 p 307
A92-25372 p 357
A92-25373 p 372
A92-25374 p 315
A92-25501 p 406
A92-25502 p 357
A92-25503 p 387
A92-25505 p 393
A92-25506 p 315
A92-25520 p 353
A92-25521 p 350
A92-25535 p 393
A92-25575 p 307
A92-25576 * p 315
A92-25577 p 316
A92-25578 p 414
A92-25636 p 316
A92-25655 p 353
A92-25676 * # p 316
A92-25677 * # p 316
A92-25680 p 418
A92-25682 * # p 316
A92-25683 # p 350
A92-25685 * # p 317
A92-25687 # p 357
A92-25691 # p 317
A92-25693 # p 393
A92-25696 * # p 372
A92-25712 * # p 357
A92-25716 # p 394
A92-25719 * # p 369
A92-25720 # p 394
A92-25723 # p 317
A92-25724 * # p 369
A92-25725 # p 317
A92-25726 * # p 317
A92-25727 # p 317
A92-25728 * # p 318
A92-25729 # p 318
A92-25730 # p 318
A92-25731 * # p 318
A92-25732 # p 318
A92-25733 * # p 379
A92-25734 * # p 318
A92-25735 # p 318
A92-25736 # p 319
A92-25737 # p 319
A92-25738 # p 319
A92-25739 # p 319
A92-25740 # p 319
A92-25743 * # p 350
A92-25744 * # p 351
A92-25745 * # p 369
A92-25746 * # p 369
A92-25747 * # p 407
A92-25748 # p 319
A92-25749 # p 351
A92-25750 * # p 351
A92-25751 # p 351
A92-25752 # p 369
A92-25753 # p 369
A92-25754 # p 320
A92-25755 * # p 320
A92-25756 # p 387
A92-25757 # p 320
A92-25758 # p 320
A92-25759 * # p 320
A92-25761 # p 320
A92-25762 * # p 320
A92-25763 # p 321
A92-25764 # p 321
A92-25765 # p 321
A92-25766 # p 321
A92-25767 # p 321
A92-25768 # p 321
A92-25769 # p 321
A92-25770 # p 322
A92-25771 * # p 322
A92-25772 * # p 322
A92-25774 * # p 383
A92-25775 # p 322
A92-25776 * # p 383
A92-25777 * # p 322
A92-25778 * # p 383
A92-25779 * # p 322
A92-25786 * # p 394
A92-25787 # p 388
A92-25846 p 394
A92-25997 p 388
A92-26152 p 388
A92-26216 * p 323
A92-26219 * p 394
A92-26227 * # p 394
A92-26232 * # p 414
A92-26234 * # p 372
A92-26235 # p 395
A92-26240 # p 323
A92-26241 * # p 323
A92-26242 # p 323
A92-26243 * # p 323
A92-26244 * # p 323
A92-26245 # p 357
A92-26247 # p 372
A92-26248 # p 323
A92-26249 # p 395
A92-26250 p 307
A92-26252 # p 373
A92-26253 * # p 373
A92-26254 # p 324
A92-26255 * # p 324
A92-26256 # p 324
A92-26257 # p 324
A92-26258 * # p 324
A92-26259 # p 324
A92-26260 * # p 325
A92-26261 * # p 325
A92-26262 # p 325
A92-26263 * # p 325
A92-26264 * # p 325
A92-26265 * # p 325
A92-26266 * # p 326
A92-26267 * # p 326
A92-26268 # p 326
A92-26274 # p 326
A92-26275 # p 326
A92-26276 # p 326
A92-26277 # p 326
A92-26280 # p 327
A92-26281 # p 327
A92-26283 * # p 327
A92-26284 # p 327
A92-26285 # p 327
A92-26288 * # p 328
A92-26291 * # p 328
A92-26302 # p 395
A92-26317 # p 328
A92-26318 # p 328
A92-26322 * # p 328
A92-26323 # p 328
A92-26324 # p 329
A92-26325 * # p 329
A92-26326 * # p 329
A92-26327 * # p 329
A92-26328 * # p 414
A92-26351 p 388
A92-26353 p 415
A92-26356 p 329
A92-26357 p 329
A92-26359 p 351
A92-26360 p 383
A92-26361 p 351
A92-26362 p 415
A92-26363 p 415
A92-26364 p 329
A92-26368 p 411
A92-26370 p 330
A92-26371 p 383
A92-26376 p 373
A92-26381 p 330
A92-26383 p 415
A92-26401 p 330
A92-26402 * p 330
A92-26403 * p 330
A92-26405 * p 415
A92-26406 * p 415
A92-26410 p 330
A92-26411 p 330
A92-26413 p 395
A92-26416 p 330
A92-26433 p 395
A92-26435 * p 330
A92-26436 * p 395
A92-26437 * p 395
A92-26441 p 415
A92-26442 p 331
A92-26443 p 331
A92-26550 p 357
A92-26667 p 389
A92-26776 p 395
A92-26779 p 395
A92-26780 p 354
A92-26792 p 308
A92-26793 p 308
A92-26795 p 395
A92-26797 p 331
A92-26799 p 396
A92-26848 p 354
A92-26849 p 357
A92-26850 p 389
A92-26920 p 373
A92-26930 * # p 415
A92-26931 * # p 416
A92-26932 * # p 331
A92-26935 * # p 396
A92-26939 # p 396
A92-26940 # p 373
A92-26941 # p 373
A92-26942 # p 373
A92-26943 # p 331
A92-26944 # p 331
A92-26945 # p 331
A92-26946 * # p 332
A92-26947 * # p 332
A92-26948 * # p 332
A92-26949 # p 351
A92-26950 * # p 357
A92-26951 # p 358
A92-26952 # p 396
A92-26957 # p 332
A92-26964 # p 332
A92-26965 # p 333
A92-26968 # p 411
A92-26970 # p 411
A92-26974 * # p 383
A92-26975 # p 384
A92-26976 # p 384
A92-26978 * # p 333
A92-26980 * # p 333
A92-26984 # p 407
A92-26992 # p 411
A92-27007 * # p 374
A92-27009 * # p 396
A92-27010 # p 333
A92-27011 # p 333
A92-27012 # p 333
A92-27013 # p 334
A92-27014 # p 334
A92-27016 * # p 334
A92-27017 # p 334
A92-27021 * # p 334
A92-27023 * # p 334
A92-27029 # p 396
A92-27031 * # p 334
A92-27032 # p 397
A92-27034 # p 411
A92-27036 # p 335
A92-27042 # p 384
A92-27043 # p 379
A92-27050 # p 389
A92-27051 # p 389
A92-27052 # p 389
A92-27053 # p 389
A92-27054 # p 390
A92-27082 # p 379
A92-27083 # p 379
A92-27088 # p 335
A92-27092 # p 335
A92-27093 # p 335
A92-27094 # p 335
A92-27095 # p 335
A92-27097 # p 336
A92-27098 # p 336
A92-27099 # p 336
A92-27102 # p 384
A92-27107 # p 387
A92-27108 # p 374
A92-27114 # p 374
A92-27347 * p 411
A92-27354 p 374
A92-27381 p 336
A92-27384 p 336
A92-27394 p 358
A92-27448 p 308
A92-27450 p 417
A92-27482 p 397
A92-27531 p 336
A92-27532 p 336
A92-27533 p 337
A92-27537 p 337
A92-27593 p 337
A92-27594 p 337
A92-27596 p 337
A92-27597 p 337
A92-27645 p 338
A92-27770 p 397
A92-27773 p 397
A92-27776 p 370
A92-27777 p 370
A92-27783 p 397
A92-27785 p 370
A92-27801 p 338
A92-27802 p 338
A92-27803 p 338
A92-27826 p 379
A92-27827 p 338
A92-27828 p 338
A92-27829 p 338
A92-27831 p 338
A92-27832 p 370
A92-27833 p 339
A92-27836 p 358
A92-27837 p 370
A92-27838 p 397
A92-27851 p 339
A92-27855 p 416
A92-27856 p 397
A92-27857 p 374
A92-27858 p 411
A92-27859 p 412
A92-27865 p 398
A92-27901 p 358
A92-27902 p 358
A92-27903 p 398
A92-27905 p 339
A92-27906 p 370
A92-27908 p 398
A92-27909 p 339
A92-27913 p 374
A92-27914 p 379
A92-27939 p 407
A92-27953 p 407
A92-27958 * p 407
A92-27960 p 407
A92-27961 p 407
A92-27962 p 408
A92-27963 p 408
A92-27991 * p 408
A92-28005 p 339
A92-28006 p 339
A92-28026 p 339
A92-28027 p 340
A92-28031 * p 398
A92-28032 * p 416
A92-28033 p 398
A92-28035 p 398
A92-28036 * p 340
A92-28037 * p 416
A92-28039 p 340
A92-28041 * p 340
A92-28042 p 340
A92-28043 * p 340
A92-28044 * p 340
A92-28047 p 340
A92-28062 * p 340
A92-28063 * p 398
A92-28136 p 412
A92-28142 p 412
A92-28151 * p 379
A92-28152 * p 380
A92-28153 p 380
A92-28154 p 380
A92-28183 p 417
A92-28186 * # p 341
A92-28190 # p 416
A92-28191 * # p 374
A92-28192 * # p 341
A92-28193 * # p 341
A92-28194 * # p 341
A92-28196 # p 341
A92-28197 * # p 341
A92-28199 * # p 341
A92-28200 * # p 342
A92-28201 * # p 398
A92-28202 * # p 342
A92-28204 * # p 342
A92-28213 * # p 342
A92-28215 * # p 342
A92-28217 * # p 342
A92-28218 # p 343
A92-28223 * # p 343
A92-28224 * # p 343
A92-28226 * # p 398
A92-28251 p 390
A92-28419 p 375
A92-28433 p 390
A92-28434 p 375
A92-28435 p 375
A92-28436 p 375
A92-28459 p 375
A92-28464 p 399
A92-28476 p 343
A92-28477 p 343
A92-28478 p 343
A92-28479 p 375
A92-28480 p 375
A92-28489 p 358
A92-28492 p 308
A92-28493 p 358
A92-28494 p 412
A92-28495 p 399
A92-28501 p 343
A92-28503 p 390
A92-28513 p 399
A92-28517 p 375
A92-28519 p 344
A92-28522 p 344
A92-28523 * p 344
A92-28524 p 344
A92-28526 * p 344
A92-28527 p 344
A92-28528 p 399
A92-28529 p 399
A92-28531 p 375
A92-28533 * p 376
A92-28534 * p 376
A92-28535 * p 376
A92-28536 p 376
A92-28537 * p 399
A92-28538 * p 376
A92-28556 p 490
A92-28588 p 490
A92-28592 p 490
A92-28633 p 490
A92-28655 * p 491
A92-28669 p 491
A92-28672 p 491
A92-28682 p 510
A92-28684 p 491
A92-28686 p 491
A92-28690 p 491

A92-28720 p 510
A92-28725 p 492
A92-28737 p 492
A92-28745 p 492
A92-28747 p 492
A92-28748 p 492
A92-28750 p 492
A92-28874 p 467
A92-28875 p 457
A92-28941 p 419
A92-28943 p 421
A92-28949 p 421
A92-29037 p 506
A92-29052 p 506
A92-29061 p 476
A92-29066 p 506
A92-29093 * p 476
A92-29094 p 477
A92-29101 p 507
A92-29102 p 477
A92-29115 p 477
A92-29116 p 468
A92-29117 * p 477
A92-29118 * p 477
A92-29119 * p 477
A92-29120 * p 478
A92-29124 p 478
A92-29127 p 478
A92-29128 p 478
A92-29132 p 507
A92-29134 p 507
A92-29155 p 507
A92-29171 p 478
A92-29177 p 507
A92-29188 p 478
A92-29189 p 507
A92-29237 p 507
A92-29248 p 508
A92-29280 p 508
A92-29291 p 508
A92-29304 * p 485
A92-29313 p 508
A92-29315 p 508
A92-29316 * p 508
A92-29324 p 508
A92-29326 p 509
A92-29327 p 509
A92-29330 * p 478
A92-29331 p 478
A92-29332 * p 479
A92-29355 p 421
A92-29356 p 468
A92-29360 p 453
A92-29361 p 479
A92-29368 p 509
A92-29374 p 509
A92-29375 p 468
A92-29376 p 469
A92-29418 p 457
A92-29472 p 421
A92-29504 p 492
A92-29505 p 483
A92-29506 p 453
A92-29507 p 448
A92-29508 p 448
A92-29516 p 479
A92-29517 p 421
A92-29518 p 457
A92-29521 p 421
A92-29557 p 457
A92-29595 # p 421
A92-29596 # p 422
A92-29603 # p 422
A92-29604 # p 422
A92-29609 # p 493
A92-29610 *# p 493
A92-29639 *# p 487
A92-29669 p 457
A92-29670 p 458
A92-29671 p 458
A92-29672 p 458
A92-29673 * p 419
A92-29674 p 483
A92-29675 p 458
A92-29709 p 469
A92-29710 p 422
A92-29711 p 469
A92-29712 p 483
A92-29714 p 422
A92-29716 p 422
A92-29717 p 469
A92-29718 p 469
A92-29719 p 422
A92-29720 p 423
A92-29721 p 469
A92-29722 p 493
A92-29725 p 487
A92-29726 p 504
A92-29728 p 487
A92-29729 p 469
A92-29731 p 470
A92-29732 p 448
A92-29733 p 470
A92-29736 p 470
A92-29737 p 470
A92-29739 p 470
A92-29740 p 470
A92-29741 p 470
A92-29742 p 470
A92-29743 p 471
A92-29760 # p 453
A92-29856 # p 453
A92-29889 *# p 453
A92-29944 # p 471
A92-29956 # p 485
A92-29972 *# p 423
A92-29973 p 471
A92-29999 p 423
A92-30000 p 423
A92-30023 * p 454
A92-30091 p 458
A92-30092 p 419
A92-30126 p 423
A92-30127 p 423
A92-30128 p 423
A92-30129 p 424
A92-30130 p 509
A92-30131 p 479
A92-30132 p 479
A92-30133 p 471
A92-30134 p 458
A92-30135 p 424
A92-30136 p 424
A92-30138 p 424
A92-30139 p 486
A92-30140 p 458
A92-30141 p 419
A92-30143 p 511
A92-30144 p 424
A92-30145 p 424
A92-30146 p 424
A92-30147 p 493
A92-30149 p 479
A92-30150 p 479
A92-30152 p 493
A92-30153 p 424
A92-30154 p 425
A92-30157 p 425
A92-30158 p 425
A92-30159 p 425
A92-30160 p 425
A92-30161 p 493
A92-30162 p 493
A92-30167 p 425
A92-30170 p 494
A92-30171 p 425
A92-30172 p 425
A92-30173 p 426
A92-30180 p 426
A92-30181 p 426
A92-30185 p 426
A92-30186 p 426
A92-30187 p 426
A92-30188 p 426
A92-30190 p 480
A92-30191 p 480
A92-30192 p 480
A92-30196 p 426
A92-30197 p 427
A92-30199 p 427
A92-30200 p 427
A92-30201 p 427
A92-30202 p 427
A92-30203 p 427
A92-30204 p 427
A92-30205 p 511
A92-30206 p 427
A92-30207 p 428
A92-30208 p 494
A92-30209 p 459
A92-30210 p 428
A92-30211 p 428
A92-30212 p 428
A92-30311 p 509
A92-30318 p 511
A92-30319 p 428
A92-30371 p 428
A92-30373 p 428
A92-30375 p 428
A92-30381 p 471
A92-30409 p 483
A92-30476 p 494
A92-30498 p 419
A92-30501 p 494
A92-30502 p 429
A92-30517 p 429
A92-30520 p 429
A92-30522 p 429
A92-30523 p 429
A92-30526 p 429
A92-30527 p 429
A92-30528 p 429
A92-30530 p 429
A92-30531 p 429
A92-30532 p 429
A92-30538 p 429
A92-30539 p 430
A92-30540 p 430
A92-30541 p 430
A92-30542 p 430
A92-30549 p 480
A92-30550 p 430
A92-30551 p 430
A92-30552 p 430
A92-30557 p 430
A92-30558 p 430
A92-30559 p 430
A92-30560 p 430
A92-30596 p 487
A92-30603 p 494
A92-30611 p 488
A92-30624 # p 431
A92-30651 p 454
A92-30685 p 486
A92-30850 p 431
A92-30995 p 480
A92-31021 p 480
A92-31063 p 454
A92-31071 p 494
A92-31084 p 494
A92-31151 p 431
A92-31152 p 431
A92-31154 p 431
A92-31155 * p 431
A92-31156 * p 431
A92-31157 * p 431
A92-31158 p 431
A92-31160 p 432
A92-31163 * p 432
A92-31164 p 494
A92-31165 * p 432
A92-31167 * p 432
A92-31169 * p 432
A92-31172 p 432
A92-31173 p 495
A92-31174 p 483
A92-31183 p 432
A92-31185 p 432
A92-31186 * p 432
A92-31187 p 432
A92-31188 p 433
A92-31194 * p 495
A92-31198 p 495
A92-31325 p 459
A92-31425 p 433
A92-31430 p 509
A92-31468 p 433
A92-31486 p 495
A92-31487 * p 433
A92-31489 p 433
A92-31491 * p 433
A92-31492 p 434
A92-31495 p 434
A92-31496 p 434
A92-31525 p 419
A92-31547 p 434
A92-31549 p 434
A92-31552 p 495
A92-31564 p 495
A92-31606 p 459
A92-31630 * p 496
A92-31639 * p 435
A92-31640 * p 435
A92-31652 # p 435
A92-31653 # p 435
A92-31655 # p 496
A92-31660 # p 471
A92-31661 # p 435
A92-31663 # p 435
A92-31668 # p 459
A92-31669 # p 459
A92-31670 *# p 459
A92-31675 # p 459
A92-31676 *# p 486
A92-31677 # p 436
A92-31678 *# p 436
A92-31679 *# p 436
A92-31680 *# p 436
A92-31683 # p 471
A92-31685 # p 471
A92-31686 # p 483
A92-31687 *# p 436
A92-31688 # p 437
A92-31689 # p 472
A92-31690 *# p 437
A92-31691 # p 459
A92-31692 *# p 480
A92-31696 # p 472
A92-31697 # p 486
A92-31698 # p 486
A92-31700 # p 472
A92-31778 p 496
A92-31853 p 437
A92-31854 p 437
A92-31855 p 437
A92-31857 p 437
A92-31858 p 496
A92-31860 p 437
A92-31861 p 437
A92-31862 p 438
A92-31863 p 438
A92-31865 p 480
A92-31867 p 438
A92-31868 p 438
A92-31869 p 438
A92-31870 p 438
A92-31871 p 438
A92-31872 p 438
A92-31873 p 439
A92-31874 p 439
A92-31875 p 439
A92-31876 p 480
A92-31877 p 439
A92-31878 p 460
A92-31879 p 439
A92-31880 p 439
A92-31881 p 460
A92-31882 p 439
A92-31883 p 439
A92-31884 p 440
A92-31885 p 440
A92-31886 p 440
A92-31887 p 440
A92-31890 p 440
A92-31892 p 496
A92-31893 p 460
A92-31894 p 460
A92-31896 p 460
A92-31897 p 440
A92-31898 p 440
A92-31899 p 440
A92-31951 p 454
A92-31955 p 454
A92-31961 p 440
A92-31962 p 441
A92-31963 p 441
A92-31969 p 441
A92-31988 p 496
A92-32052 p 504
A92-32056 p 484
A92-32060 p 467
A92-32062 p 467
A92-32064 p 467
A92-32073 * p 505
A92-32080 p 467
A92-32082 p 467
A92-32089 p 467
A92-32090 p 467
A92-32091 p 467
A92-32095 p 468
A92-32097 p 468
A92-32129 * p 505
A92-32130 p 496
A92-32140 p 468
A92-32177 * p 496
A92-32178 p 441
A92-32181 * p 441
A92-32182 * p 441
A92-32183 * p 497
A92-32184 * p 441
A92-32196 * p 441
A92-32232 * p 497
A92-32233 p 460
A92-32234 p 441
A92-32235 * p 441
A92-32236 * p 442
A92-32237 * p 442
A92-32238 p 448
A92-32239 * p 442
A92-32240 p 497
A92-32241 p 442
A92-32242 p 481
A92-32243 p 442
A92-32245 p 442
A92-32247 * p 460
A92-32248 p 481
A92-32250 * p 461
A92-32251 * p 442
A92-32253 * p 488
A92-32264 p 497
A92-32265 p 497
A92-32296 p 472
A92-32297 p 472
A92-32298 p 472
A92-32299 p 472
A92-32300 p 472
A92-32323 p 442
A92-32324 p 442
A92-32325 p 461
A92-32394 p 488
A92-32411 p 497
A92-32500 *# p 442
A92-32501 p 443
A92-32502 p 511
A92-32504 p 443
A92-32507 p 497
A92-32508 p 497
A92-32509 p 498
A92-32523 p 498
A92-32524 p 498
A92-32542 p 599
A92-32553 p 535
A92-32554 p 535
A92-32555 p 579
A92-32556 p 579
A92-32562 p 579
A92-32564 p 576
A92-32578 p 579
A92-32636 p 580
A92-32662 p 576
A92-32746 * p 580
A92-32942 * p 580
A92-32979 p 535
A92-32980 p 603
A92-32982 p 529
A92-32983 p 529
A92-32984 p 529
A92-32988 p 580
A92-32998 p 529
A92-32999 p 529
A92-33182 # p 535
A92-33185 # p 580
A92-33191 # p 600
A92-33193 *# p 535
A92-33194 # p 536
A92-33196 *# p 536
A92-33198 # p 515
A92-33204 # p 531
A92-33206 # p 517
A92-33208 *# p 536
A92-33209 *# p 580
A92-33218 # p 553
A92-33219 # p 536
A92-33221 # p 605
A92-33230 # p 553
A92-33239 # p 536
A92-33240 *# p 517
A92-33244 # p 573
A92-33245 # p 563
A92-33246 # p 563
A92-33247 # p 563
A92-33248 # p 563
A92-33249 # p 536
A92-33250 # p 536
A92-33251 # p 537
A92-33252 # p 537
A92-33253 # p 537
A92-33254 # p 515
A92-33256 *# p 605
A92-33257 # p 605
A92-33261 # p 581
A92-33269 # p 605
A92-33271 # p 537
A92-33277 # p 563
A92-33278 # p 563
A92-33279 # p 577
A92-33280 # p 537
A92-33281 # p 537
A92-33282 # p 581
A92-33287 # p 574
A92-33300 # p 600
A92-33301 # p 600
A92-33302 # p 600
A92-33303 # p 600
A92-33304 *# p 600
A92-33306 # p 600
A92-33307 # p 537
A92-33313 *# p 537
A92-33314 # p 517
A92-33320 *# p 517

A92-33326 # p 538
A92-33327 # p 538
A92-33333 # p 538
A92-33336 # p 553
A92-33337 # p 553
A92-33339 # p 515
A92-33342 # p 538
A92-33343 # p 538
A92-33345 # p 601
A92-33426 p 531
A92-33427 p 531
A92-33428 p 606
A92-33429 p 531
A92-33430 p 515
A92-33431 p 531
A92-33432 p 531
A92-33433 p 532
A92-33434 p 532
A92-33435 p 532
A92-33436 p 532
A92-33437 p 532
A92-33438 p 532
A92-33439 p 532
A92-33440 p 532
A92-33441 p 533
A92-33460 p 515
A92-33461 p 515
A92-33462 p 516
A92-33463 p 606
A92-33602 p 574
A92-33603 p 601
A92-33607 * p 601
A92-33622 p 533
A92-33632 p 533
A92-33639 p 574
A92-33754 p 601
A92-33770 p 603
A92-33771 p 603
A92-33778 p 581
A92-33790 p 603
A92-33799 p 529
A92-33800 p 538
A92-33847 p 581
A92-33918 * p 577
A92-33919 p 538
A92-34219 p 571
A92-34253 * p 529
A92-34289 * # p 581
A92-34292 # p 581
A92-34297 * # p 582
A92-34307 * # p 582
A92-34320 # p 582
A92-34332 p 582
A92-34354 # p 582
A92-34357 * # p 582
A92-34358 * # p 539
A92-34359 # p 564
A92-34360 * # p 583
A92-34362 * # p 539
A92-34363 * # p 583
A92-34373 # p 539
A92-34374 # p 583
A92-34376 # p 583
A92-34381 * # p 583
A92-34382 * # p 584
A92-34389 p 584
A92-34390 * # p 539
A92-34391 # p 539
A92-34392 * # p 539
A92-34393 # p 540
A92-34394 # p 540
A92-34403 # p 584
A92-34410 # p 584
A92-34411 # p 540
A92-34412 # p 540
A92-34413 * # p 540
A92-34414 * # p 541
A92-34415 # p 541
A92-34417 # p 541
A92-34451 p 584
A92-34452 # p 584
A92-34465 * # p 585
A92-34466 # p 517
A92-34467 # p 585
A92-34468 # p 541
A92-34469 * # p 517
A92-34470 # p 564
A92-34471 # p 541
A92-34472 * # p 585
A92-34473 * # p 585
A92-34474 * # p 577
A92-34475 # p 585
A92-34476 * # p 541
A92-34477 * # p 542
A92-34478 # p 564
A92-34479 # p 564
A92-34480 * # p 564
A92-34481 # p 564
A92-34482 * # p 565
A92-34497 # p 518
A92-34498 * # p 518
A92-34499 # p 518
A92-34500 # p 542
A92-34501 # p 518
A92-34517 # p 518
A92-34522 p 585
A92-34524 # p 585
A92-34525 * # p 586
A92-34542 # p 601
A92-34543 # p 542
A92-34544 * # p 542
A92-34545 # p 542
A92-34546 * # p 542
A92-34547 # p 565
A92-34548 # p 586
A92-34554 # p 601
A92-34591 # p 586
A92-34592 * # p 543
A92-34593 # p 543
A92-34596 * # p 571
A92-34597 * # p 518
A92-34598 * # p 556
A92-34599 # p 543
A92-34603 * # p 586
A92-34604 # p 601
A92-34650 p 543
A92-34683 * p 519
A92-34688 p 565
A92-34692 p 606
A92-34759 p 586
A92-34770 p 606
A92-34771 p 606
A92-34775 p 516
A92-34825 p 587
A92-34826 * p 519
A92-34878 p 597
A92-34893 * p 574
A92-34908 p 597
A92-34976 p 554
A92-35028 * p 597
A92-35055 p 587
A92-35109 p 598
A92-35132 * p 598
A92-35142 p 587
A92-35276 p 554
A92-35428 p 572
A92-35434 p 543
A92-35436 p 543
A92-35437 p 544
A92-35441 p 544
A92-35443 p 572
A92-35444 p 519
A92-35452 p 544
A92-35454 p 554
A92-35465 p 577
A92-35475 p 577
A92-35479 p 587
A92-35541 p 557
A92-35543 p 519
A92-35544 p 519
A92-35546 p 587
A92-35551 p 557
A92-35554 p 587
A92-35555 p 587
A92-35556 p 588
A92-35560 p 557
A92-35561 p 557
A92-35564 p 588
A92-35567 p 588
A92-35569 p 557
A92-35570 p 557
A92-35571 p 519
A92-35572 p 588
A92-35573 p 588
A92-35574 p 516
A92-35575 p 516
A92-35610 p 574
A92-35651 p 565
A92-35652 * # p 565
A92-35653 * # p 572
A92-35654 * # p 565
A92-35655 * # p 565
A92-35656 * # p 572
A92-35666 * # p 566
A92-35667 * # p 566
A92-35668 * # p 566
A92-35669 # p 566
A92-35670 * # p 566
A92-35671 # p 567
A92-35672 # p 588
A92-35673 * # p 588
A92-35674 # p 589
A92-35675 # p 567
A92-35676 # p 567
A92-35677 * # p 567
A92-35678 * # p 567
A92-35679 # p 544
A92-35680 # p 544
A92-35681 # p 544
A92-35682 # p 544
A92-35687 * # p 557
A92-35688 # p 558
A92-35689 * # p 520
A92-35690 * # p 520
A92-35691 * # p 589
A92-35692 # p 572
A92-35693 # p 567
A92-35694 # p 520
A92-35695 * # p 589
A92-35696 * # p 589
A92-35697 * # p 589
A92-35699 # p 589
A92-35726 p 533
A92-35727 p 516
A92-35728 p 520
A92-35729 p 590
A92-35731 p 545
A92-35732 p 567
A92-35733 p 545
A92-35734 p 545
A92-35735 p 545
A92-35736 p 545
A92-35737 p 545
A92-35738 p 546
A92-35739 p 602
A92-35740 p 533
A92-35741 * p 603
A92-35742 p 554
A92-35743 p 554
A92-35744 p 546
A92-35745 p 590
A92-35746 p 590
A92-35747 p 568
A92-35748 p 568
A92-35749 p 568
A92-35750 p 546
A92-35751 * p 546
A92-35752 p 546
A92-35753 p 520
A92-35754 p 546
A92-35755 p 520
A92-35756 p 568
A92-35757 p 568
A92-35758 p 521
A92-35759 p 530
A92-35760 p 530
A92-35762 p 568
A92-35763 p 554
A92-35764 p 554
A92-35765 p 554
A92-35766 p 546
A92-35767 p 547
A92-35768 p 568
A92-35769 p 569
A92-35770 * p 569
A92-35771 p 547
A92-35772 * p 547
A92-35773 p 555
A92-35774 p 547
A92-35775 p 569
A92-35776 p 569
A92-35777 * p 569
A92-35778 * p 604
A92-35779 p 547
A92-35780 p 547
A92-35781 p 547
A92-35782 p 604
A92-35783 p 521
A92-35784 p 521
A92-35785 p 569
A92-35786 p 570
A92-35787 p 521
A92-35788 p 521
A92-35847 p 590
A92-35911 p 558
A92-35912 p 558
A92-35913 p 521
A92-35914 p 558
A92-35915 p 558
A92-35916 p 577
A92-35917 p 558
A92-35918 p 516
A92-35919 p 558
A92-35921 p 558
A92-35926 p 516
A92-35927 p 555
A92-35928 p 533
A92-35929 p 548
A92-35931 p 533
A92-35932 p 555
A92-35933 p 570
A92-35934 p 548
A92-35936 * p 548
A92-35937 p 548
A92-35938 p 548
A92-35939 p 570
A92-35940 p 548
A92-35941 p 555
A92-35942 p 555
A92-35943 p 602
A92-35944 p 549
A92-35945 p 549
A92-35947 p 570
A92-35948 p 549
A92-35949 p 555
A92-35950 p 555
A92-35952 p 549
A92-35953 p 556
A92-35977 p 590
A92-35988 p 521
A92-35992 p 522
A92-35995 p 522
A92-35997 p 522
A92-36006 * p 604
A92-36007 * p 591
A92-36021 p 522
A92-36023 p 522
A92-36026 p 522
A92-36028 p 522
A92-36029 p 523
A92-36030 p 523
A92-36032 p 591
A92-36033 p 523
A92-36035 p 523
A92-36036 p 523
A92-36037 p 591
A92-36038 p 523
A92-36076 p 534
A92-36100 p 524
A92-36124 p 534
A92-36125 p 556
A92-36126 p 558
A92-36127 p 574
A92-36151 p 524
A92-36156 p 591
A92-36186 * p 524
A92-36194 p 591
A92-36200 p 530
A92-36349 p 530
A92-36351 p 591
A92-36357 p 524
A92-36358 p 558
A92-36359 * p 524
A92-36377 p 577
A92-36380 p 577
A92-36416 p 604
A92-36417 p 602
A92-36420 p 524
A92-36421 p 559
A92-36549 p 609
A92-36550 p 609
A92-36552 p 610
A92-36600 p 610
A92-36606 p 670
A92-36611 p 670
A92-36826 p 610
A92-36827 p 610
A92-36828 p 641
A92-36830 p 610
A92-36834 * p 610
A92-36835 p 610
A92-36836 p 610
A92-36838 p 610
A92-36839 p 610
A92-36840 * p 611
A92-36842 p 611
A92-36843 p 611
A92-36844 p 670
A92-36846 * p 670
A92-36848 * p 611
A92-36851 p 670
A92-36855 p 641
A92-36861 * p 611
A92-36888 p 653
A92-36889 p 653
A92-36890 p 653
A92-36891 p 653
A92-36892 p 653
A92-36893 p 670
A92-36895 p 690
A92-36897 p 607
A92-36899 p 670
A92-36900 p 668
A92-36901 p 670
A92-36948 p 671
A92-36950 p 697
A92-36952 p 665
A92-36964 p 668
A92-36965 p 666
A92-36966 p 666
A92-36967 p 666
A92-36972 p 611
A92-36974 p 611
A92-36977 p 653
A92-36979 * p 611
A92-36990 p 660
A92-37061 p 607
A92-37072 p 637
A92-37073 p 637
A92-37074 p 642
A92-37075 p 637
A92-37077 p 660
A92-37168 p 634
A92-37188 * p 671
A92-37375 p 666
A92-37389 p 611
A92-37390 p 654
A92-37391 p 642
A92-37394 p 660
A92-37395 p 671
A92-37423 p 654
A92-37424 p 654
A92-37534 p 690
A92-37537 * p 611
A92-37539 * p 612
A92-37549 p 612
A92-37550 p 612
A92-37551 p 612
A92-37552 * p 612
A92-37553 p 613
A92-37554 p 613
A92-37559 p 671
A92-37576 p 642
A92-37577 p 642
A92-37791 p 690
A92-37824 p 654
A92-37825 p 642
A92-37868 p 671
A92-37875 p 607
A92-37933 p 613
A92-37950 p 690
A92-38000 p 634
A92-38025 p 654
A92-38101 p 607
A92-38111 * p 668
A92-38128 p 650
A92-38129 p 663
A92-38163 p 671
A92-38201 p 607
A92-38206 p 642
A92-38207 p 634
A92-38208 p 634
A92-38213 p 666
A92-38216 p 671
A92-38217 p 607
A92-38218 p 607
A92-38220 p 608
A92-38225 p 672
A92-38266 p 608
A92-38267 p 654
A92-38269 p 613
A92-38270 p 613
A92-38273 p 690
A92-38275 p 672
A92-38316 p 642
A92-38370 * p 613
A92-38373 p 613
A92-38374 p 634
A92-38375 p 634
A92-38380 p 637
A92-38381 p 638
A92-38383 p 685
A92-38384 p 638
A92-38456 p 614
A92-38478 * # p 666
A92-38569 * # p 666
A92-38636 # p 690
A92-38699 * # p 690
A92-38770 p 672
A92-38851 p 672
A92-38856 p 614
A92-38858 p 614
A92-38859 p 614
A92-38860 p 614
A92-38861 p 614
A92-38863 p 615
A92-38866 p 672
A92-38867 p 672
A92-38906 p 615
A92-38907 p 615

A92-38908 p 615
A92-38909 p 615
A92-38910 p 615
A92-38913 p 615
A92-38916 p 616
A92-38917 p 616
A92-38918 p 616
A92-38919 p 616
A92-38920 p 616
A92-38922 p 672
A92-38923 p 693
A92-38924 p 616
A92-38925 p 616
A92-39009 * p 673
A92-39042 p 693
A92-39044 p 686
A92-39045 p 686
A92-39046 p 686
A92-39050 p 686
A92-39051 p 686
A92-39052 p 686
A92-39053 p 686
A92-39054 p 687
A92-39055 p 687
A92-39056 p 687
A92-39057 p 687
A92-39058 p 687
A92-39059 p 687
A92-39060 p 693
A92-39061 p 687
A92-39062 p 693
A92-39063 p 688
A92-39064 p 688
A92-39065 p 688
A92-39066 p 693
A92-39068 p 693
A92-39082 p 642
A92-39083 p 643
A92-39084 p 643
A92-39085 p 694
A92-39086 p 694
A92-39087 p 643
A92-39088 p 694
A92-39089 p 643
A92-39099 p 688
A92-39100 p 688
A92-39101 p 688
A92-39102 p 688
A92-39103 p 689
A92-39104 p 694
A92-39106 p 694
A92-39109 p 694
A92-39111 p 695
A92-39226 p 695
A92-39228 * p 695
A92-39229 * p 663
A92-39235 p 689
A92-39236 p 689
A92-39237 p 689
A92-39238 * p 695
A92-39239 p 689
A92-39240 p 689
A92-39241 * p 695
A92-39243 p 695
A92-39244 p 697
A92-39245 p 697
A92-39281 p 673
A92-39301 p 634
A92-39302 p 634
A92-39303 p 635
A92-39304 p 643
A92-39305 p 635
A92-39308 p 673
A92-39309 p 654
A92-39310 p 635
A92-39333 * p 616
A92-39338 p 617
A92-39340 * p 617
A92-39480 p 695
A92-39514 p 664
A92-39558 p 673
A92-39560 p 638
A92-39561 * p 650
A92-39563 p 697
A92-39565 p 638
A92-39567 p 638
A92-39569 p 638
A92-39570 p 651
A92-39672 p 668
A92-39682 p 668
A92-39725 p 643
A92-39852 * p 668
A92-39854 * p 668
A92-39861 p 669
A92-39893 p 661
A92-39894 p 661
A92-39900 p 661
A92-39902 p 661
A92-39903 * p 661
A92-39904 p 661
A92-39905 * p 661
A92-39908 p 661
A92-39909 p 661
A92-39910 p 661
A92-39913 p 643
A92-39930 p 673
A92-39934 p 617
A92-39940 p 617
A92-39941 p 617
A92-39944 p 673
A92-39949 p 617
A92-39951 p 654
A92-39952 p 651
A92-39958 p 673
A92-39959 p 674
A92-39960 p 691
A92-39961 p 691
A92-39963 p 651
A92-39964 * p 617
A92-39965 * p 618
A92-39966 * p 643
A92-39967 * p 618
A92-39968 * p 608
A92-39969 * p 608
A92-39970 p 635
A92-39971 p 635
A92-39973 p 618
A92-39974 p 618
A92-39975 p 618
A92-39976 p 618
A92-39977 p 635
A92-39980 * p 651
A92-39981 p 651
A92-39982 p 651
A92-39983 p 608
A92-39984 p 661
A92-39985 p 662
A92-39986 p 619
A92-39987 p 674
A92-39988 p 619
A92-39989 p 644
A92-39990 p 644
A92-39991 * p 664
A92-39992 * p 644
A92-39993 p 655
A92-39995 p 655
A92-39998 p 655
A92-39999 p 644
A92-40000 p 644
A92-40001 p 655
A92-40002 p 655
A92-40003 p 655
A92-40004 p 644
A92-40005 p 655
A92-40006 p 656
A92-40007 p 656
A92-40008 p 656
A92-40009 p 644
A92-40010 p 644
A92-40012 p 674
A92-40013 p 656
A92-40014 p 651
A92-40015 p 651
A92-40016 p 635
A92-40017 p 652
A92-40018 p 674
A92-40020 p 674
A92-40021 p 635
A92-40022 p 636
A92-40023 p 636
A92-40024 * p 674
A92-40027 p 638
A92-40028 p 645
A92-40029 p 645
A92-40030 p 645
A92-40031 p 645
A92-40032 p 645
A92-40033 * p 666
A92-40034 p 645
A92-40035 p 645
A92-40036 p 645
A92-40037 p 646
A92-40038 p 646
A92-40039 p 662
A92-40040 p 646
A92-40041 p 646
A92-40042 p 646
A92-40043 p 646
A92-40051 p 675
A92-40052 * p 675
A92-40055 * p 619
A92-40056 p 619
A92-40059 * p 619
A92-40063 p 619
A92-40068 p 620
A92-40080 p 675
A92-40081 p 620
A92-40084 p 620
A92-40085 p 620
A92-40086 p 620
A92-40087 p 620
A92-40093 p 675
A92-40102 p 675
A92-40103 p 675
A92-40104 p 620
A92-40105 * p 621
A92-40106 p 621
A92-40111 p 621
A92-40119 p 621
A92-40121 p 621
A92-40125 p 621
A92-40126 p 621
A92-40127 p 622
A92-40128 p 622
A92-40132 p 676
A92-40134 * p 622
A92-40140 p 622
A92-40143 p 622
A92-40144 p 656
A92-40148 p 676
A92-40151 * p 656
A92-40171 p 622
A92-40172 p 676
A92-40173 p 622
A92-40175 p 623
A92-40177 p 623
A92-40180 p 623
A92-40182 p 623
A92-40187 p 639
A92-40188 p 639
A92-40189 p 676
A92-40199 p 639
A92-40226 p 639
A92-40232 p 639
A92-40239 p 639
A92-40262 p 652
A92-40383 p 608
A92-40384 p 646
A92-40385 p 646
A92-40386 p 608
A92-40387 p 646
A92-40388 p 647
A92-40389 p 647
A92-40390 * p 696
A92-40391 p 623
A92-40392 p 608
A92-40393 p 647
A92-40394 * p 609
A92-40395 p 662
A92-40396 p 609
A92-40397 p 609
A92-40398 p 609
A92-40400 p 676
A92-40409 p 669
A92-40545 p 647
A92-40548 p 656
A92-40549 p 623
A92-40580 p 623
A92-40588 p 696
A92-40598 p 623
A92-40599 p 624
A92-40600 p 624
A92-40602 p 624
A92-40605 p 624
A92-40606 p 657
A92-40607 p 657
A92-40608 p 657
A92-40609 p 657
A92-40610 p 657
A92-40611 p 657
A92-40615 p 657
A92-40621 p 657
A92-40622 p 664
A92-40746 p 624
A92-40866 p 696
A92-40869 p 676
A92-40880 p 609
A92-40882 p 676
A92-40883 p 652
A92-40884 p 647
A92-40885 * p 647
A92-40897 p 647
A92-40898 p 676
A92-40943 p 658
A92-41034 p 757
A92-41060 p 757
A92-41082 p 757
A92-41091 p 754
A92-41119 p 754
A92-41176 p 729
A92-41177 p 699
A92-41178 p 700
A92-41179 p 700
A92-41180 p 757
A92-41184 p 751
A92-41186 p 757
A92-41188 p 700
A92-41190 p 758
A92-41193 p 752
A92-41195 p 775
A92-41196 p 701
A92-41197 p 701
A92-41199 p 776
A92-41207 p 701
A92-41208 p 724
A92-41209 p 747
A92-41210 p 747
A92-41211 * p 701
A92-41212 p 743
A92-41213 p 701
A92-41214 p 701
A92-41215 * p 747
A92-41217 * p 701
A92-41218 * p 729
A92-41219 * p 701
A92-41220 * p 725
A92-41221 p 747
A92-41222 p 729
A92-41223 p 701
A92-41224 * p 702
A92-41225 * p 736
A92-41226 p 743
A92-41227 * p 702
A92-41228 * p 702
A92-41229 p 702
A92-41230 p 747
A92-41231 p 702
A92-41232 p 702
A92-41233 p 729
A92-41235 p 702
A92-41236 p 702
A92-41237 p 699
A92-41238 * p 758
A92-41239 * p 729
A92-41240 p 778
A92-41241 p 758
A92-41242 p 758
A92-41243 p 729
A92-41244 p 758
A92-41246 p 703
A92-41247 p 703
A92-41261 * p 703
A92-41262 * p 723
A92-41263 * p 730
A92-41264 * p 703
A92-41265 * p 703
A92-41266 p 778
A92-41267 * p 703
A92-41268 * p 703
A92-41269 p 703
A92-41271 p 703
A92-41276 * p 703
A92-41278 p 703
A92-41279 p 703
A92-41282 p 758
A92-41289 p 704
A92-41291 p 704
A92-41296 * p 758
A92-41297 p 758
A92-41314 # p 704
A92-41317 # p 704
A92-41318 # p 704
A92-41320 # p 704
A92-41322 # p 704
A92-41323 # p 758
A92-41324 # p 778
A92-41331 # p 778
A92-41332 # p 779
A92-41336 # p 747
A92-41340 # p 779
A92-41344 # p 752
A92-41348 # p 705
A92-41359 p 779
A92-41419 p 776
A92-41431 p 733
A92-41472 p 725
A92-41528 p 744
A92-41534 p 699
A92-41535 * p 752
A92-41536 p 705
A92-41537 p 705
A92-41538 * p 705
A92-41539 * p 705
A92-41540 * p 705
A92-41541 * p 705
A92-41542 p 705
A92-41545 p 705
A92-41653 p 705
A92-41658 p 759
A92-41781 p 699
A92-41801 p 759
A92-41817 p 705
A92-41819 p 736
A92-41820 p 782
A92-41822 p 736
A92-41824 p 782
A92-41834 p 759
A92-41835 p 759
A92-41836 p 759
A92-41874 p 754
A92-41926 p 706
A92-41928 p 734
A92-41929 p 747
A92-42040 p 754
A92-42051 p 759
A92-42052 p 759
A92-42054 p 699
A92-42057 p 759
A92-42071 p 760
A92-42073 p 776
A92-42077 p 760
A92-42084 p 760
A92-42086 p 760
A92-42095 p 774
A92-42097 p 775
A92-42124 p 706
A92-42145 p 760
A92-42172 p 776
A92-42313 p 725
A92-42315 p 760
A92-42317 p 760
A92-42320 p 761
A92-42345 p 754
A92-42400 p 736
A92-42486 p 725
A92-42500 p 723
A92-42501 p 754
A92-42502 p 761
A92-42529 p 761
A92-42531 p 706
A92-42533 p 706
A92-42601 p 779
A92-42602 * p 734
A92-42603 p 734
A92-42604 p 725
A92-42605 p 744
A92-42606 p 779
A92-42607 p 761
A92-42634 p 725
A92-42653 p 761
A92-42654 p 761
A92-42655 p 754
A92-42665 p 761
A92-42680 p 706
A92-42682 p 706
A92-42683 p 707
A92-42684 p 707
A92-42726 p 707
A92-42730 p 707
A92-42732 p 779
A92-42735 p 707
A92-42736 p 707
A92-42737 p 708
A92-42738 p 708
A92-42777 p 708
A92-42778 p 779
A92-42780 p 776
A92-42785 p 775
A92-42789 p 725
A92-42797 p 761
A92-42798 p 755
A92-42800 p 736
A92-42949 p 762
A92-43046 p 730
A92-43055 p 708
A92-43060 p 708
A92-43065 p 708
A92-43067 p 708
A92-43071 p 708
A92-43072 p 709
A92-43073 p 709
A92-43095 p 699
A92-43096 p 747
A92-43097 p 747
A92-43098 p 748
A92-43099 p 748
A92-43100 * p 730
A92-43101 p 709
A92-43102 p 709
A92-43103 p 709

A92-43104 p 748
A92-43105 p 748
A92-43107 p 762
A92-43109 p 762
A92-43110 p 748
A92-43112 p 744
A92-43113 p 748
A92-43115 p 744
A92-43118 p 730
A92-43119 p 709
A92-43120 p 744
A92-43121 p 744
A92-43122 p 726
A92-43123 p 726
A92-43124 p 748
A92-43125 p 748
A92-43126 p 762
A92-43127 p 744
A92-43128 p 744
A92-43129 p 744
A92-43131 p 744
A92-43132 p 709
A92-43133 p 762
A92-43134 p 745
A92-43135 p 745
A92-43136 p 748
A92-43137 p 699
A92-43138 p 730
A92-43139 p 734
A92-43140 p 730
A92-43141 p 700
A92-43142 p 730
A92-43143 p 730
A92-43144 p 709
A92-43145 p 709
A92-43146 p 745
A92-43147 p 700
A92-43148 p 700
A92-43149 p 730
A92-43150 p 734
A92-43151 p 734
A92-43153 p 700
A92-43155 p 723
A92-43156 p 762
A92-43157 p 700
A92-43158 p 748
A92-43159 p 745
A92-43160 p 780
A92-43161 p 723
A92-43162 p 723
A92-43163 p 723
A92-43164 p 723
A92-43166 p 710
A92-43167 p 710
A92-43169 p 710
A92-43170 p 710
A92-43171 p 748
A92-43172 p 749
A92-43174 p 710
A92-43178 p 776
A92-43180 p 745
A92-43181 p 776
A92-43182 p 745
A92-43183 p 745
A92-43184 p 745
A92-43185 p 745
A92-43187 p 776
A92-43189 p 731
A92-43190 p 752
A92-43191 p 710
A92-43192 p 752
A92-43194 p 710
A92-43195 p 737
A92-43196 p 737
A92-43197 p 711
A92-43198 p 711
A92-43199 p 749
A92-43200 p 752
A92-43201 p 711
A92-43202 p 711
A92-43203 p 711
A92-43204 p 711
A92-43205 p 711
A92-43206 p 762
A92-43208 p 734
A92-43209 p 734
A92-43210 p 749
A92-43211 p 752
A92-43212 p 752
A92-43213 p 762
A92-43217 p 734
A92-43218 p 745
A92-43219 p 723
A92-43220 p 735
A92-43221 p 735
A92-43222 p 735
A92-43224 p 735
A92-43225 p 735
A92-43226 p 711
A92-43227 p 711
A92-43228 p 711
A92-43229 p 711
A92-43230 p 712
A92-43231 p 712
A92-43233 p 737
A92-43237 p 755
A92-43239 p 737
A92-43240 p 763
A92-43241 p 781
A92-43242 p 731
A92-43243 p 731
A92-43244 p 731
A92-43246 p 700
A92-43247 p 700
A92-43248 p 700
A92-43269 p 752
A92-43356 p 753
A92-43399 * p 777
A92-43446 p 723
A92-43447 p 712
A92-43545 p 737
A92-43546 p 731
A92-43548 p 781
A92-43679 p 755
A92-43684 p 755
A92-43685 p 755
A92-43881 p 726
A92-43884 p 745
A92-43885 p 763
A92-43937 p 726
A92-44070 p 775
A92-44081 p 775
A92-44084 p 775
A92-44121 p 712
A92-44125 p 712
A92-44127 p 712
A92-44197 p 780
A92-44326 p 763
A92-44327 p 763
A92-44328 p 712
A92-44363 * p 712
A92-44367 p 713
A92-44368 * p 713
A92-44371 p 713
A92-44372 p 713
A92-44377 p 780
A92-44380 * p 763
A92-44381 p 763
A92-44428 p 726
A92-44501 p 755
A92-44511 p 737
A92-44512 * p 780
A92-44513 * p 713
A92-44514 * p 737
A92-44515 p 713
A92-44517 p 737
A92-44518 p 713
A92-44519 p 713
A92-44520 * p 713
A92-44524 p 737
A92-44525 * p 737
A92-44526 * p 737
A92-44528 p 714
A92-44531 p 714
A92-44545 p 738
A92-44547 # p 731
A92-44617 p 755
A92-44618 p 763
A92-44630 p 763
A92-44671 * p 714
A92-44732 p 764
A92-44733 p 764
A92-44734 p 738
A92-44850 p 726
A92-44865 p 714
A92-44895 p 783
A92-44898 p 860
A92-44909 p 916
A92-44915 p 916
A92-44919 p 839
A92-44920 p 839
A92-44922 p 855
A92-44923 p 855
A92-44929 p 855
A92-44931 p 833
A92-44932 p 839
A92-44967 p 896
A92-44969 p 839
A92-44976 p 879
A92-44981 p 879
A92-44982 p 916
A92-44985 * p 833
A92-44993 p 834
A92-44994 p 928
A92-44995 p 834
A92-44996 p 834
A92-44997 p 834
A92-44998 p 834
A92-44999 p 834
A92-45000 p 834
A92-45002 p 916
A92-45025 p 880
A92-45026 p 880
A92-45027 p 880
A92-45028 p 880
A92-45041 p 834
A92-45042 p 880
A92-45044 p 835
A92-45048 p 835
A92-45052 p 835
A92-45054 * p 835
A92-45055 p 835
A92-45064 p 916
A92-45080 p 835
A92-45081 p 835
A92-45096 p 880
A92-45130 p 896
A92-45202 p 896
A92-45226 p 896
A92-45234 p 891
A92-45236 p 891
A92-45242 p 897
A92-45260 p 897
A92-45261 p 897
A92-45263 * p 787
A92-45265 * p 880
A92-45266 * p 880
A92-45267 p 881
A92-45275 p 881
A92-45302 p 783
A92-45303 p 783
A92-45304 * p 841
A92-45305 p 841
A92-45306 p 860
A92-45307 p 860
A92-45308 p 841
A92-45309 p 783
A92-45310 p 842
A92-45311 p 842
A92-45312 p 842
A92-45313 * p 842
A92-45314 p 881
A92-45315 p 842
A92-45316 * p 860
A92-45317 p 860
A92-45318 p 787
A92-45319 p 871
A92-45320 p 872
A92-45321 p 860
A92-45322 p 872
A92-45323 p 881
A92-45324 p 787
A92-45325 * p 861
A92-45373 p 839
A92-45374 p 855
A92-45376 p 783
A92-45380 p 881
A92-45381 p 842
A92-45382 p 872
A92-45383 p 843
A92-45384 p 872
A92-45385 p 788
A92-45386 p 788
A92-45387 p 843
A92-45388 p 881
A92-45390 * p 788
A92-45391 p 788
A92-45392 p 788
A92-45393 p 788
A92-45394 p 788
A92-45395 p 789
A92-45396 p 843
A92-45397 p 843
A92-45401 p 789
A92-45403 p 897
A92-45404 p 789
A92-45405 p 789
A92-45406 p 843
A92-45407 * p 783
A92-45408 p 789
A92-45409 p 789
A92-45410 p 843
A92-45412 p 789
A92-45413 p 790
A92-45414 p 790
A92-45416 p 897
A92-45417 p 790
A92-45418 p 790
A92-45419 p 790
A92-45421 p 784
A92-45422 p 881
A92-45424 p 835
A92-45425 p 836
A92-45426 p 836
A92-45427 p 790
A92-45428 p 791
A92-45429 p 791
A92-45430 p 861
A92-45431 p 861
A92-45432 p 861
A92-45434 p 861
A92-45435 p 861
A92-45436 p 843
A92-45437 p 843
A92-45438 p 844
A92-45439 p 844
A92-45440 p 897
A92-45441 p 862
A92-45442 * p 889
A92-45443 p 791
A92-45445 p 791
A92-45449 p 855
A92-45450 p 872
A92-45451 p 891
A92-45454 p 917
A92-45455 p 844
A92-45456 p 917
A92-45476 p 791
A92-45477 # p 791
A92-45478 * # p 792
A92-45479 * # p 792
A92-45480 * # p 792
A92-45482 * # p 792
A92-45483 # p 792
A92-45484 # p 792
A92-45485 * # p 793
A92-45487 # p 793
A92-45488 # p 873
A92-45489 * # p 917
A92-45490 # p 793
A92-45491 # p 844
A92-45492 # p 917
A92-45493 * # p 793
A92-45494 * # p 793
A92-45495 # p 794
A92-45496 # p 794
A92-45497 # p 794
A92-45498 # p 794
A92-45499 # p 794
A92-45500 # p 795
A92-45501 # p 844
A92-45502 * # p 795
A92-45503 # p 795
A92-45504 # p 795
A92-45505 * # p 795
A92-45506 # p 795
A92-45507 # p 796
A92-45508 * # p 796
A92-45509 # p 796
A92-45510 * # p 796
A92-45513 # p 796
A92-45514 # p 796
A92-45515 # p 797
A92-45516 # p 797
A92-45517 * # p 797
A92-45518 * # p 797
A92-45519 # p 844
A92-45520 # p 797
A92-45522 # p 797
A92-45523 # p 798
A92-45524 # p 798
A92-45525 * # p 798
A92-45526 # p 798
A92-45528 * # p 798
A92-45529 # p 798
A92-45530 * # p 799
A92-45531 # p 799
A92-45532 # p 799
A92-45534 * # p 799
A92-45535 # p 799
A92-45536 # p 799
A92-45537 * # p 800
A92-45538 # p 800
A92-45539 * # p 800
A92-45540 * # p 800
A92-45541 * # p 800
A92-45542 * # p 800
A92-45543 * # p 801
A92-45544 # p 801
A92-45545 # p 801
A92-45546 # p 801
A92-45548 # p 801
A92-45549 # p 801
A92-45550 * # p 802
A92-45551 # p 802
A92-45552 * # p 802
A92-45553 * # p 802
A92-45554 # p 802
A92-45555 * # p 803
A92-45556 # p 803
A92-45557 * # p 803
A92-45558 # p 803
A92-45559 # p 803
A92-45560 * # p 803
A92-45561 * # p 803
A92-45562 # p 804
A92-45563 # p 804
A92-45564 # p 804
A92-45565 # p 804
A92-45566 # p 804
A92-45567 # p 805
A92-45568 * # p 805
A92-45569 # p 805
A92-45570 # p 805
A92-45571 # p 805
A92-45572 # p 805
A92-45573 # p 845
A92-45574 * # p 806
A92-45575 * # p 806
A92-45576 * # p 806
A92-45578 # p 806
A92-45580 # p 845
A92-45581 # p 928
A92-45582 # p 806
A92-45583 * # p 806
A92-45584 * # p 806
A92-45585 # p 807
A92-45588 # p 807
A92-45589 # p 917
A92-45590 # p 807
A92-45592 # p 807
A92-45593 # p 807
A92-45595 # p 807
A92-45596 * # p 808
A92-45597 # p 808
A92-45598 * # p 808
A92-45600 p 891
A92-45606 p 897
A92-45629 p 891
A92-45630 p 891
A92-45699 p 784
A92-45774 p 898
A92-45826 p 898
A92-45827 p 808
A92-45828 p 808
A92-45829 p 808
A92-45831 * p 924
A92-45833 p 898
A92-45835 * p 924
A92-45839 p 808
A92-45840 * p 808
A92-45845 * p 808
A92-45858 p 809
A92-45859 p 809
A92-45876 p 924
A92-45879 p 924
A92-45883 * p 898
A92-45885 p 898
A92-45921 p 925
A92-45929 p 925
A92-46201 p 929
A92-46202 p 784
A92-46227 p 855
A92-46243 p 855
A92-46244 * p 856
A92-46246 * p 856
A92-46247 p 856
A92-46248 p 925
A92-46252 p 898
A92-46262 * p 915
A92-46264 * p 809
A92-46426 p 862
A92-46427 p 862
A92-46428 p 889
A92-46429 p 862
A92-46430 p 925
A92-46431 * p 809
A92-46441 p 809
A92-46449 p 856
A92-46498 p 898
A92-46519 p 809
A92-46595 p 929
A92-46626 p 809
A92-46629 p 917
A92-46631 p 892
A92-46660 p 836
A92-46726 p 889
A92-46736 p 856
A92-46737 p 873
A92-46739 * p 873

A92-46741 p 873
A92-46742 * p 873
A92-46748 p 917
A92-46749 p 873
A92-46750 p 873
A92-46751 * p 873
A92-46752 p 873
A92-46761 p 873
A92-46762 p 918
A92-46765 p 874
A92-46766 p 889
A92-46776 p 874
A92-46777 p 874
A92-46778 p 810
A92-46779 p 836
A92-46780 p 882
A92-46781 p 810
A92-46782 p 810
A92-46783 * p 810
A92-46784 p 836
A92-46785 p 810
A92-46786 * p 810
A92-46787 * p 810
A92-46788 p 915
A92-46790 p 810
A92-46791 * p 810
A92-46792 p 856
A92-46793 p 811
A92-46794 p 874
A92-46797 p 811
A92-46798 * p 811
A92-46799 * p 925
A92-46800 p 845
A92-46801 p 899
A92-46802 * p 874
A92-46803 p 915
A92-46804 p 811
A92-46805 p 811
A92-46806 p 845
A92-46807 p 845
A92-46808 p 811
A92-46809 p 925
A92-46810 p 874
A92-46811 p 811
A92-46812 p 845
A92-46813 p 845
A92-46814 p 811
A92-46815 p 845
A92-46816 p 811
A92-46817 p 918
A92-46818 p 812
A92-46820 p 812
A92-46825 p 899
A92-46838 p 892
A92-46882 * p 812
A92-46883 p 812
A92-46884 p 846
A92-46886 p 812
A92-46887 * p 812
A92-46889 p 812
A92-46890 p 812
A92-46891 p 812
A92-46892 * p 812
A92-46894 * p 812
A92-46895 p 813
A92-46897 * p 813
A92-46899 * p 813
A92-46900 p 813
A92-46901 p 813
A92-46902 * p 813
A92-46903 p 813
A92-46913 p 813
A92-46916 p 899
A92-46919 p 846
A92-46921 p 846
A92-46922 p 846
A92-46923 p 874
A92-46924 * p 846
A92-46925 p 846
A92-46926 p 846
A92-46927 p 847
A92-46930 p 847
A92-46931 * p 874
A92-46932 * p 847
A92-46933 p 875
A92-46934 p 813
A92-46935 * p 813
A92-46936 p 899
A92-46940 p 899
A92-46943 p 847
A92-46944 p 814
A92-46945 * p 847
A92-46946 p 899
A92-46947 p 814
A92-46948 p 814
A92-46949 p 814
A92-46950 p 814
A92-46951 * p 814
A92-46952 * p 814
A92-46953 * p 815
A92-46954 * p 815
A92-46955 p 815
A92-46956 p 815
A92-46957 * p 815
A92-46958 p 815
A92-46959 * p 816
A92-46960 p 847
A92-46985 * # p 816
A92-46986 * # p 816
A92-46996 # p 899
A92-47028 # p 925
A92-47035 p 918
A92-47038 p 816
A92-47041 p 816
A92-47042 p 816
A92-47043 p 918
A92-47045 * p 817
A92-47050 p 918
A92-47051 * p 918
A92-47053 p 918
A92-47054 p 817
A92-47055 * p 919
A92-47057 p 817
A92-47060 p 817
A92-47061 p 817
A92-47064 p 817
A92-47066 p 919
A92-47069 p 919
A92-47071 p 900
A92-47078 p 919
A92-47079 p 817
A92-47081 p 919
A92-47083 p 919
A92-47089 p 919
A92-47090 p 818
A92-47096 p 818
A92-47100 p 818
A92-47122 p 847
A92-47128 * p 900
A92-47153 p 818
A92-47155 p 818
A92-47176 p 900
A92-47188 p 900
A92-47267 p 900
A92-47303 p 882
A92-47338 p 892
A92-47340 p 892
A92-47341 p 892
A92-47365 p 882
A92-47403 p 784
A92-47404 p 848
A92-47405 p 784
A92-47406 p 848
A92-47407 p 784
A92-47408 p 848
A92-47410 p 784
A92-47412 p 900
A92-47413 p 784
A92-47414 p 785
A92-47416 p 785
A92-47417 p 785
A92-47511 p 839
A92-47522 p 882
A92-47528 p 900
A92-47534 p 920
A92-47535 p 920
A92-47537 p 920
A92-47538 p 856
A92-47560 p 857
A92-47562 p 882
A92-47566 p 839
A92-47567 p 882
A92-47574 p 839
A92-47584 p 882
A92-47591 p 848
A92-47592 p 785
A92-47628 p 928
A92-47629 p 848
A92-47630 p 840
A92-47631 p 840
A92-47655 p 785
A92-47656 p 901
A92-47657 p 848
A92-47660 p 785
A92-47663 p 901
A92-47664 p 848
A92-47666 p 848
A92-47667 p 849
A92-47670 p 785
A92-47671 p 901
A92-47684 p 818
A92-47686 p 818
A92-47690 p 819
A92-47691 p 819
A92-47692 p 862
A92-47694 p 819
A92-47695 p 819
A92-47697 p 862
A92-47757 p 785
A92-47758 p 785
A92-47759 p 849
A92-47774 p 786
A92-47775 p 836
A92-47777 p 875
A92-47779 p 875
A92-47782 p 819
A92-47783 p 875
A92-47784 p 875
A92-47785 p 875
A92-47786 p 875
A92-47791 p 862
A92-47821 p 786
A92-47835 # p 892
A92-47839 # p 819
A92-47853 # p 901
A92-47856 # p 819
A92-47858 # p 820
A92-47860 # p 820
A92-47872 * # p 820
A92-47873 * # p 820
A92-47875 # p 820
A92-47876 # p 820
A92-47892 * # p 821
A92-47894 * # p 821
A92-47913 # p 901
A92-47915 * # p 821
A92-47917 # p 821
A92-47925 p 836
A92-47958 p 893
A92-47969 p 849
A92-47971 p 786
A92-47975 p 849
A92-48019 p 821
A92-48021 p 862
A92-48022 p 849
A92-48026 * p 901
A92-48041 p 857
A92-48042 p 857
A92-48043 p 857
A92-48044 p 857
A92-48046 p 857
A92-48047 p 857
A92-48160 * p 876
A92-48201 p 901
A92-48207 p 821
A92-48220 p 920
A92-48268 p 862
A92-48269 p 893
A92-48308 p 840
A92-48352 p 849
A92-48353 p 901
A92-48354 p 902
A92-48408 p 849
A92-48416 p 840
A92-48426 p 786
A92-48427 p 858
A92-48440 p 920
A92-48446 p 902
A92-48447 p 920
A92-48448 p 902
A92-48460 p 902
A92-48465 p 902
A92-48470 p 840
A92-48473 p 858
A92-48475 p 858
A92-48477 p 858
A92-48480 p 840
A92-48481 p 863
A92-48485 p 921
A92-48487 p 876
A92-48488 p 876
A92-48489 p 921
A92-48490 p 876
A92-48491 p 876
A92-48492 p 876
A92-48493 p 876
A92-48494 p 877
A92-48495 p 877
A92-48496 p 877
A92-48499 p 877
A92-48500 p 926
A92-48501 p 858
A92-48502 p 921
A92-48506 p 921
A92-48513 p 921
A92-48515 p 921
A92-48518 p 922
A92-48520 p 922
A92-48527 p 922
A92-48555 p 928
A92-48557 p 922
A92-48565 p 922
A92-48567 p 858
A92-48569 p 922
A92-48577 p 821
A92-48578 p 893
A92-48579 p 822
A92-48585 p 822
A92-48586 p 849
A92-48587 p 786
A92-48589 p 849
A92-48592 p 902
A92-48597 p 926
A92-48600 p 882
A92-48601 p 926
A92-48602 p 926
A92-48607 p 902
A92-48608 p 877
A92-48610 p 893
A92-48618 p 926
A92-48701 # p 822
A92-48702 # p 822
A92-48703 # p 822
A92-48704 # p 822
A92-48705 # p 822
A92-48712 # p 889
A92-48713 # p 893
A92-48714 # p 893
A92-48720 # p 823
A92-48722 # p 903
A92-48723 * # p 823
A92-48724 * # p 823
A92-48729 * # p 823
A92-48730 * # p 823
A92-48734 * # p 903
A92-48735 * # p 903
A92-48737 * # p 877
A92-48738 * # p 824
A92-48739 # p 849
A92-48740 # p 824
A92-48741 * # p 824
A92-48742 # p 824
A92-48743 * # p 863
A92-48744 * # p 824
A92-48780 * # p 890
A92-48790 # p 863
A92-48792 # p 903
A92-48793 # p 836
A92-48794 # p 922
A92-48800 # p 824
A92-48801 # p 863
A92-48802 # p 923
A92-48803 # p 903
A92-48804 # p 825
A92-48805 # p 863
A92-48817 # p 825
A92-48832 # p 863
A92-48844 * # p 903
A92-48845 # p 904
A92-48846 # p 893
A92-48847 # p 904
A92-48848 # p 894
A92-48849 * # p 890
A92-48855 # p 864
A92-48856 # p 864
A92-48857 # p 825
A92-48858 * # p 864
A92-48859 # p 864
A92-48872 # p 904
A92-48876 * # p 904
A92-48878 # p 864
A92-48879 # p 864
A92-48881 # p 882
A92-48896 # p 904
A92-48897 # p 825
A92-48898 # p 825
A92-48899 # p 825
A92-48902 * # p 877
A92-48903 # p 923
A92-48904 # p 864
A92-48906 # p 825
A92-48907 # p 904
A92-48908 * # p 883
A92-48909 * # p 826
A92-48910 # p 923
A92-48911 # p 865
A92-48915 # p 850
A92-48916 # p 850
A92-48917 # p 850
A92-48919 * # p 894
A92-48923 * # p 905
A92-48927 # p 894
A92-48936 * # p 905
A92-48937 * # p 905
A92-48938 # p 905
A92-48939 * # p 905
A92-48940 * # p 865
A92-48941 # p 850
A92-48979 # p 865
A92-48984 * # p 865
A92-48986 # p 894
A92-49014 # p 865
A92-49015 # p 905
A92-49016 # p 906
A92-49018 # p 906
A92-49019 # p 865
A92-49020 # p 865
A92-49021 # p 866
A92-49022 # p 859
A92-49023 # p 866
A92-49024 # p 866
A92-49025 # p 878
A92-49028 # p 906
A92-49031 # p 906
A92-49048 # p 906
A92-49049 # p 786
A92-49063 * # p 826
A92-49064 # p 906
A92-49076 # p 826
A92-49085 # p 906
A92-49087 # p 907
A92-49088 # p 826
A92-49096 # p 907
A92-49098 # p 866
A92-49105 # p 894
A92-49106 # p 894
A92-49109 * # p 878
A92-49110 * # p 866
A92-49111 * # p 866
A92-49112 # p 867
A92-49113 # p 867
A92-49114 # p 867
A92-49115 # p 867
A92-49117 # p 928
A92-49118 # p 826
A92-49119 # p 867
A92-49120 # p 867
A92-49126 * # p 907
A92-49128 * # p 867
A92-49134 * # p 894
A92-49136 # p 895
A92-49139 # p 868
A92-49188 p 827
A92-49251 p 964
A92-49252 p 964
A92-49254 p 964
A92-49255 p 954
A92-49258 p 984
A92-49261 p 1005
A92-49264 p 974
A92-49269 p 1012
A92-49271 p 964
A92-49272 * p 954
A92-49273 * p 964
A92-49274 p 989
A92-49275 p 989
A92-49276 p 989
A92-49277 p 989
A92-49278 p 1005
A92-49279 p 989
A92-49287 p 964
A92-49288 p 1005
A92-49289 p 1005
A92-49291 p 955
A92-49294 p 974
A92-49296 p 974
A92-49297 * p 965
A92-49299 p 1005
A92-49300 p 1005
A92-49302 p 1006
A92-49303 p 965
A92-49304 p 990
A92-49305 p 931
A92-49306 p 955
A92-49308 p 965
A92-49310 p 965
A92-49312 p 965
A92-49313 p 965
A92-49315 p 965
A92-49317 p 1006
A92-49318 p 966
A92-49324 p 974
A92-49325 * p 975
A92-49326 p 975
A92-49327 p 966
A92-49329 p 1006
A92-49330 p 975
A92-49331 p 966
A92-49332 p 966
A92-49333 p 957

A92-49336 p 966
A92-49339 p 1006
A92-49340 p 966
A92-49380 p 1012
A92-49382 p 955
A92-49383 p 955
A92-49475 p 1010
A92-49498 p 933
A92-49508 p 933
A92-49510 p 933
A92-49515 p 933
A92-49516 p 990
A92-49556 p 933
A92-49574 p 990
A92-49578 p 990
A92-49579 p 990
A92-49580 p 990
A92-49582 p 984
A92-49585 p 1006
A92-49771 p 1003
A92-49790 p 991
A92-49827 p 968
A92-49830 p 968
A92-49832 p 933
A92-49833 p 968
A92-49834 p 969
A92-49835 p 1012
A92-49836 p 969
A92-49841 p 969
A92-50007 p 985
A92-50008 p 975
A92-50009 p 957
A92-50010 p 975
A92-50013 p 1006
A92-50033 p 955
A92-50039 p 991
A92-50040 * p 991
A92-50121 p 934
A92-50122 p 955
A92-50137 p 991
A92-50203 p 958
A92-50204 p 991
A92-50206 p 1010
A92-50207 p 955
A92-50210 p 934
A92-50211 p 934
A92-50212 p 975
A92-50214 p 955
A92-50215 p 934
A92-50216 p 934
A92-50233 p 934
A92-50235 p 975
A92-50236 p 958
A92-50237 p 976
A92-50239 p 991
A92-50252 p 969
A92-50255 p 985
A92-50269 p 934
A92-50270 * p 980
A92-50272 p 934
A92-50273 * p 935
A92-50278 p 969
A92-50293 p 935
A92-50296 * p 1010
A92-50301 p 935
A92-50302 p 935
A92-50303 p 935
A92-50304 p 935
A92-50307 * p 935
A92-50309 * p 935
A92-50310 * p 935
A92-50311 p 969
A92-50312 p 935
A92-50313 * p 935
A92-50314 * p 935
A92-50315 p 958
A92-50322 p 936
A92-50325 p 936
A92-50327 p 936
A92-50401 p 1011
A92-50448 p 992
A92-50466 * p 1007
A92-50471 p 1007
A92-50473 p 936
A92-50478 p 969
A92-50490 * p 1007
A92-50497 p 976
A92-50498 * p 984
A92-50499 p 1007
A92-50503 p 976
A92-50504 p 969
A92-50505 * p 1007
A92-50508 p 976
A92-50513 p 1007
A92-50520 p 976
A92-50528 p 970
A92-50553 p 992
A92-50611 p 992
A92-50771 p 992
A92-50785 p 992
A92-50795 p 992
A92-50860 p 993
A92-51003 p 967
A92-51004 p 976
A92-51006 p 955
A92-51007 p 956
A92-51009 * p 956
A92-51011 p 967
A92-51012 p 956
A92-51014 p 993
A92-51311 p 993
A92-51316 p 993
A92-51328 p 1007
A92-51348 p 980
A92-51398 p 980
A92-51399 p 931
A92-51400 p 931
A92-51401 p 980
A92-51402 p 980
A92-51403 * p 980
A92-51404 * p 980
A92-51405 p 981
A92-51406 p 981
A92-51407 * p 981
A92-51409 * p 993
A92-51424 p 1012
A92-51438 p 993
A92-51439 p 951
A92-51440 * p 951
A92-51450 p 1012
A92-51505 p 993
A92-51506 p 958
A92-51512 p 985
A92-51513 p 994
A92-51527 p 958
A92-51537 p 994
A92-51538 p 958
A92-51545 p 994
A92-51546 p 994
A92-51555 p 985
A92-51565 p 1012
A92-51569 p 958
A92-51580 p 958
A92-51593 p 936
A92-51626 p 994
A92-51649 p 994
A92-51808 p 931
A92-51845 p 995
A92-51895 p 995
A92-51896 p 936
A92-51901 p 985
A92-51906 p 985
A92-51921 p 985
A92-51922 p 986
A92-51925 p 995
A92-51940 p 976
A92-51942 p 959
A92-51943 p 936
A92-51945 p 977
A92-51946 p 977
A92-51947 p 959
A92-51948 p 959
A92-51950 p 995
A92-52018 p 967
A92-52022 p 931
A92-52028 p 936
A92-52029 p 937
A92-52034 p 937
A92-52035 p 937
A92-52041 p 977
A92-52043 p 977
A92-52300 p 959
A92-52426 p 981
A92-52427 # p 959
A92-52428 * # p 981
A92-52433 * # p 967
A92-52434 # p 959
A92-52440 # p 1007
A92-52441 * # p 959
A92-52442 # p 959
A92-52446 # p 981
A92-52447 # p 982
A92-52448 * # p 1007
A92-52450 # p 1008
A92-52451 # p 1008
A92-52454 # p 1008
A92-52455 # p 1008
A92-52456 # p 1008
A92-52457 # p 977
A92-52458 * # p 982
A92-52459 * # p 960
A92-52460 * # p 982
A92-52465 * p 967
A92-52470 * p 995
A92-52645 p 951
A92-52650 p 956
A92-52682 p 937
A92-52722 p 995
A92-52726 p 937
A92-52730 * p 937
A92-52734 p 937
A92-52748 p 937
A92-52749 p 938
A92-52750 p 938
A92-52751 p 938
A92-52752 p 938
A92-52753 p 938
A92-52754 p 938
A92-52755 p 938
A92-52757 * p 939
A92-52761 * p 939
A92-52763 p 995
A92-52764 p 939
A92-52766 p 939
A92-52767 p 939
A92-52770 p 939
A92-52772 p 939
A92-52775 * p 940
A92-52777 * p 940
A92-52797 p 940
A92-52818 p 940
A92-52821 p 940
A92-52844 p 940
A92-52847 p 1011
A92-52848 p 941
A92-52849 p 960
A92-52890 p 970
A92-52973 p 941
A92-52981 p 996
A92-52982 p 986
A92-52983 p 986
A92-53007 p 960
A92-53009 p 941
A92-53010 p 941
A92-53011 p 996
A92-53012 p 960
A92-53013 p 996
A92-53015 p 996
A92-53018 p 951
A92-53021 p 941
A92-53022 p 941
A92-53023 p 1008
A92-53055 p 996
A92-53056 p 960
A92-53067 p 996
A92-53069 p 1009
A92-53070 p 996
A92-53071 p 996
A92-53074 p 997
A92-53078 p 941
A92-53079 p 941
A92-53080 * p 942
A92-53087 p 942
A92-53088 p 977
A92-53089 p 977
A92-53090 p 960
A92-53091 p 1011
A92-53092 p 960
A92-53093 p 1009
A92-53094 p 977
A92-53095 p 978
A92-53096 p 986
A92-53097 p 942
A92-53099 p 997
A92-53100 p 997
A92-53102 p 956
A92-53107 p 997
A92-53109 p 1009
A92-53111 p 931
A92-53120 p 970
A92-53121 p 961
A92-53181 p 970
A92-53236 p 951
A92-53239 p 956
A92-53240 p 956
A92-53250 p 932
A92-53253 p 942
A92-53257 p 1011
A92-53258 p 970
A92-53263 p 997
A92-53276 p 970
A92-53288 p 942
A92-53290 p 942
A92-53292 p 997
A92-53293 p 997
A92-53297 p 998
A92-53330 p 986
A92-53332 p 998
A92-53336 p 970
A92-53340 p 952
A92-53381 p 942
A92-53382 p 1009
A92-53386 p 943
A92-53388 p 978
A92-53389 p 971
A92-53394 p 978
A92-53434 p 1015
A92-53486 p 1065
A92-53487 p 1065
A92-53490 p 1065
A92-53491 p 1066
A92-53492 p 1066
A92-53493 p 1066
A92-53516 p 1105
A92-53545 p 1102
A92-53546 p 1073
A92-53547 p 1017
A92-53549 p 1017
A92-53550 p 1111
A92-53552 p 1017
A92-53553 p 1018
A92-53555 p 1018
A92-53556 p 1018
A92-53557 p 1018
A92-53558 p 1018
A92-53559 p 1018
A92-53560 p 1018
A92-53561 p 1019
A92-53564 p 1089
A92-53565 p 1102
A92-53578 p 1102
A92-53579 p 1019
A92-53580 p 1019
A92-53596 p 1130
A92-53603 p 1103
A92-53635 p 1103
A92-53639 p 1103
A92-53640 p 1103
A92-53641 p 1019
A92-53755 p 1111
A92-53758 p 1111
A92-53785 p 1130
A92-53786 p 1112
A92-53867 p 1019
A92-53875 p 1105
A92-53878 p 1105
A92-53882 p 1019
A92-53997 p 1019
A92-53998 p 1020
A92-54003 * # p 1020
A92-54004 * # p 1020
A92-54005 * # p 1020
A92-54006 * # p 1130
A92-54009 * # p 1066
A92-54011 * # p 1066
A92-54012 * # p 1020
A92-54013 * # p 1020
A92-54016 * # p 1021
A92-54019 # p 1103
A92-54020 * # p 1066
A92-54025 * # p 1067
A92-54026 * # p 1051
A92-54029 # p 1112
A92-54035 * # p 1067
A92-54036 * # p 1112
A92-54044 # p 1112
A92-54057 # p 1112
A92-54058 * # p 1090
A92-54059 * # p 1067
A92-54060 * # p 1067
A92-54075 # p 1112
A92-54090 * # p 1021
A92-54091 # p 1021
A92-54092 # p 1021
A92-54093 # p 1113
A92-54104 # p 1067
A92-54105 # p 1113
A92-54108 # p 1113
A92-54110 * # p 1021
A92-54111 * # p 1022
A92-54113 # p 1022
A92-54116 # p 1022
A92-54117 * # p 1022
A92-54118 # p 1022
A92-54132 * # p 1113
A92-54134 # p 1067
A92-54135 # p 1067
A92-54146 # p 1068
A92-54147 # p 1068
A92-54148 # p 1068
A92-54149 # p 1068
A92-54151 # p 1068
A92-54152 # p 1141
A92-54159 * # p 1068
A92-54160 # p 1022
A92-54161 * # p 1023
A92-54168 * # p 1069
A92-54169 * # p 1069
A92-54171 * # p 1069
A92-54177 # p 1069
A92-54178 # p 1069
A92-54179 * # p 1023
A92-54180 * # p 1090
A92-54198 # p 1113
A92-54199 # p 1113
A92-54223 p 1114
A92-54285 * # p 1130
A92-54301 p 1114
A92-54304 p 1114
A92-54307 p 1090
A92-54308 p 1023
A92-54311 p 1090
A92-54314 * p 1114
A92-54315 p 1090
A92-54317 * p 1114
A92-54319 * p 1090
A92-54321 p 1115
A92-54322 p 1090
A92-54323 p 1091
A92-54324 p 1063
A92-54325 p 1091
A92-54326 p 1091
A92-54330 p 1115
A92-54333 p 1115
A92-54334 p 1115
A92-54336 p 1091
A92-54337 p 1115
A92-54338 * p 1115
A92-54341 p 1091
A92-54342 p 1091
A92-54343 p 1092
A92-54344 * p 1116
A92-54345 p 1116
A92-54347 * p 1092
A92-54348 * p 1116
A92-54351 p 1092
A92-54484 p 1135
A92-54489 p 1023
A92-54496 p 1116
A92-54498 p 1023
A92-54546 p 1069
A92-54550 p 1052
A92-54563 p 1116
A92-54569 p 1023
A92-54571 p 1024
A92-54630 * p 1129
A92-54650 p 1116
A92-54660 * p 1135
A92-54678 p 1116
A92-54754 p 1045
A92-54867 p 1116
A92-54868 p 1117
A92-54902 p 1045
A92-54905 * p 1024
A92-54906 * p 1024
A92-54908 p 1135
A92-54909 * p 1135
A92-54910 p 1024
A92-54911 * p 1024
A92-54914 p 1024
A92-54916 * p 1024
A92-54918 p 1024
A92-54919 * p 1024
A92-54921 * p 1117
A92-54922 * p 1024
A92-54931 p 1117
A92-54932 p 1117
A92-54933 p 1025
A92-54934 * p 1117
A92-54935 p 1025
A92-54936 p 1025
A92-54938 p 1117
A92-54981 p 1052
A92-55098 p 1103
A92-55099 p 1015
A92-55100 p 1092
A92-55102 p 1015
A92-55103 p 1015
A92-55104 p 1052
A92-55127 p 1117
A92-55128 * p 1052
A92-55131 * p 1052
A92-55134 * p 1105
A92-55151 p 1130
A92-55170 * # p 1073
A92-55171 # p 1073
A92-55172 # p 1073
A92-55173 * # p 1073
A92-55174 * # p 1074
A92-55182 # p 1131

A92-55191 # p 1074
A92-55192 # p 1074
A92-55193 # p 1074
A92-55194 # p 1074
A92-55196 * # p 1074
A92-55199 * # p 1075
A92-55200 # p 1075
A92-55203 # p 1075
A92-55204 # p 1075
A92-55205 * # p 1075
A92-55206 # p 1076
A92-55211 * # p 1045
A92-55212 * # p 1063
A92-55229 # p 1076
A92-55230 * # p 1076
A92-55231 # p 1076
A92-55232 * # p 1076
A92-55233 # p 1076
A92-55237 # p 1131
A92-55246 # p 1077
A92-55262 * # p 1131
A92-55265 # p 1131
A92-55267 # p 1131
A92-55271 * # p 1131
A92-55272 # p 1141
A92-55280 # p 1077
A92-55281 * # p 1069
A92-55282 * # p 1131
A92-55283 * # p 1077
A92-55284 # p 1077
A92-55296 # p 1077
A92-55300 * # p 1052
A92-55302 # p 1077
A92-55303 # p 1077
A92-55304 # p 1078
A92-55305 # p 1078
A92-55306 # p 1132
A92-55310 # p 1103
A92-55311 # p 1104
A92-55326 p 1078
A92-55327 * # p 1078
A92-55328 * # p 1063
A92-55329 # p 1078
A92-55330 * # p 1078
A92-55331 # p 1079
A92-55332 # p 1079
A92-55333 # p 1079
A92-55334 # p 1079
A92-55340 # p 1079
A92-55341 # p 1079
A92-55342 # p 1079
A92-55343 * # p 1080
A92-55344 # p 1025
A92-55345 # p 1025
A92-55346 # p 1080
A92-55347 # p 1080
A92-55348 * # p 1092
A92-55349 # p 1080
A92-55350 * # p 1025
A92-55351 # p 1080
A92-55352 * # p 1080
A92-55353 * # p 1025
A92-55354 * # p 1081
A92-55355 * # p 1026
A92-55363 * # p 1081
A92-55364 # p 1026
A92-55365 * # p 1026
A92-55366 # p 1081
A92-55367 # p 1026
A92-55368 # p 1026
A92-55369 # p 1026
A92-55370 # p 1081
A92-55371 # p 1081
A92-55372 # p 1027
A92-55373 # p 1027
A92-55375 * # p 1027
A92-55376 * # p 1132
A92-55377 * # p 1027
A92-55380 # p 1081
A92-55382 # p 1027
A92-55387 # p 1027
A92-55393 * # p 1082
A92-55394 # p 1028
A92-55395 # p 1028
A92-55396 # p 1082
A92-55397 * # p 1028
A92-55426 p 1132
A92-55453 p 1118
A92-55500 p 1070
A92-55902 p 1070
A92-55906 p 1082
A92-55907 p 1063
A92-55908 p 1063
A92-55910 p 1082
A92-55911 p 1082
A92-55955 p 1045
A92-55968 * p 1046
A92-55973 p 1046
A92-56001 p 1015
A92-56002 p 1106
A92-56003 p 1092
A92-56005 p 1092
A92-56006 p 1028
A92-56007 p 1028
A92-56008 p 1028
A92-56009 p 1029
A92-56010 p 1029
A92-56011 p 1092
A92-56012 p 1093
A92-56013 p 1093
A92-56014 p 1052
A92-56015 p 1052
A92-56016 p 1052
A92-56017 p 1053
A92-56018 p 1053
A92-56019 p 1053
A92-56020 p 1053
A92-56021 p 1082
A92-56022 p 1083
A92-56023 p 1093
A92-56024 p 1118
A92-56025 p 1083
A92-56026 p 1083
A92-56027 p 1083
A92-56028 p 1083
A92-56029 p 1083
A92-56030 p 1083
A92-56032 p 1083
A92-56033 p 1083
A92-56034 p 1118
A92-56035 p 1118
A92-56036 p 1118
A92-56038 p 1118
A92-56039 p 1118
A92-56040 p 1029
A92-56042 p 1029
A92-56043 p 1093
A92-56044 p 1029
A92-56045 p 1029
A92-56046 p 1029
A92-56047 p 1029
A92-56048 p 1030
A92-56049 p 1030
A92-56050 p 1030
A92-56051 p 1053
A92-56052 p 1030
A92-56053 p 1030
A92-56054 p 1030
A92-56055 p 1135
A92-56057 p 1084
A92-56058 p 1030
A92-56059 p 1064
A92-56061 p 1053
A92-56062 p 1084
A92-56066 p 1084
A92-56067 p 1132
A92-56068 p 1084
A92-56069 p 1104
A92-56070 p 1084
A92-56072 p 1053
A92-56073 p 1053
A92-56074 p 1135
A92-56075 p 1053
A92-56076 p 1093
A92-56077 p 1053
A92-56078 p 1030
A92-56079 p 1084
A92-56080 p 1015
A92-56081 p 1046
A92-56082 p 1064
A92-56083 p 1015
A92-56084 p 1118
A92-56085 p 1016
A92-56086 p 1084
A92-56087 p 1016
A92-56088 p 1046
A92-56089 p 1046
A92-56090 p 1046
A92-56091 p 1046
A92-56092 p 1046
A92-56093 p 1046
A92-56094 p 1118
A92-56100 p 1016
A92-56102 p 1106
A92-56103 p 1106
A92-56105 p 1106
A92-56107 p 1118
A92-56109 p 1119
A92-56110 p 1047
A92-56111 p 1093
A92-56112 p 1054
A92-56113 p 1132
A92-56114 p 1093
A92-56115 p 1054
A92-56116 p 1047
A92-56117 p 1047
A92-56118 p 1047
A92-56119 p 1084
A92-56120 p 1047
A92-56121 p 1104
A92-56122 p 1070
A92-56141 # p 1119
A92-56143 # p 1119
A92-56151 p 1084
A92-56154 * p 1030
A92-56156 p 1054
A92-56157 * p 1030
A92-56158 * p 1054
A92-56159 p 1030
A92-56160 * p 1054
A92-56161 p 1031
A92-56162 p 1136
A92-56163 * p 1031
A92-56164 * p 1031
A92-56165 * p 1031
A92-56166 p 1031
A92-56169 p 1136
A92-56170 p 1031
A92-56171 p 1054
A92-56172 * p 1064
A92-56173 * p 1031
A92-56174 p 1054
A92-56176 * p 1054
A92-56178 p 1055
A92-56179 p 1031
A92-56180 p 1043
A92-56181 p 1119
A92-56201 p 1119
A92-56202 p 1119
A92-56209 p 1119
A92-56212 p 1141
A92-56215 p 1119
A92-56220 p 1055
A92-56221 p 1016
A92-56222 p 1120
A92-56225 p 1120
A92-56241 * p 1120
A92-56252 p 1120
A92-56254 p 1120
A92-56257 * p 1120
A92-56276 p 1121
A92-56277 p 1016
A92-56278 p 1132
A92-56279 p 1055
A92-56280 p 1093
A92-56281 p 1070
A92-56282 p 1084
A92-56283 p 1085
A92-56284 p 1085
A92-56285 * p 1055
A92-56286 * p 1055
A92-56287 p 1055
A92-56288 p 1056
A92-56289 p 1056
A92-56290 p 1056
A92-56292 p 1064
A92-56293 p 1132
A92-56295 p 1064
A92-56296 p 1121
A92-56297 p 1056
A92-56298 * p 1056
A92-56299 p 1016
A92-56300 p 1070
A92-56301 p 1056
A92-56302 p 1056
A92-56303 p 1085
A92-56304 p 1016
A92-56306 p 1016
A92-56307 p 1056
A92-56308 p 1085
A92-56309 p 1057
A92-56310 p 1057
A92-56311 p 1057
A92-56312 p 1057
A92-56313 p 1094
A92-56314 p 1085
A92-56315 * p 1085
A92-56316 * p 1057
A92-56317 p 1085
A92-56318 p 1086
A92-56320 p 1121
A92-56322 p 1121
A92-56324 * p 1121
A92-56325 p 1057
A92-56326 p 1106
A92-56327 p 1016
A92-56328 p 1057
A92-56329 p 1057
A92-56330 p 1058
A92-56331 p 1032
A92-56332 p 1032
A92-56333 p 1086
A92-56334 p 1086
A92-56335 p 1058
A92-56336 p 1058
A92-56337 p 1058
A92-56338 p 1070
A92-56339 * p 1133
A92-56340 p 1058
A92-56341 p 1058
A92-56342 p 1058
A92-56343 p 1059
A92-56344 * p 1136
A92-56345 p 1136
A92-56346 p 1059
A92-56347 p 1059
A92-56348 p 1059
A92-56349 p 1032
A92-56350 p 1059
A92-56351 p 1032
A92-56352 p 1032
A92-56353 p 1059
A92-56354 * p 1060
A92-56371 * p 1121
A92-56374 p 1121
A92-56602 * p 1141
A92-56607 p 1122
A92-56726 # p 1094
A92-56727 * # p 1094
A92-56729 # p 1094
A92-56735 # p 1122
A92-56736 # p 1017
A92-56738 # p 1094
A92-56743 * # p 1094
A92-56744 * # p 1094
A92-56745 * # p 1094
A92-56746 # p 1095
A92-56747 * # p 1032
A92-56748 * # p 1095
A92-56749 # p 1095
A92-56750 # p 1032
A92-56752 # p 1033
A92-56753 * # p 1095
A92-56754 # p 1133
A92-56755 # p 1095
A92-56756 * # p 1095
A92-56757 # p 1096
A92-56758 # p 1096
A92-56759 # p 1070
A92-56760 # p 1096
A92-56761 * # p 1096
A92-56765 # p 1122
A92-56767 * # p 1096
A92-56768 * # p 1096
A92-56770 * # p 1096
A92-56771 * # p 1033
A92-56772 # p 1104
A92-56773 # p 1097
A92-56774 # p 1097
A92-56775 # p 1097
A92-56776 * # p 1033
A92-56781 # p 1133
A92-56784 # p 1097
A92-56788 # p 1122
A92-56789 # p 1097
A92-56790 # p 1097
A92-56791 # p 1098
A92-56795 # p 1098
A92-56796 * # p 1098
A92-56797 # p 1098
A92-56798 # p 1098
A92-56802 # p 1098
A92-56803 # p 1071
A92-56805 # p 1071
A92-56806 # p 1098
A92-56807 # p 1099
A92-56809 # p 1060
A92-56810 # p 1033
A92-56815 # p 1099
A92-56816 # p 1099
A92-56818 # p 1099
A92-56824 # p 1122
A92-56825 * # p 1099
A92-56826 # p 1122
A92-56828 * # p 1122
A92-56829 # p 1123
A92-56831 # p 1099
A92-56832 * # p 1033
A92-56834 * # p 1033
A92-56835 # p 1033
A92-56836 * # p 1034
A92-56838 # p 1100
A92-56839 # p 1100
A92-56840 # p 1100
A92-56841 # p 1100
A92-56842 # p 1141
A92-56843 # p 1100
A92-56844 * # p 1141
A92-56845 * # p 1034
A92-56846 * # p 1034
A92-56847 * # p 1104
A92-56850 # p 1100
A92-56851 * # p 1034
A92-56854 * # p 1100
A92-56855 * # p 1034
A92-56856 * # p 1101
A92-56857 * # p 1035
A92-56858 * # p 1035
A92-56860 # p 1123
A92-56861 * # p 1035
A92-56862 # p 1035
A92-56866 p 1123
A92-57034 * # p 1035
A92-57035 # p 1035
A92-57039 p 1123
A92-57098 p 1071
A92-57099 p 1071
A92-57100 * p 1106
A92-57101 p 1106
A92-57102 p 1104
A92-57254 p 1104
A92-57258 p 1105
A92-57259 * p 1105
A92-57288 p 1123
A92-57399 p 1123
A92-57444 p 1133
A92-57445 p 1133
A92-57446 p 1133
A92-57499 p 1035

N92-10002 * # p 2
N92-10003 * # p 2
N92-10006 * # p 11
N92-10007 p 11
N92-10008 * # p 11
N92-10009 # p 11
N92-10010 # p 11
N92-10011 * # p 11
N92-10015 # p 12
N92-10016 # p 12
N92-10017 * # p 17
N92-10018 # p 18
N92-10019 # p 18
N92-10020 # p 19
N92-10022 # p 21
N92-10024 * # p 23
N92-10028 # p 29
N92-10053 * # p 33
N92-10062 # p 33
N92-10066 * # p 35
N92-10100 # p 35
N92-10141 # p 41
N92-10157 # p 41
N92-10163 # p 41
N92-10164 # p 41
N92-10174 # p 41
N92-10185 * p 42
N92-10206 # p 42
N92-10347 * # p 53
N92-10598 * # p 54
N92-10599 * # p 54
N92-10600 * # p 54
N92-10601 * # p 54
N92-10602 * # p 54
N92-10603 * # p 55
N92-10604 * # p 55
N92-10605 * # p 55
N92-10606 * # p 55
N92-10607 * # p 55
N92-10608 * # p 55
N92-10972 # p 2
N92-10975 * # p 12
N92-10976 * # p 12
N92-10979 * # p 12
N92-10980 # p 12
N92-10981 * # p 13
N92-10982 * # p 13
N92-10983 * # p 13
N92-10985 # p 13
N92-10986 # p 13
N92-10989 # p 13
N92-10990 * # p 14
N92-10991 # p 18
N92-10992 # p 18
N92-10993 # p 18
N92-10994 * # p 18
N92-10996 # p 19
N92-10997 # p 20
N92-11000 * # p 21
N92-11001 # p 22

N92-11002 # p 22
N92-11004 # p 22
N92-11005 # p 22
N92-11006 # p 22
N92-11007 # p 23
N92-11008 # p 23
N92-11009 # p 23
N92-11010 * # p 23
N92-11011 # p 23
N92-11012 p 25
N92-11014 * # p 26
N92-11015 # p 26
N92-11016 * # p 26
N92-11017 * # p 26
N92-11018 # p 29
N92-11019 # p 30
N92-11020 # p 31
N92-11021 # p 31
N92-11022 * # p 31
N92-11023 * # p 31
N92-11024 * # p 31
N92-11025 # p 31
N92-11028 # p 31
N92-11029 # p 32
N92-11030 * # p 32
N92-11070 * # p 33
N92-11149 * # p 35
N92-11203 # p 35
N92-11213 # p 35
N92-11235 # p 42
N92-11237 # p 42
N92-11287 # p 42
N92-11297 * # p 42
N92-11307 # p 43
N92-11309 # p 43
N92-11310 # p 43
N92-11311 # p 43
N92-11312 # p 43
N92-11319 * # p 43
N92-11328 * # p 44
N92-11367 # p 44
N92-11376 # p 44
N92-11377 * # p 44
N92-11378 * # p 44
N92-11379 * # p 44
N92-11383 # p 44
N92-11391 * # p 45
N92-11578 # p 45
N92-11593 * # p 46
N92-11642 * # p 53
N92-11706 * # p 53
N92-11737 # p 53
N92-11758 * # p 56
N92-11759 * # p 56
N92-11765 * # p 56
N92-11963 # p 57
N92-11969 p 80
N92-11970 p 81
N92-11972 # p 81
N92-11973 # p 81
N92-11975 # p 81
N92-11976 # p 81
N92-11977 * # p 81
N92-11980 # p 82
N92-11981 # p 82
N92-11982 # p 82
N92-11983 * # p 82
N92-11984 * # p 82
N92-11985 * # p 82
N92-11988 # p 102
N92-11989 p 114
N92-11990 # p 114
N92-11991 # p 114
N92-11992 * # p 114
N92-11993 # p 114
N92-11994 * # p 118
N92-11996 # p 129
N92-11997 # p 129
N92-11998 # p 130
N92-11999 # p 130
N92-12000 # p 130
N92-12001 # p 130
N92-12003 # p 134
N92-12004 # p 135
N92-12006 # p 138
N92-12007 * # p 138
N92-12025 * # p 140
N92-12033 * # p 140
N92-12049 * # p 140
N92-12060 # p 143
N92-12153 # p 155
N92-12154 # p 155
N92-12173 * # p 156
N92-12199 p 156
N92-12201 p 156
N92-12203 p 156
N92-12206 p 157
N92-12216 # p 157
N92-12231 * # p 157
N92-12270 p 157
N92-12286 * # p 157
N92-12312 # p 157
N92-12313 # p 158
N92-12373 # p 161
N92-12440 * # p 163
N92-12451 # p 163
N92-12452 # p 163
N92-12458 # p 135
N92-12461 # p 164
N92-12466 # p 135
N92-12469 # p 164
N92-12517 # p 164
N92-12520 # p 164
N92-12528 * # p 164
N92-12529 # p 102
N92-12530 # p 103
N92-12531 # p 118
N92-12534 # p 114
N92-12536 # p 118
N92-12538 # p 61
N92-12539 # p 118
N92-12540 # p 119
N92-12542 # p 164
N92-12598 * # p 166
N92-12988 # p 61
N92-12989 * # p 61
N92-12991 # p 62
N92-12992 # p 62
N92-12994 * # p 82
N92-12995 p 83
N92-12996 # p 83
N92-12997 # p 83
N92-12998 # p 83
N92-12999 # p 83
N92-13000 # p 84
N92-13001 # p 84
N92-13002 * # p 84
N92-13003 # p 84
N92-13004 # p 84
N92-13005 # p 84
N92-13006 # p 85
N92-13007 * # p 85
N92-13008 # p 85
N92-13009 * # p 85
N92-13010 # p 85
N92-13011 # p 85
N92-13012 # p 86
N92-13014 # p 86
N92-13015 # p 86
N92-13016 # p 86
N92-13017 * # p 86
N92-13018 # p 87
N92-13019 * # p 87
N92-13020 * # p 87
N92-13021 # p 87
N92-13022 # p 87
N92-13023 # p 87
N92-13024 # p 87
N92-13025 # p 88
N92-13026 # p 88
N92-13027 # p 88
N92-13028 # p 88
N92-13029 p 88
N92-13030 p 89
N92-13031 p 89
N92-13032 p 89
N92-13034 # p 89
N92-13035 # p 89
N92-13036 p 90
N92-13037 # p 90
N92-13038 * # p 90
N92-13039 # p 92
N92-13040 # p 92
N92-13041 # p 92
N92-13042 # p 93
N92-13043 # p 93
N92-13044 * # p 93
N92-13045 # p 93
N92-13046 # p 93
N92-13049 # p 103
N92-13051 # p 103
N92-13052 # p 103
N92-13053 p 115
N92-13054 * # p 115
N92-13055 # p 115
N92-13056 # p 115
N92-13057 * # p 115
N92-13058 # p 116
N92-13059 # p 116
N92-13060 # p 116
N92-13061 # p 116
N92-13062 # p 116
N92-13063 # p 116
N92-13064 * # p 117
N92-13065 * # p 119
N92-13066 # p 119
N92-13067 # p 119
N92-13069 # p 130
N92-13071 * # p 130
N92-13072 # p 131
N92-13073 * # p 135
N92-13075 # p 135
N92-13076 # p 139
N92-13077 # p 139
N92-13078 # p 139
N92-13079 # p 139
N92-13080 # p 139
N92-13351 # p 158
N92-13406 # p 158
N92-13409 # p 158
N92-13410 # p 158
N92-13434 # p 158
N92-13453 # p 159
N92-13454 # p 159
N92-13455 * # p 159
N92-13458 * # p 159
N92-13460 * # p 159
N92-13470 # p 160
N92-13746 # p 164
N92-13757 * # p 166
N92-13758 * # p 166
N92-13759 * # p 166
N92-13822 # p 166
N92-13835 * # p 165
N92-13838 * # p 90
N92-13842 * # p 117
N92-13848 * # p 90
N92-13849 * # p 90
N92-13857 * # p 167
N92-13858 * # p 119
N92-13861 * # p 90
N92-13867 * # p 160
N92-13868 * # p 91
N92-13926 # p 169
N92-13927 # p 170
N92-13928 * # p 170
N92-13929 * # p 193
N92-13930 * # p 193
N92-13931 * # p 193
N92-13932 * # p 193
N92-13933 * # p 193
N92-13938 * # p 201
N92-13939 * # p 201
N92-13948 * # p 194
N92-13949 * # p 194
N92-13950 * # p 220
N92-13951 * # p 176
N92-13953 * # p 176
N92-13954 * # p 194
N92-13955 * # p 194
N92-13956 * # p 202
N92-13958 * # p 194
N92-13959 * # p 194
N92-13960 * # p 177
N92-13961 * # p 177
N92-13962 * # p 220
N92-13969 * # p 177
N92-13970 * # p 177
N92-13973 * # p 202
N92-13974 * # p 177
N92-13977 # p 202
N92-13979 # p 177
N92-13981 # p 194
N92-13982 # p 207
N92-13985 # p 220
N92-13991 # p 170
N92-13992 # p 170
N92-13993 # p 170
N92-13994 p 178
N92-13995 * # p 178
N92-13996 * # p 178
N92-13997 * # p 178
N92-13998 * # p 179
N92-13999 * # p 179
N92-14001 * # p 179
N92-14002 * # p 179
N92-14006 # p 187
N92-14007 # p 187
N92-14009 p 189
N92-14012 # p 189
N92-14015 # p 189
N92-14018 # p 189
N92-14025 # p 190
N92-14027 # p 207
N92-14028 # p 190
N92-14029 # p 190
N92-14033 # p 190
N92-14034 # p 191
N92-14036 * # p 191
N92-14037 * # p 195
N92-14038 * # p 195
N92-14039 * # p 195
N92-14042 # p 195
N92-14043 # p 195
N92-14044 # p 196
N92-14045 # p 196
N92-14047 # p 198
N92-14048 # p 198
N92-14049 # p 198
N92-14050 # p 199
N92-14051 # p 199
N92-14052 # p 199
N92-14053 # p 199
N92-14054 # p 199
N92-14055 # p 199
N92-14056 # p 200
N92-14058 # p 200
N92-14059 # p 202
N92-14060 # p 202
N92-14063 * # p 202
N92-14064 # p 202
N92-14065 # p 205
N92-14066 * # p 205
N92-14087 * # p 210
N92-14101 # p 211
N92-14103 # p 211
N92-14108 * # p 211
N92-14210 * # p 220
N92-14217 * # p 220
N92-14262 * # p 221
N92-14263 * # p 221
N92-14270 # p 221
N92-14309 # p 221
N92-14310 * # p 221
N92-14313 * # p 221
N92-14344 * # p 221
N92-14345 # p 222
N92-14346 * # p 222
N92-14348 * # p 222
N92-14349 * # p 222
N92-14350 * # p 222
N92-14351 * # p 222
N92-14354 * # p 223
N92-14356 * # p 223
N92-14357 * # p 223
N92-14360 * # p 223
N92-14361 * # p 223
N92-14362 * # p 224
N92-14363 * # p 224
N92-14364 * # p 224
N92-14366 * # p 224
N92-14367 * # p 224
N92-14370 * # p 224
N92-14371 * # p 224
N92-14373 * # p 225
N92-14374 * # p 225
N92-14382 # p 225
N92-14386 # p 225
N92-14391 * # p 225
N92-14397 # p 225
N92-14405 # p 226
N92-14411 # p 214
N92-14413 # p 214
N92-14414 # p 226
N92-14424 # p 226
N92-14425 # p 226
N92-14428 # p 226
N92-14431 # p 226
N92-14598 * # p 234
N92-14673 # p 234
N92-14674 # p 234
N92-14677 # p 234
N92-14779 * # p 235
N92-14780 * # p 236
N92-14782 * # p 236
N92-14783 * # p 236
N92-14784 * # p 236
N92-14785 * # p 236
N92-14786 * # p 236
N92-14787 * # p 236
N92-14788 * # p 236
N92-14789 * # p 237
N92-14791 # p 237
N92-14795 * # p 237
N92-14797 * # p 237
N92-14798 # p 237
N92-14923 # p 238
N92-14925 # p 238
N92-14927 # p 238
N92-14933 # p 238
N92-14966 # p 170
N92-14968 * # p 179
N92-14969 * # p 180
N92-14972 # p 180
N92-14973 # p 180
N92-14974 # p 180
N92-14975 # p 211
N92-14977 # p 211
N92-14980 # p 211
N92-14981 # p 180
N92-14984 # p 211
N92-14985 # p 181
N92-14986 # p 181
N92-14987 # p 181
N92-14990 # p 181
N92-14992 # p 181
N92-14993 # p 181
N92-14994 # p 182
N92-14995 # p 182
N92-14996 # p 182
N92-14998 # p 182
N92-14999 # p 208
N92-15000 # p 182
N92-15001 # p 208
N92-15002 # p 208
N92-15003 # p 208
N92-15004 # p 227
N92-15005 # p 182
N92-15006 # p 183
N92-15008 # p 183
N92-15009 # p 208
N92-15013 # p 238
N92-15014 # p 183
N92-15016 # p 183
N92-15017 # p 183
N92-15020 * # p 183
N92-15021 # p 208
N92-15025 # p 184
N92-15027 # p 227
N92-15029 # p 227
N92-15030 # p 227
N92-15031 # p 184
N92-15032 # p 184
N92-15033 # p 227
N92-15035 # p 184
N92-15037 # p 211
N92-15039 * # p 184
N92-15040 # p 184
N92-15041 # p 184
N92-15042 # p 184
N92-15043 # p 209
N92-15045 # p 185
N92-15047 * # p 185
N92-15048 * # p 185
N92-15049 * # p 185
N92-15050 * # p 185
N92-15051 * # p 185
N92-15052 * # p 186
N92-15053 # p 187
N92-15054 # p 187
N92-15055 # p 187
N92-15058 # p 191
N92-15060 * # p 191
N92-15061 # p 191
N92-15065 # p 196
N92-15066 # p 196
N92-15067 # p 196
N92-15068 # p 196
N92-15069 # p 197
N92-15070 * # p 197
N92-15072 # p 205
N92-15073 # p 206
N92-15074 # p 206
N92-15075 * # p 206
N92-15076 * # p 206
N92-15077 * # p 209
N92-15083 * # p 227
N92-15084 * # p 228
N92-15089 * # p 228
N92-15092 * # p 228
N92-15093 * # p 228
N92-15094 * # p 228
N92-15095 * # p 228
N92-15191 * # p 214
N92-15203 * p 228
N92-15272 # p 229
N92-15367 # p 229
N92-15385 # p 229
N92-15392 # p 229
N92-15402 * # p 229
N92-15406 * # p 230
N92-15658 * # p 234
N92-15761 # p 238
N92-15870 * # p 234
N92-15877 * # p 212
N92-15937 # p 238
N92-15938 # p 239
N92-15962 # p 241
N92-15963 # p 242
N92-15964 # p 257

N92-15965 * # p 257
N92-15966 * # p 258
N92-15967 * # p 258
N92-15968 * # p 258
N92-15969 * # p 258
N92-15970 p 258
N92-15971 p 259
N92-15972 p 259
N92-15973 p 259
N92-15974 * # p 259
N92-15975 # p 259
N92-15978 # p 263
N92-15979 # p 263
N92-15980 # p 268
N92-15981 # p 268
N92-15983 # p 268
N92-15986 * # p 272
N92-15987 p 272
N92-15988 p 272
N92-15990 # p 272
N92-15991 * # p 276
N92-15992 # p 279
N92-15993 * # p 279
N92-15998 * # p 284
N92-16012 * # p 286
N92-16128 # p 289
N92-16174 p 296
N92-16181 # p 297
N92-16225 # p 297
N92-16243 * p 297
N92-16265 * # p 297
N92-16281 # p 297
N92-16283 * # p 297
N92-16325 # p 298
N92-16326 # p 298
N92-16336 * # p 298
N92-16458 # p 301
N92-16605 * # p 303
N92-16705 * # p 304
N92-16789 # p 304
N92-16973 * # p 286
N92-16978 # p 298
N92-16986 # p 263
N92-17002 * # p 298
N92-17004 * # p 289
N92-17006 * # p 298
N92-17011 # p 279
N92-17019 * # p 282
N92-17024 # p 299
N92-17028 # p 301
N92-17033 * # p 299
N92-17034 * # p 299
N92-17061 * # p 279
N92-17070 * # p 289
N92-17071 * # p 273
N92-17088 # p 304
N92-17096 # p 282
N92-17097 # p 284
N92-17114 # p 260
N92-17128 * # p 276
N92-17130 * # p 303
N92-17133 # p 263
N92-17149 # p 264
N92-17153 # p 273
N92-17154 # p 273
N92-17155 # p 273
N92-17157 # p 273
N92-17158 # p 273
N92-17159 # p 274
N92-17160 # p 274
N92-17161 # p 274
N92-17162 # p 274
N92-17163 # p 274
N92-17164 # p 274
N92-17165 # p 274
N92-17166 # p 282
N92-17167 * # p 286
N92-17168 # p 299
N92-17204 # p 279
N92-17213 # p 264
N92-17214 * # p 286
N92-17216 # p 299
N92-17217 # p 264
N92-17221 # p 277
N92-17222 # p 260
N92-17234 # p 275
N92-17243 # p 283
N92-17258 # p 300
N92-17259 # p 264
N92-17260 # p 285
N92-17266 # p 275
N92-17281 # p 260
N92-17297 # p 285
N92-17300 # p 275
N92-17303 # p 260
N92-17310 # p 290
N92-17313 # p 275
N92-17316 * # p 275
N92-17325 # p 287
N92-17339 # p 260
N92-17344 # p 300
N92-17346 * # p 242
N92-17347 * # p 261
N92-17350 * # p 287
N92-17369 # p 305
N92-17387 # p 300
N92-17393 * # p 301
N92-17404 # p 261
N92-17438 # p 303
N92-17442 # p 283
N92-17477 # p 242
N92-17478 # p 264
N92-17498 # p 303
N92-17506 # p 304
N92-17509 * # p 261
N92-17512 * # p 268
N92-17513 # p 275
N92-17537 # p 305
N92-17546 * # p 279
N92-17547 * # p 261
N92-17552 # p 280
N92-17565 # p 275
N92-17568 # p 268
N92-17587 # p 264
N92-17629 # p 300
N92-17653 # p 290
N92-17674 * # p 300
N92-17681 # p 261
N92-17682 # p 290
N92-17687 # p 305
N92-17707 # p 268
N92-17729 # p 280
N92-17748 # p 283
N92-17754 # p 287
N92-17755 # p 261
N92-17756 # p 285
N92-17757 # p 300
N92-17843 p 276
N92-17844 p 268
N92-17847 p 276
N92-17849 # p 262
N92-17855 # p 280
N92-17874 # p 262
N92-17875 # p 302
N92-17917 # p 283
N92-17932 # p 290
N92-17984 * # p 242
N92-17985 * # p 265
N92-17986 * # p 265
N92-17987 * # p 265
N92-17988 * # p 265
N92-17989 * # p 277
N92-17990 * # p 265
N92-17994 * # p 269
N92-17995 * # p 266
N92-17996 * # p 266
N92-17998 * # p 303
N92-17999 * # p 266
N92-18002 * # p 303
N92-18007 # p 344
N92-18012 # p 384
N92-18014 # p 370
N92-18024 * # p 358
N92-18037 # p 384
N92-18038 * # p 359
N92-18053 * # p 399
N92-18069 # p 385
N92-18073 # p 359
N92-18074 p 416
N92-18091 p 399
N92-18096 p 359
N92-18112 # p 354
N92-18116 # p 399
N92-18120 p 400
N92-18125 * # p 412
N92-18182 # p 352
N92-18187 # p 400
N92-18193 p 344
N92-18221 # p 400
N92-18230 # p 376
N92-18231 # p 344
N92-18232 # p 345
N92-18233 # p 345
N92-18239 # p 345
N92-18242 # p 352
N92-18244 # p 400
N92-18252 # p 412
N92-18259 # p 352
N92-18269 # p 345
N92-18280 * # p 387
N92-18282 * # p 416
N92-18290 # p 385
N92-18293 # p 345
N92-18294 # p 380
N92-18309 # p 417
N92-18316 # p 345
N92-18317 # p 400
N92-18318 # p 345
N92-18321 # p 380
N92-18322 # p 308
N92-18333 # p 359
N92-18341 # p 385
N92-18345 # p 346
N92-18347 * # p 359
N92-18415 # p 385
N92-18416 # p 385
N92-18482 # p 359
N92-18483 # p 400
N92-18484 # p 346
N92-18485 # p 400
N92-18515 # p 401
N92-18550 # p 401
N92-18571 # p 360
N92-18572 # p 360
N92-18573 # p 401
N92-18574 # p 360
N92-18575 # p 360
N92-18576 # p 360
N92-18577 # p 390
N92-18578 # p 360
N92-18579 # p 360
N92-18580 # p 361
N92-18581 # p 361
N92-18582 # p 361
N92-18584 # p 361
N92-18585 # p 361
N92-18586 # p 361
N92-18587 # p 362
N92-18588 * # p 362
N92-18589 * # p 362
N92-18590 # p 362
N92-18591 # p 363
N92-18592 # p 363
N92-18593 # p 363
N92-18594 # p 363
N92-18595 # p 363
N92-18647 # p 412
N92-18705 # p 401
N92-18728 # p 376
N92-18729 # p 354
N92-18760 * # p 346
N92-18778 # p 363
N92-18779 # p 363
N92-18780 * # p 364
N92-18781 # p 364
N92-18782 # p 364
N92-18783 # p 346
N92-18784 # p 364
N92-18785 # p 364
N92-18786 # p 364
N92-18787 # p 364
N92-18788 # p 365
N92-18789 # p 365
N92-18790 # p 365
N92-18791 * # p 380
N92-18792 # p 380
N92-18793 # p 380
N92-18794 # p 365
N92-18795 # p 381
N92-18814 # p 417
N92-18825 # p 346
N92-18826 # p 365
N92-18867 # p 376
N92-18877 * # p 401
N92-18893 # p 381
N92-18895 # p 346
N92-18897 # p 401
N92-18933 # p 402
N92-18940 # p 402
N92-18942 # p 387
N92-18956 * # p 385
N92-18959 # p 402
N92-18965 * # p 402
N92-18967 # p 354
N92-18969 # p 308
N92-18971 * # p 402
N92-19002 * # p 346
N92-19004 # p 402
N92-19005 # p 402
N92-19006 # p 403
N92-19030 # p 365
N92-19041 # p 354
N92-19042 # p 354
N92-19043 # p 354
N92-19044 # p 355
N92-19045 # p 355
N92-19046 # p 355
N92-19047 # p 355
N92-19048 # p 355
N92-19049 # p 355
N92-19050 # p 355
N92-19052 # p 403
N92-19080 # p 403
N92-19085 # p 347
N92-19097 # p 376
N92-19121 * # p 408
N92-19122 * # p 408
N92-19123 * # p 408
N92-19125 * # p 409
N92-19126 * # p 409
N92-19127 * # p 409
N92-19151 # p 403
N92-19154 # p 403
N92-19155 # p 404
N92-19174 * # p 381
N92-19175 * # p 347
N92-19178 # p 366
N92-19183 # p 404
N92-19184 # p 377
N92-19185 # p 366
N92-19192 # p 366
N92-19195 # p 409
N92-19217 * # p 404
N92-19218 * # p 385
N92-19225 # p 366
N92-19231 # p 409
N92-19235 # p 377
N92-19241 # p 381
N92-19247 # p 412
N92-19250 * # p 347
N92-19252 # p 347
N92-19258 * # p 404
N92-19259 # p 352
N92-19276 * # p 352
N92-19277 * # p 404
N92-19290 * # p 390
N92-19292 # p 410
N92-19295 # p 381
N92-19296 # p 347
N92-19304 # p 347
N92-19328 # p 377
N92-19329 # p 377
N92-19335 # p 412
N92-19336 # p 417
N92-19349 # p 404
N92-19350 # p 353
N92-19354 * # p 347
N92-19359 * # p 348
N92-19367 # p 348
N92-19374 * # p 366
N92-19384 # p 404
N92-19386 # p 405
N92-19391 # p 356
N92-19394 # p 348
N92-19397 # p 413
N92-19422 * # p 413
N92-19423 * # p 413
N92-19428 * # p 413
N92-19432 * # p 413
N92-19437 * # p 348
N92-19466 # p 417
N92-19490 # p 405
N92-19491 # p 356
N92-19496 * # p 367
N92-19499 * # p 381
N92-19505 # p 382
N92-19538 p 405
N92-19545 * # p 348
N92-19563 * # p 367
N92-19596 * # p 405
N92-19604 # p 356
N92-19621 p 382
N92-19623 p 349
N92-19633 # p 410
N92-19642 # p 386
N92-19662 # p 308
N92-19667 # p 410
N92-19672 * # p 416
N92-19675 * # p 386
N92-19679 # p 349
N92-19682 # p 349
N92-19698 p 349
N92-19701 p 367
N92-19726 * # p 377
N92-19764 # p 405
N92-19775 * # p 406
N92-19841 * # p 382
N92-19844 * # p 406
N92-19846 * # p 367
N92-19847 * # p 368
N92-19871 * # p 368
N92-19873 # p 406
N92-19925 # p 349
N92-19930 * # p 308
N92-19934 * # p 387
N92-19938 # p 378
N92-19939 # p 378
N92-19940 # p 386
N92-19976 # p 406
N92-19978 # p 386
N92-19993 * # p 350
N92-20026 # p 382
N92-20029 * # p 356
N92-20033 * # p 378
N92-20038 * # p 350
N92-20064 * # p 461
N92-20072 * # p 498
N92-20132 # p 488
N92-20143 # p 498
N92-20147 p 498
N92-20148 p 481
N92-20156 # p 448
N92-20164 # p 488
N92-20179 # p 472
N92-20193 * # p 488
N92-20194 * # p 499
N92-20195 * # p 481
N92-20196 * # p 473
N92-20197 * # p 499
N92-20198 * # p 499
N92-20204 # p 420
N92-20205 # p 420
N92-20229 # p 443
N92-20235 * # p 499
N92-20245 # p 505
N92-20265 # p 499
N92-20267 * # p 461
N92-20280 * # p 461
N92-20283 * # p 443
N92-20301 # p 499
N92-20303 p 448
N92-20318 # p 449
N92-20329 # p 488
N92-20332 p 443
N92-20341 # p 500
N92-20356 p 454
N92-20360 p 511
N92-20376 * # p 481
N92-20378 p 443
N92-20388 # p 511
N92-20417 * # p 461
N92-20428 p 511
N92-20436 # p 473
N92-20448 # p 484
N92-20455 # p 484
N92-20459 # p 473
N92-20460 # p 473
N92-20461 # p 512
N92-20468 # p 444
N92-20473 # p 444
N92-20475 # p 481
N92-20479 * # p 512
N92-20480 * # p 444
N92-20485 p 500
N92-20491 # p 500
N92-20494 * # p 444
N92-20497 # p 500
N92-20498 # p 444
N92-20500 # p 461
N92-20523 * # p 473
N92-20525 * # p 473
N92-20545 * # p 444
N92-20573 # p 474
N92-20574 # p 505
N92-20586 * # p 481
N92-20590 p 509
N92-20629 p 513
N92-20650 * # p 474
N92-20653 # p 500
N92-20654 * # p 445
N92-20664 * # p 462
N92-20665 * # p 462
N92-20666 * # p 486
N92-20677 * # p 501
N92-20679 * # p 489
N92-20695 # p 489
N92-20776 # p 487
N92-20794 # p 449
N92-20797 # p 445
N92-20818 # p 455
N92-20834 # p 455
N92-20849 # p 482
N92-20858 # p 489
N92-20898 # p 484
N92-20902 # p 455
N92-20905 p 510
N92-20909 # p 501
N92-20928 # p 505
N92-20934 * # p 445
N92-20951 * # p 462

N92-20954 * # p 501
N92-20997 # p 501
N92-21012 # p 445
N92-21015 # p 489
N92-21018 # p 489
N92-21040 # p 505
N92-21046 # p 512
N92-21063 # p 490
N92-21159 # p 490
N92-21162 * # p 484
N92-21173 * # p 512
N92-21188 * # p 445
N92-21201 # p 455
N92-21210 # p 462
N92-21232 # p 501
N92-21233 # p 501
N92-21234 # p 502
N92-21253 * # p 482
N92-21263 # p 455
N92-21279 # p 455
N92-21287 # p 445
N92-21297 # p 502
N92-21333 # p 446
N92-21356 * # p 446
N92-21357 * # p 482
N92-21360 # p 482
N92-21385 * # p 502
N92-21392 # p 510
N92-21404 # p 456
N92-21410 * # p 482
N92-21429 p 446
N92-21432 * # p 446
N92-21433 * # p 502
N92-21440 * # p 482
N92-21456 * # p 446
N92-21459 * # p 456
N92-21460 * # p 502
N92-21465 * # p 447
N92-21489 * # p 462
N92-21501 # p 420
N92-21502 * # p 420
N92-21503 * # p 449
N92-21504 # p 447
N92-21509 # p 456
N92-21510 # p 463
N92-21511 # p 484
N92-21513 # p 449
N92-21514 # p 447
N92-21519 * # p 474
N92-21520 * # p 474
N92-21521 * # p 474
N92-21522 * # p 474
N92-21523 * # p 475
N92-21526 * # p 487
N92-21527 * # p 475
N92-21528 * # p 447
N92-21529 * # p 475
N92-21531 * # p 475
N92-21532 * # p 475
N92-21533 * # p 475
N92-21534 * # p 475
N92-21535 * # p 476
N92-21540 * # p 463
N92-21546 * # p 506
N92-21565 * # p 463
N92-21566 * # p 463
N92-21567 * # p 463
N92-21587 * p 463
N92-21588 * p 447
N92-21679 # p 449
N92-21680 # p 449
N92-21681 # p 449
N92-21682 # p 450
N92-21683 # p 450
N92-21684 * # p 450
N92-21685 # p 502
N92-21686 * # p 450
N92-21687 # p 450
N92-21688 * # p 450
N92-21689 # p 451
N92-21690 # p 451
N92-21691 * # p 451
N92-21692 # p 451
N92-21693 # p 451
N92-21694 * # p 452
N92-21695 # p 452
N92-21696 # p 452
N92-21697 # p 452
N92-21698 # p 452
N92-21699 # p 503
N92-21703 # p 447
N92-21719 # p 512
N92-21720 # p 485
N92-21730 # p 503
N92-21736 # p 513
N92-21740 # p 476
N92-21741 # p 503
N92-21743 # p 506
N92-21744 # p 490
N92-21746 p 452
N92-21752 # p 483
N92-21753 # p 447
N92-21777 # p 485
N92-21784 # p 448
N92-21828 # p 503
N92-21833 # p 452
N92-21834 # p 420
N92-21839 p 456
N92-21847 # p 510
N92-21848 # p 476
N92-21850 # p 476
N92-21856 p 463
N92-21870 # p 485
N92-21873 # p 453
N92-21951 # p 464
N92-21952 # p 464
N92-21953 # p 503
N92-21954 # p 503
N92-21955 # p 504
N92-21956 * # p 464
N92-21957 # p 456
N92-21958 # p 456
N92-21959 # p 457
N92-21960 # p 457
N92-21961 # p 464
N92-21962 # p 464
N92-21963 # p 464
N92-21964 # p 465
N92-21965 # p 465
N92-21966 # p 465
N92-21967 # p 465
N92-21968 # p 465
N92-21969 # p 465
N92-21970 # p 466
N92-21971 # p 466
N92-21973 # p 466
N92-21974 # p 466
N92-22000 # p 466
N92-22028 # p 504
N92-22029 # p 504
N92-22096 # p 572
N92-22098 # p 559
N92-22099 # p 591
N92-22104 # p 534
N92-22105 # p 534
N92-22106 # p 534
N92-22132 p 592
N92-22137 p 604
N92-22157 p 570
N92-22179 # p 524
N92-22181 # p 525
N92-22182 # p 525
N92-22184 # p 525
N92-22193 # p 525
N92-22194 * # p 570
N92-22195 * # p 573
N92-22196 * # p 525
N92-22205 p 578
N92-22209 # p 592
N92-22210 # p 534
N92-22211 * # p 574
N92-22215 * # p 525
N92-22216 # p 602
N92-22228 * # p 592
N92-22232 * # p 525
N92-22233 # p 526
N92-22237 # p 573
N92-22239 * # p 592
N92-22240 * # p 526
N92-22241 # p 604
N92-22249 * # p 526
N92-22268 # p 575
N92-22277 # p 575
N92-22296 # p 592
N92-22298 # p 592
N92-22315 p 592
N92-22320 * # p 602
N92-22389 # p 534
N92-22395 * # p 556
N92-22397 # p 593
N92-22406 # p 559
N92-22408 # p 530
N92-22426 * # p 593
N92-22436 * # p 534
N92-22437 * # p 573
N92-22451 * # p 593
N92-22486 * # p 578
N92-22491 * # p 593
N92-22492 * # p 559
N92-22493 * # p 602
N92-22495 * # p 593
N92-22503 # p 573
N92-22504 * # p 556
N92-22506 * # p 526
N92-22507 * # p 526
N92-22510 * # p 559
N92-22511 * # p 559
N92-22513 * # p 578
N92-22514 * # p 593
N92-22515 * # p 578
N92-22517 * # p 578
N92-22518 * # p 559
N92-22519 * # p 560
N92-22520 * # p 560
N92-22523 * # p 593
N92-22526 * # p 594
N92-22527 * # p 594
N92-22529 * # p 570
N92-22530 * # p 560
N92-22531 * # p 560
N92-22532 * # p 560
N92-22533 * # p 560
N92-22534 * # p 549
N92-22535 * # p 561
N92-22536 * # p 561
N92-22538 * # p 561
N92-22539 * # p 561
N92-22540 * # p 561
N92-22541 * # p 561
N92-22543 * # p 561
N92-22562 p 594
N92-22572 p 594
N92-22573 p 594
N92-22577 p 594
N92-22598 * # p 575
N92-22605 p 549
N92-22625 * # p 575
N92-22637 * # p 578
N92-22641 # p 595
N92-22643 * # p 602
N92-22644 * # p 602
N92-22645 * # p 556
N92-22647 * # p 562
N92-22648 * # p 526
N92-22649 * # p 595
N92-22659 * # p 516
N92-22662 * # p 595
N92-22673 p 603
N92-22678 * # p 578
N92-22688 * # p 595
N92-22692 * # p 595
N92-22720 * # p 595
N92-22770 * # p 598
N92-22785 # p 550
N92-22863 * # p 562
N92-22864 * # p 550
N92-22865 * # p 527
N92-22966 # p 573
N92-22971 # p 598
N92-23095 * # p 527
N92-23096 # p 535
N92-23103 * # p 527
N92-23105 * # p 527
N92-23116 * # p 527
N92-23119 # p 598
N92-23122 p 562
N92-23154 * # p 596
N92-23168 # p 528
N92-23223 # p 579
N92-23227 # p 550
N92-23228 * # p 550
N92-23229 * # p 571
N92-23230 * # p 550
N92-23231 # p 550
N92-23232 # p 550
N92-23233 # p 551
N92-23234 # p 571
N92-23235 # p 551
N92-23236 # p 551
N92-23237 # p 551
N92-23238 # p 571
N92-23239 # p 551
N92-23251 # p 596
N92-23254 * # p 562
N92-23267 * # p 596
N92-23295 * # p 605
N92-23352 * # p 596
N92-23383 # p 599
N92-23387 # p 599
N92-23391 # p 599
N92-23393 # p 599
N92-23402 # p 599
N92-23403 # p 599
N92-23435 * # p 596
N92-23441 # p 599
N92-23496 # p 597
N92-23533 * # p 528
N92-23537 * # p 562
N92-23560 * # p 597
N92-23563 * # p 528
N92-23588 # p 605
N92-23596 # p 530
N92-23597 # p 530
N92-23671 p 562
N92-23705 # p 575
N92-23717 p 528
N92-23726 p 605
N92-23778 # p 573
N92-23820 # p 575
N92-23821 # p 576
N92-23822 # p 551
N92-23836 # p 576
N92-23881 # p 603
N92-23919 * # p 576
N92-23928 # p 606
N92-23950 # p 552
N92-23951 # p 552
N92-23952 # p 552
N92-23953 # p 552
N92-23954 # p 552
N92-23955 # p 552
N92-23956 * # p 528
N92-23957 # p 552
N92-23997 p 597
N92-24009 p 553
N92-24010 p 553
N92-24053 * # p 579
N92-24095 * # p 676
N92-24096 * # p 677
N92-24097 * # p 677
N92-24098 * # p 677
N92-24099 * # p 677
N92-24163 * # p 677
N92-24164 * # p 677
N92-24165 * # p 677
N92-24167 * # p 678
N92-24194 * # p 678
N92-24229 * # p 624
N92-24242 * # p 678
N92-24251 * # p 696
N92-24302 * # p 639
N92-24336 # p 658
N92-24337 # p 658
N92-24338 # p 658
N92-24340 # p 658
N92-24344 * # p 678
N92-24345 * # p 678
N92-24393 # p 624
N92-24394 # p 624
N92-24395 # p 625
N92-24397 * # p 691
N92-24400 * # p 691
N92-24411 * # p 691
N92-24419 * # p 691
N92-24424 * # p 691
N92-24428 * # p 692
N92-24454 # p 667
N92-24472 # p 667
N92-24514 * # p 678
N92-24531 * # p 678
N92-24539 * # p 658
N92-24547 * p 679
N92-24556 # p 648
N92-24678 * # p 609
N92-24680 * # p 625
N92-24681 * # p 625
N92-24688 * # p 696
N92-24689 * # p 652
N92-24713 # p 636
N92-24735 # p 640
N92-24760 # p 667
N92-24797 * # p 679
N92-24799 # p 640
N92-24800 * # p 696
N92-24803 * # p 625
N92-24849 # p 625
N92-24850 # p 626
N92-24853 # p 626
N92-24854 # p 626
N92-24856 # p 626
N92-24857 # p 626
N92-24858 # p 626
N92-24859 # p 627
N92-24860 # p 627
N92-24861 * # p 627
N92-24862 # p 627
N92-24863 # p 628
N92-24864 # p 628
N92-24865 # p 628
N92-24866 # p 628
N92-24869 # p 628
N92-24870 # p 629
N92-24871 # p 629
N92-24872 # p 629
N92-24873 # p 679
N92-24874 # p 679
N92-24876 # p 629
N92-24877 # p 629
N92-24882 * # p 630
N92-24885 * # p 630
N92-24888 # p 640
N92-24892 # p 679
N92-24898 * # p 630
N92-24956 * # p 630
N92-24958 * # p 630
N92-24959 * # p 680
N92-24964 # p 648
N92-24966 # p 648
N92-24977 * # p 630
N92-24984 * # p 680
N92-25049 # p 689
N92-25054 # p 680
N92-25090 * # p 664
N92-25091 * # p 664
N92-25098 # p 640
N92-25133 * # p 631
N92-25137 * # p 680
N92-25162 * # p 664
N92-25164 * # p 658
N92-25175 * # p 631
N92-25190 * # p 692
N92-25202 * # p 631
N92-25204 # p 697
N92-25223 # p 669
N92-25259 # p 669
N92-25261 * # p 631
N92-25262 p 636
N92-25263 * # p 648
N92-25264 * # p 692
N92-25267 * # p 680
N92-25276 * # p 631
N92-25279 * # p 632
N92-25297 # p 636
N92-25306 # p 692
N92-25315 # p 667
N92-25342 # p 680
N92-25350 # p 636
N92-25365 # p 665
N92-25366 # p 632
N92-25368 * # p 697
N92-25374 # p 667
N92-25376 * # p 681
N92-25401 # p 662
N92-25402 # p 665
N92-25403 # p 681
N92-25410 p 632
N92-25413 # p 698
N92-25449 * # p 665
N92-25470 # p 640
N92-25498 # p 689
N92-25510 * # p 632
N92-25518 # p 640
N92-25547 p 681
N92-25555 p 662
N92-25569 p 632
N92-25571 p 681
N92-25589 p 682
N92-25590 # p 640
N92-25591 # p 648
N92-25592 # p 652
N92-25593 # p 665
N92-25594 # p 648
N92-25595 # p 641
N92-25596 # p 648
N92-25597 # p 641
N92-25598 # p 652
N92-25599 # p 662
N92-25600 # p 641
N92-25601 # p 641
N92-25603 # p 652
N92-25606 # p 698
N92-25607 * # p 662
N92-25648 * # p 663
N92-25649 * # p 682
N92-25660 # p 682
N92-25667 # p 682
N92-25712 * # p 659
N92-25713 * # p 632
N92-25714 * # p 649
N92-25716 * # p 659
N92-25717 * # p 659
N92-25718 * # p 659
N92-25719 * # p 659
N92-25720 * # p 659
N92-25722 * # p 682
N92-25723 * # p 633
N92-25726 * # p 692
N92-25727 * # p 682
N92-25733 # p 665
N92-25734 * # p 663

N92-25752 * # p 633
N92-25808 * # p 660
N92-25809 * # p 682
N92-25814 * # p 633
N92-25816 * # p 669
N92-25911 * # p 683
N92-25912 * # p 683
N92-25913 * # p 692
N92-25914 * # p 683
N92-25915 * # p 683
N92-25916 * # p 683
N92-25917 * # p 684
N92-25918 * # p 684
N92-25919 * # p 649
N92-25920 * # p 649
N92-25921 * # p 649
N92-25922 * # p 649
N92-25924 * # p 684
N92-25926 * # p 684
N92-25927 * # p 684
N92-25928 * # p 684
N92-25930 * # p 684
N92-25931 * # p 649
N92-25933 * # p 660
N92-25934 * # p 660
N92-25935 * # p 649
N92-25959 * # p 633
N92-25960 * # p 685
N92-25962 * # p 685
N92-25964 * # p 685
N92-25967 * # p 633
N92-25982 * # p 663
N92-25995 * # p 650
N92-26017 * # p 650
N92-26018 * # p 692
N92-26028 # p 637
N92-26039 # p 650
N92-26086 # p 698
N92-26101 # p 641
N92-26104 * # p 633
N92-26125 * p 685
N92-26128 * # p 685
N92-26129 * # p 667
N92-26130 * # p 697
N92-26155 # p 650
N92-26258 # p 764
N92-26291 # p 726
N92-26349 # p 724
N92-26350 # p 775
N92-26362 # p 753
N92-26383 # p 755
N92-26405 * # p 738
N92-26435 * # p 731
N92-26441 # p 764
N92-26458 # p 777
N92-26480 p 738
N92-26521 # p 756
N92-26524 # p 777
N92-26527 # p 749
N92-26553 * # p 738
N92-26555 * # p 764
N92-26560 * # p 764
N92-26561 * # p 738
N92-26581 p 775
N92-26585 p 714
N92-26586 p 739
N92-26592 # p 765
N92-26612 * # p 714
N92-26613 * # p 739
N92-26616 p 714
N92-26620 # p 777
N92-26623 p 726
N92-26651 * # p 715
N92-26652 * # p 715
N92-26655 * # p 731
N92-26673 # p 731
N92-26680 * # p 765
N92-26697 # p 739
N92-26698 # p 765
N92-26720 # p 749
N92-26733 p 780
N92-26756 # p 727
N92-26765 # p 781
N92-26795 # p 727
N92-26816 # p 765
N92-26830 # p 781
N92-26853 # p 765
N92-26863 # p 781
N92-26896 # p 731
N92-26908 # p 766
N92-26909 # p 766
N92-26911 # p 766
N92-26913 # p 766
N92-26915 # p 766
N92-26922 # p 767
N92-26944 # p 732
N92-26947 # p 715
N92-26948 # p 727
N92-27037 * # p 739
N92-27038 # p 767
N92-27039 # p 739
N92-27040 # p 740
N92-27041 # p 740
N92-27042 # p 740
N92-27043 # p 740
N92-27044 # p 756
N92-27045 # p 767
N92-27054 p 715
N92-27062 # p 740
N92-27171 # p 780
N92-27172 # p 715
N92-27185 # p 732
N92-27188 p 732
N92-27191 * # p 715
N92-27193 * # p 767
N92-27217 # p 727
N92-27335 # p 732
N92-27344 # p 716
N92-27352 # p 767
N92-27376 * # p 716
N92-27377 * # p 716
N92-27378 * # p 756
N92-27379 * # p 740
N92-27394 # p 767
N92-27399 * # p 716
N92-27403 * # p 753
N92-27407 # p 768
N92-27422 # p 741
N92-27424 * # p 735
N92-27428 # p 749
N92-27429 # p 732
N92-27452 # p 768
N92-27459 * # p 768
N92-27460 # p 768
N92-27461 # p 741
N92-27462 # p 741
N92-27463 # p 741
N92-27464 # p 741
N92-27466 # p 741
N92-27467 * # p 768
N92-27468 # p 768
N92-27469 # p 742
N92-27470 # p 768
N92-27471 # p 769
N92-27472 # p 769
N92-27475 # p 769
N92-27478 # p 769
N92-27479 # p 769
N92-27480 # p 769
N92-27482 # p 770
N92-27484 # p 742
N92-27486 # p 756
N92-27490 # p 770
N92-27505 # p 745
N92-27518 # p 781
N92-27519 * # p 742
N92-27528 # p 781
N92-27531 # p 756
N92-27546 # p 770
N92-27558 * # p 716
N92-27577 # p 746
N92-27587 * # p 742
N92-27600 # p 770
N92-27613 # p 753
N92-27615 p 770
N92-27624 # p 716
N92-27645 # p 749
N92-27649 * # p 770
N92-27652 * # p 742
N92-27653 * # p 770
N92-27669 * # p 742
N92-27670 * # p 750
N92-27671 # p 771
N92-27680 # p 771
N92-27682 # p 724
N92-27706 # p 717
N92-27707 # p 717
N92-27708 # p 717
N92-27709 * p 717
N92-27710 # p 717
N92-27711 # p 717
N92-27712 # p 717
N92-27713 * # p 717
N92-27714 # p 718
N92-27715 # p 771
N92-27719 # p 732
N92-27723 * # p 771
N92-27731 * # p 771
N92-27735 * # p 771
N92-27737 * # p 772
N92-27738 * # p 772
N92-27739 * # p 772
N92-27740 * # p 772
N92-27749 # p 757
N92-27750 # p 724
N92-27752 # p 757
N92-27753 # p 750
N92-27760 # p 772
N92-27788 * # p 753
N92-27789 * # p 772
N92-27792 * # p 750
N92-27794 * # p 773
N92-27799 * # p 773
N92-27800 * # p 773
N92-27801 * # p 750
N92-27802 * # p 750
N92-27803 * # p 751
N92-27804 * # p 751
N92-27817 # p 743
N92-27830 * # p 777
N92-27831 * # p 777
N92-27836 # p 751
N92-27864 # p 773
N92-27870 # p 733
N92-27879 * # p 773
N92-27880 * # p 773
N92-27886 # p 774
N92-27894 * # p 727
N92-27895 # p 727
N92-27897 # p 728
N92-27898 # p 728
N92-27901 # p 728
N92-27903 # p 778
N92-27904 # p 728
N92-27905 # p 728
N92-27906 # p 735
N92-27914 # p 724
N92-27916 # p 728
N92-27918 # p 774
N92-27924 # p 780
N92-27925 # p 735
N92-27936 # p 718
N92-27937 * # p 718
N92-27938 * # p 718
N92-27939 # p 718
N92-27940 # p 718
N92-27941 # p 719
N92-27942 # p 719
N92-27943 # p 719
N92-27944 # p 719
N92-27945 # p 719
N92-27946 # p 719
N92-27947 # p 720
N92-27948 # p 720
N92-27949 # p 720
N92-27950 # p 720
N92-27951 # p 720
N92-27952 # p 720
N92-27953 # p 720
N92-27954 # p 721
N92-27955 * # p 721
N92-27956 # p 746
N92-27957 * # p 721
N92-27958 # p 746
N92-27959 # p 721
N92-27960 * # p 721
N92-27961 # p 721
N92-27962 # p 722
N92-27964 # p 729
N92-27973 # p 736
N92-27976 * # p 751
N92-27977 * # p 751
N92-27978 * # p 751
N92-27980 # p 778
N92-27994 # p 753
N92-28004 # p 736
N92-28052 # p 724
N92-28073 # p 743
N92-28076 # p 743
N92-28079 # p 729
N92-28084 # p 774
N92-28093 # p 736
N92-28102 * # p 722
N92-28114 * # p 782
N92-28118 # p 733
N92-28123 # p 733
N92-28132 # p 729
N92-28150 * # p 778
N92-28151 # p 722
N92-28152 # p 722
N92-28153 # p 733
N92-28154 # p 746
N92-28162 # p 743
N92-28171 # p 774
N92-28183 * # p 782
N92-28190 # p 722
N92-28191 # p 733
N92-28192 # p 722
N92-28209 * # p 746
N92-28245 # p 923
N92-28248 # p 883
N92-28253 # p 907
N92-28292 # p 926
N92-28294 # p 868
N92-28302 # p 926
N92-28344 * # p 929
N92-28348 # p 786
N92-28361 * # p 907
N92-28374 * # p 895
N92-28376 # p 859
N92-28377 # p 859
N92-28379 # p 859
N92-28380 # p 859
N92-28388 # p 883
N92-28398 # p 895
N92-28407 # p 883
N92-28418 * # p 868
N92-28419 * # p 868
N92-28425 # p 908
N92-28426 # p 895
N92-28434 * # p 908
N92-28435 * # p 850
N92-28457 * # p 878
N92-28458 # p 868
N92-28459 # p 869
N92-28460 # p 869
N92-28461 # p 869
N92-28462 # p 869
N92-28463 # p 869
N92-28464 * # p 869
N92-28465 # p 869
N92-28466 * # p 870
N92-28467 # p 870
N92-28468 # p 850
N92-28469 # p 851
N92-28470 # p 851
N92-28471 # p 851
N92-28472 # p 851
N92-28473 * # p 851
N92-28474 # p 851
N92-28477 * # p 827
N92-28511 * # p 827
N92-28522 # p 786
N92-28523 # p 883
N92-28524 # p 883
N92-28525 # p 883
N92-28526 # p 884
N92-28527 # p 884
N92-28528 # p 884
N92-28530 # p 837
N92-28531 # p 852
N92-28532 # p 884
N92-28533 # p 884
N92-28535 # p 884
N92-28536 # p 884
N92-28537 # p 884
N92-28539 # p 885
N92-28540 # p 885
N92-28543 # p 885
N92-28544 # p 885
N92-28545 * # p 885
N92-28546 # p 886
N92-28547 # p 886
N92-28548 # p 886
N92-28549 # p 886
N92-28550 # p 886
N92-28551 * # p 886
N92-28552 # p 886
N92-28556 * # p 927
N92-28579 # p 887
N92-28581 # p 923
N92-28584 * # p 878
N92-28635 # p 923
N92-28644 # p 859
N92-28649 # p 852
N92-28652 # p 878
N92-28653 # p 879
N92-28654 # p 859
N92-28655 # p 837
N92-28657 # p 827
N92-28658 # p 827
N92-28659 # p 827
N92-28660 # p 828
N92-28661 # p 887
N92-28669 # p 887
N92-28673 * # p 887
N92-28674 * # p 828
N92-28686 # p 870
N92-28687 # p 852
N92-28689 # p 915
N92-28692 # p 828
N92-28694 # p 908
N92-28695 # p 927
N92-28696 * # p 828
N92-28709 # p 828
N92-28711 # p 870
N92-28712 # p 908
N92-28713 # p 829
N92-28714 # p 852
N92-28718 * # p 840
N92-28720 * # p 852
N92-28721 * # p 852
N92-28729 * p 829
N92-28771 # p 853
N92-28772 # p 887
N92-28788 # p 908
N92-28789 # p 829
N92-28801 # p 879
N92-28802 # p 853
N92-28814 # p 909
N92-28820 * # p 829
N92-28829 # p 887
N92-28833 # p 888
N92-28835 # p 888
N92-28836 # p 909
N92-28865 # p 829
N92-28879 # p 909
N92-28883 # p 829
N92-28888 # p 830
N92-28900 # p 837
N92-28901 # p 853
N92-28909 * # p 927
N92-28910 * # p 853
N92-28912 # p 895
N92-28921 # p 895
N92-28923 # p 927
N92-28926 * # p 853
N92-28980 * # p 830
N92-28985 * # p 870
N92-29095 # p 927
N92-29099 * p 909
N92-29103 * # p 841
N92-29104 * # p 890
N92-29105 * # p 909
N92-29110 * # p 853
N92-29118 # p 909
N92-29136 * # p 910
N92-29148 * p 916
N92-29159 # p 830
N92-29180 # p 854
N92-29182 # p 837
N92-29188 # p 923
N92-29191 # p 910
N92-29201 # p 927
N92-29204 # p 888
N92-29206 # p 830
N92-29218 # p 929
N92-29222 # p 859
N92-29329 * # p 830
N92-29343 * # p 890
N92-29344 # p 910
N92-29352 * # p 888
N92-29361 * # p 830
N92-29402 * # p 831
N92-29408 # p 896
N92-29417 * # p 854
N92-29425 * # p 871
N92-29427 * # p 871
N92-29445 * # p 831
N92-29505 # p 888
N92-29511 # p 854
N92-29539 # p 831
N92-29580 # p 896
N92-29603 # p 910
N92-29604 # p 924
N92-29605 # p 841
N92-29615 # p 841
N92-29616 # p 854
N92-29625 * # p 831
N92-29629 # p 890
N92-29648 # p 831
N92-29649 # p 831
N92-29650 # p 854
N92-29654 * # p 879
N92-29655 * # p 888
N92-29657 * # p 832
N92-29659 * # p 871
N92-29661 * # p 871
N92-29680 # p 890
N92-29683 # p 910
N92-29691 * # p 832
N92-29703 # p 837
N92-29709 # p 888
N92-29713 # p 832
N92-29741 # p 832
N92-29830 * # p 910
N92-29870 # p 859
N92-29873 # p 910
N92-29874 # p 787
N92-29877 # p 911

N92-29884 # p 832
N92-29889 # p 833
N92-29916 # p 833
N92-29927 # p 871
N92-29933 # p 911
N92-29954 * # p 911
N92-29997 # p 928
N92-30025 * # p 879
N92-30028 * # p 911
N92-30042 * # p 912
N92-30044 * # p 912
N92-30064 * # p 912
N92-30065 * # p 912
N92-30076 # p 889
N92-30082 * # p 912
N92-30099 * # p 912
N92-30106 * # p 912
N92-30107 * # p 913
N92-30108 * # p 837
N92-30109 * # p 913
N92-30110 * # p 913
N92-30111 * # p 913
N92-30112 * # p 913
N92-30113 * # p 914
N92-30114 * # p 914
N92-30115 * # p 914
N92-30116 * # p 914
N92-30117 * # p 914
N92-30118 * # p 914
N92-30119 * # p 914
N92-30120 * # p 915
N92-30121 * # p 915
N92-30122 * # p 787
N92-30123 * # p 838
N92-30124 * # p 838
N92-30128 * # p 838
N92-30129 * # p 838
N92-30130 * # p 838
N92-30131 * # p 838
N92-30132 * # p 915
N92-30133 * # p 838
N92-30182 * # p 833
N92-30207 * # p 924
N92-30209 * # p 854
N92-30232 # p 787
N92-30239 # p 943
N92-30253 # p 932
N92-30256 # p 986
N92-30258 # p 932
N92-30295 * # p 943
N92-30298 * # p 943
N92-30303 # p 971
N92-30304 * # p 961
N92-30307 * # p 984
N92-30321 # p 986
N92-30322 # p 1009
N92-30323 # p 978
N92-30329 # p 982
N92-30335 # p 1009
N92-30367 # p 943
N92-30380 * # p 998
N92-30390 * # p 998
N92-30392 * # p 944
N92-30393 * # p 944
N92-30394 * # p 944
N92-30395 * # p 952
N92-30396 * # p 998
N92-30414 # p 987
N92-30418 # p 952
N92-30423 # p 998
N92-30424 # p 961
N92-30439 # p 978
N92-30474 # p 952
N92-30508 * # p 982
N92-30514 # p 944
N92-30518 * # p 971
N92-30524 # p 967
N92-30547 # p 982
N92-30551 # p 952
N92-30569 * # p 971
N92-30570 * # p 944
N92-30583 # p 999
N92-30654 * # p 999
N92-30675 # p 932
N92-30676 # p 944
N92-30691 * # p 945
N92-30713 # p 945
N92-30733 * # p 1013
N92-30740 * # p 945
N92-30741 * # p 945
N92-30742 * # p 945
N92-30747 * # p 945
N92-30752 * # p 961
N92-30753 * # p 971
N92-30755 # p 999
N92-30766 # p 999
N92-30767 # p 987
N92-30768 # p 1013
N92-30769 # p 983
N92-30777 # p 983
N92-30837 # p 1004
N92-30849 # p 983
N92-30874 # p 987
N92-30878 # p 961
N92-30893 # p 999
N92-30898 * # p 1009
N92-30903 # p 1000
N92-30907 * # p 1010
N92-30909 * # p 945
N92-30922 * # p 978
N92-30923 * # p 1000
N92-30947 # p 946
N92-30954 # p 1010
N92-30957 # p 1012
N92-30965 * # p 967
N92-30969 # p 987
N92-30972 * # p 972
N92-30976 # p 983
N92-30977 * # p 946
N92-30978 * # p 957
N92-30980 # p 952
N92-30988 * # p 1000
N92-30998 * # p 972
N92-31023 * # p 1000
N92-31043 * # p 1000
N92-31059 * # p 1000
N92-31067 * # p 1001
N92-31068 * # p 1001
N92-31122 # p 946
N92-31155 * # p 1001
N92-31156 * # p 1001
N92-31157 * # p 946
N92-31159 # p 953
N92-31165 # p 961
N92-31171 # p 947
N92-31172 * # p 972
N92-31174 * # p 962
N92-31175 * # p 978
N92-31192 # p 983
N92-31193 # p 953
N92-31208 * # p 962
N92-31211 # p 953
N92-31239 * # p 947
N92-31240 * # p 979
N92-31246 * # p 947
N92-31248 * # p 1011
N92-31250 * # p 972
N92-31252 * # p 983
N92-31261 * # p 962
N92-31264 * # p 962
N92-31267 * # p 932
N92-31275 * # p 973
N92-31276 * # p 947
N92-31281 * # p 1001
N92-31300 # p 947
N92-31349 * # p 1002
N92-31350 * # p 962
N92-31351 * # p 962
N92-31360 # p 987
N92-31362 # p 1004
N92-31399 # p 987
N92-31419 # p 987
N92-31439 # p 973
N92-31453 # p 953
N92-31454 # p 1011
N92-31462 # p 988
N92-31469 # p 1002
N92-31484 * # p 1002
N92-31485 * # p 1002
N92-31498 # p 1004
N92-31508 # p 947
N92-31514 # p 948
N92-31515 # p 963
N92-31532 * # p 948
N92-31533 * # p 948
N92-31534 * # p 973
N92-31549 * # p 953
N92-31555 # p 948
N92-31615 # p 932
N92-31617 # p 1002
N92-31619 * # p 1003
N92-31622 # p 948
N92-31640 * # p 983
N92-31656 * # p 979
N92-31716 # p 988
N92-31746 # p 957
N92-31767 # p 1011
N92-31777 # p 949
N92-31793 # p 963
N92-31813 # p 953
N92-31817 # p 973
N92-31823 # p 988
N92-31824 # p 1003
N92-31838 # p 957
N92-31852 * # p 1013
N92-31853 # p 949
N92-31861 # p 932
N92-31862 # p 953
N92-31863 # p 949
N92-31864 # p 1010
N92-31865 # p 979
N92-31868 # p 968
N92-31880 # p 963
N92-31881 # p 963
N92-31886 # p 1003
N92-31888 # p 949
N92-31889 # p 949
N92-31900 * # p 984
N92-31910 * # p 973
N92-31928 # p 954
N92-31933 # p 1003
N92-31942 # p 988
N92-31943 # p 954
N92-31967 # p 979
N92-32051 # p 968
N92-32054 # p 957
N92-32059 # p 974
N92-32062 # p 949
N92-32066 # p 988
N92-32076 # p 989
N92-32103 # p 1004
N92-32111 * # p 963
N92-32114 * # p 950
N92-32147 * # p 1004
N92-32162 * # p 950
N92-32175 * # p 979
N92-32177 * # p 950
N92-32201 * # p 984
N92-32213 * # p 950
N92-32219 # p 954
N92-32226 * # p 950
N92-32228 * # p 951
N92-32229 # p 1010
N92-32240 * # p 951
N92-32241 * # p 979
N92-32265 * # p 1124
N92-32268 * # p 1124
N92-32270 * # p 1124
N92-32292 * # p 1124
N92-32338 # p 1142
N92-32422 * # p 1036
N92-32424 * # p 1047
N92-32435 # p 1086
N92-32447 # p 1064
N92-32452 * # p 1071
N92-32453 # p 1142
N92-32455 # p 1043
N92-32479 p 1036
N92-32480 * # p 1036
N92-32487 p 1086
N92-32494 * # p 1036
N92-32505 # p 1141
N92-32507 * # p 1133
N92-32513 * # p 1106
N92-32514 * # p 1107
N92-32522 * # p 1107
N92-32523 * # p 1107
N92-32525 * # p 1107
N92-32527 * # p 1107
N92-32528 * # p 1107
N92-32536 * # p 1060
N92-32537 # p 1047
N92-32575 * # p 1107
N92-32576 * # p 1108
N92-32577 * # p 1108
N92-32579 * # p 1108
N92-32586 * # p 1108
N92-32595 # p 1136
N92-32606 * # p 1043
N92-32629 # p 1108
N92-32632 # p 1124
N92-32648 * # p 1036
N92-32651 # p 1036
N92-32673 # p 1037
N92-32686 # p 1124
N92-32697 # p 1136
N92-32730 # p 1037
N92-32732 # p 1037
N92-32734 # p 1101
N92-32742 # p 1125
N92-32769 # p 1037
N92-32773 # p 1037
N92-32776 # p 1125
N92-32778 * # p 1086
N92-32780 p 1087
N92-32782 p 1037
N92-32788 * # p 1087
N92-32791 # p 1109
N92-32811 # p 1038
N92-32830 # p 1047
N92-32845 # p 1048
N92-32846 # p 1109
N92-32849 # p 1048
N92-32850 # p 1064
N92-32851 # p 1134
N92-32856 p 1125
N92-32861 # p 1048
N92-32863 * # p 1109
N92-32864 * # p 1087
N92-32865 * # p 1134
N92-32866 * # p 1065
N92-32880 * # p 1134
N92-32887 * # p 1060
N92-32900 # p 1038
N92-32903 # p 1101
N92-32941 # p 1043
N92-32948 * # p 1136
N92-32949 * # p 1136
N92-32950 * # p 1137
N92-32951 * # p 1137
N92-32952 * # p 1137
N92-32955 * # p 1137
N92-32956 * # p 1137
N92-32957 * # p 1137
N92-32958 * # p 1137
N92-32960 * # p 1137
N92-32961 * # p 1138
N92-32962 * # p 1138
N92-32963 * # p 1138
N92-32964 * # p 1125
N92-32988 # p 1087
N92-33005 # p 1043
N92-33033 # p 1109
N92-33036 # p 1109
N92-33044 # p 1109
N92-33048 # p 1110
N92-33049 # p 1110
N92-33050 # p 1110
N92-33054 * # p 1110
N92-33063 * # p 1038
N92-33066 # p 1125
N92-33080 * # p 1044
N92-33098 # p 1048
N92-33102 # p 1071
N92-33104 * # p 1125
N92-33105 # p 1071
N92-33107 * # p 1087
N92-33139 * # p 1125
N92-33147 # p 1142
N92-33149 * # p 1060
N92-33160 * # p 1138
N92-33176 # p 1017
N92-33194 * # p 1044
N92-33220 # p 1129
N92-33237 * # p 1142
N92-33238 # p 1142
N92-33249 # p 1044
N92-33271 # p 1129
N92-33277 # p 1065
N92-33288 # p 1044
N92-33304 * # p 1038
N92-33305 # p 1142
N92-33306 * # p 1038
N92-33307 * # p 1126
N92-33308 # p 1048
N92-33339 * # p 1134
N92-33340 * # p 1065
N92-33351 * # p 1049
N92-33352 * # p 1049
N92-33353 * # p 1049
N92-33354 * # p 1049
N92-33355 * # p 1049
N92-33356 * # p 1050
N92-33358 * # p 1050
N92-33381 * # p 1050
N92-33398 # p 1101
N92-33404 * # p 1060
N92-33407 * # p 1050
N92-33413 * # p 1039
N92-33414 # p 1061
N92-33423 * # p 1110
N92-33424 * # p 1039
N92-33434 # p 1101
N92-33440 p 1126
N92-33479 * # p 1072
N92-33480 # p 1126
N92-33483 * # p 1134
N92-33484 * # p 1039
N92-33498 # p 1126
N92-33499 # p 1017
N92-33501 # p 1126
N92-33502 # p 1061
N92-33536 * # p 1088
N92-33537 * # p 1088
N92-33538 # p 1127
N92-33581 * # p 1039
N92-33582 p 1061
N92-33585 p 1061
N92-33596 # p 1050
N92-33609 * # p 1051
N92-33613 * # p 1110
N92-33618 * # p 1040
N92-33624 # p 1111
N92-33625 * # p 1040
N92-33627 # p 1127
N92-33631 * # p 1040
N92-33645 # p 1072
N92-33656 * # p 1040
N92-33678 # p 1040
N92-33693 # p 1051
N92-33694 # p 1143
N92-33696 * # p 1127
N92-33699 # p 1041
N92-33706 * # p 1041
N92-33719 * # p 1138
N92-33743 # p 1138
N92-33746 * # p 1072
N92-33748 # p 1072
N92-33749 # p 1072
N92-33750 # p 1061
N92-33751 # p 1129
N92-33763 # p 1105
N92-33794 # p 1129
N92-33809 # p 1051
N92-33815 # p 1072
N92-33826 * # p 1101
N92-33837 p 1041
N92-33839 p 1041
N92-33851 p 1041
N92-33874 * # p 1061
N92-33876 * # p 1138
N92-33877 * # p 1139
N92-33878 * # p 1139
N92-33879 * # p 1139
N92-33880 * # p 1139
N92-33881 * # p 1139
N92-33882 * # p 1140
N92-33883 * # p 1140
N92-33884 * # p 1140
N92-33885 * # p 1140
N92-33894 * # p 1134
N92-33916 # p 1127
N92-33920 # p 1135
N92-33948 * # p 1143
N92-33952 p 1061
N92-33953 p 1062
N92-33968 p 1127
N92-33994 # p 1111
N92-34017 * # p 1128
N92-34019 # p 1111
N92-34029 p 1042
N92-34036 p 1128
N92-34039 * # p 1062
N92-34043 * # p 1128
N92-34081 # p 1044
N92-34105 * # p 1044
N92-34107 * # p 1088
N92-34109 * # p 1065
N92-34112 * # p 1128
N92-34131 # p 1088
N92-34141 * # p 1102
N92-34144 * # p 1042
N92-34147 * # p 1042
N92-34148 * # p 1140
N92-34151 # p 1045
N92-34161 # p 1088
N92-34162 # p 1088
N92-34163 # p 1089
N92-34164 # p 1089
N92-34165 # p 1089
N92-34166 # p 1089
N92-34167 # p 1089
N92-34168 # p 1089
N92-34169 # p 1089
N92-34172 * p 1042
N92-34178 * # p 1128
N92-34182 # p 1062
N92-34192 * # p 1045
N92-34193 * # p 1042
N92-34202 * # p 1062
N92-34203 * # p 1051
N92-34207 * # p 1128
N92-34213 * # p 1102
N92-34222 * # p 1102
N92-34236 * # p 1073
N92-34243 * # p 1043
N92-34247 # p 1102

SPECIAL NOTICE

The abstract sections of the monthly supplements of *Aeronautical Engineering* can be bound separately. Individual abstracts can be located readily by means of the page numbers given at each entry, e.g., p 309 A92-24412. To assist the user in binding Supplements SP-7037(275) through SP-7037(286), a title page is included in this Cumulative Index.

AERONAUTICAL ENGINEERING

A CONTINUING BIBLIOGRAPHY

Abstracts
January — December 1992

TABLE OF CONTENTS

SP-7037 Supplement	*Page*
275	1
276	59
277	169
278	241
279	307
280	419
281	515
282	607
283	699
284	783
285	931
286	1015

1. Report No.	2. Government Accession No.	3. Recipient's Catalog No.
NASA SP-7037 (287)		

4. Title and Subtitle	5. Report Date
AERONAUTICAL ENGINEERING A Cumulative Index to the 1992 Issues	February 1993
	6. Performing Organization Code JTT
7. Author(s)	8. Performing Organization Report No.
	10. Work Unit No.
9. Performing Organization Name and Address NASA Scientific and Technical Information Program	11. Contract or Grant No.
	13. Type of Report and Period Covered Special Publication
12. Sponsoring Agency Name and Address National Aeronautics and Space Administration Washington, DC 20546-0001	14. Sponsoring Agency Code

15. Supplementary Notes

16. Abstract

This is a cumulative index to the abstracts contained in NASA SP-7037 (275) through NASA SP-7037 (286) of Aeronautical Engineering: A Continuing Bibliography. NASA SP-7037 and its supplements have been compiled through the cooperative efforts of the American Institute of Aeronautics and Astronautics (AIAA) and the National Aeronautics and Space Administration (NASA). This cumulative index includes subject, personal author, corporate source, foreign technology, contract number, report number, and accession number indexes.

17. Key Words (Suggested by Authors(s))	18. Distribution Statement
Aerodynamics Aeronautical Engineering Aeronautics Bibliographies	Unclassified - Unlimited Subject Category - 01

19. Security Classif. (of this report)	20. Security Classif. (of this page)	21. No. of Pages	22. Price
Unclassified	Unclassified	700	A99 HC

NASA-Langley, 1993

FEDERAL REGIONAL DEPOSITORY LIBRARIES

ALABAMA

AUBURN UNIV. AT MONTGOMERY LIBRARY
Documents Dept.
7300 University Drive
Montgomery, AL 36117-3596
(205) 244-3650 FAX: (205) 244-0678

UNIV. OF ALABAMA
Amelia Gayle Gorgas Library
Govt. Documents
Box 870266
Tuscaloosa, AL 35487-0266
(205) 348-6046 FAX: (205) 348-8833

ARIZONA

DEPT. OF LIBRARY, ARCHIVES, AND PUBLIC RECORDS
Federal Documents
Third Floor State Capitol
1700 West Washington
Phoenix, AZ 85007
(602) 542-4121 FAX: (602) 542-4400; 542-4500

ARKANSAS

ARKANSAS STATE LIBRARY
State Library Services
One Capitol Mall
Little Rock, AR 72201
(501) 682-2869

CALIFORNIA

CALIFORNIA STATE LIBRARY
Govt. Publications Section
914 Capitol Mall - P.O. Box 942837
Sacramento, CA 94237-0001
(916) 322-4572 FAX: (916) 324-8120

COLORADO

UNIV. OF COLORADO - BOULDER
Norlin Library
Govt. Publications
Campus Box 184
Boulder, CO 80309-0184
(303) 492-8834 FAX: (303) 492-2185

DENVER PUBLIC LIBRARY
Govt. Publications Dept. BS/GPD
1357 Broadway
Denver, CO 80203
(303) 571-2135

CONNECTICUT

CONNECTICUT STATE LIBRARY
231 Capitol Avenue
Hartford, CT 06106
(203) 566-4971 FAX: (203) 566-3322

FLORIDA

UNIV. OF FLORIDA LIBRARIES
Documents Dept.
Library West
Gainesville, FL 32611-2048
(904) 392-0366 FAX: (904) 392-7251

GEORGIA

UNIV. OF GEORGIA LIBRARIES
Govt. Documents Dept.
Jackson Street
Athens, GA 30602
(404) 542-8949 FAX: (404) 542-6522

HAWAII

UNIV. OF HAWAII
Hamilton Library
Govt. Documents Collection
2550 The Mall
Honolulu, HI 96822
(808) 948-8230 FAX: (808) 956-5968

IDAHO

UNIV. OF IDAHO LIBRARY
Documents Section
Moscow, ID 83843
(208) 885-6344 FAX: (208) 885-6817

ILLINOIS

ILLINOIS STATE LIBRARY
Reference Dept.
300 South Second
Springfield, IL 62701-1796
(217) 782-7596 FAX: (217) 524-0041

INDIANA

INDIANA STATE LIBRARY
Serials/Documents Section
140 North Senate Avenue
Indianapolis, IN 46204
(317) 232-3678 FAX: (317) 232-3728

IOWA

UNIV. OF IOWA LIBRARIES
Govt. Publications Dept.
Washington & Madison Streets
Iowa City, IA 52242
(319) 335-5926 FAX: (319) 335-5830

KANSAS

UNIV. OF KANSAS
Govt. Documents & Map Library
6001 Malatt Hall
Lawrence, KS 66045-2800
(913) 864-4660 FAX: (913) 864-5380

KENTUCKY

UNIV. OF KENTUCKY LIBRARIES
Govt. Publications/Maps Dept.
Lexington, KY 40506-0039
(606) 257-3139 FAX: (606) 257-1563; 257-8379

LOUISIANA

LOUISIANA STATE UNIV.
Middleton Library
Govt. Documents Dept.
Baton Rouge, LA 70803
(504) 388-2570 FAX: (504) 388-6992

LOUISIANA TECHNICAL UNIV.
Prescott Memorial Library
Govt. Documents Dept.
305 Wisteria Street
Ruston, LA 71270-9985
(318) 257-4962 FAX: (318) 257-2447

MAINE

TRI-STATE DOCUMENTS DEPOSITORY
Raymond H. Fogler Library
Govt. Documents & Microforms Dept.
Univ. of Maine
Orono, ME 04469
(207) 581-1680

MARYLAND

UNIV. OF MARYLAND
Hornbake Library
Govt. Documents/Maps Unit
College Park, MD 20742
(301) 454-3034 FAX: (301) 454-4985

MASSACHUSETTS

BOSTON PUBLIC LIBRARY
Govt. Documents Dept.
666 Boylston Street
Boston, MA 02117
(617) 536-5400 ext. 226
FAX: (617) 267-8273; 267-8248

MICHIGAN

DETROIT PUBLIC LIBRARY
5201 Woodward Avenue
Detroit, MI 48202-4093
(313) 833-1440; 833-1409
FAX: (313) 833-5039

LIBRARY OF MICHIGAN
Govt. Documents Unit
P.O. Box 30007
Lansing, MI 48909
(517) 373-0640 FAX: (517) 373-3381

MINNESOTA

UNIV. OF MINNESOTA
Wilson Library
Govt. Publications Library
309 19th Avenue South
Minneapolis, MN 55455
(612) 624-5073 FAX: (612) 626-9353

MISSISSIPPI

UNIV. OF MISSISSIPPI
J.D. Williams Library
Federal Documents Dept.
106 Old Gym Bldg.
University, MS 38677
(601) 232-5857 FAX: (601) 232-5453

MISSOURI

UNIV. OF MISSOURI - COLUMBIA
Ellis Library
Govt. Documents
Columbia, MO 65201
(314) 882-6733 FAX: (314) 882-8044

MONTANA

UNIV. OF MONTANA
Maureen & Mike Mansfield Library
Documents Div.
Missoula, MT 59812-1195
(406) 243-6700 FAX: (406) 243-2060

NEBRASKA

UNIV. OF NEBRASKA - LINCOLN
D.L. Love Memorial Library
Documents Dept.
Lincoln, NE 68588
(402) 472-2562

NEVADA

UNIV. OF NEVADA
Reno Library
Govt. Publications Dept.
Reno, NV 89557
(702) 784-6579 FAX: (702) 784-1751

NEW JERSEY

NEWARK PUBLIC LIBRARY
U.S. Documents Div.
5 Washington Street - P.O. Box 630
Newark, NJ 07101-0630
(201) 733-7812 FAX: (201) 733-5648

NEW MEXICO

UNIV. OF NEW MEXICO
General Library
Govt. Publications Dept.
Albuquerque, NM 87131-1466
(505) 277-5441 FAX: (505) 277-6019

NEW MEXICO STATE LIBRARY
325 Don Gaspar Avenue
Santa Fe, NM 87503
(505) 827-3826 FAX: (505) 827-3820

NEW YORK

NEW YORK STATE LIBRARY
Documents/Gift & Exchange Section
Federal Depository Program
Cultural Education Center
Albany, NY 12230
(518) 474-5563 FAX: (518) 474-5786

NORTH CAROLINA

UNIV. OF NORTH CAROLINA - CHAPEL HILL
CB#3912, Davis Library
BA/SS Dept.—Documents
Chapel Hill, NC 27599
(919) 962-1151 FAX: (919) 962-0484

NORTH DAKOTA

NORTH DAKOTA STATE UNIV. LIBRARY
Documents Office
Fargo, ND 58105
(701) 237-8886 FAX: (701) 237-7138
In cooperation with Univ. of North Dakota, Chester Fritz Library Grand Forks

OHIO

STATE LIBRARY OF OHIO
Documents Dept.
65 South Front Street
Columbus, OH 43266
(614) 644-7051 FAX: (614) 752-9178

OKLAHOMA

OKLAHOMA DEPT. OF LIBRARIES
U.S. Govt. Information Div.
200 NE 18th Street
Oklahoma City, OK 73105-3298
(405) 521-2502, ext. 252, 253
FAX: (405) 525-7804

OKLAHOMA STATE UNIV.
Edmon Low Library
Documents Dept.
Stillwater, OK 74078
(405) 744-6546 FAX: (405) 744-5183

OREGON

PORTLAND STATE UNIV.
Millar Library
934 SW Harrison - P.O. Box 1151
Portland, OR 97207
(503) 725-3673 FAX: (503) 725-4527

PENNSYLVANIA

STATE LIBRARY OF PENN.
Govt. Publications Section
Walnut St. & Commonwealth Ave. - P.O. Box 1601
Harrisburg, PA 17105
(717) 787-3752

SOUTH CAROLINA

CLEMSON UNIV.
Cooper Library
Public Documents Unit
Clemson, SC 29634-3001
(803) 656-5174 FAX: (803) 656-3025
In cooperation with Univ. of South Carolina, Thomas Cooper Library, Columbia

TENNESSEE

MEMPHIS STATE UNIV. LIBRARIES
Govt. Documents
Memphis, TN 38152
(901) 678-2586 FAX: (901) 678-2511

TEXAS

TEXAS STATE LIBRARY
United States Documents
P.O. Box 12927 - 1201 Brazos
Austin, TX 78711
(512) 463-5455 FAX: (512) 463-5436

TEXAS TECH. UNIV. LIBRARY
Documents Dept.
Lubbock, TX 79409
(806) 742-2268 FAX: (806) 742-1920

UTAH

UTAH STATE UNIV.
Merrill Library & Learning Resources Center, UMC-3000
Documents Dept.
Logan, UT 84322-3000
(801) 750-2684 FAX: (801) 750-2677

VIRGINIA

UNIV. OF VIRGINIA
Alderman Library
Govt. Documents
Charlottesville, VA 22903-2498
(804) 924-3133 FAX: (804) 924-4337

WASHINGTON

WASHINGTON STATE LIBRARY
Document Section
MS AJ-11
Olympia, WA 98504-0111
(206) 753-4027 FAX: (206) 753-3546

WEST VIRGINIA

WEST VIRGINIA UNIV. LIBRARY
Govt. Documents Section
P.O. Box 6069
Morgantown, WV 26506
(304) 293-3640

WISCONSIN

ST. HIST. SOC. OF WISCONSIN LIBRARY
Govt. Publications Section
816 State Street
Madison, WI 53706
(608) 262-2781 FAX: (608) 262-4711
In cooperation with Univ. of Wisconsin-Madison, Memorial Library

MILWAUKEE PUBLIC LIBRARY
Documents Div.
814 West Wisconsin Avenue
Milwaukee, WI 53233
(414) 278-2167 FAX: (414) 278-2137

National Aeronautics and
Space Administration
Code JTT
Washington DC 20546

Official Business
Penalty for Private Use, $300

FOURTH CLASS

SPECIAL FOURTH-CLASS RATE
POSTAGE & FEES PAID
NASA
PERMIT No. G27

L1 001 SP7037-28793021 2S090569A
NASA
CENTER FOR AEROSPACE INFORMATION
ACCESSIONING
P O BOX 8757 BWI ARPRT
BALTIMORE MD 21240

NASA

POSTMASTER: If Undeliverable (Section 158 Postal Manual) Do Not Return